SPRINGER
REFERENCE

Hans Gerhard Vogel
Editor

VOLUME 1

Drug Discovery and Evaluation: Pharmacological Assays

3rd Edition

Springer

Drug Discovery and Evaluation: Pharmacological Assays

H. Gerhard Vogel (Ed.)

Drug Discovery and Evaluation: Pharmacological Assays

Third Completely Revised, Updated and Enlarged Edition

With 5 Figures and 66 Tables

Springer

Hans Gerhard Vogel
Bohl Str. 28
73430 Aalen
Germany

ISBN: 978-3-540-70995-4

This publication is available also as:
Print publication under ISBN 978-3-540-71420-0 and
Print and electronic bundle under ISBN 978-3-540-71419-4

Library of Congress Control Number: 2007936031

Springer is part of Springer Science+Business Media

springer.com

Printed on acid-free paper SPIN: 11733775 2109 - 5 4 3 2 1 0

Preface to the Third Edition

The third edition of the book *Drug Discovery and Evaluation. Pharmacological Assays* is presented here.

The volume of data has risen considerably compared to the second edition. In particular, a large number of assays have been added. Meanwhile, data on Safety Pharmacology have been removed from this edition. An extended discussion of that important aspect of pharmacology was published in the book *Drug Discovery and Evaluation. Safety and Pharmacokinetic Assays*, edited by H. G. Vogel, F. J. Hock, J. Maas, and D. Mayer, by Springer in 2006.

Several of my colleagues provided essential contributions to this edition. In particular I am indebted to S. A. Mousa for rewriting the chapter Pharmacological Assays in Thrombosis and Hemostasis, S. G. E. Hart, for rewriting the chapter Activity on Urinary Tract, G. Müller for rewriting and amending the chapter Antidiabetic Activity, B. Schultz for amending the chapter Ophthalmologic Activity, and J. Sandow for rewriting the chapter Endocrinology. All chapters have been revised and thoroughly updated as well.

The approach to drug discovery is changing continuously. Decades ago, many drugs were found by serendipity in clinical trials. Most new drugs, however, were found by the classical approach in animal experiments. This approach has the advantage of relatively high predictability, but it also has the disadvantage that little information is provided about the molecular mechanisms involved in the observed effects, and the detection of drugs with new mechanisms always required new models.

It is generally believed that the costs of developing new pharmaceutical drugs are exploding, while the output of new drugs is actually decreasing. A change in paradigm, the *target-based or mechanism-based drug discovery approach*, was therefore welcomed with great enthusiasm. The techniques of combinatorial chemistry could generate thousands of compounds to be tested against thousands of targets using high-throughput and ultra-high-throughput technology with tremendous capacity. This made it highly effective for the identification of target-selective compounds. However, despite the fact that this approach is very advantageous from a scientific and practical viewpoint, it did not translate into a high success rate in the discovery of new drugs. This has naturally led to questions regarding the success of target-based drug discovery and, more importantly, a search for alternatives.

The target-based approach has therefore been replaced again by the *physiology-based approach*, the classical drug discovery paradigm, or the *function-based approach*, which seeks to induce a therapeutic effect by normalizing a disease-specific abnormality.

On top of this, important changes in the management of some of the larger drug companies have taken place in recent years. Modern managers were installed as chief executive officers and other high-level executives, quite often with little or no biological and technical experience. They were more interested in blockbusters

and in shareholders' value than finding new drugs, especially for rare diseases. Research workers were confronted with cumbersome and inflexible organizational structures characterized by regimentation, control, conformity, and excessive bureaucracy. Consequently, creativity and productivity decreased in this environment. Recently, however, there are signs that the situation is changing.

In this book we ask the question: "Quo vadis, pharmacology?" We suggest giving pharmacologists the freedom, time, and money to carry out their own ideas. We also describe animal models of rare diseases that enable the medically trained pharmacologist to find appropriate drugs.

We are well aware that the rapid progress in biology will once again change the methodological approach in the coming years, and that electronic media will continuously help the researcher to access and share information. However, it is becoming more and more evident that many young pharmacologists have only limited training in classical pharmacological methodologies. When searching for these methods, researchers will only find insufficient information on the methodological details in the electronic databases currently available. To this end, we hope the current book may bridge this gap by comprehensively covering those pharmacological methods utilized for over more than a hundred years.

At this point I would like to express my sincere thanks to all colleagues who contributed to the new and to the earlier editions of this book. Their names and affiliations are given in alphabetical order.

Spring 2007 *H. Gerhard Vogel*

Preface to the Second Edition

The first edition of "Drug Discovery and Evaluation – Pharmacological Assays" has been well accepted by a broad readership ranging from experienced pharmacologists to students of pharmacology. Therefore, already after a short period of time the question for a second edition arose.

The first edition was mainly centered around the personal laboratory experience of the editors and the contributors. The second edition tries to close evident gaps. The input of biochemistry to pharmacology has grown. Molecular pharmacology puts more emphasis on the mode of action of drugs, albeit it becomes clear that the activities of most drugs are not confined to one single mode of action. Studies in single cells become more and more popular, however, they do not cover the complexity of a whole organism. Possible side effects of drugs can be better detected in whole animals than in single cells. Therefore, the new requirements of the health authorities on safety pharmacology put emphasis on experiments not only in whole anesthetized animals but in conscious ones. The second edition of this book takes note of these requirements and devotes special chapters for each indication to safety pharmacology.

Molecular biology also introduced new methods to pharmacology, such as the polymerase chain reaction (PCR), reverse PCR, Northern, Western and Southern blotting. Very recently, microarray technology, proteomics, and mass spectroscopy were added as novel in vitro methods. Furthermore, genetically modified animals have been created which resemble human diseases. Pharmacogenomics has already begun to influence pharmacology and even will have greater input in the future. Special attention is given to these new achievements in various chapters of the book.

The editor and the co-editors are well aware that the rapid progress in biology during the next decades will change the methodological approach. Electronic media will help the researcher for continuous information. However, it becomes more and more evident, that young pharmacologists have only insufficient training in the classical pharmacological methodology. Searching for these methods, e.g., for safety pharmacology, the researchers cannot find sufficient information on the methodological details in the electronic data bases currently available. This hook covering the pharmacological methods of more than hundred years may be of help.

The guidelines concerning the care and use of laboratory animals have been updated.

A change in paradigm of pharmacological research has been claimed but superiorities of these new approaches compared to the old ones have still to be proven. To address this, an introductory chapter on new strategies in drug discovery and evaluation has been added, including combinatorial chemistry; high throughput screening, ultrahigh throughput screening and high content screening; pharmacogenomics, proteomics and array technology. Some critical thoughts on errors in screening procedures have been added.

At this place, we would like to express our sincere thanks to all colleagues who contributed to the new and to the first edition of this book. Their names and their positions are given alphabetically.

March 2002

H. Gerhard Vogel
Also in the name of the co-editors

Preface to the First Edition

This hook is intended to be an aid for experienced pharmacologists as well as for newcomers in the field of experimental pharmacology. The student in pharmacology, the pharmacist and the medicinal chemist will find a survey of pharmacological assays that can be used for a given indication and for which methods have demonstrated their relevance. The researchers working in special fields of pharmacology will find assays in other, unfamiliar areas which might help to expand their own research.

Certain therapeutic domains, such as cardiovascular, respiratory and renal disorders, psychiatry and neurology, peripheral nerve function, pain and rheumatic diseases, metabolic and endocrine diseases including diseases of the gastrointestinal tract, are discussed in this hook.

Each chapter is divided into pharmacological classes, e.g., anxiolytics, antiepileptics, neuroleptics, antidepressants, or anti-Parkinson drugs. For each class, in vitro methods, tests on isolated organs and in vivo methods are described.

For each method the purpose and rationale are given first, followed by a description of the procedure, evaluation of the data, modifications of the method described in the literature, and the relevant references. If possible, a critical assessment of the method based on personal experience is added. The hints for modifications of the method and the extended reference list will be of value for the experienced pharmacologist.

A few words for the justification for a book of this kind: In 1959, A.J. Lehman, Director of the Division of Pharmacology at the Food and Drug Administration, USA, wrote:

> ... Pharmacologists are individualists. Like most scientists they are seldom willing to copy each other's techniques in detail, and so their methods vary from one to the other. Nevertheless, there are basic principles and techniques which must be applied to establish the safety of a new drug.

Visitors could also read a sticker in his office:

> You too can learn pharmacology, in only three lessons: each of them lasting ten years.

Pharmacologists have always used methods from neighboring disciplines; in the past, e.g. from anatomy, pathology, surgery, zoology and predominantly physiology. Useful methods also came from electrophysiology and the behavioral sciences. Earlier drug discovery was almost exclusively based on animal experiments, clinical observations and serendipity.

In recent years, a major input has come from biochemistry. The effect of many drugs in human therapy could be explained biochemicaly as effects on specific enzymes or receptors. With the detection of more and more receptor subtypes, the

activity spectrum of a single compound became more and more complicated. At present, molecular biology provides pharmacologists with human receptors and ion channels expressed in mammalian cells in culture. This avoids the apparently existing species differences, hut the multitude of natural and perhaps artificial subtypes raises the question of physiological and pathological relevance.

The challenge for the pharmacologist always will be to correlate in vitro data with in vivo findings, bearing in mind the old saying: "*In vitro simplicitas, in vivo veritas*". The effects found in tissue cultures are quite often not typical for an intact organism.

Pharmacologists, especially in industry, have the task to find new drugs for human therapy by using appropriate models. Pharmacological models have to be relevant, that means they should predict the intended therapeutic indications. A pharmacological model can be considered relevant or correlational, if the effects obtained correlate with results observed in human therapy.

To be relevant or "correlational", a model has to fulfill some basic criteria:

- First, the model must be sensitive in a dose-dependent fashion to standard compounds that are known to possess the desired therapeutic property.
- Second, the relative potency of known active agents in the model should be comparable to their relative potency in clinical use.
- Third, the model should be selective, i.e. the effects of known agents in this therapeutic indication should be distinguishable from effects of drugs for other indications. Positive data with a new compound allow the prediction of a therapeutic effect in patients.

If new assays are applied to indications for which no effective drug is known, there must be sufficient evidence that this model is relevant for the pathological status in this indication.

The methods presented in this book have been selected according to these criteria.

Considerable discussion is going on about the necessity of animal experiments. One has to accept that only the whole animal can reflect the complexity of a human being. Even an experiment with human volunteers is only a model, albeit a highly relevant one, to investigate therapeutic effects in patients. The degree of relevance increases from isolated molecules (e.g. receptors or enzymes) to organelles, to organs up to conscious animals and human volunteers.

Without any doubt, animal experiments are necessary for the discovery and evaluation of drugs. However, they should be performed only if they are necessary and well conceived.

In Chapter N, regulations existing in various countries concerning the care and use of laboratory animals are listed. Furthermore, guidelines for anesthesia, blood collection and euthanasia in laboratory animals are given. In carrying out animal experiments, one must adhere strictly to these guidelines. Following these rules and planing the experiments well, will eliminate or minimize pain and discomfort to the animal. The methods described in this hook had the welfare of the animals as well as the benefit of the procedure for the well-being of mankind in mind.

Here, we would like to express our sincere thanks to all colleagues who contributed to this book. Their names and positions are given alphabetically below.

Autumn 1996

H. Gerhard Vogel,
Wolfgang H. Vogel

Contents

Volume 1

Volume 2

Contributors

Editor

Prof. emer. Dr. Dr. H. Gerhard Vogel,
Johann Wolfgang Goethe Universität,
Frankfurt,
Germany

Contributors to the third edition

Albus, Udo,
Sanofi-Aventis Pharma Research,
65926 Frankfurt,
Germany

Bickel, Martin,
Sanofi-Aventis Pharma Research,
Metabolism Research,
65926 Frankfurt,
Germany

Gögelein, Heinz,
Sanofi-Aventis Pharma Research,
Cardiovascular Research,
65926 Frankfurt,
Germany

Hart, Susan G. Emeigh,
Genaera Corporation,
5110 Campus Drive Plymouth Meeting,
PA 19462,
USA

Herling, Andreas W.,
Sanofi-Aventis Pharma Research,
Metabolism Research,
65926 Frankfurt,
Germany

Huwiler, Andrea,
Institute of Pharmacology University of Bern,
Friedbühlstrasse 49,
3010 Bern,
Switzerland

Juretschke, Paul,
Sanofi-Aventis Pharma Research,
65926 Frankfurt,
Germany

Mousa, Shaker A.,
The Pharmaceutical Research Institute at Albany,
Albany College of Pharmacy,
106 New Scotland Avenue,
Albany,
NY 12208,
USA

Müller, Günter,
Sanofi-Aventis Pharma Research,
Metabolism Research,
65926 Frankfurt,
Germany

Sandow, Jürgen,
Sanofi-Aventis Pharma Research,
Metabolism Research,
65926 Frankfurt,
Germany

Schäfer, Hans-Ludwig,
Sanofi-Aventis Pharma Research,
Metabolism Research,
65926 Frankfurt,
Germany

Schultz, Beth,
College of Optometry Philadelphia,
60 Tennis Ave Ambler,
PA 19002,
USA

Vogel, Wolfgang F.,
Department of Laboratory Medicine and Pathobiology,
Faculty of Medicine,
University of Toronto,
Canada

Vogel, Wolfgang H.,
Jefferson Medical College,
Thomas Jefferson University,
Department of Pharmacology,
Philadelphia,
USA

Wirth, Klaus J.,
Sanofi-Aventis Pharma Research,
Cardiovascular Research,
65926 Frankfurt,
Germany

Contributors to the second edition

Albus, Udo,
Aventis Pharma Research,
65926 Frankfurt,
Germany

Bickel, Martin,
Aventis Pharma Research,
Metabolism Research,
65926 Frankfurt,
Germany

Bleich, Markus,
Aventis Pharma Research,
Cardiovascular Research,
65926 Frankfurt,
Germany

Dere, Ekrem,
Institute of Physiological Psychology,
Heinrich Heine Universität Düsseldorf,
Germany

Gögelein, Heinz,
Aventis Pharma Research,
Cardiovascular Research,
65926 Frankfurt,
Germany

Herling, Andreas W.,
Aventis Pharma Research,
Metabolism Research,
65926 Frankfurt,
Germany

Hropot, Max,
Aventis Pharma Research,
Cardiovascular Research,
65926 Frankfurt,
Germany

Laux, Volker,
Aventis Pharma Research,
Cardiovascular Research,
65926 Frankfurt,
Germany

Just, Melitta,
Aventis Pharma Research,
Cardiovascular Research,
65926 Frankfurt,
Germany

Müller, Günter,
Aventis Pharma Research,
Metabolism Research,
65926 Frankfurt,
Germany

Rieß, Günther,
Aventis Pharma Research,
65926 Frankfurt,
Germany

Sandow, Jürgen,
Aventis Pharma Research,
Metabolism Research,
65926 Frankfurt,
Germany

Schäfer, Hans-Ludwig,
Aventis Pharma Research,
Metabolism Research,
65926 Frankfurt,
Germany

Vogel, Wolfgang F.,
Assistant Professor,
Department of Laboratory Medicine and Pathobiology,
Faculty of Medicine,
University of Toronto,
Canada

Vogel, Wolfgang H.,
Jefferson Medical College,
Thomas Jefferson University,
Department of Pharmacology,
Philadelphia,
USA

Wirth, Klaus J.,
Aventis Pharma Research,
Cardiovascular Research,
65926 Frankfurt,
Germany

Contributors to the first edition

Albus, Udo,
Hoechst-Marion-Roussel,
Cardiovascular Research,
65926 Frankfurt,
Germany

Bartlett, Robert R.,
Hoechst-Marion-Roussel,
Immunopharmacology,
65174 Wiesbaden,
Germany

Bickel, Martin,
Hoechst-Marion-Roussel,
Metabolism Research,
65926 Frankfurt,
Germany

Brioni, Jorge D.,
Abbott Laboratories,
Neuroscience Research,
Abbott Park,
IL 60064,
USA

Gögelein, Heinz,
Hoechst-Marion-Roussel,
Cardiovascular Research,
65926 Frankfurt,
Germany

Greger, R.,
Institute of Physiology,
University of Freiburg,
79104 Freiburg,
Germany

Herling, Andreas W.,
Hoechst-Marion-Roussel,
Metabolism Research,
65926 Frankfurt,
Germany

Hock, Franz Jakob,
Hoechst-Marion-Roussel,
General Pharmacology,
65926 Frankfurt,
Germany

Hropot, Max,
Hoechst-Marion-Roussel,
Cardiovascular Research,
65926 Frankfurt,
Germany

Huger, Francis P.,
Hoechst-Marion-Roussel,
Neuroscience Research,
Sommerville,
NJ,
USA

Jablonka, Bernd,
Hoechst-Marion-Roussel,
Cardiovascular Research,
65926 Frankfurt,
Germany

Just, Melitta,
Hoechst-Marion-Roussel,
Cardiovascular Research,
65926 Frankfurt,
Germany

Linz, Wolfgang,
Hoechst-Marion-Roussel,
Cardiovascular Research,
65926 Frankfurt,
Germany

Maas, Jochen,
Hoechst-Marion-Roussel,
Preclinical Development,
65926 Frankfurt,
Germany

McGaugh, James L.,
University of California at Irvine,
Irvine,
CA 92717,
USA

Müller, Günter,
Hoechst-Marion-Roussel,
Metabolism Research,
65926 Frankfurt,
Germany

Raiss, Ruth X.,
Hoechst-Marion-Roussel,
Osteoarthritis Research,
65174 Wiesbaden,
Germany

v. Rechenberg, Wolfrad,
Hoechst-Marion-Roussel,
Metabolism Research,
65926 Frankfurt,
Germany

Rudolphi, Karl A.,
Hoechst-Marion-Roussel,
Cardiovascular Research,
65926 Frankfurt,
Germany

Schölkens, Bernward A.,
Hoechst-Marion-Roussel,
Cardiovascular Research,
65926 Frankfurt,
Germany

Seeger, Karl,
Hoechst-Marion-Roussel,
Pharma Research,
65926 Frankfurt,
Germany

Weithmann, K.U.,
Hoechst-Marion-Roussel,
Immunopharmacology,
65174 Wiesbaden,
Germany

Wirth, Klaus J.,
Hoechst-Marion-Roussel,
Cardiovascular Research,
65926 Frankfurt,
Germany

Introduction
Strategies in Drug Discovery and Evaluation[1]

0.1 Historical Approaches in Drug Discovery

Today's medicine is based on traditional medicine. Traditional medicines exist in every continent of the globe and in every cultural area of the world. The most famous ones are traditional Chinese medicine in East Asia, Ayurvedic medicine in India, and formerly Galenic medicine in Europe, all of which have some resemblance to one other (Vogel 1991).

Each of these traditional medicines has its own origins and an individual basic philosophy. The art of practicing **Chinese medicine** stretches back over several thousand years. The legendary culture hero, Shen-nong, is said to have tested many herbs for their medical properties. *Pen-ts'ao*, the first compilation of herbal medicines, is connected with his name (Unschuld 1973, 1986). Since Ancient times, the Chinese have divided the world into five symbolic elements: Wood, Fire, Earth, Metal and Water. Everything in the world is dominated by one of these elements, and their constant interplay, combined with those of yin and yang, explain all change and activity in nature. The positive, generative cycle proceeds as follows: Wood burns to generate Fire; Fire produces ashes which generate Earth; Earth generates Metal, which can be mined from the ground; when heated Metal becomes molten like Water; Water promotes the growth of plants, thereby generating Wood. The negative subjugable cycle is complementary to the positive, generative one. Chinese medical views regarding the vital internal organs are based on the theories of *yin* and *yang*, the five elements (which are each related to body organs and colors), and the meridians. With medicines consisting mainly of herbal drugs and minerals, Chinese doctors manipulate these natural relationships to adjust energy imbalances caused by the excess or deficiency of these forces in the body. Chinese physicians and philosophers developed a special system of physiology describing vital organs as storage houses and vital connections as meridians that became the basis of acupuncture (Porkert 1973).

In India *Ayurveda*, *Siddha* and *Unani* systems of medicine provide healthcare for a large part of the population. The word **Ayurveda** is composed of two parts: Ayu (= life) and Veda (= knowledge). Scholars of Ayurveda had placed the origins of this science of life at some time around 6000 BC. They were orally transmitted by successive generations. The principles were recorded in great detail in compendia, which are called *Samhitas* (Dash and Junius 1987; Da-

[1] With contributions by P. Juretschke, W.F. Vogel, and G. Riess.

hanukar and Thatte 1989; Mazars 1994). Compared with modern anatomy and physiology Ayurveda is based on certain fundamental doctrines, known as the *Darshanas*, such as the seven *Dhatus*. They can be described not exactly as organs but as body constituents. The three *Doshas: vata*, *pitta* and *kapha* are regulators of cell function in various ways. A balance of the three doshas is essential for maintaining health. Imbalance of the doshas creates disease. Drug therapy in Ayurveda is highly individualized. The choice of drugs as well as the dose is not only influenced by the disease process, but also by the constitution of individuals and environmental conditions which affect the balance of the doshas and therefore the response to drugs.

Both traditional Chinese and Ayurvedic medicine developed further in terms of formulations. There is also the tendency to adopt the modern forms of clinical trials, but there has never been a change in paradigm as far as the basic philosophy is concerned.

Traditional European medicine goes back to the time of Egyptian and Babylonian-Assyrian culture. About 3000 BC the Sumerians developed a system of cuneiform writing that enabled them to write on clay tablets. At the time of King Assurbanipal 2000 BC a first comprehensive Materia Medica was written containing approximately 250 vegetable drugs and 120 mineral drugs (Koecher 1963). Around 1500 BC, the famous Egyptian papyrus *Ebers* was written, describing more than 700 drugs drawn from plants, animals, and minerals. Some are still used in our time, such as garlic and poppy seeds.

Greek philosophers such as Empedocles, Aristoteles and Pythagoras, all from around 500 BC, influenced European medicine a great deal. They created the theory of the Four Elements, which were proposed to be the components of all matter, including animals and Man. These Four Elements were Water, Air, Fire and Earth (Schöner 1964). The most famous physicians were Hippocrates (around 400 BC) and Galenus, living in the second century after Christ. In medieval times the system of pathology and therapy, originating from Galenus, dominated Western medicine. The fundamental principle in so-called Galenism was the transformation of humoral pathology into a rigid dogma (Siegel 1968). The school of Hippocrates had already formulated the theory of the Four Humours (paralleling the Four Elements), the correct balance of which meant health, while every disturbance of this balance caused disease. There were Four Humours: Blood (coming from the heart), Phlegm (supposed to come from the brain), Yellow Bile (supposed to be secreted from the liver), and Black Bile (supposed to come from the spleen and the stomach). Each of these humours had definite qualities. Blood was moist and warm; Phlegm, moist and cold; Yellow Bile, warm and dry; Black Bile, cold and dry. Furthermore, there was a definite connection between the predominance of one humour in the metabolic system and an individual's temperament, such as sanguine, phlegmatic, choleric, and melancholic.

European medicine has been influenced by Arabian medicine, mainly by the physician Ali Ibn Sina, who was known in Europe under the name Avicenna. His books were translated into Latin and his *Canon Medicinae* has influenced European medicine for centuries (Gruner 1930).

Saint Hildegard of Bingen, the abbess of a monastery, was one of the most famous physicians and pharmacists in the twelfth century (Müller 1982). She wrote many books on human nature and the use of herbal drugs. Theophrastus Bombastus von Hohenheim, also called Paracelsus and who lived in the fifteenth century, was a reformer of European medicine (Temkin 1941). One of his ideas was that in nature a remedy could always be found against every disease. The Latin sentence "*Ubi malum, ibi remedium*" was the core idea of the signature theory that the shape or the color of a plant indicates against which disease the herbal drug can be used.

European medicine has undergone a great change in paradigm. In contrast to traditional Chinese medicine and Ayurveda, traditional European medicine no longer exists and is only a matter of history of medicine. Even the self-understanding of modern phytotherapy in Europe is completely based on the allopathy that means modern Western medicine.

REFERENCES AND FURTHER READING

Dahanukar SH, Thatte UM (1989) Ayurveda Revisited. Popular Prakashan, Bombay

Dash VB, Junius AMM (1987) A handbook of Ayurveda. Concept, New Delhi

Gruner OC (1930) A treatise on the canon of medicine of Avicenna. Luzac, London

Koecher F (1963) Die babylonisch-assyrische Medizin in Texten und Untersuchungen, Vols 1–6. Walter de Gruyter, Berlin

Mazars G (1994) Traditional veterinary medicine india. Rev Sci Techn 13:433–451

Müller J (1982) Die pflanzlichen Heilmittel bei Hildegard von Bingen. Otto Müller, Salzburg

Porkert M (1973) Die theoretischen Grundlagen der Chinesischen Medizin. Franz Steiner, Wiesbaden

Schöner E (1964) Das Viererschema in der antiken Humoralpathologie. Beiheft zu Sudhoffs Archiv für Geschichte der Medizin und Naturwissenschaften, No. 4. Franz Steiner, Wiesbaden

Siegel RE (1968) Galen's system of physiology and medicine: his doctrines and observations on blood flow, respiration, humors, and internal diseases.Karger, Basel
Temkin L (1941) Four Treatises of Theophrastus von Hohenheim, called Paracelsus. Johns Hopkins University Press, Baltimore
Unschuld PU (1973) *Pen-ts'ao* – 2000 Jahre traditionelle pharmazeutische Literatur Chinas. Heinz Moos, Munich
Unschuld PU (1986) Medicine in China. A history of pharmaceutics. University of California Press, Berkeley
Vogel HG (1991) Similarities between various systems of traditional medicine. Considerations for the future of ethnopharmacology. J Ethnopharmacology 35:179–190

0.2 Classical Pharmacological Approaches

The most important achievements of **modern Western medicine** were made in several areas such as diagnosis, infectious diseases, endocrinology and medicinal chemistry. Virchow founded cellular pathology in the nineteenth century (Pagel 1906). The intensive use of the microscope in medicine with histological comparison of diseased and normal organs allowed the change from humoral to **cellular pathology**.

Medicinal chemistry as an important science started less than 100 years ago. The active principles of plants, mostly alkaloids, were isolated and were the starting point for syntheses, such as:

morphine and papaverine from *Papaver somniferum* for synthetic analgesics and spasmolytics; atropine from *Atropa belladonna* for synthetic spasmolytics; cocaine from *Erythroxylon coca* for synthetic local anesthetics; quinine and quinidine from *Cinchona succirubra* for synthetic anti-malaria drugs and antiarrhythmics; ephedrine from *Ephedra sinica* for synthetic sympathomimetics and sympatholytics including β-blockers, xanthines such as caffeine; theobromine and theophylline from *Coffea arabica*, *Theobroma cacao*, *Camellia sinensis* for vasotherapeutics such as pentoxyphylline; ergot alkaloids from *Claviceps purpurea* for semi-synthetic ergot derivatives; reserpine and ajmaline from *Rauwolfia serpentina* for synthetic antihypertensives and antiarrhythmics; physostigmine from *Physostigma venenosum* for potential antidementic drugs; glycosides from *Digitalis lanata* and *Digitalis purpurea* for semi-synthetic cardiac glycosides; anthraquinones from *Senna angustifolia* or *Rhamnus frangula* or *Rheum officinale* for synthetic laxatives.

Pharmacological research started in Europe in the second half of the nineteenth century when its founders, Rudolf Buchheim and Oswald Schmiedeberg, investigated the action of existing drugs in animal experiments (Kochweser and Schechter 1978).

With the emergence of synthetic chemistry the pharmacological evaluation of these products for therapeutic indications became necessary. Many new drugs were discovered by this classical approach during the twentieth century.

The **classical way of pharmacological screening** involves sequential testing of new chemical entities or extracts from biological material in **isolated organs** followed by **tests in whole animals**, mostly rats and mice but also higher animals if indicated. Most drugs in use nowadays in therapy have been found and evaluated with these methods.

The chemistry and pharmacology of drugs found and used in therapy until 1970 are described in the five volumes of the book by Ehrhart and Ruschig H (eds), *Arzneimittel. Entwicklung*, *Wirkung Darstellung* (1972).

In the mid 1970s **receptor binding assays** were introduced as an approach for compound evaluation by the development of radioligand binding assays, based on evaluation procedures and mathematical calculations provided by Schild (1947), Scatchard (1949), Stephenson (1956), Ariëns and van Rossum (1957), Arunlakshana and Schild (1959), Furchgott (1966), Cheng and Prusoff (1973), Rodbard and Frazier (1975), Lefkowitz and Williams (1977), Bennett (1978), Creese (1978), Munson and Rodbard (1980), McPherson (1985a,b), Tallarida and Murray (1987), and Greenstein (1991). Receptor binding assays were described for various transmitters as well as assays for ion channels and neurotransmitter reporters (e. g., by Snyder et al. 1975; Bylund and Snyder 1976; Enna 1978; U'Prichard et al. 1978, 1979; Bruns et al. 1980; Starke 1987; Dohlman et al. 1991; Krogsgaard-Larsen et al. 1991; Snider et al. 1991; Betz 1992; Wisden and Seeburg 1992; Amara and Arriza 1993; Bowery 1993; Wess 1993; Isom et al. 1994; Köhr et al. 1994; Goto and Yamada 1998; Chittajallu et al. 1999; Bormann 2000).

Characterization and classification of receptors is a continuous procedure (William 1991; Kebabian and Neumeyer 1994; Angeli and Guilini 1996; Trist et al. 1997; Godfraind and Vanhoutte 1998; Watling 1998; Alexander et al. 2001).

The use of radioligand-binding assays has facilitated the design of new chemical entities, especially as the information obtained has been used in deriving molecular models for the structure–activity relationship. The receptor technology provides a rapid means to evaluate small amounts of compound (5–10 mg) di-

rectly for their ability to interact with a receptor or enzyme, independent of its efficacy. But as new assays are developed, it also provides a means to profile the activity of compounds against a battery of binding sites, thereby yielding an *in vitro* radioligand binding profile (Shaw 1992). Receptors have been divided into an increasing number of subclasses (Vanhoutte et al. 1996) so that full characterization of a new chemical entity by receptor pharmacology also needs time and material.

DNA sequencing technology has identified many receptors, mostly belonging to the G-protein-coupled receptor superfamily. Reverse molecular pharmacology and functional genomic strategies are recommended to identify the activating ligands for these receptors (Wilson et al. 1998). The reverse molecular pharmacological methodology includes cloning and expression of G-protein-coupled receptors in mammalian cells and screening these cells for a functional response to cognate or surrogate agonists present in biological extract preparations, peptide libraries, and complex compound preparations.

The ligand-binding assay is a powerful tool in the search for agonists and antagonists for novel receptors, and for identification of novel classes of agonists and antagonists of known receptors. However, it does not differentiate between agonist and antagonist. Ligand-binding mass screening can be adapted for very high throughput. However, well-defined criteria have to be fulfilled to avoid blind alleys (Burch 1991).

REFERENCES AND FURTHER READING

Alexander S, Mathie A, Peteres J, MacKenzie G, Smith A (2001) 2001 Nomenclature Supplement. Trends Pharmacol Sci Toxicol Sci, Special Issue

Amara SG, Arriza JL (1993) Neurotransmitter transporters: three distinct gene families. Curr Opin Neurobiol 3:337–344

Angeli P, Guilini U (1996) Perspectives in receptor research. Il Farmaco 51:97–106

Ariëns EJ, van Rossum JM (1957) pD_x, pA_x and pD_x' values in the analysis of pharmacodynamics. Arch Int Pharmacodyn 110:275–299

Arunlakshana O, Schild HO (1959) Some quantitative uses of drug antagonists. Br J Pharmacol 14:48–58

Bennett JP Jr (1978) Methods in binding studies. In: Yamamura et al. (eds) Neurotransmitter receptor binding. Raven, New York, pp 57–90

Betz H (1992) Structure and function of inhibitory glycine receptors. Q Rev Biophys 25:381–394

Bormann J (2000) The 'ABC' of GABA receptors. Trends Pharmacol Sci 21:16–19

Bowery NG (1993) $GABA_B$ receptor pharmacology. Annu Rev Pharmacol Toxicol 33:109–147

Bruns RF, Daly JW, Snyder SH (1980) Adenosine receptors in brain membranes: binding of N^6-cyclohexyl [^{3}H]adenosine and 1,3-diethyl-8-[^{3}H]phenylxanthine. Proc Natl Acad Sci 77:5547–5551

Burch RM (1991) Mass ligand binding screening for receptor antagonists: prototype new drugs and blind alleys. J Receptor Res 11:1–4

Bylund DB, Snyder SH (1976) Beta adrenergic receptor binding in membrane preparations from mammalian brain. Mol Pharmacol 12:568–580

Cheng YC, Prusoff WH (1973) Relationship between the inhibition constant (K_i) and the concentration of inhibitor which causes 50 per cent inhibition (I_{50}) of an enzymatic reaction. Biochem Pharmacol 22:3099–3108

Chittajallu R, Braithwaite SP, Clarke VJR, Henley JM (1999) Kainate receptors: subunits, synaptic localization and function. Trends Pharmacol Sci 20:26–35

Creese I (1978) Receptor binding as a primary drug screening device. In: Yamamura et al. (eds) Neurotransmitter receptor binding. Raven, New York, pp 141–170

Dohlman HG, Thorner J, Caron MG, Lefkowitz RJ (1991) Model systems for the study of seven-transmembrane-segment receptors. Annu Rev Biochem 60:653–688

Ehrhart G, Ruschig H (eds) (1972) Arzneimittel. Entwicklung, Wirkung Darstellung, vols 1–5. Verlag Chemie, Weinheim/Bergstrasse

Enna SJ (1978) Radioreceptor assay techniques for neurotransmitters and drugs. In: Yamamura et al. (eds) Neurotransmitter receptor binding. Raven, New York, pp 127–139

Furchgott RF (1966) The use of β-haloalkylamines in the differentiation of receptors and in the determination of dissociation constants of receptor-agonist complexes. Adv Drug Res 3:21–55

Godfraind T, Vanhoutte PM (1998) The IUPHAR compendium of receptor characterization and classification. IUPHAR, London

Goto A, Yamada K (1998) An approach to the development of novel antihypertensive drugs: potential role of sodium pump inhibitors. Trends Pharmacol Sci 19:201–204

Greenstein BD (1991) Some uses of Scatchard plot and other parameters of ligand binding. In: Greenstein B (ed) Neuroendocrine research methods, Vol 2. Harwood Academic, Chur, pp 617–629

Isom LL, DeJongh KS, Catterall WA (1994) Auxiliary subunits of voltage-gated ion channels. Neuron 12:1183–1194

Kebabian JW, Neumeyer JL (1994) The RBI handbook of receptor classification. Research Biochemicals International, Natick, Mass.

Kochweser J, Schechter PJ (1978) Schmiedeberg in Strassburg 1872–1918: the making of modern pharmacology. Life Sci 22:13–15

Köhr G, Eckhardt S, Luddens H, Monyer H, Seeburg PH (1994) NMDA receptor channels: subunit-specific potentiation by reducing agents. Neuron 12:1031–1040

Krogsgaard-Larsen P, Ferkany JW, Nielsen E, Madsen U, Ebert B, Johansen JS, Diemer NH, Bruh T, Beattie DT, Curtis DR (1991) Novel class of amino acid antagonists at non-*N*-methyl-D-aspartic acid excitatory amino acid receptors. Synthesis, *in vitro* and *in vivo* pharmacology, and neuroprotection. J Med Chem 34:123–130

Lefkowitz RJ, Williams LT (1977) Catecholamine binding to the β-adrenergic receptor. Proc Natl Acad Sci 74:515–519

McPherson GA (1985a) Analysis of radioligand binding experiments. A collection of computer programs for the IBM PC. J Pharmacol Methods 14:213–228

McPherson GA (1985b) KINETIC, EBDA, LIGAND, LOWRY. A collection of radioligand binding analysis programs. Elsevier, Amsterdam

Munson PJ, Rodbard D (1980) LIGAND: a versatile computerized approach for characterization of ligand-binding system. Anal Biochem 107:220–239

Pagel J (1906) Rudolf Virchow. Weicher, Leipzig
Rodbard D, Frazier GR (1975) Statistical analysis of radioligand assay data, vol 37. Academic Press, New York, pp 3–22
Scatchard G (1949) The attractions of proteins for small molecules and ions. Ann NY Acad Sci 51:660–672
Schild HO (1947) pA, a new scale for the measurement of drug antagonism. Br J Pharmacol 2:189–206
Shaw I (1992) Receptor-based assays in screening of biologically active substances. Curr Opin Biotech 3:55–58
Snider RM, Constantine JW, Lowe JA III, Longo KP, Lebel WS, Woody HA, Drozda SE, Desai MC, Vinick FJ, Spencer RW, Hess HJ (1991) A potent nonpeptide antagonist of the substance P (NK_1) receptor. Science 215:435–437
Snyder SH, Creese I, Burt DR (1975) The brain's dopamine receptor: labeling with [^{3}H]dopamine. Psychopharmacol Commun 1:663–673
Starke K (1987) Presynaptic α-autoreceptors. Rev Physiol Biochem Pharmacol 107:73–146
Stephenson RP (1956) A modification of receptor theory. Br J Pharmacol 11:379–393
Tallarida RJ, Murray RB (1987) Manual of pharmacologic calculations with computer programs, 2nd edn. Springer, Berlin Heidelberg New York
Trist DG, Humphrey PPA, Leff P, Shankley NP (1997) Receptor classification. The integration of operational, structural, and transductional information. Ann NY Acad Sci 812:1–244
U'Prichard DC, Bylund DB, Snyder SH (1978) (±)-^{3}H-Epinephrine and (–)-^{3}H-dihydroalprenolol binding to β_1 and β_2 noradrenergic receptors in brain, heart and lung membranes. J Biol Chem 253:5090–5102
U'Prichard DC, Bechtel WD, Rouot B, Snyder SH (1979) Multiple apparent alpha-noradrenergic receptor binding sites in rat brain: effect of 6-hydroxydopamine. Mol Pharmacol 15:47–60
Vanhoutte PM, Humphrey PPA, Spedding M (1996) International Union of Pharmacology. XI. Recommendations for nomenclature of new receptor subtypes. Pharmacol Rev 48:1–2
Watling KJ (1998) The RBI handbook of receptor classification, 3rd edn. Research Biochemicals International, Natick, Mass.
Wess J (1993) Molecular basis of muscarinic acetylcholine receptor function. Trends Pharmacol Sci 14:308–313
William M (1991) Receptor binding in the drug discovery process. Med Res Rev 11:147–184
Wilson S, Bergsma DJ, Chambers JK, Muir AI, Fantom KGM, Ellis C, Murdock PR, Herrity NC, Stadel JM (1998) Orphan G-protein-coupled receptors: the next generation of drug targets? Br J Pharmacol 125:1387–1392
Wisden W, Seeburg PH (1992) $GABA_A$ receptor channels: from subunits to functional entities. Cur Opin Neurobiol 2:263–269

0.3 Quo Vadis, Pharmacology?

It is universally bemoaned that development costs for new pharmaceutical drugs are exploding, whilst the output of new drugs is decreasing (Horrobin 2001, 2002, 2003; Warr 2003; Sams-Dodd 2005, 2006; Rishton 2005; Schmid and Smith 2005; Lundkvist et al. 2006).

Sams-Dodd (2006) analyzed the strength and limitations of various drug discovery approaches. The *target-based drug discovery approach*, once welcomed as a change in paradigm, has for the past 10–15 years been the dominating approach in drug discovery. However, in the past few years the commercial value of novel targets in licensing deals has fallen dramatically, reflecting the fact that the probability of reaching a clinical drug candidate for a novel target is very low. This has naturally led to questions regarding the success of target-based drug discovery and, more importantly, a search for alternatives.

The *mechanism-based approach*, which corresponds to the target-based approach, screens for compounds with a specific mode of action. The focus on a single mechanism that permits the use of high-throughput screening (HTS) and ultra-HTS technology for screening makes it highly effective for the identification of target-selective compounds. However, despite the fact that this approach is highly advantageous from a scientific and practical viewpoint, it does not translate into a high success rate for novel targets. A success rate of 3% for reaching preclinical development is not attractive. Each drug discovery project usually lasts 2–4 years, and if 33 targets on average have to be evaluated to identify one that can proceed into preclinical development, it means that at least 66 years of research is needed to produce one successful drug discovery project for a novel target. Considering that the attrition rate caused by toxicological effects and lack of clinical effects are also substantial, it means that novel unvalidated targets are not attractive for the pharmaceutical industry.

The *physiology-based approach* was the first drug discovery paradigm, and this has resulted in many effective treatments. It seeks to induce a therapeutic effect by reducing disease-specific symptoms or physiological changes and screens compounds for these properties in animal models that mimic specific aspects of disease symptomatology. The screening is conducted in isolated organ systems or in whole animals. The physiology-based approach suffers from low screening capacity and difficulty in identifying the mode of action of drugs.

The *function-based approach* seeks to induce a therapeutic effect by normalizing a disease-specific abnormality. Compared with the mechanism-based approach, functional parameters represent a higher level of organism complexity because function requires the integrated action of many mechanisms. However, unlike the physiology-based approach, the parameters cannot be compared to the symptoms observed in pa-

tients. The screening capacity cannot be used for library screening.

In **summary**, no clear advantage of one drug discovery paradigm over the others could be demonstrated, because all of them have their specific strengths and weaknesses. The classical approaches cannot be abandoned.

Cuatrecasas (2006) analyzed the reasons for insufficiency of drug discovery and development. The low productivity is certainly not related to available budgets, which have increased 30-fold since 1970. The Food and Drug Administration (FDA) or regulatory issues are not fundamental barriers and contribute only marginally to the decline in drug productivity. Likewise, one cannot blame the current state of scientific advances, which in the last 20 years have been revolutionary.

Much more important are **changes in the approach to management**. Foremost among the issues that cripple drug research and development (R&D) is that while utmost creativity and innovation are required, the R&D is conducted in traditional for-profit corporations that are virtually indistinguishable operationally from those that conduct little or no R&D. Most corporations' top management does not understand the complexities of science, its mode of conduct or objectives, and runs the companies in ways that stifle creativity and innovation.

0.3.1 Managers, Not Leaders

In the 1970s things began to change. Modern managers entered as chief executive officers (CEOs) and other high-level executives, mostly with little or no technical experience. Freedom, spontaneity, flexibility, nimbleness, tolerance, compassion, humor, and diversity were replaced by bulky and inflexible organizational structures characterized by regimentation, control, conformity, and excessive bureaucracy. There are still companies that try to focus on excellent science and that attract first-rate scientists. These are, however, exceptional situations.

Drug R&D thrives in a creative, flexible, and nonautocratic environment. Success depends on individual freedom and inspiration rather than dogmatic leadership.

0.3.2 Pressures From Shareholders

The ownership of public companies consists mainly of shareholders who expect rapid (and substantive) returns on their investments. This contrasts (and often conflicts) with the nature of the business objectives, which must be based on long-term investments in science and technology.

0.3.3 Merger Mania

The decreasing earnings have stimulated mergers and acquisitions, driven by the desire to acquire existing sales (products) while decreasing costs via layoffs. This has created conditions that catalyze further inefficiencies and suffocation of innovation. The merged megacompanies' research organizations must be integrated rapidly and redundancies eliminated, oftentimes in haste.

0.3.4 Blockbuster Mania

Companies have become much less interested in developing drugs that will sell less than $1 billion a year. Without these "blockbusters" they cannot maintain the traditionally high profits. Berkowitz and Sachs (2002) described discovery and development of the blockbuster drug omeprazole.

0.3.5 Orphan Drugs and Drug Pricing

In the 1960s through the 1990s, orphan diseases were simply rare diseases for which drug companies did not wish to initiate discovery programs, for commercial reasons. It was understood that prices could not be adjusted out of line with the prevailing standards. In 1983, the US Congress passed The Orphan Drug Act to provide tax, funding, and exclusivity incentives to companies developing drugs for low-prevalence diseases (defined as fewer than 200,000 cases) that were not expected to provide investment returns. However, many drugs that have become blockbusters had early histories of major disinterest and skepticism.

There are many publications on orphan drugs and drugs for rare diseases (Von Oehsen 1989; Weinstein 1991; Haffner 2002; Rados 2003; Thoene 2004; Fischer et al. 2005; Gericke et al. 2005; Hughes et al. 2005; Moran 2005; Sheehan 2005; McCabe et al. 2006; Reidenberg 2006; Stolk et al. 2006), but they concern mainly cost-effectiveness and funding of clinical trials, but not pharmacological methods. It seems necessary that experimental pharmacologists know rare diseases and think about methods to evaluate drugs against rare diseases.

Researchers are now looking back to the **golden age of drug discovery in the 1950s and 1960s** of the last century. What was different at that time?

A few personal remarks: in the 1960s, we were looking for analgesics in a special chemical series. However, we were afraid of addictive and hallucinogenic potential. In animal experiments we found a compound almost as effective as methadone. After 2 weeks of toxicity tests, we gave it to one of our behavior cats. The results were unequivocal. So, without informing anybody, one of us took a rather high dose orally. He did not hallucinate. So we gave the compound to patients. There were no side-effects after oral dosing, but hallucinogenic side-effects were reported after intravenous dosing. We had to drop development.

Another example: we were looking for an effective and highly tolerable local anesthetic.

One pharmacologist performed animal experiments, but he injected interesting compounds into his forearm to evaluate pain and the local anesthetic effect. An excellent compound was found this way (R. Muschaweck, pers. comm. 2007).

One further example: one of our colleagues was testing sedative and hypnotic compounds. After some toxicological studies, he gave the compound to a colleague in charge of first clinical trials. He took the compound himself, but then collapsed behind his desk (E. Lindner, pers. comm. 2007).

Conclusion: we were not afraid to take our compounds ourselves even flaunting regulations. Thus **compounds were tested by the pharmacologists themselves.**

If we look back to the great breakthroughs in the 1950s and 1960s, we see that many important ones came from **serendipitous** findings.

Horace Walpole (1717–1797) coined the term serendipity in 1754 in allusion to an ancient oriental legend of the "Three Princes of Serendip". "Serendipity" in drug discovery implies the finding of one thing while looking for something else (Holubar 1991; Ban 2006).

The diuretic action of sulfanilamide and **acetazolamide** as inhibitors of carbonic anhydrase was found in clinical trials (Schwartz 1949; Maren 1960, 1967; Relman et al. 1960).

Sulfonylureas were tested as antibiotic drugs to be compared with sulfonamides. The blood sugar-lowering-effect of **sulfonylureas** designed as antibacterial agents (Loubatières 1946; Franke and Fuchs 1955; Achelis and Hardebeck 1955) was found just by chance. Then it turned out that the amino group was not necessary, resulting in **tolbutamide**. On the other hand, one has to keep in mind that millions of diabetics were treated successfully with sulfonylureas over decades, whereby only the release of insulin from the pancreatic β-cell, but not the molecular mechanism, was known (Pfeiffer et al. 1959; Bänder et al. 1969).

The antipsychotic activity of phenothiazines (**chlorpromazine**) originally tested as antihistaminic drugs was found in clinical studies (Delay and Deniker 1952; Laborit et al. 1952; Courvoisier 1956), as was the antidepressant effect of **imipramine** (Kuhn 1958).

The antidepressant effect of the monoamine oxidase inhibitor **iproniazid** was found in clinical trials (Kline 1958; Bailey et al. 1959; Dick 1959).

Valproic acid was used as an organic solvent in research laboratories for eight decades, until the observation of action against pentylenetetrazol-induced convulsions in rodents. Clinical experience emphasized therapy for absence seizures in primary generalized epilepsies. Anecdotal observations in patients with both epilepsy and migraine headaches led to the discovery of its antimigraine efficacy. More than a decade later, clinical trials established a significant efficacy of valproate in mania (Henry 2003).

Butazolidin was used as an additive to increase the solubility of aminopyrine resulting in a combination product (Wilhelmi 1949, 1950). The therapeutic value of butazolidin as single drug was recognized later (Kuzell and Schafferzick 1952; Belart 1953).

The blood-pressure-lowering effect of **clonidine** was found when tested as a vasoconstrictive drug for nasal application. The mechanism of action was clarified in animal experiments (Kobinger and Walland 1967; Callingham 1971; Timmermans and van Zwieten 1980, 1981; Langer and Hicks 1984).

Furosemide was found to be a potent diuretic and saluretic drug comparable to other substances. But animal experiments and studies in volunteers showed an effect at doses at which other diuretic drugs were no longer effective. Thus the name "**high-ceiling diuretic**" was coined.

The discovery of **sildenafil**, a highly selective inhibitor of phosphodiesterase-5 (PDE-5), was the result of research on chemical agents that might be useful in the treatment of coronary heart disease. Initial clinical studies on sildenafil were not promising with respect to its anti-anginal potential. However, the incidental discovery of its anti-impotence effect led to its approval for the treatment of erectile dysfunction (Campbell 2000; Enna 2000; Raja and Nayak 2004).

Most new drugs, however, were found by the **classical approach**, which has the advantage of relatively high relevance. If a compound has blood-pressure-

lowering activity in hypertensive rats after oral dosage, the chances of activity in humans are high. Measurement of dose–response curves, effects over a given period of time, and comparison of the effects after intravenous and oral administration have already given hints for pharmacokinetic data. This approach had the disadvantage that it was time-consuming and required relatively large amounts of the new compound (usually about 5 g). Furthermore, this approach provided little information about the molecular mechanisms involved in the observed effects.

What were the **deficiencies of the classical approach**?

We did not know the exact mode of action of our drugs in spite of the fact that we could treat patients effectively.

This **situation has changed.**

Molecular biology has a significant impact on drug discovery, offering us over 30,000 genes and their protein products as potential drug targets, and revolutionizing the processes involved in seeking drug targets, testing hypotheses, and screening for activity. In addition, the techniques of combinatorial chemistry are available, which generate thousands of compounds to test against the thousands of targets. The search for new lead compounds involves intricate high-throughput screening technology with tremendous capacity, and the use of cell culture and recombinant human cells and enzymes (In Vivo Pharmacology Training Group 2002). So we have many hypotheses and we know many biochemical steps that could be the mode of action of a new drug, but we do not know the new drug. The biochemical approach reduced the use of animals. When animal experiments are performed at a later stage, quite often the results of *in vitro* experiments cannot be validated *in vivo*.

In all countries we have regulations for the care and use of laboratory animals (see Chap. Q of this book). Animal rights extremists have created an atmosphere where students are reluctant to perform whole-animal studies. Our experience tells us that only a research worker who loves animals and is not afraid of them should perform animal experiments.

What can be **recommended** from experimental pharmacology to **increase the efficacy of drug development?**

- Looking for **short-cuts**, even neglecting the present rules when performing self experiments.
- To give pharmacologists the freedom, time and money to **realize their own ideas**.
- Giving room for **serendipity**.
- Performing **animal experiments** in parallel to *in vitro* studies.
- In respect to **orphan drugs**, it seems necessary that experimental pharmacologists know rare diseases and think about methods to evaluate drugs against these diseases.
- Pharmacologists should have **training in medicine**, not only in biochemistry.
- Outstanding pharmacologists should be selected as **leaders in research and development.**

REFERENCES AND FURTHER READING

Achelis JD, Hardebeck K (1955) Eine neue Blutzuckersenkende Substanz! Vorläufige Mitteilung. Dtsch Med Wochenschr 80:1452–1455

Bailey SD, Bucci L, Gosline E, Kline NS, Park ICH, Rochlin D, Saunders JC, Vaisberg M (1959) Comparison of iproniacid with other amino oxidase inhibitors, including W-1544, JB-516, RO 4-1018 and RO 5-0700. Ann N Y Acad Sci 80:652–668

Ban TA (2006) The role of serendipity in drug discovery. Dialogues Clin Neurosci 8:335–344

Bänder A, Pfaff W, Schmidt FH, Stork H, Schröder HG (1969) Zur Pharmakologie von HB 419, einem neuen, stark wirksamen oralen Antidiabeticum. Arzneimittelforschung 19:1363–1372

Belart W (1953) Butazolidine als Antirheumaticum im Vergleich mit Irgapyrin. Dtsch Med Wschr 78:129–131

Berkowitz BA, Sachs G (2002) Life cycle of a blockbuster drug. Discovery and development of omeprazole (Prilosec™). Mol Interventions 2:6–11

Callingham BA (1971) Current aspects of pharmacology, clonidine. Pharm J 207:431–433

Campbell SF (2000) Science, art and drug discovery: a personal perspective. Clin Sci (Lond) 99:255–260

Courvoisier S (1956) Pharmacodynamic basis for the use of chlorpromazine in psychiatry. J Clin Exp Psychopathol 17:25–37

Cuatrecasas P (2006) Drug discovery in jeopardy. J Clin Invest 116:2837–2842

Delay J, Deniker P (1952) Trente-huit cas de psychoses traitées par le cure prolongée et continue de 4560 RP. Le Congrès de Al. et Neurol. de Langue Fr. In: Compte rendu du Congrès. Masson et Cie, Paris

Dick P (1959) Therapeutic action of a monoamino oxidas inhobitot, marsilid (iproniazid) on depressive states. Schweiz Med Wschr 89:1288–1291

Enna SJ (2000) Drug stories of origins and uses. In: Stone T, Darlington G (eds) Pills, potions and poisons. How drugs work. Oxford University Press, New York, pp 492–493

Fischer A, Borensztein P, Roussel C (2005) The European rare disease therapeutic initiative. PLoS Med 2:2243

Franke H, Fuchs J (1955) Über ein neues antidiabetisches Prinzip. Ergebnisse klinischer Untersuchungen. Dtsch Med Wschr 80:1449–1452

Gericke CA, Riesberg A, Busse R (2005) Ethical issues in funding orphyn drug research and development. J Med Ethics 31:164–168

Haffner ME (2002) Orphan drug product regulation – United States. Int J Clin Pharmacol 40:84–88

Henry TR (2003) The history of valproate in clinical neuroscience. Psychopharm Bull 37 [Suppl 2]:5–16

Holubar K (1991) Serendipity: its basis and importance. Wien Klin Wschr 103:533–535
Horrobin DF (2000) Innovation in the pharmaceutical industry. J R Soc Med 93:341–345
Horrobin DF (2001) Realism in drug discovery – could Cassandra be right? Nature Biotechnol 19:1099–1100
Horrobin DF (2002) Effective clinical innovation: an ethical imperative. Lancet 359:1857–1858
Horrobin DF (2003) Modern biomedical research: an internally self-consistent universe with little contact with medical reality? Nature Rev Drug Discov 2:151–154
Hughes DA, Tunnage B, Yeo ST (2005) Drugs for exceptionally rage diseases. Do they deserve special status of funding? Q J Med 98:829–836
In vivo Pharmacology Training Group (2002) The fall and rise of *in vivo* pharmacology. Trends Pharmacol Sci 23:13–18
Kline NS (1958) Clinical experience with iproniazid (MARSILID). J Clin Exp Psychopathol Suppl 19:72–78
Kobinger W, Walland A (1967) Investigations into the mechanism of the hypotensive effect of 2-(2,6-dichlorphenylamino)-2-imidazoline-HCl. Eur J Pharmacol 2:155–162
Kuhn R (1958) The treatment of depressive states with G22355 (imipramine hydrochloride). Am J Psychiatry 115:459–464
Kuzell WC, Schaffarzick RW (1952) Phenylbutazone (butazolidin) and Butapyrin. Calif Med 77:319–325
Laborit H, Huguenard P, Allaume R (1952) Un noveau stabilisateur végétatif (LE 4560 RP). Presse Med 60:206–208
Langer SZ, Hicks PE (1984) Alpha-adrenoceptor subtypes in blood vessels. Physiology and pharmacology. J Cardiovasc Pharmacol 6 [Suppl 4]:S547–S548
Loubatières A (1946) Étude physiologique et pharmacodynamique de certains dérivés sulfonamidés hypoglycémiants. Arch Intern Physiol 54:174–177
Lundkvist J, Jonsson S, Rehnberg C (2006) The costs and benefits of regulation for reimbursement of new drugs. Health Policy 79:337–244
Maren TH (1960) A simplified micromethod for the determination of carbonic anhydrase and its inhibitors. J Pharmacol Exp Ther 130:26–29
Maren TH (1967) Carbonic anhydrase: chemistry, physiology, and inhibition. Physiol Rev 47:595–781
McCabe C, Tsuchiya A, Claxton K, Raftery J (2006) Orphan drugs revisited. Q J Med 99:341–345
Moran M (2005) A breakthrough in R&D for neglected diseases: new ways to get the drugs we need. PloS Med 2:e302
Pfeiffer EF, Pfeiffer M, Ditschuneit H, Ahn CS (1959) Clinical and experimental studies of insulin secretion following tolbutamide and metahexamide administration. Ann N Y Acad Sci 82:479–495
Rados C (2003) Orphan products: hope for people with rare diseases. FDA Consumer Magazine, November-December
Raja SG, Nayak SH (2004) Sildenafil: emerging cardiovascular indications. Ann Thorac Surg 78:1496–1506
Reidenberg MM (2006) Are drugs for rare diseases "essential"? Bull World Health Org 84:9
Relman AS, Porter R, Tobias JF, Schwartz WB (1960) The diuretic effects of large doses of acetazolamide and an analog lacking carbonic anhydrase inhibiting activity. J Clin Invest 39:1551–1559
Rishton GM (2005) Failure and success in modern drug discovery: guiding principles in the establishment of high probability of success drug discovering organizations. Med Chem 2005:519–527
Sams-Dodd F (2005) Target-based drug discovery: is something wrong? Drug Discov Today 10:139–147
Sams-Dodd F (2006) Drug discovery: selecting the optimal approach. Drug Discov Today 11:465–472
Schmid EF, Smith DA (2005) Keynote review: is declining innovation in the pharmaceutical industry a myth? Drug Discov Today 10:1031–1039
Schwartz WB (1949) New Engl J Med 240:173
Sheehan M (2005) Orphan drugs and the NHS. Fairness in health care entails more that cost effectiveness. Br Med J 331:1144–1145
Stolk P, Willeman MJC, Leufkens HGM (2006) "Rare essentials": drugs for rare diseases as essential medicines. Bull World Health Organ 84
Thoene JG (2004) Orphan drugs and orphan tests in the USA. Community Genet 7:169–172
Timmernans PB, van Zwieten PA (1980) Vasoconstriction mediated by postsynaptic alpha 2-adrenoceptor stimulation. Naunyn-Schmiedbergs Arch Pharmacol 313:17–20
Timmernans PB, van Zwieten PA (1981) Mini-review: the postsynaptic alpha 2-adrenoceptor. J Auton Pharmacol 1:171–183
Von Oehsen (1989) Orphan Drug Act on congressional agenda. Physician Exec 15:34–35
Warr WA (2003) Strategies for improving pharmaceutical R&D productivity. Drug Discov Design 7:1–15
Weinstein MC (1991) The cost-effectiveness of orphan drugs. Am J Publ Health 81:414–415
Wilhelmi G (1949) Über die pharmakologischen Wirkungen von Irgapyrin, einem neuen Präparat aus der Pyrazolonreihe. Schweiz Med Wschr 79:577
Wilhelmi G (1950) Über die antiphlogistische Wirkung von Pyrazolonen, speziell von Irgayrin, 'bei peroraler and parenteraler Verabreichung. Schweiz Med Wschr 80:936

0.4 New Approaches in Drug Discovery

0.4.1 Combinatorial Chemistry

It was always due to the ingenuity of the chemist that new chemical entities in pharmaceutical research were created (Schapira et al. 2000; Schreiber 2000). For some period of time, computer-based molecular modeling was thought to be the most effective approach. With the increasing characterization of the three-dimensional structures of receptors and enzymes, the design of molecules that interact with these biological targets was thought to be an intellectual approach using modern computer technology (Stigers et al. 1999).

This attitude to the development of **combinatorial chemistry** has changed. It has been defined as the systematic and repetitive covalent connection of a set of different "building blocks" of varying structures to each other to yield a large array of diverse molecular entities (Gallop et al. 1994; Gordon et al. 1994; Fecik et al. 1998).

An interim analysis (Adang and Hermkens 2001) showed only limited success of combinatorial chemistry approaches in terms of delivering leads. The interest in natural products has been regained (Ortholand and Ganesan 2004; Piggott and Karuso 2004).

It has become possible to use solid- or solution-phase syntheses with different chemistries and scaffolds to produce libraries tailor-made for finding or optimizing a lead directed at almost any class of target (Hogan 1996; Maclean et al. 1997; Appleton 1999; Dooley and Houghten 1999; Lukas et al. 1999; Beeley and Berger 2000; Houghten 2000; Lazo and Wipf 2000; Rademann and Jung 2000).

Several suggestions were made to enhance the success of the hit to lead process (Goodnow 2001; Goodnow et al. 2003; Alanine et al. 2003; Bleicher et al. 2003). Golebiowski et al. (2003) reviewed lead compounds discovered from libraries at various research institutes. Design of screening libraries targeted at macromolecules, such as synthetic and G-protein-coupled receptors, was described by Juliano et al. (2001), Crossley (2004), Jimonet and Jäger (2004), and Srinivasan and Kilburn (2004). Purification strategies for combinatorial and parallel chemistry were discussed by Edwards (2003).

New tools, such as molecular docking algorithms (Burkhard et al. 1999), mapping of protein-binding sites by nuclear magnetic resonance (Shuker et al. 1996), preparation of highly enantioselective selectors for chiral HPLC (Lewandowski et al. 1999), microfluidic systems (Watts and Haswell 2003; Cullen et al. 2004), light-directed synthesis (LeProust et al. 2000), and homology modeling of proteins (Kiyama et al. 1999), allow an unprecedented level of rational design to guide the synthesis of prospective drugs.

Spectroscopic methods, including especially mass spectrometry (Mathur et al. 2003; Schefzick et al. 2004) and to a lesser extent infrared and nuclear magnetic resonance, have been applied at different levels of combinatorial library synthesis: in the rehearsal phase to optimize the chemistry prior to library generation, to confirm library composition, and to characterize after screening each structure that exhibits positive response (Dancík et al. 1999; Hajduk et al. 1999; Loo et al. 1999; Scherer et al. 1999; Cancilla et al. 2000; Enjalbal et al. 2000; Kyranos et al. 2001). Schmid et al. (2000), Heeren et al. (2004), and Zhang et al. (2005) discussed the application of mass spectrometry using high-performance Fourier transform ion cyclotron resonance mass spectrometry (FTICR-MS) methods.

Blundell and Patel (2004) underlined the value of high-throughput X-ray crystallography for drug discovery.

REFERENCES AND FURTHER READING

Adang AEP, Hermkens PHH (2001) The contribution of combinatorial chemistry to lead generation: an interim analysis. Curr Med Chem 8:985–998

Alanine A, Nettekoven M, Roberts E, Thomas AW (2003) Lead generation – enhancing the success of drug discovery by investing in the hit to lead process. Comb Chem High Throughput Screen 6:51–66

Appleton T (1999) Combinatorial chemistry and HTS – feeding a voracious process. Drug Discov Today 4:398–400

Beeley N, Berger A (2000) A revolution in drug discovery. Br Med J 321:581–582

Bleicher KH, Böhm HJ, Müller K, Alanine AI (2003) Hit and lead generation: beyond high-throughput screening. Nature Rev Drug Discov 2:369–378

Blundell TL, Patel S (2004) High-throughput X-ray crystallography for drug discovery. Curr Opin Pharmacol 4:490–496

Burkhard P, Hommel U, Sanner M, Walkinshaw MD (1999) The discovery of steroids and other FKBP inhibitors using a molecular docking program. J Mol Biol 287:853–858

Cancilla MT, Leavell MD, Chow J, Leary JA (2000) Mass spectrometry and immobilized enzymes for the screening of inhibitor libraries. Proc Natl Acad Sci USA 97:12008–12013

Crossley R (2004) The design of screening libraries targeted at G-protein coupled receptors. Curr Top Med Chem 4:581–588

Cullen CJ, Wooton RCR, de Mello AJ (2004) Microfluidic systems for high-throughput and combinatorial chemistry. Curr Opin Drug Discov Dev 7:798–806

Dancík V, Addona TA, Clauser KR, Vath JE, Pevzner P (1999) De novo peptide sequencing via tandem mass spectroscopy. J Comput Biol 6:327–342

Dooley CT, Houghten RA (1999) New opioid peptides, peptidomimetics, and heterocyclic compounds from combinatorial libraries. Biopolymers (Peptide Science) 51:379–390

Edwards PJ (2003) Purification strategies for combinatorial and parallel chemistry. Comb Chem High Throughput Screen 6:11–27

Enjalbal C, Martinez J, Aubagnac JL (2000) Mass spectrometry in combinatorial chemistry. Mass Spectrometry Rev 19:139–161

Fecik RA, Frank KE, Gentry EJ, Menin SR, Mitscher LA, Telikepalli H (1998) The search for orally active medications through combinatorial chemistry. Med Res Rev 18:149–185

Gallop MA, Barrett RW, Dower WJ, Fodor SPA, Gordon EM (1994) Application of combinatorial technologies to drug discovery. 1. Background and peptide combinatorial libraries. J Med Chem 37:1233–1251

Golebiowski A, Klopfenstein SR, Portlock DE (2003) Lead compounds discovered from libraries: Part 2. Curr Opin Chem Biol 7:308–305

Goodnow RA Jr (2001) Current practices in generation of small molecule new leads. J Cell Biochem Suppl 37:13–21

Goodnow RA Jr, Guba W, Haap W (2003) Library design practices for success in lead generation with small molecule libraries. Comb Chem High Throughput Screen 6:649–660

Gordon EM, Barrett RW, Dower WJ, Fodor SPA, Gallop MA (1994) Application of combinatorial technologies to drug discovery. 2. Combinatorial organic synthesis, library screening strategies, and future directions. J Med Chem 37:1385–1401

Hajduk PJ, Gerfin T, Boehlen JM, Häberli M, Marek D, Fesik SE (1999) High-throughput nuclear magnetic resonance-based screening. J Med Chem 42:2315–2317

Heeren RMA, Kleinnijenhuis AJ, McDonnell LA, Mize TH (2004) A mini-review of mass spectrometry using high-performance FTICR-MS methods. Anal Bioanal Chem 378:1048–1058

Hogan JC Jr (1996) Directed combinatorial chemistry. Nature 384 [Suppl 17–19]:6604

Houghten RA (2000) Parallel array and mixture-based synthetic combinatorial chemistry: tools for the next millennium. Annu Rev Pharmacol Toxicol 40:273–282
Jimonet P, Jäger R (2004) Strategies for designing GPCR-focused libraries and screening sets. Curr Opin Drug Discov Dev 7:325–333
Juliano RL, Astriab-Fisher A, Falke D (2001) Macromolecular therapeutics: emerging strategies for drug discovery in the postgenome era. Mol Interv 1:40–54
Kiyama R, Tamura Y, Watanabe F, Tsizuki H, Ohtani M, Yodo M (1999) Homology modelling of gelatinase catalytic domains and docking simulations of novel sulfonamide inhibitors. J Med Chem 42:1723–1738
Kyranos JN, Cai H, Wie D, Goetzinger WK (2001) High-throughput high-performance liquid chromatography/mass spectrometry for drug discovery. Curr Opin Biotechnol 12:105–111
Lazo JS, Wipf P (2000) Combinatorial chemistry and contemporary pharmacology. J Pharmacol Exp Ther 293:705–709
LeProust E, Pellois JP, Yu P, Zhang H, Gao X, Srivannavit O, Gulari E, Zhou X (2000) Digital light-directed synthesis. A microarray platform that permits rapid reaction optimization on a combinatorial basis. J Comb Chem 2:349–354
Lewandowski K, Murer P, Svec F, Frechet JMJ (1999) A combinatorial approach to recognition of chirality: preparation of highly enantioselective aryl-dihydropyrimidine selectors for chiral HPLC. J Comb Chem 1:105–112
Loo JA, DeJohn DA, Du P, Stevenson TI, Loo RRO (1999) Application of mass spectrometry for target identification and characterization. Med Res Rev 19:307–319
Lukas TJ, Mirzoeva S, Slomczynska U, Watterson DM (1999) Identification of novel classes of protein kinase inhibitors using combinatorial peptide chemistry. J Med Chem 42:910–919
Maclean D, Schullek JR, Murphy MM, Ni Z-J, Gordon EM, Gallop MA (1997) Encoded combinatorial chemistry: synthesis and screening of a library of highly functionalized pyrrolidines. Proc Natl Acad Sci USA 94:2805–2810
Mathur S, Hassel M, Steiner F, Hollemeyer K, Hartmann RW (2003) Development of an new approach for screening combinatorial libraries using MALDI-TOF-MS and HPLC-ESI-MS/MS. J Biomol Screen 8:136–148
Ortholand JY, Ganesan A (2004) Natural products and combinatorial chemistry: back to the future. Curr Opin Chem Biol 8:271–280
Piggott AM, Karuso P (2004) Quality, not quantity: the role of natural products and chemical proteomics in modern drug discovery. Comb Chem High Throughput Screen 7:607–630
Rademann J, Jung G (2000) Integrating combinatorial synthesis and bioassays. Science 287:1947–1948
Schapira M, Raaka BM, Samuels HH, Abagyan R (2000) Rational discovery of nuclear hormone receptor antagonists. Proc Natl Acad Sci USA 97:1008–1013
Schefzick S, Kibbey C, Bradley MP (2004) Prediction of HPLC conditions using QSPR techniques: an effective tool to improve combinatorial library design. J Comb Chem 6:916–927
Scherer JR, Kheterpal I, Radhakrishnan A, Ja WWW, Mathies RA (1999) Ultra-high throughput rotary capillary array electrophoresis scanner for fluorescent DNA sequencing and analysis. Electrophoresis 20:1508–1517
Schmid DG, Grosche P, Bandel H, Jung G (2000) FTICR-mass spectroscopy for high-resolution analysis in combinatorial chemistry. Biotechnol Bioeng 71:149–161
Schreiber SI (2000) Target-oriented and diversity-oriented organic synthesis in drug discovery. Science 287:1964–1969
Shuker SB, Hajduk PJ, Meadows RP, Fesik SW (1996) Discovery of high affinity ligands for proteins. SAR by NMR. Science 274:1531–1534
Srinivasan N, Kilburn JD (2004) Combinatorial approaches to synthetic receptors. Curr Opin Chem Biol 8:305–310
Stigers KD, Soth MJ, Nowick JS (1999) Designed molecules that fold to mimic protein secondary structure. Curr Opin Chem Biol 3:714–723
Watts P, Haswell SJ (2003) Microfluidic combinatorial chemistry. Curr Opin Chem Biol 7:380–387
Zhang J, McCombie G, Guenat C, Knochemmuss R (2005) FT-ICR mass spectrometry in the drug discovery process. Drug Discov Today 10:635–642

0.4.2
High-Throughput Screening, Ultra-High-Throughput Screening, and High-Content Screening

The logical development of receptor technology was high-throughput screening (HTS) (Bolger 1999; Broach, Thorner 1996; Cox et al. 2000; Major 1999). This evolution was closely connected with the changes in strategy of chemical synthesis. The vast number of compounds produced by combinatorial chemistry and the possibility of testing many compounds, including natural products (Harvey 2000), in a short period of time by HTS stimulated each other.

High-throughput screening is the process of testing a large number of diverse chemical structures against disease targets to identify "hits". Compared to traditional drug screening methods, HTS is characterized by its simplicity, rapidness, taking the ligand–target interactions as the principle, as well as leading to a relatively high information harvest. As a multidisciplinary field, HTS involves an automated operation platform, a highly sensitive testing system, specific screening models (*in vitro*), an abundant components library, and a data acquisition and processing system. Various technologies, especially technologies such as fluorescence, nuclear magnetic resonance, affinity chromatography, surface plasmon resonance, and DNA microarray, are available, and the screening of more than 100,000 samples per day is possible. Fluorescence-based assays include the scintillation proximity assay, time-resolved energy transfer, fluorescence anisotropy, fluorescence correlation spectroscopy, and fluorescence fluctuation spectroscopy.

With the introduction of robotics, automation and miniaturization techniques, it became feasible to screen 50,000 compounds a day with complex workstations. Full automation of all assay steps, from compound addition to data collection, ultimately allows screens to be run continuously – 24 h a day, 7 days a week. Another progress is the development of 1536-well microtiter plate formats (Berg et al. 2000; Dunn

et al. 2000). Multiple types of formats are emerging beside the 96-, 384-, and 1536-, even 3456- and 9600-well plates (Sills 1998).

The trend toward assay miniaturization for high-throughput and ultra-high-throughput screening intensified the development of homogenous, fluorescence-based assays in higher density, smaller volume microplate formats. Microfluidic devices have been designed to perform continuous-flow biochemical and cell-based assays providing orders of magnitude reduction in reagent consumption (Sundberg 2000; Cullen et al. 2004). Harding et al. (1997) described the development of an automated HTS system involving two systems, the first handling isotopic assay ("hot" system), the second non-isotopic assays ("cold" system).

An ultra-high-throughput screen based on fluorescence isotropy and performed entirely using 1536-well assay plates was published by Turconi et al. (2001). Further studies on miniaturized HTS technologies were published by Wolcke and Ullmann (2001) and Brandish et al. (2006).

Target validation should not be underestimated in the drug research and development process (Williams 2003).

Enzyme assays for HTS were evaluated by Goddard and Reymond (2004). Assaying enzyme-catalyzed transformation in high throughput is crucial to enzyme discovery, enzyme engineering and the drug development process. In enzyme assays, catalytic activity is detected using labeled substrates or indirect sensor systems that produce a detectable spectroscopic signal upon reaction.

High-content screening was proposed by Giuliano et al. (1997) as a new approach to easing key bottlenecks in the drug discovery process. High-content screening defines the role of targets in cell function by combining fluorescence-based reagents with the ArrayScan™ to automatically extract temporal and spatial information about target activities within cells. High-content screening integrates cell-based assays, high-resolution fluorescence microscopy, and proprietary image processing algorithms for the automated analysis of cellular and subcellular events. It delivers the potential to screen using targets that previously were minimally used or avoided due to a lack of a robust way to measure them, such as morphology changes, cellular differentiation and cytoskeletal changes, cell-to-cell interactions, chemotaxis and motility, as well as spatial distribution changes such as receptor trafficking or complex formation.

Clark and Pickett (2000) underlined the importance of computational methods for the prediction of "drug-likeness", in particular for the prediction of intestinal absorption and blood–brain barrier penetration.

Several authors expressed their thoughts on the future of HTS (Divers 1999; Eglen 1999; Fox et al. 1999, 2001; Stahl 1999; Mander 2000). Valler and Green (2000) expressed some doubts on diversity screening in drug discovery and proposed focused screening using three-dimensional information about the target which may improve the hit rate 10- to 100-fold over random screening.

Nevertheless, this technical progress has led to a new concept in drug discovery: "a change in paradigm". Large numbers of hypothetical targets are incorporated into *in vitro* or cell-based assays and are exposed to large numbers of compounds of natural or synthetic origin.

This change in paradigm created new areas, such as bioinformatics, cheminformatics, and functional genomics (Ohlstein et al. 2000, 2006; Ryu and Nam 2000; Blake 2004).

Many compounds can elicit a positive response in a particular assay, which is called a hit. In this new terminology "**hit**" is a molecule with confirmed activity from the primary HTS assay, a good profile in secondary assays and a confirmed structure.

The hits have to be structurally defined and may give rise to leads (Lahana 1999). "**Lead**" is a hit series for which the structure–activity relationship is shown and activity demonstrated both *in vitro* and *in vivo*.

The implementation of these methods is being complemented by an increase in the use of automation and robotics. Automation may be defined as the use of stand-alone instrumentation (work stations) that performs a given task, whereas robotics uses a robot arm or track systems to move microplates between these instruments. These technologies are continuously improved (Brown and Proulx 1997; Lightbody and Alderman 2001; Ruch 2001; Alanine et al. 2003).

High-throughput screening methods are also used to characterize metabolic and pharmacokinetic data about new drugs (Watt et al. 2000; White 2000). Kansy et al. (1998) recommended parallel artificial membrane permeation assays for the description of passive absorption processes early in HTS.

High-throughput screening assays have been used for the assessment of cytochrome P450 isoenzyme metabolism using fluorogenic Vivid substrates (Marks et al. 2002, 2003, 2004).

A large pharmaceutical company has the potential to screen up to 100,000,000 compounds per year (Drews 2000). In any case, the leads or derivatives of them have to be tested in more complex mod-

els, isolated organs or animals. Only compounds active in classical pharmacological tests can be taken into preclinical and clinical development. Since only a few drug candidates, originally screened in HTS, have reached the market, the searching for higher productivity of HTS is continuing (Fox et al. 2001, 2004; Liu et al. 2004), especially because development costs for new drugs have increased tremendously (DiMasi et al. 2003).With the completion of the human genome sequencing, bioinformatics will be an essential tool in target discovery, and the *in silico* analysis of gene expression and gene function will be an integral part of it, facilitating selection of the most important targets for a disease under study (Terstappen and Reggiani 2001).

Optimistic papers on the value of virtual screening of virtual libraries were written by Green (2003) as well as by Davies et al. (2006). Some doubts were expressed on the philosophy of research management in the pharmaceutical industry neglecting the influence of creative scientists, failing to understand biological complexity, and overestimating the outcome of the "change in paradigm" (Horrobin 2000, 2001, 2002, 2003). Nevertheless, the race to test more and more compounds in a shorter time in ultra-HTS with more automation is continuing.

0.4.2.1 Errors in HTS

As for every screening procedure, HTS suffers from type 1 and type 2 errors. Type 1 errors are false positives. In HTS, a poor candidate or an artifact gives an anomalously high signal, exceeding an established threshold. Type 2 errors are the false negatives. In HTS, a perfectly good candidate compound is not flagged as a hit, because it gives an anomalously low signal. Moreover, a low degree of relevance of the test may induce a high failure rate of type 2 (see also the discussion at the end of this chapter).

Much more attention is given in the literature to false-positive results in HTS than to type 2 errors (Fowler et al. 2002; Lin et al. 2002; Bader and Hogue 2003; Colinge et al. 2003; Francis and Friedman 2003; Glover et al. 2003; Jenkins et al. 2003; Turek-Etienne et al. 2003; Deng et al. 2004; Diller and Hobbs 2004; Vidalain et al. 2004; Huth et al. 2005). Some of the false positives are promiscuous compounds that act noncompetitively and show little relationship between structure and function. McGovern et al. (2002, 2003) and Seidler et al. (2003) found that one mechanism of inhibitor promiscuity is aggregate formation: individual molecules group together to form particles 30–1000 nm in diameter and these aggregates are the active inhibitory species.

0.4.2.2 Statistical Evaluation of HTS

The ability to identify active compounds ("hits") from large libraries accurately and rapidly is the ultimate goal of HTS assays, which depends on the suitability and quality of the assay.

The *Z*-factor and the Z' factor were introduced to characterize the reliability of high-throughput assays (Zhang et al. 1999, 2000b).

The *Z*-factor is a dimensionless, simple statistical characteristic, which reflects the assay signal dynamic range and the data variation associated with the signal measurements. The *Z*-factor is defined as a screening window coefficient, which uses the formula

$$Z = 1 - \frac{3\sigma_s + 3\sigma_c}{|\mu_s - \mu_c|}$$

in which μ_s and μ_c denote the means of the population and control (usually background) signals, respectively, and the signal standard deviations are denoted as σ_s and σ_c, respectively. This coefficient takes into account the assay signal's dynamic range, the data variation associated with the sample measurement in the presence of the test library, and the data variation associated with the reference control measurement.

The Z'-factor has been defined as the ratio of the separation band to the dynamic range of the assay, based on the positive control and negative control data of the assay. It takes the formula

$$Z' = 1 - \frac{3\sigma_{c+} + 3\sigma_{c-}}{|\mu_{c+} - \mu_{c-}|}$$

in which μ_{c-} and μ_{c+} denote the means of the negative control signal and positive control signal, respectively. The standard deviations of the signals are denoted as σ_{c-} and σ_{c+}, respectively. The Z'-factor is a simple, dimensionless, and characteristic parameter for the quality of each assay.

Values of 0.7 or higher are considered to indicate a valuable assay.

CRITICAL ASSESSMENT OF THE METHOD

The *Z*-factor and the Z'-factor have been used by various authors to characterize the quality of assays (Zhang et al. 2000a; Drake et al. 2002; Lin et al. 2002; Kotarsky et al. 2003; Hamid et al. 2004).

REFERENCES AND FURTHER READING

Alanine A, Nettekoven M, Roberts E, Thomas AW (2003) Lead-generation-enhancing the success of drug discovery by investing in the hit to lead process. Comb Chem High Throughput Screen 6:51–66

Bader GD, Hogue CW (2003) An automated method for finding molecular complexes in large protein interaction networks. BMC Bioinformatics 4:2

Berg M, Undisz K, Thiericke R, Moore T, Posten C (2000) Miniaturization of a functional transcription assay in yeast (human progesterone receptor) in the 384- and 1536-well plate format. J Biomol Screen 5:71–76

Blake JF (2004) Integrating cheminformatic analysis in combinatorial chemistry. Curr Opin Chem Biol 8:407–411

Bolger R (1999) High-throughput screening: new frontiers for the 21st century. Drug Discov Today 4:251–253

Brandish PE, Chiu CS, Schneeweis J, Brandon NJ, Leech CL, Kornienko O, Scolnick EM, Strulovici B, Zheng W (2006) A cell-based ultra-high-throughput screening assay for identifying inhibitors of D-amino acid oxidase. J Biomol Screen 11:481–487

Broach JR, Thorner J (1996) High throughput screening for drug discovery. Nature 384 [Suppl. 14–16]:6604

Brown RK, Proulx A (1997) Accelerating the discovery process with automation and robotics: a sure bet or a risky venture? In: Devlin JP (ed) High throughput screening. The discovery of bioactive substances. Dekker, New York, pp 509–523

Clark DE, Pickett SD (2000) Computational methods for the prediction of "drug-likeness". Drug Discov Today 5:49–58

Colinge J, Masselot A, Giroin M Dessingy T, Magnin J (2003) OLAV: towards high-throughput tandem mass spectroscopy data identification. Proteomics 3:1454–1463

Cox B, Denyer JC, Binnie A, Donnelly MC, Evans B, Green DVS, Lewis JA, Mander TH, Merritt AT, Valler MJ, Watson SP (2000) Application of high-throughput screening techniques to drug discovery. Progr Med Chem 37:83–133

Cullen CJ, Wootton RC, de Mello AJ (2004) Microfluidic systems for high-throughput and combinatorial chemistry. Curr Opin Drug Discov Dev 7:798–806

Davies JW, Glick M, Jenkins JL (2006) Streamlining discovery by aligning in silico and high-throughput screening. Curr Opin Chem Biol 10:343–351

Deng G, Gu RF, Marmor S, Fisher SL, Jahic H, Sanyal G (2004) Development of an LC-MS based enzyme activity assay for MurC: application to evaluation of inhibition and kinetic analysis. J Pharm Biomed Anal 35:817–828

Diller DJ, Hobbs DW (2004) Deriving knowledge through data mining high-throughput screening data. J Med Chem 47:6373–6383

DiMasi JA, Hansen RW, Grabowski HG (2003) The price of innovation: new estimates of drug development costs. J Health Econom 22:151–185

Divers M (1999) What is the future of high throughput screening? J Biomol Screen 4:177–178

Drake KA, Zhang JH, Harrison RK, McGeehan GM (2002) Development of a homogeneous, fluorescence resonance energy transfer-based *in vitro* recruitment assay for peroxisome proliferators-activated receptor δ via selection of active LXXLL coactivator peptides. Anal Biochem 304:63–69

Drews J (2000) Drug discovery: a historical perspective. Science 287:1960–1964

Dunn D, Orlowski M, McCoy P, Gastgeb F, Appell K, Ozgur L, Webb M, Burbaum J (2000) Ultra-high throughput screen of two-million-member combinatorial compound collection in a miniaturized 1536-well assay format. J Biomol Screen 5:177–187

Eglen RM (1999) High throughput screening: myths and future realities. J Biomol Screen 4:179–181

Fowler A, Swift D, Longman E, Acornley A, Hemsley P, Murray D, Unitt J, Dale I, Sullivan E, Coldwell M (2002) An evaluation of fluorescence polarization and lifetime discriminated polarization for high throughput screening of serine/threonine kinases. Anal Biochem 308:223–231

Fox S, Farr-Jones S, Yund MA (1999) High throughput screening for drug discovery: continually transitioning into new technology. J Biomol Screen 4:183–186

Fox S, Wang H, Sopchak L, Khoury R (2001) Increasing the changes of lead discovery. Drug Disc World 2:35–44

Fox S, Farr-Jones S, Sopchak L, Boggs A, Comley J (2004) High-throughput screening: searching for higher productivity. J Biomol Screen 9:354–358

Francis R, Friedman SH (2003) An interference-free fluorescent assay of telomerase for the high-throughput analysis of inhibitors. Anal Biochem 323:65–73

Giuliano KA, DeBiasio RL, Dunlay RT, Gough A, Volosky JM, Zock J, Pavlakis GN, Taylor DL (1997) High-content screening: a new approach to easing key bottlenecks in the drug discovery process. J Biomol Screen 2:249–259

Glover CJ, Hite K, DeLosh R, Scudiero DA, Fivash MJ, Smith LR, Fisher RJ, Wu JW, Shi Y, Kipp RA, McLendon GL, Sausville EA, Shoemaker RH (2003) A high-throughput screen for identification of molecular mimics of Smac/DIABLO utilizing a fluorescence polarization assay. Anal Biochem 320:157–169

Goddard JP, Reymond JL (2004) Enzyme assays for high-throughput screening. Curr Opin Biotechnol 15:314–322

Green DV (2003) Virtual screening of virtual libraries. Prog Med Chem 41:61–97

Hamid R, Rotshteyn Y, Rabadi L, Parikh R, Bullock P (2004) Comparison of alamar blue and MTT assays for high through-put screening. Toxicol In Vitro 18:703–710

Harding D, Banks M, Fogarty S, Binnie A (1997) Development of an automated high-throughput screening system: a case history. Drug Descov Today 2:385–390

Harvey A (2000) Strategies for discovering drugs from previously unexplored natural products. Drug Descov Today 5:294–300

Horrobin DF (2000) Innovation in the pharmaceutical industry. J R Soc Med 93:341–345

Horrobin DF (2001) Realism in drug discovery – could Cassandra be right? Nature Biotechnol 19:1099–1100

Horrobin DF (2002) Effective clinical innovation: an ethical imperative. Lancet 359:1857–1858

Horrobin DF (2003) Modern biomedical research: an internally self-consistent universe with little contact with medical reality? Nat Rev Drug Discov 2:151–154

Huth JR, Mendoza R, Olejniczak ET, Johnson RW, Cothron DA, Liu Y, Lerner GC, Chen J, Hajduk PJ (2005) ALARM NMR: a rapid and robust experimental method to detect reactive false positives in biochemical screens. J Am Chem Soc 127:217–224

Jenkins JL, Kao RY, Shapiro R (2003) Virtual screening to enrich hit lists from high-throughput screening: a case study on small-molecule inhibitors of angiogenin. Proteins 50:81–83

Kansy M, Senner F, Gubernator K (1998) Physicochemical high throughput screening: parallel artificial membrane permeation assay in the description of passive absorption processes. J Med Chem 41:1007–1010

Kotarsky K, Antonsson L, Owman C, Olde B (2003) Optimized reporter gene assays based on a synthetic multifunc-

tional promoter and a secreted luciferase. Anal Biochem 316:208–215
Lahana R (1999) How many leads from HTS? Drug Discov Today 4:447–448
Lightbody B, Alderman EM (2001) Robotics development simplified. New Drugs 1:30–32
Lin S, Bock CL, Gardner DB, Webster JC, Favata MF, Trzaskos JM, Oldenburg KR (2002) A high-throughput fluorescent polarization assay for nuclear receptor binding utilizing crude receptor extract. Anal Biochem 300:15–21
Liu B, Li S, Hu J (2004) Technological advances in high-throughput screening. Am J Pharmacogenomics 4:263–276
Major J (1999) What is the future of high throughput screening? J Biomol Screen 4:119
Mander T (2000) Beyond uHTS? Ridiculously HTS? Drug Discov Today 6:223–225
Marks BD, Smith RW, Braun HA, Goossesn TA, Christenson M, Ozers MS, Lebakken CS, Trubetskoy OV (2002) A high throughput screening assay to screen for CYP2E1 metabolism and inhibition using a fluorogenic Vivid P450 substrate. Assay Drug Dev Technol 1:73–81
Marks BD, Goossens TA, Braun HA, Ozers MS, Smith RW, Lebakken C, Trubetskoy OV (2003) High-throughput screening assays for CYP2B6 metabolism and inhibition using fluorogenic Vivid substrates. AAPS Pharm Sci 5, Article 18
Marks BD, Thompson DV, Goossens TA. Trubetskoy OV (2004) High-throughput screening assays for the assessment of CYP2C9*1, CYP2C9*2, and CYP2C9*3 metabolism using fluorogenic Vivid substrates. J Biomol Screen 9:439–449
McGovern SL, Caselli E, Grigorieff N, Shoichet BK (2002) A common mechanism underlying promiscuous inhibitors from virtual and high-throughput screening. J Med Chem 45:1712–1722
McGovern SL, Helfand BT, Feng B, Shoichet BK (2003) A specific mechanism of nonspecific inhibitors. J Med Chem 46:4265–4272
Ohlstein EH, Ruffolo RR Jr, Elliot JD (2000) Drug discovery in the next millennium. Annu Rev Pharmacol Toxicol 40:177–191
Ohlstein EH, Johnson AG, Romanic AM (2006) New strategies in drug discovery. Methods Mol Biol 316:1–11
Ruch E (2001) The flexible approach to high throughput screening. New Drugs 1:34–36
Ryu DDY, Nam D-H (2000) Recent progress in biomolecular engineering. Biotechnol Prog 16:2–16
Seidler J, McGovern SL, Doman TN, Shoichet BK (2003) Identification and prediction of promiscuous aggregating inhibitors among known drugs. J Med Chem 46:4477–4486
Sills MA (1998) Future considerations in HTS: the acute effect of chronic dilemmas. Drug Discov Today 3:304–312
Stahl W (1999) What is the future of high throughput screening? J Biomol Screen 4:117–118
Sundberg SA (2000) High-throughput and ultra-high-throughput screening: solution- and cell-based approaches. Curr Opin Biotechnol 11:47–53
Terstappen GC, Reggiani A (2001) *In silico* research in drug discovery. Trends Pharmacol Sci 22:23–26
Turconi S, Shea K, Ashman S, Fantom K, Ernshaw DL, Bingham RP, Haupts UM, Brown MJB, Pope AJ (2001) Real experiences of uHTS: a prototypic 1536-welll fluorescence anisotropy-based uHTS screen and application of well-level quality control procedures. J Biomol Screen 6:275–290
Turek-Etienne TC, Small EC, Soh SC, Gaitonde TA, Barrabee PV, Hart EB, Bryant RW (2003) Evaluation of fluorescent compound interference in 4 fluorescence polarization assays: 2 kinases, 1 protease, and 1 phosphatase. J Biomol Screen 8:176–184
Valler MJ, Green D (2000) Diversity screening versus focussed screening in drug discovery. Drug Discov Today 5:286–293
Vidalain PO, Boxem M, Ge H, Li S, Vidal M (2004) Increasing specificity in high-throughput yeast two-hybrid experiments. Methods 32:363–370
Watt AP, Morrison D, Evans DC (2000) Approaches to higher-throughput pharmacokinetics (HTPK) in drug discovery. Drug Discov Today 5:17–24
White RE (2000) High-throughput screening in drug metabolism and pharmacokinetic support of drug discovery. Annu Rev Pharmacol Toxicol 40:133–157
Williams M (2003) Target validation. Curr Opin Pharmacol 3:571–577
Wolcke J, Ullmann D (2001) Miniaturized HTS technologies – uHTS. Drug Discov Today 6:637–646
Zhang JH, Chung TDY, Oldenburg KR (1999) A simple statistic parameter for use in evaluation and validation of high throughput screening assays. J Biomol Screen 4:67–73
Zhang JH, Chen T, Nguyen SH, Oldenburg KR (2000a) A high-throughput homogeneous assay for the reverse transcriptase using generic reagents and time-resolved fluorescence detection. Anal Biochem 281:182–186
Zhang HJ, Chung TDY, Oldenburg KR (2000b) Confirmation of primary active substances from high throughput screening of chemical and biological populations: a statistical approach and practical considerations. J Comb Chem 2:258–265

0.4.3 Technologies for High-Throughput Screening

Fundamental changes in assay technologies have facilitated the development of high-throughput screening (HTS) (Major 1995; Pazhanisamy et al. 1995; Devlin 1997; Harding et al. 1997; Houston and Banks 1997; Sittampalam et al. 1997; Su et al. 1997; Brandt 1998; Fernandes 1998; González and Negulescu 1998; Kenny et al. 1998; Pasini et al. 1998; Sills 1998; Silverman et al. 1998; Wingfield 1998; Zysk and Baumbach 1998; Bolger 1999; Labute 1999; Winkler et al. 1999; Bosse et al. 2000; Cox et al. 2000; Feiglin et al. 2000; Gauglitz 2000; Landro et al. 2000; Meza 2000; Parker et al. 2000; Schuster et al. 2000; Sundberg 2000; Liu et al. 2004).

Zehender et al. (2004) recommended SpeedScreen as the "missing ling" between genomics and lead discovery. SpeedScreen is a label-free, in-solution, affinity-based selection methodology for HTS. The protocol compromises in-solution affinity selection, followed by size exclusion chromatography in combination with microbore-liquid-chromatography/electrospray-ionization mass spectroscopy.

A versatile platform for nuclear receptor screening using AlphaScreen™ has been developed by Rouleau et al. (2003)

Abraham et al. (2004) discussed high-content screening applied to large-scale cell biology.

In **multiplexing assays**, more than one component is studied in a single sample. Advantages of this strategy include economy, since theoretically the same sample may be used for many measurements (Beske and Goldbard 2002). Also, because the exact same sample is used for different assays, sample errors caused by heterogeneity are minimized (Charter 2004). Nieuwenhuijsen et al. (2003) published a dual luciferase multiplexed HTS platform for protein–protein interactions. Maley et al. (2004) used multiplexed real-time reverse transcriptase-polymerase chain reaction (RT-PCR) for HTS applications.

Grépin (2004) recommended multiplexed cell-based assays as an intermediary screening format between HTS and high content screening.

0.4.3.1 Dispensing Technologies

Several systems for fluid dispensing are in use: the piezo- and inkjet, the "air displacement", and the "pintool" systems (Vollert et al. 2000). Piezoelectric and inkjet systems were the first introduced to the market (Lemmo et al. 1998; Rose 1999). There are three types of inkjet dispensers: thermal, solenoid, and piezoelectric. All of these use some means of compressing a liquid against a small orifice to create sufficient linear velocity to eject the fluid in the form of a drop.

The "pintool" systems use pins (needles) to transfer liquid. Up to 1536 needles are immersed into the fluid and withdrawn, taking up a few nanoliters and transferring the fluid into the wells of a microtiter plate.

Utilization of syringes and syringe needles as a contact tool enables multiple dispensing from a single fill. Generally, syringe dispensing has a higher degree of accuracy and repeatability compared with pin dispensing tools (Vollert 1998; Dunn and Feygin 2000).

Microfluidic arrays for high-throughput submicroliter assays using capillary electrophoresis were described by Gibbons (2000). Capillary electrophoresis is an analytical technique that can achieve rapid high-resolution separation of water-soluble components present in small sample volumes. Separations are based on the electrically driven movement of ions. In HTS, analytes are separated according to differences in electrophoretic mobility, depending on the charge-to-size ratio.

The most common "no contact" delivery format is piezoelectric acoustic delivery. This technique delivers a powerful sonic or ultrasonic pulse, which accelerates a tiny droplet from the surface of liquid in the stock vessel, through the air and onto the dry capture of a microplate. Hsieh et al. (2004) used disposable piezoelectric ejectors for liquid dispensing in ultra-high-throughput microarray screening.

0.4.3.2 Cell-Based Assays

Cell-based assays are increasingly attractive alternatives to *in vitro* biochemical assays for HTS (Wallace and Goldman 1997; Silverman et al. 1998). They fall into three broad categories: second messenger assays that monitor signal transduction following activation of cell-surface receptors; reporter gene assays that monitor cellular responses at the transcription/translation level; and cell proliferation assays to monitor the overall growth/no growth response of cells to external stimuli (Sundberg 2000).

Hynes et al. (2003) described a luminescence-based assay for screening the viability of mammalian cells, based on the monitoring of cell respiration by means of a phosphorescent water-soluble oxygen probe that responds to changes in the concentration of dissolved oxygen by changing its emission intensity and lifetime.

Yan et al. (2002) described a cell-based HTS assay system for monitoring G-protein-coupled receptor activation using β-galactosidase enzyme complementation technology. This technology uses a pair of inactive β-galactosidase deletion mutants as fusion partners to the protein targets of interest. To monitor G-protein-coupled receptor activation, stable cell lines expressing both G-protein-coupled receptor and β-arrestin-β-galactosidase fusion proteins are generated. Following ligand stimulation, β-arrestin binds to the activated G-protein-coupled receptor, and this interaction drives functional complementation of the β-galactosidase mutant fragments. G-protein-coupled receptor activation is measured directly by quantitating restored β-galactosidase activity with the chemoluminescent Gal-Screen reagent.

Cell-based reporter assays are used where human receptors are transfected into null cell lines either alone, or as part of receptor systems constructed to show alterations in light production (luciferin-luciferase) or light transmission (melanophore), which can be measured independently of radioactivity within minutes (Broach and Thorner 1996).

Pathirna et al. (1995) developed a transient transfection HTS assay to identify nonsteroidal human progesterone receptor modulators using luciferase expression. Zhu et al. (2004) found a good correlation be-

tween high-throughput pregnane X receptor (PXR) transactivation and binding assays.

Another reporter gene, green fluorescent protein, can be measured by fluorescence techniques in real time so that kinetic parameters can be determined from a single well of a microtiter plate (Chalfie et al. 1994; Chalfie 1995; Kain 1999; Meng et al. 2000; Arun et al. 2005).

Scheirer (1997) reviewed the various reporter genes and their applications.

Ting et al. (2001) described genetically encoded fluorescent reporters of protein tyrosine kinase activities in living cells.

González and Negulescu (1998) described intracellular detection assays for HTS which employ either fluorescent or luminescent readouts. The method is particularly suitable for measuring calcium mobilization (Akong et al. 1995; Burbaum and Sigal 1997).

Using receptor selection and amplification technology (R-SAT), it is possible to rapidly quantify specific pharmacological responses as a function of changes in cell proliferation rates (Messier et al. 1995). NIH3T3 cells (or other cell lines) are transfected with the plasmid coding for the receptor of interest and pSV-β-Gal. Cells are then transferred to 96-well microtiter plates and test compounds are added. Several days later, β-Gal activity is measured via a simple, inexpensive colorimetric assay. As a result of compound treatment, the changes in enzyme activity are a function of the proliferative activity of the cells. This functional assay can quantitatively differentiate between full agonists, partial agonists, neutral antagonists, and negative antagonists (inverse agonists). An interesting aspect of this technology is that many genes in a related family can be combined in the same cell population for convenient assay.

Bailey et al. (2002) discussed the applications of transfected cell microarrays in high-throughput drug discovery. Transfected cell microarrays are a complementary technique in which array features comprise clusters of cells overexpressing defined cDNAs. Complementary DNAs cloned in expression vectors are printed on microscope slides, which become living arrays after the addition of a lipid transfection reagent and adherent mammalian cells.

Dupriez et al. (2002) and Le-Poul et al. (2002) described aequorin-based functional assays for G-protein-coupled receptors, ion channels, and tyrosine kinase receptors.

AequoScreen is a cellular-based functional assay in which the cells are loaded with the apoaequorin cofactor coelenterazine, diluted in assay buffer, and injected into plates containing the samples to be tested.

Kunz-Schughart et al. (2004) recommended the multicellular spheroid model and the use of 3-D cultures for HTS.

Gaspari et al. (2004) described the quantification of the proliferation index of human dermal fibroblast cultures with the ArrayScan™ high-content screening reader.

Isailovic et al. (2005) presented a high-throughput method for measuring single-cell fluorescence spectra. Upon excitation with a 488 nm argon-ion laser many bacterial cells were imaged by a 20 × microscope objective while they moved through a capillary tube. Fluorescence was dispersed by a transmission diffraction grating, and an intensified charge-coupled device (ICCD) camera simultaneously recorded the zero and the first orders of the fluorescence from each cell.

Flow cytometry was recommended for high-throughput, high-content screening by Edwards et al. (2004). Flow cytometry is a platform for quantitative multi-parameter measurements of cell fluorescence. Homogeneous discrimination between free and cell-bound fluorescent probe eliminates wash steps to streamline sample processing. Waller et al. (2004) used flow cytometry as a technique for studying GPCR assembly, pharmacology, and screening.

0.4.3.3 High-Throughput Assay Technologies for Ion Channels

Ion channels represent a class of membrane-spanning protein pores that mediate the flux of ions in a variety of cell types. To date, > 400 ion channels have been cloned and characterized, and some of these channels have emerged as attractive drug targets. Zheng et al. (2004b) reviewed the technologies that are currently used for the screening of ion channels. The technologies discussed are binding assays, ion flux assays, fluorescence-based assays, and automated patch-clamp instrumentation.

Gill et al. (2003) described flux assays in HTS of ion channels in drug discovery. Technologies based on flux assays are available in a fully automated high-throughput format for efficient screening. This application offers sensitive, precise, and reproducible measurements giving accurate drug rank orders matching those of patch-clamp data.

Treherne (2006) reviewed high-throughput ion channel screening technologies in integrated drug discovery.

Automated patch-clamp systems useful for HTS techniques, such as Qpatch, have been recommended by several authors (Asmild et al. 2003; Lepple-Wienhues et al. 2003; Stett et al. 2004; Willumsen et al. 2003; Brueggemann et al. 2004; Shieh 2004; Zheng et al. 2004b; Mathes 2006).

0.4.3.4 Detection Methods

Fluorescence-based assay technologies play an increasing role in HTS. When compared to other biochemical and cell-based techniques, fluorescence has a significant advantage over such methods as isotopic labeling, colorimetry, and chemiluminescence.

Sensitivity

It is relatively simple for modern instrumentation to reliably detect a signal being emitted from a single fluorescent molecule. In biological applications, this level of sensitivity means molecules that may be present only in very small numbers can be easily detected. In the case of imaging application, such as high-content screening, their intracellular location can be determined. This high level of sensitivity also means that transient biological events can be detected very quickly, hence enabling the measurement and understanding of events that occur very rapidly inside living cells. The inherent sensitivity of fluorescence technology also permits the use of very low concentrations of fluorescent label.

Specificity

Fluorescent probes are readily available for labeling virtually any biomolecule, structure, or cell type. Immunofluorescent probes can be directed to bind not only to specific proteins but also to specific conformations, cleavage products, or site modifications, such as phosphorylation. Individual peptides and proteins can be engineered to autofluorescence by expressing them as AFP chimeras inside cells. Such high levels of specificity enable the use of several different fluorescent labels – each emitting at a unique color – and the subsequent understanding of the complex interactions that occur among and between subcellular constituents.

Accuracy

Reagents used for fluorescence labeling are well understood and their performance has been characterized under a wide variety of biological environments.

Flexibility

Fluorescence technologies have matured to the point where an abundance of useful dyes is now commercially available. Many dyes have been developed and optimized for labeling specific cell compartments and components, as well as for labeling proteins (antibodies, ligands, toxins, etc.), which can be used as probes. Other fluorescent sensors have been designed to report on biological activities or environmental changes (pH, calcium concentration, electrical potential, proximity to other probes, etc.). Multiple fluorescent labels can be used on the same sample and individually detected quantitatively, permitting measurement of multiple cellular responses simultaneously. Many quantitative techniques have been developed to harness unique properties of fluorescence, including:

- fluorescence resonance energy transfer (FRET)
- fluorescence polarization or anisotropy (FP)
- time-resolved fluorescence (TRF)
- fluorescence lifetime measurements (FLM)
- fluorescence correlation spectroscopy (FCS)
- fluorescence photobleaching recovery (FPR)
- molecular beacons (MB)

Mere et al. (1999) reported miniaturized **fluorescence resonance energy transfer (FRET)** assays and microfluidics as key components for ultra-HTS. An ultra-HTS system (UHTSS™) platform integrates several microfluidic dispensing devices, which have been developed to deliver nanoliter to microliter volumes at high speed into the appropriate wells of 384-well NanoWell™ assay plates. The activity of the compounds dispensed into the assay wells is quantified via a highly sensitive dual-wavelength emission fluorescence detector.

Pope et al. (1999) discussed the advantages and disadvantages/limitations of fluorescence techniques for the establishment of miniaturized homogeneous screening assays, including prompt intensity assay (FLINT), anisotropy assay (FA), prompt energy transfer assay (FRET), fluorescence correlation spectroscopy (mass-dependent FCS), and fluorescent correlation spectroscopy (mass-independent FCS).

Nagai et al. (2004) used FRET technology to develop genetically encoded fluorescent indicators for various cell functions.

Chin et al. (2003) described miniaturization of cell-based beta-lactamase-dependent FRET assays to ultra-high-throughput formats to identify agonists of human liver X receptors.

Wallrabe and Periasami (2005) reviewed imaging protein molecules using Förster (or fluorescence) resonance energy transfer (FRET) and fluorescence lifetime imaging measurements (**FLIM**).

Dynamics of fluorescence fluctuations in green fluorescent protein observed by **fluorescence correlation spectroscopy (FCS)** were described by Haupts et al. (1998). Auer et al. (1999) recommended fluorescence correlation spectroscopy for lead discovery by miniaturized HTS. By monitoring interactions "of single molecules in femtoliter volumes, fluorescence correlation spectroscopy offers the highest potential as the detection technique at the nanoscale. Schwille et al. (2000) reported that fluorescence correlation spectroscopy reveals fast optical excitation-driven intramolecular dynamics of yellow fluorescent proteins.

Haupts et al. (2000) compared macroscopic versus microscopic fluorescence techniques in (ultra)-HTS.

Rüdiger et al. (2001) reviewed single-molecule detection technologies in miniaturized HTS and studied binding assays for G-protein-coupled receptors using fluorescence intensity distribution analysis (**FIDA**) and fluorescence anisotropy. As a confocal detection technology, FIDA inherently allows reduction of the assay volume to the microliter range and below without any loss of signal.

Palo et al. (2002) introduced a method that combines the benefits of both fluorescence intensity distribution analysis (**FIDA**) and fluorescence lifetime analysis. It is based on fitting the two-dimensional histogram of the number of photons detected in counting time intervals of given width and the sum of excitation to detection delay times of these photons. Referred to as fluorescence intensity and lifetime distribution analysis (**FILDA**), the technique distinguishes fluorescence species on the basis of both their specific molecular brightness and the lifetime of the excited state and is also able to determine absolute fluorophore concentrations.

Jäger et al. (2003a) reviewed fluorescence techniques for high-throughput drug discovery. In particular, the family of fluorescence techniques, Fluorescence Intensity Distribution Analysis (FIDA), which is based on confocal single-molecule detection, has opened up a new field of HTS applications.

Eggeling et al. (2005) recommended the combination of Förster resonance energy transfer (FRET) and two-color global fluorescence correlation spectroscopy (2CG-FCS) for high-throughput applications in drug screening.

Sportsman and Leytes (2000) discussed miniaturization of homogenous assays using **fluorescence polarization** (**FP**), which can detect changes in molecule size as well as quantify the binding of small molecules to larger molecules. Polarization of fluorescence occurs when a fluorescent molecule is illuminated with plane-polarized light, provided that the molecule does not move during the course of fluorescent lifetime. For typical fluorescent molecules such as fluorescein, the polarization is not observed if the molecule is rotating rapidly in solution under conditions typically used in biological assays. Thus, if the polarization of fluorescence of a fluorescein-labeled ligand is measured, a low polarization will be observed when the ligand is free in solution, and a high polarization will be observed when the ligand is bound to a macromolecule such as a specific receptor or antibody.

Banks et al. (2000) described fluorescence polarization assays for HTS of G-protein-coupled receptors in 384-well microtiter plates.

Parker et al. (2000) used fluorescence polarization to develop HTS assays for nuclear receptor-displacement and kinase inhibition. This method is a solution-based, homogeneous technique, requiring no immobilization or separation of reaction components. As an example, the authors described the fluorescence polarization-based estrogen receptor assay based on the competition of fluorescein-labeled estradiol and estrogen-like compounds for binding to the estrogen receptor.

Li et al. (2000) developed an assay for measuring the activity of an enzyme that transfers multiple adenine-containing groups to an acceptor protein, based on fluorescence polarization technology in a 1536-well plate format. Texas red (rhodamine) was covalently conjugated to the adenine of the donor substrate through a C_6 spacer arm. As a result of the transfer of the adenine-containing moieties to the acceptor protein substrate, the rotational correlation time of the Texas red conjugate increased, hence increasing the degree of fluorescence polarization.

Owicki (2000) compared the perspectives of fluorescence polarization and anisotropy in HTS.

Qian et al. (2004) used fluorescence polarization to discover novel inhibitors of Bcl-xL, a factor preventing apoptosis.

Lu et al. (2004) developed a fluorescence polarization bead-based coupled assay to target activity/conformation states of a protein kinase. This assay is based on the principle of the Immobilized Metal Assay for Phosphochemicals (IMAP™) (Mole™cular Devices, Sunnyvale, Calif., USA), a fluorescence polarization assay based on the affinity capture of phosphorylated peptides (Gaudet et al. 2003; Sportsman et al. 2003).

Kolb et al. (1997) and Grépin and Pernelle (2000) described the evolution of **homogeneous time resolved fluorescence (HTRF)** technology for HTS. HTRF uses the europium (Eu^{3+}) ion caged into polycyclic cryptate (Eu-cryptate) as a donor. Laser excitation at 337 nm transfers the energy from the Eu-cryptate complex to an allophycocyanin acceptor molecule (XL665), the APC. This results in the emission of light at 665 nm over a prolonged time (milliseconds). Uncoupled or free XL665 emits at 665 nm, but with a short decay. The light emission is recorded in a time-resolved fashion over a 400-µs period, starting 50 µs after the excitation pulse, so that the autofluorescence from the media and the short-lived fluorescence of the free APC are not recorded. Eu-cryptate emits at 620 nm and is discriminated from XL665 by wavelength.

The labeling of macromolecules for HTRF assay can be done in a number of ways, depending on the type of screen, using direct, indirect or semi-direct types of labeling. Direct labeling is characterized by having the (Eu)K and XL665 covalently bound to the molecule or molecules of interest. Indirect labeling is when the (Eu)K and XL665 are bound to macromolecules through secondary interactions, such as biotin-streptavidin interaction or antibody binding. Other indirect methods, such as (Eu)K or XL665-labeled lectin, can be used for binding to membranes. The semi-direct method is a combination of direct and indirect methods and is frequently used in HTRF.

HTRF immunoassays generally use a direct labeling strategy in which two antibodies against different antigenic sites are used. One antibody is labeled with (Eu)K and another is labeled with XL665. When both bind to the antigen, energy transfer occurs and the long-lived XL665 signal is generated. Europium-labeled recombinant protein G as a fast and sensitive immunoreagent for time-resolved immunofluorometry had been described by Markela et al. (1993).

Merk et al. (2004) described time-resolved fluorescence measurements using a microlens array and area imaging devices. For applications in the TRF mode the Plate::Vision(2) 96-microlens array reader (Carl Zeiss Jena, Germany) was compared with the LEADseeker Generation IV multimodality imaging system (Amersham Biosciences UK).

Selvin (2002) discussed the principles and biophysical applications of lanthanide-based probes. Using luminescent lanthanides, instead of conventional fluorophores, as donor molecules in resonance energy transfer measurements offers many technical advantages and opens up a wide range of applications including farther measurable distances with greater accuracy, insensitivity to incomplete labeling, and the ability to use generic relatively large labels.

Karvinen et al. (2002) developed a homogenous time-resolved fluorescence quenching assay (LANCE) for caspases. The assay uses a peptide labeled with both a luminescent europium chelate and a quencher. Cleavage of the peptide by caspase-3 separates the quencher from the chelate and thus recovers europium fluorescence.

To study the interaction of two proteins, the JUN FOS dimerization was used as a model assay. The JUN protein was biotinylated. Streptavidin:(Eu)K was used to bind that label to the JUN-biotin protein via SA-biotin binding. The FOS peptide was directly labeled with XL665. Signal is only generated when JUN-biotin:SA-(Eu)K and FOS-XL665 dimerize to form the activated AP1 transcription complex.

The binding of ligands to membrane receptors and the competitive displacement by unknown molecules is one of the most common screening assays in drug discovery. To test the applicability of HTRF for receptor binding, the interaction of epidermal growth factor (EGF) with its receptor (EGFR) was studied (Mathis et al. 1994). To generate a HTRF signal, a semi-direct labeling method was developed. EGF was labeled directly with (Eu)K, and a monoclonal antibody against a nonbinding portion of the EGF receptor was used. The anti-EGRF antibody was labeled with XL665. The IC_{50} of displacement could be determined.

The phosphorylation of enzymes, proteins and receptors is a major mechanism of cell regulatory pathways and is therefore a frequent target for drug discovery. The EGFR-intrinsic tyrosine kinase activity was used to develop an HTRF assay. Biotin-labeled $(glutamine\text{-}alanine\text{-}tyrosine)_n$ (poly GAT) was used as a substrate. The EGF receptor was isolated from A431 cells after partial purification of a cell homogenate. After the phosphorylation reaction, the HTRF signal was generated by adding streptavidin-XL665 and (Eu)-K-antiphosphotyrosine antibody. To establish the biological function of HTRF in this assay, inhibition of tryphostin-47 was assayed.

Homogeneous **time-resolved fluorescence resonance energy transfer (TR-FRET) assays** represent a highly sensitive and robust HTS method for the quantification of kinase activity (Lundin et al. 2001). Moshinski et al. (2003) reported a widely applicable high-throughput TR-FRET assay for the measurement of kinase autophosphorylation. Inhibition of the vascular endothelial growth factor receptor 2 (VEGRF-2) was used as prototype.

Glickman et al. (2002) published a comparison of ALPHAScreen, TR-FRET and TRF as assay methods for FXR nuclear receptors.

Newman and Josiah (2004) described utilization of fluorescence polarization and time-resolved fluorescence resonance energy transfer assay formats for structure–activity relationship studies. Src kinase was used as a model system.

Beasley et al. (2003) described the evaluation of compound interference in immobilized metal ion affinity-based fluorescence polarization (IMAP) detection with a four million member compound collection. IMAP is a non-separation-based, antibody-independent FP assay that can be applied to many types of protein kinases and phosphatases. In this technology, a fluorescently labeled peptide substrate is phosphorylated and then captured on immobilized metal nanoparticles. The binding of the phosphorylated peptide to the nanoparticles is detected using FP.

Loomans et al. (2003) reported HTS with immobilized metal ion affinity-based fluorescence polarization detection as a homogeneous assay for protein kinases.

Klumpp et al. (2006) discussed the development of homogeneous, miniaturized assays for the identification of novel kinase inhibitors from very large compound collections. In particular, the suitability of TR-FRET based on phospho-specific antibodies, an antibody-independent fluorescence polarization (FP) approach using metal-coated beads (IMAP technology), and the determination of adenosine triphosphate consumption through chemiluminescence was evaluated.

The **Acumen Explorer** is a laser-scanning system that measures fluorescence and luminescence, combining the ability to detect sub-micron events and features with ultra-fast acquisition and data management. Different parts of the cell can be localized by labeling with Hoechst 33342, Alexa™ 488, Alexa™ 546, Alexa™ 594, or Cys™ 5. Many different colors (readouts) can be used simultaneously.

The **fluorometric imaging plate reader (FLIPR™)** permits rapid, kinetic measurements of intracellular fluorescence. Simultaneous measurements in 96 wells and in real time can be made every second: before, during and after the addition of test compounds. The detection optics of FLIPR are based on cooled charge-coupled device (CCD) technology. With each kinetic update, the system takes a picture of the bottom of a microplate, recording a signal for all the individual cells simultaneously. Enhanced sensitivity for cell-based assays is accomplished via an optical detection scheme, which allows for signal isolation on a cell monolayer. The system is ideal for monitoring intracellular calcium fluxes that occur within seconds of activation of G-coupled receptors. Using calcium-sensitive dyes such as Fluo-3 permits the derivation of full dose–response (or dose–inhibition) curves in a matter of minutes (Kuntzweiler et al. 1998; Coward et al. 1999; Miller et al. 1999; Milligan and Rees 1999; Sullivan et al. 1999).

Hodder et al. (2004) reported miniaturization of intracellular calcium functional assays to the 1536-well plate format using a fluorometric imaging plate reader. An intracellular calcium functional assay against the rat muscarinic acetylcholine receptor subtype 1 G-protein-coupled receptor was miniaturized and executed in modified instruments.

Robinson et al. (2004) used a fluorescence microplate reader to compare ratiometric and nonratiometric Ca^{2+} indicators for the assessment of intracellular free Ca^{2} in a breast cancer line.

Bednar et al. (2004) used fluorescence detection of calcium flux for kinetic characterization of novel NR2B antagonists.

Swartzman et al. (1999) developed a simple, homogeneous bead-based immunoassay for use with **fluorometric microvolume assay technology (FMAT)**.

Koltermann et al. (1998) proposed rapid assay processing by integration of **dual-color fluorescence cross-correlation spectroscopy (RAPID FCS)** as an ideal tool for ultra-HTS when combined with nanotechnology, which can probe up to 10^5 samples per day. Auer et al. (1999) used fluorescence correlation spectroscopy for lead discovery by miniaturized HTS.

Winkler et al. (1999) presented **confocal fluorescence coincidence analysis** as an alternative to HTS. Confocal fluorescence coincidence analysis extracts fluorescence fluctuations that occur coincidentally in two different spectral ranges from a tiny observation volume of less than 1 fl. This procedure makes it possible to monitor whether an association between molecular fragments labeled with different fluorophores is established or broken, providing access to the characterization of a variety of cleavage and ligation reactions in biochemistry.

Jäger et al. (2003b) published a modular, fully integrated ultra-HTS system based on **confocal fluorescence analysis techniques**. The goal was to achieve high-data quality in small assay volumes (1–4 µl) combined with reliable and unattended operation. Two new confocal fluorescence readers have been designed. One of the instruments is a four-channel confocal fluorescence reader, measuring with four objectives in parallel. The fluorescence readout is based on single-molecule detection methods, allowing high sensi-

tivity at low tracer concentrations and delivering an information-rich output. The other instrument is a confocal fluorescence imaging reader, where the images are analyzed in terms of generic patterns and quantified in units of intensity per pixel. Both readers span the application range from assays with isolated targets in homogenous solution or membrane vesicle-based assays (four-channel reader) to cell-based assays (imaging reader). Results from a comprehensive test on these assay types demonstrate the high quality and robustness of this screening system.

Heilker et al. (2005) recommended confocal fluorescence microscopy for HTS of G-protein-coupled receptors.

For HTS, Schmid et al. (1998) proposed a method to reversibly attach receptor proteins via an affinity tag to a quartz surface and subsequently detect with high sensitivity the real-time binding of ligands by **total internal reflection fluorescence**.

The **CytoFluor Fluorescence Multi-Well Plate Reader**is a versatile fluorescence intensity measurement instrument that detects and quantifies fluorescent molecules over a five-log dynamic range. The system has a sensitivity of better than 8 fmol/well for fluorescein.

Ramm (1999) described the technique of **image-based screening in the LEADseeker™ system**, which contains a cooled CCD camera and a telecentric lens with integral epifluorescence illumination.

Laser scanning imaging systems have been developed to measure cellular and subcellular quantitation of fluorescence in whole cells (Conway et al. 1999; Zuck et al. 1999; Hertzberg and Pope 2000).

Chemiluminescence is a photometric technique that is applicable to HTS. Detection of chemiluminescence is a convenient adjunct to fluorescence, since most plate readers capable of measuring fluorescence will measure luminescence as well. This technique has been used predominantly with luciferase reporter genes in cell-based assays and in high-sensitivity enzyme-linked immunosorbent assays (ELISA), employing chemolumogenic substrates for alkaline phosphatase and horseradish peroxidase (Bronstein et al. 1994, 1996). The Luc-Screen assay system with extended-glow light emission was designed for sensitive detection of the firefly luciferase reporter enzyme. Liochev and Fridovich (1997) recommended lucigenin luminescence as a measure of intracellular superoxide dismutase activity in *Escherichia coli*.

The NorthStar™ HTS workstation has been developed as a chemiluminescence analyzer for the HTS laboratory. Featuring online injection, a broad dynamic range, and an extremely low crosstalk, the NorthStar™ HTS workstation allows the routine analysis of more than 500,000 samples a day.

Grépin et al. (2001) presented an assay for precise and direct quantification of specific endogenous mRNAs in cell lysates. The technology is based on the bioluminescence detection of multiple biotinylated ssDNA probe/endogenous mRNA hybrids, which are captured onto a streptavidin-coated multi-well plate. Using the Xpress-Screen™ technology, an assay was developed aimed to monitor the induction of endogenous cFos mRNA expression in NGF-treated PC12 cells and the miniaturization of the assay in a 384-well format, which is adapted to HTS.

Pommereau et al. (2004) compared the performance of two HTS assays for a serine/tyrosin kinase: a microplate-based, bioluminescent assay that uses the luciferin/luciferase system to monitor ATP consumption, and a microfluidic assay that measures the change in mobility in an electric field of a fluorescently labeled peptide upon phosphorylation.

O'Brien et al. (2005) described homogenous, bioluminescent protease assays using caspases-3 as a model that are significantly faster and more sensitive than the fluorescent caspases-3 assays.

David et al. (2002), Gopalakrishnan et al. (2002), and Anderson et al. (2004) used **microarrayed compound screening (μARCS)**, a well-less, high-density, ultra-HTS format, for various assays. In μARCS, the reagents are incorporated into agarose gels and layered over compounds arrayed on polystyrene sheets, mimicking the pipetting steps in a microplate assay. μARCS is a very flexible format and eliminates the requirement for complex liquid handling instruments and avoids problems associated with evaporation and plate edge effects.

Bioluminescence resonance energy transfer (BRET) was developed as a technique to study protein–protein interactions. BRET is a natural phenomenon, observed in marine organisms, in which energy transfer occurs between luminescent donor and fluorescent acceptor proteins. Oxidation of cœlenterazine by *Renilla* luciferase produces light with a wavelength of 480 nm. In the sea pansy *Renilla*, the close proximity of a green fluorescent protein allows a non-radiative energy transfer that results in light emission at 509 nm by the green fluorescent protein. In the BRET technology, the first protein partner is fused to *Renilla* luciferase, whereas the second protein is fused to a fluorescent protein, e. g., yellow fluorescent protein. If the two partners do not interact, only one signal, emitted by the luciferase, can be

detected after addition of its substrate cœlenterazine. If the distance between the two partners is less than 10 nm (100 Å) and the partners interact, resonance energy transfer occurs between the luciferase and the yellow fluorescent protein and an additional signal can be detected. The method was used to study the dimerization of G-protein-coupled receptors (Angers et al. 2000, 2001; Cheng and Miller 2001; Kroeger et al. 2001; McVey et al. 2001; Ayoub et al. 2002). Based on BRET technology, Boute et al. (2002) developed a test to monitor the activation state of the insulin receptor. BRET technology was recommended for HTS assays.

A BRET2 assay was recommended by Bertrand et al. (2002). *Renilla* luciferase was used as the donor protein, while the green fluorescent protein 2 was used as the acceptor protein. In the presence of the cell-permeable substrate DeepBlueC, *Renilla* luciferase emits blue light at 395 nm. If the green fluorescent protein 2 is brought into close proximity to *Renilla* luciferase via a specific biomolecular interaction, it will absorb the blue light energy and re-emit green light at 510 nm.

Vrecl et al. (2004) described the development of a BRET2 screening assay using β-arrestin 2 mutants.

Pfleger and Eidne (2004) used BRET for the detection of real-time interactions involving G-protein-coupled receptors.

Heding (2004) described the BRET 7TM receptor/beta-arrestin assay in drug discovery and screening that can be used to screen all seven-transmembrane receptors independent of their signaling pathway.

Electrochemiluminescence has been recommended as a diagnostic and research tool (Yang et al. 1994). Electrochemiluminescence is a means of converting electrical energy into radiative energy. It involves the production of reactive intermediates from stable precursors at the surface of an electrode. These intermediates then react under various conditions to form excited states that emit light (Richter 2003).

Golla and Seethal (2004) reported a sensitive, robust, high-throughput electrochemiluminescence assay for rat insulin.

The introduction of the **scintillation proximity assay (SPA)** obviated the need to separate bound from free radioactivity in the conventional radioligand-binding assay (Bosworth and Towers 1989; Picardo and Hughes 1997; Game et al. 1998; Wu and Liu 2005). One version of the scintillation proximity assay utilized polyvinyltoluene microspheres or beads into which a scintillant has been incorporated. When a radiolabeled ligand is captured on the surface of the bead, the radioactive decay occurs in close proximity to the bead, and effectively transfers energy to the scintillant, which results in light emission (Sittampalam et al. 1997).

Zheng et al. (2004a) reported high-throughput cell-based screening using the scintillation proximity assay for the discovery of inositol phosphatase inhibitors.

FlashPlate™ technology has been described by Brown et al. (1997). FlashPlates are white 96-well polystyrene microplates coated on the inside with solid scintillant in a polystyrene polymer. The polystyrene surface provides a hydrophobic surface for absorption of proteins, such as antibodies and receptors. When the binder molecule is coated on the FlashPlate, the reaction of the mixture of radiolabeled tracer and unlabeled ligand of interest with the binder molecule, and detection of the bound radioactivity can be done in one step. Due to the microplate surface scintillation effect, only the bound radioactivity will be detected by a scintillation counter.

Dillon et al. (2003) used a FlashPlate assay for the identification of PARP-1 inhibitors.

The use of **high-performance microphysiometry** in drug discovery has been discussed by Alajoki et al. (1997). Microphysiometry measures the extracellular acidification rate. It is governed by catabolism, via the excretion of acidic end-products, such as carbon dioxide and lactic acid. In addition, it is substantially influenced in a complementary fashion by the regulation of intracellular pH, a process sensitive to physiological changes such as receptor activation (see also Sects. A.1.1.7 and E.5.1.2). The light-addressable potentiometric sensor (LAPS) uses a light-generated alternating current to probe the electrical potential at the interface between an electrolyte and the insulated surface of an appropriately biased silicon chip; the surface potential depends on pH in a Nernstian fashion. This system has been optimized for HTS.

Microarray compound screening (μARCS) was used by David et al. (2002), Gopalakrishnan et al. (2002), and Anderson et al. (2004).

Abassi et al. (2004), Atienza et al. (2005), and Yu et al. (2006) described dynamic monitoring of cell adhesion and spreading and real-time monitoring of morphological changes in living cells on **microelectronic sensor arrays**. Special microplates are integrated with electronic sensor arrays.

A promising probe for quantitative genomic studies is the **molecular beacon (MB)**, a single-stranded DNA molecule composed of a hairpin-shaped oligonucleotide that contains both a fluorophore and

a quencher group. Molecular beacons act like switches that are normally closed – when the fluorophore and the quencher are together, fluorescence is "off". Conformational changes open the hairpin, separate the fluorophore and the quencher, and the fluorescence is turned "on". These sensitive fluorescent DNA probes can be used for real-time biomolecular recognition of unseparated target species (Fang et al. 2000). Molecular beacons are useful for studies with proteins, molecular beacon aptamers (Yamamoto and Kumar 2000; Hamaguchi et al. 2001; Tan et al. 2004). Santangelo et al. (2004) described dual FRET molecular beacons for mRNA detection in living cells.

Surface plasmon resonance (Myszka and Rich 200; McDonnel 2001) is a method for characterizing macromolecular interactions. It is an optical technique that uses the evanescent wave phenomenon to measure changes in refractive index very close to a sensor surface. The binding between an analyte in solution and its ligand immobilized on the sensor surface results in a change in the refractive index. The interaction is monitored in real time and the amount of bound ligand and rates of association and dissociation can be measured with high precision. Since there is no need for fluorescent or radioisotopic labels, surface plasmon resonance biosensors are amenable to characterizing unmodified biopharmaceuticals, studying the interaction of drug candidates with macromolecular targets and identifying binding partners.

REFERENCES AND FURTHER READING

Abassi YA, Jackson JA, Zhu J, O'Connell J, Wang X, Xu X (2004) Label-free, real-time monitoring of IgE-mediated mast cell activation on microelectronic cell sensor arrays. J Immunol Methods 292:195–205

Abraham VC, Taylor DL, Haskins JR (2004) High-content screening applied to large-scale cell biology. Trends Biotechnol 22:15–22

Akong M, Siegel R, Vasserman E, Row B, Karlton D, McNeil J, Varney M, Stauderman K, Velicelebi G (1995) High-throughput measurement of intracellular calcium by fluorescence imaging of a 96-well microtiter plate. Soc Neurosci Abstr 21:577

Alajoki ML, Baxter GT, Bemiss WR, Blau D, Bousse LJ, Chan SDH, Dawes TD, Hahnenberger KM, Hamilton JM, Lam P, McReynolds RJ, Stevenson DN, Wada GH, Williams J (1997) High-performance microphysiometry in drug discovery. In: Devlin JP (ed) High throughput screening. The discovery of bioactive substances. Dekker, New York, pp 427–442

Anderson SN, Cool BL, Kifle L, Chiou W, Egan DA, Barrett LW, Richardson PL, Frevert EU, Warrior U, Kofron JL, Burns DJ (2004) Microarrayed compound screening (μARCS) to identify activators and inhibitors of AMP-activated protein kinase. J Biomol Screen 9:112–121

Angers S, Salahpour A, Joly E, Hilairet S, Chelsky D, Dennis M, Bouvier M (2000) Detection of β_2-adrenergic receptor dimerization in living cells using bioluminescence resonance energy transfer (BRET). Proc Natl Acad Sci USA 97:3684–3689

Angers S, Salahpour A, Bouvier M (2001) Biochemical and biophysical demonstration of GPCR oligomerization in mammalian cells. Life Sci 68:2243–2250

Arun KH, Kaul CL, Ramarao P (2005) Green fluorescent proteins in receptor research: an emerging tool for drug discovery. J Pharmacol Toxicol Methods 51:1–23

Asmild M, Oswald N, Krzywkowski FM, Friis S, Jacobsen BR, Reuter D, Taboryski R, Kutchinsky J, Vestergaard RK, Schrøder RL, Sørensen CB, Bech M, Korsgard MPG, Willumsen NJ (2003) Upscaling and automation of electrophysiology: toward high throughput screening in ion channel drug discovery. Receptor Channels 9:49–58

Atienza JM, Zhu J, Wang X, Xu X, Abassi Y (2005) Dynamic monitoring of cell adhesion and spreading on microelectronic sensor arrays. J Biomol Screen 10:795–805

Auer M, Moore KJ, Meyer-Almes FJ, Guenther R, Pope AJ, Stoeckli KA (1999) Fluorescence correlation spectroscopy: lead discovery by miniaturized HTS. Int J Immunopharmacol 2:457–465

Ayoub MA, Couturier C, Lucas-Meunier E, Angers S, Fossier P, Bouvier M, Jockers R (2002) Monitoring of ligand-independent dimerization and ligand-induced conformational changes of melatonin receptors in living cells by bioluminescence resonance energy transfer. J Biol Chem 277:21522–21528

Bailey SN, Wu RZ, Sabatini DM (2002) Applications of transfected cell microarrays in high-throughput drug discovery. Drug Discov Today Suppl 7:S113–S118

Banks P, Gosselin M, Prystay L (2000) Fluorescence polarization assays for high throughput screening of G protein-coupled receptors. J Biomol Screen 5:158–168

Beasley JR, Dunn DA, Walker TL, Parlato SM, Lehrach JM, Auld DS (2003) Evaluation of compound interference in immobilized metal ion affinity-based fluorescence polarization detection with a four million member compound collection. Assay Drug Dev Technol 1:455–459

Bednar B, Cunningham ME, Kiss L, Cheng G, McCauley JA, Liverton NJ, Koblan KS (2004) Kinetic characterization of novel NR2B antagonists using fluorescence detection of calcium flux. J Neurosci Methods 137:247–255

Bertrand L, Parent S, Caron M, Legault M, Joly E, Angers S, Bouvier M, Houle B, Ménard L (2002) The BRET2/arrestin assay in stable recombinant cells: a platform screen for compounds that interact with G protein-coupled receptors. J Receptor Signal Transduct Res 22:533–541

Beske OE, Goldbard S (2002) High-throughput cell analysis using multiplexed array technologies. Drug Discov Today Suppl 7:S131–S135

Bolger R (1999) High-throughput screening: new frontiers for the 21st century. Drug Discov Today 4:251–253

Bosse R, Illy C, Elands J, Chelsky D (2000) Miniaturizing screening: how low can we go today? Drug Discov Today HTS Suppl 1:42–47

Bosworth N, Towers P (1989) Scintillation proximity assay. Nature 341:167–168

Boute N, Pernet K, Issad T (2001) Monitoring the activation of the insulin receptor using bioluminescence resonance energy transfer. Mol Pharmacol 60:640–645

Boute N, Jockers R, Issad T (2002) The use of resonance energy transfer in high-throughput screening: BRET versus FRET. Trends Pharmacol Sci 23:351–354

Brandt DW (1998) Core system model: understanding the impact of reliability on high-throughput screening systems. Drug Discov Today 3:61–68

Broach JR, Thorner J (1996) High throughput screening for drug discovery. Nature 384:14–16

Bronstein I, Fortin J, Stanley E, Stewart GS, Kricka LJ (1994) Chemiluminescence and bioluminescence reporter gene assays. Anal Biochem 219:169–181

Bronstein I, Martin CS, Fortin JJ, Olesen CE, Voyta JC (1996) Chemiluminescence: sensitive detection technology for reporter gene assays. Clin Chem 42:1542–1546

Brown BA, Cain M, Broadbent J, Tomkins S, Henrich G, Joseph R, Casto S, Harney H, Greene R, Delmondo R, Ng S (1997) Flash Plate™ technology. In: Devlin JP (ed) High throughput screening. The discovery of bioactive substances. Dekker, New York, pp 317–328

Brueggemann A, George M, Klau M, Beckler M, Steindl J, Behrends JC, Fertig N (2004) The channel drug discovery and research: the automated Nano-Patch-Clamp technology. Curr Drug Discov Technol 1:91–96

Burbaum JJ, Sigal NH (1997) New technologies for high-throughput screening. Curr Opin Chem Biol 1:72–78

Chalfie M (1995) Green fluorescent protein. Photochem Photobiol 62:651–656

Chalfie M, Tu Y, Euskirchen G, Ward WW, Prasher CD (1994) Green fluorescent protein as a marker for gene expression. Science 263:802–805

Charter JM (2004) A guide to HTS assay development. D&MD Publications, Westborough, Mass.

Cheng ZJ, Miller LJ (2001) Agonist-dependent dissociation of oligomeric complexes of G-protein-coupled cholecystokinin receptors demonstrated in living cells using bioluminescence resonance energy transfer. J Biol Chem 276:48040–48047

Chin J, Adams AD, Bouffard A, Green A, Lacson RG, Smith T, Fischer PA, Menke JG, Sparrow CP, Mitnaul LJ (2003) Miniaturization of cell-based beta-lactamase-dependent FRET assays to ultra-high throughput formats to identify agonists of human liver X receptors. Assay Drug Dev Technol 1:777–787

Conway BR, Minor LK, Xu JZ, Gunnet HW, DeBiasio R, D'Andrea MR, Rubin R, Giuliano K, Zhou LB, Demarest KT (1999) Quantification of G-protein coupled receptor internalization using G-protein coupled receptor-green fluorescent protein conjugates with the ArrayScan™ high-content screening system. J Biomol Screen 4:75–86

Coward P, Chan SD, Wada HG, Humphries GM, Conklin BR (1999) Chimeric G proteins allow a high-throughput signaling assay of Gi-coupled receptors. Anal Biochem 270:242–248

Cox B, Denyer JC, Binnie A, Donnelly MC, Evans B, Green DVS, Lewis JA, Mander TH, Merritt AT, Valler MJ, Watson SP (2000) Application of high-throughput screening techniques to drug discovery. Progr Med Chem 37:83–133

David CA, Middleton T, Montgomery D, Lim HB, Kati W, Molla A, Xuei X, Warrior U, Kofron JL, Burns DJ (2002) Microarray compound screening (μARCS) to identify inhibitors of HIV integrase. J Biomol Screen 7:259–266

Devlin JP (ed) (1997) High throughput screening. The discovery of bioactive substances. Dekker, New York

Dillon KJ, Smith GCM, Martin NMB (2003) A FlashPlate assay for the identification of PARP-1 inhibitors. J Biomol Screen 8:347–552

Dunn DA, Feygin I (2000) Challenges and solutions to ultra-high-throughput screening assay miniaturization: submicroliter fluid handling. Drug Discov Today HTS Suppl 5:S84–S91

Dupriez VJ, Maes K, Le-Poul E, Burgeon E, Detheux M (2002) Aequorin-based functional assays for G-protein-coupled receptors, ion channels, and tyrosine kinase receptors. Receptors Channels 8:319–330

Edwards BS, Oprea T, Prossnitz ER, Sklar LA (2004) Flow cytometry for high-throughput, high-content screening. Curr Opin Chem Biol 8:392–398

Eggeling C, Kask P, Winkler D, Jäger S (2005) Rapid analysis of Förster resonance energy transfer by two-color global fluorescence correlation spectroscopy: trypsin proteinase reaction. Biophys J 89:605–618

Fang X, Li JJ, Perlette J, Tan W, Wang K (2000) Molecular beacons. Novel fluorescent probes. Anal Chem 72:747A–753A

Feiglin MN, Skwish S, Laab M, Heppel A (2000) Implementing multilevel dynamic scheduling for a highly flexible 5-rail high throughput screening system. J Biomol Screen 5:39–48

Fernandes PB (1998) Technological advances in high-throughput screening. Curr Opin Chem Biol 2:597–603

Game SM, Rajapurohit PK, Clifford M, Bird MI, Priest R, Bovin NV, Nifantev NE, O'Beirne G, Cook ND (1998) Scintillation proximity assay for E-, P-, and L-selectin utilizing polyacrylamide-based neoglycoconjugates as ligands. Anal Biochem 258:127–135

Gaspari F, Mariani M, Sola F, Galvani A (2004) Quantification of the proliferation index of human dermal fibroblast cultures with the ArrayScan™ high-content screening reader. J Biomol Screen 9:232–243

Gaudet EA, Huang KS, Zhang Y, Huang W, Mark D, Sportsman JR (2003) A homogeneous fluorescence polarization assay adaptable for a range of protein serine/threonine and tyrosine kinases. J Biomol Screen 8:164–175

Gauglitz G (2000) Optical detection methods for combinatorial libraries. Curr Opin Chem Biol 4:351–355

Gibbons I (2000) Microfluidic arrays for high-throughput submicroliter assays using capillary electrophoresis. Drug Discov Today HTS Suppl 1:33–38

Gill S, Gill R, Lee S, Hesketh JC, Fedida D, Rezazadeh S, Stankovich L, Liang D (2003) Flux assays in high throughput screening of ion channels in drug discovery. Assay Drug Dev Technol 1:709–717

Glickman JF, Wu X, Mercuri R, Illy C, Bowen R, He Y, Sills M (2002) A comparison of ALPHAScreen, TR-FRET and TRF as assay methods for FXR nuclear receptors. J Biomol Screen 7:3–10

Golla R, Seethal R (2004) A sensitive, robust high-throughput electrochemiluminescence assay for rat insulin. J Biomol Screen 9:62–70

González JE, Negulescu PA (1998) Intracellular detection assays for high-throughput screening. Curr Opin Biotechnol 9:624–631

Gopalakrishnan SM, Karvinen J, Kofron JL, Burns DJ, Warrior U (2002) Application of Micro Array Compound Screening (μARCS) to identify inhibitors of caspase-3. J Biomol Screen 7:317–323

Grépin C (2004) Multiplexed cell-based assays: an intermediary screening format between high throughput screening and high content screening. ICP Conference San Diego 2004

Grépin C, Pernelle C (2000) High-throughput screening. Evolution of homogeneous time resolved fluorescence (HTRF) technology for HTS. Drug Discov Today 5:212–214

Grépin C, Lionne B, Borie C, Palmer M, Pernelle C (2001) High throughput quantification of the endogenous cFos. New Drugs 1:38–41

Hamaguchi N, Ellington A, Stanton M (2001) Aptamer beacons for the direct detection of proteins. Anal Biochem 294:126–131

Harding D, Banks M, Fogarty S, Binnie A (1997) Development of an automated high-throughput screening system: a case history. Drug Discov Today 2:385–390

Haupts U, Maiti S, Schwille P, Webb WW (1998) Dynamics of fluorescence fluctuations in green fluorescent protein observed by fluorescence correlation spectroscopy. Proc Natl Acad Sci USA 95:13573–13578

Haupts U, Rüdiger M, Pope AJ (2000) Macroscopic versus microscopic fluorescence techniques in (ultra)-high-throughput screening. Drug Discov Today HTS Suppl 1:3–9

Heding A (2004) Use of the BRET 7TM receptor/beta-arrestin assay in drug discovery and screening. Expert Rev Mol Diagn 4:403–411

Heilker R, Zemanova L, Valler MJ, Nienhaus GU (2005) Confocal fluorescence microscopy for high-throughput screening of G-protein coupled receptors. Curr Med Chem 12:2551–2559

Hertzberg RP, Pope AJ (2000) High-throughput screening: new technology for the 21th century. Curr Opin Chem Biol 4:445–451

Hodder P, Mull R, Cassaday J, Berry K, Strulovici B (2004) Miniaturization of intracellular calcium functional assays to 1536-well plate format using a fluorometric imaging plate reader. J Biomol Screen 9:417–426

Houston JG, Banks M (1997) The chemical-biological interface: developments in automated and miniaturized screening technology. Curr Opin Biotechnol 8:734–740

Hsieh HB, Fitch J, White D, Torres F, Roy J, Matusiak R, Krivacic B, Kowalski B, Bruce R, Elrod S (2004) Ultra-high-throughput microarray generation and liquid dispensing using disposable piezoelectric ejectors. J Biomol Screen 9:85–94

Hynes J, Floyd S, Soini A, O'Connor R, Papkovsky D (2003) Fluorescence-based cell viability screening assays using water-soluble oxygen probes. J Biomol Screen 8:264–272

Isailovic D, Li HW, Phillips GJ, Yeung ES (2005) High-throughput single-cell fluorescence spectroscopy. Appl Spectrosc 59:221–226

Jäger S, Brand L, Eggeling C (2003a) New fluorescence techniques for high-throughput drug discovery. Curr Pharm Biotechnol 4:463–476

Jäger S, Garbow N, Kirsch A, Preckel H, Gandenberger FU, Herrenknecht K, Rüdiger M, Hutchinson JP, Bingham RP, Ramon F, Bardera A, Martin J (2003b) A modular, fully integrated ultra-high-throughput screening system based on confocal fluorescence analysis techniques. J Biomol Screen 8:648–659

Kain SR (1999) Green fluorescent protein (GRP): applications in cell-based assays for drug discovery. Drug Discov Today 4:304–312

Karvinen J, Hurskainen P, Gopalakrishnan S, Burns D, Warrior U, Hemmila I (2002) Homogenous time-resolved fluorescence quenching assays (LANCE) for caspases-3. J Biomol Screen 7:223–231

Kenny BA, Bushfiled M, Parry-Smith DJ, Fogarty S, Treherne JM (1998) The application of high-throughput screening to novel lead discovery. Prog Drug Res 51:245–269

Klumpp M, Boettcher A, Becker D, Meder G, Blank J, Leder L, Forstner M, Ottl J, Mayr LM (2006) Readout technologies for highly miniaturized kinase assays applicable to high-throughput screening in a 1536-well format. J Biomol Screen 11:617–633

Kolb AJ, Burke JW, Mathis G (1997) Homogeneous, time-resolved fluorescence method for drug discovery. In: Devlin JP (ed) High throughput screening. The discovery of bioactive substances. Dekker, New York, pp 345–360

Koltermann A, Kettling U, Bieschke J, Winkler T, Eigen M (1998) Rapid assay processing by integration of dual-color fluorescence cross-correlation spectroscopy: high throughput screening for enzyme activity. Proc Natl Acad Sci USA 95:1421–1426

Kroeger KM, Hanyaloglu AC, Seeber EM, Miles LE, Eidne KA (2001) Constitutive and agonist-dependent homo-oligomerization of the thyrotropin-releasing hormone receptor. Detection in living cells using bioluminescence resonance energy transfer. J Biol Chem 276:12736–12743

Kuntzweiler TA, Arneric SP, Donnelly-Roberts DL (1998) Rapid assessment of ligand actions with nicotinic acetylcholine receptors using calcium dynamics and FLIPR. Drug Dev Res 44:14–20

Kunz-Schughart LA, Freyer JP, Hofstaedter F, Ebner R (2004) The use of 3-D cultures for high-throughput screening: the multicellular spheroid model. J Biomol Screen 9:273–285

Labute P (1999) Binary QSAR: a new method for the determination of quantitative structure assay. Pacific Symp Biocomput 4:444–455

Landro JA, Taylor ICA, Stirtan WG, Osterman DG, Kristie J, Hunnicutt EJ, Rae PMM, Sweetman PM (2000) HTS in the new millennium. The role of pharmacology and flexibility. J Pharmacol Toxicol Methods 44:273–289

Lemmo AV, Rose DJ, Tisone TC (1998) Inkjet dispensing technology: applications for drug discovery. Curr Opin Biotechnol 9:615–617

Le-Poul E, Hisada S, Mizuguchi Y, Dupriez VJ, Burgeon E, Detheux M (2002) Adaptation of aequorin functional assay to high throughput screening. J Biomol Screen 7:57–65

Lepple-Wienhues A, Ferlinz K, Seeger A, Schäfer A (2003) Flip the tip: an automated, high quality, cost-effective patch clamp screen. Receptor Channels 9:13–17

Li Z, Mehdi S, Patel I, Kawooya J, Judkins M, Zhang W, Diener K, Lozada A, Dunnington D (2000) An ultra-high throughput screening approach for an adenine transferase using fluorescence polarization. J Biomol Screen 5:31–38

Liochev SI, Fridovich I (1997) Lucigenin luminescence as a measure of intracellular superoxide dismutase activity in *Escherichia coli*. Proc Natl Acad Sci USA 94:2891–2896

Liu B, Li S, Hu J (2004) Technological advances in high-throughput screening. Am J Pharmacogenomics 4:263–276

Loomans EE, van Doormalen AM, Wat JW, Zaman GJ (2003) High-throughput screening with immobilized metal ion affinity-based fluorescence polarization detection, a homogeneous assay for protein kinases. Assay Drug Dev Technol 1:445–453

Lu Z, Yin Z, James L, Syto R, Stafford JM, Koseoglu S, Mayhood T, Myers J, Windsor W, Kirschmeier P, Samatar AA, Malcolm B, Turek-Etienne TC, Kumar CC (2004) Development of a fluorescence polarization bead-based coupled assay to target activity/conformation states of a protein kinase. J Biomol Screen 9:309–321

Lundin K, Blomberg K, Nordström T, Lindqvist C (2001) Development of a time-resolved fluorescence resonance energy transfer assay (cell TR-FRET) for protein detection in intact cells. Anal Biochem 299:92–97

Major JS (1995) Challenges of high throughput screening against cell surface receptors. J Recept Signal Transduction Res 15:595–607

Maley D, Mei J, Lu H, Johnson DL, Ilyin S (2004) Multiplexed RT-PCR for high throughput screening applications. Comb Chem High Throughput Screen 7:727–732

Markela E, Ståhlberg TH, Hemmilä I (1993) Europium-labelled recombinant protein G. A fast and sensitive immunoreagent for time resolved immunofluorometry. J Immunol Methods 161:1–6

Mathes C (2006) QPatch: the past, present and future of automated patch clamp. Expert Opin Ther Targets 10.319–327

Mathis G, Preaudat M, Trinquet E (1994) Homogeneous EGF receptor binding assay using rare earth cryptates, amplification by nonradiative energy transfer and time resolved fluorescence. CHI Proceedings of High Throughput Screening for Drug Development, Philadelphia

McDonnel JM (2001) Surface plasmon resonance: towards an understanding of the mechanisms of biological molecular recognition. Curr Opin Chem Biol 5:572–577

McVey M, Ramsay D, Kellett E, Rees S, Wilson S, Pope AJ, Milligan G (2001) Monitoring receptor oligomerization using time-resolved fluorescence resonance energy transfer and bioluminescence resonance energy transfer. The human δ-opioid receptor displays constitutive oligomerization at the cell surface, which is regulated by receptor occupancy. J Biol Chem 276:14092–14099

Meng YG, Liang J, Wong WL, Chisholm V (2000) Green fluorescent protein as a second selectable marker for selection of high producing clones from transfected CHO cells. Gene 242:201–207

Mere L, Bennett T, Casssin P, England P, Hamman B, Rink T, Zimmerman S, Negulescu P (1999) Miniaturized FRET assays and microfluidics: key components for ultra-high-throughput screening. Drug Discov Today 4:363–369

Merk S, Lietz A, Kroner M, Valler M, Heilker R (2004) Time-resolved fluorescence measurements using microlens array and area imaging devices. Comb Chem High Throughput Screen 7:45–54

Messier TL, Dorman CM, Brauner-Osborne H, Eubanks D, Brann RM (1995) High throughput assays of cloned adrenergic, muscarinic, neurokinin, and neurotropin receptors in living mammalian cells. Pharmacol Toxicol 76:308–311

Meza MB (2000) Bead-based HTS applications in drug discovery. Drug Discov Today HTS Suppl 1:38–41

Miller TR, Witte DG, Ireland LM, Kang CH, Roch JM, Masters JN, Esbenshade TA, Hancock AA (1999) Analysis of apparent noncompetitive responses to competitive H_1-histamine receptor antagonists in fluorescent imaging plate reader-based calcium assays. J Biomol Screen 4:249–258

Milligan G, Rees S (1999) Chimeric Gα proteins: their potential use in drug discovery. Trends Pharmacol Sci 20:118–124

Moshinski DJ, Ruslim L, Blake RA, Tang F (2003) A widely applicable high-throughput TR-FRET assay for the measurement of kinase autophosphorylation: VEGRF-2 as prototype. J Biomol Screen 8:447–452

Myszka DG, Rich RL (2000) Implementing surface plasmon resonance biosensors in drug discovery. Pharm Sci Technol Today 3:310–317

Nagai T, Yamada S, Tominaga T, Ichikawa M, Miyawaki A (2004) Expanded dynamic range of fluorescent indicators for Ca^{2++} by circularly permuted yellow fluorescent proteins. Proc Natl Acad Sci USA 101:10554–19559

Newman M, Josiah S (2004) Utilization of fluorescence polarization and time resolved fluorescence resonance energy transfer assay formats for SAR studies: Src kinase as a model system. J Biomol Screen 9:525–532

Nieuwenhuijsen BW, Huang Y, Wang Y, Ramirez F, Kalgaonkar G, Young KH (2003) A dual luciferase multiplexed high-throughput screening platform for protein-protein interactions. J Biomol Screen 8:676–684

O'Brien MA, Daily WJ, Hesselberth PE, Moravc RA, Scurria MA, Klaubet DH, Bulleit RF, Wood KV (2005) Homogenous, bioluminescent protease assays: caspases-3 as a model. J Biomol Screen 10:137–148

Owicki JC (2000) Fluorescence polarization and anisotropy in high throughput screening: perspectives and primer. J Biomol Screen 5:297–306

Palo K, Brand L, Eggeling C, Jäger S, Kask P, Gall K (2002) Fluorescence intensity and lifetime distribution analysis: towards higher accuracy in fluorescence fluctuation spectroscopy. Biophys J 83:605–618

Parker GJ, Law TL, Lenoch FJ, Bolger RE (2000) Development of high throughput screening assays using fluorescence polarization: nuclear receptor-ligand-binding and kinase-phosphatase assays. J Biomol Screen 5:77–88

Pasini P, Musiani M, Russo C, Valenti P, Aicardi G, Crabtree JE, Baraldini M, Roda A (1998) Chemiluminescence imaging in bioanalysis. J Pharm Biomed Anal 18:555–564

Pathirna C, Stein RB, Berger TS, Fenical W, Ianiro T, Torres A, Goldman ME (1995) Nonsteroidal human progesterone receptor modulators from the marine algae *Cymopolia barbata*. Mol Pharmacol 476:630–635

Pazhanisamy S, Stuver CM, Livingston DJ (1995) Automation of high-performance liquid chromatography-based enzyme assay: evaluation of inhibition constants for human immunodeficiency virus-1 protease inhibitors. Anal Biochem 229:48–53

Pfleger KDG, Eidne KA (2004) New technologies: bioluminescence resonance energy transfer (BRET) for the detection of real time interactions involving G-protein coupled receptors. Pituitary 6:141–151

Picardo M, Hughes KT (1997) Scintillation proximity assays. In: Devlin JP (ed) High throughput screening. The discovery of bioactive substances. Dekker, New York, pp 307–316

Pommereau A, Pap E, Kannt A (2004) Two simple and generic antibody-independent assays: comparison of a bioluminescent and a microfluidic assay format. J Biomol Screen 9:409–416

Pope AJ, Haupts UM, Moore KJ (1999) Homogeneous fluorescence readouts for miniaturized high-throughput screening. Drug Discov Today 4:350–362

Qian J, Voorbach MJ, Huth JR, Coen ML, Zhang H, Ng SC, Comess KM, Petros AM, Rosenberg SH, Warrior U, Burns DJ (2004) Discovery of novel inhibitors of Bcl-xL using multiple high-throughput screening platforms. Anal Biochem 328:131–138

Ramm P (1999) Imaging systems in assay screening. Drug Discov Today 4:401–410

Richter MM (2004) Electrochemiluminescense (ECL). Chem Rev 104:3003–3036

Robinson JA, Jenkins NS, Holman NA, Roberts-Thomson SJ, Monteith GR (2004) Ratiometric and nonratiometric Ca^{2+} indicators for the assessment of intracellular free Ca^{2+} in a breast cancer line using a fluorescence microplate reader. J Biochem Biophys Methods 31:227–237

Rose D (1999) Microdispensing technologies in drug discovery. Drug Discov Today 4:411–419

Rouleau N, Turcotte S, Mondou MH, Roby P, Bossé R (2003) Development of a versatile platform for nuclear receptor screening using AlphaScreen™. J Biomol Screen 8:191–197

Rüdiger M, Haupts U, Moore KJ, Pope AJ (2001) Single-molecule detection technologies in miniaturized high throughput screening: binding assays for G protein-coupled receptors using fluorescence intensity distribution analysis and fluorescence anisotropy. J Biomol Screen 6:29–37

Santangelo PJ, Nix B, Tsourkas A, Boa G (2004) Dual FRET molecular beacons for mRNA detection in living cells. Nucleic Acids Res 32:e57

Scheirer W (1997) Reporter gene assay applications. In: Devlin JP (ed) High throughput screening. The discovery of bioactive substances. Dekker, New York, pp 401–412

Schmid EL, Tairi AP, Hovius R, Vogel H (1998) Screening ligands for membrane protein receptors by total internal reflection fluorescence: the 5-HT_3 serotonin receptor. Anal Chem 70:1331–1338

Schuster M, Wasserbauer E, Einhauer A, Ortner C, Jungbauer A, Hammerschmid F, Werner G (2000) Protein expression strategies for identification of novel target proteins. J Biomol Screen 5:89–97

Schwille P, Kummer S, Heikal AA, Webb WW (2000) Fluorescence correlation spectroscopy reveals fast optical excitation-driven intramolecular dynamics of yellow fluorescent proteins. Proc Natl Acad Sci USA 97:151–156

Selvin PR (2002) Principles and biophysical applications of lanthanide-based probes. Annu Rev Biophys Biomol Struct 31:275–302

Shieh CC (2004) Automated high-throughput patch clamp techniques. Drug Discov Today 9:551–552

Sills (1998)

Silverman L, Campbell R, Broach JR (1998) New assay techniques for high throughput screening. Curr Opin Chem Biol 2:397–403

Sittampalam GS, Kahl SD, Janzen WP (1997) High throughput screening: advances in assay technologies. Curr Opin Chem Biol 1:384–391

Sportsman JR, Leytes LJ (2000) Miniaturization of homogenous assays using fluorescence polarization. Drug Discov Today HTS Suppl 1:27–32

Sportsman JR, Daijo J, Gaudet EA (2003) Fluorescence polarization assays in signal discovery. Comb Chem High Throughput Screen 6:195–200

Stett A, Burkhardt C, Weber U, van Stiphout P, Kott T (2004) CYTOCENTERING. A novel technique enabling automated cell-by-cell patch clamping with the CYTOPATCH chip. Receptor Channels 9:59–66

Su S, Vivier RG, Dickson MC, Kendrick MK, Williamson NM, Anson JG, Houston JG, Craig FF (1997) High throughput PT-PCR analysis of multiple transcripts using a microplate RNA isolation procedure. Biotechniques 22:1107–1113

Sullivan E, Tucker EM, Dale IL (1999) Measurement of Ca^{2+} using the Fluorometric Imaging Plate Reader (FLIPR). Methods Mol Biol 114:125–133

Sundberg SA (2000) High-throughput and ultra-high-throughput screening: solution- and cell-based approaches. Curr Opin Biotechnol 11:47–53

Swartzman EE, Miraglia SJ, Mellentin-Michelotti J, Evangelista L, Yuan PM (1999) A homogeneous and multiplexed immunoassay for high throughput screening using fluorometric microvolume assay technology. Anal Biochem 271:143–151

Tan W, Wang K, Drake TJ (2004) Molecular beacons. Curr Opin Chem Biol 8:547–553

Ting AY, Kain KH, Klemke RL, Tsien RY (2001) Genetically encoded fluorescent reporters of protein tyrosine kinase activities in living cells. Proc Natl Acad Sci USA 98:15003–15008

Treherne JM (2006) Exploiting high-throughput ion channel screening technologies in integrated drug discovery. Curr Pharm Des 12:497–406

Vollert H (1998) Development of a robust miniaturized screening system. Proceeding, IBC, Practical Aspects for Assay Miniaturization and Design for Drug Discovery, Boston, Mass., USA

Vollert H, Jordan B, Winkler I (2000) Wandel in der Wirkstoffsuche – Ultra-High-Throughput-Screening-Systeme in der Pharmaindustrie. Transkript Laborwelt 1:5–10

Vrecl M, Jorgennsen R, Pogačnik A, Heiding A (2004) Development of a $BRET^2$ screening assay using β-arrestin 2 mutants. J Biomol Screen 9:322–333

Wallace RW, Goldman ME (1997) Bioassay design and implementation. In: Devlin JP (ed) High throughput screening. The discovery of bioactive substances. Dekker, New York, pp 279–305

Waller A, Simons PC, Biggs SM, Edwards BS, Prossnitz ER (2004) Techniques: GPCR assembly, pharmacology and screening by flow cytometry. Trends Pharmacol Sci 25:663–669

Wallrabe H, Periasami A (2005) Imaging protein molecules using FRET and FLIM microscopy. Curr Opin Biotechnol 16:19–29

Willumsen NJ, Bech M, Olesen SP, Jensen BS, Korsgaard MPG, Christophersen P (2003) High throughput electrophysiology: new perspectives for ion channel discovery. Receptor Channels 9:3–12

Wingfield J (1998) Developing effective assays on HTS. Drug Discov Today 3:97–99

Winkler T, Kettling U, Koltermann E, Eigen M (1999) Confocal fluorescence coincidence analysis: an approach to ultra high-throughput screening. Proc Natl Acad Sci USA 96:1375–1378

Wu S, Liu B (2005) Application of scintillation proximity assay in drug discovery. BioDrugs 19:383–392

Yamamoto R, Kumar PKR (2000) Molecular beacon aptamer fluoresces in the presence of Tat protein of HIV-1. Genes Cells 5:389–396

Yan YX, Boldt-Houle DM, Tillotson BP, Gee MA, D'Eon BJ, Chang XJ, Olesen CEM, Palmer MAJ (2002) Cell-based high-throughput screening assay system for monitoring G protein-coupled receptor activation using β-galactosidase enzyme complementation technology. J Biomol Screen 7:451–459

Yang H, Leland IK, Yost D, Mssey RJ (1994) Electrochemiluminescence: a new diagnostic and research tool. Biotechnology 12:193–194

Yu N, Atienza JM, Bernard J, Blanc S, Zhu J, Wang X, Xu X, Abassi YA (2006) Real-time monitoring of morphological changes in living cells by electronic cell sensor arrays. Anal Chem 78:35–43

Zehender H, le Goff F, Lehmann N, Filipuzzi I, Mayr LM (2004) SpeedScreen: the "missing ling" between genomics and lead discovery. J Biomol Screen 9:498–505

Zheng W, Brandish PE, Kolodin DG, Scolnick EM, Strulovici B (2004a) High-throughput cell-based screening using scintillation proximity assay for the discovery of inositol phosphatase inhibitors. J Biomol Screen 9:132–140

Zheng W, Spencer RH, Kiss L (2004b) High throughput assay technologies for ion channel drug discovery. Assay Drug Dev Technol 2:543–552

Zhu Z, Chen T, Lin JH, Bell A, Bryson J, Dubaquie Y, Yan N, Yanchunas J, Xie D, Stoffel R, Sinz M, Dickinson K (2004) Correlation of high-throughput pregnane X receptor (PXR) transactivation and binding assays. J Biomol Screen 9:533–540

Zuck P, Lao ZG, Skwish S, Glickman JF, Yang K, Burbaum J, Inglese J (1999) Ligand-receptor binding measured by laser-scanning imaging. Proc Natl Acad Sci USA 96:11122–11127

Zysk JR, Baumbach WR (1998) Homogeneous pharmacologic and cell-based screens provide diverse strategies in drug discovery. Somatostatin antagonists as a case study. Comb Chem High Throughput Screen 1:171–183

0.4.4 Pharmacogenomics

The concept of an altered response based on genetic background is not new. In 510 BC, Pythagoras recognized that some individuals developed hemolytic anemia with fava bean consumption (Nebert 1999). In 1914, Garrod expanded this observation, stating that enzymes detoxified foreign agents so that they were excreted harmlessly. However, some people lack these enzymes and experience adverse effects (Weber 1999). Hemolytic anemia due to fava bean consumption was later determined to occur in glucose-6-phosphate-deficient individuals (Mager et al. 1965; Podda et al. 1969).

The term pharmacogenetics was first used by Friedrich Vogel in 1959. The dawn of pharmacogenetics continued by combining Mendelian genetics with observed phenotypes. In 1932, Snyder performed the first global study of ethnic variation and deduced that taste deficiency was inherited. He proposed that the phenylthiourea nontaster phenotype was an inherited recessive trait and that the frequency of occurrence differed between races (Snyder 1932). Other genetic differences, such as aldehyde dehydrogenase and alcohol dehydrogenase, were discovered. These deficiencies are common in Asians and cause them to have less alcohol tolerance (Goedde et al. 1983; Inoue et al. 1984). Similarly, polymorphisms in the *N*-acetyl transferase enzyme are also segregated by ethnicity and correlate to the latitude of the country (Weber 1999).

These genetic differences were originally thought to be caused by genetic variance, but it was not until the advent of molecular biology that disease states could be carefully analyzed. The following dogma:

$$\text{gene} \longrightarrow \text{protein} \longrightarrow \text{biochemical process} \longrightarrow \text{disease state}$$

became the model for examining human diseases. Following this scheme, sickle cell anemia was the first trait to reveal that a single point mutation can change protein structure and lead to a disease phenotype (Murayama 1966; Bookchin et al. 1970). Single nucleotide polymorphisms (SNPs) are responsible for many diseases (Kleyn and Vesell 1998; Vesell 2000; Weaver 2001; Wieczorek and Tsongalis 2001). SNPs can change receptors, transport proteins, and drug-metabolizing enzymes. The advances in genetic technology to detect polymorphisms have caused an explosion in pharmacogenetic research and many of these discoveries have been employed in clinical practice.

Many thousands of polymorphisms can be determined simultaneously in a patient. These SNPs are selected as markers evenly distributed in the genome, in the hope that functionally relevant polymorphisms can be associated with specific markers by virtue of their proximity to the chromosome. Such genome-wide association studies are used in the discovery of susceptibility genes for diseases, such as asthma and prostate cancer, but they are equally suitable for determining the genes in drug response (Sadée 1999).

Disorders such as Huntington's disease or cystic fibrosis are associated with defects in a single gene product identified by positional cloning. This involves the isolation of a gene with the information on its subchromosomal localization and the phenotypic expression of a mutation of this gene that results in a particular disease state. Positional cloning is based on the unique, inheritable DNA fingerprint associated with each individual, from which the inheritance of identified polymorphisms can be tracked, along with the inheritance of the disease. While this approach has been more or less successful in diseases involving a single gene defect, more complex diseases, such as Alzheimer's disease, cancer, asthma or cardiovascular diseases, appear to result from the influence of multiple gene defects.

The next step is to identify the function of the protein expressed by the DNA using functional genomics. This technique involves the use of sequence comparisons with known proteins, using computer databases, transgenic expression or expression in surrogate systems; gene knockouts in mice (Rudolph and Möhler 1999; West et al. 2000; Zambrowicz et al. 2003), or relatively simple organisms such as *Drosophila melanogaster*, *Caenorhabditis elegans*, Zebrafish (Link et al. 2000; Haberman 2003; Artal-Sanz et al. 2006) or *Saccharomyces cerevisiae*. A two-hybrid system to identify molecular binding partners can be used to identify proteins that are associated with the gene product of interest.

Progress in genomics technology, especially the elucidation of the human genome (International Genome Sequencing Consortium 2001; Venter et al. 2001), has created an unique opportunity to significantly impact on the pharmaceutical drug development processes (Carulli et al. 1998; van Oosterhout 1998; Debouck and Goodfellow 1999; Farber 1999; Vidal and Endoh 1999; Wilson et al. 1998; Jones and Fitzpatrick 1999; Zweiger 1999; Beeley et al. 2000; Bentley 2000; Broder and Venter 2000; Debouck and Metcalf 2000; Harris 2000; Marshall 2000; Meldrum 2000a, 2000b; Rockett and Dix 2000; Schuster et al.

2000; Steiner and Anderson 2000; Peet and Bey 2001; Winkelmann 2001, Hemmilä and Hurskainen 2002).

Genetic polymorphism in drug-metabolizing enzymes, transporters, receptors, and other drug targets are linked to individual differences in the efficacy and toxicity of many medications. Pharmacogenomic studies can elucidate the inherited nature of these differences, thereby enhancing the possibilities of drug discovery and providing a stronger scientific basis for optimizing drug therapy on the basis of each patient's genetic constitution (Evans and Relling 1999; Grant 2001).

Receptor polymorphism is also the reason for differences in drug effects among patients. Two genetic variants of the angiotensin-converting enzyme (ACE) are described, depending on an insertion (I-form) or deletion (D-form) of a base pair at position 287 in the gene, which are equally distributed in the Caucasian population. Individuals with the D/D-form express ACE levels much higher than I/I individuals. They have an increased risk for myocardial infarction and may respond better to therapy with ACE inhibitors (Samani et al. 1996; Danser and Schunkert 2000). Another example is the association between β_2-adrenergic receptor polymorphisms and asthma (Liggett 1997). There are three polymorphisms that alter receptor function, which may influence the therapeutic success.

Genomics will introduce a new dimension in drug research. The number of molecular targets modified by the complete armamentarium of modern drugs is not greater than 500. The number of genes that contribute to multifactorial diseases might not be very high; the numbers reported for different forms of diabetes and hypertension are 5–10 per disease (Guillausseau et al. 1997; Shimkets and Lifton 1996). There are 100–150 disease entities that present an epidemiological and economical problem to industrialized societies. If one assumes 10 contributing genes for 100 multifactorial diseases (including different forms of cancer, asthma, diabetes, hypertension, atherosclerosis and osteoporosis), one arrives at 1000 "disease genes" that dispose patients to the most important multigenetic conditions (Drews 2000, 2001). It appears reasonable to assume that each of these disease genes, or rather proteins that are specified by the disease genes, connects with at least 5–10 proteins that are feasible levels for drug intervention. On the basis of these calculations, one can assume that 5000–10,000 can be used as targets for drug interventions.

Lennon (2000) discussed the methods for high-throughput gene expression analysis applicable to drug discovery, including differential display of eukaryotic mRNA, the modification thereof called restriction enzyme analysis of differentially expressed sequences (READS), expression sequence tags (EST) methodology, serial analysis of gene expression, filter arrays, and DNA microarrays.

Celis et al. (2000) gave an excellent survey on microarray technology.

Gene expression analyses and genetic polymorphisms are important not only for determining predisposition to disease and for drug discovery, but also for predicting the incidence of adverse drug reactions (Meyer 2000). In the past, several drugs had to be withdrawn from the market due to rare, but severe, adverse events. Some drug metabolic enzyme variants have been found to cause severe adverse events. They form qualitatively or quantitatively different metabolites with toxicological implications (Bullingham 2001).

Most of the enzymes involved in both drug metabolism and the elimination of many therapeutic agents are members of the cytochrome P450 (CYP) family that includes more than 30 isoforms (Gonzales 1990). One drug-metabolizing enzyme, resulting in numerous drugs being withdrawn from the market, is CYP3A, which is involved in the oxidative biotransformation of up to 50% of clinically important therapeutic agents. The expression of CYP3A is regulated by genetic and non-genetic factors that can result in a 5- to 20-fold interindividual variability in metabolic clearance. Another enzyme, CYP2D6 (debrisoquine hydroxylase), metabolizes one-quarter of all prescribed drugs and is inactive in 6% of the Caucasian population (Wolf and Smith 1999). A principal molecular defect in poor metabolizers is a single base pair mutation in exon 5 of CYP2C19 (De Morais et al. 1994; Sadée 1999). These enzymes are being screened at the earliest stages of the drug development process. The single nucleotide point mutation profile of an individual can indicate a predisposition for adverse side-effects. Furthermore, drug transport protein polymorphisms and their drug interactions may provide another valuable tool in screening for potential toxic effects of drugs. The pharmacogenomic approach should reduce the number of compounds failing during late clinical development (Adam et al. 2000).

A detailed knowledge of the genetic basis of individual drug response is of major clinical and economic importance and can provide the basis for a rational approach to drug prescription. In the sense of a "personalized medicine", prospective genotyping will lead to patients being prescribed drugs that are both safer

and more effective (Sadée 1999; March 2000; Murphy 2000; Spear et al. 2001; Dietel and Sers 2006).

Winkelmann et al. (2001) initiated the Ludwigshafen Risk and Cardiovascular Health (LURIC) study, which aims to provide a resource for the study of environmental and genetic risk factors and their interactions, and of the functional relationship between gene variation and biochemical phenotype (functional genomics), or response to medication (pharmacogenomics) and long-term prognosis of cardiovascular disease.

A vision for the future of genomics research was given by Collins et al. (2003).

Rolling-cycle amplification (RCA) is a system for amplification, which may be used for detection of proteins or nucleic acid targets (Lizardi et al. 1998; Zhong et al. 2001). Rolling-circle amplification driven by DNA polymerase can replicate circularized oligonucleotide probes with either linear or geometric kinetics under isothermal conditions. In the presence of two primers, one hybridizing to the positive strand and the other to the negative strand of DNA, a complex pattern of DNA strand displacement ensues that generates 10^9 or more copies of each circle in 90 min, enabling detection of point mutations in human genomic DNA. Using a single primer, RCA generates hundreds of tandemly linked copies of a covalently closed circle in a few minutes. I-matrix-associated, the DNA product remains bound to the site of synthesis, where it may be tagged, condensed, and imaged as a point light source. The target DNA can be attached to an antibody, biotin, or other protein probe.

Vanhecke and Janitz (2005) discussed functional genomics using high-throughput RNA interference. **RNA interference** (RNAi) describes the post-transcriptional silencing of gene expression that occurs in response to the introduction of double-stranded RNA into cells. To facilitate large-scale functional genomics studies using RNAi, several high-throughput approaches have been developed based on microarray or microwell assays. The RNAi silencing mechanism is based on the fact that long double-stranded RNA is processed to short interfering RNA (**siRNA**) duplexes by the enzyme Dicer, which exhibits RNase-III-like activity. A single strand of the siRNA is incorporated into the group of cytoplasmic proteins to form an RNA-induced silencing complex (**RISC**). Activated RISC, guided by the antisense siRNA strand, performs endonucleolytic cleavage of target mRNA. Thus produced mRNA fragments are rapidly degraded by cytoplasmic nucleases (Tijsterman and Plasterk 2004).

Rondinone (2006) dicussed the therapeutic potential of RNAi in metabolic diseases.

Aza-Blanc et al. (2003) described the identification of modulators of TRAIL-induced apoptosis via RNAi-based phenotypic screening. TRAIL is a TNF superfamily member that induces selective cytotoxicity of tumor cells when bound to its cognate receptors (Lee et al. 2002).

Using RNAi, Kamath et al. (2003) performed a systematic functional analysis of the *Caenorhabditis elegans* genome. Mousses et al. (2003) describe a microarray analysis in cultured mammalian cells.

Paddison et al. (2004) described a resource for large-scale RNA-interference-based screens in mammals; Berns et al. (2004), a large-scale RNAi screen in human cells to identify new components of the p53 pathway.

Promega Protocols and Applications Guide is a published survey on RNA interference.

The use of siRNA in therapy and drug target discovery is discussed by Cocks and Theriault (2004), Hannon and Rossi (2004), Jones et al. (2004), Kurreck (2004), Meister and Tuschi (2004), Siuod (2004), Bartz and Jackson (2005), and Catterjee-Kishore (2006).

Xin et al. (2004) discussed high-throughput siRNA-based functional target validation. They initiated a project with a functional cell-based screen for a biological process of interest using libraries of small interfering RNA (siRNA) molecules. In this protocol, siRNAs function as potent gene-specific inhibitors. SiRNA-mediated knockdown of the target gene is confirmed by TaqMan analysis, and genes with impacts on biological functions of interest are selected for further analysis. Once the genes are confirmed and further validated, they may be used for HTS to yield lead compounds.

Tang (2005) discussed two classes of short RNA molecules, siRNA and microRNA (miRNA), which are incorporated into related RNA-induced silencing complexes (RISCs), termed siRISC and miRISC, respectively. They are distinct complexes that regulate mRNA stability and translation.

MicroRNAs (miRNAs) are generated via a two-step processing pathway to yield ~22 nucleotide small RNAs that regulate gene expression at the post-transcriptional level (Lee et al. 2002). Initial cleavage is catalyzed by Drosha, a nuclease of the RNase III family, which acts on primary miRNA transcripts (pri-miRNAs) in the nucleus (Lee et al. 2003).

MicroRNAs play important regulatory roles in animals and plants by targeting mRNAs for cleavage

or translational repression (Bartel 2004). The microRNAs of *Caenorhabditis elegans* are described by Lim et al. (2003).

Denli et al. (2004) showed that Drosha exists in a multi-protein complex, the microprocessor, and begins the process of destructing that complex into its constituent components. Along with Drosha, the microprocessors also contains Pasha (partner of Drosha), a double-stranded RNA binding protein. Han et al. (2004) dissected the mechanisms of action of human Drosha by generating mutants and beycharacterizing its interacting partner, DGCR8.

Berezikov et al. (2005) described phylogenetic shadowing and computational identification of human microRNA genes.

Barad et al. (2004) reported microRNA expression detected by oligonucleotide microarray system establishment and expression profiling in human tissue. Liang et al. (2005) described a miRNA profiling microarray, in which miRNAs are directly labeled at the 3′ terminus with biotin and hybridized with complementary oligo-DNA probes immobilized on glass slides, and subsequently detected by measuring the fluorescence of quantum dots labeled with streptavidin bound to miRNAs through streptavidin–biotin interaction.

Locked nucleic acids (LNA) were reported in 1998 (Obidia et al. 1998; Koshkin et al. 1998). LNA is a nucleic acid analog containing one more LNA nucleotide monomers with a bicyclic furanose unit locked in an RNA-mimicking sugar confirmation. LNA nucleotides display unprecedented hybridization affinity toward complementary single-stranded RNA and complementary single- or double-stranded DNA (Braasch and Corey 2001; Vester and Wengel 2004). They are considered as a versatile tool for therapeutics and genomics (Petersen and Wengel 2003; Jepsen et al. 2004).

Tolstrup et al. (2003) reported the development of a software package, OligoDesign, which provides optimal design of LNA oligonucleotide capture probes for gene expression profiling.

Válóczi et al. (2004) described sensitive and specific detection of microRNAs by Northern blot analysis using LNA-modified oligonucleotide probes.

Elmén et al. (2005) reported LNA-mediated improvements in siRNA stability and functionality.

Thomassin et al. (2004) presented MethylQuant, a sensitive method for quantifying methylation of specific cytosines within the genome. The presence of a locked nucleic acid at the 3′ end of the discriminative primer provides the specificity necessary for accurate and sensitive quantification.

Nucleic acid "**lariats**" have been of great interest since their discovery (Wallace and Edmonds 1983). The synthesis of lariat RNA and DNA via template-mediated chemical ligation of Y-shaped oligonucleotides was reported by Carriero and Damha (2003). Deoxyribozymes that synthesize branched and lariat RNA were studied by Wang and Silverman (2003). RNAse III-mediated degradation of unspliced pre-mRNAs and lariat introns was reported by Danin-Kreiselman et al. (2003). Coombes and Boeke (2005) evaluated the detection methods for large lariat RNAs.

REFERENCES AND FURTHER READING

Adam GI, Reneland R, Andersson M, Risinger C, Nilsson M, Lewander T (2000) Pharmacogenomics to predict drug response. Pharmacogenomics 1:5–14

Artal-Sanz M, de Jong L, Tavenarakis N (2006) *Caenorhabditis elegans*: a versatile platform fore drug discovery. Biotechnol J 1:1405–1418

Aza-Blanc P, Cooper CL, Wagner K, Batalov S, Deveraux QL, Cooke MP (2003) Identification of modulators of TRAIL-induced apoptosis via RNAi-based phenotypic screening. Mol Cell 12:627–637

Barad O, Meiri E, Avniel A, Aharonpv R, Barzilai A, Bentwich E, Gilad S, Hurban P, Karov Y, Lobenhofer EK, Sharon E, Shiboleth Y, Shtutman M, Bentwich Z, Einat P (2004) MicroRNA expression detected by oligonucleotide microarray system establishment and expression profiling in human tissue. Genome Res 14:2486–2494

Bartel DP (2004) MicroRNAs: genomics, biogenesis, mechanism, and function. Cell 116:281–297

Bartz S, Jackson AL (2005) How will RNAi facilitate drug development? Sci STKE eg7 (available online at http://stke.sciencemag.org/cgi/content/abstract/2005/295/pe39

Beeley LJ, Duckworth DM, Southan C (2000) The impact of genomics on drug discovery. Prog Med Chem 37:1–43

Bentley DR (2000) Decoding the human genome sequence. Human Mol Genet 9:2353–2358

Berezikov E, Guryev V, van de Belt J, Wienholds E, Plasterk RHA, Cuppen E (2005) Phylogenetic shadowing and computational identification of human microRNA genes. Cell 120:21–24

Berns K, Hijmans EM, Mullenders J, Brummelkamp TR, Velds A, Heimerikx M, Kerkhovem RM, Madiredjo M, Nijkamp W, Weigelt B, Agami R, Ge W, Cavet G, Linsley PS, Beijersbergen RL, Bernards R (2004) A large-scale RNAi screen in human cells identifies new components of the p53 pathway. Nature 428:431–437

Bookchin RM, Nagel RI, Ranney HM (1970) The effect of beta 73 Asn on the interactions of sickling hemoglobin. Biochim Biophys Acta 221:373–375

Braasch DA, Corey DR (2001) Locked nucleic acid (LNA): fine tuning the recognition of DNA and RNA. Chem Biol 8:1–7

Broder S, Venter JC (2000) Sequencing the entire genomes of free-living organisms: the foundation of pharmacology in the new millennium. Annu Rev Pharmacol Toxicol 40:97–132

Bullingham R (2001) Pharmacogenomics: how gene variants can ruin good drugs. Curr Drug Discov 1:17–20

Carriero S, Damha MJ (2003) Template-mediated synthesis of laraiat RNA and DNA. J Org Chem 68:8328–8338

Carulli JP, Artinger M, Swain PM, Root CD, Chee L, Tulig C, Guerin J, Osborne M, Stein G, Lian J, Lomedico PT (1998)

High throughput analysis of differential gene expression. J Cell Biochem Suppl 30–31:286–296
Catterjee-Kishore M (2006) From genome to phenome – RNAi library screening and hit characterization using signaling pathway analysis. Curr Opin Drug Discov Dev 9:231–239
Celis JE, Kruhøffer M, Gromova I, Frederiksen C, Østergaard M, Thykjaer T, Gromov P, Yu J, Pálsdóttir H, Magnusson N, Ørntoft TF (2000) Gene expression profiling: monitoring transcription and translation using DNA microarrays and proteomics. FEBS Lett 480:2–16
Cocks BG, Theriault TP (2004) Development in effective application of small inhibitory RNA (siRNA) technology in mammalian cells. Drug Discov Today Targets 3:165–171
Collins FS, Green ED, Guttmacher AE, Guyer MS (2003) A vision for the future of genomics research. A blueprint for the genomic era. Nature 422:835–847
Coombes CE, Boeke JD (2005) An evaluation of detection methods for large lariat RNAs. RNA 11:323–331
Danin-Kreiselman M, Lee CY, Chanfreau G (2003) RNAse III-mediated degradation of unspliced pre-mRNAs and lariat introns. Mol Cell 11:1279–1289
Danser AHJ, Schunkert H (2000) Renin-angiotensin system gene polymorphisms: potential mechanisms for their association with cardiovascular disease. Eur J Pharmacol 410:303–316
De Morais SM, Wilkinson GR, Blaisdell J, Nakamura K, Meyer UA, Goldstein JA (1994) The major genetic defect responsible for the polymorphism of S-mephentoin metabolism in humans. J Biol Chem 269:15419–15422
Debouck C, Goodfellow PN (1999) DNA microarrays in drug discovery and development. Nat Genet 21 [1 Suppl]:48–50
Debouck C, Metcalf B (2000) The impact of genomics on drug discovery. Annu Rev Pharmacol Toxicol 40:193–208
Denli AM, Tops BBJ, Plasterk RAH, Ketting RF, Hannon GJ (2004) Processing of primary microRNAs by the microprocessor complex. Nature 432:231–235
Dietel M, Sers C (2006) Personalized medicine and development of targeted therapies: the upcoming challenge for diagnostic molecular pathology. A review. Virchows Arch 448:744–755
Drews J (2000) *Quo vadis*, biotech? (Part 1). Drug Discov Today 5:547–553
Drews J (2001) *Quo vadis*, biotech? (Part 2). Drug Discov Today 6:21–26
Elmén J, Thonberg H, Ljungberg K, Frieden M, Westergaard M, Xu Y, Wahren B, Liang Z, Ørum H, Koch T, Wahlestedt C (2005) Locked nucleic acid (LNA) mediated improvements in siRNA stability and functionality. Nucleic Acids Res 33:439–447
Evans WE, Relling MV (1999) Pharmacogenomics: translating functional genomics into rational therapeutics. Science 286:487–491
Farber GK (1999) New approaches to rational drug design. Pharmacol Ther 84:327–332
Goedde HW, Argwal DP, Harada S (1983) Pharmacogenetics of alcohol sensitivity. Pharmacol Biochem Behav 18 [Suppl 1]:161–166
Gonzales FJ (1990) Molecular genetics of the P-450 superfamily. Pharmacol Ther 45:1–38
Grant SF (2001) Pharmacogenetics and pharmacogenomics: tailored drug therapy for the 21th century. Trends Pharmacol Sci 22:3–4
Guillausseau PJ, Tielmans D, Virally-Monod M, Assayag M (1997) Diabetes: from phenotypes to genotypes. Diabetes Metab Res 23 [Suppl 2]:14–21
Haberman AB (2003) Model organisms: tools for drug discovery and development. Drug Discov Des 9:1–16
Han J, Lee Y, Yeom KH, Kim YK, Jin H, Kim VN (2004) The Drosha-DGCR8 complex in primary microRNA processing. Genes Dev 18:3016–3027
Hannon GJ, Rossi JJ (2004) Unlocking the potential of the human genome with RNA interference. Nature 431:371–378
Harris T (2000) Genetics, genomics and drug discovery. Med Res Rev 20:203–211
Hemmilä IA, Hurskainen P (2002) Novel strategies in drug discovery. Drug Discov Today Suppl 7:S150–S156
Inoue K, Fukunaga M, Kiriyama T, Komura S (1984) Accumulation of acetaldehyde in alcohol-sensitive Japanese: relation to ethanol and acetaldehyde oxidizing capacity. Alcohol Clin Exp Res 8:319–322
International Human Genome Sequencing Consortium (2001) Initial sequencing and analysis of the human genome. Nature 409:860–921
Jepsen JS, Sorensen MD, Wengel J (2004) Locked nucleic acid: a potent nucleic acid analog in therapeutics and biotechnology. Oligonucleotides 14:130–146
Jones DA, Fitzpatrick FA (1999) Genomics and the discovery of new drug targets. Curr Opin Chem Biol 3:71–76
Jones SW, de Souza PM, Lindsay MA (2004) siRNA gene silencing: a route to drug target discovery. Curr Opin Pharmacol 4:522–527
Kamath RS, Fraser AG, Dong Y, Poulin G, Durbin R, Gotta M, Kanapin A, Le Bot N, Moreno S, Sohrmann M, Welchman DP, Zipperlen P, Ahringer J (2003) Systematic functional analysis of *Caenorhabditis elegans* genome using RNAi. Nature 421:231–237
Kleyn PW, Vesell ES (1998) Genetic variation as a guide to drug development. Science 281:1820–1821
Koshkin AA, Singh S, Nielsen P, Rajwanshi VK, Kumar R, Meldgaard M, Olsen CE, Wengel J (1998) LNA (locked nucleic acids): synthesis of the adenosine, cytosine, guanine, 5-methylcytosine, thymine and uracil bicyclonucleoside monomers, oligomerisation, and unprecedented nucleic acid recognition. Tetrahedron 54:3607–3630
Kurrek J (2004) Expediting target identification and validation through RNAi. Expert Opin Biol Ther 4:427–429
Lee HO, Herndon JM, Barriero R, Griffith TS, Ferguson TA (2002) TRAIL: a mechanism of tumor surveillance in an immune privileged site. J Immunol 169:4739–4744
Lee Y, Jeon K, Lee Jt, Kim S, Kim VN (2002) MicroRNA maturation: stepwise processing and subcellular localization. EMBO J 21:4663–4670
Lee Y, Ahn C, Han J, Choi H, Kim J, Yim J, Lee J, Provost P, Radmark O, Kim S, Kim VN (2003) The nuclear RNase III Drosha initiates microRNA processing. Nature 425:415–419
Lennon GG (2000) High-throughput gene expression analysis for drug discovery. Drug Discov Today 5:59–66
Liang RQ, Li W, Li Y, Tan CY, Li JX, Jin YX, Ruan KC (2005) An oligonucleotide microarray for microRNA expression analysis based on labeling RNA with quantum dot and nanogold probes. Nucleic Acids Res 33:e17
Liggett SB (1997) Polymorphisms of the β_2-adrenergic receptor and asthma. Am J Respir Crit Care Med 156:S156–S162
Lim LP, Lau NC, Weinstein EG, Abdelhakim A, Yekta S, Rhoades MW, Burge CB, Bartel DP (2003) The microRNAs of *Caenorhabditis elegans*. Genes Dev 17:991–1008
Link EM, Hardiman G, Sluder AE, Johnson CD, Liu LX (2000) Therapeutic target discovery using *Caenorhabditis elegans*. Pharmacogenomics 1:203–207
Lizardi PM, Huang X, Zhu Z, Bray-Ward P, Thomas DC (1998) Mutation detection and single-molecule counting

using isothermal rolling-circle amplification. Nature Genet 19:225–232
Mager J, Glaser G, Razin A, Izak G, Bien S, Noam M (1965) Metabolic effects of pyrimidines derived from fava bean glycosides on human erythrocytes deficient in glucose-6-phosphate dehydrogenase. Biochem Biophys Res Commun 20:235–240
March R (2000) Pharmacogenomics: the genomics of drug response. Yeast 17:16–21
Marshall E (2000) Human genome: rival genome sequencers celebrate a milestone together. Science 288:2294–2295
Meister G, Tuschi T (2004) Mechanisms of gene silencing by double-stranded RNA. Nature 431:343–349
Meldrum D (2000a) Automation for genomics, part one: preparation for sequencing. Genome Res 10:1081–1092
Meldrum D (2000b) Automation for genomics, part two: sequencers, microarrays, and future trends. Genome Res 10:1288–1303
Meyer UA (2000) Pharmacogenomics and adverse drug reactions. Lancet 356:1667–1671
Mousses S, Caplen NJ, Cornelison R, Weaver D, Basik M, Hautaniemi S, Elkahloun AG, Lotufo RA, Choudary A, Dougherty ER, Suh E, Kallioniemi O (2003) RNAi microarray analysis in cultured mammalian cells. Genome Res 13:2341–2347
Murayama M (1966) Tertiary structure of sickle cell hemoglobin and its functional significance. J Cell Physiol 67 [Suppl. 1]:21–32
Murphy MP (2000) Current pharmacogenomic approaches to clinical drug development. Pharmacogenomics 1:115–123
Nebert D (1999) Pharmacogenetics and pharmacogenomics: why is this relevant to the clinical geneticist? Clin Genet 56:247–258
Obida S, Nanbu D, Hari Y, Andoh JI, Morio KI, Doi T, Imashini T (1998) Stability and structural features of the duplexes containing nucleoside analogues with a fixed N-type conformation, $2'-O,4'-C$-methylenribonucleosides. Tetrahedron Lett 39:5401–5404
Paddison PJ, Silva JM, Conklin DS, Schlabach M, Li M, Aruleba S, Balija V, O'Shaughnessy A, Gnoj L, Scobia K, Chang K, Westbrook T, Clery M, Sachidamandam R, McCombie WR, Elledge SJ, Hannon GJ (2004) A resource for large-scale RNA-interference-based screens in mammals. Nature 428:427–431
Peet NP, Bey P (2001) Pharmacogenomics: challenges and opportunities. Drug Discov Today 6:495–498
Petersen M, Wengel J (2003) LNA: a versatile tool for therapeutics and genomics. Trends Biotechnol 21:74–81
Podda M, Fiorelli G, Ideo G, Spano G, Dioguardi N (1969) *In vitro* effect of a fava bean extract and its fractions on reduced glutathione in glucose-6-phosphate dehydrogenase deficient red cells. Folia Haematol Int Mag Klin Morphol Blutforsch 91:51–55
Rockett JC, Dix DJ (2000) DNA arrays: technology, options and toxicological applications. Xenobiotica 30:155–177
Rondinone CM (2006) Therapeutic potential of RNAi in metabolic diseases. Biotechniques 40:S31–S36
Rudolph U, Möhler H (1999) Genetically modified animals in pharmacological research: future trends. Eur J Pharmacol 375:327–337
Sadée W (1999) Pharmacogenomics. Br Med J 319:1286–1290
Samani NJ, O'Toole L, Channer K, Woods KL (1996) A meta-analysis of the association of the deletion allele of the angiotensin-converting enzyme gene with myocardial infarction. Circulation 94:708–712
Schuster M, Wasserbauer E, Einhauer A, Ortner C, Jungbauer A, Hammerschmid F, Werner G (2000) Protein expression strategies for identification of novel target proteins. J Biomol Sci 5:89–97
Shimkets RA, Lifton RP (1996) Recent advances in the molecular genetics of hypertension. Curr Opin Nephrol Hypertens 2:162–165
Sioud M (2004) Therapeutic siRNAs. Trends Pharmacol Sci 25:22–28
Snyder LH (1932) Studies in human inheritance: IX. The inheritance of taste deficiency in man. Ohio J Sci 32:436–468
Spear BB, Heath-Chiozzi M, Huff J (2001) Clinical applications of pharmacogenetics. Trends Mol Med 7:201–204
Steiner S, Anderson NL (2000) Expression profiling in toxicology – potentials and limitations. Toxicol Lett 112–113:467–471
Tang G (2005) siRNA and miRNA: an insight into RISCs. Trends Biochem Sci 30:106–114
Thomassin H, Kress C, Grange T (2004) MethylQuant: a sensitive method for quantifying methylation of specific cytosines within the genome. Nucleic Acids Res 32:e168
Tijsterman M, Plasterk RHA (2004) Dicers at RISC: the mechanism of RNAi. Cell 117:1–4
Tolstrup N, Nielsen PS, Kolberg JG, Frankel AM, Vissing H, Kauppinen S (2003) OligoDesign: optimal design of LNA (locked nucleic acid) oligonucleotide capture probes for gene expression profiling. Nucleic Acids Res 31:3758–3762
Válóczi A, Hornyik C, Varga N, Burgyán J, Kauppinen S, Havelda Z (2004) Sensitive and specific detection of microRNAs by northern blot analysis using LNA-modified oligonucleotide probes. Nucleic Acids Res 32:e175
Van Oosterhout AJM (1998) Genomics and drug discovery. Trends Pharmacol Sci 19:157–160
Vanhecke D, Janitz M (2005) Functional genomics using high-throughput RNA interference. Drug Discov Today 10:205–212
Venter JC et al (2001) The sequence of the human genome. Science 291:1304–1351
Vesell ES (2000) Advances in pharmacogenetics and pharmacogenomics. J Clin Pharmacol 40:930–938
Vester B, Wengel J (2004) LNA (locked nucleic acid): high-affinity targeting of complementary RNA and DNA. Biochemistry 43:13233–13241
Vogel F (1959) Moderne Probleme der Humangenetik. Erg Inn Med Kinderheilkd 12:52–125
Wallace JC, Edmonds M (1983) Polyadenylated nuclear RNA contains branches. Proc Natl Acad Sci USA 80:950–954
Wang Y, Silverman SK (2003) Deoxyribozymes that synthesize branched and lariat RNA. J Am Chem Soc 125:6880–6881
Weaver TA (2001) High-throughput SNP discovery and typing for genome-wide genetic analysis. New technologies for life sciences: a trends guide 1:36–42
Weber WW (1999) Populations and genetic polymorphisms. Mol Diagn 4:299–307
West DB, Iakougova O, Olsson C, Ross D, Ohmen J, Chatterjee A (2000) Mouse genetics/genomics: an effective approach for drug target discovery and validation. Med Res Rev 20:216–230
Wieczorek SJ, Tsongalis GJ (2001) Pharmacogenomics: will it change the field of medicine? Clin Chim Acta 308:1–8
Wilson S, Bergsma DJ, Chambers JK, Muir AI, Fantom KG, Ellis C, Murdock PR, Herrity NC, Stadel JM (1998) Orphan G-protein-couples receptors: the next generation of drug targets? Br J Pharmacol 125:1387–1392
Winkelmann BR (2001) Genomics and large scale phenotypic databases. Pharmacogenomics 2:3–5

Winkelmann BR, Marz W, Boehm BO, Zotz R, Hager J, Hellstern P, Senges J (2001) Rationale and design of the LURIC study – a resource for functional genomics, pharmacogenomics and long-term prognosis of cardiovascular disease. Pharmacogenomics 2 [Suppl 1]:S1–S73

Wolf CR, Smith G (1999) Pharmacogenetics. Br Med Bull 55:366–386

Xin H, Bernal A, Amato FA, Pinhasov A, Kauffman J, Brenneman DE, Derian CK, Anrade-Gordon P, Plata-Salamán CR, Ilyin SE (2004) High-throughput siRNA-based functional target validation. J Biomol Screen 9:286–293

Zambrowicz BP, Turner CA, Sands AT (2003) Predicting drug efficacy: knockouts model pipeline drugs of the pharmaceutical industry. Curr Opin Pharmacol 3:563–570

Zhong XB, Lizardi PM, Huang XH, Bray-Ward PL, Ward DC (2001) Visualization of oligonucleotides probes and point mutations in interphase nuclei and DNA fibers using rolling circle amplification. Proc Natl Acad Sci USA 98:3940–3945

Zweiger G (1999) Knowledge discovery in gene-expression-microarray data: mining the information output of the genome. Trends Biotechnol 17:429–436

0.4.5 Proteomics

The term "proteome" was coined by Wilkins et al. (1995) to describe the protein complement of the genome. The term proteomics was first used to describe the complexity of proteins expressed in an organism using two-dimensional gel electrophoresis (2-DE) followed by quantitative analysis. 2-DE remains the highest resolution protein separation method available, but the ability to concentrate and identify low abundance proteins has always been an extremely difficult problem. Mass spectrometry (MS) has been an integral part of approaching this problem (de Hoog and Mann 2004; Lane 2005). Although improvements in 2-D gel technology have been made since its introduction, three enabling technological advances have provided the basis for the foundation of the field of proteomics (Patterson 2000). The first advance was the introduction of large-scale nucleotide sequencing of both expressed sequence tags (ESTs) and genomic DNA. The second was the development of mass spectrometers able to ionize and mass-analyze biological molecules and the widespread introduction of mass spectrometers, capable of data-dependent ion selection for fragmentation (MS/MS) (i. e., without the need for user intervention). The third was the development of computer algorithms able to match uninterpreted (or partially interpreted) MS/MS spectra with translations of the nucleotide sequence databases, thereby tying together the first technological advances. The mass spectrometer instruments are named for their type of ionization source and mass analyzer (Patterson and Abersold 1995; Carr and Annan 1997; Patterson 1998). To measure the mass of molecules, the test material must be charged (ionized) and desolvated. The two most successful mechanisms for ionization of peptides and proteins are matrix-assisted laser desorption ionization (MALDI) and electrospray ionization (ESI). In MALDI the analyte of interest is embedded in a matrix that is dried and then volatilized in a vacuum under ultraviolet laser irradiation. This is a relatively efficient process that ablates only a small portion of the analyte with each laser shot. Typically, the mass analyzer coupled with MALDI is a time-of-flight (TOF) mass analyzer, that measures the elapsed time from acceleration of the charged (ionized) molecules through a field-free drift region (Kowalski and Stoerker 2000). The other common ionization source is ESI, in which the analyte is sprayed from a fine needle at high voltage toward the inlet of the mass spectrometer (which is under vacuum) at a lower voltage. The spray is typically either from a reversed-phase HPLC column or a nanospray device (Wilm and Mann 1994), similar to a microinjection needle. The ions formed during this process are directed into the mass analyzer, which could be a triple-quadrupole, an ion trap, a Fourier-transform ion cyclotron resonance (FT-ICR), or a hybrid quadrupole TOF (Qp-TOF) type (Morris et al. 1996). Although unambiguous identification of a protein cannot always be derived from the masses of a few of its peptides in the tandem mass spectrometer, peptide ions from the first mass spectrometer run are fragmented and identified in a second run to yield a more valuable commodity of a peptide sequence.

Annis et al. (2004) and Whitehurst et al. (2006) proposed affinity selection-mass spectroscopy (AS-MS) as a useful high-throughput assay system for the discovery and characterization of all classes of integral membrane protein ligands, including allosteric modulators.

The goal of proteomics is a comprehensive, quantitative description of protein expression and its change under the influence of biological perturbations, such as disease and drug treatment (Anderson and Anderson 1998, 2002; Müller et al. 1998; Blackstock and Weir 1999; Dove 1999; Hatzimanikatis et al. 1999; Jungblut et al. 1999; Williams 1999). A combination of mRNA and protein expression patterns has to be simultaneously considered to develop a conceptual understanding of the functional architecture of genomes and gene networks (Kreider 2000). New methods are created such as automated proteomics platforms (Quadroni and James 1999; Nielsen et al. 1999), combining two-dimensional electrophoresis, automated spot picking and mass spectrometry (Binz et al. 1999; Dancik et al.

1999; Loo et al. 1999; Dutt and Lee 2000; Feng 2000; Patterson et al. 2000; Ryu and Nam 2000; Service 2000; Yates 2000; James 2001; Jain 2001; Rabilloud 2001).

Improvements in quality, ability and utility of large-scale tertiary and quarternary protein structural information are enabling a revolution in rational design, having a particular impact on drug discovery and optimization (Maggio and Ramnarayan 2001).

Disease proteomics will give a better understanding of disease processes, develop new biomarkers for diagnosis and early detection of disease, and accelerate drug development (Hanash 2003).

One may expect that with the new approach of drug research, including combinatorial chemistry, genomics, pharmacogenomics, proteomics, and bioinformatics, unprecedented results will be generated (Browne 2000; Burley et al. 1999; Debouck and Metcalf 2000; Drews 2000; Haystead 2001).

The difficulties arising in proteomic experiments from data analysis are discussed by Patterson (2003).

Duncan and Hunsucker (2005) discussed the value of proteomics as a tool for clinically relevant biomarker discovery and validation. A critical review on the impact of "OMIC" technology in drug development is given by Bilello (2005).

REFERENCES AND FURTHER READING

Anderson NL, Anderson NG (1998) Proteome and proteomics: new technologies, new concepts, and new words. Electrophoresis 19:1853–1861

Anderson NL, Anderson NG (2002) The human plasma proteome. History, character, and diagnostic prospects. Mol Cell Proteomics 1:845–856

Annis DA, Nazef N, Chung CC, Scott MP, Nash HM (2004) A general technique to rank protein-ligand binding affinities and determine allosteric versus direct binding site competition in compound mixtures. J Am Chem Soc 126:15495–15503

Bilello JA (2005) The agony and ecstasy of "OMIC" technology in drug development. Curr Mol Med 5:39–52

Binz PA, Müller M, Walther D, Bienvenut WV, Gras R, Hoogland C, Bouchet G, Gasteiger E, Fabbretti R, Gay S, Palagi P, Wilkins MR, Rouge V, Tonella L, Paesano S, Rossellat G, Karmime A, Bairoch A, Sanchez JC, Appel RD, Hochstrasser DF (1999) A molecular scanner to automate proteomic research and to display proteome images. Anal Chem 71:4981–4988

Blackstock WP, Weir MP (1999) Proteomics: quantitative and physical mapping of cellular proteins. Trends Biotechnol 17:121–127

Browne MJ (2000) Analysis of large gene databases for discovery of novel therapeutic agents. J Biotechnol 78:247–259

Burley SK, Almo SC, Bonanno JB, Capel M, Chance MR, Gaasterland T, Lin D, Sali A, Studier FW, Swaminathan S (1999) Structural genomics: beyond the human gene project. Nature Genet 23:151–157

Carr SA, Annan RS (1997) Overview of peptide and protein analysis by mass spectrometry. In: Ausubel FM, Brent R, Kingston RE, Moore DD, Seidman JG, Smith JA, Struhl K (eds) Current protocols in molecular biology. Wiley, New York, pp 10.21.1–10.21.27

Dancik V, Addona TA, Clauser KR, Vath JE, Pevzner PA (1999) De novo peptide sequencing via tandem mass spectrometry. J Comput Biol 6:327–342

De Hoog CL, Mann M (2004) Proteomics. Annu Rev Genomics Hum Genet 5:267–293

Debouck C, Metcalf B (2000) The impact of genomics on drug discovery. Annu Rev Pharmacol Toxicol 40:193–208

Dove A (1999) Proteomics: translating gene into products? Nature Biotechnol 17:233–236

Drews J (2000) Drug discovery: a historical perspective. Science 287:1960–1964

Duncan MW, Hunsucker SW (2005) Proteomics as a tool for clinically relevant biomarker discovery and validation. Exp Biol Med 230:808–817

Dutt MJ, Lee KH (2000) Proteomic analysis. Curr Opin Biotechnol 11:176–179

Feng HP (2000) A protein microarray. Nature Struct Biol 7:829–830

Hanash S (2003) Disease proteomics. Nature 422:226–232

Hatzimanikatis V, Choe LH, Lee KH (1999) Proteomics: theoretical and experimental considerations. Biotechnol Prog 15:312–318

Haystead TAJ (2001) Proteome mining: exploiting serendipity in drug discovery. Curr Drug Discov 1:22–24

Jain KK (2001) Proteomics: new technologies and their applications. Drug Discov Today 6:457–459

James P (2001) Proteome research: mass spectrometry. Springer, Berlin Heidelberg New York

Jungblut PR, Zimny-Arndt U, Zeindl-Eberhart E, Stulik J, Koupilova K, Pleissner KP, Otto A, Müller EC, Sokolowska-Kohler W, Grabner G, Stoffler G (1999) Proteomics in human disease: cancer, heart and infectious diseases. Electrophoresis 20:2100–2110

Kowalski P, Stoerker J (2000) Accelerating discoveries in the proteome and genome with MALDI TOF MS. Pharmacogenomics 1:359–366

Kreider BL (2000) PROfusion: genetically tagged proteins for functional proteomics and beyond. Med Res Rev 20:212–215

Lane CS (2005) Mass-spectrometry-based proteomics in the life sciences. Cell Mol Life Sci 62:848–869

Loo JA, DeJohn DE, Du P, Stevenson TI, Ogorzalek-Loo RR (1999) Application of mass spectrometry for target identification and characterization. Med Res Rev 19:307–319

Maggio ET, Ramnarayan K (2001) Recent developments in computational proteomics. Trends Biotechnol 19:266–272

Morris HR, Paxton C, Langhorne J, Berg M, Bordoli RS, Hoyes J, Bateman RH (1996) High sensitivity collisionally-activated decomposition tandem mass flight mass spectrometer, the Q-TOF, for low fentomole/attomole-range biopolymer sequencing. J Protein Chem 16:469–479

Müller S, Neumann T, Lottspeich F (1998) Proteomics – a new way for drug target discovery. Arzneimittelforschung 48:93–95

Nielsen H, Brunak S, van Heijne G (1999) Machine learning approaches for the prediction of signal peptides and other protein sorting signals. Protein Eng 12:3–9

Patterson SD (1998) Protein identification and characterization by mass spectrometry. In: Ausubel FM, Brent R, Kingston RE, Moore DD, Seidman JG, Smith JA, Struhl K (eds) Current protocols in molecular biology. Wiley, New York, pp 10.22.1–10.22.24

Patterson SD (2000) Mass spectrometry and proteomics. Physiol Genomics 2:59–65

Patterson SD (2003) Data analysis – the Achilles heel of proteomics. Nature Biotechnol 21:221–222
Patterson SD, Aebersold R (1995) Mass spectrometric approaches for the identification of gel-separated proteins. Electrophoresis 16:1791–11814
Patterson SD, Spahr CS, Daugas E, Susin SA, Irinopoulou T, Koehler C, Kroemer G (2000) Mass spectrometric identification of proteins released from mitochondria undergoing permeability transition. Cell Death Differ 7:137–144
Quadroni M, James P (1999) Proteomics and automation. Electrophoresis 20:664–677
Rabilloud T (2001) Proteome research: two-dimensional gel electrophoresis and identification methods. Springer, Berlin Heidelberg New York
Ryu DD, Nam DH (2000) Recent progress in biomolecular engineering. Biotechnol Prog 16:2–16
Service RF (2000) Proteomics. Can Celera do it again? Science 287:2136–2138
Whitehurst CE, Nazef N, Annis DA, Hou Y, Murphy DM, Spacciapoli P, Yao Z, Ziebell MR, Cheng CC, Shipps GW Jr, Felsch JS, Lau D, Nash HM (2006) Discovery and characterization of orthosteric and allosteric muscarinic M2 acetylcholine receptor ligands by affinity selection-mass spectrometry. J Biomol Screen 11:194–207
Wilkins MR, Sanchez JC, Gooley AA, Appel RD, Humphery-Smith I, Hochstrasser DF, Williams KL (1995) Progress with proteome projects: why all proteins expressed by a genome should be identified and how to do it. Biotechnol Genet Eng Rev 13:19–50
Williams KL (1999) Genomes and proteomes: toward a multidimensional view of biology. Electrophoresis 20:678–688
Wilm MS, Mann M (1994) Electrospray and Taylor-Cone theory, Dole's beam of macromolecules at last? Int J Mass Spectrom Ion Processes 136:167–180
Yates JR 3rd (2000) Mass spectrometry. From genomics to proteomics. Trends Genet 16:5–8

0.4.6 Array Technology

Array technology is based on the RNA and DNA hybridization reaction previously used in Northern and Southern expression analysis. However, these traditional approaches allowed the detection of only one single gene. In contrast, gene arrays and microarrays allow the analysis of hundreds or thousands of genes simultaneously (DeRisi and Iyer 1999; Diehn et al. 2000; Epstein and Butow 2000; Deyholos et al. 2001; Jordan 2001; Rocket 2000; Taniguchi 2001; Hardiman 2004; Imbeaud and Auffray 2005). Gene chips can be global, containing the entire genome of one species on the slide. Besides the miniaturization, the greatest leap of technology was the development of fluorescence-labeled nucleotides, which can be detected by laser scanning. They have now replaced the use of radioactively labeled DNA.

Two different methods are used in array production: chips are loaded with either synthetic oligonucleotides (Lipshutz et al. 1999) or with a DNA fragment isolated directly from the respective gene. A specific process allows the synthesis of oligonucleotides directly onto the glass surface. Normally, every gene is represented by about 20 oligonucleotides from different regions of the gene. Each oligonucleotide is 25–30 base pairs in length and is synthesized next to a control oligonucleotide with a mismatch.Whole genome arrays were pioneered by Affymetrix using a proprietary chip technology but are now available from other suppliers as well.

The development of DNA chips was pioneered by researchers at Stanford University (Brown and Botstein 1999; Sherlock et al. 2001). Along with the Stanford Microarray Database a number of additional centers voted for an open online access to their array databases: http://genome-www.stanford.edu.

Killion et al. (2003) created the Longhorn Array Database (LAD), which is an open-source, MIAME-compliant implementation of the Stanford Microarray Database. LAD is available at http://www.longhornarraydatabase.org/.

The standard MIAME (minimum information about a microarray experiment) was proposed by Brazma et al. (2001).

Kamb and Ramaswami (2001) presented a simple method for statistical analysis of intensity differences in microarray-derived gene expression data which does not require multiple replicates. The difference-averaging method enables determination of variances as a function of signal intensities by averaging over the entire dataset.

Novoradovskaya et al. (2004) recommended Universal Reference RNA (URR) as a standard for microarray experiments, a useful tool for monitoring intra- and inter-experimental variation. A variety of microassays were used to determine the percentage of spots hybridizing with URR and producing signal above a user defined threshold (microarray coverage). Microarray coverage was consistently greater than 80% for all arrays tested.

Regardless of using oligonucleotides or DNA arrays, one always needs two RNA samples for chip analysis. The RNA can be isolated from treated versus untreated cell lines, from the serum of an animal before or after drug administration, or from tumor versus normal tissue. Standard protocols require about 100 µg total RNA, from which poly A^+ RNA is extracted. Next, the RNA is converted by reverse transcription into cDNA in the presence of fluorescence-labeled dyes. Commonly, the sample is labeled with Cy-5 and the control with Cy-3. Both cDNAs are combined and hybridized against the array (Rautenstrauss and Liehr 2001). Since DNA–DNA binding

reactions are thermodynamically slow, the chip is incubated overnight at temperatures above 60°C. Chip analysis is performed by scanning with two lasers at 562 nm (Cy-3) and 644 nm (Cy-5). The overlay of both scans shows genes that are deregulated. By convention, overexpressed genes are shown in green, repressed genes in red and unchanged expression in yellow. Data are evaluated by scatter blot analysis, where the relative expression of each gene is indicated by logarithmic axes. Sophisticated bioinformatic protocols are used for further annotation and data comparison (Zhang 1999; Gaasterland and Berikanow 2000).

The best approach to microarray analysis is to begin with a small number of the elements in the microarray known to be a pattern and ask questions of the other elements in the microarray; i. e., perform instantaneous scientific experiments regarding whether each of the other elements in the microarray is related to the known pattern (Burke 2000).

Emerging technologies and perspectives for microarray applications are reviewed by Gebauer (2004).

Epstein and Walt (2003) described fluorescence-based fibre optic arrays as a universal platform for sensing. Optical fibres provide a universal sensing platform as they are easily integrated with a multitude of different sensing schemes. Such schemes enable the preparation of a multitude of sensors including high-density oligonucleotide arrays and high-throughput cell-based arrays. Imaging fibre bundles comprised of thousands of fused optical fibres are the basis for an optically connected, individually addressable parallel sensing platform. Fibre optic imaging bundles possess miniature feature sizes (3- to 10-μm-diameter fibres), allowing high-density sensor packing ($\sim 2 \times 10^7$ sensors per cm^2).

Ge (2000) described the development of a universal protein array (UPA) system that provides a sensitive, quantitative, multipurpose, effective and easy technology to determine not only specific protein–protein interactions, but also specific interactions of proteins with DNA, RNA, ligands and other small chemicals.

The application of biochip and microarray systems in pharmacogenomics is discussed by Jain (2000).

MacBeath et al. (1999) discussed the possibilities of printing small molecules as microassays and detecting protein–ligand interactions en masse.

Firestein and Pisetsky (2002) published guidelines for studies using DNA microarray technology. The criteria for evaluating microarray studies are: (1) reproducibility must be demonstrated, including rigorous evaluation of the run-to-run variability of each gene; (2) detailed statistical analysis is required; including appropriate corrections for repeated multiple measurements; (3) homogeneous cell populations should be optimally studied, to reduce the complexity of analysis; (4) a non-array method must confirm changes in the expression of key genes.

Ziauddin and Sabatini (2001) developed a microarray-driven gene expression system for the functional analysis of many gene products in parallel. Mammalian cells are cultured on a glass slide printed in defined locations with different DNAs. Cells growing on the printed areas take up the DNA, creating spots of localized transfection within a lawn of non-transfected cells. By printing sets of complementary DNAs cloned in expression vectors, microarrays are made, whose features are clusters of live cells that express a defined cDNA at each location.

Feldman et al. (2002) described advantages of mRNA amplification for microarray analysis and recommended routine mRNA amplification for all cDNA microarray-based analysis of gene expression.

Nielsen et al. (2005) developed a ready-to-spot polymer microarray slide, which is coated with a uniform layer of reactive electrophilic groups using anthraquinone-mediated photo-coupling chemistry. The slide coating reduces the hydrophobicity of the native polymer significantly, thereby enabling robust and efficient one-step coupling of spotted 5′-amino-like oligonucleotides onto the polymer slide. The coated polymer microarray slide represents a robust and cost-effective platform for pre-spotted oligonucleotide arrays.

Luo and Geschwind (2001) reviewed microarray applications in neuroscience with reference to applications in neurologic diseases in humans and the use of animal models.

Bunney et al. (2003) reviewed new strategies to discover candidate vulnerability genes in psychiatric disorders by microarray technology.

Templin et al. (2002) discussed the possibilities offered by protein microarray technology. Recent developments in the field of protein microarrays show applications for enzyme–substrate, DNA–protein and different types of protein–protein interactions. The authors discuss theoretical advantages and limitations of any miniaturized capture-molecule-ligand assay system.

Salisbury et al. (2002) described peptide microarrays for the determination of protease substrate specificity using fluorogenic peptidyl coumarin substrates.

The technology, the materials and the methods used for antibody microarrays are described by Lal et al. (2002) and Kusnezow et al. (2003).

Gopalakrishnan et al. (2002) described the application of Micro Arrayed Compound Screening (microARCS) to identify inhibitors of caspase-3. In this format, 8,640 discrete compounds are spotted and dried onto a polystyrene sheet, which has the same footprint as a 96-well plate. A homogeneous time-resolved fluorescence assay format (LANCE) was applied to identify the inhibitors of caspase-3 using a peptide substrate labeled with a fluorescent europium chelate and a dabcyl quencher. The caspase-3 enzyme was cast into a thin agarose gel, which was placed on a sheet containing test compounds. A second gel containing caspase substrate was then laid above the enzyme gel to initiate the reaction. Caspase-3 cleaves the substrate and separates the europium from the quencher, giving rise to a time-resolved fluorescence signal, which was detected using a ViewLux charge-coupled device imaging system.

Protein chip technology has been addressed by Zhu and Snyder (2003). Protein microarray technology has shown its great potential in basic research, diagnostics, and drug discovery. It has been applied to analyze antibody–antigen, protein–protein, protein–nucleic acid, protein–lipid and protein–small molecule interactions, as well as enzyme–substrate interactions. Progress in the field of protein chips includes surface chemistry, capture molecule attachment, protein labeling and detection methods, high-throughput protein–antibody production, and applications to analyze entire proteomes.

Lenigk et al. (2002) recommended plastic biochannel hybridization devices as a new concept for microfluidic DNA arrays.

Lee et al. (2004) described high-throughput screening of novel peptide inhibitors of an integrin receptor from the hexapeptide library by using a protein microarray chip. Novel peptide ligands with high affinity to the integrin were identified from the peptide libraries with this chip-based screening system by a competitive inhibition assay in a simultaneous and high-throughput fashion.

Hsieh et al. (2004) described an ultra-high-throughput microarray generation and liquid dispensing using multiple disposable piezoelectric ejectors.

Lim et al. (2005) used microarray analysis to show that some microRNAs downregulate a large number of target mRNAs.

Howbrook et al. (2003) reviewed developments in microarray technologies including gene expression analysis, DNA microarrays, protein and peptide microarrays, glycomics, tissue and cell microarrays as well as progress in microarray technology, such as microfluids, molecular imprintation, and nanotechnology.

Gosalia and Diamond (2003) developed a method that performs enzymatic assays in nanoliter volumes in the liquid phase with minimal evaporation, no cross-contamination, and high reproducibility, and that has the capability to rapidly assemble multicomponent reactions with minimal usage in a microarray format. Chemical compounds within individual nanoliter droplets of glycerol are microarrayed onto glass slides at 400 spots/cm^2. Using aerosol deposition, subsequent reagents and water are metered into each reaction center to rapidly assemble diverse multicomponent reactions without cross-contamination or the need for surface linkage. This proteomics technique allows the kinetic profiling of protease mixtures, protease–substrate interactions, and high-throughput screening reactions.

Kusnezow and Hoheisel (2002) discussed promises and problems of antibody microarrays and compared this approach with the achievements of DNA microarrays.

Rondelez et al. (2005) developed microfabricated arrays of femtoliter chambers that allow single molecule enzymology. The microchip ensures that the chambers are uniform and precisely positioned.

Rougemont and Hingamp (2003) provided a method for automatically determining relevant gene clusters among the many genes monitored with microarrays.

Forster et al. (2004) described triple-target microarray experiments as a novel experimental strategy. There are two main dye-labeling strategies for microarray studies based on custom-spotted cDNA or oligonucleotide arrays: (1) dye-labeling of a single target sample with a particular dye, followed by subsequent hybridization to a single microarray slide, (2) dye-labeling of two different target samples with two different dyes, followed by subsequent co-hybridization to a single microarray slide. The two dyes most frequently used for either method are Cy3 and Cy5. The authors proposed and evaluated a novel experimental set-up utilizing three differently labeled targets co-hybridized to one microarray slide. In addition to Cy3 and CY5, Alexa 594 was incorporated as a third dye label.

Sharma et al. (2004) developed software called "ArrayD" that offers various alternative design solutions for a microassay given a set of user requirements.

Watson et al. (2004) published methods for high-throughput validation of amplified fragment pools of bacterial artificial chromosome (BAC) DNA for con-

structing high-resolution CHG assays. The development of array based on comparative genomic hybridization (CGH) technology provides improved resolution for detection of alterations in genomic DNA copy number. In array CHG, generating spotting solution is a multi-step process where BAC clones are converted to replenishable PCR-amplified fragment pools (AFP) for use as spotting solution in a microarray format on glass substrate. Current methods for identifying initial BAC clones can be adapted to verify the identity of AFP spotting solutions used in printing assays. Of these methods, AFP sequencing is considered to be the most efficient for large-scale identification of spotting solution in a high-throughput manner.

Daly et al. (2005) presented a statistical method based on propagation of error to evaluate concentration estimation errors in an ELISA microarray process.

Do and Choi (2006) gave a review of normalization techniques of microarray data from single-labeled platforms such as the Affymetrix GeneChip array to dual-labeled platforms, e. g., spotted array, focusing on their principles and assumptions.

Ma and Horiuchi (2006) recommended chemical microarray as a new tool for drug screening and discovery in order to find new ways in HTS to profile the activity of large numbers of chemicals against hundreds of biological targets in a fast, low-cost fashion.

Uttamchandani et al. (2005) reviewed recent advances and applications of small molecule microarrays. Small molecule microarrays (SMM) are of value in high-throughput exploration, both in the identification of biologically significant natural and synthetic small molecules and in harnessing their vast potential towards medicinal and diagnostic applications.

Sobek et al. (2006) recommended microarray technology as a universal tool for high-throughput analysis of biological systems and reviewed the recent developments in surface chemistry and derivatization.

REFERENCES AND FURTHER READING

Brazma A, Hingamp P, Quackenbush J, Sherlock G, Spellman P, Stoeckert C, Aach J, Ansorge W, Ball CA, Causton HC, Gaasterland T, Glenisson P, Holstege FC, Kim IF, Markowitz V, Matese JT, Parkinson H, Robinson A, Sarkans U, Schulze-Kremer S, Stewart J, Taylor R, Vilo J, Vingron M (2001) Minimum information about a microarray experiment (MIAME) – towards standards for microarray data. Nature Genet 29:365–371

Brown PO, Botstein D (1999) Exploring the new world of the genome with DNA microarrays. Nature Genet 21 [Suppl 1]:33–37

Bunney WE, Bunney BG, Vawter MP, Tomita H, Li J, Evans SJ, Choudary PVPV, Myers RM, Jones EG, Watson SJ, Akil H (2003) Microarray technology: a review of new strategies to discover candidate vulnerability genes in psychiatric disorders. Am J Psychiatry 160:657–666

Burke HB (2000) Discovering patterns in microarray data. Mol Diagn 5:349–357

Daly DS, White AM, Varnum SM, Anderson KK, Zangar RC (2005) Evaluation concentration estimation errors in ELISA microarray experiments. BMC Bioinformatics 6:17

DeRisi JL, Iyer VR (1999) Genomics and array technology. Curr Opin Oncol 11:76–79

Deyholos M, Wang H, Galbraith D (2001) Microarrays for gene discovery and metabolic pathway analysis in plants. Origins 2:6–8

Diehn M, Eisen MB, Botstein D, Brown PQ (2000) Large-scale identification of secreted and membrane-associated gene products using DNA microarrays. Nat Genet 25:58–62

Do JH, Choi DK (2006) Normalization of microarray data: single-labeled and dual-labeled arrays. Mol Cell 22:254–261

Epstein CB, Butow RA (2000) Microarray technology – enhanced versatility, persistent challenge. Curr Opin Biotechnol 11:36–41

Epstein JR, Walt DR (2003) Fluorescence-based fibre optic arrays: a universal platform for sensing. Chem Soc Rev 32:203–214

Feldman AL, Costouros NG, Wang E, Qian M, Marincola FM, Alexander HR, Libutti SK (2002) Advantages of mRNA amplification for microarray analysis. Biotechniques 33:906–914

Firestein GS, Pisetsky DS (2002) DNA microarrays: boundless technology of bound by technology? Guidelines for studies using microarray technology. Arthritis Rheum 46:859–861

Forster T, Costa Y, Roy D, Cooke HJ, Maratu K (2004) Triple-target microarray experiments: a novel experimental strategy. BMC Genomics 5:13

Gaasterland D, Berikanow S (2000) Making the most of microarray data. Nature Genet 24:204–206

Ge H (2000) UPA, a universal protein array system for quantitative detection of protein-protein, protein-DNA, protein-RNA, and protein-ligand interactions. Nucleic Acids Res 28:e3

Gebauer M (2004) Microarray applications: emerging technologies and perspectives. Drug Discov Today 9:915–917

Gopalakrishnan SM, Karvinen J, Kofron JL, Burns DJ, Warrior U (2002) Application of Micro Arrayed Compound Screening (microARCS) to identify inhibitors of caspase-3. J Biomol Screen 7:317–323

Gosalia DN, Diamond SL (2003) Printing chemical libraries on microarrays for fluid phase nanoliter reactions. Proc Natl Acad Sci USA 110:8721–8726

Hardiman G (2004) Microarray platforms – comparisons and contrasts. Pharmacogenomics 5:487–502

Howbrook DN, van der Valk AM, O'Shaughnessy MC, Sarker DK, Baker SC, Lloyd AW (2003) Developments in microarray technologies. Drug Discov Today 8:642–651

Hsieh HB, Fitch J, White D, Torres F, Roy J, Matusiak R, Krivacic B, Bruce R, Elrod S (2004) Ultra-high-throughput microarray generation and liquid dispensing using multiple disposable piezoelectric ejectors. J Biomol Screen 9:85–94

Imbeaud S, Auffray C (2005) "The 39 steps" in gene expression profiling: critical issues and proposed best practices for microarray experiments. Drug Discov Today 10:1175–1182

Jain KK (2000) Application of biochip and microarray systems in pharmacogenomics. Pharmacogenomics 1:289–307

Jordan B (2001) DNA microarrays: gene expression applications. Springer, Berlin Heidelberg New York

Kamb A, Ramaswami M (2001) A simple method for statistical analysis of intensity differences in microarray-derived gene expression data. BMC Biotechnol 1:8

Killion PJ, Sherlock G, Iyer VR (2003) The Longhorn Array Database (LAD): an open-source, MIAME compliant im-

plementation of the Stanford Microarray Database. BMC Informatics 4:32–38
Kusnezow W, Hoheisel JD (2002) Antibody microarrays: promises and problems. BioTechniques 33:S14–S23
Kusnezow W, Jacob A, Waijew A, Diehl F, Hoheisel JD (2003) Antibody microarrays: an evaluation of production parameters. Proteomics 3:254–264
Lal SP, Christopherson RI, dos Remedios CG (2002) Antibody arrays: an embryonic but rapidly growing technology. Drug Discov Today Suppl 7:S143–S149
Lee Y, Kang DK, Chang SI, Han MH, Kang IC (2004) High-throughput screening of novel peptide inhibitors of an integrin receptor from the hexapeptide library by using a protein microarray chip. J Biomol Screen 9:687–694
Lenigk R, Liu RH, Athavale M, Chen Z, Ganser D, Yang J, Rauch C, Liu Y, Chan B, Yu H, Ray M, Marrero R, Grodzinski P (2002) Plastic biochannel hybridization devices: a new concept for microfluidic DNA arrays. Anal Biochem 311:40–49
Lim LP, Lau NC, Garrett-Engele P, Grimson A, Schelter JM, Castle J, Bartel DP, Linsley PS, Johnson JM (2005) Microarray analysis show that some microRNAs downregulate large number of target mRNAs. Nature 433:769–773
Lipshutz RJ, Fodor SPA Gingeras TR, Lockhart DJ (1999) High density synthetic oligonucleotide arrays. Nature Genetics 21 [Suppl 1]:20–24
Luo Z, Geschwind DH (2001) Microarray applications in neuroscience. Neurobiol Dis 8:163–193
Ma H, Horiuchi KY (2006) Chemical microarray: a new tool for drug screening and discovery. Drug Discov Today 11:551–668
MacBeath G, Koehler AN, Schriber SL (1999) Printing small molecules as microassays and detecting protein-ligand interactions en masse. J Am Chem Soc 121:7967–7968
Nature Office (2000) Microarrays on the slide. Compiled by the Nature Office from information provided by the manufacturers. New gadgets, including some of the latest in microarray technology. Nature 406:659–600
Nielsen PS, Ohlsson H, Alsbo C, Andersen MS, Kauppinen S (2005) Expression profiling by oligonucleotide microarrays spotted on coated polymer slides. J Biotechnol 116:125–134
Novoradovskaya N, Whitfield ML, Basehore LS, Novoradovsky A, Pesich R, Usary J, Karaca M, Wong WK, Aprelikova O, Fero M, Perou CM, Botstein D, Braman J (2004) Universal Reference RNA as a standard for microarray experiments. BMC Genomics 5:20
Rautenstrauss BW, Liehr T (2001) FISH technology. Springer, Berlin Heidelberg New York
Rockett JC, Dix DJ (2000) DNA arrays: technology, options and toxicological applications. Xenobiotica 30:155–177
Rondelez Y, Tresset G, Tabata KV, Arata H, Fujita H, Takeuchi S, Noji H (2005) Microfabricated arrays of femtoliter chambers allow single molecule enzymology. Nature Biotechnol 433
Rougemont J, Hingamp P (2003) DNA microarray data and contextual analysis of correlation graphs. BMC Bioinformatics 4:15
Salisbury CM, Maly DJ, Ellman JA (2002) Peptide microarrays for the determination of protease substrate specificity. J Am Chem Soc 124:14868–14870
Sharma A, Srivastava GP, Sharma VK, Ramachandran S (2004) ArrayD: a general purpose software for microarray design. BMC Bioinformatics 5:142–150
Sherlock G, Hernandez-Boussard T, Kasarskis A, Binkley G, Matese JC, Dwight SS, Kaloper M, Weng S, Jin H, Ball CA, Eisen MB, Spellman PT, Brown PO, Botstein D, Cherry JM (2001) The Stanford microarray database. Nucleic Acids Res 29:152–155
Sobek J, Bartscherer K, Jacob A, Hoheisel JD, Angenendt P (2006) Microarray technology as a universal tool for high-throughput analysis of biological systems. Comb Chem High Throughput Screen 9:365–380
Taniguchi M, Mura K, Iwao H, Yamanaka S (2001) Quantitative assessment of DNA microarrays – comparison with Western blot analyses. Genomics 71:34–39
Templin MF, Stoll D, Schrenk M, Traub PC, Vöhringer CF, Joos TO (2002) Protein microarray technology. Drug Discov Today 7:815–822
Uttamchandani M, Walsh DP, Yao SQ, Chang YT (2005) Small molecule microarrays: recent advances and applications. Curr Opin Chem Biol 9:4–13
Watson SK, deLeeuw RJ, Ishkanian AS, Malloff CA, Lam WL (2004) Methods for high throughput validation of amplified fragment pools of BAC DNA for constructing high resolution of CHG assays. BMC Genomics 5:6
Zhang MQ (1999) Large-scale gene expression data analysis: a new challenge to computational biologists. Genome Res 9:681–688
Zhu H, Snyder M (2003) Protein chip technology. Curr Opin Chem Biol 7:55–63
Ziauddin J, Sabatini DM (2001) Microarrays of cells expressing defined cDNAs. Nature 411:107–110

0.4.7 NMR Technology

Magnetic resonance imaging (**MRI**) and spectroscopy (**MRS**) have become established technologies in modern biomedical research, providing relevant information on the various stages of the drug discovery and development process and are an important tool in drug discovery and metabolism (Hoult et al. 1974; Rudin et al. 1999, 2004a, 2004b, 2006; Rudin and Weissleder 2003; Beckmann et al. 2001, 2005, 2006; Beckmann and Rudin 2006). Several successful and potential applications of MRI and MRS in stroke, rheumatoid arthritis, osteoarthritis, respiratory diseases, oncology and cardiovascular diseases are described.

Strengths of MRI are: (1) *high soft tissue contrast*, which is governed by a multitude of parameters; (2) *noninvasiveness*, which is relevant when studying chronic diseases and allows for the translation of study protocols from animals to humans; and (3) *the high chemical specificity* of MRS, allowing the identification of individual analytes based on compound-specific resonance frequencies, an important prerequisite for the *in vivo* study of tissue metabolism. The main disadvantage of MRI/MRS is the *inherently low sensitivity* due to the low quantum energy involved as compared to optical spectroscopy, leading to a low degree of spin polarization. Only nuclei with high natural abundance and high intrinsic magnetic moment, such as protons, provide sufficient signal intensity for imaging applications. In addition, exogenous contrast

agents (CA, paramagnetic or superparamagnetic compounds) with different levels of specificity are often used to modulate local signal intensities. MRI is a multidimensional technique providing cross-sectional images as well as full three-dimensional (3D) data of body regions.

Bammer et al. (2005) gave a review on the foundations of advanced MRI. The mathematical and physical basics as well as the medical applications of MRI are described by Hornak (2007).

Using time domain NMR techniques, slice selection with shaped pulses, special encoding by pulsed field gradients, gradient echo detection and Fourier transform methods, highly resolved images of anatomy can be generated in almost real time. The most frequently used parameters are the spin-lattice relaxation time (T_1) and the spin-spin relaxation time (T_2). MRI is routinely used as a tomographic imaging technique, where anatomical pictures are created of 1-mm-thick tissue sections. The contrast differences between brain structures in most MRI techniques are determined by the different densities and diffusion of protons, as well as differences in relaxation times. T_2 images are sensitive to water and, because all pathological alterations in brains are associated with altered distribution of tissue water (edema), this technique is highly useful for visualizing the spatial distribution of lesions. Contrast in T_1 images is determined mainly by different lattice densities. Dense structures, such as compact white matter, have low T_1 values, whereas relatively loose structures, such as gray matter or lesions, have higher T_1 values. To distinguish inflammatory active from inactive lesions, the paramagnetic dye gadolinium-DTPA is intravenously injected (0.1–0.3 mmol kg^{-1}) and, in areas of increased blood–brain barrier permeability, leaks into the brain parenchyma, causing local enhancement of the T_1-weighted signal intensity. Srijkers et al. (2007) reviewed the current status of MRI contrast agents.

Detailed descriptions on the use of MRI are reported in Chap. A, Sects. 3.2.6, 3.2.7, 8.1.13 and Chap. E, Sects. 10.1, 10.2, 10.2.1, 10.2.2, 10.2.3, 10.3, 10.3.1, and 10.3.2.

Sillerud and Larson (2006) reviewed screening methods for drug discovery based on nuclear magnetic resonance (NMR), which were boosted by the introduction of sophisticated computational techniques for reducing the time for the acquisition of the primary NMR data for multidimensional studies.

Further non-invasive radiological techniques, such as **BOLD-MRI** (blood-oxygen-level-dependent MRI; Ogawa et al. 1992; Keogh et al. 2005; Burke and Bührle 2006), positron emission tomography (**PET**; Fowler et al. 1999) and **^{31}P MRS** (Braun et al. 1997), have been evaluated.

With BOLD-MRI, brain function has been successfully probed and has initiated the widely practiced field of functional MRI (**fMRI**) (Andersen et al. 2002; Schwarz et al. 2003). Mirsattari et al. (2005) described physiological monitoring of small animals during fMRI. Sauter et al. (2002) applied fMRI to study functional recovery following cytoprotective treatment in a rat model of human embolic stroke.

In addition, spectroscopic imaging with *in vivo* magnetic resonance ^{1}H-spectroscopy MRI, known as **MRSI**, enables the quantification of relative concentrations of specific metabolites, such as intramyocellular lipid content, at predetermined locations in organs (Kurhanewicz et al. 1996, 2000; Kuhlmann et al. 2003; Neumann-Haefelin et al. 2004; Schoelch et al. 2004).

Another important MRI technique is magnetization transfer ratio (**MTR**) imaging. The MTR of a given tissue is defined as the ratio of free protons to protons bound to tissue macromolecules (Deloire-Grassin et al. 2000; Smith et al. 2006).

Among other methodologies in functional imaging is the use of electron paramagnetic resonance (**EPR**), a technique almost identical in principle and practice to NMR (Eaton et al. 1991). EPR addresses unpaired spins, and in a given magnetic field the resonance frequency of an ensemble of electrons is 658 times higher than that of protons. There are two approaches of EPR imaging (**ERPI**), namely the continuous-wave (CW) modality (constant frequency with a field sweep) or the time-domain (termed Fourier transform, FT) modality (acquisition of an impulse response of the system at constant field). Devasahayam et al. (2004) described tailored sinc pulses for uniform excitation and artifact-free radiofrequency time-domain EPR imaging. A truncated sinc [sin (x)/x] pulse, tailored to compensate for the Q-profile (RF frequency response) of the resonator, was shown to yield images from phantom objects as well as *in vivo* images, with minimal distortion.

Another very closely related modality known by two alternate names, **PEDRI** (proton electron double resonance imaging; Lurie et al. 1988, 2005) and **OMRI** (Overhauser-enhanced magnetic resonance imaging; Golman et al. 1998, 2002), utilizes the Overhauser effect, by which protons are polarized in the presence of stable free radicals to provide highly enhanced MR images at very low fields. The principle behind OMRI is the saturation of free radical resonance by continuous (or pulsed) irradiation

at the electron resonance frequency, which leads to an Overhauser enhancement of the proton magnetization (also known as dynamic nuclear polarization, DNP) via mainly the time-dependent dipolar interactions between the unpaired electrons and the water protons. This may lead to a high enhancement factor (Ardenkjær-Larsen et al. 1998). This technique has been shown to produce useful functional proton images that can be used to perform non-invasive quantitative *in vivo* oximetry. The sensitivity of OMRI can be additionally improved by field cycling (Lurie et al. 1989; Subramanian et al. 2004).

Krishna et al. (2002) used OMRI for tumor oximetry and co-recording of tumor anatomy and tissue oxygen concentration.

Post (2003) used exchange-transferred nuclear Overhauser effect spectroscopy (**et-NOESY**) to probe the conformation of a ligand while bound to its macromolecular receptor.

REFERENCES AND FURTHER READING

Andersen AH, Zhang Z, Barber T, Rayens WS, Zhang J, Grondin R, Hardy P, Gerhardt GA, Gash DM (2002) Functional MRI studies in awake rhesus monkeys. methodological and analytical strategies. J Neurosci Methods 118:141–152

Ardenkjær-Larsen HJ, Laursen I, Leunbach I, Ehnholm GI, Wistrand LG, Petersson JS, Golman K (1998) EPR and DNP properties of certain novel single electron contrast agents intended for oximetric imaging. J Magn Reson 133:1–12

Bammer R, Skare S, Newbould R, Liu C, Thijs V, Ropele S, Clayton DB, Krueger G, Moseley ME, Glover GH (2005) Foundations of advanced magnetic resonance imaging. NeuroRX 2:167–196

Beckmann N, Rudin M (2006) The drug discovery and development process: opportunities and challenges for MR techniques. In: Beckmann N (ed) In vivo MR techniques in drug discovery and development. Taylor and Francis, New York, pp 7–28

Beckmann N, Mueggler T, Allegrini PR, Laurent D, Rudin M (2001) From anatomy to the target: contributions of magnetic resonance imaging to preclinical pharmaceutical research. Anat Rec 265:85–100

Beckmann N, Laurent D, Tigani B, Panizzutti R, Rudin M (2004) Magnetic resonance imaging in drug discovery: lessons from disease areas. Drug Discov Today 9:35–42

Braun KPJ, Dijkhuizen RM, de Graff RA, Nicolay K, Vandertop WP, Gooskens RHJM, Tulleken KF (1997) Cerebral ischemia and white matter edema in experimental hydrocephalus. A combined *in vivo* MRI and MRS study. Brain Res 757:295–298

Burke M, Bührle CH (2006) BOLD response during uncoupling of neuronal activity and CBF. Neuroimage 32:1–8

Deloire-Grassin MS, Brochet B, Quesson B, Delalande C, Canioni P, Petry KG (2000) In vivo evaluation of remyelinization in rat brain by magnetic transfer imaging. J Neurol Sci 178:10–16

Devasahayam N, Murugesan R, Matsumoto K, Mitchell JB, Cook JA, Subramanian S, Krishna MC (2004) Tailored sinc pulses for uniform excitation and artefact-free radio frequency time-domain EPR imaging. J Magn Reson 168:110–117

Eaton GR, Eaton SE, Ohno K (eds) (1991) EPR imaging and in vivo EPR. CRC, Boca Raton, Fla.

Fowler JS, Volkow ND, Wang GI, Ding YS, Dewey SL (1999) PET and rug research and development. J Nucl Med 40:1154–1163

Golman K, Leunbach I, Ardenkjaer-Larsen JH, Ehnholm GI, Wistrand LG, Peterson JS, Jarvi A, Vahasalo S (1998) Overhauser-enhanced MR imaging (OMRI). Acta Radiol 39:10–17

Golman K, Leunbach I, Petersson JS, Holz D, Overweg J (2002) Overhauser-enhanced MRI. Acad Radiol 9 [Suppl 1]:S104–S108

Hornak JP (2007) The basics of MRI. Magnetic Resonance Laboratory, Center of Imaging Service, Rochester Institute of Technology, Rochester, N.Y.

Hoult DI, Busby SJ, Gadian DG, Radda GK, Richards RE, Seeley PJ (1974) Observation of tissue metabolites using 31P nuclear magnetic resonance. Nature252:285–287

Keogh BP, Cordes D, Stanberry L, Figler DB, Robbins CA, Tempel BL, Green CG, Emmi A, Maravilla KM, Schwartzkroin PA (2005) BOLD-fMRI of PTZ-induced seizures in rats. Epilepsy Res 66:75–90

Krishna MC, English S, Yamda K, Yoo J, Murugesan R, Devasahayam N, Cook JA, Golman K, Ardenkjær-Larsen HJ, Subramanian S, Mitchell JB (2002) Overhauser enhanced magnetic resonance imaging for tumor oximetry: coregistration of tumor anatomy and tissue oxygen concentration. Proc Natl Acad Sci USA 99:2216–2221

Kuhlmann J, Neumann-Haefelin C, Belz U, Kalisch J, Juretschke HP, Stein M, Kleinschmidt E, Kramer W, Herling AW (2003) Intramyocellular lipid and insulin resistance: a longitudinal in vivo ^{1}H-spectroscopic study in Zucker diabetic fatty rats. Diabetes 52:138–144

Kurhanewicz J, Vigneron D, Hricak H, Carroll P, Narayan P, Nelson S (1996) Three-dimensional H-1 MR spectroscopic imaging of the in situ human prostate with high ((0.24–0.1 CM(3)) spatial resolution. Radiology 198:795–805

Kurhanewicz J, Vigneron DB, Nelson SJ (2000) Three-dimensional magnetic resonance spectroscopic imaging of brain and prostate cancer. Neoplasia 2:166–189

Lurie DJ, Bussell DM, Bell LH, Maillard JR (1988) Proton-electron double magnetic resonance imaging of free radical solutions. J Magn Reson 76:366–370

Lurie DH, Hutchinson JMS, Bell JH Nicholsin I, Bussell DM, Mallerd JL (1989) Field cycled proton-electron double resonance imaging of free radicals in large aqueous samples. J Magn Reson 84:431–437

Lurie DJ, Davies GR, Foster MA, Hutchinson JMS (2005) Field-cycled PEDRI imaging of free radicals with detection at 450 mT. Magn Res Imag 23:175–181

Mirsattari SM, Bihari F, Leung LS, Menon RS, Wang Z, Ives JR, Bartha R (2005) Physiological monitoring of small animals during magnetic resonance imaging. J Neurosci Methods 144:207–213

Neumann-Haefelin C, Beha A, Kuhlmann J, Belz U, Gerl M, Quint M, Biemer-Daub G, Broenstrup M, Stein M, Kleinschmidt E, Schaefer HL, Schmoll D, Kramer W, Juretschke HP, Herling AW (2004) Muscle type specific intramyocellular and hepatic lipid metabolism during starvation in Wistar rat. Diabetes 53:528–634

Ogawa S, Tank DW, Menson R, Ellerman JM, Kim SG, Merkle H, Ugurbil K (1992) Intrinsic signal changes accompanying sensory stimulation – functional brain mapping with magnetic resonance imaging. Proc Natl Acad Sci USA 89:5951–5955

Post CB (2003) Exchange-transferred NOE spectroscopy and bound ligand structure determination. Curr Opin Struct Biol 13:581–588
Rudin M, Weissleder R (2003) Molecular imaging in drug discovery and development. Nature Res Drug Discov 2:132–131
Rudin M, Beckmann R, Porszasz R, Reese T, Bochelen T, Sauter A (1999) In vivo magnetic resonance methods in pharmaceutical research: current status and perspectives. NMR Biomed 12:69–97
Rudin M, Beckmann N, Rausch M (2004a) Magnetic resonance imaging in biomedical research: Imaging of drugs and drug effects. Methods Enzymol 385:240–256
Rudin M, Allegrini P, Beckmann N, Gremlich HU, Kneuer R, Laurent D, Rausch M, Stoeckli M (2004b) Noninvasive imaging in drug discovery and development. Workshop Ernst Schering Research Foundation 48:47–75
Rudin M, Tausch M, Stoeckli M (2005) Molecular imaging in drug discovery and development: potential and limitations of nonnuclear methods. Mol Imaging Biol 7:5–13
Rudin M, Allegrini PR, Rausch M (2006) MRI and MRS in animal models of focal cerebral ischemia. In: Beckmann N (ed): In vivo MR techniques in drug discovery and development. Taylor and Francis, New York, pp 123–145
Sauter A, Reese T, Pórszász R, Baumann D, Rausch M, Rudin M (2002) Recovery of function in cytoprotected cerebral cortex in rat stroke model assessed by functional MRI. Magn Reson Med 47:759–765
Schoelch C, Kuhlmann J, Gossel M, Mueller G, Neumann-Haefelin C, Belz U, Kalisch J, Biemer-Daub G, Kramer W, Juretschke HP, Herling AW (2004) Characterization of adenosine-A1 receptor–mediated antilipolysis in rats by tissue microdialysis, ^{1}H-spectroscopy, and glucose clamp studies. Diabetes 53:1920–1926
Schwarz AJ, Reese T, Gozzi A, Bifone A (2003) Functional MRI using intravascular contrast agents. Detrending of the relative cerebrovascular (rCBV) time course. Magn Reson Imaging 21:1191–1200
Sillerud LO, Larson RS (2006) Nuclear magnetic resonance-based screening methods for drug discovery. Methods Mol Biol 316:227–289
Smith SA, Farrell JAD, Jones CK, Reich DS, Calabresi PA, van Zijl PCM (2006) Pulsed magnetization transfer imaging with body coil transmission at 3 Tesla: feasibility and application. Magnet Reson Med 56:8566–875
Srijkers GJ, Mulder WJ, van Tilborg GA, Nikolay K (2007) MRI contrast agents: current status and future perspectives. Anticancer Agents Med Chem 7:291–305
Subramanian S, Matsumoto KI, Mitchell JB, Krishna MC (2004) Radio frequency continuous-wave and time-dependent EPR imaging and Overhauser-enhanced magnetic resonance imaging of small animals: instrumental developments and comparison of relative merits for functional imaging. NMR Biomed 17:263–294

0.5 Errors in Screening Procedures

Any screening procedure has a characteristic error rate. This is inevitable because in high-throughput screening it is necessary to sacrifice some accuracy or precision to achieve the requisite speed. Thus when a large number of compounds is carried through a particular screen, some of the compounds will be classified incorrectly. A screen may be used in an absolute sense, so that compounds that pass a certain criterion are termed positives, whereas those that fail to meet the criterion are termed negatives. Compounds that pass, but should have failed, are false positives. In general, false positives are tolerable, if they are not too numerous, because they will be rectified later. Compounds that fail, but should have passed, are false negatives. False negatives are lost forever if the failure eliminates them from further testing.

All screening procedures are based on assumptions of analogy. They have different degrees of relevance or predictability. Studies in phase II clinical trials will predict with high probability the results in large clinical trails. But even here there is the possibility of false-positive or false-negative results. The relevance of a test is much less in early pharmacological tests, such as used in high-throughput screening. Generally, the relevance is inversely proportional to the simplicity of the test.

In any case, one is confronted with the problem of false-positive results (type I errors) and false-negative results (type II errors).

In each step two sources of error for **false-positive results** have to be taken in account:

1. a = error of the first type due to the model
2. α = error of the first type due to statistics

For definition: In the error of the first type a compound is considered to be active, but is actually ineffective. This type of error will be clarified during further development, after negative clinical trials at the latest.

However, there are also two sources of error for **false-negative results**:

1. b = error of the second type due to the model
2. β = error of the second type due to statistics

In the error of the second type a compound is considered to be ineffective, but is actually effective.

This type of error will never be clarified; an effective drug has just been missed. Perhaps another investigator will test this compound under different aspects.

The statistical errors derive from the fact that a pharmacological test is performed only several times or in a limited number of animals. One can specify the probability that a decision made is incorrect, i. e., a drug candidate is erroneously identified as effective when it is actually ineffective. Usually this risk is set to 5% ($P < 0.05$) and is called the statistical error of the first type or type I error. The error of the second type or type II error is connected to the type I error by statistical rules.

Usually, screening is performed sequentially. Tests in high-throughput screening are followed by tests in

isolated organs, then in small animals, and special tests in higher animals, until the compound is recommended for further development and for studies in human beings. From each step errors of type I, but also from type II, arise. As a consequence, many effective compounds will be lost.

There are two ways to circumvent this obstacle: (1) to increase the number of compounds entering the screening procedure dramatically, hope for a reasonable number of true positives, and accept a high rate of false-negative results (White 2000) as followed in the ultra high-throughput screening, or (2) to perform tests with high relevance, meaning tests with high predictive value in whole animals at an early stage (Vogel and Vanderbeeke 1990).

The literature on high-throughput screening includes some publications dealing with false-negative results (Jones and King 2003; Colland and Daviet 2004; Heller-Uszynska and Kilian 2004).

Zhang et al. (1999, 2000) studied the role of false-negative results in high-throughput screening procedures. They presented a statistical model system that predicts the reliability of hits from a primary test as affected by the error in the assay and the choice of the hit threshold. The hit confirmation rate, as well as false-positive (representing substances that initially fall above the hit limit but whose true activity is below the hit limit) and false-negative (representing substances that initially fall below the hit limit but whose true activity is in fact greater than the hit limit) rates have been analyzed by computational simulation. The *Z*-factor and the *Z′*-factor were introduced to characterize the reliability of high-throughput assays.

The problem of type II errors, i. e., false-negative results, also exists in many other physiological and pharmacological studies (Martorana et al. 1982; Barros et al. 1991; Sandkühler et al. 1991; Waldeck 1996; Williams et al. 1997). For example, Pollard and Howard (1986) re-investigated the staircase test, a well-accepted primary screening method for anxiolytics, and found several false-negative results for clinically active anxiolytics.

REFERENCES AND FURTHER READING

Barros HM, Tannhauser MA, Tannhauser SL, Tannhauser M (1991) Enhanced detection of hyperactivity after drug withdrawal with a simple modification of the open-field apparatus. J Pharmacol Methods 26:269–275

Colland F, Daviet L (2004) Integrating a functional proteomic approach into the target discovery process. Biochemie 86:625–632

Heller-Uszynska K, Kilian A (2004) Microarray TRAP – a high-throughput assay to quantitate telomerase activity. Biochem Biophys Res Commun 323:465–472

Jones PA, King AV (2003) High throughput screening (HTS) for phototoxicity hazard using the in vitro 3T3 neutral red uptake assay. Toxicol In Vitro 17:703–708

Martorana PA, Göbel H, Kettenbach P, Nitz RE (1982) Comparison of various methods for assessing infarct-size in the dog. Basic Res Cardiol 77:301–308

Pollard GT, Howard JL (1986) The staircase test: some evidence of nonspecificity for anxiolytics. Psychopharmacol Berl 89:14–19

Sandkühler J, Willmann E, Fu QG (1991) Characteristics of midbrain control of spinal nociceptive neurons and nonsomatosensory parameters in the pentobarbital-anesthetized rat. J Neurophysiol 65:33–48

Vogel HG, Vanderbeeke O (1990) "*In vitro / in vivo*" pharmacology. Mathematical models for screening strategy. Internal Presentation at Hoechst AG

Waldeck B (1996) Some pharmacodynamic aspects on long-acting beta-adrenoceptor agonists. Gen Pharmacol 27:575–580

White RE (2000) High-throughput screening in drug metabolism and pharmacokinetic support of drug discovery. Annu Rev Pharmacol Toxicol 40:133–157

Williams JL, Hathaway CA, Kloster KL, Layne BH (1997) Low power, type-II errors, and other statistical problems in recent cardiovascular research. Am J Physiol 273:H487–H493

Zhang JH, Chung TDY, Oldenburg KR (1999) A simple statistic parameter for use in evaluation and validation of high throughput screening assays. J Biomol Screen 4:67–73

Zhang JH, Chung TDY, Oldenburg KR (2000) Confirmation of primary active substances from high throughput screening of chemical and biological populations: a statistical approach and practical considerations. J Comb Chem 2:285–265

Chapter A
Cardiovascular Activity[1]

[1] With contributions to this and the former editions by B.A. Schölkens, H. Gögelein, F.P. Huger, W. Linz, K.A. Rudolphi, K. Wirth.

A.1 Cardiovascular Analysis

A.1.1 In Vitro Methods

A.1.1.1 α_1-Adrenoreceptor Binding

PURPOSE AND RATIONALE

α_1-adrenoceptors are widely distributed and are activated either by norepinephrine released from sympathetic nerve terminals or by epinephrine released from the adrenal medulla. Receptor activation mediates a variety of functions, including contraction of smooth muscle, cardiac stimulation, cellular proliferation and activation of hepatic gluconeogenesis and glycolysis. In the CNS, the activation of α_1-adrenoceptors results in depolarization and increased neuronal firing rate.

The α-adrenoreceptor population of plasma membranes from rat heart ventricles consists only of the α_1-adrenoreceptor subtype. A constant concentration of the radioligand ^{3}H-prazosin (0.2–0.3 nM) is incubated with increasing concentrations of a non-labeled test drug (0.1 nM–1 mM) in the presence of plasma membranes from rat heart ventricles. If the test drug exhibits any affinity to α-adrenoceptors, it is able to compete with the radioligand for receptor binding äsites. Thus, the lower the concentration range of the test drug, in which the competition reaction occurs, the more potent is the test drug. The assay is used to evaluate the concentrationbinding characteristics of drugs atria the α_1-adrenoceptor.

PROCEDURE

Solutions

preparation buffer A:

$MgCl_2 \times 6H_2O$	5 mM
$MgCl_2 \times 6H_2O$	1 mM

D(+)-sucrose 250 mM

pH 7.4

preparation buffer B (= rinse buffer):

Tris-HCl 50 mM

$MgCl_2 \times 6H_2O$ 10 mM

pH 7.4

incubation buffer:

Tris-HCl 50 mM

$MgCl_2 \times 6H_2O$ 10 mM

ascorbic acid 1.6 mM

catechol 0.3 mM

pH 7.4

radioligand:

^{3}H-prazosin × HCl

specific activity

0.37–1.11 TBq/mmol

(10–30 Ci/mmol) (NEN)

Tissue Preparation

Male Sprague-Dawley rats (200–300 g) are sacrificed by decapitation and the dissected hearts are placed in ice-cold preparation buffer A. After removal of the atria, ventricles (approx. 30 g from 40 rats) are minced with a scalpel into 2–3 mm pieces.

Membrane Preparation

Ventricles are homogenized by Ultra-Turrax (1 g tissue/20 ml preparation buffer A), the homogenate is filtered through gauze, and centrifuged at 2000 *g* (4°C) for 10 min. The pellets are discarded; the supernatant is collected, and centrifuged again at 40,000 *g* for 20 min. The resulting pellets are resuspended in approx. 300 ml preparation buffer B, homogenized by Ultra-Turrax and centrifuged as before. The final pellets are dissolved (by Ultra-Turrax) in preparation buffer B, corresponding to 1 g ventricle wet weight/4 ml buffer. The membrane suspension is immediately stored in aliquots of 5–20 ml at –77°C. Protein content of the membrane suspension is determined according to the method of Lowry et al. with bovine serum albumin as a standard.

At the day of the experiment the required volume of the membrane suspension is slowly thawed and centrifuged at 40,000 *g* (4°C) for 20 min. The pellets are resuspended in a volume of ice-cold rinse buffer, yielding a membrane suspension with a protein content of 1.0–1.5 mg/ml. After homogenization by Ultra-Turrax, the membrane suspension is stirred under cooling for 20–30 min until the start of the experiment.

Experimental Course

For each concentration samples are prepared in triplicate.

The total volume of each incubation sample is 200 µl (microtiter plates).

Saturation Experiments

total binding:

- 50 µl ^{3}H-prazosin (12 concentrations, 5×10^{-11}–5×10^{-9} M)
- 50 µl incubation buffer

non-specific binding:

- 50 µl ^{3}H-prazosin (4 concentrations, 5×10^{-11}–$\times 10^{-9}$ M)
- 50 µl phentolamine (10^{-5} M)

Competition Experiments

- 50 µl ^{3}H-prazosin (1 constant concentration, 2–3 × 10^{-10} M)
- 50 µl incubation buffer without or with non-labeled test drug (15 concentrations, 10^{-10}–10^{-3} M)

The binding reaction is started by adding 100 µl membrane suspension per incubation sample (1.0–1.5 mg protein/ml). The samples are incubated for 30 min in a shaking bath at 25°C. The reaction is stopped by withdrawing the total incubation volume by rapid vacuum filtration over glass fiber filters. Thereby the membrane-bound radioactivity is separated from the free activity. Filters are washed immediately with approx. 20 ml ice-cold rinse buffer per sample. The retained membrane-bound radioactivity on the filter is measured after addition of 2 ml liquid scintillation cocktail per sample in a liquid scintillation counter.

EVALUATION

The following parameters are calculated:

- total binding
- non-specific binding
- specific binding = total binding–non-specific binding

The dissociation constant (K_i) of the test drug is determined from the competition experiment of ^{3}H-prazosin versus non-labeled drug by a computer-supported analysis of the binding data.

$$K_i = \frac{K_D\ ^3H \times IC^{50}}{K_D\ ^3H + [^3H]}$$

IC_{50} = concentration of the test drug, which competes 50% of specifically bound ^{3}H-prazosin in the competition experiment

[^{3}H] = concentration of ^{3}H-prazosin in the competition experiment.

$K_D\ ^3H$ = dissociation constant of ^{3}H-prazosin, determined from the saturation experiment.

The K_i-value of the test drug is the concentration, at which 50% of the receptors are occupied by the test drug. The affinity constant K_i [mol/l] is recorded and serves as a parameter to assess the efficacy of the test drug.

MODIFICATION OF THE METHOD

Binding of ^{3}H-WB 4101 to α_1-adrenergic receptors in brain is used to test hypotensive activity as a possible side effect of neuroleptic drugs. The test E.5.1.6 is described in the chapter on neuroleptic activity.

Couldwell et al. (1993) found that the rat prostate gland possesses a typical α_1-adrenoceptor similar to that found in the vas deferens.

SUBTYPES OF THE α_1-ADRENOCEPTOR

Several subtypes of the α_1-adrenoceptor have been identified by pharmacological means (α_{1A} and α_{1B}, α_{1C}, α_{1D}; α_{1H}, α_{1L} and α_{1N} adrenoceptors; Endoh et al. 1992; García-Sáinz et al. 1992, 1993; Ohmura et al. 1992; Regan and Cotecchia 1992; Satoh et al. 1992; Schwinn and Lomasney 1992; Veenstra et al. 1992; Aboud et al. 1993; Oshita et al. 1993; Vargas et al. 1993; Ruffolo et al. 1994; Minneman and Esbenshade 1994; Alexander et al. 2001) or by recombinant technology ($\alpha_{1a/d}$, α_{1b}, α_{1c} adrenoceptors). They correspond to the pharmacologically defined α_{1A}, α_{1B},and α_{1D} adrenoceptors in native tissues (Bylund et al. 1994, 1998; Hieble et al. 1995; Graham et al. 1996; Hieble and Ruffolo 1996; Alexander et al. 2001; Hawrylyshyn et al. 2004; Waitling 2006).

Binding of the radioligand [^{3}H]-prazosin to the α_{1A}-adrenoceptor subtype can be measured in membranes prepared from male Wistar rat submaxillary glands (Michel et al. 1989).

Binding of the radioligand [^{3}H]-prazosin to the α_{1B}-adrenoceptor subtype can be measured in membranes prepared from male Wistar rat livers (Adolfo et al. 1989).

According to Eltze and Boer (1992), the adrenoceptor agonist SDZ NVI 085 discriminates between α_{1A}- and α_{1B}-adrenoceptor subtypes in vas deferens, kidney and aorta of the rat and may therefore be used as a tool either to detect (rat vas deferens or kidney) or exclude (rat aorta) the functional involvement of "α_{1A}-adrenoceptors in smooth muscle contraction.".

Stam et al. (1998) found that (+)-cyclazosin, which behaves as a selective, high-affinity α_{1B}-adrenoceptor ligand in binding experiments, did not show the profile of a α_{1B}-adrenoceptor antagonist in functional tissues.

Decreased blood pressure response in mice deficient of the α_{1b}-adrenergic receptor was found by Cavalli et al. (1997).

Kenny et al. (1995) used the contractile response of rat aorta to adrenaline after the application of various α_1-adrenoceptor antagonists for characterization of a α_{1D}-adrenoceptor.

REFERENCES AND FURTHER READING

Aboud R, Shafii M, Docherty JR (1993) Investigation of the subtypes of α_1-adrenoceptor mediating contractions of rat aorta, vas deferens and spleen. Br J Pharmacol 109:80–87

Adolfo JA et al (1989) Species heterogeneity of hepatic α_1-adrenoceptors: α_{1A}-, α_{1B}-, and α_{1C}-subtypes. Biochem Biophys Res Comm 186:760–767

Ahlquist RP (1948) A study of the adrenotropic receptors. Am J Physiol 153:586–600

Alexander S, Peters J, Mathie A, MacKenzie G, Smith A (2001) TiPS Nomenclature Supplement 2001

Bylund DB, Eikenburg DC, Hieble JP, Langer SZ, Lefkowitz RJ, Minneman KP, Molinoff PB, Ruffolo RR, Trendelenburg U (1994) IV. International Union of Pharmacology Nomenclature of Adrenoceptors. Pharmacol Rev 46:121–136

Bylund DB, Bond RA, Clarke DE, Eikenburg DC, Hieble JP, Langer SZ, Lefkowitz RJ, Minneman KP, Molinoff PB, Ruffolo RR, Strosberg AD, Trendelenburg U (1998) Adrenoceptors. The IUPHAR Compendium of Receptor Characterization and Classification

Cavalli A, Lattion AL, Hummler E, Nenniger M, Pedrazzini T, Aubert JF, Michel MC, Yang M, Lembo G, Vecchione C, Mostardini M, Schmidt A, Beermann F, Cotecchia S (1997) Decreased blood pressure response in mice deficient of the α_{1b}-adrenergic receptor. Proc Natl Acad Sci USA 94:11589–11594

Cheng YC, Prusoff WH (1973) Relationship between the inhibition constant (K_i) and the concentration of inhibitor which causes 50 per cent inhibition (I_{50}) of an enzymatic reaction. Biochem Pharmacol 22:3099–3108

Couldwell C, Jackson A, O'Brien H, Chess-Williams R (1993) Characterization of the α_1-adrenoceptors of rat prostate gland. J Pharm Pharmacol 45:922–924

Eltze M, Boer R (1992) The adrenoceptor agonist, SDZ NVI 085, discriminates between α_{1A}-and α_{1B}-adrenoceptor-subtypes in vas deferens, kidney and aorta of the rat. Eur J Pharmacol 224:125–136

Endoh M, Takanashi M, Norota I (1992) Role of alpha$_{1A}$ adrenoceptor subtype in production of the positive inotropic effect mediated via myocardial alpha$_1$ adrenoceptors in the rabbit papillary muscle: influence of selective alpha$_{1A}$ subtype antagonists WB 4101 and 5-methylurapidil. Naunyn-Schmiedeberg's Arch Pharmacol 345:578–585

García-Sáinz JA (1993) α_1-adrenergic action: receptor subtypes, signal transduction and regulation. Cell Signal 5:539–547

García-Sáinz JA, Romero-Avila MT, Hernandez RA, Macias-Silva M, Olivares-Reyes A, González-Espinosa C (1992) Species heterogeneity of hepatic α_1-adrenoceptors: α_{1A}-, α_{1B}- and α_{1C}-subtypes. Biochem Biophys Res Commun 186:760–767

Gleason MM, Hieble JP (1992) The α_2-adrenoreceptors of the human retinoblasoma cell line (Y79) may represent an additional example of the α_{2C}-adrenoceptor. Br. J Pharmacol 107:222–225

Graham RM, Perez DM, Hawa J (1996) Alpha1 adrenergic receptor subtypes. Molecular structure, function and signaling. Circ Res 78:737–749

Greengrass P, Bremner R (1979) Binding characteristics of ^{3}H-prazosin to rat brain α-adrenergic receptors. Eur J Pharmacol 55:323–326

Guicheney P, Meyer P (1981) Binding of [^{3}H]-prazosin and [^{3}H]-dihydroergocryptine to rat cardiac α-adrenoceptors. Br J Pharmac 73:33–39

Hawrylyshyn KA, Michelotti GA, Cogé F, Guénin SP, Schwinn DA (2004) Update on human α_1-adrenoceptor subtype signaling and genomic organization. Trends Pharmacol Sci 25 :449–455

Hieble JP, Ruffolo RR Jr (1997) Recent advances in the identification of α_1- and α_2-adrenoceptor subtypes. Therapeutic implications. Expert Opin Invest Drugs 6:367–387

Hieble JP, Bylund DB, Clarke DE, Eikenburg DC, Langer SZ, Lefkowitz RJ, Minneman KP, Ruffolo RR Jr (1995) International Union of Pharmacology: X. Recommendation for nomenclature of α_1-adrenoceptors. Consensus update. Pharmacol Rev 47:267–270

Hoffman BB, de Lean A, Wood CL, Schocken DD, Lefkowitz RJ (1979) Alpha-adrenergic receptor subtypes: Quantitative assessment by ligand binding. Life Sci 24:1739–1746

Kenny BB, Chalmers DH, Philpott PC, Naylor AM (1995) Characterization of an α_{1D}-adrenoceptor mediating the contractile response of rat aorta to adrenaline. Br J Pharmacol 115:981–986

Miach PJ, Dausse JP, Cardot A, Meyer P (1980) ^{3}H-prazosin binds specifically to 'α_1'-adrenoceptors in rat brain. Naunyn-Schmiedeberg's Arch Pharmacol 312:23–26

Michel AD, et al (1989) Identification of a single α_{1A}-adrenoceptor corresponding to the α_{1A}-subtype in rat submaxillary gland. Br J Pharmacol 98:833–889

Minneman KP, Esbenshade TA (1994) α_1-adrenergic receptor subtypes. Ann Rev Pharmacol Toxicol 34:117–133

Ohmura T, Oshita M, Kigoshi S, Muramatsu I (1992) Identification of α_1-adrenoceptor subtypes in the rat vas deferens: binding and functional studies. Br J Pharmacol 107:697–704

Oshita M, Kigoshi S, Muramatsu I (1993) Pharmacological characterization of two distinct α_1-adrenoceptor subtypes in rabbit thoracic aorta. Br J Pharmacol 108:1071–1076

Regan JW, Cotecchia S (1992) The α-adrenergic receptors: new subtypes, pharmacology, and coupling mechanisms. In: Brann MR (ed) Molecular Biology of G-Protein-coupled receptors. Birkhäuser, Boston Basel Berlin, pp 76–112

Ruffolo RR, Stadel JM, Hieble JP (1994) α-adrenoceptors: recent developments. Med Res Rev 14:279–270

Satoh M, Kojima C, Takayanagi I (1992) Characterization of α_1-adrenoceptor subtypes labeled by [^{3}H]prazosin in single cells prepared from rabbit thoracic aorta. Eur J Pharmacol 221:35–41

Schwinn DA, Lomasney JW (1992) Pharmacologic characterization of cloned α_1-adrenoceptor subtypes: selective antagonists suggest the existence of a fourth subtype. Eur J Pharmacol – Mol Pharmacol Sect 227:433–436

Stam WB, Van der Graaf PH, Saxena PR (1998) Functional characterization of the pharmacological profile of the putative α_{1B}-adrenoceptor antagonist, (+)-cyclazosin. Eur J Pharmacol 361:79–83

Timmermans PBMWM, Karamat Ali F, Kwa HY, Schoop AMC, Slothorst-Grisdijk FP, van Zwieten PA (1981) Identical antagonist selectivity of central and peripheral alpha$_1$ adrenoceptors. Mol Pharmacol 20:295–301

Vargas HM, Cunningham D, Zhou L, Hartman HB, Gorman AJ (1993) Cardiovascular effects of chloroethylclonidine, a irreversible α_{1B}-adrenoceptor antagonist, in the unanesthetized rat: a pharmacological analysis *in vivo* and *in vitro*. J Pharm Exp Ther 266:864–871

Veenstra DMJ, van Buuren KJH, Nijkamp FP (1992) Determination of α_1-adrenoceptor subtype selectivity by [^{3}H]-prazosin displacement studies in guinea-pig cerebral cortex and rat spleen membranes. Br J Pharmacol 107:202–206

Waitling KJ (ed) (2006) The Sigma-RBI handbook of receptor classification and signal transduction, 5th edn. Sigma-Aldrich, St Louis, Mo., pp 88–89

A.1.1.2 α_2-Adrenoreceptor Binding

PURPOSE AND RATIONALE

α_2-adrenoceptors are widely distributed and are activated by norepinephrine released from sympathetic nerve terminals or by epinephrine released from the adrenal medulla or from some neurons in the CNS. The most extensively characterized action is the prejunctionally mediated inhibition of the release of neurotransmitters from many peripheral and central neurons. α_2-adrenoceptors are also present at postjunctional sites, where they mediate actions such as smooth muscle contraction, platelet aggregation and inhibition of insulin secretion. Activation of postsynaptic α_2-adrenoceptors in the brainstem results in an inhibition of sympathetic outflow in the periphery.

Clonidine is a centrally-acting antihypertensive agent, which lowers blood pressure mostly through reducing sympathetic tone by acting at the nucleus tractus solitarius in the brain stem (Kobinger and Walland 1967). Clonidine can, however, act at both peripheral and central α_2-receptors. Peripherally administered clonidine causes a brief increase in blood pressure followed by a prolonged decrease (Rand and Wilson 1968). Functional studies (^{3}H-NE release) indicate a presynaptic mechanism for clonidine (Langer 1977,

1981; Starke 1977). However, lesioning studies fail to confirm a presynaptic location for clonidine receptors in either the CNS or periphery (U'Prichard et al. 1979; Bylund and Martinez 1981; U'Prichard et al. 1980). No change in clonidine receptor sites was seen after 6-hydroxydopamine lesions in cerebral cortex. This may be due to the fact that α_2-receptors are both pre- and postsynaptic (Hieble et al. 1988).

Alpha-adrenergic agonists most potently displace ^{3}H-clonidine. Ergot compounds, dopamine agonists and mianserin are also fairly potent (U'Prichard et al. 1977). A survey on functions mediated by alpha-2 adrenergic receptors was given by Ruffolo et al. (1988) and on the role of neurotransmitters in the central regulation of the cardiovascular system by McCall (1990). Although clonidine relieves the autonomic symptoms of morphine withdrawal (Gold et al. 1978), there is no evidence for a direct α_2/opiate-receptor interaction.

The purpose of this assay is to assess the interaction of hypotensive agents with central α_2-receptors and determine possible clonidine-like mechanisms of action. Clonidine binding may also be relevant to the activity of other classes of drugs such as antidepressants that interact with α_2-receptors.

PROCEDURE

Reagents

1. Tris buffer pH 7.7
   a) 57.2 g Tris HCl q.s. to 1 liter
      (0.5 M Tris buffer, pH 7.7)
      16.2 g Tris base
   b) make a 1:10 dilution in distilled H_2O
      (0.05 M Tris buffer, pH 7.7)
2. Tris buffer containing physiological ions
   a) Stock buffer

NaCl	7.014 g
KCl	0.372 g
$CaCl_2$	0.222 g
$MgCl_2$	0.204 g

   q.s to 100 ml in 0.5 M Tris buffer
   b) Dilute 1:10 in distilled H_2O.
      This yields 0.05 M Tris HCl, pH 7.7; containing NaCl (120 mM), KCl (5 mM), $CaCl_2$ (2 mM) and $MgCl_2$ (1 mM)
3. [4-^{3}H]-Clonidine hydrochloride (20–30 Ci/mmol) is obtained from New England Nuclear.
   For IC_{50} determinations: ^{3}H-Clonidine is made up to a concentration of 120 nM and 50 µl are added to each tube (yielding a final concentration of 3 nM in the 2 ml volume assay).
4. Clonidine-HCl is obtained from Boehringer Ingelheim.
   A stock solution of 0.1 mM clonidine is made up to determine non-specific binding. This yields a final concentration of 1 µM in the assay (20 µl to 2 ml).
5. Test compounds:
   For most assays, a 1 mM stock solution is made up in a suitable solvent and serially diluted, so that the final concentrations in the assay range from 10^{-5} to 10^{-8} M. Seven concentrations are used for each assay and higher or lower concentrations can be used, depending on the potency of the drug.

Tissue Preparation

Male Wistar rats are sacrificed by decapitation and the cortical tissue is rapidly dissected. The tissue is homogenized in 50 volumes of 0.05 M Tris buffer pH 7.7 (buffer 1b) with the Brinkman Polytron, and centrifuged at 40,000 *g* for 15 min. The supernatant is discarded and the final pellet rehomogenized in 50 volumes of buffer 2b. This tissue suspension is then stored on ice. The final tissue concentration is 10 mg/ml. Specific binding is 1% of the total added ligand and 80% of total bound ligand.

Assay

100 µl	0.5 M Tris – physiological salts pH 7.7 (buffer 2a)
830 µl	H_2O
20 µl	Vehicle (for total binding) or 0.1 mM clonidine (for nonspecific binding) or appropriate drug concentration.
50 µl	^{3}H-clonidine stock solution
1000 µl	tissue suspension.

Tissue homogenates are incubated for 20 min at 25°C with 3 nM ^{3}H-clonidine and varying drug concentrations, and immediately filtered under reduced pressure on Whatman GF-B filters. The filters are washed with 3 five ml volumes of 0.05 M Tris buffer pH 7.7, and transferred to scintillation vials. Specific clonidine binding is defined as the difference between total bound radioactivity and that bound in the presence of 1 µM clonidine.

EVALUATION

IC_{50} calculations are performed using log-probit analysis. The percent inhibition at each drug concentration is the mean of triplicate determinations.

MODIFICATIONS OF THE METHOD

Perry and U'Prichard (1981) described [^{3}H]rauwolscine (α-yohimbine) as a specific radioligand for brain α_2-adrenergic receptors.

Goldberg and Robertson (1983) reviewed yohimbine as a pharmacological probe for the study of the α_2-adrenoreceptor.

Pimoule et al. (1983) characterized [^{3}H]RX 781094 [(imidazolinyl-2)-2benzodioxane-1,4] as a specific α_2-adrenoceptor antagonist radioligand.

Murphy and Bylund (1988) characterized alpha-2 adrenergic receptors in the OK cell, an opossum kidney cell line.

Binding of the radioligand [^{3}H]-rauwolscine to the α_{2A}-adrenoceptor subtype can be measured in membranes prepared from rabbit spleens (Michel et al. 1989).

Binding of the radioligand [^{3}H]-yohimbine to the α_{2B}-adrenoceptor subtype can be measured in membranes prepared from male Wistar rat kidney cortices (Connaughton and Docherty 1989).

SUBTYPES OF THE α_2-ADRENOCEPTOR

Using ^{3}H-rauwolscine as ligand Broadhurst et al. (1988) studied the existence of two alpha$_2$-adrenoreceptor subtypes.

Bylund et al. (1988) used [^{3}H]-yohimbine and [^{3}H]-rauwolscine to study alpha-2A and alpha-2B adrenergic subtypes in tissues and cell lines containing only one subtype.

Brown et al. (1990) found that [^{3}H]-yohimbine labels at α_{2A}- and α_{2B}-adrenoceptors whereas [^{3}H]-idazoxan labels the α_{2A}-adrenoceptor and, in addition, an imidazoline binding site.

Several subtypes of the α_2-adrenoceptor have been identified by pharmacological means (α_{2A}-, α_{2B}-, α_{2C}-, and α_{2D}-adrenoceptors; Ruffulo 1990; Uhlén and Wikberg 1990; Gleason and Hieble 1992; Satoh and Takayanagi 1992; Takano et al. 1992; Ruffolo et al. 1993) or by recombinant technology as α_{2a}-, α_{2b}-, α_{2c}-adrenoceptors (Bylund et al. 1994; Hieble et al. 1995; Hieble and Ruffolo 1996; Alexander et al. 2001; Waitling 2006).

Gleason and Hieble (1992) reported that the α_2-adrenoreceptors of the human retinoblastoma cell line (Y79) may represent an additional example of the α_{2C}-adrenoceptor.

Marjamäki et al. (1993) recommended the use of recombinant human α_2-adrenoceptors to characterize subtype selectivity of antagonist binding.

All three α_2-adrenoceptor types serve as autoreceptors in postganglionic sympathetic neurons (Trendelenburg et al. 2003).

Uhlén et al. (1994) found that the α_2-adrenergic radioligand [^{3}H]-MK912 is α_{2C}-selective among human α_{2A}-, α_{2B}- and α_{2C}-adrenoceptors.

Uhlén et al. (1998) tested the binding of the radioligand [^{3}H]RS79948–197 to human, guinea pig and pig α_{2A}-, α_{2B}- and α_{2C}-adrenoceptors and compared the values with MK912, RX821002, rauwolscine and yohimbine. [^{3}H]RS79948–197 was non-selective for the α_2-adrenoceptor subtypes, showing high affinity for all three.

REFERENCES AND FURTHER READING

Alexander S, Peters J, Mathie A, MacKenzie G, Smith A (2001) TiPS Nomenclature Supplement 2001

Boyajian CL, Leslie FM (1987) Pharmacological evidence for alpha-2 adrenoceptor heterogeneity: Differential binding properties of [^{3}H]rauwolscine and [^{3}H]idazoxan in rat brain. J Pharmacol Exp Ther 241:1092–1098

Brasch H (1991) No influence of prejunctional α_2-adrenoceptors on the effects of nicotine and tyramine in guinea-pig atria. J Auton Pharmacol 11:37–44

Broadhurst AM, Alexander BS, Wood MD (1988) Heterogeneous ^{3}H-rauwolscine binding sites in rat cortex: two alpha$_2$-adrenoreceptor subtypes or an additional non-adrenergic interaction? Life Sci 43:83–92

Brown CM, MacKinnon AC, McGrath JC, Spedding M, Kilpatrick AT (1990) α_2-adrenoceptors subtypes and imidazoline-like binding sites in the rat brain. Br J Pharmacol 99:803–809

Bylund DB (1978) Subtypes of α_2-adrenoceptors: pharmacological and molecular biological evidence converge. Trends Pharmacol Sci 9:356–361

Bylund DB, Eikenberg DC, Hieble JP, Langer SZ, Lefkowitz RJ, Minneman KP, Molinoff PB, Ruffolo RR, Trendelenburg U (1994) IV. International union of pharmacology nomenclature of adrenoceptors. Pharmacol Rev 46:121–136

Bylund DB, Martinez JR (1981) Postsynaptic localization of α_2-adrenergic receptors in rat submandibular gland. J Neurosci 1:1003–1007

Bylund DB, Ray-Prenger C, Murphy TJ (1988) Alpha-2A and alpha-2B adrenergic receptor subtypes: antagonist binding in tissues and cell lines containing only one subtype. J Pharmacol Exp Ther 245:600–607

Connaughton S, Docherty R (1989) Functional evidence for heterogeneity of peripheral prejunctional α_2-adrenoceptors. Br J Pharmacol 101:285–290

Gleason MM, Hieble JP (1992) The α_2-adrenoceptors of the human retinoblastoma cell line (Y79) may represent an additional example for the α_{2C}-adrenoceptor. Br J Pharmacol 107:222–225

Gold MS, Redmond DE, Kleber HD (1978) Clonidine blocks acute opiate withdrawal symptoms. Lancet 2:599–602

Goldberg MR, Robertson D (1983) Yohimbine: a pharmacological probe for the study of the α_2-adrenoreceptor. Pharmacol Rev 35:143–180

Hieble JP, Sulpicio AC, Nichols AJ, Willette RN, Ruffulo RR (1988) Pharmacologic characterization of SK&F

104078, a novel alpha-2 adrenoceptor antagonist which discriminates between pre- and postjunctional alpha-2 adrenoceptors. J Pharm Exp Ther 247:645–652
Hieble JP, Ruffolo RR Jr, Sulpicio AC (1995) Functional subclassification of α_2-adrenoreceptors. Pharmacol Commun 6:91–97
Hieble JP, Ruffolo RR Jr, Sulpicio AC, Naselsky DP, Conway TM, Ellis C, Swift AM, Ganguli S, Bergsma DJ (1996) Subclassification and nomenclature of α_1- and α_2-adrenoceptors. In: Jucker E (ed) Progress in Drug Research. Birkhäuser Verlag, pp 81–130
Kobinger W, Walland A (1967) Investigations into the mechanism of the hypotensive effect of 2-(2,6-dichlorphenylamino)-2-imidazoline-HCl. Eur J Pharmacol 2:155–162
Langer SZ (1977) Presynaptic receptors and their role in the regulation of transmitter release. Br J Pharmacol 60:481–497
Langer SZ (1981) Presynaptic regulation of the release of catecholamines. Pharmacol Rev 32:337–362
Marjamäki A, Luomala K, Ala-Uotila S, Scheinin M (1993) Use of recombinant human α_2-adrenoceptors to characterize subtype selectivity of antagonist binding. Eur J Pharmacol, Mol Pharmacol Sect 246:219–226
McCall RB (1990) Role of neurotransmitters in the central regulation of the cardiovascular system. Progr Drug Res 35:25–84
Michel AD, Loury DN, Withing RL (1989) Differences between the α_2-adrenoceptor in rat submaxillary gland and the α_{2A}- and α_{2B}-adrenoceptor subtypes. Br J Pharmacol 98:890–897
Murphy TJ, Bylund DB (1988) Characterization of alpha-2 adrenergic receptors in the OK cell, an opossum kidney cell line. J Pharmacol Exp Ther 244:571–578
Perry BD, U'Prichard DC (1981) [^{3}H]rauwolscine (α-yohimbine): a specific radioligand for brain α_2-adrenergic receptors. Eur J Pharmacol 76:461–464
Pimoule C, Scatton B, Langer SZ (1983) [^{3}H]RX 781094: a new antagonist ligand labels α_2-adrenoceptors in the rat brain cortex. Eur J Pharmacol 95:79–85
Rand MJ, Wilson J (1968) Mechanisms of the pressor and depressor actions of St 155 (2-(2,6-dichlorophenylamino-2-imidazoline hydrochloride) (Catapres). Eur J Pharmacol 3:27–33
Ruffulo RR (1990) α_2-adrenoceptor agonists and antagonists. Neurotransmissions 6 (2):1–5
Ruffulo RR, Nichols AJ, Hieble JP (1988) Functions mediated by alpha-2 adrenergic receptors. Humana Press, Clifton, pp 187–280
Ruffolo RR, Nichols AJ, Stadel JM, Hieble JP (1993) Pharmacologic and therapeutic applications of α_2-adrenoceptor subtypes. Annu Rev Pharmacol Toxicol 33:243–279
Satoh M, Takayanagi I (1992) Identification and characterization of the α_{2D}-adrenoceptor subtype in single cells prepared from guinea pig tracheal smooth muscle. Japan J Pharmacol 60:393–395
Starke K (1977) Regulation of noradrenaline release by presynaptic receptor systems. Rev Physiol Biochem Pharmacol 77:1–124
Summers RJ, Barnett DB, Nahorski SR (1983) Characteristics of adrenoceptors in homogenates of human cerebral cortex labelled with (^{3}H)-rauwolscine. Life Sci 33:1105–1112
Takano Y, Takano M, Yaksh TL (1992) The effect of intrathecally administered imiloxan and WB4101: possible role of α_2-adrenoceptor subtypes in the spinal cord. Eur J Pharmacol 219:465–468
Trendelenburg AU, Philipp M, Meyer A, Klebroff W, Hein L, Starke K (2003) All three alpha2-adrenoceptor types serve as autoreceptors in postganglionic sympathetic neurons. Naunyn-Schmiedebergs Arch Pharmacol 368:504–512
U'Prichard DC, Greenberg DA, Snyder SH (1977) Binding characteristics of a radiolabeled agonist and antagonist at central nervous system alpha noradrenergic receptors. Mol Pharmacol 13:454–473
U'Prichard DC, Bechtel WD, Rouot B, Snyder SH (1979) Multiple apparent alpha-noradrenergic receptor binding sites in rat brain: Effect of 6-hydroxydopamine. Mol Pharmacol 15:47–60
U'Prichard DC, Reisine TD, Mason ST, Fibiger MC, Yamamura HI (1980) Modulation of rat brain α- and β-adrenergic receptor populations by lesion of the dorsal noradrenergic bundle. Brain Res 187:143–154
Uhlén S, Wikberg JES (1990) Spinal cord α_2-adrenoceptors are of the α_{2A}-subtype: comparison with α_{2A}- and α_{2B}-adrenoceptors in rat spleen, cerebral cortex and kidney using [^{3}H]-RX821002 ligand binding. Pharmacol Toxicol 69:341–350
Uhlén S, Porter AC, Neubig RR (1994) The novel α_2-adrenergic radioligand [^{3}H]-MK912 is α_{2C}-selective among human α_{2A}-, α_{2B}- and -α_{2C} adrenoceptors. J Pharmacol Exp Ther 271:1558–1565
Uhlén S, Dambrova M, Näsman J, Schiöth HB, Gu Y, Wikberg-Mattson A, Wikberg JE (1998) [^{3}H]RS79948–197 binding to human, guinea pig and pig α_{2A}-, α_{2B}- and -α_{2C} adrenoceptors. Comparison with MK912, RX821002, rauwolscine and yohimbine. Eur J Pharmacol 343:93–101
Waitling KJ (2006) The Sigma RBI handbook of receptor classification and signal transduction, 5th edn. Sigma-Aldrich, St Louis, Mo., pp 90–91

A.1.1.3 Electrically Stimulated Release of [^{3}H]Norepinephrine from Brain Slices

PURPOSE AND RATIONALE

The existence of presynaptic receptors which regulate the evoked release of neurotransmitters has been functionally demonstrated in both peripheral and central nervous system (Langer 1981; Starke 1981; Raiteri et al. 1984; Miller 1998). Presynaptic adrenergic α_2-receptors regulate the evoked release of norepinephrine, comprising a short negative feedback loop. Alpha-2 agonists, such as clonidine and guanabenz, inhibit evoked release and alpha-2 antagonists, such as yohimbine and idazoxan, enhance evoked release.

The assay is used as a biochemical screen for agents which enhance or inhibit release of [^{3}H]norepinephrine (^{3}H-NE) and is particularly useful for testing receptor function of α_2-adrenergic agonists and antagonists.

The procedures used emphasize delicate care of slices. By treating slices with great care, one is able to incubate at low tracer concentrations of ^{3}H-NE (25 nM), thus minimizing nonspecific labeling of releasable pools other than those in noradrenergic nerve terminals. It also permits the use of low (and more physiological) stimulation parameters, which allow the

neurons to recover easily between stimulations and do not flood the synaptic cleft with released NE, which would compete with any applied drug thus decreasing sensitivity.

PROCEDURE

This assay is based on the method described by Zahniser et al. (1986).

A Reagents

1. Krebs-Henseleit bicarbonate buffer, pH 7.4 (KHBB):

NaCl	118.4 mM
KCl	4.7 mM
$MgSO_4 \times 7\ H_2O$	1.2 mM
KH_2PO_4	2.2 mM
$NaHCO_3$	24.9 mM
$CaCl_2$	1.3 mM
dextrose (added prior to use)	11.1 mM

   The buffer is aerated for 60 min with 95% O_2, 5% CO_2 on ice and pH is checked.
2. Levo-[Ring-2,5,6-^{3}H]-norepinephrine (specific activity 40–50 Ci/mmol) is obtained from New England Nuclear.
   The final desired concentration of ^{3}H-NE is 25 nM. 0.125 nmol is added to 5 ml KHBB.
3. Test compounds
   For most assays, a 1 mM stock solution of the test compound is made up in a suitable solvent and diluted such that the final concentration in the assay is 1 µM. Higher or lower concentrations may be used depending on the potency of the drug.

B Instrumentation

Neurotransmitter release apparatus consisting of:

- oscilloscope B8K, Precision Model 1420, dual-trace microscope (Dynascan Corp.)
- constant current unit, Grass model CCU1 (Grass Instr. Co.)
- stimulator, model S44, solid state square wave stimulator (Grass Instr. Co.)
- pump, Watson-Marlow, model 502 SHR, standard drive module; model 501 M multichannel pumphead (Bacon Technical Instr.)
- circulator, Haake D8 immersion circulator (Haake Buchler Instr. Inc.)
- fraction collector, Isco Retriever IV fraction collector (Isco Inc.)

C Tissue Preparation

Male Wistar rats (100–150 g) are decapitated, cortical tissue removed on ice and 0.4 mm slices are prepared with a McIlwain tissue chopper. The slices are made individually and removed from the razor blade by twirling an artist's paint brush underneath the slice. Care should be taken not to compress the slice or impale it on the bristles. The slices are placed in cold, oxygenated buffer (10–20 ml) and incubated at 35°C for 30 min under oxygen. After this incubation, the buffer is decanted, leaving the slices behind. Then 5 ml of cold oxygenated buffer is added, and enough [^{3}H]NE to bring the final concentration to 25 nM. This is then incubated and shaken for 30 min at 35°C under oxygen. After this step, the buffer is decanted and the "loaded" slices are rapidly placed on the nylon mesh in the stimulation chambers using a cut-off pipetman tip.

D Assay

To establish a stable baseline, control buffer is pumped through the chamber for 1 h at a flow rate of 0.7 ml/min before the first stimulation. One hour is allowed to pass before the second stimulation. When drugs are used, each concentration is prepared in a separate flask in control buffer and allowed to equilibrate with the tissue slice 20 min before the second stimulation. The experiment is stopped 40 min after the second stimulation.

Stimulation parameters are set at 5 Hz (2 ms duration) for 60 s, with 1 ms delay and voltage setting of 440 SIU (250 Ω).

After the experiment is completed, the chambers are washed with distilled water for at least 20 min, then 200 ml of 20% methanol in distilled water, then distilled water again for at least 20 min.

EVALUATION

After conversion of dpm, percent fractional release is calculated for each fraction, using the spreadsheet program.

Percent fractional release is defined as the amount of radiolabeled compound released divided by the amount present in the tissue at that moment in time. "Spontaneous release" (SP) values are the average of the two fractions preceding and the first fraction in that range after the stimulation period. "Stimulated" (S) are the summed differences between the percent fractional release during stimulation and the appropriate SP value.

The effects of drugs can be reported as S_2/S_1 ratios. To normalize the data, drug effects can be estimated by first calculating S_2/S_1 values for control and drug-treated slices and then expressing the S_2/S_1 value for the drug-treated slices as a percentage of the

S_2/S_1 value for the control slices for each experiment. Each condition should be tested in slices from each animal.

REFERENCES AND FURTHER READING

Langer SZ (1981) Presynaptic regulation of the release of catecholamines. Pharmacol Rev 32:337–362

Miller RJ (1998) Presynaptic receptors. Ann Rev Pharmacol Toxicol 38:201–227

Raiteri M, et al (1984) In: Handbook of Neurochemistry, Vol. 6, Plenum Publishing Corporation, New York, pp 431–462,

Starke K (1981) Presynaptic receptors. Ann. Rev. Pharmacol. Toxicol. 21:7–30

Zahniser NR, et al (1986) In: Chemical and Functional Assays of Receptor Binding, 1986, Short Course 1, Syllabus, published by Society for Neuroscience, Washington D.C., pp 73–81

A.1.1.4 Imidazoline Receptor Binding

PURPOSE AND RATIONALE

Imidazoline receptors constitute a family of nonadrenergic high-affinity binding sites for clonidine, idazoxan, and allied drugs. Drugs selectively binding to imidazoline receptors are expected to have less side effects than clonidine (Ernsberger et al. 1992, 1997; Molderings et al. 1992; Limon et al. 1992). One major subclass, the I_1 receptors, being mainly distributed in the brain and brain stem, partly mediates the central hypotensive action of clonidine-like drugs. The I_2 receptors, an other subclass, are mitochondrial, not G protein coupled, and have diversified functions. They may be involved in neuroprotection for cerebral ischemia. Two binding sites of [^{3}H]p-aminoclonidine, α_2-adrenoceptors and imidazoline binding sites, could be separated (Ernsberger et al. 1987; Bricca et al. 1988; Kamisaki et al. 1990). At least 3 subtypes of imidazoline/guanidinium-receptive sites have been found by photoaffinity labeling (Lanier et al. 1993).

Several endogenous ligands for imidazoline receptors, collectively termed clonidine displacing substances (CDSs), have been detected in tissues and serum (Reis et al. 1995; Chan et al. 1997).

An endogenous substance with clonidine-like properties originally isolated from brain which binds selectively to imidazoline receptors was described by Atlas and Burstein (1984), Ernsberger et al. (1988), Atlas (1991), Meeley et al. (1992), Dontenwill et al. (1992, Ragunathan and Reis 1996). The endogenous substance agmatine, a decarboxylated arginine, may be the physiological agonist at imidazoline receptors acting as neurotransmitter (Li et al. 1994; Gonzales et al. 1996; Head et al. 1997; Herman 1997; Reis and Regunathan 2000). Further candidates of endogenous ligands are discussed (Reis and Ragunathan 1998).

A critical review on imidazoline binding sites is given by Eglen et al. (1998).

PROCEDURE

Tissue Preparation

Whole bovine brains and adrenal glands are obtained from a local slaughterhouse. The lateral medulla oblongata is isolated by a sagittal section through the lateral margin of the pyramids and then bisected. The ventral half is defined as the ventrolateral medulla.

Fresh bovine adrenal glands are perfused retrogradely through the adrenal vein twice with 25 ml ice-cold Krebs-Henseleit bicarbonate buffer. The glands are perfused again with 25 ml ice-cold Krebs-Henseleit buffer containing 0.025% collagenase (type I, Sigma Chemical), incubated at room temperature for 1 h, then perfused with 25 ml fresh buffer containing collagenase and incubated for 30 min at 35°C. The digested glands are split, and the medulla is removed from the cortex. Adrenal medullae are minced and incubated while being stirred for 30 min at 37°C. The digest is filtered and centrifuged at 200 *g* for 30 min at 20°C. The cell pellet is resuspended in 30 ml Krebs' solution without collagenase, recentrifuged, flash-frozen, and stored at –70°C.

Membrane Preparation

Fresh bovine ventrolateral medulla and collagenase-digested rat renal medulla are homogenized with a Polytron (Tekmar Tissumizer; setting 80 for 15 s twice) in 20 vol of ice-chilled HEPES-buffered isotonic sucrose (pH 7.4) containing the protease inhibitors 1,10-phenanthroline (100 µM) and phenylmethylsulfonyl fluoride (50 µM). Bovine adrenomedullary chromaffin cells are homogenized in 15 ml HEPES-buffered isotonic sucrose by 10 strokes in a glass/glass handhold homogenizer. The homogenates are centrifuged at 1000 *g* for 5 min at 4°C to remove nuclei and debris. The pellets (P1) are resuspended in 20 ml of homogenization buffer and centrifuged again at 1000 *g* for 5 min. The supernatants are centrifuged at 48,000 *g* for 18 min at 4°C, and the resulting pellet (P2) is resuspended in 10–25 vol 50 mM Tris-HCl buffer (pH 7.7) containing 5 mM EDTA. After recentrifugation at 48,000 *g* for 18 min, the resulting membrane pellet is resuspended in Tris-HCl containing 25 mM NaCl, preincubated for 30 min at 25°C, chilled on ice, centrifuged again, resuspended a final time in Tris-HCl alone, centrifuged, flash-frozen, and stored at –70°C.

Binding Assays

For determination of specific binding to I_1-imidazoline sites and α_2-adrenergic receptors radioligand binding assays are performed with [^{3}H]clonidine, [^{3}H]*p*-iodoclonidine, or [^{3}H]moxonidine. Membranes are slowly thawed and resuspended in Tris-HCl or Tris-HEPES buffer (pH 7.7, 25°C). Assays are conducted in a total volume of 250 µl in polypropylene 96 well plates (Beckman Macrowell). Each well contains 125 µl membrane suspension, 25 µl radioligand, and 100 µl drug or vehicle. Incubations are initiated by the addition of membrane suspension and carried out for 40 min at 25°C. Nonspecific binding is defined in the presence of either piperoxan or phentolamine (0.1 mM), which are imidazoline-adrenergic agents. Specific α_2-adrenergic binding is defined by epinephrine (0.1 mM). In experiments with catecholamines, all samples contain ascorbic acid in a final concentration of 0.001%. Incubations are terminated by vacuum filtration over Reeves-Angel or Whatman GF/C fiberglass filters using a cell harvester (Brandel). The filters are washed four times with 5 ml ice-cold Tris-HCl, placed in scintillation vials, covered with 4 ml scintillation cocktail and counted at 50% efficiency. Protein is assayed by a modified Lowry et al. method (Peterson 1977) using a deoxycholate-trichloroacetic acid protein precipitation technique which provides a rapid quantitative recovery of soluble and membrane proteins from interfering substances even in very dilute solutions. Sodium dodecyl sulfate is added to alleviate possible nonionic and cationic detergent and lipid interferences, and to provide mild conditions for rapid denaturation of membrane and proteolipid proteins.

EVALUATION

Data are obtained as disintegrations per min and transferred to the Equilibrium Binding Data Analysis program (McPherson 1985). Then, several experiments are analyzed simultaneously with the LIGAND program for non-linear curve fitting (Munson and Rodbard 1980). IC_{50} values are estimated from inhibition curves by non-linear curve fitting (Mutolsky and Ransnas 1987). Protein assay data are also analyzed by non-linear curve fitting (McPherson 1985).

MODIFICATIONS OF THE METHOD

Tesson et al. (1991) defined the subcellular localization of imidazoline-guanidinium-receptive sites by performing binding studies with the radioligand [^{3}H]idazoxan.

Lanier et al. (1993) visualized multiple imidazoline/guanidinium-receptive sites with the photoaffinity adduct 2-[3-azido-4-[^{125}I]iodo-phenoxy]methyl imidazoline.

Molderings et al. (1991) characterized imidazoline receptors involved in the modulation of noradrenaline release in the rabbit pulmonary artery pre-incubated with [^{3}H]noradrenaline.

Molderings and Göthert (1995) determined electrically or K^+-evoked tritium overflow from superfused rabbit aortic strips pre-incubated with [^{3}H]noradrenaline in order to characterize presynaptic imidazoline receptors which mediate noradrenaline release and compared them with I_1- and I_2-imidazoline radioligand binding sites.

Ernsberger et al. (1995) described optimization of radioligand binding assays for I_1 imidazoline sites.

Munk et al. (1996) reported the synthesis and pharmacological evaluation of a potent imidazoline-1 receptor specific agent.

Piletz et al. (1996) compared the affinities of several ligands for [^{125}I]p-iodoclonidine binding at human platelet I_1 imidazole binding sites.

Several selective ligands for imidazoline I_2 receptors have been identified, such as:

- LSL 60101 (Alemany et al. 1995; Menargues et al. 1995),
- RS-45041–190 (MacKinnon et al. 1995; Brown et al. 1995),
- RX801077 (= 2-BFI = 2-(2-benzofuranoyl)-2-imidazoline and analogues (Jordan et al. 1996; Lione et al. 1996; Alemany et al. 1997; Hosseini et al. 1997; Wiest and Steinberg 1997; Hudson et al. 1997).

REFERENCES AND FURTHER READING

Alemany R, Olmos G, Escriba PV, Menargues A, Obach R, Garcia-Sevilla JA (1995) LSL, 60101, a selective ligand for imidazoline I_2 receptors, on glial fibrillary acidic protein concentration. Eur J Pharmacol 280:205–210

Alemany R, Olmos G, Garcia-Sevilla JA (1997) Labeling of I2B-imidazoline receptors by [^{3}H]2-(2-benzofuranyl)-2-imidazoline (2-BFI) in rat brain and liver. Characterization, regulation and relation to monoamine oxidase enzymes. Naunyn-Schmiedeberg's Arch Pharmacol 356:39–47

Atlas D (1991) Clonidine-displacing substance (CDS) and its putative imidazoline receptor. New leads for further divergence of α_2-adrenergic receptor activity. Biochem Pharmacol 41:1541–1549

Atlas D, Burstein Y (1984) Isolation and partial purification of a clonidine-displacing endogenous brain substance. Eur J Biochem 144:287–293

Bricca G, Dontenwill M, Molines A, Feldman J, Belcourt A, Bousquet P (1989) The imidazoline preferring receptor: binding studies in bovine, rat and human brainstem. Eur J Pharmacol 162:1–9

Brown CM, MacKinnon AC, Redfern WS, William A, Linton C, Stewart M, Clague RU, Clark R, Spedding M (1995) RS-45041–190: A selective, high affinity ligand for I_2 imidazoline receptors. Br J Pharmacol 116:1737–1744

Bousquet P (1995) Imidazoline receptors: From basic concepts to recent developments. J Cardiovasc Pharmacol 26/Suppl 2:S1–S6

Bousquet P (1998) Imidazoline receptors: how many, where and why? Naunyn-Schmiedeberg's Arch Pharmacol 358, Suppl 1, R 195

Chan SLF, Atlas D, James RFL, Morgan NG (1997) The effect of the putative endogenous imidazoline receptor ligand, clonidine-displacing substance, on insulin secretion from rat and human islets of Langerhans. Br J Pharmacol 120:926–932

Dontenwill M, Molines A, Verdun A, Bricca G, Belcourt A, Bousquet P (1992) A circulating imidazoline-like substance cross-reacts with anti-clonidine antibodies: high levels in hypertensive patients. Fundam Clin Pharmacol 6, Suppl 6:49s

Eglen RM, Hudson AL, Kendall DA, Nutt DJ, Morgan NG, Wilson VC, Dillon MP (1998) 'Seeing through a glass darkly': casting light on imidazoline 'I' sites. Trends Pharmacol Sci 19:381–390

Ernsberger P, Meeley MP, Mann JJ, Reis DJ (1987) Clonidine binds to imidazoline binding sites as well as α_2-adrenoceptors in the ventrolateral medulla. Eur J Pharmacol 134:1–13

Ernsberger P, Meeley MP, Reis DJ (1988) An endogenous substance with clonidine-like properties: selective binding to imidazole sites in the ventrolateral medulla. Brain Res 441:309–318

Ernsberger P, Giuliano R, Willette RN, Reis DJ (1990) Role of imidazole receptors in the vasodepressor response to clonidine analogs in the rostral ventrolateral medulla. J Pharm Exp Ther 253:408–418

Ernsberger PR, Westbrooks KL, Christen MO, Schäfer SG (1992) A second generation of centrally acting antihypertensive agents act on putative I_1-imidazoline receptors. J Cardiovasc Pharmacol 20, Suppl 4:S1–S10

Ernsberger P, Piletz JE, Graff LM, Graves ME (1995) Optimization of radioligand binding assays for I_1 imidazoline sites. Ann New York Acad Sci 763:163–168

Ernsberger P, Friedman JE, Koletsky RJ (1997) The I_1-imidazoline receptor: From binding site to therapeutic target in cardiovascular disease. J Hypertens/Suppl 15:S9–S23

Gonzalez C, Regunathan S, Reis DJ, Estrada C (1996) Agmatine, an endogenous modulator of noradrenergic transmission in the rat tail artery. Br J Pharmacol 119:677–684

Hamilton CA (1995) Imidazoline receptors, subclassification, and drug-induced regulation. Ann New Acad Sci 763:57–65

Head GA, Chan CKS, Godwin SJ (1997) Central cardiovascular actions of agmatine, a putative clonidine-displacing substance, in conscious rabbits. Neurochem Int 30:37–45

Herman ZS (1997) Agmatine – a novel endogenous ligand of imidazoline receptors. Pol J Pharmacol 49:85–88

Hieble JP, Ruffolo RR (1992) Imidazoline receptors: historical perspective. Fundam Clin Pharmacol 6 (Suppl 1):7s–13s

Hieble JP, Ruffolo RR (1995) Possible structural and functional relationships between imidazoline receptors and α_2-adrenoceptors. Ann New Acad Sci 763:8–21

Hosseini AR, King PR, Louis WJ, Gundlach AL (1997) [^{3}H]2-(2-Benzofuranyl)-2-imidazoline, a highly selective radioligand for imidazoline I_2 receptor binding sites. Naunyn Schmiedeberg's Arch Pharmacol 355:131–138

Hudson AL, Chapleo CB, Lewis JW, Husbands S, Grivas K, Mallard NJ, Nutt DJ (1997) Identification of ligands selective for central I_2 imidazoline binding sites. Neurochem Int 30:47–53

Jordan S, Jackson HC, Nutt DJ, Handley SL (1996) Discrimination stimulus produced by the imidazoline I_2 site ligand, 2-BFI. J Psychopharmacol 10:273–278

Kamisaki Y, Ishikawa T, Takao Y, Omodani H, Kuno N, Itoh T (1990) Binding of [^{3}H]*p*-aminoclonidine to two sites, α_2-adrenoceptors and imidazoline binding sites: distribution of imidazoline binding sites in rat brain. Brain Res 514:15–21

Lanier SM, Ivkovic B, Singh I, Neumeyer JL, Bakthavachalam V (1993) Visualization of multiple imidazoline/guanidinium-receptive sites. J Biol Chem 268:16047–16051

Li G, Regunathan S, Barrow CJ, Eshraghi J, Cooper R, Reis DJ (1994) Agmatine: an endogenous clonidine-displacing substance in the brain. Science 263:966–969

Limon I, Coupry I, Tesson F, Lachaud-Pettiti V, Parini A (1992) Renal imidazoline-guanidinium receptive site: a potential target for antihypertensive drugs. J Cardiovasc Pharmacol 20, Suppl 4:S21–S23

Lione LA, Nutt DJ, Hudson AL (1996) [^{3}H]2-(2-benzofuranyl)-2-imidazoline: A new selective high affinity radioligand for the study of rabbit brain imidazoline I_2 receptors. Eur J Pharmacol 304:221–229

MacKinnon AC, Stewart M, Olverman HJ, Spedding M, Brown CM (1993) [^{3}H]p-aminoclonidine and [^{3}H]idazoxan label different populations of imidazoline sites on rat kidney. Eur J Pharmacol 232:79–87

MacKinnon AC, Redfern WS, Brown CM (1995) [^{3}H]-RS-45041–190: A selective high affinity ligand for I_2 imidazoline receptors. Br J Pharmacol 116:1729–1736

Mc Pherson GA (1985) Analysis of radioligand binding experiments: A collection of computer programs for the IBM PC. J Pharmacol Meth 14:213–218

Meeley MP, Hensley ML, Ernsberger P, Felsen D, Reis DJ (1992) Evidence for a bioactive clonidine-displacing substance in peripheral tissues and serum. Biochem Pharmacol 44:733–740

Menargues A, Cedo M, Artiga O, Obach R, Garcia-Sevilla JA (1995) Effects of the I_2 imidazoline receptor ligand LSL 60101 on various models of anorexia in rats. Ann New York Acad Sci 763:494–496

Molderings GJ, Göthert M (1995) Inhibitory presynaptic imidazoline receptors on sympathetic nerves in the rabbit aorta differ from I_1- and I_2-imidazoline binding sites. Naunyn-Schmiedeberg's Arch Pharmacol 351:507–516

Molderings GJ, Hentrich F, Göthert M (1991) Pharmacological characterization of the imidazoline receptor which mediates inhibition of noradrenaline release in the rabbit pulmonary artery. Naunyn-Schmiedeberg's Arch Pharmacol 344:630–638

Molderings GJ, Michel MC, Göthert M, Christen O, Schäfer SG (1992) Imidazolrezeptoren: Angriffsort einer neuen Generation von antihypertensiven Arzneimitteln. Dtsch Med Wschr 117:67–71

Munk SA, Lai RK, Burke JE, Arasasingham PN, Kharlamb AB, Manlapaz CA, Padillo EU, Wijono MK, Hasson DW, Wheeler LA, Garst ME (1996) Synthesis and pharmacological evaluation of 2-endo-amino-3-exo-isopropylbicyclo[2.2.1]heptane: a potent imidazoline-1 receptor specific agent. J Med Chem 39:1193–1195

Munson PJ, Rodbard D (1980) LIGAND, a versatile computerized approach for characterization of ligand binding systems. Anal Biochem 107:220–239

Musgrave IF, Krautwurst D, Schulz G (1996) Imidazoline binding sites and signal transduction pathways. Clin Exp Pharmacol Physiol 23:990–994
Mutolsky HJ, Ransnas LA (1987) Fitting curves for data using non-linear regression: a practical and non mathematical review. FASEB J 1:365–374
Peterson GL (1977) A simplification of the protein assay method of Lowry et al. which is more generally applicable. Anal Biochem 83:346–356
Piletz JE, Zhu H, Chikkala DN (1996) Comparison of ligand binding affinities at human I_1 imidazole binding sites and the high affinity state of α_2 adrenoceptor subtypes. J Pharmacol Exper Ther 279:694–702
Regunathan S, Reis DJ (1996) Imidazoline receptors and their endogenous ligands. Annu Rev Pharmacol Toxicol 36:511–544
Regunathan S, Evinger MJ, Meeley MP, Reis DJ (1991) Effects of clonidine and other imidazole-receptor binding agents on second messenger systems and calcium influx in bovine adrenal chromaffin cells. Biochem Pharmacol 42:2011–2018
Reis DJ, Ragunathan S (1998) Endogenous ligands of imidazoline receptors. Naunyn-Schmiedeberg's Arch Pharmacol 358, Suppl 1, R 195
Reis DJ, Regunanthan S (2000) Is agmatine a novel neurotransmitter in brain? Trends Pharmacol Sci 21:187–193
Reis DJ, Li G, Regunathan S (1995) Endogenous ligands of imidazoline receptors: Classic and immunoreactive Clonidine-displacing substance and agmatine. Ann New York Acad Sci 763:295–313
Tesson F, Prip-Buus C, Lemoine A, Pegorier JP, Parini A (1991) Subcellular distribution of imidazoline-guanidinium-receptive sites in human and rabbit liver. J Biol Chem 266:155–160
Van Zwieten (1997) Central imidazoline (I_1) receptors as targets of centrally acting antihypertensives: Moxonidine and rilmenidine. J Hypertens 15:117–125
Wang H, Regunathan S, Ruggiero DA, Milner TA, Meeley MP, Reis DJ (1993) Biochemical and immunohistochemical characterization of imidazoline receptor protein. Am J Hypertens 6:77A
Wiest SA, Steinberg MI (1997) Binding of [^{3}H]2-(2-benzofuranyl)-2-imidazoline (BFI) to human brain: Potentiation by tranylcypromine. Life Sci 60:605–615
Yu A, Frishman WH (1996) Imidazoline receptor agonist drugs: A new approach to the treatment of systemic hypertension. J Clin Pharmacol 36:98–111

A.1.1.5 β-Adrenoreceptor Binding

PURPOSE AND RATIONALE

β-adrenoceptors are widely distributed, found at both central and peripheral sites, and are activated either via norepinephrine released from sympathetic nerve terminals or via epinephrine released from the adrenal medulla. Important physiological consequences of β-adrenoceptor activation include stimulation of cardiac rate and force, relaxation of vascular, urogenital and bronchial smooth muscle, stimulation of renin secretion from the juxtaglomerular apparatus, stimulation of insulin and glucagon secretion from the endocrine pancreas, stimulation of glycogenolysis in liver and skeletal muscle and stimulation of lipolysis in the adipocyte.

Three β-adrenoceptor proteins have been cloned, and the characteristics of these recombinant receptors correspond with those of the three well characterized β-adrenoceptors on native tissue, designated as β_1, β_2 and β_3. The possible roles of β_3-adrenoceptors in the cardiovascular system were discussed by Gauthier et al. (2000). An additional β-adrenoceptor modulatingcardiac contractility has been designated as the β_4-adrenoceptor (Kaumann et al. 1998).

While it was initially thought that cardiac stimulation involved primarily the β_1-adrenoceptor, it now appears that all of the receptor subtypes may be involved. Bronchodilation appears to be mediated by the β_2-adrenoceptor. The β_3-adrenoceptor is responsible for lipolysis in white adipose tissue and thermogenesis in the brown adipose tissue found in rodents. Renin release appears to be mediated by the β_1-adrenoceptor (Waitling 2006).

The β-adrenoceptor population of plasma membranes from bovine heart ventricles consists of 75–80% β_1- and 20–25% β_2-adrenoceptors. The use of this tissue allows a parallel investigation of the binding characteristics of drugs at both the β_1- and β_2-adrenoceptors. Both, the β_1- and β_2-adrenoceptors coexist in rat ventricular myocytes, but stimulation of these receptor subtypes elicits qualitatively different cell responses at the levels of ionic channels, the myofilaments, and sarcoplasmic reticulum (Xiao and Lakatta 1993).

A constant concentration of the radioligand ^{3}H-dihydroalprenolol (^{3}H-DHA) (4–6 nM) is incubated with increasing concentrations of a non-labeled test drug (0.1 nM–1 mM) in the presence of plasma membranes from bovine heart ventricles. If the test drug exhibits any affinity to β-adrenoceptors, it is able to compete with the radioligand for receptor binding sites. Thus, the lower the concentration range of the test drug, in which the competition reaction occurs, the more effective is the test drug.

PROCEDURE

Materials and Solutions

preparation buffer:

Tris-HCl	5 mM
$MgCl_2 \times 6\,H_2O$	1 mM
D(+)-sucrose	250 mM
pH 7.4	

310 mOsm sodium phosphate buffer:

pH 7.4	rinse buffer:
Tris-HCl	50 mM
$MgCl_2 \times 6\,H_2O$	10 mM
pH 7.4	

incubation buffer:

Tris-HCl	50 mM
$MgCl_2 \times 6\,H_2O$	10 mM
ascorbic acid	1.6 mM
catechol	0.3 mM
pH 7.4	

radioligand:

(–)^{3}H-dihydroalprenolol × HCl

(^{3}H-DHA) specific activity 1.48–2.59 TBq/mmol (40–70 Ci/mmol) (NEN)

for inhibition of ^{3}H-dihydroalprenolol binding in non-specific binding experiments:

(–)isoprenaline(+)bitartrate salt (Sigma)

Bovine hearts are obtained freshly from the local slaughter house. The lower part of the left ventricle from 5 hearts is separated and kept in ice-cold preparation buffer. In the laboratory, approx. 60 g wet weight from the five ventricle pieces are minced with a scalpel into 2–3 mm pieces.

Membrane Preparation

Ventricles are homogenized by Ultra-Turrax (1 g tissue/10 ml buffer), the homogenate is filtered through gauze and centrifuged at 500 *g* (4°C) for 10 min. The pellets are discarded, the supernatant is collected, and centrifuged at 40,000 *g* for 20 min. The resulting pellets are resuspended in approx. 300 ml 310 mOsm sodium phosphate buffer, homogenized by Ultra-Turrax, and centrifuged as before. The final pellets are dissolved (by Ultra-Turrax) in sodium phosphate buffer corresponding to 1 g ventricle wet weight/2 ml buffer. The membrane suspension is immediately stored in aliquots of 5–20 ml at –77°C. Protein concentration of the membrane suspension is determined according to the method of Lowry et al. with bovine serum albumin as a standard.

At the day of the experiment, the required volume of the membrane suspension is slowly thawed and centrifuged at 40,000 *g* (4°C) for 20 min. The pellets are resuspended in a volume of ice-cold rinse buffer, yielding a membrane suspension with a protein content of approx. 2.0 mg/ml. After homogenizing by Ultra-Turrax, the membrane suspension is stirred under cooling for 20–30 min until the start of the experiment.

Experimental Course

All incubation samples are performed in triplicate.

The total volume of each incubation sample is 200 µl (microtiter plates).

Saturation Experiments

total binding:

- 50 µl ^{3}H-DHA
  (12 concentrations, 3×10^{-10}–4×10^{-8} M)
- 50 µl incubation buffer

non-specific binding:

- 50 µl ^{3}H-DHA
  (4 concentrations, 3×10^{-10}–4×10^{-8} M)
- 50 µl (–)isoprenaline (10^{-5} M)

Competition Experiments

- 50 µl ^{3}H-DHA
  (1 constant concentration, 4–6 × 10^{-9} M)
- 50 µl incubation buffer without or with non-labeled test drug
  (15 concentrations 10^{-10}–10^{-3} M)

The binding reaction is started by adding 100 µl membrane suspension per incubation sample (approx. 2 mg protein/ml). The samples are incubated for 60 min in a shaking water bath at 25°C. The reaction is stopped by rapid vacuum filtration of the total incubation volume over glass fiber filters. Thereby the membrane-bound radioactivity is separated from the free activity. Filters are washed immediately with approx. 20 ml ice-cold rinse buffer per sample. The retained membrane-bound radioactivity on the filter is measured after addition of 2 ml liquid scintillation cocktail per sample in a Packard liquid scintillation counter.

EVALUATION

The following parameters are calculated:

- total binding
- non-specific binding
- specific binding = total binding–non-specific binding

The dissociation constant (K_i) of the test drug is determined from the competition experiment of ^{3}H-DHA versus non-labeled drug by a computer-sup-

ported analysis of the binding data.

$$K_i = \frac{K_D\ ^3H \times IC_{50}}{K_D\ ^3H + [^3H]}$$

IC_{50} = concentration of the test drug, which competes with 50% of specifically bound ^{3}H-DHA in the competition experiment

$[^3H]$ = concentration of ^{3}H-DHA in the competition experiment.

$K_D\ ^3H$ = dissociation constant of ^{3}H-DHA, determined from the saturation experiment.

The K_i-value of the test drug is the concentration, at which 50% of the receptors are occupied by the test drug.

The affinity constant K_i [mol/l] is recorded and serves as a parameter to assess the efficacy of the test drug.

Standard data

propranolol hydrochloride $K_i = 6–8 \times 10^{-9}$ mol/l

MODIFICATIONS OF THE METHOD

Abrahamsson et al. (1988) performed a receptor binding study on the β_1- and β_2-adrenoceptor affinity of atenolol and metoprolol in tissues from the rat, the guinea pig and man with various radioligands, such as [^{125}I](±)hydroxybenzylpindolol, [^{125}I](–)pindolol, [^{3}H](–)dihydroalprenolol, and [^{3}H](–)CGP 12177.

Fleisher and Pinnas (1985) used specific binding of (–)[^{3}H]dihydroalprenolol to rat lung membranes for *in vitro* studies on the relative potency of bronchodilator agents.

REFERENCES AND FURTHER READING

Abrahamsson T, Ek B, Nerme V (1988) The β_1- and β_2-adrenoceptor affinity of atenolol and metoprolol: a receptor-binding study performed with different ligands in tissues from the rat, the guinea pig and man

Cheng YC, Prusoff WH (1973) Relationship between the inhibition constant (K_I) and the concentration of inhibitor which causes 50 per cent inhibition (I_{50}) of an enzymatic reaction. Biochem Pharmacol 22:3099–3108

Fleisher JH, Pinnas JL (1985) *In vitro* studies on the relative potency of bronchodilator agents. Lung 163:161–171

Gauthier C, Langin D, Balligand JL (2000) β_3-adrenoceptors in the cardiovascular system. Trends Pharmacol Sci 21:426–431

Hedberg A, Minneman KP, Molinoff PB (1980) Differential distribution of beta-1 and beta-2 adrenergic receptors in cat and guinea-pig heart. J Pharmacol Exp Ther 212:503–508

Kaumann AJ, Preitner F, Sarsero D (1998), Molenaar P, Revelli JP, Giacobino JP (–)CGP 12177 causes cardiostimulation and binds to cardiac putative β_4-adrenoceptors in both wild-type and β_3-adrenoceptor knockout mice. Mol Pharmacol 53:670–675

Minneman KP, Hegstrand LR, Molinoff PB (1979) The pharmacological specificity of beta-1 and beta-2 adrenergic receptors in rat heart and lung *in vitro*. Mol Pharmacol 16:21–33

Waitling KJ (2006) The Sigma RBI handbook of receptor classification and signal transduction, 5th edn. Sigma-Aldrich, St Louis, Mo., pp 92–93

Wiemer G, Wellstein A, Palm D, Hattingberg HM v, Brockmeier D (1982) Properties of agonist binding at the β-adrenoceptor of the rat reticulocyte. Naunyn-Schmiedeberg's Arch Pharmacol. 321:11–19

Xiao RP, Lakatta EG (1993) β_1-adrenoceptor stimulation and β_2-adrenoceptor stimulation differ in their effect on contraction, cytosolic Ca^{2+}, and Ca^{2+} current in single rat ventricular cells. Circ Res 73:286–300

A.1.1.6 β_1-Adrenoreceptor Binding

PURPOSE AND RATIONALE

β-adrenergic receptors were differentiated from α-receptors (Ahlquist 1948) and subsequently divided into 2 distinct subtypes, β_1 and β_2 (Lands et al. 1967) based on differing pharmacology in different tissues. β-receptors have been labelled in a number of tissues including heart, lung, erythrocytes and brain using the β-agonists [^{3}H]-epinephrine (U'Prichard et al. 1978), or [^{3}H]-hydroxybenzylisoproterenol (Lefkowitz and Williams 1977) or the β-receptor antagonists [^{3}H]-alprenolol (Mukherjee et al. 1975), [^{3}H]-dihydroalprenolol (DHA) (U'Prichard et al. 1978; Bylund and Snyder 1976) and (^{125}I)-iodohydroxypindolol (Weiland et al. 1980). DHA is a potent β-antagonist (Mukherjee et al. 1975), which labels both β_1 and β_2 adrenergic receptors. The binding characteristics of this ligand in brain were described by Bylund and Snyder (1976), who showed that antagonists competed potently and agonists less potently although stereospecificity was maintained. The pharmacology of binding was consistent with β_1-receptor occupancy. Lesioning studies (Wolfe et al. 1982), combined with non-linear regression analysis of data have shown that while β-receptors in rat cerebellum are primarily of the β_2 subtype, the β_1 occurring in rat cerebral cortex are physiologically more significant. The assay can be used to evaluate the direct interaction of drugs with β-receptors labelled by [^{3}H]-dihydroalprenolol.

PROCEDURE

Reagents

Tris buffer, pH 8.0

1. a) 44.4 g Tris HCl q.s. to 1 liter (0.5 M Tris, pH 8.0) 26.5 g Tris base
   b) Dilute 1:10 in distilled water. (0.05 M Tris, pH 8.0)

2. (–)-[propyl-1,2,3-^{3}H] Dihydroalprenolol hydrochloride (45–52 Ci/mmol) is obtained from New England Nuclear.
   For IC_{50} determinations: A stock solution of 20 nM ^{3}H-DHA is made up in distilled H_2O and 50 µl is added to each tube (this yields a final concentration of 1 nM in the 1 ml assay).
3. (±)-propranolol HCl is obtained from Ayerst.
   A 1 mM propranolol stock solution is made up in distilled water and further diluted 1:20 in distilled water to give 50 µM propranolol solution. Twenty µl of dilute stock solution is added to 3 tubes to determine nonspecific binding (yields a final concentration of 1 µM in a 1 ml assay).
4. Test compounds:
   For most assays, a 1 mM stock solution is made up in a suitable solvent and serially diluted, such that the final concentration in the assay ranges from 10^{-5} to 10^{-8} M. Seven concentrations are used for each assay. Higher or lower concentrations may be used depending on the potency of the compound.

Tissue Preparation

Male rats are decapitated and the brains rapidly removed. The cerebral cortices are dissected free, weighed and homogenized in 50 ml of ice-cold 0.05 Tris buffer, pH 8.0. This homogenate is centrifuged at 40,000 *g*, the supernatant decanted and the pellet resuspended and recentrifuged at 40,000 *g*. The final pellet is resuspended in the initial volume of fresh 0.05 Tris buffer, pH 8.0. This tissue suspension is then stored on ice. The final tissue concentration in the assay is 10 mg/ml. Specific binding is about 3% of the total added ligand and 80% of the total bound ligand.

Assay

380 µl	H_2O
50 µl	0.5 Tris buffer, pH 8.0
20 µl	Vehicle (for total binding) or 50 µM (±) propranolol (for nonspecific binding) or appropriate drug concentration
50 µl	^{3}H-DHA stock solution
500 µl	tissue suspension.

The tissue homogenates are incubated for 15 min at 25°C with 1 nM ^{3}H-DHA and varying drug concentrations. With each binding assay, triplicate samples are incubated with 1 µM (±)-propranolol under identical conditions to determine nonspecific binding. The assay is stopped by vacuum filtration through Whatman GF/B filters which are washed 3 times with 5 ml of ice-cold 0.05 Tris buffer, pH 8.0. The filters are counted in 10 ml of Liquiscint scintillation cocktail.

EVALUATION

The percent inhibition of each drug concentration is the mean of triplicate determinations. IC_{50} values are obtained by computer-derived log-probit analysis.

MODIFICATIONS OF THE METHOD

Dooley et al. (1986) recommended CGP 20712 A as a useful tool for quantitating β_1 and β_2 adrenoceptors.

REFERENCES AND FURTHER READING

Ahlquist RP (1948) Study of adrenotropic receptors. Am J Physiol 153:586–600

Bylund DB, Snyder SH (1976) Beta adrenergic receptor binding in membrane preparations from mammalian brain. Mol Pharmacol 12:568–580

Dooley DJ, Bittiger H, Reymann NC (1986) CGP 20712 A: A useful tool for quantitating β_1 and β_2 adrenoceptors. Eur J Pharmacol 130:137–139

Haeusler G (1990) Pharmacology of β-blockers: classical aspects and recent developments. J Cardiovasc Pharmacol 16 (Suppl 5):S1–S9

Lands AM, Arnold A, McAuliff JP, Luduena FP, Brown TG (1967) Differentiation of receptor systems activated by sympathomimetic amines. Nature 214:597–598

Lefkowitz RJ, Williams LT (1977) Catecholamine binding to the β-adrenergic receptor. Proc Nat Acad Sci 74:515–519

Mukherjee C, Caron MG, Coverstone M, Lefkowitz RJ (1975) Identification of adenylate cyclase-coupled β-adrenergic receptors in frog erythrocytes with (–)-[^{3}H]-alprenolol. J Biol Chem 250:4869–4876

U'Prichard DC, Bylund DB, Snyder SH (1978) (±)-[^{3}H]Epinephrine and (–)-[^{3}H] dihydroalprenolol binding to β_1- and β_2-noradrenergic receptors in brain, heart and lung membranes. J Biol Chem 253:5090–5102

Weiland GA, Minneman KD, Molinoff PB (1980) Thermodynamics of agonist and antagonist interaction with mammalian β-adrenergic receptors. Mol Pharmacol 18:341–347

Wolfe BB, Minneman KP, Molinoff PB (1982) Selective increases in the density of cerebellar β_1-adrenergic receptors. Brain Res 234:474–479

A.1.1.7 β_2-Adrenoreceptor Binding

PURPOSE AND RATIONALE

Lands et al. (1967) classified β-receptors into β_1 and β_2 subtypes according to differences in the action of various catecholamines. Synthesis of more selective β-antagonists has helped to confirm the existence of receptor subtypes. Based on catecholamine pharmacology and differences in the tissue distribution, it has been suggested that the β_1-receptor serves as the receptor for norepinephrine acting as a neurotransmitter and the β_2-receptor serves as a receptor for epinephrine acting as a hormone. (Nahorski 1981;

Ariens and Simonis 1983; Lefkowitz et al. 1983; Minneman 1983). Since [^{3}H]-dihydroalprenolol is a nonspecific ligand, it is necessary to select a tissue which is enriched in β_2-receptors in order to convey specificity to this assay. Tissues with predominantly β_2-receptors include lung (U'Prichard et al. 1978; Ariens and Simonis 1983; Lefkowitz et al. 1983), cerebellum (Lefkowitz et al. 1983; Minneman et al. 1983), rat and frog erythrocytes (Mukherjee et al. 1975; Lefkowitz et al. 1983) and ciliary process (Nathanson 1985) whereas, forebrain, heart and avian erythrocytes are relatively enriched in the β_1-subtype (Lefkowitz et al. 1983). Due to poor binding characteristics in cerebellum, rat lung is chosen as the tissue for β_2-adrenergic receptors.

A compound with β_2-selectivity would be less likely to produce cardiac effects but more likely to produce bronchiolar constriction. The test is used to determine the affinity of compounds for the β_2-adrenergic receptor subtype. A measure of receptor subtype selectivity can be determined when data are compared with those obtained in the β_1-adrenergic assay in rat cerebral cortex.

The present nomenclature of β_1, β_2, and β_3 receptors was reviewed by Alexander et al. (2001).

PROCEDURE

Reagents

1. Tris buffers, pH 8.0
   a) 44.4 g Tris HCl q.s. to 1 liter (0.5 M Tris, pH 8.0) 26.5 g Tris base
   b) Dilute 1:10 in distilled water (0.05 M Tris, pH 8.0)
2. (–)-[propyl-1,2,3-^{3}H] Dihydroalprenolol hydrochloride (45–52 Ci/mmol) is obtained from New England Nuclear.
   For IC_{50} determinations: A stock solution of 20 nM ^{3}H-DHA is made up in distilled water and 50 µl is added to each tube (this yields a final concentration of 1 nM in the assay)
3. (±)-propranolol HCl is obtained from Ayerst.
   A 1 mM propranolol stock solution is made up in distilled water and further diluted 1:20 in distilled water to give 50 µM propranolol solution. Twenty µl of dilute stock solution are added to 3 tubes to determine nonspecific binding (yielding a final concentration of 1 µM in a 1 ml assay).
4. Test compounds:
   For most assays, a 1 mM stock solution is made up in a suitable solvent and serially diluted, such that the final concentrations in the assay range from 10^{-5} to 10^{-8} M. Seven concentrations are used for each assay. Higher or lower concentrations may be used depending on the potency of the compound to be tested.

Tissue Preparation

Male Wistar rats are sacrificed by decapitation and the lungs removed, weighed and homogenized in 50 volumes of ice-cold 0.05 M Tris buffer, pH 8.0 using a Tekmar homogenizer. The homogenate is passed through a cheese cloth and centrifuged at 40,000 *g* for 15 min. The final membrane pellet is resuspended in the original volume of Tris buffer, pH 8.0, and used in the assay.

Assay

380 µl	H_2O
50 µl	0.5 Tris buffer, pH 8.0
20 µl	Vehicle (for total binding) or 50 µM (±)-propranolol (for nonspecific binding) or appropriate drug concentration
50 µl	^{3}H-DHA stock solution
500 µl	tissue suspension.

The tissue homogenates are incubated for 15 min at 25°C with 1 nM ^{3}H-DHA and varying drug concentrations. In each binding assay, triplicate samples are incubated with 1 µM (±)-propranolol under identical conditions to determine nonspecific binding. The assay is stopped by vacuum filtration through Whatman GF/B filters which are washed 3 times with 5 ml of ice-cold 0.05 Tris buffer, pH 8.0. The filters are counted in 10 ml of Liquiscint scintillation cocktail.

EVALUATION

The percent inhibition of each drug concentration is the mean of triplicate determinations. IC_{50} values are obtained by computer-derived log-probit analysis.

MODIFICATIONS OF THE METHOD

Dooley et al. (1986) recommended CGP 20712 as a useful tool for quantitating β_1- and β_2-adrenoceptors.

McCrea and Hill (1993) described salmeterol as a long-acting β-adrenoceptor agonist mediating cyclic AMP accumulation in the B50 neuroblastoma cell line.

Sarsero et al. (1998) recommended (–)[^{3}H]-CGP 12177A as radioligand for the putative β_4-adrenoceptor.

McConnell et al. (1991, 1992; Owicki and Parce 1992) used a special apparatus, the 'cytosensor microphysiometer' which measures the rate of proton excretion from cultured cells. Chinese hamster ovary cells

were transfected with human β_2-adrenergic receptors. The β_2-adrenergic receptor activates adenylate cyclase resulting in an increase in the cyclic AMP concentration within the cell which can be measured as acidification. Addition of 10 µM isoproterenol, 500 µM 8-bromo cyclic AMP, or 10 µg/ml forskolin induced a reversible acidification.

Hoffmann et al. (2004) compared human β-adrenergic receptor subtypes using characterization of stably transfected receptors in CHO cells.

PROCEDURE

cDNA of human β-adrenergic receptors cDNAs coding for human β-adrenergic receptors in pcDNA3 expression vectors were verified by sequencing and comparison with the respective GeneBank entries. The translated amino acid sequences corresponded to the published sequences for the β_1-adrenergic receptor (Frielle et al. 1987), β_2-adrenergic receptor (Schofield et al. 1987), and β_3-adrenergic receptor (Emorine et Y al. 1989). With respect to polymorphisms, the β-adrenergic receptors used in this study corresponded to the following variants: β_1-receptor 49-Ser, 389-Gly; β_2-receptor 16-Arg, 27-Gln, 164-Thr; β_3-receptor 64-Trp. All of the variants correspond to the sequences originally termed wild-type.

Stable Transfection of Cells

Chinese hamster ovary cells (CHO-K1 cells; CCL61, American Type Culture Collection, Rockville, Md., USA) were transfected with plasmid DNA for stable expression using the calcium phosphate precipitation method (Chen and Okayama 1987) as described for the rat A_1 adenosine receptor (Freund et al. 1994). Positive clones were selected with 600 µg/ml of the neomycin analog G-418, and single clonal lines were isolated by limiting dilution. Expression of the receptor was verified by radioligand binding.

Cell culture and membrane preparation Chinese hamster ovary cells stably transfected with human β-adrenergic receptor subtypes were grown adherently and maintained in Dulbecco's Modified Eagle's Medium with nutrient mixture F12 (DMEM/F12), containing 10% fetal calf serum, penicillin (100 U/ml), streptomycin (100 µg/ml), L-glutamine (2 mM) and geneticin (G-418, 0.2 mg/ml) at 37°C in 5% CO_2/95% air. Cells were split 2 or 3 times weekly at a ratio of between 1:5 and 1:15. In order to harvest cells the culture medium was removed, cells were washed twice with PBS and membranes were prepared or cells were frozen on the dishes for later preparation of membranes. Crude membrane fractions were prepared from fresh (measurement of adenylyl cyclase) or frozen cells (radioligand binding). The resulting membrane pellets were resuspended in 50 mM Tris/HCl buffer pH 7.4 to give a final protein concentration of 1–2 mg/ml.

Radioligand Binding Studies and Adenylyl Cyclase Activity

The radioligand binding experiments were performed with membranes prepared as described above. Assays were done in a volume of 200 µl in 50 mM Tris/HCl, pH 7.4 (assay buffer) in the presence of 100 µM GTP to ensure monophasic binding curves for agonists. For saturation binding experiments at human β_1- and β_2-receptors up to 400 pM ^{125}I-CYP and for β_3-receptors up to 1,500 pM ^{125}I-CYP were used. Non-specific binding was determined in the presence of 10 µM alprenolol. For competition binding, 50 pM ^{125}I-CYP in the case of β_1- and β_2-receptors, or 80 pM ^{125}I-CYP for β_3-receptors were used. For most of the competition binding experiments membranes with intermediate receptor expression (β_1: 367 ± 75 fmol/mg protein, β_2: 282 ± 19 fmol/mg protein, β_3: 377 ± 82 fmol/mg protein) were used. For selected compounds it was demonstrated that higher receptor expression did not affect K_i values (data not shown). Membranes were incubated for 90 min at 30°C, filtered through Whatman GF/C filters, and washed 3 times with ice-cold assay buffer. Samples were counted in a γ-counter (Wallac 1480 wizard 3). K_D-values for ^{125}I-CYP were calculated by non-linear curve fitting with the program SCTFIT. Ligand IC_{50} values were calculated using Origin 6.1 (OriginLab Corporation, Northampton, Mass., USA) and were transformed to K_i values according to Cheng and Prusoff (1973).

Adenylyl cyclase activity in cell membranes was determined according to Jakobs et al. (1976). Membrane protein (50 µg) was added to an incubation mixture with final concentrations of 50 mM Tris/HCl pH 7.4, 100 µM cAMP, 0.2% BSA, 10 µM GTP, 100 µM ATP, 1 mM $MgCl_2$, 100 µM IBMX, 15 mM phosphocreatine, and 300 U/ml of creatine kinase. Membranes were incubated with about 200,000 cpm of [α-^{32}P]-ATP for 20 min in the incubation mixture as described (Klotz et al. 1985). Accumulation of [α-^{32}P]-cAMP was linear over at least 20 min under all conditions. The reaction was stopped by addition of 400 µl of 125 mM ZnAc-solution and 500 µl of 144 mM Na_2CO_3. Samples were centrifuged for 5 min at 14,000 rpm in a laboratory microcentrifuge. Then, 800 µl of the resulting supernatant wase finally applied to alumina WN-6 (Sigma) columns that were eluted twice with 2 ml of 100 mM Tris/HCl pH 7.4.

The eluates were counted in a β-counter (Beckmann LS 1801).

Niclauss et al. (2006) compared the ability of three radioligands, [^{125}I]-cyanopindolol, [^{3}H]-CGP 12,177 and [^{3}H]-dihydroalprenolol, to label the three human β-adrenoceptor subtypes. Saturation and competition binding experiments were performed using membrane preparations from Chinese hamster ovary cells stably transfected with the three subtypes. While [^{3}H]-CGP 12,177 had very similar affinity for β_1- and β_2-adrenoceptors (about 40 pM), [^{125}I]-cyanopindolol and [^{3}H]-dihydroalprenolol had four- to sixfold higher affinity for β_2- as compared to β_1-adrenoceptors (10 vs. 45 and 187 vs. 1,021 pM, respectively). The affinity of [^{125}I]-cyanopindolol at β_3-adrenoceptors was considerably lower (440 pM) than at the other two subtypes. The β_3-adrenoceptor affinity of [^{3}H]-CGP 12,177 and [^{3}H]-dihydroalprenolol was so low that it could not be estimated within the tested range of radioligand concentrations (up to 4,000 pM and 30,000 pM for [^{3}H]-CGP 12,177 and [^{3}H]-dihydroalprenolol, respectively). All three radioligands were ill-suited to labeling β_3-adrenoceptors, particularly in preparations co-expressing multiple subtypes. In the absence of alternatives, [^{125}I]-cyanopindolol appears the least unsuitable for labeling β_3-adrenoceptors. At present, there is still a need for high-affinity radioligands that are selective for β_3-adrenoceptors.

REFERENCES AND FURTHER READING

Alexander S, Peters J, Mathie A, MacKenzie G, Smith A (2001) TiPS Nomenclature Supplement 2001

Ariens EJ, Simonis AM (1983) Physiological and pharmacological aspects of adrenergic receptor classification. Biochem Pharmacol 32:1539–1545

Chen C, Okayama H (1987) High-efficiency transformation of mammalian cells by plasmid DNA. Mol Cell Biol 7:2745–2752

Cheng YC, Prusoff WH (1973) Relationship between the inhibition constant (K_i) and the concentration of inhibitor which causes 50 per cent inhibition (I_{50}) of an enzymatic reaction. Biochem Pharmacol 22:3099–3108

Collis MG (1983) Evidence for an A_1 adenosine receptor in the guinea pig atrium. Br J Pharmac78:207–212

Deighton NM, Motomura S, Bals S, Zerkowski HR, Brodde OE (1992) Characterization of the beta adrenoceptor subtype(s) mediating the positive inotropic effects of epinine, dopamine, dobutamine, denopamine and xamoterol in isolated human right atrium. J Pharm Exp Ther 262:532–538

Dooley DJ, Bittiger H, Reymann NC (1986) CGP 20712: A useful tool for quantitating β_1- and β_2-adrenoceptors. Eur J Pharmacol 130:137–139

Emorine LJ, Marullo S, Briend-Sutren MM, Patey G, Tate K, Delavier-Klutchko C, Strosberg AD (1989) Molecular characterization of the human beta 3-adrenergic receptor. Science 245:1118–1121

Freund S, Ungerer M, Lohse MJ (1994) A_1 adenosine receptors expressed in CHO-cells couple to adenylyl cyclase and phospholipase C. Naunyn-Schmiedebergs Arch Pharmacol 350:49–56

Frielle T, Collins S, Daniel KW, Caron MG, Lefkowitz RJ, Kobilka BK (1987) Cloning of the cDNA for the human β_1-adrenergic receptor. Proc Natl Acad Sci USA 84:7290–7294

Hoffmann C, Leitz MR, Ober-dorf-Maass S, Lohse MJ, Klotz KN (2004) Comparative pharmacology of human β-adrenergic receptor subtypes – characterization of stably transfected receptors in CHO cells. Naunyn Schmiedbergs Arch Pharmacol 369:151–159

Jakobs KH, Saur W, Schultz G (1976) Reduction of adenylyl cyclase activity in lysates of human platelets by the alpha-adrenergic component of epinephrine. J Cyclic Nucleotide Res 2:381–392

Klotz K-N, Cristalli G, Grifantini M, Vittori S, Lohse MJ (1985) Photoaffinity labeling of A_1-adenosine receptors. J Biol Chem 260:14659–14664

Klotz K-N, Hessling J, Hegler J, Owman C, Kull B, Fredholm BB, Lohse MJ (1998) Comparative pharmacology of human adenosine receptor subtypes – characterization of stably transfected receptors in CHO cells. Naunyn-Schmiedebergs Arch Pharmacol 357:1–9

Lands AM, Arnold A, McAuliffe JP, Luduena FP, Brown TG (1967) Differentiation of receptor systems activated by sympathomimetic amines. Nature (London) 214:597–598

Lefkowitz RJ, Stadel JM, Caron MG (1983) Adenylate cyclase coupled beta-adrenergic receptors: Structure and mechanisms of activation and desensitization. Ann Rev Biochem 52:159–186

McConnell HM, Rice P, Wada GH, Owicki JC, Parce JW (1991) The microphysiometer biosensor. Curr Opin Struct Biol 1:647–652

McConnell HM, Owicki JC, Parce JW, Miller DL, Baxter GT, Wada HG, Pitchford S (1992) The Cytosensor Microphysiometer: biological applications of silicon technology. Science 257:1906–1912

McCrea KE, Hill SJ (1993) Salmeterol, a long acting β-adrenoceptor agonist mediating cyclic AMP accumulation in a neuronal cell line. Br J Pharmacol 110:619–626

Minneman KP, Wolfe BB, Pittman RN, Molinoff PB (1983) β-adrenergic receptor subtypes in rat brain. In: Segawa T (ed) Molecular Pharmacology of Neurotransmitter Receptors. Raven Press, New York

Mukherjee C, Caron MG, Coverstone M, Lefkowitz RJ (1975) Identification of adenylate cyclase-coupled β-adrenergic receptors in frog erythrocytes with (–)-^{3}H-Alprenolol. J Biol Chem 250:4869–4876

Nahorski SR (1981) Identification and significance of beta-adrenoceptor subtypes. TIPS, April 1981:95–98

Nathanson JA (1985) Differential inhibition of beta adrenergic receptors in human and rat ciliary process and heart. J Pharmacol Exp Ther 232:119–126

Niclauss N, Michel-Reher MB, Alewijnse AE, Michel MC (2006) Comparison of three radioligands for the human b-adrenoceptor types. Naunyn-Schmiedebergs Arch Pharmacol 374:99–105

Owicki JC, Parce JW (1992) Biosensors based on the energy metabolism of living cells: The physical chemistry and cell biology of extracellular acidification. Biosensors Bioelectronics 7:255–272

Sarsero D, Molenaar P, Kaumann AJ (1998) Validity of (–)-[^{3}H]-CGP 12177A as radioligand for the putative β_4-adrenoceptor in rat striatum. Br J Pharmacol 123:371–380

Schofield PR, Rhee LM, Peralta EG (1987) Primary structure of the human beta-adrenergic receptor gene. Nucleic Acids Res 15:3636

U'Prichard DC, Bylund DB, Snyder SH (1978) (±)-^{3}H-Epinephrine and (–)-^{3}H-dihydroalprenolol binding to β_1 and β_2 noradrenergic receptors in brain, heart and lung membranes. J Biol Chem 253:5090–5102

A.1.1.8 Adenosine A_1 Receptor Binding

GENERAL CONSIDERATIONS

Adenosine receptors belong to the class of purinoceptors (Burnstock 1972, 1981; Olsson and Pearson 1990). Purinoceptors are divided into two general types on the basis of recognized natural ligands:

P_1 receptors recognize adenosine and AMP and P_2 receptors recognize ATP and AMP. Fredholm et al. (1994), Abbracchio and Burnstock (1994, Jacobson et al. 2000) proposed a nomenclature system which is now widely accepted: two families of P2 purinoceptors, P2X ionotropic ligand-gated ion channel receptors (North 2002) and P2Y metabotropic G-protein-coupled receptors (Costanzi et al. 2004). The nomenclature of seven subtypes of P2X receptors and six subtypes of P2Y receptors has been agreed by the NC-IUPHAR Subcommittee (Burnstock 2001; Alexander et al. 2001; Waitling 2006).

The effects of adenosine are mediated effects through cAMP (Sattin and Rall 1970; VanCalker et al. 1978). It was discovered that adenosine could either inhibit or stimulate the formation of cAMP. The discovery of dual effects on adenylate cyclase led to the proposal of two distinct adenosine receptors referred to as the A_1 and A_2 receptors. The A_1 subtype of adenosine receptor mediates the inhibition of adenylate cyclase; whereas, the A_2 subtype mediates stimulation of adenylate cyclase. The methylxanthines are relatively nonselective inhibitors of adenosine receptor subtypes and their pharmacological properties are thought to be mostly due to antagonism of these receptors.

Comparison of adenosine receptors with other G-protein linked receptors indicates that they comprise a family of G protein coupled receptors that can be grouped by subtypes or by species. Thus, in addition to A_1 and A_2, several authors described A_{1a}, A_{1b}, A_{2a}, A_{2b}, A_3, and A_4 receptors with species dependent differences (Jacobson et al. 1992 1996; Zhou et al. 1992; Linden et al. 1993; Salvatore et al. 1993; Linden et al. 1994; Fredholm et al. 1994; Alexander et al. 2001). The nomenclature and classification of adenosine receptors were published by Fredholm et al. (2001) and Waitling (2006). Klotz (2000) reviewed adenosine receptors and their ligands. The four subtypes of adenosine receptors referred to as A_1, A_{2A}, A_{2B}, and A_3 are members of the superfamily of G-protein-coupled receptors. The most recently discovered member of the adenosine receptor family, the A3 receptor, has a unique pharmacological profile (Salvatore et al. 1993; Avila et al. 2002).

PURPOSE AND RATIONALE

The purpose of this assay is to measure the affinity of test compounds for adenosine (A_1) receptors. Evidence for an A_1 adenosine receptor in the guinea pig atrium was given by Collis (1983). Adenosine plays a physiological role in many systems, including platelet aggregation, lipolysis, steroidogenesis and smooth muscle tone (Daly 1982).The vasodilatory and cardiac depressant effects of adenosine are well known. In addition to cardiovascular effects, adenosine has marked effects in the CNS including depression of electrophysiological activity (Siggins and Schubert 1981), anticonvulsant activity, analgesic properties (Ahlijanian and Takemori 1985) and inhibition of neurotransmitter release (Harms et al. 1979).

The agonist, [^{3}H]cyclohexyladenosine (CHA), has affinity for the A_1 receptor in the nanomolar concentration range and has proven to be a suitable ligand for A_1 receptor assays (Bruns et al. 1980; Bruns et al. 1986). Selective A_1 (Schingnitz et al. 1991) and A_2 antagonists (Shimada et al. 1992; Jacobson et al. 1993) have been described. Adenosine and its nucleotides have not only a cardiovascular but predominantly a cerebral activity (Phillis and Wu 1981; Daly 1982; Fredholm et al. 1982).

PROCEDURE

Reagents

1. a) 0.5 M Tris buffer, pH 7.7
   b) 0.05 M Tris buffer, pH 7.7
2. Adenosine deaminase is obtained from Sigma Chemical Co.
   Adenosine deaminase is added to 0.05 M Tris-HCl buffer, pH 7.7 for final resuspension of the membrane pellet, such that the concentration in the assay is 0.1 U/ml of tissue.
3. Cyclohexyladenosine, N^6-[Adenine-2,8-^{3}H] (specific activity 34 mCi/mmol) is obtained from New England Nuclear.
   For IC_{50} determinations: [^{3}H]CHA is made up to a concentration of 40 nM and 50 µl are added to each tube. This yields a final concentration of 1 nM in the assay.
4. Theophylline is obtained from Regis Chemical Co.
   A 100 mM stock solution is made up in deionized water. 20 µl are added to each of 3 tubes for the de-

termination of nonspecific binding, yielding a 1 mM final concentration in the assay.

5. Test compounds
   For most assays, a 1 mM stock solution is prepared in DMSO and serially diluted, such that the final concentrations in the assay range from 10^{-5} to 10^{-8} M. Seven concentrations are used for each assay. Higher or lower concentrations may be used depending on the potency of the drug.

Tissue Preparation

Male Wistar rats are sacrificed by decapitation. Whole brains minus cerebellum are removed, weighed and homogenized in 10 volumes of ice-cold 0.05 M Tris buffer, pH 7.7. The homogenate is centrifuged at 48,000 *g* for 10 min, the supernatant decanted, the pellet resuspended in the same volume of buffer and centrifuged again as before. The final pellet is resuspended in 0.05 M Tris buffer containing 0.1 U/ml of adenosine deaminase.

Assay

1000 µl	tissue suspension
930 µl	H_2O
20 µl	vehicle
	or theophylline
	or appropriate concentration of test compound
50 µl	^{3}H-CHA

The tubes are incubated for 2 hours at 25°C. The assay is stopped by vacuum filtration through Whatman GF/B filters which are then washed 3 times with 5 ml of 0.05 M Tris buffer. The filters are then placed into scintillation vials with 10 ml liquiscintillation cocktail, left to soak overnight and counted.

EVALUATION

Specific binding is defined as the difference between total binding and binding in the presence of 1 mM theophylline. IC_{50} values are calculated from the percent specific binding at each drug concentration.

The complexity of interaction of adenosine ligands with receptors (Bruns et al. 1986) precludes the simple calculation of K_i values by the Cheng–Prusoff equation.

MODIFICATIONS OF THE METHOD

Stiles et al. (1985) used ^{125}I-labeled N^6-2-(4-aminophenyl)ethyladenosine as a selective ligand to probe the structure of A_1 receptors.

Lohse et al. (1987) described 8-cyclopentyl-1,3-dipropylxanthine (DPCPX) as a high affinity antagonist radioligand for A_1 adenosine receptors.

Klotz et al. (1989) described 2-chloro-N^6-[^{3}H]cyclopentyladenosine ([^{3}H]CCPA) as a high affinity agonist radioligand for A_1 adenosine receptors.

Von Lubitz et al. (1995) studied the therapeutic implications of chronic NMDA receptor stimulation on adenosine A_1 receptors.

The partial agonism of theophylline-7-riboside on the adenosine A_1 receptor has been reported by Ijzerman et al. (1994).

Libert et al. (1992) reported the cloning and functional characterization of a human A_1 adenosine receptor.

REFERENCES AND FURTHER READING

Abbracchio MP, Burnstock G (1994) Purinoceptors: are there families of P2X and P2Y purinoceptors? Pharmacol Ther 64:445–475

Ahlijanian MK, Takemori AE (1985) Effects of (–)-N^6-R-phenylisopropyladenosine (PIA) and caffeine on nociception and morphine-induced analgesia, tolerance and dependence in mice. Eur J Pharmacol 112:171–179

Alexander S, Peters J, Mathie A, MacKenzie G, Smith A (2001) TiPS Nomenclature Supplement 2001

Avila MY, Stone RA, Civan MM (2002) Knockout of A_3 adenosine receptors reduces mouse intraocular pressure. Invest Ophthalmol Vis Sci 43:3021–3026

Bruns RF, Daly JW, Snyder SH (1980) Adenosine receptors in brain membranes: Binding of N^6-cyclohexyl [^{3}H]adenosine and 1,3-diethyl-8-[^{3}H]phenylxanthine. Proc Natl Acad Sci 77:5547–5551

Bruns RF, Lu GH, Pugsley TA (1986) Characterization of the A_2 adenosine receptor labeled by [^{3}H]NECA in rat striatal membranes. Mol Pharmacol 29:331–346

Burnstock G (1972) Purinergic nerves. Pharmacol Rev 24:509–581

Burnstock G (ed) (1981) Purinergic receptors. Receptors and recognition. Chapman & Hall, London, Ser. B, Vol. 12

Burnstock G (2001) Purine-mediated signalling in pain and visceral perception. Trends Pharmacol Sci 22:182–188

Costanzi S, Mamedova L, Gao ZG, Jacobson KA (2004) Architecture of P2Y nucleotide receptors: structural comparison based on sequence analysis, mutagenesis and homology modelling. J Med Chem 47:5393–5404

Daly JW (1982) Adenosine receptors: Targets for future drugs. J Med Chem 25:197–207

Fredholm BB, Jonzon B, Lindgren E, Lindström K (1982) Adenosine receptors mediating cyclic AMP production in the rat hippocampus. J Neurochem 39:165–175

Fredholm BB, Abbracchio MP, Burnstock G, Daly JW, Harden TK, Jacobson KA, Leff P, Williams M (1994) Nomenclature and classification of purinoceptors. Pharmacol Rev 46:143–156

Fredholm BB, Ijzerman AP, Jacobson KA, Klotz KN, Linden J (2001) International Union of Pharmacology. XXV. Nomenclature and classification of adenosine receptors. Pharmacol Rev 53:527–552

Hamilton HW, Taylor MD, Steffen RP, Haleen SJ, Bruns RF (1987) Correlation of adenosine receptor affinities and cardiovascular activity. Life Sci 41:2295–2302

Harms HH, Wardeh G, Mulder AH (1979) Effects of adenosine on depolarization-induced release of various radiolabelled

neurotransmitters from slices of rat corpus striatum. Neuropharmacol 18:577–580
Ijzerman AP, van der Wenden EM, von Frijtag Drabbe Künzel JK, Mathôt RAA, Danhof M, Borea PA, Varani K (1994) Partial agonism of theophylline-7-riboside on adenosine receptors. Naunyn Schmiedeberg's Arch Pharmacol 350:638–645
Jacobson KA (1996) Specific ligands for the adenosine receptor family. Neurotransmissions 12:1–6
Jacobson KA, van Galen PJ, Williams M (1992a) Adenosine receptors: Pharmacology, structure-activity relationships, and therapeutic potential. J Med Chem 35:407–422
Jacobson KA, van Galen PJM, Williams M (1992b) Adenosine receptors: pharmacology, structure-activity relationships, and therapeutic potential. J Med Chem 35:409–422
Jacobson KA, Gallo-Rodriguez C, Melman N, Fischer B, Maillard M, van Bergen A, van Galen P, Karton Y (1993) Structure-activity relationships of 8-styrylxanthines as A_2-selective antagonists. J Med Chem 36:1333–1342
Jacobson KA, King BF, Burnstock GF (2000) Pharmacological characterization of P2 (nucleotide) receptors. Celltransmissions 16:3–16
Klotz KN, Lohse MJ, Schwabe U, Cristalli G, Vittori S, Grifantini M (1989) 2-Chloro-N^6-[^{3}H]cyclopentyladenosine ([^{3}H]CCPA) – a high affinity agonist radioligand for A_1 adenosine receptors. Naunyn-Schmiedeberg's Arch Pharmacol 340:679–683
Klotz KN (2000) Adenosine receptors and their ligands. Naunyn-Schmiedebergs Arch Pharmacol 362:382–391
Libert F, Van Sande J, Lefort A, Czernilofsky A, Dumont JE, Vassart G, Ensinger JA, Mendia KD (1992) Cloning and functional characterization of a human A_1 adenosine receptor. Biochem Biophys Res Commun 187:919–926
Linden J, Taylor HE, Robeva AS, Tucker AL, Stehle JH, Rivkees SA (1993) Molecular cloning and functional expression of a sheep A_3 adenosine receptor with widespread tissue distribution. Mol Pharmacol 44:524–532
Linden J, Jacobson ME, Hutchins C, Williams M (1994) Adenosine receptors. In: Peroutka SJ (ed) Handbook of Receptors and Channels. G Protein Coupled Receptors. CRC Press, Boca Raton, Vol 1, pp 29–44
Lohse MJ, Klotz KN, Lindenborn-Fotinos J, Reddington M, Schwabe U, Olsson RA (1987) 8-Cyclopentyl-1,3-dipropylxanthine (DPCPX) – a high affinity antagonist radioligand for A_1 adenosine receptors. Naunyn-Schmiedeberg's Arch Pharmacol 336:204–210
Murphy KMM, Snyder SH (1982) Heterogeneity of adenosine A_1 receptor binding in brain tissue. Mol Pharmacol 22:250–257
North RA (2002) Molecular physiology of P2X receptors. Physiol Rev 82:1013–1067
Olsson RA, Pearson JC (1990) Cardiovascular purinoceptors. Pharmacol Rev 70:761–845
Phillis JW, Wu PH (1981) The role of adenosine and its nucleotides in central synaptic transmission. Prog Neurobiol 16:178–239
Salvatore CA, Jacobson ME, Taylor HE, Linden J (1993) Molecular cloning and characterization of the human A_3 adenosine receptor. Proc Natl Acad Sci 90:10365–10369
Sattin A, Rall TW (1970) The effect of adenosine and adenine nucleotides on the adenosine 3′, 5′-phosphate content of guinea pig cerebral cortical slices. Mol Pharmacol 6:13–17
Schingnitz G, Küfner-Mühl U, Ensinger H, Lehr E, Kühn FJ (1991) Selective A_1-antagonists for treatment of cognitive deficits. Nucleosides and Nucleotides 10:1067–1076
Schwabe U, Trost T (1980) Characterization of adenosine receptors in rat brain by (–)[^{3}H]N^6-phenylisopropyladenosine. Naunyn Schmiedeberg's Arch Pharmacol 313:179–187
Shimada J, Suzuki F, Nonaka H, Ishii A, Ichikawa S (1992) (*E*)-1,3-Dialkyl-7-methyl-8-(3,4,5-trimethoxystyryl)xanthines: Potent and selective A_2 antagonists. J Med Chem 35:2342–2345
Siggins GR, Schubert P (1981) Adenosine depression of hippocampal neurons *in vitro*: An intracellular study of dose-dependent actions on synaptic and membrane potentials. Neurosci Letters 23:55–60
Stiles GL, Daly DT, Olsson RA (1985) The A_1 receptor. Identification of the binding subunit by photoaffinity crosslinking. J Biol Chem 260:10806–10811
VanCalker D, Müller M, Hamprecht B (1978) Adenosine inhibits the accumulation of cyclic AMP in cultured brain cells. Nature 276:839–841
Von Lubitz DKJE, Kim J, Beenhakker M, Carter MF, Lin RCS, Meshulam Y, Daly JW, Shi D, Zhou LM, Jacobson KA (1995) Chronic NMDA receptor stimulation: therapeutic implications of its effect on adenosine A_1 receptors. Eur J Pharmacol 283:185–192
Waitling KJ (2006) The Sigma RBI handbook of receptor classification and signal transduction, 5th edn. Sigma-Aldrich, St Louis, Mo., pp 86–87, 130–137
Zhou QY, Li C, Olah ME Johnson RA, Stiles GL (1992) Molecular cloning and characterization of an adenosine receptor: The A_3 adenosine receptor. Proc Natl Acad Sci 89:7432–7436

A.1.1.9 Adenosine A_2 Receptor Binding

PURPOSE AND RATIONALE

The A_2 receptor is a low-affinity binding site for adenosine (Daly et al. 1981). Activation of the A_2 receptor subtype by agonists mediates an increase in adenylate cyclase activity, while the A_1 receptor has the opposite effect. Although many of the physiological effects of adenosine seem to correlate with activity at the A_1 receptor, the effect on coronary blood flow correlates with activation of A_2 receptors (Hamilton et al. 1987).

This assay uses ^{3}H-NECA (5′-N-ethylcarboxamido[8-^{3}H]adenosine) to label A_2 receptors in rat striatum by the method described by Bruns et al. (1986). Comparison of data from this assay and the A_1 receptor assay provides a measure of selectivity for these two receptors.

PROCEDURE

Reagents

1. a) 0.5 M Tris buffer, pH 7.7
   b) 0.05 M Tris buffer, pH 7.7
   c) 0.05 M Tris buffer, pH 7.7, containing 12 mM $CaCl_2$ (final assay concentration: 10 mM)
2. Adenosine deaminase is obtained from Sigma Chemical Co.

Adenosine deaminase is added to 0.05 M Tris-HCl buffer, pH 7.7, containing 12 mM $CaCl_2$ for final resuspension of the membrane pellet, such that the concentration in the assay is 0.1 U/ml of tissue.

3. 5′-N-Ethylcarboxamido[8-^{3}H]adenosine (specific activity 23–40 mCi/mmol) is obtained from Amersham.
   For IC_{50} determinations: ^{3}H-NECA is made up to a concentration of 80 nM and 50 µl is added to each tube. This yields a final concentration of 4 nM in the assay.
4. Cyclopentyladenosine (CPA) is obtained from Research Biochemicals Inc.
   A 5 mM stock solution is made up in DMSO. 20 µl are added to each of 3 tubes for the determination of nonspecific binding, yielding a 100 µM final concentration in the assay.
   Since [^{3}H]NECA is not a specific ligand for A_2 receptors, CPA is added to all other tubes to mask the A_1 receptors at a final concentration of 50 nM.
5. Test compounds
   For most assays, a 1 mM stock solution is made up in a suitable solvent and serially diluted, such that the final concentration in the assay ranges from 2×10^{-5} to 2×10^{-8} M. Seven concentrations are used for each assay. Higher or lower concentrations may be used depending on the potency of the drug.

Tissue Preparation

Male Wistar rats are sacrificed by decapitation. Striata are removed, weighed and homogenized in 10 volumes of ice-cold 0.05 M Tris buffer, pH 7.7. The homogenate is centrifuged at 48,000 *g* for 10 min, the supernatant decanted, the pellet resuspended in the same volume of buffer and centrifuged again as before. The final pellet is resuspended in 100 volumes of 0.05 M Tris buffer containing 10 mM $CaCl_2$ and 0.1 U/ml of adenosine deaminase.

Assay

830 µl	tissue suspension
100 µl	CPA
20 µl	vehicle or CPA or appropriate concentration of test compound
50 µl	^{3}H-NECA

The tubes are incubated at 25°C for 2 hours. The assay is stopped by vacuum filtration through Whatman GF/B filters which are then washed 3 times with 5 ml of 0.05 M Tris buffer. The filters are then placed into scintillation vials with 10 ml Liquiscint scintillation cocktail, left to soak overnight and counted.

EVALUATION

Specific binding is defined as the difference between total binding and binding in the presence of 100 µM CPA. IC_{50} values are calculated from the percent specific binding at each drug concentration.

The complexity of interaction of adenosine ligands with receptors precludes the simple calculation of K_i values by the Cheng–Prusoff equation.

MODIFICATIONS OF THE METHOD

Jarvis et al. (1989) reported on [^{3}H]CGS 21 680, a selective A_2 adenosine receptor agonist which directly labels A_2 receptors in rat brain. [^{3}H]CGS 21 680 binding was greatest in striatal membranes with negligible specific binding obtained in rat cortical membranes.

Gurden et al. (1993) described the functional characterization of three adenosine receptor types.

Hutchinson et al. (1990) described 2-(arylalkylamino)adenosin-5′-uronamides as a new class of highly selective adenosine A_2 receptor ligands.

A_{2A} Adenosine receptors from rat striatum and rat pheochromocytoma PC12 cells have been characterized with radioligand binding and by activation of adenylate cyclase (Hide et al. 1992).

Nonaka et al. (1994) reported on KF17837 ((E)-8-(3,4-dimethoxystyryl)-1,3-dipropyl-7-methylxantine), a potent and selective adenosine A_2 receptor antagonist.

The *in vitro* pharmacology of ZM 241385, a potent, non-xanthine, A_{2a} selective adenosine receptor antagonist has been reported by Poucher et al. (1955).

Monopoli et al. (1994) described the pharmacology of the selective $A_{2\alpha}$ adenosine receptor agonist 2-hexynyl-5′-N-ethylcarboxamidoadenosine.

Jacobson et al. (1993) described structure-activity relationships of 8-styrylxanthines as A_2-selective adenosine antagonists.

Varani et al. (1996) reported pharmacological and biochemical characterization of purified A_{2a} adenosine receptors in human platelet membranes by [^{3}H]-CGS 21680 binding.

Van der Ploeg et al. (1996) characterized adenosine A_2 receptors in human T-cell leukemia Jurkat cells and rat phaeochromocytoma PC12 cells using adenosine receptor agonists.

REFERENCES AND FURTHER READING

Bruns RF, Lu GH, Pugsley TA (1986) Characterization of the A_2 adenosine receptor labeled by [^{3}H]NECA in rat striatal membranes. Mol Pharmacol 29:331–346

Daly JW, Bruns RF, Snyder SH (1981) Adenosine receptors in the central nervous system: relationship to the central actions of methylxanthines. Life Sci 28:2083–2097

Gurden MF, Coates J, Ellis F, Evans B, Foster M, Hornby E, Kennedy I, Martin DP, Strong P, Vardey CJ, Wheeldon A (1993) Functional characterization of three adenosine receptor types. Br J Pharmacol 109:693–698

Hamilton HW, Taylor MD, Steffen RP, Haleen SJ, Bruns RF (1987) Correlation of adenosine receptor affinities and cardiovascular activity. Life Sci 41:2295–2302

Hide I, Padgett WL, Jacobson KA, Daly JW (1992) A_{2A} Adenosine receptors from rat striatum and rat pheochromocytoma PC12 cells: Characterization with radioligand binding and by activation of adenylate cyclase. Mol Pharmacol 41:352–359

Hutchinson AJ, Williams M, de Jesus R, Yokoyama R, Oei HH, Ghai GR, Webb RL, Zoganas HC, Stone GA, Jarvis MF (1990) 2-(Arylalkylamino)adenosin-5′-uronamides: a new class of highly selective adenosine A_2 receptor ligands. J Med Chem 33:1919–1924

Jacobson KA, Gallo-Rodriguez C, Melman N, Fischer B, Maillard M, van Bergen A, van Galen PJM, Karton Y (1993) Structure-activity relationships of 8-styrylxanthines as A_2-selective adenosine antagonists. J Med Chem 36:1333–1342

Jarvis MF, Schulz R, Hutchison AJ, Do UH, Sills MA, Williams M (1989) [^{3}H]CGS 21 680, a selective A_2 adenosine receptor agonist directly labels A_2 receptors in rat brain. J Pharm Exp Ther 251:888–893

Monopoli A, Conti A, Zocchi C, Casati C, Volpini R, Cristalli G, Ongini E (1994) Pharmacology of the new selective $A_{2\alpha}$ adenosine receptor agonist 2-hexynyl-5′-N-ethylcarboxamidoadenosine. Arzneim Forsch/Drug Res 44:1296–1304

Nonaka H, Ichimura M, Takeda M, Nonaka Y, Shimada J, Suzuki F, Yamaguchi K, Kase H (1994) KF17837 ((E)-8-(3,4-dimethoxystyryl)-1,3-dipropyl-7-methylxantine), a potent and selective adenosine A_2 receptor antagonist. Eur J Pharmacol Mol Pharmacol Sect 267:335–341

Poucher SM, Keddie JR, Singh P, Stoggall SM, Caulkett PWR, Jones G, Collis MG (1955) The *in vitro* pharmacology of ZM 241385, a potent, non-xanthine, A_{2a} selective adenosine receptor antagonist. Br J Pharmacol 115:1096–1102

Parkinson FE, Fredholm BB (1991) Effects of propentofylline on adenosine A_1 and A_2 receptors and nitrobenzylthioinosine-sensitive nucleoside transporters: quantitative autoradiographic analysis. Eur J Pharmacol 202:361–366

Van der Ploeg I, Ahlberg, Parkinson FE, Olsson RA, Fredholm BB (1996) Functional characterization of adenosine A_2 receptors in Jurkat cells and PC12 cells using adenosine receptor agonists. Naunyn Schmiedebergs Arch Pharmacol 353:250–260

Varani K, Gessi S, Dalpiaz A, Borea PA (1996) Pharmacological and biochemical characterization of purified A_{2a} adenosine receptors in human platelet membranes by [^{3}H]-CGS 21680 binding. Br J Pharmacol 117:1693–1701

A.1.1.10 Adenosine A_3 Receptor Binding

PURPOSE AND RATIONALE

The A_3 adenosine receptor has been cloned and characterized by Zhou et al. (1992). A possible role in reproduction has been discussed. The role of central A_3 adenosine receptors may be the mediation of behavioral depressant effects (Jacobson et al. 1993). The design of selective ligands of A_3 adenosine receptors and the therapeutic concepts including effects on locomotor activity, cardiovascular effects, effects in cerebral ischemia (von Lubitz et al. 1994), in cardiac preconditioning and as antagonists in inflammation and asthma has been discussed by Jacobson et al. (1995). Von Lubitz et al. (1995) noticed some anticonvulsive activity of the adenosine A_3 receptor selective agonist IB-MECA (N^6-(3-iodobenzyl) adenosine-5′-N-methyl-carboxamide). Stimulation of the A_3 adenosine receptor facilitates release of allergic mediators in mast cells (Ramkumar et al. 1993) inducing hypotension in the rat (Hannon et al. 1995). A binding site model and structure-activity relationships for the rat A_3 adenosine receptor are described by van Galen et al. (1994).

PROCEDURE

Cell culture and membrane preparation

Chinese hamster ovary (CHO) cells stably expressing the rat A_3 adenosine receptor are grown in F-12 medium containing 10% fetal bovine serum and penicillin/streptomycin (100 units/ml and 100 µg/ml, respectively) at 37° in a 5% CO_2 atmosphere. When cells reach confluency, they are washed twice with 10 ml of ice-cold lysis buffer (10 mM EDTA, pH 7.4). After addition of 5 ml of lysis buffer, cells are mechanically scraped and homogenized in an ice-cold Dounce homogenizer. The suspension is centrifuged at 43,000 *g* for 10 min. The pellet is suspended in the minimum volume of ice-cold 50 mM Tris/10 mM $MgCl_2$/1 mM EDTA (pH 8.26 at 5°C) buffer required for the binding assay and homogenized in a Dounce homogenizer. Aminodeaminase (ADA, Boehringer Mannheim) is added to a final concentration of 3 units/ml and the suspension is incubated at 37°C for 15 min; the membrane suspension is subsequently kept on ice until use.

Radioligand binding assay

Binding of [^{125}I]APNEA (N^6-2-(4-aminophenyl)-ethyladenosine) to CHO cells stably transfected with the rat A_3 adenosine receptor clone is performed according to Stiles et al. (1985). Assays are performed in 50/10/1 buffer in glass tubes and contain 100 µl of the membrane suspension, 50 µl of inhibitor. Incubations are carried out in duplicate for 1 h at 37°C and are terminated by rapid filtration over Whatman GF/B filters, using a Brandell cell harvester. Tubes are washed three times with 3 ml of buffer. Radioactivity is determined in a Beckman γ -counter. Non-specific binding is determined in the presence of 40 µM R-PIA = N^6-[(R)]-1-methyl-2-phenylethyl]adenosine.

EVALUATION

K_i values are calculated according to Cheng and Prusoff (1973), assuming a K_d for [^{125}I]APNEA of 17 nM.

MODIFICATIONS OF THE METHOD

^{125}I-4-aminobenzyl-5′-N-methylcarboxamidoadenosine has been recommended as a high affinity radioligand for the rat A_3 adenosine receptor (Olah et al. 1994).

Molecular cloning and functional expression of a sheep A_3 adenosine receptor has been reported by Linden et al. (1993).

G protein-dependent activation of phospholipase C by adenosine A_3 receptors in rat brain was reported by Abbracchio et al. (1995).

Molecular cloning and characterization of the human A_3 adenosine receptor was reported by Salvatore et al. (1993).

The differential interaction of the rat A_3 adenosine receptor with multiple G-proteins has been described by Palmer et al. (1995).

Baraldi and Borea (2000) described new potent and selective human adenosine A_3 receptor antagonists using radioligand binding studies to the human A_3 receptor.

REFERENCES AND FURTHER READING

Abbracchio MP, Brambilla R, Ceruti S, Kim HO, von Lubitz DKJE, Jacobson KA, Cattabeni F (1995) G protein-dependent activation of phospholipase C by adenosine A_3 receptors in rat brain. Mol Pharmacol 48:1038–1045

Baraldi PG, Borea PA (2000) New potent and selective human adenosine A_3 receptor antagonists. Trends Pharmacol Sci 21:456–459

Cheng YC, Prusoff WH (1973) Relationship between the inhibition constant (K_i) and the concentration of the inhibitor which causes 50% inhibition (IC_{50}) of an enzyme reaction. Biochem Pharmacol 22:3099–3108

Hannon JP, Pfannkuche HJ, Fozard JR (1995) A role for mast cells in adenosine A_3 receptor-mediated hypotension in the rat. Br J Pharmacol 115:945–952

Jacobson KA, Nikodijevic O, Shi D, Gallo-Rodriguez C, Olah ME, Stiles GR, Daly JW (1993) A role of central A_3 adenosine receptors. Mediation of behavioral depressant effects. FEBS Lett 336:57–60

Jacobson KA, Kim HO, Siddiqi SM, Olah ME, Stiles GL, von Lubitz DKJE (1995) A_3 adenosine receptors: design of selective ligands of and therapeutic concepts. Drugs Future 20:689–699

Linden J, Taylor HE, Robeva AS, Tucker AL, Stehle JH, Rivkees SA (1993) Molecular cloning and functional expression of a sheep A_3 adenosine receptor with widespread tissue distribution. Mol Pharmacol 44:524–552

Olah ME, Gallo-Rodriguez C, Jacobson KA, Stiles GL (1994) ^{125}I-4-aminobenzyl-5′-N-methylcarboxamidoadenosine, a high affinity radioligand for the rat A_3 adenosine receptor. Mol Pharmacol 45:978–982

Palmer TM, Gettys TW, Stiles GL (1995) Differential interaction with and regulation of multiple G-proteins by the rat A_3 adenosine receptor. J Biol Chem 270:16895–16902

Ramkumar V, Stiles GL, Beaven M, Ali H (1993) The A_3 adenosine receptor is the unique adenosine receptor which facilitates release of allergic mediators in mast cells. J Biol Chem 268:16887–16890

Salvatore CA, Jacobson MA, Taylor HE, Linden J, Johnson RG (1993) Molecular cloning and characterization of the human A_3 adenosine receptor. Proc Natl Acad Sci USA 90:10365–10369

Stiles GL, Daly DT, Olsson RA (1985) The adenosine A_1 receptor. Identification of the binding subunit by photoaffinity cross-linking. J Biol Chem 260:10806–10811

van Galen PJM, van Bergen AH, Gallo-Rodriguez C, Melman N, Olah ME, Ijzerman AP, Stiles GL, Jacobson KA (1994) A binding site model and structure-activity relationships for the rat A_3 adenosine receptor. Mol Pharmacol 45:1101–1111

Von Lubitz DKJE, Lin RCS, Popik P, Carter MF, Jacobson KA (1994) Adenosine A_3 receptor stimulation and cerebral ischemia. Eur J Pharmacol 263:59–67

Von Lubitz DKJE, Carter MF, Deutsch SI, Lin RCS, Mastropaolo J, Meshulam Y, Jacobson KA (1995) The effects of adenosine A_3 receptor stimulation on seizures in mice. Eur J Pharmacol 275:23–29

Zhou QY, Li C, Olah ME, Johnson RA, Stiles GL (1992) Molecular cloning and characterization of the adenosine receptor: The A_3 adenosine receptor. Proc Natl Acad Sci USA 89:7432–7336

A.1.1.11 Inhibition of Adenosine Uptake in Human Erythrocytes

PURPOSE AND RATIONALE

Adenosine regulates multiple physiological functions in animals and humans. It plays a potent neuromodulatory role mainly by inhibiting the presynaptic transmitter release, e. g. of glutamate and aspartate. It is released by synaptic stimulation and during hypoxia in the central and peripheral nervous system. Adenosine plays a neuroprotective role in hypoxia and ischemia since it reduces the excessive stimulation of the NMDA receptors. The use of adenosine uptake inhibitors has been proposed as a new therapeutic strategy for hypoxic/ischemic disease. Due to its vasodilatory action adenosine plays a key role in the regulation of coronary and cerebral blood flow. The rapid cellular uptake of adenosine by erythrocytes is a reason for the short duration of action of adenosine.

Human erythrocytes are used as a cellular model to detect adenosine uptake inhibitors. Erythrocytes are treated with test compound and thereafter incubated with ^{3}H-adenosine. The uptake of ^{3}H-adenosine is evaluated in relation to the untreated control group.

Dipyridamole is a potent inhibitor of adenosine uptake (IC_{50} of 3×10^{-7} M).

Standard compounds:

- theophylline
- dipyridamole (Persantin)
- propentofylline (HWA 285)

PROCEDURE

Materials and solutions

isotonic glycyl-glycine buffer, pH 7.4

KCl	5.0 mM
NaCl	119.5 mM
$MgCl_2$	2.0 mM
glycyl-glycine	50 mM
Na_2HPO_4	2.0 mM
2-[^{3}H]-adenosine (specific activity 0.2 μCi/μmol)	5 μM

Buffer-washed fresh human erythrocytes are depleted of ATP by incubation in an isotonic glycyl-glycine buffer at 37°C. Aliquots of the erythrocyte suspensions are incubated for 2 min in fresh glycyl-glycine buffer solution containing additional 10 mM glucose and test- or standard compound. In screening assays, test compounds are added at a concentration of 5×10^{-4} M. Drugs showing an effect in this assays, are further tested at a concentration range of 10^{-5}–5×10^{-4} M to determine IC_{50} values (triplicate samples for each concentration).

The suspension is then incubated with 5 μM radioactively labelled 2-[^{3}H]-adenosine for 30 s. The adenosine uptake is stopped by adding cold buffer (4°C) containing 5 μM adenosine, 10 μM glucose and 7.4 μM dipyridamole. After centrifugation, the tritium radioactivity is determined in the supernatant.

EVALUATION

The percent change of ^{3}H-adenosine uptake relative to the vehicle control group is determined. The ^{3}H-adenosine uptake of the control group is taken as 100%; subsequent results are expressed as percentages of this.

IC_{50} values are determined by plotting the percent inhibition against test compound concentration; IC_{50} is defined as the dose of drug leading to a 50% inhibition of adenosine uptake.

Statistical evaluation is performed by means of the Student's *t*-test.

Standard data:

- IC_{50} of dipyridamole 3×10^{-7} M

MODIFICATIONS OF THE METHOD

Marangos et al. (1982), Verma and Marangos (1985) recommended [^{3}H]nitrobenzylthioinosine binding as a probe for the study of adenosine uptake sites in brain of various species. The highest density of binding sites were found in the caudate and hypothalamus of human and rat brain.

REFERENCES AND FURTHER READING

Bowmer CJ, Yates MS (1989) Therapeutic potential for new selective adenosine receptor ligands and metabolism inhibitors. Trends Pharmacol Sci 10:339–341

Geiger JD, Fyda DM (1991) Adenosine transport in nervous system tissues. In: Stone TW (ed) Adenosine in the Nervous System. Academic Press, London, San Diego, New York, pp 1–23

Marangos PJ, Patel J, Clark-Rosenberg R, Martino AM (1982) [^{3}H]Nitrobenzylthioinosine binding as a probe for the study of adenosine uptake sites in brain. J Neurochem 39:184–191

Porsche E (1982) Effects of methylxanthine derivates on the adenosine uptake in human erythrocytes. IRCS Med Sci 10:389

Rudolphi KA, Schubert P, Parkinson FE, Fredholm BB (1992) Adenosine and brain ischemia. Cerebrovasc Brain Metab Rev 4:346–369

Verma A, Marangos PJ (1985) Nitrobenzylthioinosine binding in brain: an interspecies study. Life Sci 36:283–290

Winn HR, Rubio GR, Berne RM (1981) The role of adenosine in the regulation of cerebral blood flow. J Cerebr Blood Flow Metab 1:239–244

A.1.1.12 Inhibition of Vasopeptidases

GENERAL CONSIDERATIONS

Vasopeptidase inhibitors (VPIs) inhibit both angiotensin converting enzyme (ACE) and neprilysin (NEP) and can thus reduce the activity of the renin-angiotensin system and potentiate the vasodilatory, natriuretic and antiproliferative effects of bradykinin and natriuretic peptides (Burnett 1999; Bralet and Schwartz 2001). Combined inhibition of neutral endopeptidase 24.11 (NEP) and ACE is a candidate therapy for hypertension and cardiac failure (Duncan et al. 1999). Heath et al. (1995) described the quantification of a dual ACE-I-converting enzyme-neutral endopeptidase inhibitor and the active thiol metabolite in dog plasma by high-performance liquid chromatography with ultraviolet absorption detection. Dumoulin et al. (1995) studied the metabolism of bradykinin by the rat coronary vascular bed and found that combined treatment with the ACE inhibitor enalaprilate and the NEP inhibitor retrothiorphan reduced bradykinin degradation to lower values than enalaprilate alone.

Hubner et al. (2001) reported *in-vitro* and *in-vivo* inhibition of rat neutral endopeptidase and ACE with the vasopeptidase inhibitor gemopatrilat. Dumoulin et

al. (2001) compared the effects of a vasopeptidase inhibitor with those of neutral endopeptidase and ACE inhibitors on bradykinin metabolism in the rat coronary bed.

Crackower et al. (2002) described type-2 ACE (ACE2) as an essential regulator of heart function. In three different rat models of hypertension, ACE2 messenger RNA and protein expression were markedly reduced. Targeted disruption of ACE2 in mice resulted in a severe cardiac contractility defect.

REFERENCES AND FURTHER READING

Bralet J, Schwartz J-C (2001) Vasopeptidase inhibitors: an emerging class of cardiovascular drugs. Trends Pharmacol Sci 22:106–109

Burnett JC (1999) Vasopeptidase inhibition: a new concept in blood pressure management. J Hypertens 17 [Suppl 1]:S37–S43

Crackower MA, Sarao R, Oudit GY, Yagil C, Kozieradzki I, Scanga SE, Oliveira-dos-Santos AJ, da Costa J, Zhang L, Pei Y, Scholey J, Ferrario CM, Manoukian AS, Chappell MC, Backx PH, Yagil Y, Penninger JM (2002) Angiotensin-converting enzyme 2 is an essential regulator of heart function. Nature 417:822–828

Dumoulin MJ, Adam A, Blais C Jr, Lamontagne D (1998) Metabolism of bradykinin by the rat coronary vascular bed. Cardiovasc Res 38:229–236

Dumoulin MJ, Adam A, Rouleau JL, Lamontagne D (2001) Comparison of a vasopeptidase inhibitor with neutral endopeptidase and angiotensin-converting enzyme inhibitors on bradykinin metabolism in the rat coronary bed. J Cardiovasc Pharmacol 37:359–366

Duncan AM, James GM, Anastasopoulos F, Kladis A, Briscoe TA, Campbell DJ (1999) Interaction between neutral endopeptidase and angiotensin converting enzyme in rats with myocardial infarction: effects on cardiac hypertrophy and angiotensin and bradykinin peptide levels. J Pharmacol Exp Ther 289:295–303

Heath TG, Massad DD, Carroll JI, Mathews BS, Chang J, Scott DO, Kuo BS, Toren PC (1995) Quantification of a dual angiotensin I-converting enzyme-neutral endopeptidase inhibitor and the active thiol metabolite in dog plasma by high-performance liquid chromatography with ultraviolet absorption detection. J Chromatogr B670:91–101

Hubner RA, Kubota E, Casley DJ, Johnston CI, Burrell LM (2001) In-vitro and in vivo inhibition of rat neutral endopeptidase and angiotensin converting enzyme with the vasopeptidase inhibitor gemopatrilat. J Hypertens 19:941–946

A.1.1.12.1 Inhibition of the Angiotensin-Converting Enzyme in Vitro

PURPOSE AND RATIONALE

An *in vitro* system can be used to screen potential angiotensin-converting enzyme inhibitors. Fluorescence generated by an artificial substrate in presence or absence of the inhibitor is measured to detect inhibitory activity.

PROCEDURE

Reagents

1. 50 mM Tris-HCl buffer, pH 8.0 + 100 mM NaCl
2. 10 mM potassium phosphate buffer, pH 8.3
3. Substrate: O-aminobenzoylglycyl-p-nitro-L-phenylalanyl-L-proline (molecular weight 482) (Bachem Gentec. Inc., Torrance, California, USA)
   a) stock solution: 10 mg substrate in 10 ml 50 mM Tris-HCl buffer, pH 8.0 + 100 mM NaCl
   b) working solution: 2 ml stock solution is added to 18 ml 50 mM Tris-HCl buffer, pH 8.0 + 100 mM NaCl; final concentration in the assay is 170.2 µM.
4. Test compounds
   Compounds are made up to a concentration of 1 mM in 50 mM Tris-HCl buffer, pH 8.0 + 100 mM NaCl or 10% methanol in Tris/NaCl if insoluble in aqueous buffer alone. This will give a final concentration in the assay of 0.1 mM. If inhibition is seen, further dilution in Tris/NaCl should be made.

Enzyme preparation

Lung tissue from 10 rats is diced and homogenized in a blender with 3 pulses of 15 s each. The homogenate is centrifuged at 5000 *g* for 10 min. The pellet is discarded, the supernatant is dialyzed against three 1 liter changes of 10 mM potassium phosphate buffer, pH 8.3 overnight in the cold and then centrifuged at 40,000 *g* for 20 min. The pellet is discarded, 390 mg $(NH_4)_2SO_4$ is added for each ml of supernatant. This will give 60% saturation. The solution is stirred on ice for 15 min. The pellet formed is dissolved in 15 ml potassium phosphate buffer, pH 8.3 and dialyzed against the same buffer overnight in the cold with three 1 liter changes. Some protein will precipitate during dialysis. The suspension is centrifuged at 40,000 *g* for 20 min and the supernatant is discarded. The final solubilized enzyme preparation can be aliquoted and stored at –20°C at least 6 months.

Enzyme inhibition studies

1. Enzyme activity is measured with a Perkin Elmer LS-5 Fluorescence Spectrophotometer or equivalent at an excitation wavelength of 357 nm and an emission wavelength of 424 nm.
2. Enzyme assay
   50 µl vehicle or inhibitor solution and 40 µl enzyme are preincubated for 5 min, then 410 µl substrate working solution is added.

Samples are mixed by drawing fluid back up into the pipette and by pipetting into the cuvette. For the initial

control run of the day, the auto zero is pushed immediately after placing the sample in the cuvette.

EVALUATION

The individual fluorescence slope is measured and % inhibition is calculated as follows:

$$\%\,\text{inhibition} = \%\,\text{inhibition} = \left(100 - \frac{\text{slope in presence of inhibitor}}{\text{control slope}}\right) \times 100$$

Inhibitor concentrations on either side of the IC_{50} should be tested to generate a dose-response curve. The IC_{50} is calculated using Litchfield-Wilcoxon log-probit analysis.

Standard data:

- IC_{50} values for inhibition of angiotensin I-converting enzyme
- Compound IC_{50} [M]
- Captopril 6.9×10^{-9}

MODIFICATIONS OF THE METHOD

Other assays use the cleavage of hippuric acid from tripeptides (Hip-Gly-Gly or Hip-His-Leu) whereby hippuric acid is either tritium labelled or determined spectrophotometrically (Cushman and Cheung 1969, 1971; Friedland and Silverstein 1976; Santos et al. 1985; Hecker et al. 1994).

Bünning (1984) studied the binding and inhibition kinetics of ramipril and ramiprilate (Hoe 498 diacid) with highly purified angiotensin converting enzyme using furanacryloyl-Phe-Gly-Gly as substrate.

The importance of tissue converting enzyme inhibition in addition to inhibition in plasma has been verified in several studies (Unger et al. 1984, 1985; Linz and Schölkens 1987).

Eriksson et al. (2002), Oudit et al. (2003), and Danilczyk et al. (2003, 2004) discussed the role of the homolog of angiotensin-converting enzyme ACE2 in cardiovascular physiology. ACE2 appears to negatively regulate the renin-angiotensin system and cleaves Ang I and Ang II into the inactive Ang 1–9 and Ang 1–7. ACE2 differs in its specificity and physiological role from ACE.

REFERENCES AND FURTHER READING

Bünning P (1984) Inhibition of angiotensin converting enzyme by 2-[N-[(S)-1-carboxy-3-phenylpropyl]-L-alanyl]-(1S,3S,5S)-2-azabicyclo[3.3.0]octane-3-carboxylic acid (Hoe 489 diacid). Arzneim Forsch Drug Res 34:1406–1410

Cushman DW, Cheung HS (1969) A simple substrate for assay of dog lung angiotensin converting enzyme. Fed Proc 28:799

Cushman DW, Cheung HS (1971) Spectrophotometric assay and properties of the angiotensin converting enzyme of rabbit lung. Biochem Pharmacol 20:1637–1648

Danilczyk U, Eriksson U, Crackower MA, Penninger JM (2003) A story of two ACEs. J Mol Med 61:227–234

Danilczyk U, Eriksson U, Oudit GY, Penninger JM (2004) Physiological roles of the angiotensin-converting enzyme 2. Cell Mol Life Sci 61:2714–2719

Dzau VJ, Pratt RE (1986) Renin-angiotensin system: Biology, physiology, and pharmacology. In: Fozzard HA, Haber E, Jennings RB, Katz AM, Morgan MD (eds) The Heart and Cardiovascular System. Vol. 2, Chapter 69, pp 1631–1662. Raven Press New York

Eriksson U, Danilczyk U, Penninger JM (2002) Just the beginning: novel functions for angiotensin-converting enzymes. Curr Biol 12:R745–R7542

Friedland J, Silverstein E (1976) A sensitive fluorimetric assay for serum angiotensin converting enzyme. Am J Clin Path 66:416–424

Hayakari M, Kondo Y, Izumi H (1978) A rapid and simple spectrophotometric assay of angiotensin-converting enzyme. Analyt Biochem 84:361–369

Hecker M, Pörtsi I, Bara AT, Busse R (1994) Potentiation by ACE inhibitors of the dilator response to bradykinin in the coronary microcirculation: interaction at the receptor level. Br J Pharmacol 111:238–244

Linz W, Schölkens BA (1987) Influence of local converting enzyme inhibition on angiotensin and bradykinin effects in ischemic hearts. J Cardiovasc Pharmacol 10 (Suppl 7):S75–S82

Oudit GY, Crackower MA, Backx PH, Penninger JM (2003) The role of ACE2 in cardiovascular physiology. Trends Cardiovasc Med 13:93–1101

Pre J, Bladier D (1983) A rapid and sensitive spectrophotometric method for routine determination of serum angiotensin I converting enzyme activity. IRCS Medical Sci 11:220–221

Santos RAS, Krieger EM, Greene LJ (1985) An improved fluorimetric assay of rat serum and plasma converting enzyme. Hypertension 7:244–252

Unger T, Fleck T, Ganten D, Rettig F (1984) 2-[N-[(S)-1-Ethoxycarbonyl-3-phenylpropyl-L-alanyl]-(1S,3S,5S)-2-azabicyclo[3.3.0]octane-3-carboxylic acid (Hoe 498): antihypertensive action and persistent inhibition of tissue converting enzyme activity in spontaneously hypertensive rats. Arzneim Forsch/Drug Res 34:1426–1430

Unger T, Ganten D, Lang RE, Schölkens BA (1985) Persistent tissue converting enzyme inhibition following chronic treatment with Hoe 498 and MK 421 in spontaneously hypertensive rats. J Cardiovasc Pharmacol 7:36–41

A.1.1.12.2 Inhibition of Neutral Endopeptidase (Neprilysin)

PURPOSE AND RATIONALE

Neutral endopeptidase cleaves various peptides, such as enkephalins, kinins, chemotactic peptide, atrial natriuretic factor, and substance P. Reviews on neutral endopeptidase 24.11 (enkephalinase) were given by Erdös and Skidgel (1989) and by Roques et al. (1993). Structural requirements were investigated by Santos et al. (2002).

Several enzymatic assays have been developed for measuring neutral endopeptidase (NEP) activity, such as radiolabeled methods (Vogel and Altstein 1977; Llorens et al. 1982) and colorimetric assays (Almenoff et al. 1981; Almenoff and Orlowsky 1984); fluorometric assay (Florentin et al. 1984; Goudreau et al. 1994). Burell et al. (1997) and Hubner et al. (2001) used the selective NEP inhibitor radioligand ^{125}I-labelled RB104.

Cavalho et al. (1995, 1996) described a highly selective assay for neutral endopeptidase based on the cleavage of a fluorogenic substrate related to Leu-enkephalin.

PROCEDURE

A recombinant soluble form of NEP (rNEP) was expressed using a baculovirus/insect-cell system and purified by immunoaffinity.

The substrate (10 nmol) was incubated with rNEP (100 ng) in a final volume of 100 µl of 50 mM Tris-HCl buffer, pH 7.4, at 37°C for 30 min. For the inhibition assays, the enzyme was preincubated with 1 µM thiorphan or 1 µM captopril for 20 min before its incubation with the substrate. The reaction was stopped by heating for 5 min at 100°C. After centrifugation at 10,000 *g* for 10 min, the supernatant fraction was injected into an HPLC column and eluted with a 20%–40% gradient of acetonitrile containing 0.05% trifluoroacetic acid over a period of 30 min, at a flow rate of 1 ml/min. The substrate and products, detected by both UV absorbance (220 nm) and fluorescence (λ_{em} = 420 nm, λ_{ex} = 320 nm) with the detectors arranged in series, were collected to identify the cleavage site by amino acid analysis.

EVALUATION

Kinetic parameters for the NEP-catalyzed hydrolysis were determined from the double-reciprocal Lineweaver-Burkq plots.

MODIFICATIONS OF THE METHOD

Sulpizio et al. (2004) described the determination of **NEP activity in tissues** after *in vivo* treatment of rats with ACE inhibitors. After sacrifice of the animals, approximately 250 mg of kidney tissue was homogenized in 6 volumes of 0.1 M KH_2PO_4, pH 8.3, 0.3 M NaCl, and 1 µM $ZnSO_4$, using a Teflon-glass motor-driven pestle. NEP activity was measured by adding 35 µl of homogenate to wells containing 5 µl buffer or 10 phosphoramidon. Next, 10 µl of 2.5 mM *N*-dansyl-D-ala-gly-p-nitro-phe-gly substrate (Florentin et al. 1984) was added to each sample to yield a 0.5 mM final concentration and incubated for 4 min at 37°C. Subsequently, 100 µl of 10% TCA was added and plates were centrifuged to pellet precipitated proteins. Then 50 µl of supernatant was added to 100 µl of 100% ethanol and 50 µl of 1 N NaOH in a black fluorometric plate. After 10 min, plates were read at 590 nm emission, 320 nm excitation in a fluorometer.

Zhang et al. (1994) described an ELISA for the neuropeptide endopeptidase 3.4.24.11 in human serum and leukocytes.

Gros et al. (1989) studied the protection of atrial natriuretic factor against degradation and the diuretic and natriuretic responses after *in vivo* inhibition of enkephalinase (EC 3.4.24.11) by acetorphan. Increased tissue neutral endopeptidase 24.11 activity in spontaneously hypertensive hamsters was reported by Vishwanata et al. (1998). Graf et al. (1998) studied regulation of neutral endopeptidase 24.11 in human vascular smooth muscle cells by glucocorticoids and protein kinase C.

Pham et al. (1992) described the effects of a selective endopeptidase inhibitor on renal function and blood pressure in conscious normotensive Wistar and hypertensive DOCA-salt rats.

NEP is involved in organ systems other than the cardiovascular system, for example the brain and lung.

Ratti et al. (2001) studied the correlation between neutral endopeptidase (NEP) in serum and the degree of bronchial hyperreactivity.

Shirotani et al. (2001) found that neprilysin degrades both amyloid β peptides 1–40 and 1–42 very rapidly and efficiently. Newell et al. (2003) found that thiorphan-induced neprilysin inhibition raises amyloid β levels in rabbit cortex and cerebrospinal fluid.

Facchinetti et al. (2003) described the ontogeny, regional and cellular distribution of metalloprotease neprilysin 2 (**NEP2**) in the rat in comparison with neprilysin and endothelin-converting enzyme-1.

REFERENCES AND FURTHER READING

Almenoff J, Orlowsky M (1984) Biochemical and immunological properties of a membrane-bound brain metalloendopeptidase: comparison with thermolysin-like kidney neutral metalloendopeptidase. J Neurochem 42:151–157

Almenoff J, Wilk S, Orlowsky M (1981) Membrane bound pituitary metalloendopeptidase: apparent identity to enkephalinase. Biochem Biophys Res Commun 102:206–214

Burrell LM, Farina M, Risvanis J, Woollard D, Casely D, Johnston CI (1997) Inhibition of neutral endopeptidase, the degradative enzyme for natriuretic peptides, in rat kidney after oral SCH 42495. Clin Sci (Lond) 93:43–50

Cavalho KM, Boilleau G, Franca MS, Medeiros MA, Camargo AC, Juliano L (1995) A new fluorometric assay for neutral endopeptidase (EC 3.4.24.11). Braz J Med Biol Res 28:1055–1059

Cavalho KM, Boileau G, Camargo ACM, Juliano L (1996) A highly selective assay for neutral endopeptidase based on the cleavage of a fluorogenic substrate related to Leu-enkephalin. Anal Biochem 237:167–173

Erdös EG, Skidgel RA (1989) Neutral endopeptidase 24.11 (enkephalinase) and related regulatory peptide hormones. FASB J 3:145–151

Facchinetti P, Rose C, Schwartz JC, Ouimet T (2003) Ontogeny, regional and cellular distribution of the novel metalloprotease neprilysin 2 in the rat: a comparison with neprilysin and endothelin-converting enzyme-1. Neuroscience 118:627–639

Florentin D, Sassi A, Roques BP (1984) A highly sensitive fluorometric assay for "enkephalinase", a neutral metalloendopeptidase that releases tyrosine-glycine-glycine from enkephalins. Anal Biochem 141:62–69

Goudreau N, Guis C, Soleilhac JM, Roques BP (1994) Dns-gly-(*p*-NO_2)phe-βala, a specific fluorogenic substrate for neutral endopeptidase 24.11. Anal Biochem 219:87–95

Graf K, Schäper C, Gräge M, Fleck E, Kunkel G (1998) Glucocorticoids and protein kinase C regulate neutral endopeptidase 24.11 in human vascular smooth muscle cells. Basic Res Cardiol 93:11–17

Gros C, Souque A, Schwarzt JC, Duchier J, Cournot A, Baumer O, Lecomte JM (1989) Protection of atrial natriuretic factor against degradation: diuretic and natriuretic responses after *in vivo* inhibition of enkephalinase (EC 3.4.24.11) by acetorphan. Proc Natl Acad Sci USA 86:7580–7584

Hubner RA, Kubota E, Casley DJ, Johnston CI, Burrell LM (2001) In-vitro and in vivo inhibition of rat neutral endopeptidase and angiotensin converting enzyme with the vasopetidase inhibitor gemopatrilat. J Hypertens 19:941–946

Llorens C, Malfroy B, Schwartz JC, Gacel G, Roques BP, Morgat JL, Javoy-Agid F, Agid Y (1982) Enkephalin dipeptidyl carboxypeptidase (enkephalinase) activity: selective radioimmunoassay, properties and regional distribution in human brain. J Neurochem 39:1081–1089

Newell AJ, Sue LI, Scott S, Rauschkolb PK, Walker DG, Potter PE, Beach TG (2003) Thiorphan-induced neprilysin inhibition raises amyloid β levels in rabbit cortex and cerebrospinal fluid. Neurosci Lett 350:178–180

Pham I, el Amrani AI, Fournie-Zaluski MC, Corvol P, Roques B, Michel JB (1992) Effects of the selective endopeptidase inhibitor, retrothiophan, on renal function and blood pressure in conscious normotensive Wistar and hypertensive DOCA-salt rats. J Cardiovasc Pharmacol 20:847–857

Ratti H, Zhang M, Kunkel G (2001) Correlation between neutral endopeptidase (NEP) 3.4.24.11 in serum and the degree of bronchial hyperreactivity. Regul Pept 97:181–186

Roques BP, Noble F, Dauge V, Fournie-Zaluski MC, Beaumont A (1993) Neutral endopeptidase 24:11: structure, inhibition, and experimental and clinical pharmacology. Pharamcol Rev 45:87–146

Santos AN, Wulfänger J, Helbing G, Blosz T, Langner J, Riemann D (2002) Two C-terminal cysteines are necessary for proper folding of the peptidase neprilysin/CD10. Biochem Biophys Res Commun 295:423–427

Shirotani K, Tsubuki S, Iwata N, Takaki Y, Harigaya W, Maruyama K, Kiryu-Seo S, Kiyama H, Iwata H, Tomita T, Iwatsubo T, Saido TC (2001) Neprilysin degrades both amyloid β peptides 1–40 and 1–42 most rapidly and efficiently among thiorphan- and phosphoramidon-sensitive endopeptidases. J Biol Chem 276:21895–21901

Sulpizio AC, Pullen MA, Edward RM, Brooks DP (2004) The effect of acute angiotensin-converting enzyme and neutral endopeptidase 24.11 inhibition on plasma extravasation in the rat. J Pharmacol Exp Ther 309:1141–1147

Vishwanata JK, Davis RC, Blumberg S, Gao XP, Rubinstein I (1998) Increased tissue neutral endopeptidase 24.11 activity in spontaneously hypertensive hamsters. Am J Hypertens 11:585–590

Vogel Z, Altstein M (1977) The adsorption of enkephalin to porous polystyrene beads: a simple assay for enkephalin hydrolysis: FEBS Lett 80:332–335

Zhang M, Niehus J, Schnellbacher T, Müller S, Graf K, Schultz KD, Baumgarten CR, Lucas C, Kunkel G (1994) ELISA for the neuropeptide endopeptidase 3.4.24.11 in human serum and leukocytes. Peptides 15:843–848

A.1.1.13 Quantitative Autoradiographic Localization of Angiotensin-Converting Enzyme

PURPOSE AND RATIONALE

Cardiac angiotensin converting enzyme can be quantified in tissue, such as in rat hearts with chronic infarction after left coronary ligation, by computerized *in vitro* autoradiography (Kohzuki et al. 1996)

PROCEDURE

Myocardial infarction is induced in Wistar rats by left coronary artery ligation (see A.3.2.2). After various time intervals (1–8 months) the animals are decapitated, the hearts rapidly removed, and snap-frozen in isopentane at –40°C. Frozen section (20 µm) are cut in a cryostat at –20°C. The sections are thaw-mounted onto gelatin-coated slides, dried in a desiccator for 2 h at 4°C and then stored at –80°C.

Quantitative autoradiography

Radioligand: MK351A is a tyrosyl derivative of lisinopril, a potent competitive inhibitor of ACE. MK351A is iodinated by the chloramine T method and separated free from ^{125}I by SP Sephadex C25 column chromatography.

^{125}I-MK351A binding: The sections are preincubated in 10 mmol/L sodium phosphate buffer, pH 7.4, containing 150 mmol/L NaCl and 2% bovine serum albumin for 15 min at 20°C. The sections are then incubated with 11.1 KBq/ml ^{125}I-MK351A in the same buffer for 60 min at 20°C. Nonspecific binding is determined in the presence of 10^{-6} mol/L MK351A or lisinopril. Binding isotherms are determined using a set of serial sections incubated with 10^{-12}–10^{-6} mol/L lisinopril for 60 min.

After incubation, the sections are rapidly dried under a stream of cold air, placed in X-ray cassettes, and exposed to Agfa Scopix CR3 X-ray film for 12–72 h

at room temperature. After exposure, the sections are fixed in formaldehyde and stained with haematoxylin and eosin. The optical density of the X-ray films is quantified using an imaging device controlled by a personal computer.

EVALUATION

The optical density of the autoradiographs is calibrated in terms of the radioactivity density in dpm/mm^2 with reference standards maintained through the procedure. The apparent binding site concentration (B_{max}) and binding affinity constant (K_A) in all the areas (excluding coronary arteries) of the right ventricle, intraventricular septum, the infarcted area in the left ventricle and the non-infarcted area in the left ventricle are estimated by an iterative non-linear model-fitting computer program LIGAND (Munson and Rodbard 1980).

REFERENCES AND FURTHER READING

Kohzuki M, Johnston CI, Chai SY, Jackson B, Perich R, Paxton D, Mendelson FAO (1991) Measurement of angiotensin converting enzyme induction and inhibition using quantitative *in vitro* autoradiography: tissue selective induction after chronic lisinopril treatment. J Hypertens 9:579–587

Kohzuki M, Kanazawa M, Yoshida K, Kamimoto M, Wu XM, Jiang ZL, Yasujima M Abe K, Johnston CI, Sato T (1996) Cardiac angiotensin converting enzyme and endothelin receptor in rats with chronic myocardial infarction. Jpn Circ J 60:972–980

Mendelsohn FAO, Chai S, Dunbar SY et al (1984) *In vitro* autoradiographic localization of angiotensin-converting enzyme in rat brain using ^{125}I-labelled MK351A. J Hypertens 2, Suppl 3:41–44

Munson PJ, Rodbard D (1980) LIGAND, a versatile computerized approach for characterization of ligand-binding systems. Anal Biochem 107:220–239

A.1.1.14 Angiotensin Antagonism

The renin-angiotensin-aldosterone hormonal axis is the major long-term control for regulation of both arterial blood pressure and sodium balance. It supports normotension or hypertension via angiotensin vasoconstriction and angiotensin plus aldosterone-induced renal sodium retention (Laragh 1993; Unger and Schölkens 2004).

Volpe et al. (1995) Wagner et al. (1996) showed that regulation of aldosterone biosynthesis by adrenal renin is mediated through AT_1 receptors in renin transgenic rats.

Easthope and Jarvis (2002) reviewed pharmacological, pharmacokinetic and clinical data on the angiotensin II antagonist candesartan cilexetil.

REFERENCES AND FURTHER READING

Easthope SE, Jarvis B (2002) Candesartan Cilexetil. An update of its use in essential hypertension. Drugs 62:1253–1287

Laragh JH (1993) The renin system and new understanding of the complications of hypertension and their treatment. Arzneim Forsch/Drug Res 43:247–254

Unger T, Schölkens BA (eds) (2004) Angiotensin. Handbook of experimental pharmacology, Vol 1 (548 pp) and Vol II (603 pp). Springer, Berlin Heidelberg New York, p 163Volpe M, Rubattu S, Gigante B, Ganten D, Porcellini A, Russo R, Romano M, Enea E, Lee MA, Trimarco B (1995) Regulation of aldosterone biosynthesis by adrenal renin is mediated through AT_1 receptors in renin transgenic rats. Circ Res 77:73–79

Wagner J, Thile F, Ganten D (1996) The renin-angiotensin system in transgenic rats. Pediatr Nephrol 10:108–112

A.1.1.14.1 Angiotensin II Receptor Binding

PURPOSE AND RATIONALE

Angiotensin II receptor subtypes, AT_1 and AT_2, have been identified by structurally dissimilar antagonists, by different distribution in organs of various species and with specific radioligands (Chiu et al. 1989, 1990, 1992, 1993; Chang and Lotti 1991; Gibson et al. 1991; Chansel et al. 1992; Steckelings et al. 1992; Aiyar et al. 1993; Barnes et al. 1993; Bossé et al. 1993; Bottari et al. 1993; Dzau et al. 1993; Feuillan et al. 1993; van Meel et al. 1993; Alexander et al. 2001). These two types of receptors have been cloned (Sasaki et al. 1991; Murphy et al. 1991; Mukoyama et al. 1993; Kambayashi et al. 1993). Two other mammalian receptors named AT_3 and AT_4 have been described (de Gasparo et al. 1998).

The functional correlates of angiotensin II receptors have been discussed by Timmermans et al. (1992, 1993; Bernstein and Berk 1993). Most effects of angiotensin are mediated via the AT_1 receptors, but a possible role of angiotensin II subtype AT_2 receptors in endothelial cells and isolated ischemic rat hearts has been suggested (Wiemer et al. 1993a, b). Clearance studies in dogs indicated that the angiotensin type 2 receptor may be related to water handling in the kidney (Keiser et al. 1992).

Evidence for AT_1 receptor subtypes (AT_{1A} and AT_{1B}) has been reported (Iwai and Inagami 1992; Kakar et al. 1992; Balmforth et al. 1994; Matsubara et al. 1994; Bauer and Reams 1995; de Gasparo et al. 1998).

Chai et al. (2004) described the properties of the angiotensin IV/AT_4 receptor.

The assay described below is used to determine the affinity of test compounds to the angiotensin II receptor by measuring their inhibitory activity on the bind-

ing of ^{3}H-angiotensin II to a plasma membrane preparation from rat or bovine adrenal cortex.

PROCEDURE

Fresh bovine adrenal glands are obtained from the local slaughter house. For rat adrenal glands, male Sprague-Dawley rats weighing 250–300 g are sacrificed. The adrenals are separated from fat tissue and the medullae removed. The cortices are minced and homogenized in 5 mM Tris buffer containing 1 mM $MgCl_2$ and 250 mM sucrose, pH 7.4, using a chilled Potter homogenizer. The homogenate is centrifuged at 3000 *g* and 4°C for 10 min. The supernatant is recentrifuged at 39,000 *g* and 4°C for 10 min. The pellets are resuspended in 75 mM Tris buffer containing 25 mM $MgCl_2$, pH 7.4, and recentrifuged twice at 39,000 *g* and 4°C for 10 min. After the last centrifugation, the pellets are suspended in 75 mM Tris buffer containing 25 mM $MgCl_2$ and 250 mM sucrose, pH 7.4. Samples of 0.5 ml are frozen in liquid nitrogen and stored at –70°C.

In the competition experiment, 50 µl ^{3}H-angiotensin II (one constant concentration of $0.5–1 \times 10^{-9}$ M), and 50 µl test compound (6 concentrations, $10^{-5}–10^{-10}$ M) and 100 µl membrane suspension from rat or bovine adrenal cortex (approx. 250 mg wet weight/ml) per sample are incubated in a bath shaker at 25°C for 60 min. The incubation buffer contains 50 mM HEPES, 0.1 mM EDTA, 100 mM NaCl, 5 mM $MgCl_2$ and 0.2% bovine serum albumin, pH 7.4.

Saturation experiments are performed with 12 concentrations of ^{3}H-angiotensin II ($15–0.007 \times 10^{-9}$ M). Total binding is determined in the presence of incubation buffer, non-specific binding is determined in the presence of non-labeled angiotensin II (10^{-6} M).

The reaction is stopped by rapid vacuum filtration through glass fiber filters. Thereby the membrane-bound radioactivity is separated from the free one. The retained membrane-bound radioactivity on the filter is measured after addition of 3 ml liquid scintillation cocktail per sample in a liquid scintillation counter.

EVALUATION OF RESULTS

The following parameters are calculated:

- total binding of ^{3}H-angiotensin II
- non-specific binding: binding of ^{3}H-angiotensin II in the presence of mepyramine or doxepine
- specific binding = total binding–non-specific binding
- % inhibition of ^{3}H-angiotensin II binding: 100–specific binding as percentage of control value

The dissociation constant (K_i) and the IC_{50} value of the test drug are determined from the competition experiment of ^{3}H-angiotensin II versus non-labeled drug by a computer-supported analysis of the binding data (McPherson 1985).

MODIFICATIONS OF THE METHOD

Olins et al. (1993) performed competition studies in rat uterine smooth muscle membranes and rat adrenal cortex membranes using [^{125}I] labeled angiotensin II.

Membranes from cultured rat aortic smooth muscle cells and from human myometrium were used for binding studies with [^{125}I] labeled angiotensin II by Criscone et al. (1993).

Wiener et al. (1993) used membrane preparations from rat lung and adrenal medulla for binding studies with [^{125}I] labeled angiotensin II.

Bradbury et al. (1993) used a guinea pig adrenal membrane preparation to study nonpeptide angiotensin II receptor antagonists.

Cazaubon et al. (1993) prepared purified plasma membranes from rat livers for [^{125}I] AII binding assays.

Noda et al. (1993) described the inhibition of rabbit aorta angiotensin II (AII) receptor by a non-peptide AII antagonist.

Kushida et al. (1995) tested AT II receptor binding in particulate fractions of rat mesenteric artery and rat adrenal cortex and medulla with ^{125}I-AT II.

Chang et al. (1995) used rabbit aorta, rat adrenal and human AT_1 receptors in CHO cells and AT_2 receptors from rat adrenal and brain to characterize a non-peptide angiotensin antagonist.

Aiyar et al. (1995) tested inhibition of [^{125}I]-angiotensin II or [^{125}I]angiotensin II (Sar^1,Ile^8) binding in various membrane and cell preparations, such as rat mesenteric artery, rat adrenal cortex, rat aortic smooth muscle cell, human liver, recombinant human AT_1 receptor, bovine cerebellum, and bovine ovary.

Caussade et al. (1995) tested [^{125}I]Sar^1,Ile^8-angiotensin II binding to rat adrenal membranes and rat aortic smooth muscle cells.

Using [^{125}I]Sar^1,Ile^8-angiotensin II as radioligand, de Gasparo and Whitebread (1995) compared the affinity constants of valsartan and losartan in liver and adrenal of rat and marmoset, human adrenal and in rat aortic smooth muscle cells.

Webb et al. (1993) transfected the vascular angiotensin II receptor cDNA (AT_{1A}) into Chinese hamster ovary cells to generate the stable cell line CHO-AT_{1A} and recommended these cells as a useful model

to study AT_{1A} receptor domains, which are critical to signaling pathways.

Kiyama et al. (1995) used COS cells transfected with a cDNA encoding a human AT_1 angiotensin II receptor to evaluate nonpeptide angiotensin II receptor antagonists.

Mizuno et al. (1995) used bovine adrenal cortical membranes, Nozawa et al. (1997) membrane fractions from rat aorta, bovine cerebellum and human myocardium and [^{125}I]angiotensin II as radioligand.

Renzetti et al. (1995a, b) used membranes from rat adrenal cortex and bovine cerebellum for binding assays with [^{3}H]angiotensin II as radioligand.

Inter-species differences in angiotensin AT_1 receptors were investigated by Kawano et al. (1998).

The angiotensin II receptor subtype having a high affinity for lorsatan has been designated angiotensin AT_1 receptor and the receptor having a high affinity for PD123177 (1-(3-methyl-4-aminophenyl) methyl-5-diphenylacetyl-4,5,6,7-tetrahydro-1H-imidazo[3,5-c]pyridine-6-carboxylic acid) as angiotensin AT_2 receptor (Bumpus et al. 1991; Nozawa et al. 1994; Chang et al. 1995).

In order to determine affinity for the angiotensin AT_1 subtype in a radioligand binding assay with ^{125}I-sarcosine^1, isoleucine^8 angiotensin II, Chang and Lotti (1991), Chang et al. 1995), Wong et al. (1995) incubated membranes of tissues with both AT_1 and AT_2 receptors in the presence of 1 μM PD121981 (which occupied all the AT_2 binding sites) and for the angiotensin AT_2 subtype in the presence of 1 μM lorsatan (which occupied all the AT_1 binding sites).

Hilditch et al. (1995) used membranes from rat livers and [^{3}H]-AT II for the determination of binding affinity at AT_1 receptors, or membranes from bovine cerebellum and [^{125}I]-Tyr^4-AT II for AT_2 receptors.

Lu et al. (1995) studied the influence of freezing on the binding of ^{125}I-sarcosine^1, isoleucine^8 angiotensin II to angiotensin II receptor subtypes in the rat. The results suggested that studies of AII receptor subtypes that involve freezing of the tissue underestimate the density and affinity of the AT_1 receptor subtype.

REFERENCES AND FURTHER READING

Aiyar N, Griffin E, Shu A, Heys R, Bergsma DJ, Weinstock J, Edwards R (1993) Characterization of [^{3}H]SK&F 108655 as a radioligand for angiotensin type-1 receptor. J Recept Res 13:849–861

Aiyar N, Baker E, Vickery-Clark L, Ohlstein EH, Gellai M, Fredrickson TA, Brooks DP, Weinstock J, Weidley EF, Edwards RM (1995) Pharmacology of a potent long-acting imidazole-5-acrylic acid angiotensin AT_1 receptor antagonist. Eur J Pharmacol 283:63–72

Alexander S, Peters J, Mathie A, MacKenzie G, Smith A (2001) TiPS Nomenclature Supplement 2001

Balmforth AJ, Bryson SE, Aylett AJ, Warburton B, Ball SG, Pun KT, Middlemiss D, Drew GM (1994) Comparative pharmacology of recombinant AT_{1A}, AT_{1B} and human AT_1 receptors expressed by transfected COS-M6 cells. Br J Pharmacol 112:277–281

Barnes JM, Steward LJ, Barber PC, Barner NM (1993) Identification and characterization of angiotensin II receptor subtypes in human brain. Eur J Pharmacol 230:251–258

Bauer JH, Reams GP (1995) The angiotensin II Type 1 receptor antagonists. A new class of antihypertensive drugs

Bernstein KE, Berk BC (1993) The biology of angiotensin II receptors. Am J Kidney Dis 22:745–754

Bossé R, Servant G, Zhou LM, Boulay G, Guillemette G, Escher E (1993) Sar^1-p-Benzoylphenylalanine-angiotensin, a new photoaffinity probe for selective labeling of the type 2 angiotensin receptor. Regul Peptides 44:215.223

Bottari SP, de Gasparo M, Steckelings UM, Levens NR (1993) Angiotensin II receptor subtypes: characterization, signalling mechanisms, and possible physiological implications. Front Neuroendocrin 14:123–171

Bradbury RH, Allott CP, Dennis M, Girdwood JA, Kenny PW, Major JS, Oldham AA, Ratcliffe AH, Rivett JE, Roberts DA, Robins PJ (1993) New nonpeptide angiotensin II receptor antagonists. 3. Synthesis, biological properties, and structure-activity relationships of 2-alkyl-4-(biphenylmethoxy)pyridine derivatives. J Med Chem 36:1245–1254

Bürgisser E, Raine AEG, Erne P, Kamber B, Bühler FR (1985) Human cardiac plasma concentrations of atrial natriuretic peptide quantified by radioreceptor assay. Biochem Biophys Res Comm 133:1201–1209

Caussade F, Virone-Oddos A, Delchambre C, Cazes M, Versigny A, Cloarec A (1995) *In vitro* pharmacological characterization of UP 269–6, a novel nonpeptide angiotensin II receptor antagonist. Fundam Clin Pharmacol 9:119–128

Cazaubon C, Gougat J, Bousquet F, Guiraudou P, Gayraud R, Lacour C, Roccon A, Galindo G, Barthelmy G, Gautret B, Bernhart C, Perreaut P, Breliere JC, le Fur G, Nisato D (1993) Pharmacological characterization of SR 47436, a new non-peptide AT_1 subtype angiotensin II receptor antagonist. J Pharmacol Exp Ther 265:826–834

Chai S, Fernando R, Peck G, Ye S, Mendelson F, Jenkins T, Albiston A (2004) What's new in the renin-angiotensin system? The angiotensin IV/AT_4 receptor. Cell Mol Life Sci 61:2728–2737

Chang RSL, Lotti VJ (1991) Angiotensin receptor subtypes in rat, rabbit and monkey tissues: relative distribution and species dependency. Life Sci 49:1485–1490

Chang RSL, Lotti VJ, Chen TB, O'Malley SS, Bedensky RJ, Kling PJ, Kivlighn SD, Siegl PKS, Ondeyka D, Greenlee WJ, Mantlo NB (1995) *In vitro* pharmacology of an angiotensin AT_1 receptor antagonist with balanced affinity for AT_2 receptors. Eur J Pharmacol 294:429–437

Chansel D, Czekalski S, Pham P, Ardaillou R (1992) Characterization of angiotensin II receptor subtypes in human glomeruli and mesangial cells. Am J Physiol 262:F432–F441

Chiu AT, Herblin WF, McCall DE, Ardecky RJ, Carini DJ, Duncia JV, Pease LJ, Wong PC, Wexler RR, Johnson AL, Timmermans PBMWM (1989) Identification of angiotensin II receptor subtypes. Biochem Biophys Res Commun 165:196–203

Chiu AT, McCall DE, Ardecky RJ, Duncia JV, Nguyen TT, Timmermans PBMWM (1990) Angiotensin II receptor

subtypes and their selective nonpeptide ligands. Receptor 1:33–40

Chiu AT, Carini DJ, Duncia JV, Leung KH, McCall DE, Price WA, Wong PC, Smith RD, Wexler RR, Timmermans PBMWM (1991) DuP 532: A second generation of nonpeptide angiotensin II receptor antagonists. Biochem Biophys Res Comm 177:209–217

Chiu AT, McCall DE, Roscoe WA (1992) [^{125}I]EXP985: a highly potent and specific nonpeptide radioligand for the AT_1 angiotensin receptor. Biochem Biophys Res Commun 188:1030–1039

Chiu AT, Leung KH, Smith RD, Timmermans PBMWM (1993) Defining angiotensin receptor subtypes. In: Raizada MK, Phillips MI, Sumners C (eds) Cellular and Molecular Biology of the Renin-Angiotensin System. CRC Press, Boca Raton, pp 245–271

Criscione L, de Gasparo M, Bühlmayer P, Whitebread S, Ramjoué HPR, Wood J (1993) Pharmacological profile of valsartan: a potent, orally active, nonpeptide antagonist of angiotensin II AT_1-receptor subtype. Br J Pharmacol 110:761–771

Cox HM, Munday KA, Poat JA (1984) Inactivation of [^{125}I]angiotensin II binding sites in rat renal cortex epithelial membranes by dithiothreitol. Biochem Pharmacol 33:4057–4062

De Gasparo M, Whitebread S (1995) Binding of valsartan to mammalian angiotensin AT_1 receptors. Regul Peptides 59:303–311

De Gasparo M, Catt KJ, Inagami T (1998) Angiotensin receptors. In: Girdlestone D (ed) The IUPHAR Compendium of Receptor Characterization and Classification. IUPHAR Media, London, pp 80–86

Dzau VJ, Sasamura H, Hein L (1993) Heterogeneity of angiotensin synthetic pathways and receptor subtypes: Physiological and pharmacological implications. J Hypertens 11:S13–S18

Entzeroth M, Hadamovsky S (1991) Angiotensin II receptors in the rat lung are of the AII-1 subtype. Eur J Pharmacol Mol Pharmacol Sec 206:237–241

Feuillan PP, Millan MA, Aguilera G (1993) Angiotensin II binding sites in the rat fetus: characterization of receptor subtypes and interaction with guanyl nucleotides. Regul Peptides 44:159–169

Gibson RE, Thorpe HH, Cartwright ME, Frank JD, Schorn TW, Bunting PB, Siegl PKS (1991) Angiotensin II receptor subtypes in renal cortex of rats and monkeys. Am J Physiol 261:F512

Hilditch A, Hunt AAE, Travers A, Polley J, Drew GM, Middlemiss D, Judd DB, Ross BC, Robertson MJ (1995) Pharmacological effects of GR138950, a novel angiotensin AT_1 receptor antagonist. J Pharm Exp Ther 272:750–757

Iwai N, Inagami T (1992) Identification of two subtypes in the rat type1 angiotensin II receptor. FEBS Lett 298:257–260

Kakar SS, Sellers JC, Devor DC, Musgrove LC, Neill JD (1992) Angiotensin II type-1 receptor subtype cDNAs: Differential tissue expression and hormonal regulation. Biochem Biophys Res Commun 183:1090–1096

Kambayashi Y, Bardhan S, Takahashi K, Tsuzuki S, Inui H, Hamakubo T, Inagami T (1993) Molecular cloning of a novel angiotensin II receptor isoform involved in phosphotyrosine phosphatase inhibition. J Biol Chem 268:24543–24546

Kawano KI, Fujishima K, Nagura J, Yasoda S, Shinki, Hachisu M, Konno F (1998) Nonpeptide angiotensin receptor antagonist recognizes inter-species differences in angiotensin AT_1 receptors. Eur J Pharmacol 357:33–39

Keiser JA, Bjork FA, Hodges JC, Taylor DG (1992) Renal hemodynamic and excretory responses to PD123319 and losartan, nonapeptide AT_1 and AT_2 subtype-specific angiotensin II ligands. J Pharm Exp Ther 262:1154–1160

Kiyama R, Hayashi K, Hara M, Fujimoto M, Kawabata T, Kawakami M, Nakajima S, Fujishita T (1995) Synthesis and evaluation of novel pyrazolo[1,5-a]pyrimidine derivatives as non-peptide angiotensin II receptor antagonists. Chem Pharm Bull 43:960–965

Kushida H, Nomura S, Morita O, Harasawa Y, Suzuki M, Nakano M, Ozawa K, Kunihara M (1995) Pharmacological characterization of the nonpeptide angiotensin II receptor antagonist, U-97018. J Pharmacol Exp Ther 274:1042–1053

Lu XY, Zhang W, Grove KL, Speth RC (1995) Influence of freezing on the binding of ^{125}I-sarcosine^{1}, isoleucine^{8} angiotensin II to angiotensin II receptor subtypes in the rat. J Pharmacol Toxicol Meth 33:83–90

McPherson GA (1985) Analysis of radioligand binding experiments. A collection of computer programs for the IBM PC. J Pharmacol Meth 14:213–228

Matsubara H, Kanasaki M, Murasawa S, Tsukaguchi Y, Nio Y, Inada M (1994) Differential gene expression and regulation of angiotensin receptor subtypes in rat cardiac fibroblasts an cardiomyocytes in culture. J Clin Invest 93:1592–1601

Mizuno M, Sada T, Ikeda M, Fukuda N, Miyamoto M, Yanagisawa H, Koike H (1995) Pharmacology of CS-866, a novel nonpeptide angiotensin II receptor antagonist. Eur J Pharmacol 285:181–188

Mukoyama M, Nakajima M, Horiuchi M, Sasamura H, Pratt RE, Dzau VJ (1993) Expression cloning of type-2 angiotensin II receptor reveals a unique class of seven-transmembrane receptors. J Biol Chem 268:24539–24542

Murphy TJ, Alexander RW, Griendling KK, Runge MS, Bernstein KE (1991) Isolation of a cDNA encoding the vascular type-1 angiotensin II receptor. Nature 351:233–236

Noda M, Shibouta Y, Inada Y, Ojima M, Wada T, Sanada T, Kubo K, Kohara Y, Naka T, Nishikawa K (1993) Inhibition of rabbit aorta angiotensin II (AII) receptor by CV-11974, a new nonpeptide AII antagonist. Biochem Pharmacol 46:311–318

Nozawa Y, Haruno A, Oda N, Yamasaki Y, Matsuura N, Yamada S, Inabe K, Kimura R, Suzuki H, Hoshino T (1994) Angiotensin II receptor subtypes in bovine and human ventricular myocardium. J Pharmacol Exp Ther 270:566–571

Nozawa Y, Haruno A, Oda N, Yamasaki Y, Matsuura N, Miyake H, Yamada S, Kimura R (1997) Pharmacological profile of TH-142177, a novel orally active AT_1-receptor antagonist. Fundam Clin Pharmacol 11:395–401

Olins GM, Corpus VM, Chen ST, McMahon EG, Paloma MA, McGraw DE, Smits GJ, Null CL, Brown MA, Bittner SE, Koepke JB, Blehm DJ, Schuh JR, Baierl CS, Schmidt RE, Cook CS, Reitz DB, Penick MA, Manning RE, Blaine EH (1993) Pharmacology of SC-52458, an orally active, nonpeptide angiotensin AT_1 receptor antagonist. J Cardiovasc Pharmacol 22:617–625

Renzetti AR, Criscuoli M, Salimbeni A, Subissi A (1995a) Molecular pharmacology of LR-B/081, e new non-peptide angiotensin AT_1 receptor antagonist. Eur J Pharmacol Mol Pharmacol Sect 290:151–156

Renzetti AR, Cucchi P, Guelfi M, Cirillo R, Salimbeni A, Subissi A, Giachetti A (1995b) Pharmacology of LR-B/057, a novel active AT_1 receptor antagonist. J Cardiovasc Pharmacol 25:354–360

Robertson MJ, Barnes JC, Drew GM, Clark KL, Marshall FH, Michel A, Middlemiss D, Ross BC, Scopes D, Dowle MD (1992) Pharmacological profile of GR117289 *in vitro*:

a novel, potent and specific non-peptide angiotensin AT_1 receptor antagonist. Br J Pharmacol 107:1173–1180
Sasaki K, Yamono Y, Bardhan S, Iwai N, Murray JJ, Hasegawa M, Matsuda Y, Inagami T (1991) Cloning and expression of a complementary DANN encoding a bovine adrenal angiotensin II type-1 receptor. Nature 351:230–233
Steckelings UM, Bottari SP, Unger T (1992) Angiotensin receptor subtypes in the brain. TIPS 13:365–368
Timmermans PBMWM, Benfield P, Chiu AT, Herblin WF, Wong PC, Smith RD (1992) Angiotensin II receptors and functional correlates. Am J Hypertens 5:221S–235S
Timmermans PBMWM, Wong PC, Chiu AT, Herblin WF, Benfield P, Carini DJ, Lee PJ, Wexler RR, Saye JAM, Smith RD (1993) Angiotensin receptors and angiotensin receptor antagonists. Pharmacol Rev 45:205–251
van Meel JCA, Entzeroth M, Hauel N, Narr B, Ries U, Wienen W (1993) Angiotensin II receptor antagonists. Arzneim Forsch/Drug Res 43:242–246
Webb ML, Monshizadegan H, Dickinson KE, Serafino R, Moreland S, Michel I, Seiler SM, Murphy TJ (1993) Binding and signal transduction of the vascular angiotensin II (AT_{1A}) receptor cDNA stably expressed in Chinese hamster cells. Regul Pept 44:131–139
Wiemer G, Schölkens BA, Busse R, Wagner A, Heitsch H, Linz W (1993b) The functional role of angiotensin II-subtype AT_2 receptors in endothelial cells and isolated ischemic rat hearts. Pharm Pharmacol Lett 3:24–27
Wiemer G, Schölkens BA, Wagner A, Heitsch H, Linz W (1993a) The possible role of angiotensin II subtype AT_2 receptors in endothelial cells and isolated ischemic rat hearts. J Hypertens 11, Suppl 5:S234–S235
Wienen W, Hauel N, van Meel JCA, Narr B, Ries U, Entzeroth M (1993) Pharmacological characterization of the novel nonpeptide angiotensin II receptor antagonist, BIBR 277. Br J Pharmacol 110:245–252
Wong PC, Quan ML, Saye JAM, Bernard R, Crain EJ Jr, NcCall DE, Watson CA, Zaspel AM, Smith RD, Wexler RR, Timmermans PBMWM, Chiu AT (1995) Pharmacology of XR510, a potent orally active nonpeptide angiotensin II AT_1 receptor antagonist with high affinity to the AT_2 receptor subtype. J Cardiovasc Pharmacol 26:354–362

A.1.1.14.2 AT_2 Receptor Binding

PURPOSE AND RATIONALE

In addition to the AT_1 receptor, the AT_2 receptor has attracted increasing interest (Gallinat et al. 2000; Nouet and Nahmias 2000). Steckelings et al. (2005) reviewed the knowledge of AT2 receptor distribution, signaling and function with an emphasis on growth/anti-growth, differentiation, and the regeneration of neuronal tissue.

Wan et al. (2004a, 2004b) described a porcine myometrial membrane AT_2 receptor assay.

PROCEDURE

Myometrial membranes are prepared from porcine uteri. Nielsen et al. (1997) found that in myometrium from non-pregnant sows, the Ang II receptors were almost exclusively AT_2 receptors. A presumable interference by binding to AT_1 receptors was blocked by addition of 1 µM losartan. Binding of [^{125}I]Ang II to membranes was conducted in a final volume of 0.5 ml containing 50 mM Tris-HCl (pH 7.4), 100 mM NaCl, 10 mM $MgCl_2$, 1 mM EDTA, 0.025% bacitracin, 0.2% BSA, homogenate corresponding to 10 mg of the original tissue weight, [^{125}I]Ang II (80,000–85,000 cpm, 0.03 nM), and variable concentration of test substance. Samples were incubated at 25°C for 1.5 h, and binding was terminated by filtration through Whatman GF/B glass-fiber filter sheets, which had been pre-soaked overnight with 0.3% polyethylamine, using a Brandel cell harvester. The filters were washed with 3 × 3 ml of Tris-HCl (pH 7.4) and transferred to tubes. The radioactivity was measured in a γ-counter. All determinations were performed in triplicate.

EVALUATION

The characteristics of the Ang-II-binding AT_2 receptor were determined by using six different concentrations (0.03–5 nmol/l) of the labeled [^{125}I]-Ang II. Non-specific binding was determined in the presence of 1 µM Ang II. The specific binding was determined by subtracting the non-specific binding from the total bound [^{125}I]-Ang II. IC_{50} was determined by Scatchard analysis of data obtained with Ang II by using GraFit (Erithacus Software, UK).

MODIFICATIONS OF THE METHOD

Whitebread et al. (1991) described the radioligand CGP 42112A as a high-affinity and highly selective ligand for the characterization of angiotensin AT_2 receptors. Heemskerk and Saavedra (1995) performed quantitative autoradiography of Ang II AT_2 receptors with [^{125}I]CGP 42112.

Heerding et al. (1997) performed mutational analysis of the Ang II type 2 receptor in order to study the contribution of conserved extracellular amino acids.

Hoe et al. (2003) reported the molecular cloning, characterization, and distribution of the gerbil Ang II AT_2 receptor.

Utsunomiya et al. (2005) described Ang II AT_2 receptor localization in cardiovascular tissues by its antibody developed in AT_2 gene-deleted mice.

REFERENCES AND FURTHER READING

Gallinat S, Busche S, Raizada MK, Summers C (2000) The angiotensin II type 2 receptor: an enigma with multiple variation. Am J Physiol 278:E357–E374
Heemskerk FJM, Saavedra JM (1995) Quantitative autoradiography of angiotensin II AT_2 receptors with [^{125}I]CGP 42112. Brain Res 677:29–38
Heerding JN, Yee DK, Jacobs SL, Fluharty SJ (1997) Mutational analysis of the angiotensin II type 2 receptor: contri-

bution of conserved extracellular amino acids. Regul Pept 72:97–103
Hoe KL, Armando I, Baiardi G, Sreenath T, Kulkarni A, Martínez A, Saavedra JM (2003) Molecular cloning, characterization, and distribution of the gerbil angiotensin II AT_2 receptor. Am J Physiol 285:R1373–R1383
Nielsen AH, Schauser K, Winther H, Dantzer V, Poulsen K (1997) Angiotensin II receptors and renin in the porcine uterus: myometrial AT2 and endometrial AT1 receptors are down-regulated during gestation. Clin Exp Pharmacol Physiol 24:309–314
Nouet S, Nahmias C (2000) Signal transduction from the angiotensin II AT_2 receptor. Trends Endocrinol Metab 11:1–6
Steckelings UM, Kaschira E, Unger T (2005) The AT2 receptor – A matter of love and hate. Peptides 26:1401–1409
Utsunomiya H, Nakamura M, Kakudo K, Inagami T, Tamura M (2005) Angiotensin II AT_2 receptor localization in cardiovascular tissues by its antibody developed in AT_2 gene-deleted mice. Regul Pept 126:155–161
Wan Y, Wallinder C, Johansson B, Holm M, Mahalingam AK, Wu X, Botros M, Karlén A, Pettersson A, Nyberg F, Fändriks L, Hallberg A, Alterman M (2004a) First reported nonpeptide AT_1 receptor agonist (L-162,313) acts as an AT_2 receptor agonist in vivo. J Med Chem 47:1536–1540
Wan Y, Wallinder C, Plouffe B, Beaudry H, Mahalingam AK, Wu X, Johansson B, Holm M, Botros M, Karlén A, Pettersson A, Nyberg F, Fändriks L, Gallo-Payer N, Hallberg A, Alterman M (2004b) Design, synthesis and biological evaluation of the first selective nonpeptide AT_2 receptor agonist. J Med Chem 47:5995–6008
Whitebread SE, Taylor V, Bottari SP, Kamber B, de Gasparo M (1991) Radioligand CGP 42112A: a novel high affinity and highly selective ligand for the characterization of angiotensin AT_a receptors. Biochem Biophys Res Commun 181:1365–1371

A.1.1.14.3 Angiotensin II Induced Contraction in Isolated Rabbit Aorta

PURPOSE AND RATIONALE

The isolated rabbit aorta has been used to evaluate angiotensin II agonists (Liu 1993) and angiotensin II antagonists (Chang et al. 1992, 1994; Noda et al. 1993; Aiyar et al. 1995; Cirillo et al. 1995; Kushida et al. 1995; Mochizuki et al. 1995; Renzetti et al. 1995; Wong et al. 1995; Hong et al. 1998; Kawano et al. 1998).

PROCEDURE

New Zealand White male rabbits weighing 2–3 kg are sacrificed and exsanguinated. The thoracic aorta is removed and cleaned from adherent fat and connective tissue. The vascular endothelium is removed by gently rubbing the intimal surface of the vessel. Spiral aortic strips (2–3 mm wide and 30 mm long) are prepared and mounted in 5 ml organ baths containing Krebs-Henseleit solution (120 mM NaCl, 4.7 mM KCl, 4.7 mM $MgSO_4$, 1.2 mM KH_2PO_4, 2.5 mM $CaCl_2$, 25 mM $NaHCO_3$, glucose 10 mM, pH 7.4). The organ baths are kept at 37°C and gassed continuously with 95% O_2/5% CO_2. Strips are attached to isometric transducers connected to a polygraph and a resting tension of 1 g is applied to each strip. Changes in contraction are analyzed with a digital computer. Aortic strips are allowed to equilibrate for 1 h and washed every 15 min. Two consecutive contractile-response curves to cumulative addition of ATII (0.1–300 mM) are constructed. After each curve the strips are washed 4 times and allowed to relax to the baseline tension. Afterward, each strip is incubated for 30 min with the vehicle or with a single concentration of the antagonist (1 – 10 – 100 – 1000 mM) before a third concentration-response curve to angiotensin II is obtained.

EVALUATION

The result of each concentration is expressed as a percentage of maximum response to AII. The pA_2 and pD'_2 values are calculated (van Rossum 1963).

MODIFICATIONS OF THE METHOD

Isolated guinea pig aortas were used by Mizuno et al. (1995).

Cirillo et al. (1995) evaluated the antagonism against AII-induced vasoconstriction in rat isolated perfused kidney.

Chang et al. (1992, 1994) determined AII-induced aldosterone release in rat adrenal cells and AII-induced [^{3}H]inositol phosphate accumulation in cultured rat aorta smooth muscle cells.

Shibouta et al. (1993) described the pharmacological profile of a highly potent and long-acting Ang II receptor antagonist and its prodrug.

Ojima et al. (1997) studied the mechanisms of the insurmountable antagonism of candesartan, an angiotensin AT_1 receptor antagonist, on Ang-II-induced rabbit aortic contraction in contraction and binding studies.

REFERENCES AND FURTHER READING

Aiyar N, Baker E, Vickery-Clark L, Ohlstein EH, Gellai M, Fredrickson TA, Brooks DP, Weinstock J, Weidley EF, Edwards EM (1995) Pharmacology of a potent long-acting imidazole-5-acrylic acid angiotensin AT_1 receptor antagonist. Eur J Pharmacol 283:63–72
Chang RLS, Siegl PKS, Clineschmidt BV, Mantlo NB, Chakravarty PK, Greenlee WJ, Patchett AA, Lotti VJ (1992) *In vitro* pharmacology of L-158,809, a new highly potent and selective angiotensin II receptor antagonist. J Pharmacol Exp Ther 262:133–138
Chang RSL, Bendesky RJ, Chen TB, Faust KA, Kling PJ, O'Malley SA, Naylor EM, Chakravarty PK, Patchett AA,

Greenlee WJ, Clineschmidt BV, Lotti VJ (1994) *In vitro* pharmacology of MK-996, a new potent and selective angiotensin II (AT_1) receptor antagonist. Drug Dev Res 32:161–171

Cirillo R, Renzetti AR, Cucchi P, Guelfi M, Salimbeni A, Caliari S, Castellucci A, Evangeklista S, Subissi A, Giachetti A (1995) Pharmacology of LR-B/081, a new highly potent, selective and orally active, nonpeptide angiotensin II AT_1 receptor antagonist. Br J Pharmacol 114:1117–1124

Hong KW, Kim CD, Lee SH, Yoo SE (1998) The *in vitro* pharmacological profile of KR31080, a nonpeptide AT_1 receptor antagonist. Fundam Clin Pharmacol 12:64–69

Kawano KI, Fujishima K, Nagura J, Yasuda S, Hachisu SM, Konno F (1998) Nonpeptide angiotensin II receptor antagonist recognized inter-species differences in angiotensin AT_1 receptors. Eur J Pharmacol 357:33–39

Kushida H, Nomura S, Morita O, Harasawa Y, Suzuki M, Nakano M, Ozawa K, Kunihara M (1995) Pharmacological characterization of the nonpeptide angiotensin II receptor antagonist, U-97018. J Pharmacol Exp Ther 274:1042–1053

Liu YJ (1993) Evidence that [Sar^1]angiotensin II behaves differently from angiotensin II at angiotensin AT_1 receptors in rabbit aorta. Eur J Pharmacol 235:9–15

Mizuno M, Sada T, Ikeda M, Fukuda N, Miyamoto M, Yanikasawa H, Koike H (1995) Pharmacology of CS-866, a novel nonpeptide angiotensin II receptor antagonist. Eur J Pharmacol 285:181–188

Mochizuki S, Sato T, Furuta K, Hase K, Ohkura Y, Fukai C, Kosakai K, Wakabayashi S, Tomiyama A (1995) Pharmacological properties of KT3–671, a novel nonpeptide angiotensin receptor antagonist. J Cardiovasc Pharmacol 25:22–29

Noda M, Shibouta Y, Inada Y, Ojima M, Wada T, Sanada T, Kubo K, Kohara Y, Naka T, Nishikawa K (1993) Inhibition of rabbit aortic angiotensin II (AII) receptor by CV-1197, a new nonpeptide AII antagonist. Biochem Pharmacol 46:311–318

Ojima M, Inada Y, Shibouta Y, Wada T, Sanada T, Kubo K, Nishikawa K (1997) Candesartan (CV-11974) dissociates slowly from the angiotensin AT_1 receptor. Eur J Pharmacol 319:137–146

Renzetti AR, Cucchi P, Guelfi M, Cirillo R, Salimbeni A, Subissi A, Giachetti A (1995) Pharmacology of LR-B/057, a novel orally active AT_1 receptor antagonist. J Cardiovasc Pharmacol 25:354–360

Shibouta Y, Inada Y, Ojima M, Wada T, Noda M, Sanada T, Kubo K, Kohara Y, Naka T, Nishikawa K (1993) Pharmacological profile of a highly potent and long-acting angiotensin II receptor antagonist, 2-ethoxy-1-[[2′-(1H-tetrazol-5-yl)biphenyl-4- yl]methyl]-1H-benzimidazole-7-carboxylic acid (CV-11974), and its prodrug, (+/-)-1-(cyclohexyloxycarbonyloxy)-ethyl 2-ethoxy-1-[[2′-(1H-tetrazol-5- yl)biphenyl-4-yl]methyl]-1H-benzimidazole-7-carboxylate (TCV-116). J Pharm Exp Ther 266:114–120

Van Rossum JM (1963) Cumulative dose-response curves. II. Techniques for the making of dose-response curves in isolated organs and evaluation of drug parameters. Arch Int Pharmacodyn 143:299–330

Wong PC, Quan ML, Saye JM, Bernard R, Crain EJ Jr, McCall DE, Watson CA, Zaspel AM, Smith RD, Wexler RR, Timmermans PBMVM, Chiu AT (1995) Pharmacology of XR510, a potent orally active nonpeptide angiotensin II AT_1 receptor antagonist with high affinity for the AT_2 receptor subtype. J Cardiovasc Pharmacol 26:354–362

A.1.1.14.4 Angiotensin II Antagonism in Vivo

PURPOSE AND RATIONALE

The effect of ATII antagonists on blood pressure has been measured in anesthetized (Olins et al. 1993; Beauchamp et al. 1995; Kawano et al. 1998), in pithed (Cazes et al. 1995; Christophe et al. 1995; Cirillo et al. 1995; Deprez et al. 1995; Häuser et al. 1998) and in conscious (Junggren et al. 1996; Nozawa et al. 1997; Shibasaki et al. 1997; Hashimoto et al. 1998) normotensive and hypertensive rats.

PROCEDURE

Male Sprague-Dawley rats are anesthetized with 100 mg/kg i.p. Inactin and placed on servo-controlled heating pads to maintain body temperature between 37°C and 38°C. PE50 catheters are implanted in the femoral artery and vein to measure arterial blood pressure and administer compounds, respectively. A catheter is placed in the trachea to ensure airway patency. Arterial pressure is measured continuously by connecting the arterial catheter to transducer coupled to a Gould pressure transducer. The output is recorded on a polygraph. Mean arterial pressure is derived electronically. After a 30–45 min stabilization period, autonomic transmission is blocked by treatment with mecamylamine (3 mg/kg i.v.) and atropine (0.4 mg/kg i.v.). After arterial pressure has stabilized, angiotensin is infused i.v. in isotonic saline with a syringe pump. When the pressure response to angiotensin has stabilized, angiotensin II antagonists are given in increasing doses. The doses are given intravenously in a cumulative fashion, i. e., the next highest dose is given at the time of maximum response to the prior dose.

EVALUATION

Data are presented as percent inhibition of the angiotensin pressor response to each dose of the antagonists and plotted against the log of the cumulative doses of antagonist. Linear regression is used to calculate the dose at which the response to angiotensin is inhibited 50% (ID_{50}) for each rat. Means ±SEM are calculated.

MODIFICATIONS OF THE METHOD

Olins et al. (1993), Cirillo et al. (1995) determined also the antihypertensive effects in conscious spontaneously hypertensive rats and in conscious sodium-deficient dogs.

Stasch et al. (1997) studied the long-term blockade of the angiotensin II receptor in renin trangenic rats, salt-loaded Dahl rats, and stroke-prone spontaneously hypertensive rats.

Nishioka et al. (1998), Richter et al. (1998) used the (mRen-2)27 transgenic (Tg^+) rat, a hypertensive model dependent on increased expression of the renin angiotensin system, to explore the role of angiotensin AT_2 receptors in the control of cardiovascular and renal excretory function.

Simoes e Silva et al. (1998) evaluated the effects of chronic administration of an angiotensin antagonist on diuresis and natriuresis in normotensive and spontaneously hypertensive rats.

Kai et al. (1998) examined the effects of an angiotensin II type 1 antagonist on cardiac hypertrophy and nephropathy using Tsukuba hypertensive mice (THM) carrying both human renin and angiotensinogen genes.

Kivlighn et al. (1995a, b), Gabel et al. (1995), studied angiotensin II antagonists in conscious rats, dogs, rhesus monkeys and chimpancees.

Keiser et al. (1995) studied arterial blood pressure in conscious renal hypertensive rats, conscious sodium-depleted dogs, conscious sodium-depleted monkeys and conscious renal hypertensive monkeys.

Kim et al. (1997) examined the effects of an angiotensin AT_1 receptor antagonist on volume overload-induced cardiac gene expression in rats. Cardiac volume overload was prepared by abdominal aortocaval shunt. Cardiac tissue mRNA was measured by Northern blot analysis with specific probes.

Yamamoto et al. (1997), Ogilvie et al. (1998), studied angiotensin II receptor antagonists in acute heart failure induced by coronary artery ligation in anesthetized dogs and in chronic heart failure induced by left ventricular rapid-pacing in conscious dogs.

Massart et al. (1998) evaluated the cumulative hypotensive effects of angiotensin II- and endothelin-1-receptor antagonists in a model renovascular hypertension in dogs.

Hayashi et al. (1997) examined the hemodynamic effects of an angiotensin II type 1 receptor antagonist in rats with myocardial infarction induced by coronary ligation.

Kivlighn et al. (1995c) studied the effects of a nonpeptide that mimics the biological actions of angiotensin II in anesthetized rats.

Huckle et al. (1996) evaluated angiotensin II receptor antagonists for their ability to inhibit vascular intimal thickening in a porcine coronary artery model of vascular injury.

REFERENCES AND FURTHER READING

Beauchamp HT, Chang RSL, Siegl PKS, Gibson RE (1995) *In vivo* receptor occupancy of the angiotensin II receptor by nonpeptide antagonists: relationships to *in vitro* affinities and *in vivo* pharmacologic potency. J Pharmacol Exp Ther 272:612–618

Cazes M, Provost D, Versigny A, Cloarec A (1995) *In vivo* pharmacological characterization of UP 269–6, a novel nonpeptide angiotensin II receptor antagonist. Eur J Pharmacol 284:157–170

Christophe B, Libon R, Cazaubon C, Nisato D, Manning A, Chatelain B (1995) Effects of irbesartan (SR 47436/BMS-186295) on angiotensin II-induced pressor responses in the pithed rat: Potential mechanisms of action. Eur J Pharmacol 281:161–171

Cirillo R, Renzetti AR, Cucchi P, Guelfi M, Salimbeni A, Caliari S, Castellucci A, Evangelista S, Subissi A, Giachetti A (1995) Pharmacology of LR-B/081, a new highly potent, selective and orally active, nonpeptide angiotensin II AT_1 receptor antagonist. Br J Pharmacol 114:1117–1124

Deprez P, Guillaume J, Becker R, Corbier A, Didierlaurent S, Fortin M, Frechet D, Hamon G, Heckmann B, Heitsch H, Kleemann HW, Vevert JP, Vincent JC, Wagner A, Zhang J (1995) Sulfonylureas and sulfonycarbamates as new nontetrazole angiotensin II antagonists. Discovery of a highly potent orally active (imidazolylbiphenylyl)-sulfonylurea (HR 720). J Med Chem 38:2357–2377

Gabel RA, Kivlighn SD, Zingara GJ, Schorn TW, Schaffer LW, Ashton WT, Chang LL, Flanagan K Greenlee WJ, Siegl PKS (1995) *In vivo* pharmacology of L-159,913, a new highly potent and selective nonpeptide angiotensin II receptor antagonist. Clin Exp Hypertens 17:931–953

Häuser W, Denhofer A, Nguyen T, Dominiak P (1998) Effects of the AT1 antagonist HR 720 in comparison to losartan on stimulated sympathetic outflow, blood pressure, and heart rate in pithed spontaneously hypertensive rats. Kidney Blood Press Res 21:29–35

Hashimoto Y, Ohashi R, Kurosawa Y, Minami K, Kaji H, Hayashida K, Narita H, Murata S (1998) Pharmacologic profile of TA-606, a novel angiotensin II receptor antagonist in the rat. J Cardiovasc Pharmacol 31:568–575

Hayashi N, Fujimura Y, Yamamoto S, Kometani M, Nakao K (1997) Pharmacological profile of valsartan, a non-peptide angiotensin II type 1 receptor antagonist. 4th communication: Improvement of heart failure of rats with myocardial infarction by valsartan. Arzneim Forsch/Drug Res 47:625–629

Huckle WR, Drag MD, Acker WR, Powers M, McFall RC, Holder DJ, Fujita T, Stabilito II, Kim D, Ondeyka DL, Mantlo NB, Chang RSL, Reilly CF, Schwartz RS, Greenlee WJ, Johnson RG Jr (1996) Effects of subtype-selective and balanced angiotensin II receptor antagonists in a porcine coronary artery model of vascular restenosis. Circulation 93:1009–1019

Junggren IL, Zhao X, Sun X, Hedner T (1996) Comparative cardiovascular effects of the angiotensin II type 1 receptor antagonists ZD 7155 and losartan in the rat. J Pharm Pharmacol 48:829–833

Kai T, Sigimura K, Shimada S, Kurooka A, Takenaka T, Ishikawa K (1998) Inhibitory effects of a subdepressor dose of I-158,809, an angiotensin II type 1 antagonist, on cardiac hypertrophy and nephropathy via the activated human renin-angiotensin system in double transgenic mice with hypertension. Jpn Circ J 62:599–603

Kawano KI, Fujishima K, Nagura J, Yasuda S, Hachisu SM, Konno F (1998) Nonpeptide angiotensin II receptor an-

tagonist recognized inter-species differences in angiotensin AT_1 receptors. Eur J Pharmacol 357:33–39
Keiser JA, Ryan MJ, Panek RL, Hodges JC, Sircar I (1995) Pharmacological characterization of CI-996, a new angiotensin receptor antagonist. J Pharmacol Exp Ther 272:963–969
Kim S, Sada T, Mizuno M, Ikeda M, Yano M, Miura K, Yamanaka S, Koike H, Iwao H (1997) Effects of angiotensin AT_1 receptor antagonist on volume overload-induced cardiac gene expression in rats. Hypertens Res Clin Exp 20:133–142
Kivlighn SD, Zingaro GJ, Gabel RA, Broten TP, Schorn TW, SchafferLW, Naylor EM, Chakravaty PK, Patchett AA, Greenlee WJ, Siegl PKS (1995a) *In vivo* pharmacology of an novel AT_1 selective angiotensin antagonist, MK-996. Am J Hypertens 8:58–66
Kivlighn SD, Zingaro GJ, Gabel RA, Broten TP, Chang RSL, Ondeyka DL, Mantlo NB, Gibson RE, Greenlee WJ, Siegl PKS (1995b) *In vivo* pharmacology of an angiotensin AT_1 receptor antagonist with balanced affinity for angiotensin AT_2 receptors. Eur J Pharmacol 294:439–450
Kivlighn SD, Huckle WR, Zingaro GJ, Rivero RA, Lotti VJ, Chang RSL, Schorn TW, Kevin N, Johnson RG Jr, Greenlee WJ, Siegl PKS (1995) Discovery of L-162,313: a nonpeptide that mimics the biological actions of angiotensin II. Am J Physiol 286, Regul Integr Comp Physiol 37:R820–R823
Massart PE, Hodeige DG, van Mechelen H, Charlier AA, Ketelslegers JM, Heyndrickx GR, Donckier JE (1998) Angiotensin II and endothelin-1 receptor antagonists have cumulative hypotensive effects in canine Page hypertension. J Hypertens 16:835–841
Nishioaak T, Morris M, Li P, Ganten D, Ferrario CM, Callahan MF (1998) Depressor role of angiotensin AT_2 receptors in the (mRen-2)27 transgenic rat. Am J Hypertens 11:357–362
Nozawa Y, Haruno A, Oda N, Yamasaki Y, Matsuura N, Miyaka H, Yamada S, Kimura R (1997) Pharmacological profile of TH-142177, a novel orally active AT_1 receptor antagonist. Fundam Clin Pharmacol 11:395–401
Ogilvie RI, Zborowska-Sluis D (1998) Captopril and angiotensin II receptor agonist therapy in a pacing model of heart failure. Can J Cardiol 14:1025–1033
Olins GM, Smits GJ, Koepke JP, Huang HC, Reitz DB, Manning RE, Blaine EH (1993) *In vivo* pharmacology of SC-51316, a nonpeptidic angiotensin II receptor antagonist. Am J Hypertens 6:619–625
Richter C, Bruneval P, Menard J, Giudicelli JF (1998) Additive effects of enalapril and losartan in (mREN-2)27 transgenic rats. Hypertension 31:692–698
Shibasaki M, Fujimori A, Kusayama T, Tokioka T, Satoh Y, Okazaki T, Uchida W, Inagaki O, Yanagisawa I (1997) Antihypertensive activity of a nonpeptide angiotensin II receptor antagonist, YM358, in rats and dogs. Eur J Pharmacol 335:175–184
Simoes e Silva AC, Bello APC, Baracho NCV, Khosla MC, Santos RAS (1998) Diuresis and natriuresis produced by long term administration of a selective angiotensin-(1–7) antagonist in normotensive and hypertensive rats. Regul Pept 74:177–184
Stasch JP, Knorr A, Hirth-Dietrich C, Kramer T, Hubsch W, Dressel J, Fey P, Beuck M, Sander E, Frobel K, Kazda S (1997) Long-term blockade of the angiotensin II receptor in renin transgenic rats, salt-loaded Dahl rats, and stroke-prone spontaneously hypertensive rats. Arzneim Forsch/Drug Res 47:1016–1023
Yamamoto S, Hayashi N, Kometani M, Nakao K (1997) Pharmacological profile of valsartan, a non-peptide angiotensin II type 1 receptor antagonist. 5th communication: Hemodynamic effects of valsartan in dog heart failure models. Arzneim Forsch/Drug Res 47:630–634

A.1.1.15
Renin-Inhibitory Activity Using Human Kidney Renin and a Synthetic Substrate

PURPOSE AND RATIONALE

In contrast to other enzymes, renin shows a rather high species specificity. To be relevant for humans human renin has to be used. One of the reasons that human renin is specific for human angiotensinogen lies in the sequence of human angiotensinogen itself. Inhibition of renin is measured by angiotensinogen formed in the presence of angiotensinase inhibitors. The following procedure is used to determine the effect of potential renin inhibitors on purified human kidney renin without interference from plasma proteins or lipids.

PROCEDURE

The synthetic substrate represents the first fourteen amino acids of the N-terminus of human angiotensinogen: Asp-Arg-Val-Tyr-Ile-His-Pro-Phe-His-Leu-Val-Ile-His-Asn. The assay mixture is composed of phosphate buffer (pH 7.5), bovine serum albumin, 3 mM EDTA, 0.01 mM phenylmethylsulfonyl fluoride (PMSF), 0.002% Genapol PF 10, test compound (dissolved in DMSO), substrate (3 µM) and purified human kidney renin (Calbiochem GmbH, Frankfurt/M., Germany; cat. no. 553861). The mixture is incubated for two hours at 37°C. Then the reaction is stopped by transfer of 450 µl into preheated (95°C) Eppendorf tubes. The amount of angiotensin I liberated is measured by RIA (Renin MAIA kit, Serono Diagnostika GmbH, Freiburg, Germany).

Human angiotensinogen (0.2 µM) may be used as a substrate instead of the tetradekapeptide. The pH value of the incubation mixture may be lowered to 6.0 by using a maleic acid buffer; this results in higher renin activity. HEPES (N-2-hydroxyethylpiperazine-N′-2-ethane sulfonic acid) may be substituted for phosphate in the pH 7.5 buffer.

EVALUATION

Renin activity, i. e. angiotensin I production (ng/ml × 2 h), is corrected for an angiotensin I – like immunoreactivity which can be measured in the assay samples even in the absence of added renin. IC_{50} values are determined from a plot of renin activity (as per cent of control) vs. molar concentration of the test compound.

MODIFICATIONS OF THE METHOD

Wang et al. (1993) described a continuous fluorescence assay of renin activity employing a new fluorigenic peptide substrate.

Inhibition of plasma renin activity in blood samples from various species can be determined in order to evaluate the species specificity of a renin inhibitor (Linz et al. 1994)

Blood samples are obtained from dogs, sheep and rhesus monkeys by venipuncture. Wistar rats and guinea pigs are anesthetized with Nembutal (60 mg/kg intraperitoneally) and the blood is collected by puncture of the abdominal aorta. Human blood is collected from volunteers (Donafix blood collecting set, Braun Melsungen AG, Melsungen, FR Germany) in cooled bottles. All blood samples are anticoagulated with Na-EDTA (final concentration 10–15 mM). The renin is dissolved in DMSO as 10^{-2} M stock solution and diluted before each experiment in DMSO. The endogenous formation of ANG I in plasma during incubation at 37°C is determined as the measure of renin activity. Generation and quantitation of ANG I are performed using a commercial radio immunoassay kit (Renin-MAIA, Serono Diagnostika GmbH, Freiburg, FR Germany). Plasma samples are thawed on ice and centrifuged after addition of 100 µl PMSF solution (kit) per 10 ml. The assay mixture contains 450 µl plasma plus 1% (v/v) PMSF solution, 45 µl buffer (phosphate buffer, pH = 7.4, + 10^{-5} M ramiprilate) and 5 µl renin inhibitor solution (diluted in DMSO as required) or pure DMSO for controls. The assay is incubated for an appropriate time (2–3 hours) at 37°C. ANG I is measured in 100 µl samples (triplicate determinations). Basal ANG I immunoreactivity of the plasma is determined from an unincubated control assay (0°C). This pre-incubation value is subtracted from all measurements. The renin activity in the presence of the renin inhibitor is calculated as percent activity in relation to control samples containing only DMSO. The IC_{50} value is determined from a semilogarithmic plot of percent renin activity versus concentration of the renin inhibitor.

Wood et al. (1990) determined the activity of a synthetic renin inhibitor against rat, mouse, dog, guinea pig, rabbit, cat, marmoset and human renin using plasma pools from these species. Plasma from each species was collected using EDTA as an anticoagulant. Samples of plasma were incubated at 37°C in the presence or absence of varying concentrations of test compound. The ANG I formed was measured by radioimmunoassay.

Shibasaki et al. (1991) used squirrel monkeys to study the *in vivo* activity of a specific renin inhibitor after intravenous and oral application.

Bohlender et al. (1996) reconstructed the human renin-angiotensin system in transgenic rats overexpressing the human angiotensin gene TGR(hOGEN) 1623 by chronically injecting human recombinant renin intravenously using Alzet pumps.

Salimbeni et al. (1996) tested the *in vitro* inhibition of human plasma renin activity by two synthetic angiotensinogen transition state analogues.

Wood et al. (2003) determined the inhibitory potency of an orally effective renin inhibitor *in vitro* against human renin. Human recombinant renin (0.33 ng/ml) was incubated with a synthetic tetradecapeptide substrate (TDP, 13.33 µM) corresponding to the 14 terminal amino acids of human angiotensinogen, in 0.33 M Tes buffer, pH 7.2, containing 1% human serum albumin and 0.1% neomycin sulphate for 1 h at 37°C. The enzymatic reaction was stopped by adding 1 ml ice-cold 0.1 M Tris-acetate buffer, pH 7.4, containing 0.1% HSA. The angiotensin generated during the incubation was measured by radioimmunoassay. The oral activity was confirmed in hypertensive patients (Gradman et al. 2005).

REFERENCES AND FURTHER READING

Bohlender J, Ménard J, Wagner J, Luft FC, Ganten D (1996) Développement chez le rat d'un modèle d'hypertension à la rénine humaine. Arch Mal Cœur 89:1009–1011

Bolis G, Fung AKL, Greer J, Kleinert HD, Marcotte PA, Perun TJ, Plattner JJ, Stein HH (1987) Renin inhibitors. Dipeptide analogues of angiotensinogen incorporating transition state, nonpeptidic replacements at the scissile bond. J Med Chem 30:1729–1737

Corvol P, Menard J (1989) Renin inhibition: Immunological procedures and renin inhibitor peptides. Fundam Clin Pharmacol 3:347–362

Freedlender AE, Goodfriend TL (1979) Renin and the angiotensins. In: Jaffe BM, Behrman HR (eds) Methods of Hormone Radioimmunoassay. Academic Press, New York, pp 889–907

Gradman AH, Schmieder RE, Lins RL, Nussberger J, Chiang Y, Bedigian MP (2005) Aliskiren, a novel orally effective renin inhibitor, provides dose-dependent antihypertensive efficacy and placebo-like tolerability in hypertensive patients. Circulation 111:1012–1018

Greenlee WJ (1990) Renin inhibitors. Med Res Rev 10:173–236

Heitsch H, Henning R, Kleemann HW, Linz W, Nickel WU, Ruppert D, Urbach H, Wagner A (1993) Renin inhibitors containing a pyridylaminodiol derived C-terminus. J Med Chem 36:2788–2800

Kokubu T, Hiwada K, Murakami E, Muneta S, Morisawa Y, Yabe Y, Koike H, Iijima Y (1987) *In vitro* inhibition of human renin by statine-containing tripeptide inhibitor. J Cardiovasc Pharmacol 10 (Suppl. 7) S88–S90

Linz W, Heitsch H, Henning R, Jung W, Kleemann HW, Nickel WU, Ruppert D, Urbach H, Wagner A, Schölkens BA (1994) Effects of the renin inhibitor *N*-[*N*-(3-

(4-amino-1-piperidinyl-carbonyl)-2(*R*)-benzylpropionyl)-L-histidinyl]-(2*S*,3*R*,4*S*)-1-cyclohexyl-3,4-dihydroxy-6(2-pyridyl)-hexane-2-amide acetate (S 2864) in anesthetized rhesus monkeys. Arzneim Forsch/Drug Res 44:815–820

Murakami K, Ohsawa T, Hirose S, Takada K, Sakakibara S (1981) New fluorogenic substrates for renin. Analyt Biochem 110:232–239

Salimbeni A, Paleari F, Poma D, Criscuoli M, Scolastico C (1996) Synthesis and renin inhibitory activity of novel angiotensinogen transition state analogues modified at the P_2-histidine position. Eur J Med Chem 31:827–832

Shibasaki M, Asano M, Fukunaga Y, Usui T, Ichihara M, Murakami Y, Nakano K, Fujikura T (1991) Pharmacological properties of YM-21095, a potent and highly specific renin inhibitor. Am J Hypertens 4:932–938

Wang GT, Chung CC, Holzman TF, Krafft GA (1993) A continuous fluorescence assay of renin activity. Analyt Biochem 210:351–359

Wood JM, Criscione L, de Gasparo M, Bühlmayer P, Rüeger H, Stanton JL, Jupp RA, Kay J (1989) CGP 38 560: Orally active, low-molecular weight renin inhibitor with high potency and specificity. J Cardiovasc Pharmacol 14:221–226

Wood JM, Mah SC, Baum HP, de Gasparo M, Cumin F, Rüeger H, Nussberger J (1990) Evaluation of a potent inhibitor of subprimate and primate renins. J Pharmacol Exp Ther 253:513–517

Wood JM, Maibaum J, Rahuel J, Grütter MG, Cohen NC, Rasetti V, Rüger H, Göschke R, Stutz S, Fuhrer W, Schilling W, Rigollier P, Yamaguchi Y, Cumin F, Baum HP, Sdchnell CR, Herold P, Mah R, Jensen C, O'Brien E, Stanton A, Bedigian MP (2003) Structure-based design of aliskiren, a novel orally effective renin inhibitor. Biochem Biophys Res Commun 308:698–705

A.1.1.16 PAF Binding Assay

PRINCIPLE AND RATIONALE

Injection of platelet activating (PAF) factor induces a wide range of potent and specific effects on target cells, including aggregation of platelets and shock symptoms like systemic hypotension, pulmonary hypertension, increased vascular permeability, neutropenia and thrombocytopenia. Inhalation of PAF causes immediate bronchoconstriction followed by inflammation of the airways (further information see Sect. B.1.9).

Hikiji et al. (2004) showed in PAF-deficient mice that the absence of platelet-activating factor receptor protects mice from osteoporosis following ovariectomy, a model of postmenopausal osteoporosis.

PAF is also implicated in estrogen-induced angiogenesis via nuclear factor-κB activation (Seo et al. 2004) and in delaying corneal wound healing (Bazan 2005).

The PAF receptor belongs to the superfamily of G protein-coupled receptors (Chao and Olson 1993, Izumi and Shimizu 1995). Cloning studies have indicated a single human PAF receptor gene containing an intron at the 5′ flanking region, providing alternative sequences (Ishi and Shimizu 2000).

The following procedure is used to detect compounds that inhibit binding of ^{3}H-PAF (platelet activating factor) in rabbit platelets (PAF receptor).

PROCEDURE

Crude rabbit platelets are incubated in plastic tubes for 15 min at 25°C in a buffer solution (0.54 g/l KH_2PO_4, 0.6 g/l Na_2HPO_4, 5.8 g/l NaCl, 1.0 g/l BSA, pH 7.1) with 1 nM synthetic ^{3}H-labeled PAF (1-*O*-[1,2-$^3H_2$]alkyl-2-*O*-acetyl-*sn*-glycero-3-phosphocholine) and various concentrations of test compound. Non-specific binding is determined in the presence of 10 µM CV 3988. Bound ligand is separated from the incubation medium by rapid filtration through Whatman GF/C glass fibre filters. Following rinsing with ice-cold buffer (3 × 5 ml), the filters are placed in 10 ml scintillation cocktail for radioactivity determination.

EVALUATION

The following parameters are calculated:

- total binding of ^{3}H-PAF
- non-specific binding in the presence of 10 µM CV 3988
- specific binding = total binding–non-specific binding
- % inhibition: 100–specific binding as percentage of the control value

Compounds are first tested at a single high concentration (5000 nM) in triplicate. For those showing more than 50% inhibition a displacement curve is constructed using 7 different concentrations of test compound. Binding potency of compounds is expressed either as a "relative binding affinity" (RBA) with respect to the standard compound (CV 3988) which is tested in parallel or as an IC_{50}.

$$\text{RBA} = \frac{\text{IC}_{50}\text{ standard compound}}{\text{IC}_{50}\text{ compound}} \times 100\%$$

Standard data:

- CV 3988 IC_{50}: 276 nM ± 24 ($n = 20$)

MODIFICATIONS OF THE METHOD

Several authors (Casals-Stenzel et al. 1987; Dent et al. 1989a, b; Ring et al. 1992; Ukena et al. 1988) used the specific platelet activating factor receptor antagonist [^{3}H]WEB-2086 or [^{3}H]Apafant to identify and

characterize the PAF-receptors expressed on the cell surface of platelets, macrophages, and eosinophils.

Balsa et al. (1996) characterized [^{3}H]Apafant binding to the PAF receptor on rabbit platelet membranes and compared a microplate filtration system with the standard method.

REFERENCES AND FURTHER READING

Balsa D, Merlos M, Giral M, Ferrando R, García-Rafanell J, Forn J (1996) Characterization of [^{3}H]Apafant binding to PAF receptor on rabbit platelet membranes: A comparison of a microplate filtration system and a standard method. J Pharmacol Toxicol Meth 36:53–62

Bazan HE (2005) Cellular and molecular events in corneal wound healing: significance of lipid signalling. Exp Eye Res 80:453–463

Casals-Stenzel J, Muacevic G, Weber KH (1987) Pharmacological actions of WEB-2086, a new specific antagonist of platelet activating factor. J Pharmacol Exp Ther 241:974–981

Chao W, Olson MS (1993) Platelet-activating factor: Receptors and signal transduction. Biochem J 292:617–629

Dent G, Ukena D, Sybrecht GW, Barnes PJ (1989a) [^{3}H]WEB-2086 labels platelet activating factor in guinea pig and human lung. Eur J Pharmacol 169:313–316

Dent G, Ukena D, Chanez P, Sybrecht GW, Barnes J (1989b) Characterization of PAF receptors on human neutrophils using the specific antagonist WEB-2086: Correlation between binding and function. FEBS Lett 244:365–368

Handley DA (1990) Preclinical and clinical pharmacology of platelet-activating factor receptor antagonists. Medicin Res Rev 10:351–370

Hikiji H, Ishii S, Shindou H, Takato T, Shimizu T (2004) Absence of platelet-activating factor receptor protects mice from osteoporosis following ovariectomy. J Clin Invest 114:85–93

Hwang SB, Lee CSC, Cheah MJ, Shen TY (1983) Specific receptor sites for 1-O-alkyl-2-O-acetyl-sn-glycero-3-phosphocholine (platelet activating factor) on rabbit platelet and guinea pig smooth muscle membrane. Biochemistry 22:4756–4763

Ishii S, Shimizu T (2000) Platelet-activating factor (PAF) receptor and genetically engineered PAF mutant mice. Progr Lipid Res 39:41–82

Izumi T, Shimizu T (1995) Platelet-activating factor: Gene expression and signal transduction. Biochem Biophys Acta 34:317–333

Ring PC, Seldon PM, Bernes PJ, Giembycz MA (1992) Pharmacological characterization of a receptor for platelet activating factor on guinea pig peritoneal macrophages using [^{3}H]Apafant, a selective and competitive platelet activating factor antagonist: Evidence that the noncompetitive behavior of apafant in functional studies relates to slow kinetics of dissociation. Molec Pharmacol 43:302–312

Seo KH, Lee HS, Jung B, Ko HM, Cvhoi JH, Park SJ, Choi IH, Lee KH, Im SY (2004) Estrogen enhances angiogenesis through a pathway involving platelet-activating factor-mediated nuclear factor-κB activation. Cancer Res 64:6482–6488

Terashita ZI, Imura Y, Nishikawa K (1985) Inhibition by CV-3988 of the binding of [^{3}H]-platelet activating factor (PAF) to the platelet. Biochem Pharmacol 34:1491–1495

Ukena D, Dent G, Birke F, Robaut C, Sybrecht G, Barnes PJ (1988) Radioligand binding of antagonists of platelet activating factor to intact human platelets. FEBS Lett 228:285–289

A.1.1.17 Endothelin

A.1.1.17.1 General Considerations

Endothelin is an endothelium-derived peptide family consisting of three peptides (ET-1, ET-2, and ET-3) with very potent and long-lasting vasoconstrictive activity (Yanagisawa et al. 1988a, b; King et al. 1989; Miller et al. 1989; Yanagisawa and Masaki 1989; Inoue et al. 1989; Shinmi et al. 1989; Vanhoutte et al. 1992; Davenport 2002; Masaki 2004).

ET-1 is processed from prepro ET-1, pro-ET-1 to big ET-1, which is converted to ET-1 by the endothelin-converting-enzyme (ECE).

Subtypes of endothelin receptors have been described (Takayanagi et al. 1991; Miyazaki et al. 1992).

Molecular characterization of the ET_A and ET_B receptors was reported by Miyazaki et al. (1992), Sakuarai et al. (1992).

In addition, the existence of a third type, ET_C, was found in *Xenopus laevis* (Karne et al. 1993).

The comparison of recombinant endothelin receptors shows different affinity rank orders to the three endothelins (Masaki et al. 1994).

Grant et al. (1997) reported the *in vitro* expression of endothelin-1 (ET-1) and the ET_A and ET_B ET receptors by prostatic epithelium and stroma.

The ET peptides not only elicit potent and long-lasting contractions of isolated strips of various blood vessels *in vitro* but also increase blood pressure *in vivo* suggesting that this peptide family may be involved in the pathogenesis of cardiovascular diseases (Simonson and Dunn 1990; Masaki 1991; Doherty 1992; Goto et al. 1996; Gray and Webb 1996; Douglas and Ohlstein 1997). Sarafotoxin S6c, originally isolated from snake venom, is an agonist which distinguishes between endothelin subtypes (Williams et al. 1991).

Endothelin is degradeted by vascular smooth muscle cells (Bernmek et al. 1996).

REFERENCES AND FURTHER READING

Arai H, Hori S, Aramori I, Ohkubo H, Nakanishi S (1990) Cloning and expression of a cDNA encoding an endothelin receptor. Nature 348:730–732

Bernmek H, Peng KC, Angelova K, Ergul A, Puett D (1996) Endothelin degradation by vascular smooth muscle cells. Regul Pept 66:155–162

Davenport AP (2002) International Union of Pharmacology. XXIX. Update on endothelin receptor nomenclature. Pharmacol Rev 54:219–226
Doherty AM (1992) Endothelin: A new challenge. J Med Chem 35:1493–1508
Douglas SA, Ohlstein EH (1997) Signal transduction mechanisms mediating the vascular actions of endothelin. J Vasc Res 34:152–164
Goto K, Hama H, Kasuya Y (1996) Molecular pharmacology and pathophysiological significance of endothelin. Jpn J Pharmacol 72:261–290
Gray GA, Webb DJ (1996) The endothelin system and its potential as a therapeutic target in cardiovascular disease. Pharmacol Ther 72:109–148
Inoue A, Yanagisawa M, Kimura S, Kasuya Y, Miyauchi T, Goto K, Masaki T (1989) The human endothelin family: Three structurally and pharmacologically distinct isopeptides predicted by three separate genes. Proc Natl Acad Sci, USA, 86:2863–2867
Karne S, Jayawickreme CK, Lerner MR (1993) Cloning and characterization of an endothelin-3 specific receptor (ET_C receptor) from *Xenopus laevis* dermal melanophores. J Biol Chem 268:19126–19133
King AJ, Brenner BM, Anderson S (1989) Endothelin: a potent renal and systemic vasoconstrictor peptide. Am J Physiol 256 (Renal Fluid Electrolyte Physiol 25): F1051–F1058
Lerman A, Hildebrand FL, Margulies KB, O'Morchu B, Perrella MA, Heublein DM, Schwab TR, Burnett JC (1990) Endothelin: A new cardiovascular regulatory peptide. Mayo Clin Proc 65:1441–1455
Masaki T, Yanagisawa M, Goto K, Kimura S, Takuwa Y (1991) Cardiovascular significance of endothelin. In: Rubanyi GM (ed) Cardiovascular Significance of Endothelium-Derived Vasoactive Factors. Futura Publ Co, Inc., Mount Kisco, NY, pp 65–81
Masaki T, Vane JR, Vanhoutte PM (1994) V. International union of pharmacology nomenclature of endothelin receptors. Pharmacol Rev 46:137–142
Masaki T (2004) Historical review: endothelin. Trends Pharmacol Sci 25:219–224
Miller WL, Redfield MM, Burnett JC, Jr (1989) Integrated cardial, renal, and endocrine actions of endothelin. J Clin Invest 83:317–320
Miyazaki H, Kondoh M, Masuda Y, Watanabe H, Murakami K (1992) Endothelin receptors and receptor subtypes. In: Rubanyi GM (ed) Endothelin. Oxford University Press, New York, Oxford, pp 58–71
Rubanyi GM, Bothelho LHP (1991) Endothelins. FASEB J 5:2713–2720
Sakuarai T, Yanigasawa M, Masaki T (1992) Molecular characterization of endothelin receptor. Trends Pharmacol Sci 13:103–108
Shinmi O, Kimura S, Sawamura T, Sugita Y, Yoshizawa T, Uchiyama Y, Yanagisawa M, Goto K, Masaki T, Kanazawa I (1989) Endothelin-3 is a novel neuropeptide: Isolation and sequence determination of endothelin-1 and endothelin-3 in porcine brain. Biochem Biophys Res Commun 164:587–593
Simonson MS, Dunn MJ (1990) Cellular signaling by peptides of the endothelin gene family. FASEB J 4:2989–3000
Takayanagi R, Ohnaka K, Takasaki C, Ohashi M, Nawata H (1991) Multiple subtypes of endothelin receptors in porcine tissues: characterization by ligand binding, affinity labeling and regional distribution. Regul Peptides 32:23–37
Vanhoutte PM, Gräser T, Lüscher TF (1992) Endothelium-derived contracting factors. In: Rubanyi GM (ed) Endothelin. Oxford University Press, New York, Oxford. pp 3–16
Williams DL Jr, Jones KL, Pettibone DJ, Lis EV, Clineschmidt BV (1991) Sarafotoxin S6c: an agonist which distinguishes between endothelin subtypes. Biochem Biophys Res Commun 175:556–561
Yanagisawa M, Masaki T (1989) Endothelin, a novel endothelium-derived peptide. Pharmacological activities, regulation and possible role in cardiovascular control. Biochem Pharmacol 38:1877–1883
Yanagisawa M, Kurihara H, Kimura S, Tomobe Y, Kobayashi M, Mitsiu Y, Yasaki Y, Goto K, Masaki T (1988a) A novel potent vasoconstrictor peptide produced by vascular endothelial cells. Nature 332:411–415
Yanagisawa M, Inoue A, Ishikawa T, Kasuya Y, Kimura S, Kumagaye SI, Nakasjima K, Watanabe TX, Sakakibara S, Goto K, Masaki T (1988b) Primary structure, synthesis, and biological activity of rat endothelin, an endothelium-derived vasoconstrictor peptide. Proc Natl Acad Sci USA 85:6964–6967

A.1.1.17.2 Evaluation of Endothelin Activity

PURPOSE AND RATIONALE

Most investigators used isolated arteries to evaluate the activity of endothelins and derivatives. Rodman et al. (1989) compared the potency and efficacy of porcine and rat endothelin in rat aortic and pulmonary rings.

PROCEDURE

Arterial rings are obtained from male Sprague Dawley rats weighing from 300–400 g. Rats are anesthetized with 50 mg/kg i.p. pentobarbital, the chest is opened, 100 units heparin sulfate are injected into the right ventricle, and the rats are exsanguinated. Rings are then isolated from either the descending thoracic aorta or the right main pulmonary artery, cleaned of adventitia, and suspended from Grass FT03 force-displacement transducers in muscle baths containing 10 ml of physiologic salt solution of the following composition ($\times 10^{-3}$ M): $CaCl_2$ 1.80, $MgSO_4$ 0.83, KCl 5.3.6, NaCl 116.34, NaH_2PO_4 0.40, D-glucose 5.50, and $NaHCO_3$ 10.04. The solution is maintained at 37°C and bubbled with 21% O_2 and 5% CO_2. Endothelium-denuded rings are prepared by gently rubbing the intima with a roughened steel rod. Denudation is confirmed by the absence of relaxation to 10^{-5} M acetylcholine in rings precontracted with 10^{-7} M norepinephrine. Resting force is adjusted to the optimum resting tension of 0.75 g for pulmonary artery rings and 1.0 g for aortic rings. Maximum contraction to 8×10^{-2} M KCl is determined and subsequent responses to endothelin are expressed as a percentage of maximum KCl contraction for determination of maximum effectiveness or as a percentage of maximum endothelin contraction for determination of potency.

EVALUATION

Concentration-response curves are compared using the method of Carpenter (1986). Data are expressed as means ± SEM and statistical comparisons are performed using Student's *t*-test, with $P < 0.05$ considered significant.

MODIFICATIONS OF THE METHOD

Lembeck et al. (1989) studied the effects of endothelin on the cardiovascular system and on smooth muscle preparations in different species.

Reynolds and Mok (1990) studied the role of thromboxane A_2/prostaglandin H_2 receptor in the vasoconstrictor response of **rat aorta** to endothelin.

Pang et al. (1990) studied the cellular mechanisms of action of endothelin in **isolated canine coronary arteries**.

Lüscher et al. (1992) used **perfused and pressurized mesenteric resistance arteries of rats** and **human internal mammary arteries** to study the interaction between endothelin and endothelium-derived relaxing factors.

Michel et al. (2003) studied the endothelin system in various animal models of pulmonary hypertension.

Advenier et al. (1990) studied the contractile activity of three endothelins (ET-1, ET-2 and ET-3) on the **human isolated bronchus**.

Wallace et al. (1989) compared the effects of endothelin-1 and endothelin-3 on the **rat stomach**.

Aldosterone secretion in cultured calf zona glomerulosa cells was stimulated by ET-1 and sarafotoxin S6b to a similar degree, but less than by angiotensin II (Gomez-Sanchez 1990).

Brock and Danthuluri (1992) used **cultured vascular smooth muscle cells** to study the cellular actions of endothelin.

Pigment dispersion in cultured dermal melanophores from *Xenopus laevis* was used as indicator of ET_C receptor mediated responses (Karne et al. 1993).

REFERENCES AND FURTHER READING

Advenier C, Sarria B, Naline E, Puybasset L, Lagente V (1990) Contractile activity of three endothelins (ET-1, ET-2 and ET-3) on the human isolated bronchus. Br J Pharmacol 100:168–172

Brock TA, Danthuluri AR (1992) Cellular actions of endothelin in vascular smooth muscle. In: Rubanyi GM (ed) Endothelin. Oxford University Press, New York, Oxford. pp 103–124

Carpenter JR (1986) A method for presenting and comparing dose-response curves. J Pharmacol Meth 15:283–287

Gomez-Sanchez CE, Cozza EN, Foecking MF, Chiou S, Ferris MW (1990) Endothelin receptor subtypes and stimulation of aldosterone secretion. Hypertension 15:744–747

Karne S, Jayawickreme CK, Lerner MR (1993) Cloning and characterization of an endothelin-3 specific receptor (ET_C receptor) from *Xenopus laevis* dermal melanophores. J Biol Chem 268:19126–19133

Lembeck F, Decrinis M, Pertl C, Amann R, Donnerer J (1989) Effects of endothelin on the cardiovascular system and on smooth muscle preparations in different species. Naunyn-Schmiedeberg's Arch Pharmacol 340:744–751

Lüscher TF, Boulanger C, Yang Z, Dohi Y (1992) Interaction between endothelin and endothelium-derived relaxing factor(s) In: Rubanyi GM (ed) Endothelin. Oxford University Press, New York, Oxford. pp 125–136

Michel PR, Langleben D, Dupuis J (2003) The endothelin system in pulmonary hypertension. Can J Physiol Pharmacol 81:542–554

Pang DC, Johns A, Patterson K, Parker Botelho LH, Rubanyi GM (1990) Cellular mechanisms of action of endothelin in isolated canine coronary arteries. In: Rubanyi GM, Vanhoutte PM (eds) Endothelin-Derived Contracting Factors. Karger Basel, pp 66–72

Reynolds EE, Mok LLS (1990) Role of thromboxane A_2/prostaglandin H_2 receptor in the vasoconstrictor response of rat aorta to endothelin. J Pharmacol Exp Ther 252:915–921

Rodman DM, McMurty IF, Peach JL, O'Brien RF (1989) Comparative pharmacology of rat and porcine endothelin in rat aorta and pulmonary artery. Eur J Pharmacol 165:297–300

Wallace JL, Keenan CM, MacNaughton WK, McKnight GW (1989) Comparison of the effects of endothelin-1 and endothelin-3 on the rat stomach. Eur J Physiol 167:41–47

A.1.1.17.3 Endothelin Receptor Antagonism in Vitro

PURPOSE AND RATIONALE

Competitive endothelin antagonists are of therapeutic interest (Ihara et al. 1991; Fujimoto et al. 1992; Fukuroda et al. 1992; Urade et al. 1992; Breu et al. 1993; Mihara and Fujimoto 1993; Sogabe et al. 1993; Warner 1994; Opgenorth 1995; Brunner 1998).

A sensitive sandwich-enzyme immunoassay for human endothelin has been established by Suzuki et al. (1989).

PROCEDURE

The ventricles of rat hearts are minced with scissors and homogenized in 7 vol of ice-cold 20 mM $NaHCO_3$ containing 0.1 mM PMSF (Phenylmethylsulfonyl fluoride), pH 7.4, with a Polytron homogenizer (Brinkman Instruments Inc., Westberg, NY). The homogenates are centrifuged at 1000 *g* for 10 min, and then the pellet discarded. The supernatant is centrifuged at 30,000 *g* for 30 min. The pellet is washed once and resuspended in Tris buffer (50 mM, pH 7.4 at 25°C) containing 0.1 mM PMSF, and stored at –80°C until use.

For binding studies (Gu et al. 1989) cardiac membranes (0.21 mg/ml as protein) are incubated

with 25 pM [^{125}I]ET-1 or [^{125}I]ET-3 (New England Nuclear) in a final assay volume of 0.1 ml in borosilicated glass tubes, containing 50 mM Tris-HCl, 0.1 mM PMSF, 10 µg/ml aprotinin, 10 µg/ml leupeptin, 10 µg/ml pepstatin A, 250 µg/ml bacitracin, and 10 µg/ml soybean trypsin inhibitor (pH 7.4). Binding is performed for 60 min at 37°C. The binding reaction is terminated by the addition of 2.5 ml of ice-cold 50 mM Tris-HCl (pH 7.4), followed by a rapid filtration through a Whatman GF/C glass fibre filter (presoaked in 1% polyethyleneimine) under reduced pressure. The filters are then quickly washed 4 times with 2.5 ml of the buffer. Radioactivity retained on the filter is counted.

EVALUATION

Non-specific binding is defined in the presence of ET-1. Specific binding is the difference between total and non-specific binding. K_i-values and Scatchard plots are calculated.

MODIFICATIONS OF THE METHOD

The nomenclature of endothelin receptors has been reviewed by Alexander et al. (2001).

Cain et al. (1991) described an endothelin-1 receptor binding assay for high throughput chemical screening using the clonal cell line A10 of smooth muscle cells, derived from embryonic rat thoracic aorta.

Functional endothelin/sarafotoxin receptors were described in rat heart myocytes (Galron et al. 1989) and in the rat uterus (Bousso-Mittler 1989).

Mihara and Fujimoto (1993) cultured rat aortic smooth muscle A7r5 cells expressing ET_A receptors (Takuwa et al. 1990) and human Girardi heart cells expressing ET_B receptors (Mihara and Fujimoto 1992). Receptor specificity could be demonstrated.

Mihara et al. (1994) characterized the nonpeptide endothelin receptor antagonist 97–139, both *in vitro* (rat aortic smooth muscle cells and Girardi heart cells) and *in vivo* (ET1- antagonism in pithed rats) and compared it with another endothelin receptor antagonist (BQ-123). Discrepancies between *in vitro* and *in vivo* data were explained by different plasma binding.

Aramori et al. (1993) studied the receptor-binding properties and the antagonistic activities of an endothelin antagonist in transfected Chinese ovary hamster cells permanently expressing the two ET receptor subtypes (ET_A and ET_B).

De Juan et al. (1993) characterized an endothelin receptor subtype B in the retina of rats.

Clozel et al. (1994) performed binding assay on cells or membranes from baculovirus infected insect cells that expressed recombinant ET_A or ET_B receptor, CHO cells that expressed recombinant ET_A or ET_B receptor, cultured human vascular smooth muscle cells from umbilical veins, rat mesangial cells (for ET_A), microsomal membranes from human placenta and from porcine cerebellum (for ET_{B1}) and from porcine trachea (for ET_{B2}, using BQ-3020 or sarafotoxin S6C as ligand).

Williams et al. (1995) used CHO cells expressing cloned ET_A or ET_B receptors directly in binding and functional assays without preparing membranes from them.

Reynolds et al. (1995) used CHO-K1 cells expressing recombinant human ET_B receptor, Ltk^- cells expressing human ET_A receptor and rabbit renal artery vascular smooth muscle cells expressing rabbit ET_A receptor for evaluation of an ET_A receptor antagonist.

Rat or bovine cerebella were used for differentiation of receptor subtypes (Williams et al. 1991).

Peter and Davenport (1995) proposed a selective ligand for ET_A receptors.

Ihara et al. (1992), Watakabe et al. (1992) described radioligands for endothelin (ET_B) receptors.

Vigne et al. (1996) described the properties of an endothelin-3-sensitive Eta-like endothelin receptor in brain capillary endothelial cells.

The human type-B endothelin receptor was cloned from human lung poly A+RNA and expressed in CHO cells by Chiou et al. (1997). Dissociation characteristics of endothelin receptor agonists and antagonists were determined.

Stables et al. (1997) described a bioluminescent assay for agonist activity at G-protein-coupled receptors, such as the endothelin ET_A receptor. Transient expression of apoaequorin in CHO cells and reconstitution with the cofactor coelenterazine resulted in a large, concentration dependent agonist-mediated luminescent response following cotransfection with the endothelin ET_A, angiotensin AT_{II}, TRH and neurokinin NK_1 receptors, all of which interact predominantly with the $G\alpha_q$-like phosphoinositidase-linked G-proteins.

REFERENCES AND FURTHER READING

Alexander S, Peters J, Mathie A, MacKenzie G, Smith A (2001) TiPS Nomenclature Supplement 2001

Aramori I, Nirei H, Shoubo M, Sogabe K, Nakamura K, Kojo H, Notsu Y, Ono T, Nakanishi S (1993) Subtype selectivity of a novel endothelin antagonist, FR139317, for the two endothelin receptors in transfected Chinese hamster ovary cells. Mol Pharmacol 43:127–131

Banasik JL, Hosick H, Wright JW, Harding JW (1991) Endothelin binding in brain of normotensive and spontaneously hypertensive rats. J Pharmacol Exp Ther 257:302–306
Bousso-Mittler D, Kloog Y, Wollberg Z, Bdolah A, Kochva E, Sokolovsky M (1989) Functional endothelin/sarafotoxin receptors in the rat uterus. Biochem Biophys Res Commun 162:952–957
Breu V, Löffler BM, Clozel M (1993) *In vitro* characterization of RO 46–2005, a novel synthetic non-peptide endothelin antagonist of ET_A and ET_B receptors. FEBS 334:210–214
Brunner HR (1998) Endothelin inhibition as a biologic target for treating hypertension. Am J Hypertens 11, Suppl III:103S-109S
Cain MJ, Garklick RK, Sweetman PM (1991) Endothelin-1 receptor binding assay for high throughput chemical screening. J Cardiovasc Pharmacol 17 [Suppl 7]:S150–S151
Chiou WJ, Magnuson SR, Dixon D, Sundy S, Opgenorth TJ, Wu-Wong JR (1997) Dissociation characteristics of endothelin receptor agonists and antagonists in cloned human type-B endothelin receptor. Endothelium 5:179–189
Clozel M, Breu V, Gray GA, Kalina B, Löffler BM, Burri K, Cassal JM, Hirth G, Müller M, Neidhart W, Ramuz H (1994) Pharmacological characterization of bosentan, a new potent orally active nonpeptide endothelin receptor antagonist. J Pharmacol Exp Ther 270:228–235
De Juan JA, Moya FJ, Garcia de Lacoba M, Fernandez-Cruz A, Fernandez-Durango R (1993) Identification and characterization of endothelin receptor subtype B in rat retina. J Neurochem 61:1113–1119
Fujimoto M, Mihara S, Nakajima S, Ueda M, Nakamura M, Sakurai K (1992) A novel, non-peptide endothelin antagonist, isolated from bayberry, *Myrica cerifera*. FEBS Lett 305:41–44
Fukuroda T, Nishikibe M, Ohta Y, Ihara M, Yano M, Ishikawa K, Fukami T, Ikemoto F (1991) Analysis of responses to endothelins in isolated porcine blood vessels by using a novel endothelin antagonist, BQ-153. Life Sci 50: PL107–PL112
Galron R, Klog Y, Bdolah A, Sokolovsky M (1989) Functional endothelin/sarafotoxin receptors in rat heart myocytes: structure-activity relationships and receptor subtypes. Biochem Biophys Res Commun 163:936–943
Gu XH, Calsey D, Nayler W (1989) Specific high-affinity binding sites for ^{125}I-labelled porcine endothelin in rat cardiac membranes. Eur J Pharmacol 167:281–290
Hiley CR (1995) Endothelin receptor ligands. Neurotransmissions/2:1–6
Ihara M, Saeki T, Fukuroda T, Kimura S, Ozaki S, Patel AC, Yano M (1992) A novel radioligand [^{125}I]BQ-3020 selective for endothelin (ET_B) receptors. Life Sci 51:PL47–52
Mihara SI, Fujimoto M (1992) Non-isopeptide-selective endothelin receptors in human Girardi heart cells. Life Sci 50:219–226
Mihara S, Fujimoto M (1993) The endothelin ET_A receptor-specific effects of 50–235, a nonpeptide endothelin antagonist. Eur J Pharmacol 246:33–38
Mihara S, Nakajima S, Matumura S, Kohnoike T, Fujimoto M (1994) Pharmacological characterization of a potent nonpeptide endothelin receptor antagonist, 97–139. J Pharmacol Exp Ther 268:1122–1128
Opgenorth TJ (1995) Endothelin receptor antagonism. Adv Pharmacol 33:1–65
Peter MG, Davenport AP (1995) Selectivity of [^{125}I]-PD151242 for human rat and porcine ET_A receptors in the heart. Br J Pharmacol 114:297–302
Reynolds EE, Keiser JA, Haleen SJ, Walker DM, Olszewski B, Schroeder RL, Taylor DG, Hwang O, Welch KM, Flynn MA, Thompson DM, Edmunds JJ, Berryman KA, Plummer M, Cheng XM, Patt WC, Doherthy AM (1995) Pharmacological characterization of PD 156707, an orally active ET_A receptor antagonist. J Pharmac Exp Ther 273:1410–1417
Sogabe K, Nirei H, Shoubo M, Nomoto A, Ao S, Notsu Y, Ono T (1993) Pharmacological profile of FR139317, a novel, potent endothelin ET_A receptor antagonist. J Pharm Exp Ther 264:1040–1046
Stables J, Green A, Marshall F, Fraser N, Knight E, Sautel M, Milligan G, Lee M, Rees S (1997) A bioluminescent assay for agonist activity at potentially any G-protein-coupled receptor. Anal Biochem 252:115–126
Suzuki N, Matsumoto H, Kitada C, Msaki T, Fujino M (1989) A sensitive sandwich-enzyme immunoassay for human endothelin. J Immunol Meth 118:245–250
Takuwa Y, Kasuya Y, Takuwa N, Kudo M, Yanagisawa M, Goto K, Masaki T, Yamashita K (1990) Endothelin receptor is coupled to phospholipase C via a pertussis toxin-insensitive guanine nucleotide-binding regulatory protein in vascular smooth muscle cells. J Clin Invest 85:653–658
Urade Y, Fujitani Y, Oda K, Watakabe T, Umemura I, Takai M, Okada T, Sakata K, Karaki H (1992) An endothelin receptor-selective antagonist: IRL 1038, [Cys^{11}-Cys^{15}]-endothelin-1(11–21) FEBS Lett 311:12–16
Vigne P, Desmarets J, Guedin D, Frelin Ch (1996) Properties of an endothelin-3-sensitive Eta-like endothelin receptor in brain capillary endothelial cells. Biochem Biophys Res Commun 220:839–842
Warner TD (1994) Endothelin receptor antagonists. Cardiovasc Drug Dev 12:105–122
Watakabe T, Urade Y, Takai M, Umemura I, Okada T (1992) A reversible radioligand specific for the ET_B receptor: [^{125}I]Tyr^{13}-Suc-[Glu^{9},$Ala^{11,15}$]-endothelin-1(8–21), [^{125}I]IRL 1620. Biochem Biophys Res Commun 185:867–873
Williams DL Jr, Murphy KL, Nolan NA, O'Brien JA, Pettibone DJ, Kivlighn SD, Krause SM, Lis EV Jr, Zingaro GJ, Gabel RA, Clayton FC, Siegl PKS, Zhang K, Naue J, Vyas K, Walsh TF, Fitch KJ, Chakravarty PK, Greenlee WJ, Clineschmidt BV (1965) Pharmacology of L-754,142, a highly potent, orally active, nonpeptidyl endothelin antagonist. J Pharmac Exp Ther 275:1518–1526
Williams DL Jr, Jones KL, Pettibone DJ, Lis EV, Clineschmidt BV (1991) Sarafotoxin S6c: an agonist which distinguishes between endothelin receptor subtypes. Biochem Biophys Res Commun 175:556–561

A.1.1.17.4 Endothelin Receptor Antagonism in Vivo

PURPOSE AND RATIONALE

Various pharmacological models have been used for the characterization of endothelins and endothelin antagonists, such as the isolated porcine coronary artery. (Hickey et al. 1985; Yanagisawa et al. 1988, 1989; Inoue et al. 1989; Kimura et al. 1989; Ihara et al. 1991; Fukuroda et al. 1991).

Since the smooth musculature is considered to contain mainly ET_A receptors the preparation is used to test ET_A antagonists.

PROCEDURE

Left anterior descending coronary arteries are isolated from fresh porcine hearts. Connective tissues and adherent fat are removed. For removal of vascular endothelium, the intimal surface of spiral strips is rubbed gently with filter paper. The endothelium-denuded arteries are cut into spiral strips about 10 mm long and 1 mm wide. Each strip is suspended in an organ bath containing Krebs-Henseleit solution bubbled with 95% O_2/5% CO_2 at 37°C. After equilibration, reference contraction is isometrically obtained with 50 mM KCl. Concentration-response curves for ET-1 are obtained by cumulative additions of ET-1. Antagonists are added 20 min before the cumulative additions of ET-1.

EVALUATION

The pA_2 values and slopes are obtained by analysis of Schild plots.

MODIFICATIONS OF THE METHOD

Opgenorth et al. (1996) characterized an orally active and highly potent ET_A-selective receptor antagonist by *in vitro* and *in vivo* methods.

Calo et al. (1996) investigated three **rabbit vessels, the carotid, the pulmonary artery, and the jugular vein** to identify vascular monoreceptor systems, either ET(A) or ET(B), for structure-activity studies of endothelins and their antagonists.

Vedernikov et al. (1993) used **rings of the left circumflex coronary artery** from **dogs** which were denuded of endothelium and exposed to anoxic periods. August et al. (1989), Urade et al. (1992) used **rat aortic smooth muscle denuded of the epithelium** and Sogabe et al. (1993) **spirally cut strips of rabbit aorta**.

Williams et al. (1995) used **rat aorta, rabbit iliac and pulmonary artery** for contractile assays, and **anesthetized ferrets and conscious normotensive dogs** as *in vivo* models to characterize a nonpeptidyl endothelin antagonist.

Itoh et al. (1993) studied the preventive effect of an ET_A receptor antagonist on **experimental cerebral vasospasm in dogs** using a two-hemorrhage model of subarachnoid hemorrhage. Clozel et al. (1993) performed similar experiments in rats.

The **vasodilating** effect in the **isolated perfused rat mesentery** which is found after infusion of rat endothelin (Warner et al. 1989) and after the selective ET_B receptor agonist sarafotoxin S6c (Williams et al. 1991) can be antagonized by an endothelin receptor antagonist (Clozel et al. 1993).

Ercan et al. (1996) found an increase of digoxin-induced ectopic ventricular complexes by endothelin peptides in **isolated guinea pig hearts**, which could be antagonized by an endothelin-A receptor antagonist.

The **endothelin-induced sustained increase of blood pressure** in anesthetized rats was studied by Yanagisawa et al. (1988), Inoue et al. (1989), Ihara et al. (1991). Intravenous bolus injection of endothelin causes a biphasic blood pressure response: a transient decrease, probably mediated from the release of vasodilator mediators (prostacyclin and EDRF), and a sustained increase (Rubanyi and Bothelho 1991).

Nishikibe et al. (1993) examined the **antihypertensive effect** of an endothelin antagonist in a genetic hypertensive model (**stroke-prone spontaneously hypertensive rats**).

Watanabe et al. (1995) characterized the pharmacological profile of a non-selective endothelin receptor antagonist and studied the **inhibition of myocardial infarct size** in rats.

The contractile activity of the **isolated guinea pig trachea without epithelium** and of the guinea pig longitudinal muscle was used by Urade et al. (1992) for determination of **ET_B receptor** mediated responses.

Spinella et al. (1991) assessed bioactivity of a specific endothelin-1 antagonist in an **isolated perfused guinea pig lung** preparation in which pulmonary artery pressure was monitored.

Gosselin et al. (2002) demonstrated the effects of a selective ET_A-receptor antagonist in murine models of allergic asthma.

Tabrizchi and Ford (2003) studied the haemodynamic effects of the endothelin receptor antagonist tezosentan in anaesthetized rats treated with tumor necrosis factor-alpha.

REFERENCES AND FURTHER READING

August M, Delaflotte S, Chabrier PE, Braquet P (1989) Comparative effects of endothelin and phorbol 12–13- dibutyrate in rat aorta. Life Sci 45:2051–2059

Calo G, Gratton JP, Orleans-Juste P, Regoli D (1996) Pharmacology of endothelins: vascular preparations for studying ET(A) and ET(B) receptors. Mol Cell Biochem 154:31–37

Clozel M, Breu V, Burri K, Cassal JM, Fischli W, Gray GA, Hirth G, Löffler BM, Müller M, Neidhart W, Ramuz H (1993) Pathophysiological role of endothelin revealed by the first orally active endothelin receptor antagonist. Nature 365:759–761

Ercan ZS, Ilhan M, Kilinç M, Türker RK (1996) Arrhythmogenic action of endothelin peptides in isolated perfused whole hearts from guinea pigs and rats. Pharmacology 53:234–240

Gosselin M, Goulet S, Wu-Wong JR, Wessale JL, Opgenorth TJ, Boulet LP, Battistini B (2002) Effects of a selec-

tive ET_A-receptor antagonist (ABT-627), in murine models of allergic asthma: demonstration of mouse strain specificity. Clin Sci 103 [Suppl 48]:367S–370S
Ihara M, Noguchi K, Saeki T, Fukuroda T, Tsuchida S, Kimura S, Fukami TG, Ishikawa K, Nishikibe M, Yano M (1991) Biological profiles of highly potent novel endothelin antagonists selective for the ET_A receptor. Life Sci 50:247–255
Inoue A, Yanagisawa M, Kimura S, Kasuya Y, Miyauchi T, Goto K, Masaki T (1989) The human endothelin family: Three structurally and pharmacologically distinct isopeptides predicted by three separate genes. Proc Natl Acad Sci, USA, 86:2863–2867
Itoh S, Sasaki T, Ide K, Ishikawa K, Nishikibe M, Yano M (1993) A novel ET_A receptor antagonist, BQ-485, and its preventive effect on experimental cerebral vasospasm in dogs. Biochem Biophys Res Commun 195:969–975
Kimura S, Kasuya Y, Sawamura T, Shinmi O, Sugita Y, Yanagisawa M, Goto K, Masaki T (1989) Conversion of big endothelin-1 to 21-residue endothelin-1 is essential for expression of full vasoconstrictor activity: Structure-activity relationships of big endothelin-1. J Cardiovasc Pharmacol 13 (Suppl 5):S5–S7
Nishikibe M, Tsuchida S, Okada M, Fukuroda T, Shimamoto K, Yano M, Ishikawa K, Ikemoto F (1993) Antihypertensive effect of a newly synthesized endothelin antagonist, BQ123, in a genetic hypertensive model. Life Sci 52:717–724
Opgenorth TJ, Adler AL, Calzadilla SV, Chiou WJ, Daytin BT, Dixon DB, Gehrke LJ, Hernandez L, Magnuson SR, Marsh KC, Novosad EI, von Geldern TW, Wessale JL, Winn M, Wu-Wong JR (1996) Pharmacological characterization of A-127722: an orally active and highly potent ET_A-selective receptor antagonist. J Pharmacol Exp Ther 276:473–481
Shimamoto H, Kwa CY, Daniel EE (1992) Pharmacological assessment of Ca^{2+}-dependence of endothelin-1-induced response in rat aorta. Eur J Pharmacol 216:225–233
Spinella MJ, Malik AB, Evertitt J, Andersen TT (1991) Design and synthesis of a specific endothelin-1 antagonist: effects on pulmonary vasoconstriction. Proc Natl Acad Sci USA 88:7443–7446
Tabrizchi R, Ford CA (2003) Haemodynamic effects of endothelin receptor antagonist, tezosentan, in tumour necrosis factor-alpha treated anaesthetized rats. Naunyn-Schmiedebergs Arch Pharmacol 367:156–167
Urade Y, Fujitani Y, Oda K, Watakabe T, Umemura I, Takai M, Okada T, Sakata K, Karaki H (1992) An endothelin receptor-selective antagonist: IRL 1038, [Cys^{11}-Cys^{15}]-endothelin-1(11–21). FEBS Lett 311:12–16
Vedernikov YP, Goto K, Vanhoutte PM (1993) The ET_A antagonist BQ-123 inhibits anoxic contractions of canine coronary arteries without endothelium. J Cardiovasc Pharmacol 22, Suppl 8:S252–S265
Warner TD, de Nucci G, Vane JR (1989) Rat endothelin is a vasodilator in the isolated perfused mesentery of the rat. Eur J Pharmacol 159:325–326
Watanabe T, Awane Y, Ikeda S, Fujiwara S, Kubo K, Kikuchi T, Kusomoto K, Wakimasu M, Fujino M (1995) Pharmacological profile of a non-selective ET_A and ET_B receptor antagonist, TAK-044 and the inhibition of myocardial infarct size in rats. Br J Pharmacol 114:949–954
Wilkes LC, Boarder MR (1991) Characterization of the endothelin binding site on bovine adrenomedullary chromaffin cells: Comparison with vascular smooth muscle cells. Evidence for receptor heterogeneity. J Pharmacol Exp Ther 256:628–633
Williams DL Jr, Murphy KL, Nolan NA, O'Brien JA, Pettibone DJ, Kivlighn SD, Krause SM, Lis EV Jr, Zingaro GJ, Gabel RA, Clayton FC, Siegl PKS, Zhang K, Naue J, Vyas K, Walsh TF, Fitch KJ, Chakravarty PK, Greenlee WJ, Clineschmidt BV (1965) Pharmacology of L-754,142, a highly potent, orally active, nonpeptidyl endothelin antagonist. J Pharmac Exp Ther 275:1518–1526
Yanagisawa M, Masaki T (1989) Endothelin, a novel endothelium-derived peptide. Pharmacological activities, regulation and possible role in cardiovascular control. Biochem Pharmacol 38:1877–1883
Yanagisawa M, Kurihara H, Kimura S, Tomobe Y, Kobayashi M, Mitsiu Y, Yasaki Y, Goto K, Masaki T (1988) A novel potent vasoconstrictor peptide produced by vascular endothelial cells. Nature 332:411–415

A.1.1.17.5 Quantitative Autoradiographic Localization of Endothelin-1 Receptor

PURPOSE AND RATIONALE

The endothelin-1 (ET-1) receptor can be quantified in tissue, such as in rat hearts with chronic infarction after left coronary ligation, by computerized *in vitro* autoradiography (Kohzuki et al. 1996)

PROCEDURE

Myocardial infarction is induced in Wistar rats by left coronary artery ligation (see A.3.2.2). After various time intervals (1–8 months) the animals are decapitated, the hearts rapidly removed, and snap-frozen in isopentane at –40°C. Frozen section (20 µm) are cut in a cryostat at –20°C. The sections are thaw-mounted onto gelatin-coated slides, dried in a desiccator for 2 h at 4°C and then stored at –80°C.

Quantitative autoradiography

Radioligand: Endothelin-1 is iodinated with ^{125}Iodine using Iodogen (Pierce Chemical Co, IL, USA)

^{125}I-ET-1 binding: The sections are preincubated for 15 min at 20°C in 20 mmol/L Hepes buffer, pH 7.4, containing 135 mmol/L NaCl, 2 mmol/L $CaCl_2$, 0.2% BSA, and 0.01% bacitracin. The sections are then incubated with 11.1 KBq/ml ^{125}I-ET-1 in the same buffer for 60 min at 20°C. Nonspecific binding is determined in the presence of 10^{-6} mol/L ET-1. Binding isotherms are determined using a set of serial sections incubated with 10^{-12} to 10^{-6} mol/L unlabelled ET-1 for 60 min.

After incubation, the sections are rapidly dried under a stream of cold air, placed in X-ray cassettes, and exposed to Agfa Scopix CR3 X-ray film for 12–72 h at room temperature. After exposure, the sections are fixed in formaldehyde and stained with hematoxylin and eosin. The optical density of the X-ray films is

quantified using an imaging device controlled by a personal computer.

EVALUATION

The optical density of the autoradiographs is calibrated in terms of the radioactivity density in dpm/mm^2 with reference standards maintained through the procedure. The apparent binding site concentration (B_{max}) and binding affinity constant (K_A) in all the areas (excluding coronary arteries) of the right ventricle, intraventricular septum, the infarcted area in the left ventricle and the non-infarcted area in the left ventricle are estimated by an iterative non-linear model-fitting computer program LIGAND (Munson and Rodbard 1980).

REFERENCES AND FURTHER READING

Kohzuki M, Johnston CI, Chai SY, Casley DJ, Mendelson FAO (1989a) Localization of endothelin receptors in rat kidney. Eur J Pharmacol 160:193–194

Kohzuki M, Johnston CI, Chai SY, Casley DJ, Rogerson F, Mendelson FAO (1989b) Endothelin receptors in rat adrenal gland visualized by quantitative autoradiography. Clin Exp Pharmacol Physiol 16:239–242

Kohzuki M, Chai SY, Paxinos J, Karavas A, Casley DJ, Johnston CI, Mendelson FAO (1989c) Localization and characterization of endothelin receptor binding sites in rat brain visualized by *in vitro* autoradiography. Neuroscience 42:245–260

Kohzuki M, Kanazawa M, Yoshida K, Kamimoto M, Wu XM, Jiang ZL, Yasujima M Abe K, Johnston CI, Sato T (1996) Cardiac angiotensin converting enzyme and endothelin receptor in rats with chronic myocardial infarction. Jpn Circ J 60:972–980

Munson PJ, Rodbard D (1980) LIGAND, a versatile computerized approach for characterization of ligand-binding systems. Anal Biochem 107:220–239

A.1.1.17.6 Inhibition of Endothelin Converting Enzyme

PURPOSE AND RATIONALE

Endothelin converting enzyme inhibitors suppress the biosynthesis of endothelin are therefore potential antihypertensive drugs (De Lombaert et al. 1994; Trapani et al. 1995; Morita et al. 1994; Bihovsky et al. 1995; Claing et al. 1995; Descombes et al. 1995; Chackalamannil et al. 1996; Jeng 1997; Jeng and De Lombaert 1997; Brunner 1998).

Purification of rat and porcine endothelin converting enzyme (ECE) was reported by Ohmaka et al. (1993), Takahashi et al. 1993). Molecular cloning and characterization of the enzyme ECE-1 was performed from rat (Shimada et al. 1994), bovine (Ikura et al. 1994; Schmidt et al. 1994; Xu et al. 1994), and human tissue (Schmidt et al. 1994; Shimada et al. 1995; Yorimitsu et al. 1995).

A second enzyme, termed ECE-2, was cloned (Emoto and Yanagisawa 1995).

Walkden and Turner (1995) described the expression of endothelin converting enzyme and related membrane peptidases, e. g., the endopeptidase E-24.11, in the human endothelial cell line EA.hy926.

IN VITRO ASSAY

A rapid and selective *in vitro* assay for endothelin-converting enzyme was described by Fawzi et al. (1994). The assay is based on the quantitative determination of [^{125}I]endothelin-1 released from (3-[^{125}I]iodotyrosyl^{13})big endothelin-1 by binding to the membrane bound endothelin receptor.

PROCEDURE

For the **preparation of lung membranes**, frozen guinea pig lungs are weighed and homogenized in 10 times gram tissue weight of solution A (50 mM Tris-HCl, pH 7.4, 025 M sucrose, and 2 mM EDTA) using a Polytron tissue homogenizer. Homogenization is repeated 4 times with 5- to 8-min intervals between homogenization. Homogenates are spun for 30 min at 2000 *g*. Supernatants containing membranes are carefully decanted and saved. Pellets are rehomogenized in solution A and homogenates are spun at 2000 *g* for 30 min. Supernatants are removed, mixed with supernatants from the first spin and spun at 100,000 *g* for 60 min. Pellets containing membranes are suspended in solution B (10 mM Tris-HCl, pH 7.4, and 0.125 M sucrose) using a Dounce homogenizer. Samples are divided into 1-ml fractions, rapidly frozen in a dry ice-methanol bath, and stored at −80°C.

Rat liver membranes are prepared with the same method and further purified over a sucrose step gradient. The membranes are suspended in solution C (10 mM Tris-HCl, pH 7.4) containing 44% sucrose at a protein concentration of 2 mg/ml. Samples of 25 ml are placed in ultraclear centrifuge tubes for the Beckman SW 28 rotor, overlaid with 10 ml solution C containing 42.3% sucrose, and spun for 2 h at 27,000 rpm (100,000 *g*). Top layers containing membrane are collected and diluted with solution C to obtain an 8% sucrose concentration. Samples are spun in a 45 Ti rotor (100,000 *g*) for 1 h. Supernatants are discarded. Pellets containing membrane are suspended in solution B, divided into 1-ml samples, rapidly frozen in dry ice-methanol bath, and stored at −80°C.

For the **endothelin (ET) binding assay**, membrane preparations are incubated with selected concentrations of [^{125}I]endothelin-1 (final reaction volume = 500 µl) in a solution D containing 60 mM Tris-

HCl, pH 7.4, 150 mM NaCl and 6 mg/ml BSA for 90 min at 37°C. Reactions are terminated by the addition of 4 ml of solution E containing 10 mM Tris-HCl, pH 7.4, and 150 mM NaCl at 4°C followed by rapid filtration on Whatman GF/B glass microfiber filters. Filters are presoaked for 1 h at 4°C in a solution containing 50 mM Tris-HCl, pH 7.4, 10 mg/ml BSA and 0.1% sodium azide. Test tubes and filters are washed four times with 4 ml of solution E at 4°C, and radioactivity retained on the filters is counted in a gamma counter. Nonspecific binding is determined in the presence of 1 µM unlabeled ET-1 in the reaction mixture.

For the **endothelin converting enzyme assay**, samples containing 10 µg of protein are incubated in a solution containing 50 mM Tris-HCl, pH 7.0, 100 mM NaCl and 5 mg/ml BSA in a final volume of 100 µl. Conversion reactions are initiated by addition of [^{125}I]big endothelin-1 to obtain a final concentration of 500 pM. Samples are incubated for 2 h at 37°C. To measure [^{125}I]endothelin-1 released from [^{125}I]big endothelin-1 conversion, 50 µg of purified rat liver membranes (as a source of ET receptors) is added to the reaction mixture, and reaction volume is adjusted to 500 µl and solution composition is adjusted to that of solution D of the endothelin binding assay. Following a 90-min incubation at 37°C to reach equilibrium in binding, reactions are terminated by addition of a solution E at 4°C followed by rapid filtration on Whatman GF/B glass microfiber filters. Nonspecific binding is determined in the presence of 1 µM unlabeled ET-1 in the reaction mixture. Specific ET-1 binding is used as an index of endothelin converting enzyme activity.

To test the effect of endothelin converting enzyme inhibitors, endothelin converting enzyme assays are carried out in the presence of desired concentrations of the compounds.

EVALUATION

Endothelin converting enzyme activity in the presence of compounds is expressed as a percentage of control endothelin converting enzyme activity in the membrane preparation which is determined simultaneously. The concentration of compounds producing a 50% inhibition of endothelin converting enzyme activity (IC_{50} values) is determined from a plot of the percentage of control endothelin converting enzyme activity versus log concentration of compounds.

IN VIVO ASSAY

Procedure

Male Sprague Dawley rats weighing 300–400 g are anesthetized with ether, spinalized and placed under artificial respiration. The vagus nerves are cut and the carotid arteries ligated. A catheter is placed in one of the carotid arteries to allow measurement of arterial blood pressure. The second catheter in placed into the penile vein to allow infusion or injection of drugs. After stabilization, the animals receive a first injection of either ET-1, big ET-1, norepinephrine, angiotensin I or AT II, The pressor responses are recorded and after return to the baseline, a second injection of the agonist is given either in the presence or the absence of the inhibitor.

EVALUATION

Data are calculated as mean ± SEM. Student's *t*-test for paired and unpaired observations is used to analyze the results.

MODIFICATIONS OF THE METHOD

Little et al. (1994) developed a two-step protocol for high-throughput assays of endothelin converting enzyme activity. Human umbilical vein and human aorta endothelial cells were found to preferentially convert the big endothelin-1 isopeptide through a membrane-bound, thiorphan-insensitive, and phophoramidon-sensitive zinc metalloendopeptidase. Endothelins are quantified by a separate step using either enzyme immunoassays or radioceptor assays in 96-well formats. The method can be used to either characterize ECE from different tissues or screen for inhibitors of a specific ECE activity.

McMahon et al. (1993) tested the effects of endothelin converting enzyme inhibitors and endothelin receptor subtype A antagonists on blood pressure in spontaneously and renal hypertensive rats.

Changes of vascular resistance in isolated perfused kidneys were used by Descombes et al. (1995) to characterize a selective inhibitor of big ET-1 responses. The studies were performed on kidneys taken from adult male Wistar rats (300–400 g). The rats were anesthetized with sodium pentobarbital (50 mg/kg i.p.) and the left kidney was prepared for infusion with Tyrode solution. The changes in renal vascular resistance were recorded as changes in perfusion pressure monitored at constant flow (6 ml/min). After stabilization, a bolus injection of ET-1 or big ET-1 was administered and the resulting pressure responses were recorded. On return to baseline levels, a second injection of the endothelins was given either under control conditions or in presence of the putative enzyme inhibitor.

Because increasing evidence implicates that endothelin plays a role in the pathophysiology of cerebral insults, Kwan et al. (1997) studied the prevention

and reversal of cerebral vasospasm in an experimental model of subarachnoid hemorrhage. Three ml of arterial blood was withdrawn from the ear artery of rabbits and injected into the cisterna magna under anesthesia. Drugs were administered either before or 24 h after this procedure. Forty-eight hours later, the animals were anesthetized again and perfusion fixation was performed with Hank's balanced salt solution followed by a mixture with 2% paraformaldehyde and 2.5% glutaraldehyde. Cross sections of the basilar arteries were analyzed by computer-assisted morphometry.

A review on the knowledge of molecular pharmacology of endothelin converting enzymes was given by Turner and Murphy (1996).

Johnson and Ahn (2000) developed an internally quenched fluorescent substrate selective for endothelin-converting enzyme-1.

Luciani et al. (2001) described highly sensitive and selective fluorescence assays for rapid screening of endothelin-converting enzyme inhibitors.

REFERENCES AND FURTHER READING

Bigaud M, Hauss B, Schalk C, Jauch MF, D'Orchymont H (1994) Structure activity relationship of phosphoramidon derivatives for *in vivo* endothelin converting-enzyme inhibition. Fundam Clin Pharmacol 8:155–161

Bihovsky R, Levinson BL, Loewi R, Erhardt PW, Polokoff MA (1995) Hydroxamic acids as potent inhibitors of endothelin-converting enzyme from human bronchiolar smooth muscle. J Med Chem 38:2119–2129

Brunner HR (1998) Endothelin inhibition as a biologic target for treating hypertension. Am J Hypertens 11:103S–109S

Chackalamannil S, Chung S, Stamford AW, McKittrick BA, Wang Y, Tsai H, Cleven R, Fawzi A, Czarniecki M (1996) Highly potent and selective inhibitors of endothelin converting enzyme. Bioorganic Medic Chem Lett 6:1257–1260

Claing A, Neugebauer W, Yano M, Rae GA, D'Orléans-Juste P (1995) [Phe^{22}]-big endothelin-1[19–37]: a new and potent inhibitor of the endothelin-converting enzyme. J Cardiovasc Pharmacol 26/Suppl 3:S72–S74

De Lombaert S, Ghai RD, Jeng AY, Trapani AJ, Webb RL (1994) Pharmacological profile of a non-peptide dual inhibitor of neutral endopeptidase 24.11 and endothelin converting enzyme. Biochem Biophys Res Commun 204:407–412

Descombes JJ, Mennecier P, Versluys D, Barou V, de Nanteuil G, Laubie M, Verbeuren TJ (1995) S 17162 is a novel selective inhibitor of big ET-1 responses in the rat. J Cardiovasc Pharmacol 26/Suppl 3:S61–S64

Emoto N, Yanagisawa M (1995) Endothelin-converting enzyme is a membrane bound, phosphoramidon sensitive metalloprotease with acidic pH optimum. J Biol Chem 270:15262–15268

Fawzi AB, Cleven RM, Wright DL (1994) A rapid and selective endothelin-converting enzyme assay: characterization of a phosphoramidon-sensitive enzyme from guinea pig lung membrane. Anal Biochem 222:342–350

Ikura T, Sawamura T, Shiraki T, Hosokawa H, Kido T, Hoshikawa H, Shimada K, Tanzawa T, Kobayashi S, Miwa S, Masaki T (1994) cDNA cloning and expression of bovine endothelin-converting enzyme. Biochem Biophys Res Commun 203:1417–1422

Jeng AY (1997) Therapeutic potential of endothelin converting enzyme inhibitors. Exp Opin Ther Patents 7:1283–1295

Jeng AY, DeLombaert S (1997) Endothelin converting enzyme inhibitors. Curr Pharmac Design 3:597–614

Johnson GD, Ahn K (2000) Development of an internally quenched fluorescent substrate selective for endothelin-converting enzyme-1. Anal Biochem 286:112–118

Kwan AL, Bavbek M, Jeng AY, Maniara W, Toyoda T, Lappe RW, Kassell NF, Lee KS (1997) Prevention and reversal of cerebral vasospasm by an endothelin converting enzyme inhibitor, CGS 26303, in an experimental model of subarachnoid hemorrhage. J Neurosurg 87:281–286

Little DK, Floyd DM, Tymiak AA (1994) A rapid and versatile method for screening endothelin converting enzyme activity. J Pharm Toxicol Meth 31:199–205

Luciani N, de Rocquigny H, Turcaud S, Romieu A, Roques BP (2001) Highly sensitive and selective fluorescence assays for rapid screening of endothelin-converting enzyme inhibitors. Biochem J 356:813–819

McMahon EG, Palomo MA, Brown MA, Bertenshaw SR, Carter JS (1993) Effect of phosphoramidon (endothelin converting enzyme inhibitor) and BQ-123 (endothelin receptor subtype A antagonist) on blood pressure in hypertensive rats. Am J Hypertens 6:667–673

Morita A, Nomizu M, Okitsu M, Horie K, Yokogoschi H, Roller PP (1994) D-Val^{22} containing human big endothelin-1 analog, [D-Val^{22}]Big ET-1[16–38], inhibits the endothelin converting enzyme. FEBS Lett 353:84–88

Ohnaka K, Takayanagi R, Nishikawa M, Haji M, Nawata H (1993) Purification and characterization of phosphoramidon sensitive endothelin-converting enzyme in porcine aortic endothelium. J Biol Chem 268:26759–26766

Opgenorth JJ, Wu-Wong JR, Shiosaki K (1992) Endothelin-converting enzymes. FASEB J 6:2653–2659

Schmidt M, Kröger B, Jacob E, Seulberger H, Subkowski T, Otter R, Meyer T, Schmalzling G, Hillen H (1994) Molecular characterization of human and bovine endothelin converting enzyme (ECE-1). FEBS Lett 356:238–243

Shimada K, Takahashi M, Tanzawa K (1994) Cloning and functional expression of endothelin-converting enzyme from rat endothelial cells. J Biol Chem 269:18275–18278

Shimada K, Matsushita Y, Wakabayashi K, Takahashi M, Matsubara A, Iijima Y, Tanzawa K (1995) Cloning and functional expression of human endothelin-converting enzyme cDNA. Biochem Biophys Res Commun 207:807–812

Takahashi M, Matsiushita Y, Iijima Y, Tanzawa K (1993) Purification and characterization of endothelin-converting enzyme from rat lung. J Biol Chem 268:21394–21398

Turner AJ, Murphy LJ (1996) Molecular pharmacology of endothelin converting enzymes. Biochem Pharmacol 51:91–102

Trapani AJ, De Lombaert S, Kuzmich S, Yeng AY (1995) Inhibition of big ET-1-induced pressure response by an orally active dual inhibitor of endothelin-converting enzyme and neutral endopeptidase 24.11. J Cardiovasc Pharmacol 26/Suppl 3:S69–S71

Walkden BJ, Turner AJ (1995) Expression of ECE and related membrane peptidases in the EA.hy926 cell line. J Cardiovasc Pharmacol 26/Suppl 3:S50–S60

Xu D, Emoto N, Giaid A, Slaughter C, Kaw S, deWit D, Yanagisawa M (1994) ECE-1: a membrane bound metalloprotease that catalyzes the proteolytic activation of big endothelin-1. Cell 78:473–485

Yorimitsu K, Moroi K, Inagaki N, Saito T, Masuda Y, Masaki T, Seino S, Kimura S (1995) Cloning and sequencing of a human endothelin converting enzyme in renal adenocarcinoma (ACHN) cells producing endothelin-2. Biochem Biophys Res Commun 208:721–927

A.1.1.18 Nitric Oxide

A.1.1.18.1 General Considerations on Nitric Oxide

PURPOSE AND RATIONALE

The endothelium releases a labile, diffusable vasorelaxing substance that has been termed endothelium-derived relaxing factor = EDRF endothelium-derived relaxing factor. (Furchgott and Zawadszki 1980). Nitric oxide release accounts for the biological activity of endothelium-derived relaxing factor (Palmer et al. 1987; Vanhoutte 1999).

Nitric oxide plays a role in a wide range of physiological processes including regulation of blood flow and arterial pressure via endothelium-dependent relaxation of blood vessels (Rees et al. 1989; Moncada et al. 1991; Umans and Levi 1995; Huraux et al. 1999; McIntyre et al. 1999; Zanzinger 1999; Hropot et al. 2003), ischemia/reperfusion injury (Gao et al. 2002; Schulz et al. 2004), peripheral nitregric transmission at smooth muscle (Rand and Li 1995), intracellular communication in the CNS with activation of guanylyl cyclase in target neurons (Southam and Garthwaite 993), experimental stroke (Willmot et al. 2005), learning and memory (Susswein et al. 2004), in neurogenic inflammation (Kajekar et al. 1995), in the regulation of leukocyte recruitment (Hickey 2001), and macrophage defense mechanisms following exposure to bacterial products (Förstermann et al. 1992; Förstermann and Kleinert 1995; Knowles and Moncada 1994). Fiorucci et al. (2002) discussed the effects of nitric oxide-releasing NSAIDs.

NO-donor drugs, such as sodium nitrite, sodium nitroprusside, *S*-nitroso-*N*-acetyl-D,L-penicillamine (SNAP), 3-morpholino-sydnonimine (SIN-1) are used as vasodilators (Schör et al. 1989; Megson 2000). N^G-Nitro-L-arginine was described as an antagonist of endothelium-dependent dilator responses by inhibiting endothelium-derived relaxing factor release (Moore et al. 1990; Lamontagne et al. 1991). Ribero et al. (1992) proposed inhibition of nitric oxide synthesis by long-term treatment of rats with nitro-L-arginine as a new model of arterial hypertension.

Excessive production of NO damages DNA and activates poly(ADP-ribose)polymerase (PARP) (Pieper et al. 1999). In cases of massive NO production, neurons enter the PARP-suicide pathway. NO damages DNA via to major pathways: the first involves nitrosation of primary or secondary amines and nucleic acid bases, whereas the second involves the combination of NO with superoxide to from peroxinitrite (Szabó et al. 1996, 1997). The most likely reactive oxidant intermediate responsible for DNA breakage is peroxynitrous acid which rapidly oxidizes sulphydryl groups, and also nitrates and hydroxylates aromatic compounds including tyrosine, tryptophan, and guanosine (Halliwell 1997). Downstream DNA damage that follows excessive NO production results in significant activation of poly(ADP-ribose)polymerase which leads to rapid energy depletion and cell death (Feihl et al. 2001).

Davis et al. (2001) reviewed the non-3′,5′-cyclic-guanosine-monophosphate-mediated effects of NO including modifications of proteins, lipids, and nucleic acids.

Andreadis et al. (2003) described oxidative and nitrosative events in asthma.

REFERENCES AND FURTHER READING

Andreadis AA, Hazen SL, Comhair SAA, Erzurum SC (2003) Oxidative and nitrosative events in asthma. Free Radical Biol Med 15:213–225

Davis KL, Martin E, Turko IV, Murad F (2001) Novel effects of nitric oxide. Annu Rev Pharmacol Toxicol 41:203–236

Feihl F, Waeber B, Liaudet L (2001) Is nitric overproduction the target of choice for management of septic shock? Pharmacol Ther 91:179–213

Fiorucci S, Antonelli E, Burgaud JL, Morelli A (2002) Nitric oxide-releasing NSAIDs. Drug Safety 24:801–811

Förstermann U, Kleinert H (1995) Nitric oxide synthase: Expression and expressional control of the three isoforms. Naunyn-Schmiedeberg's Arch Pharmacol 352:351–364

Förstermann U, Schmidt HHHW, Pollock JS, Sheng H, Mitchell JA, Warner TD, Murad F (1992) Characterization and classification of constitutive and inducible isoforms of nitric oxide synthase in various cell types. In: Moncada S, Marletta MA, Hibbs JB Jr, Higgs EA (eds) The Biology of Nitric Oxide. 2 Enzymology, Biochemistry and Immunology. Portland Press, London and Chapel Hill, pp 21–23

Furchgott RF, Zawadzki JV (1980) The obligatory role of endothelial cells in the relaxation of arterial smooth muscle by acetylcholine. Nature 288:373–376

Gao F, Gao E, Yue TL, Ohlstein EH, Lopez BL, Christopher TA, Ma XL (2002) Nitric oxide mediates the antiapoptotic effect of insulin in myocardial ischemia-reperfusion. The roles of PI3-kinase, *Akt*, and endothelial nitric oxide synthase phosphorylation. Circulation 105:1497–1502

Halliwell B (1997) What nitrates tyrosine? Is nitrotyrosine specific as biomarker of peroxynitrite? FFEBS Lett 411:157–160

Hickey MJ (2001) Role of inducible nitric oxide synthase in the regulation of leucocyte recruitment. Clin Sci 100:1–11

Hropot M, Langer KH, Wiemer G, Grötsch H, Linz W (2003) Angiotensin II subtype AT_1 receptor blockade prevents hy-

pertension and renal insufficiency induced by chronic NO-synthase inhibition in rats. Naunyn-Schmiedebergs Arch Pharmacol 367:312–317
Huraux C, Makita T, Kurz S, Yamaguchi K, Szlam F, Tarpey MM, Wilcox JN, Harrison DG, Levy JH (1999) Superoxide production, risk factors, and endothelium-dependent relaxations in human internal mammary arteries. Circulation 99:53–59
Kajekar R, Moore PK, Brain SD (1995) Essential role for nitric oxide in neurogenic inflammation in rats cutaneous microcirculation. Evidence for endothelium-independent mechanism. Circ Res 76:441–447
Lamontagne D, Pohl U, Busse R (1991) N^G-Nitro-L-arginine antagonizes endothelium-dependent dilator responses by inhibiting endothelium-derived relaxing factor release in the isolated rabbit heart. Pflüger's Arch 418:266–270
McIntyre M, Bohr DF, Dominiczak AF (1999) Endothelial function in hypertension. The role of superoxide anion. Hypertension 34:539–545
Megson IL (2000) Nitric oxide donor drugs. Drugs Future 25:701–715
Moncada S, Palmer RMJ, Higgs SA (1991) Nitric oxide: physiology, pathophysiology and pharmacology. Pharmacol Rev 43:109–142
Moore PK, al-Swayeh OA, Chong NWS, Evans RA, Gibson A (1990) L-N^G-nitro arginine (L-NOARG), a novel, L-arginine-reversible inhibitor of endothelium-dependent vasodilatation *in vitro*. Br J Pharmacol 99:408–412
Palmer RMJ, Ferrige AG, Moncada S (1987) Nitric oxide release accounts for the biological activity of endothelium-derived relaxing factor. Nature 327:524–526
Pieper AA, Verma A, Zhang J, Snyder SH (1999) Poly(ADP-ribose)polymerase, nitric oxide and cell death. Trends Pharmacol Sci 20:171–181
Rand MJ, Li CG (1995) Nitric oxide as a neurotransmitter in peripheral nerves: Nature of transmitter and mechanism of transmission. Ann Rev Physiol 57:659–682
Rees DD, Palmer RMJ, Moncada S (1989) Role of endothelium-derived nitric oxide in the regulation of blood pressure. Proc Natl Acad Sci USA 86:3375–3378
Ribero MO, Antunes E, de Nucci G, Lovisolo SM, Zatz R (1992) Chronic inhibition of nitric oxide synthesis. A new model of arterial hypertension. Hypertension 20:298–303
Schrör K, Förster S, Woditsch I, Schröder H (1989) Generation of NO from molsidomine (SIN-1) *in vitro* and its relationship to changes in coronary vessel tissue. J Cardiovasc Pharmacol 14, Suppl 11:S29–S34
Schulz R, Kelm M, Heusch G (2004) Nitric oxide in myocardial ischemia/reperfusion injury. Cardiovasc Res 61:L402–L413
Southam E, Garthwaite J (1993) The nitric oxide-cyclic GMP signalling pathway in the rat brain. Neuropharmacol 32:1267–1277
Susswein AJ, Katzoff A, Miller N, Hurwitz I (2004) Nitric oxide and memory. Neuroscientist 10:153–162
Szabó C (1996) DNA strand breakage and activation of poly-ADP ribosyltransferase: A cytotoxic pathway triggered by peroxynitrite. Free Radic Biol Med 21:855–869
Szabó C, Cuzzocrea S, Zingarelli B, O'Connor M, Salzman AL (1997) Endothelial dysfunction in a rat model of endotoxic shock. Importance of the activation of poly(ADP-ribose) synthetase by peroxynitrite. J Clin Invest 100:723–735
Umans JG, Levi R (1995) Nitric oxide in the regulation of blood flow and arterial pressure. Ann Rev Physiol 57:771–790
Vanhoutte PM (1999) How to assess endothelial function in human blood vessels. J Hypertens 17:1047–1058
Willmot M, Gray L, Gibson C, Murphy S, Bath PMW (2005) A systematic review of nitric oxide donors and l-arginine in experimental stroke; effects on infarct size and cerebral blood flow. Nitric Oxide 12:141–149
Zanzinger J (1999) Role of nitric oxide in the neural control of cardiovascular function. Cardiovasc Res 43:639–649

A.1.1.18.2 Bioassay of EDRF Release

PURPOSE AND RATIONALE

EDRF release from arterial endothelium can be studied by a sandwich technique using donor tissue with intact endothelium facing with its intimal side the intimal side of a detector tissue.

PROCEDURE

Rabbits are subjected to various kinds of treatment, e. g., atherogenic diet or drug treatment for prevention of arteriosclerosis. Aorta segments, about 2 cm in length, are prepared, cut open along their longitudinal axis and pinned to a tissue suspender without damaging the endothelium. These segments serve as donor tissue for EDRF. Circumferential aorta strips from the abdominal aorta of untreated control rabbits are de-endothelialized by gently blotting their luminal surfaces on wet filter paper. These denuded abdominal aorta strips are pinned opposite the donor segments (intimal surface facing intimal surface) and function as detector for luminally released EDRF. Each sandwich preparation is suspended in a 40-ml organ bath, filled with oxygenated Krebs-Ringer buffer at 37°C containing 10 mM indomethacin. After connecting the detector strip to a force transducer, the angle between the detector strip and the donor segment is minimized and the distance between donor and detector tissue standardized. After one hour stabilization, the strips are brought to their optimum length-tension relationship by repeated exposure to 80 mM KCl. When a stable contractile response is established, the strips are precontracted with phenylephrine to 80–100% of their KCl-induced contraction. After stabilization of plateau phase, cumulative doses of acetylcholine (0.01–10 mM) are added to induce EDRF release from donor tissues.

EVALUATION

Relaxations of the detector strip induced by EDRF release from treated donor rabbit aortas are compared with aortas from control rabbits.

MODIFICATIONS OF THE METHOD

An other bioassay for measuring function of cultured endothelial cells using a computer system for the acquisition and analysis of vascular contractility has been published by Winn et al. (1992).

REFERENCES AND FURTHER READING

Riezebos J, Vleeming W, Beems RB, van Amsterdam JGC, Meijer GW, de Wildt DJ, Porsius AJ, Wemer J (1994) Comparison of Israpidine and Ramipril in cholesterol-fed rabbits: effect on progression of atherosclerosis and endothelial dysfunction. J Cardiovasc Pharmacol 23:415–423

Winn MJ, Panus PC, Norton P, Dai J (1992) Computer system for the acquisition and analysis of vascular contractility. Application to a bioassay of endothelial cell function. J Pharmacol Toxicol Meth 28:49–55

A.1.1.18.3 Isolated Arteries with and Without Endothelium

PURPOSE AND RATIONALE

Endothelial cells are able to synthesize and release potent vasoconstrictive agents, such as endothelin and angiotensin as well as vasodilating agents, such as EDRF. In isolated arterial segments the endothelial surface can be functionally destroyed allowing a differentiation between a direct action of drugs on the smooth muscle cells and an indirect effect via the endothelium. Isolated rings of rabbit or rat aorta are useful models to study the effects of endothelium derived factors such as EDRF or endothelins and their antagonists (Linz et al. 1986; Tracey et al. 1990; Fujimoto et al. 1992; Fukuroda et al. 1992; Wiemer et al. 1992). A survey of the history and on techniques leading to the discovery of endothelium-dependent relaxation was given by Furchgott (1993).

PROCEDURE

The descending thoracic aorta from rabbits of either sex (weighing 2.5–3.5 kg) is excised and dissected free from connective tissue. Care is taken to avoid damage of the endothelium. The aorta is divided into 2 mm wide rings and cut off in small strips. From some strips, the endothelium is removed by gently rubbing the intimal surfaces between the fingers for approximately 30 s. The strips are suspended in a 25 ml organ bath containing Krebs-bicarbonate solution at 37°C being gassed continuously with 5% CO_2/95% O_2. Contractions of the strips are recorded isometrically with a load of 2 g on the tissues. After an equilibration period of 2 h a stable baseline tone is reached.

To study the vasodilating effects of a compound, the strips are contracted with norepinephrine (10^{-8} M), or angiotensin II (10^{-7} M), or potassium chloride (20 mM). When a stable contraction plateau has been reached, the vasodilating agent is added in various concentrations. In these concentrations, norepinephrine, angiotensin II and KCl evoke a response of 60–80% of maximal contraction in intact rings of rabbit aorta. Rings without endothelium exhibit a response which is significantly enhanced in comparison with the response of the intact preparation after norepinephrine and angiotensin II precontraction.

To indicate the functional removal of the endothelium, the responsiveness of each preparation is tested with the known endothelium-dependent dilator, acetylcholine. In endothelium-intact rings, acetylcholine relaxes contractions induced by norepinephrine or angiotensin II. In precontracted rings devoid of endothelium, acetylcholine does not show any relaxing effect or causes contractions by itself at higher concentrations (Furchgott and Zawadzki 1980). As an example, atriopeptin III causes a similar concentration-dependent relaxation of all precontracted preparations with intact and with functionally destroyed endothelium indicating a direct effect on the smooth muscle cells. The relaxation is accompanied by an increase of cGMP.

EVALUATION

Statistical analyses are performed by regression analysis of dose response curves to determine EC_{50} values. Data are given as means ± standard deviation.

CRITICAL ASSESSMENT OF THE METHOD

The isolated aortic ring of rabbits with and without functionally intact endothelium is a useful tool to differentiate direct effects on the arterial smooth musculature from effects mediated by the endothelium.

MODIFICATIONS OF THE METHOD

Fujimoto et al. (1992) used the thoracic aorta from rats to study the effects between endothelin and an endothelin receptor antagonist. In transverse strips from **rat**thoracic aorta, 2 mm wide and 4–5 mm long, the endothelium was removed by gently rubbing the interior surface of the aorta. Concentration-response curves of contractions after ET-1 in the presence and the absence of the inhibitor were compared.

Pellisier et al. (1992) perfused the isolated mesenteric vascular bed of the **rat** with Tyrode solution and measured the perfusion pressure after injection of graded doses of norepinephrine and the dose-dependent relaxation due to acetylcholine in the vascular bed precontracted by norepinephrine infusion. In order to destroy the endothelial layer, the perfusate was

changed to a hypotonic Tyrode solution containing all of the constituents present in normal Tyrode solution but in one-tenth of the concentration resulting in disruption of more than 95% of the endothelial cells. The effect of norepinephrine was enhanced, whereas the effect of acetylcholine was abolished.

Legan and Sisson (1990) described a method to denude **rat** aortic endothelium *in vitro* with saponin.

Bohn and Schönafinger (1989) used helical strips of pulmonary arteries of **guinea pigs** in which the endothelium has been removed for biological detection of NO.

Fukuroda et al. (1992) used spiral strips from **porcine** coronary artery and vein and from intrapulmonary artery and vein removing the intimal surface by lightly rubbing with wet filter paper. Concentration-contraction curves for ET-1 and ET-3 were obtained with and without an endothelin antagonist.

Hayashi et al. (1988) described functional and anatomical recovery of endothelium after balloon denudation of the left circumflex coronary artery in **dogs**.

Endothelial denudation of the left circumflex coronary artery was used by Chu and Cobb (1987) to study the vasoactive effects of serotonin on proximal coronary arteries in awake **dogs**.

Experiments in isolated rings of the left circumflex or left anterior descending coronary artery of **dogs** with and without endothelium were performed by Desta et al. (1995).

Terrón (1996) analyzed the effects of 5-HT_1-receptor antagonists on 5-HT and sumatriptan induced isometric contractions in endothelium denuded segments of **canine** coronary arteries.

Ren et al. (1993) isolated coronary arteries from Japanese **monkeys** (*Macaca fuscata*) with and without endothelium to study muscarinic receptor subtypes mediating vasodilatation and vasoconstriction.

REFERENCES AND FURTHER READING

Bohn H, Schönafinger K (1989) Oxygen and oxidation promote the release of nitric oxide from sydnonimines. J Cardiovasc Pharmacol 14 (Suppl 11):S6–S12

Chu A, Cobb FR (1987) Vasoactive effects of serotonin on proximal coronary arteries in awake dogs. Circ Res 61 (Suppl II):II81–II87

Desta B, Nakashima M, Kirchengast M, Vanhoutte PM, Boulanger CM (1995) Previous exposure to bradykinin unmasks an endothelium-dependent relaxation to the converting enzyme inhibitor Trandolaprilat in isolated canine coronary arteries. J Pharm Exp Ther 272:885–891

Fujimoto M, Mihara S, Nakajima S, Ueda M, Nakamura M, Sakurai K (1992) A novel, non-peptide endothelin antagonist, isolated from bayberry, Myrica cerifera. FEBS Lett 305:41–44

Fukuroda T, Nishikibe M, Ohta Y, Ihara M, Yano M, Ishikawa K, Fukami T, Ikemoto F (1992) Analysis of responses to endothelins in isolated porcine blood vessels by using a novel endothelin antagonist, BQ-153. Life Sci 50:PL-107–PL-112

Furchgott RF (1993) The discovery of endothelium-dependent relaxation. Circulation 87: Suppl V:V3–V8

Furchgott RF, Zawadzki JV (1980) The obligatory role of endothelial cells in the relaxation of arterial smooth muscle by acetylcholine. Nature 288:373–376

Hayashi Y, Tomoike H, Nagasawa K, Yamada A, Nishijima H, Adachi H, Nakamura M (1988) Functional and anatomical recovery of endothelium after denudation of coronary artery. Am J Physiol 254:H1081–H1090

Jeremy JY, Dandona P (1989) Effect of endothelium removal on stimulatory and inhibitory modulation of rat aortic prostaglandin synthesis. Br J Pharmacol 96:243–250

Legan E, Sisson JA (1990) Method to denude rat aortic endothelium with saponin for phosphoinositide analysis in vascular smooth muscle. J Pharmacol Meth 23:31–39

Linz W, Albus U, Wiemer G, Schölkens BA, König W (1986) Atriopeptin III induces endothelium-independent relaxation and increases cGMP levels in rabbit aorta. Klin Wschr 64 (Suppl VI):27–30

Peach MJ, Singer HA, Loeb AL (1985) Mechanism of endothelium-dependent vascular smooth muscle relaxation. Biochem Pharmacol 34:1867–1874

Pelissier T, Miranda HF, Bustamante D, Paelle C, Pinardi G (1992) Removal of the endothelial layer in perfused mesenteric vascular bed of the rat. J Pharmacol Meth 27:41–44

Pörsti I, Bara AT, Busse R, Hecker M (1994) Release of nitric oxide by angiotensin-(1–7) from porcine coronary endothelium: implications for a novel angiotensin receptor. Br J Pharmacol 111:652–654

Ren LM, Nakane T, Chiba S (1993) Muscarinic receptor subtypes mediating vasodilation and vasoconstriction in isolated, perfused simian coronary arteries. J Cardiovasc Pharmacol 22:841–846

Reynolds EE, Mok LLS (1990) Role of thromboxane A_2/prostaglandin H_2 receptor in the vasoconstrictor response of rat aorta to endothelin. J Pharmacol Exp Ther 252:915–921

Scivoletto R, Carvalho MHC (1984) Cardionatrin causes vasodilation *in vitro* which is not dependent on the presence of endothelial cells. Eur J Pharmacol 101 :143–145

Terrón JA (1996) GR127935 is a potent antagonist of the 5-HT_1-like receptor mediating contraction in the canine coronary artery. Eur J Pharmacol 300:109–112

Tracey WR, Linden J, Peach MJ, Johns RA (1990) Comparison of spectrophotometric and biological assays for nitric oxide (NO) and endothelium-derived relaxing factor (EDRF): Nonspecificity of the diazotization reaction for NO and failure to detect EDRF. J Pharmacol Exp Ther 252:922–928

Wiemer G, Becker RHA, Jablonka B, Rosenkranz G, Schölkens BA, Linz W (1992) Effects of converting enzyme inhibitors and the calcium antagonist nifedipine alone and in combination on precontracted isolated rabbit aortic rings. Arzneim Forsch /Drug Res 42:795–797

A.1.1.18.4 Nitric Oxide Formation by Cultured Endothelial Cells

PURPOSE AND RATIONALE

Endothelial cells are able to synthesize and to release not only potent vasoconstrictor peptides such as an-

giotensin and endothelin but also potent dilators such as nitric oxide (NO), ATP, substance P, and bradykinin.

NO-formation can be assessed by determination of intracellular cyclic GMP in cultured endothelial cells, whereas release of NO from these cells can be measured by the stimulatory effect of NO on the activity of soluble guanylyl cyclase (Lückhoff et al. 1988; Wiemer et al. 1991; Linz et al. 1992; Bogle et al. 1992; review by Moncada et al. 1991).

PROCEDURE

Endothelial cell culture

Bovine or porcine aorta is obtained from local slaughter houses. Endothelial cells are isolated by digestion with dispase (Lückhoff et al. 1988). The cells are seeded on 6- or 24-well plates (e. g., Nunc Intermed, Wiesbaden, Germany) and grown to confluence. Dulbecco's modified Eagle's/Ham's F-12 medium containing 20% fetal calf serum is supplemented with penicillin (10 U/ml), streptomycin (10 µg/ml), L-glutamate (1 mM/l), glutathione (5 mg/ml), and L(+)ascorbic acid (5 mg/ml); (Biotect protection medium).

Measurement of cyclic GMP

Primary cultures of endothelial cells are used. After removal of the culture medium by aspiration, the monolayer is washed twice with 2 ml HEPES-Tyrode's solution (37°C). Thereafter, the cells are preincubated for 15 min at 37°C with 3-isobutyl-1-methylxanthine (IBMX), (10^{-4} M/l). After this time, drugs or solvents are added. After predetermined periods, the incubation medium is quickly removed. The cells are then immediately extracted with 0.6 ml 6% trichloroacetic acid and scraped off with a rubber scraper. The cell suspension is sonicated for 10 s before being centrifuged for 5 min at 4000 *g*. The supernatants are extracted with four volumes of water saturated diethylether, and the samples frozen (–20°C) until analysis. The protein contents of the samples are measured according to Lowry et al. (1951). Cyclic GMP can be determined in the acetylated samples by various methods (Heath et al. 1992), e. g., using a commercially available radioimmunoassay (New England Nuclear). Cyclic GMP content is expressed as picomoles GMP per milligram protein.

Measurement of NO release

Release of NO from endothelial cells is assayed on the basis of the stimulatory effect of NO on the activity of soluble guanylyl cyclase (purified from bovine lung) (Gerzer et al. 1981). The activity of the enzyme is determined in terms of the formation of cyclic [^{32}P]GMP from α-[^{32}P]GTP. Reactions are carried out in a reaction mixture containing 30 mM triethanolamine-HCl (pH 7.4), 1 mM reduced glutathione, 4 mM $MgCl_2$, 1 mM cGMP and 0.1 mg/ml bovine γ-globulin (total volume of 0.18 ml) at 37°C in the presence of α-[^{32}P]GTP (0.03 mM; 0.2 µCi) and soluble guanylyl cyclase (4 µg). Ten-µl samples are quickly transferred to the reaction mixture. Enzymatic formation of cGMP is allowed to proceed for 60 s and then stopped by the addition of 450 µl zinc acetate (120 mM) and 500 µl sodium carbonate (120 mM). A complete inhibition of cGMP formation can be achieved by preincubation of the monolayers for 30 min with the stereospecific inhibitor of NO synthase, N^G-nitro-L-arginine.

EVALUATION

Time-response curves and dose-response curves after addition of various activators or inhibitors of NO synthase are established. Data are reported as mean values ±SEM of cGMP (pmol/mg protein) or guanylyl cyclase activity (nmol/mg/min). Statistical evaluation is performed with Student's *t*-test.

MODIFICATIONS OF THE METHOD

The clinical pharmacology of L-arginine has been reviewed by Böger and Bode-Böger (2001).

Isolation of porcine cerebral capillary endothelial cells has been described by Wiemer et al. (1994).

Feelisch and Noack (1987) and Nakazawa et al. (1992) used chemiluminescence techniques for determination of NO.

A method for on-line detection of nitric oxide formation in liquid aqueous phase by electron paramagnetic resonance spectroscopy was described by Mordvintcev et al. (1991). Similar methods were used by Ichimori et al. (1992), Lancester et al. (1992), Steel-Goodwin et al. (1992).

Hecker et al. (1995) used a cascade superfusion bioassay to characterize a stable L-arginine-derived relaxing factor released from cytokine-stimulated vascular smooth muscle cells.

Electrochemical microprobes for direct measurement of NO in tissues have been developed (Shibuki 1990; Ishida et al. 1996; Smits and Lefebvre 1997).

Malinski and Taha (1992), Linz et al. (1999) measured nitric oxide release by a porphyrinic-based microsensor with a detection limit of 10 nmol/L. The amperometric signal at a constant potential of 0.67 V was measured with a voltametric analyzer (PAR model 273, Princeton Applied Research) interfaced

with an IBM 80486 computer with data acquisition and software.

Gabriel et al. (1997) developed a method for the detection of intracellular nitric oxide generation in dissociated cerebellar granule cells using dichlorofluorescin diacetate and flow cytometry.

Sumpio et al. (1987) found that cyclic mechanical stress stimulates cultured bovine aortic endothelial cells to proliferate.

Using this method, Rosales et al. (1997) found that exposure of endothelial cells to cyclic strain induces elevations of cytosolic Ca^{2+} concentration through mobilization of intracellular and extracellular pools.

REFERENCES AND FURTHER READING

Böger RH, Bode-Böger SM (2001) The clinical pharmacology of L-arginine. Annu Rev Pharmacol Toxicol 41:79–99

Bogle RG, Coade SB, Moncada S, Pearson JD, Mann GE (1992) Bradykinin stimulates L-arginine transport and nitric oxide release in vascular endothelial cells. formation in cytokine-treated rat hepatocytes and in blood and liver during sepsis. In: Moncada S, Marletta MA, Hibbs JB Jr, Higgs EA (eds) The Biology of Nitric Oxide. 1 Physiological and Clinical Aspects. Portland Press, London and Chapel Hill, pp 80–84

Busse R, Lamontagne D (1991) Endothelium-derived bradykinin is responsible for the increase in calcium produced by angiotensin-converting enzyme inhibitors in human endothelial cells. Naunyn-Schmiedeberg's Arch Pharmacol 344:126–129

Feelisch M, Noack E (1987) Nitric oxide (NO) formation from nitrovasodilators occurs independently of hemoglobin or non-heme iron. Eur J Pharmacol 142:465–469

Gabriel C, Camins A, Sureda FX, Aquirre L, Escubedo E, Pallàs M, Camarasa J (1997) Determination of nitric oxide generation in mammalian neurons using dichlorofluorescin diacetate and flow cytometry. J Pharmacol Toxicol Meth 38:93–98

Gerzer R, Hofmann F, Schultz G (1981) Purification of a soluble, sodium-nitroprussidestimulated guanylate cyclase from bovine lung. Eur J Biochem 116:479–486

Griffiths MJD, Messent M, McAllister RJ, Evans TW (1993) Aminoguanidine selectively inhibits inducible nitric oxide synthase. Br J Pharmacol 110:963–968

Heath R, Brynat B, Horton JK (1992) Which cyclic GMP assay? In: Moncada S, Marletta MA, Hibbs JB Jr, Higgs EA (eds) The Biology of Nitric Oxide. 2 Enzymology, Biochemistry and Immunology. Portland Press, London and Chapel Hill, pp 98–102

Hecker M, Boese M, Schini-Kerth VB, Mülsch A, Busse R (1995) Characterization of the stable L-arginine-derived relaxing factor released from cytokine-stimulated vascular smooth muscle cells as an N^G-hydroxy-L-arginine-nitric oxide adduct. Proc Natl Acad Sci USA 92:4671–4675

Hock FJ, Wirth K, Albus U, Linz W, Gerhards HJ, Wiemer G, Henke S, Breipohl G, König W, Knolle J, Schölkens BA (1991) Hoe 140 a new potent and long acting bradykinin antagonist: *in vitro* studies. Br J Pharmacol 102:769–773

Holzmann S, Kukovetz WR, Windischhofer W, Paschke E, Graier WF (1994) Pharmacologic differentiation between endothelium-dependent relaxations sensitive and resistant to nitro-L-arginine in coronary arteries. J Cardiovasc Pharmacol 23:747–756

Ichimori K, Pronai L, Fukahori M, Arroyo CM, Nakzawa H (1992) Spin trapping/electron paramagnetic spectroscopy analysis of endothelium-derived relaxing factors and their intermediates in human platelets. In: Moncada S, Marletta MA, Hibbs JB Jr, Higgs EA (eds) The Biology of Nitric Oxide. 2 Enzymology, Biochemistry and Immunology. Portland Press, London and Chapel Hill, pp 68–69

Ishida Y, Hashimoto M, Fukushima S, Masumura S, Sasaki T, Nakayama K, Tamura K, Murakami E, Isokawa S, Momose K (1996) A nitric oxide-sensitive electrode: requirement of lower oxygen concentration for detecting nitric oxide from the tissue. J Pharmacol Toxicol Meth 35:19–24

Jaffe EA, Nachman RL, Becker CG, Minick CR (1973) Culture of human endothelial cells derived from umbilical veins. J Clin Invest 52:2745–2756

Lancester JR Jr, Stadler J, Billiar TR, Bergonia HA, Kim YM, Piette LH, Simmons RL (1992) Electron-paramagnetic resonance detection of iron-nitrosyl formation in cytokine-treated rat hepatocytes and in blood and liver during sepsis. In: Moncada S, Marletta MA, Hibbs JB Jr, Higgs EA (eds) The Biology of Nitric Oxide. 2 Enzymology, Biochemistry and Immunology. Portland Press, London and Chapel Hill, pp 76–80

Linz W, Wiemer G, Schölkens BA (1992) ACE-inhibition induces NO-formation in cultured bovine endothelial cells and protects isolated ischemic rat hearts. J Mol Cell Cardiol 24:909–919

Linz W, Wohlfart P, Schoelkens BA, Becker RHA, Malinski T, Wiemer G (1999) Late treatment with ramipril increases survival in old spontaneously hypertensive rats. Hypertension 34:291–295

Lowry OH, Rosebrough NJ, Farr AL, Randall RJ (1951) Protein measurement with phenol reagent. J Biol Chem 193:265–275

Lückhoff A, Pohl U, Mülsch A, Busse R (1988) Differential role of extra- and intracellular calcium in the release of EDRF and prostacyclin from cultured endothelial cells. Br J Pharmacol 95:189–196

Malinski T, Taha Z (1992) Nitric oxide release from a single cell measured *in situ* by a porphyrinic-based microsensor. Nature 358:676–678

Moncada S, Palmer RMJ, Higgs EA (1991) Nitric oxide: physiology, pathophysiology, and pharmacology. Pharmacol Rev 43:109–142

Mordvintcev P, Mülsch A, Busse R, Vanin A (1991) On-line detection of nitric oxide formation in liquid aqueous phase by electron paramagnetic resonance spectroscopy. Anal Biochem 19:142–146

Mülsch A, Böhme E, Busse R (1987) Stimulation of soluble guanylate cyclase by endothelium-derived relaxing factor from cultured endothelial cells. Eur J Pharmacol 135:247–250

Nakazawa H, Fukahori M, Murata T, Furuya T (1992) On-line monitoring of nitric oxide generation from isolated perfused rat lung using decrease in superoxide-dependent chemiluminescence. In: Moncada S, Marletta MA, Hibbs JB Jr, Higgs EA (eds) The Biology of Nitric Oxide. 2 Enzymology, Biochemistry and Immunology. Portland Press, London and Chapel Hill, pp 69

Nathan C (1992) Nitric oxide as a secretory product of mammalian cells. FASEB J 6:3051–3064

Rosales OR, Isales CM, Barrett PQ, Brophy C, Sumpio BE (1997) Exposure of endothelial cells to cyclic strain induces elevations of cytosolic Ca^{2+} concentration through mobilization of intracellular and extracellular pools. Biochem J 326:385–392

Shephard JT, Vanhoutte PM (1991) Endothelium-derived relaxing (EDRF) and contracting factors (EDCF) in the control of cardiovascular homeostasis: the pioneering observations. In: Rubanyi GM (ed) Cardiovascular Significance of Endothelium-Derived Vasoactive Factors. Futura Publ Comp, Inc., Mount Kisco, NY, pp 39–64

Shibuki K (1990) An electrochemical microprobe for detecting nitric oxide release in brain tissue. Neurosci Res 9:69–76

Smits GJM, Lefebvre RA (1997) Evaluation of an electrochemical microprobe for direct NO measurement in the rat gastric fundus. J Pharmacol Toxicol Meth 37:97–103

Steel-Goodwin L, Arroyo CM, Gray B, Carmichael AJ (1992) Electron paramagnetic resonance detection of nitric oxide-dependent spin adducts in mouse jejunum. In: Moncada S, Marletta MA, Hibbs JB Jr, Higgs EA (eds) The Biology of Nitric Oxide. 2 Enzymology, Biochemistry and Immunology. Portland Press, London and Chapel Hill, pp 80–84

Sumpio BE, Banes AJ, Levin LG, Johnson G Jr (1987) Mechanical stress stimulates aortic endothelial cells to proliferate. J Vasc Surg 6:252–256

Wiemer G, Schölkens BA, Becker RHA, Busse R (1991) Ramiprilat enhances endothelial autacoid formation by inhibiting breakdown of endothelium derived bradykinin. Hypertension 18:558–563

Wiemer G, Popp R, Schölkens BA, Gögelein H (1994) Enhancement of cytosolic calcium, prostaglandin and nitric oxide by bradykinin and the ACE inhibitor ramiprilate in porcine brain capillary endothelial cells. Brain Res 638:261–266

A.1.1.18.5 Expression of Nitric Oxide Synthase

PURPOSE AND RATIONALE

Properties of various forms of nitric oxide synthase (NOS) have been described by Mayer et al. (1992), Leone et al. (1992), Hevel et al. (1992), Förstermann et al. (1992, 1995), (Salter et al. 1992), Pollock et al. (1992), Schmidt et al. (1992), and Mungrue et al. (2003), among them type I, which is constitutively expressed in neurons; the inducible type II which is found in macrophages and hepatocytes, but also in the brain (Moro et al. 1998), where it may contribute to NO-mediated neurotoxicity; and type III, which is constitutively expressed in endothelial cells (Knowles and Moncada 1994). NOS can be inhibited by several routes, e. g., competition with L-arginine, NADPH, flavin or tetrahydrobiopterin, interaction of the haeme group of NOS, interference with Ca^{2+} availability or calmodulin binding to the enzyme (Fukuto and Chaudhuri 1995). A widely used inhibitor is L-NAME (Vargas et al. 1991). Selective inhibition of constitutive NOS can by achieved by 7-nitroindazole (Moore et al. 1993); of the inducible NOS by aminoguanidine hydrochloride (Griffiths et al. 1993) and by 2-amino-5,6-dihydro-6-methyl-4H-1,3-thiazine (= AMT) (Nakane et al. 1995). Linz et al. (1999) determined NOS in the left cardiac ventricle of hypertensive rats.

PROCEDURE

Tissues are ground at the temperature of liquid nitrogen using a microdismembranator (Braun). The powders are extracted for 1 h on ice with 10 mmol/l Tris-HCl, pH 7.4, containing 1% SDS and protease inhibitors (complete, Boehringer Mannheim). Debris is removed by a 30-min centrifugation at 4°C (>100,000 *g*). 100 µg of total of the protein extracts are subjected to SDS-PAGE electrophoresis and transferred to nitrocellulose membranes (Hybond, Amersham). The eNOS protein is detected by use of a specific antibody (monoclonal anti-NOS III), Transduction Laboratories) and visualized by enhanced chemifluorescence with a commercially available kit (Amersham). As a secondary antibody, an anti-mouse IgG antibody coupled to alkaline phosphatase is used (Jackson ImmunoResearch Laboratories). Chemifluorescence is analyzed and quantified by scanning with a Fluorimager 595-system (Molecular Dynamics).

EVALUATION

The data are given as mean ± SEM. ANOVA is used followed by Tuckey's test for post-ANOVA multiple pair comparisons.

MODIFICATIONS OF THE METHOD

Linz et al. (1997) measured expression of ecNOS in the carotid artery of hypertensive rats by Western blot analysis. Frozen (–70°C) vessels were thawed and extracted with guanidium isothiocyanate/phenol/chloroform (Chomczynski and Sacchi 1987). Crude protein fractions were obtained by alcohol precipitation of the phenol phase. A total of 100 µg of the protein extracts was subjected to SDS-PAGE and transferred to nitrocellulose membranes (Bio-Rad). Ponceau staining was performed to verify the quality of the transfer and the equipartition of protein in each lane. EcNOS protein was detected with a specific antibody (mouse NOS III, Transduction Laboratories) and visualized by enhanced chemifluorescence with a commercially available kit (Amersham). The autoradiographs were analyzed by scanning densitometry.

McCall et al. (1991) identified N-iminoethyl-L-ornithine as an irreversible inhibitor of nitric oxide synthase.

Bauersachs et al. (1998, 1999) measured vascular reactivity in isolated rat aortic rings mounted in an organ bath (Föhr Medical Instruments, Seeheim Germany) for isometric force measurement and determined superoxide anion production by lucigenin-enhanced chemiluminescence and endothelial nitric ox-

ide synthase and soluble guanylyl cyclase expression by reverse transcription-polymerase chain reaction.

Von der Leyen et al. (1995) reported gene therapy inhibiting neointimal vascular lesions in rats. After denudation of the endothelium of carotid arteries by balloon injury, endothelial cell nitric oxidase expression in the vessel wall was restored by using the Sendai virus/liposome *in vivo* gene transfer technique.

Lund et al. (2000) found that gene transfer of endothelial nitric oxide synthase improves relaxation of carotid arteries from diabetic rabbits.

Mungrue et al. (2002) discussed lessons from murine genetic models on the role of NOS in heart failure.

REFERENCES AND FURTHER READING

Bauersachs J, Bouloumié A, Fraccarollo D, Hu K, Busse R, Ertl G (1998) Hydralazine prevents endothelial dysfunction, but not the increase in superoxide production in nitric oxide-deficient hypertension. Eur J Pharmacol 362:77–81

Bauersachs J, Bouloumié A, Fraccarollo D, Hu K, Busse R, Ertl G (1999) Endothelial dysfunction in chronic myocardial infarction despite increased vascular endothelial nitric oxide synthase and soluble guanylate cyclase expression. Role of enhanced vascular superoxide production

Chomczynski P, Sacchi N (1987) Single-step method for RNA isolation by acid guanidium thiocyanatephenolchloroform extraction. Anal Biochem 162:156–159

Förstermann U, Schmidt HHHW, Pollock JS, Sheng H, Mitchell JA, Warner TD, Murad F (1992) Characterization and classification of constitutive and inducible isoforms of nitric oxide synthase in various cell types. In: Moncada S, Marletta MA, Hibbs JB Jr, Higgs EA (eds) The Biology of Nitric Oxide. 2 Enzymology, Biochemistry and Immunology. Portland Press, London and Chapel Hill, pp 21–23

Förstermann U, Kleinert H (1995) Nitric oxide synthase: Expression and expressional control of the three isoforms. Naunyn-Schmiedeberg's Arch Pharmacol 352:351–364

Fukuto JM, Chaudhuri G (1995) Inhibition of constitutive and inducible nitric oxide synthase: Potential selective inhibition. Annu Rev Pharmacol Toxicol 35:165–194

Hevel JM, White KA, Marletta MA (1992) Purification of the inducible murine macrophage nitric oxide synthase: identification as a flavoprotein and detection of enzyme-bound tetrahydrobiopterin. In: Moncada S, Marletta MA, Hibbs JB Jr, Higgs EA (eds) The Biology of Nitric Oxide. 2 Enzymology, Biochemistry and Immunology. Portland Press, London and Chapel Hill, pp 19–19–21

Knowles RG, Moncada S (1994) Nitric oxide synthases in mammals. Biochem J 298:249–258

Leone AM, Palmer RMJ, Knowles RG, Francis PL, Ashton DS, Moncada S (1992) Molecular oxygen is incorporated in nitric oxide and citrulline by constitutive and inducible nitric oxide synthases. In: Moncada S, Marletta MA, Hibbs JB Jr, Higgs EA (eds) The Biology of Nitric Oxide. 2 Enzymology, Biochemistry and Immunology. Portland Press, London and Chapel Hill, pp 7–14

Linz W, Jessen T, Becker RHA, Schölkens BA, Wiemer G (1997) Long-term ACE inhibition doubles lifespan of hypertensive rats. Circulation 96:3164–3172

Linz W, Wohlfart P, Schoelkens BA, Becker RHA, Malinski T, Wiemer G (1999) Late treatment with ramipril increases survival in old spontaneously hypertensive rats. Hypertension 34:291–295

Lund DD, Faraci FM, Miller FJ, Jr, Heistad DD (2000) Gene transfer of endothelial nitric oxide synthase improves relaxation of carotid arteries from diabetic rabbits. Circulation 101:1027–1033

Mayer B, John M, Heinzel B, Klatt P, Werner ER, Böhme E (1992) Properties of Ca^{2+}-regulated brain nitric oxide synthase. In: Moncada S, Marletta MA, Hibbs JB Jr, Higgs EA (eds) The Biology of Nitric Oxide. 2 Enzymology, Biochemistry and Immunology. Portland Press, London and Chapel Hill, pp 4–6

McCall TB, Feelisch M, Palmer RMJ, Moncada S (1991) Identification of N-iminoethyl-L-ornithine as an irreversible inhibitor of nitric oxide synthase in phagocytic cells. Br J Pharmacol 102:234–238

Moore PK, Wallace P, Gaffen Z, Hart SL, Babbedge RC (1993) Characterization of the novel nitric oxide synthase inhibitor 7-nitroindazole and related indazoles: Antinociceptive and cardiovascular effects. Br J Pharmacol 110:219–224

Moro MA, de Alba J, Leza JC, Lorenzo P, Fernández AP, Bentura ML, Boscá L, Lizasoain I (1998) Neuronal expression of inducible nitric oxide synthase after oxygen and glucose deprivation in rat forebrain slices. Eur J Neurosci 10:445–456

Mungrue IN, Husain M, Stewart DJ (2002) The role of NOS in heart failure. Lessons from murine genetic models. Heart Failure Rev 7:407–422

Mungrue IN, Bredt DS, Stewart DJ, Husain M (2003) From molecules to mammals: what's NOS got to do with it ? Acta Physiol Scand 179:123–135

Nakane M, Klinghöfer V, Kuk JE, Donnelly JL, Budzik GP, Pollock JS, Basha F, Carter GW (1995) Novel potent and selective inhibitors of inducible nitric oxide synthase. Mol Pharmacol 47:831–834

Pollock JS, Mitchell JA, Warner TD, Schmidt HHHW, Nakana M, Förstermann U, Murad F (1992) Purification of nitric oxide synthases from endothelial cells. In: Moncada S, Marletta MA, Hibbs JB Jr, Higgs EA (eds) The Biology of Nitric Oxide. 2 Enzymology, Biochemistry and Immunology. Portland Press, London and Chapel Hill, pp 108–111

Salter M, Knowles RG, Moncada S (1992) Widespread tissue distribution, species distribution and changes in activity of Ca^{2+}-dependent and Ca^{2+}-independent nitric oxide synthases. In: Moncada S, Marletta MA, Hibbs JB Jr, Higgs EA (eds) The Biology of Nitric Oxide. 2 Enzymology, Biochemistry and Immunology. Portland Press, London and Chapel Hill, pp 193–197

Schmidt HHHW, Smith RM, Nakana M, Gagne GD, Miller MF, Pollock JS, Sheng H, Förstermann U, Murad F (1992) Type I nitric oxide synthase: purification, characterization and immunohistochemical localization. In: Moncada S, Marletta MA, Hibbs JB Jr, Higgs EA (eds) The Biology of Nitric Oxide. 2 Enzymology, Biochemistry and Immunology. Portland Press, London and Chapel Hill, pp 112–114

Vargas HM, Cuevas JM, Ignarro LJ, Chaudhuri G (1991) Comparison of the inhibitory potencies of N(G)-methyl-, N(G)-nitro- and N(G)-amino-L-arginine on EDRF formation in the rat: Evidence for continuous basal EDRF release. J Pharm Exp Ther 257:1208–1215

Von der Leyen HE, Gibbbons GH, Morishita R, Lewis NP, Zhang L, Nakajima M, Kaneda Y, Cooke JP, Dzau VJ (1995) Gene therapy inhibiting neointimal vascular lesion: *In vivo* transfer of endothelial cell nitric oxide synthase gene. Proc Natl Acad Sci USA 92:1137–1141

A.1.1.19 Inhibition of Rho Kinase

PURPOSE AND RATIONALE

Rho is a member of the Ras-related family of small molecular weight GTP-binding proteins, and Rho works as a molecular switch by shuttling between the GDP-bound inactive form and the GTP-bound active form. Rho is involved in cell motility, cell adhesion, cytokinesis, Ras-induced transformation, transcriptional activation, and cell cycle progression. These actions, through Rho signaling, are mediated by downstream Rho effectors, such as the ROCK family of Rho-associated serine/threonine protein kinases. Studies with ROCK-specific inhibitors indicate that the ROCK pathway works in the contraction of vascular smooth muscle. Several studies indicate that Rho-kinase may be a novel therapeutic target in the treatment of cardiovascular disease (Kobayashi et al. 2002; Shimokawa 2002; Ito et al. 2003, 2004; Nakakuki et al. 2005; Budzyn et al. 2006; Winaver et al. 2006).

Ishizaki et al. (2000) described the pharmacological properties of a specific inhibitor of Rho-associated kinases.

PROCEDURE

Kinase assay

Recombinant ROCK-I, ROCK-II, PKN, or citron kinase was expressed in HeLa cells as a Myc-tagged protein by transfection using lipofectamine, and was precipitated from the cell lysates by the use of 9E10 monoclonal anti-Myc antibody coupled to G protein-Sepharose (Ishizaki et al. 1997). Recovered immunocomplexes were incubated with various concentrations of [^{32}P]ATP and 10 µg of histone type 2 as substrates, in the absence or presence of various concentrations of test compounds at 30°C for 30 min in a total volume of 30 µl of the kinase buffer containing 50 mM HEPES-NaOH, pH 7.4, 10 mM $MgCl_2$, 5 mM $MnCl_2$, 0.02% Briji 35, and 2 mM dithiothreitol. PKCα was incubated with 5 µM [^{32}P]ATP and 200 µg/ml histone type 2 as substrates in the absence or presence of various concentrations of test compounds at 30°C for 10 min in a kinase buffer containing 50 mM Tris-HCl, pH 7.5, 0.5 mM $CaCl_2$, 5 mM magnesium acetate, 25 µg/ml phosphatidyl serine, 50 ng/ml 12-*O*-tetradecanoylphorbol-13-acetate and 0.001% leupeptin in a total volume of 30 µl. Incubation was terminated by the addition of 10 µl of 4× Laemmli sample buffer. After boiling for 5 min, the mixture was subjected to SDS-polyacrylamide gel electrophoresis on a 16% gel. The gel was stained with Coomassie Brilliant Blue, and then dried. The bands corresponding to histone type 2 were excised, and the radioactivity was measured.

EVALUATION

K_i values were either determined by the double reciprocal plot or calculated from the equation $K_i = IC_{50}/(1 + S/K_m)$, where S and K_m are the concentration of ATP and the K_m value for ATP, respectively.

REFERENCES AND FURTHER READING

Budzyn K, Marley PD, Sobey CG (2006) Targeting Rho and Rho-kinase in the treatment of cardiovascular disease. Trends Pharmacol Sci 27:97–104

Ishizaki T, Naito M, Fujisawa K, Maekawa M, Watanabe N, Saito Y, Narumiya S (1997) p160ROCK, a Rho-associated coiled-coil forming protein kinase, works downstream of Rho and induces focal adhesions. FEBS Lett 404:118–124

Ishizaki T, Uehata M, Tamechika I, Keel J, Nonomura K, Maekawa M, Narumiya S (2000) Pharmacological properties of Y-27632, a specific inhibitor of Rho-associated kinases. Mol Pharmacol 57:976–983

Ito K, Hirooka Y, Sakai K, Kishi T, Kaibuchi K, Shimokawa H, Takeshita A (2003) Rho/Rho-kinase pathway in brain stem contributes to blood pressure regulation via sympathetic nervous system. Possible involvement of neural mechanisms of hypertension. Circ Res 92:1337–13343

Ito K, Hirooka Y, Kishi T, Kimura Y, Kaibuchi K, Shimokawa H, Takeshita A (2004) Rho/Rho-kinase pathway in the brain stem contributes to hypertension caused by chronic nitric oxide synthase inhibition. Hypertension 43:156–162

Kobayashi N, Horinaka S, Mita SI, Nakano S, Honda T, Yoshida K, Kobayashi T, Matsuoka H (2002) Critical role of Rho-kinase pathway for cardiac performance and remodeling in failing rat hearts. Cardiovasc Res 55:757–767

Nakakuki T, Ito M, Iwasaki H, Kureishi Y, Okamoto R, Moriki N, Kongo M, Kato S, Yamada N, Isaka N, Nakano T (2005) Rho/Rho-kinase pathway contributes to C-reactive protein-induced plasminogen activator inhibitor-1 expression in endothelial cells. Arterioscler Thromb Vasc Biol 25:2088–2093

Shimokawa H (2002) Rho-kinase as a novel therapeutic target in treatment of cardiovascular disease. J Cardiovasc Pharmacol 39:319–327

Winaver J, Ovcharenko E, Rubinstein I, Gurbanov K, Pollesello P, Bishara B, Hoffman A, Abassi Z (2006) Involvement of Rho kinase pathway in the mechanisms of renal vasoconstriction and cardiac hypertrophy in rats with experimental heart failure.. Am J Physiol 290:H2007–H2014

A.1.1.20 Inhibition of Na^+/H^+ Exchange

PURPOSE AND RATIONALE

Na^+/H^+ exchange was first described by Murer et al. (1976) in a study of intestinal and renal brush border vesicles. The plasma membrane Na^+/H^+ exchanger is an ubiquitous pH regulating cellular ion transport system. It is driven by the Na^+ gradient and extrudes

protons from the cytosol in exchange for extracellular Na^+ ions (Aronson 1985; Frelin et al. 1988; Fliegel and Dyck 1995; Orlowski and Grinstein 1997; Wakabayashi et al. 1997; Dibrov and Fliegel 1998). Six mammalian Na^+/H^+ exchangers: NHE1, NHE2, NHE3; NHE4, NHE5 (Attaphitaya et al. 1999; Szabo et al. 2000), and NHE6 have been described (Tse et al. 1994; Orlowski 1999; Counillon and Pouysségur 2000).

In cardiac tissue the exchanger has a major role in the control of intracellular pH. At the onset of cardiac ischemia and during reperfusion, Na^+/H^+ exchange is excessively activated by low intracellular pH. Since the deleterious Na^+ influx in this condition was found to originate mainly from Na^+/H^+ exchange (Frelin et al. 1984; Schömig et al. 1988), the exchanger seems to be responsible for an increase of cytosolic sodium in ischemic cells. The accumulation of intracellular Na^+ causes an activation of Na^+/K^+ ATPase (Frelin et al. 1984; Rasmussen et al. 1989) which in turn increases ATP consumption.

During ischemia the aerobic metabolism of glucose terminates in lactic acid. A vicious circle leads to a further decrease of intracellular pH and to a further activation of Na^+/H^+ exchange, resulting in energy depletion, cellular Na^+ overload and finally due to the coupling of Na^+ and Ca^{2+} transport via Na^+/Ca^{2+} exchange, cellular Ca^{2+} overload (Lazdunski et al. 1985; Tani and Neely 1990; Scholz and Albus 1993). Especially in ischemic cardiac tissue, where Na^+/H^+ exchange is the predominant pH regulating ion transport system (Weissenberg et al. 1989), these pathological events can lead to increased excitability and precipitation of cellular death. Therefore, it is desirable to find potent and well tolerated inhibitors of Na^+/H^+ exchange which should be able to interrupt this vicious cycle, to conserve cellular energy stores and to diminish cellular excitability and necrosis during cardiac ischemia. Such effects have been found with relatively weak inhibitors of Na^+/H^+ exchange at high toxic doses, such as amiloride and ethyl isopropyl amiloride (Scholz et al. 1992).

The myocardial Na^+/H^+ exchanger is regarded as a therapeutic target for the prevention of myocardial ischemic and reperfusion injury and attenuation of postinfarction heart failure (Karmazyn et al. 2001).

More potent Na^+/H^+ exchange inhibitors showed beneficial effects on ischemia/reperfusion injury (see A.5.0.7 and A.5.0.8) in rats (Aye et al. 1997; Myers et al. 1998; Aihara et al. 2000), dogs (Gumina et al. 1998, 2000) and pigs (Portman et al. 2001). Heart hypertrophy and heart failure after myocardial infarction is reduced (Yoshida and Karmazyn 2000; Kusumoto et al. 2001). Ischemia-induced apoptosis in isolated rat hearts is attenuated by sodium-hydrogen exchange inhibitors (Chakrabarti et al. 1997).

Linz and Busch (2003) demonstrated the effects of NHE-1 inhibition from protection during acute ischemia/reperfusion to prevention of myocardial remodeling.

REFERENCES AND FURTHER READING

Aihara K, Hisa H, Sato T, Yoneyama F, Sasamori J, Yamaguchi F, Yoneyama S, Mizuno Y, Takahashi A, Nagai A, Kimura T, Kogi K, Sato S (2000) Cardioprotective effect of TY-12533, a novel Na^+-H^+ exchange inhibitor on ischemia/reperfusion injury. Eur J Pharmacol 404:221–229

Aronson PS (1985) Kinetic properties of the plasma membrane Na^+-H^+ exchanger. Ann Rev Pharmacol 47:545–560

Attaphitaya S, Park K, Melvin JE (1999) Molecular cloning and functional expression of a rat Na^+/H^+ exchanger (NHE5) highly expressed in brain. J Biol Chem 274:4383–4388

Aye NN, Xue YX, Hashimoto K (1997) Antiarrhythmic effects of cariporide, a novel Na^+/H^+ exchange inhibitor, on reperfusion ventricular arrhythmias in rat hearts. Eur J Pharmacol 339:121–127

Chakrabarti S, Hoque ANE, Karmazy M (1997) A rapid ischemia-induced apoptosis in isolated rat hearts and its attenuation by the sodium-hydrogen exchange inhibitor HOE 642 (Cariporide) J Mol Cell Cardiol 29:3169–3174

Counillon L, Pouysségur J (2000) The expanding family of eukaryotic Na^+-H^+ exchangers. J Biol Chem 275:1–4

Dibrov P, Fliegel L (1998) Comparative molecular analysis of Na^+/H^+ exchangers: a unified model for Na^+/H^+ antiport? FEBS Letters 424:1–5

Fliegel L, Dyck JRB (1995) Molecular biology of the cardiac sodium/hydrogen exchanger. Cardiovasc Res 29:155–159

Frelin C, Vigne P, Lazdunski M (1984) The role of Na^+/H^+ exchange system in cardiac cells in relation to the control of the internal Na^+ concentration. J Biol Chem 259:8880–8885

Frelin C, Vigne P, Ladoux A, Lazdunski M (1988) The regulation of intracellular pH in cells from vertebrates. Eur J Biochem 174:3–14

Gumina RJ, Mizumura T, Beier N, Schelling P, Schultz JJ, Gross GJ (1998) A new sodium/hydrogen exchange inhibitor, EMD 85131, limits infarct size in dogs when administered before or after coronary artery occlusion. J Pharmacol Exp Ther 286:175–183

Gumina RJ, Daemmgen J, Gross GJ (2000) Inhibition of the Na^+/H^+ exchanger attenuates phase 1b ischemic arrhythmias and reperfuion-induced ventricular fibrillation. Eur J Pharmacol 396:119–124

Karmazyn M, Sostaric JV, Gan XT (2001) The myocardial Na^+/H^+ exchanger: a therapeutic target for the prevention of myocardial ischaemic and reperfusion injury and attenuation of postinfarction heart failure. Drugs 61:375–389

Kusumoto K, Haist JV, Karmazyn M (2001) Na^+/H^+ exchange inhibition reduces hypertrophy and heart failure after myocardial infarction in rats. Am J Physiol 280 (Heart Circulatory Physiol): H738–H745

Lazdunski M, Frelin C, Vigne P (1985) The sodium/hydrogen exchange system in cardiac cells: its biochemical and pharmacological properties and its role in regulation internal concentrations of sodium and internal pH. J Mol Cell Cardiol 17:1029–1042

Linz WJ, Busch AE (2003) NHE-1 inhibition: from protection during acute ischaemia/reperfusion to prevention of myocardial remodelling. Naunyn-Schmiedebergs Arch Pharmacol 368:239–246
Myers ML, Farhangkhoee P, Karmazyn M (1998) Hydrogen peroxide induced impairment of postischemic ventricular function is prevented by the sodium-hydrogen exchange inhibitor HOE &42 (cariporide). Cardiovasc Res 40:290–296
Murer H, Hopfer U, Kinne R (1976) Sodium/proton antiport in brush-border-membranes isolated from rat small intestine and Kidney. Biochem J 154:597–604
Orlowski J (1999) Na^+/H^+ exchangers. Molecular diversity and relevance to the heart. Ann NY Acad Sci 874:346–353
Orlowski J, Grinstein S (1997) Na^+/H^+ exchangers in mammalian cells. J Biol Chem 272:22373–22776
Portman MA, Panos AL, Xiao Y, Anderson DL, Ning X-H (2001) HOE-642 (cariporide) alters pH_i and diastolic function after ischemia during reperfusion in pig hearts *in situ*. Am J Physiol 280 (Heart Circulatory Physiol): H830–H834
Rasmussen HH, Cragoe EJ, Ten Eick RE (1989) Na^+-dependent activation of Na^+-K^+ pump in human myocardium during recovery from acidosis. Am J Physiol 256:H431–H439
Schömig A, Kurz T, Richardt G, Schömig E (1988) Neuronal sodium homeostasis and axoplasmic amine concentration determine calcium-independent noradrenaline release in nor-moxic and ischemic rat heart. Circ Res 63:214–226
Scholz W, Albus U (1993) Na^+/H^+ exchanger exchange and its inhibition in cardiac ischemia and reperfusion. Basic Res Cardiol 88:443–455
Szabo EZ, Numata M, Shull GE, Orlowski J (2000) Kinetic and pharmacological properties of a human brain Na^+/H^+ exchanger isoform 5 stably expressed in Chinese hamster ovary cells. J Biol Chem 275:6302–6307
Tse CM, Levine SA, Yun CHC, Brant SR, Nath S, Pouysségur J, Donowitz M (1994) Molecular properties, kinetics and regulation of mammalian Na^+/H^+ exchangers. Cell Physiol Biochem 4:282–300
Tani M, Neely JR (1990) Na^+ accumulation increases Ca^{+2} overload and impairs function in anoxic rat heart. J Mol Cell Cardiol 22:57–72
Wakabayshi S, Shigekawa M, Pouysségur J (1997) Molecular physiology of vertebrate Na^+/H^+ exchangers. Physiol Rev 77:51–74
Weissberg PL, Little PJ, Cragoe EJ, Bobik A (1989) The pH of spontaneously beating cultured rat hearts is regulated by an ATP-calmodulin-dependent Na^+/H^+ antiport. Circ Res 64:676–685
Yoshida H, Karmazyn M (2000) Na^+/H^+ exchange inhibition attenuates hypertrophy and heart failure in 1-wk postinfarction rat myocardium. Am J Physiol 278 (Heart Circulatory Physiol): H300-H304

A.1.1.20.1 Inhibition of Na^+/H^+ Exchange in Thrombocytes

PURPOSE AND RATIONALE

The inhibition of Na^+/H^+ exchange has been studied in platelets by measuring the optical density after osmotic cell swelling (Rosskopf et al. 1991).

PROCEDURE

About 5 ml blood is withdrawn by venipuncture from human donors or from the vena jugularis externa of Beagle dogs or from the aorta of anesthetized Wistar rats (weighing 250–350 g). Coagulation is inhibited by 0.8 ml citrate acid dextrose (65 mM citric acid, 11 mM glucose, 85 mM trisodium citrate). Platelet-rich plasma (PRP) is obtained by centrifugation of whole blood at 90 *g* for 10 min at room temperature. Platelet count is measured, e. g., with a Casey 1 multichannelyser (Schärfe System, Reutlingen, Germany).

Each of the experiments is performed with 10–50 µl PRP containing 20×10^6 platelets in a volume of 100 µl with saline. To activate Na^+/H^+ exchange in the platelets by intracellular acidification, 500 µl propionate buffer (135 mM Na-propionate, 1 mM HCl, 1 mM $CaCl_2$, 1 mM $MgCl_2$, 10 mM glucose, 20 mM HEPES, pH 6.7, 22°C) are added to the PRP/NaCl solution. Swelling of the platelets results in a decrease of optical density which can be measured with an aggregometer, e. g. with a Turbitimer (Behringwerke, Marburg, Germany). The system is activated photometrically by the addition of the propionate buffer to the cuvette. The experiments are performed with and without the addition of the Na^+/H^+ exchange inhibitor to be tested. The inhibitors are added in concentrations between 10^{-4} and 10^{-8} mol/l. 5-(N-ethyl-N-isopropyl)amiloride (EIPA) is used as standard. During the experiments all solutions are kept at 22°C in a temperature controlled water bath.

EVALUATION

Results are given as means ± SD. Student's *t*-test is employed for statistical evaluation. IC_{50} values are calculated from dose-response curves.

REFERENCES AND FURTHER READING

Rosskopf D, Morgenstern E, Scholz W, Osswald U, Siffert W (1991) Rapid determination of the elevated Na^+-K^+exchange in platelets of patients with essential hypertension using an optical swelling assay. J Hypertens 9:231–238

A.1.1.20.2 Inhibition of Na^+/H^+ Exchange in Cholesterol Activated Rabbit Erythrocytes

PURPOSE AND RATIONALE

The inhibition of Na^+/H^+ exchange has been studied in cholesterol activated rabbit erythrocytes by flame photometry of sodium (Scholz et al. 1992, 1993).

PROCEDURE

White rabbits (New Zealand strain, Ivanovas) are fed with a rabbit standard chow with 2% cholesterol for

6 weeks to increase the Na^+/H^+ exchange (Scholz et al. 1990) and to make the erythrocytes suitable for measurement of sodium influx via Na^+/H^+ exchange by flame photometry. Blood is drawn from the ear artery of the rabbits and coagulation prevented with 25 IU/ml potassium heparin. The hematocrit of the samples is determined in duplicate by centrifugation. Aliquots of 100 µl are taken to measure the initial sodium content of the erythrocytes.

To determine the amiloride sensitive sodium influx into erythrocytes, 100 µl of each blood sample are added to 5 ml of buffer made hyperosmolar by sucrose (140 mM NaCl, 3 mM KCl, 150 mM sucrose, 0.1 mM ouabain, 20 mM tris-hydroxymethylaminomethane, pH 7.4) and incubated for 60 min at 37°C. Subsequently, the erythrocytes are washed three times in ice-cold $MgCl_2$-ouabain-solution (112 mM $MgCl_2$, 0.1 mM ouabain).

For determination of intracellular sodium content, the cells are hemolyzed in distilled water, the cell membranes are centrifuged and the sodium concentration of the haemolysate is measured by flame photometry. Net influx of sodium into the erythrocytes is calculated from the difference between the initial sodium content and the sodium content after incubation. Amiloride-sensitive sodium influx is calculated from the difference between sodium content of erythrocytes incubated with and without amiloride (3×10^{-4} M). Each experiment is done with the erythrocytes from 6 different animals. In each case, the comparison of Na^+ contents is based on erythrocytes from the same animal. Doses between 10^{-4} and 10^{-7} M of the inhibitor are tested.

EVALUATION

Statistical analysis of the data obtained is performed with Student's *t*-test for paired groups. IC_{50} values are calculated from dose-response curves.

REFERENCES AND FURTHER READING

Scholz W, Albus U, Hropot M, Klaus E, Linz W, Schölkens BA (1990) Zunahme des Na^+/H^+-Austausches an Kaninchenerythrozyten unter atherogener Diät. In: Assmann G, Betz E, Heinle H, Schulte H (eds) Arteriosklerose – Neue Aspekte aus Zellbiologie und Molekulargenetik. Epidemiologie und Klinik. Vieweg, Braunschweig, Wiesbaden. pp 296–302

Scholz W, Albus U, Linz W, Martorana P, Lang HJ, Schölkens BA (1992) Effects of Na^+/H^+ exchange inhibitors in cardiac ischaemia. J Mol Cell Cardiol 24:731–740

Scholz W, Albus U, Lang HJ, Linz W, Martorana PA, Englert HC, Schölkens BA (1993) Hoe 694, a new Na^+/H^+ exchange inhibitor and its effects in cardiac ischemia. Br J Pharmacol 109:562–568

A.1.1.20.3 Sodium Influx into Cultured Cardiac Myocytes

PURPOSE AND RATIONALE

The inhibition of Na^+/H^+ exchange has been studied in cultured cardiac myocytes (Scholz et al. 1992).

PROCEDURE

Rat myocardial cells are isolated from hearts of neonatal rats by trypsin digestion. The cells are cultured in 35 mm dishes and grown to confluence in Dulbecco's Minimum Essential Medium (DMEM, GIBCO) in an atmosphere containing 10% CO_2. After confluence, the cells are used for measurement of $^{22}Na^+$ influx. The cells are washed twice with Krebs-Ringer-solution buffered with HEPES/Tris (KRB) in which sodium chloride has been replaced by choline chloride (Choline chloride 130 mM, $CaCl_2$ 1.5 mM, KCl 5 mM, $MgCl_2$ 1 mM, HEPES 20 mM, pH 7.0 with Tris) and then incubated for 20 min at 37°C in the same buffer with added 0.1% bovine serum albumin (BSA) and 10 mM/l glucose. The culture dishes are then incubated for another 10 min with Na^+-propionate for cytosolic acidification and stimulation of Na^+/H^+ exchange. The compounds are dissolved in 500 µl/dish KRB in which 50% of the sodium chloride has been replaced by choline chloride containing additionally 2 µCi/ml $^{22}Na^+$-bicarbonate, and 5-(N-ethyl-N-isopropyl)amiloride (EIPA). After the stimulation period, sodium influx is terminated by washing the cells twice with ice-cold stop solution (0.1 mM $MgCl_2$, 10 mM Tris, pH 7.0). Subsequently, the cells are lyzed with 250 µl trichloroacetic acid and scraped from the dishes. Radioactivity is determined in a Packard gamma counter. Doses between 3×10^{-4} and 10^{-8} mM/l of standard and new compounds are tested. Six dishes are used for each concentration of test compounds.

EVALUATION

Mean values ± SD are compared with Student's *t*-test. IC_{50} values are calculated from dose-response curves.

REFERENCES AND FURTHER READING

Scholz W, Albus U, Linz W, Martorana P, Lang HJ, Schölkens BA (1992) Effects of Na^+/H^+ exchange inhibitors in cardiac ischaemia. J Mol Cell Cardiol 24:731–740

A.1.1.20.4 Inhibition of Na^+/H^+ Exchange into Cultured Aortic Endothelial Cells

PURPOSE AND RATIONALE

The inhibition of Na^+/H^+ exchange has been studied in endothelial cells (Scholz et al. 1993) by measuring the $^{22}Na^+$ influx.

PROCEDURE

Bovine aortic endothelial cells (BAEC) are isolated by dispase digestion form bovine aorta obtained from animals killed at the local slaughter house. The cells are cultured in 35 mm dishes and grown to confluence in Dulbecco's Minimum Essential Medium (DMEM, GIBCO) in an atmosphere with 10% CO_2. Three days after confluence the cells are used for measurement of $^{22}Na^+$ influx. The cells are washed twice with Krebs-Ringer solution buffered with HEPES/Tris (KRB) in which sodium chloride has been replaced by choline chloride (Choline chloride 130 mM, $CaCl_2$ 1.5 mM, KCl 5 mM, $MgCl_2$ 1 mM, HEPES 20 mM, pH 7.0 with Tris) and then incubated for 20 min at 37°C in the same buffer with added 0.1% bovine serum albumin (BSA) and 10 mM glucose. To stimulate Na^+/H^+ exchange the culture dishes are incubated for another 10 min with 500 µl/dish KBR in which all sodium chloride has been replaced by 65 mM each of choline chloride and Na^+-propionate or with KBR in which 50% of the sodium chloride has been replaced by choline chloride for unstimulated controls. In addition, the buffer contains 2 µCi/ml $^{22}Na^+$ and the test compounds or the standard. After the stimulation period, the sodium influx is terminated by washing the cells twice with ice-cold stop solution (0.1 mM $MgCl_2$, 10 mM Tris, pH 7.0). Subsequently, the cells are lyzed with 250 µl trichloroacetic acid and scraped from the dishes. Radioactivity is determined in a Packard gamma counter. Doses between 10^{-5} and 10^{-7} mM/l of standard and new compounds are tested. Six dishes are used for each concentration of test compounds.

EVALUATION

Mean values ± SD are compared with Student's *t*-test. IC_{50} values are calculated from dose-response curves.

MODIFICATIONS OF THE METHOD

Ewart et al. (1997) studied lipoprotein lipase activity in cultured rat cardiomyocytes in the presence of insulin and dexamethasone.

REFERENCES AND FURTHER READING

Benos DJ, Cunningham S, Baker RR, Beason KB, Oh Y, Smith PR (1992) Molecular characteristics of amiloride-sensitive sodium channels. Rev Physiol Biochem Pharmacol 120:31–113

Ewart HS, Carroll R, Severson DL (1997) Lipoprotein lipase activity in rat cardiomyocytes is stimulated by insulin and dexamethasone. Biochem J 327:439–442

Frelin C, Vigne P, Lazdunski M (1985) The role of Na^+/H^+ exchange system in the regulation of internal pH in cultured cardiac cells. Eur J Biochem 149:1–4

Frelin C, Vigne P, Breittmayer JP (1990) Mechanism of the cardiotoxic action of palytoxin. Mol Pharmacol 38:904–909

Jean T, Frelin C, Vigne P, Lazdunski M (1986) The Na^+/H^+ exchange system in glial cell lines. Properties and activation by an hyperosmotic shock. Eur J Biochem 160:211–219

Scholz W, Albus U (1993) Na^+/H^+ exchange and its inhibition in cardiac ischemia and reperfusion. Bas Res Cardiol 88:443–455

A.1.1.20.5 NHE Activity Measured by Intracellular pH in Isolated Ventricular Myocytes

PURPOSE AND RATIONALE

Changes of the intracellular pH of cultured bovine endothelial cells have been fluorometrically monitored using the pH-dye 2′,7′-bis(carboxyethyl)carboxyfluorescein (BCECF) by Kitazano et al. (1988). This method has been used to study the activity of inhibitors of Na^+/H^+ exchange (Scholz et al. 1995).

PROCEDURE

For preparation of isolated rat ventricular muscular cells (Yazawa et al. 1990), hearts of male Wistar rats are dissected, mounted on a Langendorff apparatus and perfused first at 37°C for 3 min with Tyrode solution adjusted to pH 7.4, second for 5–7 min with nominally calcium free Tyrode solution and finally with calcium free Tyrode solution containing 0.12–0.2 mg/ml collagenase (Sigma type I). After 15–20 min collagenase treatment, the heart is washed with storage solution (composition in mmol/L: KOH 70, l-glutamic acid 50, KCl 40, taurine 20, KH_2PO_4 20, $MgCl_2$ 3, glucose 20, HEPES 10, and EGTA 0.5, pH 7.4). The ventricles are cut into small pieces and myocytes are dispersed by gently shaking and finally by filtration through a nylon mesh (365 µm). Thereafter, the cells are washed twice by centrifugation at 600–1000 rpm for 5 min and kept at 4°C until use. For the pH recovery experiment the cells are loaded with the membrane permeable acetoxymethyl ester (AM) form of the fluorescent indicator 2′,7′-bis(carboxyethyl)-5(6)-carboxyfluorescein (BCECF). BCECF-AM is dissolved in DMSO and diluted to a 1.25 µM storage solution. Cardiomyocytes are loaded in this solution for 30 min at room temperature and are then centrifuged and resuspended in storage solution. The measure-

ments are performed in bicarbonate-free NaCl solution (NaCl 140, KCl 4.7, $CaCl_2$ 1.3, $MgCl_2$ 1, glucose 10, and HEPES 10 mM/L, pH 7.4) at 34°C using an apparatus according to Nitschke et al. (1991). The pH-dependent signal of BCECF is obtained by illuminating at 490 and 437 nm and dividing the emitted light signals (520–560 nm). The background signal, determined by closing the shutter, is subtracted from the total signal. The autofluorescence determined by illuminating unloaded cells can be ignored. In order to investigate the function of the Na^+/H^+ exchange system, the intracellular pH (pH_i) of the cells is decreased by the NH_4Cl prepulse technique and the rate of return to resting pH_i is determined. Test compounds are dissolved in the incubation medium. For each test concentration, the recovery of pH_i is first recorded in control NaCl solution.

EVALUATION

Data are analyzed by fitting a straight line to the initial (5 min) data points of the pH recovery curve. For statistical presentation, the slopes of the linear curves are demonstrated. All reported data are presented as means ± SEM. Statistical comparisons are made using either a paired or unpaired *t*-test.

MODIFICATIONS OF THE METHOD

The pH-sensitive fluorescence dye C-SNARF-1 (= carboxy-semi-naphtho-rhoda-fluor 1) was used by Yatsutake et al. (1996), Shipolini et al. (1997), and Yokoyama et al. (1998).

Fischer et al. (1999) tested new drugs for the Na^+/H^+ exchanger in Chinese hamster ovary cells which are enriched with the NHE-1 isoform of the Na^+/H^+ anti-porter. The Na^+/H^+ exchanger was stimulated with NaCl and the rate of extracellular acidification was quantified with the Cytosensor.

REFERENCES AND FURTHER READING

Fischer H, Seelig A, Beier N, Raddatz P, Seelig J (1999) New drugs for the Na^+/H^+ exchanger. Influence of Na^+ concentration and determination of inhibition constants with a microphysiometer. J Membr Biol 1:39–45

Kitazono T, Takeshige K, Cragoe EJ, Minakami S (1988) Intracellular pH changes of cultured bovine aortic endothelial cells in response to ATP addition. Biochem Biophys Res Commun 152:1304–1309

Nitschke R, Fröbe U, Greger R (1991) Antidiuretic hormone acts via V_1 receptor in intracellular calcium in the isolated perfused rabbit cortical thick ascending limb. Pflüger's Arch 417:622–632

Scholz W, Albus U, Counillon L, Gögelein H, Lang H-J, Linz W, Weichert A, Schölkens BA (1995) Protective effects of HOE642, a selective sodium-hydrogen exchange subtype 1 inhibitor, on cardiac ischaemia and reperfusion. Cardiovasc Res 29:260–268

Shipolini AR, Yokoyama H, Galiñanes M, Edmondson SJ, Hearse DJ, Avkiran M (1997) Na^+/H^+ exchanger activity does not contribute to protection by ischemic preconditioning in the isolated rat heart. Circulation 96:3617–3625

Yasutake M, Haworth RS, King A, Avkiran M (1996) Thrombin activates the sarcolemmal Na^+/H^+ exchanger: evidence for a receptor-mediated mechanism involving protein kinase C. Circ Res 79:705–715

Yazawa K, Kaibara M, Ohara M, Kamayama M (1990) An improved method for isolating cardiac myocytes useful for patch-clamp studies. Jpn J Physiol 40:157–163

Yokoyama M, Yasutake M, Avkiran M (1998) α_1-adrenergic stimulation of sarcolemnal Na^+/H^+ exchanger activity in rat ventricular myocytes: evidence for selective mediation by the α_{1A}-adrenoceptor subtype. Circ Res 82:1078–1985

A.1.1.20.6 NHE Subtype Specificity

PURPOSE AND RATIONALE

Molecular identification of mammalian Na^+/H^+ exchanger subtypes has been pioneered by Pouysségour and coworkers (Sardet et al. 1989) who used genetic complementation of fibroblast cell lines that lack all endogenous NHEs. Schwark et al. (1998) studied an inhibitor of Na^+/H^+ exchanger subtype 3 in various cell types.

PROCEDURE

cDNAs for the NHE subtypes human NHE1, rabbit NHE2, rat NHE3 (Pouysségour) or cloned by reverse transcriptase-polymerase chain reaction from human kidney mRNA are used. These cDNAs are cloned into the mammalian expression vector pMAMneo and transferred into the NHE-deficient mouse fibroblast cell line LAP1. Cells expressing the NHE subtypes are selected by the acid load survival method (Sardet et al. 1989). Clonal cell lines for each subtype are used for intracellular pH (pH_i) recovery after acid load. For studies of pH_i recovery (Faber et al. 1996), cells are scraped off the culture dishes washed and incubated with 5 µmol/l BCECF-AM [2′,7′-bis(2-carboxyethyl)-5,6-carboxy-fluorescein-acetoxy-methyl ester] for 20 min at 37°C in a buffer containing 20 mM NH_4Cl. The cells are then washed to remove extracellular dye and resuspended in the loading buffer without BCECF-AM. Intracellular acidification is induced by addition of 975 µl NH_4Cl-free and HCO_3^--free solution (so-called recovery medium: HCO_3^--free to inhibit the Na^+-dependent Cl^-/HCO_3^- exchanger of LAP1 cells) to an 25-µl aliquot of cells (≅25,000 cells). The pH_i recovery is recorded with a dual-grating Deltascan single-photon counting fluorometer (Photon Technology International, South Brunswick, NJ, USA) with exci-

tation wavelength of 505 nm and 440 nm and an emission wavelength of 535 nm. The measurement time varies between subtypes (120 s for NHE1, 300 s for NHE2, 180 s for NHE3). The inhibitors are first dissolved in DMSO, diluted in recovery medium and added in a volume of 975 µl to this medium.

A cloned opossum kidney cell line (Helmle-Kolb et al. 1990) is used additionally. Cells are grown as a monolayer in growth medium (1:1 mixture of nutrient mixture Ham F12 and Dulbecco's modified medium Eagle with 10% fetal calf serum). For subcultivation and pH-recovery experiments, the cells are detached from the surface of the culture vessels with trypsin-EDTA solution (2.5 g trypsin+0.2 g EDTA per liter in Dulbecco's phosphate-buffered saline) and suspended in growth medium. Measurement time in pH_i recovery experiments is 400 s.

Porcine renal brush-border membrane vesicles (BBMV) prepared by a Mg^{2+} precipitation technique are loaded with 150 mmol/l NaCl, 5 mmol/l HEPES/Tris, pH 7.0, and pre-incubated for 10 min at 37°C with various concentrations of NHE inhibitors. Intravesicular acidification through Na^+/H^+ exchange is started by diluting BBMV into Na^+-free buffer (150 mmol/l tetramethylammonium chloride, 5 mmol HEPES/Tris, pH 7.0) containing the appropriate concentrations of the NHE inhibitors and the fluorescent Δ pH indicator acridine orange (12 µmol/l). The fluorescence changes of acridine orange are recorded continuously by a Hitachi F-2000 spectrofluorometer at 495 nm excitation and 525 nm emission wavelength. The initial acridine orange fluorescence quenching in controls (no inhibitor) is set to 100%.

EVALUATION

Values are presented as means ± SD (four measurement per concentration). The IC_{50} values and Hill coefficients are calculated using the Sigma plot software. Statistical significance is calculated by means of the distribution-independent *H*-test and non-parametric *U*-test. $P < 0.05$ is considered as significant.

MODIFICATIONS OF THE METHOD

Counillon et al. (1993), Scholz et al. (1995) determined the NHE subtype specificity of Na^+/H^+ antiporters by their ability to inhibit initial rates of amiloride sensitive $^{22}Na^+$ uptake in fibroblast cell lines separately expressing the NHE-1, NHE-2 and NHE-3 isoforms.

Ko et al. (2004) determined the inhibitory effects of flavonoids on phosphodiesterase isozymes from guinea pig and their structure–activity relationships.

REFERENCES AND FURTHER READING

Counillon LT, Scholz W, Lang HJ, Pouysségour J (1993) Pharmacological characterization of stably transfected Na^+/H^+ antiporter isoforms using amiloride analogs and a new inhibitor exhibiting anti-ischemic properties. Mol Pharmacol 44:1041–1045

Faber S, Lang HJ, Hropot M, Schölkens BA, Mutschler E (1996) A novel screening assay of the Na^+-dependent $Cl^-/HCO3^-$ exchanger (NCBE) and its inhibitors. Cell Physiol Biochem 6:39–49

Helmle-Kolb C, Montrose MH, Stange G, Murer H (1990) Regulation of Na^+/H^+ exchange in opossum kidney cells by parathyroid hormone, cyclic AMP and phorbol esters. Pflüger's Arch 415:461–470

Ko WC, Shih CM, Lai YH, Chen JH, Huang HL (2004) Inhibitory effects of flavonoids on phosphodiesterase isozymes from guinea pig and their structure–activity relationships. Biochem Pharmacol 68:2087–2094

Sardet C, Franchi A, Pouysségour J (1989) Molecular cloning, primary structure, and expression of the human growth factor-activable Na^+/H^+ antiporter. Cell 56:271–280

Scholz W, Albus U, Counillon L, Gögelein H, Lang H-J, Linz W, Weichert A, Schölkens BA (1995) Protective effects of HOE642, a selective sodium-hydrogen exchange subtype 1 inhibitor, on cardiac ischaemia and reperfusion. Cardiovasc Res 29:260–268

Schwark JR, Jansen HW, Lang HJ, Krick W, Burckhardt G, Hropot M (1998) S3226, a novel inhibitor of Na^+/H^+ exchanger subtype 3 in various cell types. Pflüger's Arch Eur J Physiol 436:797–800

A.1.1.21 Phosphodiesterases

Cyclic nucleotide phosphodiesterases (PDEs) catalyze the hydrolysis of cAMP and/or cGMP. They function with adenyl and guanylyl cyclases to regulate the amplitude and duration of responses triggered by the second messengers cAMP and cGMP. The enzyme phosphodiesterase (PDE) exists in various forms. At least 11 families of phosphodiesterases have been identified (Torphy and Page 2000; Francis et al. 2001; Maurice et al. 2003; Lugnier 2006). The properties and functions of GAF domains in cyclic nucleotide phosphodiesterases are reviewed by Zoraghi et al. (2004).

Hofmann et al. (2006) reviewed the nomenclature and structure–function relationships of cyclic nucleotide-regulated channels.

Mongillo et al. (2004) reported fluorescence resonance energy transfer-based analysis of cAMP dynamics in live neonatal rat cardiac myocytes, revealing distinct functions of compartmentalized phosphodiesterases. Studying real-time monitoring of PDE2 activity in live cells, Nikolaev et al. (2005) found that hormone-stimulated cAMP hydrolysis is faster than hormone-stimulated cAMP synthesis.

Snyder et al. (2005) studied the role of cyclic nucleotide phosphodiesterases in the regulation of adipocyte lipolysis.

Zhang et al. (2004) desribed a glutamine switch mechanism for nucleotide selectivity by phosphodiesterases.

REFERENCES AND FURTHER READING

Francis SH, Turko IV, Corbin JD (2001) Cyclic nucleotide phosphodiesterases: relating structure and function. Prog Nucleic Acid Res Mol Biol 65:1–52

Hofmann F, Biel M, Kaupp UB (2006) International Union of Pharamcology. LI. Nomenclature and structure-function relationships of cyclic nucleotide-regulated channels. Pharmacol Rev 57:455–462

Lugnier C (2006) Cyclic nucleotide phosphodiesterase (PDE) superfamily: a new target for the development of specific therapeutic agents. Pharmacol Ther 109:366–398

Maurice DH, Palmer D, Tilley DG, Dunkerley HA, Netherton SJ, Raymond DR, Elbatarny HS, Jimmo SL (2003) Cyclic nucleotide phosphodiesterase activity, expression, and targeting in cells of the cardiovascular system. Mol Pharmacol 64:533–546

Mongillo M, McSorley T, Evellin S, Sood A, Lissandron V, Terrin A, Huston E, Hannawacker A, Lohse MJ, Pozzan T, Houslay MD, Zaccolo M (2004) Fluorescence resonance energy transfer-based analysis of cAMP dynamics in live neonatal rat cardiac myocytes reveals distinct functions of compartmentalized phosphodiesterases. Circ Res 95:67–75

Snyder PB, Esselstyn JM, Loughney K, Wolda SL, Florio VA (2005) The role of cyclic nucleotide phosphodiesterases in the regulation of adipocyte lipolysis. J Lipid Res 46:494–503

Torphy TJ, Page C (2000) Phosphodiesterases: the journey towards therapeutics. Trends Pharmacol Sci 21:157–159

Zhang KYJ, Card GL, Suzuki Y, Artis DR, Fong D, Gillette S, Hsieh D, Neiman J, West BL, Zhang C, Milburn MV, Kim SH, Schlessinger J, Bollag G (2004) A glutamine switch mechanism for nucleotide selectivity by phosphodiesterases. Mol Cell 15:279–286

Zoraghi R, Corbin JD, Francis SH (2004) Properties and functions of GAF domains in cyclic nucleotide phosphodiesterases and other proteins. Mol Pharmacol 65:267–278

A.1.1.21.1 Inhibition of Phosphodiesterase

PURPOSE AND RATIONALE

The inhibition of cAMP-PDE and cGMP-PDE by various test compounds can be measured using a two-step radioisotopic procedure.

PROCEDURE

Materials

[8-^{3}H]cAMP (28 Ci/mmol), [8-^{3}H]-cGMP (15 Ci/mmol) and [U^{14}C]guanosine (528 mCi/mmol) are obtained from Du Pont de Nemours (Paris, France). Unlabelled cyclic nucleotides, 5′-nucleotidase (Ophiophagus hannah venom) are from the Sigma Chemical Co. (La Verpillére, France).

Tissue preparations

Male Sprague-Dawley rats (250–300 *g*) are decapitated. Hearts are perfused with 0.15 M NaCl through the aorta to remove the blood. The ventricles are minced in 5 vol. of 10 mM Tris-HCl buffer containing 0.32 M sucrose, 1 mM EDTA, 5 nM DTT and 0.1 mM PMSF at pH 7.5. The suspension is homogenized in a glass-glass Potter-Elvejhem. The homogenate is then centrifuged at 105,000 *g* for 60 min. The 105,000 *g* supernatant is stored at –75°C until injection on the HPLC column.

Isolation of PDEs

The cytosolic fraction from rat ventricles (5–8 mg of protein) is loaded at the rate of 1 ml/min on a Mono Q HPLC column which has been previously equilibrated with buffer A (50 mM Tris-HCl, 2 mM EDTA, 14 mM 2-mercaptoethanol, 0.1 mM PMSF, pH 7.5). Under these conditions, greater than 95% of the PDE activity is bound to the column. PDE activity is eluted at a flow rate of 1 ml/min using the following step by step and linear gradients of NaCl in buffer A: 25 ml of 0.16 M NaCl, 20 ml of 0.23 M NaCl, 30 ml from 0.23 to 0.29 M NaCl, 15 ml of 0.29 M NaCl, 30 ml from 0.29 to 0.50 M NaCl. The separation is done at 4°C. Fractions of 1 ml are collected and stored at –75°C in the presence of 20% glycerol. The fractions are tested for PDE activity, and the peaks containing the different isoenzymes are identified. Fractions containing preferentially one isoenzyme are pooled.

PDE Assay

PDE activity is assayed by a two-step radioisotopic procedure according to Thompson et al. (1974), Boudreau and Drummond (1975), Prigent et al. (1981). cAMP-PDE and cGMP-PDE activities are measured with a substrate concentration of 0.25 µM. To evaluate the cGMP-stimulated PDE activity, assays are performed with 5 µM cAMP in the absence or presence of 5 µM cGMP. Xanthine derivates are dissolved in DMSO. The stock solutions are appropriately diluted with 40 mM Tris-HCl buffer so that the final DMSO concentration in the PDE assay does not exceed 1%. At this concentration, DMSO has no significant effect on the PDE activity of any of the fractions. The inhibitory potency of the xanthine derivates is examined on each separated isoform.

EVALUATION

The IC_{50} values (concentration of a drug which inhibit 50% of the enzymatic activity) are calculated by plotting the percentage of residual enzymatic activity ver-

sus the logarithmic concentration of the drug. Confidence limits (95%) for the IC_{50} values are determined by linear regression analysis.

MODIFICATIONS OF THE METHOD

Phosphodiesterase activity can be determined using ^{32}P-labelled GPT (Reinsberg 1999). The reaction is performed using an Eppendorf cup with 10 mM GTP, the test solution and [^{32}P]GTP. The reaction is started with 1 mM sodium nitroprusside solution. After an incubation period of 20 min at 37°C, the reaction is stopped with 500 µl of 120 mM sodium carbonate and 400 µl of zinc acetate, whereby the zinc carbonate and the substrate GTP are almost (about 90%) all precipitated, and so separated from cGMP. The precipitate is separated by centrifugation and the supernatant submitted to chromatography on an aluminum oxide column. The column is first treated with Tris HCl buffer. From the supernatant, 900 ml is applied. After two washing periods, the cGMP is eluted in five fractions. These fractions are measured and the highest activities are pooled.

The PDE activity is calculated from the difference between applied [^{32}P]GTP minus unaltered [^{32}P]GTP.

REFERENCES AND FURTHER READING

Boudreau RJ, Drummond GI (1975) A modified assay of 3′,5′-cyclic-AMP phosphodiesterase. Anal Biochem 63:388–399

Meskini N, Némoz G, Okyayuz-Baklouti I, Lagarde M, Prigent AF (1994) Phosphodiesterase inhibitory profile of some related xanthine derivatives pharmacologically active on the peripheral microcirculation. Biochem Pharmacol 47:781–788

Pichard AL, Cheung WY (1976) Cyclic 3′:5′-nucleotide phosphodiesterase. Interconvertible multiple forms and their effects on enzyme activity and kinetics. J Biol Chem 251:5726–5737

Prigent AF, Némoz G, Yachaoui Y, Pageaux JF, Pacheco H (1981) Cyclic nucleotide phosphodiesterase from a particulate fraction of rat heart. Solubilization and characterization of a single enzymatic form. Biochem Biophys Res Commun 102:355–364

Prigent AF, Fougier S, Nemoz G, Anker G, Pacheco H, Lugnier C, Lebec A, Stoclet JC (1988) Comparison of cyclic nucleotide phosphodiesterase isoforms from rat heart and bovine aorta. Separation and inhibition by selective reference phosphodiesterase inhibitors. Biochem Pharmacol 37:3671–3681

Reinsberg L (1999) Personal Communication

Terai M, Furihata C, Matsushima T, Sugimura T (1976) Partial purification of adenosine 3′, 5′-cyclic monophosphate phosphodiesterase from rat pancreas in the presence of excess protease inhibitors. Arch Biochem Biophys 176:621–629

Thompson WJ, Brooker G, Appleman MM (1974) Assay of cyclic nucleotide phosphodiesterases with radioactive substrates. In: Hardman JG, O'Malley BW (eds) Methods in enzymology, Vol 38. Academic Press, New York, pp 205–212

Description of Phosphodiesterase Isoforms

Phosphodiesterase 1

PDE1 family variants are activated upon Ca^{2+}/calmodulin binding (Kakkar et al. 1999; Goraya and Cooper 2005; Sharma et al. 2006). The PDE1 subfamily consists of three different gene products (PDFE1A, PDE1B, and PDE1C) which differ in their regulatory properties, substrate affinities, specific activities for calmodulin, tissue distribution, and molecular weights (Yan et al. 1996; Yu et al. 1997). PDE1 is present in brain, cardiomyocytes, vascular smooth muscle cells, and vascular endothelial cells (Maurice et al. 2003). Inhibition has been described for nimodipine (Epstein et al. 1982) and for vinpocetine (Hagiwara et al. 1984).

Phosphodiesterase 2

A single *PDE2* gene encodes three PDE2 variants (Rosman et al. 1997). Martinez et al. (2002) studied the crystal structure of murine PD2A and found that the two GAF domains in phosphodiesterase 2A have distinct roles in dimerization and cGMP binding. PDE2 is found in various areas of the brain (Lugnier 2006), in adrenal medulla, heart, rat ventricle (Yanaka et al. 2003), liver, and brown adipose tissue (Coudray et al. 1999). Erythro-9-(2-hydroxy-3-nonyl) adenine (EHNA) was shown to specifically act on PDE2 by inhibiting cCMP-activated PDE2 (Podzuweit et al. 1995).

Chambers et al. (2006) described a new chemical tool for exploring the physiological function of the PDE2 isozyme.

Phosphodiesterase 3

The PDE3 family is composed of two genes, *PDE3A* and *PDE3B*. *PDE3A* mRNA is enriched in blood vessels, heart, megakaryocytes and oocytes, whereas *PDE3B* is highest in in adipocytes, hepatocytes, brain, renal collecting duct epithelium, and developing spermatocytes (Reinhardt et al. 1995). PDE3 inhibitors have been extensively investigated and developed as non-glycoside, non-sympathomimetic, cardiotonic agents for the treatment of heart failure. Milrinone is the most studied and most extensively used PDE3 inhibitor and is used in the acute treatment of heart failure (Cruickshank 1993). Trequinsin (HL 725) inhibits PDE3 in a nanomolar range (Ruppert and Weithmann 1982); it also inhibits PDE1, PDE2, and PDE4 in submicromolar concentrations (Stoclet et al. 1995).

Boswell-Smith et al. (2006) studied the pharmacology of two long-acting trequinsin-like phosphodiesterase 3/4 inhibitors, RPL554 and RPL565.

Hambleton et al. (2005) studied isoforms of cyclic nucleotide phosphodiesterase PDE3 and their contribution to cAMP hydrolytic activity in subcellular fractions of human myocardium.

Masciarelli et al. (2004) described mice deficient of cyclic nucleotide phosphodiesterase 3A as a model of female infertility.

Adachi et al. (2005) reported the effects of a phosphodiesterase 3 inhibitor, olprinone, on rhythmical change in the tension of human gastroepiploic artery.

Abbott and Thompson (2006) performed analysis of anti-PDE3 activity of 2-morpholinochromone derivates revealing multiple mechanisms of antiplatelet activity.

Phosphodiesterase 4

PDE4 is mainly present in the brain (Houslay et al. 1998), inflammatory cells (Tenor and Schudt 1996), cardiovascular tissues (Stoclet et al. 1995), and smooth muscles, but is lacking in the platelets. Four *PDE4* genes (*PDE4A–D*) yield a large number of distinct PDE4 varaints. These enzymes, which result from the use of alternate promoters and extensive splicing of PDE4 mRNAs, are stratified into long or short forms (Conti et al. 2003).

One *PDE4A*, three *PDE4B* (PDE4B1, PDE4B2, and PDE4B3), and three *PDE4D* (PDE4D1, PDE4D2, PDE4D3) variants are expressed in rat and human cardiac tissue (Houslay and Adams 2003). Two *PDE4D* gene-derived variants, PDE4D3 and PDE4D6, are expressed in human and rat aortic, mesenteric, and femoral contractile/quiescent and synthetic/activated vascular smooth muscle cells (Liu et al. 2000).

The role of cAMP-specific PDE4 phosphodiesterases in cellular signaling was reviewed by Houslay and Adams (2003) and Conti et al. (2003).

Huai et al. (2003) studied the three-dimensional structures of PDE4D in a complex with roliprams and the implication for inhibitor selectivity.

Baillie et al. (2003) found that β-arrestin-mediated PDE4 cAMP phosphodiesterase recruitment regulates β-adrenoceptor switching from G_s to G_i.

The antidepressant compound rolipram (ZK 62711) is a selective inhibitor of PDE4 (Schwabe et al. 1976; Komas et al. 1989). O'Donnell and Zhang (2004) described the antidepressant effects of inhibitors of cAMP phosphodiesterase (PDE4). Many analogs were studied as PDE4 inhibitors for treatment of asthma and chronic obstructive pulmonary disease (COPD) as well as anti-inflammatory drugs; however, most failed due to emetic side-effects (Giembycz 2002).

Phosphodiesterase 5

Selective inhibitors of cyclic guanosine monophosphate (cGMP) phosphodiesterase type 5 (**PDE5**) were found to be effective in the treatment of erectile dysfunction in men (Jeremy et al. 1997; Ballard et al. 1998; Chuang et al. 1998; Stief et al. 1998; Corbin and Francis 1999; Turko et al. 1999; Wallis et al. 1999; Hosogai et al. 2001; Rotella 2001; Saenz de Tejada et al. 2001; Ukita et al. 2001).

The PDE5 family consists of a single *PDE5* gene that can encode three distinct proteins (PDE5A1–3) (Loughney et al. 1998).

Wang et al. (2001) characterized type 5 phosphodiesterases in the corpus cavernosum of several species.

Qiu et al. (2000) demonstrated that rabbit corpus cavernosum smooth muscle shows a different phosphodiesterase profile than human corpus cavernosum.

Kim et al. (2001) compared the inhibition of cyclic GMP hydrolysis in human corpus cavernosum smooth muscle cells by vardenafil with that by sildenafil.

The discovery of novel, potent, and selective PDE5 inhibitors was reported by Bi et al. (2001).

Corbin et al. (2004) described the structural basis for the higher potency of vardenafil compared with sildenafil in inhibiting cCMP-specific phosphodiesterase-5 (PDE5).

PDE5 inhibitors such as sildenafil can be used in the treatment of pulmonary arterial hypertension (Galié et al. 2005).

Cohen et al. (1996) found that inhibition of cGMP-specific phosphodiesterase selectively vasodilates the pulmonary circulation in rats made chronically hypoxic by exposure to a simulated high altitude. Chronic hypoxia augments protein kinase G-mediated Ca^{2+} desensitization in pulmonary vascular smooth muscle through inhibition of RhoA/Rho kinase signaling (Jernigan et al. 2004).

Thompson et al. (2001) studied the effect of sildenafil on corpus cavernosal smooth muscle relaxation and cGMP formation in the diabetic rabbit.

Tantini et al. (2005) found an antiproliferative effect of sildenafil on human pulmonary artery smooth muscle cells.

Other Phosphodiesterases

The families of **PDE6 to PDE11** have been identified as a result of bioinformatics-based genomic screening (Soderling and Beavo 2000). The search for inhibitors is just beginning.

Gillespie and Beavo (1989) discussed inhibition and stimulation of photoreceptor phosphodiesterases (later on termed **PDE6**) by dipyridamole and M&B 22,948.

D'Armours et al. (1999) investigated the potency and mechanism of action of E4021, a type 5 phosphodiesterase isozyme-selective inhibitor, on the photoreceptor phosphodiesterase.

Zhang et al. (2005) described the efficacy and selectivity of phosphodiesterase-targeted drugs in inhibiting photoreceptor phosphodiesterase (**PDE6**) in retinal photoreceptors.

Smith et al. (2004) reported the discovery of a selective inhibitor of **phosphodiesterase 7**.

The discovery of thiadiazoles as a novel structural class of potent and selective **PDE7 inhibitors** was reported by Vergne et al. (2004a, 2004b).

Lorthiois et al. (2004) and Bernadelli et al. (2004) described spiroquinazolinones as potent and selective **PDE7** inhibitors.

The first potent and selective **PDE9** inhibitor was characterized by Wunder et al. (2005) using a cGMP reporter cell line.

REFERENCES AND FURTHER READING

Abbott BM, Thompson PE (2006) Analysis of anti-PDE3 activity of 2-morpholinochromone derivates reveals multiple mechanisms of anti-platelet activity. Bioorg Med Chem Lett 16:969–973

Adachi H, Kakiki M, Kishi Y (2005) Effects of a phosphodiesterase 3 inhibitor, olprinone, on rhythmical change in tension of human gastroepiploic artery. Eur J Pharmacol 528:137–143

Baillie GS, Sood A, McPhee I, Gall I, Perry SJ, Lefkowitz RJ, Houslay MD (2003) β-Arrestin-mediated PDE4 cAMP phosphodiesterase recruitment regulates β-adrenoceptor switching from G_s to G_i. Proc Natl Acad Sci USA 100:940–945

Ballard SA, Gingell CJ, Tang K, Turner LA, Price ME, Naylor AM (1998) Effects of sildenafil on the ralaxation of human corpus cavernosum tissue in vitro and the activities of cyclic nucleotide phosphodiesterase isozymes. J Urol 159:2164–2171

Bernadelli P, Lorthiois E, Vergne F, Oliveira C, Mafroud AK, Proust E, Pham N, Ducrot P, Moreau F, Idrissi M, Tertre A, Bertin B, Coupe M, Chevalier E, Descours A, Berliozseux F, Berna P, Li M (2004) Spiroquinazolinones as novel, potent and selective PDE7 inhibitors. Part 2: Optimization of 5,8-disubstituted derivatives. Bioorg Med Chem Lett 14:4627–4631

Bi Y, Stoy P, Adam L, He B, Krupinski J, Normandin D, Pongrac R, Seliger L, Watson A, Macor JE (2001) The discovery of novel, potent and selective PDE5 inhibitors. Bioorg Med Chem Lett 11:2461–2464

Boswell-Smith V, Spina D, Oxford AW, Comer MB, Seeds EA, Page CP (2006) The pharmacology of two novel long-acting phosphodiesterase 3/4 inhibitors, RPL554 [9,10-dimethoxy-2(2,4,6-trimethylphenylimino)-3-(n-carbamoyl-2-aminoethyl)-3,4,6,7-tetrahydro-2H-pyrimido[6,1-a]isoquinolin-4-one] and RPL565 [6,7-dihydro-2-(2,6-diisopropylphenoxy)-9,10-dimethoxy-4H-pyrimido[6,1-a]isoquinolin-4-one]. J Pharmacol Exp Ther 318:840–848

Chambers RJ, Abrams K, Garceau NY, Kamath AV, Manley CM, Lilley SC, Otte DA, Scott DO, Sheils AL, Tess DA, Vellekoop AS, Zhang Y, Lam KT (2006) A new chemical tool for exploring the physiological function of the PDE2 isozyme. Bioorg Med Chem Lett 16:307–310

Chuang AT, Strauss JD, Murphy RA, Steers WD (1998) Sildenafil, a type-5 cGMP phosphodiesterase inhibitor, specifically amplifies cGMP-dependent relaxation in rabbit corpus cavernosum muscle *in vitro*. J Urol 160:257–261

Cohen AH, Hanson K, Morris K, Fouty B, MacMurty IF, Clarke W, Rodman DM (1996) Inhibition of cyclic 3′-5′-guanosine monophosphate-specific phosphodiesterase selectively vasodilates the pulmonary circulation in chronically hypoxic rats. J Clin Invest 97:172–179

Conti M, Richter W, Mehats C, Livera G, Park JY, Jin G (2003) Cyclic AMP-specific PDE4 phosphodiesterases as critical components of cyclic AMP signaling. J Biol Chem 278:5493–5496

Corbin JD, Francis SH (1999) Cyclic GMP phosphodiesterase-5: Target of sildenafil. J Biol Chem 274:13729–13732

Corbin JD, Beasley A, Blount MA, Francis SH (2004) Verdenafil: structural basis for higher potency over sildenafil in inhibiting cCMP-specific phosphodiesterase-5 (PDE5). Neurochem Int 45:859–863

Coudray C, Charon C, Komas N, Mory G, Diot-Dupuy F, Manganiello V, Ferre P, Bazin R (1999) Evidence for the presence of several phosphodiesterase isoforms in brown adipose tissue of Zucker rats: modulation of PDE2 by the fa gene expression. FEBS Lett 456:207–210

Criuckshank JM (1993) Phosphodiesterase III inhibitors: long-term risks and short-term benefits. Cardiovasc Drugs Ther 7:655–660

D'Armours MR, Granovsky AE, Artemyev NO, Cote RH (1999) Potency and mechanism of action of E4021, a type 5 phosphodiesterase isozyme-selective inhibitor, on the photoreceptor phosphodiesterase depend on the state of activation of the enzyme. Mol Pharmacol 3:508–514

Epstein PM, Fiss K, Hachisu R, Andrenyak DM (1982) Interaction of calcium antagonists with cyclic AMP phosphodiesterase and calmodulin. Biochem Biophys Res Commun 105:1142–1149

Galié N, Ghofrani HA, Torbicki A, Barst RJ, Rubin LJ, Badesch D, Fleming T, Parpia T, Burgess G, Branzi A, Grimminger F, Kurzyna M, Simmoneau G (2005) Sildenafil citrate therapy for pulmonary arterial hypertension. N Engl J Med 353:2148–2157

Giembycz MA (2002) Development status of second generation PDE4 inhibitors for asthma and COPD: the story so far. Monaldi Arch Chest Dis 57:48–64

Gillespie PG, Beavo JA (1989) Inhibition and stimulation of photoreceptor phosphodiesterases by dipyridamole and M&B 22,948. Mol Pharmacol 36:773–781

Goraya TA, Cooper DMF (2005) Ca^{2+}-calmodulin-dependent phosphodiesterase (PDE1): current perspectives. Cell Sign 17:789–797

Hagiwara M, Endo T, Hidaka H (1984) Effects of vinpocetine on cyclic nucleotide metabolism in vascular smooth muscle. Biochem Pharmacol 33:453–457

Hambleton R, Krall, Tikishvili E, Honeggar M, Ahmad F, Manganiello VC, Movsesian MA (2005) Isoforms of cyclic nucleotide phosphodiesterase PDE3 and their contribution to cAMP hydrolytic activity in subcellular fractions of human myocardium. J Biol Chem 280:39168–39174

Hosogai N, Hamada K, Tomita M, Nagashima A, Takahashi T, Sekizawa T, Mizutani T, Urano Y, Kuroda A, Sawada K,

Ozaki T, Seki J, Goto T (2001) FR226807: a potent and selective phosphodiesterase type 5 inhibitor. Eur J Pharmacol 428:295–302

Houslay MD, Sullivan M, Bolger GB (1998) The multienzyme PDE4 cyclic adenosine monophosphate-specific phosphodiesterase family: intracellular targeting, regulation, and selective inhibition by compounds exerting anti-inflammatory and antidepressant actions. Adv Pharmacol 44:225–342

Houslay MD, Adams DR (2003) PDE4 cAMP phosphodiesterases: modular enzymes that orchestrate signaling cross-talk, desensitization and compartmentalization. Biochem J 370:1–18

Huai G, Wang H, Sun Y, Kim HY, Liu Y, Ke H ((2003) Three-dimensional structures of PDE4D in complex with roliprams and implication on inhibitor selectivity. Structure 11:865–873

Jeremy JY, Ballard SA, Naylor AM, Miller MAW, Angelini GD (1997) Effects of sildenafil, a type-5 cGMP phosphodiesterase inhibitor, and papaverine on cyclic GMP and cyclic AMP levels in the rabbit corpus cavernosum *in vitro*. Br J Urol 79:958–963

Jernigan NL, Walker BR, Resta TC (2004) Chronic hypoxia augments protein kinase G-mediated Ca^{2+} desensitization in pulmonary vascular smooth muscle through inhibition of RhoA/Rho kinase signaling. Am J Physiol 287:L1220–L1229

Kakkar R, Raju RVS, Sharma RK (1999) Calmodulin-dependent cyclic nucleotide phosphodiesterase (PDE1). Cell Mol Life Sci 55:1164–1185

Kim NN, Huang YH, Goldstein I, Bischoff E, Traish AM (2001) Inhibition of cyclic GMP hydrolysis in human corpus cavernosum smooth muscle cells by vardenafil, a novel, selective phosphodiesterase type 5 inhibitor. Life Sci 69:2249–2256

Komas N, Lugnier C, Le Bed A, Serradeil-Le Gal C, Barthelemy G, Stoclet JC (1989) Differential sensitivity to cardiotonic drugs of cyclic AMP phosphodiesterases isolated from canine ventricular and sinoatrial-enriched tissues. J Cardiovasc Pharmacol 14:213–220

Liu H, Palmer D, Jimmo SL, Tilley DG, Dunkerley HA, Pang SC, Maurice DH (2000) Expression of phosphodiesterase 4D (PDE4D) is regulated by both the cyclic AMP-dependent protein kinase and mitogen-activated protein kinase signaling pathways. A potential mechanism allowing for the coordinated regulation of PDE4D activity and expression in cells. J Biol Chem 275:26615–26624

Lorthiois E, Bernadelli P, Vergne F, Oliveira C, Mafroud AK, Proust E, Heuze L, Moreau F, Idrissi M, Tertre A, Bertin B, Coupe M, Wrigglesworth R, Decours A, Soulard P, Berna P (2004) Spiroquinazolinones as novel, potent and selective PDE7 inhibitors. Part 1. Bioorg Med Chem Lett 14:4623–4626

Loughney K, Hill TR, Florio VA, Uher L, Rosman GJ, Wolda SL, Jones BA, Howard ML, McAllister-Lucas LM, Sonnenburg WK, Francis SH, Corbin JD, Beavo JA, Ferguson K (1998) Isolation and characterization of cDNAs encoding PDE5A, a human cGMP-binding cGMP-specific 3′, 5′-cyclic nucleotide phosphodiesterase. Gene 216:139–147

Lugnier C (2006) Cyclic nucleotide phosphodiesterase (PDE) superfamily: a new target for the development of specific therapeutic agents. Pharmacol Ther 109:366–398

Martinez SE, Wu AY, Glavas NA, Tang XB, Turley S, Hol WGJ (2002) The two GAF domains in phosphodiesterase 2A have distinct roles in dimerization and cGMP binding. Proc Natl Acad Sci USA 99:13260–13265

Masciarelli S, Horner K, Liu C, Park SH, Hinckley M, Hockman S, Nedachi T, Jin C, Conti M, Manganiello V (2004) Cyclic nucleotide phosphodiesterase 3A-deficient mice as a model of female infertility. J Clin Invest 114:196–205

Maurice DH, Palmer D, Tilley DG, Dunkerley HA, Netherton SJ, Raymond DR, Elbatarny HS, Jimmo SL (2003) Cyclic nucleotide phosphodiesterase activity, expression, and targeting in cells of the cardiovascular system. Mol Pharmacol 64:533–546

Mongillo M, McSorley T, Evellin S, Sood A, Lissandron V, Terrin A, Huston E, Hannawacker A, Lohse MJ, Pozzan T, Houslay MD, Zaccolo M (2004) Fluorescence resonance energy transfer-based analysis of cAMP dynamics in live neonatal rat cardiac myocytes reveals distinct functions of compartmentalized phosphodiesterases. Circ Res 95:67–75

Nikolaev VO, Gambaryan S, Engelhardt S, Walter U, Lohse MJ (2005) Real-time monitoring of the PDE2 activity of live cells. J Biol Chem 280:1716–1719

O'Donnell JM, Zhang HT (2004) Antidepressant effects of inhibitors of cAMP phosphodiesterase (PDE4). Trends Pharmacol Sci 26:158–163

Podzuweit T, Nennstiel P, Müller A (1995) Isozyme selective inhibition of cCMP-stimulated cyclic nucleotide phosphodiesterases by erythro-9-(2-hdroxy-3-nonyl) adenine. Cell Signal 7:733–738

Qiu Y, Kraft P, Lombardi E, Clancy J (2000) Rabbit corpus cavernosum smooth muscle shows a different phosphodiesterase profile than human corpus cavernosum. J Urol 164:882–886

Reinhardt RR, Chin E, Zhou J, Taira M, Murata T, Manganiello VC, Bondy CA (1995) Distinctive anatomical patterns of gene-expression for cCMP-inhibited cyclic nucleotide phosphodiesterases. J Clin Invest 95:1528–1538

Rosman GJ, Martins TJ, Sonnenburg WK, Beavo JA, Ferguson K, Loughney K (1997) Isolation and characterization of human cDNAs encoding a cGMP-stimulated 3′, 5′-cyclic nucleotide phosphodiesterase. Gene 191:89–95

Rotella DP (2001) Phosphodiesterase type 5 inhibitors: discovery and therapeutic utility. Drugs Future 26:153–162

Ruppert D, Weithmann KU (1982) HL 725, an extremely potent inhibitor of platelet phosphodiesterase and induced platelet aggregation. Life Sci 31:2037–2043

Saenz de Tejada I, Angulo J, Cuevas P, Fernández A, Moncada I, Allona A, Lledó E, Körschen I, Niewöhner U, Haning H, Pages E, Bischoff E (2001) The phosphodiesterase inhibitory selectivity and the in vitro and in vivo potency of the new PDE5 inhibitor vardenafil. Int J Impot Res 13:282–290

Schwabe U, Miyake M, Ohga Y, Daly JW (1976) 4-(3-Cyclopentyloxy-4-methoxyphenyl)-2-pyrrolidone (ZK 62711): a potent inhibitor of adenosine cyclic 3′,5′-monophosphate phosphodiesterases in homogenates and tissue slices from rat brain. Mol Pharmacol 11:900–911

Sharma RK, Das SB, Lakshmikuttyamma A, Selvakumar P, Shrivastav A (2006) Regulation of calmodulin-stimulated cyclic nucleotide phosphodiesterase (PDE1): Review. Int J Mol Med 18:95–105

Smith SJ, Cieslinski LB, Newton R, Donnelly LE, Fenwick PS, Nicholson AG, Barnes PJ, Barnette MS, Giembycz MA (2004) Discovery of BRL 50481 [3-(N,N-dimethylsulfonamido)-4-methyl-nitrobenzene], a selective inhibitor of phosphodiesterase 7: In vitro studies in human monocytes, lung macrophages, and $CD8^+$ T-lymphocytes. Mol Pharmacol 66:1679–1689

Soderling SH, Beavo SH (2000) Regulation of cAMP and cGMP signaling: new phosphodiesterases and new functions. Curr Opin Cell Biol 12:174–179

Stief CG, Uckert S, Becker AJ, Truss MC, Jonas U (1998) The effect of the specific phosphodiesterase (PDE) inhibitors on human and rabbit cavernous tissue in vitro and in vivo. J Urol 159:1390–1393

Stoclet JC, Keravis T, Komas N, Lugnier C (1995) Cyclic nucleotide phosphodiesterases as therapeutic targets in cardiovascular diseases. Expert Opin Invest Drugs 4:1081–1100

Tantini B, Manes A, Fiumana E, Pignatti C, Guarnieri C, Zannoli R, Branzi A, Galié N (2005) Antiproliferative effect of sildenafil on human pulmonary artery smooth muscle cells. Basic Res Cardiol 100:131–138

Tenor H, Schudt C (1996) Analysis of isoenzyme profiles in cells and tissues by pharmacological methods. In: Schudt C, Dent G, Rabe KF (eds) Phosphodiesterase inhibitors. Handbook of Immunopharmacology. Academic Press, London, pp 21–40

Thompson CS, Mumtaz FH, Khan MA, Wallis RM, Mikhailidis DP, Morgan RJ, Angelini CD, Jeremy JY (2001) The effect of sildenafil on corpus cavernosal smooth muscle relaxation and cyclic GMP formation in the diabetic rabbit. Eur J Pharmacol 425:57–64

Turko IV, Ballard SA, Francis SH, Corbin JD (1999) Inhibition of GMP-binding cyclic GMP-specific phosphodiesterase (Type 5) by sildenafil and related compounds. Mol Pharmacol 56:124–130

Ukita T, Nakamura Y, Kubo A, Yamamoto Y, Moritani Y, Saruta K, Higashijima T, Kotera J, Kikawa K, Omori K (2001) Novel, potent, and selective phosphodiesterase 5 inhibitors: synthesis and biological activities of a series of 4-ary-1-isochinoline derivatives. J Med Chem 44:2204–2218

Vergne F, Bernadelli P, Lorthiois E, Pham N, Proust E, Oliveira C (2004a) Discovery of thiadiazoles: a novel structural class of potent and selective PDE7 inhibitors: Part 2: Metabolism-directed optimization studies towards orally bioavailable derivatives. Bioorg Med Chem Lett 14:4615–4621

Vergne F, Bernadelli P, Lorthiois E, Pham N, Proust E, Oliveira C, Mafroud AK, Royer F, Wrigglesworth R, Schellhaas JK, Barvian MR, Moreau F, Idrissi M, Tertre A, Bertin B, Coupe M, Berna P, Soulard P (2004a) Discovery of thiadiazoles as a novel structural class of potent and selective PDE7 inhibitors. Part 1: Design, synthesis and structure-activity relationship studies. Bioorg Med Chem Lett 14:4607–4613

Vergne F, Bernadelli P, Lorthiois E, Pham N, Proust E, Oliveira C, Mafroud AK, Ducrot P, Wrigglesworth R, Berlioz-Seux F, Coleon F, Chevalier E, Moreau F, Idrissi M, Tertre A, Descours A, Berna P, Li M (2004b) Discovery of thiadiazoles as a novel structural class of potent and selective PDE7 inhibitors. Part 2: Metabolism-directed optimization studies towards orally bioavailable derivatives. Bioorg Med Chem Lett 14:4615–4621

Wallis RM, Corbin JD, Francis SH (1999) Tissue distribution of phosphodiesterase families and the effect of sildenafil on tissue cyclic nucleotides, platelet function, and the contractile responses of trabeculae carneae and aortic rings *in vitro*. Am J Cardiol 83:3C–12C

Wang P, Wu P, Myers JG, Stamford A, Egan RW, Billah MM (2001) Characterization of human, dog and rabbit corpus cavernosum type 5 phosphodiesterases. Life Sci 68:1977–1987

Wunder F, Tersteegen A, Rebmann A, Erb C, Fahrig T, Hendrix M (2005) Characterization of the first potent and selective PDE9 inhibitor using a cGMP reporter cell line. Mol Pharmacol 68:1775–1781

Yan C, Zhao AZ, Bentley JK, Beavo JA (1996) The calmodulin-dependent phosphodiesterase gene *PDE1C* encodes several functionally different splice variants in a tissue-specific manner. J Biol Chem 271:25699–25706

Yanaka N, Kurosawa Y, Minami K, Kawai E, Omori K (2003) CGMP-phosphodiesterase activity is upregulated in response to pressure overload of rat ventricles. Biosci Biochem 67:073–079

Yu S, Wolda SL, Frazier ALB, Florio VA, Martins TJ, Snyder PB, Harris EAS, McCaw KN, Farell CA, Steiner B, Bentley JK, Beavo JA, Ferguson K, Gelinas R (1997) Identification and characterisation of a human calmodulin-stimulated phosphodiesterase PDEB1. Cell Signal 9:519–529

Zhang X, Feng Q, Cote RH (2005) Efficacy and selectivity of phosphodiesterase-targeted drugs in inhibiting photoreceptor phosphodiesterase (PDE6) in retinal photoreceptors. Invest Ophthalmol Vis Sci 46:3060–3066

A.1.1.22
Stimulation of Heart Membrane Adenylate Cyclase

PURPOSE AND RATIONALE

Metzger and Lindner (1981) discovered that the positive inotropic and vasodilatory effects of forskolin were correlated with the stimulation of adenylate cyclase and cAMP-dependent protein kinase. Subsequent studies by Seamon (1981) demonstrated that forskolin, unlike hormones, guanine nucleotides, fluoride or cholera toxin could stimulate cyclase activity in the absence of the guanine nucleotide regulatory protein. Since those reports, hundreds of papers have been published on the effects of forskolin in numerous mammalian organ and cell systems. Several comprehensive review articles have also been published (Seamon and Daly 1981, 1983; Daly 1984).

While forskolin has proven to be an invaluable research tool for investigations of adenylate cyclase systems (Salomon et al. 1974; Seamon et al. 1981, 1983), reports on its effects on cardiovascular (Lindner et al. 1978), pulmonary (Chang et al. 1984) and ocular physiology (Caprioli and Sears 1983; Caprioli 1985) suggest a therapeutic potential (Seamon 1984) as well.

Described here is an *in vitro* assay which can be used to compare the potency of forskolin, forskolin analogs or other direct or indirect adenylate cyclase activators for the stimulation of adenylate cyclase in heart membranes. The purpose of this assay is to determine and compare the potency of direct or indirect activators of adenylate cyclase for an ability to stimulate heart membrane adenylate cyclase *in vitro*.

PROCEDURE

The hearts of the Wistar rat, Hartley guinea pig, golden Syrian hamster or cardiomyopathic hamster (CHF-146) are used as a source of adenylate cyclase for this assay.

Reagents

1. 0.5 M Tris buffer, pH 7.4
2. 0.05 M Tris buffer, pH 7.4, containing 0.1 M $CaCl_2$
3. Tris buffer mixture
   0.05 M Tris buffer, containing 1 mM IMBX (isobutylmethylxanthine), 0.2 mM EGTA, 5 mM $MgCl_2$, 0.5 mM ATP ($Na_2ATP \times 3\,H_2O$) and 20 mM creatine phosphate (Na_2 Creatine-$PO_4 \times 5\,H_2O$) (final concentrations in the incubation media).
4. Creatine phosphokinase (ATP:Creatine N-Phosphotransferase, EC 2.73.2), type I, from rabbit muscle is obtained from Sigma Chemical Co.
   The concentration of enzyme in the incubation media is 40 U/ml.
5 Test compounds
   For most assays, a 30 mM stock solution is made up in a suitable solvent (ethanol, ethyl acetate or DMSO for most forskolin analogs). Serial dilutions are made such that the final concentration in the assay ranges from 3×10^{-4} to 3×10^{-7} M. The concentration of vehicle in the assay is 1%.

Tissue Preparation

One entire heart from rat, guinea pig or hamster is dissected, weighed and homogenized in 50 volumes of ice-cold 0.05 M Tris buffer, pH 7.4 containing 0.1 mM $CaCl_2$ (reagent 2) using a Brinkman Polytron (setting 7 for 15 s). The homogenate is centrifuged at 10,000 *g* for 20 min at 4°C. The resulting pellet is resuspended in 50 volumes of homogenizing buffer and recentrifuged as before. The supernatant of this spin is discarded and the resulting pellet is finally resuspended in 10 volumes of the homogenizing buffer, for rat and hamster and 60 volumes for guinea pig tissue. This final preparation is filtered through a thin layer of gauze and kept on ice until used in the assay. The protein concentration is approximately 250–350 mg/ml.

Protein concentrations from an aliquot of the tissue suspension are determined on the day of the experiment by the method of Bradford (1976) using the Bio-Rad assay kit.

Assay

300 µl	Tris buffer mixture, pH 7.4 (reagent 3)
50 µl	creatine phosphokinase
5 µl	vehicle or appropriate concentration of test drug
95 µl	H_2O
50 µl	tissue suspension

The tubes are incubated for 5 min at 37°C and the reaction is then stopped by placing the tubes into a boiling water bath for 4 min. The tubes are then centrifuged at 1000 *g* for 10 min and cAMP levels determined in a 15 µl aliquot of the supernatant using a radioimmunoassay kit (Code TRK432) obtained from Amersham according to the manufacturer's protocol.

Test principle: The method is based on the competition between unlabeled cAMP and a fixed quantity of ^{3}H-labelled cAMP for binding to a protein which has high specificity and affinity for cyclic AMP. The amount of labelled cAMP–protein complex formed is inversely related to the amount of unlabelled cAMP present in the assay sample. The concentration of cAMP in the unknown is determined by comparison with a linear standard curve.

EVALUATION

The data are expressed as pmol cAMP/mg protein/min and dose-response stimulation curves are subjected to logic analysis to determine the concentration of compound which exhibits 50% of maximal stimulation (ED_{50}).

The β-blocking activities of compounds can be determined by their activities, by which they counteract the isoproterenol and GTP induced stimulation of rat heart membrane bound adenylate cyclase (Greenslade et al. 1979).

REFERENCES AND FURTHER READING

Bradford M (1976) A rapid and sensitive method for the quantitation of microgram quantities of protein utilizing the principle of protein-dye binding. Analyt Biochem 72:248–254

Caprioli J (1985) The pathogenesis and medical management of glaucoma. Drug Dev Res 6:193–215

Caprioli J, Sears M (1983) Forskolin lowers intraocular pressure in rabbits, monkeys and man. Lancet 1:958–960

Chang J, Hand JM, Schwalm S, Dervinis A, Lewis AJ (1984) Bronchodilating activity of forskolin *in vitro* and *in vivo*. Eur J Pharmacol 101:271–274

Daly JW (1984) Forskolin, adenylate cyclase and cell physiology: An overview. In: Greengard P et al (eds) Advances in Cyclic Nucleotide and Protein Phosphorylation Research 17:81–89

Greenslade FC, Tobia AJ, Madison SM, Krider KM, Newquist KL (1979) Labetalol binding to specific alpha- and beta-adrenergic sites *in vitro* and its antagonism of adrenergic responses *in vivo*. J Mol Cell Cardiol 11:803–811

Hubbard JW, Conway PG, Nordstrom LC, Hartman HB, Lebedinsky Y, O'Malley GJ, Kosley RW (1992) Cardiac adenylate cyclase activity, positive chronotropic and inotropic effects of forskolin analogs with either low, medium or high binding site activity. J Pharm Exp Ther 256:621–627

Kebabian JW (1992) The cyclic AMP cascade: A signal transduction system. Neurotransmiss 8(2):1–4

Lebedinsky Y, Nordstrom ST, Aschoff SE, Kapples JF, O'Malley GJ, Kosley RW, Fielding S, Hubbard JW (1992) Cardiotonic and coronary vasodilator responses to milrinone, forskolin, and analog P87–7692 in the anesthetized dog. J Cardiovasc Pharmacol 19:779–789

Lindner E, Dohadwalla AN, Bhattacharya BK (1978) Positive inotropic and blood pressure lowering activity of a diterpene derivative isolated from Coleus forskohli: Forskolin. Arzneim Forsch/Drug Res 28:284–289
Metzger H, Lindner E (1981) The positive inotropic-acting forskolin, a potent adenylate-cyclase activator. Arzneim Forsch/Drug Res 31:1248–1250
Salomon Y, Londos C, Rodbell M (1974) A highly sensitive adenylate cyclase assay. Analyt Biochem 58:541–548
Seamon KB (1984) Forskolin and adenylate cyclase: new opportunities in drug design. Ann Rep Med Chem 19:293–302
Seamon KB, Daly JW (1981a) Activation of adenylate cyclase by the diterpene forskolin does not require the guanine nucleotide regulatory protein. J Biol Chem 256:9799–9801
Seamon KB, Daly JW (1981b) Forskolin: A unique diterpene activator of cyclic AMP-generating systems. J Cycl Nucl Res 7:201–224
Seamon KB, Daly JW (1983) Forskolin, cyclic AMP and cellular physiology. Trends Pharmacol Sci 4:120–123
Seamon KB, Padgett W, Daly JW (1981) Forskolin: Unique diterpene activator of adenylate cyclase in membranes and in intact cells. Proc Natl Acad Sci USA 78:3363–3367
Seamon KB, Daly JW, Metzger H, de Souza NJ, Reden J (1983) Structure activity relationships for activation of adenylate cyclase by the diterpene forskolin and its derivates. J Med Chem 26:436–439
Seamon KB, Vaillancourt R, Edwards M, Daly JW (1984) Binding of [^{3}H]forskolin to rat brain membranes. Proc Natl Acad Sci USA 81:5081–5085

A.1.1.23 ^{3}H-Forskolin Binding Assay

PURPOSE AND RATIONALE

This assay is used to identify compounds which demonstrate high affinity [nM] for association with forskolin binding sites *in vitro* as a preliminary screen in conjunction with stimulation of adenylate cyclase to determine the potential for cardiac chronotropic and inotropic and other effects of forskolin. Guinea pig heart tissue and rat brain tissue are used as sources of binding assays.

PROCEDURE FOR GUINEA PIG HEART TISSUE

A. Reagents
1. 0.05 M Tris-HCl buffer, pH 7.4
2. 0.05 M Tris-HCl, pH 8.0 containing 1 mM EGTA, 1 mM $MgCl_2$ and 0.32 M sucrose
3. [^{3}H]-Forskolin (specific activity 31.6 Ci/mmol) is obtained from New England Nuclear.
   Final concentration in the assay is approximately 15 nM.
4. Forskolin and test compounds
   Forskolin and forskolin analogs are diluted to 40 µM. A 100 µl addition of this solution to the final incubate of 200 µl tissue and 100 µl ^{3}H-forskolin results in a final concentration of 10^{-5} M.
   Appropriate serial dilutions of this stock solution are made such that the final concentrations in the assay range from 10^{-5} to 10^{-11} M with each concentration being done in triplicate.

B. Tissue preparation
Male Hartley guinea pigs (300–350 g) are sacrificed by decapitation. The heart is immediately removed, weighed, rinsed, diced and homogenized in 10 volumes of ice-cold 0.05 M buffer(reagent 2) using a Polytron homogenizer (setting 10, 30 s). The resulting homogenate is centrifuged at 12,000 *g* for 15 min at 4°C. The clear supernatant of this spin is discarded, the remaining pellet (P_2) is resuspended in 5 volumes of the same ice-cold buffer and rehomogenized. This final suspension (approximately 0.8–1.0 mg protein/ml) is kept on ice until use. Protein concentrations are estimated according to the method of Lowry et al. (1951).

C. Binding assay
To generate a dose-response inhibition curve, ^{3}H-forskolin binding is performed according to the method of Seamon et al. (1984) with minor modifications.
200 µl tissue suspension
100 µl ^{3}H-forskolin
100 µl appropriate concentration of forskolin or forskolin analog, or buffer
Tubes are incubated at 30°C for 10 min. The incubate is then diluted with 5 ml of ice-cold 0.05 M Tris-HCl buffer, pH 7.4 (reagent 1) and immediately vacuum filtered through glass fiber filters (Whatman GF/B) by using a Brandel Cell Harvester. The filters are rapidly washed 3 times with 5 ml aliquots of Tris-HCl buffer (reagent 1), added to 10 ml scintillation cocktail and analyzed for radioactivity.

PROCEDURE FOR RAT BRAIN TISSUE

A. Reagents
1. 0.32 M sucrose buffer
2. 0.05 M Tris-HCl buffer, pH 7.5
3. [^{3}H]-Forskolin (specific activity 31.6 Ci/mmol) is obtained from New England Nuclear.
   Final concentration in the assay is approximately 10 nM.
4. Forskolin and test compounds
   Forskolin and forskolin analogs are diluted to 40 µM. A 100 µl addition of this solution to the final incubate of 200 µl tissue and 100 µl ^{3}H-forskolin results in a final concentration of 10^{-5} M.

Appropriate serial dilutions of this stock solution are made such that the final concentrations in the assay range from 10^{-5} to 10^{-11} M with each concentration being done in triplicate.

B. Tissue preparation

Male Sprague-Dawley rats (200–250 g) are sacrificed by decapitation. The brain is rapidly removed and dissected on ice. Striata are homogenized in 50 volumes of ice-cold 0.32 M sucrose buffer (reagent 1) using a Polytron homogenizer (setting 7, 15 s). The resulting homogenate is centrifuged at 1000 *g* for 10 min at 0–4°C. The supernatant is retained and recentrifuged at 20,000 *g* for 10 min at 0–4°C. The clear supernatant of this spin is discarded and the remaining pellet (P_2) is resuspended in ice-cold Tris-HCl buffer, pH 7.5 such that the final protein concentration is approximately 3.0–4.0 mg/ml. Protein concentrations are estimated according to the method of Lowry et al. (1951).

C. Binding assay

To generate a dose-response inhibition curve, ^{3}H-forskolin binding is performed according to the method of Seamon et al. (1984) with minor modifications.

200 µl tissue suspension

100 µl ^{3}H-forskolin

100 µl appropriate concentration of forskolin or forskolin analog or buffer

Tubes are incubated at 23°C for 60 min. The incubate is then diluted with 5 ml of ice-cold 0.05 M Tris-HCl buffer, pH 7.4 (reagent 2) and immediately vacuum filtered through glass fiber filters (Whatman GF/B) by using a Brandel Cell Harvester. The filters are rapidly washed three times with 5 ml aliquots of Tris-HCl buffer (reagent 2), added to 10 ml scintillation cocktail and analyzed for radioactivity.

EVALUATION

Specific binding is defined as the difference between binding of ^{3}H-forskolin in the absence and presence of 10 µM forskolin and represents 85–90% of total binding at 10 nM ^{3}H-forskolin.

Results of the dose-response inhibition curves are analyzed by determining the concentration of competing compound which inhibits 50% of the ^{3}H-forskolin binding sites (IC_{50}). This value is determined by computer-derived log-probit analysis.

The activity of various forskolin analogs are based on IC_{50} values and are categorized as follows:

	IC_{50}[M]
0 = Not determined	
1 = No activity	$>10^{-5}$
2 = Slight activity	10^{-5}–10^{-6}
3 = Moderate activity	10^{-6}–10^{-7}
4 = Marked activity	$<10^{-7}$

To compare the activity of various compounds from experiment to experiment, an inhibition constant (K_I) is determined as described by Cheng and Prusoff (1973). The K_I is determined from the equation:

$$K_I = IC_{50}/1 + LC/K_D$$

IC_{50} = concentration of competing compound which inhibits 50% of the ^{3}H-forskolin binding sites

LC = determined ^{3}H-forskolin concentration (approximately 10 nM)

K_D = dissociation of affinity constant for ^{3}H-forskolin determined previously to be approximately 13.4 nM for rat striatum and 196 nM for guinea pig heart

Standard data:

Binding inhibition values for forskolin

	Striatum	Heart
IC_{50}	43.1 ± 4.9 nM	34.2 ± 5.0 nM
K_I	26.0 ± 3.1 nM	31.6 ± 4.6 nM

REFERENCES AND FURTHER READING

Cheng YC, Prusoff WH (1973) Relationship between the inhibition constant (K_I) and the concentration of inhibitor which causes 50 percent inhibition (IC_{50}) of an enzymatic reaction. Biochem Pharmacol 22:3099–3108

Lowry OH, Rosebrough NJ, Farr AL, Randall RJ (1951) Protein measurement with phenol reagent. J Biol Chem 193:265–275

Seamon KB, Vaillancourt R, Edwards M, Daly JW (1984) Binding of [^{3}H]forskolin to rat brain membranes. Proc Natl Acad Sci USA 81:5081–5085

A.1.1.24 Patch Clamp Technique[2]

PURPOSE AND RATIONALE

The introduction of the patch clamp technique (Neher and Sakmann 1976) revolutionized the study of cellular physiology by providing a high-resolution method of observing the function of individual ionic channels in a variety of normal and pathological cell types. By

[2]Contributions by H. Gögelein.

the use of variations of the basic recording methodology, cellular function and regulation can be studied at a molecular level by observing currents through individual ionic channels (Liem et al. 1995; Sakmann and Neher 1995).

The most intriguing method is called the "on-cell" or "cell-attached" configuration, because ion channels can be recorded on an intact cell (Jackson 1993). This mode is well suited for investigation of ion channels that are activated by hormonal stimulation and triggered by intracellular second messengers.

Another versatile mode is the "cell-excised" configuration (Hamill 1993). It is obtained by suddenly removing the patch pipette from the cell, so that the membrane patch is pulled off the cell. This mode easily allows the investigator to expose the channel proteins to drugs by changing the bath solution. The single channel currents are recorded on a videotape and are analyzed off-line by a computer system. Various parameters are evaluated, such as the single channel conductance, open and closed times of the channel, and the open-state probability, which is the percentage of time the channel stays in its open state.

In addition to these modes, which enable the recording of single channel currents, it is also possible to measure the current flowing through the entire cell. This "whole-cell mode" is obtained by rupturing the membrane patch in the cell-attached mode (Hamill et al. 1981; Dietzel et al. 1993). This is achieved by applying suction to the interior of the patch pipette. The "whole-cell mode" allows not only the recording of electrical current, but also the measurement of cell potential. Moreover, the cell interior is dialyzed by the electrolyte solution contained in the patch pipette.

The fabrication of patch clamp pipettes has been described by Sakmann and Neher (1995) and Cavalié et al. (1993).

Variations of the patch clamp technique have been used to study neurotransmitter transduction mechanisms (Smith 1995).

High throughput methods are required when developing drugs that work on ion channel function (Mathes 2003; Bennett and Guthrie 2003). Patch clamping suffers from low throughput, which is not acceptable for drug screening.

Fertig et al. (2002) and Brueggemann et al. (2004, 2006) presented nanopatch clamp technology, which is based on a planar, microstructured glass chip, which enables automatic whole-cell patch clamp experiments. Planar glass substrates containing a single microaperture produced by ion track etching are used to record currents through ion channels in living mammalian cells.

Falconer et al. (2002) reported high throughput screening for ion channel modulators setting up a Beckman/Sagian core system to fully automate functional fluorescence-based assays that measure ion channel function. Voltage-sensitive fluorescent probes were applied and the activity of channels was measured using Aurora's Voltage/Ion Probe Reader (VIPR). The system provides a platform for fully automated high throughput screening as well as pharmacological characterization of ion channel modulators.

Schroeder et al. (2003) described a high throughput electrophysiology measurement platform consisting of computer-controlled fluid handling, recording electronics, and processing tools capable of voltage clamp whole-cell recordings from thousands of individual cells per day. The system uses a planar, multiwell substrate (a PatchPlate). The system positions one cell into a hole separating two fluid compartments in each well of the substrate. Voltage control and current recordings from the cell membrane are made subsequent to gaining access to the cell interior by applying a permeabilizing agent to the intracellular side.

Willumsen's group recommended ion channel screening with QPatch (Asmild et al. 2003; Kutchisky et al. 2003; Krzywkowski et al. 2004). This system claims to allow fast and accurate electrophysiological characterization of ion channels, e. g., for determination of IC_{50} values for ion channel blockers. The system comprises 16 parallel patch clamp sites, each based on a silicon chip with a micro-etched patch clamp hole. Intra- and extra-cellular fluids are administered by laminar flow through integrated miniature flow channels.

REFERENCES AND FURTHER READING

Asmild M, Oswald N, Krzywkowski FM, Friis S, Jacobsen RB, Reuter D, Taboryski R, Kutchinsky J, Vestergaard RK, Schroder RL, Sorensen CB, Bech M, Korsgaard MP Willumsen NJ (2003) Upscaling and automation of electrophysiology: toward high throughput screening in ion channel drug discovery. Receptor Channels 9:49–58

Bennett PB, Guthrie HRE (2003) Trends in ion channel drug discovery: advances in screening technologies. Trends Biotechnol 21:563–569

Brueggemann A, George M, Klau M, Beckler M, Steimdl J, Behrends JC, Fertig N (2004) Ion channel drug discovery and research. The automated nano-patch-clamp technology. Curr Drug Discover Technol 1:91–96

Brüggemann A, Stoelzle S, George M, Behrends JC, Fertig N (2006) Microchip technology for automated and parallel patch-clamp recording. Small 2:840–646

Cavalié A, Grantyn R, Lux HD (1993) Fabrication of patch clamp pipettes. In: Kettenmann H, Grantyn R (eds) Practical electrophysiological methods. Wiley, New York, pp 235–240
Dietzel ID, Bruns D, Polder HR, Lux HD (1993) Voltage clamp recording. In: Kettenmann H, Grantyn R (eds) Practical electrophysiological methods. Wiley, New York, pp 256–262
Falconer M, Smith F, Surah-Narwal S, Congrave G, Liu Z, Hayter P, Ciaramella G, Keighley W, Haddock P, Waldron G, Sewing A (2002) High-throughput screening for ion channel modulators. J Biomol Screen 7:460–465
Fertig N, Klau M, George M, Blick RH, Behrends JC (2002) Activity of single ion channel proteins detected with a planar microstructure. Appl Physics Lett 81:4865–4867
Hamill OP (1993) Cell-free patch clamp. In: Kettenmann H, Grantyn R (eds) Practical electrophysiological methods. Wiley, New York, pp 284–288
Hamill OP, Marty A, Neher E, Sakmann B, Sigworth FJ (1981) Improved patch-clamp techniques for high-resolution current recording from cells and cell-free membrane patches. Pflügers Arch 391:85–100
Jackson MB (1993) Cell-attached patch. In: Kettenmann H, Grantyn R (eds) Practical electrophysiological methods. Wiley, New York, pp 279–283
Krzywkowski K, Schroder RL, Ljungstrom T, Kutchinsky J, Friis S, Vestergaard RK, Jacobsen RB, Pedersen S, Helix N, Sorensen CB, Bech M, Willumsen NJ (2004) Automatation of the patch-clamp technique: technical validation through identification and characterization of potassium channel blockers. Biophys J 86:483a
Kutchinsky J, Friis S, Asnild M, Taboryski R, Pedersen S, Vestergaard RK, Jacobsen RB, Krzywkowski K, Schroder RL, Ljungstrom T, Helix N, Sorensen CB, Bech M, Willumsen NJ (2003) Characterization of potassium channel modulators with QPatch automated patch-clamp technology system characteristics and performance. Assay Drug Dev Technol 1:685–693
Liem LK, Simard JM, Song Y, Tewari K (1995) The patch clamp technique. Neurosurgery 36:382–392
Mathes C (2003) Ion channels in drug discovery and development. Drug Discover Today 8:1022–1024
Neher E, Sakmann B (1976) Single-channel currents recorded from membranes of denervated frog muscle fibres. Nature 260:799–802
Sakmann B, Neher E (1995) Single-cell recording. Plenum, New York
Schroeder K, Neagle B, Trezise DJ, Worley J (2003) IonWorks™ HT: A new high-throughput electrophysiology measurement platform. J Biomol Screen 8:50–64
Smith PA (1995) Methods for studying neurotransmitter transduction mechanisms. J Pharmacol Toxicol Meth 33:63–73

A.1.1.24.1 Patch Clamp Technique in Isolated Cardiac Myocytes

PURPOSE AND RATIONALE

The generation of an action potential in heart muscle cells depends on the opening and closing of ion-selective channels in the plasma membrane. The patch clamp technique enables the investigation of drug interactions with ion-channel-forming proteins at the molecular level.

PROCEDURE

Isolated cells from ventricular muscle of rat and guinea pig are prepared as described by Yazawa et al. (1990). Animals are sacrificed by cervical dislocation. Hearts are dissected and mounted on a Langendorff-type apparatus and perfused first with Tyrode solution (in mM: 143 NaCl, 5.4 KCl, 1.8 $CaCl_2$, 0.5 $MgCl_2$, 0.25 NaH_2PO_4, 5 HEPES, pH adjusted to 7.4 with NaOH) at 37°C for 3 min at a hydrostatic pressure of 60–70 cmH_2O, then with nominally Ca^{2+}-free Tyrode solution (no Ca^{2+} is added) for 5–7 min, and finally with nominally Ca^{2+}-free Tyrode solution containing 0.12–0.2 mg/ml collagenase (Sigma, type I). After 15–20 min of collagenase treatment, the heart is now soft and is washed with storage solution (in mM: 70 KOH, 50 L-glutamic acid, 40 KCl, 20 taurine, 20 KH_2PO_4, 3 $MgCl_2$, 10 glucose, 10 HEPES, 0.5 EGTA, pH adjusted to 7.4 with KOH). The ventricles are cut into pieces (about 5mm × 5 mm) and poured into a beaker. The myocytes are dispersed by gently shaking the beaker and filtration through a nylon mesh (365 µm). Then, the myocytes are washed twice by centrifugation at 600–1000 rpm (about 90 *g*) for 5 min and kept at room temperature. The rod shape of the cell and the clear striations of sarcomeres are important criteria for selecting viable cells for the assay. Experiments are performed at 35°C–37°C.

For investigation with the patch clamp technique (Neher and Sakmann 1976; Hamill et al. 1981), the isolated cells are placed into a thermostat-controlled chamber, mounted on the stage of an inverted microscope equipped with differential interference contrast optics. Under optical control (magnification 400×) a glass micropipette, having a tip opening of about 1 µm, is placed onto the cell. The patch pipettes are fabricated from borosilicate glass tubes (outer diameter 1.5 mm, inner diameter 0.9 mm) by means of an electrically heated puller. In order to prevent damage of the cell membrane, the tip of the micropipette is fire polished, by moving a heated platinum wire close to the tip. The patch pipette is filled with either high-NaCl or KCl solution and is mounted on a micro manipulator. A silver chloride wire connects the pipette solution to the head stage of an electronic amplifier. A second silver chloride wire is inserted into the bath and serves a ground electrode.

After establishing contact with the cell membrane, a slight negative pressure is applied to the inside of the patch pipette by means of a syringe. Consequently, a small patch of membrane is slightly pulled into the opening of the micro pipette and close contact

between the glass and membrane is formed, leading to an increase of the electrical input resistance into the giga-ohm range (about 10^{10} Ohm). This high input resistance enables the recording of small electrical currents in the range of picosiemens (10^{-12} S), which flow through channel-forming proteins situated in the membrane patch. The electrical current is driven by applying an electrical potential across the membrane patch, and/or by establishing an appropriated chemical gradient for the respective ion species.

The patch clamp methods allows one to investigate the interaction of drugs with all ion channels involved in the functioning of the heart muscle cell (K^+, Na^+, Ca^{2+} and eventually Cl^- channels). Moreover, the different types of K^+ channels existing in cardiomyocytes can be distinguished by their different single-channel characteristics or by appropriate voltage-pulse protocols in the whole-cell mode.

EVALUATION

Concentration–response curves of drugs which inhibit or activate ion channels can be recorded either at the single channel level or by measuring the whole-cell current. IC_{50} and EC_{50} values (50% inhibition or activation, respectively) can be obtained with both methods.

MODIFICATIONS OF THE METHOD

The patch clamp technique has been used for evaluation of anti-arrhythmic agents (Bennett et al. 1987; Anno and Hondeghem 1990; Gwilt et al. 1991).

Gögelein et al. (1998) used isolated ventricular myocytes from guinea pigs to study a cardioselective inhibitor of the ATP-sensitive potassium channel.

Multiple types of calcium channels have been identified by patch clamp experiments (Tsien et al. 1988).

The effects of potassium channel openers have been measured (Terzic et al. 1994).

Ryttsén et al. (2000) characterized electroporation of single NG108–15 cells with carbon-fiber microelectrodes by patch clamp recordings and fluorescence microscopy.

Monyer and Lambolez (1995) reviewed the molecular biology and physiology at the single cell level, discussing the value of the polymerase chain reaction at the single cell level and the use of patch pipettes for collecting the contents of a single cell on which the reverse transcription is performed.

The patch clamp technique was found to be very versatile in the investigation of ion channels in atrial myocytes, especially from dogs or humans. Cell were obtained from atria either in sinus rhythm or in atrial fibrillation (reviewed in Bosch et al. 1999).

REFERENCES AND FURTHER READING

Anno T, Hondeghem LM (1990) Interaction of flecainide with guinea pig cardiac sodium channels. Circ Res 66:789–803

Bennett PB, Stroobandt R, Kesteloot H, Hondeghem LM (1987) Sodium channel block by a potent, new antiarrhythmic agent, Transcainide, in guinea pig ventricular myocytes. J Cardiovasc Pharmacol 9:661–667

Bosch RF, Zeng X, Grammer JB, Popovic K, Mewis C, Kühlkamp V (1999) Ionic mechanisms of electrical remodeling in human atrial fibrillation. Cardiovasc Res 44:121–131

Gögelein H, Hartung J, Englert HC, Schölkens BA (1998) HMR 1883, a novel cardioselective inhibitor of the ATP-sensitive potassium channel. Part I. Effects on cardiomyocytes, coronary flow and pancreatic β-cells. J Pharmacol Exp Ther 286:1453–1464

Gwilt M, Dalrymple HW, Burges RA, Blackburn KJ, Dickinson RP, Cross PE, Higgins AJ (1991) Electrophysiologic properties of UK-66,914, a novel class III antiarrhythmic agent. J Cardiovasc Pharmacol 17:376–385

Hamill OP, Marty A, Neher E, Sakmann B, Sigworth FJ (1981) Improved patch-clamp techniques for high-resolution current recording from cells and cell-free membrane patches. Pflugers Arch 391:85–100

Monyer H, Lambolez B (1995) Molecular biology and physiology at the single-cell level. Curr Opin Neurobiol 5:382–387

Neher E, Sakmann B (1976) Single-channel currents recorded from membranes of denervated frog muscle fibres. Nature 260:799–802

Pallotta BS (1987) Patch-clamp studies of ion channels. In: Meltzer HY (ed) Psychopharmacology: The third generation of progress. Raven, New York, pp 325–331

Ryttsén F, Farre C, Brennan C, Weber SG, Nolkrantz K, Jardemark K, Chiu DT, Orwar O (2000) Characterization of single-cell electroporation by using patch-clamp and fluorescence microscopy. Biophys J 79:1993–2001

Terzic A, Jahangir A, Kurachi Y (1994) HOE-234, a second generation K^+ channel opener, antagonizes the ATP-dependent gating of cardiac ATP-sensitive K^+ channels. J Pharmacol Exp Ther 268:818–825

Tsien RW, Lipscombe D, Madison DV, Bley RK, Fox AP (1988) Multiple types of neuronal calcium channels and their selective modulation. TINS 11:431–438

Yazawa K, Kaibara M, Ohara M, Kameyama M (1990) An improved method for isolating cardiac myocytes useful for patch-clamp studies. Jpn J Physiol 40:157–163

A.1.1.24.2 Voltage Clamp Studies on Sodium Channels

PURPOSE AND RATIONALE

The epithelial Na^+ channel plays an important role in epithelial Na^+ absorption in the distal colon, urinary bladder, salivary and sweat ducts, respiratory tract and, most importantly, in the distal tubules of the kidney (Catterall 1986; Palmer 1992). Regulation of this epithelial Na^+ channel has a major impact on Na^+ balance, blood volume, and blood pressure. Inhibition of epithelial Na^+ channel expression is used for the treatment of hypertension (Endou and Hosoyamada 1995).

Busch et al. (1995) studied the blockade of epithelial Na^+ channels by triamterenes using two-microelectrode voltage clamp experiments in *Xenopus* oocytes expressing the three homologous subunits (α, β, and γ) of the rat epithelial Na^+ channel (rENaC).

PROCEDURE

Xenopus laevis oocytes are injected with the appropriate cRNA encoding for the α, β, and γ-subunits (Canessa et al. 1993) of the rat epithelial Na^+ channel (rENaC). The cRNA for the wild-type α-subunit and its deletion mutant Δ278–273 is always coinjected with an equal amount of β and γ-subunit cRNA (10 ng/oocyte).

Then, 2–8 days after cRNA injection, the two-microelectrode voltage clamp method is used to record currents from *Xenopus* oocytes. Recordings are performed at 22°C using a Geneclamp amplifier (Axon Instruments, Foster City, Calif., USA), and MacLab D/A converter and software for data acquisition and analysis (AD Instruments, Castle Hill, Australia). The ND 96 solution (control) contains (mM): NaCl 96, KCl 2, $CaCl_2$ 1.8, $MgCl_2$ 1, HEPES 5, pH 7.0. In some experiments, Na^+ is replaced by *N*-methyl-D-glucamine (NMDG) solution. The microelectrodes are filled with 3 M KCl solution and have resistances in the range 0.5–0.9 MΩ. Chemicals (e. g., triamterene as standard) are added at concentrations between 0.2 and 100 µM. The amplitude of the induced currents varies considerably, depending on the day of channel expression and the batch of oocytes. The mutant channel induces considerably smaller currents than the wild-type channel. The total Na^+ current amplitude is determined at least once for each experimental day by superfusion with NMDG solution, or with 3 µM or 5 µM amiloride solution at the beginning and at the end of each set of experiments.

EVALUATION

Data are presented as means ± SEM. A paired Student's *t*-test is used. The level of statistical significance is set at $P < 0.05$.

MODIFICATIONS OF THE METHOD

Nawada et al. (1995) studied the effects of a sodium, calcium, and potassium antagonistic agent on the sodium current by the whole cell voltage clamp technique (tip resistance = 5 MΩ[Na]$_i$ and [Na]$_o$ 10 mmol/l at 20°C) in guinea pig isolated ventricular cells.

Sunami and Hiraoka (1996) studied the mechanism of cardiac Na^+ channel block by a charged class I antiarrhythmic agent, in guinea pig ventricular myocytes using patch clamp techniques in the whole-cell, cell-attached and inside-out configurations.

Erdõ et al. (1996) compared the effects of *Vinca* derivatives on voltage-gated Na^+ channels in cultured cells from rat embryonic cerebral cortex. Effects on Na^+ currents were measured by applying voltage steps (20 ms duration) to –10 mV from a holding potential of –70 mV every 20 s. Steady-state inactivation curves were obtained by clamping the membrane at one of a series of 15-s prepulse potentials, followed 1 ms later by a 20-ms test pulse to –10 mV.

Ragsdal et al. (1993) examined the actions of a Na^+ channel blocker in whole-cell voltage clamp recordings from Chinese hamster ovary cells transfected with a cDNA encoding the rat brain type IIA Na^+ channel and from dissociated rat brain neurons.

Taglialatela et al. (1996) studied cloned voltage-dependent Na^+ currents expressed in *Xenopus* oocytes upon injection of the cRNA encoding α-subunits from human and rat brain.

Wang et al. (1997) investigated pharmacological targeting of long QT mutant sodium channels.

Eller et al. (2000) measured the effects of a calcium antagonist on inward Na^+ currents (I_{Na}) in GH3-cells with the whole-cell configuration of the patch clamp technique. I_{Na} was recorded after depolarization from a holding potential of –80 mV to a test potential of +5 mV. Initial "tonic" block (resting state-dependent block) was defined as peak I_{Na} inhibition during the first pulse 2 min after drug application as compared with I_{Na} in the absence of drug. "Use-(frequency-) dependent" block of I_{Na} was measured during trains of 5- or 50-ms test pulses (3 Hz) applied from –80 mV to a test potential of +5 mV after a 2-min equilibrium period in the drug-containing solution. Use-dependent block was expressed as the percentage decrease of peak I_{Na} during the last pulse of the train as compared with I_{Na} during the first pulse.

Khalifa et al. (1999) characterized the effects of an antidepressant agent on the fast inward current (I_{Na}) in isolated guinea pig ventricular myocytes. Currents were recorded in the whole-cell configuration of the patch clamp technique in the presence of Ca^{2+} and K^+ channel blockers.

Haeseler et al. (1999) measured the effects of 4-chloro-*m*-cresol, a preservative added to a wide variety of drugs, on heterologously expressed wild-type, Paramyotonia congenita (R1448H) and hyperkalemic periodic paralysis (M1360V) mutant α-subunits of human muscle sodium channels using whole-cell and inside-out voltage clamp experiments.

Song et al. (2000) studied the effects of *N*-ethyl-maleimide, an alkylating agent to protein sulfhydryl groups, on tetrodotoxin-sensitive (TTX-S) and tetrodotoxin-resistant (TTX-R) sodium channels in rat dorsal root neurons using the whole-cell configuration of the patch clamp technique. Rats at the age of 2–6 days were anesthetized with isoflurane and the spinal cord was removed and cut longitudinally. Dorsal root ganglia were plucked from the area between the vertebrae of the spinal column, and incubated in phosphate-buffered saline solution containing 2.5 mg/ml trypsin at 37°C for 30 min. After enzyme treatment, ganglia were rinsed with Dulbecco's Modified Eagle Medium supplemented with 10% horse serum. Single cells were mechanically dissociated by trituration with a fire-polished Pasteur pipette and plated on poly-L-lysine-coated glass coverslips. Cells attached to the coverslips were transferred into a recording chamber on the stage of an inverted microscope. Ionic currents were recorded under voltage clamp conditions by the whole-cell patch clamp technique. The solution in the pipette contained (in mM): CsCl 125, NaF 20, HEPES 5, EGTA 5. The pH was adjusted to 7.2 with CsOH and the osmolarity was 279 mosmol/l on average. The external solution contained (in mM): NaCl 50, choline chloride 90, tetramethylammonium chloride 20, D-glucose 5, HEPES 5, $MgCl_2$ 1, $CaCl_2$ 1. Lanthanum ($LaCl_3$, 10 µM) was used to block calcium channel current. The solution was adjusted to pH 7.4 with tetramethylammonium hydroxide and the osmolarity was 304 mosmol/l on average. An Ag–AgCl pellet/3 M KCl-agar bridge was used for the reference electrode. Membrane currents were recorded using an Axopatch-1D amplifier. Signals were digitized by a 12-bit analog-to-digital interface, filtered with a low-pass Bessel filter at 5 kHz and sampled at 50 kHz using pCLAMP6 software (Axon Instruments) on an IBM-compatible PC. Series resistance was compensated 60%–70%. Capacitative and leakage currents were subtracted by using a P + P/4 procedure (Bezanilla and Armstrong 1977). The liquid junction potential between internal and external solutions was on average –1.7 mV. TTX (100 nM) was used to separate TTX-R sodium currents from TTX-S sodium currents. For the study of TTX-S sodium channels, cells that expressed only TTX-S sodium channels were used. TTX-S sodium channels were completely inactivated within 2 ms when currents were evoked by depolarizing steps to 0 mV, while TTX-R sodium channels persisted for more than 20 ms. The difference in kinetics was used to identify the type of sodium current.

Abriel et al. (2000) described the molecular pharmacology of the sodium channel mutation DI790G linked to long QT syndrome.

Makielski et al. (2003) showed that a ubiquitous splice variant and a common polymorphism affect heterologous expression of recombinant human SCN5AS heart sodium channels.

Viswanathan et al. (2001) studied gating mechanisms for flecainide action in *SNCN5A*-linked arrhythmia syndromes.

REFERENCES AND FURTHER READING

Abriel H, Wehrens XHT, Benhorin J, Kerem B, Kass RS (2000) Molecular pharmacology of the sodium channel mutation DI790G linked to the long-QT- syndrome. Circulation 102:921–925

Bezanilla F, Armstrong CM (1977) Inactivation of the sodium channel: I. Sodium current experiments. J Gen Physiol 70:549–566

Busch AE, Suessbrich H, Kunzelmann K, Hipper A, Greger R, Waldegger S, Mutschler E, Lindemann B, Lang F (1995) Blockade of epithelial Na^+ channels by triamterenes – underlying mechanisms and molecular basis. Pflügers Arch 432:760–766

Canessa CM, Schild L, Buell G, Thorens B, Gautschi I, Horisberger JD, Rossier BC (1994) Amiloride-sensitive N^+ channel is made of three homologous subunits. Nature 367:463–467

Catterall WA (1986) Molecular properties of voltage-sensitive sodium channels. Annu Rev Biochem 55:953–985

Eller P, Berjukov S, Wanner S, Huber I, Hering S, Knaus HG, Toth G, Kimball SD, Striessnig J (2000) High affinity interaction of mibefradil with voltage-gated calcium and sodium channels. Br J Pharmacol 130:699–677

Endou H, Hosoyamada M (1995) Potassium-retaining diuretics: aldosterone antagonists. In: Greger RH, Knauf H, Mutschler E (eds) Handbook of experimental pharmacology, Vol 117. Springer, Berlin Heidelberg New York, pp 335–362

Erdõ SL, Molnár P, Lakics V, Bence JZ, Tömösközi Z (1996) Vincamine and vincanol are potent blockers of voltage-gated Na^+ channels. Eur J Pharmacol 314:69–73

Haeseler G, Leuwer M, Kavan J, Würz A, Dengler R, Piepenbrock S (1999) Voltage-dependent block of normal and mutant muscle sodium channels by 4-Chloro-m-Cresol. Br J Pharmacol 128:1259–1267

Khalifa M, Daleau P, Turgeon J (1999) Mechanism of sodium channel block by venlafaxine in guinea pig ventricular myocytes. J Pharmacol Exp Ther 291:280–284

Makielski JC, Ye B, Valdivia CR, Pagel MD, Pu J, Tester DJ, Ackerman MJ (2003) A ubiquitous splice variant and a common polymorphisms affect heterologous expression of recombinant human SCN5AS heart sodium channels. Circ Res 93:821–828

Nawada T, Tanaka Y, Hisatome I, Sasaki N, Ohtahara A, Kotake H, Mashiba H, Sato R (1995) Mechanism of inhibition of the sodium current by bepridil in guinea-pig isolated ventricular cells. Br J Pharmacol 116:1775–1780

Palmer LG (1992) Epithelial Na channels: function and diversity. Annu Rev Physiol 54:51–66

Ragsdal DS, Numann R, Catterall WA, Scheuer T (1993) Inhibition of Na^+ channels by the novel blocker PD85,639. Mol Pharmacol 43:949–954

Song J-H, Jang Y-Y, Shin Y-K, Lee C-S, Chung S (2000) *N*-Ethyl-maleimide modulation of tetrodotoxin-sensitive and tetrodotoxin-resistant sodium channels in rat dorsal root neurons. Brain Res 855:267–273

Sunami A, Hiraoka M (1996) Blockade of cardiac Na^+ channels by a charged class I antiarrhythmic agent, bisaramil: possible interaction of the drug with a pre-open closed state. Eur J Pharmacol 312:245–255

Taglialatela M, Ongini E, Brown AM, di Renzo G, Annunziato L (1996) Felbamate inhibits cloned voltage-dependent Na^+ channels from human and rat brain. Eur J Pharmacol 316:373–377

Viswanathan PV, Bezzina CR, George AL, Jr, Roden DM, Wilde AAM, Balser JR (2001) Gating mechanisms for flecainide action in *SNCN5A*-linked arrhythmia syndromes. Circulation 104:1200–1205

Wang DW, Yazawa K, Makita N, George AL, Jr, Bennett PB (1997) Pharmacological targeting of long QT mutant sodium channels. J Clin Invest 99:1714–1720

A.1.1.24.3 Voltage Clamp Studies on Potassium Channels

PURPOSE AND RATIONALE

Potassium channels represent a very large and diverse collection of membrane proteins which participate in important cellular functions regulating neuronal and cardiac electrical patterns, release of neurotransmitters, muscle contractility, hormone secretion, secretion of fluids, and modulation of signal transduction pathways. The main categories of potassium channels are gated by voltage or an increase of intracellular calcium concentration (Escande and Henry 1993; Kaczorowski and Garcia 1999; Alexander et al. 2001). For ATP-sensitive potassium channels see Sect. K.6.6.12.

The delayed outward potassium current in heart muscle cells of several species is made up of a **rapidly** (I_{Kr}) and a **slowly** (I_{Ks}) activating component (Sanguinetti and Jurkiewicz 1990; Wang et al. 1994; Gintant 1996; Lei and Brown 1996; Carmeliet and Mubagawa 1998). Several potent and selective blockers of the I_{Kr} channel have been shown to prolong the effective refractory period, but have a reverse rate-dependent activity with both normal and elevated extracellular potassium concentrations (Colatsky et al. 1990). Inhibitors of the slow component I_{Ks} were developed in order to circumvent the negative rate dependence of I_{Kr} channel blockers in the effective refractory period (Busch et al. 1996; Suessbrich et al. 1996, 1997; Bosch et al. 1998). Gögelein et al. (2000) studied the effects of a potent inhibitor of I_{Ks} channels in *Xenopus* oocytes and guinea pig ventricular myocytes.

PROCEDURE

Studies in *Xenopus* oocytes are performed with the two-microelectrode voltage clamp method. For isolation of the oocytes, the toads are anesthetized using a 1 g/l solution of 3-aminobenzoic acid ethyl ester and placed on ice. A small incision is made to retrieve sacs of oocytes and is subsequently closed with absorbable surgical suture. On waking up, the toads are placed back into the aquarium. The ovaries are cut up into small pieces and the oocytes are washed in Ca^{2+}-free Or-2 solution (82.5 mM NaCl, 2 mM KCl, 1 mM $MgCl_2$, 5 mM HEPES; pH 7.4) and subsequently digested in Or-2 containing collagenase A (1 mg/ml, Worthington, type II) until follicles are not longer detectable on the oocyte's surface. The oocytes are stored at 18°C in recording solution ND-96 (NaCl 96 mM, KCl 2 mM, $CaCl_2$ 1.8 mM, $MgCl_2$ 1 mM, HEPES 5 mM, pH 7.4) with added sodium pyruvate (275 mg/l), theophylline (90 mg/l), and gentamicin (50 mg/l).

For electrophysiological recordings, the two-microelectrode voltage clamp configuration is used to record ion currents from *Xenopus* oocytes. Injection of cRNA is performed according to Methfessel et al. (1986) and Golding (1992). Oocytes are injected individually with cRNA encoding for the human protein minK, guinea pig Kir2.1, human H*erg*, human Kv1.5, mouse Kv1.3, or human HNC2. In the case of minK the functional potassium channel is a heteromultimer composed of the endogenous (*Xenopus*) KvLQT1 and the injected human minK. This heteromultimeric potassium current in then called I_{Ks} (Barhanin et al. 1996; Sanguinetti et al. 1996).

The electrophysiological recordings are performed at room temperature, using a Geneclamp amplifier (Axon Instruments), and MacLab D/A converter. The amplitudes of the recorded currents are measured at the end of the test voltage steps. To amplify the inward potassium current through Kir2.1 and HNC2, the external potassium concentration is raised to 10 mM KCl and the NaCl concentration lowered to 88 mM (ND-88). The microelectrodes are filled with 3 M KCl and have a resistance between 0.5 MΩ and 1 MΩ. During the recordings the oocytes are continuously perfused with ND-96 (or ND-88 in the case of Kir2.1 and HCN2). The test compounds are dissolved in dimethylsulfoxide (DMSO) and added to the buffer ND-96 or ND-88. The current amplitude is determined after 5 min of wash-in time.

For the isolation of *ventricular myocytes*, guinea pigs (weight about 400 g) or Sprague-Dawley rats of either sex are sacrificed by cervical dislocation. The hearts are dissected and perfused retrogradely via the aorta at 37°C: first with nominally Ca^{2+}-free Tyrode solution (in mmol/l): 143 NaCl, 5.4 KCl, 0.5 $MgCl_2$, 0.25 NaH_2PO_4, 10 glucose, 5 HEPES, pH 7.2, then

with Tyrode solution containing 20 mmol/l Ca^{2+} and 3 mg/ml collagenase type CLS II (Biochrom, Berlin Germany). After 5–10 min collagenase treatment the ventricles are cut up into small pieces in the storage solution (in mmol/l): 50 L-glutamic acid monopotassium salt, 40 KCl, 20 taurine, 20 KH_2PO_4, 1 $MgCl_2$, 10 glucose, 0.2 EGTA, pH 7.2. The myocytes are then dispersed by gentle shaking followed by filtration through a nylon mesh (365 μm). The cells are finally washed twice by centrifugation at 90 *g* for 5 min and kept in the storage solution at room temperature.

Whole-cell currents are recorded in the tight-seal whole-cell mode of the patch clamp technique, using an EPC-9 amplifier (HEKA Elektronik, Lambrecht, Germany). Patch pipettes are pulled from borosilicate glass capillaries (wall thickness 0.3 mm, outer diameter 1.5 mm) and their tips are fire-polished. Series resistance is in the range of 1–10 MΩ and 50% compensated by means of the EPC's compensation circuit.

The I_{Ks}, I_{Kr}, and I_{K1} currents in guinea pig ventricular myocytes are investigated. The voltage pulses for recording the current components are as follows: I_{Ks} current: holding potential –80 mV to –50 mV (200 ms) to +60 mV (3 s) to –40 mV (2 s) to –80 mV; I_{Kr} current: holding potential –80 mV to –50 mV (200 ms) to –10 mV (3 s) to –40 mV (2 s) to –80 mV. I_{Kr} is evaluated as the tail current evoked by a voltage pulse from –10 mV to –40 mV; I_{K1}: holding potential –80 mV to –120 mV (200 ms) to –80 mV. In order to suppress the L-type Ca^{2+} current, 5 mmol/l nifedipine is added to the bath solution.

EVALUATION

All average data are presented as means ±SEM. Student's *t*-test is used to determine the significance of paired observations. Differences are considered as significant at $P < 005$.

MODIFICATIONS OF THE METHOD

Using the whole-cell configuration of the patch clamp technique, Grissmer et al. (1994) analyzed the biophysical and pharmacological properties of five cloned voltage-gated K^+ channels stably expressed in mammalian cell lines.

Sanchez-Chapula (1999) studied the block of the transient outward K^+ channel (I_{to}) by disopyramide in isolated rat ventricular myocytes using whole-cell patch clamp techniques.

Using the patch clamp technique, Cao et al. (2001) investigated the effects of a centrally acting muscle relaxant and structurally related compounds on recombinant small-conductance Ca^{2+}-activated K^+ channels (rSK2 channels) in HEK mammalian cells.

Tagliatela et al. (2000) discussed the block of the K^+ channels encoded by the human *ether-á-go-go-related* gene (HERG), termed $K_{V(r)}$, which are the molecular determinants of the rapid component of the cardiac repolarizing current $I_{K(Vr)}$, involved in the cardiotoxic potential and CNS effects of first-generation antihistamines and may be therapeutic targets for antiarrhythmic agents (Vandenberg et al. 2001; Zhou et al. 2005).

Chabbert et al. (2001) investigated the nature and electrophysiological properties of Ca^{2+}-independent depolarization-activated potassium currents in acutely isolated mouse vestibular neurons using the whole-cell configuration of the patch clamp technique. Three types of currents were identified.

Furthermore, Longobardo et al. (1998) studied the effects of a quaternary bupivacaine derivative on delayed rectifier K^+ currents stably expressed in *Ltk*$^-$ cells using the whole-cell configuration of the patch clamp technique.

Moreno et al. (2003) studied the effects of a selective angiotensin II type 1 receptor antagonist on cloned potassium channels involved in human cardiac repolarization.

Sanchez-Chapula et al. (2002) investigated the voltage-dependent block of wild-type and mutant HERG K^+ channels by the antimalarial compound chloroquine.

Anson et al. (2004) published molecular and functional characterization of common polymorphism in HERG (KCNH2) potassium channels.

For more information on the evaluation of HERG potassium channels in safety pharmacology see Chap. I.D by Brian D. Guth.

REFERENCES AND FURTHER READING

Alexander S, Peters J, Mathie A, MacKenzie G, Smith A (2001) TiPS Nomenclature Supplement 2001

Anson BD, Ackerman MJ, Tester DJ, Will ML, Delisle BP, Anderson CL, January CT (2004) Molecular and functional characterization of common polymorphism in HERG (KCNH2) potassium channels. Am J Physiol 286:H2434–H2441

Barhanin J, Lesage F, Guillemare E, Fink M, Lazdunski M, Romey G (1996) KvLQT1 and IsK (minK) proteins associate to form the IKs cardiac potassium current. Nature 384:78–80

Bosch RF, Gaspo R, Busch AE, Lang HJ, Li R-G, Nattel S (1998) Effects of the chromanol 293B, a selective blocker of the slow component of the delayed rectifier K^+ current, on repolarization in human and guinea pig ventricular myocytes. Cardiovasc Res 38:441–450

Busch AE, Suessbrich H, Waldegger S, Sailer E, Greger R, Lang HJ, Lang F, Gibson KJ, Maylie JG (1996) Inhibition of I_{Ks} in guinea pig cardiac myocytes and guinea pig I_{sK} channels by the chromanol 293B. Pflügers Arch 432:1094–1096

Cao Y-J, Dreixler JC, Roizen JD, Roberts MT, Houamed KM (2001) Modulation of recombinant small-conductance Ca^{2+}-activated K^+ channels by the muscle relaxant chlorzoxazone and structurally related compounds. J Pharmacol Exp Ther 296:683–689

Carmeliet A, Mubagawa K (1998) Antiarrhythmic drugs and cardiac ion channels: mechanism of action. Prog Biophys Mol Biol 70:1–71

Chabbert C, Chambard JM, Sans A, Desmadryl G (2001) Three types of depolarization-activated potassium currents in acutely isolated mouse vestibular neurons. J Neurophysiol 85:1017–1026

Colatsky TJ, Follmer CH, Starmer CF (1990) Channel specificity in antiarrhythmic drug action. Mechanism of potassium channel block and its role in suppressing and aggravating cardiac arrhythmias. Circulation 82:2235–2242

Escande D, Henry P (1993) Potassium channels as pharmacological targets in cardiovascular medicine. Eur Heart J 14 [Suppl B]:2–9

Gintant GA (1996) Two components of delayed rectifier current in canine atrium and ventricle. Does I_{Ks} play a role in the reverse rate dependence of class III agents? Circ Res 78:26–37

Gögelein H, Brüggemann A, Gerlach U, Brendel J, Busch AE (2000) Inhibition of I_{Ks} channels by HMR 1556. Naunyn-Schmiedebergs Arch Pharmacol 362:480–488

Golding AL (1992) Maintenance of *Xenopus laevis* and oocyte injection. Methods Enzymol 207:266–279

Grissmer S, Nguyen AN, Aiyar J, Hanson DC, Mather RJ, Gutman GA, Karmilowicz MJ, Auperin DD, Chandy KG (1994) Pharmacological characterization of five cloned voltage-gated K^+ channels, types Kv1.1, 1.2, 1.3, 1.5, and 3.1, stably expressed in mammalian cell lines. Mol Pharmacol 45:1227–1234

Kaczorowski GJ, Garcia ML (1999) Pharmacology of voltage-gated and calcium-activates potassium channels. Curr Opin Chem Biol 3:448–458

Lei M, Brown HF (1996) Two components of the delayed rectifier potassium current, IK, in rabbit sinoatrial node cells. Exp Physiol 81:725–741

Longobardo M, Delpón E, Caballero R, Tamargo J, Valenzuela C (1998) Structural determinants of potency and stereoselective block of hKv1.5 channels induced by local anesthetics. Mol Pharmacol 54:162–169

Methfessel C, Witzemann V, Takahashi T, Mishina M, Numa S, Sakmann B (1986) Patch clamp measurements on *Xenopus laevis* oocytes: currents through endogenous channels and implanted acetylcholine receptor. Pflügers Arch 407:577–588

Moreno I, Caballero R, Ganzález T, Arias C, Valenzuela C, Iriepa I, Gálvez E, Tamargo J, Delpón E (2003) Effects of irbesartan on cloned potassium channels involved in human cardiac repolarization. J Pharmacol Exp Ther 304:862–873

Sanchez-Chapula JA (1999) Mechanisms of transient outward K^+ channel block by disopyramide. J Pharmacol Exp Ther 290:515–523

Sanchez-Chapula JA, Navarro-Polanco RA, Culberson C, Chen J, Sanguinetti MC (2002) Molecular determinants of voltage-dependent human ether-a-go-go related gene (HERG) K^+ channel block. J Biol Chem 277:23587–23595

Sanguinetti MC, Jurkiewicz NK (1990) Two components of cardiac delayed rectifier K^+ currents: differential sensitivity to block by class III antiarrhythmic agents. J Gen Physiol 96:195–215

Sanguinetti MC, Curran ME, Zou A, Shen J, Spector PS, Atkinson DL, Keating MD (1996) Coassembly of KvLTQ1 and minK (IsK) proteins form cardiac IKs potassium channel. Nature 384:80–83

Suessbrich H, Busch A, Ecke D, Rizzo M, Waldegger S, Lang F, Szabo I, Lang HJ, Kunzelmann K, Greger R, Busch AE (1996) Specific blockade of slowly activating channels by chromanols – impact on the role of I_{sK} channels in epithelia. FEBS Lett 396:271–275

Suessbrich H, Busch AE, Scherz MW (1997) The pharmacology of cloned cardiac potassium channels. Ion Channel Modulators 2:432–439

Tagliatela M, Timmerman H, Annunziato L (2000) Cardiotoxic potential and CNS effects of first-generation antihistamines. Trends Pharmacol Sci 21:52–65

Vandenberg JI, Walker BD, Campbell TC (2001) HERG K^+ channels: friend and foe. Trends Pharmacol Sci 22:240–246

Wang Z, Fermini B, Nattel S (1994) Rapid and slow components of delayed rectifier current in human atrial myocytes. Cardiovasc Res 28:1540–1546

Zhou J, Angelli-Szafran CE, Bradley JA, Chen X, Koci BJ, Volberg WA, Sun Z, Cordes JS (2005) Novel potent human *Ether-à-Go-Go*-related gene (*h*ERG) potassium channel enhancers and their in vitro antiarrhythmic activity. Mol Pharmacol 68:876–884

A.1.1.24.3.1 Studies on Kv1.5 Channel

PURPOSE AND RATIONALE

Treatment of atrial fibrillation/flutter with available potassium channel blockers (Class III antiarrhythmic agents which mainly block the delayed rectifier current I_{kr}) is associated with ventricular proarrhythmia. Prolongation of ventricular repolarization leads to early after-depolarization from which torsades de pointes can evolve. Therefore, blockade of a cardiac current of exclusive relevance in the atria is highly desirable as it is expected to be devoid of ventricular proarrhythmic effects. The ultrarapid delayed rectifier potassium current (I_{kur}) seems an ideal atrial antiarrhythmic target since it is found to contribute to the action potential in the atrium but not in the ventricle. The molecular correlate of the human cardiac ultrarapid delayed rectifier potassium current is the potassium channel Kv1.5, which therefore gained much interest (Li et al. 1996; Longobardo et al. 1998; Perchenet and Clément-Chomienne 2000; Caballero et al. 2000, 2001, 2004; Bachmann et al. 2001; Kobayashi et al. 2001; Matsuda et al. 2001; Choi et al. 2002; Moreno et al. 2003; Choe et al. 2003; Fedida et al. 2003; Godreau et al. 2002, 2003; Peukert et al. 2003, 2004; Plane et al. 2005).

For *in vivo* studies on atrial fibrillation see A.5.0.9, A.5.0.9.1, A.5.0.9.2, A.5.0.9.3.

Gögelein et al. (2004) studied the effects of the antiarrhythmic drug AVE0118 on cardiac ion channels.

PROCEDURE

Molecular Biology and Cell Culture

Human Kv1.5 cDNA was subcloned into the eukaryotic expression vectors pcDNA3.1 and pcDNA3.1/zeo (Invitrogen, Groningen, the Netherlands), cDNA encoding human Kv4.3 long (Kv4.3l; Dilks et al. 1999) was subcloned into pcDNA3.1, and the cDNA encoding human KChIP2 short (KChIP2.2; Decher et al. 2001) was subcloned into pcDNA3.1/zeo expression vector. Chinese hamster ovary (CHO) cells were transfected with either hKv1.5 or hKv4.3 and KChIP2.2 expression constructs. Transfection was carried out using lipofectamine (Life Technologies/Gibco BRL, Karlsruhe, Germany) according to the manufacturer's instructions. To boost Kv1.5 channel expression, CHO cells were consecutively transfected with both Kv1.5 expression constructs. Both hKv1.5 and hKv4.3 + hKChIP2.2 were stably expressed in CHO cells, which were maintained in ISCOVE's medium (Biochrom KG, Berlin, Germany), supplemented with 10% fetal bovine serum, 2 mM L-glutamine, 350 µg/ml Zeocin (Invitrogen) and 400 µg/ml G418 (PAA Laboratories). HERG, the potassium channel underlying I_{Kr} currents in human hearts, was cloned and transfected into CHO cells as described previously (Rampe et al. 1997). Cells used for patch clamping were seeded on glass or plastic coverslips 12–36 h before use.

Northern blot analysis of Kv1.5 in the pig heart and cloning of pig Kv1.5

Polyadenylated RNA was isolated from pig cardiac tissues with the Oligotex mRNA purification kit (Qiagen) and 10 µg per tissue was resolved by denaturing formaldehyde electrophoresis and blotted on a positively charged nylon membrane. The membrane was hybridized with a DIG-labeled riboprobe (DIG RNA labeling kit, Roche) encompassing the entire coding sequence of human Kv1.5 and exposed on a Lumi-Imager (Roche). The pig Kv1.5 was cloned by 5′-rapid amplification and 3′-rapid amplification of cDNA ends (RACE) reactions. An adapter ligated, double-stranded cDNA library was prepared from pig heart mRNA with the Marathon cDNA amplification kit (Clontech). The 5′-RACE and 3′-RACE reactions were performed with oligonucleotide primers derived from a partial pig Kv1.5 nucleotide sequence (GenBank accession number AF348084). Overlapping cDNA clones were obtained by repeated reactions and the DNA sequence determined by automated DNA sequencing on both strands (ABI 310, Perkin Elmer). A full-length cDNA clone was established by recombinant PCR. It encodes an open reading frame of 1,083 bp and a protein with 86% overall sequence similarity to the human Kv1.5 protein. The sequence of the pig Kv1.5 cDNA was submitted to GenBank (accession number: AY635585).

For *Xenopus* oocyte expression, cDNAs encoding Kv1.5, Kv4.3, and KChip2.2 were cloned into the oocyte expression vector pSGEM (Villmann et al. 1997), and capped cRNA was synthesized using the T7 mMessage mMachine kit (Ambion, Austin, Tex., USA).

Voltage-clamp experiments in Xenopus Oocytes

Handling and injection of *Xenopus* oocytes were performed according to Bachmann et al. (2001). Adult female *Xenopus laevis* frogs were anesthetized with 3-aminobenzoic acid ethyl ester solution (1 g/l) and intact ovary lobes were removed. The oocytes were defolliculated by treatment with 40 mg collagenase dissolved in 20 ml buffer (in mM: NaCl 82.5, KCl 2, $MgCl_2$ 1, HEPES 5, titrated to pH 7.5 with NaOH) for 120–150 min at 18°C. Oocytes were injected with 50 nl cRNA using a microinjector (World Precision Instruments, Sarasota, Fla., USA). Oocytes were stored under gentle shaking at 18°C in a buffer containing (in mM): NaCl 96, KCl 2, $CaCl_2$ 1.8, $MgCl_2$ 1, HEPES 5, Na-pyruvate 2.5, theophylline 0.5, gentamicin 50 µg/ml, titrated to pH 7.5 with NaOH. They were used for experiments 1–3 days after injection.

Two-electrode voltage clamp recordings were performed at room temperature in a medium containing (in mM): NaCl 96, KCl 2, $CaCl_2$ 1.8, $MgCl_2$ 1, HEPES 5, pH 7.5 with NaOH. Microelectrodes were pulled from filament borosilicate glass capillaries (Hilgenberg, Malsfeld, Germany) using a horizontal microelectrode puller (Zeitz, Augsburg, Germany). After filling with 3 M KCl, pipettes had a resistance of 0.3–1.3 MΩ. To activate hKv1.5 and hKv4.3 channels, oocytes were clamped from a holding potential of –80 mV to 40 mV for 500 ms. Data were recorded with a Turbo Tec 10CX amplifier (NPI, Tamm, Germany) using an ITC-16 interface (Instrutech Corporation, Long Island, USA) and the Pulse software (HEKA Elektronik, Lambrecht, Germany).

Patch Clamp Experiments with CHO Cells

Cells expressing Kv1.5 or Kv4.3 plus KChIP2.2 were assayed using the standard whole-cell patch clamp technique (Hamill et al. 1981). Cells were mechanically removed from the tissue culture flask and placed in a perfusion chamber with a solution containing (in

mM): NaCl 140, KCl 4.7, $CaCl_2$ 2, $MgCl_2$ 1.1, HEPES 10, pH adjusted to 7.4 with NaOH. Patch pipettes were pulled from borosilicate glass capillaries and heat polished. After filling with (in mM): NaCl 10, KCl 120, EGTA 1, HEPES 10, $MgCl_2$ 1.1 (pH 7.2 with potassium hydroxide, KOH), pipettes had resistances of 2–3 MΩ. Experiments were carried out at 36 ± 1°C. For the recording of hKv1.5, voltage pulses of 450 ms duration were applied from the holding potential of –30 mV to +20 mV at a frequency of 1 Hz. For recording of the hKv4.3+KChIP2.2, the holding potential was –50 mV and test pulses of 200 ms duration were applied to –10 mV at a frequency of 1 Hz. Data were recorded with an EPC-9 patch clamp amplifier (HEKA Elektronik) and the Pulse software (HEKA Elektronik) and stored on a PC for later analysis. Series resistance was in the range of 4–9 MΩ and was compensated by 80% by means of the EPC9's compensation circuit. The experiments were performed under continuous superfusion of the cells with solution heated to 36 ± 1°C.

HERG channel currents were recorded at room temperature using the whole-cell configuration of the patch clamp technique with an Axopatch 200B amplifier (Axon Instruments). Briefly, electrodes (3–6 MΩ resistance) were fashioned from TW150F glass capillary tubes (World Precision Instruments) and filled with pipette solution (in mM: potassium aspartate 120, KCl 20, Na_2ATP 4, HEPES 5, $MgCl_2$ 1, pH 7.2 adjusted with KOH). HERG currents were initiated by a positive voltage pulse (20 mV) followed by a negative pulse (–40 mV) and were recorded for off-line analyses. Once HERG current from a cell perfused with control external solution (in mM: NaCl 130, KCl 5, sodium acetate 2.8, $MgCl_2$ 1, HEPES 10, glucose 10, $CaCl_2$ 1 at pH 7.4 adjusted with NaOH) was stabilized, the cell was perfused with external solution containing the compound at a specific concentration for percentage inhibition. For each concentration from each cell, peak amplitude of the steady-state HERG tail current at –40 mV was measured. The peak amplitude for each concentration was compared with that for the control solution from the same cell and expressed as percent control.

Isolation of Porcine Atrial Myocytes

Male pigs weighing 15–30 kg of the German Landrace were anesthetized with pentobarbital exactly as described previously (Wirth and Knobloch 2001). After a left thoracotomy the lung was retracted, the pericardium incised and the heart was quickly removed and placed in oxygenated nominally Ca^{2+}-free Tyrode solution containing (in mM): NaCl 143, KCl 5.4, $MgCl_2$ 0.5, NaH_2PO_4 0.25, HEPES 5 and glucose 10, pH adjusted to 7.2 with NaOH. The hearts were then mounted on a Langendorff apparatus and perfused via the left circumflex coronary artery with Tyrode solution (37°C) with constant pressure (80 cmH_2O). All coronary vessels descending to the ventricular walls were ligated, ensuring sufficient perfusion of the left atrium. When the atrium was clear of blood and contraction had ceased (≈5 min), perfusion was continued with the same Tyrode solution, which now contained 0.015 mM $CaCl_2$ and 0.03% collagenase (type CLS II, Biochrom KG, Berlin, Germany), until atrial tissue softened (≈20 min). Thereafter, left atrial tissue was cut into small pieces and mechanically dissociated by trituration. Cells were then washed with storage solution containing (in mM): L-glutamic acid 50, KCl 40, taurine 20, KH_2PO_4 20, $MgCl_2$ 1, glucose 10, HEPES 10, EGTA 2 (pH 7.2 with KOH) and filtered through a nylon mesh. The isolated cells were kept at room temperature in the storage solution.

Isolation of Guinea Pig Ventricular Myocytes

Ventricular myocytes were isolated by enzymatic digestion according to Gögelein et al. (1998). Dunkin Hardley Pirbright White guinea pigs (weight about 400 g) were sacrificed by cervical dislocation. The hearts were dissected and perfused retrogradely via the aorta at 37°C with the same solutions as used for isolation of pig atrial myocytes.

Electrophysiological Recordings from Cardiac Myocytes

Whole-cell currents were recorded with an EPC-9 patch clamp amplifier (HEKA Elektronik) as described above for CHO cells. A small aliquot of cell-containing solution was placed in a perfusion chamber and after a brief period allowing for cell adhesion to the chamber, the cells were perfused with (in mM): NaCl 140, KCl 4.7, $CaCl_2$ 1.3, $MgCl_2$ 1.0, HEPES 10, glucose 10, pH adjusted to 7.4 with NaOH. Patch pipettes were pulled from borosilicate glass capillaries and heat polished. After filling with (in mM) KCl 130, $MgCl_2$ 1.2, HEPES 10, EGTA 10, K_2ATP 1, GTP 0.1, and phosphocreatine 5 (pH 7.2 with KOH) pipettes had a resistance of 2–3 MΩ. Series resistance was in the range of 6–12 MΩ and was compensated by 60%–70%. Offset voltages generated when the pipette was inserted in NaCl solution (1–5 mV) were zeroed before formation of the seal.

Effects of AVE0118 on the I_{KACh} were recorded from pig left atrial myocytes by applying voltage pulses of 500 ms duration from the holding potential of –80 mV to –100 mV. Carbachol (10 µM) was added

in order to evoke the I_{KACh}. After stabilization of the I_{KACh} (3 min), AVE0118 was added in increasing concentrations in the continuous presence of carbachol. The current was measured at the end of the pulse after 3 min of incubation at each concentration and inhibition of the carbachol-activated current was calculated. In some experiments, AVE0118 was washed out before application of the next higher concentration.

Also the L-type Ca^{2+} current was investigated in pig left atrial cells. In these experiments, KCl in the pipette was replaced by CsCl and voltage pulses of 300 ms duration were applied from the potential of –40 mV to 0 mV. Possible effects of AVE0118 on the currents I_{K1}, I_{Ks}, I_{Kr} and I_{KATP} were investigated in guinea pig ventricular myocytes. I_{K1} currents were recorded by a voltage step from –80 mV to –120 mV lasting for 200 ms. When I_{Ks} and I_{Kr} currents were recorded, 1 µM nisoldipine was added to the bath to block the L-type Ca^{2+} current. I_{Ks} was assessed by voltage pulse to +60 mV for 3 s, starting from –40 mV. I_{Kr} was evaluated as the tail current evoked by a voltage pulse from –10 mV to –40 mV. I_{KATP} was evoked by adding 1 µM rilmakalim (Krause et al. 1995) to the bath and by applying voltage ramps from –130 mV to +80 mV for 500 ms. The rilmakalim-activated current was recorded at the potential 0 mV. All patch clamp experiments were performed under continuous superfusion of the cells with solution heated to 36±1°C.

EVALUATION

All averaged data are presented as the mean ± SEM. The Student's *t*-test was used to determine the significance of paired or unpaired observations. Differences were considered significant at $P < 0.05$. The values for half-maximal inhibition (IC_{50}) and the Hill coefficient were calculated by fitting the data points of the concentration–response curves to the logistic function:

$$f(x) = (a - d)/\left[1 + (x/c)^n\right] + d$$

where a represents the plateau value at low drug concentration and d the plateau value at high drug concentration; c represents the IC_{50} value and n the Hill coefficient. The curve-fitting and the Student's *t*-test were performed with the computer program *Sigma-Plot* 5.0.

REFERENCES AND FURTHER READING

Bachmann A, Gutcher I, Kopp K, Brendel J, Bosch RF, Busch AE, Gögelein H (2001) Characterization of a novel Kv1.5 channel blocker in Xenopus oocytes, CHO cells, and human cardiomyocytes. Naunyn-Schmiedebergs Arch Pharmacol 364:472–478

Caballero R, Delpón E, Valenzuela C, Longobardo M, Tamargo J (2000) Losartan and its metabolite E3174 modify cardiac delayed rectifier K^+ currents. Circulation 101:1199–1205

Caballero R, Delpón E, Valenzuela C, Longobardo M, González T, Tamagro J (2001) Direct effects of candesartan and eprosartan in human cloned potassium channels involved in cardiac repolarization. Mol Pharmacol 59:825–836

Caballero R, Gómez R, Núòez L, Moreno I, Tamargo J, Delpón E (2004) Diltiazem inhibits hKv1.5 and Kv4.3 currents in therapeutic concentrations. Cardiovasc Res 64:457–466

Choe H, Lee YK, Lee YT, Choe H, Ko SH, Joo CU, Kim MH, Kim GS, Eun JS, Kim JH, Chae SW, Kwak YG (2003) Papaverine blocks hKv1.5 channel current und human atrial ultrarapid delayed rectifier K^+ currents. J Pharmacol Exp Ther 304:706–712

Choi BH, Choi JS, Rhie DJ, Yoon SH, Min DS, Jo YH, Kim MS, Hahn SJ (2002) Direct inhibition of the cloned Kv1.5 channel by AG-1478, a tyrosine kinase inhibitor. Am J Physiol 282:C1461–C1468

Decher N, Uyguner O, Scherer CR, Karaman B, Yükselapak M, Busch AE, Steinmeyer K, Wollnik B (2001) hKChIP2 is a functional modifier of hKv4.3 potassium channels: cloning and expression of a short hKChIP2 splice variant. Cardiovasc Res 52:255–264

Dilks D, Ling H-P, Cockett M, Sokol P, Numann R (1999) Cloning and expression of the human Kv4.3 potassium channel. J Neurophysiol 81:1974–1977

Fedida D, Eldstrom J, Hesketh C, Lamorgese M, Castel L, Steele DF, van Wagoner DR (2003) Kv1.5 is an important component of repolarizing K^+ current in canine atrial myocytes. Circ Res 93:744–751

Godreau D, Vranckx R, Hatem SN (2002) Mechanism of action of antiarrhythmic agent bertosamil on hKv1.5 channels and outward current in human atrial myocytes. J Pharmacol Exp Ther 300:612–620

Godreau D, Vranckx R, Maguy A, Goyenvalle C, Hatem SN (2003) Different isoforms of synapse-associated protein, SAP97, are expressed in the heart and have distinct effects on the voltage-gated K^+ channel Kv1.5. J Biol Chem 278:47046–47052

Gögelein H, Hartung J, Englert HC, Schölkens BA (1998) HMR 1883, a novel cardioselective inhibitor of the ATP-sensitive potassium channel. I. Effects on cardiomyocytes, coronary flow and pancreatic β-cells. J Pharmacol Exp Ther 286:1453–1464

Gögelein H, Brendel J, Steinmeyer K, Strübing C, Picard N, Rampe D, Kopp K, Busch AE, Bleich M (2004) Effects of the antiarrhythmic drug AVE0118 on cardiac ion channels. Naunyn-Schmiedebergs Arch Pharmacol 370:183–192

Hamill OP, Marty M, Neher E, Sakmann B, Sigworth FJ (1981) Improved patch-clamp techniques for high-resolution current recording from cells and cell-free membrane patches. Pflügers Arch 391:85–100

Kobayashi S, Reien Y, Ogura T, Saito T, Masuda Y, Nakaya H (2001) Inhibitory effect of bepridil on hKv1.5 channel current; comparison with amidarone and E-4031. Eur J Pharmacol 430:149–157

Krause E, Englert H, Gögelein H (1995) Adenosine triphosphate-dependent K currents activated by metabolic inhibition in rat ventricular myocytes differ from those elicited by the channel opener rilmakalim. Pflügers Arch 429:625–635

Li GR, Feng J, Wang Z, Fermine B, Nattel S (1996) Adrenergic modulation of ultrarapid rectifier K^+ current in human atrial myocytes. Circ Res 78:903–915

Longobardo M, González T, Navarro-Polanco R, Calballero R, Delpón E, Tamargo J, Snyders DJ, Tamkum MM, Valen-

zuela C (2000) Effects of a quaternary bupivacaine derivative on delayed rectifier K^+ currents. Br J Pharmacol 130:391–401
Matsuda T, Masumiya H, Tanaka N, Yamashita T, Tsuruzoe N, Tanaka Y, Tanaka H, Shigenoba K (2001) Inhibition by a novel anti-arrhythmic agent, NIP-142, of cloned human cardiac K^+ channel Kv1.5 current. Life Sci 68:2017–2024
Moreno I, Caballero R, González T, Arias C, Valenzuela C, Iriepa I, Gálvez E, Tamargo J, Delpón E (2003) Effects of irbesartan on cloned potassium channels involved in human cardiac repolarization. J Pharmacol Exp Ther 304:862–873
Perchenet L, Clément-Chomienne O (2000) Characterization of the mibefradil block of the human heart delayed rectifier hKv1.5. J Pharmacol Exp Ther 295:771–778
Peukert S, Brendel J, Pirad B, Bruggemann A, Below P, Kleemann HW, Hemmerle H, Schmidt W (2003) Identification, synthesis, and activity of novel blockers of the voltage-gated potassium channel Kv1.5. J Med Chem 46:486–498
Peukert S, Brendel J, Pirard B, Strübing C, Kleemann HW, Böhme T, Hemmerle H (2004) Pharmacophore-based search, synthesis, and biological evaluation of anthranilic amides as novel blockers of the Kv1.5 channel. Bioorg Med Chem Lett 14 :2823–2827
Plane F, Johnson R, Kerr P, Wiehler W, Thorneloe K, Ishii K, Chen T, Cole W (2005) Heteromultimeric Kv1 channels contribute to myogenic control of arterial diameter. Circ Res 96:216–224
Rampe D, Roy ML, Dennis A, Brown AM (1997) A mechanism for the proarrhythmic effects of cisapride (Propulsid): high affinity blockade of the human cardiac potassium channel HERG. FEBS Lett 417:28–32
Villmann C, Bull L, Hollmann M (1997) Kainate binding proteins possess functional ion channel domains. J Neurosci 17:7634–7643
Wirth KJ, Knobloch K (2001) Differential effects of dofetilide, amiodarone, and class Ic drugs on left and right atrial refractoriness and left atrial vulnerability in pigs. Naunyn-Schmiedebergs Arch Pharmacol 363:166–174

A.1.1.24.4 Voltage Clamp Studies on Calcium Channels

PURPOSE AND RATIONALE

Calcium influx through voltage-gated Ca^{2+} channels mediates a range of cytoplasmatic responses, including muscle contraction, release of neurotransmitters, Ca^{2+} dependent gene transcription and the regulation of neuronal excitability has been reviewed by several authors (Augustine et al. 1987; Bean 1989; Miller 1987; Zamponi 1997; Snutch et al. 2001). In addition to their normal physiological function, Ca^{2+} channels as calcium antagonists are also implicated in a number of human disorders (see also A.4.0.1).

Using patch clamp techniques, the structure and regulation of voltage-gated Ca^{2+} channels has been studied by many authors (Sculptoreanu et al. 1993; Peterson et al. 1997; Catterall 2000).

Berjukow et al. (2000) analyzed the role of the inactivated channel conformation in molecular mechanism of Ca^{2+} channel block by a dihydropyridine derivative in L-type channel constructs and mutants in *Xenopus* oocytes and described the electrophysiological evaluation.

PROCEDURE

Inward barium currents (I_{Ba}) are studied with two microelectrode voltage-clamp of *Xenopus* oocytes 2–7 days after microinjection of approximately equimolar cRNA mixtures of constructs of L-channel mutants. All experiments are carried out at room temperature in a bath solution with the following composition: 40 mM $Ba(OH)_2$, 50 mM NaOH, 5 mM HEPES, 2 mM CsOH (pH adjusted to 7.4 with methanesulfonic acid). Voltage recording and current injecting microelectrodes are filled with 2.8 M CsCl, 0.2 M CsOH, 10 mM EGTA, 10 mM HEPES (pH 7.4) with resistances of 0.3–2 MΩ. Resting channel block is estimated as peak I_{Ba} inhibition during 100-ms test pulses from -80 to 20 mV at a frequency of 0.033 Hz until steady state is reached. The dose response curves of I_{Ba} inhibition were fitted using the Hill equation:

$$\frac{I_{\text{Ba, drug}}}{I_{\text{Ba, control}}}(\%) = \frac{100 - A}{1 + \left(\frac{C}{\text{IC}_{50}}\right)^{nH}} + A$$

where IC_{50} is the concentration at which I_{Ba} inhibition is half-maximal, C is the applied drug concentration, A is the fraction of I_{Ba} that is not blocked, and nH is the Hill coefficient.

Recovery from inactivation is studied at a holding potential of -80 mV after depolarizing Ca^{2+} channels during a 3-s prepulse to 20 mV by applying 30-ms test pulses (to 20 mV) at various time intervals after the conditioning prepulse. Peak I_{Ba} values are normalized to the peak current measured during the prepulse, and the time course of I_{Ba} recovery from inactivation is fitted to a mono- or biexponential function

$$I_{\text{Ba, recovery}} = A \times \exp\left(\frac{-t}{\tau_{\text{fast}}}\right) + B \times \exp\left(\frac{-t}{\tau_{\text{slow}}}\right) + C$$

Voltage dependence of inactivation under quasi-steady state conditions is measured using a multi step protocol to account for run-down (less than 10%). A control test pulse (50 ms to 20 mV) is followed by a 1.5-s step to -100 mV followed by a 30-s conditioning step, a 4-ms step to -100 mV, and a subsequent test pulse to 20 mV (corresponding to the peak potential of the I-V curves).

Inactivation during the 30 s conditioning pulse is calculated as follows.

$$I_{\text{Ba, inactivation}} = \frac{I_{\text{Ba, test}}(20\,\text{mV})}{I_{\text{Ba, control}}(20\,\text{mV})}$$

The pulse sequence is applied every 3 min from a holding potential of -100 mV. Inactivation curves are drawn according to the following Boltzmann equation.

$$I_{\mathrm{Ba,inactivation}} = I_{\mathrm{SS}} + (1 - I_{\mathrm{SS}}) \left(1 + \exp \left(\frac{V - V_{0.5}}{k} \right) \right)$$

where V is the membrane potential, $V_{0.5}$ is the midpoint voltage, k is the slope factor, and I_{SS} is the fraction of non inactivating current.

Steady state inactivation of the mutate channels at -80 mV is estimated by shifting the membrane holding potential from -80 to -100 mV. Subsequent monitoring of the corresponding changes in I_{Ba} amplitudes until steady state reveals the fraction of Ca^{2+} channels in the inactivated state at -80 mV. Steady state inactivation of different L-type channel constructs at -30 mV is estimated by fitting time course of current inactivation to a biexponential function.

The I_{Ba} inactivation time constants are estimated by fitting the I_{Ba} decay to a mono- or biexponential function.

EVALUATION

Data are given as the means ± SE. Statistical significance is calculated according to Student's unpaired *t*-test.

MODIFICATIONS OF THE METHOD

Besides *Xenopus* oocytes (Waard and Campell 1995; Hering et al. 1997; Kraus et al. 1998), several other cell types and constructs, such as CHO cells (Sculptoreanu et al. 1993; Stephens et al. 1997), HEK293 (human embryonic kidney) cells (Lacinová et al. 1999), tsA-201 cells, a subclone of HEK293, (Peterson et al. 1997; McHugh et al. 2000), cardiac myocytes from rats (Scamps et al. 1990; Tohse et al. 1992; Gomez et al. 1994) and rabbits (Xu et al. 2000), isolated atrial myocytes from failing and non-failing human hearts (Cheng et al. 1996), skeletal muscle myotubes from mice and rabbits, (Johnson et al. 1994), myocytes of guinea pig mesentery artery (Morita et al. 1999), dendrites from rat pyramidal and olfactory bulb neurons (Markram and Sakmann 1994; Stuart and Spruston 1995; Koester and Sakmann 1998; Margie et al. 2001), rat amygdala neurons (Foehring and Srcoggs 1994; Young et al. 2001) were used to study the function of calcium channels.

Using the whole-cell variation of the patch-clamp technique, Yang et al. (2000) studied cellular T-type and L-type calcium channel currents in mouse neuroblastoma N1E115 cells. The cells were cultured in Dulbecco's modified Eagle's medium containing 10% fetal bovine serum at 37°C in a humidified atmosphere of 5% CO_2 in air. The medium was changed every 3–4 days. After mechanical agitation, 3×10^4 cells were replanted in 35-mm tissue culture dishes containing 4 ml of bath solution. After cell attachment, the dish was mounted on the stage of an inverted phase-contrast microscope for Ca^{2+} channel current recording. These cells expressed predominantly T channel currents. In experiments where L channels were specifically sought, the cells were grown and maintained at confluence for 3–4 weeks under the same culture conditions with the addition of 2% dimethylsulfoxide (Narahash et al. 1987). Three to 5 days before use, the cells were replanted with the same medium. These cells expressed predominantly L channel currents. A small number of these cells also expressed T channel currents. Hence, cells were selected so that at a holding potential of –40 mV, the T channel component was very small and the inward current measured was conducted predominantly by L channels.

By using whole-cell and perforated patch-clamp techniques, Wu et al. (2000) showed that mifrabidile, a non-dihydropyridine compound, has an inhibitory effect on both T- and L-type Ca^{2+} currents in pancreatic β-cells.

REFERENCES AND FURTHER READING

Augustine GJ, Charlton MP, Smith RJ (1987) Calcium action in synaptic transmitter release. Ann Rev Neurosci 10:633–693

Bean BP, Classes of calcium channels in vertebrate cells. Annu Rev Physiol 51:376–384

Berjukom S, Marksteiner R, Gapp F, Sinneger MJ, Hering S (2000) Molecular mechanism of calcium channel block by israpidine. Role of a drug-induced inactivated channel configuration. J Biol Chem 275:22114–22120

Catterall WA (2000) Structure and regulation of voltage-gated Ca^{2+} channels. Ann Rev Cell Dev Biol 16:521–555

Cheng T-H, Lee F-Y, Wei J, Lin C-I (1996) Comparison of calcium-current in isolated atrial myocytes from failing and nonfailing human hearts. Mol Cell Biochem 157:157–162

Gomez JP, Potreau D, Branka JE, Raymond G (1994) Developmental changes in Ca^{2+} currents from newborn rat cardiomyocytes in primary culture. Pflügers Arch 428:214–249

Foehring RC, Srcoggs RS (1994) Multiple high-threshold calcium currents in acutely isolated rat amygdaloid pyramidal cells. J Neurophysiol 71:433–436

Hering S, Aczél S, Klaus RL, Berjukow S, Striessnig J, Timin EN (1997) Molecular mechanism of use-dependent calcium channel block by phenylalkylamines: role of inactivation. Proc Natl Acad Sci USA 94:13323–13328

Hockerman GH, Peterson BZ, Sharp E, Tanada TN, Scheuer T, Catterall (1997) Constriction of a high-affinity receptor site for dihydropyridine agonists and antagonists by single amino acid substitution in a non-L-type Ca^{2+} channel. Proc Natl Aced Sci USA 94:14906–14911

Johnson BD, Scheuer T, Catterall WA (1994) Voltage-dependent potentiation of L-type Ca^{2+} channels in skeletal muscles cells requires anchored cAMP-dependent protein kinase. Proc Natl Acad Sci 91:11492–11406

Koester HJ, Sakmann B (1998) Calcium dynamics in single spines during coincident pre- and postsynaptic activity depend on relative timing of back-propagation action potentials and subthreshold excitatory potentials. Proc Natl Acad Sci USA 95:9596–9601

Kraus RL, Hering S, Grabner M, Ostler D, Striessnig J (1998) Molecular mechanisms of diltiazem interaction with L-type Ca^{2+} channels. J Biol Chem 273:27205–27212

Lacinová L, An HR, Xia J, Ito H, Klugbauer N, Triggle E, Hofmann F, Kass RS (1999) Distinction in the molecular determinants of charged and neutral dihydropyridine block of L-type calcium channels. J Pharmacol Exp Ther 289:1472–1479

Lacinová L, Klugbauer N, Hofmann F (2000) State- and isoform-dependent interaction of israpidine with the α_{1C} L-type calcium channel. Pflügers Arch Eur J Physiol 440:50–60

Margrie TW, Sakmann B, Urban NN (2001) Action potential propagation in mitral cell lateral dendrites is decremental and controls recurrent and lateral inhibition in the mammalian olfactory bulb. Proc Natl Acad Sci USA 98:319–324

Markram H, Sakmann B (1994) Calcium transients in dendrites of neocortical neurons evoked by single subthreshold excitatory postsynaptic potentials via low-voltage-activated calcium channels. Proc Natl Acad Sci USA 91:5207–5211

McHugh D, Sharp EM, Scheuer T, Catterall WA (2000) Inhibition of L-type calcium channels by protein kinase C phophorylation of two sites in the N-terminal domain. Proc Natl Acad Sci USA 97:12334–12338

Miller RJ (1987) Multiple calcium channels and neuronal function. Science 235:46–52

Morita H, Cousins H, Inoue H, Ito Y, Inoue R (1999) Predominant distribution of nifedipine-insensitive, high voltage-activated Ca^{2+} channels in the terminal mesenteric artery of guinea pig. Circ Res 85:596–605

Narahash T, Tsunoo A, Yoshii M (1987) Characterization of two types of calcium channels in mouse neuroblastoma cells. J Physiol 38:231–249

Peterson BZ, Johnson BD, Hockerman GH, Acheson M, Scheuer T, Catterall WA (1997), Analysis of the dihydropyridine receptor site of L-type calcium channels by alanine-scanning mutagenesis. J Biol Chem 272:18752–18758

Scamps F, Mayoux E, Charlemagne D, Vassort G (1990) Calcium current in single cells isolated from normal and hypertrophied rat heart. Circ Res 67:199–208

Sculptoreanu A, Rotman E, Takahasi M, Scheuer T, Catterall WA (1993) Voltage-dependent potentiation of the activity of cardiac L-type calcium channel $\alpha 1$ subunits due to phophorylation by cAMP-dependent protein kinase. Proc Natl Acad Sci USA 90:10135–10139

Snutch TP, Sutton KG, Zamponi GW (2001) Voltage-dependent calcium channels – beyond diydropyridine antagonists. Curr Opin Pharmacol 1:11–16

Stephens GJ, Page KM, Burley JR, Berrow NS, Dolphin AC (1997) Functional expression of brain cloned $\alpha 1$E calcium channels in COS-7 cells. Pflügers Arch 433:525–532

Stuart G, Spruston N (1995) Probing dendritic function with patch pipettes. Curr Opin Neurobiol 5:389–394

Tohse N, Masuda H, Sperelakis N (1992) Novel isoform of Ca^{2+} channel in rat fetal cardiomyocytes. J Physiol (Lond.) 451:295–306

Waard MD, Campell KP (1995) Subunit regulation of the neuronal α_{1A} Ca^{2+} channel expressed in *Xenopus* oocytes. J Physiol (Lond) 485:619–634

Wu S, Zhang M, Vest PA, Bhattacharjee A, Liu L, Li M (2000) A mifrabidile metabolite is a potent intracellular blocker of L-type Ca^{2+} currents in pancreatic β-cells. J Pharmacol Exp Ther 292:939–943

Xu X, Rials SJ, Wu Y, Liu T, Marinchak RA, Kowey PR (2000) Effects of captopril treatment of renovascular hypertension on β-adrenergic modulation of L-type Ca^{2+} current. J Pharmacol Exp Ther 292:196–200

Yang JC, Shan J, Ng KF, Pang P (2000) Morphine and methadone have different effects on calcium channel currents in neuroblastoma cells. Brain Res 870:199–203

Young C, Huang Y-C, Lin C-H, Shen Y-Z, Gean P-W (2001) Selective enhancement of L-type calcium currents by corticotropin in acutely isolated rat amygdala neurons. Mol Pharmacol 59:604–611

Zamponi GW (1997) Antagonist sites of voltage-dependent calcium channels. Drug Dev Res 42:131–143

A.1.1.24.5
Patch Clamp Studies on Chloride Channels

PURPOSE AND RATIONALE

Cl^- channels are a large, ubiquitous and highly diverse group of ion channels involved in many physiological key processes including: regulation of electrical excitability; muscle contraction; secretion; and sensory signal transduction. Cl^- channels belong to several distinct families characterized in detail: voltage-gated Cl^- channels, the cAMP-regulated channel CFTR (cystic fibrosis transmembrane conductance regulator), ligand-gated Cl^- channels that open upon binding to the neurotransmitters GABA or glycine, and Cl^- channels that are regulated by the cytosolic Ca^{2+} concentration (Jentsch and Günther 1997; Frings et al. 2000).

Cliff and Frizel (1990) studied the cAMP- and Ca^{2+}-activated secretory Cl^- conductances in the Cl^- secreting colonic tumor epithelial cell line T84 using the whole-cell voltage-clamp technique.

PROCEDURE

T84 cells are used 1–3 days after plating on collagen-coating coverslips. The cells are maintained at 37°C. At this temperature, the responsiveness of the cells to secretagogues, particularly to cAMP-dependent agonists, is improved. Increases in Cl^- and K^+ conductances are the major electrical events during stimulation of Cl^- secretion. Accordingly, bath-pipette ion gradients are chosen so that transmembrane Cl^- and K^+ currents can be monitored independently at clamp voltages equal to the reversal potentials of these ions. The pipette solution is: 115 MM KCl, 25 mM *N*-methyl-D-glucamine (NMDG) glutamate, 0.5 mM

EGTA, 0.19 mM $CaCl_2$, 2 mM $MgCl_2$, 2 mM Na_2ATP, 0.05 mM Na_3GPT, 5 mM HEPES, pH 7.2. The bath solution is: 115 mM NaCl, 40 mM NMDG glutamate, 5 mM potassium glutamate, 2 mM $MgCl_2$, 1 mM $CaCl_2$, 5 mM HEPES, pH 7.2. Bath Na^+ and Cl^- concentrations are reduced by substituting NMDG chloride or sodium glutamate for NaCl. When Na^+ and K^+ free solutions are used, Na^+ and K^+ are replaced by $NMDG^+$, and Cl^- is reduced by replacing Cl^- by glutamate.

During whole-cell recording, the membrane potential is clamped alternately to three different voltages, each for 500-msec duration. Computer-controlled voltage-clamp protocols are used to generate current-voltage (I-V) relations when the transmembrane currents are relatively stable by stepping the clamp voltage between −100 and +100 mV at 20 mV intervals.

Test drugs (e. g., 8-(4-chlorophenylthio) adenosine 3′,5′-cyclic monophosphate, A23187, forskolin, or ionomycin) are solubilized in stock solutions (ethanol of DMSO) and diluted.

EVALUATION

Instantaneous relations are constructed from currents recorded 6 msec after a voltage step.

MODIFICATIONS OF THE METHOD

Maertens et al. (2000) used the whole-cell patch-clamp technique to study the effect of an antimalarial drug on the volume-regulated anion channel (VRAC) in cultured bovine pulmonary artery endothelial cells. They also examined the effects on other Cl^- channels, i. e., the Ca^{2+} activated Cl^- channel and the cystic fibrosis transmembrane conductance regulator to assess the specificity for VRAC.

Pusch et al. (2000) characterized chloride channels belonging to the ClC family. Chiral clofibric acid derivates were tested on the human ClC-1 channel, a skeletal muscle chloride channel, after heterologous expression in *Xenopus laevis* oocytes by means of two microelectrode voltage clamp recordings.

REFERENCES AND FURTHER READING

Frings S, Reuter D, Kleene SJ (2000) Neuronal Ca^{2+} activated Cl^- channels – homing in on an elusive channel species. Progr Neurobiol 60:247–289

Jentsch TJ, Günther W (1997) Chloride channels: an emerging molecular picture. BioAssays 19:117–126

Maertens C, Wie L, Droogmans G, Nilius B (2000) Inhibition of volume-regulated and calcium-activated chloride channels by the antimalarial mefloquine. J Pharmacol Exp Ther 295:29–36

Pusch M, Liantonio A, Bertorello L, Accardi A, de Lucca A, Pierno S, Tortorella V, Camerino DC (2000) Pharmacological characterization of chloride channels belonging to the ClC family by the use of chiral clofibric acid derivates. Mol Pharmacol 58:498–507

A.1.1.25 Inhibition of Hyperpolarization-Activated Channels

PURPOSE AND RATIONALE

The hyperpolarization-activated cation currents (termed I_f, I_h, or I_q) play a key role in the initiation of cardiac and neuronal pacemaker depolarizations. Unlike most voltage-gated channels, they are activated by hyperpolarizing voltage steps to potentials negative to –60 mV, near the resting potential of most cells. This property earned them the designation of I_f for "funny" or I_q for "queer." The funny current, or pacemaker (I_f) current, was first described in cardiac pacemaker cells of the mammalian sino-atrial node as a current that slowly activates on hyperpolarization at voltages in the diastolic voltage range, and contributes to the generation of cardiac rhythmic activity and to its control by sympathetic and parasympathetic innervations (DiFrancesco et al. 1986; Accili et al. 1997, 2002; Robinson and Siegelbaum 2003}; Baruscotti et al. 2005). In sino-atrial cells, f-channels are modulated by cAMP independently of phosphorylation, through a mechanism involving direct interaction of cAMP with the intracellular side of the channels (DiFrancesco and Tortora 1991; Bois et al. 1996). A significant advancement in the study of molecular properties of pacemaker channels was achieved when a new family of channels was cloned, the HCN (hyperpolarization-activated, cyclic nucleotide gated) channels (Ishii et al. 1999; Kaupp and Seifert 2001; Biel et al. 2002; Macri et al. 2002). The HCN family is related to the cyclic nucleotide-gated channel and *eag* potassium channel family and belongs to the superfamily of voltage-gated cation channels. HCN channels are characterized by six membrane-spanning segments (S1–S6) including voltage-sensing (S4) and pore (between S5 and S6) regions. In the C-terminal region they contain a consensus sequence for binding of cyclic nucleotides. In the heart, neurotransmitter-induced control of cardiac rhythm is mediated by I_f through its second-messenger cAMP, whose synthesis is stimulated and inhibited by β-adrenoceptor and muscarinic agonists, respectively.

Inhibition of the I_f channel was recommended for induction of bradycardia and treatment of coronary disease (Thollon et al. 1994, 1997; Simon et al. 1995; Bois et al. 1996; Deplon et al. 1996; Acilli et al. 1997;

Rocchetti et al. 1999; Monnet et al. 2001, 2004; Bucchi et al. 2002; Cerbai et al. 2003; Rigg et al. 2003; Vilaine et al. 2003; Albaladejo et al. 2004; Colin et al. 2004; DiFrancesco and Camm 2004; Moreno et al. 2004; Mulder et al. 2004; Vilaine 2004; Chatelier et al. 2005; Leoni et al. 2005; Romanelli et al. 2005; Schipke et al. 2006).

Romanelli et al. (2005) reported the design, synthesis and preliminary biological evaluation of zatebradine analogs as potential blockers of hyperpolarization-activated current and Chatelier et al. (2005) described that a calmodulin antagonist directly inhibits f-type current in rabbit sino-atrial cells.

PROCEDURE

Sino-atrial Cell Isolation

Sino-atrial node myocytes of the rabbit were isolated (DiFrancesco et al. 1986). Cells were allowed to settle in Petri dishes, and were superfused with normal Tyrode solution containing (mM): NaCl 140, KCl 5.4, $CaCl_2$ 1.8, $MgCl_2$ 1, D-glucose 5.5, Hepes–NaOH 5; pH 7.4.

Electrophysiology

In macro-patch experiments the temperature was kept at 27°C–28°C and the patch pipette solution contained (mM): NaCl 70, KCl 70, $CaCl_2$ 1.8, $MgCl_2$ 1, $BaCl_2$ 1, $MnCl_2$ 2, Hepes–KOH 5; pH 7.4. The control solution perfusing the intracellular side of the membrane patches contained (mM): potassium aspartate 130, NaCl 10, $CaCl_2$ 2, EGTA 5, Hepes–KOH 10; pH 7.2, pCa = 7. In some experiments, the calcium concentration of the bath solution was reduced to 0.1 nM according to the calculation of Fabiato and Fabiato (1979) and the correction of Tsien and Rink (1980).

Macro-patches containing hundreds of f-channels were formed using a large-tipped pipette (0.5 to 2 MΩ) (DiFrancesco and Tortora 1991). The test compound or calmodulin (Calbiochem) was dissolved in either distilled water and ethanol (50/50) or distilled water, respectively, divided into aliquots, and stored at −20°C until use. Ethanol was added to control solutions at the same concentration used in test solutions (lower than 0.1%).

EVALUATION

The time course of macro-patch I_f under the influence of the modifying compounds was recorded by applying hyperpolarizing steps of 3 s duration at a frequency of 1/15 Hz. At steady-state, the voltage dependence of I_f was described by the equation: $I_f(E) = g_f(E) \cdot (E - vE_f) = g_{fmax} \cdot y_\infty(E) \cdot (E - E_f)$, where g_f is the conductance, g_{fmax} the fully activated conductance, y_∞ (E) the steady-state activation parameter and E_f the reversal potential (DiFrancesco and Noble 1985). Steady-state current/voltage (I/V) curves were measured by applying 1-min-long hyperpolarizing voltage ramps with a rate of −115 mV/min from a holding potential of −35 mV. Conductance–voltage (g_f/E) relations were then obtained from the above equation as ratios between steady-state I/V curves (i_f/E) and $E-E_f$, where E_f was set to −12.24 mV (DiFrancesco and Mangoni 1994). Conductance curves were fitted by Boltzmann function: $g_f(E) = g_{fmax} \cdot y_\infty(E) = g_{fmax} \cdot 1/[1 + \exp(E - E_{1/2})/p]$ where $E_{1/2}$ is the half-maximal voltage of activation and p is the inverse-slope factor. This allowed estimation of the shifts of the voltage dependence of conductance (i. e., of the activation parameter y_∞) measured as changes in $E_{1/2}$. Shifts of the I_f activation curve caused by cAMP were also determined by a quicker method not requiring measurement of the conductance–voltage relation (Accili and DiFrancesco 1996). Shifts were obtained by applying hyperpolarizing steps from −35 mV to near the mid-point of the I_f activation curve and adjusting the holding potential (−35 mV in the control solution) until the cAMP-induced change in I_f was compensated and the control I_f magnitude fully restored. Since the compensation involved a change of the test voltage (from E to $E + s_m$, where s_m is the measured displacement of the holding potential in mV), a correction was introduced to obtain the shift of the activation curve (s, mV), according to the relation: $s = s_m \cdot [+ (y_\infty / (dy_\infty / dE)] / (E - E_f)$.

When comparing different sets of data, statistical analysis was performed with either the Student's t-test or analysis of variance (ANOVA). Values of $P < 0.05$ were considered significant. Statistical data were given as mean ± SEM values.

REFERENCES AND FURTHER READING

Albaladejo P, Challande P, Kakou A, Benetos A, Labat C, Louis H, Safar ME, Lacolley P (2004) Selective reduction of heart rate by ivabradine: effect on the visco-elastic arterial properties in rats.. J Hypertens 22:1739–1745

Accili EA, DiFrancesco D (1996) Inhibition of the hyperpolarization-activated current (if) of rabbit SA node myocytes by niflumic acid. Pflügers Arch 431:757–762

Accili EA, Robinson RB, DiFrancesco D (1997) Properties and modulation of I_f in newborn versus adult SA node. Am J Physiol 272:H1549–H1552

Accili EA, Proenza C, Baruscotti M, DiFrancesco D (2002) From funny current to HCN channels: 20 years of excitation. News Physiol Sci 17:32–37

Baruscotti M, Bucchi A, DiFrancesco D (2005) Physiology and pharmacology of the cardiac pacemaker ("funny") current. Pharmacol Ther 107:59–79

Biel M, Schneider A, Wahl C (2002) Cardiac HCN channels: structure, function, and modulation. Trends Cardiovasc Med 12:206–2134
Bois P, Bescond J, Renaudon B, Lenfant J (1996) Mode of action of bradycardic agent, S-16257, on ionic currents of rabbit sinoatrial node cells. Br J Pharmacol 118:1051–1057
Bucchi A, Baruscotti M, DiFrancesco D (2002) Current-dependent block of rabbit sino-atrial node I_f channels by Ivabradine. J Gen Physiol 120:1–13
Cerbai E, de Paoli P, Sartiani L, Lonardo G, Mugelli A (2003) Treatment with Irbesartan counteracts the functional remodeling of ventricular myocytes from hypertensive rats. J Cardiovasc Pharmacol 41:804–812
Chatelier A, Renaudon B, Bescond J, El Chemaly A, Demion M, Bois P (2005) Calmodulin antagonist W7 directly inhibits f-type current in rabbit sino-atrial cells. Eur J Pharmacol 521:29–33
Colin P, Ghaleb B, Monnet X, Hittinger L, Berdeaux A (2004) Effect of graded heart rate reduction with Ivabradine on myocardial oxygen consumption and diastolic time in exercising dogs. J Pharmacol Exp Ther 308:236–240
Deplon E, Valenzuela C, Perez O, Franqueza L, Gay P, Snyders DJ, Tamargo J (1996) Mechanisms of block of human cloned potassium channel by the enantiomers of a new bradycardic agent: S-16257–2 and S-1620–2. Br J Pharmacol 117:1293–1301
DiFrancesco D, Ferroni A, Mazzanti M, Tromba C (1986), Properties of the hyperpolarizing-activated current (i_f) in cells isolated from the rabbit sino-atrial node. J Physiol (Lond) 377:61–88
DiFrancesco P, Tortora D (1991) Direct activation of cardiac pacemaker channels by intracellular cyclic AMP. Nature 351:145–147
DiFrancesco D, Mangoni M (1994) Modulation of single hyperpolarization-activated channels i_f by cAMP in the rabbit sino-atrial node. J Physiol (Lond) 474:473–482
DiFrancesco D, Camm JA (2004) Heart rate lowering by specific and selective I_f current inhibition with Ivabradine. Drugs 64:1757–1765
Fabiato A, Fabiato F (1979) Calcium programs for computing the composition of the solutions containing multiple metals and ligands used for experiments in skinned muscle cells. J Physiol (Lond) 75:463–505
Ishii TM, Takano M, Xie LH, Noma A, Ohmori H (1999) Molecular characterization of the hyperpolarization-activated cation channel in rabbit heart sinoatrial node. J Biol Chem 274:12835–12839
Kaupp UB, Seifert R (2001) Molecular diversity of pacemaker channels. Annu Rev Physiol 63:235–257
Leoni AL, Marionneau C, Demolombe S, Le Bouter S, Mangoni ME, Escande D, Charpentier F (2005) Chronic heart rate reduction remodels ion channel transcripts in the mouse sinoatrial node but not in the ventricle. Physiol Genomics 24:4–12
Macri V, Proenza C, Agranovich E, Angoli D, Accili EA (2002) Separable gating mechanisms in a mammalian pacemaker channel. J Biochem Chem 277:35939–35946
Monnet X, Ghaleb B, Colin P, de Curzon OP, Guidicelli JF, Berdeaux A (2001) Effects of heart rate reduction with Ivabradine on exercise-induced myocardial ischemia and stunning. J Pharmacol Exp Med 299:1133–1139
Monnet X, Colin P, Ghaleb B, Hittinger L, Giudicelli JF, Berdeaux (2004) Heart rate reduction during exercise-induced myocardial ischemia and stunning. Eur Heart J 25:579–586
Moreno AP (2004) Biophysical Properties of homomeric and heteromultimeric channels formed by cardiac connexins. Cardiovasc. Res. 62:276–286
Mulder P, Barbier S, Chagraoui A, Richard V, Henry JP, Lallemand F, Renet S, Lerebours G, Mahlberg-Gaudin F, Thuillez C (2004) Long-term heart rate reduction induced by the selective If current inhibitor Ivabradine improves left ventricular function and intrinsic myocardial structure in congestive heart failure. Circulation 109:1674–1679
Rigg L, Mattick PAD, Heath BM, Terrar DA (2003) Modulation of the hyperpolarization-activated current (I_f) by calcium and calmodulin in the guinea-pig sino-atrial node. Cardiovasc Res 57:497–504
Robinson RB, Siegelbaum SA (2003) Hyperpolarization-activated cation currents: from molecules to physiological function. Annu Rev Physiol 65:453–480
Rocchetti M, Armato A, Cavalieri B, Micheletti M, Zaza A (1999) Lidocaine inhibition of the hyperpolarization-activated current in sinoatrial myocytes. J Cardiovasc Pharmacol 34:434–439
Romanelli MN, Cerbai E, Dei S, Guandalini L, Martelli C, Martini E, Scapecchi S, Teodori E, Mugelli A (2005) Design, synthesis and preliminary biological evaluation of zatebradine analogues as potential blockers of hyperpolarization-activated current. Bioorg Med Chem 13:1211–1220
Schipke JD, Büter I, Hohlfeld T, Schmitz-Spanke S, Gams E (2006) Selektive I_f-Kanal-Hemmung: eine Alternative in der Behandlung der koronaren Herzkrankheit? Herz 31:55–74
Simon L, Ghaleb B, Puybasset L, Giudicelli JF, Berdeaux (1995) Coronary and hemodynamic effects of S 16257, a new bradycardic agent, in resting and exercising conscious dogs. J Pharmacol Exp Ther 275:659–665
Thollon C, Cambarrat C, Vian J, Prost JF, Peglion JL, Vilaine JP (1994) Electrophysiological effects of S 16257, a novel sino-atrial node modulator, on rabbit and guinea-pig cardiac preparations: comparison with UL-FS 49. Br J Pharmacol 112:37–42
Thollon C, Bidouard JP, Cambarrat C, Lesage L, Reure H, Delescluse I, Vian J, Peglion JL, Vilaine JP (1997) Stereospecific in vitro and in vivo effects of the new sinus node inhibitor (+)-S 16257. Eur J Pharmacol 339:43–51
Tsien RW, Rink J (1980) Neutral carrier ion-selective microelectrodes for measurements of intracellular free calcium. Biochim Biophys Acta 599:623–638
Vilaine JP, Bidouard JP, Lesage L, Reure H, Péglion JL (2003) Anti-ischemic effects of Ivabradine, a selective heart rate-reducing agent, in exercise-induced myocardial ischemia in pigs. J Cardiovasc Pharmacol 42:688–696
Vilaine JP (2004) Selection et caracterisation pharmacologique de Procorolan, un inhibiteur selectif du courant pacemaker If. Therapie 59:495–505

A.1.1.26 Measurement of Cytosolic Calcium with Fluorescent Indicators

PURPOSE AND RATIONALE

Intracellular free Ca-concentration can be measured in cultured endothelial cells with a fluorometric methods (Tsien et al. 1982; Grynkiewicz et al. 1985; Lückhoff et al. 1988; Busse and Lamontagne 1991; Hock et al. 1991).

PROCEDURE

Cultured endothelial cells from the pig are seeded on quartz coverslips and grown to confluence. The cells

are loaded with the fluorescent probe indo-1 by incubation with 2 µmol indo-1/AM and 0.025% Pluronic F-127, a non-ionic detergent. Thereafter, the coverslips are washed and transferred to cuvettes, filled with HEPES buffer.

EVALUATION

Fluorescence is recorded in a temperature controlled (37°C) spectrofluorophotometer (excitating wavelength 350 nm, emission wavelength simultaneously measured at 400 and 450 nm).

MODIFICATIONS OF THE METHOD

Lee et al. (1987) measured cytosolic calcium transients from the beating rabbit heart using indo-1 AM as indicator.

Yangisawa et al. (1989) measured intracellular Ca^{2+} concentrations in coronary arterial smooth muscle of dogs with fura-2.

Makujina et al. (1995) measured intracellular calcium by fura-2 fluorescence simultaneously with tension in everted rings of porcine coronary artery denuded of endothelium.

Hayashi and Miyata (1994) described the properties of the commonly used fluorescent indicators for intracellular calcium: Fura-2, Indo-1, and Fluo-3.

Monteith et al. (1994) studied the Ca^{2+} pump-mediated efflux in vascular in spontaneously hypertensive rats.

REFERENCES AND FURTHER READING

Busse R, Lamontagne D (1991) Endothelium-derived bradykinin is responsible for the increase in calcium produced by angiotensin-converting enzyme inhibitors in human endothelial cells. Naunyn-Schmiedeberg's Arch Pharmacol 344:26–129

Grynkiewicz G, Poenie M, Tsien RY (1985) A new generation of Ca^{+2} indicators with improved fluorescence properties. J Biol Chem 260:3440–3450

Hayashi H, Miyata H (1994) Fluorescence imaging of intracellular Ca^{2+}. J Pharmacol Toxicol Meth 31:1–10

Hock FJ, Wirth K, Albus U, Linz W, Gerhards HJ, Wiemer G, Henke S, Breipohl G, König W, Knolle J, Schölkens BA (1991) Hoe 140 a new potent and long acting bradykinin antagonist: *in vitro* studies. Br J Pharmacol 102:769–773

Lee HC, Smith N, Mohabir R, Clusin WT (1987) Cytosolic calcium transients from the beating mammalian heart. Proc Natl Acad Sci USA 84:7793–7797

Lückhoff A, Pohl U, Mülsch A, Busse R (1988) Differential role of extra- and intracellular calcium in the release of EDRF and prostacyclin from cultured endothelial cells. Br J Pharmacol 95:189–196

Makujina SR, Abebe W, Ali S, Mustafa SJ (1995) Simultaneous measurement of intracellular calcium and tension in vascular smooth muscle: validation of the everted ring preparation. J Pharmacol Toxicol Meth 34:157–163

Monteith GR, Chen S, Roufogalis BD (1994) Measurement of Ca^{2+} pump-mediated efflux in hypertension. J Pharmacol Toxicol Meth 31:117–124

Tsien RY, Pozzan T, Rink TJ (1982) Calcium homeostasis in intact lymphocytes: Cytoplasmic free calcium monitored with a new intracellularly trapped fluorescent indicator. J Cell Biol 94:325–334

Wiemer G, Popp R, Schölkens BA, Gögelein H (1994) Enhancement of cytosolic calcium, prostaglandin and nitric oxide by bradykinin and the ACE inhibitor ramiprilat in porcine brain capillary endothelial cells. Brain Res 638:261–266

Yanagisawa T, Kawada M, Taira N (1989) Nitroglycerine relaxes canine coronary arterial smooth muscle without reducing intracellular Ca^{2+} concentrations measured with fura-2. Br J Pharmacol 98:469–482

A.1.1.27 Measurement of Contractile Force of Isolated Cardiac Myocytes

PURPOSE AND RATIONALE

Eschenhagen et al. (1997) developed a method for culturing embryonic cardiomyocytes in a collagen matrix to produce a coherently contracting 3-dimensional model heart tissue that allows direct measurement of isometric contractile force.

PROCEDURE

Ventricles from 9–11 day incubated chicken embryos (Cavanaugh 1955) are minced in Dulbecco's minimal essential medium (DMEM), washed once with 0.25% trypsin/0.1% EDTA in phosphate buffered saline (PBS), pH 7.45, and then digested in fresh trypsin/EDTA for 15 min at 37°C. The supernatant is discarded and the pellet is subjected to digestion with 0.1% collagenase (144 U/mg) in PBS, pH 7.45, for 30 min at 37°C. This supernatant is discarded and the pellet digested further with several cycles of collagenase for 10–20 min each until the pellet is completely digested. DNase I (40 µl, 1 mg/ml in PBS) is added between cycles depending on the presence of viscous DNA. The isolated cells are kept in Petri dishes in DMEM supplemented with 15% heat-inactivated fetal calf serum in the CO_2 incubator. After completion of the digestion, the cells are incubated for another 30–60 min in the CO_2 incubator (preplating). The cell suspension is centrifuged at 250 rpm (12 *g*). The pellet is resuspended in 10 ml culture medium (DMEM, 10% inactivated horse serum, 2% chicken embryo extract (Gibco BRL), 2 mmol/l glutamine, 10 µg/ml streptomycin, and 100 U/ml penicillin G, recentrifuged at 250 rpm, and finally resuspended in culture medium at $2–3 \times 10^6$ cells per ml.

For casting cardiomyocyte-populated collagen gels, strips of Velcro are glued with silicone rubber to glass

tubes (13 mm length, 3 mm outer diameter, 2 mm inner diameter). Pairs of Velcro-coated tubes, kept at a fixed distance by a stainless steel wire spacer, are placed in rectangular wells ($15 \times 17 \times 4$ mm) cut into a layer of silicone rubber in a 100 mm polymethylenepentene Petri dish. This assembly is autoclaved before use. For each gel, 1 ml of an ice-cold collagen/cell mixture is poured into each well between the Velcro-coated glass tubes. This mixture has the same composition as the culture medium and contains in addition to 1 mg neutralized collagen I from rat tail (Upstate Biotechnology, Inc.), 1×10^6 cardiomyocytes, the acetic acid in the collagen solution, and the NaOH to neutralize it. The mixture is allowed to gel at 37°C for 60 min before culture medium is added to the dish. Medium changes are performed after overnight and then every other day.

After 6–11 days in culture, the gels are removed from the culture dish, the spacers are withdrawn, and one of the glass tubes is mounted on a fixed electrode; the other tube is connected by an inelastic silk string to an isometric force transducer attached to a Wekagraph thermal array recorder (Föhr Instruments, Heidelberg, Germany). The preparation is adjusted to its original (spacer) length before it is immersed in a convential water bath filled with modified Tyrode's solution maintained at 35°C and continuously gassed with 95% O_2 and 5% CO_2.

After a 30–60 min equilibration period without pacing, force and frequency reaches a stable value. Gels are then electrically stimulated with rectangular pulses (10 ms, 20–40 V) at a standard frequency of 1.5 Hz. Preload is stepwise adjusted to L_{max}, the length at which the preparation develops maximal force. Cumulative doses of inotropic compounds, e. g. isoprenaline or forskoline, are added. All gels are exposed to a concentration-response curve for calcium (1.8–12.6 mmol/l) and one or two additional inotropic stimuli.

EVALUATION

All values are presented as arithmetic means ± SEM. Student's *t*-test for paired observations is used to compare force of contraction, resting tension, or beating frequency before and after other interventions.

MODIFICATIONS OF THE METHOD

Ferrara et al. (1997) studied the role of Gi-proteins and β-adrenoceptors in the age-related decline of contraction in guinea-pig ventricular myocytes. The isolated myocytes were placed in Krebs-Henseleit solution in a Perspex chamber on the stage of a Zeiss IM inverted microscope and superfused with Krebs-Henseleit solution containing 1 mmol/l Ca^{2+} at 2 ml/min and 32°C. Cells were selected using the following criteria: rod shaped, without sarcolemmal blebs, no spontaneous contractions, stable baseline contraction to electrical stimulation at 0.5 Hz and sarcomere length not shorter than 1.67 µm. The image of the cells was displayed on a TV monitor and the length change measured with a video motion detector. Contraction amplitude and velocity was expressed as change in sarcomere length, calculated from the change in length of the myocyte and its original sarcomere length.

Using a similar technique, Harding et al. (1988) studied contractile responses of isolated rat and rabbit myocytes to isoproterenol and calcium, and Harding et al. (1992) isolated ventricular myocytes from failing and non-failing human heart.

REFERENCES AND FURTHER READING

Cavanaugh MW (1955) Growth of chick heart cells in monolayer culture. J Exp Zool 128:573–581

Eschenhagen T, Fink C, Remmers U, Scholz H, Wattchow J, Weil J, Zimmermann W, Dohmen HH, Schäfer H, Bishopric N, Wakatsuki T, Elson EL (1997) Three-dimensional reconstitution of embryonic cardiomyocytes in a collagen matrix: a new heart muscle model. FASEB J 11:683–694

Ferrara N, Böhm M, Zolk O, O'Gara P, Harding SE (1997) The role of Gi-proteins and β-adrenoceptors in the age-related decline of contraction in guinea-pig ventricular myocytes. J Mol Cell Cardiol 29:439–448

Harding SE, Vescovo G, Kirby M, Jones SM, Gurden J, Poole-Wilson PA (1988) Contractile responses of isolated rat and rabbit myocytes to isoproterenol and calcium. J Mol Cell Cardiol 20:635–647

Harding SE, Jones SM, O'Gara P, del Monte F, Vescovo G, Poole-Wilson PA (1992) Isolated ventricular myocytes from failing and non-failing human heart; the relation of age and clinical status of patients to isoproterenol response. J Mol Cell Cardiol 24:549–564

A.1.1.28 Adrenomedullin

A.1.1.28.1 General Considerations

Adrenomedullin is a 52-amino acid peptide originally discovered in human adrenal pheochromocytoma by monitoring the elevating activity of platelet cAMP (Kitamura et al. 1993). Molecular cloning of rat adrenomedullin was reported by Sakata et al. (1993). The genomic structure of human adrenomedullin gene was reported by Ishimitsu et al. (1994). Adrenomedullin and **proadrenomedullin N-terminal 20 peptide (PAMP)** which are both hypotensive and bronchodilating, are derived from **preproadrenomedullin** (Kanazawa et al. 1995; Iwasaki et al.

1996; Shimosawa and Fujita 1996; Hinson et al. 1998; Samson 1998; Autelitano and Tang 1999; Jimenez et al. 1999; Lopez et al. 1999; Tajima et al. 1999).

Adrenomedullin is found ubiquitously in tissues and organs, especially in cardiovascular tissues and in the kidney, lung, brain and endocrine glands (Wimalawansa 1996; Van Rossum et al. 1997; Eto et al. 1999; Jougasaki and Burnett 2000; Kitamuro et al. 2000). The main biological effect is vasodilatation (Ishiyama et al. 1993; Nikitenko et al. 2002). A hypotensive effect has been found in rats (Khan 1997), rabbits (Fukuhara et al. 1995), and man (Lainchbury et al. 1997). Adrenomedullin belongs to the calcitonin gene-related peptide/calcitonin peptide family as it shares approximately 25% homology with calcitonin gene-related peptide (Kitamura et al. 1993). Several pharmacological studies are related to the vasodilating effect of adrenomedullin, e. g., in mouse aorta (Ashton et al. 2000), in the mesenteric vascular bed (see A.8.2.5), (Santiago et al. 1995), in the hind limb vascular bed (see A.8.2.1), (Santiago et al. 1994; Champion et al. 1996, 1997), in the pulmonary vascular bed (see A.8.2.6), (DeWitt et al. 1994; Lippton et al. 1994; Heaton et al. 1995; Nossaman et al. 1995), on cerebral blood flow in dogs (Baskaya et al. 1995) and in cats (Takao et al. (1999), on renal hemodynamics in dogs (see A.8.2.3) (Ebara et al. 1994; Yukawa 1998), or on vasodilation in perfused rat kidneys (Hayakawa et al. 1999). Intravenous infusion of adrenomedullin exerted diuresis and natriuresis without major changes in blood pressure and produced beneficial hemodynamic and renal vasodilator effects in rats with compensated heart failure (Vari et al. 1996; Nagaya et al. 1999). In isolated perfused, paced rat heart preparations, adrenomedullin showed a dose-dependent inotropic effect (Szokodi et al. 1998). Pulmonary vasodilator responses and vasorelaxant effects in isolated pulmonary artery rings were found by Gumusel et al. (1998). Adrenomedullin is a growth-promoting factor for cultured vascular smooth muscle cells (Iwasaki et al. 1998) and fibroblasts (Isumi et al. 1998).

Willenbrock et al. (1999) showed a beneficial effect of adrenomedullin on renal function in rats with aortocaval shunt.

Adrenomedullin inhibits gastric secretion in rats with chronic gastric fistula (see J.3.1.3), (Rossowski et al. 1997) and inhibits reserpine-induced gastric lesions in rats (Clementi et al. 1998). Tsuchida et al. (1999) found an inhibition of cholecystokinin-stimulated amylase secretion by adrenomedullin in rat pancreatic acini.

Rademaker et al. (2003) discussed the role of adrenomedullin in the pathophysiology of heart failure.

Lewis et al. (1998) described a specific and sensitive radioimmunoassay for human adrenomedullin.

Ohta et al. (1999) developed an one-step direct assay for adrenomedullin with monoclonal antibodies.

N-terminal fragments of adrenomedullin show vasopressor activities (Watanabe et al. 1996).

Adrenotensin, an other adrenomedullin gene product, contract in an endothelium-dependent manner pulmonary blood vessels (Gumusel et al. 1996).

REFERENCES AND FURTHER READING

Ashton D, Hieble P, Gout B, Aiyar N (2000) Vasodilatory effect of adrenomedullin in mouse aorta. Pharmacology 61:101–105

Autelitano DJ, Tang F (1999) Coexpression of preproadrenomedullin with a putative adrenomedullin receptor gene in vascular smooth muscle. Clin Sci 96:493–498

Baskaya MK, Suzuki Y, Anzai M, Seki Y, Saito K, Takayasu M, Shibuya M, Sugita K (1995) Effects of adrenomedullin, calcitonin gene-related peptide, and amylin on cerebral circulation in dogs. J Cerebr Blood Flow Metab 15:827–834

Champion HC, Duperier CD, Fitzgerald WE, Lambert DG, Murphy WA, Coy DH, Kadowitz PJ (1996) [Mpr^{14}]-rADM(14–50), a novel analog of adrenomedullin, possesses potent vasodilator activity in the hindlimb vascular bed of the cat. Life Sci 59: PL1–7

Champion HC, Akers DL, Santiago JA, Lambert DG, McNamara DB, Kadowitz PJ (1997) Analysis of the responses to human synthetic adrenomedullin and calcitonin gene-related peptides in the hindlimb vascular bed of the cat. Mol Cell Biochem 176:5–11

Clementi G, Caruso A, Cutuli VCM, de Bernardis E, Prato A, Mangano NG, Amico-Roxas M (1998) Effect of centrally or peripherally injected adrenomedullin on reserpine-induced gastric lesions. Eur J Pharmacol 360:51–54

DeWitt BJ, Cheng DY, Caminiti GN, Nossaman BD, Coy DH, Murphy WA, Kadowitz PJ (1994) Comparison of responses to adrenomedullin and calcitonin gene-related peptide in the pulmonary vascular bed of the cat. Eur J Pharmacol 257:303–306

Ebara T, Miura K, Okumura M, Matsuura T, Kim S, Yukimura T, Iwao H (1994) Effect of adrenomedullin on renal hemodynamics and function in dogs. Eur J Pharmacol 263:69–73

Eto T, Kitamura K, Kato J (1999) Biological and clinical roles of adrenomedullin in circulation control and vascular diseases. Clin Exp Pharmacol Physiol 26:371–380

Fukuhara M, Tsuchihashi T, Abe I, Fujishima M (1995) Cardiovascular and neurohormonal effects of intravenous adrenomedullin in conscious rabbits. Am J Physiol 269, Regul Integr Comp Physiol 38:R1289–1293

Gumusel B, Chang JK, Hao Q, Hyman A, Lippton H (1996) Adrenotensin: An adrenomedullin gene product contracts pulmonary blood vessels. Peptides 17:461–465

Gumusel B, Hao Q, Hyman AL, Kadowitz PJ, Champion HC, Chang JK, Mehta JL, Lippton H (1998) Analyses of responses to adrenomedullin-(-3.52) in the pulmonary vascular bed of rats. Am J Physiol 274; Heart Circ Physiol 43:H1255–H1263

Hayakawa H, Hirata Y, Kakoki M, Suzuki Y, Sugimoto T, Omata M (1999) Role of nitric oxide-cAMP pathway in

adrenomedullin-induced vasodilation in the rat. Hypertension 33:689–693

Heaton J, Lin B, Chang J-K, Steinberg S, Hyman A, Lippton H (1995) Pulmonary vasodilation to adrenomedullin: A novel peptide in humans. Am J Physiol 268, Heart Circ Physiol 37:H2211–H2215

Hinson JP, Hagi-Pavli E, Thomson LM, Kapas S (1998) Pro-adrenomedullin N-terminal 20 peptide (PAMP) receptors and signal transduction in the rat adrenal gland. Life Sci 62:439–443

Ishimitsu T, Kojima M, Kangawa K, Hino J, Matsuoka H, Kitamura K, Eto T, Matsuo H (1994) Genomic structure of human adrenomedullin gene. Biochem Biophys Res Commun 203:631–639

Ishiyama Y, Kitamura K, Ichiki Y, Nakamura S, Kida O, Kangawa E, Eto T (1993) Hemodynamic effects of a novel hypotensive peptide, human adrenomedullin, in rats. Eur J Pharmacol 241:271–273

Isumi Y, Minamino N, Katafuchi T, Yoshioka M, Tsujii T, Kangawa K, Matsuo H (1998) Adrenomedullin production in fibroblasts: Its possible function as a growth regulator of Swiss 3T3 cells. Endocrinology 139:2552–2563

Iwasaki H, Hirata Y, Iwashina M, Sato K, Marumo F (1996) Specific binding sites for proadrenomedullin N-terminal 20 peptide (PAMP) in the rat brain. Endocrinology 137:3045–3050

Iwasaki H, Eguchi S, Shichiri M, Marumo F, Hirata Y (1998) Adrenomedullin as a novel growth-promoting factor for cultured vascular smooth muscle cells: Role of tyrosine kinase-mediated mitogen-activated protein kinase activation. Endocrinology 139:3432–3441

Jimenez N, Calvo A, Martinez A, Rosell D, Cuttitta F, Montuenga LM (1999) Expression of adrenomedullin and proadrenomedullin N-terminal 20 peptide in human and rat prostate. J Histochem Cytochem 47:1167–1177

Jougasaki M, Burnett JC Jr (2000) Adrenomedullin: Potential in physiology and pathophysiology. Life Sci 66:855–872

Kanazawa H, Kawaguchi T, Fujii T, Kudoh S, Hirata K, Kurihara N, Takeda T (1995) Comparison of bronchodilator responses to adrenomedullin and proadrenomedullin N-terminal 20 peptide. Life Sci 57: PL241-PL245

Khan AI, Kato J, Kitamura K, Kanagawa K, Eto T (1997) Hypotensive effect of chronically infused adrenomedullin in conscious Wistar–Kyoto and spontaneously hypertensive rats. Clin Exp Pharmacol Physiol 24:139–142

Kitamura K, Kangawa K, Kawamoto M, Ichiki Y, Nakamura S, Matsuo H (1993) Adrenomedullin: a novel hypotensive peptide isolated from human pheochromocytoma. Biochem Biophys Res Commun 192:553–560

Kitamuro T, Takahashi K, Nakayama M, Murakami O, Hida W, Shirato K, Shibahara S (2000) Induction of adrenomedullin during hypoxia in cultures human glioblastoma cells. J Neurochem 75:1826–1833

Lainchbury JG, Cooper GJS, Coy DH, Jiang N-Y, Lewis LK, Yandle TG, Richards AM, Nicholls MG (1997) Adrenomedullin: A hypotensive hormone in man. Clin Sci 92:467–472

Lewis LK, Smith MW, Yandle TG, Richards AM, Nicholls MG (1998) Adrenomedullin (I-52) measured in human plasma by radioimmunoassay: Plasma concentration, adsorption, and storage. Clin Chem 44:571–577

Lippton H, Chang J-K, Hao Q, Summer W, Hyman AL (1994) Adrenomedullin dilates the pulmonary vascular bed *in vivo*. J Appl Physiol 76:2154–2156

Lopez J, Cuesta N, Martinez A, Montuenga L, Cuttitta F (1999) Proadrenomedullin N-terminal 20 peptide (PAMP) immunoreactivity in vertebrate juxtaglomerular cells identified by both light and electron microscopy. Gen Comp Endocrinol 116:192–203

Nagaya H, Nishikimi T, Horio T, Yoshihara F, Kanazawa A, Matsuo H, Kangawa K (1999) Cardiovascular and renal effects of adrenomedullin in rats with heart failure. Am J Physiol 276; Regul Integr Comp Physiol 45:R213–R218

Nikitenko LL, Smith DM, Hague S, Wilson CR, Bicknell R, Rees MCP (2002) Adrenomedullin and the microvasculature. Trends Pharmacol Sci 23:101–103

Nossaman BD, Feng CJ, Cheng DY, Dewitt BJ, Coy DH, Murphy WA, Kadowitz PJ (1995) Comparative effects of adrenomedullin, an adrenomedullin analog, and CGRP in the pulmonary vascular bed of the cat and the rat. Life Sci 56:63–66

Ohta H, Tsuji T, Asai S, Sasakura K, Teraoka H, Kitamura K, Kangawa K (1999) One-step direct assay for mature-type adrenomedullin with monoclonal antibodies. Clin Chem 45:244–251

Rademaker MT, Cameron VA, Charles CJ, Lainchbury JG, Nicholls MG, Richards AM (2003) Adrenomedullin and heart failure. Regul Pept 112:51–60

Rossowski WJ, Jing N-Y, Coy DH (1997) Adrenomedullin, amylin, calcitonin-gene related peptide and their fragments are potent inhibitors of gastric secretion in rats. Eur J Pharmacol 336:51–63

Sakata J, Shimokubo T, Kitamura K, Nakamura S, Kangawa K, Matsuo H, Eto T (1993) Molecular cloning and biological activities of rat adrenomedullin, a hypotensive peptide. Biochem Biophys Res Commun 195:921–927

Samson WK (1998) Proadrenomedullin-derived peptides. Front Neuroendocrinol 19:100–127

Santiago JA, Garrison E, Ventura VL, Coy DH, Bitar K, Murphy WA, McNamara DB, Kadowitz PJ (1994) Synthetic human adrenomedullin and adrenomedullin 15–52 have potent short-lived vasodilator activity in the hindlimb vascular bed of the cat. Life Sci 55: PL85–PL90

Santiago JA, Garrison E, Purnell WL, Smith RE, Champion HC, Coy DH, Murphy WA, Kadowitz PJ (1995) Comparison of responses to adrenomedullin and adrenomedullin analogs in the mesenteric vascular bed of the cat. Eur J Pharmacol 272:115–118

Shimosawa T, Fujita T (1996) Hypotensive effect of a newly identified peptide, proadrenomedullin N-terminal 20 peptide. Hypertension 28:325–329

Szokodi T, Kinnunen P, Tavi P, Weckstrom M, Toth M, Ruskoaho H (1998) Evidence for cAMP-independent mechanisms mediating the effects of adrenomedullin, a new inotropic peptide. Circulation 97:1062–1070

Tajima A, Osamura RY, Takekoshi S, Itoh Y, Sanno N, Mine T, Fujita T (1999) Distribution of adrenomedullin (AM), proadrenomedullin N-terminal 20 peptide, and AM mRNA in the rat gastric mucosa by immunocytochemistry and *in situ* hybridization. Histochem Cell Biol 112:139–146

Takao M, Tomita M, Tanahashi N, Kobari M, Fukuuchi Y (1999) Transient vasodilatory effects of adrenomedullin on cerebral parenchymal microvessels in cats. Neurosci Lett 268:147–150

Tsuchida T, Ohnishi H, Tanaka Y, Mine T, Fujita T (1999) Inhibition of stimulated amylase secretion by adrenomedullin in rat pancreatic acini. Endocrinology 140:865–870

Van Rossum D, Hanisch UK, Quirion R (1997) Neuroanatomical localization, pharmacological characterization and functions of CGRP, related peptides and their receptors. Neurosci Biobehav Rev 21:649–678

Vari RC, Adkins SD, Samson WK (1996) Renal effects of adrenomedullin in the rat. Proc Soc Exp Biol Med 211:178–183

Watanabe TX, Itahara Y, Inui T, Yoshizawa-Kumagaye K, Nakajima K, Sakakibara S (1996) Vasopressor activities of N-terminal fragments of adrenomedullin in anesthetized rats. Biochem Biophys Res Commun 219:59–63

Willenbrock R, Pagel I, Krause EG, Scheuermann M, Dietz R (1999) Acute hemodynamic and renal effects of adrenomedullin in rats with aortocaval shunt. Eur J Pharmacol 369:195–203

Wimalawansa SJ (1996) Calcitonin gene-related peptide and its receptors: molecular genetics, physiology, pathophysiology, and therapeutic potentials. Endocrine Rev 17:533–585

Yukawa H (1998) Effect of adrenomedullin on systemic and regional hemodynamics in dogs. Teikyo Med J 25:381–388

A.1.1.28.2 Receptor Binding of Adrenomedullin

PURPOSE AND RATIONALE

Muff et al. (1995), Poyer (1997) reviewed the binding characteristics of the structurally related hormones calcitonin, calcitonin gene-related peptide, amylin, and adrenomedullin. Vine et al. (1996) compared *in vitro* binding of adrenomedullin, calcitonin gene-related peptide and amylin.

Specific adrenomedullin binding sites were described in human brain (Sone et al. 1997), in the rat spinal cord (Owji et al. 1996), in cultured brain cells (Zimmermann et al. 1996), and in cultured rat mesangial cells (Osajima et al. 1996).

PROCEDURE

Human brain is obtained at autopsy. For preparation of membranes, tissues are homogenized in ice-cold 50 mM HEPES buffer, pH 7.6; containing 0.25 M sucrose, 10 µg/ml soybean trypsin inhibitor, 0.5 µg/ml pepstatin, 0.5 µg/ml leupeptin, 0.5 µg/ml antipain, 0.1 mg/ml benzamidine, 0.1 mg/ml bacitracin, and 30 µg/ml aprotinin. The homogenates are centrifuged at 1500 *g* for 20 min at 4°C. The pellets are resuspended in 10 vol of the above buffer without sucrose and centrifuged at 100,000 *g* for 1 h at 4°C. The final pellets are resuspended to a concentration of 2–10 mg protein/ml, aliquoted, and stored at –80°C.

For the receptor binding assay, brain membranes (100 µg protein) are incubated at 4°C in 0.5 ml binding buffer (20 mM HEPES buffer, pH 7.4, containing 5 mM $MgCl_2$, 10 mM NaCl, 4 mM KCl, 1 mM EDTA, and 0.3% BSA) containing 0.3 nM ^{125}I- human adrenomedullin in siliconized microcentrifuge tubes. Pellets are washed with 0.5 ml binding buffer at 4°C and counted in a γ-counter.

EVALUATION

Nonspecific binding is determined in the presence of 200 nM unlabeled human adrenomedullin. Specific binding is defined as total binding minus nonspecific binding. Data are calculated as mean ± SEM.

MODIFICATIONS OF THE METHOD

Eguchi et al. (1994) studied the binding of human adrenomedullin and analogs and the adenylate cyclase activity in cultured rat vascular smooth muscle cells.

Zimmermann et al. (1995) showed that adrenomedullin and calcitonin gene-related peptide interact with the same receptor in cultured human neuroblastoma SK-N-MC cells.

Moody et al. (1997) investigated the binding affinity of adrenomedullin in C6 glioma cells.

Findings of Belloni et al. (1998) suggested the existence of different receptor subtypes for adrenomedullin in the human adrenal cortex.

Mazzocchi et al. (1999) found abundant [^{125}I]-adrenomedullin binding sites in both zona glomerulosa and adrenal medulla in the rat adrenal gland.

REFERENCES AND FURTHER READING

Belloni AS, Meneghelli V, Champion HC, Murray WA, Coy DH, Kadowitz PJ, Nussdorfer GG (1998) Autoradiographic evidence that zona glomerulosa and capsular vessels of the human adrenal cortex are provided with different subtypes of adrenomedullin receptors. Peptides 19:1581–1584

Eguchi S, Hirata Y, Iwasaki H, Sato K, Watanabe TX, Inui T, Nakajima K, Sakakibara S, Marumo F (1994) Structure-activity relationship of adrenomedullin a novel vasodilatory peptide, in cultured rat vascular smooth muscle cells. Endocrinology 135:2454–2458

Mazzocchi G, Albertin G, Andreis PG, Neri G, Malendowicz LK, Champion HC, Bahceliouglu M, Kadowitz PJ, Nussdorfer GG (1999) Distribution, functional role, and signaling mechanisms of adrenomedullin receptors in the rat adrenal gland. Peptides 20:1479–1487

Moody TW, Miller MJ, Martinez A, Unsworth E, Cuttitta F (1997) Adrenomedullin binds with high affinity, elevates cyclic AMP, and stimulates c-fos mRNA in C6 glioma cells. Peptides 18:1111–1115

Muff R, Born W, Fischer JA (1995) Receptors for calcitonin, calcitonin gene related peptide, amylin, and adrenomedullin. Can J Physiol Pharmacol 73:963–967

Osajima A, Uezono Y, Tamura M, Kitamura K, Mutoh Y, Ueta Y, Kangawa K, Kawamura M, Tanenao E, Yamashita H, Izumi F, Tagasugi M, Kuroiwa H (1996) Adrenomedullin-sensitive receptors are preferentially expressed in cultured rat mesangial cells. Eur J Pharmacol 315:319–325

Owji AA, Gardiner JV, Upton PD, Mahmoodi M, Ghatei MA, Bloom SR, Smith DM (1996) Characterization and molecular identification of adrenomedullin binding sites in the spinal cord: A comparison with calcitonin gene-related peptide receptors. J Neurochem 67:2172–2179

Poyner DR (1997) Molecular pharmacology of receptors for calcitonin-gene-related peptide, amylin and adrenomedullin. Biochem Soc Transact 25:1032–1036

Sone M, Takahashi K, Satoh F, Murakami O, Totsune K, Ohneda M, Sasano H, Ito H, Mouri T (1997) Specific adrenomedullin binding sites in the human brain. Peptides 18:1125–1129

Vine W, Beaumont K, Gedulin B, Pittner R, Moore CX, Rink TJ, Young AA (1996) Comparison of the *in vitro* and *in vivo* pharmacology of adrenomedullin, calcitonin gene-related peptide and amylin in rats. Eur J Pharmacol 314:115–121

Zimmermann U, Fischer JA, Muff R (1995) Adrenomedullin and calcitonin gene-related peptide interact with the same receptor in cultured human neuroblastoma SK-N-MC cells. Peptides 16:421–424

Zimmermann U, Fischer JA, Frei K, Fischer AH, Reinscheid RK, Muff R (1996) Identification of adrenomedullin receptors in cultured rat astrocytes and in neuroblastoma × glioma hybrid cells (NG108–15). Brain Res 724:238–245

A.1.1.29 Atrial Natriuretic Factor (ANF)

A.1.1.29.1 General Considerations

PURPOSE AND RATIONALE

The atria of mammalian hearts synthesize and secrete peptides with potent natriuretic and vasoactive properties known as ANF = atrial natriuretic factor (de Bold et al. 1981). The atrial natriuretic peptide hormonal system consists of a 126-amino acids prohormone synthesized within myocytes of the heart and stored in storage granules within the heart before release into circulation (Kangawa and Matsuo 1984; Oikawa et al. 1984; Vesely 1992). This hormonal system contains several peptides from the 126-amino acid-prohormone with blood pressure lowering, natriuretic, diuretic and/or kaliuretic properties (Martin et al. 1990; Vesely et al. 1994). Thus, peptides consisting of amino acid 1 to 30 (LANP = long-acting natriuretic peptide), 31 to 67 (vessel dilator), 79 to 98 (kaliuretic peptide) and 99 to 126 (ANF) each have blood pressure lowering, natriuretic, diuretic and/or kaliuretic properties both in humans and in animals. Human and rat atria predominantly secrete a peptide of 28 amino acid residues, ANF-(99–126), which represents the C-terminus of a precursor sequence of 126 amino acid residues. In addition, vessel dilator and LANP circulate as distinct entities after having been proteolytically cleaved from the rest of the amino terminus by proteases (Ackerman et al. 1997).

Plasma immunoreactive ANF-(99–126) concentration increases in normal rats after volume expansion, while infusion of the peptide lowers blood pressure in several animal models of hypertension.

An international standard for atrial natriuretic factor was established by an international collaborative study (Poole et al. 1988). Human ANF-(99–126) was synthesized, highly purified and distributed to several laboratories, who performed radioimmunoassays, radioreceptor assays and an *in vitro* assay using the vasorelaxant activity in precontracted rat aortic strips.

The C-type natriuretic peptide is a 22-amino acid peptide that was initially identified in the central nervous system (Ogawa et al. 1992; Barr et al. 1996; Amin et al. 1996). The distribution of C-type natriuretic peptide, which has structural homology with atrial and brain natriuretic peptides and also similar activities, is wide and includes the endothelium, myocardium, gastrointestinal and genitourinary tracts. **Brain natriuretic peptide** has been described as a novel cardiac hormone (Nakao et al. 1991). Yasue et al. (1994) studied the localization and mechanism of secretion of B-type natriuretic peptide in comparison with those of A-type natriuretic peptide in normal subjects and patients with heart failure. N-terminal pro-brain natriuretic peptide became a diagnostic screening tool to differentiate between patients with normal and left ventricular systolic function (Bay et al. 2003; Gardner et al. 2003).

Jiao and Baertschi (1993) reviewed the neural control of the endocrine rat heart. Stimulation of cardiac sympathetic nerves potently stimulates ANF secretion.

ANF inhibits proliferation in non-myocardial cells and is anti-hypertrophic in cardiomyocytes. Silberbach et al. (1999) reported that activation of an extracellular signal-regulated protein kinase is required for the anti-hypertrophic effect of atrial natriuretic factor in neonatal rat ventricular myocytes.

REFERENCES AND FURTHER READING

Ackerman BH, Overton RM, McCormick MT, Schocken DD, Vesely DL (1997) Disposition of vessel dilator and long-acting natriuretic peptide in healthy humans after one-hour infusion. J Pharm Exp Ther 282:603–608

Amin J, Carretero OA, Ito S (1996) Mechanism of action of atrial natriuretic factor and C-type natriuretic peptide. Hypertension 27:684–687

Barr CS, Rhodes P, Struthers AD (1996) C-type natriuretic peptide. Peptides 17:1243–1251

Bay M, Kirk V, Parner J, Hassager C, Nielsen H, Krogsgaard K, Trawinski J, Boesgaard S, Aldershvile J (2003) NT-proBNP: a new diagnostic screening tool to differentiate between patients with normal and left ventricular systolic function. Heart 89:150–154

De Bold AJ, Borenstein HB, Veress AT, Sonnenberg HA (1981) A rapid and potent natriuretic response to intravenous injection of atrial myocardial extract in rats. Life Sci 28:89–94

Gardner RS, Özlalp F, Murday AJ, Robb SD, McDonagh TA (2003) N-terminal pro-brain natriuretic peptide. A new gold standard in predicting mortality in patients with advanced heart failure. Eur Heart J 24:1735–1743

Jiao J-H, Baertschi AJ (1993) Neural control of the endocrine rat heart. Proc Natl Acad Sci 90:7799–7803

Kangawa K, Matsuo H (1984) Purification and complete amino acid sequence of a α-human atrial natriuretic polypeptide (α-hANP) Biochem Biophys Res Commun 118:131–138

Martin DR, Pevahouse JB, Trigg DJ, Vesely DL, Buerkert JE (1990) Three peptides from the ANF prohormone NH_2-terminus are natriuretic and/or kaliuretic. Am J Physiol 258:F1401–F1408

Nakao K, Mukoyama M, Hosoda K, Suga S, Ogawa Y, Saito Y, Shirakai G, Arai H, Jougasaki M, Imura H (1991) Biosynthesis, secretion, and receptor selectivity of human brain natriuretic peptide. CanJ Physiol Pharmacol 69:1500–1506

Ogawa Y, Nakao K, Nakagawa O, Komatsu Y, Hosoda K, Suga S, Arai H, Nagata K, Yoshida N, Imura H (1992) Human C-type natriuretic peptide. Characterization of the gene and peptide. Hypertension 19:809–813

Oikawa S, Imai M, Ueno A (1984) Cloning and sequence analysis of cDNA encoding a precursor for human atrial natriuretic polypeptide. Nature 309:724–726

Poole S, Gaines Das RE, Dzau VJ (1988) The international standard for atrial natriuretic factor. Calibration by an international collaborative study. Hypertension 12:629–634

Silberbach M, Gorenc T, Hershberger RE, Stork PJS, Steyger PS, Roberts CT Jr (1999) Extracellular signal-regulated protein kinase activation is required for the anti-hypertrophic effect of atrial natriuretic factor in neonatal ventricular myocytes. J Biol Chem 274:24858–24864

Vesely DL (1992) Atrial Natriuretic Hormones. Prentice Hall: Englewood Cliffs, NJ

Vesely DL, Douglass MA, Dietz JR, Gower WR Jr, McCormick MD, Rodriguez-Paz G, Schocken DD (1994) Three peptides from the atrial natriuretic factor prohormone amino terminus lower blood pressure and produce a diuresis, natriuresis, and/or kaliuresis in humans. Circulation 90:1129–1140

Yasue H, Yoshimura M, Sumida H, Kikuta H, Kugiyama K, Jougasaki M, Ogawa H, Okumura K, Mukoyama M, Nakao K (1994) Localization and mechanism of secretion of B-type natriuretic peptide in comparison with those of A-type natriuretic peptide in normal subjects and patients with heart failure. Circulation 90:195–203

A.1.1.29.2 Bioassay for ANF

PURPOSE AND RATIONALE

Matsui et al. (1987) described a rapid bioassay for quantification of atrial natriuretic polypeptides in rats with continuous recording of the conductivity of the urine, urine flow and blood pressure.

PROCEDURE

Male Sprague Dawley rats weighing 180–240 g are anesthetized with 60 mg/kg i.p. pentobarbital sodium. Anesthesia is maintained by injection of supplemental doses of pentobarbital sodium. After tracheotomy, catheters are placed into the left jugular vein and the right carotid artery for injection of samples or infusion of 10% mannitol in 0.9% saline and for blood pressure recording. Through a small suprapubic incision the bladder is cannulated for collection of urine, and the cannula is connected to a device for continuous measurement of urine conductivity, by which the electrolyte concentration is estimated. Urine flow rate is recorded using a drop counter, and urine samples are collected in a plastic tube.

After completion of surgery, 0.6–0.8 ml of 10% mannitol in 0.9% saline is administered into the jugular vein and is continuously infused at a rate of 4.0 ml/h by a syringe pump. Following an equilibration of 45–60 min, the bioassay is started when the urine flow is increased to 50–75 µl/min. All test samples with a volume of 100 µl are directly injected into the jugular vein followed by a wash injection of ~30 µl of saline. Mean arterial blood pressure, urine conductivity, and urine flow rate are simultaneously recorded.

For dose-response curves, serial dilutions of human ANF (α-hANP) and of test substance are prepared. Vehicle and various doses of α-hANP or test substance are injected in a randomized sequence. Immediately after the injection, urine is collected for 10 min. Urine volumes are determined by weighing, and urinary sodium and potassium concentrations are measured by flame photometry.

EVALUATION

Linear-regression analyses by the method of least squares are used for evaluating dose-response relationship. One-way analysis of variance for repeated measures and the Newman-Keuls test are used to detect statistical differences.

MODIFICATIONS OF THE METHOD

Petersen et al. (1988) determined atrial content and plasma levels of atrial natriuretic peptides in rats with chronic renal failure. The natriuretic activity in the bioassay was estimated as the increase in Na excretion in urine samples from the control period to the maximal natriuretic response.

Allen and Gellai (1987) measured cardioinhibitory effects of atrial peptide in conscious chronically instrumented rats. The hemodynamic and renal excretory responses were measured with and without replacement of urinary fluid losses.

Thibault et al. (1984) characterized the biological activities of atrial natriuretic factor-related peptides *in vivo* by a natriuretic bioassay and *in vitro* by relaxation of contracted intestinal smooth muscle (chick rectum).

Schiller et al. (1986) tested synthetic analogs of atrial natriuretic peptide in the rabbit aorta assay and in a bioassay monitoring suppression of aldosterone secretion from bovine zona glomerulosa cells.

Dlouha and McBroom (1986) measured diuretic and natriuretic activity of atrial extracts of taurine-treated normal and cardiomyopathic hamsters by urine flow and Na^+ excretion in the rat bioassay.

St.-Louis and Schiffrin (1988) measured vasorelaxant effects of different atrial natriuretic peptides on rat aortic and mesenteric artery rings and compared the results with the potency of the same peptides to displace ^{125}I-labeled ANP on membrane preparations of aorta and of mesenteric vein bed.

Kohse et al. (1992) described a bioassay for quantitative determination of natriuretic peptides in human biological samples using bovine aortic and bovine kidney epithelial cultured cells. The amount of cyclic AMP produced by these cells was measured by radioimmunoassay.

Kecskemeti et al. (1996) studied the effects of atrial natriuretic peptide (ANP) on action potential characteristics in various (human, rabbit, guinea-pig) atrial and guinea pig ventricular papillary muscles. The data suggested that ANP inhibits the slow inward Ca^{2+} channel activity and facilitates the K^+ channel activity.

Salt-sensitive hypertension was found in ANP knockout mice (Melo et al. 1998).

REFERENCES AND FURTHER READING

Allen DE, Gellai M (1987) Cardioinhibitory effect of atrial peptide in conscious rats. Am J Physiol 252 (Regul Integr Comp Physiol 21): R610–616

Dlouha H, McBroom (1986) Atrial natriuretic factor in taurine-treated normal and cardiomyopathic hamsters. Proc Soc Exp Biol Med 181:411–415

Kecskemeti V, Pacher P, Pankucsi C, Nanasi P (1996) Comparative study of electrophysiological effects of atrial natriuretic peptide. Mol Cell Biochem 160/161:53–59

Kohse KP, Feifel K, Wisser H (1992) Quantitative determination of natriuretic peptides in human biological samples with a bioassay using cultured cells. Eur J Clin Chem Clin Biochem 30:837–845

Matsui K, Kimura T, Ota K, Shoji M, Inoue M, Iitake K, Yoshinaga K (1987) A rapid bioassay for quantification of atrial natriuretic polypeptides. Am J Physiol 252 (Regul Integr Comp Physiol 21): R1009–R1014

Melo LG, Veress AT, Chong CK, Pang SC, Flynn TG, Sonnenberg H (1998) Salt-sensitive hypertension in ANP knockout mice: potential role of abnormal plasma renin activity. Am J Physiol 274 (Regul Intergr Comp Physiol 43): R255–R261

Petersen JS, Bech OM, Steiness E, Kirstein D, Korsgaard N, Baanrup U, Christensen S (1988) Atrial content and plasma levels of atrial natriuretic peptides in rats with chronic renal failure. Scand J Clin Lab Invest 48:431–439

Schiller PW, Bellini F, Dionne G, Maziak LA, Garcia L, DeLéan A, Cantin M (1986) Synthesis and activity profiles of atrial natriuretic peptide (ANP) analogs with reduced ring size. Biochem Biophys Res Commun 138:880–886

St.-Louis JU, Schiffrin EL (1988) Vasorelaxant effects of and receptors for atrial natriuretic peptides in the mesenteric artery and aorta of the rat. Can J Physiol Pharmacol 66:951–956

Thibault G, Garcia R, Carrier F, Seidah NG, Lazure C, Chrétien M, Cantin M, Genest J (1984) Structure-activity relationships of atrial natriuretic factor (ANF). I. Natriuretic activity and relaxation of intestinal smooth muscle. Biochem Biophys Res Commun 125:938–046

A.1.1.29.3 Receptor Binding of ANF

PURPOSE AND RATIONALE

Schiffrin et al. (1985) described receptors for atrial natriuretic factor in the rat.

PROCEDURE

Synthetic ANF-(99–126) is iodinated with ^{125}I by a modification (Gutskowska et al. 1984) of the chloramine T method (Greenwood and Hunter 1963). Separation of radiolabeled ANF from free iodine is achieved by immunoaffinity chromatography followed by C-18 reverse phase high pressure liquid chromatography.

For preparation of membranes, Sprague Dawley rats weighing 300 g are sacrificed by decapitation. The atria, ventricles, renal arteries, mesentery, the mesentery vascular bed, and adrenals are processed for binding studies. Adrenal capsules are separated by manual compression. The tissues are immersed in 0.25 M sucrose solution, finely minced with scissors, and homogenized in a Polytron (setting 8, 10 s twice). The homogenate is centrifuged at 1550 *g* for 10 min at 4°C; the supernatant is decanted and recentrifuged. The final supernatant is filtered through a cheesecloth, then centrifuged at 10,400 *g* for 30 min. The pellet is resuspended in a 0.05 M Tris-HCl buffer, pH 7.4, containing 120 mM NaCl, 5 mM $MgCl_2$, 0.5 mM phenyl methyl sulfonyl fluoride, 0.1% bacitracin, and 1 μM aprotinin. Proteins are measured by the Coomassie blue method (Spector 1978). Next, bovine serum is added at a concentration of 0.2%, and the membranes are diluted to a protein concentration of 0.25 to 1 mg/ml in the Tris-buffer containing 0.2% albumin.

The ^{125}I-AFN binding assay uses 30–50 pM of labeled ANF and 10^{-13} to 10^{-6} unlabeled ANF in competition experiments. In saturation experiments, increasing concentrations of ^{125}I-AFN (6–200 pM) are used, and nonspecific binding is determined by incubation in the presence of 1 μM unlabeled ANF for each point of the saturation curves. Incubation is done with 25–100 μg of receptor protein per tube, at 4°C for 60 min. All assays are performed in duplicate. Separation of bound and free radioactivity is achieved by rapid filtration through polyethylenimine-treated Whatman GF/C filters soaked with the assay buffer. The filters are washed twice with 3 ml of 0.9% NaCl,

then are allowed to dry and are counted in a gamma counter.

EVALUATION

Binding data are analyzed by computer assisted nonlinear regression analysis using the LIGAND program (Munson and Rodbard 1980). The inhibition constant K_i is calculated according the Cheng and Prussoff equation.

MODIFICATIONS OF THE METHOD

Misono (2000) found that the binding of atrial natriuretic factor to its receptor is dependent on chloride concentration.

REFERENCES AND FURTHER READING

Greenwood FC, Hunter WM (1963) The preparation of ^{131}I-labelled human growth hormone of high specific radioactivity. Biochem J 89:114–123

Gutkowska J, Thibault G, Januszewicz P, Cantin M, Genest J (1984) Direct radioimmunoassay of atrial natriuretic factor. Biochem Biophys Res Commun 122:593–601

Misono KS (2000) Atrial natriuretic factor binding to its receptor is dependent on chloride concentration. A possible feedback-control mechanisms in renal salt regulation. Circ Res 86:1135

Munson PJ, Rodbard D (1980) LIGAND: a versatile computerized approach for characterization of ligand-binding systems. Anal Biochem 107:220–239

Schiffrin EL, Chartier L, Thibault G, St-Louis J, Cantin M, Genest J (1985) Vascular and adrenal receptors for atrial natriuretic factor in the rat. Circ Res 56:801–807

Spector T (1978) Refinement of the Coomassie blue method of protein quantitation. Anal Biochem 86:142–146

A.1.1.29.4 ANF Gene Expression

PURPOSE AND RATIONALE

Production of atrial natriuretic factor and brain natriuretic peptide can be measured by gene expression using total RNA extraction and Northern blot analysis and the quantitative competitive reverse transcription polymerase chain reaction (Hama et al. 1995; Ogawa et al. 1996, 1997, 1998, 1999).

PROCEDURE

Extraction of Plasma and Tissue Samples

Plasma samples are acidified by adding 100 µl/ml of 1 mol/l HCl and passed through Sep-Pak C_{18} cartridges (Millipore) that are pre-wetted with 5 ml of 80% acetonitrile in 0.1% trifluoroacetic acid (TFA) and 10 ml of 0.1% TFA. The cartridges with the absorbed peptides are washed with 20 ml of 0.1% TFA and eluted with 3 ml of 60% acetonitrile in 0.1% TFA. Tissue samples are homogenized in 10 vol of an extracting mixture consisting of 0.1 N HCl, 1.0 mol/l acetic acid, and 1% NaCl and centrifuged at 10,000 *g* for 30 min at 4°C. The supernatants are then extracted with the use of Sep-Pak C_{18} cartridges by elution with 80% acetonitrile in 0.1% TFA. The eluates from tissue or plasma are freeze-dried and processed for RIA.

Total RNA Extraction and Northern Blot Analysis

Atrial and ventricular tissue samples from individual rats are extracted using Trizol (GIBCO BRL). Total RNA from the atrium (10 µg) and ventricle (20 µg) are electrophoretically separated in an agarose-formaldehyde gel followed by blotting to nylon membranes (Hybond N+, Amersham) overnight. Membranes are prehybridized in 2.5 × Denhardt's solution, 5 × SSC, 50% formamide, 25 mmol/l KH_2PO_4, pH 6.4, 0.2% SDS, and 0.2 mg/mL herring sssDNA for 3 h at 42°C for cDNA probes, or prehybridized in 5 × Denhardt's solution, 6 × SSC, 50 mmol/l NaH_2PO_4, 0.5% SDS, and 0.2 mg/ml herring sssDNA for 3 h at 5°C below the calculated T_m for oligonucleotide probes. Hybridization is then carried out for 16 h at the same temperature and the same solution as the prehybridization condition except for the presence of the radiolabeled probes. Five cDNA probes and two oligonucleotide probes are used. The cDNA probes used are as follows: (1) a 900-bp *Eco*RI/*Hin*dIII fragment containing the full-length rat ANF cDNA, (2) a 595-bp *Sal*I fragment containing full-length rat BNP cDNA, (3) a 5-kb *Eco*RI/*Sal*I fragment of the mouse 28S rRNA cDNA probe, (4) a 2-kb *Bam*HI/*Bgl*II fragment of the mouse PGK gene cDNA, and (5) rat α_1-III collagen cDNA containing 1300 bp of the 3′ noncoding and coding regions. The two oligonucleotide probes are 39 and 24 base fragments specific for unique regions in the 3′ untranslated regions of the rat α-MHC and β-MHC genes. The α-sequence is 5′GGGATAGCAACAGCGAGGCTCT TTCTGCTGGACAGGTTA-3′(T_m = 60°C),and the β-sequence is 5′-CTCCAGGTCTCAGGGCTTCACA GG-3′ (T_m = 52°C).

The cDNAs are labeled with 5′-[α^{32}P]dCTP (3000 Ci/mmol, Amersham) using the Megaprime DNA labeling system (Amersham). The oligonucleotides are labeled with [γ-^{32}P]ATP (3000 Ci/mmol, Amersham) using a 5′-end-labeling kit (Amersham). At the end of hybridization, the membranes are washed twice at 42°C with 2 × SSC and 1% SDS and twice at 55°C with 1 × SSC and 0.1% SDS for the cDNA probes or are washed once at 30°C with 5 × SSC and 0.1% SDS and twice at the same temperature as the hybridization with 1 × SSC and 0.1% SDS for

the oligonucleotide probes. Before additional probing, bound counts are completely stripped from the membranes by washing twice in 10 mmol/l sodium citrate, pH 6.8, 0.25% SDS for 10 min at 100°C. Autoradiographs are scanned with an Ultrascan XL laser densitometer (LKB Produckter) and LKB 2400 Gelscan XL software package. The scanning values of ANF, BNP, collagen-III, and α-MHC and β-MHC mRNAs are normalized to 28S ribosomal RNA or PGK mRNA as internal controls to correct for differences in the amount of RNA applied and transfer efficiency.

Plasma and cardiac tissue concentrations of immunoreactive ANF and BNP are determined by RIA with anti-rat $ANF_{99–126}$ and anti-rat $BNP_{64–95}$ sera, respectively, from Peninsula Laboratories.

Quantitative competitive reverse transcription polymerase chain reaction

RNA samples are reverse transcribed with Super Script II RNase H 2 Reverse Transcriptase and oligo(dT)12–18 primer with the use of a reverse transcription kit (GIBCO BRL). An aliquot of the cDNA product is used for PCR amplification with ANF primers. A dilution series of total RNA (5 mg) aliquots is prepared for each sample. Each dilution is spiked with competitor RNA. After the PCR, aliquots (5 ml) of the PCR product are electrophoresed on a 2% agarose gel and visualized by ethidium bromide staining. Photographs are taken with Polaroid 55 film, and the negatives are scanned with the use of an Ultrascan XL laser densitometer and Gelscan XL 2000 software package. The ratio of the density of the competitor RNA to the target RNA is plotted against the amount of the competitor RNA added to each reaction.

EVALUATION

All results are expressed as mean $\pm$ SEM. A level of $P < 0.5$ is considered significant. ANOVA is performed to determine statistical differences among multiple groups. When significance is obtained by ANOVA, Fisher's least squares difference post hoc analysis is used to determine pairwise differences.

MODIFICATIONS OF THE METHOD

Ramirez et al. (1997) reported that the nuclear δ_B isoform of Ca^{2+}/calmodulin-dependent protein kinase II regulates atrial natriuretic gene expression in cultured neonatal rat ventricular myocytes.

Thuerauf et al. (1998) found that the p38 mitogen-activated protein kinase mediates the transcriptional induction of the atrial natriuretic factor gene through a serum response element and discussed the potential role for the transcription factor ATF6.

Kakita et al. (1999) studied p300 protein as a coactivator of the transcription factor GATA-5 in the transcription of cardiac-restricted atrial natriuretic factor gene.

Bianciotti and de Bold (2000) investigated the effect of selective ET_A receptor blockade on natriuretic peptide gene expression in DOCA-salt hypertension in rats.

REFERENCES AND FURTHER READING

Bianciotti LG, de Bold AJ (2000) Effect of selective ET_A receptor blockade on natriuretic peptide gene expression in DOCA-salt hypertension. Am J Physiol 279 (Heart Circ Physiol):H93–H101

Hama N, Itoh H, Shirakami G, Nakagawa O, Suga S-I, Ogawa Y, Masuda I, Nakanishi K, Yoshimasa T, Hashimoto Y, Yamaguchi M, Hori R, Yasue H, Nakao K (1995) Rapid ventricular induction of brain natriuretic peptide gene expression in experimental acute myocardial infarction. Circulation 92:1558–1564

Kakita T, Hasegawa K, Morimoto T, Kaburagi S, Wada H, Sasayama S (1999) p300 Protein as a coactivator of GATA-5 in the transcription of cardiac-restricted atrial natriuretic factor gene. J Biol Chem 274:34096–34102

Ogawa T, Linz W, Stevenson M, Bruneau BG, Kuroski de Bold ML, Chen J-H, MD, Eid H, Schölkens BA, de Bold AJ (1996) Evidence for load-dependent and load-independent determinants of cardiac natriuretic peptide production. Circulation 93:2059–2067

Ogawa T, Bruneau BG, Yokota N, Kuroski de Bold ML, de Bold AJ (1997) Tissue-specific regulation of renal and cardiac atrial natriuretic gene expression in desoxycorticosterone acetate-salt rats. Hypertension 30:1342–1347

Ogawa T, Linz W, Schölkens BA, de Bold AJ (1998) Regulation of aortic atrial natriuretic factor and angiotensinogen in experimental hypertension. J Cardiovasc Pharmacol 32:1001–1008

Ogawa T, Linz W, Schölkens BA, de Bold AJ (1999) Variable renal atrial natriuretic factor gene expression in hypertension. Hypertension 33:1342–1347

Ramirez MT, Zhao X-L, Schulman H, Brown JH (1997) The nuclear δ_B isoform of Ca^{2+}/calmodulin-dependent protein kinase II regulates atrial natriuretic gene expression in ventricular myocytes. J Biol Chem 272:31203–31208

Thuerauf DJ, Arnold ND, Zechner D, Hanford DS, DeMartin KM, McDonough PM, Prywes R, Glembotski CC (1998) p38 Mitogen-activated protein kinase mediates the transcriptional induction of the atrial natriuretic factor gene through a serum response element. A potential role for the transcription factor ATF6. J Biol Chem 273:20636–20643

A.1.1.29.5 Radioimmunoassay for ANF

PURPOSE AND RATIONALE

Gutkowska et al. (1984) developed a direct radioimmunoassay of atrial natriuretic factor (ANF). The

method uses a synthetic 26-amino-acid fragment (8–33 ANF) of the native peptide.

PROCEDURE

Because 8–33 ANF is a small molecule, it is necessary to covalently conjugate the peptide to a larger protein (bovine thyroglobulin) for immunization. To 50 mg thyroglobulin dissolved in 2 ml distilled water, pH 7.4, 30 mg CDI [1-ethyl-3-(3-dimethylaminopropyl) carbodiimide HCl] is added in 1 ml distilled water, pH 7.4. Then 5 mg 8–33 ANF in water is added dropwise while stirring. The solution is kept overnight at 4°C, then another 30 mg CDI is added and the mixture is kept for 2 h at room temperature with constant stirring. The cloudy mixture is dialyzed for 24 h at 4°C against 0.9% saline. The dialyzed material is then fractionated and stored at –70°C.

For immunization, 100 µg of the ANF-thyroglobulin complex are suspended in 1 ml saline, thoroughly mixed with 1 ml complete Freund's adjuvant and injected into the shaved backs of New Zealand white rabbits. Each animal receives also 0.5 ml *Bordetella pertussis* vaccine subcutaneously with the primary immunization. The animals are reimmunized at monthly intervals with 100 µg of antigen in incomplete Freund's adjuvant and bled by ear artery 10 days after the booster injection.

For iodination, 5 µg ANF in 5 µl 0.01 M ammonium acetate, pH 5.0 is introduced in a 1.5 ml Eppendorf vial followed by the addition of 1 mCi Na ^{125}I in a volume of 25 µl. Chloramine T 10 µg/10 µl is added to the reaction vial and 30 s later sodium metabisulfide (20 µg/10 µl) is added. Each addition is followed by mixing. Purification of the iodinated tracer is achieved by HPLC on a µBondapax C_{18} column, eluted with a linear gradient of 20 to 50% acetonitrile with 0.1% trifluoroacetic acid with a slope of 0.5%/min and a flow rate of 1 ml/min.

The radioimmunoassay procedure is performed in polystyrene tubes at 4°C by mixing 100 µl of standard or sample, 100 µl of antiserum diluted 1:4000, 100 µl of ^{125}I-ANF and 300 µl of the same buffer containing 1% BSA. After incubation for 24 h at 4°C the free from antigen-bound ^{125}I-ANF is separated by dextran-coated charcoal. One ml of dextran-charcoal suspension is added to each tube. After 5 s agitation the tubes are centrifuged at 4000 rpm at 4°C for 10 min. The supernatant is decanted and the radioactivity counted in a gamma counter.

EVALUATION

Dose-response curves are prepared and Scatchard analysis is performed.

MODIFICATIONS OF THE METHOD

Radioimmunoassays were also developed for long-acting natriuretic peptide and vessel dilator (Vesely et al. 1994; Winters et al. 1989).

REFERENCES AND FURTHER READING

Gutkowska J, Thibault G, Januszewicz P, Cantin M, Genest J (1984) Direct radioimmunoassay of atrial natriuretic factor. Biochem Biophys Res Commun 122:593–601

Vesely DL, Douglass MA, Dietz JR, Giordano AT, McCormick MT, Rodriguez-Paz G, Schocken DD (1994) Negative feedback of atrial natriuretic peptides. J Clin Endocrinol Metab 78:1128–1134

Winters CJ, Sallman AL, Baker BJ, Meadows J, Rico DM, Vesely DL (1989) The N-terminus and a 4000 molecular weight peptide from the mid portion of the N-terminus of the atrial natriuretic factor prohormone each circulate in humans and increase in congestive heart failure. Circulation 80:438–449

A.1.1.30 Urotensin II

A.1.1.30.1 General Considerations

PURPOSE AND RATIONALE

Urotensin II is a cyclic peptide originally isolated from the urophysis, the hormone storage-secretion organ of the caudal neurosecretory system of teleost fishes, such as *Gillichthys mirabilis* (Pearson et al. 1980; Maguire and Davenport 2002).

Several structural forms of urotensin II have been reported in different species (Grieco et al. 2004). These peptides show smooth muscle contracting activity. Itoh et al. (1987) reported contraction of major artery segments of rat, especially of the thoracic aorta, by urotensin II.

Human urotensin II is an 11-amino-acid peptide that retains the cyclic portion typical of fish urotensin II. It has been found in vascular and cardiac tissues and is a very potent constrictor of certain human isolated arteries and veins as well as of several vessels of other species (Douglas et al. 2000; Douglas 2003).

The potency of urotensin II as a vasoconstrictor is an order of magnitude greater than that of endothelin-1, making human urotensin II the most potent vasoconstrictor identified so far.

Human urotensin II is also a potent endothelium-dependent relaxant in rat precontracted arteries (Katano

et al. 2000) and in human small pulmonary and systemic abdominal resistance arteries (Stirrat et al. 2001).

Bottrill et al. (2000) found that human urotensin II contracted endothelium-intact rat isolated left anterior descending coronary arteries. The contractile response was significantly enhanced by removal of the endothelium. However, human urotensin II caused concentration-dependent relaxation of 5-HT-precontracted arteries, which was abolished by *N*-nitro-L-arginine methyl ester (L-NAME) or removal of the endothelium.

Using merino ewes as experimental animals, Watson et al. (2003) found that urotensin II acts centrally to increase epinephrine and adrenocorticotrophic hormone (ACTH) release and causes potent inotropic and chronotropic actions.

Coy et al. (2002) investigated structural requirements at the N-terminus of urotensin II octapeptides.

Carotenuto et al. (2004) investigated the active conformation of urotensin II by CD spectroscopy and NMR analysis in SDS micelles.

Watson and May (2004) reviewed the role of urotensin II in central and peripheral cardiovascular control.

REFERENCES AND FURTHER READING

Bottrill FE, Douglas FE, Hiley CR, White R (2000) Human urotensin II is an endothelium-dependent vasodilator in rat small arteries. Br J Pharmacol 130:1865–1870

Carotenuto A, Grieco P, Campiglia P, Novellino E, Rovero P (2004) Unravelling the active conformation of urotensin II. J Med Chem 47:1652–1661

Coy DH, Rossowski WJ, Cheng BL, Taylor JE (2002) Structural requirements at the N-terminus of urotensin II octapeptides. Peptides 23:2259–2264

Douglas SA, Sulpizio AC, Piercy V, Sarau HM, Ames RS, Aiyar NV, Ohlstein EH, Wilette RN (2000) Differential vasoconstrictor activity of human urotensin II in vascular tissue isolated from the rat, mouse, dog, pig, marmoset and cynomolgus monkey. Br J Pharmacol 131:1262–1274

Douglas SA (2003) Human urotensin-II as a novel cardiovascular target: "heart" of the matter or simply a fishy "tail"? Curr Opin Pharmacol 3:159–167

Grieco P, Rovero P, Novellino E (2004) Recent structure-activity studies of the peptide hormone urotensin II, a potent vasoconstrictor. Curr Med Chem 11:969–979

Itoh H, Itoh Y, Rivier J, Lederis K (1987) Contraction of major artery segments of rat by fish neuropeptide urotensin II. Am J Physiol 252(2Pt2):R361–R366

Katano Y, Ishihata A, Aita T, Ogaki T, Horie T (2000) Vasodilator effect of urotensin II, one of the most potent vasoconstricting factors, on rat coronary arteries. Eur J Pharmacol 402:209–211

Magzire JJ, Davenport AP (2002) Is urotensin-II the new endothelin? Br J Pharmacol 137:579–588

Pearson D, Shively JE, Clark BR, Geschwing II, Barkley M, Nishioka RS, Bern HA (1980) Urotensin II: a somatostatin-like peptide in the caudal neurosecretory system of fishes. Proc Natl Acad Sci USA 77:5021–5024

Stirrat A, Gallagher M, Douglas SA, Ohlstein EH, Berry C, Kirk A, Richardson M, MacLean MR (2001) Potent vasodilator responses to human urotensin-II in human pulmonary and abdominal resistance arteries. Am J Physiol 280:H925–H928

Watson AMD, Lambert GW, Smith KJ, May CN (2003) Urotensin II acts centrally to increase epinephrine and ACTH release and cause potent inotropic and chronotropic actions. Hypertension 42:373–379

Watson AM, May CN (2004) Urotensin II, a novel peptide in central and peripheral cardiovascular control. Peptides 25:1759–1766

A.1.1.30.2 Rat Thoracic Aorta Bioassay for Urotensin II

PURPOSE AND RATIONALE

Most studies on urotensin analogs, agonists and antagonists used the isolated thoracic aorta of rats as a pharmacological model (Itoh et al. 1988; Nothacker et al. 1999; Sauzeau et al. 2001; Camarda et al. 2002a; Grieco et al. 2002a, 2002b; Rossowski et al. 2002). Several urotensin II antagonists have been tested in this model (Behm et al. 2002; Herold et al. 2003).

Patacchine et al. (2003) tested urantide, an ultrapotent urotensin II antagonist peptide, in the rat aorta.

PROCEDURE

Male albino rats (Wistar strain, 275–350 g) are decapitated under ether anesthesia. The thoracic aorta is cleared of surrounding tissue and excised from the aortic arch to the diaphragm. From each vessel, a helically cut strip is prepared, and then it is cut into two parallel strips. The endothelium is removed by gently rubbing the vessel intimal surface with a cotton-tip applicator; the effectiveness of this maneuver is assessed by the loss of relaxation response to acetylcholine (1 μM) in preparations precontracted with noradrenaline (1 μM). All preparations are placed in 5-ml organ baths filled with oxygenated normal Krebs–Henseleit solution. Motor activity of the strips is recorded isotonically (load 5 mN). A cumulative concentration–response curve to hU-II is constructed on one of the two strips, which serves as control. The other strip receives the antagonist peptide under examination and, after a 30-min incubation period, hU-II is administered cumulatively. Maximal contractile responses of preparations to hU-II are obtained by administration of KCl (80 mM) at the end of the cumulative curves.

EVALUATION

Antagonist activity is expressed in terms of pK_B (negative logarithm of the antagonist dissociation constant) and, assuming a slope of –1.0, is estimated as the mean

of the individual values obtained with the equation: pK_B = log[dose ratio–1]–log[antagonist concentration] (Kenakin 1997). Competitive antagonism is checked by the Schild plot method: a plot with linear regression line and slope not significantly different from unity is considered as proof of simple reversible competition (Kenakin 1997).

MODIFICATIONS OF THE METHOD

Gibson et al. (1988) studied the influence of urotensin II on calcium flux in rat aorta. Urotensin II caused an increase in uptake of ^{45}Ca by segments of rat aorta. This increase was abolished by calcium channel blocking drugs.

Douglas et al. (2000) found differential vasoconstrictor activity of human urotensin II in vascular tissue isolated from the rat, mouse, dog, pig, marmoset and cynomolgus monkey depending on species and anatomical localization.

Camarda et al. (2002b) studied the effects of human urotensin II in isolated vessels (aorta, large arteries, veins) of various species (rats, guinea pigs, rabbits, pigs, human) and compared them with other vasoactive agents (noradrenaline, angiotensin II, endothelin I).

Watanabe et al. (2001) found a synergistic effect of urotensin II with serotonin on rabbit vascular smooth muscle cell proliferation.

Tamura et al. (2003) examined the effects of urotensin II on activation of extracellular signal-regulated kinase and focal adhesion kinase in cultured vascular smooth muscle cells.

Tzanidis et al. (2003) studied direct actions of urotensin II on the heart in a rat model of heart failure after myocardial infarction and the implications for cardiac fibrosis and hypertrophy.

Matsushita et al. (2003) showed that urotensin II is an autocrine/paracrine growth factor for the porcine renal epithelial cell line LLCPK1.

Behm et al. (2004) investigated the role of urotensin II in the etiology of essential hypertension. Intravenous injection in anesthetized cats induced an increase in systemic blood pressure and peripheral vascular resistance.

REFERENCES AND FURTHER READING

Behm DJ, Herold CL, Ohlstein EH, Knight SD, Dhanak D, Douglas SA (2002) Pharmacological characterization of SB-710411 (Cpa-c[D-Cys-Pal-D-Trp-Lys-Val-Cys]-Cpa-amide), a novel peptidic urotensin-II receptor antagonist. Br J Pharmacol 137:449–458

Behm DJ, Doe CPA, Johns DG, Maniscalco K, Stankus GP, Wibberley A, Willette RN, Douglas SA (2004) Urotensin-II: a novel systemic hypertensive factor in the cat. Naunyn Schmiedebergs Arch Pharmacol 369:274–280

Camarda V, Guerrini R, Kostenis E, Rizzi A, Calo G, Hattenberger A, Zucchini M, Salvadori S, Reguli D (2002a) A new ligand for the urotensin II receptor. Br J Pharmacol 137:311–314

Camarda V, Rizzi A, Calò G, Gendron G, Perron SI, Kostenis E, Zamboni P, Mascoli F, Regoli D (2002b) Effects of human urotensin II in isolated vessels of various species: comparison with other vasoactive agents. Naunyn-Schmiedebergs Arch Pharmacol 365:141–149

Douglas SA, Ashton DJ, Sauermelch CF, Coatney RW, Ohlstein DH, Ruffolo MR, Ohlstein EH, Aiyar NV, Willette RN (2000) Human urotensin II is a potent vasoactive peptide: pharmacological characterization in the rat, mouse, dog and primate. Cardiovasc Pharmacol 36/Suppl1:S163–166

Gibson A, Conyers S, Bern HA (1988) Influence of urotensin II on calcium flux in rat aorta. J Pharm Pharmacol 40:893–985

Grieco P, Carotenuto A, Patacchini R, Maggi CA, Novellino E, Rovero P (2002a) Design, synthesis, conformational analysis and biological studies of urotensin-II lactam analogues. Bioorg Med Chem 10:3731–3739

Grieco P, Carotenuto A, Campiglia P, Zampelli E, Patacchini R, Maggi CA, Novellino E, Rovero P (2002b) A new potent urotensin II receptor peptide agonist containing a pen residue at the disulfide bridge. J Med Chem 45:4391–4394

Herold CL, Behm DJ, Buckley PT, Foley JJ, Wixted WE, Sarau HM, Douglas SA (2003) The neuromedin B receptor antagonist, BIM-23127, is a potent antagonist at human and rat urotensin-II receptors. Br. J Pharmacol 139:203–207

Itoh H, McMaster D, Lederis K (1988) Functional receptors for fish neuropeptide urotensin II in major rat arteries. Eur J Pharmacol 149:61–66

Kenakin P (1997) Pharmacologic analysis of drug – receptor interaction, 3rd edn. Lippincott-Raven, Philadelphia, Pa.

Matsushita M, Shichiri M, Fukai N, Ozawa N, Yoshimoto T, Takasu N, Hirata Y (2003) Urotensin II is an autocrine/paracrine growth factor for the porcine renal epithelial cell line, LLCPK1. Endocrinology 144:1825–1831

Nothacker HP, Wang Z, McNeil AM, Saito Y, Merten S, O'Dowd B, Duckles SP, Civelli O (1999) Identification of the natural ligand of an G-protein-coupled receptor involved in the regulation of vasoconstriction. Nature Cell Biol 1:383–385

Patacchini R, Santicioli P, Giuliani S, Grieco P, Novellino E, Rovero P, Maggi CA (2003) Urantide: an ultrapotent urotensin II antagonist peptide in the rat aorta. Br J Pharmacol 140:1155–1158

Rossowski WJ, Cheng BL, Taylor JE, Datta R, Coy DH (2002) Human urotensin II-induced aorta ring contractions are mediated by protein kinase C, tyrosine kinases and Rho-kinase: inhibition by somatostatin receptor antagonists. Eur J Pharmacol 438:159–170

Sauzeau V, Le Mellionnec E, Bertoglio J, Scalbert E, Pacaud P, Loirand G (2001) Human urotensin II-induced contraction and arterial smooth muscle cell proliferation are mediated by RhoA and Rho-Kinase. Circ Res 88:1102–1104

Tamura K, Okazaki M, Tamura M, Isozumi K, Tasaki H, Nakashima Y (2003) Urotensin II-induced activation of extracellular signal-regulated kinase in cultured vascular smooth muscle cells: involvement of cell adhesion-mediated integrin signaling. Life Sci 72:1049–1060

Tzanidis A, Hannan RD, Thomas WG, Onan D, Autelitano DJ, See F, Kelly DJ, Gilbert RE, Krum H (2003) Direct actions of urotensin II on the heart. Implications for cardiac fibrosis and hypertrophy. Circ Res 93:246–253

Watanabe T, Pakala R, Katagiri T, Benedict CR (2001) Synergistic effect of urotensin II with serotonin on vascular smooth muscle cell proliferation. J Hypertens 19:2191–2196

A.1.1.30.3 Intracellular Calcium Mobilization Assay

PURPOSE AND RATIONALE

Human urotensin II induces concentration-dependent increases in intracellular calcium in HEK-293 cells expressing human GPR14 (Ames et al. 1999). Herold et al. (2003) used this assay to test a synthetic antagonist at human and rat urotensin II receptors.

PROCEDURE

Cell Culture

HEK293 cells stably expressing the hUT or rUT receptors are generated and propagated as described previously (Ames et al. 1999).

Intracellular Calcium ($Ca^{2+}{}_i$) Mobilization Assay

hUT-HEK293 cells or rUT-HEK293 cells are seeded in blackwalled, clear-bottomed 96-well Biocoat plates (Beckton-Dickinson, Bedford, Mass., USA, Herold et al. 2004) at a density of 45,000 cells/well, grown in the incubator at 37°C for 18–24 h, and prepared for $Ca^{2+}{}_i$ measurements (Ames et al. 1999). Plates are placed into the Fluorometric Imaging Plate Reader (Molecular Devices, Sunnyvale, Calif., USA) where cells, loaded with Fluo 3 (Molecular Probes, Eugene, Ore., USA), are exposed to excitation (488 nm) from a 6-W argon laser. Fluorescence is monitored at 566 nm emission for all 96 wells simultaneously, and data are read every 1 s for 1 min and then every 3 s thereafter. Agonist is added after 10 s and concentration–response curves are obtained by calculating the maximal fluorescence counts above background after the addition of each concentration of agonist. For antagonist studies, BIM-23127 (Bachem, King of Prussia, Pa., USA) is added 10 min prior to the addition of hU-II (California Peptide Research, Napa, Calif., USA).

EVALUATION

Concentration–response curves are analyzed by nonlinear regression using GraphPad Prism 3.0 software (GraphPad, San Diego, Calif., USA).

MODIFICATIONS OF THE METHOD

Flohr et al. (2002) performed structure–activity relationship studies on urotensin II by investigating peptide analogs and their ability to mobilize calcium in GPR14-transfected CHO cells.

Camarda et al. (2002) evaluated a new ligand for the urotensin II receptor ([Orn^8]U-II) in calcium functional assays performed on HEK293 cells expressing the recombinant rat and human UT receptor.

Croston et al. (2002) used a functional mammalian cell-based R-SAT assay (ACADIA Pharmaceuticals, San Diego, Calif., USA) to identify non-peptide agonists of the CRP14/urotensin II receptor in high-throughput screening. According to Shapiro et al. (2002) NIH-3T3 cells were grown in 96-well tissue culture plates to 70%–80% confluence in Dulbecco's modified Eagle's medium supplemented with 10% calf serum and 1% penicillin/streptomycin/Gln. Cells were transfected for 12–16 h with plasmid DNAs using Superfect Reagent (Qiagen, Valencia, Calif., USA) according to the manufacturer's protocols. R-SATs were performed with 0.5–50 ng/well receptor and 20 ng/well β-galactosidase plasmid DNA. After overnight transfection, medium was replaced with serum-free Dulbecco's modified Eagle's medium containing 2% cyto-sf3 (Kemp Biotechnologies, Frederick, Md., USA) and 1% penicillin/streptomycin/Gln and varying concentrations of drug. Cells were grown in a humidified atmosphere with 5% ambient CO_2 for 4–6 days. Medium was removed from the plates, and β-galactosidase activity was measured by the addition of *o*-nitrophenyl β-D-galactopyranoside (in phosphate-buffered saline with 5% Nonidet P-40 detergent). The resulting colorimetric reaction was measured using a spectrophotometric plate reader (Titertek, Huntsville, Ala., USA) at 420 nM. For HTS, NIH-3T3 cells transiently transfected with the urotensin II receptor expression vector and plasmid were frozen and for the assay thawed, plated and exposed to drug.

REFERENCES AND FURTHER READING

Ames RS, Sarau HM, Chambers JK, Willette RN, Aiyar NV, Romanic AM, Louden CS, Foley JJ, Sauermelch CF, Coatney RW, Ao Z, Dias J, Holmes SD, Stadel JM, Martin JD, Liu WS, Glover GI, Wilson S, McNulty DE, Ellis CE, Elshourbagy NA, Shabon U, Trill JJ, Hay DWP, Ohlstein EN, Bergsma DJ, Douglas SA (1999) Human urotensin-II is a potent vasoconstrictor and agonist for the orphan receptor GPR14. Nature 401:282–286

Camarda V, Guerrini R, Kostenis E, Rizzi A, Calo G, Hattenberger A, Zucchini M, Salvadori S, Reguli D (2002) A new ligand for the urotensin II receptor. Br J Pharmacol 137:311–314

Croston GE, Olsson R, Currier EA, Burstein ES, Weiner D, Nash N, Severance D, Allenmark SG, Thunberg L, Ma JN, Mohell N, O'Dowd B, Brann MR, Hacksell U (2002) Discovery of the first nonpeptide agonist of the CRP14/urotensin II receptor: 3-(4-chlorophenyl)-3-(2-(dimethylamino)ethyl)isochroman-1-one (AC-7954). J Med Chem 45:4950–4953

Flohr S, Kurz M, Kostenis E, Brkovic A, Fournier A, Klabunde T (2002) Identification of nonpeptide urotensin II receptor antagonists by virtual screening on a pharmacophore model derived from structure-activity relationships and nuclear magnetic resonance studies on urotensin II. J Med Chem 45:1799–1805

Herold CL, Behm DJ, Buckley PT, Foley JJ, Wixted WE, Sarau HM, Douglas SA (2003) The neuromedin B receptor antagonist, BIM-23127, is a potent antagonist at human and rat urotensin-II receptors. Br J Pharmacol 139:203–207

Shapiro DA, Kristiansen K, Weinert DM, Kroeze WK, Roth BL (2002) Evidence for a model of agonist-induced activation of 5-hydroxytryptamine 2A serotonin receptors that involves the interruption of a strong ionic interaction between helices 3 and 6. J Biol Chem 277:11441–11449

A.1.1.30.4 Receptor Binding of Urotensin II

PURPOSE AND RATIONALE

The G-protein-coupled receptor GPR14/SENR was described by Marchese et al. (1995) and Tal et al. (1995). Liu et al. (1999) and Mori et al. (1999) identified urotensin II as the endogenous ligand for the orphan G-protein-coupled receptor GPR14. It was renamed as urotensin II (UT) receptor by UPHAR (Douglas and Ohlstein 2000). Human, rat, mouse and monkey receptors have been cloned. The amino acid sequence identity of the monkey UT receptor is 97% and 77% identical to the human and rat sequences respectively, while the mouse UT receptor is 76% and 93% identical to the human and rat sequences, respectively.

Brkovic et al. (2003) performed functional and binding characterizations of urotensin-II-related peptides in human and rat urotensin II receptor assays.

PROCEDURE

Reagents and Solvents

The following fluorenylmethyloxycarbonyl-protected amino acids were purchased from Chem-Impex International (Wood Dale, Ill., USA): Ala, Cys(Trt), His(Trt), Phe, Trp, Lys-(Boc), Tyr(tBu), Asp(OtBu), Glu(OtBu), Pro, Gln(Trt), Thr(tBu), Arg(Pbf), Orn(Boc), HomoCys(Trt), Cys(Acm), and D-Trp. Biograde TFA was obtained from Halocarbon (River Edge, N.J., USA). Diisopropylethylamine was from Aldrich (Milwaukee, Wis., USA). Wang resin and benzotriazol-1-yl-oxy-tris(dimethylamino)-phosphonium hexafluorophosphate were purchased from Albatross (Montreal, QC).

Basal ISCOVE medium and fetal calf serum (FCS) were from Biochrom (Berlin, Germany). The GC-melt PCR kit as well as the human and rat genomic DNA were purchased from CLONTECH (Palo Alto, Calif., USA). The pEAK8 mammalian episomal expression vector and the selection marker puromycin were from Edge Biosystems (Gaithersburg, Md., USA). Dulbecco's modified Eagle's medium (DMEM), L-glutamine, HEPES, LipofectAMINE reagent, and penicillin-streptomycin were from Invitrogen (Carlsbad, Calif., USA). The pCDNA3.1(+) mammalian expression vector was from Invitrogen. The calcium-sensitive fluorescence dye Fluo-4 and Pluronic F-127 were obtained from Molecular Probes (Eugene, Ore., USA). Flashplates PLUS and monoiodinated human [^{125}I-Tyr9]urotensin II for radioligand binding assays were from Perkin Elmer Life Sciences (Boston, Mass., USA). Gentamicin, the transfection reagent FuGene 6, and Complete protease inhibitor were purchased from Roche (Basel, Switzerland). Bacitracin, EDTA-disodium salt, probenecid, $MgCl_2$, NaCl, and sucrose were obtained from Sigma-Aldrich (St. Louis, Mo., USA).

Cloning of Human and Rat Urotensin II Receptor

As the putative human urotensin II receptor sequence is intronless, this protein was cloned from human genomic DNA via PCR. PCR conditions, established to amplify the human GPR14 sequence, were 94°C; 10 min followed by 35 cycles of 94°C, 1 min, 60°C, 1 min, 72°C, and 2 min using the GC-melt kit. Primers designed to amplify the coding sequence contained a *Bam*HI site in the forward and a *Xba*I site in the reverse primer, respectively. The urotensin receptor coding region, flanked by *Bam*HI/*Xba*I sites, was cloned into the pCDNA3.1(+) mammalian expression vector and sequenced in both directions. For generation of stable cell lines, the human U-II receptor coding sequence flanked by a 5′*Eco*RI site and a 3′*Eco*RV site was cloned into the mammalian episomal expression vector pEAK8.

The rat U-II receptor coding sequence flanked by a 5′ *Eco*RI and 3′ *Not*I site was amplified via PCR from rat kidney cDNA and cloned into the mammalian pEAK8 expression vector. Sequences of all urotensin-II-receptor-expressing plasmids were verified by dideoxy sequencing in both directions.

Cell Culture and Transfection

CHO K1-cells were grown in basal ISCOVE medium supplemented with 10% FCS, 2 mM L-glutamine, penicillin-streptomycin (10,000 IU/ml – 10,000 µg/ml), and 25 mg/ml gentamicin at 37°C in a humidified 5% CO_2 incubator. Cells were transiently transfected with the U-II receptor cDNAs using the LipofectAMINE reagent according to the manufacturer's protocol. After 18–24 h following the

transfection, cells were split into blackwalled 96-well plates at a density of 50,000 cells/well and cultured for an additional 18- to 24-h period before being used in the functional fluorescence imaging plate reader (FLIPR) assay (described below in detail) measuring intracellular Ca^{2+} release upon receptor activation.

FLIPR ASSAY

Cells were loaded in 96-well plates for 1 h (37°C, 5% CO_2) with 100 µl of PBS (without Ca^{2+}, Mg^{2+} and $NaHCO_3$) containing 4 µM of the fluorescent calcium indicator Fluo-4, 0.22% Pluronic F-127 in dimethyl sulfoxide, 2.5 mM probenecid, 1 mM EGTA, and 1% FCS. Cells were then washed three times with PBS (without Ca^{2+}, Mg^{2+} and $NaHCO_3$) containing 1 mM EDTA, 0.5 mM $MgCl_2$, and 2.5 mM probenecid. After the final wash, a 100-µl residual volume remained on the cells. Peptides were aliquoted as 2× solutions in 96-well plates and transferred by the instrument from the ligand plate to the cell plate. Fluorescence was recorded with the fluorometric imaging plate reader FLIPR (Molecular Devices, Sunnyvale, Calif., USA) over a period of 3 min. Fluorescence was recorded simultaneously in all wells at 3-s intervals during the first minute and at 10-s intervals during the last 2 min. Fluorescence data were generated in duplicate and repeated at least three times.

Generation of Stable Human and Rat U-II Receptor Expressing Cell Lines

For the generation of stable cell lines expressing the human and rat urotensin II receptor, HEK293 cells were transfected with human- and rat-pEAK8 constructs using the FuGene 6 transfection reagent according to the supplier's protocol. Two days after transfection, cells were selected in DMEM, supplemented with 10% FCS, 20 mM HEPES, penicillin-streptomycin (10,000 IU/ml – 10,000 µg/ml), and 1 µg/ml puromycin for a period of 4 weeks (37°C, 5% CO_2, 95% relative humidity). Functional activity of the urotensin-II-receptor-expressing cell population was verified with a FLIPR assay recording urotensin-II-mediated intracellular Ca^{2+} release, as described above.

Membrane Preparation and Radioligand Binding Assays

HEK293 cells stably expressing human or rat urotensin II receptors were cultured up to 80% confluency in DMEM, supplemented with 10% FCS, 20 mM HEPES, penicillin-streptomycin (10,000 IU/ml – 10,000 µg/ml), and 1 µg/ml puromycin (37°C, 5% CO_2, 95% relative humidity). Cells were washed once with ice-cold PBS and a second time with PBS containing the protease inhibitor cocktail (Complete). Cells were scraped off and centrifuged gently. The pellet was resuspended in a buffer containing 5 mM HEPES, 1 mM EDTA-disodium salt, and the cocktail of protease inhibitor Complete and then incubated on ice for 15 min. Cells were pelleted again and resuspended with a homogenizer (Unit F8B, Constant cell disruption systems; Honiley, Warwickshire, UK). The supernatant and resuspended pellet were combined and centrifuged at 50,000 *g* (Beckman Avanti J251). The cell membrane pellet was resuspended in a buffer consisting of 20 mM HEPES, 1 mM EDTA-disodium salt, 150 mM NaCl, and 10% sucrose. Membrane aliquots were stored at –80°C. One day before the binding assay, membranes were thawed, pelleted, and resuspended in the assay buffer consisting of 20 mM HEPES, 150 mM NaCl, 1 mM EDTA-disodium salt, 160 µg/ml bacitracin, and Complete protease inhibitor (two tablets per 100 ml).

Membranes were distributed into 96-well wheat-germ-agglutinin Flashplates PLUS, incubated overnight for adsorption, and then the Flashplates PLUS were washed twice with the assay buffer. For equilibrium binding assays, 0.2 nM human [^{125}I-Tyr9]urotensin II (initial specific activity 2200 Ci/mmol, or 81,400 GBq/mmol) was incubated with the indicated amounts of unlabeled competitors for 4 h and radioactivity counted in a 1450 Microbeta Wallac Jet (Wallac, Turku, Finland).

EVALUATION

Data of the FLIPR assay were analyzed by non-linear curve fitting using GraphPad Prism version 3.0 (GraphPad Software, San Diego, Calif., USA).

Non-specific binding was determined in the radioligand binding assays in the presence of 10 µM human U-II and corresponded to 31 ± 2% ($n = 5$, mean ± SEM) of the total binding for membranes expressing the human urotensin II receptor and to 8 ± 1% ($n = 5$, mean ± SEM) of the total binding for membranes expressing the rat urotensin II receptor. Data analysis was performed with GraphPad Prism 3.0.

MODIFICATIONS OF THE METHOD

Flohr et al. (2002) identified non-peptide urotensin II receptor antagonists by virtual screening on a phamacophore model derived from structure–activity relationships and nuclear magnetic resonance studies on urotensin II.

REFERENCES AND FURTHER READING

Brkovic A, Hattenberger A, Kostenis E, Klabunde T, Flohr S, Kurz M, Bourgault S, Fournier A (2003) Functional and binding characterizations of urotensin II-related peptides in human and rat urotensin II- receptor assay. J Pharmacol Exp Ther 306:1200–1209

Douglas SA, Ohlstein EH (2000) Urotensin receptors. In: Girdlestone D (ed) The IUPHAR compendium of receptor characterization and classification. IUPHAR Media, London, pp 365–372

Flohr S, Kurz M, Kostenis E, Brkovic A, Fournier A, Klabunde T (2002) Identification of nonpeptide urotensin II receptor antagonists by virtual screening on a phamacophore model derived from structure-activity relationships and nuclear magnetic resonance studies on urotensin II. J Med Chem 45:1799–1805

Liu Q, Pong SS, Zeng Z, Zhang Q, Howard AD, Williams DL, Jr, Davidoff M, Wang R, Austin CP, McDonald TP, Bai C, George SR, Evans JF, Caskey CT (1999) Identification of urotensin II as the endogenous ligand for the orphan G-protein-coupled receptor GPR14. Biochem Biophys Res Commun 266:174–178

Maguire JJ, Kuc RE, Davenport AP (2000) Orphan-receptor ligand human urotensin II: receptor localization in human tissues and comparison of vasoconstrictor responses with endothelin-1. Br J Pharmacol 131:441–446

Marchese A, Heiber M, Nguyen T, Heng HH, Saldivia VR, Cheng R, Murphy PM, Tsui LC, Shi X, Gregor P (1995) Cloning and chromosomal mapping of three novel genes, GPR9, GPR10 and GPR14, encoding receptors related to interleukin 8, neuropeptide Y, and somatostatin receptors. Genomics 29:335–344

Mori M, Sugo T, Abe M, Shimomura Y, Kurihara M, Kitada C, Kikuchi K, Shintani Y, Kurokawa T, Onda H, Nishimura O, Fujino M (1999) Urotensin II is the endogenous ligand of a G-protein-coupled orphan receptor, SENR (GPR14). Biochem Biophys Res Commun 265:123–129

Nothacker HP, Wang Z, McNeil AM, Saito Y, Merten S, O'Dowd B, Duckles SP, Civelli O (1999) Identification of the natural ligand of an G-protein-coupled receptor involved in the regulation of vasoconstriction. Nature Cell Biol 1:383–385

Tal M, Ammar DA, Karpuj M, Krizhanovsky V, Naim M, Thompson DA (1995) A novel putative neuropeptide receptor expressed in neural tissue, including sensory epithelia. Biochem Biophys Res Commun 209:752–759

A.1.1.30.5 Urotensin II Gene Expression

PURPOSE AND RATIONALE

The UT receptor is expressed in vascular tissue (Ames et al. 1999; Maguire et al. 2000). A direct link between U-II, the UT receptor and vasoconstriction has to be assumed (Ames et al. 1999; Douglas and Ohlstein 2001). Behm et al. (2003) used homologous recombination in embryonic stem (ES) cells to generate mice lacking the UT receptor coding region to determine the effect(s) of this receptor on vascular reactivity both *in vivo* and *in vitro* and to verify that U-II exerts its effects on vascular smooth muscle tone via an interaction with UT.

PROCEDURE

Targeting the UT Gene and Generation of Mutant Mice

Gene targeting was performed in murine E14.1 ES cells, replacing the single coding exon of the UT receptor locus with a positive selection cassette containing the neomycin phosphotransferase gene (Neo) driven by the phosphoglycerate kinase I (PGK) promoter. 5′- and 3′-homology arms, both of ∼4.0 kb, were cloned from a 129SVJ mouse genomic bacterial artificial chromosome (BAC) library and placed on either side of the positive selection cassette. Homologous recombination in neomycin-resistant ES cells was confirmed by Southern blot of *Bam*HI-digested genomic DNA using an ∼800-bp *Bam*HI/ *Sma*I restriction fragment as the 5′ external probe (which detects 6.5- and 6.0-kb bands at the wild-type and targeted locus, respectively). Approximately 1 in 80 G418-resistant clones had undergone homologous recombination. Homologous recombination at the 3′ end was confirmed in these ES cell clones by Southern blot of *Hind*III-digested genomic DNA using a ∼700-bp *Xmn*I/*Hind*III restriction fragment as the 3′-external probe (which detects 5.5- and 5.0-kb bands at the wild-type and targeted locus, respectively). Three targeted clones were injected into C57B16/J-derived blastocysts. Male chimeras were crossed with C57B16/J females to give N1F0 offspring, which were subsequently intercrossed to generate N1F1 offspring. In addition, N1F0 offspring were successively backcrossed to C57B16/J females to generate N5F0 mice. These were intercrossed to create an N5F1 population.

Genotyping of Study Populations

N1F1 and N5F1 study populations were genotyped by polymerase chain reaction (PCR) and Southern blot of genomic DNA isolated from the hearts of animals used in the studies. Hearts of wild-type ($UT^{(+/+)}$) and UT receptor knockout ($UT^{(-/-)}$) mice were cut into small pieces (∼1 mm) and placed into polypropylene tubes. Extraction buffer [2 ml; 10 mM Tris-HCl pH 8.0, 50 mM NaCl, 100 mM ethylenediaminetetraacetic acid (EDTA), 0.5% SDS, 20 µg ml^{-1} RNase, 100 µg ml^{-1} proteinase K] was added and samples were incubated at 50°C–55°C for 4 h until completely lysed. The mixture was then extracted two times each with phenol, phenol/chloroform and chloroform (Maniatis et al. 1989). Genomic DNA was precipitated by adding 2.5 vols of cold ethanol, washed with 70% v/v ethanol (–20°C) and dissolved in 200 µl of 10 mM Tris-HCl, 1 mM EDTA TE, pH 8.0. Once dissolved, the purity and concentration of the DNA

were measured by spectrophotometry (absorbency at 260 and 280 nm wavelength).

PCR amplification was performed using 50-µl aliquots (50 mM KCl, 10 mM Tris-HCl, pH 8.3, 17 mM $MgCl_2$, 200 nM 2′-deoxynucleotide 5′-triphosphates (dNTPs), 10% v/v dimethylsulfoxide, 1.25U *Taq* DNA polymerase; (Perkin-Elmer, Norwalk, Conn., USA) using 200 ng of genomic DNA as the template and PCR primers specific to the neomycin resistance gene present at the targeted locus (5′-TGA ACA AGA TGG ATT GCA CGC AGG TTC TCC GGC-3′ and 5′-GCC AAG CTC TTC AGC AAT ATC ACG GGT AGC-3′, yielding an ∼700-bp product)) and mouse UT gene-specific primers (5′-CTG GCT GAC CTG CTG TAT CTG CT-3′ and 5′-CAG GGT CAC ACA AAG CAC TCT CA-3′, yielding an ∼900-bp product). A 500-bp mouse glyceraldehyde-3-phosphate dehydrogenase (GAPDH) amplicon was used as the internal control (5′-TGG CCA AGG TCA TCC ATG AC-3′ and 5′-GTC CAC CAC CCT GTT GCT GTA G-3′, yielding an ∼500-bp product). Amplification was performed for 30 cycles at 60°C annealing for 30 s, 72°C extension for 90 s and 94°C denaturing for 30 s. Amplification of a 500-bp (GAPDH)/700-bp doublet alone corresponded to a $UT^{(-/-)}$ genotype and a 500-bp (GAPDH)/900-bp doublet alone corresponded to a $UT^{(+/+)}$ genotype.

Genomic DNA (20 µg) was digested with *Bam*HI and run on an agarose gel (1%). The agarose gel was then treated with denaturing solution (0.5 M NaOH, 1.5 M NaCl) for 45 min, followed by neutralization with 0.5 M Tris-HCl (pH 7.5), 1.5 M NaCl for 30–40 min. The DNA was transferred to a nylon membrane (GeneScreen Plus, NEN Life Science Products, Mass., USA) and probed with cDNA corresponding to the full-length mouse UT receptor open reading frame (ORF). cDNA fragments were labeled with [α-^{32}P] 2′-deoxycytidine 5′-triphosphate (dCTP) using standard random primed methods (T7 QuickPrime; Pharmacia Biotech, Piscataway, N.J., USA). Membranes were prehybridized for 2 h at 42°C and incubated overnight at 42°C with 1×10^9 cpm μg^{-1} denatured radiolabeled probe in standard buffer [50% deionized formamide, 6 × sodium chloride, sodium citrate (SSC), 5 × Denhardt's reagent, 0.5% sodium dodecyl sulfate (SDS), 100 µg ml^{-1} denatured, fragmented salmon sperm DNA]. Membranes were washed under conditions of low stringency (three 15-min washes in 1 × SSC, 0.1% SDS at 28°C) followed by a high stringency wash in 0.1 × SSC/0.1% SDS for 30 min at 55°C. Hybridization signals were detected by conventional X-ray autoradiography (Hyper film, Amersham Life Science, UK) and phosphor imaging (Storm 860, Molecular Dynamics, Sunnyvale, Calif., USA).

Hemodynamics and Echocardiography

Male wild-type ($UT^{(+/+)}$) and homozygous UT receptor knockout ($UT^{(-/-)}$) mice, anesthetized with 1.5% isoflurane, underwent transthoracic echocardiographic determination of left ventricular end-diastolic volume (EDV), end-systolic volume (ESV), stroke volume (SV), cardiac output (CO) and ejection fraction (EF). Further to this, mice were re-anesthetized the following day for hemodynamic evaluation where a fluid-filled catheter was inserted into the left carotid artery for the measurement of mean arterial blood pressure (MAP) and heart rate (HR). The catheter was then advanced into the left ventricle (LV) to obtain measurements of left ventricular end-systolic (LVESP) and end-diastolic pressure (LVEDP). At the end of the study, selected organs (right and left kidney, heart, right and left ventricle and lungs) were isolated and wet weights were measured.

Preparation and Utilization of Mouse Isolated Aortae and Mesenteric Arteries

Male (4 months; 27 g) wild-type ($UT^{(+/+)}$) and UT receptor knockout ($UT^{(-/-)}$) mice were anesthetized with inhaled isoflurane (5% in O_2) and killed by cervical dislocation. Proximal descending thoracic aortae were isolated and cleaned of adherent tissue. Vessels approximately 3 mm in length were suspended in 10-ml organ baths containing Krebs solution of the following composition (mM): NaCl 112.0, KCl 4.7, KH_2PO_4 1.2, $MgSO_4$ 1.2, $CaCl_2$ 2.5, $NaHCO_3$ 25.0, dextrose 11.0. Krebs solution was maintained at 37 ± 1°C and aerated with 95% O_2, 5% CO_2 (pH 7.4). For contraction studies, vessels were denuded of endothelium by rubbing with a fine forceps and indomethacin (10 mM) was added to the buffer. Changes in isometric force were measured under 0.5 *g* optimal resting tension using FT03 force-displacement transducers (Grass Instruments, Quincy, Mass., USA) coupled to Model 7D polygraphs.

The Halpern–Mulvany wire myograph (Model 610M; Danish Myo Technology, Denmark) was used for measurement of isometric force development of endothelium-intact superior mesenteric arteries (optimal resting tension of 0.5 *g*) and data were recorded using a Grass 7400 direct thermal recorder.

Following a 60-min equilibration period, vessels were treated with standard concentrations of KCl (60 mM) and phenylephrine (1 mM) to which subsequent agonist-induced responses were normalized.

Once the contractile response to phenylephrine had plateaued, carbachol (10 μM) was added to the vessels in order to evaluate endothelial integrity.

Cumulative concentration–response curves to phenylephrine (0.1 nM to 10 μM), angiotensin II (0.1 nM to 10 μM), endothelin-1 (0.1 nM to 1 mM) and hU-II (0.01 nM to 3 μM) were obtained for each vessel by adding the spasmogen to the tissue bath in half-log increments. During relaxation studies, vessels were preconstricted with an EC_{80} concentration of phenylephrine and contractile tone was reversed by adding cumulative amounts of carbachol (1 nM to 30 μM) or sodium nitroprusside (0.1 nM to 1 μM). Each response was allowed to plateau before the addition of subsequent agonist concentrations. Vessels were allowed to recover for at least 30 min between subsequent agonist–response curves, and were not exposed to subsequent agonists after treatment with either endothelin-1 or hU-II.

EVALUATION

All values are expressed as mean ± SEM and *n* represents the total number of animals from which the vessels were isolated. Statistical comparisons were made using an unpaired, two-tailed *t*-test or Fisher's exact tests and differences were considered significant when $P < 0.05$. Concentration–response curves were fitted to a logistic equation as previously described (Douglas et al. 1995).

MODIFICATIONS OF THE METHOD

Coulouarn et al. (1998) reported cloning of the cDNA encoding the urotensin II precursor (Prepro-UII cDNA) in frog and human. Intense expression of the urotensin gene in motoneurons of the spinal cord was found indicating important physiological functions of urotensin II.

Elshourbagy et al. (2002) reported molecular and pharmacological characterization of genes encoding urotensin II peptides and their cognate G-protein-coupled receptors from the mouse and monkey. Monkey and mouse preproU-II genes were identified to encode 123 and 125 amino acids. Monkey and mouse UT receptors were 389, and 386 amino acids, respectively. Expression of mouse and monkey U-II/UT receptor mRNA was found also in extravascular tissues, including lung, pancreas, skeletal muscle, kidney and liver.

REFERENCES AND FURTHER READING

Ames RS, Sarau HM, Chambers JK, Willette RN, Aiyar NV, Romanic AM, Louden CS, Foley JJ, Sauermelch CF, Coatney RW, Ao Z, Dias J, Holmes SD, Stadel JM, Martin JD, Liu WS, Glover GI, Wilson S, McNulty DE, Ellis CE, Elshourbagy NA, Shabon U, Trill JJ, Hay DWP, Ohlstein EN, Bergsma DJ, Douglas SA (1999) Human urotensin-II is a potent vasoconstrictor and agonist for the orphan receptor GPR14. Nature 401:282–286

Behm DJ, Harrison SM, Ao Z, Maniscalco K, Pickering SJ, Grau EV, Woods TN, Coatney RM, Doe CPA, Willette RN, Johns DG, Douglas SA (2003) Deletion of the UT receptor gene results in the selective loss of urotensin-II contractile activity in aortae isolated from UT receptor knockout mice. Br J Pharmacol 139:464–472

Coulouarn Y, Lihrmann I, Jegou S, Anouar Y, Tostivint H, Beauvillain JC, Conlon JM, Bern HA, Vaudry H (1998) Cloning of the cDNA encoding the urotensin II precursor in frog and human reveals intense expression of the urotensin gene in motoneurons of the spinal cord. Proc Natl Acad Sci USA 95:15803–15808

Douglas SA, Beck GR, Elliott JD, Ohlstein EH (1995) Pharmacological evidence for the presence of three distinct functional endothelin receptor subtypes in the rabbit lateral saphenous vein. Br J Pharmacol 114:1529–1540

Douglas SA, Ohlstein EH (2000) Urotensin receptors. In: Girdlestone D (ed) The IUPHAR compendium of receptor characterization and classification. IUPHAR Media, London, pp 365–372

Elshourbagy NA, Douglas SA, Shabon U, Harrison S, Duddy G, Sechler JL, AO, Z, Maleeff BE, Naselsky D, Disa J, Aiyar NV (2002) Molecular and pharmacological characterization of genes encoding urotensin-II peptides and their cognate G-protein-coupled receptors from the mouse and monkey. Br J Pharmacol 136:9–22

Maguire JJ, Kuc RE, Davenport AP (2000) Orphan-receptor ligand human urotensin II: receptor localization and comparison of vasoconstrictor responses with endothelin-1. Br J Pharmacol 131:441–446

Maniatis T, Fritsch EF, Sambrook J (1989) Molecular cloning. A laboratory manual. Cold Spring Harbor, New York

A.1.1.31 Apelin

A.1.1.31.1 General Considerations

PURPOSE AND RATIONALE

The peptide apelin, consisting of 36 amino acids, is found increasingly to play a role in biology and medicine (Kleinz and Davenport 2005; Masri et al. 2005). The family of apelin peptides is derived from a single gene and activates the 7-transmembrane G-protein-coupled receptor APJ. In the search for an endogenous ligand of the orphan G-protein-coupled receptor APJ, Tatemoto et al. (1998) isolated and characterized endogenous peptide ligands, designated apelin, from bovine stomach extracts. Apelin-13, consisting of 13 amino acids, was more active than apelin-36. APJ was first identified in a human gene by O'Dowd et al. (1993), sharing close identity to the angiotensin receptor. In rats, the greatest expression of APJ mRNA was detected in the lung, suggesting that APJ and its ligand play an important role in the pulmonary system

(Hosoya et al. 2000). Cloning, pharmacological characterization and brain distribution of the rat apelin receptor were reported by De Mota et al. (2000), and the physiological role of apelin and its receptor in rat brain by Reaux et al. (2001). The hypothalamic and hypophyseal distribution of the receptor suggested an involvement of apelin in the control of neuro- and adenohypophyseal hormone release, whereas the presence in the pineal gland and in discrete higher brain structures pointed to possible roles in the regulation of circadian rhythms and of water and food intake behavior. Studying the distribution of apelin-synthesizing neurons in the adult rat brain, Reaux et al. (2002) suggested multiple roles of apelin especially in the central control of ingestive behaviors, pituitary hormone release and circadian rhythms. Studying apelin immunoreactivity in the rat hypothalamus and pituitary, Brailoiu et al. (2002) concluded that apelin may be a signaling peptide released from the hypothalamic-hypophyseal axis. De Mota et al. (2004) found that apelin is a potent diuretic neuropeptide counteracting vasopressin actions through inhibition of vasopressin neuron activity and vasopressin release. Masri et al. (2002) reported that apelin activates extracellular signal-regulated kinases via a system sensitive to pertussis toxin (PTX). Pharmacological and immunohistochemical characterization of the APJ receptor and its endogenous ligand apelin were reviewed by Medhurst et al. (2003). Jászberény et al. (2004) studied the behavioral, neuroendocrine, and thermoregulatory actions of apelin-13. Wang et al. (2004) investigated the localization of apelin in the gastrointestinal tract, ontogeny, and stimulation of gastric cell proliferation and of cholecystokinin secretion. Boucher et al. (2005) found in isolated mouse and human adipocytes that apelin is upregulated by insulin and obesity.

REFERENCES AND FURTHER READING

Boucher J, Masri B, Daviaud D, Gesta S, Guigné C, Mazzucotelli A, Castan-Laurell I, Tack I, Knibiehler B, Carpéné C, Audigier Y, Saulnier-Blache JS, Valet P (2005) Apelin, a newly identified adipokine up-regulated by insulin and obesity. Endocrinology 146:1764–1771

Brailoiu GC, Dun SL, Yang J, Ohsawa M, Chang JK, Dun NJ (2002) Apelin-immunoreactivity in the rat hypothalamus and pituitary. Neurosci Lett 327:193–197

De Mota N, Lenkei Z, Llorens-Cortès C (2000) Cloning, pharmacological characterization and brain distribution of the rat apelin receptor. Neuroendocrinology 72:400–407

De Mota N, Reaux-le Goazigo A, el Messari S, Chartrel N, Roesch D, Gujardin C, Kordon C, Vaudry H, Moos F, Llorens-Cortès C (2004) Apelin, a potent diuretic neuropeptide counteracting vasopressin actions through inhibition of vasopressin neuron activity and vasopressin release. Proc Natl Acad Sci USA 101:10464–10469

Hosoya M, Kawamata Y, Fukusumi S, Fujii R, Habata Y, Hinuma S, Kitada C, Honda S, Kurukawa T, Onda H, Nishimura O, Fujino M (2000) Molecular and functional characterization of APJ. J Biol Chem 275:21061–21067

Jaszberenyi M, Bujdoso E, Telegdy G (2004) Behavioral, neuroendocrine and thermoregulatory actions of apelin-13. Neuroscience 129:811–816

Kleinz MJ, Davenport AP (2005) Emerging roles of apelin in biology and medicine. Pharmacol Ther 107:198–211

Masri B, Knibiehler B, Audigier Y (2005) Apelin signalling: a promising pathway from cloning to pharmacology. Cell Signal 17:415–426

Masri B, Lahlou H, Mazarguil H, Knibiehler B, Audigier Y (2002) Apelin (65–77) activates extracellular signal-regulated kinases via a PTX-sensitive system. Biochem Biophys Res Commun 290:539–545

Medhurst AD, Jennings CA, Murdock P, Darker JG (2003) Pharmacological and immunohistochemical characterization of the APJ receptor and its endogenous ligand apelin. J Neurochem 84:1162–1172

O'Dowd BF, Heiber M, Chan A, Heng HHQ, Tsui LC, Kennedy JL, Shi X, Petronis A, George SR, Nguyen T (1993) A human gene that shows identity with the gene encoding the angiotensin receptor in located on chromosome 11. Gene 136:355–360

Reaux A, de Mota N, Skultetyova I, Lenkei Z, el Messari S, Gallatz K, Corvol P, Palkovits M, Llorens-Cortès (2001) Physiological role of a novel neuropeptide, apelin, and its receptor in the rat brain. J Neurochem 77:1085–1096

Reaux A, Gallatz K, Palkovits M, Llorens-Cortès C (2002) Distribution of apelin-synthesizing neurons in the adult rat brain. Neuroscience 113:653–662

Tatemoto K, Hosoya M, Habata Y, Fujii R, Kakegawa T, Zou MX, Kawamata Y, Fukusumi S, Hinuma S, Kitada T, Kurukawa T, Onda H, Fujino M (1998) Isolation and characterization of a novel endogenous peptide ligand for the human APJ receptor. Biochem Biophys Res Commun 251:471–476

Wang G, Anini Y, Wei W, Qi X, O'Carroll AM, Mochizuki T, Wang HQ, Hellmich MR, Englander EW, Greeley GH Jr (2004) Apelin, a new enteric peptide: localization in the gastrointestinal tract, ontogeny, and stimulation of gastric cell proliferation and of cholecystokinin secretion. Endocrinology 145:1342–1348

A.1.1.31.2 Cardiovascular Actions of Apelin

PURPOSE AND RATIONALE

Most reports concentrate on the functional role of apelin in the cardiovascular system (Tatemoto et al. 2001; Katugampola et al. 2002; Sokodi et al. 2002; Katugampola and Davenport 2003; Chen et al. 2003; Berry et al. 2004; Kleinz and Davenport 2004; Kagiyama et al. 2005; Losano 2005).

Cheng et al. (2003) studied the venous dilator effect of apelin in conscious rats using a method for measurement of body venous tone published by Pang (2000).

Ashley et al. (2005) found that apelin improves cardiac contractility and reduces cardiac loading *in vivo* in mice.

PROCEDURE

Male C57Bl/ 6 mice were used. The following studies were performed: magnetic resonance imaging of the heart, pressure–volume hemodynamics, effects of chronic apelin infusion, assessment of ventricular hypertrophy after sacrifice, and expression of the APJ receptor.

Pressure–volume hemodynamics were assessed using the Aria system (Millar Instruments, Houston, Tex., USA), This measurement platform, specifically designed for small rodents, comprises an ultra-miniature 1.4 F (0.47 mm outer diameter) catheter, which incorporates pressure and conductance sensors, possessing hardware including analog-digital conversion and analysis software. Pressure is measured directly in mmHg, while the conductivity of blood is used to estimate volume and allow construction of pressure–volume relationships in real time.

Male mice aged 8–16 weeks were anesthetized with 1%–2% isoflurane in oxygen. The internal jugular vein was cannulated with PE tubing and a 10% albumin solution infused at 5 µl/min following a bolus of 150 µl over 5 min. After tracheostomy, a 19-gauge cannula was inserted into the trachea and the animal was ventilated at a tidal volume of 200 µl at 100 breaths per minute. Following an incision just dorsal to the xyphoid cartilage, the diaphragm was visualized from below, and after diaphragmatic incision, the left ventricular apex was visualized. The pressure–volume catheter was inserted along the long axis of the left ventricle, from where it was adjusted to obtain rectangular-shaped pressure–volume loops. Baseline loops were recorded following volume replacement, at which point the inferior vena cava was visualized within the chest and occlusion parameters were recorded during and after a 5-s manual occlusion of the vessel. Next, the albumin solution was replaced by one containing 100 nM apelin, which was infused at 5 µl/min for 20 min, following which baseline and occlusion loops were recorded once again.

Signals from the catheter were digitized using the Powerlab system and stored for offline analysis using the PVAN software. This allows analyses of pressure (e. g., end-systolic pressure, end-diastolic pressure) and derivation of pressure–time and volume–time parameters at steady state.

For **magnetic resonance imaging**, male C57Bl/6 mice aged 16 weeks were scanned twice on subsequent days. The animals underwent general anesthesia while breathing spontaneously via a nose cone fitted carefully to minimize escape of anesthetic into the environment. Two percent isoflurane was administered with an oxygen flow rate of 1–2 l/min. Platinum needle ECG leads were inserted subcutaneously. Respiration was monitored by means of a pneumatic pillow sensor positioned against the abdomen. Mouse body temperature was maintained during scanning at 37°C by a flow of heated air thermostatically controlled by a rectal temperature probe. Magnetic resonance images were acquired on a 4.7 T Oxford magnet controlled by a Varian Inova console (Varian, Palo Alto, Calif., USA) using a transmit–receive, quadrature, volume coil with an inner diameter of 3.5 cm. Image acquisition was gated to respiration and to the ECG R wave (SA Instruments, Stony Brook, N.Y., USA). Coronal and sagittal scout images led to the acquisition of multiple contiguous 1-mm-thick, short axis slices orthogonal to the interventricular septum. Nine cine frames were taken at each slice level with the following sequence parameters: TE = 2.8 ms, NEX = 12, FOV = 3 × 3 cm, matrix = 128 × 128, flip angle = 60°. Cine frames were spaced 16 ms apart and acquired through slightly more than one cardiac cycle guaranteeing acquisition of systole and diastole. On the second day of scanning, mice received 300 µg/kg body weight of apelin as an intraperitoneal injection 1 h prior to scanning. A pilot study had previously identified 1 h as an appropriate time within which to identify apelin effects resulting from peritoneal absorption. Planimetry measurements of end-diastolic and end-systolic dimensions were derived offline from short axis views of the left ventricle at the level of the papillary muscles using ImageJ software (National Institutes of Health, Bethesda, Md., USA). Ejection fraction was calculated as [LVEDA-LVESA]/LVEDA, where LVEDA is left ventricular end-diastolic area and LVESA is left ventricular end-systolic area.

EVALUATION

Data were analyzed using Student's *t* statistic (paired) or repeated measures analysis of variance using the post hoc comparison of Fisher.

MODIFICATIONS OF THE METHOD

Katugampola et al. (2001, 2002) described [^{125}I](Pyr^{1})apelin as a radioligand for localizing the APJ orphan receptor in human and rat tissues.

Kasai et al. (2004) found that apelin worked as an angiogenic factor in the retinal endothelial cell line RF/6A.

REFERENCES AND FURTHER READING

Ashley EA, Powers J, Chen M, Kundo R, Finsterbach T, Caffarelli A, Deng A, Eichorn J, Mahajan R, Agrawal R,

Greve J, Robbins R, Patterson AJ, Bernstein D, Quertermous T (2005) The endogenous peptide apelin potently improves cardiac contractility and reduces cardiac loading in vivo. Cardiovasc Res 65:73–82

Berry MF, Pirolli TJ, Jayasankar V, Burdick J, Morine KJ, Gardner TJ, Woo YJ (2004) Apelin has in vivo inotropic effects in normal and failing hearts. Circulation 110[suppl II]:II187–II193

Chen MM, Ashley EA, Deng DXF, Tsalenko A, Deng A, Tabibiazar R, Ben-Dor A, Fenster B, Yang E, King JY, Fowler M, Robbins R, Johnson FL, Bruhn L, McDonagh T, Dargie H, Yakhini Z, Tsao PS, Quertermous T (2003) Novel role for the potent endogenous inotrope apelin in human cardiac dysfunction. Circulation 108:1432–1439

Cheng X, Cheng XS, Pang CCY (2003) Venous dilator effect of apelin, an endogenous peptide ligand for the orphan APJ receptor, in conscious rats. Eur J Pharmacol 470:171–175

Ishida J, Hashimoto T, Hashimoto Y, Nishiwak S, Iguchi T, Harada S, Sugaya T, Matsuzaki H, Yamamoto R, Shiota N, Okunishi H, Kihara M, Umemura S, Sugiyama F, Yagami KI, Kasuya Y, Mochizuki N, Fukamizu A (2004) Regulatory roles for APJ, a seven-transmembrane receptor related to angiotensin-type 1 receptor in blood pressure *in vivo*. J Biol Chem 279:262674–26279

Kagiyama S, Fukuhara M, Matsumara K, Lin Y, Fujii K, Iida M (2005) Central and peripheral cardiovascular actions of apelin in conscious rats. Regul Peptídes 125:55–59

Kasai A, Shintani N, Oda M, Kakuda M, Hashimoto H, Matsuda T, Hinuma S, Baba A (2004) Apelin is a novel angiogenic factor in retinal endothelial cells. Biochem Biophys Res Commun 325:395–400

Katugampola SD, Maguire JJ, Matthewson SR, Davenport AP (2001) [^{125}I](Pyr^{1})Apelin-13 is a novel radioligand for localizing the APJ orphan receptor in human and rat tissues. Br J Pharmacol 132:1255–1260

Katugampola SD, Maguire JJ, Kuc RE, Wiley KE, Davenport AP (2002) Discovery of recently adopted orphan receptors for apelin, urotensin II, and ghrelin identified using novel radioligands and functional role in the human cardiovascular system. Can J Physiol Pharmacol 80:369–374

Katugampola SD, Davenport AP (2003) Emerging roles for orphan G-protein-coupled receptors in the cardiovascular system. Trend Pharmacol Sci 24:30–35

Kleinz MJ, Davenport AP (2004) Immunocytochemical localization of the endogenous vasoactive peptide apelin to human vascular and endothelial cells. Regul Peptides 118:119–125

Losano GA (2005) On the cardiovascular activity of apelin. Cardivasc Res 65:8–9

Pang CCY (2000) Measurement of body venous tone. J Pharmacol Toxicol Meth 44:341–360

Szokodi I, Tavi P, Földes G, Voutilainen-Myllylä S, Ilves M, Tokola H, Pikkarainen S, Piuhola J, Rysä J, Tóth M, Ruskoaho H (2002) Apelin, the novel endogenous ligand of the orphan receptor APJ, regulates cardiac contractility. Circ Res 91:434–440

Tatemoto K, Takayama K, Zou MX, Kumaki I, Zhang W, Kumano K, Fujimiya M (2001) The novel peptide apelin lowers blood pressure via a nitric oxide-dependent mechanism. Regul Peptides 99:87–92

A.1.1.32 TRP Channels

A.1.1.32.1 General Considerations

The transient receptor potential (TRP[1]) ion channels are named after the role of the channels in *Drosophila* phototransduction (Montell 2001). The mammalian genes are encoded by at least 28 channel subunit genes (Clapham 2003; Moran et al. 2004; Clapham et al. 2005). Six protein families comprise the mammalian TRP superfamily: the classic TRPs (TRPCs), the vanilloid receptor TRPs (TRPVs), the melastatin or long TRPs (TRPMs), the mucolipins (TRPMLs), the polycystins (TRPPs), and ankyrin transmembrane protein 1 (ANKTM1, TRPA1). The TRP channel primary structures predict six transmembrane (TM) domains with a pore domain between the fifth (S5) and sixth (S6) segments and both C and N termini presumably located intracellularly (Vannier et al. 1998).

The TRP superfamily includes >20 related cation channels that play critical roles in processes ranging from sensory physiology to vasorelaxation and male fertility. Defects in TRP channels have been associated with changes in growth control and one TRP-related protein may be a tumor suppressor. Moreover, mutations in a member of the TRP superfamily are a common cause of polycystic kidney disease, while disruption of another is responsible for mucolipidosis, a neurodegenerative disease. TRP proteins are widely expressed in the nervous system, and, in non-excitable cells, TRP-related channels may be the primary mode of Ca^{2+} entry. TRP proteins are cation channels; however, they vary significantly in their selectivity and mode of activation. Nevertheless, members of the TRP superfamily share significant sequence homology and predicted structural similarities.

Based on primary amino acid homology, the conventional TRP proteins can be classified into three subfamilies: TRPC, TRPV, and TRPM (Birnbaumer et al. 2003). Three additional, more distantly related subfamilies have recently been defined: ANKTM1, a Ca^{2+}-permeant, non-selective cation channel, is the only mammalian member of the TRPA branch of TRP proteins. It is activated by noxious cold temperature, pungent mustard oil compounds and may additionally serve as a mechanosensitive transduction channel in auditory hair cells as well as an ionotropic cannabinoid receptor. The three mucolipins, TRPML1, 2, and 3, appear to be ion channels in intracellular vesicles. Mutations in TRPML1 cause mucolipidosis type IV,

a neurodegenerative lysosomal storage disorder, while genetic defects in TRPP2, a member of the TRPP subfamily, are frequently encountered in patients suffering from autosomal dominant polycystic kidney disease.

REFERENCES AND FURTHER READING

Albert AP, Large WA (2003) Store-operated Ca^{2+}-permeable non-selective cation channels in smooth muscle cells. Cell Calcium 33:345–356

Birnbaumer L, Yidirim E, Abramowitz J (2003) A comparison of the genes coding for canonical TRP channels and their M, V and P relatives. Cell Calcium 33:419–432

Clapham DE (2003) TRP channels as cellular sensors. Nature (Lond) 426:517–524

Clapham DE, Julius D, Montell C, Schultz G (2005) International Union of Pharmacology. XLIX. Nomenclature and structure-function relationships of transient receptor potential channels. Pharamcol Rev 57:427–450

Flockerzi V (2007) An introduction to TRP channels. Handb Exp Pharmacol 179:1–19

Gudermann T, Flockerzi V (2005) TRP channels as new pharmacological targets. Naunyn-Schmiedebergs Arch Pharmacol 371:241–244

Harteneck C (2003) Proteins modulating TRP channel function. Cell Calcium 33:303–310

Kumar B, Dreja K, Shah SS, Cheong A, Xu SZ, Sukumar P, Naylor J, Forte A, Cipollaro M, McHugh D, Kingston PA, Heagerty AM, Munsch CM, Bergdahl A, Hultgårdh-Nilsson A, Gomez MF, Porter KE, Hellstrand P, Beech DJ (2006) Upregulated TRPC1 channel in vascular injury in vivo and its role in human neointimal hyperplasia. Circ Res 98:557–563

Li S, Westwick J, Poll C (2003) Transient receptor potential (TRP) channels as potential drug targets in respiratory disease. Cell Calcium 33:551–558

Montell C (2001) The venerable invertebrate TRP channels. Cell Calcium 31:409–417

Montell C, Birnbaumer L, Flockerzi V (2002) The TRP channels, a remarkable functional family. Cell 108:595–598

Moran MM, Xu H, Clapham DE (2004) TRP ion channels in the nervous system. Curr Opin Neurobiol 14:362–369

Nilius B (2003) From TRPs to SOCs, CCEs, and CRACs. Consensus and controversies. Cell Calcium 33:293–298

Schilling WP (2001) TRP proteins. Novel therapeutic targets for regional blood pressure control? Circ Res 88:256–259

Vannier B, Zhu X, Brown D, Birnbaumer L (1998) The membrane topology of human transient receptor potential 3 as inferred from glycosylation-scanning mutagenesis and epitope immunocytochemistry. J Biol Chem 273:8675–8679

Voets T, Nilius B (2003) The pore of TRP channels: trivial or neglected? Cell Calcium 33:299–302

A.1.1.32.2 TRPC Channels

The TRPC family can be divided into three subgroups by sequence homology as well as functional similarities: C1/C4/C5, C3/C6/C7, and C2. **TRPC1** was the first member of the mammalian TRP family purported to form an ion channel (Zitt et al. 1996). Given the widespread expression of TRPC1 and its ability to coassemble with other TRPC subunits (Xu et al. 1997; Lintschinger et al. 2000; Strübing et al. 2003), TRPC1 might be a component of different heteromeric TRP complexes. The subgroup most closely related to TRPC1 comprises TRPC4 and TRPC5. TRPC4 and TRPC5 are PDZ motif-containing proteins that can form homomeric cation channels that are activated following stimulation of G_q-coupled receptors (Okada et al. 1999) as well as receptor tyrosine kinases (Schaefer et al. 2000).

Xu and Beech (2001) found that TRPC1 is a membrane-spanning subunit of store-operated Ca^{2+} channels in native vascular smooth muscle cells.

Vandebrouck et al. (2002) described involvement of TRPC in the abnormal calcium influx observed in dystrophic (*mdx*) mouse skeletal muscle fibers.

Venkatachalam et al. (2003) discussed regulation of canonical transient receptor potential (TRPC) channel function by diacylglycerol and protein kinase C.

Bergdahl et al. (2003) found that cholestrerol depletion impairs vascular reactivity to endothelin-1 by reducing store-operated Ca^{2+} entry dependent on TRPC1.

Amiri et al. (2003) published FRET-based analysis of TRPC subunit stoichiometry.

Jho et al. (2005) reported that angiopoietin-1 opposes VEGF-induced increase in endothelial permeability by inhibiting TRPC1-dependent Ca^{2+} influx.

Rao and Kaminski (2006) found that induction of intracellular elevation by Δ^9-tetrahydrocannabinol in T cells involves TRPC1 channels.

Takai et al. (2004) distinguished two types of non-selective cation channels by muscarinic stimulation with carbachol in bovine muscle cells.

Kumar et al. (2006) studied upregulated TRPC1 channel in vascular injury *in vivo* and its role in human neointimal hyperplasia.

Less information is available about **TRPC2**, which shares approximately 30% sequence identity with the TRPC3/6/7 subfamily. Full-length TRPC2 mRNA and several N-terminal splice variants have been found in mouse and rat tissue, but TRPC2 seems to be a pseudogene in humans (Vannier et al. 1999; Liman 2003). TRPC2 protein was localized to neuronal micovilli in rat vomeronasal organ (Liman 2003) and in the head of mouse sperm (Jungnickel et al. 2001).

TRPC3, **TRPC6**, and **TRPC7** are 75% identical. When expressed they constitute non-selective cation currents that rectify in both the inward (- voltages) and outward (+ voltages) directions. TRPC3, TRPC6, and TRPC7 are inwardly and outwardly rectifying, have relatively low selectivity for Ca^{2+} over Na^+, and are ac-

tivated by diacylglycerol (DAG) (Hofmann et al. 1999; Okada et al. 1999; Putney et al. 2004). These channels seem to play important roles in vascular and airway smooth muscle (Trebak et al. 2003; Yu et al. 2003; Corteling et al. 2004).

Groschner and Rosker C (2005) described TRPC3 as a versatile transducer molecule that serves integration and diversification of cellular signals.

Graziani et al. (2006) investigated the potential role of membrane cholesterol as a regulator of cellular TRPC3 conductance.

Smyth et al. (2006) found a dissociation of regulated trafficking of TRPC3 channels in the plasma membrane from their activation by phospholipase C.

TRPC4 and TRPD5 are receptor-operated Ca^{2+}-permeable non-selective cation channels (Plant and Schaefer 2003).

Odell et al. (2005) found that epidermal growth factor induces tyrosine phosphorylation, membrane insertion and activation of transient receptor potential channel 4.

Saleh et al. (2006) described that angiotensin II activates two cation channels with distinct TRPC1 and TRCP6 channel properties in rabbit mesenteric artery myocytes.

Shimizu et al. (2006) reported that Ca^{2+}-calmodulin-dependent myosin light chain kinase is essential for activation of TRPC5 channels expressed in HEK293 cells.

Shi et al. (2004) described multiple regulation by calcium of murine homologs of transient receptor potential proteins TRP6 and TRP7 expressed in HEK293 cells.

Xu et al. (2006) identified sphingosine-1-phosphate as an activator of the calcium channel TRPC5, which controls vascular smooth muscle activity.

Estacion et al. (2004) studied activation of human TRPC6 channels by receptor stimulation.

Basora et al. (2003) reported that 20-hydroxyeicosatetraenoic acid (20-HETE) activates mouse TRPC6 channels expressed in HEK293 cells.

Maruyama et al. (2006) found that heteromultimeric TRPC6-TRPC7 channels contribute to arginine vasopressin-induced cation current of A7r5 vascular smooth muscle cells.

REFERENCES AND FURTHER READING

Amiri H, Schultz G, Schäfer M (2003) FRET-based analysis of TRPC subunit stoichiometry. Cell Calcium 33:461–470

Basora N, Boulay G, Bilodeau L, Rousseau E, Payett MD (2003) 20-Hydroxyeicosatetraenoic adid (20-HETE) activates mouse TRPC6 channels expressed in HEK293 cells. J Biol Chem 278:31709–31716

Bergdahl A, Gomez MF, Dreja K, Xu SZ, Adner M, Beech DJ, Broman J, Hellstrand P, Swärd K (2003) Cholesterol depletion impairs vascular reactivity to endothelin-1 by reducing store-operated Ca^{2+} entry dependent on TRPC1. Circ Res 93:839–847

Corteling RL, Li S, Giddings J, Westwick J, Poll C, Hall IP (2004) Expression of transient receptor potential C6 and related transient receptor potential family members in human airway smooth muscle and lung tissue. Am J Respir Cell Mol Biol 30:145–154

Estacion M, Li S, Sinkins WG, Gosling M, Bahra P, Poll C, Westwick J, Schilling WP (2004) Activation of human TRPC6 channels by receptor stimulation. J Biol Chem 279:22047–22056

Graziani A, Rosker C, Kohlwein SD, Zhu MX, Romanin C, Sattler W, Groschner K, Poteser M (2006) Cellular cholesterol controls TRPC3 function: evidence for a novel dominant-negative knockdown strategy. Biochem J 396:147–155

Groschner K, Rosker C (2005) TRPC3: a versatile transducer molecule that serves integration and diversification of cellular signals. Naunyn-Schmiedebergs Arch Pharmacol 371:251–256

Hofmann T, Obukhov AG, Schaefer M, Harteneck C, Gudermann T, Schultz G (1999) Direct activation of human TRPC6 and TRPC3 channels by diacylglycerol. Nature (Lond) 397:259–263

Jho D, Mehta D, Ahmmed G, Gao XP, Tiruppathi C, Broman M, Malik AB (2005) Angiopoietin-1 opposes VEGF-induced increase in endothelial permeability by inhibiting TRPC1-dependent Ca^{2+} influx. Circ Res 96:1282–1290

Jungnickel MK, Marrero H, Birnbaumer L, Lemos JR, Florman HM (2001) Trp2 regulates entry of Ca^{2+} into mouse sperm triggered by egg ZP3. Nat Cell Biol 3:499–502

Kumar B, Dreja K, Shah SS, Cheong A, Xu SZ, Sukumar P, Naylor J, Forte A, Cipollaro M, McHugh D, Kingston PA, Heagerty AM, Munsch CM, Bergdahl A, Hultgårdh-Nilsson A, Gomez MF, Porter KE, Hellstrand P, Beech DJ (2006) Upregulated TRPC1 channel in vascular injury in vivo and its role in human neointimal hyperplasia. Circ Res 98:557–563

Lee J, Cha SK, Sun TJ, Huang CL (2005) PIP2 activates TRPV5 and releses its inhibition by intracellular Mg^{2+}. J Gen Physiol 126:439–451

Liman ER (2003) Regulation by voltage and adenine nucleotides of a Ca^{2+}-activated cation channel from hamster vomeronasal sensory neurons. J Physiol (Lond) 548:777–787

Lintschinger B, Balzer-Geldsetzer M, Baskaran T, Graier WF, Romanin C, Zhu MX, Groschner K (2000) Coassembly of Trp1 and Trp3 proteins generates diacylglycerol- and Ca^{2+}-sensitive cation channels. J Biol Chem 275:27799–27805

Maruyama Y, Nakanishi Y, Walsh EJ, Wilson DP, Welsh DG, Cole WC (2006) Heteromultimeric TRPC6-TRPC7 channels contribute to arginine vasopressin-induced cation current of A7r5 vascular smooth muscle cells. Circ Res 98:1520–1527

Odell AF, Scott JL, Van Helden DF (2005) Epidermal growth factor induces tyrosine phosphorylation, membrane insertion and activation of transient receptor potential channel 4. J Biol Chem 280:37974–37987

Okada T, Inoue R, Yamazaki K, Maeda A, Kurosaki T, Yamakuni T, Tanaka I, Shimizu S, Ikenaka K, Imoto K (1999) Molecular and functional characterization of a novel mouse transient receptor potential protein homologue TRP7. Ca^{2+}-permeable cation channel that is constitutively activated and enhanced by stimulation of G protein-coupled receptor. J Biol Chem 274:27359–27370

Plant TD, Schaefer M (2003) TRPC4 and TRPD5: receptor-operated Ca^{2+}-permeasble nonselective cation channels. Cell Calcium 33:441–450

Putney JW Jr, Trebak M, Vazquez G, Wedel B, Bird GS (2004) Signalling mechanisms for TRPC3 channels. Novartis Found Symp 258:123–133

Rao GK, Kaminski NE (2006) Induction of intracellular elevation by Δ^9-tetrahydrocannabinol in T cells involves TRPC1 channels. J Leukoc Biol 79:202–213

Saleh SN, Albert AP, Peppiat CM, Large WA (2006) Angiotensin II activates two cation channels with distinct TRPC1 and TRCP6 channel properties in rabbit mesenteric artery myocytes. J Physiol (Lond) 577:479–495

Schaefer M, Plant TD, Obukhov AG, Hofmann T, Gudermann T, Schultz G (2000) Receptor-mediated regulation of the nonselective cation channels TRPC4 and TRPC5. J Biol Chem 275:17517–17526

Shi J, Mori E, Mori Y, Mori M, Li J, Ito Y, Inoue R (2004) Multiple regulation by calcium of murine homologues of transient receptor potential proteins TRP6 and TRP7 expressed in HEK293 cells. J Physiol (Lond) 561:415–437

Shimizu S, Yoshida T, Wakamori M, Ishii M, Okada T, Takahashi M, Seto M, Sakurada K, Kiuchi Y, Mori Y (2006) Ca^{2+}-calmodulin-dependent myosin light chain kinase is essential for activation of TRPC5 channels expressed in HEK293 cells. J Physiol (Lond) 570:219–235

Smyth JT, Lemonnier L, Vazquez G, Bird GS, Putney JW (2006) Dissociation of regulated trafficking of TRPC3 channels in the plasma membrane from their activation by phospholipase C. J Biol Chem 281:11712–11720

Strübing C, Krapivinsky G, Krapivinsky L, Clapham DE (2003) Formation of novel TRPC channels by complex subunit interactions in embryonic brain. J Biol Chem 278:39014–39019

Takai Y, Sugawara R, Ohinata H, Takai A (2004) Two types of non-selective cation channels by muscarinic stimulation with carbachol in bovine muscle cells. J Physiol (Lond) 559(3):899–922

Trebak M, Vazquez G, Bird GS, Putney JW (2003) The TRPC3/6/7 subfamily of cation channels. Cell Calcium 33:451–461

Vandebrouck C, Martin D, Colson-Van Schoor M, Debaix H, Gailly P (2002) Involvement of TRPC in the abnormal calcium influx observed in dystrophic (*mdx*) mouse skeletal muscle fibers. J Cell Biol 158:1089–1096

Vannier B, Peyton M, Boulay G, Brown D, Qin N, Jiang M, Zhu X, Birnbaumer L (1999) Mouse trp2, the homologue of the human trpc2 pseudogene, encodes mTrp2, a store depletion-activated capacitative Ca^{2+} entry channel. Proc Natl Acad Sci USA 96:2060–2064

Venkatachalam K, Zheng F, Gill DL (2003) Regulation of canonical transient receptor potential (TRPC) channel function by diacylglycerol and protein kinase C. J Biol Chem 278:29031–29040

Xu XZ, Li HS, Guggino WB, Montell C (1997) Coassembly of TRP and TRPL produces a distinct store-operated conductance. Cell 89:1155–1164

Xu SZ, Beech DJ (2001) TrpC1 is a membrane-spanning subunit of store-operated Ca^{2+} channels in native vascular smooth muscle cells. Circ Res 88:84–87

Xu SZ, Muraki K, Zeng F, Li J, Sukumar P, Shah S, Dedman AM, Flemming OK, McHugh D, Naylor J, Cheong A, Bateson AN, Munsch CM, Porter KLE, Beech DJ (2006) A sphingosine-1-phosphate-activated calcium channel controlling vascular smooth muscle activity. Circ Res 98:1381–1389

Yu Y, Sweeney M, Zhang S, Platoshyn O, Landsberg J, Rothman A, Yuan JX (2003) PDGF stimulates pulmonary vascular smooth muscle cell proliferation by upregulating TRPC6 expression. Am J Physiol 284:C316–C330

Zitt C, Zobel A, Obukhov AG, Harteneck C, Kalkbrenner F, Lückhoff A, Schultz G (1996) Cloning and functional expression of a human Ca^{2+}-permeable cation channel activated by calcium store depletion. Neuron 16:1189–1196

A.1.1.32.3 TRPM Channels

The TRPM subfamily has eight members divided into four groups: M1 (melastatin)/M3, M7 (TRP-PLIK)/M6, M2/M8, and M4/M5 (Hartzeneck 2005; Fonfria et al. 2006). **TRPM1** may be regulated through direct interaction with a cytosolic isoform generated by alternative RNA splicing (Xu et al. 2001). **TRPM2** is a 1503-amino-acid protein that is highly expressed in brain (Nagamine et al. 1998) and present in blood cells.

Perraud et al. (2003) reviwed TRPM2 Ca^{2+}-permeable cation channels.

Hill et al. (2004a, 2004b) reported inhibition of TRPM2 channels by the antifungal agents clotrimazole and econazole as well as by flufenamic acid; Kraft et al. (2006) by *N*-(*p*-amylcinnamoyl)anthranilic acid.

Identified first by sequencing projects, the function of **TRPM3** is poorly understood. The hTRPM3 gene maps to human chromosome 9q-21.12 and encodes a 1555-amino-acid protein.

TRPM4 and **TRPM5** have similar characteristics. TRPM4b, a splice variant of TRPM4, and TRPM5 are Ca^{2+}-activated, voltage-modulated, monovalent-selective cation channels with 25-pS single-channel conductances (Launay et al. 2002; Hofmann et al. 2003; Nilius et al. 2003). Pérez et al. (2003) studied the ion channel TRPM5 in taste receptor cells.

TRPM6 and **TRPM7** comprise a unique subfamily of TRP proteins with both channel and kinase activities. TRPM7, which has 1863 amino acid residues, was identified in a yeast two-hybrid screen as a protein interacting with phospholipase C (PLC) (Runnels et al. 2001; Schmitz et al. 2003). It seems to be ubiquitously expressed. Takezawa et al. (2004) described receptor-mediated regulation of the TPRM7 channel through its endogenous protein kinase domain.

TRPM8 is a 1104-amino-acid protein that does not seem to contain associated enzymatic domains. TRPM8 is a non-selective, voltage-modulated conductance. At colder temperatures (8°C–28°C) or in the presence of menthol, TRPM8 current is activated at a more physiological range of voltages (Brauchi et al. 2004; Voets et al. 2004). This channel is expressed in

small-diameter primary sensory neurons, where it presumably functions as a thermosensor (McKemy et al. 2002; Peier et al. 2002).

REFERENCES AND FURTHER READING

Brauchi S, Orio P, Latorre R (2004) Clues to understanding cold sensation: thermodynamics and electrophysiological analysis of the cold receptor TRPM8. Proc Natl Acad Sci USA 101:15494–15499

Fonfrai E, Murdock PR, Cusdin FS, Benham CD, Kelsell RE, McNulty S (2006) Tissue distribution profiles of the human TRPM cation channel family. J Recept Signal Transduct Res 26:159–178

Hartzeneck C (2005) Function and pharmacology of TRPM cation channels. Naunyn-Schmiedebergs Arch Pharmacol 371:307–314

Hill K, McNuty S, Randall AD (2004a) Inhibition of TRPM2 channels by the antifungal agents clotrimazole and econazole. Naunyn-Schmiedebergs Arch Pharmacol 370:227–237

Hill K, Benham CD, McNulty S, Randall AD (2004b) Flufenamic acid is a pH-dependent antagonist of TRPM2 channels. Neuropharmacol ogy 47:450–460

Hofmann T, Chubanov V, Gudermann T, Montell C (2003) TRPM5 is a voltage-modulated and Ca^{2+}-activated monovalent selective cation channel. Curr Biol 13:1153–1158

Kraft R, Grimm C, Frenzel H, Harteneck C (2006) Inhibition of TRPM2 cation channels by N-(p-amylcinnamoyl) anthranilic acid. Br J Pharmacol 148:264–273

Launay P, Fleig A, Perraud AL, Scharenberg AM, Penner R, Kinet JP (2002) TRPM4 is a Ca^{2+}-activated nonselective cation channel mediating cell membrane depolarization. Cell 109:397–407

McKemy DD, Neuhausser WM, Julius D (2002) Identification of a cold receptor reveals a general role for TRP channels in thermosensation. Nature (Lond) 416:52–58

Nagamine K, Kudoh J, Minoshima S, Kawasaki K, Asakawa S, Ito F, Shimizu N (1998) Molecular cloning of a novel putative Ca^{2+} channel protein (TRPC7) highly expressed in brain. Genomics 54:124–131

Nilius B, Prenen J, Droogmans G, Voets T, Vennekens R, Freichel M, Wissenbach U, Flockerzi V (2003) Voltage dependence of the Ca^{2+}-activated cation channel TRPM4. J Biol Chem 278:30813–30820

Peier AM, Moqrich A, Hergarden AC, Reeve AJ, Andersson DA, Story GM, Earley TJ, Dragoni I, McIntyre P, Bevan S, Patapoutian A (2002) A TRP channel that senses cold stimuli and menthol. Cell 108:705–715

Pérez CA, Margolskee RF, Kinnamon SC, Ogura T (2003) Making sense with TRP channels: store-operated calcium entry and the ion channel Trpm5 in taste receptor cells. Cell Calcium 33:541–549

Perraud AL, Schmitz C, Scharenberg AM (2003) TRPM2 C^{a2+} permeable cation channels. From gene to biological function. Cell Calcium 33:519–531

Runnels LW, Yue L, Clapham DE (2002) The TRPM7 channel is inactivated by PIP_2 hydrolysis. Nat Cell Biol 4:329–336

Schmitz C, Perraud AL, Johnson CO, Inabe K, Smith MK, Penner R, Kurosaki T, Fleig A, Scharenberg AM (2003) Regulation of vertebrate cellular Mg^{2+} homeostasis by TRPM7. Cell 114:191–200

Takezawa R, Schmitz C, Demeuse P, Scharenberg AM, Penner R, Fleig A (2004) Receptor-mediated regulation of the TPRM7 channel through its endogenous protein kinase domain. Proc Natl Acad Sci USA 101:6009–6014

Voets T, Droogmans G, Wissenbach U, Janssens A, Flockerzi V, Nilius B (2004) The principle of temperature-dependent gating in cold- and heat-sensitive TRP channels. Nature (Lond) 430:748–754

Xu XZ, Moebius F, Gill DL, Montell C (2001) Regulationn of melastatin, a TRP-realted protein, through interaction with a cytoplasmic isoform. Proc Natl Acad Sci U S A. 98(19):10692–7

A.1.1.32.4 TRPV Channels

The TRPV subfamily is named after the first mammalian member of the subfamily, vanilloid receptor 1 (Caterina et al. 1997; Benham et al. 2002; Montell et al. 2002; Clapham 2003; Mutai and Heller 2003). TRPV5 and TRPV6 are highly Ca^{2+}-selective TRP channels that mediate trans-epithelial Ca^{2+} transport in kidney and intestine (Hoenderop et al. 2003).

The TRPV channel subfamily has six members divided into two groups: V1/V2/V3/V4 and V5/V6. The vanilloid receptor, TRPV1, is the best understood ion channel in this class (Caterina et al. 1997; Caterina and Julius 2001).

TRPV channels as temperature sensors were revived by Benham et al. (2003).

The expressed **TRPV1** capsaicin receptor is a heat/proton/lipid/voltage-modulated Ca^{2+}-permeant (P_{Ca}/P_{Na} 10) ion channel. A more voltag-gating-centric explanation is that at warmer temperatures (> 37°C) or in the presence of capsaicin, TRPV1 current is activated by a more physiological range of voltages (Brauchi et al. 2004). TRPV1 is desensitized by internal Ca^{2+}; it is not activated by store depletion. TRPV1, V2, and V3 are activated by the synthetic compound 2-aminoethoxydiphenylborate (2-APB) (Chung et al. 2004; Hu et al. 2004). Endogenous cannabinoid receptor ligands, such as anandamide, are potential TRPV1 agonists.

The vanilloid receptor-like channel **TRPV2** is 50% identical to TRPV1, but is insensitive to capsaicin (Caterina et al. 1999). Like TRPV1 it is more permeable to Ca^{2+} than to Na^+ ($P_{Ca}/P_{Na} = 3:1$). It has been proposed to mediate high-threshold noxious heat sensation, perhaps in the lightly myelinated A nociceptors, but its presence in non-sensory tissue suggests other functions as well.

TRPV3 is expressed widely but most strikingly in skin. Increasing temperature from 22 to 40°C in mammalian cells transfected with hTRPV3 elevates intracellular calcium by activating a non-selective cationic conductance (P_{Ca}/P_{Na} 10:1) (Peier et al. 2002; Smith et al. 2002; Xu et al. 2002). As in sensory neurons, the current is steeply dependent on temperature, sen-

sitizes with repeated heating, and displays a striking hysteresis on heating and cooling, but the extent of expression in sensory neurons is controversial. Based on these properties, TRPV3 is thermosensitive in the physiological range of temperatures between TRPM8 and TRPV1 and may play a role in pain.

TRPV4 is 40% identical to TRPV1 and TRPV2 (Liedtke et al. 2000; Strotmann et al. 2000). When expressed in mammalian cells it comprises a moderately selective cation channel ($P_{Ca}/P_{Na} = 6$), which, like TRPV1, displays a gently outwardly rectifying *I–V* relation. TRPV4 is 40% identical to TRPV1 and TRPV2 (Liedtke et al. 2000; Strotmann et al. 2000). When expressed in mammalian cells it comprises a moderately selective cation channel ($P_{Ca}/P_{Na} = 6$), which, like TRPV1, displays a gently outwardly rectifying *I–V* relation.

TRPV5 and TRPV6 comprise a separate subfamily of TRPVs with only 30% identity with TRPV1. The expressed channels strongly inwardly rectify and are the most Ca^{2+}-selective ($P_{Ca}/P_{Na} > 100$) (Nilius et al. 2000; Vennekens et al. 2000; Yue et al. 2001; Den Dekker et al. 2003) of all TRP channels. These properties are consistent with proposed mechanisms for Ca^{2+}-selective channels in which negatively charged glutamic or aspartic acid residues provide a binding site for divalents within the pore. Intra- and extracellular [Ca^{2+}] (Yue et al. 2001; Hirnet et al. 2003; Bödding and Flockerzi 2004) and calmodulin (Lambers et al. 2004) regulate TRPV6 activity. The localization of TRPV5 and TRPV6 to the proximal small intestine and collecting duct of the kidney, along with mouse knockout data, suggests that this family is important in calcium uptake via epithelial cells (Hoenderop et al. 2005).

Lee et al. (2005) reported that PIP_2 activates TRPV5 and releases its inhibition by intracellular Mg^{2+}.

REFERENCES AND FURTHER READING

Benham CD, Davis JB, Randall AD (2002) Vanilloid and TRP channels: a family of lipid-gated cation channels. Neuropharmacology 42:873–888

Benham CD, Gunthorpe MJ, Davis JB (2003) TRPV channels as temperature sensors. Cell Calcium 33:479–487

Bödding M, Flockerzi V (2004) Ca^{2+} dependence of the Ca^{2+}-selective TRPV6 channel. J Biol Chem 279:36546–36552

Brauchi S, Orio P, Latorre R (2004) Clues to understanding cold sensation: thermodynamics and electrophysiological analysis of the cold receptor TRPM8. Proc Natl Acad Sci USA 101:15494–15499

Caterina MJ, Schumacher MA, Tominaga M, Rosen TA, Levine JD, Julius D (1997) The capsaicin receptor: a heat-activated ion channel in the pain pathway. Nature (Lond) 389:816–824

Caterina MJ, Rosen TA, Tominaga M, Brake AJ, Julius D (1999) A capsaicin-receptor homologue with a high threshold for noxious heat. Nature (Lond) 398:436–441

Caterina MJ, Julius D (2001) The vanilloid receptor: a molecular gateway to the pain pathway. Annu Rev Neurosci 24:487–517

Chung MK, Lee H, Mizuno A, Suzuki M, Caterina MJ (2004) 2-Aminoethoxydiphenyl borate activates and sensitizes the heat-gated ion channel TRPV3. J Neurosci 24:5177–5182

Clapham DE (2003) TRP channels as cellular sensors. Nature 426:517–524

Den Dekker E, Hoenderop JGJ, Nilius B, Bindels RJM (2003) The epithelial calcium channels, TRPV5 & TRPV6: from identification towards regulation. Cell Calcium 33:497–507

Hirnet D, Olaussson J, Fecher-Trost C, Bödding M, Nastainczyk W, Wissenbach U, Flockerzi V, Freichel M (2003) The TRPV6 gene, cDNA,and protein. Cell Calcium 33:509–518

Hoenderop JG, Voets T, Hoefs S, Weidema F, Prenen J, Nilius B, Bidels RJ (2003) Homo- and heterotetrameric architecture of the epithelial Ca^{2+} channels TRPV5 and TRPV6. EMBO J 22:776–785

Hoenderop JG, Nilius B, Bindels RJ (2005) Calcium absorption across epithelia. Physiol Rev 85:373–422

Hu HZ, Gu Q, Wang C, Colton CK, Tang J, Kinoshita-Kawada M, Lee LY, Wood JD, Zhu MX (2004) 2-Aminoethoxydiphenyl borate is a common activator of TRPV1, TRPV2 and TRPV3. J Biol Chem 279:35741–35748

Lambers TT, Weidema AF, Nilius B, Hoenderop JG, Bindels RJ (2004) Regulation of the mouse epithelial Ca^{2+} channel TRPV6 by the Ca^{2+}-sensor calmodulin. J Biol Chem 279:28855–28861

Lee J, Cha SK, Sun TJ, Huang CL (2005) PIP_2 activates TRPV5 and releases its inhibition by intracellular Mg^{2+}. J Gen Physiol 126:439–451

Liedtke W, Choe Y, Marti-Renom MA, Bell AM, Denis CS, Sali A, Hudspeth AJ, Friedman JM, Heller S (2000) Vanilloid receptor-related osmotically activated channel (VR-OAC), a candidate vertebrate osmoreceptor. Cell 103:525–535

Montell C, Birnbaumer L, Flockerzi V, Bindels RJ, Bruford EA, Caterina MJ, Clapham DE, Harteneck C, Heller S, Julius D (2002) A unified nomenclature for the superfamily of TRP cation channels. Mol Cell 92:229–231

Mutai M, Heller S (2003) Vertebrate and invertebrate TRPV-like mechanoreceptors. Cell Calcium 33:471–478

Nilius B, Vennekens R, Prenen J, Hoenderop JG, Bindels RJ, Droogmans G (2000) Whole-cell and single channel monovalent cation currents through the novel rabbit epithelial Ca^{2+} channel ECaC. J Physiol (Lond) 527 (Pt 2):239–248

Peier AM, Reeve AJ, Andersson DA, Moqrich A, Earley TJ, Hergarden AC, Story GM, Colley S, Hogenesch JB, McIntyre P, Bevan S, Patapoutian A (2002) A heat-sensitive TRP channel expressed in keratinocytes. Science 296:2046–2049

Smith GD, Gunthorpe MJ, Kelsell RE, Hayes PD, Reilly P, Facer P, Wright JE, Jerman JC, Walhin JP, Ooi L et al (2002) TRPV3 is a temperature-sensitive vanilloid receptor-like protein. Nature (Lond) 418:186–190

Strotmann R, Harteneck C, Nunnenmacher K, Schultz G, Plant TD (2000) OTRPC4, a nonselective cation channel that confers sensitivity to extracellular osmolarity. Nat Cell Biol 2:695–702

Vennekens R, Hoenderop GJ, Prenen J, Stuiver M, Willems PHGM, Droogmans G, Nilius B, Bindels RJM (2000) Permeation and gating properties of the novel epithelial Ca^{2+} channel. J Biol Chem 275:3963–3969

Xu H, Ramsey I, Kotecha SA, Moran M, Chong JA, Lawson D, Ge P, Lilly J, Silos-Santiago I, Xie Y et al (2002) TRPV3 is a calcium-permeable temperature-sensitive cation channel. Nature (Lond) 418:181–186

Yue L, Peng JB, Hediger MA, Clapham DE (2001) CaT1 manifests the pore properties of the calcium-release-activated calcium channel. Nature (Lond) 410:705–709

A.1.1.32.5 TRPV1 Receptor Assay

PURPOSE AND RATIONALE

The vanilloid receptor-1 (TRPV1) is a non-selective cation channel, predominantly expressed by peripherally sensory neurons, which is known to play a key role in the detection of noxious painful stimuli, such as capsaicin and heat. Smart et al. (2000, 2001) found that the endogenous lipid anandamide is a full agonist at the human vanilloid receptor and characterized human vanilloid VR1 pharmacology using FLIPR. With these methods, Gunthorpe et al. (2004) identified and characterized a potent and selective vanilloid receptor (VR1/TRPV1) antagonist.

PROCEDURE

Cloning and Expression of VR1 Receptors in HEK293 Cells

Human VR1 cDNA was identified using the published rat VR1 sequence (GenBank accession AF029310) to search public nucleotide databases. Expressed sequence tag T48002 was identified and its sequence extended by rapid amplification of the cDNA ends using cDNA templates from a number of tissue sources. The full cDNA was amplified from brain cDNA, inserted into the expression vector pcDNA3.1, double-strand sequenced, and stably expressed in HEK293 cells. Rat VR1 cDNA was amplified from rat DRG cDNA and similarly expressed in HEK293 cells.

Cell Culture

hVR1-HEK293 cells were grown as monolayers in minimum essential medium (MEM) supplemented with non-essential amino acids, 10% fetal calf serum, and 0.2 mM L-glutamine, and maintained under 95%/5% O_2/CO_2 at 37°C. Cells were passaged every 3–4 days and the highest passage number used was 20. Dissociated rat neonatal DRG cultures were prepared as described by Skaper et al. (1990).

Electrophysiological Studies

Cells were plated and cultured on glass coverslips at 26,000 cells cm^{-2} and whole-cell voltage clamp recordings were performed at room temperature (20–24°C), using standard methods. The extracellular solution consisted of (mM): NaCl 130, KCl 5, $CaCl_2$ 2, $MgCl_2$ 1, glucose 30, HEPES-NaOH 25, pH 7.3. For anandamide application this solution was supplemented with 0.2% lipid-free bovine serum albumin. Patch pipettes of resistance 2–5 MΩ were fabricated on a Sutter Instruments P-87 electrode puller and were filled with the following solution (mM): CsCl 140, $MgCl_2$ 4, EGTA 10, HEPES-CsOH 10, pH 7.3. All recordings were made from single, well isolated, phase-bright cells. Currents were recorded at a holding potential of –70 mV using an Axopatch 200B amplifier. Data acquisition and analysis were performed using the pClamp7 software suite. Drug applications were affected with an automated fast-switching solution exchange device (Warner Instruments SF-77B; time for solution exchange ≈30 ms).

Measurements of $[Ca^{2+}]_i$ Using the FLIPR

hVR1-HEK293 cells were seeded into black-walled clear-base 96-well plates (Costar, UK) at a density of 25,000 cells per well in MEM, supplemented as above, and cultured overnight. The cells were then incubated with MEM containing the cytoplasmic calcium indicator Fluo-3AM (4 μM; Teflabs, Austin, Tex., USA) at 25°C for 120 min. The cells were washed four times with, and finally cultured in, Tyrode's medium containing 0.2% BSA, before being incubated for 30 min at 25°C with either buffer alone (control) or buffer containing various antagonists. The plates were then placed into a FLIPR (Molecular Devices, UK) to monitor cell fluorescence ($\lambda_{EX} = 488$ nM, $\lambda_{EM} = 540$ nM) (Sullivan et al. 1999) before and after the addition of various agonists.

EVALUATION

Responses were measured as peak fluorescence intensity (FI) minus basal FI, and where appropriate were expressed as a percentage of a maximum capsaicin-induced response. Data are expressed as mean ± SEM unless otherwise stated. Curve-fitting and parameter estimation were carried out using Graph Pad Prism 3.00 (GraphPad Software, Calif., USA). pK_B values were generated from IC_{50} curves for the antagonist vs a fixed EC_{80} concentration of agonist using the Cheng–Prusoff equation.

MODIFICATIONS OF THE METHOD

Rao and Kaminski (2006) reported that induction of intracellular elevation by Δ^9-tetrahydrocannabinol in T cells involves TRPC1 channels.

REFERENCES AND FURTHER READING

Gunthorpe MJ, Benham CD, Randall A, Davis JB (2002) The diversity in the vanilloid (TRPV) receptor family of ion channels. Trends Pharmacol Sci 23:191

Gunthorpe MJ, Rami HK, Jerman JC, Smart D, Gill CH, Soffin EM, Hanna SL, Lappin SC, Egerton J, Smith GD, Worby A, Howett L, Owen D, Nasir S, Davies CH, Thompson M, Wyman PA, Randall AD, Davis JB (2004) Identification and characterization of SB-366971, a potent and selective vanilloid receptor (VR1/TRPV1) antagonist. Neuropharmacology 46:133–149

Rao GK, Kaminski NE (2006) Induction of intracellular elevation by Δ^9-tetrahydrocannabinol in T cells involves TRPC1 channels. J Leukoc Biol 79:202–213

Skaper SD, Facci L, Milani D, Leon A, Toffano G (1990) Culture and use of primary and clonal neural cells. In: Conn PM (ed) Methods in neurosciences, Vol 2. Academic Press, New York, pp 17–33

Smart D, Gunthorpe MJ, Jerman JC, Nasir S, Gray J, Muir AI, Chambers JK, Randall AD, Davus JB (2000) The endogenous lipid anandamide is a full agonist at the human vanilloid receptor (hVR1). Br J Pharmacol 129:227–230

Smart D, Jerman JC, Gunthorpe MJ, Brough SJ, Ranson J, Cairns W, Hayes PD, Randall AD, Davis JH (2001) Characterisation using PLIPR of human vanilloid receptor pharmacology. Eur J Pharmacol 417:51–58

Sullivan E, Tucker EM, Dale IL (1999) Measurement of $[Ca^{2+}]_i$, usuing the fluorometric imaging plate reader (FLIPR). In: Lambert DG (ed) Calcium signaling protocols. Humana Press, New Jersey, pp 125–136

A.1.2 Studies in Isolated Organs

A.1.2.1 α-Sympatholytic Activity in Isolated Vascular Smooth Muscle

PURPOSE AND RATIONALE

Noradrenaline and other sympathomimetic drugs increase vascular smooth muscle tone by stimulation of α-adrenergic receptors. Contractions can be antagonized by α-adrenergic receptor blocking agents such as phentolamine. Drugs can be tested for their capacity of reducing vascular smooth muscle contractions induced by the adrenergic receptor-activating agent noradrenaline. Moreover, effects of peptides, such as bradykinin, can be tested with strips of aorta or pulmonary artery.

PROCEDURE

As donor animals Pirbright White guinea pigs of either sex weighing about 400 g, or Chinchilla rabbits weighing about 3.5 kg, or Sprague-Dawley rats weighing 200–300 g are used. The vessels to be tested are the thoracic aorta or the arteria pulmonalis. The animals are sacrificed by stunning and exsanguination. The pulmonary artery or the thoracic aorta is quickly removed and cut into helical strips of 1–2 mm width and 15–20 mm length. The strips are mounted in an organ bath with a preload of 1 g. Krebs-Henseleit buffer solution containing 11.5 M glucose is maintained at 37°C and oxygenated with 95% O_2, 5% CO_2. Isotonic or isometric registration is performed. Changes in length are recorded isotonically using a lever transducer (368 type B, Hugo Sachs Elektronik Freiburg). Isometric force is measured with a force transducer (UC-2 Gould-Statham, Oxnard, USA).

Experimental Course

Following an equilibration period of 60 min, contractions are induced by repeated administrations of (–)noradrenaline HCl in concentrations of 2×10^{-6} M for testing the contractions of the pulmonary artery and in concentrations of 2×10^{-8} M for testing the contractions of the aorta. After obtaining a stable plateau of identically sized contractions, cumulative doses of the test compound are added into the organ bath. Consecutive concentrations are given when the response of the previous dose has reached a plateau.

Controls at the end of the experiment: If a compound does not show vasorelaxing activity at any dose, the sensitivity of the preparation is tested by adding phentolamine (1×10^{-7} M).

If a compound shows vasorelaxing activity, the reversibility of the relaxation is tested by increasing the noradrenaline concentration.

EVALUATION

The contractile force is determined before and after drug administration.

Percent inhibition of spasmogen-induced contraction by test drug is calculated as compared to the maximal contraction with a spasmogen alone (= 100%).

IC_{50} values are determined from the individual dose-response curves. IC_{50} is defined as the dose of drug leading to a 50% relaxation of noradrenaline-induced contraction.

MODIFICATIONS OF THE METHOD

The isolated vena cava of rabbits can be used for assaying α-adrenolytic activity. The rabbit is sacrificed by CO_2 anesthesia. The vena cava inferior is removed and cut into strips. The percent inhibition of epinephrine or norepinephrine induced contractions is determined.

The effects of bradykinin and bradykinin antagonists can be tested in isolated guinea pig artery and isolated rabbit aorta which contains predominantly the BK_1-receptor type (Regoli and Barabé 1980; Hock et al. 1991).

Wisskirchen et al. (1998) tested agonists of calcitonin gene-related peptide, homologues and antagonists in rat isolated pulmonary artery. Endothelium-intact pulmonary artery rings were contracted with 3×10^{-8} M phenylephrine and a cumulative dose-response curve of relaxation was constructed.

REFERENCES AND FURTHER READING

Furchgott RF (1967) Techniques for studying antagonism and potentiation of sympathomimetic drugs an isolated tissues. In: Siegler PE, Moyer JH (eds) Animal and clinical pharmacologic techniques in drug evaluation. pp 256–266. Year Book Medical Publishers, Inc., Chicago

Green AF, Boura ALA (1964) Sympathetic nerve blockade. In: Laurence DR, Bacharach AL (eds) Evaluation of drug activities: Pharmacometrics. Academic Press, London and New York, pp 370–430

Hock FJ, Wirth K, Albus U, Linz W, Gerhards HJ, Wiemer G, Henke S, Breipohl G, König W, Knolle J, Schölkens BA (1991) Hoe 140 a new potent and long acting bradykinin antagonist: *in vitro* studies. Br J Pharmacol 102:769–773

Rajagopalan R, Ghate AV, Subbarayan P, Linz W, Schoelkens BA (1993) Cardiotonic activity of the water soluble forskolin derivative 8,13-epoxy-6β-(piperidinoacetoxy)-1α,7β,9α-trihydroxy-labd-14-en-11-one. Arzneim Forsch/Drug Res 43(I):313–319

Regoli D, Barabé J (1980) Pharmacology of bradykinin and related peptides. Pharmacol Rev 32:1–46

Wisskirchen FM, Burt RP, Marshall I (1998) Pharmacological characterization of CGRP receptors of the rat pulmonary artery and inhibition of twitch responses of the rat vas deferens. Br J Pharmacol 123:1673–1683

A.1.2.2 α-Sympatholytic Activity in the Isolated Guinea Pig Seminal Vesicle

PURPOSE AND RATIONALE

The seminal vesicles of guinea pigs and rats are tubular organs whose longitudinal and annular muscles are innervated by the sympathetic system. The inhibition of contractions induced by norepinephrine or the α_1-selective agonist phenylephrine indicates α-sympatholytic activity. Sharif and Gokhale (1986) recommended the use the isolated rat seminal vesicle as a rather sensitive and specific model.

PROCEDURE

Male guinea pigs weighing 300 to 600 g are sacrificed by a blow to the neck. Both seminal vesicles are prepared and placed in Ringer's solution in an organ bath maintained at 32°C and being oxygenated with 95% O_2/5% CO_2. Isotonic or isometric registration is performed. Changes in length are recorded isotonically using a lever transducer (368 type B, Hugo Sachs Elektronik Freiburg). Isometric force is measured with a force transducer (UC-2 Gould-Statham, Oxnard, USA).

Following an equilibration period of 30 min, contractions are induced by repeated administration of (–)norepinephrine HCl in concentrations of 1 to 5 µg/ml or phenylephrine HCl in concentrations of 10 to 50 µg/ml. After obtaining a stable plateau of identical contractions, the test compound is added into the organ bath. Three min later, the previous concentration of norepinephrine or phenylephrine is added. As standard phentolamine is used in concentrations of 3 to 30×10^{-7} M.

EVALUATION

Contractions of the seminal vesicle induced by the α-adrenergic agonists after addition of the test compound are compared with the initial values and expressed as percentage thereof. For in depth analysis, full dose-response curves of the agonist are recorded before and after addition of various doses of the antagonist. A parallel shift to the right indicates competitive antagonism which can be evaluated as pA_x – values according to Schild (1947)

MODIFICATION OF THE METHOD

Leitch (1954) recommended the use of isolated seminal vesicles of rats for the assay of sympatholytic drugs.

REFERENCES AND FURTHER READING

Brügger J (1945) Die isolierte Samenblase des Meerschweinchens als biologisches Testobjekt zur quantitativen Differenzierung der sympathikolytischen Wirkung der genuinen Mutterkornalkaloide und ihrer Dihydroderivate. Helv Physiol Acta 3:117–134

Green AF, Boura ALA (1964) Depressants of peripheral sympathetic nerve function. I Sympathetic nerve blockade. In: Laurence DR, Bacharach AL (eds) Evaluation of drug activities: Pharmacometrics. Academic Press, London New York, pp 370–430

Leitch JL (1954) The use of the rat's isolated seminal vesicle for the assay of sympatholytic drugs. Br J Pharmacol 9:236–239

Schild HO (1947) pA, a new scale for the measurement of drug antagonism. Br J Pharmacol 2:189–206

Sharif SI, Gokhale SD (1986) Pharmacological evaluation of the isolated rat seminal vesicle preparation. J Pharmacol Meth 15:65–75

A.1.2.3 α-Sympatholytic Activity in the Isolated Vas Deferens of the Rat

PURPOSE AND RATIONALE

The vas deferens of the guinea pig or preferably the rat is used for quantitative evaluation of adrenergic antagonists. The response of this organ to α-adrenergic agonists consists of a strong rapid contraction followed

by quick relaxation on washing the agonists out of the tissue.

PROCEDURE

Male Wistar rats weighing about 300 g are used. The animals are sacrificed by a sharp blow to the neck, the vasa deferentia are dissected free from the extraneous tissues and suspended in a organ bath containing Tyrode solution being oxygenated with a 95% O_2 and 5% CO_2 mixture at 32°C. Isotonic registration is performed at a preload of 0.5 g. Changes in length are recorded isotonically using a lever transducer (e. g., 368 type B, Hugo Sachs Elektronik, Freiburg, FRG).

Following an equilibration period of 30 min, contractions are induced by repeated administration of (–)norepinephrine HCl in concentrations of 0.5, 1.0, 2.0, or 4.0 µg/ml. After obtaining a stable plateau of identical contractions, the test compound is added into the organ bath. Three min later, the previous concentration of norepinephrine is added. As standard phentolamine is used in concentrations of 3 to 30×10^{-7} M.

EVALUATION

Contractions of the vas deferens induced by the α-adrenergic agonist after addition of the test compound are compared with the initial values and expressed as percentage thereof. For in depth analysis, full dose-response curves of the agonist are recorded before and after addition of various doses of the antagonist. A parallel shift to the right indicates competitive antagonism which can be evaluated as pA_x – values according to Schild (1947).

MODIFICATIONS OF THE METHOD

Electrical stimulation of the isolated ductus deferens results in the release of norepinephrine. Stimulation induced contractions of this organ are inhibited by clonidine which impairs adrenergic neurotransmission by activating inhibitory α-receptors. The ductus deferens is suspended in an organ bath bubbled with carbogen and maintained at 37°C. Tension is adjusted to 25 mN. Following a 45 min equilibration period, supramaximal amplitude stimulation by a HSE type 2 stimulator (Hugo Sachs Elektronik, Freiburg) is applied. After stabilization of the response, clonidine is added to the organ bath in accumulated doses. Test compounds are added 5 min prior to clonidine administration. The percent potentiation of clonidine induced inhibition of contractions is determined.

Taylor et al. (1983) used the rat deferens for pharmacological characterization of purinergic receptors.

Nerve-muscle preparations of the vas deferens have been reviewed by Holman (1975).

Hughes et al. (1974) used the electrically stimulated mouse vas deferens for assessment of the agonistic and antagonistic activities of narcotic analgesic drugs.

Ross et al. (2001) used the mouse vas deferens to study structure-activity relationship for the endogenous cannabinoid, anadamide, and certain of its analogues at vanilloid receptors.

Oka et al. (1980) recommended the vas deferens from rabbits as a specific bioassay for opioid κ-receptor agonists.

Mutafova-Yambolieva and Radmirov (1993) studied the effects of endothelin-1 on electrically- or drug-induced contractile responses mediated by purinergic or adrenergic receptors in the isolated prostatic portion of rat vas deferens.

Ward et al. (1990) used isolated vasa deferentia preparations from rat and mouse to study the pharmacological profile of the analgesic pravadoline.

Hukovic (1961) described an isolated ductus deferens preparation together with the sympathetic hypogastric nerve of the guinea pig.

Cordellini and Sannomiya (1984) pretreated guinea pigs with reserpine. In the isolated vasa deferentia concentration-effects curves to phenylephrine were established in the presence of cocaine. The antagonistic effect of phenoxybenzamine was used for receptor occupancy studies.

Donoso et al. (1992) studied neurotransmission in epididymal and prostatic segments of isolated superfused rat vas deferens preparations.

Vaupel and Su (1987) used the vas deferens preparation of guinea pigs to study sigma and phencyclidine receptors.

Eltze (1988) used the field-stimulated (95% of maximum voltage, 0.1 Hz, 0.5 ms) portion of rabbit vas deferens to study muscarinic M_1 and M_2-receptors.

Dumont et al. (1997) used the isolated guinea pig heart and the isolated rat vas deferens for *in vitro* bioassays of calcitonin gene-related peptide (CGRP) agonists and antagonists.

Poyner et al. (1999) found concentration-dependent inhibitions of the electrically stimulated twitch responses of guinea pig vas deferens by calcitonin gene-related peptide, amylin and adrenomedullin.

Couldwell et al. (1993) found that the rat prostate gland possesses a typical α_1-adrenoceptor similar to that found in the vas deferens.

Wisskirchen et al. (1998) tested agonists of calcitonin gene-related peptide, homologues and antagonists in rat isolated vas deferens. The prostatic half was

suspended under 0.5 g resting tension and equilibrated in Krebs solution at 37°C. Contractile responses of the prostatic vas were induced by electrical field stimulation at 0.2 Hz, 1.0 ms and 60 V through parallel platinum electrodes either side of the tissue.

REFERENCES AND FURTHER READING

Cordellini S, Sannomiya P (1984) The vas deferens as a suitable preparation for the study of α-adrenoreceptor molecular mechanisms. J Pharmacol Meth 11:97–107

Couldwell C, Jackson A, O'Brien H, Chess-Williams R (1993) Characterization of the α_1-adrenoceptors of rat prostate gland. J Pharm Pharmacol 45:922–924

Donoso MV, Montes CG, Lewin J, Fournier A, Calixto JB, Huidobro-Toro JP (1992) Endothelin-1 (ET)-induced mobilization of intracellular Ca^{2+} stores from the smooth muscle facilitates sympathetic cotransmission by potentiation of adenosine 5′-triphosphate (ATP) motor activity: studies in the rat vas deferens. Peptides 13:831–840

Dumont Y, Fournier A, St-Pierre S, Quirion R (1997) A potent and selective $CGRP_2$ agonist, [Cys(Et)^{2,7}]hCGRPα: comparison in prototypical $CGRP_1$ and $CGRP_2$ *in vitro* bioassays. Can J Physiol Pharmacol 75:671–676

Eltze M (1988) Muscarinic M_1 and M_2-receptors mediating opposite effects on neuromuscular transmission in rabbit vas deferens. Eur J Pharmacol 151:205–221

Holman ME (1975) Nerve-muscle preparations of the vas deferens. In: Daniel EE, Paton DM (eds) Methods in Pharmacology, Vol 3, Smooth Muscle. Plenum Press, New York and London, pp 403–417

Hughes J, Kosterlitz HW, Leslie FM (1974) Assessment of the agonistic and antagonistic activities of narcotic analgesic drugs by means of the mouse vas deferens. Br J Pharmacol 51:139P–140P

Hukovic S (1961) Responses of the isolated sympathetic nerve-ductus deferens preparation of the guinea pig. Br J Pharmacol 16:188–194

Lindner E (1963) Untersuchungen über das Verhalten des N-(3′-phenylpropyl-(2′))-1,1-diphenylpropyl-(3)-amins (Segontin) gegenüber den Wirkungen des Noradrenalins. Arch Int Pharmacodyn 146:475–484

Lotti VJ, Taylor DA (1982) α_2-adrenergic agonist and antagonist activity of the respective (–)- and (+)-enantiomers of 6-ethyl-9-oxaergoline (EOE). Eur J Pharmacol 85:211–215

Moore PK, Griffiths RT (1982) Pre-synaptic and post-synaptic effects of xylazine and naphazoline on the bisected rat vas deferens. Arch Int Pharmacodyn 260:70–77

Mutafova-Yambolieva V, Radomirov R (1993) Effects of endothelin-1 on postjunctionally-mediated purinergic and adrenergic components of rat vas deferens contractile responses. Neuropeptides 24:35–42

Ohlin P, Stromblad BCR (1963) Observations on isolated vas deferens. Br J Pharmacol 20:299–306

Oka T, Negishi K, Suda M, Matsumiya T, Inazu T, Ueki M (1980) Rabbits vas deferens: a specific bioassay for opioid κ-receptor agonists. Eur J Pharmacol 73:235–236

Poyner DR, Taylor GM, Tomlinson AE, Richardson AG, Smith DM (1999) Characterization of receptors for calcitonin gene-related peptide and adrenomedullin on the guinea pig vas deferens. Br J Pharmacol 126:1276–1282

Ross RA, Gibson TM, Brockie HC, Leslie M, Pashmi G, Craib SJ, DiMarzo V, Pertwee RC (2001) Structure-activity relationship for the endogenous cannabinoid, anadamide, and certain of its analogues at vanilloid receptors in transfected cells and vas deferens. Br J Pharmacol 132:631–640

Schild HO (1947) pA, a new scale for the measurement of drug antagonism. Br J Pharmacol 2:189–206

Taylor DA, Wiese S, Faison EP, Yarbrough GGl (1983) Pharmacological characterization of purinergic receptors in the rat deferens. J Pharmacol Exp Ther 224:40–45

van Rossum JM (1965) Different types of sympathomimetic α-receptors. J Pharm Pharmacol 17:202–216

Vaupel DB, Su TP (1987) Guinea pig vas deferens preparation may contain both sigma receptors and phencyclidine receptors. Eur J Pharmacol 139:125–128

Wisskirchen FM, Burt RP, Marshall I (1998) Pharmacological characterization of CGRP receptors of the rat pulmonary artery and inhibition of twitch responses of the rat vas deferens. Br J Pharmacol 123:1673–1683

A.1.2.4 α-Sympatholytic Activity in the Isolated Rat Spleen

PURPOSE AND RATIONALE

α-Stimulant agents (such as epinephrine, norepinephrine) or electrical stimulation induce contractions in sympathetically innervated organs such as spleen smooth muscle. These effects can be antagonized by drugs with α-blocking activities such as phentolamine.

PROCEDURE

Male Sprague-Dawley rats weighing 180–220 g are used. The animal is sacrificed in CO_2 anesthesia. The spleen is removed and cut longitudinally into two halves. Each part is placed in an organ bath containing nutritive solution. The bath solution is bubbled with carbogen and maintained at 37°C. Following a 30 min incubation period under a tension of 0.5 g, contractions are elicited by administration of epinephrine (10^{-6} g/ml) or norepinephrine 10^{-6} g/ml). After obtaining 3 approximately identical spasms, the test compound is administered followed by the addition of the spasmogen 5 min later. The contractile response is allowed to plateau and recorded.

Standard compound:

- phentolamine

EVALUATION

The contractile force is recorded at its maximal level before and after drug administration. The percent inhibition of epinephrine or norepinephrine induced contraction is determined.

REFERENCES AND FURTHER READING

DiPalma (1964) Animal techniques for evaluating sympathomimetic and parasympathomimetic drugs. In: Nodine JH,

Siegler PE (eds) Animal and pharmacologic techniques in drug evaluation. Vol I, pp 105–110. Year Book Medical Publ., Inc. Chicago

Swamy VC (1971) α-adrenergic blocking agents. In: Turner RA, Hebborn P (eds) Screening Methods in Pharmacology, Vol II, pp 1–19, Academic Press, New York and London

Turner RA (1965) Sympatholytic agents. In: Screening methods in pharmacology, Vol I, pp 143–151, Academic Press, New York and London

A.1.2.5 α-Sympatholytic Activity in the Isolated Rat Anococcygeus Muscle

PURPOSE AND RATIONALE

The rat anococcygeus muscle as pharmacological tool was introduced by Gillespie (1972, 1980), Gibson and Gillespie (1973). This smooth muscle has a dense adrenergic innervation and contracts to noradrenaline, acetylcholine, 5-hydroxytryptamine, but not to histamine. Moreover, the muscle contracts to field stimulation or stimulation of extrinsic nerves. The preparation can be used to assess the pre- and post-synaptic α-adrenoceptor blocking activity of drugs (Doggrell 1980, 1983).

PROCEDURE

The two anococcygeus muscles arise from the upper coccygeal vertebra close to one another in the midline of the pelvic cavity. The muscles pass caudally, lying first behind and the to one side of the colon, finally joining together to form a ventral bar in front of the colon a few mm from the anus. The extrinsic nerves pass in a branch of the perineal nerve on either side to enter the deep surface of each muscle just before the formation of the ventral bar.

After sacrifice, the abdomen of rats is opened in the mid-line, the pelvis split and the bladder and urethra removed. Care is required in clearing the lower part of the urethra to avoid damage to the ventral bar of muscle, the only region lying ventral to the colon. The colon is then cut through at the pelvic brim, the pelvic portion pulled forward and the delicate connective tissue behind cleared until the anococcygeus muscles come into view. The muscles are isolated, in some instances with the extrinsic nerve intact. The extrinsic nerves on either side run in the posterior scrotal branch of the perineal nerve and leave it to enter the deep surface of the anococcygeal muscles as the lie on the lateral surface of the colon. The ventral bar is cut through and each muscle mounted in a 100 ml bath containing Krebs solution at 36°C. The solution is gassed with 95% O_2+5% CO_2. Tension is measured with isometric transducers and displayed on a polygraph. Field stimulation of the intramural nerves is applied after drawing the muscles through a pair of electrodes similar to those described by Burn and Rand (1960); when the muscles are stimulated through their extrinsic nerves the nerves are drawn through similar electrodes. Stimulation of either intramural or extrinsic nerves is with 1 ms pulses at 20 Hz, and at a supramaximal voltage.

Dose-response curves are established with doses of 2×10^{-7} to 4×10^{-6} M noradrenaline, 4×10^{-7} to 4×10^{-5} M acetylcholine or with graded frequencies of electrical stimulation.

The effect of noradrenaline is abolished by α-adrenergic antagonists, such as 10^{-6} M phentolamine. Dose-response curves show a parallel shift characteristic of competitive antagonism.

EVALUATION

Contractions of the anococcygeus muscle induced by an α-adrenergic agonist after addition of the test compound are compared with the initial values and expressed as percentage thereof. For in depth analysis, full dose-response curves of the agonist are recorded before and after addition of various doses of the antagonist. A parallel shift to the right indicates competitive antagonism which can be evaluated as pA_x – values according to Schild (1947).

MODIFICATIONS OF THE METHOD

Gibson et al. (1990) found L-N^G-nitroarginine to be a potent inhibitor of non-adrenergic, non-cholinergic relaxations in the rat anococcygeus muscle.

Oliveira and Bendhack (1992) found that dopamine has a dual effect in the rat anococcygeus muscle: a partial effect due to an indirect sympathomimetic action and a partial effect due the interaction with postjunctional receptors.

Brave et al. (1993) investigated the interaction between motor sympathetic and inhibitory non-adrenergic, non-cholinergic nerves in the rat anococcygeus muscle using L-N^G-nitroarginine, an inhibitor of L-arginine:NO synthase.

Cakici et al. (1993) described a coaxial bioassay system consisting of guinea pig trachea as donor organ for epithelial derived-relaxing factors and phenylepinephrine-precontracted rat anococcygeus muscle as assay tissue.

Iravani and Zar (1993) found differential effects of nifedipine on nerve-mediated and noradrenaline-evoked contractions of rat anococcygeus muscle.

Rand and Li (1993) studied the modulation of acetylcholine-induced contractions of the rat anococcygeus muscle by activation of nitrergic nerves.

Mudumbi and Leighton (1994) investigated the mechanisms of action of relaxation induced by bradykinin and by electrical field stimulation in isolated rat anococcygeus muscle, where contractile tone had been elevated with clonidine.

Gwee et al. (1995) investigated the prejunctional and postjunctional inhibition of adrenergic transmission in the rat isolated anococcygeus muscle by cimetidine.

Najbar et al. (1996) found that smooth muscle cells in the rat anococcygeus muscle are endowed with two distinct P-2-purinoreceptors which subserve contractions.

De Godoy et al. (2003) evaluated the inhibitory effects of atropine and hexamethonium on the angiotensin-II-induced contraction of rat anococcygeus muscles. Pettibone et al. (1993) examined the inhibitory potency and selectivity of an oxytocin antagonist against oxytocin-stimulated contractions if the **mouse** anococcygeus muscle.

Dehpour et al. (1993) and Radjaee et al. (1996) used isolated anococcygeus muscles from **rabbits** and found an extremely regular activity induced by methoxamine or clonidine.

REFERENCES AND FURTHER READING

Brave SR, Bhat S, Hobbs AJ, Tucker JF, Gibson A (1993) Influence of L-N^G-nitroarginine on sympathic nerve induced contraction and noradrenaline release in the rat anococcygeus muscle. J Auton Pharmacol 13:219–225

Burn HJ, Rand MJ (1960) The relation of circulating noradrenaline to the effect of sympathetic stimulation. J Physiol 150:295–305

Cakici I, Tunctan B, Abacioglu N, Kanzik I (1993) Epithelium-dependent responses of serotonin in a coaxial bioassay system. Eur J Pharmacol 236:97–105

De Godoy MAF, Accorsi-Mendonça D, de Oliviera AM (2003) Inhibitory effects of atropine and hexamethonium on the angiotensin II-induced contraction of the rat anococcygeus muscles. Naunyn-Schmiedebergs Arch Pharmacol 367:176–182

Dehpour AR, Tajkhorshid E, Radjaee-Behbahani N, Kheirollahi K (1993) Methoxamine-induced rhythmic activity in rabbit anococcygeus muscle. Gen Pharmacol 24:841–845

Doggrell SA (1980) The assessment of pre- and post-synaptic a-adrenoceptor blocking activity of drugs using the rat anococcygeus muscle. J Pharmacol Meth 3:323–331

Doggrell SA (1983) On the assessment of the potency of antagonists using the rat isolated anococcygeus muscle. J Pharmacol Meth 10:243–254

Gibson A, Hobbs AJ, Mirzazadeh D (1990) L-N^G-nitroarginine is a potent inhibitor of non-adrenergic, non-cholinergic relaxations in the rat anococcygeus muscle. Eur J Pharmacol 183:1793

Gillespie JS (1972) The rat anococcygeus muscle and its response to nerve stimulation and to some drugs. Br J Pharmacol 45:404–416

Gillespie JS (1980) The physiology and pharmacology of the anococcygeus muscle. Trends Pharmacol Sci 1:453–457

Gibson A, Gillespie JS (1973) The effect of immunosympathectomy and of 6-hydroxydopamine on the response of the rat anococcygeus muscle to nerve stimulation and to some drugs. Br J Pharmacol 47:261–267

Gwee MCE, Cheahj LS, Shoon ML (1995) Prejunctional and postjunctional inhibition of adrenergic transmission in the rat isolated anococcygeus muscle by cimetidine. J Auton Pharmacol 15:177–185

Iravani MM, Zar MA (1993) Differential effects of nifedipine on nerve-mediated and noradrenaline-evoked contractions of rat anococcygeus muscle. Eur J Pharmacol 250:193–195

Kulkarni SK, Sharma A (1994) Rat anococcygeus: A dynamic smooth muscle preparation for experimental pharmacology. Methods Find Exp Clin Pharmacol 16:379–385

Mudumbi RV, Leighton HJ (1994) Analysis of bradykinin-induced relaxations in the rat isolated anococcygeus muscle. Life Sci 54:813–821

Najbar ATZ, Li CG, Rand MJ (1996) Evidence for two distinct P-2-purinoreceptors subserving contraction of the rat anococcygeus smooth muscle. Br J Pharmacol 118:537–542

Oliveira AM, Bendhack LM (1992) Dopamine-induced contractile responses of the rat anococcygeus muscle. Arch Int Pharmacodyn Ther 316:97–104

Pettibone DJ, Clineschmidt BV, Guidotti MT, Lis EV, Reiss DR, Woyden CJ, Bock MG, Evans BE, Freidinger RM, Hobbs DW, Veber DF, Williams PD, Chiu SHL, Thompson KL, Schorn TW, Siegl PKS, Kaufman MJ, Cukierski MA, Haluska GJ, Cook MJ, Novy MJ (1993a) L-368,899, a potent orally active oxytocin antagonist for potential use in preterm labor. Drug Dev Res 30:129–142

Radjaee-Behbahani N, Dehpour AR, Tajkhorshid E, Kheirollahi K (1993) Clonidine-induced rhythmic activity in rabbit anococcygeus muscle. Gen Pharmacol 27:525–528

Rand MJ, Li CG (1993) Modulation of acetylcholine-induced contractions of the rat anococcygeus muscle by activation of nitrergic nerves. Br J Pharmacol 110:1479–1482

Schild HO (1947) pA, a new scale for the measurement of drug antagonism. Br J Pharmacol 2:189–206

A.1.2.6 β_1-Sympatholytic Activity in Isolated Guinea Pig Atria

PURPOSE AND RATIONALE

The β-agonist isoprenaline (isoproterenol) induces an increase in the frequency and force of contraction of spontaneously beating isolated right atrias and potentiates contractions of electrically stimulated isolated left atria. Drugs with β-sympatholytic activity inhibit these isoprenaline-induced effects. β-receptor blocking activity of drugs can be evaluated in isolated right (a) and left (b) guinea pig atria. Since the heart contains predominantly β_1-adrenoreceptors, β_1-blocking activity is assessed by this test.

PROCEDURE

Pirbright White guinea pigs of either sex weighing 250–300 g are used. The animal is sacrificed by stunning and exsanguination. The heart is removed, the right or the left atrium is cut off and mounted in a 50 ml organ bath with a preload of 100 mg. The Krebs-

Henseleit solution is maintained at 32°C and aerated with 95% O_2/5% CO_2. Contractions are recorded isotonically using a lever transducer (368 type B, Hugo Sachs Elektronik, Freiburg).

Right Atrium

After an equilibration period of 30 min, isoprenaline is administered into the organ bath to potentiate inotropy and frequency of the isolated right atrium. Cumulative doses of isoprenaline are added starting from a concentration of 0.05 µg/ml; consecutive doses are administered at 3 min intervals.

When a stable maximum plateau of the effect is achieved, the organ bath is thoroughly flushed for 1 min; flushing is repeated twice 5 and 20 min later. The whole procedure is repeated with the same isoprenaline concentrations (control baseline values = 100%).

The test compound is then added into the organ bath and 5 min later, again isoprenaline is given at cumulative doses.

If the test compound has β-receptor blocking activity (β-sympatholytic),

1. higher isoprenaline concentrations are necessary to induce the same potentiation of inotropy and frequency or
2. at the same isoprenaline concentrations added as before, the increase in inotropy and frequency is reduced.

At the end of the experiment, again a cycle without test drug is performed.

Left Atrium

The left atrium is stimulated by a square wave stimulator with 2 impulses/s at a voltage of 15 V and an impulse duration of 1 ms. After an equilibration period of 30 min, the β-agonist isoprenaline is added at concentrations of 0.05–0.1 mg/ml. The organ bath is then thoroughly flushed for 1 min. Flushing is repeated twice 5 and 20 min later. The whole procedure is repeated with the same cumulative isoprenaline concentrations (control baseline values = 100%) and flushing procedure.

When a stable plateau of contractions is achieved, the test compound is added into the organ bath and 3 min later, isoprenaline is added again at cumulative concentrations.

If the test compound has β-receptor blocking activity (β-sympatholytic), the isoprenaline-induced effects are inhibited.

In addition, refractory period is determined before and after drug administration.

EVALUATION

a) Percent inhibition of (a) isoprenaline-induced or (b) electrically-induced and isoprenaline-potentiated increased inotropy and frequency by test drug is calculated as compared to pre-drug activity (= 100%).
b) Percent change in refractory period is calculated.

IC_{50} values are determined from the individual dose-response curves.

Statistical evaluation is performed by means of the paired *t*-test.

Standard compounds:

- propranolol HCl,
- amrinon,
- nifedipine,
- and milrinone.

MODIFICATIONS OF THE METHOD

A detailed description of the use of isolated atrial preparations has been given by Levy (1971).

Instead of the right atrium, Doggrell and Hughes (1986) used the isolated right ventricle of the rat for the assessment of the β-adrenoreceptor blocking activity of propranolol and investigated the competitive nature of the isoproterenol antagonism at various doses with Schild-plot analysis. Doggrell (1988) used the isolated left atria of the rat for simultaneous assessment of membrane-stabilizing and β-adrenoreceptor blocking activity.

Berthold et al. (1990) described a method for testing cardiotonic sodium channel activators in isolated, electrically stimulated left guinea pig atria after potassium depolarization.

Olson et al. (1995) studied the function of isolated rat left atria and papillary muscles and quantified the voltage-response relationship between punctate and field electrical stimulation after pretreatment with reserpine or β-blockers.

REFERENCES AND FURTHER READING

Berthold H, Scholtysik G, Schaad A (1990) Identification of cardiotonic sodium channel activators by potassium depolarization in isolated guinea pig atria. J Pharmacol Meth 24:121–135

Doggrell DH (1988) Simultaneous assessment of membrane-stabilizing and β-adrenoreceptor blocking activity of drugs with the rat isolated left atria. J Pharmacol Meth 19:93–107

Doggrell S, Hughes EW (1986) On the assessment of the β-adrenoreceptor blocking activity of propranolol using the rat isolated right ventricle. J Pharmacol Meth 15:119–131

Furchgott RF (1967) Techniques for studying antagonism and potentiation of sympathomimetic drugs an isolated tissues. In: Siegler PE, Moyer JH (eds) Animal and clinical phar-

macologic techniques in drug evaluation. pp 256–266. Year Book Medical Publishers, Inc., Chicago
Grodzinska L, Gryglewski R (1971) Action of beta-adrenolytics on the isolated guinea pig atria. Arch Int Pharmacodyn 191:133–141
Grupp IL, Grupp G (1984) Isolated heart preparations perfused or superfused with balanced salt solutions. In: Schwartz A (ed) Methods in Pharmacology, Vol 5: Myocardial Biology. pp 111–128. Plenum Press, New York London
Levy JV (1971) Isolated atrial preparations. In: Schwartz A (ed) Methods in Pharmacology Vol 1, pp 77–104. Appleton-Century-Crofts, Meredith Corporation, New York
Olson RD, Vestal RE, Mednhall WA, Mudumbi RV (1995) Quantification of the voltage-response relationship between punctate and field electrical stimulation and the function of isolated rat left atria and papillary muscles. J Pharmacol Toxicol Meth 34:225–230

A.1.2.7 β_2-Sympatholytic Activity in the Isolated Tracheal Chain

PURPOSE AND RATIONALE

Contraction of bronchial smooth muscle is induced by the cholinergic agonist carbachol. The carbachol effect can be antagonized by the β-agonist isoprenaline (isoproterenol). A compound has β-sympatholytic activity if the spasmolytic action of isoprenaline is inhibited. The β-sympatholytic effect of drugs can be evaluated in an *in vitro* model. Since the trachea contains predominantly β_2-adrenoreceptors, β_2-blocking activity can be assessed by this test.

PROCEDURE

Male Pirbright White guinea pigs weighing 250–300 g are used. The animals are sacrificed by stunning and exsanguination. The trachea is removed and cut into individual rings. Six rings are connected in series by means of short loops of silk thread. The tracheal chain is mounted in an 50 ml organ bath with a preload of 1 g for isotonic registration. To the nutritive solution (Tyrode) containing ascorbic acid and 1.0 g/L glucose, the α-receptor blocking agent phentolamine (0.1 µg/ml) and the spasmogen carbachol (80 ng/ml) are added. The solution is maintained at 34°C and aerated with 95% O_2, 5% CO_2

Experimental Course

After an equilibration period of 30 min, cumulative doses of 10^{-10} to 10^{-7} M of the spasmolytic agent isoprenaline are added. When maximal relaxation is obtained, the organ bath is flushed and the procedure repeated. After the two control relaxations with isoprenaline, the tissue is rinsed thoroughly and the first dose of the test compound is administered. Three min later, cumulative doses of isoprenaline are administered as before. Following a 10 min washout and recovery period, the next dose of the test compound is given. Up to 10 drug concentrations can be tested with one organ.

Standard compounds:

- propranolol
- practolol

EVALUATION

Percent inhibition of isoprenaline-induced relaxation under drug treatment is calculated compared to maximal relaxation induced by isoprenaline alone (control = 100%).

A competitive antagonism of test compound is evaluated and can be quantitated from the dose-response curve.

MODIFICATIONS OF THE METHOD

O'Donnell and Wanstall (1980) used guinea pig tracheal preparations, where K^+-depolarization was achieved by replacing all the Na^+ in Krebs solution by an equivalent amount of K^+ causing a sustained contraction of the preparations. A dose-dependent relaxation effect of isoprenaline could be obtained provided that the preparations were repolarized by washing in normal Krebs solution between curves. pA_2 values were in good agreement with values obtained in other types of tracheal preparations.

Guinea pig superfused trachea and dispersed tracheal cells have been used by Buckner et al. (1995) to compare the effects of isoproterenol and forskolin on immunologic and nonimmunologic histamine release.

Lundblad and Persson (1988) found that epithelial removal is of little consequence for the pharmacology of the guinea pig tracheal open ring preparation *in vitro*.

The rat portal vein has been recommended as model for assessment of β_2 adrenoceptor blocking activity of drugs by Doggrell (1990).

REFERENCES AND FURTHER READING

Buckner CK, Fishleder RI, Conklin R, Graziano FM (1995) A comparison of the effects of isoproterenol and forskolin on immunologic and nonimmunologic release of histamine from guinea-pig superfused trachea and dispersed tracheal cells. J Pharmacol Toxicol Meth 33:47–52
Castillo JC, de Beer EJ (1947). The tracheal chain. I. A preparation for the study of antispasmodics with particular reference to bronchodilator drugs. J Pharmacol Exp Ther 90:104–109
Doggrell SA (1990) Assessment of the β_2 adrenoceptor and Ca^{2+} channel-blocking activity of drugs with the rat portal vein. J Pharmacol Meth 24:145–156

Foster RW (1965) The nature of the adrenergic receptors of the trachea of the guinea-pig. J Pharm Pharmac 18:1–12
Green AF, Boura ALA (1964) Sympathetic nerve blockade. In: Laurence DR, Bacharach AL (eds) Evaluation of drug activities: Pharmacometrics. Academic Press, London and New York, pp 370–430
Longmore J, Miller M, Trezise DJ, Weston AL (1991) Further studies on the mechanism of action of isoprenaline in bovine tracheal smooth muscle. Br J Pharmacol 102:Proc Suppl 182P
Lundblad KA, Persson CG (1988) The epithelium and the pharmacology of guinea-pig tracheal tone *in vitro*. Br J Pharmacol 93:909–917
O'Donnell SR, Wanstall JC (1980) The use of guinea pig K^+-depolarized tracheal chain preparations in β-adrenoreceptor studies. J Pharmacol Meth 4:43–50
Trendelenburg P (1912) Physiologische und pharmakologische Untersuchungen an der isolierten Bronchialmuskulatur. Naunyn-Schmiedeberg's Arch Exp Pathol Pharmakol 69:79–107
Van Rossum JM (1963) Cumulative dose-response curves. II. Technique for the making of dose-response curves in isolated organs and the evaluation of drug parameters. Arch Int Pharmacodyn 143:299–300
Waldeck B, Widmark E (1985) Comparison of the effects of forskolin and isoprenaline on tracheal, cardiac and skeletal muscle from guinea-pig. Eur J Pharmacol 112:349–353

A.1.2.8 Angiotensin Converting Enzyme Inhibition in the Isolated Guinea Pig Ileum

PURPOSE AND RATIONALE

The angiotensin-converting enzyme (ACE) is responsible for the formation of the active angiotensin II from the inactive angiotensin I. The same enzyme is responsible for the degradation of the active peptide bradykinin to inactive products. ACE activity can therefore be measured in two ways: activity of the newly formed angiotensin II and inhibition of the activity of bradykinin. ACE inhibition results in decreased activity of the precursor angiotensin I and potentiation of the bradykinin effect. The guinea pig ileum contracts in response to both peptides, angiotensin II and bradykinin, and can be used for quantitative determination of ACE inhibiting activity.

PROCEDURE

Guinea pigs of either sex weighing 300 to 500 g are used. They are sacrificed by stunning and exsanguination. The abdomen is opened with scissors. Just distal to the pylorus, a cord is tied around the intestine which is then severed above the cord. The intestine is gradually removed, and the mesentery is being cut away as necessary. When the colon is reached, the intestine is cut free. Below the cord, the intestine is cut halfway through, so that a glass tube can be inserted. Tyrode's solution is passed through the tube and the intestine until the effluent is clear. Mesentery is cut away from the intestine that was joined to the colon. Pieces of 3 cm length are cut. Preferably, the most distal piece is used being the most sensitive one. This piece is fixed with a tissue clamp and brought into an organ bath with Tyrode's solution at 37°C being oxygenated with O_2. The other end is fixed to an isometric force transducer (UC 2 Gould-Statham, Oxnard USA). Responses are recorded on a polygraph.

Angiotensin I Antagonism

After an equilibrium time of 30 min, angiotensin I is added in a concentration of 10 ng/ml bath solution. The force of contraction is recorded and the angiotensin I dosage is repeated once or twice until the responses are identical. Then the potential ACE inhibitor is added. After 5 min incubation time, again angiotensin I is added. The contraction is diminished depending on the activity of the ACE inhibitor.

Bradykinin Potentiation

Pieces of guinea pig ileum are prepared as described before. After an equilibrium time of 30 min bradykinin is added in a concentration of 15 ng/ml bath solution. The force of contraction is recorded and bradykinin additions are repeated once or twice until the response is identical. Then the potential ACE inhibitor is added. After 5 min incubation time, again bradykinin is added. The contraction is potentiated depending on the activity of the ACE inhibitor.

EVALUATION

Angiotensin I Antagonism

The contraction after addition of the ACE inhibitor is expressed as percentage of contraction without the ACE inhibitor. Using various doses of the ACE inhibitor IC_{50} values (concentrations inducing 50% inhibition) are calculated. As standards ramipril, enalapril, and captopril are used.

Bradykinin Potentiation

The increase of the contraction after addition of the ACE inhibitor is expressed as percentage of contraction without the ACE inhibitor. As standard ramiprilate is used.

CRITICAL ASSESSMENT OF THE METHOD

The classical method of the isolated guinea pig ileum has been proven to be a reliable method for screening of potential ACE inhibitors.

REFERENCES AND FURTHER READING

Rubin B, Laffan RJ, Kotler DG, O'Keefe EH, Demaio DA, Goldberg ME (1978) SQ 14,225 (D-3-mercapto-2-methylpropanoyl-L-proline), a novel orally active inhibitor of angiotensin I-converting enzyme. J Pharmacol Exp Ther 204:271–280

A.1.2.9 Contractile and Relaxing Activity on Isolated Blood Vessels Including Effects of Potassium Channel Openers

PURPOSE AND RATIONALE

The contractile process within the vascular smooth muscle results from an increase in the concentration of intracellular Ca^{2+}. Inhibition of vasoconstriction occurs by addition of calcium antagonists or by removal of extracellular calcium. The vasorelaxing effects of compounds can be tested in isolated rodent arteries (pulmonary artery, thoracic aorta). Arterial rings or strips with or without endothelial lining are contracted with different agents, e. g., extracellular K^+ and Ca^{2+}, the α-adrenoceptor agonists phenylephrine and noradrenaline, the Ca^{2+} ionophore A23187 or the thromboxane receptor agonist U46619. Compounds with vasodilating activity antagonize the induced contractions.

Potassium channel openers such as cromakalin, nicorandil, pinacidil or HOE 234 induce relaxation of contracted smooth musculature (Bolton et al. 1998). These effects are explained by data from patch clamp technique and ion flux experiments as well as by antagonism against potassium channel blockers. They indicate the potential use as antihypertensive and anti-asthmatic drugs (Hamilton and Weston 1989; Edwards and Weston 1990, 1993; Weston and Edwards 1992). The studies are complicated by the high diversity of potassium channels including ATP-sensitive, voltage-sensitive and Ca^{2+}-activated channels (Mourre et al. 1986; Blatz and Magleby 1987; Ashcroft and Ashcroft 1990; Jan and Jab 1990; Pongs 1992; Wann 1993). Since each functional channel appears to consist of four different subunits, the possibility exists that there may be hundreds of different voltage-sensitive K channels, depending on their subunit composition. Ashcroft and Gribble (2000) discussed new windows on the mechanism of action of K_{ATP} channel openers.

Glibenclamide is an antagonist of the ATP-modulated K^+ channel allowing the localization of the binding sites (Eltze 1989; French et al. 1990; Mourre et al. 1990; Miller et al. 1991).

PROCEDURE

Male Pirbright White guinea pigs weighing about 400 g, or Chinchilla rabbits weighing about 3.5 kg, or Sprague-Dawley rats weighing 250–400 g are used as donor animals. The tested vessels are the thoracic aorta or the arteria pulmonalis.

Materials and solutions

Physiological salt solutions (PSS) [mM]			
	PSS I	PSS II	PSS III
NaCl	122	112	72 (92)
KCl	5.0	5	40 (20)
$CaCl_2$	1.2	–	–
$MgSO_4$	0.56	0.56	0.56
KH_2PO_4	1.2	1.2	1.2
$NaHCO_3$	25	25	25
EDTA	–	0.2	–
glucose	12	12	12

Contracting agents	
$K^+ + Ca^{2+}$	40 mM + 0.5 mM
$K^+ + Ca^{2+}$	20 mM + 0.5 mM
U 46619 (thromboxane A_2 analogue)	1 µM
A 23187 (calcium ionophore)	5 µM
noradrenaline	1 µM
phenylephrine	0.1 µM
acetylcholine	1 µM
oxyhemoglobin	10 µM
methylene blue	10 µM

Animals are sacrificed by stunning and exsanguination. At least 4 isolated organs are tested per drug. The heart and the pulmonary artery are quickly removed and immersed in PSS I at room temperature. The artery is dissected into rings and endothelial cells are removed by gently rubbing the intimal surface. Spirally cut strips of 15–20 mm length and 1–1.5 mm width are suspended at a resting force of 380 mg in an organ bath containing 20 ml oxygenated (95% O_2, 5% CO_2) PSS I at 37°C. Changes in length are recorded isotonically using a lever transducer (368 type B, Hugo Sachs Elektronic, Freiburg).

To test the effect of compounds on vessels with intact endothelial lining, the thoracic aorta of rats is isolated and dissected free from surrounding tissue. Rings of 3 mm width are cut and suspended in the organ bath containing PSS I. Isometric force is measured with a force transducer (UC-2, Gould-Statham, Oxnard, USA) under a resting tension of 500 mg.

The functional integrity of the endothelium is tested before drug administration. One µM acetylcholine in the organ bath should result in a transient relaxation.

After an equilibration period of 1 h, contraction of each vessel strip or ring is induced by addition of one of the contracting agents into the organ bath.

To induce contractions of potassium-depolarized vessels, three different PSS solutions are used (PSS I for 30 min, PSS II for 3×15 min and PSS III). Contraction is induced in the presence of PSS III by adding 0.5 mM Ca^{2+} into the organ bath.

When a stable plateau of contraction is achieved, cumulative concentrations of the test compound are added into the organ bath to obtain drug-response curves. Consecutive concentrations are added either at 1 h-intervals or when the response of the previous dose has reached a steady state level.

In order to study the time course of relaxation and the duration of action, only one concentration is tested.

To test whether the mechanism of action of a vasorelaxing agent is related to the liberation of nitric oxide, methylene blue or oxyhemoglobin (10 μM) are added to the organ bath 15–30 min prior to the cumulative administration of the test compound. Methylene blue or oxyhemoglobin block selectively NO induced relaxation.

EVALUATION

Mean values of relaxation ± SEM are calculated. The height of contraction before the first drug administration is taken as 100%.

IC^{50} values are determined from the individual dose-response curves. IC^{50} is defined as the dose of drug leading to a 50% relaxation of the contraction induced by KCl or other agonists.

Statistical evaluation is performed by means of the *t*-test.

MODIFICATIONS OF THE METHOD

Calderone et al. (1996) compared four **rat** aortic preparation (single ring, spiral strip, zig-zag strip, and multiple ring) on the basis of responses to noradrenaline and acetylcholine. They recommended the multiple ring preparation as the most suitable of all four for the study of vasoactive drugs because of the reproducibility of both contracturant and relaxing responses.

Kent et al. (1982) used rat aortic strips contracted to a stable tension by either phenylephrine or barium chloride for comparison of vasodilators.

Wilson et al. (1988) studied in isolated rings of rat aorta precontracted with noradrenaline the antagonism of glibenclamide against the vasorelaxation induced by cromakalin.

Löhn et al. (2002) cannulated cerebral arteries from mice with glass cannulas on both sides, allowing an application of hydrostatic pressure to the vessel. Diameter was measured by using a videomicroscopic system (Nikon Diaphot, Düsseldorf, Germany) connected to a personal computer with appropriate software for detection of changes of vessel diameter (TSE, Bad Homburg, Germany).

Nishimura and Suzuki (1995) tested the contractile responses to 5-HT in basilar arteries, superior mesenteric arteries and thoracic aortas from **stroke-prone spontaneously hypertensive rats** in comparison to normal Wistar–Kyoto rats and found that that the hyperresponsiveness to 5-HT is mediated by different 5-HT receptor subtypes.

Fouda et al. (1991) used **the isolated tail arteries from rats**. Differences of the vasoconstrictor response to potassium and norepinephrine between tail arteries from spontaneously hypertensive, renovascular hypertensive, and various strains of normotensive rats were found.

Hamilton et al. (1986), Dacquet et al. (1987) studied the effects of calcium entry blockers in **rat portal vein**.

Bråtveit and Helle (1984) studied the inhibition of vascular smooth muscle by vasoactive intestinal peptide (VIP) in the isolated rat portal vein.

Shetty and Weiss (1987) studied the inhibition of spontaneous rhythmic movements and norepinephrine-induced tension responses in the rat portal vein.

Edwards et al. (1991) compared the effects of several potassium-channel openers on rat bladder and rat portal vein *in vitro*.

Smith et al. (1993) tested the ability of C-terminally truncated fragments of human α-calcitonin gene-related peptide to relax **mesenteric arteries** precontracted with norepinephrine

Chen et al. (1996) studied the contractile effects of noradrenaline and neuropeptide Y given alone or in combination on isolated rat mesenteric resistance vessels.

Gurden et al. (1993) used **guinea pig** aorta relaxation for functional characterization of adenosine receptor types.

Eltze (1989) studied the antagonism of glibenclamide against potassium channel openers in the isolated **guinea pig pulmonary artery**.

Szentmiklósi et al. (1995) used circular segments from the proximal part of the main pulmonary artery of guinea pigs to study contractile and relaxant effects of adenosine receptors.

Pikkers and Hughes (1995) examined the effect of hydrochlorothiazide on intracellular calcium concentration $[Ca^{2+}]_i$ and tone in **guinea pig mesenteric arteries**. Vessels were mounted on a microvascular myograph and loaded with the Ca^{2+}-sensitive fluorescent dye, Fura-2.

Nishimura et al. (1998) used isolated aorta rings from **Syrian hamsters**. Contractile responses were recorded with an isometric transducer (TSE, Bad Homburg, Germany) and stored (TSE Data acquisition software).

Meisheri et al. (1990) recommended the use of the isolated **rabbit mesentery artery** as a sensitive *in vitro* functional assay to detect K^+-channel-dependent vasodilators.

Mironneau and Gargouil (1979) studied the influence on electrophysiological and mechanical parameters of longitudinal smooth muscle strips isolated from **rabbit portal vein** by means of a double sucrose gap method associated with a photoelectric device for recording contractions.

Lauth et al. (2001) performed superfusion assays with **rabbit jugular vein**. Four venous ring segments (3–4 mm long) were tested simultaneously by mounting them between force transducers and a rigid support for measurement of isometric force. Increasing doses of bradykinin were applied as bolus injections and the ensuing constrictor response was monitored with the aid of a PC-operated analysis System (Biosys, TSE, Bad Homburg, Germany).

McBean et al. (1986, 1988) used isolated segments of the arteria basilaris of **pigs** to detect compounds with antivasoconstrictive properties. Contraction is elicited by $PGF_{2\alpha}$, serotonin or norepinephrine. Specimens are obtained from adult pigs (strain: Deutsche Landrasse) within 30 min after slaughter from the local slaughter house and stored in nutritive solution. The vessels are trimmed to a length of 4 mm, and the segments are suspended between 2 L-shaped metal hooks in a bath containing 20 ml modified Krebs Henseleit solution (NaCl 148 mM, KCl 5.4 mM, $CaCl_2$ 2.2 mM, $NaHCO_3$ 12 mM, glucose 12 mM). The bath solution is maintained at 37°C and continuously gassed with carbogen to produce a resulting pH of 7.35–7.45. The preparation is incubated under a tension of 37.28 mN (optimal passive load producing the largest contractile response to 3×10^{-6} M $PGF_{2\alpha}$). Following a 60 minute stabilization period, the vessels are sensitized with 30 mM KCl for 10 min. The vessels are washed for 1 minute, and allowed to recover for 30 min with additional 1 minute washes at 15 and 30 min. Thereafter, contractions of the vessels are induced by adding $PGF_{2\alpha}$ at 3×10^{-6} M. The contractile response is allowed to plateau, then the test compound is administered at cumulative doses.

For each test compound a dose-response curve is recorded. The EC_{50} is obtained graphically or by means of a Hill plot. The EC_{50} is defined as the dose of drug producing half maximal response.

Werner et al. (1991) studied the vascular selectivity of calcium antagonists using **porcine** isolated ventricular trabeculae and right **coronary arteries**.

Merkel et al. (1992) used isolated porcine coronary artery rings precontracted with prostaglandin $F_{2\alpha}$ to demonstrate the vasorelaxant activity of an A_1-selective adenosine agonist.

Miwa et al. (1993) compared the effect of a K^+-channel opener with cromakalim, nitroglycerin and nifedipine on endothelin-1-induced contraction of porcine coronary artery.

Satoh et al. (1993) investigated in isolated porcine large coronary arteries whether or not the vasorelaxant actions of nicorandil and cromakalim would be selective using seven different vasoconstrictor agonists.

Yokoyama et al. (1994) studied the vasodilating mechanisms of several pyridinecarboximidamide derivatives in isolated porcine coronary arteries.

Makujina et al. (1995) described a procedure that facilitates the eversion of vascular smooth muscle. Vascular segments of porcine coronary artery, approximately 2 cm in length, were sutured to portions of polyethylene tubing inserted into the lumen of the vessel. After being secured and stabilized by the tubing, the vessel was everted while immersed in physiological buffer. Intracellular calcium concentrations (measured by fura-2AM fluorometry) and tension were registered simultaneously in everted rings denuded of endothelium.

Izumi et al. (1996) tested a K^+-channel opener and related compounds in isolated porcine coronary arteries contracted with 25 mM KCl.

Frøbert et al. (1996) described impedance planimetry as a new catheter-based technique to measure porcine coronary artery pharmacodynamics and compared the results with the commonly used wire-mounted isometric tension technique after *in vitro* application of nifedipine in various concentrations. A four-electrode impedance measuring system was located inside a 12-mm long balloon which was introduced into 3–4 cm long segments of the left anterior descending coronary artery obtained from 70–90-kg Danish Landrace-Yorkshire pigs.

Hamel et al. (1993) dissected segments (3–4 mm long) of temporal ramifications of the middle cerebral

artery from **bovine** brains and mounted them between two L-shaped metal prongs in a tissue bath containing Krebs-Ringer solution at 37°C. Changes in muscle tension were measured by a force displacement transducer and recorded on a polygraph. Several 5-HT receptor agonists were tested for their ability to induce vasoconstriction and their potencies were compared to that of 5-HT. The authors concluded that bovine pial arteries appear to be the best available model for the human cerebrovascular 5-HT_{1D} receptor.

De la Lande et al. (1996) used isolated segments from proximal (4.5 mm i.d.) and distal (0.5 mm i.d.) bovine coronary arteries and found a heterogeneity of response to glyceryl trinitrate.

The isolated **human** coronary artery was used to study the vasoconstriction by acutely acting antimigraine drugs (Saxena et al. 1996a, b, 1997)

REFERENCES AND FURTHER READING

Ashcroft JH, Ashcroft FM (1990) Properties and functions of ATP-sensitive K-channels. Cell Signal 2:197–214

Ashcroft FM, Gribble FM (2000) New windows on the mechanism of action of K_{ATP} channel openers. Trends Pharmacol Sci 21:439–445

Barhanin J, Duprat F, Fink M, Guillemare E, Heurteaux C, Honoré E, Lesage F, Patel A, Reyes R, Romey G, Lazdunski M (1998) Novel structural and functional types of K^+ channels. Naunyn-Schmiedeberg's Arch Pharmacol 358, Suppl 1, R 23

Blatz AL, Magleby KL (1987) Calcium-activated potassium channels. Trends Neurosci 10:463–467

Bolton TB, Prestwich SA, Zhang HL (1998) The target channel for potassium channel opener drugs in vasodilatation. Naunyn-Schmiedeberg's Arch Pharmacol 358, Suppl 1, R 200

Bråtveit M, Helle KB (1984) VIP inhibition of vascular smooth muscle: complementary to β_2-adrenoceptor mediated relaxation in the isolated rat portal vein. Acta Physiol Scand 121:269–276

Calderone V, Martinotti E, Scatizzi R, Pelegrini A, Breschi MC (1996) A modified aortic multiple-ring preparation for functional studies. J Pharmacol Toxicol Meth 35:131–138

Cheng H, Fetscher C, Schäfers RF, Wambach G, Philipp Th, Michel MC (1996) Effects of noradrenaline and neuropeptide Y on rat mesenteric microvessel contraction. Naunyn-Schmiedeberg's Arch Pharmacol 353:314–323

Cook NS (1988) The pharmacology of potassium channels and their therapeutic potential. TIPS 9:21–28

Dacquet C, Mironneau C, Mironneau J (1987) Effects of calcium entry blockers on calcium-dependent contractions of rat portal vein. Br J Pharmac 92:203–211

De la Lande IS, Stafford I, Horowitz JD (1996) Heterogeneity of glyceryl trinitrate response in isolated bovine coronary arteries. Eur J Pharmacol 318:65–71

Edwards G, Weston AH (1990) Potassium channel openers and vascular smooth muscle relaxation. Pharmac Ther 48:237–258

Edwards G, Henshaw M, Miller M, Weston AH (1991) Comparison of the effects of several potassium-channel openers on rat bladder and rat portal vein in vitro. Br J Pharmacol 102:679–680

Edwards G, Weston AH (1993) The pharmacology of ATP-sensitive potassium channels. Annu Rev Pharmacol Toxicol 33:597–637

Eltze M (1989) Glibenclamide is a competitive antagonist of cromakalim, pinacidil and RP 49356 in guinea-pig pulmonary artery. Eur J Pharmac 165:231–239

Fouda AK, Capdeville C, Henrion D, Thorin-Trescases N, Thorin E, Atkinson J (1991) Differences between the *in vitro* vasoconstrictor responses of the tail artery to potassium and norepinephrine between spontaneously hypertensive, renovascular hypertensive, and various strains of normotensive rats. J Pharmacol Meth 25:61–68

French JF, Riera LC, Sarmiento JG (1990) Identification of high and low (GTP-sensitive) affinity [^{3}H]glibenclamide binding sites in cardiac ventricular membranes. Biochem Biophys Res Comm 167:1400–1405

Frøbert O, Mikkelsen EO, Gregersen H, Nyborg NBC, Bagger JP (1996) Porcine coronary artery pharmacodynamics *in vitro* evaluated by a new intravascular technique: relation to axial stretch. J Pharmacol Toxicol Meth 36:13–19

Gurden MF, Coates J, Ellis F et al (1993) Functional characteristics of three adenosine receptor types. Br J Pharmacol 109:693–698

Hamel E, Grégoire L, Lau B (1993) 5-HT_1 receptors mediating contractions in bovine cerebral arteries: a model for human cerebrovascular '5-$HT_{1D\beta}$' receptors. Eur J Pharmacol 242:75–82

Hamilton TC, Weston AH (1989) Cromakalim, nicorandil and pinacidil: novel drugs which open potassium channels in smooth muscle. Gen Pharmacol 20:1–9

Hamilton TC, Weir SW, Weston AH (1986) Comparison of the effects of BRL 34915 and verapamil on electrical and mechanical activity in rat portal vein. Br J Pharmac 88:103–111

Izumi H, Tanaka Y, Okada N, Izawa T (1996) Structure-activity relationship of a novel K^+-channel opener and related compounds in porcine coronary artery. Gen Pharmacol 27:985–989

Jan LY, Jan YN (1990) How might the diversity of potassium channels be generated? Trends Neurosci 13:415–419

Kent RL, Harakal C, Santamore WP, Carey RA, Bove AA (1982) An index for comparing the inhibitory action of vasodilators. Eur J Pharmac 85:85–91

Kurachi Y (1998) Molecular pharmacology of potassium channels. Naunyn-Schmiedeberg's Arch Pharmacol 358, Suppl 1, R 6

Langer SZ, Trendelenburg U (1969) The effect of a saturable uptake mechanism on the slopes of dose-response curves for sympathomimetic amines and on the shifts of dose-response curves produced by a competitive antagonist. J Pharmacol. Exp Ther 167:117–142

Lauth M, Cattaruzza M, Hecker M (2001) ACE inhibitor and AT_1 antagonist blockade of deformation-induced gene expression in the rabbit jugular vein through B_2 receptor activation. Arterioscler Thromb Vasc Biol 21:61–66

Löhn M, Kämpf D, Gui-Xuan C, Haller H, Luft FC, Goll Nishimura H, Buikema H, Baltatu O, Ganten D, Urata H (1998) Regulation of arterial tone by smooth muscle myosin type II. Am J Physiol 283:C1383–C1389

Makujina SR, Abebe W, Ali S, Mustafa SJ (1995) Simultaneous measurement of intracellular calcium and tension in vascular smooth muscle: validation of the everted ring preparation. J Pharmacol Toxicol Meth 34:157–163

Martin W, Villani GM, Jothianandan D, Furchgott RF (1985) Selective blockade of endothelium-dependent and glyceryl trinitrate-induced relaxation by hemoglobin and by

methylene blue in the rabbit aorta. J Pharmacol Exp Ther 232:708–716
McBean DE, Harper AM, Rudolphi KA (1986) Effects of adenosine and its analogues on the cerebrovasculature and their antagonism by 8-phenyltheophylline: Identification of the receptor(s) involved. Pfluegers Arch 407 Suppl. 1:31
McBean DE, Harper AM, Rudolphi KA (1988) Effects of adenosine and its analogues on porcine basilar arteries: Are only A_2 receptors involved? J Cerebr Blood Flow Metab 8:40–45
Meisheri KD, Dubray LAC, Olynek JJ (1990) A sensitive *in vitro* functional assay to detect K^+-channel-dependent vasodilators. J Pharm Meth 24:251–261
Merkel LA, Lappe RW, Rivera LM, Cox BF, Perrone MH (1992) Demonstration of vasorelaxant activity with an A_1-selective adenosine agonist in porcine coronary artery: Involvement of potassium channels. J Pharmacol Exp Ther 260:437–443
Miller JA, Velayo NL, Dage RC, Rampe D (1991) High affinity [^{3}H]glibenclamide binding sites in rat neuronal and cardiac tissue: localization and development characteristics. J Pharm Exp Ther 256:358–364
Mironneau J, Gargouil YM (1979) Action of indapamide on excitation-contraction coupling in vascular smooth muscle. Eur J Pharmacol 57:57–67
Miwa A, Kasai H, Motoki K, Jinno Y, Yokoyama T, Fukushima H, Ogawa N (1993) Effect of KRN2391, a novel vasodilator, on endothelin-1-induced contraction of porcine coronary artery. Comparison with cromakalim, nitroglycerin and nifedipine. Arch Int Pharmacodyn Ther 326:52–61
Mourre C, Hugues M, Lazdunski M (1986) Quantitative autoradiographic mapping in rat brain of the receptor of apamin, a polypeptide toxin specific for one class of Ca^{2+}-dependent K^+ channels. Brain Res 382:239–249
Mourre C, Widman C, Lazdunski M (1990) Sulfonylurea binding sites associated with ATP-regulated K^+ channels in the central nervous system: autoradiographic analysis of their distribution and ontogenesis, and their localization in mutant mice cerebellum. Brain Res 519:29–43
Nishimura H, Buikema H, Baltatu O, Ganten D, Urata H (1998) Functíonal evidence for alternative ANG II-forming pathways in hamster cardiovascular system. Am J Physiol 275:H1307–H1312
Nishimura Y, Suzuki A (1995) Enhanced contractile responses mediated by different 5-HT receptor subtypes in basilar arteries, superior mesenteric arteries and thoracic aortas from stroke-prone spontaneously hypertensive rats. Clin Exper Pharmacol Physiol Suppl 1:S99–S101
O'Donnell SR, Wanstall JC (1987) Choice and concentration of contractile agent influence responses of rat aorta to vascular relaxant drugs. J Pharm Pharmacol 39:848–850
Pikkers P, Hughes AD (1995) Relaxation and decrease in $[Ca^{2+}]_i$ by hydrochlorothiazide in guinea pig isolated mesenteric arteries. Br J Pharmacol 114:703–707
Pongs O (1992) Structural basis of voltage-gated K^+ channel pharmacology. TIPS 13:359–365
Rehm H, Lazdunski M (1988) Purification and subunit structure of a putative K^+-channel protein identified by its binding properties for dendrotoxin I. Proc Natl Acad Sci USA 85:4919–4923
Satoh K, Mori T, Yamada H, Taira N (1993) Nicorandil as a nitrate, and cromakalim as a potassium channel opener, dilate isolated porcine large coronary arteries in an agonist-nonselective manner. Cardiovasc Drugs Ther 7:691–699
Saxena PR, Maassen van den Brink A, Heiligers JPC, Scalbert E, Guardiola-Lemaitire B (1996a) Effects of S20794, a close analogues of sumatripan, on porcine carotid haemodynamics and human isolated coronary artery. Pharmacol Toxicol 79:199–204
Saxena PR, De Vries P, Heiligers JPC, Maassen van den Brink A, Bax WA, Barf T, Wikström H (1996b) Investigations with GMC2021 in experimental models predictive of antimigraine activity and coronary side-effect potential. Eur J Pharmacol 312:53–62
Saxena PR, De Vries P, Wang W, Heiligers JPC, Maassen van den Brink A, Bax WA, Yocca FD (1997) Effects of avitriptan, a new 5-$HT_{1B/1D}$ receptor agonist, in experimental models predictive of antimigraine activity and coronary side-effect potential. Naunyn-Schmiedeberg's Arch Pharmacol 355:295–302
Scherf H, Pietsch R, Landsberg G, Kramer HJ, Düsing R (1986) Converting enzyme inhibitor ramipril stimulates prostacyclin synthesis by isolated rat aorta: evidence for a kinin-dependent mechanism. Klin Wschr 64:742–745
Shetty SS, Weiss GB (1987) Dissociation of actions of BRL 34915 in the rat portal vein. Eur J Pharmacol 141:485–488
Smith DD, Li J, Wang Q, Murphy RF, Adrian TE, Elias Y, Bockman CS, Abel PW (1993) Synthesis and biological activity of C-terminally truncated fragments of human α-calcitonin gene-related peptide. J Med Chem 36:2536–2541
Szentmiklósi AJ, Ujifalusi A, Cseppentö A, Nosztray K, Kovács P, Szabó JZ (1995) Adenosine receptors mediate both contractile and relaxant effects of adenosine in main pulmonary artery of guinea pigs. Naunyn-Schmiedeberg's Arch Pharmacol 351:417–425
Wann KT (1993) Neuronal sodium and potassium channels: structure and function. Br J Anaesth 71:2–14
Werner G, Klaus W, Kojda G, Fricke U (1991) Hydrophobic properties of novel dihydronaphthyridine calcium antagonists and biological activity in porcine isolated cardiac and vascular smooth muscle. Naunyn-Schmiedeberg's Arch Pharmacol 344:337–344
Weston AH, Edwards G (1992) Recent progress in potassium channel opener pharmacology. Biochem Pharmacol 43:47–54
Wilson C, Buckingham RE, Mootoo S, Parrott LS, Hamilton TC, Pratt SC, Cawthorne MA (1988) *In vivo* and *in vitro* studies of cromakalim (BRL 34915) and glibenclamide in the rat. Br J Pharmacol 93:126P
Yokoyama T, Okada Y, Jinno Y, Izumi H, Izawa T, Ogawa N (1994) Comparative analysis of vasodilating mechanisms of Ki1769, Ki3315 and KRN2391, pyridinecarboximidamide derivatives, in porcine isolated coronary artery. Gen Pharmacol 25:941–945

A.1.2.10 Isolated Guinea Pig Ureter

PURPOSE AND RATIONALE

The isolated guinea pig ureter shows phasic-rhythmic contractions after addition of KCl to the organ bath. Inhibition of this effect can be explained as a modulation of potassium channels.

PROCEDURE

Male unfasted guinea pigs weighing 400–500 g are sacrificed and both ureters removed immediately without the part directly connected to the pelvis in order to exclude the pacemaker region responsible for spontaneous activity. Each segment of 2 cm length is

placed in a Petri dish containing Tyrode solution at 37°C, freed of surrounding connective tissue and then suspended at a baseline tension of 0.5 p in a 25 ml organ bath containing Tyrode solution at 37°C being aerated with 5% CO_2/95% O_2, pH 7.4. Contractions are measured isometrically using Gould/Statham UC 2 transducers. After a 15 min equilibration period, KCl is added to the bath in a final concentration of 3×10^{-2} Mol/l and left in the bath for 2 min. KCl induces a constant series of phasic-rhythmic contractions without a rise in baseline tone. Subsequent washing causes the immediate disappearance of the rhythmic contractions. This addition of KCl is repeated and the values of these two experiments are used as initial values. The antagonistic activity is studied by addition of the test drug one min prior to the KCl challenge. Percentage of the following parameters are determined: mean height of contractions, frequency of contractions and the product of mean height and frequency of contractions. For interaction studies the potassium channel blocker glibenclamide 10^{-6} mol/l is added 1 min prior to the test drug.

EVALUATION

Arithmetic means and standard deviations of the data are calculated and compared with initial values using Student's *t*-test.

CRITICAL ASSESSMENT OF THE METHOD

The isolated guinea pig ureter stimulated with KCl can be used for studies on the modulation of potassium channels.

MODIFICATIONS OF THE METHOD

Yoshida and Kuga (1980) recorded electrical activities in a preparation consisting of the pelvic region and the upper ureter of the guinea pig. Train field stimulation of the pelvic region evoked a train of nerve action potentials followed by a multiphasic smooth muscle action potential after a latency of about 2.5–8.0 s. This smooth muscle response was abolished by tetrodotoxin and dibucaine, and also by cholinergic blocking agents.

The effects of veratridine and of yohimbine on the efflux of norepinephrine from electrically stimulated guinea pig ureters were studied by Kalsner (1992).

Maggi and Giuliani (1994) studied the excitability and refractory period of the guinea pig ureter to electrical field stimulation.

Roza and Laird (1995), Laird and Cervero (1996) studied the pressor responses to distension of the ureter in anesthetized rats as a model of acute visceral pain.

A simple method for measurement of ureteric peristaltic function *in vivo* in anesthetized rats was published by Kontani et al. (1993).

REFERENCES AND FURTHER READING

Kalsner S (1992) Adrenergic presynaptic antagonists and their mechanism of action in smooth muscle. Am J Physiol 262 (Regul Intergr Comp Physiol 31):R400–R406

Kontani H, Ginkawa M, Sakai T (1993) A simple method for measurement of ureteric peristaltic function *in vivo* and the effects of drugs acting on ion channels applied from the ureter lumen in anesthetized rats. Jap J Pharmacol 62:331–338

Laird JMA, Cervero F (1996) Effects of metamizol on nociceptive responses to stimulation of the ureter and on ureter motility in anaesthetized rats. Inflamm Res 45:150–154

Linz W, Englert H, Kaiser J, Klaus E, Metzger H, Wirth K, Schölkens BA (1992) Evidence for an involvement of potassium channels in the action of forskolin and 1,9-dideoxyforskolin. Pharm Pharmacol Lett 1:99–102

Maggi CA, Giuliani S (1994) Calcitonin gene-related peptide (CGRP) regulates excitability and refractory period of the guinea pig ureter. J Urology 152:520–524

Roza C, Laird JMA (1995), Pressor responses to distension of the ureter in anaesthetized rats: characterization of a model of acute visceral pain. Neurosci Lett 198:9–12

Susano S, Moriyama K, Shimamura K (1992) Potentiation of twitch contraction in guinea pig ureter by sodium vanadate. Am J Physiol Cell Physiol 263:C953–C958

Yoshida S, Kuga T (1980) Effects of field stimulation on cholinergic fibers of the pelvic region in the isolated guinea pig ureter. Jap J Physiol 30:415–426

Young CJ, Attele A, Toledano A, Núñez R, Moss J (1994) Volatile anesthetics decrease peristalsis in the guinea pig ureter. Anesthesiology 81:452–458

A.1.2.11 Isolated Corpus Cavernosum

PURPOSE AND RATIONALE

The isolated corpus cavernosum of rabbits has gained interest as pharmacological model since selective inhibitors of cyclic guanosine monophosphate (cGMP) phosphodiesterase type 5 (PDE5) were found to be effective in the treatment of erectile dysfunction in man (Ballard et al. 1996; Jeremy et al. 1997; Chuang et al. 1998; Liu et al. 1998; Turko et al. 1999; Wallis 1999; Wallis et al. 1999; Stief 2000; Aydin et al. 2001; Thompson et al. 2001; Lin et al. 2002).

PROCEDURE

Male New Zealand White rabbits weighing 3–4 kg are sedated with an intramuscular injection of 25 mg/kg ketamine+6 mg/kg xylazine. Anesthesia is maintained by intravenous injection of 25 mg/kg nembutal. The penis is removed at the level of the attachment of the corporal bodies to the ischium. The corpus cavernosum (total length about 20 mm) is sharply dissected from tunica albuginea and two longitudinal strips with

unstretched length about 10 mm are made from the proximal, more muscular portion.

Corporal strips are placed in organ baths containing 10 ml Tyrode's buffer (NaCl 124.9 mmol/l, KCl 12.5 mmol/l, $MgCl_2 \cdot 6H_2O$ 0.5 mmol/l, NaH_2PO_4 H_2O 0.4 mmol/l, $CaCl_2$ 1.8 mmol/l and glucose 5.5.mmol/l) at 37°C. Each tissue is equilibrated with a mixture of 95% O_2 and 5% CO_2 at pH 7.4. One end of each strip is connected to a force displacement transducer, and changes in muscle tension are measured and recorded with a polygraph. After zeroing and balancing transducers and strip chart, 2.0 g of tension is placed on each strip, and the strips are allowed to equilibrate for 30 min.

Each strip is prestimulated with 10 µM phenylephrine, then relaxed by electrical field stimulation with square wave pulses of 80 V, 1 ms duration at 2–16 Hz frequency. Then sodium nitroprusside (0.01–100 µM) is added ad NO donor. Finally, the standard (sildenafil 1 nM to 1 µM) or the test compound is added.

EVALUATION

The dose-dependent increase of relaxation after test compound and standard is measured. From dose-response curves activity ratios can be calculated.

MODIFICATIONS OF THE METHOD

Wallis et al. (1999) studied the inhibition of human phosphodiesterases PDE1 to PDE6 by sildenafil in various tissues, such as cardiac ventricle, corpus cavernosum, skeletal muscle and retina.

Park et al. (1997) reported functional characterization of angiotensin II receptors in rabbit corpus cavernosum.

Yildirim et al. (1997) investigated the effects of castration and testosterone on the constricting effect of phenylephrine and endothelium-dependent and -independent relaxing effects of different agonists in the corpus cavernosum of male rabbits.

Liu et al. (1998) analyzed the pharmacological effects of *in vitro* ischemia on rabbit corpus cavernosum.

Gupta et al. (1998) found that activation of G_i-coupled postsynaptic α_2-adrenoceptors causes contraction of smooth muscles in the corpus cavernosum of rabbits.

Teixeira et al. (1998) used a bioassay cascade to study the effect of *Tityus serrulatus scorpion* venom on the rabbit isolated corpus cavernosum.

Cellec and Moncada (1998) used the clitoral corpus cavernosum of female rabbits to study the role of nitrergic neurotransmission in non-adrenergic non-cholinergic relaxation responses.

The isolated corpus cavernosum of **rats** has been used by Tong and Cheng (1997), Gemalmaz et al. (2001), and Wingard et al. (2003), of **mice** by Gocmen et al. (1997) and Mizusawa et al. (2001), of **dogs** by Hayashida et al. (1996), Comiter et al. (1997), of **monkeys** by Okamura et al. (1998), of **horses** by Recio et al. (1997).

Studies in isolated **human** corpus cavernosum were performed by Holmquist et al. (1992), Bush et al. (1992), Rajfer et al. (1992), Cellek and Moncada (1997), Ballard et al. (1998), Omote (1999), Wallis et al. (1999), Lin et al. (2000), and Stief et al. (1998, 2000).

***In vivo*studies** measuring intracavernous pressure in **rats** were performed by Ari et al. (1996), Chan et al. (1996), Moody et al. (1997), Reilly et al. (1997), Chang et al. (1998), Mills et al. (1998), Gemalmaz et al. (2001), Takagi et al. (2001), Rajasekaran et al. (2005), and Wingard et al. (2006).

Cashen et al. (2002) measured intracavernous pressure in anesthetized mice.

In vivo studies on penile erection were performed in **cats** by Champion et al. (1997).

Intracavernous pressure was measured *in vivo* in anesthetized **dogs** by Ayajiki et al. (1997), Sarikaya et al. (1997), Carter et al. (1998), and Noto et al. (2000).

Bischoff and Schneider (2000) decribed a simple and quantitative model to study agents that influence penile erection in **conscious rabbits**. Erection was assessed by measuring the length of uncovered mucosa before and after the intravenous administration of agents. Anmals did not require anesthesia during the course of the study.

REFERENCES AND FURTHER READING

Ari G, Vardi Y, Hoffman A, Finberg JPM (1996) Possible role of endothelins in penile erection. Eur J Pharmacol 307:69–74

Ayajiki K, Hayashida H, Okamura T, Toda N (1997) Pelvic nerve stimulation-induced pressure responses in corpus cavernosum of anesthetized dogs. Am J Physiol 273, Heart Circ Physiol 42:H2141–H2145

Aydin S, Ozbeck H, Yilmaz Y, Atilla MK, Bayrakli H, Catin H (2001) Effects of sildenafil citrate, acetylcholine, and sodium nitroprusside on the relaxation of rabbit cavernosal tissue in vitro. Urology 58:119–124

Ballard SA, Turner LA, Naylor AM (1996) Sildenafil, a potent selective inhibitor of type 5 phosphodiesterase, enhances nitric oxide-dependent relaxation of rabbit corpus cavernosum. Br J Pharmacol 118, Proc Suppl: 153P

Ballard SA, Gingell CJ, Tang K, Turner LA, Price ME, Naylor AM (1998) Effects of sildenafil on the relaxation of human corpus cavernosum tissue in vitro and the activities of cyclic nucleotide phosphodiesterase isozymes. J Urol 159:2164–2171

Bischoff E, Schneider K (2000) A conscious-rabbit model to study verdenafil hydrochloride and other agents that influence penile erection. Int J Impot Res 13:230–235

Bush PA, Aronson WJ, Buga GM, Ignarro LJ (1992) Nitric oxide is a potent relaxant of human and rabbit corpus cavernosum. J Urol 147:1650–1655

Carter AJ, Ballard SA, Naylor AM (1998) Effect of the selective phosphodiesterase type5 inhibitor sildenafil on erectile function in the anesthetized dog. J Urol 160:242–246

Cashen DE, McIntyre DE, Martin WJ (2002) Effects of sildenafil on erectile activity in mice lacking endothelial nitric oxide synthase. Br J Pharmacol 136:693–700

Cellec S, Moncada S (1997) Nitrergic control of peripheral sympathetic responses in the human corpus cavernosum. Proc Natl Acad Sci USA 94:8226–8231

Cellec S, Moncada S (1998) Nitrergic transmission mediates the non-adrenergic non-cholinergic responses in the clitoral corpus cavernosum of the rabbit. Br J Pharmacol 125:1627–1629

Champion HC, Wang R, Hellstrom WJG, Kadowitz PJ (1997) Nociceptin, a novel endogenous ligand for the ORL_1 receptor, has potent erectile activity in the cat. Am J Physiol 273, Endocrinol Metab 36:E214–E219

Chan YH, Huang C-L, Chan SHH (1996) Nitric oxide as a mediator of cocaine-induced penile erection in the rat. Br J Pharmacol 118:155–161

Chang AYW, Chan JYH, Chan SHH (1998) Participation of hippocampal formation in negative feedback inhibition of penile erection in rats. Brain Res 788:160–168

Chuang AT, Strauss JD, Murphy RA, Steers WD (1998) Sildenafil, a type-5 cGMP phosphodiesterase inhibitor, specifically amplifies cGMP-dependent relaxation in rabbit corpus cavernosum muscle *in vitro*. J Urol 160:257–261

Comiter CV, Sullivan MP, Yalla SV, Kifor I (1997) Effect of angiotensin II on corpus cavernosum smooth muscle in relation to nitric oxide environment: *In vitro* studies in canines. Int J Impotence Res 9:135–140

Gemalmaz H, Waldeck K, Chapman TN, Tuttle JB, Steers WD, Andersson KE (2001) In vivo and in vitro investigation of the effects of sildenafil on rat cavernous smooth muscle. J Urol 165:1010–1014

Gocmen C, Ucar P, Singirik E, Dikmen A, Baysal F (1997) An *in vitro* study of nonadrenergic-noncholinergic activity on the cavernous tissue of mouse. Urol Res 25:269–275

Gupta S, Moreland RB, Yang S, Gallant CM, Goldstein I, Traish A (1998) The expression of functional postsynaptic α_2-adrenoceptors in the corpus cavernosum smooth muscle. Br J Pharmacol 123:1237–1245

Hayashida H, Okamura T, Tomoyoshi T, Toda N (1996) Neurogenic nitric oxide mediates relaxation of canine corpus cavernosum. J Urol 155:1122–1127

Holmquist F, Hedlund H, Andersson KE (1991) L-*NG*-nitro arginine inhibits non-adrenergic, non-cholinergic relaxation of human isolated corpus cavernosum. Acta Physiol Scand 141:441–442

Jeremy JY, Ballard SA, Naylor AM, Miller MAW, Angelini GD (1997) Effects of sildenafil, a type-5 cGMP phsophodiesterase inhibitor, and papaverine on cyclic GMP and cyclic AMP levels in the rabbit corpus cavernosum *in vitro*. Br J Urol 79:958–963

Lin C-S, Lau A, Tu R, Lue TF (2000) Expression of three isoforms of cGMP-binding cGMP-specific phsophodiesterase (PDE5) in human penile cavernosum. Biochem Biophys Res Commun 268:628–635

Lin RJ, Wu BN, Lo YC, Shen KP, Lin YT, Huang CH, Chen IJ (2002) KMUP-1 relaxes rabbit corpus cavernosum smooth muscle in vitro and in vivo: involvement of cyclic GMP and K^+ channels. Br J Pharmacol 135:1159–1166

Liu S-P, Horan P, Levin RM (1998) Digital analysis of the pharmacological effects of *in vitro* ischemia of rabbit corpus cavernosum. Pharmacology 56:216–222

Mills TM, Lewis RW, Stopper VS, Reilly CM (1998) Loss of alpha-adrenergic effect during the erectile response in the long-term diabetic rat. J Androl 19:473–478

Mizusama H, Hedlund P, Håkansson A, Alm P, Andersson KE (2001) Morphological and functional in vitro and in vivo characterization of the mouse corpus cavernosum. Br J Pharmacol 132:1333–1341

Moody JA, Vernet D, Laidlaw S, Rajfer J, Gonzalez-Cadavid HF (1997) Effects of long-term oral administration of L-arginine on the rat erectile response. J Urol 158:942–947

Noto T, Inoue H, Ikeo T, Kikkawa K (2000) Potentiation of penile tumescence by T-1032, a new potent and specific phosphodiesterase type V inhibitor, in dogs. J Pharmacol Exp Ther 294:870–675

Okamura T, Ayajiki K, Toda N (1998) Monkey corpus cavernosum relaxation mediated by NO and other relaxing factor derived from nerves. Am J Physiol 274, Heart Circ Physiol 43:H1075–H1081

Omote M (1999) Pharmacological profiles of sildenafil (VIAGRA^{TM}) in the treatment of erectile dysfunction: Efficacy and drug interaction with nitrate. Folia Pharmacol Jpn 114:213–218

Park J-K, Kim S-Z, Kim S-H, Park Y-K, Cho K-W (1997) Renin angiotensin system in rabbit corpus cavernosum: Functional characterization of angiotensin II receptors. J Urol 158:653–658

Rajfer J, Aronson WJ, Bush PA, Dorey FJ, Ignarro LJ (1992) Nitric oxide as a mediator of relaxation of the corpus cavernosum response to nonadrenergic, noncholinergic neurotransmission. N Engl J Med 326:90–94

Rajasekaran M, White S, Baquir A, Wilkes N (2005) Rho-kinase inhibition improves erectile function in aging male Brown-Norway rats. J Androl 26:182–188

Recio P, Lopez JLG, Garcia-Sacristan A (1997) Pharmacological characterization of adrenoceptors in horse corpus cavernosum penis. J Auton Pharmacol 17:191–198

Reilly CM, Zamorano P, Stopper VS, Mills TM (1997) Androgenic regulation of NO availability in rat penile erection. J Androl 18:110–115

Sarikaya S, Asci R, Aybek Z, Yilmaz AF, Buyukalpelli R, Yildiz S (1997) Effect of intracavernous calcium blockers in dogs. Int Urol Nephrol 29:673–680

Stief CG, Uckert S, Becker AJ, Truss MC, Jonas U (1998) The effect of the specific phosphodiesterase (PDE) inhibitors on human and rabbit cavernous tissue in vitro and in vivo. J Urol 159:1390–1393

Stief CG (2000) Phosphodiesterase inhibitors in the treatment of erectile dysfunction. Drugs Today 36:93–99

Stief CG, Uckert S, Becker AJ, Harringer W, Truss MC, Forssmann WG, Jonas U (2000) Effects of sildenafil on cAMP and cGMP levels in isolated human cavernous and cardiac tissue. Urology 55:146–150

Takagi M, Mochida H, Noto T, Yano K, Inoue H, Ikeo T, Kikkawa K (2001) Pharmacological profile of T-1032, a novel specific phosphodiesterase type 5 inhibitor, in isolated rat aorta and rat corpus cavernosum. Eur J Pharmacol 411:161–168

Teixeira CE, Bento AC, Lopes-Martins RAB, Teixeira SA, von Eickestedt V, Muscará MN, Arantes EC, Giglio JR, Antunes E, de Nucci G (1998) Effect of *Tityus serrulatus scorpion* venom on the rabbit isolated corpus cavernosum and

the involvement of NANC nitrergic nerve fibres. Br J Pharmacol 123:435–442
Thompson CS, Mumtaz FH, Khan MA, Wallis RM, Mikhailidis DP, Morgan RJ, Angelini GD, Jereremy JY (2001) The effect of sildenafil on corpus cavernosal smooth muscle relaxation and cyclic GMP formation in the diabetic rabbit. Eur J Pharmacol 425:57–64
Tong Y-C, Cheng J-T (1997) Subtyping of α_1-adrenoceptors responsible for the contractile response in the rat corpus cavernosum. Neurosci Lett 228:159–162
Turko IV, Ballard SA, Francis SH, Corbin JD (1999) Inhibition of cyclic GMP-binding cyclic GMP-specific phosphodiesterase (type 5) by sildenafil and related compounds. Mol Pharmacol 56:124–130
Wallis RM (1999) The pharmacology of sildenafil, a novel and selective inhibitor of phosphodiesterase (PDE) type 5: Folia Pharmacol Jpn 114/Suppl 1:22P–26P
Wallis RM, Corbin JD, Francis SH (1999) Tissue distribution of phosphodiesterase families and the effect of sildenafil on tissue cyclic nucleotides, platelet function, and the contractile responses of trabeculae carneae and aortic rings *in vitro*. Am J Cardiol 83:3C–12C
Wingard CJ, Johnson JA, Holmes A, Prikosch A (2003) Improved erectile function after Rho-kinase inhibition in a rat castrate model of erectile dysfunction. Am J Physiol 284:R1572–R1578
Yildirim MK, Yildirim S, Utkan T, Sarioglu Y, Yalman Y (1997) Effects of castration on adrenergic, cholinergic and nonadrenergic, noncholinergic responses of isolated corpus cavernosum from rabbit. Br J Urol 79:964–970

A.1.3
Cardiovascular Analysis in Vivo

A.1.3.1
Hemodynamic Screening in Anesthetized Rats

PURPOSE AND RATIONALE

The test is used to detect the effect of compounds on blood pressure and heart rate of anesthetized rats and to check for possible interference with adrenergic receptors. Antihypertensive agents with different mechanisms of action can be detected with this test.

PROCEDURE

Male Sprague-Dawley rats weighing 250–400 g are used. At least 2 animals are necessary for screening of one compound. The rats are anesthetized by intraperitoneal injection of 8 ml/kg of a solution of 8% urethane and 0.6% chloralose. The trachea is cannulated to facilitate spontaneous respiration. Body temperature is maintained at 38°C by placing the animal on a heating pad.

The left femoral vein is cannulated for drug administration, which is standardized to injections of 0.2 ml/100 g body weight over a period of 1 min. For measurement of hemodynamic parameters and for intra-arterial administration of test compound, a cannula is inserted retrogradely into the right carotid artery. The tip of the catheter is positioned close to the origin of the subclavian artery. This allows most of the injected substances to reach the CNS via the vertebral artery before going into the general circulation.

For continuous monitoring of blood pressure (systolic and diastolic pressure) and heart rate, the catheter is connected to a pressure transducer (Statham DB 23).

When stable hemodynamic conditions are achieved for at least 20 min (control values), test boli of adrenaline (1 mg/kg) and isoprenaline (0.25 mg/kg) are administered. When baseline values are again established, increasing doses of the test substance (0.01, 0.1, 3.0 mg/kg) are given intra-arterially. In case of no effect, the interval between successive doses is 15 min, otherwise 60 min. To check for α- or β-blocking activity, adrenaline and isoprenaline administration is repeated after injection of the highest dose of test compound. If the test compound shows no effect, a standard antihypertensive compound is administered for control purpose.

Hemodynamic parameters are recorded continuously during the whole experiment.

EVALUATION

Changes in blood pressure and heart rate after drug administration are compared to control values obtained during the 20 min pre-drug period.

Maximal changes in BP and HR and duration of the effect are reported.

The results are scored relative to the efficacy of standard compounds for the degree of the effect and the duration of the effect.

Statistical significance is not tested because of the small number of animals used ($n = 2$, sometimes 3 or 4) but larger numbers of animals have to be used for quantitative evaluation.

CRITICAL ASSESSMENT OF THE METHOD

Due to the administration of the test compounds via the right common carotid artery not only peripherally acting vasodilators and neuron blockers but also compounds affecting the blood pressure regulating mechanisms in the CNS are detected. Bolus injections of adrenaline and isoprenaline reveal possible α- or β-antagonistic effects.

Standard data:

The following compounds at the doses indicated lead to a strong decrease in blood pressure:

- Clonidine 0.008 mg/kg
- Dihydralazine 1.0 mg/kg
- Phentolamine 3.0 mg/kg

- Prazosin 0.1 mg/kg
- Propranolol 1.0 mg/kg
- Urapidil 1.0 mg/kg
- Verapamil 0.1 mg/kg

MODIFICATIONS OF THE METHOD

Several authors (Mervaala et al. 1999; Wallerath et al. 1999; Rothermund et al. 2000; Baltatu et al. 2001) monitored arterial pressure and heart rate using a pressure transducer system and continuously recorded on a computer-based registration system (TSE, Bad Homburg, Germany).

A procedure for differential intra-arterial pressure recordings from different arteries in the rat was described by Pang and Chan (1985).

DeWildt and Sangster (1983) described the evaluation of derived aortic flow parameters measured by means of electromagnetic flowmetry as indices of myocardial contractility in anesthetized rats.

Using a special Millar ultraminiature catheter pressure transducer and a thermodilution microprobe, Zimmer et al. (1987, 1988) measured right ventricular functional parameters in anesthetized, closed-chest rats.

Veelken et al. (1990) published improved methods for baroreceptor investigations in chronically instrumented rats.

Salgado and Krieger (1988), de Abreu and Salgado (1990), Da Silva et al. (1994) studied the function of the**baroreceptor reflex** in thiopental anesthetized rats. The left aortic nerve was isolated and supported by a bipolar stainless steel electrode and carefully insulated with silicone rubber. Carotid pressure was recorded simultaneously with aortic nerve discharges on an oscilloscope and monitored with a loudspeaker.

King et al. (1987) developed a cross circulation technique in rats to distinguish central from peripheral cardiovascular actions of drugs. The right common carotid arteries were ligated, and the left common carotid arteries and left and right external jugular veins of two phenobarbital-anesthetized rats were connected with polyethylene tubing so that peripheral blood from one rat, A, supplied the head of another rat, B, and then returned to the body of A, and vice versa, for peripheral blood from rat B. Each rat was artificially ventilated with O_2, the chest was opened, and both subclavian arteries were ligated. Prior to the ligation of the subclavian arteries, blood flow from rat A supplied its own brain and both brain hemispheres but not the brain stem of rat B. Following subclavian artery ligation, blood flow from rat A did not supply A's brain, but supplied both hemispheres and brain stem of rat B. The head of each rat was, therefore, rendered dependent on the carotid arterial blood supply from another rat. This rat cross-circulation preparation can be used to separate the central and peripheral cardiovascular actions of drugs.

Zavisca et al. (1994) studied the hypertensive responses to defined electrical and mechanical stimuli in anesthetized rats. Rats were given etomidate, 3.8 mg/kg/h intravenously following carotid artery and jugular vein cannulation. At 15 min after beginning the infusion, 4 types of noxious stimuli were administered sequentially at 1-min intervals: Type 1: Square electrical waves 125 cps, 1.6 ms, 2-s duration, varying current from 0.4 to 12 mA; Type 2: A single 10-mA electrical stimulus, 5-s train duration; Type 3: Tail clamping; Type 4: Skin incision. After each stimulus, maximum change in systolic blood pressure was measured. Graded electrical stimulation allowed the best quantitative evaluation of the hypertensive response to noxious stimuli.

Hyman et al. (1998) described a novel catheterization technique for the *in vivo* measurements of **pulmonary vascular responses** in rats. Male Charles River rats weighing 26–340 g were anesthetized and strapped in supine position to a fluoroscopic table. They breathed air enriched with oxygen through an endotracheal tube inserted by tracheostomy. Catheters were inserted into the femoral blood vessels. The venous catheters were passed to the right atrium under fluoroscopy. A F-1 thermistor catheter was passed from the left carotid artery into the ascending aorta under fluoroscopy, and a PE-50, 150-mm plastic catheter with a specially constructed curved tip was passed fluoroscopically from the left jugular vein into the main pulmonary artery. A plastic radiopaque 22-gauge catheter 100 mm in length with a curved tip was passed with a 0.025 mm soft-tip coronary guiding catheter from the right jugular vein through the right atrium to the inferior vena cava. The coronary soft-tip guide was then withdrawn. A specially curved 102.5-mm transseptal needle, 0.4 mm in diameter, was then passed though the catheter. Both the needle and catheter were withdrawn into the superior portion of the right atrium under fluoroscopic guidance so that the needle and catheter both rotated freely. With the rat in a slight left anterior oblique position, the catheter and needle were carefully rotated anteriorly to the intra-atrial septum. With gentle pressure, the catheter and needle can be felt and seen fluoroscopically to pass through the atrial septum. As the needle was withdrawn, the curve of the catheter permitted passage of the tip into the vein draining either the left or right

lower lobe. The catheter was carefully positioned near the pulmonary venoatrial junction and fixed in place. Mean pressures in the femoral artery, pulmonary artery and pulmonary vein at the venoatrial junction were measured with pressure transducers and recorded on a polygraph. Cardiac output was obtained in triplicate by delivering 0.1 ml normal saline at room temperature into the femoral venous catheter at the right venoatrial junction and determining thermodilution cardiac output with the thermistor catheter in the ascending aorta.

Hayes (1982) described a technique for determining contractility, intraventricular pressure, and heart rate in the **anesthetized guinea pig** by inserting a needle, attached to a pressure transducer, through the chest wall into the left ventricle.

Williams et al. (1995) used **castrated male ferrets** anesthetized by intramuscular injection of a mixture of 55 mg/kg ketamine and 4 mg/kg xylazine to measure the effects of a nonpeptidyl endothelin antagonist on endothelin-induced pressor responses.

REFERENCES AND FURTHER READING

Baltatu O, Fontes MAP, Campagnole-Santos MJ, Caligiorni S, Ganten D, Santos RAS, Bader M (2001) Alterations in the renin-angiotensin system, at the RVLM of transgenic rats with low brain angiotensinogen. Am J Physiol 280:R428–R433

Chu D, Hofmann A, Stürmer E (1978) Anesthetized normotensive rats for the detection of hypotensive activity of a β-adrenoceptor antagonist and other anti-hypertensive agents. Arzneim Forsch/Drug Res 28:2093–2097

Da Silva VJD, da Silva SV, Salgado MCO, Salgado HC (1994) Chronic converting enzyme inhibition facilitates baroreceptor resetting to hypertensive levels. Hypertension 23 (Suppl I):I-68–I-72

de Abreu GR, Salgado HC (1990) Antihypertensive drugs distinctly modulate the rapid resetting of the baroreceptors. Hypertension 15 (Suppl 1):I-63–I-67

DeWildt DJ, Sangster B (1983) An evaluation of derived aortic flow parameters as indices of myocardial contractility in rats. J Pharmacol Meth 10:55–64

Hayes JS (1982) A simple technique for determining contractility, intraventricular pressure, and heart rate in the anesthetized guinea pig. J Pharmacol Meth 8:231–239

Hyman AL, Hao Q, Tower A, Kadowitz PJ, Champion HC, Gumusel B, Lippton H (1998) Novel catheterization technique for the *in vitro* measurements of pulmonary vascular responses in rats. Am J Physiol 274 (Heart Circ Physiol 43):H1218–H1229

King KA, Tabrizchi R, Pang CCY (1987) Investigation of the central and peripheral actions of clonidine and methoxamine using a new *in vivo* rat preparation. J Pharmacol Meth 17:283–295

Mervaala E, Dehmel B, Gross V, Lippoldt A, Bohlender J, Milia AF, Ganten D, Luft FC (1999) Angiotensin-converting enzyme inhibition and AT_1 receptor blockade modify the pressure-natriuresis relationship by additive mechanisms in rats with human renin and angiotensinogen genes. J Am Soc Nephrol 10:1669–1680

Pang CCY, Chan TCK (1985) Differential intraarterial pressure recordings from different arteries in the rat. J Pharmacol Meth 13:325–330

Rothermund L, Friebe A, Paul M, Koesling D, Kreutz R (2000) Acute blood pressure effects of YC-1-induced activation of soluble guanylyl cyclase in normotensive and hypertensive rats. Br J Pharmacol 130:205–208

Salgado HC, Krieger EM (1988) Extent of baroreceptor resetting in response to sodium nitroprusside and verapamil. Hypertension 11 (Suppl 1):I-121–I-125

Veelken R, Unger Th, Medvedev OS (1990) Improved methods for baroreceptor investigations in chronically instrumented rats. J Pharmacol Meth 23:247–254

Wallerath T, Witte K, Schäfer SC, Schwarz PM, Prellwitz W, Wohlfart P, Kleinert H, Lehr HA, Lemmer B, Förstermann U (1999) Down-regulation of the expression of endothelial NO synthase is likely to contribute to glucocorticoid-mediated hypertension. Proc Natl Acad Sci USA 96:13357–13362

Williams DL Jr, Murphy KL, Nolan NA, O'Brien JA, Pettibone DJ, Kivlighn SD, Krause SM, Lis EV Jr, Zingaro GJ, Gabel RA, Clayton FC, Siegl PKS, Zhang K, Naue J, Vyas K, Walsh TF, Fitch KJ, Chakravarty PK, Greenlee WJ, Clineschmidt BV (1965) Pharmacology of L-754,142, a highly potent, orally active, nonpeptidyl endothelin antagonist. J Pharmac Exp Ther 275:1518–1526

Zavisca FG, David Y, Kao J, Cronau LH, Stanley TH, David T (1994) A new method to evaluate cardiovascular response in anesthetized rats. Hypertension after variable intensity, brief electrical stimuli. J Pharmacol Toxicol Meth 31:99–105

Zimmer HG, Zierhut W, Marschner G (1987) Combination of ribose with calcium antagonist and β-blocker treatment in closed-chest rats. J Mol Cell Cardiol 19:635–639

Zimmer HG, Zierhut W, Seesko RC, Varekamp AE (1988) Right heart catheterization in rats with pulmonary hypertension and right ventricular hypertrophy. Basic Res Cardiol 83:48–57

A.1.3.2 Blood Pressure in Pithed Rats

PURPOSE AND RATIONALE

The pithed rat has been proposed for assessing pressor substances by Shipley and Tilden (1947). The preparation is frequently used to evaluate drug action on the cardiovascular system since this preparation is devoid of neurogenic reflex control that may otherwise modulate the primary drug effect.

PROCEDURE

Male rats weighing 250–350 g are prepared for pithing under halothane anesthesia. The left carotid artery is cannulated for blood pressure monitoring and blood sampling. Furthermore, the trachea and the right jugular vein are cannulated. The rats are pithed inserting a steel rod, 2.2 mm in diameter and about 11 cm in length, through the orbit and foramen magnum down the whole length of the spinal canal. Via the tra-

cheotomy tube, the animals are ventilated with a small animal ventilation pump. Inspirated air is oxygen-enriched by providing a flow of oxygen across a T-piece attached to the air intake of the ventilation pump (Harvard Apparatus model 680). The rats are ventilated at a frequency of 60 cycles/min with a tidal volume of 2 ml/100 body weight. Thirty min after pithing, a 0.3 ml blood sample is withdrawn from the carotid cannula and immediately analyzed for pO_2, pCO_2, pH, and derived bicarbonate concentration using an automatic blood gas analyzer. By alterations of the respiratory stroke volume of the pump, the values are adjusted to: pCO_2 30–43 mm Hg, pH 7.36–7.50, pO_2 87–105 mm Hg.

Continuous registration of blood pressure and cardiac frequency (Hellige He 19 device and Statham P 23 Db transducer) is performed via the left carotid artery.

In order to measure α_1 and α_2 antagonism, first dose-response curves are registered using doses of 0.1–30 µg/kg i.v. phenylephrine (a selective α_1 agonist), and 1–1000 µg/kg i.v. BHT 920, (a selective α_2 agonist). The test drug is administered intravenously and the agonist dose-response curves are repeated again 15 min later.

EVALUATION

If the curve of blood pressure response to the agonists is shifted, dose-response curves are plotted on a logarithmic probit scale and potency ratios are calculated.

MODIFICATIONS OF THE METHOD

Gillespie and Muir (1967) described a method of stimulating the complete sympathetic outflow from the spinal cord to blood vessels in the pithed rat by coating those parts of the pithing rod which lay in the sacral and cervical region of the spinal cord with high-resistance varnish to restrict stimulation to the thoracolumbar region. The steel rod is insulated with an adhesive throughout its length except for a 5 cm section which provides sufficient a stimulation area of the lower thoracolumbar nerves. For stimulating nerves fibers supplying exclusively the heart, a pithing rod is used which is insulated throughout its length except for a 0.5 cm section 7 cm proximal to the tip. The spinal cord is stimulated electrically using the pithing rod as the cathode and a hypodermic needle which is inserted under the skin near the right hind-limb, as the anode. Varying the intensity and/or the duration of the stimulation, dose-response curves can be registered which are altered after treatment with drugs.

Curtis et al. (1986) described an improved pithed rat method by mounting the preparation vertically with the head pointing downward resulting in considerably higher blood pressure and heart rate.

MacLean and Hiley (1988) studied the effect of artificial respiratory volume on the cardiovascular responses to an α_1- and α_2-adrenoceptor agonist in the air-ventilated pithed rat using microsphere technique and analysis of arterial blood gases and pH.

Trolin (1975) used decerebrated rats to study the clonidine-induced circulatory changes.

Balt et al. (2001) compared the angiotensin II type 1 (AT1) receptor blockers losartan, irbesartan, telmirsatan and the ACE inhibitor captopril on inhibition of angiotensin-II-induced facilitation of sympathetic neurotransmission in the pithed rat.

REFERENCES AND FURTHER READING

Balt JC, Mathy MJ, Pfaffendorf M, van Zwieten PA (2001) Inhibition of angiotensin II-induced facilitation of sympathetic neurotransmission in the pithed rat: a comparison between losartan, irbesartan, telmirsatan and captopril. J Hypertens 19:465–273

Curtis MJ, McLeod BA, Walker MJA (1986) An improved pithed rat preparation: the actions of the optical enantiomers of verapamil. Asia Pacific J Pharmacol 1:73–78

Fluharty SJ, Vollmer RR, Meyers SA, McCann MJ, Zigmond MJ, Stricker EM (1987) Recovery of chronotropic responsiveness after systemic 6-hydroxydopamine treatment: Studies in the pithed rat. J Pharm Exp Ther 243:415–423

Gillespie JS, Muir TC (1967) A method of stimulating the complete sympathetic outflow from the spinal cord to blood vessels in the pithed rat. Br J Pharmacol Chemother 30:78–87

Gillespie S, MacLaren A, Pollock D (1970) A method of stimulating different segments of the autonomic flow from the spinal column to various organs in the pithed cat and rat. Br J Pharmacol 40:257–267

MacLean MR, Hiley CR (1988) Effect of artificial respiratory volume on the cardiovascular responses to an α_1- and α_2-adrenoceptor agonist in the air-ventilated pithed rat. Br J Pharmacol 93:781–790

Majewski H, Murphy TV (1989) Beta-adrenoreceptor blockade and sympathetic neurotransmission in the pithed rat. J Hypertension 7:991–996

Milmer KE, Clough DP (1983) Optimum ventilation levels for maintenance of normal arterial blood pO_2, pCO_2, and pH in the pithed rat preparation. J Pharmacol Meth 10:185–192

Nichols AJ, Hamada A, Adejare A, Miller DD, Patil PN, Ruffolo RR (1989) Effect of aromatic fluorine substitution on the *alpha* and *beta* adrenoreceptor mediated effects of 3,4-dihydroxy-tolazoline in the pithed rat. J Pharmacol Exp Ther 248:617–676

Schneider J, Fruh C, Wilffert B, Peters T (1990) Effects of the selective β_1-adrenoreceptor antagonist, Nebivolol, on cardiovascular parameters in the pithed normotensive rat. Pharmacology 40:33–41

Shipley RE, Tilden JH (1947) A pithed rat preparation suitable for assaying pressor substances. Proc Soc Exp Med 64:453–455

Trolin G (1975) Effects of pentobarbitone and decerebration on the clonidine-induced circulatory changes. Eur J Pharmacol 34:1–7

Tung LH, Jackman G, Campell B, Louis S, Iakovidis D, Louis WJ (1993) Partial agonist activity of celiprolol. J Cardiovasc Pharmacol 21:484–488

Van Meel JCA, Wilfert B, De Zoeten K, Timmermans PBMWM, Van Zwieten PA (1982) The inhibitory effect of newer calcium antagonists (Nimodipine and PY-108–068) on vasoconstriction *in vivo* mediated by postsynaptic α_2-adrenoreceptors. Arch Int Pharmacodyn 260:206–217

Vargas HM, Zhou L, Gorman AJ (1994) Role of vascular alpha-1 adrenoceptor subtypes in the pressor response to sympathetic nerve stimulation in the pithed rat. J Pharm Exp Ther 271:748–754

A.1.3.3 Antihypertensive Vasodilator Activity in Ganglion-Blocked, Angiotensin II Supported Rats

PURPOSE AND RATIONALE

The method is used to demonstrate direct vasodilator activity of potential antihypertensive agents. The experimental model is an anesthetized, ganglion-blocked rat whose blood pressure is maintained by an intravenous infusion of angiotensin II. The test allows to differentiate between centrally acting antihypertensives and peripheral vasodilators.

PROCEDURE

Male Wistar rats weighing 275–450 g are anesthetized with a combination of urethane (800 mg/kg) and chloralose (60 mg/kg) administered intraperitoneally in a volume of 10 ml/kg. Following induction of anesthesia, chlorisondamine (2.5 mg/kg) is injected into the peritoneal cavity to abolish sympathetic and parasympathetic nerve activity. The right femoral artery is cannulated to monitor blood pressure (Statham pressure transducer P23Db) and heart rate. Both femoral veins are cannulated to administer drugs or infuse angiotensin II. The trachea is intubated and animals are allowed to breathe spontaneously. Following a stabilization interval of 10–15 min, angiotensin II is infused at a rate of 0.25 or 3.5 µg/min in a volume equivalent to 0.05 ml/min (Harvard infusion pump).

After an increase of blood pressure, a new elevated steady-state pressure is established within 15–20 min. Drugs are subsequently injected intravenously over an interval of 3 min in a volume of 2 ml/kg. Mean arterial pressure is recorded on a polygraph at 5, 10, 15, 20 and 30 min after initiation of drug administration. Seven to 9 animals are used for each drug and dose level studied.

α-adrenoreceptor blockade can be determined in ganglion-blocked rats. Pressor responses to graded doses of phenylephrine injected intravenously are obtained before and 15 min after administration of test compounds. Sufficient concentrations of phenylephrine have to be given to ensure a rise in mean arterial blood pressure of 50 mm Hg or more. Data obtained from 5 or 6 animals are averaged and resultant dose-response curves plotted. The dose of phenylephrine required to elicit a 50 mm Hg increase in mean arterial blood pressure is interpolated from dose response curves.

Standard data:

The following compounds are used as standards and, at the doses indicated, lower mean arterial blood pressure by about 50 mm Hg:

- Cinnarizine 3.0 mg/kg, i.v.
- Hydralazine 1.0 mg/kg, i.v.
- Minoxidil 10.0 mg/kg, i.v.
- Saralasine 0.03 mg/kg, i.v.
- Molsidomine 0.1 mg/kg, i.v.

EVALUATION

Mean values ± SEM are given for mean arterial blood pressure and heart rate. Changes of these parameters after drug administration are compared to control values obtained immediately before the application of the test compound. Statistical significance is assessed by means of the paired *t*-test.

CRITICAL ASSESSMENT OF THE METHOD

A hypotensive response in this model appears to correlate more closely with antihypertensive activity in DOCA-salt hypertensive rats than does a vasodilator response in the perfused hind limb of anesthetized dogs and allows a distinction between central anti-hypertensive and vasodilators.

MODIFICATIONS OF THE METHOD

Santajuliana et al. (1996) developed a standard ganglionic blockade protocol to assess neurogenic pressor activity in conscious rats. Rats were instrumented with arterial and venous catheters for measurement of arterial pressure and heart rate and for administration of three different ganglionic blockers (trimethaphan, hexamethonium, and chlorisondamine).

REFERENCES AND FURTHER READING

Deitchman D, Braselton JP, Hayes DC, Stratman RL (1980) The ganglion-blocked, angiotensin II-supported rat: A model for demonstrating antihypertensive vasodilator activity. J Pharmacol Meth 3:311–321

Santajuliana D, Hornfeldt BJ, Osborn JW (1996) Use of ganglionic blockers to assess neurogenic pressor activity in conscious rats. J Pharmacol Toxicol Meth 35:45–54

A.1.3.4 Blood Pressure in Conscious Hypertensive Rats (Tail Cuff Method)

PURPOSE AND RATIONALE

Rats with spontaneous or experimentally induced hypertension are widely used for screening of potentially antihypertensive compounds. The indirect tail cuff method allows the determination of systolic blood pressure according to the following principle: The cuff is quickly inflated to well above suspected systolic blood pressure; the pulse will then be obliterated. Thereafter, pressure in the cuff is slowly released and, as the pressure falls below systolic blood pressure, the pulse will reappear. The method is analogous to sphygmomanometry in human and can be applied not only at the tail of awake rats but also in dogs and small primates. The indirect tail cuff method is widely used to evaluate the influence of antihypertensive drugs in spontaneously and experimentally hypertensive rats.

PROCEDURE

Male spontaneous hypertensive rats (Charles River) weighing 300–350 g or rats with experimentally induced hypertension are used.

Surgical Procedure to Induce Renal Hypertension

Male Sprague-Dawley rats weighing 80–100 g are anesthetized by intraperitoneal injection of 0.8 ml 4% chloralhydrate solution. Both kidneys are exposed retroperitoneally. To induce renal hypertension, a silver clip (0.2 mm diameter, 4 mm length) is placed onto both renal arteries, the kidneys are reposed and the wound is closed by suture.

Within 5–6 weeks, operated animals attain a renal hypertension with a systolic blood pressure (BPs) of 170–200 mm Hg (mean normal physiological BPs for rats is 100 mm Hg). Only animals with a BPs = 180 mm Hg are used for the tests.

Test Procedure

The procedure is the same for spontaneously and experimentally hypertensive rats. Groups of 6 animals are used per dose. The control group receives saline only. To reduce spontaneous variations in blood pressure, animals are adjusted to the experimental cage by bringing them into the restraining cage which is enclosed in a 31–32°C measuring chamber 3–4 times before the start of the experiment for a period of 30–60 min.

To measure blood pressure, a tubular inflatable cuff is placed around the base of the tail and a piezoelectric pulse detector is positioned distal to the cuff. The cuff is inflated to approximately 300 mm Hg. As the pressure in the cuff is slowly released, the systolic pressure is detected and subsequently recorded on a polygraph.

The test substance is administered intraperitoneally or by gavage once per day over a period of 5 days. The usual screening dose of a new compound is 25 mg/kg. Blood pressure and heart rate measurements are taken at the following times:

day 1: predose and 2 h postdrug
day 3: predose and 2 h postdrug
day 5: predose, 2 h postdrug and 4 h postdrug.

Between measurements, animals are returned to their home cages.

Standard compounds:

- endralazine (3 mg/kg p.o.)
- nifedipine (3 mg/kg p.o.)
- urapidil (5 mg/kg p.o.)

EVALUATION

Mean values in systolic blood pressure before and after drug administration and the duration of the effect are determined. Percent decrease in systolic blood pressure under drug treatment is calculated. Statistical significance is assessed by the Student's *t*-test.

Scores for % decrease in systolic blood pressure and for the duration of the effect are allotted.

CRITICAL ASSESSMENT OF THE METHOD

The indirect tail-cuff method is being used in many laboratories with many modifications of the devices. Pfeffer et al. (1971) found a good correlation between values obtained with the indirect tail-cuff method and values measured directly with indwelling carotid arterial cannulae, whereas Buñag et al. (1971) reported a lack of correlation between direct and indirect measurement of arterial pressure in unanesthetized rats and Patten and Engen (1971) found difficulties to measure accurate systolic values at higher blood pressure. A good correlation between direct blood pressure data from the carotid artery in rats and readings with the tail cuff method was found by Matsuda et al. (1987) who developed a six-channel automatic blood pressure measuring apparatus with a highly sensitive photoelectric sensor for the detection of tail arterial blood flow and a microcomputer system for automatic measurement of systolic blood pressure and heart rate and for data acquisition and processing.

MODIFICATIONS OF THE METHOD

Details of the tail-cuff method in rats have been discussed by Stanton (1971).

Special equipment for measuring blood pressure in rats is commercially available (e. g., TSE GmbH, Bad Homburg, Germany).

Widdop and Li (1997) described a simple versatile method for measuring tail cuff systolic blood pressure in conscious rats. A tail cuff consisting of a metal T-piece tube with latex rubber inside the tube is placed around the tail at the proximal end. A piezoelectric transducer (model MLT1010) is strapped to the ventral surface of the tail to record the pulse signal from the caudal artery and connected directly to a MacLab data-acquisition system ADInstruments Pty Ltd.).

The tail-cuff method for measurement blood pressure has been adapted for dogs, monkeys (Wiester and Iltis 1976), and cats (Mahoney and Brody 1978).

Blood pressure can be measured from the hind leg of the rat using a leg cuff and a photoelectric cell situated at the dorsal surface of the foot (Kersten et al. 1947). When the leg is occluded, the foot swells and the amount of light striking the photocell is reduced. When the pressure in the cuff is released, the arterial blood flow is restored, the increase of foot volume is decreased and the amount of light transversing the paw increases.

REFERENCES AND FURTHER READING

Buñag RD (1984) Measurement of blood pressure in rats. In: de Jong W (ed) Handbook of Hypertension. Vol 4. Experimental and Genetic Models of Hypertension. Elsevier Science Publ., New York, pp 1–12

Buñag RD, McCubbin JW, Page IH (1971) Lack of correlation between direct and indirect measurement of arterial pressure in unanesthetized rats. Cardiovasc Res 5:24–31

Kersten H, Brosene WG Jr, Ablondi F, Subba Row Y (1947) A new method for the indirect measurement of blood pressure in the rat. J Lab Clin Med 32:1090–1098

Mahoney LT, Brody MJ (1978) A method for indirect recording of arterial pressure in the conscious cat. J Pharmacol Meth 1:61–66

Matsuda S, Kurokawa K, Higuchi K, Imamura N, Hakata H, Ueda M (1987) A new blood pressure measuring apparatus equipped with a microcomputer system for conscious rats. J Pharmacol Meth 17:361–376

Patten JR, Engen RL (1971) The comparison of an indirect method with a direct method for determining blood pressure on rats. Cardiovasc Res Center Bull 9:155–159

Pernot F (1991) Blood pressure on conscious rats, non-invasive method: tail-cuff. In: 7th Freiburg Focus on Biomeasurement. Cardiovascular and Respiratory *in vivo* Studies. Biomesstechnik-Verlag March GmbH, 79232 March, Germany, pp 30–32

Pfeffer JM, Pfeffer MA, Frohlich ED (1971) Validity of an indirect tail-cuff method for determining systolic arterial pressure in unanesthetized normotensive and spontaneously hypertensive rats. J Lab Clin Med 78:957–962

Stanton HC (1971) Experimental hypertension. In: Schwartz A (ed) Methods in Pharmacology, Vol 1, pp 125–150. Appleton-Century-Crofts, Meredith Corporation. New York

Widdop RE, Li XC (1997) A simple versatile method for measuring tail cuff systolic blood pressure in conscious rats. Clin Sci 93:191–194

Wiester MJ, Iltis R (1976) Diastolic and systolic blood pressure measurements in monkeys determined by a non invasive tail-cuff technique. J Lab Clin Med 87:354–361

A.1.3.5 Direct Measurement of Blood Pressure in Conscious Rats with Indwelling Catheter

PURPOSE AND RATIONALE

The method first described by Weeks (1960) allows the direct measurement of arterial pressure in conscious rats eliminating the influence of anesthesia on cardiovascular regulation.

PROCEDURE

Preparation of Cannulae

In order to prepare the cannulae 7 cm and 12 cm long pieces are cut from PE 10 and PE 20 tubings respectively. A stylet wire is inserted into the PE 10 tubing and the PE 20 tubing is also slipped over the stylet wire. The ends of the tubings are heated in a current of hot air and fused together. Ridges are made to anchor the cannula in the animal's tissue. In order to make a ridge, the stylet wire is left inside the cannula and the cannula is heated in a fine jet of hot air. When the polyethylene at the point of heating becomes soft, the cannula is pressed slightly and thus a ridge is formed. One ridge is formed at the PE 20 tubing, about 0.5 cm away from the junction with the PE 10 tubing, and 3 more ridges are formed on the PE 20 tubing at a distance of about 1 cm from each other, first one being situated about 3 cm away from the free end of the PE 20 tubing. The stylet wire is then removed from the cannula and the PE 10 portion of the cannula near the junction with the PE 20 tubing is wound around a glass rod with a diameter of 4 mm. Two rounds are made. Then it is dipped in a boiling water bath for about 5 s. When taken out of the bath, the cannula retains its circles, forming a spring-like structure.

Implantation of Cannulae

Male Sprague-Dawley rats weighing about 300 g are used. The rat is anesthetized with 45 mg/kg pentobarbital i.p. The area of the neck and the abdomen are shaved and cleaned with 70% alcohol. The viscera are exposed through a midline abdominal incision. A segment of the abdominal aorta is exposed just above the bifurcation. A trocar is passed through the psoas muscles adjacent to this segment of the aorta, through the muscles of the back and under the skin until it emerges

from the skin of the neck. Then the cannula is inserted into the trocar and the trocar is withdrawn from the body. The end of the cannula thus comes out from the neck, being anchored by silk sutures to the neck skin and to the psoas muscle. The cannula is filled with heparin solution and the end which is projecting out from the neck skin is blocked with a tight fitting stainless steel needle. Then the other end of the cannula is implanted into the aorta. The aorta is wiped with a cotton-tipped applicator stick above the bifurcation, occluded above this segment and punctured with a bent 27 gauge hypodermic needle. The tip of the PE 10 catheter is inserted through the needle and advanced up the aorta. The intestines are replaced and the wound sutured. The rats are allowed to recover for one week.

Measurement of Blood Pressure

The occluding stainless steel needle is removed and the cannula flushed with diluted heparin solution. The rat is placed in a small cage to restrict its movements, even so it is free to move. The cannula is connected to a Statham P 23 Db pressure transducer and blood pressure is recorded on a polygraph. Test drugs or standards are administered either subcutaneously or orally. Recordings are taken before and after administration of drug over a period of 1 h.

EVALUATION

Changes of blood pressure are measured for degree and duration. Five rats are used for each dose and compound. The maximal changes of each group are averaged and compared with the standard.

CRITICAL ASSESSMENT OF THE METHOD

Direct measurement of arterial blood pressure in unanesthetized rats originally introduced by Weeks (1960) has become a valuable and widely used tool in cardiovascular research.

MODIFICATIONS OF THE METHOD

A detailed description of a slightly modified Week's method has been given by Stanton (1971).

Improvements of the method for continuous direct recording of arterial blood pressure and heart rate in rats have been described by Buñag et al. (1971), Laffan et al. (1972), Buckingham (1976), Garthoff and Towart (1981), Garthoff (1983). A detailed description of permanent cannulation of the iliolumbar artery was given by Remie et al. (1990).

Wixson et al. (1987) described a technique for chronic catheterization of the carotid artery in the rat.

Prepared cannulas are commercially available (IRC Life Science, Woodland Hills CA).

A newer modification uses the access to the aorta via the common carotid artery (Linz et al. 1992). Rats are prepared under thiopental anesthesia with arterial PE-50 lines (Intramedic from Clay Adams, USA). The lines are introduced into the ascending aorta via the right carotid artery for direct measurement of arterial blood pressure and into the jugular vein for i.v. application of test compounds. Both lines, filled with saline containing heparin, are surfaced on the neck. The animals are allowed to recover for at least 2 days. Blood pressure is monitored through Statham R P23 Db transducers connected to a recording device. During measurements the lines are kept open with counter current saline infusion at a rate of 1 ml/h.

Bao et al. (1991) placed one catheter via the right femoral artery in the abdominal aorta in rats for recording mean arterial pressure and two additional catheters via the left carotid artery into the descending aorta for application of bradykinin and bradykinin antagonists.

Arterial pressure was recorded in unanesthetized rats after induction of severe hypertension by complete ligation of the aorta between the origin of the renal arteries by Sweet and Columbo (1979).

Hilditch et al. (1978) described a device for the direct recording of blood pressure in conscious dogs.

Akrawi and Wiedlund (1987) described a method for chronic portal vein infusion in unrestrained rats. Hepatic drug metabolism can be studied by infusion into the portal vein and blood collection from the femoral vein.

Robineau (1988) described a method for recording electrocardiograms in conscious, unrestrained rats. Electrodes were implanted subcutaneously and a socket connector was sutured on the head of the animal. A flexible cord leading to a swivel collector was linked to an ECG amplifier.

Kurowski et al. (1991) reported on an improved method to implant, maintain, and protect arterial and venous catheters in conscious rats for extended periods of time.

Schenk et al. (1992) measured cardiac left ventricular pressure in conscious rats using a fluid-filled catheter.

Tsui et al. (1991) recommended a reliable technique for chronic carotid arterial catheterization in the rat.

Hagmüller et al. (1992) described a tail-artery cannulation method for the study of blood parameters in freely moving rats.

Liebmann et al. (1995) described an *in vivo* long-term perfusion system which is based on au-

tomated, computer-controlled high-frequency heparin (10 U/ml) flushing of a cannula inserted into the tail artery of freely moving rats.

Santajuliana et al. (1996) used conscious rats instrumented with arterial and venous catheters to assess neurogenic pressor activity after administration of ganglionic blockers.

Rezek and Havlicek (1975) described simple cannula systems for the infusion of experimental substances in chronic, unrestrained animals. A cannula with a removable cap is used for infusions into various parts of the digestive tract. Intravenous infusions can be performed through a closed system cannula which avoids a possible introduction of air into the circulation.

Kimura et al. (1988) described a method for chronic portal venous, aortic, and gastric cannulation to determine portal venous and aortic glucose and lactate levels in conscious rats.

REFERENCES AND FURTHER READING

Akrawi SH, Wiedlund PJ (1987) A method for chronic portal vein infusion in unrestrained rats. J Pharmacol Meth 17:67–74

Bao G, Qadri F, Stauss B, Stauss H, Gohlke P, Unger T (1991) HOE 140, a new highly potent and long-acting bradykinin antagonist in conscious rats. Eur J Pharmacol 200:179–182

Buckingham RE (1976) Indwelling catheters for direct recording of arterial blood pressure and intravenous injection of drugs in the conscious rat. J Pharm Pharmac 28:459–461

Buñag RD, McCubbin JW, Page IH (1971) Lack of correlation between direct and indirect measurement of arterial pressure in unanesthetized rats. Cardiovasc Res 5:24–31

Garthoff B (1983) Twenty-four hour blood pressure recording in aortic coarctation hypertensive rats. Naunyn Schmiedeberg's Arch Pharmacol 322:R22

Garthoff B, Towart R (1981) A new system for the continuous direct recording of blood pressure and heart rate in the conscious rat. J Pharmacol Meth 5:275–278

Hagmüller K, Liebmann P, Porta S, Rinner I (1992) A tail-artery cannulation method for the study of blood parameters in freely moving rats. J Pharm Toxicol Meth 28:79–83

Hilditch A, Newberry A, Whithing S (1978) An improved device for the direct recording of blood pressure in conscious dogs. J Pharmacol Meth 1:89–90

Kimura RE, Lapine TR, Gooch III WM (1988) Portal venous and aortic glucose and lactate changes in a chronically catheterized rat. Pediat Res 23:235–240

Kurowski SZ, Slavik KJ, Szilagyi JE (1991) A method for maintaining and protecting chronic arterial and venous catheters in conscious rats. J Pharmacol Meth 26:249–256

Laffan RJ, Peterson A, Hitch SW, Jeunelot C (1972) A technique for prolonged, continuous recording of blood pressure of unrestrained rats. Cardiovasc Res 6:319–324

Liebmann PM, Hofer D, Absenger A, Zimmermann P, Weiss U, Porta S, Schauenstein K (1995) Computer-controlled flushing for long-term cannulation in freely moving rats. J Pharmacol Toxicol Meth 34:211–214

Linz W, Klaus E, Albus U, Becker R, Mania D, Englert HC, Schölkens BA (1992) Cardiovascular effects of the novel potassium channel opener (3S,4R)-3-hydroxy-2,2-dimethyl-4-(2-oxo-1-pyrrolidinyl)-6-phenylsulfonylchromane hemihydrate. Arzneim Forsch/Drug Res 42:1180–1185

Remie R, van Dongen JJ, Rensema JW (1999) Permanent cannulation of the iliolumbar artery. In: Van Dongen, Remie, Rensema, van Wunnik (eds) Manual of Microsurgery on the Laboratory Rat. Elsevier Science Publ, pp 231–241

Rezek M, Havlicek V (1975) Chronic multipurpose cannulas and a technique for the cannulation of small veins and arteries. Physiol Behav 15:623–626

Robineau F (1988) A simple method for recording electrocardiograms in conscious, unrestrained rats. J Pharmacol Meth 19:127–133

Santajuliana D, Hornfeldt BJ, Osborn JW (1966) Use of ganglionic blockers to assess neurogenic pressor activity in conscious rats. J Pharmacol Toxicol Meth 35:45–54

Schenk J, Hebden A, McNeill JH (1992) Measurement of cardiac left ventricular pressure in conscious rats using a fluid-filled catheter. J Pharm Toxicol Meth 27:171–175

Stanton HC (1971) Experimental hypertension. In: Schwartz A (ed) Methods in Pharmacology, Vol 1, pp 125–150. Appleton-Century-Crofts, Meredith Corporation. New York

Sweet CS, Columbo JM (1979) Cardiovascular properties of antihypertensive drugs in a model of severe renal hypertension. J Pharmacol Meth 2:223–239

Tsui BCH, Mosher SJ, Yeung PKF (1991) A reliable technique for chronic carotid arterial catheterization in the rat. J Pharm Meth 25:343–352

Weeks JR, Jones JA (1960) Routine direct measurement of arterial pressure in unanesthetized rats. Proc Soc Exp Biol Med 104:646–648

Wixson SK, Murray KA, Hughes HC Jr (1987) A technique for chronic arterial catheterization in the rat. Lab Anim Sci 37:108–110

A.1.3.6 Cannulation Techniques in Rodents

PURPOSE AND RATIONALE

Cardiovascular pharmacology requires special techniques for catheterization and permanent cannulation of vessels. A few methods are described below.

A comprehensive literature survey on methods for vascular access and collection of body fluids from the laboratory rat was written by Cocchetto and Bjornsson (1983).

REFERENCES AND FURTHER READING

Cocchetto DM, Bjornsson TD (1983) Methods for vascular access and collection of body fluids from the laboratory rat. J Pharmaceut Sci 72:465–492

A.1.3.6.1 Permanent Cannulation of the Jugular Vein in Rats

PURPOSE AND RATIONALE

Permanent cannulation of the jugular vein in rats in combination with a head attachment apparatus allowing easy connection of cannulae was first introduced by Steffens (1969). Modifications were described by Brown and Hege (1972), Nicolaidis et al. (1974) and

by Dons and Havlik (1986). A detailed description was given by Remie et al. (1990).

PROCEDURE

Rats are anesthetized with N_2O_2/O_2/halothane. The shaven neck of the animal on the right side is disinfected with chlorhexidine solution. The incision is made just above the right clavicle. Connective and adipose tissue are pushed aside with blunt forceps and the jugular vein is exposed. The external jugular vein is followed and the division into the maxillary vein, the facial and the linguofacial vein identified. The largest vein is chosen and mobilized for a distance of about 5 mm. Small artery forceps are used to clamp the vessel. The vein is then ligated rostral to the clamp with 6–0 silk, and a second ligature is put loosely around the vessel, but not tightened. Using iridectomy scissors, a V-shaped hole is cut in the vein 2 mm rostral from the bifurcation. Prior to its insertion into the vessel, a sterile cannula is connected to a 1 ml syringe filled with a heparinized saline solution. The vessel is dilated by means of a sharp pointed jeweler's forceps, the cannula slit between the legs of the forceps and gently pushed into the vessel until the tip is at the level of the right atrium. Then the forceps is removed, the caudal ligature gently tied, and the rostral ligature used to anchor the cannula to the vessel. The cannula is tunneled to emerge at the top of the head. While the skin in the neck is held firmly, the artery forceps is inserted subcutaneously in caudal direction over a distance of about 3 cm, then turned anti-clockwise in the direction of the incision in the neck. The cannula is grasped with the forceps. Then the forceps is pulled back until the cannula emerges at the crown of the head and closed by a small microvascular clamp. The cannula is slid over the short end of a 20G stainless steel needle bent to a 90° angle. The catheter is flushed with saline and filled with polyethylene/heparin solution. The long end of the L-shaped stainless steel adapter is closed with a piece of heat-sealed PE-tubing and the wounds are closed with sutures.

MODIFICATIONS OF THE METHOD

Hutchaleelaha et al. (1997) described a simple apparatus for serial blood sampling from the external jugular vein which permits simultaneous measurement of locomotor activity in freely moving rats.

REFERENCES AND FURTHER READING

Brown MR, Hedge GA (1972) Thyroid secretion in the unanesthetized, stress-free rat and its suppression by pentobarbital. Neuroendocrinology 9:158–174

Dons RF, Havlik R (1986) A multilayered cannula for long-term blood sampling in unrestrained rats. Lab Anim Sci 36:544–547

Hutchaleelaha A, Sukbuntherng J, Mayersohn (1997) Simple apparatus for serial blood sampling in rodents permitting simultaneous measurement of locomotor activity as illustrated with cocaine. J Pharmacol Toxicol Meth 37:9–14

Nicolaidis S, Rowland N, Meile MJ, Marfaing-Jallat P, Pesez A (1974) A flexible technique for long term infusion in unrestrained rats. Pharmacol Biochem Behav 2:131–136

Remie R, van Dongen JJ, Rensema JW (1990) Permanent cannulation of the jugular vein (acc. to Steffens). In: Van Dongen, Remie, Rensema, van Wunnik (eds) Manual of Microsurgery on the Laboratory Rat. Elsevier Science Publ., pp 159–169

Steffens AB (1969) A method for frequent sampling of blood and continuous infusion of fluids in the rat without disturbing the animal. Physiol Behav 4:833–936

A.1.3.6.2 Permanent Cannulation of the Renal Vein in Rats

PURPOSE AND RATIONALE

A detailed description for permanent cannulation of the renal vein in rats was given by Remie et al. (1990).

PROCEDURE

Rats are anesthetized with N_2O_2/O_2/halothane. After opening the abdominal wall, the intestines are lifted out and laid next to the animal on the right side (as viewed by the surgeon) on gauze moistened with warm saline solution. This provides an excellent view to the vena cava. At its confluence with the vena cava, the right renal vein is stripped of its adipose tissue and the peritoneum is opened. Using small anatomical forceps the peritoneum is detached from the vena cava by making small spreading movements with the forceps just beneath the peritoneum. Subsequently, the vena cava and the renal vein are mobilized for approximately 1.5 cm, to allow for clamping of the vessel. A four or five fine-stitch purse-string is placed in the vessel at the confluence of the vena cava and the right renal vein. Using a Barraquer needle holder and a cotton-wool stick, the 7–0 silk suture, armed with a BV-1 needle, is guided through the vessel. After each stitch, any bleeding has to be immediately arrested by applying light pressure using a cotton-wool stick. Having completed the suture a single knot is made with the drawstrings. Three microvascular clips are then placed on the vena cava and the renal vein; first the proximal clip on the vena cava, followed by the clip on the renal vein and finally the distal vena cava clip. A small aperture is cut immediately inside the purse-string suture using iridectomy scissors and jeweler's forceps. The cannula, which is filled with a heparinized saline solution, is pushed into the opening as far as possible. Subse-

quently, the purse-string suture is pulled taut and the clip of the renal vein removed, while pushing the cannula further. The proximal clip on the vena cava is now removed as quickly as possible. The patency of the cannula is checked and the drawstrings of the purse-string suture are used to anchor the cannula. The cannula is laid kink-free in the abdominal cavity and sutured to the internal abdominal cavity near the xiphoid cartilage. The abdomen is closed in two layers and the cannula tunneled to the top of the head. The cannula together with a L-shaped adapter is fixed to the skull.

REFERENCES AND FURTHER READING

Remie R, Rensema JW, van Dongen JJ (1990) Permanent cannulation of the renal vein. In: Van Dongen, Remie, Rensema, van Wunnik (eds) Manual of Microsurgery on the Laboratory Rat. Elsevier Science Publ., pp 223–230

A.1.3.6.3 Permanent Cannulation of the Portal Vein in Rats

PURPOSE AND RATIONALE

Several techniques have been described for cannulation of the portal vein in rats (Hyun et al. 1967; Pelzmann and Havemeyer 1971; Suzuki et al. 1973; Sable-Amplis and Abadie 1973; Helman et al. 1984). A detailed description for permanent cannulation of the portal vein in rats was given by Remie et al. (1990). After additional application of platinum electrodes around the portal vein in close proximity to the catheter tip, this model can also be used to study the presynaptic regulation of neurotransmitter release from nonadrenergic nerve terminals (Remie and Zaagsma 1986; Remie et al. 1988, 1989).

PROCEDURE

Rats are anesthetized with N_2O_2/O_2/halothane. After opening the abdominal wall, the intestines are lifted out and laid next to the animal on the right side (as viewed by the surgeon) on gauze moistened with warm saline solution. Using a micro needle holder and a cotton-wool stick, a four or five, fine stitch purse-string suture (7–0 silk suture armed with a BV-1 needle) is placed in the wall of the portal vein at the side opposite the gastroduodenal vein. The diameter of the purse-string should be about 1 mm. After the suture has been completed a single knot is made with the drawstrings. The portal vein is clamped with a small curved hemostatic bulldog clamp. Using iridectomy scissors and a pair of jeweler's forceps the center of the purse-string is cut, a cannula filled with heparinized saline is inserted into the vessel and pushed upwards. The purse-string is gently tightened taking care not to obstruct the cannula. The drawstrings of the suture are used to anchor the cannula. The cannula is laid kink-free in the abdominal cavity and sutured to the internal abdominal cavity near the xiphoid cartilage. The abdomen is closed in two layers and the cannula tunneled to the top of the head. The cannula together with a L-shaped adapter is fixed to the skull.

REFERENCES AND FURTHER READING

Helman A, Castaing D, Morin J, Pfister-Lemaire N, Assan R (1984) A new technique for hepatic portal vein catheterization in freely moving rats. Am J Physiol 246 (Endocrinol Metab 9):E544–E547

Hyun SA, Vanhouny GV, Treadwell CR (1967) Portal absorption of fatty acids in lymph and portal vein cannulated rats. Biochem Biophys Acta 137:296–305

Pelzmann KS, Havemeyer RN (1971) Portal blood vein sampling in intestinal drug absorption studies. J Pharm Sci 60:331–332

Remie R, Zaagsma J (1986) A new technique for the study off vascular presynaptic receptors in freely moving rats. Am J Physiol 251:H463–H467

Remie R, Knot HJ, Kolker HJ, Zaagsma J (1988) Pronounced facilitation of endogenous noradrenaline release by presynaptic β_2-adrenoceptors in the vasculature of freely moving rats. Naunyn-Schmiedeberg's Arch Pharmacol 338:215–220

Remie R, Coppes RP, Zaagsma J (1989) Presynaptic muscarinic receptors inhibiting endogenous noradrenaline release in the portal vein of the freely moving rat. Br J Pharmacol 97:586–590

Remie R, van Dongen JJ, Rensema JW, van Wunnik GHJ (1990) Permanent cannulation of the portal vein. In: Van Dongen, Remie, Rensema, van Wunnik (eds) Manual of Microsurgery on the Laboratory Rat. Elsevier Science Publ., pp 213–221

Sable-Amplis R, Abadie D (1975) Permanent cannulation of the hepatic portal vein in rats. J Appl Physiol 38:358–359

Suzuki T, Sattoh Y, Isozaki S, Ishida R (1973) Simple method for portal vein infusion in the rat. J Pharm Sci 62:345–347

A.1.3.6.4 Permanent Cannulation of the Thoracic Duct in Rats

PURPOSE AND RATIONALE

Collection of lymph is rather difficult and has performed mainly in dogs (Biedl and Offer 1907; Gryaznova 1962, 1963; Vogel 1963). Some techniques have been described for the rat (Bollman et al. 1948; Girardet 1975). Remie et al. (1990) did not obstruct the duct by placing a purse-string suture in the wall of the duct, by which the cannula is secured. The animal's lymph can be collected during the experiment, and after refilling the cannula the lymph flow remains undisturbed.

PROCEDURE

Rats are anesthetized with N_2O_2/O_2/halothane. After opening the abdominal cavity, the intestines are placed

in gauze moistened with warm saline and laid to the left of the animal. The suprarenal abdominal artery is located and mobilized by gently tearing the connective tissue. Using blunt dissection technique, the thoracic duct is mobilized along the dorsolateral surface of the aorta. A small three to four fine stitch purse-string suture is placed in the wall of the duct, using a 9–0 Ethilon suture. A hole is cut inside the purse-string with a very fine pair of scissors, while holding the wall with angled jeweler's forceps. The cannula which is filled with heparinized saline solution and is inserted into the duct using anatomical forceps. After the tip of the cannula has been inserted into the thoracic duct, the curved forceps are removed and the total tip is pushed into the duct. The ligature is then closed and some lymph will flow into the cannula. The cannula is secured within the abdominal cavity by attaching it to the abdominal muscle near the xiphoid cartilage with a 7–0 silk suture. Following the closure of the abdominal wall and the tunneling of the cannula to the crown of the head, a L-shaped adapter is placed on the cannula, filled with PVP-solution and closed with a heat-sealed polyethylene cap.

REFERENCES AND FURTHER READING

Biedl A, Offer TR (1907) Über Beziehungen der Ductuslymphe zum Zuckerhaushalt. Hemmung von Adrenalinwirkung durch die Lymphe. Wien Kin Wschr

Bollman JL, Cain JC, Grindlay JH (1948) Techniques for the collection of lymph from the liver, small intestine, or thoracic duct of the rat. J Lab Clin Med 33:1349–1352

Girardet RE (1975) Surgical technique for long-term studies of thoracic duct circulation in the rat. J Appl Physiol 39:682–688

Gryaznova AV (1962) Ligation of the thoracic duct in dogs. Arkhiv Anatomii, Gistologii i Embriologii 42:90–95

Gryaznova AV (1963) Ligation of the thoracic duct in dogs. Fed Proc 22/II,T886

Remie R, van Dongen JJ, Rensema JW (1990) Permanent cannulation of the thoracic duct. In: Van Dongen, Remie, Rensema, van Wunnik (eds) Manual of Microsurgery on the Laboratory Rat. Elsevier Science Publ., pp 243–253

Vogel HG (1963) Unpublished data

A.1.3.6.5 Portacaval Anastomosis in Rats

PURPOSE AND RATIONALE

In 1877 the Russian surgeon Eck reported the achievement of successful portacaval shunts in dogs. Lee and Fischer (1961), Funovics et al. (1975), de Boer et al. (1986), described portacaval shunt in the rat. A detailed description of surgery for portacaval anastomosis in rats was given by van Dongen et al. (1990).

PROCEDURE

Rats are anesthetized with N_2O_2/O_2 in combination with either enflurane, methoxyflurane or isoflurane. After opening the abdominal wall, the intestines are placed left to the animal on gauze moistened with warm saline solution. Proximally and distally to the animal's right renal vein, the vena cava is then stripped of its adipose and connective tissue, and the retroperitoneal cavity is opened. Using anatomical forceps the peritoneum is dissected from the vena cava by making small spreading movements with the forceps just above the vena cava. The portal vein is pulled slightly to the left using straight anatomical forceps and freed from the hepatic artery and the gastroduodenal artery with curved anatomical forceps. Rostral to the celiac artery, the abdominal artery which is covered with peritoneum is freed from its lateral muscle bed over a length of approximately 5 mm providing enough space for placing a small bulldog clamp at a later stage of the operation. Without occlusion a six fine-stitch purse-string is placed in the wall of the vena cava close to its confluence with the right renal vein. Using a Barraquer needle holder and a cotton wool stick, the 7–0 silk suture armed with a BV-1 needle is guided through the vessel. After each stitch, bleeding has to be arrested immediately, by applying light pressure on the area, again using the cotton wool stick. After the suture has been completed, a single knot is made with the drawstrings. The drawstrings should come together at the rostral part of the purse-string. A bulldog clamp, modified to resemble a Satinsky vascular clamp, is then placed on the vena cava.

Before clamping the abdominal aorta rostral to the celiac artery with a small bulldog clamp, a ligature (7–0 silk) is placed around the portal vein as close as possible to the hilus of the liver. Subsequently, the clamp is placed on the aorta and the ligature tightened. A Heifetz clip is then placed transversely onto the portal vein at its confluence with the gastroduodenal vein. The portal vein is cut just distally from the ligature. A prepared button is slipped over the left-hand straight small anatomical forceps, while the right-hand forceps are used to pass the portal vein to the left-hand anatomical forceps. The vein is then grasped and pulled through the button. Subsequently, the button is pushed as close as possible to the Heifetz clip, and clamped to the clip using a Pilling bulldog clamp.

Using small straight, and curved anatomical forceps the portal vein is reversed around the button and fixed with a previously prepared 7–0 silk suture. The Pilling bulldog clamp is then removed and replaced at the end of the Satinsky clamp for reasons of stability. The vena

cava is then somewhat elevated, bringing it into closer contact with the portal vein button.

A longitudinal cut is made in the purse-string suture using iridectomy scissors and jeweler's forceps. One drawstring of the suture is clamped with a small hemostat and put under slight tension in a rostral direction. The button manipulated by its grip, is pushed into the vena cava. The purse-string is tightened with the left hand whilst the right hand still holds the button in position. The button is released and two additional knots tied. The Satinsky clamp is removed first followed by the Heifetz clamp and the bulldog clamp on the aorta. After replacing the intestines the abdominal wall is closed in two layers.

REFERENCES AND FURTHER READING

De Boer JEG, Janssen MA, van Dongen JJ, Blitz W, Oostenbroek RJ, Wesdorp RIC, Soeters PB (1986) Sequential metabolic characteristics following portacaval shunt in rats. Eur Soc Surg Res 18:96–106

Eck NV (1877) On the question of ligature of the portal vein. Voen Med J; St. Petersburg 130:1–2

Funovics JM, Cummings MG, Shuman L, James JH, Fischer JE (1975) An improved non suture method for portacaval anastomosis in the rat. Surgery 77:668–672

Lee SH, Fischer B (1961) Portacaval shunt in the rat. Surgery 50:668–672

van Dongen JJ, Remie R, Rensema JW, van Wunnik GHJ (1990) Portacaval anastomosis. In: Van Dongen, Remie, Rensema, van Wunnik (eds) Manual of Microsurgery on the Laboratory Rat. Elsevier Science Publ., pp 171–199

A.1.3.7 Cardiovascular Analysis in Anesthetized Mice

PURPOSE AND RATIONALE

To fully utilize the potential of mouse models with specific gene mutations, it is necessary to study the functional consequences of genetic manipulations in fully intact mice. Lorenz and Robbins (1997) developed and validated a methodology to study cardiovascular parameters in closed-chest mice.

PROCEDURE

Adult mice of either sex weighing 25–35 g are anesthetized by intraperitoneal injection of 50 mg/kg ketamine and 100 mg/kg thiobutabarbital. After the mice are placed on a thermally controlled surgical table with body temperature continually monitored via a rectal probe, a tracheotomy is performed with a short length (< 1 cm) of PE-90 tubing. The right femoral artery is then cannulated with polyethylene tubing which is pulled over a flame to a small diameter (∼0.4 mm OD). The catheter is advanced ∼1 cm, near the level of the aorta, and connected directly to a low-compliance COBE CDXIII fixed-dome pressure transducer for the measurement of arterial blood pressure. The right femoral vein is then cannulated with the same type of small-diameter tubing and connected to a microinjection pump for the infusion of experimental drugs. To assess myocardial performance, the right carotid artery is cannulated with a 2F Millar MIKRO-TIP transducer (Model SPR-407, Millar Instruments, Houston TX). This high-fidelity transducer, which has a tip diameter of ∼0.67 mm, has a reported frequency response that is flat up to 10,000 Hz and therefore can be used to accurately monitor the high frequency of the mouse ventricular pulse pressure. During continual monitoring of the blood pressure wave to ascertain the anatomic position of the catheter, the tip of the transducer is carefully advanced through the ascending aorta and into the left ventricle. When the stable waveform of the ventricular pressure profile is achieved, the transducer is anchored in place with 7–0 silk sutures. After completion of the surgery, all wounds are closed with cyanoacrylate to minimize evaporative loss of fluid, and the animals are allowed to stabilize for 30–45 min.

EVALUATION

Blood pressure signals from the COBE transducer and from the Millar transducer are amplified and the output is recorded and analyzed with a MacLab 4/s data acquisition system connected to a Macintosh 7100/80 computer which allows the calculation of the following parameters:

dP/dt	first derivative of the ventricular pressure wave,
MAP	mean arterial pressure,
HR	heart rate,
LVP	systolic and diastolic left ventricular pressure,
LVEDP	left ventricular enddiastolic pressure.

Further indices of ventricular performance can be calculated from dP/dt.

MODIFICATIONS OF THE METHOD

Champion et al. (2000) described a **right-heart catheterization technique** for *in vivo* measurement of vascular responses in lungs of intact mice. CD1 mice weighing 25–38 g were anesthetized with thiopentobarbital (85–95 mg/kg i.p.) and ketamine 3 mg/kg i.p.) and were strapped in supine position to a thermoregulated fluoroscopic table. The trachea was cannulated and the animals breathed with room air enriched with 95% O_2/5% CO_2. A femoral artery was cannulated

for the measurement of systemic arterial pressure. Heart rate was electronically monitored from the systolic pressure pulses with a tachometer (Grass model 7P44A). The left jugular vein was cannulated for the administration of agonists and antagonists.

For measuring pulmonary arterial pressure, a special single lumen catheter was constructed. The catheter was 145 mm in length and 0.25 mm in outer diameter, with a specially curved tip to facilitate passage through the right heart, main pulmonary artery, and the left or right pulmonary artery. Before the catheter was introduced, the catheter curve was initially straightened with a 0.010-in. straight angioplastic guide wire to facilitate passage from the right jugular vein into the right atrium at the tricuspid valve under fluoroscopic guidance. As the straight wire was removed, the natural curve facilitated entry of the catheter into the right ventricle. A 0.010-in. soft-tip coronary artery guide wire was then inserted, and the catheter was passed over the guide wire into the main pulmonary artery under fluoroscopic guidance. Pressure in the main pulmonary artery was measured with a pressure transducer, and mean pulmonary artery pressure was derived electronically and recorded continuously.

Cardiac output was measured by the thermodilution technique. A known volume (20 µl plus catheter dead space) of 0.9% NaCl solution at 23°C was injected into the right atrium, and changes in blood temperature were measured at the root of the aorta. A cardiac output computer equipped with a small-animal interface was used. The thermistor microprobe was inserted into the right carotid artery and advanced to the aortic arch, where changes in aortic blood temperature were measured. A catheter placed in the right jugular vein was advanced to the right atrium or main pulmonary artery for rapid bolus injection of saline. The saline solution was injected with a constant-rate syringe to ensure rapid and repeatable injection of the saline indicator solution. Thermodilution curves were recorded on a chart recorder and pulmonary and systemic blood pressure monitored continuously. Catheter placement was verified by postmortem examination.

REFERENCES AND FURTHER READING

Champion HC, Villnave DJ, Tower A, Kadowitz PJ, Hyman AL (2000) A novel right-heart catheterization technique for *in vivo* measurement of vascular responses in lungs of intact mice. Am J Physiol, Heart Circ Physiol 278:H8–H15

Lorenz JN, Robbins J (1997) Measurement of intraventricular pressure and cardiac performance in the intact, closed-chest mouse. Am J Physiol 272 (Heart Circ Physiol 41):H1137–H1146

A.1.3.8 Blood Pressure in Anesthetized Cats

PURPOSE AND RATIONALE

Cats are the most sensitive species of cardiovascular regulation. They were used extensively for cardiovascular screening. Recently, experiments in dogs are preferred since this species can be bred more easily in homogeneous strains.

PROCEDURE

Adult cats of either sex weighing 2.5 to 4 kg are anesthetized by intraperitoneal injection of 35 mg/kg pentobarbital sodium. Tracheotomy is performed and a tracheal cannula is inserted so that the cat can be mechanically ventilated with room air. A femoral artery and two femoral veins are cannulated for measurement of arterial blood pressure and systemic administration of drugs. The arterial cannula is connected to a Statham model P23Gb transducer. All recordings are made on a polygraph. Heart rate is determined with a Beckman Cardiotach connected to a voltage/pressure-pulse coupler. Rectal temperature is monitored and maintained between 37°C and 38°C with a heating pad.

The following drugs are injected i.v. as challenges:

- epinephrine 0.1, 0.3, 0.5 µg/kg,
- norepinephrine 0.1, 0.3, 0.5 µg/kg,
- isoproterenol 0.1, 0.2, 0.4 µg/kg,
- carbachol 0.1, 0.2, 0.5 µg/kg.

At least 5 min are allowed between challenge doses to permit the measured parameters to return to baseline.

Test drugs are injected at various doses followed by injections of the challenging drugs.

EVALUATION

Dose-response curves of challenging drugs are established before and after injections of the test drugs.

CRITICAL ASSESSMENT OF THE METHOD

Blood pressure experiments in anesthetized cats are very valuable as screening techniques for cardiovascular agents. Moreover, potentiation of norepinephrine response has been used as screening procedure for antidepressants with norepinephrine uptake inhibiting activity.

MODIFICATIONS OF THE METHOD

Sander (1965) investigated the vasoconstrictor and vasodilator effects of procaine in spinal cats. The animals

were anesthetized with ether and ventilated with a positive pressure pump via a tracheal cannula. The spinal cord was then cut between the second and third vertebrae, and ether administration stopped. The remaining portion of the spinal cord above the transection was destroyed by passing a curette through the spinal canal.

Yardley et al. (1989) studied cardiovascular parameters in spinal cats. The animals were anesthetized with 80 mg/kg intravenously administered α-chloralose. The spinal cord was transected or crushed at the first cervical segment after tetracaine hydrochloride (0.125 mg in 0.1 ml) had been injected into this region of the cord. Systemic blood pressure was supported at a level sufficient to maintain constricted pupils (mean value 45 ± 5 mm Hg) by volume expansion with blood from a donor (10–20 ml) or an infusion of dextran.

REFERENCES AND FURTHER READING

Chen K, Hernandez Y, Dertchen KI, Gillis RA (1994) Intravenous NBQX inhibits spontaneously occurring sympathetic nerve activity and reduces blood pressure in cats. Eur J Pharmacol 252:155–160

Corman LE, diPalma JR (1967) Animal techniques for measuring drug effects on various peripheral vascular beds. In: Siegler PE, Moyer JH (eds) Animal and clinical pharmacologic techniques in drug evaluation, Vol II, pp 434–443. Year Book Medical Publ., Inc., Chicago

Crumb WJ Jr, Kadowitz PJ, Xu YQ, Clarkson CW (1990) Electrocardiographic evidence for cocaine cardiotoxicity in cat. Canad J Physiol Pharmacol 68:622–625

Henderson TR, DeLorme EM, Takahashi K, Gray AP, Dretchen KI (1988) Cardiovascular effects of 1-methyl-4-(1-naphthyl-vinyl)piperidine hydrochloride. Eur J Pharmacol 158:149–152

Mian MA, Malta E, Raper C (1986) Cardiovascular actions of Xamoterol (ICI 118,587) in anaesthetized cats, rats, and guinea pigs. J Cardiovasc Pharmacol 8:314–323

Pichler L, Kobinger W (1985) Possible function of α_1-adrenoceptors in the CNS in anesthetized and conscious animals. Eur J Pharmacol 107:305–311

Sander HD (1965) The vasoconstrictor and vasodilator effects of procaine. Can J Physiol Pharmacol 43:39–46

Yardley CP, Fitzsimonis CL, Weaver LC (1989) Cardiac and peripheral vascular contributions to hypotension in spinal cats. Am J Physiol 257 (Heart Circ Physiol 26): H1347–H1353

A.1.3.9 Cardiovascular Drug Challenging Experiments in Anesthetized Dogs

PURPOSE AND RATIONALE

Sympathomimetic and cholinomimetic compounds as well as angiotensin II and carotid occlusion exert characteristic responses in blood pressure of anesthetized dogs. Antagonism or potentiation of these responses allow to characterize the cardiovascular activity of a new compound.

PROCEDURE

Adult Beagle dogs of either sex weighing between 8 and 15 kg are anesthetized with 15 mg/kg sodium thiopental, 200 mg/kg sodium barbital and 75 mg/kg sodium pentobarbital. Additional doses of sodium pentobarbital are given as needed. The dogs are intubated with a cuffed endotracheal tube and placed on a Harvard respirator (20 ml/kg, 10–15 cycles/min). A femoral vein and artery are cannulated using polyethylene tubing for drug administration and determination of arterial blood pressure, respectively. The animals are bilaterally vagotomized.

The arterial cannula is connected to a Statham model P23Gb transducer. All recordings are made on a polygraph. Heart rate is determined with a Beckman Cardiotach connected to a voltage/pressure-pulse coupler.

Drug challenges: One of the following combinations of drugs is administered i.v. to the dogs. The challenges are given in a fixed order: at least twice prior to test drug administration to insure consistent responses and again starting 15 min post test drug. Epinephrine and norepinephrine (1 µg/kg), isoproterenol (0.25 µg/kg), carbachol (0.25 µg/kg), tyramine (100 µg/kg) are used; bilateral carotid occlusion (45 s), phenylephrine (10 µg/kg), isoproterenol (0.25 µg/kg) angiotensin II (0.2 µg/kg) and carbachol (0.25 µg/kg) for cardiovascular drugs. At least 5 min are allowed between challenge doses to permit the measured parameters to return to baseline. Challenge drug doses are sometimes varied to keep the mean arterial pressure within the following limits: epinephrine (+30 to +60 mm Hg), norepinephrine (–30 to +70 mm Hg), tyramine (+30 to +70 mm Hg), isoproterenol (–30 to –50 mm Hg), carbachol (–30 to –50 mm Hg), phenylephrine (–30 to +70 mm Hg), angiotensin II (+30 to +50 mm Hg), and bilateral carotid occlusion (+30 to +70 mm Hg).

EVALUATION

The recordings are studied to detect any changes in the arterial pressure response to the challenge drug before and after test-drug administration and to observe any changes in blood pressure and heart rate. Results are expressed as the percentage change from the predrug response.

REFERENCES AND FURTHER READING

Corman LE, diPalma JR (1967) Animal techniques for measuring drug effects on various peripheral vascular beds.

In: Siegler PE, Moyer JH (eds) Animal and clinical pharmacologic techniques in drug evaluation, Vol II, pp 434–443. Year Book Medical Publ., Inc., Chicago

Hoppe JO, Brown Jr TG (1964) Animal techniques for evaluating autonomic blocking agents, antihypertensive and vasodilator drugs. In: Nodine JE, Siegler PE (eds) Animal and clinical pharmacologic techniques in drug evaluation. Vol I, pp 116–121. Year Book Medical Publ., Inc., Chicago

A.1.3.10 Hemodynamic Analysis in Anaesthetized Dogs

PURPOSE AND RATIONALE

The hemodynamic effects of compounds supposed to affect the cardiovascular system are evaluated by measuring preload and afterload of the heart, contractility, heart rate, cardiac output and peripheral or coronary flow. To measure these cardiovascular parameters accurately, the use of larger animals such as dogs or pigs is necessary.

This experimental model allows the classification of test drugs according to their action as having:

- positive inotropic effects
- negative inotropic effects (Ca^{2+}-antagonist, anti-arrhythmic?)
- hypertensive effects
- hypotensive effects
- coronary-dilating effects
- β-blocking effects
- α-blocking effects
- anti-anginal effects
- peripheral-vasodilating effects

PROCEDURE

Male or female inbred Beagle or Labrador-Harrier dogs weighing between 15 and 25 kg are used. They are anesthetized with a bolus injection of 35–40 mg/kg pentobarbital, and continued with an infusion of 4–6 mg/kg/h. A catheter is placed into the cephalic vein for intravenous injections. Another catheter is placed into the duodenum for enteral administration. Respiration is maintained with room air through a tracheal tube using a positive pressure respirator, e. g., Bird-Mark-7-respirator. Blood gas analyses are performed at regular time intervals. Oxygen is supplied via the respirator as needed.

Preparation for Hemodynamic Measurements

Blood pressure is recorded through a cannula inserted into the left femoral artery and connected to a Statham pressure transducer (Statham P 23 DB).

For determination of LVP, a Millar microtip catheter (type PC 350) is inserted via the left common carotid artery into the left ventricle. LVEDP is measured on a high-sensitivity scale. From the pressure curve, dp/dt_{max} is differentiated and heart rate is counted. The LVP-signal also triggers a cardiotachometer.

Cardiac output, pulmonary artery pressure (PAP) and stroke volume are measured by a thermodilution technique using a Cardiac Output Computer (Gould/Statham SP 1245) and a balloon-tip triple lumen catheter (Gould SP 5105, 5F) with the thermistor positioned in the pulmonary artery via the jugular vein.

Myocardial oxygen consumption (MVO_2) is calculated as pressure-work-index according to Rooke and Feigl (1982).

Femoral blood flow and coronary flow are measured with electromagnetic flow probes attached to the femoral artery and the circumflex branch of the left coronary artery (LCX), respectively.

Experimental Course

When stable hemodynamic conditions and blood gas values of pO_2>100 mm Hg and pCO_2 < 35 mm Hg are achieved for at least 20 min (control values), the test substance is administered through a catheter inserted into a cephalic vein in doses of 0.1, 0.3, 1.0, and 3.0 mg/kg or into the duodenum in doses of 0.3, 1.0, 3.0, and 10.0 mg/kg.

All parameters are recorded continuously during the whole experiment.

Characteristics

- blood pressure
  - systolic, BPs
  - diastolic, BPd
- left ventricular pressure, LVP
- left ventricular enddiastolic pressure, LVEDP
- maximal rate of pressure rise, dp/dt max
- heart rate, HR
- peripheral blood flow in A. femoralis, PF
- blood pressure A. pulmonalis, PAP
- coronary flow, CF
- cardiac output, CO
- stroke volume, SV
- total peripheral resistance, TPR
- left ventricular stroke work, LVSW
- left ventricular minute work, LVMW
- left ventricular myocardial oxygen consumption, MVO_2

CALCULATION OF RESULTS AND EVALUATION

Besides the different directly measured hemodynamic parameters, the following data are calculated according to the respective formulae

- stroke volume [ml/beat],

$$SV = \frac{CO}{HR}$$

- total peripheral resistance [dyns/cm^5],

$$TPR = \frac{BPm}{CO} \times 79.9$$

- left ventricle stroke work [J/beat],

$$LVSW = (BPm - LVEDP) \times SV \times 0.333 \times 10^{-3}$$

- left ventricular minute work [J/min],

$$LVMW = LVSW \times HR$$

- left ventricular myocardial oxygen consumption [ml O_2/min/100 g],

$$MVO_2 = K_1(BPs \times HR) + K_2 \times \frac{(0.8BPs + 0.2BPd) \times HR + SV}{BW} + 1.43$$

$K_1 = 4.08 \times 10^{-4}$
$K_2 = 3.25 \times 10^{-4}$
BPs = systolic blood pressure [mm Hg]
BPd = diastolic blood pressure [mm Hg]
BPm = mean blood pressure [mm Hg]
HR = heart rate [beats/min]
CO = cardiac output [ml/min]
SV = stroke volume [ml/beat]
$LVEDP$ = left ventricular enddiastolic pressure [mm Hg]
BW = body weight [kg]

Changes in parameters measured after drug administration are compared to control values obtained during the 20 min pre-drug period.

Results are presented as mean ± SEM with $n > 3$.

Statistical significance is assessed by means of the paired *t*-test.

MODIFICATIONS OF THE METHOD

The effect of drugs on the carotid artery occlusion effect can be studied in anesthetized dogs. The occlusion of right and left common carotid arteries is performed by squeezing them between a polyethylene tubing and a twine which is passed inside the tubing and around the carotid artery. An occlusion of the carotid arteries for 30 s causes an increase of systolic blood pressure by 40–50 mm Hg. Inhibition of this effect by drugs is tested.

Studies in anesthetized dogs can be used to determine the influence of cardiotonic drugs on propranolol induced cardiac insufficiency (Rajagopalan et al. 1993)

Instead of dogs, **pigs (German landrace)** weighing between 20–35 kg can be used. They are pretreated with ketamine 500 mg/5 ml i.m., methomidate hydrochloride 200 mg/4 ml i.p., xylazine 60 mg/3 ml i.m., and anaesthetized with 15–20 mg/kg pentobarbital sodium, followed by continuous infusion of 12 mg/kg/h. The parameters are evaluated similarly to the experiments in dogs.

Measurement of cardiac output by the thermodilution method in **rats** was described by Richardson et al. (1962) and Müller and Mannesmann (1981).

Thermodilution methods were used by Rosas et al. (1964) in anesthetized rats, by Carbonell et al. (1985) and by Salyers et al. (1988) in conscious rats to determine hemodynamic parameters.

Oxygen pressure, carbon dioxide pressure and pH in coronary venous and common carotid arterial blood of anesthetized dogs has been measured using a blood gas analyzer (Aisaka et al. 1988).

Acute ischemic left ventricular failure can be induced in anesthetized dogs by repeated injections of plastic microspheres into the left coronary artery (Smiseth and Mjøs 1982; Sweet et al. 1984; Schölkens et al. 1986). A coronary catheter was introduced through the right femoral artery and advanced under fluoroscopy to the left coronary ostium, guided by injection of small amounts of contrast medium. After reaching baseline values, acute left ventricular failure was induced by subsequent intra-coronary injections of plastic microspheres (52.9 ±2.48 µm non-radioactive tracer microspheres). The microspheres were suspended in saline with a drop of Tween 80 and sonified before use, 1 mg microspheres/1 ml saline corresponding to approximately 12,000 microspheres. (13–16 injections of microspheres or 3.4–5.0 mg/kg). Microspheres were injected every 5 min for 70–90 min. Each microsphere injection effected an immediate and stepwise increase in LVEDP. With this procedure, LVEDP can be increased to a desired level in a very controlled manner. In the 30 min following embolization, LVEDP continued to increase by approximately 5 mm Hg. Animal with arrhythmias had to be excluded from the study. Thirty min after the end of embolization, when hemodynamic parameters had stabilized, drug administrations were started.

Valdes-Cruz et al. (1984) developed an **open-chest preparation in dogs** to validate the accuracy of a two-dimensional Doppler echocardiographic method for

estimating pressure drops across discrete stenotic obstructions.

In order to assess the potential of a single breath technique (using freon-22) as an effective way to estimate cardiac output non-invasively, Franks et al. (1990) measured simultaneously with the single breath technique the aortic flow using an electromagnetic flowmeter in anesthetized dogs.

REFERENCES AND FURTHER READING

Aisaka K, Hidaka T, Hattori Y, Inomata N, Ishihara T, Satoh F (1988) General pharmacological studies on N-(2,6-dimethyl-phenyl)-8-pyrrolizidineacetamide hydrochloride hemihydrate. 3rd Communication: Effect on cardiovascular system. Arzneim Forsch/Drug Res 38:1417–1425

Bohn H, Martorana PA, Schönafinger K (1992) Cardiovascular effects of the new nitric oxide donor, pirsidomine. Hemodynamic profile and tolerance studies in anesthetized and conscious dogs. Eur J Pharmacol 220:71–78

Carbonell LF, Salom MG, Salazar FJ, Garcia-Estañ J, Ubeda M, Queseda T (1985) Normal hemodynamic parameters in conscious Wistar rats. Revista Española Fisiologia 41:437–442

Franks PJ, Hooper RH, Humphries RG, Jones PR, O'Connor SE (1990) Effective pulmonary flow, aortic flow and cardiac output: *in vitro* and *in vivo* comparisons in the dog. Exp Physiol 75:95–106

Martorana PA, Kettenbach B, Bohn H, Schönafinger K, Henning R (1994) Antiischemic effects of pirsidomine, a new nitric oxide donor. Eur J Pharmacol 257:267–273

Millard RW (1984) Cardiac and vascular measurements in conscious and anesthetized animals. In: Schwartz A (ed) Methods in Pharmacology, Vol 5, Myocardial Biology., Plenum Press, New York and London, pp 167–174

Müller B, Mannesmann G (1981) Measurement of cardiac output by the thermodilution method in rats. II. Simultaneous measurement of cardiac output and blood pressure in conscious rats. J Pharmacol Meth 5:29–34

Rajagopalan R, Ghate AV, Subbarayan P, Linz W, Schoelkens BA (1993) Cardiotonic activity of the water soluble forskoline derivative 8,13-epoxy-6β-(piperidinoacetoxy)-1α,7β,9α-tri-hydroxy-labd-14-en-11-one. Arzneim Forsch/Drug Res 43(I):313–319

Richardson AW, Cooper T, Pinakatt T (1962) Thermodilution method for measuring cardiac output of rats by using a transistor bridge. Science 135:317–318

Rooke GA, Feigl EO (1982) Work as a correlate of canine left ventricular oxygen consumption, and the problem of catecholamine oxygen wasting. Circ Res 50:273–286

Rosas R, Montague D, Gross M, Bohr DF (1964) Cardiac action of vasoactive polypeptides in the rat. I. Bradykinin. II Angiotensin. Circ Res 16:150–161

Salyers AK, Rozek LF, Bittner SE, Walsh GM (1988) Simultaneous determination of ventricular function and systemic hemodynamics in the conscious rat. J Pharmacol Meth 19:267–274

Schölkens BA, Becker RHA, Kaiser J (1984) Cardiovascular and antihypertensive activities of the novel non-sulfhydryl converting enzyme inhibitor 2-[N-[(S)-1-ethoxycarbonyl-3-phenylpropyl]-L-alanyl]-(1S,3S,5S)-2-azabicyclo[3.3.0]octane-3-carboxylic acid (Hoe 498). Arzneim Forsch/Drug Res 34:1417–1425

Schölkens BA, Martorana PA, Göbel H, Gehring D (1986) Cardiovascular effects of the converting enzyme inhibitor ramipril (Hoe 498) in anesthetized dogs with acute ischemic left ventricular failure. Clin Exper Theory and Practice A8 (6) 1033–1048

Smiseth OA, Mjøs OD (1982) A reproducible and stable model of acute ischemic left ventricular failure in dogs. Clin Physiol 2:225–239

Sweet CS, Ludden CT, Frederick CM, Ribeiro LGT (1984) Hemodynamic effects of angiotensin and renin inhibition in dogs with acute left ventricular failure. Amer J Med 77:7–12

Valdes-Cruz LM, Horowitz S, Sahn DJ, Larson D, Lima CO, Mesel E (1984) Validation of a Doppler echocardiographic method for calculating severity of discrete stenotic obstructions in a canine preparation with a pulmonary arterial band. Circulation 69:1177–1181

A.1.3.11 Hemodynamic Measurements in Conscious Dogs

PURPOSE AND RATIONALE

The potency of a cardiovascular drug depends on the direct effects at the cellular level and on the response of the cardiovascular control mechanisms. The latter are often markedly influenced by anesthesia. The chronically instrumented conscious dog with renal hypertension is therefore a more realistic test model to evaluate the effects of antihypertensive, anti-anginal and cardiotonic compounds. The test is used to evaluate hemodynamic drug effects in conscious dogs, an experimental model with chronic arterial and ventricular catheterization and renal artery constriction.

PROCEDURE

Male or female Labrador-Harrier dogs weighing 15–25 kg are used. They are anaesthetized with 1 mg/kg xylazine i.m., followed by 1 mg/kg xylazine i.v. and 18 mg/kg pentobarbital sodium i.v. For chronic instrumentation and induction of renal hypertension, fluid-filled catheters are implanted into the abdominal aorta and into the left ventricle. The catheters are tunneled subcutaneously and exteriorized on the nape of the neck dorsally. Renal hypertension is induced by placing silastic constrictors around both renal arteries. Hemodynamic measurements are performed after a two-week recovery period or later.

To familiarize the dogs to the test surroundings, they are brought into the laboratory 2–3 times before the start of the study. Thus, drug testing is possible without sedation. During the experiment the animal rests quietly on a laboratory table.

Experimental Protocol

Hemodynamic measurements are performed by connecting the two implanted catheters to Statham pressure transducers. Pressure signals, electronically dif-

ferentiated LVP d*p*/d*t* max and heart rate are recorded with a polygraph.

After reaching stable hemodynamic conditions for at least 20 min (control baseline values), the test compound is administered either orally in a gelatin capsule or by intravenous injection into the cephalic vein.

Hemodynamic parameters are recorded continuously starting 30 min before to 120 min after drug administration, and thereafter at 1 h intervals until 6 h after dosage.

EVALUATION

The following parameters are monitored:

- systolic blood pressure [mm Hg]
- diastolic blood pressure [mm Hg]
- left ventricular enddiastolic blood pressure, LVEDP [mm Hg]
- left ventricular pressure at d*p*/d*t* max [mm Hg/s]
- heart rate [beats/min]

Mean values ± SEM are calculated with $n > 3$ as differences to pre-drug control values.

MODIFICATIONS OF THE METHOD

Mann et al. (1987) described a simple procedure for direct blood pressure measurement in conscious dogs using the Vascular-Access-Port™, consisting of a 33 × 13 mm reservoir body affixed to a silicon rubber catheter.

Müller-Schweinitzer (1984) described a method for the assessment of vasoconstrictor agents by recording venous compliance in the conscious dog. Changes in the diameter of the canine saphenous vein, produced by inflation to 45 mm Hg of a sphygmomanometer cuff placed on the upper hind leg, were recorded.

Hintze and Vatner (1983) compared the effects of nifedipine and nitroglycerin in conscious dogs, instrumented for instantaneous and continuous measurements of coronary arterial and left ventricular diameters with an ultrasonic dimension gauge, arterial and left ventricular pressure with implanted miniature gauges, and coronary blood flow with an electromagnetic flowmeter or a Doppler ultrasonic flowmeter.

Shimshak et al. (1986) studied the recovery of regional myocardial contractile function after a 10 min coronary artery occlusion in chronically instrumented conscious dogs.

Wright et al. (1987) described a minimally invasive technique which allows assessment of histamine H_1-receptor antagonist activity in conscious dogs based on the inhibition of tachycardia caused by intravenous administration of the H_1-receptor agonist, 2-pyridylethylamine.

Hashimoto et al. (1991) studied the coronary effects of nicorandil in comparison with nitroglycerin in chronic conscious dogs instrumented with ultrasonic crystals and electromagnetic flowmeters in the circumflex coronary artery.

Hartman and Warltier (1990) described a model of multivessel coronary artery disease using conscious, chronically instrumented dogs. A hydraulic occluder and Ameroid constrictor were implanted around the left anterior descending and the left circumflex coronary arteries. Pairs of piezoelectric crystals were implanted within the subendocardium of the left anterior descending and the left circumflex coronary artery perfusion territories to measure regional contractile function. A catheter was placed in the left atrial appendage for injection of radioactive microspheres to measure regional myocardial perfusion.

Hof et al. (1990) used the Doppler method for measuring cardiac output in **conscious rabbits**.

Grohs et al. (1993) simultaneously assessed cardiac output with pulsed Doppler and electromagnetic flowmeters during cardiac stimulation.

REFERENCES AND FURTHER READING

Bohn H, Rosenstein B (1986) Technical notes on chronic fluid-filled catheters and renal artery constrictors for testing hemodynamic drug effects in conscious hypertensive dogs. J Pharmacol Meth 16:227–238

Grohs JG, Huber S, Raberger G (1993) Simultaneous assessment of cardiac output with pulsed Doppler and electromagnetic flowmeters during cardiac stimulation. J Pharmacol Toxicol Meth 30:33–38

Hartman JC, Warltier DC (1990) A model of multivessel coronary artery disease using conscious, chronically instrumented dogs. J Pharmacol Meth 24:297–310

Hashimoto K, Kinoshita M, Ohbayashi Y (1991) Coronary effects of nicorandil in comparison with nitroglycerin in chronic conscious dogs. Cardiovasc Drugs Ther 5:131–138

Hintze TH, Vatner SF (1983) Comparison of effects of nifedipine and nitroglycerin on large and small coronary arteries and cardiac function in dogs. Circ Res 52 (Suppl I):139–146

Hof RP, Hof A, Stürm RP (1990) The Doppler method for measuring cardiac output in conscious rabbits: Validation studies, uses, and limitations. J Pharmacol Meth 24:263–276

Mann WA, Landi MS, Horner E, Woodward P, Campbell S, Kinter LB (1987) A simple procedure for direct blood pressure measurement in conscious dogs. Lab Anim Sci 37:105–108

Müller-Schweinitzer E (1984) The recording of venous compliance in the conscious dog: A method for the assessment of vasoconstrictor agents. J Pharmacol Meth 12:53–58

Rajagopalan R, Ghate AV, Subbarayan P, Linz W, Schoelkens BA (1993) Cardiotonic activity of the water soluble forskoline derivative 8,13-epoxy-6β-(piperidinoacetoxy)-1α,7β,9α-trihydroxy-labd-14-en-11-one. Arzneim Forsch/Drug Res 43(I) 313–319

Sarazan RD (1991) The chronically instrumented conscious dog model. In: 7th Freiburg Focus on Biomeasurement. Cardiovascular and Respiratory *in vivo* Studies. Biomesstechnik-Verlag March GmbH, 79232 March, Germany. pp 37–44

Shimshak TM, Preuss KC, Gross GJ, Brooks HL, Warltier DC (1986) Recovery of contractile function in postischemic reperfused myocardium of conscious dogs: influence of nicorandil, a new antianginal agent. Cardiovasc Res 20:621–626

Vatner SF, Higgins CB, Franklin D, Braunwald E (1971) Effect of a digitalis glycoside on coronary and systemic dynamics in conscious dogs. Circ Res 28:470–479

Wright A, Raval P, Eden RJ, Owen DAA (1987) Histamine H_1-receptor antagonist activity assessed in conscious dogs. J Pharm Meth 18:123–129

A.1.3.12 Hemodynamic Studies in Monkeys

PURPOSE AND RATIONALE

Prior to studies in human beings, studies of cardiovascular effects of new drugs in monkeys are necessary in some instances.

PROCEDURE

Rhesus monkeys of either sex, weighing between 5 and 8 kg are anesthetized with 20 mg/kg ketamine hydrochloride followed by 50 mg/kg pentobarbital-Na given slowly i.v. A small side-branch of the femoral or radial artery is surgically exposed and cannulated for blood pressure recordings using a blood pressure transducer (P23 ID). Heart rate is determined from a conventional ECG lead by a biotachometer. Compounds are administered either intravenously or via a gastric fibroscope, e. g., Olympus XP 10, into the duodenum under visual control. The cardiovascular parameters are registered for a pretest period of 30 min and then during 60 min after intravenous administration or 2 h after intragastric administration of the test drug. Three to 6 animals are used for evaluation.

EVALUATION

Mean values ± SD are calculated for the pretest period and for the cardiovascular effects every min for 5 min after i.v. administration and then every 5 min. After intragastric administration the values are registered every 5 min up to 30 min and then every 10 min. The values after administration of the test compound are compared statistically with the pretest values using the Student's *t*-test.

MODIFICATIONS OF THE METHOD

Lacour et al. (1993) studied cardiovascular parameters in conscious **cynomolgus monkeys** (*Macaca fascicularis*). A silicone catheter (internal and external diameter 0.64 and 1.19 mm, respectively) was implanted under aseptic conditions into the thoracic aorta via a carotid artery after the monkeys had been anesthetized with 40 mg/kg ketamine and 0.5 mg/kg acepromazine intramuscularly. The vascular catheter (filled with an aqueous solution of 40% polyvinylpyrolidone and 20% heparin) was inserted into a carotid artery. A patch of silicone was sewn around the artery to maintain the catheter in position, the latter being routed subcutaneously and exteriorized at the top of the head into a stainless steel connector. This connector was fixed to the skull with screws and dental cement, and sealed with a plug to protect the catheter from damage. The monkeys were permitted a 3-week minimum recovery period. Before the experiment was performed the monkeys were placed in a primate-restraining chair on several occasions, of gradually increasing duration, for experiment acclimatization.

Pulsatile arterial pressure was recorded by connecting the arterial catheter to a polygraph via a Statham P23Id pressure transducer. Mean arterial pressure and heart rate were derived from the pulse pressure signal and recorded. A catheter was inserted acutely into a saphenous vein for administration of compounds.

REFERENCES AND FURTHER READING

Lacour C, Roccon A, Cazaubon C, Segondy D, Nisato D (1993) Pharmacological study of SR 47436, a non-peptide angiotensin II AT^1-receptor antagonist, in conscious monkeys. J Hypertens 11:1187–1194

Linz W, Klaus E, Albus U, Becker R, Mania D, Englert HC, Schölkens BA (1992) Cardiovascular effects of the novel potassium channel opener (3S,4R)-3-hydroxy-2,2-dimethyl-4-(2-oxo-1-pyrrolidinyl)-6-phenylsulfonyl-chromane hemihydrate. Arzneim-Forsch/Drug Res 42:1180–1185

A.1.3.13 Measurement of Cardiac Output and Regional Blood Flowwith Microspheres

PURPOSE AND RATIONALE

The microsphere technique allows the measurement of cardiac output and regional blood flow. Using different radionuclides, repeated determinations are possible. The method is applicable not only for dogs, cats, and minipigs (Hof et al. 1980) but also for rats (McDevitt and Nies 1976; Bonnacrossi et al. 1978; Ishise et al. 1980; Stanek et al. 1985) using microspheres of appropriate size.

PROCEDURE

Male Sprague-Dawley rats weighing 265–375 g are anesthetized with 35 mg/kg i.p. pentobarbital. The

right carotid and right femoral arteries are cannulated. Using pressure monitoring, a carotid cannula is manipulated into the left ventricle. Carbonized microspheres ($15 \pm 5\,\mu$ diameter) labelled with ^{85}Sr are drawn into a glass injection chamber and suspended in 0.3 ml 6% dextran so that each chamber contains 60000 to 80,000 microspheres. The radioactivity in each chamber is determined by gamma scintillation counting before and after microsphere injection, the difference being the amount of radioactivity injected. The microspheres are injected into the left ventricle in a total volume of 0.8 ml 6% dextran over 20 s. Simultaneously, arterial blood from the femoral artery is withdrawn at 0.8 ml/min for 90 s with a syringe withdrawal pump.

EVALUATION

This reference blood sample is used to calculate the cardiac output by the formula:

$$\text{cardiac output} = \text{counts injected} \times \frac{\text{reference sample withdrawal rate}}{\text{reference sample counts}}$$

After obtaining the reference sample, the animals are sacrificed with pentobarbital and the organs dissected, placed in counting vials, and counted for 5 min. Regional distribution of the cardiac output is calculated by comparing the radioactivity in each organ with the total injected radioactivity. Organ flow is determined by multiplying the cardiac output by the fractional distribution of the cardiac output to the organ.

CRITICAL ASSESSMENT OF THE METHOD

Problems associated with the microsphere technique in rats are the hemodynamic effects of the solutions used to inject the microspheres and the effects of blood withdrawal after repeated determinations (Stanek et al. 1985).

MODIFICATIONS OF THE METHOD

For repeated determinations, other nuclides have been used, such as ^{46}Sc, ^{51}Cr, ^{141}Ce, ^{125}I (Hof et al. 1980).

Kovách et al. (1992) used up to 5 radiolabelled microspheres (^{57}Co, ^{113}Sn, ^{85}Sr, ^{95}Nb and ^{46}Sc) for measurement of regional cerebral blood flow in cats.

Faraci and Heistad (1992) measured blood flow with radioactive microspheres (15 μ diameter) labeled with ^{46}Sc, ^{95}Nb, ^{153}Gd, ^{85}Sr, and ^{141}Ce in anesthetized rabbits.

Grover et al. (1990), Gross et al. (1992) measured myocardial blood flow in dogs with the radioactive microsphere technique.

Kowallik et al. (1991) measured regional myocardial blood flow with multiple colored microspheres. The method yielded values very similar to those obtained with radioactive microspheres.

REFERENCES AND FURTHER READING

Bonnacrossi A, Dejana E, Qunintana A (1978) Organ blood flow measured with microspheres in the unanesthetized rat: effects of three room temperatures. J Pharmacol Meth 1:321–328

Faraci FM, Heistad DD (1992) Does basal production of nitric oxide contribute to regulation of brain-fluid balance? Am J Physiol 262:H340–H344

Flaim SF, Nellis SH. Toggart EJ, Drexler H, Kanda K, Newman ED (1984) Multiple simultaneous determinations of hemodynamics and flow distribution in conscious rats. J Pharmacol Meth 11:1–39

Gross GJ, Auchampach JA, Maruyama M, Warltier DC, Pieper GM (1992) Cardioprotective effects of nicorandil. J Cardiovasc Pharmacol 20 (Suppl 3):S22–S28

Grover GJ, Sleph PG, Dzwonczyk S (1990) Pharmacological profile of chromakalim in the treatment of myocardial ischemia in isolated rat hearts and anesthetized dogs. J Cardiovasc Pharmacol 16:853–864

Heymann MA, Payne BD, Hoffmann JIE, Rudolph AM (1977) Blood flow measurements with radionuclide-labeled particles. Prog Cardiovasc Dis 20:55–79

Hof RP, Wyler F, Stalder G (1980) Validation studies for the use of the microsphere method in cats and young minipigs. Basic Res Cardiol 75:747–756

Ishise S, Pegram BL, Yamamoto J, Kitamura Y, Frohlich ED (1980) Reference sample microsphere method: cardiac output and blood flows in conscious rat. Am J Physiol 239:H443–449

Kovách AGB, Szabó C, Benyó Z, Csaki C, Greenberg JH, Reivich M (1992) Effects of N^G-nitro-L-arginine and L-arginine on regional cerebral blood flow in the cat. J Physiol 449:183–196

Kowallik P, Schulz R, Guth BD, Schade A, Pfaffhausen W, Gross R, Heusch G (1991) Measurement of regional myocardial blood flow with multiple colored microspheres. Circulation 83:974–982

McDevitt DG, Nies AS (1976) Simultaneous measurement of cardiac output and its distribution with microspheres in the rat. Cardiovasc Res 10:494–498

Stanek KA, Coleman TG, Smith TL, Murphy WR (1985) Two hemodynamic problems commonly associated with the microsphere technique for measuring regional blood flow in rats. J Pharmacol Meth 13:117–124

A.1.3.14 Carotid Artery Loop Technique

PURPOSE AND RATIONALE

The carotid loop method, originally described by van Leersum (1911) for rabbits has been used by several authors (e. g., Child and Glenn 1938; Valli et al. 1967; O'Brien et al. 1971; Meyer et al. 1989) for measurement of blood pressure or blood sampling in conscious dogs and sheep (Lagutchik et al. 1992).

PROCEDURE

Male or female inbred Beagle or Labrador-Harrier dogs weighing between 15 and 25 kg are used. They are anesthetized with a bolus injection of 35–40 mg/kg pentobarbital, continued with an infusion of 4–6 mg/kg/h. The animal is placed on a heated operating table. The skin on the ventral side of the neck is carefully shaved and disinfected. The course of the carotid artery is outlined by palpation along the tracheal border. About 2 cm of skin is taken on each side marking the width of the flap. The medial incision is made slightly above the thyroid cartilage and is extended caudal to a point about 1 cm lateral and 1 cm above the manubrium sterni. The lateral incision again lies about 2 cm from the line of the carotid artery and parallel to it. The lateral incision is only half as long as the medial one. The incisions are made down to the subcutaneous tissue over the platysma muscle. Between the skin and the muscle, the flap is undermined. All bleeding points are carefully clamped and tied.

The subcutaneous tissue, the platysma myoides muscle and the anterior fascia of the neck are incised in the course of the midline incision down to the plane of cleavage between the sternohyoid and sternomastoid muscle. By blunt dissection, these muscles are separated, disclosing at their depth the neurovascular bundle over which lies the internal jugular vein. The floor of the space so isolated is formed by the longus capitis muscle. By careful dissection, these muscles are separated at least 1 cm above and below the limits of the incision in the skin. The superior thyroid artery marks the uppermost portion of the carotid artery suitable for exteriorization. The plane of cleavage is followed caudal to the origin of the sternocleidomastoid muscle at the manubrium sterni. Throughout the limits of the incision the artery is dissected free from the internal jugular vein and then from the vagus nerve.

The first step in the exteriorization of the artery is the reapproximation of the muscle borders beneath the vessel by mattress sutures. In order to prevent tension on the completed loop due to contraction of the sternomastoid and sternohyoid muscle, it is important to reapproximate these muscles throughout their course. Sutures are placed at the edges of skin. The tubular flap of skin is then approximated loosely around the carotid artery. It is essential that the skin flap fits loosely around the artery. A continuous suture of fine silk is started at the place where the vessel emerges from the muscle borders. The suture is so placed as to include the artery in a sling of skin which isolates the vessel from the line of suture of the underside of the completed loop. Finally, the proximal and distal quarters of the flap are closed with sutures, while the skin tube is closed with a continuous suture. Antibiotics are given locally and systemically.

One thickness of gauze is placed beneath the loop and along each border a strip of gauze in order to relieve the loop from the pressure caused by the reminder of dressings. Around the neck is wrapped a gauze bandage several turns of which have passed behind the forelimbs in order to prevent the dressing from riding upwards on the animal's neck. Over this is placed a plaster roll protecting the loop from the animal's efforts of scratching. The dressings are changed on the fifth and seventh day when the sutures can be removed.

Blood pressure measurements can be made according to Riva-Rocci's principle by placing a inflatable cuff around the loop.

CRITICAL ASSESSMENT OF THE METHOD

The carotid artery loop method needs some surgical experience and very meticulous caretaking of the animals.

MODIFICATIONS OF THE METHOD

Lewis et al. (1980) placed a CO_2 sensor using mass spectrometry and its through flow cuvette in a common carotid artery-to-jugular vein loop in anesthetized cats.

Meyer et al. (1989a, b) studied pulmonary gas exchange in panting dogs with an exteriorized carotid artery loop.

Kaczmarczyk et al. (1979) used conscious, chronically instrumented dogs with electric flow probes around the left renal artery and a carotid loop to study postprandial volume regulation.

REFERENCES AND FURTHER READING

Child CG, Glenn F (1938) Modification of van Leersum carotid loop for determination of systolic blood pressure in dogs. Arch Surg 36:381–385

Kaczmarczyk G, Schimmrich B, Mohnhaupt R, Reinhardt HM (1979) Atrial pressure and postprandial volume regulation in conscious dogs. Pflüger's Arch Eur J Physiol 38:143–150

Lagutchik MS, Sturgis JW, Martin DG, Bley JA (1992) Review of the carotid loop procedure in sheep. J Invest Surg 5:79–89

Lewis G, Ponte J, Purves MJ (1980) Fluctuations of P(a), (CO_2) with the same period as respiration in the cat. J Physiol (London) 298:1–11l

Meyer M, Hahn G, Buess Ch, Mesch U, Piiper J (1989) Pulmonary gas exchange in panting dogs. J Appl Physiol 66:1258–1263

Meyer M, Hahn G, Piiper J (1989) Pulmonary gas exchange in panting dogs: a model for high frequency ventilation. Acta Anaesthesiol Scand 33, Suppl 90:22–27

O'Brien DJ, Chapman WH, Rudd FV, McRoberts JW (1971) Carotid artery loop method of blood pressure measurement in the dog. J Appl Physiol 30:161–163
Valli VEO, McSherry BJ, Archibald J (1967) The preparation and use of carotid loops. Can Vet Jour 8:209–211
van Leersum EC (1911) Eine Methode zur Erleichterung der Blutdruckmessung bei Tieren. Arch ges Physiol 142:377–395

A.1.3.15 Measurement of Heart Dimensions in Anesthetized Dogs

PURPOSE AND RATIONALE

The measurement of the heart dimensions allows to localize the effect of a drug on the activity of the heart. An ultrasonic technique is used for continuous measurement of left ventricular dimensions. Compounds are tested with potential anti-anginal activity due to the reduction of left ventricular diameter. The test is used to evaluate the influence of drugs on left ventricular external and internal diameter in anesthetized dogs.

PROCEDURE

Male or female Beagle or Labrador-Harrier dogs weighing 15–25 kg are used for the test. The dog is anesthetized by intravenous injection of 35–40 mg/kg pentobarbital sodium followed by subcutaneous injection of 2 mg/kg morphine. Respiration is maintained through a tracheal tube with N_2O/O_2 (3:1) using a positive pressure respirator.

Implantation of Ultrasonic Transducers

Ultrasonic transducers are constructed and implanted as described by Stinson et al. (1974).

To measure left ventricular external diameter (LVED), two ultrasonic transducers are fixed to the left ventricular wall. One crystal is sutured to the posterior wall within the rectangular area formed by the left circumflex coronary artery and the left posterior descending artery. The other one is placed near the first diagonal branch of the left anterior descending coronary artery. Exact positioning is assured with an oscilloscope.

To measure left ventricular internal diameter (LVID), the transducers are placed in the same anatomical area as for the epicardial crystals. However, they are pushed through the wall of the left ventricle through stab wound incisions. The crystals are positioned across the greatest transverse diameter of the left ventricle, one on the anterior and the other on the posterior endocardial wall.

Bleeding during the implantation procedure is controlled by umbilical tapes around the cranial and caudal veins and by purse string sutures at the implantation sites. The pericardial incision and the chest is closed by sutures and the transducer wires are connected to the recording equipment.

In each dog, either LVED or LVID is measured together with the other hemodynamic parameters.

Preparation for Hemodynamic Measurements

Blood pressure is recorded through a cannulated femoral artery by a pressure transducer (Statham P 23 DB).

For determination of LVP, a Millar microtip catheter (type PC 350) is inserted via the left A. carotis communis. LVEDP is measured on a high-sensitivity scale. From the pressure curve, dp/d$t$max is differentiated and heart rate is calculated.

Hemodynamic parameters are recorded continuously during the whole experiment.

Experimental Course

When stable hemodynamic conditions are achieved for at least 30 min (control values), the test substance is administered by intravenous or intraduodenal injection.

Readings are taken at times 0, 15, 30, 45, 60, 75, 90 and 120 after drug administration. Left ventricular dimensions are measured at the end of the diastole and systole.

Characteristics:

- blood pressure
  - systolic blood pressure
  - diastolic blood pressure
- left ventricular pressure, LVP
- left ventricular enddiastolic pressure
- left ventricular contractility, dp/dt
- heart rate, HR
- left ventricular external diameter, LVED
- left ventricular internal diameter, LVID

EVALUATION

Hemodynamic parameters, LVED and LVID [mm] are determined.

Changes in parameters after drug administration are compared to control values obtained during the 30 min pre-drug period.

Statistical significance is assessed by means of the paired t-test.

Since a change in the diameter of the left ventricle is a reasonable accurate index of left ventricular volume, a reduction of LVED or LVID with no change in dp/dt and HR can be considered as a strong indicator

for "venous pooling" and thus an anti-anginal activity of a compound.

Scores are allotted relative to the efficacy of standard compounds assessing the intensity as well as the duration of the effect.

Standard data:

		LVED [mm]		LVID [mm]	
Nitroglycerin	0.005 mg/kg, i.v.	–0.9	20 min	–1.2	30 min
Isosorbide-dinitrate	0.1 mg/kg, i.v.			–0.6	120 min
Molsidomine	0.2 mg/kg, i.v.	–2.1	>60 min	–1.4	>120 min
Nifedipine	0.1 mg/kg, i.v.			+1.2	120 min

MODIFICATIONS OF THE METHOD

Novosel et al. (1992) measured the dimensions of the right ventricle with microsonometry in anesthetized rabbits.

REFERENCES AND FURTHER READING

Barnes GE, Horwith LD, Bishop VS (1979) Reliability of the maximum derivatives of left ventricular pressure and internal diameter as indices of the inotropic state of the depressed myocardium. Cardiovasc Res 13:652–662

Bishop VS, Horwitz LD (1971) Effects of altered autonomic control on left ventricular function in conscious dogs. Am J Physiol 221:1278–1282

Fiedler VB, Oswald S, Göbel H, Faber W, Scholtholt J (1980) Determination of left ventricular dimensions with ultrasound. J Pharmacol Meth 3:201–219

Horwitz LD, Bishop VS (1972) Left ventricular pressure-dimension relationships in the conscious dog. Cardiovasc Res 6:163–171

Novosel D, Hof A, Evenou JP, Hof PP (1992) Assessment of right ventricle dimensions with microsonometry in anesthetized rabbits. J Pharmacol Toxicol Meth 28:73–77

Stinson EB, Rahmoeller G, Tecklenberg PL (1974) Measurement of internal left ventricular diameter by tracking sonomicrometer. Cardiovasc Res 8:283–289

Suga H, Sagawa K (1974) Assessment of absolute volume from diameter of the intact canine left ventricular cavity. J Appl Physiol 36:496–499

A.1.3.16 Telemetric Monitoring of Cardiovascular Parameters in Rats

PURPOSE AND RATIONALE

Radiotelemetry allows the recording of cardiovascular parameters in conscious, free-moving animals. Several authors (Brockway et al. 1991; Mattes and Lemmer 1991; Guiol et al. 1992; Morimoto et al. 1992; Basil et al. 1993; Brockway and Hassler 1993; Lemmer et al. 1993, 1994, 1995; Calhoun et al. 1994; Diamant et al. 1993; Kramer et al. 1993a, 1995; Griffin et al. 1994; Kuwahara et al. 1994; Sato et al. 1994, 1995; van den Buuse et al. 1994; Kinter 1996; Becker et al. 1997; Witte et al. 1998) used commercially available systems with some modifications to study the circadian rhythm of blood pressure and the influence of drugs on heart rate, blood pressure and motility in rats.

PROCEDURE

The telemetry and data acquisition system (e. g., Data Sciences International, Inc., St Paul MN) consists of four parts:

1. the implantable transmitter, which measures the pressure. This device contains a highly stable, ion-implant, semiconductor, strain-gauge sensor and battery-powered electronics to process the information from the pressure sensor and to telemeter it from within the animal. Arterial pressure is transmitted to the sensor via a 0.7-mm diameter, fluid-filled catheter;
2. the receiver which detects the signal from the implanted transmitter and converts it to a form readable by computer;
3. the pressure reference module, which measures atmospheric pressure to allow for the telemetered absolute pressure to be converted to a gauge pressure;
4. the data acquisition software, which accepts data from the reference module and the receivers, filters corrupt samples from the incoming data stream, converts the telemetered pressure to millimeters of mercury, subtracts atmospheric pressure from the telemetered pressure, and stores the data for retrieval, plotting, and analysis.

Under pentobarbital anesthesia, the telemetry transmitter is implanted into rats. The descending aorta is exposed between the renal arteries. A vascular clamp is made by putting two surgical threads on the proximal and distal part of the artery. The catheter tip is inserted through an incision in the vessel. A drop of cyanoacrylate glue is applied to the dried entry point. The transmitter is sutured to the abdominal musculature.

EVALUATION

Data from individual animals are recorded over long periods of time which allow the investigator to follow the circadian rhythm under several experimental conditions.

MODIFICATIONS OF THE METHOD

Hess et al. (1996) monitored pulmonary arterial pressure in freely moving **rats** by inserting the sensing

catheter of a telemetric system through a small hole and pushing it into the pulmonary artery.

Further cardiovascular studies in rats using the telemetric system were reported by Sgoifo et al. (1998), Webb et al. (1998).

Kramer et al. (1993b) used telemetry to record electrocardiogram and heart rate in freely moving **mice**.

Carlson and Wyss (2000) used small telemetry probes for long term recording of arterial pressure and heart rate in mice after implantation to the carotid artery or the abdominal aorta.

DePasquale et al. (1994) used radiotelemetry to monitor cardiovascular function in conscious **guinea pigs**.

Telemetric ECG recordings in **cardiomyopathic hamsters** were reported by Desjardins et al. (1996).

Van den Buuse and Malpas (1997) studied cardiovascular parameters in **rabbits** by radiotelemetry.

Astley et al. (1991), Smith et al. (1993) used telemetric systems to monitor cardiovascular responses in **baboons**.

Schnell and Wood (1993) measured blood pressure and heart rate by telemetry in conscious, unrestrained **marmosets**.

An ultrasonic blood flowmeter telemetry system for **cats** and rabbits has been described by Yonezawa et al. (1989, 1992).

Telemetry was used by Symons et al. (1992) to monitor the severity of events representing myocardial dysfunction in **miniswine**.

Savory and Kostal (1997) applied the telemetric system for chronic measurement of cardiovascular and other parameters in **chicken**.

Radiotelemetry has also been used for other pharmacological experiments, such as field potential analysis by radioelectroencephalography (see Sect. E.1.2.6), step through passive avoidance (see Sect. F.3.1.2), shock-prod burying test in rats (see Sect. E.2.5.3), measurement of body temperature (see Sect. H.4.0.2) and motility in rats and mice (Clement et al. 1989; Guillet et al. 1990; Diamant et al. 1993; van den Buuse 1994).

REFERENCES AND FURTHER READING

Astley CA, Smith OA, Ray RD, Golanov EV, Chesney MA, Chalyan VG, Taylor DJ, Bowden DM (1991) Integrating behavior and cardiovascular response: the code. Am J Physiol, Regul Integr Comp Physiol 261:R172–R181

Basil MK, Krulan C, Webb RL (1993) Telemetric monitoring of cardiovascular parameters in conscious spontaneously hypertensive rats. J Cardiovasc Pharmacol 22:897–905

Becker RHA, Baldes L, Furst U, Schulze KJ (1997) Sustained diurnal blood pressure reduction in SHR with ramipril assessed by telemetric monitoring. Clinical and Experimental Hypertension. Vol 19:1233–1246

Brockway BP, Medvedev OS (1991) Circulatory studies on rats using telemetry instrumentation and methodology. In: 7th Freiburg Focus on Biomeasurement. Cardiovascular and Respiratory *in vivo* Studies. Biomesstechnik-Verlag March GmbH, 79232 March, Germany. pp 142–147

Brockway BP, Hassler CR (1993) Application of radiotelemetry to cardiovascular measurements in pharmacology and toxicology. In: Salem H, Baskin SI (eds) New Technologies and Concepts for Reducing Drug Toxicities. CRC Press, Boca Raton, pp 109–132

Brockway BP, Mills PA, Azar SH (1991) A new method for continuous chronic measurement and recording of blood pressure, heart rate and activity via radiotelemetry. Clin Exp Hyper Theory Pract A13:885–895

Calhoun DA, Zhu S, Wyss JM, Oparil S (1994) Diurnal blood pressure variations and dietary salt in spontaneously hypertensive rats. Hypertension 24:1–7

Carlson SH, Wyss JM (2000) Long-term telemetric recording of arterial pressure and heart rate in mice fed basal and high NaCl diets. Hypertension 35:e1–e5

Clement JG, Mills P, Brockway B (1989) Use of telemetry to record body temperature and activity in mice. J Pharmacol Meth 21:129–140

DePasquale MJ, Ringer LW, Winslow RL, Buchholz R, Fossa AA (1994) Chronic monitoring of cardiovascular function in the conscious guinea pig using radiotelemetry. Hypertension 16:245–260

Desjardins S, Cauchy MJ, Kozliner A (1996) The running cardiomyopathic hamster with continuous telemetric ECG: A new heart failure model to evaluate 'symptoms', cause of death and heart rate. Exper Clin Cardiol 1:29–36

Diamant M, von Wolfswinkel L, Altorffer B, de Wied D (1993) Biotelemetry: Adjustment of a telemetry system for simultaneous measurement of acute heart rate changes and behavioral events in unrestrained rats. Physiol Behav 53:1121–1126

Griffin KA, Picken M, Bidani AK (1994) Radiotelemetric BP monitoring, antihypertensives and glomeruloprotection in remnant kidney model. Kidney Internat 46:1010–1018

Guillet MC, Molinié B, Laduron PM, Terlain B (1990) Effects of ketoprofen in adjuvant-induced arthritis measured in a new telemetric model test. Eur J Pharmacol 183:2266–2267

Guiol C, Ledoussal C, Surgé JM (1992) A radiotelemetry system for chronic measurement of blood pressure and heart rate in the unrestrained rat. Validation of the method. J Pharmacol Toxicol Meth 28:99–105

Hess P, Clozel M, Clozel JP (1996) Telemetric monitoring of pulmonary pressure in freely moving rats. J Appl Physiol 81:1027–1032

Kinter L (1996) Cardiovascular Telemetry and Laboratory Animal Welfare: New Reduction and Refinements Alternatives. SMD, Data Sciences International, Inc., pp 1–10

Kramer K, Dijkstra H, Bast A (1993a) Control of physical exercise in rats in a swimming basin. Physiol Behav 53:271–276

Kramer K, van Acker SABE, Voss HP, Grimbergen JA, van der Vijgh WJF, Bast A (1993b) Use of telemetry to record electrocardiogram and heart rate in freely moving mice. J Pharm Toxicol Meth 30:209–215

Kramer K, Grimbergen JA, van der Gracht L, van Jeperen DJ, Jonker RJ, Bast A (1995) The use of telemetry to record electrocardiogram and heart rate in freely swimming rats. Meth Find Exp Clin Pharmacol 17:107–112

Kuwahara M, Yayou KI, Ishii K, Hashimoto SI, Tsubone H, Sugano S (1994) Power spectral analysis of heart rate vari-

ability as a new method for assessing autonomic activity in the rat. J Electrocardiol 27:333–337
Lee JY, Brune ME, Warner RB, Buckner SB, Winn M, De B, Zydowsky TM, Opgenorth TJ, Kerkman DJ, DeBerhardis JF (1993) Antihypertensive activity of ABBOTT-81282, a nonpeptide angiotensin II antagonist, in the renal hypertensive rat. Pharmacology 47:176–187
Lemmer B, Mattes A, Böhm M, Ganten D (1993) Circadian blood pressure variation in transgenic hypertensive rats. Hypertension 22:97–101
Lemmer B, Witte K, Makabe T, Ganten D, Mattes A (1994) Effects of enalaprilat on circadian profiles in blood pressure and heart rate of spontaneously and transgenic hypertensive rats. J Cardiovasc Pharmacol 23:311–314
Lemmer B, Witt K, Minors D, Waterhouse J (1995) Circadian rhythms of heart rate and blood pressure in four strains of rat: Difference due to, and separate from locomotor activity. Biol Rhythm Res 26:493–504
Mattes A, Lemmer B (1991) Effects of amlodipine on circadian rhythms in blood pressure, heart rate, and motility: a telemetric study in rats. Chronobiol Internat 8:526–538
Morimoto K, Morimoto A, Nakamori T, Tan N, Minagawa T, Murakami N (1992) Cardiovascular responses induced in free-moving rats by immune cytokines. J Physiol 448:307–320
Rubini R, Porta A, Baselli G, Cerutti S, Paro M (1993) Power spectrum analysis of cardiovascular variability monitored by telemetry in conscious unrestrained rats. J Autonom Nervous System 45:181–190
Sato K, Kandori H, Sato SH (1994) Evaluation of a new method using telemetry for monitoring the left ventricular pressure in free-moving rats. J Pharmacol Toxicol Meth 31:191–198
Sato K, Chatani F, Sato S (1995) Circadian and short-term variabilities in blood pressure and heart rate measured by telemetry in rabbits and rats. J Auton Nerv Syst 54:235–246
Savory CJ, Kostal L (1997) Application of a telemetric system for chronic measurement of blood pressure, heart rate, EEG and activity in the chicken. Physiol Behav 61:963–969
Schnell CR, Wood JM (1993) Measurement of blood pressure and heart rate by telemetry in conscious, unrestrained marmosets. Am J Physiol 264 (Heart Circ Physiol 33):H1509–H1516
Sgoifo A, Stilli D, deBoer SF, Koolhaas JM, Musso E (1998) Acute social stress and cardiac electrical activity in rats. Aggress Behav 24:287–296
Smith OA, Astley CA, Spelman FA, Golanov EV, Chalyan VG, Bowden DM, Taylor DJ (1993) Integrating behavior and cardiovascular responses: posture and locomotion. I. Static analysis. Am J Physiol 265 (Regul Integr Comp Physiol 34): R1458–R1568
Symons JD, Pitsillides KF, Longhurst CJ (1992) Chronic reduction of myocardial ischemia does not attenuate coronary collateral development in miniswine. Circulation 86:660–671
Tornatzky W, Miczek KA (1993) Long-term impairment of autonomic circadian rhythms after brief intermittent social stress. Physiol Behav 53:983–993
van den Buuse M (1994) Circadian rhythms of blood pressure, heart rate, and locomotor activity in spontaneously hypertensive rats as measured with radiotelemetry. Physiol Behav 55:783–786
van den Buuse M, Malpas SC (1997) 24-Hour recordings of blood pressure, heart rate and behavioural activity in rabbits by radiotelemetry: effects of feeding and hypertension. Physiol Behav 62:83–89
Webb RL, Navarrete AE, Davis S, de Gasparo M (1998) Synergistic effects of combined converting enzyme inhibition and angiotensin II antagonism on blood pressure in conscious telemetered spontaneously hypertensive rats. J Hypertens 16:843–852
Witte K, Schnecko A, Buijs R, van der Vliet J, Scalbert E, Delagrange P, Guardiola-Lemaître B, Lemmer B (1998) Effects of SCN lesions on circadian blood pressure rhythm in normotensive and transgenic hypertensive rats. Chronobiol Intern 15:135–145
Yonezawa Y, Caldwell WM, Schadt JC, Hahn AW (1989) A miniaturized ultrasonic flowmeter and telemetry transmitter for chronic animal blood flow measurements. Biomed Sci Instrument 25:197–111
Yonezawa Y, Nakayama T, Ninomija I, Caldwell WM (1992) Radiotelemetry directional ultrasonic blood flowmeter for use with unrestrained animals. Med Biol Eng Comput 30:659–665

A.1.3.17 Cardiovascular Effects After Intracerebroventricular Administration

PURPOSE AND RATIONALE

Several drugs, like α_2-adrenergic agonists, act primarily at central sites. Their effects can be most clearly demonstrated after injection into the cerebroventricular system. The first experiments have been performed in cats. The method has been adapted to rats.

PROCEDURE

Rats of either sex weighing 250–350 g are anesthetized with 100 mg/kg hexobarbital i.p. The scalp is cut in a sagittal line. With a dental drill a hole of 1–1.5 mm diameter is drilled through the cranial bone 1 mm lateral and 2 mm caudal of the bregma. A PVC-catheter is introduced perpendicular to the bone to a depth of 3 mm in order to reach the lateral cerebral ventricle. The catheter is fixed with dental cement and the wound closed. Test substances are administered through the catheter. To measure blood pressure one catheter is placed in one carotid artery and connected to a Statham transducer. Blood pressure and heart rate are recorded on a polygraph over a period of at least 30 min. For long acting drugs registration periods up to 2 h are necessary. After the experiment, the animal is sacrificed and the brain removed to confirm the site of injection.

EVALUATION

Systolic and diastolic blood pressure as well as heart rate after intracerebroventricular injection are expressed as percentage of pretreatment values. The response is compared with the standard clonidine which is effective in doses of 4–60 µg.

MODIFICATIONS OF THE METHOD

Based on the work of Feldberg et al. (1954) and Hayden et al. (1966), Mastrianni et al. (1986) developed an

intracerebroventricular perfusion system for the study of centrally acting antihypertensive drugs in the rat. The antihypertensive effect of clonidine could be observed over several hours.

Methods used to detect central hypotensive activity of drugs have been reviewed by Timmermans (1984).

REFERENCES AND FURTHER READING

Feldberg W, Sherwood SL (1954) Injections of drugs into the lateral ventricle of the cat. J Physiol 123:148–167

Hayden JF, Johnson LR, Maickel RP (1966) Construction and implantation of a permanent cannula for making injections into the lateral ventricle of the rat brain. Life Sci 5:1509–1515

Mastrianni JA, Harris TM, Ingenito AJ (1986) An intracerebroventricular perfusion system developed for the study of centrally acting antihypertensive drugs in the rat. J Pharmacol Meth 16:63–72

Timmermans PBMWM (1984). Centrally acting hypotensive drugs. In: van Zwieten (ed) Handbook of Hypertension, Vol 3, Pharmacology of Antihypertensive Drugs. Elsevier Amsterdam, pp 102–153

A.1.3.18 Influence on Orthostatic Hypotension

PURPOSE AND RATIONALE

Orthostatic hypotension with dizziness up to unconsciousness is a syndrome occurring in many human individuals. Moreover, several drugs are known to cause orthostatic hypotension. In several animal species, such as rabbit, cat and dog, this syndrome can be evoked by changing the usual horizontal position into a vertical position with the head upwards using a tilting table.

PROCEDURE

Cats of either sex weighing 2.0–3.0 kg are temporarily anesthetized with ether. Anesthesia is maintained by intravenous injection of 70 mg/kg chloralose. The animal is fixed with its legs on a heated operating table which can be tilted by 90 degrees. The carotid artery is cannulated for measuring blood pressure through a Statham P 23 Db transducer on a 6 channel Hellige recorder. The femoral vein is cannulated for injection of the test compound. After the blood pressure is stabilized for 30 min, the animal is quickly tilted to a vertical position for 1 minute. Due to the change of position and gravitational force, there is a rapid fall in blood pressure which recovers as soon as the animal is restored to its original position. After taking the control reading, the test compound is administered intravenously and the same procedure is repeated. The fall in blood pressure is recorded.

EVALUATION

A significant increase in postural hypotension with respect to the control would indicate that the test compound may produce orthostatic hypotension in human. Moreover, some compounds, like sympathomimetics, can reduce or prevent postural hypotension.

MODIFICATIONS OF THE METHOD

Sponer et al. (1981) described a method for evaluating postural hypotension in conscious **rabbits** placed on a tilting table whereby blood pressure was measured from the central artery of the ear.

Takata et al. (1999) reported a rabbit model for evaluation of chlorpromazine-induced orthostatic hypotension.

Humphrey and McCall (1982) described a model for predicting orthostatic hypotension during acute and chronic antihypertensive drug therapy in **rats** anesthetized with chloralose, urethane and pentobarbital using a heated tilting table.

Lee et al. (1982) evaluated postural hypotension induced by drugs in conscious restrained normotensive rats. Blood pressure was recorded after cannulation of the femoral artery under light ether anesthesia. A special tilting table was build for simultaneous studies in four rats.

Martel et al. (1996, 1998) studied the phenomenon of cardiovascular deconditioning observed in crew members of space flights in rats after tail suspension.

Socci et al. (2000) studied cardiovascular responses to simulated microgravity in Sprague-Dawley rats. Microgravity is known to induce orthostatic intolerance and baroreflex impairment in astronauts. The authors used 30° head-down tilt, 24-h whole-body suspension or 7-day tail suspension to mimic microgravity and to find treatment ameliorating the symptoms.

Baum et al. (1981) studied antihypertensive and orthostatic responses to drugs in conscious **dogs**. A catheter was placed in the subclavian artery for measurement of blood pressure and exteriorized at the back of the neck some days prior to the experiment. The animals were placed into a sling and tilted to the 90° upright position for periods of 60 s. every hour by lifting their forelimbs. Blood pressure response before and after treatment with test drugs was measured.

A none human **primate** model for evaluating the potential of antihypertensive drugs to cause orthostatic hypotension was described by Pals and Orley (1983) Polyvinyl catheters were implanted in the abdominal aorta and the vena cava via an external iliac artery and vein to **cynomolgus monkeys** during ketamine anesthesia. The catheters were routed subcutaneously from

the groin area to the top of the head and exteriorized. After recovery the animals were placed in restraining chairs allowing the change from vertical to horizontal position.

REFERENCES AND FURTHER READING

Baum Th, Vliet GV, Glennon JC, Novak PJ (1981) Antihypertensive and orthostatic responses to drugs in conscious dogs. J Pharmacol Meth 6:21–32

Boura ALA, Green AF (1959) The actions of bretylium: Adrenergic neuron blocking and other effects. Br J Pharmacol 14:536–548

Humphrey SJ, McCall RB (1982) A rat model for predicting orthostatic hypotension during acute and chronic antihypertensive drug therapy. J Pharmacol Meth 25:25–34

Lee CH, Strosber AM, Roszkowski AP, Warren LA (1982) A model for evaluation of postural hypotension induced by drugs in conscious restrained normotensive rats. J Pharmacol Meth 7:15–24

Martel E, Champeroux P, Lacolley P, Richard S, Safar M, Cuche JL (1996) Central hypervolemia in the conscious rat: a model of cardiovascular deconditioning. J Appl Physiol 80:1390–1396

Martel E, Ponchon P, Champeroux P, Elghozi JL, Renaud de la Faverie JF, Dabire H, Pannier B, Richard S, Safar M, Cuche JL (1998) Mechanism of cardiovascular deconditioning induced by tail suspension in the rat. Am J Physiol 274 (5 Pt2):H1667–H1673

Pals DT, Orley J (1983) A none human primate model for evaluating the potential of antihypertensive drugs to cause orthostatic hypotension. J Pharmacol Meth 9:183–192

Socci RR, Wang M, Thierry-Palmer M, Emmett N, Bayorh MA (2000) Cardiovascular responses to simulated microgravity in Sprague-Dawley rats. Clin Exp Hypertens 22:155–164

Sponer G, Mannesmann G, Bartsch W, Dietmann K (1981) A method for evaluating postural hypotension in conscious rabbits as a model to predict effects of drugs in man. J Pharmacol Meth 5:53–58

Takata Y, Kurihara J, Suzuki S, Okubo Y, Kato H (1999) A rabbit model for evaluation of chlorpromazine-induced orthostatic hypotension. Biol Pharm Bull 22:457–462

A.1.3.19 Bezold-Jarisch Reflex

PURPOSE AND RATIONALE

The circulatory collapse after intravenous injection of veratrine has been first described in cats and is known as BEZOLD-JARISCH-reflex (Bezold and Hirt 1867; Jarisch and Richter 1939a, b, Jarisch 1940; Aviado and Guavera-Aviado 2001). Fleckenstein et al. (1950) recommended this as a suitable animal model of shock.

The original observation was a triphasic blood pressure response in cats or dogs characterized by a short lasting fall in blood pressure accompanied by bradycardia, followed by a short lasting increase and than a long-lasting decrease of blood pressure after intravenous injection of veratridin or other veratrum alkaloids.

Kalkman et al. (1984) showed that three distinct subtypes of serotonergic receptors mediate the triphasic blood pressure response to serotonin observed in the Bezold-Jarisch reflex.

The Bezold-Jarisch reflex has been studied in several species, such as **cats** (Takei et al. 1995; Vayssettes-Couchay et al. 1997), **dogs** (Zucker and Cornish 1981; Barron and Bishop 1982; Harron and Kobinger 1984; Giles and Sander 1986; Baugh et al. 1989; Watson et al. 1995), **ferrets** (Andrews and Bhandari 1993), **rabbits** (Chen 1979), guinea pigs, **rats** (Fozard 1984; Gylys et al. 1988; Cohen et al. 1989; Blower 1990; Miyata et al. 1991; Turconi et al. 1991; Matsumoto et al. 1992; Meller et al. 1992; Robertson et al. 1992; Kishibayashi et al. 1993; Geissler et al. 1993; Haga et al. 1994; Hegde et al. 1994; Eglen et al. 1995; Göthert et al. 1995; Delagrange et al. 1996; De Vries 1997; Malinowska et al. 2001; Godlewski et al. 2003) and **mice** (Eglen et al. 1994; Middlefell et al. 1996), whereby species differences have been observed (Yamono et al. 1995).

In cats and dogs, the Bezold-Jarisch reflex was elicited by veratrine and veratridine, but also by capsaicin and the 5-HT_3 receptor agonists 2-methyl-5-HT, phenylbiguanide, chlorophenylbiguanide and serotonin itself.

In rats, mostly 5-HT or 2-methyl-5-HT were used as stimuli to characterize 5-HT_3 receptor antagonists.

PROCEDURE

Male Sprague Dawley rats weighing 250–380 g are given food and water ad libitum, except those used for intraduodenal drug administration; these rats are deprived of food overnight. The animals are anesthetized by intraperitoneal injection of 1.5 g/kg urethane. Body temperature is maintained at 37°C by placing the animal on a heating pad. The left jugular vein or duodenum, trachea and left femoral vein are cannulated for drug administration (i.v. or i.d.), facilitation of respiration and injection of 2-methyl 5-HT, respectively. Heart rate is derived from a limb lead II ECG monitored via subdermal platinum electrodes and is recorded with amplifiers on a polygraph. A dose-response curve to 2-methyl 5-HT (5–100 µg/kg, i.v.) is constructed in each rat to establish a submaximal dose (usually 10 or 20 µg/kg, i.v.) which elicits a reproducible bradycardic response. Each rat receives then a single dose of test drug or standard and is then challenged with 2-methyl 5-HT at 5, 15, 30, 60, 120, 180, 240, 300, 360, 420, and 480 min post dosing. A separate group of rats receiving vehicle (saline for i.v.,

deionized water for i.d.) is similarly tested in each study.

EVALUATION

Duration of action of the compounds is assessed by determining the period of time for which the inhibitory effects remain significantly different from vehicle controls. Statistical analysis of the data is performed by a repeated measure analysis of variance (ANOVA) followed by pairwise comparisons against control at each time period using Fisher's multiple comparison test.

MODIFICATIONS OF THE METHOD

Harron and Kobinger (1984) used capsaicin to elicit the Bezold-Jarisch reflex in anesthetized artificially respirated dogs pretreated with a beta-adrenoceptor antagonist to evaluate the activity of clonidine-like drugs on central alpha$_2$ adrenoceptors after intracisternal administration.

The Bezoold-Jarisch reflex in rats has been used for evaluation of 5-HT$_3$ receptor agonists (Rault et al. 1996; López-Tudanca et al. 2003).

Rocha et al. (2003) found an enhancement of the Bezold-Jarisch reflex in the acute phase of myocardial infarction of the anesthetized rabbit.

REFERENCES AND FURTHER READING

Andrews PLR, Bhandari P (1993) Resinferatoxin, an ultrapotent capsaicin analogue, has anti-emetic properties in the ferret. Neuropharmacology 32:799–806

Aviado DM, Guavera-Aviado D (2001) The Bezold-Jarisch reflex. A historical perspective of cardiopulmonary reflexes. Ann NY Acad Sci 940:48–58

Barron KW, Bishop VS (1982) Reflex cardiovascular changes with veratridine in the conscious dog. Am J Physiol, Heart Circ Physiol 11:H810–H817

Baugh L, Abraham W, Matthews E, Lahr P (1989) Pharmacological profile of MDL 26,024GO: A novel antiasthmatic agent. Agents Actions 27:431–434

Blower PR (1990) The role of specific 5-HT$_3$ receptor antagonism in the control of cytostatic drug induced emesis. Eur J Cancer 26, Suppl 1:S8–S11

Chen HI (1979) Interaction between the baroreceptor and Bezold-Jarisch reflexes. Am J Physiol 6:H655–H661

Cohen ML, Bloomquist W, Gidda JS, Lacefield W (1989) Comparison of the 5-HT$_3$ receptor antagonist properties of ICS 205–930, GR38032 and zacopride. J Pharmacol Exp Ther 248:197–201

Delagrange P, Emerit MB, Merahi N, Abraham C, Morain P, Rault S, Renard P, Pfeiffer B, Guardiola-Lemaitre P, Hamon M (1996) Interaction of S 21007 with 5-HT$_3$ receptors. *In vitro* and *in vivo* characterization. Eur J Pharmacol 316:195–203

De Vries P, Apaydin S, Villalon CM, Heiligers JPC, Saxena PR (1997) Interaction of GR127935, a 5-HT$_{1B/D}$ receptor ligand with functional 5-HT receptors. Naunyn-Schmiedeberg's Arch Pharmacol 355:423–430

Eglen RM, Lee CH, Khabbaz M, Fontana DJ, Daniels S, Kilfoil T, Wong EHF (1994) Comparison of potencies of 5-HT$_3$ receptor antagonists at inhibiting aversive behavior to illumination and the von Bezold-Jarisch reflex in the mouse. Neuropharmacol 33:227–234

Eglen RM, Lee CH, Smith WL, Johnson LG, Clark R, Whiting RL, Hedge SS (1995) Pharmacological characterization of RS 25259–197, a novel and selective 5-HT$_3$ receptor antagonist, *in vivo*. Br J Pharmacol 114:860–866

Fleckenstein A, Muschaweck R, Bohlinger F (1950) Weitere Untersuchungen über die pharmakologische Ausschaltung des BEZOLD-JARISCH-Reflexes. Naunyn Schmiedeberg's Arch exper Path Pharmakol 211:132–142

Fozard JR (1984) MDL 72222: A potent and highly selective antagonist at neuronal 5-hydroxytryptamine receptors. Naunyn-Schmiedeberg's Arch Pharmacol 326:36–44

Geissler MA, Torrente JR, Elson AS, Gylys JA, Wright RN, Iben LG, Davis HH, Yocca FD (1993) Effects of BMY 33462, a selective and potent serotonin type-3 receptor antagonist, on mesolimbic dopamine mediated behavior. Drug Dev Res 29:16–24

Giles TD, Sander GE (1986) Comparative cardiovascular responses to intravenous capsaicin, phenyldiguanide, veratrum alkaloids and enkephalins in the conscious dogs. J Auton Pharmacol 6:1–7

Godlewski G, Göthert M, Malinowska B (2003) Cannabinoid receptor-independent inhibition of cannabinoid agonists of the peripheral 5-HT$_3$ receptor-mediated Bezold-Jarisch reflex. Br J Pharmacol 138:767–774

Göthert M, Hamon M, Barann M, Bönisch H, Gozlan H, Laguzzi R, Metzenauer P, Nickel B, Szelenyi I (1995) 5-HT3 antagonism by anpirtoline, a mixed 5-HT$_1$ receptor agonist/5-HT$_3$ receptor antagonist. Br J Pharmacol 114:269–274

Gylys JA, Wright RN, Nicolosi WD, Buyniski JP, Crenshaw RR (1988) BMY 25801, an anti-emetic agent free of D$_2$ dopamine antagonist properties. J Pharmacol Exp Ther 244:830–837

Haga K, Asano K, Inaba K, Morimoto Y, Setoguchi M (1994) Effect of Y-25130, a selective 5-hydroxytryptamine-3 receptor antagonist, on gastric emptying in mice. Arch Int Pharmacodyn Ther 328:344–355

Harron DWG, Kobinger W (1984) Facilitation of the Bezold-Jarisch reflex by central stimulation of alpha-2 adrenoceptors in dogs. Naunyn-Schmiedeberg's Arch Pharmacol 325:193–197

Hegde SS, Wong AG, Perry MR, Ku P, Moy TM, Loeb M, Eglen RM (1995) 5-HT$_4$ receptor mediated stimulation of gastric emptying in rats. Naunyn-Schmiedeberg's Arch Pharmacol 351:589–595

Jarisch A (1940) Vom Herzen ausgehende Kreislaufreflexe. Arch Kreislaufforsch 7:260–274

Jarisch A, Richter H (1939a) Die Kreislaufwirkung des Veratrins. Naunyn Schmiedeberg's Arch exp Path Pharmakol 193:347–354

Jarisch A, Richter H (1939b) Der Bezold-Effekt – Eine vergessene Kreislaufreaktion. Klin Wochschr 18:185–187

Kalkman HO, Engel G, Hoyer D (1984) Three distinct subtypes of serotonergic receptors mediate the triphasic blood pressure response to serotonin in rats. J Hypertens 2, Suppl 3:143–145

Kishibayashi N, Ichikawa S, Yokoyama T, Ishii A, Karasawa A (1993) Pharmacological properties of KF19259, a novel 5-HT$_3$ receptor antagonist, in rats: Inhibition of the distal colonic function. Jpn J Pharmacol 63:495–502

López-Tudanca PL, Labeaga L, Innerárity A, Alonso-Cires L, Tapia I, Mosquera R, Orjales A (2003) Synthesis and pharmacological characterization of a new benzoxazole derivative as a potent 5-HT_3 receptor agonist. Bioorg Med Chem 11:2709–2714

Malinowska B, Kwolek G, Göthert M (2001) Anandamide and methanandamide induce both vanilloid VR_1 and cannabinoid CB_1 receptor mediated changes in heart rate and blood pressure in anesthetized rats. Naunyn-Schmiedebergs Arch Pharmacol 364:562–569

Matsumoto M, Yoshioka M, Togashi H, Saito H (1992) Effects of ondasentron on cardiovascular reflex to exogenous serotonin in anesthetized rats. Biog Amines 8:443–449

Meller ST, Lewis SJ, Brody MJ, Gebhart GF (1992) Vagal afferent-mediated inhibition of a nociceptive reflex by i.v. serotonin in the rat. II. Role of 5-HT receptor subtypes. Brain Res 585:71–86

Middlefell VC, Bill DJ, Brammer NT, Coleman J, Fletcher A, Hallett I, Rhodes KF, Wainwright TL, Ward TJ (1996) WAY-SEC-579: A novel 5-HT_3 receptor antagonist. CNS Drug Rev 2:269–293

Miyata K, Kamato T, Yamano M, Nishida A, Ito H, Katsuyama Y, Yuki H, Tsutsumi R, Ohta M, Takeda M, Honda K (1991) Serotonin 5-HT_3 receptor blocking activities of YM060, a novel 4,5,6,7-tetrahydrobenzimidazole derivative and its enantiomer in anesthetized rats. J Pharmacol Exp Ther 259:815–819

Rault S, Lancelot JC, Prunier H, Robba M, Renard P, Delagrange P, Pfeiffer B, Caignard DH, Guardiola-Lemaitre B, Hamon M (1996) Novel selective and partial agonists of 5-HT_3 receptors. Part 1. Synthesis and biological evaluation of piperazinopyrrolothienopyrazines. J Med Chem 39:2068–2080

Robertson DW, Bloomquist W, Wong DT, Cohen ML (1992) MCPP but not TFMPP is an antagonist at cardiac 5-HT_3 receptors. Life Sci 50:599–605

Rocha I, Rosario LB, de Oliviera EI, Barros MA, Silva-Carvallho L (2003) Enhancement of carotid chemoreceptor reflex and cardiac chemosensitive reflex in the acute phase of myocardial infarction of the anesthetized rabbit. Basic Res Cardiol 98:175–180

Takei N, Takei S, Tomomatsu S, Suzuki K, Yagi S (1995) Augmentation of clonidine on Bezold-Jarisch reflex control of renal sympathetic nerve activity in cats. Jpn J Nephrol 37:12–16

Turconi M, Donetti A, Schiavone A, Sagrada A, Montagna E, Nicola M, Cesana R, Rizzi C, Micheletti R (1991) Pharmacological properties of a novel class of 5-HT_3 receptor antagonists. Eur J Pharmacol 203:203–211

Vayssettes-Couchay C, Bouysset F, Laubie M, Verbeuren TJ (1997) Central integration of the Bezold-Jarisch reflex in the cat. Brain Res 74:272–278

von Bezold A, Hirt L (1867) Über die physiologischen Wirkungen des essigsauren Veratrin's. Untersuchungen aus dem physiologischen Laboratorium Würzburg 1:75–156

Watson JW, Gonsalves SF, Fossa AA, McLean S, Seeger T, Obach S, Andrews PLR (1995) The anti-emetic effects of CP-99,994 in the ferret and the dog: Role of the NK_1 receptor. Br J Pharmacol 115:84–94

Yamono M, Ito H, Kamoto T, Miyata K (1995) Species difference in the 5-hydroxytryptamine$_3$ receptor associated with the Bezold-Jarisch reflex. Arch Int Pharmacodyn Ther 330:177–189

Zucker IH, Cornish KG (1981) The Bezold-Jarisch reflex in the conscious dog. Circ Res 49:940–948

A.1.3.20 Endotoxin Induced Shock

PURPOSE AND RATIONALE

Many bacterial infections as well as allergic reactions are known to induce pathophysiological events that may lead to shock in man. When experimental animals are injected with endotoxin and galactosamine, shock and death occur in all untreated animals 5–7 h after injection. The endotoxin induced shock is marked by pulmonary embolism, bronchospasm and renal failure. Bacterial liposaccharides (endotoxins) play an important role in the pathogenicity of Gram-negative infections.

The reactivity of animals to endotoxin may be enhanced by simultaneous administration of galactosamine. Galactosamine is a specific hepatotoxic agent that leads to early metabolic alterations and consequent cellular liver damage. The following procedure is used to detect compounds that prevent the occurrence of endotoxin-induced shocks.

Cardiovascular parameters of endotoxin induced shock are greatly influenced by various anesthetics. For this reason, a model was proposed by Brackett et al. (1985) and Schaefer et al. (1987) to study the circulatory shock pattern after endotoxemia in conscious unrestrained rats.

PROCEDURE

Male Sprague-Dawley rats weighing 300 ± 10 g are anesthetized with 5% enflurane. A tracheal cannula is connected to a rodent respirator delivering 2% enflurane. Via the right jugular vein the tip of one catheter is placed just adjacent to the right atrium for injection of endotoxin, monitoring of central venous pressure, and rapid injection of room-temperature saline to produce thermodilution curves for calculation of cardiac output. The right carotid artery is cannulated with a thermistor-catheter combination for measurement of thermodilution cardiac output curves and aortic blood pressure. The thermistor tip is placed in the aortic arch just distal to the aortic valve. The catheters are guided under the skin exiting through the back of the neck just below the base of the skull.

The animals are allowed to regain consciousness and are then placed in cages that allow unrestrained movements about the cage at all times throughout the study with no further handling. The experimental animals receive a 20-sec infusion of 40 mg/kg endotoxin (*E. coli*, Difco) being paired with sham animals with identical catheters but receiving an equal volume of saline. Test compounds are injected intravenously

10 min prior to endotoxin injection. Cardiac outputs are measured using the thermodilution technique by rapidly injecting a volume calculated to deliver 100 µl of room temperature saline to the circulatory system. Central venous and aortic blood pressure and heart rate are continuously monitored for the following 4 h. Cardiac output measurements are made 5, 15, 30, 60, 120, 180, and 240 min after endotoxin. At the end of the study, the animals are sacrificed and the catheters checked visually to ensure proper placement.

EVALUATION

Central venous pressure, arterial pressure, and cardiac output of drug treated animals receiving endotoxin are compared with animals receiving endotoxin only and saline sham treated animals. Furthermore, cardiac index, total peripheral resistance, and stroke volume are calculated. The small intestines of all rats are examined for severity of hemorrhage using a five point scale. Repeated-measures analysis of variance is used to analyze the data.

MODIFICATIONS OF THE METHOD

Lindenbaum et al. (1990) studied the effect of *E. coli* endotoxin on cardiovascular parameters of anesthetized **dogs**. Inhibition of the detoriation of metabolic functions and improvement of cardiovascular parameters were found after cocarboxylase treatment.

Endotoxin induced shock has been tested in **mice** (Galanos et al. 1979). Groups of 10 male C57 BL/6 mice weighing 20–22 g are injected intravenously with a mixture of 0.01 µg of Salmonella abortus equi lipopolysaccharide and 7.5–15 mg galactosamine in 0.02 ml phosphate buffered saline. The test compound is administered either intravenously at the same time or orally 45 min prior challenge. Twenty-four hours later, the number of surviving mice is determined.

Metz and Sheagren (1990) reviewed the effects of ibuprofen in animal models of septic shock.

Von Asmuth et al. (1990), Luongo et al. (1998), and Cuzzocrea et al. (2004) described a zymosan-induced shock model in **mice**. Male CD mice (20–22 g) were treated intraperitoneally with zymosan (500 mg/kg, suspended in saline solution) or with zymosan and drug (rosiglitazone 3 mg/kg, intraperitoneally) at 1 and 6 h after zymosan. Eighteen hours after administration of zymosan, animals were assessed for non-septic shock. Clinical severity of systemic toxicity was scored for the whole experimental period (12 days) in the mice after zymosan or saline injection on a subjective scale ranging from 0 to 3: 0 = absence, 1 = mild, 2 = moderate, 3 = serious. The ranging scale was used for each of the toxic signs (conjunctivitis, ruffled fur, diarrhea, and lethargy) observed in the animals. The final score was the sum of the single evaluation (maximum value 12).

Overbergh et al. (2003) studied acute shock induced by antigen in NOD mice. The 8-week-old NOD, BALB/c, and C57BL/6 mice were immunized by injection of 100 µg antigen [Hen egg white lysozyme (HEL), GAD65 (p524–542) (SRLSKVAPVIKARMMEYGTT), bovine insulin B (ins-B) chain, heat shock protein (hsp)-65, PLP peptide (amino acids 135–151), ovalbumin, keyhole limpet hemocyanine (KLH), and tetanus toxin] emulsified at a 1:1 concentration in complete Freund's adjuvant (CFA) or incomplete Freund's adjuvant (Difco Laboratories, Detroit, Mich., USA) in the hind footpads. NOD-*scid* mice were injected with 100 µg HEL antigen suspended in CFA. All mice were reinjected with the same antigen 3 weeks later in a similar manner. Clinical evolution and survival rate after sensitization with various peptides were monitored in different mouse strains. Shock was characterized by pilo-erection, prostration, erythema of the tail, ears, and footpads, and dyspnea with shallow breathing. Serum for antibody measurement and spleens for quantification of mRNA levels were collected before immunization and again before booster administration.

Baldwin et al. (1991) tested the effect of Polymyxin B on experimental shock from meningococcal lipooligosaccharide and *Escherichia coli* lipopolysaccharide endotoxins in anesthetized **rabbits**.

Muacevic and Heuer (1992) tested the effect of platelet-activating factor antagonists in anesthetized rats.

Otterbein et al. (1993) tested the effects of peptides on survival of mice injected with 50 mg/kg lipopolysaccharide endotoxin in mice and on survival of rats with fecal peritonitis.

Mountz et al. (1995) reported an increased susceptibility of fas mutant **MRL-Ipr/Ipr mice** to Staphylococcal enterotoxin B-induced septic shock.

REFERENCES AND FURTHER READING

Baldwin G, Alpert G, Caputo GL, Baskin M, Parsonnet J, Gillis ZA, Thompson C, Silber GR, Fleisher GR (1991) Effect of Polymyxin B on experimental shock from meningococcal and *Escherichia coli* endotoxins. J Infect Dis 164:542–549

Brackett DJ, Schaefer CF, Tompkins P, Fagraeus L, Peters LJ, Wilson MF (1985) Evaluation of cardiac output, total peripheral vascular resistance, and plasma concentrations of vasopressin in the conscious, unrestrained rat during endotoxemia. Circulat Shock 17:273–284

Cuzzocrea S, Pisano B, Dugo L, Ianaro A, Patel NSA, di Paola R, Genovese T, Chatterjee PK, Fulia F, Cuzzocrea E, di Rosa M, Caputi AP, Thiemermann C (2004) Rosiglitazone, a ligand of peroxisome proliferator-activated receptor-γ, reduces development of nonseptic shock in mice. Crit Care Med 32:457–466

Galanos C, Freudenberg MA, Reutter W (1979) Galactosamine-induced sensitization to the lethal effects of endotoxin. Proc Natl Acad Sci USA 76:5939–5943

Lindenbaum GA, Lerrieu AJ, Carrol SF, Kapusnick RA (1990) Efectos de la cocarboxilasa en perros sometidos a choque septico experimental. Compend Invest Clin Latinoam 10:18–26

Luongo C, Imperatore F, Cuzzocrea S, Filippelli A, Scafuro MA, Mangoni G, Portolano F, Rossi F (1998) Effects of hyperbaric oxygen exposure on a zymosan-induced shock model. Crit Care Med 26:1972–1976

Metz CA, Sheagren JN (1990) Ibuprofen in animal models of septic shock. J Crit Care 5:206–212

Mountz JD, Baker TJ, Borcherding DR, Bluethmann H, Zhou T, Edwards CK (1995) Increased susceptibility of fas mutant MRL-Ipr/Ipr mice to staphylococcal enterotoxin B-induced septic shock. J Immunol 155:4829–4837

Muacevic G, Heuer HO (1992) Platelet-activating factor antagonists in experimental shock. Arzneim Forsch/Drug Res 42:1001–1004

Otterbein L, Lowe VC, Kyle DJ, Noronha-Blob L (1993) Additive effects of a bradykinin antagonist, NPC 17761, and a leumedin, NPC 15669, on survival in animal models. Agents Actions 39, Special Conference Issue: C125–C127

Overbergh L, Decallonne B, Branisteanu DD, Valckx D, Kasran A, Bouillon R, Mathieu C (2003) Acute shock induced by antigen in NOD mice. Diabetes 52:335–342

Schäfer CF, Biber B, Brackett DJ, Schmidt DD, Fagraeus L, Wilson MF (1987) Choice of anesthetic alters the circulatory shock as gauged by conscious rat endotoxemia. Acta Anaesthesiol Scand 31:550–556

Von Asmuth EJ, Maessen JG, van der Linden CJ, Buurman WA (1990) Tumor necrosis factor alpha (TNF-α) and interleukin 6 in a zymosan-induced shock model. Scand J Immunol 32:313–319

A.1.3.21 Hemorrhagic Shock

PURPOSE AND RATIONALE

Hemorrhagic shock is one of the most severe consequences of accidents. Several animal models in various species have been developed to resemble the conditions in man and to test therapeutic or prophylactic measures (Lamson and de Turk 1945; Selkurt and Rothe 1961; Mills 1976). A method for hemorrhagic shock in anesthetized as well as in unanesthetized rats has been described by van der Meer et al. (1987). Experimental hemorrhagic shock is defined as a situation in which the cardiovascular system, after a period of hypovolemia followed by complete re-infusion of the shed blood, gradually detoriates ending in the death of the animal.

PROCEDURE

Female rats weighing 170–190 g are anesthetized by i.p. injection of sodium pentobarbital, 25 m/kg, followed after 20 min by 20 mg/kg, and kept in a chamber at 30°C and relative humidity over 80%. The left femoral vein is cannulated for application of the test drug. The right common iliac artery is cannulated and the cannula (polyvinyl chloride, 14 cm long, inner diameter 2 mm) is filled with heparin and exteriorized in the neck. After intraarterial injection of 0.2 ml heparin 500 IU/ml, the cannula is connected to a siliconized calibrated glass reservoir (inner diameter 18 mm), the height of which can be changed to adjust the surface of the shed blood to a fixed level.

The test drug is injected i.v. 5 min prior to bleeding. Bleeding is performed against (at heart level) 30 mm Hg for 1 h, 25 mm Hg for 0.5 h, 30 mm Hg for 1 h, 25 mm Hg for 0.5 h, and finally 30 mm Hg for 1 h. The shed blood is partially taken up again spontaneously. After 4 h, re-infusion is started by increasing the pressure to 60 mm Hg for 5 min, to 80 mm Hg for 5 min, and (if necessary) to 100 mm Hg. During the hypovolemic phase respiration becomes gradually slower. If respiration arrest is imminent 0.5 ml 5% glucose are injected intra-arterially, thus avoiding death during the period of hypovolemia. Practically all rats die at an average of 4 h after complete re-infusion.

EVALUATION

Survival time is taken as the time between complete re-infusion and death. Average survival time of treated animals is compared with that of controls. Furthermore, after autopsy the number of gastrointestinal lesions, subendocardial hemorrhage, kidney tubular necrosis and liver cell necrosis are registered by histological examination.

CRITICAL ASSESSMENT OF THE METHOD

In spite of the fact that hemorrhagic shock does not reflect the situation of traumatic shock in man in every aspect, the condition is close enough to use the model for testing compounds which potentially inhibit or ameliorate shock in man.

MODIFICATIONS OF THE METHOD

A method to study hemorrhagic shock in dogs has been described in detail by Mills (1967). Large dogs weighing 20–30 kg are anesthetized by an i.v. injection of 25 mg/kg sodium pentobarbital. The animals are respirated by means of a Harvard respirator set at a stroke volume of 400 ml and a rate of 20 respiration/min. Blood pH is regulated between 7.37 and 7.42

by varying the gas flow between 100% O_2 and a mixture of 95% O_2 and 5% CO_2. Central arterial blood pressure is recorded by inserting a catheter through one femoral artery to the aortic arch. Pulmonary artery pressure is measured by inserting a PE 50 catheter through a small neck vein, reaching the right ventricle and allowing to float into the pulmonary artery. The right atrial catheter is also inserted through a small neck vein. After the chest is opened, the left atrial catheter is tied in place through a small opening in the left atrial appendage. Blood flow is measured in the ascending aorta (cardiac output), carotid, superior mesenteric, renal and femoral arteries using electromagnetic flowmeters. Furthermore, pulse rate is monitored from the electrocardiogram.

The test drug is injected i.v. 10 min prior bleeding. Blood is removed either at a specific volume or until a selected reduction of blood pressure has occurred. The cardiovascular parameters of treated animals are compared with those of controls.

Shock associated with hemoconcentration was produced in dogs by Davis (1941) by bleeding from the carotid artery and injections of 25% sodium chloride solution subcutaneously in doses of 25 ml.

The effect of insulin on glucose uptake in the soleus muscle of rats during hemorrhagic shock was studied by Chaudry et al. (1975).

Bauer et al. (1995) used hemorrhagic shock in rats to evaluate the influence of interleukin-1 on leukocyte-endothelial cell interactions and the microcirculation in the liver by means of intravital microscopy after application of an interleukin-1 receptor antagonist.

Kitajima et al. (1995) studied gastric mucosal injury induced by hemorrhagic shock in rats.

REFERENCES AND FURTHER READING

Bauer C, Marci I, Bauer M, Fellger H, Larsen R (1995) Interleukin-1 receptor antagonist attenuates leukocyte-endothelial interactions in the liver after hemorrhagic shock in the rat. Crit Care Med 23:1099–1105

Chaudry IH, Sayeed MM, Baue AE (1975) The effect of insulin on glucose uptake in soleus muscle during hemorrhagic shock. Can J Physiol Pharmacol 53:67–73

Davis HA (1941) Physiologic effects of high concentrations of oxygen in experimental secondary shock. Arch Surg 43:1–13

Kitajima T, Tani K, Yamaguchi T, Kubota Y, Okuhira M, Mizuno T, Inoue K (1995) Role of endogenous endothelin in gastric mucosal injury by hemorrhagic shock in rats. Digestion 56:111–116

Lamson PD, de Turk (1945) Studies on shock induced by hemorrhage. XI. A method for the accurate control of blood pressure. J Pharmacol Exp Ther 83:250–252

Mills LC (1967) Animal and clinical techniques for evaluating drugs in various types of shock. In: Siegler PF, Moyer JH (eds) Animal and clinical pharmacologic techniques in drug evaluation. Year Book Medical Publ. Inc., Chicago, pp 478–492

Selkurt EE, Rothe CF (1961) Critical analysis of experimental shock models. In: Seeley SF, Weisiger JR (eds) Recent progress and present problems in the field of shock. Fed Proc 20, Suppl 9, part III, pp 30–37

Van der Meer C, Valkenburg PW, Snijders PM, Wijnans M, van Eck P (1987) A method for hemorrhagic shock in the rat. J Pharmacol Meth 17:75–82

A.1.3.22 Tourniquet Shock

PURPOSE AND RATIONALE

Compression of extremities in man by heavy objects for periods of several hours results in the so-called crush syndrome. The rescued individual shows immediately a favorable response to therapy, but within a few hours symptoms of shock develop followed by signs of progressive renal damage leading to death (Duncan and Blalock 1942). Moreover, arterial bleeding after accidents needs the applications of tourniquets. During surgical procedures on extremities a tourniquet may be necessary (Wilgis 1971), the time of which has to be limited in order to avoid fatal consequences. The pathophysiological mechanisms of tourniquet induced shock remain still to be elucidated. Nevertheless, animal models in rats (Chandra and Dave 1970), rabbits (Little 1974), and dogs (Goto et al. 1988) had to be developed to evaluate drugs capable to inhibit the fatal consequences of crush and tourniquet shock.

PROCEDURE

Wistar rats of either sex weighing 250–280 g are anesthetized with phenobarbital. The tourniquets consist of rubber tubes (internal diameter 4 mm, external diameter 5.8 mm). Both tights are fastened by the rubber tubes and the pressure which is monitored by a miniature pressure sensor and an amplifier (e. g. Kyowa Electronic Instruments Co, Tokyo) is adjusted to 1.5 kg/cm^2. The rubber tubes are knotted and the sensor removed. After 3 h the animals are treated with the test compound or the control solution. The tourniquet is left in place for 6 h while the animals remain under pentobarbital anesthesia. Then, the rubber tubes are removed, and the rats are returned to their cages. Within a few min, the reperfused hind limbs, which have been pale blue, turn pink. The animals are then allowed free access to food and water. Blood is withdrawn at different intervals during the tourniquet and afterwards for measurement of hematocrit, transaminases, urea nitrogen and total protein. Time to death is registered.

EVALUATION

Statistical evaluation of the survival intervals is performed with the log rank test according to Peto et al. (1976). Blood chemical data are analyzed using the Kruskal-Wallis (1952) rank sum test. Multiple comparisons are corrected by the Bonferroni's method (1980).

CRITICAL EVALUATION OF THE METHOD

These methods are valuable to find drugs effective in this life-threatening situation.

MODIFICATIONS OF THE METHOD

Ghussen et al. (1979) studied the effect of methylprednisolone on the experimental tourniquet shock in **dogs**.

Haugan and Kirkebo (1984) used a model in anesthetized **rats** with tourniquet shock by bilateral hindlimb occlusion for 3 1/2 h, and burn shock by scalding the hind 50% of the body surface for 30 s in 90°C water.

Horl and Horl (1985) investigated the effect of tourniquet ischemia on carbohydrate metabolism in **dog** skeletal muscle

Sáez et al. (1982) followed the time course of appearance of lactic dehydrogenase enzymes in the serum of **rats** after different periods of ischemia by bilateral application of rubber band tourniquets to the hind legs.

Sáez et al. (1986) studied the effects of allopurinol on biochemical changes of the gastrocnemius muscle in rats subjected to tourniquet shock followed by reperfusion.

REFERENCES AND FURTHER READING

Aoki Y, Nata M, Odaira T, Sagisaka K (1992) Suppression of ischemia-reperfusion injury by liposomal superoxide dismutase in rats subjected to tourniquet shock. Int J Leg Med 105:5–9

Chandra P, Dave PK (1970) Effect of dipyrone on tourniquet shock. Arzneim Forsch (Drug Res) 20:409–412

Duncan GW, Blalock A (1942) The uniform production of experimental shock by crush injury: possible relationship to clinical crush syndrome. Ann Surg 115:684–694

Ghussen F, Stock W, Bongartz R (1979) The effect of methylprednisolone on the experimental tourniquet shock in dogs. Res Exp Med 176:87–95

Goto H, Benson KT, Katayama H, Tonooka M, Tilzer LL, Arakawa K (1988) Effect of high-dose of methylprednisolone on tourniquet ischaemia. Can J Anaesth 35:484–488

Haugan A, Kirkebo A (1984) Local blood flow changes in the renal cortex during tourniquet and burn shock in rats. Circ Shock 14:147–157

Horl M, Horl WH (1985) Effect of tournique ischemia on carbohydrate metabolism in dog skeletal muscle. Eur Surg Res 17:53–60

Kruskal JB, Wallis WA (1952) Use of ranks in one-criterion variance analysis. J Am Stat Assoc 47:583–621

Little RA (1974) The compensation of post-traumatic oedema in the rabbit at different ages. J Physiol 238:207–221

Paletta FX, Willman V, Ship AG (1960) Prolonged tourniquet ischemia of extremities. An experimental study on dogs. J Bone Joint Surg 42:945–950

Peto R, Pike MC, Armitage P, Breslow NE, Cox DR, Howard SV, Mantel N, McPherson K, Peto J, Smith PG (1976) Design and analysis of randomized clinical trials requiring prolonged observation of the patient. I. Introduction and design. II. Analysis and examples. Br J Cancer 585–612

Sáez JC, Vivaldi E, Günther B (1982) Tourniquet shock in rats: Appearance of lactic dehydrogenase isoenzymes in serum. IRCS Med Sci 10:191–192

Sáez JC, Cifuentes F, Ward PH, Günther B, Vivaldi E (1986) Tourniquet shock in rats: Effects of allopurinol on biochemical changes of the gastrocnemius muscle subjected to ischemia followed by reperfusion. Biochem Med Metabol Biol 35:199–209

Sen PK (1980) Nonparametric simultaneous inference for some MANOVA models. In: Krishnaiah PR (ed) Handbook of Statistics. Vol 1; North-Holland, Amsterdam, New York, pp 673–702

Van der Meer C, Valkenburg PW, Ariëns AT, van Benthem MJ (1966) Cause of death in tourniquet shock in rats. Am J Physiol 210:513–525

Vujnov St, Prostran M, Savic JD, Varagic VM, Lovric M (1992) Beta-adrenergic receptors and catecholamines in the rat heart during tourniquet trauma. Circulat Shock 36:38–44

Wilgis EFS (1971) Observations on the effects of tourniquet ischemia. J Bone Joint Surg 53 A:1343–1346

A.1.3.23 Heat Stroke

PURPOSE AND RATIONALE

Heat stroke is a medical emergency where quick diagnosis and treatment of victims are essential for positive prognosis. Several animal models have been established by investigators in heat related studies. Rats (Francesconi and Mager 1978; Hubbard et al. 1977, 1979; Kielblock et al. 1982), rabbits (Shih et al. 1984), dogs (Bynum et al. 1977) and sheep (Tayeb and Marzouki 1990) are considered to be the most suitable models because of their similarity to man in response to high temperature.

PROCEDURE

Male Sprague Dawley rats weighing 450 to 550 g are fasted 18–24 h before the experiment. For prevention studies the animals are treated subcutaneously 1 h before either being restrained in an appropriate wire cage which is placed into an environmental chamber set at 41.5°C ambient temperature or being exercised in a motor-driven treadmill. Core temperature (rectal probe inserted 6.5 cm) are measured using copper/constantan thermocouples in conjunction with a thermocouple reference oven and a 10-channel data acquisition system with a teletype printout. After

reaching exhaustion or a predetermined core temperature, all rats are monitored at 26°C ambient temperature while resting in plastic cages lined with wood shavings. After recovery, animals are returned to their cages and allowed water but no food for 24 h.

EVALUATION

LD_{50} values are determined in treated and control animals.

MODIFICATIONS OF THE METHOD

Kielblock et al. (1982) analyzed cardiovascular function by direct recording of arterial blood pressure and ECG-analysis.

Francesconi and Mager (1978) studied pathochemical indices, such as serum lactate concentration, potassium levels and plasma creatine phosphokinase.

Kregel et al. (1988) investigated peripheral vascular responses to hyperthermia in the rat by implantation of Doppler flow probes on the superior mesenteric, left iliac or left renal, and external caudal arteries. They concluded that a selective loss of compensatory vasoconstriction triggers the cascade of events that characterize heat stroke.

Shido and Nagasaka (1990) studied thermoregulatory responses to acute body heating in rats acclimated to continuous heat exposure. Indirect external warming was performed by raising the jacket water temperature surrounding the calorimeter from 24 to 39°C. Intraperitoneal heating was made through an electric heater implanted chronically in the peritoneal cavity.

Chiu et al. (1995) reported an increased survival in rat heatstroke by reducing hypothalamic serotonin release after administration of interleukin-1 receptor antagonist.

REFERENCES AND FURTHER READING

Bynum G, Patton J, Bowers W, Leav I, Wolfe D, Hamlet M, Marsili M (1977) An anesthetized dog heat stroke model.J Appl Physiol: Resp Environ Exercise Physiol 43:292–296

Chiu WT, Kao TY, Lin MT (1995) Interleukin-1 receptor antagonist increases survival in rat heatstroke by reducing hypothalamic serotonin release. Neurosci Lett 202:33–36

Damanhouri ZA, Tayeb OS (1992) Animal models for heat stroke studies. J Pharmacol Toxicol Meth 28:119–127

Francesconi RP, Mager M (1978) Heat-injured rats: pathochemical indices and survival time. J Appl Physiol: Resp Environ Exercise Physiol 45:1–6

Hubbard RW, Bowers WD, Matthew WT, Curtis FC, Criss REL, Sheldon GM, Ratteree JW (1977) Rat model of acute heatstroke mortality. J Appl Physiol: Resp Environ Exercise Physiol 42:809–816

Hubbard RW, Criss REL, Elliott LP, Kelly C, Matthew WT, Bowers WD, Mager M (1979) Diagnostic significance of selected serum enzymes in a rat heatstroke model. J Appl Physiol: Respirat Environ Exercise Physiol 46:334–339

Kielblock AJ, Strydom NB, Burger FJ, Pretorius PJ, Manjoo M (1982) Cardiovascular origins of heatstroke pathophysiology: an anesthetized rat model. Aviat Space Environ Med 53:171–178

Kregel KC, Wall PT, Gisolfi CV (1988) Peripheral vascular responses to hyperthermia in the rat. J Appl Physiol 64:2582–2588

Shido O, Nagasaka T (1990) Thermoregulatory responses to acute body heating in rats acclimated to continuous heat exposure. J Appl Physiol 68:59–65

Shih CJ, Lin MS, Tsai SH (1984) Experimental study on the pathogenesis of heat stroke. J Neurosurg 60:1252–1264

Tayeb OS, Marzouki ZM (1990) Effect of dantrolone pretreatment on heat stroke in sheep. Pharmacol Res 22:565–572

A.1.3.24
α- and β-Adrenoreceptors in the Mouse Iris

PURPOSE AND RATIONALE

A simple method to test mydriatic substances is the test on the mouse pupil as described by Pulewka (1932). The diameter of the pupil is narrowed by intensive light illumination. A dose-dependent increase of pupil diameter can be achieved by intraperitoneal application of atropine and synthetic mydriatics (Ing et al. 1950; Burn et al. 1950). The mydriatic effect of hexamethonium analogues has been measured by Blackman et al. (1956). Mydriasis is induced by norepinephrine, epinephrine and isoproterenol and can be antagonized by α- or β-blockers (Freundt 1965).

PROCEDURE

Male mice weighing 15–20 g are used. They are kept for at least 30 min in separate beakers under bright illumination before the pupil diameters are measured with a dissecting microscope containing an arbitrary scale in the eyepiece. To make the illumination as uniform as possible, the beakers containing the mice are placed beneath long low-power fluorescent tubes and on top of glossy white paper. The pupil diameter is measured in mm before and at various time intervals after treatment. Groups of 5–10 mice are used for each dose of compound and for vehicle control.

To test sympatholytic activity, various doses of the α- or β-blocker are injected subcutaneously 30 min prior to intravenous injection of 0.1 mg/kg norepinephrine, or 0.05 mg/kg epinephrine, or 20 mg/kg isoproterenol. The effect of norepinephrine is blocked by α-blockers, but not by β-blockers, the effect of epinephrine by both α- and β-blockers, and the effect of isoproterenol by β-blockers, but not by α-blockers.

EVALUATION

The mean values of diameters in the groups treated with α- or β-blockers are compared with those of an-

imals treated with norepinephrine, epinephrine or isoproterenol only.

MODIFICATIONS OF THE METHOD

Edge (1953) used mydriasis in the mouse as a quantitative method of estimating parasympathetic ganglion block.

Håkanson et al. (1987) used the isolated iris sphincter of pigmented rabbits to test multiple tachykinin pools in sensory nerve fibres. The eyes were taken out within 1 min after sacrifice and opened by an incision 2–3 mm posterior to the limbus, followed by excision of the iris from the ciliary margin. The iris sphincter muscle was then opened, cut in half and mounted vertically on a Perspex holder in a 7 ml tissue bath maintained at 35°C. The mechanical activity after electrical stimulation was recorded isometrically using a force displacement transducer and a polygraph.

Kern (1970) used isolated sphincter and dilator muscles from human eyes obtained at autopsy for studies on sympathomimetics and adrenergic blocking agents. Cholinotropic and α- and β-adrenergic receptors were identified.

Responses to bradykinin and or capsaicin of the isolated iris sphincter were considered to be mediated by substance P released from the trigeminal nerve (Ueda et al. 1984).

Pupillary dilatation can be used as an index for central nervous system α_2-adrenoreceptor activation (Koss 1986).

Clonidine induces mydriasis which is mediated by α_2-adrenoreceptors located in the brain (Berridge et al. 1983; Hey et al. 1985). Blockade of presynaptically located α_2-adrenoreceptors is considered as a possible mechanism for antidepressant drugs. Mianserin was able to antagonize clonidine-induced mydriasis in the rat.

Gower at al (1988) studied a large number of psychotropic drugs in this model with the aim to reveal *in vivo* α_2-adrenoreceptor blocking effects of new compounds.

Male Wistar rats weighing 230–300 g were anesthetized with pentobarbital, 60 mg/kg i.p., and a polyethylene catheter was inserted into the femoral vein for drug administration. The rat's head rested on the base platform of a binocular Olympus microscope positioned so that the pupil diameter of the right eye could be measured by means of a micrometer inserted into one eyepiece of the microscope. A constant light intensity was maintained throughout the experiment. Rats were first injected with saline 25 min after anesthesia induction. The pupil diameter was measured 1 min after injection. Five min after measurement, mydriasis was induced by clonidine (0.1 mg/kg, i.v.) and the diameter was measured 1 min after injection. This was followed by the test compound, injected at 6 min intervals at increasing doses. The pupil was measured at 1 min after each injection. The dose inhibiting 50% of the clonidine-induced mydriasis (ID_{50}) was determined per rat from the cumulative dose-response curve.

Savontaus et al. (1997) studied the effect of an imidazoline derivative against detomidine-induced mydriasis in anesthetized rats.

REFERENCES AND FURTHER READING

Berridge TL, Sadie B, Roach AG, Tulloch IF (1983) α_2-adrenoceptor agonists induce mydriasis in the rat by an action within the CNS. Br J Pharmacol 78:507–515

Blackman JG, Fastier FN, Patel CM, Wong LCK (1956) Assessment of depressor activity and mydriatic activity of hexamethonium analogues. Br J Pharmacol 11:282–288

Burn JH, Finney DJ, Goodwin LG (1950) Biological Standardization. Oxford University Press, London, pp 320–324

Bynke G, Håkanson R, Hörig J, Leander S (1983) Bradykinin contracts the pupillary sphincter and evokes ocular inflammation through release of neuronal substance P. Eur J Pharmacol 91:469–475

Edge ND (1953) Mydriasis in the mouse: a quantitative method of estimating parasympathetic ganglion block. Br J Pharmacol Chemother 8:10–14

Freundt KJ (1965) Adrenergic alpha- and beta-receptors in the mouse iris. Nature 206:725–726

Gower AJ, Broekkamp CLE, Rijk HW, van Delft AME (1988) Pharmacological evaluation of *in vivo* tests for α_2-adrenoceptor blockade in the central nervous system and the effects of mianserin and its aza-analog ORG 3770. Arch Int Pharmacodyn 291:185–201

Håkanson R, Beding B, Erkman R, Heilig M, Wahlestedt C, Sundler F (1987) Multiple tachykinin pools in sensory nerve fibres in the rabbit iris. Neurosci 21:943–950

Hey JA, Gherezghiher T, Koss MC (1985) Studies on the mechanism of clonidine-induced mydriasis in the rat. Naunyn-Schmiedeberg's Arch Pharmacol328:258–263

Ing HR, Dawes GS, Wajda I (1945) Synthetic substitutes for atropine. J Pharm Exp Ther 85:85–105

Kern R (1970) Die adrenergischen Receptoren der intraoculären Muskeln des Menschen. Graefes Arch klin exp Ophthal 180:231–248

Koss MC (1986) Pupil dilatation as an index of central nervous system α_2-adrenoceptor activation. J Pharmacol Meth 15:1–19

Pulewka P (1932) Das Auge der weißen Maus als pharmakologisches Testobjekt. I. Mitteilung: Eine Methode zur quantitativen Bestimmung kleinster Mengen Atropin und anderer Mydriatika. Naunyn Schmiedeberg's Arch exp Path Pharmak 168:307–315

Savontaus E, Raasmaja A, Rouru J, Koulu M, Pesonen U, Virtanen R, Savola JM, Huupponen R (1997) Anti-obesity effect of MPV-1743 A III, a novel imidazoline derivative, in genetic obesity. Eur J Pharmacol 328:207–215

Ueda N, Muramatsu I, Fujiwara M (1984) Capsaicin and bradykinin-induced substance P-ergic Koss MC (1986) Pupillary dilatation as an index for central nervous system α_2-adrenoreceptor activation. J Pharmacol Meth 15:1–19

A.1.3.25
α_2-Adrenoreceptor Blockade Measured in Vivo by Clonidine-Induced Sleep in Chicks

PURPOSE AND RATIONALE

In young chicks, clonidine causes a loss of righting reflex which is antagonized by mianserin (Pommier et al. 1982). This phenomenon was used to measure α_2-adrenoceptor blockade *in vivo* by Gower et al. (1988).

PROCEDURE

Male white Leghorn chicks are used either a few hours after hatching or 1 or 2 days later. Clonidine-induced loss of righting reflex (sleep) is determined with 8 animals at a time. Two animals are treated with placebo and 2 with each of 3 dose levels of the test compound. Tests with groups of 8 animals are continued until 10 animals are tested per dose level or placebo treatment. The chicks are marked with ink and injected intraperitoneally with placebo or the test compound. Ten min later, 1.2 mg/kg clonidine is injected into a leg muscle and the animals are placed individually in small Macrolon cages. The beginning of sleep time is defined as the moment at which the animals can be placed on their back and remain in this position. Sleep time is recorded until they return to their feet spontaneously or another attempt to put them on their back fails. Sleep time is recorded for a maximum period of 30 min.

EVALUATION

Statistical evaluations of differences in median sleeping times are done with the Mann-Whitney *U*-test. Dose-response relations for various drugs can be calculated.

CRITICAL ASSESSMENT OF THE METHOD

Compounds with known α_2-adrenoceptor blocking activity antagonize clonidine-induced sleep in chicks dose-dependently. Yohimbine is one of the most active compounds. However, also other centrally active compounds of which their main effect is not α_2-blockade, reduce clonidine-induced sleeping time. One of the most potent is apomorphine acting on dopamine D_2-receptors. Therefore, the clonidine-induced sleeping test in chicks can not be regarded as highly specific for α_2-adrenoceptors.

REFERENCES AND FURTHER READING

Gower AJ, Broekkamp CLE, Rijk HW, van Delft AME (1988) Pharmacological evaluation of *in vivo* tests for α_2-adrenoceptor blockade in the central nervous system and the effects of mianserin and its aza-analog ORG 3770. Arch Int Pharmacodyn 291:185–201

Pommier Y, Andréjak M, Mouillé P, Dabiré H, Lucet B, Schmitt H (1982) Interaction between mianserin and clonidine at α_2-adrenoceptors. Naunyn-Schmiedeberg's Arch Pharmacol 318:288–294

A.1.3.26
Activity at β_1- and β_2-Adrenoreceptors in the Rat

PURPOSE AND RATIONALE

The relative potency of catecholamines as stimulants of β-adrenoreceptor mediated responses vary in different tissues indicating the existence of two subtypes of β-receptors (β_1 and β_2) (Lands et al. 1967). β-adrenoreceptors in the heart have been classified as being of the β_1-subtype. β-adrenoreceptors in the uterus, diaphragm, bronchioles and small intestine have been classified as being of the β_2-subtype, since in these tissues, epinephrine is more potent than norepinephrine. These observations led to the development of selective agonists and antagonists. Isolated organs (see below) having predominantly one receptor subtype, such as the isolated heart and the isolated atrium for β_1, and the isolated uterus or the isolated tracheal chain for β_2, are used to test compounds for selective activity. Assessing both activities in the same animal *in vivo* results in the advantage that pharmacokinetic and metabolic influences of the drug being tested are the same for both parameters.

PROCEDURE

Female Sprague-Dawley rats (200–220 g) are anesthetized with 60 mg/kg pentobarbital i.p. prior to pithing (Gillespie and Muir 1967). The animals are artificially respired with room air using a Harvard small animal ventilator (90 strokes/min at a pressure of 7 cm H_2O). Body temperature is maintained by placing the animals on a heated operating table. The left carotid artery is cannulated for continuous monitoring of blood pressure via a Statham p23Id pressure transducer. The blood pressure signal is used to trigger an instantaneous rate meter for continuous monitoring of heart rate. A femoral vein is cannulated for intravenous administration of drugs.

A midline incision is made to expose one horn of the uterus. The ovarian artery is cut, tied and one horn dissected free from the ovary leaving the myometrial blood supply intact. A cotton thread is attached to the free end of the uterine horn, passed through a glass-jacketed organ bath and connected to an isometric (Pioden UF1) transducer for measurement of spontaneous contractions. A cannula is inserted into the peritoneal

cavity for administration of drugs by the i.p. route. The organ bath is positioned such that it surrounds the uterine horn without touching it. The tissue is perifused with Krebs-Henseleit solution being gassed with 95% O_2/5% CO_2 and maintained at 37°C. A resting tension of 0.2 g is applied to the tissue, which is allowed to stabilize until spontaneous contractions are constant over a period of 5–10 min. All recordings are made on a polygraph.

EVALUATION OF AGONISTS

Dose-response curves after i.v. injection are established for isoprenaline (nonselective between β_1- and β_2-adrenoreceptors), salbutamol (selective for β_2-adrenoreceptors), and noradrenaline (selective for β_1-adrenoreceptors) in increasing heart rate (beats/min) and decreasing the height of uterine contraction (calculated as percentage of the original amplitude). Animals given noradrenaline are pretreated with phenoxybenzamine (3.3 mmol/kg i.v.) in order to antagonize irreversibly the α-adrenoreceptors. Agonist dose-response curves ($n > 4$) on heart rate and uterine relaxation are carried out by assessing the activity of at least 3 doses of each agonist. New synthetic compounds can be tested after intraperitoneal administration additionally.

EVALUATION OF ANTAGONISTS

The ability of a non-selective β-blocker, such as propranolol (1 mmol/kg i.v.), a β_1-selective β-blocker, such as atenolol, and a β_2-selective β-blocker to inhibit responses to isoprenaline on both heart rate and uterine relaxation is assessed by comparing the log linear portion of the dose-response curve to isoprenaline in the absence and in the presence of the β-adrenoreceptor antagonist in the same animal. Dose ratios for each antagonist are calculated.

CRITICAL ASSESSMENT OF THE METHOD

The method described by Piercy (1988) has the advantage to measure both agonistic and antagonistic activity and to differentiate between effects on β_1- and β_2-adrenoreceptors. Compared to tests in isolated organs, *in vivo* activity can be determined after intraperitoneal or intraduodenal administration.

MODIFICATIONS OF THE METHOD

Härtfelder et al. (1958) studied the influence of various agents on the contractions of electrically stimulated **isolated uteri of rabbits and guinea pigs**.

Nathason (1985) evaluated the activity of beta-blockers to inhibit the cardio-acceleratory effect of systemically administered isoproterenol in **unanesthetized, restrained albino rabbits** together with the effect on membrane bound adenylate cyclase in homogenized ciliary process villi in order to find compounds selectively lowering intraocular pressure.

REFERENCES AND FURTHER READING

Gillespie JS, Muir TC (1967) A method of stimulating the complete sympathetic outflow from the spinal cord to blood vessels in the pithed rat. Br J Pharmacol Chemother 30:78–87

Härtfelder G, Kuschinsky G, Mosler KH (1958) Über pharmakologische Wirkungen an elektrisch gereizten glatten Muskeln. Naunyn-Schmiedeberg's Arch exp Path Pharmak 234:66–78

Lands AM, Arnold A, McAuliff JP, Ludena FP, Brown TG (1967a) Differentiation of receptor systems activated by sympathetic amines. Nature 214:597–598

Lands AM, Ludena FP, Buzzo HD (1967b) Differentiation of receptors responsive to isoproterenol. Life Sci 6:2241–2249

Lish PM, Weikel JH, Dungan KW (1965) Pharmacological and toxicological properties of two new β-adrenergic receptor antagonists. J Pharmacol Exp Ther 149:161–173

Nathason JA (1985) Differential inhibition of beta adrenergic receptors in human and rabbit ciliary process and heart. J Pharmacol Exper Ther 232:119–126

Piercy V (1988a) Method for assessing the activity of drugs at β_1- and β_2-adrenoreceptors in the same animal. J Pharmacol Meth 20:125–133

Piercy V (1988b) The β-adrenoreceptors mediating uterine relaxation throughout the oestrus cycle of the rat are predominantly of the β_2-subtype. J Autonom Pharmacol 8:11–18

A.1.3.27
β_1- and β_2-Sympatholytic Activity in Dogs

PURPOSE AND RATIONALE

Intravenous administration of isoprenaline (isoproterenol) stimulates β_1-receptors of the heart which can be detected as an increase in contractility (dp/dt max). Intraarterial injection of isoprenaline stimulates β_2-receptors of peripheral blood vessels leading to an increased peripheral blood flow. Therefore, a β_1- or β_2-blocking activity of a compound is revealed by the inhibition of the effects of isoprenaline. The following tests are used to evaluate β-blocking activity of drugs. A β-blocker screening is done in anesthetized dogs (a); in addition, the test allows a differentiation between β_1- and β_2-receptor activity and the determination of ED_{50} values (b).

PROCEDURE

Male or female Beagle dogs weighing about 20 kg are used. Animals are premedicated with 1 g Inactin(i.v.) and anesthetized by intravenous administration of 20 mg/kg chloralose and 250 mg/kg urethane. In addition, they receive a subcutaneous injection of 2 mg/kg morphine 1 h after the start of anesthesia. Animals are

heparinized. Respiration is maintained through a tracheal tube using a positive pressure respirator. End-expiratory CO_2 content is measured continuously; respiratory rate and depth of respiration are adjusted to 4.5–6 vol% end-expiratory CO_2. For administration of isoprenaline, a peripheral vein is cannulated.

Preparation for Hemodynamic Measurements

For recording of peripheral systolic and diastolic blood pressure, a cannula inserted into a femoral artery is connected to a pressure transducer (Statham p 23 DB). For determination of LVP, a Millar microtip catheter (PC 350) is inserted via the left arteria carotis communis. LVEDP is measured from a high-sensitivity scale. From the pressure curve, d*p*/d*t* max is differentiated and heart rate is counted. Peripheral blood flow in the femoral artery is measured with an electromagnetic flow probe.

Screening for β-Blocking Effects in Anesthetized Dogs

Following a steady-state period of 30–60 min, isoprenaline is administered intravenously 2–3 times to the anesthetized animal and hemodynamic parameters are recorded (control values = 100%). Then, the test substance is injected intravenously at cumulative doses (final concentrations of 0.01, 0.05 and 0.15 mg/kg). For each dose, 10 min "drug effects" are monitored by measuring hemodynamic parameters. Then the effect of isoprenaline is tested again (3 times).

In other experiments, a single dose of the drug is administered to determine the duration of action.

If a test compound does not show an inhibitory influence on isoprenaline effects, a second test compound is administered.

All hemodynamic parameters are registered continuously during the whole experiment.

Testing for β_1- and β_2-Blocking Effects; Determination of ED_{50}

Following a steady-state period of 30–60 min, isoprenaline is administered for i.v. administration (β_1-test) twice at a dose of 0.5 µg/kg and for intraarterial administration (β_2-test) twice at a dose of 0.05 µg/kg. Hemodynamic parameters are recorded (control values = 100%). Then, the test substance is injected intravenously at cumulative doses. Consecutively increasing doses are given at 15-min intervals. For each dose, 10 min "drug effects" are monitored by measuring hemodynamic parameters. Thereafter isoprenaline is given intravenously and 5 min later intra-arterially.

All hemodynamic parameters are registered continuously during the whole experiment.

Characteristics:

- blood pressure
  - systolic, BPs
  - diastolic, BPd
- heart rate
- left ventricular pressure, LVP
- left ventricular enddiastolic pressure, LVEDP
- d*p*/d*t* max
- peripheral flow, A. femoralis
- ECG, lead II

Standard compounds:

- propranolol HCl
- practolol
- metoprolol tartrate

EVALUATION

β_1-receptor antagonism is measured as a decrease in contractility (d*p*/d*t* max).

Inhibition of the isoprenaline-induced elevation of heart rate is considered as an indicator for non-selective β-blockade. For cardioselective β-receptor blockers the increase in d*p*/d*t* max is inhibited with lower doses of test drug than the rise in heart rate.

β_2-receptor blockade by a test drug is measured as inhibition of the isoprenaline-induced increase in peripheral blood flow.

The different hemodynamic parameters are determined.

Percent inhibition of the isoprenaline-induced effects by a test compound is calculated and compared to the isoprenaline effects before drug administration (= 100%).

ED_{50} values for β_1- and β_2-antagonism are calculated by log-probit analyses. ED_{50} is defined as the dose of drug leading to a 50% inhibition of the isoprenaline effects.

An ED_{50} β_1/ED_{50} β_2-ratio of < 1 indicates that a β-blocking agent predominantly influences β_1-receptors (cardioselectivity).

REFERENCES AND FURTHER READING

Turner RA (1971) β-adrenergic blocking agents. In: Turner RA, Hebborn P (eds) Screening methods in pharmacology. Vol II. pp 21–40. Academic Press, New York and London

A.1.3.28 Intrinsic β-Sympathomimetic Activity in Reserpine-Pretreated Dogs

PURPOSE AND RATIONALE

β-blocking agents can be classified as

- β-blocking agents with intrinsic sympathomimetic activity (ISA),
- β-blocking agents with membrane stabilizing activity (MSA),
- β-blocking agents with organ selectivity (high affinity to heart β_1-receptors).

In the following procedure with reserpine-pretreated dogs, β-blocking agents with intrinsic sympathomimetic activity can be identified. Reserpine administration 24 h before the start of the experiment leads to a depletion of catecholamine depots. Thus, it is possible to differentiate between indirectly acting sympathomimetics such as tyramine and directly acting ones such as noradrenaline.

This test is used to identify β-blocking drugs with intrinsic sympathomimetic activity.

PROCEDURE

Male or female Beagle dogs weighing about 15 kg are used. Twenty-four h before the test, dogs receive an intramuscular injection of 0.3 mg/kg reserpine. At the day of the experiment, the animals are anesthetized by intravenous administration of 10–20 mg/kg pentobarbital sodium. Respiration through a tracheal tube using a positive pressure respirator is controlled by measuring end-expiratory CO_2 concentrations (4–5 vol%).

Preparation for Hemodynamic Measurements

For recording of peripheral systolic and diastolic blood pressure, a femoral artery is cannulated and connected to a pressure transducer (Statham p 23 DB). For determination of LVP, a Millar microtip catheter (PC 350) is inserted into the left ventricle via the left common carotid artery. LVEDP is measured from a high-sensitivity scale. From the pressure curve, dp/dt max is differentiated and heart rate is counted.

Experimental Course

The test substance is administered by continuous intravenous infusion of 0.02 mg/kg (1 ml/min) until a cumulative dose of 3 mg/kg is achieved (within approximately 150 min). Thereafter, the velocity of infusion is doubled (0.04 mg/kg, 2 ml/min). The test is finished when a cumulative dose of 7 mg/kg is achieved (after a total time of approximately 250 min).

Hemodynamic parameters are registered continuously during the entire experiment.

Characteristics:

- blood pressure
  - systolic blood pressure
  - diastolic blood pressure
- left ventricular pressure, LVP
- left ventricular enddiastolic pressure, LVED
- dp/dt max
- heart rate, HR

EVALUATION

The different hemodynamic parameters are determined. As a measure for intrinsic sympathomimetic activity (ISA), the increase in dp/dt max and in heart rate are evaluated. Absolute and relative differences of these parameters in drug-treated animals are compared to vehicle control values.

Statistical evaluations are performed by means of the Student's t-test if $n > 4$.

Scores are allotted relative to the efficacy of standard compounds for intensity as well as for duration of the effect.

REFERENCES AND FURTHER READING

DiPalma (1964) Animal techniques for evaluating sympathomimetic and parasympathomimetic drugs. In: Nodine JH, Siegler PE (eds) Animal and pharmacologic techniques in drug evaluation. Vol I, pp 105–110. Year Book Medical Publ., Inc. Chicago

Green AF, Boura ALA (1964) Depressants of peripheral sympathetic nerve function. In: Laurence DR, Bacharach AL (eds) Evaluation of Drug Activities: Pharmacometrics. Academic Press, London and New York, 369–430

A.1.3.29 Cat Nictitating Membrane Preparation (Ganglion Blocking Activity)

PURPOSE AND RATIONALE

Nicotinic acetylcholine receptors are involved in the ganglionic neurotransmission. Various subtypes are described for nicotinic acetylcholine receptors (Sargent 1993; McGehee and Role 1995; Karlin and Akabas 1995; Alexander et al. 2001).

The nictitating membrane of the cat has been used extensively in pharmacological studies to evaluate ganglion blocking activity because of the ease with which its movements can be recorded, because of the simplicity of its innervation (the purely adrenergic fibres have their cell bodies in the easily accessible superior cervical ganglion of the same site) and because its blood supply (via the external carotid artery) is accessible for intraarterial injections. Preganglionic and postganglionic stimulation allow the interpretation of the mode of action of vasoactive drugs.

PROCEDURE

The animal is anesthetized with 35 mg/kg pentobarbitalsodium i.p. Tracheostomy is performed and a tra-

cheal cannula is inserted. On one side, the sympathetic nerve is exposed, separated from the vagus nerve and prepared in order to place electrodes for preganglionic and postganglionic stimulation. Preferably, the vagus nerve at this site is severed at the central end. The head of the animal is fixed in a head holder to prevent head movements. A linear transducer is fixed at the mid of the border of the nictitating membrane allowing the registration of the contractions on a polygraph. Preganglionic and postganglionic stimuli are exerted by a square wave stimulator, with a pulse width of 0.3 to 0.5 ms, an amplitude of 1–3 V, and a frequency of 20/min. The amplitude and pulse width varies from animal to animal. The sympathetic nerve is stimulated before and after the administration of the compound and the changes in the contraction of the nictitating membrane are noted. Furthermore, the response of the nictitating membrane to exogenous adrenaline is registered.

EVALUATION

The decrease of the response after drug application is expressed as percentage of the control before drug. Ganglionic blockers decrease the response to preganglionic stimulation but have no influence on postganglionic stimulation or exogenous adrenaline. Neuronal blockers decrease the response to both preganglionic and postganglionic stimulation but do not affect the response to exogenous adrenaline which may even be enhanced. α-receptor blockers decrease the response to both preganglionic and postganglionic stimulation as well as decrease the effect of exogenous adrenaline. Catecholamine uptake inhibitors increase the response to both preganglionic and postganglionic stimulation as well as enhance the response to exogenous adrenaline.

CRITICAL ASSESSMENT OF THE METHOD

The nictitating membrane preparation has been widely used for differentiation of cardiovascular effects. Since the use of higher animals such as cats has been limited to a great extent, this model is now being used only exceptionally.

As alternative, the contraction of the inferior eyelid of anesthetized **rats** after preganglionic electrical stimulation of the superior cervical ganglion has been recommended (Gertner 1956; Steinbrecher and Schmid-Wand 1986). In the modification used by Steinbrecher and Schmid-Wand (1986) the method is suitable for testing compounds with potential adrenergic and antiadrenergic activity but not for testing ganglion blocking activities.

Male Sprague Dawley rats are anesthetized with 100 mg/kg thiobutabarbital i.p. and kept on a heated operation table at a rectal temperature of 37°C. One femoral vein is cannulated and filled with 4% heparin solution. One femoral artery is cannulated for registration of blood pressure. Tracheotomy is performed and a polyethylene catheter of 5 cm length inserted. The head of the animal is fixed carefully. The vibrissae at the lower eyelid on the right side are cut, a thread attached at the margin of this eyelid and attached to a strain-gauge. To immobilize the musculature of the face, the mouth of the animal is sutured and the head support attached. The right sympathetic nerve is exposed, separated from the vagus nerve and prepared in order to place electrodes for preganglionic stimulation. For calibration, stimulation is performed twice with an interval until contraction is back to baseline. Furthermore, a dose of 0.001 mg/kg adrenaline is given as bolus injection. Eyelid contraction and blood pressure increase are recorded. Then the putative adrenergic blocker or the standard 1.0 mg/mg phentolamine are injected intravenously. Eyelid contraction after electrical stimulation or after adrenaline is reduced dose-dependently.

MODIFICATIONS OF THE METHOD

Quilliam and Shand (1964) assessed the selectivity of drugs by comparing the effects on ganglionic transmission and on the pre- and post-ganglionic nerves in the isolated superior cervical ganglion preparation of the rat.

Langer and Trendelenburg (1969) performed experiments with normal nictitating membranes of pithed cats as well as with isolated normal nictitating membranes.

Koss and Hey (1992) used frequency-dependent nictitating membrane responses by sympathetic nerve stimulation in anesthetized cats to determine the potential role of prejunctional histamine H_3 receptors.

Gurtu et al. (1992) used contractions of the cat nictitating membrane to explore the effects of calcium channel blockers on neurotransmission *in vivo*, by comparing the effects of verapamil and nifedipine on contractions of nictitating membrane following either electrical stimulation of the superior cervical ganglion or intravenous injection of phenylephrine.

Koss (1992) compared the peripheral and central nervous system sympatholytic actions of prazosin using the cat nictitating membrane. Submaximal contractions of the nictitating membranes were evoked by electrical stimulation of the preganglionic cervical

sympathetic nerve trunk and by stimulation of the posterior hypothalamus in anesthetized cats.

Badio et al. (1996) evaluated spiropyrrolizidines, a new structural class of blockers of nicotinic receptor channels with selectivity for ganglionic type receptors in rat pheochromocytoma PC12 cells (with an $\alpha_3\beta_{4(5)}$-nicotinic receptor) and human medulloblastoma TE671 cells (with an $\alpha_1\beta_1\gamma\delta$-nicotinic receptor).

REFERENCES AND FURTHER READING

Alexander S, Peters J, Mathie A, MacKenzie G, Smith A (2001) TiPS nomenclature Supplement 2001, pp 7–12

Badio B, Shi D, Shin Y, Hutchinson KD, Padgett WL, Daly JW (1996) Spiropyrrolizidines, a new class of blockers of nicotinic receptors. Biochem Pharmacol 52:933–939

Boura AL, Green AF (1959) The actions of brethylium: Adrenergic neuron blocking and other effects. Br J Pharmacol 14:536–548

Bowman WC, Webb SN (1972) Neuromuscular blocking and ganglion blocking activities of some acetylcholine antagonists in the cat. J Pharm Pharmacol 24:762–772

Claßen HG, Marquardt P, Späth M (1968) Sympathicomimetische Wirkungen von Cyclohexylamin. Arzneim Forsch/Drug Res 18:590–594

Fleckenstein A, Burn JH (1953) The effect of denervation on the action of sympathicomimetic amines on the nictitating membrane. Br J Pharmacol 8:69–78

Gertner SB (1956) Pharmacological studies on the inferior eyelid of the anaesthetized rat. Br J Pharmacol 11:147

Green AF, Boura ALA (1964) Depressants of peripheral sympathetic nerve function. I Sympathetic nerve blockade. In: Laurence DR, Bacharach AL (eds) Evaluation of drug activities: Pharmacometrics. Academic Press, London and New York, pp 370–430

Gurtu S, Seth S, Roychoudhary AK (1992) Evidence of verapamil-induced functional inhibition of noradrenergic neurotransmission *in vivo*. Naunyn-Schmiedeberg's Arch Pharmacol 345:172–175

Isola W, Bacq ZM (1946) Innervation symapthique adrénergique de la musculature lisse des paupières. Arch Internat Physiol 54:30–48

Karlin A, Akabas MH (1995) Toward a structural basis for the function of nicotinic acetylcholine receptors and their cousins. Neuron 15:1231–1244

Koss MC (1992) Comparison of peripheral and central nervous system sympatholytic actions of prazosin using the cat nictitating membrane. Eur J Pharmacol 211:61–67

Koss MC, Hey JA (1992) Activation of histamine H_3 receptors produces presynaptic inhibition of neurally evoked cat nictitating membrane responses *in vivo*. Naunyn-Schmiedeberg's Arch Pharmacol 346:208–212

Langer SZ, Trendelenburg U (1969) The effect of a saturable uptake mechanism on the slopes of dose-response curves for sympathomimetic amines and on the shifts of dose-response curves produced by a competitive antagonist. J Pharm Exp Ther 167:117–142

McGehee DS, Role LW (1995) Physiological diversity of nicotinic acetylcholine receptors expressed by vertebrate neurons. Annu Rev Physiol 57:521–546

Quilliam JP, Shand DG (1964) The selectivity of drugs blocking ganglionic transmission in the rat. Br J Pharmacol 23:273–284

Sargent PB (1995) The diversity of neuronal nicotinic acetylcholine receptors. Annu Rev Neurosci 16:403–443

Steinbrecher W, Schmid-Wand M (1986) Das elektrisch gereizte Unterlid der narkotisierten Ratte. Eine alternative Methode zur elektrisch gereizten Nickhaut der narkotisierten Katze. Personal Commun 2000

Trendelenburg U, Haeusler G (1975) Nerve-muscle preparations of the nictitating membrane. In: Daniel EE, Paton DM (eds) Methods in Pharmacology, Vol 3, Smooth muscle, Plenum Press New York and London pp 457–468

A.1.3.30 Assessment of Ganglion-Blocking Activity in the Isolated Bovine Retractor Penis Muscle

PURPOSE AND RATIONALE

The use of the bovine retractor penis muscle for the assessment of ganglion-blocking activity of neuromuscular blocking drugs has been recommended by Alaranta et al. (1990) and Klinge et al. (1993). Klinge and Sjöstrand (1974) performed not only extensive studies on the physiology and pharmacology of the retractor penis in the bull, but also discussed the various hypotheses on inhibitory and excitatory innervation of this muscle, which is present in many vertebrates such as horses, cats, dogs and rats, but not in men and rabbits. They also found that the effects on the isolated retractor penis muscle and on penile arteries are rather similar. The excitatory innervation was found to be predominantly α-adrenergic (Klinge et al. 1970; Klinge and Sjöstrand 1977) whereas other transmitters such as histamine and bradykinin were effective only in some species. Relaxation of the isolated retractor penis muscle could be elicited by nicotine and other nicotinic agonists (Klinge et al. 1988). In the studies on ganglion-blocking activity, strips of the retractor penis muscle are precontracted by 5-hydroxytryptamine. Relaxation induced by nicotine is antagonized by ganglion-blockers.

PROCEDURE

Retractor penis muscles are obtained from bulls of different breeds weighing 250–500 kg. Samples are dissected 10–30 cm distal to the points where the paired muscle bundles pass the anal orifice. Immediately after slaughter, the samples are freed from fat and other surrounding tissue and placed into Tyrode solution at 2–4°C. Strips, 15–25 mm in length and 2–3 mm wide, are prepared and mounted in 20-ml organ baths containing Tyrode solution at 35°C aerated with 95% O_2 and 5% CO_2. An equilibrium time of 2 to 4 h is allowed. During the equilibrium period washed are performed at about 60-min intervals. Changes in tension are recorded by means of Grass FT 03 force displacement transducers coupled to a polygraph.

A high-enough tone for studying the nicotine-induced relaxation, usually 8–15 g, is generated by adding 5-HP in a concentration between 0.1 and 6 µM to the organ bath. Washing is performed 2 min after application of nicotine; 60–80 min later the tone is again raised and the application of nicotine is repeated. The effect of a neuromuscular blocking drug is studied only if the relaxations caused by nicotine in two consecutive controls are equal in size.

EVALUATION

The blocking activity of a certain concentration of a drug is expressed as % reduction in the relaxation of the muscle strip, according to the following equation:

$$\frac{A - B}{A} \times 100$$

Where A is the size of the control relaxation in millimeters, and B is the size of the relaxation of the blocking drug. In order to construct regression lines, the activity of four or five dose levels from the assumed linear part of the concentration-effect curve is studied. The activity of each dose level is studied in at least 5 strips obtained from different animals. IC_{50} values are calculated from the regression lines. The parallelism of the regression lines is tested by covariance analysis.

CRITICAL ASSESSMENT OF THE METHOD

Molar potency ratios of known ganglion-blocking agents obtained with this method were compared with the results of other methods, such as inhibition of contraction of cat nictitating membrane evoked by preganglionic sympathetic stimulation (Bowman and Webb 1972; see 1.3.29), inhibition of nicotine-induced contraction of the isolated guinea pig ileum (Feldberg 1951), inhibition of contraction of guinea pig vas deferens evoked by preganglionic stimulation of the hypogastric nerve *in vitro* (Birmingham and Hussain 1980), depression of postganglionic action potentials evoked by preganglionic stimulation of the superior cervical ganglion of the rat *in vitro* (Quilliam and Shand 1964), induction of mydriasis in mouse by blocking the ciliary ganglion (Edge 1953). A fair but not a complete agreement between the results obtained with various methods was found.

MODIFICATIONS OF THE METHOD

Gillespie and Sheng (1990) studied the effects of pyrogallol and hydroquinone on the response to non-adrenergic, non-cholinergic nerve stimulation in the rat anococcygeus and the bovine retractor penis muscles.

Parkkisenniemi and Klinge (1996) used samples of retractor penis muscles and penile arteries from bulls for functional characterization of endothelin receptors.

La et al. (1997) studied the inhibition of nitrergic nerve-induced relaxations in rat anococcygeus and bovine retractor penis muscles by hydroxycobalamin.

REFERENCES AND FURTHER READING

Alaranta S, Klinge E, Pätsi T, Sjöstrand NO (1990) Inhibition of nicotine-induced relaxation of the bovine retractor penis muscle by compounds known to have ganglion-blocking activity. Br J Pharmacol 101:472–476

Birmingham AT, Hussain SZ (1980) A comparison of the skeletal neuromuscular and autonomic ganglion-blocking potencies of five non-depolarizing relaxants. Br J Pharmacol 70:501–506

Bowman WC, Webb SN (1972) Neuromuscular blocking and ganglion blocking activities of some acetylcholine antagonists in the cat. J Pharm Pharmacol 24:762–772

Edge ND (1953) Mydriasis in the mouse: a quantitative method of estimating parasympathetic ganglion block. Br J Pharmacol Chemother 8:10–14

Feldberg W (1951) Effects of ganglion-blocking substances on the small intestine. J Physiol (Lond) 113:483–505

Gillespie JS, Sheng H (1990) The effects of pyrogallol and hydroquinone on the response to NANC nerve stimulation in the rat anococcygeus and the bovine retractor penis muscles. Br J Pharmacol 99:194–196

Klinge E, Sjöstrand NO (1974) Contraction and relaxation of the retractor penis muscle and the penile artery in the bull. Acta Physiol Scand, Suppl 420:5–88

Klinge E, Sjöstrand NO (1977) Comparative study of some isolated mammalian smooth muscle effectors of penile erection. Acta Physiol Scand 100:354–365

Klinge E, Potho P, Solatunturi E (1970) Adrenergic innervation and structure of the bull retractor penis muscle. Acta Physiol Scand 78:110–116

Klinge E, Alaranta S, Sjöstrand NO (1988) Pharmacological analysis of nicotinic relaxation of bovine retractor penis muscle. J Pharmacol Exp Ther 245:280–286

Klinge E, Alaranta S, Parkkisenniemi UM, Kostiainen E, Sjöstrand NO (1993) The use of the bovine retractor penis muscle for the assessment of ganglion-blocking activity of neuromuscular blocking and other drugs. J Pharmacol Toxicol Meth 30:197–202

La M, Paisley K, Martin W, Rand MJ (1997) Effects of hydroxycobalamin on nitrergic transmission in rat anococcygeus and bovine retractor penis muscles: sensitivity to light. Eur J Pharmacol 321:R5–R6

Parkkisenniemi UM, Klinge E (1996) Functional characterization of endothelin receptors in the bovine retractor penis muscle and penile artery. Pharmacol Toxicol 79:73–79

Quilliam JP, Shand DG (1964) The selectivity of drugs blocking ganglion transmission in the rat. Br J Pharmacol 23:273–284

A.1.3.31 Angiotensin II Antagonism

PURPOSE AND RATIONALE

Angiotensin II antagonists can be tested in rats after elimination of cardiovascular reflexes by vagotomy and ganglionic blockade. Several angiotensin II

antagonists possess intrinsic agonistic activity. This can be tested by injection of various doses to the vagotomized, ganglion-blocked animal. The antagonistic activity of the angiotensin II antagonist can be evaluated by antagonism against graded doses of angiotensin II. The duration of activity can be tested during continuous infusion of angiotensin II.

PROCEDURE

Male Sprague-Dawley rats weighing about 300 g are used. They are anesthetized with 60 mg/kg pentobarbital sodium i.v. One carotid artery is cannulated and connected with a Statham transducer P 23 Db. Blood pressure is recorded on a polygraph. Both jugular veins are cannulated for application of test compounds and for infusion. Both vagal nerves are cut 3 mm dorsal of the larynx. For ganglionic blockade, 10 mg/kg pentolinium tartrate are injected intravenously. At least 5 animals are used for evaluation of one test drug.

Intrinsic Agonistic Activity

After the blood pressure has reached a constant value, doses of 1, 2, 4 and 16 µg/kg of the test compound are injected via the jugular vein. Blood pressure is recorded.

Antagonistic Activity

In 10 min intervals doses of 0.5; 1.0; and 2.0 µg/kg angiotensin II are injected to establish dose-response curves. After 10 min, continuous infusion is started of the potential angiotensin II blocker in a dosage of 10 µg/kg/0.1 ml/min. Ten min after beginning of the infusion, again doses of 0.5; 1.0; and 2.0 µg/kg angiotensin II are injected.

Duration of Activity

In this set-up, angiotensin II is administered as continuous infusion at a dosage of 1 µg/kg/0.02 ml/min. When blood pressure has reached an elevated steady state level, 0.1 mg/kg of the angiotensin II antagonist is administered.

Intensity and duration of the fall of blood pressure are recorded.

EVALUATION

Intrinsic Agonistic Activity

An increase of blood pressure indicates the intrinsic agonistic activity.

Antagonistic Activity

Increases of blood pressure after graduated doses of angiotensin II during the infusion is expressed as percentage of the increase before infusion. The results are compared with known angiotensin II antagonists.

CRITICAL ASSESSMENT OF THE METHOD

In this test not only potency and duration of activity but also the intrinsic agonistic activity of an angiotensin II antagonist can be tested.

MODIFICATIONS OF THE METHOD

Various other pharmacological models have been used to test angiotensin II antagonists:

Blood pressure in conscious unrestrained rats with chronically implanted catheters with normal blood pressure, spontaneous hypertension and chronic renal hypertension (Vogel et al. 1976; Chiu et al. 1989; Brooks et al. 1992; Aiyar et al. 1995; Deprez et al. 1995; Gabel et al. 1995; Hilditch et al. 1995; Keiser et al. 1995; Nagura et al. 1995; Nozawa et al. 1995; Renzetti et al. 1995; Wong 1995; Junggren et al. 1996),

Blood pressure in conscious spontaneously hypertensive and in anesthetized ganglion-blocked rats (Olins et al. 1993),

Blood pressure in pithed and in conscious renovascular hypertensive rats (Criscone et al. 1993; Wienen et al. 1993; Deprez et al. 1995; Kivlighn et al. 1995a; Kushida et al. 1995),

Blood pressure in rats after intracerebroventricularly injected angiotensin II (Vogel et al. 1976; Batt et al. 1988),

Blood pressure in conscious angiotensin I-infused and renin-dependent **hypertensive dogs** (Brooks et al. 1992; Cazaubon et al. 1993; Aiyar et al. 1995; Deprez et al. 1995; Gabel et al. 1995; Keiser et al. 1995; Wong et al. 1995),

Blood pressure and heart rate in conscious sodium-depleted and sodium-repleted **cynomolgus monkeys** (Lacour et al. 1993; Cazaubon et al. 1993; Keiser et al. 1995),

Angiotensin II induced pressor responses in **marmosets** (Nagura et al. 1995),

Blood pressure and heart rate in conscious **rhesus monkeys** and anesthetized **chimpanzees** (Gabel et al. 1995; Kivlighn et al. 1995b; Kivlighn et al. 1995c).

Inhibition of angiotensin II-induced contraction in isolated **aorta** rings or strips from **rabbits** (Chui et al. 1989, 1990; Criscione et al. 1993; Cazaubon et al. 1993; Olins et al. 1993; Wienen et al. 1993; Aiyar et al. 1995; Caussade et al. 1995; Hilditch et al. 1995; Keiser et al. 1995; Kushida et al. 1995; Nagura et al. 1995; Renzetti et al. 1995; Wong et al. 1995), from **rats** (Nozawa et al. 1997), from **neonatal rats** (Keiser et al. 1993), from **guinea pigs** (Mizuno et al. 1995),

Inhibition of angiotensin II-induced contraction in isolated rat pulmonary artery (Chang et al. 1995),

Antagonism against angiotensin II in isolated strips of rabbit aorta, rabbit jugular vein, rabbit pulmonary artery, rat portal vein, rat stomach, rat urinary bladder, human urinary bladder, human colon, human ileum (Rhaleb et al. 1991),

Contractions of **guinea pig ileum** *in situ* (Khairallah and Page 1961),

Antagonism against angiotensin II in the **isolated rat uterus** (Wahhab et al. 1993),

Contractile force and prostaglandin E synthesis in electrically stimulated **rabbit isolated vas deferens** (Trachte et al. 1990),

Antagonism against angiotensin II-induced aldosterone release in **bovine adrenal glomerulosa cells**. (Criscione et al. 1993), and in rat dispersed adrenal capsular cells (Chang et al. 1995),

Antagonism against angiotensin II-induced inhibition of guanylate cyclase activity in the **rat pheochromocytoma cell line** PC12W (Brechler et al. 1993).

Brooks et al. (1995) compared the cardiovascular and renal effects of an angiotensin II receptor antagonist and captopril in **rats with chronic renal failure** induced by 5/6 nephrectomy. Under sodium pentobarbital anesthesia the right kidney was removed and approximately two thirds of the left kidney was infarcted by ligating two or three branches of the left renal artery.

Kim et al. (1997) studied the effects of an angiotensin AT_1 receptor antagonist on volume overload-induced cardiac gene expression in rats. An abdominal aortacaval shunt was prepared in 9-weeks old male Wistar rats under sodium pentobarbital anesthesia. The vena cava and the abdominal aorta were exposed by opening the abdominal cavity via a midline incision. The aorta was punctured at the union of the segment two thirds caudal to the renal artery and one third cephalic to the aortic bifurcation with a 18-gauge disposable needle. The needle was advanced into the aorta, perforating its adjacent wall and penetrating the vena cava. After the aorta was clamped, the needle was withdrawn, and a drop of cyanoacrylate glue was used to seal the aortic puncture point. The patency of the shunt was verified visually by swelling of the vena cava and mixing of arterial and venous blood. The rats were treated either with vehicle or the angiotensin antagonist. Four days after the preparation of the AC shunt, 24 h-urine volume, electrolytes and aldosterone were measured. Six days after the AC shunt blood was collected by puncture of a tail vein and plasma renin activity and aldosterone were measured. Seven days after AC shunt, hemodynamic studies were performed in pentobarbital anesthesia. Afterwards, the heart was rapidly excised, left and right atria and ventricles were separated and frozen in liquid nitrogen for the extraction and measurement of cardiac tissue RNA.

Shibasaki et al. (1997) tested the effect on the renin-angiotensin-aldosterone system in **conscious rats** after cannulation of the abdominal aorta under anesthesia 3–4 days before the experiment. After oral dosing of the angiotensin II receptor antagonist blood samples were withdrawn and plasma renin and aldosterone determined by radioimmunoassay.

Similar to the effects of ACE inhibitors, lifespan of hypertensive rats could be doubled by long-term treatment with an angiotensin II type 1 receptor blocker (Linz et al. 2000).

Ledingham and Laverty (1996) treated **genetically hypertensive New Zealand rats** with a specific AT_1 receptor antagonist via osmotic minipumps for several weeks and measured the effects on blood pressure, cardiac hypertrophy and the structure of resistance arteries.

Transgenic animals were recommended for further studies to influence the human renin-angiotensin system (Müller et al. 1995; Wagner et al. 1995; Bohlender et al. 1996).

REFERENCES AND FURTHER READING

Aiyar N, Baker E, Vickery-Clark L, Ohlstein EH, Gellai M, Fredrickson TA, Brooks DP, Weinstock J, Weidley EF, Edwards RM (1995) Pharmacology of a potent long-acting imidazole-5-acrylic acid angiotensin AT_1 receptor antagonist. Eur J Pharmacol 283:63–72

Batt CM, Klein EW, Harding JW, Wright JW (1988) Pressor responses to amastatin, bestatin and Plummer's inhibitors are suppressed by pretreatment with the angiotensin receptor antagonist Sarthran. Brain Res Bull 21:731–735

Bohlender J, Ménard J, Wagner J, Luft FC, Ganten D (1996) Hypertension 27:535–540

Brechler V, Jones PW, Levens NR, de Gasparo M, Bottari SP (1993) Agonistic and antagonistic properties of angiotensin analogs at the AT_2 receptor in PC12W cells. Regul Pept 44:207–213

Brooks DP, Fredrickson TA, Weinstock J, Ruffolo RR Jr, Edwards RM, Gellai M (1992) Antihypertensive activity of the nonpeptide angiotensin II receptor antagonist, SK&F 108566, in rats and dogs. Naunyn Schmiedeberg's Arch Pharmacol 345:673–678

Brooks DP, Contino LC, Short BG, Gowan Ch, Trizna W, Edwards RM (1995) SB 203220: A novel angiotensin II receptor antagonist and renoprotective agent. J Pharmacol Exp Ther 274:1222–1227

Caussade F, Virone-Oddos A, Delchambre C, Cazes M, Versigny A, Cloarec A (1995) *In vitro* pharmacological characterization of UP 269–6, a novel nonpeptide angiotensin II receptor antagonist. Fundam Clin Pharmacol 9:119–128

Cazaubon C, Gougat J, Bousquet F, Guiraudou P, Gayraud R, Lacour C, Roccon A, Galindo G, Barthelmy G, Gautret B,

Bernhart C, Perreaut P, Breliere JC, le Fur G, Nisato D (1993) Pharmacological characterization of SR 47436, a new non-peptide AT_1 subtype angiotensin II receptor antagonist. J Pharmacol Exp Ther 265:826–834

Chang RSL, Lotti VJ, Chen TB, O'Malley SS, Bedensky RJ, Kling PJ, Kivlighn SD, Siegl PKS, Ondeyka D, Greenlee WJ, Mantlo NB (1995) *In vitro* pharmacology of an angiotensin AT_1 receptor antagonist with balanced affinity for AT_2 receptors. Eur J Pharmacol 294:429–437

Chiu AT, Duncia JV, McCall DE, Wong PC, Price WA, Thoolen MJMC, Carini DJ, Johnson AL, PBMWM Timmermans (1989) Nonapeptide angiotensin II receptor antagonists. III. Structure-function studies. J Pharmacol Exp Ther 250:867–874

Chui AT, McCall DE, Price WA, Wong PC, Carini DJ, Duncia JV, Wexler RR, Yoo SE, Johnson AL, PBMWM Timmermans (1990) Nonapeptide angiotensin II receptor antagonists: Cellular and biochemical pharmacology of DuP 753, an orally active antihypertensive agent. J Pharm Exp Ther 252:711–718

Criscione L, de Gasparo M, Bühlmayer P, Whitebread S, Ramjoué HPR, Wood J (1993) Pharmacological profile of valsartan: a potent, orally active, nonpeptide antagonist of angiotensin II AT_1-receptor subtype. Br J Pharmacol 110:761–771

Deprez P, Guillaume J, Becker R, Corbier A, Didierlaurent S, Fortin M, Frechet D, Hamon G, Heckmann B, Heitsch H, Kleemann HW, Vevert JP, Vincent JC, Wagner A, Zhang J (1995) Sulfonylureas and sulfonylcarbamates as new non-tetrazole angiotensin II receptor antagonists. Discovery of the highly potent orally active (imidazolylbiphenyl)sulfonylurea (HR 720). J Med Chem 38:2357–2377

Gabel RA, Kivlighn SD, Zingaro GJ, Schorn TW, Schaffer LW, Ashton WT, Chang LL, Flanagan K, Greenlee WJ, Siegl PKS (1995) *In vivo* pharmacology of L-159,913, a new highly potent and selective nonpeptide angiotensin II receptor antagonist. Clin Exp Hypertens 17:931–953

Hilditch A, Hunt AAE, Travers A, Polley J, Drew GM, Middlemiss D, Judd DB, Ross BC, Robertson MJ (1995) Pharmacological effects of GR138950, a novel angiotensin AT_1 receptor antagonist. J Pharm Exp Ther 272:750–757

Junggren IL, Zhao X, Sun X, Hedner Th (1996) Comparative cardiovascular effects of the angiotensin II type 1 receptor antagonists ZD 7155 and losartan in the rat. J Pharm Pharmacol 48:829–833

Keiser JA, Major TC, Lu GH, Davis LS, Panek RL (1993) Is there a functional cardiovascular role for the AT_2 receptors? Drug Dev Res 29:94–99

Keiser JA, Ryan MJ, Panek RL, Hedges JC, Sircar I (1995) Pharmacologic characterization of CI-996, a new angiotensin receptor antagonist. J Pharm Exp Ther 272:963–969

Khairallah PA, Page IH (1961) Mechanism of action of angiotensin and bradykinin on smooth muscle *in situ*. Am J Physiol 200:51–54

Kim S, Sada T, Mizuno M, Ikeda M, Yano M, Miura K, Yamanaka S, Koike H, Iwao H (1997) Effects of angiotensin AT_1 receptor antagonist on volume overload-induced cardiac gene expression in rats. Hypertens Res 20:133–142

Kivlighn SD, Huckle WR, Zingaro GJ, Rivero RA, Lotti VJ, Chang RSL, Schorn TW, Kevin N, Johnson RG Jr, Greenlee WJ, Siegl PKS (1995a) Discovery of L-162,313: a nonpeptide that mimics the biological actions of angiotensin II. Am J Physiol 268 (Regul Integr Comp Physiol 37): R820–R823

Kivlighn SD, Zingaro GJ, Gabel RA, Broten TB, Schorn TW, Schaffer LW, Naylor EM, Chakravarty PK, Patchett AA, Greenlee WJ, Siegl PKS (1995b) *In vivo* pharmacology of a novel AT_1 selective angiotensin II receptor antagonist, MK-996. Am J Hypertension 8:58–66

Kivlighn SD, Zingaro GJ, Gabel RA, Broten TB, Chang RSL, Ondeyka DL, Mantlo NB, Gibson RE, Greenlee WJ, Siegl PKS (1995c) *In vivo* pharmacology of an angiotensin AT_1 receptor antagonist with balanced affinity for angiotensin AT_2 receptors. Eur J Pharmacol 294:439–450

Kushida H, Nomura S, Morita O, Harasawa Y, Suzuki M, Nakano M, Ozawa K, Kunihara M (1995) Pharmacological characterization of the nonpeptide angiotensin II receptor antagonist, U-97018. J Pharmacol Exp Ther 274:1042–1053

Lacour C, Roccon A, Cazaubon C, Segondy D, Nisato D (1993) Pharmacological study of SR 47436, a non-peptide angiotensin II AT_1-receptor antagonist, in conscious monkeys. J Hypertens 11:1187–1194

Ledingham JM, Laverty R (1996) Remodelling of resistance arteries in genetically hypertensive rats by treatment with valsartan, an angiotensin II receptor antagonist. Clin Exper Pharmacol Physiol 23:576–578

Linz W, Heitsch H, Schölkens BA, Wiemer G (2000) Lonterm angiotensin II type 1 receptor blockade with fonsartan doubles lifespan of hypertensive rats. Hypertension 35:908–913

Mizuno M, Sada T, Ikeda M, Fukuda N, Miyamoto M, Yanagisawa H, Koike H (1995) Pharmacology of CS-866, a novel nonpeptide angiotensin II receptor antagonist. Eur J Pharmacol 285:181–188

Müller D, Hilgers K, Bohlender J, Lippoldt A, Wagner J, Fischli W, Ganten D, Mann JFE, Luft FC (1995) Effects of human renin in the vasculature of rats transgenic for human angiotensinogen. Hypertension 26:272–278

Nagura J, Yasuda S, Fujishima K, Yamamoto M, Chui C, Kawano KI, Katano K, Ogino H, Hachisu M, Konno F (1995) Pharmacological profile of ME3221, a novel angiotensin II receptor antagonist. Eur J Pharmacol 274:210–221

Nozawa Y, Haruno A, Oda N, Yamasaki Y, Matsuura N, Miyake H, Yamada S, Kimura R (1997) Pharmacological profile of TH-142177, a novel orally active AT_1-receptor antagonist. Fundam Clin Pharmacol 11:395–401

Olins GM, Corpus VM, Chen ST, McMahon EG, Paloma MA, McGraw DE, Smits GJ, Null CL, Brown MA, Bittner SE, Koepke JB, Blehm DJ, Schuh JR, Baierl CS, Schmidt RE, Cook CS, Reitz DB, Penick MA, Manning RE, Blaine EH (1993) Pharmacology of SC-52458, an orally active, nonpeptide angiotensin AT_1 receptor antagonist. J Cardiovasc Pharmacol 22:617–625

Renzetti AR, Cucchi P, Guelfi M, Cirillo R, Salimbeni A, Subissi A, Giachetti A (1995) Pharmacology of LR-B/057, a novel active AT_1 receptor antagonist. J Cardiovasc Pharmacol 25:354–360

Rhaleb NE, Rouissi N, Nantel F, D'Orléans-Juste P, Regoli D (1991) DuP 753 is a specific antagonist for the angiotensin receptor. Hypertens 17:480–484

Siegl PKS (1993) Discovery of losartan, the first specific nonpeptide angiotensin II receptor antagonist. J Hypertension 11 (Suppl 3):S19–S22

Shibasaki M, Fujimori A, Kusayama T, Tokioka T, Satoh Y, Okazaki T, Uchida W, Inagaki O, Yangisawa I (1997) Antihypertensive activity of a nonpeptide angiotensin II receptor antagonist, YM358, in rats and dogs. Eur J Pharmacol 335:175–184

Smits GJ, Koepke JP, Blaine EH (1991) Reversal of low dose angiotensin hypertension by angiotensin receptor antagonists. Hypertension 18:17–21

Trachte GJ, Ferrario CM, Khosla MC (1990) Selective blockade of angiotensin responses in the rabbit isolated vas deferens by angiotensin receptor antagonists. J Pharm Exp Ther 255:929–934

Vogel HG, Jung W, Schoelkens BA (1976) Hypotensive action of central injection of angiotensin II antagonist in conscious rats with experimental hypertension. Abstr. No. 286, p 117, V. Intern Congr Endocin, Hamburg

Wagner J, Thiele F, Ganten D (1996) The renin-angiotensin system in transgenic rats. Pediatr Nephrol 10:108–112

Wahhab A, Smith JR, Ganter RC, Moore DM, Hondrelis J, Matsoukas J, Moore GJ (1993) Imidazole based non-peptide angiotensin II receptor antagonists. Investigation of the effects of the orientation of the imidazole ring on biological activity. Arzneim Forsch/Drug Res 43:1157–1168

Wienen W, Hauel N, van Meel JCA, Narr B, Ries U, Entzeroth M (1993) Pharmacological characterization of the novel non-peptide angiotensin II receptor antagonist, BIBR 277. Br J Pharmacol 110:245–252

Wong PC, Price WA Jr, Chiu AT, Thoolen MJMC, Duncia JV, Johnson AL, Timmermans PBMWM (1989) Nonapeptide angiotensin II receptor antagonists. IV. EXP6155 and EXP6803. Hypertension 13:489–497

Wong PC, Hart SH, Zaspel AM, Chiu AT, Ardecky RJ, Smith RD, Timmermans PBMWM (1990) Functional studies on nonpeptide angiotensin II receptor subtype-specific ligands: DuP 753 (A ll-1) and PD 123177 (A ll-2) J Pharmac Exp Ther 255:584–592

Wong PC, Hart SD, Chiu AT, Herblin WF, Carini DJ, Smith RD, Wexler RR, Timmermans PBMWM (1991a) Pharmacology of DuP 5323, a selective and noncompetitive AT1 receptor antagonist. J Pharm Exp Ther 259:861–870

Wong PC, Price WA, Chiu AT, Duncia JV, Carini DJ, Wexler RR, Johnson AL, Timmermans PBMWM (1991b) *In vivo* pharmacology of DuP 753. Am J Hypertens 4:288S–298S

Wong PC, Quan ML, Saye JAM, Bernard R, Crain EJ Jr, NcCall DE, Watson CA, Zaspel AM, Smith RD, Wexler RR, Timmermans PBMWM, Chiu AT (1995) Pharmacology of XR510, a potent orally active nonpeptide angiotensin II AT_1 receptor antagonist with high affinity to the AT_2 receptor subtype. J Cardiovasc Pharmacol 26:354–362

A.1.3.32 ACE Inhibition Measured in Vivo in the Rat

PURPOSE AND RATIONALE

The angiotensin-converting enzyme (ACE) is responsible for the cleavage of the almost inactive angiotensin I to the active angiotensin II. The same enzyme (kininase II) is responsible for the degradation of the active peptide bradykinin to inactive products. ACE activity can therefore be measured in two ways: activity of the newly formed angiotensin II and diminution of the activity of bradykinin. ACE inhibition results in decreased activity of the precursor angiotensin I and potentiation of the bradykinin effect. The cardiovascular system is sensitive to both peptides, reacting with an increase of blood pressure to angiotensin II and with a decrease to bradykinin. These reactions can be used for quantitative determination of ACE inhibiting activity.

PROCEDURE

Male Sprague-Dawley rats weighing 300–400 g are used. The animals are anesthetized by i.p. injection of 70 mg/hg pentobarbital. After intubation of the trachea they are artificially respirated with 30 strokes/min and a stroke volume of 6–8 ml. The right carotid artery is cannulated and blood pressure registered with a Statham-element (P 23 Db) and a polygraph. One jugular vein is cannulated for i.v. injections. After laparotomy a catheter is inserted into the duodenum for enteral administration and the wound closed again. Blood pressure is stabilized 30% below the normal level by i.m. injection of 5 mg/kg pentolinium. In order to prevent excessive mucus production in the bronchial system, 40 µg/kg atropine sulfate are injected intramuscularly.

Inhibition of Angiotensin I Cleavage

After stabilization of blood pressure, 310 ng/kg angiotensin I is injected intravenously in 0.1 ml saline. The injection is repeated in 5-min intervals until an identical pressure reaction occurs. The test compounds are administered at doses of 1 and 10 mg/kg intravenously or 25 mg/kg intraduodenally. 3 min after iv. injection or 10 min after i.d. administration, again 310 ng/kg angiotensin I is injected. Standards are ramipril, enalapril or captopril.

Potentiation of Bradykinin-Induced Vasodepression

A low dose of bradykinin has to be chosen in order to visualize the bradykinin potentiation. One µg/kg, eventually 3 µg/kg bradykinin are injected intravenously at 5 min intervals until a stable reaction is achieved. Three min after i.v. injection or 10 min after intraduodenal administration of the test substance, the bradykinin injection is repeated.

EVALUATION

Inhibition of Angiotensin I Cleavage

The diminution of the pressure reaction to angiotensin I after administration of a potential ACE inhibitor is the parameter for the activity of the new compound. The inhibition is calculated as percent of controls. Using various doses of the ACE inhibitor, dose-response curves can be established and ID_{50} values be calculated.

Potentiation of Bradykinin-Induced Vasodepression

Potentiation of bradykinin induced vasodepression is expressed as percentage of controls. Using various doses of the test compound and the standard, dose-response curves can be established and potency ratios calculated.

CRITICAL ASSESSMENT OF THE METHOD

Both parameters, inhibition of angiotensin I response and potentiation of bradykinin-induced vasodepression have been proven as reliable parameters for evaluation of ACE inhibitors.

MODIFICATIONS OF THE METHOD

Natoff et al. (1981) used the ratio of responses to angiotensin I and angiotensin II in spontaneously hypertensive rats, either pithed or anesthetized with urethane, to determine the degree and the duration of effect of captopril.

Blood levels of angiotensin II can also be measured by radioimmunoassay.

Several studies in rats showed the beneficial effects of prolonged treatment with ACE inhibitors. Postoperative mortality in rats with left ventricular hypertrophy and myocardial infarction was decreased by ACE inhibition (Linz et al. 1996).

Inhibition of angiotensin I-induced pressure response by administration of ACE-inhibitors can be measured not only in anesthetized rats, but also in anesthetized dogs, conscious rats and conscious dogs (Becker et al. 1984).

Life-long ACE inhibition doubles lifespan of hypertensive rats not only if the treatment is started at the age of one month (Linz et al. 1997), but ramipril also increases survival in old spontaneously hypertensive rats if treatment is started at the age of 15 months (Linz et al. 1999).

Panzenbeck et al. (1995) reported that captopril-induced hypotension is inhibited by the bradykinin blocker HOE 140 in Na^+ depleted **marmosets.**

REFERENCES AND FURTHER READING

Becker RHA, Schölkens BA, Metzger M, Schulze KJ (1984) Pharmacological activities of the new orally active angiotensin converting enzyme inhibitor 2-[N-[(S)-1-ethoxycarbonyl-3-phenylpropyl-L-alanyl]-(1S,3S,5S)-2-azabicyclo[3.3.0]octane-3-carboxylic acid (Hoe 498). Arzneim Forsch/Drug Res 34:1411–1416

Linz W, Wiemer G, Schmidts HL, Ulmer W, Ruppert D, Schölkens BA (1996) ACE inhibition decreases postoperative mortality in rats with left ventricular hypertrophy and myocardial infarction. Clin Exper Hypertension 18:691–712

Linz W, Jessen T, Becker RHA, Schölkens BA, Wiemer G (1997) Long-term ACE inhibition doubles lifespan of hypertensive rats. Circulation 96:3164–3172

Linz W, Wohlfart P, Schoelkens BA, Becker RHA, Malinski T, Wiemer G (1999) Late treatment with ramipril increases survival in old spontaneously hypertensive rats. Hypertension 34:291–295

Natoff IL, Brewster M, Patel AT (1981) Method for measuring the duration of inhibition of angiotensin I-converting enzyme *in vivo*. J Pharmacol Meth 5:305–312

Panzenbeck M, Loughnan CL, Madwed JB, Winquist RJ, Fogal SE (1995) Captopril-induced hypotension is inhibited by the bradykinin blocker HOE 140 in Na^+ depleted marmosets. Am J Physiol 269(4 Pt 2): H1221–H1228

Pettinger W, Sheppard H, Palkoski Z, Renyi E (1973) Angiotensin antagonism and antihypertensive activity of phosphodiesterase inhibiting agents. Life Sci 12:49–62

Rubin B, Laffan RJ, Kotler DG, O'Keefe EH, Demaio DA, Goldberg ME (1978) SQ 14,225 (D-3-mercapto-2-methylpropanoyl-L-proline), a novel orally active inhibitor of angiotensin I-converting enzyme. J Pharmacol Exp Ther 204:271–280

A.1.3.33
Evaluation of Renin Inhibitors in Dogs

PURPOSE AND RATIONALE

Highly specific inhibitors of the enzyme renin are considered to be potential antihypertensive agents. These agents cause a fall in blood pressure of sodium-deficient dogs and decrease plasma renin activity as well as angiotensin II level.

PROCEDURE

Animal Experiment

Adult mongrel dogs (8–14 kg) of either sex are given water ad libitum and maintained on a low sodium diet for 1–2 weeks before the experiment. A single intramuscular injection of 5 mg/kg furosemide is given 48 h before the experiment. On the day of the experiment the dogs are anesthetized with sodium pentobarbital (30 mg/kg i.v.) and a cuffed endotracheal tube is positioned to allow artificial respiration. To measure arterial blood pressure a femoral artery is catheterized with polyethylene tubing. The right and left femoral veins are catheterized for drug administration and delivery of a maintenance infusion of sodium pentobarbital (5 mg/kg/h). Blood pressure is measured directly through the catheter, which is connected to a Gould-Statham pressure transducer. Blood samples are collected from the arterial catheter.

Increasing doses of the potential renin inhibitor are infused over 30 min followed by a 30 min recovery period. Immediately after the last recovery period, the dogs are given an i.v. infusion of the angiotensin receptor antagonist saralasin (20 µg/kg/min) for 30 min. For measurement of plasma renin activity and an-

giotensin II levels, the dogs are infused over a period of 30 min with the test compound and blood is withdrawn at 0, 15, 30, 60, 90, 120, 180, and 240 min after the start of the infusion. After the final blood drawing, 20 µg/kg/min saralasin is infused for 30 min.

Analytical Procedures

The antibody-trapping method is preferred to measure plasma renin activity (PRA). In this procedure PRA is determined at pH 7.4 by RIA quantification of angiotensin I (ANG I) generated and then trapped by excess anti-ANG I antibody (Poulsen and Jorgensen 1973; Nussberger et al. 1987). In tubes coated with rabbit anti-ANG I antibody (Gamma Coat™ ^{125}I Plasma renin activity RIA kit; Baxter Travenol Diagnostics) and incubated in an ice-water bath, 75 µl plasma are mixed with 7 µl 3 M TRIS base buffer (pH 7.2) containing 200 mM EDTA, and 3 µl 0.2 M TRIS base (pH 7.5) containing 3 g/L human serum albumin (fraction V, Sigma). Tubes are vortexed and incubated at 37°C for 60 min. The incubation is terminated by placing the tubes in an ice-water bath. Next, 75 µl of the TRIS albumin buffer are added, followed by 1 ml phosphate RIA buffer (Gamma Coat™) containing 15,000 cpm of ^{125}I ANG I. Standard ANG I (0.2–50 ng/ml) is also incubated at 37°C for 60 min with 10 µl TRIS/albumin buffer. In an ice-water bath, low renin plasma (75 µl) is added to the standards before the addition of a 1 ml tracer solution. Samples and standards are incubated for 24 h at 4°C. Tubes are then aspirated and counted in a gamma counter.

Levels of immunoreactive angiotensin II (ir-ANG II) are measured using a procedure described by Nussberger et al. (1985). Two–three ml of whole blood are collected in prechilled glass tubes containing 125 µl of the following "inhibitor" solution: 2% ethanol, 25 mM phenanthroline, 125 mM EDTA, 0.5 mM pepstatin A, 0.1 mM captopril, 2 g/l neomycin sulfate, and 0.1 mM of the renin inhibitor CGP 38560. The tubes are then centrifuged and the plasma quickly frozen in liquid nitrogen and stored at –70°C. For extraction of angiotensin peptides, Bond-Elut cartridges (Bond-Elut-pH) containing 100 mg phenylsilica are used, along with a Vac Elut SPS24 vacuum manifold (Analytichem; Harbor City, CA). Each cartridge is preconditioned with 1.0 ml methanol (HPLC grade) followed by 1.0 ml of water (HPLC grade) at a vacuum pressure of 5 mm Hg. One ml of the thawed sample is then applied to the cartridge and washed with 3 ml HPLC grade water. The angiotensin peptides retained at the columns are eluted with 0.5 ml methanol (HPLC grade, vacuum pressure less than 5 mm Hg) into polypropylene tubes coated with a buffer containing 0.2 M TRIS, 0.02% NaN_3, and 2.5 mg/ml fatty acid-free bovine serum albumin (pH 7.4 with glacial acetic acid). The methanol is evaporated at 40°C and ir-ANG II measured using an antibody (IgG Corp., Nashville, TN) with greater than 1000-fold selectivity for ANG II.

EVALUATION

All data are expressed as mean ± SEM. The hypotensive responses after various doses of the renin antagonist are compared with the inhibition of plasma renin activity and the decrease of immunoreactive angiotensin II.

CRITICAL ASSESSMENT OF THE METHOD

The antibody-trapping method, reported here, gives a better correlation with the blood pressure lowering effect in dogs than the conventional method based on RIA for generated ANG I (Palmer et al. 1993).

MODIFICATIONS OF THE METHOD

Pals et al. (1990) described a rat model for evaluating inhibitors of human renin using anesthetized, nephrectomized, ganglion-blocked rats. The blood pressure rise induced by sustained infusion of renin was dose-dependently decreased by a renin inhibitor.

REFERENCES AND FURTHER READING

Nussberger J, Brunner DB, Waeber B, Brunner HR (1985) True versus immunoreactive angiotensin II in human plasma. Hypertension 7 (Suppl I):I1–I17

Nussberger J, d'Amore TF, Porchet M, Waeber B, Brunner DB, Brunner HR, Kler L, Brown AN, Francis RJ (1987) Repeated administration of the converting enzyme inhibitor Cilazapril to normal volunteers. J Cardiovasc Pharmacol 9:39–44

Palmer RK, Rapundalo ST, Batley BL, Barnes AE, Singh S, Ryan MJ, Taylor DG (1993) Disparity between blood pressure and PRA inhibition after administration of a renin inhibitor to anesthetized dogs: Methodological considerations. Clin Exper Hypertens 15:663–681

Pals DT, Lawson JA, Couch SJ (1990) Rat model for evaluating inhibitors of human renin. J Pharmacol Meth 23:230–245

Poulsen K, Jørgensen J (1973) An easy radioimmunological assay of renin activity, concentration and substrate in human and animal plasma and tissue based on angiotensin I trapping by antibody. J Clin Endocrin Metab 39:816–825

Sealey JE, Laragh JH (1975) Radioimmunoassay of plasma renin activity. Semin Nucl Med 5:189–202

A.1.3.34 Evaluation of Renin Inhibitors in Monkeys

PURPOSE AND RATIONALE

The renin-angiotensin-system as the main regulator of blood pressure can be influenced in several ways.

One approach involves the inhibition of renin. Renin is an aspartyl protease that hydrolyzes angiotensinogen to release the dekapeptide angiotensin I, which is subsequently converted to angiotensin II by angiotensin-converting-enzyme. Sequencing of renin and angiotensinogen from various species revealed marked species differences for both the enzyme and the substrate. Inhibitors developed for human renin show a high specificity for primate renin and show only weak inhibition of renin from subprimate species. This means that the most common laboratory animals, such as rats and dogs, are not suitable for the *in vivo* evaluation of renin inhibitors. The marmoset was chosen by Wood et al. (1985, 1989) as a primate model.

PROCEDURE

Marmosets (*Callithrix jacchus*) of both sexes weighing between 300 and 400 g are fed a pellet diet supplemented with fruit. Two days prior to the experiment the animals are anesthetized and catheters are implanted in a femoral artery for measurement of blood pressure and in a lateral tail vein for injection or infusion of test substances. Thirty min before the experiment, the animals receive an intravenous injection of 5 mg/kg furosemide in order to stimulate renin release. During the experiment, the marmosets are sedated with diazepam (0.3 mg/kg i.p.) and kept in restraining boxes. Mean blood pressure is recorded continuously, and heart rate is measured at fixed intervals. The test compound or the standard are injected at various doses by intravenous infusion or administered orally.

EVALUATION

Blood pressure is recorded after 30 min of intravenous infusion and 30 min after stopping the infusion. Comparing the changes from pretreatment values after various doses, dose-response curves can be established.

MODIFICATIONS OF THE METHOD

Fischli et al. (1991) monitored arterial pressure in conscious and chronically instrumented monkeys using a telemetry system. One week before the experiment, the animals were anesthetized, and a 3F high fidelity pressure tip transducer (Millar Instruments, Inc.) was inserted into the abdominal aorta through the right femoral artery. Then the catheter was tunneled subcutaneously to the back of the monkey in the interscapular region. The proximal part of the catheter was connected to a transmitter located in a jacket worn by the monkey. The blood pressure was transmitted continuously to a receiver, which transformed the signal to an analogue value of blood pressure.

Linz et al. (1994) reported on the effects of renin inhibitors in anesthetized rhesus monkeys weighing between 5 and 13 kg. The animals are sodium-depleted by administration of 10 mg/kg/day furosemide-Na for 6 consecutive days. At day 7, 10 mg/kg furosemide is given i.v. 30 min before the start of the experiment. Anesthesia is induced with 20 mg/kg ketamine-hydrochloride i.m. and continued with 40 mg/kg pentobarbitone-Na, slow i.v. drip. After completion of surgical procedures and after insertion of catheters under fluoroscopic control, the following hemodynamic parameters are measured: Pulse rate, and systolic and diastolic blood pressures are registered with a transducer (Statham P23 ID) in one femoral artery. A catheter tip manometer (Millar Instruments, Houston, Texas, USA) is introduced into the left ventricular cavity for the determination of left ventricular pressure. Contractility is electronically deduced from left ventricular pressure with appropriate amplifiers (Hellige GmbH, Freiburg, Germany). The electrocardiogram (ECG) from conventional lead II is taken using an ECG transducer (Hellige GmbH). Heart rate is measured from QRS-peaks using a biotachometer (Hellige GmbH). Cardiac output is determined using the thermodilution method. Thermodilution is integrated and converted to cardiac output readings by commercially available equipment (HMV 7905, Hoyer, Bremen). To determine cardiac output, 2 ml chilled 0–5°C isotonic glucose solution (5%) is injected rapidly into the right ventricle by a catheter via the right jugular vein. A thermistor is placed into the aortic arch via the right carotid artery.

Hemodynamics are monitored for 30 min following i.v. injection of various doses of the potential renin inhibitor. At the end of the experiments the ACE inhibitor ramiprilat 100 µg/kg is given i.v. to probe for an additional blood pressure lowering effect. Blood samples for the determination of ANG II concentration, renin inhibition and plasma drug levels are withdrawn at 10, 30 and 60 min after i.v. injection of the renin inhibitor. The volume is replaced by i.v. injections of isotonic glucose solution (5%). After all data and blood samples have been obtained, animals are sacrificed by an overdose of pentobarbitone-Na.

For experiments after intraduodenal administration sodium depletion and anesthesia are done as described above. A small side branch of the femoral or radial artery is surgically exposed and cannulated for blood pressure measurements using a pressure transducer (P23 ID). Heart rate is determined from a conventional

ECG lead by a biotachometer. Blood samples are withdrawn via a catheter placed into the saphenous vein. A gastric fiberscope (Olympus XP 10) is introduced into the duodenum under visual control and the renin inhibitor is administered intraduodenally through the service channel of the fiberscope in a volume of 5 ml. Blood samples are withdrawn before and at 15, 30, 45, 60, 90 and 120 min after intraduodenal administration.

Wood et al. (2005) tested an orally effective renin inhibitor (aliskiren) in marmosets. Blood pressure and heart rate were measured by telemetry in conscious animals moving freely in their home cages. Pressure transmitters (AM Unit, model TA11PA-C40Data Sciences, USA) were implanted into the peritoneal cavity under aseptic conditions and light anesthesia. The sensor catheter was placed in the aorta below the renal artery pointing upstream.

CRITICAL ASSESSMENT OF THE METHOD

Due to the high species specificity of renin and its substrate, angiotensinogen, renin inhibitors for treatment of hypertension have to be tested in primate models. The marmoset as well as the rhesus monkey have been proven to be suitable models.

REFERENCES AND FURTHER READING

Evans DB, Cornette JC, Sawyer TK, Staples DJ, de Vaux AE, Sharma SK (1990) Substrate specificity and inhibitor structure-activity relationships of recombinant human renin: implications in the *in vivo* evaluation of renin inhibitors. Biotechnol Appl Biochem 12:161–175

Fischli W, Clozel JP, Amrami KE, Wostl W, Neidhart W, Stadler H, Branca Q (1991) RO 42–5892 is a potent orally active renin inhibitor in primates. Hypertension 18:22–31

Greenlee WJ (1990) Renin inhibitors. Med Res Rev 10:173–236

Hiwada K, Kobuko T, Murakami E, Muneta S, Morisawa Y, Yabe Y, Koike H, Iijima Y (1988) A highly potent and long-acting oral inhibitor of human renin. Hypertension 11:707–712

Linz W, Heitsch H, Henning R, Jung W, Kleemann HW, Nickel WU, Ruppert D, Urbach H, Wagner A, Schölkens BA (1994) Effects of the renin inhibitor *N*-[*N*-(3-(4-amino-1-piperidinylcarbonyl)-2(*R*)-benzylpropionyl)-L-histidinyl]-(2*S*,3*R*,4*S*)-1-cyclohexyl-3,4-dihydroxy-6(2-pyridyl)-hexane-2-amide acetate (S 2864) in anesthetized rhesus monkeys. Arzneim Forsch/Drug Res 44:815–820

Wood JM, Gulati N, Forgiarini P, Fuhrer W, Hofbauer KG (1985) Effects of a specific and long-acting renin inhibitor in the marmoset. Hypertension 7:797–803

Wood JM, Baum HP, Forgiarini P, Gulati N, Jobber RA, Neisius D, Hofbauer KG (1989a) Haemodynamic effects of acute and chronic renin inhibition in marmosets. J Hypertension 7, Suppl 2:S37–S42

Wood JM, Criscione L, de Gasparo M, Bühlmayer P, Rüeger H, Stanton JL, Jupp RA, Kay J (1989b) CGP 38 560: orally active, low-molecular-weight renin inhibitor with high potency and specificity. J Cardiovasc Pharmacol 14:221–226

Wood JM, Schnell CR, Cumin F, Menard J, Webb RL (2005) Aliskiren, a novel, orally effective renin inhibitor, lowers blood pressure in marmosets and spontaneously hypertensive rats. J Hypertens 23:417–426

A.1.3.35 Penile Erection in Rabbits

PURPOSE AND RATIONALE

The discovery of inhibitors of phosphodiesterase as effective drugs for patients with erectile dysfunction (Klotz et al. 2001; Porst et al. 2001) has stimulated the use of appropriate *in vivo* animal models. In particular, rabbits have been recommended as models for impotence research (Bischoff and Schneider 2000, 2001; Bischoff 2001; Bischoff et al. 2001; Saenz de Tejada et al. 2001) confirming earlier work in this area (Thielen et al. 1969; Sjöstrand and Kline 1979; Naganuma et al. 1993; Lin and Lin 1996).

PROCEDURE

Adult male Chinchilla rabbits weighing 3.5–4.5 kg are housed in individual cages for at least 1 week after arrival, at room temperature with water and food ad libitum.

For the study, an indwelling catheter filled with saline is inserted into a marginal ear vein and taped in position. The drugs are injected into the ear vein, followed by a small volume of saline. The time is noted and at appropriate times the animal gently removed from the cage and held by one research worker. The rabbit penis is not visible when it is not erect (Naganuma et al. 1993). However, when erection occurs, it is possible to examine the pudendal area and measure the length of the uncovered penile mucosa with sliding calipers.

EVALUATION

Penile erection is evaluated by measuring the length to the nearest millimeter of the uncovered penile mucosa with a sliding caliper at 5, 10, 15, 30, 50, 60, 90, and 120 min after administration of the test compounds and continued hourly for up to 5 h. Mean values are calculated and results expressed as means ± SEM. The area under the curve is calculated by an integration program.

MODIFICATIONS OF THE METHOD

Choi et al. (2002) compared the efficacy of verdenafil and sildenafil in facilitating penile erection in **anesthetized rabbits**. Penile erections were elicited by submaximal pelvic nerve stimulation every 5 min for 30 min. Response was assessed by continuously

recording intracavernosal pressure and systemic arterial pressure.

Min et al. (2000) tested the augmentation of pelvic-nerve-mediated sexual arousal in anesthetized **female rabbits** by sildenafil. The following parameters were measured before, during and after pelvic nerve stimulation at 4, 16, and 32 Hz: (1) hemoglobin concentration and oxygen saturation in female genital (vaginal, labial, clitoral) tissues by laser oximetry; (2) clitoral blood flow by laser Doppler flowmetry; (3) vaginal luminal pressure by a balloon catheter pressure transducer; (4) vaginal lubrication by tampon.

Carter et al. (1998) tested the effect of the selective phosphodiesterase type 5 inhibitor sildenafil on erectile dysfunction in **pentobarbital-anesthetized dogs**. Increases in intracavernosal pressure in the corpus cavernosum and penile blood flow were induced by pelvic nerve stimulation over a frequency range of 1–16 Hz. The effects of increasing doses of sildenafil on electric-stimulated intracavernosal pressure, penile blood flow, blood pressure, and heart rate were evaluated.

REFERENCES AND FURTHER READING

Bischoff E (2001) Rabbits as models for impotence research. Int J Impot Res 13:146–148

Bischoff E, Niewoehner U, Haning H, Es Sayed M, Schenke T, Schlemmer KH (2001) The oral efficacy of verdenafil hydrochloride for inducing penile erection in a conscious rabbit model. J Urol 165:1316–1318

Bischoff E, Schneider K (2000) A conscious rabbit model is able to demonstrate the efficacy of verdenafil and sildenafil on penile erection. Int J Impot Res Suppl 12:65

Bischoff E, Schneider K (2001) A conscious-rabbit model to study verdenafil hydrochloride and other agents that induce penile erection. Int J Impot Res 13:230–235

Carter AJ, Ballard SA, Naylor AM (1998) Effect of the selective phosphodiesterase type 5 inhibitor sildenafil on erectile dysfunction in the anaesthetized dog. J Urol 160:242–246

Choi S, O'Connell L, Min K, Kim NN, Munarriz R, Goldstein I, Bischoff E, Traisch AM (2002) Efficacy of verdenafil and sildenafil in facilitating penile erection in an animal model. J Androl 23:332–337

Klotz T, Sachse R, Heidrich A, Jockenhövel F, Rhode G, Wensing G, Horstmann R, Engelmann R (2001) Verdenafil increases penile rigidity and tumescence in erectile dysfunction patients: a RigiScan and pharmacokinetic study. World J Urol 19:32–39

Lin YM, Lin JS (1996) The rabbit as an intracavernous injection study model. Urol Res 24:27–32

Min K, Kim NN, McAuley I, Stankowicz M, Goldstein I, Traisch AM (2000) Sildenafil augments pelvic nerve-mediated female sexual arousal in the anesthetized rabbit. Int J Impot Res 12 [Suppl 3]:S32–S39

Naganuma H, Egashira T, Fujii I (1993) Neuroleptics induce penile erection in the rabbit. Clin Exp Pharmacol Physiol 20:177–183

Porst H, Rosen R, Padma-Nathan H, Goldstein I, Giuliano F, Ulbrich E, Bandel T (2001) The efficacy and tolerability of vardenafil, a new, oral, selective phosphodiesterase type 5 inhibitor, in patients with erectile dysfunction: the first at-home clinical trial. Int J Impot Res 13(4):192–199

Saenz de Tejada I, Angulo J, Cuevas P, Fernández A, Moncada I, Allona A, Lledó E, Körschen HG, Niewöhner U, Haning H, Pages E, Bischoff E (2001) The phosphodiesterase inhibitory selectivity and the in vitro and in vivo potency of the new PDE5 inhibitor verdenafil. Int J Impot Res 13:282–290

Sjöstrand NO, Klinge E (1979) Principal mechanisms controlling penile retraction and protrusion in rabbits. Acta Physiol Scand 106:199–214

Thielen P, Renders M, Rectem D (1969) Medullary regions controlling the erection and retraction of the penis in rabbits. Arch Int Physiol Biochim 77:340–342

A.1.4 Cardiovascular Safety Studies

See:
Brian D. Guth
Methods in Cardiovascular Safety Pharmacology
Chapter I. D.
In:
Drug Discovery an Evaluation
Safety and Pharmacokinetic Assays
By: H.G: Vogel (Ed), F.J. Hock, J. Maas, D. Mayer (CoEds)
Springer Verlag Berlin Heidelberg New York, 2006

A.2 Methods to Induce Experimental Hypertension

A.2.0.1 Acute Renal Hypertension in Rats

PURPOSE AND RATIONALE

Since the classical experiments of Goldblatt et al. (1934) there is clear evidence that the ischemia of the kidneys causes elevation of blood pressure by activation of the renin-angiotensin system. The principle can be used both for acute and chronic hypertension. In rats acute renal hypertension is induced by clamping the left renal artery for 4 h. After reopening of the vessel, accumulated renin is released into circulation. The protease renin catalyzes the first and rate-limiting step in the formation of angiotensin II leading to acute hypertension. The test is used to evaluate antihypertensive activities of drugs.

PROCEDURE

Male Sprague-Dawley rats weighing 300 g are used. The animals are anesthetized by intraperitoneal injection of 100 mg/kg hexobarbital sodium. A PVC-coated Dieffenbach clip is placed onto the left hilum of the kidney and fixed to the back muscles. The renal artery is occluded for 3.5–4 h.

3.5 h following the surgery, the animals are anesthetized by intraperitoneal injection of 30–40 mg/kg pentobarbital sodium. The trachea is cannulated to facilitate spontaneous respiration. To measure systolic and diastolic blood pressure, the cannula in the carotid artery is connected to a pressure transducer (Statham P 23 Db).

For administration of the test compound, a jugular vein is cannulated.

Following a stable blood pressure state, ganglionic blockade is performed with pentolinium (10 mg/kg i.v.). After obtaining stable reduced blood pressure values, the renal arterial clip is removed. This leads to a rise in blood pressure as a consequence of elevated plasma renin level. Within 15 min a stable hypertension is achieved (control = 100%).

The test substance is then administered by intravenous injection at doses of 10 and 100 µg/kg.

Blood pressure is monitored continuously until a renewed increase to the starting level is obtained.

Ten–twelve animals are used per compound.

EVALUATION

Increase in blood pressure after reopening of the renal artery and reduction in blood pressure after administration of the test drug are determined [mm Hg]. Percent inhibition of hypertensive blood pressure values under drug treatment are calculated as compared to pretreatment hypertension values. Duration of the effect is determined [min]. Statistical significance is assessed by the paired *t*-test.

MODIFICATIONS OF THE METHOD

A sharp and transient in systemic arterial blood pressure associated with reflex bradycardia can be elicited by injection of 5-hydroxytryptamine, cyanide, nicotine or lobeline into the coronary artery blood stream of dogs (Berthold et al. 1989). The phenomenon is named the cardiogenic hypertensive chemoreflex and 5-HT proved to be the most powerful agent for its initiation (James et al. 1975).

REFERENCES AND FURTHER READING

Berthold H, Scholtysik G, Engel G (1989) Inhibition of the 5-HT-induced cardiogenic hypertensive chemoreflex by the selective 5-HT_3 receptor antagonist ICS 205–930. Naunyn-Schmiedeberg's Arch Pharmacol 339:259–262

Boura ALA, Green AF (1964) Antihypertensive agents. In: Laurence DR, Bacharach AL (eds) Evaluation of drug activities: Pharmacometrics. Academic Press London and New York pp 431–456

Goldblatt H, Lynch J, Hanzal RF, Summerville WW (1934) Studies on experimental hypertension. I. The production of persistent evaluation of systolic blood pressure by means of renal ischemia. J exper Med 59:347–379

James TN, Isobe JH, Urthaler F (1975) Analysis of components in a cardiogenic hypertensive chemoreflex. Circulation 52:179–192

A.2.0.2 Chronic Renal Hypertension in Rats

PURPOSE AND RATIONALE

On the basis of the findings of Goldblatt et al. (1934) that ischemia of the kidneys induces hypertension, various modifications of the technique have been described for several animal species. One of the most effective modifications in rats is the so called 1-kidney-1-clip method.

PROCEDURE

Male Sprague-Dawley rats weighing 200–250 g are anaesthetized with 50 mg/kg i.p. pentobarbital. The fur on the back is shaved and the skin disinfected. In the left lumbar area a flank incision is made parallel to the long axis of the rat. The renal pedicel is exposed with the kidney retracted to the abdomen. The renal

artery is dissected clean and a U-shaped silver clip is slipped around it near the aorta. Using a special forceps (Schaffenburg 1959) the size of the clip is adjusted so that the internal gap ranges from 0.25–0.38 mm. The right kidney is removed through a flank incision after tying off the renal pedicle. The skin incisions are closed by wound clips.

4–5 weeks after clipping blood pressure is measured and rats with values higher than 150 mm Hg selected for the experiments. Blood pressure readings are taken on each of 3 days prior to drug treatment. Drugs are administered orally in volumes of 10 ml/kg. The rats are divided into 4 animals per dose and each animal is used as his own control. Compounds are administered for 3 days and predrug and 2 h postdrug blood pressure readings are taken.

EVALUATION

Changes in systolic blood pressure are expressed in mm Hg. Activity is determined by comparing treatment blood pressure values with the control blood pressure value (Day 1, predrug blood pressure). Comparisons are made using the paired *t*-test for evaluation of statistical significance.

MODIFICATIONS OF THE METHOD

Duan et al. (1996) induced renal hypertension in male Hartley **guinea pigs** by a two-step procedure consisting of ligation of the left caudal renal artery and right nephrectomy. Arterial blood pressure and heart rate were monitored in conscious animals. ACE-inhibitors reduced blood pressure in sham-operated and in renal hypertensive guinea pigs, whereas renin inhibitors were effective only in renal hypertensive animals.

REFERENCES AND FURTHER READING

Boura ALA, Green AF (1964) Antihypertensive agents. In: Laurence DR, Bacharach AL (eds) Evaluation of drug activities: Pharmacometrics. Academic Press London and New York pp 431–456

Duan J, Jamarillo J, Jung GL, McLeod AL, Fernades BH (1996) A novel renal hypertensive guinea pig model for comparing different inhibitors of the renin-angiotensin system. J Pharmacol Toxicol Meth 35:83–89

Goldblatt H, Lynch J, Hanzal RF, Summerville WW (1934) Studies on experimental hypertension. I. The production of persistent evaluation of systolic blood pressure by means of renal ischemia. J exper Med 59:347–379

Leite R, Salgado MCO (1992) Increased vascular formation of angiotensin II in one-kidney, one clip hypertension. Hypertension 19:575–581

Schaffenburg CA (1959) Device to control constriction of main renal artery for production of hypertension in small animals. Proc Soc Exp Biol Med 101:676–677

Zandberg P (1984) Animal models in experimental hypertension: relevance to drug testing and discovery. In: van Zwieten (ed) Handbook of Hypertension, Vol 3, Pharmacology of Antihypertensive Drugs. Elsevier Amsterdam, pp 102–153

A.2.0.3 Chronic Renal Hypertension in Dogs

PURPOSE AND RATIONALE

Production of hypertension by clamping renal arteries has been first described by Goldblatt et al. (1934) in dogs. Later on, the method has been modified, e. g., as the "wrapping" technique (Abram and Sobin 1947).

PROCEDURE

Dogs weighing 8–12 kg are anesthetized with i.v. injection of 15 mg/kg thiopental. Anesthesia is maintained with a halothane-oxygen mixture. Under aseptic conditions, a midline abdominal incision is made. One kidney is exposed and wrapped in cellophane and then replaced. The contralateral kidney is exposed. The artery, vein and ureter are ligated and the kidney is removed. The abdomen is closed by sutures and clips. On the day of surgery and for 3 days following, the dogs are given antibiotics. Body temperature is measured twice daily for 4 days following surgery.

Six weeks following surgery, blood pressure is measured using a tail-cuff method. For recording, the tail-cuff is attached to a polygraph. Only animals with a systolic blood pressure higher than 150 mm Hg are considered to be hypertensive and can participate in studies evaluating potential antihypertensive compounds.

For the experiment, blood pressure is recorded either by the indirect tail-cuff method or by direct measurement via an implanted arterial cannula. On day 1 readings are made every 2 h, just before, and 2 and 4 h after oral treatment with the potential antihypertensive compound. Drug administration is repeated for 5 days. On days 3 and 5 blood pressure readings are taken before and 2 and 4 h after treatment. At least 3 dogs are used per dose and compound.

EVALUATION

The starting value is the average of the 2 readings before application of the drug. Each of the following readings is subtracted from this value and recorded as fall of blood pressure at the various recording times.

MODIFICATIONS OF THE METHOD

Renal hypertension in rats has been achieved by many modifications of the method (Stanton 1971) such as the

technique according to Grollman (1944). The kidney is exposed through a lumbar incision, the renal capsule is removed by gentle traction, and a figure-8 ligature is applied being tight enough to deform the kidney but not tight enough to cut the tissue.

Renal hypertension may be induced in the **rat** by encapsulating both kidneys with latex rubber capsules (Abrams and Sobin 1947). Moulds are formed from plastic using a rat kidney as a model. The capsules are prepared by dipping the moulds in liquid latex allowing them to dry in the air. Three applications of latex are applied before the capsules are toughened by placing them under warm running tap water. The kidney is exposed by lumbar incision, the renal capsule gently removed and the capsule applied.

REFERENCES AND FURTHER READING

Abrams M, Sobin S (1947) Latex rubber capsule for producing hypertension in rats by perinephritis. Proc Soc Exp Biol Med 64:412–416

Goldblatt H, Lynch J, Hanzal RF, Summerville WW (1934) Studies on experimental hypertension. I. The production of persistent evaluation of systolic blood pressure by means of renal ischemia. J exper Med 59:347–379

Grollman A (1944) A simplified procedure for inducing chronic renal hypertension in the mammal. Proc Soc Exp Biol Med 57:102–104

Schaffenburg CA (1959) Device to control constriction of main renal artery for production of hypertension in small animals. Proc Soc exper Biol Med 101:676–677

Sen S, Tarazi RC, Bumpus FM (1981) Reversal of cardiac hypertrophy in renal hypertensive rats: medical vs. surgical therapy. Am J Physiol 240:H408–H412

Stanton HC (1971) Experimental hypertension. In: Schwartz A (ed) Methods in Pharmacology, Vol 1, pp 125–150. Appleton-Century-Crofts, Meredith Corporation. New York

A.2.0.4 Neurogenic Hypertension in Dogs

PURPOSE AND RATIONALE

Vasodilator and depressor reflexes, originating in the baroreceptor areas of the carotid sinus and aortic arch, play an important part in the regulation of blood pressure. Stimulation of the afferent buffer fibres exerts an inhibitory influence on the vasomotor center, and their sectioning leads to a persistent rise in blood pressure. In this way, acute neurogenic hypertension can be induced in dogs.

PROCEDURE

Adult dogs of either sex weighing 10–15 kg are anesthetized using 15 mg/kg sodium thiopental, 200 mg/kg sodium barbital and 60 mg/kg sodium pentobarbital i.v. A femoral vein and artery are cannulated using polyethylene tubing to administer compounds i.v. and record arterial pressure and heart rate, respectively. Left ventricular pressure and dp/dt are recorded via the left common carotid artery (post-deafferentiation) using a Millar microtip pressure transducer. P_{max} is recorded by speeding up the chart paper. Cardiac output is determined by introducing a Swan-Ganz catheter into the right heart and pulmonary artery via a jugular vein. Five ml of cold 5% dextrose is injected into the right atrium and an Edwards Cardiac output computer is used to calculate the cardiac output from the temperature change in the pulmonary artery. All recordings are made with a polygraph.

Both of the carotid arteries are cleared up to the bifurcation of the internal and external carotid arteries. The carotid sinus nerves are isolated, ligated and sectioned and a bilateral vagotomy is performed to produce neurogenic hypertension (mean arterial pressure more than 150 mm Hg). The dog is allowed to equilibrate for approximately 30 min and a bolus of the test compound is administered by intravenous injection. Heart rate, arterial pressure, left ventricular pressure, Pmax and dp/dt are monitored for 90 min. A minimum of 3 dogs are used for each compound.

EVALUATION

Changes of the cardiovascular parameters are expressed as percentage of the values before administration of the drug.

MODIFICATIONS OF THE METHOD

Neurogenic hypertension through baroreceptor denervation has also been described in **rabbits** (Angell-James 1984) and in rats (Krieger 1984).

CRITICAL ASSESSMENT OF THE METHOD

The neurogenic hypertension is useful for acute experiments. However, it is less useful for chronic experiments since the elevated blood pressure caused by buffer nerve section is more labile than that caused by renal ischemia.

REFERENCES AND FURTHER READING

Angell-James JE (1984) Neurogenic hypertension in the rabbit. In: de Jong (ed) Handbook of Hypertension, Vol. 4: Experimental and Genetic Models of Hypertension. Elsevier Science Publ, pp 364–397

Boura ALA, Green AF (1964) Antihypertensive agents. In: Laurence DR, Bacharach AL (eds) Evaluation of drug activities: Pharmacometrics. Academic Press London and New York pp 431–456

Grimson KS (1941) The sympathetic nervous system in neurogenic and renal hypertension. Arch Surg, Chicago, 43:284–305
Krieger EM (1984) Neurogenic hypertension in the rat. In: de Jong (ed) Handbook of Hypertension, Vol. 4: Experimental and Genetic Models of Hypertension. Elsevier Science Publ, pp 350–363
Maxwell RA, Plummer AJ, Schneider F, Povalski H, Daniel AI (1960) Pharmacology of [2-(octahydro-1-azocinyl)-ethyl]-guanidine sulfate (SU-5864). J Pharmacol 128:22–29

A.2.0.5 DOCA-salt Induced Hypertension in Rats

PURPOSE AND RATIONALE

Mineralocorticoid-induced hypertension is thought to be due to the sodium retaining properties of the steroid causing increases in plasma and extracellular volume. The hypertensive effect is increased by salt loading and unilateral nephrectomy in rats.

PROCEDURE

Male Sprague Dawley rats weighing 250–300 g are anesthetized with ether. Through a flank incision the left kidney is removed. The rats are injected twice weekly with 20 mg/kg s.c. desoxycorticosteroneacetate in olive oil for 4 weeks. Drinking water is replaced with a 1% NaCl solution. Blood pressure starts to rise after one week and reaches systolic values between 160 and 180 mm Hg after 4 weeks.

MODIFICATIONS OF THE METHOD

The regimen to induce DOCA-salt hypertension has been modified by many authors (Stanton 1971).

DOCA pellets (Peterfalvi and Jequier 1960; Passmore and Jimenez 1990) or implants in silastic devices (Ormsbee and Ryan 1973; King and Webb 1988) were used instead of repeated injections.

DOCA-salt hypertension can also be achieved without nephrectomy (Bockman et al. 1992).

Using kininogen-deficient Brown Norway Katholiek (BN-Ka) rats, Majima et al. (1991, 1993) showed suppression of rat desoxycorticosterone-salt hypertension by the kallikrein-kinin system.

Li et al. (1996) examined small-artery structure on a wire myograph and quantified endothelin-1 messenger RNA by Northern blot analysis in DOCA-salt hypertensive rats after administration of an ACE-inhibitor, a calcium channel antagonist and a nitric oxide synthase inhibitor.

Ullian (1997) described the **Wistar–Furth rat** as a model of mineralocorticoid resistance. These rats developed two-kidney, one-clip hypertension to the same degree as did Wistar rats and reacted to glucocorticoid treatment with a rapid onset of hypertension, but were resistant to the development of DOCA-NaCl hypertension.

Studies in DOCA-salt hypertensive **mice** were reported by Gross et al. (1998, 1999), Honeck et al. (2000), Peng et al. (2001).

REFERENCES AND FURTHER READING

Bockman ChS, Jeffries WB, Pettinger WA, Abel PW (1992) Enhanced release of endothelium-derived relaxing factor in mineralocorticoid hypertension. Hypertension 20:304–313
Codde JP, Croft KD, Beilin LJ (1987) Dietary suppression of prostaglandin synthesis does not accelerate DOCA/salt hypertension in rats. Clin Exp Pharm Physiol 14:513–523
Dardik BN, Di Bello PM, Chatelain RE (1988) Elevated arterial cyclic AMP levels during the development of one kidney, one clip and DOCA hypertension in rats. Eur J Pharmacol 158:139–143
Friedman SM, McIndoe RA, Tanaka M (1988) The relation of cellular sodium to the onset of hypertension induced by DOCA-saline in the rat. J Hypertension 6:63–69
Gross V, Lippoldt A, Bohlender J, Bader M, Hansson A, Luft FC (1998) Cortical and medullary hemodynamics in desoxycorticosterone acetate-salt hypertensive mice. J Am Soc Nephrol 9:346–354
Gross V, Schneider W, Schunk WH, Mervaala E, Luft FC (1999) Chronic effects of lovastatin and bezafibrate on cortical and medullary hemodynamics in desoxycorticosterone acetate-salt hypertensive mice. J Am Soc Nephrol 10:1430–1439
Hasnain Q, MacDonald G (1993) Metabolic studies of uridine in rats with DOCA-salt hypertension and on high sodium diet. Clin Exper Pharm Physiol 20:384–387
Honeck H, Gross V, Erdmann B, Kärgel E, Neunaber R, Milia AF, Schneider W, Luft FC, Schunk WH (2000) Cytochrome P450-dependent renal arachidonic acid metabolism in desoxyxcorticosterone acetate-salt hypertensive mice. Hypertension 36:610
King CM, Webb RC (1988) The endothelium partially obscures enhanced microvessel reactivity in DOCA hypertensive rats. Hypertension 12:420–427
Li JS, Sventek P, Schiffrin EL (1996) Effect of antihypertensive treatment and N^{ω}-nitro-L-arginine methyl ester on cardiovascular structure in deoxycorticosterone acetate-salt hypertensive rats. J Hypertension 14:1331–1339
Majima M, Katori M, Hanazuka M, Mizogami S, Nakano T, Nakao Y, Mikami R, Uryu H, Okamura R, Mohsin SSJ, Oh-Ishi S (1991) Suppression of rat desoxycorticosterone-salt hypertension by the kallikrein-kinin system. Hypertension 17:806–813
Majima M, Yoshida O, Mihara H, Muto T, Mitsogami S, Kuribayashi Y, Katori M, Oh-Ishi S (1993) High sensitivity to salt in kininogen-deficient Brown Norway Katholiek rats. Hypertension 22:705–714
Opoku J, Kalimi M (1992) Role of the antiglucocorticoid RU 486 in the prevention of steroid-induced hypertension. Acta Endocrin 127:258–261
Ormsbee HS, Ryan CF (1973) Production of hypertension with desoxycorticosterone acetate-impregnated silicone rubber implants. J Pharmacol Sci 62:255–257
Passmore JC, Jimenez AE (1990) Separate hemodynamic roles for chloride and sodium in deoxycorticosterone acetate-salt hypertension. Proc Soc Exp Biol Med 194:283–288

Peng H, Carretero OA, Alfie ME, Masura JA, Rhaleb NE (2001) Effects of angiotensin-converting enzyme inhibitor and angiotensin type 1 receptor antagonist in deoxycorticosterone acetate-salt hypertensive mice lacking *Ren-2 gene*. Hypertension 37:974

Peterfalvi M, Jequier R (1960) La 10-methoxy deserpidine. Étude pharmacologique. Arch Int Pharmacodyn 124:237–254

Schenk J, McNeill JH (1992) The pathogenesis of DOCA-salt hypertension. J Pharm Toxicol Meth 27:161–170

Stanton HC (1971) Experimental hypertension. In: Schwartz A (ed) Methods in Pharmacology, Vol 1, pp 125–150. Appleton-Century-Crofts, Meredith Corporation. New York

Ullian ME (1997) The Wistar–Furth rat as a model of mineralocorticoid resistance. Kidney Internat 52: Suppl 61:S10–S13

A.2.0.6 Fructose Induced Hypertension in Rats

PURPOSE AND RATIONALE

Increases in dietary carbohydrate intake can raise blood pressure in experimental animals. The increased intake of either sucrose or glucose was shown to enhance the development of either spontaneous hypertension or salt hypertension in rats (Hall and Hall 1966; Preuss and Preuss 1980; Young and Landsberg 1981). Hwang et al. (1987) first reported that hypertension could be induced in normal rats by feeding a high-fructose diet. Fructose feeding was also found to cause insulin resistance, hyperinsulinemia, and hypertriglyceridemia in normal rats (Zavaroni et al. 1980; Tobey et al. 1982). Dai and McNeill (1995) studied the concentration- and duration-dependence of fructose-induced hypertension in rats.

PROCEDURE

Groups of 8 male Wistar rats weighing 210–250 g are used. The are housed two per cage on a 12-h light 12-h dark cycle and are allowed free access to standard laboratory diet (Purina rat chow) and drinking fluid. Drinking fluid consists either of tap water or 10%-fructose solution. Body weight, food intake and fluid intake of each rat are measured every week during treatment. Using the tail-cuff method, systolic blood pressure and pulse rate is measured before and every week during treatment. Blood samples are collected before and every second week during treatment for determination of plasma glucose, insulin, and triglycerides.

EVALUATION

Since maximum effects on the chosen parameters are achieved after 6 weeks, the duration of treatment can be limited to this time. Statistical analysis is performed using a one-way or two-way analysis of variance, followed by the Newman-Keuls test.

MODIFICATIONS OF THE METHOD

Reaven et al. (1988, 1989) found an attenuation of fructose-induced hypertension by exercise training and an inhibition by somatostatin treatment.

Brands et al. (1991, 1992) found an increase of arterial pressure during chronic hyperinsulinemia in conscious rats.

Hall et al. (1995) reported the effects of 6 weeks of a high-fat diet on cardiovascular, renal, and endocrine functions in chronically instrumented conscious **dogs**. Body weight increased by approximately 16.9 kg, whereas MAP, cardiac output, and heart rate increased by 28%, 77%, and 68%, respectively.

REFERENCES AND FURTHER READING

Brands MW, Hildebrandt DA, Mizelle HL, Hall JE (1991) Sustained hyperinsulinemia increases arterial pressure in conscious rats. Am J Physiol 260:R764–R768

Brands MW, Hildebrandt DA, Mizelle HL, Hall JE (1992) Hypertension during chronic hyperinsulinemia in rats is not salt sensitive. Hypertension 19 (Suppl I):I83–I89

Dai S, McNeil JH (1995) Fructose-induced hypertension in rats is concentration- and duration-dependent. J Pharmacol Toxicol Meth 33:101–107

Hall CE, Hall O (1966) Comparative effectiveness of glucose and sucrose in enhancement of hyperalimentation and salt hypertension. Proc Soc Exp Biol Med 123:370–374

Hall JE, Brands MW, Zappe DH, Dixon WN, Mizelle HL, Reinhart GA, Hildebrandt DA (1995) Hemodynamic and renal responses to chronic hyperinsulinemia in obese, insulin-resistant dogs. Hypertension 25:994–1002

Hwang IS, Ho H, Hoffman BB, Reaven GM (1987) Fructose-induced insulin resistance and hypertension in rats. Hypertension 10:512–516

Hwang IS, Huang WC, Wu JN, Reaven GM (1989) Effect of fructose-induced hypertension on the renin-angiotensin-aldosterone system and atrial natriuretic factor. Am J Hypertens 2:424–427

Preuss MB, Preuss HG (1980) The effects of sucrose and sodium on blood pressures in various substrains of Wistar rats. Labor Invest 43:101–107

Reaven GM, Ho H, Hoffman BB (1988) Attenuation of fructose-induced hypertension in rats by exercise training. Hypertension 12:129–132

Reaven GM, Ho H, Hoffman BB (1989) Somatostatin inhibition of fructose-induced hypertension. Hypertension 14:117–120

Tobey TA, Mondon CE, Zavaroni I, Reaven GM (1982) Mechanism of insulin resistance in fructose-fed rats. Metabolism 31:608–612

Young JB, Landsberg L (1981) Effect of sucrose on blood pressure in the spontaneously hypertensive rat. Metabolism 30:421–424

Zavaroni I, Sander S, Scott A, Reaven GM (1980) Effect of fructose feeding on insulin secretion and insulin action in the rat. Metabolism 29:970–973

A.2.0.7 Genetic Hypertension in Rats

SURVEY

Inherited hypertension in rats has been described by Smik and Hall 1958; Phelan and Smirk 1960; Laverty and Smirk 1961; Phelan 1968 as **genetically hypertensive (GH) rats** (Simpson and Phelan 1984).

Okamoto et al. (1963, 1966) reported the development of a strain of spontaneously hypertensive rats from mating one Wistar male rat with spontaneously occurring high blood pressure with a female with slightly elevated blood pressure. By inbreeding over several generations a high incidence of hypertension with blood pressure values of 200 mm Hg or more was achieved. These strains were called "**Spontaneously hypertensive rats (Akamoto-Aoki)**" = **SHR** or **"Wistar–Kyoto rats**" = **WKY**. Hypertension in these rats is clearly hereditary and genetically determined, thus comparable to primary hypertension in humans. Cardiac hypertrophy (Sen et al. 1974) and cellular ionic transport abnormalities have been observed (Yamori 1984).

Inbred strains being **salt-hypertension-sensitivey** and **salt-hypertension-resistant (RD)** have been developed by Dahl et al. (1962, 1963), Rapp (1984), Cicila et al. (1993). Inoko et al. (1994) reported the transition from compensatory hypertrophy to dilated, failing left ventricles in Dahl salt-sensitive rats.

Two strains of rats with inbred dissimilar sensitivity to DOCA-salt hypertension (**"Sabra strain"**) have been separated by Ben-Ishay et al. (1972, 1984).

Another hypertensive strain derived from Wistar rats was produced by brother-sister mating in the group of Bianchi et al. (1974, 1986) at the University of Milan called **"Milan hypertensive strain**" = **MHS**. These rats show a cell membrane defect resulting in abnormal kidney function. Salvati et al. (1990) studied the diuretic effect of bumetanide in isolated perfused kidneys of Milan hypertensive rats.

Furthermore, the **"Lyon"** strains of hypertensive, normotensive and low-blood-pressure rats were developed (Dupont et al. 1973; Vincent et al. 1984; Dubay et al. 1993). These rats show a genetically determined defect in central nervous function.

Spontaneously hypertensive rats which develop failure before 18 months have been selectively bred. Several substrains of spontaneous hypertensive rats were separated by the group of Okamoto et al. (1974) including the **stroke-prone strain SHR = SHRSP**. These rats have an increased sympathetic tone and show a high incidence of hemorrhagic lesions of the brain with motor disturbances followed by death (Yamori 1984; Feron et al. 1996).

A strain of obese spontaneously hypertensive rats has been described by Koletsky (1975), Ernsberger et al. (1993).

With new techniques of genetic engineering, **transgenic rats with hypertension** could be created. Increase of blood pressure of spontaneously hypertensive rat is determined by multiple genetic loci (Deng and Rapp 1992; Dubay et al. 1993). With new technology not only these loci could be defined but also new models in hypertension research and models to detect antihypertensive drugs could be established (Bohlender et al. 1997; Pinto et al. 1998).

Mullins et al. (1990) reported fulminant hypertension in transgenic rats harboring the mouse Re-2 gene.

A **rat strain TGR(mREN2)27** as a monogenetic model in hypertension research was described by Peters et al. (1993), Lee et al. (1996), Langheinrich et al. (1996), and Ohta et al. (1996).

Bohlender et al. (1996) reconstructed the human renin-angiotensin system in transgenic rats overexpressing the human angiotensin gene TGR(hOGEN) 1623 by chronically injecting human recombinant renin intravenously using Alzet pumps.

Zolk et al. (1998) described the effects of quinapril, losartan and hydralazine on cardiac hypertrophy and β-adrenergic neuroeffector mechanisms in transgenic TGR(mREN2)27 rats.

CRITICAL ASSESSMENT OF THE METHOD

The use of spontaneously hypertensive rats to detect potential antihypertensive compounds is well established. On the basis of available data no preference can be given to a particular strain. The most abundant experience has been gained with the Wistar–Kyoto strain. Transgenic rats with well defined genomes are gaining more importance.

MODIFICATIONS OF THE METHOD

Pijl et al. (1994) described streptozotocin-induced diabetes mellitus in spontaneously hypertensive rats as a pathophysiological model for the combined effects of hypertension and diabetes.

Rosenthal et al. (1997) used rats of the Cohen-Rosenthal diabetic hypertensive strain to examine the effects of an ACE-inhibitor, an ATII antagonist and a calcium antagonist on systolic pressure and spontaneous blood glucose levels.

Holycross et al. (1997) used hypertensive SHHF/Mcc-facp rats to study plasma renin activity during development of heart failure.

Linz et al. (1997) compared the outcome of lifelong treatment with the ACE inhibitor ramipril in young prehypertensive stroke-prone spontaneously hypertensive rats and age-matched normotensive Wistar–Kyoto rats. Lifelong ACE inhibition doubled the lifespan in hypertensive rats matching that of normotensive rats.

Studies in **genetically hypertensive mice** were reported by Rosenberg et al. (1985), Hamet et al. (1990) Meneton et al. (2000). Ohkubo et al. (1990) generated transgenic mice with elevated blood pressure by introduction of the rat renin and angiotensinogen genes.

REFERENCES AND FURTHER READING

Ben-Ishay D (1984) The Sabra hypertension-prone and -resistant strain. In: de Jong W (ed) Handbook of Hypertension. Vol 4. Experimental and Genetic Models of Hypertension. Elsevier Science Publ., New York, pp 296–313

Ben-Ishay D, Saliternik R, Welner A (1972) Separation of two strains of rats with inbred dissimilar sensitivity to DOCA-salt hypertension. Experientia 28:1321–1322

Berthelot A (1991) Hypertension models and screening of antihypertensive drugs. In: 7th Freiburg Focus on Biomeasurement. Cardiovascular and Respiratory *in vivo* Studies. Biomesstechnik-Verlag March GmbH, 79232 March, Germany, pp 106–109

Bianchi G, Fox U, Imbasciati E (1974) The development of a new strain of spontaneously hypertensive rats. Life Sci 14:339–347

Bianchi G, Ferrari P, Barber BR (1984) The Milan hypertensive strain. In: de Jong W (ed) Handbook of Hypertension, Vol 4: Experimental and Genetic Models of Hypertension. pp 328–340

Bianchi G, Ferrari P, Cusi D, Salardi S, Giudi E, Niutta E, Tripodi G (1986) Genetic and experimental hypertension in the animal model – Similarities and dissimilarities to the development of human hypertension. J Cardiovasc Pharmacol 8 (Suppl 5) S64–S70

Bohlender J, Ménard J, Wagner J, Luft FC, Ganten D (1996) Développement chez le rat d'un modèle d'hypertension à la rénine humaine. Arch Mal Cœur 89:1009–1011

Bohlener J, Fukamizu, Lippoldt A, Nomura T, Dietz R, Ménard J, Muarakami K, Luft FC, Ganten D (1997) High human renin hypertension in transgenic rats. Hypertension 29(part 2):428–434

Cicila GT, Rapp JP, Wang JM, Lezin ES, Ng SC, Kurtz TW (1993) Linkage of 11β-hydroxylase mutations with altered steroid biosynthesis and blood pressure in the Dahl rat. Nature Genetics 3:346–353

Dahl LK, Heine M, Tassinari L (1962) Role of genetic factors in susceptibility to experimental hypertension due to chronic salt ingestion. Nature 194:480–482

Dahl LK, Heine M, Tassinari L (1962a) Effects of chronic salt ingestion. Evidence that genetic factors play an important role in susceptibility to experimental hypertension. J Exper Med 115:1173–1190

Dahl LK, Heine M, Tassinari L (1963b) Effects of chronic excess salt ingestion: role of genetic factors in both DOCA-salt and renal hypertension. J Exper Med 118:605

Deng Y, Rapp JP (1992) Cosegregation of blood pressure with angiotensin converting enzyme and atrial natriuretic receptor genes using Dahl salt-sensitive rats. Nature Genetics 1:267–272

Dubay Ch, Vincent M, Samani NJ, Hilbert P, Kaiser MA, Beressi JP, Kotelevtsev Y, Beckmann JS, Soubrier F, Sassard J, Lathorp GM (1993) Genetic determinants of diastolic and pulse pressure map to different loci in Lyon hypertensive rats. Nature Genetics 3:354–357

Dupont J, Dupont JC, Fromnet A, Milon H, Vincent M (1973) Selection of three strains of rats with spontaneously different levels of blood pressure. Biomedicine 19:36–41

Ernsberger P, Koletsky RJ, Collins LA, Douglas HC (1993) Renal angiotensin receptor mapping in obese spontaneously hypertensive rats. Hypertension 21:1039–1045

Feron O, Salomone S, Godfraind T (1996) Action of the calcium channel blocker lacidipine on cardiac hypertrophy and endothelin-1 gene expression in stroke-prone hypertensive rats. Br J Pharmacol 118:659–664

Ganten D (1987) Role of animal models in hypertension research. Hypertension, Suppl. 9:1:I2–I4

Gouyon B, Julier C, Takahashi S, Vincent M, Ganten D, Georges M, Lathrop GM (1991) Chromosomal mapping of two genetic loci associated with blood-pressure regulation in hereditary hypertensive rats. Nature 353:521–529

Hamet P, Malo D, Tremblay J (1990) Increased transcription of a major stress gene in spontaneously hypertensive mice. Hypertension 15:904–908

Hilbert P, Lindpaintner K, Beckmann JS, Serikawa T, Soubrier F, Dubay C, Cartwright P, Ganten D, Lindpainter K, Ganten U, Peters J, Zimmermann F, Bader M,. Mullins J (1991) Transgenic animals: New animal models in hypertension research. Hypertension 17:843–855

Holycross BJ, Summers BM, Dunn RB, McCune SA (1997) Plasma renin activity in heart failure-prone SHHF/Mcc-facp rats. Am J Physiol 273(1 Pt2):H228–H233

Inoko M, Kihara Y, Morii I, Fujiwara H, Saayama S (1994) Transition from compensatory hypertrophy to dilated, failing left ventricles in Dahl salt-sensitive rats. Am J Physiol 267:H2471–H2482

Jacob HJ, Lindpainter K, Lincoln SE, Kusumi K, Bunker RK, Mao YP, Ganten D, Dzau VJ, Lander ES (1991) Genetic mapping of a gene causing hypertension in the stroke-prone spontaneously hypertensive rat. Cell 67:213–224

Koletsky S (1975) Pathologic findings and laboratory data in a new strain of obese hypertensive rats. Am J Pathol 80:129–140

Langheinrich M, Jee MA, Böhm M, Pinto YM, Ganten D, Paul M (1996) The hypertensive *Ren-2* transgenic rat TGR(mREN2)27 in hypertension research. Characteristics and functional aspects. Am J Hypertens 9:506–512

Laverty R, Smirk FH (1961) Observations on the pathogenesis of spontaneous inherited hypertension and constricted renal-artery hypertension in rats. Circ Res 9:455–464

Lee MA, Böhm M, Paul M, Bader M, Ganten U, Ganten D (1996) Physiological characterization of the hypertensive transgenic rat TGR(mREN2)27. Am J Physiol 270(6 Pt 1):E919–E929

Linz W, Ganten D (1992) Contributions of animal models to understanding hypertension. In: Zipes DP,. Rowlands DJ (eds) Progress in Cardiology, pp 25–36, Lea and Febiger, Philadelphia

Linz W, Jessen T, Becker RHA, Schölkens BA, Wiemer G (1997) Long-term ACE inhibition doubles lifespan of hypertensive rats. Circulation 96:3164–3172

Meneton P, Ichikawa I, Inagami T, Schnermann J (2000) Renal physiology of the mouse. Am J Physiol 278:339–351

Mullins JJ, Ganten D (1990) Transgenic animals: new approaches to hypertension research. J Hypertension 8 (Suppl 7):S35–S37

Mullins JJ, Peters J, Ganten D (1990) Fulminant hypertension in transgenic rats harboring the mouse Re-2 gene. Nature 344:541–544

Ohkubo H, Kawakami H, Kakehi Y, Takumi T, Arai H, Yokota Y, Iwai M, Tanabe Y, Masu M, Hata J, Iwao H, Okamoto H, Yokoyama M, Nomura T, Katsuki M, Nakanishi S (1990) Generation of transgenic mice with elevated blood pressure by introduction of the rat renin and angiotensinogen genes. Proc Natl Acad Sci USA 87:5153–5156

Ohta K, Kim S, Wanibuchi H, Ganten D, Iwao K (1996) Contribution of local renin-angiotensin system to cardiac hypertrophy, phenotypic modulation, and remodelling in TGR(mREN2)27 transgenic rats. Circulation 94:785–791

Okamoto K, Aoki K (1963) Development of a strain of spontaneously hypertensive rats. Jap Circulat J 27:282–293

Okamoto K, Tabei R, Fukushima M, Nosaka S, Yamori Y, Ichijima K, Haebara H, Matsumoto M, Maruyama T, Suzuki Y, Tamegai M (1966) Further observations of the development of a strain of spontaneously hypertensive rats. Jap Circulat J 30:703–716

Okamoto K, Yamori Y, Nagaoka A (1974) Establishment of the stroke-prone spontaneously hypertensive rat (SHR) Circ Res 34/35 Suppl: I143–I153

Peters J, Münter K, Bader M, Hackenthal E, Mullins JJ, Ganten D (1993) Increased adrenal renin in transgenic hypertensive rats, TGR(mREN2)27, and its regulation by cAMP, angiotensin II, and calcium. J Clin Invest 91:742–747

Phelan EL (1968) The New Zealand strain of rats with genetic hypertension. NZ Med J 67:334–344

Phelan EL, Smirk FH (1960) Cardiac hypertrophy in genetically hypertensive rats. J Path Bact 80:445–448

Pijl AJ, van der Wal AC, Mathy MJ, Kam KL, Hendriks MGC, Pfaffendorf M, van Zwieten PA (1994) Streptozotocin-induced diabetes mellitus in spontaneously hypertensive rats: a pathophysiological model for the combined effects of hypertension and diabetes. J Pharmacol Toxicol Meth 32:225–233

Pinto YM, Paul M, Ganten D (1998) Lessons from rat models of hypertension: from Goldblatt to genetic engineering. Cardiovasc Res 39:77–88

Pravenec M, Klír P, Kren V, Zicha J, Kuneš J (1989) An analysis of spontaneous hypertension in spontaneously hypertensive rats by means of new recombinant inbred strains. J Hypertension 7:217–222

Rapp JP (1984) Characteristics of Dahl salt-susceptible and salt-resistant rats. In: de Jong W (ed) Handbook of Hypertension. Vol 4. Experimental and Genetic Models of Hypertension. Elsevier Science Publ., New York, pp 286–295

Rapp JP, Wang SM, Dene H (1989) A genetic polymorphism in the renin gene of Dahl rats cosegregates with blood pressure. Science 242:542–544

Rosenberg WL, Schlager G, Gennaro JF Jr (1985) Glomerular filtration and fluid balance in genetically hypertensive mice. Proc Soc Exp Biol Med 178:629–634

Rosenthal T, Erlich Y, Rosenmann E, Cohen A (1997) Effects of enalapril, losartan, and verapamil on blood pressure and glucose metabolism in the Cohen-Rosenthal diabetic hypertensive rat. Hypertension 29:1260–1264

Salvati P, Ferrario RG, Bianchi G (1990) Diuretic effect of bumetanide in isolated perfused kidneys of Milan hypertensive rats. Kidney Internat 37:1084–1089

Samani NJ, Brammar WJ, Swales JD (1989) A major structural abnormality in the renin gene of the spontaneously hypertensive rat. J Hypertension 7:249–254

Sen S, Tarazi RC, Khairallah PA, Bumpus FM (1974) Cardiac hypertrophy in spontaneously hypertensive rats. Circ Res 35:775–781

Simpson FO, Phelan EL (1984) Hypertension in the genetically hypertensive rat strain. In: de Jong W (ed) Handbook of Hypertension, Vol 4: Experimental and Genetic Models of Hypertension. pp 200–223. Elsevier Science Publ., New York

Smirk FH, Hall WH (1958) Inherited hypertension in rats. Nature 182:727–728

Vincent M, Sacquet J, Sassard J (1984) The Lyon strains of hypertensive, normotensive and low-blood-pressure rats. In: de Jong W (ed) Handbook of Hypertension, Vol 4: Experimental and Genetic Models of Hypertension. pp 314–327. Elsevier Science Publ., New York

Yamori Y (1984a) Development of the spontaneously hypertensive rat (SHR) and of various spontaneous rat models, and their implications. In: de Jong W (ed) Handbook of Hypertension, Vol 4: Experimental and Genetic Models of Hypertension. pp 224–239. Elsevier Science Publ., New York

Yamori Y (1984b) The stroke-prone spontaneously hypertensive rat: contributions to risk factor analysis and prevention of hypertensive diseases. In: de Jong W (ed) Handbook of Hypertension. Vol 4. Experimental and Genetic Models of Hypertension. Elsevier Science Publ., New York, pp 240–255

Yamori Y, Horie R, Nara Y, Kihara M (1983) Pathogenesis, prediction and prevention of stroke in stroke-prone SHR In: Stefanovich V (ed) Stroke: Animal models. pp 99–113. Pergamon Press Oxford, New York, Paris, Kronberg

Zolk O, Flesch M, Schnabel P, Teisman AC, Pinto YM, van Gilst WH, Paul M, Böhm M (1998) Effects of quinapril, losartan and hydralazine on cardiac hypertrophy and β-adrenergic neuroeffector mechanisms in transgenic TGR(mREN2)27 rats. Br J Pharmacol 123:405–412

A.2.0.8 Hypertension Induced by Chronic NO-Synthase Inhibition

PURPOSE AND RATIONALE

Tonic basal release of nitric oxide (NO) by vascular endothelial cells controls blood pressure in the basal state. Chronic blockade of NO synthesis in the rat produces systemic hypertension and glomerular damage (Baylis et al. 1992). This was recommended by Ribeiro et al. (1992) as a model of hypertension. Yang et al. (1996) found an increase of vascular angiotensin II receptor expression after chronic inhibition of NO synthase in spontaneously hypertensive rats. The detrimental sequels of chronic NO synthase inhibition in rats can be inhibited by treatment with ACE inhibitors (Hropot et al. 1994; Küng et al. 1995). Hsieh et al. (2004) reported that NO inhibition by L-NAME accelerates hypertension and induces perivascular inflammation in rats.

Hropot et al. (2003) reported that angiotensin II subtype AT_1 receptor blockade prevents hypertension and renal insufficiency induced by chronic NO synthase inhibition in rats.

PROCEDURE

Male Wistar rats at an age of 7–8 weeks weighing 210 ± 10 g were placed at random in metabolic cages,

divided in four to six groups of six to eight rats each. Group 1 (control) had free access to tap water and food. Groups 2–4 were treated with 0.02% L-NAME water solution for 6 weeks in a daily dose of 25 mg/kg. Groups 3 and 4 received the angiotensin receptor antagonists fonsartan (10 mg/kg) or lorsatan (30 mg/kg) for 6 weeks daily per stomach tube. Groups 5 and 6 received fonsartan and lorasatan alone. At the end of the study, 24-h urine samples were collected and retrobulbar blood samples were taken in short inhalation anesthesia. Plasma values of creatine, PRA and electrolytes were determined. For clearance evaluation rats were anesthetized with 50 mg/kg thiopentone i.p. In order to determine glomerular filtration rate and renal plasma flow, clearances of inulin and *para*-aminohippurate were performed. After the clearance experiments, the rats were sacrificed and hearts and kidneys removed. Hearts were perfused in the isolated working heart preparation via the aorta with modified Krebs-Henseleit buffer containing solvents or drugs. After a preischemic period of 20 min, acute regional myocardial ischemia was produced by clamping the left coronary artery close to its origin for 15 min (ischemic period). Thereafter, the clip was removed and changes during reperfusion were monitored (reperfusion period). The following cardio-dynamic and cardio-metabolic parameters were measured: incidence and duration of ventricular fibrillation, left ventricular pressure, contractility (d*P*/d*t* max), heart rate and coronary flow; in the coronary effluent lactate dehydrogenase, creatine kinase and lactate; in the myocardial tissue lactate, glycogen, ATP and creatine phosphate. Left ventricular pressure was measured with a Statham pressure transducer (P 23 DB) which on differentiation yielded LV d*P*/d*t* max and heart rate. Coronary flow was determined by electromagnetic flow probes in the aortic cannula. For the determination of lactate release, lactate dehydrogenase (LDH) and creatine kinase (CK) activities in the perfusate samples were taken from the coronary effluent and analyzed spectrophotometrically.

EVALUATION

Results are presented as arithmetical means ± SEM. A one-way ANOVA was calculated with SYSTAT for Windows (SYSTAT, Evanston, Ill., USA) followed by multiple pairwise comparisons according to Tukey.

MODIFICATIONS OF THE METHOD

Arnal et al. (1993) measured cardiac weight of rats in hypertension induced by NO synthase blockade.

Linz et al. (1999) reviewed the interactions between ACE, kinins and NO.

Sampaio et al. (2002) reported that hypertension plus diabetes mimics the cardiomyopathy induced by NO inhibition in rats.

Rossi et al. (2003) found that chronic inhibition of NO synthase induces hypertension and cardiomyocyte mitochondrial and myocardial remodeling in the absence of hypertrophy.

REFERENCES AND FURTHER READING

Arnal JF, el Amrani AI, Chatellier G, Menard J, Michel JB (1993) Cardiac weight in hypertension induced by nitric oxide synthase blockade. Hypertension 22:380–387

Baylis C, Mitruka B, Deng A (1992) Chronic blockade of nitric oxide synthesis in the rat produces systemic hypertension and glomerular damage. J Clin Invest 90:276–281

Hropot M, Grötsch H, Klaus E, Langer KH, Linz W, Wiemer G, Schölkens BA (1994) Ramipril prevents the detrimental sequels of chronic NO synthase inhibition in rats: hypertension, cardiac hypertrophy and renal insufficiency. Naunyn-Schmiedebergs Arch Pharmacol 350:646–652

Hropot M, Langer KH, Wiemer G, Grötsch H, Linz W (2003) Angiotensin II subtype AT_1 receptor blockade prevents hypertension and renal insufficiency induced by chronic NO-synthase inhibition in rats. Naunyn-Schmiedebergs Arch Pharmacol 367:312–317

Hsieh NK, Wang JY, Liu JC, Wang SD, Chen HI (2004) Nitric oxide inhibition accelerates hypertension and induces perivascular inflammation in rats. Clin Exp Pharmacol Physiol 31:212–218

Küng CF, Moreau P, Takase H, Lüscher TF (1995) L-NAME hypertension alters endothelial and smooth muscle function in rat aorta. Prevention by trandolapril and verapramil. Hypertension 26:744–751

Linz W, Wohlfart P, Schölkens BA, Malinski T, Wiemer G (1999) Interactions between ACE, kinins and NO. Cardiovasc Res 43:549–561

Ribeiro MO, Anuntes E, de Nucci G, Lovisolo SM, Zatz R (1992) Chronic inhibition of nitric oxide synthesis. A new model of arterial hypertension. Hypertension 20:298–303

Rossi MA, Ramos SG, Prado CM (2003) Chronic inhibition of nitric oxide synthase induces hypertension and cardiomyocyte mitochondrial and myocardial remodeling in the absence of hypertrophy. J Hypertens 21:993–1001

Sampaio RC, Tanus-Santos JE, Melo SESFC, Hyslop S, Franchinini KG, Luca IM, Moreno H Jr (2002) Hypertension plus diabetes mimics the cardiomyopathy induced by nitric oxide inhibition in rats. Chest 122:1412–1420

Yang Y, Macdonald GJ, Duggan KA (1996) A study of angiotensin II receptors after chronic inhibition of nitric oxide synthase in the spontaneously hypertensive rat. Clin Exp Pharmacol Physiol 23:441–443

A.2.0.9 Pulmonary Hypertension Induced by Monocrotaline

PURPOSE AND RATIONALE

The pyrrolizidine alkaloid monocrotaline, derived from *Crotalaria spectabilis*, is hepatotoxic and pneumotoxic in the rat. A single injection of monocrotaline

leads to progressive pulmonary hypertension resulting in right ventricular hypertrophy and cardiac failure (Gillespie et al. 1986, 1988; Todorovich-Hunter et al. 1988). Pathologic changes and hemodynamic changes associated with monocrotaline administration include blebbing of the lung, degeneration and fragmentation of endothelial cells, perivascular edema, extravasation of red blood cells, and muscularization of the pulmonary arteries and arterioles (Valdiva et al. 1967; Lalich et al. 1977; Huxtable et al. 1978; Hislop and Reid 1979; Meyrick and Reid 1979; Meyrick et al. 1980; Ghodsi and Will 1981; Hilliker et al. 1982; Sugita et al. 1983; Hilliker and Roth 1985; Stenmark et al. 1985; Altieri et al. 1986; Molteni et al. 1986; Lai et al. 1996). Rats given monocrotaline develop severe right ventricular hypertrophy often accompanied by ascites and pleural effusions (Ceconi et al. 1989).

Amelioration by angiotensin-converting enzyme inhibitors and by penicillamine has been demonstrated (Molteni et al. 1985, 1986).

PROCEDURE

Treatment of male Sprague Dawley rats weighing 200–225 g with the test drug (angiotensin converting enzyme inhibitor or vehicle) is started one week prior to a single subcutaneous injection of 100 mg/kg monocrotaline up to sacrifice 4, 7, or 14 days later by pentobarbital anesthesia and exsanguination. Heart and lungs are excised from thoracic cavity. After removing atria from the heart, the right ventricle is separated from the left ventricle plus septum which are blotted and weighed separately. Left lung is blotted, weighed, minced and reweighed after drying at room temperature for 14 days. Three pulmonary artery segments, main pulmonary artery, right extrapulmonary artery and an intrapulmonary artery from the from the right lower lobe, are isolated for study of vascular responsiveness. Cylindrical segments of each vessel are suspended between stainless steel hooks in 10-ml isolated tissue baths containing modified Krebs-Henseleit buffer aerated with 95% O_2/5% CO_2 at 37°C. At the end of each experiment, vessel segments are blotted and weighed and their dimensions measured. Cross-sectional area of each artery is determined from tissue weight and diameter.

Arteries are equilibrated for 1 h at 1 g of passive applied load and then are made to contract to KCl (6×10^{-2} M). After washout, the procedure is repeated with applied loads increased by 1 g increments. Responses are normalized to the maximum active force development generated by an artery in each experiment and the data are plotted as a function of applied force. Changes in isometric force are monitored through force displacement transducers (Grass FT03) and recorded on a polygraph.

Responsiveness to contractile and relaxant agonists is assessed in pulmonary arteries from saline- and monocrotaline-treated rats both in verum- and placebo-treated groups. Cumulative concentration-response curves to hypertonic KCl, angiotensin II and norepinephrine are generated sequentially in vessels at resting tone. Arteries are then contracted submaximally with norepinephrine and cumulative concentration-response curves to the vasorelaxants isoproterenol and acetylcholine are determined.

EVALUATION

Contractions are expressed as active tension development, force generated per cross-sectional area and relaxations are normalized to precontraction tone. Both contractile and relaxation responses are plotted as a function of the negative logarithm of agonist concentration. Differences in mean responses are compared by a *t*-test for grouped data.

MODIFICATIONS OF THE METHOD

Molteni et al. (1986) treated rats continuously with monocrotaline in the drinking water at a concentration of 2.4 mg/kg/day for a period of 6 weeks. Test rats received an ACE-inhibitor during this time in the drinking water and controls the vehicle only. At the end of the experiment, hearts and lungs were weighed and examined by light and electron microscopy.

Madden et al. (1995) determined L-arginine-related responses to pressure and vasoactive agents in monocrotaline-treated rat pulmonary arteries.

Ono et al. (1995) studied the effects of prostaglandin E_1 (PGE_1) on pulmonary hypertension and lung vascular remodelling in the rat monocrotaline model of human pulmonary hypertension.

Yamauchi et al. (1996) studied the effects of an orally active endothelin antagonist on monocrotaline-induced pulmonary hypertension in rats.

Gout et al. (1999) evaluated the effects of adrenomedullin in isolated vascular rings from rats treated with monocrotaline (60 mg/kg s.c.) causing pulmonary hypertension and ventricular hypertrophy within 3 to 4 weeks.

Kanno et al. (2001) studied the effect of an angiotensin-converting enzyme inhibitor on pulmonary arterial hypertension and endothelial nitric oxide synthase expression in monocrotaline-treated rats. For evaluation of right ventricular hypertrophy as a result of pulmonary arterial hypertension, multislice spin-

echo MRI images were acquired at 8–12 time points in a cardiac cycle with respiratory and ECG gating (Kanno et al. 2000) at 2, 3, 4, and 5 weeks after monocrotaline treatment.

Kang et al. (2003) reported that a phosphodiesterase-5 inhibitor attenuated monocrotaline-induced pulmonary hypertension in rats.

REFERENCES AND FURTHER READING

Altiere RJ, McIntyre MJ, Petrenka J, Olson JW, Gillespie MN (1986) Altered pulmonary vascular smooth muscle responsiveness in monocrotaline-induced pulmonary hypertension. J Pharmacol Exp Ther 236:390–395

Ceconi C, Condorelli ER, Quinzanini M, Rodella A, Ferrari R, Harris P (1989) Noradrenaline, atrial natriuretic peptide, bombesin and neurotensin in myocardium and blood of rats in congestive cardiac failure. Cardiovasc Res 23:674–682

Ghodsi F, Will JA (1981) Changes in pulmonary structure and function induced by monocrotaline intoxication. Am J Physiol 240:H149–H155

Gillespie MN, Olson JW, Reinsel CN, O'Connor WN, Altiere RJ (1986) Vascular hyperresponsiveness in perfused lungs from monocrotaline-treated rats. Am J Physiol 251:H109–H114

Gillespie MN, Goldblum SE, Cohen DA, McClain CJ, (1988) Interleukin-1 bioactivity in the lungs of rats with monocrotaline-induced pulmonary hypertension. Proc Soc Exp Biol Med 187:26–32

Gout B, Quiniou MJ, Khandoudi N, Le Dantec C, Saiag B (1999) Impaired endothelium-dependent relaxation by adrenomedullin in monocrotaline-treated rat arteries. Eur J Pharmacol 380:23–30

Hilliker KS, Roth RA (1985) Increased vascular responsiveness in lungs of rats with pulmonary hypertension induced by monocrotaline pyrrole. Am Rev Resp Dis 131:46–50

Hilliker KS, Bell TG, Roth RA (1982) Pneumotoxicity and thrombocytopenia after single injection of monocrotaline. Am J Physiol 242:H573–H579

Hislop A, Reid L (1979) Arterial changes in Crotalaria spectabilis-induced pulmonary hypertension in rats. Br J Exp Pathol 55:153–163

Huxtable RD, Ciaramitaro D, Eisenstein D (1978) The effect of a pyrrolizidine alkaloid, monocrotaline, and a pyrrole, dehydroretronecine, on the biochemical functions of the pulmonary endothelium. Mol Pharmacol 14:1189–1203

Kang KK, Ahn GJ, Sohn YS, Ahn BO, Kim WB (2003) DA-8159, a potent cGMP phosphodiesterase inhibitor, attenuates monocrotaline-induced pulmonary hypertension in rats. Arch Pharm Res 26:612–619

Kanno S, Lee PC, Zhang Y et al (2000) Attenuation of myocardial ischemia/reperfusion injury by superinduction of inducible nitric oxide synthase. Circulation. 101:2742–2748

Kanno S, Wu YJ, Lee PC, Billiar TR, Ho C (2001) Angiotensin-converting enzyme inhibitor preserves p21 and endothelial nitric oxide synthase expression in monocrotaline-induced pulmonary arterial hypertension in rats. Circulation 104:945–950

Lai YL, Thacker AA, Diana JN (1996) Hypoxemia and elevated tachykinins in rat monocrotaline pneumotoxicity. Lung 174:195–203

Lalich JJ, Johnson WD, Raczniak JJ, Shumaker RC (1977) Fibrin thrombosis in monocrotaline pyrrole induced cor pulmonale in rats. Arch Path Lab Med 101:69–73

Madden JA, Keller PA, Choy JS, Alvarez TA, Hacker AD (1995) L-arginine-related responses to pressure and vasoactive agents in monocrotaline-treated rat pulmonary arteries. J Appl Physiol 79:589–593

Meyrick B, Reid L (1979) Development of pulmonary arterial changes in rats fed Crotalaria spectabilis. Am J Pathol 94:37–50

Meyrick B, Gamble W, Reid L (1980) Development of Crotonolaria pulmonary hypertension: A hemodynamic and structural study. Am J Physiol 239:H692–H702

Molteni A, Ward WF, Ts'Ao CH, Solliday NH, Dunne M (1985) Monocrotaline-induced pulmonary fibrosis in rats: Amelioration by captopril and penicillamine. Proc Soc Exp Biol Med 180:112–120

Molteni A, Ward WF, Ts'Ao CH, Solliday NH (1986) Monocrotaline-induced cardiopulmonary damage in rats: amelioration by the angiotensin-converting enzyme inhibitor CL242817. Proc Soc Exp Biol Med 182:483–493

Ono S, Tanita T, Hoshikawa Y, Song C, Maeda S, Tabata T, Noda M, Ueda S, Ashino Y, Fujimura S (1995) Effects of prostaglandin E_1 (PGE_1) on pulmonary hypertension and lung vascular remodelling in a rat monocrotaline model of human pulmonary hypertension. Jpn J Thorac Dis 33:862–867

Pelá G, Missale C, Raddino R, Condorelli E, Spano PF, Visioli O (1990) β_1-and β_2-receptors are differentially desensitized in an experimental model of heart failure. J Cardiovasc Pharmacol 16:839–846

Stenmark KR, Morganroth ML, Remigo LK, Voelkel NF, Murphy RC, Henson PM, Mathias MM, Reeves JT (1985) Alveolar inflammation and arachidonate metabolism in monocrotaline-induced pulmonary hypertension. Am J Physiol 248:859–866

Sugita T, Hyers TM, Dauber IM, Wagner WW, McMurtry IF, Reeves JT (1983) Lung vessel leak precedes right ventricular hypertrophy in monocrotaline-treated rats. J Appl Physiol 54:371–374

Todorovich-Hunter L, Johnson DJ, Ranger P, Keeley FW, Rabinovitch M (1988) Altered elastin and collagen synthesis associated with progressive pulmonary hypertension induced by monocrotaline. A biochemical and ultrastructural study. Lab Invest 58:184–195

Valdiva E, Lalich JJ, Hayashi Y, Sonnard J (1967) Alterations in pulmonary alveoli after a single injection of monocrotaline. Arch Pathol 84:64–76

Yamauchi R, Hoshino T, Ban Y, Kikkawa K, Murata S, Nawano M, Toriumi W (1996) Effects of T-0115, a novel orally active endothelin antagonist, on monocrotaline-induced pulmonary hypertension in rats. Jpn J Pharmacol 71 (Suppl 1): 236P

A.2.0.10 Portal Hypertension in Rats

PURPOSE AND RATIONALE

Portal hypertension is associated with hyperdynamic splanchnic circulation and reduced vascular resistance (Vorobioff et al. 1983). Tanoue et al. (1991) developed a method for inducing portal hypertension and esophageal varices in rats – partial ligation of the portal vein after devascularization of the circumference of the left renal vein and complete ligation of the portal vein on the fifth day thereafter. Tsugawa et al. (2000)

used this model to study the role of nitric oxide and endothelin-1 in rat portal hypertension.

PROCEDURE

Male Sprague-Dawley rats were anesthetized with 50 mg/kg Nembutal intraperitoneally. The portal vein was isolated and stenosis created by a single ligature of 3–0 silk placed around the portal vein and a 20-gauge blunt-tipped needle after devascularization of the left renal vein. This devascularization is indispensable in preventing the development of excess collateral vessels, which inhibit the formation of esophageal varices and the portal hypertensive state. The needle was then removed from the ligature. In addition, 3–0 silk was also placed at the area of partial ligation (loose ligation), and both ends were then drawn out through the abdominal wall. Five days after the operation, the ends of the silk that had been placed in the flank were simultaneously pulled to induce complete portal vein ligation. Two weeks later, this portal hypertension model was completed.

Portal venous pressure, blood flow volume in the intra-abdominal viscera, plasma NO and plasma endothelin-1 were measured.

EVALUATION

Results were expressed as mean ± standard deviation. The Student's *t*-test was used to determine significance between portal hypertension rats and sham-operated controls.

MODIFICATIONS OF THE METHOD

Portal hypertension by portal vein ligation without devascularization of the left renal vein was used by Lee et al. (1985), Braillon et al. (1986), Oren et al. (1995), Fernandez et al. (1996), Moreno et al. (1996), Connolly et al. (1999), Hilzenrat et al. (1999), Chagneau et al. (2000), Yu et al. (2000), and Sakurabayashi et al. (2002).

Dieguez et al. (2002) used a surgical technique based on the development of a triple stenosing ligation to worsen the complications inherent to the prehepatic chronic portal hypertension.

Jaffe et al. (1994) and Li et al. (1998) used injection of different sized microspheres into the portal vein of male Wistar rats to induce portal hypertension.

REFERENCES AND FURTHER READING

Braillon A, Lee SS, Girod C, Peignoux-Martinot M, Valla D, Lebrec D (1986) Role of portasystemic shunts in the hyperkinetic circulation of the portal hypertensive rat. J Lab Clin Med 108:543–548

Chagneau C, Tazi KA, Heller J, Sogni P, Poirel O, Moreau R, Lebrec D (2000) The role of nitric oxide in the reduction of protein kinase C-induced contractile response in aortae from rats with portal hypertension. J Hepatol 33:26–32

Connolly C, Cawley T, McCormick PA, Docherty JR (1999) Portal hypertension increases vasoconstrictor responsiveness of rat aorta. Clin Sci 96:41–47

Dieguez B, Aller MA, Nava MP, Palma MD, Arias JL, Lopez L, Arias J (2002) Chronic portal hypertension in the rat by triple-portal stenosis ligation. J Invest Surg 15:329–336

Fernandez M, Garcia-Pagan JC, Casadevall M, Mourelle MI, Pique JM, Bosch J, Rodes J (1996) Acute and chronic cyclooxygenase blockage in portal-hypertensive rats: influence on nitric oxide biosynthesis. Gastroenterology 110:1529–1535

Jaffe V, Alexander B, Mathie RT (1994) Intrahepatic portal occlusion by microspheres: a new model of portal hypertension in the rat. Gut 35:815–819

Hilzenrat N, Arish A, Sikuler E (1999) Acute hemodynamic changes following hemorrhage and volume restitution, using a low viscosity plasma expander, in anesthetized portal hypertensive rats. J Hepatol 31:874–879

Lee SS, Girod C, Valla D, Geoffroy P, Lebrec D (1985) Effect of pentobarbital anesthesia on splanchnic hemodynamics of normal and portal-hypertensive rats. Am J Physiol 249:G528–G532

Li X, Benjamin IS, Alexander B (1998) The relationship between intrahepatic portal systemic shunts and microsphere induced portal hypertension in the rat liver. Gut 42:276–282

Moreno L, Martinez-Cuesta MA, Pique JM, Bosch J, Esplugues JV (1996) Anatomical differences in responsiveness to vasoconstrictors in the mesenteric veins from normal and portal hypertensive rats. Naunyn-Schmiedebergs Arch Pharmacol 354:474–480

Oren R, Hilzenrat N, Maaravi Y, Yaari A, Sikuler R (1995) Hemodynamic effects of hypothyroidism induced by methimidazole in normal and portal hypertensive rats. Dig Dis Sci 40:1941–1945

Sakurabayashi S, Koh KC, Chen L, Groszmann RJ (2002) Octreotide ameliorates the increase in collateral blood flow during postprandial hyperemia in portal hypertensive rats. J Hepatol 36:507–512

Tanoue K, Kitano S, Hshizume M, Wada H, Sugimachi K (1991) A rat model of esophageal varices. Hepatology 13:353–358

Tsugawa K, Hashizume M, Migou S, Kisihara F, Kawanaka H, Tomikawa M, Tanoue K (2000) Role of nitric oxide and endothelin-1 in a portal hypertensive rat model. Scand J Gastroenterol 35:1097–1105

Vorobioff J, Bredfeldt JE, Groszmann RJ (1983) Hyperdynamic circulation in portal-hypertensive rat model: a primary factor of maintenance of chronic portal hypertension. Am J Physiol 244:G52–G57

Yu Q, Shao R, Qian HS, George SE, Rockey DC (2000) Gene transfer of the neuronal NO synthase isoforms to cirrhotic rat liver ameliorates portal hypertension. J Clin Invest 105:741–748

A.3
Coronary (Cardiac) Drugs

A.3.1
Isolated Organs

A.3.1.1
Heart-Lung Preparation

PURPOSE AND RATIONALE

The isolated heart-lung of the dog was introduced by Knowlton and Starling (1912). Since then, the dog model has been used for many physiological and pharmacological studies (Krayer 1931; Krayer and Mendez 1942; Somani and Blum 1966; Takeda et al. 1973; Ishikawa et al. 1978, 1983; Ono et al. 1984a, b; Caffrey et al. 1986; Hausknecht et al. 1986; Fessler et al. 1988; Seifen et al. 1987, 1988; Naka et al. 1989). More recently, the rat model has been preferred (Dietz 1984, 1987; Onwochei et al. 1987, 1988; Kashimoto et al. 1987, 1990, 1994,1995, Fukuse et al. 1995).

PROCEDURE

Wistar rats weighing 300–320 g are anesthetized with 50 mg/kg pentobarbitone i.p. Tracheotomy is performed and intermittent positive pressure ventilation is instituted with air. The chest is opened and flooded with ice-cold saline and the heart arrested. Cannulae are inserted into the aorta and the superior (for measurement of central venous pressure) and inferior venae cavae. The heart-lung preparation is perfused with a solution containing rat blood cells from another rat and Krebs-Ringer bicarbonate buffer, with hematocrit and pH of 25% and 7.4, respectively. Concentration of the buffer constituents (mM): NaCl 127, KCl 5.1, $CaCl_2$ 2.2, KH_2PO_4 1.3, $MgSO_4$ 2.6, $NaHCO_3$ 15, glucose 5.5 and heparin. The perfusate pumped from the aorta passes through a pneumatic resistance and is collected in a reservoir maintained at 37°C and then returned to the inferior vena cava. In this model, no other organs except the heart and lung are perfused. Cardiac output is determined by the inflow as long as the heart does not fail. Mean arterial pressure is regulated by the pneumatic resistance. Heart rate is recorded by a bioelectric amplifier and cardiac output is measured with an electromagnetic blood flow meter. Arterial pressure and right atrial pressure are measured with transducers and amplifiers. The heart is perfused initially with cardiac output of 30 ml/min and mean arterial pressure of 80 mm Hg. Test drugs are administered into the perfusate 5 min after start of the experiment.

EVALUATION

Hemodynamic data within groups are analyzed by two-way analysis of variance (ANOVA) with repeated measures. Recovery time is measured by the Kruskal-Wallis test. The other data are analyzed by one-way ANOVA followed by the Dunnett test for multiple comparisons.

MODIFICATIONS OF THE METHOD

Using the Starling heart-lung preparation in dogs, Wollenberger (1947) studied the energy-rich phosphate supply of the failing heart.

Shigei and Hashimoto (1960) studied the mechanism of the heart failure induced by pentobarbital, quinine, fluoroacetate and dinitrophenol in dog's heart-lung preparation and effects of sympathomimetic amines and ouabain on it.

Imai et al. (1961) used heart-lung preparations of the dog to study the cardiac actions of methoxamine with special reference to its antagonistic action to epinephrine.

Capri and Oliverio (1965), Beaconsfield et al. (1974) used the heart-lung preparation of the **guinea pig**.

Robicsek et al. (1985) studied the metabolism and function of an autoperfused heart-lung preparation of the **dog**.

The **dog heart-lung preparation** was used by Seifen et al. (1988) to study the interaction of a calcium channel agonist with the effects of digoxin, by Somani and Blum (1966) to study blockade of epinephrine- and ouabain-induced cardiac arrhythmias in the dog,
by Riveron et al. (1988) to investigate the energy expenditure of an autoperfusing heart-lung preparation,
by Namakura et al. (1987) to study the role of pulmonary innervation in an *in situ* lung-perfusion preparation as a new model of neurogenic pulmonary edema,
by Hausknecht et al. (1986) to investigate the effects of lung inflation on blood flow during cardiopulmonary resuscitation,
by Caffrey et al. (1986) to evaluate the effect of naloxone on myocardial responses to isoproterenol,
by Ono et al. (1984) to estimate the cardiodepressant potency of various beta-blocking agents,
by Ishikawa et al. (1983) for a graphical analysis of drug effects in the dog heart-lung preparation – with particular reference to the pulmonary circulation and effects of norepinephrine and 5-hydroxytryptamine,
by Iizuka (1983) to study the cardiac effects of acetylcholine and its congeners,

by Fessler et al. (988) to investigate the mechanism of reduced LV afterload by systolic and diastolic positive pleural pressure,
by Takeda et al. (1973) to study the cardiac actions of oxprenolol.

Beaconsfield et al. (1974) used the heart-lung preparation of **guinea pigs** to study the cardiac effect of delta-9-tetrahydrocannabinol.

The **rabbit** autoperfusing heart-lung preparation was used by Muskett et al. (1986, 1988).

The isolated heart-lung preparation in the **cat** was described by Beaufort et al. (1993).

Kontos et al. (1987, 1988) harvested heart-lung blocks from **calves**.

REFERENCES AND FURTHER READING

Beaconsfield P, Oakley C, Carpi A, Rainsbury R, del Basso P (1974a) Cardiac effect of delta-9-tetrahydrocannabinol on a heart-lung preparation and on the intact animal. Eur J Cardiol 2:167–173

Beaconsfield P, Oakley C, Carpi A (1974b) Cardiac effect of delta-9-tetrahydrocannabinol on a heart-lung preparation and on the intact animal. Eur J Cardiol 2:167–173

Beaufort AM, Wierda JMKH, Houwertjes MC, Kleef UW, Meijer DKF (1993) The isolated heart-lung preparation in the cat. An *in situ* model to study the role of the lungs in the disposition of drugs. J Pharmacol Toxicol Meth 29:147–156

Caffrey JL, Wooldridge CB, Gaugl JF (1986) Naloxone enhances myocardial responses to isoproterenol in dog isolated heart-lung. Am J Physiol 250 (Heart Circ Physiol 19): H749–H754

Capri A, Oliverio A (1965) Effect of reserpine on the heart-lung preparation of guinea pig. Arch Int Pharmacodyn Ther 157:470–486

Dietz JR (1984) Release of natriuretic factor from rat heart-lung preparation by atrial distension. Am J Physiol 247 (Regulatory Integrative Comp Physiol 16) R1093–R1096

Dietz JR (1987) Control of atrial natriuretic factor release from a rat heart-lung preparation. Am J Physiol 252 (Regulatory Integrative Comp Physiol 21): R498–R502

Fessler HE, Brower RG, Wise RA, Permutt S (1988) Mechanism of reduced LV afterload by systolic and diastolic positive pleural pressure. J Appl Physiol 65:1244–1250

Fukuse T, Albes JM, Takahashi Y, Brandes H, Hausen B, Schäfers HJ (1995) Influence of red blood cells in an ex vivo rat heart-lung model. J Surg Res 59:399–404

Hausknecht MJ, Wise RA, Brower RG, Hassapoyannes C, Weisfeldt ML, Suzuki J, Permutt S (1986) Effects of lung inflation on blood flow during cardiopulmonary resuscitation in the canine isolated heart-lung preparation. Circ Res 59:676–683

Iizuka H (1983) Cardiac effects of acetylcholine and its congeners as assessed in canine heart-lung preparation. Folia Pharmacol Jpn 81:441–449

Imai S, Shigei T, Hashimoto K (1961) Cardiac actions of methoxamine with special reference to its antagonistic action to epinephrine. Circ Res 9:552–560

Jerusalem E, Starling EH (1910) On the significance of carbon dioxide for the heart beat. J Physiol 40:279–294

Ishikawa N, Taki K, Hojo Y, Hagino Y, Shigei T (1978) Direct recording of cardiac output- and venous return-curves in the dog heart-lung preparation for a graphical analysis of the effects of cardioactive drugs. Jpn Heart J 19:775–782

Ishikawa N, Taki K, Hojo Y, Hagino Y, Shigei T (1983) Graphical analysis of drug effects in the dog heart-lung preparation – with particular reference to the pulmonary circulation and effects of norepinephrine and 5-hydroxytryptamine. Jpn J Pharmacol 33:785–794

Kashimoto S, Tsuji Y, Kumazawa T (1987) Effects of halothane and enflurane on myocardial metabolism during postischaemic reperfusion in the rat. Acta Anaesth Scand 31:44–47

Kashimoto S, Kume M, Kumazawa T (1990) Functional and metabolic effects of bupivacaine and lignocaine in the rat heart-lung preparation. Br J Anaesth 65:521–526

Kashimoto S, Nakamura T, Kume M, Nonaka A, Kumazawa T (1994) Effects and interaction of nicardipine and volatile anesthetics in the rat heart-lung preparation. J Anesth 8:78–83

Kashimoto S, Namakura T, Furuya A, Kume M,. Kumazawa T (1995) Alteration of cardiac function and metabolism in the rat heart-lung preparation by methyl methacrylate and their protection by ulinastatin. Jpn J Anesth 44:1477–1481

Knowlton FP, Starling EH (1912) The influence of variations in temperature and blood pressure on the performance of the isolated mammalian heart. J Physiol 44:206–219

Kontos GJ Jr, Borkon AM, Adachi H, Baumgartner WA, Hutchins GM, Brawn J, Reitz BA (1987) Successful extended cardiopulmonary preservation in the autoperfused working heart-lung preparation. Surgery 102:269–276

Kontos GJ Jr, Borkon AM, Baumgartner WA, Fonger JD, Hutchins GM, Adachi H, Galloway E, Reitz BA (1988) Improved myocardial and pulmonary preservation by metabolic substrate enhancement in the autoperfused working heart-lung preparation. J Heart Transplant 7:140–144

Krayer O (1931) Versuche am isolierten Herzen. Naunyn Schmiedeberg's Arch exper Path Pharmakol 162:1–28

Krayer O, Mendez R (1942) Studies on veratrum alkaloids. I. The action of veratrine upon the isolated mammalian heart. J Pharmacol Exper Ther 74:350–364

Merin RG (1988) The isolated heart preparation. Br J Anesth 60:28S–34S

Muskett AD, Burton NA, Gay WA, Miller M, Rabkin MS (1986) Preservation in the rabbit autoperfusing heart-lung preparation: a potential role of indomethacin. Surgical Forum 37:252–254

Muskett AD, Burton NA, Grossman M, Gay WA Jr (1988) The rabbit autoperfusing heart-lung preparation. J Surg Res 44:104–108

Namakura J, Zhang S, Ishikawa N (1987) Role of pulmonary innervation in canine *in situ* lung-perfusion preparation: a new model of neurogenic pulmonary edema. Clin exp Pharmacol Physiol 14:535–543

Naka Y, Hirose H, Matsuda H, Nakano S, Shirakura R, Kawaguchi A, Miyamoto Y, Miyagawa S, Fukushima N, Kawashima Y (1989) Prevention of pulmonary edema in autoperfusing heart-lung preparations by FUT-175 and leukocyte depletion. Transplant Proc 21:1353–1356

Ono H, Kanazawa Y, O'Hara N, Hashimoto K (1984a) Estimation of cardiodepressant potency of nadolol, alprenololol, propranolol and pindolol, β-blocking agents, in heart-lung preparation and blood-perfused excised papillary muscle preparation of the dog. Japan J Pharmacol 36:507–517

Ono H, O'Hara N (1984b) A study of the cardiodepressant action of a β-blocking agent carteolol in heart-lung preparation of the dog. Jpn Circ J 86:1030–1044

Onwochei MO, Rapp JP (1988) Biochemically stimulated release of atrial natriuretic factor from heart-lung preparation in Dahl rats. Proc Soc Exper Biol Med 188:395–404
Onwochei MO, Snajdar RM, Rapp JP (1987) Release of atrial natriuretic factor from heart-lung preparations of inbred Dahl rats. Am J Physiol 253 (Heart Circ Physiol 22):H1044–1052
Riveron FA, Ross JH, Schwartz KA, Casey G, Sanders ON, Eisiminger R, Magilligan DJ Jr (1988) Energy expenditure of autoperfusing heart-lung preparation. Circulation 78, II Suppl III-103–III-109
Robicsek F, Masters TN, Duncan GD, Denyer MH, Rise HE, Etchison M (1985) An autoperfused heart-lung preparation: metabolism and function. Heart Transplant 4:334–338
Seifen E, Seifen AB, Kennedy RH, Bushman GA, Loss GE, Williams TG (1987) Comparison of cardiac effects of enflurane, isoflurane, and halothane in the dog heart-lung preparation. J Cardiothor Anesth 1:543–553
Seifen E, Kennedy RH, Seifen AB (1988) Interaction of BAY K-8644 with effects of digoxin in the dog heart-lung preparation. Eur J Pharmacol 158:109–117
Shigei T, Hashimoto K (1960) Study on the mechanism of the heart failure induced by pentobarbital, quinine, fluoroacetate and dinitrophenol in dog's heart-lung preparation and effects of sympathomimetic amines and ouabain on it. Jpn J Pharmacol 9:109–122
Somani P, Blum BK (1966) Blockade of epinephrine- and ouabain-induced cardiac arrhythmias in the dog heart-lung preparation. J Pharmacol Exp Ther 152:235–242
Takeda K, Iizuka K, Imai S (1973) Cardiac actions of oxprenolol as studied in dog heart-lung preparations. Arzneim Forsch/Drug Res 23:1446–1450
Wollenberger A (1947) On the energy-rich phosphate supply of the failing heart. Am J Physiol 150:733–745

A.3.1.2 Isolated Heart According to Langendorff

PURPOSE AND RATIONALE

More than 100 years ago Langendorff (1895) described studies on isolated surviving mammalian hearts using mainly cats as donors. Since then, the method has been improved from the technical site and is nowadays used for studies with guinea-pig, rabbit or rat hearts. In principle, the heart is perfused in retrograde direction from the aorta either at constant pressure or at constant flow with oxygenated saline solutions. Retrograde perfusion closes the aortic valves, just as in the *in situ* heart during diastole. The perfusate is displaced through the coronary arteries flowing off the coronary sinus and the opened right atrium. In this original set-up the ventricles do not fill with perfusate and therefore do not perform pressure-volume work. Parameters usually measured are: contractile force, coronary flow and cardiac rhythm.

PROCEDURE

Guinea pigs of either sex weighing 300–500 g are sacrificed by stunning. For studies of biochemical parameters in tissue and perfusate, removal of the heart during barbiturate anesthesia and artificial respiration is recommended. The heart is removed as quickly as possible and placed in a dish containing Ringer's solution at 37°C. Associated pericardial and lung tissue are removed. The aorta is located and cut just below the point of its division. A glass or plastic cannula is introduced into the aorta, tied with two threads and perfusion is started with oxygenated Ringer's solution or Krebs-Henseleit buffer. The heart is transferred to a double walled plexiglass perfusion apparatus which is kept at 37°C by the water from a thermostat. Oxygenated Ringer's solution is perfused at a constant pressure of 40 mm Hg and at a temperature of 37°C from a reservoir. A small steel hook with a string is attached to the apex of the heart. Contractile force is measured isometrically by a force transducer with a preload of 2.5 g and recorded on a polygraph. Coronary flow is measured by a drop counter. Alternatively, flow measurements can be performed using a mechanic-electronic flow meter consisting of a vertical pipe and a magnetic valve (Hugo Sachs Electronic KG, Germany). Heart rate is measured through a chronometer coupled to the polygraph. Drugs are injected into the perfusion medium just above the aortic cannula.

CRITICAL ASSESSMENT OF THE METHOD

A reappraisal of the LANGENDORFF heart preparation was given by Broadley (1979) underlining the usefulness to test coronary vasodilating drugs. The value of the LANGENDORFF method can be best assessed by demonstrating a few of its applications in physiology and pharmacology. Direct effects can be measured as well as the antagonism against various physiological and pharmacological agents.

MODIFICATIONS OF THE METHOD

A survey on various modifications of the LANGENDORFF-technique and the **isolated working heart preparation** has been given by Ross (1972).

Neely et al. (1967) inserted a second cannula into a pulmonary vein or the left atrium. Perfusate from a reservoir flows via this cannula through the mitral valve into the left ventricle. During the systole of the heart, the left ventricle repumps the perfusate through the aorta into the reservoir. The perfusate flowing through the coronary arteries and dripping off from the outside of the heart is collected in a vessel below the heart and recirculated into the reservoir with a roller pump.

Flynn et al. (1978) underlined the difference of this working heart preparation to the original LAN-

GENDORFF method and reported the effects of histamine and noradrenaline on peak left ventricular systolic pressure, contractility, sinus rate, coronary flow, aortic flow, total cardiac output, and external pressure-volume work. Therefore, this method is reported separately.

Ishiu et al. (1996) measured simultaneously Ca^{2+}-dependent indo-1 fluorescence and left ventricular pressure on a beat-to-beat basis in Langendorff guinea pig hearts and investigated the changes in Ca^{+2} transient and left ventricular function during positive inotropic stimulation and myocardial ischemia.

Hukovic and Muscholl (1962) described the preparation of the isolated **rabbit** heart with intact sympathic nervous supply from the right stellate ganglion.

Hendrikx et al. (1994) used the isolated perfused rabbit heart to test the effects of an Na^+/H^+ exchange inhibitor on postischemic function, resynthesis of high-energy phosphate and reduction of Ca^{2+} overload.

Michio et al. (1985) modified the Langendorff method in rabbits to a working heart preparation by cannulating the left atrium. At a pressure of 20 cm H_2O in the left atrium, the heart pumped the solution against a hydrostatic pressure of 100 cm H_2O. Aortic flow, systolic aortic pressure, coronary flow, and heart rate were measured.

The influence of an ACE-inhibitor on heart rate, lactate in the coronary effluate and GTP-level in the myocardium after 60-min hypothermic cardiac arrest was studied in working heart preparation of rabbits by Zegner et al. (1996).

Gottlieb and Magnus (1904) introduced the so called **"balloon method"**. A small balloon fixed to the tip of a catheter is filled with water and inserted into the left ventricle via one of the pulmonary veins, the left atrium and the mitral valve. The balloon size has to fit the volume of the left ventricle and therefore its size depends on the animal species and body weight. The catheter can be fixed by tying the pulmonary vein stems. Via a three-way valve, the balloon can be extended to a given preload. The beating heart now exerts a rhythmic force to the balloon and thus to the membrane of a pressure transducer. The advantages of this method are that force development and preload can be stated reproducibly in pressure units [mm Hg], left ventricular contraction curves can be used for further calculations, and continuous heart rate recordings can be carried out without any problems when using a rate meter.

Sakai et al. (1983) reported a similar method adapted to **mice**.

Bardenheuer and Schrader (1983) described a method whereby the balloon is inserted into the left ventricle as described above. However, isovolumetric pressure in the left ventricle is not measured. Instead, the fluid in the balloon is pumped through the cannula into a closed extra corporal circulation. The fluid is forced into one direction by 2 recoil valves. The balloon is made of silicone material using a Teflon form (Linz et al. 1986). The dimensions of the form are derived from casts of the left ventricle of K^+-arrested heart by injection of dental cement (Palavit 55, Kulzer and Co, GmbH, Germany). During each heart beat the fluid volume expelled from the balloon corresponding to the stroke volume of the heart, can be recorded by means of a flow meter probe and an integrator connected in series. Preload and afterload can be adjusted independently from each other. The perfusate flow (retrograde into the aorta and through the coronary arteries) is recorded separately.

The following parameters were measured in isolated **rat** hearts (Linz et al. 1986; Linz et al. 1990):

- LVP (left ventricular pressure) with Statham pressure transducer P 23 DB, which on differentiation yielded LV dp/dt_{max} and HR (heart rate). Cardiac output and coronary flow (CF) are determined by electromagnetic flow probes in the outflow system and in the aortic cannula, respectively. Coronary venous pO_2 is measured with a catheter placed in the pulmonary artery by a type E 5046 electrode connected to a PMH 73 pH/blood gas monitor (Radiometer). An epicardial electrocardiogram recording is obtained via two silver electrodes attached to the heart. All parameters are recorded on a Brush 2600 recorder.
- Myocardial oxygen consumption (MWO_2) [ml/min/g wet weight] is calculated according to the equation:

$$MVO_2 = CF \times (P_a = P_v) \times (c/760) \times 100$$

where CF is the coronary flow [ml/min/g], P_a is the oxygen partial pressure of arterial perfusate (650 mm Hg), P_v is the oxygen partial pressure of the venous effluent perfusate [mm Hg], and c is the 0.0227 ml O_2/ml perfusate representing the Bunsen solubility coefficient of oxygen dissolved in perfusate at 37°C (Zander and Euler 1976).

For the determination of lactate dehydrogenase (LDH) and creatine kinase (CK) activities in the perfusate, samples are taken from the coronary effluent.

After the experiments, hearts are rapidly frozen in liquid nitrogen and stored at –80°C. Of the left ventricle, 500 mg are taken, put into 5 ml ice-cold $HClO_4$ and disrupted with an Ultra-Turrax (Junke and Kunkel, Ika-Werk, Type TP). Glycogen is hydrolyzed with amyloglycosidase (pH 4.8) and determined as glucose. Furthermore, ATP and creatine phosphate are measured.

Avkiran and Curtis (1991) constructed a dual lumen aortic cannula which permits independent perfusion of left and right coronary beds in isolated rat hearts without necessitating the cannulation of individual arteries.

Igic (1996) described a modification of the isolated perfused working rat heart. A special double cannula was designed consisting of an outer cannula that is inserted into the aorta and an inner cannula that is advanced into the left ventricle. The perfusion fluid flows through the inner cannula into the left ventricle, and is ejected from there into the aorta. If the outer cannula system is closed, the fluid perfuses the coronary vessels and drips off outside the heart. When the outer cannula is open and certain pressure resistance is applied, a fraction of the ejected fluid perfuses coronary vessels and the rest is expelled. Because the inner cannula can be easily retracted into the outer cannula, which is placed in the aorta, the preparation provides an opportunity to use the same heart as a "working" or "non-working" model for investigating functions of the heart.

By labeling glucose, lactate, or fatty acids in the perfusate with ^{3}H or ^{14}C, Barr and Lopaschuk (1997) directly measured energy metabolism in the isolated rat heart.

Krzeminski et al. (1991) described a new concept of the isolated heart preparation with on-line computerized data evaluation. Left ventricular pressure was recorded by means of a balloon-catheter, while special suction electrodes obtained the high-amplitude, noise-free electrogram recordings. The coronary effluent partial pressure of oxygen was continuously monitored, which enabled the calculation of myocardial oxygen consumption (MVO_2). The effluent partial pressure of carbon dioxide and pH value were also measured simultaneously. A computerized system of data acquisition, calculation, storage, and end report was described.

Döring and Dehnert (1988) described continuous simultaneous **ultrasonic recording** of two cardiac diameters in an isolated perfused guinea-pig heart. For the measurement of the left ventricular transversal diameter the ultrasonic transmitter was positioned at the epicardium at the largest cardiac diameter. The corresponding ultrasonic receiver was inserted through the right atrium into the right ventricle to approximately the same height as the transmitter. In the right ventricle, which is empty in the isolated perfused LANGENDORFF-heart, it was automatically positioned opposite to the transmitter. Additional transducers were placed both at the heart's base and apex for assessment of the ventricular longitudinal diameter.

Several authors used the **isolated perfused mouse heart**.

Bittner et al. (1996) described a work-performing heart preparation for myocardial performance analysis in murine hearts using a modified Langendorff apparatus.

Sumaray and Yellon (1998a, b) constructed a specially designed Langendorff apparatus that allows perfusion of the isolated **mouse** heart. These authors reported that ischemic preconditioning reduces infarct size following global ischemia in the murine myocardium.

Brooks and Apstein (1996) measured left ventricular systolic and diastolic pressures in the isovolumically contracting (balloon in the left ventricle) mouse hearts.

Sutherland et al. (2003) reviewed characteristics and cautions in the use of the isolated perfused heart of mice.

Wang et al. (2001) studied the relationship between ischemic time and ischemia/reperfusion injury in isolated Langendorff-perfused mouse hearts.

Tejero-Taldo et al. (2002) reported that α-adrenergic receptor stimulation produces late preconditioning through inducible nitric oxide synthase in mouse heart.

Ross et al. (2003) found that the α_{1B}-adrenergic receptor decreases the inotropic response in the mouse Langendorff heart model.

Bratkovsky et al. (2004) measured coronary flow reserve in isolated hearts from mice.

Plumier et al. (1995) generated **transgenic mice** expressing the human heart heat shock protein 70. Upon reperfusion of the hearts after 30 min of ischemia in the Langendorff preparation, transgenic hearts versus non transgenic hearts showed significantly improved recovery of contractile force.

Hannan et al. (2000) compared ENOS knockout and wild-type mouse hearts which were perfused in a Langendorff apparatus with Krebs bicarbonate buffer and subjected to 20 min of global normothermic ischemia followed by 30 min of reperfusion. Myocardial function was measured using a ventricular balloon to determine time to onset of contraction, left ventricular

developed pressure (LVDP), left ventricular end-diastolic pressure (LVEDP), and heart rate-pressure product (RPP).

Sheikh et al. (2001) generated transgenic mice overexpressing fibroblast growth factor (FGF)-2 protein in the heart. An isolated mouse heart model of ischemia-reperfusion injury was used to assess the potential of endogenous FGF-2 for cardioprotection.

APPLICATIONS

Positive Inotropic Effects

While negative inotropic substances can be tested in a heart beating with normal force, the evaluation of a positive inotropic compound usually requires that cardiac force is first reduced. Acute experimental heart failure can be induced by an overdose of barbiturates, such as sodium thiopental, or calcium antagonists. This kind of cardiac failure can be reversed by β-sympathomimetic drugs, cardiac glycosides, or increased Ca^{+2} concentration. In this way, the potential β-sympathomimetic activity of a new drug can be measured using isoproterenol as standard. After thiopental-Na treatment, left ventricular pressure (LVP) and dp/dt_{max} decrease considerably, whereas coronary flow is slightly enhanced. β-Sympathomimetic drugs restore LVP and dp/dt_{max} and keep coronary blood flow elevated.

Cardiac glycosides increase LVP and dp/dt_{max} and leave coronary flow unchanged.

Negative Inotropic Effects

The effects of a β-sympathomimetic drug such as isoproterenol at doses of 0.05 to 0.2 µg increasing contractile force as well as heart frequency are registered. After injection of a β-blocker, the effects of isoproterenol are attenuated. The effects of a potential β-blocking agent can be tested comparing the isoproterenol inhibition versus a standard such as propranolol (0.1 mg).

Coronary Vessel Dilating Effect

The LANGENDORFF heart has been extensively used for assessing the coronary dilating activity of drugs (Broadley 1979). Rothaul and Broadley (1982) demonstrated the release of coronary vasodilator mediators from guinea pig isolated hearts by a technique employing donor and recipient hearts in series.

Calcium-Antagonism

In order to demonstrate the effect of calcium-antagonists, 1 to 5 mg $BaCl_2$ are injected which induce a pronounced spasm of the coronary arteries thereby reducing the coronary flow. Five min later, the test drug is injected. Active compounds have a relaxing effect on coronary arteries indicated by an increase of coronary flow. After this effect has weaned, $BaCl_2$ is injected again and the test drug or a standard drug, e. g. nifedipine, is tested. The increase of coronary flow is expressed as percentage of flow during $BaCl_2$ spasm and compared with the effect of the standard. Using various doses, dose-response curves can be established.

Effect on Potassium Outflow Induced by Cardiac Glycosides

Lindner and Hajdu (1968) described a method using the LANGENDORFF heart in which contractile force, coronary flow, and the potassium content in the coronary outflow was determined by flame photometry. Increase in potassium outflow correlates well with the positive inotropic effect.

Gradual Determination of Hypoxic Damage

Lindner and Grötsch (1973) measured the enzymes creatine phosphokinase (CPK), lactate dehydrogenase (LDH), α-hydroxybutyrate dehydrogenase (α-HBDH), and glutamicoxalacetic transaminase (GOT) in the effluent of a guinea pig heart preparation under varying degrees of hypoxia. Potassium content and oxygen tension in the inflowing and outflowing solution were determined. The heart rate, the amplitude of contraction and the rate of coronary vessel perfusion were recorded additionally.

Metabolic Studies with Nuclear Magnetic Resonance

Using ^{31}P, studies on metabolism of nucleotides and phosphorylated intermediates of carbohydrates in isolated hearts have been performed (Garlick et al. 1977; Jacobus et al. 1977; Hollis et al. 1978; Matthews and Radda 1984).

Arrhythmogenic, Anti-Arrhythmic and Antifibrillatory Effects

The LANGENDORFF heart preparation is also used to test the influence of compounds on cardiac rhythm. For recording monophasic action potentials, suction electrodes are applied on the heart. Ventricular fibrillation can be induced by simultaneous injection of digitoxin (12.5–25.0 µg) and aconitine (12.5–25.0 µg) into the perfusion fluid (Lindner 1963). Cardiac glycosides shorten the refractory period, decrease the conduction velocity and increase heterotopic stimulus generation. Aconitine increases markedly heterotopic stimulus generation. Both compounds together induce invariably ventricular fibrillation. Anti-arrhythmic com-

pounds can be tested in this way. Fibrillation is inhibited, at least partially, by 20 µg prenylamine, 10–20 µg quinidine or 20 µg ajmaline.

Takeo et al. (1992) described protective effects of anti-arrhythmic agents on oxygen-deficiency-induced contractile dysfunction of isolated perfused hearts. Hypoxia in isolated rabbit hearts was induced by perfusing the heart for 20 min with Krebs-Henseleit buffer saturated with a gas mixture of 95% N_2 and 5% CO_2 containing 11 mM mannitol. After hypoxic perfusion, the heart was reoxygenated for 45 min with oxygenated buffer containing glucose.

Dhein et al. (1989) studied the pathway and time course of the epicardial electrical activation process by means of a computer-assisted epicardial potential mapping, using a matrix of 256 unipolar AgCl electrodes (1 mm spatial and 0.25 ms temporal resolution) in isolated rabbit hearts perfused according to the Langendorff technique. From the activation times of the surrounding electrodes, the direction and velocity of activation for each electrode were calculated, thereby allowing construction of an epicardial vector field. The method was used for the assessment of arrhythmogenic and anti-arrhythmic drug activity.

Electrical Stimulation and Antifibrillatory Effect

Ventricular fibrillation can be induced in the LANGENDORFF preparation by reducing the glucose content of the perfusion medium to 0.25 g/1000 ml and the KCl content to 0.12 g/1000 ml. (Burn et al. 1957, 1960; Lindner 1963). After a perfusion period of 20 min, 10 µg epinephrine are injected into the perfusion cannula. Immediately afterwards, the heart is stimulated with a current of 40 Hz and 5 mA for 2 min. This procedure is repeated every 10 min. Standard conditions are achieved when the fibrillation continues without further electrical stimulation. Hearts treated in this way serve as controls. Other hearts stimulated in the same way are treated with continuous infusion of the test drug or the standard via the perfusion medium. Differences in the incidence of fibrillations are calculated using the χ^2 test.

Electrophysiological Evaluation of Cardiovascular Agents

Balderston et al. (1991) modified the Langendorff technique in rabbit hearts in order to perform electrophysiologic studies. His bundle electrograms were measured with a plunge electrode and allowed atrioventricular nodal physiology to be evaluated directly. Atrial conduction and refractoriness, atrioventricular node conduction and refractoriness, His-Purkinje conduction, and ventricular conduction and refractoriness could be accurately measured. The effects of verapamil and flecainide were described.

EDRF Release from the Coronary Vascular Bed

Lamontagne et al. (1992) isolated platelets from blood of healthy human donors and injected platelets boluses into the perfusion line of the Langendorff preparation of a rabbit heart. In the effluent cyclic GMP was determined as an index for EDRF release.

REFERENCES AND FURTHER READING

Avkiran M, Curtis MJ (1991) Independent dual perfusion of left and right coronary arteries in isolated rat hearts. Am J Physiol 261 (Heart Circ Physiol 30): H2082–H2090

Balderston SM, Johnson KE, Reiter MJ (1991) Electrophysiologic evaluation of cardiovascular agents in the isolated intact rabbit heart. J Pharmacol Meth 25:205–213

Bardenheuer H, Schrader J (1983) Relationship between myocardial oxygen consumption, coronary flow, and adenosine release in an improved isolated working heart preparation of guinea pigs. Circ Res 51:263–271

Barr RL, Lopaschuk GD (1997) Direct measurement of energy metabolism in the isolated rat heart. J Pharmacol Toxicol Meth 38:11–17

Bittner HB, Chen EP, Peterseim DS, Van Trigt P (1996) A work-performing heart preparation for myocardial performance analysis in murine hearts. J Surg Res 64:57–62

Bratkovsky S, Aasum E, Birkeland CH, Riemersma RA, Myrhe ESP, Larsen TS (2004) Measurement of coronary flow reserve in isolated hearts from mice. Acta Physiol Scand 181:167–172

Broadley KJ (1979) The Langendorff heart preparation – Reappraisal of its role as a research and teaching model for coronary vasoactive drugs. J Pharmacol Meth 2:143–156

Brooks WW, Apstein CS (1996) Effect of treppe on isovolumic function in the isolated blood-perfused mouse heart. J Mol Cell Cardiol 28:1817–1822

Brown TG, Lands AM (1964) Cardiovascular activity of sympathomimetic amines. In: Laurence DR, Bacharach AL (eds) Evaluation of Drug Activities: Pharmacometrics. Academic Press, London and New York, pp 353–368

Burn HJ, Hukovic S (1960) Anoxia and ventricular fibrillation: With a summary of evidence on the cause of fibrillation. Br J Pharmacol 15:67–70

Burn HJ, Goodford PJ (1957) Effect of lack of glucose and of lack of oxygen on ventricular fibrillation. J Physiol 137:20P–21P

Chevalier B, Mouas C, Mansier P, Aumont MC, Swynghedauw B (1987) Screening of inotropic drugs on isolated rat and guinea pig hearts. J Pharmacol Meth 17:313–326

Dhein S, Müller A, Klaus W (1989) The potential of epicardial activation mapping in isolated hearts for the assessment of arrhythmogenic and antiarrhythmic drug activity. J Pharmacol Meth 22:197–206

Döring HJ (1990) The isolated perfused warm-blooded heart according to LANGENDORFF. Technique – Function – Application. Physiologie bohemoslovaca 39:481–496

Flynn SB, Gristwood RW, Owen DAA (1978) Characterization of an isolated, working heart guinea-pig heart including effects of histamine and noradrenaline. J Pharmacol Meth 1:183–195

Garlick PP, Radda GK, Seeley PJ, Chance B (1977) Phosphorus NMR studies on perfused heart. Biochem Biophys Res Commun 74:1256–1262

Gottlieb R, Magnus R (1904) Digitalis und Herzarbeit. Nach Versuchen an überlebenden Warmblüterherzen. Naunyn-Schmiedeberg's Arch exper Path Pharmakol 51:30–63

Hannan RL, John MC, Kouretas PC, Hack BD, Matherne GP, Laubach VE (2000) Deletion of endothelial nitric oxidase exacerbates myocardial stunning in an isolated mouse heart model. J Surg Res 93:127–132

Hendrikx M, Mubagawa K, Verdonk F, Overloop K, Van Hecke P, Vanstapel F, Van Lommel A, Verbeken E, Lauweryns J, Flameng W (1994) Na^+-H^+ exchange inhibitor HOE 694 improves postischemic function and high-energy phosphate resynthesis and reduces Ca^{2+} overload in isolated perfused rabbit heart. Circulation 89:2787–2798

Hollis DP, Nunnally RL, Taylor GJ, Weisfeldt ML, Jacobus WE (1978) Phosphorus NMR studies of heart physiology. J Mag Reson 29:319–330

Hukovic S, Muscholl E (1962) Die Noradrenalin-Abgabe aus dem isolierten Kaninchenherzen bei sympathischer Nervenreizung und ihre pharmakologische Beeinflussung. Naunyn-Schmiedeberg's Arch exp Path Pharmak 244:81–96

Igic R (1996) The isolated perfused "working" rat heart: a new method. J Pharmacol Toxicol Meth 35:63–67

Ishiu R, Abe Y, Onishi K, Ueda Y, Sekioka K, Nakano T (1996) Changes in calcium transient and left ventricular function during inotropic stimulation and myocardial ischemia in indo-1-loaded beating guinea pig heart. J Pharmacol Toxicol Meth 35:55–61

Jacobus WE, Taylor GJ, Hollins DP, Nunnally RL (1977) Phosphorus nuclear magnetic resonance of perfused working rat hearts. Nature 265:756–758

Krzeminski T, Kurcok A, Kapustecki J, Kowalinski J, Slowinski Z, Brus R (1991) A new concept of the isolated heart preparation with on-line computerized data evaluation. J Pharm Meth 25:95–110

Lamontagne D, König A, Bassenge E, Busse R (1992) Prostacyclin and nitric oxide contribute to the vasodilator action of acetylcholine and bradykinin in the intact rabbit coronary bed. J Cardiovasc Pharmacol 20:652.657

Langendorff O (1895) Untersuchungen am lebenden Säugethierherzen. Pflüger's Arch ges Physiol 61:291–332

Lindner E (1963) Untersuchungen über die flimmerwidrige Wirkung des N-(3′-phenylpropyl-(2′))-1,1-diphenylpropyl-(3)-amins (Segontin). Arch Int Pharmacodyn 146:485–500

Lindner E, Grötsch H (1973) Methode zur graduellen Bestimmung hypoxischer Schädigung am isolierten Meerschweinchenherzen nach Langendorff. Arzneim Forsch/Drug Res 23:926–929

Lindner E, Hajdu P (1968) Die fortlaufende Messung des Kaliumverlustes des isolierten Herzens zur Bestimmung der Wirkungsstärke digitalisartiger Körper. Arch Int Pharmacodyn 175:365–372

Linz W, Schölkens BA, Han YF (1986) Beneficial effects of the converting enzyme inhibitor, ramipril, in ischemic rat hearts. J Cardiovasc Pharmacol 8 (Suppl 10):S91–S99

Linz W, Martorana PA, Schölkens BA (1990) Local inhibition of bradykinin degradation in ischemic hearts. J Cardiovasc Pharmacol 15 (Suppl 6): S99–S109

Matthews PM, Radda GK (1984) Applications of nuclear magnetic resonance to the study of myocardial metabolism and pharmacology. In: Schwartz A (ed) Methods in Pharmacology, Vol 5, Myocardial Biology., Plenum Press, New York and London, pp 175–228

Michio F, Hideo I, Tetsuya A (1985) *In vitro* assessment of myocardial function using a working rabbit heart. J Pharmacol Meth 14:49–60

Neely JR, Liebermeister H, Batterbsy EJ, Morgan HE (1967) Effect of pressure development on oxygen consumption by isolated rat heart. Am J Physiol 212:804–814

Plumier JCL, Ross BM, Currie RW, Angelidis CA, Kazlaris H, Kollias G, Pagoulatos GN (1995) Transgenic mice expressing the human heart heat shock protein 70 have improved postischemic myocardial recovery. J Clin Invest 95:1854–1860

Ross BD (1972) Perfusion techniques in biochemistry. A laboratory manual in the use of isolated perfused organs in biochemical experimentation. Clarendon Press, Oxford, Chapter 5: Heart and skeletal muscle. pp 258–320

Ross SA, Rorabaugh BR, Chalothorn D, Yun J, Gonzalez-Cabrera PJ, McCune DF, Piasik MT, Perez DM (2003) The α_{1B}-adrenergic receptor decreases the inotropic response in the mouse Langendorff heart model. Cardiovasc Res 60:598–607

Rothaul AL, Broadley KJ (1982) Measurements of oxygen tension in perfusates from guinea pig isolated hearts and the demonstration of coronary vasodilator material. J Pharmacol Meth 7:91–103

Sakai K, Akima M, Tsuyama K (1983) Evaluation of the isolated perfused heart of mice, with special reference to vasoconstriction caused by intracoronary acetylcholine. J Pharmacol Meth 10:263–270

Sheikh F, Sontag DP, Fandrich RR, Kardami E, Cattini PA (2001) Overexpression of FGF-2 increases cardiac myocyte viability after injury in isolated mouse hearts. Am J Physiol, Heart Circ Physiol 280:H1030–H1050

Sumaray MS, Yellon DM (1998a) Characterization and validation of a murine model of global ischaemia-reperfusion injury. Mol Cell Biochem 186:61–68

Sumaray MS, Yellon DM (1998b) Ischemic preconditioning reduces infarct size following global ischemia in the murine myocardium. Bas Res Cardiol 93:384–390

Sutherland FJ, Shattock MJ, Baker KE, Hearse DJ (2003) Mouse isolated perfused heart: characteristics and cautions. Clin Exp Pharmacol Physiol 30 :867–898

Takeo S, Tanonaka K, Liu JX, Ohtsuka Y (1992) Protective effects of antiarrhythmic agents on oxygen-deficiency-induced contractile dysfunction of isolated perfused hearts. In: Yasuda H, Kawaguchi H (eds) New Aspects in the Treatment of Failing Heart. Springer, Tokyo, Berlin, Heidelberg, pp 13–219

Tejero-Taldo MI, Gursoy E, Zhao TC, Kukreja RC (2002) α-Adrenergic receptor stimulation produces late preconditioning through inducible nitric oxide synthase in mouse heart. J Mol Cell Cardiol 34:185–195

Wang QD, Swärdh A, Sjöquist PO (2001) Relationship between ischemic time and ischemia/reperfusion injury in isolated Langendorff-perfused mouse hearts. Act Physiol Scand 171:123–128

Xiang JZ, Linz W, Becker H, Ganten D, Lang RE, Schölkens B, Unger Th (1985) Effects of converting enzyme inhibitors: Ramipril and enalapril on peptide action and neurotransmission in the isolated heart. Eur J Pharmacol 113:215–223

Zander B, Euler H (1976) Concentration measurements of physically dissolved oxygen by the classical van Slyke principle. In: Deng H, Balslen J, Brook R (eds) Measurement of oxygen. Elsevier Scientific Publ. C., Amsterdam, pp 271–276

Zegner M, Podesser B, Koci G, Weisser J, Hallström S, Schima H, Wollenek GH (1996) Evaluation of the in-

fluences of ramiprilat on the reperfusion. – Studied on the isolated working heart model. Acta Chir Austriatica 28:343–346

A.3.1.3 Coronary Artery Ligation in Isolated Working Rat Heart

PURPOSE AND RATIONALE

In working heart preparations of rats, ischemia can be induced by clamping the left coronary artery close to its origin. After removal of the clip, changes in the reperfusion period can be observed. Prevention of these symptoms can be an indicator of the efficacy of coronary drugs.

PROCEDURE

The preparation used is a modification of an isolated working heart preparation originally used for guinea pig hearts (Bardenheuer and Schrader 1983). Wistar rats of either sex weighing 280–300 g are sacrificed by decapitation. The hearts are removed and dissected free from the epicard and surrounding connective tissue. A cannula is introduced into the aorta from where the coronary vessels are perfused with the non-recirculated perfusion medium according to the Langendorff technique. In the left ventricle a balloon closely fitting the ventricular cavity is placed and connected to an artificial systemic circulation. The fluid in the balloon is pumped through a cannula into the closed extra corporal circulation being forced into one direction by 2 recoil valves. The balloon is made of silicone material using a Teflon form (Linz et al. 1986). The dimensions of the form are derived from casts of the left ventricle of K^+-arrested heart by injection of dental cement (Palavit 55, Kulzer and Co, GmbH, Germany). During each heart beat the fluid volume pressed from the balloon, corresponding to the stroke volume of the heart, can be recorded by means of a flow meter probe and an integrator connected in series. Preload and afterload can be adjusted independently from each other. The perfusate flow (retrograde into the aorta and through the coronary arteries) is recorded separately.

The following parameters were measured in isolated rat hearts (Linz et al. 1986):

LVP (left ventricular pressure) with Statham pressure transducer P 23 DB, which on differentiation yielded LV dp/dt_{max} and HR (heart rate). Cardiac output and coronary flow (CF) are determined by electromagnetic flow probes in the outflow system and in the aortic cannula, respectively. Coronary venous pO_2 is measured with a catheter placed in the pulmonary artery by a type E 5046 electrode connected to a PMH 73 pH/blood gas monitor (Radiometer). An epicardial electrocardiogram recording is obtained via two silver electrodes attached to the heart. All parameters are recorded on a Brush 2600 recorder.

Myocardial oxygen consumption (MWO_2) [ml/min/g wet weight] is calculated according to the equation:

$$MVO_2 = CF \times (P_a - P_v) \times (c/760) \times 100$$

where CF is the coronary flow [ml/min/g], P_a is the oxygen partial pressure of arterial perfusate (650 mm Hg), P_v is the oxygen partial pressure of the venous effluent perfusate [mm Hg], and c is the 0.0227 ml O_2/ml perfusate representing the Bunsen solubility coefficient of oxygen dissolved in perfusate at 37°C (Zander and Euler 1976).

Coronary Artery Ligation

For coronary artery occlusion experiment (Scholz et al. 1992, 1993), the isolated working hearts are perfused for a period of 20 min (pre-ischemic period) with modified Krebs-Henseleit buffer at a constant pressure of 65 mm Hg. Thereafter, acute myocardial ischemia is produced by clamping the left coronary artery close to is origin for 15 min (ischemic period). The clip is then reopened, and changes during reperfusion are monitored for 30 min (reperfusion period). After coronary artery ligation and reperfusion the hearts develop ventricular fibrillation.

From the coronary effluent samples are taken for lactate, lactate dehydrogenase (LDH), and creatine kinase (CK) determinations. After the experiment, glycogen, lactate, ATP, and creatine phosphate in myocardial tissue are measured.

The test drugs are given into the perfusion medium either before occlusion or 5 min before reperfusion. For *ex vivo* studies, the rats are treated orally with the test drug 1 h before sacrifice and preparation of the isolated working heart.

EVALUATION

The incidence and duration of ventricular fibrillation after treatment with coronary drugs is compared with controls. Left ventricular pressure, LV dP/dt max, and coronary flow are reduced after coronary constriction by angiotensin II, whereas enzyme activities in the effluent are increased and the myocardial content of glycogen, ATP and creatine phosphate are decreased. Cardiac protective drugs have the opposite effects. The values of each parameter are statistically compared with controls.

MODIFICATIONS OF THE METHOD

Vogel and Lucchesi (1980) described an isolated, blood perfused, **feline** heart preparation for evaluating pharmacological interventions during myocardial ischemia. Ventricular function was measured with a fluid-filled latex balloon within the left ventricle.

Vleeming et al. (1989) ligated the left coronary artery in rats after thoracotomy in ether anesthesia. Forty-eight hours after the operation, the hearts were prepared for retrograde constant pressure perfusion, according to the Langendorff technique.

Igic (1996) presented a new method for the isolated working rat heart. A special double cannula was designed consisting of an outer cannula that is inserted in the aorta and an inner cannula that is advanced into the left ventricle. The perfusion fluid flows through the inner cannula into the left ventricle, and is ejected from there into the aorta. If the outer cannula system is closed, the fluid perfuses the coronary vessels and drips off outside the heart. When the outer cannula is open and certain pressure resistance is applied, a fraction of the ejected fluid perfuses the coronary vessels and the rest is expelled. Because the inner cannula can easily be retracted into the outer cannula, which is placed in the aorta, this preparation provides an opportunity to use the same heart as a "working" or "non-working" model for investigating functions of the heart.

Pepe and McLennan (1993) described a maintained afterload model of ischemia in erythrocyte-perfused isolated working hearts of rats.

Further characterization of the pathophysiological reactions or the isolated working heart was performed by Linz et al. (1999). The external heart power (EHP) [mJ/min/g] was calculated using the formula:

$$\begin{aligned} EHP_{\mathrm{LV}} &= \text{pressure} - \text{volume} + \text{acceleration work} \\ &= [SV(MAP - LAP)] \\ &\quad + [1/2SV \times d \times (SV/\pi r^2 e^2)]HR\, g_{\mathrm{LVwwt}}^{-1} \end{aligned}$$

SV indicates stroke volume; *MAP*, mean aortic pressure; *LAP*, mean left arterial pressure; *d*, specific weight perfusate (1.004 g/cm^3); *r*, inner radius of aortic cannula; *e*, ejection time; *HR*, heart rate; LV, left ventricle; LVwwt, left ventricular wet weight.

The function of the left ventricle was altered by changing the aortic pressure (afterload) at constant left atrial filling load (preload). By adjusting the Starling resistance, the aortic outflow could be switched during 1 min from the fixed baseline afterload to a preset higher afterload producing step-wise rises in mean arterial pressure.

Lee et al. (1988) studied the effects of acute global ischemia on cytosolic calcium transients in perfused isolated **rabbit** hearts with the fluorescent calcium indicator indo 1. Indo 1-loaded hearts were illuminated at 360 nm, and fluorescence was recorded simultaneously at 400 and 550 nm from the epicardial surface of the left ventricle. The F_{400}/F_{550} ratio was calculated by an analog circuit, which allowed cancellation of optical motion artifact. The resulting calcium transients were registered simultaneously with the ventricular pressure and demonstrated a rapid upstroke and slow decay similar to those recorded in isolated ventricular myocytes. Global ischemia rapidly suppressed contraction, but it produced a concurrent increase in the systolic and diastolic levels of calcium transients, together with an increase in the duration of the peak.

REFERENCES AND FURTHER READING

Grupp IL, Grupp G (1984) Isolated heart preparations perfused or superfused with balanced salt solutions. In: Schwartz A (ed) Methods in Pharmacology, Vol 5: Myocardial Biology. pp 111–128. Plenum Press, New York and London

Igic R (1996) The isolated perfused "working" rat heart: a new method. J Pharmacol Toxicol Meth 35:63–67

Kannengieser GJ, Lubbe WF, Opie LH (1975) Experimental myocardial infarction with left ventricular failure in the isolated perfused rat heart. Effects of isoproterenol and pacing. J Mol Cell Cardiol 7:135–151

Linz W, Schölkens BA, Han YF (1986) Beneficial effects of the converting enzyme inhibitor, ramipril, in ischemic rat hearts. J Cardiovasc Pharmacol 8 (Suppl 10):S91–S99

Linz W, Schölkens BA, Manwen J, Wilhelm M, Ganten D (1986) The heart as a target for converting enzyme inhibitors: Studies in ischaemic isolated working hearts. J Hypertension 4, Suppl 6:S477–S479

Linz W, Schölkens BA, Kaiser J, Just M, Bei-Yin Q, Albus U, Petry P (1989) Cardiac arrhythmias are ameliorated by local inhibition of angiotensin formation and bradykinin degradation with the converting-enzyme inhibitor ramipril. Cardiovasc Drugs Ther 3:873–882

Linz W, Wohlfart P, Schoelkens BA, Becker RHA, Malinski T, Wiemer G (1999) Late treatment with ramipril increases survival in old spontaneously hypertensive rats. Hypertension 34:291–295

Martorana PA, Linz W, Göbel H, Petry P, Schölkens BA (1987) Effects of nicainoprol on reperfusion arrhythmia in the isolated working rat heart and on ischemia and reperfusion arrhythmia and myocardial infarct size in the anesthetized rat. Eur J Pharmacol 143:391–401

Pepe S, McLennan PL (1993) A maintained afterload model of ischemia in erythrocyte-perfused isolated working hearts. J Pharm Toxicol Meth 29:203–210

Rajagopalan R, Ghate AV, Subbarayan P, Linz W, Schoelkens BA (1993) Cardiotonic activity of the water soluble forskoline derivative 8,13-epoxy-6β-(piperidinoacetoxy)-1α,7β,9α-trihydro-xy-labd-14-en-11-one. Arzneim Forsch/Drug Res 43:313–319

Schölkens BA, Linz W, Lindpaintner K, Ganten D (1987) Angiotensin deteriorates but bradykinin improves cardiac function following ischaemia in isolated rat hearts. J Hypertens 5: Suppl 5:S7–S9

Scholz W, Albus U, Linz W, Martorana P, Lang HJ, Schölkens BA (1992) Effects of Na^+/H^+ exchange inhibitors in cardiac ischaemia. J Mol Cell Cardiol 24:731–740
Scholz W, Albus U, Lang HJ, Linz W, Martorana PA, Englert HC, Schölkens BA (1993) Hoe 694, a new Na^+/H^+ exchange inhibitor and its effects in cardiac ischemia. Br J Pharmacol 109:562–568
van Gilst WH, de Graeff PA, Wesseling H, de Langen CDJ (1986) Reduction of reperfusion arrhythmias in the ischemic isolated rat heart by angiotensin converting enzyme inhibitors: A comparison of captopril, enalapril, and HOE 498. J Cardiovasc Pharmacol 8:722–728
Vleeming W, van der Wouw PA, van Rooij HH, Wemer J, Porsius AJ (1989) *In vitro* method for measurement of cardiac performance and responses to inotropic drugs after experimentally induced myocardial infarction in the rat. J Pharmacol Meth 21:95–102
Vogel WM, Lucchesi BR (1980) An isolated, blood perfused, feline heart preparation for evaluating pharmacological interventions during myocardial ischemia. J Pharmacol Meth 4:291–303

A.3.1.4 Isolated Working Heart Model in Infarcted Rat Heart

PURPOSE AND RATIONALE

The model of chronic heart failure in spontaneously hypertensive rats described by Itter et al. (2004a) (see A.6.0.1.2) has been used by the same group to study the isolated working heart in rats after chronic infarction (Itter et al. 2004b).

PROCEDURE

Animals and Methods

WKY/NHsd and SHR/NHsd rats at an age of 4 months were randomized into two groups – sham and myocardial infarction (MI). The sham procedure consisted of opening the pericardium and placing a superficial suture in the epicardium of the left ventricle (LV). Chronic heart failure (CHF) was induced by permanent (8 weeks) occlusion of the left coronary artery 2 mm distal to the origin from the aorta resulting in a large infarction of the free left ventricular wall.

Eight weeks after surgery, parameters indicating CHF were measured. Cardiac hypertrophy, function and geometric properties were determined by the "working heart" mode and *in vivo* determinations by MRI and heart weight.

Surgery

The rats were anesthetized with a mixture of ketamine/xylazine (35/2 mg/kg i.p.). The left ventrolateral thorax was shaved and prepared to create a disinfected surgical access area. When stable anesthesia was achieved the animals were placed on a small animal operation table, intubated and ventilated with room air using a small animal ventilator (KTR-4, Hugo Sachs Elektronik, March-Hugstedten, Germany). The level of anesthesia was deemed as adequate following loss of the pedal withdrawal reflex and absence of the palpebral reflex. Reflexes were evaluated before surgery. The operation took 5 min. The tidal volume was adjusted at 3–5 ml and the ventilation rate was 40 breaths/min. Left thoracotomy was performed via the third intercostal space. The heart was exposed and the pericardium opened. The left main coronary artery was ligated with Perma-Hand silk 4–0 USP (Ethicon, Nordersredt, Germany) near its origin at the aorta (2 mm distal to the edge of the left atrium). Ligation resulted in infarction of the free left ventricular wall. Ligation was deemed successful when the anterior wall of the left ventricle turned pale. At this point the lungs were hyperinflated by increasing the positive end-expiratory pressure, and the chest was closed. The rats were placed on a heating pad and covered with a layer of unbleached tissue paper. The rats were extubated following return of reflexes. They were continuously monitored until they started moving in their cages. To avoid ventricular arrhythmias, lidocaine (2 mg/kg i.m.) was given before surgery. To prevent acute lung edema, the rats received furosemide (Lasix, 2 mg/kg body weight twice daily for 3 days) via the drinking water. To avoid pain and distress the rats received metamizol treatment (Novalgin, 0.1 mg/kg body weight i.m.) once, directly after the recovery period.

Before killing the animals 8 weeks after MI, non-invasive sequential nuclear magnetic resonance (NMR) measurements of heart geometric properties were done. Thereafter the animals were anesthetized with pentobarbitone (180 mg/kg i.p. Pentobarbital) and subsequently heparinized (Heparin Natrium 500 I.U./100 g body weight i.p.). Once stable anesthesia was achieved (stage III 3, reflexes absent), the animals were connected to an artificial respirator via a PE (polyethylene) tube inserted into the trachea and ventilated with room air. A transverse laparotomy and a right anterolateral thoracotomy were performed, and the heart was rapidly removed for the evaluation of its function in the working heart mode. The heart was immersed in physiological buffer chilled to 4°C. The aorta was dissected free and mounted onto a cannula (internal diameter: 1.4 mm) attached to perfusion apparatus. The hearts were perfused according to the method of Langendorff with an oxygenated (95% O2/5% CO_2) non-circulating Krebs–Henseleit solution of the following compositions (mM): NaCl, 118; KCl, 4.7; $CaCl_2$, 2.52; $MgSO_4$, 1.64; $NaHCO_3$,

24.88; KH_2PO_4, 1.18; glucose, 5.55; and Na pyruvate, 2.0 at a perfusion pressure of 60 mmHg. Any connective tissue, thymus or lung was carefully removed. A catheter placed into the pulmonary artery drained the coronary effluent perfusate that was collected for the determination of coronary flow and venous pO_2 measurements. The left atrium was cannulated via an incision of the left auricle. All pulmonary veins were ligated close to the surface of the atria.

When a tight seal with no leaks had been established and after a 15-min equilibration period, the hearts were switched into the working mode, using a filling pressure (preload) of 12 mmHg in WKY/NHsd and 18 mmHg in SH rats. The afterload pressure was 60 mmHg in WKY/NHsd and 80 mmHg in SH rats. After validation of the basis parameters the afterload pressure was enhanced in a cumulative manner from an additional 20 mmHg to 140 mmHg. Thereafter the isovolumetric maxima were determined by enhancing the preload pressure in steps of 5 mmHg to 30 mmHg.

Flow and pressure signals for computation were obtained from the PLUGSYS-measuring system (Hugo Sachs Elektronik, March-Hugstedten, Germany). Computation of data was performed with a sampling rate of 500 Hz, averaged every 2 s, using the software Aquire Plus V1.21f (PO-NE-MAH, Hugo Sachs Elektronik, March-Hugstedten, Germany).

Determination of Infarct Size

After the evaluation of the external heart work, the total heart weight, and the left and right ventricular weights were determined. The left ventricle was then sectioned transversely into four slices from the apex to the base. Eight pictures were taken of each rat heart, two from each slice. Total infarct size was determined by planimetry of the projected and magnified slices. The areas of infarcted tissue as well as the intact myocardium of each slice were added together and averaged. The infarcted fraction of the left ventricle was calculated from these measurements and expressed as a percentage of the left ventricular mass. The left ventricular perimeter, diameter, infarct scar length, as well as wall thickness and infarct wall thinning were determined as well.

EVALUATION

The data are given as mean ± SEM. Statistics were performed using the SAS system statistics package (SAS Insititute, Cary, N.C., USA) with a sequential rejection *t*-test according to Holm (1979).

REFERENCES AND FURTHER READING

Holm S (1979) A simple sequential rejective multiple test procedure. Scand J Stat 6:65–70

Itter G, Jung W, Juretschke P, Schölkens BA, Linz W (2004a) A model of chronic heart failure in spontaneous hypertensive rats (SHR). Lab Anim 38:138–148

Itter G, Jung W, Schölkens BA, Linz W (2004b) The isolated working heart model in infarcted rat hearts. Lab Anim 39:178–193

A.3.1.5 Relaxation of Bovine Coronary Artery

PURPOSE AND RATIONALE

Eicosanoids can regulate the tonus of coronary arteries. Prostacyclin induces relaxation, whereas thromboxane A_2 causes contraction. Spiral strips from bovine coronary artery can be used for assaying relaxation activity of test compounds (Dusting et al. 1977)

PROCEDURE

Freshly slaughtered beef hearts are immersed in cold oxygenated Krebs solution and immediately transported in a thermos flask to the laboratory. The left descending coronary artery and several of its primary branches are cut into spiral strips (about 20 mm long and 2–3 mm wide). The specimens can be stored up to 48 h at 4°C. The artery strips are suspended in a 4 ml organ bath under an initial tension of 2 g and immersed in a Krebs' bicarbonate solution at 37°C being gassed with oxygen containing 5% CO_2 throughout the experiment. The Krebs solution contains a mixture of antagonists to inhibit any actions from endogenous acetylcholine, 5-hydroxytryptamine, histamine or catecholamines (hyoscine hydrobromide 10^{-7} g/ml, methysergide maleate 2×10^{-7} g/ml, mepyramine maleate 10^{-7} g/ml, propranolol hydrochloride 2×10^{-6} g/ml). The strips are superfused with a solution of the test compounds in concentrations of 0.01, 0.1, 1.0 µg/ml at a rate of 10–20 ml/min with oxygenated Krebs solution containing the mixture of antagonists. Isometric contractions are recorded with Grass force-displacement transducers (type FT 03 C) on a Grass polygraph. The strips are superfused with Krebs' solution 3 h prior to the experiment. Standard compounds are 100 ng/ml PGE_2 inducing contraction and 100 ng/ml PGI_2 inducing pronounced relaxation.

EVALUATION

The relaxation induced by the test compound is expressed as percentage of maximal response to 100 ng/ml PGI_2.

MODIFICATIONS OF THE METHOD

Campell and Paul (1993) measured the effects of diltiazem on isometric force generation, $[Ca^{2+}]_i$, and energy metabolism in the isolated **porcine** coronary artery.

Li et al. (1997) determined the ability of analogues of human α-calcitonin gene-related peptide to relax isolated porcine coronary arteries precontracted with 20 mM KCl.

REFERENCES AND FURTHER READING

Dusting GJ, Moncada S, Vane JR (1977) Prostacyclin (PGX) is the endogenous metabolite responsible for relaxation of coronary arteries induced by arachidonic acid. Prostaglandins 13:3–15

Gilmore N, Vane JR, Wyllie JH (1968) Prostaglandins released by the spleen. Nature 218:1135–1140

Li J, Matsuura JE, Waugh DJJ, Adrian TE, Abel PW, Manning MC, Smith DD (1997) Structure – activity studies on position 14 of human α-calcitonin gene-related peptide. J Med Chem 40:3071–3076

A.3.2 In Vivo Methods

A.3.2.1 Isoproterenol Induced Myocardial Necrosis in Rats

PURPOSE AND RATIONALE

Cardiac necrosis can be produced by injection of natural and synthetic sympathomimetics in high doses. Infarct-like myocardial lesions in the rat by isoproterenol have been described by Rona et al. (1959). These lesions can be totally or partially prevented by several drugs such as sympatholytics or calcium-antagonists.

PROCEDURE

Groups of 10 male Wistar rats weighing 150–200 g are pretreated with the test drug or the standard either s.c. or orally for 1 week. Then, they receive 5.25 and 8.5 mg/kg isoproterenol s.c. on two consecutive days. Symptoms and mortality in each group are recorded and compared with those of rats given isoproterenol alone. Forty-eight hours after the first isoproterenol administration, the rats are sacrificed and autopsied. The hearts are removed and weighed, and frontal sections are embedded for histological examination.

EVALUATION

Microscopic examination allows the following grading:

Grade 0: no change

Grade 1: focal interstitial response

Grade 2: focal lesions in many sections, consisting of mottled staining and fragmentation of muscle fibres

Grade 3: confluent retrogressive lesions with hyaline necrosis and fragmentation of muscle fibres and sequestrating mucoid edema

Grade 4: massive infarct with occasionally acute aneurysm and mural thrombi

For each group the main grade is calculated with the standard deviation to reveal significant differences.

CRITICAL ASSESSMENT OF THE METHOD

The test has been used by many authors for evaluation of coronary active drugs, such as calcium-antagonists and other cardioprotective drugs like nitroglycerin and molsidomine (Vértesy et al. 1991; Classen et al. 1993).

MODIFICATIONS OF THE METHOD

Yang et al. (1996) reported a protective effect of human adrenomedullin$^{13–52}$, a C-terminal fragment of adrenomedullin$^{10–52}$ on the myocardial injury produced by subcutaneous injection of isoproterenol into rats.

REFERENCES AND FURTHER READING

Bhargava AS, Preus M, Khater AR, Günzel P (1990) Effect of iloprost on serum creatine kinase and lactate dehydrogenase isoenzymes after isoprenaline-induced cardiac damage in rats. Arzneim Forsch/Drug Res 40:248–252

Brodowicz GR, Lamb DR (1991) Exercise training, indomethacin, and isoproterenol-induced myocardial necrosis in rats. Bas Res Cardiol 86:40–48

Campell JD, Paul RJ (1993) Effects of diltiazem on force, $[Ca^{2+}]_i$, and energy metabolism in porcine coronary artery. J Cardiovasc Pharmacol 22:408–415

Ciplea AG, Kretschmar R, Heimann W, Kirchengast M, Safer A (1988) Protective effect of the new calcium antagonist Anipamil against isoprenaline-induced cardionecrosis in rats. Arzneim-Forsch/Drug Res 38:215–221

Classen L, Michalsky G, Kammermeier H (1993) Catecholamine-induced cardiac necroses: Protective effect of leucocytopenia, influence of an S2 antagonist, thromboxan-synthetase inhibitor and prostacyclin analogue. Bas Res Cardiol 88:52–59

Ferrans VJ, Hibbs RG, Black WC, Weilbaecher DG (1964) Isoproterenol-induced myocardial necrosis. A histochemical and electron microscopic study. Am Heart J 68:71–90

Genovese A, Chiariello M, de Alfieri W, Latte S, Ferro G, Condorelli M (1982) Quantitative assessment of infarct size in isoproterenol-infarcted rats. Jpn Heart J 23:997–1006

Handforth CP (1962) Isoproterenol-induced myocardial infarction in animals. Arch Path 73:161–165

Joseph X, Bloom S, Pledger G, Balazs T (1983) Determinants of resistance to the cardiotoxicity of isoproterenol in rats. Toxicol Appl Pharmacol 69:199–205

Knufman NMJ, van der Laarse A, Vliegen HW, Brinkman CJJ (1987) Quantification of myocardial necrosis and cardiac hypertrophy in isoproterenol-treated rats. Res Commun Chem Pathol Pharmacol 57:15–32

Meijer AEFH, Hettwer H, Ciplea AG (1988) An enzyme histochemical study of isoproterenol-induced myocardial necroses in rats. Histochem J 20:697–707

Preus M, Bhargava AS, Khater AER, Günzel P (1988) Diagnostic value of serum creatine kinase and lactate dehydrogenase isoenzyme determinations for monitoring early cardiac damage in rats. Toxicol Letters 42:225–253

Rona G (1967) Experimental drug-induced myocardial infarction for animal pharmacologic screening. In: Siegeler PE, Moyer JH (eds) Animal and clinical pharmacologic techniques in drug evaluation. Vol II, pp 464–470, Year Book Medical Publ. Chicago

Rona G, Chappel CI, Balazs T, Gaudry R (1959) An infarct-like myocardial lesion and other toxic manifestations produced by isoproterenol in the rat. Arch Path 76:443–455

Rona G, Chappel CI, Kahn DS (1963) The significance of factors modifying the development of isoproterenol-induced myocardial necrosis. Am Heart J 66:389–395

Vértesi C, Knopf E, Gaál, Körmöczy PS (1991) Comparison of the cardioprotective effects of nitroglycerin, molsidomine, and SIN-1 in rats. J Cardiovasc Pharmacol 17 (Suppl 3) S141–S144

Wexler BC (1985) Prolonged protective effects following propranolol withdrawal against isoproterenol-induced myocardial infarction in normotensive and hypertensive rats. Br J exp Path 66:143–154

Yang J, Zhao D, Chang YZ, Tin Q, Zhao YT, Shi XY, Zhang ZK, Tang CS (1996) Protective effect of adrenomedullin$^{10–52}$ on isoproterenol-induced myocardial injury in rats. Chin Pharmacol Bull 12:530–533

A.3.2.2 Myocardial Infarction After Coronary Ligation in Rodents

PURPOSE AND RATIONALE

Ligation of the left coronary artery in rats as described by Selye (1960) induces an acute reduction in pump function and a dilatation of left ventricular chamber. The method has been used to evaluate beneficial effects of drugs after acute (Chiariello et al. 1980; Flaim and Zelis 1981; Bernauer 1985) or chronic (Innes and Weisman 1981; Pfeffer et al. 1985; Linz et al. 1996) treatment.

PROCEDURE

Male Sprague Dawley rats weighing 200–300 g are anesthetized with diethylether. The chest is opened by a left thoracotomy, and a thread is inserted near the middle of the lateral margin of the cutaneous wound and carried through a tunnel of the left pectoral muscle around the cranial half of the incision. The heart is gently exteriorized by pressure on the abdomen. A ligature is placed around the left coronary artery, near its origin, and is tightened. Within seconds, the heart is repositioned in the thoracic cavity, and the ends of the musculocutaneous thread are tightened to close the chest wall and enable the animal to breathe spontaneously. The speed of the procedure renders mechanical respiration unnecessary.

To evaluate drug effects, the rats are treated 5 min after and 24 h after occlusion by subcutaneous injection (standard 5 mg/kg propranolol).

Two days after surgery, the rats are anesthetized with 60 mg/kg i.p. pentobarbital and the right carotid artery is cannulated with a polyethylene catheter connected to a pressure transducer. The fluid-filled catheter is then advanced into the left ventricle through the aortic valve for measurement of left ventricular systolic and end-diastolic pressure.

After hemodynamic measurements, the heart is arrested by injecting 2 ml of 2.5 M potassium chloride. The chest is opened, and the hearts are isolated and rinsed with 300 mM KCl to maintain a complete diastole. A double-lumen catheter is advanced into the left ventricle through the ascending aorta, the right and left atria are tied off with a ligature, and the right ventricle is opened. The left ventricular chamber is filled with a cryostatic freeze medium through the smaller of the two catheter lumens and connected to a hydrostatic pressure reservoir maintained at a level corresponding to the end-diastolic pressure measured *in vivo*. The outlet (larger lumen) is then raised to the same level as the inlet to allow fluid in the two lumens to equilibrate. The heart is rapidly frozen with hexane and dry-ice.

The hearts are serially cut with a cryostat into 40-µm-thick transverse sections perpendicularly to the longitudinal axis from apex to base. At a fixed distance, eight sections are obtained from each heart and collected on gelatin-coated glass slides. Sections are air-dried and incubated at 25°C for 30 min with 490 µM nitroblue tetrazolium and 50 mM succinic acid in 0.2 M phosphate buffer (pH 7.6), rinsed in cold distilled water, dehydrated in 95% ethyl alcohol, cleared in xylene, and mounted with a synthetic resin medium. Viable tissue appears dark blue, contrasting with the unstained necrotic tissue.

EVALUATION

The infarct size can be determined by planimetry and expressed as percentage of left ventricular area, and thickness can be expressed as percentage of non-infarcted ventricular wall thickness (MacLean et al. 1978; Chiariello 1980; Roberts et al. 1983). An automatic method for morphometric analysis with image acquisition and computer processing was described by Porzio et al. (1995).

CRITICAL ASSESSMENT OF THE METHOD

Myocardial infarction following coronary artery ligation in Sprague-Dawley rats is a widely used rat model of heart failure. If the left coronary artery is not completely ligated, heart failure may occur as a consequence of chronic myocardial ischemia (Kajstura et al. 1994).

MODIFICATIONS OF THE METHOD

Johns and Olson (1954) described the coronary artery patterns for mouse, rat, hamster and guinea pig.

Kaufman et al. (1959), Fishbein et al. (1978, 1980) used various histochemical methods for identification and quantification of border zones during the evolution of myocardial infarction.

Sakai et al. (1981) described an **experimental model of angina pectoris in the intact anesthetized rat**. In anesthetized rats the tip of a special carotid cannula was placed closely to the right and left coronary ostium. Single intra-aortic injections of methacholine or acetylcholine (in the presence of physostigmine) developed a reproducible elevation of the ST segment and the T wave of the electrocardiogram. Coronary drugs were tested to prevent these changes.

Ytrehus et al. (1994) analyzed the effects of anesthesia, perfusate, risk zone, and method of infarct sizing in rat and rabbit heart infarction.

Leprán et al. (1981) placed a loose ligature of atraumatic silk around the left anterior descending coronary artery under ether anesthesia in **rats**. Ten days later, acute myocardial infarction was produced by tightening the ligature.

Kouchi et al. (2000) found an increase in $G_{i\alpha}$ protein accompanying progression of post-infarction remodelling in hypertensive cardiomyopathy in **rats.** G protein α subunits were studied with immunoblotting techniques (Böhm et al. 1990). The polyclonal antiserum MB1 was raised in rabbits against the carboxyl-terminal decapeptide of retinal transduction (KENLKDCGLF) coupled to keyhole limpet hemocyanine. The MB1 recognized $G_{i\alpha 1}$ and $G_{i\alpha 2}$ but not $G_{0\alpha}$ and $G_{i\alpha 3}$ (Böhm et al. 1994). The membrane fractions were electrophoresed in SDS-polyacrylamide gels and were transferred to nitrocellulose filters. The filters were incubated with the first antibodies for $G_{i\alpha}$ (MB1) or $G_{s\alpha}$ (RM/1) and then with the second antibody (horseradish peroxidase-conjugated goat anti-rabbit IgG, Amersham). Immunoreactive signals were detected by means of the ECL kit (Amersham).

Liu et al. (1997) found that ligation of the left descending coronary artery in Lewis inbred **rats** produces an uniformly large infarct with low mortality. The model may be superior to the usual model in Sprague-Dawley rats with a marked variability in infarct size and cardiac dysfunction.

Coronary artery ligation induces left ventricular remodeling with cardiomyocyte apoptosis, myocardial fibrosis indicated by morphological studies and by collagen accumulation, which can be prevented by drug treatment (Yang et al. 1992; Belichard et al. 1994; Nguyen et al. 1998; Sia et al. 2002; Bäcklund et al. 2004).

The naturally occurring peptide ***N*-acety-seryl-aspartyl-lysyl-proline (Ac-SDKP)** is a inhibitor of pluripotent hematopoietic stem cell proliferation and is normally present in human plasma and circulating mononuclear cells. It is cleaved to an inactive form by the NH_2-terminal catalytic domain of ACE (Azizi et al. 1996). Acute angiotensin converting enzyme inhibition increases the plasma level of *N*-acetyl-seryl-aspartyl-lysyl-proline (Azizi et al. 1996). By morphological studies and collagen determinations, Rasoul et al. (2004) found an antifibrotic effect of Ac-SDKP and angiotensin converting enzyme inhibition in hypertension in rats. Similarly, Yang et al. (2004) found that Ac-SDKP reverses inflammation and fibrosis in rats with heart failure after myocardial infarction.

Moreover, Azizi et al. (1997) and Le Meur et al. (1998) discussed whether the plasma Ac-SDKP level is a reliable marker of chronic angiotensin converting enzyme inhibition in hypertensive patients. An AcSDKP EIA Kit is available from Cayman, Ann Arbor, Mich., USA.

Chen et al. (2004) found inhibition and reversal of myocardial -infarction-induced hypertrophy and heart failure by NHE-1 inhibition.

Johns and Olson (1954) described a method of experimental **myocardial infarction by coronary occlusion in small animals**, such as **mouse**, **hamster**, **rat** and **guinea pig**.

Scholz et al. (1995) described a dose-dependent reduction of myocardial infarct size in **rabbits** by a selective sodium-hydrogen exchange subtype 1 inhibitor.

Gomoll and Lekich (1990) tested the **ferret** for a myocardial ischemia/salvage model. Varying combinations of duration of left anterior descending coronary occlusion and reperfusion were evaluated.

Coronary artery ligation in mice

Michael et al. (1995, 1999), and Gould et al. (2001) described the surgical procedure to induce myocardial ischemia in **mice** by ligation of the left anterior descending branch of the left coronary artery.

Infarct and Reperfusion Model

Male C57BL/6 mice 12–16 weeks of age (22.5–30.5 g body weight) were used. Anesthesia was produced by an intraperitoneal injection of pentobarbital sodium (4 mg/ml; 10 µl/g body weight). Mice were placed in a supine position with paws taped to the operating table. With direct visualization of the trachea, an endotracheal tube was inserted and connected to a Harvard rodent volume-cycled ventilator cycling at 100/min with volume sufficient to adequately expand the lungs but not overexpand. The inflow valve was supplied with 100% oxygen.

For studies of the myocardial response to permanent occlusion, ligation of the anterior descending branch of the left coronary artery was achieved by tying an 8–0 silk suture around the artery. The suture was passed under the artery at a position ~ 1 mm from the tip of the normally positioned left auricle.

For studies of the effect of reperfusion after coronary artery occlusion, the ligature was tied at the same location on the coronary artery used for the permanent occlusion. However, to allow subsequent reestablishment of blood flow, occlusion was produced by placing a 1-mm length of polyethylene (PE) tubing (OD = 0.61 mm) on the artery and fixing it in place with the ligature. The artery was then compressed by tightening the ligature, producing myocardial blanching and electrocardiographic (ECG) S-T segment elevation as observed in permanent ligations. After occlusion for the desired time, blood flow was restored by removing the ligature and PE tubing. The chest wall was then closed by a 6–0 Ticron suture with one layer through the chest wall and muscle and a second layer through the skin and subcutaneous layer.

After surgical closing of the chest, the endotracheal tube was removed, warmth was provided by a heat lamp, and 100% oxygen was provided via a nasal cone. The animal was given 0.1 mg/kg butorphanol tartrate as an analgesic, and it became sternally recumbent within 1 h. After surviving the experimental infarct the mice recovered, and this allowed postoperative physiological measurement. Sham-operated mice underwent an identical procedure with placement of the ligature but did not undergo coronary artery occlusion.

MODIFICATIONS OF THE METHOD

Guo et al. (1998) demonstrated the effects of an early and a late phase of ischemic preconditioning in mice. The results demonstrated that, in the mouse, a robust infarct-sparing effect occurred during both the early and the late phases of ischemic preconditioning, although the early phase was more powerful.

Guo et al. (2005) found that late preconditioning induced by NO donors, adenosine A_1 receptor agonists, and δ_1-opioid receptor agonists is mediated by inducible NO synthase.

Lutgens et al. (1999) reported cardiac structural and functional changes after chronic myocardial infarction in the mouse.

Scherrer-Crosbie et al. (1999) described echocardiographic determination of risk area in a murine model of myocardial ischemia. Myocardial contrast echocardiography was performed before and after coronary artery ligation in anesthetized mice by intravenous injection of contrast microbubbles and transthoracic echo imaging. Time-video intensity curves were obtained for the anterior, lateral, and septal myocardial walls. After myocardial ischemia, myocardial contrast echocardiography defects were compared with the area of no perfusion measured by Evans blue staining.

Jones and Lefer (2001) described cardioprotective actions of acute HMG-CoA reductase inhibition in the setting of myocardial infarction.

Janssens et al. (2004) reported that cardiomyocyte-specific overexpression of NO synthase 3 (NOS3) improves left ventricular (LV) performance and reduces compensatory hypertrophy after myocardial infarction. The effect of cardiomyocyte-restricted overexpression of one NO synthase isoform, NOS3, on LV remodeling after myocardial infarction in mice was tested. LV structure and function before and after permanent left anterior descending (LAD) coronary artery ligation were compared in transgenic mice with cardiomyocyte-restricted NOS3 overexpression (NOS3-TG) and their wild-type littermates (WT). Before myocardial infarction, systemic hemodynamic measurements, echocardiographic assessment of LV fractional shortening (FS), heart weight, and myocyte width (as assessed histologically) did not differ in NOS3-TG and WT mice. The inotropic response to graded doses of isoproterenol was significantly reduced in NOS3-TG mice. One week after LAD ligation, the infarcted fraction of the LV did not differ in WT and NOS3-TG mice. Four weeks after myocardial infarction, however, end-systolic LV internal diameter (LVID) was greater, and FS and maximum and minimum rates of LV pressure development were less in WT than in NOS3-TG mice. LV weight/body weight ratio was greater in WT than in NOS3-TG mice.

LaPointe et al. (2004) found that inhibition of cyclooxygenase-2 (COX-2) improves cardiac function after myocardial infarction in the mouse. Myocardial infarction was produced by ligation of the LAD coro-

nary artery in mice. Two days later, mice were treated with a selective COX-2 inhibitor, or vehicle in drinking water for 2 weeks. After the treatment period, mice were subjected to two-dimensional M-mode echocardiography to determine cardiac function. Hearts were then analyzed for determination of infarct size, interstitial collagen content, brain natriuretic peptide (BNP) mRNA, myocyte cross-sectional area, and immunohistochemical staining for transforming growth factor (TGF)β and COX-2.

Shibuya et al. (2005) reported that *N*-acetyl-seryl-aspartyl-lysine-proline prevents renal insufficiency and matrix expansion in diabetic d*b*/d*b* **mice**.

Weinberg et al. (2005) found in coronary ligation experiments in mice, that rosuvastatin reduces experimental left ventricular infarct size after ischemia-reperfusion injury but not total coronary occlusion.

Yang et al. (2005) found that the infarct-sparing effect of A_{2A}-adenosine receptor activation is due primarily to its action on lymphocytes. Chimeric mice were created by bone marrow transplantation from A_{2A}AR-knockout or green fluorescent protein (GFP) donor mice to irradiated congenic C57BL/6 (B6) recipients. In the GFP chimeras, we were unable to detect GFP-producing cells in the vascular endothelium, indicating that bone-marrow-derived cells were not recruited to endothelium at appreciable levels after bone marrow transplantation and/or acute myocardial infarction. Injection of 5 or 10 µg/kg of a potent and selective agonist of A_{2A} adenosine receptor had no effect on hemodynamic parameters but reduced infarct size in B6 mice after 45 min of LAD artery occlusion followed by 24 h of reperfusion.

Kanno et al. (2003) found **connexin**43 to be a determinant of myocardial infarct size following coronary occlusion in mice.

Regulation of myocardial connexins during hypertrophic remodeling was reviewed by Teunissen et al. (2004).

Kuhlmann et al. (2006) reported that granulocyte colony stimulating factor (G-CSF), alone or in combination with stem cell factor (SCF), can improve hemodynamic cardiac function after myocardial infarction in mice and reduces inducible arrhythmias in the infarcted heart potentially via increased connexin43 expression and arteriogenesis.

REFERENCES AND FURTHER READING

Azizi M, Rousseau A, Ezan E, Guyene TT, Michelet S, Grognet JM, Lefant M, Corvol P, Ménard J (1996) Acute angiotensin-converting enzyme inhibition increases the plasma level of the natural stem cell regulator *N*-acetyl-seryl-aspartyl-lysyl-proline. J Clin Invest 97:839–844

Azizi M, Rousseau A, Ezan E, Guyene TT, Michelet S, Grognet JM, Lenfant M, Corvol P, Menard J (1997) Acute angiotensin-converting enzyme inhibition increases the plasma level of the natural stem cell regulator *N*-acetyl-seryl-aspartyl-lysyl-proline. J Clin Invest 97.839–844

Azizi M, Ezan E, Nicolet L, Grognet JM, Ménard J (1997) High plasma level of *N*-acetyl-seryl-aspartyl-lysyl-proline. A new marker of chronic angiotensin-converting enzyme inhibition. Hypertension 30:1015–1019

Bäcklund T, Palojoki E, Saraste A, Eriksson A, Finkenberg P, Kytö V, Lakkisto P, Mervaala E, Voipio-Pulkki LM, Laine M, Tikkanen L (2004) Sustained cardiomyocyte apoptosis and left ventricular remodelling after myocardial infarction in experimental diabetes. Diabetologia 47:325–330

Belichard P, Savard P, Cardinal R, Naddeau R, Gosselin H, Paradis P, Rouleau JL (1994) Markedly different effects on ventricular remodelling result in a decrease in inducibility of ventricular arrhythmias. J Am Coll Cardiol 23:505–513

Bernauer W (1985) The effect of β-adrenoreceptor blocking agents on evolving myocardial necrosis in coronary ligated rats with and without reperfusion. Naunyn-Schmiedeberg's Arch Pharmacol 328:288–294

Böhm M, Gierschik P, Jakobs KH, Pieske B, Schnabel P, Ungerer M, Erdmann E (1990) Increase of $G_{i\alpha}$ in human hearts with dilated but not ischemic cardiomyopathy. Circulation 82:1249–1265

Böhm M, Eschenhagen T, Gierschik P, Larisch K, Lensche H, Mende U, Schmitz W, Schnabel P, Scholz H, Steinfath M, Erdmann H (1994) Radioimmunochemical quantification of $G_{i\alpha}$ in right and left ventricles from patients with ischemic and dilated cardiomyopathy and predominant left ventricular failure. J Mol Cell Cardiol 26:133–149

Chen L, Chen CX, Gan XT, Beier N, Scholz W, Karmazyn M (2004) Inhibition and reversal of myocardial infarction-induced hypertrophy and heart failure by NHE-1 inhibition. Am J Physiol 286:H381–H387

Chiariello M, Brevetti G, DeRosa G, Acunzo F, Petillo F, Rengo F, Condorelli M (1980) Protective effects of simultaneous alpha and beta adrenergic receptor blockade on myocardial cell necrosis after coronary arterial occlusion in rats. Am J Cardiol 46:249–254

Colatsky Th (1989) Models of myocardial ischemia and reperfusion injury: Role of inflammatory mediators in determining infarct size. Pharmacological Methods in the Control of Inflammation, pp 283–320, Alan R. Liss, Inc.

Fishbein MC, MacLean D, Maroko PR (1978) Experimental myocardial infarction in the rat. Qualitative and quantitative changes during pathologic evolution. Am J Pathol 90:57–70

Fishbein MC, Hare AC, Gissen SA, Spadaro J, MacLean D, Maroko PR (1980) Identification and quantification of histochemical border zones during the evolution of myocardial infarction in the rat. Cardiovasc Res 14:41–49

Flaim SF, Zelis R (1981) Diltiazem pretreatment reduces experimental myocardial infarct size in rat. Pharmacology 23:281–286

Gomoll AW, Lekich RF (1990) Use of the ferret for a myocardial ischemia/salvage model. J Pharmacol Meth 23:213–223

Gould KE, Taffet GE, Michael LH, Christie RM, Konkol DL, Pocius JS, Zachariah JP, Chaupin DF, Daniel SL, Sandusky GE, Jr, Hartley CJ, Entman ML (2001) Heart failure and greater infarct expansion in middle-aged mice: a relevant model for postinfarction failure. Am J Physiol 282:H615–H621

Guo Y, Wu WJ, Qiu Y, Tang XL, Yang Z, Bolli R (1998) Demonstration of an early and a late phase of ischemic preconditioning in mice. Am J Physiol 275:H1375–H1387

Guo Y, Stein AB, Wu WJ, Zhu X, Tan W, Li Q, Bolli R (2005) Late preconditioning induced by NO donors, adenosine A_1 receptor agonists, and δ_1-opioid receptor agonists is mediated by iNOS. Am J Physiol 289:H2251–H2257

Innes IR, Weisman H (1981) Reduction in the severity of myocardial infarction by sulfinpyrazone. Am Heart J 102:153–157

Janssens S, Pokreisz P, Schoonjans L, Pellens M, Vermeersch P, Tjwa M, Jans P, Scherrer-Crosbie M, Picard MH, Szelid Z, Gillijns H, Van de Werf F, Collen D, Bloch KD (2004) Cardiomyocyte-specific overexpression of nitric oxide synthase 3 improves left ventricular performance and reduces compensatory hypertrophy after myocardial infarction. Circ Res 94:1256–1262

Johns TNP, Olson BJ (1954) Experimental myocardial infarction. I. A method of by coronary occlusion in small animals. Ann Surg 140:675–682

Jones SP, Lefer DJ (2001) Cardioprotective actions of acute HMG-CoA reductase inhibition in the setting of myocardial infarction. Acta Physiol Scand 173:139–143

Kajstura J, Zhang X, Reiss K, Szoke E, Li P, Lagastra C, Cheng W, Darzynkiewicz Z, Olivetti G, Anversa P (1994) Myocyte cellular hyperplasia and myocyte cellular hypertrophy contribute to chronic ventricular remodeling in coronary artery narrowing-induced cardiomyopathy in rats. Circ Res 74:382–400

Kanno S, Kovacs A, Yamada KA, Saffitz JE (2003) Connexin43 as a determinant of myocardial infarct size following coronary occlusion in mice. J Am Coll Cardiol 41:681–686

Kaufman N, Gavan TL, Hill RW (1959) Experimental myocardial infarction in the rat. Arch Pathol 57:482–488

Kouchi I, Zolk O, Jockenhövel F, Itter G, Linz W, Cremers B, Böhm M (2000) Increase in $G_{i\alpha}$ protein accompanies progression of post-infarction remodelling in hypertensive cardiomyopathy. Hypertension 36:42–47

Kuhlmann MT, Kirchhof P, Klocke R, Hasib L, Stypmann J, Fabritz L, Stelljes M, Tian W, Zwiener M, Mueller M, Kienast J, Breithardt G, Nikol S (2006) G-CSF/SCF reduces inducible arrhythmias in the infracted heart potentially via increased connexin43 expression and arteriogenesis. J ExpMed 203:87–97

LaPointe MC, Mendez M, Leung A, Tao Z, Yang XP (2004) Inhibition of cyclooxygenase-2 improves cardiac function after myocardial infarction in the mouse. Am J Physiol 286:H1416–H1424

Le Meur Y, Aldigier JC, Praloran V (1998) Is plasma Ac-SDKP level is a reliable marker of chronic angiotensin-converting enzyme inhibition in hypertensive patients? Hypertension 31:1201–1202

Leprán I, Koltai M, Szekeres L (1981) Effect of non-steroid anti-inflammatory drugs in experimental myocardial infarction in rats. Eur J Pharmacol 69:235–238

Linz W, Wiemer G, Schmidts HL, Ulmer W, Ruppert D, Schölkens BA (1996) ACE inhibition decreases postoperative mortality in rats with left ventricular hypertrophy and myocardial infarction. Clin Exper Hypertension 18:691–712

Liu YH, Yang XP, Nass O, Sabbah HN, Peterson E, Carretero OA (1997) Chronic heart failure induced by coronary artery ligation in Lewis inbred rats. Am J Physiol 272 (2 Pt2):H722–H727

Lutgens E, Daemen MJ, de Muinck ED, Debets J, Leenders P, Smits JF (1999) Chronic myocardial infarction in the mouse: cardiac structural and functional changes. Cardiovasc Res 41:586–593

MacLean D, Fishbein MC, Braunwald E, Maroko PR (1978) Long-term preservation of ischemic myocardium after experimental coronary artery occlusion. J Clin Invest 61:541–551

Michael LH, Entman ML, Hartley CJ, Youker KA, Zhu J, Hall SR, Hawkins HK, Berens K Balantyne CM (1995) Myocardial ischemia and reperfusion: a murine model. Am J Physiol 269 (Heart Circ Physiol 38): H2147–H2154

Michael LH, Ballantyne CM, Zachariah JP, Gould KE, Pocius JS, Taffet GE, Hartley CJ, Pham TT, Daniel SL, Funk E, Entman ML (1999) Myocardial infarction and remodeling in mice: effect of reperfusion. Am J Physiol 277:H660–H668

Nguyen T, Salibi EE, Rouleau JL (1998) Postinfarction survival and inducibility of ventricular arrhythmias in the spontaneously hypertensive rat. Effects of ramipril and hydralazine. Circulation 98:2074–2080

Pfeffer JM, Pfeffer MA, Braunwald E (1985) Influence of chronic captopril therapy on the infarcted left ventricle of the rat. Circ Res 57:84–95

Porzio S, Masseroli M, Messori A, Forloni G, Olivetti G, Jeremic G, Riva E, Luvara G, Latini R (1995) A simple, automatic method for morphometric analysis of the left ventricle in rats with myocardial infarction. J Pharmacol Toxicol Meth 33:221–229

Rasoul S, Carretero OA, Peng H, Cavasin MA, Zhuo J, Sanchez-Mendoza A, Brigstock DR, Rhaleb NE (2004) Antifibrotic effect of Ac-SDKP and angiotensin converting enzyme inhibition in hypertension. J Hypertens 22:593–603

Roberts CS, MacLean D, Braunwald E, Maroko PR, Kloner RA (1983) Topographic changes in the left ventricle after experimentally induced myocardial infarction in the rat. Am J Cardiol 51:873–876

Sakai K, Akima M, Aono J (1981) Evaluation of drug effects in a new experimental model of angina pectoris in the intact anesthetized rat. J Pharmacol Meth 5:325–336

Scherrer-Crosbie M, Steudel W, Ullrich R, Hunziker PR, Liel-Cohen N, Newell J, Zaroff J, Zapol WM, Picard MH (1999) Echocardiographic determination of risk area in a murine model of myocardial ischemia. Am J Physiol 277:H986–H992

Scholz W, Albus U, Counillon L, Gögelein H, Lang HJ, Linz W, Weichert A, Schölkens BA (1995) Protective effects of HOE 642, a selective sodium-hydrogen exchange subtype 1 inhibitor, on cardiac ischemia and reperfusion. Cardiovasc Res 29:260–268

Selye H, Bajusz E, Grasso S, Mendell P (1960) Simple techniques for the surgical occlusion of coronary vessels in the rat. Angiology 11:398–407

Shibuya K, Kanasaki K, Isono M, Sato H, Omata M, Sugimoto T, Araki SI, Isshiki K, Kashiwagi A, Haneda M, Koya D (2005) *N*-Acetyl-seryl-aspartyl-lysine-proline prevents renal insufficiency and matrix expansion in diabetic d*b*/d*b* mice. Diabetes 54:838–835

Sia YT, Lapointe N, Parker TG, Tsoporis JN, Deschepper CP, Calderose A, Pourdjabbar A, Jasmin JF, Sarrazin JF, Liu P, Asam A, Butany J, Rouleau JL (2002) Beneficial effects of long-term use of the antioxidant probucol in heart failure in the rat. Circulation 105:2549–2555

Teunissen BEJ, Jongsma HJ, Bierhuizen MFA (2004) Regulation of myocardial connexins during hypertrophic remodelling. Eur Heart J 25:1979–1989

Walker MJA, MacLeod BA, Curtis MJ (1991) Myocardial ischemia and infarction. Comp Pathol Bull 23:3–4

Weinberg EO, Scherrer-Crosbie M, Picard MH, Nasseri BA, MacGillivray C, Gannon J, Lian Q, Bloch KD, Lee RT (2005) Rosuvastatin reduces experimental left ventricular infarct size after ischemia-reperfusion injury but not total coronary occlusion. Am J Physiol 288:H1802–H1809

Yang XP, Sabbah HN, Liu YH, Sharov VG, Mascha EJ, Alwan I, Carretero OA (1992) Ventriculographic evaluation in three rat models of cardiac dysfunction, Am J Physiol 265(6 Pt 2):H1946–1952

Yang F, Yang XP, Liu YH, Xu J, Cingolani O, Rhaleb NE, Carretero OA (2004) Ac-SDKP reverses inflammation and fibrosis in rats with heart failure after myocardial infarction. Hypertension 43:229–236

Yang Z, Day YJ, Toufektsian MC, Ramos SI, Marshall M, Wang XQ, French BA, Linden J (2005) Infarct-sparing effect of A_{2A}-adenosine receptor activation is due primarily to its action on lymphocytes. Circulation 111:2190–2197

Ytrehus K, Liu Y, Tsuchida A, Miura T, Liu GS, Yang XM, Herbert D, Cohen MV, Downey JM (1994) Rat and rabbit heart infarction: effects of anesthesia, perfusate, risk zone, and method of infarct sizing. Am J Physiol 267 (Heart Circ Physiol 36):H2383–H2390

A.3.2.3 Occlusion of Coronary Artery in Anesthetized Dogs and Pigs

PURPOSE AND RATIONALE

The size of infarcts is studied after proximal occlusion of the left anterior descending coronary artery in open-chest dogs. Compounds potentially reducing infarct-size are tested. To delineate the post-mortem area at risk, coronary arteriograms are made after injection of a $BaSO_4$-gelatin mass into the left coronary ostium. The infarct's area is visualized with nitro-blue tetrazolium chloride in myocardial sections.

PROCEDURE

Dogs of either sex weighing approximately 30 kg are used. The animals are anesthetized by intravenous injection of pentobarbital sodium (bolus of 35 mg/kg followed by continuous infusion of 4 mg/kg/h). The animals are placed in the right lateral position. Respiration is maintained through a tracheal tube using a positive pressure respirator. Arterial blood gases are checked, and the ventilation rate and/or oxygen flow rate are adjusted to achieve physiological blood gas values (P_{O2}: 100–140 mm Hg, P_{CO2}: 32–40 mm Hg, and pH 7.47). A peripheral vein (saphenous vein) is cannulated for the administration of test compound. The ECG is recorded continuously from lead II (Einthoven).

Preparation for Hemodynamic Measurements

For recording of peripheral systolic and diastolic blood pressure, the cannula of a femoral vein is connected to a pressure transducer (Statham P 23 DB). For determination of left ventricular pressure (LVP), a Millar microtip catheter (PC 350) is inserted via the left carotid artery. Left ventricular enddiastolic pressure (LVEDP) is measured from a high-sensitivity scale. From the pressure curve, d*p*/d*t* max is differentiated and heart rate is counted.

Experimental Procedure

The heart is exposed through a left thoracotomy between the fourth and fifth intercostal space, the pericard is opened and the left anterior descending coronary artery (LAD) is exposed. After reaching steady state conditions for the hemodynamic parameters (approx. 45 min), the LAD is ligated just below the first diagonal branch for 360 min. No attempt is made to suppress arrhythmic activity after the ligation.

The test substance or the vehicle (controls) is administered by intravenous bolus injection and/or continuous infusion. The schedule of administration may vary. Hemodynamic parameters are registered continuously during the whole experiment. At the end of the experiment, the animals are sacrificed with an overdose of pentobarbital sodium and the heart is dissected.

Preparation to Determine Area at Risk

Coronary arteriograms are made according to Schaper et al. (1979) to delineate the anatomic post-mortem area at risk. A purse-string suture is placed around the left coronary ostium in the sinus of Valsalva; a cannula is then placed in the ostium and the purse-string suture is tightened. Micronized $BaSO_4$ suspended in 12% gelatin solution (37°C) is injected under increasing pressure (2 min at 100 mm Hg, 2 min at 150 mm Hg and 2 min at 200 mm Hg). The heart is placed in crushed ice to gel the injectate. The right ventricle is removed and the left ventricle plus septum is cut into transverse sections (approx. 1 cm thick) from the apex to the level of the occlusion (near the base). From each slice angiograms are made with a X-ray tube at 40 kV to assess the post-mortem area at risk (by defect opacity: reduction of $BaSO_4$-filled vessels in infarct tissue).

Preparation to Determine Infarct Size

The slices are then incubated in p-nitro-blue tetrazolium solution (0.25 g/L in Sörensen phosphate buffer, pH 7.4, containing 100 mM D,L-maleate) in order to visualize the infarct tissue (blue/violet-stained healthy tissue, unstained necrotic tissue). The slices are photographed on color transparency film for the determination of the infarct area.

Left ventricle and infarct area, and area at risk are measured by planimetry from projections of all slices with the exclusion of the apex and of the slice containing the ligature.

EVALUATION

Mortality and the different hemodynamic parameters are determined. Changes of parameters in drug-treated animals are compared to vehicle controls. The different characteristics are evaluated separately. Mean values ± SEM of infarct area and of area at risk are calculated. Statistical analyses consist of regression and correlation analyses and of the Student's *t*-test. Results are considered significant at $p < 0.05$.

MODIFICATIONS OF THE METHOD

Nachlas and Shnitka (1963) described the macroscopic identification of early myocardial infarcts by alterations in dehydrogenase activity in dogs by staining the cardiac tissue with Nitro-BT [2,2′-di-p-nitrophenyl-5,5′ diphenyl-3,3′-(3,3′-dimethoxy-4,4′-biphenylene) ditetrazolium chloride] yielding a dark blue formazan in viable muscle but not in necrotic muscle fibers.

Chiariello et al. (1976) compared the effects of nitroprusside and nitroglycerin on ischemic injury during acute myocardial infarction in dogs.

Black et al. (1995) studied the cardioprotective effects of heparin or *N*-acetylheparin in an *in vivo* dog model of myocardial and ischemic reperfusion injury. The hearts were removed after 90 min of coronary occlusion and a 6 h-reperfusion period. Area at risk was determined by the absence of Evans blue dye after perfusion of the aorta in a retrograde fashion and infarct zone by the absence of formazan pigment within the area at risk after perfusion of the circumflex coronary artery with triphenyltetrazolium chloride.

Reimer et al. (1985) tested the effect of drugs to protect ischemic myocardium in unconscious and conscious dogs. In the conscious model, dogs of either sex weighing 10–25 kg were anesthetized with thiamyal sodium (30–40 mg/kg i.v.) and underwent thoracotomy through the 4th intercostal space. Heparin-filled polyvinyl chloride catheters were positioned in the aortic root, the left atrium via the left atrial appendage, and a systemic vein. A mechanical adjustable snare type occluder was placed around the proximal left circumflex coronary artery above or below the first marginal branch, so that temporary occlusion resulted in cyanosis of at least 75% of the inferior wall. The catheters and snare were either exteriorized or positioned in a subcutaneous pocket at the back of the neck. Penicillin, 1000,000 units, and streptomycin, 1.0 g, were given i.m. for the first 4 postoperative days, and at least 7 days were allowed for recovery from surgery.

Dogs were fasted overnight prior to the study. After exteriorization and flushing of the catheters, 30–40 min were allowed for the animals to adjust to laboratory conditions. Morphine sulfate, 0.25 mg/kg, i.m., was given 30 min before occlusion, and an additional 0.25 mg/kg, i.v., was given 20 min later. Heart rate and aortic and left atrial pressures were monitored continuously. Permanent coronary occlusion was produced by a sudden one-stage tightening of the snare occluder. Drugs were administered by continuous i.v. infusion over 6 h. Hemodynamic measurements were taken 5 min before occlusion and 10, 25, 105, 180, and 360 min after occlusion.

Raberger et al. (1986) described a model of **transient myocardial dysfunction in conscious dogs**. Mongrel dogs, trained to run on a treadmill, were chronically instrumented with a miniature pressure transducer in the left ventricle and a hydraulic occluder placed around the circumflex branch of the left coronary artery. Two pairs of piecoelectrical crystals for sonomicrometry were implanted subendocardially to measure regional myocardial functions. Comparable episodes of regional dysfunction of the left coronary artery area during treadmill runs were found after partial left coronary artery stenosis induced by external filling of the occluder.

Hartman and Warltier (1990) described a model of **multivessel coronary artery disease** using conscious, chronically instrumented dogs. A hydraulic occluder was implanted around the left anterior descending coronary artery (LAD) and an Ameroid constrictor around the left circumflex coronary artery (LCCA). Pairs of piecoelectric crystals were implanted within the subendocardium of the LAD and LCCA perfusion territories to measure regional contractile function. A catheter was placed in the left atrial appendage for injection of radioactive microspheres to measure regional myocardial perfusion. Bolus injections of adenosine were administered daily via the left atrium to evaluate LAD and LCCA coronary reserve. After stenosis by the Ameroid constrictor, radioactive microspheres were administered to compare regional perfusion within normal myocardium to flow in myocardium supplied by the occluded or stenotic coronary arteries.

Holmborn et al. (1993) compared triphenyltetrazolium chloride staining versus detection of fi-

bronectin in experimental myocardial infarction in **pigs**.

Klein et al. (1995) used intact **pigs** and found myocardial protection by Na^+/H^+ exchange inhibition in ischemic reperfused hearts.

Klein et al. (1997) measured the time delay of cell death by Na^+/H^+ exchange inhibition in regionally ischemic, reperfused **porcine** hearts.

Garcia-Dorado et al. (1997) determined the effect of Na^+/H^+ exchange blockade in ischemic rigor contracture and reperfusion-induced hypercontracture in *pigs* submitted to 55 min of coronary occlusion and 5 h reperfusion. Myocardial segment length analysis with ultrasonic microcristals was used to detect ischemic rigor (reduction in passive segment length change) and hypercontracture (reduction in end-diastolic length).

Symons et al. (1998) tested the attenuation of regional dysfunction in response to 25 cycles of ischemia (2 min) and reperfusion (8 min) of the left circumflex coronary artery in **conscious swine** after administration of a Na^+/H^+ exchange inhibitor. The animals were instrumented to measure arterial blood pressure, regional myocardial blood flow (colored microspheres), systolic wall thickening in the normally perfused left anterior descending and left circumflex coronary artery regions (sonomicrometry), left circumflex coronary artery blood flow velocity (Doppler) and reversibility to occlude the left circumflex coronary artery (hydraulic occluder).

Etoh et al. (2001) studied myocardial and interstitial matrix metalloproteinase activity after acute myocardial infarction in **pigs**.

REFERENCES AND FURTHER READING

Abendroth RR, Meesmann W, Stephan K, Schley G, Hübner H (1977) Effects of the β-blocking agent Atenolol on arrhythmias especially ventricular fibrillation and fibrillation threshold after acute experimental coronary artery occlusion. Z Kardiol 66:341–350

Black SC, Gralinski MR, Friedrichs GS, Kilgore KS, Drsicoll EM, Lucchesi BR (1995) Cardioprotective effects of heparin or *N*-acetylheparin in an *in vivo* model of myocardial and ischemic reperfusion injury. Cardiovasc Res 29:629–636

Chiariello M, Gold HL, Leinbach RC, Davis MA, Maroko PR (1976) Comparison between the effects of nitroprusside and nitroglycerin on ischemic injury during acute myocardial infarction. Circulation 54:766–773

Etoh T, Joffs C, Deschamps AM, Davis J, Dowdy K, Hendrick J, Baicu S, Mukherjee R, Manhaini M, Spinale FG (2001) Myocardial and interstitial matrix metalloproteinase activity after acute myocardial infarction in pigs. Am J Physiol 281:H987–994

Garcia-Dorado D, Ganzález MA, Barrabés JA, Ruiz-Meana M, Solares J, Lidon RM, Blanco J, Puigfel Y, Piper HM, Soler-Soler J (1997) Prevention of ischemic rigor contracture during coronary occlusion by inhibition of Na^+-H^+ exchange. Cardiovasc Res 35:80–89

Hartman JC, Warltier DC (1990) A model of multivessel coronary artery disease using conscious, chronically instrumented dogs. J Pharmacol Meth 24:297–310

Holmborn B, Näslund U, Eriksson A, Virtanen I, Thornell LE (1993) Comparison of triphenyltetrazolium chloride (TTC) staining versus detection of fibronectin in experimental myocardial infarction. Histochemistry 99:265–275

Klein HH, Pich S, Bohle RM, Wollenweber J, Nebendahl K (1995) Myocardial protection by Na^+/H^+ exchange inhibition in ischemic, reperfused porcine hearts. Circulation 92:912–917

Klein HH, Bohle RM, Pich S, Lindert-Heimberg S, Wollenweber J, Nebendahl K (1997) Time delay of cell death by Na^+/H^+ exchange inhibition in regionally ischemic, reperfused porcine hearts. J Cardiovasc Pharmacol 30:235–240

Martorana PA, Göbel H, Kettenbach B, Nitz RE (1982) Comparison of various methods for assessing infarct-size in the dog. Basic Res Cardiol 77:301–308

Martorana PA, Kettenbach B, Breipohl G, Linz W (1990) Reduction of infarct size by local angiotensin-converting enzyme inhibition is abolished by a bradykinin antagonist. Eur J Pharmacol 182:395–396

Nachlas MN, Shnitka TK (1963) Macroscopic identification of early myocardial infarcts by alterations in dehydrogenase activity. Am J Pathol 42:379–396

Raberger G, Krumpl G, Mayer N (1986) A model of transient myocardial dysfunction in conscious dogs. J Pharmacol Meth 16:23–37

Reimer KA, Jennings RB, Cobb FR, Murdock RH, Greenfield JC, Becker LC, Bulkley BH, Hutchins GM, Schwartz RP, Bailey KR, Passamani ER (1985) Animal models for protecting ischemic myocardium: Results of the NHLBI cooperative study. Comparison of unconscious and conscious dog models. Circ Res 56:651–665

Schaper W, Frenzel H, Hort W (1979) Experimental coronary artery occlusion. I. Measurement of infarct size. Basic Res Cardiol. 74:46–53

Scherlag BJ, El-Sherif N, Hope R, Lazzara R (1974) Characterization and localization of ventricular arrhythmias resulting from myocardial ischemia and infarction. Circ Res 35:372–383

Symons JD, Correa SD, Schaefer S (1998) Na-H exchange inhibition with cariporide limits functional impairment due to repetitive ischemia. J Cardiovasc Pharmacol 32:

A.3.2.4 Acute Ischemia by Injection of Microspheres in Dogs

PURPOSE AND RATIONALE

Severe left ventricular failure is induced by repeated injections of 50 µm plastic microspheres into the left main coronary artery of anesthetized dogs. Hemodynamic measurements are performed under theses conditions testing drugs which potentially improve cardiac performance. The test can be used to evaluate the influence of drugs on myocardial performance during acute ischemic left ventricular failure in dogs.

PROCEDURE

Dogs of either sex weighing approximately 30 kg are anesthetized by an intravenous bolus injection of 35–40 mg/kg pentobarbital sodium continued by an infusion of 4 mg/kg/h. The animals are placed in the right lateral position. Respiration is maintained through a tracheal tube using a positive pressure respirator and controlled by measuring end-expiratory CO_2 concentration as well as blood gases. Two peripheral veins are cannulated for the administration of narcotic (brachial vein) and test compounds (saphenous vein). The ECG is recorded continuously in lead II (Einthoven).

Preparation for Hemodynamic Measurements

For recording of peripheral systolic and diastolic blood pressure, the cannula of the right femoral vein is connected to a pressure transducer (Statham P 23 DB). For determination of left ventricular pressure (LVP), a Millar microtip catheter (Gould PC 350) is inserted via the left carotid artery. Left ventricular enddiastolic pressure (LVEDP) is measured on a high-sensitivity scale. From the pressure curve, dp/dt max is differentiated and heart rate (HR) is counted. To measure right ventricular pressure, a Millar microtip catheter is inserted via the right femoral vein. Systolic, diastolic and mean pulmonary artery pressure (PAP), mean pulmonary capillary pressure, and cardiac output are measured by a thermodilution technique using a Cardiac Index Computer (Gould SP 1435) and a balloon-tip triple lumen catheter (Gould SP 5105, 5F) with the thermistor positioned in the pulmonary artery via the jugular vein.

The heart is exposed through a left thoracotomy between the fourth and fifth intercostal space, the pericard is opened and the left circumflex coronary artery (LCX) is exposed. To measure coronary blood flow, an electromagnetic flow probe (Hellige Recomed) is placed on the proximal part of the LCX.

Polystyrol microspheres (3M Company, St. Paul, Minnesota, USA) with a diameter of $52.5 \pm 2.24\,\mu m$ are diluted with dextran 70, 60 mg/ml and saline at a concentration of 1 mg microspheres/ml (1 mg = approx. 12,000 beads). For administration of microspheres, an angiogram catheter (Judkins-Schmidt Femoral-Torque, William Cook, Europe Aps. BP 7) is inserted into the left ostium via the left femoral artery.

Induction of Failure

The microspheres are injected through the angiogram catheter into the left ostium initially as 10 ml and later as 5 ml boluses about 5 min apart. The microsphere injections produce stepwise elevations of LVEDP. Embolization is terminated when LVEDP has increased to 16–18 mm Hg and/or PAPm has increased to 20 mm Hg and/or heart rate has reached 200 beats/min. The embolization is completed in about 70 min and by injection of an average dose of 3–5 mg/kg microspheres. Hemodynamic variables are allowed to stabilize after coronary embolization for at least 30 min.

Experimental Course

The test substance or the vehicle (controls) is then administered by intravenous bolus injection or continuous infusion, or by intraduodenal application.

Recordings are obtained

- before embolization
- after embolization
- before administration of test compound
- 5, 30, 45, 60, 90, 120 and, eventually, 150 and 180 min following administration of test drug. At the end of the experiment, the animal is sacrificed by an overdose of pentobarbital sodium.

EVALUATION

Besides the different directly measured hemodynamic parameters, the following data are calculated according to the respective formula:

stroke volume [ml/s],

$$SV = \frac{\text{cardiac output}}{\text{heart rate}}$$

tension index [mmHgs],

$$IT = \frac{BPs \times \text{heart rate}}{1000}$$

Coronary vascular resistance [mm Hgmin/ml],

$$CVR = \frac{BPm \times RAPm}{CBF}$$

total peripheral resistance [dyns/cm^5],

$$TPR = \frac{BPm \times RAPm}{\text{cardiac output}} \times 79.9$$

Pulmonary artery resistance [dyn s/cm^5],

$$PAR = \frac{PAPm - PCPm}{\text{cardiac output}} \times 79.9$$

right ventricle work [kgm/min],

$$RVW = (PAPm - RAPm) \times \text{cardiac output} \times 0.0136$$

left ventricle work [kgm/min],

$$LVW = (BPm - LVEDP) \times \text{cardiac output} \times 0.0136$$

left ventricular myocardial oxygen consumption [ml O_2/min/100 g],

$$MVO_2 = K_1(BPs \times HR) + K_2 \frac{(0.8BPs + 0.2BPd) \times HR \times SV}{BW} + 1.43$$

$K_1 = 4.08 \times 10^{-4}$
$K_2 = 3.25 \times 10^{-4}$
BPs = systolic blood pressure [mm Hg]
BPd = diastolic blood pressure [mm Hg]
BPm = mean blood pressure [mm Hg]
CBF = coronary blood flow in left circumflex coronary artery [ml/min]
RAPm = mean right atrial pressure [mm Hg]
PAPm = mean blood pressure A. pulmonalis [mm Hg]
PCPm = mean pulmonary capillary pressure
HR = heart rate [beats/min]
SV = stroke volume [ml]
BW = body weight [kg]

Changes of parameters in drug-treated animals are compared to vehicle controls; statistical significance of the differences is calculated with the Student's *t*-test.

Mean embolization times, doses of microspheres and number of microsphere applications are evaluated.

MODIFICATIONS OF THE METHOD

Gorodetskaya et al. (1990) described a simple method to produce acute heart failure by coronary vessel embolization with microspheres in rats.

REFERENCES AND FURTHER READING

Gorodetskaya EA, Dugin SF, Medvedev OS, Allabergenova AE (1990) A simple method to produce acute heart failure by coronary vessel embolization in closed chest rats with microspheres. J Pharmacol Meth 24:43–51

Rooke GA, Feigl EO (1982) Work as a correlate of canine left ventricular oxygen consumption, and the problem of catecholamine oxygen wasting. Circ Res 50:273–286

Schölkens BA, Martorana PA, Göbel H, Gehring D (1986) Cardiovascular effects of the converting enzyme inhibitor ramipril (Hoe 498) in anesthetized dogs with acute ischemic left ventricular failure. Clin and Exp Theory and Practice A8(6):1033–1048

Smiseth OA (1983) Effects of the β-adrenergic receptor agonist pirbuterol on cardiac performance during acute ischaemic left ventricular failure in dogs. Eur J Pharmacol 87:379–386

Smiseth OA, Mjøs OD (1982) A reproducible and stable model of acute ischemic left ventricular failure in dogs. Clin Physiol 2:225–239

A.3.2.5 Influence on Myocardial Preconditioning

PURPOSE AND RATIONALE

Damage to the mammalian heart produced by prolonged ischemia and reperfusion can be reduced by "preconditioning" the myocardium via a brief cycle of ischemia and reperfusion prior to the protracted ischemic event. Ischemic preconditioning has been shown to decrease infarct size and increase recovery of post-ischemic ventricular function (Murray et al. 1986), and to reduce leakage of cellular marker proteins indicative for cardiac myocyte death (Volovsek et al. 1992). In addition, preliminary preconditioning also attenuates cardiac arrhythmia associated with subsequent occlusion and reperfusion (Vegh et al. 1990).

The mechanistic basis of this phenomenon is under discussion (Parratt 1994; Parratt and Vegh 1994). Adenosine receptor involvement in myocardial protection after ischemic preconditioning in rabbits has been shown by Baxter et al. (1994). Adenosine (A_1 receptor) antagonists have been demonstrated to block the protection produced by preconditioning (Liu et al. 1991), and short term administration of adenosine was shown to simulate the protective effects of ischemic preconditioning (Toombs et al. 1993). These observations together suggest that adenosine is generated by the short preconditioning ischemia. Other recent pharmacological studies (Gross and Auchampach 1992; Yao and Gross 1994) indicate the involvement of the ATP-sensitive potassium channel. Recent investigations indicate that an increase of NO production after ACE inhibitors may be a part of the protective mechanism (Linz et al. 1992, 1994). Moreover, the involvement of prostanoids and bradykinin in the preconditioning process has been discussed (Wiemer et al. 1991). Gho et al. (1994) found a limitation of myocardial infarct size in the rat by transient renal ischemia, supporting the hypothesis that the mechanism leading to cardiac protection by ischemic preconditioning may not only reside in the heart itself.

PROCEDURE

New Zealand rabbits of either sex weighing 2.5–3.5 kg are initially anesthetized with an intramuscular injection of ketamine (50 mg/ml) /xylazine (10 mg/ml) solution at a dose of 0.6 ml per kg body weight. A tracheotomy is performed to facilitate artificial respiration. The left external jugular vein is cannulated to permit a constant infusion (0.15–0.25 ml/min) of xylazine (2 mg/ml in heparinized saline) to assist in

maintaining anesthesia and fluid volume. Anesthesia is also maintained by i.m. injections (0.4–0.6 ml) of ketamine (80 mg/ml) and xylazine (5 mg/ml) solution. After the xylazine infusion is started, animals are respired with room air at a tidal volume of 10 ml/kg and a frequency of 30 inflations per min (Harvard Apparatus, USA). Thereafter, ventilation is adjusted or inspiratory room air is supplemented (5% CO_2/95% O_2) to maintain arterial blood chemistry within the following ranges: pH 7.35–7.45, P_{CO2} 25–45 mm Hg, P_{O2} 90–135 mm Hg. The right femoral artery and vein are isolated and catheterized for measurement of arterial pressure and administration of drugs, respectively.

A thoracotomy is performed in the fourth intercostal space, and the lungs are retracted to expose the heart. The pericardium is cut to expose the left ventricle, and a solid-state pressure transducer catheter (e. g., MicroTip 3F, Millar Instruments, Houston, USA) is inserted through an apical incision and secured to enable measurement of pulsatile left ventricular pressure. The maximal rate of increase in left ventricular pressure (LVdP/dt max) is determined by electronic differentiation of the left ventricular pressure wave form. A segment of 4–0 prolene suture is looped loosely around a marginal branch of the left main coronary artery to facilitate coronary occlusion during the experiment. Needle electrodes are inserted subcutaneously in a lead II configuration to enable recording of an ECG in order to determine heart rate and help confirm the occurrence of ischemia (ST segment elevation) and reperfusion of the myocardium distal to the coronary occlusion. Continuous recording of pulsatile pressure, ECG, heart rate, and LVdP/dt are simultaneously displayed on a polygraph (e. g. Gould chart recorder, Gould Inc., Valley View, USA) and digitized in real time by a personal computer. Hemodynamic data are condensed for summary and later statistical analysis.

Ischemic preconditioning is induced by tightening the prolene loop around the coronary artery for 5 min and then loosening to reperfuse the affected myocardium for 10 min prior to a subsequent 30 min occlusion. After surgical preparation, and prior to 30 min of occlusion, rabbits are randomly selected to receive ischemic preconditioning, no preconditioning, or ischemic preconditioning plus treatment with test drugs. After 30 min of occlusion, the ligature is released and followed by 120 min of reperfusion. Occlusion is verified by epicardial cyanosis distal to the suture, which is usually accompanied by alterations in hemodynamics and ECG. Reperfusion is validated by return of original color. Systemic hemodynamics are summarized for each experimental period. The experiment is terminated after 120 min of reperfusion, and the heart is excised for determinations of infarct size and area at risk.

Immediately before the animal is sacrificed, the marginal branch of the left coronary artery is reoccluded and India ink is rapidly injected by syringe with a 18-g needle into the left ventricular chamber to demarcate blackened normal myocardium from unstained area at risk. After the rabbits are sacrificed, the heart is removed and sectioned in a breadloaf fashion from apex to base perpendicular to the long axis. The right ventricle is removed from each slice leaving only the left ventricle and septum. After each slice is weighed, the portions are washed and incubated in a phosphate buffered saline solution of triphenyl tetrazolium chloride (1 g/ml, Sigma) for 10–15 min. Salvaged myocardium in the area at risk stains brick red, whereas infarcted tissue remains unaltered in color. Slices are then placed between sheets of Plexiglas and the areas (normal, risk, infarct) of each slice are traced on a sheet of clear acetate. Traces are then digitized and analyzed using computerized planimetry to compare the relative composition of each slice with respect to normal tissue, area at risk, and infarcted myocardium. Planimetry is performed with a computerized analysis system, e. g., Quantimet 570C image analysis system (Leica, Deerfield, USA).

Surface areas of normal tissue, area at risk, and infarcted myocardium on both sides of each slide are averaged for the individual slide. The contribution of each slide to total infarcted and area at risk (%) and area at risk as a percentage of total left ventricular mass for the entire left ventricle is prorated by the weight of each slice (Garcia-Dorado et al. 1987). By adding the adjusted contributions from each slice to infarcted tissue, area at risk, and left ventricular mass, a three-dimensional mathematical representation of total myocardial infarct size and risk zone can be calculated for each rabbit, and a mean tabulated for each treatment group for statistical comparison.

EVALUATION

All data are presented as mean ± SD. Systemic hemodynamic data are analyzed by ANOVA using Statistica/W software. Means are considered significantly different at $p < 0.05$.

MODIFICATIONS OF THE METHOD

Li et al. (1990) found in dog experiments that preconditioning with one brief ischemic interval is as effective as preconditioning with multiple ischemic periods.

In contrast, Vegh et al. (1990) found in other dog experiments that two brief preconditioning periods of coronary occlusion, with an adequate period of reperfusion between, reduce the severity of arrhythmias.

Yang et al. (1996) found a second window of protection after ischemic preconditioning in conscious rabbits which minimizes both infarction and arrhythmias.

Late preconditioning against myocardial stunning in conscious pigs together with an increase of heat stress protein (HSP) 70 was described Sun et al. (1995).

Szilvassy et al. (1994) described the anti-ischemic effect induced by ventricular overdrive pacing as a conscious rabbit model of preconditioning. Rabbits were equipped with right ventricular electrode catheters for pacing and intracavital recording and polyethylene cannulae in the left ventricle and right carotid artery to measure intraventricular pressure and blood pressure. One week after surgery in conscious animals, ventricular overdrive pacing at 500 beats/min over 2, 5, or 10 min resulted in an intracavital S-T segment elevation, shortening of ventricular effective refractory period, decrease in maximum rate of pressure development and blood pressure, and increase in left ventricular end-diastolic pressure proportional to the duration of stimulus. A 5-min preconditioning ventricular overdrive pacing applied 5 or 30 min before a 10-min ventricular overdrive pacing markedly attenuated ischemic changes, whereas a 2-min ventricular overdrive pacing had no effect.

The ventricular overdrive pacing induced preconditioning effect was lost in atherosclerotic rabbits (Szilvassy et al. 1995), however, delayed cardiac protection could be induced in these animals (Szekeres et al. 1997).

REFERENCES AND FURTHER READING

Baxter GF, Marber MS, Patel VC, Yellon DM (1994) Adenosine receptor involvement in a delayed phase of myocardial protection 24 h after ischemic preconditioning. Circulation 90:2993–3000

Garcia-Dorado D, Théroux P, Elizaga J, Galiñanes M, Solares J, Riesgo M, Gomez MJ, Garcia-Dorado A, Aviles FF (1987) Myocardial reperfusion in the pig heart model: infarct size and duration of coronary occlusion. Cardiovasc Res 21:537–544

Gho BC, Schoemaker RG, van der Lee C, Sharma HS, Verdouw PC (1994) Myocardial infarct size limitation in rat by transient renal ischemia. Circulation 90: I-476/2557

Gross JG, Auchampach JA (1992) Blockade of ATP-sensitive potassium channels prevents myocardial preconditioning in dogs. Circ Res 70:223–233

Hoff PT, Tamura Y, Lucchesi BR (1990) Cardioprotective effects of amlodipine on ischemia and reperfusion in two experimental models. Am J Cardiol 66:10H–16H

Li GC, Vasquez JA, Gallagher KP, Lucchesi BR (1990) Myocardial protection with preconditioning. Circulat 82:609–619

Linz W, Wiemer G, Schölkens BA (1992) ACE-inhibition induces NO-formation in cultured bovine endothelial cells and protects isolated ischemic rat hearts. J Mol Cell Cardiol 24:909–919

Linz W, Wiemer G, Gohlke P, Unger T, Schölkens BA (1994) Kardioprotektive Effekte durch Ramipril nach Ischämie und Reperfusion in tierexperimentellen Studien. Z Kardiol 83: Suppl 4:53–56

Liu GS, Thornton J, Van Winkle DM, Stanley WH, Olsson RA, Downey JM (1991) Protection against infarction afforded by preconditioning is mediated by A_1 adenosine receptors in rabbit heart. Circulation 84:350–356

Mickelson JK, Simpson PJ, Lucchesi BR (1989) Streptokinase improves reperfusion blood flow after coronary artery occlusion. Intern J Cardiol 23:373–384

Murry CE, Jennings RB, Reimer KA (1986) Preconditioning with ischaemia: a delay of lethal cell injury in ischaemic myocardium. Circulation 74:1124–1136

Parratt JR (1994) Protection of the heart by ischemic preconditioning: mechanisms and possibilities for pharmacological exploitation. TIPS 15:19–25

Parratt J, Vegh A (1994) Pronounced antiarrhythmic effects of ischemic preconditioning. Cardioscience 5:9–18

Simpson PJ, Fantone JC, Mickelson JK, Gallagher KP, Lucchesi BR (1988) Identification of a time window for therapy to reduce experimental canine myocardial injury: suppression of neutrophil activation during 72 h of reperfusion. Circ Res 63:1070–1079

Sun JZ, Tang XL, Knowton AA, Park SW, Qiu Y, Bolli R (1995) Late preconditioning against myocardial stunning. An endogenous protective mechanism that confers resistance to post-ischemic dysfunction 24 h after brief ischemia in conscious pigs. J Clin Invest 95:388–403

Szekeres L, Szilvássy Z, Fernandy P, Nagy I, Karcsu S, Scáti S (1997) Delayed cardiac protection against harmful consequences of stress can be induced in experimental atherosclerosis in rabbits. J Mol Cell Cardiol 29:1977–1983

Szilvássy Z, Fernandy P, Bor P, Jakab I, Lonovics J, Koltai M (1994) Ventricular overdrive pacing-induced anti-ischemic effect: a conscious rabbit model of preconditioning. Am J Physiol 266 (Heart Circ Physiol 35): H2033–H2041

Szilvássy Z, Fernandy P, Szilvássy J, Nagy I, Karcsu S, Lonovics J, Dux L, Koltai M (1995) The loss of pacing-induced preconditioning in atherosclerotic rabbits: role of hypercholesterolaemia. J Mol Cell Cardiol 27:2559–2569

Tamura Y, Chi L, Driscoll EM, Hoff PT, Freeman BA, Gallagher KP, Lucchesi BR (1988) Superoxide dismutase conjugated to polyethylene glycol provides sustained protection against myocardial ischemia/reperfusion injury in canine heart. Circ Res 63:944–959

Toombs CF, McGee DS, Johnston WE, Vinten-Johansen J (1993) Protection from ischaemic-reperfusion injury with adenosine pretreatment is reversed by inhibition of ATP sensitive potassium channels. Cardiovasc Res 27:623–629

van Gilst WH, de Graeff PA, Wesseling H, de Langen CDJ (1986) Reduction of reperfusion arrhythmias in the ischemic isolated rat heart by angiotensin converting enzyme inhibitors: A comparison of captopril, enalapril, and HOE 498. J Cardiovasc Pharmacol 8:722–728

Vegh A, Szekeres L, Parrat JR (1990) Protective effects of preconditioning of the ischaemic myocardium involve cyclooxygenase products. Cardiovasc Res 24:1020–1023

Volovsek A, Subramanian R, Reboussin D (1992) Effects of duration of ischaemia during preconditioning on mechanical function, enzyme release and energy production in the isolated working rat heart. J Mol Cell Cardiol 24:1011–1019

Wiemer G, Schölkens BA, Becker RHA, Busse R (1991) Ramiprilat enhances endothelial autacoid formation by inhibiting breakdown of endothelium-derived bradykinin. Hypertension 18:585–563

Yang XM, Baxter GF, Heads RJ, Yellon DM, Downey JM, Cohen MV (1996) Infarct limitation of the second window of protection in a conscious rabbit model. Cardiovasc Res 31:777–783

Yao Z, Gross GJ (1994) A comparison of adenosine-induced cardioprotection and ischemic preconditioning in dogs. Efficacy, time course, and role of K_{ATP} channels. Circulation 89:1229–1236

A.3.2.6 MRI Studies of Cardiac Function

PURPOSE AND RATIONALE

Magnetic resonance imaging (MRI) is the preferred technique for the visualization of lesions in the brain and spinal cord of patients with MS. It visualizes the resonance signals of tissue protons when they are placed in a time-varying strong magnetic field. The most frequently used parameters measured in MS are the spin-lattice relaxation time (T_1) and the spin-spin relaxation time (T_2). MRI is routinely used as a tomographic imaging technique, where anatomical pictures are created of 1-mm-thick tissue sections. The contrast differences between brain structures in most MRI techniques are determined by the different densities and diffusion of protons, as well as differences in relaxation times. T_2 images are sensitive to water and, because all pathological alterations in MS brains are associated with altered distribution of tissue water (edema), this technique is highly useful for visualization of the spatial distribution of lesions. Contrast in T_1 images is determined mainly by different lattice densities. Dense structures, such as compact white matter, have low T_1 values, whereas relatively loose structures, such as grey matter or lesions, have higher T_1 values.

To distinguish inflammatory active from inactive lesions, the paramagnetic dye gadolinium-DTPA is intravenously injected (0.1–0.3 mmol kg^{-1}) and, in areas of increased blood–brain barrier permeability, leaks into the brain parenchyma, causing local enhancement of the T_1-weighted signal intensity.

A third important MRI technique in MS is magnetization transfer ratio (MTR) imaging. The MTR of a given tissue is defined as the ratio of free protons versus protons bound to tissue macromolecules.

MRI has emerged as a highly accurate and quantitative tool for the evaluation of cardiac function (Peshock et al. 1996).

Al-Shafei et al. (2000a, 2002b) performed MRI analysis of cardiac cycle events in diabetic rats and tested the effect of angiotensin-converting enzyme inhibition.

PROCEDURE

Diabetes was induced in Wistar rats at an age of 7, 10, and 13 weeks. The rats were anesthetized using 1%–2% halothane in oxygen, their blood glucose levels were checked. They were then given a single intraperitoneal injection of streptozotocin 65 mg/kg body weight. The control rats received sham injections of the citrated buffer when they were 7 weeks old. One diabetic group was treated with 2 g/l captopril in the drinking water

For **MR imaging**, rats were anesthetized using 1%–2% halothane in oxygen, weighed and their systolic blood pressures measured non-invasively using a rat tail blood pressure monitor both before and after imaging sessions to confirm physiological stability. Electrocardiographic (ECG) monitoring used shielded subcutaneous electrodes and a Tektronix 2225 oscilloscope. The cine imaging protocols were performed with the anesthetized animal placed in a specially designed home-built half-sine-spaced birdcage radiofrequency (RF) probe unit contained within a cylindrical plastic holder fitted within a gradient set of internal diameter 11 cm. The RF probe unit was made up of a half-sine spaced birdcage RF probe of internal diameter of 4.5 cm with open ends, an RF shield consisting of a cylinder of copper gauze surrounding and sliding over the birdcage, a tuning capacitor and a coaxial cable to carry the RF (Ballon et al. 1990). The assembly included ECG leads, attachment plugs for the ECG leads and a unit to anchor anesthetic delivery tubes near the nose of the animal. All experiments used a 2 T Oxford Instruments (UK) superconducting magnet with a horizontal internal bore of 31 cm. A gated cine protocol synchronized line acquisition to set times following alternate electrocardiographic R waves. This acquisition was then repeated at the same slice position at 12 equally incremented times through the cardiac cycle. This sequence in turn was repeated for each of the 128 lines to generate each 128×128 image, which itself was acquired twice for signal averaging. The preceding procedure was in turn repeated 12 times to obtain signal-averaged images for every one of the 12 contiguous transverse slices examined. Each imaging session therefore required ($128 \times 12 \times 2 \times 2$) times the

cardiac cycle duration. The effective repeat time (TR) was approximately 13 ms. The short echo time (TE) of 4.3 ms reduced motion artifacts and ensured good contrast between blood and myocardium.

EVALUATION

The image data were transferred from the MRI console using in-house hardware and software to remote UNIX workstations for quantitative analysis using in-house software based on CaMReS libraries (CaMReS, Dr N. J. Herrod, Herchel Smith Laboratory for Medicinal Chemistry, University of Cambridge).

MODIFICATIONS OF THE METHOD

Itter et al. (2004) used non-invasive MRI techniques in a model of chronic heart failure in spontaneously hypertensive rats.

Bryant et al. (1998) and Franco et al. (1999) described MRI and invasive evaluation of development of heart failure in transgenic **mice** with myocardial expression of tumor necrosis factor-α.

Wiesmann et al. (2002) reported analysis of right ventricular function in healthy mice and a murine model of heart failure by*in vivo* MRI.

Kraitchman et al. (2003) described quantitative ischemia detection during cardiac magnetic resonance stress testing by use of fast harmonic phase MTI (FastHARP) in dogs.

Reddy et al. (2004) discussed the feasibility of a porcine model of healed myocardial infarction by integration of cardiac MRI with three-dimensional electroanatomic mapping to guide left ventricular catheter manipulation.

Pelzer et al. (2005) reported that the estrogen receptor-α agonist 16α-LE2 inhibits cardiac hypertrophy and improves hemodynamic function in estrogen-deficient spontaneously hypertensive rats. Improved left ventricular function upon 16α-LE2 treatment was also observed in cardiac MRI studies.

REFERENCES AND FURTHER READING

Al-Shafei AIM, Wise RG, Gresham GA, Bronns G, Carpenter TA, Hall LD, Huang CHL (2002a) Non-invasive magnetic resonance assessment of myocardial changes and the effects of angiotensin-converting enzyme inhibition in diabetic rats. J Physiol (Lond) 538:541–553

Al-Shafei AIM, Wise RG, Gresham GA, Carpenter TA, Hall LD, Huang CHL (2002b) Magnetic resonance imaging analysis of cardiac cycle events in diabetic rats: the effect of angiotensin-converting enzyme inhibition. J Physiol (Lond) 538:555–572

Ballon D, Graham MC, Midownik S, Koutcher JA (1990) A 64 MHz half-birdcage resonator for clinical imaging. Journal of Magnetic Resonance 90:131–140

Bryant D, Becker L, Richardson J, Shelton J, Franco F, Peshock R, Thompson M, Giroir B (1998) Cardiac failure in transgenic mice with myocardial expression of tumor necrosis factor-α. Circulation 97:1375–1381

Franco F, Thomas GD, Giroir B, Bryant D, Bullock MC, Chwialkowski MC, Victor RG, Peshock RM (1999) Magnetic resonance imaging and invasive evaluation of development of heart failure in transgenic mice with myocardial expression of tumor necrosis factor-α. Circulation 99:448–454

Itter G, Jung W, Juretschke P, Schölkens BA, Linz W (2004) A model of chronic heart failure in spontaneous hypertensive rats (SHR) Lab Anim 38:138–146

Kraitchman DL, Sampath S, Castillo E, Derbyshire JA, Boston RC, Bluemke DA, Gerber BL, Pronce JL, Osman NF (2003) Quantitative ischemia detection during cardiac magnetic resonance stress testing by use of FastHARP. Circulation 107:2025–2030

Pelzer T, Jazbutyte V, Hu K, Segerer S, Nahrendorf M, Nordbeck P, Bonz AW, Muck J, Fritzemeier KH, Hegele-Hartung C, Ertl G, Neyses L (2005) The estrogen receptor-α agonist 16α-LE2 inhibits cardiac hypertrophy and improves hemodynamic function in estrogen-deficient spontaneously hypertensive rats. Cardiovasc Res 67:604–612

Peshock RM, Willet DL, Sayad DE, Hundley WG, Chwialkowski MC, Clarke GD, Parkey RW (1996) Quantitative MR imaging of the heart. Magn Reson Imaging Clin N Am 4:267–305

Reddy VY, Malchano ZJ, Holmvang G, Schmidt EJ, d'Avila A, Houghtaling C, Chan RC (2004) Integration of cardiac magnetic resonance imaging with three-dimensional electroanatomic mapping to guide left ventricular catheter manipulation. Feasibility of a porcine model of healed myocardial infarction. J Am Coll Cardiol 44:2202–2213

Wiesmann F, Frydrychowicz A, Rautenberg J, Illinger R, Rommel E, Haase A, Neubauer S (2002) Analysis of right ventricular function in healthy mice and a murine model of heart failure by in vivo MRI. Am J Physiol 283:H1065–H1071

A.3.2.7 MRI Studies After Heart and Lung Transplantation

PURPOSE AND RATIONALE

Acute cardiac allograft rejection continues to be the cause of graft loss and contributes to the morbidity and mortality after cardiac transplantation. Endomyocardial biopsy is used routinely for cardiac transplant rejection surveillance. A sensitive and non-invasive method for detecting rejection is desirable. Kanno et al. (2001) developed a rat model of heterotopic heart and lung transplantation for MRI experiments. Allotransplantations were performed with syngeneic transplantations serving as controls. MR images were obtained with a gradient echo method.

PROCEDURE

Animals

All rats used in the experiments were male, 2–3 months of age, and weighed 220–250 g each. Ani-

mals were housed individually and provided with food and water ad libitum. Inbred Brown Norway (BN; $RT1^n$) and DA ($RT1^a$) rats were obtained from Harlan Sprague Dawley (Indianapolis, Ind).

Heart and Lung Transplantation

Under anesthesia with injection of 35 mg/kg body weight of sodium pentobarbital IP, 500 U/kg body weight of heparin was injected. In the syngeneic group, an en bloc donor heart and lung were taken from a BN rat and transplanted to another BN rat. In the allogeneic group, a graft from a DA rat was transplanted to a BN rat. This group was divided into two groups: one group was treated with 3 mg/kg per day ciclosporin (CsA), and the other group was not given CsA. Graft survival was monitored every day by palpating contraction of the transplanted heart.

Operative procedures have been described by Kanno et al. (2000). In brief, after the chest wall of the donor rat was opened, the left lung was ligated and excised. The azygos vein with the left superior and right superior venae cavae was ligated and divided. The descending thoracic aorta was transected, and 10 ml of cold University of Wisconsin solution (UW solution, Dupont Pharma) was infused into the inferior vena cava until the fluid draining from the aorta was clear, followed by ligation and division of the inferior vena cava. The ascending aorta was dissected and transected at the portion between the left common carotid artery and the left subclavian artery, followed by ligation and division of the right brachiocephalic artery and the left common carotid artery. After removal of the heart and lung from the donor, the right lung was washed 3 times through the bronchus with UW solution containing penicillin G. The grafts were then placed into cold UW solution for ≈5 min until transplantation. Next, the left inguinal portion of the recipient rat was opened and dissected to make enough space for the transplanted organs. The left lower part of the abdominal wall was opened in a transverse fashion from the left femoral vessels to the midline. The abdominal organs were retracted to the right, and both the aorta and the inferior vena cava just beyond the bifurcation were dissected. The vessels were clamped, and an appropriate opening of the aorta was made to receive the aorta of the graft in an end-to-side fashion. Rhythmic heartbeats commenced spontaneously as the heart and the lung regained circulation after removal of the clamp. After hemostasis of the surgical field, the abdominal wall was sutured, with care taken not to kink or obstruct the aorta of the graft.

MRI EXPERIMENTS

MRI measurements were carried out on a 4.7-T/40-cm Bruker AVANCE DRX MR instrument equipped with 15-cm, 10-gauss/cm shielded gradients. *In vivo* MR images of transplanted heart-lung were obtained over a period of 24 h after infusion of dextran-coated ultrasmall superparamagnetic iron oxide (USPIO) particles. The imaging sequence consisted of a gradient echo sequence, triggered to ECG and ventilator (60 strokes/min, 10 ml/kg), with TR/TE 500/10 ms, flip angle equal to Ernst angle, slice thickness 1 mm, field of view 6.0 cm, data matrix size 256 × 130 (zero-filled to 256 × 256), and scan time 5 min. ECG leads were placed on both of the hind limbs of the rat with the transplant to pick up the heartbeat from the transplanted heart more effectively. The change of MRI signal intensity was measured in whole ventricular wall in each transplanted heart. The MR signal intensity of the heart was normalized to that of the leg muscle, because USPIO particles are not readily taken up by muscular tissue, according to Gellissen et al. (1999)

Dextran-coated USPIO particles were synthesized according to the method of Palmacci and Josephson (1993) with slight modifications (Dodd et al. 1999) The MR relaxivities R_1 (spin-lattice relaxation rate constant, $1/T_2$, per mol of Fe in USPIO) and R_2 (spin-spin relaxation rate constant, $1/T_2$, per mol of Fe in USPIO) measured at 4.7 T were 3.8×10^4 and 9.1×10^4 (mol/l)/s, respectively. For *in vivo* studies, dextran-coated USPIO particles were dialyzed against PBS solution and diluted to a concentration of 18 μmol Fe/ml, and 0.8 ml of the suspension (i. e., ≈3 mg Fe/kg body weight) was injected intravenously for each study.

At 6 days after transplantation, dextran-coated USPIO particles were injected intravenously as mentioned above, and the animals were subjected to MRI. Then 24 h later, these animals were again placed inside the magnet and scanned. The regions of interest were defined manually with Bruker software. MR signal intensity in the entire ventricular wall in the plane was measured. After injection of USPIO particles at postoperative day (POD) 6, animals with allotransplants were given CsA for 4 (POD 7 to 10) or 7 (POD 7 to 13) days and reinjected with USPIO particles on POD 14.

Pathological Analysis and Immunohistochemistry

After an MR experiment was completed, the transplanted hearts were extirpated, fixed in 3.7% formaldehyde, and embedded in paraffin for 5-μm sections. Hematoxylin-eosin staining and Perl's Prussian blue staining were performed in the Transplantation Pathol-

ogy Laboratory of the University of Pittsburgh Medical Center. Histological analysis for pathological grading of heart rejection, which is based on the criteria established by the International Society for Heart and Lung Transplantation, was also performed by this laboratory in a blinded manner. Monoclonal anti-rat macrophage antibody (ED1, Serotec) was used as a primary antibody for macrophages. Immunohistochemistry was carried out with the ABC staining system (Santa Cruz Biotechnology) according to the manufacturer's protocol.

EVALUATION

The results are presented as mean ± SD. The results were analyzed by ANOVA with StatView software (SAS Institute). A value of $P < 0.05$ was considered to be statistically significant.

REFERENCES AND FURTHER READING

Dodd SJ, Williams M, Suhan JP et al (1999) Detection of single mammalian cells by high-resolution magnetic resonance imaging. Biophys J 76:103–109

Gellissen J, Axmann C, Prescher A et al (1999) Extra- and intracellular accumulation of ultrasmall superparamagnetic iron oxides (USPIO) in experimentally induced abscesses of the peripheral soft tissues and their effects on magnetic resonance imaging. Magn Reson Imaging 17:557–567

Kanno S, Lee PC, Dodd SJ et al (2000) A novel approach using magnetic resonance imaging for the detection of lung allograft rejection. J Thorac Cardiovasc Surg 120:923–934

Kanno S, Wu YJ, Lee PC, Dodd SJ, Williams M, Griffith HP, Ho C (2001) Macrophage accumulation associated with rat cardiac allograft rejection detected by magnetic resonance imaging with ultrasmall superparamagnetic iron oxide particles. Circulation 104:934–938

Palmacci S, Josephson L (1993) Synthesis of polysaccharide covered superparamagnetic oxide colloids. US Patent 5262176 Example 1. November 16, 1993

A.3.3 Ex Vivo Methods

A.3.3.1 Plastic Casts from Coronary Vasculature Bed

PURPOSE AND RATIONALE

Prolonged administration of coronary drugs has been shown to increase the number and size of interarterial collaterals of dogs and pigs after coronary occlusion (Vineberg et al. 1962; Meesmann and Bachmann 1966). An increased rate of development of collateral arteries was observed after physical exercise in dogs (Schaper et al. 1965), as well as after chronic administration of coronary dilating drugs (Lumb and Hardy 1963). An even more effective stimulus for collateral development is an acute or gradual occlusion of one or several major coronary branches. Filling the arterial coronary bed with a plastic provides the possibility to make the collaterals visible and to quantify them (Schmidt and Schmier 1966; Kadatz 1969).

PROCEDURE

Dogs weighing 10–15 kg are anesthetized with pentobarbital sodium 30 mg/kg i.v. They are respirated artificially and the thorax is opened. After opening of the pericard, Ameroid cuffs are placed around major coronary branches. Gradual swelling of the plastic material occludes the lumen within 3–4 weeks. The dogs are treated daily with the test drug or placebo. After 1 week recovery period they are submitted to exercise on a treadmill ergometer. After 6 weeks treatment, the animals are sacrificed, the heart removed and the coronary bed flushed with saline. The liquid plastic Araldite is used to fill the whole coronary tree from the bulbus aortae. The aortic valves are glued together in order to prevent filling of the left ventricle. Red colored Araldite is used to fill the arterial tree. The venous part of the coronary vasculature can be filled with blue colored Araldite from the venous sinus. The uniformity of the filling pressure, the filling time, and the viscosity of the material are important. Polymerization is complete after several hours. Then, the tissue is digested with 35% potassium hydroxide. The method gives stable preparations which can be preserved for a long time.

EVALUATION

Plastic casts from drug treated animals are compared with casts from dogs submitted to the same procedure without drug treatment.

CRITICAL ASSESSMENT OF THE METHOD

The procedure allows impressive demonstration of the formation of arterial collaterals. The results of post mortem Araldit impletion agree with the functional results of experimental coronary occlusion.

MODIFICATIONS OF THE METHOD

Boor and Reynolds (1977) described a simple planimetric method for determination of left ventricular mass and necrotic myocardial mass in postmortem hearts.

REFERENCES AND FURTHER READING

Boor PJ, Reynolds ES (1977) A simple planimetric method for determination of left ventricular mass and necrotic myocardial mass in postmortem hearts. Am J Clin Pathol 68:387–392

Kadatz R (1969) Sauerstoffdruck und Durchblutung im gesunden und koronarinsuffizienten Myocard des Hundes und ihre Beeinflussung durch koronarerweiternde Pharmaka. Arch Kreislaufforsch 58:263–293

Kadatz R (1971) Agents acting on coronary blood vessels. In Turner RA, Hebborn P (eds) Screening methods in pharmacology, Vol II. Academic Press, New York London, pp 41–60

Meesman W (1982) Early arrhythmias and primary ventricular fibrillation after acute myocardial ischemia in relation to pre-existing collaterals. In: Parratt JR (ed) Early Arrhythmias Resulting from Myocardial Ischemia. Mechanisms and Prevention by Drugs. McMillan London, pp 93–112

Meesmann W, Bachmann GW (1966) Pharmakodynamisch induzierte Entwicklung von Koronar-Kollateralen in Abhängigkeit von der Dosis. Arzneim Forsch 16:501–509

Meesmann W, Schulz FW, Schley G, Adolphsen P (1970) Überlebensquote nach akutem experimentellem Coronarverschluß in Abhängigkeit von Spontankollateralen des Herzens. Z ges exp Med 153:246–264

Schaper W, Xhonneux R, Jageneau AHM (1965) Stimulation of the coronary collateral circulation by Lidoflazine (R 7904) Naunyn-Schmiedeberg's Arch exp Path Pharmak 252:1–8

Schmidt HD, Schmier J (1966) Eine Methode zur Herstellung anatomischer Korrosionspräparate – dargestellt am Koronargefäßsystem des Hundes. Zschr Kreislaufforsch 55:297–305

Vineberg AM, Chari RS, Pifarré R, Mercier C (1962) The effect of Persantin on intercoronary collateral circulation and survival during gradual experimental coronary occlusion. Can Med Ass J 87:336–345

A.4 Calcium Uptake Inhibiting Activity

A.4.0.1 General Considerations

Cellular calcium flux is regulated by receptor-operated and voltage-dependent channels, which are sensitive to inhibition by calcium entry blockers. The term calcium antagonist was introduced by Fleckenstein (1964, 1967) when two drugs, prenylamine and verapamil, originally found as coronary dilators in the LANGENDORFF-experiment, were shown to mimic the cardiac effects of simple Ca^{2+}-withdrawal, diminishing Ca^{2+}-dependent high energy phosphate utilization, contractile force, and oxygen requirement of the beating heart without impairing the Na^+-dependent action potential parameters. These effects were clearly distinguishable from β-receptor blockade and could promptly be neutralized by elevated Ca^{2+}, β-adrenergic catecholamines, or cardiac glycosides, measures that restore the Ca^{2+} supply to the contractile system. In the following years many Ca^{2+}-antagonists were introduced to therapy. Specific Ca^{2+}-antagonists interfere with the uptake of Ca^{2+} into the myocardium and prevent myocardial necrotization arising from deleterious intracellular Ca^{2+} overload. They act basically as specific inhibitors of the slow transsarcolemnal Ca^{2+} influx but do not or only slightly affect the fast Na^+ current that initiates normal myocardial excitation.

Calcium channels and the sites of action of drugs modifying channel function have been classified (Bean 1989; Porzig 1990; Tsien and Tsien 1990; Spedding and Paoletti 1992).

Nomenclature and structure–function relationships of voltage-gated calcium channels were reviewed by Catterall et al. (2005).

Kochegarow (2003) reviewed the therapeutic application of modulators of voltage-gated calcium channels.

Four main types of voltage dependent calcium channels are described:

1. L type (for long lasting),
2. T type (for transient),
3. N type (for neuronal), and
4. P type (for Purkinje cells).

They differ not only by their function (Dolphin 1991) and localization in tissues and cells but also by their sensitivity to pharmacological agents (Ferrante and Triggle 1990; Dascal 1990; Kitamura et al. 1997) and by their specificity to radioligands.

The widely distributed **L-type channels** exist in isoforms (L1, 2, 3, 4) and consist of several subunits, known as α_1, α_2, β, γ, δ. They are sensitive to dihydropyridines, phenylalkylamines or benzothiazepines, but insensitive to ω-conotoxin and ω-agatoxin. The segments required for antagonist binding have been analyzed (Peterson et al. (1996, Schuster et al. 1996; Mitterdorfer et al. 1996; Hockerman et al. 1997; Striessnig et al. 1998; Catterall 1998).

Berjukow et al. (2000) discussed the molecular mechanism of calcium channel block by israpidine.

Striessnig et al. (2004) described the role of L-type Ca^{2+} channels in Ca^{2+} channelopathies.

The **T-type channels** are located mainly in the cardiac sinoatrial node and have different electrophysiological characteristics from L-type channels (Massie 1997; Perez-Reyes et al. 1998).

Reviews of molecular physiology of low-voltage-activated T-type calcium channels were given by Perez-Reyes (2003, 2006).

N- and P-type calcium channels blockers occur in neuronal cells and are involved in neurotransmitter release (Olivera et al. 1987; Bertolino and Llinás 1992; Mintz et al. 1992; Woppmann et al. 1994; Diversé-Pierluissi et al. 1995; Miljanich and Ramachandran 1995; Fisher and Bourque 1996; Ikeda 1996; Ertel et al. 1997; Sinnegger et al. 1997).

REFERENCES AND FURTHER READING

Barhanin J, Borsotto M, Coppola T, Fosset M, Hosey MM, Mourre C, Pauron D, Qar J, Romey G, Schmid A, Vandaele S, Van Renterghem C, Lazdunski M (1989) Biochemistry, molecular pharmacology, and functional control of Ca^{2+}-channels. In: Wray DW, Norman RI, Hess P (eds) Calcium Channels: Structure and Function. Ann NY Acad Sci 560:15–26

Bean BP (1989) Classes of calcium channels in vertebrate cells. Annu Rev Physiol 51:367–384

Berjukow S, Marksteiner R, Gapp F, Sinnegger MJ, Hering S (2000) Molecular mechanism of calcium channel block by israpidine. J Biol Chem 275:22114–22120

Bertolino M, Llinás RR (1992) The central role of voltage-activated and receptor-operated calcium channels in neuronal cells. Annu Rev Pharmacol Toxicol 32:399–421

Catterall WA (1998) Receptor sites for blockers of L-type calcium channels. Naunyn-Schmiedeberg's Arch Pharmacol 358, Suppl 2, R 582

Catterall WA, Saegar MJ, Takahashi M, Nunoki K (1989) Molecular properties of dihydropyridine-sensitive calcium channels. In: Wray DW, Norman RI, Hess P (eds) Calcium Channels: Structure and Function. Ann NY Acad Sci 560:1–14

Catterall WA, Perez-Reyes E, Snutch TP, Striennig J (2005) International Union of Pharmacology. XLVIII. Nomenclature and structure-function relationships of voltage-gated calcium channels. Pharmacol Rev 57:411–425

Dascal N (1990) Analysis and functional characteristics of dihydropyridine-sensitive and -insensitive calcium channel proteins. Biochem Pharmacol 40:1171–1178

Diversé-Pierluissi M, Goldsmith PK, Dunlap K (1995) Transmitter-mediated inhibition of N-type calcium channels in sensory neurons involves multiple GTP-binding proteins and subunits. Neuron 14:191–200

Dolphin AC (1991) Regulation of calcium channel activity by GTP binding proteins and second messengers. Biochim Biophys Acta 1091:68–80

Ertel SI, Ertel EA, Clozel JP (1997) T-Type calcium channels and pharmacological blockade: Potential pathophysiological relevance. Cardiovasc Drugs Ther 11:723–739

Ferrante J, Triggle DJ (1990) Drug- and disease-induced regulation of voltage-dependent calcium channels. Pharmacol Rev 42:29–44

Fisher TE, Bourque CW (1996) Calcium-channel subtypes in the somata and axon terminals of magnocellular neurosecretory cells. Trends Neurosci 19:440–444

Fleckenstein A (1964) Die Bedeutung der energiereichen Phosphate für Kontraktilität und Tonus des Myocards. Verh Dtsch Ges Inn Med 70:81–99

Fleckenstein A (1983) History of calcium antagonists. Circ Res 52 (Suppl I):3–16

Fleckenstein A, Kammermeier H, Döring HJ, Freund HJ (1967) Zum Wirkungsmechanismus neuartiger Koronardilatatoren mit gleichzeitig Sauerstoff einsparenden Myocardeffekten, Prenylamin, Irpoveratril. Z Kreislaufforsch 56:716–744,839–853

Fleckenstein A, Frey M, Fleckenstein-Grün G (1983) Consequences of uncontrolled calcium entry and its prevention with calcium antagonists. Eur Heart J 4 (Suppl H):43–50

Fleckenstein A, Frey M, Fleckenstein-Grün G (1986) Antihypertensive and arterial anticalcinotic effects of calcium antagonists. Am J Cardiol 57:1D–10D

Galizzi JP, Quar J, Fosset M, Van Renterghem C, Lazdunski M (1987) Regulation of calcium channels in aortic muscle cells by protein kinase C activators (diacylglycerol and phorbol esters) and by peptides (vasopressin and bombesin) that stimulate phosphoinositide breakdown. J Biol Chem 262:6947–6950

Hockerman GH, Peterson BZ, Johnson BD, Catterall WA (1997) Molecular determinants of drug binding and action on L-type calcium channels. Annu Rev Pharmacol Toxicol 37:361–396

Hosey MM, Chang FC, O'Callahan CM, Ptasienski J (1989) L-type channels in cardiac and skeletal muscle: purification and phosphorylation. In: Wray DW, Norman RI, Hess P (eds) Calcium Channels: Structure and Function. Ann NY Acad Sci 560:27–38

Ikeda SR (1996) Voltage-dependent modulation of N-type calcium channels by G-protein $\beta\gamma$-subunits. Nature 380:255–258

Kitamura N, Ohta T, Ito S, Nakazato Y (1997) Calcium channel subtypes in porcine adrenal chromaffin cells. Pflügers Arch – Eur J Physiol 434:179–187

Kochegarow AA (2003) Pharmacological modulators of voltage-gated calcium channels and their therapeutic application. Cell Calcium 33:145–162

Maggi CA, Tramontana M, Cecconi R, Santicioli P (1990) Neurochemical evidence of N-type calcium channels in transmitter secretion from peripheral nerve endings of sensory nerves in guinea pigs. Neurosci Lett 114:203–206

Massie BM (1997) Mibefradil: A selective T-type calcium antagonist. Am J Cardiol 80A:231–321

Miljanich GP, Ramachandran J (1995) Antagonists of neuronal calcium channels: structure, function and therapeutic implications. Annu Rev Pharmacol Toxicol 35:707–734

Mintz IM, Adams ME, Bean BP (1992) P-Type calcium channels in rat central and peripheral neurons. Neuron 9:85–95

Mitterdorfer J, Wang Z, Sinnegger MJ, Hering S, Striessnig J, Grabner M, Glossmann H (1996) Two amino acid residues in the IIIS5 segment of L-type calcium channels differentially contribute to 1,4-dihydropyridine sensitivity. J Biol Chem 271:30330–30335

Moresco RM, Govoni S, Battaini F, Trivulzio S, Trabucchi M (1990) Omegaconotoxin binding decreases in aged rat brain. Neurobiol Aging 11:433–436

Nakao SI, Ebata H, Hamamoto T, Kagawa Y, Hirata H (1988) Solubilization and reconstitution of voltage-dependent calcium channel from bovine cardiac muscle. Ca^{2+} influx assay using the fluorescent dye Quin2. Biochim Biophys Acta 944:337–343

Olivera BM, Cruz LJ, de Santos V, LeCheminant GW, Griffin D, Zeikus R, McIntosh JM, Galyean R, Varga J, Gray WR, Rivier J (1987) Neuronal calcium channel antagonists. Discrimination between calcium channel subtypes using ω-conotoxin from *Conus magnus* venom. Biochemistry 26:2086–2090

Perez-Reyes E, Cribbs L, Daud A, Jung-Ha Lee (1998) Molecular characterization of T-type calcium channels. Naunyn-Schmiedeberg's Arch Pharmacol 358, Suppl 2:R583

Perez-Reyes E (2003) Molecular physiology of low-voltage-activated T-type calcium channels. Physiol Rev 83:117–161

Perez-Reyes E (2006) Molecular characterization of T-type calcium channels. Cell Calcium 40:89–96

Peterson BZ, Tanada TN, Catterall WA (1996) Molecular determinants of high affinity dihydropyridine binding in L-type calcium channels. J Biol Chem 271:5293–5296

Porzig (1990) Pharmacological modulation of voltage-dependent calcium channels in intact cells. Rev Physiol Biochem Pharmacol 114:209–262

Rampe D, Triggle DJ (1993) New synthetic ligands for L-type voltage-gated calcium channels. Progr Drug Res 40:191–238
Reuter H, Porzig H, Kokubun S, Prod'Hom B (1988) Calcium channels in the heart. Properties and modulation by dihydropyridine enantiomers. Ann NY Acad Sci 522:16–24
Rosenberg RL, Isaacson JS, Tsien RW (1989) Solubilization, partial purification, and properties of ω-conotoxin receptors associated with voltage-dependent calcium channels. In: Wray DW, Norman RI, Hess P (eds) Calcium Channels: Structure and Function. Ann NY Acad Sci 560:39–52
Schuster A, Lacinová L, Klugbauer N, Ito H, Birnbaumer L, Hofmann F (1996) The IVS6 segment of the L-type calcium channel is critical for the action of dihydropyridines and phenylalkylamines. EMBO J 15:2365–2370
Sinnegger MJ, Wang Z, Grabner M, Hering S, Striessnig J, Glossmann H, Mitterdorfer J (1997) Nine L-type amino acid residues confer full 1,4-dihydropyridine sensitivity to the neuronal calcium channel α_{1A} subunit. J Bill Chem 272:27686–27693
Spedding M, Paoletti R (1992) Classification of calcium channels and the sites of action of drugs modifying channel function. Pharmacol Rev 44:363–376
Striessnig J, Grabner M, Mitterdorfer J, Hering S, Sinneger MJ, Glossmann H (1998) Structural basis of drug binding to L Ca^{2+} channels. Trends Pharmacol Sci 19:108–115
Striessnig J, Hoda JC, Koschak A, Zaghetto F, Müllner C, Sinnegger-Brauns MJ, Wild C, Watschinger K, Trockenbacher A, Pelster G (2004) L-type Ca^{2+} channels in Ca^{2+} channelopathies. Biochem Biophys Res Commun 322:1341–1346
Tsien RW, Tsien RY (1990) Calcium channels, stores and oscillations. Annu Rev Cell Biol 6:715–760
Woppmann A, Ramachandran J, Miljanich GP (1994) Calcium channel subtypes in rat brain: Biochemical characterization of the high-affinity receptors for ω-conopeptides SNX-230 (synthetic MVIIC), SNX-183 (SVIB), and SNX-111 (MVIIA). Mol Cell Neurosci 5:350–357

A.4.1
In Vitro Methods

A.4.1.1
^{3}H-Nitrendipine Binding in Vitro

PURPOSE AND RATIONALE

Radiolabeled dihydropyridine calcium channel antagonists such as ^{3}H-nitrendipine (Salter and Grover 1987; Campiani et al. 1996) are selective ligands for a drug receptor site associated with the voltage-dependent calcium channel. A constant concentration of the radioligand ^{3}H-nitrendipine (0.3–0.4 nM) is incubated with increasing concentrations of a non-labeled test drug (0.1 nM–1 mM) in the presence of plasma membranes from bovine cerebral cortices. If the test drug exhibits any affinity to calcium channels, it is able to compete with the radioligand for channel binding sites. Thus, the lower the concentration range of the test drug, in which the competition reaction occurs, the more potent is the test drug.

PROCEDURE

Materials and solutions:

Preparation buffer	Tris-HCl pH 7.4	50 mM
Incubation buffer	Tris-HCl Genapol pH 7.4	50 mM 0.001%
Radioligand	^{3}H-nitrendipine Specific activity 2.59–3.22 TBq/mmol (70–87 Ci/mmol) (NEN)	
For inhibition of ^{3}H-ni-trendipine binding in non-specific binding Experiments	Nifedipine (Sigma)	

Two freshly slaughtered bovine brains are obtained from the slaughterhouse and placed in ice-cold preparation buffer. In the laboratory, approx. 5 g wet weight of the two frontal cerebral cortices are separated from the brains.

Membrane Preparation

The tissue is homogenized (glass Teflon potter) in ice-cold preparation buffer, corresponding to 1 g cerebral wet weight/50 ml buffer, and centrifuged at 48,000 *g* (4°C) for 10 min. The resulting pellets are resuspended in approx. 270 ml preparation buffer, and the homogenate is centrifuged as before. The final pellets are dissolved in preparation buffer, corresponding to 1 g cerebral cortex wet weight/30 ml buffer. The membrane suspension is immediately stored in aliquots of 5–10 ml at –77°C. Protein content of the membrane suspension is determined according to the method of Lowry et al. (1951) with bovine serum albumin as a standard.

At the day of the experiment, the required volume of the membrane suspension is slowly thawed and centrifuged at 48,000 *g* (4°C) for 10 min. The resulting pellets are resuspended in a volume of ice-cold incubation buffer, yielding a membrane suspension with a protein content of 0.6–0.8 mg/ml. After homogenization (glass Teflon potter), the membrane suspension is stirred under cooling for 20–30 min until the start of the experiment.

Experimental Course

As 1,4-dihydropyridines tend to bind to plastic material, all dilution steps are done in glass tubes.

For each concentration samples are prepared in triplicate. The total volume of each incubation sample is 200 µl (microtiter plates).

Saturation Experiments

total binding:

- 50 µl ^{3}H-nitrendipine (12 concentrations, 5×10^{-11}–4×10^{-9} M)
- 50 µl incubation buffer

non-specific binding:

- 50 µl ^{3}H-nitrendipine (4 concentrations, 5×10^{-11}–4×10^{-9} M)
- 50 µl nifedipine (5×10^{-7} M)

Competition Experiments

- 50 µl ^{3}H-nitrendipine (1 constant concentration, 3–4×10^{-10} M)
- 50 µl incubation buffer without or with non-labeled test drug (15 concentrations, 10^{-10}–10^{-3} M)

The binding reaction is started by adding 100 µl membrane suspension per incubation sample (0.6–0.8 mg protein/ml). The samples are incubated for 60 min in a bath shaker at 25°C. The reaction is stopped by subjecting the total incubation volume to rapid vacuum filtration over glass fibre filters. Thereby the membrane-bound is separated from the free radioactivity. Filters are washed immediately with approx. 20 ml ice-cold rinse buffer per sample. The retained membrane-bound radioactivity on the filter is measured after addition of 2 ml liquid scintillation cocktail per sample in a Packard liquid scintillation counter.

EVALUATION

The following parameters are calculated:

- total binding
- non-specific binding
- specific binding = total binding - non-specific binding

The dissociation constant (K_i) of the test drug is determined from the competition experiment of ^{3}H-nitrendipine versus non-labeled drug by a computer-supported analysis of the binding data.

$$\frac{K_D\ ^3\mathrm{H} \times \mathrm{IC}_{50}}{K_D\ ^3\mathrm{H} + [^3\mathrm{H}]}$$

IC_{50} = concentration of the test drug, which displaces 50% of specifically bound ^{3}H-nitrendipine in the competition experiment

[^{3}H] = concentration of ^{3}H-nitrendipine in the competition experiment.

K_D ^{3}H = dissociation constant of ^{3}H-nitrendipine, determined from the saturation experiment.

The K_i-value of the test drug is the concentration, at which 50% of the receptors are occupied by the test drug.

The affinity constant K_i [mol/l] is recorded and serves as a parameter to assess the efficacy of the test drug.

Standard data:

- nifedipine $K_i = 2$–4×10^{-9} mol/l

MODIFICATIONS OF THE METHOD

[^{3}H](+)-PN200–100 (israpidine) has been used by many authors as the labeled ligand for binding experiments (Grassegger et al. 1989; Nokin et al. 1990; Striessnig et al. 1991; Yaney et al. 1991; Miwa et al. 1992; Ichida et al. 1993; Kalasz et al. 1993; Ikeda et al. 1994; Rutledge and Triggle 1995; Shimasue et al. 1996; He et al. 1997; Natale et al. 1999; Matthes et al. 2000; Peri et al. 2000).

Yaney et al. (1991) performed binding experiments with [^{3}H](+)-PN200–110 to membranes of RINm5F cells.

The RINm5F pancreatic β-cells were grown on plastic culture flasks in medium RPMI 1640 supplemented with 10% fetal bovine serum, 100 µg/ml of streptomycin and 100 U/ml penicillin. The cells were kept in humidified incubators at 37°C in 5% CO_2-95% air. Maintenance flasks were subcultured every 4–5 days at ~80% confluency. For binding experiments of [^{3}H](+)-PN200–110 to membranes, cells were removed from the flasks by incubation for 15–20 min in 10 mM MOPS [3-(*N*-morpholino)propanesulfonic acid] and 1 mM EGTA (pH 7.4) at 4°C. The osmotically ruptured cells were homogenized with a Brinkmann Polytron followed by centrifugation at 20,000 *g* for 15 min. The pellet was resuspended and washed twice. The final pellet was resuspended in 1 mM $CaCl_2$ and 20 mM MOPS (pH 7.4) at a protein concentration of 0.2–0.4 mg/ml. Membranes were incubated at room temperature with (+)-[^{3}H]PN200–110 in a final volume of 500 µl (Weiland and Oswald 1985). Bound and free radioligand were separated by vacuum filtration through a glass fiber filter (no. 32, Schleicher and Schüll) followed by three washes of the filter with 3 ml incubation buffer. Non-specific binding was determined in the presence of 1 µM nitrendipine. Radioactivity retained by the filters was determined by liquid scintillation counting. The concentration of free radioligand was calculated by scintillation counting of aliquots of incubation mixtures under nonspecific conditions before and after centrifugation.

Several other calcium entry blockers, such as nimodipine, diltiazem, verapamil and desmethoxyverapamil, have been labeled and used for binding studies in order to elucidate the calcium channel recognition sites and may be used for further classification of calcium antagonists (Ferry and Glossmann 1982; Glossmann et al. 1983; Goll et al. 1984; Lee et al. 1984; Glossmann et al. 1985; Schoemaker and Langer 1985; Ruth et al. 1985; Reynolds et al. 1986).

Vaghy et al. (1987) identified of a 1,4-dihydropyridine- and phenylalkylamine-binding polypeptide in calcium channel preparations.

Naito et al. (1989) described photoaffinity labeling of the purified skeletal muscle calcium antagonist receptor by [^{3}H]azidobutyryl diltiazem.

Watanabe et al. (1993) reported that azidobutyryl clentiazem labels the benzothiazepine binding sites in the α_1 subunit of the skeletal muscle calcium channel. Tissue heterogeneity of calcium channel antagonist binding sites has been demonstrated by Gould et al. (1983).

Photoaffinity labeling of the cardiac calcium channel with 1,4-dihydropyridine(–)-[3H]azidopine was described by Ferry at al (1987).

Knaus et al. (1992) described a unique fluorescent phenylalkylamine probe for L-type Ca^{2+} channels.

Binding sites for ω-conotoxin appear to be primarily associated with the N-type of voltage-dependent calcium channels (Feigenbaum et al. 1988; Wagner et al. 1988).

Cohen et al. (1992) recommended the peptide ω-agatoxin IIIA as a valuable pharmacological tool being the only known ligand that blocks L-type calcium channels with high affinity at all voltages and causes, unlike the 1,4-dihydropyridines, no block of T-type calcium channels.

REFERENCES AND FURTHER READING

Balwierczak JL, Grupp IL, Grupp G, Schwartz A (1986) Effects of bepridil and diltiazem on [^{3}H] nitrendipine binding to canine cardiac sarcolemma. Potentiation of pharmacological effects of nitrendipine by bepridil. J Pharmacol Exp Ther 237:40–48

Bellemann P, Ferry D, Lübbecke F, Glossmann H (1981) [^{3}H]-Nitrendipine, a potent calcium antagonist, binds with high affinity to cardiac membranes. Arzneim Forsch/Drug Res 31:2064–2067

Boles RG, Yamamura HI, Schoemaker H, Roeske WR (1984) Temperature-dependent modulation of [^{3}H]nitrendipine binding by the calcium channel antagonists verapamil and diltiazem in rat brain synaptosomes. J Pharmacol Exp Ther 229:333–339

Bolger GT, Skolnick P (1986) Novel interactions of cations with dihydropyridine calcium antagonist binding sites in brain. Br J Pharmacol 88:857–866

Bolger GT, Genko P, Klockowski R, Luchowski E, Siegel H, Janis RA, Triggle AM, Triggle DJ (1983) Characterization of binding of the Ca^{2+} channel antagonist, [^{3}H]nitrendipine, to guinea pig ileal smooth muscle. J Pharmacol Exp Ther 225:291–309

Campiani G, Fiorini I, De Filippis MP, Ciani SM, Garofalo A, Nacci V, Giorgi G, Sega A, Botta M, Chiarini A, Budriesi R, Bruni G, Romeo MR, Manzoni C, Mennini T (1996) Cardiovascular characterization of pyrrolo[2,1-*d*] [1,5]benzothiazepine derivatives binding selective to the peripheral-type benzodiazepine receptor (PBR): from dual PBR affinity and calcium antagonist activity to novel and selective calcium entry blockers. J Med Chem 39:2922–2938

Cheng YC, Prusoff WH (1973) Relationship between the inhibition constant (K_I) and the concentration of inhibitor which causes 50 per cent inhibition (I_{50}) of an enzymatic reaction. Biochem Pharmacol 22:3099–3108

Cohen CJ, Ertel EA, Smith MM, Venam VJ, Adams ME, Leibowitz MD (1992) High affinity block of myocardial L-type calcium channels by the spider toxin ω-agatoxin IIIA: advantages over 1,4-dihydropyridines. Mol Pharmacol 42:947–951

Ehlert FJ, Itoga E, Roeske WR, Yamamura HI (1982) The interaction of [^{3}H]nitrendipine with receptors for calcium antagonists in the cerebral cortex and heart of rats. Biochem Biophys Res Commun 104:937–943

Ehlert FJ, Roeske WR, Itoga E, Yamamura HI (1982) The binding of [^{3}H]nitrendipine to receptors for calcium channel antagonists in the heart, cerebral cortex, and ileum of rats. Life Sci 30:2191–2202

Feigenbaum P, Garcia ML, Kaczorowski GJ (1988) Evidence for distinct sites coupled with high affinity ω-conotoxin receptors in rat brain synaptic plasma membrane vesicles. Biochem Biophys Res Commun 154:298–305

Ferry DR, Glossmann H (1982) Identification of putative calcium channels in skeletal muscle microsomes. FEBS Lett 148:331–337

Ferry DR, Goll A, Gadow C, Glossmann H (1984) (–)-^{3}H-desmethoxyverapamil labelling of putative calcium channels in brain: autoradiographic distribution and allosteric coupling to 1,4-dihydropyridine and diltiazem binding sites. Naunyn Schmiedeberg's Arch Pharmacol 327:183–187

Ferry DR, Goll A, Glossmann H (1987) Photoaffinity labelling of the cardiac calcium channel. Biochem J 243:127–135

Fleckenstein A (1977) Specific pharmacology of calcium in myocardium, cardiac pacemakers and vascular smooth muscle. Ann Rev Pharmacol Toxicol 17:149–177

Glossmann H, Ferry DR (1985) Assay for calcium channels. Meth Enzymol 109:513–550

Glossmann H, Linn T, Rombusch M, Ferry DR (1983) Temperature-dependent regulation of d-*cis*-[^{3}H]diltiazem binding to Ca^{2+} channels by 1,4-dihydropyridine channel agonists and antagonists. FEBS Letters 160:226–232

Glossmann H, Ferry DR, Goll A, Striessnig J, Schober M (1985a) Calcium channels: Basic properties as revealed by radioligand binding studies. J Cardiovasc Pharmacol 7 (Suppl 6):S20–S30

Glossmann H, Ferry DR, Goll A, Striessnig J, Zernig G (1985b) Calcium channels and calcium channel drugs: Recent biochemical and biophysical findings. Arzneim Forsch./Drug Res 35:1917–1935

Glossmann H, Ferry DR, Striessnig J, Goll A, Moosburger K (1987) Resolving the structure of the Ca^{2+} channel by photoaffinity labelling. Trends Pharmacol Sci 8:95–100

Goll A, Ferry DR, Striessnig J, Schober M, Glossmann H (1984) (–)-[^{3}H]Desmethoxyverapamil, a novel Ca^{2+} channel probe. FEBS Lett 176:371–377

Gould RJ, Murphy KMM, Snyder SH (1982) [^{3}H]Nitrendipine-labeled calcium channels discriminate inorganic calcium agonists and antagonists. Proc Nat Acad Sci, USA 79:3656–3660

Gould RJ, Murphy KMM, Snyder SH (1983) Tissue heterogeneity of calcium channel antagonist binding sites labeled by [^{3}H]nitrendipine. Mol Pharmacol 25:235–241

Grassegger A, Striessnig J, Weiler M, Knaus HG, Glossmann H (1989) [^{3}H]HOE 166 defines a novel calcium antagonist drug receptor – distinct from the 1,4-dihydropyridine binding domain. Naunyn Schmiedebergs Arch Pharmacol 340:752–759

He M, Bodi I, Mikala G, Schwartz A (1997) Motif III S5 of L-type channels is involved in the dihydropyridine binding site. J Biol Chem 272:2629–2633

Ichida S, Wada T, Nakazaki S, Matsuda N, Kishino H, Akimoto T (1993) Specific bindings of [^{3}H](+)PN200–110 and [^{125}]omega-conotoxin to crude membranes from differentiated NG 108–15 cells. Neurochem Res 18:633–638

Ikeda S, Amano Y, Adachi-Akahane S, Nagao T (1994) Binding of [^{3}H](+)PN200–110 to aortic membranes from normotensive and spontaneously hypertensive rats. Eur J Pharmacol 264:223–226

Janis RA, Sarmianto JG, Maurer SC, Bolger GT, Triggle DJ (1984) Characteristics of the binding of [^{3}H]nitrendipine to rabbit ventricular membranes: Modification by other Ca^{2+} channel antagonists and by the Ca^{2+} channel agonist Bay K 8644. J Pharmacol Exp Ther 231:8–15

Kalasz H, Watanabe T, Yabana H, Itagaki K, Naito K, Nakayama H, Schwartz A, Vaghy PL (1993) Identification of 1,4-dihydropyridine binding domains within the primary structure of the α_1 subunit of the skeletal muscle L-type calcium channel. FEBS Lett 331:177–181

Knaus HG, Moshammer T, Kang HC, Haugland RP, Glossmann H (1992) A unique fluorescent phenylalkylamine probe for L-type Ca^{2+} channels. J Biol Chem 267:2179–2189

Lee HR, Roeske WR, Yamamura HI (1984) High affinity specific [^{3}H](+)PN 200–110 binding to dihydropyridine receptors associated with calcium channels in rat cerebral cortex and heart. Life Sci 35:721–732

Matthes J, Huber I, Haaf O, Antepohl W, Striessnig J, Herzig S (2000) Pharmacodynamic interaction between mibefradil and other calcium channel blockers. Naunyn-Schmiedebergs Arch Pharmacol 361:578–583

Miwa K, Miyagi Y, Araie E, Sasayama S (1992) Effects of diltiazem and verapamil on (+)-PN 200–110 binding kinetics in dog cardiac membranes. Eur J Pharmacol 213:127–132

Marangos PJ, Patel J, Miller Ch, Martino AM (1982) Specific calcium antagonist binding sites in brain. Life Sci 31:1575–1585

Naito K, McKenna E, Schwartz A, Vaghy PI (1989) Photoaffinity labeling of the purified skeletal muscle calcium antagonist receptor by a novel benzodiazepine, [^{3}H]azidobutyryl diltiazem. J Biol Chem 264:21211–21214

Natale NR, Rogers ME, Staples R, Triggle DJ, Rutledge A (1999) Lipophilic 4-isoxazolyl-1,4-dihydropyridines: synthesis and structure-activity relationships. J Med Chem 42:3087–3093

Nokin P, Clinet M, Beaufort P, Meysman L, Laruel R, Chatelain P (1990) SR 33557, a novel calcium entry blocker. II Interactions with 1,4-dihydropyridine, phenylalkylamine, and benzodiazepine binding sites in rat heart sarcolemmal membranes. J Pharmacol Exp Ther 255:600–607

Peri R, Padmanabhan S, Rutledge A, Singh S, Triggle DJ (2000) Permanently charged chiral 1,4-dihydropyridines: molecular probes of L-type calcium channels. Synthesis and pharmacological characterization of methyl-(ω-trimethylalkylammonium 1,4-dihydro-2,6-dimethyl-4-(3-nitro-phenyl)-3,5-pyridinecarboxylate iodide, calcium channel antagonists. J Med Chem 43:2906–2914

Reynolds IJ, Snowman AM, Snyder SH (1986) (–)-[^{3}H]Desmethoxyverapamil labels multiple calcium channel modulator receptors in brain and skeletal muscle membranes: Differentiation by temperature and dihydropyridines. J Pharmacol Exp Ther 237:731–738

Ruth P, Flockerzi V, von Nettelblatt V, Oeken J, Hoffmann F (1985) Characterization of binding sites for nimodipine and (–)-desmethoxyverapamil in bovine sarcolemma. Eur J Biochem 150:313–322

Rutledge A, Triggle DJ (1995) The binding interactions of Ro 40–5967 at the L-type Ca^{2+} channel in cardiac tissue. Eur J Pharmacol 280:155–158

Salter F, Grover AK (1987) Characterization and solubilization of the nitrendipin binding protein from canine small intestinal circular smooth muscle. Cell Calcium 8:145–166

Schoemaker H, Langer SZ (1985) [^{3}H]diltiazem binding to calcium channel antagonists recognition sites in rat cerebral cortex. Eur J Pharmacol 111:273–277

Shimasue K, Urushidani T, Hagiwara M, Nagao T (1996) Effects of anadamide and arachidonic acid on specific binding of (+)-PN200–110 and (?)-desmethoxyverapamil to L-type Ca^{2+} channel. Eur J Pharmacol 296:347–350

Striessnig J, Murphy BJ, Catterall WA (1991) Dihydropyridine receptor of L-type Ca^{2+} channels: identification of binding domains for [^{3}H](+)-PN200–110 and [^{3}H]azidopine within the α1 subunit. Proc Natl Acad Sci USA 88:10769–10773

Vaghy PI, Striessnig J, Miwa K, Knaus HG, Itagati K, McKenna E, Glossmann H, Schwartz A (1987) Identification of a novel 1,4-dihydropyridine- and phenylalkylamine-binding polypeptide in calcium channel preparations. J Biol Chem 262:14337–14342

Wagner JA, Snowman AM,. Biswas A, Olivera BM, Snyder SH (1988) ω-Conotoxin GVIA binding to a high-affinity receptor in brain: Characterization, calcium sensitivity, and solubilization. J Neurosci 8:3354–3359

Watanabe T, Kalasz H, Yabana H, Kuniyasu A, Mershon J, Itagaki K, Vaghy PL, Naito K, Nakayama H, Schwartz A (1993) Azidobutyryl clentiazem, a new photoactivable diltiazem analog, labels benzothiazepine binding sites in the α_1 subunit of the skeletal muscle calcium channel. FEBS Lett 334:261–264

Weiland GA, Oswald RE (1985) The mechanism of binding of dihydropyridine calcium channel blockers to rat brain membranes. J Biol Chem 260:8456–8464

Yaney GC, Stafford A, Henstenberg JD, Sharp GWG, Weiland GA (1991) Binding of the dihydropyridine calcium channel blocker (+)-[^{3}H]isopropyl-4-(2,1,3-benzoxadiazol-4-yl)-1,4-dihydro-5-methoxy-carbonyl-2,6-dimethyl-3- pyridinecarboxylate (PN200–110) to RINm5F membranes and cells. Characterization and functional significance. J Pharmacol Exp Ther 258:652–662

A.4.2
Calcium Antagonism in Isolated Organs

A.4.2.1
Calcium Antagonism on Action Potential of Isolated Guinea Pig Papillary Muscle

PURPOSE AND RATIONALE

Intracellular action potential in the guinea pig papillary muscle is recorded. Partial depolarization is achieved by potassium enriched Ringer solution and by addition of isoproterenol. Resting potential is increased to 40 mV resulting in inactivation of the fast sodium channel. Under these conditions, upstroke velocity is an indicator for calcium flux through the membrane, which is decreased by calcium blockers.

PROCEDURE

Guinea pigs of either sex (Pirbright White strain) weighing 300–400 g are sacrificed by stunning, the carotid arteries are severed, and the thoracic cage is opened immediately. The heart is removed, placed in a container of prewarmed, pre-oxygenated Ringer solution, and the pericardium and the atria are trimmed away. The left ventricle is opened and the two strongest papillary muscles removed. They are fixed between a suction electrode for electrical stimulation and a force transducer for registration of contractions. Initially, normal Ringer solution oxygenated with carbogen (95% O_2/5% CO_2) at a temperature of 36°C is used. A standard micro electrode technique is applied to measure the action potential via a glass micro electrode containing 3 M KCl solution, which is inserted intracellularly. The papillary muscle is stimulated with rectangular pulses of 1 V and of 1 ms duration at intervals of 500 ms. The interval between two stimuli is variable in order to determine refractory periods. The intensity of the electrical current is just below the stimulation threshold. The intracellular action potential is amplified, differentiated for registration of upstroke velocity (Hugo Sachs micro electrode amplifier), together with the contraction force displayed on an oscilloscope (Gould digital storage oscilloscope OS 4000), and recorded (Gould 2400 recorder).

After an incubation period of 30 min the Ringer solution is changed to the following composition containing 5 times more potassium and 10% less sodium.

- NaCl 8,1 g/L
- KCl 1,0 g/L
- $CaCl_2$ 0,2 g/L
- $NaHCO_3$ 0,1 g/L
- glucose 5,0 g/L

For further depolarization, isoproterenol (1.0 mg per 100 ml) is added. By this measure, resting potential is increased to about 40 mV, resulting in inactivation of the fast inward sodium channel. The resulting slow rising action potential is sensitive to calcium antagonistic drugs (Kohlhardt and Fleckenstein 1977).

The test compound is added at a concentration of 1 µg/ml. Effective compounds are tested at lower concentrations and compared with the standard (nifedipin at concentrations of 0.01 and 0.1 µg/ml)

EVALUATION

The decrease of upstroke velocity is tested at various concentrations of the test compound and compared with the standard.

REFERENCES AND FURTHER READING

Grupp IL, Grupp G (1984) Isolated heart preparations perfused or superfused with balanced salt solutions. In: Schwartz A (ed) Methods in Pharmacology, Vol 5: Myocardial Biology. Plenum Press, New York and London, pp 111–128

Kohlhardt M, Fleckenstein A (1977) Inhibition of the slow inward current by nifedipine in mammalian ventricular myocardium. Naunyn Schmiedeberg's Arch Pharmacol 298:267–272

Linz W, Schölkens BA, Kaiser J, Just M, Bei-Yin Q, Albus U, Petry P (1989) Cardiac arrhythmias are ameliorated by local inhibition of angiotensin formation and bradykinin degradation with the converting-enzyme inhibitor ramipril. Cardiovasc Drugs Ther 3:873–882

Striessnig J, Meusburger E, Grabner M, Knaus HG, Glossmann H, Kaiser J, Schölkens B, Becker R, Linz W, Henning R (1988) Evidence for a distinct Ca^{2+} antagonist receptor for the novel benzothiazinone compound Hoe 166. Naunyn-Schmiedeberg's Arch Pharmacol 337:331–340

A.4.2.2
Calcium Antagonism in the Isolated Guinea Pig Atrium

PURPOSE AND RATIONALE

k-Strophanthine (and other cardiac glycosides) inhibit the membrane-bound Na^+/K^+-activated ATP-ase which leads to an increase in intracellular Ca^{2+}-concentration. Ca^{2+} ions activate the contractile apparatus, causing a distinctive enhancement of contractions. The procedure can be used to evaluate a compound's calcium channel blocking activity by measuring its ability to decrease atrial contractions induced by k-strophanthine.

PROCEDURE

Apparatus

HSE-stimulator 1 (Hugo Sachs Elektronik, D-79232 March-Hugstetten, Germany)

Stimulation data:

- frequency 1.5 Hz
- duration 3 ms
- voltage 3–8 V

Experiment

Guinea pigs of either sex weighing 200–500 g are sacrificed with a blow to the nape of the neck and exsanguinated. The left atrium is removed, placed in an organ bath and attached to an isotonic strain gauge, its base being wired to an electrode of the stimulator. The Ringer-solution is aerated with carbogen and kept at 36°C. The atrium is continuously stimulated via stimulator 1, the voltage being slowly increased up to the threshold level. Contractions are recorded on a polygraph. Prior to drug administration, two prevalues are obtained by adding 2 µg/ml k-strophanthine-α (Cymarin) to the organ bath and measuring the increase in contractile force. Following a 15 min washout and recovery period, the test drug is added to the bath followed by administration of k-strophanthine-α 10 min later. The change in contractile force is always measured 10 min after the addition of k-strophanthine-α.

Standard compounds:

- Verapamil hydrochloride
- Nifedipine

EVALUATION

The percent inhibition of k-strophanthine-α induced contraction is determined.

MODIFICATIONS OF THE METHOD

Calcium antagonists can also be evaluated in the LANGENDORFF heart preparation (Lindner and Ruppert 1982).

Leboeuf et al. (1992) reported the protective effect of bepridil and flunarizine against veratrine-induced contracture in rat atria concluding from the results in this model that these agents may be more effective as L-type calcium ion-channel blockers in protecting against calcium overload during ischaemia and reperfusion injury.

REFERENCES AND FURTHER READING

Church J, Zsotér TT (1980) Calcium antagonistic drugs. Mechanism of action. Can J Physiol Pharmacol 58:254–264

Grupp IL, Grupp G (1984) Isolated heart preparations perfused or superfused with balanced salt solutions. In: Schwartz A (ed) Methods in Pharmacology, Vol 5: Myocardial Biology. pp 111–128. Plenum Press, New York and London

Leboeuf J, Baissat J, Massingham R (1992) Protective effect of bepridil and against veratrine-induced contracture in rat atria. Eur J Pharmacol 216:183–189

Lindner E, Ruppert D (1982) Effects of calcium antagonists on coronary spasm and pulmonary artery contraction in comparison to their antagonistic action against K-strophanthin in isolated guinea-pig atria. Pharmacology 24:294–302

Rajagopalan R, Ghate AV, Subbarayan P, Linz W, Schoelkens BA (1993) Cardiotonic activity of the water soluble forskoline derivative 8,13-epoxy-6β-(piperidinoacetoxy)-1α,7β,9α-trihydroxy-labd-14-en-11-one. Arzneim Forsch/ Drug Res 43(I) 313–319

Salako LA, Vaugham Williams EM, Wittig JH (1976) Investigations to characterize a new anti-arrhythmic drug, ORG 6001, including a simple test for calcium antagonism. Br J Pharmacol 57:251–262

A.4.2.3 Calcium Antagonism in the Isolated Rabbit Aorta

PURPOSE AND RATIONALE

Contraction of aorta rings is induced by adding potassium chloride or norepinephrine to the organ bath containing slightly modified Krebs bicarbonate buffer. Test drugs with calcium channel blocking activity have a relaxing effect.

PROCEDURE

Rabbits of either sex weighing 3–4 kg are sacrificed with an overdose of pentobarbital sodium. The chest cavity is opened and the descending thoracic aorta (from the level of the aortic arch to the level of the diaphragm) is rapidly removed and placed in a beaker of oxygenated Krebs bicarbonate buffer at 37°C.

The content of magnesium and calcium is slightly diminished in the Krebs bicarbonate buffer resulting in the following composition:

- NaCl 118.4 mMol
- KCl 4.7 mMol
- KH_2PO_4 1.2 mMol
- $MgSO_4 \cdot 2H_2O$ 1.2 mMol
- $CaCl_2 \cdot 2H_2O$ 1.9 mMol
- $NaHCO_3$ 25.0 mMol
- dextrose 10.0 mMol
- EDTA 0.013 mMol

The tissue is then transferred to a dish containing fresh oxygenated, warmed Krebs solution. Fat and loose connective tissue are carefully removed while keeping the tissue moist with the solution. Eight rings of 4–5 mm width are obtained and each is mounted in a 20 ml tissue bath which contains the oxygenated warmed Krebs solution. Initial tension is set at 1.0 g. The tissue is allowed to incubate over a period of 2 h, during which time the Krebs solution is changed every 15 min. Also during this time, tension is maintained at 1.0 g. Just prior to the end of the 2 h equilibration period, the Krebs solution is changed again and the tissue

is allowed to stabilize at 1.0 g tension. A sustained contraction is then generated by addition of either 40 mM KCl or 2.9×10^{-3} mM norepinephrine.

Twenty min after addition of the agonist, the test drug is added so that the final concentration in the bath is 1×10^{-5} M. The percent relaxation reading is taken 30 min after addition of the test drug. If at least 30% relaxation occurs, an accumulative concentration-relaxation curve is established. There is a 30 min period of time between the addition of each concentration of test compound.

EVALUATION

Active tension is calculated for the tissue at the time point just prior to the addition of the test compound and also at the point 30 min after the addition of each concentration of test compound. Active tension is defined as the difference between the generated tension and the baseline tension. The percent relaxation from the predrug, precontracted level is calculated for each concentration of test compound. A number of 5 experiments constitutes a dose range. An ID_{50} is calculated by linear regression analysis.

MODIFICATIONS OF THE METHOD

Hof and Vuorela (1983) compared three methods for assessing calcium antagonism on rabbit aorta smooth muscle.

Matsuo et al. (1989) reported a simple and specific screening method for Ca-entry blockers. In the presence of various Ca-channel blockers, 1×10^{-4} M Ca^{2+} causes relaxation of rat uterine smooth muscle that has been tonically contracted with oxytocin in calcium-free medium after prolonged preincubation with 3 mM EGTA.

Micheli et al. (1990) used spirally cut preparations of rat aorta and rings of rabbit ear artery to test calcium entry blocker activity.

Rüegg et al. (1985) described a smooth muscle cell line originating from fetal rat aorta to be suitable for the study of voltage sensitive calcium channels. Calcium channel antagonists inhibited both the basal and the potassium chloride stimulated $^{45}Ca^{2+}$ uptake.

REFERENCES AND FURTHER READING

Hof RP, Vuorela HJ (1983) Assessing calcium antagonism on vascular smooth muscle: comparison of three methods. J Pharmacol Meth 9:41–52

Matsuo K, Morita S, Uchida MK, Sakai K (1989) Simple and specific assessment of Ca-entry-blocking activities of drugs by measurement of Ca reversal. J Pharmacol Meth 22:265–275

Micheli D, Collodel A, Semerano C, Gaviraghi G, Carpi C (1990) Lacidipine: A calcium antagonist with potent and long-lasting antihypertensive effects in animal studies. J Cardiovasc Pharmacol 15:666–675

Rüegg UT, Doyle VM, Zuber JF, Hof RP (1985) A smooth muscle cell line suitable for the study of voltage sensitive calcium channels. Biochem Biophys Res Commun 130:447–453

Robinson CP, Sastry BVR (1976) The influence of mecamylamine on contraction induced by different agonists and the role of calcium ions in the isolated rabbit aorta. J Pharmacol Exp Ther 197:57–65

Striessnig J, Meusburger E, Grabner M, Knaus HG, Glossmann H, Kaiser J, Schölkens B, Becker R, Linz W, Henning R (1988) Evidence for a distinct Ca^{2+} antagonist receptor for the novel benzothiazinone compound Hoe 166. Naunyn-Schmiedeberg's Arch Pharmacol 337:331–340

Towart R (1982) Effects of nitrendipine (Bay e 5009), nifedipine, verapamil, phentolamine, papaverine, and minoxidil on contractions of isolated rabbit aortic smooth muscle. J Cardiovasc Pharmacol 4:895–902

Turner RA (1965) Cardiotonic agents; The aortic strip of the rabbit. In: Turner RA (ed) Screening methods in pharmacology. pp 203–209. Academic Press, New York and London

A.4.2.4 Calcium Antagonism in the Isolated Guinea Pig Pulmonary Artery

PURPOSE AND RATIONALE

Contraction of the pulmonary artery is induced by changing the normal Tyrode solution in the organ bath against a potassium enriched solution. This contraction can be inhibited by calcium blockers.

PROCEDURE

The following solutions are used:

	Normal Tyrode solution [mMol]	Potassium Enriched Tyrode solution [mMol]
NaCl	135.0	89.0
KCl	3.7	50.0
$MgSO_4$	0.81	0.81
NaH_2PO_4	0.41	0.41
$NaHCO_3$	11.0	11.0
$CaCl_2$	2.25	2.25
Glucose	5.6	5.6

Guinea pigs (Pirbright White strain) of either sex weighing 400–500 g are sacrificed by stunning. The pulmonary artery is removed and cut spirally at an angle of 45°. The resulting strip is cut to lengths of 2 cm and one piece is suspended in oxygenated normal Tyrode solution in an organ bath at 37°C with a preload of 1 g. Contractions are registered with an isotonic strain transducer and recorded on a polygraph.

After 1 h equilibrium time, normal solution is exchanged with potassium enriched Tyrode solution. The artery strip reacts with a contraction which achieves after 10 min 90–95% of its maximum. After an additional 10 min, exchange to normal Tyrode solution is performed. Ten min later again a contraction is induced by potassium enriched solution. When the height of the contraction has reached a constant level, the test substance is added and again potassium induced contraction recorded. The height of the contraction is expressed as percent of initial potassium induced contraction.

After lavage, the procedure is repeated with a higher dose or the standard.

EVALUATION

For calculation of a regression line, the decrease of contraction versus control after various doses is measured in mm. The percentage of inhibition after various doses is taken for calculation of an ED_{50}.

REFERENCES AND FURTHER READING

Green AF, Boura ALA (1964) Sympathetic nerve blockade. In: Laurence DR, Bacharach AL (eds) Evaluation of drug activities: Pharmacometrics. Academic Press, London and New York, pp 370–430

Lindner E, Ruppert D (1982) Effects of Ca^{2+} antagonists on coronary spasm and pulmonary artery contraction in comparison to their antagonistic action against k-strophanthin in isolated guinea-pig atria. Pharmacology 24:294–302

Striessnig J, Meusburger E, Grabner M, Knaus HG, Glossmann H, Kaiser J, Schölkens B, Becker R, Linz W, Henning R (1988) Evidence for a distinct Ca^{2+} antagonist receptor for the novel benzothiazinone compound Hoe 166. Naunyn-Schmiedeberg's Arch Pharmacol 337:331–340

A.4.3 In Vivo Methods

A.4.3.1 Evaluation of Calcium Blockers in the Pithed Rat

PURPOSE AND RATIONALE

Using the cardioaccelerator response in pithed rats, calcium entry blockers can be distinguished from other agents which have modes of action not involving direct blockade of calcium entry (Clapham 1988).

PROCEDURE

Male Sprague-Dawley rats (250–350 g) are anaesthetized with methohexitone sodium (50 mg/kg i.p.). Following cannulation of the trachea, the rats are pithed through one orbit with a stainless steel rod and immediately artificially respired with room air (78 strokes/min, 1 ml/100 g body weight) via a Palmer small animal respiration pump. A jugular vein is cannulated for administration of drugs. Arterial blood pressure is recorded from a carotid artery using a pressure transducer. Heart rate is derived from the phasic arterial pressure signal with a phase lock loop rate-meter (BRL Instrument Services). Both parameters are displayed on a recorder. The animals are kept warm by an incandescent lamp positioned about 25 cm above them. The pithing rod is withdrawn so that the tip lays in the thoracic portion of the spinal cord. All rats then receive (+)tubocurarine (1.5 mg/kg i.v.) and are bilaterally vagotomized.

The cardioaccelerator response is obtained by continuous electrical stimulation of the thoracic spinal cord with square wave pulses of 0.5 ms duration, at supramaximal voltage at a frequency of 0.5 Hz using the pithing rod as a stimulating electrode. An indifferent electrode is inserted subcutaneously in the femoral region. Only rats with a resulting tachycardia of more than 100 beats/min are included into the experiments.

When the cardioaccelerator response has stabilized for about 3–5 min, cumulative intravenous doses of drug or corresponding vehicle are administered. Succeeding doses are given when the response to the previous dose has stabilized.

Calcium antagonists and β-blockers inhibit dose-dependent the tachycardia elicited by electrical stimulation of the spinal cord, whereas lignocaine and nicorandil are not effective.

Doses of β-blockers or calcium-antagonists, which reduce the tachycardia to 50% are tested again. Three min after administration of the drug, calcium gluconate (1 mg/min) or water (0.1 ml/min) are infused using a Harvard apparatus compact infusion pump. The effects of calcium entry blockers, but not of β-adrenoreceptor blockers, are antagonized.

EVALUATION

The level of tachycardia immediately prior to drug administration is taken as 100% and responses to drugs are expressed as a percentage of this predose tachycardia. If an inhibitory effect > 50% is seen, then an ID_{50} (with 95% confidence limits) is interpolated from linear regression analysis. Significance of differences between the groups receiving calcium gluconate and their parallel vehicle controls is calculated by Student's *t*-test.

CRITICAL ASSESSMENT OF THE METHOD

Differentiation between the effects of β-blockers and calcium-antagonists can be achieved in a relatively simple *in vivo* model.

REFERENCES AND FURTHER READING

Clapham JC (1988) A method for *in vivo* assessment of calcium slow channel blocking drugs. J Cardiovasc Pharmacol 11:56–60

A.5 Anti-Arrhythmic Activity

A.5.0.1 General Considerations

Guidelines for the study of arrhythmias in man and animals regarding the experimental design as well as the classification, quantification, and analysis were given as the Lambeth Conventions by Walker et al. (1988).

Classification

Anti-arrhythmic drugs have been classified into various groups and subgroups (Vaughan Williams 1970, 1975, 1984, 1988, 1991, 1992; Borchard et al. 1989; Frumin et al. 1989; Harumi et al. 1989; Colatsky and Follmer 1990; Podrid 1990; Coromilas 1991; Nattel 1991; Rosen and Schwartz 1991; Scholz 1991; Woosley 1991; Ravens 1992; Sanguinetti 1992; Grant 1992; Nattel 1993; Scholz 1994). This classification is based on electrophysiological effects (e. g., action potential) and on interaction with membrane receptors and ion channels. The heterogeneity of classification criteria resulted in vivid discussions (The Sicilian Gambit 1991; Vaughan Williams 1991, 1992). In particular, a clinical study (CAST investigators 1990) challenged the therapeutic value of some anti-arrhythmic drugs.

Weirich and Antoni (1990, 1991) proposed a subdivision of class-1-anti-arrhythmic drugs according to the saturation behavior of frequency-dependent block and its onset-kinetics.

Class I anti-arrhythmic drugs directly alter membrane conductance of cations, particularly those of Na^+ and K^+. They reduce upstroke velocity, V_{max}, of the cardiac action potential by blockade of the fast Na^+ channel. This leads to a depression of conduction velocity, a prolongation of the voltage- and time-dependent refractory period and an increase in the threshold of excitability in cardiac muscle. Class I anti-arrhythmic drugs are subclassified according their effect on the action potential duration.

Class I A anti-arrhythmic drugs (Quinidine-like substances, e. g., disopyramide, procainamide, ajmaline) lengthen the action potential duration which is reflected in the ECG as lengthening of the QT-interval. This effect is added to that on fast sodium channel resulting in delayed recovery from inactivation.

Class I B anti-arrhythmic drugs (lidoacaine-like drugs, e. g., mexiletine, phenytoin, tocainide), in contrast, shorten the action potential duration.

Class I C anti-arrhythmic drugs (e. g., encainide, flecainide, propafenone, indecainide) produce quinidine- and lidocaine-like effects and exert differential actions on the duration of action potential in Purkinje fibres (shortening) and ventricular muscle.

Class II anti-arrhythmic drugs are β-adrenergic antagonists. They exert their anti-arrhythmic effects by antagonizing the electrophysiological effects of catecholamines which are mainly mediated by an increase in slow calcium inward current.

Class III anti-arrhythmic drugs (e. g., amiodarone, bretylium, sotalol) prolong the action potential and lead to a corresponding increase in the effective refractory period. The action is mainly due to a block of outward repolarizing currents. However, activation of sodium and calcium inward currents that prolong the plateau of the action potential may also be involved.

Class IV anti-arrhythmic drugs (e. g., verapamil, diltiazem) are slow calcium channel blockers suppressing the slow calcium inward current and calcium-dependent slow action potentials.

Experimentally Induced Arrhythmias

Winslow (1984) reviewed the methods for the detection and assessment of antiarrhythmic activity.

Szekeres (1979) suggested a rational screening program for the selection of effective antiarrhythmic drugs.

Arrhythmia models in the rat were reviewed by Cheung et al. (1993).

Arrhythmogenic stimuli can be divided into three groups: chemical, electrical and mechanical (Szekeres and Papp 1975; Wilson 1984).

Chemically Induced Arrhythmias

A large number of chemical agents alone or in combination are capable of inducing arrhythmias. Administration of anesthetics like chloroform, ether, halothane (sensitizing agents) followed by a precipitating stimulus, such as intravenous adrenaline, or cardiac glycosides (usually ouabain), aconitine, and veratrum alkaloids cause arrhythmias. The sensitivity to these arrhythmogenic substances differs among various species.

Electrically Induced Arrhythmias

The possibilities to produce arrhythmias by electrical stimulation of the heart and the difficulties for evaluation of anti-arrhythmic drugs by this approach have

been discussed by Szekeres (1971). Serial electrical stimulation result in flutter and fibrillation and it is possible to reproduce some of the main types of arrhythmias of clinical importance. The flutter threshold or the ventricular multiple response threshold may be determined in anesthetized dogs before or after the administration of the test drug.

Mechanically Induced Arrhythmias

Arrhythmias can be induced directly by ischemia or by reperfusion. After ischemia either by infarction or by coronary ligation several phases of arrhythmias are found. The two stage coronary artery ligation technique described by Harris (1950) focuses on late arrhythmias.

Curtis and Walker (1988) examined seven scores in an attempt to validate the use of arrhythmia scores in an *in vivo* model of conscious rats.

The influence on reperfusion arrhythmias can be tested in various species, e g., rat, pig, dog and cat (Bergey et al. 1982; Winslow 1984; Curtis et al. 1987; Brooks et al. 1989).

REFERENCES AND FURTHER READING

Bergey JL, Nocella K, McCallum JD (1982) Acute coronary artery occlusion-reperfusion-induced arrhyhythmias in rats, dogs, and pigs: antiarrhythmic evaluation of quinidine, procainamide and lidocaine. Eur J Pharmacol 81:205–216

Borchard U, Berger F, Hafner D (1989) Classification and action of antiarrhythmic drugs. Eur Heart J 10 (Suppl E):31–40

Brooks RR, Miller KE, Carpenter JF, Jones SM (1989) Broad sensitivity of rodent arrhythmia models to class I, II, III, and IV antiarrhythmic agents. Proc Soc Exp Biol Med 191:201–209

Cheung PH, Pugsley MK, Walker MJA (1993) Arrhythmia models in the rat. J Pharmacol Toxicol Meth 29:179–184

Colatsky TJ, Follmer CH (1990) Potassium channels as targets for antiarrhythmic drug action. Drug Dev Res 19:129–140

Coromilas J (1991) Classification of antiarrhythmic agents: electropharmacologic basis and clinical relevance. Cardiovasc Clin 22:97–116

Curtis MJ, Walker MJA (1988) Quantification of arrhythmias using scoring systems: an examination of seven scores in an *in vivo* model of regional myocardial ischemia. Cardiovasc Res 22:656–665

Curtis MJ, Macleod BA, Walker MJA (1987) Models for the study of arrhythmia in myocardial ischaemia and infarction: the use of the rat. J Mol Cell Cardiol 19:399–419

Ellis CH (1956) Screening of drugs for antiarrhythmic activity. Ann NY Acad Sci 64:552–563

Frumin H, Kerin NZ, Rubenfire M (1989) Classification of antiarrhythmic drugs. J Clin Pharmacol 29:387–394

Grant (1992) On the mechanism of action of antiarrhythmic agents. Am Heart J 123:1130–1136

Harris AS (1950) Delayed development of ventricular ectopic rhythms following experimental coronary occlusion. Circ Res 1:1318–1328

Harumi K, Tsutsumi T, Sato T, Sekiya S (1989) Classification of antiarrhythmic drugs based on ventricular fibrillation threshold. Am J Cardiol 64:10J–14J

Nattel S (1991) Antiarrhythmic drug classifications. A critical appraisal of their history, present status, and clinical relevance. Drugs 41:672–701

Nattel S (1993) Comparative mechanisms of action of antiarrhythmic drugs. Am J Cardiol 72:13F–17F

Podrid PJ, Mendes L, Beau SL, Wilson JS (1990) The oral antiarrhythmic drugs. Progr Drug Res 35:151–247

Ravens U (1992) Einteilungsprinzipien der Antiarrhythmika bei Herzrhythmusstörungen. Z Kardiol 81: Suppl 4:119–125

Rosen MR, Schwartz PJ (1991) The Sicilian Gambit. A new approach to the classification of antiarrhythmic drugs based on their actions on arrhythmogenic mechanisms. Circulation 84:1831–1851

Sanguinetti MC (1992) Modulation of potassium channels by antiarrhythmic and antihypertensive drugs. Hypertension 19:228–236

Scholz H (1991) New classification of antiarrhythmic drugs. The modulated receptor hypothesis. New Trends Antiarrhythm 7:275–289

Scholz H (1994) Classification and mechanism of action of antiarrhythmic drugs. Fundam Clin Pharmacol 8:385–390

Sugimoto T, Murakawa Y, Toda I (1989) Evaluation of antifibrillatory effects of drugs. Am J Cardiol 64:33J–36J

Szekeres L (1979) Experimental models for the study of antiarrhythmic agents. In: Progress in Pharmacology Vol 2/4, pp 25–31, Gustav Fischer Verlag, Stuttgart

Szekeres L, Papp JG (1971) Production of experimental arrhythmias and methods for evaluating antiarrhythmic action. In: Experimental Cardiac Arrhythmias and Antiarrhythmic drugs. Académiai Kladó, Budapest, pp 24–92

Szekeres L, Papp JG (1975) Experimental cardiac arrhythmias. In: Schmier J, Eichler O (eds) Experimental Production of Diseases, Part 3, Heart and Circulation, Handbook of Experimental Pharmacology Vol XVI/3, Springer-Verlag New York Berlin Heidelberg, pp 131–182

The cardiac arrhythmia suppression trial (CAST) investigators (1990) Preliminary report: Effect of encainide and flecainide on mortality in a randomized trial of arrhythmia suppression after myocardial infarction. New Engl J Med 321:406–412

Vaughan-Williams EM (1970) Classification of antiarrhythmic drugs. In: Sandøe E, Flensted-Jensen E, OLesen KH (eds) Symposium on cardiac arrhythmias. Elsinore, Denmark, April 23–25, 1970, Publ. by AB Astra, Södertälje, Sweden, pp 449–472

Vaughan Williams EM (1975) Classification of antidysrhythmic drugs. Pharmacol Ther B1:115–138

Vaughan Williams EM (1984) A classification of antiarrhythmic actions reassessed after a decade of new drugs. J Clin Pharmacol 24:129–147

Vaughan Williams EM (1988) Classification of antiarrhythmic actions. In: Handbook of Experimental Pharmacology Vol 89:45–67, Springer, Heidelberg

Vaughan Williams EM (1991) Significance of classifying antiarrhythmic actions since the cardiac arrhythmia suppression trial. J Clin Pharmacol 31:123–135

Vaughan Williams EM (1992) Classifying antiarrhythmic actions: by facts or speculation. J Clin Pharmacol 32:964–977

Walker MJA, Curtis MJ, Hearse DJ, Campbell RWF, Janse MJ, Yellon DM, Cobbe SM, Coker SJ, Harness JB, Harron DWG, Higgins AJ, Julian DG, Lab MJ, Manning AS, Northover BJ, Parratt JR, Riemersma RA, Riva E, Russell DC, Sheridan DJ, Winslow E, Woodward B (1988) The Lambeth Conventions: guidelines for the study of arrhyth-

mias in ischemia, infarction, and reperfusion. Cardiovasc Res 22:447–455
Weirich J, Antoni H (1990) Differential analysis of the frequency-dependent effects of class 1 antiarrhythmic drugs according to periodical ligand binding: implications for antiarrhythmic and proarrhythmic activity. J Cardiovasc Pharmacol 15:998–1009
Weirich J, Antoni H (1991) Neue Aspekte zur frequenzabhängigen Wirkung von Klasse-1-Antiarrhythmika. Eine kritische Analyse der gebräuchlichen Subklassifikation. Z Kardiol 80:177–186
Wilson E (1984) Methods for detection and assessment of antiarrhythmic activity. Pharmacol Ther 24:401–433
Winbury MM (1956) Relation between atrial and ventricular anti-arrhythmic assay methods: rationale for a screening program. Ann NY Acad Sci 64:564–573
Woosley RL (1991) Antiarrhythmic drugs. Annu Rev Pharmacol Toxicol 31:427–455

A.5.0.2 Electrocardiography in Animals

PURPOSE AND RATIONALE

Recording of the electrocardiogram is an essential tool in the evaluation of anti-arrhythmic drugs (Johnston et al. 1983; Curtis and Walker 1986; Adaikan et al. 1992). Similar to the heart rate, the electrocardiogram is different between various species (Bazett 1920; Kisch 1953; Heise and Kimbel 1955; Beinfield and Lehr 1968; Budden et al. 1981; Driscoll 1981; Osborn 1981; Hayes et al. 1994). Many authors used the bipolar lead II between right foreleg and left hindleg, which is in line with the neutrally placed heart. Additionally, lead I (between right and left foreleg) stated to lie in the axis of the horizontal heart, and lead III (between left foreleg and left hindleg) in line with the vertical heart, may be used as well as unipolar leads (usually designed as V_1 to V_6) and the unipolar leads designed as aVL, aVR, and aVF. Out of several species being used the procedure for rats (Penz et al. 1992; Hayes et al. 1994) is described.

PROCEDURE

Male Sprague Dawley rats weighing 250–300 g are anesthetized by intraperitoneal injection of 60 mg/kg pentobarbitone. The right jugular vein is cannulated for injections, while the left coronary artery is cannulated for recording blood pressure on a polygraph. The ECG is recorded using a Lead type II of configuration along the anatomical axis of the heart as determined by palpation. ECGs are recorded at a standard chart speed of 100 mm/s on a polygraph and simultaneously on a storage oscilloscope. Measurements of intervals are made on the chart recorder and from the memory trace of the monitor.

Since in the rat it is difficult to detect a T-wave that corresponds exactly with the T-wave seen in other species (Beinfeld and Lehr 1968; Driscoll 1981; Surawicz 1987) T-wave calculations are made on the basis of the repolarization wave that follows the QRS complex. The following variables are measured:

σ *T* = time for the depolarization wave to cross the atria, *P-R* interval, *QRS* interval, *Q-T* interval, and *RSh* (the height between the peak of R and S wave). The *RSh* magnitude is taken as a measure of the extent of S-wave depression as exerted by class I sodium channel blocking antiarrhythmics.

EVALUATION

Statistical analyses are based on ANOVA followed by Duncan's test for differences of means. In order to demonstrate the relationships between and drug effects, standard cumulative dose-response curves are constructed.

MODIFICATIONS OF THE METHOD

Osborne (1973, 1981) described a restraining device facilitating electrocardiogram recording in **conscious rats**.

Curtis and Walker (1986), Johnston et al. (1983) studied the responses to ligation of a coronary artery and the actions of antiarrhythmics in conscious rats.

Hayes et al. (1994) studied the ECG in **guinea pigs**, rabbits and primates.

Stark et al. (1989) described an epicardic surface and stimulation technique (SST-ECG) in Langendorff perfused guinea pig hearts.

Epicardial His bundle recordings in the guinea pig *in vivo* were described by Todt and Raberger (1992).

Chronic recording from the His bundle in awake nonsedated **dogs** was reported by Karpawich et al. (1983) and by Atlee et al. (1984).

Van de Water et al. (1989) reported a formula to correct the QT interval of the electrocardiogram in dogs for changes in heart rate.

Wu et al. (1990) described a dual electrophysiologic test for atrial anti-reentry and ventricular antifibrillatory studies in anesthetized dogs. The reentry portion of the model was created surgically by a Y-shaped crushing around the tissue between the superior and inferior vena cava and tissue parallel to the AV groove. The pacing induced tachycardia that results from circus movements around the tricuspid ring was very persistent in duration and regular in cycle length. The antifibrillatory activities were assessed by determination of the ventricular fibrillation threshold using a train-stimuli method.

Weissenburger et al. (1991) developed an experimental model of the long QT syndrome in conscious dogs for screening the bradycardia-dependent proarrhythmic effects of drugs and for studying the electrophysiology of "torsades de pointes."

Bauer et al. (2004) described pro- and antiarrhythmic effects of fast cardiac pacing in a canine model of acquired long QT syndrome.

Holter monitoring in conscious dogs was described by Krumpl et al. (1989a, b).

Coker (1989) recommended the anesthetized **rabbit** as a model for ischemia- and reperfusion-induced arrhythmias.

Baboons and **monkeys** *(Macaca sp.)* were used by Adaikan et al. (1992).

REFERENCES AND FURTHER READING

Adaikan G, Beatch GN, Lee TL, Ratnam SS, Walker MJA (1992) Antiarrhythmic actions of Tedisamil: Studies in rats and primates. Cardiovasc Drugs Therapy 6:345–352

Atlee JL, Dayer AM, Houge JC (1984) Chronic recording from the His bundle in the awake dog. Basic Res Cardiol 79:627–638

Bauer A, Donahue JK, Voss F, Becker R, Kraft P, Senges JC, Kelemn K, Katus HA, Schoels W (2004) Pro- and antiarrhythmic effects of fast cardiac pacing in a canine model of acquired long QT syndrome. Naunyn Schmiedebergs Arch Pharmacol 369:447–454

Bazett HC (1920) An analysis of the time-relations of electrocardiograms. Heart 7:353–370

Beinfield WH, Lehr D (1968) QRS-T variations in the rat electrocardiogram. Am J Physiol 214:197–204

Budden R, Buschmann G, Kühl UG (1981) The rat ECG in acute pharmacology and toxicology. In: Budden R, Detweiler DK, Zbinden G (eds) The Rat Electrocardiogram in Pharmacology and Toxicology. Pergamon Press, Oxford, New York, pp 41–81

Coker SJ (1989) The anesthetized rabbit as a model for ischemia- and reperfusion-induced arrhythmias: Effects of quinidine and bretylium. J Pharmacol Meth 21:263–279

Curtis MJ, Walker MJA (1986) The mechanisms of action of the optical enantiomers of verapamil against ischaemia-induced arrhythmias in the conscious rat. Br J Pharmac 89:137–147

Driscoll P (1981) The normal rat electrocardiogram. In: Budden R, Detweiler DK., Zbinden G (eds) The Rat Electrocardiogram in Pharmacology and Toxicology. Pergamon Press, Oxford, New York, pp 1–14

Hayes E, Pugsley MK, Penz WP, Adaikan G, Walker MJA (1994) Relationship between QaT and RR intervals in rats, guinea pigs, rabbits and primates. J Pharmacol Toxicol Meth 32:201–207

Heise E, Kimbel KH (1955) Das normale Elektrokardiogramm der Ratte. Z Kreislaufforsch 44:212–221

Johnston KM, McLeod BA, Walker JMA (1983) Responses to ligation of a coronary artery in conscious rats and the actions of antiarrhythmics. Can J Physiol Pharmacol 61:1340–1353

Karpawich PP, Gillette PC, Lewis RM, Zinner A, McNamara DG (1983) Chronic epicardial His bundle recordings in awake nonsedated dogs: a new method. Am Heart J 105:16–21

Kisch B (1953) The heart rate and the electrocardiogram of small animals. Exp Med Surg 11:117–130

Krumpl G, Todt H, Schunder-Tatzber S, Raberger G (1989a) Holter monitoring in conscious dogs. Assessment of arrhythmias occurring during ischemia and in the early reperfusion phase. J Pharmacol Meth 22:77–91

Krumpl G, Todt H, Schunder-Tatzber S, Raberger G (1989b) Holter monitoring in conscious dogs. Assessment of arrhythmias occurring in the late reperfusion phase after coronary occlusion. J Pharmacol Meth 22:93–102

Osborne BE (1973) A restraining device facilitating electrocardiogram recording in rats. Lab Anim 7:185–188

Osborn BE (1981) The electrocardiogram (ECG) of the rat. In: Budden R, Detweiler DK., Zbinden G (eds) The Rat Electrocardiogram in Pharmacology and Toxicology. Pergamon Press, Oxford, New York, pp 15–28

Penz W, Pugsley M, Hsieh MZ, Walker MJA (1992) A new ECG measure (RSh) for detecting possible sodium channel blockade *in vivo* in rats. J Pharmacol Meth 27:51–58

Stark G, Stark U, Tritthart HA (1989) Assessment of the conduction of the cardiac impulse by a new epicardic surface and stimulation technique (SST-ECG) in Langendorff perfused mammalian hearts. J Pharmacol Meth 21:195–209

Surawicz B (1987) The QT interval and cardiac arrhythmias. Ann Rev Med 38:81–90

Todt H, Raberger G (1992) Epicardial His bundle recordings in the guinea pig *in vivo*. J Pharmacol Toxicol Meth 27:191–195

Van de Water A, Verheyen J, Xhonneux R, Reneman RS (1989) An improved method to correct the QT interval of the electrocardiogram for changes in heart rate. J Pharmacol Meth 22:207–217

Weissenburger J, Chezalviel F, Davy JM, Lainée P, Guhennec C, Penin E, Engel F, Cynober L, Motté G, Cheymol G (1991) Methods and limitations an experimental model of the long QT syndrome. J Pharmacol Meth 26:23–42

Wu KM, Hunter TL, Proakis AG (1990) A dual electrophysiologic test for atrial antireentry and ventricular antifibrillatory studies. Effects of bethanidine, procainamide and WY-48986. J Pharmacol Meth 23:87–95

A.5.0.3 Aconitine Antagonism in Rats

PURPOSE AND RATIONALE

The plant alkaloid aconitine persistently activates sodium channels. Infusion of aconitine in the anesthetized rat causes ventricular arrhythmias. Drugs considered to have anti-arrhythmic properties can be tested in aconitine-intoxicated rats.

PROCEDURE

Male Ivanovas rats weighing 300–400 g are used. The animals are anesthetized by intraperitoneal injection of 1.25 g/kg urethane. Five µg/kg aconitine dissolved in 0.1 N HNO_3 is administered by continuous infusion into the saphenous vein of 0.1 ml/min and the ECG in lead II is recorded every 30 seconds. The test compound is injected orally or intravenously at a screening dose of 3 mg/kg 5 min before the start of the aconitine infusion. Eight–ten animals are used per compound.

EVALUATION

The anti-arrhythmic effect of a test compound is measured by the amount of aconitine/100 g animal (duration of infusion) which induces

- ventricular extrasystoles
- ventricular tachycardia
- ventricular fibrillation
- and death.

Higher doses of aconitine in the treated group as compared to an untreated control group are an indication of anti-arrhythmic activity.

Statistical significance between the groups is assessed by the Student's *t*-test.

The scores are allotted for the intensity and the duration of the effect relative to the efficacy of standard compounds.

Standard data:

- Procainamid, 5 mg/kg i.v. and lidocaine, 5 mg/kg, i.v. lead to an increase in LD_{100} by 65% (corresponds to LD_{100} of approximately 9 µg/100 g).

CRITICAL ASSESSMENT OF THE METHOD

Aconitine – antagonism *in vivo* has been proven as a valuable screening method for anti-arrhythmic activity.

MODIFICATIONS OF THE METHOD

Scherf (1947) studied the auricular tachycardia caused by aconitine administration in **dogs**.

Scherf et al. (1960) provoked atrial flutter and fibrillation in anesthetized dogs by application of a few crystals of aconitine or delphinine to the surface of the right atrium in the appendix area near the head of the sinus node.

Mc Leod and Reynold (1962) induced arrhythmia by aconitine in the isolated **rabbit** atrium.

Nwangwu et al. (1977) used aconitine as arrhythmogenic agent for screening of anti-arrhythmic agents in **mice**.

Yamamoto et al. (1993) used urethane-anesthetized rats under artificial respiration with tubocurarine pretreatment. After thoracotomy and incision of the pericardium, a piece of filter paper soaked with aconitine solution was applied to the right atrium. Test drugs were applied by continuous i.v. infusion. In addition to ECG lead II, intra-atrial ECG was monitored.

Aconitine-antagonism in conscious mice as screening procedure has been recommended by Dadkar and Bhattacharya (1974) and in anesthetized mice by Winslow (1980).

Nakayama et al. (1971) described the topical application of aconitine in a small cup placed on the right atrium of dogs to induce supraventricular arrhythmias.

A method using the **cat** has been developed by Winslow (1981).

Other Arrhythmogenic Agents

In addition to the aconitine model Vaille et al. (1992) demonstrated the selectivity of a $CaCl_2$ continuous infusion screening method in rats for the evaluation of antiarrhythmic calcium antagonists.

A mouse chloroform model was recommended by Lawson (1968).

Vargaftig et al. (1969) induced ventricular fibrillation in mice by inhalation of chloroform.

Papp et al. (1967) proposed the experimental $BaCl_2$-arrhythmia as a quantitative assay of anti-arrhythmic drugs.

Al-Obaid et al. (1998) used calcium chloride-induced arrhythmias for anti-arrhythmic activity evaluation in anesthetized male rats. Cardiac arrhythmias were induced by a single intravenous injection of 10% $CaCl_2$ (50 mg/kg). The induced arrhythmias were then analyzed for magnitude of initial bradycardia, onset, incidence and duration of the induced fibrillations. After the induction of the arrhythmia, the animal was allowed to recover completely (15–20 min) and the test compound was injected in different doses intravenously. The effect of the test compound on the basal heart rate was then examined and the percentage change in the heart rate was calculated. Seven min later, the arrhythmogenic dose of $CaCl_2$ was readministered and the effect of the treatment on the induced arrhythmia parameters was evaluated as percentage change in the measured parameters or as protection or non-protections against the induced fibrillations.

Tripathi and Thomas (1986) described a method for the production of ventricular tachycardia in the rat and guinea pig by exposing the animals to benzene vapors for 2 min followed by an intravenous adrenaline injection.

Arrhythmias could be induced by changing the medium of cultured rat heart muscle cells (Wenzel and Kloeppel 1978).

In isolated rat hearts ventricular fibrillation was induced by isoprenaline and a catechol-O-methyl transferase inhibitor at high perfusion temperature (Sono et al. 1985).

Takei (1994) described experimental arrhythmia in guinea pigs induced by grayanotoxin-I, a biologically active diterpenoid from the plant family of Ericaceae.

REFERENCES AND FURTHER READING

Al-Obaid AM, El-Subbagh HI, Al-Shabanah OA, Mahran MA (1998) Synthesis and biological evaluation of new cyclopenteno[b]-thiophene derivatives as local anesthetic and antiarrhythmic agents. Pharmazie 53:24–28

Bazzani C, Genedani S, Tagliavini S, Bertolini A (1989) Putrescine reverses aconitine-induced arrhythmia in rats. J Pharm Pharmacol 41:651–653

Brooks RR, Carpenter JF, Jones SM, Gregory CM (1989) Effects of dantrolene sodium in rodent models of cardiac arrhythmia. Eur J Pharmacol 164:521–530

Dadkar NK, Bhattacharya BK (1974) A rapid screening procedure for antiarrhythmic activity in the mouse. Arch Int Pharmacodyn Ther 212:297–301

Lawson JW (1968) Antiarrhythmic activity of some isoquinoline derivatives determined by a rapid screening procedure in the mouse. J Pharmacol Exp Ther 160:22–31

Lu HR, De Clerk F (1993) R 56 865, a Na^+/Ca^{2+}-overload inhibitor, protects against aconitine-induced cardiac arrhythmias *in vivo*. J Cardiovasc Pharmacol 22:120–125

Nakayama K, Oshima T, Kumakura S, Hashimoto K (1971) Comparison of the effects of various β-adrenergic blocking agents with known antiarrhythmic drugs on aconitine-arrhythmia produced by the cup method. Eur J Pharmacol 14:9–18

Nwangwu PU, Holcslaw TL, Stohs JS (1977) A rapid *in vivo* technique for preliminary screening of antiarrhythmic agents in mice. Arch Int Pharmacodyn 229:219–226

Papp G, Szekeres L, Szmolenszky T (1967) The effects of quinidine, ajmaline, papaverine and adrenergic beta-receptor inhibitors in experimental $BaCl_2$-arrhythmia developed for the quantitative assay of antiarrhythmic drugs. Acta Phys Acad Sci Hung 32:365–375

Paróczai M, Kárpáti E, Solti F (1990) The effect of bisaramil on experimental arrhythmias. Pharmacol Res 22:463–480

Scherf D (1947) Studies on auricular tachycardia caused by aconitine administration. Proc Soc Exp Biol Med 64:233–239

Scherf D, Blumenfeld S, Taner D, Yildiz M (1960) The effect of diphenylhydantoin (Dilantin) on atrial flutter and fibrillation provoked by focal application of aconitine or delphinine. Am Heart J 60:936–947

Sono K, Akimoto Y, Magaribuchi T, Kurahashi K, Fujiwara M (1985) A new model of ventricular fibrillation induced by isoprenaline and catechol-O-methyl transferase inhibitor at high perfusion temperature in isolated rat hearts. J Pharmacol Meth 14:249–254

Takei (1994) Grayanotoxin-I induced experimental arrhythmia in guinea pig. J Aichi Med Univ Assoc 22:495–512

Tripathi RM, Thomas GP (1986) A simple method for the production of ventricular tachycardia in the rat and guinea pig. J Pharmacol Meth 15:279–282

Vaille A, Scotto di Tella AM, Maldonado J, Vanelle P (1992) Selectivity of a $CaCl_2$ continuous infusion screening method in rats. Meth Find Exp Clin Pharmacol 14:183–187

Vargaftig BV, Coignet JL, Walmetz JL, Lefort J (1969) A critical evaluation of three methods for the study of adrenergic beta-blocking and anti-arrhythmic agents. Eur J Pharmacol 6:49–55

Wenzel DG, Kloeppel JW (1978) Arrhythmias induced by changing the medium of cultured rat heart muscle cells: a model for assessment of antiarrhythmic agents. J Pharmacol Meth 1:269–276

Winslow E (1980) Evaluation of antagonism of aconitine-induced dysrhythmias in mice as a method of detecting and assessing antidysrhythmic activity. Br J Pharmac 71:615–622

Winslow E (1981) Hemodynamic and arrhythmogenic effects of aconitine applied to the left atria of anesthetized cats. Effects of amiodarone and atropine. J Cardiovasc Pharmac 3:87–100

Yamamoto T, Hosoki K, Karasawa T (1993) Anti-arrhythmic effects of a new calcium antagonist, Monopetil, AJ-2615, in experimental arrhythmic models. Clin Exper Pharmacol Physiol 20:497–500

A.5.0.4 Digoxin-Induced Ventricular Arrhythmias in Anesthetized Guinea Pigs

PURPOSE AND RATIONALE

Overdose of cardiac glycosides, such as digoxin, induces ventricular extrasystoles, ventricular fibrillation, and finally death. The occurrence of these symptoms can be delayed by anti-arrhythmic drugs.

PROCEDURE

Male guinea pigs (Marioth strain) weighing 350–500 g are anesthetized with 35 mg/kg pentobarbital sodium intraperitoneally. Trachea, one jugular vein and one carotid artery are catheterized. Positive pressure ventilation is applied with a respiratory pump (Rhema GmbH, Germany) at 45 breaths/min. The carotid artery is used for monitoring systemic blood pressure via a pressure transducer. Digoxin is infused into the jugular vein with a perfusion pump (ASID BONZ PP 50) at a rate of 85 µg/kg in 0.266 ml/min until cardiac arrest. The electrocardiogram (lead III) is recorded with subcutaneous steel-needle electrodes (Hellige 19).

Treated groups ($n = 5$–10 animals) receive the test drug either orally 1 h or intravenously 1 min prior to the infusion. The control group ($n =$ at least 5 animals) receives the digoxin infusion only. The period until the onset of ventricular extrasystoles, ventricular fibrillation, and cardiac arrest is recorded. The total amount of infused digoxin (µg/kg) to induce ventricular fibrillation is calculated. Standard drugs are lidocaine (3 mg/kg i.v.) or ramipril (1 mg/kg p.o.).

EVALUATION

Using Student's *t*-test the doses of digoxin needed to induce ventricular extrasystoles, or ventricular fibrillation, or cardiac arrest, respectively, after treatment with anti-arrhythmic drugs are compared statistically with controls receiving digoxin only.

REFERENCES AND FURTHER READING

Brooks RR, Carpenter JF, Jones SM, Gregory CM (1989) Effects of dantrolene sodium in rodent models of cardiac arrhythmia. Eur J Pharmacol 164:521–530

Dörner J (1955) Zur Frage der Beziehungen zwischen Strophanthintoxicität und der Größe der Coronardurchblutung. Arch exp Path Pharmakol 226:152–162

Lindner E (1963) Untersuchungen über die flimmerwidrige Wirkung des N-(3′-phenyl-propyl-(2′))-1,1-diphenylpropyl-(3)-amins (Segontin). Arch Int Pharmacodyn 146:485–500

Linz W, Schölkens BA, Kaiser J, Just M, Bei-Yin Q, Albus U, Petry P (1989) Cardiac arrhythmias are ameliorated by local inhibition of angiotensin formation and bradykinin degradation with the converting-enzyme inhibitor ramipril. Cardiovasc Drugs Ther 3:873–882

Windus H (1952) Die Beeinflussung der Glykosidwirkung am Herzen durch coronargefässwirksame Medikamente. Klin Wschr 30:215–217

A.5.0.5
Strophanthin or Ouabain Induced Arrhythmia

PURPOSE AND RATIONALE

Acute intoxication with the cardiac glycoside strophanthin K induces ventricular tachycardia and multifocal ventricular arrhythmias in dogs. This can be used as a test model to evaluate the effect of potential antiarrhythmic drugs on ventricular arrhythmias.

PROCEDURE

Male or female dogs of either sex weighing approximately 20 kg are used. The animals are anesthetized by intravenous injection of 30–40 mg/kg pentobarbital sodium. Two peripheral veins are cannulated for the administration of the arrhythmia-inducing substance (*V. brachialis*) and the test compound (*V. cephalica antebrachii*). For intraduodenal administration of the test drug, the duodenum is cannulated. Electrocardiogram is registered with needle electrodes from lead II. Heart frequency is derived from R-peaks of ECG. Two–three animals are used for one compound.

Strophanthin K is administered by continuous i.v.-infusion at a rate of 3 µg/kg/min. Thirty–fourty min later, signs of cardiac glycoside intoxication appear leading to ventricular tachycardia or to multifocal ventricular arrhythmias. When this state is achieved, the strophanthin infusion is terminated. When the arrhythmias are stable for 10 min, the test substance is administered intravenously in doses between 1.0 and 5.0 mg/kg or intraduodenally in doses between 10 and 30 mg/kg.

ECG II recordings are obtained at times: -0.5, 1, 2, 5 and 10 min following administration of test drug.

For i.v. administration: A test compound is considered to have an anti-arrhythmic effect if the extrasystoles immediately disappear. If the test compound does not show a positive effect, increasing doses are administered at 15 min-intervals. If the test substance does reverse arrhythmias, the next dose is administered after the reappearance of stable arrhythmias.

For i.d. administration: A test compound is considered to have a definite anti-arrhythmic effect if the extrasystoles disappear within 15 min. The test drug is considered to have "no effect" if it does not improve strophanthin intoxication within 60 min following drug administration.

EVALUATION

Evaluation of the therapeutic effect of a drug is difficult and somewhat arbitrary since there is no clear-cut correlation between effectiveness of a test compound and duration of its effect, i. e. return to normal ECGs. The standard drugs ajmaline, quinidine and lidocaine re-establish normal sinus rhythm at doses of 1 and 3 mg/kg (i.v.) and 10 mg/kg (i.d.). Arrhythmias are eliminated for 20 min (i.v.) and for > 60 min (i.d.) following drug administration.

MODIFICATIONS OF THE METHOD

Ettinger et al. (1969) used arrhythmias in dogs induced by ouabain to study the effects of phentolamine in arrhythmia.

Garrett et al. (1964) studied the antiarrhythmic activity of *N,N*-diisopropyl-*N*'-diethylaminoethylurea hydrochloride in anesthetized dogs with arrhythmias induced by ouabain, aconitine or acetylcholine. Furthermore, ultra-low frequency ballistocardiograms with ECG registration were performed in dogs.

Raper and Wale (1968) studied the effects on ouabain- and adrenaline-induced arrhythmias in **cats**.

Kerr et al. (1985) studied the effects of a vasodilator drug on ouabain-induced arrhythmias in anesthetized dogs.

A modified method for the production of cardiac arrhythmias by ouabain in anesthetized cats was published by Rao et al. (1988).

Brooks et al. (1989) infused ouabain intravenously to **guinea pigs** and determined the onset of ventricular extrasystoles and of fibrillation.

Thomas and Tripathi (1986) studied the effects of α-adrenoreceptor agonists and antagonists with different affinity for α_1- and α_2-receptors on ouabain-induced arrhythmias and cardiac arrest in guinea pigs.

Krzeminski (1991) and Wascher et al. (1991) used of ouabain-induced arrhythmia in guinea pigs for the evaluation of potential antidysrhythmic agents.

Al-Obaid et al. (1998) used ouabain-induced arrhythmias in anesthetized **Wistar rats** for evaluation of cyclopenteno[b]thiophene derivatives as antiarrhythmic agents.

REFERENCES AND FURTHER READING

Al-Obaid AM, El-Subbagh HI, Al-Shabanah OA, Mahran MA (1998) Synthesis and biological evaluation of new cyclopenteno[b]thiophene derivatives as local anesthetic and antiarrhythmic agents. Pharmazie 53:24–28

Brooks RR, Miller KE, Carpenter JF, Jones SM (1989) Broad sensitivity of rodent arrhythmia models to class I, II, III, and IV antiarrhythmic agents. Proc Soc Exp Biol Med 191:201–209

Dörner J (1955) Zur Frage der Beziehungen zwischen Strophanthintoxicität und Größe der Coronardurchblutung. Arch exper Path Pharmakol 226:152–162

Duce BR, Garberg L, Johansson B (1967) The effect of propranolol and the dextro and laevo isomers of H 56/28 upon ouabain-induced ventricular tachycardia in unanaesthetized dogs. Acta Pharmacol Toxicol 25: Suppl 2:41–49

Ettinger S, Gould L, Carmichael JA, Tashjian RJ (1969) Phentolamine: use in digitalis-induced arrhythmias. Am Heart J 77:636–640

Garrett J, Gonçalves Moreira M, Osswald W, Guimarães S (1964) Antiarrhythmic activity of N,N-diisopropyl-N′-diethylamino-ethylurea hydrochloride. J Pharmacol Exp Ther 143:243–251

Kerr MJ, Wilson R, Shanks RG (1985) Suppression of ventricular arrhythmias after coronary artery ligation by Pinacidil, a vasodilator drug. J Cardiovasc Pharmacol 7:875–883

Krzeminski T (1991) A rapid *in vivo* technique for the screening of potential anti-dysrhythmic agents. In: 7th Freiburg Focus on Biomeasurement. Cardiovascular and Respiratory *in vivo* Studies. Biomesstechnik-Verlag March GmbH, 79232 March, Germany, pp 131–135

Rao TS, Seth SD, Nayar U, Manchanda SC (1988) Modified method for the production of cardiac arrhythmias by ouabain in anesthetized cats. J Pharmacol Meth 20:255–263

Raper C, Wale J (1968) Propranolol, MJ-1999 and Ciba-39089-Ba in ouabain and adrenaline induced cardiac arrhythmias. Eur J Pharmac 4:1–12

Thomas GP, Tripathi RM (1986) Effects of α-adrenoreceptor agonists and antagonists on ouabain-induced arrhythmias and cardiac arrest in guinea pig. Br J Pharmac 89:385–388

Wascher TC, Dittrich P, Kukovetz WR (1991) Antiarrhythmic effects of two new propafenone related drugs. A study on four animals models of arrhythmia. Arzneim Forsch/Drug Res 41:119–124

A.5.0.6 Ventricular Fibrillation Electrical Threshold

PURPOSE AND RATIONALE

The use of anti-arrhythmic drugs in the treatment of ventricular arrhythmias aims to prevent the development of ventricular fibrillation. Several electrical stimulation techniques have been used to measure ventricular fibrillation threshold such as single pulse stimulation, train of pulses stimulation, continuous 50-Hz stimulation and sequential pulse stimulation.

PROCEDURE

Adult dogs weighing 8–12 kg are anesthetized with sodium pentobarbital (35 mg/kg) and ventilated with air using a Harvard respiratory pump. Systolic arterial pressure is monitored and body temperature maintained by a thermal blanket. The chest is opened by a midline sternotomy and the heart suspended in a pericardial cradle. The sinus node is crushed and a 2.0 mm diameter Ag-AgCl stimulating electrode is embedded in a Teflon disc sutured to the anterior surface of the left ventricle. The heart is then driven by 3-ms square anodal constant current pulses for 400 ms of the basic cycle and is prematurely stimulated by one 3-ms test stimulus through the driving electrode. Electrical stimulation is programmed by a digital stimulator. A recording electrode is placed on the surface of each ventricle. A silver plate is implanted under the skin in the right femoral region as indifferent electrode. Lead II of the body surface electrocardiogram is monitored. To determine ventricular fibrillation threshold (VFT), a 0.2- to 1.8-second train of 50-Hz pulses is delivered 100 ms after every eighteenth basic driving stimulus. The current intensity is increased from the diastolic threshold in increments of 10 µA to 1.0 mA or until ventricular fibrillation occurs. The minimal current intensity of the pulse train required to induce sustained ventricular fibrillation is defined as the VFT. When ventricular fibrillation occurs, the heart is immediately defibrillated and allowed to recover to control conditions for 15 to 20 min. Anti-arrhythmic drugs are administered through the femoral vein.

EVALUATION

Ventricular fibrillation threshold (VFT) is determined before and after administration of test drugs at given time intervals. The mean values of 10 experiments are compared using Student's *t*-test.

MODIFICATIONS OF THE METHOD

Marshall et al. (1981) and Winslow (1984) suggested to determine VFT in the pentobarbitone anesthetized rat.

Wu et al. (1989) recommended a conscious dog model for re-entrant atrial tachycardia.

Wu et al. (1990) described a dual electrophysiologic test for atrial anti-re-entry and ventricular antifibrillatory studies in dogs. The re-entry portion of the model was created surgically by a Y-shaped crushing around the tissue between the superior and inferior vena cava and tissue parallel to the AV groove. The antifibrillatory activities were assessed by determination of the ventricular fibrillation threshold using a train-stimuli method.

A chronically prepared rat model of electrically induced arrhythmias was described by Walker and Beatch (1988).

REFERENCES AND FURTHER READING

Burgess MJ, Williams D, Ershler P (1977) Influence of test site on ventricular fibrillation threshold. Am Heart J 94:55–61

Harumi K, Tsutsumi T, Sato T, Sekiya S (1989) Classification of antiarrhythmic drugs based on ventricular fibrillation threshold. Am J Cardiol 64:10J–14J

Jaillon P, Schnittger I, Griffin JC, Winkle RA (1980) The relationship between the repetitive extrasystole threshold and the ventricular fibrillation threshold in the dog. Circ Res 46:599–605

Marshall RJ, Muir AW, Winslow E (1981) Comparative antidysrhythmic and hemodynamic effects of orally or intravenously administered mexiletine and Org 6001 in the anesthetized rat. Br J Pharmacol 74:381–388

Murakawa Y, Toda I, Nozaki A, Kawakubo K, Sugimoto T (1989) Effects of antiarrhythmic drugs on the repetitive extrasystole threshold and ventricular fibrillation threshold. Cardiology 76:58–66

Papp JG, Szekeres L (1968) Analysis of the mechanism of adrenaline actions on ventricular vulnerability. Eur J Pharmacol 3:5–26

Sugimoto T, Murakawa Y, Toda I (1989) Evaluation of antifibrillatory effects of drugs. Am J Cardiol 64:33J–36J

Vanremoortere E, Wauters E (1986) Fibrillation threshold curves and anti-arrhythmic drugs. Arch Int Pharmacodyn 176:476–479

WalkerMJA, Beatch GN (1988) Electrically induced arrhythmias in the rat. Proc West Pharmacol Soc 31:167–170

Wilson E (1984) Methods for detection and assessment of antiarrhythmic activity. Pharmacol Ther 24:401–433

Wu KM, Proakis AG, Hunter TL, Shanklin JR (1989) Effects of AHR-12234 on cardiac transmembrane action potentials, *in situ* cardiac electrophysiology and experimental models of arrhythmia. Arch Int Pharmacodyn 301:131–150

Wu KM, Hunter TL, Proakis AGl (1990) A dual electrophysiologic test for atrial anti-re-entry and ventricular antifibrillatory studies. J Pharmacol Meth 23:87–95

A.5.0.7
Coronary Artery Ligation, Reperfusion Arrhythmia and Infarct Size in Rats

PURPOSE AND RATIONALE

Coronary artery ligation in anesthetized rats results in arrhythmias and myocardial infarction. Following occlusion of the left main coronary artery, very marked ventricular dysrhythmias occur. Electrocardiogram is recorded during ligation and subsequent reperfusion. The amount of infarcted tissue is measured by means of p-nitro-blue tetrazolium chloride-staining in myocardial sections. The model is used to test drugs with potential anti-arrhythmic activities.

PROCEDURE

Groups of 8–10 male Sprague-Dawley rats weighing 350–400 g are used. The animals are anesthetized by intraperitoneal injection of 60 mg/kg pentobarbital sodium. The trachea is intubated to allow artificial ventilation (Starling pump). A catheter is placed in an external jugular vein for administration of test compounds. Peripheral blood pressure is recorded from the common carotid artery using a pressure transducer and a polygraph. The chest is opened by left thoracotomy at the forth intercostal space. After opening the pericard, the heart is exteriorized by gentle pressure on the chest walls and a thin silk thread (Ethicon 1.5 metric, 4–0) attached to an atraumatic needle is placed around the left coronary artery about 2–3 mm distal of the origin of the left coronary artery for later ligation. From that point on, the animal is ventilated with room air using a stroke volume of 1 ml/100 g body weight at a rate of 54 strokes/min. The heart is then placed back in the chest cavity. Any animal in which this procedure itself produces dysrhythmias or a sustained fall in mean arterial blood pressure to less than 70 mm Hg has to be discarded from the study.

After an equilibration time of approx. 45 min, the test substance or the vehicle (control) is administered by intravenous injection. Five min later, the ligature at the left coronary artery is closed either for 15 or 90 min (in case infarct-size is assessed) and subsequently reperfused for 30 min. For oral application, the test compounds are dissolved or suspended in the vehicle 30 min before occlusion. Peripheral blood pressure and ECG lead II are recorded continuously during the whole experiment. Rectal temperature is maintained at 38°C. The numbers of ventricular premature beats (VPB), ventricular tachycardia (VT) and ventricular fibrillation (VF) are counted in the occlusion and reperfusion periods and evaluated according to the guidelines of the Lambeth Convention (Walker et al. 1988).

Preparation to Determine Infarct Size

At the end of the reperfusion period, the animal is sacrificed with an overdose of pentobarbital sodium, the heart is dissected and cut into transversal sections (approx. 1 mm thick) from the apex to the base. The slices are stained with p-nitro-blue tetrazolium chloride solution (0.25 g/L p-nitro-blue tetrazolium chloride in Sörensen phosphate buffer, containing 100 mM D, L-maleate) in order to visualize the infarct tissue (blue/violet-stained healthy tissue, unstained necrotic tissue). The slices are photographed on color transparency film for the determination of infarct area. Left ventricle and infarct area are measured by planimetry from projections of all slices with the exclusion of the apex and the slice containing the ligature.

EVALUATION

The following parameters are evaluated:

- mortality
- hemodynamics
  - peripheral blood pressure [mm Hg]
  - heart rate [beats/min]
  - pressure rate index (PRI) (BPs × HR) [mm Hg × beats/1000]
- arrhythmias
  - ventricular extrasystoles (= premature ventricular contractions) (PVC)
    - percent animals with PVC
    - number of PVC/5 or 30 min
  - ventricular tachycardia (VT) (VT defined as any run of seven or more consecutive ventricular extrasystoles)
    - percent animals with VT
    - duration [s] of VT/5 or 30 min
  - ventricular fibrillation (VF)
    - percent animals with VF
    - duration [s] of VF/5 or 30 min
- infarct size (area)

The different characteristics are evaluated separately and compared with a positive control (5 mg/kg nicainoprol i.v.).

Changes of parameters in drug-treated animals are compared to vehicle control values.

Statistical significance is assessed by the Student's *t*-test.

MODIFICATIONS OF THE METHOD

Leprán et al. (1983) placed a loose silk loop around the left coronary artery and passed the thread through a cylinder shaped polyethylene tube outside the thorax. The rats were allowed to recover from primary surgery. The loose ligature was tightened 7–10 days thereafter and arrhythmias recorded by ECG tracings.

Johnston et al. (1983) described the responses to ligation of a coronary artery in conscious rats and the actions of anti-arrhythmics.

As reported in Sect. A.3.1.2 and A.3.1.3, the isolated heart according to LANGENDORFF and the isolated working rat heart preparation can be used for ligation experiments inducing arrhythmias. Lubbe et al. (1978) reported ventricular arrhythmias associated with coronary artery occlusion and reperfusion in the isolated perfused rat heart as a model for assessment of anti-fibrillatory action of anti-arrhythmic agents.

Bernier et al. (1986) described reperfusion-induced arrhythmias in the isolated perfused rat heart. The isolated rat heart was perfused according the LANGENDORFF-technique. A ligature was placed around the left anterior descending coronary artery close to its origin. The arterial occlusion was maintained for 10 min followed by reperfusion. Test compounds were included in the perfusion medium. With epicardial ECG-electrodes the number of premature ventricular complexes, the incidence and duration of ventricular fibrillation, and the incidence of ventricular tachycardia were recorded.

Abraham et al. (1989) tested antiarrhythmic properties of tetrodotoxin against occlusion-induced arrhythmias produced by ligation of the left anterior descending coronary artery in the rat.

MacLeod et al. (1989) tested a long acting analogue of verapamil for its actions against arrhythmias induced by ischemia and reperfusion in conscious and anesthetized rats, as well as for effects on epicardial intracellular action potentials.

Harper et al. (1993) found that the inhibition of Na^+/H^+ exchange preserves viability, restores mechanical function, and prevents the pH paradox in reperfusion injury to rat neonatal myocytes.

Scholz et al. (1993, 1995) reported protective effects of HOE642, a selective sodium-hydrogen exchange subtype 1 inhibitor, on cardiac ischaemia and reperfusion in rats.

Likewise, Yasutake et al. (1994) found protection against reperfusion-induced arrhythmias in rats by intracoronary infusion of a Na^+/H^+ exchange inhibitor.

Aye et al. (1997) tested the effects of a Na^+/H^+ exchange inhibitor on reperfusion ventricular arrhythmias in rat hearts.

Ferrara et al. (1990) studied the effect of flecainide acetate on reperfusion- and barium-induced ventricular tachyarrhythmias in the isolated perfused rat heart by monitoring heart rate, coronary flow rate, left ventricular systolic pressure, dp/dt_{max}, and the voltage of the epicardial electrogram.

Heterogeneity of ventricular remodeling after acute myocardial infarction in rats has been reported by Capasso et al. (1992).

Bellemin-Baurreau et al. (1994) described an *in vitro* method for evaluation of antiarrhythmic and antiischemic agents by using programmed electrical stimulation of the isolated rabbit heart after ligation of the left ventricular branch of the coronary artery and a reperfusion period of 15 min.

The use of the rat in models for the study of arrhythmias in myocardial ischemia and infarction has been reviewed by Curtis et al. (1987).

Black and Rodger (1996), Black (2000) reviewed the methods used to study experimental myocardial ischemic and reperfusion injury in various animal species.

Linz et al. (1997) reported that in isolated rat hearts with ischemia-reperfusion injuries, perfusion with bradykinin reduces the duration and incidence of ventricular fibrillations, improves cardiodynamics, reduces release of cytosolic enzyme, end preserves energy-rich phosphate and glycogen stores.

Mulder et al. (1998) studied the effects of chronic treatment with calcium antagonists in rats with chronic heart failure induced by coronary artery ligation.

The effect of antihypertensive agents on cardiac and vascular remodelling was discussed by Mallion et al. (1999).

REFERENCES AND FURTHER READING

Abraham S, Beatch GN, MacLeod BA, Walker MJA (1989) Antiarrhythmic properties of tetrodotoxin against occlusion-induced arrhythmias in the rat: a novel approach to the study of antiarrhythmic effects of ventricular sodium channel blockade. J Pharmacol Exp Ther 251:1166–1173

Aye NN, Xue YX, Hashimoto K (1997) Antiarrhythmic effects of cariporide, a novel Na^+-H^+ exchange inhibitor, on reperfusion ventricular arrhythmias in rat hearts. Eur J Pharmacol 339:121–127

Bellemin-Baurreau J, Poizot A, Hicks PE, Armstrong JM (1994) An *in vitro* method for evaluation of antiarrhythmic and antiischemic agents by using programmed electrical stimulation of rabbit heart. J Pharmacol Toxicol Meth 31:31–40

Bernier M, Hearse DJ, Manning AS (1986) Reperfusion-induced arrhythmias and oxygen-derived free radicals. Studies with "anti-free radical" interventions and a free radical-generating system in the isolated perfused rat heart. Circ Res 58:331–340

Black SC, Rodger IW (1996) Methods for studying experimental myocardial ischemic and reperfusion injury. J Pharmacol Toxicol Meth 35:179–190

Black SC (2000) *In vivo* models of myocardial ischemia and reperfusion injury. Application to drug discovery and evaluation. J Pharmacol Toxicol Meth 43:153–167

Brooks RR, Carpenter JF, Jones SM, Gregory CM (1989) Effects of dantrolene sodium in rodent models of cardiac arrhythmia. Eur J Pharmacol 164:521–530

Capasso JM, Li P, Zhang X, Anversa P (1992) Heterogeneity of ventricular remodeling after acute myocardial infarction in rats. Am J Physiol 262 (Heart Circ Physiol 31):H486–H495

Clark C, Foreman MI, Kane KA, McDonald FM, Parratt JR (1980) Coronary artery ligation in anesthetized rats as a method for the production of experimental dysrhythmias and for the determination of infarct size. J Pharmacol Meth 3:357–368

Colatsky Th (1989) Models of myocardial ischemia and reperfusion injury: Role of inflammatory mediators in determining infarct size. Pharmacological Methods in the Control of Inflammation, pp 283–320, Alan R. Liss, Inc

Curtis MJ, Macleod BA, Walker MJA (1987) Models for the study of arrhythmias in myocardial ischaemia and infarction: the use of the rat. J Mol Cell Cardiol 19:399–419

Ferrara N, Abete P, Leosco D, Caccese P, Orlando M, Landino P, Sederino S, Tedeschi C, Rengo F (1990) Effect of flecainide acetate on reperfusion- and barium-induced ventricular tachyarrhythmias in the isolated perfused rat heart. Arch Int Pharmacodyn 308:104–114

Harper IS, Bond JM, Chacon E, Reece JM, Herman B, Lemasters JJ (1993) Inhibition of Na^+/H^+ exchange preserves viability, restores mechanical function, and prevents the pH paradox in reperfusion injury to rat neonatal myocytes. Basic Res Cardiol 88:430–442

Harris N, Kane KA, Muir AW, Winslow E (1982) Influences of hypothermia, cold, and isolation stress on the severity of coronary artery ligation-induced arrhythmias in rats. J Pharmacol Meth 7:161–171

Harris S (1950) Delayed development of ventricular ectopic rhythms following experimental coronary occlusion. Circ Res 1:1318–1328

Johnston KM, MacLeod BA, Walker MJA (1983) Responses to ligation of a coronary artery in conscious rats and the actions of antiarrhythmics. Can J Physiol Pharmacol 61:1340–1353

Krzeminski T (1991) Reperfusion – induced arrhythmias in anaesthetized rats; The essential model for the study of potential anti-dysrhythmic and cytoprotective drugs according to the LAMBETH conventions. 7th Freiburg Focus on Biomeasurement. Cardiovascular and Respiratory *in vivo* Studies. Biomesstechnik-Verlag March GmbH, 79232 March, Germany, pp 125–130

Leprán I, Koltai M, Siegmund W, Szekeres L (1983) Coronary artery ligation, early arrhythmias, and determination of the ischemic area in conscious rats. J Pharmacol Meth 9:219–230

Linz W, Wiemer G, Schölkens BA (1997) Beneficial effects of bradykinin on myocardial energy metabolism and infarct size. Am J Cardiol 80:118A–123A

Lubbe WF, Daries PS, Opie LH (1978) Ventricular arrhythmias associated with coronary artery occlusion and reperfusion in the isolated perfused rat heart: a model for assessment of antifibrillatory action of antiarrhythmic agents. Cardiovasc Res 12:212–220

Mallion JM, Baguet JP, Siche JP, Tremel F, de Gaudemaris R (1999) Cardiac and vascular remodelling: effect of antihypertensive agents. J Human Hypertens 13 [Suppl 1]:S35–S41

Manning AS, Hearse DJ (1984) Review: Reperfusion-induced arrhythmias: Mechanism and prevention. J Mol Cell Cardiol 16:497–518

MacLeod BA, Moult M, Saint KM, Walker MJA (1989) The antiarrhythmic efficacy of anipamil against occlusion and reperfusion arrhythmias. Br J Pharmacol 98:1165–1172

Martorana PA, Linz W, Göbel H, Petry P, Schölkens BA (1987) Effects of nicainoprol on reperfusion arrhythmia in the isolated working heart and on ischemia and reperfusion arrhythmia and myocardial infarct size in the anesthetized rat. Eur J Pharmacol 143:391–401

Mulder P, Richard V, Thuillez C (1998) Different effects of calcium antagonists in a rat model of heart failure. Cardiology 89, Suppl 1:33–37

Paróczai M, Kárpáti E, Solti F (1990) The effect of bisaramil on experimental arrhythmias. Pharmacol Res 22:463–480

Schölkens BA, Linz W, König W (1988) Effects of the angiotensin converting enzyme inhibitor, ramipril, in isolated ischaemic rat heart are abolished by a bradykinin antagonist. J Hypertens 6, Suppl 4:S25–S28

Scholz W, Albus U, Linz W, Martorana P, Lang HJ, Schölkens BA (1992) Effects of Na^+/H^+ exchange inhibitors in cardiac ischaemia. J Mol Cell Cardiol 24:731–740

Scholz W, Albus U, Lang HJ, Linz W, Martorana PA, Englert HC, Schölkens BA (1993) Hoe 694, a new Na^+/H^+ exchange inhibitor and its effects in cardiac ischemia. Br J Pharmacol 109:562–568

Scholz W, Albus U, Lang HJ, Linz W, Martorana PA, Englert HC, Schölkens BA (1993) Hoe 694, a new Na^+/H^+

exchange inhibitor and its effects in cardiac ischaemia. Br J Pharmacol 109:562–568
Scholz W, Albus U, Counillon L, Gögelein H, Lang HJ. Linz W, Weichert A, Schölkens BA (1995) Protective effects of HOE642, a selective sodium-hydrogen exchange subtype 1 inhibitor, on cardiac ischaemia and reperfusion. Cardiovasc Res 29:260–268
Selye H, Bajusz E, Grasso S, Mendell P (1960) Simple techniques for the surgical occlusion of coronary vessels in the rat. Angiology 11:398–407
Sun W, Wainwright CL (1994) The potential antiarrhythmic effects of exogenous and endogenous bradykinin in the ischaemic heart *in vivo*. Coron Artery Dis 5:541–550
Uematsu T, Vozeh S, Ha HR, Hof RP, Follath F (1986) Coronary ligation-reperfusion arrhythmia models in anesthetized rats and isolated perfused rat hearts. Concentration-effect relationships of lidocaine. J Pharmacol Meth 16:53–61
van Gilst WH, de Graeff PA, Wesseling H, de Langen CDJ (1986) Reduction of reperfusion arrhythmias in the ischemic isolated rat heart by angiotensin converting enzyme inhibitors: A comparison of captopril, enalapril, and HOE 489. J Cardiovasc Pharmacol 8:722–728
Walker MJA, Curtis MJ, Hearse DJ, Campbell RWF, Janse MJ, Yellon DM, Cobbe SM, Coker SJ, Harness JB, Harron DWG, Higgins AJ, Julian DG, Lab MJ, Manning AS, Northover BJ, Parratt JR, Riemersma RA, Riva E, Russell DC, Sheridan DJ, Winslow E, Woodward B (1988) The Lambeth Conventions; guidelines for the study of arrhythmias in ischaemia, infarction and reperfusion. Cardiovasc Res 22:447–455
Yasutake M, Ibuki C, Hearse DJ, Avkiran M (1994) Na+/H+ exchange and reperfusion arrhythmias: protection by intracoronary infusion of a novel inhibitor. Am J Physiol:H2430–H2440

A.5.0.8
Ventricular Arrhythmia After Coronary Occlusion

A.5.0.8.1
Ventricular Fibrillation After Coronary Occlusion and Reperfusion in Anesthetized Dogs

PURPOSE AND RATIONALE

Coronary artery occlusion in anesthetized dogs is accompanied by an increase in heart rate, heart contractility, left ventricular end-diastolic pressure, and blood pressure as well as by ventricular arrhythmias. During a subsequent reperfusion period, a high percentage of control animals die from ventricular fibrillation. Drugs with potential protective effects are tested which reduce both hemodynamic and electrical changes.

PROCEDURE

Dogs of either sex weighing 20–25 kg are used. Anesthesia is induced by intravenous injection of 30 mg/kg thiobutobarbital sodium and maintained by i.v. administration of 20 mg/kg chloralose and 250 mg/kg urethane followed by subcutaneous administration of 2 mg/kg morphine. The animals are placed in the right lateral position. Respiration is maintained through a tracheal tube using a positive pressure respirator (Bird Mark 7). A peripheral vein (saphenous vein) is cannulated for the administration of test compound. The ECG is recorded continuously in lead II (Einthoven).

Preparation for Hemodynamic Measurements

For recording of peripheral systolic and diastolic blood pressure, the cannula of a femoral artery is connected to a pressure transducer (Statham P 23 DB). For determination of left ventricular pressure (LVP), a Millar microtip catheter (PC 350) is inserted via the left carotid artery. Left ventricular end-diastolic pressure (LVEDP) is measured on a high-sensitivity scale; heart rate (HR) is determined from the LVP wave form. Myocardial contractility is measured as the rate of rise of LVP (dp/dt max). The sum of ST-segment elevations is calculated from five values of the peripheral limbs in ECG lead II. The pressure-rate index ($PRI = BPs \times HR$) serves as a measure of oxygen consumption.

Experimental Course

The heart is exposed through a left thoracotomy between the fourth and fifth intercostal space, the pericard is opened and the left anterior descending coronary artery (LAD) is prepared. A silk suture is placed around the LAD, just below the first diagonal branch. After an equilibration period of approx. 45 min., the test substance or the vehicle (controls) is administered as an intravenous bolus. Twenty min later, the ligature at the coronary artery is closed for 90 min. During the occlusion period, the test compound or the vehicle (controls) are given by continuous infusion. After release of the coronary obstruction, the animal is monitored for a 30 min reperfusion period. All parameters are recorded during the whole experiment. At the end of the test, surviving animals are sacrificed by an overdose of pentobarbital sodium.

EVALUATION

The following parameters are evaluated:

- mortality
- hemodynamics
- arrhythmias
  - ventricular extrasystoles (= premature ventricular contractions) (PVC)
  - percent animals with PVC
  - number of PVC/5 or 30 min

- ventricular tachycardia (VT) (VT defined as any sequence of seven or more consecutive ventricular extrasystoles)
- duration [s] of VT/5 or 30 min
- ventricular fibrillation (VF)
- percent animals with VF

The different characteristics are evaluated separately. Changes of parameters in drug-treated animals are compared to vehicle controls. Statistical significance of the differences is calculated by means of the Student's *t*-test.

Standard data:

Mortality: In an representative experiment, 10 out of 12 of control animals died from ventricular fibrillation during the 30 min reperfusion period. One out of 8 molsidomine-treated animals died and the death was also from ventricular fibrillation during the reperfusion phase. (Molsidomine was given as a continuous infusion of 0.5 mg/kg/ml/min during the occlusion period; controls received saline).

MODIFICATIONS OF THE METHOD

Varma and Melville (1963) described ventricular fibrillation induced by coronary occlusion during hypothermia in **dogs**.

Wilkerson and Downey (1978) described a technique for producing ventricular arrhythmias in dogs through coronary occlusion by an embolus (glass beads) being introduced into the coronary circulation via a rigid cannula which is inserted through the carotid artery.

Weissenburger et al. (1991) described a model in dogs suitable for screening the bradycardia-dependent proarrhythmic effects of drugs and for studying the electrophysiology of "torsades de pointes".

Coker (1989) recommended the anesthetized **rabbit** as a model for ischemia- and reperfusion-induced arrhythmias.

Thiemermann et al. (1989) described a rabbit model of experimental myocardial ischemia and reperfusion. Drugs were administered by intravenous infusion 5 min after the occlusion of the left anterior-lateral coronary artery and continued during the 60 min occlusion and subsequent 3 h reperfusion periods.

Hendrikx et al. (1994) reported that the Na^+-H^+ exchange inhibitor HOE 694 improves post-ischemic function and high-energy phosphate resynthesis and reduced Ca^{2+} overload in the isolated perfused rabbit heart.

Barrett et al. (1997) described a method of recording epicardial monophasic action potentials and ischemia-induced arrhythmias following coronary artery ligation in intact rabbits.

Naslund et al. (1992) described a closed chest model in *pigs*. Occlusion was induced in pentobarbitone anesthetized, mechanically ventilated **pigs** by injection of a 2 mm ball into a preselected coronary artery. Reperfusion was achieved by retraction of the ball via an attached filament.

D'Alonzo et al. (1994) evaluated the effects of potassium channel openers on pacing- and ischemia-induced ventricular fibrillation in anesthetized pigs.

Sack et al. (1994) described the effects of a Na^+/H^+ antiporter inhibitor on post-ischemic reperfusion in pig heart.

Premaratne et al. (1995) used a **baboon** open chest model of myocardial ischemia and reperfusion. Baboons underwent occlusion of the left anterior descending coronary artery for 2 h. Fifteen min after occlusion, the treated group received hyaluronidase i.v. over a 10-min period. The ischemic period was followed by 22 h of reperfusion. At the end of the reperfusion period, the hearts were excised and the perfusion bed at risk for infarction was determined by infusion of a microvascular dye.

REFERENCES AND FURTHER READING

Barrett TC, MacLeod BA, Walker MJA (1997) A model of myocardial ischemia for the simultaneous assessment of electrophysiological changes and arrhythmias in intact rabbits. J Pharmacol Toxicol Meth 37:27–36

Coker SJ (1989) Anesthetized rabbit as a model for ischemia- and reperfusion-induced arrhythmias. Effects of quinidine and bretylium. J Pharmacol Meth 21:263–279

Colatsky TJ (1989) Models of myocardial ischemia and reperfusion injury: Role of inflammatory mediators in determining infarct size. In: Pharmacological Methods in the Control of Inflammation. Alan R. Liss, Inc., pp 283–320

D'Alonzo AJ, Hess TA, Darbenzio RB, Sewter JC, Conder ML, McCullough JR (1994) Effects of cromakalim or pinacidil on pacing- and ischemia-induced ventricular fibrillation in the anesthetized pig. Basic Res Cardiol 89:163–176

Hendrikx M, Mubagwa K, Verdonck F, Overloop K, Van Hecke P, Vanstapel F, Van Lommel A, Verbeken E, Laurweryns J, Flameng W (1994) New Na^+-H^+ exchange inhibitor HOE 694 improves postischemic function and high-energy phosphate resynthesis and reduced Ca^{2+} overload in isolated perfused rabbit heart. Circulation 89:2787–2798

Krumpl G, Todt H, Schunder-Tatzber S, Raberger G (1990) Programmed electrical stimulation after myocardial infarction and reperfusion in conscious dogs. J Pharmacol Meth 23:155–169

Linz W, Schölkens BA (1992) Role of bradykinin in the cardiac effects of angiotensin-converting enzyme inhibitors. J Cardiovasc Pharmacol 20(Suppl 9):S83–S90

Linz W, Wiemer G, Gohlke P, Unger T, Schölkens BA (1994) The contribution of bradykinin to the cardiovascular actions of ACE inhibitors. In Lindpaintner K, Ganten D (eds) The Cardiac Renin Angiotensin System. Futura Publ Co., Inc., Armonk, NY, pp 253–287

Martorana PA, Mogilev AM, Kettenbach B, Nitz RE (1983) Effect of molsidomine on spontaneous ventricular fibrillation following myocardial ischemia and reperfusion in the dog. In: Chazov E, Saks V, Rona G (eds) Advances in Myocardiology. Plenum Publishing Comp., New York, Vol. 4, pp 605–613

Martorana PA, Kettenbach B, Breipohl G, Linz W, Schölkens BA (1990) Reduction of infarct size by local angiotensin-converting enzyme inhibition is abolished by a bradykinin antagonist. Eur J Pharmacol 182:395–396

Naslund U, Haggmark S, Johansson G, Pennert K, Reiz S, Marklund SL (1992) Effects of reperfusion and superoxide dismutase on myocardial infarct size in a closed chest pig model. Cardiovasc Res 26:170–178

Premaratne S, Watanabe BI, LaPenna WF, McNamara JJ (1995) Effects of hyaluronidase on reducing myocardial infarct size in a baboon model of ischemia-reperfusion. J Surg Res 58:205–210

Sack S, Mohri M, Schwarz ER, Arras M, Schaper J, Ballagi-Pordány G, Scholz W, Lang HJ, Schölkens BA, Schaper W (1994) Effects of a new Na^+/H^+ antiporter inhibitor on postischemic reperfusion in pig heart. J Cardiovasc Pharmacol 23:72–78

Thiemermann C, Thomas GR, Vane JR (1989) Defibrotide reduces infarct size in a rabbit model of experimental myocardial ischaemia and reperfusion. Br J Pharmacol 97:401–408

Varma DR, Melville KI (1963) Ventricular fibrillation induced by coronary occlusion during hypothermia in dogs and the effects of quinidine, quinacrine and oxytocin. Canad J Biochem Physiol 41:511–517

Weissenburger J, Chezalviel F, Davy JM, Lainée P, Guhennec C, Penin E, Engel F, Cynober L, Motté G, Cheymol G (1991) Methods and limitations of an experimental model of long QT syndrome. J Pharmacol Meth 26:23–42

Wilkerson DR, Downey JM (1978) Ventricular arrhythmias produced by coronary artery occlusion in closed-chest dogs. J Pharmacol Meth 1:39–44

A.5.0.8.2 Harris Dog Model of Ventricular Tachycardia

PURPOSE AND RATIONALE

In 1950, Harris found that the mortality in dogs after coronary occlusion with a 2-stage ligation procedure was lower than with 1-stage ligation. The left descending coronary artery is partially occluded for 30 min after which time total ligation is performed. Under these conditions arrhythmias develop within 4–7 h, reach a peak between 24 and 48 h and abate within 3–5 days.

PROCEDURE

Surgical Procedure

Dogs of either sex are anesthetized by intravenous injection of methohexitone sodium (10 mg/kg), an endotracheal tube is inserted, and anesthesia maintained with halothane. The heart is exposed through an incision in the fourth or fifth intercostal space. The anterior descending branch of the left coronary artery is dissected free below its second branch and ligated in two stages. Two ligatures are placed around the artery and a 21 gauge needle. The first ligature is tied round the artery and the needle, which is then removed. Thirty min later, the second ligature is tied tightly round the artery. The chest is closed in layers 30 min after the second ligature has been tied, and the dog is allowed to recover.

Test Procedure

Further observations are made when the dogs are conscious, e. g., 22–24 h after ligation of the coronary artery. The dogs are positioned to lie on their side and remain in this position throughout the experiment. Mean blood pressure is recorded from a catheter placed in the femoral artery. Lead II and aV_L of the electrocardiogram and blood pressure are continuously recorded for a control period of 30 min before and during drug administration. Drugs are administered either by injection or by continuous infusion via a hind leg vein.

EVALUATION

The number of sinus and ectopic beats are counted for each successive 5-min period. Beats with a distinct P wave preceding a mean frontal QRS vector of normal duration are counted as sinus in origin; all others are denoted as ectopic.

MODIFICATIONS OF THE METHOD

The model which resembles late arrhythmias occurring in postinfarction patients has been used with modifications by many authors (e. g., Kerr et al. 1985; Reynolds and Brown 1986; Gomoll 1987; Garthwaite et al. 1989; Krumpl et al. 1989a, b; Trolese-Mongheal et al. 1985, 1991; Spinelli et al. 1991).

Methods for producing experimental complete atrioventricular block in dogs were described and reviewed by Dubray et al. (1983) and by Boucher and Duchene-Marullaz (1985).

REFERENCES AND FURTHER READING

Boucher M, Duchene-Marullaz P (1985) Methods for producing experimental complete atrioventricular block in dogs. J Pharmacol Meth 13:95–107

Clark BB, Cummings JR (1956) Arrhythmias following experimental coronary occlusion and their response to drugs. Ann NY Acad Sci 64:543–551

Dubray C, Boucher M, Paire M, Duchene-Marullaz P (1983) A method for determining the atrial effective refractory period in the unanaesthetized dog. J Pharmacol Meth 9:157–164

Garthwaite SM, Hatley FR, Frederik LG, Cook C (1989) Efficacy and plasma concentrations of SC-36602 in canine models of ventricular arrhythmia. J Cardiovasc Pharmacol 13:218–226

Gomoll AW (1987) Assessment of drug effects on spontaneous and induced ventricular arrhythmias in a 24-h canine infarction model. Arzneim Forsch/Drug Res 37:787–794
Harris AS (1950) Delayed development of ventricular ectopic rhythms following experimental coronary occlusion. Circ Res 1:1318–1328
Kerr MJ, Wilson R, Shanks RG (1985) Suppression of ventricular arrhythmias after coronary artery ligation by Pinacidil, a vasodilator drug. J Cardiovasc Pharmacol 7:875–883
Krumpl G, Todt H, Schunder-Tatzber S, Raberger G (1989a) Holter monitoring in conscious dogs. Assessment of arrhythmias occurring during ischemia and in the early reperfusion phase. J Pharmacol Meth 77–91
Krumpl G, Todt H, Schunder-Tatzber S, Raberger G (1989b) Holter monitoring in conscious dogs. Assessment of arrhythmias occurring in the late reperfusion phase after coronary occlusion. J Pharmacol Meth 22:92–102
Menken U, Wiegand V, Bucher P, Meesmann W (1979) Prophylaxis of ventricular fibrillation after acute coronary occlusion by chronic beta-adrenoceptor blockade with atenolol. Cardiovasc Res 13:588–594
Reynolds RD, Brown BS (1986) Antiarrhythmic activity of flestolol, a novel ultra-short-acting β-adrenoceptor antagonist, in the dog. Eur J Pharmacol 131:55–66
Spinelli W, Hoffman B, Hoffman BF (1991) Antiarrhythmic drug action in the Harris dog model of ventricular tachycardia. J Cardiovasc Electrophysiol 2:21–33
Trolese-Mongheal Y, Trolese JF, Lavarenne J, Duchene-Marullaz P (1985) Use of experimental myocardial infarct to demonstrate arrhythmogenic activity of drugs. J Pharmacol Meth13:225–234
Trolese-Mongheal Y, Barthelemy J, Trolese JF, Duchene-Marullaz P (1991) Time course of spontaneous ventricular arrhythmias following acute coronary occlusion in the dog. J Pharmacol Meth 26:125–137
Vegh A, Papp JG, Parratt J (1994) Attenuation of the antiarrhythmic effects of ischaemic preconditioning by blockade of bradykinin B_2 receptors. Br J Pharmacol 113:1167–1172

A.5.0.8.3 Protection against Sudden Coronary Death

PURPOSE AND RATIONALE

The group of Lucchesi described an experimental dog model to test protection against sudden coronary death (Patterson et al. 1982; Uprichard et al. 1989a, b; Chi et al. 1990a, b, 1991; Kitzen et al. 1990; Black et al. 1991, 1993).

Surgical Preparation

Purpose-bred male mongrel dogs weighing 14–22 kg are anesthetized with 30 mg/kg pentobarbital i.v. The dogs are ventilated with room air through a cuffed endotracheal tube and a Harvard respirator. A cannula is inserted in the left external jugular vein. A left thoracotomy is performed between the fourth and fifth ribs, and the heart is exposed and suspended in a pericardial cradle. The left anterior descending coronary artery (LAD) is isolated at the tip of the left atrial appendage, and the left circumflex coronary artery (LCX) is isolated ~1 cm from its origin. After a 20-gauge hypodermic needle has been placed on the LAD, a ligature is tied around the artery and the needle. The needle is then removed, resulting in critical stenosis of the vessel. The LAD is perfused for 5 min in the presence of the critical stenosis. Ischemic injury of the anterior ventricular myocardium is achieved by 2-h occlusion of the LAD by a silicon rubber snare. The vessel is reperfused after 2 h in the presence of the critical stenosis. During the period of LAD reperfusion, an epicardial bipolar electrode (1-mm silver posts, 3-mm interelectrode separation) is sutured on the left atrial appendage for subsequent atrial pacing. A bipolar plunge electrode (25-gauge stainless steel, 5 mm long, 3 mm separation) is sutured on the interventricular septum, adjacent to the occlusion site and overlying the right ventricular outflow tract (RVOT). Two similar stainless steel bipolar plunge electrodes are sutured to the left ventricular (LV) wall: one at the distribution of the LAD distal to the occlusion (infarct zone, IZ), and the second in the distribution of the LCX (non-infarct zone, NZ). A 30-gauge silver-coated copper wire electrode is passed through the wall and into the lumen of the LCX and sutured to the adjacent surface of the heart. Silver disc electrodes are implanted subcutaneously for ECG monitoring. The surgical incision is closed and the animals are allowed to recover.

Drug Treatment

The animals are treated after the recovery period during the 3 days of programmed electrical stimulation either with the test drug or with the solvent.

Electrophysiologic Studies and Programmed Electrical Stimulation

Programmed electrical stimulation (PES) is performed between days 3 and 5 after induction of anterior myocardial infarction by occlusion/perfusion of the LAD. Animals are studied while conscious and unsedated. Heart rate, ECG intervals and other electrophysiologic parameters (for details see original publications) are determined before PES is started. Premature ventricular stimuli are introduced in the region of the right ventricular outflow tract. The extra stimuli are triggered from the R-wave of the ECG, and the R-S_2 coupling interval is decreased from 350 ms until ventricular refractoriness occurs. At this time, double and triple ventricular extra stimuli are introduced during sinus rhythm. Ventricular tachyarrhythmias are defined as 'non- sustained', if five or more repetitive ventricular responses are initiated reproducibly, but terminated spontaneously. Ventricular tachyarrhythmias are

defined as 'sustained', if they persist for at least 30 s or, in the event of hemodynamic compromise, require ventricular burst pacing for their termination.

Sudden Cardiac Death

A direct anodal 15 µA current from a 9-V nickel-cadmium battery is passed through a 250 Ohm resistor and applied to the electrode in the lumen of the left circumflex coronary artery. The cathode of the battery is connected to a s.c. implanted disc electrode. Lead II ECG is recorded for 30 s every 15 min on a cardiocassette recorder. After 24 h of constant anodal current or development of ventricular fibrillation, the animals are sacrificed, the hearts are excised and the thrombus mass in the LCX is removed and weighed. The heart is sectioned transversely and incubated for 15 min at 37°C in a 0.4% solution of tetrazolium triphenyl chloride for identification of infarcted areas. Time of onset of ventricular ectopy and of lethal arrhythmia is provided from recordings of the cardiocassette.

EVALUATION

Non-sustained and sustained tachyarrhythmias are evaluated.

CRITICAL ASSESSMENT OF THE METHOD

Sudden coronary death is one of the leading causes of death in developed countries. These facts warrant the use of complicated models in higher animals for search of active drugs.

MODIFICATIONS OF THE METHOD

Schwartz et al. (1984) described an experimental preparation for sudden cardiac death in dogs. The animals were chronically instrumented and studied 1 month after an anterior myocardial infarction. A balloon catheter around the circumflex coronary artery was inflated to produce acute myocardial ischemia and the occlusion was maintained for 2 min. Several days later, the animals were subjected to a submaximal stress on a motor-driven treadmill for 12–18 min. During the last minute of exercise the left coronary artery was occluded, the treadmill stopped, and the occlusion was maintained for a second minute.

Schwartz et al. (1988) analyzed the baroreceptor reflexes in conscious dogs with and without a myocardial infarction to get insights in the mechanisms of sudden death.

Cahn and Cervoni (1990) reviewed of the use of animal models of sudden cardiac death for drug development.

Pak et al. (1997) found that canine tachycardia-induced cardiomyopathy is a useful model for studying mechanisms and therapy of sudden cardiac death in heart failure. Adamson et al. (1994) performed a longitudinal study in dogs at high and low risk for sudden death and found an unexpected interaction between β-adrenergic blockade and heart rate variability before and after myocardial infarction.

Basso et al. (2004) recommended arrhythmogenic right ventriculopathy causing sudden death in boxer dogs as an animal model of human disease.

REFERENCES AND FURTHER READING

Adamson PB, Huang MH, Vanoli E, Foreman RD, Schwartz PJ, Hull SS (1994) Unexpected interaction between β-adrenergic blockade and heart rate variability before and after myocardial infarction. A longitudinal study in dogs at high and low risk for sudden death. Circulation 90:976–982

Basso C, Fox PR, Meurs KM, Towbin JA, Spier AW, Calabrese F, Maron BJ, Thiene G (2004) Arrhythmogenic right ventriculopathy causing sudden death in boxer dogs. A new animal model of human disease. Circulation 109:1180–1185

Black SC, Chi L, Mu DX, Lucchesi RR (1991) The antifibrillatory actions of UK 68,798, a class III antiarrhythmic agent. J Pharm Exp Ther 258:416–423

Black SC, Butterfield JL, Lucchesi BR (1993) Protection against programmed stimulation-induced ventricular tachycardia and sudden coronary death by NE-10064, a class III antiarrhythmic drug. J Cardiovasc Pharmacol 22:810–818

Cahn PS, Cervoni P (1990) Current concepts and animal models of sudden cardiac death for drug development. Drug Dev Res 19:199–207

Chi L, Mu DX, Driscoll EM, Lucchesi BR (1990a) Antiarrhythmic and electrophysiologic actions of CK-3579 and sematilide in a conscious canine model of sudden coronary death. J Cardiovasc Pharmacol 16:312–324

Chi L, Uprichard ACG, Lucchesi BR (1990b) Profibrillatory actions of pinacidil in a conscious canine model of sudden coronary death. J Cardiovasc Pharmacol 15:452–464

Chi L, Mu DX, Lucchesi BR (1991) Electrophysiology and antiarrhythmic actions of E-4031 in the experimental animal model of sudden coronary death. J Cardiovasc Pharmacol 17:285–295

Kitzen JM, Chi L, Uprichard ACG, Lucchesi BR (1990) Effects of combined thromboxane synthase inhibition/thromboxane receptor antagonism in two models of sudden cardiac death in the canine: limited role of thromboxane. J Cardiovasc Pharmacol 16:68–80

Pak PH, Nuss HB. Tunin RS, Kaab S, Tomaselli GF, Marban E, Kass DA (1997) Repolarization, abnormalities, arrhythmia and sudden death in canine tachycardia-induced cardiomyopathy. J Am Coll Cardiol 30:576–584

Patterson E, Holland K, Eller BT, Lucchesi BR (1982) Ventricular fibrillation resulting from a site remote from previous myocardial infarction. A conscious canine model for sudden coronary death. Am J Cardiol 50:1414–1423

Schwartz PJ, Billman GE, Stone HL (1984) Autonomic mechanisms in ventricular fibrillation induced by myocardial ischemia during exercise in dogs with healed myocardial infarction. An experimental preparation for sudden cardiac death. Circulation 69:790–800

Schwartz PJ, Vanoli EV, Stramba-Badiale M, de Ferrari GM, Billman GE, Foreman RD (1988) Autonomic mechanisms and sudden death. New insights from analysis of baroreceptor reflexes in conscious dogs with and without a myocardial infarction. Circulation 78:969–979

Uprichard ACG, Chi L, Kitzen JM, Lynch JJ, Frye JW, Lucchesi BR (1989a) Celiprolol does not protect against ventricular tachycardia or sudden death in the conscious canine: a comparison with pindolol in assessing the role of intrinsic sympathomimetic activity. J Pharm Exp Ther 251:571–577

Uprichard ACG, Chi L, Lynch JJ, Frye JW, Driscoll EM, Frye JW, Lucchesi BR (1989b) Alinidine reduces the incidence of ischemic ventricular fibrillation in a conscious canine model, a protective effect antagonized by overdrive atrial pacing. J Cardiovasc Pharmacol 14:475–482

A.5.0.8.4 Ventricular Fibrillation Induced by Cardial Ischemia During Exercise

PURPOSE AND RATIONALE

Billman and his group developed methods to evaluate antiarrhythmic drugs for their activity in cardiovascular parameters in an exercise-plus-ischemia test.

PROCEDURE

Surgical Preparation

Mongrel dogs, weighing 15.4 to 19.1 kg, are anesthetized and instrumented to measure left circumflex CBF, left ventricular pressure and ventricular electrogram (Billman and Hamlin 1996; Billman et al. 1993, 1997; Schwartz et al. 1984). The animals are given Innovar Vet (0.02 mg/kg fentanyl citrate and 1 mg/kg hydroperidol i.v.) as a preanesthetic, whereas a surgical plane of anesthesia is induced with sodium pentobarbital (10 mg/kg i.v.). A left thoracotomy is made in the fourth intercostal space, and the heart is exposed and supported by a pericardial cradle. A 20-MHz pulsed Doppler flow transducer and a hydraulic occluder are placed around the left circumflex artery. A pair of insulated silver-coated wires are sutured to the epicardial surface of both the left and right ventricles. These electrodes are used for ventricular pacing or to record a ventricular electrogram from which HR is determined using a Gould Biotachometer (Gould Instruments, Cleveland, OH). A precalibrated solid-state pressure transducer (Konigsberg Instruments, Pasadena, CA) is inserted into the left ventricle via a stab wound in the apical dimple. Finally, a two-stage occlusion of the left anterior descending coronary artery is performed approximately one third the distance from the origin to induce an anterior wall myocardial infarction. This vessel is partially occluded for 20 min and then tied off. All leads from the cardiovascular instrumentation are tunneled under the skin to exit on the back of the animal's neck. A transdermal fentanyl patch that delivers 75 µg/h for 72 h is placed on the back of the neck (secured with adhesive tape) to decrease postoperative discomfort. In addition, bupivacaine HCl, a long-acting local anesthetic, is injected to block the intercostal nerves (i. e., pain fibers) in the area of the incision. Each animal is placed on prophylactic antibiotic therapy (amoxicillin 500 mg p.o.) three times daily for 7 days. The animals are placed in an "intensive care" setting for the first 24 h and placed on antiarrhythmic therapy (Billman and Hamlin 1996; Billman et al. 1993, 1997; Schwartz et al. 1984).

Exercise-Plus-Ischemia Test

The studies begin 3 to 4 weeks after the production of the myocardial infarction. The animals are walked on a motor-driven treadmill and trained to lie quietly without restraint on a laboratory table during this recovery period. Susceptibility to VF is then tested. The animals run on a motor-driven treadmill while workload is increased every 3 min for a total of 18 min. The protocol begins with a 3-min warm-up period, during which the animals run at 4.8 km/h at 0% grade. The speed is increased to 6.4 km/h, and the grade is increased every 3 min as follows: 0%, 4%, 8%, 12% and 16%. During the last minute of exercise, the left circumflex coronary artery is occluded, the treadmill is stopped and the occlusion is maintained for 1 additional min (total occlusion time, 2 min). Large metal plates (diameter, 11 cm) are placed across the animal's chest so that electrical defibrillation can be achieved with minimal delay but only after the animal is unconscious (10–20 s after VF begin). The occlusion is immediately released if VF occur.

The animals then receive one or more of the following treatments:

1 the exercise-plus-ischemia test is repeated after pretreatment with the standard drug glibenclamide (1.0 mg/kg i.v.). The drug is injected in a cephalic vein; 3 min before exercise begins.
2 The exercise-plus-ischemia test is repeated after pretreatment with the test drug
3 Finally, a second control (saline) exercise plus ischemia test is performed 1 week after the last drug test. At least 5 days are intermitted between drug treatments. Drugs are given in a random order.

Refractory Period Determination

On a subsequent day, the effective refractory period is determined using a Medtronic model 5325 programmable stimulator, both at rest and during myocardial ischemia. The heart is paced for 8 beats (S_1; in-

trastimulus interval, 300 ms; pulse duration, 1.8 ms at twice-diastolic threshold of ~6 mA). The intrastimulus interval is progressively shortened between the last paced beat and a single extrastimulus (S_2). The refractory period represents the shortest interval capable of generating a cardiac response and is measured using either the left or right ventricular electrodes. This procedure is completed within 30 s. Once the control values are determined, refractory period measurements are repeated after the standard drug glibenclamide (1.0 mg/kg i.v.), or the test drug. After the completion of these studies, refractory period is determined during myocardial ischemia (2-min occlusion of the left circumflex coronary artery) ~60 s after the onset of the coronary occlusion.

Reactive Hyperemia Studies

The K_{ATP} has been implicated in vascular regulation, particularly CBF (Aversano et al. 1991; Belloni and Hintze 1991; Daut et al. 1990). Therefore, the effects of standard and test drug on the response to brief interruptions in CBF are also evaluated. Animals are placed on a laboratory table, and the left circumflex coronary is occluded three or four times for 15 s. At least 2 min (or until CBF had returned to preocclusion base line) elapse between occlusions. The occlusions are then repeated 5 min after standard and test drug. On the subsequent day, the studies are repeated with the drug that had not been given the previous day.

EVALUATION

All hemodynamic data are recorded on a Gould model 2800S eight-channel recorder (Cleveland, OH) and a Teac model MR-30 FM tape recorder (Tokyo, Japan). Coronary blood flow is measured with a University of Iowa Bioengineering flowmeter model 545 C-4 (Iowa City, IA). The rate of change of left ventricular pressure [$d(LVP)/dt$] is obtained by passing the left ventricular pressure through a Gould differentiator that has a frequency response linear to > 300 Hz. The data are averaged over the past 5 s of each exercise level. The coronary occlusion data are averaged over the last 5 s before and at the 60-s line point (or VF onset) after occlusion onset. The total area between the peak CBF and return to base line is measured for each 15-s occlusion, and the percent repayment is calculated. The reactive hyperemia response to each occlusion is then averaged to obtain one value for each animal. The data are then analyzed using analysis of variance for repeated measures. When the F ratio is found to exceed a critical value ($P < 0.05$), Scheffe's test is used to compare the mean values. The effects of the drug intervention on arrhythmia formation are determined using a χ^2 test with Yates' correction for continuity. All data are reported as mean ± SEM. Cardiac arrhythmias, PR interval and QT interval are evaluated at a paper speed of 100 mm/s. QT interval is corrected for HR using Bazett's method.

CRITICAL ASSESSMENT OF THE METHOD

Tests combining coronary constriction with physical exercise may resemble most closely the situation in coronary patients.

REFERENCES AND FURTHER READING

Aversano T, Ouryang P, Silverman H (1991) Blockade of the ATP-sensitive potassium channel modulates reactive hyperemia in the canine coronary circulation. Circ Res 69:618–622

Belloni FI, Hintze TH (1991) Glibenclamide attenuates adenosine-induced bradycardia and vasodilation. Am J Physiol 261:H720–H727

Billman GE (1994) Role of ATP sensitive potassium channel in extracellular potassium accumulation and cardiac arrhythmias during myocardial ischaemia. Cardiovasc Res 28:762–769

Billman GE, Hamlin RL (1996) The effects of mifebradil, a novel calcium channel antagonist on ventricular arrhythmias induced by ischemia and programmed electrical stimulation. J Pharmacol Exp Ther 277:1517–1526

Billman GE, Avendano CE, Halliwill JR, Burroughs JM (1993) Effects of the ATP-dependent potassium channel antagonist, glyburide, on coronary blood flow and susceptibility to ventricular fibrillation in unanesthetized dogs. J Cardiovasc Pharmacol 21:197–204

Billman GE, Castillo LC, Hensley J, Hohl CM, Altschuld RA (1997) Beta$_2$-adrenergic receptor antagonists protect against ventricular fibrillation: *in vivo* and *in vitro* evidence for enhanced sensitivity to beta$_2$-adrenergic stimulation in animals susceptible to sudden death. Circulation 96:1914–1922

Billman GE, Englert HC, Schölkens BA (1998) HMR 1883, a novel cardioselective inhibitor of the ATP-sensitive potassium channel. Part II: Effects on susceptibility to ventricular fibrillation induced by myocardial ischemia in conscious dogs. J Pharmacol Exp Ther 286:1465–1473

Collins MN, Billman GE (1989) Autonomic response to coronary occlusion in animals susceptible to ventricular fibrillation. Am J Physiol 257 (Heart Circ Physiol 26): H1886–H1889

Daut J, Meier-Rudolph W, von Beckenrath N, Merke G, Gunther K, Godel-Meinen I (1990) Hypoxic dilation of coronary arteries is mediated by ATP-sensitive potassium channels. Science 247:1341–1344

Schwartz PJ, Billman GE, Stone HL (1984) Autonomic mechanisms in ventricular fibrillation induced by myocardial ischemia during exercise in dogs with healed myocardial infarction. Circulation 69:790–800

A.5.0.9 Experimental Atrial Fibrillation

A.5.0.9.1 Atrial Fibrillation by Atrial Pacing in Dogs

PURPOSE AND RATIONALE

Morillo et al. (1995) published a model of sustained atrial fibrillation by chronic rapid atrial pacing in dogs. Halothane-anesthetized mongrel dogs underwent insertion of a transvenous lead at the right atrial appendage that was continuously paced at 400 beats/min for 6 weeks. Two-dimensional echocardiography was performed to assess the effects of rapid atrial pacing on atrial size. Atrial vulnerability was defined as the ability to induce sustained repetitive atrial responses during programmed electrical stimulation. Effective refractory period (ERP) was measured at two endocardial sites of the right atrium. Sustained atrial fibrillation (AV) was defined as AF $\geq$15 min. In animals with sustained AF, 10 quadripolar epicardial electrodes were surgically attached to the left and right atria. The local atrial fibrillatory cycle length (AFCL) was measured in a 20-s window. Marked biatrial enlargement was documented after 6 weeks of continuous rapid atrial pacing. An increase in atrial area of at least 40% was necessary to induce sustained AF.

More studies using this method were performed by Gaspo et al. (1997a, 1997b), Yue et al. (1997), Sun et al. (1998), and Nattel and Li (2000).

Shiroshita-Takeshita et al. (2004) studied the effect of drugs on atrial fibrillation promotion by atrial-tachycardia remodeling on dogs.

PROCEDURE

Mongrel dogs were anesthetized with ketamine (5.3 mg/kg i.v.), diazepam (0.25 mg/kg i.v.) and halothane (1.5%). Unipolar leads were inserted through jugular veins into the right ventricular apex and the right atrial appendage and connected to pacemakers (Medtronic) in subcutaneous pockets in the neck. A bipolar electrode was inserted into the right atrium for stimulation and recording during serial electrophysiological study. AV block was created by radiofrequency ablation of control ventricular response during atrial tachypacing. The right ventricular pacemaker was programmed to 80 beats/min.

After 24 h for recovery, a baseline closed-chest serial electrophysiological study was performed under ketamine/diazepam/isoflurane anesthesia, and then atrial tachypacing (400 beats/min) was initiated. The closed-chest electrophysiological study was repeated at 2, 4, and 7 days of atrial tachypacing, and a final open-chest electrophysiological study was performed on day 8 under morphine-chloralose anesthesia.

Results of atrial tachypacing in drug-treated dogs were compared with results of dogs without treatment (controls).

Study Protocol

Dogs were anesthetized and ventilated mechanically. The atrial pacemaker was deactivated and a right atrium appendage effective refractory period was measured at basic lengths of 150, 200, 250, 300, and 360 ms with 10 basic stimuli (S_1) followed by a premature extra-stimulus (S_2) with 5-ms decrements. The longest S_1-S_2 failing to capture defined the effective refractory period. AF was induced by atrial burst pacing at 10 Hz and 4 times threshold current. To estimate mean AF duration in each dog, AF was induced 10 times if AF duration was $<$20 min and 5 times if AF lasted 20–30 min and then averaged. If AF lasted longer than 30 min, it was considered sustained and was terminated by DC cardioversion. A 20-min rest period was then allowed before continuing measurements.

For open-chest electrophysiological studies, dogs were anesthetized and ventilated mechanically. A femoral artery and both femoral veins were cannulated for pressure monitoring and drug administration. A median sternotomy was performed, and bipolar electrodes were hooked to the right atrial and left atrial appendages for recording and stimulation. A programmable stimulator (Digital Cardiovascular Instruments) was used to deliver twice-threshold currents. Five silicon sheets containing 240 bipolar electrodes were sutured onto the atrial surface (Fareh et al. 2001). Atrial effective refractory periods were measured as multiple basic cycle lengths in the right and left atrial appendages and at basic cycle length 300 ms in six additional sites: right and left atrium posterior wall, right and left atrium inferior wall, and right and left atrium Bachmann's bundle. Atrial fibrillation vulnerability was determined as the percentage of atrial sites at which AF could be induced by single extra-stimuli.

EVALUATION

Data are presented as mean $\pm$ SEM. Multiple-group comparisons were obtained by ANOVA. AF duration data were analyzed after logarithmic transformation. Bonferroni-corrected *t* tests were used to evaluate individual-mean differences.

MODIFICATIONS OF THE METHOD

Verheule et al. (2004) described a canine model of atrial fibrillation due to chronic atrial dilatation.

Courtemanche et al. (1999) and Ramirez et al. (2000) published mathematical models of fibrillation-induced electrical remodeling and of canine atrial action potentials.

Pinto and Boyden (1999) reviewed electrical remodeling in ischemia and infarction.

Cabo and Boyden (2003) performed a computational analysis of electrical remodeling of the epicardial border zone in the canine infarcted heart.

Sakabe et al. (2004) reported that enalapril prevents perpetuation of atrial fibrillation by suppressing atrial fibrosis and over-expression of connexin43 in a canine model of atrial pacing-induced left ventricular dysfunction.

Baartscheer et al. (2005) induced combined volume and pressure overload in New Zealand white **rabbits**. In a first surgical procedure, volume overload was produced by rupture of the aortic valve until pulse pressure increased by about 100%, and after 3 weeks, pressure overload was created by suprarenal abdominal aortic constriction of 50%. In these animals, chronic inhibition of the Na^+/H^+ exchanger attenuated cardiac hypertrophy and prevented cellular remodeling in heart failure.

Using **cultured atrial myocytes** (HL-1 cells), Yang et al. (2005) found that rapid field stimulation (300 beats/min) causes electrical remodeling.

REFERENCES AND FURTHER READING

Baartscheer A, Schumacher CA, van Borren MMGJ, Belterman CNW, Coronel R, Opthof T, Fiolet JWT (2005) Chronic inhibition of Na^+/H^+-exchanger attenuates cardiac hypertrophy and prevents cellular remodelling in heart failure. Cardiovasc Res 65:83–92

Cabo C, Boyden PA (2003) Electrical remodelling of the epicardial border zone in the canine infracted heart: a computational analysis. Am J Physiol 284:H372–H384

Courtemanche M, Ramirez RJ, Nattel S (1999) Ionic targets for drug therapy and atrial-fibrillation-induced electrical remodelling: insights from a mathematical model. Cardiovasc Res 42:477–489

Fareh S, Bardeau A, Nattel S (2001) Differential efficacy of L- and T-type calcium channel blockers in preventing tachycardia-induced atrial remodelling in dogs. Cardiovasc Res 49:762–770

Gaspo R, Bosch RF, Bou-Abboud E, Nattel S (1997a) Tachycardia-induced changes in Na^+ current in a chronic dog model of atrial fibrillation. Circ Res 81:1045–1052

Gaspo R, Bosch RF, Talajic M, Nattel S (1997b) Functional mechanisms underlying tachycardia-induced sustained atrial fibrillation in a chronic dog model. Circulation 96:4027–4035

Morillo CA, Klein GJ, Jones DL, Guiraudon CM (1995) Chronic rapid atrial pacing. Structural, functional, and electrophysiological characteristics of a new model of sustained atrial fibrillation. Circulation 91:1588–1595

Nattel S, Li D (2000) Ionic remodelling in the heart. Pathophysiological significance and therapeutic opportunities for atrial fibrillation. Circ Res 87:440–447

Pinto JMB, Boyden PA (1999) Electrical remodelling in ischemia and infarction. Cardiovasc Res 42:284–297

Ramirez RJ, Nattel S, Courtmanche M (2000) Mathematical analysis of canine atrial action potentials: rate, regional factors, and electrical remodelling. Am J Physiol 279:H1767–H1785

Sakabe M, Fujiki A, Nishida K, Sugao M, Nagasawa H, Tsuneda T, Mizumaki K, Inoue H (2004) Enalapril prevents perpetuation of atrial fibrillation by suppressing atrial fibrosis and over-expression of connexion43 in a canine model of atrial pacing-induced left ventricular dysfunction. J Cardiovasc Pharmacol 43:851–859

Shiroshita-Takeshita A, Schram G, Lavoie J, Nattel S (2004) Effect of simvastatin and antioxidant vitamins on atrial fibrillation promotion by atrial-tachycardia remodelling on dogs. Circulation 110:2313–2319

Sun H, Gaspo R, Leblanc N, Nattel S (1998) Cellular mechanisms of atrial dysfunction caused by sustained atrial tachycardia. Circulation 98:719–727

Verheule S, Wilson E, Banthia S, Everett TH, Shanbhag S, Sih HJ, Olgin J (2004) Direction-dependent conduction abnormalities on a canine model of atrial fibrillation due to chronic atrial dilatation. Am J Physiol 287:H634–H644

Yang Z, Shen W, Rottman JN, Wikswo JP, Murray KT (2005) Rapid stimulation causes electrical remodelling in cultured atrial myocytes. J Mol Cell Cardiol 38:299–308

Yue L, Feng J, Gaspo R, Li GR, Wang Z, Nattel S (1997) Ionic remodelling underlying action potential changes in a canine model of atrial fibrillation. Circ Res 81:512–525

A.5.0.9.2 Atrial Fibrillation in Chronically Instrumented Goats

PURPOSE AND RATIONALE

Atrial fibrillation is the most common tachyarrhythmia in humans. It causes palpitations, decreased cardiac output, heart failure and systemic thromboembolism, and is associated with significant mortality. Wijffels et al. (1995) demonstrated in a chronically instrumented conscious goat model, that episodes of atrial fibrillation may be self-perpetuating ("Atrial fibrillation begets atrial fibrillation") and have suggested that there may be a purely electrophysiological explanation (termed atrial electrical remodeling) for the increase of atrial fibrillation with time. This model has been extensively used to study pathophysiological mechanism and the influence of drugs (Wijffels et al. 1997, 1999, 2000; Allessie et al. 1998; Tieleman et al. 1999; Duytschaever et al. 2000, 2005; Garratt and Fynn 2000; Van der Velden 2000a, 2000b; Veloso 2001; Brendel and Peukert 2003; Shan et al. 2004; Blaauw et al. 2004a).

Blaauw et al. (2004b) studied the efficacy and atrial selectivity of a blocker of the early ultrarapid compo-

nent of the delayed rectifier (I_{kur}) in remodeled atria of the goat.

PROCEDURE

Female goats weighing 52 ± 2 kg were used. According to the method of Duytschaever et al. (2001), Teflon-felt plaques with multiple electrodes were sutured onto the free wall of each atrium, Bachmann's bundle, and the left ventricle. All leads were tunnelled subcutaneously to the neck and exteriorized by four 30-pole connectors. Experiments were started 3–4 weeks after surgery. Atrial fibrillation was induced by a fibrillation pacemaker (Wijffels et al. 1995).

The atria were paced with biphasic stimuli of 2 ms duration and $4 \times$ threshold. The atrial effective refractory period was measured at the free wall of the right and left atria during regular pacing (interval, 400–200 ms). Single interpolated stimuli were applied after eight basic stimuli, starting within the refractory period. The longest interval that failed to capture the atria (2-ms increments) was taken as the atrial effective refractory period. Atrial conduction velocity was measured along Bachmann's bundle during right atrial pacing. The distance over which conduction velocity was measured ranged from 3.5 to 5 cm.

The length of the fibrillation waves was determined at the right atrial free wall by measuring the refractory period and conduction velocity during AF. The refractory period was measured by slow, fixed-rate pacing (1 Hz), resulting in a series of single, randomly coupled, premature stimuli. Local capture of AF was evidenced by radial spread of activation from the pacing site and a short delay between stimulus and response. For each coupling interval, the percentage of capture was determined. The shortest interval capturing the atrium $\geq$50% was taken as the refractory period. Conduction velocity was determined with a mapping electrode containing 5×6 electrodes (interelectrode distance, 4 mm) from the local conduction vectors within areas of 3×3 electrodes. At least 50 AF cycles were used to determine conduction velocity.

Inducibility of AF was measured at the right and left atria by single premature stimuli applied during regular pacing (400 ms). In case a premature beat induced a rapid irregular rhythm lasting > 1 s, AF was considered inducible. The AF cycle length was measured automatically by an algorithm detecting the negative intrinsic deflection of the fibrillation electrogram. A median value of 300 consecutive intervals was calculated. QT duration was measured during atrial pacing and persistent AF from either an epicardial electrogram or a precordial ECG. Because Bazett's formula cannot be applied during AF, another approach was used to correct QT duration. In each goat, the relationship between the RR interval and QT duration was determined during 20 s of AF. The RR-QT relationship after drug administration was compared with the normal RR-QT relation.

The electrophysiological effects of the test drug and a conventional class III drug were measured before and after 48 h (1–4 days) of AF. The drugs were infused intravenously over 1 h, during which time AF cycle length was monitored. After 30 min of infusion, refractory period, conduction velocity, median RR interval, and QT duration were measured. Successful cardioversion was defined as termination of AF within $\leq$1 h of drug administration.

EVALUATION

Differences between groups were evaluated by paired Student's *t*-test or by two-way repeated ANOVA with post hoc Bonferroni's *t*-test. McNemar's test was used to compare AF inducibility. Changes in corrected QT duration were calculated by the one-sample *t*-test. Differences were considered significant at $P < 0.05$. Results are presented as mean $\pm$ SEM.

REFERENCES AND FURTHER READING

Allessie MA, Wijffels MCEF, Dorland R (1998) Mechanisms of pharmacological cardioversion of atrial fibrillation by Class I drugs. J Cardiovasc Electrophysiol 9 [8 Suppl]:S69–S77

Blaauw Y, Beier N, van der Voort P, van Hunnik A, Schotten U, Allessie MA (2004a) Inhibitors of the Na^+/H^+ exchanger cannot prevent atrial electrical remodeling in the goat. J Cardiovasc Electrophysiol 15:440–446

Blaauw Y, Gögelein H, Tieleman RG, van Hunnik A, Schotten U, Allessie MA (2004) "Early" class III drugs for the treatment of atrial fibrillation. Efficacy and atrial selectivity of AVE0118 in remodeled atria of the goat. Circulation 110:1717–1724

Brendel J, Peukert S (2003) Blockers of the Kv1.5 channel for the treatment of atrial hypertension. Curr Med Chem Cardiovasc Hematol Agents 1:273–287

Duytschaever MF, Garratt CJ, Allessie MA (2000) Profibrillatory effects of verapamil but not of digoxin in the goat model of atrial fibrillation. J Cardiovasc Electrophysiol 11:1375–1385

Duytschaever MF, Mast F, Killian M, Blaauw Y, Wijffels M, Allessie M (2001) Methods for determining the refractory period and excitable gap during persistent atrial fibrillation in the goat. Circulation 104:947–962

Duytschaever MF, Blaauw Y, Allessie MA (2005) Consequences of atrial electrical remodeling for the anti-arrhythmic action of class IC and class III drugs. Cardiovasc Res 67:69–76

Garratt CJ, Fynn SP (2000) Atrial electrical remodeling and atrial fibrillation. Q J Med 93:563–565

Shan Z, van der Voort PH, Blaauw Y, Duytschaever M, Allessie MA (2004) Fractionation of electrograms and linking of activation during pharmacological cardioversion of persistent atrial fibrillation in the goat. J Cardiovasc Electrophysiol 15:572–580

Tieleman RG, Blaauw Y, Van Gelder IC, De Langen CDJ, de Kam PJ, Grandjean JG, Patberg KW, Bel KJ, Allessie MA, Crijns HJGM (1999) Digoxin delays recovery from tachycardia-induced electrical remodeling of the atria. Circulation 100:1836–1842

Van der Velden HMW, Ausma J, Rook MB, Hellemons AJCGM, van Veen TAAB, Allessie MA, Jongsma HJ (2000a) Gap junctional remodeling on relation to stabilization of atrial fibrillation in the goat. Cardiovasc Res 46:476–486

Van der Velden HMW, van der Zee, Wijffels MC, van Leuven C, Dorland R, Vos MA, Jongsma HJ, Allessie MA (2000b) Atrial fibrillation in the goat induces changes in monophasic action potential and mRNA expression of ion channels involved in repolarization. J Cardiovasc Electrophysiol 11:1262–1269

Veloso HH (2001) Electrophysiologic effects of digoxin in the goat model of atrial fibrillation and its clinical implications. J Cardiovasc Electrophysiol 12:735–736

Wijffels MCEF, Kirchhof CJHJ, Dorland R, Allessie MA (1995) Atrial fibrillation begets atrial fibrillation. A study in awake chronically instruments goats. Circulation 92:1954–1968

Wijffels MCEF, Kirchhof CJHJ, Dorland R, Power J, Allessie MA (1997) Electrical remodeling due to atrial fibrillation in chronically instrumented conscious goats. Roles of neurohumoral changes, ischemia, atrial stretch, and high rate of electrical activation. Circulation 96:3710–3720

Wijffels MCEF, Kirchhof CJHJ, Dorland R, Allessie MA (1999) Pharmacological cardioversion of chronic atrial fibrillation in the goat by class IA, IC, and III drugs: a comparison between hydroquinidine, cibenzoline, flecainide, and *d*-sotalol. J Cardiovasc Electrophysiol 10:178–193

Wijffels MCEF, Dorland R, Mast F, Allessie MA (2000) Widening the excitable gap during pharmacological cardioversion of atrial fibrillation in the goat. Effects of cibenzoline, hydroquinidine, flecainide, and *d*-sotalol. Circulation 102:260–267

A.5.0.9.3 Influence on Ultrarapid Delayed Rectifier Potassium Current in Pigs

PURPOSE AND RATIONALE

Blockade of cardiac potassium channels and the resulting prolongation of repolarization and refractoriness is the mode of action of class III antiarrhythmic drugs. In the human heart, the ultrarapid delayed rectifier potassium current (I_{Kur}) was identified in atrial, but not in ventricular tissue. It appears to contribute to action potential repolarization (Wang et al. 1993; Li et al. 1996) in the atrium but not the ventricle. The molecular correlate of the human cardiac ultrarapid delayed rectifier potassium current seems to be the Kv1.5 protein (Fedida et al. 1993; Wang et al. 1993; Feng et al. 1997, 1998).

Since prolongation of ventricular repolarization seems to be invariably associated with proarrhythmia (early afterdepolarizations leading to torsades de pointes arrhythmia) as shown with available potassium channel blockers (class III drugs) such as the highly selective and potent I_{Kr}-channel blocker dofetilide (Torp-Pedersen et al. 1999), blockade of a cardiac current that is exclusively present in the atria is highly desirable as it is expected to be devoid of ventricular proarrhythmic effects. Therefore, the atrial Kv1.5 channel is a highly attractive target in the search for new and safer atrial antiarrhythmic drugs (Nattel and Singh 1999).

In a series of studies, Wirth and Knobloch (2001), Knobloch et al. (2002, 2004), and Wirth et al. (2003) investigated electrophysiological and antiarrhythmic effects of I_{Kur} channel blockers on left versus right pig atrium *in vivo* in comparison with I_{Kr} blockers in pigs.

PROCEDURE

Surgery

Castrated male pigs (24–30 kg) of the German Landrace were premedicated with 3 ml Rompun 2% i.m. (xylacine HCL, 23.3 mg/ml = 3 mg/kg i.m.) and 6 ml Hostaket (ketamine HCl, 115 mg/ml = 20 mg/kg i.m.) and anesthetized with an i.v. bolus of 5 ml Narcoren (pentobarbital, 160 mg/ml = 25–30 mg/kg i.v.) followed by a continuous intravenous infusion of 12–17 mg/kg per h pentobarbital. Animals were ventilated with room air and oxygen by a respirator (ABV-Intensiv; Stephan, Gackenbach, Germany). After a left thoracotomy the lung was retracted, the pericardium incised and the heart suspended in a pericardial cradle. Bipolar body surface ECG was recorded using subcutaneous needle electrodes in the classical lead II or lead III arrangement.

Atrial Effective Refractory Period Measurements

Atrial effective refractory period (ERP) measurements at different basic cycle lengths (BCL 240/300/400 ms) were performed (Wirth and Knobloch 2001). Atrial responses to the pacing procedure were visualized via monophasic action potential (MAP) from the left and right atrium as will be described below. A conditioning train of ten basic stimuli (S1) at twice-diastolic pacing threshold was followed by a diastolic extrastimulus (S2, pulse duration 1 ms) starting about 30 ms above the expected ERP with a 5-ms decrement (UHS 20, universal heart stimulator; Biotronik, Berlin, Germany). The longest coupling interval unable to elicit a propagated atrial response was taken as the atrial ERP.

MAP Recording Sites and Atrial Pacing Electrodes

Left atrial ERP was measured via a MAP pacing catheter (EP Technologies, Model 1675; Boston Scientific, La Garenne-Colombes, France), which was fixed in each pig in the middle of the left atrial free wall in

an approximately perpendicular position by a holding device (Yuan et al. 1994). The tip of the MAP pacing catheter was covered by a sponge. Programmed stimulation was performed by the MAP pacing catheter.
Right atrial MAP for ERP measurement was taken from the endocardium of the right atrium also via a steerable MAP pacing catheter. The catheter, inserted via the V. femoralis, was used for atrial stimulation too. Its position in the right atrium was checked by palpitation and by the typical atrial MAP morphology and duration and, additionally, by short rapid atrial pacing at a BCL of 240 ms, which the ventricle was not able to follow 1:1 as indicated by frequent *p*-waves dissociated from the QRS complex. There were no significant differences between endocardial and epicardial ERP measurements in the free walls of either atrium at baseline and after drug.

Left Atrial Vulnerability

During the ERP measurement procedure the mere S2-extrastimulus, which followed the ten conditioning S1 stimuli during the ERP-measurement procedure, frequently triggered runs of atrial tachycardia in the left, not the right, atrium. The occurrence of tachycardias was primarily unintended, but then exploited as a parameter for the judgement of the antiarrhythmic efficacy of compounds (referred to as left atrial vulnerability). Whether or not a run of S2-triggered atrial tachyarrhythmia occurred during the ERP-measurement procedure at a given BCL was noted. The occurrences of triggered tachyarrhythmias were summed up for the three BCLs tested over three time points (during a 30-min period before or after a drug). Thus, the maximal occurrence of S2-tachyarrhythmias during the control or drug period in an individual animal was nine.

Drugs

Drugs were dissolved in polyethyleneglycol (PEG) 400 (Riedel-de Haen, Seelze, Germany) and administered i.v. over 5 min in a volume of 3 ml. Vehicle was injected at least 30 min before each drug. For each drug a separate group of pigs was used.

EVALUATION

All data were presented as means ± SEM. Two-way ANOVA for repeated measures followed by Student's *t*-test was used for the calculation of statistically significant differences between left and right atrial ERP prolongations at the three basic cycle lengths and the inhibition of left atrial vulnerability. A value of $P < 0.05$ was accepted as significant. The longest ERP at each pacing rate after drug administration was taken and expressed as absolute or percent increase from vehicle control. Interatrial difference in refractoriness was calculated as the difference between the left and right atrial ERP.

REFERENCES AND FURTHER READING

Fedida D, Wible B, Wang Z, Fermini B, Faust F, Nattel S, Brown AM (1993) Identity of a novel delayed rectifier current from human heart with a cloned K^+ channel current. Circ Res 73:210–216

Feng J, Wible B, Li GR, Wang Z, Nattel S (1997) Antisense oligodeoxynucleotides directed against Kv1.5 mRNA specifically inhibit ultrarapid delayed rectifier K^+ current in cultured adult human atrial myocytes. Circ Res 80:572–579

Feng J, Xu D, Wang Z, Nattel S (1998) Ultrarapid delayed rectifier current inactivation in human atrial myocytes: properties and consequences. Am J Physiol 275:H1717–H1725

Knobloch K, Brendel J, Peukert S, Rosenstein B, Busch AE, Wirth KJ (2002) Electrophysiological and antiarrhythmic effects of the novel I_{Kur} channel blockers, S9947 and S20951, on left vs. right pig atrium in vivo in comparison with the I_{Kr} blockers dofetilide, azimilide, d,l-sotalol and ibutilide. Naunyn-Schmiedebergs Arch Pharmacol 366:482–487

Knobloch K, Brendel J, Rosenstein B, Bleich M, Busch AE, Wirth KJ (2004) Atrial-selective antiarrhythmic actions of novel I_{Kur} vs. I_{Kr}, I_{Ks}, and I_{Kach} class Ic drugs and β-blockers in pigs. Med Sci Monit 10:BR221–BR228

Li GR, Feng J, Wang Z, Fermini B, Nattel S (1996) Adrenergic modulation of ultrarapid delayed rectifier K^+ current in human atrial myocytes. Circ Res 78:903–915

Nattel S, Singh BN (1999) Evolution, mechanisms, and classification of antiarrhythmic drugs: focus on class III actions. Am J Cardiol 84:11R–19R

Torp-Pedersen C, Moller M, Bloch-Thomsen PE, Kober L, Sandoe E, Egstrup K, Agner E, Carlsen J, Videbaek J, Marchant B, Camm AJ (1999) Dofetilide in patients with congestive heart failure and left ventricular dysfunction. N Engl J Med 341:857–865

Wang Z, Fermini B, Nattel S (1993) Sustained depolarization-induced outward current in human atrial myocytes: evidence for a novel delayed rectifier K^+ current similar to Kv1.5 cloned channel currents. Circ Res 73:1061–1076

Wirth KJ, Knobloch K (2001) Differential effects of dofetilide, amiodarone, and class Ic drugs on left and right atrial refractoriness and left atrial vulnerability in pigs. Naunyn-Schmiedebergs Arch Pharmacol 363:166–174

Wirth KJ, Paehler T, Rosenstein B, Knobloch K, Maier T, Frenzel J, Brendel J, Busch AE, Bleich M (2003) Atrial effects of the novel K^+-channel-blocker AVE0118 in anesthetized pigs. Cardiovasc Res 60:298–306

Yuan S, Blomstrom-Lundqvist C, Olsson SB (1994) Monophasic action potentials: concepts to practical applications. J Cardiovasc Electrophysiol 5:287–308

A.5.0.10 Characterization of Anti-Arrhythmic Activity in the Isolated Right Ventricular Guinea Pig Papillary Muscle

PURPOSE AND RATIONALE

According to Vaughan-Williams (1970) anti-arrhythmic drugs are divided into 4 different classes depending on their mode of action. Class I anti-arrhythmic

agents decrease the upstroke velocity of the action potential through blockade of Na^+ channels. Class II drugs block β-receptors. Class III anti-arrhythmic agents prolong action potential duration, presumably through blockade of K^+ channels. Class IV anti-arrhythmic agents inhibit the slow calcium influx during the plateau of the action potential through Ca^{2+} channel blockade. These electrophysiological actions also have functional manifestations, e. g., Na^+ channel blockade decreases excitability, K^+ channel blockade lengthens refractory period, and Ca^{2+} channel blockade decreases tension of cardiac muscle. A simple and accurate non-microelectrode method is necessary to identify and classify potential anti-arrhythmic drugs into the classes I, III, and IV. In right ventricular guinea pig papillary muscle developed tension (DT), excitability (EX), and effective refractory period (ERP) are measured.

PROCEDURE

Guinea pigs of either sex weighing 200–400 g are stunned, the carotid arteries are severed, and the thoracic cage is opened immediately. The heart is removed, placed into a container of prewarmed, preoxygenated physiologic solution and the pericardium, atria, and other tissues are removed. The heart is then pinned to a dissection dish, and the right ventricle is opened. The tendinous end of the papillary muscle is ligated with a silk thread, and the chordae tendinae are freed from the ventricle. The opposite end of the papillary muscle is then cut free close to the ventricular wall. The non-ligated end of the papillary muscle is clamped into a tissue holder, the end of which is a leucite block containing platinum wire field electrodes.

The preparation is transferred to a tissue bath containing 75 ml of a physiological salt solution that is gassed continuously with 95% O_2/5% CO_2 and maintained at a temperature of 35°C and a pH of 7.4. The silk thread is used to connect the muscle to a Grass FT03C force transducer. An initial resting tension of 1 g is established. Muscles are field stimulated to contract isometrically. The stimulus duration is 1 ms, the frequency 1 Hz, and the voltage twice threshold. Pulses are delivered with the use of a Grass S88 constant voltage stimulator, and developed tension is recorded with the use of a polygraph recorder. The preparation is equilibrated in this manner for 90 min with bath solution changes every 15 min. Control measurements of the force-frequency curve, stimulus strength-duration curve and the effective refractory period are made following the 75 min bath exchange, i. e., during the last 15 min of equilibration.

The force-frequency curve is obtained by measuring developed tension over a range of stimulation frequencies (0.3, 0.5, 0.8, 1.0, and 1.2 Hz). The tissue is contracted for 90 s at each of these frequencies with a brief period of stimulation at 1.5 Hz inserted between increments. The purpose of the 1.5 Hz insert is to keep "pacing history" constant as well as to minimize progressive, nonspecific depression during the lower frequency stimulation series. Both pre- and postdrug developed tension (at each frequency) are expressed as a percentage of the predrug developed tension at 1 Hz. The percent change in post treatment (versus pretreatment) developed tension at 1 Hz is used to quantitate an agent's inotropic effect.

The stimulus strength-duration curves are determined by varying the stimulus duration (0.1, 0.4, 0.8, 1.0, 1.5, 3.0, and 3.4 ms) and finding the threshold voltage that produced a 1:1 correspondence between stimulus and response at each duration. The degree of shift in the strength-duration curve is measured by computing the area between the pre- and post-treatment curves. The boundaries for the area are determined by the first (x-axis parallel) and the last (x-axis perpendicular) durations and by lines from the origin to the second and fourth durations.

Effective refractory period (ERP) is measured at 1 Hz using twin pulse stimuli. After every 8–10 pulses, a second delayed stimulus (S_2) identical to the basic drive pulse (S_1) is introduced. This procedure is repeated, shortening the delay (S_1–S_2) by 5 ms increments. The value of the ERP is taken as the longest delay (S_1–S_2) for which there is a single response to twin pulses. The change in ERP is computed as the difference (ms) between the pre- and post-treatment ERP values.

At the conclusion of the 90 min predrug equilibration period, an aliquot of the test drug designed to achieve the desired final concentration is added to the bath. The tissue must equilibrate for 1 h in the drug solution before postdrug measurements of the force-frequency curve, stimulus strength-duration curve, and effective refractory period are obtained.

EVALUATION

The changes in effective refractory period (ERP) (post treatment minus pretreatment), the degree of shift in the strength-duration curve (geometrical area between pre- and post-treatment curves), and the percent changes in post treatment developed tension at 1 Hz are calculated. The results of these calculations are used to classify the compound as a class I, III, or IV anti-arrhythmic agent on the basis of its effect on de-

veloped tension, excitability, and effective refractory period. An upward and right shift of the strength-duration curve (decrease in excitability) is characteristic for a class I anti-arrhythmic agent, such disopyramide. Selective prolongation of effective refractory period is characteristic for class III anti-arrhythmic agents, such as sotalol. Depression of developed tension, and/or flattening or reversal of the force-frequency curve is characteristic for a class IV anti-arrhythmic agent, such as verapamil.

CRITICAL ASSESSMENT OF THE METHOD

The model of the electrically stimulated isolated guinea pig papillary muscle is a simple method to classify anti-arrhythmic agents. Some drugs have multiple actions and, therefore, belong in more than one class. For further characterization analysis of the action potential is necessary.

MODIFICATIONS OF THE METHOD

O'Donoghue and Platia (1991) recommended the use of monophasic action potential recordings for the evaluation of anti-arrhythmic drugs.

Shibuya et al. (1993) studied the effects of the local anesthetic bupivacaine on contraction and membrane potential in isolated canine right ventricular papillary muscles. From analysis of action potential it is concluded that at low concentrations contraction is depressed mainly due to a Na^+ channel block, whereas at high concentrations also Ca^{2+} channels may be blocked.

Kodama et al. (1992), Maryuama et al. (1995) studied the effects of potential antiarrhythmics on maximum upstroke velocity and duration of action potential in isolated right papillary muscles of guinea pigs as well as the influence of these agents on single ventricular myocytes.

Borchard et al. (1982) described a method for inducing arrhythmias or asystolia by the application of 50 Hz alternating current (ac) to electrically driven isolated left atria and right papillary muscles of the guinea pig. An increase in driving frequency from 1 to 3 Hz effected a significant reduction of the threshold of ac-arrhythmia in guinea pig papillary muscle, but no change in atria. A decrease in temperature from 31°C to 25°C and an increase in Ca^{2+} from 1.25 to 5 mmol/l elevated the threshold for ac-arrhythmia and -asystolia. Fast sodium channel inhibitors increased threshold of ac-arrhythmia in left atria and papillary muscles, whereas the slow channel inhibitor verapamil was ineffective in concentrations up to 6 µmol/l.

REFERENCES AND FURTHER READING

Arnsdorf MF, Wasserstrom JA (1986) Mechanism of action of antiarrhythmic drugs: A matrical approach. In: Fozzard HA, Haber E, Jennings RB, Katz AM, Morgan HE (eds) The Heart and Cardiovascular System. Scientific Foundations. Vol 2. Raven Press, New York, pp 1259–1316

Borchard U, Bösken R, Greef K (1982) Characterization of antiarrhythmic drugs by alternating current induced arrhythmias in isolated heart tissues. Arch Int Pharmacodyn 256:253–268

Hackett AM, McDonald SJ, Schneider P, Schweingruber F, Garthwaite SM (1990) Simple *in vitro* method to characterize anti-arrhythmic agents. J Pharmacol Meth 23:107–116

Kodama I, Suzuki R, Honjio H, Toyama J (1992) Electrophysiological effects of diprafenone, a dimethyl congener of propafenone on guinea pig ventricular cells. Br J Pharmacol 107:813–820

Maruyama K, Kodama I, Anno T, Suzuki R, Toyama J (1995) Electrophysiological effects of Ro 22–9194, a new antiarrhythmic agent, on guinea pig ventricular cells. Br J Pharmacol 114:19–26

O'Donoghue S, Platia EV (1991) Monophasic action potential recordings: evaluation of antiarrhythmic drugs. Progr Cardiovasc Dis 34:1–14

Sanguinetti MC, Jurkiewitz NK (1990) Two components of cardiac delayed rectifier K^+ current. J Gen Physiol 96:195–215

Shibuya N, Momose Y, Ito Y (1993) Effects of bupivacaine on contraction and membrane potential in isolated canine papillary muscles. Pharmacology 47:158–166

Vaughan-Williams EM (1970) Classification of antiarrhythmic drugs. In: Sandøe E, Flensted-Jensen E, OLesen KH (eds) Symposium on cardiac arrhythmias. Elsinore, Denmark, April 23–25, 1970, Publ. by AB Astra, Södertälje, Sweden, pp 449–472

A.5.0.11
Action Potential and Refractory Period in Isolated Left Ventricular Guinea Pig Papillary Muscle

PURPOSE AND RATIONALE

Intracellular action potential in the left ventricular guinea pig papillary muscle is recorded after electrical stimulation. The stimulation frequency is varied in order to determine the refractory period. Resting potential, upstroke velocity, duration of action potential, threshold, refractory period and contractile force can be measured *in vitro*. Compounds which affect the duration of the effective refractory period may have anti-arrhythmic or pro-arrhythmic effects. In addition, the inotropic effect (positive or negative) of the test compound is determined.

PROCEDURE

Guinea pigs of either sex (Marioth strain) weighing 250–300 g are sacrificed by stunning, the carotid arteries are severed, and the thoracic cage is opened immediately. The heart is removed, placed in a container of prewarmed, pre-oxygenated Ringer solution, and the pericardium and the atria are trimmed away. The

left ventricle is opened and the two strongest papillary muscles removed. They are fixed between a suction electrode for electrical stimulation and a force transducer for registration of contractions. Ringer solution oxygenated with carbogen (95% O_2/5% CO_2) at a temperature of 36°C is used.

A standard micro electrode technique is applied to measure the action potential via a glass micro electrode containing 3 M KCl solution, which is inserted intracellularly. The papillary muscle is stimulated with rectangular pulses of 1 V and of 1 ms duration at an interval of 500 ms. The interval between two stimuli is variable in order to determine refractory periods. The intensity of the electrical current is just below the stimulation threshold.

The intracellular action potential is amplified, differentiated for registration of upstroke velocity (dV/dt) (Hugo Sachs micro electrode amplifier), together with the contraction force displayed on an oscilloscope (Gould digital storage oscilloscope OS 4000), and recorded (Gould 2400 recorder).

The effects on fast sodium channels as well as on calcium channels can be studied. The former requires measurement of the normal action potential and the latter the slow action potential obtained at 30 mM K^+. To estimate the relative refractory periods, the second stimuli are set in decremental intervals until contraction ceases. Relative refractory period is defined as the minimum time interval of two stimuli at which each of the stimuli is answered by a contraction. The stimulation threshold is also measured.

After an equilibrium time of 30 min the test compound is added. After 15 and 30 min the following parameters are compared with the predrug values:

- Resting potential mV
- upstroke velocity V/s
- duration of action potential ms
- stimulation threshold V
- refractory period ms
- contraction force mg

The organ bath is flushed thoroughly between two consecutive applications of increasing test drug doses.

EVALUATION

Contractile force [mm] and relative refractory period [ms] are determined before and after drug administration. $ED_{25\,ms}$- and $ED_{50\,ms}$-values are determined. ED_{25ms} or ED_{50ms} is defined as the concentration of test drug in the organ bath at which the relative refractory period is reduced or prolonged by 25 ms or 50 ms.

Since many anti-arrhythmic agents possess additionally negative inotropic effects, changes in the force of contraction are also determined.

ED_{50} values are calculated from log-probit analyses. Scores are allotted relative to the efficacy of standard compounds (lidocaine, propranolol, quinidine).

The following changes are indicators for anti-arrhythmic activity:

- increase of stimulation threshold
- decrease of upstroke velocity
- prolongation of action potential
- increase of refractory period.

Upstroke velocity and duration of action potential are used for **classification purposes**.

MODIFICATIONS OF THE METHOD

Tande et al. (1990) studied the electromechanical effects of a class III anti-arrhythmic drug on guinea pig and rat papillary muscles and atria using conventional microelectrode technique.

Shirayama et al. (1991) studied with a similar technique the electrophysiological effects of sodium channel blockers in isolated guinea pig left atria.

Dawes (1946) described a method of examining substances acting on the refractory period of cardiac muscle using isolated rabbit auricles.

The same method was recommended as first step of a screening program for quinidine-like activity by Schallek (1956).

Wellens et al. (1971) studied the decrease of maximum driving frequency of isolated guinea pig auricles after antiarrhythmic drugs and beta-blockers.

Salako et al. (1976) recorded electropotentials along the conducting system after stimulation of the proximal part of the His bundle in rabbits.

Brown (1989), Wu et al. (1989), Gwilt et al. (1991a, b) measured *in vitro* transmembrane action potential in Purkinje fibers and endocardial ventricular muscles from dogs.

Voltage clamp techniques in isolated cardiac myocytes from guinea pigs have been used by Wettwer et al. (1991).

Nygren et al. (2004) described heterogeneity of action potential durations in isolated mouse left and right atria recorded using voltage-sensitive dye mapping.

REFERENCES AND FURTHER READING

Adaniya H, Hiraoka M (1990) Effects of a novel class III anti-arrhythmic agent, E-4031, on reentrant tachycardias in rabbit right atrium. J Cardiovasc Pharmacol 15:976–982

Brown BS (1989) Electrophysiological effects of ACC-9358, a novel class I antiarrhythmic agent, on isolated canine

Purkinje fibers and ventricular muscle. J Pharmac Exp Ther 248:552–558
Dawes GS (1946) Synthetic substitutes for quinidine. Br J Pharmacol 1:90–112
Gwilt M, Dalrymple HW, Burges RA, Blackburn KJ, Dickinson RP, Cross PE, Higgins AJ (1991a) Electrophysiologic properties of UK-66,914, a novel class III antiarrhythmic agent. J Cardiovasc Pharmacol 17:376–385
Gwilt M, Arrowsmith JE, Blackburn KJ, Burges RA, Cross PE, Dalrymple HW, Higgins AJ (1991b) UK-68–798: A novel, potent and highly selective class III antiarrhythmic agent which blocks potassium channels in cardiac cells. J Pharmacol Exp Ther 256:318–324
Linz W, Schölkens BA, Kaiser J, Just M, Bei-Yin Q, Albus U, Petry P (1989) Cardiac arrhythmias are ameliorated by local inhibition of angiotensin formation and bradykinin degradation with the converting-enzyme inhibitor ramipril. Cardiovasc Drugs Ther 3:873–882
Nygren A, Lomax AE, Giles WR (2004) Heterogeneity of action potential durations in isolated mouse left and right atria recorded using voltage-sensitive dye mapping. Am J Physiol 287:H26134–H2643
Salako LA, Vaughan Williams EM, Wittig JH (1976) Investigations to characterize a new anti-arrhythmic drug, ORG 6001, including a simple test for calcium antagonism. Br J Pharmacol 57:251–262
Schallek W (1956) A screening program for quinidine-like activity. Arch Int Pharmacodyn 105:221–229
Shirayama T, Inoue D, Inoue M, Tatsumi T, Yamahara Y, Asayama J, Katsume H, Nakegawa M (1991) Electrophysiological effects of sodium channel blockers on guinea pig left atrium. J Pharm Exp Ther 259:884–893
Tande PM, Bjørnstad, Yang T, Refsum H (1990) Rate-dependent class III antiarrhythmic action, negative chronotropy, and positive inotropy of a novel I_k blocking drug, UK-68,798: potent in guinea pig but no effect in rat myocardium. J Cardiovasc Pharmacol 16:401–410
Wellens D, Dessy F, de Klerk L (1971) Antiarrhythmic drugs and maximum driving frequency of isolated guinea pig auricles. Arch Int Pharmacodyn 190:411–414
Wettwer E, Scholtysik G, Schaad A, Himmel H, Ravens U (1991) Effects of the new class III antiarrhythmic drug E-4031 on myocardial contractility and electrophysiological parameters. J Cardiovasc Pharmacol 17:480–487
Wu KM, Proakis AG, Hunter TL, Shanklin JR (1989) Effects of AHR-12234 on cardiac transmembrane action potentials, *in situ* cardiac electrophysiology and experimental models of arrhythmia. Arch Int Pharmacodyn 301:131–150

A.6 Methods to Induce Cardiac Hypertrophy and Insufficiency

Animal models of cardiac hypertrophy and insufficiency have been reviewed by Hasenfuss (1988), Muders and Elsner (2000), and Vanoli et al. (2004).

REFERENCES AND FURTHER READING

Hasenfuss G (1988) Animal models of human cardiovascular disease, heart failure and hypertrophy. Cardiovasc Res 39:60–76
Muders F, Elsner F (2000) Animal models of chronic heart failure. Pharmacol Res 41:605–612
Vanoli E, Bacchini S, Panigada S, Pentimalli F, Adamson PB (2004) Experimental models of heart failure. Eur Heart J Suppl 6 (Suppl F):F7–F15

A.6.0.1 Cardiac Hypertrophy and Insufficiency in Rats

A.6.0.1.1 Aortic Banding in Rats

PURPOSE AND RATIONALE

Blood flow restriction of the aorta in rats induces not only hypertension but also cardiac hypertrophy within several weeks. Angiotensin converting enzyme inhibitors, even at subantihypertensive doses, but not other antihypertensive drugs, inhibit cardiac hypertrophy (Linz et al. 1991; Schölkens et al. 1991; Gohlke et al. 1992; Linz 1992a; Linz et al. 1996; Bruckschlegel et al. 1995; Ogawa et al. 1998).

PROCEDURE

Male Sprague Dawley rats weighing 270–280 g are fasted 12 h before surgery. Anesthesia is induced by i.p. injection of 200 mg/kg hexobarbital. The abdomen is shaved, moistened with a disinfectant and opened by a cut parallel to the linea alba. The intestine is moistened with saline and placed in a plastic cover to prevent desiccation. The aorta is prepared free from connective tissue above the left renal artery and underlaid with a silk thread. Then, a cannula no. 1 (0.9×40 mm) is placed longitudinally to the aorta and both aorta and cannula are tied. The cannula is removed, leaving the aortic lumen determined by the diameter of the cannula. The intestine is placed back into the abdominal cavity with the application of 5.0 mg rolitetracycline (Reverin). In sham-operated controls no banding is performed. The skin is closed by clipping.

The animals are treated once daily over a period of 6 weeks with doses of the ACE-inhibitor or other antihypertensive drugs found previously effective to lower blood pressure in rats. At the end of the experiment blood pressure is measured under hexobarbital anesthesia (200 mg/kg i.p.) via indwelling catheters in the left carotid artery. Blood pressure measurement in conscious rats with the convential tail-cuff method is not possible due to the large pressure difference across the ligature. Therefore, only one measurement at the end of the study is possible. The hearts are removed, rinsed in saline until free of blood and gently blotted to dryness. Total cardiac mass is determined by weighing on an electronic balance to the nearest 0.1 mg. The atria and all adjacent tissues are trimmed off and the weight of the left ventricle including the septum as well as the

remaining cardiac tissue representing the right ventricle are determined separately. Weights are calculated per 100 g body weight.

EVALUATION

Total cardiac mass, weight of left and right ventricle of treated rats are compared with operated controls and sham-operated controls.

MODIFICATIONS OF THE METHOD

Uetmasu et al. (1989) described a simple method for producing graded aortic insufficiencies in rats and subsequent development of cardiac hypertrophy. Selective perforation of the right cup of the aortic valve or in combination with that of the left valve cup was performed using a plastic rod inserted from the right common carotid artery. Hypertrophy of the heart, but no hypertension or cardiac insufficiency, was observed.

Similar methods were used by Yamazaki et al. (1989) to study the alterations of cardiac adrenoceptors and calcium channels subsequent to aortic insufficiency, by Umemura et al. (1992) to study baroreflex and β-adrenoceptor function and by Ishiye et al. (1995) to study the effects of an angiotensin II antagonist on the development of cardiac hypertrophy due to volume overload.

Hyperplastic growth response of vascular smooth muscle cells in the thoracic aorta was found following induction of acute hypertension in rats by aortic coarctation by Owens and Reidy (1985). Changes in cardiac gene expression during compensated hypertrophy and the transition to cardiac decompensation in rats with aortic banding were studied by Feldman et al. (1993). Muders et al. (1995) produced aortic stenosis in rats by placing a silver clip (inner diameter 0.6 mm) on the ascending aorta. Schunkert et al. (1995) studied alteration of growth responses in established cardiac pressure overload hypertrophy in rats with aortic banding. **Prevention of cardiac hypertrophy after aortic banding** by ACE inhibitors probably mediated by bradykinin could be shown (Linz et al. 1989, 1992a, b, 1993, 1994; Linz and Schölkens 1992; Schölkens et al. 1991; Weinberg et al. 1994).

Weinberg et al. (1997) studied the effect of angiotensin AT_1 receptor inhibition on hypertrophic remodelling and ACE expression in rats with pressure-overload hypertrophy due to ascending aortic stenosis.

REFERENCES AND FURTHER READING

Bruckschlegel G, Holmer SR, Jandeleit K, Grimm D, Muders F, Kromer EP, Riegger GA, Schunkert H (1995) Blockade of the renin-angiotensin system in cardiac pressure-overload hypertrophy in rats. Hypertension 25:250–259

Feldman AM, Weinberg EO, Ray PE, Lorell BH (1993) Selective changes in cardiac gene expression during compensated hypertrophy and the transition to cardiac decompensation in rats with aortic banding. Circ Res 73:184–192

Gohlke P, Stoll M, Lamberty V, Mattfeld T, Mall G, van Even P, Martorana P, Unger T (1992) Cardiac and vascular effects of chronic angiotensin converting enzyme inhibition at subantihypertensive doses. J Hypertens 10 (Suppl 6):S141–S145

Ishiye M, Umemura K, Uematsu T, Nakashima M (1995) Effects of losartan, an angiotensin II antagonist, on the development of cardiac hypertrophy due to volume overload. Biol Pharm Bull 18:700–704

Linz W, Schölkens BA (1992) A specific B_2-bradykinin receptor antagonist Hoe 140 abolishes the antihypertrophic effect of ramipril. Br J Pharmacol 105:771–772

Linz W, Schölkens BW, Ganten D (1989) Converting enzyme inhibition specifically prevents the development and induces regression of cardiac hypertrophy in rats. Clin Exper Hypert. Theory and Practice A11 (7):1325–1350

Linz W, Henning R, Schölkens BA (1991) Role of angiotensin II receptor antagonism and converting enzyme inhibition in the progression and regression of cardiac hypertrophy in rats. J Hypertens 9 (Suppl 6):S400–S401

Linz W, Schaper J, Wiemer G, Albus U, Schölkens BW (1992a) Ramipril prevents left ventricular hypertrophy with myocardial fibrosis without blood pressure reduction: a one year study in rats. Br J Pharmacol 107:970–975

Linz W, Wiemer G, Schölkens BA (1992b) Contribution of bradykinin to the cardiovascular effects of ramipril. J Cardiovasc Pharmacol 22 (Suppl 9):S1–S8

Linz W, Wiemer G, Schölkens BA (1993) Bradykinin prevents left ventricular hypertrophy in rats. J Hypertension 11 (Suppl 5):S96–S97

Linz W, Wiemer G, Gohlke P, Unger T, Schölkens BA (1994) The contribution of bradykinin to the cardiovascular actions of ACE inhibitors. In Lindpaintner K, Ganten D (eds) The Cardiac Renin Angiotensin System. Futura Publ Co., Inc., Armonk, NY, pp 253–287

Linz W, Wiemer G, Schmidts HL, Ulmer W, Ruppert D, Schölkens BA (1996) ACE inhibition decreases postoperative mortality in rats with left ventricular hypertrophy and myocardial infarction. Clin Exper Hypertension 18:691–712

Muders F, Kromer EP, Bahner U, Elsner D, Ackermann B, Schunkert H, Plakovits M, Riegger GAJ (1995) Central vasopressin in experimental aortic stenosis in the rat. Cardiovasc Res 29:416–421

Ogawa T, Linz W, Schölkens BA, de Bold AJ (1998) Regulation of aortic atrial natriuretic factor and angiotensinogen in experimental hypertension. J Cardiovasc Pharmacol 32:1001–1008

Owens GK, Reidy MA (1985) Hyperplastic growth response of vascular smooth muscle cells following induction of acute hypertension in rats by aortic coarctation. Circ Res 57:695–705

Schölkens BA, Linz W, Martorana PA (1991) Experimental cardiovascular benefits of angiotensin-converting enzyme inhibitors: Beyond blood pressure reduction. J Cardiovasc Pharmacol 18 (Suppl 2):S26–S30

Schunkert T, Weinberg EO, Bruckschlegel G, Riegger AJ, Lorell BH (1995) Alteration of growth responses in established cardiac pressure overload hypertrophy in rats with aortic banding. J Clin Invest 96:2768–2774

Uetmatsu T, Yamazaki T, Matsuno H, Hayashi Y, Nakashima M (1989) A simple method for producing graded aortic insufficiencies in rats and subsequent development of cardiac hypertrophy. J Pharmacol Meth 22:249–257

Umemura K, Zierhut W, Quast U, Hof RP (1992) Baroreflex and β-adrenoceptor function are diminished in rat cardiac hypertrophy due to volume overload. Basic Res Cardiol 87:263–271

Weinberg EO, Min Ae Lee, Weigner M, Lindpaintner K, Bishop SP, Benedict CR, Ho KKL, Douglas PS, Chafizadeh E, Lorell BH (1997) Angiotensin AT_1 receptor inhibition: Effects on hypertrophic remodelling and ACE expression in rats with pressure-overload hypertrophy due to ascending aortic stenosis. Circulation 95:1592–1600

Weinberg EO, Schoen FJ, George D, Kagaya Y, Douglas PS, Litwin SE, Schunkert H, Benedict CR, Lorell BH (1994) Angiotensin-converting enzyme inhibition prolongs survival and modifies the transition to heart failure in rats with pressure overload hypertrophy due to ascending aortic stenosis. Circulation 90:1410–1422

Yamazaki T, Uematsu T, Mizuno A, Takiguchi Y, Nakashima M (1989) Alterations of cardiac adrenoceptors and calcium channels subsequent to production of aortic insufficiency in rats. Arch Int Pharmacodyn Ther 299:155–168

A.6.0.1.2 Chronic Heart Failure in Rats

PURPOSE AND RATIONALE

Rat models of heart failure were reviewed by Muders and Elsner (2000). Chronic heart failure can be induced in rats by occlusion of coronary arteries. One of the first reports was by Selye et al. (1960). More recent reports are by Pfeffer et al. (1979), Hodsman et al. (1988), Van Veldhuisen et al. (1994, 1995), Kajstura et al. (1994), Gómez et al. (1997), Liu et al. (1997a, 1997b), and Jadavo et al. (2005).

Itter et al. (2004) described a model of chronic heart failure (CHF) in spontaneously hypertensive rats.

PROCEDURE

Study Design

Adult male 4-month-old SHR/NHsd and WKY/NHsd rats (Harlan Sprague Dawley, Winkelmann, Germany) weighing 250–300 g were used. Cardiovascular failure was induced by permanent (8 weeks) occlusion of the left coronary artery 2 mm distal to the origin from the aorta resulting in a large infarction of the free left ventricular wall.

Eight weeks after surgery, parameters indicating CHF were measured. Cardiac hypertrophy, function, and geometric properties were determined by the "working heart" mode and *in vivo* determinations by MRI and heart weight. Hydroxyproline/proline ratio was measured as an indicator of heart fibrosis.

Surgery

The rats were anesthetized with a mixture of ketamine/xylazine (35/2 mg/kg) i.p. The left ventrolateral thorax was shaved and prepared to create a disinfected surgical access area. When a stable anesthesia was achieved the animals were placed on a small animal operation table, intubated and ventilated with room air using a small animal ventilator (KTR-4, Hugo Sachs Elektronik, March-Hugstedten, Germany). The level of anesthesia was deemed as adequate following loss of the pedal withdrawal reflex and absence of the palpebral reflex. The tidal volume was adjusted at 3–5 ml and the ventilation rate was 40 breaths/min. Left thoracotomy was performed via the third intercostal space. The heart was exposed and the pericardium opened. The left main coronary artery was ligated with Perma-Hand silk 4–0 USP (Ethicon, Norderstedt, Germany) near its origin at the aorta (2 mm distal to the edge of the left atrium). Ligation resulted in infarction of the free left ventricular wall. Ligation was deemed successful when the anterior wall of the left ventricle turned pale. At this point the lungs were hyperinflated by increasing the positive endexpiratory pressure, and the chest was closed. The rats were placed on a heating pad. They were continuously monitored until they start moving in their cages. To avoid ventricular arrhythmias, lidocaine (2mg/kg i.m.) was given before surgery. The sham procedure consisted of opening the pericardium and placing a superficial suture in the epicardium of the LV. To prevent acute lung edema, the rats received furosemide 2 mg/kg twice daily for 3 days via the drinking water.

Measurements at the End of the Study

Before killing the animals 8 weeks after MI, non-invasive sequential nuclear magnetic resonance (NMR) measurements of heart geometric properties were done. Thereafter the animals were anesthetized with pentobarbitone (180 mg/kg i.p.) and subsequently heparinized (Heparin sodium 500 IU/100 g body weight i.p.). Once stable anesthesia was achieved (stage III 3, reflexes absent), the animals were connected to an artificial respirator via a PE tube inserted into the trachea and ventilated with room air. The right carotid artery was cannulated with a polyethylene catheter to monitor mean blood pressure, systolic blood pressure, diastolic blood pressure and heart rate over a stable time course of 10 min.

A transverse laparotomy and a right anterolateral thoracotomy were performed, and the heart was rapidly removed for the evaluation of its function in the working heart mode. Thereafter the heart weight, and

the left and right ventricular weights were determined. For infarct size determination the left ventricle was sectioned transversely into four slices from the apex to the base. The infarct size was determined by planimetry and expressed as a percentage of LV mass. Lung weight and further lung histology sections were evaluated. Hydroxyproline/proline ratio was determined in paraffin-embedded slices of the left ventricle.

Magnetic Resonance Imaging

The animals were monitored by MRI at day 7 and day 42 post-MI. The rats were anesthetized with a mixture of 1% halothane and 30/70 N_2O/oxygen with a specially manufactured rat mask. The fully anesthetized rats (phase III 3) were placed on a cradle made of Plexiglas in a supine position. Respiration and ECG were monitored continuously. MRI experiments were performed according to Rudin et al. (1991). The images were acquired by a spinecho sequence SE (500/20), the field of view was 50 mm, the image resolution was 256×256 pixels with a dimension of 0.2×0.2 mm. Four adjacent transverse slices were recorded; slice thickness was 1.5 mm. Before the acquisition of data, a coronary pilot scan was measured for adequate positioning of the transverse slices. MRI data acquisition was gated to the cardiac cycle by a Physiograd SM 785 MR monitoring system (Bruker, Karlsruhe, Germany). Two sets of transverse images were acquired, one at end-systole and another at end-diastole. End-diastole was defined as the image obtained 8 ms after the onset of the R wave of the ECG, corresponding to the largest cavity area. End-systole was defined as the image with the smallest LV cavity area. The image analysis was done using Bruker software (Karlsruhe, Germany). The parameters of left ventricular end-diastolic volume (LVEDV), left ventricular end-systolic volume (LVESV), septum size, infarct size, ejection fraction (EF), left ventricular chamber diameter (r) and circumference were measured. EF was estimated in percentage terms by the subtraction LVEDV–LVESV. After the procedure the rats were ventilated with oxygen, the mask was replaced, and they were brought back into their cages. They were monitored until they started moving in the cage.

Blood Pressure/Heart Rate

The animals were anesthetized with pentobarbitone (180 mg/kg i.p.) and subsequently heparinized (Heparin sodium 500 IU/100 g body weight i.p.). Once stable anesthesia was achieved, the animals were connected to an artificial respirator via a PE tube inserted into the trachea and ventilated with room air. The right carotid artery was cannulated with a polyethylene catheter. The catheter was connected to a PLUGSYS measuring system (Hugo Sachs Elektronik, March-Hugstedten, Germany) to monitor mean blood pressure, systolic blood pressure, diastolic blood pressure and heart rate over a stable time course of 10 min.

Working Heart

For the final investigations, the heart of the anesthetized rat was rapidly removed and immersed in physiological buffer chilled to 4°C. The aorta was dissected free and mounted onto a cannula (internal diameter: 1.4 mm) attached to a perfusion apparatus. The hearts were perfused according to the method of Langendorff with an oxygenated (95% O_2/5% CO_2) noncirculating Krebs–Henseleit solution of the following compositions (mM): NaCl, 118; KCl, 4.7; $CaCl_2$, 2.52; $MgSO_4$, 1.64; $NaHCO_3$, 24.88; KH_2PO_4, 1.18; glucose, 5.55; and Na-pyruvate, 2.0 at a perfusion pressure of 60 mmHg. Any connective tissue, thymus or lung was carefully removed. A catheter placed into the pulmonary artery drained the coronary effluent perfusate that was collected for the determination of coronary flow and venous pO_2 measurements. The left atrium was cannulated via an incision of the left auricle. All pulmonary veins were ligated close to the surface of the atria. When a tight seal with no leaks had been established and after a 15-min equilibration period, the hearts were switched into the working mode, using a filling pressure (preload) of 12 mmHg in WKY/NHsd and 18 mmHg in SH rats. The afterload pressure was 60 mmHg in WKY/NHsd and 80 mmHg in SH rats. After validation of the basis parameters the afterload pressure was enhanced in a cumulative manner from an additional 20 mmHg to 140 mmHg. Thereafter the isovolumetric maxima were determined by enhancing the preload pressure in steps of 5 mmHg to 30 mmHg. Flow and pressure signals for computation were obtained from the PLUGSYS-measuring system. Computation of data was performed with a sampling rate of 500 Hz, averaged every 2 s, using the software Aquire Plus V1.21f (PO-NE-MAH, Hugo Sachs Elektronik, March-Hugstedten, Germany).

Determination of Infarct Size

After the evaluation of the external heart work, the total heart weight, the left and right ventricular weights were determined. The left ventricle was then sectioned transversely into four slices from the apex to the base. Eight pictures were taken of each rat heart, two from each slice. Total infarct size was determined by planimetry of the projected and magnified slices.

The area of infarcted tissue as well as the intact myocardium of each slice were added together and averaged. The infarcted fraction of the left ventricle was calculated from these measurements and expressed as a percentage of the LV mass. The left ventricular perimeter, diameter, infarct scar length, as well as wall thickness and infarct wall thinning were determined as well. According to Pfeffer et al. (1985) and Pfeffer and Pfeffer (1987), rats with infarct sizes < 20% and > 40% were excluded from the study.

Lung Histological Determination

After lung weight determination, the organ was immersed in 4% formalin (pH 7.0–7.5; 0.1 M). The lung was cut into small pieces, dehydrated and embedded in paraffin. Hematoxylin and eosin (HE) sections were evaluated by light microscopy.

Hydroxyproline/Proline Ratio

After embedding, the rest of the fixed left ventricular tissue was freeze-dried. Proline and hydroxyproline was then analyzed according to the method of López de León and Rojkind (1985) and the ratio of both were calculated.

REFERENCES AND FURTHER READING

The data are given as mean ± SEM. Statistics were performed using the SAS system statistics package (SAS Institute, Cary, N.C., USA) with a sequential rejection *t*-test.

MODIFICATIONS OF THE METHOD

Jain et al. (2000) studied the effects of angiotensin II receptor blockade after coronary ligation and exercise training on treadmill in rats.

Medvedev and Gorodetskaya (1993) induced heart failure in rats by microembolization of coronary vessels with 15-µm plastic microspheres.

Katona et al. (2004) found that selective sensory denervation by capsaicin aggravates adriamycin-induced cardiomyopathy in rats.

A simple and rapid method of developing high output heart failure and cardiac hypertrophy in rats by producing **aortacaval shunts** was described by Garcia and Diebold (1990). Rats weighing 180–200 g were anesthetized with 30 mg/kg i.p. pentobarbitone. The vena cava and the abdominal aorta were exposed by opening the abdominal cavity via a midline incision. The aorta was punctured at the union of the segment two-thirds caudal to the renal artery and one-third cephalic to the aortic bifurcation with an 18-gauge disposable needle. The needle was advanced into the aorta, perforating its adjacent wall and penetrating in the vena cava. A bulldog vascular clamp was placed across the aorta caudal to the left renal artery. Once the aorta was clamped, the needle was fully withdrawn and a drop of cyanoacrylate glue was used to seal the aorta-punctured point. The clamp was removed 30 s later. The patency of the shunt was verified visually by swelling vena cava and the mixing of arterial and venous blood. The peritoneal cavity was closed with silk thread stitches and the skin with metallic clips. Rats with aorta-caval shunts developed cardiac hypertrophy with significantly higher absolute and relative heart weights.

Other studies with aortocaval shunts in rats were published by Flaim et al. (1979) and Liu et al. (1991).

Isoyama et al. (1988) studied myocardial hypertrophy after creating aortic insufficiency in rats.

Terlink et al. (1998) studied ventricular dysfunction in rats with diffuse isoproterenol-induced myocardial necrosis.

Sabbah et al. (1991) described a model of chronic heart failure produced by multiple sequential coronary microembolizations in **dogs.**

REFERENCES AND FURTHER READING

Flaim SF, Minteer WJ, Nellis SH, Clark DP (1979) Chronic arteriovenous shunt: evaluation of a model for heart failure in rat. Am J Physiol 236:H698–H704

Garcia R, Diebold S (1990) Simple, rapid, and effective method of producing aortacaval shunts in the rat. Cardiovasc Res 24:430–432

Gómez AM, Valdivia HH, Cheng H, Lederer MR, Santana LF, Cannell MB, McCune SA, Altschuld REA, Lederer WJ (1997) Defective excitation-contraction coupling in experimental cardiac hypertrophy and heart failure. Science 276:800–806

Hodsman GP, Kohzuki M, Howes LG, Sumithran E, Tsunoda K, Johnston CI (1988) Neurohumoral responses to chronic myocardial infarction in rats. Circulation 78:376–381

Itter G, Jung W, Juretschke P, Schölkens BA, Linz W (2004) A model of chronic heart failure in spontaneous hypertensive rats (SHR). Lab Anim 38:138–148

Isoyama S, Grossman W, Wei JY (1988) The effect of myocardial adaptation to volume overload in the rat. J Clin Invest 81:1850–1857

Jadavo S, Huang C, Kirshenbaum L, Karmazyn M (2005) NHE-1 inhibition improves impaired mitochondrial permeability transition and respiratory function during postinfarction remodelling in the rat. J Mol Cell Cardiol 38:135–143

Jain M, Liao R, Ngoy S, Whittaker P, Apstein CS, Eberli FR (2000) Angiotensin II receptor blockade attenuates the deleterious effects of exercise training on post-MI ventricular remodelling in rats. Cardiovasc Res 46:66–72

Kajstura J, Zhang X, Reiss K, Szoke E, Li P, Lagrasta C, Cheng W, Darzynkiewicz Z, Olivetti G, Anversa P (1994) Myocyte cellular hyperplasia and myocytes cellular hypertrophy contribute to chronic ventricular remodelling in coronary artery narrowing-induced cardiomyopathy in rats. Circ Res 74:383–400

Katona M, Boros K, Sántha P, Ferdinandy P, Dux M, Jancsó G (2004) Selective sensory denervation by capsaicin aggra-

vates adriamycin-induced cardiomyopathy in rats. Naunyn-Schmiedebergs Arch Pharmacol 370:436–443
Liu Z, Hilbelink DR, Crockett WB, Gerdes AM (1991) Regional changes in hemodynamics and cardiomyocyte size in rats with aortacaval fistulas. 1. Developing and established hypertrophy. Circ Res 69:52–58
Liu YH, Yang XP, Sharov VG, Nass O, Sabbah HN, Peterson E, Carretero OA (1997a) Effects of angiotensin-converting enzyme inhibitors and angiotensin II type 1 receptor antagonists in rats with heart failure. J Clin Invest 99:1926–1935
Liu YH, Yang XP, Nass O, Sabbah HN, Petersen E, Carretero OA (1997b) Chronic heart failure induced by coronary artery ligation in Lewis inbred rats. Am J Physiol 272 (2 Pt2):H722–H727
López de León A, Rojkind M (1985) A simple method for collagen and total protein determination in formalin-.fixed paraffin-embedded sections. J Histochem Cytochem 33:737–743
Medvedev OS, Gorodetskaya EA (1993) Systemic and regional hemodynamic effects of perindopril in experimental heart failure. Am Heart J 126(3 Pt2):764–769
Muders F, Elsner F (2000) Animal models of chronic heart failure. Pharmacol Res 41:605–612
Pfeffer MA, Pfeffer JM, Fishbein MC, Fletcher PJ, Spadaro J, Kloner RA, Braunwald E (1979) Myocardial infarct size and ventricular function in rats. Circ Res 44:593–512
Pfeffer MA, Pfeffer JM (1987) Ventricular enlargement and reduced survival after myocardial infarction. Circulation 7 [Suppl. IV]:93–97
Pfeffer MA, Pfeffer JM, Steinberg C, Finn P (1985) Survival after an experimental myocardial infarction: beneficial effects of long-term therapy with captopril. Circulation 72:406–412
Rudin M, Pedersen B, Umemura K, Zierhut W (1991) Determination of rat heart morphology and function *in vivo* in two models of cardiac hypertrophy by means of magnetic resonance imaging. Basic Res Cardiol 8:165–74
Sabbah HN, Stein PD, Kono T, Gheorghiade M, Levine TB, Jafri S, Hawkins ED, Goldstein S (1991) A canine model of chronic heart failure produced by multiple sequential coronary microembolizations. Am J Physiol 260(4 Pt 2):H1379–H1384
Selye H, Bajusz E, Grasso S, Mendell P (1960) Simple techniques for the surgical occlusion of coronary vessels in the rat. Angiology 11:398–407
Terlink JR, Pfeffer JM, Pfeffer MA (1998) Effect of left ventricular sphericity on the evolution of ventricular dysfunction in rats with diffuse isoproterenol-induced myocardial necrosis. J Cardiac Fail 4:45–56
Van Veldhuisen DJ, van Gilst WH, de Smet BJ, de Graeff PA, Scholtens E, Buikema H, Girbes AR, Wesseling H, Lie KI (1994) Neurohumoral and hemodynamic effects of ibopamine in a rat model of chronic myocardial infarction and heart failure. Cardiovasc Drugs Ther 8:245–250
Van Veldhuisen DJ, Brodde OE, van Gilst WH, Schulze C, Hegeman H, Anthonio RL, Scholtens E, de Graeff PA, Wesseling H, Lie KI (1995) Relation between myocardial β-adrenoceptor density and hemodynamic and neurohumoral changes in a rat model of chronic myocardial infarction: effects of ibopamine and captopril. Cardiovasc Res 30:386–393

A.6.0.2
Cardiac Hypertrophy and Insufficiency in Mice

A.6.0.2.1
Cardiac Hypertrophy in Mice

PURPOSE AND RATIONALE

Rockman et al. (1991, 1993) developed a model of ventricular hypertrophy in the intact mouse by use of microsurgical techniques.

PROCEDURE

Eight-week-old adult mice weighing 18–22 g are anesthetized by intraperitoneal injection of a mixture of 100 mg/kg ketamine, 5 mg/kg xylazine, and 2.5 mg/kg morphine. Animals are placed under a dissecting microscope in the supine position and a midline cervical incision is made to expose the trachea and carotid arteries. After endotracheal intubation, the cannula is connected to a volume cycled rodent ventilator on supplemental oxygen with a tidal volume of 0.2 ml and a respiratory rate of 110 per min. Both left and right carotid arteries are cannulated with flame stretched PE50 tubing. Catheters are connected to modified P50 Statham transducers.

The chest cavity is entered in the second intercostal space at the left upper sternal border through a small incision and the thymus is gently deflected out of the field of view to expose the aortic arch. After the transverse aorta is isolated between the carotid arteries, it is constricted by a 7.0 nylon suture ligature against a 27-gauge needle, the latter being promptly removed to yield a constriction of 0.4 mm diameter and provide a reproducible transverse aortic constriction of 65–75%.

The hemodynamic effects of acute and chronic constriction are followed by monitoring the pressure gradient between the two carotid arteries in anesthetized animals. Systolic and mean arterial pressure at baseline, during total occlusion when the ligature is tied, and early (15 min) and late (7 days) after transverse aortic constriction are recorded. The increase in systolic pressure provides an adequate mechanical stimulus for the development of cardial hypertrophy.

To confirm myocardial hypertrophy, both sham-operated and aortic-constricted hearts are examined 7 days after operation. Hearts examined for *cell size* are perfused with 4% paraformaldehyde/1% glutaraldehyde through the apex, immersed in osmium tetroxide, dehydrated in graded alcohols, and embedded in araldite. Tissue blocks are sectioned at a thickness of 1 μm, mounted on slides, and stained with tolu-

idine blue. Cell areas are measured by manually tracing the cell outline on an imaging system connected to a computer.

At the end of the experiment, mice were sacrificed in anesthesia, heart excised and weighed, the atria and ventricles separately frozen in liquid nitrogen for Northern blot analysis. Total RNA is extracted by a single step extraction with guanidinium thiocyanate. The RNA is size fractionated by agarose gel electrophoresis, transferred to nylon membranes by vacuum blotting, and hybridized with the appropriate complementary DNA probes labeled with ^{32}P by random priming to a specific activity of $0.95–1.2 \times 10^6$ cpm/ng.

EVALUATION

Variables measured are expressed as mean $\pm$ SD. Statistical significance of differences between sham-operated and thoracic aortic-constricted animals is assessed by Student's *t*-test.

MODIFICATIONS OF THE METHOD

Dom et al. (1994) studied myosin heavy chain regulation and myocytes' contractile depression after LV hypertrophy in aortic-banded mice.

Okada et al. (2004) subjected mice to transverse aortic constriction. Echocardiographic analysis demonstrated cardiac hypertrophy and failure 1 and 4 weeks after surgery. Cardiac expression of endoplasmatic reticulum chaperones was significantly increased indicating that pressure overload by transverse aortic constriction induced prolonged endoplasmatic reticulum stress.

REFERENCES AND FURTHER READING

Dom GW, Robins J, Ball N, Walsh RA (1994) Myosin heavy chain regulation and myocytes contractile depression after LV hypertrophy in aortic-banded mice. Am J Physiol 267(1 Pt2):H400–H406

Okada KI, Minamino T, Tsukamoto Y, Liao Y, Tsukamoto O, Takashima S, Hirata A, Fujita M, Nagamachi Y, Nakatani T, Yutani C, Ozawa K, Ogawa S, Tomoike H, Hori M, Kitakaze M (2004) Prolonged endoplasmatic reticulum stress in hypertrophic and failing heart after aortic constriction. Possible contribution of endoplasmatic reticulum stress to cardiac myocyte apoptosis. Circulation 110:705–712

Rockman HA, Ross RS, Harris AN, Knowlton KU, Steinhelper ME, Field LJ, Ross J Jr, Chien KR (1991) Segregation of atrial-specific and inducible expression of an atrial natriuretic factor transgene in an *in vivo* murine model of cardiac hypertrophy. Proc Natl Acad Sci USA 88:8277–8281

Rockman HA, Knowlton KU, Ross J Jr, Chien KR (1993) *In vivo* murine cardiac hypertrophy. A novel model to identify genetic signaling mechanisms that activate an adaptive physiological response. Circulation 87 (Suppl VII):VII-14–VII-21

A.6.0.2.2 Chronic Heart Failure in Mice

PURPOSE AND RATIONALE

Several authors reported the development of murine models of cardiac failure (Kaplan et al. 1994; Rockman et al. 1994; Balasubramaniam et al. 2004; Suzuki et al. 2004; Walther et al. 2004; Wang et al. 2004; Liao et al. 2005).

Xu et al. (2004) studied cardioprotection in mice with heart failure by dual inhibition of angiotensin converting enzyme (ACE) and neutral endopeptidase (NEP).

PROCEDURE

Mice with a targeted deletion of the B_2 kinin receptor gene or C57BL/6J mice at an age of 10–12 weeks were anesthetized with 50 mg/kg sodium pentobarbital i.p., intubated and ventilated with room air using a positive-pressure respirator. A left thoracotomy was performed via the fourth intercostal space; the lungs were retracted to expose the heart, and the pericardium was opened. The left anterior descending coronary artery was ligated with an 8–0 nylon suture near its origin between the pulmonary outflow tract and the edge of the left atrium. Acute myocardial ischemia was considered successful when the anterior wall of the left ventricle turned pale and an obvious ST segment elevation was observed. The lungs were inflated by increasing positive end-expiratory pressure and the thoracotomy site was closed. Sham-operated mice were subjected to the same procedure except that the suture around the left anterior coronary artery was not tied.

Systolic blood pressure was measured in conscious mice using a non-invasive computerized tail-cuff system. Cardiac geometry and function were evaluated with a Doppler echocardiographic system. LV diastolic dimension was measured and ejection fraction was calculated from

$[(LVAd - LVAs)/LVAd] \times 100$, where LVAd is LV diastolic area and LVAs is LV systolic area.

Four weeks after surgery, each strain was separated into one group treated with an ACE inhibitor, one group treated with a NEP inhibitor, one group treated with both inhibitors and one control group. All drugs were administered in drinking water for 20 weeks.

At the end of the study, all mice were anesthetized with pentobarbital and the heart stopped at diastole

by intraventricular injection of 15% KCl. The heart, lungs, and liver were weighed to assess hypertrophy and congestion. Infarct size was determined by Gomori trichrome staining and expressed as the ration of the infarcted portion to total LV circumference.

Sections (6 µm) from each slice were double-stained with fluorescein-labeled peanut agglutinin to delineate the myocyte cross-sectional area and interstitial space and rhodamine-labeled *Griffonia simplicifolia* lectin I to show the capillaries. To calculate interstitial collagen fraction, the total surface area (microscopic field), interstitial space (collagen plus capillaries), and area occupied by capillaries alone were measured by computer-assisted videodensometry.

After 20 weeks of treatment, plasma renin was measured.

EVALUATION

Data were expressed as mean ± SE. Mortality rates were compared using χ^2 tests. For the echo, blood pressure, heart weight, lung weight, infarct size, plasma renin concentration, and histology data, paired or two-sample tests using non-parametric methods were used to perform all comparisons of interest.

REFERENCES AND FURTHER READING

Balasubramaniam R, Chawla S, Mackenzie L, Schwiening CJ, Grace AA, Huang CLH (2004) Nifedipine and diltiazem suppress ventricular arrhythmogenesis and calcium release in mouse hearts. Pflügers Arch 449:150–158

Kaplan ML, Cheslow Y, Vikstrom K, Malhotra A, Geenen DL, Nakouzi A, Leinwand LA, Buttrik PM (1994) Cardiac adaptations to chronic exercise in mice. Am J Physiol 267(3 Pt2):H1167–H1173

Liao Y, Asakura M, Takashima S, Ogai A, Asano Y, Asanuma H, Minamino T, Tomoike H, Hori M, Kitakaze M (2005) Benidipine, a long-acting calcium channel blocker, inhibits cardiac remodeling in pressure-overloaded mice. Cardiovasc Res 65:879–888

Rockman HA, Ono S, Ross RS, Jones LR, Karimi M, Bhargava V, Ross J, Jr, Chien KR (1994) Molecular and physiological alterations in murine ventricular dysfunction. Proc Natl Acad Sci USA 91:2694–2698

Suzuki Y, Nakano K, Sugiyama M, Imagawa JI (2004) βARK1 inhibition improves survival in a mouse model of heart failure induced by myocardial infarction. J Cardiovasc Pharmacol 44:329–334

Walther T, Steendijk P, Westermann D, Hohmann C, Schulze K, Heringer-Walther S, Schultheiss HP, Tschöpe C (2004) Angiotensin deficiency in mice leads to dilated cardiomyopathy. Eur J Pharmacol 493:161–165

Wang D, Liu YH, Yang XP, Rhaleb NE, Xu J, Peterson E, Rudolph AE, Carretero OA (2004) Role of a selective aldosterone blocker in mice with chronic heart failure. J Cardiac Fail 10:67–73

Xu J, Carretero OA, Liu YH, Yang F, Shesley EG, Oja-Tebbe N, Yang XP (2004) Dual inhibition of ACE and NEP provides greater cardioprotection in mice with heart failure. J Cardiac Fail 10:83–89

A.6.0.2.3 Transgenic Mice and Heart Failure

PURPOSE AND RATIONALE

Several hundreds of papers on transgenic mice and heart failure are published. Only a few can be mentioned here.

Chien (1995) described cardiac muscle diseases in genetically engineered mice.

Edwards et al. (1996) described severe cardiomyopathy in transgenic mice overexpressing the skeletal muscle myogenic regulator *myf5*.

Arber et al. (1997) found that MLP-deficient mice exhibit a disruption of cardiac cytoarchitectural organization, dilated cardiomyopathy, and heart failure.

Graham et al. (1997) described a mouse model for mitochondrial myopathy and cardiomyopathy resulting from a deficiency in the heart/muscle isoforms of the adenine nucleotide translocator.

Iwase et al. (1997) studied cardiomyopathy in transgenic mice induced by overexpression of the cardiac stimulatory G protein α subunit.

Knollmannn et al. (2000) reported remodeling of ionic currents in hypertrophied and failing hearts of transgenic mice overexpressing calsequestrin.

Beggah et al. (2002) described reversible cardiac fibrosis and heart failure induced by conditional expression of an antisense mRNA of the mineralocorticoid receptor in cardiomyocytes.

Verheule et al. (2004) found increased vulnerability to atrial fibrillation in transgenic mice with selective atrial fibrosis caused by overexpression of TGF-β1.

Duncan et al. (2005) found that chronic xanthine oxidase inhibition prevents myofibrillar protein oxidation and preserves cardiac function in a transgenic mouse model of cardiomyopathy.

Hartil and Charron (2005) reviewed mouse models where transgenic technology has been utilized to alter expression of genes involved in cardiac uptake and metabolism of either lipid or carbohydrate.

Hilfiker-Kleiner et al. (2005) reported that STAT3-knockout mice harboring a cardiomyocyte-restricted deletion of STAT3 showed enhanced susceptibility to cardiac injury caused by myocardial ischemia, systemic inflammation, or drug toxicity.

Sanbe et al. (2005) studied reversal of amyloid-induced heart disease in desmin-related cardiomyopathy.

REFERENCES AND FURTHER READING

Arber S, Hunter JJ, Ross J, Jr, Hongo M, Sansig G, Borg J, Perriard JC, Chien KR, Caroni P (1997) MLP-deficient mice exhibit a disruption of cardiac cytoarchitectural organization, dilated cardiomyopathy, and heart failure. Cell 88:393–403

Beggah AT, Escoubert B, Puttini S, Cailmail S, Delage V, Ouvrard-Pascaud A, Bocchi B, Peuchmaur M, Delcayre C (2002) Reversible cardiac fibrosis and heart failure induced by conditional expression of an antisense mRNA of the mineralocorticoid receptor in cardiomyocytes. Proc Natl Acad Sci USA 99:7160–7165

Chien KR (1995) Cardiac muscle diseases in genetically engineered mice: evolution of molecular physiology. Am J Physiol 269:H755–H766

Duncan JG, Ravi R, Stull LB, Murphy AM (2005) Chronic xanthine oxidase inhibition prevents myofibrillar protein oxidation and preserves cardiac function in a transgenic mouse model of cardiomyopathy. Am J Physiol 289:H1512–H1518

Edwards JG, Lyons GE, Micales BK, Malhotra A, Factor S, Leinwand LA (1996) Cardiomyopathy in transgenic *myf5* mice. Circ Res 78:379–387

Graham BH, Waymire KG, Cottrell B, Trounce IA, MacGregor GR, Wallace DC (1997) A mouse model for mitochondrial myopathy and cardiomyopathy resulting from a deficiency in the heart/muscle isoforms of the adenine nucleotide translocator. Nat Genet 16:226–234

Hartil K, Charron MJ (2005) Genetic modification of the heart: transgenic modification of cardiac lipid and carbohydrate utilization. J Mol Cell Cardiol 39:581–593

Hilfiker-Kleiner D, Hilfiker A, Drexler H (2005) Many good reasons to have STAT3 in the heart. Pharmacol Ther 107:131–137

Iwase M, Uechi M, Vatner DA, Asai K, Shannon RP, Kudej RK, Wagner TE, Wight DC, Patrick TA, Ishikawa Y, Homcy CJ, Vatner SF (1997) Cardiomyopathy induced by cardiac Gs α overexpression. Am J Physiol 272 (1 Pt2):H585–H589

Knollmannn BC, Knollmann-Ritschel BEC, Weissman NJ, Jones LR, Morad M (2000) Remodelling of ionic currents in hypertrophied and failing hearts of transgenic mice overexpressing calsequestrin. J Physiol (Lond) 525.2:483–498

Sanbe A, Osinska H, Villa C, Gulick J, Klevitsky R, Glabe CG, Kayed R, Robbins J (2005) Reversal of amyloid-induced heart disease in desmin-related cardiomyopathy. Proc Natl Acad Sci USA 102:13592–13597

Verheule S, Sato T, Everett T, Engle SK, Otten D, Rubart-von der Lohe M, Nakajima HO, Nakajima H, Field LJ, Olgin FE (2004) Increased vulnerability to atrial fibrillation in transgenic mice with selective atrial fibrosis caused by overexpression of TGF-β1. Circ Res 94:1458–1465

A.6.0.3 Cardiac Insufficiency in Guinea Pigs

PURPOSE AND RATIONALE

Congestive heart failure in man is characterized by cardiac hypertrophy, peripheral edema, lung and liver congestion, dyspnea, hydrothorax and ascites. Effective treatment is achieved by cardiac glycosides. Based on techniques reported by Selye et al. (1960) a method was developed to induce congestive heart failure in guinea pigs with symptoms very close to human pathology (Vogel and Marx 1964; Vogel et al. 1965).

PROCEDURE

Male guinea pigs weighing 250–400 g are used. The fur at the ventral thorax is shaved and the skin disinfected. The animal is anesthetized with ether. The skin is cut with scissors on the left side at a length of 4 cm. The left musculus pectoralis is cut at the costal insertion and elevated. The forth intercostal space is opened with two blunted forceps. The heart is pressed against the opening with the left hand. The pericardium is opened with a fine forceps and pulled back to the basis of the heart. The beating heart is extruded from the thorax wound by pressure with the left hand on the right thorax wall. A ring-shaped clamp covered with a thin rubber tube is placed around the basis of the heart keeping the heart outside of the thorax without closing off the blood circulation. A thread soaked with diluted disinfectant solution is placed as a loop around the apex of the heart and tightened so that the apical third of both ventricles is tied off. The degree of tightening of the loop is essential. Complete interruption of blood supply to the apical third resulting in necrosis has to be avoided as well as the loop's slipping off. Technical skill is necessary to place the loop around the beating heart into the correct position. After removal of the clamp the heart is placed back, the incision between the forth and fifth costal rib closed and the musculus pectoralis placed over the wound. Intrathoracal air forming a pneumothorax is removed by pressure on both sides of the thorax. After application of an antibiotic emulsion the skin wound is closed. The surgical procedure has to be finished within a short period of time.

The animals develop symptoms of severe congestive heart failure with a death rate of 80% within 14 days. Lung weight and relative heart weight are significantly increased. Exudate in the thorax cavity and ascites amount between 3.5 and 7.5 ml with extreme values of 17.5 ml. Lung edema and liver congestion are found histologically. Peripheral edema and preterminal dyspnea and tachypnea are observed. When treated with various doses (0.1 to 100 µg/kg) of cardiac glycosides s.c. or i.m. over a period of 14 days the symptoms of cardiac insufficiency, e. g., volumes of transudate as well as death rate, are dose-dependent diminished.

EVALUATION

From survival rate, ED_{50} values of cardiac glycosides can be calculated which are in the same dosage range as therapeutic doses in man.

CRITICAL ASSESSMENT OF THE METHOD

The experimental model in guinea pigs reflects very closely the symptoms of cardiac insufficiency in man, e. g., lung congestion, hydrothorax, liver congestion, ascites, peripheral edema and cardiac hypertrophy. The

therapeutic potency of cardiac glycosides can be evaluated with this method. Additional factors being known to enhance the symptoms of congestive heart failure in man, like salt load and diphtheria toxin, further increase mortality and hydropic symptoms. The method can be used for special purposes, however, it needs considerable training and technical skill.

MODIFICATIONS OF THE METHOD

Siri et al. (1989, 1991) produced left ventricular hypertrophy in the guinea pig by gradually increasing ventricular afterload. A mildly constricting band was placed around the ascending aorta of very young guinea pigs (225–275 g). With growth to 500–1000 g, left ventricular systolic pressure increased and ventricular hypertrophy developed. Only some of the animals developed dyspnea and severe ventricular dysfunction.

Kiss et al. (1995) studied the effects on Ca^{2+} transport and mechanics in compensated pressure-overload hypertrophy and congestive heart failure in guinea pigs. The descending aorta was banded for 4 and 8 weeks in adult guinea pigs.

Tweedle et al. (1995) assessed subrenal banding of the abdominal aorta as a method of inducing cardiac hypertrophy in the guinea pig.

Pfeffer et al. (1987) induced myocardial infarction in **rats** by ligation of the left coronary artery and found hemodynamic benefits and prolonged survival with long-term captopril therapy.

Acute ischemic left ventricular failure can be induced in anesthetized **dogs** by repeated injections of plastic microspheres into the left coronary artery (see A.3.2.4).

Huang et al. (1997) created congestive heart failure in **sheep** by selective sequential intracoronary injection of 90 µm microspheres under 1.5% isofluorane injection.

REFERENCES AND FURTHER READING

Huang Y, Kawaguchi O, Zeng B, Carrington RAJ, Horam CJ, Yuasa T, Abdul-Hussein N, Hunyor SN (1997) A stable ovine congestive heart failure model. A suitable substrate for left ventricular assist device assessment. ASAIO J 43:M408–M413

Kiss E, Ball NA, Kranias EG, Walsh RA (1995) Differential changes in cardiac phospholamban and sarcoplasmic reticular Ca^{2+}-ATPase protein levels. Effects on Ca^{2+} transport and mechanics in compensated pressure-overload hypertrophy and congestive heart failure. Circ Res 77:759–764

Pfeffer JM, Pfeffer MA, Braunwald E (1987) Hemodynamic benefits and prolonged survival with long-term captopril therapy in rats with myocardial infarction and heart failure. Circulation 75:I-149–I-155

Selye H, Bajusz E, Grasso S, Mendell P (1960) Simple techniques for the surgical occlusion of coronary vessels in the rat. Angiology 11:398–407

Siri FM, Nordin C, Factor SM, Sonnenblick E, Aronson R (1989) Compensatory hypertrophy and failure in gradual pressure-overloaded guinea pig heart. Am J Physiol 257(3 Pt2):H1016–H1024

Siri FM, Krueger J, Nordin C, Ming Z, Aronson RS (1991) Depressed intracellular calcium transients and contraction in myocytes from hypertrophied and failing guinea pig hearts. Am J Physiol 261 (2 Pt2):H514–H530

Tweedle D, Henderson CG, Kane KA (1995) Assessment of subrenal banding of the abdominal aorta as a method of inducing cardiac hypertrophy in the guinea pig. Cardioscience 6:115–119

Vogel HG, Marx KH (1964) Untersuchungen an der experimentellen hydropischen Herzinsuffizienz des Meerschweinchens. Naunyn Schmiedeberg's Arch Path Pharm 247:337

Vogel HG, Marx KH, Ther L (1965) Über die experimentelle hydropische Herzinsuffizienz am Meerschweinchen. Operationstechnik, Einfluß zusätzlicher Faktoren und Effekt von Herzglykosiden. Arzneim Forsch/Drug Res 15:542–548

A.6.0.4 Cardiomyopathic Syrian Hamster

PURPOSE AND RATIONALE

Cardiomyopathy in Syrian hamsters has been described by Bajusz et al. (1966), Bajusz and Lossnitzer (1968), Bajusz (1969), Bajusz et al. (1969a, b), Homburger and Bajusz (1970), Gertz (1972). The disease originates from an autosomal, recessively transmissible disorder, which leads to degenerative lesions in all striated muscles and in particular in the myocardium. Histopathological changes consist of myocytolytic necrosis followed by fibrosis and calcification. The evolution of the cardiomyopathic disease can be characterized by five distinct phases: A prenecrotic stage, in which no pathology is evident, a time of active myocytolysis and cellular necrosis, a phase of fibrosis and calcium deposition, an overlapping period of reactive hypertrophy of the remaining viable myocytes, and a final stage of depressed myocardial performance and failure.

PROCEDURE

The model of cardiomyopathy in Syrian hamsters has been used by several authors. One has to note, that several strains of cardiomyopathic hamsters have been used: strain Bio 53:58 by Capasso et al. (1989, 1990) and by Chemla et al. (1992, 1993), strain BIO 14.6 by Tapp et al. (1989) and by Sen et al. (1990), strain CHF 146 CM by van Meel et al. (1989) and by Haleen et al. (1991), strain BIO82.62 by ver Donck et al. (1991), strain J-2-N by Kato et al. (1992), strain CHF 147 by Desjardins et al. (1989), Hanton et al. (1993).

Various experimental protocols have been described. Most authors use survival rate and heart weight as end point (e. g., van Meel et al. 1989; ver Donck et al. 1991; Hanton et al. 1993). Generally, the experiments are started with animals at an age of 120 to 200 days.

Capasso et al. (1989, 1990) studied the mechanical and electrical properties of cardiomyopathic hearts of Syrian hamsters using isolated left ventricular posterior papillary muscles.

Tapp et al. (1989) tested stress-induced mortality in cardiomyopathic hamsters by five consecutive daily 2-h periods supine immobilizations at 4°C.

Sen et al. (1990) tested the inotropic and calcium kinetic effects of calcium channel agonists and antagonists in primary cultures of isolated cardiac myocytes.

Haleen et al. (1991) tested the effects of an angiotensin converting enzyme inhibitor not only on survival, but also on left ventricular failure in the isolated Langendorff heart by measurement of left ventricular end-diastolic pressure, dP/dt_{max} and mean coronary flow.

Dixon et al. (1997) tested the effect of an AT_1 receptor antagonist on cardiac collagen remodelling in the cardiomyopathic Syrian hamster.

In addition to the effects on left ventricular papillary muscles strips, Chemla et al. (1992) tested the effects on diaphragm contractility in the cardiomyopathic Syrian hamster.

Whitmer et al. (1988) and Kuo et al. (1992) tested sarcolemmal and sarcoplasmatic reticulum calcium transport in the cardiomyopathic Syrian hamster.

Nigro et al. (1997) identified the Syrian hamster cardiomyopathy gene.

Tanguay et al. (1997) tested the coronary and cardiac sensitivity to a vasoselective benzothiazepine-like calcium antagonist in isolated, perfused failing hearts of Syrian hamsters.

Bilate et al. (2003) recommended the Syrian hamster as a model for the dilated cardiomyopathy of Chagas' disease. Female hamsters were infected via the intraperitoneal route with *Trypanosoma cruzi* Y strain blood trypomastigotes. Survival was monitored, echocardiography was performed after 4 and 12 months, and histopathological examinations were carried out at the end of the study period.

CRITICAL ASSESSMENT OF THE METHOD

Positive effects of various drugs have been found in the cardiomyopathic hamster, such as cardiac glycosides, inotropic compounds, beta-blockers, calcium antagonists, and ACE-inhibitors. The specificity of the effects has to be challenged.

MODIFICATIONS OF THE METHOD

The **tight-skin (TSK) mouse** is a genetic model of pulmonary emphysema connected with right ventricular hypertrophy (Martorana et al. 1990; Gardi et al. 1994).

REFERENCES AND FURTHER READING

Bajusz E (1969) Hereditary cardiomyopathy: a new disease model. Am Heart J 77:686–696

Bajusz E, Lossnitzer A (1968) A new disease model of chronic congestive heart failure: Studies on its pathogenesis. Trans NY Acad Sci 30:939–948

Bajusz E, Homburger F, Baker JR, Opie LH (1966) The heart muscle in muscular dystrophy with special reference to involvement of the cardiovascular system in the hereditary myopathy of the hamster. Ann NY Acad Sci 138:213–229

Bajusz E, Baker JR, Nixon CW, Homburger F (1969a) Spontaneous hereditary myocardial degeneration and congestive heart failure in a strain of Syrian hamsters. Ann NY Acad Sci 156:105–129

Bajusz E, Homburger F, Baker JR, Bogdonoff P (1969b) Dissociation of factors influencing myocardial degeneration and generalized cardiocirculatory failure. Ann NY Acad Sci 156:396–420

Bilate AMB, Salemi VMC, Ramirez FJA, de Brito T, Silva AM, Umezawa ES, Mady C, Kalil J, Cunha-Neto E (2003) The Syrian hamster as a model for the dilated cardiomyopathy of Chagas' disease: a quantitative echocardiographical and histopathological analysis. Microb Infect 5:1116–1124

Capasso JM, Olivetti G, Anvera P (1989) Mechanical and electrical properties of cardiomyopathic hearts of Syrian hamsters. Am J Physiol, Heart Circ Physiol 257:H1836–H1842

Capasso JM, Sonnenblick EH, Anversa P (1990) Chronic calcium channel blockade prevents the progression of myocardial contractile and electrical dysfunction in the cardiomyopathic Syrian hamster. Circ Res 67:1381–1393

Chemla D, Scalbert E, Desché P, Pourny JC, Lambert F, Lecarpentier Y (1992) Effects of perindopril on myocardial inotropy, lusitropy and economy, and on diaphragm contractility in the cardiomyopathic Syrian hamster. J Pharm Exp Ther 262:515–525

Chemla D, Scalbert E, Desché P, Pourny JC, Lambert F, Lecarpentier Y (1993) Myocardial effects of early therapy with perindopril during experimental cardiomyopathy. Am J Cardiol 71:41E–47E

Desjardins S, Mueller RW, Hubert RS, Cauchy MJ (1989) Effects of milrinone treatment in cardiomyopathic hamsters (CHF 147) with severe congestive heart failure. Cardiovasc Res 23:620–630

Devaux JY. Cabane L, Elser M, Flaouters H, Duboc D (1993) Non-invasive evaluation of the cardiac function in golden retriever dogs by radionuclide angiography. Neuromuscular Disord 3:429–432

Dixon IMC, Ju H, Reidl NL, Scammell-La-Fleur T, Werner JP, Jasmin G (1997) Cardiac collagen remodelling in the cardiomyopathic Syrian hamster and the effect of losartan. J Mol Cell Cardiol 29:1837–1850

Factor SM, Sonnenblick EH (1985) The pathogenesis of clinical and experimental congestive cardiomyopathy: recent concepts. Prog Cardiovasc Dis 27:395–420

Factor SM, Minase T, Cho S, Dominitz R, Sonnenblick EH (1982) Microvascular spasm in the cardiomyopathic Syrian hamster: a preventable cause of focal myocardial necrosis. Circ 66:342–354
Forman R, Parmley WW, Sonnenblick EH (1972) Myocardial contractility in relation to hypertrophy and failure in myopathic Syrian hamsters. J Mol Cell Cardiol 4:203–211
Gardi C, Martorana PA, Calzoni P, Cavarra E, Marcolongo P, de Santi MM, van Even P, Lungarella G (1994) Cardiac collagen changes during the development of right ventricular hypertrophy in tight-skin mice with emphysema. Exp Mol Pathol 60:100–107
Gertz EW (1972) Cardiomyopathic Syrian hamster: A possible model of human disease. Prog Exp Tumor Res 16:242–260
Haleen SJ, Weishaar RE, Overhiser RW, Bousley RF, Keiser JA, Rapundalo SR, Taylor DG (1991) Effects of Quinapril, a new angiotensin converting enzyme inhibitor, on left ventricular failure and survival in the cardiomyopathic hamster. Circ Res 68:1302–1312
Hanton G, Barnes P, Shepperson NB, Walley R (1993) Effects of hydrochlorothiazide and captopril on the survival and heart weight of cardiomyopathic hamsters. Res Commun Chem Pathol Pharmacol 81:159–166
Homburger F (1979) Myopathy of hamster dystrophy: history and morphological aspects. Ann NY Acad Sci 317:2–17
Homburger F, Bajusz E (1970) New models of human disease in Syrian hamsters. J Am Med Ass 212:604–610
Jasmin G, Proscheck L (1982) Hereditary polymyopathy and cardiomyopathy in the Syrian hamster: I. Progression of heart and skeleton muscle lesions in the UM-X7.1 line. Muscle Nerve 5:20–25
Jasmin G, Proschek L (1984) Calcium and myocardial cell injury. An appraisal in the cardiomyopathic hamster. Canad J Physiol Pharmacol 62:891–898
Kato M, Takeda N, Yang J, Nagano M (1992) Effects of angiotensin converting enzyme inhibitors and the role of the renin-angiotensin-aldosterone system in J-2-N cardiomyopathic hamsters. Jpn Circ J 56:46–51
Kuo TH, Tsang W, Wang KK, Carlock L (1992) Simultaneous reduction of the sarcolemmal and SR calcium APTase activities and gene expression in cardiomyopathic hamster. Biochim Biophys Acta 1138:343–349
Malhotra A, Karell M, Scheuer J (1985) Multiple cardiac contractile protein abnormalities in myopathic Syrian hamsters (Bio 53:58). J Mol Cell Cardiol 17:95–107
Martorana PA, Wilkinson M, van Even P, Lungarella G (1990) Tsk mice with genetic emphysema. Right ventricular hypertrophy occurs without hypertrophy of muscular pulmonary arteries or muscularization of arterioles. Am Rev Resp Dis 142:333–337
Nigro V, Okazaki Y, Belsito A, Piluso G, Matsuda Y, Politano L, Nigro G, Ventura C, Abbondanza C, Molinari AM, Acampora D, Nishimura A, Hayashizaki Y, Puca GA (1997) Identification of the Syrian hamster cardiomyopathy gene. Hum Mol Genet 6:601–607
Sen L, O'Neill M, Marsh JD, Smith TW (1990) Inotropic and calcium kinetic effects of calcium channel agonist and antagonist in isolated cardiac myocytes from cardiomyopathic hamsters. Circ Res 67:599–608
Strobeck JE, Factor SM, Bhan A, Sole M, Liew CC, Fein F, Sonnenblick EH (1979) Hereditary and acquired cardiomyopathies in experimental animals: Mechanical, biochemical and structural features. Ann NY Acad Sci 317:59–68
Tanguay M, Jasmin G, Blaise G, Dumant L (1997) Coronary and cardiac sensitivity to the vasoselective benzothiazepine-like calcium antagonist, clentiazem, in experimental heart failure. Cardiovasc Drugs Ther 11:71–79
Tapp WN, Natelson BH, Creighton D, Khazam C, Ottenweller JE (1989) Alprazolam reduces stress-induced mortality in cardiomyopathic hamsters. Pharmacol Biochem Behav 32:331–336
Van Meel JC, Mauz ABM, Wienen W, Diederen W (1989) Pimobendan increases survival of cardiomyopathic hamsters. J Cardiovasc Pharmacol 13:508–509
Ver Donck L, Wouters L, Olbrich HG, Mutschler E, Brogers M (1991) Nebivolol increases survival in cardiomyopathic hamsters with congestive heart failure. J Cardiovasc Pharmacol 18:1–3
Whitmer JT, Kumar P, Solaro RJ (1988) Calcium transport properties of cardiac sarcoplasmic reticulum from cardiomyopathic Syrian hamsters (BIO 53.58 and 14.6): evidence for a quantitative defect in dilated myopathic hearts not evident in hypertrophic hearts. Circ Res 62:81–85
Wiederhold KF, Nilius B (1986) Increased sensitivity of ventricular myocardium to intracellular calcium-overload in Syrian cardiomyopathic hamster. Biomed Biochim Acta 45:1333–1337

A.6.0.5 Cardiac Failure in Rabbits

PURPOSE AND RATIONALE

Rabbit models of heart failure were reviewed by Mudders and Elsner (2000).

Rapid pacing was used by Masaki et al. (1994), Porsa et al. (1994), Eble et al. (1998), Li et al. (2003), and Rose et al. (2005); coronary artery ligation by Pennock et al. (1997), Currie and Smith (1999), Romanic et al. (2001), and Miller et al. (2004); combined pressure and volume overload by Ezzaher et al. (1991), Mohammadi et al. (1997), Dekker et al. (1998), and Baartscheer et al. (2003a, 2003b); aortic insufficiency and aortic constriction by Bouanani et al. (1991) and Pogwizd et al. (1999); regurgitation after damage of the mitral valve by Gunawardena et al. (1999); regurgitation after aortic valve destruction by Magid et al. (1988, 1994), Yoshikawa et al. (1993), King et al. (1997), and Liu et al. (1998); Luchner et al. (2001) used a rabbit model of progressive left ventricular dysfunction to investigate differential expression of cardiac atrial natriuretic peptide and brain natriuretic peptide. Ventricular pacing-induced heart failure could be induced with a transvenously implanted pacemaker system.

PROCEDURE

Male rabbits (chinchilla bastard) underwent implantation of a programmable cardiac pacemaker (Medtronic Minix 8340, Minneapolis, Mn., USA). Under anesthesia (ketamine 60 mg/kg xylazine 5 mg/kg i.m.), the right internal jugular vein was dissected and cannulated with a single-lumen central venous catheter (Braun, Germany). The catheter was then advanced

into the right ventricle under pressure guidance. A transvenous screw-in pacemaker lead (Medtronic) was advanced through the catheter into the ventricular apex and implanted endocardially. The pacemaker was implanted subcutaneously into the right abdominal wall and the pacemaker lead was connected subcutaneously with the pacemaker. Rapid ventricular pacing-induced heart failure could be induced with a transvenously implanted pacemaker system. All rabbits were allowed to recover for at least 10 days after surgery before the pacemaker was started for the induction of heart failure. Proper pacemaker function was checked intraoperatively, at the time of programming, and subsequently all 10 days.

Rabbits (CHF group) underwent pacing with a stepwise increase of stimulation frequencies over 30 days. During the first 10 days, animals were paced at 330 beats/min (bpm). This protocol results in ELVD, as defined by significant LV systolic dysfunction with cardiac enlargement and decreased perfusion pressure but no clinical signs failure The pacing rate was then increased to 360 bpm for 10 days and 380 bpm for another 10 days and ELVD evolved to CHF with further cardiac enlargement and further decreased perfusion pressure together with clinical signs of fluid retention (ascites). At baseline (control), after being paced at 330 bpm for 10 days (ELVD) and at the end of the protocol (CHF), conscious arterial pressure was measured invasively via the medial ear artery and a 2-D guided M-mode echocardiogram was obtained. At the end of the pacing protocol, rabbits were killed by i.v. euthanasia and tissue was rapidly harvested. Hearts were trimmed on ice, snap frozen in liquid nitrogen and stored at –80°C until further processing.

Echocardiography

A long and short-axis echocardiogram (HP Sonos 5500, 12 MHz probe) was performed under light sedation (5 mg midazolam i.m.) in a supine position from the left parasternal window. LV end-diastolic (LVEDd) and end-systolic (LVESd) dimensions and diastolic and systolic thickness of the left ventricular anterior wall (AEDth and AESth) and posterior wall (PEDth and PESth) as well as left atrial diameter (LAd) were determined from three repeated 2-D guided M-mode tracings using the ASE convention. From those measurements, fractional shortening (FS) was calculated as: FS = (LVEDd– LVESd) /LVEDd.

Analytical methods

For analysis of cardiac natriuretic peptide expression, mRNA was extracted from all atrial and left ventricular samples utilizing a commercial kit (Fasttrack, Invitrogen).

As a probe for brain natriuretic peptide (BNP), a 750-bp *Eco*R1/*Hind*III DNA restriction fragment containing the gene for rabbit BNP was used.

EVALUATION

Results of the quantitative studies were expressed as mean ± SEM. Comparisons between the control, ELVD and CHF groups were performed by analysis of variance (ANOVA) followed by Fisher's least significant difference test. Comparison between the atrial and LV tissues as well as between atrial natriuretic peptide (ANP) and BNP were performed by paired Student's *t*-test. Statistical significance was defined as $P < 0.05$.

MODIFICATIONS OF THE METHOD

Arnolda et al. (1985) studied adriamycin cardiomyopathy in the rabbit.

Klimtova et al. (2002) performed a comparative study of chronic toxic effects of daunorubicin and doxorubicin in rabbits.

Alexander et al. (1993) studied electrographic changes following corona-virus-induced myocarditis and dilated cardiomyopathy in rabbits.

Sanbe et al. (2005) described a transgenic model for human troponin I-based hypertrophic cardiomyopathy in the rabbit.

REFERENCES AND FURTHER READING

Alexander IK, Keene BW, Small JD, Yount B Jr, Baric RS (1993) Electrographic changes following rabbit corona-virus-induced myocarditis and dilated cardiomyopathy. Adv Exp Med Biol 342:365–370

Arnolda L, McGrath B, Cocks M, Sumithran E, Johnston C (1985) Adriamycin cardiomyopathy in the rabbit: an animal model of low output cardiac failure with activation of vasoconstrictor mechanisms. Cardiovasc Res 19:378–382

Baartscheer A, Schumacher CA, Belterman CNW, Coronel R, Fiolet JWT (2003a) SR calcium handling and calcium after-transients in a rabbit model of heart failure. Cardiovasc Res 58:99–108

Baartscheer A, Schumacher CA, van Borren MMGJ, Belterman VNW, Coronel R, Fiolet JWT (2003b) Increased Na^+/H^+-exchange activity is the cause of increased $[Na^+]_i$ and underlies disturbed calcium handling in the rabbit pressure and volume overload heart failure model. Cardiovasc Res 57:1015–1024

Bouanani N, Cosin A, Gilson N, Crotazier B (1991) Beta-adrenoceptors and adenylate cyclase activity in hypertrophied and failing rabbit left ventricle. J Mol Cell Cardiol 23:573–581

Currie S, Smith GL (1999) Enhanced phosphorylation of phospholamban and downregulation of sarco/endoplasmatic reticulum Ca^{2+} ATPase type 2 SERCA2) in cardiac sarcoplasmatic reticulum from rabbits with heart failure. Cardiovasc Res 41:135–146

Dekker LR, Rademaker H, Vermeulen JT, Opthof T, Coronel R, Spaan JA, Janse MJ (1988) Cellular uncoupling during ischemia in hypertrophied and failing rabbit ventric-

ular myocardium: effects of preconditioning. Circulation 97:1724–1730
Eble DM, Walker JD, Samarei AM, Spinale FG (1998) Myosin heavy chain synthesis during progression of chronic tachycardia induced heart failure in rabbits. Bas Res Cardiol 93:50–55
Ezzaher A, el Houda-Bouanani N, Su JB, Hittinger L, Crozatier B (1991) Increased negative inotropic effect of calcium-channel blockers in hypertrophied and failing rabbit heart. J Pharmacol Exp Ther 257:466–471
Gunawardena S, Bravo E, Kappagoda CT (1999) Rapidly adapting receptors in a rabbit model of mitral regurgitation. J Physiol (Lond) 521:739–748
King RK, Magid NM, Opio G, Borer JS (1997) Protein turnover in compensated chronic aortic regurgitation. Cardiology 88:518–525
Klimtova I, Simunek T, Mazurova Y, Hrdina R, Gersi V, Adamcova M (2002) Comparative study of chronic toxic effects of daunorubicin and doxorubicin in rabbits. Hum Exp Toxicol 21:649–657
Li YL, Sun YS, Overholt JL, Prabhakar NR, Rozanski GJ, Zucker IH, Schultz HD (2003) Attenuated outward potassium currents in carotid body glomus cells of heart failure rabbit: involvement of nitric oxide. J Physiol (Lond) 555:219–229
Liu SK, Magid NR, Fox PR, Goldfine SM, Borer JS (1998) Fibrosis, myocyte degeneration and heart failure in chronic aortic regurgitation. Cardiology 90:101–109
Luchner A, Muders F, Dietl O, Friedrich E, Blumberg F, Protter AA, Riegger GAJ, Elsner D (2001) Differential expression of cardiac ANP and BNP in a rabbit model of progressive left ventricular dysfunction. Cardiovasc Res 51:601–607
Magid NM, Young MS, Wallerson DC, Goldweit RS, Carter JN, Deveraux RB, Borer JS (1988) Hypertrophic and functional response to experimental chronic aortic regurgitation. J Mol Cell Cardiol 20:239–246
Magid NM, Opio G, Wallerson DC, Young MS, Borer JS (1994) Heart failure due to chronic aortic regurgitation. Am J Physiol 267(2 Pt2): H556–H562
Masaki H, Imaizumi T, Harasawa Y, Takeshita A (1994) Dynamic arterial baroreflex in rabbits with hear failure induced by rapid pacing. Am J Physiol 267(1 Pt2): H92–H99
Miller DJ, MacFarlane NG, Wilson G (2004) Altered oscillatory work by ventricular myofilaments from a rabbit coronary artery ligation model of heart failure. Cardiovasc Res 61:94–104
Mohammadi K, Rouet-Benzineb P, Laplace M, Crozatier B (1997) Protein kinase C activity and expression in rabbit left ventricular hypertrophy. J Mol Cell Cardiol 29:1687–1694
Muders F, Elsner F (2000) Animal models of chronic heart failure. Pharmacol Res 41:605–612
Pennock GD, Yun DD, Agarwal PG, Spooner PH, Goldman S (1997) Echocardiographic changes after myocardial infarction in a model of left ventricular dysfunction. Am J Physiol 273(4 Pt2):H2018–2029
Pogwizd SM, Qi M, Yuan W, Samaral AM, Bers DM (1999) Upregulation of Na^+/Ca^{2+} exchanger expression and function in an arrhythmogenic rabbit model of heart failure. Circ Res 85:1009–1019
Porsa E, Freeman GL, Herlihy JT (1994) Tachycardia heart failure alters rabbit aortic smooth muscle responsiveness to angiotensin II. Am J Physiol 266(3 PT2):H1228–1232
Romanic AM, Burns-Curtis CL, Gout B, Berrebi-Bertrand I, Ohlstein EH (2001) Matrix metalloproteinase expression in cardiac myocytes following myocardial infarction in the rabbit. Life Sci 68:799–814
Rose J, Armoundas AA, Tian Y, DeSilvestre D, Burysek M, Halperin V, O'Rourke B, Kass DA, Marban E, Tomaselli GF (2005) Molecular correlates to altered expression of potassium currents in failing rabbit myocardium. Am J Physiol 288:H2077–H2087
Sanbe DM, James J, Tuzcu V, Nas S, Martin L, Gulick J, Osinka H, Sakthivel S, Klevitsky R, Ginsburg KS (2005) Transgenic model for human troponin I-based hypertrophic cardiomyopathy. Circulation 111:2330–2338
Yoshikawa T, Handa S, Yamada T, Wainai Y, Suzuki M, Nagami K, Tani M, Nakamura Y (1993) Sequential changes in sympatho-neuronal regulation and contractile function following aortic regurgitation in rabbit heart. Eur Heart J 14:1404–1409

A.6.0.6 Congestive Heart Failure in Dogs

PURPOSE AND RATIONALE

Several methods are described, to induce congestive heart failure in dogs, such as rapid ventricular pacing (Armstrong et al. 1986; Freeman et al. 1987; Wilson et al. 1987; Komamura et al. 1992, 1993; Perreault et al. 1992; Travill et al. 1992; Cheng et al. 1993; Redfield et al. 1993; Cory et al. 1994; Kiuchi et al. 1994; Ohno et al. 1994; Vatner et al. 1994; Wang et al. 1994; Williams et al. 1994; Eaton et al. 1995; Spinale et al. 1995; Wolff et al. 1995; Zile et al. 1995; Ravens et al. 1996; Shinbane et al. 1997; O'Rourke et al. 1999; Winslow et al. 1999).

Luchner et al. (1996) assessed circulating, renal, cardiac, and vascular angiotensin II in a canine model of rapid ventricular pacing-induced heart failure that evolves from early left ventricular dysfunction to overt congestive heart failure.

PROCEDURE

Male mongrel dogs underwent implantation of a programmable cardiac pacemaker (Medtronic). Under pentobarbital sodium anesthesia and artificial respiration, the heart was exposed via a small left lateral thoracotomy and pericardiotomy, and a screw-in epicardial pacemaker lead was implanted into the right ventricle. The pacemaker was implanted subcutaneously into the left chest wall and connected to the pacemaker lead. The dogs were allowed to recover for at least 10 days after surgery before the pacemaker was started. During the first 10 days dogs were paced at 180 beats/min (bpm), resulting in early left ventricular dysfunction as defined by significant systolic dysfunction with decreased cardiac output, cardiac enlargement, and increased filling pressures but maintained systemic perfusion pressure and renal sodium

excretion and no clinical signs of heart failure. The pacing rate was then increased weekly to 200, 210, 220 and 240 bpm, and early left ventricular dysfunction evolved to overt congestive heart failure with avid sodium retention and clinical signs of congestion. At baseline (control), after dogs had been paced at 180 bpm for 10 days and at the end of the protocol (overt CHF), urine was collected for measurement of sodium excretion; conscious mean arterial pressure was measured via a port catheter; a 2-D guided M-mode echogram was obtained; and arterial blood was drawn. Cardiac filling pressures and cardiac output were measured by the thermodilution method at baseline and at the end of the protocol. Arterial blood was collected in EDTA tubes for measurement of ANP, BNP, cGMP, PRA, aldosterone, and Ang II. After euthanasia, hearts were rapidly trimmed and left ventricles weighted for calculation of the index LV weight to body weight.

EVALUATION

Results were expressed as mean ± SE. Comparison between the control, early LV dysfunction, and overt CHF were performed by ANOVA followed by Fisher's least significant difference test.

MODIFICATIONS OF THE METHOD

Kleaveland et al. (1988) and Nagatsu et al. (1994) used the technique of experimental **mitral regurgitation** in dogs to induce left ventricular dysfunction. A 30-cm, 7F sheath was introduced across the aortic valve through the carotid artery. A urologic calculus retrieval forceps was advanced through the sheath to the mitral valve apparatus and was used to sever chordae tendineae. When pulmonary capillary wedge pressure rose to 20 mmHg and forward stroke volume was reduced to 50% of its baseline, a ventriculogram was performed to confirm angiographically that severe mitral regurgitation had been created.

Dell'Italia et al. (1995) and Su et al. (1999) induced mitral regurgitation by percutaneous chordal rupture in dogs.

Kinney et al. (1991) published a method to induce acute, reversible tricuspid insufficiency in anesthetized dogs. A wire spiral is advanced through the atrioventricular canal from the right atrium. The spiral causes regurgitation by preventing complete apposition of the valve leaflets while permitting retrograde flow to occur through the spiral lumen. The degree of regurgitation can be controlled by the use of spirals of different size. Creation of tricuspid insufficiency was demonstrated by onset of right atrial pressure V waves, a ballooning of the right atrium during ventricular systole, palpation of an atrial thrill, or by color Doppler echocardiography. The model is reversible and allows repeated trials of various grades of regurgitation.

Carlyle and Cohn (1983) described a non-chirurgical model of chronic left ventricular dysfunction. The method is accomplished by repetitive DC shock with a guidewire introduced percutaneously and positioned in the left ventricle along the intraventricular septum and an external paddle at the left ventricular apex.

McDonald et al. (1992) produced localized left ventricular necrosis without obstruction of the coronary blood flow in dogs by transmyocardial direct-current shock.

Sabbah et al. (1991, 1993, 1994) and Gengo et al. (1992) produced chronic heart failure in dogs by multiple sequential intracoronary **embolizations with microspheres**. The dogs underwent three to nine intracoronary embolizations with polystyrene latex microspheres (70–102 μm in diameter) performed 1–3 weeks apart. Embolizations were discontinued when left ventricular ejection fraction was less than 35%.

Vanoli et al. (2004) used multiple coronary microembolizations in dogs, whereby three to nine embolizations were performed 1 week apart. The first three embolizations consisted of 2 ml of microsphere suspension injected subselectively into either the left anterior descending or left circumflex coronary artery in an alternating fashion. Subsequent embolizations consisted of 3–6 ml of microspheres divided equally between the left anterior descending or left circumflex coronary artery until LV ejection fraction was < 35%.

Magovern et al. (1992) described a canine model of left ventricular dysfunction caused by five weekly intracoronary infusions of **adriamycin**.

Koide (1997) described premorbid determinants of left ventricular dysfunction in a model of gradually induced pressure overload in dogs. Mongrel dogs were studied through 8 weeks of gradually imposed ascending aortic constriction with the use of a **novel banding technique**. During banding, an initial gradient of 30 mmHg was created. Before banding, at 2, 4, and 6 weeks after banding, hemodynamics and left ventricular mechanics were examined at cardiac catheterization; then the pressure overload was increased by tightening the band.

Valentine et al. (1988) and Devaux et al. (1993) described **X-linked muscular dystrophy in dogs** with cardiac insufficiency similar to Duchenne muscular dystrophy in men and recommended this as an animal model for cardiac insufficiency.

REFERENCES AND FURTHER READING

Armstrong PW, Stopps TP, Ford SE, de Bold AJ (1986) Rapid ventricular pacing in the dog: pathophysiological studies of heart failure. Circulation 74:1075–1084

Carlyle PF, Cohn JN (1983) A nonchirurgical model of chronic left ventricular dysfunction. Am J Physiol 244:H769–H774

Cheng CP, Noda T, Nozawa T, Little WD (1993) Effect of heart failure on the mechanism of exercise-induced augmentation of mitral valve flow. Circ Res 72:795–806

Cory CR, Shen H, O'Brien PJ (1994) Compensatory asymmetry in down-regulation and inhibition of the myocardial Ca^{2+} cycle in congestive heart failure in dogs by idiopathic dilated cardiomyopathy and rapid ventricular pacing. J Mol Cell Cardiol 26:173–184

Dell'Italia LJ, Meng QC, Balcells E, Straeter-Knowlen IM, Hankes GH, Dillon R, Cartee RE, Orr R, Bishop SP, Oparil S (1995) Increased ACE and chymase-like activity in cardiac tissue of dogs with chronic mitral regurgitation. Am J Physiol 269(6 Pt2):H2065–H2073

Eaton GM, Cody RJ, Nunziata E, Binkley PF (1995) Early left ventricular dysfunction elicits activation of sympathetic drive and attenuation of parasympathetic tone in the paced canine model of congestive heart failure. Circulation 92:555–561

Freeman GL, Little WC, O'Rourke RA (1987) Influence of heart rate on left ventricular performance in conscious dogs. Circ Res 61:455–464

Gengo PJ, Sabbah HN, Steffen RP, Sharpe KJ, Kono T, Stein PD, Goldstein S (1992) Myocardial beta receptor and voltage sensitive calcium channel changes in a canine model of chronic heart failure. J Mol Cell Cardiol 24:1361–1369

Kinney TE, Olinger GN, Sgar KB, Boerboom LE (1991) Acute, reversible tricuspid insufficiency: creation of a canine model. Am J Physiol 260:H638–H641

Kiuchi K, Shannon RP, Sato N, Bigaud M, Lajoie C, Morgan KG, Vatner SF (1994) Factors involved in delaying the rise in peripheral resistance in developing heart failure. Am J Physiol 267 (1 Pt2):H211–H216

Kleaveland JP, Kussmaul WG, Vinciguerra T, Diters R, Carabello BA (1988) Volume overload hypertrophy in a closed-chest model of mitral regurgitation. Am J Physiol 254(6 Pt2):H1034–H1041

Koide M, Nagatsu M, Zile MR, Hamakawi M, Swindle MM, Keech G, DeFreyte G, Tagawa H, Cooper G, Carabello BA (1997) Premorbid determinants of left ventricular dysfunction in a novel model of gradually induced pressure overload in the adult canine. Circulation 95:1601–1610

Komamura K, Shannon RP, Pasipoularides A, Ihara T, Lader AS, Patrick TA, Bishop SP, Vatner SF (1992) Alterations in left ventricular diastolic function in conscious dogs with pacing-induced heart failure. J Clin Invest 89:1825–1838

Komamura K, Shannon RP, Ihara T, Shen YT, Mirsky I, Bishop SP, Vatner SF (1993) Exhaustion of Frank-Starling mechanism in conscious dogs with heart failure. Am J Physiol 265 (4 Pt2):H1119–H1131

Luchner A, Stevens TL, Borgeson DD, Redfield MM, Bailey JE, Sandberg SM, Heublein DM, Burnett JC Jr (1996) Angiotensin II in the evolution of experimental heart failure. Hypertension 28:472–477

Magovern JA, Christlieb IY, Badylak SF, Lantz GC, Kao RL (1992) A model of left ventricular dysfunction caused by intracoronary adriamycin. Ann Thoracic Surg 53:861–863

McDonald KM, Francis GS, Carlyle PF, Hauer K, Matthews J, Hunter DW, Cohn JN (1992) Hemodynamic, left ventricular structural and hormonal changes after discrete myocardial damage in the dog. J Am Coll Cardiol 19:460–467

Nagatsu M, Zile MR, Tsutsui H, Schmid PG, DeFreyte G, Cooper IV G, Carabello BA (1994) Native β-adrenergic support for left ventricular dysfunction in experimental mitral regurgitation normalizes indexes of pump and contractile function. Circulation 89:818–826

Ohno M, Cheng CP, Little WC (1994) Mechanism of altered patterns of left ventricular filling during the development of congestive heart failure. Circulation 89:2241–2250

O'Rourke B, Kass DA, Tomaselle GF, Kääb S, Tunin R, Marbán E (1999) Mechanisms of altered excitation-contraction coupling in canine tachycardia-induced heart failure. I: experimental studies. Circ Res 84:562–570

Ravens U, Davia K, Davies CH, O'Gara P, Drake-Holland AJ, Hynd JW, Noble MIM, Harding SE (1996) Tachycardia-induced failure alters contractile properties of canine ventricular myocytes. Cardiovasc Res 32:613–621

Perreault CL, Shannon RP, Komamura K, Vatner SF, Morgan JP (1992) Abnormalities in intracellular calcium regulation and contractile function in myocardium from dogs with pacing-induced heart failure. J Clin Invest 83:932–938

Redfield MM, Aarhus LL, Wright RS, Burnett JC (1993) Cardiorenal and neurohumoral function in a canine model of left ventricular dysfunction. Circulation 87:2016–2022

Sabbah HN, Stein PD, Kono D, Gheorghiade M, Levine TB, Jafri S, Hawkins ET, Goldstein S (1991) A canine model of chronic heart failure produced by multiple sequential coronary microembolizations. Am J Physiol 260(4 Pt2):H1379–H1384

Sabbah HN, Hansen-Smith F, Sharov VG, Kono T, Lesch M, Gengo PJ, Steffen RP, Levine TB, Goldstein S (1993) Decreases proportion of type I myofibers in skeletal muscle of dogs with chronic heart failure. Circulation 87:1729–1737

Sabbah HN, Shimoyama H, Kono T, Gupta RC, Sharov VG, Scicli G, Levine TB, Doldstein S (1994) Effects of long-term monotherapy with enalapril, metoprolol, and digoxin on the progression of left ventricular dysfunction and dilation in dogs with reduced ejection fraction. Circulation 89:2852–2859

Shinbane JS, Wood Ma, Jensen DN, Ellenbogen KA, Fitzpatrick AP, Scheinman MM (1997) Tachycardia-induced cardiomyopathy: a review of animal models and clinical studies. J Am Coll Cardiol 29:709–715

Spinale FG, Holzgrefe HH, Mukherjee R, Hird B, Walker JD, Armin-Baker A, Powell JR, Koster WH (1995) Angiotensin-converting enzyme inhibition and the progression of congestive cardiomyopathy. Circulation 92:562–578

Su X, Wei CC, Machida N, Bishop SP, Hankes GH, Dillon AR, Oparil S, Dell'Italia LJ (1999) Differential expression of angiotensin-converting enzyme and chymase in dogs with chronic mitral regurgitation. J Mol Cell Cardiol 31:1033–1045

Travill CM, Williams TD, Pate P, Song G, Chalmers J, Lightman SL, Sutton R, Noble MI (1992) Hemodynamic and neurohumoral response in heart failure produced by rapid ventricular pacing. Cardiovasc Res 26:783–790

Valentine BA, Cooper BJ, DeLahunta A, O'Quinn R, Blue JT (1988) Canine X-linked muscular dystrophy. An animal model of Duchenne muscular dystrophy: Clinical studies. J Neurol Sci 88:69–81

Vanoli E, Bacchini S, Panigada S, Pentimalli F, Adamson PB (2004) Experimental models of heart failure. Eur Heart J Suppl 6 (Suppl F):F7–F15

Vatner DE, Sato N, Kiucho K, Shannon RP, Vatner SF (1994) Decrease in myocardial ryanodine receptors and altered ex-

citation-contraction coupling early in the development of heart failure. Circulation 90:1432–1430
Wang J, Seyedi N, Xu XB, Wolin MS, Hintze TH (1994) Defective endothelium-mediated control of coronary circulation in conscious dogs after heart failure. Am J Physiol 266(2Pt2):H670–H680
Williams RE, Kass DA, Kawagoe Y, Pak P, Tunin RS, Shah R, Hwang A, Feldman AM (1994) Endomyocardial gene expression during development of pacing tachycardia-induced heart failure in the dog. Circ Res 75:615–623
Wilson JR, Douglas P, Hickey WF, Lanoce V, Ferraro N, Muhammad A, Reicheck N (1987) Experimental congestive heart failure produced by rapid ventricular pacing in the dog: cardiac effects. Circulation 75:857–867
Winslow RL, Rice J, Jafri S, Marbán E, O'Rourke B (1999) Mechanisms of altered excitation-contraction coupling in canine tachycardia-induced heart failure, II: model studies. Circ Res 84:571–586
Wolff MR, Whitesell LF, Moss RL (1995) Calcium sensitivity of isometric tension is increased in canine experimental heart failure. Circ Res 76:781–789
Zile MR, Mukherjee R, Clayton C, Kato S, Spinale FG (1995) Effects of chronic supraventricular pacing tachycardia on relaxation rate in isolated cardiac muscle cells. Am J Physiol 268(5 Pt2):H2104–H2113

A.6.0.7 Cardiac Failure in Pigs

PURPOSE AND RATIONALE

Cardiac failure was studied in pigs using several experimental procedures.

Chow et al. (1990) recommended rapid ventricular pacing in pigs as an experimental model of congestive heart failure.

Farrar et al. (1993) studied pacing-induced dilated cardiomyopathy in pigs. Congestive heart failure was produced by rapid ventricular pacing at 230 bpm for 1 week.

Spinale et al. (1990a, 1990b, 1991, 1992) examined the consequences of chronic supraventricular tachycardia on various parameters of ventricular dysfunction and subendocardial changes in pigs.

Carroll et al. (1995) investigated gene expression in a swine model of ventricular hypertrophy during pressure overload.

Multani et al. (2001) studied long-term angiotensin converting enzyme and angiotensin I-receptor inhibition in pacing-induced heart failure in pigs. Heart failure was induced by rapid atrial pacing (240 bpm for 3 weeks).

Kassab et al. (1993, 2000) investigated remodeling of right ventricular branches after hypertrophy in pigs.

Krombach et al. (1999) studied the effects of amlodipine in congestive heart failure in pigs at rest and after treadmill exercise.

PROCEDURE

Left thoracotomy was performed in Yorkshire pigs in anesthesia. Catheters connected to a vascular access port were placed in the thoracic aorta, the pulmonary artery, and the left atrium. The access ports were then placed in a subcutaneous pocket. A 20-mm flow probe was placed around the pulmonary artery immediately distal to the pulmonary catheter and the electrical connection exteriorized through the thoracolumbar fascia. A shielded stimulating electrode was sutured onto the left atrium, connected to a programmable pacemaker and buried in a subcutaneous pocket. The thoracotomy was closed in layers and the pleural space evacuated of air. After a 14- to 21-day recovery, measurements were performed under normal resting conditions and after exercise. The pacemakers were activated to 240 bpm for a period of 21 days. During the last 3 days, one group was treated with drug, the other served as control. At the day of the study, electrocardiograms were performed, and the pacemakers deactivated. After a 30-min stabilization period, 2-D and M-mode echocardiographic studies were used to image the left ventricle from the parasternal approach. Left ventricular fractional shortening was calculated as (end-diastolic dimension – end-systolic dimension)/diastolic dimension, and was expressed as a percentage. The access ports were entered and pressures obtained using externally calibrated transducers. The flow probe was connected to a digital flowmeter. From the digitized flow signal, stroke volume was computed on a beat-to-beat basis and averaged for a minimum of 25 ejections. Pulmonary and systemic vascular resistances were computed as the mean pressure divided by cardiac output multiplied by the constant 80 to convert to resistance units of dyne$\cdot s \cdot$cm^{-5}. Samples were drawn from the pulmonary artery and atrial catheters for measurement of oxygen saturation and hemoglobin content. The plasma samples were assayed for renin activity, endothelin concentration, and catecholamine levels.

EVALUATION

Results were presented as mean $\pm$ SEM. Pairwise tests of individual group means were compared using Bonferroni probabilities.

MODIFICATIONS OF THE METHOD

Zhang et al. (1996) studied functional and bioenergetic consequences of post-infarction left remodeling in a porcine model. Proximal left coronary artery occlusion was used to generate a myocardial infarction in young pigs. The animals were then followed over sev-

eral months while remodeling of the left ventricle developed. Left ventricular wall thickness, ejection fraction, and wall stress were measured by MRI. Myocardial ATP, creatine phosphate, and inorganic phosphate levels were measured by spatially localized ^{31}P-NMR spectroscopy, and regional myocardial blood flow was measured with radioactive microspheres.

PROCEDURE

MRI Protocols

All MRI studies were performed on the standard Siemens Medical System VISION operating at 1.5 T. The animals were anesthetized with sodium pentobarbital. A catheter was placed into the femoral artery and advanced into the LV chamber for LV pressure recording. Animals then were placed on their left side in a Helmholtz coil with a diameter of 18 cm, which was used to improve signal to noise. To compute LV wall stress, the image acquisition was triggered by the LV pressure through the fluid-filled LV catheter. All of the imaging sequences were synchronized to the LV pressure trace. The electronic LV pressure signal was recorded and fed to a comparator set to a threshold level of 10% of the upslope of the LV pressure curve at the beginning of systole. The signal from the comparator was sent to a pulse former and then fed to the ECG port of the magnetic resonance system, where it was treated like the standard electrographic input to run the pulse sequences. Scout images were taken in the axial plane with a single-shot, ultrafast gradient echo sequence (McDonald et al. 1992; Wilke et al. 1993; Geiger et al. 1995). From the axial image, both horizontal and vertical long-axis images were obtained. By alternating back and forth several times, a true vertical long axis of the left ventricle was obtained. From the long-axis scout image, short-axis segmented cine turboflash slices were prescribed to cover the myocardium from apex to base. The double-oblique, short-axis turboflash images cover the heart from apex to base with a slice thickness of 10 mm, with no interslice gap.

MRI Cine Technique

The parameters of the segmented cine sequence were TR/TE/flip angle = 33 ms/6.1 ms/25 degrees with an FOV = 17.5 cm and a matrix of 87 × 128 (pixel size, 2 mm × 1.4 mm) and slice thickness of 7–10 mm (Atkinson et al. 1991). The sequence used segmented k-space acquisition such that three phase-encoded lines were gathered per cardiac phase per heartbeat. Total image acquisition required approximately 52 heartbeats for each slice location. The temporal image resolution (data acquisition window) of this sequence was 33 ms per cardiac image. Each myocardial level took < 1.5 min to acquire, since two acquisitions were used and the average heart rate of the animals was 120 bpm. The average number of short-axis slices needed to image the entire myocardium from apex to base was six to eight. This 10-min protocol provided high signal-to-noise cine sequences covering the entire heart.

Spin-Echo Images

To obtain high-resolution anatomic heart images, multislice, single-phase spin-echo images trigged in the systolic phase were acquired to cover the entire heart. These images permitted the precise delineation of the extent of the scar region of the heart. Images were taken with a slice thickness of 5 mm and a FOV of 17.5 cm, resulting in a true spatial resolution of 2 mm × 1.4 mm pixel size. The TR for this sequence equals the RR interval (500 ms) and the echo time TE was set to 30 ms. Total measurement time for an average of 10–14 slices was 5 min.

Image Analysis of the MRI Cine Studies

The imaging data were archived to optical disk and copied to a SUN SPARC 10 workstation for evaluation with the use of an automatic segmentation program (ImageView, Siemens Cooperate Research). The program is based on robust deformable models of endocardial and epicardial border segmentation of ventricular boundaries in cardiac magnetic resonance images. This segmentation technique has been combined with a user interface that allows one to load, sort, visualize, and analyze a cardiac study in < 20 min. The segmentation algorithm is based on the steepest descent as well as dynamic programming strategies integrated via multiscale analysis for minimizing the energy function of the resulting contour. The ventricular boundaries are used to construct a three-dimensional model for visualization and to compute hemodynamic parameters. Automatic segmentation of endocardial and epicardial boundaries was performed for calculation of ventricular volumes, EF, LV diastolic and systolic volumes, and absolute myocardial mass from multislice, multiphase magnetic resonance cine images. Starting with a user-specified approximate boundary or an interior point of the ventricle for one starting image in one slice, the algorithm generated automatic contours corresponding to the epicardium and the endocardium and automatically propagated them to other slices in the cardiac phase (spatial propagation) and to other phases for a given slice location (temporal propagation) of

the cardiac study. The observer then could make some manual corrections to the six or seven pairs of contours in the first column of the temporal-spatial matrix. Manual modifications generally were made on the apex and base levels.

EVALUATION

Mean LV wall thickness for each short-axis ring was averaged from three measurements of the remote zone (anterior wall and septum wall). The thickness of the scar was averaged from three measurements of the scar area. LVSA measurement in each slice was computed by subtracting the total area enclosed by the endocardium from that enclosed by the subepicardium; the resultant area was multiplied by the slice thickness to obtain the volume of each slice; the total LV mass volume was calculated by adding up the volumes of all the short-axis slices. The total LVSA was obtained by dividing the total LV wall mass volume by the mean of LV wall thickness of each slice. Similarly, the LVSSA was obtained by dividing the total scar volume, which was the sum of the scar volume of each short axis, by the mean of the scar thickness of each short axis. LV mass was computed by the total LV wall mass volume multiplied by 1.05 (specific gravity of myocardium) to calculate the LV mass. The LV end-diastolic volume (V_d) and end-systolic volume (V_s) of each slice were represented by the area enclosed by the endocardium. The total LV volume was computed by adding the volumes of all slices. LVEF was calculated by $100 \times (V–V_s)/V_d\%$. Interobserver and intraobserver errors for the calculations of LV mass and LV volumes have been shown to be < 3 mg and 3 ml, respectively (McDonald et al. 1994). Meridional wall stress was computed from the LV pressure and simultaneously obtained short-axis view of LV MRI (LV cavity diameter and average thickness the remote LV wall) as described by Grossman et al. (1975).

Spatially Localized ^{31}P-NMR Spectroscopic Technique

Measurements were performed in a 40-cm-bore, 4.7-T magnet interfaced with a SISCO (Spectroscopy Imaging Systems Corporation) console. The LV pressure signal was used to gate NMR data acquisition to the cardiac cycle, while respiratory gating was achieved by triggering the ventilator to the cardiac cycle between data acquisitions (Robitaille et al. 1990). ^{31}P- and ^{1}H-NMR frequencies were 81 and 200.1 MHz, respectively. Spectra were recorded in late diastole with a pulse repetition time of 6–7 s. This repetition time allowed full relaxation for ATP and P_i resonances and ≈90% relaxation for the CP resonance (Zhang and McDonald 1995). CP resonance intensities were corrected for this minor saturation; the correction factor was determined for each heart from two spectra recorded consecutively without transmural differentiation, one with 15-s repetition time to allow full relaxation and the other with the 6- to 7-s repetition time used in all the other measurements.

Radiofrequency transmission and signal detection were performed with a 25-mm-diameter surface coil. The coil was cemented to a sheet of silicone rubber 0.7 mm in thickness and ≈50% larger in diameter than the coil itself. A capillary containing 15 µl of 3 M phosphonoacetic acid was placed at the coil center to serve as a reference. The proton signal from water detected with the surface coil was used to homogenize the magnetic field and to adjust the position of the animal in the magnet so that the coil was at or near the magnet and gradient isocenters. This was accomplished with a spin-echo experiment and a readout gradient. The information gathered in this step also was used to determine the spatial coordinates for spectroscopic localization. Chemical shifts were measured relative to CP, which was assigned a chemical shift of –2.55 ppm relative to 85% phosphoric acid at 0 ppm.

Spatial localization across the LV wall was performed with the RAPP-ISIS/FSW method (Hendrich et al. 1991). Signal origin was restricted with the use of B_0 gradients and adiabatic inversion pulses to a column coaxial with the surface coil perpendicular to the LV wall. The column dimensions were 17 × 17 mm. Within this column, the signal was further localized using the B_1 gradient to five voxels centered about 45°, 60°, 90°, 120°, and 135° spin rotation increments. FSW localization used a nine-term Fourier series expansion. The Fourier coefficients, the number of free induction decays acquired for each term in the Fourier expansion, and the multiplication factors used to construct the voxels have been reported previously. The position of the voxels relative to the coil was set using the B_1 magnitude at the coil center, which was experimentally determined in each case by measurement of the 90° pulse length for the phosphonoacetic acid reference located in the coil center. Each set of spatially localized transmural spectra were acquired in 10 min. A total of 96 scans was accumulated within each 10-min block.

EVALUATION

Resonance intensities were quantified with the use of integration routines provided by the SISCO software. ATPγ resonance was used for ATP determination. Since data were acquired with the transmitter fre-

quency being positioned between the ATPγ and CP resonance, the off-resonance effects on these peaks were negligible. The numeric values for CP and ATP in each voxel were expressed as ratios of CP/ATP. P_i levels were measured as changes from baseline values (ΔP_i) with the use of integrals obtained in the region covering the P_i resonance.

REFERENCES AND FURTHER READING

Atkinson DJ, Edelman RR.(1991) Cineangiography of the heart in a single breath hold with segmented turboflash sequence. Radiology 178:357–360

Carroll SM, Nimmo LE, Knoepfler PS, White FC, Bloor CM (1995) Gene expression in a swine model of ventricular hypertrophy: Intercellular adhesion molecule, vascular endothelial growth factor and plasminogen activators are upregulated during pressure overload. J Mol Cell Cardiol 27:1427–1441

Chow E, Woodard JC, Farrar DJ (1990) Rapid ventricular pacing in pigs: an experimental model of congestive heart failure. Am J Physiol 258:H1603–H1605

Farrar DJ, Woodard JC, Chow E (1993) Pacing-induced dilated cardiomyopathy increases left-to-right ventricular systolic interaction. Circulation 88:720–725

Geiger D, Gupta A, Costa LA, Vlontzos J (1995) Dynamic programming for detecting, tracking and matching deformable contours. IEEE Trans Pattern Analysis Machine Intelligence 17:294–302

Grossman W, Jones D, McLaurin LP.(1975) Wall stress and patterns of hypertrophy in human left ventricle. J Clin Invest 56:56–64

Hendrich K, Merkle H, Weisdorf S, Vine W, Garwood M, Ugurbil K (1991) Phase modulated rotating frame spectroscopic localization using an adiabatic plane rotation pulse and a single surface coil. J Magn Reson 92:258–275

Kassab GS, Imoto K, White FC, Rider CA, Fung YC, Bloor CM (1993) Coronary arterial tree remodelling in right ventricular hypertrophy. Am J Physiol 265(1 Pt2):H366–H375

Kassab GS, Schatz A, Imoto K, Fung YC (2000) Remodeling of the bifurcation asymmetry of right ventricular braches in hypertrophy. Ann Biomed Eng 28:424–430

Krombach RS, Clair MJ, Hendrick JW, Mukherjee R, Houck WV, Hebbar L, Kribbs SB, Dodd MG, Spirale FG (1999) Amlodipine therapy in congestive heart failure: hemodynamic and neurohormonal effects at rest and after treadmill exercise. Am J Cardiol 84:3L–15L

McDonald K, Parrish T, Wennberg P, Stillman AE, Francis GS, Cohn JN.(1992) Rapid, accurate and simultaneous noninvasive assessment of right and left ventricular mass with nuclear magnetic resonance imaging using the snapshot gradient method. J Am Coll Cardiol 19:1601–1607

McDonald KM, Yoshiyama M, Francis GS, Ugurbil K, Cohn JN, Zhang J (1994) Abnormal myocardial bioenergetics in canine asymptomatic left ventricular dysfunction. J Am Coll Cardiol. 23:786–793

Multani MM, Krombach RS, Hednrick JW, Baicu SC, Joffs C, Sample JA, deGasparo M, Spinale FG (2001) Long-term angiotensin-converting enzyme and angiotensin I-receptor inhibition in pacing-induced heart failure. Effects on myocardial interstitial bradykinin levels. J Cardiac Fail 7:348–354

Robitaille PM, Lew B, Merkle H, Path G, Sublett E, Hendrich K, Lindstrom P, From AHL, Garwood M, Bache RJ, Ugurbil K (1990) Transmural high energy phosphate distribution and response to alterations in workload in the normal canine myocardium as studied with spatially localized 31P NMR spectroscopy. Magn Reson Med 16:91–116

Spinale FG, Hendrick DA, Crawford FA, Smith AC, Hamada Y, Carabello BA (1990a) Chronic supraventricular tachycardia causes ventricular dysfunction and subendocardial injury in swine. Am J Physiol 259(1 Pt2):H218–H229

Spinale FG, Hendrick DA, Crawford FA, Carabello BA (1990b) Relationship between bioimpedance, thermodilution, and ventriculographic measurements in experimental congestive heart failure. Cardiovasc Res 24:423–429

Spinale FG, Tomita M, Zellner JL, Cook JC, Crawford FA, Zile MR (1991) Collagen remodelling and changes in LV function during development and recovery from supraventricular tachycardia. Am J Physiol 261(2 Pt2):H308–H318

Spinale FG, Fulbright BM, Mukherjee R, Tanaka R, Hu J, Crawford FA, Zile MR (1992) Relation between ventricular and myocytes function with tachycardia-induced cardiomyopathy. Circ Res 71:174–187

Wilke N, Simm C, Zhang J, Ellermann J, Ya X, Merkle H, Path G, Ludemann H, Bache RJ, Ugurbil K (1993) Contrast-enhanced first pass myocardial perfusion imaging: correlation between myocardial blood flow in dogs at rest and during hyperemia. Magn Reson Med 29:485–497

Zhang J, McDonald K (1995) Bioenergetic consequence of left ventricular remodeling secondary to discrete myocardial infarction. Circulation 92:1011–1019

Zhang J, Wilke N, Wang Y, Zhang Y, Wang C, Eijgelshoven MHJ, Cho YK, Murakami Y, Ugurbil K, Bache RJ, From AHL (1996) Functional and bioenergetic consequences of postinfarction left remodelling in a new porcine model. Circulation 94:1089–1100

A.6.0.8 Cardiac Failure in Sheep

PURPOSE AND RATIONALE

Various methods have been used to induce cardiac failure in sheep: pressure overload after aortic banding (Aoyagi et al. 1993; Charles et al. 1996), volume loading after myocardial infarction (Charles et al. 2003), rapid ventricular pacing (Rademaker 1997, 2002b, 2005; Byrne et al. 2002; Moreno et al. 2005), coronary microembolization (Huang et al. 2004; Monreal et al. 2004).

Rademaker et al. (2002a) studied combined angiotensin converting enzyme inhibition and adrenomedullin in an ovine model of heart failure induced by rapid ventricular pacing.

PROCEDURE

Surgical Preparation

Coopworth ewes (38 ± 47 kg) were instrumented via a left lateral thoracotomy. Under general anesthesia (induced by 17 mg/kg thiopentone; maintained with halothane/nitrous oxide), two polyvinyl chloride catheters were inserted in the left atrium for blood sampling and left atrial pressure (LAP) determination; a Konigsberg pressure-tip transducer was inserted in

the aorta to record mean arterial pressure (MAP); an electromagnetic flow probe was placed around the ascending aorta to measure cardiac output (CO); a 7 French Swan-Ganz catheter was inserted in the pulmonary artery for infusions; and a 7 French His-bundle electrode was stitched subepicardially to the wall of the left ventricle for left ventricular pacing. All leads were externalized through incisions in the back. A bladder catheter was inserted per urethra for urine collections.

The animals were allowed to recover for 14 days before commencing the study protocol. During the experiments, the animals were held in metabolic cages, had free access to water and ate a diet of chaff and sheep pellets (containing 40 mmol/day sodium and 200 mmol/day potassium). A further 40 mmol of sodium was administered orally daily as NaCl tablets using an applicator.

Study Protocol

Heart failure was induced by 7 days of rapid left ventricular pacing (225 bpm) [15] and maintained by continuous pacing for the duration of the study. On four separate days with a rest day between each, the sheep received, in random order, a vehicle control (Haemaccel), human adrenomedullin alone (50 ng/min per kg infusion for 3 h), an ACE inhibitor alone (captopril: 25 mg bolus + 2 mg/h infusion for 3 h), and both agents combined. Infusions were administered in a total volume of 60 ml via the pulmonary artery catheter, commencing at 10:00 hours.

Mean arterial pressure, left atrial pressure, cardiac output and calculated total peripheral resistance

(CTPR = mean arterial pressure/cardiac output) were recorded at 15-min intervals in the 1-h prior to infusion (baseline), and at 15, 30, 45, 60, 90, 120 and 180 min during both the 3-h infusion and post-infusion periods. Hemodynamic measurements were determined by on-line computer-assisted analysis.

Blood samples were drawn from the left atrium at 30 min and immediately pre-infusion (baseline), and at 30, 60, 120 and 180 min during the 3-h infusion and post-infusion periods. Samples were taken into tubes on ice, centrifuged at 3939 *g* for 10 min at 4°C and stored at either –20°C or –80°C before assay for immunoreactive (ir-) adrenomedullin, cAMP, plasma renin activity, angiotensin II, aldosterone, atrial natriuretic peptide, brain natriuretic peptide, endothelin-1, catecholamines and cortisol.

All samples from individual animals were measured in the same assay to avoid inter-assay variability. Plasma electrolytes and hematocrit were measured in every sample taken. Urine volume and samples for the measurement of urine cAMP, sodium, potassium and creatinine excretion were collected every 1 h. Creatinine clearance was calculated as urine creatinine/plasma creatinine.

EVALUATION

Results are expressed as mean ± SEM. Baseline hemodynamic and hormone values represent the means of the four and two measurements respectively made in the 1 h immediately pre-infusion. Statistical analysis was performed by repeated-measures ANOVA. Baseline data from all treatments were compared. Treatment- and time-related differences between all four study limbs were determined using a two-way ANOVA (treatment–time interactions are quoted in the text). Statistical significance was assumed when $P < 0.05$

REFERENCES AND FURTHER READING

Aoyagi T, Fujii AM, Flaganan MF, Arnold LW, Brathwaite KW, Colan SD, Mirsky I (1993) Transition from compensated hypertrophy to intrinsic myocardial dysfunction during development of left ventricular pressure-overload hypertrophy in conscious sheep. Systolic dysfunction precedes diastolic dysfunction. Circulation 88:2415–2425

Byrne MJ, Raman JS, Alferness CA, Elser MD, Kaye DM, Power JM (2002) An ovine model of tachycardia-induced degenerative dilated cardiomyopathy and heart failure with prolonged onset. J Cardiac Fail 8:108–115

Charles CJ, Kaaja RJ, Espiner EA, Nicholls MG, Pemberton CJ, Richards AM, Yandle TG (1996) Natriuretic peptides in sheep with pressure overload left ventricular hypertrophy. Clin Exp Hypertens 18:1051–1071

Charles CJ, Elliott JM, Nicholls MG, Rademaker MT, Richards AM (2003) Natriuretic peptides maintain sodium homoeostasis during chronic volume loading post-myocardial infarction in sheep. Clin Sci 104:429–436

Huang Y, Hunyor SN, Liang L, Kawaguchi O, Shirota K, Ikeda Y, Yuasa T, Gallagher G, Zeng B, Zheng X (2004) Remodeling of chronic severely failing ischemic sheep heart after coronary microembolization: functional, energetic, structural, and cellular responses. Am J Physiol 286:H2141–H2150

Monreal G, Gerhardt MA, Kambara A, Abrishamchian AR, Bauer JA, Goldstein AH (2004) Selective microembolization of the circumflex coronary artery in an ovine model: dilated, ischemic cardiomyopathy and left ventricular dysfunction. J Cardiac Fail 10:174–183

Moreno J, Zaitsev AV, Warren M, Berenfeld O, Kalifa J, Lucca E, Mironov S, Guha P, Jalife J (2005) Effect of remodelling, stretch and ischemia on ventricular fibrillation frequency and dynamics in a heart failure model. Cardiovasc Res 65:158–166

Rademaker MT, Charles CJ, Lewis LK, Yandle TG, Cooper GJS, Coy DH, Richards AM, Nicholls MG (1997) Beneficial hemodynamic and renal effects of adrenomedullin in an ovine model of heart failure. Circulation 96:1983–1990

Rademaker MT, Charles CJ, Cooper JS, Coy DH, Espiner EA, Lewis LK, Nicholls MG, Richards AM (2002b)

Combined angiotensin-converting enzyme inhibition and adrenomedullin in an ovine model of heart failure. Clin Sci 102:653–660

Rademaker MT, Charkles CJ, Espiner EA, Frampton CM, Lainchbury JG, Richards AM (2005) Four-day urocortin-I administration has sustained beneficial hemodynamic, hormonal, and renal effects in experimental heart failure. Eur Heart J 26:2055–2062

A.6.0.9 Cardiac Failure in Monkeys

PURPOSE AND RATIONALE

Several authors used monkeys for studies of cardiac failure. Hollander et al. (1977) investigated the role of hypertension in ischemic heart disease in the **cynomolgus monkey** with coarctation of the aorta. Sieber et al. (1980) studied cardiotoxic effects of adriamycin in **macaques.**

Various studies were performed by the group of Hoit and Walsh in **baboons** (Hoit et al. 1955a, 1955b, 1997a, 1997b; Khoury et al. 1996). Hoit et al. (1997a) studied the effects of thyroid hormone on cardiac β-adrenergic responsiveness in conscious baboons.

PROCEDURE

Animal Instrumentation

Adult male baboons (*Papio anubis*) weighing 21–30 kg were pre-instrumented for physiological monitoring in a lightly anesthetized, sedated state. Animals were pre-instrumented with a Konigsburg micromanometer and a polyvinyl catheter in the LV apex, miniaturized sonomicrometer pairs (3 MHz, 6 mm) across the LV anteroposterior minor axis, a polyvinyl catheter in the right atrium for central venous access, and pacing wires on the right atrial appendage. Wires and tubes were tunneled subcutaneously into the interscapular area for later use. Postoperative pain was reduced by the use of Buprenex (0.01 mg/kg i.m., q 6 h), and postoperative antibiotic (Monocid 25 mg/kg) was administered for 5 days to reduce the risk of infection. Baseline hemodynamic studies were performed after a minimum of 1 week for postoperative recovery.

Hemodynamic data acquisition and analysis The micromanometers and fluid-filled catheters were calibrated with a mercury manometer. Zero drift of the micromanometer was corrected by matching the LV end-diastolic pressure measured simultaneously through the LV catheter. The fluid-filled LV catheter was connected to a pre-calibrated Statham 23 dB transducer with zero pressure at the level of the mid right atrium. The transit time of ultrasound between the ultrasonic dimension crystals was measured with a multichannel sonomicrometer (Triton Technology) and converted to distance assuming a constant velocity of sound in blood of 1.55 mm/ms.

The analog LV dP/dI signal was obtained on-line by electronic differentiation of the high-fidelity LV pressure signal. τ was derived from the high-fidelity LV pressure tracing by the method of Weiss et al. (1976), which assumes a monoexponential decay of LV pressure to a zero asymptote and has been shown to be directionally equivalent to other mathematical approaches for quantification of isovolumic pressure decay. τ is equal to the time in milliseconds for LV pressure to decay to $1/e$; thus, decreases in τ reflect improved isovolumic ventricular relaxation.

Fractional shortening of the LV minor axis was calculated as (EDD–ESD)/EDD, where EDD is LV end-diastolic dimension and ESD is LV end-systolic dimension. LV end-diastole was defined as the time in which LV dP/dt_{max} increased by $\geq$ 150 mmHg/s for 50 ms, and LV end-systole was defined as the time of the maximum ratio of LV pressure to LV minor-axis dimension. LV volumes were derived from minor-axis diameter (D) measurements: LV volume $= \pi/6(D)^3$.

V_{cf} was calculated as LV fractional shortening divided by LV ejection time; LV ejection time was defined as the time from peak positive to peak negative dP/dt.

Analog signals for high-fidelity and fluid-filled LV pressures, LV short-axis dimension, LV dP/dt, and the ECG were recorded on-line on a Gould multichannel recorder at 25 and 100 mm/s paper speed and digitized through an analog-to-digital board (Dual Control Systems) interfaced to an IBM AT computer at 500 Hz and stored on a floppy disk. Data were analyzed using an algorithm and software developed in our laboratory. Steady-state data were acquired over 5–10 s during spontaneous respiration and averaged.

Experimental Protocols

Hemodynamic studies were performed a minimum of 1 week after instrumentation and were repeated after 22–30 (26.8 ± 2.7) days of thyroid T_4 administration. Animals were tranquilized with Valium (1–5 mg) and ketamine (100 mg), and cholinergic blockade was achieved with atropine (0.4–0.8 mg i.v.); additional ketamine was administered as necessary, to a maximum cumulative dose of 40 mg/kg. Animals were atrially paced at a rate 40% to 50% greater than the control heart rate in order to obtain data at matched heart rates after thyrotoxicosis was produced.

Dobutamine Group

After hemodynamic stability was ensured and baseline data were recorded, intravenous dobutamine was infused at 5-min intervals at upwardly titrated rates of 2.5, 5.0, 7.5, and 10.0 $\mu g \cdot kg^{-1} \cdot min^{-1}$ to examine the effects of β_1-adrenergic stimulation. The dose range of catecholamine for these studies was chosen to alter inotropic and lusitropic states without causing an untoward increase in heart rate. Steady-state hemodynamic measurements were made during minutes 4 and 5 of each infusion period. At each level, the pacemaker was briefly turned off to determine the effect of dobutamine on the heart rate.

Four of the animals in this group were studied with incremental pacing both before and after β-adrenergic blockade with esmolol (0.3 $mg \cdot kg^{-1} \cdot min^{-1}$ i.v.V). The pacing protocol and the results from a larger group of animals studied before β-adrenergic blockade were detailed in a previous report. Briefly, atrial pacing was instituted at a rate above the intrinsic heart rate to avoid competing rhythms and was increased at 0.2-Hz increments until the critical heart rate was achieved. The critical heart rate was defined as the rate at which dP/dt_{max} and τ reached a maximum and minimum, respectively, during progressive increases in heart rate. We showed previously that hyperthyroidism significantly increases the critical heart rates for both dP/dt_{max} and τ.

The EC_{50} of dobutamine for LV dP/dt_{max} was determined by fitting log(dose)-transformed data to a sigmoidal relation with software from Graph Pad.

Terbutaline Group

Additional animals were chronically instrumented so that we could examine the effects of β_2-adrenergic stimulation. One animal died suddenly after receiving thyroid hormone for 20 days. In the remaining three animals, the β_2-adrenergic agonist terbutaline was infused both before and after production of the hyperthyroid state. Incremental doses of terbutaline (15 min/dose) were infused over a dosing range of 25 to 300 $ng \cdot kg^{-1} \cdot min^{-1}$.

Thyroid Function Tests

Thyroid function tests were performed before the baseline experiment in the euthyroid state and before the terminal experiment (within 24 h of the last dose of T_4) in the hyperthyroid state. T_3 radioimmunoassay, T_4, and free T_4 levels were measured at each state.

EVALUATION

Paired mean data were compared by Student's *t*-test. The effects of thyroid status, catecholamine dose, and β-blockade on hemodynamic and dimension variables were examined with repeated-measures ANOVA (SuperAnova, Abacus Concepts). When significant differences were found, group means were compared with contrasts. A value of $P < 0.05$ was considered significant. Unless specified, data are expressed as mean $\pm$ SD.

REFERENCES AND FURTHER READING

Hoit BD, Shao Y, Gabel M, Walsh RA (1995a) Disparate effects of early pressure overload hypertrophy and force-dependent indices of ventricular performance in the conscious baboon. Circulation 91:1213–1220

Hoit BD, Shao Y, Kinoshita A, Gabel M, Husain A, Walsh RA (1995b) Effects of angiotensin II generated by an angiotensin converting enzyme-independent pathway on left ventricular performance in the conscious baboon. J Clin Invest 95:1519–1527

Hoit BD, Khoury SF, Shao Y, Gabel M, Liggett SB, Walsh RA (1997a) Effects of thyroid hormone on cardiac β-adrenergic responsiveness in conscious baboons. Circulation 96:592–598

Hoit BD, Pawlowski-Dam CM, Shao Y, Gabel M, Walsh RA (1997b) The effects of a thyroid hormone analog on left ventricular performance and contractile and calcium cycling proteins in the baboon. Proc Assoc Am Physicians 109:136–145

Hollander W, Prusty S, Kirkpatrick B, Paddok J, Nagraj S (1977) Role of hypertension in ischemic heart disease and cerebral vascular disease in the cynomolgus monkey with coarctation of the aorta. Circ Res 40 [5 Suppl 1]: I70–I80

Khoury SF, Hoit BD, Dave V, Pawlowski-Dahm CM, Shao Y, Gavel M, Periasamy M, Walsh RA (1996) Effects of thyroid hormone on left ventricular performance and regulation of contractile and Ca^{2+}-cycling proteins in the baboon. Circ Res 79:727–735

Sieber SM, Correa P, Young DM, Dalgard DW, Adamson RH (1980) Cardiotoxic and possible leukemogenic effects of adriamycin in nonhuman primates. Pharmacology 20:9–14

Weiss JL, Frederickson JW, Weisfeldt ML.(1976) Hemodynamic determinants of the time course of fall in canine left ventricular pressure. J Clin Invest 58:751–760

A.6.0.10 Cardiac Failure in Other Species

PURPOSE AND RATIONALE

Various species have been used to study experimental cardiac failure.

Breisch et al. (1984) studied the effects of pressure-overload hypertrophy in the left myocardium of young adult **cats**. Hypertrophy was induced by a 90% constriction of the ascending aorta.

Genao et al. (1996) recommended dilated cardiomyopathy in **turkeys** as an animal model for the study of human heart failure.

Do et al. (1997) studied energy metabolism in normal and hypertrophied right ventricle of the **ferret** heart.

Wang et al. (1994) studied Ca^{2+} handling and myofibrillar Ca^{2+} sensitivity in **ferret** cardiac myocytes with pressure-overload hypertrophy.

Bovine hereditary cardiomyopathy was recommended as an animal model of human dilated cardiomyopathy by Eschenhagen et al. (1995).

REFERENCES AND FURTHER READING

Breisch EA, White FC, Bloor CM (1984) Myocardial characteristics of pressure overload hypertrophy. A structural and functional study. Lab Invest 51:333–342

Do E, Baudet S, Verdys M, Touzeau C, Bailly F, Lucas-Héron B, Sagniez M, Rossi A, Noireaud J (1997) Energy metabolism in normal and hypertrophied right ventricle of the ferret heart. J Mol Cell Cardiol 29:1903–1913

Eschenhagen T, Dieterich M, Kluge SH, Magnussen O, Mene U, Muller F, Schmitz W, Scholz H, Weil J, Sent U (1995) Bovine hereditary cardiomyopathy: an animal model of human dilated cardiomyopathy. J Mol Cell Cardiol 27:357–370

Genao A, Seth K, Schmnidt U, Carles M, Gwathmey JK (1996) Dilated cardiomyopathy in turkeys: an animal model for the study of human heart failure. Lab Animal Sci 46:399–404

Wang J, Flemal K, Qiu Z, Ablin L, Grossman W, Morgan JP (1994) Ca^{2+} handling and myofibrillar Ca^{2+} sensitivity in ferret cardiac myocytes with pressure-overload hypertrophy. Am J Physiol 267(3 Pt2):H918–H924

A.6.0.11 Hypertrophy of Cultured Cardiac Cells

PURPOSE AND RATIONALE

Kojima et al. (1994), Komuro et al. (1990, 1991, 1993), Yamazaki et al. (1993, 1994, 1996) described a method to induce hypertrophy of cardiomyocytes by mechanical stress *in vitro*.

PROCEDURE

Primary cultures from cardiomyocytes are prepared from ventricles of 1-day-old neonatal Wistar Kyoto rats. According to the method of Simpson and Savion (1982), the cultures are treated for 3 days with 0.1 mM bromodeoxyuridine to suppress proliferation of nonmyocardial cells. Elastic culture dishes ($2 \times 4 \times 1$ cm) are made by vulcanizing liquid silicone rubber consisting of methylvinyl polysiloxane and dimethyl hydrogen silicone resin using platinum as a catalyst. The bottom of the disc is 1-mm thick, and it is highly transparent because of no inorganic filler in either component. Cells are plated in a field density of 1×10^5 cells/cm^2 in culture medium consisting of Dulbecco's modified Eagle's medium with 10% fetal bovine serum. Mechanical stress on cardiac cells is applied by gently pulling and hanging the dish on pegs. A 10% change in length of the dish results in an almost identical change in the length of the cell along a single axis (Kimuro et al. 1990). Cardiocytes are stretched by 5%, 10%, or 20%. Drugs, e. g., an angiotensin-II receptor antagonist, are added 30 min before stretch.

For protein analysis, the silicone dishes are stretched for 24 h after 2 days of serum starvation and [^{3}H]phenylalanine (1 µCi/ml) is added for 60 min. At the end of each stress, the cells are rapidly rinsed four times with ice-cold phosphate-buffered saline and incubated for 20 min on ice with 1 ml of 5% trichloroacetic acid. The total trichloroacetic acid-insoluble radioactivity in each dish is determined by liquid scintillation counting.

For determination of mitogen-activated protein kinase, cardiomyocytes are lysed on ice and centrifuged. Aliquots of the supernatants of myocyte extracts are incubated in kinase buffer (25 mM/l Tris-HCl, pH 7.4, 10 mM/l $MgCl_2$, 1 mM/l dithiothreitol, 40 µM/l APT, 2 µCi [γ-^{32}P]ATP, 2 µM/l protein kinase inhibitor peptide, and 0.5 mM/l EGTA) and substrates (25 µg myelin basic protein). The reaction is stopped by adding stopping solution containing 0.6% HCl, 1 mM/l ATP, and 1% bovine serum albumin. Aliquots of the supernatant are spotted on P81 paper (Whatman), washed in 0.5% phosphoric acid, dried and counted.

For determination of*c-fos mRNA*, Northern blot analysis is performed.

EVALUATION

Values are expressed as mean ± SEM. Comparisons between groups are made by one-way ANOVA followed by Dunnett's modified *t*-test.

CRITICAL ASSESSMENT OF THE METHOD

The interesting approach to induce hypertrophy of cardiac cells *in vitro* has been used predominantly by one research group. Confirmation by other research groups including modifications of the mechanical procedures seems to be necessary.

REFERENCES AND FURTHER READING

Kojima M, Shiojima I, Yamazaki T, Komuro I, Yunzeng Z, Ying W, Mizuno T, Ueki K, Tobe K, Kadowaki T, Nagai R, Yazaki Y (1994) Angiotensin II receptor antagonist TCV-116 induces regression of hypertensive left ventricular hypertrophy *in vivo* and inhibits the intercellular signaling pathway of stretch-mediated cardiomyocyte hypertrophy *in vitro*. Circulation 89:2204–2211

Komuro I, Yazaki Y (1993) Control of cardiac gene expression by mechanical stress. Annu Rev Physiol 55:55–75

Komuro I, Kaida T, Shibazaki Y, Kurabayashi M, Katoh Y, Hoh E, Takaku F, Yazaki Y (1990) Stretching cardiac myocytes stimulates protooncogene expression. J Biol Chem 265:3595–3598

Komuro I, Katoh Y, Kaida T, Shibazaki Y, Kurabayashi M, Hoh E, Takaku F, Yazaki Y (1991) Mechanical loading stimulates cell hypertrophy and specific gene expression in cultured rat cardiac myocytes. J Biol Chem 266:1265–1268

Simpson P, Savion A (1982) Differentiation of rat myocytes in single cell cultures with and without proliferating nonmyocardial cells. Circ Res 50:101–116

Yamazaki T, Tobe K, Hoh E, Maemura K, Kaida T, Komuro I, Tamamoto H, Kadowaki T, Nagai R, Yazaki Y (1993) Mechanical loading activates mitogen-activated protein kinase and S6 peptide kinase in cultured cardiac myocytes. J Biol Chem 268:12069–12076

Yamazaki T, Komuro I, Shiojima I, Mizuno T, Nagai R, Yazaki Y (1994) *In vitro* methods to study hypertrophy of cardiac cells. J Pharmacol Toxicol Meth 32:19–23

Yamazaki T, Komuro I, Yazaki Y (1996) Molecular aspects of mechanical stress-induced hypertrophy. Mol Cell Biochem 163/164:197–201

A.7 Positive Inotropic Activity (Cardiac Glycosides)

A.7.0.1 General Considerations

Biological standardization of cardiac glycosides was necessary as long as the drugs used in therapy were plant extracts or mixtures of various glycosides. They were standardized in units of an international standard. Some of the pharmacological methods used for these purposes and adopted by many pharmacopoeias have nowadays *historical interest* only. This holds true for the frog method and the pigeon method (Burn et al. 1950).

Particularly, the **frog method** was used for standardization. The method adopted by the U.S Pharmacopoeia X was the 1 h test. Healthy frogs (*Rana pipiens*) weighing 20–30 g were selected from the cold storage room. One hour before assay, their weight was recorded and they were placed in wire cages with a water depth of 1 cm. The doses of digitalis were calculated so that they approximated 0.015 ml/g body weight. Injections were made into the ventral lymph sac. One hour later, the animals were pithed and the heart removed and examined. Systolic arrest of the ventricle and widely dilated atrium indicated the typical result. Calculations of activity in terms of International Units were made from the percentage of dead animals in the test group versus those in the group receiving the international standard.

The **pigeon method** introduced by Hanzlik (1929) and adopted by USP XVII depends on the observation that intravenously injected cardiac glycosides have an emetic action in pigeons. In the original test, adult pigeons weighing 300–400 g are injected with a solution of the cardiac glycoside into a suitable wing vein in the axillary region. Vomiting occurring within 15 min is regarded as positive result. Two doses of test solution and standard are injected and percentage of vomiting pigeons registered. This 4 point assay allows calculation of ED_{50} values and of the potency ratio compared with the standard.

Modifications of other methods, such as the **cat method** introduced by Hatcher and Brody (1910) and described in detail by Lind van Wijngarden (1926), the **guinea pig method** described by Knaffl-Lenz (1926) and the **isolated cat papillary muscle** method introduced by Catell and Gold (1938) still being used for evaluation of synthetic cardioglycosides and other positive inotropic compounds are referenced in detail below.

Surveys on the evaluation of cardiac glycosides have been given by Bahrmann and Greef (1981), for the use of the isolated papillary muscle by Reiter (1981) and for other isolated heart preparations by Greef and Hafner (1981). Moreover, the influence on Na^+/K^+-ATPase, an *in vitro* model specific for cardiac glycosides (Gundert-Remy and Weber 1981), is described.

The mechanisms of action have been reviewed by Scholz (1984) and Grupp (1987).

Analogous to antiarrhythmic agents, Feldmann (1993) proposed a classification system that categorizes inotropic agents according to their supposed mode of action:

Class I: Inotropic agents that increase intracellular cyloAMP, including β-adrenergic agonists and phosphodiesterase inhibitors,

Class II: Inotropic agents affecting sarcolemmal ion pumps and channels, in particular cardiac glycosides inhibiting Na^+/K^+-ATPase,

Class III: Agents that modulate intracellular calcium mechanisms (no therapeutic inotropic agents in this kind yet available),

Class IV: Inotropic agents having multiple mechanisms of action

REFERENCES AND FURTHER READING

Bahrmann H, Greeff K (1981) Evaluation of cardiac glycosides in the intact animal. Handbook of Experimental Pharmacology 56/I:118–152, Springer, Berlin, Heidelberg, New York

Burn JH, Finney DJ, Goodwin LG (1950) Digitalis, strophanthus, and squill. In: Biological Standardization, Chapter XIII, pp 294–310, Oxford University Press, London, New York, Toronto

Cattell M, Gold H (1938) Influence of digitalis glycosides on the force of contraction of mammalian cardiac muscle. J Pharmacol Exp Ther 62:116–125

Di Palma JR (1964) Animal techniques for evaluating digitalis and its derivatives. In: Nodine JH, Siegler PE (eds) Animal and Clinical Pharmacologic Techniques in Drug Evaluation. Chapter 15, pp 154–159, Year Book Medical Publishers, Inc., Chicago
Feldman AM (1993) Classification of positive inotropic agents. J Am Coll Cardiol 22:1223–1227
Greef K (1963) Zur Pharmakologie der herzwirksamen Glykoside. Klin Physiol 1:340–370
Greef K, Hafner D (1981) Evaluation of cardiac glycosides in isolated heart preparations other than papillary muscle. Handbook of Experimental Pharmacology 56/I:161–184. Springer, Berlin, Heidelberg, New York
Grupp G (1987) Selective updates on mechanisms of action of positive inotropic agents. Mol Cell Biochem 76:97–112
Gundert-Remy U, Weber E (1981) ATPase for the determination of cardiac glycosides. Handbook of Experimental Pharmacology 56/I:83–94. Springer, Berlin, Heidelberg, New York
Hanzlik JP (1929) New method of estimating the potency of digitalis in pigeons: *Pigeon emesis*. J Pharmacol Exp Ther 35:363–391
Hatcher RA, Brody JG (1910) The biological standardization of drugs. Am J Pharm 82:360–372
Knaffl-Lenz E (1926) The physiological assay of preparations of digitalis. J Pharmacol Exp Ther 29:407–425
Lind van Wijngaarden C de (1926) Untersuchungen über die Wirkungsstärke von Digitalispräparaten. II. Mitteilung: Über die Genauigkeit der Dosiseichung an der Katze. Arch exp Path Pharmak 113:40–58
Reiter M (1981) The use of the isolated papillary muscle for the evaluation of positive inotropic effects of cardioactive steroids. Handbook of Experimental Pharmacology 56/I:153–159. Springer, Berlin, Heidelberg, New York
Scholz H (1984) Inotropic drugs and their mechanisms of action. J Am Coll Cardiol 4:389–397

A.7.1
In Vitro Tests

A.7.1.1
Ouabain Binding

PURPOSE AND RATIONALE

Cardiac glycosides can be characterized by their binding kinetics (association process, equilibrium binding, and dissociation process) on the ouabain receptor.

PROCEDURE

Heart sarcolemma preparations are obtained from rat or dog heart. From a canine heart or from rat hearts submitted to coronary perfusion myocytes are isolated by collagenase digestion. The isolated membrane fractions consist mainly of myocyte sarcolemma. [^{3}H]ouabain with a specific radioactivity of about 20 Ci/mmol is incubated with ligands to be tested in 10 ml of binding medium consisting of 1 mM $MgCl_2$, 1 mM inorganic phosphate, and 50 mM Tris-HCl, pH 7.4 at 37°C for 10 min.

Association process: After temperature equilibration in the presence of either 10 or 100 nM [^{3}H]ouabain, 200 µg of membrane preparation are added to initiate the reaction. At various times, 4.5 ml are removed and rapidly filtered.

Equilibrium binding: At the end of the temperature equilibration carried out in the presence of increasing concentrations of [^{3}H]ouabain ranging from 10 nM to 3 µM, 40 µg of membranes are added. After 30 min, duplicate aliquots of 4.5 ml are removed and filtered.

Dissociation process: Once equilibrium has been achieved under the experimental conditions used to study association, 10 ml of prewarmed Mg^{2+} plus P_i Tris-HCl solution supplemented with 0.2 mM unlabeled ouabain are added to initiate dissociation of [^{3}H]ouabain. At various times, aliquots of 0.9 ml are removed and rapidly filtered.

All aliquots are filtered under vacuum on HAWP Millipore filters (0.45 µm) and rinsed three times with 4 ml of ice-cold buffer. The radioactivity bound to the filters and the specific binding measurements are determined.

EVALUATION

Kinetic parameters for the association and the dissociation process are calculated. The results of equilibrium binding are analyzed by Scatchard plots.

REFERENCES AND FURTHER READING

Erdmann E, Schoner W (1973) Ouabain-receptor interactions in (Na^++K^+)-ATPase preparations from different tissues and species. Determination of kinetic constants and dissociation constants. Biochim Biophys Acta 307:386–398
Erdmann E, Schoner W (1974) Ouabain-receptor interactions in (Na^++K^+)-ATPase preparations. IV. The molecular structure of different cardioactive steroids and other substances and their affinity to the glycoside receptor. Naunyn Schmiedeberg's Arch Pharmacol 283:335–356
Erdmann E, Philipp G, Scholz H (1980) Cardiac glycoside receptor, (Na^++K^+)-ATPase activity and force of contraction in rat heart. Biochem Pharmacol 29:3219–3229
Lelievre LG, Charlemagne D, Mouas C, Swynghedauw B (1986) Respective involvements of high- and low-affinity digitalis receptors in the inotropic response of isolated rat heart to ouabain. Biochem Pharmacol 35:3449–3455
Maixent JM, Charlemagne D, de la Chapelle B, Lelievre LG (1987) Two Na,K-ATPase isoenzymes in canine cardiac myocytes. Molecular basis of inotropic and toxic effects of digitalis. J Biol Chem 262:6842–6848
Maixent JM, Gerbi A, Berrebi-Bertrand I, Correa PE, Genain G, Baggioni A (1993) Cordil reversibly inhibits the Na,K-ATPase from outside the cell membrane. Role of K-dependent dephosphorylation. J Receptor Res 13:1083–1092

A.7.1.2
Influence on Na^+/K^+ ATPase

PURPOSE AND RATIONALE

The enzyme Na^+/K^+ ATPase is the transport system for Na^+ and K^+ in the cell membranes. The membrane

bound enzyme couples ATP hydrolysis to the translocation of Na^+ and K^+ ions across the plasma membrane through a series of conformational transitions between the E_1 and E_2 states of the enzyme. The enzyme is a heterodimer consisting of a catalytic subunit (110 kDa) associated with a glycosylated β subunit (55 kDa). Three alpha (α_1, α_2, α_3) subunits have been identified by cDNA cloning. In the heart, enzyme Na^+/K^+ ATPase is the target of the positive inotropic glycosides. Therefore, it is of interest for the characterization of positive inotropic compounds. The test is based on the determination of phosphate generated from ATP under special conditions. Inhibition of bovine cerebral Na^+/K^+ ATPase prepared according to Schoner et al. (1967) is measured after addition of various concentrations of the test compound compared with those of the standard (Erdmann et al. 1980).

PROCEDURE

Solutions

1.00 ml 133 mM imidazole pH 7.3
0.04 ml 160 mM $MgCl_2$
0.02 ml DPNH (10 mg/ml)
0.04 ml 310 mM NH_4Cl
0.04 ml 100 mM ATP
0.02 ml 40 mM phosphoenol-pyruvate
0.05 ml pyruvate-kinase (1 mg/ml = 150 U/ml)
0.04 ml lactate-dehydrogenase
(0.5 mg/ml = 180 U/ml)
0.20 ml 1 M NaCl
0.01–0.02 ml bovine cerebral ATPase (depending on activity of the enzyme) up to 2.0 ml distilled water

Test

The enzyme activity is started by addition of the ATP solution at 37°C. After 4 min the inhibitor (various concentrations of the cardiac glycoside) is added. Na^+/K^+ ATPase activity is measured by a coupled optical assay. The reaction is continuously recorded and corrected for Mg^{2+}-activated ATPase by inhibition of Na^+/K^+ ATPase with 10^{-3} M ouabain.

EVALUATION

Inhibition of ATPase is measured after addition of various concentrations of the test compound. Dose-response curves are established and compared with the standard (k-strophanthin). Potency ratios can be calculated.

MODIFICATIONS OF THE METHOD

Brooker and Jelliffe (1972) and Marcus et al. (1975) described an *in vitro* assay based on displacement of radiolabeled ouabain bound to ATPase by various glycosides. Another method is based on the inhibition of rubidium uptake into erythrocytes (Lowenstein 1965; Belz 1981).

Erdmann et al. (1980) prepared (Na^++K^+)-ATPase-containing cardiac cell membranes from rat hearts.

Maixent et al. (1987, 1991) described two Na,K-ATPase isoenzymes in canine cardiac myocytes as the molecular basis of inotropic and toxic effects of digitalis.

The effect of ouabain on Na^+/K^+ATPase activity in cells of the human rhabdomyosarcoma cell line TE671 was studied by Miller et al. (1993) with a special equipment, the microphysiometer (McConnell et al. 1992).

CRITICAL ASSESSMENT OF THE METHOD

The *in vitro* methods being used for determinations of plasma levels of glycosides (Maixent et al. 1995) have been largely substituted by radioimmunoassays specific for individual glycosides. Nevertheless, the inhibition of Na^+/K^+ ATPase can be used as an indicator of activity of new semisynthetic cardiac glycosides.

REFERENCES AND FURTHER READING

Anner B, Moosmayer M (1974) Rapid determination of inorganic phosphate in biological systems by a highly sensitive photometric method. Analyt Biochem 65:305–309

Akera T, Brody T (1978) The role of Na^+, K^+-ATPase in the inotropic action of digitalis. Pharmacol Rev 29:197–201

Belz GG (1981) Rubidium uptake in erythrocytes. Handbook of Experimental Pharmacology 56. Springer, Berlin Heidelberg New York, pp 95–113

Borsch-Galetke E, Dransfeld H, Greef K (1972) Specific activity of Na^++K^+- activated ATPase in rats and guinea pigs with hypoadrenalism. Naunyn-Schmiedeberg's Arch Pharmacol 274:74–80

Brooker G, Jelliffe RW (1972) Serum cardiac glycoside assay based upon displacement of ^{3}H-ouabain from Na-K ATPase. Circulation 45:20–36

Burnett GH, Conklin RL (1968) The enzymatic assay of plasma digitoxin levels. J Lab Clin Med 71:1040–1049

Charlemagne D, Maixent JM, Preteseille M, Lelievre LG (1986) Ouabain binding sites and Na^+,K^+)-ATPase activity in rat cardiac hypertrophy. Expression of the neonatal forms. J Biol Chem 261:185–189

Erdmann E, Philipp G, Scholz H (1980) Cardiac glycoside receptor, (Na^++K^+)-ATPase activity and force of contraction in rat heart. Biochem Pharmacol 29:3219–3229

Gundert-Remy U, Weber E (1981) ATPase for the determination of cardiac glycosides. Handbook of Experimental Pharmacology 56/I:83–94. Springer, Berlin, Heidelberg, New York

Lelievre LG, Maixent G, Lorente P, Mouas C, Charlemagne D, Swynghedauw B (1986) Prolonged responsiveness to ouabain in hypertrophied rat heart: physiological and biochemical evidence. Am J Physiol 250:H923–H931

Lindner E, Schöne HH (1972) Änderungen der Wirkungsdauer und Wirkungsstärke von Herzglykosiden durch Abwandlungen der Zucker. Arzneim Forsch/Drug Res 22:428–435
Lindner E, v. Reitzenstein G, Schöne HH (1979) Das 14,15-β-oxido-Analoge des Proscillaridins (HOE 040) Arzneim Forsch/Drug Res 29:221–226
Lowenstein JM (1965) A method for measuring plasma levels of digitalis glycosides. Circulation 31:228–233
Maixent JM, Charlemagne D, de la Chapelle B, Lelievre LG (1987) Two Na,K-ATPase isoenzymes in canine cardiac myocytes. Molecular basis of inotropic and toxic effects of digitalis. J Biol Chem 262:6842–6848
Maixent JM, Fénard S, Kawamoto RM (1991) Tissue localization of Na,K-ATPase isoenzymes by determination of their profile of inhibition with ouabain, digoxin, digitoxigenin and LND 796, a new aminosteroid cardiotonic. J Receptor Res 11:687–698
Maixent JM, Gerbi A, Berrebi-Bertrand I, Correa PE, Genain G, Baggioni A (1993) Cordil reversibly inhibits the Na,K-ATPase from outside the cell membrane. Role of K-dependent dephosphorylation. J Receptor Res 13:1083–1092
Maixent JM, Gerbi A, Barbey O, Fenard S, Kawamoto RM, Baggioni A (1995) Relation of plasma concentrations to positive inotropic effect of intravenous administration of cordil in dogs. Pharm Pharmacol Lett 1:1–4
Mansier P, Lelievre LG (1982) Ca^{2+}-free perfusion of rat heart reveals a $(Na^+ + K^+)$ATPase form highly sensitive to ouabain. Nature 300:535–537
Marcus FI, Ryan JN, Stafford MG (1975) The reactivity of derivatives of digoxin and digitoxin as measured by the Na-K-ATPase displacement assay and by radioimmunoassay. J Lab Clin Med 85:610–620
McConnell HM, Owicki JC, Parce JW, Miller DL, Baxter GT, Wada HG, Pitchford S (1992) The Cytosensor microphysiometer. Science 257:1906–1912
Miller DL, Olson JC, Parce JW, Owicki JC (1993) Cholinergic stimulation of the Na^+/K^+ adenosine triphosphatase as revealed by microphysiometry. Biophys J 64:813–823
Noel F, Godfraind T (1984) Heterogeneity of ouabain specific binding sites and $(Na^+ + K^+)$-ATPase inhibition in microsomes from rat heart. Biochem Pharmacol 33:47–53
Schoner W, v. Illberg C, Kramer R, Seubert W (1967) On the mechanism of Na^+- and K^+- stimulated hydrolysis of adenosine triphosphate. Eur J Biochem 1:334–343
Schwarz A, Nagano K, Nakao M, Lindenmayer GE, Allen JC, Matsoi HM (1971) The sodium- and potassium activated adenosine-triphosphatase system. In: Schwartz (ed) Methods in pharmacology Vol 1, Appleton-Century-Crofts, Meredith Corporation, New York, pp 361–388
Skou JC, Esmann M (1992) The Na_2K-ATPase. J Bioenerg Biomembr 24:249–261
Thomas R, Allen J, Pitts BJR, Schwartz A (1974) Cardenolide analogs. An explanation for the unusual properties of AY 22241. Eur J Pharmacol 53:227–237

A.7.2
Tests in Isolated Tissues and Organs

A.7.2.1
Isolated Cat Papillary Muscle

PURPOSE AND RATIONALE

Isolated cardiac tissue has been chosen to study the decrease of performance after prolonged electrical stimulation and during restoration of force under the influence of cardiac glycosides. Cattell and Gold (1938) described a method using cat papillary muscle.

PROCEDURE

Cats of either sex weighing 2.5–3 kg are used. The animal is anesthetized with ether and the thorax is opened rapidly. The heart is removed and a papillary muscle from the right ventricle is isolated and fixed in an organ bath containing oxygenated Ringer's solution at 36°C. One end of the muscle is tied to an tissue holder and the other one to a strain gauge. The muscle is stimulated electrically with 4–6 V, 2 ms duration and a rate of 30/min. The contractions are recorded on a polygraph. After 1 h, the muscle begins to fail and the force of contraction diminishes to a fraction of control. At this point, the cardiac glycoside is added to the bath, restoring the contractile force to levels approaching control. The standard dose is 300 ng/ml ouabain. The potency of natural and semisynthetic glycosides can be determined with this method. Catecholamines, like adrenaline (10 ng/ml) or isoprenaline (10 ng/ml), are active as well.

EVALUATION

The increase of contractile force is calculated as percentage of the predose level. Dose-response curves can be established using various doses.

CRITICAL ASSESSMENT OF THE METHOD

The use of isolated papillary muscle strips can be recommended for evaluation of inotropic compounds of various chemical classes.

MODIFICATIONS OF THE METHOD

Instead of cat papillary muscle the isolated left atrium of guinea pigs can be used (see Sect. A.1.2.6). For testing cardiac glycosides, the calcium content in the Ringer solution is reduced to 50%.

Andersom (1983) compared responses of guinea pig paced left atria to various positive inotropic agents at two different calcium concentrations (1.25 and 2.50 mM). Consistently good results were obtained at the lower calcium concentration with isoproterenol, ouabain, amrinone, and 3-isobutyl-1-methylxanthine.

Böhm et al. (1989) studied positive inotropic substances like isoprenaline and milrinone in isolated cardiac preparations from different sources. They used isolated papillary muscles from Wistar–Kyoto rats and from spontaneously hypertensive rats, but also human papillary muscle strips from patients with moderate

heart failure (NYHA II–III) and compared the effects with papillary muscle strips from patients with severe heart failure (NYHA IV). They recommended that new positive inotropic agents should be screened in human myocardial tissue from patients with heart failure.

Labow et al. (1991) recommended a human atrial trabecular preparation for evaluation of inotropic substances.

Böhm et al. (1989) tested positive inotropic agents in isolated cardiac preparations from different sources, e. g., human papillary muscle strips from patients with severe heart failure (NYHA IV), human papillary muscle strips from patients with moderate heart failure (NYHA II–III), human atrial trabeculae, isolated papillary muscles from Wistar–Kyoto rats, and isolated papillary muscles from spontaneous hypertensive rats. They suggested that positive inotropic effects should be screened in isolated myocardium from patients with heart failure.

REFERENCES AND FURTHER READING

Anderson WG (1983) An improved model for assessment of positive inotropic activity *in vitro*. Drug Dev Res 3:443–451

Böhm M, Diet F, Pieske B, Erdmann E (1989) Screening of positive inotropic agents in isolated cardiac preparations from different sources. J Pharmacol Meth 21:33–44

Brown TG, Lands AM (1964) Cardiovascular activity of sympathomimetic amines. In: Laurence DR, Bacharach AL (eds) Pharmacometrics Vol 1, Academic Press New York, pp 353–368

Cattell M, Gold H (1938) Influence of digitalis glycosides on the force of contraction of mammalian cardiac muscle. J Pharmacol Exp Ther 62:116–125

Di Palma JR (1964) Animal techniques for evaluating digitalis and its derivatives. In: Nodine JH, Siegler PE (eds) Animal and Clinical Pharmacologic Techniques in Drug Evaluation. Chapter 15, Year Book Medical Publishers, Inc., Chicago, pp 154–159

Grupp IL, Grupp G (1984) Isolated heart preparations perfused or superfused with balanced salt solutions. In: Schwartz A (ed) Methods in Pharmacology, Vol 5: Myocardial Biology. pp 111–128. Plenum Press, New York and London

Labow RS, Desjardins S, Keon WJ (1991) Validation of a human atrial trabecular preparation for evaluation of inotropic substances. J Pharm Meth 26:257–268

Rajagopalan R, Ghate AV, Subbarayan P, Linz W, Schoelkens BA (1993) Cardiotonic activity of the water soluble forskoline derivative 8,13-epoxy-6β-(piperidinoacetoxy)-1α,7β,9α-trihydroxy-labd-14-en-11-one. Arzneim Forsch/Drug Res 43:313–319

Reiter M (1981) The use of the isolated papillary muscle for the evaluation of positive inotropic effects of cardioactive steroids. Handbook of Experimental Pharmacology 56/I:153–159. Springer, Berlin, Heidelberg, New York

Turner RA (1965) Cardiotonic agents. In: Screening Methods in Pharmacology. pp 203–209. Academic Press, New York, London

A.7.2.2 Isolated Hamster Cardiomyopathic Heart

PURPOSE AND RATIONALE

Special strains of Syrian hamsters develop cardiomyopathy. These animals can be used for evaluation of cardiotonic drugs (see Sect. A.6.0.4).

PROCEDURE

Hamsters with cardiomyopathy (Bio 14/6) at the age of 50 weeks are used. Controls are normal Syrian hamsters (FIB hybrids) at the same age. The animals are pretreated with heparin (5 mg/kg i.p.) and 20 min later the heart is prepared according the method of Langendorff and perfused with heart Ringer solution under 75 mm H_2O hydrostatic pressure. The preparation is allowed to equilibrate in the isolated state for 60 min at 32°C with a diastolic preload of 1.5 g. The force of contractions is recorded isometrically by a strain gauge transducer on a polygraph, e. g., Heliscriptor He 19 recorder (Hellige GmbH, Freiburg, Germany). From these signals, the heart rate is measured by a chronometer. The coronary flow is measured by an electromagnetic flowmeter. Compounds are injected via the aortic cannula into the inflowing heart-Ringer solution.

EVALUATION

The contractile force and the coronary flow in hearts from diseased and normal animals is registered before and after application of the test drugs. Mean values and standard deviation are calculated before and after drug application and statistically compared using Student's *t*-test.

MODIFICATION OF THE METHOD

Jasmin et al. (1979) showed after prolonged *in vivo* administration beneficial effects of a variety of cardiovascular drugs, including verapamil, prenylamine, dibenamine and propranolol.

After chronic administration (4 or 12 weeks subcutaneously), Weishaar et al. (1987) found beneficial effects of the calcium channel blocker diltiazem, but not by the administration of digitalis.

In contrast, in the experiments of Ottenweller et al. (1987) hamsters treated orally with digoxin survived and showed significant amelioration of the pathological syndrome of heart failure.

REFERENCES AND FURTHER READING

Jasmin G, Solymoss B, Proscheck L (1979) Therapeutic trials in hamster dystrophy. Ann NY Acad Sci 317:338–348

Ottenweller JE, Tapp WN, Natelson BH (1987) The effect of chronic digitalis therapy on the course of heart failure and on endocrine function in cardiomyopathic hamsters. Res Commun Chem Pathol Pharmacol 58:413–416

Rajagopalan R, Ghate AV, Subbarayan P, Linz W, Schoelkens BA (1993) Cardiotonic activity of the water soluble forskoline derivative 8,13-epoxy-6β-(piperidinoacetoxy)-1α,7β,9α-trihydroxy-labd-14-en-11-one. Arzneim Forsch/Drug Res 43(I) 313–319

Weishaar RE, Burrows SD, Kim SN, Kobylarz-Singer DC, Andrews LK, Quade MM, Overhiser R, Kaplan HR (1987) Protection of the failing heart: comparative effects of chronic administration of digitalis and diltiazem on myocardial metabolism in the cardiomyopathic hamster. J Appl Cardiol 2:339–360

A.7.2.3
Potassium Loss from the Isolated Guinea Pig Heart

PURPOSE AND RATIONALE

Cardiac glycosides induce a net loss of potassium from cardiac tissue due to their inhibition of the Na^+/K^+ ATPase. Therefore, potassium is increased in the effluent of the isolated guinea pig heart. This phenomenon can be used as parameter for the activity of digitalis-like compounds (Lindner and Hajdu 1968).

PROCEDURE

The isolated heart of guinea pigs according to LANGENDORFF is prepared as described in Sect. A.3.1.1. The coronary outflow is measured by counting the drops of the effluent by a photocell. The effluent is collected in a funnel with a thin upwards shaped outlet allowing to withdraw small fluid samples for analysis by a flame photometer. A pump attached to a 4-way valve changes the samples to the flame photometer every 15 s in the following sequence: effluent Tyrode-solution from the heart, distilled water, Tyrode-solution used for perfusion, distilled water. The potassium content of affluent and effluent Tyrode-solution is compared and registered on a Varian-recorder. The difference is attributed to the potassium outflow from the heart. The dose-response curve is flat in the therapeutic range, much steeper in the toxic range.

EVALUATION

The following parameters are recorded and calculated:

- coronary flow [ml/min]
- contractile force
- potassium loss [mVal/min]

CRITICAL ASSESSMENT OF THE METHOD

A good correlation was found between the measured potassium loss and the positive inotropic effect of cardiac glycosides. The method is suitable for the quick determination of efficacy of digitalis-like substances and facilitates the discrimination from other positive inotropic compounds like adrenaline.

REFERENCES AND FURTHER READING

Greef K, Hafner D (1981) Evaluation of cardiac glycosides in isolated heart preparations other than papillary muscle. Handbook of Experimental Pharmacology 56/I:161–184. Springer, Berlin, Heidelberg, New York

Lindner E, Hajdu P (1968) Die fortlaufende Messung des Kaliumverlustes des isolierten Herzens zur Bestimmung der Wirkungsstärke digitalisartiger Körper. Arch Int Pharmacodyn 175:365–372

A.7.3
In Vivo Tests

A.7.3.1
Cardiac Toxicity in Cats (Hatcher's Method)

PURPOSE AND RATIONALE

The purpose of the method, originally introduced by Hatcher and Brody (1910) and described in detail by Lind van Wijingaarden (1926), was to establish "cat units" for cardiac glycoside preparations. Hatcher and Brody defined "the cat unit as the amount of crystalline ouabain which is fatal within about ninety minutes to a kilogram of a cat when the drug in injected slowly and almost continuously into the femoral vein". Time to cardiac arrest after intravenous infusion of a solution with defined concentration of the standard was used as reference and the unknown solution of the test preparation compared with the standard. The method can be used for testing natural and semisynthetic glycosides.

PROCEDURE

Cats of either sex weighing 2–3.5 kg are temporarily anesthetized with ether. Anesthesia is maintained with 70 mg/kg chloralose given intravenously. The animal is fixed on its legs on a heated operating table. Tracheostomy is performed and a tracheal cannula is inserted. ECG is recorded from lead II. Then, intravenous infusion of the test solution is started. The endpoint is cardiac arrest which should be reached within 30–60 min by proper adjustment of the concentration of the infused solution.

MODIFICATIONS OF THE METHOD

Hatcher's original method has been modified by many authors. The method using **guinea pigs**, introduced by Knaffl-Lenz (1926) is in its essentials similar to the cat method.

Guinea pigs weighing 400–600 g are anesthetized with urethane (1.75 g/kg i.m.) The animal is secured

on a operating table and the trachea is cannulated. The jugular vein is cannulated for infusion of the test preparation. Cardiac arrest is recorded from ECG lead II.

Dogs and guinea pigs were used by Dörner (1955).

REFERENCES AND FURTHER READING

Bahrmann H, Greeff K (1981) Evaluation of cardiac glycosides in the intact animal. Handbook of Experimental Pharmacology 56/I: 118–152, Springer, Berlin, Heidelberg, New York

Burn JH, Finney DJ, Goodwin LG (1950) Digitalis, strophanthus, and squill. In: Biological Standardization, Chapter XIII, pp 294–310, Oxford University Press, London, New York, Toronto

Dörner J (1955) Zur Frage der Beziehungen zwischen Strophanthintoxicität und Größe der Coronardurchblutung. Arch exper Path Pharmakol 226:152–162

Hatcher RA, Brody JG (1910) The biological standardization of drugs. Am J Pharm 82:360–372

Knaffl-Lenz E (1926) The physiological assay of preparations of digitalis. J Pharmacol Exp Ther 29:407–425

Lind van Wijngaarden C de (1926) Untersuchungen über die Wirkungsstärke von Digitalispräparaten. II. Mitteilung: Über die Genauigkeit der Dosiseichung an der Katze. Arch exp Path Pharmak 113:40–58

A.7.3.2 Decay Rate and Enteral Absorption Rate of Cardiac Glycosides

PURPOSE AND RATIONALE

The basic principle of Hatcher's or Knaffl-Lenz's method is suitable to determine decay rates of cardiac glycosides. The decay of efficacy can by due to excretion or metabolic degradation of the glycoside.

PROCEDURE

Beagle dogs of either sex weighing 8–20 kg are anesthetized with 35 mg/kg pentobarbital sodium i.v. The animal is fixed on its legs on a heated operating table. Tracheostomy is performed and a tracheal cannula inserted. The vena femoralis is cannulated for continuous infusion of a defined concentration (µg/kg/min) of the test compound. ECG is recorded from lead II. The signs of first toxic effects, e. g., extra systoles, AV-block) are recorded. At this time, the infusion is terminated and the total dose/kg of the applied glycoside registered. After 4, 8, 12, or 24 h the infusion procedure is repeated. Within this period of time the glycoside administered with the first dose is only partially metabolized or excreted. Therefore, the dose needed for observation of ECG changes during the second infusion will be lower than in the first experiment.

EVALUATION

The dose required in the second experiment for induction of ECG changes is equal to the amount of metabolized or excreted glycoside. This value is expressed as percentage of the amount required in the first experiment and indicates the decay rate of the glycoside. Testing after various time intervals, the decay rate can be visualized graphically and half life times be calculated.

MODIFICATIONS OF THE METHOD

Rhesus monkeys have been used since their response to cardiac glycosides is more similar to that of man than that of dogs (Lindner et al. 1979).

The basic principle of Hatcher's or Knaffl-Lenz's method is also suitable to determine *enteral absorption of cardiac glycosides*. Again, for this purpose dogs are preferred instead of cats or guinea pigs. The dose to induce cardiac arrest is determined in 3–6 dogs. To other dogs, the same test compound is given intraduodenally at a dose below the intravenous lethal dose. Ninety or 180 min afterwards, the intravenous infusion with the same infusion speed and the same concentration of the test compound as in the previous experiments is started and time until cardiac arrest determined. The higher the duodenal resorption of the compound, the lower the dose of the intravenous infusion will be. For evaluation, the intravenous dose needed in the second experimental series (with enteral predosing) is subtracted from the dose of the first series (without enteral predosing) and indicates the amount of absorbed compound. This value is expressed as percentage of the value of the first series and indicates the absorption rate.

The efficacy and safety of a novel Na^+,K^+-ATPase inhibitor has been tested in dogs with propranolol-induced heart failure by Maixent et al. (1992).

REFERENCES AND FURTHER READING

Bahrmann H, Greeff K (1981) Evaluation of cardiac glycosides in the intact animal. Handbook of Experimental Pharmacology 56/I:118–152, Springer, Berlin

Kleemann A, Lindner E, Engel J (1985) Herzglykoside und deren Aglykone. In: Arzneimittel, Fortschritte 1972–1985. pp 213–226. Verlag Chemie, Weinheim, Germany

Lindner E, Schöne HH (1972) Änderungen der Wirkungsdauer und Wirkungsstärke von Herzglykosiden durch Abwandlungen der Zucker. Arzneim Forsch/Drug Res 22:428–435

Lindner E, v. Reitzenstein G, Schöne HH (1979) Das 14,15-β-oxido-Analoge des Proscillaridins (HOE 040) Arzneim Forsch/Drug Res 29:221–226

Maixent JM, Bertrand IB, Lelièvre LG, Fénard S (1992) Efficacy and safety of the novel Na^+,K^+-ATPase inhibitor 20R 14β-amino 3β-rhamnosyl 5β-pregnan 20β-ol in a dog model of heart failure. Arzneim Forsch/Drug Res 42:1301–1305

A.8
Effects on Blood Supply and on Arterial and Venous Tonus

A.8.1
Models for Stroke and Multi-Infarct Cerebral Dysfunction

A.8.1.1
Cerebral Ischemia by Carotid Artery Occlusion in Mongolian Gerbils

PURPOSE AND RATIONALE

The Mongolian gerbil (*Meriones unguiculatus*) is extremely susceptible to carotid occlusion because of the peculiar anatomical occurrence of an incomplete circle of Willis without posterior communicating artery and a frequently rudimentary anterior communicating artery. Clamping of both carotid arteries induces a bilateral temporary brain ischemia (Levine and Sohn 1969; Bosma et al. 1981; Mršulja et al. 1983; Hossmann et al. 1983; Chandler et al. 1985). This pathological animal model allows the simulation of circulatory disturbances in the human brain. The hippocampus is one of the most vulnerable regions of the brain to ischemia and anoxia. The gerbil is known to develop selective neuronal damage in the CA1 sector of the hippocampus following brief periods of forebrain ischemia. This damage differs from conventionally described ischemic neuronal injury because of its slow development (Ito et al. 1975; Kirino 1982; Hossmann et al. 1983). The occlusion time can be varied allowing determination of various parameters, e. g. ischemia induced amnesia (see Sect. F.3.1.8).

PROCEDURE

Male Mongolian gerbils (strain: Hoe GerK jirds) weighing 48–88 g are randomly divided into groups (10–15 animals for each test and control group). Prior to testing, the animals are housed in a climate-controlled environment (21°C) with food and water available ad libitum. Fifteen minutes before surgery, the gerbils receive the test compound by oral or intraperitoneal administration. The control group is treated with vehicle alone.

The exposure of the common carotid arteries is performed under anesthesia with sodium pentobarbital (32 mg/kg i.p.), chloralhydrate (100 mg/kg i.p.) and atropine sulfate (0.8 mg/kg i.p.). The carotid arteries are isolated from surrounding tissue and a loop of unwaxed dental floss is placed around each artery. A 2 cm length of double lumen catheter is passed from the level of carotid artery through the muscle layers of the dorsal surface of the neck. Each end of dental floss is threaded through a separate lumen, leaving a loose loop around the artery. Two days later, occlusion of each artery is produced by gently pulling the dental floss until the artery is completely occluded between the floss and the center wall of the catheter. Heifitz clips are placed on the floss against the exterior end of the tubing to maintain occlusion. After various intervals (5 to 30 min), the clips are removed and circulation is restored.

Complete bilateral occlusion of the arteries is confirmed by behavioral symptoms, i. e., depression of spontaneous motor activity, shallow and rapid respiration, and ptosis. Care is taken to avoid a drop of body temperature during any stage of the experiment. After experimental manipulations, animals are placed on a heating pad until complete recovery of motor activity.

Subjects are placed in individual observation glasses which are kept at a temperature of 29°C. They are observed for neurological symptoms (such as circling behavior, jumping and rolling seizures, opisthotonus, tonic convulsions, etc.) for 90 min.

After various intervals, the gerbils are sacrificed and their brains are removed.

EVALUATION

The following parameters are measured two hours after occlusion:

Degree of brain edema: water content (difference in weight of wet and dry brain)

Content of sodium and potassium. The hemispheres are separated and put on pre-weighted watch glasses to determine the wet weight. Then the hemispheres are dried in an open Petri dish for 2 days at a temperature of 95°C. After cooling off, the dry weight is noted. Sodium and potassium concentrations in the dried brain hemispheres are determined by flame photometry. The Na^+/K^+-ratio is calculated.

For *histological examinations*, the animals are sacrificed at 2 or 4 days after ischemia under ether anesthesia by decapitation. The brains are then removed and frozen in CO_2. Hippocampi are sectioned coronally with a cryostat at –14°C. The section thickness for Nissl and glial fibrillary acid protein (GFAP) staining is 20 µm and for the histochemical localization of calcium 30 µm.

Nissl staining and its quantitative evaluation. The sections are mounted by thawing on glass slides, Nissl

stained, and cover slipped with Permount. In order to standardize the histological procedure and to rule out the possibility that differences in the staining intensity were due to technical inconsistency, slides from control and experimental groups are processed together, stained for 5 min, and differentiated in a series of alcohols for 3 min each. The extent of hippocampal nerve cell damage (as reflected by cell loss and decreased stainability) is assessed by measuring the amount of Nissl-stained material in a predetermined representative region of the CA1 area with the aid of a guided densitometer (Leitz Texture Analysis System). The measuring field is 50 × 500 µm, fitting to the width of the CA1 soma layer (about 40 µm).

Calcium localization. A modification of technique described by Kashiwa and Atkinson (1963) is used for the cytochemical localization of ionic calcium. The principle of the technique is that calcium complexes with a chelating agent producing an insoluble chromophore.

Stock solutions: Two solutions were used: a) glyoxalbis-(2-hydroxyanil) (GBHA), 0.4 g/100 ml absolute ethanol (2 ml 0.4% GBHA); and b) NaOH, 5 g/100 ml distilled water (0.3 ml 5% NaOH).

Staining procedure: First, cryostat sections are placed immediately in cold absolute acetone for rapid fixation for 5 min. Next, floating sections are transferred into 96% alcohol for 5 min and then transferred to staining solution for 3–4 min. Sections are then placed in 96% alcohol and mounted on glass slides. Because of quenching, it is necessary to view and photograph immediately.

GFAP (glial fibrillary acid proteinglial fibrillary acid protein) fluorescencemicroscopy. Following slide mounting, cryostat sections are fixed for 15 min in 3.5% formaldehyde solution in 0.01 M phosphate-buffered saline (PBS). The sections are incubated with mouse primary antibody against GFAP (Boehringer, Mannheim, FRG) for 30 min diluted 1:50 PBS. This antibody shows cross reactions also with GFAP from pigs and rats, indicating low species selectivity (Graber and Kreutzberg, 1986). The sections are rinsed in PBS and incubated to tetramethylrhodamine isothiocyanate (TRITC) specific for mouse immunoglobulin G (T-5393 from Sigma) diluted 1:50 in PBS. Control sections are incubated with PBS instead of primary antibody.

Measurements, expressed as extinction units per measuring field, are taken from three slides of each animal and averaged. Statistical analysis is done by Student's *t*-test.

MODIFICATIONS OF THE METHOD

"Sensitive" gerbils can be selected according to the method of Delbarre et al. (1988). In this method, pupil dilatation is obtained with atropine sulfate (1%) 20 min before anesthesia. Ocular fundus is examined with direct ophthalmoscope (Heine) before ligation and 5 min later. Only animals with an absence of retinal blood flow after ligation are considered as positive.

Using ^{31}P nuclear magnetic resonance spectroscopy, Sasaki et al. (1989) studied energy metabolism of the ischemic brain of gerbils *in vivo*.

An unanesthetized-gerbil model of cerebral ischemia was described by Chandler et al. (1985).

Using microdialysis, adenosine and its metabolites were measured directly in the brain of male gerbils by Dux et al. (1990). Two microdialysis probes (CMA/10, Carnegie Medicine, Sweden) were implanted stereotactically in the brain of the animals, one in the left dorsal hippocampus and one in the right striatum. The fibres were fixed to the cranium using dental wax. The dialysate was collected in 5 min intervals, and the concentrations of adenosine, hypoxanthine and inosine were determined by HPLC (Zetterström et al. 1982; Fredholm et al. 1984).

Kindy et al. (1992) measured glial fibrillary acid protein and vimentine on mRNA level by Northern blot analysis and protein content by immunoblot analysis in the gerbil neocortex, striatum and hippocampus after transient ischemia.

McRae et al. (1994) studied the effect of drug treatment on activated microglial antigens in hippocampal sections after ischemia in gerbils with cerebral fluid from patients with Alzheimer's disease and the amyloid precursor protein.

Nurse and Corbett (1996) found neuroprotection in gerbils with global cerebral ischemia after several days of mild, drug-induced hypothermia. The protection by the AMPA-antagonist NBQX may be due to a decrease in body temperature. A protracted period of subnormal temperature during the postischemic period can obscure the interpretation of preclinical studies.

REFERENCES AND FURTHER READING

Bosma HJ, Paschen W, Hossman KA (1981) Cerebral ischemia in gerbils using a modified vascular occlusion model. In: Meyer JS, Lechner H, Reivich M, Ott EO, Aranibar A (1981) Cerebral Vascular Disease 3, Excerpta Medica, Amsterdam, pp 280–285

Chandler MJ, DeLeo J, Carney JM (1985) An unanesthetized-gerbil model of cerebral ischemia-induced behavioral changes. J Pharmacol Meth 14:137–146

Delbarre G, Delbarre B, Barrau Y (1988) A suitable method to select gerbils with incomplete circle of Willis. Stroke 19:126

DeLeo J, Toth L, Schubert P, Rudolphi K, Kreutzberg GW (1987) Ischemia-induced neuronal cell death, calcium accumulation, and glial response in the hippocampus of the Mongolian gerbil and protection by propentofylline (HWA 285). J Cerebr Blood Flow Metab 7:745–751

Dux E, Fastbo J, Ungerstedt U, Rudolphi K, Fredholm BB (1990) Protective effect of adenosine and a novel xanthine derivative propentofylline on the cell damage after bilateral carotid occlusion in the gerbil hippocampus. Brain Res 516:248–256

Fredholm BB, Dunwiddie TV, Bergman B, Lindström K (1984) Levels of adenosine and adenine nucleotides in slices of rat hippocampus. Brain Res 295:127–136

Graeber MB, Kreutzberg GW (1986) Astrocytes increase in glial fibrillary acidic protein during retrograde changes of facial motor neurons. J Neurocytol 15:363–373

Hossman KA, Mies G, Paschen W, Matsuoka Y, Schuier FJ, Bosma HJ (1983) Experimental infarcts in cats, gerbils and rats. In: Stefanovich V (ed) Stroke: Animal Models, Pergamon Press; Oxford, New York, pp 123–137

Ito M, Spatz M, Walker JT, Klatzo I (1975) Experimental cerebral ischemia in Mongolian gerbils. 1. Light microscopic observations. Acta neuropathol (Berl) 32:209–223

Kashiwa HK, Atkinson WG (1963) The applicability of a new Schiff base glyoxal bis (2-hydroxy-anil), for the cytochemical localization of ionic calcium. J Histochem Cytochem 11:258–264

Kindy MA, Bhat AN, Bhat NR (1992) Transient ischemia stimulates glial fibrillary acid protein and vimentine gene expression in the gerbil neocortex, striatum and hippocampus. Mol Brain Res 13:199–206

Kirono T (1982) Delayed neuronal death in the gerbil hippocampus following ischemia. Brain Res 239:57–69

Levine S, Sohn D (1969) Cerebral ischemia in infant and adult gerbils. Arch Pathol 87:315–317

Lundy EF, Solik BS, Frank RS, Lacy PS, Combs DJ, Zelenok GB, D'Alecy LG (1986) Morphometric evaluation of brain infarcts in rats and gerbils. J Pharmacol Meth 16:201–214

McRae A, Rudolphi KA, Schubert P (1994) Propentofylline depresses amyloid and Alzheimer's CSF antigens after ischemia. Neuro Report 5:1193–1196

Mršulja BB, Micíc DV, Djuricic BM (1983) Gerbil stroke model: an approach to the study of therapeutic aspects of postischemic brain edema. In: Stefanovich V (ed) Stroke: Animal Models, Pergamon Press; Oxford, New York, pp 45–62

Nurse S, Corbett D (1996) Neuroprotection after several days of mild, drug-induced hypothermia. J Cerebr Blood Flow Metab 16:474–480

Rudolphi KA, Keil M, Hinze HJ (1987) Effect of theophylline on ischemically induced hippocampal damage in Mongolian gerbils: A behavioral and histopathological study. J Cerebr Blood Flow Metab 7:74–81

Sasaki M, Naritomi H, Kanashiro M, Nishimura H, Sawada T (1989) Effects of propentofylline on energy metabolism of the ischemic brain studied by *in vivo* ^{31}P nuclear magnetic resonance spectroscopy. Arzneim Forsch/Drug Res 39:886–889

Zetterström T, Vernet L, Ungerstedt U, Tossman U, Jonzon B, Fredholm BB (1982) Purine levels in the intact rat brain. Studies with an implanted hollow fibre. Neurosci Lett 29:111–115

A.8.1.2 Forebrain Ischemia in Rats

PURPOSE AND RATIONALE

Smith et al. (1984) described a model of forebrain ischemia in rats induced by transient occlusion of both carotid arteries and exsanguination to a blood pressure of 40 mm Hg. This method has been used extensively (Nuglisch et al. 1990; Oberpichler et al. 1990; Rischke and Krieglstein 1990; Krieglstein and Peruche 1991; Nuglisch et al. 1991; Prehn et al. 1991; Rischke and Krieglstein 1991; Seif el Nasr et al. 1992; Peruche et al. 1995).

PROCEDURE

Male Wistar rats weighing 250–300 g are anesthetized with 3.5% halothane and then connected to a Starling type respirator delivering 0.8% halothane and 30% O_2 in N_2O. The jugular vein and the tail artery are catheterized for withdrawal of blood and for monitoring blood pressure. Anticoagulation is achieved by intravenous heparin (200 IU/kg) application. Blood gases, blood pH, blood pressure, and blood glucose are measured 5 min prior to ischemia and 10 min after ischemia.

Halothane, but not N_2O, is discontinued and the rats are allowed to recover for 30 min. During this period, muscle paralysis is maintained with 5 mg/kg suxamethonium chloride, repeated every 15 min. After injection of trimethaphan camphor sulfonate (5 mg/kg), forebrain ischemia is induced by clamping of both carotid arteries and exsanguination to a blood pressure of 40 mm Hg. To prevent decay of intra-ischemic brain temperature, the environmental temperature is adjusted to 30°C by means of a infrared heating lamp. After 10 min of ischemia, the carotid clamps are removed and blood pressure is restored by re-infusing the shed blood. To minimize systemic acidosis, the rats receive intravenously 50 mg/kg $NaHCO_3$. The animals are removed from the respirator when they regain spontaneous respiration.

EVALUATION

Various parameters are used to evaluate the consequences of transient forebrain ischemia and the effectiveness of drug treatment:

- Local cerebral blood flow determination with the [^{14}C]iodoantipyrine method (Sakurada et al. 1978),
- Histological assessment of ischemic cell damage in the hippocampus on day 7 after ischemia (Seif el Nasr et al. 1990; Nuglisch et al. 1990),

- Local cerebral glucose utilization using the [^{14}C]deoxyglucose method described by Sokoloff et al. (1977),
- Quantitative analysis of the electrocorticogram (Peruche et al. 1995).

MODIFICATIONS OF THE METHOD

Kochhar et al. (1988) used two focal cerebral ischemia models in **rabbits**: a multiple cerebral embolic model by injection of microspheres into the internal carotid circulation and a spinal chord ischemia model by occluding the aorta for predetermined periods.

Gilboe et al. (1965) described the isolation and mechanical maintenance of the **dog** brain.

Andjus et al. (1967) and Krieglstein et al. (1972) described the preparation of the isolated perfused rat brain for studying effects on cerebral metabolism.

A cerebral ischemia model with conscious **mice** was described by Himori et al. (1990).

REFERENCES AND FURTHER READING

Andjus RK, Suhara K, Sloviter HA (1967) An isolated, perfused rat brain preparation, its spontaneous and stimulated activity. J Appl Physiol 22:1033–1039

Gilboe DD, Cotanch WW, Glover MB (1965) Isolation and mechanical maintenance of the dog brain. Nature 206:94–96

Himori N, Watanabe H, Akaike N, Kurasawa M, Itoh J, Tanaka Y (1990) Cerebral ischemia model with conscious mice. Involvement of NMDA receptor activation and derangement of learning and memory ability. J Pharmacol Meth 23:311–327

Kochhar A, Zivin JA, Lyden PD, Mazzarella V (1988) Glutamate antagonist therapy reduces neurologic deficits produced by focal central nervous system ischemia. Arch Neurol 45:148–153

Krieglstein G, Krieglstein J, Stock R (1972) Suitability of the isolated perfused rat brain for studying effects on cerebral metabolism. Naunyn-Schmiedeberg's Arch Pharmacol 275:124–134

Krieglstein J, Peruche B (1991) Pharmakologische Grundlagen der Therapie der zerebralen Ischämie. Arzneim Forsch/Drug Res 31:303–309

Nuglisch J, Karkoutly C, Mennel HD, Roßberg C, Krieglstein J (1990) Protective effect of nimodipine against neuronal damage in rat hippocampus without changing postischemic cerebral blood flow. J Cerebr Blood Flow Metab 10:654–659

Nuglisch J, Rischke R, Krieglstein J (1991) Preischemic administration of flunarizine or phencyclidine reduces local cerebral glucose utilization in rat hippocampus seven days after ischemia. Pharmacology 42:333–339

Oberpichler H, Sauer D, Roßberg C, Mennel HD, Krieglstein J (1990) PAF antagonist ginkgolide B reduces postischemic neuronal damage in rat brain hippocampus. J Cerebr Blood Flow Metab 10:133–135

Peruche B, Klaassens H, Krieglstein J (1995) Quantitative analysis of the electrocorticogram after forebrain ischemia in the rat. Pharmacology 50:229–237

Prehn JHM, Backhauß C, Karkoutly C, Nuglisch J, Peruche B, Roßberg C, Krieglstein J (1991) Neuroprotective properties of 5-HT$_{1A}$ receptor agonists in rodent models of focal and global cerebral ischemia. Eur J Pharmacol 203:213–222

Rischke R, Krieglstein J (1990) Effects of Vinpocetin on local cerebral blood flow and glucose utilization seven days after forebrain ischemia in the rat. Pharmacology 41:153–160

Rischke R, Krieglstein J (1991) Postischemic neuronal damage causes astroglial activation and increase in local cerebral glucose utilization in rat hippocampus. J Cerebr Blood Flow Metab 11:106–113

Sakurada O, Kennedy C, Jehle J, Brown JD, Carbin O, Sokoloff L (1978) Measurement of local cerebral blood flow with iodo[^{14}C]-antipyrine. Am J Physiol 234:H59–H66

Seif el Nasr M, Peruche B, Roßberg C, Mennel HD, Krieglstein J (1990) Neuroprotective effect of memantine demonstrated *in vivo* and *in vitro*. Eur J Pharmacol 185:19–24

Seif el Nasr M, Nuglisch J, Krieglstein J (1992) Prevention of ischemia-induced cerebral hypothermia by controlling the environmental temperature. J Pharmacol Meth 27:23–26

Smith ML, Auer RN, Siesjö BK (1984a) The density and distribution of ischemic brain injury in the rat following 2–10 min of forebrain ischemia. Acta Neuropathol (Berl) 64:319–332

Smith ML, Bendek G, Dahlgren N, Rosén I, Wieloch T, Siesjö BK (1984b) Models for studying long-term recovery following forebrain ischemia in the rat. 2. A 2-vessel occlusion model. Acta Neurol Scand 69:385–401

Sokoloff L, Reivich M, Kennedy C, DesRosiers MH, Patlak CS, Pettigrew KD, Sakurada O, Shinohara M (1977) The [^{14}C]deoxyglucose method for the measurement of local cerebral glucose utilization: Theory, procedure, and normal values in the conscious and anesthetized albino rat. J Neurochem 28:897–916

A.8.1.3 Hypoxia Tolerance Test in Rats

PURPOSE AND RATIONALE

The electrical activity of the brain is dependent on a continuous energy supply. Hypoxia is induced in test animals by inhalation of nitrogen. Marked hypoxia depresses cerebral metabolism resulting in an electrical failure of the brain. The procedure is used to investigate the ability of test compounds to antagonize the hypoxia-induced electrical failure of the brain by measuring the hypoxia-tolerance and the EEG recovery.

PROCEDURE

Male Sprague Dawley rats or stroke-prone rats weighing 250–300 g are used. They are anesthetized with hexobarbital sodium (100–120 mg/kg, i.p) and surgically implanted with 2 epidural EEG-electrodes and a reference electrode to the parietal frontal cortex. After a minimum of a one week recovery period, testing can be started. The rats receive the test compound by intravenous or intraperitoneal administration. The control group is treated with vehicle alone. Thirty to 60 min after i.p. administration (immediately after i.v. administration) the animals are anaesthetized by

hexobarbital sodium at 100–120 mg/kg, i.p. When the stage of surgical anesthesia is reached, the animals are placed in a hypoxia chamber. EEG and ECG are recorded using a Hellige recorder.

Hypoxia is induced by inhalation of nitrogen (1200 l/h). On reaching an isoelectric EEG, the nitrogen inhalation is terminated and the animals are allowed to breath room air. The recording is continued until EEG potentials can again be registered.

EVALUATION

The following parameters are measured in the test and control groups

- Hypoxia tolerance (HT): The time from the start of nitrogen inhalation until the onset of isoelectric EEG.
- Latency of EEG recovery: The time from the end of nitrogen inhalation until the onset of EEG potentials.
- The values of test and control groups are compared.

The percent change is calculated.
Statistics: Student's *t*-test by unpaired comparison.

REFERENCES AND FURTHER READING

Hossman KA, Mies G, Paschen W, Matsuoka Y, Schuier FJ, Bosma HJ (1983) Experimental infarcts in cats, gerbils and rats. In: Stefanovich V (ed) Stroke: Animal Models, Pergamon Press; Oxford, New York, pp 123–137

A.8.1.4 Middle Cerebral Artery Occlusion in Rats

PURPOSE AND RATIONALE

The permanent middle cerebral artery (MCA) occlusion technique in rats has been widely employed to evaluate various kinds of neuroprotective agents in cerebral ischemia (Ginsberg and Busto 1989). Focal cerebral infarction is achieved using a modification of the MCA occlusion model described by Tamura et al. (1981) and Pak et al. (1992).

PROCEDURE

Adult male Sprague-Dawley rats weighing 300–400 g are used in the experiments. The animals are anesthetized with a nitrous oxide-oxygen mixture (70:30%) containing 1.0 to 1.2% halothane. A mask is put on the nose and self-respiration is maintained during surgery, which takes around 20 to 30 min. The right femoral artery and vein are catheterized for monitoring blood pressure, blood sampling and administration of the drug. Left MCA occlusion is performed via a subtemporal approach without removal of zygomatic arch or temporal muscle. Under high magnification of a surgical microscope, the left MCA is coagulated with a microbipolar coagulator from the olfactory tract to the most proximal portion of the MCA through a cranial window, about 3 to 4 mm in diameter, and cut afterward. Anesthesia is stopped just after MCA occlusion. The arterial catheter is removed soon after MCA occlusion, but the venous catheter is maintained for constant infusion of the drug by a swivel system (Harvard Apparatus, UK.). The animals are maintained normothermic (37°C) by a homeothermic system (Homeothermic Blanket System, Harvard Apparatus, UK.). During the surgery, mean arterial blood pressure (MABP) is recorded continuously (Model 7E polygraph, Grass, USA). Arterial gases and pH (178 pH/blood gas analyzer, Corning, USA) as well as hematocrit and blood glucose are measured twice, once about 15 min before MCA occlusion and the other just following MCA occlusion. Bilateral temporal muscle temperature (Therm 2250–1, Ahlborn Mess- und Regelungstechnik, Germany) is monitored during the surgery and several minutes before sacrifice.

Two, six, twelve and twenty-four hours after discontinuing anesthesia, each rat's level of consciousness and motor activity are evaluated using a grading scale of 0 to 3 (0: normal activity; 1: spontaneous activity+/–; 2: not arousable by tactile stimulation; 3: not arousable by painful stimulation, no spontaneous activity). Immediately before sacrifice, neurological status is examined using a grading scale of 0 to 3 (0: no observable deficit; 1: forelimb flexion; 2: decreased resistance to lateral push without circling; 3: the same status as grade 2, with circling). Four groups of rats are studied: vehicle-treated controls, and drug-treated animals at 3 different doses.

All the rats are re-anesthetized 24 h after MCA occlusion and sacrificed by intravenous injection of KCl. Immediately after sacrifice the brain is removed and frozen at –10°C for 10 min. The forebrain is cut into eight coronal slices by a rat brain slicer which are processed with the tetrazolium chloride (TTC) emulsion technique. Areas of brain not stained by TTC are drawn on a diagram at 8 preselected coronal levels of forebrain without knowledge of the experimental treatment. The areas of ischemic damage in the cerebral hemisphere, cerebral cortex, and caudate nucleus, drawn in the diagram are measured with a planimeter (KP-21, Koizumi, Japan) and integrated to determine the volumes.

REFERENCES AND FURTHER READING

Significance of the differences between the control and the treated groups is assessed by analysis of variance with subsequent inter group comparison by Student's *t*-test with Bonferroni correction. $P < 0.05$ is required for significance.

MODIFICATIONS OF THE METHOD

Hossmann (1982) reviewed the experimental models of cerebral ischemia.

Yamamoto et al. (1992) studied the inhibition of NO biosynthesis on the volume of focal ischemic infarction produced by occlusion of the middle cerebral artery in spontaneously hypertensive rats.

Shigeno et al. (1985) described a recirculation model following middle cerebral artery occlusion in rats. The trunk of the middle cerebral artery was isolated between the rhinocortical branch and the lenticulostriate artery and encircled with a loose-fitting suture of nylon thread. The thread was exteriorized through a small polyethylene catheter, which was previously introduced into the craniectomy site through a burr hole in the zygoma. The artery was occluded by retraction of the thread, which was then fixed with biological glue. Recirculation was achieved by cutting and removing the thread.

Bederson et al. (1986a) occluded the middle cerebral artery at different sites in six groups of normal rats and characterized the anatomical sites that produce uniform cerebral infarction. A neurological system was developed that can be used to evaluate the effects of cerebral ischemia.

Bederson et al. (1986b) evaluated the use of 2,3,5-triphenyltetrazolium chloride as a histopathological stain for identification and quantification of infarcted brain tissue after middle cerebral artery occlusion in rats.

Yang et al. (1992) found a reduction of Na,K-ATPase activity in the ischemic hemisphere shortly after middle cerebral artery occlusion in rats.

Du et al. (1996) induced transient focal cerebral ischemia in rats by a 90 min period of ligation of the right middle cerebral artery and both common carotid arteries.

Germano et al. (1987) found a decrease of stroke size and deficits in rats with middle cerebral artery occlusion after treatment with kynurenic acid, a broad spectrum antagonist of excitatory amino acid receptors.

Wu et al. (1999) reported that propentofylline attenuates microglial reaction in the rat spinal cord induced by middle cerebral artery occlusion.

Gotti et al. (1988) found a reduction of the volume of infarcted tissue due to occlusion of the middle cerebral artery in **rats** and **cats** after administration of NMDA receptor antagonists.

Hossmann and Schuier (1980) studied experimental brain infarcts in **cats** after occlusion of the left middle cerebral artery.

Retro-orbital occlusion of the middle cerebral artery in cats was performed by Sundt and Waltz (1966) and by Gotti et al. (1988).

Welsh et al. (1987), Backhauß et al. (1992) described focal cerebral ischemia in **mice** after permanent occlusion of the middle cerebral artery.

Hara et al. (1997) found a reduction of ischemic and excitotoxic neuronal damage by inhibition of interleukin 1β-converting enzyme family proteases after occlusion of the middle cerebral artery in **mice** and **rats**. Nylon filaments were introduced from the carotid artery which were withdrawn after 2 h. One day later, the animals were tested for neurological deficits and the brains analyzed for infarct size and interleukin 1β levels.

Huang et al. (1994) produced **knock-out mice** deficient in the neuronal isoform of NO synthase by targeted disruption of the neuronal nitric oxide synthase gene. In these mice, Hara et al. (1996) found reduced brain edema and infarction volume after transient middle coronary artery occlusion.

Nishimura et al. (1998) described an experimental model of thromboembolic stroke without craniotomy in **cynomolgus monkeys** by delivering an autologous blood clot to the middle cerebral artery. A chronic catheter was implanted in the left carotid artery in male cynomolgus monkeys. A 5 cm long piece of an autologous blood clot was flushed into the internal carotid artery with physiological saline. A neurological score was assigned at 0.167, 0.5, 1, 2, 4, 6, and 24 h after embolization. In the acute phase after embolization, typical behavior consisted of circling gait and moderate deviation towards the side of embolization, long-lasting and strong extensor hypotonia of the contralateral lower and upper limbs, and mild to severe incoordination. Contralateral hemiplegia was observed over the following 24 h. At 24 h the animals were sacrificed immediately after the last neurological scoring, and the cerebral vasculature was inspected for the location of the clot. The brain was then cut into 2 mm thick coronal sections. Cerebral infarction size and location were ascertained by the triphenyl-2H-tetrazolium chloride staining method. The lesions involved mostly the caudate nucleus, internal capsule, putamen and thalamus.

Salom et al. (1999) subjected female **goats** to 20 min global cerebral ischemia under halothane/N_2O anesthesia. An episode of transient global ischemia was achieved by occlusion of the two external carotid arteries and simultaneous external compression of the jugular veins by a neck tourniquet. A reperfusion period started when the occlusions were released, and it was monitored for 2 h.

De Ley et al. (1988) studied experimental thromboembolic stroke induced by injection of a single autologous blood clot into the internal cerebral artery in dogs by**positron emission tomography**.

REFERENCES AND FURTHER READING

Backhauß C, Karkoutly C, Welsch M, Krieglstein J (1992) A mouse model of focal cerebral ischemia for screening neuroprotective drug effects. J Pharmacol Meth 27:27–32

Bederson JB, Pitts LH, Tsuji M, Nishimura MC, Davis RL, Bartkowski H (1986a) Rat middle cerebral artery occlusion: Evaluation of the model and development of a neurologic examination. Stroke 17:472–476

Bederson JB, Pitts LH, Germano SM, Nishimura MC, Davis RL, Bartkowski HM (1986b) Evaluation of 2,3,5-triphenyltetrazolium chloride as a stain for detection and quantification of experimental cerebral infarction in rats.Stroke 17:1304–1308

De Ley G, Weyne J, Demeester G, Stryckman K, Goethals P, Van de Velde E, Leusen I (1988) Experimental thromboembolic stroke studied by positron emission tomography: immediate versus delayed reperfusion by fibrinolysis. J Cerebr Blood Flow Metab 8:539–545

Du C, Hu R, Csernansky CA, Liu XZ, Hsu CY, Choi DW (1996) Additive neuroprotective effects of dextrorphan and cycloheximide in rats subjected to transient focal cerebral ischemia. Brain Res 718:233–236

Germano IM, Pitts LH, Meldrum BS, Bartkowski HM, Simon RP (1987) Kynurenate inhibition of cell excitation decreases stroke size and deficits. Ann Neurol 22:730–734

Ginsberg MD, Busto R (1989) Rodent models of cerebral ischemia. Stroke 20:1627–1642

Gotti B, Duverger G, Bertin J, Carter C, Dupont R, Frost J, Gaudilliere B, MacKenzie ET, Rousseau J, Scatton B, Wick A (1988) Ifenprodil and SL 82.0715 as cerebral antiischemic agents. I. Evidence for efficacy in models of focal cerebral ischemia. J Pharm Exp Ther 247:1211–1221

Hara H, Huang PL, Panahian N, Fishman MC, Moskowitz MA (1996) Reduced brain edema and infarction volume in mice lacking the neuronal isoform of nitric oxide synthase after transient MCA occlusion. J Cerebr Blood Flow Metab 16:605–611

Hara H, Friedlander RM, Gagliardini V, Ayata C, Fink K, Huang Z, Shimizu-Sasamata M, Yuan J, Moskowitz MA (1997) Inhibition of interleukin 1β converting enzyme family proteases reduces ischemic and excitotoxic neuronal damage. Proc Natl Acad Sci USA 94:2007–2012

Hossmann KA (1982) Treatment of experimental cerebral ischemia. J Cerebr Blood Flow Metab 2:275–297

Hossmann KA, Schuier FJ (1980) Experimental brain infarcts in cats. I. Pathophysiological observations. Stroke 11:583–592

Huang PL, Dawson PM, Bredt DS, Snyder SH, Fishman MC (1994) Targeted disruption of the neuronal nitric oxide synthase gene. Cell 75:1273–1286

Nsihimura A, Hamada T, Fukuzaki K, Miyajima H, Nagata R, Kito G (1998) A new model of experimental thromoboembolic stroke in cynomolgus monkey. Naunyn-Schmiedeberg's Arch Pharmacol 358, Suppl 1:R70

Park CK, Rudolphi KA (1994) Antiischemic effects of propentofylline (HWA 285) against focal cerebral infarction in rats. Neurosci Lett 178:235–238

Park CK, McCulloch J, Kang JK, Choi CR (1992) Efficacy of D-CPPene, a competitive *N*-methyl-D-aspartate antagonist in focal cerebral ischemia in the rat. Neurosci Lett 147:41–44

Salom JB, Barberá MD, Centeno JM, Ortí M, Torregrosa G, Alborch E (1999) Relaxant effects of sodium nitroprusside and NONOates in goat middle cerebral artery: Delayed impairment by global ischemia-reperfusion. Nitric Oxide: Biol Chem 3:85–93

Shigeno T, Teasdale GM, McCulloch J, Graham DI (1985) Recirculation model following MCA occlusion in rats. Cerebral blood flow, cerebrovascular permeability, and brain edema. J Neurosurg 63:272–277

Smith SE, Meldrum BS (1992) Cerebroprotective effect of a non-N-methyl-D-aspartate antagonist, GYKI 52466, after focal ischemia in the rat. Stroke 23:861–864

Sundt TM, Waltz AG (1966) Experimental cerebral infarction: Retro-orbital, extradural approach for occluding the middle cerebral artery. Mayo Clin Proc 41:159–168

Tamura A, Graham DI, McCulloch J, Teasdale GM (1981) Focal cerebral ischaemia in the rat: 1. Description of technique and early neuropathological consequences following middle cerebral artery occlusion. J Cerebr Blood Flow Metab 1:53–60

Welsh FA, Sakamoto T, McKee AE, Sims RE (1987) Effect of lactacidosis on pyridine nucleotide stability during ischemia in mouse brain. J Neurochem 49:846–851

Wu YP, McRae A, Rudolphi K, Ling EA (1999) Propentofylline attenuates microglial reaction in the rat spinal cord induced by middle cerebral artery occlusion. Neurosci Lett 280:17–20

Yamamoto S, Golanov EV, Berger SB, Reis DJ (1992) Inhibition of nitric oxide synthesis increases focal ischemic infarction in rat. J Cerebr Blood Flow Metab 12:717–726

Yang GY, Chen SF, Kinouchi H, Chan PH, Weinstein PR (1992) Edema, cation content and ATPase activity after middle cerebral artery occlusion in rats. Stroke 23:1331–1336

A.8.1.5 Photochemically Induced Focal Cerebral Ischemia in Rats

PURPOSE AND RATIONALE

Focal cerebral ischemia in rats can be induced by irradiation with intensive green light via a fibre optic through the skull after injection of the dye Rose Bengal. The resulting cerebral infarct can be studied for various parameters, such as infarct volume, water content, local cerebral blood flow and glucose utilization.

PROCEDURE

Male Sprague-Dawley rats (300–350 g) are used. Anesthesia is induced with 3% halothane in oxygen and is maintained with 1% halothane in oxygen applied via a face mask. A small incision is made in the skin over the right femoral vein and a thin catheter is

inserted. One ml of the dye Rose Bengal (in a concentration of 5 mg/ml of saline) is injected. A midline head incision is made and the right side of the skull is exposed. An intense green light, produced by a xenon lamp (75W, Zeiss, FRG) and then passed through a filter (wavelength 570 nm, Schott, Mainz, FRG) and a heat filter (Schott, Mainz, FRG), is directed on the skull at the level of the bregma for 15 min. The 3 mm diameter of the illuminated circle is determined by passing the light through a fibre optic (Schott, Mainz, FRG) while in close contact to the skull. The temperature of the skull underneath the fibre optic does not change during the time of illumination. At the end of the induction period, the temporary catheter is removed from the femoral vein which remains patent following the closure of the catheterization site with liquid suture (Histoacryl, Braun, Melsungen, FRG), and the incisions in the leg and head are likewise sutured after liberal application of local anesthetic. The anesthetic gas mixture is discontinued and the rats are allowed to recover consciousness in a warm environment until such times as the appropriate experiment is to be performed. Due to the non-invasive nature of this technique it is not possible to measure blood pressure or blood gases during the ischemic period. However, rectal temperature and plasma glucose concentrations are controlled.

Measurement of Infarct Volume

Osmotically controlled mini-pumps (Model 2ML1 Alzet, USA) are placed into the peritoneum of two groups of six male Sprague Dawley rats (body weight 300–350 g). The mini-pumps are fitted via thin polyethylene catheters to the femoral vein of the rats. Each pump contains either 2 ml of physiological saline or 2 ml of a solution of the drug to be studied. The animals are then given an ischemic insult as described in the previous section. Seventy-two hours after the induction of ischemia, the rats are sacrificed by decapitation and the brains removed and frozen at –50°C. Coronal sections (20 µ) are cut in a cryotome at –20°C, fixed in Haidenhain's Susa and stained with Cresyl Violet. The ischemic area on 90 sections is measured and the volume of ischemic change is then calculated using a linear trapezoidal extrapolation of the areas measured.

Measurement of Brain Water Content

Three groups each of six rats are used. One group receives no ischemic lesion (the illumination with green light is omitted from the experimental protocol) and two groups are lesioned as described above. One lesioned group receives the test drug orally at 15 min, 30 min, 1, 3 and 5 h after the induction of the ischemia or sham operation. The other group is treated with saline at the same time-points. Twenty-four hours later the rats are sacrificed by decapitation. The brains are rapidly removed and placed on a cutting block with 1 mm gradations. Two cuts are made 1 mm or less anterior and posterior to the lesion. The thick section so produced is then divided into left (non-lesioned) and right (lesioned) halves and placed in pre-weighed vials and the wet weights of the tissue samples are carefully measured. The tissue is then frozen in liquid nitrogen and then left under vacuum (less than 0.1 Torr) for 24 h. On removal the vials are sealed to prevent rehydration and reweighed to obtain the dry weight of tissue from which the water content (expressed as percentage of wet weight of tissue) is calculated.

EVALUATION

All data are presented as mean ± SD of the mean. For left (contralateral to the lesion) against right (ipsilateral to the lesion) comparisons, a *t*-test with paired comparison was used ($P < 0.05$). Statistical differences between groups were calculated using the unpaired *t*-test.

MODIFICATIONS OF THE METHOD

Boquillon et al. (1992) produced cerebral infarction in mice by intravenous injection of 10 mg/kg rose bengal, and by focal illumination of the intact skull surface for 3 min with a laser source, operating at 570 nm with power levels of 2, 5, 10, and 20 mW.

Matsuno et al. (1993) used a similar model to induce cerebral ischemia in rats based on middle cerebral artery occlusion by the photochemical reaction of rose bengal after irradiation with high intensity green light.

Stieg et al. (1999) studied neuroprotection by the NMDA receptor-associated open-channel blocker memantine in a photothrombotic model of cerebral focal ischemia in neonatal rat. An excellent correlation between infarct size determined by magnetic resonance imaging (MRI) and histopathological analysis in the same animals was found.

REFERENCES AND FURTHER READING

Boquillon M, Boquillon JP, Bralet J (1992) Photochemically induced, graded cerebral infarction in the mouse by laser irradiation. Evolution of brain edema. J Pharm Meth 27:1–6

Grome JJ, Gojowczyk G, Hofmann W (1990) Effect of chronic intravenous administration of propentofylline (HWA 285) on the volume of focal ischemic damage in the rat. Stroke 21, Suppl I:I-134–I-135, PS-12–11

Matsuno H, Uematsu T, Umemura K, Tagiguchi Y, Asai Y, Murakana Y, Nakashima M (1993) A simple and reproducible cerebral thrombosis model in rats induced by a photochemical reaction and the effect of a plasmin-plasminogen activator chimera in this model. J Pharm Toxicol Meth 29:165–173

Stieg PE, Sathi S, Warach S, Le DA, Lipton SA (1999) Neuroprotection by the NMDA receptor-associated open-channel blocker memantine in a photothrombotic model of cerebral focal ischemia in neonatal rat. Eur J Pharmacol 375:115–120

A.8.1.6 Microdialysis and Neuroprotection Experiments After Global Ischemia in Rats

PURPOSE AND RATIONALE

Transient global ischemia can be induced in rats by electrocauterization of the vertebral arteries followed by clamping of the carotid arteries.

PROCEDURE

Male Wistar rats weighing 280–340 g are used. The rats are anesthetized with methohexital sodium (60 mg/kg i.v.) and the vertebral arteries are electrocauterized (Pulsinelli and Brierley 1979). The rats are fasted overnight and re-anesthetized on the following day with halothane and intubated. The femoral artery and vein are cannulated to allow blood sampling, blood withdrawal and recording of mean arterial pressure (MAP). Samples of blood are taken at regular time intervals and blood gas/acid base status is analyzed (Instrumentation Laboratory, 1306). Rectal temperature is measured with a thermistor and controlled at 37°C by means of a heating lamp. Four-vessel occlusion ischemia is induced for 20 min by bilateral carotid clamping followed by a period of reflow.

Microdialysis Experiments

The head of the rat is fixed in a stereotactic frame. The skin is incised over the head, pulled apart and a 3 × 3 mm hole is drilled through the cranium. A microdialysis probe (Sandberg et al. 1986) is implanted into CA1 region of the hippocampus (2.2 mm lateral and 3.8 mm dorsal to bregma, and the window of the dialysis membrane 1.4–2.9 mm below the cortical surface). The electroencephalogram (EEG) is measured continuously with a tungsten electrode attached to the dialysis probe. The probe is perfused at a rate of 2.5 µl/min with a modified Ringer solution. Dialysates are sampled every 10 min and analyzed for purines (Hagberg et al. 1987) and amino acids (Lindroth et al. 1985). One group receives the test drug i.p. 15 min prior to ischemia whereas the control group obtains saline. The animals are followed during 20 min of ischemia and 2 h of reflow.

HPLC analyses are carried out using a reverse-phase C_{18} column (Waters 10 µm µBondapak) with isocratic elution, a flow rate of 1.0 ml/min and at ambient temperature. For adenosine, inosine and hypoxanthine the mobile phase is 10 mM $NH_4H_2PO_4$, pH 6.0, 13% methanol.

Neuroprotection Experiments

During ischemic insult and for 20 min of reflow, the temperature of the temporalis muscle is controlled at 37°C. Immediately following ischemia the rats are divided into two groups. One group is treated with the test drug and the other with saline. A bolus injection is administered i.p. 15 min after ischemia and a mini-osmotic pump is implanted into the abdominal cavity which delivers the test drug for 7 days. Control animals receive a bolus of saline and mini-osmotic pumps filled with saline. Seven days later the rats are anesthetized with pentobarbital and perfusion-fixed with formol saline. The histological evaluation is done "blind". The hippocampal damage is semiquantified according to the following scoring system:

0 = no damage
1 = scanty damage,
2 = moderate damage
3 = severe damage
4 = complete loss of pyramidal cells in the hippocampus.

EVALUATION

The purine and amino acid data are expressed as means ± SEM and differences are evaluated with the non-parametric Mann-Whitney test. The neuroprotective efficacy of the test drug is evaluated with two-tailed Student's *t*-test.

MODIFICATIONS OF THE TEST

In addition to the assessment of neuronal damage, Block et al. (1996) tested spatial learning of treated rats one week after 4-vessel occlusion in a Morris water maze.

REFERENCES AND FURTHER READING

Benveniste H, Drejer J, Schousboe A, Diemer NH (1984) Elevation of the extracellular concentrations of glutamate and aspartate in rat hippocampus during transient cerebral ischemia monitored by intracerebral microdialysis. J Neurochem 43:1396–1374

Block F, Schmitt W, Schwarz M (1996) Pretreatment but not post-treatment with GYKI 52466 reduces functional

deficits and neuronal damage after global ischemia in rats. J Neurol Sci 139:167–172
Choi DW (1990) Methods for antagonizing glutamate neurotoxicity. Cerebrovasc Brain Metab 2:105–147
Hagberg H, Andersson P, Lacarewicz J, Jacobson I, Butcher S, Sandberg M (1987) Extracellular adenosine, inosine, hypoxanthine, and xanthine in relation to tissue nucleotides and purines in rat striatum during transient ischemia. J Neurochem 49:227–231
Hagberg H, Andiné P, Fredholm B, Rudolphi K (1990) Effect of the adenosine uptake inhibitor propentofylline on the extracellular adenosine and glutamate and evaluation of its neuroprotective efficacy after ischemia in neonatal and adult rats. In: Krieglstein J, Oberpichler (eds) Pharmacology of Cerebral Ischemia. Wissenschaftliche Verlagsgesellschaft mbH, Stuttgart, pp 427–437
Lindroth P, Hamberger A, Sandberg M (1985) Liquid chromatographic determination of amino acids after precolumn fluorescence derivatization. In: Boulton AA, Baker GB, Wood JD (eds) Neuromethods, Vol 3, Amino acids. HUMANA Press Inc., pp 97–116
Pulsinelli WA, Brierley JB (1979) A new model of bilateral hemispheric ischemia in the unanesthetized rat. Stroke 10:267–272
Sandberg M, Butcher SP, Hagberg H (1986) Extracellular overflow of neuroactive amino acids during severe insulin-induced hypoglycemia: *In vivo* dialysis of the rat hippocampus. J Neurochem 47:178–184

A.8.1.7 Hypoxia/Hypoglycemia in Hippocampal Slices

PURPOSE AND RATIONALE

The *in vitro* release of adenosine, inosine, and hypoxanthine from rat hippocampal slices can be determined with and without drug.

PROCEDURE

Male Sprague-Dawley rats weighing 150–275 g are decapitated, the hippocampi isolated and cut into 400 µm thick slices which are placed into KRB (4°C) containing (mM) NaCl (118), KCl (4.85), $MgSO_4$ (1.15), KH_2PO_4 (1.15), $NaHCO_3$ (25), glucose (5.5), $CaCl_2$ (1.3) equilibrated with 95% O_2/5% CO_2. The incubation medium is brought up to room temperature over a period of 30 min. The KRB is then replaced with fresh medium and the slices are incubated for a further 30 min at room temperature, followed by 30 min at 37°C in fresh KRB. Following the initial incubations, slices are labelled for 45 min with ^{3}H-adenine (5 µCi/ml) at 37°C. Two labelled slices are transferred into plastic cylinders which have nylon net bases and these, together with the slices, are placed into glass superfusion chambers. Slices are superfused at a flow rate of 0.5 ml/min with KRB at 37°C. After a 60 min wash, collection of 5 min fractions begins, which continues throughout the remainder of the experiment. A 1.25 ml aliquot of the fractions is taken for determination of radioactivity using scintillation spectrometry (scintillation fluid: Picofluor 15). The remaining 1.25 ml is taken for HPLC analysis of purines and amino acids.

Hypoxia/hypoglycemia is induced by superfusion with KRB containing no glucose and 95% N_2 and 5% CO_2 for 35 min followed by recovery. All other procedures are as described above. The test drug is added to the perfusion fluid at an appropriate concentration. The 1.25 ml aliquots taken for HPLC analysis are pooled with two other aliquots (total 3.75 ml), lyophilized and concentrated 10 fold before analysis. Samples are analyzed for adenosine, inosine and hypoxanthine with HPLC. The radioactivity associated with each of these fractions is also determined by collecting the eluent from the column at the appropriate times. HPLC analyses are carried out using a reverse-phase C_{18} column (Waters 10 µm µBondapak) with isocratic elution, a flow rate of 1.0 ml/min and at ambient temperature. For adenosine, inosine and hypoxanthine the mobile phase is 10 mM $NH_4H_2PO_4$, pH 6.0, 13% methanol.

EVALUATION

Values for adenosine, inosine and hypoxanthine can be expressed in two ways: (1) release rate per slice (pmol/min × slice); (2) percentage of the total amount of released radioactivity (% total $_3$H-label released). The purine data are expressed as means ± SEM and differences are evaluated with the non-parametric Mann-Whitney test.

REFERENCES AND FURTHER READING

Dunwiddie TV (1986) The use of *in vitro* brain slices in neuropharmacology. In: Electrophysiological Techniques in Pharmacology. Alan R Liss, Inc., pp 65–90
Hagberg H, Andiné P, Fredholm B, Rudolphi K (1990) Effect of the adenosine uptake inhibitor propentofylline on the extracellular adenosine and glutamate and evaluation of its neuroprotective efficacy after ischemia in neonatal and adult rats. In: Krieglstein J, Oberpichler (eds) Pharmacology of Cerebral Ischemia. Wissenschaftliche Verlagsgesellschaft mbH, Stuttgart, pp 427–437

A.8.1.8 Measurement of Local Cerebral Blood Flow and Glucose Utilization in Rats

PURPOSE AND RATIONALE

Cerebral glucose utilization can be determined using [^{14}C]-2-deoxyglucose according to Sokoloff et al. (1977). Local cerebral blood flow using [^{14}C]-iodoantipyrine is measured as described by Sakurada et al. (1978).

PROCEDURE

Animal Preparation

The experiments are performed on male Sprague-Dawley rats (260–300 g). Catheters are placed, under light halothane (1%) anesthesia, into the femoral vein and artery of each hind limb (for the measurement of mean arterial pressure, the sampling of arterial blood and the intravenous administration of drugs and radioisotopic tracer). The wound sites are then infused with local anesthetic, sutured, and protected by pads. The lower abdomen is covered by an elastic stocking, followed by a loose-fitting plaster coat. Anesthesia is discontinued and the rats are allowed at least two hours to recover before any further manipulations are performed.

Experimental Protocol

The rats are given an intravenous infusion (50 µl/min) of either saline or the test drug dissolved in saline. This infusion is maintained throughout the measurement of local cerebral blood flow or local cerebral glucose utilization.

Local Cerebral Glucose Utilization

A full description of the method for measuring local cerebral glucose utilization using [^{14}C]-2-deoxyglucose has been published (Sokoloff et al. 1977). Five minutes after the administration of the test drug, the experiment is started with the intravenous administration of [^{14}C]-2-deoxyglucose (125 µCi/kg). Fourteen timed arterial blood samples are taken during the following forty-five minutes. These samples are centrifuged and the plasma is measured for glucose concentration (using an automated glucose analyzer) and [^{14}C] levels (by liquid scintillation counting). At the end of this period the rats are sacrificed by decapitation, the brain rapidly removed and frozen at –45°C. Twenty micron thick coronal sections are cut in a cryostat (–22°C) and autoradiograms are prepared by placing these sections in an array against Kodak SB-5 X-ray film along with pre-calibrated plastic standards range (55–851 nCi/g) for seven days in light-tight cassettes.

Local Cerebral Blood Flow

The autoradiographic measurement of local cerebral blood flow using [^{14}C]-iodoantipyrine is carried out as described by Sakurada et al. (1978). [^{14}C]-iodoantipyrine (125 µCi/kg) is administered fifteen minutes after the infusion of the test drug has commenced. In a period of sixty seconds, eighteen timed arterial samples are collected in pre-weighed filter-paper discs from a free flowing arterial catheter. The discs are reweighed and the [^{14}C] concentration of each is measured by liquid scintillation counting. At the end of one minute, the rat is decapitated and autoradiograms are prepared in the same manner as for the measurement of local cerebral glucose utilization.

Densitometric Analysis of Autoradiograms

Tissue [^{14}C] concentrations were determined using a densitometer system (Zeiss, FRG) by reference to the images of the precalibrated standards. For each structure of interest, bilateral determination of optical densities are made on six different autoradiographic images in which the structure is best defined.

The mean optical density is used to calculate [^{14}C] concentrations. From this value, and the history of [^{14}C] in the blood, values of local cerebral blood flow and glucose utilization are obtained using the respective operational equations of these methods (Sakurada et al. 1978; Sokoloff et al. 1977).

EVALUATION

Groups of data are statistically compared by *t*-test with unpaired comparison using the BONFERRONI correction factor for multiple group analyses. Linear regression data for comparing cerebral blood flow (CBF) and glucose utilization (GU) undergo log transformation as recommended by McCulloch et al. (1982).

MODIFICATIONS OF THE METHOD

Ito et al. (1990) measured glucose utilization in the mouse brain by the simultaneous use of [^{14}C]2-deoxyglucose and [^{3}H]3-O-methylglucose.

High-resolution animal positron emission tomography was recommended by Magata et al. (1995) for noninvasive measurement of cerebral blood flow with ^{15}O-water and glucose metabolic rate with ^{18}F-2-fluoro-2-deoxyglucose.

The effect of ginseng pretreatment on cerebral glucose metabolism in ischemic rats using animal positron emission tomography (PET) with [^{18}F]-2 fluoro-2-deoxy-D-glucose ([^{18}F]-FDG) was described by Choi et al. (1997).

Hawkins et al. (1993) developed a method for evaluating tumor glycolytic rates *in vivo* with nude mice injected with 2-[^{18}F]fluoro-2-deoxy-D-glucose and a dedicated animal positron emission tomography scanner.

Positron emission tomography has been used with specific ligands for CNS imaging (de la Sayette 1991; Jones et al. 1991; Kung 1993).

Rogers et al. (1994) synthesized ^{18}F-labelled vesamicol derivates to be evaluated in small animal positron emission tomography.

Hume et al. (1997) measured *in vivo* saturation kinetics of two dopamine transporter probes using a small animal positron emission tomography scanner.

REFERENCES AND FURTHER READING

Choi SR, Magata Y, Saji H, Tajima K, Kitano H, Konishi J, Yokoyama A (1997) Effect of ginseng pretreatment on cerebral glucose metabolism in ischemic rats using animal positron emission tomography (PET) and ([^{18}F]-FDG). Phytother Res 11:437–440

De la Sayette T, Chavoix C, Brouillet A, Hantraye P, Kunimoto M, Khalili-Varasteh M, Guibert B, Prenant C, Mazière M (1991) *In vivo* benzodiazepine receptor occupancy by CL 218,872 visualized by positron emission tomography in the brain of the living baboon: Modulation by GABAergic transmission and relation with anticonvulsant activity. Exp Brain Res 83:397–402

Grome J, Stefanovich V (1985) Differential effects of xanthine derivatives on local cerebral blood flow and glucose utilization in the conscious rat. In: Stefanovich V, Rudolphi K, Schubert P (eds) Adenosine: Receptors and Modulation of Cell Function. IRL Press Ltd., Oxford, England, pp 453–458

Hawkins RA, Choi Y, Scates S, Rege S, Hoh CK, Glaspy J, Phelps ME (1993) An animal model for *in vivo* evaluation of tumor glycolytic rates with positron emission tomography. J Surg Oncol 53:104–109

Hume SP, Brown DJ, Ashwoth S, Hirani E, Luthra SK, Lammertsma AA (1997) *In vivo* saturation kinetics of two dopamine transporter probes measured using a small animal positron emission tomography scanner. J Neurosci Meth 76:45–51

Ito K, Sawada Y, Ishizuka H, Sugiyama Y, Suzuki H, Iga T, Hanano M (1990) Measurement of cerebral glucose utilization from brain uptake of [^{14}C]2-deoxyglucose and [^{3}H]3-O-methylglucose in the mouse. J Pharmacol Meth 23:129–140

Jones HA, Rhodes CR, Law MP, Becket JM, Clark JC, Boobis AR, Taylor GW (1991) Rapid analysis of ^{11}C-labelled drugs: fate of [^{11}C]-*S*-4-(*tert*.-butylamino-2-hydroxypropoxy)-benzimidazol-2-one in the dog. J Chromatogr Biomed Appl 570:361–370

Kung HF (1993) SPECT and PET ligands for CNS imaging. Neurotransmissions 9/4:1–6

Lacombe B, Meric P, Seylaz J (1980) Validity of cerebral blood flow measurements obtained with quantitative tracer techniques. Brain Res Rev 2:105–169

Magata Y, Saji H, Choi SR, Tajima K, Takagaki T, Sasayama S, Yonekura Y, Kitano H, Watanabe M, Okada H, Yoshikawa E, Yamashita T, Yokoyama A, Konishi J (1995) Noninvasive measurement of cerebral blood flow and glucose metabolic rate in the rat with high-resolution animal positron emission tomography (PET): A novel *in vivo* approach for assessing drug action in the brains of small animals. Biol Pharm Bull 18:753–756

McCulloch J, Kelly PAT, Ford I (1982) Effect of apomorphine on the relationship between local cerebral glucose utilization and local cerebral blood flow. (with an appendix on its statistical analysis). J Cerebr Blood Flow Metab 2:487–499

Rogers GA, Stone-Elander S, Ingvar M, Eriksson L, Parsons SM, Widen L (1994) ^{18}F-labelled vesamicol derivates: Syntheses and preliminary *in vivo* small animal positron emission tomography evaluation. Nucl Med Biol 21:219–230

Sakurada O, Kennedy C, Jehle J, Brown JD, Carbin O, Sokoloff L (1978) Measurement of local cerebral blood flow with iodo(^{14}C)-antipyrine. Am J Physiol 234:H59–H66

Smith CB (1981) Age-related changes in local rates of cerebral glucose utilization in the rat. In: Enna SJ et al (eds) Brain. Neurotransmitters and Receptors in Aging and Age-Related Disorders (Aging, Vol 17) Raven Press, New York, pp 195–201

Sokoloff L, Reivich M, Kennedy C, DesRosiers MH, Patlak CS, Pettigrew KD, Sakurada O, Shinohara M (1977) The [^{14}C]deoxyglucose method for the measurement of local cerebral glucose utilization: Theory, procedure, and normal values in the conscious and anesthetized albino rat. J Neurochem 28:897–916

Winn HR, Rubio GR, Berne RM (1981) The role of adenosine in the regulation of cerebral blood flow. J Cerebr Blood Flow Metab 1:239–244

Wolfson LI, Sakurada O, Sokoloff L (1977) Effects of γ-butyrolactone on local cerebral glucose utilization in the rat. J Neurochem 29:777–783

A.8.1.9 Cerebrovascular Resistance in Anesthetized Baboons

PURPOSE AND RATIONALE

Cerebral blood flow and cerebrovascular resistance can be measured by injection of inert radioactive gas (^{133}Xenon) and evaluation of the ^{133}Xe clearance curve in anesthetized baboons.

PROCEDURE

Animal Preparation

The experiments are performed on baboons (*Papio* or *cynocephalus*) weighing 9–13 kg. Initial sedation with phencyclidine (10 mg i.m.) is followed by an intravenous injection of sodium thiopental (75 mg/kg). The animals are intubated to a positive pressure ventilator delivering 70:30% nitrous oxide and oxygen in open circuit. A continuous intravenous infusion of phencyclidine (0.01 mg/kg/min) is given throughout the course of the experiment. Suxamethonium (50 mg i.m.) is administered every 30 min in order to assist control of ventilation with the respiratory pump.

During the experiments, the end tidal concentration of CO_2 is continuously measured and the ventilating pump adjusted to maintain an arterial CO_2 tension ($PaCO_2$) of between 37 and 40 mm Hg for the control measurements. Arterial blood samples are taken during every measurement of cerebral blood flow (CBF) to measure $PaCO_2$, PaO_2, and pH by direct reading electrodes (Corning). Body temperature is maintained around 37°C by means of an electrically heated blanket and infrared heating lamps.

Catheters are inserted into the aorta via femoral arteries for the continuous measurement of arterial blood pressure and for the withdrawal of arterial blood samples. Both femoral veins are cannulated, one for the continuous infusion of phencyclidine and the other for the infusion of the test drug. A catheter is inserted into the right lingual artery so that its tip lays just distal to the carotid bifurcation. This catheter is flushed at regular intervals with heparinized saline to prevent platelet aggregation at the tip. In the studies with required intravenous administration of test drug, the other branches of the external carotid artery are ligated. Where the requirement is for intracarotid administration of test drug, another catheter is retrogradely advanced into the external carotid artery so that its tip lays next to the tip of the lingual catheter. This catheter is then attached to a constant-rate infusion pump (Sage Instruments). Heparinized saline is infused at a rate of 0.2 ml/min to act as a control for drug infusion.

A burr hole is made over the midline fissure and a catheter inserted into the sagittal sinus for the withdrawal of cerebral venous blood samples. The hole is sealed with plaster of Paris. The scalp and temporalis muscle are removed with diathermy down to the level of the zygomatic arch.

Measurement of Cerebral Blood Flow, Cerebral Oxygen Utilization, and Cerebrovascular Resistance

A collimated scintillation crystal is placed over the temporal region of the exposed skull on the right side and angled in such a way that viewed only brain and overlying skull.

Approximately 260 µCi of ^{133}Xenon dissolved in 0.5 ml sterile heparinized saline (500 IU) is injected over 1 s into the catheter in the lingual branch of the carotid artery. The gamma-ray emission of the $_{133}$Xe are detected by the scintillation counter attached to a photomultiplier. The pulses are amplified and subjected to pulse height analysis (peak 81 KeV ± 8 KeV) to reduce Compton scatter before fed into a rate meter and scaler. The output from the rate meter is displayed on a chart recorder. Cerebral blood flow is calculated from the height/area equation (Høedt-Rasmussen et al. 1966). The formula used is

$$F = (H_2 - H_{10}) \times 100/\lambda A_{10}\,,$$

where F is CBF in ml blood per 100 g brain tissue per min; λ = brain tissue/blood partition coefficient for ^{133}Xe (the figure of 1.1 is used [Veall and Mallett 1966]); H_i = maximum initial height of the ^{133}Xe clearance curve in counts per min as taken from the chart recorder; H_{10} = height of the clearance curve 10 min after the peak height in counts per s; A_{10} = total integrated counts over the 10 min of clearance as taken from the scaler and corrected for background activity over that period.

Cerebral oxygen consumption is measured from the product of the DBF and the difference in oxygen content between the arterial blood and cerebral venous blood sampled from the sagittal sinus. Blood oxygen is measured by a charcoal-fuel cell system (Lex-O_2-Con).

An estimate of cerebrovascular resistance is obtained by subtracting the mean sagittal sinus pressure from the mean arterial pressure and dividing this pressure difference by the CBF.

EEG Recording

Electroencephalographic readings are recorded bilaterally throughout the experiment. A series of holes are drilled in the calvarium 10 mm apart in two rows. Each row is 14 mm lateral to the sagittal suture. The holes are threaded to receive nylon screws in which silver-silver chloride ball electrodes are fixed loosely. The electrodes are positioned epidurally and the free ends are soldered to a multi-channel socket which is mounted on the calvarium with plaster of Paris.

Experimental Procedure

Following completion of the surgery, the animals are left undisturbed for 1 h. At least three control estimations of CBF and other parameters are made until steady conditions of flow, arterial blood pressure, and blood gas tensions are obtained.

Protocols

Intravenous administration. After stable control values have been established, the infusion is started. The CBF is measured at 5 min after the start and again at 25 min. The infusion is stopped 10 min after this flow period, giving a total infusion time of 35 min. Further flow measurements are made at 10, 30, and 50 min after stopping the infusion.

Intracarotid administration. After establishing control values, the intracarotid infusion of the test drug is begun. The CBF is measured at 10, 30, 50 and 70 min. The infusion is stopped 80 min after commencing, and post infusion measurements are made after 20, 40, and 60 min.

EVALUATION

Data are presented as mean values ± SEM Evaluation of statistical significance is performed by means of Student's *t*-test with Bonferroni correction.

MODIFICATIONS OF THE METHOD

Kozniewska et al. (1992), Wang et al. (1992) measured cerebral blood flow in **rats** by intracarotid injection of ^{133}Xe.

Solomon et al. (1985) and Clozel and Watanabe (1993) induced cerebral vasoconstriction by injection of autologous blood in the cisterna magna of rats. Cerebral blood flow was measured with the radioactive microsphere technique.

Lin et al. (2003) described a model of subarachnoid hemorrhage-induced cerebral vasospasm in **mice**. Adult mice received injections of autologous blood into the cisterna magna. The diameters of large intracranial vessels were measured 1 h to 7 days after the subarachnoid hemorrhage. A diffuse blood clot was evident in both the anterior and posterior circulations. Vascular wall thickening, lumenal narrowing, and corrugation of the internal elastic lamina were observed. Both acute (6–12 h) and delayed (1–3 days) phases of vasoconstriction occurred after subarachnoid hemorrhage. Overall mortality was only 3%. The model is recommended for screening of therapeutic candidates.

Delayed cerebral vasospasm was induced in anesthetized **dogs** by removal of 4 ml cerebrospinal fluid and injection of the same volume of fresh autologous arterial nonheparinized blood into the cisterna magna by Varsos et al. (1983) as a model of subarachnoid hemorrhage. The procedure was repeated on the third day and angiograms were taken of the vertebral-basilar vessels. The reduction of diameter of the basilar artery was taken as endpoint.

Imaizumi et al. (1996) produced experimental subarachnoid hemorrhage by intracisternal injection of arterial blood in **rabbits**. The degree of vasospasm and the effect of calcitonin gene-related peptide were evaluated angiographically by measuring the basilar artery diameter.

Inoue et al. (1996) produced experimental subarachnoid hemorrhage in **cynomolgus monkeys** by placing a clot around the internal carotid artery. A series of angiographic analyses were performed, before subarachnoid hemorrhage and on days 7 and 14 after treatment with calcitonin gene-related peptide to examine changes in the diameter of the ipsilateral internal carotid artery, middle cerebral artery, and anterior cerebral artery.

Hughes et al. (1994) adapted the ^{133}xenon clearance technique for simultaneous measurement of cutaneous blood flow in **rabbits** at a large number of skin sites within the same animal.

REFERENCES AND FURTHER READING

Clozel M, Watanabe H (1993) BQ-123, a peptidic endothelin ET_A receptor antagonist, prevents the early cerebral vasospasm following subarachnoid hemorrhage after intracisternal but not after intravenous injection. Life Sci 52:825–834

Grome JJ, Rudolphi K, Harper AM (1985) Cerebrovascular effects of a xanthine derivative propentofylline (HWA 285). Drug Dev Res 5:111–121

Høedt-Rasmussen K, Sveinsdottir E, Lassen NA (1966) Regional cerebral blood flow in man determined by intra-arterial injection of radioactive inert gas. Circ Res 18:237

Hughes S, Brain S, Williams G, Williams T (1994) Assessment of blood flow changes at multiple sites in rabbit skin using a ^{133}xenon clearance technique. J Pharmacol Toxicol Meth 32:41–47

Imaizumi S, Shimizu H, Ahmad I, Kaminuma T, Tajima M, Yoshimoto T, Megyesi J, Findlay JM, Kikuchi H, Nozaki K (1996) Effect of calcitonin gene-related peptide on delayed vasospasm after experimental subarachnoid hemorrhage in rabbits. Surg Neurol 46:263–271

Inoue T, Shimizu H, Kaminuma T, Tajima M, Watabe K, Yoshimoto T, Dacey RG Jr, Solomon RA, Selman WR (1996) Prevention of cerebral vasospasm by calcitonin gene-related peptide slow-release tablet after subarachnoidal hemorrhage in monkeys. Neurosurgery 39:984–990

Kozniewska E, Oseka M, Stys (1992) Effects of endothelium-derived nitric oxide on cerebral circulation during normoxia and hypoxia in the rat. J Cerebr Blood Flow Metab 12:311–317

Lacombe P, Meric P, Seylaz J (1980) Validity of cerebral blood flow measurements obtained with quantitative tracer techniques. Brain Res Rev 2:105–169

Lin CL, Calisaneller T, Utica N, Dumont AS, Kassell NF, Lee KS (2003) A murine model of subarachnoid hemorrhage-induced cerebral vasospasm. J Neurosci Meth 123 :89–97

Nielsen SL, Lassen NA, Elmqvist D (1975) Muscle blood flow in man studied with the local radioisotope method. In: Kunze K, Desmedt JE (eds) Studies on Neuromuscular Diseases. Proc Intern Sympos, Giessen 1973, Karger, Basel, pp 79–81

Solomon RA, Antunes JL, Chen RYZ, Bland L, Chien S (1985) Decrease in cerebral blood flow in rats after experimental sub-archnoid hemorrhage: a new animal model. Stroke 16:58–64

Varsos VG, Liszczak TM, Han DH, Kistler JP, Vielma J, Black PM, Heros RC, Zervas NT (1983) Delayed cerebral vasospasm is not reversible by aminophylline, nifedipine, or papaverine in a "two-hemorrhage" canine model. J Neurosurg 58:11–17

Veall N, Mallett BL (1966) Regional cerebral blood flow determination by ^{133}Xe inhalation and external recording: The effect of arterial recirculation. Clin Sci 30:353

Wang Q, Paulson OB, Lassen NA (1992) Effect of nitric oxide blockade by N^G-nitro-L-arginine on cerebral blood flow response to changes in carbon dioxide tension. J Cerebr Blood Flow Metab 12:947–953

A.8.1.10 Effect on Cerebral Blood Flow in Cats (Fluvography)

PURPOSE AND RATIONALE

Cerebral blood flow in anaesthetized cats an be measured by fluvography. The heat transfer coefficient of

the brain can be measured with a probe representing an indirect blood flow value.

In this method, the measuring device consists of a thermo probe, which is attached to the tissue in order to record continually the heat transport (Hensel, 1956). The device depends on having an electrically heated part and an unheated reference point. The difference in temperature between the heated part of the device and the unheated reference point is a function of local blood flow. An increase in flow tends to lower the local temperature by carrying away the heat gain and vice versa.

PROCEDURE

Cats of either sex weighing 2.5–4.0 kg are anaesthetized by intraperitoneal administration of pentobarbital sodium (35 mg/kg) and intubated with a tracheal tube. The left femoral vein and the right femoral artery are cannulated for i.v. drug administration and determination of arterial blood pressure, respectively. The arterial cannula is connected to a Statham transducer P 23 Db.

For intraduodenal drug administration the duodenum is cannulated following laparotomy.

Before actually starting the experiment, the arterial blood gas concentrations are determined.

Animals are only used for further testing if they show normal blood gas concentrations. During the course of the experiment, blood flow, blood pressure and blood gas concentrations are regularly monitored.

The head of the animal is fixed in a stereotactic device. The skull cap and the dura are opened, the probes are placed on the surface of the cortex in the region of the marginal frontal gyrus, and the exposed brain is covered with moist swabs. The Fluvograph (Hartmann+Braun, Frankfurt) is used with the appropriate thermo probes.

To test the correct position of the thermocouple and the response of the animal, inhalations of carbon dioxide/ air or injections of epinephrine (adrenaline) are used, leading to a distinctive increase in cerebral blood flow. Following stabilization of the parameters mentioned above, the standard compound is administered and the change in blood flow is recorded. Five min after obtaining the original values, the test compound is administered.

Standard compound:

- pentoxifylline
  1 and 3 mg/kg (i.v. administration)
  10 and 30 mg/kg (i.d. administration)

EVALUATION

The percent change in the heat transfer coefficient is used as an indirect measure for the change of cerebral blood flow. Statistics: Student's *t*-test is performed by unpaired comparison.

REFERENCES AND FURTHER READING

Betz E (1965) Local heat clearance from the brain as a measure of blood flow in acute and chronic experiments. Acta Neurol Scand Suppl 14:29–37

Golenhofen K, Hensel H, Hildebrandt G (1963) Durchblutungsmessungen mit Waerme-Elementen. Georg Thieme Verlag, Stuttgart

Lacombe P, Meric P, Seylaz J (1980) Validity of cerebral blood flow measurements obtained with quantitative tracer techniques. Brain Res Rev 2:105–169

A.8.1.11
Effect on Cerebral Blood Flow and in Ischemic Skeletal Muscle in Rats (Laser-Doppler-Effect)

PURPOSE AND RATIONALE

The principle of the Laser Doppler effect is based on the fact that a laser light beam directed on tissue is scattered in static structures as well as in moving cells. Light beams scattered in moving red cells undergo a frequency shift according to the Doppler effect, while beams scattered in static tissue alone remain unshifted in frequency. The number of Doppler shifts per time is recorded as a measure for erythrocyte flow in a given volume. This means, that the direction of flow cannot be determined, but relative changes in micro circulatory blood flow can be recorded. The procedure can be used to detect test compounds that improve the blood supply of the brain or the flow of red blood cells in the ischemic skeletal muscle.

PROCEDURE

Male Sprague-Dawley rats weighing 300–500 g are anaesthetized with pentobarbital sodium (60 mg/kg i.p.). The trachea is exposed and intubated with a short tracheal tube to allow ventilation. The following vessels have to be cannulated: The femoral vein is cannulated for test drug administration. The femoral artery is cannulated for blood pressure recording and blood gas analysis.

Before actually starting the experiment, the arterial blood gas concentrations are determined. Animals are only used for further testing if they show normal blood gas concentrations (pa CO_2: 32–42 mm Hg; pa O_2: 70–110 mm Hg). The mean arterial blood pressure should not drop below 100 mm Hg. During the course of the experiment, blood flow, blood pressure and blood gas concentrations are regularly monitored.

For Cerebral Blood Flow

The head of the animal is fixed in a stereotactic device. After trepanation of the skull (opening 3 mm in diameter), the Laser Doppler probe is placed 1 mm above the surface of the brain. Values are measured with the Laser Doppler apparatus (Periflux F2, Perimed KB, Stockholm).

Following stabilization of the parameters mentioned above, the standard compound is administered and the change in blood flow is recorded. Five min after obtaining the original values, the test compound is infused. Following two administrations of the test compound, the standard compound is administered again. Duration of the effect is measured as half life in seconds.

For Peripheral Blood Flow

A small area of the femoral artery of the right hind limb is exposed and the Laser Doppler probe is placed 1 mm above the muscle surface. Before actually starting the experiment, the arterial blood gas concentrations are determined. Animals are only used for further proceeding if they show normal blood gas concentrations. During the course of the experiment, the blood pressure is recorded. The RBC flux is recorded continuously and after stabilization of the output signal, the femoral artery is occluded leading to underperfusion of the muscles of the right pelvic limb. At this stage, the test compound is administered by intravenous infusion for 10 min (0.05 ml/min).

Standard compound for cerebral blood flow is propentofylline (1 mg/kg, i.v.). The percent increase in blood flow produced by propentofylline ranges between 40% and 60%.

EVALUATION

The percent increase in blood flow after test drug administration is determined (compared to the value before drug administration).

Statistics: Student's *t*-test by unpaired comparison, test substance versus standard.

MODIFICATIONS OF THE METHOD

Iadecola (1992), Prado et al. (1992), Raszkiewicz et al. (1992) measured the influence of nitric oxide on cortical cerebral blood flow in anesthetized rats by Laser-Doppler flowmetry.

Benessiano et al. (1985) measured aortic blood flow with range-gated Doppler flowmeter in anesthetized rats.

Partridge (1991) measured nerve blood flow in the sciatic nerve of anesthetized rats with a Laser Doppler Flowmeter after application of local anesthetics and of epinephrine.

REFERENCES AND FURTHER READING

Benessiano J, Levy BI, Michel JB (1985) Instantaneous aortic blood flow measurement with range-gated Doppler flowmeter in anesthetized rat. J Pharmacol Meth 14:99–110

Iadecola C (1992) Does nitric oxide mediate the increases in cerebral blood flow elicited by hypercapnia? Proc Natl Acad Sci USA 89:3913–3916

Kunze K, Berk H (1975) Oxygen supply and muscle blood flow in normal and diseased muscle. In: Kunze K, Desmedt JE (eds) Studies on Neuromuscular Diseases. Proc Intern Sympos, Giessen 1973, Karger, Basel, pp 82–91

LeNoble JLML, Struyker-Boudier HAJ, Smits JFM (1987) Differential effects of general anesthetics on regional vasoconstrictor responses in the rat. Arch Int Pharmacodyn 289:82–92

Partridge BL (1991) The effects of local anesthetics and epinephrine on rat sciatic nerve blood flow. Anesthesiology 75:243–251

Prado R, Watson BD, Kuluz J, Dietrich WD (1992) Endothelium-derived nitric oxide synthase inhibition. Effects on cerebral blood flow, pial artery diameter, and vascular morphology in rats. Stroke 23:1118–1124

Raszkiewicz JL, Linville DG, Kerwin JF, Wagenaar F, Arneric SP (1992) Nitric oxide synthase is critical in mediating basal forebrain regulation of cortical cerebral circulation. J Neurosci Res 33:129–135

Rudquist I, Smith QR, Michel ME, Ask P, Öberg P, Rapoport SI (1985) Sciatic nerve blood flow measured by laser Doppler flowmetry and [^{14}C]iodoantipyrine. Am J Physiol 248:H311–H317

A.8.1.12 Traumatic Brain Injury

PURPOSE AND RATIONALE

A major goal in research into mechanisms of brain damage and dysfunction in patients with severe head injury and in discovery of potential therapies is the development of a suitable animal model. While a variety of experimental techniques have been developed (Denny-Brown and Russell 1941; Gurdjian et al. 1954; Ommaya and Gennarelli 1974; Sullivan et al. 1976; Nilsson et al. 1977; Hayes et al. 1984; Marmarou et al. 1994; Mésenge et al. 1996), the most widely employed technique is fluid percussion, which produces brain injury by rapid injection of fluid into the closed cranial cavity (Sullivan et al. 1976; McIntosh et al. 1989, 1990; Faden et al. 1989; Dixon et al. 1991; Sun and Faden 1995; Petty et al. 1996; Laurer et al. 2000; Maegele et al. 2005). Most authors used rats, however, other species, such ad cats (Sullivan et al. 1976; Hayes et al. 1983, 1984), rabbits (Lindgren and Rinder 1969) and mice (Hall et al. 1988; Mésenge et al. 1996) were employed.

PROCEDURE

Surgical Preparation

Male Sprague Dawley rats weighing from 400 to 500 g are anesthetized with ketamine (80 mg/kg, i.m.) and sodium pentobarbital (20 mg/kg, i.p.). During surgical preparation and throughout the experiment, all wounds are infused with a topical anesthetic (lidocaine hydrochloride 2.0%). Catheters are inserted into the femoral vein for drug administration and into the femoral artery for blood pressure/blood gas monitoring. A 2.0 mm hollow female Leur-Loc fitting (to induce trauma) is rigidly fixed with dental cement to the animal's skull in a craniectomy centered over the left parietal cortex 5 mm from lambda, 5 mm from bregma, 4 mm from sagittal suture. The dura is left intact at this opening. Immediately following surgical preparation, a constant i.v. infusion of sodium barbital (15 mg/kg/h) is begun and maintained for the duration of the studies.

Drug Administration

Drugs or equal volumes of saline are administered through the femoral vein over 10 min by constant infusion beginning 15 min before trauma.

Fluid-Percussion Injury

The fluid-percussion device consists of a Plexiglas cylindrical reservoir, 60 cm long and 4.5 cm in diameter, bounded at one end by a Plexiglas, cork-covered piston mounted on O-rings. The opposite of the reservoir is fitted with a 2-cm-long metal housing on which a transducer is mounted and connected to a 5-mm tube (2 mm inner diameter) that terminates with a male Luer-Loc fitting. At the time of injury the tube is connected with the female Luer-Loc fitting that has been chronically implanted over the exposed dura of the rat. After the entire system is filled with 37°C isotonic saline, injury is induced by a metal pendulum which strikes the piston of the device from a predetermined height. The device produces a pulse of increased intracranial pressure of fairly constant duration (21–23 ms) by injecting various volumes of saline into the closed cranial cavity. Brief displacement and deformation of neural tissue results from the rapid epidural injection of saline. The magnitude of injury is regulated by varying the height of the pendulum, which results in corresponding variations of the intracranial pressure expressed in atmospheres. The pressure pulses are measured extracranially by a transducer and recorded on a storage oscilloscope.

EVALUATION

Behavioral Outcome

Posttraumatic deficits are evaluated at 24 h, 1 week and 2 weeks following trauma. Outcomes include forelimb flexion (right and left), lateral pulsion (right and left) and angle score (left, right and vertical position). Scores range from 0 (maximal deficits) to 5 (normal) for each task, By combining scores of all tests, a composite neuroscore is determined, ranging from 0 to 35 (Faden 1993).

Histopathology

At 2 weeks, following final neurological scoring, the rats are sacrificed by decapitation. The brain is removed, quickly frozen in isopentane and stored in a –80°C freezer until sectioning. Coronal brain sections are selected to span the longitudinal axis of the dorsal hippocampus between –3.2 and –3.8 Bregma. Sections (16 mm thick) are cut at –18°C in a microtome-cryostat and thaw-mounted onto chrome-gelatin rubbed microscope glass slides and kept at –80°C for histological study.

Sections are stained with Crystal violet. CA1 and CA3 pyramidal cells with a distinct nucleus and nucleolus are counted as viable neurons, in one reticle within CA3 and in three reticles (R1, R2 and R3) within the subfield of the hippocampus, in both right and left hemispheres. The number of viable neurons is counted twice at 400 × microscope field.

An immunochemical method is used to detect glial fibrillary acidic protein (GFAP)-positive astrocytes in the hippocampus (Faddis and Vijayan 1988). Counting of the number of cells is done under 400 × light microscopy in the dorsal CA1 subfield between medial and lateral regions.

Statistical Analysis

Neuroscores from forelimb flexion tests, lateral pulsion tests and angle board tests are statistically analyzed by non-parametric Mann-Whitney U-tests. Histological data are analyzed by one way ANOVA test, followed by Scheffe's test.

MODIFICATIONS OF THE METHOD

Shohami et al. (1995) tested the effect of a non-psychotropic cannabinoid which acts as a non-competitive NMDA antagonist on motor and memory functions after closed head injury in the **rat**.

Fox et al. (1998) developed a **mouse** model of traumatic brain injury using a device that produces controlled cortical impact, permitting independent manipulation of tissue deformation and impact velocity and

resulting in sustained sensory/motor and cognitive defects.

Tang et al. (1997) reported impairment in learning and memory in an experimental model of concussive brain injury in **mice**.

Bemana and Nago (1998) induced acute intercranial hypertension in **cats** by continuous inflation of an extradural balloon with physiological saline at a constant rate of 0.5 ml/h for 3 h. At this point, inflation was discontinued and the balloon remained expanded for an additional hour after which it was deflated.

A model of **traumatic injury to the spinal cord** was used by Springer et al. (1997). Female Long Evans rats weighing 200–250 g were anesthetized with pentobarbital and a dorsal laminectomy was performed to expose the spinal cord at thoracic level T 10. The vertebral column was stabilized by clamping the column at vertebra 8 and 11. The New York University (NYU) impactor device was used which produces accurate and reproducible damage to the rat spinal cord (Gruner 1992; Basso et al. 1996). This device is a weight drop apparatus that uses optical potentiometers to record the movement of a 10-g impact rod and the vertebral column following impact and is connected to a PC that monitors rod and vertebral movements during impact.

REFERENCES AND FURTHER READING

Basso DM, Beattie MS, Bresnahan JC (1996) Graded histological and locomotor outcomes after spinal cord contusion using the NYU weight-drop device versus transection. Exp Neurol 139:244–256

Bemana I, Nagao S (1998) Effects of Niravoline (RU 51599), a selective kappa-opioid receptor agonist on intracranial pressure in gradually expanding extradural mass lesion. J Neurotrauma 15:117–124

Denny-Brown D, Russell WR (1941) Experimental cerebral percussion. Brain 64:93–164

Dixon CE, Clifton GL, Lighthall JW, Yagjmai AA, Haynes RL (1991) A controlled cortical impact model of traumatic brain injury in the rat. J Neurosci Meth 39:253–262

Faddis B, Vijayan VK (1988) Application of glial fibrillary acidic protein histochemistry in the quantification of astrocytes in the rat brain. Am J Anat 183:316–322

Faden AI (1993) Comparison of single and combination drug treatment strategies in experimental brain trauma. J Neurotrauma 10:91–100

Faden AI, Demediuk P, Panter SS, Vink R (1989) The role of excitatory amino acids and NMDA receptors in traumatic brain injury. Science 244:798–800

Fox GB, Fan L, Lavasseur RA, Faden AI (1998) Sustained sensory/motor and cognitive deficits with neuronal apoptosis following controlled impact brain injury in the mouse. J Neurotrauma 15:599–614

Gruner JA (1992) A monitored contusion model of spinal cord injury in the rat. J Neurotrauma 9:123–128

Gurdjian ES, Lissner HR, Webster JE (1954) Studies on experimental concussion. Relation of physiological effect to time duration of intracranial pressure increase at impact. Neurology 4:674–681

Hall ED, Yonkers PA, McCall JM (1988) Effects of the 21-amino-steroid U74006F on experimental head injury in mice. J Neurosurg 68:456–461

Hayes RL, Lewelt W, Yeatts ML (1983) Metabolic, behavioral and electrophysiological correlates of experimental brain injury in the cat. J Cerebr Blood Flow Metab 3:38–40

Hayes RL, Pechura CM, Katayama Y, Povlishock JT, Giebel ML, Becker DP (1984) Activation of pontine cholinergic sites implicated in unconsciousness following cerebral percussion in cats. Science 223:301–303

Laurer HL, Lenzlinger PM, McIntosh TK (2000) Models of traumatic brain injury. Eur J Trauma 26:95–100

Lindgren S, Rinder L (1969) Production and distribution of intracranial and intraspinal pressure changes at sudden extradural fluid volume input in rabbits. Acta Physiol Scand 76:340–351

Maegele M, Gruener-Lippert M, Ester-Bode T, Garbe J, Bouillon B, Neugebauer E, Klug N, Lefering R, Neiss WF, Angelov DN (2005) Multimodal early onset stimulation combined with enriched environment is associated with reduced CNS lesion volume and enhanced reversal of neuromotor dysfunction after traumatic brain injury in rats. Eur J Neurosci 21:2406–2418

Marmarou A, Foda MAAE, van den Brink W, Campell J, Kita H, Demetriadu K (1994) A new model of diffuse brain injury in rats. J Neurosurg 80:291–300

McIntosh TK, Vink R, Noble L, Yamakami I, Fernyak S, Soares H, Faden AL (1989) Traumatic brain injury in the rat: characterization of a lateral fluid-percussion model. Neurosci 28:233–244

McIntosh TK, Vink R, Soares H, Hayes R, Simon R (1990) Effect of noncompetitive blockade of N-methyl-D-aspartate receptors on the neurochemical sequelae of experimental brain injury. J Neurochem 55:1170–1179

Mésenge Ch, Verrecchia C, Allix M, Boulu RR, Plotkine M (1996) Reduction of the neurological deficit in mice with traumatic brain injury by nitric oxide synthase inhibitors. J Neurotrauma 13:209–214

Nilsson B, Ponten U, Voigt G (1977) Experimental head injury in the rat. Part 1. Mechanics,

Ommaya AK, Gennarelli TA (1974) Cerebral concussion and traumatic unconsciousness. Correlation of experimental and clinical observations on blunt head injuries. Brain 97:633–654

Petty MA, Poulet P, Haas A, Namer IJ, Wagner J (1996) Reduction of traumatic brain injury-induced cerebral oedema by a free radical scavenger. Eur J Pharmacol 307:149–155

Shohami E, Novikov M, Bass R (1995) Long-term effect of HU211, a novel non-competitive NMDA antagonist, on motor and memory functions after closed head injury in the rat. Brain Res 674:55–62

Springer JE, Azbill RD, Mark RJ, Begley JG, Waeg G, Mattson MP (1997) 4-Hydroxynonenal, a lipid peroxidation product, rapidly accumulates following traumatic spinal cord injury and inhibits glutamate uptake. J Neurochem 68:2469–2476

Sullivan HG, Martinez J, Becker DP, Miller JD, Griffith R, Wist AO (1976) Fluid-percussion model of mechanical brain injury in the cat. J Neurosurg 45:520–534

Sun FY, Faden AI (1995) Neuroprotective effects of 619C89, a use-dependent sodium channel blocker, in rat traumatic brain injury. Brain Res 673:133–140

Tang Y-P, Noda Y, Hasegawa T, Nabeshima T (1997) A concussive-like brain injury model in mice: impairment in learning and memory. J Neurotrauma 14:851–862

A.8.1.13 Cerebral Blood Flow Measured by NMRI

PURPOSE AND RATIONALE

Over the past several years, magnetic resonance imaging (MRI) has become an established tool in the drug discovery and development process. The main advantages of MRI are its high resolution, non-invasiveness and versatility, which allow comprehensive characterization of a disease state and the effects of drug intervention. Recent advances now allow the application of this technique to the characterization of models of lung inflammation in rats and to the profiling of anti-inflammatory drugs. Repeated measurements can be carried out on the same animal, and time-courses of events can be easily assessed. Furthermore, the prospect of using MRI to detect non-invasively a sustained mucus hypersecretory phenotype induced by endotoxin brings an important new perspective to models of chronic obstructive pulmonary disease in animals. Importantly, it might be possible to extend the use of this technique to the clinical study of inflammation in the lung and the consequences of drug treatment (Beckmann et al. 2003, 2004).

Functional magnetic resonance imaging has been developed as pharmacological magnetic resonance imaging for pharmacodynamic assays and to establish brain-penetrating parameters (Leslie and James 2000). Although the regional cerebral metabolic rate of glucose is strongly increased during cerebral activity, the cerebral metabolic rate of O_2 is not increased in direct proportion. The result is that the relative uptake of O_2 from blood actually decreases. The veins and capillaries draining from the activated region are "arterialized" and their deoxyhemoglobin concentration is reduced. Deoxygenated and oxygenated hemoglobin have different magnetization properties; thus the changes in the ratio of these two entities can be detected by blood-oxygen-level-dependent (BOLD) magnetic resonance imaging. At least for studies in animals, these methods may be preferred to positron emission tomography (Cherry and Phelps 1996).

Petty et al. (2003) studied the *in vivo* neuroprotective effects of a systemically active antagonist of the NMDA receptor glycine site by magnetic resonance imaging in ischemic stroke in rats.

PROCEDURE

Transient Model of Focal Ischemia in Rats

In the right common carotid artery was ligated. The transient model of middle cerebral artery occlusion was based on techniques described by Zea Longa et al. (1989) and Belayev et al. (1996). By means of an operating microscope, the right common carotid artery was exposed through a midline neck incision. The right superior thyroid, occipital, and pterygopalatine arteries were ligated and cut. A poly-L-lysine-coated 3–0 nylon monofilament with a heat-blunted tip was inserted through the proximal external carotid artery into the internal carotid artery and pushed forward a distance of 19 or 20 mm from the carotid bifurcation, depending on the weight of the rat, so as to occlude the origin of the middle cerebral artery. After suture placement, the neck incision was closed and the animal was allowed to regain consciousness. Two hours following occlusion of the artery, the rats were tested on a standard neurological battery to confirm the presence of a neurological deficit. Animals that did not exhibit a forelimb flexion were excluded from further study. At this time, the rats were re-anesthetised and the intraluminal suture was completely withdrawn to restore the blood supply.

Magnetic Resonance Imaging (MRI) Measurements

Measurements were performed 30 min, 3 h, and 24 h after the onset of ischemia on a 7-T Bruker BIOSPEC experimental scanner (DBX; Bruker Medical, Ettlingen, Germany) with a 30-cm bore magnet and actively shielded gradient coils (200 mT/m; rise time < 80 µs).

A 72-mm resonator was used for *rf* transmission; signals were detected with a 35-mm inductively coupled surface coil placed over the skull of the animal. The *rf* coils were decoupled from each other – the transmitter coil actively and the receiver coil passively.

Using gradient-echo imaging, sagittal pilot scans were performed to ensure accurate positioning of the animal in the magnet. For this purpose, the coronal plane 5.9 mm posterior to the rhinal fissure was placed in the isocenter of the magnet, thus focusing on the center of the ischemic territory resulting from the middle cerebral artery occlusion.

For the determination of the temporal evolution of the ischemic lesion, two NMR imaging modalities were used. A field of view of 3.2 cm, a slice thickness of 1.5 mm, and an interslice distance of 2 mm were used for both sequences. Multislice packages were recorded by placing the center of the multislice imaging packet 5.9 mm posterior to the rhinal fissure.

Diffusion-weighted imaging was performed using a Stejskal–Tanner spin-echo sequence [echo time (TE) = 37.2 ms, repetition time (TR) = 2325 ms, eight slices] in six rats per group. To enable quantification of the apparent diffusion coefficient (ADC) of brain water, three b values were used (b = 50, 825,

and 1600 s/mm^2). ADC maps were calculated pixelwise using the monoexponential model (Le Bihan et al. 1986).

Perfusion-weighted imaging was performed with an ultrafast version of the arterial spin tagging technique (Kerskens et al. 1996; Franke et al. 2000) in four rats per group. In independent experiments, three coronal slices were recorded, thus covering the central part of the ischemic lesion. Measurement parameters were: TE = 3.5 ms, TR = 7.4 ms, MATRIX = 128 × 64, AVERAGE = 8. Each experiment consisted of two image acquisitions separated by a recovery period. During the first acquisition, blood flowing through the neck was adiabatically inverted (preparation TIME = 3 s; *z*-gradient = 5 mT/m; B1 FIELD = 150 mG; off-resonance FREQUENCY = 6000 Hz; mean preparation DISTANCE = 2.8 cm upstream from the imaging plane); in the second acquisition, inflowing spins were left undisturbed. Both phases were separated by a recovery period of 10 s. In each perfusion experiment, the two images suffered the same signal loss due to magnetization transfer effects but differed in the magnetization of the inflowing blood. Perfusion-weighted images were obtained by subtraction of the acquisitions with and without prior adiabatic spin inversion. In the second acquisition, inflowing spins were left undisturbed. Perfusion-weighted images were obtained by subtraction of the acquisitions with and without prior adiabatic spin inversion.

EVALUATION

Data were transferred to a PC and image analysis was carried out using the image processing software Scion Image for Windows (Scion Corporation, Frederick, Md., USA). Lesion volumes were calculated using ADC maps, as the ischemic lesion area was estimated by summing up all pixels with a relative ADC < 80% compared to the healthy, contralateral hemisphere (Hoehn-Berlage et al. 1995). Perfusion signal intensities are referred to the homologous contralateral regions and given as ratios of ipsilateral to contralateral values.

MODIFICATIONS OF THE METHOD

Edema following middle cerebral artery occlusion in spontaneously hypertensive rats was measured by magnetic resonance imaging (Seega and Elger 1993; Elger et al. 1994a). Magnetic resonance imaging was also used to determine the size of intracerebral hemorrhage in rats induced by stereotactic microinfusion of collagenase into the caudate putamen (Elger et al. 1994b).

Reese et al. (2000) visualized regional brain activation by bicucculine by functional magnetic resonance imaging. Time-resolved assessment of bicucculine-induced changes in local cerebral blood volume was achieved using magnetite nanoparticles as an intravascular contrast agent.

Pevsner et al. (2001) described a photothrombotic method of acute small stroke induction in rats with histopathologic and *in vivo* magnetic resonance imaging (MRI) observations from 3 to 6 h after irradiation, which is homologous to a human autopsy specimen. Utilizing 30 min of irradiation with minimal beam intensity (0.1 W/cm^2) cold white light in conjunction with 20 mg of intravenous (i.v.) rose bengal as a rapid infusion, small infarcts were induced photochemically in the frontal lobes of rats.

Using *in vivo* and *ex vivo* magnetic resonance imaging, Ohlstein et al. (2000) evaluated the effects of tranilast, an antiallergic drug, on neointima formation following balloon angioplasty of the rat coronary artery.

Swain et al. (2003) employed T-two-star (T_2*)-weighted and flow-alternating inversion recovery (FAIR) functional magnetic resonance imaging to assess chronic changes in blood volume and flow as a result of exercise in rats. Prolonged exercise induced angiogenesis and increased cerebral blood flow in primary motor cortex.

Using MRI evaluation of brain damage, Banfi et al. (2004) demonstrated that pentoxifylline prevents spontaneous brain ischemia in stroke-prone rats.

Henderson et al. (2004) studied functional magnetic resonance imaging during hypotension in young and adult cats.

In a magnetic resonance imaging study Shirhan et al. (2004) found that spermine reduces infarction and neurological deficit a rat model of middle cerebral artery occlusion.

Paczynski et al. (2000) studied the effects of fluid management on edema volume and midline shift in a rat model of ischemic stroke. MRI were obtained 24 h after the onset of ischemia so that the ratio of hemispheric volumes ipsilateral and contralateral to the infarct and the extent of midline shift could be obtained.

Cash et al. (2001) evaluated the effectiveness of aminoguanidine as a neuroprotective agent in a rat model of transient middle cerebral artery occlusion using serial magnetic resonance imaging.

The MRI protocol consisted of three interleaved imaging regimens: proton density-weighted imaging (PDWI), T_2-weighted imaging (T_2WI) and diffusion-weighted imaging (DWI). Repetition time (TR) was 3 s for each of the three regimens and echo times (TE)

were 70 ms for the T_2WI and DWI and 28 ms for the PDWI. For DWI, diffusion-sensitizing gradients (*b*-value 590×10^{-3} s/mm^2) were applied along the inferior to superior axis of the brain. Two averages were acquired per phase encode step. The images were collected at an in-plane resolution of 0.31×0.31 mm from 18 contiguous, 1-mm-thick slices, with a total acquisition time of 43 min.

REFERENCES AND FURTHER READING

Banfi C, Sironi L, de Simoni G, Gelosa P, Barcella S, Perego C, Gianazza E, Guetrini U, Tremoli E, Mussoni L (2004) Pentoxifylline prevents spontaneous brain ischemia in stroke-prone rats. J Pharmacol Exp Ther 310:890–895

Beckmann N, Tigani B, Mazzoni L, Fozzard JR (2003) Techniques: magnetic resonance imaging of the lung provides potential for non-invasive preclinical evaluation of drugs. Trends Pharmacol Sci 24:550–554

Beckmann N, Laurent D, Tigani B, Panizzutti R, Rudin M (2004) Magnetic resonance imaging in drug discovery: lessons from disease areas. Drug Dis Today 9:35–42

Belayev L, Alonso OF, Busto R, Zhao W, Ginsberg MD (1996) Middle cerebral artery occlusion in the rat by intraluminal suture: neurological and pathological evaluation of an improved model. Stroke 27:1616–1623

Cash D, Beech JS, Rayne RC, Bath PMW, Meldrum BS, Williams SCR (2001) Neuroprotective effect of aminoguanidine on transient focal ischaemia in the rat brain. Brain Res 905:91–103

Cherry SR, Phelps ME (1996) Imaging brain function with positron emission tomography. In: Toga AW, Mazziotta JC (eds) Brain mapping: the methods. Academic Press, New York, pp 191–221

Elger B, Seega J, Raschack M (1994a) Oedema reduction by levemopamil in focal cerebral ischaemia of spontaneously hypertensive rats studied by magnetic resonance imaging. Eur J Pharmacol 254:65–71

Elger B, Seega J, Brendel R (1994b) Magnetic resonance imaging study on the effect of levemopamil on the size of intracerebral hemorrhage in rats. Stroke 25:1836–1841

Franke C, van Dorsten FA, Olah L, Schwindt W, Hoehn M (2000), Arterial spin tagging perfusion imaging of rat brain: dependency on magnetic field strength. Magn Reson Imaging 18:1109–1113

Henderson LA, Macey PM, Richard CA, Runquist ML, Harper RM (2004) Functional magnetic resonance imaging during hypotension in the developing animal. J Appl Physiol 97:2248–2257

Hoehn-Berlage M, Norris DG, Kohno K, Mies G, D. Leibfritz D, Hossmann KA (1995) Evolution of regional changes in apparent diffusion coefficient during focal ischemia of rat brain: the relationship of quantitative diffusion NMR imaging to reduction of cerebral blood flow and metabolic disturbances. J Cereb Blood Flow Metab 15:1002–1011

Kerskens CM, Hoehn-Berlage M, Schmitz B, Busch E, Bock C, Gyngell ML, Hossmann KA (1996) Ultrafast perfusion-weighted MRI of functional brain activation in rats during forepaw stimulation: comparison with T_2*-weighted MRI. NMR Biomed. 8:20–23

Le Bihan D, Breton E, Lallemand D, Grenier P, E. Cabanis E, Laval-Jeantet M (1986) MR imaging of intravoxel incoherent motions: application to diffusion and perfusion in neurologic disorders. Radiology 161:401–407

Leslie RA, James MF (2000) Pharmacological magnetic resonance imaging: a new application for functional MRI. Trends Pharmacol Sci 21:314–318

Ohlstein EH, Romanic AM, Clark LV, Kapadia RD, Sarkar SK, Gagnon R, Chandra S (2000) Application of in vivo and ex vivo magnetic resonance imaging for the evaluation of tranilast on neointima formation following balloon angioplasty of the rat coronary artery. Cardiovasc Res 47:759–768

Paczynski RP, Venkatesan R, Diringer MN, He YY, Hsu CY, Lin W (2000) Effects of fluid management on edema volume and midline shift in a rat model of ischemic stroke. Stroke 31:1702–1708

Petty MA, Neumann-Haefelin C, Kalisch J, Sarhan S, Wettstein JG, Juretschke HP (2003) In vivo neuroprotective effects of ACEA 1021 confirmed by magnetic resonance imaging in ischemic stroke. Eur J Pharmacol 474:53–62

Pevsner PH, Eichenbaum JW, Miller DC, Pivawer G, Eichenbaum KD, Stern A, Zakian KL, Koutcher JA (2001) A photothrombotic model of small early ischemic infarcts in the rat brain with histologic and MRI correlation. J Pharm Toxicol Meth 45:227–233

Reese T, Bjelke B, Porszacz R, Baumann D, Bochelen D, Sauter A, Rudin M (2000) Regional brain activation by bicucculine visualized by functional magnetic resonance imaging. Time-resolved assessment of bicucculine-induced changes in local cerebral blood volume using an intravascular contrast agent. NMR Biomed 13:43–49

Seega J, Elger B (1993) Diffusion- and *T*2-weighted imaging: evaluation of oedema reduction in focal cerebral ischaemia by the calcium and serotonin antagonist levemopamil. Magnet Reson Imag 11:401–409

Shirhan MD, Moochala SM, Ng PY, Lu J, Ng KC, Teo L, Yap E, Ng I, Hwang P, Lim T, Sitoh YY, Rumpel H, Jose R, Ling E (2004) Spermine reduces infarction and neurological deficit following a rat model of middle cerebral artery occlusion: a magnetic resonance imaging study. Neuroscience 124:299–304

Swain RA, Harris AB, Wiener EC, Dutka MV, Morris HD, Theien BE, Konda S, Engberg K, Lauterbur PC, Greenough WT (2003) Prolonged exercise induces angiogenesis and increases cerebral blood flow in primary motor cortex of the rat. Neuroscience 117:1037–1046

Zea Longa E, Weinstein PR, Carlson S, Cummins RW (1989) Reversible middle cerebral artery occlusion without craniectomy in rats. Stroke 20:84–91

A.8.2 Peripheral Blood Supply

A.8.2.1 Perfused Hindquarter Preparation with Sympathetic Nerve Stimulation in Rats

PURPOSE AND RATIONALE

Perfusion of the hindquarter in rats with a constant flow rate allows the evaluation of the effect of drugs on the peripheral vascular bed. Since constant blood flow is maintained, changes in the vascular resistance of the perfused bed are directly proportional to changes in the perfusion pressure.

PROCEDURE

Male Wistar rats weighing between 250 and 300 g are pre-treated with heparin (1000 units/kg i.v.) and anesthetized with pentobarbital sodium (50 mg/kg i.p.) The animals are intubated with a tracheal tube and positive pressure ventilation is maintained with a Harvard Rodent Respirator at 4–6 ml/stroke and 50 strokes/min. The right jugular vein is cannulated with polyethylene tubing for administration of drugs.

The lumbar sympathetic chain is isolated dorsal to the inferior mesenteric branches via an abdominal midline incision. The aorta is freed from the vena cava and two silk ligatures are placed around the aorta. The aorta is ligated and cannulated proximal as well as distally with polyethylene tubings. A short piece of rubber tubing is inserted at the distal end to allow intraarterial injections of drugs. Two "T" junctions allow the measurement of arterial pressure and perfusion pressure by Statham P 23 Db pressure transducers being recorded through a Hellige physiological recorder. From the proximal part of the aorta, blood is forced to its distal part by a peristaltic pump (Desaga) through a glass coil kept at 40°C. Flow rate is adjusted to produce a stable perfusion pressure as close to the systemic pressure as possible. After initial adjustment, flow rate is not altered for the remainder of the experiment.

Following perfusion pressure stabilization, the sympathetic chain is isolated and a small (1 mm wide, 2 mm long) curved bipolar electrode is placed around the nerve for electrical stimulation. Square-wave pulses from a Grass stimulator are used to activate the nerve with a constant current of 2.5 milliamps, supramaximal voltage and varying frequencies of 5 ms duration.

A dose-response curve is established for norepinephrine by giving doses of 0.01 µg, 0.03 µg, 0.1 µg, 0.3 µg, 1.0 µg, and 3.0 µg intra-arterially and measuring perfusion pressure changes. Similarly, a frequency-response curve to nerve stimulation is established by stimulation at 3 Hz, 6 Hz, and 10 Hz for 30 s. Two predrug readings are taken to insure consistent responses.

A minimum of four animals is used for each test compound.

EVALUATION

The first predrug dose-response curves are compared with the second predrug, 5 min and 60 min postdrug dose-response curves. From regression equations for norepinephrine and nerve stimulation, mean responses and potency values with 95% confidence limits are calculated.

MODIFICATIONS OF THE METHOD

Folkow et al. (1970) perfused the hindquarters of spontaneously hypertensive rats and control rats at a constant rate of flow with an oxygenated plasma substitute in order to study the increased flow resistance and vascular reactivity. The hindquarters were isolated from the upper part of the body by standardized mass ligatures at identical levels until the aorta and the inferior caval vein provided the only intact circulatory connections between the two parts of each animal.

Thimm et al. (1984) described reflex increases in heart-rate induced by perfusing the hind leg of the rat with solutions containing lactic acid.

Thimm and Baum (1987) obtained spike recordings from chemosensitive nerve fibres of group III and IV of the rat nervus peroneus. Applications were performed either by perfusion of the circulatory isolated hindleg or by superfusion of the isolated musculus extensor digitorum longus.

Kitzen et al. (1978) used the perfused hind limb of the **dog** with sympathetic nerve stimulation for cardiovascular analysis.

Reitan et al. (1991) developed a near anesthetic-free isolated hindlimb model in the **dog** and studied the effects of halothane and atropine sulfate on vascular resistance.

Wiegershausen and Deptalla (1969) used the isolated perfused hindlimb of the **cat** to study the influence of local anesthetics on the vasoconstrictor actions induced by bradykinin, epinephrine and histamine.

Santiago et al. (1994) analyzed the responses to bradykinin in the hindquarters vascular bed of the cat.

Champion et al. (1996, 1997) analyzed the responses of human synthetic adrenomedullin, an analog of adrenomedullin and calcitonin gene-related peptides in the hindlimb vascular bed of the cat.

REFERENCES AND FURTHER READING

Bhattacharya BK, Dadkar NK, Dohadwalla AN (1977) Vascular reactivity of perfused vascular bed in spontaneously hypertensive and normotensive rats. Br J Pharmacol 59:243–246

Bomzon A, Naidu SG (1985) Perfusion of the isolated rat hind limb. An analysis of the technique. J Pharmacol Meth 14:285–296

Brody MJ, Shaffer RA, Dixon RL (1963) A method for the study of peripheral vascular responses in the rat. J Appl Physiol 18:645–647

Champion HC, Duperier CD, Fitzgerald WE, Lambert DG, Murphy WA, Coy DH, Kadowitz PJ (1996) [Mpr^{14}]-rADM(14–50), a novel analog of adrenomedullin, possesses potent vasodilator activity in the hindlimb vascular bed of the cat. Life Sci 59: PL1–7

Champion HC, Akers DL, Santiago JA, Lambert DG, McNamara DB, Kadowitz PJ (1997) Analysis of the responses to human synthetic adrenomedullin and calcitonin gene-

related peptides in the hindlimb vascular bed of the cat. Mol Cell Biochem 176:5–11
Dadkar NK, Dohadwalla AN, Bhattacharya BK (1977) The effect of tyramine on peripheral vasculature of the spontaneously hypertensive rat. J Pharm Pharmacol 29:48–49
Folkow B, Hallbäck M, Lundgren Y, Weiss L (1970) Background of increased flow resistance and vascular reactivity in spontaneously hypertensive rats. Acta Physiol Scand 80:93–106
Kitzen JM, Long JP, Cannon JG (1978) Pharmacology of 6,7-dihydroxy-2-dimethylaminotetralin (TL-99). I. Cardiovascular activity in the dog and cat. J Pharm Exp Ther 206:239–247
Reitan JA, Kien ND, Martucci RW, Thorup SJ, Dennis PJ (1991) Development of a near anesthetic-free isolated canine hindlimb model. The effects of halothane and atropine sulfate on vascular resistance. J Pharmacol Meth 26:223–232
Ross BD (1972) Hind-limb perfusion. In: Perfusion techniques in biochemistry. A laboratory manual in the use of isolated perfused organs in biochemical experimentation. Clarendon Press, Oxford, pp 308–320
Ruderman NB, Houghton CRS, Hems R (1971) Evaluation of the isolated perfused rat hind-quarter for the study of muscle metabolism. Biochem J 124:639–651
Santiago JA, Garrison EA, Kadowith PJ (1994) Analysis of responses to bradykinin: effects of Hoe-140 in the hindquarters vascular bed of the cat. Am J Physiol 267 (Heart Circ Physiol 36): H828–H836
Thimm F, Baum K (1987) Response of chemosensitive nerve fibres of group III and IV to metabolic changes in rat muscles. Pflügers Arch 410:143–152
Thimm F, Carvalho M, Babka M, Meier zu Verl E (1984) Reflex increases in heart-rate induced by perfusing the hind leg of the rat with solutions containing lactic acid. Pflügers Arch 400:286–293
Werber AH, Fink GD (1985) Continuous measurement of hindquarter resistance changes to nerve stimulation and intra-arterial drug administration in rats. J Pharmacol Meth 13:67–82
Wiegershausen B, Deptalla H (1969) Der Einfluß einiger Lokalanästhetika auf die erregende Wirkung von Bradykinin am glatten Muskel. 1. Mitteilung: Die Verstärkung der vasokonstriktorischen Wirkung von Bradykinin an der isolierten Hinterpfote der Katze. Arch Int Pharmacodyn 177:278–286

A.8.2.2 Effect on Peripheral Blood Flow in Rats

PURPOSE AND RATIONALE

Various methods exist to measure peripheral blood flow in rats, such as the microsphere technique, electromagnetic flowmetry and Doppler ultrasonic flowmetry.

Radioactive microspheres are used to calculate the distribution of blood from the heart to various organs and tissues before and after the administration of test compounds. In this method, microspheres are injected into the left cardiac ventricle. It is postulated that the first contraction of the cardiac muscle will expel these spheres into the circulation. Consequently the microspheres can be trapped in different organs according to the organ's perfusion rate. It is not a primary screening method but it is a useful test for distinguishing compounds with blood flow altering activities.

The microspheres used are 14 µ in diameter. They are marked with isotopes. In this test, four different radioactive elements are used (Cr^{51}, Sr^{85}, Sc^{46}, Ce^{141}), allowing the determination of blood flow before dosing and after the administration of 3 different compounds or 3 different doses (of the same compound).

PROCEDURE

Male Wistar rats weighing 500–550 g are anaesthetized with pentobarbital. The trachea is exposed and intubated with a short endotracheal tube to allow ventilation. Prior to testing the jugular vein is cannulated for administration of test drugs. The carotid artery is cannulated and later on the catheter is passed retrograde into the ventricle. Ventricular pressure is recorded to assure the correct emplacement of the catheter tip in the ventricle. This catheter is connected to another catheter allowing the injection of microspheres into the left ventricle later on. The right arteria brachialis is cannulated and connected to a Hellige blood pressure recorder. During the course of the test, blood pressure will be measured continuously. The left femoral artery is cannulated and connected to an infusion pump. During the experiment blood will be withdrawn from this artery.

After these preparations the rat is allowed 15–30 min to recover. Before actually starting the experiment, the arterial blood gas concentration of each animal is measured. Animals are only used for the experiment if they show normal blood gas concentrations. During the following procedure blood pressure, ventricular pressure and the heart rate are continuously recorded. To determine baseline blood flow animals receive 0.2 ml vehicle/min over a 3 min period. In the 4th minute rats receive the first injection of microspheres (Cr^{51}). Simultaneously 0.5 ml/min blood is withdrawn from the femoral artery catheter for one minute, the pump thus being used as a reference organ. The animals are allowed 20 min to recover before the administration of drugs. The test compound is infused into the jugular vein at a rate of 0.2 ml/min for 3 min followed by injection of the second microsphere (Sr^{85}). The same procedure is repeated using the other two microspheres (Sc^{46} and Ce^{141}) following administration of the second and third test compound.

At the end of the experiment blood gas concentrations are measured. The animals are killed and their organs are removed. Usually blood flow is determined in the following organs:

- brain (right and left hemisphere; right hemisphere showing slight ischemia due to cannulation of carotis)
- cerebellum
- lungs
- heart
- kidney (right and left)
- skeletal muscle (right hind extremity)
- duodenum
- stomach
- spleen
- diaphragm
- adrenal gland (right and left)

To determine effects of test compounds on the blood flow in the underperfused skeletal muscle the same experiment can be performed with the right femoral artery being clamped. In this way effects of the test drug on the ischemic and normal skeletal muscle (left thoracic limb) can be compared in the same animal.

EVALUATION

The rate of blood flow/tissue at a certain time is determined by measuring radioactivity in the different tissues and comparing the results to that of the blood sample.

MODIFICATIONS OF THE METHOD

Blood flow in various peripheral organs, e. g., renal blood, flow can be measured with electromagnetic flowmeters (e. g., Transflow 601, Skalar Medical, Holland) or with Doppler ultrasonic flowmetry (Shaffer and Medvedev 1991).

Lappe et al. (1986) studied regional vascular resistance in conscious spontaneously hypertensive rats which were chronically instrumented with pulse Doppler flow probes to allow measurement of renal, mesenteric and hind quarters blood flow.

Hartman et al. (1994) validated a transit-time ultrasonic volume flow meter by simultaneous measurements with an electromagnetic flow metering method.

Lepore et al. (1999) used electron paramagnetic resonance to investigate the time course of nitric oxide generation and its susceptibility of nitric oxide synthase in ischemia-reperfusion injury to rat skeletal muscle *in vivo*. Total hind limb ischemia was applied for 2 h using a rubber band tourniquet method. At the end of ischemia the tourniquet was removed and the limb allowed to reperfuse for various time intervals.

Beattie et al. (1995) measured carotid arterial vascular resistance in anesthetized **rabbits**. Carotid blood flow was measured by a Doppler flow probe placed around the right common carotid artery. Dose-response curves of reduction of carotid arterial vascular resistance were constructed after injection of various doses of substance P-methyl ester via the right lingual artery. Intravenous injection of various doses of a selective tachykinin NK_1 receptor antagonist inhibited this effect dose-dependently.

REFERENCES AND FURTHER READING

Beattie DT, Beresford IJM, Connor HE, Marshall FH, Hawcock AB, Hagen RM, Bowers J, Birch PJ, Ward P (1995) The pharmacology of GR203040, a novel, potent and selective tachykinin NK_1 receptor antagonist. Br J Pharmacol 116:3149–3157

Hartman JC, Olszanski DA, Hullinger TG, Brunden MN (1994) *In vivo* validation of a transit-time ultrasonic volume flow meter. J Pharmacol Toxicol Meth 31:153–160

Heiss WD, Traupe H (1981) Comparison between hydrogen clearance and microsphere technique for rCBF measurement. Stroke 12:161–167

Hof RP, Wyler F, Stalder G (1980) Validation studies for the use of the microsphere method in cats and young minipigs. Basic Res Cardiol 75:747–756

Lappe RW, Todt JA, Wendt RL (1986) Effect of fenoldopam on regional vascular resistance in conscious spontaneously hypertensive rats. J Pharm Exp Ther 236:187–191

Lepore DA, Kozlov AV, Stewart AG, Hurley JV, Morrison WA, Tomasi A (1999) Nitric oxide synthase-independent generation of nitric oxide in rat skeletal muscle ischemic-perfusion injury. Nitric Oxide: Biol Chem 3:75–84

Marcus ML, Heistad DD, Ehrhardt JC, Abboud FM (1976) Total and regional cerebral blood flow measurements with 7–10, 15, 25 and 50 µm microspheres. J Appl Physiol 40:501–507

Shaffer RA, Medvedev OS (1991) New applications of a 20-Mhz Doppler ultrasonic flowmeter. In: 7th Freiburg Focus on Biomeasurement. Cardiovascular and Respiratory *in vivo* Studies. Biomesstechnik-Verlag March GmbH, 79232 March, Germany, pp 142–147

Vetterlein F, Halfter R, Schmidt G (1979) Regional blood flow determination in rats by the microsphere method during i.v. infusion of vasodilating agents. Arzneim-Forsch/Drug Res 29:747–751

A.8.2.3 Effect on Peripheral Blood Flow in Anesthetized Dogs

PURPOSE AND RATIONALE

Effects on blood pressure have to be analyzed whether they are mediated by central, cardial, or peripheral action. By injecting small doses of the test compound directly into a vascular bed, thus avoiding changes of central hemodynamics, peripheral vasodilating activity of a compound can be tested. This test is used to evaluate direct vasodilating or constricting activities of drugs *in vivo*-measurements of blood flow.

PROCEDURE

Male or female Beagle or Labrador-Harrier dogs weighing 15–25 kg are used. The dogs are premedi-

cated intravenously with heparin (bolus of 500 IU/kg and successive injections of 50 IU/kg every 30 min) and anesthetized by intravenous injection of thiobarbital sodium (0.5 mg/kg i.v.), chloralose (20 mg/kg i.v.) and urethane (250 mg/kg i.v.). Respiration is maintained with room air through a tracheal tube using a positive pressure respirator. Blood gas analysis is performed at regular time intervals. Oxygen is supplied via the respirator as needed.

Preparation for Hemodynamic Measurements

To measure peripheral blood flow and to administer the test substance, a bypass is inserted into a femoral artery incorporating an electromagnetic flow probe and a port for injections. The other femoral artery is also equipped with a bypass used for the administration of a reference compound or a second test drug.

For recording of peripheral blood pressure and heart rate, one of the bypasses is connected to a pressure transducer (Statham P 23 BD).

All parameters are recorded continuously during the whole experiment.

Experimental Course

When stable hemodynamic conditions are achieved for at least 20 min, the vehicle is administered (control), and 10 min later the test compound. Immediately after each administration, the port is flushed with physiological saline. Successive doses are administered after recovery to baseline values.

Readings are taken at times 0, 0.5, 1, 2, 5 and 10 min, and, if necessary, at additional 10 min-intervals following drug administration.

Standard compound:

- carbocromene 1 mg/kg

Characteristics:

- blood pressure
  – systolic, BPs
  – diastolic, BPd
- heart rate, HR
- peripheral blood flow, PF

EVALUATION

Changes in blood pressure, heart rate and peripheral blood flow at different times after drug administration are compared to vehicle control values obtained in the 10 min pre-drug period.

With $n > 2$, results are presented as mean $\pm$ SEM. Statistical significance is assessed by means of the paired *t*-test. Scores are compared to the efficacy of standard compounds for intensity and for duration of the effect.

MODIFICATIONS OF THE METHOD

Regional blood flow can be determined by the use of microspheres (Rudolph and Heyman 1967). The method is based on the principle that biologically inert microspheres will be trapped due their diameter in the microvasculature (Hales and Cliff 1977). The use of radioactive microspheres has some disadvantages (Buckberg et al. 1971). The use of fluorescent labeled microspheres for measurement of regional organ perfusion has been recommended (Glenny et al. 1993; Prinzen and Glenny 1994; van Oosterhout et al. 1995). Raab et al. (1999), Thein et al. (2000) described the automation of the use of fluorescent microspheres using a special sample processing unit. A Zymate-Robotic System (Zymark, Idstein, Germany) was modified to handle a special filtration device.

Ebara et al. (1994) measured renal blood flow in dogs after intrarenal arterial infusion of adrenomedullin.

REFERENCES AND FURTHER READING

Buckberg GD, Luck JC, Payne DB, Hoffmann JIE, Archie JP, Fixler DE (1971) Some sources of error in measuring blood flow with radioactive microspheres. J Appl Physiol 31:589–604

Ebara T, Miura K, Okumura M, Matsuura T, Kim S, Yukimura T, Iwao H (1994) Effect of adrenomedullin on renal hemodynamics and function in dogs. Eur J Pharmacol 263:69–73

Glenny RW, Bernard S, Brinkley M (1993) Validation of fluorescent-labeled microspheres for measurement of regional organ perfusion. J Appl Physiol 74:2585–2597

Hales JRS, Cliff WJ (1977) Direct observations of the behavior of microspheres in the microvasculature. Bibliotheca Anatom 15:87–91

Prinzen FW, Glenny RW (1994) Development of non-radioactive microsphere technique for blood flow measurement. Cardiovasc Res 28:1467–1475

Raab S, Thein N, Harris AG, Messmer K (1999) A new sample-processing unit for the fluorescent microsphere method. Am J Physiol 276 (Heart Circ Physiol 45): H1801–H1806

Rudolph A, Heyman MA (1967) The circulation of the fetus in utero; methods for studying distribution of cardiac output and organ blood flow. Circ Res 21:163–184

Thein E, Raab S, Harris AG, Messmer K (2000) Automation of the use of fluorescent microspheres for the determination of blood flow. Comp Meth Progr Biomed 61:11–21

Turner RA (1971) β-adrenergic blocking agents. In: Turner RA, Hebborn P (eds) Screening methods in pharmacology. Vol II, pp 21–40. Academic Press, New York and London

Van Oosterhout MF, Willigers HM, Reneman RS (1995) Fluorescent microspheres to measure organ perfusion: validation of o simplified sample processing technique. Am J Physiol 269 (Heart Circ Physiol 38):H725–H733

A.8.2.4
Effect on Peripheral Blood Supply Measured by Local Oxygen Pressure

PURPOSE AND RATIONALE

Local oxygen pressure is directly related to oxygen supply to peripheral organs, e. g., muscle (Luebbers 1969; Kessler 1969). The local oxygen pressure (PO_2) is recorded directly on the muscle surface. In the following procedure the effect of test compounds on the local oxygen pressure (PO_2) of the normal and the ischemic skeletal muscle is determined.

PROCEDURE

Male Beagle dogs weighing 15–20 kg are used. The dog is anesthetized by intraperitoneal administration of pentobarbital sodium (Nembutal). Prior to testing, the following vessels have to be cannulated: The V. femoralis of the left pelvic limb is cannulated for administration of test compounds. The A. femoralis of the left pelvic limb is cannulated for blood pressure recording. The V. femoralis of the right pelvic limb is cannulated. During the course of this test blood will be withdrawn from this vein to monitor lactate concentrations.

Small areas of muscles of the right pelvic limb and the right thoracic limb are exposed. Muscle relaxation is induced by intravenous injection of 0.1 mg/kg alcuronium chloride (Alloferin) and maintained by i.p. administration of 0.05 mg/kg Alloferin at 30 min intervals. The trachea is exposed and intubated to assist the dog's respiration.

A PO_2 electrode is placed on the exposed muscle area of the right hind limb. After stabilization of PO_2 curves, the femoral artery of the right hind limb is occluded by putting a clip around the vessel. Muscle PO_2 drops rapidly. Following stabilization, test compounds are given by intravenous infusion for 10 min or by intraduodenal administration at this stage. The PO_2 of the non ischemic muscle is recorded simultaneously via a second electrode on the right thoracic extremity. The clip is removed after maximally one hour. This procedure can be repeated up to four times in one animal. Blood gas concentrations and pH are determined at the beginning and end of each experiment.

Standard compound:

- pentoxifylline

EVALUATION

The following parameters are determined:

- Maximal increase in PO_2 (mm Hg) after administration of test drug
- duration of effect by determining the half life

REFERENCES AND FURTHER READING

Dawson JM, Okyayuz-Baklouti I, Hudlická O (1990) Skeletal muscle microcirculation: the effects of limited blood flow and treatment with torbafylline. Int J Microcirc Exp 9:385–400

Ehrly AM, Schroeder W (1976) Sauerstoffdruckwerte im ischaemischen Muskelgewebe von Patienten mit chronischen arteriellen Verschlußerkrankungen. Verh Dtsch Ges Kreislaufforsch 42:380–384

Kessler M, Grunewald W (1969) Possibilities of measuring oxygen pressure fields in tissue by multiwire platinum electrodes. Progr Resp Res 3:147–152

Kessler M, Hoeper J, Krumme BA (1976) Monitoring of tissue perfusion and cellular function. Anesthesiology 45:184–197

Kunze K, Berk H (1975) Oxygen supply and muscle blood flow in normal and diseased muscle In: Kunze K, Desmedt JE (eds) Studies on Neuromuscular Diseases. Karger, Basel p 82–91

Luebbers DW, Baumgärtl H, Fabel H, Huch A, Kessler M, Kunze K, Riemann H, Seiler D, Schuchardt S (1969) Principle of construction and application of various platinum electrodes. Progr Resp Res 3:136–146

A.8.2.5
Effect on Mesenteric Blood Flow in Rats

PURPOSE AND RATIONALE

Blood flow in the mesenteric vascular bed *in situ* (Bhattacharya et al. 1977; Eikenburg 1984; Randall et al. 1989; Jackson and Inagami 1990) can be studied in rats in a way similar to that of the perfused hindquarter.

PROCEDURE

Wistar rats of either sex weighing 250–300 g are anesthetized with a combination of urethane (500 mg/kg i.v.) and sodium pentobarbitone (30 mg/kg). The abdomen is opened by a midline incision and a segment of the superior mesenteric artery is exposed by careful dissection of the surrounding tissue. Care is taken to avoid damage to the accompanying nerve terminals. One cannula is inserted into the carotid artery and the other into the superior mesenteric artery. Blood from the carotid artery is forced by a peristaltic pump (Desaga) into the superior mesenteric artery, using a glass coil kept at 40°C. Blood required to fill the tubing initially is obtained from donor rats. Heparin is administered intravenously to the animals prior to cannulation of the mesenteric artery. The blood pressure and the perfusion pressure are measured by Statham P 23 Db pressure transducers and recorded through a 2-channel Hellige recorder. The pump speed is initially

adjusted so that the perfusion pressure equals the systemic blood pressure. Intraarterial injections into the mesenteric vascular bed are made by puncturing the tubing going towards the periphery. Intravenous injections are made through a cannula inserted into the external jugular vein.

EVALUATION

Changes in the vascular resistance are measured by comparing perfusion pressure before and after drug administration. If constant blood flow is maintained, changes in the vascular resistance of the perfused bed are directly proportional to changes in the perfusion pressure.

MODIFICATIONS OF THE METHOD

Reactivity in the mesenteric vascular bed can be tested in an isolated preparation (McGregor 1965; Kawasaki and Takasaki 1984; Laher and Triggle 1984; McAdams 1984; Foy and Nuhu 1985; Longhurst and Head 1985; Soma et al. 1985; Hsueh et al. 1986; Longhurst et al. 1986; Manzini and Perretti 1988; Nassar et al. 1988; Randall and Hiley 1988). The abdomen of anesthetized rats is opened and the superior mesenteric artery is separated from surrounding tissue in the region of the aorta. A cannula is inserted into the superior mesenteric artery at its origin from the abdominal aorta. The cannula is filled with heparinized Krebs solution. The ileocoeliac branch of the artery is tied off and the intestine separated from the mesentery by cutting close to the intestinal border of the mesentery. The cannulated artery and its vascular bed are dissected out and mounted in an organ bath. The preparation is perfused with oxygenated Krebs-bicarbonate buffer (pH 7.4) at 37°C. Perfusion pressure is recorded via a side arm of the arterial cannula using a Statham pressure transducer. The flow rate is adjusted to give a baseline perfusion pressure of 20–30 mm Hg. The test substances are infused into another side arm of the arterial cannula for 15 s using an infusion pump. After three stimuli with norepinephrine (1 µg) or potassium chloride (1 mg), the test drugs are infused followed by further stimulation. The inhibition of increase of perfusion pressure after test drugs is expressed as percentage of control.

Nuki et al. (1994) compared the vasodilating activity of chicken calcitonin gene-related peptide with human α-CGRP and rat CGRP in the precontracted mesenteric vascular bed of rats.

The **rabbit** isolated arterially perfused intestinal segment preparation was used by Brown et al. (1983) as a model for vascular dopamine receptors.

Komidori et al. (1992) recommended the isolated rat mesenteric vascular-intestinal loop preparation as an excellent model fort demonstrating resistance changes in isolated vascular beds while simultaneously measuring endogenous catecholamine overflow.

Pelissier et al. (1992) showed that perfusion with hypotonic solutions removed the endothelial layer in the isolated perfused mesenteric vascular bed of the rat, allowing the study of endothelial-dependent vascular responses.

Santiago et al. (1993) used the mesenteric vascular bed of the **cat** to study the inhibitory effects of the bradykinin receptor antagonist Hoe 140 on vascular responses to bradykinin.

The responses of adrenomedullin and adrenomedullin analogs in the mesenteric vascular bed of the cat were compared by Santiago et al. (1995).

Chu and Beilin (1994) studied the mesenteric vascular reactivity which is reduced in pregnant rats after application of bradykinin and the bradykinin receptor antagonist Hoe 140.

Mulavi and Halpern (1977), Qiu et al. (1995) studied the mechanical and contractile properties of *in situ* localized mesenteric arteries in normotensive and spontaneously hypertensive rats.

REFERENCES AND FURTHER READING

Bhattacharya BK, Dadkar NK, Dohadwalla AN (1977) Vascular reactivity of perfused mesenteric vascular bed in spontaneously hypertensive and normotensive rats. Br J Pharmacol 59:243–246

Brown RA, O'Connor SE, Smith GW, Verity A (1983) The rabbit isolated arterially perfused intestinal segment preparation: A model for vascular dopamine receptors. J Pharmacol Meth 9:137–145

Chu ZM, Beilin LJ (1994) Effects of HOE 140 on systemic depressor responses to bradykinin and mesenteric vascular reactivity *in vivo* in pregnant Wistar–Kyoto rats. Clin Exp Pharmacol Physiol 21:137–140

Eikenburg DC (1984) Functional characterization of the pre- and postjunctional α-adrenoceptors in the *in situ* perfused rat mesenteric vascular bed. Eur J Pharmacol 105:161–165

Foy JM, Nuhu SZ (1985) Effect of three 'loop' diuretics and prostaglandins E_2 & I_2 on the isolated perfused rat mesenteric vasculature. Arch Int Pharmacodyn 273:237–250

Hsueh W, Gonzalez-Crussi F, Arroyave JL (1986) Release of leukotriene C_4 by isolated, perfused rat small intestine in response to platelet-activating factor. J Clin Invest 78:108–114

Jackson EK, Inagami T (1990) Blockade of the pre- and postjunctional effects of angiotensin *in vivo* with a non-peptide angiotensin receptor antagonist. Life Sci 46:945–953

Kawasaki H, Takasaki K (1984) Vasoconstrictor response induced by 5-hydroxytryptamine released from vascular adrenergic nerves by periarterial nerve stimulation. J Pharm Exp Ther 229:816–822

Komidori H, Yamamoto R, Nickols GA, Takasaki K (1992) Characterization of the isolated rat mesenteric vascular-intestinal loop preparation. J Pharmacol Meth 27:59–65
Laher I, Triggle CR (1984) Pharmacological studies of smooth muscle from Dahl salt-sensitive and salt-resistant rats. Can J Physiol Pharmacol 62:101–104
Longhurst PA, Head JH (1985) Responses of the isolated perfused mesenteric vasculature from diabetic rats: the significance of appropriate control tissues. J Pharm Exp Ther 235:45–49
Longhurst PA, Stitzel RE, Head RJ (1986) Perfusion of the intact and partially isolated mesenteric vascular bed: Application to vessels from hypertensive and normotensive rats. Blood Vessels 23:288–296
Manzini S, Perretti F (1988) Vascular effects of capsaicin in isolated perfused rat mesenteric bed. Eur J Pharmacol 148:153–159
McAdams RP (1984) The effect of temperature on the α-adrenoreceptor antagonist potency of indoramin and labetalol in the rat perfused mesenteric vascular bed. J Pharm Pharmacol 36:628–629
McGregor DD (1965) The effect of sympathetic nerve stimulation on vasoconstrictor responses in perfused mesenteric blood vessels of the rat. J Physiol (London) 177:21–30
Mulavi NJ, Halpern W (1977) Contractile properties of small arterial resistance vessels in spontaneously hypertensive and normotensive rats. Circ Res 41:19–26
Nassar BA, Huang YS, McDonald ATJ, Jenkins KD, Horrobin DF (1988) The influence of phenelzine and tranylcypromine on the release of prostaglandins from the rat mesenteric vascular bed. Can J Physiol Pharmacol 66:1206–1209
Nuki C, Kawasaki H, Takasaki K, Wada A (1994) Structure-activity study of chicken calcitonin gene-related peptide (CGRP) on vasorelaxation in rat mesenteric resistance vessels
Pelissier T, Miranda HF, Bustamante D, Paeile C, Pinardi G (1992) Removal of the endothelial layer in perfused mesenteric vascular bed of the rat. J Pharmacol Meth 27:41–44
Qiu HY, Valtier B, Struyker-Boudier HAJ, Levy BI (1995) Mechanical and contractile properties of *in situ* localized mesenteric arteries in normotensive and spontaneously hypertensive rats. J Pharmacol Toxicol Meth 33:159–170
Randall MD, Hiley CR (1988) Effect of phenobarbitone pretreatment upon endothelium-dependent relaxation to acetylcholine in rat superior mesenteric arterial bed. Br J Pharmacol 94:977–983
Randall MD, Douglas SA, Hiley CR (1989) Vascular activities of endothelin-1 and some alanyl substituted analogues in resistance beds of the rat. Br J Pharmacol 98:685–699
Santiago JA, Osei SY, Kadowith PJ (1993) Inhibitory effects of Hoe 140 on vascular responses to bradykinin in the mesenteric vascular bed of the cat. Eur J Pharmacol 236:315–318
Santiago JA, Garrison E, Purnell WL, Smith RE, Champion HC, Coy DH, Murphy WA, Kadowitz PJ (1995) Comparison of responses to adrenomedullin and adrenomedullin analogs in the mesenteric vascular bed of the cat. Eur J Pharmacol 272:115–118
Soma M, Manku DK, Horrobin DF (1985) Prostaglandins and thromboxane outflow from the perfused mesenteric vascular bed in spontaneously hypertensive rats. Prostaglandins 29:323–333

A.8.2.6
Effect on Pulmonary Blood Flow

PURPOSE AND RATIONALE

During controlled pulmonary blood flow, lobar arterial pressure can be measured in anesthetized cats (Lippton et al. 1984; Hyman et al. 1989; McMahon and Kadowitz 1993; deWitt et al. 1994).

PROCEDURE

Adult cats of either sex weighing 2.5 to 4.5 kg are sedated with ketamine hydrochloride (10–15 mg/kg i.m.) and anesthetized with pentobarbital sodium (30 mg/kg i.v.). The animals are fixed in supine position and supplemental doses of anesthetic are administered to maintain a uniform level of anesthesia. The trachea is intubated and the animals breath room air enriched with 95% O_2/5% CO_2. Systemic arterial pressure is measured from a catheter inserted into the aorta from a femoral artery, and intravenous injections are made from a catheter positioned in the inferior vena cava from a femoral vein.

For perfusion of the left lower lung lobe, a special designed 28-cm 6F triple-lumen balloon perfusion catheter (Arrow International, Reading, PA) is passed under fluoroscopic guidance from the left external jugular vein into the artery to the left lower lobe. The animal is heparinized by 1000 IU/kg i.v., and the lobar artery is isolated by distension of the balloon cuff on the perfusion catheter. The lobe is then perfused by way of the catheter lumen beyond the balloon cuff, with blood withdrawn from a femoral artery with a perfusion pump. Lobar arterial pressure is measured from a second port 5 mm from the cuff on the perfusion catheter. The perfusion rate is adjusted so that lobar arterial perfusion pressure approximates mean pressure in the main pulmonary artery. Left atrial pressure is measured with a 6F double-lumen catheter passed transseptally into the vein draining the left lower lobe. The catheter tip is positioned so that the left atrial pressure port on the distal lumen is 1–2 cm into the lobar vein and the second catheter port is near the venoatrial junction.

Lobar arterial pressure can be elevated to an high steady state level by the administration of N^{ω}-nitro-L-arginine$^{\omega}$, followed by an intralobar infusion of the stable prostaglandin/endoperoxide analogue U-46619.

EVALUATION

Dose-response curves after administration of graded doses of drugs, e. g., decrease of lobar arterial pressure

after various doses of bradykinin, are established. The effects of antagonists, e. g. HOE 140, can be studied.

MODIFICATIONS OF THE METHOD

Liu et al. (1992) used a blood-perfused rat lung preparation to study pulmonary vasoconstriction or endothelium-dependent relaxation.

Byron et al. (1986) studied the deposition and airway-to-perfusate transfer of disodium fluorescein from 3–4 μm solid aerosols in an isolated perfused lung preparation of rats.

Mor et al. (1990) determined angiotensin-converting enzyme activity in the isolated perfused **guinea pig** lung.

Franks et al. (1990) used in Beagle **dogs** a single breath technique employing freon-22 as the soluble marker gas simultaneously with measurement of aortic blood flow by an electromagnetic flowmeter.

Tanaka et al. (1992) measured lung water content in dogs with acute pulmonary hypertension induced by injection of glass beads.

Drake et al. (1978) studied filtration characteristics of the exchange vessels in isolated dog lung by calculating the volume conductance with use of different components of the weight-gain curve following changes in capillary pressure.

Heaton et al. (1995) studied the effects of human adrenomedullin on the pulmonary vascular bed of isolated, blood perfused rat lung.

DeWitt et al. (1994), Lippton et al. (1994) investigated the effects of adrenomedullin in the pulmonary and systemic vascular bed of the **cat**.

Nossaman et al. (1995) compared the effects of adrenomedullin, an adrenomedullin analog, and CGRP in the pulmonary vascular bed of the cat and the rat.

REFERENCES AND FURTHER READING

Baum MD, Kot PA (1972) Responses of pulmonary vascular segments to angiotensin and norepinephrine. J Thorac Cardiovasc Surg 63:322–328

Byron PR, Roberts NSR, Clark AR (1986) An isolated perfused rat lung preparation for the study aerosolized drug deposition and absorption. J Pharmaceut Sci 75:168–171

DeWitt BJ, Cheng DY, McMahon TJ, Nossaman BD, Kadowitz PJ (1994a) Analysis of responses to bradykinin in the pulmonary vascular bed of the cat. Am J Physiol, Heart Circ Physiol 266:H2256–H2267

DeWitt BJ, Cheng DY, Caminiti GN, Nossaman BD, Coy DH, Murphy WA, Kadowitz PJ (1994b) Comparison of responses to adrenomedullin and calcitonin gene-related peptide in the pulmonary vascular bed of the cat. Eur J Pharmacol 257:303–306

Drake R, Gaar KA, Taylor AE (1978) Estimation of the filtration coefficient of pulmonary exchange vessels. Am J Physiol 234:H266–H274

Franks PJ, Hooper RH, Humphries RG, Jones PRM, O'Connor SE (1990) Effective pulmonary flow, aortic flow and cardiac output: *in vitro* and *in vivo* comparison in the dog. Exper Physiol 75:95–106

Heaton J, Lin B, Chang J-K, Steinberg S, Hyman A, Lippton H (1995) Pulmonary vasodilation to adrenomedullin: A novel peptide in humans. Am J Physiol 268, Heart Circ Physiol 37:H2211–H2215

Hyman AL, Kadowitz PJ, Lippton HL (1989) Methylene blue selectively inhibits pulmonary vasodilator response in cats. J Appl Physiol 66:1513–1517

Lippton H, Chang J-K, Hao Q, Summer W, Hyman AL (1994) Adrenomedullin dilates the pulmonary vascular bed *in vivo*. J Appl Physiol 76:2154–2156

Lippton HL, Nandiwada PA, Hyman AL, Kadowitz PJ (1984) Influence of cyclo-oxygenase blockade on responses to isoproterenol, bradykinin and nitroglycerin in the feline pulmonary vascular bed. Prostaglandins 28:253–270

Liu SF, Dewar A, Crawley DE, Barnes PJ, Evans TW (1992) Effect of tumor necrosis factor on hypoxic pulmonary vasoconstriction. J Appl Physiol 72:1044–1049

McMahon TJ, Kadowitz PJ (1993) Analysis of responses to substance P in the pulmonary vascular bed of the cat. Am J Physiol 264 (Heart Circ Physiol 33): H394–H402

Mor L, Bomzon A, Frenkel R, Youdim MBH (1990) Angiotensin-converting enzyme activity in the isolated perfused guinea pig lung. J Pharmacol Meth 23:141–153

Nossaman BD, Feng CJ, Cheng DY, Dewitt BJ, Coy DH, Murphy WA, Kadowitz PJ (1995) Comparative effects of adrenomedullin, an adrenomedullin analog, and CGRP in the pulmonary vascular bed of the cat and the rat. Life Sci 56:63–66

Tanaka H, Tajimi K, Matsumoto A, Kobayashi K (1992) Effects of milrinone on lung water content in dogs with acute pulmonary hypertension. J Pharmacol Toxicol Meth 28:201–208

A.8.2.7 Effect on Contractile Force of Ischemic Muscle

PURPOSE AND RATIONALE

Skeletal muscle is stimulated until it reaches its maximal force of contraction. This means that the muscle is forced to function at a level near exhaustion and has to use maximally the substrate supplied by the circulation. Then, the femoral artery is occluded, leading to underperfusion and a subsequent lack of substrate. As a consequence, the muscle's force of contraction decreases rapidly. Measuring the change in contractile force caused by drug administration reveals a drug's ability to restore ischemic muscle functions. In the following procedure, the drugs are tested for their effect on the force of contraction of the ischemic skeletal muscle.

PROCEDURE

Male Wistar rats weighing 400–450 g are anaesthetized by intraperitoneal administration of pentobarbital (Nembutal) (35 mg/kg). A tracheal tube is placed

to assist the rat's ventilation. The left carotid artery is cannulated for blood pressure recording and the left jugular vein is cannulated for the i.v. administration of test drugs. An incision is made to the skin of the right pelvic limb distal to the groin and the skeletal muscle is exposed down to the ankle. The skin is carefully trimmed away from the muscle to assure that contractions cannot be impaired by retraction of the skin. The major nerve supply is severed and a small length of the descending branch of the femoral artery is prepared free. The freely hanging muscle is attached to the force transducer (range 0–500 g, Z 6, Rhema, Germany) and a resting tension of 50 g is placed on the muscle. To prevent dehydration, the skin is left attached to the muscle and the muscle is kept moist by the continuous drip of a 0.9% NaCl-solution.

After these preparations, the rat is allowed to recover at least 30 min. Two needle electrodes are inserted into the muscle. Square impulses of 40 ms are generated with Stimulator 1 (Hugo Sachs Elektronik, Freiburg, Germany). The muscle is stimulated with a frequency of about 80 contractions per minute. The amplitude is increased gradually up to the muscle's maximal contractile force (usually between 2.0 and 3 mA). Following stabilization, the femoral artery is occluded with a clip for 5 min and subsequently reopened. After at least 15 min, test drugs are administered by intravenous infusion (0.075 ml/min) for 10 min. Five minutes after starting drug infusion, the artery is clamped again (for 5 min) while drug infusion is still going on. The force of contraction is continuously recorded. After declamping the artery, the rat is allowed to recover for at least 30 min before the whole procedure is repeated with another test drug. In this way, 3 different compounds can be tested in the same animal.

Standard compound:

- pentoxifylline

EVALUATION

The following parameters are measured:

- the percent inhibition of contractile force before drug administration (artery being clamped)
- the percent inhibition of contractile force after drug administration (artery being clamped)

The percent increase in contractile force after drug administration is calculated.

CRITICAL ASSESSMENT OF THE METHOD

An attempt is made to measure not only the effects of the drug on vasculature tonus but also on muscle metabolism.

MODIFICATIONS OF THE METHOD

Weselcouch and Demusz (1990) studied drug effects in the ischemic hindlimbs of **ferrets**. The hindlimb was stimulated to contract isometrically via supramaximal electrical stimulation of the sciatic nerve. Ischemia was induced by partial occlusion of the abdominal aorta. Pentoxifylline attenuated the loss of function in a dose-related manner.

Okyayuz-Baklouti et al. (1992) studied the functional, histomorphological and biochemical changes in atrophying skeletal muscle using a novel immobilization model in the rat.

Le Tallec et al. (1996) reported the effects of dimethylformamide on *in vivo* fatigue and metabolism in rat skeletal muscle measured by 31P nuclear magnetic resonance spectroscopy.

REFERENCES AND FURTHER READING

Angersbach D, Ochlich P (1984) The effect of 7-(2′-oxopropyl)-1,3-di-n-butyl-xanthine (BRL 30892 on ischaemic skeletal muscle pO_2, pH and contractility in cats and rats. Arzneim. Forsch/Drug Res 34:1274–1278

Le Tallec N, Lacroix P, de Certaines JD, Chagneau F, Lavasseur R, Le Rumeur E (1996) Effects of dimethylformamide on *in vivo* fatigue and metabolism in rat skeletal muscle measured by 31P-NMR. J Pharmacol Toxicol Meth 35:139–143

Okyayuz-Baklouti I (1989) The effects of torbafylline on blood flow, pO_2, and function of rat ischemic skeletal muscle. Eur J Pharmacol 166:75–86

Okyayuz-Baklouti I, Konrad-Clement S, Reifert P, Schmitt T, Schuck D (1992) Novel immobilization model in the rat: functional, histomorphological and biochemical changes in atrophying skeletal muscle. J Musc Res Mot 14:259–260

Ward A, Clissold SP (1987) Pentoxifylline, a review of its pharmacodynamic and pharmacokinetic properties. Drugs 34:50–97

Weselcouch EO, Demusz (1990) Drug effects on function in the ferret ischemic hindlimb. J Pharmacol Meth 23:255–264

A.8.2.8 Effect on Perfusion of Rabbit Ear (Pissemski Method)

PURPOSE AND RATIONALE

The procedure was described as early as 1914 by Pissemski, based on experiments of Krawkow (1913) in fish gills. It can be used to elucidate vasoactive properties (both vasoconstrictive and vasodilating) of

compounds. The isolated rabbit's ear is used to determine the effect of test compounds on its perfusion rate. Administration of norfenephrine induces vasoconstriction leading to a decrease in perfusion rate. A compound with vasodilatory properties will inhibit the norfenephrine induced fall in perfusion rate whereas a vasoconstrictor will potentiate this effect.

PROCEDURE

A rabbit of either sex weighing 1.5–3 kg is sacrificed by CO_2 narcosis and its ears are severed immediately. The ear is placed on a glass disc, the posterior auricular artery is exposed and cannulated. The cannula is connected to a tubing with a T-branch allowing the infusion of different solutions. Ringer's solution, kept at room temperature, is infused under 40 cm water column pressure via the cannula. The perfusion flow volume is recorded using a time ordinate recorder and a CONDON tipper or a photoelectric drop counter.

Prior to drug administration, the pH of the Ringer solution (containing test compound) must be determined. If the pH is greater than 8.5 or smaller than 6.5, it should be adjusted by adding a diluted NaOH- or HCl-solution.

Testing for Vasodilatory (Norfenephrine Antagonistic) Activity

Norfenephrine is infused at a concentration of 0.5 µg/ml until the maximal contraction is reached. The test compound is prepared in Ringer's solution at a concentration of 100 µg/ml. A volume of 30 ml is infused via the cannula over a 15 min period under constant pressure. The change of perfusion rate is determined. If there is a positive response (increase in perfusion rate), the test may be repeated using lower concentrations. If there is a negative response (further decrease in perfusion rate), the compound can be tested for vasoconstrictive activity.

Testing for Vasoconstrictive Activity

This test is repeated as described above without administration of norfenephrine.

Standard compounds:

- as vasodilator
  - dihydralazine
  - theophylline
  - pentoxyfylline 100 µg/ml
- as vasoconstrictor
  - norfenephrine (Novadral)

EVALUATION

Testing for Vasodilatory Activity

The perfusion rate of the ear vessel is determined during the course of the test:

R = perfusion rate of vehicle perfused vessel

RN = perfusion rate of norfenephrine constricted vessel

RNP = perfusion rate of norfenephrine constricted vessel following compound administration

The percent inhibition of norfenephrine induced decrease in perfusion pressure is calculated using the following formula:

$$\% \text{ inhibition} = \frac{(RN - RNP)}{R - RN} \times 100$$

Testing for Vasoconstrictive Activity

The normal perfusion rate (ear vessel perfused with Ringer's solution) is taken as 100%. The percent inhibition of perfusion rate following compound administration is determined.

MODIFICATIONS OF THE METHOD

Schlossmann (1927) used the isolated rabbit ear preparation according to Pissemski for determination of the adrenaline content in blood.

De la Lande and Rand (1965), de la Lande et al. (1967) described a method of perfusing the isolated central artery of the rabbit ear. Small segments of the artery, taken from the base of the ear, were perfused at a constant rate with Krebs solution at 37°C. To enable drugs to be applied either to the intima or the adventitia, the artery was double cannulated so that the intraluminal and extraluminal perfusion media did not mix. Constrictor responses were measured by the maximum rise in perfusion pressure.

Steinsland et al. (1973) studied the inhibition of adrenergic transmission by parasympathicomimetics in the isolated central ear artery of the rabbit. Perfusion was performed at a constant flow rate with Krebs' solution and perfusion pressure was recorded with a transducer.

Allen et al. (1973) incubated isolated segments of rabbit ear artery with (^{3}H)-(–)-noradrenaline and measured the amount of tritium released into the luminal perfusate and into the extraluminal superfusate.

Budai et al. (1990) used isolated proximal 3–4-cm segments of the rabbit ear artery or rat tail artery in a low volume perfusion-superfusion system for measurement of transmitter release from blood vessels *in vitro*.

Miyahara et al. (1993) used arterial rings rabbit ear arteries *in vitro* which were contracted by perivascular nerve stimulation, or 5×10^{-7} noradrenaline or high potassium (29.6 mM) solution. High doses of dexamethasone or clobetasol-17-propionate decreased the amplitude of contractions. Furthermore, the authors performed *in vivo* experiments in albino rabbits, whereby the fur was removed from the distal parts of the ear by applying a depilatory cream at least 24 h before the experiments. The apical regions of the ear were then stripped with adhesive tape 7 times to remove the keratinous epidermal layer. The rabbit was anesthetized and the experimental parts of the ear were placed under a high resolution magnifying camera and immobilized using bilayer adhesive tapes. The vascular reactions induced by topical application of corticosteroids were recorded chronically using videotapes.

Aoki and Chiba (1993) described a method for separate intraluminal and extraluminal perfusion of the **basilar artery** in dogs. A polyethylene roof was designed to cover the canine basilary artery so that an extraluminal superfusion stream could pass over the artery that simultaneously received an intraluminal perfusion.

REFERENCES AND FURTHER READING

Allen GS, Rand MJ, Story DF (1973) Techniques for studying adrenergic transmitter release in an isolated perfused artery. Cardiovasc Res 7:423–428

Aoki T, Chiba S (1993) A new cannula-inserting method for measuring vascular responsiveness. Separate intraluminal and extraluminal perfusion of canine basilar artery. J Pharmacol Toxicol Meth 29:21–27

Budai D, Buchholz JN, Duckles SP (1990) Low volume perfusion-superfusion system for measurement of transmitter release from blood vessels *in vitro*. J Pharmacol Meth 23:41–49

De la Lande IS, Rand MJ (1965) A simple isolated nerve-blood vessel preparation. Aust J Exp Biol Med 43:939–656

De la Lande IS, Frewin D, Waterson JG (1967) The influence of sympathetic innervation on vascular sensitivity to noradrenaline. Br J Pharmac Chemother 31:82–93

Green AF, Boura ALA (1964) Depressants of peripheral sympathetic nerve function. In: Laurence DR, Bacharach AL (eds) Evaluation of Drug Activities: Pharmacometrics. Academic Press, London and New York, 369–430

Griesbacher T, Lembeck F (1987) Actions of bradykinin antagonists on bradykinin-induced plasma extravasation, venoconstriction, prostaglandin E_2 release, nociceptor stimulation and contraction of the iris sphincter muscle of the rabbit. Br J Pharmacol 92:333–340

Krawkow NP (1913) Über die Wirkung von Giften auf die Gefässe isolierter Fischkiemen. Pflüger's Arch 151:583–603

Lembeck F, Griesbacher T, Eckhardt M, Henke S, Breipohl G, Knolle J (1991) New, long-acting, potent bradykinin antagonists. Br J Pharmacol 102:297–304

Miyahara H, Imayama S, Hori Y, Suzuki H (1993) Cellular mechanisms of the steroid-induced vascular responses in the rabbit ear artery. Gen Pharmacol 24:1155–1162

Pissemski SA (1914) Über den Einfluss der Temperatur auf die peripherischen Gefässe. Pflüger's Arch 156:426–442

Schlossmann H (1927) Untersuchungen über den Adrenalingehalt des Blutes. Naunyn Schmiedeberg's Arch Exp Path Pharmakol 121:160–203

Schneider G (1935) Einfluß von Novalgin und kolloidalem Eisen auf die Ödembildung am isolierten Kaninchenohr. Naunyn-Schmiedeberg's Arch exp Path Pharmakol 179:56–60

Steinsland OS, Furchgott RF, Kirpekar SM (1973) Inhibition of adrenergic transmission by parasympathicomimetics in the rabbit ear artery. J Pharmacol Exp Ther 184:346–356

Turner RA (1965) The perfused rabbit ear. In: Screening methods in pharmacology. Chapter 12: Sympatholytic agents. pp 150–151. Academic Press New York, London

A.8.2.9 Effect on Venous Tonus In Situ in Dogs

PURPOSE AND RATIONALE

Veins can be classified into two groups: those that respond and those that do not respond to epinephrine, acetylcholine and sympathetic nerve stimulation. As studies in dogs have shown (Rice et al. 1966) the reactive veins have a considerable amount of smooth muscle whereas the nonreactive ones lack any appreciable amount of smooth muscle fibres in the tunica media. A special preparation allows the registration of localized venous vasoconstriction.

PROCEDURE

Dogs weighing 20–30 kg are anesthetized with 35 mg/kg pentobarbital sodium i.v. The trachea is cannulated and the dog ventilated with a respiration pump. The femoral vein is cannulated for systemic injections. After administration of 5 mg/kg heparin sodium i.v., the saphenous vein and the femoral artery are cannulated. The venous cannula is placed approximately 1 cm distal to its junction with another vein. After the non-perfused branch of the junction is ligated, constant blood flow is maintained from the femoral artery by using a Sigmamotor pump. The flow is adjusted so that a normal physiologic pressure in the vein is maintained. Perfusion pressure is measured between the pump and the vein so that any changes in pressure reflect changes in venous resistance. The peak changes in perfusion pressure are used to measure pressure changes from recorded data. The blood flow is maintained on a constant level. Therefore, changes in pressure must reflect changes in resistance. Pressure is recorded with a polygraph using an Statham pressure transducer (P23AA). In addition to recording perfusion pressure, venous pressure is measured at two additional points along the vein. In order to

record venous pressure centrally from the site of perfusion, the shaft of a 27-gauge needle is placed into the end of a 10 cm piece of a thin Silastic tubing. At the other end, a 27 gauge needle is inserted and attached to a Statham pressure transducer (P23B). Pressure is recorded on a polygraph. One needle is inserted into the vein just proximal of the junction of the two veins. The second needle is placed into the vein so that the distance between the tip of the perfusion cannula and the first needle is the same as the distance between the two needles. In this way pressure decreases across the junction and an adjacent segment can be measured simultaneously. Injections of test compounds are made into the cannula between the pump and the saphenous vein. Changes in pressure measured by the three transducers are recorded. As standard, doses of 0.1–1.0 µg norepinephrine are injected.

EVALUATION

Responses to test drugs are measured in mm Hg and calculated as percentage of response to norepinephrine.

REFERENCES AND FURTHER READING

Rice AJ, Leeson CR, Long JP (1966) Localisation of venoconstrictor responses. J Pharmacol Exp Ther 154:539–545

A.8.3 Arterial Aneurysms

A.8.3.1 General Considerations

Abdominal aortic aneurysms represent a life-threatening condition characterized by chronic inflammation, destructive remodeling of the extracellular matrix and segmental dilatation of the aortic wall (Dobrin 1989; Ernst 1993). Several authors described animal models of aneurysms (Carrell et al. 1999; Dobrin 1999; Daugherty and Cassis 2004). Most studies were performed in mice. Abdominal aortic aneurysms are evoked by genetically defined defects in extracellular matrix maturation, increased degradation of elastin and collagen, aberrant cholesterol homeostasis, or enhanced production of angiotensin peptides.

The **Blotchy mouse** has an X-linked trait that leads to aortic aneurysms and subsequent fatal rupture in nearly all affected male mice (Brophy et al. 1988; Reilly et al. 1990).

Maki et al. (2002) showed that inactivation of the **lysyl oxidase gene Lox** leads to aortic aneurysms, cardiovascular dysfunction, and perinatal death in mice.

Aneurysm development has been noted in a number of mice with deficiencies in the components of the matrix metalloproteinase system (Silence et al. 2001, 2002).

The use of mice in atherosclerosis research was escalated by the development of mice that are deficient in either apoE or LDL receptors susceptible to aneurysm development (Ishibashi et al. 1994; Prescott et al. 1999).

Accelerated atherosclerosis, aortic aneurysms formation, and ischemic heart disease were found in apolipoprotein E and endothelial nitric oxide synthase double-knockout mice (Kuhlencordt et al. 2001). ACE inhibition reduces some symptoms of vascular pathology in apoE and eNOS compound-deficient mice (Knowles et al. 2000). Mice with deficiency of the LDL receptor-related protein (LRP) showed pathological changes in the aortic arch and abdominal aorta with substantial lengthening, dilatation, thickening and large aneurysms (Herz and Strickland 2001; Boucher et al. 2003).

Salt-sensitive aortic aneurysms and rupture in hypertensive transgenic mice that overproduce angiotensin II were described by Nishijo et al. (1998).

The infusion of elastase into the infrarenal segment has been used as model for abdominal aorta aneurysms in rats (Anidjar et al. 1990) and mice (Pyo et al. 2000).

Lee et al. (2001) described abdominal aortic aneu rysms in mice lacking expression of inducible nitric oxide synthase.

Periarterial application of calcium chloride was used to induce aneurysms of the **rabbit** common carotid artery (Gertz et al. 1988) and in the rabbit aorta (Freestone et al. 1997).

This technique has been used in **mice** by Chiou et al. (2001) and Longo et al. (2002).

MODIFICATIONS OF THE METHOD

Nomoto et al. (2003) described the effects of two inhibitors of renin-angiotensin system on attenuation of postoperative remodeling after **left ventricular aneurysm** repair in rats.

REFERENCES AND FURTHER READING

Anidjar S, Salzmann JL, Gentric D, Lagneau P, Camilleri JP, Michel JB (1990) Elastase-induced experimental aneurysms in rats. Circulation 82:973–981

Boucher P, Gotthardt M, Li WP, Anderson RG, Herz J (2003) LRP: role in vascular wall integrity and protection from atherosclerosis. Science 3000:329–332

Brophy CM, Tilson JE, Braverman IM, Tilson MD (1988) Age of onset, pattern of distribution, and histology of aneurysm development in a genetically predisposed mouse. J Vasc Surg 8:45–48

Carrell TW, Smith A, Bumand KG (1999) Experimental techniques and models in the study of the development and treatment of abdominal aortic aneurysm. Br J Surg 86:305–312
Chiou AC, Chiu B, Pearce WH (2001) Murine aortic aneurysm produced by periarterial application of calcium chloride. J Surg Res 99:371–376
Daugherty A, Cassis LA (2004) Mouse models of abdominal aortic aneurysms. Arterioscler Thromb Vasc Biol 24:429–434
Dobrin PB (1989) Pathophysiology and pathogenesis of aortic aneurysms. Current concepts. Surg Clin North Am 69:687–703
Dobrin PB (1999) Animal models of aneurysms. Ann Vasc Surg 13:641–648
Ernst CB (1993) Abdominal aortic aneurysm. N Engl J Med 328:1167–1172
Freestone T, Turner RJ, Higman DJ, Lever MJ, Powell JT (1997) Influence of hypercholesterolemia and adventitial inflammation on the development of aortic aneurysms in rabbits. Arterioscler Thromb Vasc Biol 17:10–17
Gertz SD, Kurgan A, Eisenberg D (1988) Aneurysms of the rabbit common carotid artery induced by periarterial application of calcium chloride in vivo. J Clin Invest 81:649–656
Herz J, Strickland DK (2001) LRP: a multifunctional scavenger and signaling receptor. J Clin Invest 108:779–784
Ishibashi S, Goldstein JL, Brown MS, Herz J, Burns DK (1994) Massive xanthomatosis and atherosclerosis in cholesterol-fed low density lipoprotein receptor-negative mice. J Clin Invest 93:1885–1893
Knowles JW, Reddick RL, Jenette JC, Smithies O, Maeda N (2000) Enhanced atherosclerosis and kidney dysfunction in *eNOS(-)/(-)Apo(-)/(-)* mice are ameliorated by enalapril treatment. J Clin Invest 105:451–458
Kuhlencordt PJ, Gyurko R, Han F, Scherrer-Crosbie M, Aretz TH, Hajjar R, Picard MH, Huang PL (2001) Accelerated atherosclerosis, aortic aneurysms formation, and ischemic heart disease in apolipoprotein E/endothelial nitric oxide synthase double-knockout mice. Circulation 104:44–454
Lee JK, Borhani M, Ennis TL, Upchurch GR Jr, Thompson RW (2001) Experimental abdominal aortic aneurysms in mice lacking expression of inducible nitric oxide synthase. Arterioscler Thromb Vasc Biol 21:1391–1401
Longo GW, Xiong W, Greiner TC, Zhao Y, Fiotti N, Baxter BT (2002) Matrix metalloproteinases 2 and 9 work in concert to produce aortic aneurysms. J Clin Invest 110:625–632
Maki JM, Rasanen J, Tikkanen H, Sormunen R, Makikallio K, Kivirikko KI, Soininen R (2002) Inactivation of the lysyl oxidase gene Lox leads to aortic aneurysms, cardiovascular dysfunction, and perinatal death in mice. Circulation 106:2503–2509
Nishijo N, Sugiyama F, Kimoto K, Taniguchi K, Murakami K, Suzuki S, Fukamizu A, Yagami K (1998) Salt-sensitive aortic aneurysms and rupture in hypertensive transgenic mice that overproduce angiotensin II. Lab Invest 78:1059–1066
Nomoto T, Nishina T, Tsuneyoshi H, Miwa S, Nishimura K, Komeda M (2003) Effects of two inhibitors of renin-angiotensin system on attenuation of postoperative remodeling after left ventricular aneurysm repair in rats. J Card Surg 18 [Suppl 2]:S61–S68
Prescott MF, Sawyer WK, Von Linden Reed J, Jeune M, Chou M, Caplan SL, Jeng AY (1999) Effect of matrix metalloproteinase inhibition on progression of atherosclerosis and aneurysm in LDL receptor-deficient mice overexpressing MMP-3, MMP-12, and MMP-13 and on restenosis in rats after balloon injury. Ann N Y Acad Sci 878:179–190
Pyo R, Lee HK, Shipley M, Curci JA, Mao D, Ziporin SJ, Ennis TL, Shapiro SD, Senior RM, Thompson RW (2000) Targeted disruption of matrix metalloproteinase-9 (gelatinase B) suppresses development of experimental aortic aneurysms. J Clin Invest 105:1641–1649
Reilly JM, Savage EB, Brophy CM, Tilson MD (1990) Hydrocortisone rapidly induces aortic rupture in a genetically susceptible mouse. Arch Surg 125:707–709
Silence J, Lupu F, Collen D, Lijnen HR (2001) Persistence of atherosclerotic plaque but reduced aneurysm formation in mice with stromelysin-1 (MMP-3) gene inactivation. Arterioscler Thromb Vasc Biol 21:1440–1445
Silence J, Collen D, Lijnen HR (2002) Reduced atherosclerotic plaque but enhanced aneurysm formation in mice with inactivation of the tissue inhibitor of metalloproteinase-1 (*TIMP-1*) gene. Circ Res 90:897–903

A.8.3.2 Angiotensin II-Induced Aortic Aneurysm in Mice

PURPOSE AND RATIONALE

Angiotensin II promotes atherosclerotic lesions and aneurysms in apolipoprotein E-deficient mice (Daugherty et al. 2000, 2001; Knowles et al. 2000; Wang et al. 2001; Manning et al. 2002, 2003; Deng et al. 2003; Martin-McNulty et al. 2003; Saraff et al. 2003).

Wang et al. (2005) reported that a Rho-kinase inhibitor attenuated angiotensin II-induced abdominal aortic aneurysm in apolipoprotein E-deficient mice by inhibiting apoptosis and proteolysis.

PROCEDURE

Animal Preparation

Osmotic minipumps (model 2004, Alzet) containing either PBS or Ang II (1.44 mg/kg per day) in PBS were implanted subcutaneously in 6-month-old apoE-KO male mice (Jackson Laboratories). Two days before saline and Ang II infusion, mice were provided with water (Ang IIgroup) or water containing test compound at a concentration of 0.5 mg/ml (low-dose group) or 1.0 mg/ml (high-dose group). Age-matched apoE-KO mice without any treatment were used as naïve controls. At the end of the 30-day treatment period, mice were euthanized, and the hearts were perfused with DEPC in saline. The arterial tree was rapidly dissected from fat and connective tissue and snap-frozen in liquid nitrogen.

MORPHOLOGICAL EXAMINATION

Quantification of Aneurysm Formation

After the aorta was dissected free from the surrounding connective tissue, images were recorded with a digital camera and later used to measure the outer diameter of the suprarenal aorta at the midpoint between the diaphragm and right renal artery. A commonly used

clinic standard to diagnose abdominal aortic aneurysm is an increase in aortic diameter of ≈50% (Johnston et al. 1991). The average diameter of the normal suprarenal aorta in naïve control mice is 0.8 mm. A threshold of 1.22 mm was set as evidence of an incidence of aneurysm formation. Aneurysm severity was assessed with a scoring system described by Daugherty et al. (2001): type 0, no aneurysm (the suprarenal region of the aorta was not obviously different from naïve apoE-KO mice without Ang II treatment); type I, a dilated lumen with no thrombus; type II, remodeled tissue often containing thrombus; type III, a pronounced bulbous form of type II containing thrombus; and type IV, multiple aneurysms containing thrombus. To analyze this measurement semiquantitatively, the numerical score assigned to the type of aneurysm for each animal in a group was averaged to generate a pathology score for statistical comparison.

Quantification of Atherosclerotic Lesion Area

The left and right carotid arteries and the aortic arch were dissected, excised, opened longitudinally, and pinned down on wax-coated Petri dishes. Atherosclerotic lesions were visible without staining. Images of the open luminal surface of the vessels were captured with a digital camera (Sony) mounted on a dissecting microscope. The atherosclerotic lesion area was quantified by use of the C-Simple system (Compix) and expressed as a percentage of the total luminal surface area (Wang et al. 2000, 2001; Martin-McNulty et al. 2003).

Histology and Immunohistochemical Staining

Two representative suprarenal aortas from each group were fixed in formalin, embedded in paraffin, and cut into 5-μm-thick sections. The adjacent sections were stained with hematoxylin and eosin or by the immunohistochemical method. To identify macrophages in the aortic wall, a purified rat anti-mouse Mac-3 monoclonal antibody (BD Pharmingen) was used for immunochemistry staining (PhenoPath Laboratories). To localize cells undergoing nuclear DNA fragmentation, *in situ* terminal deoxynucleotidyl transferase–mediated dUTP nick-end labeling (TUNEL) was performed using an *in situ* apoptosis detection kit (Roche Biochemicals) (Song et al. 2000; Feng et al. 2002). Paraffin sections were deparaffinized and rehydrated. Sections were then washed with PBS and incubated with proteinase K (20 μg/ml) for 20 min. Endogenous peroxidase was inactivated with 3% hydrogen peroxide in methanol at room temperature. TdT, which catalyzes a template-independent addition of deoxyribonucleotide to 3-OH ends of DNA, was used to incorporate digoxigenin-conjugated dUTP to the ends of DNA fragment *in situ*. The TUNEL signal was then detected with an anti-digoxigenin antibody conjugated with peroxidase and developed with diaminobenzidine as a chromogen. Sections were counterstained with hematoxylin, dehydrated, and cleared before coverslips were placed. Both positive and negative control slides were processed at the same time in each experiment. The presence of apoptotic cells was scored as nuclear staining, with a distinctive morphological appearance associated with cell shrinkage and chromatin condensation.

EVALUATION

Results are presented as mean ± SE for the number of animals used. Statistical comparison for the incidence of abdominal aortic aneurysms was performed by χ^2 analysis. Multiple comparison of mean values was performed by ANOVA, followed by a subsequent Student-Newman-Keuls test for repeated measures. Differences were considered statistically significant at a value of $P < 0.05$.

REFERENCES AND FURTHER READING

Daugherty A, Manning MW, Cassis LA (2000) Angiotensin II promotes atherosclerotic lesions and aneurysms in apolipoprotein E-deficient mice. J Clin Invest 195:1605–1612

Daugherty A, Manning MW, Cassis LA (2001) Antagonism of AT2 receptors augments angiotensin II-induced abdominal aortic aneurysms and atherosclerosis. Br J Pharmacol 134:865–870

Deng GG, Martin-McNulty B, Sukovich DA, Freay A, Halks-Miller M, Thinnes T, Loskutoff DJ, Carmeliet P, Dole WP, Wang YX (2003) Urokinase-type plasminogen activator plays a critical role in angiotensin II-induced abdominal aortic aneurysm. Circ Res 92:510–517

Feng Q, Song W, Lu X, Hamilton JA, Lei M, Peng T, Yee SP (2002) Development of heart failure and congenital septal defects in mice lacking endothelial nitric oxide synthase. Circulation 106:873–879

Johnston KW, Rutherford RB, Tilson MD, Shah DM, Hollier L, Stanley JC (1991) Suggested standards for reporting on arterial aneurysms: Subcommittee on Reporting Standards for Arterial Aneurysms, Ad Hoc Committee on Reporting Standards, Society for Vascular Surgery and North American Chapter, International Society for Cardiovascular Surgery. J Vasc Surg 13:452–458

Knowles JW, Reddick RL, Jenette JC, Smithies O, Maeda N (2000) Enhanced atherosclerosis and kidney dysfunction in *eNOS(-)/(-)Apo(-)/(-)* mice are ameliorated by enalapril treatment. J Clin Invest 105:451–458

Manning MW, Cassis LA, Huang J, Szilvassy SJ, Daugherty A (2002) Abdominal aortic aneurysms: fresh insights from a novel animal model of the disease. Vasc Med 7:45–54

Manning MW, Cassis LA, Daugherty A (2003) Differential effects of doxycycline, a broad-spectrum matrix metalloproteinase inhibitor, on angiotensin II-induced atherosclerosis

and abdominal aortic aneurysms. Arterioscler Thromb Vasc Biol 23:483–488
Martin-McNulty B, Tham DM, da Cunha V, Ho JJ, Wilson DW, Rutledge JC, Deng GG, Vergona R, Sullivan ME, Wang YX (2003) 17 β-estradiol attenuates development of angiotensin II-induced aortic abdominal aneurysm in apolipoprotein E-deficient mice. Arterioscler Thromb Vasc Biol 23:1627–1632
Saraff K, Babamusta F, Cassis LAS, Daugherty A (2003) Aortic dissection precedes formation of aneurysms and atherosclerosis in angiotensin II-infused, apolipoprotein E-deficient mice. Arterioscler Thromb Vasc Biol 23:1621–1626
Song W, Lu X, Feng Q (2000) Tumor necrosis factor-alpha induces apoptosis via inducible nitric oxide synthase in neonatal mouse cardiomyocytes. Cardiovasc Res 45:595–602
Wang YX, Halks-Miller M, Vergona R, Sullivan ME, Fitch R, Mallari C, Martin-McNulty B, da Cunha V, Freay A, Rubanyi GM, Kauser K (2000) Increased aortic stiffness assessed by pulse wave velocity in apolipoprotein E–deficient mice. Am J Physiol 278:H428–H434
Wang YX, Martin-McNulty B, Feay AD, Sujowich DA, Halks-Miller M, Li AA, Vergona R, Sullivan ME, Morser J, Dole WP, Deng GG (2001) Angiotensin II increases urokinase-type plasminogen activator expression and induces aneurysms in the abdominal aorta of apolipoprotein E-deficient mice. Am J Pathol 159:1455–1464
Wang YX, Martin-McNulty B, da Cinha V, Vincelette J, Lu X, Feng Q, Hlaks-Miller M, Mahmoudo M, Schroeder M, Subramanyam B, Tseng JL, Deng GD, Schirm S, Johns A, Kauser K, Dole WP, Light DR (2005) Fasudil, a Rho-kinase inhibitor, attenuates angiotensin II-induced abdominal aortic aneurysm in apolipoprotein E-deficient mice by inhibiting apoptosis and proteolysis. Circulation 111:2219–2226

A.8.4 Angiogenesis and Anti-Angiogenesis

A.8.4.1 General Considerations

Regulation of new blood vessel formation, angiogenesis, is precisely programmed throughout the lifetime of vertebrates. Besides the role of angiogenesis in normal function, it is an essential component of disease processes, including tumor growth, rheumatoid arthritis, psoriasis, and diabetic retinopathy (Folkman and Klagsbrun 1987; Klagsbrun and D'Amore 1991; Folkman and Shing 1992). Multiple factors that stimulate angiogenesis either directly or indirectly have been described, including the fibroblast growth factor family (Esch et al. 1985), vascular endothelial growth factor (Leung et al. 1990; Thomas 1996; Ferrara and Davis-Smyth 1997), epidermal growth factor (Gospadarowicz et al. 1979), transforming growth factor-α and -β (Schreiber et a 1986; Yang and Moses 1990), tumor necrosis factor-α (Leibovich et al. 1987), angiogenin (Fett et al. 1985), CYR61, a product of a growth factor-inducible immediate early gene (Babic et al. 1998) ect. The pharmacological inhibition of angiogenesis is of considerable interest in the development of new therapeutic modalities for the treatment of diseases such as diabetic retinopathy, atherosclerosis, hemangiomas, rheumatoid arthritis and cancer, in which pathological angiogenesis occurs (Ezekowitz et al. 1992; Folkman and Shing 1992; Fan and Brem 1992; O'Brien et al. 1994). Several natural inhibitors of angiogenesis were described, such as thrombospondin (Good et al. 1990), somatostatin (Barrie et al. (1993), angiostatin, isolated from a subclone of Lewis lung carcinoma, (O'Reilly et al. 1994, 1996), endostatin, a 20 kDa angiogenesis inhibitor from a murine hemangioendothelioma which is a C-terminal fragment of collagen XVIII (O'Reilly et al. 1997; Dhanabal et al. 1999), vasostatin (Pike et al. 1998).

Angiogenesis was studied *ex vivo* by culturing rat or mouse aortic rings in collagen gel (Zhu et al. 2003). Unlike rat aorta explants, unstimulated mouse aortic rings were unable to spontaneously produce an angiogenic response under serum-free conditions. They, however, responded to basic fibroblast growth factor (bFGF) and vascular endothelial growth factor (VEGF), generating networks of branching neovessels.

Couffinhal et al. (1998) published a mouse model of angiogenesis. The femoral artery of one hind-limb was ligated and excised. Laser Doppler perfusion imaging was employed to document the consequent reduction in hind-limb blood-flow, which typically persisted for up to 7 days. Neovascularization was shown to develop in association with augmented expression of VEGF mRNA and protein from skeletal myocytes as well as endothelial cells from the ischemic hind-limb.

REFERENCES AND FURTHER READING

Babic AM, Kireeva ML, Kolesnikova TV, Lau LF (1998) CYR61, a product of a growth factor-inducible immediate early gene, promotes angiogenesis and tumor growth. Proc Natl Acad Sci USA 95:6355–6360
Barrie R, Woltering EA, Hajarizadeh H, Mueller C, Ure T, Fletcher WS (1993) Inhibition of angiogenesis by somatostatin and somatostatin-like compounds is structurally dependent. J Surgical Res 55:446–450
Couffinhal T, Siver M, Zheng LP, Kearney M, Witzenbichler B, Isner JM (1998) Mouse model of angiogenesis.. Am J Pathol 152:1667–1679
Dhanabal M, Volk R, Ramchandran R, Simons M, Sukhatme VP (1999) Cloning, expression, and *in vitro* activity of human endostatin. Biochem Biophys Res Commun 258:345–352
Esch F, Baird A, Ling N, Ueno N, Hill F, Denoroy L, Klepper R, Gospodarowicz D, Bohlen P, Gillemin R (1985) Primary structure of bovine pituitary basic fibroblast growth factor (FGF) and comparison with the amino-terminal sequence of bovine brain acidic FGF. Proc Natl Acad Sci USA 82:6507–6511

Ezekowitz RA, Mulliken JB, Folkman J (1992) Interferon alfa-2a therapy for life-threatening hemangiomas in infancy. New Engl J Med 326:1456–1463
Fan TPD, Brem S (1992) in: Waring MJ, Ponder B (eds) The Search for New Anticancer Drugs: Cancer Biology Series, Vol 3, pp 185–229, Kluwer Publ., Lancaster
Ferrara N, Davis-Smyth T (1997) The biology of vascular endothelial growth factor. Endocr Rev 18:4–25
Fett JW, Strydom DJ, Lobb RR, Aldeman EM, Bethune JL, Riordan JF, Vallee BL (1985) Isolation and characterization of angiogenin, an angiogenic protein from human carcinoma cells. Biochemistry 24:5480–5486
Folkman J, Klagsbrun M (1987) Angiogenic factors. Science 235:442–447
Folkman J, Shing Y (1992) Angiogenesis. J Biol Chem 267:10931–10934
Good DJ, Polverini PJ, Rastinejad F, Le Beau MM, Lemons RS, Frazier WA, Bouck NP (1990) A tumor suppressor-dependent inhibitor of angiogenesis is immunologically and functionally indistinguishable from a fragment of thrombospondin. Proc Natl Acad Sci USA 87:6624–6628
Gospodarowicz D, Bialecki H, Thakral GK (1979) The angiogenic activity of the fibroblast and epidermal growth factor. Exp Eye Res 28:501–514
Klagsbrun M, D'Amore PA (1991) Regulators of angiogenesis. Ann Rev Physiol 53:217–239
Leibovich SJ, Polverini PJ, Shepard HM, Wiseman DM, Shively V, Nuseir N (1987) Macrophage-induced angiogenesis is mediated by tumor necrosis factor alpha. Nature 329:630–632
Leung DW, Cachianes G, Kuang WJ, Goeddel DV, Ferrara N (1990) Vascular endothelial growth factor is a secreted angiogenic mitogen. Science 246:1306–1309
O'Brien ER, Garvin MR, Dev R, Stewart DK, Hinohara T, Simpson JB, Shwartz SM, (1994) Angiogenesis in human coronary atherosclerotic plaques. Am J Pathol 145:883–894
O'Reilly MS, Holmgren L, Shing Y, Chen C, Rosenthal RA, Moses M, Lane WS, Cao Y, Sage EH, Folkman J (1994) Angiostatin, a novel angiogenesis inhibitor that mediates the suppression of metastases by a Lewis lung carcinoma. Cell 79:315–328
O'Reilly MS, Holmgren L, Chen C, Folkman J (1996) Angiostatin induces and sustains dormancy of human primary tumors in mice. Nature Med 2:689–692
O'Reilly MS, Boehm T, Shing Y, Fukai N, Vasios G, Lane WS, Flynn E, Birkhead JR, Olsen BR, Folkman J (1997) Endostatin: an endogenous inhibitor of angiogenesis and tumor growth. Cell 88:277–285
Pike SE, Yao L, Jones KD, Cherney B, Appella E, Sakaguchi K, Nakhasi H, Teruya-Feldstein J, Wirth P, Gupta G, Tosato G (1998) Vasostatin, a calreticulin fragment, inhibits angiogenesis and suppresses tumor growth. J Exp Med 188:2349–2356
Schreiber AB, Winkler ME, Derynk R (1986) Transforming growth factor-alpha: a more potent angiogenic mediator than epidermal growth factor. Science 232:1251–1253
Thomas KA (1996) Vascular endothelial growth factor, a potent and selective angiogenic agent. J Biol Chem 271:603–606
Yang EY, Moses HL (1990) Transforming growth factor 1-induced changes in cell migration, proliferation, and angiogenesis in the chicken chorioallantoic membrane. J Cell Biol 111:731–741
Zhu WH, Iurlaro M, MacIntyre A, Fogel E, Nicosia RF (2003) The mouse aorta model: Influence of genetic background and aging on bFG- and VEGF-induced angiogenic sprouting. Angiogenesis 6:193–199

A.8.4.2 Endothelial Cell Proliferation

PURPOSE AND RATIONALE

Human umbilical vein endothelial cells (HUVEC) were used by various authors to study endothelial cell proliferation (Bussolino et al. 1992; Benelli et al. 1995; Danesi et al. 1997; Hu 1998; Iurlaro et al. 1998; Vacca et al. 1999; Xin et al. 1999).

PROCEDURE

The HUV-EC-C human endothelial cells (American Type Culture Collection, Rockville, MD) are cultured at 37°C and 5% CO_2 in 90% Ham's F12K, 10% fetal bovine serum, 30 µg/ml endothelial cell growth factor, 100 µg/ml heparin, and 4 mM L-glutamine. The effect of test compound on HUV-EC-C cell proliferation is evaluated on 3×10^3 cells/well in 24-well plates. After 24 h, the test compound in various concentrations of the vehicle are added, and plates are incubated for 72 h. Cells are then harvested with trypsin/EDTA and counted by an hemocytometer.

EVALUATION

Results are expressed as number of cells in vehicle and compound-treated cultures and are the mean of three separate experiments ± SE.

MODIFICATIONS OF THE METHOD

In addition to human umbilical veil endothelial cells, Pike et al. (1998) used fetal bovine heart endothelial cells and measured DNA synthesis by [^{3}H]thymidine deoxyribose uptake.

Oikawa et al. (1991) used vascular cells from bovine carotid arteries and tested cell proliferation in a collagen gel and cell migration in a Boyden chamber.

Bovine capillary endothelial cells were used by Folkman et al. (1979), Clapp et al. (1993), O'Reilly et al. (1997), Cao et al. (1999).

REFERENCES AND FURTHER READING

Benelli U, Lepri A, Nardi M, Danesi R, Del Tacca M (1995) Tradipil inhibits endothelial cell proliferation and angiogenesis in the chick chorioallantoic membrane and in the rat cornea. J Ocular Pharmacol 11:157–166
Bussolino F, Di Renzo MF, Ziche M, Bocchietto E, Olivero M, Naldini R, Gaudino G, Tamagnone L, Coffer A, Comoglio PM (1992) Hepatocyte growth factor is a potent angiogenic growth factor which stimulates endothelial cell motility and growth. J Cell Biol 119:629–641
Cao R, Wu HL, Veitonmäki N, Linden P, Farnebo J, Shi G Y, Cao Y (1999) Suppression of angiogenesis and tumor growth by the inhibitor K1–5 generated by plasmin-mediated proteolysis. Proc Natl Acad Sci 96:5728–5733
Clapp C, Martial JA, Guzman RC, Rentier-Delrue F, Weiner RI (1993) The 16-kilodalton N-terminal fragment of human

prolactin is a potent inhibitor of angiogenesis. Endocrinology 133:1292–1299
Danesi R, Agen C, Benelli U, Di Paolo A, Nardini D, Bocci G, Basolo F, Camapgni A, Del Tacca M (1997) Inhibition of angiogenesis by the somatostatin analogue octreotide acetate (SMS 201–995). Clin Cancer Res 3:265–272
Folkman J, Haundenschild CC, Zetter BR (1979) Long-term culture of capillary endothelial cells. Proc Natl Acad Sci USA 76:5217–5221
Hu G-F (1998) Neomycin inhibits angiogenin-induced angiogenesis. Proc Natl Acad Sci USA 95:9791–9795
IurlaroM, Vacca A, Minischetti M, Ribatti D, Pellegrino A, Sardanelli A, Giacchetta F, Dammacco F (1998) Antiangiogenesis by cyclosporine. Exp Hematology 26:1215–1222
Oikawa T, Hasegawa M, Shimamura M, Ashino H, Murota SI, Morita I (1991) Eponemycin, a novel antibiotic, is a highly powerful angiogenesis inhibitor. Biochem Biophys Res Commun 181:1070–1076
O'Reilly MS, Boehm T, Shing Y, Fukai N, Vasios G, Lane WS, Flynn E, Birkhead JR, Olsen BR, Folkman J (1997) Endostatin: an endogenous inhibitor of angiogenesis and tumor growth. Cell 88:277–285
Pike SE, Yao L, Jones KD, Cherney B, Appella E, Sakaguchi K, Nakhasi H, Teruya-Feldstein J, Wirth P, Gupta G, Tosato G (1998) Vasostatin, a calreticulin fragment, inhibits angiogenesis and suppresses tumor growth. J Exp Med 188:2349–2356
Vacca A, Iurlaro M, Ribatti D, Minischetti M, Nico B, Ria R, Pellegrino A, Dammacco F (1999) Antiangiogenesis is produced by nontoxic doses of vinblastine. Blood 94:4143–4155
Xin X, Yang S, Kowalski J, Gerritsen ME (1999) Peroxisome proliferator-activated receptor γ ligands are potent inhibitors of angiogenesis *in vitro* and *in vivo*. J Biol Chem 274:9116–9121

A.8.4.3 Chorioallantoic Membrane Assay

PURPOSE AND RATIONALE

The chick chorioallantoic membrane assay, originally described by Auerbach et al. (1974), has been used with some modifications by several authors to test angiogenesis and inhibition of angiogenesis, e. g., by Taylor and Folkman (1982), Crum et al. (1985), Vu et al. (1985), McNatt et al. (1992, 1999), Barrie et al. (1993), Clapp et al. (1993), Gagliardi and Collins (1993), Benelli et al. (1995), Ribatti et al. (1995), Klauber et al. (1996), Oikawa and Shimamura (1996), Danesi et al. (1997), O'Reilly et al. (1997), Iurlaro et al. (1998), Cao et al. (1999), Vacca et al. (1999).

PROCEDURE

Fertilized White Leghorn chicken eggs are incubated at 37°C at constant humidity. On incubation day 3, a square window is opened in the shell and 2 to 3 ml of albumen is removed to allow detachment of the developing chorioallantoic membrane (CAM). The window is sealed with a glass and the eggs are returned to the incubator. On day 8, 1 mm^3 gelatin sponges loaded with 3 µl phosphate-buffered saline alone as the negative control or containing 3 µg (1 mg/ml) of the angiogenic recombinant basic fibroblast growth factor alone as positive control, or together with various doses of test compound, are implanted on top of the CAM. The sponge traps the sample and allows slow release of the product. CAM are examined daily until day 12, when the angiogenic response peaks. On day 12, blood vessels entering the sponge within the focal plane of the CAM are recognized microscopically, counted by two observers in a double-blind fashion under a Zeiss SR stereomicroscope, and photographed in ovo with the MC63 Camera system (Zeiss, Oberkochen, Germany). To better highlight vessels, the CAM are injected into a large allantoic vein with India ink solution, fixed in Serra's fluid, dehydrated in graded ethanols, and rendered transparent in methylbenzoate. On day 12, after microscopic counting, the embryos and their membranes are fixed in ovo in Bouin's fluid. The sponges and the underlying and immediately adjacent CAM portions are removed, embedded in paraffin, sectioned at 8 µm along a plane parallel to the CAM surface, and stained with a 0.5% aqueous solution of toluidine blue.

EVALUATION

Angiogenesis is measured by a planimetric point count method (Ribatti et al. 1999): four to six 250× magnification fields covering almost the whole of every third section within 30 serial slides of each sponge per sample are analyzed within a superimposed 144 intersection point square reticulum of 0.125 mm^2. Only transversely sectioned microvessels, ie, capillaries and venules with or without a 3 to 10 µm lumen occupying the intersection points, are counted and calculated as the mean ± 1 SD per section, per CAM, and groups of CAM. Statistical significance of differences is calculated by comparing the data from each experiment to their controls using Student's *t*-test.

MODIFICATIONS OF THE METHOD

Oh et al. (1997) studied the lymphatics of differentiated avian chorioallantoic membrane using microinjection of Mercox resin, semi- and ultrathin sectioning, immunohistochemical detection of fibronectin and α-smooth muscle actin, and *in situ* hybridization with vascular endothelial growth factor VEGFR-2 and VEGFR-3 probes.

Using the chick chorioallantoic membrane assay, Giannopoulou et al. (2003) showed that amifostine, an inorganic thiophosphate-cytoprotective agent, inhibits angiogenesis *in vivo*.

REFERENCES AND FURTHER READING

Auerbach R, Kubai L, Knighton D, Folkman J (1974) A simple procedure for the long-term cultivation of chicken embryos. Dev Biol 41:391–394

Barrie R, Woltering EA, Hajarizadeh H, Mueller C, Ure T, Fletcher WS (1993) Inhibition of angiogenesis by somatostatin and somatostatin-like compounds is structurally dependent. J Surgical Res 55:446–450

Benelli U, Lepri A, Nardi M, Danesi R, Del Tacca M (1995) Tradipil inhibits endothelial cell proliferation and angiogenesis in the chick chorioallantoic membrane and in the rat cornea. J Ocular Pharmacol 11:157–166

Cao R, Wu HL, Veitonmäki N, Linden P, Farnebo J, Shi G Y, Cao Y (1999) Suppression of angiogenesis and tumor growth by the inhibitor K1–5 generated by plasmin-mediated proteolysis. Proc Natl Acad Sci 96:5728–5733

Clapp C, Martial JA, Guzman RC, Rentier-Delrue F, Weiner RI (1993) The 16-kilodalton N-terminal fragment of human prolactin is a potent inhibitor of angiogenesis. Endocrinology 133:1292–1299

Crum R, Szabo S, Folkman J (1985) A new class of steroids inhibits angiogenesis in the presence of heparin or a heparin fragment. Science 230:1375–1378

Danesi R, Agen C, Benelli U, Di Paolo A, Nardini D, Bocci G, Basolo F, Camapgni A, Del Tacca M (1997) Inhibition of angiogenesis by the somatostatin analogue octreotide acetate (SMS 201–995). Clin Cancer Res 3:265–272

Gagliardi A, Collins DC (1993) Inhibition of angiogenesis by antiestrogens. Cancer Res 53:533–535

Giannopoulou E, Katsoris P, Kardamakin D, Papadimitiou E (2003) Amifostine inhibits angiogenesis in vivo. J Pharmacol Exp Ther 304:729–737

Klauber N, Browne F, Anand-Apte B, D'Amato RJ (1996) New activity of spironolactone. Inhibition of angiogenesis *in vitro* and *in vivo*. Circulation 94:2566–2571

IurlaroM, Vacca A, Minischetti M, Ribatti D, Pellegrino A, Sardanelli A, Giacchetta F, Dammacco F (1998) Antiangiogenesis by cyclosporine. Exp Hematology 26:1215–1222

McNatt LG, Lane D, Clark AF (1992) Angiostatic activity and metabolism of cortisol in the chorioallantoic membrane (CAM) of the chick embryo. J Steroid Biochem Molec Biol 42:687–693

McNatt LG, Weimer L, Yanni J, Clark AF (1999) Angiostatic activity of steroids in the chick embryo CAM and rabbit cornea models of neovascularization. J Ocular Pharmacol 15:413–423

Oh SJ, Jeltsch MM, Birkenhäger R, McCarthy JEG, Weich HA, Christ B, Alitalo K, Wilting J (1997) VEGF and VEGF-C: Specific induction of angiogenesis and lymphangiogenesis in the differentiated avian chorioallantoic membrane. Dev Biol 188:96–109

Oikawa T, Shimamura M (1996) Potent inhibition of angiogenesis by wortmannin, a fungal metabolite. Eur J Pharmacol 318:93–96

O'Reilly MS, Boehm T, Shing Y, Fukai N, Vasios G, Lane WS, Flynn E, Birkhead JR, Olsen BR, Folkman J (1997) Endostatin: an endogenous inhibitor of angiogenesis and tumor growth. Cell 88:277–285

Ribatti D, Urbinati C, Nico B, Rusnati M,. Roncali L, Presta M (1995) Endogenous basic fibroblast growth factor is implicated in the vascularization of the chick chorioallantoic membrane. Dev Biol 170:39–49

Ribatti D, Presta M, Vacca A, Ria R, Giulani R, Dell'Era P, Nico B, Roncali R, Damacco F (1999) Human erythropoietin induces a proangiogenic phenotype in cultured endothelial cells and stimulates neovascularization *in vivo*. Blood 93:2627–2636

Taylor S, Folkman J (1982) Protamine is an inhibitor of angiogenesis. Nature 297:307–312

Vacca A, Iurlaro M, Ribatti D, Minischetti M, Nico B, Ria R, Pellegrino A, Dammacco F (1999) Antiangiogenesis is produced by nontoxic doses of vinblastine. Blood 94:4143–4155

Vu MT, Smith CF, Burger PC, Klintworth GK (1985) An evaluation of methods to quantitate the chick chorioallantoic membrane assay in angiogenesis. Lab Invest 53:499–508

A.8.4.4 Cornea Neovascularization

PURPOSE AND RATIONALE

Neovascularization of the rabbit cornea has been used by several authors to study inhibition of angiogenesis (Gimbrone et al. 1974; Crum et al. 1985; BenEzra et al. 1987, 1997; Klauber et al. 1996; McNatt et al. 1999; Joussen et al. 1999).

PROCEDURE

New Zealand White rabbits are anesthetized for surgery and quantification of newly developed blood vessels with 5 mg/kg xylazine hydrochloride and 35 mg/kg ketamine hydrochloride i.m. Corneal blood vessels are induced by basic fibroblast growth factor which is applied in carrier pellets. These pellets are produced by dispersing 50 µl of 2% methylcellulose containing 500 ng human recombinant basic fibroblast growth factor diluted in 10 µl phosphate-buffered saline in plastic rods with a diameter of 4 mm. Dried pellets are folded twice and implanted intrastromally in the 12 o'clock position into a corneal tunnel. This tunnel is created by a central cut of approximately 50% depth and extended into the peripheral cornea to a point 2.0 mm away from the limbus. Following implantation, the central entrance of the tunnel is closed with a single 10–0 nylon suture in order to ensure that the tear film does not dissolve the pellet and uncontrolled liberation of the growth factor is prevented.

The test substance is dissolved in a viscous gel containing 0.002% polyacrylic acid, 0.04% sorbitol, and 0.001% cetrimide in a watery base. The eyes are treated once daily with 0.1 ml of this gel which is applied in the lower conjunctiva sac. The eyes are closed for several seconds to avoid loss of the substance. Each animal's contralateral eye receives gel without test substance and serves as control. Control animals receive the viscous gel without test substance.

Animals are observed daily under an operating microscope, and vascular growth is documented on days 6, 9, 12, and 16 after surgery. The number of blood vessels, their length and the dimension of the

vascularized area are quantified with a caliper under the operating microscope as well as on standardized photographs. On every observation day corneas are stained with fluorescein in order to show epithelial irregularities due to the topical treatment.

EVALUATION

Differences between treated eyes and controls are tested for significance using unpaired Student's *t*-test.

MODIFICATIONS OF THE METHOD

Damms et al. (1997) characterized the neovascularization that follows the intracorneal injection of bovine albumin in rabbits as a model of angiogenesis. New Zealand white rabbits received intracorneal injections of phosphate buffered saline with and without various amounts of bovine albumin. The rabbits were co-sensitized or pre-sensitized by intramuscular bovine albumin. The corneal response was quantified by ranking photographs taken periodically after the injection.

Babic et al. (1998) tested an angiogenesis promotor in the corneal pocket angiogenesis assay in **rats**.

Xin et al. (1999) studied inhibitors of angiogenesis in the corneal angiogenesis assay in rats. A 1.5 mm incision was made approximately 1 mm from the center of the cornea in anesthetized Sprague Dawley rats. Using a curved spatula, the incision was bluntly dissected through the stroma toward the outer canthus of the eye. A hydron pellet (2×20 mm) containing 200 ng vascular endothelial growth factor and 100 ng sucralfrate was inserted into the base of the pocket.

Foschi et al. (1994), Benelli et al. (1995), Danesi et al. (1997) studied neovascularization of rat cornea induced by **chemical injury**. Both eyes of ether-anesthetized rats were cauterized by applying a $AgNO_3$/KNO_3 (1:1, w/w) applicator to the surface of the cornea eccentrically at a point approximately 2 mm from the corneoscleral limbus. Rats were treated 4 times daily for 6 days with eye drops. The eyes were examined by slit-lamp microscopy daily for 6 days to the evaluate the growth of the vessels. On the 6th day after cauterization, the rats were anesthetized and the upper body perfused through a cannula inserted in the ascending aorta with Ringer's solution until the normal pink color of the fundi disappeared and then with a mixture of 10% India ink/6% gelatin in Ringer's solution. The eyes were enucleated and placed in 4% formaldehyde. The cornea and a 1 mm rim of adjacent scleral tissue were dissected from the rest of the globe and three full thickness peripheral radial cuts were made to allow flattening of the cornea. The corneas were then placed on a glass slide in mounting media, magnified, and photographed. The area occupied by blood vessels was calculated and the area vascularization of drug treated animals was compared to that of control rats.

Kenyon et al. (1996), Cao et al. (1999) performed the corneal micropocket assay in **mice**.

REFERENCES AND FURTHER READING

Babic AM, Kireeva ML, Kolesnikova TV, Lau LF (1998) CYR61, a product of a growth factor-inducible immediate early gene, promotes angiogenesis and tumor growth. Proc Natl Acad Sci USA 95:6355–6360

BenEzra D, Hemo I, Maftzir G (1987) The rabbit cornea. A model for the study of angiogenic factors. In: Ezra D, Ryan SJ, Glaser B, Murphy R (eds) Ocular Circulation and Neovascularization. Documenta Ophthalmologia Proceedings, Series 50, Martinus Nijhoff, Dordrecht, The Netherlands, pp 335–340

BenEzra D, Griffin BW, Maftzir G, Aharanov O, Sharif NA, Clark AF (1997) Topical formulations of novel angiostatic steroids inhibit rabbit corneal neovascularization. Invest Ophthalmol Vis Sci 38:1954–1962

Cao R, Wu HL, Veitonmäki N, Linden P, Farnebo J, Shi G Y, Cao Y (1999) Suppression of angiogenesis and tumor growth by the inhibitor K1–5 generated by plasmin-mediated proteolysis. Proc Natl Acad Sci 96:5728–5733

Crum R, Szabo S, Folkman J (1985) A new class of steroids inhibits angiogenesis in the presence of heparin or a heparin fragment. Science 230:1375–1378

Damms T, Ross JR, Duplessie MD, Klintwort GK (1997) Intracorneal bovine albumin: an immunologic model of corneal angiogenesis. Graefe's Arch Clin Exp Ophthalmol 235:662–666

Foschi D, Castoldi L, Corsi F, Radaelli E, Trabucchi E (1994) Inhibition of inflammatory angiogenesis in rats by locoregional administration of hydrocortisone and protamine. Agents Actions 42:40–43

Gimbrone MA, Cotran RS, Leapman SB, Folkman J (1974) Tumor growth and neo-vascularization: an experimental model using the rabbit cornea. J Nat Cancer Inst 52:413–427

Joussen AM, Kruse FE, Völcker HE, Kirchhof B (1999) Topical application of methotrexate for inhibition of corneal angiogenesis. Graefe's Arch Clin Exp Ophthalmol 237:920–927

Kenyon BM, Voest EE, Chen CC, Flynn E, Folkman J, D'Amato RJ, (1996) A model of angiogenesis in the mouse cornea. Invest Ophthalmol Vis Sci 37:1625–1632

Klauber N, Browne F, Anand-Apte B, D'Amato RJ (1996) New activity of spironolactone. Inhibition of angiogenesis *in vitro* and *in vivo*. Circulation 94:2566–2571

McNatt LG, Weimer L, Yanni J, Clark AF (1999) Angiostatic activity of steroids in the chick embryo CAM and rabbit cornea models of neovascularization. J Ocular Pharmacol 15:413–423

Xin X, Yang S, Kowalski J, Gerritsen ME (1999) Peroxisome proliferator-activated receptor γ ligands are potent inhibitors of angiogenesis *in vitro* and *in vivo*. J Biol Chem 274:9116–9121

A.8.4.5
Rat Subcutaneous Air Sac Model

PURPOSE AND RATIONALE

Lichtenberg et al. (1997, 1999) recommended the subcutaneous air sac model in rats as a simple method for *in vivo* screening of antiangiogenesis. Subcutaneous injection of air in the rat results in the formation of an air pouch. If air pouches are kept inflated by repeated injections of air the develop a structure of synovial lining (Edwards et al. 1981). The subcutaneous air pouch appears more like a bursal cavity than a synovial joint (Kowanko et al. 1986) and after 8–10 days the cells of the air sac appear as a transparent membrane on which the formation of new vessels can be studied.

PROCEDURE

Under anesthesia 10–15 ml of air is introduced dorsally to female Sprague Dawley rats weighing 150–180 g by subcutaneous injections using a 25 gauge needle to produce an air sac located approximately 4–5 cm behind the head of the animal. The air sacs are re-inflated every forth day. The wall of the air sac becomes progressively thicker with time and after approximately 10 days a sufficient lining of cells has been established. For sponge implantation, the animals are anesthetized again. A 1.5 cm incision is made through the clipped skin covering the air sac and blunt dissection is used to open a 2 cm deep cavity towards the cranial base of the air sac by careful separation of the skin from the membrane. A cellulose implant (Spontex sponge) with a diameter of 8 mm is carefully pressed into the cavity of the membrane away from the incision site and the incision closed by sutures. The animals are treated for 10 days with various doses of test compound in a volume of 10 ml/kg or vehicle. The subcutaneous injection is made under light CO_2/O_2 anesthesia into the hind leg 5–7 cm away from the air sac. This injection site is chosen to eliminate any risk of inducing irritative side-effects on the membrane. After 10 days treatment, the animals are sacrificed after having received 20 min before an injection of 1 μCi of ^{125}I-labelled immunoglobulin via the tail vein. The overlying skin of the air sac is removed to expose the transparent membrane. The extent of vascular proliferation is scored *in situ*:

1+: slight background vascularization;
2+: few new vessels reach the sponge;
3+: many new vessels reach and penetrate the implant;
4+: very intense formation of new vessels which reach and penetrate the implant.

Following *in situ* scoring, the implant and the membrane from each animal are placed in the same plastic vial containing 10% formalin and the radioactivity is measured in a γ-counter. The implants are examined microscopically after staining with haematoxylin and eosin.

EVALUATION

The extent of vascular proliferation scored *in situ* is compared between vehicle and treated animals by the Wilcoxon test. The angiogenic response measured by ^{125}I-activity in cpm is subjected to analysis of variance followed by Dunnett's *t*-test to compare each dose with the vehicle. The cpm's are log-transformed to obtain variance homogeneity. The correlation between *in situ* scores and cpm is estimated by Spearman's rank correlation coefficient after ranking cpm values.

MODIFICATIONS OF THE METHOD

In a further study, Lichtenberg et al. (1999) inoculated vascular endothelial growth factor producing tumor cells subcutaneously directly on the membrane, and the formation of vessels was measured 8 days later. Furthermore, slow-release pellets containing angiogenic factors, basic fibroblast growth factor or vascular endothelial growth factor, were implanted on the subcutaneous membrane.

Nakamura et al. (1999) studied suppression of angiogenesis induced by S-180 mouse tumor cells in the dorsal air sac assay in **mice**.

Funahashi et al. (1999) developed a mouse dorsal air sac model for quantifying *in vivo* tumor-induced angiogenesis which is determined by measuring the blood volume in an area of skin held in contact with a tumor cell-containing chamber, using ^{51}Cr-labeled red blood cells.

Schreiber et al. (1986) described the **hamster cheek pouch assay** for testing angiogenic/antiangiogenic activity.

REFERENCES AND FURTHER READING

Edwards JC, Sedgwick AD, Willoughby DA (1981) The formation of a structure with the features of synovial lining by subcutaneous injection of air. An *in vivo* tissue culture system. J Pathol 134:147–156

Funahashi Y, Wakabayashi T, Semba T, Sonoda J, Kitoh K, Yoshimatsu K (1999) Establishment of a quantitative mouse dorsal air sac model and its application to evaluate a new angiogenesis inhibitor. Oncol Res 11:319–329

Kowanko IC, Gordon TP, Rosenbilds AM, Brooks PM, Roberts-Thompson PJ (1986) The subcutaneous air pouch model of synovium and the inflammatory response to heat aggregated gammaglobulin. Agents Actions 18:421–428

Lichtenberg J, Hansen CA, Skak-Nilsen T, Bay C, Mortensen JT, Binderup L (1997) The rat subcutaneous air sac model:

a new and simple method for *in vivo* screening of antiangiogenesis. Pharmacol Toxicol 81:280–284
Lichtenberg J, Hjarnaa P JV, Kristjansen PEG, Hansen D, Binderup L (1999) The rat subcutaneous air sac model: A quantitative assay of antiangiogenesis in induced vessels. Pharmacol Toxicol 84:34–40
Nakamura M, Katsuki Y, Shibutani Y, Oikawa T (1999) Dienogest, a synthetic steroid, suppresses both embryonic and tumor-cell-induced angiogenesis. Eur J Pharmacol 386:33–40
Schreiber AB, Winkler ME, Derynk R (1986) Transforming growth factor-α: a more potent angiogenic factor than epidermal growth factor. Science 232:1250–1253

A.8.4.6 Mesenteric Window Angiogenesis Model

PURPOSE AND RATIONALE

Norrby et al. (1986, 1990, 1995) described the mesenteric window assay in rats for quantitative measurement of induction and inhibition of angiogenesis. The tissue being used is the membranous, 'window'-like parts of the mesentery which is normally vascularized and appears to lack significant physiologic angiogenesis. Since the mesenteric window natively measures only 5–10 µm in thickness, the vasculature is virtually two-dimensional. Due to the structural and metabolic simplicity of the test tissue, the mesenteric window microvasculature is regarded as an ideal test system for establishing the functional influences of defined factors (Zweifach 1973).

PROCEDURE

Angiogenesis is induced by i.p. injection of the mast-cell secretagogue compound 48/80 twice daily for 4.5 days to male Sprague Dawley rats weighing about 225 g. Test compounds or saline are injected s.c. 1 h before each injection of compound 48/80.

Angiogenesis is quantified by microscopically counting the number of vessel profiles per unit length of the mesenteric window in 4 microtome sections per specimen, cut perpendicularly to the surface, from the central part of the window. This reflects the degree of branching, the degree of tortuosity and the degree of spatial expansion of the vasculature. Four specimens per animal are analyzed.

Four mesenteric window specimens are spread, fixed on objective slides and stained with toluidine blue to measure the relative vascularized area. Three randomly selected vascular view fields per mesenteric-window spread are analyzed for microvascular length per unit area of vascularized tissue. The total microvascular length is computed from the vascularized area of each animal multiplied by the mean microvascular length for the corresponding treatment group.

EVALUATION

The non-parametric two-tailed Mann-Whitney U rank sum test for unpaired observations is used for statistical analysis.

REFERENCES AND FURTHER READING

Norrby K (1995) Evidence of a dual role of endogenous histamine in angiogenesis. Int J Exp Pathol 76:87–92
Norrby K, Jakobsson A, Sörbo J (1986) Mast cell-mediated angiogenesis. A novel experimental model using the rat mesentery. Virchow's Arch B. Cell Pathol 52:195–206
Norrby K, Jakobsson A, Sörbo J (1990) Quantitative angiogenesis in spreads of intact mesenteric windows. Microvasc Res 39:341–348
Zweifach BW (1973) The microcirculation in the intestinal mesentery. Microvasc Res 5:363–367

A.8.4.7 Quantification of Vascular Endothelial Growth Factor-C

PURPOSE AND RATIONALE

Vascular endothelial growth factor (VEGF) has achieved considerable therapeutic interest (Clauss 1998; Enholm et al. 1998; Ferrara et al. 2004).

Weich et al. (2004) described an ELISA for quantification of vascular endothelial growth factor-C.

PROCEDURE

Materials and Methods

The fully processed rat protein dNdC-VEGF-C and dNdC-VEGF-D were produced in insect cells and purified from supernatants (Kirkin et al. 2001). Human dNdC-VEGF-C and soluble VEGFR-3 production was achieved according to (Joukov et al. 1997; Hornig et al. 1999). A polyclonal antibody against rat VEGF-C was developed in rabbits (antibody 4080; BioGenes Berlin). A total amount of 1.2 mg rat VEGF-C (containing a C-terminal 6His-tag) was used for immunization of two New Zealand white rabbits. After immunization with 0.1 mg protein, each rabbit was boosted on days 7, 14, 28, 56 and 84 with the same amount. The dilution of the serum for half-maximal titer was 1:10,000. Total IgG from rabbit serum was isolated using HiTrap Protein A Sepharose columns (Amersham Bioscience, Freiburg).

Generations of Cell Lines, Serum-Free Cell Culture Supernatants, Lysates and Tissue Sample Preparation

Experiments were conducted using three human (PC-3 cells, 293 cells, COLO 800 cells) and four rat (10AS, ARIP, BRL3A, MT-450) tumour cell lines and 1640 medium (Gibco-BRL, Bethesda, Md., USA). Stable transfected clones were selected and tested for VEGF-

C expression and secretion using a polyclonal anti-VEGF-C antiserum.

The cells were grown to 80% confluence in 75-cm^2 tissue culture flasks (Nunc, Roskilde, Denmark). Conditioned media was collected under low-serum (2%) growth conditions. Tumor tissues were snap-frozen in liquid nitrogen and homogenized in RIPA buffer (0.1% SDS, 1% IGEPAL CA-630, 0.5% Na-deoxycholate, protease-inhibitor cocktail in phosphate-buffered saline).

VEGF-C Sandwich-ELISA

The VEGF-C antibody 4080 was isolated from serum using HiTrap Protein-A Sepharose columns. Then, depletion of the anti-his antibody fraction was done by antigen-affinity purification using 10 mg of immobilized 6H-tagged TxnTb protein [Tryparedoxin (Txn) from *Trypanosoma brucei* (Tb)]. Antigen-affinity purification for the antibody 4080 was performed by immobilizing 1 mg rat VEGF-C on an NHS-activated HiTrap column (Amersham Bioscience, Freiburg). The development of a highly sensitive and specific sandwich ELISA for VEGF-C was done using standard methods. Rabbit IgG 4080 (10 µg/ml) was used for coating and the antigen-affinity purified and biotinylated antibody 4080 at 1 µg/ml was used as a detector antibody. Biotinylation of antibody 4080 was done with 6 mg IgG in 100 mM carbonate buffer, pH 8.5 at 3 mg/ml with using biotin-amidohexanoic acid NHS (Sigma, St. Louis, Mo., USA). The molecular ratio biotin:protein was 30:1. As a standard, human and rat dNdC-VEGF-C was used over a concentration range between 0.1 and 6.25 ng/ml. For visualization of the detector, streptavidin-enzyme conjugate was used (Endogen, Woburn, Mass., USA) followed by the addition of TMB (tetra-methyl-benzidine; Roche Mannheim, Germany).

EVALUATION

After stopping the reaction with 1 M H_2SO_4, the absorbance was measured at 450 and 620 nm with an ELISA plate reader (Labsystems, Finland). Generally, the samples were analyzed in different dilutions, measuring each dilution in duplicate. Samples were diluted at least 1:2 with sample diluent (BenderMedSystems, Vienna).

MODIFICATIONS OF THE METHOD

Rissanen et al. (2003) found that VEGF-D is the strongest angiogenesis and lymphangiogenetic factor among VEGFs delivered into skeletal muscle via adenoviruses.

REFERENCES AND FURTHER READING

Clauss M (1998) Functions of the VEGF receptor-1 (FLT-1) in the vasculature. Trends Cardiovasc Med 8:241–245

Enholm B, Jussila L, Karkkainen M, Alitalo K (1998) Vascular endothelial growth factor-C: A growth factor for lymphatic and blood vascular endothelial cell. Trends Cardiovasc Med 8:292–297

Ferrara N, LeCouter J, Lin R, Peale F (2004) EG-VEGF and Bv8: a novel family of tissue-restricted angiogenic factors. Biochim Biophys Acta 1654:69–78

Hamada K, Oike Y, Takakura N, Ito Y, Jussila L, Dumont DJ, Alitalo K, Suda T (2000) VEGF-C signaling pathways through VEGFR-2 and VEGFR-3 in vasculoangiogenesis and hematopoiesis. Blood 96:3793–3800

Hornig C, Behn T, Bartsch W, Yayon A, Weich HA (1999) Detection and quantification of complexed and free soluble human vascular endothelial growth factor receptor-1 (sVEDFR-1) by ELISA. J Immunol Meth 226:169–177

Joukov V, Kaipainen A, Jeltsch M, Jajusola K, Olofsson B, Kumar V, Erikssan U, Alitalo K (1997) Vascular endothelial growth factors VEGF-B and VEGF-C. J Cell Physiol 1732:211–215

Kirkin V, Mazitschek R, Krishnan J, Steffen A, Waltenberger J, Pepper MS, Giannis A, Sleeman J (2991) Characterization of indolines which preferentially inhibit VEGF-Cand VEGF-D-induced activation of VEGFR-3 rather than VEGFR-2. Eur J Biochem 286:5530–5540

Rissanen TT, Markkanen JE, Gruchala M, Heikura T, Puranen A, Kettunen MI, Kholová I, Keuppinen RAS, Achan MG, Stacker SA, Alitalo K, Ylä-Herttula S (2003) VeGF-D is the strongest angiogenesis and lymphangiogenetic factor among VEGFs delivered into skeletal muscle via adenoviruses. Circ Res 92:1098–1106

Weich HA, Bando H, Brokelmann M, Baumann P, Toi M, Barleon B, Alitalo K, Sipos B, Sleeman J (2004) Quantification of vascular endothelial growth factor-C (VEGF-C) by a novel ELISA: J Immunol Meth 285:145–155

A.8.4.8 Inhibitors of Vascular Endothelial Growth Factor

PURPOSE AND RATIONALE

Inhibitors of vascular endothelial growth factor have gained therapeutic interest (Whittles et al. 2002; Gingrich et al. 2003; Hamma-Kourbali et al. 2003; Verheul and Pinedo 2003;

Fernandez et al. 2004; Roberts et al. 2004; Baka et al. 2006). In particular, VEGF Trap, a soluble decoy receptor comprising portions of VEGF receptors 1 and 2, has been studied (Wulff et al. 2001; Holash et al. 2002; Kim et al. 2002; Hood and Cheresh 2003; Saishin et al. 2003; Fukasawa and Korc 2004; Fraser et al. 2005; Hu et al. 2005; Lau et al. 2005).

Byrne et al. (2003) found that vascular endothelial growth factor-Trap decreases tumor burden, inhibits ascites, and causes dramatic vascular remodeling in an ovarian cancer model.

PROCEDURE

Cell Lines

Ascites fluid from athymic mice previously inoculated with OVCAR-3 cells was used. Cells from the SKOV-3 human cystadenocarcinoma cell line were grown in McCoy's 5a medium with 1.5 mM L-glutamine, penicillin, and streptomycin, supplemented with 10% FCS. Cells were grown to confluence and harvested by trypsinization with 0.25 mg/ml trypsin/EDTA and suspended in PBS before inoculation into mice.

Animals

Athymic Balb c *nu/nu* mice were housed under pathogen-free conditions and fed autoclaved pellets and water.

Retroviral Constructs

The pLZR Phoenix vector was modified by the addition of a MCS followed by an internal ribosome entry sequence-GFP cassette (Rommel et al. 1999). Thus, genes subcloned into the MCS produce bicistronic constructs under the control of the viral 5′ long terminal repeat. The entire coding sequence of $mVEGF_{164}$ was inserted into the MCS for the construct used to transduce cells with VEGF, whereas the MCS was left empty for the GFP-only vector. Constructs were transfected into Amphotrophic packaging lines to produced infective virus using standard techniques (Grignani et al. 1998).

SKOV-3 MODEL

SKOV-3 cell lines were infected with Amphotrophic viruses encoding either $mVEGF_{164}$ and GFP or GFP only. Cells that were successfully transduced with the retroviruses were collected by FACS using a Cytomation MoFlo (Fort Collins, Colo., USA) with fluorescence emission from GFP measured with a 530/540 nm bandpass filter. More than 50% of the cells were GFP positive after infection, allowing $> 4.0 \times 10^5$ cells to be collected and used to establish cell lines. To verify viral transduction, cells were resorted several days later and found to be > 80% positive for GFP expression. Cells were then expanded, aliquoted, and frozen. All experiments were performed with an aliquot expanded by four to five passages and tested for viability before injection.

In Vivo Adenoviral and SKOV-3 Studies

Adenoviral constructs were achieved according to Thurston et al. (2000). Adenoviral plaque-forming units (5.0×10^8) or 1.0×10^7 SKOV-3 cells were suspended in a volume of 300–400 µl of PBS or serum-free cell culture medium and injected i.p. into female nude mice. VEGF-Trap or control buffer was delivered twice weekly at 25 mg/kg via s.c. injection in a volume of 50–200 µl. Mice were assessed daily for general health and development of ascites and weighed at least twice weekly. Animals were sacrificed if they had lost > 10% of body weight or had persistent ascites on three consecutive assessments. After sacrifice, ascites was removed with a sterile thin caliber plastic transfer pipette and quantified, and hematocrit was measured.

OVCAR-3 MODEL

OVCAR-3 cells obtained from ascites fluid were prepared (Hu et al. 2002). Briefly, 2×10^6 cells in 500 µl of RPMI 1640 were injected i.p. into athymic Balb/C nude (*nu/nu*) mice. Fourteen days after inoculation, blinded administration of VEGF-Trap or human Fc as control was initiated at a dose of 25 mg/kg. Injections were given s.c. in the nape of the neck using a 28.5-gauge needle and a 0.5-ml insulin syringe. Injections (0.05 ml) were administered twice weekly throughout the experimental period. Body weight and abdominal circumference were quantified twice weekly. In addition, animals were monitored daily for evidence of advanced disease (listlessness, extensive swelling of the abdominal cavity). At the end of the experiment, all remaining mice underwent euthanasia with CO_2 followed by cervical dislocation. The volume of ascites was measured, and tumors were excised and weighed. Immediately before sacrifice, mice received i.v. injection with FITC lycopersicon lectin (see below).

Tumor Vasculature

According to Holash et al. (2002) s.c. tumors were established. After small s.c. tumors became palpable (1 week after implantation), treatment with the VEGF-Trap was initiated. VEGF-Trap or an equivalent volume of vehicle was delivered twice weekly s.c. at the nape of the neck. Tumor vasculature was visualized by using antibodies to platelet-endothelial cell adhesion molecule for immunohistochemistry.

VEGF-Trap-treated OVCAR-3 tumor-bearing mice and control, untreated tumor-bearing mice were anesthetized by i.m. injection with ketamine (87 mg/kg) and xylazine (13 mg/kg), followed by i.v. injection with 100 µl of FITC lycopersicon lectin or 100 µg of Cy3 albumin (Jackson Immunology Research, West Grove, Pa., USA). Then 10 min later, mice were perfused through the ascending aorta with 4% paraformaldehyde in PBS for 2 min. Tumors and control organs were extracted and placed in fixative for 1–2 h followed by immersion in 30% sucrose/PBS

overnight, embedded in OCT, cryostat sectioned, and viewed by fluorescence microscopy.

REFERENCES AND FURTHER READING

Baka S, Clamp AR, Jayson GC (2006) A review on the latest clinical compounds that inhibit VEGF in pathological angiogenesis. Expert Opin Ther Targets 10.867–876

Byrne AT, Ross L, Holash J, Nakanishi M, Hu L, Hofmann JI, Yancopoulos GD, Jaffe RB (2003) Vascular endothelial growth factor-Trap decreases tumor burden, inhibits ascites, and causes dramatic vascular remodeling in an ovarian cancer model. Clin Cancer Res 9:5721–5728

Fernandez M, Vizzutti F, Garcia-Pagan JC, Rodes J, Bosch J (2004) Anti-VEGF receptor-2 monoclonal antibody prevents portal-system collateral vessel formation in hypertensive mice. Gastrooenterology 126:886–894

Fraser HM, Wilson H, Morris KD, Swanston I, Wiegand SJ (2005) Vascular endothelial growth factor Trap suppresses ovarian function at all stages of the luteal phase in the macaque. J Clin Endocrinol Metab 90:5811–5818

Fukusawa M, Korc M (2004) Vascular endothelial growth factor-Trap suppresses tumorigenicity of multiple pancreatic cancer cell lines. Clin Cancer Res 10:3327–3332

Gingrich DE, Reddy DR, Iqbal MA, Singh J, Almone LD, Angeles TS, Albom M, Yang S, Ator MA, Meyer SL, Robinson C, Ruggeri BA, Dionne CA, Vaught Jl, Mallamo JP, Hudkins RL (2003) A new class of potent vascular endothelial growth factor receptor tyrosine kinase inhibitors. Structure-activity relationships for a series of 9-alkoxymethyl-12-(3-hydroxypropyl)indeno[2,1-*a*]pyrrolo[3,4-c]carbazole-5-ones and the identification of CEP-52144 and its dímethylglycine ester prodrug clinical candidate CEP-7055. J Mol Chem 46:5375–5388

Grignani F, Kinsella T, Mencarelli A, Valtieri M, Riganelli D, Grignani F, Lanfrancone L, Peschle C, Nolan GP, Pelicci PG (1998). High-efficiency gene transfer and selection of human hematopoietic progenitor cells with a hybrid EBV/retroviral vector expressing the green fluorescence protein. Cancer Res 58:14–19

Hamma-Kourbali Y, Di Benedetto M, Ledoux D, Oudar O, Leroux Y, Lecouvey M, Kraemer M (2003) A novel noncontaiining-nitrogen biphosphonate inhibits both in vitro and in vivo angiogenesis. Biochem Biophys Res Commun 310:816–823

Holash J, Davis S, Papadopoulos N, Croll SD, Ho L, Russell M, Boland P, Leidich R, Hylton D, Buorova E, Ioffe E, Huang T, Radziejewski C, Bailey K, Fandl JP, Daly T, Wiegand SJ, Yankopoulos GD, Rudge JS (2002) VEGF-Trap: a VEGF blocker with potent antitumor effects. Proc Natl Acad Sci USA 99:11393–11398

Hood JD, Cheresh DA (2003) Building a better trap. Proc Natl Acad Sci USA 100:8624–8625

Hu L, Hofmann J, Lu Y, Mills GB, Jaffe RB (2002) Inhibition of phosphatidylinositol 3′-kinase increases efficacy of paclitaxel in *in vitro* and *in vivo* ovarian cancer models. Cancer Res 62:1087–1092

Hu L, Hofmann J, Holash J, Yancopoulos GD, Sood AK, Jaffe RB (2005) Vascular endothelial growth factor Trap combined with Paclitaxel strikingly inhibits tumor and ascites, prolonging survival in a human ovarian cancer model. Clin Cancer Res 11:6966–6971

Kim ES, Serur A, Huang J, Manley CA, McCrudden KW, Frischer JS, Soffer SZ, Ring L, New T, Zabski S, Rudge JS, Holash J, Yancopoulos GD, Kandel JJ, Yamashiro DJ (2002) Potent VEGF blockade causes regression of coopted vessels in a model of neuroblastoma. Proc Natl Acad Sci USA 99:11399–11404

Lau SC, Rosa DD, Jayson G (2005) Technology evaluation: VEGF Trap (cancer). Regeneron/Sanofi-aventis.

Roberts DM, Anderson AL, Hidaka M, Swetenburg RL, Patterson C, Stanford WL, Bautch VL (2004) A vascular gene trap screen defines RasGRP3 as an angiogenesis-regulated gene required for the endothelial response to phorbol esters. Mol Cell Biol 24:10515–10528

Rommel C, Clarke B, Zimmermann S, Nunez L, Rossman R, Reid K, Moelling K, Yancopoulos GD, Glass DJ (1999) Differentiation stage-specific inhibition of the Raf-MEK-ERK pathway by Akt. Science 286:1738–1741

Saishin Y, Saishin Y, Takahashi K, Lima-e-Silva R, Hylton D, Rudge JS, Wiegand SJ, Campochiaro PA (2003) VEGF-Trap (R1R2) suppresses choroidal neovascularization and VEGF-induced breakdown of the blood-retinal barrier. J Cell Physiol 195:241–248

Thurston G, Rudge JS, Ioffe E, Zhou H, Ross L, Croll SD, Glazer N, Holash J, McDonald DM, Yancopoulos G (2000). Angiopoietin-1 protects the adult vasculature against plasma leakage. Nat Med 6:460–463

Verheul HMW, Pinedo HM (2003) Vascular endothelial growth factor and its inhibitors. Drug Today 39 [Suppl C]:81–93

Whittles CE, Pocock TM, Wedge SR, Kendrew J, Hennequin LF, Harper SJ, Bates DO (2002) ZM32881, a novel inhibitor of vascular endothelial growth factor-receptor-2 tyrosine kinase activity. Microcirculation 9:513–522

Wulff C, Wilson H, Rudge JS, Wiegand SJ, Lunn SF, Fraser HM (2001) Luteal angiogenesis: prevention and intervention by treatment with vascular endothelial growth factor $Trap_{A40}$. J Lin Endocrinol Metab 86:3377–3386

Chapter B
Pharmacological Assays in Thrombosis and Haemostasis[1]

[1] Contributed by Shaker A. Mousa based on contributions by M. Just and V. Laux.

B.1 General Introduction

Cardiovascular, cerebrovascular, and venous thromboembolic disorders continue to be the leading causes of death throughout the world. Over the past two decades, great advances have been made in the pharmacological treatment and prevention of arterial and venous thrombotic disorders (e. g., tissue plasminogen activators, platelet GPIIb/IIIa antagonists, and ADP receptor antagonists such as clopidogrel, low-molecular weight heparins, and direct thrombin inhibitors). New research is leading to the next generation of antithrombotic compounds such as direct coagulation FVIIa inhibitors, tissue factor pathway inhibitors, gene therapy, and orally active direct thrombin inhibitors and coagulation factor Xa (FXa) inhibitors. In vitro assays as well as animal models of thrombosis have played and will continue to play crucial roles in the discovery and validation of novel drug targets, the selection of new agents for clinical evaluation, and the provision of dosing and safety information for clinical trials. In addition, these models have provided valuable information regarding the mechanisms of these new agents and the interactions between antithrombotic agents that work by different mechanisms. This comprehensive manual presents the pivotal models that led to the development of drugs that have proven to be effective clinically. The major issues regarding the use of animal models of thrombosis—such as the use of positive controls, appropriate pharmacodynamic markers of activity, safety evaluation, species-specificity, and pharmacokinetics—are highlighted. Finally, the use of genetic models in thrombosis/hemostasis research and pharmacology is also presented.

B.2 In Vitro Tests

B.2.1 Blood Coagulation Tests

PURPOSE AND RATIONALE

The coagulation cascade consists of a complex network of interactions resulting in thrombin-mediated conversion of fibrinogen to fibrin, which is one major component of a thrombus. The coagulation cascade can be initiated either by the "exogenous pathway," the release of thromboplastin (tissue factor) leading to activation of factor VII to the tissue factor/factor VIIa complex, or by the "endogenous pathway," so-called contact activation leading via factors XII, XI and IX to the assembly of the tenase complex consisting of activated factors VIII and IX and Ca^{2+} on a phospholipid surface. Both complexes can activate factor X, which induces the formation of the prothrombinase complex consisting of factor X_a, factor Va and Ca^{2+} on a phospholipid surface. The latter leads to the activation of thrombin, which, in turn, cleaves fibrinogen to fibrin. The three coagulation tests (prothrombin time [PT], activated partial thromboplastin time [APTT], and thrombin time [TT]) allow one to differentiate between effects on the exogenous or endogenous pathway or on fibrin formation. The influence of compounds on the plasmatic blood coagulation is determined by measuring the coagulation parameters PT, APTT, and TT *ex vivo*.

PROCEDURE

Male Sprague-Dawley rats weighing 200–220 g receive the test compound or the vehicle (controls) by oral, intraperitoneal, intravenous, or other route of administration. After the end of the absorption time, they are anesthetized by intravenous injection of 60 mg/kg sodium pentobarbital. The caudal caval vein is exposed by a midline incision or by cardiac puncture and 1.8 ml blood is collected into a plastic syringe containing 0.2 ml 100 mM citrate buffer pH 4.5 (Behring Werke, Marburg). The sample is immediately agitated and centrifuged in a plastic tube at 1500 × *g* for 10 min. Plasma is transferred to another plastic tube and the coagulation tests for the determination of TT, PT, and APTT are performed within 3 h.

In general, citrated plasma is coagulated by the addition of the respective compounds (see below), and the time to clot formation is determined in the coagulometer (= coagulation time).

For detailed laboratory diagnosis of bleeding disorders and assessment of blood coagulation see Palmer (1984) and Nilsson (1987).

Prothrombin Time (PT). An aliquot of 0.1 ml of citrated plasma is incubated for 1 min at 37°C. Then 0.2 ml of human thromboplastin (Thromborel, Behring Werke, Marburg) is added and the coagulometer (Schnittger+Gross coagulometer, Amelung, Brake) is started. The time to clot formation is determined. The PT measures effects on the exogenous pathway of coagulation.

Activated Partial Thromboplastin Time (APTT). To 0.1 ml of citrated plasma 0.1 ml of human placenta lipid extract (Pathrombin, Behring Werke, Marburg) is added and the mixture is incubated for 2 min at 37°C.

The coagulation process is initiated by the addition of 0.1 ml 25 mM calcium chloride when the coagulometer is started and the time to clot formation is determined. The APTT measures effects on the endogenous pathway of coagulation.

Thrombin Time (TT). To 0.1 ml of citrated plasma 0.1 ml of diethylbarbiturate-citrate buffer, pH 7.6 (Behring Werke Marburg) is added and the mixture is incubated for 1 min at 37°C. Then 0.1 ml of bovine test-thrombin (30 IU/ml, Behring Werke Marburg) is added and the coagulometer is started. The time to clot formation is determined. The TT measures effects on fibrin formation.

EVALUATION

Mean values of TT, PT, and PTT are calculated in dosage groups and vehicle controls. Statistical evaluation is performed by means of the unpaired Student's *t*-test.

REFERENCES AND FURTHER READING

Demers C, Derzko C, David M, Douglas J (2005) Gynaecological and obstetric management of women with inherited bleeding disorders. J Obstet Gynaecol Can. 27(7):707–732

Nilsson IM (1987) Assessment of blood coagulation and general haemostasis. In: Bloom AL, Thomas DP (eds) Haemostasis and Thrombosis. 2nd ed. Longman Group (UK) Limited 1987, pp 922–932

Palmer RL (1984) Laboratory diagnosis of bleeding disorders: basic screening tests. Postgrad Med 76:137–148

Viale PH (2005) Abnormal clotting in cancer: an overview of pathophysiology and etiology. Semin Oncol Nurs. 21(4 Suppl 1):12–20

B.2.2 Thrombelastography

PURPOSE AND RATIONALE

Thrombelastography (TEG) was developed first by Hartert (1948). The thrombelastograph (Haemoscope Corp, Skokie, Illinois, USA) is a device that provides a continuous recording of the process of blood coagulation and subsequent clot retraction. The blood samples are transferred to cuvettes and maintained at 37°C. The cuvettes are set in motion around their vertical axes. Originally, a torsion-wire suspended mirror in the plasma remains immobile as long as the plasma is fluid. The cuvette and the mirror become dynamically related as fibrin forms, resulting in transmission of cuvette motion to the mirror. The mirror then oscillates with an amplitude governed by the specific mechanical properties of the clot and reflects its light to a thermopaper. The modern thrombelastograph transfers the analogous recording to a digital signal that is evaluated by a computer program.

PROCEDURE

TEG can be performed in either whole blood or in citrated platelet-rich or platelet-poor plasma after recalcification. Blood samples are obtained from Beagle dogs weighing 12–20 kg, from rabbits weighing 1.7–2.5 kg, from Wistar rats weighing 150–300 g, or from humans. The test subjects receive the compound by intravenous (i.v.), subcutaneous (s.c.), or oral administration. Ten or 20 min post dosing (i.v., s.c. administration) or 60, 90 or 180 min post dosing (oral administration) blood is collected. The blood samples are mixed with 3.8% trisodium citrate solution (1 part citrate solution to 9 parts blood) as anticoagulant. The citrated whole blood is recalcified by adding 0.4 ml isotonic calcium chloride solution. An aliquot of 0.36 ml of the recalcified whole blood is transferred to the prewarmed cup of the thrombelastograph. After the apparatus has been correctly adjusted and the samples sealed with liquid paraffin to prevent drying, the time for the whole procedure is noted. The thrombelastogram is recorded for 2 h.

EVALUATION

The following measurements are the standard variables of TEG:

1. Reaction time (*r*): the time from sample placement in the cup until onset of clotting (defined as amplitude of 1 mm). This represents the rate of initial fibrin formation.
2. Clot formation time (*k*): the difference from the 1 mm *r* to 20 mm amplitude. *k* represents the time taken for a fixed degree of viscoelasticity achieved by the forming clot, caused by fibrin build up and cross linking.
3. Alpha angle ($\alpha°$): angle formed by the slope of the TEG tracing from the *r* to *k* value. It denotes speed at which solid clot forms.
4. Maximum amplitude (*MA*): greatest amplitude on the TEG trace. *MA* represents the absolute strength of the fibrin clot and is a direct function of the maximum dynamic strength of fibrin and platelets.
5. Clot strength (*G* in dynes per square centimeter): defined by $G = (5000\,MA)/(96 - \mathrm{s}MA)$. In a tissue factor-modified TEG (Khurana et al. 1997), clot strength is clearly a function of platelet concentration.
6. Lysis 30, Lysis 60 (*Ly30*, *Ly60*): Reduction of amplitude relative to maximum amplitude at 30 and 60 min after time of maximum amplitude. These parameters represent the influence of clot retraction and fibrinolysis.

TEG Parameters	TF (25 ng)	LPS (0.63 ug)	Xa (0.25 nM)	Thrombin (0.3 mU)
		Mean ± SEM		
R (minutes)	29.7 ± 2.3	23.4 ± 1.4	15.6 ± 2.9	3.4 ± 0.6
K (minutes)	5.8 ± 1.0	7.6 ± 0.9	4.8 ± 0.5	5.5 ± 0.8
α (angle)	45.0 ± 2.6	47.8 ± 3.2	61.5 ± 2.1	57.8 ± 2.9
MA (mm)	58.2 ± 1.7	50.0 ± 2.0	65.0 ± 0.8	50.1 ± 2.4

Citrated human whole blood plus 2 mM calcium. Data represent mean for n = 6 ± SEM.

Table 1 Effect of various stimulus on platelet/fibrin clot dynamics as shown by Mousa et al. (2000)

MODIFICATIONS OF THE METHOD

Bhargava et al. (1980) compared the anticoagulant effect of a new potent heparin preparation with a commercially available heparin by TEG *in vitro* using citrated dog and human blood. Barabas et al. (1993) used fibrin plate assay and TEG to assess the antifibrinolytic effects of synthetic thrombin inhibitors. Scherer et al. (1995) described an endotoxin-induced rabbit model of hyper-coagulability for the study of the coagulation cascade and the therapeutic effects of coagulation inhibitors using various parameters, including TEG.

Khurana et al. (1997) introduced tissue factor-modified TEG to study platelet glycoprotein IIb/IIIa function and to establish a quantitative assay of platelet function. With this modification, Mousa et al. (2000) found two classes of glycoprotein IIb/IIIa (GPIIb/IIIa) antagonists, one with high binding affinity for resting and activated platelets and slow platelet dissociation rates (class I) demonstrating potent inhibition of platelet function, in contrast to those with fast platelet dissociation rates (class II). Additionally, Mousa et al. (2005) utilized the TEG in phase II clinical trial in monitoring the efficacy of oral platelet GPIIb/IIIa antagonist on platelet/fibrin clot dynamics.

CRITICAL ASSESSMENT OF THE METHOD

Zuckerman et al. (1981) compared TEG with other common coagulation tests (fibrinogen, prothrombin time, activated thromboplastin time, platelet count, and fibrin split products) and found that there is a strong relationship between the thrombelastographic variables and these common laboratory tests. Mousa et al. (2005) and others expanded the use of TEG in differentiating among different antiplatelets, anticoagulants, and optimal combinations of both. Moreover, TEG has an increased sensitivity for detecting blood clotting anomalies; it contains additional information on the hemostatic process. This is due to the following: (1) the fact that most laboratory measurements end with the formation of the first fibrin strands while TEG measures the coagulation process on whole blood from initiation of clotting to the final stages of clot lysis and retraction, and (2) the ability of TEG to use whole non-anticoagulated blood without influence of citrate or other anticoagulants.

REFERENCES AND FURTHER READING

Barabas E, Szell E, Bajusz S (1993) Screening for fibrinolysis inhibitory effect of synthetic thrombin inhibitors. Blood Coagul Fibrinolysis 4:243–248

Bhargava AS, Freihuber G, Guenzel P (1980) Characterization of a new potent heparin. III. Determinations of anticoagulant activity of a new potent heparin preparation by thrombelastography *in vitro* using citrated dog and human blood. Arzneim Forsch/Drug Res 30:1256–1258

Hartert H (1948) Blutgerinnungsstudien mit der Thrombelastographie, einem neuen Untersuchungsverfahren. Klin Wschr 26:577–583

Khurana S, Mattson JC, Westley S et al (1997) Monitoring platelet glycoprotein IIb/IIIa-fibrin interaction with tissue factor-activated thromboelastography. J Lab Clin Med 130:401–411

Mousa SA, Khurana S, Forsythe MS (2000) Comparative *in vitro* efficacy of different platelet glycoprotein IIb/IIIa antagonists on platelet-mediated clot strength induced by tissue-factor with use of thromboelastography – Differentiation among glycoprotein IIb/IIIa antagonists. Arterioscler Thromb Vasc Biol 20:1162–1167

Mousa SA, Bozarth JM, Seiffert D, Feuerstein GZ (2005) Using thrombelastography to determine the efficacy of the platelet GPIIb/IIIa antagonist, roxifiban, on platelet/fibrin-mediated clot dynamics in humans. Blood Coagulation Fibrinolysis 16:165–171

Scherer RU, Giebler RM, Schmidt U et al (1995) Short-time rabbit model of endotoxin-induced of hypercoagulability. Lab Anim Sci 45:538–546

Zuckerman L, Cohen E, Vagher JP et al (1981) Comparison of thrombelastography with common coagulation tests. Thromb Haemost 46:752–756

B.2.3 Chandler Loop

PURPOSE AND RATIONALE

The Chandler loop technique allows the production of *in vitro* thrombi in a moving column of blood (Chandler 1958). The thrombi generated in the Chandler device show morphology very similar to that of human thrombi formed *in vivo* (Robbie et al. 1997), with platelet-rich upstream sections (“white heads”) that are

relatively resistant to t-PA-mediated thrombolysis in contrast to the red blood-cell-rich downstream parts ("red tails") (Stringer et al. 1994).

PROCEDURE

One millimeter of non-anticoagulated whole blood is drawn directly into a polyvinyl tube with a length of 25 cm and an internal diameter of 0.375 cm (1 mm = 9.9 cm tubing). The two ends of the tube are then brought together and closed by an outside plastic collar. The circular tube is placed and centered on a turntable, tilted to an angle of 23°, and rotated at 17 rpm. At the moment the developing thrombus inside the tube becomes large enough to occlude the lumen, the blood column becomes static and moves around in the direction of rotation of the tube.

EVALUATION

Time to occlusion of the tube by the thrombus establishes a definite end point in this system.

MODIFICATIONS OF THE METHOD

Stringer et al. (1994) used this method to determine the influence of an anti-PAI-1 antibody (CLB-2C8) on the t-PA-induced lysis of Chandler thrombi *in vitro*. They used citrated blood and supplemented it with 5.8 µM [^{125}I]-labeled fibrinogen prior to recalcification. After generation in the Chandler loop, the thrombi were washed with isotonic saline and then cut transversally into an upstream (head) and a downstream part (tail). The radioactivity of both parts was determined in a gamma counter (pre-value). The head and the tail were then subjected to thrombolysis by adding 300 µl phosphate-buffered saline containing plasminogen (2 µM) and t-PA (0.9 nM). During the observation time of 240 min, aliquots of 10 µl were taken at 30, 60, 120, 180 and 240 min, and the radioactivity was determined. The relation of the measured radioactivity to the pre-value was expressed as percentage of clot lysis.

Van Giezen et al. (1998) used this method to differentiate the effect of an anti-PAI-1 polyclonal antibody (PRAP-1) on human or rat thrombi.

REFERENCES AND FURTHER READING

Chandler AB (1958) *In vitro* thrombotic coagulation of the blood. A method for producing a thrombus. Lab Invest 7:110–114

Munch K, Wolf MF, Gruffaz P, Ottenwaelter C, Bergan M, Schroeder P, Fogt EJ (2000) Use of simple and complex in vitro models for multiparameter characterization of human blood-material/device interactions. J Biomater Sci Polym Ed. 11(11):1147–1163

Robbie LA, Young SP, Bennett B, Booth NA (1997) Thrombi formed in a Chandler loop mimic human arterial thrombi in structure and PAI-1 content in distribution. Thromb Haemost 77:510–515

Stringer HAR, Van Swieten P, Heijnen HFG et al (1994) Plasminogen activator inhibitor 1 released from activated platelets plays a key role in thrombolysis resistance. Studies with thrombi generated in the Chandler loop. Arterioscler Thromb 14:1452–1458

Van Giezen JJJ, Nerme V, Abrahamsson T (1998) PAI-1 inhibition enhances the lysis of the platelet-rich part of arterial-like thrombi formed *in vitro*. A comparative study using thrombi prepared from rat and human blood. Blood Coagul Fibrinol 9:11–18

B.2.4 Platelet Aggregation and Deaggregation in Platelet-Rich Plasma or Washed Platelets (Born Method)

PURPOSE AND RATIONALE

Platelets play a crucial role in primary hemostasis by forming hemostatic plugs at sites of vascular injury. Moreover, they contribute to intravascular thrombus formation mostly upon rupture of an atherosclerotic plaque. The contact of unactivated platelets to exposed subendothelial tissue leads to adhesion via two main mechanisms: binding of subendothelial von Willebrand factor (vWF) to the platelet GPIb-IX-V-complex at high shear rates and binding of collagen to two receptors, integrin $\alpha 2\beta 1$ and GPVI. Platelet adhesion initiates the reactions of shape change, secretion, and activation of GPIIb-IIIa-ligand binding sites. These reactions result in the formation of platelet aggregates. Activation of GPIIb-IIIa is also achieved through signaling by a number of agonists that bind to G-protein-coupled receptors. Consequently, for the measurement of platelet aggregation, platelets are activated by the addition of one of the following agonists to platelet-rich plasma (PRP) or washed platelets: ADP, arachidonic acid (forming thromboxane A2) or U 46619, collagen, thrombin or TRAP, serotonin, epinephrine, PAF. The formation of platelet aggregates with stirring leads to changes in optical density that are monitored photometrically, usually for 4 min. The test has been developed originally by Born (1962a, and 1962b) and is used to evaluate quantitatively the effect of compounds on induced platelet aggregation *in vitro* or *ex vivo*. For *in vitro* studies, human PRP is preferred.

PROCEDURE

The test is carried out either *ex vivo* or *in vitro*. There are other commercial sources for the various agonists listed.

Table 2 Materials and solutions

Anticoagulating substances	
Hirudin (Sigma) or PPAK	200 µg/ml
Trisodium citrate	0.11 M
ACD solution	
Citric acid	38 mM
Sodium citrate	75 mM
Glucose	124 mM
Platelet-aggregating substances (final concentrations in the test)	
ADP: for reversible or biphasic aggregation	0.1–5 µM
ADP: for irreversible aggregation (Sigma)	3–10 µM
Sodium arachidonate (Biodata)	0.3–1 mM
Calcium ionophore A 23187 (Calbiochem)	10 µM
Collagen (Hormonchemie)	3 µg/ml
PAF-acether (C 16-PAF, Bachem)	0.1 µM
Thrombin (Sigma)	0.02–0.05 IU/ml
TRAP (SFLLRNP, Bachem)	1–10 µM
U 46619 (ICN)	1–10 µM
Ristocetin	0.1–1 mg/ml
GPRP (fibrin antipolymerant, Bachem)	0.5 mM
4-channel aggregometer (PAP 4, Bio Data)	

For *ex vivo* assays, mice, rats, or guinea pigs from either sex receive the test compound or the vehicle (for controls) by oral, intraperitoneal or intravenous administration. At the end of the absorption time, blood is collected by caval venipuncture under pentobarbital sodium anesthesia and xylazine (8 mg/kg i.m.) premedication.

From rabbits (Chinchilla strain, weighing 3 kg), blood is withdrawn by cardiopuncture under xylazine (20 mg/kg i.m.) sedation. The first blood sample (control) is collected before administration of the test compound, the second sample at the end of the absorption time of the test agent.

For *in vitro* assays, human blood is collected from the antecubital vein of adult volunteers who had not received any medication for the last two weeks.

PREPARATION OF PRP, PPP, AND WP

The entire procedure is performed in plastic (polystyrene) tubes and carried out at room temperature. Freshly collected venous blood is anticoagulated with hirudin (1 volume + 9 volumes of animal blood) or ACD solution (1 volume + 9 volumes of human blood) and centrifuged at 150 × *g* for 15 min to obtain platelet-rich plasma (PRP). The PRP-supernatant is carefully removed, and the rest is further centrifuged at 1500 × *g* for 10 min to obtain platelet-poor plasma (PPP). PRP is diluted with PPP to a platelet count of 3×10^8/ml before use in the aggregation assays. To obtain washed platelets (WP), 8.5 volumes of human blood are collected into 1.5 volumes of ACD and centrifuged as for PRP. PRP is acidified to a pH of 6.5 by addition of approximately 1 ml ACD to 10 ml PRP. Acidified PRP is centrifuged for 20 min at 430*g*. The pellet is resuspended in the original volume with Tyrode's solution (mM: NaCl 120, KCl 2.6, $NaHCO_3$ 12, NaH_2PO_4 0.39, HEPES 10, glucose 5.5; albumin 0.35%) and set to platelet count of 3×10^8/ml.

For *ex vivo* assays, duplicate samples of 320µl PRP from drug-treated and vehicle control subjects (for rabbits: control samples before drug administration) are inserted into the aggregometer at 37°C under continuous magnetic stirring at 1000 rpm. After the addition of 40 µl physiological saline and 40 µl aggregating agent, changes in optical density are monitored continuously at 697 nm.

For *in vitro* assays, 40 µl of the test solution are added to samples of 320 µl PRP or WP from untreated subjects. The samples are inserted into the aggregometer and incubated at 37°C for 2 min under continuous magnetic stirring at 1000 rpm. After the addition of 40 µl aggregating agent, changes in optical density are monitored continuously at 697 nm either for 4 min or until constant values for aggregation are achieved. In cases of thrombin activation of PRP, glycine-proline-aspartate-proline (GPRP) is added in order to avoid fibrin formation. In order to measure deaggregation, experimental compounds are added to stimulated PRP at 70 or 100% of control aggregation and monitoring is performed for further 10 min. Deaggregation is measured by the decrease of light transmission (see Haskel et al. 1989).

Studies should be completed within 3 hours after blood withdrawal.

EVALUATION

The transmission maximum serves as a scale for platelet aggregation (0% = transmission of PRP, 100% = transmission of PPP).

For *in vitro* assays:

1. Percent inhibition of platelet aggregation is determined in concentration groups relative to vehicle controls. Statistical significance is evaluated by means of the unpaired Student's t-test.
2. IC_{50} values are determined from the non-linear curve fitting of concentration-effect relationships.

IC_{50} is defined as the concentration of test drug for half maximal inhibition of aggregation.

3. Percent deaggregation is determined at 10 min after addition of compound; IC_{50} is calculated from the concentration-effect relationship.

For *ex vivo* assays:

1. Mean values for aggregation in dosage groups are compared to the vehicle control groups (for rabbits: control values before drug administration). Statistical significance is evaluated by means of the Student's *t*-test (paired for rabbits; unpaired for others).
2. ED_{50} values are determined from the dose-response curves. ED_{50} is defined as the dose of drug leading to 50% inhibition of aggregation in the animals.

CRITICAL ASSESSMENT OF THE METHOD

The assay, introduced by Born (1962a and 1962b), has become a standard method in clinical diagnosis of platelet function disorders and of aspirin intake. Furthermore, the method is used in the discovery of antiplatelet drugs with the advantage of rapid measurement of a functional parameter in intact human platelets. However, processing of platelets during the preparation of PRP, washed or filtered platelets from whole blood results in platelet activation and separation of large platelets. Additionally, there is no standardization among the different laboratories due to variation in use of different tubes, different final agonist concentrations, and other technical differences.

MODIFICATIONS OF THE METHOD

Several authors have described modifications of the assay procedure. Breddin et al. (1975) described spontaneous aggregation of platelets from vascular patients in a rotating cuvette. Klose et al. (1975) measured platelet aggregation under laminar flow conditions using a thermostated cone-plate streaming chamber in which shear rates are continuously augmented and platelet aggregation is measured from light transmission through a transilluminating system. Marguerie et al. (1979, 1980) developed a method of measuring two phases of platelet aggregation after gel filtration of a platelet suspension (see below). Lumley and Humphrey (1981) described a method to measure platelet aggregation in whole blood (see below). Fratantoni and Poindexter (1990) performed aggregation measurements using a microtiter plate reader with specific modification of the agitation of samples. Comparison of the 96-well microtiterplate method with conventional aggregometry showed similar dose-response curves for thrombin, ADP, and arachidonic acid.

Ammit and O'Neil (1991) used a quantitative bioassay of platelet aggregation for rapid and selective measurement of platelet-activating factor. Mousa et al. (1994, 1998) and others utilized this assay for *in vitro* screening and *ex vivo* and antiplatelet efficacy in various species and in humans for platelet GPIIb/IIIa antagonists.

Yamanaka et al. (2005) performed platelet aggregations assays using an eight channel aggregometer (NBS HEMA TRACER 801, Nikobioscience, Tokyo, Japan) to test structure-activity relationships of potent GPIb/IIIA antagonists.

Francischetti et al. (2000) used the Microplate Reader for studying a platelet aggregation inhibitor from the salivary gland of the blood-sucking bug, *Rhodnius prolixus*.

REFERENCES AND FURTHER READING

Ammit AJ, O'Neill C (1991) Rapid and selective measurement of platelet-activating factor using a quantitative bioassay of platelet aggregation. J Pharmacol Meth 26:7–21

Born GVR (1962a) Quantitative investigations into the aggregation of blood platelets. J Physiol (London) 162:67P–68P

Born GVR (1962b) Aggregation of blood platelets by adenosine diphosphate and its reversal. Nature 194:927–929

Breddin K, Grun H, Krzywanek HJ, Schremmer WP (1975) Zur Messung der "spontanen" Thrombocytenaggregation. Plättchenaggregationstest III. Methodik. Klin Wschr 53:81–89

Francischetti IMB, Ribeiro JMC, Champagne D, Andersen J (2000) Purification, cloning, expression, and mechanism of action of a novel platelet aggregation inhibitor from the salivary gland of the blood-sucking bug, *Rhodnius prolixus.* J Biol Chem 275(17):12639–12650

Fratatoni JC, Poindexter BJ (1990) Measuring platelet aggregation with microplate reader. Am J Clin Pathol 94:613–617

Haskel E, Abendschein DR (1989) Deaggregation of human platelets *in vitro* by an RGD analog antagonist of platelet glycoprotein IIb/IIIa receptors. Thromb Res 56:687–695

Klose HJ, Rieger H, Schmid-Schönbein H (1975) A rheological method for the quantification of platelet aggregation (PA) *in vitro* and its kinetics under defined flow conditions. Thrombosis Res 7:261–272

Lumley P, Humphrey PP (1981) A method for quantitating platelet aggregation and analyzing drug-receptor interactions on platelets in whole blood in vitro. J Pharmacol Methods 6(2):153–166

Marguerie GA, Plow EF, Edgington TS (1979) Human platelets possess an inducible and saturable receptor specific for fibrinogen. J Biol Chem 254(12):5357–5363

Marguerie GA, Edgington TS, Plow EF (1980) Interaction of fibrinogen with its platelet receptor as part of a multistep reaction in ADP-induced platelet aggregation. J Biol Chem 255(1):154–161

Mousa SA, Bozarth JM, Forsythe MS, et al (1994) Antiplatelet and antithrombotic efficacy of DMP 728, a novel platelet GPIIb/IIIa receptor antagonist. Circulation. 89(1):3–12

Mousa SA, Bozarth JM, Lorelli W, et al (1998) Antiplatelet efficacy of XV459, a novel nonpeptide platelet GPIIb/IIIa antagonist: comparative platelet binding profiles with c7E3. J Pharmacol Exp Therapeutics 286(3):1277–1284

Yamanaka T, Ohkubo M, Kuroda S, Nakamura H, Takahashi Aoki T, Mihara K, Seki J, Kato M (2005) Design, synthesis, and structure-activity relationships of potent GPIb/IIIA antagonists: discovery of FK419. Bioorg Med Chem 13:4343–4352

B.2.5 Platelet Aggregation After Gel Filtration (Gel-Filtered Platelets, GFP)

PURPOSE AND RATIONALE

Triggering of platelet activation by low concentrations of ADP, epinephrine or serotonin—so-called weak platelet agonists—in plasma- and fibrinogen-free platelet suspensions does not result in platelet aggregation unless exogenous fibrinogen is added. As opposed to this, platelet aggregation induced by thrombin, collagen or prosta-glandin-endoperoxide—so-called strong agonists—is independent of exogenous fibrinogen because these substances lead to the secretion of intracellular platelet ADP and fibrinogen. Studies of platelet aggregation in gel-filtered platelets are performed in cases where the adhesive ligand fibrinogen or vWF is needed in a defined concentration or where plasma proteins could negatively interfere with the effect of compounds. The assay is mostly used to evaluate the influence of compounds on platelet GPIIb-IIIa or other integrins or on GPIb-IX-V. Mousa et al. (1994, 1998) and others have extensively utilized this assay to determine the impact of plasma protein binding on antiplatelet efficacy by comparing inhibition of platelet aggregation in GFP versus PRP.

PROCEDURE

Preparation of Gel-Filtered Platelets

The entire procedure is performed in plastic (polystyrene) tubes at room temperature according to Marguerie et al. (1979).

Blood is drawn from healthy adult volunteers who had no medication for the last two weeks. Venous blood (8.4 ml) is collected into 1.4 ml ACD-solution and centrifuged for 10 min at 120 *g*. The platelet-rich plasma (PRP) is carefully removed, the pH adjusted to 6.5 with ACD-solution, and centrifuged at 285 *g* for 20 min. The resulting pellet is resuspended in Tyrode's buffer (approx. 500 µl buffer/10 ml PRP). The platelet suspension is applied immediately to a Sepharose CL 2B column; equilibration and elution at 2 ml/min flow rate is done with Tyrode's buffer without hirudin and apyrase. Platelets are recovered in the void volume. Final platelet suspension is adjusted to 4×10^8/ml. Gel filtered platelets (GFP) are kept at room temperature for 1 h until the test is started.

Table 3 Materials and solutions

Acid-citrate-dextrose (ACD) solution	
Citric acid	0.8%
Sodium citrate	2.2%
Glucose	2.45%
Hirudin	0.6 U/ml
Tyrode's solution	
NaCl	137 mM
KCl	2.7 mM
$MgCl_2$	5.5 mM
NaH_2PO_4	3.0 mM
HEPES	3.5 mM
Glucose	5.5 mM
Albumin	0.2%
Hirudin	0.06 U/ml
Apyrase	40 µg/ml
pH	7.2
ADP	10 µM
Thrombin	0.02–0.05 U/ml
$CaCl_2$	0.5 mM
Fibrinogen (American Diagnostica)	1 mg/ml
von Willebrand factor	10 µg/ml
Sepharose CL 2B (Pharmacia)	
Acrylic glass column (Reichelt Chemietechnik, 3 cm inner diameter, 18 cm length)	
Aggregometer (PAP 4, Biodata)	

Experimental Course

For the aggregation studies, GFP in Tyrode's buffer is incubated with $CaCl_2$ (final concentration 0.5 mM) with or without fibrinogen (final conc. 1 mg/ml) in polystyrene tubes. After 1 min, 20 µl of the test compound or the vehicle (controls) are added, and the samples are incubated for another 2 min. After the addition of 20 µl platelet agonist, changes in light transmission are recorded. The whole procedure is done under continuous magnetic stirring at 37°C (1000 rpm) in the aggregometer. Samples with added $CaCl_2$ but without fibrinogen identify proper exclusion of plasma proteins if neither spontaneous aggregation occurs nor aggregation in the presence of weak agonists. Full aggregatory response of GFP to 10 µM ADP shows intact platelets (with only minor pre-activation with gel filtration).

EVALUATION

The transmission maximum serves as a scale for platelet aggregation. Each test compound is assayed with at least two different donor-GFPs; in the case of an anti-aggregating effect, the test is performed with 4–6 GFPs.

Mean values of the dosage groups are compared to the controls. Statistical significance is evaluated by means of the Student's *t*-test.

The percent inhibition of platelet aggregation in the dosage groups is calculated relative to the vehicle controls.

IC_{50} values (50% inhibition of aggregation) are determined from the concentration-effect curves.

For detailed methodology and evaluation of different agents see Marguerie et al. (1979 and 1980), Markell et al. (1993), and Mousa et al. (1994 and 1998).

REFERENCES AND FURTHER READING

Marguerie GA, Edgington TS, Plow EF (1980) Interaction of fibrinogen with its platelet receptor as part of a multistep reaction in ADP-induced platelet aggregation. J Biol Chem 255:154–161

Marguerie GA, Plow EF, Edgington TS (1979) Human platelets possess an inducible and saturable receptor specific for fibrinogen. J Biol Chem 254:5357–5363

Markell MS, Fernandez J, Naik UP et al (1993) Effects of cyclosporine-A and cyclosporine-G on ADP-stimulated aggregation of human platelets. Ann NY Acad Sci 969:404–407

Mousa SA, Bozarth JM, Forsythe MS, et al (1994) Antiplatelet and antithrombotic efficacy of DMP 728, a novel platelet GPIIb/IIIa receptor antagonist. Circulation. 89(1):3–12

Mousa SA, Bozarth JM, Lorelli W, et al (1998) Antiplatelet efficacy of XV459, a novel nonpeptide platelet GPIIb/IIIa antagonist: comparative platelet binding profiles with c7E3. J Pharmacol Exp Therapeutics 286(3):1277–1284

B.2.6 Platelet Aggregation in Whole Blood

PURPOSE AND RATIONALE

The method uses a whole blood platelet counter that counts single platelets and does not require their separation from other blood cell types. Platelet aggregation is induced in anti-coagulated human whole blood samples by the addition of the aggregating agents arachidonic acid or collagen. The number of platelets is determined in drug-treated and vehicle control samples; the percentage of inhibition of aggregation and IC_{50} values are calculated in dosage groups. The effect of compounds on other blood cells that secondarily can influence platelet aggregation is included in this test system. The method has been described by Lumley and Humphrey (1981) and by Cardinal and Flower (1980).

PROCEDURE

The entire procedure is performed in plastic (polystyrene) tubes and carried out at room temperature. Blood is drawn from healthy adult volunteers who had not received medication for the last 2 weeks; 9 ml venous blood is anti-coagulated with 1 ml of sodium citrate and kept in a closed tube at room temperature for 30–60 min until the start of the test.

Table 4 Materials and solutions

Anticoagulant: sodium citrate to induce platelet aggregation	3.8%
Sodium arachidonate (Biodata)	3.6×10^{-4} M
Collagen (Hormonchemie)	10 µg/ml
Serono Hematology System 9000 or Sysmex Micrcellcounter F 800	

For the aggregation studies, 10 µl test substance or vehicle (control) is added to 480 µl citrated blood. Samples in closed tubes are pre-incubated for 5 min in a 37°C water shaker bath at 75 strokes/min. Then, 10 µl aggregating agent are added, and samples are incubated for another 10 min. The number of platelets (platelet count) is determined in 10 µl samples immediately before and 10 min after the addition of the aggregating agent ('initial platelet count', '10-min-platelet count' after adding platelet agonist ± antagonist) in a hematology cell counter.

The following samples for the determination of the platelet count are prepared in duplicate:

- control aggregation = spontaneous aggregation (without aggregating agent): 480 µl blood + 20 µl vehicle. Blood samples with >20% spontaneous aggregation are not used to test for induced aggregation.
- maximal aggregation: 480 µl blood + 10 µl vehicle + 10 µl aggregating agent. Values represent the maximal induced aggregation rate of the blood sample.
- test substance aggregation: 480 µl blood + 10 µl test substance + 10 µl aggregating agent.

EVALUATION

From the samples for maximal aggregation (vehicle), the percentage of maximal aggregation is calculated according to the following formula:

$$\%\ \text{maximal aggregation} = 100 - \frac{\text{10-min-platelet count} \times 100}{\text{initial plateletcount}}$$

From the samples for test substance induced aggregation, the percentage of aggregation in dosage groups is

calculated according to the following formula:

$$\%\ \text{aggregation} = \frac{\text{10-min-platelet count} \times 100}{\text{initial platelet count}}$$

IC_{50} values (50% inhibition of aggregation) are determined from the dose-response curves (log concentration test substance versus % inhibition of aggregation).

REFERENCES AND FURTHER READING

Cardinal DC, Flower RJ (1980) The electronic aggregometer: a novel device for assessing platelet behavior in blood. J Pharmacol Meth 3:135–158

Lumley P, Humphrey PPA (1981) A method for quantitating platelet aggregation and analyzing drug-receptor interactions on platelets in whole blood *in vitro*. J Pharmacol Meth 6:153–166

B.2.7 Platelet Micro- and Macro-Aggregation Using Laser Scattering

PURPOSE AND RATIONALE

- A new highly sensitive method to study platelet aggregation based on the measurement of mean radius or particle size makes it possible to record kinetics of formation of micro- and macro-aggregates in real time
- Sensitivity in measurements of spontaneous aggregation is higher than in routine light transmittance.

A new platelet aggregometer (AG-10; Kowa, Japan) that uses a laser-light-scattering beam has been introduced (Tohgi et al. 1996). Platelet aggregates, the size of which can be measured as total voltage of light-scatter intensity at 1.0-sec intervals for a 10-min period, can be divided into 3 ranges: small aggregates (diameter 9 to 25 µm), medium (26 to 50 µm), and large (>50 µm). Using laser scatter aggregation, it was found that young smokers had an increased number of small platelet aggregates, which cannot be detected with a conventional aggregometer based on the turbidometric method (Matsuo et al. 1997). This device detects platelet aggregation in the small-aggregate size range by the addition of unfractionated heparin (UFH), and the aggregates are disaggregable in incubation with protamine sulfate. When platelet aggregation induced by UFH at a final concentration of 0.5 U/mL was observed in 36 normal subjects with no history of heparin exposure, 13 had a positive response in excess of 0.5 V of light intensity in the small-aggregate size range. In chronic hemodialysis patients in whom heparin had been used regularly for many years, a positive response with heparin-induced aggregates was noted in 37 of 59 patients, which was increased compared with that of normal subjects. The light intensity in the small-aggregate size range was enhanced during heparinized dialysis. In patients with a positive heparin response, the intensity of aggregates after heparin was significantly increased compared with that in nonresponders to heparin. Also, we obtained the same results by this system: that enhanced platelet aggregation response to heparin was not inhibited by aspirin or argatroban but was inhibited by anti-glycoprotein IIb/IIIa antibodies or small molecule antagonists. The findings of enhanced platelet aggregation during heparin infusion could be directly obtained without the addition of ADP or TRAP using laser aggregometry (Xiao and Théroux 1998).

LIMITATIONS

This technique can not be applied in whole blood yet but can be used with PRP, washed platelet, or GFP

MODIFICATIONS OF THE METHOD

For functional characterization of an acid platelet aggregation inhibitor and hypotensive phopsholipase A_2 from *Bothrops jararacussu* snake venom, Andrião-Escarso et al. (2002) measured platelet aggregation in rabbit blood using a whole blood Lumi-Aggregometer.

REFERENCES AND FURTHER READING

Andrião-Escarso SH, Soares Am, Fontes MRM, Fuly AL, Corrêa FMA, Rosa JC, Greene LJ, Giglio JR (2002) Structural and functional characterization of an acid platelet aggregation inhibitor and hypotensive phopsholipase A_2 from *Bothrops jararacussu* snake venom. Biochem Pharmacol 64:723–732

Kudoh T, Sakamoto T, Miyamoto S, Matsui K, Kojima S, Sugiyama S, Yoshimura M, Ozaki Y, Ogawa H (2006) Relation between platelet microaggregates and ankle brachial index in patients with peripheral arterial disease. Thromb Res 117(3):263–9

Mousa SA, Forsythe M, Bozarth J, Jin F, Confalone PN (2000) Human platelet αIIbβ3 integrin binding affinity and specificity of SJ874: antiplatelet efficacy versus aspirin. Coron Artery Dis 11:563–570

Tohgi H, Takahashi H, Watanabe K et al (1996) Development of large platelet aggregates from small aggregates as determined by laser-light scattering: effects of aggregant concentration and antiplatelet medication. Thromb Haemost 75:838–843

Xiao Z, Théroux P (1998) Platelet activation with unfractionated heparin at therapeutic concentrations and comparisons with a low-molecular-weight heparin and with a direct thrombin inhibitor. Circulation 97:251–256

B.2.8 Fibrinogen Receptor Binding

PURPOSE AND RATIONALE

The assay is used to evaluate the binding characteristics of drugs at the fibrinogen receptor. A constant concentration of the radioligand ^{125}I-fibrinogen (30–50 nM) is incubated with increasing concentrations of a non-labeled test drug (0.1 nM–1 mM) in the presence of gel-filtered human platelets. If the test drug exhibits any affinity to fibrinogen receptors, it is able to compete with the radioligand for receptor binding sites. Thus, the lower the concentration range of the test drug, in which the competition reaction occurs, the more potent the test drug. Platelets are activated with 10 mmol/l ADP to stimulate the ^{125}I-fibrinogen binding at the GPIIb/IIIa receptor.

PROCEDURE

Preparation of Gel-Filtered Platelets

From a healthy volunteer, 200 ml blood is collected. Ana aliquot of 8.4 ml blood is mixed with 1.4 ml ACD-buffer in polystyrol tubes and centrifuged at $150 \times g$ for 15 min. The resulting platelet-rich plasma (PRP) is collected, and an aliquot is taken for platelet counting. Then, 10 ml PRP are mixed with 1 ml ACD-buffer (ACD-PRP, pH ~ 6.5); 5 ml portions of ACD-PRP are transferred to plastic tubes and centrifuged at $1500 \times g$ for 15 min. The resulting supernatant is decanted, and each pellet is resuspended in 500 µl Tyrode buffer C. An aliquot is taken for platelet counting to calculate the loss of platelets. The platelet suspension is then transferred to a Sepharose-packed column that has been eluted with approx. 100 ml degassed Tyrode buffer B (2 ml/min). The column is closed and eluted with degassed Tyrode buffer B (2 ml/min). The first platelets appear after 18–20 min and are then collected for 10 min in a closed plastic cup. Gel-filtered platelets (GFP) are set to 4×10^8 platelets/ml with Tyrode buffer B and kept at room temperature until the start of the test (Mousa et al. 1994 and 2001).

EXPERIMENTAL COURSE

For each concentration, samples are tested in triplicate (test tubes No. 72708, Sarstedt).The total volume of each incubation sample is 500 µl. The concentration of ^{125}I-fibrinogen is constant for all samples (10 µg/500 µl).

COMPETITION EXPERIMENTS

The competition reaction is characterized by one buffer value (bidistilled water) and various concentrations of non-labeled fibrinogen or test compound.

- 100 µl ^{125}I-fibrinogen
- 100 µl non-labeled fibrinogen or test drug (various concentrations, 10^{-10}–10^{-3} M)
- 5 µl ADP.

Non-specific-binding: The non-specific binding of ^{125}I-fibrinogen is defined as the radioligand binding in the presence of 10^{-5} M of non-labeled fibrinogen.

The binding reaction is started by adding 250 µl GFP (4×10^8 platelets/ml). The samples are incubated for 30 min at room temperature. Subsequently, a 100 µl aliquot of the incubation sample is transferred to a microtainer tube containing 400 µl glucose solution. The tubes are centrifuged at $1{,}500 \times g$ for 2 min to separate ^{125}I-fibrinogen bound at the platelet glycoprotein IIb–IIIa receptor from free radioligand. The supernatant is carefully decanted and is allowed to run off for approx. 30 min. Radioactivity of the platelet pellets is counted for 1 min in a gamma counter with an efficiency of 65.3%.

MATERIALS AND SOLUTIONS

See Table 5.

EVALUATION

The quantity of the specific ^{125}I-fibrinogen binding results from the difference between the total and the non-specific binding.

Platelet glycoprotein IIb-IIIa receptor binding is given as fmol ^{125}I-fibrinogen/10^8 platelets or ^{125}I-fibrinogen molecules bound per platelet.

The dissociation constant (K_i) of the test drug is determined from the competition experiment of ^{125}I-fibrinogen versus non-labeled drug by a computer-supported analysis of the binding data.

$$K = \frac{K_D^{125}\mathrm{I} \times IC_{50}}{K_D^{125}\mathrm{I} + [^{125}\mathrm{I}]}$$

IC_{50} = concentration of the test drug, which displaces 50% of the specifically glycoprotein IIb-IIIa receptor bound ^{125}I-fibrinogen in the competition experiment.

[^{125}I] = concentration of ^{125}I-fibrinogen in the competition experiment.

$K_D{}^{125}$I = dissociation constant of ^{125}I-fibrinogen, determined from the saturation experiment.

The K_i-value of the test drug is the concentration, at which 50% of the fibrinogen receptors are occupied by the test drug.

For detailed methodology and evaluations of various mechanisms and agents see the following selected

Table 5 Materials and solutions

Solutions for platelet preparation		
Stock solution I	Citrate	0.8%
	Sodium citrate	2.2%
Stock solution II	NaCl	120 mM
	KCl	2.8 mM
	NaH_2PO_4	10.0 mM
	HEPES	10.0 mM
ACD-buffer	Stock solution I	2.45%
	+ glucose	
	+ hirudin	0.06 U/ml
Tyrode buffer A	Stock solution II	
	+ $NaHCO_3$	12 mM
Tyrode buffer B	Stock solution II	
	+ $NaHCO_3$	12 mM
	+ glucose	5.5 mM
	+ bovine albumin	0.35%
Tyrode buffers A and B are degassed by aspiration for approx. 1 h after setting the pH to 7.2.		
Tyrode buffer C	Tyrode buffer B (degassed)	
	+ apyrase	40 µg/ml
	+ hirudin	0.06 U/ml
Chromatography column	Acryl glass column (200 × 170 mm, 30 mm diameter), closed with 3 perlon filters, pore sizes 63, 90 and 230 µm, and gauze 50 µm filled with degassed Sepharose CL2B-suspen-sion (Pharmacia LKB); equilibrated with 500 ml degassed Tyrode buffer A (2 ml/min)	
Incubation buffer		
Stock solution	NaCl	120 mM
	KCl	2.6 mM
	NaH_2PO_4	0.39 mM
	HEPES	10.0 mM
	$CaCl_2$	0.5 mM
Incubation buffer, pH 7.2	stock solution	
	+ $NaHCO_3$	12 mM
	+ glucose	5.5 mM
	+ human albumin	0.35%
Glucose solution (in incubation buffer)		
Radioligand	^{125}I-fibrinogen specific activity 3.7 Mbq/mg fibrinogen (100 µCi/mg fibrinogen) (Amersham), 1 mg radio-labeled fibrinogen is dissolved in 10 ml incubation buffer	
Non-labeled fibrinogen (mw 340000, grade L, Sigma; in bidistilled water)		10^{-3}–10^{-10} M
ADP (in incubation buffer)		10 µM
Gamma-counter (1282 Compugamma CS, LKB)		

references: Bennett, Vilaire (1979); Kornecki et al. (1981); Marguerie et al. (1979 and 1980); Mendelsohn et al. (1990), and Mousa et al. (1994).

REFERENCES AND FURTHER READING

Bennett JS, Vilaire G (1979) Exposure of platelet fibrinogen receptors by ADP and epinephrine. J Clin Invest 64:1393–1401

Kornecki E, Niewiarowski S, Morinelli TA, Kloczewiak M (1981) Effects of chymotrypsin and adenosine diphosphate on the exposure of fibrinogen receptors on normal human and Glanzmann's thrombasthenic platelets. J Biol Chem 256:5696–5701

Marguerie GA, Edgington TS, Plow EF (1980) Interaction of fibrinogen with its platelet receptor as part of a multistep reaction in ADP-induced platelet aggregation. J Biol Chem 255:154–161

Marguerie GA, Plow EF, Edgington TS (1979) Human platelets possess an inducible and saturable receptor specific for fibrinogen. J Biol Chem 254:5357–5363

Mendelsohn ME, O'Neill S, George D, Loscalzo J (1990) Inhibition of fibrinogen binding to human platelets by *S*-nitroso-*N*-acetylcysteine. J Biol Chem 265:19028–19034

Mousa SA, Bozarth JM, Naik UP, Slee A (2001) Platelet GPIIb/IIIa binding characteristics of small molecule RGD mimetic: distinct binding profile for Roxifiban. Br J Pharmacol 133:331–336

Mousa SA, Bozarth JM, Forsythe MS, Slee A (2000) Differential antiplatelet efficacy for various GPIIb/IIIa antagonists: role of plasma calcium levels. Cardiovasc Res 47:819–826

B.2.9 Euglobulin Clot Lysis Time

PURPOSE AND RATIONALE

The euglobulin lysis time is used as an indicator for the influence of compounds on the fibrinolytic activity in rat blood according to Gallimore et al. (1971). The euglobulin fraction of plasma is separated from inhibitors of fibrinolysis by acid precipitation and centrifugation. Euglobulin predominantly consists of plasmin, plasminogen, plasminogen activator and fibrinogen. By addition of thrombin to this fraction, fibrin clots are formed. The lysis time of these clots is determined as a measurement of the activity of activators of fibrinolysis (e. g. plasminogen activators). Thus, compounds that stimulate the release of tissue-type plasminogen activator from the vessel wall can be detected.

PROCEDURE

Rats are anesthetized by intraperitoneal injection of 60 mg/kg pentobarbital sodium and placed on a heating pad (37°C). At the same time, the test solution or the vehicle (controls) is administered intravenously or intraperitoneally. Twenty-five minutes later, the animals receive another intraperitoneal injection of 12 mg/kg sodium pentobarbital to keep them in deep narcosis for 45 min.

Plasma Preparation

After the test compound is absorbed, blood is withdrawn from the inferior caval vein exposed by a midline excision. Blood (1.8 ml) is removed with a plastic syringe containing 0.2 ml 3.8% sodium citrate solution. The sample is thoroughly mixed, transferred to a plastic tube and immediately immersed in ice. Plasma is prepared by centrifugation at 2000 *g* for 10 min at 2°C.

Euglobulin Preparation

A 0.5 ml portion of plasma is added to 9.5 ml of ice-cold distilled water; the pH is brought to 5.3 by the addition of 0.13 ml of 1% acetic acid. The diluted plasma is kept on ice for 10 min, and the precipitated euglobulin fraction is collected by centrifugation at 2000 *g* for 10 min at 2°C. The supernatant is discharged, and the remaining fluid is removed by drying the tube on a filter paper for 1 min. The euglobulin precipitate is dissolved in 1 ml of 0.12 M sodium acetate solution.

Euglobulin Lysis Assay

Aliquots (0.45 ml) of the euglobulin solution are transferred to test tubes, and 0.05 ml thrombin (Test Thrombin, Behring Werke) (25 U/ml) are added. The tubes are transferred to a water bath at 37°C. The time interval between the addition of thrombin and the complete lysis of the clots is measured. For details see Gallimore et al. (1971) and Singh et al. (2005).

EVALUATION

The lysis time (min) is determined. Euglobulin lysis test (ELT) is shortened when activators of fibrinolysis are increased.

Percent lysis time is calculated in dosage treated groups as compared to controls.

Statistical evaluation is performed by means of the Student's *t*-test.

REFERENCES AND FURTHER READING

Gallimore MJ, Harris SL, Tappenden KA, Winter M, Jones DW (2005) Urokinase induced fibrinolysis in thromboelastography: a model for studying fibrinolysis and coagulation in whole blood. J Thromb Haemost 3(11):2506–2513

Gallimore MJ, Tyler HM, Shaw JTB (1971) The measurement of fibrinolysis in the rat. Thromb Diath Haemorrh 26:295–310

Singh U, Devaraj S, Jialal I (2005) C-reactive protein decreases tissue plasminogen activator activity in human aortic endothelial cells: evidence that C-reactive protein is a procoagulant. Arterioscler Thromb Vasc Biol 25(10):2216–2221

B.2.10 Flow Behavior of Erythrocytes

PURPOSE AND RATIONALE

The deformation of erythrocytes is an important rheological phenomenon in blood circulation according to Teitel (1977) and Nash (1990). It allows the passage of normal red cells through capillaries with diameters

smaller than that of the discoid cells and reduces the bulk viscosity of blood flowing in large vessels. In the following test, the initial flow of filtration is taken as a criterion for erythrocyte deformability. A prolonged time of filtration can be due to 2 basic pathologic phenomena: an increased rigidity of the individual red cells or an increased tendency of the cells to aggregate. To simulate decreased red blood cell deformability, the erythrocytes are artificially modified by one (or by the combination) of the following stress factors:

- addition of calcium ions (increase in erythrocyte rigidity)
- addition of lactic acid (decrease in pH value)
- addition of 350–400 mmol NaCl (hyperosmolarity)
- storing the sample for at least 4 h (cellular ageing, depletion of ADP)

The following procedure can be used to evaluate the effect of test compounds on the flow behavior of erythrocytes.

PROCEDURE

Apparatus

Erythrocyte filtrometer MF 4 (Fa. Myrenne, 52159 Roetgen, Germany) Membrane filter (Nuclepore Corp.) pore diameter: 5–10 µm, pore density: 4×10^5 pores/cm^2.

Ex Vivo

Blood is collected from Beagle dogs weighing 12–20 kg, from rabbits weighing 1.2–2.5 kg, or from Wistar rats weighing 150–300 g. The test subjects receive the test compound by oral, subcutaneous or intravenous administration 15, 60, 90 or 180 min before the withdrawal of blood.

In Vitro

Following addition of the test compound, blood is incubated at 37°C for 5 or 30 min.

Freshly collected venous blood is anticoagulated with K-EDTA (1 mg/ml blood) or heparin (5 IU/ml heparin sodium) and centrifuged at $250 \times g$ for 7 min. The supernatant (plasma) and the buffy coat are removed and discarded. The packed erythrocytes are resuspended in autologous plasma containing 0.25% human albumin, and the haematocrit value is fixed at 10%. The red blood cells are altered by one or several of the stress factors mentioned above.

A sample of 2 ml of the stressed suspension is applied to the filtrometer and the initial flow rate is determined. The filtration curve is plotted automatically.

EVALUATION

The cumulative volume of the filtered suspension is recorded per time unit (10 min)

The slope of the curve is determined at different time intervals.

The initial flow rate (10% of the cell suspension having passed the filter) is recorded.

Statistics

Data of each set are first tested for normal distribution using the Kolmogoroff/Smirnow test. The normal distribution hypothesis is eliminated if the data having a significance level of 5% are not normally distributed. In case that both data sets to be compared are normally distributed, the F-test is applied. The hypothesis of homogeneity of variance of both test series is eliminated when the significance level for homogeneity of variance is 5%. The *t*-test for paired and non-paired data is performed when homogeneity of variance is present. In any case, a paired difference test (for paired data) or the U-test (for non-paired data) is likewise carried out (paired of difference test = Wilcoxon test; U-test = Wilcoxon-Mann-Whitney or Mann-Whitney test, respectively).

REFERENCES AND FURTHER READING

Nash GB (1990) Filterability of blood cells: methods and clinical applications. Biorheology. 27(6):873–882

Teitel P (1977) Basic principles of the 'filterability test' (FT) and analysis of erythrocyte flow behavior. Blood Cells 3:55–70

B.2.11 Filterability of Erythrocytes

PURPOSE AND RATIONALE

The Single Erythrocyte Rigidometer (SER) allows the measurement of deformability of individual red blood cells by determining their passage time through a pore under constant shear stress. In this test, the passage times of single erythrocytes through one pore in a synthetic membrane are determined according to Kiesewetter et al. (1982), Roggenkamp et al. (1983), and Seiffge et al. (1986). The pore in the membrane practically represents a capillary with defined diameter and length. The driving pressure is produced by the constant shear stress. The passage of the red blood cells is measured with the help of an electrical device. A constant current of 50–200 nA is applied. When an erythrocyte passes through the pore, the current is interrupted. The test is used to detect compounds that improve filterability of erythrocytes. To simulate decreased red blood cell deformability, the erythrocytes

are artificially modified either by one or by a combination of the following stress factors:

- addition of calcium ions (increase in erythrocyte rigidity)
- addition of lactic acid (decrease in pH value)
- addition of 350–400 mmol NaCl (hyperosmolarity)
- storing the sample for at least 4 h (cellular ageing, depletion of ADP).

PROCEDURE

Apparatus

Single erythrocyte rigidometer (Myrenne, 52159 Roetgen, Germany)

Data: driving pressure: $dp = 70$ Pa (dog, rabbit, rat), $dp = 100$ Pa (man); wall shear stress: $\tau = 3$ Pa.

Single pore membrane: length: 30 µm; diameter: 3.5 µm (rat), 4.0 µm (rabbit, dog), 4.5 µm (man)

Ex Vivo

Blood is collected from Beagle dogs weighing 12–20 kg, from rabbits weighing 1.2–2.5 kg, from Wistar rats weighing 150–300 g, or from humans. The test subjects receive the test compound by oral, subcutaneous or intravenous administration 15, 60, 90 or 180 min before the withdrawal of blood.

In Vitro

Following addition of the test compound, the blood samples are incubated at 37°C for 5 or 30 min.

The blood samples are mixed with K-EDTA (1 mg/ml blood) or heparin (5 IE/ml heparin sodium) to prevent clotting. The blood is centrifuged at $250 \times g$ for 7 min. The plasma and the buffy coat are removed and discarded. The packed erythrocytes are resuspended in filtrated HEPES-buffer containing 0.25% human albumin, and the haematocrit value is fixed to <1%. The red blood cells are altered by one or several stress factors mentioned above. A sample of 2 ml of the stressed suspension is applied to the measuring device, and the passage time of a population of 250 erythrocytes (tm) is determined. Cells remaining in the pore for more than 100 ms (tm >100 ms) lead to a rheological occlusion.

Untreated red blood cell suspensions serve as control.

EVALUATION

The mean passage time of 250 single erythrocytes and the number of rheological occlusions/250 erythrocytes is determined.

Statistics

The statistical significance is evaluated according to the procedure described for flow behavior of erythrocytes described above.

REFERENCES AND FURTHER READING

Kiesewetter H, Dauer M, Teitel P et al (1982) The single erythrocyte rigidometer (SER) as a reference for RBC deformability. Biorheology 19:737–753

Nash GB (1990) Filterability of blood cells: methods and clinical applications. Biorheology 27(6):873–82

Roggenkamp HG, Jung F, Kiesewetter H (1983) Ein Gerät zur elektrischen Messung der Verformbarkeit von Erythrocyten [A device for the electrical measurement of the deformability of red blood cells]. Biomed Techn 28:100–104

Seiffge D, Behr S (1986) Passage time of red blood cells in the SER; their distribution and influences of various extrinsic and intrinsic factors. Clin Hemorheol 6:151–164

B.2.12 Erythrocyte Aggregation

PURPOSE AND RATIONALE

The aggregation of red blood cells into rouleaux and from rouleaux into 3-dimensional cell networks is a rheological parameter that decisively influences the flow behavior of blood, especially in disturbed microcirculation. In the following procedure, an apparatus (erythrocyte aggregometer) is used to measure erythrocyte aggregation. The transparent measuring chamber (cone/plate configuration) is transilluminated by light of a defined wave length. The intensity of the transmitted light, which is modified by the aggregation process, is recorded. The method can be used to determine the effect of test compounds on erythrocyte aggregation according to Kiesewetter et al. (1982) and Schmid-Schoenbein et al. (1973).

PROCEDURE

Apparatus

Selective Erythrocyte Rigidometer (Fa. Myrenne, 52159 Roetgen, Germany)

Ex Vivo

Blood is collected from Beagle dogs weighing 12–20 kg, from rabbits weighing 1.2–2.5 kg, or from Wistar rats weighing 150–300 g. The test subjects receive the test compound by oral, subcutaneous or intravenous administration 15, 60, 90 or 180 min before the withdrawal of blood.

In Vitro

Following addition of the test compound, the blood sample is incubated at 37°C for 5 or 30 min.

Blood is obtained from the test subjects by venipuncture and mixed with K-EDTA (1 mg/ml) or heparin (5 IU/ml heparin sodium) to prevent clotting. Erythrocyte aggregation is determined in whole blood. A sample of 40 µl blood is transferred to the measuring device. The red cells are dispersed at a shear rate of 600/s. After 20 s, flow is switched to stasis, and the extent of erythrocyte aggregation is determined photometrically.

EVALUATION

Statistics

The statistical significance is evaluated according to the procedure described for flow behavior of erythrocytes (see above).

REFERENCES AND FURTHER READING

Ben Assayag E, Bova I, Berliner S, Peretz H, Usher S, Shapira I, Bornstein NM (2006) Gender differences in the expression of erythrocyte aggregation in relation to B beta-fibrinogen gene polymorphisms in apparently healthy individuals. Thromb Haemost 95(3):428–433

Kiesewetter H, Radtke H, Schneider R et al (1982) Das Mini-Erythrozyten-Aggregometer: Ein neues Gerät zur schnellen Quantifizierung des Ausmaßes der Erythrocytenaggregation [Mini Erythrocyte Aggregometer: A new apparatus for rapid quantification of the extent of erythrocyte aggregation]. Biomed Tech 27:209–213

Ricart JM, Vaya A, Todoli J, Santaolaria ML, Calvo J, Aznar J (2005) Erythrocyte aggregation in Behcet's disease determined with the Sefam and Myrenne aggregometer: lack of association with thrombosis and uveitis. Clin Hemorheol Microcirc. 33(4):389–396

Schmid-Schoenbein H, van Gosen J, Heinich L et al (1973) A counter-rotating "Rheoscope chamber" for the study of the microrheology of blood cell aggregation by microscopic observation and microphotometry. Microvasc Res 6:366–376

B.2.13 Determination of Plasma Viscosity

PURPOSE AND RATIONALE

One of the principal methods for measuring viscosity is based on the rate of flow of a liquid through an orifice according to Harkness (1971). In this test, a defined volume of plasma is transferred into a capillary viscometer, and the efflux time required for the plasma to flow from the upper to the lower mark is measured. Using this procedure, the effect of test compounds on the viscosity of blood plasma can be determined. The test can be carried out either *ex vivo* or *in vitro.*

PROCEDURE

Ex Vivo

Beagle dogs weighing 12–20 kg, rabbits weighing 2.0–3.0 kg, or Wistar rats weighing 150–300 g of either sex are used as test animals. Likewise, the test procedure can be performed in humans. The test subjects receive the test compound by oral, subcutaneous or intravenous administration 15, 60, 90 or 180 min before the withdrawal of blood.

In Vitro

Following addition of the test compound, plasma (obtained as described below) is incubated at 37°C for 5 or 30 min.

Freshly collected venous blood is anticoagulated with 1 mg/ml blood K^+-EDTA or heparin sodium (5 IU/ml blood) and centrifuged at $250 \times g$ for 5 min. The supernatant (plasma) is removed, and a sample of 0.9 ml plasma is transferred into a capillary viscometer (Coulter Harkness, Coulter Electr., LTD, England) provided with a glass capillary of 0.5 mm inside diameter. The temperature during measurement is 37°C. The flow time, t, required for the plasma to flow through the capillary is measured. Untreated plasma serves as control.

EVALUATION

The viscosity of each sample can be determined using the following formula:

$$\eta = K \times t \times \rho$$

where η = viscosity of plasma, K = calibration constant of viscometer, t = flow time of 0.9 ml plasma, and ρ = density of plasma.

The change in viscosity relative to the control group is determined.

Statistical evaluation is carried out using the Student's t-test.

REFERENCES AND FURTHER READING

Bax BE, Richfield L, Bain MD, Mehta AB, Chalmers RA, Rampling MW (2005) Haemorheology in Gaucher disease. Eur J Haematol. 75(3):252–258

Harkness J (1971) The viscosity of human blood plasma; its measurement in health and disease. Biorheology 8:171–179

Holdt B, Lehmann JK, Schuff-Werner P (2005) Comparative evaluation of two newly developed devices for capillary viscometry. Clin Hemorheol Microcirc. 33(4):379–387

B.3 In Vitro Models of Thrombosis

PURPOSE AND RATIONALE

There is abundant evidence suggesting that platelets play a pivotal role in the pathogenesis of arterial

thrombotic disorders, including unstable angina (UA), myocardial infarction (MI) and stroke. The underlying pathophysiological mechanism of these processes has been recognized as the disruption or erosion of a vulnerable atherosclerotic plaque leading to local platelet adhesion and subsequent formation of partially or completely occlusive platelet thrombi.

The specific platelet surface receptors that support these initial adhesive interactions are determined by the local fluid dynamic conditions of the vasculature and the extracellular matrix constituents exposed at the sites of vascular injury. Konstantopoulos et al. (1998) and Alveriadou et al. (1993) demonstrated that under high shear conditions, the adhesion of platelets to exposed subendothelial surfaces of atherosclerotic or injured vessels presenting collagen and von Willebrand factor (vWF) is primarily mediated by the platelet glycoprotein (GP)Ib/IX/V complex. This primary adhesion to the matrix activates platelets, leading ultimately to platelet aggregation mediated predominantly by the binding of adhesive proteins such as fibrinogen and vWF to GPIIb/IIIa. In addition, direct platelet aggregation in the bulk phase under conditions of abnormally elevated fluid shear stresses, analogous to those occurring in atherosclerotic or constricted arterial vessels, as shown by Turitto (1982), may be important. Shear-induced platelet aggregation is dependent upon the availability of vWF and the presence of both GPIb/IX and GPIIb/IIIa on the platelet membrane. It has been postulated that at high shear stress conditions, the interaction of vWF with the GPIb/IX complex is the initial event leading to platelet activation, which also triggers the binding of vWF to GPIIb/IIIa to induce platelet aggregate formation.

A variety of methods have been utilized to assess the *ex vivo* and/or *in vitro* efficacy of platelet antagonists, including photometric aggregometry, whole blood electrical aggregometry and particle counter methods, as described in the above segments. In photometric aggregometry, a sample is placed in a stirred cuvette in the optical light path between a light source and a light detector. Aggregate formation is monitored by a decrease in turbidity, and the extent of aggregation is measured as percent of maximal light transmission. The major disadvantage of this technique is that it cannot be applied in whole blood since the presence of erythrocytes interferes with the optical responses. Furthermore, it is insensitive to the formation of small aggregates. Particle counters are used to quantitate the size and the number of particles suspended in an electrolyte solution by monitoring the electrical current between two electrodes immersed in the solution. Aggregation in this system is quantitated by counting the platelets before and after stimulation, and it is usually expressed as a percentage of the initial count, as shown by Jen and McIntire (1984). However, the disadvantage of this technique is that it cannot distinguish platelets and platelet aggregates from other blood cells of the same size. Thus, one is limited to counting only a fraction of single platelets, as well as aggregates that are much larger than erythrocytes and leukocytes. The technique of electrical aggregometry allows the detection of platelet aggregates as they attach to electrodes immersed in a stirred cuvette of whole blood or platelet suspensions. Such an attachment results in a decrease in conductance between the two electrodes that can be quantitated in units of electrical resistance. However, a disadvantage of this method is that it is not sensitive in the detection of small aggregates, as demonstrated by Sweeney et al. (1989).

This segment discusses two complementary *in vitro* flow models of thrombosis that can be used to accurately quantify platelet aggregation in anticoagulated whole blood specimens and to evaluate the inhibitory efficacy of platelet antagonists: (1) a viscometric-flow cytometric assay to measure direct shear-induced platelet aggregation in the bulk phase, as demonstrated by Konstantopolous et al. (1995); and (2) a parallel-plate perfusion chamber coupled with a computerized videomicroscopy system to quantify the adhesion and subsequent aggregation of human platelets in anticoagulated whole blood flowing over an immobilized substrate (e. g. collagen I), as shown by Konstantopolous et al. (1995), and Mousa et al. (2002). Furthermore, Mousa et al. (2002) demonstrated a third *in vitro* flow assay in which surface-anchored platelets are pre-incubated with a GPIIb/IIIa antagonist, and unbound drug is washed away prior to the perfusion of THP-1 monocytic cells, thereby enabling one to distinguish agents with markedly distinct affinities and receptor-bound lifetimes.

PROCEDURE

Isolation of Human Platelets

The steps described in subsequent subheadings outline the procedure for isolation and purification of platelets from whole blood obtained by venipuncture from human volunteers. Obtain blood sample by venipuncture from an antecubital vein into polypropylene syringes containing either sodium citrate (0.38% final concentration) or heparin (10 U/ml final concentration). Centrifuge anticoagulated whole blood at $160 \times g$ for 15 min to prepare platelet-rich plasma (PRP).

Isolation of Washed Platelets

PRP specimens are subjected to a further centrifugation (1,100 *g* for 15 min) in the presence of 2 μM PGE_1 (Evangelista et al. 1996).

The platelet pellet is resuspended in HEPES-Tyrode buffer containing 5 mM EGTA and 2 μM PGE_1.

Platelets are then washed via centrifugation (1,100 *g* for 10 min), resuspended at 2×10^8/mL in HEPES-Tyrode buffer, and kept at room temperature for no longer than 4 hours before use in aggregation/adhesion assays.

MATERIALS

- Anticoagulant solution (sodium citrate, porcine heparin, PPACK etc.)
- Fluorescently labeled platelet-specific antibody
- Dulbecco's phosphate-buffered saline (D-PBS) (with and without Ca^{2+}/Mg^{2+}).
- Formaldehyde
- Type I collagen, from bovine Achille's tendon
- 0.5 mol/L glacial acetic acid in water
- Glass coverslips (24 × 50 mm; Corning; Corning, NY)
- Silicone sheeting (gasket) (0.005-in or 0.010-in thickness; Specialty Manufacturing Inc; Saginaw, MI)
- Quinacrine dihydrocholride
- Prostaglandin E_1 (PGE_1) and EGTA
- Thrombin
- Bovine serum albumin
- HEPES-Tyrode buffer (129 mM NaCl, 9.9 mM $NaHCO_3$, 2.8 mM KCl, 0.8 mM K_2PO_4, 0.8 mM $MgCl_2 \cdot 6H_2O$, 1 mM $CaCl_2$, 10 mM HEPES, 5.6 mM dextrose)
- 3-aminopropyltriethoxysilane (APES)
- Acetone
- 70% nitric acid in water
- THP-1 monocytic cells
- Platelet antagonists such as abciximab

EVALUATIONS

The methods described below (Sections 2.1–2.3) outline different dynamic adhesion/aggregation assays used to assess the *in vitro* and/or *ex vivo* efficacy of platelet antagonists: (1) a viscometric-flow cytometric assay to measure shear-induced platelet-platelet aggregation in the bulk phase, (2) a perfusion chamber coupled with a computerized videomicroscopy system to visualize in real time and quantify (a) the adhesion and subsequent aggregation of platelets flowing over an immobilized substrate (e. g. extracellular matrix protein) and (b) free-flowing monocytic cell adhesion to immobilized platelets.

REFERENCES AND FURTHER READING

Abulencia JP, Tien N, McCarty OJT, Plymire D, Mousa SA, Konstantopoulos K (2001) Comparative antiplatelet efficacy of anovel, nonpeptide GPIIb/IIIa antagonists (XV454) and abciximab (c7E3) in flow models of thrombosis. Arterioscler Thromb Vasc Biol 21:149–156

Alveriadou BR, Moake JL, Turner NA, Ruggeri ZM, Folie BJ, Phillips MD, Schreiber Ab, Hrinda ME, McEntire LV (1993) Real-time analysis of shear dependent thrombus formation and its blockade by inhibitors of von Villebrand factor binding to platelets. Blood 81:1263–1276

Evangelista V, Manarini S, Rotondo S et al (1996) Platelet/polymorphonuclear leukocyte interaction in dynamic conditions: evidence of adhesion cascade and cross talk between P-selectin and the beta 2 integrin CD11b/CD18. Blood 88:4183–4194

Jen CJ, McIntire LV (1984) Characteristics of shear-induced aggregation in whole blood. J Lab Clin Med 103:115–124

Konstantopoulos K, Kamat SG, Schafer AI et al (1995) Shear-induced platelet aggregation is inhibited by in vivo infusion of an anti-glycoprotein IIb/IIIa antibody fragment, c7E3 Fab, in patients undergoing coronary angioplasty. Circulation 91:1427–1431

Konstantopoulos K, Kukreti S, McIntire LV (1998) Biomechanics of cell interactions in shear fields. Adv Drug Delivery Rev 33:141–164

Mousa SA, Abulencia JP, McCarty OJ et al (2002) Comparative efficacy between glycoprotein IIb/IIIa antagonists roxifiban and orbofiban in inhibiting platelet responses in flow models of thrombosis. J Cardiovasc Pharmacol 39:552–560

Sweeney JD, Labuzzetta JW, Michielson CE, Fitzpatrick JE (1989) Whole blood aggregation using impedance and particle counter methods. Am J Clin Pathol 92:794–797

Turitto VT (1982) Blood viscosity, mass transport, and thrombogenesis. Prog Hemost Thromb 6:139–177

B.3.1 Cone-and-Plate Viscometry Under Shear-Flow Cytometry

PURPOSE AND RATIONALE

The cone-and-plate viscometer is an *in vitro* flow model used to investigate the effects of bulk fluid shear stress on suspended cells. Anticoagulated whole blood specimens (or isolated cell suspensions) are placed between the two platens (both of stainless steel) of the viscometer. Rotation of the upper conical platen causes a well-defined and uniform shearing stress to be applied to the entire fluid medium, as described by Konstantopolous et al. (1998). The shear rate (γ) in this system can be readily calculated from the cone angle and the speed of the cone using the formula:

$$\gamma = \left(\frac{2\pi\omega}{60\theta_{cp}} \right)$$

where γ is the shear rate in sec^{-1}, ω is the cone rotational rate in revolutions per minute (rev/min) and θ_{cp} is the cone angle in radians. The latter is typically in the range of 0.3 to 1.0°. The shear stress, τ, is proportional to shear rate, γ, as shown by: $\tau = \mu \cdot \gamma$, where μ is the viscosity of the cell suspension (the viscosity of anticoagulated whole blood is ~0.04 cp at 37°C). This type of rotational viscometer is capable of generating shear stresses from ~2 dyn/cm^2 (venous level) to greater than 200 dyn/cm^2 (stenotic arteries).

PROCEDURE

Single platelets and platelet aggregates generated upon shear exposure of blood specimens are differentiated from other blood cells on the basis of their characteristic forward-scatter and fluorescence (by the use of fluorophore-conjugated platelet specific antibodies) profiles by flow cytometry, as described by Konstantopolous et al. (1995). This technique requires no washing or centrifugation steps that may induce artifactual platelet activation, and it allows the study of platelet function in the presence of other blood elements. The procedure used to quantify platelet aggregation induced by shear stress is as follows:

- Incubate anticoagulated whole blood with platelet antagonist or vehicle (control) at 37°C for 10 min.
- Place a blood specimen (typically ~500 µl) on the stationary platen of a cone-and-plate viscometer maintained at 37°C.
- Take a small aliquot (~3 µl) from the pre-sheared blood sample, fix it with 1% formaldehyde in D-PBS (~30 µl).
- Expose the blood specimen, in the presence or absence of a platelet antagonist, to well-defined shear levels (typically 4000 sec^{-1} to induce significant platelet aggregation in the absence of a platelet antagonist) for prescribed periods of time (typically 30 to 60 sec).
- Take a small aliquot (~3 µl) from the sheared blood specimen, and immediately fix it with 1% formaldehyde in D-PBS (~30 µl).
- Incubate the fixed blood samples with a saturating concentration of a fluorescently labeled platelet-specific antibody, such as anti-GPIb(6D1)-FITC, for 30 min in the dark.
- Dilute specimens with 2 ml of 1% formaldehyde, and analyze them by flow cytometry.

Flow cytometric analysis is used to distinguish platelets from other blood cells on the basis of their characteristic forward scatter and fluorescence profiles, as shown in Fig. 1. Data acquisition is then carried out on each sample for a set period (usually 100 sec), thereby allowing equal volumes for both the pre-sheared and sheared specimens to be achieved. As a result, the percent platelet aggregation can be determined by the disappearance of single platelets into the platelet aggregate region using the formula: $\%\ Platelet\ Aggregation = (1 - Ns/Nc \times 100)$, where *Ns* represents the single platelet population of the sheared specimen and *Nc* represents the single platelet population of the pre-sheared specimen. By comparing the extents of platelet aggregation in the presence and absence of a platelet antagonist, its antiplatelet efficacy can be readily determined.

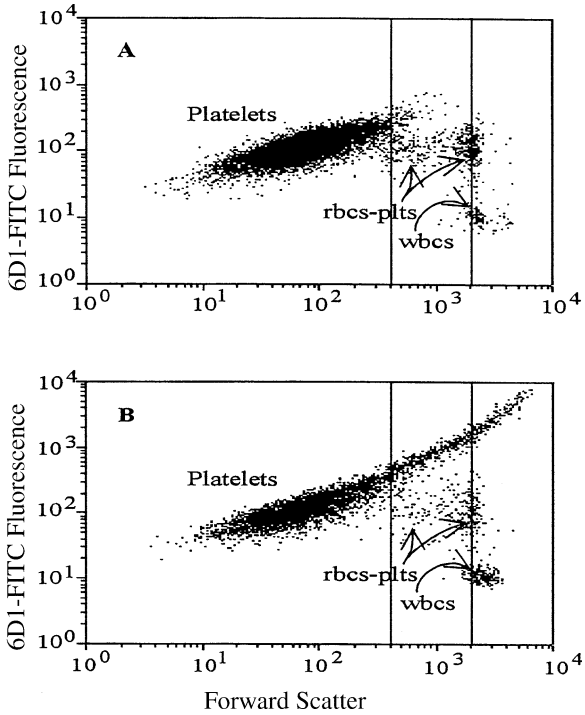

Figure 1 Quantification of shear-induced platelet aggregation by flow cytometry. Panel A corresponds to an unsheared blood specimen. Panel B corresponds to a blood specimen that has been subjected to a pathologically high level of shear stress for 30 sec. As can be seen in the figure, there are three distinct cell populations. The upper population consists of platelets and platelet aggregates. The "rbcs-plts" population corresponds to platelets associated with erythrocytes and leukocytes. The "wbcs" population consists of some leukocytes that have elevated levels of FITC autofluorescence. The left vertical line separates single platelets (≤ 4.5 µm in diameter) from platelet aggregates, whereas the right vertical line separates "small" from "large" platelet aggregates. The latter were defined to be larger than 10 µm in equivalent sphere diameter

REFERENCES AND FURTHER READING

Konstantopoulos K, Kamat SG, Schafer AI et al (1995) Shear-induced platelet aggregation is inhibited by in vivo infusion

of an anti-glycoprotein IIb/IIIa antibody fragment, c7E3 Fab, in patients undergoing coronary angioplasty. Circulation 91:1427–1431
Konstantopoulos K, Kukreti S, McIntire LV (1998) Biomechanics of cell interactions in shear fields. Adv Drug Delivery Rev 33:141–164

B.3.2 Platelet Adhesion and Aggregation Under Dynamic Shear

PURPOSE AND RATIONALE

The steps described and outlined an *in vitro* flow model of platelet thrombus formation, which can be used to evaluate the *ex vivo* and/or *in vitro* efficacy of platelet antagonists. Thrombus formation may be initiated by platelet adhesion from rapidly flowing blood onto exposed subendothelial surfaces of injured vessels containing collagen and von Willebrand factor (vWF), with subsequent platelet activation and aggregation. Konstantopolous et al. (1995) described the use of a parallel-plate flow chamber that provides a controlled and well-defined flow environment based on the chamber geometry and the flow rate through the chamber. The wall shear stress, τ_w, assuming a Newtonian and incompressible fluid, can be calculated using the formula:

$$\tau_w = \frac{6\mu Q}{wh^2}$$

where Q is the volumetric flow rate, μ is the viscosity of the flowing fluid, h is the channel height, and b is the channel width. A flow chamber typically consists of a transparent polycarbonate block, a gasket whose thickness determines the channel depth, and a glass coverslip coated with an extracellular matrix protein such as type I fibrillar collagen. The apparatus is held together by vacuum. Shear stress is generated by flowing fluid (e. g. anticoagulated whole blood or isolated cell suspensions) through the chamber over the immobilized substrate under controlled kinematic conditions using a syringe pump. Mousa et al. (2002) combined the parallel-plate flow chamber with a computerized epi-fluorescence videomicroscopy system that enables one to visualize in real time and separately quantify the adhesion and subsequent aggregation of human platelets in anticoagulated whole blood (or isolated platelet suspensions) flowing over an immobilized substrate.

PROCEDURE

Preparation of Collagen-Coated Surfaces

- Dissolve 500 mg collagen type I from bovine Achille's tendon into 200 ml of 0.5 mol/L acetic acid in water, pH 2.8.
- Homogenize for 3 hours.
- Centrifuge the homogenate at 200*g* for 10 min, collect supernatant, and measure collagen concentration by a modified Lowry analysis.
- Coat glass coverslips with 200 µl of fibrillar collagen I suspension on all but first 10 mm of the slide length (coated area = 12.7 × 23), and place in a humid environment at 37°C for 45 min.
- Rinse excess collagen with 10 ml of D-PBS maintained at 37°C before assembly into the flow chamber (Folie et al. 1988).

Platelet Perfusion Studies

- Add the fluorescent dye quinacrine dihydrochloride to anticoagulated whole blood samples at a final concentration of 10 µM immediately after blood collection.
- Prior to the perfusion experiment, incubate blood with either a platelet antagonist or vehicle (control) at 37°C for 10 min.
- Perfuse anticoagulated whole blood through the flow chamber for 1 min at wall shear rates ranging from 100 sec^{-1} (typical of venous circulation) to 1500 sec^{-1} (mimicking partially constricted arteries) for prescribed periods of time (e. g. 1 min). Platelet-substrate interactions are monitored in real time using an inverted microscope equipped with an epifluorescent illumination attachment and silicon-intensified target video camera, and recorded on videotape. The microscope stage and flow chamber are maintained at 37°C by an incubator heating module and incubator enclosure during the experiment.

EVALUATION

Videotaped images are digitized and computer analyzed at 5, 15 and 60 sec for each perfusion experiment. The number of adherent individual platelets in the microscopic field of view during the initial 15 sec of flow is determined by image processing and used as the measurement of platelet adhesion that initiates platelet thrombus formation. The number of platelets in each individual thrombus is calculated as the total thrombus intensity (area × fluorescence intensity) divided by the average intensity of single platelets determined in the 5-sec images. By comparing the extents of platelet aggregation in the presence and absence of a platelet antagonist, its antiplatelet efficacy can be de-

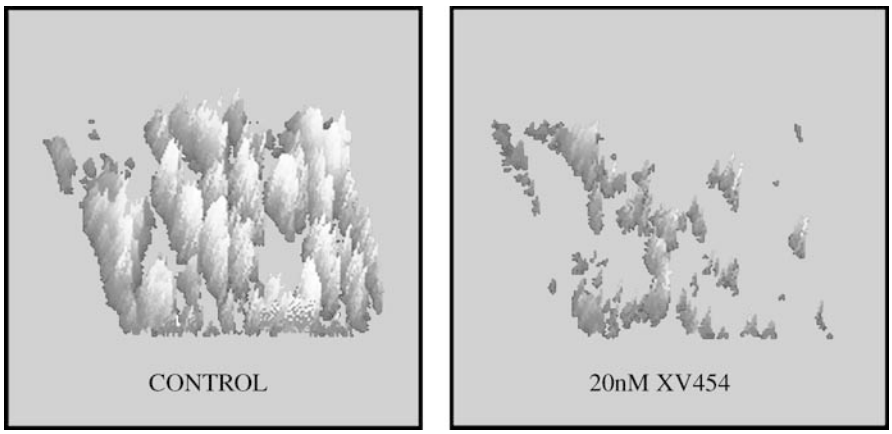

Figure 2 Three-dimensional computer-generated representation of platelet adhesion and subsequent aggregation on collagen I/von Willebrand factor from normal heparinized blood perfused in the absence (control) or presence of a GPIIb/IIIa antagonist (XV454) at 37°C for 1 min at 1,500 sec^{-1}

termined (Fig. 2). Along these lines, any potential inhibitory effects of a platelet antagonist on platelet adhesion can be readily assessed.

REFERENCES AND FURTHER READING

Folie BJ, McIntire LV, Lasslo A (1988) Effects of a novel antiplatelet agent in mural thrombogenesis on collagen-coated glass. Blood 72:1393–1400

Konstantopoulos K, Kamat SG, Schafer AI et al (1995) Shear-induced platelet aggregation is inhibited by in vivo infusion of an anti-glycoprotein IIb/IIIa antibody fragment, c7E3 Fab, in patients undergoing coronary angioplasty. Circulation 91:1427–1431

Mousa SA, Abulencia JP, McCarty OJ et al (2002) Comparative efficacy between glycoprotein IIb/IIIa antagonists roxifiban and orbofiban in inhibiting platelet responses in flow models of thrombosis. J Cardiovasc Pharmacol 39:552–560

B.3.3 Cell Adhesion to Immobilized Platelets: Parallel-Plate Flow Chamber

PURPOSE AND RATIONALE

In this assay, immobilized platelets are pretreated with a GPIIb/IIIa antagonist, and any unbound drug is washed away before the perfusion of monocytic THP-1 cells. Mousa et al. (1998) demonstrated that agents with slow platelet off-rates such as XV454 ($t_{1/2}$ of dissociation = 110 min; K_d = 1 nM) and abciximab ($t_{1/2}$ of dissociation = 40 min; K_d = 9.0 nM) that are distributed predominantly as receptor-bound entities with little unbound in the plasma, can effectively block these heterotypic interactions as shown by Abulencia et al. (2001) and by Mousa et al. (2002). In contrast, agents with relatively fast platelet dissociation rates such as orbofiban ($t_{1/2}$ of dissociation = 0.2 min; K_d >110 nM), whose antiplatelet efficacy depends on the plasma concentration of the active drug, do not exhibit any inhibitory effects, as described by Mousa et al. (2002).

PROCEDURE

Preparation of 3-Aminopropyltriethoxysilane (APES)-Treated Glass Slides

- Soak glass coverslips overnight in 70% nitric acid.
- Wash coverslips with tap water for 4 hours.
- Dry coverslips by washing once with acetone, followed by immersion in a 4% solution of APES in acetone for 2 min.
- Repeat the step above, followed by a final rinse of the glass coverslips with acetone.
- Wash coverslips three times with water, and allow them to dry overnight.

Immobilization of Platelets on 3-APES-Treated Glass Slides

- Layer washed platelets or platelet-rich plasma (2×10^8 cells/ml) on the surface of a coverslip at ~30 µl/cm^2.
- Allow platelets to bind to APES-treated coverslip in a humid environment at 37°C for 30 min.

Monocytic THP-1 Cell-Platelet Adhesion Assay

- Assemble the platelet-coated coverslip on a parallel-plate flow chamber, which is then mounted on the stage of an inverted microscope equipped with a CCD camera connected to a VCR and TV monitor.
- Perfuse the antiplatelet antagonist at the desirable concentration or vehicle (control) over surface-bound platelets, and incubate for 10 min. The extent of platelet activation can be further modulated by the presence of chemical agonists such as thrombin (0.02–2 U/ml) during the 10 min incubation. The microscope stage and flow chamber are maintained

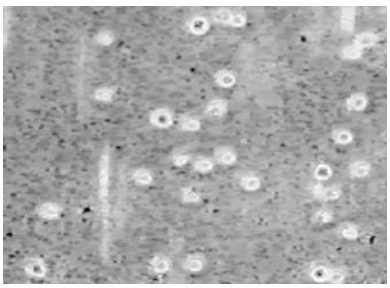

Figure 3 Phase-contrast photomicrograph of THP-1 cells (phase bright objects) attached to a layer of thrombin-treated platelets (phase dark objects) after THP-1 cell perfusion for 3 min at a shear stress level of 1.5 dyn/cm^2

at 37°C by an incubator heating module and incubator enclosure during the experiment.

- In some experiments, unbound platelet antagonist is removed by a brief washing step (4 min) prior to the perfusion of the cells of interest over the platelet layer. In others, the desirable concentration of the platelet antagonist is continuously maintained in the perfusion buffer during the entire course of the experiment.
- Perfuse cells (e. g. THP-1 monocytic cells, leukocytes, tumor cells, protein-coated beads, etc.) over surface-bound platelets, either in the presence or absence of a platelet antagonist (see above), at the desirable flow rate for prescribed periods of time. THP-1 cell binding to immobilized platelets is monitored in real time and recorded on videotape.
- Determine the extent of THP-1 cell tethering, rolling and stationary adhesion to immobilized platelets, as well as the average velocity of rolling THP-1 cells. By comparing the corresponding extents of THP-1 cell tethering, rolling and stationary adhesion to immobilized platelets in the presence and absence of a platelet antagonist (Fig. 3), its antiplatelet efficacy can be determined as shown by Mousa et al. (1995).

EVALUATION

Low-speed centrifugation results in the separation of platelets (top layer) from larger and more dense cells such as leukocytes and erythrocytes (bottom layer). To minimize leukocyte contamination in PRP specimens, slowly aspirate the uppermost two thirds of the platelet layer. Furthermore, certain rare platelet disorders, such as Bernard-Soulier Syndrome (BSS), are characterized by larger than normal platelets which must therefore be isolated by allowing whole blood to gravity separate for 2 hours post-venipuncture.

The mechanical force most relevant to platelet-mediated thrombosis is shear stress. The normal time-averaged levels of venous and arterial shear stresses range between 1–5 dyn/cm^2 and 6–40 dyn/cm^2, respectively. However, fluid shear stress may reach levels well over 200 dyn/cm^2 in small arteries and arterioles partially obstructed by atherosclerosis or vascular spasm. The cone-and-plate viscometer and parallel-plate flow chamber are two of the most common devices used to simulate fluid mechanical shearing stress conditions in blood vessels.

Due to the large concentration of platelets and erythrocytes in whole blood, small aliquots (~3µl) of pre-sheared and post-sheared specimens must be obtained and processed prior to the flow cytometric analysis. This will minimize an artifact produced as a platelet and an erythrocyte pass through the light beam of a flow cytometer at the same time.

The "rbcs-plts" population represents 3–5% of the displayed cells. A small fraction (~5%) of this population seems to be leukocyte-platelet aggregates, as evidenced by the use of an anti-CD45 monoclonal antibody. The remaining events correspond to erythrocytes associated with platelets. However, it appears that the majority of the latter population is an artifact generated by the simultaneous passage of a platelet and an erythrocyte through the beam of a flow cytometer. This concept is corroborated by the fact that further dilution of pre-sheared and sheared blood specimens and/or reduction of the sample flow rate during the flow cytometric analysis results in a dramatic relative decrease of the "rbcs-plts" population.

The collagen density remaining on glass coverslips after D-PBS rinsing can be measured by the difference in weight of 20 clean uncoated slides versus 20 collagen-treated slides.

Experiments are optimally monitored ~100–200 µm downstream from the collagen/glass interface using a 60 × FLUOR objective and 1 × projection lens, which gives a 3.2×10^4 µm^2 field of view. A field of view closer to the interface may lead to non-reproducible results due to variations in the collagen layering in that region. In contrast, positions farther downstream are avoided in order to minimize the effects of upstream platelet adhesion and subsequent aggregation on both the fluid dynamic environment as well as bulk platelet concentration.

The digitization of a background image (at the onset of perfusion prior to platelet adhesion to the collagen I surface) and its subtraction from a subsequent image acquired 5 sec after an initial platelet adhesion event allows the determination of the fluorescence in-

tensity emitted by a single platelet. The intensity level of each single platelet is measured as a mean gray level between 0 (black) and 255 (white) through the use of an image processing software (e. g. OPTIMAS; Agris-Schoen Vision Systems, Alexandria, VA), and is multiplied by its corresponding area (total number of pixels covered by each single platelet). The aforementioned products are then averaged for all single platelet events detected at the 5-sec time point, thus enabling us to calculate the average intensity of single platelets.

A single field of view ($10 \times 0.55\,mm^2$) is monitored during the 3 min period of the experiment; at the end, five additional fields of view ($0.55\,mm^2$) are monitored for 15 sec each. The following parameters can be quantified: (a) the number of total interacting cells per mm^2 during the entire 3-min perfusion experiment; (b) the number of stationary interacting cells per mm^2 after 3 min of shear flow; (c) the percentage of total interacting cells that are stationary after 3 min of shear flow; and (d) the average rolling velocity (μm/sec) of interacting cells. The number of interacting cells per mm^2 is determined manually by reviewing the videotapes. Stationary interacting cells per mm^2 are considered as those that move <1-cell radius within 10 sec at the end of the 3-min attachment assay. To quantify their number, images can be digitized from a videotape recorder using an imaging software package (e. g. OPTIMAS). Rolling velocities can be computed as the distance traveled by the centroid of the rolling THP-1 cell divided by the time interval using image processing.

REFERENCES AND FURTHER READING

Abulencia JP, Tien N, McCarty OJT et al (2001) Comparative antiplatelet efficacy of a novel, nonpeptide GPIIb/IIIa antagonist (XV454) and abciximab (c7E3) in flow models of thrombosis. Arterioscler Thromb Vasc Biol 21:149–156

Mousa SA, Forsythe M, Bozarth J, Youssef A, Wityak J, Olson R, Sielecki T (1998) XV454, a novel nonpeptide small-molecule platelet GIIb/IIIa antagonist with comparable platelet alpha(IIb)beta3-binding kinetics to c7E3. J Cardiovasc Pharmacol 32(5):736–44

Mousa SA, Abulencia JP, McCarty OJ et al (2002) Comparative efficacy between glycoprotein IIb/IIIa antagonists roxifiban and orbofiban in inhibiting platelet responses in flow models of thrombosis. J Cardiovasc Pharmacol 39:552–560

B.4 In Vivo or Ex Vivo Models

PURPOSE AND RATIONALE

The general understanding of the pathophysiology of thrombosis is based on the observations of Virchow in 1856. He proposed three factors responsible for thrombogenesis: obstruction of blood flow, changes in the properties of blood constituents (hypercoagulability), and vessel wall injury. Experimental models of thrombosis focus on one, two or all three factors of Virchow's triad. Therefore, they differ with respect to the prothrombotic challenge—either stenosis, stasis, vessel wall injury (mechanical, electrical, chemical, photochemical, laser light), insertion of foreign surface, or injection of a prothrombotic factor, and they differ with respect to the vessel type and with respect to the animal species.

Roughly, two types of models can be differentiated (Didisheim 1972; Kaiser et al. 1999; Mousa et al. 1998; Perzborn et al. 2005): (1) models in which thrombi are produced in veins by stasis and/or injection of a procoagulant factor, resulting in fibrin-rich "red" venous type thrombi; or (2) models in which thrombi are produced in arteries by vessel wall injury and/or stenosis, resulting in platelet-rich "white" mural thrombi. But the differentiation is not strict because platelets and the coagulation system influence each other. Drugs preventing fibrin formation may well act in arterial models and vice versa. Thrombosis models are usually performed in healthy animals. The underlying chronic diseases in humans, namely atherosclerosis or thrombophilias, are not included in the models. Thus, any model is limited regarding its clinical relevance. The pharmacological effectiveness of a new antithrombotic drug should be studied in more than one animal model. In spite of these limitations, animal models predict clinical effectiveness of drugs for the treatment and prevention of thrombotic diseases fairly well. A list of such drugs is presented in a recent review by Leadley et al. (2000). Furthermore, the clinical usefulness of an antithrombotic drug is determined by its safety/efficacy ratio regarding the bleeding risk. Assessment of a parameter of the hemostatic system should therefore be included in the models if possible.

The development of antithrombotic agents requires pre-clinical assessment of the biochemical and pharmacologic effects of these drugs. It is important to note that the second- and third-generation antithrombotic drugs are devoid of *in vitro* anticoagulant effects, yet *in vivo*, by virtue of endogenous interactions, these drugs produce potent antithrombotic actions. The initial belief that an antithrombotic drug must exhibit *in vitro* anticoagulant activity is no longer valid. This important scientific observation has been possible only because of the availability of animal models.

Several animal models utilizing species such as rats, rabbits, dogs, pigs and monkeys have been made available for routine use. Other animal species such as the hamster, mouse, cat and guinea pig have also been uti-

lized. Species variations are an important consideration in selecting a model and interpreting the results as these variations can result in different antithrombotic effects. Rats and rabbits are the most commonly used species in which both arterial and venous thrombosis has been investigated. Both pharmacologic and mechanical means have been used to produce a thrombogenic effect in these models. Both rat and rabbit models for studying bleeding effects of drugs have also been developed. The rabbit ear blood loss model is most commonly used to test the hemorrhagic effect of drugs. The rat tail bleeding models have also been utilized for the study of several antithrombotic drugs.

These animal models have been well established and can be used for the development of antithrombotic drugs. It is also possible to use the standardized bleeding and thrombosis models to predict the safety and efficacy of drugs. Thus, in addition to the evaluation of *in vitro* potency, the endogenous effect of antithrombotic drugs can also be investigated. Such standardized methods can be recommended for inclusion in pharmacopoeial screening procedures. Numerous models have now been developed to mimic a variety of clinical conditions where antiplatelet and antithrombotic drugs are used, including myocardial infarction, stroke, cardiopulmonary bypass, trauma, peripheral vascular diseases and restenosis. While dog and primate models are relatively expensive, they have also provided useful information on the pharmacokinetics and pharmacodynamics of antithrombotic drugs. The primate models, in particular, have been extremely useful, as the hemostatic pathways in these species are comparable to those in humans. The development of such agents as the specific glycoprotein IIb/IIIa inhibitor antibodies relies largely on these models. These models are, however, of pivotal value in the development of antithrombotic drugs and provide extremely useful data on the safety and efficacy of new drugs developed for human usage.

PROCEDURE

Animal Models of Thrombosis

In most animal models of thrombosis, healthy animals are challenged with thrombogenic (pathophysiologic) stimuli and/or physical stimuli to produce thrombotic or occlusive conditions. These models are useful for the screening of antithrombotic drugs.

I. Stasis-Thrombosis Model: Since its introduction by Wessler et al. (1959), the rabbit model of jugular stasis thrombosis has been extensively used for the pharmacologic screening of antithrombotic agents. This model has also been adapted for use in rats (Meuleman et al. 1991). In the stasis thrombosis model, a hypercoagulable state is mimicked by administration of one of a number of thrombogenic challenges, including human serum (Carrie et al. 1994), thromboplastin (Walenga et al. 1986), activated prothrombin complex concentrates (Vlasuk et al. 1991), factor Xa (Millet et al. 1994) and recombinant relipidated tissue factor (Callas et al. 1995). This administration serves to produce a hypercoagulable state. Diminution of blood flow achieved by ligating the ends of the vessel segments serves to augment the prothrombotic environment. The thrombogenic environment produced in this model simulates venous thrombosis where both blood flow and the activation of coagulation play a role in the development of a thrombus.

II. Models Based on Vessel Wall Damage: The formation of a thrombus is not solely induced by a plasmatic hypercoagulable state. In the normal vasculature, the intact endothelium provides a nonthrombogenic surface over which the blood flows. Disruption of the endothelium not only limits the beneficial effects enumerated above, but also exposes subendothelial tissue factor and collagen that serve to activate the coagulation and platelet aggregation processes, respectively. Endothelial damage can be induced experimentally by physical means (clamping, catheter), chemical means (FITC, Rose Bengal, ferrous chloride), thermal injury or electrolytic injury.

EVALUATION

Each setting in the design of an animal model can answer specific question in relation to certain thrombotic disorders in human. However, the ultimate model of human thrombosis is in human.

REFERENCES AND FURTHER READING

Callas DD, Bacher P, Fareed J (1995) Studies on the thrombogenic effects of recombinant tissue factor: in vivo versus ex vivo findings. Semin Thromb Hemost 21(2):166–176

Carrie D, Caranobe C, Saivin S et al (1994) Pharmacokinetic and antithrombotic properties of two pentasaccharides with high affinity to antithrombin III in the rabbit: comparison with CY 216. Blood 84(8):2571–2577

Didisheim P (1972) Animal models useful in the study of thrombosis and antithrombotic agents. Prog Haemostas Thromb 1:165–197

Kaiser B, Kirchmaier CM, Breddin HK, Fu K, Fareed J (1999) Preclinical biochemistry and pharmacology of low molecular weight heparins in vivo–studies of venous and arterial thrombosis. Semin Thromb Hemost. 25 Suppl 3:35–42

Leadley RJ, Chi L, Rebello SS, Gagnon A (2000) Contribution of *in vivo* models of thrombosis to the discovery and devel-

opment of novel antithrombotic agents. J Pharmacol Toxicol Methods 43:101–116
Meuleman DG, Hobbelen PM, Van Dinther TG et al (1991) Antifactor Xa activity and antithrombotic activity in rats of structural analogues of the minimum antithrombin III binding sequence: discovery of compounds with a longer duration of action than the natural pentasaccharide. Semin Thromb Hemost 17(Suppl 1):112–117
Millet J, Theveniaux J, Brown NL (1994) The venous antithrombotic profile of naroparcil in the rabbit. Thromb Haemost 72(6):874–879
Mousa SA, Bozarth JM, Edwards S, Carroll T, Barrett J (1998) Novel technetium-99m-labeled platelet GPIIb/IIIa receptor antagonists as potential imaging agents for venous and arterial thrombosis. Coronary Artery Dis 9(2–3):131–41
Perzborn E, Strassburger J, Wilmen A, Pohlmann J, Roehrig S, Schlemmer KH, Straub A (2005) In vitro and in vivo studies of the novel antithrombotic agent BAY 59–7939–an oral, direct Factor Xa inhibitor. J Thromb Haemost 3(3):514–21
Virchow R (1856) Über die Verstopfung der Lungenarterie. In: Gesammelte Abhandlungen zur wissenschaftlichen Medizin. Frankfurt, Meidinger Sohn, S 221
Vlasuk GP, Ramjit D, Fujita T et al (1991) Comparison of the in vivo anticoagulant properties of standard heparin and the highly selective factor Xa inhibitors antistasin and tick anticoagulant peptide (TAP) in a rabbit model of venous thrombosis. Thromb Haemost 65(3):257–262
Walenga JM, Fareed J, Petitou M et al (1986) Intravenous antithrombotic activity of a synthetic heparin pentasaccharide in a human serum induced stasis thrombosis model. Thromb Res 43(2):243–248
Wessler S, Reimer SM, Sheps MC (1959) Biologic assay of a thrombosis-inducing activity in human serum. J Appl Physiol 14:943–946

B.4.1 Stenosis- and Mechanical Injury-Induced Coronary Thrombosis: Folts Model

PURPOSE AND RATIONALE

Thrombosis in stenosed human coronary arteries is one of the most common thrombotic diseases leading to unstable angina, acute myocardial infarction or sudden death. Treatment with angioplasty, thrombolysis, or by-pass grafts can expose new thrombogenic surfaces and re-thrombosis may occur. The mechanisms responsible for this process include interactions of platelets with the damaged arterial wall and platelet aggregation.

In order to study new drugs for their antithrombotic potential in coronary arteries, Folts and Rowe (1974) developed the model of periodic acute platelet thrombosis and cyclic flow reductions (CFRs) in stenosed canine coronary arteries. Uchida et al. described a similar model in 1975. The model includes various aspects of unstable angina pectoris (i. e. critical stenosis, vascular damage, downstream vasospasm induced by vasoconstrictors released or generated by platelets). The cyclic variations in coronary blood flow are a result of acute platelet thrombi that may occlude the vessel but that either embolize spontaneously or can easily be embolized by shaking the constricting plastic cylinder. They are not a result of vasospasm (Folts et al. 1982). Clinically, aspirin can reduce the morbidity and mortality of coronary thrombotic diseases but its effect is limited. Similarly, CFRs in the Folts model are abolished by aspirin but the effect can be reversed by increases in catecholamines and shear forces (Folts and Rowe 1988). As part of an expert meeting on animal models of thrombosis, a review of the Folts model has been published (Folts 1991).

Five different protocols are described in the following section for the induction of coronary thrombosis.

Coronary Thrombosis Induced by Stenosis

The described preparations are characterized by episodic, spontaneous decreases in coronary blood flow interrupted by restorations of blood flow. CFRs, which are alterations in coronary blood flow, are associated with transient platelet aggregation at the site of the coronary constriction and abrupt increase in blood flow after embolization of platelet-rich thrombi.

Damage of the vessel wall is produced by placing a hemostatic clamp on the coronary artery; a fixed amount of stenosis is produced by an externally applied obstructive plastic cylinder upon the damaged part of the vessel. In dogs, the stenosis is critical, i. e. the reactive hyperemic response to a 10-sec occlusion is abolished (protocol 1); in pigs, the stenosis is subcritical, i. e. there is a partial reactive hyperemia left (Just and Schönafinger 1991; protocol 2).

For some animals, especially for young dogs, damage of the vessel wall and stenosis is not sufficient to induce thrombotic cyclic flow variations. In these cases, an additional activation of platelets by infusion of epinephrine (protocol 3) is required, leading to the formation of measurable thrombi. In another preparation (protocol 4), thrombus formation is induced by subcritical stenosis without prior clamping of the artery and infusion of platelet activating factor (PAF), according to the model described by Apprill et al. (1985). In addition to these protocols, coronary spasms induced by released platelet components can influence coronary blood flow. Therefore, this model includes the main pathological factors of unstable angina pectoris.

Coronary Thrombosis Induced by Electrical Stimulation

In this preparation, coronary thrombosis is induced by delivery of low-amperage electrical current to the inti-

mal surface of the artery, according to the method described by Romson et al. (1980a). In contrast to the stenosis protocols, an occluding thrombosis is formed gradually without embolism after some hours (protocol 5). As a consequence of this time course, the thrombi formed are of the mixed type and contain more fibrin than the platelet thrombi with critical stenosis.

PROCEDURE

Coronary Thrombosis Induced by Stenosis

Protocol 1: Critical Stenosis Dogs of either sex weighing 15–40 kg, at least 8 months of age, are anesthetized with pentobarbital sodium (bolus of 30–40 mg/kg and continuous infusion of approx. 0.1 mg/kg/min); respiration is maintained through a tracheal tube using a positive pressure respirator. The heart is exposed through a left thoracotomy at the fourth or fifth intercostal space, the pericardium is opened and the left circumflex coronary artery (LCX) is exposed. An electromagnetic or Doppler flowprobe is placed on the proximal part of the LCX to measure coronary blood flow. Distal to the flowprobe, the vessel is squeezed with a 2-mm hemostatic clamp for 5 sec. A small cylindrical plastic constrictor, 2–4 mm in length and with an internal diameter of 1.2–1.8 mm (depending on the size of the LCX) is then placed around the artery at the site of the damage. Usually, the constrictor has to be changed several times (2–5 times) until the appropriate narrowing of the vessel is achieved, and cyclic flow variations are observed. In case of an occlusion of the artery without spontaneous embolization of the formed thrombus, reflow is induced by shortly lifting the vessel with a thread placed beneath the stenotic site.

Only dogs with regularly repeated CFRs of similar intensity within a pre-treatment phase of 60 min are used in these experiments.

The test substance is then administered by intravenous bolus injection or continuous infusion, or by intraduodenal application. CFRs are registered for 2–4×60 min and compared to pre-treatment values.

Prior to testing, preparations for additional hemodynamic measurements are performed (see below).

Protocol 2: Subcritical Stenosis Male castrated pigs (German landrace, weighing 20–40 kg) are anesthetized with ketamine (2 mg/kg i.m.), metomidate (10 mg/kg i.p.) and xylazine (1–2 mg/kg i.m.). In order to maintain the stage of surgical anesthesia, animals receive a continuous i.v. infusion of 0.1–0.2 mg/kg/min pentobarbital sodium. Respiration is maintained through a tracheal tube using a positive pressure respirator. The heart is exposed through a left thoracotomy at the fourth and fifth intercostal space, the pericardium is opened and the left descending coronary artery (LAD) is exposed. An electromagnetic or Doppler flowprobe is placed on the proximal part of the LAD to measure coronary blood flow. Distal to the flowprobe, the vessel is squeezed with a 1-mm hemostatic clamp for 5 sec. A small cylindrical plastic constrictor, 2 mm in length, is then placed around the artery at the site of the damage. Usually, the constrictor has to be changed several times until the appropriate narrowing of the vessel is achieved, which produces cyclic flow reductions. CFRs are similar to those in dogs; pigs, however, show a reactive hyperemic response. If embolization does not occur spontaneously, the formed thrombus is released at reduction of blood flow by shortly lifting the vessel with forceps.

Only pigs with regularly repeated CFRs of similar intensity within a pre-treatment phase of 60 min are used in these experiments.

The test substance is then administered by intravenous bolus injection or continuous infusion, or by intraduodenal application. CFRs are registered for 2×60 min and compared to pre-treatment values.

Protocol 3: Stenosis+Epinephrine Infusion If protocol 1 does not lead to CFRs, additionally epinephrine (0.2 µg/kg/min) is infused into a peripheral vein for twice over 60 minutes (60 min before and 60 min following drug administration). CFRs are registered and compared in the 60 min post-drug phase to the 60 min pre-drug phase.

Protocol 4: Stenosis+PAF Infusion The LCX is stenosed without prior mechanical wall injury. This preparation does not lead to thrombus formation (subcritical stenosis). For the induction of CFRs, PAF (C 16-PAF, Bachem) (0.2 nmol/kg/min) is infused into a cannulated lateral branch of the coronary artery.

After 30 min, PAF infusion is terminated and blood flow returns to its normal, continuous course. Thirty minutes later, the test substance is concomitantly administered and a second PAF infusion is started for 30 min.

CFRs are registered and compared in the drug-treated, second PAF phase to the pre-drug, first PAF phase.

Coronary Thrombosis Induced by Electrical Stimulation

Protocol 5 The LCX is punctuated distal to the flow probe with a chrome-vanadium-steel electrode (3-

mm length, 1-mm diameter). The electrode (anode) is placed in the vessel in contact with the intimal lining and connected over a Teflon coated wire to a 9 V battery, a potentiometer and an amperemeter. A disc electrode (cathode) is secured to a subcutaneous thoracal muscle layer to complete the electrical circuit. The intima is stimulated with 150 µA for 6 hours. During this time, an occluding thrombosis is gradually formed.

The test substance or the vehicle (control) is administered either at the start of the electrical stimulation or 30 min following the start.

The time interval until the thrombotic occlusion of the vessel occurs and the thrombus size (wet weight measured immediately after removal at the end of the experiment) are determined.

Prior to testing, preparations for additional hemodynamic measurements are performed (see below).

For all protocols, the following preparations and measurements are performed:

- To measure peripheral arterial blood pressure (BP [mm Hg]), the right femoral artery is cannulated and connected to a Statham pressure transducer.
- Left ventricular pressure (LVP [mm Hg]) is determined by inserting a microtip-catheter via the carotid artery retrogradely.
- Left ventricular end-diastolic pressure (LVEDP [mm Hg]) is evaluated through sensitive amplification of the LVP.
- Contractility (LV dp/dt max [mm Hg/s]) is determined from the initial slope of the LVP curve.
- Heart rate (min^{-1}) is determined from the pulsatile blood pressure curve.
- The ECG is recorded in lead II.
- Arterial pH and concentrations of blood gases are kept at physiological levels by adjusting respiration and infusion of sodium bicarbonate.
- Blood hematocrit values (37%–40%) and number of erythrocytes are kept constant by infusion of oxypolygelatine in dogs and electrolyte solution in pigs.
- Body temperature is monitored with a rectal thermistor probe and kept constant by placing the animals on a heated metal pad with automatic regulation of temperature.
- Template buccal mucosal bleeding time is carried out using the Simplate$^{\hat{a}}$ device.

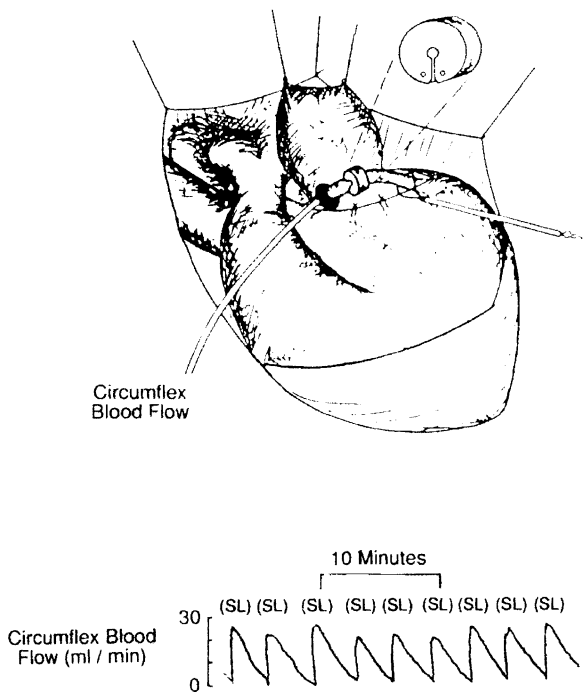

Figure 4 Technique for monitoring platelet aggregation in the partially obstructed left circumflex coronary artery of the dog. Electromagnetic flow probes measure blood flow. Partial obstruction of the coronary artery with a plastic Lexan cylinder results in episodic cyclical reductions in coronary blood flow that are due to platelet-dependent thrombus formation. Every 2–3 mm the thrombus must be mechanically shaken loose to restore blood. For detailed application of the Folts model, see Folts, Rowe (1974, 1988); and Folts et al. (1976, 1982)

EVALUATION

For all protocols, the mean maximal reduction of blood pressure (systolic/diastolic [mm Hg]) is determined.

Protocols 1–4 The following parameters are determined to quantify stenosis-induced coronary thrombosis:

- Frequency of CFRs = cycle number per time
- Magnitude of CFRs = cycle area (mm^2)

Percent change in cycle number and cycle area after drug treatment is calculated compared to pre-treatment controls.

Statistical significance is assessed by the paired Student's t-test.

Protocol 5 The following parameters are determined to quantify electrically-induced coronary thrombosis:

- Occlusion time (min) = time to zero blood flow
- Thrombus size (mg) = wet weight of the thrombus immediately after removal.

Percent change in mean values for occlusion time and thrombus size in drug-treated groups is compared to the control group.

Statistical significance is assessed by the non-paired Student's *t*-test.

CRITICAL ASSESSMENT

Both, the stenosis (Folts) and the electrical (Romson/Lucchesi) model of coronary thrombosis are widely used to study the role of mediators in the thrombotic process and the effect of new antithrombotic drugs. Bush and Patrick (1986) reviewed the role of the endothelium in arterial thrombosis and the effect of some inhibitors and mediators in the Folts model, e. g. thromboxane, prostacyclin, cyclooxygenase, serotonin, NO-donors and other vasodilators. The effect of an NO-donor could be reversed by the NO-scavenger oxyhemoglobin indication that indeed NO was responsible for the anti-thrombotic action (Just and Schönafinger 1991). Recent mechanisms of antithrombotic drug action that have been studied in either of the two coronary thrombosis models are the oral GP IIb/IIIa antagonist DMP 728 (Mousa et al. 1996); the LMWH enoxaparin (Leadley et al. 1998), which inhibited CFRs in contrast to unfractionated heparin; the thrombin inhibitors PEG-hirudin (Ruebsamen and Kirchengast 1998) and melagatran (Mehta et al. 1998); an anti-P-selectin antibody (Ikeda et al. 1999); and activated protein C (Jackson et al. 2000).

The clinical relevance of studies in the Folts model has been questioned because the model is very sensitive to antithrombotic compounds. However, the lack of a reversal of the effect by epinephrine or increase in degree of stenosis differentiates any new drug from aspirin. Electrical coronary thrombosis is less sensitive: e. g. aspirin has no effect, and with some drugs higher dose levels are required; however, in principle, most drug mechanisms act in both models if at all.

MODIFICATIONS OF THE METHOD

Romson et al. (1980b) described a simple technique for the induction of coronary artery thrombosis in the conscious dog by delivery of low-amperage electric current to the intimal surface of the artery.

Benedict et al. (1986) modified the electrical induction of thrombosis by use of two Doppler flow probes proximal and distal to the needle electrode in order to measure changes in blood flow velocity. The electrical current was stopped at 50% increase in flow velocity, and thrombosis then occurred spontaneously. The important role of serotonin was demonstrated by increases in coronary sinus serotonin levels just prior to occlusion.

Warltier et al. (1987) described a canine model of thrombin-induced coronary artery thrombosis, as well as the effects of intracoronary streptokinase on regional myocardial blood flow, contractile function, and infarct size.

Al-Wathiqui et al. (1988) described the induction of cyclic flow reduction in the coronary, carotid, and femoral arteries of conscious chronically instrumented dogs.

The method of Folts thrombosis has also been applied to carotid arteries in monkeys. Coller et al. (1989) induced CFRs in carotid arteries of anesthetized cynomologus monkeys and showed abolition by the GP IIb/IIIa antibody abciximab.

REFERENCES AND FURTHER READING

Al-Wathiqui MH, Hartman JC, Brooks HL, Warltier DC (1988) Induction of cyclic flow reduction in the coronary, carotid, and femoral arteries of conscious chronically instrumented dogs: a model for investigating the role of platelets in severely constricted arteries. J Pharmacol Meth 20:85–92

Apprill P, Schmitz JM, Campbell WB et al (1985) Cyclic blood flow variations induced by platelet-activating factor in stenosed canine coronary arteries despite inhibition of thromboxane synthetase, serotonin receptors, and α-adrenergic receptors. Circulation 72:397–405

Benedict CR, Mathew B, Rex KA et al (1986) Correlation of plasma serotonin changes with platelet aggregation in an *in vivo* dog model of spontaneous occlusive coronary thrombus formation. Circ Res 58:58–67

Bush LR, Patrick D (1986) The role of the endothelium in arterial thrombosis and the influence of antithrombotic therapy. Drug Dev Res 7:319–340

Coller BS, Smith SR, Scudder LE et al (1989) Abolition of *in vivo* platelet thrombus formation in primates with monoclonal antibodies to the platelet GP IIb/IIIa receptor: correlation with bleeding time, platelet aggregation and blockade of GP IIb/IIIa receptors. Circulation 80:1766–1774

Folts JD (1991) An *in vivo* model of experimental arterial stenosis, intimal damage, and periodic thrombosis. Circulation 83 (Suppl IV):IV-3–IV-14

Folts JD, Crowell EB, Rowe GG (1976) Platelet aggregation in partially obstructed vessels and its elimination with aspirin. Circulation 54:365–370

Folts JD, Gallagher K, Rowe GG (1982) Blood flow reductions in stenosed canine coronary arteries: vasospasm or platelet aggregation? Circulation 65:248–255

Folts JD, Rowe GG (1974) Cyclical reductions in coronary blood flow in coronary arteries with fixed partial obstruction and their inhibition with aspirin. Fed Proc 33:413

Folts JD, Rowe GG (1988) Epinephrine reverses aspirin inhibition of *in vivo* platelet thrombus formation in stenosed dog coronary arteries. Thromb Res 50:507–516

Ikeda H, Ueyama T, Murohara T et al (1999) Adhesive interaction between P-selectin and sialyl Lewis X plays an important role in recurrent coronary arterial thrombosis in dogs. Arterioscler Thromb Vasc Biol 19:1083–1090

Jackson CV, Bailey BD, Shetler TJ (2000) Pharmacological profile of recombinant human activated protein C (LY203638) in a canine model of coronary artery thrombosis. J Pharmacol Exp Ther 295:957–971

Just M, Schönafinger K (1991) Antithrombotic properties of a novel sydnonimine derivative. J Cardiovasc Pharmacol 17 (Suppl 3):S121–S126

Leadley RJ, Kasiewski CJ, Bostwick JS et al (1998) Inhibition of repetitive thrombus formation in the stenosed canine coronary artery by enoxaparin, but not by unfractionated heparin. Arterioscler Thromb Vasc Biol 18:908–914

Mehta JL, Chen L, Nichols WW et al (1998) Melagatran, an oral active-site inhibitor of thrombin, prevents or delays formation of electrically induced occlusive thrombus in the canine coronary artery. J Cardiovasc Pharmacol 31:345–351

Mousa SA, DeGrado WF, Mu D-X et al (1996) Oral antiplatelet antithrombotic efficacy of DMP 728, a novel platelet GPIIb/IIIa antagonist. Circulation 93:537–543

Romson JL, Hook BG, Lucchesi BR (1980a) Potentiation of the antithrombotic effect of prostacyclin by simultaneous administration of aminophylline in a canine model of coronary artery thrombosis. J Pharmacol Exp Ther 227:288–294

Romson JL, Haack DW, Lucchesi BR (1980b) Electrical induction of coronary artery thrombosis in the ambulatory canine: a model for *in vivo* evaluation of anti-thrombotic agents. Thromb. Res 17:841–853

Ruebsamen K, Kirchengast M (1998) Thrombin inhibition and intracoronary thrombus formation: effect of polyethylene glycol-coupled hirudin in the stenosed, locally injured canine coronary artery. Coron Artery Dis 9:35–42

Uchida Y, Yoshimoto N, Murao S (1975) Cyclic fluctuations in coronary blood pressure and flow induced by coronary artery constriction. Jpn Heart J 16:454–464

Warltier DC, Lamping KA, Pelc LR, Gross GJ (1987) A canine model of thrombin-induced coronary artery thrombosis: effects of intracoronary streptokinase on regional myocardial blood flow, contractile function, and infarct size. J Pharmacol Meth 18:305–318

B.4.2 Stenosis- and Mechanical Injury-Induced Arterial and Venous Thrombosis: Harbauer-Model

PURPOSE AND RATIONALE

Harbauer et al. (1984) and Harbauer and Allendorf (1988) first described a venous model of thrombosis induced by mechanical injury and stenosis of the jugular vein. In a modification, both arterial and venous thrombosis is produced in rabbits by stenosis of the carotid artery and the jugular vein with simultaneous mechanical damage of the endothelium. This activates platelets and the coagulation system and leads to changes in the bloodstream pattern. As a consequence, occluding thrombi are formed as detected by blood flow measurement. The dominant role of platelets in this model is shown by the inhibitory effect of an antiplatelet serum in both types of vessels (Just 1986). The test is used to evaluate the antithrombotic capacity of compounds in an *in vivo* model of arterial and venous thrombosis where thrombus formation is highly dependent on platelet activation.

PROCEDURE

Male Chinchilla rabbits weighing 3–4 kg receive the test compound or the vehicle (controls) by oral, intravenous or intraperitoneal administration. The first ligature (vein, preparation see below) is performed at the end of absorption (i.p. approx. 30 min, p.o. approx. 60 min, i.v. variable).

Sixty-five minutes before stenosis, the animals are sedated by intramuscular injection of 8 mg/kg xylazine (Rompun) and anesthetized by intravenous injection of 30–40 mg/kg pentobarbital sodium 5 min later. During the course of the test, anesthesia is maintained by continuous infusion of pentobarbital sodium (30–40 mg/kg/h) into one femoral vein. A Statham pressure transducer is placed into the right femoral artery for continuous measurement of blood pressure. Spontaneous respiration is maintained through a tracheal tube. One jugular vein and one carotid artery are exposed on opposite sides. Small branches of the vein are clamped to avoid blood flow in spite of vessel occlusion. Electromagnetic or Doppler flow probes are placed on the vein (directly central to the vein branching) and on the artery (as far central as possible). Blood flow (ml/min) is measured continuously. After reaching steady state (approx. 15–30 min), a metal rod with a diameter of 1.3 mm is placed on the jugular vein (2 cm central to the vein branching) and a ligature is tightened. After 1 min, the rod is removed from the ligature. Immediately thereafter (approx. 1.5 min), the carotid artery is damaged by briefly squeezing it with forceps. Then a small plastic constricting cylinder 1.2 mm wide and 2 mm long is placed around the site of the endothelial damage.

In addition, the template bleeding time is measured at various time interval before and after drug treatment (depending on the route of administration) in the shaved inner ear using the Simplate device. Care is taken to select parts of the skin without larger vessels.

EVALUATION

Percent thrombus formation (= thrombosis incidence) is judged by determination of the number of occluded vessels (blood flow = 0).

Percent inhibition of thrombosis incidence is calculated in dosed groups as compared to vehicle controls. Thrombosis incidence is always 100% in vehicle controls.

Statistical significance is assessed by means of the Fisher exact test.

If initial values for blood flow do not significantly differ in dosage and control groups, the area below the blood flow curves is measured by planimetry in addition, and mean values in dosed groups are compared to controls by means of the unpaired Student's *t*-test. Mean values of occlusion times [min] in dosage and

control groups are calculated and compared by means of the t-test.

The maximal change in systolic and diastolic blood pressure during the period of stenosis as compared to the initial values before drug administration is determined. There is no standardized assessment score. As an example, a reduction of systolic blood pressure by 30 mm Hg and of diastolic blood pressure by 20 mm Hg is quoted as a strong reduction in blood pressure.

CRITICAL ASSESSMENT OF THE METHOD

Two main factors of arterial thrombosis are essential in this model: high-grade stenosis and vessel wall damage. In the absence of either, no thrombus is found. The occlusive thrombus is formed fast and in a highly reproducible manner. In both vessels thrombus formation is equally dependent on platelet function, as shown by antiplatelet serum. Therefore, the jugular vein thrombosis in this model differs from stasis-induced deep vein thrombosis with predominant fibrin formation. On the other hand, these occlusive thrombi are more stable than the pure platelet thrombi in the Folts model since carotid blood flow cannot be restored by shaking the constrictor. The following antithrombotic drugs are effective: (i) antiplatelet drugs like ticlopidine, prostacyclin/iloprost, NO-donors (SNP, molsidomine) but not aspirin, thromboxane-synthase-inhibitors; (ii) anticoagulants like hirudin, high-dose heparin, warfarin; and (iii) streptokinase/t-PA (Bevilacqua et al. 1991, Just 1986). In contrast, drugs that only lower blood pressure—such as hydralazine, clonidine, and prazosin—have no effect on thrombus formation in this model.

MODIFICATIONS OF THE METHOD

Bevilacqua et al. (1991) performed the same model in rabbit carotid arteries but compared the procedure in one artery before drug treatment with the contralateral artery after drug treatment. Heparin, the synthetic thrombin inhibitor FPRCH2Cl, iloprost and t-PA inhibited carotid occlusion in this model but not aspirin.

Spokas and Wun (1992) produced venous thrombosis in the vena cava of rabbits by vascular damage and stasis. The vascular wall was damaged by crushing with hemostat clamps. A segment of the vena cava was looped with two ligatures, 2.5 cm apart. At 2 h after ligation, the isolated venous sac was dissected and the clot removed for determination of dry weight.

Lyle et al. (1995) searched for an animal model mimicking the thrombotic reocclusion and restenosis occurring in several cases after successful coronary angioplasty in man. The authors developed a model of angioplasty-induced injury in atherosclerotic rabbit femoral arteries. Acute ^{111}indium-labelled platelet deposition and thrombosis were assessed 4 hours after balloon injury in arteries subjected to prior endothelial damage (air desiccation) and cholesterol supplementation (1 month). The effects of inhibitors of factor X_a or platelet adhesion, heparin, and aspirin on platelet deposition were studied.

Thrombosis Induced by Cooling

Lindenblatt et al. (2005), Meng (1975), Meng and Seuter (1977) and Seuter et al. (1979) described a method to induce arterial thrombosis in rats by chilling of the carotid artery. Rats were anesthetized; the left carotid artery was exposed and occluded proximal by means of a small clamp. The artery was placed for 2 min into a metal groove which was cooled to –15°C. The vessel was compressed by a weight of 200 g. In addition, a silver clip was fixed to the vessel distally from the injured area to produce a disturbed and slow blood flow. After 4 min, the proximal clamp was removed and the blood flow reestablished in the injured artery. In the rabbit, slightly different conditions were used: the chilling temperature was –12°C for a period of 5 min, and the compressing weight was 500 g. The wound was closed, and the animal was allowed to recover from anesthesia. Antithrombotic compounds were administered in various doses at different time intervals before surgery. After 4 hours, the animals received heparin and were reanesthetized. The lesioned carotid artery was removed and thrombus wet-weight was immediately measured.

REFERENCES AND FURTHER READING

Bevilacqua C, Finesso M, Prosdocimi M (1991) Acute carotid artery occlusive thrombosis and its pharmacological prevention in the rabbit. Thromb Res 62:263–273

Harbauer G, Allendorf A (1988) Experimental investigations on the thrombosis-preventing effect of low-molecular-weight heparins. Haemostasis 18 Suppl 3:69–72

Harbauer G, Hiller W, Hellstern P (1984) Ein experimentelles Modell der venösen Thrombose am Kaninchen: Überprüfung seiner Brauchbarkeit mit Low Dose Heparin. [An experimental model of venous thrombosis in the rabbit: test of its usefulness with low-dose heparin.] In: Koslowski L (ed) Chirurgisches Forum ‘84 für experimentelle und klinische Forschung. Springer-Verlag, Berlin, Heidelberg, New York, Tokyo, pp 69–72

Just M (1986) Pharmakologische Beeinflussung einer experimentellen Thrombose beim Kaninchen. [Influence of various agents on experimental thrombosis in the rabbit.] In: Wenzel E, Hellstern P, Morgenstern E et al (eds) Rationelle Therapie und Diagnose von hämorrhagischen und thrombophilen Diathesen. Schattauer Verlag, Stuttgart – New York, pp 4.95–4.98

Lindenblatt N, Menger MD, Klar E, Vollmar B (2005) Sustained hypothermia accelerates microvascular thrombus formation in mice. Am J Physiol Heart Circ Physiol 289(6):H2680–7
Lyle EM, Fujita T, Conner MW et al (1995) Effect of inhibitors of factor X_a or platelet adhesion, heparin, and aspirin on platelet deposition in an atherosclerotic rabbit model of angioplasty injury. J Pharmacol Toxicol Meth 33:53–61
Meng K (1975) Tierexperimentelle Untersuchungen zur antithrombotischen Wirkung von Acetylsalicylsäure. Therap Ber 47:69–79
Meng K, Seuter F (1977) Effect of acetylsalicylic acid on experimentally induced arterial thrombosis in rats. Naunyn-Schmiedeberg's Arch Pharmacol 301:115–119
Seuter F, Busse WD, Meng K et al (1979) The antithrombotic activity of BAY g 6575. Arzneim Forsch/Drug Res 29:54–59
Spokas EG, Wun TC (1992) Venous thrombosis produced in the vena cava of rabbits by vascular damage and stasis. J Pharm Toxicol Meth 27:225–232

B.4.3 Electrical-Induced Thrombosis

PURPOSE AND RATIONALE

The use of electrical current to induce thrombosis in hamster and dog has been described in the early 1950s by Lutz et al. (1951) and Sawyer et al. (1953a, b). In general, two different approaches exist. One method produces electrical damage by means of two externally applied hook-like electrodes (Hladovec 1973, Philp et al. 1978). The other method uses a needle electrode that is advanced through the walls of the blood vessels and positioned in their lumen; the second electrode is placed into a subcutaneous site completing the circuit (Salazar 1961, Romson et al. 1980, Benedict et al. 1986).

PROCEDURE

Anaesthetized rats weighing 200–300 g are intubated, and a femoral artery is cannulated for administration of drugs. One carotid artery is isolated from surrounding tissues over a distance of 10–15 mm.

A pair of rigid stainless-steel wire hook-like electrodes with a distance of 4 mm are adjusted to the artery by means of a rack and pinion gear manipulator. The artery is raised slightly away from the surrounding tissue. Isolation of the electrodes is achieved by the insertion of a small piece of parafilm under the artery. Blood flow is measured with an ultrasonic Doppler flowmeter (Transonic, Ithaca NY, USA); the flow probe (1RB) is placed proximal to the damaged area.

Thrombus formation is induced in the carotid arteries by the application of an electrical current (350 V, DC, 2 mA) delivered by an electrical stimulator (Stoelting Co, Chicago, Cat. No 58040) for 5 min to the exterior surface of the artery.

EVALUATION

- Blood flow before and after induction of thrombus for 60 min
- Time to occlusion (min): the time between onset of the electrical current and the time at which blood flow decreases under 0.3 ml/min
- Patency of the blood vessel over 30 min.

CRITICAL ASSESSMENT OF THE METHOD

The electrical-induced thrombus is composed of densely packed platelets with some red cells. Moreover, the electrical injury causes extensive damage to intimal and subintimal layers. The endothelium is completely destroyed, and this damage extends to subendothelial structures including smooth muscle cells. The deep damage could reduce the possibility of discrimination between drugs on the basis of their antithrombotic activity. However, Philp et al. (1978) could show that unfractionated heparin completely blocked thrombus formation, whereas other antiplatelet agents displayed differentiated antithrombotic action. He concluded that this relatively simple model of arterial thrombosis might prove a useful screening test for drugs with antithrombotic potential.

MODIFICATIONS OF THE METHOD

The technique described by Salazar et al. (1961) uses a stainless steel electrode that is inserted into a coronary artery in the dog and that delivers anodal current to the intravascular lumen. The electrode is positioned under fluoroscopic control, which complicates the method. The technique was modified by Romson et al. (1980). They placed the electrode directly into the coronary artery of open-chest anaesthetized dogs.

Rote et al. (1993, 1994) used a carotid thrombosis model in dogs. A calibrated electromagnetic flow meter was placed on each common carotid artery proximal to both the point of insertion of an intravascular electrode and a mechanical constrictor. The external constrictor was adjusted with a screw until the pulsatile flow pattern decreased by 25% without altering the mean blood flow. Electrolytic injury to the intimal surface was accomplished with the use of an intravascular electrode composed of a Teflon-insulated silver-coated copper wire connected to the positive pole of a 9-V nickel-cadmium battery. The cathode was connected to a subcutaneous site. Injury was initiated in the right carotid artery by application of a 150 µA continuous pulse anodal direct current to the intimal sur-

face of the vessel for a maximum duration of 3 hours or for 30 min beyond the time of complete vessel occlusion, as determined by the blood flow recording. Upon completion of the study on the right carotid, the procedure for induction of vessel wall injury was repeated on the left carotid artery after administration of the test drug.

Benedict et al. (1986) introduced a procedure in which anodal current is discontinued when mean distal coronary flow velocity increased by approximately 50%, reflecting disruption of normal flow by the growing thrombus. Occlusive thrombosis occurred within 1 hour after stopping the electrical current. It was observed that the final phase of thrombosis occurred independently of electrical injury.

A ferret model of acute arterial thrombosis was developed by Schumacher et al. (1996). A 10-min anodal electrical stimulation of 1 mA was delivered to the external surface of the carotid artery while measuring carotid blood flow. This produced an occlusive thrombus in all vehicle-treated ferrets within 41 ± 3 min, with an average weight of 8 ± 1 mg. Thrombus weight was reduced by aspirin or a thromboxane receptor antagonist.

Guarini (1996) produced a completely occlusive thrombus in the common carotid artery of rats by applying an electrical current to the arterial wall (2 mA for 5 min) while simultaneously constricting the artery with a hemostatic clamp placed immediately downstream from the electrodes.

Sturgeon et al. (2006) adapted the Folts and the electric methods of arterial thrombosis in small animals. Mousa et al. (1999) used the same animal pre- and post-treatment by using left and right arterial sides.

REFERENCES AND FURTHER READING

Benedict CR, Mathew B, Rex KA et al (1986) Correlation of plasma serotonin changes with platelet aggregation in an *in vivo* dog model of spontaneous occlusive coronary thrombus formation. Circ Res 58:58–67

Guarini S (1996) A highly reproducible model of arterial thrombosis in rats. J Pharmacol Toxicol Meth 35:101–105

Hladovec J (1973) Experimental arterial thrombosis in rats with continuous registration. Thromb Diath Haemorrh 29:407–410

Lutz BR, Fulton GP, Akers RP (1951) White thromboembolism in the hamster cheek pouch after trauma, infection and neoplasia. Circulation III:339–351

Mousa SA, Kapil R, Mu DX (1999) Intravenous and oral antithrombotic efficacy of the novel platelet GPIIb/IIIa antagonist roxifiban (DMP754) and its free acid form, XV459. Arterioscler Thromb Vasc Biol 19(10):2535–41

Philp RB, Francey I, Warren BA (1978) Comparison of antithrombotic activity of heparin, ASA, sulfinpyrazone and VK 744 in a rat model of arterial thrombosis. Haemostasis 7:282–293

Romson JL, Haack DW, Lucchesi BR (1980) Electrical induction of coronary artery thrombosis in the ambulatory canine: a model for *in vivo* evaluation of anti-thrombotic agents. Thromb Res 17:841–853

Rote WE, Mu DX, Roncinske RA et al (1993) Prevention of experimental carotid artery thrombosis by Applagin. J Pharm Exp Ther 267:809–814

Rote WE, Davis JH, Mousa SA et al (1994) Antithrombotic effects of DMP 728, a platelet GPIIb/IIIa receptor antagonist, in a canine model of arterial thrombosis. J Cardiovasc Pharmacol 23:681–689

Salazar AE (1961) Experimental myocardial infarction, induction of coronary thrombosis in the intact closed-chest dog. Circ Res 9:135–136

Sawyer PN, Pate JW (1953a) Bioelectric phenomena as an etiologic factor in intravascular thrombosis. Am J Physiol 175:103–107

Sawyer PN, Pate JW, Weldon CS (1953b) Relations of abnormal and injury electric potential differences to intravascular thrombosis. Am J Physiol 9:108–112

Schumacher WA, Steinbacher TE, Megill JR, Durham SK (1996) A ferret model of electrical-induction of arterial thrombosis that is sensitive to aspirin. J Pharmacol Toxicol Meth 35:3–10

Sturgeon SA, Jones C, Angus JA, Wright CE (2006) Adaptation of the Folts and electrolytic methods of arterial thrombosis for the study of anti-thrombotic molecules in small animals. J Pharmacol Toxicol Methods. 53(1):20–9

B.4.4 $FeCl_3$-Induced Thrombosis

PURPOSE AND RATIONALE

A variety of chemical agents has been used to induce thrombosis in animals. Topical $FeCl_3$ was described by Reimann-Hunziger (1944) and recently by Wang et al. (2006) as thrombogenic stimulus in veins. Kurz et al. (1990) showed that the thrombus produced with this method in the carotid arteries of rats is composed of platelets and red blood cells enmeshed in a fibrin network. This model is used as a simple and reproducible test for evaluation of antithrombotic (Broersma et al. 1991) and profibrinolytic test compounds (van Giezen et al. 1997).

PROCEDURE

Rats weighing between 250 and 300 g are anaesthetized with Inactin (100 mg/kg), and a polyethylene catheter (PE-205) is inserted into the trachea via a tracheotomy to facilitate breathing. Catheters are also placed in the femoral artery for blood samples and measurement of arterial blood pressure and in the jugular vein for administration of test agents. The right carotid artery is isolated and an ultrasonic Doppler flowprobe (probe 1RB, Transonic, Ithaca NY, USA) is placed on the vessel to measure blood flow. A small piece of Parafilm "M" (American Can Co, Greenwich,

CT) is placed under the vessel to isolate it from surrounding tissues throughout the experiment.

The test agent is administered by gavage or as an intravenous injection at a defined time prior to initiation of thrombus formation. Thrombus formation is induced by the application of filter paper (2 × 5 mm), saturated with 25% $FeCl_3$ solution, to the carotid artery. The paper is allowed to remain on the vessel 10 min before removal. The experiment is continued for 60 min after the induction of thrombosis. At that time, the thrombus is removed and weighed.

EVALUATION

- Blood flow before and after induction of thrombus for 60 min
- Time to occlusion (min): the time between $FeCl_3$ application and the time at which blood flow decreases under 0.3 ml/min
- Thrombus weight after blotting the thrombus on filter paper

REFERENCES AND FURTHER READING

Broersma RJ, Kutcher LW, Heminger EF (1991) The effect of thrombin inhibition in a rat arterial thrombosis model. Thromb Res 64:405–412

Kurz KD, Main BW, Sandusky GE (1990) Rat model of arterial thrombosis induced by ferric chloride. Thromb Res 60:269–280

Reimann-Hunziger G (1944) Über experimentelle Thrombose und ihre Behandlung mit Heparin. Schweiz Med Wschr 74:66–69

Van Giezen JJ, Wahlund G, Nerme J, Abrahamsson T (1997) The Fab-fragment of a PAI-1 inhibiting antibody reduces thrombus size and restores blood flow in a rat model of arterial thrombosis. Thromb Haemost 77:964–969

Wang X, Smith PL, Hsu MY, Ogletree ML, Schumacher WA (2006) Murine model of ferric chloride-induced vena cava thrombosis: evidence for effect of potato carboxypeptidase inhibitor. J Thromb Haemost 4(2):403–10

Tang Z, Wang Y, Xiao Y, Zhao M, Peng S (2003) Antithrombotic activity of PDR, a newly synthesized L-Arg derivative, on three thrombosis models in rats. Thromb Res 110(2–3):127–33

B.4.5 Thrombin-Induced Clot Formation in Canine Coronary Artery

PURPOSE AND RATIONALE

A canine model of thrombin-induced clot formation was developed by Gold et al. (1984) in which localized coronary thrombosis was produced in the LAD. This is a variation of the technique described by Collen et al. (1983) who used radioactively labeled fibrinogen to monitor the occurrence and extent of thrombolysis of rabbit jugular veins clots. The vessel was intentionally de-endothelialized by external compression with blunt forceps. Snare occluders were then placed proximal and distal to the damaged site, and thrombin (10 U) was injected into the isolated LAD segment in a small volume via a previously isolated side branch. Autologous blood (0.3–0.4 ml) mixed with calcium chloride (0.05 M) also was injected into the isolated LAD segment, producing a stasis-type red clot superimposed on an injured blood vessel. The snares were released 2–5 min later, and total occlusion was confirmed by selective coronary angiography. This model of coronary artery thrombosis relies on the conversion of fibrinogen to fibrin by thrombin. The fibrin-rich thrombus contains platelets, but at no greater concentration than in a similar volume of whole blood. Once the thrombus is formed, it is allowed to age for 1–2 hours, after which a thrombolytic agent can be administered to lyse the thrombus and restore blood flow.

PROCEDURE

In the initial study described by Gold et al. (1984), recombinant t-PA was characterized for its ability to lyse 2-hour-old thrombi. Tissue plasminogen activator was infused at doses of 4.3, 10, and 25 µg/kg/min, i.v, and resulted in reperfusion times of 40, 31, and 13 min, respectively. Thus, in this model of canine coronary thrombosis, t-PA exhibited dose-dependent coronary thrombolysis. Furthermore, it is possible to study the effect of different doses of t-PA on parameters of systemic fibrinolytic activation, such as fibrinogen, plasminogen, and a_2-antiplasmin, as well as to assess myocardial infarct size. For example, Kopia et al. (1988) demonstrated that streptokinase (SK) elicited dose-dependent thrombolysis in this model.

Subsequently, Gold et al. (1986 and 1988) modified the model to study not only reperfusion but also acute reocclusion. Clinically, reocclusion is a persistent problem after effective coronary thrombolysis, which is reported to occur in 15–45% of patients (Goldberg et al. 1985). Thus, an animal model of coronary reperfusion and reocclusion would be important from the standpoint of evaluating adjunctive therapies to t-PA to hasten and/or increase the response rate to thrombolysis as well as prevent acute reocclusion.

Thrombin-Induced Rabbit Femoral Artery Thrombosis: Localized thrombosis can also be produced in rabbit peripheral blood vessels such as the femoral artery by injection of thrombin, calcium chloride, and fresh blood via a side branch (Shebuski et al. 1988).

Either femoral artery is isolated distal to the inguinal ligament and traumatized distally from the lateral circumflex artery by rubbing the artery with the

jaws of forceps. An electromagnetic flow probe is placed distal to the lateral circumflex artery to monitor femoral artery blood flow (FABF). The superficial epigastric artery is cannulated for induction of the thrombus and subsequent infusion of thrombolytic agents. Localized thrombi distal to the lateral circumflex artery with snares approximately 1 cm apart are induced by the sequential injection of thrombin, $CaCl_2$ (1.25 mmol), and a volume of blood sufficient to distend the artery. After 30 min, the snares are released and FABF is monitored for 30 mm to confirm total obstruction of flow by the thrombus.

EVALUATION

The model of thrombin-induced clot formation in the canine coronary artery was modified such that a controlled high-grade stenosis was produced with an external constrictor. Blood flow was monitored with an electromagnetic flow probe. In this model of clot formation with superimposed stenosis, reperfusion in response to t-PA occurs with subsequent reocclusion. The monoclonal antibody against the human GPIIb/IIIa receptor developed by Coller et al. (1983) and tested in combination with t-PA in the canine thrombosis model hastened t-PA-induced thrombolysis and prevented acute reocclusion (Yasuda et al., 1988). These actions *in vivo* were accompanied by abolition of ADP-induced platelet aggregation and markedly prolonged bleeding time.

REFERENCES AND FURTHER READING

Collen D, Stassen JM, Verstraete M (1983) Thrombolysis with human extrinsic (tissue-type) plasminogen activator in rabbits with experimental jugular vein thrombosis. J Clin Invest 71:368–376

Coller BS, Peerschke EI, Scudder LE, Sullivan CA (1983) A murine monoclonal antibody that completely blocks the binding of fibrinogen to platelets produces a thrombasthenic-like state in normal platelets and binds to glycoproteins IIb and/or IIIa. J Clin Invest 72:325–338

Gold HK, Coller BS, Yasuda T et al (1988) Rapid and sustained coronary artery recanalization with combined bolus injection of recombinant tissue-type plasminogen activator and monoclonal antiplatelet Gp IIb/IIIa antibody in a canine preparation. Circulation 77:670–677

Gold HK, Fallon JT, Yasuda T et al (1984) Coronary thrombolysis with recombinant human tissue-type plasminogen activator. Circulation 70:700–707

Gold HK, Leinbach RC, Garabedian HD et al (1986) Acute coronary reocclusion after thrombolysis with recombinant human tissue-type plasminogen activator: prevention by a maintenance infusion. Circulation 73:347–352

Goldberg RK, Levine S, Fenster PE (1985) Management of patients after thrombolytic therapy for acute myocardial infarction. Clin Cardiol 8:455–459

Kopia GA, Kopaciewicz LJ, Ruffolo RR (1988) Coronary thrombolysis with intravenous streptokinase in the anesthetized dog: a dose-response study. J Pharmacol Exp Ther 244:956–962

Shebuski RJ, Storer BL, Fujita T (1988) Effect of thromboxane synthetase inhibition on the thrombolytic action of tissue-type plasminogen activator in a rabbit model of peripheral arterial thrombosis. Thromb Res 52:381–392

Yasuda T, Gold HK, Fallon JT et al (1988) Monoclonal antibody against the platelet glycoprotein (GP) IIb/IIIa receptor prevents coronary artery reocclusion after reperfusion with recombinant tissue type plasminogen activator. J Clin Invest 81:1284–1291

B.4.6 Laser-Induced Thrombosis

PURPOSE AND RATIONALE

Thrombus formation in rat or rabbit mesenteric arterioles or venules is induced by laser beams. The test can be performed in normal or pretreated (induction of arteriosclerosis or adjuvant arthritis) animals. The mediators for thrombus formation in this method are platelet adhesion to the injured endothelial vessel wall on one hand and ADP-induced platelet aggregation on the other. Most probably, ADP is primarily released by laser beam-lysed erythrocytes, due to the fact that erythrocyte hemoglobin exerts strong adsorbability to frequencies emitted by laser beams. There is a further, secondary, aggregation stimulus following the release reaction induced by the platelets themselves.

PROCEDURE

Apparatus

- 4 W argon laser (Spectra Physics, Darmstadt, FRG); wave length: 514.5 nm; energy below the objective: 15 mW; duration of exposure: 1/30 or 1/15 sec
- Microscope ICM 405, LD-Epipland 40/0.60 (Zeiss, Oberkochen, FRG)
- Video camera (Sony, Trinicon tube)
- Recorder (Sony, U-matic 3/4")
- Videoanalyzer and correlator to determine blood flow velocity

In Vivo Experiment

Male Sprague Dawley or spontaneously hypertensive stroke-prone Wistar or Lewis rats with adjuvant induced arthritis weighing 150–300 g or New Zealand rabbits with arteriosclerosis induced by cholesterol feeding for 3 months are used. The animals receive the test compound by oral, intravenous, intraperitoneal, or subcutaneous administration. Control animals are treated with vehicle alone. Prior to thrombus induction, the animals are pretreated by s.c. injection of 0.1 mg/kg atropine sulfate solution and anaesthetized

by intraperitoneal administration of 100 mg/kg ketamine hydrochloride and 4 mg/kg xylazine.

Thrombus formation is induced 15, 30, 60 or 90 min post dosing. Investigations are performed in arterioles or venules of 13±1 µm in diameter of the fat-free ileocaecal portion of the mesentery. During the test procedure, the mesenterium is superfused with physiological saline solution or degassed paraffin liquid (37°C). The ray of the argon laser is led into the inverted ray path of the microscope by means of a ray adaptation and adjusting device. The frequency of injuries is 1 per 2 min. The exposure time for a single laser shot is 1/30 or 1/15 sec. The number of injuries necessary to induce a defined thrombus is determined. All thrombi formed during the observation period with a minimum length of 13 µm or an area of at least 25 μm^2 are evaluated. All measuring procedures are photographed by a video system.

Standard compounds:

- acetylsalicylic acid (10 mg/kg, per os)
- pentoxifylline (10 mg/kg, per os)

For detailed description and evaluation of various agents and mechanisms see the following references: Arfors et al. (1968), Herrmann (1983), Seiffge and Kremer (1984 and 1986), Seiffge and Weithmann (1987), and Weichert et al. (1983).

EVALUATION

The number of laser shots required to produce a defined thrombus is determined. Mean values and SEM are calculated.

REFERENCES AND FURTHER READING

Arfors KE, Dhall DP, Engeset J et al (1968) Biolaser endothelial trauma as a means of quantifying platelet activity in vivo. Nature 218:887–888

Herrmann KS (1983) Platelet aggregation induced in the hamster cheek pouch by a photochemical process with excited fluorescein-isothiocyanate-dextran. Microvasc Res 26:238–249

Seiffge D, Kremer E (1984) Antithrombotic effects of pentoxifylline on laser-induced thrombi in rat mesenteric arteries. IRCS Med Sci 12:91–92

Seiffge D, Kremer E (1986) Influence of ADP, blood flow velocity, and vessel diameter on the laser-induced thrombus. Thromb Res 42:331–341

Seiffge D, Weithmann U (1987) Surprising effects of the sequential administration of pentoxifylline and low dose acetylsalicylic acid on thrombus formation. Thromb Res 46:371–383

Weichert W, Pauliks V, Breddin HK (1983) Laser-induced thrombi in rat mesenteric vessels and antithrombotic drugs. Haemostasis 13:61–71

B.4.7 Photochemical-Induced Thrombosis

PURPOSE AND RATIONALE

In 1977, Rosenblum and El-Sabban reported that ultraviolet light can produce platelet aggregation in cerebral microvessels of the mouse after intravascular administration of sodium fluorescein. They found that in contrast to heparin, both aspirin and indomethacin prolonged the time to first platelet aggregate. Herrmann (1983) provided a detailed study in which he showed that scavengers of singlet oxygen, not of hydroxyl radicals, inhibited platelet aggregation induced by the photochemical reaction. He postulated that by exciting the intravascularly administrated fluorescein, singlet oxygen damages endothelial cells, which subsequently leads to platelet adhesion and aggregation.

PROCEDURE

Studies are performed in mesenteric arteries of 15–30 µm diameter in anesthetized rats. After intravenous injection of fluorescein isothiocyanate-dextran 70 (FITC-dextran, Sigma, 10%, 0.3 ml), the FITC-dextran in arterioles is exposed to ultraviolet light (wavelength of excitation 490 nm, wavelength of emission 510 nm).

EVALUATION

Thrombus formation is quantitated by determining the time between onset of excitation and appearance of the first platelet aggregate adhering to the vessel wall.

CRITICAL ASSESSMENT OF THE METHOD

In contrast to other thrombosis induction methods, photochemically induced thrombosis can be easily used in smaller animals. Thrombi are composed primarily of platelets; however, the primary target of the photochemical insult is the endothelial cells by means of oxygen radical damage.

MODIFICATIONS OF THE METHOD

Matsuno et al. (1991) report a method to induce thrombosis in the rat femoral artery by means of a photochemical reaction after injection of a fluorescent dye (rose Bengal, 10 mg/kg i.v.) and transillumination with a filtered xenon lamp (wave length: 540 nm). Blood flow is monitored by a pulsed Doppler flow meter. Occlusion is achieved after approximately 5–6 min. Pretreatment with heparin dose-dependently prolongs the time required to interrupt the blood flow. The model also enables one to study thrombolytic mechanisms, which had been evaluated with t-PA. A comparative

data for hirudin in various models was carried out by Just et al. (1991).

REFERENCES AND FURTHER READING

Herrmann KS (1983) Platelet aggregation induced in the hamster cheek pouch by a photochemical process with excited fluorescein isothiocyanate-Dextran. Micovasc Res 26:238–249

Just M, Tripier D, Seiffge D (1991) Antithrombotic effects of recombinant hirudin in different animal models. Haemostasis 21(Suppl 1):80–87

Matsuno H, Uematsu T, Nagashima S, Nakashima M (1991) Photochemically induced thrombosis model in rat femoral artery and evaluation of effects of heparin and tissue-type plasminogen activator with use of this model. J Pharmacol Methods 25:303–317

Rosenblum WI, El-Sabban F (1977) Platelet aggregation in the cerebral microcirculation: effect of aspirin and other agents. Circ Res 40:320–328

B.4.8 Foreign-Surface-Induced Thrombosis

The presence of foreign materials in the circulation produces activation of the coagulation and the platelet system. Various prothrombotic surfaces have been used to develop experimental animal models. In contrast to many other thrombosis models, the thrombosis induced by foreign surfaces does not presuppose endothelial damage.

B.4.8.1 Wire Coil-Induced Thrombosis

PURPOSE AND RATIONALE

A classical method to produce thrombosis is based on the insertion of wire coils into the lumen of blood vessels. The model was first described by Stone and Lord (1951) in aorta of dogs and was further modified to be used in arterial coronary vessels of opened-chest dogs. The use in venous vessels was described by Kumada et al. (1980).

The formation of thrombotic material around the coil is reproducible and can be easily standardized to study pharmacological agents (Just and Schönafinger 1991, Mellott et al. 1993, Rübsamen and Hornberger 1996).

Venous thrombosis is produced in rats by insertion of a stainless steel wire coil into the inferior caval vein. Platelets as well as plasmatic coagulation are activated on the wire coil. Thrombus formation onto the wire is quantitated by measuring the protein content of the thrombotic material isolated. The kinetics of thrombus formation show an increase in weight and protein content within the first 30 min, followed by a steady state between thrombus formation and endogenous thrombolysis leading to a constant protein content of thrombi between 1 and up to 48 hours following implantation of the wire coil. Thrombosis incidence in untreated control animals in this model is 100%. The test is used to evaluate antithrombotic and thrombolytic properties of compounds in an *in vivo* model of venous thrombosis in rats.

PROCEDURE

Male Sprague-Dawley rats weighing 260–300 g receive the test compound or the vehicle (controls) by oral, intravenous or intraperitoneal administration. At the end of absorption (i.v. 1 min, i.p. 30 min, p.o. 60 min), the animals are anesthetized by intraperitoneal injection of 1.3 g/kg urethane. Through a midline incision the caudal caval vein is exposed and a stainless steel wire coil (a dental pate carrier, Zipperer size 40(st), Zdarsky Erler KG, München) is inserted into the lumen of the vein just below the left renal vein branching by gently twisting of the wire toward the iliac vein. The handle of the carrier is cut off so as to hold the back end of the wire at the vein wall. The incision is sutured and the animal is placed on its back on a heating pad (37°C). The wound is reopened after 2 hours; the wire coil is carefully removed together with the thrombus on it and rinsed with 0.9% saline. The thrombotic material is dissolved in 2 ml alkaline sodium carbonate solution (2% Na_2CO_3 in 0.1 N NaOH) in a boiling water bath for 3 min. The protein content is determined in 100 µl aliquots by the colorimetric method of Lowry. See figure below (Fig. 5).

Thrombolysis

In addition to the described preparation, for continuous infusion of a thrombolytic test solution a polyethylene catheter is inserted in the jugular vein. One and a half hours after implantation of the wire coil, the test compound or the vehicle (controls) is infused for up to 2.5 hours. The wire coil is then removed and the protein content of thrombi is determined (see above). Bernat et al. (1986) demonstrated the fibrinolytic activity of urokinase and streptokinase-human plasminogen complex in this model.

EVALUATION

Thrombosis incidence (= number of animals with thrombi in dosage groups as compared to vehicle controls) is assessed.

The mean protein content (mg) of the thrombotic material in dosage groups and vehicle controls is deter-

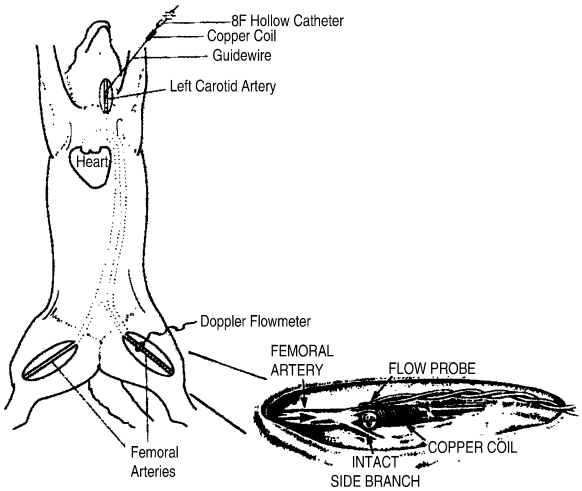

Figure 5 Schematic diagram of the canine femoral artery copper coil model of thrombolysis. A thrombogenic copper coil is advanced to either femoral artery via the left carotid artery. By virtue of the favorable anatomical angles of attachment, a hollow polyurethane catheter advanced down the left carotid artery nearly always enters the descending aorta, and with further advancement, into either femoral artery without fluoroscopic guidance. A flexible, Teflon-coated guidewire is then inserted through the hollow catheter and the latter is removed. A copper coil is then slipped over the guidewire and advanced to the femoral artery (see inset). Femoral artery flow velocity is measured directly and continuously with a Doppler flow probe placed just proximal to the thrombogenic coil and distal to a prominent sidebranch, which is left patent to dissipate any dead space between the coil and the next proximal sidebranch. Femoral artery blood flow declines progressively to total occlusion over the next 10–12 mm after coil insertion

mined. Percent change in protein content is calculated in dosage groups as compared to controls.

Statistical significance is assessed by means of the unpaired Student's *t*-test.

REFERENCES AND FURTHER READING

Bernat A, Vallee E, Maffrand JP (1986) A simple experimental model of thrombolysis in the rat: effect of urokinase and of the complex human plasminogen-streptokinase. Thromb Res 44(Suppl VI):112

Just M, Schönafinger K (1991) Antithrombotic properties of a novel sydnonimine derivative. J Cardiovasc Pharmacol 17 (Suppl 3):S121–S126

Kumada T, Ishihara M, Ogawa H, Abiko Y (1980) Experimental model of venous thrombosis in rats and effect of some agents. Thrombosis Res 18:189–203

Mellot MJ, Stranieri MT, Sitko GR et al (1993) Enhancement of recombinant tissue plasminogen activator-induced reperfusion by recombinant tick anticoagulant peptide, a selective factor X_a inhibitor, in a canine model of femoral artery thrombosis. Fibrinolysis 7:195–202

Rübsamen K, Hornberger W (1996) Prevention of early reocclusion after thrombolysis of copper-coil-induced thrombi in the canine coronary artery: comparison of PEG-hirudin and unfractionated heparin. Thromb Haemost 76:105–110

Stone P, Lord JW (1951) An experimental study of the thrombogenic properties of magnesium-aluminum wire in the dog's aorta. Surgery 30:987–993

B.4.8.2 Eversion Graft-Induced Thrombosis

PURPOSE AND RATIONALE

The eversion graft model for producing thrombosis in the rabbit artery was first described by Hergrueter et al. (1988) and later modified by Jang et al. (1989, 1990) and Gold et al. (1991). A 4- to 6-mm segment of the rabbit femoral or the dog left circumflex artery is excised, everted and then reimplanted into the vessel by end-to-end anastomoses. After restoration of the blood flow, a platelet-rich occlusive thrombus forms rapidly, leading to complete occlusion of the vessel. This model mimics a deep arterial injury since the adventitial surface is a non-endothelial tissue containing tissue factor and collagen. The rabbit model described here uses a carotid graft inserted into the femoral graft to avoid vasoconstriction often occurring in the inverted femoral segments.

PROCEDURE

In anaesthetized New Zealand White rabbits, the right carotid artery is exposed. After double ligation, a 3-mm segment of the artery is excised, everted and immersed in prewarmed (37°C) isotonic saline. Thereafter, the right femoral artery is exposed and occluded by means of a double-occluder (2-cm distance). The femoral artery is transected and the everted graft from the carotid artery is inserted by end-to-end anastomosis using 12 sutures with 9–0 nylon (Prolene, Ethicon, Norderstedt, Germany) under a surgical microscope (Wild M650, Leitz, Heerbrugg, Switzerland). Perfusion of the graft is measured by means of an ultrasonic flowmeter (Model T106, Transonic, Ithaca, NY, USA). The flow probe is positioned 2 cm distal from the graft. After a stabilization period of 15 min, the test substance is given intravenously through the catheterized right jugular vein. Ten minutes after substance administration, the vessel clamps are released and the blood flow is monitored by the flowmeter for 120 min.

Arterial blood is collected from the left carotid artery at baseline (immediately before substance administration), 10 min, 60 min and 120 min after substance administration.

EVALUATION

- Time until occlusion (time after restoring of vessel

blood flow until occlusion of the vessel, indicated by a flow less than 3.0 ml/min)
- Patency (time during which perfusion of graft is measured related to an observation period of 120 min after administration of test compounds).

Statistical Analysis

Time until occlusion and patency are expressed as median and the interquartile range/2 (IQR/2). Significant differences ($p < 0.05$) are calculated by the non-parametric Kruskal-Wallis test.

CRITICAL ASSESSMENT OF THE METHOD

The eversion graft is very thrombogenic, although technically difficult and time consuming. The deep occlusive thrombi can prevented only by intraarterially administered thrombolytics or aggressive antithrombotic treatments such as recombinant hirudin at high dosages, or PEG-hirudin. The adventitial surface is a non-endothelial tissue containing tissue factor and collagen. Thus, both the coagulation system and blood platelets are activated.

MODIFICATIONS OF THE METHOD

Gold et al. (1991) modified the model to be used in thoracotomized dogs in partial obstructed left circumflex coronary arteries. The combination of reduced blood flow due to the constrictor, along with an abnormal non-endothelial surface, produces total thrombotic occlusion within 5 min.

REFERENCES AND FURTHER READING

Gold HK, Yasuda T, Jang IK et al (1991) Animal models for arterial thrombolysis and prevention of reocclusion: erythrocyte-rich versus platelet-rich thrombus. Circulation 83:IV26–IV403

Hergrueter CA, Handren J, Kersh R, May JW (1988) Human recombinant tissue-type plasminogen activator and its effect on microvascular thrombosis in the rabbit. Plast Reconstr Surg 81:418–424

Jang IK, Gold HK, Ziskind AA et al (1989) Differential sensitivity of erythrocyte-rich and platelet-rich arterial thrombi to lysis with recombinant tissue-type plasminogen activator. Circulation 79:920–928

Jang IK, Gold HK, Ziskind AA et al (1990) Prevention of platelet-rich arterial thrombosis by selective thrombin inhibition. Circulation 81:219–225

B.4.8.3 Arteriovenous Shunt Thrombosis

PURPOSE AND RATIONALE

A method for the direct observation of extracorporal thrombus formation was introduced by Rowntree and Shionoya (1927) and extensively utilized by others (Rushkin et al. 2003; Tang et al. 2003). These first studies could provide evidence that anticoagulants like heparin and hirudin do inhibit thrombus development in arteriovenous shunts. Since today, the A-V-shunt thrombosis models have been often used to evaluate the antithrombotic potential of new compounds in different species including rabbits (Knabb et al. 1992), rats (Hara et al. 1995), pigs (Scott et al. 1994), dogs and cats (Best et al. 1938), and non-human primates (Yokoyama et al. 1995).

PROCEDURE

Rats are anaesthetized and fixed in supine position on a temperature-controlled heating plate to maintain body temperature. The left carotid artery and the right jugular vein are catheterized with short polyethylene catheters. The catheters are filled with isotonic saline solution and clamped. The two ends of the catheters are connected with a 2-cm glass capillary with an internal diameter of 1 mm. This glass capillary provides the thrombogenic surface. At a defined time after administration of the test compound, the clamps that are occluding the A-V-shunt are opened.

The measurement of the patency of the shunt is performed indirectly with a NiCrNi-thermocouple, which is fixed distal to the glass capillary. If blood is flowing, the temperature rises from room temperature to body temperature. In contrast, decreases of temperature indicate the formation of an occluding thrombus. The temperature is measured continuously over 30 min after opening of the shunt.

CRITICAL ASSESSMENT OF THE METHOD

It has been shown by Best et al. (1938) that the thrombi formed in the AV-shunt are to a greater part white arterial thrombi. This might be due to the high pressure and shear rate inside the shunts; in those cases, the thrombi tend to be more arterial in character (Chi et al. 1999).

REFERENCES AND FURTHER READING

Best CH, Cowan C, MacLean DL (1938) Heparin and the formation of white thrombi. J Physiol 92:20–31

Chi L, Rebello S, Lucchesi BR (1999) *In vivo* models of thrombosis. In: U'Prichard ACG and Gallagher KP (eds) Anti-thrombotics. Springer-Verlag, Berlin Heidelberg, pp 101–127

Hara T, Yokoyama A, Tanabe K et al (1995) DX-9065a, an orally active, specific inhibitor of factor X_a, inhibits thrombosis without affecting bleeding time in rats. Thromb Haemost 74:635–639

Knabb RM, Ketenner CA, Timmermanns PB, Reilly TM (1992) *In vivo* characterization of a new thrombin inhibitor. Thromb Haemost 67:56–59

Rowntree LG, Shionoya T (1927) Studies in extracorporeal thrombosis. I. A method for the direct observation of extracorporal thrombus formation. II. Thrombosis formation in normal blood in the extracorporeal vascular loop. III. Effects of certain anticoagulants (heparin and hirudin) on extracorporeal thrombosis and on the mechanism of thrombus formation. J Exp Med 46:7–26

Rukshin V, Azarbal B, Finkelstein A, Shah PK, Cercek B, Tsang V, Kaul S (2003) Effects of GP IIb/IIIa receptor inhibitor tirofiban (aggrastat) in ex vivo canine arteriovenous shunt model of stent thrombosis. J Cardiovasc Pharmacol 41(4):615–24

Scott NA, Nunes GL, King SB III et al (1994) Local delivery of an antithrombin inhibits platelet-dependent thrombosis. Circulation 90:1951–1955

Tang Z, Wang Y, Xiao Y, Zhao M, Peng S (2003) Antithrombotic activity of PDR, a newly synthesized L-Arg derivative, on three thrombosis models in rats. Thromb Res 110(2–3):127–33

Yokoyama T, Kelly AB, Marzec UM et al (1995) Antithrombotic effects of orally active synthetic antagonist of activated factor X in nonhuman primates. Circulation 92:485–491

B.4.8.4 Thread-Induced Venous Thrombosis

PURPOSE AND RATIONALE

Compared to the arterial system, it seems to be more difficult to develop a thrombosis model in venous blood vessels with respect to reproducibility and variability (Chi et al. 1999). Complete stasis together with a thrombogenic stimulus (Wessler-type) is used by numerous investigators to evaluate the effect of compounds on venous thrombosis. Hollenbach et al. (1994) developed a rabbit model of venous thrombosis by inducing cotton threads into the abdominal vena cava of rabbits. The cotton threads serve as a thrombogenic surface, and a thrombus forms around it, growing to a maximum mass after 2–3 hours. The prolonged non-occlusive character of thrombogenesis in this model focuses on progression of thrombus formation rather than initiation. Therefore, the conditions more closely resemble pathophysiology in humans because blood continues to flow throughout the experiment (Chi et al. 1999).

PROCEDURE

Rabbits weighing between 2.5 and 3.5 kg are anaesthetized with isofluorane inhalation anesthesia, and a polyethylene catheter is inserted into the left carotid artery. A polyethylene tube (PE 240, inner diameter 1.67 mm) of 14 cm length is filled with isotonic saline, and a copper wire with 5 fixed cotton threads (length 6 cm) is inserted into the tube (after determination of the net weight of the cotton threads). A laparotomy is performed and the vena cava and iliac vein are dissected free from surrounded tissue. The test agent is administered by a rabbit intragastric tube 60 min (depending on the *ex vivo* study) prior to initiation of thrombus formation. Blood samples will be measured at 60, 90, 120, 150 and 210 min after oral administration of the test compound.

Thrombus formation is induced by the inserting the thrombosis catheter into the caval vein via the iliac vein (7 cm). Then the copper wire is pushed forward 3 cm to liberate the cotton threads into the vessel lumen. One hundred fifty minutes after thrombus initiation, the caval segment containing the cotton threads and the developed thrombus will be removed, longitudinally opened and the content blotted on filter paper. After weighing the cotton thread with the thrombus, the net thread weight will be subtracted to determine the corrected thrombus weight.

EVALUATION

- Corrected thrombus weight after blotting the thrombus on filter paper and subtraction of the net weight of the cotton thread
- Mean arterial blood pressure
- APTT, HepTest, antiFIIa and antiFXa activity.

CRITICAL ASSESSMENT OF THE METHOD

The composition of the cotton-threaded thrombus shows a composition of fibrin together with tightly aggregated and distorted erythrocytes, thus being in accordance with human deep-vein thrombosis structure. Non-occlusive thrombus formation has been successfully inhibited by heparins, prothrombinase complex inhibitors and thrombin inhibitors (Hollenbach et al. 1994, 1995).

MODIFICATIONS OF THE METHOD

In addition to the originally described method, it is possible to measure blood flow by means of an ultrasonic flow probe, attached distally to the position of the cotton threads on the vein.

REFERENCES AND FURTHER READING

Chi L, Rebello S, Lucchesi BR (1999) *In vivo* models of thrombosis. In: Uprichard ACG and Gallagher KP (eds) Antithrombotics. Springer Berlin, Heidelberg, pp 101–127

Hollenbach S, Sinha U, Lin PH et al (1994) A comparative study of prothrombinase and thrombin inhibitors in a novel rabbit model of non-occlusive deep vein thrombosis. Thromb Haemostast 71:357–362

Hollenbach SJ, Wong AG, Ku P et al (1995) Efficacy of FXa inhibitors in a rabbit model of venous thrombosis. Circulation 92:I486–I487

B.4.8.5 Thrombus Formation on Superfused Tendon

PURPOSE AND RATIONALE

In all models that include vessel wall damage, blood gets in contact with adhesive proteins of the subendothelial matrix, i. e. von Willebrand factor, collagens, fibronectin, laminin and others. Gryglewski et al. (1978) described an *in vivo* method where blood of an unanesthetized animal is in contact *ex vivo* with a foreign surface consisting mainly of collagen. The foreign surface is produced out of the tendon of another animal species. After superfusion of the tendon, blood is recirculated to the unanesthetized animal. The method aims at the quantitation of the antiplatelet potency of drugs based on the formation of platelet thrombi onto the surface of the tendons or of aortic strips from atherosclerotic rabbits.

PROCEDURE

Blood was withdrawn from the carotid artery of anesthetized and heparinized cats by a roller pump at a speed of 6 ml/min. After a passage through a warmed jacket (37°C), blood was separated into 2 streams, each flowing at a speed of 3 ml/min superfusing in parallel 2 twin strips of the central part of longitudinally cut rabbit Achilles tendon (30 × 3 mm). The blood superfusing the strips dripped into collectors and by its gravity was returned to the venous system of the animals through the left jugular vein. The tissue strips were freely suspended in air and the upper end was tied to an auxotonic lever of a smooth muscle/heart Harvard transducer, while the lower end was loaded with a weight (1–2 g) to keep the lever with its counterweight in a neutral position. When superfused with blood, the strips were successively covered with clots changing the weight of the strips. The weight changes were continuously recorded. After a control period of 30 min, the formed thrombi were gently removed and fixed in formalin for histological examination. Then, the strips were superfused with Tyrode solution and the animals injected with the antithrombotic drug. After 10 min, blood superfusion was renewed for another 30 min.

EVALUATION

The ratio of an increase in weight of the strips after the drug treatment to the increase in weight before drug treatment was considered as an index of antiaggregatory activity.

REFERENCES AND FURTHER READING

Gryglewski RJ, Korbut R, Ocetkiewicz A, Stachura J (1978) *In vivo* method for quantitation of anti-platelet potency of drugs. Naunyn-Schmiedeberg's Arch Pharmacol 302:25–30

B.4.9 Stasis-Induced Thrombosis (Wessler Model)

PURPOSE AND RATIONALE

The "Wessler model" is a classical method of inducing venous thrombosis in animals. Wessler (1952, 1953, 1955a & b, 1957) and Wessler et al. (1959) combined local venous stasis with hypercoagulability produced by injection of human or dog serum into the systemic circulation of dogs or rabbits. The jugular vein of these animals is occluded by clamps 1 min after the injection of the procoagulatory stimulus into the circulation. Within a few minutes after clamping, a red clot is formed in the isolated venous segment. Fareed et al. (1985) summarized a variety of substances that can be used as pro-coagulatory stimuli. Aronson and Thomas (1985) found an inverse correlation between the duration of stasis and the amount of the hypercoagulating agents to produce the clot.

PROCEDURE

Anaesthetized rabbits are fixed in supine position on a temperature-controlled (37°C) heating table. Following cannulation of both carotid arteries (the left in cranial direction) and the right femoral vein, segments of 2 cm length of the two external jugular veins are exposed and isolated between two loose sutures. Then, 0.3 ml/kg calcium thromboplastin (SIGMA, Deisenhofen, Germany, FRG) is administered via the left carotid artery. Meticulous care is taken to maintain a standard injection time of 30 sec followed by injection of 0.5 ml physiological saline within 15 sec; 45 sec later, both jugular vein segments are occluded by distal and proximal sutures. Stasis is maintained for 30 min. Blood samples are taken immediately before occlusion and 30 sec before end of stasis. After excision, the occluded vessel segments are placed on a soaked sponge and opened by a longitudinal incision.

EVALUATION

The size of the clots is assessed using a score system: (0: blood only; 1: very small clot piece[s], filling out at most 1/4 of the vessel; 2: larger clot piece[s], filling out at most 1/2 of the vessel; 3: very large clot[s], filling out at most 3/4 of the vessel; 4: one large clot, filling out the whole vessel). The scores of the left and the right jugular vein are added, forming the thrombus size value of one animal. Additionally, the thrombus weight is measured after blotting the thrombus on filter paper.

Thrombus score is expressed as median (minimum–maximum). Thrombus weight is given as mean ± SEM. For the statistical evaluation of the antithrombotic effect, the nonparametric U-Test of Mann and Whitney (thrombus score) or Student's *t*-test for unpaired samples (thrombus weight) is used. Significance is expressed as $p < 0.05$.

CRITICAL ASSESSMENT OF THE METHOD

Breddin (1989) described the Wessler model because of its static character as the retransformation of an *in vitro* experiment into a very artificial test situation. One of the major drawbacks is the relative independence of platelet function and hemodynamic changes that largely influence thrombus formation *in vivo*. However, the model has been shown to be very useful for evaluation of the antithrombotic effect of compounds like heparin and hirudin.

MODIFICATIONS OF THE METHOD

There are a number of different procoagulant agents that had been used to induce thrombosis in this model, such as human serum, Russel viper venom, thromboplastin, thrombin, activated prothrombin complex concentrates and factor X_a (Aronson and Thomas 1985, Fareed et al. 1985). The sensitivity and accuracy of the model can be improved by injecting iodinated fibrinogen into the animals before injecting the thrombogenic agent and then measuring the specific radioactivity in the clot.

The general drawback of the Wessler model is the static nature of the venous thrombus development. To overcome this problem some investigators have developed more dynamic models with reperfusion of the occluded vessel segments after clot development. Depending on the time of test compound administration (pre- or post-thrombus initiation), the effect on thrombus growth and fibrinolysis can be evaluated. Levi et al. (1992) have used this model to assess the effects of a murine monoclonal anti-human PAI-1 antibody, and Biemond et al. (1996) compared the effect of thrombin-and factor X_a-inhibitors with a low molecular weight heparin.

Venous reperfusion model: New Zealand white rabbits weighing 2.5 kg are anesthetized with 0.1 ml atropine, 1.0 mg/kg diazepam, and 0.3 ml Hypnorm (Duphar, 10 mg/ml fluanisone and 0.2 ml fentanyl). Further anesthesia is maintained with 4 mg/kg i.v. thiopental. The carotid artery is cannulated after exposition through an incision in the neck. The jugular vein is dissected free from tissue, and small side branches are ligated over a distance of 2 cm. The vein is clamped proximally and distally to isolate the vein segment. Citrated rabbit blood (from another rabbit) is mixed with ^{131}I-radiolabeled fibrinogen (final radioactivity, approximately 25 mCi/ml). Then, 150 µl of this blood is aspirated in a 1-ml syringe containing 25 µl thrombin (3.75 IU) and 45 µl 0.25 mol $CaCl_2$, and 200 µl of the clotting blood is immediately injected into the isolated segment. The vessel clamps are removed 30 min after clot injection, and blood flow is restored. ^{125}I-radio-labeled fibrinogen (approximately 5 µCi) is injected through the cannula in the carotid artery, (in case of the fibrinolysis studies immediately followed by 0.5 mg/kg recombinant tissue-type plasminogen activator). For each dosage group, four thrombi are analyzed. The extent of thrombolysis is assessed by measurement of the remaining ^{131}I-fibrinogen in the clot and compared with the initial clot radioactivity. The comparison between blood and thrombus ^{125}I-radioactivity reveals the extent of thrombus growth (blood volume accreted to the blood). The thrombus lysis and extension are monitored 60 or 120 min after thrombus formation and are expressed as percentage of the initial thrombus volume. Statistics is performed as variance analysis and the Newman-Keuls test. Statistical significance is expressed at the level of $p < 0.05$.

REFERENCES AND FURTHER READING

Aronson DL, Thomas DP (1985) Experimental studies on venous thrombosis: effect of coagulants, procoagulants and vessel contusion. Thromb Haemost 54:866–870

Biemond BJ, Friederich PW, Levi M et al (1996) Comparison of sustained antithrombotic effects of inhibitors of thrombin and factor X_a in experimental thrombosis. Circulation 93:153–160

Breddin HK (1989) Thrombosis and Virchow's triad: what is established. Semin Thromb Haemost 15:237–239

Fareed J, Walenga JM, Kumar A, Rock A (1985) A modified stasis thrombosis model to study the antithrombotic action of heparin and its fractions. Semin Thromb Hemost 11:155–175

Levi M, Biemond BJ, VanZonneveld AJ et al (1992) Inhibition of plasminogen activator inhibitor-1 activity results in promotion of endogenous thrombolysis and inhibition of thrombus extension in models of experimental thrombosis. Circulation 85:305–312

Wessler S (1952) Studies in intravascular coagulation. I. Coagulation changes in isolated venous segments. J Clin Invest 31:1011–1014

Wessler S (1953) Studies in intravascular coagulation. II. A comparison of the effect of dicumarol and heparin on clot formation in isolated venous segments. J Clin Invest 32:650–654

Wessler S (1955a) Studies in intravascular coagulation. III. The pathogenesis of serum-induced venous thrombosis. J Clin Invest 34:647–651

Wessler S (1955b) Studies in intravascular coagulation. IV. The effect of dicumarol and heparin on serum-induced venous thrombosis. Circulation 12:553–556

Wessler S (1957) Studies in intravascular coagulation. V. A dis-

tinction between the anticoagulant and antithrombotic effects of dicumarol. N Engl J Med 256:1223–1225
Wessler S, Reimer SM, Sheps MC (1959) Biological assay of a thrombosis-inducing activity in human serum. J Appl Physiol 14:943–946

B.4.10 Disseminated Intravascular Coagulation (DIC) Model

PURPOSE AND RATIONALE

DIC is another model that is also used widely in rats and mice. It is a model of systemic thrombosis or disseminated intravascular coagulation (DIC), which is induced by tissue factor, endotoxin (lipopolysaccharide), or FXa (Herbert et al. 1996, Yamazaki et al. 1994, Sato et al. 1998). After systemic administration of the thrombogenic stimulus, this model can be performed with or without mechanical vena caval stasis. When stasis is used, the major parameter is the thrombus mass, but when stasis is not used, the readouts are fibrin degradation products, fibrinogen, platelet count, PT, and APTT, among others. As shown by the many and varied parameters, when used without stenosis, the post-experimental analysis can be time-consuming and technically demanding. Although rodents are useful as a primary efficacy model, limitations such as the ability to withdraw multiple blood samples over the course of the experiment and the difference in activity of at least some FXa inhibitors in human compared to rat plasma *in vitro* require that compounds be characterized further in more advanced *in vivo* models of thrombosis.

REFERENCES AND FURTHER READING

Herbert JM, Bernat A, Dol F et al (1996) DX 9065A, a novel, synthetic selective and orally active inhibitor of factor Xa: in vitro and in vivo studies. J Pharmacol Exp Therapeutics 276:1030–1038
Sato K, Kawasaki T, Hisamichi N et al (1998) Antithrombotic effects of YM-60828, a newly synthesized factor Xa inhibitor, in rat thrombosis models and its effects on bleeding time. Br J Pharmacol 123:92–96
Yamazaki M, Asakura H, Aoshima K et al (1994) Effects of DX-9065a, an orally active, newly synthesized and specific inhibitor of factor Xa, against experimental disseminated intravascular coagulation in rats. Thromb Haemostasis 72:393–396

B.4.11 Microvascular Thrombosis in Trauma Models

PURPOSE AND RATIONALE

Successful replantation of amputated extremities is dependent in large degree on maintaining the microcirculation. A number of models have been developed in which blood vessels are subjected to crush injury with or without vascular avulsion and subsequent anastomosis (Fu et al. 1997, Korompilias et al. 1997, Stockmans et al. 1997). In the model of Stockmans (1997), both femoral veins are dissected from the surrounding tissue. A trauma clamp, which has been adjusted to produce a pressure of 1,500 g/mm^2, is positioned parallel to the long axis of the vein. The anterior wall of the vessel is grasped between the walls of the trauma clamp and the two endothelial surfaces are rubbed together for a period of 30 sec as the clamp is rotated. Formation and dissolution of platelet-rich mural thrombi are monitored over a period of 35 min by transillumination of the vessel. By using both femoral veins, the effect of drug therapy can be compared to control in the same animal, minimizing intra-animal variations.

The models of Korompilias et al. (1997) and Fu et al. (1997) examine the formation of arterial thrombosis in rats and rabbits, respectively. In these models, either the rat femoral artery or the rabbit central ear artery is subjected to a standardized crush injury. The vessels are subsequently divided at the midpoint of the crushed area and then anastomosed. Vessel patency is evaluated by milking the vessel at various time points post-anastomosis. These models have been used to demonstrate the effectiveness of topical administration of LMWH in preventing thrombotic occlusion of the vessels. Such models, while effectively mimicking the clinical situation, are limited by the necessity of a high degree of surgical skill to effectively anastomose the crushed arteries.

REFERENCES AND FURTHER READING

Fu K, Izquierdo R, Vandevender D, Warpeha RL, Wolf H, Fareed J (1997) Topical application of low molecular weight heparin in a rabbit traumatic anastomosis model. Thromb Res 86(5):355–61
Korompilias AV, Chen LE, Seaber AV, Urbaniak JR (1997) Antithrombotic potencies of enoxaparin in microvascular surgery: influence of dose and administration methods on patency rate of crushed arterial anastomoses. J Hand Surg [Am]. 22(3):540–6
Stockmans F, Stassen JM, Vermylen J, Hoylaerts MF, Nystrom A (1997) A technique to investigate microvascular mural thrombus formation in arteries and veins: II. Effects of aspirin, heparin, r-hirudin, and G-4120. Ann Plast Surg. 38(1):63–8

B.4.12 Cardiopulmonary Bypass Models

PURPOSE AND RATIONALE

Cardiopulmonary bypass (CPB) models have been described in baboons (Van Wyk et al. 1998), swine (De-

wanjee et al. 1996) and dogs (Henny et al. 1985). In each model, the variables that can affect the hemostatic system—such as anesthesia, shear stresses caused by the CPB pumps and the exposure of plasma components and blood cells to foreign surfaces (catheters, oxygenators, etc)—are comparable to that observed with human patients. With these models, it is possible to examine the potential usefulness of novel anticoagulants in preventing thrombosis under relatively harsh conditions where both coagulation and platelet function are altered. The effectiveness of direct thrombin inhibitors (Van Wyk et al. 1998), LMWHs (Murray 1985) and heparinoids (Henny et al. 1985) has been compared to standard heparin. Endpoints have included the measurement of plasmatic anticoagulant levels, the histological determination of microthrombi deposition in various organs, the formation of blood clots in the components of the extracorporeal circuit and the deposition of radiolabeled platelets in various organs and on the components of the extracorporeal circuit. These models, therefore, can be used to assess the antithrombotic potential of new agents for use in CPB surgery and also to assess the biocompatability of components used to maintain extracorporeal circulation. For detailed protocols and evaluations see Callas et al. (1995), Carrie et al. (1994), Fu et al. (1997), Korompilias et al. (1997), Meuleman et al. (1991), Millet et al. (1994), Stockmans et al. (1997), Vlasuk et al. (1991), Walenga et al. (1987), and Wessler et al. (1959).

REFERENCES AND FURTHER READING

Callas DD, Bacher P, Fareed J (1995) Studies on the thrombogenic effects of recombinant tissue factor: in vivo versus ex vivo findings. Semin Thromb Hemost 21(2):166–176

Carrie D, Caranobe C, Saivin S et al (1994) Pharmacokinetic and antithrombotic properties of two pentasaccharides with high affinity to antithrombin III in the rabbit: comparison with CY 216. Blood 84(8):2571–2577

Dewanjee MK, Wu S, Kapadvanjwala M et al (1996) Reduction of platelet thrombi and emboli by L-arginine infusion during cardiopulmonary bypass in a pig model. J Thromb Thrombolysis 3:339–356

Fu K, Izquierdo R, Vandevender D et al (1997) Topical application of low molecular weight heparin in a rabbit traumatic anastomosis model. Thromb Res 86(5):355–361

Henny ChP, TenCate H, TenCate JW (1985) A randomized blind study comparing standard heparin and a new low molecular weight heparinoid in cardiopulmonary bypass surgery in dogs. J Clin Lab Med 106:187–196

Korompilias AV, Chen LE, Seaber AV, Urbaniak JR (1997) Antithrombotic potencies of enoxaparin in microvascular surgery: influence of dose and administration methods on patency rate or crushed arterial anastomoses. J Hand Surg 22(3):540–546

Meuleman DG, Hobbelen PM, Van Dinther TG et al (1991) Antifactor Xa activity and antithrombotic activity in rats of structural analogues of the minimum antithrombin III binding sequence: discovery of compounds with a longer duration of action than the natural pentasaccharide. Semin Thromb Hemost 17(Suppl 1):112–117

Millet J, Theveniaux J, Brown NL (1994) The venous antithrombotic profile of naroparcil in the rabbit. Thromb Haemost 72(6):874–879

Murray WG (1985) A preliminary study of low molecular weight heparin in aortocoronary bypass surgery. In: Murray WG (ed) Low molecular weight heparin in surgical practice [Master of surgery thesis]. London: University of London, p 266

Stockmans F, Stassen JM, Vermylen J et al (1997) A technique to investigate mural thrombus formation in arteries and veins: II. Effects of aspirin, heparin, r-hirudin and G-4120. Ann Plastic Surg 38(1):63–68

Van Wyk V, Neethling WML, Badenhorst PN, Kotze HF (1998) r-Hirudin inhibits platelet-dependent thrombosis during cardiopulmonary bypass in baboons. J Cardiovasc Surg 39:633–639

Vlasuk GP, Ramjit D, Fujita T et al (1991) Comparison of the in vivo anticoagulant properties of standard heparin and the highly selective factor Xa inhibitors antistasin and tick anticoagulant peptide (TAP) in a rabbit model of venous thrombosis. Thromb Haemost 65(3):257–262

Walenga JM, Petitou M, Lormeau JC et al (1987) Antithrombotic activity of a synthetic heparin pentasaccharide in a rabbit stasis thrombosis model using different thrombogenic challenges. Thromb Res 46(2):187–198

Wessler S, Reimer SM, Sheps MC (1959) Biologic assay of a thrombosis-inducing activity in human serum. J Appl Physiol 14:943–946

B.4.13 Extracorporeal Thrombosis Models

PURPOSE AND RATIONALE

These models employ passing blood over a section of damaged vessel (or other selected substrates) and recording the thrombus accumulation on the damaged vessel histologically or by scintigraphic detection of radiolabeled platelets or fibrin (Badimon and Badimon 1989). This model is interesting because the results can be directly compared to the *in vivo* deep arterial injury model (Wysokinski et al. 1996) results and to results from a similar extracorporeal model used in humans (Dangas et al. 1998; Ørvim et al. 1995). Dangas et al. (1998) used this model to characterize the antithrombotic efficacy of abciximab, a monoclonal antibody-based platelet glycoprotein IIb/IIIa inhibitor, after administration to patients undergoing percutaneous coronary intervention. They demonstrated that abciximab reduces both the platelet and fibrin components of the thrombus, thereby providing further insight into the unique long-term effectiveness of short-term administration of this drug. Ørvim et al. (1995) also used this model in humans to evaluate the antithrombotic efficacy of rTAP, but instead of evaluating the compound after administration of rTAP to the

patient, the drug was mixed with the blood immediately as it flowed into the extracorporeal circuit prior to flowing over the thrombogenic surface. By changing the thrombogenic surface, they were able to determine that rTAP was more effective at inhibiting thrombus formation on a tissue-factor coated surface compared to a collagen-coated surface. These results suggest that optimal antithrombotic efficacy requires an antiplatelet approach along with an anticoagulant. Although this model does not completely represent pathological intravascular thrombus formation, the use of this "human model" of thrombosis may be very useful in developing new drugs because it directly evaluates the *ex vivo* antithrombotic effect of a drug in flowing human blood.

REFERENCES AND FURTHER READING

Badimon L, Badimon JJ (1989) Mechanism of arterial thrombosis in non-parallel streamlines: platelet thrombi grow on the apex of stenotic severely injured vessel wall. J Clin Invest 84:1134–1144

Dangas G, Badimon JJ, Coller BS et al (1998) Administration of abciximab during percutaneous coronary intervention reduces both ex vivo platelet thrombus formation and fibrin deposition. Arterioscler Thromb Vasc Biol 18:1342–1349

Ørvim U, Brastad RM, Vlasuk GP, Sakariassen KS (1995) Effect of selective factor Xa inhibition on arterial thrombus formation triggered by tissue factor/factor VIIa or collagen in an ex vivo model of shear-dependent human thrombogenesis. Arterioscler Thromb Vasc Biol 15:2188–2194

Wysokinski W, McBane R, Chesebro JH, Owen WG (1996) Reversibility of platelet thrombosis in vivo. Thromb Haemost 76:1108–1113

B.4.14 Experimental Thrombocytopenia or Leucocytopenia

PURPOSE AND RATIONALE

Intravenous administration of collagen, arachidonic acid, ADP, platelet activating factor (PAF) or thrombin activates thrombocytes leading to a maximal thrombocytopenia within a few minutes. The effect is reinforced by additional injections of epinephrine. Activation of platelets leads to intravasal aggregation and temporary sequestration of aggregates in the lungs and other organs. Depending on the dose of agonist, this experimentally induced reduction of the number of circulating platelets is reversible within 60 min after induction. Following administration of PAF, a leucocytopenia is induced in addition. The assay is used to test the inhibitory capacity of drugs against thrombocytopenia or leucocytopenia as a consequence of *in vivo* platelet or leukocyte stimulation.

PROCEDURE

Male guinea pigs (Pirbright White) weighing 300–600 g, or male NMRI mice (25–36 g), or Chinchilla rabbits of either sex weighing 2–3 kg are used. Animals receive the test compound or the vehicle (controls) by oral, intraperitoneal or intravenous administration. After the end of the absorption time (p.o. 60 min, i.p. 30 min, i.v. variable), the marginal vein of the ear of rabbits is cannulated and the thrombocytopenia-inducing substances collagen or arachidonic acid are injected slowly. Blood is collected from the ear artery.

Guinea pigs, hamsters, or mice are anesthetized with pentobarbital sodium (i.p.) and Rompun (i.m.) and placed on an electrically warmed table at 37°C. The carotid artery is cannulated for blood withdrawal and the jugular vein is cannulated to administer the thrombocytopenia-inducing substances collagen+adrenaline (injection of the mixture of both within 10 sec) or PAF or thrombin. In mice, collagen + adrenaline are injected into a tail vein.

Approximately 50–100 µl blood is collected into potassium-EDTA-coated tubes at times –1, 1 and 2 min (guinea pigs and mice) or 5, 10 and 15 min (rabbits) following the injection of the inducer. The number of platelets and leukocytes is determined within 1 hour after withdrawal in 10 µl samples of whole blood using a microcellcounter suitable for blood of various animal species.

EVALUATION

The percentage of thrombocytes (or leukocytes) is determined in vehicle control and dosage groups at the different times following injection of the inducer relative to the initial value of control or dosage group, respectively. Calculated percent values of controls are taken as 100%.

Percent inhibition of thrombocytopenia (or leucocytopenia) is calculated in dosage groups relative to controls.

Statistical significance is evaluated by means of the unpaired Student's *t*-test.

CRITICAL ASSESSMENT OF THE METHOD

The method of collagen+epinephrine-induced thrombocytopenia is presently widely used to study the phenotype of mice knocked out for a specific gene with suspected role in hemostasis/thrombosis. A recent example is the *Gas* 6 –/– mouse (Angelillo-Scherrer et al. 2001) and mice lacking the gene for the G protein G(z) (Yang et al. 2000). The advantage of the method for this purpose is the simple experimental procedure

and the small volume of blood necessary. In general, application of the method in small animals (mice, hamsters) needs only small amounts of drug substance. The model is a useful first step of *in vivo* antithrombotic efficacy of antiplatelet drugs.

REFERENCES AND FURTHER READING

Angelillo-Scherrer A, deFrutos PG, Aparicio C et al (2001) Deficiency or inhibition of Gas6 causes platelet dysfunction and protects mice against thrombosis. Nature Med 7:215–221

Yang J, Wu J, Kowalska MA et al (2000) Loss of signaling through the G protein, Gz, results in abnormal platelet activation and altered responses to psychoactive drugs. Proc Natl Acad Sci USA 97:9984–9989

B.4.15 Collagenase-Induced Thrombocytopenia

PURPOSE AND RATIONALE

Intravenous administration of the proteolytic enzyme collagenase leads to formation of endothelial gaps and to exposure of deeper layers of the vessel wall. This vascular endothelial injury is mainly involved in triggering thrombus formation by activation of platelets through contact with the basal lamina. As a consequence, thrombocytopenia is induced, which is maximal within 5–10 min following collagenase injection and reversible within 30 min after induction. The model is used to test the inhibitory capacity of compounds against thrombocytopenia in a model of collagenase-induced thrombocytopenia in rats as an alternative to the model described before.

PROCEDURE

Male Sprague-Dawley rats weighing 260–300 g are used. The animals receive the test compound or the vehicle (controls) by oral, intraperitoneal or intravenous administration. After the end of the absorption time (i.p. 30 min, p.o. 60 min, i.v. variable), rats are anesthetized with pentobarbital sodium (i.p.). One carotid artery is cannulated for blood withdrawal and one jugular vein is cannulated for inducer injection. The animals receive an intravenous injection of heparin and 20 min later, approximately 100 µl blood is collected (initial value). Ten minutes later, the thrombocytopenia-inducing substance collagenase is administered intravenously.

At times 5, 10, 20 and 30 min following the injection of collagenase, samples of approximately 100 µl blood are collected into potassium-EDTA-coated tubes. The number of platelets is determined in 10 µl samples of whole blood within 1 hour after blood withdrawal, using a microcellcounter. See Völkl and Dierichs (1986) for details.

EVALUATION

The percentage of platelets is determined in vehicle control and dosage groups at the different times following injection of collagenase relative to the initial value of control or dosage group, respectively. Calculated percent values of controls are set at 100%.

Percent inhibition of thrombocytopenia is calculated in dosage groups relative to controls.

Statistical significance is evaluated by means of the unpaired Student's *t*-test.

REFERENCES AND FURTHER READING

Völkl K-P, Dierichs R (1986) Effect of intravenously injected collagenase on the concentration of circulating platelets in rats. Thromb Res 42:11–20

B.4.16 Reversible Intravital Aggregation of Platelets

PURPOSE AND RATIONALE

Isotopic labeling of platelets can be employed to monitor platelet aggregation and desegregation *in vivo*. Adenosine diphosphate (ADP), platelet activating factor (PAF), arachidonic acid, thrombin and collagen are known to induce platelet aggregation. In the following procedure, labelled platelets are continuously monitored in the thoracic (A) and abdominal (B) region of test animals. Administration of aggregation promoting agents produces an increase in counts in A and a fall in counts in B. This observation implies that platelets are being aggregated within the vascular system and accumulate in the pulmonary microvasculature. The *in vivo* method can be used to evaluate platelet antiaggregatory properties of test compounds.

PROCEDURE

Preparation of Labeled Platelets

Blood is obtained from rats by cardiopuncture. After centrifugation at 240 *g* for 10 min, the platelet-rich plasma (PRP) is transferred into a tube and suspended in calcium-free Tyrode solution containing 250 ng/ml PGE_1. The suspension is centrifuged at 640 *g* for 10 min. The supernatant is discarded and the sediment is suspended by gentle shaking with calcium-free Tyrode solution containing 250 ng/ml PGE_1. ^{51}Cr is added to 1 ml of the platelet suspension. Following a 20-min incubation period at 37°C, the suspension is again centrifuged at 640 *g* for 10 min. The supernatant

is removed, and the labeled platelets are finally resuspended in 1 ml calcium-free Tyrode solution containing 250 ng/ml PGE_1.

In Vivo Experiment

Male Sprague-Dawley or stroke-prone spontaneously hypertensive rats weighing 150–300 g are used. The animals are anaesthetized with pentobarbital sodium (30 mg/kg, i.p.). Following tracheotomy, the vena femoralis is exposed and cannulated. The labeled platelets are administered via the cannula. The circulating platelets are monitored continuously in the thoracic (A) and abdominal (B) region. The counts are collected using a dual-channel gamma spectrometer (Nuclear Enterprise 4681) incorporating a microcomputer (AM 9080A). One hour after administration of labeled platelets (when counts in A and B have stabilized), the aggregation-promoting agent (ADP, PAF, arachidonic acid, thrombin or collagen) is administered twice by intravenous injection. One hour is allowed to elapse between each i.v. injection.

The test compound is administered 2 hours after platelet injection concurrently with the fourth administration of the aggregating agent. Thirty minutes (ADP, PAF, arachidonic acid, thrombin), or 1 hour (collagen) after compound administration another control injection of the aggregating agent is given. This injection is either used as an additional control or it may reveal long-term efficacy of a test compound.

EVALUATION

The microcomputer continuously reveals information about aggregation and desegregation of labeled platelets.

The following parameters are recorded:
A = counts over thorax
B = counts over abdomen
Difference: *A*–*B*
ratio: *A/B*.

The time course of response is shown in a curve. The area under the curve is calculated by a computer program.

Statistical significance is calculated using the Student's *t*-test.

MODIFICATION OF THE METHOD

Oyekan and Botting (1986) described a method for monitoring platelet aggregation *in vivo* in rats, using platelets labeled with indium^{3+} oxine and recording the increase in radioactivity count in the lung after injection of adenosine diphosphate or collagen.

Smith et al. (1989) monitored continuously the intrathoracic content of intravenously injected ^{111}indium-labeled platelets in anesthetized guinea pigs using a microcomputer-based system.

REFERENCES AND FURTHER READING

Oyekan AO, Botting JH (1986) A minimally invasive technique for the study of intravascular platelet aggregation in anesthetized rats. J Pharmacol Meth 15:271–277

Smith D, Sanjar S, Herd C, Morley J (1989) *In vivo* method for the assessment of platelet accumulation. J Pharmacol Meth 21:45–59

B.5 Bleeding Models

B.5.1 Subaqueous Tail Bleeding Time in Rodents

PURPOSE AND RATIONALE

The damage of a blood vessel results in the formation of a hemostatic plug, which is achieved by several different mechanisms including vascular spasm, formation of a platelet plug, blood coagulation, and growth of fibrous tissue into the blood clot.

A diagnostic parameter for specific defects of the hemostatic system and for the influence of drugs affecting hemostasis is the length of time that it takes for bleeding to stop from a standard incision, the so-called bleeding time.

Bleeding-time measurements in animals are used to evaluate the hemorrhagic properties of antithrombotic drugs. The transection of the tail of a rodent was first established by Döttl and Ripke (1936) and is commonly used in experimental pharmacology.

PROCEDURE

Anaesthetized rats are fixed in supine position on a temperature-controlled (37°C) heating table. Following catheterization of a carotid artery (for measurement of blood pressure) and a jugular vein, the test compound is administered. After a defined latency period, the tail of the rat is transected with a razor-blade mounted on a self-constructed device at a distance of 4 mm from the tip of the tail. Immediately after transection, the tail is immersed into a bath filled with isotonic saline solution (37°C).

EVALUATION

The time until bleeding stops is determined within a maximum observation time of 600 sec.

CRITICAL ASSESSMENT OF THE METHOD

There are numerous variables that can influence rodent's bleeding time measurements, as discussed by Dejana et al. (1979): position of the tail (horizontal or vertical), the environment (air or saline), temperature, anesthesia, or procedure of injury (Simplate method, transsection). All these variables are responsible for the different results reported in literature on compounds like aspirin and heparin under different assay condition (Stella et al. 1975; Minsker and Kling 1977).

Furthermore, it is impossible to transect exactly one blood vessel, because the transected tail region consists of a few major arteries and veins with mutual interaction between one another.

REFERENCES AND FURTHER READING

Dejana E, Callioni A, Quintana A, DeGaetano G (1979) Bleeding time in laboratory animals: II – a comparison of different assay conditions in rats. Thromb Res 15:191–197

Döttl K, Ripke O (1936) Blutgerinnung und Blutungszeit. In: Medizin und Chemie, Leverkusen (Germany), Bayer, pp 267–273

Minsker DH, Kling PJ (1977) Bleeding time is prolonged by aspirin. Thromb Res 10:619–622

Stella L, Donati MB, Gaetano G (1975) Bleeding time in laboratory animals. I. Aspirin does not prolong bleeding time in rats. Thromb Res 7:709–716

B.5.2 Arterial Bleeding Time in Mesentery

PURPOSE AND RATIONALE

Arterial bleeding is induced by micropuncture of small arteries in the area supplied by the mesenteric artery. Bleeding is arrested in living blood vessels by the formation of a hemostatic plug due to the aggregation of platelets and to fibrin formation. In this test, compounds are evaluated that inhibit thrombus formation, thus prolonging arterial bleeding time. The test is used to detect agents which interfere with primary hemostasis in small arteries.

PROCEDURE

Male Sprague-Dawley rats weighing 180–240 g receive the test compound or the vehicle (controls) by oral, intraperitoneal or intravenous administration. After the end of the absorption time (i.p. 30 min, p.o. 60 min, i.v. variable), the animals are anesthetized by intraperitoneal injection of 60 mg/kg pentobarbital sodium. Rats are placed on an electrically warmed table at 37°C.

The abdomen is opened by a mid-line incision and the mesentery is lifted to display the mesenteric arteries. The mesentery is draped over a plastic plate and superfused continuously with Tyrode's solution maintained at 37°C. Bleeding times are determined with small mesenteric arteries (125–250 µm external diameter) at the junction of mesentery with intestines. Adipose tissue surrounding the vessels is carefully cut with a surgical blade.

Arteries are punctured with a hypodermic needle (25 gauge: 16 × 5/10 mm). The bleeding time of the mesenteric blood vessels is observed through a microscope at a magnification of 40×. The time in seconds is determined from the puncturing until the bleeding is arrested by a hemostatic plug.

EVALUATION

1. Mean values of bleeding times are determined for each dosage group (4–6 animals, 4–6 punctures each) and compared to the controls.
2. The significance of the results is assessed with the unpaired Student's *t*-test.
3. The percent prolongation of bleeding time in dosage groups relative to the vehicle controls is calculated.

For further details on methods and evaluations of various mechanisms or agents see the following: Butler et al. (1982), Dejana et al. (1979), and Zawilska et al. (1982).

REFERENCES AND FURTHER READING

Butler KD, Maguire ED, Smith JR et al (1982) Prolongation of rat tail bleeding time caused by oral doses of a thromboxane synthetase inhibitor which have little effect on platelet aggregation. Thromb Haemostasis 47:46–49

Dejana E, Callioni A, Quintana A, de Gaetano G (1979) Bleeding time in laboratory animals. II – A comparison of different assay conditions in rats. Thromb Res 15:191–197

Zawilska KM, Born GVR, Begent NA (1982) Effect of ADP-utilizing enzymes on the arterial bleeding time in rats and rabbits. Br J Haematol 50:317–325

B.5.3 Template Bleeding Time Method

PURPOSE AND RATIONALE

The template bleeding time method is used to produce a standardized linear incision into the skin of humans to detect abnormalities of primary hemostasis due to deficiencies in the platelet or coagulation system. The method has been modified with the development of a spring-loaded cassette with two disposable blades (Simplate II, Organon Teknika, Durham, NC). These template devices ensure reproducibility of length and depth of dermal incisions. Forsythe and Willis (1989) described a method that enables the Simplate tech-

nique to be used as a method to analyze the bleeding time in the oral mucosa of dogs.

PROCEDURE

The dog is positioned in sternal or lateral recumbency. A strip of gauze is tied around both the mandible and maxilla as a muzzle. The template device is placed evenly against the buccal mucosa, parallel to the lip margin, and triggered. Simultaneously, a stopwatch is started. Blood flow from the incision is blotted using circular filter paper (Whatman No. 1, Fisher Scientific Co, Clifton, NJ) held directly below, but not touching the wounds. The position of the filter paper is changed every 15 sec. The end point for each bleeding is determined when the filter paper no longer develops a red crescent.

EVALUATION

The time from triggering the device until blood no longer appears on the paper is recorded as the bleeding time. The normal range lies between 2 to 4 min.

CRITICAL ASSESSMENT OF THE METHOD

The template bleeding time varies considerably between laboratories as well as between species and strains. Therefore, it is important to perform the incisions and the blotting in an identical fashion. Prolonged bleeding times in dogs have been recognized with thrombocytopenia, von Willebrand's disease, uremia, treatment with aspirin, anticoagulants, and dextran (Forsythe and Willis 1989, Klement et al. 1998). Brassard and Meyers (1991) describe the buccal mucosa bleeding time as a test that is sensitive to platelet adhesion and aggregation deficits. Generally, results of antithrombotic drugs in bleeding time models in animals do not exactly predict bleeding risks in clinical situations. But the models allow comparison between drugs with different actions (Dejana et al. 1979, Lind 1991).

MODIFICATIONS OF THE METHOD

The Simplate device can also be used to perform incisions at the shaved inner ear of rabbits, taking care to avoid major vessels. The normal range of bleeding time in anaesthetized rabbits is approximately 100 sec.

Klement et al. (1998) described another ear bleeding model in anaesthetized rabbits. The shaved ear was immersed in a beaker containing saline at 37°C. Five full-thickness cuts were made with a no. 11 Bard-Parker scalpel blade, avoiding major vessels, and the ear was immediately re-immersed in saline. At different times thereafter (5 to 30 min) aliquots of the saline solution were removed, red cells were sedimented and lysed, and cyanohemoglobin was determined as a measure of blood loss. In this study, hirudin produced more bleeding than standard heparin.

A cuticle bleeding time (toenail bleeding time) measurement in dogs has been described by Giles et al. (1982). A guillotine-type toenail clipper is used to sever the apex of the nail cuticle. A clean transection of the nail is made just into the quick, to produce a free flow of blood. The nail is left to bleed freely. The time until bleeding stops is recorded as the bleeding time. Several nails can be cut at one time to ensure appropriate technique. The normal range lies between 2 to 8 min.

Kubitza et al. (2005) and others extended the use of the model in humans.

REFERENCES AND FURTHER READING

Brassard JA, Meyers KM (1991) Evaluation of the buccal bleeding time and platelet glass bead retention as assays of hemostasis in the dog: the effects of acetylsalicylic acid, warfarin and von Willebrand factor deficiency. Thromb Haemost 65:191–195

Dejana E, Calloni A, Quintana A, deGaetano G (1979) Bleeding time in laboratory animals. II. A comparison of different assay conditions in rats. Thromb Res 15:191–197

Forsythe LT, Willis SE (1989) Evaluating oral mucosa bleeding times in healthy dogs using a spring loaded device. Can Vet J 30:344–345

Giles AR, Tinlin S, Greenwood R (1982) A canine model of hemophilic (factor VIII:C deficiency) bleeding. Blood 60:727–730

Klement P, Liao P, Hirsh J et al (1998) Hirudin causes more bleeding than heparin in a rabbit ear bleeding model. J Lab Clin Med 132:181–185

Kubitza D, Becka M, Wensing G, Voith B, Zuehlsdorf M (2005) Safety, pharmacodynamics, and pharmacokinetics of BAY 59–7939–an oral, direct Factor Xa inhibitor–after multiple dosing in healthy male subjects. Eur J Clin Pharmacol 61(12):873–80

Lind SE (1991) The bleeding time does not predict surgical bleeding. Blood 77:2547–2552

B.6 Genetic Models of Hemostasis and Thrombosis

PURPOSE AND RATIONALE

Recent advances in genetic molecular biology have provided tools allowing scientists to design genetically altered animals that are deficient in certain proteins involved in thrombosis and hemostasis (so-called "knock-outs", or "nulls") (Carmeliet and Collen 1999, Pearson and Ginsburg 1999). These animals have been extremely useful for identifying and validating novel targets for therapeutic intervention. That is, by examin-

ing the phenotype (e.g, spontaneous bleeding, platelet defect, prolonged bleeding after surgical incision, etc.) of a specific knock-out strain, scientists can identify the role of the knocked-out protein. Then if the phenotype is favorable (e.g, not lethal), pharmacological agents can be designed to mimic the knock-out. More recently, novel gene medicine approaches have also benefited greatly from the availability of these models, as discussed below. The following section briefly summarizes some of the major findings in thrombosis and hemostasis using genetically altered mice and concludes with an example of how these models have been used in the drug discovery process.

The majority of these gene knock-outs result in mice that develop normally, are born in the expected Mendelian ratios, and are viable (as defined by the ability to survive to adulthood). Although seemingly normal, these knock-out mice display alterations in hemostatic regulation, especially when challenged. Deletion of FVIII, FIX, vWF, and the β_3-integrin (Bi et al. 1996, Denis et al. 1998, Hodivala-Dilke et al. 1999, Wang et al. 1997) all result in mice that bleed upon surgical challenge, and despite some minor differences in bleeding susceptibility, these mouse knock-out models mirror the human disease states quite well (hemophilia A, hemophilia B, von Willebrand disease, and Glanzmann's thrombasthenia, respectively). In addition, deletion of some hemostatic factors results in fragile mice with severe deficiencies in their ability to regulate blood loss. Prenatally, these mice appear to develop normally, but they are unable to survive the perinatal period due to severe hemorrhage, in most cases due to the trauma of birth.

Genetic knock-outs have also been useful in dissecting the role of individual signaling proteins in platelet activation. Deletion of the β_3-integrin (Hodivala-Dilke et al. 1999) or of $G_{\alpha q}$ (Offermanns et al. 1997) results in dramatic impairment of agonist-induced platelet aggregation. Alteration of the protein-coding region in the β_3-integrin carboxy-tail, β_3-DiY, at sites that are thought to be phosphorylated upon platelet activation, also results in unstable platelet aggregation (Law et al. 1999). Deletion of various receptors such as thromboxane A_2, P-selectin, P2Y1, and PAR-3 demonstrate diminished responses to some agonists while other platelet responses are intact (Thomas et al. 1998, Subramaniam et al. 1996, Leon et al. 1999, Kahn et al. 1998). Deletion of PAR-3, another thrombin receptor in mice, has little effect on hemostasis. This indicated the presence of yet another thrombin receptor in platelets and led to the identification of PAR-4 (Kahn et al. 1998).

Given that knock-outs of prothrombotic factors yield mice with bleeding tendencies, it follows that deletion of factors in the fibrinolytic pathway results in increased thrombotic susceptibility in mice. Plasminogen (Bugge et al. 1995; Ploplis et al. 1995), tissue plasminogen activator (t-PA), urokinase-type plasminogen activator (u-PA), and the combined t-PA/u-PA knock-out (Carmeliet et al. 1994) result in mice that demonstrate impaired fibrinolysis, susceptibility for thrombosis, vascular occlusion, and tissue damage due to fibrin deposition. Interestingly, due to fibrin formation in the heart, these mice may provide a good model of myocardial infarction and heart failure caused by thrombosis (Christie et al. 1999). Intriguingly, mice deficient in PAI-1, the primary inhibitor of plasminogen activator, demonstrate no spontaneous bleeding and a greater resistance to venous thrombosis due to a mild fibrinolytic state (Carmeliet et al. 1993), suggesting that inhibition of PAI-1 might be a promising approach for novel antithrombotic agents.

In addition to their role in the regulation of hemostasis, several of these genes are important in embryonic development. For example, deletion of tissue factor (Bugge et al. 1996; Toomey et al. 1996; Carmeliet et al. 1996), tissue factor pathway inhibitor (Huang et al. 1997), or thrombomodulin (Healy et al. 1995) results in an embryonic lethal phenotype. These and other (Connolly et al. 1996, Cui et al. 1996) hemostatic factors also appear to contribute to vascular integrity in the developing embryo. These data suggest that initiation of coagulation and generation of thrombin is important at a critical stage of embryonic development, yet other factors must contribute since some of these embryos are able to progress and survive to birth.

Clearly, genetically altered mice have provided valuable insight into the roles of specific hemostatic factors in physiology and pathophysiology. Results of these studies have provided rationale and impetus for attacking certain targets pharmacologically. These types of models have also provided excellent model systems for studying novel treatments for human diseases. For example, these models provided exceptional systems for studying gene therapy for hemophilia. Specifically, deletion of FIX, generated by specific deletions in the *FIX* gene and its promoter, results in mice that mimic the human phenotype of hemophilia B (Lin et al. 1997). When these mice are treated with adenoviral mediated transfer of human FIX, the bleeding diathesis is fully corrected (Kung et al. 1998). Similarly, selectively bred dogs that have a characteristic point mutation in the sequence encoding the catalytic domain of FIX also have a severe hemophilia B that is

phenotypically similar to the human disease (Evans et al. 1989). When adeno-associated virus-mediated canine FIX gene was administered to these dogs intramuscularly, therapeutic levels of FIX were measured for up to 17 months (Herzog et al. 1999). Clinically relevant partial recovery of whole blood clotting time and APTT was also observed over this prolonged period. These data provided support for initiating the first study of adeno-associated virus-mediated FIX gene transfer in humans (Kay et al. 2000). Preliminary results from this clinical study provided evidence for expression of FIX in the three hemophilia patients studied and also provided favorable safety data to substantiate studying this therapy at higher doses. Although it is likely that there are differences between the human disease and animal models of hemophilia (or other diseases), it is clear that these experiments have provided pharmacological, pharmacokinetic, and safety data that were extremely useful in developing this approach and designing safe clinical trials.

Gene therapy approaches to rescuing patients with bleeding diatheses are further advanced than gene therapy for thrombotic indications. However, promising preclinical data indicates that local overexpression of thrombomodulin (Waugh et al. 1999a) or tissue plasminogen activator (Waugh et al. 1999b) inhibits thrombus formation in a rabbit model of arterial thrombosis. Similarly, local gene transfer of tissue factor pathway inhibitor prevented thrombus formation in balloon-injured porcine carotid arteries (Zoldhelyi et al. 2000). These and other studies (Vassalli et al. 1997) suggest that novel gene therapy approaches will also be effective for thrombotic indications, but these treatments will need to be carefully optimized for pharmacokinetics, safety and, efficacy in laboratory animal studies prior to administration to humans.

Genetically Modified Animals

Development and application of animal models of thrombosis has played a crucial role in discovering and validating novel drug targets, selecting new agents for clinical evaluation, and providing dosing and safety information for clinical trials. In addition, these models have provided valuable information regarding the mechanisms of these new agents and the interactions between antithrombotic agents that work by different mechanisms. The development and application of small and large animal models of thrombosis to the discovery and development of novel antithrombotic agents is described in this review. The methods and major issues regarding the use of animal models of thrombosis, such as positive controls, appropriate pharmacodynamic markers of activity, safety evaluation, species-specificity, and pharmacokinetics, are highlighted. Finally, the use of genetic models of thrombosis/hemostasis is presented using gene-therapy for hemophilia as an example of how animal models have aided in the development of therapies that are presently being evaluated clinically.

REFERENCES AND FURTHER READING

Bi L, Sarkar R, Naas T et al (1996). Further characterization of factor VIII-deficient mice created by gene targeting: RNA and protein studies. Blood 88:3446–3450

Bugge TH, Suh TT, Flick MJ et al (1995) The receptor for urokinase-type plasminogen activator is not essential for mouse development or fertility. J Bio Chem 270:16886–16894

Bugge TH, Xiao Q, Kombrinck KW et al (1996) Fatal embryonic bleeding events in mice lacking tissue factor, the cell-associated initiator of blood coagulation. Proc Natl Acad Sci USA 93:6258–6263

Carmeliet P, Collen D (1999) New developments in the molecular biology of coagulation and fibrinolysis. In: Handbook of Experimental Pharmacology. Vol. 132, Antithrombotics. Berlin, Springer Verlag, pp 41–76

Carmeliet P, Mackman N, Moons L et al (1996) Role of tissue factor in embryonic blood vessel development. Nature 383:73–75

Carmeliet P, Schoonjans L, Kieckens L et al (1994) Physiological consequences of loss of plasminogen activator gene function in mice. Nature 368:419–424

Carmeliet P, Stassen JM, Schoonjans L et al (1993) Plasminogen activator inhibitor-1 gene-deficient mice. J Clin Invest 92:2756–2760

Christie PD, Edelberg JM, Picard MH et al (1999). A murine model of myocardial thrombosis. J Clin Invest 104:533–539

Connolly AJ, Ishihara H, Kahn ML et al (1996) Role of the thrombin receptor in development and evidence for a second receptor. Nature 381:516–519

Cui J, O'Shea KS, Purkayastha A et al (1996) Fatal haemorrhage and incomplete block to embryogenesis in mice lacking coagulation factor V. Nature 384:66–68

Denis C, Methia N, Frenette PS et al (1998) A mouse model of severe von Willebrand disease: defects in hemostasis and thrombosis. Proc Natl Acad Sci USA 95:9524–9529

Evans JP, Brinkhous KM, Brayer GD et al (1989) Canine hemophilia B resulting from a point mutation with unusual consequences. Proc Natl Acad Sci USA 86:10095–10099

Healy AM, Rayburn HB, Rosenberg RD, Weiler H (1995) Absence of the blood-clotting regulator thrombomodulin causes embryonic lethality in mice before development of a functional cardiovascular system. Proc Natl Acad Sci USA 92:850–854

Herzog RW, Yang EY, Couto LB et al (1999) Long-term correction of canine hemophilia B by gene transfer of blood coagulation factor IX mediated by adeno-associated viral vector. Nat Med 5:56–63

Hodivala-Dilke KM, McHugh KP, Tsakiris DA et al (1999) β_3-integrin-deficient mice are a model for Glanzmann thrombasthenia showing placental defects and reduced survival. J Clin Invest 103:229–238

Huang ZF, Higuchi D, Lasky N, Broze GJJ (1997) Tissue factor pathway inhibitor gene disruption produces intrauterine lethality in mice. Blood 90:944–951

Kahn ML, Zheng YW, Huang W et al (1998) A dual thrombin receptor system for platelet activation. Nature 394:690–694
Kay MA, Manno CS, Ragni MV et al (2000) Evidence for gene transfer and expression of factor IX in haemophilia B patients with an AAV vector. Nat Gen 24:257–261
Kung J, Hagstrom J, Cass D et al (1998) Human FIX corrects bleeding diathesis of mice with hemophilia B. Blood 91:784–790
Law DA, DeGuzman FR, Heiser P et al (1999) Integrin cytoplasmic tyrosine motif is required for outside-in αIIbβ3 signalling and platelet function. Nature 401:808–811
Leon C, Hechler B, Freund M et al (1999) Defective platelet aggregation and increased resistance to thrombosis in purinergic $P2Y_1$ receptor-null mice. J Clin Invest 104:1731–1737
Lin HF, Maeda N, Sithies O et al (1997) A coagulation factor IX-deficient mouse model for human hemophilia B. Blood 90:3962–3966
Offermanns S, Toombs CF, Hu YH, Simon MI (1997) Defective platelet activation in Gα_q-deficient mice. Nature 389:183–186
Pearson JM, Ginsburg D (1999) Use of transgenic mice in the study of thrombosis and hemostasis. In: Handbook of Experimental Pharmacology. Vol. 132, Antithrombotics. Berlin:Springer-Verlag, pp 157–174
Ploplis VA, Carmeliet P, Vazirzadeh S et al (1995) Effects of disruption of the plasminogen gene on thrombosis, growth, and health in mice. Circulation 92:2585–2593
Subramaniam M, Frenette PS, Saffaripour S et al (1996) Defects in hemostasis in P-selectin-deficient mice. Blood 87:1238–1242
Thomas DW, Mannon RB, Mannon PJ et al (1998) Coagulation defects and altered hemodynamic responses in mice lacking receptors for thromboxane A_2. J Clin Invest 102:1994–2001
Toomey JR, Kratzer KE, Lasky NM et al (1996) Targeted disruption of the murine tissue factor gene results in embryonic lethality. Blood 88:1583–1587
Vassalli G, Dichek DA (1997) Gene therapy for arterial thrombosis. Cardiovasc Res 35:459–469
Wang L, Zoppè M, Hackeng TM et al (1997) A factor IX-deficient mouse model for hemophilia B gene therapy. Proc Natl Acad Sci USA 94:11563–11566
Waugh JM, Yuksel E, Li J et al (1999a) Local overexpression of thrombomodulin for in vivo prevention of arterial thrombosis in a rabbit model. Circ Res 84:84–92
Waugh JM, Kattash M, Li J et al (1999b) Gene therapy to promote thromboresistance: local overexpression of tissue plasminogen activator to prevent arterial thrombosis in an in vivo rabbit model. Proc Natl Acad Sci USA 96:1065–1070
Zoldhelyi P, McNatt J, Shelat HS et al (2000) Thromboresistance of balloon-injured porcine carotid arteries after local gene transfer of human tissue factor pathway inhibitor. Circulation 101:289–295

B.6.1 Knock-Out Mice

PURPOSE AND RATIONALE

Genetically modified animals, in particular knock-out mice, help in the understanding of the role of various factors in blood clotting, thrombolysis, and platelet function. They are useful to verify the mode of action of new drugs.

Factor I (Fibrinogen)

Phenotype

Born in normal appearance, ~10% die shortly after birth and another 40% around 1–2 months after birth due to bleeding, failure of pregnancy, blood samples failing to clot or support platelet aggregation *in vitro* (Suh et al. 1995).

REFERENCES AND FURTHER READING

Suh TT, Holmback K, Jensen NJ et al (1995) Resolution of spontaneous bleeding events but failure of pregnancy in fibrinogen-deficient mice. Genes Dev 9:2020–2033

Factor II (Prothrombin)

Phenotype

Partial embryonic lethality: 50% between embryonic day (E) 9.5–11.5; at least 1/4 survive to term, but fatal hemorrhage few days after birth; factor II important in maintaining vascular integrity during development as well as postnatal life (Sun et al. 1998, Xu et al. 1998).

REFERENCES AND FURTHER READING

Sun WY, Witte DP, Degen JL et al (1998) Prothrombin deficiency results in embryonic and neonatal lethality in mice. Proc Natl Acad Sci USA 95:7597–7602
Xu J, Wu Q, Westfield L et al (1998) Incomplete embryonic lethality and fatal neonatal hemorrhage caused by prothrombin deficiency in mice. Proc Natl Acad Sci USA 95:7603–7607

Factor V

Phenotype

Half of the embryos die at E9–10, possibly as a result of abnormal yolk sac vasculature, remaining 50% progress normally to term, but die from massive hemorrhage within 2 hours of birth, more severe in mouse than in human (Cui et al. 1996; Yang et al. 2000).

REFERENCES AND FURTHER READING

Cui J, O'Shea KS, Purkayastha A et al (1996) Fatal hemorrhage and incomplete block to embryogenesis in mice lacking coagulation factor V. Nature 384:66–68
Yang TL, Cui J, Taylor JM et al (2000) Rescue of fatal neonatal hemorrhage in factor V deficient mice by low level transgene expression. Thromb Haemost 83:70–77

Factor VII

Phenotype

Develop normally but suffer fatal perinatal bleeding (Rosen et al. 1997).

REFERENCES AND FURTHER READING

Rosen ED, Chan JCY, Idusogie E et al (1997) Mice lacking factor VII develop normally but suffer fatal perinatal bleeding. Nature 390:290–294

Factor VIII

Phenotype

Mild phenotype compared with severe hemophilia A in humans; no spontaneous bleeding, illness or reduced activity during the first year of life; have residual clotting activity (APTT), as shown by Bi et al. (1995).

REFERENCES AND FURTHER READING

Bi L, Lawler AM, Antonarakis SE et al (1995) Targeted disruption of the mouse factor VIII gene produces a model of haemophilia A. Nat Genet 10:119–121

Factor IX

Phenotype

Factor IX coagulant activities (APTT): +/+ 92%, +/– 53%, –/– <5%; bleeding disorder (extensive bleeding after clipping a portion of the tail, bleeding to death if not cauterized (Kundu et al. 1998, Wang et al. 1997).

REFERENCES AND FURTHER READING

Kundu RK, Sangiorgi F, Wu LY et al (1998) Targeted inactivation of the coagulation factor IX gene causes hemophilia B in mice. Blood 92:168–174

Wang L, Zoppe M, Hackeng TM et al (1997) A factor IX-deficient mouse model for hemophilia B gene therapy. Proc Natl Acad Sci USA 94:11563–11566

Factor X

Phenotype

Partial embryonic lethality (1/3 died on E11.5–12.5); fatal neonatal bleeding between postnatal day (P) 5–20, as shown by Dewerchin et al. (2000).

REFERENCES AND FURTHER READING

Dewerchin M, Liang Z, Moons L et al (2000) Blood coagulation factor X deficiency causes partial embryonic lethality and fatal neonatal bleeding in mice. Thromb Haemost 83:185–190

Factor XI

Phenotype

APTT prolonged in –/– (158–200 sec) compared with +/+ (25–34 sec) and +/– (40–61 sec); no factor XI activity and antigen, did not result in intrauterine death, –/– similar bleeding as +/+ with a tendency to prolongation (Gailani et al. 1997).

REFERENCES AND FURTHER READING

Gailani D, Lasky NM, Broze GJ (1997) A murine model of factor XI deficiency. Blood Coagul Fibrinolysis 8:134–144

TF (Tissue Factor)

Phenotype

Abnormal circulation from yolk sac to embryo ~E8.5 leading to embryo wasting and death; TF has a role in blood vessel development (Bugge et al. 1996, Carmeliet et al. 1996, Toomey et al. 1996, 1997).

REFERENCES AND FURTHER READING

Bugge TH, Xiao Q, Kombrinck KW et al (1996) Fatal embryonic bleeding events in mice lacking tissue factor, the cell-associated initiator of blood coagulation. Proc Natl Acad Sci U S A 93:6258–6263

Carmeliet P, Mackman N, Moons L et al (1996) Role of tissue factor in embryonic blood vessel development. Nature 383:73–75

Toomey JR, Kratzer KE, Lasky NM et al (1996) Targeted disruption of the murine tissue factor gene results in embryonic lethality. Blood 88:1583–1587

Toomey JR, Kratzer KE, Lasky NM, Broze GJ (1997) Effect of tissue factor deficiency on mouse and tumor development. Proc Natl Acad Sci USA 94:6922–6926

TFPI (Tissue Factor Pathway Inhibitor)

Phenotype

None survive the neonatal period; 60% die between E9.5–11.5 with signs of yolk sac hemorrhage (Huang et al. 1997).

REFERENCES AND FURTHER READING

Huang ZF, Higuchi D, Lasky N, Broze GJ (1997) Tissue factor pathway inhibitor gene disruption produces intrauterine lethality in mice. Blood 90:944–951

Thrombin Receptor

Phenotype

50% die at E9–10; 50% survive and become grossly normal adult mice with no bleeding diathesis; –/– platelets strongly respond to thrombin; –/– fibroblast loose their ability to respond to thrombin⟶ second TR must exist, as shown by Connolly et al. (1996) and by Darrow et al. (1996).

REFERENCES AND FURTHER READING

Connolly AJ, Ishihara H, Kahn ML et al (1996) Role of the thrombin receptor in development and evidence for a second receptor. Nature 381:516–519

Darrow AL, Fung-Leung WP, Ye RD et al (1996) Biological consequences of thrombin receptor deficiency in mice. Thromb Haemost 76:860–866

Thrombomodulin

Phenotype

Embryonic lethality before development of a functional cardiovascular system; die before E9.5 due to retardation of growth; TM+/– mice develop normal without thrombotic complications (Christie et al. 1999, Healy et al. 1995, 1998, Weiler-Guettler et al. 1998).

REFERENCES AND FURTHER READING

Christie PD, Edelberg JM, Picard MH et al (1999) A murine model of myocardial microvascular thrombosis. J Clin Invest 104:533–539

Healy AM, Rayburn HB, Rosenberg RD, Weiler H (1995) Absence of the blood-clotting regulator thrombomodulin causes embryonic lethality in mice before development of a functional cardiovascular system. Proc Natl Acad Sci USA 92:850–854

Healy AM, Hancock WW, Christie PD et al (1998) Intravascular coagulation activation in a murine model of thrombomodulin deficiency: effects of lesion size, age, and hypoxia on fibrin deposition. Blood 92:4188–4197

Weiler-Guettler H, Christie PD, Beeler DL et al (1998) A targeted point mutation in thrombomodulin generates viable mice with a prethrombotic state. J Clin Invest 101:1983–1991

Protein C

Phenotype

KO mice appeared to develop normally macroscopically, but possessed obvious signs of bleeding and thrombosis; did not survive beyond 24 hours after delivery; microvascular thrombosis in the brain and necrosis in the liver; plasma clottable fibrinogen was not detectable, suggesting fibrinogen depletion and secondary consumptive coagulopathy (Jalbert et al. 1998).

REFERENCES AND FURTHER READING

Jalbert LR, Rosen ED, Moons L et al (1998) Inactivation of the gene for anticoagulant protein C causes lethal perinatal consumptive coagulopathy in mice. J Clin Invest 102:1481–1488

Plasminogen

Phenotype

Severe spontaneous thrombosis; reduced ovulation and fertility; cachexia and shorter survival; severe glomerulonephritis; impaired skin healing; reduced macrophage and keratinocyte migration (Bugge et al. 1995, Ploplis et al. 1995).

REFERENCES AND FURTHER READING

Bugge TH, Flick MJ, Daugherty CC, Degen JL (1995) Plasminogen deficiency causes severe thrombosis but is compatible with development and reproduction. Genes Dev 9:794–807

Ploplis VA, Carmeliet P, Vazirzadeh S et al (1995) Effects of disruption of the plasminogen gene on thrombosis, growth, and health in mice. Circulation 92:2585–2593

Alpha$_2$-Antiplasmin

Phenotype

Normal fertility, viability and development; no bleeding disorder; spontaneous lysis of injected clots; $\longrightarrow$ enhanced fibrinolytic potential; significant reduction of renal fibrin deposition after LPS (Lijnen et al. 1999).

REFERENCES AND FURTHER READING

Lijnen HR, Okada K, Matsuo O et al (1999) Alpha$_2$-antiplasmin gene deficiency in mice is associated with enhanced fibrinolytic potential without overt bleeding. Blood 93:2274–2281

T-PA (Tissue-Type Plasminogen Activator)

Phenotype

Extensive spontaneous fibrin deposition; severe spontaneous thrombosis; impaired neointima formation; reduced ovulation and fertility; cachexia and shorter survival; severe glomerulonephritis; abnormal tissue remodeling (Carmeliet et al. 1998, Christie et al. 1999).

REFERENCES AND FURTHER READING

Carmeliet P, Schoonjans L, Kieckens L et al (1998) Physiological consequences of loss of plasminogen activator gene function in mice. Nature 368:419–424

Christie PD, Edelberg JM, Picard MH et al (1999) A murine model of myocardial microvascular thrombosis. J Clin Invest 104:533–539

PAI-1 (Plasminogen Activator Inhibitor-1)

Phenotype

Reduced thrombotic incidence; no bleeding; accelerated neo-intima formation; reduced lung inflammation; reduced atherosclerosis. Detailed studies on PAI-1 are reported by Carmeliet et al. (1993), Eitzman et al. (1996), Erickson et al. (1990), Kawasaki et al. (2000), and Pinsky et al. (1998).

REFERENCES AND FURTHER READING

Carmeliet P, Stassen JM, Schoonjans L et al (1993) Plasminogen activator inhibitor-1 gene-deficient mice. II. Effects on hemostasis, thrombosis, and thrombolysis. J Clin Invest 92:2756–2760

Eitzman DT, McCoy RD, Zheng X et al (1996) Bleomycin-induced pulmonary fibrosis in transgenic mice that either lack or overexpress the murine plasminogen activator inhibitor-1 gene. J Clin Invest 97:232–237

Erickson LA, Fici GJ, Lund JE et al (1990) Development of venous occlusions in mice transgenic for the plasminogen activator inhibitor-1 gene. Nature 346:74–76

Kawasaki T, Dewerchin M, Lijnen HR et al (2000) Vascular release of plasminogen activator inhibitor-1 impairs fibrinolysis during acute arterial thrombosis in mice. Blood 96:153–60

Pinsky DJ, Liao H, Lawson CA et al (1998) Coordinated induction of plasminogen activator inhibitor-1 (PAI-1) and inhibition of plasminogen activator gene expression by hypoxia promotes pulmonary vascular fibrin deposition. J Clin Invest 102:919–928

TAFI (Thrombin Activatable Fibrinolysis Inhibitor)

Not described.

Vitronectin

Phenotype

Normal development, fertility, and survival; serum is completely deficient in "serum spreading factor" and PAI-1 binding activities; delayed arterial and venous thrombus formation (Eitzman et al. 2000, Zheng et al. 1995).

REFERENCES AND FURTHER READING

Eitzman DT, Westrick RJ, Nabel EG, Ginsburg D (2000) Plasminogenactivator inhibitor-1 and vitronectin promote vascular thrombosis in mice. Blood 95:577–580

Zheng X, Saunders TL, Camper SA et al (1995) Vitronectin is not essential for normal mammalian development and fertility. Proc Natl Acad Sci USA 92:12426–12430

Urokinase, U-PA (Urinary-Type Plasminogen Activator)

Phenotype

Single u-PA deficiency: viable, fertile, normal life span; occasionally spontaneous fibrin deposits in normal and inflamed tissue; higher incidence of endotoxin-induced thrombosis. Combined t-PA and u-PA deficiency: mice survive embryonic development; retarded growth, reduced fertility, shortened life span; spontaneous fibrin deposits more extensively and in more organs (Carmeliet et al. 1998, Heckel et al. 1990).

Transgenic mice carrying the u-PA gene linked to the albumin enhancer/promoter exhibit spontaneous intestinal and intraabdominal bleeding directly related to transgene expression in the liver and elevated plasma u-PA level; 50% die between 3 and 84 hours after birth; severe hypofibrinogenemia, loss of clotting function.

REFERENCES AND FURTHER READING

Carmeliet P, Schoonjans L, Kieckens L et al (1998) Physiological consequences of loss of plasminogen activator gene function in mice. Nature 368:419–424

Heckel JL, Sandgren EP, Degen JL et al (1990) Neonatal bleeding in transgenic mice expressing urokinase-type plasminogen activator. Cell 62:447–456

UPAR (Urinary-Type Plasminogen Activator Receptor)

Phenotype

Phenotype normal; attenuated thrombocytopenia and mortality associated with severe malaria (Bugge et al. 1995, 1996, Dewerchin et al. 1996, Piguet et al. 2000).

REFERENCES AND FURTHER READING

Bugge TH, Suh TT, Flick MJ et al (1995) The receptor for urokinase-type plasminogen activator is not essential for mouse development or fertility. J Biol Chem 270:16886–16894

Bugge TH, Flick MJ, Danton MJ et al (1996) Urokinase-type plasminogen activator is effective in fibrin clearance in the absence of its receptor or tissue-type plasminogen activator. Proc Natl Acad Sci USA 93:5899–5904

Dewerchin M, van Nuffelen A, Wallays G et al (1996) Generation and characterization of urokinase receptor deficient mice. J Clin Invest 97:870–878

Piguet PF, Da-Laperrousaz C, Vesin C et al (2000) Delayed mortality and attenuated thrombocytopenia associated with severe malaria in urokinase- and urokinase receptor-deficient mice. Infect Immun 68:3822–3829

Gas 6 (Growth Arrest-Specific Gene 6 Product)

Phenotype

Mice are viable, fertile, appear normal; do not suffer spontaneous bleeding or thrombosis; have normal tail bleeding time. Platelets fail to aggregate irreversibly to ADP, collagen, or U 46619. Arterial and venous thrombosis is inhibited and mice are protected from fatal thromboembolism after injection of collagen plus epinephrine (Angelillo-Scherrer et al. 2001).

REFERENCES AND FURTHER READING

Angelillo-Scherrer A, DeFrutos PG, Aparicio C et al (2001) Deficiency or inhibition of Gas6 causes platelet dysfunction and protects mice against thrombosis. Nat Med 7:215–221

GPIbalpha (Glycoprotein Ib Alpha, Part of the GP Ib-V–IX Complex)

Phenotype

Bleeding, thrombocytopenia and giant platelets (similar to human Bernard Soulier syndrome). See Ware et al. (2000) for details.

REFERENCES AND FURTHER READING

Ware J, Russell S, Ruggeri ZM (2000) Generation and rescue of a murine model of platelet dysfunction: the Bernard-Soulier syndrome. Proc Natl Acad Sci USA 97:2803–2808

GPV (Glycoprotein V, Part of the GP Ib-V–IX Complex)

Phenotype

Increased thrombin responsiveness, GpV–/– platelets are normal in size, normal amounts in GpIb-IX, functional in vWF-binding; platelets are hyperresponsive to thrombin$\longrightarrow$ increased aggregation response; shorter bleeding time;$\longrightarrow$GpV = negative modulator of platelet function (Ramakrishnan et al. 1999).

REFERENCES AND FURTHER READING

Ramakrishnan V, Reeves PS, DeGuzman F et al (1999) Increased thrombin responsiveness in platelets from mice

lacking glycoprotein V. Proc Natl Acad Sci USA 96:13336–13341

GPIIb (Integrin Alpha IIb, Glycoprotein IIb, Part of the GP IIb–IIIa Complex)

Phenotype

Bleeding disorder similar to Glanzmann thrombasthenia in man; platelets failed to bind fibrinogen, to aggregate and to retract a fibrinogen clot; α-granules do not contain fibrinogen (Tronik-Le Roux et al. 2000).

REFERENCES AND FURTHER READING

Tronik-Le Roux D, Roullot V, Poujol C et al (2000) Thrombasthenic mice generated by replacement of the integrin alpha$_{IIb}$ gene: demonstration that transcriptional activation of this megakaryocytic locus precedes lineage commitment. Blood 96:1399–1408

GP IIIa (Integrin Beta3, Glycoprotein IIIa, Part of the GP IIb–IIIa Complex)

Phenotype

Viable, fertile, increased fetal mortality; features of Glanzmann thrombasthenia in man, e. g. defective platelet aggregation, clot retraction; spontaneous bleeding, prolonged bleeding times; dysfunctional osteoclasts, development of osteosclerosis with age (Hodivala-Dilke et al. 1999, McHugh et al. 2000).

REFERENCES AND FURTHER READING

Hodivala-Dilke KM, McHugh KP, Tsakiris DA et al (1999) Beta3-integrin-deficient mice are a model for Glanzmann thrombasthenia showing placental defects and reduced survival. J Clin Invest 103:229–238

McHugh KP, Hodivala-Dilke K, Zheng MH et al (2000) Mice lacking beta3 integrins are osteosclerotic because of dysfunctional osteoclasts. J Clin Invest 105:433–440

GP IIa (Glycoprotein IIa, Integrin Beta 1, Part of the GP Ia–IIa Complex)

Phenotype

Integrin beta1 null platelets from conditional knockout mice develop normally, platelet count is normal. Collagen induced platelet aggregation is delayed but otherwise normal; tyrosine phosphorylation pattern is normal but phosphorylation is delayed. Bleeding time in bone marrow chimeric mice is normal; no major *in vivo* defects (Nieswandt et al. 2001).

REFERENCES AND FURTHER READING

Nieswandt B, Brakebusch C, Bergmeier W et al (2001) Glycoprotein VI but not alpha2beta1 integrin is essential for platelet interaction with collagen. EMBO J 20:2120–2130

VWF (von Willebrand Factor)

Phenotype

Factor VIII levels strongly reduced due to defective protection by vWF; highly prolonged bleeding time, hemorrhage, spontaneous bleeding; mice useful for investigating the role of vWF; delayed platelet adhesion in ferric-chloride-induced arteriolar injury (Denis et al. 1998, Ni et al. 2000).

REFERENCES AND FURTHER READING

Denis C, Methia N, Frenette PS et al (1998) A mouse model of severe von Willebrand disease: defects in hemostasis and thrombosis. Proc Natl Acad Sci USA 95:952–959

Ni H, Denis CV, Subbarao S et al (2000) Persistence of platelet thrombus formation in arterioles of mice lacking both von Willebrand factor and fibrinogen. J Clin Invest 106:385–392

Thromboxane A2 Receptor (TXA2r)

Phenotype

Mild bleeding disorder and altered vascular responses to TXA2 and arachidonic acid (Thomas et al. 1998).

REFERENCES AND FURTHER READING

Thomas DW, Mannon RB, Mannon PJ et al (1998) Coagulation defects and altered hemodynamic responses in mice lacking receptors for thromboxane A2. J Clin Invest 102:1994–2001

Prostacyclin Receptor (PGI2r)

Phenotype

Viable, fertile, normotensive; increased susceptibility to thrombosis; reduced inflammatory and pain responses (Murata et al. 1997).

REFERENCES AND FURTHER READING

Murata T, Ushikubi F, Matsuoka T et al (1997) Altered pain reception and inflammatory response in mice lacking prostacyclin receptor. Nature 388:678–682

PECAM (Platelet: Endothelial Cell Adhesion Molecule)

Phenotype

Normal platelet aggregation; prolonged bleeding time as described by Duncan et al. (1999) and by Mahooti et al. (2000).

REFERENCES AND FURTHER READING

Duncan GS, Andrew DP, Takimoto H et al (1999) Genetic evidence for functional redundancy of platelet/endothelial cell adhesion molecule-1 (PECAM-1) CD31-deficient mice reveal PECAM-1-dependent and PECAM-1-independent functions. J Immunol 162:3022–3030

Mahooti S, Graesser D, Patil S et al (2000) PECAM-1 (CD 31) expression modulates bleeding tome *in vivo*. Am J Pathol 157:75–81

Pallid (Pa)

Phenotype

Among 13 hypopigment mouse mutants with storage pool deficiency, the pallid mouse is a model of the human Hermansky Pudlak syndrome (the beige mouse is a model of the Chediak Higashi syndrome). Pallid mice exhibit prolonged bleeding time, pigment dilution, kidney lysosomal enzyme elevation serum alpha 1 antitrypsin deficiency and abnormal otolith formation. The gene defective in pallid mice encodes the highly charged 172-amino acid protein pallidin, which interacts with syntaxin 13, a protein mediating vesicle docking and fusion (Huang et al. 1999).

REFERENCES AND FURTHER READING

Huang L, Kuo YM, Gitschier J (1999) The pallid gene encodes a novel, syntaxin 13-interacting protein involved in platelet storage pool deficiency. Nat Genet 23:329–332

G Alpha(q) (Guanyl Nucleotide Binding Protein G Alpha q)

Phenotype

Defective aggregation in response ADP, TXA2, thrombin, collagen; shape change normal (Offermans et al. 1997, Ohlmann et al. 2000).

REFERENCES AND FURTHER READING

Offermans S, Toombs CF, Hu YH, Simon MI (1997) Defective platelet activation in G alpha(q)-deficient mice. Nature 389:183–186

Ohlmann P, Eckly A, Freund M et al (2000) ADP induces partial platelet aggregation without shape change and potentiates collagen-induced aggregation in the absence of Galphaq. Blood 96:2134–2139

G z (Member of the Gi Family of G Proteins)

Phenotype

Impaired platelet aggregation to epinephrine; resistance to fatal thromboembolism; exaggerated response to cocaine, reduced effect of morphine and antidepressant drugs (Yang et al. 2000).

REFERENCES AND FURTHER READING

Yang J, Wu J, Kowalska MA et al (2000) Loss of signaling through G protein, Gz, results in abnormal platelet activation and altered responses to psychoactive drugs. Proc Natl Acad Sci USA 97:9984–9989

Phospholipase C Gamma

Phenotype

Viable, fertile, decreased mature B cells; defective B cell and mast cell function; defective Fc_{gamma} receptor signaling, therefore, loss of collagen-induced platelet aggregation (Wang et al. 2000).

REFERENCES AND FURTHER READING

Wang D, Feng J, Wen R et al (2000) Phospholipase Cgamma2 is essential in the functions of B cell and several Fc receptors. Immunity 13:25–35

CD39 (Vascular Adenosine Triphosphate Diphosphohydrolase)

Phenotype

Viable, fertile; prolonged bleeding times but minimally perturbed coagulation parameters; reduced platelet interaction with injured mesenteric vasculature *in vivo*. Platelets fail to aggregate to standard agonists *in vitro* associated with purinergic P2Y1 receptor desensitization; fibrin deposition at multiple organ sites (Enjyoji et al. 1999).

REFERENCES AND FURTHER READING

Enjyoji K, Sevigny J, Lin Y et al (1999) Targeted disruption of cd39/ATP diphosphohydrolase results in disordered hemostasis and thromboregulation. Nat Med 5:1010–1017

Protein Kinase, cGMP-Dependent

Phenotype

Viable, fertile; unresponsive to cGMP and NO; defective VASP-phosphorylation; increased adhesion and aggregation of platelets *in vivo* in ischemic/reperfused mesenteric microcirculation; no compensation by cAMP kinase system (Massberg et al. 1999).

REFERENCES AND FURTHER READING

Massberg S, Sausbier M, Klatt P et al (1999) Increased adhesion and aggregation of platelets lacking cyclic guanosine 3′,5′-monophosphate kinase I. J Exp Med 189:1255–1264

Vasodilator-Stimulated Phosphoprotein (VASP)

Phenotype

Viable, fertile; mild platelet dysfunction with megakaryocyte hyperplasia, increased collagen/thrombin activation, impaired cyclic nucleotide mediated inhibition of platelet activation (Aszodi et al. 1999, Hauser et al. 1999).

REFERENCES AND FURTHER READING

Aszodi A, Pfeifer A, Ahmad M et al (1999) The vasodilator-stimulated phosphoprotein (VASP) is involved in cGMP- and cAMP-mediated inhibition of agonist-induced platelet aggregation, but is dispensable for smooth muscle function. EMBO J 18:37–48

Hauser W, Knobeloch KP, Eigenthaler M et al (1999) Megakaryocyte hyperplasia and enhanced agonist-induced platelet activation in vasodilator-stimulated phosphoprotein knockout mice. Proc Natl Acad Sci USA 96:8120–8125

Arachidonate 12-Lipoxygenase (P-12LO)

Phenotype

Platelets exhibit a selective hypersensitivity to ADP, manifested as a marked increase in slope and percent aggregation in *ex vivo* assays and increased mortality in an ADP-induced mouse model of thromboembolism (Chen et al. 1994, Johnson et al. 1998).

REFERENCES AND FURTHER READING

Chen XS, Sheller JR, Johnson EN, Funk CD (1994) Role of leukotrienes revealed by targeted disruption of the 5-lipoxygenase gene. Nature 372:179–182

Johnson EN, Brass LF, Funk CD (1998) Increased platelet sensitivity to ADP in mice lacking platelet-type 12-lipoxygenase. Proc Natl Acad Sci USA 95:3100–3105

Arachidonate 5-Lipoxygenase (P-5LO)

Phenotype

Develop normally and are healthy. No difference in their reaction to endotoxin shock; however, they resist the lethal effects of shock induced by platelet-activating factor. Inflammation induced by arachidonic acid is markedly reduced (Chen et al. 1994, Johnson et al. 1998).

REFERENCES AND FURTHER READING

Chen XS, Sheller JR, Johnson EN, Funk CD (1994) Role of leukotrienes revealed by targeted disruption of the 5-lipoxygenase gene. Nature 372:179–182

Johnson EN, Brass LF, Funk CD (1998) Increased platelet sensitivity to ADP in mice lacking platelet-type 12-lipoxygenase. Proc Natl Acad Sci USA 95:3100–3105

Thrombopoietin

Phenotype

TPO –/– and c-mpl –/–: both exhibit a 90% reduction in megakaryocyte and platelet levels, but even with these small platelet levels the mice do not have excessive bleeding; all platelets that are present are morphologically normal+functionally; *in vivo* TPO is required for control of megakaryocyte and platelet number but not for their maturation (Lawler et al. 1998).

REFERENCES AND FURTHER READING

Lawler J, Sunday M, Thibert V et al (1998) Thrombospondin-1 is required for normal murine pulmonary homeostasis and its absence causes pneumonia. J Clin Invest 101:982–992

Thrombospondin-1

Phenotype

Normal thrombin-induced platelet aggregation; increase in circulating number of white blood cells; TSP-1 is involved in normal lung homeostasis (Lawler et al. 1998).

REFERENCES AND FURTHER READING

Lawler J, Sunday M, Thibert V, et al (1998) Thrombospondin-1 is required for normal murine pulmonary homeostasis and its absence causes pneumonia. J Clin Invest 101:982–992

Mouse knock-out models of virtually all of the known hemostatic factors have been reported, as shown in Table 6.

REFERENCES AND FURTHER READING

Bi L, Sarkar R, Naas T et al (1996) Further characterization of factor VIII-deficient mice created by gene targeting: RNA and protein studies. Blood 88:3446–3450

Bugge TH, Suh TT, Flick MJ et al (1995) The receptor for urokinase-type plasminogen activator is not essential for mouse development or fertility. J Bio Chem 270:16886–16894

Bugge TH, Xiao Q, Kombrinck KW et al (1996) Fatal embryonic bleeding events in mice lacking tissue factor, the cell-associated initiator of blood coagulation. Proc Natl Acad Sci USA 93:6258–6263

Carmeliet P, Schoonjans L, Kieckens L et al (1994) Physiological consequences of loss of plasminogen activator gene function in mice. Nature 368:419–424

Carmeliet P, Stassen JM, Schoonjans L et al (1993) Plasminogen activator inhibitor-1 gene-deficient mice. J Clin Invest 92:2756–2760

Connolly AJ, Ishihara H, Kahn ML et al (1996) Role of the thrombin receptor in development and evidence for a second receptor. Nature 381:516–519

Cui J, O'Shea KS, Purkayastha A et al (1996) Fatal haemorrhage and incomplete block to embryogenesis in mice lacking coagulation factor V. Nature 384:66–68

Denis C, Methia N, Frenette PS et al (1998) A mouse model of severe von Willebrand disease: defects in hemostasis and thrombosis. Proc Natl Acad Sci USA 95:9524–9529

Dewerchin M, Liang Z, Moons L et al (2000) Blood coagulation factor X deficiency causes partial embryonic ylethality and fatal neonatal bleeding in mice. Thromb Haemost 83:185–190

Dewerchin M, Nuffelen AV, Wallays G, Bouche A, Moons L, Carmeliet P, Mulligan RC, Collen D (1996) Generation and characterization of urokinase receptor-deficient mice. J Clin Invest 97(3):870–8

Gailani D, Lasky NM, Broze GJ (1997) A murine model of factor XI deficiency. Blood Coagul Fibrinolysis 8:134–144

Healy AM, Rayburn HB, Rosenberg RD, Weiler H (1995) Absence of the blood-clotting regulator thrombomodulin causes embryonic lethality in mice before development of a functional cardiovascular system. Proc Natl Acad Sci USA 92:850–854

Hodivala-Dilke KM, McHugh KP, Tsakiris DA et al (1999) β_3-integrin-deficient mice are a model for Glanzmann thrombasthenia showing placental defects and reduced survival. J Clin Invest 103:229–238

Huang Z-F, Higuchi D, Lasky N, Broze GJJ (1997) Tissue factor pathway inhibitor gene disruption produces intrauterine lethality in mice. Blood 90:944–951

Jalbert LR, Rosen ED, Moons L et al (1998) Inactivation of the gene for anticoagulant protein C causes lethal peri-

Table 6 Genetic models of thrombosis and hemostasis

Knock-out	Viable	Embryonic Development / Survival	References
Coagulation			
Protein C	No	Normal Perinatal death	Jalbert et al. 1998
Fibrinogen	Yes	Normal Perinatal death	Suh et al. 1995
Fibrinogen-QAGVD	Yes	Normal	Suh et al. 1995
fV	No	Partial embryonic loss Perinatal death	Cui et al. 1996
FVII	Yes	Normal Perinatal death	Rosen et al. 1997
fVIII	Yes	Normal	Bi et al. 1996
fIX	Yes	Normal	Wang et al. 1997
fXI	Yes	Normal	Gailani et al. 1997
Tissue factor	No	Lethal	Toomey et al. 1996 Bugge et al. 1996
TFPI	No	Lethal	Huang et al. 1997
vWF	Yes	Normal	Denis et al. 1998
Prothrombin	No	Partial embryonic lossr perinatal death	Xue et al. 1998 Sun et al. 1998
Fibrinolytic			
u-Pa & t-PA	Yes	Normal Growth retardation	Carmeliet et al. 1994
uPAR	Yes	Normal	Dewerchin et al. 1996 Bugge et al. 1995
Plasminogen	Yes	Normal Growth retardation	Bugge et al. 1995 Ploplis et al. 1995
PA-I	Yes	Normal	Carmeliet et al. 1993
Thrombomodulin	No	Lethal	Healy et al. 1995
Platelet			
β_3	Yes	Normal Partial embryonic loss	Hodivala-Dilke et al. 1999
β_3-DiYF	Yes	Normal	Law et al. 1999
P-Selectin	Yes	Normal	Subramaniam et al. 1996
PAR-1	Yes	Normal	Connolly et al. 1996
PAR-3	Yes	Normal	Kahn et al. 1998
$G_{\alpha a}$	Yes	Normal Perinatal death	Offermans et al. 1997
TXA_2 receptor	Yes	Normal	Thomas et al. 1998
P2Y1	Yes	Normal	Leon et al. 1999

natal consumptive coagulopathy in mice. J Clin Invest 102:1481–1488

Kahn ML, Zheng Y-W, Huang W et al (1998) A dual thrombin receptor system for platelet activation. Nature 394:690–694

Law DA, DeGuzman FR, Heiser P et al (1999) Integrin cytoplasmic tyrosine motif is required for outside-in αIIbβ3 signalling and platelet function. Nature 401:808–811

Leon C, Hechler B, Freund M et al (1999) Defective platelet aggregation and increased resistance to thrombosis in purinergic $P2Y_1$ receptor-null mice. J Clin Invest 104:1731–1737

Offermans S, Toombs CF, Hu YH, Simon MI (1997) Defective platelet activation in G alpha(q)-deficient mice. Nature 389:183–186

Ploplis VA, Carmeliet P, Vazirzadeh S et al (1995) Effects of disruption of the plasminogen gene on thrombosis, growth, and health in mice. Circulation 92:2585–2593

Rosen ED, Chan JCY, Idusogie E et al (1997) Mice lacking factor VII develop normally but suffer fatal perinatal bleeding. Nature 390:290–294

Subramaniam M, Frenette PS, Saffaripour S et al (1996) Defects in hemostasis in P-selectin-deficient mice. Blood 87:1238–1242

Suh TT, Holmback K, Jensen NJ et al (1995) Resolution of spontaneous bleeding events but failure of pregnancy in fibrinogen-deficient mice. Genes Dev 9:2020–2033

Sun WY, Witte DP, Degen JL et al (1998) Prothrombin deficiency results in embryonic and neonatal lethality in mice. Proc Natl Acad Sci USA 95:7597–7602

Thomas DW, Mannon RB, Mannon PJ et al (1998) Coagulation defects and altered hemodynamic responses in mice lacking receptors for thromboxane A_2. J Clin Invest 102:1994–2001

Toomey JR, Kratzer KE, Lasky NM et al (1996) Targeted disruption of the murine tissue factor gene results in embryonic lethality. Blood 88:1583–1587

Xue J, Wu Q, Westfield L et al (1998) Incomplete embryonic lethality and fatal neonatal hemorrhage caused by prothrombin deficiency in mice. Proc Natl Acad Sci USA 95:7603–7607

Wang L, Zoppè M, Hackeng TM et al (1997) A factor IX-deficient mouse model for hemophilia B gene therapy. Proc Natl Acad Sci USA 94:11563–11566

B.7
Critical Issues in Experimental Models

B.7.1
The Use of Positive Control

Clearly, there are many antithrombotic agents that can be used to compare and contrast the antithrombotic efficacy and safety of novel agents. The classic antithrombotic agents are heparin, warfarin, and aspirin. However, new, more selective agents such as hirudin, low molecular weight heparins, and clopidogrel are commercially available that will either replace or augment these older treatments. Novel antithrombotic agents should certainly be demanded to demonstrate better efficacy than currently available therapy in animal models of thrombosis. This should be demonstrated by performing dose-response experiments that include maximally effective doses of each compound in the model. At the maximally effective dose, parameters such as APTT, PT, template bleeding time, or other, more sensitive measurements of systemic hypocoagulability or bleeding should be compared. A good example of this approach is a study by Schumacher et al. (1996), who compared the antithrombotic efficacy of argatroban and dalteparin in arterial and venous models of thrombosis. Consideration of potency and safety compared to other agents should be taken into account when advancing a drug through the testing funnel.

The early *in vivo* evaluation of compounds that demonstrate acceptable *in vitro* potency and selectivity requires evaluation of each compound alone in order to demonstrate antithrombotic efficacy. The antithrombotic landscape is becoming complicated by so many agents from which to choose that it will become increasingly difficult to design preclinical experiments that mimic the clinical setting in which polyantithrombotic therapy is required for optimal efficacy and safety. Consequently, secondary and tertiary preclinical experiments will need to be carefully designed in order to answer these specific, important questions.

REFERENCES AND FURTHER READING

Schumacher WA, Heran CL, Steinbacher TE (1996) Low-molecular-weight heparin (Fragmin) and thrombin active-site inhibitor (argatroban) compared in experimental arterial and venous thrombosis and bleeding time. J Card Pharmacol 28:19–25

B.7.2
Evaluation of Bleeding Tendency

Although the clinical relevance of animal models of thrombosis has been well-established in terms of efficacy, the preclinical tests for evaluating safety, i.e, bleeding tendency, have not been as predictable. The difficulty in predicting major bleeding, such as intracranial hemorrhage, resulting from antithrombotic or thrombolytic therapy stems from the complexity and lack of understanding of the mechanisms involved in this disorder. Predictors of anticoagulant-related intracranial hemorrhages are advanced age, hypertension, intensity and duration of treatment, head trauma, and prior neurologic disease (Stieg and Kase 1998, Sloan and Gore 1992). These risk factors are clearly difficult, if not impossible, to simulate in laboratory animals. Consequently, more general tests of anticoagulation and primary hemostasis have been employed.

Coagulation assays provide an index of the systemic hypocoagulability of the blood after administration of antithrombotic agents; however, as indicated earlier, the sensitivity and specificity of these assays varies from compound to compound, so these assays do not provide a consistent safety measure across all mechanisms of inhibition. Consequently, many laboratories have attempted to develop procedures that provide an indication of bleeding risk by evaluating primary hemostasis after generating controlled incisions in anesthetized animals. Some of the tests used in evaluating FXa inhibitors include template bleeding time, tail transection bleeding time, cuticle bleeding time, and evaluation of clinical parameters such as hemoglobin and hematocrit. Unfortunately, template bleeding tests, even when performed in humans, have not been good predictors of major bleeding events in clinical trials (Bernardi et al. 1993, Bick 1995, Rodgers and Levin 1990). However, these tests have been able to demonstrate relative advantages of certain mechanisms and agents over others. For example, hirudin, a direct thrombin inhibitor, appears to have a narrow therapeutic window when used as an adjunct to thrombolysis in clinical trials, producing unacceptable major bleeding when administered at 0.6 mg/kg, i.v. bolus, plus 0.2 mg/kg/hr (Antman et al. 1996, GUSTO Investigators 1996). When the dose of hirudin was adjusted to avoid major bleeding (0.1 mg/kg and 0.1 mg/kg/hr), no significant therapeutic advantage over heparin was observed. If the relative improvement in the ratio between efficacy and bleeding observed preclinically with Xa inhibitors compared to thrombin inhibitors such as hirudin is supported in future clinical trials, this will establish an important safety advantage for FXa inhibitors and provide valuable information for evaluating the safety of new antithrombotic agents in preclinical experiments.

REFERENCES AND FURTHER READING

Antman EM, TIMI 9B Investigators (1996) Hirudin in acute myocardial infarction: thrombolysis and thrombin inhibition in myocardial infarction (TIMI) 9B trial. Circulation 4:911–921

Bernardi MM, Califf RM, Kleiman N et al (1993) Lack of usefulness of prolonged bleeding times in predicting hemorrhagic events in patients receiving the 7E3 glycoprotein IIb/IIIa platelet antibody. Am J Cardiol 72:1121–1125

Bick RL (1995) Laboratory evaluation of platelet dysfunction. Clin Lab Med 15:1–38

Global Use of Strategies to Open Occluded Coronary Arteries (GUSTO) IIb/IIIa Investigators (1996) A comparison of recombinant hirudin with heparin for the treatment of acute coronary syndromes. N Engl J Med 335:775–782

Rodgers RPC, Levin J (1990) A critical reappraisal of the bleeding time. Sem Thromb Hemost 16:1–20

Sloan MA, Gore JM (1992) Ischemic stroke and intracranial hemorrhage following thrombolytic therapy for acute myocardial infarction: a risk-benefit analysis. Am J Cardiol 69:21A–38A

Stieg PE, Kase CS (1998) Intracranial hemorrhage: diagnosis and emergency management. Neurol Clin 16:373–390

B.7.3
Selection of Models Based on Species-Dependent Pharmacology/Physiology

As alluded to earlier, species selection for animal models of disease is often limited by the unique physiology of a particular disease target in different species or by the species specificity of the pharmacological agent for the target. For example, it was discovered relatively early in the development of platelet GPIIb/IIIa antagonists that these compounds were of limited use in rats (Cox et al. 1992) and that there was a dramatic species-dependent variation in the response of platelets to GPIIb/IIIa antagonists (Bostwick et al. 1996, Cook et al. 1993, Panzer-Knodle et al. 1993). This discovery lead to the widespread use of larger animals (particularly in dogs, whose platelet response to GPIIb/IIIa antagonists resembles humans) in the evaluation of GPIIb/IIIa antagonists. Of course the larger animals required more compound for evaluation, which created a resource problem for medicinal chemists. This was especially problematic for companies that generated compounds by combinatorial parallel synthetic chemistry in which many compounds can be made, but usually in very small quantities. However, some pharmacologists devised clever experiments that partially overcame this problem. Cook et al. (1996) administered a GPIIb/IIIa antagonist orally and intravenously to rats, and then mixed the platelet-rich plasma from the treated rats with platelet-rich plasma from untreated dogs. The mixture was then evaluated in an agonist-induced platelet aggregation assay and the resulting inhibition of canine platelet aggregation (rat platelets were relatively unresponsive to this GPIIb/IIIa antagonist) was due to the drug present in the plasma obtained from the rat. Using this method, only a small amount of drug is required to determine the relative bioavailability in rats. However, the animal models chosen for efficacy in that report (guinea pigs and dogs) were selected based on their favorable platelet response to the GPIIb/IIIa antagonist.

Similarly for inhibitors of FXa, there are significant variations in the activity of certain compounds against FXa purified from plasma of different species and in plasma-based clotting assays using plasma from different species. DX-9065 is much more potent against human FXa (Ki = 78 nM) than against rabbit (Ki = 102 nM) and rat (Ki = 1980 nM) FXa. Likewise, in the PT assay, DX-9065a was very potent in human plasma (concentration required to double PT, PTx2, was 0.52 μM) and in squirrel monkey plasma ($PT \times 2 = 0.46\,\mu M$), but was much less potent in rabbit, dog, and rat plasma ($PT \times 2 = 1.5$, 6.5, and 22.2 μM, respectively). Other FXa inhibitors have also demonstrated these species-dependent differences in activity (Tidwell et al. 1980, Nutt et al. 1991, Taniuchi et al. 1998). Regardless, the investigator must be aware of these differences so that appropriate human doses can be extrapolated from the laboratory animal studies.

Although in many cases the exact mechanism for the species-dependent differences in response to certain therapeutic agents remains unclear, these differences must be examined to determine the appropriate species to be used for preclinical pharmacological evaluation of each agent. This evaluation can routinely be performed by *in vitro* coagulation or platelet aggregation tests prior to evaluation in animal models.

REFERENCES AND FURTHER READING

Bostwick JS, Kasiewski CJ, Chu V et al (1996) Anti-thrombotic activity of RG13965, a novel platelet fibrinogen receptor antagonist. Thrombosis Research 82:495–507

Cook JJ, Holahan MA, Lyle EA et al (1996) Nonpeptide glycoprotein IIb/IIIa inhibitors. 8. Antiplatelet activity and oral antithrombotic efficacy of L-734,217. J Pharmacol Exp Ther 278:62–73

Cook NS, Zerwes H-G, Tapparelli C et al (1993) Platelet aggregation and fibrinogen binding in human, rhesus monkey, guinea-pig, hamster and rat blood: activation by ADP and thrombin receptor peptide and inhibition by glycoprotein IIb/IIIa antagonists. Thromb Haemostasis 70:531–539

Cox D, Motoyama Y, Seki J et al (1992) Pentamadine: a non-peptide GPIIb/IIIa antagonist—in vitro studies on platelets from humans and other species. Thromb Haemostasis 68:731–736

Nutt EM, Jain D, Lenny AB et al (1991) Purification and characterization of recombinant antistasin: a leech-derived inhibitor of coagulation factor Xa. Arch Biochem Biophys 285:37–44

Panzer-Knodle S, Taite BB, Mehrotra DV et al (1993) Species variation in the effect of glycoprotein IIb/IIIa antagonists on inhibition of platelet aggregation. J Pharm Tox Meth 30:47–53

Taniuchi Y, Sakai Y, Hisamichi N et al (1998) Biochemical and pharmacological characterization of YM-60828, a newly synthesized and orally active inhibitor of human factor Xa. Thromb Haemost 79:543–548

Tidwell RR, Webster WP, Shaver SR, Geratz JD (1980) Strategies for anticoagulation with synthetic protease inhibitors: Xa inhibitors versus thrombin inhibitors. Thromb Res 19:339–349

B.7.4 Selection of Models Based on Pharmacokinetics

Much debate surrounds the issue as to which species most resembles humans in terms of gastrointestinal absorption, clearance, and metabolism of therapeutic agents. Differences in gastrointestinal anatomy, physiology, and biochemistry between humans and commonly used laboratory animals suggest that no single animal can precisely mimic the gastrointestinal characteristics of humans (Kararli 1995). Due to resource issues (mainly compound availability) and animal care and use considerations, small rodents, such as rats, are usually considered for primary *in vivo* evaluation of pharmacokinetics for novel agents. However, there is great reservation about moving a compound into clinical trials based on oral bioavailability data derived from rat experiments alone. Usually, larger animals such as dogs or non-human primates, which have similar gastrointestinal morphology compared to humans, are the next step in the evaluation of pharmacokinetics of new agents. The pharmacokinetic characteristics of FXa inhibitor, YM-60828, have been studied extensively in a variety of laboratory animals. YM-60828 demonstrated species-dependent pharmacokinetics, with oral bioavailability estimates of approximately 4%, 33%, 7%, and 20% in rats, guinea pigs, beagle dogs, and squirrel monkeys, respectively**.** Although these results suggest that YM-60828 has somewhat limited bioavailability, evaluating the pharmacokinetic profile of novel agents in a number of species (Sanderson et al. 1998) is a well-established approach used to aid in identifying compounds for advancement to human testing. That is, acceptable bioavailability in a number of species suggests that a compound will be bioavailable in humans. Which of the laboratory species adequately represents the bioavailability of a specific compound in humans can only be determined after appropriate pharmacokinetic evaluation in humans. Nevertheless, preclinical pharmacokinetic data are important in selecting the appropriate animal model for testing the antithrombotic efficacy of compounds because the ultimate proof-of-concept experiment is to demonstrate efficacy by the intended route of administration.

REFERENCES AND FURTHER READING

Kararli TT (1995) Comparison of the gastrointestinal anatomy, physiology, and biochemistry of humans and commonly used laboratory animals. Biopharm Drug Disp 16:351–380

Sanderson PEJ, Cutrona KJ, Dorsey BD et al (1998) L-374,087, an efficacious, orally bioavailable, pyridinone acetamide thrombin inhibitor. Bioorg Med Chem Lett 8:817–822

B.7.5 Clinical Relevance of Data Derived from Experimental Models

Animal models of thrombosis have played a crucial role in the discovery and development of a number of compounds that are now successfully being used for the treatment and prevention of thrombotic diseases. The influential preclinical results using novel antithrombotics in a variety of laboratory animal experiments are listed in Table 7 below, along with the early clinical trials and results for each compound. This table intentionally omits many compounds that were tested in animal models of thrombosis, but failed to be successful in clinical trials or, for other reasons, did not become approved drugs. However, these negative outcomes would not have been predicted by animal models of thrombosis because the failures were generally due to other shortcomings of the drugs (e.g, toxicity, narrow therapeutic window, or undesirable pharmacokinetics or pharmacodynamics) that are not always clearly presented in the scientific literature due to proprietary restrictions in this highly competitive field.

Nonetheless, it is clear that animal models have supplied valuable information for investigators responsible for evaluating these drugs in humans, providing pharmacodynamic, pharmacokinetic, and safety data that can be used to design safe and efficient clinical trials. For detailed applications see the following references: Bugge et al. (1995), Bugge et al. (1996), Carmeliet et al. (1993), Carmeliet et al. (1994), Carmeliet et al. (1996), Christie et al. (1999), Connolly et al. (1996), Cui et al. (1996), Evans et al. (1989), Healy et al. (1995), Herzog et al. (1999), Hodivala-Dilke et al. (1999), Huang et al. (1997), Kahn et al. (1998), Kay et al. (2000), Kung et al. (1998), Law et al. (1999), Leon et al. (1999), Lin et al. (1997), Offermanns et al. (1997), Ploplis et al. (1995), Subramaniam et al. (1996), Thomas et al. (1998), Toomey et al.

Table 7 Animal models of thrombosis and their clinical correlates

Compound	Preclinical Animal Model	Preclinical Results	Ref	Clinical Indication	Clinical Result	Ref
Recombinant tissue plasminogen activator (Activase)	Rabbit pulmonary artery thrombosis	Lysis of preformed pulmonary thrombus	Matsuo et al. 1981	Acute myocardial infarction—thrombolysis	Improved recanalization	Collen et al. (1984)
Abciximab (ReoPro)	Canine coronary cyclic flow reduction	Significant inhibition of platelet-dependent thrombosis	Coller et al. 1986; Coller et al. 1989	High-risk coronary angioplasty	Reduction in death, myocardial infarction, refractory ischemia, or unplanned revascularization	EPIC Investigators (1994)
Tirofiban (Aggrestat)	Canine coronary cyclic flow reduction	Significant inhibition of platelet-dependent thrombosis	Lynch et al. 1995;	Unstable angina	Reduction in death, myocardial infarction, refractory ischemia	PRISM Investigators (1998)
Eptifibitide (Integrilin)	TPA-induced coronary thrombolysis	Significant improvement in lysis of occlusive thrombus	Nicolini et al. 1994	Acute myocardial infarction—thrombolysis with tPA	Improvement in incidence and speed of reperfusion	Ohman et al. 1997
Enoxaparin (Lovenox)	Canine coronary cyclic flow reduction	Significant inhibition of platelet-dependent thrombosis	Lynch et al. 1995	Unstable angina	Significant decrease in death, myocardial infarction, and need for revascularization at 30 days	Cohen et al. 1998
Hirudin (Refludan)	Rabbit jugular vein thrombus growth	Inhibition of thrombus growth compared to standard heparin	Agnelli et al., 1990	Deep vein thrombosis after total hip replacement	Significantly decreased rate of DVT	Eriksson et al. 1997
Argatroban	Canine coronary artery electrolytic-injury (TPA-induced thrombolysis)	Accelerated reperfusion and prevented reocclusion	Fitzgerald et al. 1989	Unstable angina	No episodes of MI during drug infusion	Gold et al. 1993

(1996), Vassalli et al. (1997), Waugh et al. (1999), and Zoldhelyi et al. (2000).

REFERENCES AND FURTHER READING

Bugge TH, Suh TT, Flick MJ et al (1995) The receptor for urokinase-type plasminogen activator is not essential for mouse development or fertility. J Bio Chem 270:16886–16894

Bugge TH, Xiao Q, Kombrinck KW et al (1996) Fatal embryonic bleeding events in mice lacking tissue factor, the cell-associated initiator of blood coagulation. Proc Natl Acad Sci USA 93:6258–6263

Carmeliet P, Stassen JM, Schoonjans L et al (1993) Plasminogen activator inhibitor-1 gene-deficient mice. J Clin Invest 92:2756–2760

Carmeliet P, Schoonjans L, Kieckens L et al (1994) Physiological consequences of loss of plasminogen activator gene function in mice. Nature 368:419–424

Carmeliet P, Mackman N, Moons L et al (1996) Role of tissue factor in embryonic blood vessel development. Nature 383:73–75

Christie PD, Edelberg JM, Picard MH et al (1999). A murine model of myocardial thrombosis. J Clin Invest 104:533–539

Connolly AJ, Ishihara H, Kahn ML et al (1996) Role of the thrombin receptor in development and evidence for a second receptor. Nature 381:516–519

Cui J, O'Shea KS, Purkayastha A et al (1996) Fatal haemorrhage and incomplete block to embryogenesis in mice lacking coagulation factor V. Nature 384:66–68

Evans JP, Brinkhous KM, Brayer GD et al (1989) Canine hemophilia B resulting from a point mutation with unusual consequences. Proc Natl Acad Sci USA 86:10095–10099

Healy AM, Rayburn HB, Rosenberg RD, Weiler H (1995) Absence of the blood-clotting regulator thrombomodulin causes embryonic lethality in mice before development of

a functional cardiovascular system. Proc Natl Acad Sci USA 92:850–854
Herzog RW, Yang EY, Couto LB et al (1999) Long-term correction of canine hemophilia B by gene transfer of blood coagulation factor IX mediated by adeno-associated viral vector. Nat Med 5:56–63
Hodivala-Dilke KM, McHugh KP, Tsakiris DA et al (1999) β_3-integrin-deficient mice are a model for Glanzmann thrombasthenia showing placental defects and reduced survival. J Clin Invest 103:229–238
Huang Z-F, Higuchi D, Lasky N, Broze GJJ (1997) Tissue factor pathway inhibitor gene disruption produces intrauterine lethality in mice. Blood 90:944–951
Kahn ML, Zheng Y-W, Huang W et al (1998) A dual thrombin receptor system for platelet activation. Nature 394:690–694
Kay MA, Manno CS, Ragni MV et al (2000) Evidence for gene transfer and expression of factor IX in haemophilia B patients with an AAV vector. Nat Gen 24:257–261
Kung J, Hagstrom J, Cass D et al (1998) Human FIX corrects bleeding diathesis of mice with hemophilia B. Blood 91:784–790
Law DA, DeGuzman FR, Heiser P et al (1999) Integrin cytoplasmic tyrosine motif is required for outside-in αIIbβ3 signalling and platelet function. Nature 401:808–811
Leon C, Hechler B, Freund M et al (1999) Defective platelet aggregation and increased resistance to thrombosis in purinergic $P2Y_1$ receptor-null mice. J Clin Invest 104:1731–1737
Lin H-F, Maeda N, Sithies O et al (1997) A coagulation factor IX-deficient mouse model for human hemophilia B. Blood 90:3962–3966
Offermanns S, Toombs CF, Hu Y-H, Simon MI (1997) Defective platelet activation in $G\alpha_q$-deficient mice. Nature 389:183–186
Ploplis VA, Carmeliet P, Vazirzadeh S et al (1995) Effects of disruption of the plasminogen gene on thrombosis, growth, and health in mice. Circulation 92:2585–2593
Subramaniam M, Frenette PS, Saffaripour S et al (1996) Defects in hemostasis in P-selectin-deficient mice. Blood 87:1238–1242
Thomas DW, Mannon RB, Mannon PJ et al (1998) Coagulation defects and altered hemodynamic responses in mice lacking receptors for thromboxane A_2. J Clin Invest 102:1994–2001
Toomey JR, Kratzer KE, Lasky NM et al (1996) Targeted disruption of the murine tissue factor gene results in embryonic lethality. Blood 88:1583–1587
Vassalli G, Dichek DA (1997) Gene therapy for arterial thrombosis. Cardiovasc Res 35:459–469
Waugh JM, Yuksel E, Li J et al (1999) Local overexpression of thrombomodulin for in vivo prevention of arterial thrombosis in a rabbit model. Circ Res 84:84–92
Zoldhelyi P, McNatt J, Shelat HS et al (2000) Thromboresistance of balloon-injured porcine carotid arteries after local gene transfer of human tissue factor pathway inhibitor. Circulation 101:289–295

REFERENCES AND FURTHER READING

Agnelli G, Pascucci C, Cosmi B, Nenci GG (1990) The comparative effects of recombinant hirudin (CGP 39393) and standard heparin on thrombus growth in rabbits. Thromb Haemost 63:204–207
Cohen M, Demers C, Gurfinkel EP et al (1998) Low-molecular-weight heparins in non-ST-segment elevation ischemia: the ESSENCE trial. Efficacy and Safety of Subcutaneous Enoxaparin versus intravenous unfractionated heparin, in non-Q-wave Coronary Events. Am J Cardiol 82:19L–24L
Collen D, Topol EJ, Tiefenbrunn AJ et al (1984) Coronary thrombolysis with recombinant human tissue-type plasminogen activator: a prospective, randomized, placebo-controlled trial. Circulation 70:1012–1017
Coller BS, Folts JD, Scudder LE, Smith SR (1986) Antithrombotic effect of a monoclonal antibody to the platelet glycoprotein IIb/IIIa receptor in an experimental animal model. Blood 68:783–786
Coller BS, Folts JD, Smith SR, Scudder LE, Jordan R (1989) Abolition of in vivo platelet thrombus formation in primates with monoclonal antibodies to the platelet GPIIb/IIIa receptor. Correlation with bleeding time, platelet aggregation, and blockade of GPIIb/IIIa receptors. Circulation 80(6):1766–74
EPIC Investigators (1994) Randomised trial of coronary intervention with antibody against platelet IIb/IIIa integrin for reduction of clinical restenosis: results at six months. Lancet 343:881–886
Fitzgerald DJ, Wright F, FitzGerald GA (1989) Increased thromboxane biosynthesis during coronary thrombolysis: evidence that platelet activation and thromboxane A2 modulate the response to tissue-type plasminogen activator in vivo. Circ Res 65:83–94
Leadley RJJ, Kasiewski CJ, Bostwick JS et al (1998) Inhibition of repetitive thrombus formation in the stenosed canine coronary artery by enoxaparin, but not by unfractionated heparin. Arterioscler Thromb Vasc Biol 18:908–914
Lynch JJJ, Sitko GR, Lehman ED, Vlasuk GP (1995) Primary prevention of coronary arterial thrombosis with the factor Xa inhibitor rTAP in a canine electrolytic injury model. Thromb Haemost 74:640–645
Matsuo O, Rijken DC, Collen D (1981) Thrombolysis by human tissue plasminogen activator and urokinase in rabbits with experimental pulmonary embolus. Nature 291:590–591
Nicolini FA, Lee P, Rios G et al (1994) Combination of platelet fibrinogen receptor antagonist and direct thrombin inhibitor at low doses markedly improves thrombolysis. Circulation 89:1802–1809

B.8 Safety Assays in Thrombosis and Haemostasis

See Mousa (2006).

REFERENCES AND FURTHER READING

Mousa SM (2006) Safety pharmacolgy of blood constituents.In: Vogel HG, Hock FJ, Maas J, Mayer D (eds) Drug Discovery and Evaluation – Safety and Pharmacokinetic Assays, Chapter I M. Springer-Verlag, Berlin Heidelberg New York, pp 255–318

Chapter C
Activity on Urinary Tract[1]

[1] Contribution for this edition by S.A. Hart, review of second ediktion by M. Hropot, contributions to the former editions by R. Greger, H. Gögelein, M. Hropot and M. Bleich.

C.1 Diuretic and Saluretic Activity

C.1.1 In Vitro Methods

C.1.1.1 Carbonic Anhydrase Inhibition In Vitro

PURPOSE AND RATIONALE

Acetazolamide (Diamox) was one of the first synthetic non-mercurial diuretics. The mode of action was found to be inhibition of carbonic anhydrase. Carbonic anhydrase is a zinc-containing enzyme that catalyzes the reversible hydration (or hydroxylation) of CO_2 to form H_2CO_3 which dissociates non-enzymatically into HCO_3^- and H^+. The enzyme is located within the cytoplasm and at the apical and basolateral membranes of proximal tubules as well as on the apical (lumenal) surface of distal tubules and in the thick ascending limb of the loop of Henle. Its primary function is to enhance H^+ secretion into the urine. At least three isoenzymes, designated as I, II and II or A, B and C, are known to exist..

Carbonic anhydrase inhibitors were originally used as diuretics but are no longer used for this purpose except in limited circumstances (metabolic alkalosis accompanied by edema). Chronic inhibition of carbonic anhydrase results in significant hypokalemia and metabolic acidosis due to bicarbonate wasting and thus inhibition of carbonic anhydrase may be mechanistically important if these effects are noted in *in vivo* studies or clinically (Okusa and Ellison, 2000). Numerous isoenzymes exist, of which CA II is the most abundant in proximal tubules and erythrocytes. The activity of carbonic anhydrase in erythrocytes is significantly higher than that in the kidney, and the enzyme is easily harvested by lysing mammalian whole blood. Thus, examination of the degree of inhibition of erythrocyte carbonic anhydrase may serve as a suitable surrogate for examination of effects on renal activity (Maren 1967; Armstrong et al. 1966).

In spite of the fact that newer diuretics are based on other modes of action, the test for inhibition of carbonic anhydrase should be performed for evaluation of a new compound. Moreover, the specific use of carbonic anhydrase inhibitors as antiglaucoma drugs has been described (Friedland and Maren 1984; Caprioli 1985). The mechanism by which carbonic anhydrase inhibitors lower intraocular pressure is through a reduction in aqueous humor formation, by affecting electrolyte and water balance in the nonpigmented ciliary epithelium (Friedland and Maren 1984; Caprioli 1985). Although many methods to measure carbonic anhydrase activity have been developed (Philpot and Philpot 1936), the micro method described by Maren (1960) is relatively simple, sensitive and reliable. The enzyme source are red cells, a rich source of the same isoenzymes found in the eye (Maren 1967; Armstrong et al. 1966; Wistrand et al. 1986; Wistrand and Knuutila 1980).

PROCEDURE

The analytical method is based on the catalysis of the conversion of CO_2 to H_2CO_3 by the enzyme, with resultig decrease in pH being monitored colorimetrically (Philpot and Philpot, 1936).

Materials and Solutions

- phenol red indicator solution: 12.5 mg phenol red/liter 2.6 mM $NaHCO_3$, pH 8.3 + 218 mM Na_2CO_3
- 1 M sodium carbonate/bicarbonate buffer, pH 9.8
- Enzyme: Carbonic anhydrase from dog blood; Blood is collected into a heparinized tube and diluted 1:100 with deionized water.
- Equipment
  - Reaction vessel – custom made by Labglass Inc., Vineland, NJ, USA
  - Monostat bench mounted flowmeter
  - 30% CO_2 – M& G Gases, Branchburg, NJ, USA

Assay

CO_2 flow rate is adjusted to 30 (45) ml/min. The following solutions are added to the reaction vessel:

400 µl phenol red indicator solution

100 µl enzyme

200 µl H_2O or appropriate drug concentration after 3 min for equilibration:

100 µl carbonate/bicarbonate buffer is added.

The following parameters are determined in duplicate samples:

T_u = (uncatalyzed time) = time for the color change to occur in the absence of enzyme.

T_e = (catalyzed time) = time for the color change to occur in the presence of the enzyme.

$T_u - T_e$ = enzyme rate

T_i = enzyme rate in the presence of various concentrations of inhibitor

EVALUATION

Percent inhibition of carbonic anhydrase is calculated according to the following formula:

$$\%\text{Inhibition} = 1 - \frac{(T_u - T_e) - (T_i - T_e)}{T_u - T_e} \times 100$$

Standard data:

- Compound IC_{50}[M]
- Acetazolamide 9.0×10^{-9}
- Chlorothiazide 9.0×10^{-7}

CRITICAL ASSESSMENT OF THE METHOD

Determination of carbonic anhydrase inhibition is of value to characterize the activity spectrum of sulfonamide diuretics.

MODIFICATIONS OF THE METHOD

Landolfi et al. (1997) reported a modified procedure for the measurement of carbonic anhydrase activity. The measure of carbonic anhydrase activity is based on the rate of CO_2 hydration by the enzyme. Such transformation was monitored by a procedure which consists in the measure of time necessary for the pH of an appropriate buffer to decrease from 8 to 7.5 in the presence of a constant CO_2 flow: such time period is dose-dependently reduced by the addition of the enzyme and further modified in the presence of carbonic anhydrase inhibitory compounds. The time required for a specific change in pH can be determined electrochemically as opposed to colorimetrically. This requires the use of a well-calibrated pH meter with a fast-reacting electrode. Activity is expressed in enzyme units, defined as a doubling of the time needed for the pH change in the absence of enzyme. These methods are much more sensitive than the colorimetric determination (Maren, 1960; Landolfi et al., 1997; Lukasi, 2005).

REFERENCES AND FURTHER READING

Armstrong JMD, Myers DV, Verpoorte JA, Edsall JT (1966) Purification and properties of human erythrocyte carbonic anhydrase. J Biol Chem 241:5137–5149

Caprioli J (1985) The pathogenesis and medical management of glaucoma. Drug Dev Res 6:193–215

Eveloff J, Swenson ER, Maren TH (1979) Carbonic anhydrase activity of brush border and plasma membranes prepared from rat kidney cortex. Biochem Pharmacol 28:1434–1437

Friedland BR, Maren TH (1984) Carbonic anhydrase: Pharmacology of inhibitors and treatment of glaucoma. In: Pharmacology of the Eye. Handbook Exp Pharmacol 69:279–309

Landolfi C, Marchetti M, Ciocci G, Milanese C (1997) Development and pharmacological characterization of a modified procedure for the measurement of carbonic anhydrase activity. J Pharmacol Toxicol Meth 38:169–172

Lukasi HC (2005) Low dietary zinc decreases erythrocyte carbonic anhydrase activities and impairs cardiorespiratory function in men during exercise. Am J Clin Nutr 81:1045–1051

Maren TH (1960) A simplified micromethod for the determination of carbonic anhydrase and its inhibitors. J Pharmacol Exp Ther 130:26–29

Maren TH (1967) Carbonic anhydrase: Chemistry, physiology, and inhibition. Physiol Rev 47:595–781

Okusa MD, Ellison DH (2000) Physiology and pathophysiology of diuretic action. In Seldon D. W. and Giebsich, G. (eds), "The Kidney: Physiology and Pathophysiology (3rd ed.)". Lippincott, Williams and Wilkins: Philadelphia

Philpot FJ, Philpot JSL (1936) A modified colorimetric estimation of carbonic anhydrase. Biochem J 30:2191–2193

Wistrand PJ, Knuuttila K-G (1980) Bovine lens carbonic anhydrases: Purification and properties. Exp Eye Res 30:277–290

Wistrand PJ, Schenholm M, Lönnerholm G (1986) Carbonic anhydrase isoenzymes CA I and CA II in the human eye. Invest Ophthalm Visual Sci 27:419–428

C.1.2 In Vivo Methods

C.1.2.1 Diuretic Activity in Rats (LIPSCHITZ Test)

PURPOSE AND RATIONALE

A method for testing diuretic activity in rats has been described by Lipschitz et al. (1943). The test is based on water and sodium excretion in test animals and compared to rats treated with a high dose of urea. The "Lipschitz-value" is the quotient between excretion by test animals and excretion by the urea control.

PROCEDURE

Male Wistar rats weighing 100–200 g are used. Three animals per group are placed in metabolic cages provided with a wire mesh bottom and a funnel to collect the urine. Stainless-steel sieves are placed in the funnel to retain feces and to allow the urine to pass. The rats are fed with standard diet (Altromin pellets) and water ad libitum. Fifteen hours prior to the experiment food and water are withdrawn. Three animals are placed in one metabolic cage. For screening procedures two groups of three animals are used for one dose of the test compound. The test compound is applied orally at a dose of 50 mg/kg in 5.0 ml water/kg body weight. Two groups of 3 animals receive orally 1 g/kg urea. Additionally, 5 ml of 0.9% NaCl solution per 100 g body weight are given by gavage. Urine excretion is recorded after 5 and after 24 h. The sodium content of the urine is determined by flame photometry. Active compounds are tested again with lower doses.

EVALUATION

Urine volume excreted per 100 g body weight is calculated for each group. Results are expressed as the "Lipschitz-value", i. e., the ratio T/U, in which T is the response of the test compound, and U, that of urea treatment. Indices of 1.0 and more are regarded as a positive effect. With potent diuretics, Lipschitz values of 2.0 and more can be found. Calculating this index for the 24 h excretion period as well as for 5 h indicates the duration of the diuretic effect. Similar to urine volume, quotients can be calculated for sodium excretion. Dose-response curves can be established using various doses. Loop diuretics are characterized by a steep dose-response curve. Saluretic drugs, like hydrochlorothiazide, show Lipschitz values around 1.8, whereas loop diuretics (or high ceiling diuretics) like furosemide, bumetanide or piretanide reach values of 4.0 and more.

CRITICAL ASSESSMENT OF THE METHOD

The Lipschitz test has been proven to be a standard method and a very useful tool for screening of potential diuretics.

MODIFICATIONS OF THE METHOD

The method has been modified in various ways by several authors. Cummings et al. (1960) recommended a sequential procedure with criteria for acceptance or rejection of test drugs. Kau et al. (1984) recommended a method for screening diuretic agents in the rat using normal saline (4% body weight) as hydrating fluid.

Homozygous Brattleboro rats exhibit symptoms of diabetes insipidus (Valtin et al. 1965). The condition is due to the failure of hypothalamic neurons to produce vasopressin, which is due to a single base point deletion in the vasopressin gene (Schmale and Richter 1984). The abnormal quinine drinking aversion in the Brattleboro rat with diabetes insipidus is reversed by a vasopressin agonist (Laycock et al. 1994).

These animals can be used to study vasopressin agonism and antagonism and the aquaretic effects of synthetic drugs.

Klatt et al. (1975) described a method of collecting urine excreted by cats. On the basis of urine funnel used in rats, an appropriate larger metabolism cage made out of transparent, rigid polyvinyl chloride was used. The cage was improved by a built-in sieve cone which assured good separation of urine and feces. A device to measure and record the time and amount of voided urine was attached. Urine was collected in a vessel with a hose connection from the bottom to a pressure sensor. An attached overflow tube could be occluded. The initial pressure of the sensor was fed into a linear recorder. Before the test, the recorder was calibrated with a sufficient amount of distilled water to adjust the number of division intervals for direct measurement of voided urine in milliliters. This allowed calculation of the time point of voiding from the chart speed.

REFERENCES AND FURTHER READING

Cummings JR, Haynes JD, Lipchuck LM, Ronsberg MA (1960) A sequential probability ratio method for detecting compounds with diuretic activity in rats. J Pharmacol Exp Ther 128:414–418

Kau ST, Keddie JR, Andrews D (1984) A method for screening diuretic agents in the rat. J Pharmacol Meth 11:67–75

Klatt P, Muschaweck R, Bossaller W, Magerkurth KO, Vanderbeeke O (1997) Method of collecting urine and comparative investigation of quantities excreted by cats and dogs after furosemide. Am J Vet Res 36:919–923

Laycock JF, Chatterji U, Seckl JR, Gartside IB (1994) The abnormal quinine drinking aversion in the Brattleboro rat with diabetes insipidus is reversed by the vasopressin agonist DDAVP: a possible role for vasopressin in the motivation to drink. Physiol Behav 55:407–412

Lipschitz WL, Hadidian Z, Kerpcsar A (1943) Bioassay of diuretics. J Pharmacol Exp Ther 79:97–110

Muschaweck R, Hajdu P (1964) Die saludiuretische Wirksamkeit der Chlor-N-(2-furylmethyl)-5-sulfamyl-anthranilsäure. Arzneim Forsch 14:44–47

Muschaweck R, Sturm K (1972) Diuretika. In: Ehrhart G, Ruschig H (eds) Arzneimittel. Entwicklung – Wirkung – Darstellung. Vol 2, pp 317–328. Verlag Chemie, Weinheim/Bergstrasse, Germany

Nyunt-Wai V, Laycock JF (1990) The pressor response to vasopressin is not attenuated by hypertonic NaCl in the anaesthetized Brattleboro rat. J Physiol 430:35P

Schmale H, Richter D (1984) Single base deletion in the vasopressin gene is the cause of diabetes insipidus in Brattleboro rats. Nature 308:705–709
Schmale H, Ivell M, Breindl D, Darmer D, Richter D (1984) The mutant vasopressin gene from diabetes insipidus (Brattleboro) rats is transcribed but the message is not efficiently translated. EMBO J 3:3289–3293
Szot P, Dorsa DM (1992) Cytoplasmatic and nuclear vasopressin RNA in hypothalamic and extrahypothalamic neurons of the Brattleboro rat: An *in situ* hybridization study. Mol Cell Neurosci 3:224–236
Valtin H, Sawyer WH, Sokol HW (1965) Neurohypophyseal principles in rats homozygous and heterozygous for hypothalamic diabetes insipidus (Brattleboro strain) Endocrinology 77:701–706

C.1.2.2 Saluretic Activity in Rats

PURPOSE AND RATIONALE

Excretion of electrolytes is as important as the excretion of water for treatment of peripheral edema and ascites in congestive heart failure as well as for treatment of hypertension. Potassium loss has to be avoided. As a consequence, saluretic drugs and potassium-sparing diuretics were developed. The diuresis test in rats was modified in such a way that potassium and chloride as well as osmolality are determined in addition to water and sodium. Ratios between electrolytes can be calculated indicating carbonic anhydrase inhibition or a potassium sparing effect.

PROCEDURE

Male Wistar rats weighing 100–200 g fed with standard diet (Altromin pellets) and water ad libitum are used. Fifteen hours prior to the test, food but not water is withdrawn. Test compounds are applied in a dose of 50 mg/kg orally in 0.5 ml/100 g body weight starch suspension. Three animals are placed in one metabolic cage provided with a wire mesh bottom and a funnel to collect the urine. Two groups of 3 animals are used for each dose of a test drug. Urine excretion is registered every hour up to 5 h. The 5-h urine is analyzed by flame photometry for sodium and potassium and argentometrically by potentiometrical end point titration (Chloride-Titrator Aminco) for chloride. To evaluate compounds with prolonged effects the 24 h urine is collected and analyzed. Furosemide (25 mg/kg p.o.), hydrochlorothiazide (25 mg/kg p.o.), triamterene (50 mg/kg p.o.), or amiloride (50 mg/kg p.o.) are used as standards.

EVALUATION

- The sum of Na^+ and Cl^- excretion is calculated as parameter for saluretic activity.
- The ratio Na^+/K^+ is calculated for natriuretic activity. Values greater than 2.0 indicate a favorable natriuretic effect. Ratios greater than 10.0 indicate a potassium-sparing effect.
- The ratio

$$\frac{Cl^-}{Na^+ + K^+}$$

(ion quotient) is calculated to estimate carbonic anhydrase inhibition.
- Carbonic anhydrase inhibition can be excluded at ratios between 1.0 and 0.8. With decreasing ratios slight to strong carbonic anhydrase inhibition can be assumed.

MODIFICATIONS OF THE METHOD

Adrenalectomized rats treated with DOCA or aldosterone can be utilized to test **aldosterone antagonists**. Spironolactone has no effect in the absence of a mineralocorticoid, but reverses in a dose-related manner the effect of DOCA on the Na^+/K^+ ratio in the urine (Kagawa et al. 1957; Bicking et al. 1965).

REFERENCES AND FURTHER READING

Bicking JB, Mason JW, Woltersdorf OW, Jones JH, Kwong SF, Robb CM, Cragoe EJ (1965) Pyrazine diuretics. I. N-amidino-3-amino-6-halopyrazinecarboxamides. J Med Chem 8:638–642
Kagawa CM, Cella JA, Van Arman CG (1957) Action of new steroids in blocking effects of aldosterone and desoxycorticosterone on salt. Science 126:1015–1016
Muschaweck R, Hajdu P (1964) Die saludiuretische Wirksamkeit der Chlor-N-(2-furylmethyl)-5-sulfamyl-anthranilsäure. Arzneim Forsch/Drug Res 14:44–47
Muschaweck R, Sturm K (1972) Diuretika. In: Ehrhart G, Ruschig H (eds) Arzneimittel. Entwicklung – Wirkung – Darstellung. Vol 2, pp 317–328. Verlag Chemie, Weinheim/Bergstrasse, Germany

C.1.2.3 Diuretic and Saluretic Activity in Dogs

PURPOSE AND RATIONALE

Dogs have been extensively used to study renal physiology and the action of diuretics. Renal physiology of the dog is claimed to be closer to man than that of rats. Oral absorbability of diuretic substances can appropriately be studied in dogs. Using catheters, interval collections of urine can be made with more reliability than in rats. Simultaneously, blood samples can be withdrawn to study pharmacokinetics.

PROCEDURE

Beagle dogs of either sex have to undergo intensive training to be accustomed to accept gavage feeding

and hourly catheterization without any resistance. The dogs are placed in metabolic cages. At least 4 dogs are used as controls receiving water only, as standard controls (1 g/kg urea p.o. or 5 mg/kg furosemide p.o.) or the test drug group. Twenty-four hours prior to the experiment food but not water is withheld. On the morning of the experiment, the urine bladder is emptied with a plastic catheter. The dogs receive 20 ml/kg body weight water by gavage, followed by hourly doses of 4 ml/kg body weight drinking water. The bladder is catheterized twice in an interval of 1 h and the urine collected for analysis of initial values. Then, the test compound or the standard is applied either orally or intravenously. Hourly catheterization is repeated over the next 6 h. Without further water dosage the animals are placed in metabolic cages overnight. Twenty-four hours after dosage of the test compound, the dogs are catheterized once more and this urine together with the urine collected over night in the metabolic cage registered. All urine samples are analyzed by flame photometry for sodium and potassium and by argentometry (Chloride Titrator Aminco) for chloride content. Furthermore, osmolality is measured with an Osmometer.

EVALUATION

Urine volume, electrolyte concentrations and osmolality are averaged for each group. The values are plotted against time to allow comparison with pretreatment values as well as with water controls and standards. The non-parametric U-test is used for statistical analysis.

REFERENCES AND FURTHER READING

Baer JE (1965) Animal techniques for evaluating diuretics. In: Nodin HJ, Siegler PE (eds) Animal and Clinical Pharmacologic Techniques in Drug Evaluation. pp 231–236. Year Book Medical Publ. Inc. Chicago

Muschaweck R, Hajdu P (1964) Die saludiuretische Wirksamkeit der Chlor-N-(2-furylmethyl)-5-sulfamyl-anthranilsäure. Arzneim Forsch/Drug Res 14:44–47

Muschaweck R, Sturm K (1972) Diuretika. In: Ehrhart G, Ruschig H (eds) Arzneimittel. Entwicklung – Wirkung – Darstellung. Vol 2, pp 317–328. Verlag Chemie, Weinheim/Bergstrasse, Germany

Suki W, Rector FC, Seldin DW (1965) The site of action of furosemide and other sulfonamide diuretics in the dog. J Clin Invest 44:1458–1469

C.2 Assessment of Renal Function

C.2.1 In Vitro Methods

C.2.1.1 Patch Clamp Technique in Kidney Cells[2]

PURPOSE AND RATIONALE

In the different parts of the kidney (proximal tubules, distal tubules, collecting ducts) fluid is reabsorbed and substances may be transported either from the tubule lumen to the blood side (reabsorption) or vice versa (secretion). Besides active transport and coupled transport systems, ion channels play an important role in the function of kidney cells. The various modes of the patch clamp technique (cell-attached, cell-excised, whole-cell mode) (Neher and Sakmann 1976; Hamill et al. 1981) allow the investigation of ion channels. In addition, the investigation of other electrogenic transport mechanisms, such as the sodium-coupled alanine transport can be studied.

PROCEDURE

The patch clamp technique can be applied to cultured kidney cells (Merot et al. 1988), to freshly isolated kidney cells (Hoyer and Gögelein 1991) or to cells of isolated perfused kidney tubules (Gögelein and Greger 1984). The latter method shall be described in more detail.

Segments of late superficial proximal tubules of rabbit kidney are dissected and perfused from one end with a perfusion system (Burg et al. 1966; Greger and Hampel 1981). The non-cannulated end of the tubule is freely accessible to a patch pipette. Under optical control (differential interference contrast optics with 400× magnification) the patch pipette can be moved through the open end into the tubule lumen and is brought in contact with the brush border membrane. After slight suction of the patch electrode, gigaseals form instantaneously and single potassium or sodium channels can be recorded in the cell-attached or inside-out cell-excised mode (Gögelein and Greger 1984; Gögelein and Greger 1986a).

In order to obtain exposed lateral cell membranes suitable to the application of the patch clamp method, pieces of the tubule are torn off by means of a glass pipette (diameter about 40 µm). As to facilitate the tearing off, the tubules are incubated for about 5 min in

[2] Contribution by H. Gögelein.

0.5 g/l collagenase (Sigma, C 2139) at room temperature. After tearing off part of the cannulated tubule, clean lateral cell membranes are exposed at the non-cannulated end. The patch pipette can be moved to the lateral cell membrane and gigaseals can be obtained. It was possible, to investigate potassium channels (Gögelein and Greger 1987) and nonselective cation channels (Gögelein and Greger 1986b) in these membranes.

As cells are still part of an epithelial layer and, therefore, are intracellularly coupled, the whole-cell technique is not appropriate in this preparation. On the other hand, cotransport systems can only be investigated by the whole-cell method because the transport rate of a single event is much too small to be resolved in a similar manner as single ion channel events. Consequently, cells of rabbit proximal tubules are isolated as described in detail elsewhere (Hoyer and Gögelein 1991; Heidrich and Dew 1977). After cervical dislocation the kidneys are rapidly excised and placed in ice-cold solution [mmol/l]: 150 K-cyclamate, 10 HEPES, 1 $CaCl_2$, 1 $MgCl_2$, pH 7.4. The following steps are performed on ice: After decapsulation, superficial cortical slices of about 0.5 mm thickness are dissected and minced with a scalpel. The tissue is homogenized in a Dounce homogenizer by three strokes with a loose-fitting pestle. The homogenate is then poured through graded sieves (250, 75 and 40 µm) to obtain a population of single cells. Since the predominant tubule section of the cortex of the rabbit kidney is the pars convoluta of the proximal tubule, it can be concluded that the majority of the isolated cells in the cell suspension are of proximal tubule origin. By light microscopy cells are identified by long microvilli distributed over the entire cell surface and can easily be discriminated from remaining erythrocytes, cell detritus and tubular fragments.

By application of the whole-cell mode of the patch clamp technique to freshly isolated cells of convoluted proximal tubules, the sodium-alanine cotransport system could be investigated in detail (Hoyer and Gögelein 1991).

EVALUATION

In isolated perfused renal tubules, concentration response curves of drugs which inhibit ion channels can be obtained with the patch clamp technique. In isolated cells of the proximal tubule, the whole-cell mode of the patch clamp technique enables the investigation of the sodium-alanine cotransport system. The apparent K_m values for sodium and L-alanine can be recorded.

MODIFICATIONS OF THE METHOD

Schlatter (1993) recorded membrane voltages of macula densa cells with the fast or slow whole-cell patch-clamp method. The effects of diuretics and the conductance properties of these cells were examined.

REFERENCES AND FURTHER READING

Burg M, Grantham J, Abromow M, Orloff J (1966) Preparation and study of fragments of single rabbit nephrons. Am J Physiol 210:1293–1298

Gögelein H, Greger R (1984) Single channel recordings from basolateral and apical membranes of renal proximal tubules. Pflügers Arch. 401:424–426

Gögelein H, Greger R (1986a) Na^+ selective channels in the apical membrane of rabbit late proximal tubules (pars recta). Pflügers Arch. 406:198–203

Gögelein H, Greger R (1986b) A voltage-dependent ionic channel in the basolateral membrane of late proximal tubules of the rabbit kidney. Pflügers Arch. 407 (Suppl. 2):S142–S148

Gögelein H, Greger R (1987) Properties of single K^+ channels in the basolateral membrane of rabbit proximal straight tubules. Pflügers Arch. 410:288–295

Greger R, Hampel W (1981) A modified system for *in vitro* perfusion of isolated renal tubules. Pflügers Arch. 389:175–176

Hamill OP, Marty A, Neher E, Sakmann B, Sigworth FJ (1981) Improved patch-clamp techniques for high resolution current recording from cells and cell-free membrane patches. Pflügers Arch. 391:85–100

Heidrich HG, Dew M (1977) Homogeneous cell populations from rabbit kidney cortex. Proximal, distal tubule, and renin-active cells isolated by free-flow electrophoresis. J Cell Biol 74:780–788

Hoyer J, Gögelein H (1991) Sodium-alanine cotransport in renal proximal tubule cells investigated by whole-cell current recording. J Gen Physiol 97:1073–1094

Merot J, Bidet M, Gachot B, LeMaout S, Tauc M, Poujeol P (1988) Patch clamp study on primary culture of isolated proximal convoluted tubules. Pflügers Arch. 413:51–61

Neher E, Sakmann B (1976) Single channel currents recorded from membranes of denervated frog muscle fibres. Nature 260:799–802

Schlatter E (1993) Effect of various diuretics on membrane voltage of macula densa cells. Whole-cell patch-clamp experiments. Pflügers Arch Eur J Physiol 423:74–77

C.2.1.2 Perfusion of Isolated Kidney Tubules[3]

PURPOSE AND RATIONALE

The various tubule segments: proximal tubule (PT, S1–S3); descending thin limb of the loop of Henle (DTL); ascending thin limb of the loop of Henle (ATL); thick ascending limb of the loop of Henle (TAL); distal convoluted tubule (DCT); connecting tubule (CNT); cortical collecting duct (CCD); medullary collecting duct (MCD); papillary collecting duct (PCD) have different functional properties. The *in*

[3] Contribution by R. Greger (first edition) and M. Bleich (second edition).

vitro perfusion of isolated tubule segments (Burg et al. 1966) is the method of choice if one has to identify the site and the mechanism of action of a pharmacological agent which has been shown to act on kidney function in clearance and micropuncture studies.

PROCEDURE

After its invention by Burg et al. (1966) this technique has been used successfully in the kidney tubule segments of several species: man; rabbit; rat; mouse; hamster; snake; birds etc. The tubule segments are dissected from thin kidney slices (<1 mm thickness). Usually dissection can be done using sharpened forceps or needles without the addition of proteases (collagenase). The segment is identified by its anatomical location and by its appearance. A 20–50× lens is used for dissection. Dark field illumination is helpful for the identification of the segment under study. PT, TAL, DCT, CNT, CCD, MCD can all be dissected quite easily. The dissection of DTL, ATL and PCD is much more difficult because these segments are damaged easily by the mechanical dissection. Dissection is usually performed at 4°C in a Ringer type solution.

The dissected segment is transferred into the perfusion chamber by a transfer pipette. The perfusion chamber is mounted in the stage of an inverted microscope (20–400×). The chamber is usually kept at 37°C, and the bath perfusate is also preheated to this temperature. The bath perfusate will depend on the tubule segment under study. In most instances it will contain HCO_3^- and will be bubbled with CO_2. The metabolic substrate will be acetate for PT and D-glucose for TAL, CCD etc. The actual perfusion is performed with two sets of concentric glass pipettes, one set at the perfusion end; and one at the collection end of the segment. These pipettes are manufactured with special glass forges. The most refined one has been designed by Hampel and Greger. The glass tube is rotated at approximately 1 rps, is moved in perpendicular direction by a remote control, and the heating filament is moved in xy direction also by a remote control. The shaping of the glass is observed continuously by a lens (5–50×). The pulling force is provided by weights fixed on the lower end of the glass tube. The pipettes are cut either by a diamond or by the pulling force of a small glass bead, fixed on the edge of a vertical platinum filament and melted sidewise on the pipette. When the heating current of the platinum filament is switched off the filament retracts and brakes the pipette a the desired site. Greger and Hampel (1981) have modified the original perfusion system of Burg and co-workers. Their device is optimized inasmuch as it guarantees concentric alignment of the various pipettes. The forward and backward movement is controlled by small electric motors. At the perfusion side they use 4 concentric pipettes. The outermost one contains sylgard and is driven over the perfused end of the tubule in order to seal this end. The tubule is held by a holding pipette with appropriate dimensions. The tubule is sucked into this pipette up to the constriction. Then the perfusion pipette with a tip diameter smaller than the inner diameter of the perfused segment is advanced into the segment held by the holding pipette. The perfusion pipette is put under hydrostatic pressure of a few to 100 cm to achieve a perfusion rate of 1–20 nl/min. Usually the collapsed tubule lumen opens when the perfusion pipette is advanced. The pipette is advanced in the lumen until it reaches an area of the segment where it appears intact by inspection (200–400×). Within its lumen the perfusion pipette contains yet another pipette, the fluid exchange pipette. With this pipette the composition of the perfusate can be replaced very rapidly (Greger and Schlatter 1983). The collection end of the tubule segment is sucked into a holding pipette. A sylgard pipette is advanced to seal the collection site. The holding pipette at the collection site will contain mineral oil in flux measurements. Then a collection pipette is advanced through the oil to quantitatively collect the perfusate delivered by the tubule.

The **measured parameters** can be as follows:

Flux measurements (Schafer et al. 1974). The collection rate (V_c, nl/min) can be measured by the constant bore collection pipette by timed collections. Radioactive tracers can be added to the lumen or bath fluid. For instance, radioactively labelled inulin can be added to the perfusate (In_p) and can be used to measure volume absorption (ΔV = perfusion rate (V_i–V_c). Unidirectional fluxes, bath to lumen and lumen to bath, for any given substance can be quantified, and permeabilities (P_x) can be determined:

$$P_x = (V_i - V_c)L^{-1}[\ln(x_p In_c x_c^{-1} In_p) + 1]$$

where L is the length of the segment; x_p and x_c are the concentrations of x in the perfusate and in the collected fluid; and In_c is the inulin concentration in the collected fluid. Net fluxes of x can be determined as the difference of the unidirectional fluxes or by the chemical determination of Δx (perfusate–collected fluid). This requires very sensitive methods. Electron probe analysis of Na^+, K^+, Ca^{2+}, Mg^{2+} etc. has been used to determine the net transport of these ions in various tubule segments (Wittner et al. 1988). Flux studies are usually performed at low luminal perfusion rates of a few nl/min. Substances under study can be added

to the luminal and bath perfusate, and paired data can be obtained under control and experimental conditions (Burg and Green 1973; Stoner et al. 1974; Burg 1980; Burg and Stoner 1976; Dillingham et al. 1993).

Transepithelial electrical measurements. The perfusion pipette can be connected to the high impedance input of an electrometer. The voltage is referenced to the grounded bath. The connections are usually made with agar bridges (80 g agar in 1 l Ringer's solution), and appropriate corrections for liquid junction voltages must be applied. With identical solutions in the bath and in the lumen and with high luminal perfusion rates (> 10 nl/min), any transepithelial voltage (V_{te}) must be caused by active transport = active transport potential (Frömter 1984). Hence, the effectiveness of putative inhibitors of active transport can also be examined by the measurement of V_{te}. According to Ohm's law the determination of the flux of ions also requires the measurement of transepithelial resistance. Greger (1981) has introduced a method which utilizes a dual channel perfusion pipette, made of Q-shaped glass. One channel is used for perfusion and the other for current (I_{te}) injection. The current is defined by a resistor chosen such that the deflection in V_{te} generated by this pulse is in the order of 10–20 mV. Transepithelial resistance (R_{te}) can now be calculated from ΔV_{te} and I_{te}. The ratio of V_{te} and R_{te} is called equivalent short circuit current. It is directly proportional to active transport (Greger 1985). The measurement of V_{te} and R_{te} is much more efficient than flux studies for pharmacological screening, provided that the process under study produces a transepithelial voltage. Several substances can be examined in one single tubule in strictly paired fashion (Schlatter et al. 1983; Wangemann et al. 1986). The time resolution of the measurements is on the order of 1 s, whereas that of flux studies is several minutes at best.

Intracellular electrical measurements. Greger and Schlatter (1983) have developed a method for the use of impalement techniques in the isolated perfused tubule. Very fine tip microelectrodes (Ø < 100 nm) are used to impale the tubule cell across the basolateral membrane. The actual impalement is performed by a piezo stepper which accelerates the microelectrode to high speed, which makes it possible to penetrate the rigid basal membrane. The simultaneous measurement of V_{te}, R_{te}, and basolateral membrane voltage (V_{bl}) allows for a complete analysis of voltages and resistances (Greger 1985; Ullrich and Greger 1985). Ion selective microelectrodes can also be used in impalement studies, and the cytosolic ion activities for e. g. Na^+, K^+, Cl^- can also be determined (Greger 1985). These methods are all rather difficult to perform. They are of high relevance for the understanding of the function of a given tubule segment and for the detailed description of the mechanism of action of a drug, which, in preceding studies has been shown to act in a given tubule segment.

Patch clamp studies. The combination of *in vitro* perfusion of renal tubules and patch clamp analysis of ion channels in the luminal and basolateral membranes is described in Sect. C.2.1.1.

Fluorescent dyes in the isolated perfused tubule. Several fluorescent dyes for the monitoring of Na^+, K^+, Cl^-, Ca^{2+}, pH have become available during the past few years. These dyes can be used in the *in vitro* perfused tubule (Nitschke et al. 1991). The inverted microscope is equipped with an appropriate illumination and filter wheel for excitation. The emission is measured by photon counting or by a video camera. When compared with impalement methods, these techniques are probably easier for routine use.

EVALUATION

For each of the above protocols paired measurements of one or several given parameters of tubule transport are obtained under control conditions and in the presence of a substance under study. Also concentration response curves can be obtained in one single preparation (Schlatter et al. 1983; Wangemann et al. 1986; Wittner et al. 1987). Intracellular measurements are usually required to define the mechanism of action (Greger 1985). Especially the electrical and optical measurements have a very high reproducibility. For screening usually 3 preparations are sufficient. Approximately 10 preparations are required for concentration response curves.

REFERENCES AND FURTHER READING

Burg MB, Green N (1973) Function of the thick ascending limb of Henle's loop. Am J Physiol 224:659–668

Burg MB, Orloff J (1980) Perfusion of isolated renal tubules. In: Anonymous. (ed) Handbook of Physiology. pp 145–159

Burg M, Stoner L (1976) Renal tubular chloride transport and the mode of action of some diuretics. Ann Rev Physiol 38:37–45

Burg M, Grantham J, Abramow M, Orloff J (1966) Preparation and study of fragments of single rabbit nephrons. Am J Physiol 210:1293–1298

Dillingham MA, Schrier RW, Greger R (1993) Mechanisms of diuretic action. In: Schrier RW, Gottschalk CW. (eds) Clinical Disorders of Fluid, Electrolytes, and Acid Base. Little Brown and Comp, Boston, pp 2435–2452

Frömter E (1984) Viewing the kidney through microelectrodes. Am J Physiol 247:F695–F705

Greger R (1981) Cation selectivity of the isolated perfused cortical thick ascending limb of Henle's loop of rabbit kidney. Pflügers Arch 390:30–37

Greger R (1985) Application of electrical measurements in the isolated *in vitro* perfused tubule. Mol Physiol 8:11–22
Greger R, Hampel W (1981) A modified system for *in vitro* perfusion of isolated renal tubules. Pflügers Arch 389:175–176
Greger R, Schlatter E (1983a) Cellular mechanism of the action of loop diuretics on the thick ascending limb of Henle's loop. Klin Wochenschr 61:1019–1027
Greger R, Schlatter E (1983b) Properties of the lumen membrane of the cortical thick ascending limb of Henle's loop of rabbit kidney. Pflügers Arch 396:315–324
Nitschke R, Fröbe U, Greger R (1991) ADH increases cytosolic Ca^{2+}-activity in isolated perfused rabbit thick ascending limb via a V1 receptor. Pflügers Arch 417:622–632
Schafer JA, Troutman SL, Andreoli TE (1974) Volume reabsorption, transepithelial potential differences, and ionic permeability properties in mammalian superficial proximal straight tubules. J Gen Physiol 64:582–607
Schlatter E, Greger R, Weidtke C (1983) Effect of "high ceiling" diuretics on active salt transport in the cortical thick ascending limb of Henle's loop of rabbit kidney. Correlation of chemical structure and inhibitory potency. Pflügers Arch 396:210–217
Stoner LC, Burg MB, Orloff J (1974) Ion transport in cortical collecting tubule; effect of amiloride. Am J Physiol 227:453–459
Ullrich KJ, Greger R (1985) Approaches to the study of tubule transport functions. In: Seldin DW, Giebisch G. (eds) Physiology and Pathophysiology. Raven Press, New York, pp 427–469
Wangemann P, Wittner M, Di Stefano A, Englert HC, Lang HJ, Schlatter E, Greger R (1986) Cl^--channel blockers in the thick ascending limb of the loop of Henle. Structure activity relationship. Pflügers Arch 407 (Suppl 2):S128–S141
Wittner M, Di Stefano A, Wangemann P, Delarge J, Liegeois JF, Greger R (1987) Analogues of torasemide – structure function relationships. Experiments in the thick ascending limb of the loop of Henle of rabbit nephron. Pflügers Arch 408:54–62
Wittner M, Di Stefano A, Wangemann P, Nitschke R, Greger R, Bailly C, Amiel C, Roinel N, De Rouffignac C (1988) Differential effects of ADH on sodium, chloride, potassium, calcium and magnesium transport in cortical and medullary thick ascending limbs of mouse nephron. Pflügers Arch 412:516–523

C.2.1.3 Isolated Perfused Kidney

PURPOSE AND RATIONALE

Isolated kidney is a good tool for studying proximal tubule, but of limited value for distal tubule function. The kidney can be perfused *in situ* and isolated *in vitro*. The isolated kidney can be perfused by a pump using blood or plasma-like solutions. One specific problem of the blood-perfused dog kidney *in vitro* is its instability. After only 1 h of perfusion, glomerular filtration and renal blood flow decline markedly. It was reported that *in situ*-perfused isolated dog kidney seems to be more stable. In isolated perfused rat kidney plasma-like solutions are used for perfusion. This system, by inclusion of a dialyzing unit, provides optimal conditions for maintaining a constant electrolyte composition of the perfusate. However, function of distal tubule is also grossly impaired in this rat model. The isolated kidney does not acidify tubular fluid, and the concentrating ability is reduced.

PROCEDURE

Kidneys are obtained from anaesthetized male rats with a body weight of 300 to 400 g. The donor animals are fasted overnight prior to surgery, but have free access to water. After the abdominal cavity is exposed by a ventricular incision, the right ureter is cannulated with PE-50 polyethylene tubing and heparin is injected into the vena cava (500 U/kg body weight). The venous cannula is introduced into the vena cava below the right renal vein. The right kidney is freed from the perirenal fat, not disrupting the renal capsule. The renal artery is cannulated via the superior mesenteric artery without interruption of flow. Thereafter, the kidney is continuously perfused with a perfusion solution fed from the gravity system situated 130 cm above the cannula. Ligatures around the renal artery and vena cava above the renal pedicle are tied. The kidney is then removed from the animal and placed in a Plexiglas chamber. A perfusion pressure of 80–90 mm Hg in the renal artery is maintained by adjusting the speed of the perfusion pump. For more details see references.

EVALUATION

After the equilibration period, clearance periods of 20 min are used. Urine samples are collected and perfusate is obtained at midpoint of the clearance period for the evaluation of overall kidney function. For determination of glomerular filtration rate (GFR) and fluid transport, ^{3}H-labelled polyethylene glycol is added to a modified Krebs-Henseleit bicarbonate buffer. Electrolytes are determined in urine by standard flame photometry. Fractional excretions of water, electrolytes and test compounds are calculated.

LIMITATIONS OF THE METHOD

Isolated perfused dog kidneys have been reported to be less stable than those of other species, with glomerular filtration and renal flow markedly decreasing after only one hour of perfusion. The *in situ*-perfused isolated dog kidney seems to be more stable. Distal tubule functions are impaired in isolated perfused kidneys in all species. Urine acidification, concentration and dilution functions are also abnormal, and effects on these cannot be assessed in these models (Kirkpatrick and Gandolfi 2005).

MODIFICATIONS OF THE METHOD

Tarako et al. (1991) evaluated oxygen supply and energy state in the isolated perfused rat kidney.

Metabolic activities of the isolated perfused rat kidney were described by Nishiitsutsuji-Uwo et al. (1967).

Cox et al. (1990) used the isolated perfused rat kidney as a tool in the investigation of renal handling and effects of nonsteroidal anti-inflammatory drugs.

REFERENCES AND FURTHER READING

Cox PGF, Moons MM, Slegers JFG, Russel FGM, van Ginneken CAM (1990) Isolated perfused rat kidney as a tool in the investigation of renal handling and effects of nonsteroidal anti-inflammatory drugs. J Pharmacol Meth 24:89–103

Kirkpatrick DS, Gandolfi AJ (2005) *In vitro* techniques in screening and mechanistic studies; organ perfusion, slices and nephron components. In Tarloff J B., and Lash, L. H. (eds) Toxicology of the Kidney, 3rd ed., pp 81–147. CRC Press, Boca Raton

Maack T (1980) Physiological evaluation of the isolated perfused rat kidney. Am J Physiol 238:F71–F78

Newton JF, Hook JB (1981) Isolated perfused rat kidney. Meth Enzymol 77:94–105

Nishiitsutsuji-Uwo JM, Ross BD, Krebs HA (1967) Metabolic activities of the isolated perfused rat kidney. Biochem J 103:852–862

Nizet AH (1978) Methodology for study of isolated perfused dog kidney *in vitro*. In: Martinez-Maldonado M (ed) Methods in Pharmacology, Vol 4B, Renal Pharmacology pp 369–383. Plenum Press, New York and London

Ross BD (1972) Perfusion techniques in biochemistry. 4. Kidney. Clarendon Press, Oxford, pp 228–257

Schurek HJ (1980) Application of the isolated perfused rat kidney in nephrology. In: Stolte H, Alt J (eds) Contributions to Nephrology 19:176–190. S. Karger, Basel

Tarako T, Nakata K, Kawakami T, Miyazaki Y, Muakami M, Seo Y, Suzuki E (1991) Validation of a toxicity testing model by evaluating oxygen supply and energy state in the isolated perfused rat kidney. J Pharmacol Meth 25:195–204

C.2.2 In Vivo Methods

C.2.2.1 Clearance Methods

PURPOSE AND RATIONALE

Investigations of clearance represent indirect methods for the evaluation of renal function and provide information on the site of action of diuretics and other pharmacological agents within the nephron. The discovery of the countercurrent multiplier system as the mechanism responsible for the concentration and dilution of the urine has been the prerequisite for the identification of the site of action of diuretic drugs. A drug that acts solely in the proximal convoluted tubule, by causing the delivery of the increased amounts of filtrate to the loop of Henle and the distal convolution, would augment the clearance of solute-free water (C_{H2O}) during water diuresis and the reabsorption of solute-free water (T_{CH2O}) during water restriction. In contrast, drugs that inhibit sodium reabsorption in Henle's loop would impair both C_{H2O} and T_{CH2O}. On the other hand, drugs that act only in the distal tubule would reduce C_{H2O} but not T_{CH2O}.

PROCEDURE

Clearance experiments are performed either in conscious or anaesthetized beagle dogs under conditions of water diuresis and hydropenia. The status of water diuresis and hydropenia may be accomplished as described by Suki et al. (1965). Water diuresis is induced by oral administration of 50 ml of water per kg body weight and maintained by continuos infusion into jugular vein of 2.5% glucose solution and 0.58% NaCl solution at 0.5 ml/min per kg body weight. When water diuresis is well established, the glucose infusion is discontinued and control urine samples are collected by urethral catheter. Blood samples are obtained in the middle of each clearance period. After the control period, compounds to be tested are administered and further clearance tests are performed.

Hydropenia is induced by withdrawing the drinking water 48 h before experiment. On the day before the experiment 0.5 U/kg body weight of vasopressin in oil is injected intramuscularly. On the day of the experiment 20 mU/kg vasopressin is injected i.v., followed by infusion of 50 mU/kg per hour vasopressin. To accomplish constant urine flow 5% NaCl solution is infused at 1 ml/min per kg body weight up to i.v. administration of a compound to be tested, followed by i.v. infusion of 0.9% NaCl solution at a rate equal to the urine flow. Glomerular filtration rate (GFR) and renal plasma flow (RPF) are measured by the clearance of inulin and para-aminohippurate, respectively. Therefore, appropriate infusion of inulin (bolus of 0.08 g/kg followed by infusion of 1.5 mg/kg per min) and para-aminohippurate (bolus 0.04 g/kg followed by infusion of 0.3 mg/kg per min) are initiated. Inulin and para-aminohippurate are measured according to Walser et al. (1955) and Smith and al (1945), respectively.

Tracers are administered intravenously to achieve near steady-state concentrations; a priming dose loads the plasma and extracellular compartments, and subsequent infusion replaces renal losses. Once steady state plasma tracer levels are approached, a series of timed urine collections (clearance periods) are performed, with blood samples collected at the either the midpoint or beginning and end of the clearance periods. The urine and blood (plasma or serum) samples are analyzed for tracer(s) and the test compound.

Tracers for the determination of GFR must be freely filtered and then neither secreted nor reabsorbed. This allows the assumption that the amount of plasma cleared of the tracer per unit time represents that which has been filtered through the glomeruli (i.e., GFR). The fructose polysaccharide, inulin (mw ~5200) is the most commonly used tracer in all species and serves as the 'gold standard' to which others are compared (Finco 1983; Ragan and Weller, 1999). Other indicators include isotopes of vitamin B_{12}, sodium iodothalamate, iohexol and radiolabelled metal chelates of ethylenediamintetracetate (EDTA) and diethylaminotriaminepentaacetate (DPTA) (Sarkar et al. 1988, 1991; Gaspari et al. 1997; Ragan and Weller 1999).

Tracers for the assessment of renal plasma flow must be completely cleared (combination of filtration and efficient tubular secretion to the urine) on first pass through the kidney. This allows the assumption that the volume of plasma cleared per unit time represents that which was either filtered by the glomeruli or bypassed the glomeruli and perfused the tubules. *p*-aminohippurate (PAH) is used for the assessment of RPF, because it is both freely filtered by the glomeruli and actively secreted by the organic acid transport pathway of the proximal tubule. First-pass PAH extraction by the kidneys varies from about 70% to 90% in rats, dogs, and humans (Brenner et al. 1976), but for the purpose of estimating RBF it is assumed to be 100%. Using this assumption, RPF is always slightly underestimated. Tetraethylammonium bromide (TEA), a substrate for the renal cation transporter, may also be used, and is subject to the same limitations (Ragan and Weller 1999).

Inulin is measured colorimetrically, either by acid hydrolysis to generate a green product, or by a series of enzymatic reactions based on inulinase with subsequent reduction of NADH. HPLC methods are used for the remaining exogenous GFR tracers. PAH and TEA are measured colorimetrically (Newman and Price 1999).

EVALUATION

Renal clearance (Cl) of any compound (X) can be determined by comparing the urinary excretion rate of compound X to the plasma concentration of compound X.

The urinary excretion rate is calculated as:

$$\text{Urinary excretion rate (mg/min)} = U_x\text{(mg/ml)} \times V\text{(ml/min)}$$

Where U_x represents the concentration of substance X in urine (in mg/ml) and V represents the volume of urine collected per unit time (in ml/min). Thus, the clearance equation may be constructed:

$$Cl_x\text{(ml/minute)} = U_x\text{(mg/ml)} \times V\text{(ml/min)}/P_x\text{(mg/ml)}$$

Where P_x is the concentration of compound X in plasma (in mg/ml)

GFR is estimated by calculating the clearance of the tracer or endogenous substance. RPF estimated using PAH clearance is often designated effective renal plasma flow (ERPF). Renal plasma flow is converted to renal blood flow (RBF) by dividing ERPF by the plasma fraction of whole blood, as estimated from the hematocrit (Hct):

$$RBF = ERPF/(1 - Hct)$$

The clearances of other compounds can be compared with inulin clearances to determine how the kidney functions in the elimination of the test compound. A clearance ratio is constructed by dividing the renal clearance of the test compound (X) by the renal clearance of inulin:

$$\text{Clearance Ratio} = CL_x,\ \text{(ml/min)}/Cl_{inulin},\ \text{(ml/min)}$$

A clearance ratio < 1.0 indicates reabsorption of the test substance following filtration, whereas active secretion will result in a clearance ratio of > 1.0.

MODIFICATIONS OF THE METHOD

Endogenous compounds can administered exogenously in place of tracer substances. This has been done for the dog using creatinine (Sapirstein et al. 1955; Finco et al. 2001) and for the rat using cystatin C (Tenstad et al. 1996). Either urine or plasma clearance methods can be used for the former. For the latter, plasma clearance was used to estimate GFR due to the fact that cystatin C is reabsorbed and degraded by the proximal tubule and does not appear in the urine.

Rönnhedh et al. (1996) described a simple method to perform serial renal clearance studies without urine collection in rats. This was applied to non-radiolabeled para-aminohippurate sodium and iothalamate sodium which were used respectively to estimate renal blood flow and glomerular filtration rate.

Gabel et al. (1996) described fast and accurate assays for measuring glomerular filtration rate and effective renal blood flow in conscious rats. An enzymatic method was developed for the determination of inulin

and a colorimetric method was developed for determination of p-aminohippurate in the plasma and urine of rats.

Hropot et al. (1985) described clearance methods in monkeys. Chimpanzees weighing 30.7 ± 10.6 kg were anesthetized with 1 mg/kg Sernylan i.m. Food was withdrawn 24 h prior to the experiment and the animals received only tap water ad libitum. In the morning before the experiment, the urinary bladder of the animals was emptied by catheterization. The urine was discarded. To determine the glomerular filtration rate (inulin clearance), a bolus injection of 50 mg/kg inulin i.v. was given and followed by a continuous infusion of 3 ml/min inulin dissolved in Ringer lactate solution. After an equilibrium of 60 min, urine and blood samples were collected for two control clearance periods of 30 min each. The control periods were followed by intravenous administration of the test preparation in a dose of 20 mg/kg. Thereafter, urine and blood samples were collected during 6 clearance periods. The following parameters were determined: urine excretion, inulin clearance and urate clearance [ml/kg/min], fractional excretion of urate and plasma urate [mmol/l].

Tanaka et al. (1990) evaluated uricosuric and diuretic properties of diuretic agents using clearance studies in urate-loaded dogs and urate-loaded rabbits.

LIMITATIONS OF THE METHOD

First-pass extraction of PAH is highly variable both between species and between individuals within a species, which adds to the inherent inaccuracy of the estimate of RBF by this method. Furthermore, the test compound may interfere with the extraction of either PAH or TEA by competing for transport by the organic anion or cation transporters (Newman and Price, 1999; Ragan and Weller, 1999).

The limitations of the Jaffe method for creatinine determination have been discussed in section 1.1.1. Exogenous creatinine clearance compensates for the insensitivity of the method as well as the interference by endogenous chromagens by artificially increasing the plasma creatinine concentration (Finco 1997).

REFERENCES AND FURTHER READING

Brenner BM, Zatz R, Ichikawa I (1976) In: Brenner BM, Rector, FC Jr (ed) The Kidney, 3rd edn. WB Saunders, Philadelphia, pp 93–123

Finco DR (1997) Kidney function. In Kaneko, JJ, Harvey, JW, and Bruss, ML, eds., Clinical Biochemistry of Domestic Animals, 6th ed., pp 441–485. Academic Press, San Diego

Finco DR, Braselton WE, Cooper TA (2001) Relationship between plasma iohexol clearance and urinary exogenous creatinine clearance in dogs. J Vet Intern Med 2001 Jul-Aug;15(4):368–73

Gabel RA, Ranaei RA, Kivlighn (1996) A new method of measuring renal function in conscious rats without the use of radioisotopes. J Pharmacol Toxicol Meth 36:189–197

Gaspari F, Perico N, Remuzzi G (1997) Measurement of glomerular filtration rate. Kidney Int (Suppl.63) :S151-S154

Hropot M, Klaus E, Seuring B, Lang HJ (1985) Effects of diuretics on magnesium excretion. Magnesium Bull 7:20–24

Hropot M, Klaus E, Knolle J, König W, Scholz W (1986) Effect of rat atriopeptin III on renal function in dogs during water diuresis and hydropenia. Klin Wochenschr 64 (Suppl VI):58–63

Newman DJ, Price CP (1999) Renal function and nitrogen metabolites. In Burtis CA, and Ashwood, ER, eds., Tietz Textbook of Clinical Chemistry, 3rd ed., pp 1204–1270. WB Saunders Company, Philadelphia

Ragan HA, Weller RE (1999) Markers of renal function and injury. In Loeb, WF, and Quimby, FW (eds), The Clinical Chemistry of Laboratory Animals, 2nd edition, pp 519-548, Taylor and Francis, Philadelphia

Rönnhedh C, Jaquenod M, Mather LE (1996) Urineless estimation of glomerular filtration rate and renal blood flow in the rat. J Pharmacol Toxicol Meth 36:123–129

Russel FGM, Wouterse AC, Hekman P, Grutters GJ, van Ginneken CAM (1987) Quantitative urine collection in renal clearance studies in the dog. J Pharmacol Meth 17:125–136

Sapirstein LG, Vidt DC, Mandell MJ, Hanusek G (1955) Volumes of distribution and clearances of intravenously injected creatinine in the dog. Am J Physiol 181:330–336

Sarkar SK, Holland GA, Lenkinski R, Mattingly MA, Kinter LB (1988) Renal imaging studies at 1.5 and 9.4 T: effects of diuretics. Magn Reson. Med 7:117–124

Sarkar SK, Rycyna RE, Lenkinski RE, Solleveld HA, Kinter LB (1991) Yb-DTPA, a novel contrast agent in magnetic resonance imaging: application to rat kidney. Magn. Reson. Med 17(2):328–34

Smith HW, Finkelstein N, Aliminosa L, Crawford B, Graber M (1945) The renal clearances of substituted hippuric acid derivatives and other aromatic acids in dog and man. J Clin Invest 24:388–393

Suki W, Rector FC Jr, Seldin DW (1965) The site of action of furosemide and other sulfonamide diuretics in the dog. J Clin Invest 44:1458–1469

Tanaka S, Kanda A, Ashida SI (1990) Uricosuric and diuretic activities of DR-3438 in dogs and rabbits. Japan J Pharmacol 54:307–314

Tenstad O, Roals AB, Grubb A, Aukland K (1996) Renal handling of radiolabeled cystatin C in the rat. Scand J Clin Lab Invest 56:409–414

Walser M, Davidson DG, Orloff J (1955) The renal clearance of alkali-stable inulin. J Clin Invest 34:1520–1523

C.2.2.2
Assessment of Glomerular Filtration Rate (GFR) and Renal Blood Flow (RBF)

C.2.2.2.1
Assessment of GFR by Plasma Chemistry

PURPOSE AND RATIONALE

Estimation of the glomerular filtration rate (GFR) is considered a sensitive index of functional nephron

mass (Newman and Price, 1999). Point measurements of the plasma levels of several endogenous small molecules (urea, creatinine, 2-(a-mannopyranosyl)-L-tryptophan) or small (less than 66 kDa) proteins (cystatin C (γ-trace), prostaglandin D synthase (β-trace protein), α_1-microglobulin, β_2-microglobulin, and retinol binding protein) have been used to assess GFR in many species.

PROCEDURE

Serum or plasma samples are collected from the test animals (if plasma is used, blood should be collected in heparinized tubes). Assay methods vary, and are outlined below:

Urea is most commonly assayed by combined urease methods, in which the urea is first converted to two ammonium ions. The ammonium generated is then measured by either enzymatic or chemical methods. Urea nitrogen values determined by this method (mg/ml) are converted to urea values by the use of appropriate factors (2.14 for urea in mg/ml, 0.357 for urea in mmol/L) (Emeigh Hart and Kinter 2005).

Creatinine is most commonly measured by the Jaffe reaction of creatinine with picrate to generate an orange chromogen. Several enzymatic assays (based on reactions with creatinase or creatinine deaminase) have also been developed. These are equal in sensitivity to the Jaffe method but are considered less likely to be subject to interference by endogenous or exogenous chromogens (Finco et al. 1995; Finco 1997; Newman and Price, 1999). Chromatography (HPLC or LC-MS/MS) assay methods are more sensitive than the Jaffe method and are not subject to interference by endogenous chromagens (Dunn et al. 2004; Owen and Keevil, 2007).

2-(a-mannopyranosyl)-L-tryptophan (MPT) is measured by HPLC (Takahira et al. 2001). Cystatin C assays are all antibody based (nephelometric, agglutination or sandwich ELISA) (Pergande and Jung, 1993; Finney et al. 1997; Jensen et al. 2001), and have been used successfully in dogs, rats, mice and cats (Hakansson et al. 1996; Boekenkamp et al. 2001; Braun et al. 2002; Martin et al. 2002). The other small molecular weight proteins are detected by immunoassays as well.

EVALUATION

Analyte levels are compared either to those of a concomitant control group (using appropriate statistical methods of the group size is large enough) or to laboratory-specific reference intervals for the species, strain, age and sex in question. Elevation of analyte levels outside of the reference range indicate a decrease in GFR, with the magnitude of the elevation being roughly proportional to the degree of the decrement.

Additionally, algorithms can be used to convert plasma creatinine to creatinine clearance, which provides a reasonably accurate estimate of GFR in humans (Cockroft and Gault, 1976):

$$\text{GFR} \approx (140 - \text{age}) \times \text{weight (kg)} \times K72 \times \text{Serum creatinine (mg/dL)}$$

Where $K = 0.85$ for women, 1.00 for men

A similar algorithm has been generated for dogs of either gender (Finco et al., 1995):

$$\text{GFR} \approx 2.6/\text{Serum creatinine (mg/dL)}$$

LIMITATIONS OF THE METHOD

Effects on prerenal (dehydration, blood loss, altered vasomotor tone, age-related decreases in renal blood flow in rats) and/or postrenal factors (obstruction or extravasation of urine to the peritoneal cavity) may cause elevations of the commonly measured analytes that do not reflect effects on the GFR or loss of functional nephron mass (Baum et al. 1975; Corman and Michel, 1987; Finco, 1997; Newmann and Price, 1999).

Urea and creatinine elevations in plasma are in general not sensitive enough to detect low-level alterations (less than 75% loss) of GFR, due to the contribution of renal secretion and/or reabsorption to their overall excretion, (which can compensate for their decreased filtration), to wide variations in baseline levels of some analytes, and to inherent imprecision in the assays used (Finn and Porter, 1998; Price, 2002; Starr et al. 2002; Shemesh et al. 1985). In particular, urea will underestimate GFR (due to extensive tubular reabsorption with decreased GFR) (Baum et al., 1975; Kaplan and Kohn, 1992; Newman and Price, 1999), and creatinine tends to overestimate GFR (because it is secreted by the tubule in many species and secretion increases with reduced GFR) (Shemesh et al. 1985; Andreev et al. 1999; Newman and Price, 1999; Star et al. 2002). In addition, creatinine synthesis is regulated by feedback inhibition which limits the degree of elevation than can occur in plasma (Watson et al. 2002).

The Jaffe reaction for creatinine is subject to interference by numerous endogenous substrates and drugs or compounds (Schwendenwein and Gabler, 2001; Sonntag and Scholer, 2001; Dunn et al. 2004). This effect can be minimized by using appropriate substrate extraction or by the use of kinetic assessments. The urease assay is specific for urea, but increased circulating ammonia (such as occurs in aged plasma samples,

metabolic disorders and portocaval shunting) will react with the subsequent reaction and result in falsely elevated plasma levels (Newman and Price, 1999).

Baseline levels of urea and creatinine are variable, as they are subject to influences on their extrarenal synthesis and release. Plasma urea reflects hepatic synthesis rate and will be elevated with increased protein catabolism (increased dietary protein intake, gastrointestinal hemorrhage, fever, severe burns, corticosteroid administration, sustained exercise or muscle wasting), and decreased with low or poor quality protein diets, modest food restriction in rodents or hepatic insufficiency (Pickering and Pickering, 1984; Finco 1997; Hamberg, 1997; Tauson and Wamberg, 1998; Newman and Price, 1999). Baseline creatinine reflects muscle catabolism and will be elevated in individuals with higher muscle mass or following sustained exercise or acute muscle damage; it will be lower in individuals with loss of muscle mass (Finco, 1997; Newman and Price, 1999). Drugs which compete with creatinine for renal excretion may falsely elevate plasma levels in the absence of renal injury (Andeev et al. 1999).

2-(a-mannopyranosyl)-L-tryptophan (MPT) appears to be less likely to be affected by muscle mass than creatinine. Point-in-time measurements of this tryptophan glycoconjugate correlated extremely well with the inulin clearance, suggesting it may be a superior indicator of GFR. However, the renal handling of MPT has not been examined to determine if plasma levels may be influenced by either reabsorption or secretion (Horiuchi et al. 1994; Gutsche et al. 1999; Takahira et al. 2001).

Pitt et al. (2006) reported the pharmacological profile and toxicity of fluorescein-labelled sinsitrin, a novel marker for GFR measurements.

Cystatin C does not appear to be a sensitive index of GFR in the cat (Martin et al. 2002).

The other small protein markers of GFR are detected by immunoassays with reagents specific for the human proteins; the cross-reactivity of these reagents with other species and the usefulness of these markers in animal models have not been well established (Loeb, 1998).

REFERENCES AND FURTHER READING

Andreev E, Koopman M, Arisz L (1999) A rise in plasma creatinine that is not a sign of renal failure: which drugs can be responsible? J Internal Med 246:247–25

Baum N, Dichoso CC, Carlton CE (1975) Blood urea nitrogen and serum creatinine. Physiology and interpretations. Urology 5:583–588

Boekenkamp A, Giuliano C, Christian D (2001) Cystatin C in a rat model of end-stage renal failure. Renal Failure 23:431–438

Braun J-P, Perxachs A, Péchereau D, de la Farge F (2002) Plasma cystatin C in the dog: reference values and variations with renal failure. Comp Clin Pathol 11:44–49

Cockcroft DW, Gault MH (1976) Prediction of creatinine clearance from serum creatinine. Nephron 16:31–41

Corman B, Michel JB (1987) Glomerular filtration, renal blood flow, and solute excretion in conscious aging rats. Am J Physiol 22; R555-R560

Dunn SR, Qi, Z, Bottinger EP, Breyer M, Sharma K (2004) Utility of endogenous creatinine clearance as a measure of renal function in mice. Kidney Int. 65:1959–1967

Emeigh Hart SG, Kinter LP (2005) Assessing Renal Effects of Toxicants *in vivo*. In Tarloff JB, and Lash, LH (eds) Toxicology of the Kidney, 3rd ed., pp 81–147. CRC Press, Boca Raton

Finco DR (1997) Kidney function. In Kaneko, JJ, Harvey, JW, and Bruss, ML, eds., Clinical Biochemistry of Domestic Animals, 6th ed., pp 441–485. Academic Press, San Diego

Finco DR, Brown SA, Vaden SL, Ferguson DC (1995) Relationship between plasma creatinine concentration and glomerular filtration rate in dogs. J Vet Pharmacol Ther 18;418–421

Finn WF, Porter GA (1998) Urinary biomarkers and nephrotoxicity. In DeBroe, ME, Porter, GA, Bennett, WM and Verpooten, GA, eds., Clinical Nephrotoxins, pp 61-99 Kluwer Academic Publishers, Dordrecht (Netherlands)

Finney H, Newman DJ, Gruber W, Merle P, Price CP (1997) Initial evaluation of cystatin C measurement by particle-enhanced immunonephelometry on the Behring nephelemeter systems (BNA, BN II) Clin Chem 43:1016–1022

Gutsche B, Grun C, Scheutzow D, Herderich M (1999) Tryptophan glycoconjugates in food and human urine. Biochem J 343:11–19

Hakansson K, Changgoo H, Anders G, Stefan K, Magnus A (1996) Mouse and rat cystatin C: *Escherichia coli* production, characterization, and tissue distribution. Comp Biochem Physiol – B: Comp Biochem 114:303–311

Hamberg O (1997) Regulation of urea synthesis by diet protein and carbohydrate in normal man and in patients with cirrhosis. Relationship to glucagon and insulin. Danish Med Bull 44:225–241

Horiuchi K, Yonekawa O, Iwahara K, Kanno T, Kurihara T, Fujise Y (1994) A hydrophilic tetrahydro-beta-cerboline in human urine. J Biochem 115:362–366

Jensen AL, Bomholt M, Moe L (2001) Preliminary evaluation of a particle-enhanced turbidimetric immunoassay (PETIA) for the determination of cystatin C-like immunoreactivity in dogs. Vet Clin Pathol 30:86–90

Loeb WF (1998) The measurement of renal injury. Toxicol Pathol 26:26–28

Loeb WF, Quimby FW (1999) The Clinical Chemistry of Laboratory Animals, 2nd ed. Taylor and Francis, Philadelphia

Martin C, Pechereau D, de la Farge F, Braun JP (2002) Plasma cystatin C in the cat: current techniques do not allow to use it for the diagnosis of renal failure. Rev Med Vet 153:305–310

Newman DJ, Price CP (1999) Renal function and nitrogen metabolites. In Burtis CA, and Ashwood, ER, eds., Tietz Textbook of Clinical Chemistry, 3rd ed., pp 1204–1270. WB Saunders Company, Philadelphia

Owen LJ, Keevil BG (2007) Does bilirubin cause interference in Roche creatinine methods? Clin Chem 53:370-371

Pergande M, Jung K (1993) Sandwich enzyme immunoassay of cystatin C in serum with commercially available antibodies. Clin Chem 39; 1885–1890

Pickering RG, Pickering CE (1984) The effects of reduced dietary intake upon the body and organ weights, and some clinical chemistry and haematologic variates of the young Wistar rat. Toxicol Lett 21;271–277
Pitt J, Issaeva O, Wodere S, Sadick M, Kränzlin B, Fiedler F, Klötzer HM, Krämer U, Gretz N (2006) Pharmacological profile and toxicity of fluorescein-labelled sinsitrin, a novel marker for GFR measurements. Naunyn-Schmiedeberg's Arch Pharmacol 373:204–211
Price RG (2002) Early markers of nephrotoxicity. Comp Clin Pathol 11:2–7
Schwendenwein I, Gabler C (2001) Evaluation of an enzymatic creatinine assay. Vet Clin Pathol 30:163–164
Shemesh O, Golbetz H, Kriss JP, Myers BD (1985) Limitations of creatinine as a filtration marker in glomerulonephropathic patients. Kidney Int 2:830–838
Starr R, Hostetter T, Hortin GL (2002) New markers for kidney disease. Clin Chem 48:1375–1376
Takahira R, Yonemura K, Yonekawa O, Iwahara K, Kanno T, Fujise Y, Hishida A (2002) Tryptophan glycoconjugate as a novel marker of renal function. American J Med 110; 192–197
Tauson A-H, Wamberg S (1998) Effects of protein supply on plasma urea and creatinine concentrations in female mink (*Mustela vison*). J Nutr 128; 2584S-2586S
Watson ADJ, Lefebvre HP, Concordet D, Laroute V, Ferré, J-P, Braun J-P, Conchou F, Toutain P-L (2002) Plasma exogenous creatinine clearance test in dogs: comparison with other methods and proposed limited sampling strategy. J Vet Int Med 16:22–33

C.2.2.2.2 Assessment of RBF by Intravascular Doppler Flow Probes

PURPOSE AND RATIONALE

Probes utilizing electromagnetic or Doppler technology may be positioned around or within a renal artery to allow direct measurement of renal blood flow (Yagil 1990; Haywood et al. 1981). Detection of blood flow using Doppler systems is based on changes in the emitted ultrasonic frequency, a Doppler shift, caused by reflection of the signal of moving blood cells. The Doppler shift is proportional to the velocity of blood flow, as indicated by the following equation:

$$\Delta f = \frac{2 f_0 v \cos\theta}{c}$$

Where Δf = Doppler peak frequency shift, f_0 = transmission frequency, v = instantaneous peak velocity, θ = angle of incidence of the beam to the bloodstream (assumed to be 0^o for linear probes) and c = speed of sound in blood (1570 m/sec) (Chilian et al. 1982).

This technique is particularly useful when rapid or continuous assessment of effects on renal blood flow or assessment of renal vasoreactivity need to be assessed.

PROCEDURE

Doppler probes have been applied to rats, rabbits, cats, dogs, pigs, monkeys and humans; these must be appropriately calibrated prior to experimental use. Animals are anesthetized and the probes are placed within the renal artery via the abdominal aorta, which may be accessed via the femoral or carotid arteries. The diameter of the renal artery at the placement site of the Doppler probe must be determined simultaneously to correct velocity measurements for determination of renal blood flow (see Evaluation).

EVALUATION

A number of parameters can be derived from the Doppler measurements, most commonly including average peak velocity (APV), pulsatility index (PI) and resistive index (RI). Renal blood flow (in mL/min) can be calculated as follows:

$$\mathrm{RBF} = \frac{\mathrm{APV} \times \pi \times \mathrm{D}^2 \times 60}{4}$$

Where D = renal arterial diameter (Doucette et al. 1992).

Resistive index (RI) has been shown in several species to be positively correlated with tubular disfunction or postrenal obstruction and its return to normal may serve as a prognostic indicator of resolution of tubular disease (Rivers et al. 1997; Shokeir et al. 1996; Tsuji and Taira, 2001).

LIMITATIONS OF THE METHOD

Dopper probe assessment of velocity is accurate primarily in straight blood vessels of small diameter (< 4.76 mm) and at relatively low flow rates (< 200 mL/min), both of which may be exceeded in normal renal arteries in many species (Lerman and Rodriguez-Porcel, 2001).

In dogs, acute, severe normovolaemic anaemia significantly altered renal artery Doppler parameters without having an influence on Doppler assessment of splanchnic blood flow; the technique may thus be inaccurate in anemic animals (Koma et al., 2006). Furthermore, it is invasive and the size of the test species to which it can be applied depends on the availability of appropriately sized and calibrated probes (Lerman and Rodriguez-Porcel 2001).

REFERENCES AND FURTHER READING

Chilian WM, Marcus ML (1982) Phasic coronary blood flow velocity in intramural and epicardial coronary arteries. Circ Res 50:775–781
Doucette JW, Corl D, Payne HM, Flynn AE, Goto M, Nassi M, Segal J (1992) Validation of a Doppler guide wire for in-

travascular measurement of coronary artery flow velocity. Circulation 85:1899–1911
Haywood JR, Shaffer RA, Fastenow C, Fink GD, Brody MJ (1981) Regional blood flow measurement with pulsed Doppler flowmeter in conscious rat. Am J Physiol 241: H273–8
Koma LM, Kirberger RM, Scholtz L (2006) Doppler ultrasonographic changes in the canine kidney during normovolaemic anaemia. Res Vet Sci. 80:96–102
Lerman LO, Rodriguez-Porcel M (2001) Functional assessment of the circulation of the single kidney. Hypertension 38:625–629
Rivers BJ, Walter PA, Polzin DJ, King VL (1997) Duplex doppler estimation of intrarenal pourcelot resistive index in dogs and cats with renal disease. J Vet Intern Med 11:250–60
Shokeir AA, Nijman RJ, el-Azab M, Provoost AP (1996) Partial ureteric obstruction: a study of Doppler ultrasonography and diuretic renography in different grades and durations of obstruction. Br J Urol. 78:829–35
Tsuji Y, Taira H (2001) Correlation between renal blood flow and intrarenal Doppler measurements in canine autotransplanted kidney. Int Urol Nephrol. 32:307–10
Yagil Y (1990) Acute effect of cyclosporin on inner medullary blood flow in normal and postischemic rat kidney. Am J Physiol 258: F1139–44

C.2.2.2.3 Assessment of GFR and RBF by Scintigraphic Imaging

PURPOSE AND RATIONALE

Radioactive indicators (^{99c}Tc-DPTA, ^{113m}In-DPTA, ^{99c}Tc-mercaptoacetyltriglycine) may be used to measure renal blood or plasma flows or glomerular filtration rate (Reba et al. 1968). These techniques require intraarterial or intravenous administration of the tracer followed by monitoring of the amount of tracer in the kidneys with an external gamma camera (Fommei and Volterrani 1995).

In species where extrarenal clearance of tracers used in the determination of GFR or RPF is high or variable, external detection methods may actually be more accurate than plasma clearance methods because the extrarenal component of plasma removal is elminated (Drost et al. 2003).

PROCEDURE

The selected radiotracer is injected either intravenously or intraarterially. External measurements of radioactivity retained in the kidney are made either at timed intervals (rate of accumulation, or slope method) or at a selected interval, usually corresponding to either first pass or peak level of the tracer (percent accumulation, or integral method) (Kampa et al. 2002).

LIMITATIONS OF THE METHOD

These techniques do not yield absolute flow, but rather flow per unit volume or tissue mass. However, algorithms can be developed in the species of interest to allow conversion of tissue uptake to GFR or RBF expressed in standard units by simultaneous determination of plasma clearance of the tracer in preliminary experiments (Kelleher et al. 1991; Kampa et al. 2003), as the correlations between methods for any given tracer are in general high (Delpassand et al. 2000).

In general, assessment of GFR or RBF by external detection methods is less accurate than assessment by clearance methods, although the correction algorithm used for the external detection method can influence the degree of accuracy achievable (DeSanto et al. 1993; Itoh et al. 2000; Itoh, 2003). Integral methods (calculated based on the percent of the dose accumulated) are in general more accurate because they eliminate variability resulting from variable durations of the uptake phase (Kampa et al. 2003). Manual selection of the region of interest (ROI) for the collection of the scintigraphy data also improves the accuracy (Kampa et al. 2002).

MODIFICATIONS OF THE METHOD

Depending on the tracer used, either GFR or RBF can be estimated from the results. The table below lists different tracers that can be used for the assessment of either GFR or RBF (Emeigh Hart and Kinter, 2005):

REFERENCES AND FURTHER READING

De Santo NG, Anastasio P, Cirillo M, Santoro D, Spitali L, Mansi L, Celentano L, Capodicasa D, Cirillo E, Del Vecchio E, Pascale C, Capasso G (1999) Measurement of glomerular filtration rate by the 99mTc-DTPA renogram is less precise than measured and predicted creatinine clearance. Nephron 81:36–140
Delpassand ES, Homayoon K, Madden T, Mathai M, Podoloff DA (2000) Determination of glomerular filtration rate using a dual-detector gamma camera and the geometric mean of renal activity: correlation with the Tc-99m DTPA plasma clearance method. Clin Nucl Med 25:258–262
Drost WT, McLoughlin MA, Mattoon JS, Lerche P, Samii VF, DiBartola SP, Chew DJ, Barthez PY (2003) Determination of extrarenal plasma clearance and hepatic uptake of technetium-99m-mercaptoacetyltriglycine in cats. Am J Vet Res 64:1076–1080
Emeigh Hart SG, Kinter LP (2005) Assessing Renal Effects of Toxicants *in vivo*. In Tarloff JB, and Lash, LH (eds) Toxicology of the Kidney, 3rd ed., pp 81–147. CRC Press, Boca Raton
Fommei E, Volterrani D (1995) Renal nuclear medicine. Sem. Nucl. Med 25:183–194
Itoh K, Tsushima S, Tsukamoto E, Tamaki N (2000) Reappraisal of single-sample and gamma camera methods for determination of the glomerular filtration rate with 99mTc-DTPA. Ann Nucl Med 14:143–150
Itoh K (2003) Comparison of methods for determination of glomerular filtration rate: Tc-99m-DTPA renography, predicted creatinine clearance method and plasma sample method. Ann Nucl Med 17:561–565

Table 1 Radiopharmaceuticals Used for Estimating

Glomerular Filtration Rate	Renal Blood or Plasma Flow
^{3}H-inulin	^{3}H-para-aminohippuric acid (PAH)
^{14}C-inulin	^{14}C-PAH
^{14}C-carboxy inulin	S^{99m}Tc-hippuran analogs
^{14}C-hydroxy-methyl inulin	^{99m}Tc-iminodiacetic PAH (PAHIDA)
^{131}I-chloroiodopropyl inulin	^{99m}Tc-mercaptoacetyltriglycine (^{99m}Tc-Mag3)
^{131}I-propargyl inulin	^{99m}Tc-mercaptosuccinyltriglycine (^{99m}Tc-MSG3)
^{125}I-diatrizoate	^{99m}Tc-N,N′bis(mercaptoacetyl)-2,3-diaminopropanoate (CO2-DADS-A)
^{125,131}I-iothalamate (Conray – 60)	^{125,131}I-iodopyracet (Diodrast)
^{131}I-diatrizoate (Hypaque, Renografin)	^{131}I-orthoiodohippurate (Hippuran, OIH)
^{51}Cr-,^{99m}Tc-,^{111,113m}In-,^{140}La-,^{169}Yb-EDTA	^{67,68}Ga-N-succinyl desferioxamine
^{51}Cr-,^{99m}Tc-,^{111,113m}In-,^{140}La-,^{169}Yb-DTPA	^{97}Ru-ruthenocenyl-glycine (Ruppuran)
^{57,58}Co-hydroxycobalamin	^{99m}Tc-thiodiglycolic acid
^{57,58}Co-cyanocobalamin	

Kampa N, Wennstrom U, Lord P, Twardock R, Maripuu E, Eksell P, Fredriksson SO (2002) Effect of region of interest selection and uptake measurement on glomerular filtration rate measured by 99mTc-DTPA scintigraphy in dogs. Vet Radiol Ultrasound. 2002 Jul-Aug;43(4):383-391

Kampa N, Bostrom I, Lord P, Wennstrom U, Ohagen P, Maripuu E (2003) Day-to-day variability in glomerular filtration rate in normal dogs by scintigraphic technique. J Vet Med A Physiol Pathol Clin Med 50:37–41

Kelleher JP, Anderson PJ, Gordon I, Snell ME (1991) Estimation of glomerular filtration rate in the miniature pig by kidney uptake on the gamma camera. Nucl Med Commun.12:817–822

Reba RC, Hosain F, Wagner NH (1968) Indium-113m diethylenetriaminepentaacetic acid (DTPA): a new radiopharmaceutical for study of the kidneys. Radiol. 90:147–149

C.2.2.3 Assessment of Renal Tubule Functions

C.2.2.3.1 Urinalysis

PURPOSE AND RATIONALE

More than 99% of the reabsorption of glucose, protein and electrolytes occurs in the proximal tubule. Electolyte concentrations can be affected by other tubule segments, but even low-level changes in proximal tubular function will be reflected by increased urinary excretion of protein and glucose (Stonard et al. 1987; Finco, 1997; Loeb and Quimby, 1999; Newman and Price, 1999; Aleo et al. 2002). Standard and modified urinalysis techniques can be successfully used to assess the effects of compounds on proximal tubule uptake processes (Katsuno et al. 2007).

PROCEDURE

Collection of a good quality sample from the test species is paramount to obtaining high quality data from the urinalysis. Samples must be collected in clean containers and must be kept free of contamination from food, drinking water, feces, blood and bacteria. For best results, samples should be analyzed promptly (ideally within one hour) after collection, but where analysis must be delayed, the sample must be protected from chemical degradation and evaporation, best accomplished by using collection containers that are appropriately sized for the species in question, tightly sealing the containers when possible, and keeping the specimen cold (4°C) until analysis. If chilled or frozen, samples must be allowed to slowly equilibrate to room temperature before analysis.

Point-in-time samples can easily be collected from most species, either by free-catch, urethral catheterization, manual compression of the bladder or cystocentesis (withdrawal of urine from directly from the bladder with a needle and syringe). Catheterization may require sedation or anesthesia, especially in females of all species and in male pigs whose urethral recess makes this process difficult (Van Metre and Angelos, 1999). Manual compression of the bladder can also be performed on rodents, and cystocentesis may also be performed by a skilled operator using a small (25 gauge) needle and syringe (Loeb and Quimby, 1999).

Timed urine collections in all species (including large animals) can also be obtained by the use of specially designed metabolism cages. A metabolism cage consists of an animal chamber mounted above an excrement collection system. The animal chamber must be equipped with feeder and waterer units if an animal is to be housed in the metabolism cage for more than a few hours. These need to be sized appropriately to the test species of interest (especially regarding the collection container, which must minimize surface

area available for evaporation) and designed to eliminate contamination of the urine by food, drinking water, or feces. In selecting the size of the collection container, the anticipated urine volume should be considered: a mouse will produce 0.25–1 ml in 24 hours of urine, a rat, 10 ml, a hamster, 5–8 ml, a rabbit, 600 ml and a dog or minipig, 500 ml or more (Loeb, 1998; McClure, 1999; Van Metre and Angelos, 1999). Whatever type of metabolism cage is used, the following general precautions are offered:

1. For studies of >24 hours duration, test animals should be acclimated to the metabolism cage for several days prior to study initiation. During this period, animals should be monitored frequently to insure that they learn to use the feeder and waterer systems properly. Test animals should be maintaining or gaining weight prior to study initiation.
2. Feeder and waterer systems should provide ample food and water to meet the animal's needs for the duration of urine collection and all separator systems should function properly. For chronic studies (>5–7 days duration) it is useful to have a complete exchange of feeder, waterer, and urine/feces collector and separator systems so that soiled units may be rapidly exchanged with clean, dry/filled units at regular intervals.
3. Cages should be decontaminated, cleaned, rinsed with distilled/deionized water, and thoroughly dried prior to use. Surfaces used to collect urine may be siliconized or sprayed with a suitable hydrophobic material (PAM, General Foods) to facilitate urine collection.
4. All surfaces contacting urine should be rinsed with distilled/deionized water or appropriate solvents to collect any residuals at appropriate intervals.
5. To preserve the quality of the specimens during prolonged collection times, the opening of the collection vial needs to be small to prevent evaporation and the vial should be surrounded either with wet ice or frozen cold packs to chill the sample promptly once it is deposited (Loeb, 1998; Loeb and Quimby, 1999). Urine may also be collected under mineral oil to prevent evaporative losses. For very small or antidiuretic animals (eg. hamsters, gerbils) placing the cage over a shallow pan of oil and skim feces from the surface may be necessary while collecting urine with a pipette from under the oil. To maximize the volume of the sample collected in rodents in metabolism cages, food should be withheld (this also reduces the risk of contamination of the sample) and water provided (Lee et al. 1998).

Routine urinalysis consists of visual assessment (color, clarity), volume, specific gravity or osmolality, pH, and quantitative or semiquantitative determination of total protein and glucose and microscopic evaluation of urine sediment (Weingand et al., 1996). Urine constituents can be measured semiquantitatively using commercially available "dipstick" test strips (Chemstrips, Roche Diagnostics or Multistix, Bayer Heath Care Diagnostics) which contain reagents for the determination of specific gravity, protein, glucose, ketones, bilirubin, urobilinogen, hemoglobin, nitrite and leukocyte esterases (Newman and Price, 1999). These strips may be read manually or using automated analyzers specific to each product.

If quantitative assessment of urine analytes is required (see under "Evaluation"), either urine volume or urine creatinine concentration must be measured and used to "normalize" the concentration of the measured analyte. This will negate the effects of differences in urine concentration between animals and allow for accurate comparison of the results. Creatinine can be measured by the same methods used for plasma..

EVALUATION

Urine volume, combined with assessment of urine concentration (specific gravity or osmolality) can serve as an index to renal function. With severe acute loss of functional nephron mass, urine output is decreased (oliguria) or absent (anuria), while loss of the ability of the kidney to adequately concentrate urine results in the excretion of large volumes of dilute urine.

The commercially available dipstick reagents do not detect the low levels of glucose found in normal urine and thus positive results indicate significant glucosuria in most species (the exception is the gerbil, where dipstick positive glucosuria is normal) (McClure, 1999). If glucosuria is detected, time-matched plasma glucose levels are needed to rule out that this result has not resulted from an increase in the filtered glucose load. If plasma glucose is normal, the appearance of glucose in the urine may indicate a functional deficit in the proximal tubule (Stonard et al. 1987; Finco 1997; Loeb and Quimby 1999; Newman and Price, 1999; Aleo et al. 2002).

Because of inherent inaccuracies in the dipsticks when applied to animal urine (see below under "Limitations of the Method"), positive results by dipstick for protein must be followed by detailed qualitative and quantitative assessment.

Quantitative assessment of urinary protein excretion is necessary to rule out a contribution from

glomerular malfunction. In general, excretion of markedly elevated levels of protein is indicative of glomerular disease, whereas low-level proteinuria indicates tubular damage or very early/lowgrade glomerular injury (Peterson et al. 1969; Finco, 1997).

A number of different methods have been developed for quantitative assessment, including turbidometric, colorimetric (Biuret and Lowry assays as examples) and dye binding assays. All have their advantages and limitations; in general, biuret assays tend to detect all types of proteins with equal sensitivity but require fairly large sample volumes, turbidometric assays can suffer from lack of precision with variations in urine ionic strength, and dye-based methods may suffer from interference with exogenous and endogenous urine substances. The Folin phenol (Lowry), Coomassie brilliant blue and Ponceau S methods have been recommended as being particularly precise for urine samples (Petersen et al., 1969; Dilena et al. 1983; Finco, 1997; Newman and Price, 1999).

Qualitative assessment (identification of the proteins excreted) is necessary to determine if low-level proteinuria has resulted from glomerular or tubular malfunction. Concomitant elevation of albumin and one or more of the low molecular weight proteins (which are freely filtered by the normal glomerulus) indicates that the proteinuria has resulted from decreased tubular reabsorption of proteins, while albumin elevation alone or concurrently with a high molecular weight protein (normally excluded from the filtrate by the glomerulus) indicates primary glomerular injury (Petersen et al. 1969; Finn and Porter, 1998; Gruder et al. 1998; Umbreit and Wiedemann, 2000). Commonly used filtered low molecular weight proteins include retinol binding protein (Price, 2000, 2002; Aleo et al. 2002, 2003), α_2- or β_2-microglobulin (Viau et al. 1986; Loeb, 1998; Finn and Porter, 1998; Price, 2000, 2002) or cystatin C (Finn and Porter, 1998; Herget-Rosenthal et al. 2001; Uchida and Gotoh, 2002).

LIMITATIONS OF THE METHOD

Because the commercially available dipsticks are designed for clinical use, they are inaccurate for a number of parameters in animal urine. The specific gravity reagents are completely inaccurate in all species. Dipsticks which use a glucose oxidase method for urine glucose can show a false positive result in species such as the dog and mouse with high urinary ascorbate levels or in urine contaminated with hypochlorite used as a disinfectant (Finco, 1997; Loeb and Quimby, 1999). For all glucose detection methods, test article formulations that contain glucose or other metabolizable sugars in quantities, should be avoided, as they may transiently overwhelm tubule reabsorption mechanisms and generate false positive test results. Protein detection is based on a bromphenol blue method that is most sensitive for albumin (Newman and Price, 1999), which means that proteinuria that does not result primarily from an increased albumin excretion may not be detected by this method. Furthermore, since these tests are designed for human urine, false positives are frequent in species like the dog, whose normal urine protein levels are just above the lower limits for humans (Finco, 1997), and dipstick tests are invariably positive in male rats and mice which have normal high proteinuria (Loeb and Quimby, 1999).

The sensitivity of the quantitative protein assays to the protein(s) of interest depends in large measure on which protein is used to generate the standard curve. Albumin is most commonly used because it is the most abundant protein in urine and while it is adequate for most methods (Dilena et al. 1983), it will in general underestimate the abundance of many other proteins of interest in urine (Guder and Hofman, 1992).

Qualitative assessment of urine proteins other than albumin is hampered in many species by the lack of suitable immunoassays; with the exception of cystatin C, commerically available antibodies do not cross react with the animal proteins (Loeb and Quimby, 1999; Uchida and Gotoh, 2002). Assessment of urinary retinol excretion has been shown to be a sensitive index to retinol binding protein excretion in the rat (Aleo et al. 2002, 2003).

MODIFICATIONS OF THE METHOD

Point-in-time samples from laboratory rodents may be obtained by taking advantage of the fact that these animals frequently urinate when they are handled or shortly after being removed from their home cage. A skilled, quick and prepared operator with a ready small container or plain microcapillary tube may be able to obtain a small sample in the first instance (Loeb and Quimby, 1999); in the second, the animal can be placed in a small confined space on plastic food wrap and observed carefully for urination, as it has been shown that most rodents will urinate within 20 minutes after removal from their home cages. The sample thus generated can be collected by micropipette (Kurien and Scofield, 1999).

For repeated point-in-time urine samples from rats over short periods of time (one to two weeks after the surgery), the urethra or the ureter can be cannulated. Cannulated rats can also be used to collect accurate

and complete timed urine samples (Mandavilli et al. 1991; Horst et al. 1988).

REFERENCES AND FURTHER READING

Aleo MD, Navetta KA, Emeigh Hart SG, Harrell JM, Whitman-Sherman JL, Krull DK, Wilhelms MB, Boucher GG, Jakowski AB (2002) Mechanism-based urinary biomarkers of aminoglycoside-induced phospholipidosis. Comp. Clin. Pathol. 11:193–194

Aleo MD, Navetta KA, Emeigh Hart SG, Harrell JM, Whitman-Sherman JL, Krull DK, Wilhelms MB, Boucher GG, Jakowski AB (2003) Mechanism-based urinary biomarkers of renal phospholipidosis and injury. *Toxicological Sciences* 72(Suppl):24

Dilena BA, Penberthy LA, Fraser CG (1983) Six methods for determining urinary protein compared. Clin. Chem. 29:553–557

Finco DR (1997) Kidney function. In: Kaneko JJ, Harvey JW, Bruss ML (eds) Clinical Biochemistry of Domestic Animals. Academic Press, San Diego

Finn WF, Porter GA (1998) Urinary biomarkers and nephrotoxicity. In: DeBroe ME, Porter GA, Bennett WM, Verpooten GA (eds) Clinical Nephrotoxins. Kluwer Academic Publishers, Dordrecht (Netherlands)

Guder WG, Hofmann W (1992) Markers for the diagnosis and monitoring of renal lesions. Clin Nephrol 38: S3–S7

Guder WG, Ivandic M, Hofmann W (1998) Physiopathology of proteinuria and laboratory diagnostic strategy based on single protein analysis. Clin Chem Lab Med 36:935–939

Herget-Rosenthal S, Poppen D, Pietruck F, Marggraf G, Phillip T, Kribben A (2001) Prediction of severity of acute tubular necrosis by tubular proteinuria. J Am Soc Nephrol 12:170A

Horst PJ, Bauer M, Veelken R, Unger T (1988) A new method for collecting urine directly from the ureter in conscious unrestrained rats. Ren Physiol Biochem 11:325–331

Katsuno K, Fujimori Y, Takemura Y, Hiratochi M, Itoh F, Komatsu Y, Fujikura H, Isaji M (2007) Sergliflozin, a novel selective inhibitor of low affinity sodium glucose cotransporter (SGLT2), validates the critical role of SGLT2 in renal glucose reabsorption and modulates plasma glucose level. J Pharm Exper Ther 320:323–330

Kurien BT, Scofield RH (1999) Mouse urine collection using clear plastic wrap. Lab Anim 33:83–86

Lee KM, Reed LL, Bove DL, Dill JA (1998) Effects of water dilution, housing and food on rat urine collected from the metabolism cage. Lab Anim Sci 48:520–525

Loeb WF (1998) The measurement of renal injury. Toxicol Pathol 26:26–28

Loeb WF, Quimby FW (1999) The Clinical Chemistry of Laboratory Animals. Taylor and Francis, Philadelphia

Mandavilli U, Schmidt J, Rattner DW, Watson WT, Warshaw AL (1991) Continuous complete collection of uncontaminated urine from conscious rodents. Lab. Anim. Sci. 41:258–261

McClure DE (1999) Clinical pathology and sample collection in the laboratory rodent. Vet Clin North Am 2:565–590

Newman DJ, Price CP (1999) Renal function and nitrogen metabolites. In: Burtis CA, Ashwood ER (eds) Tietz Textbook of Clinical Chemistry. W. B. Saunders Company, Philadelphia

Peterson PA, Evrin P-E, Berggård I (1969) Differentiation of glomerular, tubular and normal proteinuria: determinations of urinary excretion of .β $_2$-microglobulin, albumin, and total protein. J Clin Investig 48:1189–1198

Price RG (2000) Urinalysis to exclude and monitor nephrotoxicity. Clin Chim Acta 297:173–182

Price RG (2002) Early markers of nephrotoxicity. Comp Clin Pathol. 11:2–7

Stonard MD, Gore CW, Oliver GJA, Smith IK (1987) Urinary enzymes and protein patterns as indicators of injury to different regions of the kidney. Fundam Appl Toxicol 9:339–351

Uchida K, Gotoh A (2002) Measurement of cystatin-C and creatinine in urine. Clin Chim Acta 323:121–128

Umbreit A, Wiedemann G (2000) Determination of urinary protein fractions. A comparison with different electrophoretic methods and quantitatively determined protein concentrations. Clin Chim Acta 297:163–172

Van Metre DC, Angelos SM (1999) Miniature pigs. Vet Clin North Am 2:519–537

Viau C, Bernard A, Lauwerys R (1986) Determination of rat β_2-microglobulin in urine and serum. I. Development of an immunoassay based on latex particles agglutination. J Appl Toxicol 6:185–189

C.2.2.3.2 Electrolyte Excretion

Since one of the kidney's primary functions is maintaining electrolyte and mineral homeostasis in the face of fluctuating dietary intake and body needs, examination of plasma and urine electrolyte levels will provide some insight into renal function. Because of the large functional mass of the kidney, alteration of plasma electrolyte levels are usually not detected until the effect on renal functional is significant (pathologic). In contrast, urine electrolyte levels examined with knowledge of plasma levels and dietary intake can serve as an extremely sensitive index to the effect of drugs or chemicals on the functional state of the kidney.

In animal studies the diet can be carefully controlled and thus the intake (and hence the plasma electrolyte levels) can be assumed to be fairly constant. Provided there are no sources of significant electrolyte loss resulting from the experimental manipulations (e. g., vomiting, diarrhea, salivation), urine electrolyte levels will reflect the effects of the compound on either GFR (determines the filtered load) or tubular secretion or reabsorption (determines the final urine electrolyte composition).

C.2.2.3.3 Fractional Excretion Methods

PURPOSE AND RATIONALE

Fractional excretion (FE) is the proportion of the filtered load of any analyte that is excreted from the plasma. If both tubular function and plasma electrolyte values are normal, increases in electrolyte FE values clearly reflect a decrement in GFR. With tubular malfunction, the direction of the change in FE values depends on the net direction of electrolyte transport (i. e.,

FE will increase for electrolytes that are primarily reabsorbed and will decrease for secreted electrolytes) (Finco, 1997; Stockham and Scott, 2002).

PROCEDURE

FE assessments can be performed in any species, as it requires only carefully timed complete urine collections and a concurrent assessment of GFR. FE will be unitless if the urine collection period is expressed in minutes, thus (Finco,1997):

$$\begin{aligned}\text{FE} = &\big(\text{urine electrolyte concentration (mmol/L)}\\ &\times \text{urine (mL/collection period)}\big)\\ &/\big(\text{GFR (mL/min)}\\ &\times \text{plasma electrolyte concentration (mmol/L)}\big)\end{aligned}$$

To eliminate the need for both complete timed urine collections (difficult to do in most animals) and concurrent assessment of GFR, FE values are usually calculated based on point-in-time urine collections by using creatinine excretion during the same time period as an estimator of GFR (Finco, 1997).

Animals are placed in appropriately-sized metabolism cages for an appropriate period of time to allow collection of an adequate volume of urine. At the midpoint of the collection period a blood sample is obtained under appropriate anesthesia (note: the use of CO_2 will falsely elevate plasma potassium levels and render the method inaccurate) for determination of electrolyte and creatinine levels.

Plasma and urine electrolytes and creatinine are determined by standard methods (Durst and Siggard-Andersen, 1999; Newman and Price, 1999; Scott et al., 1999). FE is calculated from the results as outlined below (Stockham and Scott 2002):

$$\begin{aligned}\text{FE} = &\big(\text{urine electrolyte concentration}\\ &\times \text{plasma creatinine concentration urine}\big)\\ &/\big(\text{creatinine concentration}\\ &\times \text{plasma electrolyte concentration}\big)\end{aligned}$$

LIMITATIONS OF THE METHOD

If the Jaffe method for creatinine is used, the investigator must be aware of potential interference due to endogenous chromogens (the error is magnified in species where these chromogens are present in higher concentration in the plasma than in the urine (dog, mouse) (Finco, 1997; Dunn et al. 2004) or possibly the test compound (Sonntag and Scholer, 2001). Additionally, plasma electrolyte levels may fluctuate as the result of eating or due to diurnal rhythms (Finco, 1997). The impact of inaccuracies can be minimized by consistent timing of urine collection, fasting of animals before and during urine collection and the inclusion of a concurrent untreated (vehicle control) group in all studies.

MODIFICATIONS OF THE METHOD

Although FE of sodium is most commonly used to assess tubular function, FE of magnesium has been shown to be the most sensitive index in detecting low-level tubular injury in humans (Barton et al., 1987; Futrakul et al. 1999; Kang et al. 2000; Oladipo et al. 2003). Increased FE of calcium has also been shown to serve as a sensitive index of effects on renal function unrelated to overt renal injury (Lam and Adelstein 1986; Tuso and Nortman, 1992; Eliott et al. 2000)

FE of urea has been recently shown to be more useful than the FE of sodium in distinguishing between prerenal and renal azotemia in humans (Carvounis et al. 2002) and thus may also be useful in making this distinction in animal models. Changes in the FE of urea also reflect changes in urine flow rates (in general, these values move parallel to each other) and can be used as an estimate of this parameter (Finco, 1997). The methods used to detect urea in urine are the same as those used in serum (Newmann and Price, 1999).

FE of anions (ammonium, bicarbonate) can be used to determine the potential mechanism underlying systemic acid base imbalances (Rothstein et al. 1990; Kim et al. 2001).

REFERENCES AND FURTHER READING

Barton CH, Vaziri ND, Martin DC, Choi S, Alikhani S (1987) Hypomagnesemia and renal magnesium wasting in renal transplant recipients receiving cyclosporine. Am J Med 83:693–699

Carvounis CP, Nisar S, Guro-Razuman S (2002) Significance of the fractional excretion of urea in the differential diagnosis of acute renal failure. Kidney Int 62:2223–2229

Dunn SR, Qi, Z, Bottinger EP, Breyer M, Sharma K (2004) Utility of endogenous creatinine clearance as a measure of renal function in mice. Kidney Int 65:1959–1967

Durst RA, Siggard-Andersen O (1999) Electrochemistry. In Burtis CA and Ashwood ER (eds) Tietz Textbook of Clinical Chemistry, 3rd ed., pp 133–163. WB Saunders Company, Philadelphia

Eliott C, Newman N, Madan A (2000) Gentamicin effects on urinary electrolyte excretion in healthy subjects. Clin Pharmacol Ther 67:16–21

Emeigh Hart SG, Kinter LP (2005) Assessing Renal Effects of Toxicants *in vivo*. In Tarloff JB, and Lash, LH (eds) Toxicology of the Kidney, 3rd ed., pp 81–147. CRC Press, Boca Raton

Finco DR (1997) Kidney function. In Kaneko, JJ, Harvey, JW, and Bruss, ML, eds., Clinical Biochemistry of Domestic Animals, 6th ed., pp 441–485. Academic Press, San Diego

Futrakul P, Yenrudi S, Futrakul N, Sensirivatana R, Kingwatanakul P, Jungthirapanich J, Cherdkiadtikul T, Laoha-

paibul A, Watana D, Singkhwa V, Futrakul S, Pongsin P (1999) Tubular function and tubulointerstitial disease. Am J Kidney Dis 33:886–891
Kang HS, Kerstan D, Dai L, Ritchie G, Quamme GA (2000) Aminoglycosides inhibit hormone-stimulated Mg+2 uptake in mouse distal convoluted tubule cells. Can J Physiol Pharmacol 78(8):595–602
Kim HY, Han JS, Jeon US, Joo KW, Earm JH, Ahn C, Lee J S, Kim GH (2001) Clinical signficance of the fractional excretion of anions in metabolic acidosis. Clin Nephrol. 55(6):448–452
Lam M, Adelstein DJ (1986) Hypomagnesemia and renal magnesium wasting in patients treated with cisplatin. Am J Kidney Dis 8:164–169
Newman DJ, Price CP (1999) Renal function and nitrogen metabolites. In Burtis CA, and Ashwood, ER, eds., Tietz Textbook of Clinical Chemistry, 3rd ed., pp 1204–1270. WB Saunders Company, Philadelphia
Oladipo OO, Onubi J, Awobusuyi O, Afonja OA (2003) Fractional excretion of magnesium of chronic renal failure patients in Lagos Nigeria. Niger Postgrad Med J 10:131–13
Rothstein M, Obialo C, Hruska KA (1990) Renal tubular acidosis. Endocrinol Metab Clin North Am 19(4):869–887
Scott MG, Heusel JW, LeGrys VA, Siggard-Andersen O (1999) Electrolytes and blood gases. In Burtis CA and Ashwood ER (eds) Tietz Textbook of Clinical Chemistry, 3rd ed., pp 1056–1092. WB Saunders Company, Philadelphia
Sonntag O, Scholer A (2001) Drug interference in clinical chemistry: recommendation of drugs and their concentrations to be used in drug interference studies. Ann Clin Biochem 38:376–38
Stockham SL, Scott MA (2002) Fundamentals of Veterinary Clinical Pathology, 1st ed. Iowa State University Press, Ames
Tuso PJ, Nortman D (1992) Renal magnesium wasting associated with acetaminophen abuse. Conn Med 56:421–423

C.2.2.3.4 Quantitative Electrolyte Excretion

PURPOSE AND RATIONALE

Fractional excretion methods are useful in that they can identify alterations in analyte excretion with relative ease, as they require only point-in-time assessment of analyte concentration and don't require complete and timed urine collection. Greater sensitivity, however, is obtained with quantitative evaluation of electrolyte excretion. This method is more difficult, requiring carefully timed, complete urine collection, and because plasma levels are not evaluated there needs to be reasonable assurance that the changes in excretion seen do not result from alteration of the filtered load of the analyte in question (e. g., plasma levels and GFR remain consistent). In animal studies where the diet is carefully controlled these factors are not usually of concern.

PROCEDURE

The method can be used on any species, although rats are most commonly used. Animals are usually fasted but allowed access to water; if anesthetized animals are used, intravenous administration of balanced electrolyte solutions (e. g., lactated Ringer's solution) or 0.9% NaCl solution can be administered by intravenous infusion to ensure that plasma volume (and thus GFR) and electrolyte levels are maintained.

Urine is collected by any appropriate method over a specified period of time. If possible, the urinary bladder should be emptied before collection of test urine is initiatied and at the end of the collection period; this can be accomplished in dogs by catheterization and in rodents by handling or manual expression of the bladder. If metabolism cages are used, special care must be taken to avoid evaporation of urine and contamination of the vials with feces or drinking water, as accurate determination of volume is important. The volume of urine collected is determined gravimetrically, and urine electrolytes are measured by standard methods (Durst and Siggard-Andersen, 1999; Scott et al. 1999).

EVALUATION

The volume of urine collected over the time period is defined as the urine flow rate:

$$V = \text{volume collected/time period (expressed in mL/min)}$$

and electrolyte excretion (U_XV) is defined as:

$$U_X V = \{[(\text{concentration of } X \text{ in urine}) \times V] / \text{body weight in g}\} \times 100 \quad (\text{expressed in mmol/min/100 g})$$

As a general rule, $U_{Na}V + U_K V = U_{Cl}V$. If it does not, the assumption must be made that there are additional anions in the urine. Carbonic anhydrase inhibition (i. e., excess urinary bicarbonate may be the culprit if the ratio:

$$\frac{U_{Cl}V}{U_{Na}V + U_K V}$$

is less than 0.8.

Net natriuretic activity can be assessed by evaluation of the ratio:

$$\frac{U_{Na}V}{U_K V}.$$

Values greater than 2.0 indicate a favorable natriuretic effect, and values greater than 10.0 indicate a potassium-sparing effect.

REFERENCES AND FURTHER READING

Durst RA, Siggard-Andersen O (1999) Electrochemistry. In Burtis CA and Ashwood ER (eds) Tietz Textbook of Clinical Chemistry, 3rd ed., pp 133–163. WB Saunders Company, Philadelphia

Emeigh Hart SG, Kinter LP (2005) Assessing Renal Effects of Toxicants in vivo. In Tarloff JB, and Lash, LH (eds) Toxicology of the Kidney, 3rd ed., pp 81–147. CRC Press, Boca Raton

Scott MG, Heusel JW, LeGrys VA, Siggard-Andersen O (1999) Electrolytes and blood gases. In Burtis CA and Ashwood ER (eds) Tietz Textbook of Clinical Chemistry, 3rd ed., pp 1056–1092. WB Saunders Company, Philadelphia

C.2.2.3.5 Assessment of Tubular Transport Processes using Transport Substrates and Inhibitors

PURPOSE AND RATIONALE

A number of transporters for organic anions and cations are present on both the lumenal and basolateral surfaces of the proximal tubules. These are essential to the secretion and/or reabsorption of a number of endogenous substrates as well as functioning in the elimination of xenobiotics. These transporters frequently function as ion exchangers and their activity is thus bi-directional, so that the net direction of transport (i. e., secretion or reabsorption) for any given substrate depends not only on the numbers and activity of the transporters on either side of the tubule but also on the presence and concentration of competing or co-transported substrates. This feature of tubular transport has been one of the major challenges in the development of uricosuric agents for the treatment of hyperuricemia (Terkeltaub et al. 2006). Compounds that affect either the expression or activity of transporters, are competitive substrates for them, or act as inhibitors of transport thus may affect not only the clearance of therapeutic agents but also that of endogenous metabolites (Wright and Danzler, 2003).

PROCEDURE

The choice of substrate or inhibitor used depends on the transport process or specific transporter of interest. The table below lists the most commonly used substrates and their transporters (note: most inhibitors act competitively and are themselves substrates for the transporter in question).

Transport studies can be performed in any animal model from which urine and plasma may be collected readily. Inhibitors are administered 30 minutes to 1 hour before the administration of the test substance. Substrates are usually administered intravenously, and are detected in urine and plasma most commonly by colorimetric methods.

EVALUATION

Standard clearance or excretion methods are used to assess the effects.

LIMITATIONS OF THE METHOD

Significant sex differences exist in renal transporter expression and activity in rodents and rabbits (Sekine et

Compound	Most Common Use	Transporter Affected	Comments
Tetraethylammonium (TEA)	Substrate	OCT1, OCT2, OCT3	Most commonly used substrate
1-methyl-4-phenylpyridinium (MPP^+)	Substrate	OCT1, OCT2	Can be used to differentiate OCT3-mediated transport
Tributylmethylammonium (TBuMA)	Substrate	OCT3	Can be used to differentiate OCT3-mediated transport
Urate	Substrate	URAT1, OAT1, OAT3	URAT1 is selective for urate in human kidney but has other OA transport functions in other species
p-aminohippurate (PAH)	Substrate	OAT1, OAT2, OAT3(?), OAT4	Most commonly used substrate. Questionable substrate for OAT3
Estrone sulfate	Substrate	OAT3, OAT4, Oatp1	Oatps are homologs of bile acid transporters in the liver
Lucifer yellow	Substrate	OAT1	Can be detected spectrofluorometrically
Phenolsulfonphthalein (Phenol red)	Substrate	OAT3	Clearance has traditionally been used as a surrogate for urate transport
Probenecid	Inhibitor	OAT1, OAT2, OAT3, URAT1	Used therapeutically and experimentally
Cimetidine	Inhibitor	OAT3	Used to correct creatinine clearance for the contribution of tubular secretion
Benzbromarone	Inhibitor	URAT1	

al. 2006). Many of the substrates, and all of the inhibitors, are not specific enough for accurate determination of the exact transporter affected by the test compound.

MODIFICATIONS OF THE METHOD

The listed substrates and inhibitors may also be used in *in vitro* modles such as isolated tubules or kidney slices. In the latter model, net transport is usually assessed by measuring either the disappearance of the substrate from the medium or, more commonly, the degree or rate of accumulation of the substrate over time in the tissue slice (Kirkpatrick and Gandolfi, 2005).

REFERENCES AND FURTHER READING

Iwanaga T, Kobayashi K, Hirayama M, Maeda T, Tamai I (2005) Involvement of uric acid transporter in increased reanl clearance of the xanthine oxidase inhibitor oxypurinol induced by a uricosuric agent, benzabromarone. Drug Met Disp 33:1791–1795

Jonker JW, Schinkel AH (2004) Pharmacological and physiological functions of the polyspecific organic cation transporters: OCT1, 2, and 3 (SLC22A1-3) J Pharmacol Exper Ther 308:2–9

Kirkpatrick DS, Gandolfi AJ (2005) *In vitro* techniques in screening and mechanistic studies; organ perfusion, slices and nephron components. In Tarloff JB, and Lash, LH (eds) Toxicology of the Kidney, 3rd ed., pp 81–147. CRC Press, Boca Raton

Kreppel E (1959) Der Einfluß einiger Phenylbutazonderivate auf den Phenolrotblutspiegel der Ratte. Med Exp 1:285–289

Masereeuw R, Moons MM, Toomey BH, Russel FGM, Miller DS (1999) Active Lucifer Yellow secretion in renal proximal tubule: evidence for organic anion transport system rossover. J Pharm Exper Ther 289:1104–1111

Sekine T, Miyazaki H, Endou H (2006) Molecular physiology of renal organic anion transporters Am J Physiol Renal Physiol 290: F251–F261

Terkeltaub R, Bushinski DA, Becker MA (2006) Recent developments in our understanding of the renal basis of hyperuricemia and the development of novel antihyperuricemic therapies. Arth Res Ther 8 (Suppl 1): S4

Wright SH, Danzler WH (2004) Molecular and cellular physiology of organic cation and anion transport. Physiol Rev 84:987–1049

C.2.2.4
Assessment of Renal Concentrating Ability

C.2.2.4.1
Solute-Free Water Excretion and Reabsorption

PURPOSE AND RATIONALE

Investigations of the clearance of solute-free water represent indirect methods for the evaluation of several aspects of renal function and provide information on the site and mechanism of action of agents within the nephron. The discovery of the countercurrent multiplier system as the mechanism responsible for the concentration and dilution of the urine has been the prerequisite for the identification of the site of action of diuretic drugs. A drug that acts solely in the proximal convoluted tubule, by causing the delivery of the increased amounts of filtrate to the loop of Henle and the distal convoluted tubule, would augment the clearance of electrolyte-free water (EC_{H2O}) during water diuresis and the reabsorption of electrolyte-free water (ETC_{H2O}) during water restriction. In contrast, drugs that inhibit sodium reabsorption in Henle's loop would impair both EC_{H2O} and ETC_{H2O}. On the other hand, drugs that act only in the distal tubule would reduce EC_{H2O} but not ETC_{H2O}.

PROCEDURE

These tests may be performed in any species from which urine and plasma can be readily collected, although low-level changes in concentrating ability may be more readily manifest in rats than in dogs (Sharrat and Frazer 1963; Osbourne et al. 1983). The general procedure involves initially placing the animals in a metabolism cage with unlimited access to water. After collection of a urine sample (16–24 hours is best), the water is withdrawn and the urine is collected for the next 12–16 hours. The urine specific gravity (or preferentially, urine osmolality) is measured and compared both with the value from the hydrated animal and the mean values from the water-deprived control group (Ragan and Weller, 1999).

Assessment of renal urine diluting ability is more cumbersome but can be accomplished in rats by administration of an oral dose of water by gavage representing 5% of the animal's body weight. The animals are then placed in metabolic cages and the urine is collected every 30 minutes for the next 2 hours (Sharrat and Frazer 1963). In dogs, water diuresis can be induced by oral administration of 50ml of water per kg body weight and maintained by continuous infusion into jugular vein of 2.5% glucose solution and 0.58% NaCl solution at 0.5ml/min per kg body weight. When water diuresis is well established, the glucose infusion is discontinued and control urine samples are collected by urethral catheter (Suki et al. 1965). The volume and specific gravity (or osmolality) of the collected urine is measured and the results expressed as the percent of the administered dose of water excreted during the time period. Time-matched plasma samples are collected for the determination of plasma osmolality.

EVALUATION

In addition to gross assessment of renal dilution or concentrating ability (as described above), quantita-

tive evaluation of either osmolar clearance, freewater clearance (C_{H2O}), or solute-free water clearance (EC_{H2O}) may add additional sensitivity to the evaluation of these functions.

Osmolar clearance can be calculated as follows:

$$C_{osm} = (U_{osm} X\ V)/P_{osm}$$

where C_{osm} = osmolar clearance, U_{osm} = urine osmolality (in mosm/kg water), V = urine flow (measured in ml/min) and P_{osm} = plasma osmolality (measured in msom/kg water). C_{osm} is expressed in ml/min. C_{osm} less than V indicates excretion of a dilute urine (i. e., excess water is being excreted), but C_{osm} greater than V indicates excretion of concentrated urine (i. e., excretion of excess solute).

Freewater clearance (C_{H2O}) provides an estimate of the amount of urine being excreted in excess that needed to clear solutes, and is calculated traditionally as follows:

$$C_{H2O} = V\ X[(1 - U_{osm})/P_{osm}]$$
(Wesson and Anslow, 1952)

More accurate assessment of the ability of the kidney to appropriately regulate plasma tonicity and/or respond appropriately to antidiuretic hormone (ADH) can be made by calculation of electrolyte-free water clearance (EC_{H2O}). This formula takes into account only water needed to excrete excess "effective" osmolytes (in general, monovalent electrolytes and their associated anions) and is calculated as follows:

$$EC_{H_2O} = V\ X\{1 - ([Na^+ + K^+]_{urine} / [Na^+ + K^+]_{plasma})\}$$ (Shoker, 1994)

LIMITATIONS OF THE METHOD

In general the sensitivity of either urine concentration or dilution tests to detect the effects of test compounds on renal function is quite low, regardless of species (Ragan and Weller, 1999). Furthermore, these tests (especially the urine dilution test) may be significantly altered by extrarenal effects (e. g., vomiting, diarrhea, delayed GI absorption, altered adrenal cortical function). Calculation of osmolar, freewater and electrolyte-free water clearances require accurate assessment of urine flow rates, which will require accurate and complete collection of all urine produced during the time interval, not always easily accomplished in small animal species. Catheterized models should be utilized in this circumstance. In addition, calculated electrolyte-free water clearances may be influenced by the presence of excess effective osmolytes in either urine or plasma (e. g., in circumstances of hyperglycemia or metabolic acidosis/alkalosis) and the formula must be corrected to account for these if they are known to be present (Shoker 1994; Nguyen and Kurtz, 2005).

REFERENCES AND FURTHER READING

Ragan HA, Weller RE (1999) Markers of renal function and injury. In Loeb, WF, and Quimby, FW (eds), The Clinical Chemistry of Laboratory Animals, 2nd edition, pp 519-548, Taylor and Francis, Philadelphia

Nguyen MK, Kurtz I (2005) Derivation of a new formula for calculating urinary electrolyte-free water clearance based on the Edelman equation. Am J Physiol Renal Physiol 288: F1-F7

Osbourne CA, Finco DR, Low DG (1983) Pathophysiology of renal disease, renal failure and uremia. In Ettinger, SJ (ed)Textbook of Veterinary Internal Medicine, 3rd ed, pp 1733-1798. WB Saunders, Philadelphia

Sharratt M, Frazer AC (1963) The sensitivity of function tests in detecting renal damage in the rat. Toxicol Appl Pharmacol 5:36–48

Shoker AS (1994) Application of the clearance concept to hyponatremic and hypernatremic disorders: a phenomenological analysis. Clin Chem 40:1220–1227

Suki W, Rector FC Jr, Seldin DW (1965) The site of action of furosemide and other sulfonamide diuretics in the dog. J Clin Invest 44:1458–1469

Wesson LG, Anslow WP (1952) Effect of osmotic diuresis and mercurial diuresis in simultaneous water diuresis. Am J Physiol 170:255–259

C.2.2.4.2 Assessment of Medullary Osmolarity and Blood Flow

PURPOSE AND RATIONALE

The ability of the kidney to concentrate urine depends entirely on the maintenance of the renal medullary interstitium in a hypertonic state. Hypertonicity reflects two phenomena; water-uncoupled transport of osmotically active substances (sodium and urea, primarily) into the medullary interstitium, and the trapping of those solutes in the interstitium by the vasa recta countercurrent multiplier system. The hypertonic gradient is created by the active transport of sodium into the interstitium in the ascending loop of Henle, and a combination of passive and facilitated transport of urea located in the collecting duct; the magnitude and effectiveness of the gradient is determined by the rate of plasma flow through the vasa recta (Pallone et al. 2003; Sadowski and Dobrowolski 2003). The method described allows simultaneous assessment of both parameters.

PROCEDURE

Male Wistar rats have been used in these experiments. Under appropriate anesthesia, the femoral artery and vein are cannulated for measurement of aortic blood

pressure and infusion of fluids and test compounds, respectively. The left kidney is exposed and placed in a plastic cup as for micropuncture experiments (see 1.2.1.4.), except that the dorsal surface is placed at the top of the cup, facing the operator. The ureter is catheterized and a platinum-iridium admittance electrode is inserted along the corticopapillary axis from the dorsal surface of the kidney (the probe is sized to ensure correct placement of the recording surfaces within the inner renal medulla). The capsule is incised and a needle laser-Doppler (LD) probe is inserted adjacent to the admittance probe. Animals are maintained in intravenous infusions of balanced electrolyte solution to maintain plasma volume and ensure adequate renal perfusion.

Medullary blood flow (MBF) is assessed by the LD probe, which is connected to a perfusion monitor (Periflux 4001, Perimed). The number and velocity of erythrocytes moving between the two optical fibers of the LD probe is determined. Admittance (the reciprocal of impedence) is measured between the tip of the LD probe and the admittance electrode by a conductance meter connected to both of these, following the application of a measuring current at a frequency of 24 Hz. Following the experiment, the kidney is dissected to verify that the LD and electrode have been correctly placed.

EVALUATION

Medullary blood flow (MBF) is expressed in arbitrary perfusion units (PU), based on the voltage generated by the Doppler flux of the blood cells moving beneath the LD probe (roughly, the product of cell number X velocity). By definition, a 10V signal from the detector is considered 1000 PU. Admittance (Y) is expressed in millisiemens (mS), and is directly related to the ionic tonicity of the tissue (primarily due to the NaCl content). Effects in treated animals are expressed relative to those in untreated controls. If desired, urine may be collected from the ureteral cannula for excretion determinations.

LIMITATIONS OF THE METHOD

Because MBF is expressed in arbitrary units, only relative changes within a single animal can be detected, thus each animal must serve as its own control (although results between animals in the same study can be compared with the use of a calibration algorithm). Significant tissue damage, resulting in non-functional mephrons, does result from the placement of the equipment and thus the technique can only be applied to the innermost medulla (where the glomeruli originate below the depth of the damaged zone). The admittance recordings reflect only the concentration of NaCl in the medulla and thus changes in tonicity resulting strictly from changes in urea concentration cannot be detected by this method.

MODIFICATION OF THE METHOD

Regional changes in medullary tonicity and the steepness of the osmotic gradient can be detected using a system of three needle electrodes that allows assessment of admittance in the outer and inner medulla separately. This arrangement cannot be coupled with the LD probe because excessive tissue damage would result (Sadowski and Portalska, 1983).

An admittance electrode surrounded by a steel cannula fitted to syringe pumps may be used in place of the needle electrode. This setup allows for direct infusion of test substances into the medulla so that local effects may be monitored (Dowbrowolski and Sadowski, 2004).

REFERENCES AND FURTHER READING

Dobrowolski L, Badzynska B, Walkowska A, Sadowski J (1998) Osmotic hypertonicity of the renal medulla during changes in renal perfusion pressure in the rat. J Physiol 508:929–935

Dobrowolski L, Sadowski J (2004) Renal medullary infusion of indomethacin and adenosine

Pallone TL, Turner MR, Edwards A, Jamison RL (2003) Countercurrent exchange in the renal medulla. Am J Physiol Regul Integr Comp Physiol 284: R1153–R1175

Sadowski J, Portalska E (1983) Dynamic evaluation of renal electrolyte gradient by in situ impedance studies. Kidney Int 24:800–803

Sadowski J, Kompanowska-Jezierska E, Dobrowolski L, Walkowska A, Badzynska B (1997) Simultaneous recording of tissue ion content and blood flow in rat renal medulla: evidence on interdependence. Am J Physiol 273: F658-F662

Sadowski J, Dobrowolski L (2003) The renal medullary interstitium: focus on osmotic hypertonicity. Clin Exper Pharmacol Physiol 30:119–126

C.2.2.5 Micropuncture Techniques in the Rat[4]

PURPOSE AND RATIONALE

Micropuncture techniques have been applied to the direct investigation of the effect of diuretics on single nephron function. The observed changes in tubular fluid reabsorptive rates and electrolyte concentrations can be used to asses the mechanism of action. The rat is the model of choice since proximal and distal tubules as well as collecting ducts are accessible for micropuncture.

[4] Contribution by M. Hropot.

PROCEDURE

Clearance and free-flow micropuncture studies are performed in rats with a body weight of about 250 g, anaesthetized by the intraperitoneal injection of thiopentone (Trapanal 50 mg/kg). The animals are fasted for 16 h before the beginning of the experiment, but have free access to tap water. After anesthesia the animals are placed on a thermostatically heated table. Thereafter rats are tracheotomized and carotid artery and jugular vein are cannulated for blood pressure recording, blood sampling, and for infusion of compounds, respectively. The left kidney is carefully exposed by a flank incision, embedded in a small plastic vessel with cotton wool, and bathed with paraffin oil at 37°C. The ureter is cannulated and rectal temperature monitored continuously. A bolus injection of 75 µCi inulin ^{3}H in 0.7 ml NaCl solution is given, followed by 0.85% NaCl solution at a rate of 2.5 ml/min per 100 g body weight. The sustained infusion delivers 75 µCi inulin ^{3}H per hour. The control puncture of tubules is performed 45 min after beginning of the intravenous infusion. The direct collection of tubular fluid samples from proximal and distal tubules is carried out with glass capillaries of 8 to 10 µm external diameter using a micromanipulator and microscopic observation. Distal tubules are identified by intravenous injection of lissamine green. The control period is followed by the test period. After an equilibration period of 30 min with the compound to be tested, micropuncture is performed again and tubular fluid is collected. The uretral urine is collected and blood sampling is performed in the middle of each clearance period.

The infusion rate/volume is determined by the size of the animal. Distal collection is done by identification of the perfused segment by its dye content; a second micropipette is then inserted, a distal oil or wax block is placed and the infusion fluid can be collected for subsequent analysis (Knox and Marchand 1976; Ramsey et al. 1996; Lorenz et al. 1999; Wang et al. 1993, 1999).

EVALUATION

The following parameters may be determined: inulin clearance (GFR), single nephron GFR, fractional delivery of water, sodium and potassium in proximal and distal tubules and in urine.

Fluid reabsorption (J_v) is assessed by comparing the inulin concentration in the perfusate to that in the collected sample, thus (Wang et al., 1993):

$$J_v = V_0 - VL,$$

Where VL is the collected fluid volume (normalized for the length of the tubular segment over which it was collected), and:

$$V_0 = VL(INL/IN_0),$$

Where INL = concentration of inulin in the collected sample, and IN_0 is the inulin concentration in the perfusate.

The net flux of the desired analyte (J_X, where X is the anlyte of interest – Na, K, HCO_3, glucose, etc.), is calculated thus:

$$J_X = V_0[X]_0 - VL[X]_L,$$

Where $[X]_0$ is the concentration of the analyte in the perfusion fluid, and $[X]_L$ is the concentration of the analyte in the collected fluid.

All data are expressed as mean values ± SEM. Comparison of the effects of compounds to be tested with controls is performed by one way analysis of variance and by Student's *t*-test for paired and unpaired data.

MODIFICATION OF THE METHOD

Inulin conjugated to fluorescein isothiocyanate (FITC) may be used in place of the radiolabelled inulin. The inulin concentration in the sample is assessed by comparing the fluorescence in the sample to a standard curve (Lorenz and Gruenstein, 1999).

This technique can be applied to distal tubules as well as to proximal tubules. Distal tubules are identified at the surface of the isolated kidney following micropuncture and perfusion of a proximal tubule as described above. Once the dye reaches the superficial portion of the distal tubule, it is blocked with oil or wax and accessed both proximally and distally as described above (Levine 1985).

REFERENCES AND FURTHER READING

Duarte CG, Chomety F, Giebisch G (1971) Effect of amiloride, ouabain and furosemide on distal tubular function in the rat. Am J Physiol 221:632–640

Hropot M, Fowler Nicole Karlmark B, Giebisch G (1985) Tubular action of diuretics: Distal effects on electrolyte transport and acidification. Kidney Int 28:477–489

Knox FG, Marchand GR (1976) Study of renal action of diuretics by micropuncture techniques. In: Martinez-Maldonado M (ed) Methods in Pharmacology, Vol 4A, Renal Pharmacology pp 73–98. Plenum Press, New York and London

Levine DZ (1985) An in vivo microperfusion study of distal tubule bicarbonate reabsorption in normal and ammonium chloride rats. J Clin Invest 75:588–595

Lorenz JN, Gruenstein E (1999) A simple, non-radioactive method for evaluating single nephron filtration rate and fluid reabsorptio using FITC inulin. *Am J Physiol* 276:F122–F177

Lorenz JN, Schultheis PJ, Traynor T, Shull G, Schnermann J (1999) Micropuncture analysis of single-nephron function in NHE3-deficient mice. *Am J Physiol* 277: F447-F453

Ramsey CR, Knox FG (1996) in *Renal Methods in Toxicology*, LH Lash and RK Zalups, Boca Raton:CRC Press, pp. 79–9
Wang T, Malnic G, Giebisch G, Chan YL (1993) Renal Bicarbonate Reabsorption in the Rat. IV. Bicarbonate Transport Mechanisms in the Early and Late Distal Tubule. J Clin Invest 91:2776–2784
Wang T, Yang C-L, Abbiati T, Schultheis PJ, Shull GE, Giebisch G, Aronson PS (1999) Mechanism of proximal tubule bicarbonate absorption in NHE3 null mice. Am J Physiol 277: F298–F302

C.2.2.6
Stop-Flow Technique[5]

PURPOSE AND RATIONALE

This procedure is of considerable value in the localization of transport processes along the length of the nephron. During clamping of the ureter, glomerular filtration is grossly reduced. The contact time for the tubular fluid in the respective nephron segments increases, and the concentration of the constituents of tubular fluid should approximate the static-head situation. After release of the clamp, the rapid passage of the tubular fluid should modify the composition of the fluid only slightly. The first samples should correspond to the distal nephron segment, the latest to glomerular fluid. However, with introduction of the micropuncture technique, the stop-flow method appears less attractive.

PROCEDURE

This method can be performed in different animals during anesthesia and was originally described by Malvin et al. (1958). The ureter of an animal undergoing intense osmotic diuresis is clamped for several minutes allowing a relatively static column of urine to remain in contact with the various tubular segments for longer than the usual periods of time. Thus, the operation of each segment on the tubular fluid is exaggerated. Then the clamp is released, and the urine is sampled sequentially. Small serial samples are collected rapidly, the earliest sample representing fluid which had been in contact with the most distal nephron segment. Substances examined are administered along with inulin before the application of uretral occlusion. However, tubular segments downstream from the proximal segments may modify the tubular fluid during its egress.

EVALUATION

In each sample the concentration of a glomerular marker, such as inulin, and the concentration of the substance under study are measured. Fractional excretion of the substance and the glomerular marker are plotted versus the cumulative urinary volume.

MODIFICATIONS OF THE METHOD

Shinosaki and Yonetani (1989), Shinosaki et al. (1994) performed stop-flow studies on tubular transport of uric acid in rats treated with pyrazinoic acid, an inhibitor of tubular urate secretion.

Tanaka et al. (1990) used stop-flow experiments to test uricosuric and diuretic activities of new compounds in dogs.

Stop flow techniques can be performed in isolated perfused tubular segments using micropuncture techniques. The proximal and distal micropunctures are performed as described, but instead of immediately collecting fluid from the distal micropipette, pressure is applied equal to that of the perfusion pressure at the proximal pipette, until flow ceases at the infusing pipette. Sampling occurs following a period in which the perfusate remains static in the perfused tubule segment. Care must be taken, especially in mice, to prevent tubular leaking with excessive stop-flow pressures or infusion rates (Schnermann, 1999).

REFERENCES AND FURTHER READING

Malvin RL, Wilde WS, Sullivan LP (1958) Localisation of nephron transport by stop flow analysis. Am J Physiol 194:135–142
Muschaweck R, Sturm K (1972) Diuretika. In: Ehrhart G, Ruschig H (eds) Arzneimittel. Entwicklung – Wirkung – Darstellung. Vol 2, pp 317–328. Verlag Chemie, Weinheim/Bergstrasse, Germany
Schnermann J (1999) Micropuncture analysis of tubuloglomerular feedback regulation in transgenic mice. J Am Soc Nephrol 10:2614–2619
Shinosaki T, Yonetani Y (1989) Stop-flow studies on tubular transport of uric acid in rats. Adv Exp Med Biol 253A:293–300
Shinosaki T, Harada H, Yonetani Y (1991) Uricosuric property of a new diuretic compound, S-8666-S-(–)-enantiomer. Drug Dev Res 22:153–163
Tanaka S, Kanda A, Ashida SI (1990) Uricosuric and diuretic activities of DR-3438 in dogs and rabbits. Japan J Pharmacol 54:307–314

C.3
Impaired Renal Function

C.3.1
Chronic Renal Failure in the Rat

PURPOSE AND RATIONALE

Chronic renal failure is a frequent pathological condition in man. An animal model as described by Acott

[5] Contribution by M. Hropot.

et al. (1987) is of value to test new diuretics under these conditions.

PROCEDURE

Sprague-Dawley rats weighing 150–200 are anesthetized by i.m. injection of ketamine (40 mg/kg) and droperidol/fentanyl (Inovar) 0.25 mg/kg. Through a 6-cm midline incision in the abdominal wall the small bowel and cecum are lifted and placed on saline-soaked gauze sponges. The exposed right kidney is dissected from the retroperitoneal area and the vascular and ureteric pedicles are ligated with 2–0 silk sutures, transected, and the kidney is removed. The renal artery of the left kidney is dissected into the hilum to expose the three main segmental renal arteries. The kidney is not dissected out of the peritoneum. The anterior caudal branch of the artery is then temporarily ligated to establish the volume of renal tissue supplied. The area of ischemia becomes demarcated within 10–15 s. If this approximates 1/4 to 1/3 of the kidney, a permanent ligature is placed. The viscera are then carefully replaced in the abdomen and peritoneum and linea alba are closed with a continuous suture. The skin is closed with stainless-steel clips.

Blood for serum creatinine is collected by retro-orbital puncture under anesthesia at various time intervals up to 12 months. In association with this, 24-hour urines are collected for measurement of creatinine, protein, and specific gravity.

EVALUATION

Serum creatinine increases up to 500 µM/l after 12 months, whereas creatinine clearance decreases. Significantly increased urine volumes are accompanied by decreased urine specific gravity indicating a decreased concentrating ability. Proteinuria is significantly increased. Terminal uremia occurs after 14–15 months.

CRITICAL ASSESSMENT OF THE METHOD

The method may be used for special pharmacological studies as well as for evaluation of renal toxicity of new chemicals.

MODIFICATIONS OF THE METHOD

Sancho et al. (1989) used a similar procedure in rats ligating two of the three terminal branches of the left renal artery, followed by right nephrectomy.

Freeman (1971) induced azotemia combined with hypothermia in rats by ligation of the urinary bladder at the base.

William et al. (1997) described renal ischemia-reperfusion injury in rats. The animals were anesthetized and subjected to 45 min of bilateral renal occlusion using atraumatic vascular clamps before renal perfusion was reestablished. After various time interval (up to 1 week) blood urea nitrogen, creatinine and myeloperoxidase activity in the kidney were determined. The protective effects of an intracellular adhesion molecule monoclonal antibody were tested.

Ishidoya et al. (1995), Klahr and Morrissey (1997) induced interstitial renal fibrosis by unilateral ureteral obstruction in Sprague Dawley rats and tested the effect of ACE inhibitors and angiotensin II receptor antagonists.

Hartenbower and Coburn (1972) described a method for producing chronic renal insufficiency in the *chick*. By urethral ligation, the function of one kidney was completely eliminated, and the functional mass of the other was reduced by two-thirds. The method resulted in elevation of plasma concentration of uric acid, the major product of protein catabolism in avian plasma, to levels 2–4 times normal for periods as long as 3 weeks.

Two to 3 weeks old White Leghorn cockerels are anesthetized with ether, and the abdominal feathers are clipped. The chick is placed supine on a small operating board with hips flexed and legs extended over the head. An incision is made along the left side of the abdomen extending into the peritoneal cavity. Self-retaining retractors are used to maintain exposure. The right ureter is identified and ligated just proximal to its junction with the cloaca. The left ureter and renal vein are ligated with a single suture near the middle of the left kidney.

The degree of azotemia is assessed by measuring uric acid levels in blood samples 0.2–0.3 ml, obtained by cardiac puncture at intervals of 2–6 days after surgery.

Uric acid blood levels are compared between operated and sham-operated animals. Histological examination is performed after sacrifice of the animals.

REFERENCES AND FURTHER READING

Acott PD, Ogborn MR, Crocker JFS (1987) Chronic renal failure in the rat. A surgical model for long-term-toxicological studies. J Pharmacol Meth 18:81–88

Freeman RM (1971) The role of magnesium in the pathogenesis of azotemic hypothermia. Proc Soc Exp Biol Med 137:1069–1072

Hartenbower DL, Coburn JW (1972) A model of renal insufficiency in the chick. Lab Anim Sci 22:258–261

Ishidoya S, Morrissey J, McCracken R, Reyes A, Klahr S (1995) Angiotensin II receptor antagonist ameliorates re-

nal tubulo-interstitial fibrosis caused by unilateral ureteral obstruction. Kidney Intern 47:1285–1294
Klahr S, Morrissey JJ (1997) Comparative study of ACE inhibitors and angiotensin II receptor antagonists in interstitial scarring. Kidney Intern 52, Suppl 63:111–114
Sancho JJ, Duh Qy, Oms L, Sitges-Serra A, Hammond ME, Arnaud CD, Clark OH (1989) A new experimental model for secondary hyperparathyroidism. Surgery 106:1002–1008
Williams P, Lopez H, Britt D, Chan C, Ezrin A, Hottendorf R (1997) Characterization of renal ischemia-reperfusion injury in rats. J Pharmacol Toxicol Meth 37:1–7

C.3.2
Chronic Renal Failure After Subtotal (Five-Sixths) Nephrectomy in Rats

PURPOSE AND RATIONALE

Subtotal (five-sixths) nephrectomy in rats has been used by many authors as model for chronic renal failure. Levine et al. (1997) used this model to evaluate the hypothesis that under these conditions endogenous angiotensin II modulates *in vivo* bicarbonate reabsorption (J_{tCO2}) in distal tubules via H^+-adenosinetriphosphatase and Na^+H^+-exchange. Bicarbonate reabsorption (J_{tCO2}) in distal tubules is significantly increased in five-sixths nephrectomized rats.

PROCEDURE

Surgical Procedure

Male Sprague-Dawley rats weighing 230–280 g are anesthetized with halothane via a face mask. Prior to the first incision, the animal is given 20 ml/kg normal saline subcutaneously. On a heated table, a midline laparatomy is performed 2 cm below the xiphoid bone cartilage and the abdomen is opened. The right kidney is isolated and brought out of the abdomen by grasping the fat at the lower pole of the kidney. This fat is blunt dissected (sparing the adrenal gland), and three silk 4-0 ligatures are passed under the ureter, renal artery, and renal vein, tying one distally and two proximally. The ureter, renal artery and renal vein are then cut between the ligatures, the proximal ties are cut short, and the distal tie is pulled out, removing the kidney. After the area is checked for bleeding, the left kidney is the similarly isolated and brought out of the abdomen. The fat around the kidney is blunt dissected, avoiding excessive handling of the kidney or damage to the ureter, and the left and right renal poles are removed (two-thirds nephrectomy). The left remnant kidney is then returned to the abdomen and moistened with 5 ml of normal saline. The abdomen is closed with sutures and the skin with autoclips. Sham rats undergo the same procedure, except that the kidneys are only touched by the instruments. All rats are allowed 13–16 days recovery prior to microperfusion.

Microperfusion Experiments

The rats are anesthetized with 100 mg/kg thiobutabarbital sodium and placed on a heated operating table. After tracheostomy, using a PE-240 tubing, the left carotid artery is cannulated for continuous blood pressure measurement and collection of blood for acid-base and electrolyte analyses while the left jugular vein is cannulated with three lines for infusion of fluid, pentobarbital sodium anesthetic and 10% Lissamine green (Levine et al. 1996). The left kidney is exposed by flank incision, carefully dissected from the adrenal gland, and immobilized in a stainless steel cup covered with mineral oil. The ureter is catheterized with PE-50 tubing to ensure proper urine flow.

To replace surgical fluid losses, the rats are infused at 1% body wt/h for 30 min via the jugular vein with donor plasma from control rats. The animals are then maintained on 0.9% saline at 1% body wt/h for the remainder of the experiment.

Two-loop perfusable surface distal tubules are identified by injecting a bolus of 1% Lissamine green into surface proximal loops and observing its passage through the nephron. The distal tubules are perfused at 15 nl/min with a hypotonic solution containing (in mM) 28 HCO_3, 26 Cl, 56 Na, 2 K, 1.8 Ca, 22 urea, and 4 gluconate, as well as 0.05% FD and C green dye no. 3 (Keystone, Chicago, IL) and 0.1% albumin. The perfused bicarbonate load, higher than in free flow, is chosen to more easily reveal the effect of inhibitors. Sample collections are quantitative and timed. A 10-min preperfusion period precedes all collections.

Groups of five-sixths nephrectomized rats are treated with various agents, e. g., angiotensin II, angiotensin$_1$ receptor antagonists, or Na^+/H^+ antiporter inhibitors.

Analyses

Whole blood and urine pH and P_{CO2} are measured quantitatively by an electrode blood-gas system and HCO_3 concentrations are calculated. Plasma and urine Na^+ and K^+ concentrations are measured by flame photometry and Cl^- concentrations by electrotitration. Plasma total protein concentrations and urine specific gravity are measured by refractometry, and hematocrits are determined by a microcapillary reader. Urine osmolalities are determined by freezing-point osmometry. Plasma creatinine concentrations are determined by the Jaffé method without deproteinization.

Perfusate and sample total CO_2 concentrations are measured by microcalorimetry (Levine et al. 1996). A standard curve is run before sample analysis, and standard samples bracket the determination of sample and perfusate CO_2 determination.

EVALUATION

The perfusion rate (R_P) is calculated as the product of the measured collection rate (R_C) and the ratio of inulin concentration in collected tubular fluid and perfusate. Water absorption (J_V) is calculated as the difference between the calculated perfusion rate and the measured collection rate (R_P minus R_C). J_{tCO2} is calculated as

$$J_{tCO2} = [(R_P C_P) - (R_C C_C)/L$$

whereby C_P and C_C are the measured CO_2 concentrations in perfusate and collected fluid, respectively, and L is the tubular length in millimeters, measured by dissection after latex injection.

Data are expressed as the means ± SE. Statistical significance is assessed by two-tailed unpaired Student's *t*-test or one way analysis of variance (ANOVA) followed by either Dunnett's test for multiple comparisons vs. control or the Newman-Keuls test for all pairwise comparisons. Tests indicating a value of $P < 0.05$ indicate a statistically significant difference between groups.

MODIFICATIONS OF THE METHOD

Function of the remnant kidney after subtotal (5/6) nephrectomy in **rats** has been used for many purposes:

- to test the potential benefit of calcium antagonists (Tolins and Raij 1990; Jarusiripipat et al. 1992; Van den Branden et al. 1997) or antioxidants (Vaziri et al. 1998),
- to verify the effect of ACE-inhibitors (Pelayo et al. 1990; Kakinuma et al. 1992; Ashab et al. 1995; Liu et al. 1996; Ali et al. 1998; Cohen et al. 1998; MacLaughlin et al. 1998), angiotensin antagonists (Kohzuki et al. 1994, 1995; Brooks et al. 1995; Barreto-Chaves and Mello-Aires 1996; Noda et al. 1997; Lariviere et al. 1998; Roczniak et al. 1999) and endothelin receptor antagonists (Nabokov et al. 1996; Potter et al. 1997; Wolf et al. 1999; Brochu et al. 1999; Shimuzu et al. 1999), or Na^+/H^+ antiporter inhibitors (Fernandez et al. 1994),
- to study the influence of hormones, such as parathyroid hormone (Fukagawa et al. 1991; Urena et al. 1994; Yi et al. 1995; Schaefer et al. 1996), growth hormone (Santo et al. 1992; Garcia de Boto et al. 1996), insulin-like growth factor I (Hazel et al. 1994; Mak and Pak 1996; Tonshoff et al. 1997), vasopressin (Bardoux et al. 1999), atrial natriuretic factor (Wong and Wong 1991, 1992), Luk et al. 1995) or erythropoietin (Poux et al. 1995; Zhou et al. 1997), during development of chronic renal failure.

Kimura et al. (1999) reported a model of progressive chronic renal failure in *rats*, produced by a single injection of microspheres (20 to 30 µm in diameter) into the left renal artery after right nephrectomy.

Cowley et al. (1996) described the **Han:SRPD rat** strain which develops autosomal dominant polycystic kidney disease with chronic renal failure that resembles human autosomal dominant polycystic kidney disease.

Chronic renal failure can be induced by feeding a lithium containing diet (40–50 mmol/kg) to newborn *rats* until an age of 55–65 weeks (Christensen et al. 1992, 1997; Nyengaard et al. 1994).

Stockelman et al. (1998) described chronic renal failure in a **mouse** model of human adenine phosphoribo-syltransferase deficiency. Hamilton and Cotes (1994) used a partial nephrectomy model in *mice* with two-thirds of total renal mass excised to evaluate erythropoiesis and erythropoietin production from extrarenal sources such as the submandibulary salivary gland. Koumegawa et al. (1991) suggested the DBA/2FG-pcy *mouse*, which develops numerous cysts in kidney cortex and medulla, a progressive anemia and an elevation of blood urea nitrogen, as useful spontaneous model of progressive renal failure.

Brown et al. (1990) studied the metabolism of erythropoietin in normal and uremic **rabbits** with 5/6 nephrectomy. Bonilla-Felix used *rabbits* after 75% nephrectomy to study the response of cortical collecting ducts from remnant kidneys to arginine vasopressin.

Fine et al. (1990), Vaneerdeweg et al. (1992) described surgical techniques for kidney resection to produce chronic renal failure in **dogs**.

REFERENCES AND FURTHER READING

Ali SM, Laping NJ, Fredrickson TA, Contino LC, Olson BA, Anderson K, Brooks DP (1998) Angiotensin-converting enzyme inhibition attenuates proteinuria and renal $TGF_{\beta 1}$ mRNA expression in rats with chronic renal disease. Pharmacology 57:20–27

Ashab I, Peer G, Blum M, Wollman Y, Chernihovsky T, Hassner A, Schwartz D, Cabiki S, Silverberg D, Iaina A (1995) Oral administration of L-arginine and captopril in rats prevents chronic renal failure by nitric oxide production. Kidney Int 47:1515–1521

Bardoux P, Martin H, Ahoulay M, Schmitt F, Bouby N, Trinh Trang Tan M, Bankir E (1999) Vasopressin contributes to hyperfiltration, albuminuria, and renal hypertrophy in diabetes mellitus: Study in vasopressin-deficient Brattleboro rats. Proc Natl Acad Sci USA 96:10397–10402

Barreto-Chaves MLM, Mello-Aires M (1996) Effect of luminal angiotensin II and ANP on early and late cortical distal tubule HCO_3-reabsorption. Am J Physiol 271; Renal Fluid Electrolyte Physiol 40:F977–F984

Bonilla-Felix M, Hamm LL, Herndon J, Vehaskari VM (1992) Response of cortical collecting ducts from remnant kidneys to arginine vasopressin. Kidney Int 41:1150–1154

Brochu E, Lacasse MS, Moreau C, Lebel M, Kingma I, Grose JH, Laviviere R (1999) Endothelin in ET_A receptor blockade prevents the progression of renal failure and hypertension in uraemic rats. Nephrol Dial Transplant 14:1881–1888

Brooks DP, Contino LC, Short BG, Gowan C, Trizna W, Edwards RM (1995) SB 203220: A novel angiotensin II receptor antagonist and renoprotective agent. J Pharmacol Exp Ther 274:1222–1227

Brown JH, Lappin TRJ, Elder EG, Bridges MJ, McGeown MG (1990) The metabolism of erythropoietin in the normal and uremic rabbit. Nephrol Dial Transplant 5:855–859

Christensen S, Marcussen N, Petersen S, Shalmi M (1992) Effects of uninephrectomy and high protein feeding on lithium-induced chronic renal failure in rats. Renal Physiol Biochem 15:141–149

Christensen S, Shalmi M, Hansen AK, Marcussen N (1997) Effects of pepindopril and hydrochlorothiazide on the long-term progression of lithium-induced chronic renal failure in rats. Pharmacol Toxicol 80:132–141

Cohen DS, Mathis JE, Dotson RA, Graybill SR, Wosu NJ (1998) Protective effects of CGS 30440, a combined angiotensin-converting enzyme inhibitor and neutral endopeptidase inhibitor, in a model of chronic renal failure. J Cardiovasc Pharmacol 32:87–95

Cowley BD Jr, Grantham JJ, Muessel MJ, Kraybill AL, Gattone II VH (1996) Modification of disease progression in rats with inherited polycystic kidney disease. Am J Kidney Dis 27:865–879

Fernadez R, Lopes MJ, De Lira RF, Dantas WFG, Cragoe EJ Jr, Malnic G (1994) Mechanism of acidification along cortical distal tubule of the rat. Am J Physiol 266, Renal Fluid Electrolyte Physiol 35:F218–F226

Fine A, Jones D, Kaushal G, LeFal Y, Sharma G (1990) Remnant model of renal failure in the dog: Avoidance of second surgery by chemical nephrectomy. Clin Invest Med 13:152–154

Garcia de Boto MJ, Cobo A, Rodriguez J, Fernandez P, Rey C, Santos F (1996) Chronic renal failure and human growth hormone treatment do not modify endothelium-dependent reactions in the rat aorta *in vitro*. J Auton Pharmacol 16:97–103

Fukagawa M, Kaname SY, Igarashi T, Ogata E, Kurokawa K (1991) Regulation of parathyroid hormone synthesis in chronic renal failure in rat. Kidney Int 39:874–881

Hamilton DL, Cotes PM (1994) The effect of the submandibular salivary gland on the erythropoietin response to hypoxia in mice with chronic renal failure. Exp Hematol 22:256–260

Hazel SJ, Gillespie CM, Moore RJ, Clark RG, Jureidini KF, Martin AA (1994) Enhanced body growth in uremic rats treated with IGF-I and growth hormone in combination. Kidney Int 46:58–68

Jarusiripipat C, Chan L, Shapiro JI, Schrier RW (1992) Effect of long-acting calcium entry blocker (anipamil) on blood pressure, renal function and survival of uremic rats. J Pharmacol Exp Ther 260:243–247

Kakinuma Y, Kawamura T, Bills T, Yoshioka T, Ichikawa I, Fogo A (1992) Blood pressure-independent effect of angiotensin inhibition on vascular lesions of chronic renal failure. Kidney Int 42:46–55

Kimura M, Suzuki T, Hishida A (1999) A rat model of progressive renal failure produced by microembolism. Am J Pathol 155:1371–1380

Kohzuki M, Yasujima M, Yoshida K, Kanazawa M, Abe K (1994) Antihypertensive and antiproteinuric effects of losartan in spontaneously hypertensive rats with chronic renal failure. Hypertens Res Clin Exp 17:173–178

Kohzuki M, Kanazawa M, Liu PF, Kamimoto M, Yoshida K, Saito T, Yasujima M, Sato T, Abe K (1995) Kinin and angiotensin II receptor antagonists in rats with chronic renal failure: Chronic effects on cardio- and renoprotection of angiotensin converting enzyme inhibitors. J Hypertens 13:1785–1790

Koumegawa JI, Nagano N, Arai H, Wada N, Kusaka M, Takahashi A (1991) Anemia in new congenital adult type polycystic kidney mice. J Urol 146:1645–1649

Lariviere R, Lebel M, Kingma T, Grose JH, Boucher D (1998) Effects of losartan and captopril on endothelin-1 production in blood vessels and glomeruli of rats with reduced renal mass. AM J Hypertens 11:989–997

Levine DZ, Iacovitti M, Buckman S, Burns KD (1996) Role of angiotensin II in dietary modulation of rat late distal tubule bicarbonate flux *in vivo*. J Clin Invest 97:120–125

Levine DZ, Iacovitti M, Buckman S, Hinke MT, Luck B, Fryer JN (1997) ANG II-dependent HCO_3^- reabsorption in surviving rat renal tubules: expression/activation of H^+-ATPase. Am J Physiol 272; Renal Physiol 41:F799–F808

Liu DT, Turner SW, Wen C, Witworth JA (1996) Angiotensin converting enzyme inhibition and protein restriction in progression of experimental chronic renal failure. Pathology 28:156–160

Luk JKH, Wong EFC, Wong NLM (1995) Downregulation of atrial natriuretic factor clearance receptors in experimental chronic failure in rats. Am J Physiol 269; Heart Circ Physiol 38:H902–G908

MacLaughlin M, Monserrat AJ, Muller A, Matoso M, Amorena C (1998) Role of kinins in the renoprotective effect of angiotensin-converting enzyme inhibitors in experimental chronic renal failure. Kidney Blood Press Res 21:329–334

Mak RHK, Pak YK (1996) End-organ resistance to growth hormone and IGF-I in epiphyseal chondrocytes of rats with chronic renal failure. Kidney Int 50:400–406

Nabokov A, Amann K, Wagner J, Gehlen F, Munter K, Ritz E (1996) Influence of specific and non-specific endothelin receptor antagonists on renal morphology in rats with surgical renal ablation. Nephrol Dial Transplant 11:514–520

Noda M, Fukuda R, Matsuo T, Ohta M, Nagano H, Imura Y, Nishikawa K, Shibouta Y (1997) Effects of candesartan cilexetil (TCV-116) and enalapril in 5/6 nephrectomized rats. Kidney Int Suppl 51/63:S136–S139

Nyengaard JR, Bendtsen TF, Christensen S, Ottosen PD (1994) The number and size of glomeruli in long-term lithium-induced nephropathy in rats. APMIS 102:59–66

Pelayo JC, Quan AH, Shanley PF (1990) Angiotensin II control of the renal microcirculation in rats with reduced renal mass. Am J Physiol 258; Renal Fluid Electrolyte Physiol 27:F414–F422

Potter GS, Johnson RJ, Fink GD (1997) Role of endothelin in hypertension of experimental chronic renal failure. Hypertension 30:1578–1584

Poux JM, Lartigue M, Chaisemartin RA, Galen FX, Leroux-Robert C (1995) Uraemia is necessary for erythropoietin-induced hypertension in rats. Clin Exp Pharmacol Physiol 22:769–771
Roczniak A, Fryer JN, Levine DZ, Burns KD (1999) Downregulation of neuronal nitric oxide synthase in the rat remnant kidney. J Am Soc Nephrol 10:704–713
Santos F, Chan JCM, Hanna JD, Niimi K, Krieg RJ Jr, Wellons MD (1992) The effect of growth hormone on the growth failure of chronic renal failure. Pediatr Nephrol 6:262–266
Schaefer L, Malchow M, Schaefer RM, Ling H, Heidland A, Massry SG (1996) Effects of parathyroid hormone on renal tubular proteinases. Miner Electrolyte Metabol 22:182–186
Shimizu T, Hata S, Kuroda T, Mihara SI, Fujimoto M (1999) Different roles of two types of endothelin receptors in partial ablation-induced chronic renal failure in rats. Eur J Pharmacol 381:39–49
Stockelman MG, Lorenz JN, Smith FN, Boivin GP, Sahota A, Tischfield JA, Stambrook PJ (1998) Chronic renal failure in a mouse model of human adenine phosphoribosyltransferase deficiency. Am J Physiol 275; Renal Physiol 44:F154–F163
Tolins JP, Raij L (1990) Comparison of converting enzyme inhibitor and calcium channel blocker in hypertensive glomerular injury. Hypertension 10:452–461
Tonshoff B, Powell DR, Zhao D, Durham SK, Coleman ME, Domene HM, Blum WF, Baxter RC, Moore LC, Kaskel FJ (1997) Decreased hepatic insulin-like growth factor (IGF)-I and increased IGF binding protein-1 and -2 gene expression in experimental uremia. Endocrinology 138:938–946
Urena P, Kubrusly M, Mannstadt M, Hruby M, Tan MMTT, Silve C, Lacour B, Abou-Samra AB, Segre GV, Drueke T (1994) The renal PTH/PTHrP receptor is down-regulated in rats with chronic renal failure. Kidney Int 45:605–611
Van den Branden Gabriels M, Vamecq J, Houte KV, Verbeelen D (1997) Carvedilol protects against glomerulosclerosis in rat remnant kidney without general changes in antioxidant enzyme status: A comparative study of two β-blocking drugs, carvedilol and propranolol. Nephron 77:319–324
Vaneerdeweg W, Buyssens N, De Winne T, Sebrechts M, Babloyan A, Arakelian S, De Broe ME (1992) A standard surgical technique to obtain a stable and reproducible chronic renal failure model in dogs. Eur Surg Res 24:273–282
Vaziri ND, Oveisi F, Ding Y (1998) Role of increased oxygen free radical activity in the pathogenesis of uremic hypertension. Kidney Int 53:1748–1754
Wolf SC, Brehm Br, Gaschler F, Brehm S, Klaussner M, Smykowski J, Amann K, Osswald H, Erley CM, Risler T (1999) Protective effects of endothelin antagonists in chronic renal failure. Nephrol Dial Transplant 14, Suppl 4:29–30
Wong NLM, Wong EEC (1991) Increased release of atrial natriuretic peptide by the atria of rats with experimental renal failure. Nephron 57:89–93
Wong NLM, Wong EEC (1992) Effect of dietary sodium on atrial natriuretic factor released in rats with chronic renal failure. Nephron 61:464–469
Yi H, Fukagawa M, Yamamoto H, Kumagai M, Watanabe T, Kurokawa K (1995) Prevention of enhanced parathyroid hormone secretion, synthesis and hyperplasia by mild dietary phosphorus restriction in early chronic renal failure in rats. Possible direct role of phosphorus. Nephron 70:242–248
Zhou XJ, Pandian D, Wang QX, Vaziri ND (1997) Erythropoietin-induced hypertension is not mediated by alterations of plasma endothelin, vasopressin, or atrial natriuretic peptide levels. J Am Soc Nephrol 8:901–905

C.3.3
Experimental Nephritis

C.3.3.1
General Considerations

Various experimental procedures were described as models for glomerulonephritis in human beings. Most of them were developed in rats and rabbits. They involve the reactions of antibodies against renal components, such as Masugi nephritis (Masugi and Sato 1934), Heymann nephritis (Heymann 1959), nephrotoxic serum nephritis (Unanue and Dixon 1967), crescentic type anti-glomerular membrane nephritis (Nagoe et al. 1994, 1998), anti-Thy1 nephritis (Chen et al. 1999).

Moreover, MRL Mpf lpr/lpr (MRL/lpr)-mice were described which spontaneously develop a severe disease with many symptoms very similar to human systemic lupus erythematodes, i. e. hypergammaglobulinemia, and glomerulonephritis (Theofilopoulos and Dixon 1981; see also I.2.2.16).

REFERENCES AND FURTHER READING

Chen Y-M, Chien C-T, Hu-Tsai M-I, Wu K-D, Tsai C-C, Wu M-S, Tsai T-J (1999) Pentoxifylline attenuates experimental mesangial proliferative glomerulonephritis. Kidney Intern 56:932–943
Heymann W, Hackel DB, Harwood S, Wilson SGF, Hunter JLP (1959) Production of nephrotic syndrome in rats by Freund's adjuvant and rat kidney suspension. Proc Soc Exp Biol Med 100:660–664
Masugi M, Sato Y (1934) Über die allergische Gewebsreaktion der Niere. Zugleich ein experimenteller Beitrag zur Pathogenese der diffusen Glomerulonephritis und der Periarteriitis nodosa. Virchows Arch Pathol Anat Physiol Klin Med 293:615–664
Nagao T, Nagamatsu T, Suzuki Y (1994) Effect of DP-1904, a thromboxane A_2 synthetase inhibitor, on crescentic nephritis in rats. Eur J Pharmacol 259:233–242
Nagao T, Nagamatsu T, Suzuki Y (1998) Effect of lipo-prostaglandin E_1 on crescentic-type anti-glomerular basement membrane nephritis in rats. Eur J Pharmacol 348:37–44
Theofilopoulos AN, Dixon FJ (1981) Etiopathogenesis of murine SLE. Immunological Rev 55:179–216
Unanue ER, Dixon FJ (1967) Experimental glomerulonephritis: Immunological events and pathogenic mechanisms. Adv Immunol 6:1–90

C.3.3.2
Nephrotoxic Serum Nephritis

PURPOSE AND RATIONALE

Nephrotoxic serum nephritis is produced in animals by administration of heterologous antibody against glomerular basement membrane. This is regarded as an experimental model of human glomerular immune injury resulting in glomerulonephritis (Unanue

and Dixon 1967). The glomerular lesions induced by nephrotoxic serum nephritis vary with species. The Wistar–Kyoto rat is susceptible to the induction of a crescentic glomerulonephritis following small doses of nephrotoxic serum (Kushiro et al. 1998; Suzuki et al. 1998).

PROCEDURE

Preparation of Nephrotoxic Serum

Normal Wistar rat kidneys are fully perfused with physiologic saline through a catheter placed in the aorta. Renal cortical tissue is removed, homogenized and diluted with physiological saline at about 20% suspension. Two ml of renal cortical homogenate are emulsified with an equal volume of Freund's complete adjuvant. This emulsion is injected subcutaneously into rabbits twice a month for two months. Seven days after the last injection, the rabbits are bled from the carotid artery under anesthesia. The sera are decomplemented for 30 min at 56°C and absorbed with freshly harvested rat erythrocytes.

Experimental Protocol

Male Wistar–Kyoto rats weighing 150 g receive either continuous administration of the test drug by an osmotic pump (ALZA Co., Palo Alto, USA) or saline. Twenty-four hours later, the rats are injected with 1 ml of nephrotoxic serum. At 9, 12, and 14 days, urine samples are collected and urinary protein levels are measured using the Lowry method. At 14 days the rats are sacrificed under ether anesthesia, and both kidneys are removed. Portions of these tissues are processed for light microscopy, immunofluorescence staining and immunoperoxidase staining.

For light microscopy, tissues are fixed and embedded in paraffin. Sections are stained with hematoxylin and eosin, and periodic acid Schiff's reagent. Twenty glomeruli are examined per rat and number of glomeruli which forms crescent is counted.

Indirect immunofluorescence studies are performed on 3 µm-thick cryostat sections which are air dried and incubated with anti-rat intercellular adhesion molecule-1 (ICAM-1) antibody (Tamatani and Miyasaka 1990) for 60 min at room temperature. After washing the antibody binding is visualized by incubating the sections for 30 min with fluorescein isothiocyanate-labeled goat anti-mouse IgG.

Direct immunofluorescence studies are performed on 4 µm thick cryostat sections, which are incubated with fluorescein isothiocyanate-labeled goat anti-rat IgG, goat anti-rat C3, goat anti-rat fibrinogen and goat anti-rabbit IgG.

The staining intensity of 20 glomeruli per rat is semiquantitatively assessed into 4 grades.

For **immunoperoxidase staining** the distribution of leukocytes is examined using an immunoperoxidase ABC kit (Vector Lab, Burlingame, USA). Nonspecific protein binding is blocked by incubating the cryostat sections with 10% bovine serum in Tris-buffered saline for 20 min. Nonspecific staining is blocked by 15 min incubation with avidin and then biotin using the avidin-biotin blocking kit (Vector Lab). Endogenous peroxidase activity is inhibited by incubating the sections in methanol containing 0.3% H_2O_2 for 20 min. Sections are first incubated for 60 min with primary antibodies at room temperature, incubating monoclonal antibodies against rat monocytes/macrophages (ED-1), rat CD4 and rat CD8. Then the sections are incubated with biotinylated donkey anti-mouse IgG for 30 min at room temperature. Biotinylated horseradish peroxidase is applied for 30 min at room temperature. Peroxidase activity is developed in 3,3-diaminobenzidine and hydrogen peroxide. The sections are then counterstained with Mayer's hematoxylin. The number of ED-1 positive cells, CD4 positive cells and CD8 positive cells per glomerular cross-section is counted in 20 glomeruli per rat.

EVALUATION

All data are expressed as mean ± SEM. Significance of differences between groups is determined using Wilcoxon's test.

MODIFICATIONS OF THE METHOD

Masugi and Sato (1934), Krakower and Greenspon (1951), Heyman et al. (1959, 1965), Eddington et al. (1968) already described experimental allergic glomerulonephritis in rats.

Ito et al. (1983), Nagao et al. (1994, 1998) induced crescentic type antiglomerular basement membrane nephritis in male Sprague Dawley rats by injecting 6.5 mg rabbit gamma-globulin in 0.25 ml Freund's complete adjuvant into the hind foot pads, following the injection of 0.6 ml of rabbit anti-rat glomerular basement membrane serum into the tail vein.

Couser et al. (1978) studied the development of immune deposits on the subepithelial surface of the glomerular capillary wall in isolated rat kidneys perfused at controlled perfusion pressure, pH, temperature, and flow rates with recirculating oxygenated perfusate containing bovine serum albumin in buffer and sheep antibody to rat proximal tubular epithelial cell brush border antigen.

Hayashi et al. (1996) tested the effects of a flavonoid in original-type anti-glomerular basement membrane antibody associated glomerulonephritis in male Sprague Dawley rats on upregulation of intracellular adhesion molecule expression and on increase in leukocyte function-associated antigen positive cells in nephritic glomeruli.

Nagamatsu et al. (1999) found beneficial effects of an angiotensin II type I receptor antagonist in anti-glomerular basement membrane antibody-associated nephritis in rats.

Sanaka et al. (1997) evaluated the effects of a free radical scavenger on the progression of nephrotoxic serum nephritis in male Sprague Dawley rats. The rat glomerular basement membrane was prepared according to the method of Krakower and Greenspon (1951) who localized the nephrotoxic antigen within the isolated renal glomerulus.

Kawasaki et al. (1992) induced crescentic glomerulonephritis with a small dose of nephrotoxic serum in WKY rats, which was characterized by the early infiltration of CD8 positive cells in glomeruli. *In vivo* depletion of CD8 positive cells completely prevented proteinuria and crescent formation.

Okuda et al. (1990) provided evidence of an elevated expression of transforming growth factor-β, proteoglycans and fibronectin in glomerulonephritis induced in rats by injection of anti-thymocyte serum.

Hamada and Nagase (1996), Chen et al. (1999) induced anti-Thy1 nephritis with the antibody to the Thy-1 antigen which is present in the mesangial cells of the glomeruli. The early pathobiological cellular events are characterized by invasion of platelets, polymorphonuclear leukocytes, and monocytes into the glomerulus which occurs within hours after induction of nephritis. Complement-dependent mesangiolysis then ensues between day 1 and 3.

Liebler et al. (2004) induced acute anti-Thy1.1-mesangioproliferative glomerulonephritis by administering 500 µg of Moab 1-22-3 dissolved in PBS as a single-shot injection into the tail vein of the rats on day 0. Moab 1-22-3 is a monoclonal antibody directed against the Thy1.1-like antigen on the surface of rat mesangial cells.

Passive Heymann nephritis (Heymann 1959) was used a model by Hara et al. (1991), Nagao et al. (1996), Heise et al. (1998). The disease is induced in rats by heterologous antibody to crude renal border antigen Fx1A. The model is characterized by granular deposition of heterologous and homologous antibody and complement along the glomerular capillary wall and as a counterpart, extensive electron-dense subepithelial deposits are seen at the ultrastructural level. Massive proteinuria develops after a latent period of 2 to 4 days in the absence of glomerular hypercellularity.

Kawasaki et al. (1995) studied the therapeutic effect of combined treatment with monoclonal antibodies against intercellular adhesion molecule 1 (ICAM-1) and lymphocyte-function-associated antigen 1 (LFA-1) in **Masugi nephritis** of Wistar–Kyoto rats.

Thaiss et al. (1989) evaluated the effect of the immunosuppressant cyclosporin A on an active model of *in situ* immune complex glomerulonephritis. Wistar rats were preimmunized with human IgG and 2 weeks after the last antigen injection, the left kidney was perfused with cationized human IgG in order to induce unilateral *in situ* immune complex glomerulonephritis.

Okubo et al. (1990) studied the immunosuppressive effects of FK506 on active Heymann's nephritis and the autologous phase of Masugi nephritis.

Rennke et al. (1994) developed a model system of acute nephritis in the rat whereby a chemically reactive form of the hapten azobenzenearsonate is introduced directly in to the left kidney of pre-immunized Brown Norway rats.

REFERENCES AND FURTHER READING

Chen Y-M, Chien C-T, Hu-Tsai M-I, Wu K-D, Tsai C-C, Wu M-S, Tsai T-J (1999) Pentoxifylline attenuates experimental mesangial proliferative glomerulonephritis. Kidney Intern 56:932–943

Couser WG, Steinmuller DR, Stilmant MM, Salant DJ, Lowenstein LM (1978) Experimental glomerulonephritis in the isolated perfused rat kidney. J Clin Invest 62:1275–1287

Eddington TS, Glassock RJ, Dixon FJ (1968) Autologous immune complex nephritis induced with renal tubular antigen. I. Identification and isolation of the pathogenic antigen. J Exp Med 127:555–572

Hamada N, Nagase M (1996) *In vivo* effect of OPC15161, a superoxide scavenger, on anti-Thy1 nephritis. Eur J Pharmacol 317:123–128

Hara M, Batsford SR, Mihatsch MJ, Bitter-Suermann D, Vogt A (1991) Complement and monocytes are essential for provoking glomerular injury in passive Heymann nephritis in rats. Terminal complement components are not the sole mediators of proteinuria. Labor Invest 65:168–179

Hayashi K, Nagematsu T, Honda S, Suzuki Y (1996) Butein (3,4,2′,4′-tetrahydroxychalcone) ameliorates experimental anti-glomerular basement membrane antibody-associated glomerulonephritis. Eur J Pharmacol 316:279–306

Heise G, Grabensee B, Schrör K, Heering P (1998) Different actions of the cyclooxygenase 2 selective inhibitor flosulide in rats with passive Heymann nephritis. Nephron 80:220–226

Heymann W, Hackel DB, Harwood J, Wilson SGF, Hunter JLP (1959) Production of nephrotic syndrome in rats by Freund's adjuvant and rat kidney suspension. Proc Soc Exp Biol Med 100:660–668

Heymann W, Kmetec EP, Wilson SGF, Hunter JLP, Hackel DB, Okuda R, Cuppage F (1965) Experimental autoimmune renal disease in rats. Ann NY Acad Sci 124:310–315

Ito M, Yamada H, Okamoto K, Suzuki Y (1983) Crescentic type nephritis induced by anti-glomerular basement membrane (GBM) serum in rats. Jpn J Pharmacol 33:1145–1154
Kawasaki K, Yaoita E, Yamamoto T, Kihara I (1992) Depletion of CD8 positive cells in nephrotoxic serum nephritis of WKY rats. Kidney Intern 41:1517–1527
Kawasaki K, Yaoita E, Yamamoto T, Kihara I (1995) Therapeutic effect of combined treatment with monoclonal antibodies against intercellular adhesion molecule 1 and lymphocyte-function-associated antigen 1 in Masugi nephritis of Wistar–Kyoto rats. Nephron 71:101–102
Krakower CA, Greenspon SA (1951) Localization of nephrotoxic antigen within the isolated renal glomeruli. Arch Pathol 51:629–639
Kushiro M, Shikata K, Sugimoto H, Shikata Y, Miyatake N, Wada J, Miyasaka M, Makino H (1998) Therapeutic effects of prostacyclin analog on crescentic glomerulonephritis of rat. Kidney Intern 53:1314–1320
Liebler S, Überschär B, Kübert H, Brems S, Schnitger A, Tsukada M, Zouboulis CC, Ritz E, Wagner J (2004) The renal retinoid system: time dependent activation in experimental glomerulonephritis. Am J Physiol Renal Physiol 286:F458–F465
Masugi M, Sato T (1934) Virchows Arch Pathol Anat Physiol Klin Med 293:615
Nagamatsu T, Hayashi K, Oka T, Suzuki Y (1999) Angiotensin II type I receptor antagonist suppresses proteinuria and glomerular lesions in experimental nephritis. Eur J Pharmacol 374:93–101
Nagao T, Nagamatsu T, Suzuki Y (1994) Effect of DP-1904, a thromboxane A_2 synthetase inhibitor, on crescentic nephritis in rats. Eur J Pharmacol 259:233–242
Nagao T, Nagamatsu T, Suzuki Y (1996) Effect of DP-1904, a thromboxane A_2 synthetase inhibitor, on passive Heymann nephritis in rats. Eur J Pharmacol 316:73–80
Nagao T, Nagamatsu T, Suzuki Y (1998) Effect of lipoprostaglandin E_1 on crescentic-type anti-glomerular basement membrane nephritis in rats. Eur J Pharmacol 348:37–44
Okubo Y, Tsukada Y, Maezawa A, Ono K, Yano S, Naruse T (1990) FK506, a novel immunosuppressive agent, induces antigen-specific immunotolerance in active Heymann's nephritis and in the autologous phase of Masugi nephritis. Clin Exp Immunol 82:450–455
Okuda S, Languino LR, Ruoslathi E, Border WA (1990) Elevated expression of transforming growth factor-β and proteoglycan production in experimental glomerulonephritis. Possible role in expansion of the mesangial extracellular matrix. J Clin Invest 86:453–462
Rennke HG, Klein PS, Sandstrom DJ, Mendrick DL (1994) Cell-mediated immune injury in the kidney: Acute nephritis induced by azobenzenearsonate. Kidney Intern 45:1044–1056
Sanaka T, Nakano Y, Nishimura H, Shinobe M, Higuchi C, Omata M, Nihei H, Sugino N (1997) Therapeutic effect of a newly developed antioxidative agent (OPC-15161) on experimental immune complex nephritis. Nephron 76:315–322
Suzuki S, Gejyo F, Kuroda T, Kazama JJ, Imai N, Kimura H, Arakawa M (1998) Effect of a new elastase inhibitor, ONO-5046, on nephrotoxic serum nephritis in rats. Kidney Intern 53:1291–1208
Tamatani T, Miyasaka M (1990) Identification of monoclonal antibodies reactive with the rat homolog of ICAM-1 and evidence for differential involvement of ICAM-1 in the adherence of resting versus activated lymphocytes to high endothelial cells. Int Immunol 2:165–171
Thaiss F, Schoeppe W, Willaredt-Stoll JG, Batsford S, Mihatsch MJ (1989) Cyclosporin A prevents proteinuria in an active model of membranous nephropathy in rats. Labor Invest 61:661–669
Unanue ER, Dixon FJ (1967) Experimental glomerulonephritis: Immunological events and pathogenic mechanisms. Adv Immunol 6:1–90

C.3.4 Experimental Nephrosis

PURPOSE AND RATIONALE

Some compounds used in antineoplastic therapy induce nephrosis in animals, like the antibiotic adriamycin (=doxorubicin) (Milner et al. 1991, 1994; Chagnac et al. 1994; Wapstra et al. 1996; De Boer et al. 1999; Mutti et al. 1999) or daunomycin (Kimura et al. 1993), the aminonucleoside puromycin (Yayama et al. 1993; Guoji et al. 1994; Magil 1996; Ebihara et al. 1997; Nosaka et al. 1997; Park et al. 1998; Asami et al. 1999; Pedraza-Chaverri et al. 1999) or cisplatin (Abdel-Gayoum et al. 1999).

These models allow to test the protective effects of drugs even after the renal disease in established, i. e. mimic the clinical situation (Wapstra et al. 1996).

PROCEDURE

Male Wistar rats with an initial weight of about 300 g receive a single intravenous dose of 2 mg/kg adriamycin. Twice a week during a 12-weeks period, the animals are weighed, 24-h urine is collected and blood pressure is measured by the tail-cuff method.

During the first 5 weeks, all animals are kept on a low sodium diet with tap water ad libitum. After stabilization of proteinuria (5 weeks), animals are divided into 2 groups receiving either low sodium or normal sodium diet. After a week stabilization on these diets, animal receive different doses of treatment in their drinking water. These regimen is continued until the end of the study (week 12), at which time all animals are sacrificed and blood samples and kidney tissue are obtained.

During each blood pressure measurement session, five measurements are recorded for each animal. The blood pressure is taken as the mean of the last 3 recordings. Urinary protein is determined by the Pyrogallol Red-molybdate method (RA-1000 Technicon). Urinary sodium, creatinine and urea and serum electrolytes, creatinine, albumin, cholesterol and triacylglycerols are measured by a standard autoanalyser technique. Kidney samples are fixed in paraformaldehyde and embedded in paraffin. Sections

are stained with the periodic acid/Schiff technique. Focal glomerular sclerosis is scored semiquantitatively by light microscopy.

EVALUATION

Analysis of co-variance is used to compare the experimental groups (defined by diet or dose of drug) after 2 weeks of treatment (week 8) and the end of the study (week 12) with the baseline value (week 6) as a co-variable. Tuckey's method is used for comparison of groups receiving different doses of drug. The other statistical comparisons are performed using Student's *t*-test.

MODIFICATIONS OF THE METHOD

Fawn-Hooded rats develop systemic hypertension and spontaneous age-dependent glomerulosclerosis with proteinuria (Mackenzie et al. 1997).

Spontaneous nephrosis with proteinuria occurs in Dahl salt-sensitive rats fed on a normal sodium diet (Yoneda et al. 1998).

Mizuno et al. (1999) studied the ICGN mouse strain as a unique model for naturally occurring nephrotic syndrome.

Focal segmental glomerulosclerosis with heavy proteinuria has been found in mice in which the Mpv17 gene was inactivated ($Mpv17^{-/-}$ mice). Binder et al. (1999) recommended these animals as model of steroid-resistant nephrosis sensitive to radical scavenger therapy.

Kimura et al. (1993) described strain specificity in the susceptibility of mice to daunomycin-induced nephrosis.

Klahr and Morrissey (1997) described the effects of ACE inhibitors and angiotensin II receptor antagonists on various parameters associated with renal interstitial fibrosis induced by unilateral ureteral obstruction in rats.

REFERENCES AND FURTHER READING

Abdel-Gayoum AA, El Jenjan KB, Ghwarsha KA (1999) Hyperlipidaemia in cisplatin-induced nephrotic rats. Hum Exp Toxicol 18:454–459

Asami T, Toyabe S, Uchiyama M (1999) Effects of glutathione on aminonucleoside nephrosis in rats. Acta Med Biol 47:9–14

Binder CJ, Weiher H, Exner M, Kerjaschki D (1999) Glomerular overproduction of oxygen radicals in Mpv17 gene-inactivated mice causes podocyte foot process flattening and proteinuria. A model of steroid-resistant nephrosis sensitive to radical scavenger therapy. Am J Pathol 154:1967–1075

Chagnac A, Korzets A, Ben Bassat M, Zevin D, Hirsh J, Meckler J, Levi J (1994) Uninephrectomy aggravates tubulointerstitial injury in rats with adriamycin nephrosis. Nephron 66:176–180

De Boer E, Navis G, Wapstra FH, De Jong PE, De Zeeuw D (1999) Effect of proteinuria reduction on prevention of focal glomerulosclerosis by angiotensin-converting enzyme inhibition is modifiable. Kidney Intern 56, Suppl 71:S42–S46

Ebihara I, Nakamura T, Tomino Y, Koide H (1997) Effect of a specific endothelin receptor A antagonist and an angiotensin-converting enzyme inhibitor on glomerular mRNA levels for extracellular matrix components, metalloproteinases (MMP) and a tissue inhibitor of MMP in aminonucleoside nephrosis. Nephrol Dial Transplant 12:1001–1006

Guoji Y, Orita M, Tashiro K, Abe H (1994) Effects of glycyrrhetinic acid on aminonucleoside nephrosis in rats. Naunyn-Schmiedeberg's Arch Pharmacol 349:318–323

Kimura M, Takahashi H, Ohtake T, Sato T, Hishida A, Nishimura M, Honda H (1993) Interstrain differences in murine daunomycin-induced nephrosis. Nephron 63:193–198

Klar S, Morrissey JJ (1997) Comparative study of ACE inhibitors and angiotensin II receptor antagonists in interstitial scarring. Kidney Intern 52, Suppl 63: S-111–S114

Mackenzie HS, Ots M, Ziai F, Lee K-W, Kato S, Brenner BM (1997) Angiotensin receptor agonists in experimental models of chronic renal failure. Kidney Intern 52, Suppl 63:140–143

Magil A (1996) Inhibition of progression of chronic puromycin aminonucleoside nephrosis by probucol, an antioxidant. J Am Soc Nephrol 7:2340–2347

Milner LS, Wei SH, Houser MT (1991) Amelioration of glomerular injury in doxorubicin hydrochloride nephrosis by dimethylthiourea. J Lab Clin Med 118:427–434

Milner LS, Wei S, Kazakoff P, Watkins L, Houser MT (1994) Synergistic effect of fish oil diet and dimethylurea in acute adriamycin nephrosis. AM J Med Sci 308:266–270

Mizuno S, Mizuno-Horikawa Y, Yue B-F, Okamoto M, Kurosawa T (1999) Nephrotic mice (ICGN strain): A model of diffuse mesangial sclerosis in infantile nephrotic syndrome. Am J Nephrol 19:73–82

Mutti A, Coccini T, Alinovi R, Toubeau G, Broeckaert F, Bergamaschi E, Mozzoni P, Nonclercq D, Bernard A, Manzo L (1999) Exposure to hydrocarbons and renal disease: An experimental animal model. Renal Fail 21:369–385

Nosaka K, Takahashi T, Nishi T, Imaki H, Suzuki T, Suzuki K, Kurokawa K, Endou H (1997) An adenosine deaminase inhibitor prevents puromycin aminonucleoside nephrotoxicity. Free Rad Biol Med 22:597–605

Park Y-S, Guijarro C, Kim Y, Massy CA, Kasiske BL, Keane WF, O'Donnell MP (1998) Lovastatin reduces glomerular macrophage influx and expression of monocyte chemoattractant protein-1 mRNA in nephrotic rats. Am J Kidney Dis 31:190–194

Pedraza-Chaverri J, Granados-Silvestre MA, Medina-Campos ON, Hernández-Pando R (1999) Effect of the *in vivo* catalase inhibition on aminonucleoside nephrosis. Free Rad Biol Med 27:245–253

Wapstra FH, Van Goor H, Navis G, De Jong PE, De Zeeuw D (1996) Antiproteinuric effect predicts renal protection by angiotensin-converting enzyme inhibition in rats with established adriamycin nephrosis. Clin Sci 90:339–340

Yayama K, Kawao M, Tujii H, Itoh N, Okamoto H (1993) Dup 753 prevents the development of puromycin aminonucleoside-induced nephrosis. Eur J Pharmacol 236:337–338

Yoneda H, Toriumi W, Ohmachi Y, Okumura F, Fujimura H, Nishiyama S (1998) Involvement of angiotensin II in development of spontaneous nephrosis in Dahl salt-sensitive rats. Eur J Pharmacol 362:213–219

C.4
Uricosuric and Hypo-Uricemic Activity

C.4.1
In Vitro Methods

C.4.1.1
Inhibition of Xanthine Oxidase In Vitro Indicating Hypouricemic Activity

PURPOSE AND RATIONALE

Synthesis of uric acid primarily occurs in the liver, but the kidney has an important role in the pathophysiology of hyperuricemic syndromes. Because uric acid is poorly soluble, excessive amounts in the circulation may precipitate out into the tissues, particularly the joints, resulting in a painful arthropathy ("gout"). In humans, this condition is usually the result of faulty tubular transport of urate, resulting in increased net reabsorption. Attempts to treat hyperuricemia with tubular transport inhibitors (theoretically increasing urinary excretion of urate) frequently exacerbate the condition because tubular transport is bi-directional; reduction of net uric acid synthesis by inhibition of xanthine oxidase is the preferred therapeutic approach. Furthermore, in renal hypoxic conditions, xanthine oxidase contributes to renal injury by the generation of oxygen free radicals and xanthine oxidase inhibition has been shown to be useful in such conditions (Shinosaki and Yonetani, 1991; Rhoden et al. 2000;Terkeltaub et al. 2006).

Xanthine oxidase catalyzes the oxidation of hypoxanthine and xanthine to uric acid. Xanthine oxidase is a complex metalloflavoprotein containing one molybdenum, one FAD and two iron-sulfur centers of the ferredoxine type in each of its two independent subunits. Usually, the enzyme is isolated from cow's milk. The enzyme is inhibited by allopurinol and related compounds. The production of uric acid from the substrate (xanthine) can be determined by measuring the change in optical density in the UV range.

PROCEDURE

The test compound is incubated with xanthine oxidase (usually derived from milk, sometimes derived from rat liver or small intestine), EDTA and phosphate buffer solution (pH 7.8) at 37°C. Control solutions without test compound are incubated under identical conditions. Following addition of xanthine, the change in absorbance is determined.

Assay conditions:

- wavelength: 293 nm
- line path: 10 mm
- final volume: 1.0 ml

EVALUATION

The percent inhibition of xanthine oxidase is determined relative to control solutions.

IC_{50} values of test compounds are calculated.

Standard data:

- Allopurinol: IC_{50}: ca 10^{-8} mol/l

REFERENCES AND FURTHER READING

Heinz F, Reckel S (1983) Xanthine oxidase In: Bergmeyer HU (ed) Methods of Enzymatic Analysis, Vol. III, 3rd edition. Verlag Chemie Weinheim, Deerfield Beach, Basel, pp 211–216

Rhoden E, Teloken C, Lucas M, Rhoden C, Mauri M, Zettler C, Bello-Klein A, Barros E (2000) Protective effect of allopurinol in the renal ischemia-reperfusion in uninephrectomized rats. Gen Pharmacol 35:189–193

Shinosaki T, Yonetani Y (1991) Hyperuricemia induced by the uricosuric drug probenecid in rats. Jpn J Pharmacol. 55:461–468

Terkeltaub R, Bushinski DA, Becker MA (2006) Recent developments in our understanding of the renal basis of hyperuricemia and the development of novel antihyperuricemic therapies. Arth Res Ther 8 (Suppl 1): S4

C.4.1.2
Urate Uptake in Brush Border Membrane Vesicles

PURPOSE AND RATIONALE

The urate-anion exchanger system in brush border membrane vesicle, which mediates hydroxyl ion gradient-dependent urate uptake, is the most likely route for the mediation of urate transport in the first step of urate reabsorption in the proximal tubules. Luminal drugs which inhibit urate reabsorption are inhibiting the transport of urate by blocking the urate/anion exchanger.

PROCEDURE

Male Sprague Dawley rats weighing 320–380 g are sacrificed by decapitation and the kidneys are removed immediately. All steps for the preparation of brush border membrane vesicles are carried out at 4°C. Renal cortex is homogenized for 2 min in a medium containing 250 mmol/l mannitol, 10 mmol/l Tris, 16 mmol/l HEPES buffer (pH 7.5) using a Physcotron homogenizer. The homogenate is centrifuged at 2400 *g* for 10 min and the supernatant is centrifuged at 2800 *g* for 20 min. Subsequently, the supernatant is discarded and the loosely packed membrane-rich layer is flushed off from the bottom densely packed brown pellet. The membrane-rich layer is resuspended manually

in 250 mmol/l mannitol containing 10 mmol/l Tris-HEPES (pH 7.5) using a Dounce homogenizer and $MgSO_4$ is added to a final concentration of 10 mmol/l. After standing for 20 min, the suspension is centrifuged at 2400 *g* for 20 min and the supernatant containing brush border membranes is recentrifuged two more times at 2400 *g* for 20 min. The final supernatant is centrifuged at 28,000 *g* for 20 min and the pellet is suspended in a small amount of medium containing 150 mmol/l mannitol, 50 mmol/l potassium phosphate buffer (pH 7.5) and 2 mmol/l $MgSO_4$ to a final protein concentration of 4–8 mg/ml. The brush border membrane vesicle preparation is frozen and stored at –80°C until use.

After preincubation of the brush border membrane vesicle preparation for 2 h, [2-^{14}C]urate uptake is initiated by adding 200 µl of incubation medium to 20 µl of the membrane suspension. The incubation medium has the following composition (mmol/l): 150 mannitol, 2 $MgSO_4$, 50 potassium phosphate buffer, pH 6.0 or 7.5, 0.02 [2-^{14}C]urate, and various concentrations of the inhibitor. At 10 s after the addition of the incubation medium, 200 µl portions of the suspension are pipetted onto the center of prewetted cellulose acetate filters kept under suction. The vesicles retaining on the filter are washed immediately with 5 ml of an ice-cold solution containing 150 mmol/l mannitol and 50 mmol/l potassium phosphate buffer, pH 6.0 or 7.5, which is used at the same pH as the incubation medium. Preincubations and incubations are performed at 23 ± 1°C. Each experiment is performed in triplicate. Corrections are made for the radioactivity bound to the filters in the absence of membrane vesicles. The term of the OH^- gradient-dependent urate uptake is defined as the difference between the uptakes in the incubation medium at pH 6.0 and that at pH 7.5. The OH^- gradient-dependent urate uptake at 10 s is assumed to present an initial velocity.

EVALUATION

From a concentration-response curve relating log concentration of drug to the logit activity of the OH^- gradient-dependent urate uptake for 10 s, IC_{50} (concentration producing 50% of inhibition) is determined by least-squares regression analysis.

REFERENCES AND FURTHER READING

Dan T, Koga H (1990) Uricosurics inhibit urate transporter in renal brush border membrane vesicles. Eur J Pharmacol 187:303–312

Dan T, Onuma E, Tanaka H, Koga H (1991) A selective uricosuric action of AA-193 in rats. Comparison with its effect on PAH secretion *in vivo* and *in vitro*. Naunyn-Schmiedeberg's Arch Pharmacol 343:532–537

Kahn AM, Branham S, Weinman EJ (1983) Mechanism of urate and p-aminohippurate transport in rat microvillus membrane vesicle. Am J Physiol 245 (Renal Fluid Electrolyte Physiol 14):F151–158

C.4.2 In Vivo Methods

C.4.2.1 Diuretic and Uricosuric Activity in Mice

PURPOSE AND RATIONALE

Renal excretion of uric acid consists of three components: complete filterability of uric acid in the glomerulus, subsequent tubular reabsorption, and tubular secretion (Gutman and Yü 1961). Pronounced species differences have been described in uric acid metabolism including man. Mice were recommended for primary screening of uricosuric drugs.

PROCEDURE

Male NMRI mice weighing 25–30 g are used. On the evening prior to the experiment, food but not water is withheld. In the morning, the mice are orally loaded with 50 ml/kg 0.9% NaCl-solution. Together with the sodium load the test compound is applied by gavage in 2% starch suspension. Controls receive saline and starch suspension only. Groups of 5 mice are placed into metabolism cages. Urine is collected over 4 h. In the urine sodium and potassium are determined by flame photometry, chloride by argentometrically with potentiometrical end point titration (Chloride titrator, Aminco), uric acid by the Uriquant-method, creatinine by the Jaffé-reaction, as well as pH and osmolality.

EVALUATION

Urine excretion is calculated in ml/kg. Uric acid-, creatinine- and ion-excretions are calculated in mmol/kg and expressed as percent changes versus controls. The changes are evaluated statistically using Student's *t*-test.

CRITICAL ASSESSMENT OF THE METHOD

Some saluretic-diuretic agents, like ethacrynic acid, are inactive in the rat, when given orally. Moreover, uricosuric activity in mice is less reliable than that in primates.

REFERENCES AND FURTHER READING

Baker KM, Hook JB, Williamson HE (1965) Saluretic action of ethacrynic acid in the mouse. J Pharm Sci 54:1830

Fanelli GM (1976) Drugs affecting the renal handling of uric acid. In: Martinez-Maldonado M (ed) Methods in Pharmacology Vol 4A: Renal Pharmacology Chapter 9, pp 269–292, Plenum Press, New York and London
Gutman AB, Yü TF (1961) A three-component system for regulation of renal excretion of uric acid in man. Trans Assoc Am Physicians 74:353–365
Hill TWK, Randall PJ (1976) A method for screening diuretic agents in the mouse: an investigation of sexual differences. J Pharm Pharmacol 28:552–554
Sim MF, Hopcroft RH (1976) Effect of various diuretic agents in the mouse. J Pharm Pharmacol 28:609–612

C.4.2.2 Hypouricemic Activity After Allantoxanamide Treatment in Rats

PURPOSE AND RATIONALE

Most species used for pharmacological experiments have rather low blood levels of uric acid. Experimental hyperuricemia can by induced by inhibition of the enzyme uricase. In most species uricase metabolizes uric acid to allantoin. Allantoxanamide blocks uricase and increases endogenously synthesized uric acid. This increase is blocked by compounds like allopurinol.

PROCEDURE

Non fasted male Sprague Dawley rats weighing 230–280 g are treated by intraperitoneal injection of 250 mg/kg allantoxanamide suspended in 5 ml/kg sesame oil. The test compound is applied orally in a dose of 50 mg/kg in 40 ml/kg water. Likewise, the standard compound allopurinol is given in a dose of 50 mg/kg. Eight rats are used for the each dose of test drugs and standard. The animals are placed individually into metabolism cages with free access to food and water. Urine is collected during the periods of 1 to 6 and 7 to 24 h. Blood is withdrawn by retroorbital puncture prior and 2, 6 and 24 h after compound administration. Uric acid is determined with the Uric-aquant-method in plasma [mmol/l] and urine [mmol/l].

EVALUATION

Mean values of uric acid concentrations in plasma at the different time intervals and mean values of uric acid excretion after 6 and 24 h of the test group are compared with the control group (allantoxanamide treated only) using Student's *t*-test.

REFERENCES AND FURTHER READING

Hropot M, Sörgel F, v Kerékjártó B, Lang HJ, Muschaweck R (1980) Pharmacological effects of 1,3,5-triazines and their excretion characteristics in the rat. In: Rapado A, Watts RWE, De Bruyn CHMM (eds) Purine Metabolism in Man – III A, Plenum Publishing Corp., New York, pp 269–276
Hropot M, Muschaweck R, Klaus E (1984) Uricostatic effect of allopurinol in the allantoxanamide-treated rat: A new approach for evaluation antiuricopathic drugs. In: De-Bruyn CHMM, Simmonds HA, Muller MM (eds) Purine Metabolism in Man – IV, Part A, Plenum Publishing Corp., New York, pp 175–178
Johnson WJ, Chartrand A (1978) Allantoxanamide: a potent new uricase inhibitor *in vivo*. Life Sci 23:2239–2244

C.4.2.3 Hypouricemic and Uricosuric Activity After Potassium Oxonate Treatment in Rats

PURPOSE AND RATIONALE

Increase of uric acid in serum of rats is induced by a special diet and the uricase inhibitor potassium oxonate. Uric acid concentration in serum and uric acid excretion in urine prior and after three experimental days are determined.

PROCEDURE

Male Wistar rats weighing 250 g are placed individually in metabolic cages. They are offered a special diet containing 5% fructose, 3% uric acid, 2% potassium oxonate (2,4-dihydroxy-1,3-triazine-6-carbonic acid) and 0.001% artificial sweetener. Drinking water consists of a 0.5% solution of potassium oxonate. The animals are treated orally with 50 or 100 mg/kg of the test compound or the standard (allopurinol) dissolved in 5 ml/100 g body weight of 0.5% potassium oxonate solution. The treatment is repeated on the second day. On the third day 24 h urine is collected and the animals are sacrificed by exsanguination. Concentrations of uric acid and electrolytes (Na^+, K^+, Cl^-) are determined in blood and urine.

EVALUATION

Concentrations of uric acid and electrolytes in blood and urine of animals treated with the test compound are compared statistically with control and standard drug treated animals.

MODIFICATIONS OF THE METHOD

Clearance techniques in oxonate-treated rats were used by Yonetani et al. (1987), Shinosaki et al. (1991), Dan et al. (1994).

Sugino and Shimada (1995) tested uricosuric effects in oxonate-loaded rats, in the pyrazinoic acid suppression test and in the phenolsulfonphthalein test.

REFERENCES AND FURTHER READING

Bonardi G, Vidi A (1973) Action of 4-phenyl-1,2-diphenyl-3,5-pyrazolidinedione (DA 2370) on an experimental hyperuricosuria in the rat. Pharm Res Comm 5:125–129

Dan T, Yoneya T, Onoma M, Onuma E, Ozawa K (1994) Hypouricemic and uricosuric actions of AA-193 in a hyperuricemic rat model. Metabolism 43:123–128
Hropot M, Sörgel F, v Kerékjártó B, Lang HJ, Muschaweck R (1980) Pharmacological effects of 1,3,5-triazines and their excretion characteristics in the rat. In: Rapado A, Watts RWE, De Bruyn CHMM (eds) Purine Metabolism in Man – III A, Plenum Publishing Corp., New York, pp 269–276
Hropot M, Muschaweck R, Klaus E (1984) Uricostatic effect of allopurinol in the allantoxanamide-treated rat: A new approach for evaluation antiuricopathic drugs. In: DeBruyn CHMM, Simmonds HA, Muller MM (eds) Purine Metabolism in Man – IV, Part A, Plenum Publishing Corp., New York, pp 175–178
Johnson WJ, Stavric B, Chartrand A (1969) Uricase inhibition in the rat by s-triazines: an animal model for hyperuricemia and hyperuricosuria. Proc Soc Exp Biol Med 131:8–12
Kageyama N (1971) A direct colorimetric determination of uric acid in serum and urine with uricase-catalase system. Clin Chim Acta 31:421–426
Musil J (1977) Physiological characteristics of various experimental models for the study of disorders in purine metabolism. In: Müller MM, Kaiser E, Seegmiller JE (eds) Purine Metabolism in Man II – Physiology, Pharmacology and Clinical Aspects. Plenum Publishing Corp., New York, pp 179–188
Shinosaki S, Harada H, Yonetani Y (1991) Uricosuric property of a new diuretic compound, S-8666-S-(–)-enantiomer. Drug Dev Res 22:153–163
Stavric B, Clayman S, Gadd REA, Hébert D (1975) Some *in vivo* effects in the rat induced by chlorprothixene and potassium oxonate. Pharm Res Comm 7:117–124
Sugino H, Shimada H (1995) The uricosuric effect in rats of E5050, a new derivative of ethanolamine, involves inhibition of the tubular postsecretory reabsorption of urate. Jpn J Pharmacol 68:297–303
Yonetani Y, Ikawi K, Shinosaki T, Kawase-Hanafusa A, Harada H, van Es AA (1987) A new uricosuric diuretic, S-8666, in rats and chimpanzees. Japan J Pharmacol 43:389–398

C.4.2.4 Phenol Red Excretion in Rats

PURPOSE AND RATIONALE

Phenol red (= phenolsulfonphthalein) excretion is an indirect test for uricosuric activity. After intravenous injection phenol red is mainly eliminated by active secretion in the proximal tubulus of the kidney. Treatment with uricosuric agents decreases the secretory activity of tubulus cells resulting in a delayed excretion of phenol red. Plasma values of phenol red are increased in treated animals as compared to controls.

PROCEDURE

Male Wistar rats weighing 120–150 g are treated orally with the test compound or the standard 30 min prior to intravenous injection via the tail vein with 2.5 ml/kg of a 3% aqueous solution of phenolsulfonphthalein. For intravenous application, 5.0 ml/kg of the test drug solution are injected immediately after the phenolsulfonphthalein injection followed by flushing with 2.5 ml/kg saline. By retro-orbital puncture blood samples are withdrawn after 30, 60 and 180 min. Blood (0.2 ml) is diluted with 2 ml 0.9% NaCl-solution and centrifuged. To 1 ml of the supernatant 1 ml of 1% sodium carbonate solution and 8 ml of saline are added. Using a spectrophotometer (Eppendorf, Hamburg) extinction at 546 nm is determined.

EVALUATION

Extinction values are calculated for total blood. At each time interval the values in treated rats are compared statistically with those of controls.

REFERENCES AND FURTHER READING

Kreppel E (1959) Der Einfluß einiger Phenylbutazonderivate auf den Phenolrotblutspiegel der Ratte. Med Exp 1:285–289
Scarborough HC, McKinney GR (1962) Potential uricosuric agents derived from 1,3-diphenyl-barbituric acid. J Med Pharm Chem 5:175–183
Turner RA (1965) Uricosuric agents In: Screening Methods in Pharmacology Chapter 39, pp 262–263, Academic Press, New York and London

C.4.2.5 Uricosuric Activity in Dalmatian Dogs

PURPOSE AND RATIONALE

Most species have low plasma levels and low renal excretion of uric acid. The Dalmatian dog is an exception with excessive uric acid excretion, but with relatively high plasma levels. Explanations are a genetically determined defect in tubular reabsorption of the filtered urate (Friedman and Byers 1948; Kessler et al. 1959) and a defective hepatic uricase activity (Yü et al. 1971). The Dalmatian dog is being used for studies of uricosuric agents.

PROCEDURE

Conscious male Dalmatian dogs with a body weight of about 20 kg are used. Food but not water is withheld 24 h prior to the experiment. The animals are placed individually in metabolic cages. The urinary bladder is emptied by catheterization. Twenty ml/kg drinking water is applied by gavage. Every 2 h the animals are catheterized again, blood is withdrawn from a jugular vein and additional 8 ml/kg drinking water is applied by gavage. The urine and blood values obtained after the first 2 h serve as control. Then, the test compound is applied either i.v. or orally. Up to 8 h blood and urine samples are collected every 2 h. No water is given af-

ter the last sampling. The dogs stay over night in the metabolic cages. Twenty-four hours after beginning of the experiment, venous puncture and catheterization is performed once more. Blood and urine samples are analyzed for uric acid (Uricaquant-method), creatinine (Jaffé reaction), sodium and potassium (flame photometry), calcium and magnesium (atom absorption method), and chloride (argentometry) as well as for osmolality.

EVALUATION

The values after application of the drug are compared with predrug values.

CRITICAL ASSESSMENT OF THE METHOD

Dalmatian dogs bred by commercial breeders are not always homozygous. Therefore, not every dog is suitable for experiments on uric acid excretion.

REFERENCES AND FURTHER READING

Fanelli GM (1976) Drugs affecting the renal handling of uric acid. In: Martinez-Maldonado M (ed) Methods in Pharmacology, Vol 4A, Renal Pharmacology, Chapter 9, pp 269–292

Friedman M, Byers SO (1948) Observations concerning the causes of the excess excretion of uric acid in the Dalmatian dog. J Biol Chem 175:727–735

Hropot M, Klaus E, Seuring B, Lang HJ (1985) Effects of diuretics on magnesium excretion. Magnesium Bull 7:20–24

Kessler RH, Hierholzer K, Gurd RS (1959) Localization of urate transport in the nephron of mongrel and Dalmatian dog kidney. Am J Physiol 197:601–603

Muschaweck R, Hajdu P (1964) Die saludiuretische Wirksamkeit der Chlor-N-(2-furylmethyl)-5-sulfamyl-anthranilsäure. Arzneim Forsch/Drug Res 14:44–47

Yü TF, Gutman AB, Berger L, Kaung C (1971) Low uricase activity in the Dalmatian dog simulated in mongrels given oxonic acid. Am J Physiol 220:973–979

C.4.2.6 Uricosuric Activity in Cebus Monkeys

PURPOSE AND RATIONALE

The Cebus monkey is described not to possess uricase (Simkin 1971) and to have different metabolic conditions for uric acid than other experimental animals. This species is chosen for special studies of anti-uricopathic drugs since it resembles more closely human uric acid metabolism.

PROCEDURE

Cebus monkeys (*Cebus albifrons*) of either sex weighing 3.0 to 5.0 kg are used. Twenty-four h prior to the test, food is withheld, but water is available ad libitum. On the morning of the experiment, the animals receive 20 ml/kg drinking water by gavage, followed by oral application of the test compound. Control animals receive water only. The animals are placed in individual metabolism cages and the spontaneously voided urine is collected after 2, 6, and 24 h. After 2 and 6 h, additional 4 ml/kg water is given by gavage. From a cubital vein blood is withdrawn prior to the experiment and 2, 6 and 24 h after application. Urine and serum samples are analyzed for uric acid (Uricaquant-method), creatinine (Jaffé reaction), sodium and potassium (flame photometry), calcium and magnesium (atom absorption method), and chloride (argentometry) as well as for osmolality.

EVALUATION

Allopurinol and probenicide are used as standard drugs and are compared with test compounds.

CRITICAL ASSESSMENT OF THE METHOD

The use of the Cebus monkey as animal model has been proven to be the most valuable method to test putative hypouricemic compounds (Hropot 1988).

MODIFICATIONS OF THE METHOD

Onuma et al. (1988) used Cebus monkeys for evaluation of uricosuric effects of an aryloxyacetic derivative.

Yonetani et al. (1987) performed clearance experiments with uricosuric drugs in anesthetized chimpanzees.

Dan et al. (1989) tested the activity of AA-193, an uricosuric agent in rats, mice and Cebus monkeys.

REFERENCES AND FURTHER READING

Dan T, Koga H, Onuma E, Tanaka H, Sato H, Aoki B (1989) The activity of AA-193, a new uricosuric agent in animals. Adv Exp Med Biol 253:301–308

Fanelli GM (1976) Drugs affecting the renal handling of uric acid. In: Martinez-Maldonado M (ed) Methods in Pharmacology, Vol 4A, Renal Pharmacology, Chapter 9, pp 269–292

Fanelli GM, Bohn D, Stafford SH (1970) Functional characteristics of renal urate transport in the Cebus monkey. Am J Physiol 218:627–636

Hropot M (1988) Unpublished data

Onuma E, Tanaka H, Takahashi F, Tatsumi T, Akaike I, Koga H, Dan T (1988) Uricosuric effect of a new aryloxyacetic derivative (AA-193) in rats and Cebus monkeys. Jpn J Pharmacol 46(Suppl):Abst. P-250

Yonetani Y, Ikawi K, Shinosaki T, Kawase-Hanafusa A, Harada H, van Es AA (1987) A new uricosuric diuretic, S-8666, in rats and chimpanzees. Japan J Pharmacol 43:389–398

Yü TF, Gutman AB, Berger L, Kaung C (1971) Low uricase activity in the Dalmatian dog simulated in mongrels given oxonic acid. Am J Physiol 220:973–979

C.5 Influence on Lower Urinary Tract

C.5.1 In Vivo Studies

C.5.1.1 Micturition Studies

PURPOSE AND RATIONALE

Urinary incontinence is a major psychosocial, medical, and economic problem. The most common condition to be treated pharmacologically is incontinence due to detrusor instability. The response of the urinary bladder to filling with increasing volumes of fluid (cystometrogram) is a common procedure for evaluating bladder function in both animals and humans. The response of the vesico-urethral complex can be arbitrarily divided into the collection and expulsion phases. The nervous control of the detrusor, the internal and the external sphincter has been reviewed by Kuru (1965). A detailed description of the nervous control of the urinary bladder of the cat has been given by De Groat (1975). The pharmacology of lower urinary tract muscles and penile erectile tissues has been reviewed by Anderson (1993). Ferguson and Christopher (1996) reviewed urine bladder function and drug development. Urine storage and timely expulsion of bladder content are produced through the coordinated activation of a series of reflexes involving cholinergic, sympathetic, and, possibly, purinergic, serotonergic, and peptidergic innervation. In view of this complexity, *in vivo* models were developed for the quantitative analysis of the effects of drugs on the function of the vesico-urethral complex (Maggi et al. 1983, 1985, 1986, 1987a, b, 1992).

PROCEDURE

Male Wistar rats weighing 340–360 g are anesthetized by subcutaneous injection of 1.2 g/kg urethane. The left jugular vein is cannulated for drug injection. Body temperature is kept constant by means of a heating pad maintained at 37°C. Through a midline incision of the abdomen, the urinary bladder is exposed and emptied of urine by application of a slight manual pressure. A 20-gauge needle is inserted through the apex of the bladder dome for 3–4 mm into its lumen. The needle is connected to a pressure transducer by means of a polyethylene tubing (1.5 mm OD and 1.0 mm ID) and the whole system filled with saline. The tubing is provided with an internal coaxial polyethylene tubing (0.6 mm OD and 0.3 mm ID) inserted through a side hole and sealed by a drop of epoxy resin. The second tubing serves for intravesical infusion of fluid and is connected, through a peristaltic pump, to a saline reservoir.

Intraluminal pressure signals are delivered to an amplifier and displayed on a four channel polygraph. Warm saline-soaked cotton wool swabs are laid around the exteriorized organ to maintain its temperature and to keep it moist in experiments involving the topical application of substances on the bladder dome.

After a 15-min equilibration period at zero volume, variations in intraluminal pressure are recorded in response to continuous infusion of saline at a rate of 2.8 ml/h at 37°C for 30–40 min by means of a peristaltic pump connected to the polyethylene tubing inserted into the bladder. This infusion rate simulates the maximal hourly diuresis within the physiological range. In each preparation the infusion is continued until micturition occurs. Micturition is referred as the emission of several drops of fluid during a sustained phasic contraction of the detrusor muscle which is followed by return to zero or, in any case, to a value lower than that recorded just before micturition.

For both intravenous and topical administration, substances are dissolved in saline.

EVALUATION

In each experiment, the following parameters are evaluated:

1. pressure threshold = intraluminal pressure value recorded just before micturition
2. volume threshold = the volume of infused saline required to obtain micturition
3. maximal amplitude of micturition contraction
4. residual volume after micturition

The effect of substances on the compliance of the bladder wall is evaluated by comparing the volume-pressure-relationship of treated animals with that of controls.

Statistical analysis of the data is performed by means of the Student's *t*-test for paired or unpaired data, or by means of analysis of variance followed by the Tukey test. Statistical analysis of nonparametric data is made by the chi square test.

MODIFICATIONS OF THE METHOD

Either chemical (6-hydroxydopamine, reserpine) or surgical (section of hypogastric nerves) sympathectomy produces a picture of detrusor hyperreflexia and urine dropping, mimicking cystometric finding in human disease (Maggi et al. 1987a).

Postius and Szelenyi (1983) described a model for *in vivo* screening of spasmolytic compounds using the rat bladder.

Dray (1985) used the spontaneous, volume-induced contractions of the urinary bladder in the anesthetized rat to assess the central activity of substances with opioid properties.

Pietra et al. (1990) studied the effects of some antidepressants on the volume-induced reflex contractions of the rat urinary bladder. The urinary bladder of anesthetized rats was filled via the recording catheter by incremental volumes of warmed saline until bladder contractions occurred as a result of central activity. Volume-induced contractions were then recorded and occurred rhythmically and reproducibly for 2–3 h. Drug activity was assessed in each animal against the background frequency of bladder contractions, for a 15-min time period following intravenous administration of different doses.

Harada et al. (1992) proposed a method for rapid evaluation of the efficacy of pharmacologic agents and their analogs in enhancing bladder capacity and reducing the voiding frequency. Conscious rats were placed in a restrainer over a urine collector. The collector was secured to an Statham UC3 strain transducer, the output of which was amplified by a Gould bridge amplifier. Data were monitored on a polygraph. This method has been simplified by the use of an infared photodiode sensor and matched phototransistor than can detect the appearance of urine flowing from the bottom of a metabolic cage, recodrig the frequency of these events. This method produces results comparable to the original cup-fore transducer methods (Argentieri and Argentieri 2002).

Conte et al. (1991) proposed a method for simultaneous recording of vesical and the external urethral sphincter pressure in urethane-anesthetized rats.

Angelico et al. (1992) reported *in vivo* effects of different antispasmodic drugs on the rat bladder contractions induced by topically applied KCl.

Oyasu et al. (1994) measured spontaneous bladder contractions caused by raising the intravesical volume in anesthetized rats.

Yaksh et al. (1986) described a chronic model for study of micturition in unanesthetized rats. A bladder catheter was implanted chronically through laparatomy and externalized percutaneously.

Horváth et al. (1994) reported an ultrasonic method to study the influence of drugs on micturition in intact rats.

Tillig and Constantinou (1996) described videomicroscopic imaging of urethral peristaltic function in anesthetized rats. Cystometrograms were performed by recording continuously the bladder pressures while detecting micturition using a sensor placed at the orifice of the urethra. Renal pelvic pressure was measured during continuous perfusion using a nephrostomy inserted through the parenchyma. A catheter was placed in the femoral vein for intravenous drug administration. The left pyelo-ureteric junction and the upper part of the ureter were visualized using a stereomicroscope equipped with a video camera and a tape recorder. One syringe pump was used for filling the bladder to perform continuous cystometrograms. An other syringe pump was used for infusion of indigo carmine to assist the visualization of the bladder pressure.

Conte et al. (1988) developed a cystometric technique for quantitative studies on physiopharmacology of micturition in conscious, freely moving rats.

Seif et al. (2004) performed urinary bladder volumetry by means of a single retrosymphysically implantable ultrasound unit.

Peterson et al. (1989), Noronha-Blob et al. (1991) described *in vivo* cystometrogram studies in urethane-anesthetized and conscious **guinea pigs**.

Moreau et al. (1983) described simultaneous cystometry and uroflowmetry for evaluation of the caudal part of the urinary tract in **dogs**.

Imagawa et al. (1989) reported an *in vivo* procedure for functional evaluation of sympathetically mediated responses in lower urinary tract of dogs.

Häbler et al. (1990, 1992) examined the functional properties of unmyelinated and myelinated primary afferent neurons innervating the pelvic viscera in anesthetized **cats**. The axons were isolated from the intact dorsal root and the intact or chronically de-efferented ventral root of segment S2. The responses of the neurons were studied with natural stimulation of the urinary bladder using innocuous or noxious increases of intravesical pressure.

Tai et al. (2004). Decribed bladder and urethral sphincter responses evoked by microstimulation of S2 sacral spinal cord in spinal cord intact and chronic spinal cord injured **cats.**

REFERENCES AND FURTHER READING

Anderson KE (1993) Pharmacology of lower urinary tract muscles and penile erectile tissues. Pharmacol Rev 46:253–308

Angelico P, Guarneri L, Fredella B, Testa R (1992) *In vivo* effects of different antispasmodic drugs on the rat bladder contractions induced by topically applied KCl. J Pharmacol Meth 27:33–39

Argentieri TM, Argentieri MA (2002) Optical micturition interval monitor for experimental animals. J Pharmacol Toxicol Methods. 48:147–152

Conte B, D'Aranno V, Santicioli P, Giuliani S, Mancinelli A, Furio M, Maggi CA, Meli A (1988) A new method for recording cystometrograms in conscious, freely moving rats. J Pharmacol Meth 19:57–61

Conte B, Maggi CA, Parlani M, Lopez G, Manzini S, Giachetti A (1991) Simultaneous recording of vesical and urethral pressure in urethane-anesthetized rats: Effect of neuromuscular blocking agents on the activity of the external urethral sphincter. J Pharmacol Meth 26:161–171

De Groat WC (1975) Nervous control of the urinary bladder of the cat. Brain Res 87:201–211

Dray A (1995) The rat urinary bladder. A novel preparation for the investigation of central opioid activity *in vivo*. J Pharmacol Meth 13:157–165

Ferguson D, Christopher N (1996) Urine bladder function and drug development. Trends Pharmacol Sci 17:161–165

Häbler HJ, Jänig W, Koltzenburg M (1990) Activation of unmyelinated afferent fibres by mechanical stimuli and inflammation of the urinary bladder in the cat. J Physiol 425:545–562

Häbler HJ, Jänig W, Koltzenburg M (1992) Myelinated primary afferents of the sacral spinal cord responding to slow filling and distension of the cat urinary bladder. J Physiol 463:449–460

Harada T, Levounis P, Constantinou CE (1992) Rapid evaluation of the efficacy of pharmacologic agents and their analogs in enhancing bladder capacity and reducing the voiding frequency. J Pharmacol Toxicol Meth 27:119–126

Horváth G, Morvay Z, Kovács M, Szikszay M, Benedek G (1994) An ultrasonic method for the evaluation of dexmedetomidine on micturition in intact rats. J Pharmacol Toxicol Meth 32:215–218

Imagawa JI, Akima M, Sakai K (1989) Functional evaluation of sympathetically mediated responses *in vivo* lower urinary tract of dogs. J Pharmacol Meth 22:103–111

Kuro M (1965) Nervous control of micturition. Physiol Rev 45:425–494

Maggi CA (1992) Prostanoids as local modulators of reflex micturition. Pharmacol Res 25:13–20

Maggi CA, Santicioli P, Grimaldi G, Meli A (1983) The effect of peripherally administered GABA on spontaneous contractions of rat urinary bladder *in vivo*. Gen Pharmacol 14:455–458

Maggi CA, Santicioli P, Furio M, Meli A (1985) Dual effects of clonidine on micturition reflex in urethane anesthetized rats. J Pharmacol Exper Ther 235:528–536

Maggi CA, Santicioli P, Meli A (1986) The nonstop transvesical cystometrogram in urethane-anesthetized rats: A simple procedure for quantitative studies on the various phases of urinary bladder voiding cycle. J Pharmacol Meth 15:157–167

Maggi CA, Santicioli P, Meli A (1987a) Pharmacological studies on factors influencing the collecting phase of the cystometrogram in urethane-anesthetized rats. Drug Dev Res 10:157–170

Maggi CA, Giuliani S, Santicioli P, Abelli L, Regoli D, Meli A (1987b) Further studies on the mechanisms of the tachykinin-induced activation of the micturition reflex in rats: evidence for the involvement of the capsaicin-sensitive bladder mechanoreceptors. Eur J Pharmacol 136:189–205

Moreau PM, Lees GE, Gross DR (1983) Simultaneous cystometry and uroflowmetry (micturition study) for evaluation of the caudal part of the urinary tract in dogs: Reference values for healthy animals sedated with xylazine. Am J Vet Res 44:1774–1781

Noronha-Blob L, Prosser JC, Sturm BL, Lowe VC, Enna SJ (1991) (±)-Terodiline: an M1-selective muscarinic receptor antagonist. *In vivo* effects at muscarinic receptors mediating urinary bladder contraction, mydriasis and salivary secretion. Eur J Pharmacol 201:135–142

Oyasu H, Yamamoto T, Sato N, Sawada T, Ozaki R, Mukai T, Ozaki T, Nishii M, Sato H, Fujiwara T, Tozuka Z, Koibuchi Y, Honbo T, Esumi K, Ohtsuka M, Shimomura K (1994) Urinary bladder-selective action of the new antimuscarinic compound vamicamide. Arzneim Forsch/Drug Res 44:1242–1249

Peterson JS, Hanson RC, Noronha-Blob L (1989) *In vivo* cystometrogram studies in urethane-anesthetized and conscious guinea pigs. J Pharmacol Meth 21:231–241

Pietra C, Poggesi E, Angelico P, Guarneri L, Testa R (1990) Effects of some antidepressants on the volume-induced reflex contractions of the rat urinary bladder: lack of correlation with muscarinic receptors activity. Pharmacol Res 22:421–432

Postius S, Szelenyi I (1983) *In vivo* rat bladder: a new model to screen spasmolytic compounds. J Pharmacol Meth 9:53–61

Seif C, Herberger B, Cherwon E, Martinez Portillo FJ, Molitor M, Stieglitz T, Bohler G, Zendler S, Junemann KP, Braun PM (2004) Urinary bladder volumetry by means of a single retrosymphysically implantable ultrasound unit

Tai C, Booth AM, de Groat WC, Roppolo JR (2004) Bladder and urethral sphincter responses evoked by microstimulation of S2 sacral spinal cord in spinal cord intact and chronic spinal cord injured cats. Exp Neurol. 190:171-183

Tillig B, Constantinou CE (1996) Videomicroscopic imaging of ureteral peristaltic function in rats during cystometry. J Pharmacol Toxicol Meth 35:191–202

Yaksh TL, Durant PAC, Brent CR (1986) Micturition in rats: a chronic model for study of bladder function and effect of anesthetics. Am J Physiol 251 (Regulative Integrative Comp Physiol 20):R1177–R1185

C.5.2 Studies in Isolated Organs

C.5.2.1 Studies on Renal Pelvis

PURPOSE AND RATIONALE

Periodic contraction of the renal pelvic wall is important to the process of concentration of urine in the renal medulla as well as the propulsion of urine from the kidney into the bladder (Santicioli and Maggi, 1997, 1998; Knepper et al. 2003). The isolated renal pelvis of the guinea pig has been used to examine the effects of compounds an this activity. (Maggi and Giuliani 1991, 1992; Maggi et al. 1992a, b, 1992c, 1994, 1995; Giuliani and Maggi 1996; Santicioli et al. 1995, 1997; Patachini et al. 1998; Bigoni et al. 1999).

PROCEDURE

Male albino guinea pigs weighing 250–300 g are used. Following appropriate anesthesia and euthanasia, one whole kidney and attached ureter are removed and placed in oxygenated Krebs solution. The renal pelvis is carefully dissected from the renal parenchyma, separated from the ureter, cut and connected to threads

to record motility along the circular axis. The preparation is suspended in a 5 ml organ bath and mechanical activity recorded by means of an isotonic transducer (load 1 mN). Transmural electrical field stimulation is made by means of platinum wire electrodes placed at the top and the bottom of the organ bath and connected to a GRASS S 88 stimulator. Square wave pulses (pulse width 0.5 ms, 60 V) are delivered in trains of 10 s duration at frequencies of 5 to 10 Hz.

Experiments commence after a 60 to 90 min equilibrium period after which amplitude and frequency of spontaneous activity has reached a steady state. *In vitro* capsaicin desensitization is made by exposure of the preparation to 10 μM for 15 min, followed by washing out and further equilibration for 30–60 min.

Concentration response curves to noradrenaline and acetylcholine are performed by non-cumulative addition to the bath at 20 min intervals. Contact time of drugs is 15 min.

EVALUATION

The amplitude and frequency of spontaneous contractions are assessed and the Motility Index (MI) is calculated as follows:

$$MI = (\Sigma amp/5) \times F$$

where Σamp/5 is the mean amplitude of five contractions (in mN) and F is the frequency (in min^{-1}) of those five contractions. Concentration-response curves are generated by plotting the concentration versus the MI (either raw or expressed as a percent of control, using the parallel incubation as the control) (Davidson and Lang, 2000).

MODIFICATIONS OF THE METHOD

Zhang and Lang (1994), Lang et al. (1995), Lang and Zhang (1996) Teele and Lang (1998) recommended circumferentially cut strips from the proximal renal pelvis of guinea pigs since these strips contract more frequently than strips cut from the mid region.

Kimoto and Constantinou (1990, 1991) studied contractility of smooth muscle strips from the pacemaker regions and pelviureteric junction of renal pelvis from **rabbits**.

Kondo et al. (1992) determined the effects of dobutamine and terbutaline on adenylate cyclase activity and cyclic AMP content in the renal pelvis of rabbits.

Seki and Suzuki (1990) made intracellular recordings to study the electrical properties of smooth muscle cells in the rabbit renal pelvis.

Zwergel et al. (1991) developed an intact **canine** model to measure renal pelvic pressure after complete ureteral obstruction with a balloon catheter inflated in the distal ureter.

REFERENCES AND FURTHER READING

Bigoni R, Guiliani S, Calo G, Rizzi A, Guerrini R, Salvadori S, Regoli D, Maggi CA (1999) Characterization of nociceptin receptors in the periphery: *In vitro* and *in vivo* studies. Naunyn-Schmiedeberg's Arch Pharmacol 359:160–167

Davidson ME, Lang RJ (2000) Effects of selective inhibitors of cyclo-oxygenase-1 (COX-1) and cyclo-oxygenase-2 (COX-2) on the spontaneous myogenic contractions in the upper urinary tract of the guinea-pig and rat. Br. J Pharmacol. 129:661–670

Giuliani S, Maggi CA (1996) Inhibition of tachykinin release from peripheral endings of sensory nerves by nociceptin, a novel opioid peptide. Br J Pharmacol 118:1567–1569

Kimoto Y, Constantinou CE (1990) Effects of (1-desamino-8-D-arginine)vasopressin and papaverine on rabbit renal pelvis. Eur J Pharmacol 175:359–362

Kimoto Y, Constantinou CE (1991) Regional effects of indomethacin, acetylsalicylic acid and SC-19220 on the contractility of rabbit renal pelvis (pacemaker regions and pelviureteric junction). J Urol 146:433–438

Knepper MA, Saidel GM, Hascall VC, Dwyer T (2003) Concentration of solutes in the renal inner medulla: interstitial hyaluronan as a mechano-osmotic transducer. Am J Physiol Renal Physiol 284: F433–F446

Kondo S, Tashima Y, Morita T (1992) Effects of dobutamine and terbutaline on adenylate cyclase activity and cyclic AMP content in the renal pelvis of rabbits. Urol Int 49:146–150

Lang RJ, Zhang Y (1996) The effects of K^+ channel blockers on the spontaneous electrical and contractile activity in the proximal renal pelvis of the guinea pig. J Urol 155:332–336

Lang RJ, Zhang Y, Exintaris B, Vogalis F (1995) Effects of nerve stimulation on the spontaneous action potentials recorded in the proximal renal pelvis of the guinea pig. Urol Res 23:343–350

Maggi CA, Giuliani S (1991) The neurotransmitter role of CGRP in the rat and guinea pig ureter: effect of a CGRP agonist and species-related differences in the action of omega conotoxin on CGRP release from primary afferents. Neuroscience 43:261–271

Maggi CA, Giuliani S (1992) Non-adrenergic, non-cholinergic excitatory innervation of the guinea pig renal pelvis: Involvement of capsaicin-sensitive primary afferent neurons. J Urol 147:1394–1398

Maggi CA, Patacchini R, Eglezos A, Quartara L, Giuliani S, Giachetti A (1992a) Tachykinin receptors in the guinea pig renal pelvis: Activation by exogenous and endogenous tachykinins. Br J Pharmacol 107:27–33

Maggi CA, Santicioli P, Del Bianco E, Giuliani S (1992b) Local motor responses to bradykinin and bacterial chemotactic peptide formyl-methionyl-leucyl-phenylalanine (FMLP) in the guinea pig isolated renal pelvis and ureter. J Urol 14:1944–1950

Maggi CA, Theodorsson E, Santicioli P, Giuliani S (1992c) Tachykinins and calcitonin gene-related peptide as co-transmitters in local responses produced by sensory nerve activation in the guinea pig isolated renal pelvis. Neuroscience 46:549–559

Maggi CA, Giuliani S, Santicioli P (1994) Effect of cromakalim and glibenclamide on spontaneous and evoked motility of the guinea pig isolated renal pelvis and ureter. Br J Pharmacol 111:687–794

Maggi CA, Giuliani S, Santicioli P (1995) CGRP inhibits electromechanical coupling in the guinea pig isolated

renal pelvis. Naunyn-Schmiedeberg's Arch Pharmacol 352:529–537
Patacchini R, Santicioli P, Zagorodnyuk V, Lazzeri M, Turini D, Maggi CA (1998) Excitatory motor and electrical effects produced by tachykinins in the human and guinea pig isolated ureter and guinea pig renal pelvis. Br J Pharmacol 125:987–996
Santicioli P, Maggi CA (1997) Pharmacological modulation of electromechanical coupling in the proximal and distal regions of the guinea pig pelvis. J Auton Pharmacol 17:43–52
Santicioli P, Maggi CA (1998) Myogenic and neurogenic factors in the control of pyeloureteral motility and ureteral peristalsis. Pharmacol. Rev. 50:684–721
Santicioli P, Carganico G, Meini S, Giuliani S, Giachetti A, Maggi CA (1995) Modulation of stereoselective inhibition of cyclo-oxygenase of electromechanical coupling in the guinea pig isolated renal pelvis. Br J Pharmacol 114:1149–1158
Seki N, Suzuki H (1990) Electrical properties of smooth muscle cell membrane in renal pelvis of rabbits. Am J Physiol 259 (Renal, Fluid, Electrolyte Physiol 28):F888–F894
Teele ME, Lang RJ (1998) Stretch-evoked inhibition of spontaneous migrating contractions in whole mount preparation of the guinea pig upper urinary tract. Br J Pharmacol 123:1143–1153
Zhang Y, Lang RJ (1994) Effect of intrinsic prostaglandins on the spontaneous contractile and electrical activity of the proximal renal pelvis of the guinea pig. Br J Pharmacol 113:431–438
Zwergel U, Zwergel T, Ziegler M (1991) Effects of prostaglandins and prostaglandin synthetase inhibitors on acutely obstructed kidneys in the dog. Urol Int 47:64–69

C.5.2.2 Propagation of Impulses in the Guinea Pig Ureter

PURPOSE AND RATIONALE

The mammalian ureter provides one of the clearest examples of electromechanical coupling in smooth muscle. The ureter smooth muscles are electrically and mechanically quiescent but, when depolarized to threshold, they fire an action potential characterized by an unusually long-lasting potential and generate a phasic contraction (Shuba 1977; Brading et al. 1983; Meini et al. 1995). Both the action potential and the accompanying contraction critically depend upon the influx of extracellular calcium through voltage-sensitive L-type channels, which are enhanced and blocked by dihydropyridine drugs, Bay K 8644 and nifedipine, respectively. The model predicts that suppression of action potentials at any site of the ureter will suppress the propagation of contraction and peristalsis. (Weiss 1992).

PROCEDURE

A number of species (most commonly rats and guinea pigs) have been used for whole-mount or strip preparations. Following appropriate anesthesia, the whole kidney and ureter are excised and placed in a Petri dish containing oxygenated Krebs solution for dissection. A 4–5 cm long piece of ureter is dissected from the inferior renal pole and placed in a three-compartment organ bath which enables a separate superfusion of different parts of the organs. Two Perspex partitions are used to separate the renal-, middle- and bladder-sites. They include a window covered with condom rubber: a small hole (about 300 µm) is made in the rubber to enable the passage of the ureter. Proximal to each partition, the renal and bladder ends are pinned to a Sylgard support. The distal portions of the renal and bladder ends are connected via a pulley to isotonic transducers (Basile 7006, load 2 mN) for recording of mechanical activity on a two-channel polygraph. Each compartment is perfused by means of a peristaltic pump at a rate of 1 ml/min with oxygenated Krebs solution at 34°C.

The frequency and amplitude of spontaneous contractions are recorded. Alternatively, electrical field stimulation is applied to either compartment by means of two wire platinum electrodes positioned in parallel with the two sides of the ureter. Square wave pulses (5–25 ms pulse width, 20 V) are automatically delivered every 100 s by means of a GRASS S88 stimulator.

Drugs are applied by superfusion at the middle site. Amplitudes of contraction are recorded.

EVALUATION

The amplitude and frequency of contractions are assessed and the Motility Index (MI) is calculated as follows:

$$\mathrm{MI} = (\Sigma \mathrm{amp}/5) \times F$$

where Σ amp/5 is the mean amplitude of five contractions (in mN) and F is the frequency (in min^{-1}) of those five contractions.

Data are expressed as a percent of the control value and appropriate statistical analysis is performed. Concentration-response cuves may be plotted and pA_2 or pD_2 values may be calculated. Hill coefficients and EC_{50} values may also be calculated (Weiss et al. 2002).

MODIFICATIONS OF THE METHOD

Ureter preparations have been made from pig or human tissues collected at slaughter or following surgery, respectively. Ideally, no more than 20 minutes should elapse between tissue collection and incubation. Tissues are placed into cold (4°C) Krebs buffer or suitable balanced electrolyte solution and cut into rings of 0.5 to 1 cm in length. The rings are attached to a force transducer, suspended in an organ bath at 37°C, and

allowed to equilibrate for up to 1.5 hours while the frequency and amplitude of spontaneous contraction is measured. If the preparation demonstrates acceptable and stable frequenct and amplitude of spontaneous contraction within this time period it is considered suitable for experimental use. In pigs, the washout period between treatments is variable and thus the preparation is monitored for return to pre-treatment baseline before the next treatment is applied. In human tissue, spontaneous contraction seldom occurs and electrical stimulation (trains of 300 ms at an interval of 200 s and impulses of 200 mA with a duration of 6 ms at a frequency of 50 H) is required. A washout period of 20 minutes between treatments is used (Weiss et al. 2002).

The evaluation of regional differences in response, and the effect of regional responses on adjacent regions, can be evaluated in a whole ureter preparation where each region remains physically attached but can be isolated for the application of test compounds or stimuli. The entire ureter is dissected and placed in a three-compartment organ bath which enables a separate superfusion of different parts of the organs. Two Perspex partitions are used to separate the proxima (renal), middle, and distal (bladder) ends. They include a window covered with condom rubber: a small hole (about 300mm) is made in the rubber to enable the passage of the ureter. The proximal portions of each segment are pinned to a Sylgard support, and the distal portions are connected to isotonic transducers for recording of mechanical activity. Each compartment is perfused separately and electrical field stimulation can be applied to any compartment by means of two wire platinum electrodes positioned in parallel with the two sides of the ureter (Meini et al. 1995).

Tomiyama et al. (2003) characterized functional muscarinic cholinoceptors in the isolated ureter of **dogs.**

REFERENCES AND FURTHER READING

Brading AF, Burdyga ThV, Scripnyuk ZD (1983) The effects of papaverine on the electrical and mechanical activity of the guinea pig ureter. J Physiol 334:79–89

Meini S, Santicioli P, Maggi CA (1995) Propagation of impulses in the guinea pig ureter and its blockade by calcitonin-gene-related peptide. Naunyn-Schmiedeberg's Arch Pharmacol 351:79–86

Shuba MF (1977) The effect of sodium-free and potassium-free solutions, ionic current inhibitors and ouabain on electrophysiological properties of smooth muscle of guinea pig ureter. J Physiol 264:837–851

Tomiyama Y, Wanajo I, Yamazaki Y, Murakami M, Kojima M, Shibata N (2003) Functional muscarinic cholinoceptors in the isolated canine ureter. Naunyn-Schmiedeberg's Arch Pharmaacol 367:348–352

Weiss RM (1992) Physiology and pharmacology of renal pelvis and ureter. In: Walsh PC, Retik AB, Stamey TA, Vaughan ED (eds) Campell's Urology. WB Saunders Co. Philadelphia PA, Vol 1, pp 113–144

Weiss R, Mevissen M, Hauser DS, Scholtysik G, Portier CJ, Walter B, Studer UE, Danuser HJ (2002) Inhibition of human and pig ureter motility in vitro and in vivo by the K^+ channel openers PKF 217-744b and nicorandil. J Pharm Exper Ther 302:651–658

C.5.2.3 Studies on Urinary Bladder and Internal Urethral Sphincter

PURPOSE AND RATIONALE

Several authors investigated the influence of drugs on isolated parts of the lower urinary tract. Ueda et al. (1984) studied the effects on smooth muscle of the rabbit bladder dome, trigone and proximal urethra.

PROCEDURE

Male New Zealand rabbits weighing 2–3 kg are sacrificed and the abdomen is opened to remove the bladder and the urethra. After excess fat and connective tissue is removed, the bladder and the urethra are dissected into dome, trigone and proximal urethral preparations. All strips are cut transversely being approximately 2×6 mm unstretched. Ligatures are placed on both ends of the strips and one end is attached to a tissue holder and the other to a strain gauge force-displacement transducer connected to a polygraph on which isometric tension changes are recorded. Each of the strips is then placed into a 20 ml tissue bath containing Krebs-Ringer solution bubbled with 95% O_2+5% CO_2 at 37°C. Resting tension is adjusted to 1 g during an equilibrium period of at least 2 h. The contractile and relaxant responses are measured as increases or decreases from the resting tension. Doses-response curves are performed in a cumulative matter. Tissues are pretreated with an antagonist 20 min before the addition of an agonist.

EVALUATION

The values are expressed or plotted as the means ± SE and pA_2 values are calculated according to Arunlakshana and Schild (1959). Data are analyzed using the *t*-test, analysis of variance, Dunnett's test and regression analysis.

MODIFICATIONS OF THE METHOD

Rats and guinea pigs have been used for whole bladder preparations. Following appropriate anesthesia, the abdomen is opened to remove the bladder and the urethra. After excess fat and connective tissue is removed, the preparation is placed *en bloc* into appropriate bal-

anced electrolyte solution (Tyrode's or Krebs buffer) bubbled with 5% CO_2 and 95% O_2. The urethra is cannulated and connected to a pressure transducer, and the bladder is filled with a volume of solution adequate to evoke a contractile response. The bladder preparation is allowed to equilibrate for 30 minutes before any experimental manipulations are performed. The amplitude and frequency of pressure changes are recorded (Birder et al. 1999; Drake et al. 2003).

Alternatively, contractility can be assessed visually. Surface blood vessels or externally applied markings (India ink or carbon particles) are used as landmarks. Video image recording of the bladder preparations are made during the experimental manipulations. Still images from the video are evaluated and the change in linear distance between pairs of landmarks is used as an index of contractility (Drake et al. 2003).

Pietra et al. (1990) studied the effects of some antidepressants by the *in vitro* inhibition of carbachol-induced contractions of rat detrusor strip preparations. The detrusor muscle tissue (bladder dome) was cut in a semicircular direction and further dissected into strip preparations measuring approximately 2 × 20 mm.

The preparation of the isolated, innervated urinary bladder of the rat was reported by Hukovic et al. (1965). Electrical stimulation was performed by a bipolar electrode from the nerves running close to the ureter.

Mapp et al. (1990) used the isolated rat urinary bladder to study the pharmacological modulation of the contractile response to toluene diisocyanate.

Maggi et al. (1985) used isolated detrusor strips of rat bladder connected to an isometric strain gauge and stimulated by field stimulation.

Anderson (1978) recommended the **rabbit** detrusor muscle a an unique *in vitro* smooth muscle preparation. Rabbit detrusor muscles are thin and devoid of underlying submucosal tissue with parallel fiber orientation. The tissue exhibits autorhythmicity, characteristic of most single unit type smooth muscle preparations and can be employed in either isometric or isotonic organ bath recording systems.

Honda and Nakagawa (1986) studied the effects of the optical isomers of an alpha-1 adrenoceptor antagonist in rabbit lower urinary tract and prostate.

Khanna et al. (1977, 1981) evaluated the *in vitro* responses of three segments of rabbit lower urinary tract, e. g., the bladder body, the bladder base and the proximal urethra.

Ferguson and Marchant (1995) studied the inhibitory actions of GABA on rabbit urinary bladder muscle strips.

Andersson et al. (1983) studied the electrically induced relaxation of the noradrenaline contracted isolated urethra from rabbit and man. In rabbits, two circular transverse sections, each 4 mm long, were taken from the middle and upper parts of the urethra. Human urethral preparations were obtained from male patients undergoing cysto-urethrectomy en bloc because of bladder cancer. Rings of tissue were taken from the membranous and supra- and infra-collicular parts of the prostatic urethra.

Andersson et al. (1992) used transversal strips from the middle and upper part of rabbit urethra to study the involvement of nitric oxide in the electrically-induced, nerve-mediated relaxation.

Contractile responses to nervous stimulation can be assessed in whole isolated bladder preparations. The pudendal nerve remnants can be identified near the ureter and can be attached to electrodes for stimulation of the bladder. Alterations in the contractile responses by the test compound are considered to result from effects at the neuromuscular junction (Hukovic et al. 1965; Weetman, 1972; Dhattiwala and Dave, 1975).

Inci et al. (2003) used a coaxial bioassay system to test the effect of inflammation on rat urinary bladder-dependent relaxation. In this bioassay model, the bladder was the donor organ for the assays and rat anococcygeus muscle was the assay tissue. The rat bladders removed from control or treatment groups were used in its original shape after making small cuts at bladder neck and dome. The rat anococcygeus muscle was always isolated from control group of rats. The anococcygeus muscle was placed in the lumen of the bladder, so that freely enveloped by the bladder, and mounted under a resting tension of 1 g in a 20 ml organ bath filled with Krebs-Henseleit solution at 37°C and gassed with 95% O_2–5% CO_2.

Denervated urinary bladder preparations (whole or strips) can be used to determine the degree of effect on nervous system inputs. Following appropriate anesthesia, the pelvic plexus is accessed in rats by a ventral midline incision and both pelvic ganglia are obliterated by electrocauterization. The animals are allowed to recover for at least four days before the urinary bladder is harvested as described above; during this period, the neurotransmitters downstream from the nervous system inputs become inactive and only the autonomous inputs remain. Differences in response between the denervated urinary bladder preparation and one harvested from a sham-operated animal are considered to result from neural inputs. The urinary bladders of the denervated animals must be manually emptied on a daily basis during the four day

recovery period (Birder et al. 1998; Brauerman et al. 2006).

Inputs from the urothelium can be assessed in isolated urinary bladder smooth muscle preparations. Following preparation of strips from the urinary bladder, the urothelium is gently peeled away from the cut surface and the strips are mounted as described above. Effects on the capsaicin-mediated nitric oxide pathways located in the urothelium can be assessed in these preparations (Birder et al. 1998). Effects on the release of neurotransmitter substances from the epithelial strips removed from these preparations can also be examined; following isolation, the epithelial strips are incubated in Krebs buffer of suitable balanced electrolyte solution. Following a 20 minute equilibration period, the strips are stimulated either mechanically (by stoking with a glass rod or pinching with forceps) or electrically (using field stimulation of the incubation medium). The neurotransmitter substance of interest is analyzed in the bath solution and dose-response curves are generated (Downie and Karmazyn, 1984).

Ukai et al. (2006) investigated the participation of endogenous endothelin and ET_A receptor in premicturation contractions in rats with bladder outlet obstruction, a model for bladder overactivity.

Weetman (1972) described the preparation of the isolated, innervated urinary bladder in **guinea pigs**. Contractions of the tissue induced by nerve stimulation could be blocked by local anesthetics and by tetrodotoxin.

Isolated innervated, rat and guinea pig hemi-urinary bladder preparations were described by Dhattiwala and Dave (1975).

Burnstock et al. (1978) used recorded isometric tension of mucosal-free strips of the detrusor of the bladder from guinea pigs *in vitro* after electrical field stimulation.

Von Heyden et al. (1997) tested urethral relaxation after electrostimulation in guinea pigs. Male Hartley guinea pigs weighing 350–450 g were sacrificed and bladder, urethra and penis were dissected out. From each animal 4–6 urethral rings 1–2 mm thick were cut. The urethral rings were mounted according to their anatomical order: in channel 1 the most proximal ring (near the bladder neck) and in channel 6 the most distal ring (near the penile crura). The urethral rings were stretched by two spring-wire clips (Harvard Apparatus, South Natick, MA) whose tips closed in the urethral lumen. The manner in which the urethral rings were cut and mounted ensured that only the circularly oriented, mostly striated fibers contributed to the tension measured. Detrusor muscle was cut as a horizontal ring proximal to the trigone and mounted in the same way. The clips were connected with 4-O silk to a glass tissue support hook on one side and to an isometric force transducer (Föhr Medical Instruments GmbH, D-64342 Seeheim, Germany) on the other. A double-chambered bath (Föhr Medical Instruments GmbH, D-64342 Seeheim, Germany) was used in which the working chamber was connected to a second chamber, in which the gas (95% O_2 and 5% CO_2) was fed. The gas flow induced fluid circulation. Forces lower than 0.1 g could be measured without bubble artifacts in the working chamber. The transducer signals were fed into a thermal array recorder (Dash 10, Astro-Med, 63110 Rodgau, Germany). For tissue stimulation, vertical, L-shaped custom-made platinum electrodes (20 mm long, 0.3 mm diameter) 10 mm apart were used with a custom-made stimulator. The tissue was mounted parallel with the electrodes. Bipolar, monophasic balance-charged rectangular pulses of 0.8-ms duration and 75 mA current were used.

Kunisawa et al. (1985) performed a pharmacological study of alpha adrenergic receptor subtypes in smooth muscle of **human** urinary bladder base and prostatic urethra.

Wuest et al. (2005) studied the effect of a potassium channel opener on contraction of detrusor strips from **mouse, pig** and **man** in the presence and absence of urothelium..

Thornbury et al. (1992) reported on the mediation of nitric oxide of neurogenic relaxation of the urinary bladder neck muscle in **sheep**. Urinary bladders of sheep of either sex were obtained approximately 15 min after slaughter. Circularly oriented rings were cut from the region of the bladder just above the trigone. These were opened and the mucosa removed by sharp dissection to give strips with approximate dimensions of $10 \times 4 \times 4$ mm. The strips were mounted in organ baths and perfused with Krebs solution. Tension was measured with isometric transducers after field stimulation via platinum ring electrodes.

Hills et al. (1984) used isolated strips of the bladder from female **pigs**. Bladder neck strips were cut longitudinally and horizontally from the region of the bladder just below the trigone. The preparations were stripped of mucosa and trimmed to give a muscle strip of about 2×15 mm.

Klarskov (1987) studied the non-cholinergic, non-adrenergic inhibitory nerve responses of bladder outlet smooth muscle from female Danish Landrace pigs *in vitro*. Trigone strips were taken in an oblique direction from the internal urethral orifice and medially to one of the ureteric orifices, bladder neck strips transversal

from the posterior half of the borderline between bladder and urethra, and urethral strips longitudinal from the proximal posterior part.

Teramoto et al. (1997) examined the membrane potential in the proximal urethra of pigs by use of the microelectrode technique.

REFERENCES AND FURTHER READING

Anderson GF (1978) The rabbit detrusor muscle: a unique in-vitro smooth muscle preparation. J Pharmacol Meth 1:177–182

Andersson KE, Mattiasson A, Sjögren S (1983) Electrically induced relaxation of the noradrenaline contracted isolated urethra from rabbit and man. J Urol 129:210–214

Andersson KE, Pascual AG, Persson K, Forman A, Tøttrup A (1992) Electrically-induced, nerve-mediated relaxation of rabbit urethra involves nitric oxide. J Urol 147:253–259

Angelico P, Guarneri L, Fredella B, Testa R (1992) *In vivo* effects of different antispasmodic drugs on the rat bladder contractions induced by topically applied KCl. J Pharmacol Meth 27:33–39

Arunlakshana O, Schild HO (1959) Some quantitative uses of drug antagonists. Br J Pharmacol Chemother 14:48–58

Birder LA, Apodaca G, DeGroat WC, Kanai AJ (1998) Adrenergic- and capasaicin-evoked nitric oxide release from urothelium and afferent nerves in the urinary bladder. Am J Physiol 275: F226-F229

Brauerman AS, Doumanian LR, Ruggieri MR (2006) M2 and M3 muscarininc receptor activation of urinary bladder contractile signal transduction. II. Denervated rat bladder. J Pharm Exper Ther 316:875–880

Burnstock G, Cocks T, Crowe R, Kasakov L (1978) Purinergic innervation of the guinea pig urinary bladder. Br J Pharmacol 63:125–138

Dhattiwala AS, Dave KC (1975) Isolated innervated, rat and guinea pig hemi-urinary bladder preparations. Ind J Physiol Pharmacol 19:164–166

Downie JW, Karmazyn M (1984) Mechanical trauma to bladder epithelium liberates prostanoids which modulate neurotransmission in rabbit detrusor muscle. J Pharm Exper Ther 230:445–449

Drake MJ, Harvey IJ, Gillespie JI (2003) Autonomous activity in the isolated guinea pig bladder. Exp Physiol 88:19–30

Ferguson DR, Marchant JS (1995) Inhibitory actions of GABA on rabbit urinary bladder muscle strips: mediation by potassium channels. Br J Pharmacol 115:81–83

Hills J, Meldrum LA, Klarskov P, Burnstock G (1984) A novel non-adrenergic, non-cholinergic nerve-mediated relaxation of the pig bladder neck: an examination of possible neurotransmitter candidates. Eur J Pharmacol 99:287–293

Honda K, Nakagawa C (1986) Alpha-1 adrenoceptor antagonist effects of the optical isomers of YM-12617 in rabbit lower urinary tract and prostate. J Pharmacol Exper Ther 239:512–516

Hukovic S, Rand MJ, Vanov S (1965) Observations on an isolated, innervated preparation of rat urinary bladder. Br J Pharmacol 24:178–188

Inci K, Ismailoglu UB, Sahin A, Sungur A, Sahin-Erdemli I (2003) The effect of inflammation on rat urinary bladder-dependent relaxation in coaxial bioassay system. Naunyn-Schmiedebergs Arch Pharmacol 367:547–552

Khanna OP, diGregorio GJ, Sample RG, McMichael R (1977) Histamine receptors in urethrovesical smooth muscle. Urology 10:375–381

Khanna OP, Barbieri EJ, McMichael RF (1981) The effects of adrenergic agonists and antagonists on vesicourethral smooth muscle of rabbits. J Pharmacol Exp Ther 216:95–100

Klarskov P (1987) Non-cholinergic, non-adrenergic inhibitory nerve responses of bladder outlet smooth muscle *in vitro*. Br J Urology 60:337–342

Kunisawa Y, Kawabe K, Nijima T, Honda K, Takenaka T (1985) A pharmacological study of alpha adrenergic receptor subtypes in smooth muscle of human urinary bladder base and prostatic urethra. J Urol 134:396–398

Maggi CA, Santicioli P, Furio M, Meli A (1985) Dual effects of clonidine on micturition reflex in urethane anesthetized rats. J Pharmacol Exper Ther 235:528–536

Mapp CE, Chitano P, Fabbri LM, Patacchini R, Maggi CA (1990) Pharmacological modulation of the contractile response to toluene diisocyanate in the rat isolated urinary bladder. Br J Pharmacol 100:886–888

Pietra C, Poggesi E, Angelico P, Guarneri L, Testa R (1990) Effects of some antidepressants on the volume-induced reflex contractions of the rat urinary bladder: lack of correlation with muscarinic receptors activity. Pharmacol Res 22:421–432

Santicioli P, Maggi CA, Meli A (1984) $GABA_B$ receptor mediated inhibition of field stimulation-induced contractions of rabbit bladder muscle *in vitro*. J Pharm Pharmacol 36:378–381

Teramoto N, Creed KE, Brading AF (1997) Activity of glibenclamide-sensitive K^+ channels under unstimulated conditions in smooth muscle cells of pig proximal urethra. Naunyn-Schmiedeberg's Arch Pharmacol 356:418–424

Thornbury KD, Hollywood MA, McHale NG (1992) Mediation of nitric oxide of neurogenic relaxation of the urinary bladder neck muscle in sheep. J Physiol 451:133–144

Ueda S, Satakee N, Shibata S (1984) α_1- and α_2-adrenoreceptors in the smooth muscle of isolated rabbit urinary bladder and urethra. Eur J Pharmacol 103:249–254

Ukai M, Yuxama H, Noguchi Y, Someya A, Okutsu H, Watanabe M, Yoshino T, Ohtake A, Suzuki M, Sato S, Sasamata M (2006) Participation of endogenous endothelin and ET_A receptor in premicturation contractions in rats with bladder outlet obstruction. Naunyn-Schmiedeberg's Arch Pharmacol 373:197–203

Von Heyden B, Jordan U, Schmitz W, Hertle L (1997) Urethral relaxation after electrostimulation in the guinea pig is independent of nitric oxide. J Urology 157:1509–1513

Weetman DF (1972) The guinea-pig isolated, innervated bladder preparation: the effect of some autonomic drugs. Arch Int Pharmacodyn 196:383–392

Wuest M, Kaden S, Hakenberg OW, Wirth MP, Ravens U (2005) Effect of rilmakalim on detrusor contraction in the presence and absence of urothelium. Naunyn-Schmiedeberg's Arch Pharmacol 372:203–212

C.5.2.4 Effects on Isolated Urethra

PURPOSE AND RATIONALE

The relaxation response in the urethra results in a combination of decreased intraurethral pressure, increased urethral diameter and urethral shortening resulting in a flaring of the urethral orifice. A number of neurotransmitters and mediators are involved in this process, with each affecting a different stage of the process.

(Brading 1999: Andersson and Wein, 2004) The urethra is difficult to study *in situ* because of the large amount of surrounding connective tissue, which can be overcome by the use of a whole-mount preparation (Jankowski et al. 2004).

PROCEDURE

Female rats or guinea pigs have been used. Following appropriate anesthesia, the bladder and urethra are exposed via a lower midline incision, and a catheter is inserted in the urethral lumen, extending the entire axial length and exiting from a hole placed in the bladder dome. The urethra is secured to the tubing with sutures at both ends to maintain the correct *in vivo* length after dissection, and is measured. The pubic bone is then cut at a position lateral to the urethra and then separated and resected. The exposed urethra was gently removed from the ventral vaginal wall and the whole bladder-urethra unit was immediately placed in cold, oxygenated suitable balanced electrolyte solution bubbled with 21% O2-5% CO2-74% N2.

The catheter is removed so that the urethra may be secured inside the experimental apparatus, which provides a controlled fixed intraluminal pressure via an adjustable static fluid reservoir (the intraluminal pressure is controlled by adjusting the height of the reservoir). The mounted urethra is then enclosed in a bathing chamber filled with the same gassed, balanced electrolyte solution at 37°C. The preparation is allowed to equilibrate for at least 30 min before testing. A laser micrometer is positioned to measure urethral outer diameter at chosen locations along the axial length. Proximal, mid, and distal regional measurements were performed by positioning the laser at axial positions 25, 50, and 75%, respectively, from the apex of the bladder, based on *in vivo* length. Both pressure and outer diameter (OD) measurements are recorded simultaneously.

The test compound of interest is added to the bath and pressure and OD measurements are obtained following a 30 minute equilibration period. Pressure-diameter (P-D) responses are generated by incrementally increasing the pressure, in 2 mm Hg steps, from 0 to 18 mm Hg, and OD data are collected at 10 Hz over a 1-min period for each 2-mmHg step. The OD data are then averaged for each incremental increase to obtain a discrete value for each value of applied pressure.

Contractile responses can be evaluated in this preparation as well. The urethra is exposed to a fixed intraluminal pressure of 8 mmHg, which causes the tissue to be predilated and allows for a contractile response to be generated. The OD resulting from this 8-mmHg applied pressure is measured at a single axial location (i. e., proximal, mid, or distal) 30 min after pressurization. The test chemical of interest is added to the bath and the preparation is exposed for 30 minutes; at the end of this time, a series of 100 OD measurements (taken at 1 Hz) are collected at the same location and are averaged.

EVALUATION

The P-D response data are used to generate tissue compliance (C) as follows:

$$C = [D_{max} - D_{min}/D_{min}]\, X\, (P_{max} - P_{min})^{-1}$$

where D_{max} and D_{min} represent the OD at the maximum (P_{max}, 18 mm Hg) and minimum (P_{min}, 0 mm Hg) applied pressures, respectively.

Contractile responses are assessed by determining the percent change in mean OD before and after the addition of the test compound.

MODIFICATION OF THE METHOD

With careful dissection, the pudendal nerves can be identified and left intact during the diisction of the urethra from the guinea pig. These nerves can then be attached to electrodes and alterations of effects of neural inputs can be assessed. In this preparation, contractile responses were assessed by measuring changes in isometric tension and intraluminal pressure changes were also recorded (Walters et al., 2006).

Triguero et al. (2003) studied the relaxation effects of scorpion venom in the isolated urethra of **sheep**.

Michel et al. (2006) performed in vivo studies on the effects of α_1-adrenoceptor antagonists on pupil diameter and urethral tone in **rabbits**.

REFERENCES AND FURTHER READING

Andersson KE, Wein AJ (2004) Pharmacology of the lower urinary tract: basis for current and future treatments of urinary incontinence. Pharmacol Rev 56:581–631

Brading AF (1999) The physiology of the mammalian urinary outflow tract. Exper Physiol 84:215–221

Jankowski RJ, Prantil RL, Fraser MO, Chancellor MB, de Groat WC, Huard J, Vorp DA (2004) Development of an experimental system for the study of urethral biomechanical function. Am J Physiol 286: F225–F232

Michel MC, Okutsu H, Noguchi Y, Suzuki M, Ohtake A, Yuyma H, Yanai-Inamura H, Ukai M, Watanabe M, Someya A, Sasamata M (2006) In vivo studies on the effects of α_1-adrenoceptor antagonists on pupil diameter and urethral tone in rabbits. Naunyn-Schmiedeberg's Arch Pharmacol 372:346–353

Triguero D, González M, Garcia-Pascual A, Costa G (2003) Atypical relaxation of scorpion venom in the lamb urethral smooth muscle involves both NO-dependent and -independent responses. Naunyn-Schmiedeberg's Arch Pharmacol 368:151–159

Walters RD, McMurray G, Brading AF (2006) Pudendal nerve stimulation of isolated guinea-pig urethra. BJU Int. 98:1302–1306

C.5.2.5 Effects on External Urethral Sphincter

PURPOSE AND RATIONALE

In contrast to the smooth musculature of the internal urethral sphincter, the external urethral sphincter is a striate muscle and a part of the urogenital diaphragm (Kuru 1965). Judged from electromyographic studies it is generally accepted that the preponderance of continence depends on the external urethral sphincter. The external urethral sphincter shows a steady tonic discharge under resting conditions. As the bladder fills, there is initially an increase in this activity. When the rise in tension in the bladder wall leads to reflex contraction, the activity in the external urethra sphincter ceases and in remains quiescent during voiding. Parlani et al. (1992) used the external urethral sphincter of the rat as an *in vitro* model to evaluate the activity of drugs on the smooth and striated components of the urinary bladder outlet.

PROCEDURE

Male Wistar rats weighing 360–400 g are sacrificed by decapitation and exsanguination. Through a midline incision of the lower abdomen, the external urethral sphincter (Watanabe and Yamamoto 1979) is isolated from the perineal muscles and surrounding connective tissue and removed in toto. The preparation is placed in oxygenated Krebs solution, and a ring is taken from its middle region. In this area the urethra is encircled by bundles of striated muscle fibers partly interlaced with urethral smooth muscle. The rings are cut to obtain strips that are suspended in a 5-ml organ bath containing Krebs solution at 37°C. A mixture of 96% O_2 and 4% CO_2 is bubbled into the organ bath. The preparations are connected by means of a silk thread to an isometric strain gauge under a constant load of 1 g. The contractile activity is recorded on a polygraph. Field stimulation is carried out by means of two platinum wire electrodes placed at the top and the bottom of the organ bath and connected to a Grass S11 stimulator. The preparations are allowed to equilibrate for at least 60 min. Square wave pulses are delivered at an intensity between 10 and 60 V, a frequency between 0.1 and 3 Hz, and a duration between 0.1 and 1 s; trains are of 5 s every 5 min. After three consecutive reproducible responses are obtained, drugs are added to the organ bath. The effect of drugs is expressed as the percent of inhibition of contractile response before exposure to drugs and is evaluated as soon as the maximum effect is reached.

EVALUATION

Means ± standard error of the mean are calculated. Statistical evaluation is performed by using Student's *t*-test for paired or unpaired data.

MODIFICATIONS OF THE METHOD

In some studies, denervation of the external urethral sphincter was performed (Somma et al. 1989; Parlani et al. 1992). Rats were anesthetized with 30 mg/kg penthotal i.p., then the major pelvic ganglia, known to provide both sympathetic and parasympathetic innervation to the urinary bladder and the external urethral sphincter (Hulsebosh and Goggeshall 1982; Purinton et al. 1973; Watanabe and Yamamoto 1979) are isolated and bilaterally removed through a small incision of the lower abdomen.

In the same preparations, somatic denervation of the external urethral sphincter was obtained by cutting the pudendal nerves. The paravertebral muscles were carefully dissected through an incision of the skin to exteriorize the sacral plexus. The pudendal nerves were isolated, and 2–3 mm of the nerve were removed. An absorbable sponge soaked with amikain solution was left in place to prevent bleeding and infection. The muscles and the skin were sutured with cat gut. The rats were allowed to recover for 10 to 15 days in individual cages with free access to water and food.

REFERENCES AND FURTHER READING

Hulsebosh CE, Goggeshall RE (1982) An analysis of the axon population in the nerves to the pelvic viscera in the rat. J Comp Neurol 211:1–10

Kuro M (1965) Nervous control of micturition. Physiol Rev 45:425–494

Morita T, Iizuka H, Iwata T, Kondo S (2000) Function and distribution of β_3-adrenoceptors in rat, rabbit and human urinary blader and external urethral sphincter. J Smooth Muscle Res 36:21–32

Parlani M, Manzini S, Argentino-Storino A, Conte B (1992) The rat external urethral sphincter. An *in vitro* model to evaluate the activity of drugs on the smooth and striated components of the urinary bladder outlet. J Pharmacol Toxicol Meth 28:85–90

Purinton PT, Fletcher TF, Bradley WE (1973) Gross and light microscopy features of the pelvic plexus in the rat. Anat Rec 175:697–706

Somma V, Conte B, Lopez G, Astolfi Ml (1989) A method for complete removal of pelvic ganglia in female rats. J Pharmacol Meth 22:243–247

Watanabe H, Yamamoto TY (1979) Autonomic innervation of the muscle in the wall of the bladder and proximal urethra of male rats. J Anatomy 128:873–886

Chapter D
Respiratory Activity

D.1 In Vitro Tests

D.1.0.1 Histamine (H_1) Receptor Binding

PURPOSE AND RATIONALE

Histamine receptors have been classified on the basis of pharmacological analysis (Hill et al. 1997). Histamine exerts its action via at least four receptor subtypes. The H_1 receptor couples mainly to $G_{q/11}$, thereby stimulating phospholipase C, whereas the H_2 receptor interacts with G_s to activate adenylyl cyclase. The histamine H_3 and H_4 receptors couple to G_i proteins to inhibit adenylyl cyclase, and to stimulate MAPK (Hough 2001).

Histamine is considered to play a major role in asthmatic attacks (Bryce et al. 2006). H_1-antagonists have been used since decades as therapeutic agents. This as-

say is used to determine the affinity of test compounds to the histamine H_1 receptor by measuring their inhibitory activities on the binding of the H_1 antagonist ^{3}H-pyrilamine to a plasma membrane preparation from guinea pig brain.

PROCEDURE

Brains from guinea-pigs are homogenized in ice-cold Tris buffer (pH 7.5) in a Potter homogenizer (1 g brain in 30 ml buffer). The homogenate is centrifuged at 4°C for 10 min at 50,000 *g*. The supernatant is discarded, the pellet resupended in buffer, centrifuged as before, and the final pellets resupended in Tris buffer (1 g fresh weight/5 ml). Aliquots of 1 ml are frozen at –70°C.

In the competition experiment, 50 µl ^{3}H-pyrilamine (one constant concentration of 2×10^{-9} M), 50 µl test compound (>10 concentrations, 10^{-5}–10^{-10} M) and 100 µl membrane suspension from guinea pig whole brain (approx. 10 mg wet weight/ml) per sample are incubated in a shaking bath at 25°C for 30 min. Incubation buffer: 50 mM Tris-HCl buffer, pH 7.5.

Saturation experiments are performed with 11 concentrations of ^{3}H-pyrilamine ($0.1–50 \times 10^{-9}$ M). Total binding is determined in the presence of incubation buffer, non-specific binding is determined in the presence of mepyramine or doxepin (10^{-5} M).

The reaction is stopped by rapid vacuum filtration through glass fibre filters. Thereby the membrane-bound is separated from the free radioactivity. The retained membrane-bound radioactivity on the filter is measured after addition of 3 ml liquid scintillation cocktail per sample in a liquid scintillation counter.

EVALUATION OF RESULTS

The following parameters are calculated:

- total binding of ^{3}H-pyrilamine
- non-specific binding: binding of ^{3}H-pyrilamine in the presence of mepyramine or doxepin
- specific binding = total binding–non-specific binding
- % inhibition of ^{3}H-pyrilamine binding: 100–specific binding as percentage of control value

The dissociation constant (K_i) and the IC_{50} value of the test drug are determined from the competition experiment of ^{3}H-pyrilamine versus non-labeled drug by a computer-supported analysis of the binding data.

MODIFICATIONS OF THE METHOD

De Backer et al. (1993) reported genomic cloning, heterologous expression in COS-7 cells and pharmacological characterization of a human H_1-receptor.

REFERENCES AND FURTHER READING

Bryce PJ, Mathias CB, Harrison KL, Watanabe T, Geha RS, Oettgen HC (2006) The H1 histaminic receptor regulates allergic lung responses. J Clin Invest 116(6):1624–1632

Carswell H, Nahorski SR (1982) Distribution and characteristics of histamine H_1-receptors in guinea-pig airways identified by [^{3}H]mepyramine. Eur J Pharmacol 81:301–307

Chang RSL, Tran VT, Snyder SH (1979) Heterogeneity of histamine H_1-receptors: Species variations in [^{3}H]mepyramine binding of brain membranes. J Neurochem 32:1653–1663

De Backer MD, Gommeren W, Moereels H, Nobels G, Van Gompel P, Leysen JE, Luyten WH (1993) Genomic cloning, heterologous expression and pharmacological characterization of a human H_1-receptor. Biochem Biophys Res Commun 197:1601–1608

Hill SJ, Emson PC, Young JM (1978) The binding of [^{3}H]mepyramine to histamine H_1 receptors in guinea-pig brain. J Neurochem 31:997–1004

Hill SJ, Ganellin CR, Timmerman H, Schwartz JC, Shankley NP, Young JM, Schunack W, Levi R, Haas HL (1997) International Union of Pharmacology. XIII. Classification of histamine receptors. Pharmacol Rev 49:253–278

Hough LB (2001) Genomics meets histamine receptors: new subtype, new receptor. Mol Pharmacol 59:415–419

Ruat M, Schwartz JC (1989) Photoaffinity labeling and electrophoretic identification of the H_1-receptor: Comparison of several brain regions and animal species. J Neurochem 53:335–339

D.1.0.2 Muscarinic Receptor Binding

PURPOSE AND RATIONALE

Muscarinic receptors in the airways are important in both the normal physiology and the pathophysiology of pulmonary function. Acetylcholine released from parasympathetic nerve terminals causes contraction of airway smooth muscle. Animals with asthma or other chronic inflammation of the airways exhibit hypersensitivity of the airways to muscarinic agonists, and muscarinic antagonists are used therapeutically in patients with asthma and chronic obstructive pulmonary disease (Nathanson 2000). Muscarinic receptors are present in neurons in the central and peripheral nervous system, cardiac and smooth muscles, and a variety of exocrine glands. Mammals possess genes encoding five different subtypes of mAChR, termed M_1–M_5, which can be divided into two broad functional categories: the M_1, M_3, and M_5 receptors preferentially couple to the Gq family of G-proteins whereas the M_2 and M_4 receptors preferentially couple to the Gi family of G-proteins.

For involvement of acetylcholine receptors in the gastrointestinal tract see J.3.6.1.2.

Several papers deal with the distribution of muscarinic receptors in the lung, their role in pulmonary disease and the use of muscarinic antagonists for the

treatment of obstructive airways disease (Mak and Barnes 1990; Barnes 1993, 2001, 2004; Disse 2001; Disse et al. 1993, 1999; Haddad et al. 1994; Barnes et al. 1995, 1997; Patel et al. 1995; Peták et al. 1996; Alabaster 1997; Matsumoto 1997; Chelala et al. 1998; Hislop et al. 1998; Okazawa et al. 1998; Wale et al. 1999; Rees 2002; Sarria et al. 2002; Tohda et al. 2002; Costello et al. 2006).

Hirose et al. (2001) described the pharmacological properties of a muscarinic antagonist with M_2-sparing antagonistic activity.

PROCEDURE

Binding Affinity for Human and Rat Muscarinic Receptor Subtypes

In competition studies, specific binding of [^{3}H]*N*-methylscopolamine (NMS; New England Nuclear, Boston, Mass., USA) was determined using membranes from Chinese hamster ovary (CHO) cells expressing cloned human m1, m2, m3, m4, or m5 receptors (Receptor Biology, Baltimore, Md., USA), rat m1 or m3 receptors (American Type Culture Collection, Manassas, Va., USA), and rat heart tissue. These CHO cells expressing cloned rat m1 or m3 receptors, and rat heart tissue were homogenized in 3 vols of 50 mM Tris-HCl (pH 7.4) and 1 mM EDTA containing 20% sucrose with a Polytron PT-10. The homogenates were centrifuged at 10,000 *g* for 30 min at 4°C. The supernatants were centrifuged at 100,000 *g* for 60 min at 4°C. The pellets were suspended in 50 mM Tris-HCl (pH 7.4) and 5 mM $MgCl_2$ and centrifuged at 100,000 *g* for 60 min at 4°C. The pellets were resuspended in the above-mentioned buffer (25 mg/ml for CHO cells expressing cloned rat m1 or m3, and 50 mg/ml for rat heart tissue) and stored at –80°C as membrane preparations. In the binding assay, the membrane preparations were incubated with 0.19 to 0.2 nM [^{3}H]NMS in 50 mM Tris-HCl, 10 mM $MgCl_2$, and 1 mM EDTA (pH 7.4) for 2 h at room temperature. Final protein concentrations were 22 µg/ml (human m1), 70 µg/ml (human m2), 54 µg/ml (human m3), 20 µg/ml (human m4), 116 µg/ml (human m5), 481 µg/ml (rat m1 and m3), and 2500 µg/ml (rat heart). Assays were performed in a total volume of 500 µl. Non-specific binding was measured in the presence of 1 µM NMS and it was less than 2% of total binding. Free and membrane-bound [^{3}H]NMS were separated by filtration over glass filters (UniFilter-GF/C; Packard Instruments, Meriden, Conn., USA) using a cell harvester (Filtermate 196; Packard Instruments). Radioactivity was counted by a liquid scintillation counter (TopCount; Packard Instruments).

EVALUATION

For saturation studies, membranes from CHO cells expressing human m3 were incubated with an increased concentration of [^{3}H]NMS (0.1–3.2 nM) in the presence or absence of 10 nM compound A, and specific binding of [^{3}H]NMS was determined after incubation for 2 h.

Competition binding data were analyzed by a nonlinear regression fitting program using GraphPad Prism Software (San Diego, Calif., USA). Saturation binding data were transformed to make a Scatchard plot and analyzed by a linear regression fitting program using GraphPad Prism Software.

The K_i values were calculated from the IC_{50} values by using the following equation:

$$K_i = IC_{50}/(1 + [L]/K_d)$$

where K_d is the dissociation constant of [^{3}H]NMS in each receptor subtype, and [*L*] is the concentration of [^{3}H]NMS (Cheng and Prussoff 1973). K_d values of [^{3}H]NMS in each receptor subtype were determined by Scatchard plot analysis. The K_d and B_{max} values below were used in this study. Data of human cloned receptors were extracted from Receptor Biology's Product Information Sheets (Receptor Biology).

Human m1 receptor	K_d = 51 pM	B_{max} = 1.28 pmol/mg of protein
Human m2 receptor	K_d = 290 pM	B_{max} = 1 pmol/mg of protein
Human m3 receptor	K_d = 86 pM	B_{max} = 0.65 pmol/mg of protein
Human m4 receptor	K_d = 56 pM	B_{max} = 1.44 pmol/mg of protein
Human m5 receptor	K_d = 200 pM	B_{max} = 0.59 pmol/mg of protein
Rat m1 receptor	K_d = 62 pM	B_{max} = 0.039 pmol/mg of wet weight
Rat m2 receptor	K_d = 210 pM	B_{max} = 0.0090 pmol/mg of wet weight
Rat m3 receptor	K_d = 72pM	B_{max} = 0.019 pmol/mg of wet weight

In saturation studies, the K_i value was calculated using the following equation:

$$K_i = K_d/(K'_d - K_d) \times [C]$$

where K'_d or K_d is the dissociation constant of [^{3}H]NMS in human m3 receptors in the presence or absence of an inhibitor, respectively, and [*C*] is the concentration of the test drug (Nishikibe et al. 1999).

MODIFICATIONS OF THE METHOD

Struckmann et al. (2003) investigated the role of muscarinic receptor subtypes in the constriction of peripheral airways by studies on receptor-deficient mice.

REFERENCES AND FURTHER READING

Alabaster VA (1997) Discovery and development of selective M_3 antagonists for clinical use. Life Sci 60:1053–1060

Barnes PJ (1993) Muscarinic receptor subtypes: implications for therapy. Agents Actions Suppl 43:243–252

Barnes PJ (2001) Tiotropium bromide. Exp Opin Invest Drugs 10:733–740

Barnes PJ (2004) Distribution of receptor targets in the lung. Proc Am Thorac Soc 1:345–351

Barnes PJ, Belvisi MG, Mak JCW, Haddad EB, O'Connor B (1995) Tiotropium bromide (Ba 679 BR), a novel long-acting muscarinic antagonist for the treatment of obstructive airway disease. Life Sci 56:853–859

Barnes PJ, Haddad EB, Rousell J (1997) Regulation of muscarinic M_2 receptors. Life Sci 60:1015–1021

Chelala JL, Kilani A, Miller JM, Martin RJ, Ernsberger P (1998) Muscarinic receptor binding sites of the M_4 subtype in porcine lung parenchyma. Pharmacol Toxicol 83.200–207

Cheng YC, Prusoff WH (1973) Relationship between the inhibition constant (K1) and the concentration of inhibitor which causes 50 percent inhibition (I50) of an enzymatic reaction. Biochem Pharmacol 22:3099–3108

Costello RW, Jacoby DB, Fryer AD (2006) Pulmonary neuronal M_2 muscarinic receptor function in asthma and animal models of hyperreactivity. Thorax 53:613–618

Disse B (2001) Antimuscarinic treatment for lung diseases. From research to clinical practice. Life Sci 68:2557–2564

Disse B, Reichl R, Speck G, Traunecker W, Ludwig-Rominger KL, Hammer R (1993) Ba 679 BR, a novel long-acting anticholinergic bronchodilator. Life Sci 52:537–544

Disse B, Speck GA, Rominger KL, Witek TJ Jr, Hammer R (1999) Tiotropium (Spiriva™): mechanistical considerations and clinical profile in obstructive lung disease. Life Sci 64:457–464

Haddad EB, Mak JC, Barnes PJ (1994) Characterization of [^{3}H]Ba 679 BR, a slowly dissociating muscarinic antagonist, in human lung: radioligand and autoradiographic mapping. Mol Pharmacol 45:899–907

Hirose H, Aoki I, Kimura T, Fujikawa T, Numazawa T, Sasaki K, Sato A, Hasegawa T, Nishikibe M, Mitsuya M, Ohtake N, Mase T, Noguchi K (2001) Pharmacological properties of (*2R*)-*N*-[1-(6-aminopyridin-2-ylmethyl)piperidin-4-yl]-2-[(*1R*)-3,3-difluorocyclopentyl]-2-hydroxy-2-phenylacetamide: a novel muscarinic antagonist with M_2-sparing antagonistic activity. J Pharmacol Exp Ther 297:790–797

Hislop AA, Mak JCW, Reader JA, Barnes PJ, Haworth SG (1998) Muscarinic receptor subtypes in the porcine lung during postnatal development. Eur J Pharmacol 359:211–221

Mak JC, Barnes PJ (1990) Autoradiographic visualization of muscarinic receptor subtypes in human and guinea pig lung. Am Rev Respir Dis 141:1559–1568

Matsumoto S (1997) Functional evidence of excitatory M_1 receptors in the rabbit airway. J Pharmacol Exp Ther 281:531–539

Nathanson NM (2000) A multiplicity of muscarinic mechanisms: enough signaling pathways to take your breath away. Proc Natl Acad Sci USA 97:6245–6247

Nishikibe M, Ohta H, Ishikawa K, Hayama T, Fukuroda T, Noguchi K, Saito M, Kanoh T, Ozaki S, Kamei T, Hara K, William D, Kivlighn S, Krause S, Gabel R, Zingaro G, Nolan N, O'Brien J, Clayton F, Lynch J, Pettibone D, Siegl P (1999) Pharmacological properties of J-104132 (L-753,037), a potent orally active, mixed ET_A/ET_B endothelin receptor antagonist. J Pharmacol Exp Ther 289:1262–1270

Okazawa A, Cui ZH, Lötvall J, Yoshihara S, Skoogh BE, Kashimoto K, Lindén A (1998) Effect of a novel PACAP-27 analogue on muscarinic airway responsiveness in guinea-pigs *in vivo*. Eur Respir J 12:1062–1066

Patel HJ, Barnes PJ, Takahashi T, Tadjikarimi S, Yacoub MH, Belvisi MG (1995) Evidence for prejunctional muscarinic autoreceptors in human and guinea pig trachea. Am J Respir Crit Care Med 152:872–878

Peták F, Hantos Z, Adamicza A, Asztalos T, Sly PD (1996) Metacholine-induced bronchoconstriction in rats: effects of intravenous vs. aerosol delivery. J Appl Physiol 80:1841–1849

Rees PJ (2002) Tiotropium in the management of chronic obstructive pulmonary disease. Eur Respir J 19:205–206

Sarria B, Naline E, Zhang Y, Cortijo J, Molimard M, Moreau J, Therond P, Avenier C, Morcillo EJ (2002) Muscarinic M_2 receptors in acetylcholine-isoproterenol functional antagonism in human isolated bronchus. Am J Physiol L11254–L1132

Struckmann N, Schwering S, Wiegand S, Gschnell A, Yamada M, Kummer W, Wess J, Haberberger RV (2003) Role of muscarinic receptor subtypes in the constriction of peripheral airways: studies on receptor deficient mice. Mol Pharmacol 64:1444–1451

Tohda Y, Haraguchi R, Itoh M, Ohkawa K, Kubo H, Fukuoka M, Nakajima S (2002) Role of muscarinic receptors in a guinea pig model of asthma. Intern Immunopharmacol 2:1521–1527

Wale JL, Peták F, Sly PD (1999) Muscarinic blockade of methacholine induced airway and parenchymal lung responses in anaesthetized rats. Thorax 54:531–537

D.2 Effects on Air Ways

D.2.1 Tests in Isolated Organs

D.2.1.1 Spasmolytic Activity in Isolated Guinea Pig Lung Strips

PURPOSE AND RATIONALE

Several autacoids such as histamine and leukotrienes, induce bronchoconstriction. Histamine is an important mediator of immediate allergic and inflammatory reactions. It causes bronchoconstriction by activating H_1-receptors. Calcium ionophores induce the release of leukotrienes via the 5-lipoxygenase pathway. Leukotrienes are powerful bronchoconstrictors that appear to act on smooth muscles via specific receptors. In this method, drugs are tested for their capability of inhibiting bronchospasm induced by histamine or calcium ionophore. It is used to detect H_1- and leukotriene receptor blocking properties of test compounds.

PROCEDURE

Albino guinea-pigs of either sex weighing 300–450 g are sacrificed with an overdose of ether. The chest cavity is opened and the lungs are removed. They are cut into strips of 5 cm and placed into a physiological saline solution. Thereafter, the lung strips are mounted in an organ bath containing a nutritive solution. The bath is bubbled with carbogen and maintained at 37°C. Under a pre-load of 0.5 g–3 g, the tissue is left to equilibrate for 30–60 min. Prior to testing, carbachol is added to the bath to test the lung strips' ability of contraction. Twenty min later, two prevalues are obtained by adding the spasmogen

- histamine dihydrochloride 10^{-6} g/ml for 5 min, or
- Ca – ionophore 5×10^{-6} g/ml for 5 min, or
- Leukotriene LTC_4 10^{-9}–10^{-8} g/ml for 10 min, or
- Leukotriene LTD_4 10^{-9}–10^{-8} g/ml for 10 min

to the bath and recording the contractile force at its maximal level. Following a 20 min equilibration period, the spasmogen is administered again. Five minutes thereafter, the test compound is added in cumulative doses from 10^{-8} to 10^{-4} g/ml at 5 or 10 min intervals. The contractile response is determined isometrically.

Test Modification: Inhibition of Prostaglandin Synthesis

This procedure is identical to the test described above with the exception that the prostaglandin synthesis is inhibited by addition of indomethacin at 10^{-6} g/ml prior to spasmogen administration.

EVALUATION

The percent inhibition of spasmogen induced contraction is calculated.

MODIFICATIONS OF THE METHOD

Lung parenchyma strips from various species were used to measure bronchoactivity by Kleinstiver and Eyre (1979).

A descriptive model of the events occurring during an inflation-deflation cycle using excised rat lungs was proposed by Frazer et al. (1985).

Barrow (1986) measured volume-pressure cycles in air-filled or liquid-filled rabbit lungs ranging from intact lungs with the rib cage immobilized to isolated lungs.

REFERENCES AND FURTHER READING

Barrow RE (1986) Volume-pressure cycles from air and liquid-filled intact rabbit lungs. Resp Physiol 63:19–30

Foreman JC, Shelly R, Webber SE (1985) Contraction of guinea-pig lung parenchymal strips by substance P and related peptides. Arch Int Pharmacodyn 278:193–206

Frazer DG, Weber KC, Franz GN (1985) Evidence of sequential opening and closing of lung units during inflation-deflation of excised rat lungs. Resp Physiol 61:277–288

Kleinstiver PW, Eyre P (1979) Evaluation of the lung parenchyma strip preparation to measure bronchoactivity. J Pharmacol Meth 2:175–185

Lach E, Haddad EB, Gies JP (1993) Contractile effect of bombesin on guinea pig lung *in vitro*: involvement of GRP-preferring receptors. Am J Physiol 264:L80–86

Lach E, Trifilieff A, Muosli M, Landry Y, Gies JP (1994) Bradykinin-induced contraction of guinea pig lung *in vitro*. Naunyn-Schmiedeberg's Arch Pharmacol 350:201–208

Lulich KM, Papadimitriou JM, Paterson JW (1979) The isolated lung strip and single open tracheal ring: a convenient combination for characterizing Schultz-Dale anaphylactic contractions in the peripheral and central airways. Clin Exp Pharmacol Physiol 6:625–629

D.2.1.2 Spasmolytic Activity in Isolated Trachea

PURPOSE AND RATIONALE

The isolated tracheal chain of guinea pigs can be used to test for β-blocking activity (see Sect. A.1.2.7). In addition, this model can be used to test compounds which inhibit bronchospasms. It is used to detect β-sympathomimetic, H_1-receptor blocking and leukotriene receptor blocking properties of test drugs.

Carbachol is a cholinergic agonist that produces contraction of bronchial smooth muscle by muscarinic stimulation.

Histamine is an important mediator of immediate allergic (type 1) and inflammatory reactions. It causes bronchoconstriction by activating H_1-receptors.

Calcium ionophores induce the release of leukotrienes via the 5-lipoxygenase pathway. Leukotrienes are powerful bronchoconstrictors that appear to act on smooth muscle via specific receptors.

To asses a compound's ability to inhibit carbachol induced bronchospasm via β-receptor activation, a β-receptor blocking agent (for example propranolol) must be added. If relaxation of bronchial smooth muscle is brought about by β-receptor activation, the spasmolytic effect will decrease following propranolol administration.

The effect of bradykinin can be abolished by bradykinin antagonists (Hock et al. 1991).

The effects of potassium channel openers can also be studied in this test (Englert et al. 1992).

PROCEDURE

Albino guinea pigs of either sex weighing 300–550 g are sacrificed by CO_2 narcosis. The entire trachea is

dissected out and cut into individual rings (2–3 cartilaginous rings wide). Twelve–fifeteen rings are tied together with silk threads and mounted in the organ bath containing Krebs-Henseleit solution. The tissue is maintained at 37°C under a tension of 0.5 g and gassed with carbogen. Isometric contractions are recorded via a strain-gauge transduced on a polygraph. Forty-five minutes are allowed for equilibration before the addition of the spasmogen.

The following spasmogens are used:

- carbachol (2×10^{-7} g/ml)
- histamine (10^{-7} g/ml)
- Ca – ionophore for release of leukotrienes
- leukotriene LTC_4 (10^{-9}–10^{-8} g/ml)
- leukotriene LTD_4 (10^{-9}–10^{-8} g/ml)

When the contraction has reached its maximum (initial spasm) after 10–12 min, the standard drug, e. g., isoprenaline (1 ng/ml) or aminophylline (10 ng/ml) is administered. The bronchial responses are allowed to plateau and are recorded. The tissue is rinsed thoroughly and control contractions are induced again by adding spasmogen. After obtaining the initial spasm again, the test drug is added and the contractile force is recorded at its maximal level.

Determination of mechanism of action (testing for β-sympathomimetic effect). After obtaining the initial carbachol induced spasm, propranolol is administered 5 min before the addition of the test drug. Three minutes later, the tissue is challenged by carbachol administration.

EVALUATION

The percent inhibition of carbachol or other spasmogen induced contractions is calculated. From dose-response curves ED_{50} values can be calculated.

CRITICAL ASSESSMENT OF THE METHOD

The isolated guinea pig trachea has been proven to be an useful tool for several purposes, e. g., screening procedures and studies on mode of action, e. g., of potassium channel openers.

MODIFICATIONS OF THE METHOD

The molecular mechanisms of β-adrenergic relaxation of airway smooth muscle were described by Kotlikoff and Kamm (1996).

Farmer et al. (1986) studied the effects of epithelium removal on the sensitivity of **guinea-pig** isolated trachealis to bronchodilator drugs.

Wilkens et al. (1992) described a bioassay system for a tracheal smooth muscle-constricting factor using an isolated guinea pig trachea which was cannulated from both sides, mounted in an organ bath and monitored by a TV camera attached to a microscope. The picture was digitized continuously, and the diameter of the trachea calculated and displayed on a monitor throughout the experiment.

Coleman and Nials (1989) described a versatile, eight-chamber superfusion system for the evaluation of spasmogenic and spasmolytic agents using guinea pig isolated tracheal smooth muscle.

Goldie et al. (1986a) studied the influence of the epithelium on responsiveness of guinea pig isolated trachea to contractile and relaxant agonists.

Lee et al. (1997) studied the effects of bupivacaine and its isomers on guinea pig tracheal smooth muscle. The trachea from the larynx to the carina was removed and cut into single rings. Seven tracheal rings were tied together with the circular muscle running on the same side of the chain, placed into an organ bath containing Krebs Ringer's solution and connected to a force placement transducer for measurement of isometric tension.

Wong et al. (1997) tested the effects of tyrosine kinase inhibitors on antigen challenge of guinea pig lung *in vitro*. Guinea pigs were passively sensitized by a single i.p. injection of 1 mg/kg rabbit IgG antibody against ovalbumin. Bronchial rings, 3 mm in length, were obtained from the hilar bronchi of sacrificed animals and suspended isometrically in an organ bath in Krebs bicarbonate buffer with a resting load of 2 g. To determine maximum antigen-induced contractions, bronchial rings were exposed to increasing concentrations of ovalbumin. To evaluate the role of protein tyrosine kinase in mediating smooth muscle anaphylactic contraction, protein tyrosine kinase inhibitors were preincubated with bronchial rings 30 min before addition of ovalbumin.

Eltze and Galvan (1994) compared the inhibition of preganglionic and postganglionic contraction of the **rabbit** isolated bronchus/trachea by antagonists with selectivity for different muscarinic receptor subtypes with their affinities at M_1, M_2, M_3, and M_4 receptors (Barnes 1993).

For **experiments with vagus nerve stimulation**, the vagi were isolated with rings of the proximal main stem bronchi and a small portion of the distal trachea. The tissues were hung on stainless steel hooks, which passed through the lumen, and were placed in a water-jacketed organ bath filled with Krebs solution plus 2×10^{-5} M choline chloride to promote resynthesis of acetylcholine, 10^{-5} M indomethacin to prevent generation of cyclo-oxygenase products, and 10^{-6} M

DL-propranolol to block possible β-adrenoceptor-mediated effects. The preparation was fixed under a resting tension of 1 g for isometric contraction measurement using a force transducer. The vagi were passed around bipolar platinum electrodes held at the surface of the bath. Electrical stimulation was performed with trains (20 Hz, 0.3 ms at 20 V) elicited every 20 min.

For experiments with **field stimulation**, two-ring preparations from the distal trachea of the rabbit were suspended in organ bath in Krebs solution with the above mentioned additions under a resting tension of 1 g. Isometric contractions were elicited at 1 h intervals by continuous electrical field stimulation via platinum electrodes (20 Hz, 0.3 ms at 20 V) for an average 3–7 min to reach a stable plateau.

Vaali et al. (1996) studied in isolated tracheal rings of **rats** and guinea pigs the bronchorelaxing effects of nitric oxide donors. The epithelium of some rings was removed by gentle rubbing. Rat mesenteric rings were cut from the same animals as the bronchi and similarly prepared by removing the endothelium by gently rubbing of the intimate surface.

Farmer et al. (1994) used the isolated trachea from male **ferrets** weighing 1.5–2.5 kg to study the effects of bradykinin receptor agonists.

Toews et al. (1997) assessed the effects of the phospholipid mediator lysophosphatidic acid on the contractile responsiveness of isolated tracheal rings from **rabbits** and **cats**.

Tamaoki et al. (1993) used isolated rings of segmental bronchi from **dogs** to study atypical β-adrenoceptor-(β_3-adrenoceptor)mediated relaxation.

The preparation of **bovine** tracheal smooth muscle for measuring airway responsiveness *in vitro* was described by Hashjin et al. (1995).

Wali (1987) used tracheal strips from 2- to 4-week-old **chicks** to study inhibition of cholinergic and noncholinergic neural and muscular contractions by local anesthetics.

Lulich and Paterson (1980) used **human** isolated bronchial muscle preparations and compared the effects of histamine and other drugs with the effects observed on the central and peripheral airways of the rat.

Goldie et al. (1986b) measured the responses of human bronchial strip preparations to contractile and relaxant agonists in preparations from non-diseased and from asthmatic lung obtained 3–15 h post mortem.

Hulsman and de Jongste (1993) reviewed the methods to study human airways *in vitro*.

REFERENCES AND FURTHER READING

Barnes PJ (1993) Muscarinic receptor subtypes in airways. Life Sci 52:521–527

Castillo JC, de Beer EJ (1947) The tracheal chain. I. A preparation for the study of antispasmodics with particular reference to bronchodilator drugs. J Pharmacol Exp Ther 90:104–109

Coleman RA, Nials AT (1989) Novel and versatile superfusion system. Its use in the evaluation of some spasmogenic and spasmolytic agents using guinea pig isolated tracheal smooth muscle. J Pharmacol Meth 21:

Da Silva A, Amrani YS, Trifilieff A, Landry Y (1995) Involvement of B_2 receptors in bradykinin-induced relaxation of guinea-pig isolated trachea. Br J Pharmacol 114:103–108

Eltze M, Galvan M (1994) Involvement of muscarinic M_2 and M_3, but not of M_1 and M_4 receptors in vagally stimulated contractions of rabbit bronchus/trachea. Pulmon Pharmacol 7:109–120

Englert CE, Wirth K, Gehring D, Fürst U, Albus U, Scholz W, Rosenkranz B, Schölkens BA (1992) Airway pharmacology of the potassium channel opener, HOE 234, in guinea pigs: *in vitro* and *in vivo* studies. Eur J Pharmacol 210:69–75

Farmer SG, Fedan JS, Hay DWP, Raeburn D (1986) The effects of epithelium removal on the sensitivity of guinea-pig isolated trachealis to bronchodilator drugs. Br J Pharmacol 89:407–414

Farmer SG, Broom T, DeSiato MA (1994) Effects of bradykinin receptor agonists, and captopril and thiorphan in ferret isolated trachea: evidence for bradykinin generation *in vitro*. Eur J Pharmacol 259:309–313

Foster RW (1966) The nature of the adrenergic receptors of the trachea of the guinea-pig. J Pharm Pharmacol 18:1–12

Goldie RG, Papadimitriou JM, Paterson JW, Rigby PJ, Self HM, Spina D (1986a) Influence of the epithelium on responsiveness of guinea pig isolated trachea to contractile and relaxant agonists. Br J Pharmacol 87:5–14

Goldie RG, Spina D, Henry PJ, Lulich KM, Paterson JW (1986b) *In vitro* responsiveness of human asthmatic bronchus to carbachol, histamine, β-adrenoceptor agonists and theophylline. Br J Clin Pharmacol 22:669–676

Hashjin GS, Henricks PAJ, Folkerts G, Nijkamp FP (1995) Preparation of bovine tracheal smooth muscle for *in vitro* pharmacological studies. J Pharmacol Toxicol Meth 34:103–108

Hock JF, Wirth K, Albus U, Linz W, Gerhards HJ, Wiemer G, Henke St, Breipohl G, König W, Knolle J, Schölkens BA (1991) HOE 140 a new potent and long acting bradykinin-antagonist. *In vitro* studies. Br J Pharmacol 102:769–773

Hulsman AR, de Jongste JC (1993) Studies of human airways *in vitro*: A review of the methodology. J Pharm Toxicol Meth 30:117–132

Kotlikoff MI, Kamm KE (1996) Molecular mechanisms of β-adrenergic relaxation of airway smooth muscle. Ann Rev Physiol 58:115–141

Lee T-L, Adaikan PG, Lau L-C, Ratnam SS, Dambisya YM (1997) Effects of bupivacaine and its isomers on guinea pig tracheal smooth muscle. Meth Find Exp Clin Pharmacol 19:27–33

Lulich KM, Paterson JW (1980) An *in vitro* study of various drugs on central and peripheral airways of the rat: a comparison with human airways. Br. J Pharmac 68:633–636

Rhoden KJ, Barnes PJ (1989) Effect of hydrogen peroxide on guinea-pig tracheal smooth muscle *in vitro*: role of cyclo-oxygenase and airway epithelium. Br J Pharmacol 98:325–330

Sheth UK, Dadkar NK, Kamat UG (1972) Selected Topics in Experimental Pharmacology Published by Kothari Book Depot, India

Tamaoki J, Yamauchi F, Chiyotani A, Yamawaki I, Takeuchi S, Konno K (1993) Atypical β-adrenoceptor-(β_3-adrenoceptor) mediated relaxation of canine isolated bronchial muscle. J Appl Physiol 74:297–302

Toews ML, Ustinowa EE, Schultz HD (1997) Lysophosphatidic acid enhances contractility of isolated airway smooth muscle. J Appl Physiol 83:1216–1222

Vaali K, Li L, Redemann B, Paakkari I, Vapaatalo H (1996) *In vitro* bronchorelaxing effect of novel nitric oxide donors GEA 3268 and GEA 5145 in guinea pigs and rats. J Pharm Pharmacol 48:1309–1314

Waldeck B, Widmark E (1985) Comparison of the effects of forskolin and isoprenaline on tracheal, cardiac and skeletal muscles from guinea-pig. Eur J Pharmacol 112:349–353

Wali FA (1987) Local anaesthetics inhibit cholinergic and non-cholinergic neural and muscular contractions in avian tracheal smooth muscle. Acta Anaesthesiol Scand 31:148–153

Wilkens JH, Becker A, Wilkens H, Emura M, Riebe-Imre M, Plien K, Schöber S, Tsikas D, Gutzki FM, Frölich JCl (1992) Bioassay of a tracheal smooth muscle-constricting factor released by respiratory epithelial cells. Am J Physiol 263 (Lung Cell Mol Physiol 7):L137–L141

Wong WSF, Koh DSK, Koh AHM, Ting WL, Wong PTH (1997) Effects of tyrosine kinase inhibitors on antigen challenge of guinea pig lung *in vitro*. J Pharmacol Exp Ther 283:131–137

D.2.1.3 Reactivity of the Isolated Perfused Trachea

PURPOSE AND RATIONALE

The mechanism by which the epithelium affects the reactivity of tracheal musculature can be studied using the isolated perfused trachea preparation. Contractile agonists can be added either to the serosal (extraluminal) or to the mucosal (intraluminal) surface (Fedan and Frazer 1992).

PROCEDURE

A 4-cm segment of the trachea of male guinea pigs is removed after sacrifice of the animal and placed for cleaning in modified Krebs-Henseleit solution at 37°C containing (millimolar) NaCl 113.0, KCl 4.8, $CaCl_2$ 2.5, KH_2PO_4 1.2, $MgSO_4$ 1.2, $NaHCO_3$ 25.0, and glucose 5.7 (pH 7.4) being gassed with 95% O_2/5% CO_2. The trachea is then attached to a stainless-steel perfusion holder (Munakata et al. 1988), extended to its *in situ* length and placed in an organ chamber (the serosal compartment) at 37°C containing 25 ml of gassed modified Krebs-Henseleit solution. This solution is also pumped at a constant rate of 30 ml/min through the lumen (mucosal compartment). Responses of the tracheal musculature are obtained by measuring changes in inlet-outlet ΔP between the side holes of indwelling catheters, while the trachea as perfused at a constant rate of modified Krebs-Henseleit solution. The inlet and outlet catheters are connected to the positive and negative sides, respectively, of a differential pressure transducer.

Agonists are added in step-wise increasing, cumulative concentrations. Two consecutive dose-response curves are obtained after the addition either to the serosal or mucosal compartment. The second dose-response curve is obtained 1.5 h after the end of the first, the preparation being washed every 15 min during the intervening period.

EVALUATION

Responses are quantified as ΔP in centimeters of H_2O. Geometric EC_{50} values are determined from least-square analysis of a logit model and are presented along with 95% confidence intervals.

MODIFICATIONS OF THE METHOD

Baersch and Frölich (1996) measured continuously the changes of the diameter of isolated guinea pig tracheal tubes by a newly developed imaging bioassay system. The tracheal tube between larynx and bifurcation was prepared to a length of 1.8–2.5 cm, cannulated at both ends and mounted in a 15 ml organ bath filled and perfused with oxygenated Krebs solution at 37°C. The lumen of the trachea was perfused with warm (37°C) Krebs solution from a reservoir that was isolated from the tissue bath. Changes in diameter of the trachea were assessed by computerized video microscopy. The tracheal diameter was used as marker for airway size, thus allowing calculation of muscle contractions under experimental conditions. Following a 30-min equilibrium period, a contraction was induced by intraluminal application of methacholine (0.1 mmol/l) as reference contraction. After washout and return to a stable baseline, cumulative concentration-response curves were obtained by luminal or extraluminal drug application.

Yang et al. (1991) studied the role of epithelium in airway smooth muscle responses to relaxant agents. The results suggested that the epithelium is a relatively weak barrier for lipophilic agents but has a major role as a diffusion barrier to hydrophilic substances.

Munataka et al. (1988, 1989) developed an *in vitro* system to assess the role of epithelium in regulating airway tone using the intact **guinea pig** trachea. The responses to histamine, acetylcholine and hypertonic KCl when stimulated from the epithelial or serosal site were first examined in tracheae with intact epithelium. Then the responses to these agonists were registered after epithelial denudation.

Pavlovic et al. (1989) studied the role of airway epithelium in the modulation of bronchomotor tone in the isolated trachea of **rats**. An organ bath was constructed that permitted independent circulation of fluid within the lumen or around the exterior of the tracheal segment. In one-half of the preparations the epithelium was mechanically removed.

Fernandes et al. (1989) described a co-axial bioassay system, whereby rat cross-cut aorta strip preparations were set up in co-axial assemblies under 500 mg resting tension within a guinea pig tracheal segment serving as donor of the smooth muscle relaxant factor from guinea-pig tracheal epithelium.

Lewis and Broadley (1995) investigated the influence of spasmogen inhalation by guinea pigs upon subsequent demonstration of ovalbumin-induced hyperreactivity in isolated airway tissues. Guinea pigs were sensitized with ovalbumin (i.p.) 14 days before use. *In vitro* airway hyperreactivity induced by ovalbumin inhalation was determined by challenging with aerosolized spasmogen (5-HT, methacholine, the thromboxane-mimetic U-46619, or adenosine) 24 h before and again 18–24 h after the ovalbumin inhalation. One h later, the animals were sacrificed and isolated airways perfused lung halves and tracheal spirals were set up for determination of tissue sensitivity to carbachol, histamine, and adenosine.

Sparrow and Mitchell (1991) used bronchial segments obtained from the lungs of Large-white-/Landrace-cross **pigs** to study the modulation by the epithelium of the extent of bronchial narrowing produced by substances perfused through the lumen.

Mitchell et al. (1989) compared the reactions of perfused bronchial segments and bronchial strips of *pigs* to histamine and carbachol.

Hulsman et al. (1992) recommended the perfused **human** bronchiolar tube as a suitable model.

Omari et al. (1993) studied the responsiveness of human isolated bronchial segments and its relationship to epithelial loss.

REFERENCES AND FURTHER READING

Baersch G, Frölich JC (1996) A new bioassay to study contractile and relaxant effects of PGE_2 on perfused guinea pig trachea. J Pharmacol Toxicol Meth 36:63–68

Fedan JS, Frazer DG (1992) Influence of epithelium on the reactivity of guinea pig isolated, perfused trachea to bronchoactive drugs. J Pharm Exp Ther 262:741–750

Fernandes LB, Paternon JW, Goldie RG (1989) Co-axial bioassay of smooth muscle relaxant factor released from guinea-pig tracheal epithelium. Br J Pharmacol 96:117–124

Hulsman AR, Raatgeep HR, Bonta IL, Stijnen T, Kerrebijn KF, de Jongste JC (1992) The perfused human bronchiolar tube. Characteristics of a new model. J Pharm Toxicol Meth 28:29–34

Lewis CA, Broadley KJ (1995) Influence of spasmogen inhalation by guinea pigs upon subsequent demonstration of ovalbumin-induced hyperreactivity in isolated airway tissues. J Pharmacol Toxicol Meth 34:187–198

Mitchell HW, Willet KE, Sparrow MP (1989) Perfused bronchial segment and bronchial strip: narrowing vs. isometric force by mediators. J Appl Physiol 66:2704–2709

Munakata M, Mitzner W, Menkes H (1988) Osmotic stimuli induce epithelial-dependent relaxation in the guinea pig trachea. J Appl Physiol 64:466–471

Munakata M, Huang I, Mitzner W, Menkes H (1989) Protective role of epithelium in the guinea pig airway. J Appl Physiol 66:1547–1552

Omari TI, Sparrow MP, Mitchell HW (1993) Responsiveness of human isolated bronchial segments and its relationship to epithelial loss. Br J Clin Pharmacol 35:357–365

Pavlovic D, Fournier M, Aubier M, Pariente R (1989) Epithelial vs. serosal stimulation of tracheal muscle: role of epithelium J Appl Physiol 67:2522–2526

Sparrow MP, Mitchell HW (1991) Modulation by the epithelium of the extent of bronchial narrowing produced by substances perfused through the lumen. Br J Pharmacol 103:1160–1164

Yang J, Mitzner W, Hirshman C (1991) Role of epithelium in airway smooth muscle responses to relaxant agents. J Appl Physiol 71:1434–1440

D.2.1.4 Bronchial Perfusion of Isolated Lung

PURPOSE AND RATIONALE

Bronchial perfusion of the isolated lung was described by Sollmann and von Oettingen (1928) as a simple method for studying pharmacological reactions of bronchiolar muscle. The method consists in perfusing fluid down the trachea through the bronchi, and allowing it to escape from the alveoli through scratches on the surface of the lungs. Bronchoconstriction results in a reduced rate of flow, bronchodilatation is indicated by an increased flow. The method has been used to evaluate sympathomimetic drugs by Tainter et al. (1934) and by Luduena et al. (1957).

PROCEDURE

Guinea pigs weighing about 200 g are sacrificed by a head blow. The chest is opened, the trachea cut at the upper end and removed with the lung. The trachea is attached to the cannula of an perfusion apparatus. Only one lung is perfused, the other being tied off. The lower part of the lower lobe is cut off and the rest of the lung surface is scratched deeply assuring maximal pre-medication flow.

The perfusion fluid has the following composition in percentage of anhydrous salts: NaCl 0.659, $NaHCO_3$ 0.252, KCl 0.046, $CaCl_2$ 0.005, $MgCl_2$ 0.0135, NaH_2PO_4 0.01, Na_2HPO_4 0.008, glucose 5%, pH 8.0. The temperature of the perfusion medium is 37.5°C and the lung is enclosed in

a glass cylinder to be protected from variations in the environmental temperature.

The trachea is attached to the cannula of a perfusion apparatus which pumps the solution at a constant rate into a manometric tube connected with the perfused organ. Resistance to the flow (bronchoconstriction) results in an increase in the height of the column of fluid in the manometer. The intensity of bronchodilator effect is measured by the fall of the column in the manometer.

After the lung is attached to a T-shaped cannula, the pump is set in motion and the fluid, after filling the lung, flows out of the system through the third opening of the cannula. By gentle pressure air bubbles are forced out of the lung into the overflow. The lung is then treated in the aforesaid manner, and the upper outlet of the cannula closed. Histamine HCl is added in a concentration of 1:2500000 as soon as the perfusion starts and the flow is adjusted to obtain a constant progressive increase in pressure.

The drugs are injected near the cannula when the perfusion pressure reaches a level of 500–650 ml of water. The volume injected is always 0.1 ml.

Each drug is tested for bronchodilating activity against the bronchoconstriction induced by histamine in parallel with l-arterenol following a Latin square, including three doses of each drug and three doses of l-arterenol graded at 0.5 log intervals.

EVALUATION

Activity ratios of bronchodilating agents versus the standard can be calculated with a 3 + 3 point assay including confidence limits.

REFERENCES AND FURTHER READING

Luduena FP, von Euler L, Tullar BF, Lands AM (1957) Effect of the optical isomers of some sympathomimetic amines on the guinea pig bronchioles. Arch Int Pharmacodyn 111:392–400

Sollmann T, von Oettingen WF (1928) Bronchial perfusion of isolated lung as a method for studying pharmacologic reactions of bronchiolar muscle. Proc Soc Exp Biol Med 25:692–695

Tainter ML, Peddenm JR, James M (1934) Comparative actions of sympathomimetic compounds: bronchodilator actions in perfused guinea pig lungs. J Pharm Exp Ther 51:371–386

D.2.1.5 Vascular and Airway Responses in the Isolated Lung

PURPOSE AND RATIONALE

The isolated perfused rat lung allows the simultaneous registration of pulmonary vascular and airway responses to various drugs.

PROCEDURE

Male Sprague-Dawley rats weighing 300–350 g are intraperitoneally anesthetized with pentobarbital sodium (50 mg/kg). The trachea is cannulated with a short section of polyethylene tubing, connected to a rodent ventilator, and ventilated with room air enriched with 95% O_2/5% CO_2, with a tidal volume of 4–5 ml/kg and 2 cm H_2O positive end-respiratory pressure. The rats are heparinized with 1000 units of intravenous heparin and are rapidly exsanguinated by withdrawing blood from the carotid artery.

The lung is exposed by median sternotomy, and a ligature is placed around the aorta to prevent systemic loss of blood. The main pulmonary artery is catheterized, and the lung is removed en block and suspended in a warmed (39°C), humidified (100%) water-jacketed chamber. An external heat exchanger is used to maintain the temperature of the perfusate and the isolated lung chamber constant throughout the experiment. The perfusate solution (15 ml of heparinized blood and 5 ml modified Krebs-Henseleit solution) is placed in a reservoir and mixed constantly by a magnetic stirrer. The lungs are perfused with a peristaltic roller pump at a flow rate of 8–14 ml/min to maintain a physiological baseline pulmonary arterial perfusion pressure of 15 ± 0.5 mmHg. Pulmonary arterial perfusion pressure, airway pressure, and reservoir blood level are continuously monitored, electronically averaged and recorded with a polygraph.

EVALUATION

Changes (increase or decrease) in pulmonary arterial pressure and in airway pressure after injection of test compounds are measured in mm Hg and compared with baseline values.

MODIFICATIONS OF THE METHOD

Bernard et al. (1997) described an isolated perfused lung model with real time data collection and analysis of lung function. Male Sprague Dawley rats were anesthetized with 130 mg/kg pentobarbital i.p. The trachea was cannulated and then ventilated with 5% CO_2 and 95% air at e rate of 60 breath/min and a tidal volume of 2.5 ml. An injection of 650–700 units/kg of heparin was made into the right ventricle. A cannula was placed into the main pulmonary artery. The left ventricle was incised and the lungs were washed free of blood with warmed Krebs-Henseleit bicarbonate buffer with 4.5% BSA and 0.1% glucose. The left atrium was then cannulated to allow outflow of the perfusate. The lung was then removed and suspended in a chamber for perfusion. The flow rate of the perfusate

was adjusted to 8–10 ml/min/kg. Ventilation was maintained at 60 breaths/min with humidified and warmed gas. The lung was allowed to recover for 15 min at which time the lung mechanic parameters of flow, volume, transpulmonary pressure, pulmonary artery pressure, weight, resistance, elastance, and positive enddiastolic pressure were measured.

Hauge (1968) studied the conditions governing the pressor responses to ventilation hypoxia in isolated perfused rat lungs.

Uhlig and Heiny (1995) measured the weight of the isolated perfused rat lung during negative pressure ventilation for quantitating edema formation in the isolated lung.

Uhlig and Wollin (1994) described an improved setup for the isolated perfused rat lung. Breathing mechanic, such as tidal volume, pulmonary compliance, and pulmonary resistance, as well as perfusate characteristics, such as pulmonary vascular resistance, pulmonary pre- and postcapillary resistance, perfusate pH, P_{O2}, and P_{CO2}, and the capillary filtration coefficient were determined.

Byron et al. (1986) used the isolated perfused rat lung preparation for the study of aerosolized drug deposition and absorption.

Hendriks et al. (1999) published a modified technique of isolated left lung perfusion in the rat.

Riley et al. (1981) determined the tissue elastic properties of saline-filled isolated hamster lungs by measuring the pressure-volume relationships and studied the prevention of bleomycin-induced pulmonary fibrosis by *cis*-4-hydroxy-L-proline.

Lewis and Broadley (1995) tested the influence of spasmogen inhalation by **guinea pigs** upon subsequent demonstration of albumin-induced hyperreactivity in isolated airway tissues, such as perfused lung halves and tracheal spirals.

Corboz et al. (2000) used the isolated guinea pig lung to study the inhibition of capsaicin-induced bronchoconstriction by nociceptin. The lungs and the heart were removed en bloc from guinea pigs euthanized with an intraperitoneal overdose of sodium pentobarbital. The trachea and pulmonary artery were rapidly cannulated and half of the heart was cut to facilitate drainage. The lungs were then placed inside a warmed (37°C) glass chamber and suspended from a force displacement (Grass FT-03). They were mechanically ventilated with room air using a small animal ventilator. The respiratory rate was set at 60 strokes/min with a volume of 2.0 ml/stroke. Pulmonary inflation pressure was continuously monitored with a pressure transducer connected to a side arm of the tracheal cannula. Perfusion pressure was maintained with a peristaltic pump at a rate of 4.5–5.0 ml/min to produce a baseline pulmonary arterial pressure of between 6 and 14 cmH_2O. The pulmonary artery pressure was continuously monitored using a pressure transducer connected to the side arm of the pulmonary artery cannula. Transducers were connected to a polygraph for continuous monitoring of variables. The lungs were perfused with Tyrode's solution maintained at 37°C. Cumulative dose–response curves were constructed by adding increasing doses of capsaicin or the tachykinin NK_2 receptor agonist neurokinin A directly into the pulmonary artery. Test drugs were perfused 30 min before the addition of increasing doses of capsaicin or neurokinin A.

Anglade et al. (1998) measured the pulmonary capillary filtration coefficient in isolated **rabbit** lungs which were suspended by a string tied around the tracheal cannula from a counterbalanced force transducer to perform continuous weight measurement. To measure the pulmonary capillary filtration coefficient, pulmonary venous pressure was raised stepwise which results in an initial large weight gain for a few seconds followed by a slower rate of weight gain. The pulmonary capillary filtration coefficient was calculated on the slow phase of the weight curve by a time zero extrapolation or from the slope of the curve.

Nakamura et al. (1987) studied neurogenic pulmonary edema in lung perfusion preparations *in situ* in the **dog**.

Allen et al. (1993) studied the cardiovascular effects of a continuous prostacycline administration into an isolated *in situ* lung preparation in the dog.

Pogrebniak et al. (1994) investigated the influence of tumor necrosis factor in an isolated lung perfusion model in **pigs**.

The fluid filtration coefficient before and after infusion of *Escherichia coli* endotoxin was measured in excised **goat** lungs by Winn et al. (1988).

REFERENCES AND FURTHER READING

Allen DA, Schertel ER, Bailey JE (1993) Reflex cardiovascular effects of continuous prostacycline administration into an isolated *in situ* lung in the dog. J Appl Physiol 74:2928–2934

Anglade D, Corboz M, Menaouar A, Parker JC, Sanou S, Bayat S, Benchetrit G, Grimbert FA (1998) Blood flow vs. venous pressure effects on filtration coefficient in oleic-acid injured lung. J Appl Physiol 84:1011–1023

Bernard CE, Dahlby R, Hoener BA (1997) An isolated perfused lung model with real time data collection and analysis of lung function. J Pharmacol Toxicol Meth 38:41–46

Byron PR, Roberts NSR, Clark Ar (1986) An isolated perfused rat lung preparation for the study of aerosolized drug deposition and absorption. J Pharm Sci 75:168–172

Corboz MR, Rivelli MA, Egan RW, Tulshian D, Matasi J, Fawzi AB, Benbow L, Smith-Torhan A, Zhang H, Hey JA (2000) Nociceptin inhibits capsaicin-induced bronchoconstriction in isolated guinea pig lung. Eur J Pharmacol 402:171–179

Hauge A (1968) Conditions governing the pressor responses to ventilation hypoxia in isolated perfused rat lungs. Acta Physiol Scand 72:33–44

Hendriks JHM, van Schil PEY, Eyskens EJM (1999) Modified technique of isolated left lung perfusion in the rat. Eur Surg Res 31:93–96

Nakamura J, Zhang S, Ishikawa N (1987) Role of pulmonary innervation in canine *in situ* lung-perfusion preparation: a new model of neurogenic pulmonary edema. Clin Exp Pharmacol Physiol 14:535–542

Lewis CA, Broadley KJ (1995) Influence of spasmogen inhalation by guinea pigs upon subsequent demonstration of albumin-induced hyperreactivity in isolated airway tissues. J Pharmacol Toxicol Meth 34:187–198

Nossaman BD, Feng CJ, Kadowith PJ (1994) Analysis of responses to bradykinin and influence of HOE 140 in the isolated perfused rat lung. Am J Physiol Heart Circ Physiol 266:H2452–2461

Pogrebniak HW, Witt CJ, Terrill R, Kranda K, Travis WD, Rosenberg SA, Pass HI, Graeber GW, Webb WR, Mathisen DJ (1994) Isolated lung perfusion with tumor necrosis factor: A swine model in preparation of human trials. Ann Thorac Surg 57:1477–1483

Riley DJ, Kerr JS, Berg RA, Ianni BD, Pietra GG, Edelman NH, Prockop DJ (1981) Prevention of bleomycin-induced pulmonary fibrosis in the hamster by *cis*-4-hydroxy-L-proline. AM Rev Respir Dis 123:388–392

Uhlig S, Heiny O (1995) Measuring the weight of the isolated perfused rat lung during negative pressure ventilation. J Pharmacol Toxicol Meth 33:147–152

Uhlig S, Wollin L (1994) An improved setup for the isolated perfused rat lung. J Pharmacol Toxicol Meth 31:85–94

Winn R, Nickelson S, Rice CL (1988) Fluid filtration coefficient of isolated goat lungs was unchanged by endotoxin. J Appl Physiol 64:2463–2467

D.2.2 In Vivo Tests

D.2.2.1 Bronchospasmolytic Activity in Anesthetized Guinea Pigs (Konzett–Rössler method)

PURPOSE AND RATIONALE

The principle war first described by Kiese (1935). Konzett and Rössler (1940) published a method suitable for screening procedures which found worldwide acceptance. A survey on the history and further modifications was given by Döring and Dehnert (1997).

The method is based on registration of air volume changes of a living animal in a closed system consisting of the respiration pump, of the trachea and the bronchi as well as of a reservoir permitting measurement of volume or pressure of excess air. Bronchospasm decreases the volume of inspired air and increases the volume of excess air. Thus, the degree of bronchospasm can be quantified by recording the volume of excess air. Administration of spasmogens like acetylcholine, histamine, bradykinin, serotonin, ovalbumin, PAF, substance P, methacholine or leukotrienes, results in contraction of bronchial smooth muscle.

The method permits the evaluation of a drug's bronchospasmolytic effect by measuring the volume of air, which is not taken up by the lungs after bronchospasm.

PROCEDURE

Guinea-pigs of either sex weighing 250–500 g are anaesthetized with 1.25 g/kg i.p. urethane. Pentobarbital (60 mg/kg s.c.) and alcuronium chloride (1 mg/kg s.c.) are to be preferred when the bronchospasm is elicited by PAF or substance P. Anesthesia has to be deep enough in order to prevent influence of spontaneous respiration. The trachea is cannulated by means of a two way cannula, one arm of which is connected to the respiratory pump and the other to a Statham P23 Db transducer. The animal is artificially respired using a Starling pump with an inspiratory pressure set at 90–120 mm of water, an adequate tidal volume of 3 ml/100 g body weight and a frequency of 60 strokes per minute. Excess air, not taken up by the lungs, is measured and recorded on a polygraph. The internal jugular vein is cannulated for the administration of spasmogens and test compounds. The carotid artery is cannulated for measuring blood pressure.

Testing

Guinea-pigs receive the following spasmogens by i.v. administration:

- acetylcholine hydrochloride (20–40 µg/kg), or
- methacholine (20–40 µg/kg), or
- histamine dihydrochloride (5–20 µg/kg), or
- bradykinin triacetate (10–20 µg/kg), or
- ovalbumin (1 mg/kg), or
- PAF (25–50 ng/ml), or
- leukotrienes LTC_4, LTD_4 (about 1 µg/kg), or
- substance P (0.5 µg/kg).

After obtaining two bronchospasms of equal intensity, test compounds are administered i.v., p.o., s.c. or intraduodenally.

The spasmogen is given again at the following time intervals:

- 5, 15 and 30 min after i.v. administration of the drug
- 15, 30 and 60 min after intraduodenal administration of the drug
- 30 and 60 (sometimes also 120) min after p.o. administration of the drug.

The following standard compounds are used:

- atropine sulfate (0.01 mg/kg, i.v.) to inhibit acetylcholine or methacholine induced spasms
- aminophylline (6 mg/kg, i.v.) to inhibit bradykinin induced spasms
- tolpropamine-HCl (0.2 mg/kg) to inhibit histamine induced spasms
- imipramine-HCl (3–5 mg/kg) to inhibit serotonin-kreatinin-sulphate induced spasms.

EVALUATION

Results are expressed as percent inhibition of induced bronchospasm over the control agonistic responses. The ED_{50} value is calculated.

CRITICAL ASSESSMENT OF THE METHOD

The "Konzett-Roessler"-method has been proven to be a standard procedure in respiratory pharmacology being modified by several authors (Rosenthale and Dervinis 1968).

MODIFICATIONS OF THE METHOD

Forced insufflation was proposed as a simple but accurate inhalation procedure for investigating the activity of anti-asthmatic drugs in guinea pigs by Schiantarelli et al. (1982).

Lundberg et al. (1983), Belvisi et al. (1989), Miura et al. (1994) determined airway opening pressure (P_{ao}) as an index for tracheobronchial resistance to air flow.

Orr and Blair (1969) and Riley et al. (1987) sensitized rats intravenously with a potent antiserum to ovalbumin, obtained by infecting ovalbumin-sensitized donor rats with the parasitic nematode *Nippostrongylus brasiliensis* in order to boost IgE antibody production. The anesthetized animals were challenged with ovalbumin 48 h after sensitization and the subsequent increase in tracheal pressure was recorded.

Collier et al. (1993), Collier and James (1967) published a modification of the Konzett-Rössler-method using the forced re-inflation to overcome the severe bronchoconstriction occurring in sensitized guinea pigs.

Further modifications are by Schliep et al. (1986), Marano and Doria (1993).

Groeben and Brown (1996) measured changes in the cross-sectional area of conducting airways by cumulative doses of ipratropium with and without gallamine, a selective M_2 muscarinic receptor blocker, and after metaproterenol in anesthetized **dogs** using high-resolution computed tomography. Using a Somatom Plus scanner (Siemens), 50 to 55 contiguous scans were obtained, starting approximately 5 mm above the origin of the right upper lobe bronchus from the trachea and proceeding caudally using 1-mm table feed and 2-mm slice thickness. The dogs were anesthetized with thiopental. After paralysis was induced by succinylcholine, the trachea was intubated and the lungs ventilated with a volume-cycled ventilator with 100% oxygen. During the scans, the dogs were apneic at function residual capacity (approximately 2 min). Images were reconstructed using a high-spatial frequency algorithm.

REFERENCES AND FURTHER READING

Belvisi MG, Chung KF, Jackson DM, Barnes PJ (1989a) Opioid modulation of non-cholinergic neural bronchoconstriction in guinea-pig *in vivo*. Br J Pharmacol 97:1225–1231

Belvisi MG, Ichinose M, Barnes PJ (1989b) Modulation of non-adrenergic, non-cholinergic neural bronchoconstriction in guinea-pig airways via $GABA_B$-receptors. Br. J Pharmacol 97:1225–1231

Collier HOJ, Hammond AR, Whiteley B (1963) Anti-anaphylactic action of acetylsalicylate in guinea pig lung. Nature 200:176–178

Collier HOJ, James GWL (1967) Humoral factors affecting pulmonary inflation during acute anaphylaxis in the guinea pig *in vivo*. Br J Pharmacol 30:283–301

De la Motta S (1991) Simultaneous measurement of respiratory and circulatory parameters on anesthetized guinea pigs. Seventh Freiburg Focus on Biomeasurement (FFB7) Publ. by Biomesstechnik Verlag, 79232 March, Germany. B IV, pp 45–65

Döring HJ, Dehnert H (1997) Methoden zur Untersuchung der Atmungsorgane für die experimentelle Pharmakologie und Physiologie. Biomesstechnik-Verlag March GmbH, D-79323 March, Germany, pp 225–288

Groeben H, Brown RH (1996) Ipratropium decreases airway size in dogs by preferential M_2 muscarinic receptor blockade *in vivo*. Anesthesiology 85:867–873

Kiese M (1935) Pharmakologische Untersuchungen an der glatten Muskulatur der Lunge (insbesondere mit einigen ephedrinartigen Substanzen) Naunyn Schmiedeberg's Arch exp Path Pharmakol 178:342–366

Konzett H, Rössler R (1940) Versuchsanordung zu Untersuchungen an der Bronchialmuskulatur. Naunyn-Schmiedeberg's Arch Exp Path Pharmakol 192:71–74

Lau WAK, Rechtman MP, Boura ALA, King RG (1989) Synergistic potentiation by captopril and propranolol of bradykinin-induced bronchoconstriction in the guinea-pig. Clin Exp Pharmacol Physiol 16:849–857

Lefort J, Vargaftig BB (1978) Role of platelets in aspirin-sensitive bronchoconstriction in the guinea pig; interactions with salicylic acid. Br J Pharmacol 63:35–42

Lundberg JM, Brodin E, Saria A (1983) Effects and distribution of vagal capsaicin-sensitive substance P neurons with special reference to the trachea and lungs. Acta Physiol Scand 119:243–252

Marano G, Doria GP (1993) Lung constant-pressure inflation: fluid dynamic factors are the basis of airway overpressure during bronchoconstriction. Pharmacol Res 28:185–192

Miura M, Belvisi MG, Barnes PJ (1994) Modulation of non-adrenergic noncholinergic neural bronchoconstriction by bradykinin in anesthetized guinea pigs *in vivo*. J Pharm Exp Ther 268:482–486

Orr TSC, Blair AMJN (1969) Potentiated reagin response to egg albumin and conalbumin in *Nippostrongylus brasiliensis* infected rats. Life Sci 8:1073–1077

Riley PA, Mather ME, Keogh RW, Eady RP (1987) Activity of nedocromil sodium in mast-cell-dependent reactions in the rat. Int Arch Allergy Appl Immun 82:108–110

Rosenthale ME, Dervinis A (1968) Improved apparatus for measurement of guinea pig lung overflow. Arch Int Pharmacodyn 172:91–94

Schiantarelli P, Bongrani S, Papotti M, Cadel S (1982) Investigation of the activity of bronchodilators using a simple but accurate inhalation procedure: forced insufflation. J Pharmacol Meth 8:9–17

Schliep HJ, Schulze E, Harting J, Haeusler G (1986) Antagonistic effects of bisopropol on several β-adrenoceptor-mediated actions in anesthetized cats. Eur J Pharmacol 123:253–261

D.2.2.2 Effect of Arachidonic Acid or PAF on Respiratory Function In Vivo

PURPOSE AND RATIONALE

Based on the classical method of Konzett and Rössler (1940), Lefort and Vargafting (1978), Vargafting et al. (1979) studied the effects of arachidonic acid and PAF on respiratory function of guinea pigs *in vivo*.

Arachidonic acid is metabolized into thromboxane (TXA_2) and prostacyclin (PGI_2). TXA_2 produced in the lung leads to bronchoconstriction, which is independent from circulating platelets and leukotrienes; TXA_2 produced intracellularly in platelets induces a reversible thrombocytopenia. PGI_2 produced in the vessel wall leads to the reduction of systolic and diastolic blood pressure. All three effects are inhibited by drugs which block cyclo-oxygenase. In contrast, agents which block thromboxane synthetase inhibit bronchoconstriction and thrombocytopenia, but lead to a potentiation of blood pressure reduction.

In contrast to arachidonic acid, PAF as inducer leads to bronchoconstriction, which is platelet-dependent. In addition, PAF induces thrombocytopenia, leukocytopenia, reduction of blood pressure and increase of hematocrit. These effects are also reversible, but more persistent than those induced by arachidonic acid, and quickly result in tachyphylaxis. The test allows to evaluate the sites of action of drugs, which interfere with the mechanisms of bronchoconstriction and thrombocytopenia; in an *in vivo*-model guinea pigs are challenged with the spasmogens and platelet-aggregating substances arachidonic acid or PAF (platelet activating factor).

PROCEDURE

Male guinea pigs (Pirbright White) weighing 300–600 g are anesthetized with 60 mg/kg pentobarbital sodium (i.p.). One of the jugular veins is cannulated for the administration of spasmogen and test compound. Both external carotid arteries are cannulated; one is connected to a pressure transducer to register blood pressure, the other is used for blood withdrawal. The trachea is connected to a Starling pump with an inspiratory pressure set of 80 mm H_2O, an adequate tidal volume of approx. 10 ml/kg body weight and a frequency of 70–75 strokes/min. Spontaneous respiration is inhibited by intravenous injection of pancuronium (4 mg/kg) or gallamine (2 mg/kg) on time.

In some experiments, pulmonal β-receptors are blocked by intraperitoneal administration of propranolol (2 mg/kg).

Excess air, not taken up by the lungs, is conducted to a transducer with bronchotimer (Rhema, Germany) which translates changes in air flow to an electrical signal. Changes in air flow and arterial blood pressure are recorded continuously.

Animals receive multiple intravenous injections of the same dose of arachidonic acid (Sigma, 250–600 µg/kg prepared from a stock solution 10 mg/ml ethanol, 1:20 dilution with Na_2CO_3) until two bronchospasms of equal intensity are obtained. The test compound is administered intravenously and the spasmogen is given again at the following intervals: 2, 10, 20 and, if necessary, 30 min after administration of the drug.

Ordinarily, the lung has to be passively dilated (bronchotimer) after each of the bronchoconstrictions. Immediately before and 30–45 s after each of the arachidonic acid applications, approx. 50 µl blood are collected into Na-EDTA-coated tubes. The number of thrombocytes is determined with a platelet analyzer (Becton Dickinson Ultra-Flo-100 or Baker 810) in 10 µl samples of whole blood.

PAF (Paf-acether C16, Bachem, 0.03–0.04 µg/kg in 0.9% saline+0.1% human serum albumin) as inducer is injected intravenously 60 min before, 5 min and, if necessary, 60 min after intravenous drug administration. Blood samples are collected 30 s before and 15 s after each of the PAF applications. The number of leukocytes and hematocrit values are determined automatically (TOA-microcell counter CC 108, Colora Meßtechnik).

Standard compounds:

- dazoxiben HCl (inhibitor of thromboxane synthetase, TSI)
- acetylsalicylic acid (inhibitor of cyclo-oxygenase, COI)

EVALUATION

Percent inhibition or increase of bronchospasm, reduction of blood pressure, thrombocytopenia, leukocytopenia and hematocrit following test drug administration are calculated in comparison to control values before drug treatment. For the reduction of blood pressure, both the magnitude [mm Hg, systolic and diastolic] and the duration [min] are determined. Even a sole increase in duration of blood pressure reduction is considered as an increase of the effect. From the pattern profile of the influence on bronchoconstriction, thrombocytopenia and blood pressure reduction, the mechanism of action of a test drug is concluded:

- inhibitor of thromboxane synthetase
- inhibitor of cyclo-oxygenase
- other effect = no profile

In addition, the inherent action of the test substance on blood pressure is determined before arachidonic acid- or PAF-administration.

MODIFICATIONS OF THE METHODS

Kagoshima et al. (1997) used a modification of the Konzett-Rössler-method to test the suppressive effects of a PAF-antagonist on asthmatic responses in guinea pigs actively sensitized with ovalbumin. The immediate and the late asthmatic response were measured by the oscillation method according to Mead (1960).

Pauluhn (1994, 2004) described inhalation systems, mainly for toxicological studies, by which large numbers of animals can be studied simultaneously.

REFERENCES AND FURTHER READING

Kagoshima M, Tomomatsu N, Iwahisha Y, Yamaguchi S, Matsuura M, Kawakami Y, Terasawa M (1997) Suppressive effects of Y-24180, a receptor antagonist to platelet activating factor (PAF), on antigen-induced asthmatic responses in guinea pigs. Inflamm Res 46:147–153

Lefort J, Vargaftig BB (1978) Role of platelets in aspirin-sensitive bronchoconstriction in the guinea pig; interactions with salicylic acid. Br. J. Pharmac. 63:35–42

Mead J (1960) Control of respiratory frequency. J Appl Physiol 15:325–336

Pauluhn J (1994) Validation of an improved nose-only exposure system for rodents. J Appl Toxicol 14:55–63

Pauluhn J (2004) Acute inhalation studies with irritant aerosols: technical issues and relevance for risk characterization. Arch Toxicol 78:243–251

Vargaftig BB, Lefort J, Prancan AV, Chignard M, Benveniste J (1979) Platelet-lung *in vivo* interactions: An artifact of a multipurpose model?. Haemostasis 8:171–182

D.2.2.3 Bronchial Hyperreactivity

PURPOSE AND RATIONALE

Symptoms like asphyctic convulsions resembling bronchial asthma in patients can be induced by inhalation of histamine or other bronchospasm inducing agents in guinea pigs. The challenging agents are applied as aerosols produced by an ultra-sound nebulizer. The first symptoms are increased breathing frequency, forced inspiration, and finally asphyctic convulsions. The occurrence of these symptoms can be delayed by antagonistic drugs. Pre-convulsion time, i. e. time until asphyctic convulsions, can be measured.

PROCEDURE

Ten male albino guinea pigs weighing 300–400 g per group are used. The inhalation cages consist of 3 boxes each ventilated with an air flow of 1.5 l/min. The animal is placed into box A to which the test drug or the standard is applied using an ultra-sound nebulizer LKB NB108 which provides an aerosol of 0.2 ml solution of the test drug injected by an infusion pump within 1 min. Alternatively, the animal is treated orally or subcutaneously with the test drug or the standard. Box B serves as a sluice through which the animal is passed into box C. There, the guinea pig is exposed to an aerosol of a 0.1% solution of histamine hydrochloride provided by an ultra-sound nebulizer (De Vilbiss, Model 35 A). Time until appearance of asphyctic convulsions is measured. Then, the animal is immediately withdrawn from the inhalation box. The aerosols are removed from the back wall of the boxes by applying low pressure.

EVALUATION

Percent of increase of pre-convulsion time is calculated versus controls. ED_{50} values can be found, i. e. 50% of increase of pre-convulsion time.

CRITICAL ASSESSMENT OF THE METHOD

The "guinea pig asthma" has been applied as useful method in various modifications by many laboratories.

MODIFICATIONS OF THE METHODS

Simple methods to test bronchospasmolytic activity in conscious animals, called "thoracography" were described by Herxheimer (1956) Olsson (1971), Beume et al. (1985). A silicon tube with a diameter of 1 mm is filled with mercury and serves as strain gauge applied as belt around the thorax of conscious guinea pigs. Changes in electrical resistance due to breathing

movements of the thorax are registered. The animals are exposed in a Plexiglas chamber to acetylcholine nebulized by an ultrasonic device. Time until onset of coughing indicated by an increase of signal amplitude and of severe asthmatic dyspnoea is registered.

Immunological factors are involved in bronchial hyperreactivity (Reynolds 1991).

Harris et al. (1976) immunized rabbits with thermophilic actinomyces antigen (Micropolyspora faeni). Lesions resembling hypersensitivity in man were found, characterized by a mononuclear cell interstitial reaction and a marked increase in the number of intra-alveolar cells.

Ufkes et al. (1983) induced bronchial and cardiovascular anaphylaxis in Brown-Norway rats, sensitized with trinitrophenyl haptenized ovalbumin and $AlPO_4$ as adjuvant 12 days prior to challenge with trinitrophenyl haptenized bovine serum albumin intravenously.

Raeburn et al. (1992) gave a survey on techniques for drug delivery to the airways and the assessment of lung functions in animal models including parameters such as lung compliance and airway resistance.

Elwood et al. (1992) studied the effects of dexamethasone and cyclosporin A on the airway hyperresponsiveness and the influx of inflammatory cells into bronchoalveolar lavage fluid seen 18 to 24 h after exposure to aerosolized ovalbumin in actively ovalbumin-sensitized Brown-Norway rats.

Schmiedl et al. (2003) found an increase of inactive intra-alveolar surfactant subtypes in lungs of asthmatic Brown Norway rats. The volume fractions of surfactant subtypes and the epithelial surface fraction covered with alveolar edema were determined by point and intersection counting. The surface activity of surfactant from broncho-alveolar lavage was determined as the minimum surface tension at minimal bubble size with a pulsating bubble surfactometer.

Pahl et al. (2002) and Kuss et al. (2003) exposed ovalbumin-sensitized Brown Norway rats to an ovalbumin-containing aerosol in a nose-only inhalation system (TSE, Bad Homburg, Germany) for 1 h to provoke an influx of inflammatory cells into the airways. At the time of maximal influx of eosinophilic granulocytes into the airways (48 h later), the animals were sacrificed and a broncho-alveolar lavage was performed.

A model of bronchial hyperreactivity after active anaphylactic shock in conscious guinea pigs has been described by Tarayre et al. (1990). The guinea pigs were sensitized by an intramuscular injection of a large dose of ovalbumin in Freund's adjuvant. The administration of ovalbumin to induce anaphylactic shock was by aerosol. Bronchial hyperreactivity to histamine was observed 3–6 h after the anaphylactic shock.

Bolser et al. (1995) sensitized guinea pigs by intraperitoneal injection of 200 µg/kg ovalbumin mixed with 200 mg/kg aluminum hydroxide. The animals were placed 28 days later in a transparent plastic chamber and exposed to aerosols of ovalbumin (0.1%–1%) at an airflow of 4 l/min to elicit coughing. Coughs were detected by a microphone placed in the chamber and connected to an audio monitor and chart recorder. The number of coughs elicited during a 4-min exposure was counted by visual inspection of the chart record.

Pons et al. (2000) described a guinea pig model of asthma. Animals were sensitized by two intraperitoneal injections of 20 µg ovalbumin and 100 mg aluminum hydroxide given 24 h apart. The sensitized animals were anesthetized and mechanically ventilated. Air flow was measured with a pneumotachograph, along with transpulmonary pressure and arterial pressure. Lung resistance and dynamic compliance were calculated. Then, 30 min after administration of test drug, the animals were challenged by inhaled ovalbumin (5 mg/ml).

The importance of eosinophil activation for the development of allergen-induced bronchial hyperreactivity was underlined by Santing et al. (1994). A significant increase in bronchoreactivity to histamine was observed at 6 h after allergen exposure, which was associated with an increase of eosinophils in the bronchoalveolar lavage and an increase in the eosinophil peroxidase activity.

The increased pulmonary vascular permeability may be related to the adult respiratory distress syndrome in man (Snapper and Christman 1989).

The infusion of small amounts of *Escherichia coli* endotoxin into chronically instrumented awake **sheep** results in well-characterized pulmonary dysfunction (Brigham and Meyrick 1986).

One animal model associated with both increased airway responsiveness and pulmonary inflammation is endotoxemia in sheep (Hutchinson et al. 1983).

The effect of a platelet activating factor receptor antagonist on the sheep's response to endotoxin was studied by Christman et al. (1987).

Chiba and Misawa (1995) characterized muscarinic cholinoceptors in airways of antigen-induced airway hyperresponsive rats. The animals were sensitized with 2,4-dinitrophenylated *Ascaris suum* extract together with *Bordetella pertussis* (2×10^6 as an adjuvant and were boosted with 2,4-dinitrophenylated *Ascaris suum* extract 5 days later. Isometric contractions of the circu-

lar muscle of isolated bronchial rings after addition of increasing doses of acetylcholine were measured with a force-displacement transducer.

Laboratory infection of **primates** with *Ascaris suum* may provide a model of allergic bronchoconstriction (Patterson et al. 1983; Pritchard et al. 1983; Eady 1986).

Richards et al. (1986) used various models of airway hypersensitivity, such as inhalation of *Ascaris suum* antigen in monkeys and dogs.

Rylander and Marchat (1988) studied the effect of a corticosteroid on an acute inflammation in the lungs of guinea pigs exposed to an aerosol of bacterial endotoxin. The subsequent inflammatory response was evaluated counting the number of cells obtained from airway lavage and in the lung interstitium as well as the chemotactic effect of alveolar macrophages.

Hatzelmann et al. (1996) reported on automatic leukocyte differentiation in broncho-alveolar lavage fluids of guinea pigs and Brown-Norway rats using an automatic cell analyzing system (Cobas Helios 5Diff; Hoffmann-La Roche; Grenzach-Wyhlen, Germany).

Minshall et al. (1993) demonstrated that neonatal immunization of **rabbits** with *Alternia tenuis* can lead to the development of persistent airway hyperresponsiveness.

Okada et al. (1995) studied late asthmatic reactions in **guinea pigs** sensitized with *Ascaris* antigen. They evaluated interleukin-1 production by immunostaining with anti-IL-1β antibody and elucidated the action of IL-1 in late asthmatic reactions with recombinant IL-1 receptor antagonist.

Folkerts et al. (1995) found that intratracheal inoculation of *parainfluenza type 3 virus* to guinea pigs induces a marked increase of airway responsiveness to increasing doses of intravenous histamine. In spontaneously anesthetized breathing guinea pigs, inhalation of an aerosol containing the nitric oxide precursor L-arginine completely prevented the virus-induced hyperresponsiveness to histamine.

Fryer et al. (1994, 1997) measured M_2 muscarinic receptor function in anesthetized and paralyzed guinea pigs by electrical stimulation of both vagus nerves producing bronchoconstriction (measured as pulmonary inflation pressure) and bradycardia.

REFERENCES AND FURTHER READING

Beume R, Kilian U, Mussler K (1985) Die Prüfung bronchospasmolytischer Substanzen am wachen Meerschweinchen. Atemw – Lungenkrh 11:342–345

Bolser DC, DeGennaro FC, O'Reilly S, Hey JA, Chapman RW (1995) Pharmacological studies of allergic cough in the guinea pig. Eur J Pharmacol 277:159–164

Brigham KL, Meyrick B (1986) Endotoxin and lung injury: state of the art review. Am Rev Respir Dis 133:913–927

Chiba Y, Misawa M (1993) Strain differences in change in airway hyperresponsiveness after repeated antigenic challenge in three strains of rats. Gen Pharmacol 24:1265–1272

Chiba Y, Misawa M (1995) Characteristics of muscarinic cholinoceptors in airways of antigen-induced airway hyperresponsive rats. Comp Biochem Physiol 111C:351–357

Christman BW, Lefferts PL, Snapper JR (1987) Effect of a platelet activating factor receptor antagonist (SRI 63–441) on the sheep's response to endotoxin. Am Rev Respir Dis 135:A82

Eady RP (1986) The pharmacology of nedocromil sodium. Eur J Respir Dis 69: (Suppl 147):112–119

Elwood W, Lötvall JO, Barnes PJ, Chung KF (1992) Effect of dexamethasone and cyclosporin A on allergen-induced airway hyperresponsiveness and inflammatory cell responses in sensitized Brown-Norway rats. Am Rev Respir Dis 145:1289–1294

Folkerts G, van der Linde HJ, Nijkamp FP (1995) Virus-induced airway hyperresponsiveness in guinea pigs is related to a deficiency in nitric oxide. J Clin Invest 95:26–30

Fryer AD, Yarkony KA, Jacoby DB (1994) The effect of leukocyte depletion on pulmonary M_2 muscarinic receptor function in parainfluenza virus-infected guinea pigs. Br J Pharmacol 112:588–594

Fryer AD, Costello RW, Yost BL, Lobb RR, Tedder TF, Steeber DA (1997) Antibody to VLA-4, but not to L-selectin, protects neuronal M_2 muscarinic receptors in antigen-challenged guinea pig airways. J Clin Invest 99:2036–2044

Harris JO, Bice D, Salvaggio JE (1976) Cellular and humoral bronchopulmonary immune response of rabbits immunized with *thermophilic actinomyces* antigen. Am Rev Respir Dis 114:29–43

Hatzelmann A, Haefner D, Beume R, Schudt C (1996) Automatic leukocyte differentiation in bronchoalveolar lavage fluids of guinea pigs and Brown-Norway rats. J Pharmacol Toxicol Meth 35:91–99

Herxheimer H (1956) Bronchoconstrictor agents and their antagonists in the intact guinea pig. Arch Int Pharmacodyn 106:371–380

Hutchinson AA, Hinson JM, Brigham KL, Snapper JL (1983) Effect of endotoxin on airway responsiveness to aerosol histamine in sheep. J Appl Physiol 54:1463–1468

Kallos P, Pagel W (1937) Experimentelle Untersuchungen über Asthma bronchiale. Acta Med Scand 91:292–305

Kuss H, Hoefgen N, Johanssen S, Kronbach T, Rundfeldt C (2003) In vivo efficacy in airway disease models of *N*-(3,5-dichloro-pyrid-4-yl)-[1-(4-fluorobenzyl)-5-hydroxy-indole-3-yl]-glycolic acid amide (AWD 12–281), a selective phosphodiesterase 4 inhibitor for inhaled administration. J Pharmacol Exp Ther 307:373–385

Minshall EM, Riccio MM, Herd CM, Douglas GJ, Seeds EAM, McKennif MG, Sasaki M, Spina D, Page CP (1993) A novel animal model for investigating persistent airway hyperresponsiveness. J Pharmacol Toxicol Meth 30:177–188

Okada S, Inoue H, Yamauchi K, Iijima H, Okhawara Y, Takishima T, Shirato K (1995) Potential role of interleukin-1 in allergen-induced late asthmatic reactions in guinea pigs: Suppressive effect of interleukin-1 receptor antagonist on late asthmatic reaction. J Allergy Clin Immunol 95:1236–1245

Olsson OAT (1971) Histamine-induced bronchospasm in unanaesthetized guinea pigs. Acta Allergol 26:438–447

Pahl A, Zjang M, Kuss H, Szelenyi I, Brune K (2002) Regulation of IL-13 synthesis in human lymphocytes: implications for asthma therapy. Br J Pharmacol 135:1915–1926

Patterson R, Suszko IM, Harris KE (1983) The *in vivo* transfer of antigen-induced airway reactions by bronchial lumen cells. J Clin Invest 62:519–524

Pons R, Santamarïa P, Suchankova J, Cortijo J, Morcillo EJ (2000) Effects of inhaled glaucine on pulmonary responses to antigen in sensitized guinea pigs. Eur J Pharmacol 397:187–195

Pritchard DI, Eady PR, Harper ST, Jackson DM, Orr TSC, Richards IM, Trigg S, Wells E (1983) Laboratory infection of primates with *Ascaris suum* to provide a model of allergic bronchoconstriction. Clin Exp Immunol 54:469–476

Raeburn D, Underwood SL, Villamil ME (1992) Techniques for drug delivery to the airways, and the assessment of lung functions in animal models. J Pharmacol Toxicol Meth 27:143–159

Reynolds HY (1991) Immunologic system in the respiratory tract. Physiol Rev 71:1117–1133

Richards IM, Dixon M, Jackson DM, Vendy K (1986) Alternative modes of action of cromoglycate. Agents Actions 18:294–300

Rosenthale ME, Dervinis A (1968) Improved apparatus for measurement of guinea pig lung overflow. Arch Int Pharmacodyn 172:91–94

Rosenthale ME, Dervinis A, Begany AJ, Lapidus M, Gluckmann MI (1970) Bronchodilator activity of prostaglandin E_2 when administered by aerosol to three species. Experientia 26:1119–1121

Rylander R, Marchat B (1988) Modulation of acute endotoxin pulmonary inflammation by a corticosteroid. J Clin Lab Immunol 27:83–86

Santing RE, Hoekstra Y, Pasman Y, Zaagsma J, Meurs H (1994) The importance of eosinophil activation for the development of allergen-induced bronchial hyperreactivity in conscious, unrestrained guinea pigs. Clin Exp Allergy 24:1157–1163

Schmiedl A, Hoymann HG, Ochs M, Menke A, Fehrenbach A, Krug N, Tschernig T, Höhlfeld JM (2003) Increase of inactive intra-alveolar surfactant subtypes in lungs of asthmatic Brown Norway rats. Virchows Arch 442:56–65

Snapper JR, Christman BW (1989) Models of acute pulmonary inflammation. In: Pharmacological methods in the control of inflammation. Liss, New York, pp 255–281

Tarayre JP, Aliaga M, Barbara M, Tisseyre N, Vieu S, Tisne-Versailles J (1990) Model of bronchial hyperreactivity after active anaphylactic shock in conscious guinea pigs. J Pharmacol Meth 23:13–19

Ufkes JGR, Ottenhof M, Aalberse RC (1983) A new method for inducing fatal, IgE mediated, bronchial and cardiovascular anaphylaxis in the rat. J Pharmacol Meth 9:175–181

D.2.2.4 Body Plethysmography and Respiratory Parameters After Histamine-Induced Bronchoconstriction in Anesthetized Guinea Pigs

PURPOSE AND RATIONALE

Guinea pigs can be placed in a plethysmograph for measurement of respiratory parameters. Respiratory frequency and respiratory amplitude are recorded. The decrease of respiratory amplitude (diminished respiratory volume due to bronchoconstriction) and the reflectory increase of respiratory frequency after histamine inhalation are attenuated by bronchodilatatory drugs. Additional respiratory parameters can be recorded using a Fleisch tube and a catheter inserted into the pleural cavity (Englert et al. 1992). The method can be used for various purposes, e. g., to evaluate the antagonism against bradykinin-induced bronchoconstriction (Wirth et al. 1991, 1993) or the bronchodilator effects of potassium channel openers (Englert et al. 1992) or to measure the effect of morphine on respiration in rats (Kokka et al. 1965).

PROCEDURE

Guinea pigs of either sex weighing 400–600 g are anesthetized with 70 mg/kg pentobarbital i.p. The trachea, pleural cavity, jugular vein, and carotid artery are prepared and cannulated. The animals are mechanically ventilated with a Starling respiratory pump which delivers an inspiration volume that represents a tracheal pressure of 8 cm water at a rate of 60 strokes/min. Succinylcholine chloride at a dose of 1 mg/kg is given i.v. to prevent interference from spontaneous respiration. The guinea pigs are placed inside a whole body plethysmograph and tracheal, pleural, venous and arterial catheters are connected to onset ports in the wall of the plethysmograph box. The tracheal port is then connected with the respiration pump. **Airflow rate** into and out of the plethysmograph are measured as pressure difference with a No. 000 Fleisch tube and a differential pressure transducer (Fa. Hellige, PM 97 TC). Airflow is calibrated by passing compressed air through a rotameter. The **tidal volume** (V_T) is calculated from the flow signal. **Transpulmonary pressure** (P_{TP}) is measured with a differential pressure transducer (Hellige, PM 97 TC), with one side attached to a catheter inserted into the right pleural cavity and the other side connected to a side port of the tracheal cannula. P_{TP} is calibrated with a water manometer. Signals from airflow, tidal volume and transpulmonary pressure are fed into an on-line computer system (PO-NE-MAH, Model PF-1, Storrs) for calculation of **pulmonary resistance** (R_L) and **dynamic lung compliance** (C_{DYN}). These parameters are calculated for each breath with a sampling rate of $100\,s^{-1}$ for each circle. Flow and pressure signals for computation are obtained from a PLUGYS measuring system (Fa. Hugo Sachs Elektronik, Freiburg, Germany). Systemic arterial pressure is measured using a Statham pressure transducer (P 23 Db). Heart rate is computed from pressure pulses (Döring and Dehnert 1997).

Three doses of test compound or standard are injected intravenously. Saline injections serve as con-

trols. Intravenous injections of histamine (0.5–2 µg/kg) lead to a short decrease in C_{DYN} and to a short increase in R_L by approximately 200% compared with baseline. Challenges are repeated at 5-min intervals, yielding the same increase in R_L during the whole 1-h experimental period. After 3 reproducible responses the test agent is administered intravenously 1 min before the histamine injection.

To evaluate test compounds for inhalation route, aerosols are generated with an ultrasonic nebulizer (LKB, model NB 108) and are administered to the animals through a shunt in the afferent limb of the respiratory pump, allowing the inspired air to pass through the nebulizer chamber before entering the animals lungs.

EVALUATION

Inhibition of histamine induced bronchoconstriction by various doses of test compound and standard is recorded. ED_{50} values for inhibition in R_L are calculated. Furthermore, the time course of histamine antagonism can be evaluated. Compounds can be tested either after iv. injection of histamine (prevention) or during intravenous infusion of histamine (intervention).

CRITICAL ASSESSMENT OF THE METHOD

Whole body plethysmography has been proven to be a useful tool in respiratory pharmacology for studies on the antagonism against various bronchoconstrictors, such as histamine and bradykinin, as well as for airway pharmacology of potassium channel openers.

MODIFICATIONS OF THE METHOD

Several authors use body plethysmography to study respiratory functions in animals (Amdur and Mead 1958; Blümcke et al. 1967), Pennock et al. 1979; Agarwal (1981), James and Infiesto (1983), Kisagawa et al. (1984), Griffith-Johnson (1988), Danko and Chapman (1988), Ball et al. (1991), Chand et al. (1993).

The effect of β-blockers on pulmonary function and bronchoconstrictor responsiveness in **guinea pigs** and rats has been studied by Chapman et al. (1985).

Finney and Forsberg (1994) developed a technique for quantification of nasal involvement in a guinea pig plethysmograph. Nasal and lower respiratory system conductance could be measured simultaneously in anesthetized animals.

A whole body plethysmograph for conscious animals has been described by Elliott et al. (1991) and improvements by Linton (1991).

Studies of bronchospasmolytic agents with aerosol challenge in conscious guinea pigs using a double chamber plethysmograph box have been reported by Schlegelmilch (1991).

Ball et al. (1991) described a method for the evaluation of bronchoactive agents in the conscious guinea pig. The method involves the use of "head out" whole body plethysmographs from which respiratory rate can be recorded by monitoring respiration-related changes in pressure within the body chamber.

Hey et al. (1995) used a head-out, whole body plethysmograph to examine the effects of $GABA_B$ receptor agonists on minute ventilation, tidal volume and respiratory rate due to room air and carbon dioxide-enriches gas hyperventilation in conscious guinea pigs.

Murphy et al. (1998) developed a method for chronic measurement of pleural pressure in conscious **rats**. Pleural pressures were measured by surgically implanting a fluid-filled polyurethane catheter attached to a pressure-sensitive radiotelemetry transmitter (Model TA11PA-C40, Data Sciences Int., St. Paul, MN) beneath the pleural surface. A compatible receiver (Model RLA0120) and a data acquisition and analysis software system (LabPRO, Version 3) sampling at a rate of 500 Hz were used to analyze the telemetric signals.

Sinnett et al. (1981) described a fast integrated flow plethysmograph for small animals (**mice**).

Glaab et al. (2001) used tidal mid-expiratory flow in a head-out body plethysmograph as a measure of airway hyperresponsiveness in allergic mice.

Simple methods to determine respiratory parameters in small animals were described by Schütz (1960), Höbel et al. (1971).

Schlenker (1984) and Schlenker and Metz (1989) evaluated ventilatatory parameters in dystrophic **Syrian hamsters**.

Wasserman and Griffin (1977) studied bronchoactivity in the intact anesthetized **dog**.

Paré et al. (1976) determined pulmonary resistance and dynamic lung compliance in **rhesus monkeys**.

Wegner et al. (1984) measured dynamic respiratory mechanics in monkeys by forced oscillations generated by a loudspeaker in an airtight chamber.

REFERENCES AND FURTHER READING

Agrawal KP (1981) Specific airway conductance in guinea pigs: normal values and histamine induced fall. Resp Physiol 43:23–30

Amdur MO, Mead J (1958) Mechanics of respiration in unanesthetized guinea pigs. Am J Physiol 192:364–368

Arch JRS, Buckle DR, Bumstead J, Clarke GD, Taylor JF, Taylor SG (1988) Evaluation of the potassium channel activator cromakalim (BRL 34915) as a bronchodilator in the guinea pig: comparison with nifedipine. Br J Pharmacol 95:763–770

Ball DI, Coleman RA, Hartley RW, Newberry A (1991) A novel method for the evaluation of bronchoactive agents in the conscious guinea pig. J Pharmacol Meth 26:187–202

Blümcke S, Rode J, Niedorf HR (1967) Eine einfache Methode der Körper-Plethysmographie der Ratte. Naturwiss 54:343–344

Chand N, Nolan K, Pillar J, Lomask M, Diamantis W, Sofia RD (1993) Aeroallergen-induced dyspnea in freely moving guinea pigs: quantitative measurement by bias flow ventilated whole body plethysmography. Allergy 48:230–235

Chapman RW, Danko G, Siegel MI (1985) Effect of propranolol on pulmonary function and bronchoconstrictor responsiveness in guinea pigs and rats. Pharmacol Res Comm 17:149–163

Danko G, Chapman RW (1988) Simple, noninvasive method to measure antibronchoconstrictor activity of drugs in conscious guinea pigs. J Pharmacol Meth 19:165–173

Döring HJ, Dehnert H (1997) Methoden zur Untersuchung der Atmungsorgane für die experimentelle Pharmakologie und Physiologie. Biomesstechnik-Verlag March GmbH, D-79323 March, Germany, pp 267–288

Elliott RD, Fitzgerald MF, Clay TP (1991) A whole body plethysmograph for small animals. 7th Freiburg Focus on Biomeasurement. Cardiovascular and Respiratory *in vivo* Studies. Biomesstechnik-Verlag March GmbH, 79232 March, Germany, pp 66–71

Englert CE, Wirth K, Gehring D, Fürst U, Albus U, Scholz W, Rosenkranz B, Schölkens BA (1992) Airway pharmacology of the potassium channel opener, HOE 234, in guinea pigs: *in vitro* and *in vivo* studies. Eur J Pharmacol 210:69–75

Finney MJ, Forsberg KI (1994) Quantification of nasal involvement in a guinea pig plethysmograph. J Appl Physiol 76:1432–1438

Glaab T, Daser A, Brain A, Neuhaus-Steinmetz U, Fabel H, Alarie Y, Renz H (2001) Tidal midexpiratory flow as a measure of airway hyperresponsiveness in allergic mice. Am J Physiol 280:L565–L573

Griffith-Johnson DA, Nicholl PJ, McDermott M (1988) Measurement of specific airway conductance in guinea pigs. A noninvasive method. J Pharmacol Meth 19:233–242

Hey JA, Mingo G, Bolsner DC, Kreutner W, Krobatsch D, Chapman RW (1995) Respiratory effects of baclofen and 3-aminopropylphosphinic acid in guinea pigs. Br J Pharmacol 114:735–738

Höbel M, Maroske D, Eichler O (1971) Eine einfache Methode zur Bestimmung des Atemminutenvolumens von Ratten und Meerschweinchen. Arch Int Pharmacodyn 194:371–374

James JT, Infiesto BP (1983) Concurrent measurement of respiratory and metabolic parameters in rats during exposure to a test vapor: Respiratory stress test. J Pharmacol Meth 10:283–292

Kisagawa K, Saitoh K, Tanizaki A, Ohkubo K, Irino O (1984) A new method for measuring respiration in the conscious mouse. J Pharmacol Meth 12:183–189

Kokka N, Elliott HW, Way L (1965) Some effects of morphine on respiration and metabolism in rats. J Pharmacol Exp Ther 148:386–392

Linton P (1991) Improvements incorporated in the animal whole-body plethysmograph after Elliott et al. 7th Freiburg Focus on Biomeasurement. Cardiovascular and Respiratory *in vivo* Studies. Biomesstechnik-Verlag March GmbH, 79232 March, Germany, pp 72–76

Murphy DJ, Renninger JP, Gossett KA (1998) A novel method for chronic measurement of pleural pressure in conscious rats. J Pharmacol Toxicol Meth 39:137–141

Paré PD, Michoud MC, Hogg JC (1976) Lung mechanics following antigen challenge of *Ascaris suum*-sensitive rhesus monkeys. J Appl Physiol 41:668–676

Pennock BE, Cox CP, Rogers RM, Cain WA, Wells JH (1979) A noninvasive technique for measurements of changes in specific airway resistance. J Appl Physiol 46:399–406

Schlegelmilch R (1991) Respiratory measurements on conscious guinea pigs using a double chamber plethysmograph box with aerosol challenge. 7th Freiburg Focus on Biomeasurement. Cardiovascular and Respiratory *in vivo* Studies. Biomesstechnik-Verlag March GmbH, 79232 March, Germany, pp 136–140

Schlenker EH (1984) An evaluation of ventilation in dystrophic Syrian hamsters. J Appl Physiol 56:914–921

Schlenker EH, Metz TJ (1989) Ventilatory responses of dystrophic and control hamsters to naloxone. Pharmacol Biochem Behav 34:681–684

Schütz E (1960) Bestimmung der Atemgröße narkotisierter Ratten. Arzneim Forsch/Drug Res 10:52–53

Sinnett EE, Jackson AC, Leith DE, Butler JP (1981) Fast integrated flow plethysmograph for small mammals. J Appl Physiol 50:1104–1110

Wasserman MA, Griffin RL (1977) Thromboxane B_2 – comparative bronchoactivity in experimental systems. Eur J Pharmacol 46:303–313

Wegner CD, Jackson AC, Berry JD, Gillepsie JR (1984) Dynamic respiratory mechanics in monkeys measured by forced oscillations. Resp Physiol 55:47–61

Wirth K, Hock FJ, Albus U, Linz W, Alpermann HG, Anagnostopoulos H, Henke St, Breipohl W, Knolle J, Schölkens BA (1991) HOE 140, a new potent and long acting bradykinin-antagonist: *in vivo* studies. Br J Pharmacol 102:774–777

Wirth KJ, Gehring D, Schölkens BA (1993) Effect of HOE 140 on bradykinin-induced bronchoconstriction in anesthetized guinea pigs. Am Rev Resp Dis 148:702–706

D.2.2.5 Pneumotachography in Anesthetized Guinea Pigs

PURPOSE AND RATIONALE

The use of a pneumotachograph based on the principle of the Fleisch-tube and of additional pressure transducers allows simultaneous measurements of several respiratory and circulatory parameters in anesthetized guinea pigs (de la Motta 1991).

PROCEDURE

Guinea pigs (Pirbright white) weighing 300–400 g are anesthetized with 1.5 g/kg urethane i.p. The animals are shaved ventrally at the neck, placed on a heated operating table, and fixed at the upper extremities. A metal cannula with a blunted tip is inserted into the trachea and secured with a loop within the caudal section of the trachea. A thin plastic catheter is inserted into the esophagus and the tip located inside the thorax in order to register intrathoracic pressure. Furthermore, the cephalic vein at one side and the carotid artery on the opposite side are cannulated. The tracheal cannula is connected with pieces of tubing to a Fleisch tube (pneumotachograph), size 0000. In or-

der to avoid water condensation, the Fleisch tube is heated. The Fleisch tube is connected with a sensitive differential pressure transducer with a range of 2 cm H_2O (Validyne, model MP 45 -xx-871). One side of another pressure differential transducer with a range of 20 ml H_2O is connected with the esophageal catheter, the other side remaining open to room air. Both Validyne pressure transducers are connected to a separate preamplifier. For recording of the arterial blood pressure a Gould pressure transducer, Type P23Gb, is used. The signals for airflow and esophageal pressure are monitored at the output of the preamplifier with a digital 2-channel oscilloscope. To obtain various respiratory and circulatory parameters from the three primary signals they are calculated by certain formulae by an analogue computer (Buxco Pulmonary Mechanics Analyzer, Model 6). The following parameters are presented at the output of the instrument as analogue electrical signals:

Circulation

Systolic blood pressure, diastolic blood pressure, mean blood pressure

Respiration

Tidal volume, respiratory volume per minute, respiratory rate

Pulmonary Mechanics

Airway resistance, dynamic compliance, end-respiratory work.

A multi-channel recorder (Graphtec Linearcorder Mark VII) serves a functional check on the Buxco Analyzer and as analogue presentation of the calculated parameters. Data processing is performed by a 12-channel A/D converter (Buxco Data Logger, Model D/C-12 F/V) which digitizes the analogue output signals of the Buxco Analyzer and sends them through a serial interface (RS232) to an IBM PC. A special software program (Lomask 1987; Hastings 1990a, b) provides a flexible facility for data reduction and statistical evaluation.

EVALUATION

For each individual experiment the data of the last 5 min before the first substance application are averaged and used as controls. The response values after substance application are then expressed as percentages of the controls. In this way each animal serves as its own control. For an analysis of the results the response values are averaged over certain time intervals.

CRITICAL ASSESSMENT OF THE METHOD

The method described in great detail by de la Motta (1991) may be modified using different equipment according to individual needs.

MODIFICATIONS OF THE METHOD

Measurement of respiratory parameters is based on earlier studies to be mentioned for historical reasons (Gad 1880; Pflüger 1882; Zwaardemaker and Ouwehand 1904; Jaquet 1908; Rohrer 1915; Gildemeister 1922; Fleisch 1925; v. Neergaard and Wirz 1927; survey by Döring HJ 1991).

Lorino et al. (1988) assessed respiratory mechanics of histamine bronchopulmonary reactivity in guinea pigs.

O'Neil et al. (1981) published a comparative study of respiratory responses to bronchoactive agents in rhesus and cynomolgus monkeys.

Rayburn et al. (1989) described a computer-controlled pulmonary function system for studies in large animals.

Five methods of analyzing respiratory pressure-volume curves have been compared by Lai and Diamond (1986).

A specially designed pneumotachograph that is placed inside the trachea of guinea pigs was described by Santing et al. (1992) allowing the evaluation of airway functions in conscious, unstressed animals.

Lorino et al. (1993) estimated the changes in end-respiratory lung volume accompanied histamine-induced bronchoconstriction in anesthetized, paralyzed, and mechanically ventilated guinea pigs from measurements of thoracic cross-sectional area, assessed from the voltage induced by an external uniform magnetical field in a pickup coil encircling the rib cage.

Gozzard et al. (1996) evaluated the effects of PDE-inhibitors in **New Zealand White rabbits** which were immunized within 24 h of birth with *Alternaria tenuis* antigen. Spontaneously breathing rabbits were intubated in neuroleptanalgesia with a cuffed endotracheal tube connected to a thermoregulated Fleisch pneumotachograph to allow measurement of tidal air flow. An oesophageal balloon catheter was inserted to provide a measure of intra-pleural pressure and transpulmonary pressure. Antigen challenge was performed with inhaled *Alternaria tenuis* extract.

An excellent survey on various methods and equipment to measure air flow is given by Döring and Dehnert (1997).

REFERENCES AND FURTHER READING

De la Motta S (1991) Simultaneous measurement of respiratory and circulatory parameters on anesthetized guinea pigs.

Seventh Freiburg Focus on Biomeasurement (FFB7) Publ. by Biomesstechnik Verlag, 79232 March, Germany. B IV, pp 45–65
Döring HJ (1991) Historical review of methods for the measurement and evaluation of respiratory parameters, in particular airway resistance. Seventh Freiburg Focus on Biomeasurement (FFB7) Publ. by Biomesstechnik Verlag, 79232 March, Germany. B IV, pp 17–29
Döring HJ, Dehnert H (1997) Methoden zur Untersuchung der Atmungsorgane für die experimentelle Pharmakologie und Physiologie. Biomesstechnik-Verlag March GmbH, D-79323 March, Germany, pp 171–211
Fleisch A (1925) Der Pneumotachograph; ein Apparat zur Geschwindigkeitsregistrierung der Atemluft. Pflüger's Arch 209:713–722
Gad J (1880) Die Regulierung der normalen Athmung. Arch Anat Physiol, Physiol Abthlg:1–32
Gildemeister M (1922) Über die Messung der Atmung mit Gasuhr und Ventilen. Pflügers Arch 195:96–100
Gozzard N, Herd CM, Blake SM, Holbrook M, Hughes B, Higgs GA, Page CP (1996) Effects of theophylline and rolipram on antigen-induced airway responses in neonatally immunized rabbits. Br J Pharmacol 117:1405–1412
Hastings SG (1990a) An integrated system for data acquisition and analysis. Sixth Freiburg Focus on Biomeasurement (FFB6) Publ. by Biomesstechnik Verlag, 79232 March, Germany, pp 206–209
Hastings SG (1990b) Typical data reduction process. Sixth Freiburg Focus on Biomeasurement (FFB6) Publ. by Biomesstechnik Verlag, 79232 March, Germany. G IV 1–27
Jaquet A (1908) Zur Mechanik der Atembewegungen. Arch exp Path Pharmakol, Suppl, Festschr. O Schmiedeberg:309–316
Lai YL, Diamond L (1986) Comparison of five methods of analyzing respiratory pressure-volume curves. Respir Physiol 66:147–155
Lomask MR (1987) BUXCO respiratory mechanics analyzer for non invasive measurements in conscious animals. Third Freiburg Focus on Biomeasurement (FFB3) Publ. by Biomesstechnik Verlag, 79232 March, Germany, pp 212–226
Lorino AM, Bénichou M, Macquin-Mavier I, Lorino H, Harf A (1988) Respiratory mechanics for assessment of histamine bronchopulmonary reactivity in guinea pigs. Resp Physiol 73:155–162
Lorino AM, Jarreau PH, Sartene R, Mathieu M, Macquin-Mavier I, Harf A (1993) Bronchoconstriction-induced hyperinflation assessed by thoracic area measurement in guinea pigs. Am Rev Resp Dis 147:392–397
O'Neil RM, Ashack RJ, Goodman FR (1981) A comparative study of respiratory responses to bronchoactive agents in rhesus and cynomolgus monkeys. J Pharmacol Meth 5:267–273
Pflüger E (1882) Das Pneumonometer. Pflügers Arch 29:244–246
Rayburn DB, Mundie TG, Phillips YY (1989) Computer-controlled large-animal pulmonary function system. Comput Meth Progr Biomed 28:1–9
Rohrer F (1915) Der Strömungswiderstand in den menschlichen Atemwegen und der Einfluss der unregelmässigen Verzweigungen des Bronchialsystems auf den Atmungsverlauf in verschiedenen Lungenbezirken. Pflügers Arch 162:225–299
Santing RE, Meurs H, van der Mark TW, Remie R, Oosterom WC, Brouwer F, Zaagsma J (1992) A novel method to assess airway function parameters in chronically instrumented, unrestrained guinea-pigs. Pulmon Pharmacol 5:265–272
v. Neergaard K, Wirz K (1927) Über eine Methode zu Messung der Lungenelastizität am lebenden Menschen, insbesondere beim Emphysem. Z Klin Med 105:35–50
Zwaardemaker H, Ouwehand CD (1904) Die Geschwindigkeit des Athemstromes und das Athemvolum des Menschen. Arch Anat Physiol, Physiol Abthlg. Suppl:241–263

D.2.2.6 Airway Microvascular Leakage

PURPOSE AND RATIONALE

Plasma exudation in guinea-pig airways *in vivo* can be determined by Evans Blue dye and is fairly correlated with radiolabelled albumin (Rogers et al. 1989). This method can be used to study the antagonism against bradykinin- and platelet-activating factor-induced airway microvascular leakage and vagal stimulation-induced airway responses (Sakamoto et al. 1992, 1994).

PROCEDURE

Female Dunkin-Hartley guinea pigs weighing 380–600 g are anesthetized with an initial dose of 1.5 g/kg urethane injected i.p. Additional urethane is given i.v. 30 min later to achieve an appropriate level of anesthesia. A tracheal cannula is inserted into the lumen of the cervical trachea, a polyethylene catheter into the left carotid artery to monitor blood pressure and heart rate and another polyethylene catheter into the external jugular vein for administration of drugs. The animals are connected to a constant volume mechanical ventilator and then given an injection of 1.0–1.5 mg/kg suxamethonium i.v. to prevent interference with spontaneous respiration. A tidal volume of 10 ml/kg and a frequency of 60 strokes/min are used.

Lung resistance is measured as an index of airway function and monitored throughout the experiment. Transpulmonary pressure is measured with a pressure transducer with one side attached to a catheter inserted into the right pleural cavity and the other side attached to the side port of the intratracheal cannula. Airflow is measured by a pneumotachograph connected to a pressure transducer. The signals of the transducers are used for instantaneous calculation of lung resistance by an appropriate computer program.

The test compound (bradykinin receptor antagonist) is given intravenously. Ten min later, Evans Blue dye (20 mg/ml) is injected i.v. for 1 min. After 1 min, bronchoconstriction and microvascular leakage is induced by injection of bradykinin or by inhalation of bradykinin or PAF or vagal stimulation.

Six min after induction of leakage, the thoracic cavity is opened, and a cannula is inserted into the

aorta through a ventriculotomy. Perfusion is performed with 100–150 ml 0.9% saline at a pressure of 100–120 mm Hg in order to remove the intravascular dye from the systematic circulation. Blood and perfusion liquid are expelled through an incision in the right and left atrium. Subsequently, the right ventricle is opened, and the pulmonary circulation is perfused with 30 ml of 0.9% saline. The lungs are then removed, and the connective tissue, vasculature, and parenchyma are gently scraped. The airways are divided into 4 components: lower part of the trachea, main bronchi, the proximal 5 mm portion, and the distal intrapulmonary airways. The tissues are blotted dry, and then weighed. Evans Blue dye is extracted in 2 ml of formamide at 40°C for 24 h, and measured in a spectrophotometer at 620 nm.

EVALUATION

Evans Blue dye concentration, expressed as ng/mg tissue, as well as lung resistance are compared by statistical means (unpaired Student's *t*-test or Mann-Whitney U test) between treated groups and controls receiving the challenge only.

MODIFICATIONS OF THE METHOD

Boschetto et al. (1989) tested the effect of antiasthma drugs on microvascular leakage in guinea pig airways. Microvascular leakage was induced by intravenous injection of platelet-activating factor (50 ng/kg) which acts directly on venular endothelial cells, and measured by quantifying extravasation of Evans blue dye.

Xu et al. (1998) induced pulmonary edema in rats by injection of 20 µg/kg angiotensin I and studied the suppression by ACE-inhibitors, ATII antagonists and α-adrenergic receptor blockers.

Rapidly developing pulmonary edema was induced by intravenous injection of 1.2 mg/kg of the GABA agonist bicuculline in rats and the role of endogenous endothelin was examined by Herbst et al. (1995).

REFERENCES AND FURTHER READING

Boschetto P, Roberts NM, Rogers DF, Barnes PJ (1989) Effect of antiasthma drugs on microvascular leakage in guinea pig airways. Am Rev Resp Dis 139:416–421

Herbst C, Tippler B, Shams H, Simmet T (1995) A role of endothelin in bicuculline-induced neurogenic pulmonary oedema in rats. Br Pharmacol 115:753–760

Rogers DF, Boschetto P, Barnes PJ (1989) Plasma exsudation: Correlation between Evans Blue dye and radiolabelled albumin in guinea-pig airways *in vivo*. J Pharmacol Meth 21:309–315

Sakamoto T, Elwood W, Barnes PJ, Chung FK (1992) Effect of Hoe 140, a new bradykinin receptor antagonist, on bradykinin- and platelet-activating factor-induced bronchoconstriction and airway microvascular leakage in guinea pig. Eur J Pharmacol 213:367–373

Sakamoto T, Sun J, Barbnes PJ, Chung KF (1994) Effect of a bradykinin receptor antagonist, HOE 140, against bradykinin- and vagal stimulation-induced airway responses in the guinea-pig. Eur J Pharmacol 251:137–142

Xu ZH, Shimakura K, Yamamoto T, Wang LM, Mineshita S (1998) Pulmonary edema induced by angiotensin I in rats

D.2.2.7 Isolated Larynx In Situ

PURPOSE AND RATIONALE

The *in situ* isolated larynx of rats has been recommended by Willette et al. (1987) for evaluation peripheral opiate receptor antagonists. Peripheral opioid-induced laryngospasm and central opioid-induced respiratory depression can be measured simultaneously. Fentanyl citrate stimulates both peripheral and central opiate receptors, whereas [D-Ala^2-Met^5]-enkephalinamide stimulates only peripheral opiate receptors. Compounds that inhibit both laryngeal and respiratory effects of fentanyl, e. g., naloxone HCl, can be considered both central and peripheral opiate antagonists. Compounds that inhibit only the peripheral effects of fentanyl, e. g., naltrexone methylbromide, can be considered peripheral opiate receptor antagonists.

PROCEDURE

Laryngeal resistance experiments are carried out in male Sprague Dawley rats weighing 340–360 g and anesthetized with urethane (900 mg/kg, i.p.) The animals are secured in supine position and the left femoral artery and the left and right femoral veins are cannulated for recording of arterial blood pressure and administration of drugs. A right-angle polyethylene cannula (ID 1.67 mm, OD 2.42 mm) is inserted into the caudal trachea at the level of the manubrium for measuring tracheal flow via a small animal pneumotachograph. Care has to be taken to avoid damaging surrounding blood vessels or adjacent bilateral laryngeal nerves. Tracheal air flow is continually sampled (300 ml/min) for the breath to breath analysis of end tidal carbon dioxide with an infrared gas analyzer.

Laryngeal resistance in the rat is determined using a modification of the methods described by Stransky et al. (1973), Bartlett et al. (1973), and Willette et al. 1982b). The rostral portion of the trachea is cannulated with a right-angle polyethylene tube (ID 1.67 mm, OD 2.42 mm). This cannula is carefully advanced towards the larynx and secured with a suture (4–0 silk). A constant flow ($V = 30$ ml/min) of compressed air, maintained with a flow meter, is delivered through a cannula. Pre-laryngeal pressure is measured with

a needle tipped pressure transducer inserted into the lumen of the flow cannula. A 1.75-cm segment of polyethylene tubing (OD 8.4 mm, ID 4.6 mm) is placed into the mouth to retract resistive components in the nasopharyngeal region.

Laryngeal resistance (*LR*) is calculated by the following equation:

$$LR = (P_L P_i - P_L P_0)/V$$

where $P_L P_i$ is the laryngeal pressure in the cannula directing a constant flow (V) through the larynx. $P_L P_0$ is the pressure in the cannula when it is removed from the trachea.

The agonist fentanyl is administered through the left femoral vein at a dose of 12 µg/kg which is equivalent to 1.5 times the ED_{99} in the conscious rat tail flick assay. The enkephaline analogue [D-Ala^2-Met^5]-enkephalinamide is injected at a dose of 250 µg/kg which acts peripherally and increases laryngeal resistance (Willette 1982a). The opiate receptor antagonists are administered similarly into the right femoral vein.

At the conclusion of the experiment, the pulmonary afferent stimulant, phenyldiguanide (25 µg/kg, i.v.) is injected into the right femoral vein to elicit laryngospasm and to determine the viability of the preparation.

EVALUATION

All summary values are expressed as the mean plus or minus the standard error of the mean (SEM) Comparisons are made with independent and paired two-tailed *t*-tests.

MODIFICATIONS OF THE METHOD

Inagi et al. (1998) assessed the effect of botulin toxin in the rat larynx be measurement of the optical density of PAS-stained laryngeal muscle after electrical stimulation, spontaneous laryngeal muscle activity, and laryngeal movement.

O'Halloran et al. (1994) studied the effects of upper airway cooling and CO_2 on breathing and on laryngeal and supraglottic resistance in anesthetized rats.

González-Barón et al. (1989) studied the modifications of larynx resistance changing bronchial tone in cats evoked by intravenous administration of 10 µg/kg carbachol as bronchoconstrictor and by fenterol (10 µg/kg) or isoproterenol (0.1 mg/kg) as bronchodilators.

Wang et al. (1999) developed an isolated, luminally perfused laryngeal preparation in anesthetized paralyzed cats in order to compare the effects of solutions with varying levels of pH and pCO_2 on pressure-sensitive laryngeal receptor sensitivity.

REFERENCES AND FURTHER READING

Bartlett D, Remmers JE, Gautier H (1973) Laryngeal regulation of respiratory airflow. Respir Physiol 18:194–202

González-Barón S, Dawid-Miner MS, Lara JP, Clavijo E, Aguirre JA (1989) Changes in laryngeal resistance and bronchial tonus. Rev Esp Fisiol 45, Suppl:191–196

Inagi K, Connor NP, Ford CN, Schultz E, Rodriquez AA, Bless DM, Pasic D, Heisey DM (1998) Physiologic assessment of botulinum toxin effects in the rat larynx. Laryngoscope 108:1048–1054

O'Halloran KD, Curran AK, Bradford A (1994) Ventilatory and upper-airway resistance response to upper airway cooling and CO_2 in anesthetized rats. Pflüger's Arch 429:262–266

Stransky A, Szereda-Przestazewska M, Widdicombe J (1973) The effect of lung reflexes on laryngeal resistance and motoneuron discharge. J Physiol 231:517–518

Wang ZH, Bradford A, O'Regan RG (1999) Effects of CO_2 and H^+ on laryngeal receptor activity in the perfused larynx of anesthetized cats. J Physiol (Lond) 519:591–600

Willette RN, Krieger AJ, Sapru HN (1982a) Pulmonary opiate receptor activation evokes a cardiorespiratory effect. Eur J Pharmacol 78:61–70

Willette RN, Krieger AJ, Sapru HN (1982b) Opioids increase laryngeal resistance and motoneuron activity in the recurrent laryngeal nerve. Eur J Pharmacol 80:57–63

Willette RN, Evans DY, Dooley BM (1987) The *in situ* isolated larynx for evaluation peripheral opiate receptor antagonists. J Pharmacol Meth 17:15–25

D.2.2.8 Animal Models of Asthma

D.2.2.8.1 Treatment of Asthma

PURPOSE AND RATIONALE

Several authors described asthma models in mice. Hammad et al. (2004) found in a mouse model of asthma that activation of peroxisome proliferator-activated receptor-γ (PPAR-γ) in dendritic cells inhibits the development of eosinophilic airway inflammation.

PROCEDURE

Bone Marrow Dendritic Cells

OVA-TCR transgenic mice (DO10.11) on a BALB/c background, bred at the Erasmus University (Rotterdam) (Murphy et al. 1990), are used. Femurs and tibiae of female mice are removed and flushed with RPMI 1640. Vigorous pipetting disintegrates clusters within the marrow suspension. The cells are washed, enumerated, and plated in Petri dishes. Cell-culture medium (TCM) is supplemented with gentamicin (60 µg/ml), 2-mercaptoethanol (5×10^{-5} mol/l) and 5% fetal calf serum (Lutz et al. 1999). At day 0 of the culture, cells are seeded at a concentration of 2×10^6/dish in medium containing granulocyte-macrophage colony-

stimulating factor (GM-CSF, 200 IU/ml). At days 6 and 8, half of the medium is collected, centrifuged, and the pellet is resuspended in TCM containing 200 IU/ml of recombinant murine GM-CSF.

At day 9 of the culture, dendritic cells (Banchereau and Steinman 1998) are pulsed overnight with ovalbumin containing the vehicle (dimethylsulfoxide, DMSO) in which the standard PPAR-γ agonist (e. g., rosiglitazone) is suspended or with medium alone as control. Other plates are treated with the test drug or a PPAR-γ antagonist. After antigen pulsing overnight, non-adherent dendritic cells are collected, washed to remove free ovalbumin, and resuspended in phosphate-buffered saline at a concentration of 12.5×10^6 cells/ml.

Eosinophilic Airway Inflammation

For intratracheal injection of dendritic cells (Lambrecht et al. 2000), mice are anesthetized with Avertin and 80 µl of the cell suspension (1×10^6 dendritic cells) is instilled through the opening vocal cords. Mice are injected with unpulsed dendritic cells, ovalbulmin-treated dendritic cells or dendritic cells treated additionally with the PPAR-γ antagonist. From days 10–13, mice are exposed to 30-min ovalbumin aerosols. They are sacrificed 24 h after the last aerosol. Broncho-alveolar lavage is performed with 3×1 ml of Ca^{2+}- and Mg^{2+}-free buffer supplemented with 0.1 mmol/l sodium EDTA. The broncho-alveolar lavage is centrifuged; the cells are resuspended in buffer and enumerated with a hemocytometer. They are differentiated (Vremec and Shortman 1997) by staining for 30 min with anti-I-Ad/I-Ed FITC (macrophages), anti-CCR3 PE (eosinophils), antiCD3-cy-chrome, anti-B220 cytochrome (T and B cells, respectively) and anti-CD11c APC (macrophages) in PBS containing 0.5 bovine serum albumin and 0.01% sodium azide. Cells are washed and analyzed by flow cytometry (Van Rijt et al. 2002).

EVALUATION

The difference between the groups is calculated using the Mann–Whitney *U*-test for unpaired data.

MODIFICATIONS OF THE METHOD

Iwasaki et al. (2001) recommended atopic NC/Nga mice as a model for allergic asthma: after immunization with ovalbumin, severe allergic responses were elicited by a single intranasal challenge.

For testing PPAR agonists, Trifilieff et al. (2003) used a murine model of asthma using lung inflammation induced by ovalbumin or by LPS (Trifilieff et al. 2000). Female BALB/c mice (4 weeks old) were immunized with ovalbumin on days 0 and 14, exposed to an aerosol challenge of ovalbumin or phosphate-buffered saline (PBS) on day 21 and killed on day 23 for measurement of inflammatory cells in the broncho-alveolar lavage. Animals were intranasally treated with compounds 1 h before the aerosol exposure using PBS containing 2% DMSAO as vehicle.

For LPS-induced lung inflammation mice were challenged intranasally with 0.3 mg/kg of LPS (*Salmonella typhosa*) in 50 ml of sterile PBS or with sterile PBS alone and killed 3 h later for broncho-alveolar lavage. Tumor necrosis factor alpha (TNF-α) and the neutrophil chemokine KC levels were measured using an enzyme-linked immunosorbent assay kit (R&D Systems, Abingdon, UK). Animals were intranasally treated with compounds 1 h before the aerosol exposure using PBS containing 2% DMSO as vehicle.

Mueller et al. (2003) reported that **peroxisome proliferators-activated receptor γ ligands** attenuate immunological symptoms of allergic asthma. For asthma induction, Balb/c mice were injected with 10 µg of ovalbumin in Alum twice on days 1 and 5 (Zhang et al. 1999). On day 10, they were challenged intranasally with 40 µg ovalbumin in sterile saline, every day for 3 days. On the day after the last intranasal challenge, the mice were sacrificed. The degree of inflammation in the lung was evaluated by histopathology. Gene expression was tested by microarray analysis, and serum IgE determined by ELISA.

Regal et al. (2001) described trimellitic anhydride-induced eosinophilia in a mouse model of occupational asthma. Trimellitic anhydride was conjugated to mouse serum albumin. Female BALB/c mice were sensitized on days 1 and 3 intradermally with 0.1 ml of 0.3% ovalbumin suspended in corn oil. On day 12, animals were additionally sensitized intratracheally with 0.04 ml ovalbumin, trimellitic anhydride conjugated to mouse serum albumin, or mouse serum albumin dissolved in water. For elicitation of the allergic response, mice were challenged intratracheally beginning on day 19 with 0.04 ml of aqueous solutions of ovalbumin, trimellitic anhydride conjugated to mouse serum albumin, or mouse serum albumin under ketamine/xylazine anesthesia. After the last intratracheal instillation, the mice were anesthetized with pentobarbital, EDTA plasma was collected by cardiac puncture, the trachea was cannulated and the lungs were lavaged with two 0.9-ml aliquots of PBS to obtain bronchial lavage fluid. The lungs were removed for homogenization and analysis of eosinophil peroxidase and myeloperoxidase.

Churg et al. (2001) studied anti-inflammatory effects of alpha-1 antitrypsin and a metalloprotease inhibitor in C57 BL/6 mice or macrophage metalloelastase knockout mice after intratracheal instillation of a single 7-mg dose of crystalline silica (α-quartz, Minusil-5; US Silica Corporation, Clarkstown, W.Va., USA). This dose produced a rapid and persisting acute inflammatory infiltrate. Mice were euthanized 2 or 24 h after dust exposure by halothane overdose and the lungs removed from the chest cavity. A 20-gauge catheter was inserted into the trachea and the lungs lavaged six times with 1 ml of ice-cold saline. For inflammatory cell measurements, the saline lavage was centrifuged at 200 *g* at 4°C for 10 min. The supernatants were decanted, and the cell pellets were resuspended in 200 µl of saline. Total cell counts were performed using a hemocytometer and differential cell counts were performed on a 10-µl drop of the cell suspension heat-fixed on a slide and stained with hematoxylin-eosin. Lavage samples were analyzed for desmosine and hydroxyproline.

De Sanctis and Drazen (1997) discussed the genetics of native airway responsiveness in mice.

Several animal species have been used such as **rats**.

Misawa et al. (1987) found strain differences among Wistar, Lewis and Fischer 344 rats in an allergic asthma model.

Misawa and Sugiyama (1993) described an airway hyperresponsiveness model in rats, inducing allergic asthma with DNP-Ascaris extract.

Uhlig et al. (1998) reported the effects of long-term oral treatment with leflunomide on allergic sensitization, lymphocyte activation, and airway inflammation in rats.

Birrell et al. (2003) investigated the nitric-oxide synthase isoform involved in eosinophilic inflammation in a rat model of Sephadex-induced airway inflammation. The rat model of Sephadex-induced airway inflammation was also used by Belvisi et al. (2005) for preclinical studies on ciclesonide, an inhaled corticosteroid for the treatment of asthma.

Many authors used sensitized **Brown Norway rats** in experimental models of asthma (Elwood et al. 1992; Steerenberg et al. 1999; Nonaka et al. 2000; Xu et al. 2000; Blesa et al. 2002; Glaab et al. 2002; Huang et al. 2002; Belvisi et al. 2005; Valstar et al. 2006).

Guinea pigs have been used as animal models for asthma by many authors. Most studies were performed with sensitization either by injection with ovalbumin suspended in an adjuvant (Santives et al. 1976; Banner et al. 1996; Lawrence et al. 1998; Regal et al. 2000; Li et al. 2001; Santing et al. 2001; Mukaiyama et al. 2004; Boskabady and Zarei 2004; Ikezono et al. 2005; Tang et al. 2005) or by repetitive sensitization with inhaled ovalbumin (Sagara et al. 1996, 1997; Smith et al. 1996; Liu et al. 1997; Tohda et al. 1998; Cheng et al. 2001; Zhang et al. 2002) and then challenge by inhaled ovalbumin.

Fujimura et al. (1997) described a guinea pig model of ultrasonically nebulized distilled-water-induced bronchoconstriction. Guinea pigs sensitized by intradermal injection of ovalbumin in Freund's adjuvant were treated with aerosols of physiological saline generated by an ultrasonic nebulizer.

Zhou et al. (1998) reported a dose–response relationship between exposure to cockroach allergens and induction of sensitization in an experimental asthma in Hartley guinea pigs.

Larsen and Regal (2002) studied trimellitic anhydride dust-induced airway obstruction and eosinophilia in non-sensitized guinea pigs.

Nishitsuji et al. (2004) described a guinea pig model of cough variant asthma. Bronchial responsiveness to methacholine and cough reflex sensitivity to capsaicin were measured 72 h after ovalbumin inhalation in actively sensitized guinea pigs.

Dogs were used as animal models for asthma by several authors. Many studies preferred the **Basenji Greyhound dog**, which manifests various characteristics of human asthma, including airway hypersensitivity to low concentrations of methacholine (Hirshman et al. 1980; Hirshman and Downes 1981; Chan et al. 1985; Darowski et al. 1989; Emala et al. 1993, 1996).

Redman et al. (2001) studied pulmonary immunity to ragweed in a **Beagle dog** model of allergic asthma.

Some studies were reported using **cats** as an animal model for asthma. Norris et al. (2003) and Norris-Reinero et al. (2004) described an experimental model of allergic asthma in cats sensitized to the house dust mite and Bermuda grass allergen.

Several studies were performed using **monkeys** as animal models for asthma. *Ascaris suum*-sensitive monkeys were used by Mauser et al. (1995) and Zou et al. (2002). Rhesus monkeys (*Macaca mulatta*) were used by Patterson et al. (1975) and Patterson and Harris (1981, 1990, 1992). Turner et al. (1996) used *Macaca fascicularis* to demonstrate *in vitro* and *in vivo* effects of leukotriene B_4 antagonism in primates.

REFERENCES AND FURTHER READING

Banchereau J, Steinman RM (1998) Dendritic cells and the control of immunity. Nature 392:245–252

Banner KH, Paul W, Page CP (1996) Ovalbumin challenge following immunization elicits recruitment of eosinophils but

not hyperresponsiveness in guinea pigs: time course and relationship to eosinophil activation status. Pulmon Pharmacol 9:179–187

Belvisi MG, Bundschuh DS, Stoeck M, Wicks S, Underwood S, Battram CH, Haddad EB, Webber SE, Foster ML (2005) Preclinical profile of ciclesonide, a novel corticosteroid for the treatment of asthma. J Pharmacol Exp Ther 314:568–574

Birrell MA, McCluskie K, Haddad el B, Battram CH, Webber SE, Foster ML, Yacoub MH, Belvisi MG (2003) Pharmacological assessment of the nitric-oxide synthase isoform involved in eosinophilic inflammation in a rat model of sephadex-induced airway inflammation. J Pharmacol Exp Ther 304:1285–1291

Blesa S, Cortijo J, Martinez-Losa M, Mata M, Seda E, Santangelo F, Morcillo EJ (2002) Effectiveness of oral N-acetylcysteine in a rat experimental model of asthma. Pharmacol Res 45:135–140

Boskabady MH, Zarei A (2004) Increased tracheal responsiveness to beta-adrenergic agonist and antagonist in ovalbumin-sensitized guinea pigs. Pharmacology 71:73–79

Chan SC, Hanifin JM, Holden CA, Thompson WJ, Hirshman CA (1985) Elevated leukocyte phosphodiesterase as a basis for depressed cyclic adenosine monophosphate responses in the Basenji greyhound dog model of asthma. J Allergy Clin Immunol 76(2 Pt 1):148–158

Cheng G, Ueda T, Sugiyama K, Toda M, Fukuda T (2001) Compositional and functional changes of pulmonary surfactant in a guinea pig model of chronic asthma. Respir Med 95:180–186

Churg A, Dai J, Zay K, Karsan A, Hendricks S, Yee C, Martin R, MacKenzie R, Xie C, Zhang L, Shapiro S, Wright JL (2001) Alpha-1 antitrypsin and a broad metalloprotease inhibitor, RS113456, have similar acute anti-inflammatory effects. Lab Invest 81:1119–1131

Darowski MJ, Hannon VM, Hirshman CA (1989) Corticosteroids decrease airway hyperresponsiveness in the Basenji-Greyhound dog model of asthma. J Appl Physiol 66:1120–1126

De Sanctis GT, Drazen JM (1997) Genetics of native airway responsiveness in mice. Am J Respir Crit Care Med 156:S82–S88

Elwood W, Lotvall JO, Barnes PJ, Chung KF (1992) Effect of dexamethasone and cyclosporine A on allergen-induced airway hyperresponsiveness and inflammatory cell responses in sensitized Brown-Norway rats. Am Rev Respir Dis 145:1289–1294

Emala C, Black C, Curry C, Levine MA, Hirshman CA (1993) Impaired beta-adrenergic receptor activation of adenylyl cyclase in airway smooth muscle in the basenji-greyhound dog model of airway hyperresponsiveness. Am J Respir Cell Mol Biol 8:668–675

Emala CW, Aryana A, Hirshman CA (1996) Impaired activation of adenylyl cyclase in lung of the Basenji-greyhound model of airway hyperresponsiveness. Decreased numbers of high affinity beta-receptors. Br J Pharmacol 118:2009–2016

Fujimura M, Amamiya M, Myou S, Mizuguchi M, Matsuda T (1997) A guinea-pig model of ultrasonically nebulized distilled water-induced bronchoconstriction. Eur Respir J 10:2237–2242

Glaab T, Hoymann HG, Hohlfeld JM, Korolewitz R, Hecht M, Alarie Y, Tschernig T, Braun A, Krug N, Fabel H (2002) Noninvasive measurement of midexpiratory flow indicates bronchoconstriction in allergic rats. J Appl Physiol 93:1208–1214

Hammad H, Jan de Heer H, Soullié T, Angeli V, Trottein F, Hoogsteden HC, Lambrecht BN (2004) Activation of peroxisome proliferator-activated receptor-γ in dendritic cells inhibits the development of eosinophilic airway inflammation in a mouse model of asthma. Am J Pathol 164:263–271

Hirshman CA, Downes H (1981) Basenji-Greyhound dog model of asthma: influence of atropine on antigen-induced bronchoconstriction. J Appl Physiol 50:76–765

Hirshman CA, Malley A, Downes H (1980) Basenji-Greyhound dog model of asthma: reactivity to *Ascaris suum*, citric acid, and methacholine. J Appl Physiol 49:953–957

Huang TJ, Eynott P, Salmon M, Nicklin PL, Chung KF (2002) The effect of topical immunomodulators on acute allergic inflammation and bronchial hyperresponsiveness in sensitized rats. Eur J Pharmacol 437:187–194

Ikezono K, Kamata M, Mori T (2005) Adrenal influences on the inhibitory effects of procaterol, a selective β2-adrenoceptor agonist, on antigen-induced airway microvascular leakage and bronchoconstriction in guinea pigs. Pharmacology 73:209–215

Iwasaki T, Tanaka A, Itakura A, Yamashita N, Ohta K, Matsuda H, Onuma M (2001) Atopic NC/Nga mice as a model for allergic asthma: severe allergic responses by single intranasal challenge with protein antigen. J Vet Med Sci 63:413–419

Lambrecht BN, Pauwels RA, de St. Groth BF (2000) Induction of rapid T cell activation, division, and recirculation by intratracheal injection of dendritic cells in a TCR transgenic model. J Immunol 164:2937–2946

Larsen CP, Regal JF (2002) Trimellitic anhydride (TMA) dust induces airway obstruction and eosinophilia in nonsensitized guinea pigs. Toxicology 178:89–99

Lawrence TE, Millecchia LL, Fedan JS (1998) Fluticasone propionate and pentamidine isethionate reduce airway hyperreactivity, pulmonary eosinophilia and pulmonary dendritic cell response in a guinea pig model of asthma. J Pharmacol Exp Ther 284:222–227

Li Y, Martin LD, Minnicozzi M, Greenfeder S, Fine J, Pettersen CA, Chorley B, Adler KB (2001) Enhanced expression of mucin genes in a guinea pig model of allergic asthma. Am J Respir Cell Mol Biol 25:644–651

Liu M, Wang L, Holm BA, Enhorning G (1997) Dysfunction of guinea pig pulmonary surfactant and type II pneumocytes after repetitive challenge with aerosolized ovalbumin. Clin Exp Allergy 27:802–807

Lutz MB, Kukutsch N, Ogilvie ALJ, Rössner S, Koch F, Romani N, Schuler G (1999) An advanced culture method for generating large quantities of highly pure dendritic cells from mouse bone marrow. J Immunol Methods 223:77–92

Mauser PJ, Pitman AM, Fernandez X, Foran SK, Adams GK 3rd Kreutner W, Egan RW, Chapman RW (1995) Effects of an antibody to interleukin-5 in a monkey model of asthma. Am J Respir Crit Care Med 152:467–472

Misawa M, Sugiyama Y (1993) An airway hyperresponsiveness model in rat allergic asthma. Arerugi 42:107–114

Misawa M, Takenouchi K, Abiru T, Yoshino Y, Yanaura S (1987) Strain differences in an allergic asthma model in rats. Jpn J Pharmacol 45:63–68

Mueller C, Weaver V, Van den Heuvel JP, August A, Cantorna MT (2003) Peroxisome proliferators-activated receptor γ ligands attenuate immunological symptoms of allergic asthma. Arch Biochem Biophys 418:186–196

Mukaiyama O, Morimoto K, Nosaka E, Takahashi S, Yamashita M (2004) Involvement of enhanced neurokinin NK3 receptor expression in the severe asthma guinea pig model. Eur J Pharmacol 498:287–294

Murphy KM, Heimberger AB, Loh DY (1990) Induction by antigen of intrathymic apoptosis of CD4+CD8+TcRIo thymocytes in vivo. Science 250:1720–1723

Nishitsuji M, Fujimura M, Oribe Y, Nakao S (2004) A guinea pig model of cough variant asthma and role of tachykinins. Exp Lung Res 30:723–737

Nonaka T, Mitsuhashi H, Takahashi K, Sugiyama H, Kishimoto T (2000) Effect of TEI-9874, an inhibitor of immunoglobulin E production, on allergen-induced asthmatic model in rats. Eur J Pharmacol 402:287–295

Norris CR, Byerly JR, Decile KC, Berghaus RD, Walby WF, Schelegle ES, Hyde DM, Gershwin LJ (2003) Allergen-specific IgG and IgA, in serum and bronchoalveolar lavage fluid in a model of experimental feline asthma. Vet Immunol Immunopathol 96:119–127

Norris-Reinero CR, Decile KC, Berghaus RD, Williams KJ, Leutenegger CM, Walby WF, Schelegle ES, Hyde DM, Gershwin LJ (2004) An experimental model of allergic asthma in cats sensitized to house dust mite and Bermuda grass allergen. Int Arch Allergy Immunol 135:117–131

Patterson R, Harris KE (1981) Inhibition of immunoglobulin E-mediated, antigen-induced monkey asthma and skin reactions by 5,8,11,14-eicosotetraynoic acid. J Allergy Clin Immunol 67:146–152

Patterson R, Harris KE (1990) Rhesus monkey airway responses to substance P. Int Arch Allergy Appl Immunol 91:374–379

Patterson R, Harris KE (1992) IgE-mediated rhesus monkey asthma: natural history and individual animal variation. Int Arch Allergy Immunol 97:154–159

Patterson R, Irons JS, Harris KE (1975) Potentiating effect of D_2O on the ascaris-induced, reagin-mediated model of asthma in the Rhesus monkey studied by a double aerosolized antigen challenge technique. Int Allergy Appl Immunol 48:412–421

Redman TK, Rudolph K, Barr EB, Bowen LE, Muggenburg BA, Bice DE (2001) Pulmonary immunity to ragweed in a Beagle dog model of allergic asthma. Exp Lung Res 27:433–451

Regal JF, Fraser DG, Weeks CE, Greenberg NA (2000) Dietary phytoestrogens have anti-inflammatory activity in a guinea pig model of asthma. Proc Soc Exp Biol Med 223:372–378

Regal JF, Mohrman ME, Sailstadt DM (2001) Trimellitic anhydride-induced eosinophilia in a mouse model of occupational asthma. Toxicol Appl Pharmacol 175:234–242

Sagara H, Ra C, Okada T, Shinohara S, Fukuda T, Okumura K, Makino S (1996) Sialyl Lewis X analog inhibits eosinophil accumulation and late asthmatic response in a guinea pig model of asthma. Int Arch Allergy Immunol 111 [Suppl 1]:32–36

Sagara H, Matsuda H, Wada N, Yagita H, Fukuda T, Okumara K, Makino S, Ra C (1997) A monoclonal antibody against very late activation antigen-4 inhibits eosinophil accumulation and late asthmatic response in a guinea pig model of asthma. Int Arch Allergy Immunol 112:287–294

Santing RE, de Boer J, Rohof A, van der Zee NM, Zaagsma J (2001) Bronchodilatory and anti-inflammatory properties of inhaled selective phosphodiesterase inhibitors in a guinea pig model of allergic asthma. Eur J Pharmacol 429:335–344

Santives T, Roska A, Hensley GT, Moore VL, Fink JV, Abromoff P (1976) Immunologically induced lung disease in guinea pig. J Allergy Clin Immunol 57:582–594

Smith WG, Thompson JM, Kowalski DL, McKeam JP (1996) Inhaled misoprostol blocks guinea pig antigen-induced bronchoconstriction and airway inflammation. Am J Respir Crit Care Med 154(2 Pt1):295–299

Steerenberg PA, Dormans JA, van Doorn CC, Middendorp S, Vos JG, van Loveren H (1999) A pollen model in the rat for testing adjuvant activity of air pollution components. Inhal Toxicol 11:1109–1122

Tang LF, Du LZ, Zou CC, Gu WZ (2005) Levels of matrix metalloproteinase-9 and its inhibitor in guinea pig asthma model following ovalbumin challenge. Fetal Pediatr Pathol 24:81–87

Tohda Y, Kubo H, Haraguchi R, Iwanaga T, Fukuoka Nakajima S (1998) Roles of histamine receptor in a guinea pig asthma model. Int J Immunopharmacol 20:565–571

Trifilieff A, El-Hashim A, Bertrand C (2000) Time course of inflammatory and remodeling events in a mouse model of asthma: effect of steroid treatment. Am J Physiol 279:L1120–L1128

Trifilieff A, Bench A, Hanley M, Bayley D, Campbell E, Whittaker P (2003) PPAR-α and -γ, but not -δ agonists inhibit airway inflammation in a murine model of asthma: *in vitro* evidence for an NF-κB-independent effect. Br J Pharmacol 139:163–171

Turner CR, Breslow R, Conklyn MJ. Andresen CJ, Patterson DK, Lopez-Anaya A, Owens B, Lee P, Watson JW, Showell HJ (1996) In vitro and in vivo effects of leukotriene B_4 antagonism in a primate model of asthma. J Clin Invest 97:381–387

Uhlig T, Cooper D, Eber E, McMenamin C, Wildhaber JH, Sly PD (1998) Effects of long term oral treatment with leflunomide on allergic sensitization, lymphocyte activation, and airway inflammation in a rat model of asthma. Clin Exp Allergy 28:758–764

Valstar DL, Schijf MA, Nijkamp FP, Storm G, Arts JHE, Kuper CF, Bloksma N, Henricks PAJ (2006) Alveolar macrophages have a dual role in a rat model for trimellitic anhydride-induced occupational asthma. Toxicol Appl Pharmacol 211:20–29

Van Rijt LS, Prins JB, Leenen PJM, Thielemans K, de Vries VC, Hoogsteden HC, Lambrecht BN (2002) Allergen-induced accumulation of airway dendritic cells is supported by an increase in $CD31^{hi}Ly\text{-}6C^{neg}$ bone marrow precursors in a mouse model of asthma. Blood 100:3663–3671

Vremec D, Shortman K (1997) Dendritic cell subtypes in mouse lymphoid organs. Cross-correlation of surface markers, changes with incubation, and differences among thymus, spleen and lymph nodes. J Immunol 159:565–573

Xu L, Olivenstein R, Martin JG, Powell WS (2000) Inhaled budesonide inhibits OVA-induced airway narrowing, inflammation, and cys-LT synthesis in BN rats. J Appl Physiol 89:1852–1858

Zhang DH, Yang L, Cohn L, Parkyn L, Homer R, Ray P, Ray A (1999) Inhibition of allergic inflammation in a murine model of asthma by expression of a dominant-negative mutant of GATA-3. Immunity 11:473–482

Zhang M, Nomura A, Uchida Y, Iijima H, Sakamoto T, Iishii Y, Morishima Y, Mochizuki M, Masuyama K, Hirano K, Sekizawa K (2002) Ebselen suppresses late airway responses and airway inflammation in guinea pigs. Free Radic Biol Med 32:454–464

Zhou D, Chen G, Kim JT, Lee LY, Kang BC (1998) A dose-response relationship between exposure to cockroach allergens and induction of sensitization in an experimental asthma in Hartley guinea pigs. J Allergy Clin Immunol 101:653–659

Zou J, Young S, Zhu F, Xia L, Skeans S, Wan Y, Wang L, McClanahan D, Gheyas F, Wei D, Garlisi C, Jakway J, Umland S (2002) Identification of differentially expressed genes in a monkey model of allergic asthma by microarray technology. Chest 121:26S–27S

D.2.2.8.2 Prevention of Allergic Asthma Reaction

PURPOSE AND RATIONALE

Type 1 allergy is an abnormal reaction to protein substances that occur naturally. B-lymphocytes produce an antibody against the allergen. An allergic reaction occurs every time the body is exposed to the allergen causing release of histamine. Allergic reactions can be asthma, hay fever or nettle rash. Sensitization to normally harmless environmental antigens (e. g., pollen, house-dust mite) is the prerequisite for initiating the inflammatory cascade in bronchial asthma. Inflammation of the airway mucosa is orchestrated by Th-2 type T cells, which produce Th-2 cytokines (IL-4, IL-5, IL-9, IL-13, and IL-15), which regulate both IgE production and airway inflammation. At present, no cure of asthma disease is available, but primary and secondary prevention is the therapy of choice (Cieslewicz et al. 1999). Specific immunotherapy is performed by injection of increasing amounts of allergens to induce hyporesponsiveness to the respective allergen. By mucosal application of soluble antigen, mucosal tolerance can be achieved (van Halteren et al. 1997; Astori et al. 2000). Many studies have been performed in spite of the fact that no animal model is available that resembles all features of human bronchial asthma (Herz et al. 1998). In particular, models using recombinant allergens were described (Hoyne et al. 1997, 2000; Herz et al. 2004).

These studies concern specific allergens, such as **ovalbumin** (Renz et al. 1992; Marth et al. 2000; Neuhaus-Steinmetz et al. 2000; Raap et al. 2003; Reader et al. 2003; Wegmann et al. 2005), **mite dust allergen** (Hoyne et al. 1996; Clarke et al. 1999; Yasue et al. 1998a, 1998b, 1998c, 1999; Jarnicki and Thomas 2002), **pollen allergen** (Hirahara et al. 1998; Wiedermann et al. 1999, 2001; Batanero et al. 2002; Repa et al. 2004; Hufnagl et al. 2005; Winkler et al. 2006), **latex protein allergen** (Thakker et al. 1999; Woolhiser et al. 2000; Meade and Woolhiser 2002; Hufnagl et al. 2003), **bee venom allergen** (Von Garnier et al. 2000), and **cat allergen** (Briner et al. 1993; Treter and Luqman 2000).

Wegmann et al. (2005) studied involvement of distal airways in a chronic model of experimental asthma.

PROCEDURE

Animals

Pathogen-free female BALB/c mice (Harlan Winkelmann, Hannover, Germany), weighing 18–22 g and 6–8 weeks of age, were used in all experiments. The animals were maintained under standard housing conditions, fed an ovalbumin- (OVA-) free diet and supplied with food and water ad libitum.

Sensitization Protocol

Mice were sensitized to OVA by three intraperitoneal injections [10 µg OVA grade VI (Sigma, Deisenhofen, Germany) adsorbed to 1.5 mg $Al(OH)_3$ diluted in 200 µl phosphate-buffered saline (PBS)] on days 1, 14, and 21. The mice were challenged with OVA (grade V) aerosol (1% wt/vol in PBS) via the airways twice a week on two consecutive days over a period of 12 weeks (Renz et al. 1992). Sham sensitization and challenges were carried out with sterile $Al(OH)_3$ in PBS. Animals were analyzed after 1 or 12 weeks of OVA aerosol challenge. To investigate persistence of airway inflammation and lung physiological changes mice were analyzed after 6 weeks of OVA aerosol challenge discontinuation following 12 weeks of OVA aerosol challenge.

Differential Cell Counts in Broncho-Alveolar Lavage Fluid

At 48 h after the last allergen challenge broncho-alveolar lavage (BAL) was performed and analyzed (Renz et al. 1992).

Measurement of Cytokines in BAL Fluid

IL-4, IL-5 and tumor necrosis factor alpha (TNF-α) were measured in cell-free lavage fluids by cytometric bead array (CBA, BD Biosciences, San Diego, Calif., USA). The detection limit for each of the cytokines was 10 pg/ml. Complete BAL transforming growth factor beta (TGF-β) was measured after acidic activation using chicken anti-human TGF-β in a standard ELISA protocol. The detection limit for TGF-β was 20 pg/ml.

Lung Histology

Lungs were fixed *ex situ* with 4% (wt/vol) paraformaldehyde via the trachea, removed and stored in 4% paraformaldehyde. Lung tissues were embedded into paraffin, and 3 µm sections were stained with haematoxylin and eosin or periodic acid-Schiff staining. For localization of collagen fibrils, Sirius red staining was performed according to Uhal et al. (1998).

Immunohistochemistry

Indirect immunohistochemistry was used to stain lung sections for smooth muscle cells and myofibroblasts (mouse monoclonal IgG against α-SMA, clone 1A4, Immunotech, Marseilles, France), and nerve cells

(polyclonal rabbit antiserum against protein gene product 9.5, Biogenesis, Poole, UK) according to Fehrenbach et al. (2002). To distinguish smooth muscle cells from myofibroblasts a rat monoclonal IgG against fibroblast-specific peptide (clone ER-TR7; Biogenesis) was utilized.

Quantitative Morphology

Paraffin sections stained with Fast Green/Sirius Red and for α-SMA, respectively, were used to quantify changes in airway epithelial cell, collagen and smooth muscle cell layers of distal airways according to standard stereological methods. A distal airway was defined as the segment of a terminal bronchiolus that, starting at the broncho-alveolar duct transition, extended up to five alveoli along the proximal direction. Using a PC-based Olympus light microscope BX 51 equipped with a CAST-Grid System (Visiopharm, Hoersholm, Denmark), all distal airways of a given section were delineated (at a magnification of $\times 426$), and the fields of view to be analyzed (at a final magnification of $\times 1.700$) were automatically defined according to systematic uniform random sampling. The arithmetic mean thicknesses were determined as the volume of the respective component, determined by counting all points hitting airway epithelium, Sirius Red- and α-SMA-positive components, respectively. Results were referred to the reference surface determined by counting all intersections with the airway epithelial basal membrane (Reader et al. 2003). The arithmetic mean thicknesses were calculated.

Electron Microscopy and Definition of Proximal and Distal Airways

For analysis of airway wall ultrastructure, lungs of mice chronically challenged with OVA and control mice challenged with PBS ($n = 3$ per group) were fixed by instillation of 4% (wt/vol) paraformaldehyde via the trachea. Beginning at the lobar bronchus, the airways were microdissected along the axial pathway according to Plopper et al. (2001). For histopathological and ultrastructural analysis, proximal airways were defined as the lobar bronchi and the axial pathway down to the fourth intrapulmonary branch point. Mid-level airways were defined as the axial pathways between the intrapulmonary branch points 6–12. Terminal bronchioles with direct connection to the alveolar ducts were defined as distal airways (Postlethwait et al. 2000).

Non-invasive Measurement of Mid-Expiratory Airflow at Baseline and of Bronchial Responsiveness to Methacholine

The mid-expiratory airflow (EF_{50}) was measured 24 h after the last OVA aerosol challenge using head-out body plethysmography (Glaab et al. 2001).

EVALUATION

Results are presented as mean values $\pm$SD unless stated otherwise. One-way ANOVA test or Student's unpaired *t*-test was used to determine the significance of differences between animal groups.

REFERENCES AND FURTHER READING

Astori M, von Garnier C, Kettner A, Dufour N, Corradin G, Spertini F (2000) Inducing tolerance by intranasal administration of long peptides in naïve and primed CBA/J mice. J Immunol 165:3497–3505

Batanero E, Barral P, Villalba M, Rodriguez R (2002) Sensitization of mice with olive pollen allergen Ole e 1 induces Th2 responses. Int Arch Allergy Immunol 127:269–275

Briner TJ, Kuo MC, Keating KM, Rogers BL, Greenstein JL (1993) Peripheral T-cell tolerance induced in naive and primed mice by subcutaneous injection of peptides from the cat major allergen Fel d I. Proc Natl Acad Sci USA 90:7608–7612

Cieslewicz G, Tomkinson A, Adler A, Duez C, Schwarze J, Takeda K, Larson KA, Lee JJ, Irvin CG, Gelfand EW (1999) The late, but not early, asthmatic response is dependent on IL-5 and correlates with eosinophil infiltration. J Clin Invest 104:301–308

Clarke AH, Thomas WR, Rolland JM, Dow C, O'Brien RM (1999) Murine allergic respiratory responses to the major house dust mite allergen Der p 1. Int Arch Allergy Immunol 120:126–134

Fehrenbach H, Fehrenbach A, Pan T, Kasper M, Mason RJ (2002) Keratinocyte growth factor-induced proliferation of rat airway epithelium is restricted to Clara cell *in vivo*. Eur Respir J 20:1185–1197

Glaab T, Daser A, Brain A, Neuhaus-Steinmetz U, Fabel H, Alarie Y, Renz H (2001) Tidal midexpiratory flow as a measure of airway hyperresponsiveness in allergic mice. Am J Physiol 280:L565–L573

Herz U, Braun A, Rückert H, Renz H (1998) Various immunological phenotypes are associated with increased airway hyperresponsiveness. Clin Exp Allergy 28:625–634

Herz U, Renz H, Wiedermann U (2004) Animal models of type I allergy using recombinant allergens. Methods 32:271–280

Hirahara K, Saito S, Serizawa N, Sasaki R, Sakaguchi M, Inouye S, Taniguchi Y, Kaminogawa S, Shiraishi A (1998) Oral administration of a dominant T-cell determinant peptide inhibits allergen-specific TH1 and TH2 cell responses in Cry j 2-primed mice. J Allergy Clin Immunol 102:961–967

Hoyne GF, Askonas BA, Hetzel C, Thomas WR, Lamb JR (1996) Regulation of house dust mite responses by intranasally administered peptide. Transient activation of $CD4^+$ T cells precedes the development of tolerance in vivo. Int Immunol 8:335–342

Hoyne GF, Jarnicki AG, Thomas WR, Lamb JR (1997) Characterization of the specificity and duration of T cell tolerance to intranasally administered peptides in mice:

a role for intramolecular epitope suppression. Int Immunol 9:1165–1173
Hoyne GF, Le Roux I, Corsin-Jimenez M, Tan K, Dunne J, Forsyth LMG, Dallman MJ, Owen MJ, Ish-Horowicz D, Lamb JR (2000) *Serrate1*-induced *Notch* signalling regulates the decision between immunity and tolerance made by peripheral $CD4^+$ T cells. Int Immunol 12:177–185
Hufnagl K, Wagner B, Winkler B, Baier K, Hochreiter R, Thalhammer J, Kraft D, Scheiner O, Breiteneder H, Wiedermann U (2003) Induction of mucosal tolerance with recombinant Hev b 1 and recombinant Hev b 3 fpr prevention of latex allergy in BALB/c mice. Clin Exp Immunol 133:170–176
Hufnagl K, Winkler B, Focke M, Valenta R, Scheiner O, Renz H, Wiedermann U (2005) Intranasal tolerance induction with polypeptides derived from 3 noncross-reactive major aeroallergens prevents allergic polysensitization in mice. J Allergy Clin Immunol 116:370–376
Jarnicki AG, Thomas WR (2002) Stimulatory and inhibitory epitopes in the T cell responses of mice to Der p 1. Clin Exp Allergy 32:942–950
Marth T, Ring S, Schulte D, Klensch N, Strober W, Kelsall BL, Stallmach A, Zeitz M (2000) Antigen-induced mucosal T cell activation is followed by Th1 T cell suppression in continuously fed ovalbumin TCR-transgenic mice. Eur J Immunol 30:3478–3486
Meade BJ, Woolhiser M (2002) Murine models for natural rubber latex allergy assessment. Methods 27:63–68
Neuhaus-Steinmetz U, Glaab T, Daser A, Braun A, Lommatzsch M, Herz U, Kips J, Alarie Y, Renz H (2000) Sequential development of airway hyperresponsiveness and acute airway obstruction in a mouse model of allergic inflammation. Int Arch Allergy Immunol 121:57–67
Plopper CG, Van Winkle LS, Fanucchi MV, Malburg SR, Nishio SG, Chang A, Buckpitt AR (2001) Early events in naphthalene-induced acute Clara cell toxicity. II Comparison of glutathione depletion and histopathology by airway location. Am J Respir Cell Mol Biol 24:272–281
Postlethwait EM, Joad JP, Hyde DM, Schelegle ES, Bric JM, Weir AJ, Putney LF, Wong VJ, Velsor LW, Plopper CG (2000) Three-dimensional mapping of ozone-induced acute cytotoxicity in tracheobronchial airways of isolated perfused rat lung. Am J Respir Cell Mol Biol 22:191–199
Raap U, Brzoska T, Sohl S, Päth G, Emmel J, Herz U, Braun A, Luger T, Renz H (2003) α-Melanocyte-stimulating hormone inhibits allergic airway inflammation. J Immunol 170:353–359
Reader JR, Tepper JS, Schelegle ES, Aldrich MC, Putney LF. Pfeiffer JW, Hyde DM (2003) Pathogenesis of mucous cell metaplasia in a murine asthma model. Am J Pathol 162:2069–2078
Renz H, Smith HR, Henson JE, Ray BS, Irvin CG, Gelfand EW (1992) Aerosolized antigen exposure without adjuvant causes increased IgE production and increased airway responsiveness in the mouse. J Allergy Clin Immunol 89:1127–1138
Repa A, Wild C, Hufnagl K, Winkler B, Bohle B, Pollak A, Wiedermann U (2004) Influence of the route of sensitization on local and systemic immune response in a model of type I allergy. Clin Exp Immunol 137:12–18
Thakker JC, Xia JQ, Rickaby DA, Krenz GS, Kelly KJ (1999) A murine model of latex allergy-induced airway hyperresponsiveness. Lung 177:89–100
Treter S, Luqman M (2000) Antigen-specific T cell tolerance down-regulates mast cell responses in vivo. Cell Immunol 206:116–124
Uhal BD, Joshi I, Highes WF, Ramos C, Pardo A, Selman M (1998) Alveolar epithelial cell death adjacent to underlying myofibroblasts in advanced fibrotic human lung. Am J Physiol 275 (6 Pt 1):L1192–L1199
Von Garnier C, Astori M, Kettner A, Dufour N, Heusser C, Corradin G, Spertini F (2000) Allergen-derived long peptide immunotherapy down-regulates specific IgE responses and protects from anaphylaxis. Eur J Immunol 30:1638–1645
Van Halteren AG, van der Cammen MJ, Cooper D, Savelkoul HF, Kraal G, Holt PG (1997) Regulation of antigen-specific IgE, IgG1, and mast cell responses to ingested allergen by mucosal tolerance induction. J Immunol 159:3009–3015
Wegmann M, Fehrenbach H, Fehrenbach A, Held T, Schramm C, Garn H, Renz H (2005) Involvement of distal airways in a chronic model of experimental asthma. Clin Exp Allergy 35:1263–1271
Wiedermann U, Jahn-Schmid B, Lindblad M, Rask C, Holmgren J, Kraft D, Ebner C (1999) Suppressive versus stimulatory effects of allergen/cholera toxoid (CTB) conjugates depending on the nature of the allergen in a murine model of type I allergy. Intern Immunol 11:1131–1138
Wiedermann U, Herz U, Baier K, Vrtala S, Neuhaus-Steinmetz U, Bohle B, Dekan G, Renz H, Ebner C, Valenta R, Kraft D (2001) Intranasal treatment with a recombinant hypoallergenic derivative of the major birch pollen allergen Bet v 1 prevents allergic sensitization and airway inflammation in mice. Int Arch Allergy Immunol 126:68–77
Winkler B, Hufnagl K, Spittler A, Ploder M, Kállay E, Vrtala S, Valenta R, Kundi M, Renz H, Wiedermann U (2006) The role of Foxp3+ T cells in long-term efficacy of prophylactic and therapeutic mucosal tolerance induction in mouse. Allergy 61:173–180
Woolhiser MR, Munson AE, Meade BJ (2000) Immunological responses of mice following administration of natural rubber latex proteins by different routes of exposure. Toxicol Sci 55:343–351
Yasue M, Nakamura S, Yokota T, Okudaira H, Okumura Y (1998a) Experimental monkey model sensitization with mite antigen. Int Arch Allergy Immunol 115:303–311
Yasue M, Yokota T, Fukuda M, Takai T, Suko M, Okudaira H, Okumura Y (1998b) Hyposensitization to allergic reaction in rDer f 2-sensitized mice by the intranasal administration of a mutant of rDer f 2, C8/119S. Clin Exp Immunol 113:1–9
Yasue M, Yokota T, Suko M, Okudaira H, Okomura Y (1998c) Comparison of sensitization to crude and purified house dust mite allergens in inbred mice. Lab Anim Sci 48:346–352
Yasue M, Yokota T, Okudaira H, Okumura Y (1999) Induction of allergic reactions in guinea pigs with purified house dust mite allergens. Cell Immunol 192:185–193

D.2.2.9 Bleomycin-Induced Pulmonary Fibrosis

PURPOSE AND RATIONALE

Pulmonary fibrosis has been induced by bleomycin in various species: golden Syrian **hamsters** (Giri et al. 1986; Chen et al. 1997; Gurujeyalakshmi et al. 1999; Iyer et al. 1999, 2000), **mice** (Taooka et al. 1997; Tamagawa et al. 2000; Keerthisingam et al. 2001; Terasaki et al. 2000; Terasaki 2001; Atzori et al. 2004) and **rats** (Howell et al. 2001; Simler et al. 2002; Wang et al. 2002; Morcillo and Bulbena 2003).

Iyer et al. (1999) determined the effects of pirfenidone on procollagen gene expression at the transcription level in a bleomycin **hamster** model of lung fibrosis.

PROCEDURE

Treatment of Animals

Male golden Syrian hamsters weighing 90–110 g were housed in groups of four in facilities with filtered air and constant temperature and humidity. A 12-h/12-h light/dark cycle was maintained, and the animals had access to water and either pulverized Rodent Laboratory Chow 5001 or the same pulverized chow containing pirfenidone (0.5% w/w). The hamsters were fed these diets 2 days before intratracheal instillation and throughout the study period. Hamsters were instilled intratracheally with saline or bleomycin (7.5 units/kg per 5 ml). The animals were sacrificed at 3, 7, 10, 14, and 21 days after the bleomycin or saline instillation by decapitation, and their lungs were removed and freeze-clamped, dropped in liquid nitrogen, and stored at –80°C. The major portion of the sample was used for direct total RNA isolation, and the remainder was used for other biochemical studies.

Tissue Processing for Biochemical Study

The frozen lungs were thawed and homogenized in 0.1 M KCl/0.02 M Tris·HCl buffer, pH 7.6, with a Polytron homogenizer. After recording the total homogenate volume (5–6 ml), it was mixed, divided into aliquots, and stored at –80°C, except for the aliquots for lipid peroxidation and hydroxyproline assays, which were processed and assayed the same day on which the lungs were homogenized.

Determination of Lipid Peroxidation

The lung malondialdehyde equivalent (MDAE) level, an index of lipid peroxidation, was determined in the whole homogenate according to the method of Ohkawa et al. (1979)

Determination of Prolyl Hydroxylase Activity

The method for prolyl hydroxylase assay is based on the release of tritiated water from 3,4-[^{3}H]proline-labeled unhydroxylated procollagen substrate prepared *in vitro* using 10-day-old embryonic chick tibiae (Giri et al. 1983). During the reaction, tritium is released in stoichiometric proportion to prolyl hydroxylation as tritiated water, which is collected and counted as a measure of the prolyl hydroxylase activity (Hutton et al. 1966). The activity was expressed as the total dpm released/lung per 30 min.

Determination of Prolyl Hydroxylase Activity In Vitro

Control hamsters not subjected to any treatment were first anesthetized with sodium pentobarbital (80–100 mg/kg). Their lungs were perfused with ice-cold isotonic saline; then, all lung lobes were dissected out and rinsed in saline. They were immediately homogenized in buffer containing 0.1 M Tris and 0.05% Triton X. The homogenate was spun down at 6000 g for 20 min at 4°C. The supernatant was gently aspirated and used to determine prolyl hydroxylase activity and its protein content. The procedure to measure the prolyl hydroxylase activity was essentially the same as described above. Briefly, the reaction mixture in a total volume of 2.2 ml consisted of 200 µl of α-ketoglutarate (0.001 M), 200 µl of ferrous ammonium sulfate (0.005 M), 250 µl of supernatant as enzyme source, 200 µl of pirfenidone to produce the desired final concentration, 200 µl of Tris·HCl (1 M), and 20 µl of ^{3}H-unhydroxylated PC substrate (400,000 cpm). The reaction mixture was first preincubated with pirfenidone at different concentrations for 30 min at 37°C in a shaking water bath. The reaction was started by adding 200 µl of ascorbic acid (0.005 M); 30 min later, the reaction was terminated by adding 200 µl of 50% trichloroacetic acid. The tritiated water released was collected by vacuum distillation. Then 1 ml of the tritiated water was mixed with 10 ml of Ready Safe liquid scintillation cocktail (Beckman), and the radioactivity was determined at 45% counting efficiency in a scintillation counter. The protein content of the supernatant was determined according to the method of Lowry et al. (1951). The prolyl hydroxylase activity was expressed as total dpm associated with tritiated water released in the reaction mixture/mg protein per 30 min.

Determination of Hydroxyproline

For assay of lung hydroxyproline as a measure of collagen content, 1 ml of whole homogenate was precipitated with 0.25 ml of ice-cold 50% (w/v) trichloroacetic acid and centrifuged, and the precipitate was hydrolyzed in 2 ml of 6 N HCl for 18 h at 110°C. The hydroxyproline content was measured according to the method of Woessner (1961).

EVALUATION

All data are expressed as mean ± SEM. Bleomycin treatment increases the amount of proteins of extrapulmonary origin that can result in the artificial lowering of all values (Karlinski and Goldstein 1980; Goldstein and Fine 1986). Thus, the *in vivo* data are expressed on a per-lung basis. The data were compared within the groups at the corresponding times using the two-way

ANOVA where four groups were involved, and the *t* test between the two groups. A value of $P \leq 0.05$ was considered to be the minimum level of statistical significance.

MODIFICATIONS OF THE METHOD

Howell et al. (2001) induced pulmonary fibrosis in **rats**. Male Lewis rats, aged 6 weeks and weighing 140–170 g, were anesthetized by intramuscular injection of 0.75–1.0 ml/kg Hypnorm (fentanyl citrate, 0.315 mg/ml, and fluanisone, 10 mg/ml). Bleomycin sulfate was administered by a single intratracheal injection (l.5 mg/kg body weight in 0.3 ml of sterile saline). Control animals received 0.3 ml of saline alone. In initial experiments, groups of six rats were killed by pentobarbitone overdose after 6 days to allow assessment of thrombin levels in broncho-alveolar lavage fluid. Separate groups of two rats were sacrificed 1, 3, 6, and 14 days after bleomycin instillation for immunohistochemical assessment of thrombin and protease-activated receptor1. Lungs were fixed by intratracheal instillation of 4% paraformaldehyde, the trachea ligated, and the inflated lungs and heart removed *en bloc*. Tissues were fixed and transferred to 15% sucrose in phosphate-buffered saline, before alcohol dehydration and embedding in paraffin wax. An additional series of animals was killed 6 days after bleomycin or saline instillation for measurement of blood coagulation parameters, total and differential cell counts in broncho-alveolar lavage fluid, and for Northern blot analysis of lung tissue connective tissue growth factor and α_1(I) procollagen mRNA levels. For measurement of coagulation parameters, blood was collected from the inferior vena cava of animals after laparotomy, and was immediately mixed 10:1 with a solution of 3.8% trisodium citrate (w/v). For measurement of total lung collagen and connective tissue growth factor and procollagen mRNA levels, the vasculature was perfused with 5 ml of sterile saline containing 100 U/ml heparin. The lungs were removed, weighed, and immediately snap-frozen in liquid N_2 after removing the trachea and major airways.

Adachi et al. (2003) and Azoulay et al. (2003) studied the effects of granulocyte colony-stimulating factor (G-CSF) on lung injury induced by various doses of bleomycin in rats.

Sogu et al. (2004) found that endosteine, an antioxidant, prevents bleomycin-induced pulmonary fibrosis in rats.

Chen et al. (2006) reported that short courses of low-dose dexamethasone delay bleomycin-induced lung fibrosis in rats.

Chaudhary et al. (2006) described the time course of inflammation and fibrosis in the rat bleomycin model and studied the effect of timing of anti-inflammatory and antifibrotic treatments on efficacy.

Barrio et al. (2006) studied *in vitro* tracheal hyperresponsiveness to muscarinic receptor stimulation by carbachol in the rat model of bleomycin-induced pulmonary fibrosis.

Terasaki et al. (2000) and Terasaki (2001) studied the effect of epimorphin in bleomycin-induced pulmonary fibrosis in **mice**. Pulmonary fibrosis was induced in 8-week-old male ICR mice by a single intratracheal instillation of bleomycin. On selected days after injection (days 0, 3, 7, 14, 21, 28, 35, 42, and 56), the lungs were harvested and investigated. Immunohistochemical analysis was performed for epimorphin using light microscopy and confocal microscopy and also the analysis by immunoelectron microscopy and *in situ* hybridization.

Avivi-Green et al. (2006) reported that discoidin domain receptor 1-deficient mice are resistant to bleomycin-induced lung fibrosis. Matsuyama et al. (2006) found that suppression of discoidin domain receptor 1 by RNA interference attenuates lung inflammation induced by intratracheal instillation of bleomycin in mice.

Inayama et al. (2006) reported that a Iκ B kinase-β inhibitor ameliorates bleomycin-induced pulmonary fibrosis in mice.

REFERENCES AND FURTHER READING

Adachi K, Suzuki M, Sugimoto T, Yorozu K, Takai H, Uetsuka K, Nakyama H, Doi K (2003) Effects of granulocyte colony-stimulating factor (G-CSF) on bleomycin-induced lung injury of various severity. Toxicol Pathol 31:665–673

Atzori L, Chua F, Dunsmore SE, Willis D, Barbarisi M, McAnulty RJ, Laurent GJ (2004) Attenuation of bleomycin induced pulmonary fibrosis in mice using the heme oxygenase inhibitor Zn-deuteroporphyrin IX-2,4-bisethylene glycol. Thorax 59:217–223

Avivi-Green C, Singai M, Vogel WF (2006) Discoidin domain receptor 1-deficient mice are resistant to bleomycin-induced lung fibrosis. Am J Respir Crit Care Med 174:420–427

Azoulay E, Herigault S, Levame M, Brochard L, Schlemmer B, Harf A, Celclaux C (2003) Effect of granulocyte colony-stimulating factor on bleomycin-induced acute lung injury and pulmonary fibrosis. Crit Care Med 31:1442–1448

Barrio J, Cortijo J, Milara J, Mata M, Guijarro R, Blasco P, Morcillo EJ (2006) In vitro tracheal hyperresponsiveness to muscarinic receptor stimulation by carbachol in a rat model of bleomycin-induced pulmonary fibrosis. Auton Autacoid Pharmacol 26:327–333

Chaudhary NI, Schnapp A, Park JE (2006) Pharmacologic differentiation of inflammation and fibrosis in the rat bleomycin model. Am J Respir Crit Care Med 173:769–776

Chen F, Gong L, Zhang L, Wang H, Qi X, Wu X, Xiuao Y, Cai Y, Liu L, Li X, Ren J (2006) Short courses of low dose dex-

amethasone delay bleomycin-induced lung fibrosis in rats. Eur J Pharmacol 536:287–295
Chen J, Ziboh V, Giri SN (1997) Up-regulation of platelet-activating factors in lung and alveolar macrophages in the bleomycin-hamster model of pulmonary fibrosis. J Pharmacol Exp Ther 280:1219–1227
Giri SN, Chen Z, Younker WR, Schiedt MJ (1983) Effects of intratracheal administration of bleomycin on GSH shuttle enzymes, catalase, lipid peroxidation and collagen content in the lungs of hamsters. Toxicol Appl Pharmacol 71:132–141
Giri SN, Hyde DM, Nakashima JM (1986) Analysis of bronchoalveolar lavage from bleomycin-induced pulmonary fibrosis in hamsters. Toxicol Pathol 14:149–157
Goldstein RH, Fine A (1986) A fibrotic reactions in the lung: the activation of the lung fibroblast. Exp Lung Res 11:245–261
Gurujeyalakshmi G, Hollinger MA, Giri SN (1999) Pirfenidone inhibits PDGF isoforms in bleomycin hamster model of lung fibrosis at the translational level. Am J Physiol 276:L311–L318
Howell DCJ, Goldsack NR, Marshall RP, McAnulty RJ, Starke R, Purdy G, Laurent GJ, Chambers RC (2001) Direct thrombin inhibition reduced lung collagen, accumulation, and connective tissue growth factor mRNA levels in bleomycin-induced pulmonary fibrosis. Am J Pathol 159:1383–1395
Hutton JJ Jr, Tappel AL, Undenfriend SA (1966) A rapid assay for collagen proline hydroxylase. Anal Biochem 16:384–394
Inayama M, Nishioka Y, Azuma M, Muto S, Aono Y, Makino H, Tani K, Uehara H, Izumi K, Itai A, Sone S (2006) A novel Iκ B kinase-β inhibitor ameliorates bleomycin-induced pulmonary fibrosis in mice. Am J Respir Crit Care Med 173:1016–1022
Iyer SN, Gurujeyalakshmi G, Giri SN (1999) Effects of pirfenidone on procollagen gene expression at the transcription level in bleomycin hamster model of lung fibrosis. J Pharmacol Exp Ther 289:211–218
Iyer SN, Hyde DM, Giri SN (2000) Anti-inflammatory effect of pirfenidone in the bleomycin-hamster model of lung inflammation. Inflammation 24:477–491
Karlinsky JB, Goldstein RH (1980) Fibrotic lung disease–a perspective. J Lab Clin Med 96(6):939–942
Keerthisingam CB, Jenkins RG, Harrison NK, Hernandez-Rodriguez NA, Booth H, Laurent GJ, Hart SL, Foster ML, McAnulty RJ (2001) Cyclogenase-2 deficiency results in a loss of the anti-proliferative response to transforming growth factor-b in human fibrotic lung fibroblasts and promotes bleomycin-induced pulmonary fibrosis in mice. Am J Pathol 158:1411–1422
Lowry OH, Rosebrough NJ, Farr AL, Randall RJ (1951) Protein measurement with the Folin-Phenol reagents. J Biol Chem 193:265–275
Matsuyama W, Watanabe M, Shirahama Y, Hirano R, Mitsuyama H, Higashimoto I, Osame M, Arimura K (2006) Suppression of discoidin domain receptor 1 by RNA interference attenuates lung inflammation. J Immunol 176:1928–1936
Morcillo EJ, Bulbena O (2003) In vivo antioxidant treatment protects against bleomycin-induced lung damage in rats. Br J Pharmacol 138:1037–1048
Ohkawa H, Ohismi N, Yagi K (1979) Assay for lipid peroxides in animal tissues by thiobarbituric acid reaction. Anal Biochem 95:351–358
Simler NR, Howell DC, Marshall RP, Goldsack NR, Hasleton PS, Laurent GJ, Chambers RC, Egan JJ (2002) The rapamycin analogue SDZ RAD attenuates bleomycin-induced pulmonary fibrosis in rats. Eur Respir J 19:1124–11247
Sogu S, Ozyurt H, Armutcu F, Kart L, Iraz M, Akyol O, Ozen S, Kaplan S, Temel I, Yildirim Z (2004) Endosteine prevents bleomycin-induced pulmonary fibrosis in rats. Eur J Pharmacol 494:213–220
Tamagawa K, Taooka Y, Maeda A, Hiyama K, Ishioka A, Yamakido M (2000) Inhibitory effects of a lecithinized superoxide dismutase on bleomycin-induced pulmonary fibrosis in mice. Am J Respir Crit Care Med 161:1279–1284
Taooka Y, Maeda A, Hiyama K, Ishioka S, Yamakido M (1997) Effects of neutrophil elastase inhibitor on bleomycin-induced pulmonary fibrosis in mice. Am J Respir Crit Care Med 156:260–265
Terasaki Y (2001) Epimorphin in bleomycin-induced pulmonary fibrosis. Chest 120:S30–S32
Terasaki Y, Fukuda Y, Ishizaki M, Yamanka N (2000) Increased expression of epimorphin in bleomycin-induced pulmonary fibrosis in mice. Am J Respir Cell Mol Biol 23:168–174
Wang HD, Yamaya M, Okinaga S, Jia XY, Kamanaka M, Takahashi H, Guo LY, Ohrui T, Sasaki H (2002) Bilirubin ameliorates bleomycin-induced pulmonary fibrosis in rats. Am J Respir Crit Care Med 165:406–411
Woessner JF, Jr (1961) The determination of hydroxyproline in tissue and protein samples containing small proportion of this amino acid. Arch Biochem Biophys 93:440–444

D.2.2.10 Influence of Cytokines on Lung Fibrosis

PURPOSE AND RATIONALE

Several cytokines (Murphy et al. 2000) are involved in development of pulmonary fibrosis, such as granulocyte-macrophage colony-stimulating factor (GM-CSF), tumor necrosis factor alpha (TNFα), and transforming growth factor beta (TGFβ) (Kelly et al. 2003; Agostini and Gurrieri 2006).

GM-CSF is involved in fibrotic reactions of the lung (Xing et al. 1996; Adachi et al. 2002, 2003).

TGFβ is a central modulator of pulmonary and airway inflammation and fibrosis (Sime et al. 1997; Kolb et al. 2002; Gauldie et al. 2003; Xu et al. 2003; Yao et al. 2004; Hardie et al. 2006; Lee et al. 2006; Sheppard 2006).

Smad proteins are involved in the TGFβ-mediated pulmonary fibrosis (Zhao et al. 2000; Bonniaud et al. 2004, 2005; Kobayashi et al. 2006).

TNFα induces TGFβ (Sime et al. 1998; Warshamana et al. 2001; Sullivan et al. 2005).

Xing et al. (1996) reported that the **transfer of** GM-CSF **gene** to rat lung induces eosinophilia, monocytosis, and fibrotic reactions.

PROCEDURE

Construction of Recombinant Adenovirus Vectors

An 800-bp fragment of murine GM-CSF cDNA was isolated from pCDSRα by digestion with *Bam*HI and *Dra*I. The shuttle plasmid pACCMV contain-

ing 0 to 17 mu human type 5 adenovirus genome with a CMV promoter (760 bp), multicloning sites and SV40 splicing junction/polyA signal (430 bp) inserted in the E1 region of viral genome was first digested with *Sal*I, and the ends were repaired using T4 kinase and dNTPs (New England Biolabs, Beverly, Mass., USA), followed by a secondary digestion with *Bam*HI to generate the 3′ complimentary ends. The GM-CSF fragment was then subcloned into the *Bam*HI/*Sal*I site in PACCMV using T4 ligase (New England Biolabs) to generate the recombinant plasmid PACCMVmGM-CSF. The presence of the GM-CSF insert was confirmed by restriction digestions. The PACCMVmGM-CSF was co-transfected, following a standard procedure described previously (Graham and Prevec 1991), into 293 cells along with a plasmid pAdBHG10 which contained the most rightward sequences (3.7 to 100 mu) of human type 5 adenovirus genome with a partial deletion in the E3 region (Bett et al. 1994). The recombinant replication-deficient adenovirus Ad5E1PACCMVmGM-CSF (Ad5E1GM-CSF) was rescued by homologous recombination. The presence of GM-CSF cDNA in the viral genome was verified by analyzing viral genome fragments upon *Hind*III digestion and by Southern hybridization (Graham and Perec 1991). The control virus Ad5dl70–3 was constructed and characterized as previously described (Bett et al. 1994), and, similar to Ad5E1GM-CSF, this virus had the E1 region crippled, hence incapable of replication.

High titers of the above viruses were generated (Graham and Prevec 1991). Briefly, viruses purified by two rounds of CsCl gradient centrifugation were subjected to chromatography using PD-10 Sephadex columns (Pharmacia Biotech, Baie d'UrFe,Quebec, Canada) to remove CsCl. The virus fractions were collected in PBS containing 10% glycerol, measured for conductance to ensure complete removal of CsCl, pooled, titered, aliquoted and stored at –70°C until use.

Characterization of Recombinant Adenovirus Vector Expressing GM-CSF In Vitro

GM-CSF transgene mRNA was examined by Northern hybridization analysis (Xing et al. 1993) using total RNA from 293 cells infected with 10 plaque-forming units (pfu)/cell of Ad5E1GM-CSF for 24 and 48 h. The supernatants from these cells and from infected rat alveolar macrophages were assayed for GM-CSF using an ELISA kit (Endogene, Cambridge, Mass., USA). This ELISA was specific for mouse GM-CSF without crossreactivity with rat GM-CSF, with a sensitivity of 4 pg/ml.

Delivery of Recombinant Adenovirus Vectors to the Lung

Following a standard procedure (Xing et al. 1994), 300 µl of Ad5E1GM-CSF or control virus Ad5dl70–3 diluted in PBS to a concentration of 1×10^9 pfu was instilled intratracheally to the lung of Sprague Dawley male rats weighing 220–280 g (Charles River Laboratories, Ottawa, Canada). At the end of 1, 2, 4, 7, 12, 18, and 24 days after gene transfer, rats were anesthetized, blood samples were taken from the abdominal aorta, and serum preparation and bronchoalveolar lavage (BAL) were performed.

Transgene and Transgene Protein Expression in the Lung

The left lung of rats obtained at each time point was snap-frozen in liquid nitrogen. Total lung RNA extraction and Northern hybridization were performed. Reverse transcription-polymerase chain reaction (RT-PCR) was performed to examine transgene mRNA expression with total lung RNA using PCR reagents from Promega (Madison, Wis., USA) following the standard protocol. The specific primers for PCR were chosen to ensure the amplification of the transgene-specific GM-CSF mRNA but not the endogenous rat GM-CSF mRNA (Miyatake et al. 1985; Smith et al. 1994). The sense and anti-sense primer sequences were 5′-GTCTCTAACGAGTTCTCCTTCAAG-3′ and 5′-TTCAGAGGGCTATACTGCCTTCCA-3′, respectively. The primers for rat GAPDH were designed as described by Rosenfeld et al. (1992). BAL samples were collected at various times and assayed for transgene protein GM-CSF by ELISA as described above or for TNFα by ELISA specific for both murine and rat TNFα (Genzyme, Cambridge, Mass., USA). Serum samples collected from the same animals were also assayed for circulating levels of GM-CSF by ELISA.

Cytologic Examination of BAL and Blood Samples

Total cell numbers in BAL were determined using a hematocytometer. Differential cell types were determined on cytospins stained with Diff-Quik (Baxter, McGaw Park, Ill., USA) by randomly counting 300–400 cells/cytospin. To analyze the total peripheral blood leukocyte counts and differentials, blood samples were collected into heparin-coated tubes. Total leukocyte numbers were counted on a hematocytometer after lysing red blood cells with a lysis buffer containing 94% H_2O, 3% acetic acid, and 3% Diff-Quik purple stain. Differential leukocytes were determined on blood smears stained with Diff-Quik by counting 500–700 cells/blood smear.

Histopathologic Examination of Lung and other Tissues

The right lung and in some instances the whole lung of each animal were fixed by perfusion with 10% formalin (Fisher Scientific, Fairlawn, N.J., USA). Tissues from heart, liver, spleen, and kidney were also fixed in 10% formalin. Multiple sections from different lobes of the lung or from other organs were stained with hematoxylin/eosin for routine histopathology, with Congo Red for identification of tissue eosinophils, or with Elastic van Gieson for collagen and elastin.

MODIFICATIONS OF THE METHOD

Underwood et al. (2000) demonstrated in guinea pigs and rats that a p38 MAPK inhibitor reduces neutrophilia, inflammatory cytokines, MMP-9, and fibrosis in lung.

Kolb et al. (2001) reported that the proteoglycans decorin and biglycan differentially modulate TGF-β-mediated fibrotic responses in the lung of mice.

Uhal et al. (2003) showed that in rats amiodarone induced lung fibrosis and alveolitis, which could be partially inhibited by angiotensin system antagonists.

Jiang et al. (2004) described regulation of pulmonary fibrosis by the chemokine receptor CXCR3, which is the receptor for the interferon-γ-inducible C-X-C chemokines MIG/CXCL9, IP-10/CXCL10, and I-TAC/CXCL11.

Kim et al. (2006) tested the alveolar epithelial-to-mesenchymal cell transition, which develops *in vivo* during pulmonary fibrosis, and found regulation by the extracellular matrix.

Shi-Wen et al. (2006) found that constitutive ALK5-independent c-Jun N-terminal kinase activation contributes to endothelin-1 overexpression in pulmonary fibrosis and gave evidence of an autocrine endothelin loop operating through the endothelin A and B receptors.

REFERENCES AND FURTHER READING

Adachi K, Suzuki M, Sugimoto T, Suzuki S, Niki R, Oyama A, Uetsuka K, Nakamaya H, Doi K (2002) Granulocyte colony-stimulating factor exacerbates the acute lung injury and pulmonary fibrosis induced by intratracheal administration of bleomycin in rats. Exp Toxicol Pathol 53:501–510

Adachi K, Suzuki M, Sugimoto T, Uetsuka K, Nakamaya H, Doi K (2003) Effects of granulocyte colony-stimulating factor on the kinetics of inflammatory cells in the peripheral blood and pulmonary lesions during the development of bleomycin-induced lung injury in rats. Exp Toxicol Pathol 55:21–32

Agostini C, Gurrieri C (2006) Chemokine/cytokine cocktail in idiopathic pulmonary fibrosis. Proc Am Thorac Soc 3:357–363

Bett AJ, Haddara W, Prevec L, Graham FL (1994) An efficient and flexible system for construction of adenovirus vectors with insertions or deletions in early regions 1 and 2. Proc Natl Acad Sci USA 91:8802–8806

Bonniaud P, Kolb M, Galt T, Robertson J, Robbins C, Stampfli M, Lavery C, Margetts PJ, Roberts AB, Gauldie J (2004) Smad3 null mice develop airspace enlargement and are resistant to TGF-β-mediated pulmonary fibrosis. J Immunol 173:2099–2108

Bonniaud P, Margetts PJ, Ask K, Flanders K, Gauldie J, Kolb M (2005) TGF-β and *Smad3* signaling link inflammation to chronic fibrogenesis. J Immunol 175:5390–5395

Gauldie J, Galt T, Bonnioud P, Robbins C, Kelly M, Warburton T (2003) Transfer of the active form of the transforming growth factor-β1 gene to newborn rat lung induces changes consistent with bronchopulmonary dysplasia. Am J Pathol 163:2575–2584

Graham FL, Prevec L (1991) Gene transfer and expression protocols. In: Murray EJ, Walker JM (eds) Methods in molecular biology.. Humana, Clifton, N.J.. pp 109–127

Hardie WD, Le Cras TD, Jiang K, Tichelaar JW, Azhar M, Korfhagen TR (2006) A conditioned expression of transforming growth factor-α in adult mouse causes pulmonary fibrosis. Am J Physiol 286:L741–L749

Jiang D, Liang J, Hodge J, Lu B, Zhu Z, Yu S, Fan J, Gao Y, Yin Z, Homer R, Gerard C Noble PW (2004) Regulation of pulmonary fibrosis by the chemokine receptor CXCR3. J Clin Invest 114:291–299

Kelly M, Kolb M, Bonnlaud P, Gauldie J (2003) Re-evaluation of fibrinogenic cytokines in lung fibrosis. Curr Pharm Des 9:39–49

Kim KK, Kugler MC, Wolters PJ, Robillard L, Galvez MG, Brumwell AN, Sheppard D, Chapman HA (2006) Alveolar epithelial cell mesenchymal transition develops in vivo during pulmonary fibrosis and is regulated by the extracellular matrix. Proc Natl Acad Sci USA 103:13180–13185

Kobayashi T, Liu X, Wen FQ, Kohyama T, Shen L, Wang XQ, Hashimoto M, Mao L, Togo S, Kawasaki S, Sigiura H, Kamio K, Rennard SI (2006) Smad3 mediates TGF-β1-induced collagen gel contraction by human lung fibroblasts. Biochem Biophys Res Commun 339:290–295

Kolb M, Margetts PJ, Sime PJ, Gauldie J (2001) Proteoglycans decorin and biglycan differentially modulate TGF-β-mediated fibrotic responses in the lung. Am J Physiol 280:L1327–L1334

Kolb M, Bonnlaud P, Galt T, Sime PJ, Kelly MM, Margetts PJ, Gauldie J (2002) Differences in the fibrogenic response after transfer of active transforming growth factor-β1 gene to lungs of "fibrosis-prone" and "fibrosis-resistant" mouse strains. Am J Respir Cell Mol Biol 27:141–150

Lee CG, Kang HR, Homer RJ, Chupp G, Elias JA (2006) Transgenic modeling of transforming growth factor-β1. Role of apoptosis in fibrosis and alveolar remodeling. Proc Am Thorac Soc 3:418–423

Miyatake S, Otsuka T, Yokota T, Lee F, Arai K (1985) Structure of the chromosomal gene for granulocyte-macrophage colony stimulating factor: comparison of the mouse and human genes. EMBO J 4:2561–2568

Murphy PM, Baggiolini M, Charo IF, Hébert CA, Horuk R, Matsushima K, Miller LH, Oppenheim JJ, Power CA (2000) International Union of Pharmacology. XXII. Nomenclature of chemokine receptors. Pharmacol Rev 52:145–176

Rosenfeld MA, Seigfried W, Yoshimura K, Yoneyama, Fukayama KM, Stier LE, Paakko PK, Gilardi P, Stratford-Perricaudet LD, Pericaudet M, Guggino WB, Pavirani A,. Lecocq JP, Crystal RG (1992) In vivo transfer of the human cystic fibrosis transmembrane conductance regulator gene to the airway epithelium. Cell 68:143–155

Sheppard D (2006) Transforming growth factor β: a central modulator of pulmonary and airway inflammation and fibrosis. Proc Am Thoric Soc 3:413–417

Shi-Wen X, Rodrïguez-Pascual F, Lamas S, Holmes A, Howat S, Pearson JD, Dashwood MR, du Bois RM, Denton CP, Black CM, Abraham DJ, Leask A (2006) Constitutive ALK5-independent c-Jun N-terminal kinase activation contributes to endothelin-1 overexpression in pulmonary fibrosis: evidence of an autocrine endothelin loop operating through the endothelin A and B receptors. Mol Cell Biol 26:5518–5527

Sime PJ, Xing Z, Graham FL, Csaky KG, Gauldie J (1997) Adenovector-mediated gene transfer of active transforming growth factor-β1 induces prolonged severe fibrosis in rat lung. J Clin Invest 100:768–776

Sime PJ, Marr RA, Gauldie D, Xing Z, Hewlett BR, Graham FL, Gauldie J (1998) Transfer of tumor necrosis factor-α to rat lung induces severe pulmonary inflammation and patchy interstitial fibrogenesis with induction of transforming growth factor-β1 and myofibroblasts. Am J Pathol 153:825–832

Smith LR, Lundeen KA, Dively JP, Carlo DJ, Brostoff SW (1994) Nucleotide sequence of the Lewis rat granulocyte-macrophage colony-stimulating factor. Immunogenetics 39:80

Sullivan DE, Ferris MB, Pociask D, Brody AR (2005) Tumor necrosis factor-α induces transforming growth factor-β1 expression in lung fibroblasts through the extracellular signal-regulated kinase pathway. Am J Respir Cell Mol Biol 32:342–349

Uhal BD, Wang R, Laukka J, Zhuang J, Soledad-Conrad V, Filippatos G (2003) Inhibition of amiodarone-induced lung fibrosis but not alveolitis by angiotensin system antagonists. Pharmacol Toxicol 92:81–86

Underwood DC, Osborn RR, Bochnowicz S, Webb EF, Rieman DJ, Lee JC, Romnic AM, Adams JL, Hay DWP, Griswold DE (2000) SB 239063, a p38 MAPK inhibitor, reduces neutrophilia, inflammatory cytokines, MMP-9, and fibrosis in lung. Am J Physiol 279:L895–L902

Warshamana GS, Corti M, Brody AR (2001) TNF-α, PDGF, and TGF-β1 expression by primary mouse bronchiolar-alveolar epithelial and mesenchymal cells: TNF-α induces TGF-β1. Exp Mol Pathol 71:13–33

Xing Z, Jordana M, Braciak T, Ohtoshi T, Gauldie J (1993) Lipopolysaccharide induces expression of granulocyte-macrophage colony stimulating factor, interleukin-8, and interleukin-6 in human nasal, but not lung, fibroblasts: evidence for heterogeneity within the respiratory tract. Am J Respir Cell Mol Biol 9:255–263

Xing Z, Braciak T, Jordana M, Croitoru K, Graham FL, Gauldie J (1994) Adenovirus-mediated cytokine gene transfer at tissue sites: overexpression of IL-6 induces lymphocytic hyperplasia in the lung. J Immunol 153:4059–4069

Xing Z, Ohkawara Y, Jordana M, Graham FL, Gauldie J (1996) Transfer of granulocyte-macrophage colony-stimulating factor gene to rat lung induces eosinophilia, monocytosis, and fibrotic reactions. J Clin Invest 97:1102–1110

Xu YD, Hua J, Mui A, O'Connor R, Grotendorst G, Khalil N (2003) Release of biologically active TGF-β1 by alveolar epithelial cells results in pulmonary fibrosis. Am J Physiol 285:L527–L539

Yao HM, Xie QM, Chen JQ, Deng YM, Tang HF (2004) TGF-β1 induces alveolar epithelial to mesenchymal transition in vitro. Life Sci 76:29–37

Zhao J, Shi W, Chen H, Warburton D (2000) Smad7 and Smad6 differentially modulate transforming growth factor-β-induced inhibition of embryonic lung morphogenesis. J Biol Chem 275:23992–23997

D.2.2.11 Emphysema Models

PURPOSE AND RATIONALE

Several animal models of genetically determined emphysema are known, such as the **tight-skin mouse** (Rossi et al. 1984; Martorana et al. 1989; Gayraud et al. 2000), beige mutants of the C57BL6J strain (O'Donnell et al. 1999; Lucattelli et al. 2003), the **blotchy mouse** (Ranga and Kleinerman 1981; McCartney et al. 1988), and **homozygous mutant *klotho*** (***KL***$^{--}$) **mice** (Suga et al. 2000).

Hoyle et al. (1999) described emphysematous lesions, inflammation, and fibrosis in the lungs of transgenic mice overexpressing platelet-derived growth factor. Le Cras et al. (2004) reported that vascular endothelial growth factor causes pulmonary hemorrhage, hemosiderosis, and air space enlargement in neonatal mice. Tsa et al. (2004) reported that overexpression of placenta growth factor contributes to the pathogenesis of pulmonary emphysema in mice.

Blanco et al. (1989), Whitney et al. (1999), Massaro et al. (1995), Massaro and Massaro (2000, 2003), and Dirami et al. (2004) reported that in **rats** septation of gas-exchange saccules occurs during the first two postnatal weeks. Treatment with dexamethasone irreversibly impairs septation. Treatment with all-*trans*-retinoid acid prevents the dexamethasone-induced inhibition of septation.

Hind and Maden (2004) and Maden and Hind (2004) found that retinoic acid induces alveolar regeneration in the adult mouse lung after damage by disulphiram treatment. These data could not be confirmed in an elastase-induced emphysema model by Fujita et al. (2004).

Several authors used elastase instillation to produce emphysema-like lesions in **rats** (Tepper et al. 2000; March et al. 2004), **mice** (Inoue et al. 2003; Murakami et al. 2005), **rabbits** (Qi et al. 2004), and **dogs** (Morino et al. 2005).

Kuraki et al. (2002) described inhibition of human neutrophil elastase-induced emphysema in rats by an oral neutrophil elastase inhibitor.

PROCEDURE

Rat Emphysema Model

Male Wistar rats weighing 228± 15 g were divided into controls (saline treated), low-dose group (treated with 200 U human neutrophil elastase), and a high-

dose group (treated with 400 U human neutrophil elastase). Human neutrophil elastase was sprayed above the carina of the trachea using a microsprayer without tracheotomy. Eight weeks after human neutrophil elastase application, rats were sacrificed and lungs were dissected out to evaluate the morphologic changes.

Effects of Neutrophil Elastase Inhibitor

Rats were divides into four groups: saline control, human neutrophil elastase + CMC, human neutrophil elastase + low dose of inhibitor, and human neutrophil elastase + high dose of inhibitor given orally. Six hours after human neutrophil elastase, lung hemorrhage and neutrophil accumulation in the lung were determined. Eight weeks after the application, the functional and morphologic changes were determined.

Lung Hemorrhage and Neutrophil Accumulation in the Lung

After tracheostomy, broncho-alveolar lavage was performed for determination of neutrophil counts and hemoglobin in lavage fluid. In addition, neutrophil accumulation was estimated using the myeloperoxidase activity.

Lung Volume and Pulmonary Mechanics

Eight weeks after human neutrophil elastase application, rats were anesthetized and tracheotomy was performed. Using a whole-body plethysmograph for small animals, the functional residual capacity (FRC), total lung capacity and static lung compliance were determined.

EVALUATION

Data were presented as mean ± SD. Differences between groups were evaluated for statistical significance using one-way analysis of variance.

MODIFICATIONS OF THE METHOD

Boström et al. (1996) showed that platelet-derived growth factor A signaling is a critical event in lung alveolar myofibroblast development and alveogenesis.

Kirschvink et al. (2005) induced production of pulmonary MMP-2 and MMP-9 and emphysema by repeated cadmium nebulizations in rats.

Corteling et al. (2002) studied the migration and activation of neutrophils into the airway in pathological conditions such as pulmonary emphysema in BALB/c and C57BL/6 **mice** and in **golden hamsters**. The animals were sequentially treated intranasally with 0.3 mg/kg lipopolysaccharide and with 0.5 mg/kg *N*-formyl-Met-Leu-Phe.

Selman et al. (2003) induced emphysema in **guinea pigs** by exposure to the whole smoke of 20 cigarettes per day, 5 days per week, for 1 month, 2 months, and 4 months through a whole-body exposure chamber. Half of the animals received a matrix metalloproteinase inhibitor. After death, the lungs were lavaged with saline solution, and matrix metalloproteinases in the lavage fluid were determined by zymography and immunoblot. Lungs were fixed for histology, immunochemistry, and morphometry.

Lucattelli et al. (2003) described collagen phagocytosis by lung alveolar macrophages in animal models of emphysema.

REFERENCES AND FURTHER READING

Blanco LN, Massaro GD, Massaro D (1989) Alveolar dimensions and number. Developmental and hormonal regulation. Am J Physiol 257 (4 Pt 1):L240–L247

Boström H, Willetts K, Pekny M, Levéen P, Lindahl P, Hedstrand H, Pekna M, Hellström M, Gebre-Medhin S, Schalling M, Nilsson M, Kurland S, Törnell J, Heath JK, Betsholtz C (1996) PDGF-A signaling is a critical event in lung alveolar myofibroblast development and alveogenesis. Cell 85:863–873

Corteling R, Wyss D, Trifilieff A (2002) In vivo models of lung neutrophil activation. BMD Pharmacol 2:1

Dirami C, Massaro GD, Clerch LB, Ryan US, Reczek PR, Massaro D (2004) Lung retinol cells synthesize and secrete retinoic acid, an inducer of alveolus formation. Am J Physiol 286:L249–L256

Fujita M, Ye Q, Ouchi H, Nakashima M, Hamada N, Hagimoto N, Kuwano K, Mason RJ, Nakanishi Y (2004) Retinoic acid fails to reverse emphysema in adult mouse models. Thorax 59:224–230

Gayraud B, Keene DR, Sakai LY, Ramirez F (2000) New insights into the assembly of extracellular microfibrils from the analysis of the fibrillin 1 mutation in the tight skin mouse. J Cell Biol 150:667–679

Hind M, Maden M (2004) Retinoic acid induces alveolar regeneration in the adult mouse lung. Eur Respir J 23:20–27

Hoyle GW, Li J, Finkelstein JB, Eisenberg T, Liu JY, Lasky JA, Athas G, Morris GF, Brody AR (1999) Emphysematous lesions, inflammation, and fibrosis in the lungs of transgenic mice overexpressing platelet-derived growth factor. Am J Pathol 154:1763–1775

Inoue S, Nakamura H, Otake K, Saito H, Terashita K, Sato J, Takeda H, Tomoike H (2003) Impaired pulmonary inflammation response are a prominent feature of streptococcal pneumonia in mice with experimental emphysema. Am J Respir Crit Care Med 167:764–770

Kirschvink N, Vincke G, Fiévez L, Onclinx C, Wirth D, Belleflamme M, Louis R, Cataldo D, Peck MJ, Gustin P (2005) Repeated cadmium nebulizations induce pulmonary MMP-2 and MMP-9 production and emphysema in rats. Toxicology 211:36–48

Kuraki T, Ishibashi M, Takayama M, Shiraishi M, Yoshida M (2002) A novel oral neutrophil elastase inhibitor (ONO-6818) inhibits human neutrophil elastase-induced emphysema in rats. Am J Respir Crit Care Med 166:496–500

LeCras TD, Spitzmiller RE, Albertine KH, Greenberg JM, Whitsett JA, Akeson AL (2004) VEGF causes pulmonary hemorrhage, hemosiderosis, and air space enlargement in neonatal mice. Am J Lung Cell Mol Physiol 287:L134–L142

Lucattelli M, Cavarra E, de Santi MM, Tetley TD, Martorana PA, Lungarella G (2003) Collagen phagocytosis by lung alveolar macrophages in animal models of emphysema. Eur Respir J 22:728–734
Maden M, Hind M (2004) Retinoic acid in alveolar development, maintenance and regeneration. Philos Trans R Soc Lond B Biol Sci 359:799–808
March TH, Cossey PY, Esparca DC, Dix KJ, McDonald DJ, Bowen LE (2004) Inhalation administration of all-trans-retinoic acid for treatment of elastase-induced pulmonary emphysema in Fischer 344 rats. Exp Lung Res 30:383–404
Martorana PA, van Even P, Gardi C, Lungarella G (1989) A 16-month study of the development of genetic emphysema in tight-skin mouse. Am Rev Respir Dis 139:226–232
Massaro GD, Massaro D (2000) Retinoic acid treatment partially rescues failed septation in rats and mice. Am J Physiol 278:L955–L960
Massaro D, Massaro GD (2003) Retinoids, alveolus formation, and alveolar deficiency. Am Respir Cell Mol Biol 28:271–274
Massaro GD, Mortola JP, Massaro D (1995) Sexual dimorphism in the architecture of the lung's exchange region. Prod Natl Acad Sci USA 92:1105–1107
McCartney AC, Fox B, Partridge TA, Macrae KD, Tetley TD, Phillips GJ, Guz A (1988) Emphysema in the Blotchy mouse: a morphometric study. J Pathol 156:77–81
Morino S, Nakamura T, Toba T, Takahashi M, Kushibiki T, Tabata Y, Shimizu Y (2005) Fibroblast growth factor-2 induces recovery of pulmonary blood flow in canine emphysema models. Chest 128:920–926
Murakami S, Nagaya N, Itoh T, Iwase T, Fujisato T, Nishioka K, Hamada K, Kangawa K, Kimura H (2005) Adrenomedullin regenerates alveoli and vasculature in elastase-induced pulmonary emphysema in mice. Am J Respir Crit Care Med 172:581–589
O'Donnell MD, O'Connor CM, FitzGerald MX, Lungarella G, Cavarra E, Martorana PA (1999) Ultrastructure of lung elastin and collagen in mouse models of spontaneous emphysema. Matrix Biol 18:357–360
Qi Y, Zhao G, Liu D, Shriver Z, Sundaram M, Sengupta S, Venkataraman G, Langer R, Sasisekharan R (2004) Delivery of therapeutic levels of heparin and low-molecular-weight heparin through a pulmonary route. Proc Natl Acad Sci USA 101:9867–9872
Ranga V, Kleinerman J (1981) Lung injury and repair in the blotchy mouse. Effects of nitrogen dioxide inhalation. Am Rev Respir Dis 123:90–97
Rossi GA, Hunninghake GW, Gadak JE, Szapiel SV, Kawanami O, Ferrans JV, Crystal RG (1984) Hereditary emphysema in the tight-skin mouse. Evaluation of pathogenesis. Am Rev Respir Dis 129:850–855
Selman M, Cisneros-Lira J, Gaxiola M, Ramïrez R, Kudlacz EM, Mitchell PG, Pardo A (2003) Matrix metalloproteinases inhibition attenuates tobacco smoke-induced emphysema in guinea pigs. Chest 123:1633–1641
Suga T, Kurabayashi M, Sando Y, Ohyama Y, Maeno T, Maeno Y, Aizawa H, Matsumura Y, Kuwaki T, Kuro-o M, Nabeshima Y, Nagai R (2000) Disruption of the *klotho* gene causes pulmonary emphysema in mice. Defect in maintenance of pulmonary integrity during postnatal life. Am J Respir Cell Mol Biol 22:26–33
Tepper J, Pfeiffer J, Aldrich M, Tumas D, Kern J, Hoffman E, McLennan G, Hyde D (2000) Can retinoic acid ameliorate the physiologic and morphologic effects of elastase instillation in the rat? Chest 117:242–244
Tsa PN, Su YN, Li H, Huang PH, Chien CT, Lai YL, Lee CN, Chen CA, Cheng WF, Wei SC, Yo CJ, Hsieh FJ, Hsu SM (2004) Overexpression of placenta growth factor contributes to the pathogenesis of pulmonary emphysema. Am J Respir Crit Care Med 169:505–511
Whitney D, Massaro GD, Massaro D, Clerch LB (1999) Gene expression of cellular retinoid-binding proteins: modulation by retinoic acid and dexamethasone in postnatal rat lung. Pediatr Res 45:2–7

D.2.2.12 Models of Chronic Obstructive Pulmonary Disease (COPD)

PURPOSE AND RATIONALE

Chronic obstructive pulmonary disease (COPD) is a severe respiratory condition that is increasing in prevalence worldwide. The disease is characterized by airflow limitation that is not fully reversible. The airflow limitation is usually progressive and associated with abnormal inflammatory response of the lungs to noxious particles and gases. Three conditions comprise COPD, namely mucus hypersecretion, emphysema and bronchiolitis. Cigarette smoking is the major risk factor for development of COPD and accounts for the majority of cases (Donnelly and Rogers 2003). The relevance of the present animal models for COPD has been questioned (Canning 2003). Several authors used chronic cigarette-smoke exposure in mice (Hautamaki et al. 1997; Cavarra et al. 2001a, 2001b; Wright and Churg 2002; Bartalesi et al. 2005; Martorana et al. 2005), in rats (Escolar et al. 1995; Lee et al. 2005), in guinea pigs (Wright 2001; Meshi et al. 2002), or in dogs (Frasca et al. 1983).

Lee et al. (2005) reported inhibition of cigarette-smoking-induced emphysema and pulmonary hypertension in rat lungs by a HMG-CoA reductase inhibitor.

Martorana et al. (2005) found that a selective phosphodiesterase-4 (PDE4) inhibitor fully prevents emphysema in mice chronically exposed to cigarette smoke.

PROCEDURE

Six-week-old C57Bl/6J male mice were, in acute studies, exposed either to room air or the smoke of five cigarettes (Virginia filter cigarettes: 12 mg of tar and 0.9 mg of nicotine) for 20 min. In chronic studies, the mice were exposed to either room air or to the smoke of three cigarettes/day for 5 days/week for 7 months. Antioxidant capacity was assessed at the end of exposure in broncho-alveolar lavage fluid. Cytokines and chemokines were determined.

In acute studies, mice were divided in three groups of 40 animals each. These groups were then divided

into four subgroups of 10 mice: no treatment/air exposed; no treatment/smoke exposed; low dose of test compound/smoke exposed; high dose of test compound/smoke exposed.

In chronic studies, five groups of animals were used: no treatment/air exposed; drug treatment/air exposed; no treatment/smoke exposed; low dose of test compound/smoke exposed; high dose of test compound/smoke exposed. After 7 months, animals were sacrificed and the lungs fixed intratracheally with 5% formalin at a pressure of 20 cmH_2O. Lung volume was measured by water displacement. Assessment of emphysema included mean linear intercept and internal surface area. The volume density of macrophages, marked immunohistochemically with antimouse Mac-3 monoclonal antibodies, was determined by point counting.

EVALUATION

The significance of the differences was calculated using one-way analysis of variance.

MODIFICATIONS OF THE METHOD

Kumar et al. (2003) compared a selective PDE4 inhibitor with pentoxifylline (a non-selective phosphodiesterase inhibitor) and dexamethasone in ameliorating the lesions of chronic asthma in BALB/c mice sensitized to ovalbumin and chronically challenged with aerosolized antigen for 6 weeks.

Kodavanti et al. (2000) reported that the combination of elastase and sulfur dioxide exposure causes COPD-like lesions in the rat.

The potential of tachykinin receptor antagonists in airways diseases was discussed by Joos and Pauwels (2001).

Sturton and Fitzgerald (2002) reviewed PDE4 inhibitors for the treatment of COPD.

Billah et al. (2002) described the pharmacology of an orally active PDE4 inhibitor.

Pitfalls and opportunities for modeling allergic asthma in mice were discussed by Kumar and Foster (2002).

Inoue et al. (2003) described an impaired pulmonary inflammation response as a prominent feature of streptococcal pneumonia in mice with experimental emphysema.

Dual dopamine D_2 receptor and β_2-adrenoreceptor agonists were proposed for the treatment of COPD (Dougall et al. 2003; Ind et al. 2003).

Lessons from transgenic mice for the relationship between asthma and COPD were discussed by Elias (2004).

Lappalainen et al. (2005) found that interleukin-1β causes pulmonary inflammation, emphysema, and airway remodeling in the adult murine lung.

Romano (2005) discussed selectin antagonists for their therapeutic potential against asthma and COPD.

Jones et al. (2002) described a model for the continuous monitoring of polymorphonuclear leukocyte trapping in the pulmonary vasculature of the **rabbit**.

REFERENCES AND FURTHER READING

Bartalesi B, Cavarra E, Fineschi S, Lucattelli M, Lunghi B, Martorana PA, Lungarella G (2005) Different lung responses to cigarette smoke in two strains of mice sensitive to antioxidants. Eur Resp J 25:15–22

Billah MM, Cooper N, Minnicozzi M, Warneck J, Wang P, Hey JA, Kreutner W, Rizzo CA, Smith SR, Young S, Chapman RW, Dyke H, Shih NY, Piwinski JJ, Cuss FM, Montana, Ganguly AK, Egan RW (2002) Pharmacology of *N*-(3,5-dichloro-1-oxido-4-pyridinyl)-8-methoxy-2-(trifluoromethyl)-5-quinoline carboxamide (SCH 351591) a novel, orally active phosphodiesterase 4 inhibitor. J Pharmacol Exp Ther 302:127–137

Canning BJ (2003) Modeling asthma and COPD in animals: a pointless exercise? Curr Opin Pharmacol 3:244–250

Cavarra E, Lucattelli M, Gambelli F, Bartalesi B, Fineschi S, Szarka A, Giannerini F, Martorana PA, Lungarella G (2001a) Human SLPI inactivation after cigarette smoke exposure in a new in vivo model of pulmonary oxidative stress. Am J Physiol 281:L412–L417

Cavarra E, Bartalesi B, Lucattelli M, Fineschi S, Lunghi B, Gambelli F, Ortiz LA, Martorana PA, Lungarella G (2001b) Effects of cigarette smoke in mice with different levels of α_1-proteinase inhibitor and sensitivity to oxidants. Am J Respir Crit Care Med 164:886–890

Donnelly LE, Rogers DF (2003) Therapy of chronic obstructive pulmonary disease in the 21st century. Drugs 63:1973–1998

Dougall IG, Young A, Ince F, Jackson DM (2003) Dual dopamine D_2 receptor and β_2-adrenoreceptor agonists for the treatment of chronic obstructive pulmonary disease: the pre-clinical rationale. Respir Med 97 Suppl A:S3–S/

Elias J (2004) The relationship between asthma and COPD. Lessons from transgenic mice. Chest 126:111S–116S

Escolar JD, Martinez MN, Rodriguez FJ, Gonzalo G, Escolar MA, Roche PA (1995) Emphysema as a result of involuntary exposure to tobacco smoke: morphometric study in the rat. Exp Lung Res 21:255–273

Frasca JM, Auerbach O, Carter HW, Parks VR (1983) Morphologic alterations induced by short term cigarette smoking. Am J Pathol 111:11–20

Hautamaki RD, Kobayashi DK, Senior RM, Shapiro SD (1997) Requirement for macrophage elastase for cigarette smoke-induced emphysema in mice. Science 277:2002–2004

Ind PW, Laitinen L, Laursen L, Wenzel S, Wouters E, Deamer L, Nystrom P (2003) Early clinical investigations of Viozan (sibenadel HCl), a novel D_2 dopamine receptor, β_2-adrenoreceptor agonist for the treatment of chronic obstructive pulmonary disease symptoms. Respir Med 97 Suppl A:S0–S21

Inoue S, Nakamura H, Otake K, Saito H, Terashita K, Sato J, Takeda H, Tomoike H (2003) Impaired pulmonary inflammation responses are a prominent feature of streptococcal pneumonia in mice with experimental emphysema. Am J Resp Crit Care Med 167:764–770

Jones H, Paul W, Page CP (2002) A new model for the continuous monitoring of polymorphonuclear leukocyte trapping in the pulmonary vasculature of the rabbit. J Pharmacol Toxicol Meth 48:21–29
Joos GF, Pauwels RA (2001) Tachykinin receptor antagonists: potential in airways diseases. Curr Opin Pharmacol 1:235–241
Kodavanti UP, Jackson MC, Ledbetter AD, Starcher BC, Evansky PA, Harewood A, Winsett DW, Costa DL (2000) The combination of elastase and sulfur dioxide exposure causes COPD-like lesions in the rat. Chest 117:299–302
Kumar RK, Foster PS (2002) Modeling allergic asthma in mice. Pitfalls and opportunities. Am J Respir Coll Mol Biol 27:267–272
Kumar RK, Herbert C, Thomas PS, Wollin L, Beume R, Yang M, Webb DC, Foster PS (2003) Inhibition of inflammation and remodeling by Roflumilast and dexamethasone in murine chronic asthma. J Pharmacol Exp Ther 307:349–355
Lappalainen U, Whitsett JA, Wert SE, Tichelaar JW, Bry K (2005) Interleukin-1β causes pulmonary inflammation, emphysema, and airway remodeling in the adult murine lung. Am J Respir Cell Mol Biol 32:311–318
Lee JH, Lee DS, Kim EK, Choe KH, Oh YM, Shim TS, Kim SE, Lee YS, Lee SD (2005) Simvastatin inhibits cigarette smoking-induced emphysema and pulmonary hypertension in rat lungs. Am J Respir Crit Care Med 172:987–993
Martorana PA, Beume R, Lucattelli M, Wollin L, Lungarella G (2005) Roflumilast fully prevents emphysema in mice chronically exposed to cigarette smoke. Am J Respir Crit Care Med 172:848–853
Meshi B, Vitalis TZ, Ionescu D, Elliott WM, Liu C, Wang XD, Hayashi S, Hogg JC (2002) Emphysematous lung destruction by cigarette smoke. The effects of latent adenoviral infection on the lung inflammatory response. Am J Respir Cell Mol Biol 26:52–57
Romano SJ (2005) Selectin antagonists: therapeutic potential on asthma and COPD. Treatments Respir Med 4:85–94
Sturton G, Fitzgerald M (2002) Phosphodiesterase 4 inhibitors for the treatment of COPD. Chest 121.Λ 5 Suppl):192S
Wright JL (2001) The importance of ultramicroscopic emphysema in cigarette smoke-induced lung disease. Lung 179:71–81
Wright JL, Churg A (2002) Animal models of cigarette smoke-induced COPD. Chest 122 [6 Suppl]:301S

D.3 Antitussive Activity

D.3.0.1 Antitussive Activity After Irritant Inhalation in Guinea Pigs

PURPOSE AND RATIONALE

Cough is thought to be caused by a reflex. The sensitive receptors are located in the bronchial tree, particularly in the bifurcation of the trachea. These receptors can be stimulated mechanically or chemically, e. g., by inhalation of various irritants. Nerve impulses then activate the cough center in the brain. Several animals species and several irritants have been used, most frequently the citric acid induced cough in guinea pigs (Charlier et al. 1961; Karlsson et al. 1989 Braga et al. 1993). The pharmacology of cough was reviewed by Reynolds et al. (2004).

PROCEDURE

Guinea pigs of either sex weighing 300–400 g are used. The animal is placed in a cylindrical glass vessel, with 2 tubes at either ends. One serves as the entrance of the aerosol, the other for its efflux. The latter tube has a side-arm connecting to a tambour, from which changes in pressure can be registered. A pinch-clamp with a variable screw is placed on the efflux tube beyond the side arm, permitting the regulation of the sensitivity of the system, so that the normal respiration is not registered, while the displacement of air in the enclosure caused by coughing of the animal is registered. The guinea pig is exposed to the aerosol of 7.5% citric acid in water for 10 min. Each animal is tested first to obtain the control response. The number of tussive responses is registered. One hour later, the test substance is applied either s.c. or orally, and 30 min later the guinea pig is subjected to the aerosol again. The number of coughs during 10 min is recorded.

EVALUATION

The number of coughs after treatment is expressed as percentage of the control period. Using various doses, ED_{50} values can be calculated.

CRITICAL ASSESSMENT OF THE METHOD

The citric acid induced coughing in guinea pigs has been proven to be an effective method to test antitussive agents.

MODIFICATIONS OF THE METHOD

The citric cough model in guinea pigs was used by Adcock et al. (1988) to study the effects of codeine, morhine and an opioid pentapeptide, by Hay et al. (2000) to study a potent and selective neurokinin-3 receptor antagonist, and by Brown et al. (2004) to study antitussive activity of sigma-1 receptor agonists.

Cough elicited by capsaicin inhalation in guinea pigs was used by Bolser et al. (1993, 1997) to study antitussive effects of $GABA_B$ agonists or NK1 and NK2 tachykinin receptor antagonists, by McLeod et al. (1998) to study the antitussive action of antihistamines, and by Trevisani et al. (2004) to investigate the activity of iodo-resiniferatoxin, an ultra potent antagonist of the transient receptor potential vanilloid-1.

Forsberg et al. (1988) studied cough and bronchoconstriction mediated by aerosols of capsaicin or citric acid or nicotine or histamine in guinea pigs.

Püschmann and Engelhorn (1978) studied the inhibition of the coughing reflex induced by inhalation of a citric acid spray in ***rats***.

Other irritants have been used to induce cough, e. g. ammonia in dogs, guinea pigs, and cats (Rosiere et al. 1956; Källqvist and Melander 1957; Chen et al. 1960; Sallé and Brunaud 1960; Ellis et al. 1963), or nebulized sulfuric acid or sulfur dioxide in guinea pigs, rats, cats or dogs (Eichler and Smiatek 1940; May and Widdicombe 1954; Winter and Flakater 1952, 1954; Friebel et al. 1955; Reichle and Friebel 1955; Wiedemeijer et al. 1960; Chermat et al. 1966; Karttunen et al. 1982). Capsaicin aerosol was used by Forsberg and Karlsson (1986), Gallico et al. (1997).

Winter and Flakater (1955) exposed sensitized guinea pigs to aerosol of a specific antigen.

Kamei et al. (1989) induced cough in rats by a nebulized solution of capsaicin. The cough reflex was measured as airflow into or out of the chamber of a body plethysmograph by a pneumotachometer head.

Carotis sinus excitation in dogs induced by injection of lobeline resulting in coughing could be suppressed by codeine (Gross 1957).

Sanzari et al. (1968) induced cough in cats anesthetized with α-chloralose by intravenous injection of 1,1-dimethyl-4-phenylpiperazinium iodide (DMPP), a ganglionic stimulant which is more potent than lobeline and possesses only marginal ganglionic blocking properties. The number of coughs was found to be a linear function of the dose of the irritant. Coughs were recorded as spikes superimposed on the respiratory pattern. The method is suitable for quantitative evaluation of antitussive activity.

REFERENCES AND FURTHER READING

Adcock JJ, Schneider C, Smith TW (1988) Effects of codeine, morphine and a novel opioid pentapeptide BW443C, on cough, nociception, and ventilation in the unanesthetized guinea pig. Br J Pharmacol 93:93–100

Bolser DC, Aziz SM, DeGennaro FC, Kreutner W, Egan RW, Siegel MI, Chapman RW (1993) Antitussive effects of $GABA_B$ agonists in the cat and guinea pig. Br J Pharmacol 110:491–495

Bolser DC, DeGennaro FC, O'Reilly S, McLeod RL, Hey JA (1997) Central antitussive activity of the NK1 and NK2 tachykinin receptor antagonists, CP-99,994 and SR 48968, in the guinea pig and cat. Br J Pharmacol 121:165–170

Braga PC, Bossi R, Piatti G, Dal Sasso M (1993) Antitussive effect of oxatomide on citric acid-induced cough in conscious guinea pig. Arzneim Forsch/Drug Res 43:550–553

Brown C, Fezoui M, Selig WM, Schwartz CE, Ellis JL (2004) Antitussive activity of sigma-1 receptor agonists in the guinea pig. Br J Pharmacol 141:233–240

Charlier R, Prost M, Binon F, Deltour G (1961) Étude pharmacologique d'un antitussif, le fumarate acide de phénéthyl-1 (propyne-2-yl)-4-propionoxy-4 pipéridine. Arch intern Pharmacodyn 134:306–327

Charmat R, Kornowski H, Jondet A (1966) Technique de sélection rapide des substances antitussives. Application à l'évaluation de l'activité d'un dérivé de la prométhazine. Ann pharmaceut franç 24:181–184

Chen JYP, Biller HF, Montgomery EG (1960) Pharmacologic studies of a new antitussive, *alpha*-(dimetylaminomethyl)-*ortho*-chlorobenzhydrol hydrochloride (SL-501, Bayer B-186) J Pharmacol Exp Ther 128:384–391

Eichler O, Smiatek A (1940) Versuche zur Auswertung von Mitteln zur Bekämpfung des Reizhustens. Arch Exp Path Pharm 194:621–627

Ellis GP, Goldberg L, King J, Sheard P (1963) The synthesis and antitussive properties of some cyclopentane derivates. J Med Chem 6:111–117

Forsberg K, Karlsson JA (1986) Cough induced by stimulation of capsaicin-sensitive sensory neurons in conscious guinea pigs. Acta Physiol Scand 128:319–320

Forsberg K, Karlsson JA, Theodorsson E, Lundsberg JM, Persson CG (1988) Cough and bronchoconstriction mediated by capsaicin-sensitive sensory neurons in the guinea pig. Pulmon Pharmacol 1:33–39

Friebel H, Reichle C, v. Graevenitz A (1955) Zur Hemmung des Hustenreflexes durch zentral angreifende Arzneimittel. Arch exp Path Pharm 224:384–400

Gallico L, Borghi A, Dalla Rosa C, Ceserani R, Tognella S (1994) Mogusteine: a novel peripheral non-narcotic antitussive drug. Br. J Pharmacol 112:795–800

Gross A (1957) Etude expérimentale, chez le chien choralosé, de l'action antitussive de la codéine, au moyen du réflexe pleurotussigène et de la toux lobélinique. C R Soc Biol, Paris 151:704–707

Hay DWP, Giardina GAM, Griswold DE, Underwood DC, Kotzer CJ, Bush B, Potts W, Sandhu P, Lundberg D, Foley JJ, Schmidt DB, Martin LD, Kilian D, Legos JJ, Barone FC, Luttmann MA, Grugni M, Raveglia LF, Sarau HM (2002) Nonpeptide tachykinin receptor antagonists. III. SB235375, a low central nervous system-penetrant, potent and selective neurokinin-3 receptor antagonist, inhibits citric acid-induced cough and airways hyper-reactivity in guinea pigs. J Pharmacol Exp Ther 300:314–323

Källqvist I, Melander B (1957) Experimental and clinical evaluation of chlorcyclizine as an antitussive. Arzneim Forsch 7:301–304

Kamei J, Tanihara H, Igarashi H, Kasuya Y (1989) Effects of N-methyl-D-aspartate antagonists on the cough reflex. Eur J Pharmacol 168:153–158

Karlsson JA, Lanner AS, Persson CGA (1989) Airway opioid receptors mediate inhibition of cough and reflex bronchoconstriction in guinea pigs. J Pharmacol Exp Ther 252:863–868

Karttunen P, Koskiniemi J, Airaksinen MM (1982) An improvement to the use of sulfur dioxide to induce cough in experimental animals. J Pharmacol Meth 7:181–184

May AJ, Widdicombe JG (1954) Depression of the cough reflex by pentobarbitone and some opium derivatives. Br J Pharmacol 9:335–340

McLeod RL, Mingo G, O'Reilly S, Ruck LA, Bolser DC, Hey JA (1998) Antitussive action of antihistamines is independent of sedative and ventilation activity in the guinea pig. Pharmacology 52:57–64

Püschmann S, Engelhorn R (1978) Pharmakologische Untersuchungen des Bromhexin-Metaboliten Ambroxol. Arzneim Forsch/Drug Res 28:889–898

Reichle C, Friebel H (1955) Zur Hemmung des Hustenreflexes durch zentral angreifende Arzneimittel. II. Mitteilung. Arch exp Path Pharm 226:558–562

Reynolds SM, Mackenzie AJ, Spina D, Page CP (2004) The pharmacology of cough. Trends Pharmacol Sci 25:569–576
Rosiere CE, Winder CV, Wax J (1956) Ammonia cough elicited through a tracheal side tube inn unanesthetized dogs. Comparative antitussive bioassay of four morphine derivatives and methadone in terms of ammonia thresholds. J Pharmacol Exp Ther 116:296–316
Sallé J, Brunaud M (1960), Nouvelle technique d'enregistrement des mouvements de toux provoqués par l'inhalation de vapeurs irritantes chez le cobaye. Arch Int Pharmacodyn 126:120–125
Sanzari NP, Fainman FB, Emele JF (1968) Cough induced by 1,1-dimethyl-4-phenylpiperazinium iodide: a new antitussive method. J Pharmacol Exp Ther 162:190–195
Shemano I (1964) Techniques for evaluating antitussive drugs in animals. In: Nodine JH, Siegler PE (eds) Animal and clinical pharmacologic techniques in drug evaluation. Year Book Medical Publishers, Inc. Chicago, pp 456–460
Trevisani M, Milan A, Gatti R, Zanasi A, Harrison S, Fonatana G, Morice AH, Geppetti G (2004) Antitussive activity of iodo-resiniferatoxin in guinea pigs. Thorax 59:769–772
Wiedemeijer JC, Kramer HW, deJongh DK (1960) A screening method for antitussive compounds. Acta Physiol Pharmacol Neerl 9:501–508
Winter CA, Flakater L (1952) Antitussive action of *d*-isomethadone and *d*-methadone in dogs. Proc Soc Exp Biol Med 81:463–465
Winter CA, Flakater L (1954) Antitussive compounds: Testing methods and results. J Pharmacol Exp Ther 112:99–108
Winter CA, Flakater L (1955) The effects of drugs upon a graded cough response obtained in sensitized guinea pigs exposed to aerosol of specific antigen. J Exp Med 101:17–24

D.3.0.2 Cough Induced by Mechanical Stimulation

PURPOSE AND RATIONALE

Cough can be induced by mechanical stimulation of the trachea in anesthetized guinea pigs (Takagi et al. 1960; Gallico et al. 1994).

PROCEDURE

Male guinea pigs weighing 350–400 g are maintained in conditioned quarters (temperature 21 ± 2°C, relative humidity 55 ±10%, 12 h on-12 h off light cycle) with food and water ad libitum for at least 1 week before use.

After overnight fasting with water ad libitum, the guinea pigs are lightly anesthetized with 25% urethane (4 ml/kg i.p.) which induces surgical levels of analgesia without depressant effects on respiratory function. Analgesia is monitored throughout the experiment as the disappearance of head shaking in response to ear pinch. The animals are maintained at a constant body temperature of 37°C by means of a heated plate. A thin steel wire is gently inserted into the trachea through a small incision near the cricoid cartilage. Coughs are evoked by pushing the steel wire to reach the bifurcation of the trachea 35 and 5 min before oral drug administration and 30, 60 and 120 min after treatment. One violent cough occurs upon each stimulation. Only those animals that respond to both mechanical stimulations before dosing are selected and then randomly assigned to receive the test drug at various doses or the standard (codeine 15, 30 and 60 mg/kg). Ten animals per dose are used.

EVALUATION

Evaluation of the statistical significance of the results is performed with Student's *t*-test for paired data. ED_{50} values are determined by logit transformation.

MODIFICATIONS OF THE METHOD

Several other ways of mechanical stimulation have been used, e. g., by a nylon-bristled stimulator thrust into the trachea in **dogs** (Kasé 1952, 1954), or by a silver thread in **decerebrated guinea pigs** (Lemeignan et al. 1966), or by vibration of an iron slung in the trachea of a dog induced by an electromagnet (Tedeschi et al. 1959) or electrical stimulation of the trachea via a bronchoscope (Gross et al. (1958) or through implanted copper electrodes (Stefko and Benson 1953; Benson et al. 1953; Granier-Doyeux et al. 1959; Stefko et al. 1961).

Hara and Yanaura (1959), Yanaura et al. (1974, 1982) induced cough in unrestrained animals after implantation of electrodes in the trachea.

Combined mechanical and chemical stimulation has been applied by Kroepfli (1950).

Bolser et al. (1999, 2001) and McLeod et al. (2002) studied the influence of antitussive drugs on the cough motor pattern in anesthetized cats. Coughing was produced by mechanical stimulation of the intrathoracic trachea with a thin flexible polyethylene cannula for 10 s per stimulus trial. During each trial, the cannula was repetitively moved in the trachea at a frequency of ~ 2 Hz. EMGs from the diaphragm and rectus abdominis muscles were recorded with the use of bipolar tungsten-wire electrodes. The diaphragm electrodes were placed through a small midline abdominal incision, which was subsequently closed. Cough is characterized by coordinated bursts of activity in inspiratory and expiratory muscles. Cough was defined as a large burst of EMG activity in the diaphragm that is immediately followed by a burst of EMG activity in the rectus abdominis muscle. This definition differentiates augmented breaths, the aspiration reflex, or the expiration reflex from cough. The antitussive activity of selected drugs was evaluated from cumulative dose responses after intravertebral artery administration of

each compound. The protocol consisted of the application of five consecutive mechanical stimulus trials after vehicle administration. Stimulus trials were applied at 1-min intervals after each dose of compound, for a total of five stimulus trials between doses. Approximately 7 min elapsed between each dose of compound.

Kasé et al. (1976) studied the antitussive activity of d-3-methyl-N-methylmorphinan in conscious mongrel **dogs**. Coughing was induced by mechanical stimulation with a stimulator consisting of 5 hog bristles on the mucosa of tracheal bifurcation through a chronically-built tracheal fistula and in lightly anesthetized cats with a stimulator consisting of 5 whiskers of a rabbit.

REFERENCES AND FURTHER READING

Benson WM, Stefko PL, Randall LO (1953) Comparative pharmacology of levorphan, racemorphan and dextromorphan and related methyl esters. J Pharmacol Exp Ther 109:189–200

Bolser DC, Hey JA, Chapman RW (1999) Influence of central antitussive drugs on the cough motor pattern. J Appl Physiol 86:1017–1024

Bolser DC, McLeod RL, Tulshian DB, Hey JA (2001) Antinociceptive action of nociceptin in the cat. Eur J Pharmacol 430:107–111

Gallico L, Borghi A, Dalla Rosa C, Ceserani R, Tognella S (1994) Mogusteine: a novel peripheral non-narcotic antitussive drug. Br. J Pharmacol 112:795–800

Granier-Doyeux M, Horande M, Kucharski W (1959) Méthode d'évaluation quantitative des agents antitussigènes. Arch Int Pharmacodyn 121:287–296

Gross A, Lebon P, Rambert R (1958) Technique de toux expérimentale chez le Chien., par excitation faradique, sous bronchoscopie, de l'éperon trachéal. C R Soc Biol Paris 152:495–497

Hara S, Yanaura S (1959) A method of inducing and recording cough and examination of the action of some drugs with this method. Jap J Pharmacol 9:46–54

Kasé Y (1952) New methods of estimating cough depressing action. Jap J Pharmacol 2:7–13

Kasé Y (1954) The "coughing dog" – an improved method for the evaluation of an antitussive. Pharm Bull (Jpn) 2:298–299

Kasé Y, Kito G, Miyata T, Uno T, Takahama K, Ida H (1976) Antitussive activity and other related pharmacological properties of d-3-methyl-N-methylmorphinan (AT-17). Arzneim Forsch/Drug Res 26:353–360

Kroepfli P (1950) Über das Verhalten einiger Atmungsgrößen beim Husten. I. Mitteilung über den Hustenmechanismus. Helv Physiol Acta 8:33–43

Lemeignan M, Streichenberger G, Lechat P (1966) De l'utilisation du Cobaye décérébré pour l'étude des antitussifs. Thérapie 21:361–366

McLeod RL, Bolser CD, Y J, Parra LE, Mutter JC, Wang X, Tulshian DB, Egan RW, Hey JA (2002) Antitussive effect of nociceptin/orphanin FG in experimental cough models. Pulmon Pharmacol Ther 15:213–216

Stefko PL, Benson WM (1953) A method for the evaluation of antitussive agents in the unanesthetized dog. J Pharmacol Exp Ther 108:217–223

Stefko PL, Denzel J, Hickey I (1961) Experimental investigation of nine antitussive drugs. J Pharm Sci 50:216–221

Takagi F, Fukuda H, Yano K (1960) Studies on antitussives. I. Bioassay of antitussives. Yakugaku Zasshi 80:1497–1501

Tedeschi RE, Tedeschi DH, Hitchens JD, Cook L, Mattis PA, Fellows EJ (1959) A new antitussive method involving mechanical stimulation in unanesthetized dogs. J Pharmacol Exp Ther 126:338–344

Yanaura S, Iwase H, Sato S, Nishimura T (1974) A new method for induction of the cough reflex. Jap J Pharmacol 24:453–460

Yanaura S, Kitagawa H, Hosakawa T, Misawa M (1982) A new screening method for evaluating antitussives in conscious guinea pigs. J Pharm Dyn 5:965–971

D.3.0.3 Cough Induced by Stimulation of the Nervus Laryngicus Superior

PURPOSE AND RATIONALE

The probable pathways in the cough reflex arc are receptors in the area of the trachea and the large bronchi, afferent nerves mainly in the branches of the vagus nerve, a "cough center" located in the medulla oblongata, and efferent nerves closing the glottis and reinforcing the expiratory thrust. Stimulation of the Nervus laryngicus superior induces coughing. Antitussive agents with predominantly central action suppress the coughing reflex.

PROCEDURE

Cats of either sex weighing 2–3 kg are anesthetized with 40 mg/kg i.p. pentobarbital, placed on a heated operating table and their extremities secured. Since deep anesthesia suppresses coughing the dose of pentobarbital has to be adjusted. The fur is shaved ventrally at the neck. Small incisions are made at both sides of the larynx. The superior laryngeal nerves (forming a loop) are prepared carefully. After a median skin incision, the trachea is exposed and cannulated. The cannula is connected with a Fleisch-tube (size 00). One femoral artery is cannulated for registration of blood pressure via a Statham pressure transducer. One femoral vein is cannulated for intravenous application of test substances. Small hook electrodes are attached to each laryngeal nerve. At the end of an inspiration square wave impulses with a frequency of 50 Hz, an impulse width of 0.5 ms, an amplitude of 0.2–1.0 Volt, and a duration of 1–10 s are applied every 5 min. The intensity of the forced expiration is measured by the Fleisch pneumotachograph and recorded simultaneously with blood pressure on a polygraph. Prior to the intravenous application of the test compound, the response to three stimuli is recorded serving as control. After injection of the test compound or the

standard the stimuli are repeated every 5 min. Suppression or diminution of the forced expiration is recorded over 1 h. Then, the next dose or the standard (codeine phosphate 1–2 mg/kg i.v.) is applied.

EVALUATION

Total or partial suppression of the forced expiration are recorded over time and expressed as percentage of control. Intensity and duration of the effect are compared with the standard.

CRITICAL ASSESSMENT OF THE METHOD

The method described by Domenjoz (1952) is very useful to detect centrally active antitussive agents like codeine, but by definition can not determine compounds which act on cough receptors in the bronchial area. Moreover, even light anesthesia influences the cough reflex.

MODIFICATIONS OF THE METHOD

Several other assays have been described which elicit the cough reflex by central or nerve stimulation. Toner and Macko (1952) also stimulated the superior laryngeal nerve in anesthetized cats to induce a definite cough as indicated by rapid contractions of the abdominal musculature.

Mattalana and Borison (1955), Chakravarty et al. (1956) used decerebrated cats to study the central effects of antitussive drugs on cough and respiration. Cough responses were obtained by electrical stimulation of the dorsolateral region of the medulla with bipolar needle electrodes oriented by means of a stereotactic instrument.

Lindner and Stein (1959) evaluated derivatives of diphenyl-piperidono-propan, a series of antitussive drugs using a modification of the method originally described by Domenjoz (1952).

Schröder (1951) and Bobb and Ellis (1951) elicited cough in **conscious dogs** by stimulation of the vagus nerve in a surgically prepared skin loop. In anesthetized cats, coughs were elicited by electrical stimulation of the dorsolateral region in the upper medulla (Kasé et al. 1970).

REFERENCES AND FURTHER READING

Bobb JRR, Ellis S (1951) Production of cough and its suppression in the unanesthetized dog. Am J Physiol 167:768–769

Braga PC (1989) Experimental models for the study of cough. In: Braga PC, Allegra L (eds) Cough. Raven Press, Ltd. New York, pp 55–70

Chakravarty NK, Mattalana A, Jensen R, Borison HL (1956) Central effects of antitussive drugs on cough and respiration. J Pharm Exp Ther 117:127–135

Domenjoz R (1952) Zur Auswertung hustenstillender Arzneimittel. Arch exper Path Pharmakol 215:19–24

Kasé Y, Wakita Y, Kito T, Miyata T, Yuizono T, Kataoka M (1970) Centrally-induced coughs in the cat. Life Sci 9:49–59

Lindner E, Stein L (1959) Abkömmlinge des Diphenyl-piperidono-propans – eine neue Reihe hustenstillender Mittel. Arzneim Forsch/Drug Res 9:94–99

Mattalana A, Borison HL (1955) Antitussive agents and centrally-induced cough. Fed Proc 14:367–368

Schröder W (1951) Die Verwendung des Vagusschlingenhundes für die Wertbestimmung hustenstillender Substanzen. Arch Exp Path Pharmakol 212:433–439

Toner JJ, Macko E (1952) Pharmacological studies on bis-(1-carbo-β-diethyl-aminoethoxy)-1-phenylcyclopentane)-ethane disulfonate. J Pharm Exp Ther 106:246–251

van Dongen K (1956) The effect of Narcotine, Ticarda and Romilar on coughs and on the movements of the cilia in the air passages. Acta Physiol Pharmacol Neerl 4:500–507

D.4
Effects on Tracheal Cells and Bronchial Mucus Secretion and Transport

D.4.0.1
In Vitro Studies of Mucus Secretion

PURPOSE AND RATIONALE

Mucus secretion has been studied in isolated tracheas from ferrets and dogs (Borson et al. 1980; Kyle et al. 1987).

PROCEDURE

Ferrets of either sex weighing 0.6 to 1.5 kg are anesthetized with sodium barbital intraperitoneally. The trachea is exposed and cannulated with a special Perspex cannula about 5 mm below the larynx. The animal is then sacrificed with an overdose of the anesthetic and the chest is opened along the midline. The trachea is exposed to the carina, cleared of adjacent tissue, removed from the animal and cannulated just above the carina. The trachea, with its laryngeal end down, is then mounted in a water-jacketed organ bath and bathed on its submucosal site with Krebs-Henseleit solution plus 0.1% glucose at 37°C and bubbled with 95% O_2 and 5% CO_2. The lumen of the trachea remains air-filled. A plastic catheter is inserted into the lower cannula to form an airtight seal into which secretions can periodically be withdrawn and collected. Volumes of secretions are estimated by the weight difference of catheter lengths with and without secretions.

Simultaneous measurements of both mucus secretion and changes in tissue volume *in vitro* are achieved by mounting portions of ferret trachea cut longitudinally along the posterior wall, flattened out and pinned to a Perspex chamber. Krebs-Henseleit solution at

37°C and gassed with 95% O_2 and 5% CO_2, is circulated on the submucosal side of the tissue, while the luminal side is exposed to the atmosphere. The surface area of the exposed tissue is about 50 mm^2. Mucus secretion is promoted by electrical field stimulation at 50–100 V, 20 Hz, 1–2 ms duration, applied through the pins holding the tissue. Before the start of each experiment, surface fluid is gently wiped off from the luminal surface with a tissue pledglet. The epithelium is coated with a layer of powdered tantalum dust; as mucus secretion from submucosal glands occurs through gland ducts, the layer of tantalum effectively traps the secreted mucus above the duct and under the tantalum layer. Nearly hemispherical hillocks are formed. The surface is photographed at intervals through a dissecting microscope and hillock diameters are measured. Assuming the hillocks to be hemispheres, the secretion volume per unit area is calculated. Drugs are added to the submucosal bath.

EVALUATION

Secretory response after electrical stimulation in the presence or absence of drugs is recorded after 45, 90, and 135 min.

MODIFICATIONS OF THE METHOD

Quinton (1979) used isolated tracheae from cats. A segment of the trachea was mounted in a chamber such that the serosal side was constantly bathed in Ringer solution, whereas the epithelial surface was coated with water-saturated paraffin oil. Secretion was stimulated by adding appropriate drug concentrations to the bath. Under a dissecting microscope, small droplets of secretory fluid were observed to form on the tracheal epithelial surface shortly after stimulation. Timed collection of droplets secreted from three to four glands were taken up between oil blocks in constant-bore capillaries (78 µm inner diameter), and droplet volumes were measured for rate determinations usually over a period of 5 min.

CRITICAL ASSESSMENT OF THE METHODS

Both modifications of the *in vitro* methods need at least as many animals and are as time consuming as the *in vivo* methods.

REFERENCES AND FURTHER READING

Borson DB, Chinn RA, Davis B, Nadel JA (1980) Adrenergic and cholinergic nerves mediate fluid secretion from tracheal glands of ferrets. J Appl Physiol Respir Environ Exercise Physiol 49:1027–1031

Kyle H, Robinson NP, Widdicombe JG (1987) Mucus secretion by tracheas of ferret and dog. Eur J Resp Dis 70:14–22

Quinton PM (1979) Composition and control of secretions from tracheal bronchial submucosal glands. Nature 279:551–552

Robinson N, Widdicombe JG, Xie CC (1983a) *In vitro* collection of mucus from the ferret trachea. J Phys 340:7P–8P

Robinson N, Widdicombe JG, Xie CC (1983b) *In vitro* measurement of submucosal gland secretion in the ferret trachea by observation of tantalum dust-coated "hillocks". J Phys 340:8P

Widdicombe JG (1988) Methods for collecting and measuring mucus from specific sources. In: Braga PC, Allegra L (eds) Methods in Bronchial Mucology. Raven Press, Ltd., pp 21–29

D.4.0.2 Acute Studies of Mucus Secretion

PURPOSE AND RATIONALE

Many diseases of the respiratory tract cause both qualitative and quantitative changes in the mucus that covers and protects the airway epithelium. To study the influence of drugs, methods of collecting bronchial mucus are necessary (Braga 1988). Perry and Boyd (1941) described a method for collecting bronchial mucus from the rabbit.

PROCEDURE

Rabbits weighing 2.5 to 3.5 kg are anesthetized by intraperitoneal injection of 1.1 to 1.4 g/kg urethane. The trachea is exposed by blunt dissection and half opened, 2 cm below the cricoid cartilage. One arm of a T cannula with a large enough diameter to slightly distend the trachea is inserted into the trachea. The perpendicular arm is connected to an air outlet of a humidifier (temperature 35–38°C, relative humidity 80%). The other arm is connected to a collection tube. The rabbit is restrained in the supine position on a 60-degree inclined board with his head downward. Respiratory tract fluids are collected in centrifuge tubes at one hour intervals. Mucus secretion can be stimulated by vagal stimulation or by ammonium chloride given by stomach tube or by pilocarpine given i.p.

EVALUATION

Time response curves after stimulants of mucus secretion are compared with data from untreated animals.

MODIFICATIONS OF THE METHOD

A method for collecting mucus from cats, using a segment of cervical trachea about 5 cm long isolated *in situ*, with nerve and blood supplies intact and a glass cannula inserted to each end, has been described by Gallagher et al. (1975).

A method to collect mucus from the upper tract trachea and the nasopharynx in dogs in acute experiments has been proposed by Proctor et al. (1973).

Engler and Szelenyi (1984) described a new method for screening mucosecretolytic compounds using tracheal phenol red secretion in **mice**. Phenol red at a dose of 500 mg/kg was injected intraperitoneally to male mice. Thirty min later, the animals were sacrificed by carbon dioxide. The whole trachea was dissected free from surrounding tissue and excised. Each trachea was washed for 30 min in 1 ml physiological saline. Afterwards, 0.1 ml 1 M NaOH was added to the washing to stabilize the pH of the lavage fluid. The concentration of phenol red was measured photometrically. Agonists were administered subcutaneously 15 min or intragastrally 30 min before phenol red was injected. Antagonists were given 5 min prior to the administration of agonists.

Other dyes, such as Evans blue or sodium fluorescein also are reported to be eliminated in the respiratory tract fluid of mice (Graziani and Cazzulani 1981).

Dye methods reported for mice can also be used for rats (Quevauviller and Vu-Ngoc-Huyen 1966). Alcian blue was used to stain the normal bronchial tree. After chronic treatment with sulfur dioxide, there were changes in bronchial coloration. Administration of drugs protected against the effects of sulfur dioxide.

Secretion from tracheal submucosal glands can be studied in **dogs** (Davis et al. 1982; Johnson and McNee 1983, 1985). In anesthetized dogs the epithelial surface of the upper trachea is exposed and coated with powdered tantalum. Secretions from the submucosal gland ducts form elevations (hillocks) in the tantalum layer. The number of hillocks that appear in a 1.2 cm^2 field is counted.

A micropipette method for obtaining secretions from single submucosal gland ducts *in vivo* in **cat** tracheas has been described (Ueki et al. 1979, 1980; Leikauf et al. 1984). In anesthetized cats an endotracheal tube was inserted into the lower trachea and connected to a constant volume respirator. The remainder of the trachea above the endotracheal tube was then dissected open by a midline incision. Paraffin oil equilibrated with HEPES buffer was then placed on the exposed mucosa to prevent drying and to aid visualization of the gland duct openings. The secretions from the gland duct openings were collected with constant-bore (99 µm ID) glass micropipettes. The volume and the viscosity of the secreted mucus were determined.

CRITICAL ASSESSMENT OF THE METHODS

For the methods of mucus collection in rabbits, cats or dogs a rather high number of animals is necessary to achieve data suitable for statistical analysis. For screening procedures the methods using dye elimination into the trachea of mice or rats seem to be preferable.

REFERENCES AND FURTHER READING

Braga PC (1988) Methods for collecting and measuring airway mucus in animals. In: Braga PC, Allegra L (eds) Methods in Bronchial Mucology. Raven Press, Ltd., pp 3–11

Davis B, Chinn R, Gold J, Popovac D, Widdicombe JG, Nadel JA (1982) Hypoxemia reflexly increases secretion from tracheal submucosal glands in dogs. J Appl Physiol Resp Environ Exercise Physiol 52:1416–1419

Engler H, Szelenyi I (1984) Tracheal phenol red secretion, a new method for screening mucosecretolytic compounds. J Pharmacol Meth 11:151–157

Gallagher JT, Kent PW, Passatore M, Phipps RJ, Richardson PS (1975) The composition of tracheal mucus and the nervous control of its secretion in the cat. Proc Roy Soc London 192:49–76

Graziani G, Cazzulani P (1981) Su un metodo particolarmente indicato per lo studio dell'attivita espettorante nei piccoli animali. Farmaco/Ed Pr 36:167–172

Johnson HG, McNee ML (1983) Secretagogue responses of leukotriene C_4,D_4: comparison of potency in canine trachea *in vivo*. Prostaglandins 25:237–243

Johnson HG, McNee ML (1985) Adenosine-induced secretion in the canine trachea: Modification by methylxanthines and adenosine derivatives. Br J Pharmacol 86:63–67

Leikauf GD, Ueki IF, Nadel JA (1984) Autonomic regulation of viscoelasticity of cat tracheal gland secretions. J Appl Physiol Respir Environ Exercise Physiol 56:426–430

Perry WF, Boyd EM (1941) A method for studying expectorant action in animals by direct measurement of the output of respiratory tract fluids. J Pharmacol Exp Ther 73:65–77

Proctor DF, Aharonson EF, Reasor MJ, Bucklen KR (1973) A method for collecting normal respiratory mucus. Bull Physiopath Respir 9:351–358

Quevauviller A, Vu-Ngoc-Huyen (1966) Hypersecretion expérimentale du mucus bronchique chez le rat. I. Methode de appreciation anatomopathologique. C R Soc Biol 160:1845–1849

Ueki I, German V, Nadel J (1980a) Direct measurement of tracheal mucus gland secretion with micropipettes in cats. Effects of cholinergic and α-adrenergic stimulation. Clin Res 27:59A

Ueki I, German VF, Nadel JA (1980b) Micropipette measurement of airway submucosal gland secretion. Autonomic effects. Am Rev Resp Dis 121:351–357

D.4.0.3 Studies of Mucus Secretion With Chronic Cannulation

PURPOSE AND RATIONALE

Several techniques have been developed for chronic collection of mucus (Wardell et al. 1970; Yankell et al. 1970; Scuri et al. 1980).

PROCEDURE

Beagle dogs weighing 9–11 kg are anesthetized by intravenous injection of 35–40 mg/kg pentobarbital sodium. The cervical trachea is exposed by a midline skin incision and blunt dissection of the muscles. A segment approximately 10 rings in length,

with an intact blood and nerve supply, is transected. The cephalic and caudal parts of the trachea are anastomosed end-to-end with interrupted gut sutures to reestablish a patent airway. The isolated segment is loosened slightly from the surrounding tissue and turned 180° to reverse cilia movement. A funnel-shaped silicone cannula is attached to the outer surface of the proximal end of the tracheal segment with surgical mesh and sutured in place. With cannulation completed, the tracheal segment is placed in a pocket below the sternohyoid muscle and the cannula brought to the surface and exteriorized through a stab wound. Alternatively, the isolated segment is closed at its caudal end with interrupted gut sutures. The mucosal surface of the cervical end of the isolated tracheal segment is sutured with interrupted silk sutures to the overlying subcutaneous tissue through a small incision in the cervical skin. Muscles and skin are sutured normally. In two or three weeks the skin heals over the small stoma resulting in a subcutaneous pouch of functioning tracheal tissue. Mucus samples can be collected for months. In this modification, a balloon can be placed into the pouch. Pressure changes in the balloon due to contraction of the smooth tracheal muscles after physostigmine injection or vagal stimulation or relaxation after atropine injection are recorded demonstrating parasympathetic innervation.

EVALUATION

Parasympathomimetic stimulation (0.5 mg/kg pilocarpine s.c.) increases the flow rate of tracheal fluids. Pressure changes in the balloon after injection of parasympathomimetic or sympathomimetic drugs are compared with baseline values.

MODIFICATIONS OF THE METHOD

Scuri et al. (1980) inserted a T-shaped cannula into the trachea of anesthetized rabbits. The wound was sutured, the third arm was connected with a collecting tube, and after 3 days of antibiotic administration, the mucus was collected at different times to establish basal production. For the experiments, mucus was collected during a 4 h control period, then drugs were given intravenously, orally or as aerosol inhalation. Mucus was further collected during the periods of 0 to 4 and 4 to 24 h and analyzed for sialic acid, fucose, and protein content.

A tracheal pouch method in ferrets has been described by Barber and Small (1974).

Several authors published methods to determine **viscoelastic properties and rheological behavior of tracheal and bronchial mucus**: Philippoff et al. (1970), Lopez-Vidriero and Das (1977), Martin et al. (1980) Kim et al. (1982), Braga (1988), King (1988), Majima et al. (1990).

CRITICAL ASSESSMENT OF THE METHODS

The methods using pouches in dogs may be useful for physiological studies, but for pharmacological purposes the rabbit method of Scuri et al. (1980) seems preferable.

REFERENCES AND FURTHER READING

Barber WH, Smal Jr PAl (1974) Construction of an improved tracheal pouch in the ferret. Am Rev Respir Dis 115:165–169

Braga PC (1988) Dynamic methods in viscoelasticity assessment. Sinusoidal oscillation method. In: Braga PC, Allegra L (eds) Methods in Bronchial Mucology. Raven Press, Ltd. pp 63–71

Kim CS, Berkley BB, Abraham WM, Wanner A (1982) A micro double capillary method for rheological measurements of lower airway secretions. Bull Eur Physiopath Resp 18:915–927

King M (1988) Magnetic microrheometer. In: Braga PC, Allegra L (eds) Methods in Bronchial Mucology. Raven Press, Ltd, pp 73–83

Lopez-Vidriero MT, Das I, Reid LM (1977) Airway secretion: Source, biochemical and rheological properties. In: Brain JD, Proctor DF, Reid LM (eds) Respiratory Defense Mechanisms. Part I, Marcel Dekker, Inc., pp 289–356

Majima Y, Hirata K, Takeuchi K, Hattori K, Sakakura Y (1990) Effects of orally administered drugs on dynamic viscoelasticity of human nasal mucus. Am Rev Respir Dis 141:79–83

Martin M, Litt M, Marriott (1980) The effect of mucolytic agents on the rheological and transport properties of canine tracheal mucus. Am Rev Resp Dis 121:495–500

Philippoff W, Han CD, Barnett B, Dulfano MJ (1970) A method for determining the viscoelastic properties of biological fluids. Biorheology 7:55–67

Scuri R, Frova C, Fantini PL, Mondani G, Riboni R, Alfieri C (1980) Un nuovo metodo per lo studio della mucoproduzione nel coniglio. Boll Chim Farm 119:181–187

Wardell Jr, Chakrin LW, Payne BJ (1970) The canine tracheal pouch. A model for use in respiratory mucus research. Am Rev Resp Dis 101:741–754

Widdicombe JG (1988) Methods for collecting and measuring mucus from specific sources. In: Braga PC, Allegra L (eds) Methods in Bronchial Mucology. Raven Press, Ltd., pp 21–29

Yankell SL, Marshall R, Kavanagh B, DePalma PD, Resnick B (1970) Tracheal fistula in dogs. J Appl Physiol 28:853–854

D.4.0.4 Bronchoalveolar Lavage

PURPOSE AND RATIONALE

Isolation of bronchial cells from bronchoalveolar lavage was described by Myrvik et al. (1961), Bassett et al. (1988), Fryer et al. (1994, 1997), Wang et al. (1997).

PROCEDURE

After determination of mechanical respiratory parameters in anaesthetized guinea pigs, bronchoalveolar lavage is performed via the tracheal cannula. The lungs are lavaged with 5 aliquots of 10 ml phosphate-buffered saline containing 3 mM EDTA and 100 µM isoproterenol (pH 7.2–7.4). The recovered lavage fluid (40–45 ml) is centrifuged, the cells are resuspended in 20 ml of phosphate-buffered saline, and total cells are counted using a hemacytometer. The remaining aliquot is centrifuged again and cells are stained to determine cell differentials.

EVALUATION

The differences in cells recovered from bronchoalveolar lavage between treatment groups are tested by use of a one-factor analysis of variance. $P < 0.05$ is considered significant.

MODIFICATIONS OF THE METHOD

Gossart et al. (1996) determined TNF-α activity in the supernatant of bronchoalveolar lavage by the cytotoxicity against TNF-α-sensitive L929 murine fibroblasts.

REFERENCES AND FURTHER READING

Bassett DJP, Bowen Kelly E, Brewster EL, Elbon CL, Reichenbaugh SS, Bunton T, Kerr JS (1988) A reversible model of acute lung injury based on ozone exposure. Lung 166:355–369

Fryer AD, Yarkony KA, Jacoby DB (1994) The effect of leukocyte depletion on pulmonary M_2 muscarinic receptor function in parainfluenza virus-infected guinea pigs. Br J Pharmacol 112:588–594

Fryer AD, Costello RW, Yost BL, Lobb RR, Tedder TF, Steeber DA (1997) Antibody to VLA-4, but not to L-selectin, protects neuronal M_2 muscarinic receptors in antigen-challenged guinea pig airways. J Clin Invest 99:2036–2044

Gossart S, Cambon C, Orfila C, Séguélas MH, Lepert JC, Rami J, Carré P, Pipy B (1996) Reactive oxygen intermediates as regulators of TNF-α production in rat lung induced by silica. J Immunol 156:1540–1548

Myrvik QN, Leake ES, Fariss B (1961) Studies on pulmonary alveolar macrophages from the normal rabbit: A technique to produce them in a high state of purity. J Immunol 86:128–132

Wang S, Lantz RC, Rider RD, Chen GJ, Breceda V, Hays AM, Robledo RF, Tollinger BJ, Dinesh SVR, Witten ML (1996) A free radical scavenger (Lazaroid U75412E) attenuates tumor necrosis factor-alpha generation in a rabbit smoke-induced lung injury. Respiration 64:358–363

D.4.0.5 Ciliary Activity

PURPOSE AND RATIONALE

Ciliary activity is a natural defense mechanism of the mucosa in the respiratory tract against harmful extraneous agents resulting in a continuous transportation of secreted mucus. Many attempts have been made to visualize and to quantify this phenomenon. Several authors used the light beam reflex method which can be used for *in vivo* as well as for *in vitro* experiments (Dalhamn 1956, 1964; Dalhamn and Rylander 1962; Hakansson and Toremalm 1963; Mercke et al. 1974; Baldetorp et al. 1976; Lopez-Vidriero et al. 1985).

PROCEDURE

Rats are anesthetized by intraperitoneal injection of tribromo-ethanol (Avertin). The trachea is exposed and its soft parts are incised by electrocoagulation so that bleeding is avoided. The cartilaginous rings are opened sufficiently to permit microscopy. The rat is immediately placed in a moist chamber. The trachea opening is linked to a microscope (Leitz Ultropak) by means of a rubber bellows which is fitted around the lens of the microscope and is made to embrace the trachea by means of a piece of rubber tubing that is slit along its length and secured to the bellows. The beam of an illuminating lamp is concentrated to a surface of about one mm^2. By placing a heat-reflecting filter in the path of the beam the rise in temperature can be reduced. For registration of the reflected light high speed cameras with a speed of 220 exposures are used. Alternatively, the reflected light from the microscope is directed to a TV camera and amplified to be displayed on a TV screen. The frequency of ciliar beats is recorded over one hour.

EVALUATION

The beat frequency of treated animals is compared with that of controls.

MODIFICATIONS OF THE METHOD

Mercke et al. (1974) described a stroboscopic method for standardized studies of mucociliary activity in rabbit tracheal mucosa.

Lierle and Moore (1935) inserted windows into anesthetized rabbits for observation of the ciliary activity in the maxillary sinus of living animals.

With modern equipment, a similar technique has been used by Hybbinette and Mercke (1982a–c), Lindberg and Mercke (1986), Lindberg et al. (1986), Mercke et al. (1987) to study the role of several pharmacologic agents in the mucociliary defense of the rabbit maxillary sinus.

Corssen and Allen (1958) compared the toxic effects of various local anesthetic drugs on human ciliated epithelium *in vitro* by observation of rotating globes of human tracheal epithelium in tissue culture.

Cheung (1976) performed high speed cinemicrographic studies on rabbit tracheal (ciliated) epithelia.

Iravani (1967, 1971, 1975) studied the ciliary activity in the intrapulmonary airways of rats by incident light microscopy.

Lee and Verdugo (1976), Verdugo et al. (1980) recommended laser light-scattering spectroscopy for the study of ciliary activity.

Manawadu et al. (1978) studied the effects of local anesthetics on ciliary activity using ferret tracheal rings *in vitro*. The ferret possesses a long neck, and 100 or more tracheal rings can be obtained from a single ferret. The tracheal rings were maintained in sterile tubes. The ciliary activity was graded by determining the percentage of cilia beating on each ring, using transmitted light and the 10 × objective of an inverted microscope.

Rutland and Cole (1980) and Hesse et al. (1981) used a non-invasive method for obtaining nasal ciliated epithelium which is suitable for measurement of ciliary beat frequency.

Van de Donk et al. (1980) used isolated chicken embryo tracheas to measure the effects of preservatives on ciliary beat frequency. Maurer et al. (1982) studied the role of ciliary motility in acute allergic mucociliary dysfunction in cultivated ciliated cells from sheep.

Lopez-Vidriero et al. (1985) studied the effect of isoprenaline on the ciliary activity of an *in vitro* preparation of rat trachea.

Braga et al. (1986) described a simple and precise method for counting ciliary beats directly from the TV monitor screen using specimens of human ciliated epithelium obtained by brushing the nasal mucosa.

Curtis and Carson (1992) used pieces of human nasal epithelium for computer-assisted video measurement of ciliary beat frequency *in vitro*. Ciliary beat frequency was viewed with a microscope equipped with a phase contrast objective. The microscopic image was recorded by a camera and data stored by a videorecorder. For measuring ciliary beating, tapes were displayed with amplification on a monitor. A photoelectric transducer was positioned over the video image of the cilia. Movement of the cilia interrupting the light path caused changes in light intensity recorded by the photocell transducer.

REFERENCES AND FURTHER READING

Baldetorp L, Huberman D, Håkanssson CH, Toremalm NG (1976) Effects of ionizing radiation on the activity of the ciliated epithelium of the trachea. Acta Radiol Ther Phys Biol 13:225–232

Braga PC, Dall'Oglio G, Bossi R, Allegra L (1986) Simple and precise method for counting ciliary beats directly from the TV monitor screen. J Pharmacol Meth 16:161–169

Cheung ATW (1976) High speed cinemicrographic studies on rabbit tracheal (ciliated) epithelia: Determination of the beat pattern of tracheal cilia. Pediat Res 10:140–144

Corssen G, Allen CR (1958) A comparison of the toxic effects of various local anesthetic drugs on human ciliated epithelium *in vitro*. Texas Rep Biol Med 16:194–202

Curtis LN, Carson JL (1992) Computer-assisted video measurement of inhibition of ciliary beat frequency of human nasal epithelium *in vitro* by xylometazoline. J Pharm Toxicol Meth 28:1–7

Dalhamn T (1956) Mucous flow and ciliary activity in the trachea of healthy rats and rats exposed to respiratory irritant gases (SO_2, H_3N, HCHO). A functional and morphologic (light microscopic and electron microscopic) study, with special reference to technique. Acta Physiol Scand 36, Suppl 123:1–161

Dalhamn T (1964) Studies on tracheal ciliary activity. Am Rev Respir Dis 89:870–877

Dalhamn T, Rylander R (1962) Frequency of ciliary beat measured with a photo-sensitive cell. Nature 196:592–593

Hakansson CH, Toremalm NG (1963) Studies on the physiology of the trachea. I. Ciliary activity indirectly recorded by a new "light beam reflex" method. Ann Otol 74:954–969

Hesse H, Kasparek R, Mizera W, Unterholzner Ch, Konietzko N (1981) Influence of reproterol on ciliary beat frequency of human bronchial epithelium *in vitro*. Arzneim Forsch/Drug Res 31:716–718

Hybbinette JC, Mercke U (1982a) A method for evaluating the effect of pharmacological substances on mucociliary activity *in vivo*. Acta Otolaryngol 93:151–159

Hybbinette JC, Mercke U (1982b) Effects of the parasympathomimetic drug methacholine and its antagonist atropine on mucociliary activity. Acta Otolaryngol 93:465–473

Hybbinette JC, Mercke U (1982c) Effects of sympathomimetic agonists and antagonists on mucociliary activity. Acta Otolaryngol 94:121–130

Iravani J (1967) Flimmerbewegung in den intrapulmonalen Luftwegen der Ratte. Pflügers Arch 207:221–237

Iravani J (1971) Physiologie und Pathophysiologie der Cilientätigkeit und des Schleimtransports im Tracheobronchialbaum. (Untersuchungen an Ratten). Pneumonologie 144:93–112

Iravani J, Melville GN (1975) Mucociliary activity in the respiratory tract as influenced by prostaglandin E_1. Respiration 32:305–315

Lee WI, Verdugo P (1976) Laser light-scattering spectroscopy. A new application in the study of ciliary activity. Biophys J 16:1115–1119

Lierle DM, Moore PM (1935) Further study of the effects of drugs on ciliary activity: a new method of observation in the living animal. Ann Otol 44:671–684

Lindberg S, Mercke U (1986) Bradykinin accelerates mucociliary activity in rabbit maxillary sinus. Acta Otolaryngol (Stockh) 101:114–121

Lindberg S, Hybbinette JC, Mercke U (1986) Effects of neuropeptides on mucociliary activity. Ann Otol Rhinol Laryngol 95:94–100

Lopez-Vidriero MT, Jacobs M, Clarke SW (1985) The effect of isoprenaline on the ciliary activity of an *in vitro* preparation of rat trachea. Eur J Pharmacol 112:429–432

Manawadu BR, Mostow SR, LaForce FM (1978) Local anesthetics and tracheal ring ciliary activity. Anesth Analg 57:448–452

Maurer DR, Sielczak M, Oliver Jr W, Abraham WM, Wanner A (1982) Role of ciliary motility in acute allergic mucociliary dysfunction. J Appl Physiol 52:1018–1023
Mercke U, Håkanson CH, Toremalm NG (1974) A method for standardized studies of mucociliary activity. Acta otolaryng 78:118–123
Mercke U, Lindbergh S, Dolata J (1987) The role of neurokinin A and calcitonin-related peptide in the mucociliary defense of the rabbit maxillary sinus. Rhinology 25:89–93
Rutland J, Cole PJ (1980) Non-invasive sampling of nasal cilia for measurement of beat frequency and study of ultrastructure. Lancet ii, 564–565
Suzuki N (1966) Motor control of the ciliary activity in the frog's palate. J Faculty Sci, Hokkaido Univ Ser VI, 16:67–71
Van de Donk HJM, Muller-Platema IP, Zuidema J, Merkus FWHM (1980) The effects of preservatives on the ciliary beat frequency of chicken embryo tracheas. Rhinology 18:119–133
Verdugo P, Johnson NT, Tam PY (1980) β-adrenergic stimulation of respiratory ciliary activity. J Appl Physiol 48:868–871

D.4.0.6 Studies of Mucociliary Transport

PURPOSE AND RATIONALE

Mucus flow has been studied in *in vitro* and *in vivo* experiments (Iravani 1971; Ahmed et al. 1979). The rate of mucus flow can be estimated by measuring the time needed for certain particles to travel a known distance in the trachea. Numerous substances have been used such as charcoal particles (Dalhamn 1956), Teflon discs (Ahmed et al. 1979), and other pulverized materials (Deitmer 1989). The effect of local radioactivity on tracheal mucous velocity of sheep has been studied *in vitro* and *in vivo* by Ahmed et al. (1979).

PROCEDURE

For *in vitro* experiments, sheep are sacrificed during anesthesia, the trachea is exposed, clamped, and resected just below the cricoid cartilage. The chest is opened and the trachea is resected at the level of the carina. Then the trachea is slit open along the posterior membranous wall, pinned with gentle stretching on a board, and slanted upward at an angle of 25°. A metric ruler is placed along the board as a measuring reference. The board is then placed in a Plexiglas chamber with a constant temperature of 37°C and 100% humidity. Teflon discs are spread on the mucous layer. Tracheal mucus velocity is estimated by filming the movements of the radioopaque Teflon discs visualized on a television monitor connected to a camera. Disc motion is recorded for 1–2 min on a videotape, and the distance measured during the elapsed time is obtained from the videomonitor.

For *in vivo* measurements of tracheal mucus velocity, the roentgenographic method of Friedman et al. (1977), Sackner et al. (1977) is used. The sheep are restrained, and their heads are immobilized with a sling. The nasal mucosa is sprayed with a 2% lidocaine solution for topical anesthesia. A bronchofiberscope is inserted transnasally, and its tip is placed just below the vocal cords. Radioopaque Teflon discs 1.0 mm in diameter, 0.8 mm thick, and weighing 1,76 mg are blown through the inner channel of the bronchofiberscope onto the tracheal mucosa in a circumferential distribution. The cervical trachea containing the discs is visualized in the lateral projection with a television monitor. Disc motion is recorded on a videotape while the time is displayed on a digital clock. The disc image is marked to obtain the distance traveled. This distance is measured with a ruler, and the linear velocity of the disc is computed by dividing the distance by the elapsed time. This procedure is repeated for all discs in the field of view. To compute a mean tracheal mucus velocity, data from 10–15 discs are obtained in each filmed run.

EVALUATION

Disc velocities measured *in vitro* or *in vitro* are compared before and after treatment.

MODIFICATIONS OF THE METHOD

Mucociliary transport has been studied on the hard palate of decapitated frogs measuring the transport velocity of small particles, e. g., pieces of cork or charcoal (Kochmann 1930; Sadé et al. 1970).

Suzuki (1966) measured the movement of a standard object (1 mm^2 aluminum foil) on the ciliated surface of the palate of frogs.

Mucociliary clearance by the *in vitro* frog method was used by Leitch et al. (1985) to study the effects of ethanol.

Movement of poppy seeds in rabbit tracheal preparations was studied by Kensler and Battista (1966).

In chicken nasal mucosa the interaction between mucociliary transport and the ciliary beat was studied by Ukai et al. (1985).

Mucus transport in the respiratory tract of anesthetized cats was measured with uniform particles of lycopodium spores triturated with lamp black (Carson et al. 1966).

Mucociliary clearance velocities were determined by a radioisotopic method in dogs (Giordano et al. 1977, 1978).

REFERENCES AND FURTHER READING

Ahmed T, Januskiewicz AJ, Landa JF, Brown A, Chapman GA, Kenny PJ, Finn RD, Bondick J, Sackner MA (1979) Effect

of local radioactivity on tracheal mucous velocity of sheep. Am Rev Resp Dis 120:567–575
Battista SP (1971) Agents affecting mucociliary activity. In: Turner RA, Hebborn P (eds) Screening Methods in Pharmacology, Vol II. Academic Press, New York and London. pp 167–202
Carson S, Goldhamer R, Carpenter R (1966) Mucus transport in the respiratory tract. Am Rev Resp Dis 93:86–92
Dalhamn T (1956) Mucous flow and ciliary activity in the trachea of healthy rats and rats exposed to respiratory irritant gases (SO_2, H_3N, HCHO). A functional and morphologic (light microscopic and electron microscopic) study, with special reference to technique. Acta Physiol Scand 36, Suppl 123:1–161
Deitmer Th (1989) Physiology and pathology of the mucociliary system. Special regards to mucociliary transport in malignant lesions of the human larynx. Karger Basel, Chapter 5: Methods of investigation of mucociliary transport, pp 26–34, Chapter 9: Pathophysiology and pharmacology of the mucociliary system, pp 47–54
Friedman M, Stott FD, Poole DO, Dougherty R, Chapman GA, Watson H, Sackner MA (1977) A new roentgenographic method for estimating mucus velocity in airways. Am Rev Respir Dis 115:67–72
Giordano AM, Shih CK, Holsclaw DS, Khan MA, Litt M (1977) Mucus clearance: *in vivo* canine tracheal vs. *in vitro* bullfrog palate studies. J Appl Physiol 42:761–766
Giordano AM, Holsclaw D, Litt M (1978) Mucus rheology and mucociliary clearance: normal physiologic state. Am Rev Resp Dis 118:245–250
Iravani J (1971) Physiologie und Pathophysiologie der Cilientätigkeit und des Schleimtransports im Tracheobronchialbaum. (Untersuchungen an Ratten). Pneumonologie 144:93–112
Kensler CJ, Battista SP (1966) Chemical and physical factors affecting mammalian ciliary activity. Am Rev Resp Dis 93:93–102
Kochmann M (1930) Zur Pharmakologie der Expektorantien. Wirkung auf die Flimmerbewegung. Naunyn-Schmiedeberg's Arch Exp Path Pharmakol 150:23–38
Leitch GJ, Frid LH, Phoenix D (1985) Effects of ethanol on mucociliary clearance. Alcoholism Clin Exp Res 9:277–280
Sackner MA, Reinhart M, Arkin B (1977) Effects of beclomethasone diproprionate on tracheal mucus velocity. Am Rev Resp Dis 115:1069–1070
Sadé J, Eliezer N, Silberberg A, Nevo AC (1970) The role of mucus in transport by cilia. Am Rev Respir Dis 102:48–52
Ukai K, Sakakura Y, Saida S (1985) Interaction between mucociliary transport and the ciliary beat of chicken nasal mucosa. Arch otorhinolaryngol 242:225–231

D.4.0.7
Culture of Tracheal Epithelial Cells

PURPOSE AND RATIONALE

Marked morphological changes of the airway epithelium, up to severe damage, are frequently observed in inflammatory airway diseases and appear to play an important role in the pathogenesis of the broncho-obstructive symptoms (Webber and Corfield 1993; Hay et al. 1994). Freitag et al. (1996) studied the effects of lipopolysaccharides (LPS) and TNF-α on cultured rat tracheal epithelial cells and determined NO synthase activity.

PROCEDURE

Trachea of newborn rats, cut into small pieces, are explanted with the epithelial surface downwards onto 60 mm culture dishes (Lechner et al. 1985) and cultured in low-calcium (60–80 µmol/l) RPMI-1640 medium at 37°C and 5% CO_2. The medium containing 16% fetal calf serum is supplemented with epidermal growth factor and other growth promoting factors, such as 80 ng/ml cholera toxin, 2.6 ng/ml estradiol, 180 ng/ml hydrocortisone, 2.5 µg/ml insulin, 12.5 µg/ml transferrin, and 100 U/ml penicillin, 100 µg/ml streptomycin and 3.5 µg/ml amphotericin B to allow a selective outgrow of epithelial cells (Emura et al. 1990). Confluent epithelial layers are obtained after about 6–10 weeks at which time all cells show a positive staining with a pancytokeratin-antibody. Confluent cells of following passages are treated for four subsequent days with LPS (10 µg/ml) or TNF-α (500 U/ml).

The **morphology** of the cells is evaluated is evaluated by daily inspection using a phase contrast microscope with photographical documentation. Cell density in the culture is determined in each culture dish by counting daily the number of cells in four marked areas (each 2000 μm^2). For immunocytochemical staining, the cells are fixed by incubation in 100% methanol at –20°C for 20 min. The cells are washed with Ca/Mg-free phosphate buffered saline and several areas are marked of by nail-varnish. A solution of the anti-cytokeratin(pan)-antibody (monoclonal mouse IgG, Boehringer Mannheim) is added, incubated for 2 h at room temperature and after washing incubated for 30 min with a secondary antibody (FITC coupled, polyclonal rabbit anti-mouse IgG, Sigma). After washing, fluorescence microscopy is performed using a microscope with a FITC-specific filter combination. Unspecific fluorescence is excluded by performing the staining procedure in a different area of the same culture, but without the addition of the primary antibody.

For **determination of NO synthase activity**, confluent cultures are washed with oxygenated and prewarmed (37°C) Krebs-HEPES medium. Then the cells are incubated for 1 h in the same medium containing 37 kBq ^{3}H-L-arginine (100 nmol/l). After collection of the supernatants the cells are extracted in 1 ml of 0.4 mol/l $HClO_4$ for 2 h at 0–4°C.

By **HPLC analysis** ^{3}H-compounds (^{3}H-L-citrulline, ^{3}H-L-ornithine and ^{3}H-L-arginine) in incubation media and cell extracts are separated on a reverse phase column (length 250 mm, inner diameter 4.6 mm, pre-packed with Shadon ODS-Hypersil, 5 mm) using as mobile phase 0.1 mmol/l sodium phosphate buffer

(adjusted to pH 1.8) which contains octane sulphonic acid sodium salt (400 mg/l), Na_2EDTA (0.3 mmol/l) and methanol (6.25% v/v) with a flow rate of 1 ml/min (Hey et al. 1995). The eluate is collected in 1 min fractions into counting vials. After addition of a commercial scintillation cocktail the radioactivity is determined by liquid scintillation spectrophotometry. External standardization is used to correct for counting efficiency. The retention time is determined by the use of ^{14}C-labelled (L-citrulline or L-ornithine) or ^{3}H-labelled (L-arginine) standards. Protein content in cells is determined by a commercially available assay.

EVALUATION

The amounts of ^{3}H-L-citrulline in supernatants or cell extracts are expressed as DPM/µg protein. Changes in cell density are expressed as % of the density observed in each culture dish at the start of the experiment. Mean values are given ± SEM. The significance of difference is evaluated by Student's *t*-test.

REFERENCES AND FURTHER READING

Emura M, Riebe M, Ochiai M, Aufderheide M, Germann P, Mohr U (1990) New functional cell-culture approach to pulmonary carcinogenesis and toxicology. Cancer Res Clin Oncol 116:557–562

Freitag A, Reimann A, Wessler I, Racké K (1996) Effect of bacterial lipopolysaccharides (LPS) and tumor necrosis factor-α (TNF-α) on rat tracheal epithelial cells in culture: morphology, proliferation and induction of nitric oxide (NO) synthase. Pulmon Pharmacol 9:149–156

Hay DWP, Farmer SG, Goldie GR (1994) Inflammatory mediators and modulation of epithelial/smooth muscle interactions. In: Goldie RG (ed) Handbook of Immunopharmacology: Immunopharmacology of Epithelial Barriers. Academic Press, London, pp 119–146

Hey C, Wessler I, Racké K (1995) Nitric oxide (NO) synthase is inducible in rat, but not in rabbit alveolar macrophages, with a concomitant reduction in arginase activity. Naunyn Schmiedeberg's Arch Pharmacol 351:651–659

Lechner JF, LaVeck MAA (1985) A serum-free method for culturing normal bronchial cells. J Tissue Cult Meth 9:43–48

Webber SE, Corfield DR (1993) The pathophysiology of airway inflammation and mucosal damage in asthma. In: Andrews P, Widdicombe J (eds) Pathophysiology of the Gut and Airways. Portland Press, London, pp 67–77

D.4.0.8 Alveolar Macrophages

PURPOSE AND RATIONALE

Alveolar macrophages have been used for various purposes. A rat pulmonary alveolar macrophage cell line (NR8383) was initiated in culture by Helmke et al. (1987) in the presence of a gerbil lung conditioned medium and has been propagated continuously in culture. Sun et al. (1999) tested the inhibition of Ca^{2+} influx by pentoxifylline in NR8383 alveolar macrophages.

PROCEDURE

Cell Culture

The NR8383 alveolar macrophages cell line is grown in plastic tissue culture flasks in Ham's F12 medium containing 15% fetal bovine serum, 100 g/ml penicillin and 100 U/ml streptomycin sulfate. The alveolar macrophages are cultured at 37°C in an atmosphere of 5% CO_2 in air. The medium is routinely changed twice weekly. The viability of alveolar macrophages is routinely measured by trypan blue exclusion before and at 1.5 h after fura-2 loading, when all $[Ca^{2+}]_i$ determinations are completed.

Determination of $[Ca^{2+}]_i$

$[Ca^{2+}]_i$ is determined using the Ca^{2+}-sensitive fluorescent indicator fura-2 (Zhang et al. 1997; Mörk et al. 1998). NR8383 alveolar macrophages are loaded with fura-2 by incubation in PSS containing 2 mM (final concentration) fura-2/AM and 0.01% BSA for 20 min at 37°C. The cells are then rinsed twice with PSS containing 0.01% BSA and resuspended in the same medium (1.75×10^6 cells/ml). For $[Ca^{2+}]_i$ determination, a 2-ml aliquot of fura-2-loaded cells is centrifuged at 50 *g* for 2 min, resuspended in PSS containing 0.01% BSA and placed in a 4-ml cuvette. $[Ca^{2+}]_i$ is measured at 37°C using a PTI Deltascan fluorometer (PTI, South Brunswick, N.J., USA). The excitation wavelengths used are 340 and 380 nm and the emission wavelength is 505 nm. Calibration of $[Ca^{2+}]_i$ is performed for each measurement trace. Then, 1 mM $CaCl_2$ (for Ca^{2+}-free medium) and 50 mM ionomycin are added to obtain the limiting ratio for the Ca^{2+}-saturated form (R_{max}) of fura-2. Then, 0.0005% digitonin and 10 mM EGTA are added to obtain the limiting ratio for the free form of fura-2 (R_{min}. Fluorescence ratios of the 340- and 380-nm excitation and 505-nm emission are converted to $[Ca^{2+}]_i$ according to Grynkiewicz et al. (1985) using 224 nM as the K_d of fura-2 for Ca^{2+}.

Measurement of Store-Depletion-Activated Ca^{2+} Influx

The Ca^{2+} influx activated by depletion of the inositol 1,4,5-trisphosphate- (IP_3-) sensitive intracellular store is measured according to Zhang et al. (1997) and Zhu et al. (1998). Cells are exposed to either ATP or thapsigargin (TG) in Ca^{2+}-free medium for 5 min, and 1 mM Ca^{2+} is then added to initiate Ca^{2+} influx. The initial linear portion of $[Ca^{2+}]_i$ changes after addition of Ca^{2+} is used to calculate Ca^{2+} influx rate (nM/min).

EVALUATION

Results are presented as the mean± SEM of separate determinations using different cell preparations. Comparisons are made using the unpaired Student's *t*-test or the analysis of variance. *P* values <0.05 are considered significant.

MODIFICATIONS OF THE METHOD

Sirois et al. (2000) studied the influence of histamine in the cytokine network in the lung through H_2 and H_3 receptors. Alveolar macrophages from humans, Sprague Dawley rats and the alveolar macrophage cell line NR8383 were treated with different concentrations of histamine prior to their stimulation with suboptimal concentrations of lipopolysaccharide (LPS). Release of tumor necrosis factor (TNF) and interleukin-10 (IL-10) was measured.

Using the rat alveolar macrophage cell line NR8383, Gazin et al. (2004) found that uranium induces TNF-α secretion and activates the p38 mitogen-activated protein kinase (p38 MAPK).

Yang et al. (2004) studied in mice the synergy between a signal transducer and activator of transcription 3 and retinoic acid receptor-α in the regulation of the surfactant protein B gene in the lung.

REFERENCES AND FURTHER READING

Gazin V, Kerdine S, Grillon G, Pallardy M, Raoul H (2004) Uranium induces TNFα secretion and MAPK activation in rat alveolar macrophage cell line. Toxicol Appl Pharmacol 194:49–59

Grynkiewicz G, Poenie M, Tsien RY (1985) A new generation of Ca^{2+} indicators with improved fluorescence properties. J Biol Chem 260:3440–3450

Helmke RJ, Boyd RL, German VF, Mangos JA (1987) From growth factor dependence to growth factor responsiveness: the genesis of an alveolar macrophage cell line. In Vitro Cell Dev Biol 23:567–574

Mörk AC, Helmke RJ, Martinez JR, Michalek MT, Patchen MI, Zhang GH (1998) Effects of particulate and soluble (1–3)-α-glycans on Ca^{2+} influx in NR8383 alveolar macrophages. Immunopharmacology 40:77–89

Sirois J, Ménard G, Moses AS, Bissonette EY (2000) Importance of histamine in the cytokine network in the lung through H_2 and H_3 receptors: stimulation of IL-10 production. J Immunol 164:2964–2970

Sun X, Martinez JR, Zhang GH (1999) Inhibition of Ca^{2+} influx by pentoxifylline in NR8383 alveolar macrophages. Immunopharmacology 43:47–58

Yang L, Lian X, Cowen A, Xu H, Du H, Yan C (2004) Synergy between signal transducer and activator of transcription 3 and retinoic acid receptor-α in the regulation of the surfactant protein B gene in the lung. Mol Endocrinol 18:1520–1532

Zhang GH, Helmke RJ, Mörk AC, Martinez RJ (1997) Regulation of cytosolic free Ca^{2+} in cultured rat macrophages (NR8383). J Leukoc Biol 62:341–348

Zhu X, Birnbaumer L (1998) Calcium channels formed by mammalian Trp homologues. News Physiol Sci 13:211–217

D.5 Safety Pharmacology of the Respiratory System

See Murphy (2006).

REFERENCES AND FURTHER READING

Murphy DJ (2006) Respiratory function assays in safety pharmacology In: Drug Discovery and Evaluation Safety and Pharmacokinetic Assays, Chapter I.F, pp 141–149 H. G. Vogel (ed), F.J. Hock, J. Maas, D. Mayer (Co-eds) Springer-Verlag Berlin Heidelberg New York

Chapter E
Psychotropic and Neurotropic Activity

E.1
Effects on Behavior and Muscle Coordination

E.1.1
Spontaneous Behavior

E.1.1.1
General Considerations

The effects of drugs on the central and peripheral nervous systems can be easily recognized in normal animals. This does not necessarily mean that these effects can be used in therapy. Observing the global effects of drugs during LD_{50}-determinations, pharmacologists can detect psychotropic activity. Only, if these effects occur also in doses considerably below the LD_{50}, are further evaluations justified. This basic experience resulted in the development of a variety of observational tests and activity measurements.

E.1.1.2
Observational Assessment

PURPOSE AND RATIONALE

A systematic, quantitative procedure assessing the behavioral state of mice for the evaluation of drugs has been described by Irwin (1964, 1968). The method is applied in the beginning of pharmacological screening to detect psychotropic activities. It allows to identify and differentiate the profile pattern of various classes of pharmacological agents. Furthermore, observational assessment allows into the safety and potential toxicity profile of a new drug.

PROCEDURE

Mice of either sex (NMRI-strain) with a weight between 18 and 22 g are kept under standard laboratory conditions 5 days before the experiment. Animals tested for oral administration have water ad libitum but are deprived of food 16 h before the test. Animals for intravenous or intraperitoneal administration have access to food and water ad libitum until the test. For unknown substances the following doses are given:

- i.v. administration: 100, 200, 400 mg/kg
- i.p. administration: 300, 600, 1200 mg/kg
- oral administration: 500, 1000, 2000 mg/kg

Three animals are used for each dose. One group of 3 animals receiving the vehicle only, serves as control group.

Immediately after drug administration, the animals are closely observed for 2 h (following i.v. or i.p. administration) and for 5 h (following oral administra-

tion) by a "blind" observer. The following parameters are checked and compared to the vehicle control group:

Effects on CNS	Effects after manipulations
spontaneous motor activity	auditory stimulus response
restlessness	escape after touch
grooming behavior	righting reflex
squatting	paresis of hind limbs
staggering	paresis of forepaws
ataxic gait	catalepsy in induced positions
lying flat on the belly	Effects on reflexes
lying flat on the side	
lying flat on the back	pinna reflex
sleeping	corneal reflex
narcosis	pain following stimulation
bizarre behavior	Effects on autonomic nervous system
timidity	
Straubs's phenomenon	
writing	pupil diameter (constriction or dilatation)
tremors	eyelids (closure or exophthalmus)
twitches	secretion of sweat
opisthotonus	salivations
clonic convulsions	lacrimation
tonic convulsions	cyanosis
rolling and jumping convulsions	piloerection
	defecation
	urination

Depending on the route of administration, the observations are performed at different time intervals: after intravenous and after intraperitoneal administration during the first 30 min, and after 1 and 2 h; after oral administration during the first 60 min, and after 2 and 6 h. The number of deaths is counted during the first 24 h and after 7 days in order to evaluate acute and late toxicity. Arbitrary scores are chosen for each symptom. If positive effects are seen with the lowest dose, the experiment is repeated with lower doses being decreased by a factor of 3.

CRITICAL ASSESSMENT OF THE TEST

The test has been used by almost every laboratory in the world involved in screening of potential new drugs. Almost every laboratory has introduced its own modifications. In particular, the scores and the calculations differ from one laboratory to the other. Additional tests, such as grip strength or rotarod, described below, have been included into the primary screen. Graph-bar profiles have been established for known drugs in order to rate new substances accordingly. The test is definitively an useful tool for primary screening resulting in hints on psychotropic activity but also for actions on other systems. Nevertheless, this test can not substitute for more sophisticated tests for the evaluation of psychotropic activity.

MODIFICATIONS OF THE METHOD

Based on the guidelines of the United States Environmental Protection Agency (USEPA) (1991) Mattsson et al. (1996) described a performance standard for clinical and functional observational battery (FOB) for examinations of **rats.** The performance standard was an idealized composite of FOB data from experienced laboratory personnel, each person tested on a separate set of four groups of rats. The rats were examined in random order and treatments were either (a) saline, (b) chlorpromazine, (c) atropine, followed by physostigmine or (d) amphetamine.

Testing of neurotoxicity with new pharmaceuticals was reported by Haggerty (1991). He proposed a primary screen for rodents, consisting of a functional observation battery and an automated test for motor activity. In addition, a functional observation battery for dogs was developed. The rat tier I screen assesses such functions as home cage and open field activity, stimulus reactivity, and neuromuscular function. The dog tier I screen emphasizes evaluation of gait, postural reactions, and reflex function.

Rambert (2000) underlined the importance of some general conditions for general pharmacology of the CNS, such as choice of the animal species, administration route and controls of the experimental context (surroundings, temperature, schedules of the trials, interference with food-intake episodes, influence of noises and smells, expertise of the experimental staff).

Crawley and Paylor (1997), Crawley (2000) proposed a test battery and behavioral paradigms to investigate the behavioral phenotypes of transgenic and knockout mice. Several neurological and neuropsychological tests are described which can be used as first screen for behavioral abnormalities in mutant mice. Multiple behavioral paradigms are included for several categories, such as neurological reflexes, sensory abilities, motor functions, learning and memory, feeding, sexual behavior, analgesia, aggression, anxiety, depression, schizophrenia, and drug abuse.

Detailed procedure of the Irwin test performed in rats is given by Porsolt (2006).

REFERENCES AND FURTHER READING

Crawley JN (2000) Behavioral phenotyping of mutant mice. New technologies for life sciences: a trends guide 1:18–22

Crawley JN, Paylor R (1997) A proposed test battery and constellations of specific behavioral paradigms to investigate the behavioral phenotypes of transgenic and knockout mice. Hormones Behav 31:197–211

Haggerty GC (1991) Strategy for and experience with neurotoxicity testing of new pharmaceuticals. J Am Coll Toxicol 10:677–687

Irwin S (1964) Drug screening and evaluation of new compounds in animals. In: Nodin JH, Siegler PE (eds) Animal and clinical techniques in drug evaluation. Year Book Medical Publishers, Chicago, 36–54

Irwin S (1968) Comprehensive observational assessment: I a. A systematic, quantitative procedure for assessing the behavioural and physiologic state of the mouse. Psychopharmacologia (Berl.) 13:222–257

Mattsson JL, Spencer PJ, Albee RR (1996) A performance standard for clinical and functional observation battery examination of rats. J Am Coll Toxicol 15:239–254

Murray AM, Waddington JL (1990) The interaction of clozapine with dopamine D_1 versus dopamine D_2 receptor-mediated function: behavioural indices. Eur J Pharmacol 186:79–86

Porsolt RD (2006) General nervous system (CNS) safety pharmacological studies. In: Vogel HG (ed) Drug discovery and evaluation – safety and pharmacokinetic assays. Springer, Berlin Heidelberg New York

Rambert FA (2000) Pharmacologie de sécurité: système nerveux central. Thérapie 55:55–61

Silverman P (1978) Drug screening and brain pharmacology. In: Animal behaviour in the laboratory. Chapman and Hall, London, pp 58–78

United States Environmental Protection Agency (USEPA) (1991) Pesticide Assessment Guidelines. Subdivision F, Hazard Evaluation: Human and Domestic Animals. Addendum 10, Neurotoxicity Series 81, 82 and 83, PB 91–154617, Washington, DC: United States Environmental Protection Agency

E.1.1.3 Safety Pharmacology Core Battery

PURPOSE AND RATIONALE

Regulatory agencies (EMA 1997, 2000) have pointed out the necessity to perform safety pharmacology studies before application of a new drug to human beings and to assess most carefully any potential side effects. Organs or systems acutely necessary for life, i. e., the cardiovascular, respiratory and central nervous systems, are considered to be the most important to assess in safety pharmacology studies. The following parameters of CNS activity should be assessed appropriately: motor activity, behavioral changes, coordination, sensory/motor reflexes and body temperature.

Detailed descriptions of tests are found for

Observation tests:

E.1.1.2 Observational assessment

Motor activity and behavior:

E.1.2.2 Method of intermittent observations

E.1.2.3 Open field test

E.1.2.4 Hole-board test

E.1.2.5 Combined open field test

Coordination:

E.1.3.1 Inclined plane

E.1.3.2 Chimney test

E.1.3.3 Grip strength

E.1.3.4 Rotarod method

Sensory/motor reflexes:

E.1.3.6 Influence on polysynaptic reflexes

E.1.3.7 Masticatory muscle reflexes

Follow-up studies for CNS safety pharmacology are recommended, such as behavioral pharmacology, learning and memory, specific ligand binding, neurochemistry, visual, auditory and/or electrophysiology examinations. Detailed descriptions of these tests are found in the respective chapters, e. g.,

E.1.2.6 EEG analysis from rat brain by telemetry.

REFERENCES AND FURTHER READING

ICH Harmonized Tripartite Guideline (M3) (1997) "Timing of Non-clinical Safety Studies for the Conduct of Human Clinical Trial for Pharmaceuticals"

Rambert FA (2000) Pharmacologie de sécurité: système nerveux central. Thérapie 55:55–61

The European Agency for the Evaluation of Medicinal Product. Human Medicines Evaluation Unit. (2000) ICH Topic S7. Safety Pharmacology Studies for Human Pharmaceuticals. Note for Guidance on Safety Pharmacology Studies in Human Pharmaceuticals

E.1.2 Effects on Motility (Sedative or Stimulatory Activity)

E.1.2.1 General Considerations

A survey on methods to evaluate depressants of the central nervous system has been published by Turner (1965). Many of these tests are still valid in spite of the fact that new classes of drugs have been introduced since that time which have not only augmented the therapeutic armamentarium but also changed the battery of pharmacological tests.

Sedative properties of drugs are tested mostly in mice or rats. Their spontaneous motor activity depends on various factors, such as the social situation (one or more animals), familiarity with the test environment, light and temperature. The term spontaneous motor activity includes different types of movements, such as locomotion, rearing, sniffing, grooming, eating and drinking. These phenomena can be well recognized by a skilled observer, but are difficult to record over long periods of time and to quantitate. Therefore, besides procedures based on observation many methods

for automatic registration have been developed. Almost every pharmacologist working in this field has designed his/her own apparatus. Several attempts have been made to measure not only simple locomotion, but also rearing and other types of movement. The conditions to characterize drug effects by measuring locomotor activity have been surveyed by Kinnard and Watzman (1966), Geyer (1990).

A special phenomenon, called "thigmotaxis" which means that rats have the tendency to remain close to the walls of the cage, has been described by Barnett (1963). Moreover, methods to measure curiosity have been recommended. Only a few examples of prototypic methods and equipment can be given.

REFERENCES AND FURTHER READING

Barnett SH (1963) "The Rat: A Study in Behavior." Chicago: Aldine Publishing Co., pp 31–32

Geyer MA (1990) Approaches to the characterization of drug effects on locomotor activity in rodents. Modern Methods in Pharmacology, Vol. 6, Testing and Evaluation of Drugs of Abuse, pp 81–99, Wiley-Liss, Inc.

Kinnard WJ, Watzman N (1966) Techniques utilized in the evaluation of psychotropic drugs on animal activity. J Pharm Sci 55:995–1012

Silverman P (1978) Motor activity. In: Animal behaviour in the laboratory. Chapman and Hall, London, pp 79–92

Turner RA (1965) Depressants of the central nervous system. In: Turner RA (ed) Screening Methods in Pharmacology, Vol. 1, Academic Press, New York and London, pp 69–86

E.1.2.2 Method of Intermittent Observations

PURPOSE AND RATIONALE

The method described by Ther (1953) was designed to study stimulant and sedative drugs. The use of 3 mice per group implied a special social situation of the animals. For testing sedative activity, the mice are additionally treated with a stimulant, and for testing stimulant activity with a sedative drug. Each group of mice is observed repeatedly only for a short period of time during one hour and compared to a control group by a "blind" observer.

PROCEDURE

Mice of either sex with an average weight of 25 g are deprived of food and water for 24 h before the test. To avoid any influence of the circadian rhythm the experiment is performed only between 8:00 and 12:00 A.M. Twelve animals are divided into groups of 3 mice. One group of 3 mice serves as control group, the other groups receive different doses of the test drug intraperitoneally. For testing sedative activity, the mice are injected after 10 min subcutaneously with 0.5 mg/kg methamphetamine. For testing stimulant activity, the mice are treated with 800 mg/kg paraldehyde. Ten minutes afterwards, each group is placed into a glass jar of 12 cm diameter and 20 cm height which in turn are placed in a wooden box of $130 \times 50 \times 30$ cm. The glass jars are illuminated from above. Ten minutes after administration of methamphetamine or paraldehyde the observation is started.

EVALUATION

During 1 h the observer looks every minute for 1 s to each jar and registers if none, one, two or all three mice show any characteristic change in locomotion, rearing, grooming or sniffing. The maximum count in 1 h would be 180. Generally, activity decreases within 1 h. Nevertheless, methamphetamine treated animals have a total count between 120 and 150. Groups treated with an effective sedative drug show a dose dependent decrease of total counts. The number of counts in the treated groups is calculated as percentage of controls. From dose-response curves ED_{50}-values can be calculated.

CRITICAL ASSESSMENT OF THE METHOD

The method gives reliable results for sedative drugs and for compounds with central depressant activity, such as antihistaminics, neuroleptics and hypnotics. The disadvantage of the method lies in the fact that a skilled and trained observer is needed in order to get reproducible results. Therefore, several attempts have been made to automatize the method of intermittent observation.

MODIFICATIONS OF THE METHOD

Schaumann and Stoepel (1961) followed the principle of intermittent observation using a camera mounted above small wire cages (10×10 cm). The mice in the cages were photographed with an exposure time of 3 s every 7,5 min over a period of 2,5 h. Mice without movements give clear pictures, calculated as zero. Slight movements induce blurred contours, calculated as 1 point, and major movements give completely blurred pictures, calculated as 2 points. Normal mice show 20 or less points during 20 observations. Mice with more than 20 points are considered to be stimulated, mice with less than 5 points to be sedated. In this way ED_{50}-values can be calculated.

Vogel and Ther (1963) published an apparatus with automatic registration of intermittent observations. 18 cages are used which have a freely movable bottom with minimal weight which is supported by springs. A small permanent magnet attached below the floor induces an electrical current in a coil if the bottom is moved. Two mice are brought into each

cage. The control device registers during a variable period between 0.5 and 3 s if the bottom of one cage is moved or not. Within one minute, all 18 cages are registered successively. The number of movements within one hour is recorded for each cage. The sensitivity of the electric induction system is variable. A calibration is possible which picks up every movement of the animal, however, does not register the movements due to breathing. Dose-response curves can be established for stimulant and sedative drugs.

A similar apparatus was used by Hirabayashi and Tadokoro (1993) and Namina et al. (1999). The ambulatory activity of mice was measured by the tilting cage method using the Ambulometer, Model AMB-M1 (O'Hara, Tokyo, Japan).

Meyer (1962) measured the time until the exploration motility decreased to one third of the initial value.

Koek et al. (1987) used the principle of intermittent observations for various activities of rats such as locomotion, rearing, sniffing, licking, gnawing, grooming, loss of righting, Straub tail, ect. in order to compare the behavioral effects of drugs.

REFERENCES AND FURTHER READING

Hirabayashi M, Tadokoro S (1993) Effect of chlorpromazine on mouse ambulatory activity sensitization caused by (+)-amphetamine. J Pharm Pharmacol 45:481–483

Koek W, Woods JH, Ornstein P (1987) A simple and rapid method for assessing similarities among directly observable behavioural effects of drugs: PCP-like effects of 2-amino-5-phosphonovalerate in rats. Psychopharmacology 91:297–304

Meyer HJ (1962) Pharmakologie der wirksamen Prinzipien des Kawa-Rhizoms (Piper methysticum Frost) Arch Int Pharmacodyn 138:505–536

Namina M, Sugihara K, Watanabe Y, Sasa H, Umekage T, Okamoto K (1999) Quantitative analysis of the effect of lithium on the reverse tolerance and the c-Fos expression induced by methamphetamine in mice. Brain Res Prot 4:11–18

Schaumann W, Stoepel K (1961) Zur quantitativen Beurteilung von zentraler Erregung und Dämpfung im Tierversuch. Naunyn-Schmiedeberg's Arch exp Path Pharmakol 241:383–392

Ther L (1953) Über eine einfache Methode zur Bestimmung von Weck- und Beruhigungsmitteln im Tierversuch. Dtsch Apoth Ztg 93:292–294

Vogel G, Ther L (1963) Zur Wirkung der optischen Isomeren von Aethyltryptamin-acetat auf die Lagekatalepsie des Huhnes und auf die Motilität der Maus. Arzneim Forsch/Drug Res 13:779–783

E.1.2.3 Open Field Test

PURPOSE AND RATIONALE

Interruption of light beams as a measure of movements of rats or mice in a cage ("open field") has been used by many authors such as Dews (1953), Saelens et al. (1968) Nakatsu and Owen, (1980). Recently developed devices allow to register not only general motor activity but also locomotion, rearing and the speed of locomotion (Barros et al. 1991; Ericson et al. 1991).

PROCEDURE

The rats are observed in a square open field arena ($68 \times 68 \times 45$ cm) equipped with 2 rows of 8 photocells, sensitive to infrared light, placed 40 and 125 mm above the floor, respectively. The photocells are spaced 90 mm apart and the last photocell in a row is spaced 25 mm from the wall. Measurements are made in the dark in a ventilated, sound-attenuating box. Interruptions of photocell beams can be collected by a microcomputer and the following variables can be evaluated:

- Motor activity: All interruptions of photo beams in the lower rows.
- Peripheral motor activity: Activation of photo beams in the lower rows, provided that the photo beams spaced 25 mm from the wall were also activated.
- Rearing: All interruption of the photo beams in the upper rows.
- Peripheral rearing: Interruption of photo beams in the upper rows, provided that the photo beams spaced 25 mm from the wall were also activated.
- Locomotion: Successive interruptions of photocells in the lower rows when the animal is moving in the same direction.
- Speed: The time between successive photo beam interruptions during locomotion collected in 0.1 s categories.

Adult male Sprague-Dawley rats with a weight between 280 and 320 g are used. Drugs are injected subcutaneously 10 to 40 min. before test. The rats are observed for 15 min whereby counts per min. are averaged for 3 min intervals.

EVALUATION

Dose-response curves can be obtained for sedative and stimulant drugs, whereby the various parameters show different results. The effects of various doses are compared statistically with the values of controls and among themselves.

CRITICAL ASSESSMENT OF THE METHOD

Measurement of several parameters in an open field device allows to differentiate between various types of sedative or stimulant drugs, but these differences can

only be detected if dose-response curves are obtained for each parameter.

MODIFICATIONS OF THE METHOD

Besides interruption of light beams, devices based on capacitance systems such as Animex (Columbus Instruments, Ohio, USA) and Varimexhave been developed and are widely used (Crunelli and Bernasconi 1979; Liu et al. 1985; Laviola G and Alleva E 1990; Honma et al. 1990; Magnus-Ellenbroek et al. 1993; Dauge et al. 1995; Petkov et al. 1995; Surmann et al. 1995; Gillies et al. 1996; Irifune et al. 1997; Ghelardini et al. 1998).

Nikodijevic et al. (1991) studied the behavioral effects of A_1- and A_2-selective adenosine agonists and antagonists in mice using a Digiscan activity monitor (Omnitech Electronics Inc., Columbus, OH) equipped with an IBM-compatible computer. The monitor included multiple activity monitor cages ($40 \times 40 \times 30.5$ cm), each of which was surrounded by horizontal and vertical sensors not detectable by the rodent.

Steiner et al. (1997) found that D_3 receptor deficient mice enter the center of an open field significantly more than their littermates suggesting an anxiolytic-like effect of the D_3 receptor mutation.

Vorhees et al. (1992) described a locomotor activity system for rodents. The system consists of a black, ventilated test chamber, internally lighted with a ceiling mounted video camera. The camera's image is transmitted to a contrast-sensitive tracker which maps the point of highest contrast and relays the digitalized coordinates to a PC. Dedicated software stores the information and simultaneously displays a map of the tracked subject.

Rex et al. (1996, 1998) described a modified open field test sensitive to anxiolytic drugs. Food-deprived rats were placed in one corner of the open field containing food in the center. The number of rats beginning to eat within the first 5 min was increased by known anxiolytic drugs.

Several authors used computerized systems, based on interruptions of infrared light beams, on magnetic field or on video-analysis such as the VideoMot2 system developed by TSE Systems, Bad Homburg, Germany, or systems available through Bilaney Consultants Ltd., St Julians, Sevenoaks, Kent, UK. (Sillaber et al. 1998; Wellmer et al. 2000; Kuzmin et al. 2003; Sienkiewicz-Jarosz et al. 2003; Strekalova et al. 2005).

Ströhle et al. (1997) mounted a video camera connected to a computer directly above six locomotor boxes (60×60 cm each). The distance traveled by the rat in a 20-min interval was determined with a video digitizer (TSE Systems, Bad Homburg, Germany).

Spooren et al. (2000), Stobrawa et al. (2001), Heijtz et al. (2002, 2004), Abo-Salem et al. (2004), Bilkei-Gorzo et al. (2004) measured motor activity (locomotion and rearing) in several animals (rats or mice) simultaneously by means of a multi-box detection system (ActiMot; TSE Systems, Bad Homburg Germany). This system use individual photocell activity units (48 x 48 cm) connected to a control unit. Each unit consists of a base frame with two pairs of light-barrier strips (each with 16/32 pairs of infrared transmitter and receiver diodes set at a distance of 28/14 mm; XY-coordinate). An additional pair of light-barrier strips (Z-coordinate) is used to detect rearing activity. Data for the number and sequence of photocell interruptions were collected on a computer.

A novel method for counting spontaneous motor activity in rats was proposed by Masuo et al. (1997). In the "Supermex" system, a sensor detects the radiant body heat of an animal.

REFERENCES AND FURTHER READING

Abo-Salem OM, Hayallah AM, Bilkei-Gorzo A, Filipek B, Zimmer A, Müller CA (2004) Antinociceptive effects of novel A_{2B} adenosine receptor antagonists. J Pharmacol Exp Ther 308:358–366

Barros HMT, Tannhauser MAL, Tannhauser SL, Tannhauser M (1991) Enhanced detection of hyperactivity after drug withdrawal with a simple modification of the open-field apparatus. J Pharmacol Meth 26:269–275

Becker H, Randall CL (1989) Effects of prenatal ethanol exposure in C57BL mice on locomotor activity and passive avoidance behavior. Psychopharmacol 97:40–44

Bilkei-Gorzo A, Racz I, Michel K, Zimmer A, Klingmüller D, Zimmer A (2004) Behavioral phenotype of preproenkephalin-deficient mice on diverse congenic backgrounds. Psychopharmacology 176:343–352

Carlezon WA, Cornfeldt ML, Szewczak MR, Fielding S, Dunn RW (1991) Reversal of both QNX-induced locomotion and habituation decrement is indicative of M_1 agonist properties. Drug Dev Res 23:333–339

Choi OH, Shamin MT, Padgett WL, Daly JW (1988) Caffeine and theophylline analogues: correlation of behavioral effects with activity as adenosine receptor antagonists and as phosphodiesterase inhibitors. Life Sci 43:387–398

Crabbe JC, Young ER, Deutsch CM, Tam BR, Kosobud A (1987) Mice genetically selected for differences in open-field activity after ethanol. Pharmacol Biochem Behav 27:577–581

Crabbe JC, Deutsch CM, Tam BR, Young ER (1988) Environmental variables differentially affect ethanol-stimulated activity in selectively bred mouse lines. Psychopharmacology 95:103–108

Crunelli V, Bernasconi S (1979) A new device to measure different size movements: Studies on d-amphetamine-induced locomotion and stereotypy. J Pharmacol Meth 2:43–50

Dauge V, Corringer PJ, Roques BP (1995) CCK_A, but not CCK_B, antagonists suppress the hyperlocomotion induced by endogenous enkephalins, protected from enzymatic

degradation by systemic RB 101. Pharmacol Biochem Behav 50:133–139
Dews PB (1953) The measurement of the influence of drugs on voluntary activity in mice. Br J Pharmacol 8:46–48
Ericson E, Samuelsson J, Ahlenius S (1991) Photocell measurements of rat motor activity. J Pharmacol Meth 25:111–122
Fontenay M, Le Cornec J, Zaczinska M, Debarele M, Simon P, Boissier J (1970) De trois tests de comportement du rat pour l'etude des medicaments psychotropes. J Pharmacol (Paris) 1:243–254
Georgiev V, Getova D, Opitz M (1991) Mechanism of the angiotensin II effects on exploratory behavior of rats in open field. III. Modulatory role of GABA. Meth Find Exp Clin Pharmacol 13:5–9
Ghelardini C, Galeotti N, Gualtieri F, Marchese V, Bellucci C, Bartolini A (1998) Antinociceptive and antiamnesic properties of the presynaptic cholinergic amplifier PG-9. J Pharmacol Exp Ther 284:806–816
Gillies DM, Mylecharane EJ, Jackson DM (1996) Effects of 5-HT_3 receptor-selective agents on locomotor activity in rats following injection into the nucleus accumbens and the ventral tegmental area. Eur J Pharmacol 303:1–12
Heijtz RD, Beraki S, Scott L, Aperia A, Forssberg H (2002) Sex differences in the motor inhibitory and stimulatory role of dopamine D1 receptors in rats. Eur J Pharmacol 445:97–104
Heijtz RD, Scott L, Forssberg H (2004) Alteration of dopamine D1 receptor-mediated motor inhibition and stimulation during development in rats is associated with distinct patterns of c-fos mRNA expression in the frontal-striatal circuitry. Eur J Neurosci 19:945–956
Honma S, Honma KI, Hiroshige T (1991) Methamphetamine effects on rat circadian clock depend on actograph. Physiol Behav 49:787–795
Irifune M, Sato T, Nishikawa T, Masuyama T, Nomoto M, Fukada T, Kawahara M (1997) Hyperlocomotion during recovery from isoflurane anesthesia is associated with increased dopamine turnover in the nucleus accumbens and striatum in mice. Anesthesiology 86:464–475
Ivens I (1990) Neurotoxicity testing during long-term studies. Neurotoxicol Teratol 12:637–641
Kádár T, Telegdy G, Schally AV (1992) Behavioral effect of centrally administered LH-RH agonist in rats. Physiol Behav 51:601–605
Kauppila T, Tanila H, Carlson S, Taira T (1991) Effects of atipamezole, a novel α_2-adrenoreceptor antagonist, in open-field, plus-maze, two compartment exploratory, and forced swimming tests in rats. Eur J Pharmacol 205:177–182
Kulig BM (1989) A neurofunctional test battery for evaluating the effects of long-term exposure to chemicals. J Am Coll Toxicol 8:71–83
Kuzmin A, Sandin J, Terenius L, Ögren SO (2003) Acquisition, expression, and reinstatement of ethanol-induced place preference in mice: effects of opioid receptor-like 1 receptor agonists and naloxone. J Pharmacol Exp Ther 304:310–318
Laviola G, Alleva E (1990) Ontogeny of muscimol effects on locomotor activity, habituation, and pain reactivity in mice. Psychopharmacol 102:41–48
Liu HJ, Sato K, Shih HC, Shibuya T, Kawamoto H, Kitagawa H (1985) Pharmacological studies of the central action of zopiclone: effects on locomotor activity and brain monoamines in rats. Int J Clin Pharmacol Ther Toxicol 23:121–128
Magnus-Ellenbroek B, Havemann-Reinicke U (1993) Morphine-induced hyperactivity in rats – A rebound effect? Naunyn-Schmiedeberg's Arch Pharmacol 635–642
Masuo Y, Matsumoto Y, Morita S, Noguchi J (1997) A novel method for counting spontaneous motor activity in rats. Brain Res Protoc 1:321–326
Nakatsu K, Owen JA (1980) A microprocessor-based animal monitoring system. J Pharmacol Meth 3:71–82
Nieminen SA, Lecklin A, Heikkinen O, Ylitalo P (1990) Acute behavioral effects of the organophosphates Sarin and Soman in rats. Pharmacol Toxicol 67:36–40
Nikodijevic O, Sarges R, Daly JW, Jacobson KA (1991) Behavioral effects of A_1- and A_2-selective adenosine agonists and antagonists: evidence for synergism and antagonism. J Pharmacol Exp Ther 259:286–294
Okada K, Oishi R, Saeki K (1990) Inhibition by antimanic drugs of hyperactivity induced by methamphetamine-chlordiazepoxide mixture in mice. Pharmacol Biochem Behav 35:897–901
Petkov VD, Belcheva S, Konstatinova E (1995) Anxiolytic effects of dotarizine, a possible antimigraine drug. Meth Find Exp Clin Pharmacol 17:659–668
Rex A, Stephens DN, Fink H (1996) 'Anxiolytic' action of diazepam and abecarnil in a modified open field test. Pharmacol Biochem Behav 53:1005–11011
Rex A, Voigt JP, Voits M, Fink H (1998) Pharmacological evaluation of a modified open-field test sensitive to anxiolytic drugs. Pharmacol Biochem Behav 59:677–683
Rosenthal MJ, Morley JE (1989) Corticotropin releasing factor (CRF) and age-related differences in behavior of mice. Neurobiol Aging 10:167–171
Saelens JK, Kovacsics GB, Allen MP (1986) The influence of the adrenergic system on the 24-hour locomotor activity pattern in mice. Arch Int Pharmacodyn 173:411–416
Sienkiewicz-Jarosz H, Szyndler J, Czlonkowska AI, Siemiątkowski M, Maciejak P, WisłowskaA, Zeinowicz M, Lehner M, Turzyńska D, Bidziński A, Plaźnik A (2003) Rat behavior in two models of anxiety and brain [^{3}H]muscimol binding: pharmacological, correlation, and multifactor analysis. Behav Brain Res 145:17–23
Sillaber I, Montkowski A, Landgraf R, Barden N, Holsboer F, Spanagel R (1998) Enhanced morphine-induced behavioural affects and dopamine release in the nucleus accumbens in a transgenic mouse model of impaired glucocorticoid (type II) receptor function: influence of long-term treatment with the antidepressant moclobemide. Neuroscience 85:415–425
Silverman P (1978) Exploration. In: Animal behaviour in the laboratory. Chapman and Hall, London, pp 230–253
Spooren WPJM, Vassout A, Neijt HC, Kuhn R, Casparini F, Roux S, Porsolt RD, Gentsch C (2000) Anxiolytic-like effects of the prototypical metabotropic glutamate receptor 5 antagonist 2-methyl-6-(phenylethynyl)pyridine in rodents. J Pharmacol Exp Ther 295:1267–1275
Steiner H, Fuchs S, Accili D (1997) D_3 dopamine receptor-deficient mouse: Evidence of reduced anxiety. Physiol Behav 63:137–141
Stobrawa SM, Breiderhoff T, Takamori S, Engel D, Schweizer M, Zdebik AA, Bösl MR, Ruether K, Jahn H, Draguhn H, Jahn R, Jentsch TJ (2001) Disruption of ClC-3, a chloride channel expressed on synaptic vesicles, leads to a loss of the hippocampus. Neuron 28:185–196
Strekalova T, Spanagel R, Dolgov O, Bartsch D (2005) Stress-induced hyperlocomotion as a confounding factor in anxiety and depression models in mice. Behav Pharmacol 16:171–180
Ströhle A, Jahn H, Montkowski A, Liebsch G, Boll E, Landgraf R, Holsboer F, Wiedemann K (1997) Central and peripheral administration of atriopeptin is anxiolytic in rats. Neuroendocrinology 65:210–215

Strömberg C (1988) Interactions of antidepressants and ethanol on spontaneous locomotor activity and rotarod performance in NMRI and C57BL/6 mice. J Psychopharmacol 2:61–66
Sugita R, Sawa Y, Nomura S, Zorn SH, Yamauchi T (1989) Effects of reserpine on dopamine metabolite in the nucleus accumbens and locomotor activity in freely moving rats. Neurochem Res 14:267–270
Surmann A, Havemann-Reinicke U (1995) Injection of apomorphine – A test to predict individual different dopaminergic sensitivity? J Neural Transm Suppl 45:143–155
Tanger HJ, Vanwersch RAP, Wolthuis OL (1978) Automated TV-based system for open field studies: Effects of methamphetamine. Pharmacol Biochem Behav 9:557–557
VanHaaren F, Meyer ME (1991) Sex differences in locomotor activity after acute and chronic cocaine administration. Pharmacol Biochem Behav 39:923–927
Vorhees CV, Acuff-Smith KD, Mink DR, Butcher RE (1992) A method of measuring locomotor behavior in rodents: Contrast-sensitive computer-controlled video tracking activity assessment in rats. Neurotoxicol Teratol 14:43–49
Wellmer A, Noeske C, Gerber J, Munzel U, Nau R (2000) Spatial memory and learning deficits after experimental pneumococcal meningitis in mice. Neurosci Lett 296:137–140
Wolffgramm J, Lechner J, Coper H (1988) Interaction or two barbiturates and an antihistamine on body temperature and motor performance in mice. Arzneim Forsch/Drug Res 38:885–891

E.1.2.4 Hole-Board Test

PURPOSE AND RATIONALE

The evaluation of certain components of behavior of mice such as curiosity or exploration has been attempted by Boissier et al. (1964) and Boissier and Simon (1964). They used an open field with holes on the bottom into which the animals could poke their noses. The "planche à trous" or "hole-board" test has become very well recognized and has been modified and automatized by many authors.

PROCEDURE

Mice of either sex (NMRI strain) with a weight between 18 and 22 g are used. The hole-board has a size of 40 × 40 cm. Sixteen holes with a diameter of 3 cm each are distributed evenly on the floor. The board is elevated so that the mouse poking its nose into the hole does not see the bottom. Nose-poking is thought to indicate curiosity and is measured by visual observation in the earliest description and counted by electronic devices in more recent modifications. Moreover, in the newer modifications motility is measured in addition by counting interruption of light beams. Usually, 6 animals are used for each dose and for controls. Thirty minutes after administration of the test compound the first animal is placed on the hole-board and tested for 5 min.

CALCULATION

The number of counts for nose-poking of treated animals is calculated as percentage of control animals.

CRITICAL ASSESSMENT OF THE METHOD

Poking the nose into a hole is a typical behavior of mice indicating a certain degree of curiosity. Evaluation of this component of behavior has been proven to be quite useful. Benzodiazepines tend to suppress nose-pocking at relatively low doses.

MODIFICATIONS OF THE METHOD

A hole-poke measuring system is commercially available from TSE Systems, Bad Homburg, Germany.

REFERENCES AND FURTHER READING

Boissier JR, Simon P (1964) Dissociation de deux composantes dans le comportement d'investigation de la souris. Arch Int Pharmacodyn 147:372–388
Boissier JR, Simon P, Wolff J-ML (1964) L'utilisation d'une reaction particuliere de la souris (Methode de la planche atrous) pour l'etude des medicaments psychotropes. Therapie 19:571–586
Clark G, Koester AG, Pearson DW (1971) Exploratory behavior in chronic disulfoton poisoning in mice. Psychopharmacologia (Berl.) 20:169–171

E.1.2.5 Combined Open Field Test

PURPOSE AND RATIONALE

The simultaneous determination of locomotion and curiosity by using a modification of the hole-board test and a photo-beam system has been proposed as a relatively simple test (Weischer et al. 1976). Several types of such equipment are commercially available.

PROCEDURE

Male mice (NMRI-strain) with an average weight of 30 g are used. Each animal is tested individually in an automated open-field box which consists of a black Plexiglas cage (35 × 35 × 20 cm) with a post (8 × 8 × 20 cm) in the center of the cage. Two evenly spaced photo cell beams perpendicular to the wall and 2 cm above the floor divide the box into 4 compartments. Every photo cell beam interruption is registered automatically as an activity count. Each wall of the cage contains 4 evenly spaced 2 cm diameter holes in a horizontal array 7 cm above the floor. A row of 4 photocell beams is mounted 1 cm outside of the holes and automatically records every exploratory nose-poke. Thirty min. after intraperitoneal

and 60 min. after oral administration of the test compound the animal is placed into the cage and the behavior recorded for a period of 5 min. Ten mice are used for each dose as well as for controls.

EVALUATION

Counts for motility (interruption of photo cell beams inside the cage) and for curiosity (interruption of photo cell beams outside the cage due to nose-poking) are recorded individually. The mean values of the treated groups are expressed as percentage of the control group. Using different doses, dose-response curves can be obtained.

CRITICAL ASSESSMENT OF THE METHOD

A dissociation between exploratory behavior and locomotion has been found with several drugs. Even well known stimulants can reduce exploratory behavior with a concomitant increase in locomotion. Depending on the dose, tranquilizers can reduce exploration without affecting locomotion. Due to the modifications of the equipment the results of different authors are often difficult to compare.

The limitations of photocell activity cages for assessing effects of drugs were discussed by Krsiak et al. (1970).

MODIFICATIONS OF THE TEST

Geyer (1982) described a similar device and reported different effects of amphetamine, caffeine, apomorphine and scopolamine. Adams and Geyer (1982) used this device to study the LSD-induced alterations of locomotor patterns and exploration in rats.

Geyer et al. (1986) described a behavioral monitor which was designed to assess the spatial and temporal sequences of locomotor movements in rats.

Other authors, e. g. Wolffgramm et al. (1988) used video recording of the movements of mice in the evening hours at low illumination and counted the locomotor activity as the number of field crossings and the exploratory activity as the number of rearings.

Ljungberg and Ungerstedt (1977) designed a testbox for the automatic recording of eight components of behavior in rats including compulsive gnawing induced by apomorphine.

Matsumoto et al. (1990) described a system to detect and analyze motor activity in mice consisting of a doughnut-shaped cage with 36 units of detectors radially arranged from the center of the cage. Each detector unit consisted of 4 pairs of photosensors (higher-, lower-, inner-, and outer-position sensors).

Schwarting et al. (1993) described a video image analyzing system for open-field behavior which measures turning behavior, thigmotactic scanning and locomotion in rats.

REFERENCES AND FURTHER READING

Adams LM, Geyer MA (1982) LSD-induced alterations of locomotor patterns and exploration in rats. Psychopharmacology 77:179–185

Barbier P, Breteaudeau J, Autret E, Bertrand P, Foussard-Blampin O, Breteau M (1991) Effects of prenatal exposure to diazepam on exploration behavior and learning retention in mice. Dev Pharmacol Ther 17:35–43

Geyer MA (1982) Variational and probabilistic aspects of exploratory behavior in space: Four stimulant styles. Psychopharmacology Bulletin 18:48–51

Geyer MA, Rosso PV, Masten VL (1986) Multivariate assessment of locomotor behavior: Pharmacological and behavioral analyses. Pharmacol Biochem Behav 25:277–288

Krsiak M, Steinberg H, Stoleman IP (1970) Uses and limitations of photocell activity cages for assessing effects of drugs. Psychopharmacologia (Berl.) 17:258–274

Ljungberg T, Ungerstedt U (1977) Different behavioural patters induced by apomorphine: evidence that the method of administration determines the behavioural response to the drug. Eur J Pharmacol 46:41–50

Matsumoto K, Bing C, Sasaki K, Watanabe H (1990) Methylamphetamine- and apomorphine-induced changes in spontaneous motor activity using a new system to detect and analyze motor activity in mice. J Pharmacol Meth 24:111–119

Schwarting RKW, Goldenberg R, Steiner H, Fornaguera J, Huston HP (1993) A video image analyzing system for open-field behavior in the rat focusing on behavioral asymmetries. J Neurosci Meth 49:199–210

Weischer ML (1976) Eine einfache Versuchsanordnung zur quantitativen Beurteilung von Motilitaet und Neugierverhalten bei Maeusen. Psychopharmacology 50:275–279

Wolffgramm J, Lechner J, Coper H (1988) Interaction of two barbiturates and an antihistamine on body temperature and motor performance of mice. Arzneim Forsch/Drug Res, 38:885–891

E.1.2.6 EEG Analysis From Rat Brain by Telemetry

PURPOSE AND RATIONALE

Field potential analysis of freely moving rats by radioelectroencephalography from different brain areas has been developed as a sensitive method in pharmacology (Dimpfel et al. 1986, 1989, 1990, 1992; Kropf et al. 1991).

PROCEDURE

Male adult rats are implanted with four stainless steel electrodes, mounted on a base plate, into the frontal cortex, striatum, thalamus, and reticular formation. The plate carries a microplug for a four-channel radiotransmitter. During the experimental sessions, which

start 2 weeks after surgery, the transmitted field potentials are analyzed in real time using Fast Fourier Transformations. The resulting power density spectra are segmented into six frequency bands, each representing the integrated power over a certain frequency band.

EVALUATION

The data from three pre-drug periods of 15 min each are compared with those from continuously monitored 15-min postdrug periods.

MODIFICATIONS OF THE METHOD

De Simoni et al. (1990) developed a miniaturized optoelectronic system of telemetry for data obtained in freely moving animals by *in vivo* voltammetry, an electrochemical technique that uses carbon fiber microelectrodes to monitor monoamine metabolism and release continuously (Justice 1987).

Krügel et al. (2001) tested functional recovery after neuronal injury by P2 receptor blockade. The functional changes in the neuronal activity were recorded by telemetric EEG (TSE Systems, Bad Homburg, Germany).

REFERENCES AND FURTHER READING

de Simoni MG, de Luigi A, Imeri L, Algerin S (1990) Miniaturized optoelectronic system for telemetry of *in vivo* voltammetric signals. J Neurosci Meth 33:233–240

Dimpfel W, Spüler M, Nickel B (1986) Radioelectroencephalography (Tele-Stereo-EEG) in the rat as a pharmacological model to differentiate the central action of flupirtine from that of opiates, diazepam and phenobarbital. Neuropsychobiol 16:163–168

Dimpfel W, Spüler M, Nichols DE (1989) Hallucinogenic and stimulatory amphetamine derivatives: fingerprinting DOM, DOI, DOB, MDMA, and MBDB by spectral analysis of brain field potentials in the freely moving rat (Tele-Stereo-EEG). Psychopharmacol 98:297–303

Dimpfel W, Spüler M, Bonke (1990) Influence of repeated vitamin B administration on the frequency pattern analyzed from rat brain electrical activity (Tele-Stereo-EEG). Klin Wschr 68:136–141

Dimpfel W, Wedekind W, Spüler M (1992) Field potential analysis in the freely moving rat during the action of cyclandelate or flunarizine. Pharmacol Res 25:287–297

Justice JB Jr (1987) Introduction to *in vivo* voltammetry. In: J.B. Justice (ed) Voltammetry in the Neurosciences: Principles, Methods and Applications. Humana Press, Clifton, New Jersey, pp 3–102

Kropf W, Kuschinsky K, Krieglstein J (1991) Conditioning of apomorphine effects: simultaneous analysis of the alterations in cortical electroencephalogram and behaviour. Naunyn-Schmiedeberg's Arch Pharmacol 343:559–567

Krügel U, Kittner H, Franke H, Illes P (2001) Accelerated functional recovery after neuronal injury by P2 receptor blockade. Eur J Pharmacol 420:R3–R4

E.1.3 Tests for Muscle Coordination

E.1.3.1 Inclined Plane

PURPOSE AND RATIONALE

The method of Allmark and Bachinski (1949) using an inclined screen was originally developed for testing curare-like agents. Later on, it has been used by many authors (e. g. Randall et al. 1961) for testing compounds for muscle relaxant activity. The principle of an inclined plane has been used by Ther, Vogel and Werner (1959) for differentiating neuroleptics from other centrally active drugs. Rivlin and Tator (1977) also used an inclined plane to assess skeletal muscle relaxation.

PROCEDURE

The plane consists of two rectangular plywood boards connected at one end by a hinge. One board is the base, the other is the movable inclined plane. Two plywood side panels with degrees marked on their surface are fixed on the base. A rubber mat with ridges 0.2 cm in height is fixed to the inclined plane which is set at 65 degrees. Male mice (Charles River strain) with a body weight between 20 and 30 g are used. The test compound or the standard are administered to groups of 10 mice either i.p. or s.c. or orally. Thirty, 60 and 90 min thereafter, the mice are placed at the upper part of the inclined plane and are given 30 s to hang on or to fall off.

EVALUATION

The peak time is determined as the time at which a compound produces the maximum performance deficit. At this time interval, a range of doses is tested using 10 animals per group. ED_{50} values are calculated.

CRITICAL ASSESSMENT OF THE METHOD

The method has been proven to be a simple assay for muscle relaxant activity. Although the muscle relaxant tests satisfy the criteria of sensitivity and relative potency compared with clinically effective doses, the effects of anxiolytics are not clearly differentiated from neuroleptics and even from neurotoxic compounds.

MODIFICATIONS OF THE METHOD

Instead of an inclined wooden board, an inclined screen has been used by Randall et al. (1961) and Simiand et al. (1989).

REFERENCES AND FURTHER READING

Allmark MG, Bachinski WM (1949) A method of assay for curare using rats. J Am Pharm Ass 38:43–45

Randall LO, Heise GA, Schallek W, Bagdon RE, Banzinger R, Boris A, Moe RA, Abrams WB (1961) Pharmacological and clinical studies on Valium™. A new psychotherapeutic agent of the benzodiazepine class. Curr Ther Res 3:405–425

Rivlin A, Tator C (1977) Objective clinical assessment of motor function after experimental spinal cord injury in the rat. J Neurosurg 47:577–581

Ther L, Vogel G, Werner P (1959) Zur pharmakologischen Differenzierung und Bewertung von Neuroleptica. Arzneim Forsch/Drug Res 9:351–354

E.1.3.2 Chimney Test

PURPOSE AND RATIONALE

The "test de la cheminée" has been introduced by Boissier et al. (1960) as a simple test for tranquilizing and muscle relaxant activity.

PROCEDURE

Male mice (CD1, Charles River) weighing between 16 and 22 g are used in groups of 10 animals per dose. Pyrex-glass cylinders 30 cm long are required. The internal diameter varies with the animal's weight: for mice weighing 16 to 18 g, the diameter is 22 mm, for mice weighing 18 to 20 g, 25 mm; for mice weighing 20 to 22 g, 28 mm. Each tube has a mark 20 cm from its base. Initially, the tube is held in a horizontal position. At the end of the tube, near the mark, a mouse is introduced with the head forward. When the mouse reaches the other end of the tube, toward which it is pushed if necessary with a rod, the tube is moved to a vertical position. Immediately, the mouse tries to climb backwards and performs coordinated movements similar to an alpinist to pass a chimney in the mountains. This gave the name for the test. The time required by the mouse to climb backwards out at the top of the cylinder is noted.

EVALUATION

The ED_{50} (with 95% confidence limits), the dose for which 50% of the animals fail to climb backwards out of the tube within 30 s, is calculated by log-probit analysis.

CRITICAL ASSESSMENT OF THE METHOD

The chimney test can be used as an additional test with other tests determining muscle relaxant activity.

REFERENCES AND FURTHER READING

Boissier JR, Tardy J, Diverres JC (1960) Une novelle méthode simple pour explorer l'action "tranquillisante": le test de la cheminée. Med exp 3:81–84

Simiand J, Keane PE, Biziere K, Soubrie P (1989) Comparative study in mice of Tetrazepam and other centrally active skeletal muscle relaxants. Arch Int Pharmacodyn 297:272–285

Turner RA (1965) Ataractic (tranquillizing, neuroleptic) agents. In: Screening Methods in Pharmacology. Chapter 7, pp 87–100, Academic Press, New York and London

E.1.3.3 Grip Strength

PURPOSE AND RATIONALE

The test is being used to assess muscular strength or neuromuscular function in rodents which can be influenced not only by sedative drugs and muscle relaxant compounds but also by toxic agents.

PROCEDURE

The method was described as 'test de l'agrippement' by Boissier and Simon (1960). Male or female mice with an average weight of 22 g are used. In a preliminary experiment the animals are tested for their normal reactivity. The animals are exposed to a horizontal thin threat or metallic wire suspended about 30 cm into the air, which they immediately grasp with the forepaws. The mouse is released to hang on with its forelimbs. Normal animals are able to catch the threat with the hind limbs and to climb up within 5 s. Only animals who fulfill this criterion are included into the experiment. Ten mice are used in the control group and in the experimental groups. After oral or subcutaneous administration the animals are tested every 15 min. Animals which are not able to touch the threat with the hind limbs within 5 s or fall off from the threat are considered to be impaired. The test is continued for 2 h. The animals are observed for their behavior in the cages. Only if their behavior and their motility in the cage seem to be normal the disturbance of the grasping reflex can be considered as caused by central relaxation.

EVALUATION

The percentage of animals loosing the catching reflex is calculated. By use of different doses, ED_{50}-values are calculated. Likewise, time-response curves can be established.

CRITICAL ASSESSMENT OF THE METHOD

Only simultaneous observation of the animals under normal conditions gives the possibility to distinguish between central relaxation and toxic effects on neuromuscular function.

MODIFICATIONS OF THE METHOD

Kondziella (1964) described a method for the measurement of muscular relaxation in mice based on the capacity of hanging from a horizontal griddle.

Meyer et al. (1979) described a technique to measure the fore- and hind limb grip strength of rats and mice. The apparatus consists of an adjustable trough and a push-pull strain gauge with a triangular brass ring which is grasped by the animal with its forelimbs. The animal is pulled on the tail until the grip is broken. The animal continues to be pulled along the trough until the hind limbs grasp a T-shaped bar being also attached to push-pull strain gauge. The trial is completed when the grip of the hind limbs is also broken. Fore- and hind limb strength are measured. Dose-response curves could be established with various doses of chlordiazepoxide and phenobarbital.

Barcley et al. (1981) described the tight rope test for testing performance in mice.

Simiand et al. (1989) used a test originally described by Fleury (1957). A mouse held by the tail is placed on a small metallic grid which the animal gripped with its forepaws. The grid is than loaded with weights until the mouse could not longer support the weight of the grid. The endpoint is the maximal weight supported by the animal at least for 2 s. ED_{50}-values can be calculated for various centrally active skeletal muscle relaxants such as the benzodiazepines.

Deacon and Gardner (1984) described the pull-up test in rats. A rat is held by its hind legs in an inverted position. The time taken by the rat to pull itself up and grasp the hand of the experimenter is used as the test parameter.

Novack and Zwolshen (1983) tested muscle relaxants in various models, such as morphine-induced rigidity in rats, decerebrate rigidity in cats and the polysynaptic linguomandibular reflex in cats.

Montag-Sallaz and Montag (2003), Anderson et al. (2004), and Baier et al. (2004) used a Grip Strength Meter apparatus, designed by TSE Systems, Bad Homburg, Germany. If the animal releases the grip then the maximum force is shown on a digital display of a connected control unit.

REFERENCES AND FURTHER READING

Anderson KD, Abdul M, Steward O (2004) Quantitative assessment of deficits and recovery of forelimb motor function after cervical spinal cord injury in mice. Exp Neurol 190:184–191

Baier PC, Schindehütte J, Thinynane K, Flügge G, Fuchs E, Mansouri A, Paulus W, Gruss P, Trenkwalder C (2004) Behavioral changes in unilaterally 6-hydroxydopamine lesioned rats after transplantation of differentiated mouse embryonic stem cells without morphologic integration. Stem Cells 22:396–404

Barclay LL, Gibson GE, Blass JP (1981) The string test: an early behavioral change in thiamine deficiency. Pharmacol Biochem Behav 14:153–157

Boissier JR, Simon P (1960) L'utilisation du test de la traction, (Test de JULOU-COURVOISIER) pour l'etude des psycholeptiques. Therapie 15:1170–1174

Deacon RMJ, Gardner CR (1984) The pull-up test in rats: a simple method for testing muscle relaxation. J Pharmacol Meth 11:119–124

Fleury C (1957) Nouvelle technique pour mesurer l'effort musculaire de la souris, dite test de l'agrippement. Arch. Sci. 10:107–112

Kondziella W (1964) Eine neue Methode zur Messung der muskulaeren Relaxation bei weissen Maeussen. Arch Int Pharmacodyn 152:277–284

Kulig BM (1989) A neurofunctional test battery for evaluating the effects of long-term exposure to chemicals. J Am Coll Toxicol 8:71–83

Montag-Sallaz M, Montag D (2003) Severe cognitive and motor coordination deficits in Tenascin-R-deficient mice. Genes Brain Behav 2:20–31

Meyer OA, Tilson HA, Bird WC, Riley MT (1979) A method for the routine assessment of fore- and hind limb grip strength of rats and mice. Neurobehav Toxicol 1:233–236

Miquel J, Blasco M (1978) A simple technique for evaluation of vitality loss in aging mice, by testing their muscular coordination and vigor. Exp Geront 13:389–396

Novack GD, Zwolshen JM (1983) Predictive value of muscle relaxant models in rats and cats. J Pharmacol Meth 10:175–183

Simiand J, Keane PA, Biziere K, Soubrie P (1989) Comparative study in mice of Tetrazepam and other centrally active skeletal muscle relaxants. Arch Int Pharmacodyn 297:272–285

Tilson HA (1990) Behavioral indices of neurotoxicity. Toxicol Pathol 18:96–104

E.1.3.4 Rotarod Method

PURPOSE AND RATIONALE

The test is used to evaluate the activity of drugs interfering with motor coordination. In 1956, Dunham and Miya suggested that the skeletal muscle relaxation induced by a test compound could be evaluated by testing the ability of mice or rats to remain on a revolving rod. This forced motor activity has subsequently been used by many investigators. The dose which impairs the ability of 50% of the mice to remain on the revolving rod is considered the endpoint.

PROCEDURE

The apparatus consists of a horizontal wooden rod or metal rod coated with rubber with 3 cm diameter attached to a motor with the speed adjusted to 2 rotations per minute. The rod is 75 cm in length and is divided into 6 sections by plastic discs, thereby allowing the simultaneous testing of 6 mice. The rod is in a height

of about 50 cm above the table top in order to discourage the animals from jumping off the roller. Cages below the sections serve to restrict the movements of the animals when they fall from the roller. Male mice (CD-1 Charles River strain) with an weight between 20 and 30 g undergo a pretest on the apparatus. Only those animals which have demonstrated their ability to remain on the revolving rod for at least 1 minute are used for the test. The test compounds are administered intraperitoneally or orally. Thirty minutes after intraperitoneal or 60 min after oral administration the mice are placed for 1 min on the rotating rod. The number of animals falling from the roller during this time is counted.

Using different doses, ED_{50} values can be calculated. Moreover, testing at various time intervals, time-response curves can be obtained.

CALCULATION

Percent animals falling from the rotarod within the test period is calculated for every drug concentration tested. ED_{50} is defined as the dose of drug at which 50% of the test animals fall from the rotarod.

CRITICAL ASSESSMENT OF THE TEST

Many central depressive drugs are active in this test. Benzodiazepines, such as diazepam and flurazepam, have ED_{50} values below 1 mg/kg i.p. The activity of neuroleptics, such as chlorpromazine or haloperidol, is in the same range. In this way, the test does not really differentiate between anxiolytics and neuroleptics but can evaluate the muscle relaxant potency in a series of compounds such as the benzodiazepines. Moreover, the test has been used in toxicology for testing neurotoxicity.

MODIFICATIONS OF THE METHOD

A comparison of the rotarod method in rats with other tests, such as blockade of morphine-induced rigidity in rats, decerebrate rigidity in cats, and polysynaptic-monosynaptic reflex preparations in cats was published by Novack and Zwolshen (1983).

Capacio et al. (1992) used the accelerating rotarod to assess motor performance decrement in rats after administration of candidate anticonvulsant compounds in nerve agent poisoning.

The accelerating rotarod system (TSE Systems, Bad Homburg, Germany) was also used by Augustin et al. (2001), Hosseinzadeh and Asl (2003), Dere et al. (2003), and Vitali and Clarke (2004).

Rozas et al. (1997) described a drug-free rotarod test that was used to evaluate the effects of unilateral 6-hydroxydopamine lesions, nigral grafts, and subrotational doses of apomorphine. The rotarod unit was automated and interfaced with a personal computer allowing automatic recording of the time that each rat was able to stay on the rod at different rotational speeds.

REFERENCES AND FURTHER READING

Augustin I, Korte S, Rickmann M, Kretschmar HA, Südhof TC, Herms JW, Brose N (2001) The cerebellum-specific Munc13 isoform Munc13–3 regulates synaptic transmission and motor learning in mice. J Neurosci 21:10–17

Capacio BR, Harris LW, Anderson DR, Lennox WJ, Gales V, Dawson JS (1992) Use of the accelerating rotarod for assessment of motor performance decrement induced by potential anticonvulsant compounds in nerve agent poisoning. Drug Chem Toxicol 15:177–201

Cartmell SM, Gelgor L, Mitchell D (1991) A revised rotarod procedure for measuring the effect of antinociceptive drugs on motor function in the rat. J Pharmacol Meth 26:149–159

Dere E, De Souza-Silva MA, Teubner B, Söhl G, Willecke K, Huston JR (2003) Connexin30-deficient mice show increased emotionality and decreased rearing activity in the open-field along with neurochemical changes. Eur J Neurosci 18:629–638

Dunham NW, Miya TS (1957) A note on a simple apparatus for detecting neurological deficit in rats and mice. J Am Pharmaceut Assoc 46:208–210

Hosseinzadeh H, Asl MN (2003) Anticonvulsant, sedative and muscle relaxant effects of carbenoxolone in mice. BMC Pharmacology 23:1–6

Novack GD, Zwolshen JM (1983) Predictive value of muscle relaxant models in rats and cats. J Pharmacol Meth 10:175–183

Rozas G, Labandeira-Garcia JL (1997) Drug-free evaluation of rat models of Parkinsonism and nigral grafts using a new automated rotarod test. Brain Res 749:188–199

Saeed Dar M, Wooles WR (1986) Effect of chronically administered methylxanthines on ethanol-induced motor incoordination in mice. Life Sci 39:1429–1437

Vitali R, Clarke S (2004) Improved rotarod performance and hyperactivity in mice deficient in a protein repair methyltransferase. Behav Brain Res 153:129–141

E.1.3.5 Treadmill Performance

PURPOSE AND RATIONALE

Treadmill experiments have been used in pharmacology and physiology for various purposes:

1. To evaluate the influence of drugs on endurance (Snider et al. 1983; Matthew et al. 1988; Ahlenius et al. 1977a, 1997b; Soares et al. 2003; Minami et al. 2004).
2. To study muscle metabolism (Balon and Nadler 1997; Zhou and Dohm 1997; Juel 1998; Foianini et al. 2000; Gosmanov et al. 2002; Saengsirisuwan et al. 2002; Steinberg et al. 2004).
3. To study influence on the cardiovascular system (Koller et al. 1995; Roth et al. 1998; Spier et al. 1999; Sun et al. 1994, 2002; Villanueva et al. 2003).

4. To study the effect of diet (Oudot et al. 1996) and of circadian rhythm (Marchant and Mistlberger 1996).

PROCEDURE

Minami et al. (2004) studied the effect of a high-salt diet or chronic captopril treatment on exercise capacity in normotensive rats. Male Sprague Dawley rats were submitted to stepwise increasing exercise on a motor treadmill at a speed of 10, 20 and 30 m/min, 0-grade incline, for 4 min with 2-min rest intervals. Exercise was stopped when rats were unable to continue running with exhaustion despite contact with a shock at the rear of the treadmill belt. Mean arterial pressure (MAP) and heart rate (HR) were recorded continuously at rest and during the three different intensities of exercise.

EVALUATION

Values obtained for MAP and HR during the 10 s before the beginning of exercise, when all values reached a stable state, and during the last 10 s at each exercise level were used for comparison. All results are expressed as mean ± SEM. One-way ANOVA was used to assess significant differences in means across groups at rest and at each exercise level.

TREADMILL SYSTEMS

A fully computerized electronically controlled treadmill system for small laboratory animals is provided by TSE Systems, Bad Homburg, Germany : The apparatus basically consists of a rotating running belt driven by a servo-controlled motor, which provides precise operator-defined tread speed. Separating panels divide the running surface into separate exercise lanes each suited for an individual animal. The floor grids can be used to apply and electric stimulus of variable length and intensity. The incline of the running surface can be steplessly adjusted to control the labor of the animal.

Columbus Instruments, Columbus, OH, offers the animal treadmill Exer 3/6, which is a general purpose treadmill for three rats or 6 mice utilizing a single belt construction with dividing walls suspended over the tread surface supplied with or without a stimulus assembly. Speed of the belt can be adjusted in the range of 6–100 m/m.

MODIFICATIONS OF THE METHOD

Treadmill experiments in **cats** were performed by Douglas et al. (1993).

Nakai et al. (2003) and Liu et al. (2004) used treadmill experiments to study walking dysfunction in the **rat neuropathic intermittent claudication model**. In this model, male Sprague Dawley rats were anesthetized with pentobarbital. L4–L6 vertebrae were surgically exposed and two small holes were drilled, one between L4–L5 and the second between L6–L6 intervertebral spaces. Two rectangular silicone rubber strips (1.25 mm × 4 mm, thickness: 1 mm) were then placed in the L4–L6 epidural spaces. The incision was closed in two layers and penicillin was administered systemically.

Antri et al. (2005) used treadmill experiments to study long-lasting recovery of locomotor function in chronic spinal rats following combined pharmacological stimulation of serotonergic receptors with 8-OHDPAT and quipazine.

REFERENCES AND FURTHER READING

Ahlenius S, Kaur P, Salmi P (1997a) Biphasic effects of 8-OH-DPAT on endurance of treadmill performance in the male rat. Eur Neuropsychopharmacol 7:89–94

Ahlenius S, Ericson E, Hillegaart V, Nilsson LB, Salmi P, Wijkström A (1997b) *In vivo* effects of Remoxipride and aromatic ring metabolites in the rat. J Pharmacol Exp Ther 283:1356–1366

Antri M, Barthe JY, Mouffle C, Orsal D (2005) Long lasting recovery of locomotor function in chronic spinal rats following combined pharmacological stimulation of serotonergic receptors with 8-OHDPAT and quipazine. Neurosci Lett 384:162–167

Balon TW, Nadler JL (1997) Evidence that nitric oxide increases glucose transport in skeletal muscle. J Appl Physiol 82:359–363

Douglas JR, Noga BR, Dai X, Jordan LM (1993) The effect of intrathecal administration of excitatory amino acid agonists and antagonists on the initiation of locomotion in the adult cat. J Neurosci 13:990–1000

Foianini KR, Steen MS, Kinnik TR, Schmit MB, Youngblood EB, Henriksen EJ (2000) Effects of exercise training and ACE inhibition on insulin action in rat skeletal muscle. J Appl Physiol 89:687–694

Gosmanov AR, Nordtvedt NC, Brown R, Thomason DB (2002) Exercise effects on muscle β-adrenergic signaling for MAPK-dependent NKCC activity are rapid and persistent. J Appl Physiol 93:1457–1465

Juel C (1998) Skeletal muscle Na^+/H^+ exchange in rats: pH dependency and the effect of training. Acta Physiol Scand 164:135–143

Koller A, Huang A, Sun D, Kaley G (1995) Exercise training augments flow-dependent dilation in rat skeletal muscle arterioles. Circ Res 76:544–550

Liu Y, Obata K, Yamanaka H, Dai Y, Fukuoka T, Tokunaga A, Noguchi K (2004) Activation of extracellular signal-related protein kinase in dorsal horn neurons in the rat neuropathic intermittent claudication model. Pain 100:64–72

Marchant EG, Mistlberger RE (1996) Entrainment and phase shifting of circadian rhythms in mice by forced treadmill running. Physiol Behav 60:657–663

Matthew CB, Hubbard RW, Francesconi RP, Thomas GJ (1988) Carbamates, atropine, and diazbepam: effects on performance in the running rat. Life Sci 42:1925–1931

Minami N, Mori N, Nagasaka M, Harada T, Kurossawa H, Kanazawa M, Kohzuki M (2004) Effect of high-salt diet or chronic captopril treatment on exercise capacity in

normotensive rats. Clin Exp Pharmacol Physiol 31:197–201
Nakai K, Takenobu Y, Takimizu H, Akimaru S, Maegawa H, Ito H, Marsala M, Katsube N (2003) Effects of OP-1206 α-CD on walking dysfunction in the rat neuropathic intermittent claudication model: comparison with nifedipine, ticlopidine and cilostazol. Prostaglandins Lipid Mediators 71:253–263
Oudot F, Larue-Achagiotis C, Anton G, Verger P (1996) Modifications in dietary self-selection specifically attributable to voluntary wheel running and exercise training in the rat. Physiol Behav 59:1123–1128
Roth DA, White CD, Podolin DA, Mazzeo RS (1998) Alterations in myocardial signal transduction due to aging and chronic dynamic exercise. J Appl Physiol 84:177–184
Saengsirisuwan V, Perez FR, Kinnik TR, Henriksen EJ (2002) Effects of exercise training and antioxidant *R*-ALA on glucose transport in insulin-sensitive rat skeletal muscle. J Appl Physiol 92:50–58
Snider RM, Ordway GA, Gerald MC (1983) Effects of methylphenidate on rat endurance performance and neuromuscular transmission *in vitro*. Neuropharmacology 22:83–88
Soares DD, Lima NRV, Coimbra CC, Marubayashi U (2003) Evidence that tryptophan reduces mechanical efficiency and running performance in rats. Pharmacol Biochem Behav 74:357–362
Spier SA, Laughlin MH, Delp MD (1999) Effect of acute and chronic exercise on vasoconstrictor responsiveness of rat abdominal aorta. J Appl Physiol 87:1752–1757
Steinberg GR, Smith AC, Wormald S, Malenfant P, Collier C, Dyck DJ (2004) Endurance training partially reverses dietary-induced leptin resistance in rodent skeletal muscle. Am J Physiol 286:E57–E63
Sun D, Huang A, Koller A, Kaley G (1994) Short-term daily exercise activity enhances endothelial NO synthesis in skeletal muscle arterioles of rats. J Appl Physiol 76:2241–2247
Sun D, Huang A, Koller A, Kaley G (2002) Enhanced NO-mediated dilations in skeletal muscle arterioles of chronically exercised rats. Microvasc Res 64:491–496
Villanueva DS, Poirier P, Standley PR, Broderick TL (2003) Prevention of ischemic heart failure by exercise in spontaneously diabetic BB Wor rats subjected to insulin withdrawal. Metabolism 52:791–797
Zhou Q, Dohm GL (1997) Treadmill running increases phosphatidylinositol 3-kinase activity in rat skeletal muscle. Biochem Biophys Res Commun 236:647–650

E.1.3.6 Influence on Polysynaptic Reflexes

PURPOSE AND RATIONALE

Inhibition of polysynaptic reflexes is considered to be the major mode of action of muscle relaxants. Polysynaptic transmission can be measured by the flexor reflex of the hindpaw in anesthetized rats, whereas the monosynaptic Hoffmann reflex is measured by electromyographic recordings from the plantar foot muscle (Block and Schwarz 1994; Schwarz et al. 1994, 1996).

PROCEDURE

Male Wistar rats (250–280 g) are anesthetized with urethane (400 mg/kg i.p.) and α-chloralose (80 mg/kg i.p.). For the flexor reflex a hindpaw is stimulated with a pair of fine subcutaneous needle electrodes (5 square-wave shocks at 500 Hz, 0.2 ms duration and 3.0 reflex threshold). Electromyographic recordings are made with a pair of fine needle electrodes inserted into the ipsilateral tibialis muscle. Seven consecutive electromyographic recordings are amplified, and band-pass filtered (8–10 Hz), collected at a sample rate of 10 Hz, averaged and evaluated using a Signal Averager (CED, Cambridge, UK) on an IBM-compatible personal computer. Ten consecutive responses are averaged before and 20 min after i.p. application of drug.

For stimulation of the Hoffmann reflex a pair of needle electrodes is transcutaneously inserted into the surrounding of the tibial nerve (single square-wave shocks, 0.2 ms duration at 2.0 threshold). Electromyographic recordings are made with a pair of skin clip surface electrodes from the plantar foot muscle. Low intensity electrical stimulation of the tibial nerve elicits a reflex response similar to the human Hoffmann (H) reflex, which has been attributed to monosynaptic excitation of spinal α-motoneurons predominantly by primary muscle spindle afferent fibers. With increasing stimulus strength, the H-wave is preceded by an electromyographic wave, the M wave, which is due to a direct excitation of axons of α-motoneurons.

In all reflex experiments, values measured after solvent or drug application are expressed as a percentage of the corresponding pre-injection value.

EVALUATION

Statistical evaluation of group differences is performed using the Mann-Whitney U-test. Statistical analysis for dose dependency of drug effects is carried out by the Kruskal-Wallis test.

MODIFICATIONS OF THE METHOD

Ono et al. (1990), Farkas and Ono (1995), Hasegawa and Ono (1996), Otsu et al. (1998) recorded spinal reflexes from spinalized and non-spinalized rats anesthetized with α-chloralose and urethane. Laminectomy was performed in the lumbo-sacral region. Ventral and dorsal roots of the segments L4 and L5 were isolated. A skin pouch was formed at the site of the dissection to cover the exposed tissues with liquid paraffin kept at 36°C. The dorsal root of L5 was placed on bipolar silver wire electrodes for stimulation (0.2 Hz, 0.05 ms, supramaximal). The ipsilateral ventral root of L5 and the dorsal root of L4 were placed on bipolar wire electrodes for recording. Monosynaptic and polysynaptic reflexes and dorsal root-dorsal root reflexes were evoked in the L5 ventral root and in the L4 dorsal

root, respectively. These reflex potentials were amplified, displayed on an oscilloscope and averaged 8 times by an averaging computer.

Turski and Stephens (1993) recorded monosynaptic Hoffman reflexes in NMRI **mice** anesthetized with 80 mg/kg α-chloralose i.p. +400 mg/kg urethane i.p. The tibial nerve was stimulated with single square-wave pulses, 0.2 ms duration at 1.2–1.6 times the nerve threshold. Electromyogram recordings were made with a pair of skin clip surface electrodes from the plantar foot muscle. For recording polysynaptic flexor reflexes, the tibial nerve was stimulated with five square-wave pulses at 500 Hz, 0.2 ms duration at 3.0 times the nerve threshold. Electromyogram recordings were made with a pair of wire electrodes inserted percuteneously into the ipsilateral tibial muscle.

Furthermore, these authors used **genetically spastic rats**. A mutant strain of Wistar rats, which carries an autosomal recessive gene defect, is characterized by a progressive paresis of the hindlimbs with increased tone on the extensor muscles (Pittermann et al. 1976). This genetically determined syndrome of spasticity in the rat permits quantitative evaluation of the effect of drugs on muscle tone by recording activity in the electromyogram from a hindlimb extensor muscle (Klockgether et al. 1985; Turski et al. (1990).

Farkas et al. (1989), Tarnava et al. (1989) studied the effects of drugs on the reflex potentials evoked by afferent nerve stimulation and recorded from the spinal roots in unanesthetized spinal **cats**. An analog integrating method was used for quantitative evaluation of the reflex potentials. The amplified and band-pass filtered signals from the ventral root (monosynaptic reflex and polysynaptic reflex) and from the dorsal root (dorsal root reflex and dorsal root potential) were fed into signal-selectors, which transmitted the input signals only within the chosen post-stimulus intervals. Thus, the various components of the reflex potentials were separated according to their latencies.

Shakitama et al. (1997) recorded ventral root reflex potential in anesthetized rats and ventral and dorsal root potentials in anesthetized intact and spinalized cats.

Suzuki et al. (1995) studied the recovery of reflex potentials after spinal cord ischemia produced by occlusion of the thoracic aorta and the bilateral internal mammary arteries for 10 min in cats.

REFERENCES AND FURTHER READING

Block F, Schwarz M (1994) The depressant effect of GYKI 52466 on spinal reflex transmission is mediated via non-NMDA and benzodiazepine receptors. Eur J Pharmacol 256:149–153

Farkas S, Ono H (1995) Participation of NMDA and non-NMDA excitatory amino acid receptors in the mediation of spinal reflex potentials: an *in vivo* study. Br J Pharmacol 114:1193–1205

Farkas S, Tarnawa I, Berzsenyi P (1989) Effects of some centrally acting muscle relaxants on spinal root potentials: a comparative study. Neuropharmacol 21:161–170

Hasegawa Y, Ono H (1996) Effect of (±)-8-hydroxy-2-(di-n-pro-pylamino)tetralin hydrobromide on spinal motor systems in anesthetized intact and spinalized rats. Eur J Pharmacol 295:211–213

Klockgether T, Pardowitz I, Schwarz M (1985) Evaluation of the muscle relaxant properties of a novel β-carboline, ZK 93423 in rats and cats. Br J Pharmacol 86:357–366

Ono H, Saito KI, Kondo M, Morishita SI, Kato K, Hasebe Y, Nakayama M, Kato F, Nakamura T, Satoh M, Oka JI, Goto M, Fukuda H (1990) Effects of the new centrally acting muscle relaxant 7-chloro-N,N,3-trimethylbenzo[b]furan-2-carboxamide on motor and central nervous systems in rats. Arzneim Forsch/Drug Res 40:730–735

Otsu T, Nagao T, Ono H (1998) Muscle relaxant action of MS-322, a new centrally acting muscle relaxant in rats. Gen Pharmacol 30:393–398

Pittermann W, Sontag KH, Wand P, Rapp K, Deerberg F (1976) Spontaneous occurrence of spastic paresis in Han-Wistar rats. Neurosci Lett 2:45–49

Sakitama K, Ozawa Y, Aoto N, Tomita H, Ishikawa M (1997) Effects of a new centrally acting muscle relaxant, NK433 (lamperisone hydrochloride) on spinal reflexes. Eur J Pharmacol 337:175–187

Schwarz M, Block F, Pergande G (1994) N-Methyl-D-aspartate (NMDA)-mediated muscle relaxant action of flupirtine in rats. Neuroreport 5:1981–194

Schwarz M, Schmitt T, Pergande G, Block F (1995) N-Methyl-D-aspartate and α_2-adrenergic mechanisms are involved in the depressant action of flupirtine on spinal reflexes in rats. Eur J Pharmacol 276:247–255

Suzuki T, Sekikawa T, Nemoto T, Moriya H, Nakaya H (1995) Effects of nicorandil on the recovery of reflex potentials after spinal cord ischemia in cats. Br J Pharmacol 116:1815–1820

Tarnawa I, Farkas S, Berzsenyi P, Pataki A, Andrási F (1989) Electrophysiological studies with a 2,3-benzodiazepine muscle relaxant: GYKI 52466. Eur J Pharmacol 167:193–199

Turski L, Stevens DN (1993) Effect of the b-carboline Abecarnil on spinal reflexes in mice and on muscle tone in genetically spastic rats: a comparison with diazepam. J Pharmacol Exp Ther 267:1215–1220

Turski L, Klockgether T, Schwarz M, Turski WA, Sontag KH (1990) Substantia nigra: a site of action of muscle relaxant drugs. Ann Neurol 28:341–348

E.1.3.7 Masticatory Muscle Reflexes

PURPOSE AND RATIONALE

The temporomandibular joint dysfunction syndrome, characterized by pain and clicking in the temporomandibular joint and limitation of function, involves a condition caused by hypertonia combined with para-

functional habits, such as clenching or grinding of teeth and hyperreflexia (Laskin and Block 1986) which may be treated by muscle relaxants. Ozawa et al. (1996) studied the effects of a centrally acting muscle relaxant on *masticatory* muscle reflexes in rats. Both monosynaptic and polysynaptic reflexes can be studied using this model.

PROCEDURE

For recording the **monosynaptic tonic vibration reflex** of the masseter muscle, Wistar rats are anesthetized with ether, intubated with a tracheal cannula and fixed into a stereotactic apparatus. Decerebration is performed by radiofrequency lesion of the midbrain using a Lesion Generator (Radionics, RFG-4, USA) and a lesioning electrode inserted into the midbrain. After lesioning, ether anesthesia is discontinued. The tonic vibration reflex of the masseter muscle, recorded as electromyogram, is induced every 10–12 s by a sinusoidal vibration (100–500 Hz, 2 s) which is applied to the mandibula, and is delivered by a vibration generator driven by a low frequency oscillator and an amplifier. The evoked electromyogram is amplified by a biophysical amplifier and recorded on a thermal array recorder. The root mean square of the electromyogram is also recorded through an integrator.

For recording the **polysynaptic jaw opening reflex**, the animals are anesthetized by intraperitoneal pentobarbital-Na (50 mg/kg), fixed into position on their back and intubated with a tracheal cannula. Intrapulpal stimulation (0.5 Hz, 0.2 s in pulse duration, supramaximal intensity) delivered by an electrical stimulator is performed via a dental reamer inserted into the dental pulp of the mandibula. The jaw opening reflex recorded as phasic component of the electromyogram evoked in the ipsilateral digastric muscle is amplified by a biophysical amplifier and recorded on a thermal array recorder.

For recording of the **polysynaptic tonic periodontal masseteric reflex** (Funakoshi and Amano 1974) the animals are anesthetized by intraperitoneal injection of pentobarbital-Na (35 mg/kg), which is supplemented as required, intubated with a tracheal cannula and fixed onto a stereotaxic apparatus. The maxillary incisor is stimulated by pressing for 5 s every 5 min using a vibration generator driven by a trapezoid generator. The electromyogram responses to this stimulation are amplified by a biophysical amplifier and recorded on a thermal array recorder. The evoked electromyogram is transformed into square-wave pulses, fed into a staircase generator and recorded on a thermal array recorder.

EVALUATION

The significance of differences between the control and the drug-treated groups is evaluated with Dunnett's test.

MODIFICATIONS OF THE METHOD

Boucher et al. (1993) performed microinfusions of excitatory amino acid antagonists into the trigeminal sensory complex of freely moving rats while recording the long latency jaw opening reflex elicited by electrical stimulation of the dental pulp.

Bakke et al. (1998) studied in anesthetized rats neurokinin receptor mechanisms in the increased jaw muscle activity which can be evoked by injection of the small fiber excitant and inflammatory irritant mustard oil into the temporomandibular joint region.

Alia et al. (1998) preformed intra-oral administration of a NK_1 antagonist in freely moving guinea pigs during recording the short- (6–10 ms) and long-latency (18–26 ms) jaw-opening reflex elicited by electrical stimulation of the lower incisor tooth pulp.

Huopaniemi et al. (1988) determined the threshold of the tooth-pulp evoked jaw-opening reflex after naloxone in barbiturate-anesthetized cats.

REFERENCES AND FURTHER READING

Alia S, Azerad J, Pollin B (1998) Effects of RPR 100893, a potent NK_1 antagonist, on the jaw-opening reflex in the guinea pig. Brain Res 787:99–106

Bakke M, Hu JW, Sessle BJ (1998) Involvement of NK_1 and NK_2 tachykinin receptor mechanisms in jaw muscle activity reflexly evoked by inflammatory irritant application to the rat temporomandibular joint. Pain 75:219–227

Boucher Y, Pollin B, Azerad J (1993) Microinfusions of excitatory amino acid antagonists into the trigeminal sensory complex antagonize the jaw opening reflex in freely moving rats. Brain Res 614:155–163

Funakoshi M, Amano N (1974) Periodontal jaw muscle reflexes in the albino rat. J Dent Res 53:598–603

Huopaniemi T, Pertovaara A, Jyvasjavi E, Carlson C (1988) Effect of naloxone on tooth pulp-evoked jaw-opening reflex in the barbiturate-anaesthetized cat. Acta Physiol Scand 134:327–331

Laskin DM, Block S (1986) Diagnosis and treatment of myofascial pain-dysfunction (MPD) syndrome. J Prosthet Dent 56:75–83

Ozawa Y, Komai C, Sakitama K, Ishikawa M (1996) Effects of NK433, a new centrally acting muscle relaxant, on masticatory muscle reflexes in rats. Eur J Pharmacol 298:57–62

E.2 Tests for Anxiolytic Activity

E.2.0.1 General Considerations

Definitions in psychopharmacology have been coined by the activity of special compounds or chemical

classes found in patients. This is not only true for the term "neuroleptic" but also for the term "anxiolytic". Other terms have been "ataractic" or "psycholeptic". Anxiolytics are derived from "tranquilizers", such as meprobamate which was used widely until the advent of benzodiazepines. The property which these drugs have in common is the alleviation of anxiety, thus explaining the term "anxiolytic". These agents are used for the relatively minor disorders of the nonpsychotic or neurotic type, whereas the antipsychotic agents (phenothiazines, butyrophenones) are given mainly to combat the more severe psychotic or schizophrenic reactions. Thus, the terms anti-anxiety and antipsychotic indicate a qualitative distinction in the clinical use and mode of action of the drug. Pathological anxiety in man has been defined by its interference with normal functions, by manifestations of somatic disorders, emotional discomfort, interference with productivity at work, etc. This complex characterization of anxiety in man already indicates the difficulties to find appropriate pharmacological models. Therefore, several tests have to be performed to find a spectrum of activities which can be considered to be predictive for therapeutic efficacy in patients. For *in vivo* studies, most investigators use a battery of anticonvulsive tests, anti-aggressive tests and evaluation of conditioned behavior.

Most of the actions of benzodiazepines are thought to be mediated by potentiation of g-amino-butyric acid (GABA). Two subtypes of GABA receptors ($GABA_A$ and $GABA_B$) have been described. Moreover, specific binding sites for benzodiazepines have been discovered near these GABA receptors in various areas of the brain. These sites occur in a macromolecular complex that includes GABA-receptors, benzodiazepine receptors and receptors for other drugs, and a chloride channel. The benzodiazepines potentiate the neurophysiological actions of GABA at the chloride ion channel by increasing the binding of GABA to $GABA_A$ receptors. This implies that the $GABA_A$ receptor is involved in anxiety and that its direct activation would have an anxiolytic effect. Based in these findings various *in vitro* tests have been developed.

More recently, research has focused on the therapeutic potential of blocking excitatory amino acids – in particular glutamate. Excitatory amino acid receptors have been classified into at least three subtypes by electrophysiological criteria: NMDA, quisqualic acid (QA) and kainic acid (KA) (Cotman and Iversen 1987; Watkins and Olverman 1987). Some methods are described in Sect. E.3 Anti-epileptic activity.

Serotonin may play a role in anxiety, since treatment with drugs that reduce serotoninergic function, including benzodiazepines, have anxiolytic effects in animal models (Dourish et al. 1986). Several subtypes of serotonin receptors have been elucidated, e. g. 5-HT_{1A}, 5-HT_{1B}. 5-HT_{1C}, 5-HT_{1D}, 5-HT_2, 5-HT_3. Further differentiation is underway. 5-HT_{1A}, 5-HT_{1B}, and 5-HT_3 receptors are considered to be involved in the effect of anti-anxiety and novel antipsychotic drugs (Peroutka 1988; Costall et al. 1988). Some *in vitro* methods are described in Sect. E.6 Antidepressant activity and Sect. E.5 Neuroleptic activity.

REFERENCES AND FURTHER READING

Boissier JR, Simon P (1969) Evaluation of experimental techniques in the psychopharmacology of emotion. Ann NY Acad Sci 159:898–914

Costa E, Corda MG, Epstein B, Forchetti C, Guidotti A (1983) GABA-benzodiazepine interactions. In: Costa E (ed) The Benzodiazepines. From Molecular Biology to Clinical Practice. Raven Press, New York, pp 117–136

Costall B, Naylor RJ, Tyers MB (1988) Recent advances in the neuropharmacology of 5-HT_3 agonists and antagonists. Rev Neuroscience 2:41–65

Cotman CW, Iversen LL (1987) Excitatory amino acids in the brain-focus on NMDA receptors. Trends in Neurosci 10:263–265,

Fonnum F (1987) Biochemistry, anatomy, and pharmacology of GABA neurons. In: Meltzer HY (ed) Psychopharmacology: The Third Generation of Progress. Raven Press, New York, pp 173–182

Lippa AS, Priscilla A, Nash BA, Greenblatt EN (1979) Preclinical neuropharmacological testing procedures for anxiolytic drugs. In: Fielding St, Lal H (eds) Anxiolytics, Futura Publ. Comp. New York, pp 41–81

Lloyd KG, Morselli PL (1987) Psychopharmacology of GABAergic drugs. In: Meltzer HY (ed) Psychopharmacology: The Third Generation of Progress. Raven Press, New York, pp 183–195

Peroutka SJ (1988) 5-Hydroxytryptamine receptor subtypes: Molecular, biochemical and physiological characterization. Trends Neuroscience 11:496–500

Watkins JC, Olverman HJ (1987) Agonists and antagonists for excitatory amino acid receptors. Trends in Neurosci 10:265–272

Zukin SR, Young AB, Snyder SH (1974) Gamma-aminobutyric acid binding to receptor sites in the rat central nervous system. Proc Natl Acad Sci, USA, 71:4801–4807

E.2.1 In Vitro Methods

E.2.1.1 GABA Receptor Binding

E.2.1.1.1 General Considerations

γ-Aminobutyric acid (GABA) is known to be an important inhibitory neurotransmitter in the brain. Abnormalities in the GABA system have been found in neurological and psychiatric diseases such as Hunt-

ingdon's chorea, anxiety, panic attacks, schizophrenia, and epilepsy. GABA is also implicated in the mechanism of benzodiazepines and related central nervous system (CNS) drugs.

GABA receptors have been divided into $GABA_A$, $GABA_B$ and $GABA_C$ receptor subtypes which by themselves form receptor families (Enna and Möller 1987; Matsumoto 1989; Möhler 1992).

Without doubt, GABA is the most important inhibitory transmitter in the CNS. One may expect important new developments from attempts to influence the GABAergic system specifically by synthetic compounds. In general, $GABA_A$ receptor agonists are CNS depressants, muscle relaxants, and possess some nociceptive properties, whereas the receptor antagonists are convulsants. Most benzodiazepine-binding sites seem to be associated with $GABA_A$ receptors combined with a chloride channel. Among $GABA_B$ receptor agonists, baclofen has achieved success in clinical use. Results of ongoing research with receptor subtypes will result in the development of new therapeutic agents.

Studies by Urwyler et al. (2001) demonstrated that the $GABA_B$ receptor can be modulated in an allosteric manner. These compounds are not receptor agonists but they appear to act on the heptahelical region of $GABA_{B2}$ to enhance the action of the receptor agonists GABA and baclofen.

$GABA_C$ receptors are ligand-gated chloride channels that are present in many parts of the brain including the superior colliculus, cerebellum, hippocampus, and, most prominently, the retina (Ragozzino et al. 1996; Bormann 2000; Qian and Ripps 2001; Chehib 2004; Schlicker et al. 2004; Yang 2004; Pan et al. 2005; Wang and Slaughter 2005).

The formation and plasticity of GABAergic synapses, their physiological mechanisms and pathophysiological implications are discussed by Fritschy and Brünig (2003).

REFERENCES AND FURTHER READING

Bormann J (2000) The "ABC" of GABA receptors. Trends Pharmacol Sci 21:16–19

Chehib M (2004) $GABA_C$ receptor ion channels. Clin Exp Pharmacol Physiol 31:800–804

Enna SJ, Möller H (1987) γ-Aminobutyric acid (GABA) receptors and their association with benzodiazepine recognition sites. In: Meltzer HY (ed) Psychopharmacology: the third generation of progress. Raven, New York, pp 265–272

Fritschy JM, Brünig I (2003) Formation and plasticity of GABAergic synapses: physiological mechanisms and pathophysiological implications. Pharmacol Ther 98:299–323

Matsumoto RR (1989) GABA receptors: are cellular differences reflected in function? Brain Res Rev 14:203–225

Möhler H (1992) GABAergic synaptic transmission. Arzneim Forsch/Drug Res 42:211–214

Pan Y, Khalili P, Ripps H, Qian H (2005) Pharmacology of $GABA_C$ receptors: responses to agonists and antagonists distinguish A- and B-subtypes of homomeric ρ receptors expressed in *Xenopus* oocytes. Neurosci Lett 376:60–65

Qian H, Ripps H (2001) The $GABA^C$ receptors of retinal neurons. Progr Brain Res 131:295–308

Ragozzino D, Woodward RM, Murata Y, Eusebi F, Overman LE, Miledi R (1996) Design and in vitro pharmacology of a selective gamma-aminobutyric $acid_C$ receptor antagonist. Mol Pharmacol 50:1024–1030

Schlicker K, Boller M, Schmidt M (2004) $GABA_C$ receptor mediated inhibition of acutely isolated neurons of the rat dorsal lateral geniculate nucleus. Brain Res Bull 63:91–97

Urwyler S, Mosbacher J, Lingenhoehl K, Heid J, Hofstetter K, Froestl W, Bettler B, Kaupmann K (2001) Positive allosteric modulation of native and recombinant γ-amino butyric $acid_B$ receptors by 2,6-di-*tert*-butyl-4-(3-hydroxy-2,2-dimethyl-propyl)-phenol (CGP7930) and its aldehyde analog CGP13501. Mol Pharmacol 60:963–971

Wang P, Slaughter MM (2005) Effects of GABA receptor antagonists on retinal glycine receptors and on homomeric glycine receptor alpha subunits. J Neurophysiol 93:3120–3126

Yang XL (2004) Characterization of receptors for glutamate and GABA in retinal neurons. Progr Neurobiol 73:127–159

E.2.1.1.2 In Vitro Assay for GABAergic Compounds: [^{3}H]-GABA Receptor Binding

PURPOSE AND RATIONALE

Radiolabeled GABA is bound to synaptic membrane preparations of mammalian brain. The labeling of the synaptic receptor with ^{3}H-GABA requires careful attention to possible interference from nonsynaptic binding since ^{3}H-GABA can also bind nonspecifically to plasma membranes. The most prominent of which is the sodium dependent binding of GABA to brain membranes, a process which appears to be associated with the transport (uptake) sites of GABA. Sodium-independent binding of ^{3}H-GABA has characteristics consistent with the labeling of GABA receptors. In addition, the relative potencies of several amino acids in competing for these binding sites parallel their abilities to mimic GABA neurophysiologically. Therefore, the sodium-independent binding of ^{3}H-GABA provides a simple and sensitive method to evaluate compounds for GABA-mimetic properties.

PROCEDURE

Reagents

- 0.05 M Tris-maleate buffer (pH 7.1)
- 6.05 g of Tris-base are dissolved in distilled water and made up to 1000 ml. 5.93 g of Tris- maleate are dissolved in 500 ml of water. The 0.05 M Tris

maleate, pH 7.1 buffer is prepared by slowly adding Tris maleate to the Tris-base solution until the pH reaches 7.1.

- 0.32 M Sucrose: 109.5 g of sucrose are dissolved in distilled water and filled up to 1000 ml. The solution is stored at 4°C.
- ^{3}H-GABA (specific activity approximately 40 Ci/mmol) is made up to a concentration of 780 nmol in distilled water and 20 µl is added to each test tube (yielding a final concentration of 15 nmol in the assay). Isoguvacine or muscimol is prepared by dissolving 8.35 mg of isoguvacine or 6.40 mg of muscimol in 10 ml water. Twenty µl of these solutions when added to 1 ml of incubation medium give a final concentration of 0.1 mM isoguvacine or muscimol.
- Test drugs: 1 mM stock solutions are initially prepared. These are serially diluted to the required concentrations prior to the addition to the incubation mixture. Final concentrations are usually from 2×10^{-8} to 1×10^{-5} M.

Tissue Preparation

Male Charles-River rats (100–150 g) are decapitated and their whole brains rapidly removed and homogenized in 15 vol of ice-cold 0.32 M sucrose. The homogenate is centrifuged at 1000 *g* for 10 min. The pellet (nuclear fraction) is discarded and the supernatant fluid is recentrifuged at 20,000 *g* for 20 min. The supernatant is discarded and the crude mitochondrial pellet is resuspended in 15 vol distilled water using a Tekmar homogenizer. The suspension is centrifuged at 8000 *g* for 20 min. The supernatant is collected and used to carefully resuspend, using a gentle squirling motion, the pellet's soft, upper, buffy layer. This suspension is then centrifuged at 48,000 *g* for 20 min. The final crude synaptic membrane pellets are resuspended (without homogenization) in 15 volumes of distilled water and centrifuged at 48,000 *g* for 20 min. The supernatant is discarded, and the centrifuge tubes containing the pelleted membranes are capped with parafilm and stored frozen at –70°C.

Assay Procedure

A frozen membrane pellet from one whole rat brain is resuspended in 15 volumes of 0.05 M Tris-maleate buffer (pH 7.1) by homogenization at 4°C. Triton X-100 is added to a final concentration of 0.05%. This suspension is then incubated at 37°C for 30 min followed by centrifugation at 48,000 *g* for 10 min. The supernatant is discarded and the pellet resuspended by homogenization in the same volume of 0.05 Tris-maleate buffer (pH 7.1) at 4°C. The preincubation with Triton enhances specific GABA receptor binding while lowering non-specific binding.

For the standard Na-independent ^{3}H-GABA binding assay procedure, aliquots of the previously frozen, Triton treated crude synaptic membranes are incubated in triplicate at 4°C for 5 min in 0.05 M Tris-maleate buffer (pH 7.1) containing 15 nM ^{3}H-GABA alone or in the presence of 0.1 mM isoguvacine or muscimol, or the test drug.

The procedure is as follows:

- 1 ml of the 0.05 M Tris-maleate homogenate
- 20 µl of ^{3}H-GABA
- 20 µl of test drug or 20 ml of 0.1 mM isoguvacine or muscimol.

After incubation at 4°C for 5 min, the reaction is terminated by centrifugation for 15 min at 5000 rpm. The supernatant fluid is aspirated and the pellet washed twice with 1 ml of the Tris-maleate buffer. Two ml of liquiscint are added to each tube which is then vigorously vortexed. The contents of the tubes are transferred to scintillation vials, and the tubes rinsed with an additional 2 ml of cocktail. An additional 6 ml of liquiscint are added to each scintillation vial. The radioactivity is measured by liquid scintillation photometry.

EVALUATION

Specific ^{3}H-GABA binding is defined as the radioactivity which can be displaced by a high concentration of unlabeled GABA and is obtained by subtracting from the total bound radioactivity the amount of radioactivity bound in the presence of 0.1 mM isoguvacine. Results are converted to percent of specifically bound ^{3}H-GABA displaced by a given concentration of test drug. IC_{50} values with 95% confidence limits are then obtained by computer derived linear regression analysis.

REFERENCES AND FURTHER READING

Enna SJ, Snyder SH (1975) Properties of γ-aminobutyric acid (GABA) receptor binding in rat brain synaptic membrane fractions. Brain Res 100:81–97

Enna SJ, Snyder SH (1977) Influence of ions, enzymes, and detergents on γ-aminobutyric acid-receptor binding in synaptic membranes of rat brain. Mol Pharmacol 13:442–453

Enna SJ, Collins JF, Snyder SH (1977) Stereo specificity and structure-activity requirements of GABA receptor binding in rat brain. Brain Res 124:185–190

Knott C, Bowery NG (1991) Pharmacological characterization of $GABA_A$ and $GABA_B$ receptors in mammalian CNS by receptor binding assays. In: Greenstein B (ed) Neu-

roendocrine Research Methods. Vol 2, Harwood Academic Publ., Chur, pp 699–722
Lüddens H, Korpi ER (1995) Biological function of $GABA_A$/benzodiazepine receptor heterogeneity. J Psychiat Res 29:77–94
Zukin SR, Young AB, Snyder SH (1974) Gamma-aminobutyric acid binding to receptor sites in the rat central nervous system. Proc Nat Acad Sci, USA 71:4802–4807

E.2.1.1.3 $GABA_A$ Receptor Binding

PURPOSE AND RATIONALE

Two subtypes of GABA receptors have been identified:

1. $GABA_A$ receptor for which muscimol is the typical agonist, whereas bicucculine, picrotoxin, and SR 95531 are antagonists, and
2. $GABA_B$ receptor, for which baclofen is the typical agonist.

The $GABA_A$ receptor directly gates a Cl^- ionophore and has modulatory binding sites for benzodiazepines, barbiturates, neurosteroids and ethanol. By contrast, $GABA_B$ receptors couple to Ca^{2+} and K^+ channels via G proteins and second messenger systems; they are activated by baclofen and are resistant to drugs that modulate $GABA_A$ receptors.

Several subtypes of $GABA_A$ receptors have been identified by ligand binding studies (Kleingoor et al. 1991; Turner et al. 1992; Gusti et al. 1993). Molecular biology techniques revealed the $GABA_A$ receptor to be assembled as a pentameric structure from different subunit (α, β, γ and δ subunit) families making it possible that a very large number of such heteromeric $GABA_A$ receptors exist in the mammalian central and peripheral nervous system (Krogsgaard-Larsen et al. 1994; Lambert et al. 1995; Smith and Olsen 1995; Costa 1998). A total of 19 genes encoding $GABA_A$ receptor subunits are known, while several additional isoforms can occur as splicing variants of some of these (Barnard 1998). Probably more than 500 distinct $GABA_A$ receptor subtypes exist in the brain (Sieghart 2000). Sequences of six α, three β, three γ, one δ, three ρ, one ε, one π and one θ $GABA_A$ receptor subunits have been reported in mammals (Barnard 2000; Alexander et al. 2001). More insight into the pharmacological functions of $GABA_A$ receptor subtypes is expected from studies in gene-knockout mice and by knock-in point mutations (Rudolph et al. 2001).

$GABA_C$ receptors were described as a pharmacologically distinct group by Bormann and Feigenspan (1995), Johnston (1996), Bormann (2000), Zhang et al. (2001). These receptors are Cl^- pores that are insensitive to both bicucculine and baclofen. An IUPHAR Committee has recommended in 1998, that the term $GABA_C$ should be avoided and classified bicucculine- and baclofen-insensitive GABA receptors as a minor subspecies of $GABA_A$ receptors of the 'AO' type.

Subtypes of $GABA_A$ receptors were classified on the basis of subunit structure and receptor function by Barnard et al. (1998).

In rat brain membranes, only the $GABA_A$ receptor is labeled with the $GABA_A$ selective radioligand ^{3}H-SR 95531 in the given concentration range. The assay allows specifically the estimation of the test drug's binding characteristics to the $GABA_A$ receptor subpopulation.

PROCEDURE

Materials

Radioligand: ^{3}H-SR 95531 (^{3}H-2-(3-carboxypropyl)-3-amino-6-(4-methoxyphenyl)-pyridazinium bromide (New England Nuclear, Boston)

Membrane Preparation

Rats are killed by decapitation, the brains are quickly dissected and after separation from the cerebellum placed into ice-cold sucrose solution. The brains (approximately 20 g wet weight) are then homogenized in a glass Teflon potter (1 g brain weight/15 ml 320 mM D(+)-sucrose solution), and centrifuged at 1000 *g* at 4°C for 10 min. The pellets are discarded and the supernatants centrifuged at 20,000 *g* for 20 min. The resulting supernatants are discarded and the pellets are lysed by hypoosmotic shock (addition of 20 volumes of ice-cold bidistilled water). After homogenization in a glass Teflon homogenizer, the suspension is stirred under cooling for 20 min, and centrifuged at 48,000 *g* for 20 min. The resulting pellets are resuspended in ice-cold bidistilled water, the suspension is stirred and recentrifuged as before. The final pellets are resuspended in the incubation buffer (50 mM Tris-HCl and 100 mM $MgCl_2 \times 6\,H_2O$, pH 7.4) corresponding to 1 g brain wet weight/1 ml buffer. The membrane suspension is immediately stored in aliquots of 1 ml at –20°C. Protein content of the membrane suspension is determined according to the method of Lowry et al. (1951) with bovine serum albumin as standard.

At the day of the experiment, the required volume of the membrane suspension is slowly thawed and diluted 1:20 with bidistilled water. After stirring for 10 min, the membrane suspension is centrifuged at 50,000 *g* for 10 min. The resulting pellets are resuspended in ice-cold incubation buffer, yielding a membrane suspension with a protein content of 1 mg/ml.

Assay

For each concentration, assays are performed in triplicate. The total volume of each incubation sample is 200 µl (microtiter plates).

Saturation Experiments

Total binding:

- 50 ml ^{3}H-SR 95531 (12 concentrations, 2×10^{-9} to 1×10^{-7} M)
- 50 ml incubation buffer

Non-specific binding:

- 50 ml ^{3}H-SR 95531 (4 concentrations, 2×10^{-9} to 1×10^{-7} M)
- 50 ml (+) bicucculine (10^{-4} M)

Competition Experiments

- 50 ml ^{3}H-SR 95531 (1 constant concentration, $8–10 \times 10^{-9}$ M)
- 50 ml incubation buffer without or with non-labeled test drug (15 concentrations, 10^{-10} to 10^{-3} M)

The binding reaction is started by adding 100 µl membrane suspension per incubation sample. The samples are incubated for 30 min at 4°C. The reaction is stopped by subjecting the total incubation volume to rapid vacuum filtration over glass fiber filters. Thereby, the membrane-bound radioactivity is separated from the free radioactivity. Filters are washed immediately with approximately 20 ml ice-cold rinse buffer (50 mM Tris HCl, pH 7.4) per sample. The membrane-bound radioactivity is measured after addition of 2 ml liquid scintillation cocktail per sample in a Packard liquid scintillation counter.

EVALUATION

The following parameters are calculated:

- total binding
- non-specific binding
- specific binding = total binding − non-specific binding.

The dissociation constant (K_i) of the test drug is determined from the competition experiment of ^{3}H-SR 95531 versus non-labeled drug by a computer-supported analysis of the binding data.

$$K_i = \frac{K_D{}^3\mathrm{H} \times \mathrm{IC}_{50}}{K_D{}^3\mathrm{H} + [^3\mathrm{H}]}$$

IC_{50} = concentration of the test drug, which inhibits 50% of specifically bound ^{3}H-SR 95531 in the competition experiment.

$[^3H]$ = concentration of ^{3}H-SR 95531 in the competition experiment.

$K_D{}^3H$ = dissociation constant of ^{3}H-SR 95531, determined from the saturation experiment.

The K_i-value of the test drug is that concentration, at which 50% of the receptors are occupied by the test drug.

MODIFICATIONS OF THE METHOD

Binding to the agonist site of the $GABA_A$ receptor can be measured with [^{3}H]muscimol (Snodgrass 1978; Williams and Risley 1979; Martini et al. 1983).

A membrane fraction of whole brains (except cerebellum) from male Wistar rats is prepared by standard techniques. Ten mg of membrane preparation is incubated with 1 nM [^{3}H]muscimol for 10 min at 0°C. Non-specific binding is estimated in the presence of 100 nM muscimol. Membranes are filtered and washed 3 times and the filters are counted to determine specifically bound [^{3}H]muscimol.

The $GABA_A$ receptor chloride channel can be studied by binding with [^{3}H]t-butylbicycloorthobenzoate ([^{3}H]TBOB) (Schwartz and Mindlin 1988; Lewin et al. 1989).

A membrane fraction of whole brains (except cerebellum) from male Wistar rats is prepared by standard techniques. 0.4 mg of membrane preparation is incubated with 3 nM [^{3}H]TBOB for 15 min at 15°C. Non-specific binding is estimated in the presence of 200 µM picrotoxin. Membranes are filtered and washed 3 times and the filters are counted to determine [^{3}H]TBOB specifically bound.

Cromer et al. (2002) presented a model for the extracellular, ligand-binding domain of the $GABA_A$ receptor that is based on the structure of a soluble acetylcholine-binding protein.

Kittler and Moss (2003) discussed modulation of $GABA_A$ receptor activity by phosphorylation and receptor trafficking and the implications for the efficacy of synaptic inhibition.

Lambert et al. (2003) reviewed neurosteroid modulation of $GABA_A$ receptors with special emphasis on pregnane steroids.

Lüscher and Keller (2004) described regulation of $GABA_A$ receptor trafficking, channel activity, and functional plasticity of inhibitory synapses.

Macdonald et al. (2004) reviewed mutations of the $\alpha 1$, $\gamma 2$ and δ subunits of the $GABA_A$ receptor that are associated with different idiopathic generalized epilepsy syndromes.

Mody and Pearce (2004) reviewed the diversity of inhibitory neurotransmission through $GABA_A$ receptors.

Rudolph and Möhler (2004) reported analysis of $GABA_A$ receptor function and dissection of the pharmacology of benzodiazepines and general anesthetics through mouse genetics. Whereas the knockout mice have provided information primarily with respect to the regulation of subunit gene transcription, receptor assembly, and some physiological functions of individual receptor subtypes, the point-mutated knockin mice in which specific $GABA_A$ receptors are insensitive to diazepam or some general anesthetics have revealed the specific contribution of individual receptor subtypes to the pharmacological spectrum of diazepam and cerebral anesthetics.

Among $GABA_A$ agonists and partial antagonists, Krogsgaard-Larsen et al. (2004) characterized THIP (Gaboxadol) as a non-opioid analgesic and a novel type of hypnotic.

Boehm et al. (2004) described γ-aminobutyric acid receptor subunit mutant mice, which offer new perspectives on alcohol actions.

REFERENCES AND FURTHER READING

Alexander S, Peters J, Mathie A, MacKenzie G, Smith A (2001) TiPS Nomenclature Supplement 2001

Barnard EA (1998) Multiple subtypes of the $GABA_A$ receptors. Naunyn-Schmiedeberg's Arch Pharmacol 358, Suppl 2, R 570

Barnard EA (2000) The molecular architecture of $GABA_A$ receptors. In: Möhler H (ed) Handbook of Experimental Pharmacology, Pharmacology of GABA and Glycine Neurotransmission (Vol 150). pp 79–100, Springer Heidelberg

Barnard EA, Langer SZ (1998) $GABA_A$ receptors. NC-IUPHAR Subcommittee on $GABA_A$ receptors. The IUPHAR Compendium of Receptor Characterization and Classification 1998

Barnard EA, Skolnick P, Olsen RW, Mohler H, Sieghart W, Biggio G, Braestrup C, Bateson AN, Langer SZ (1998) International Union of Pharmacology. XV. Subtypes of γ-aminobutyric $acid_A$ receptors: classification on the basis of subunit structure and receptor function. Pharmacol Rev 50:291–313

Beaumont K, Chilton WS, Yamamura HI, Enna SJ (1978) Muscimol binding in rat brain: Association with synaptic GABA receptors. Brain Res 148:153–162

Boehm SL, Ponomarev I, Jennings AW, Withing PJ, Rosahl TW, Garrett EM, Blednow YA, Harris RA (2004) γ-Aminobutyric acid: a receptor subunit mutant mice: new perspectives on alcohol actions. Biochem Pharmacol 68:1581–1602

Bormann J (2000) The 'ABC' of GABA receptors. Trends Pharmacol Sci 21:16–19

Bormann J, Feigenspan A (1995) $GABA_C$ receptors. Trends Neurosci 18:515–519

Chambon JP, Feltz P, Heaulme M, Restle S, Schlichter R, Biziere K, Wermuth CG (1985) An arylaminopyridazine derivative of γ-aminobutyric acid (GABA) is a selective and competitive antagonist of the $GABA_A$ receptor site. Proc. Natl. Acad. Sci. USA 82:1832–1836

Cheng YC, Prusoff WH (1973) Relationship between the inhibition constant (K_i) and the concentration of inhibitor which causes 50 per cent inhibition (I_{50}) of an enzymatic reaction. Biochem Pharmacol 22:3099–3108

Costa E (1998) From $GABA_A$ receptor diversity emerges a unified vision of GABAergic inhibition. Ann Rev Pharmacol Toxicol 38:321–350

Cromer BA, Morton CJ, Parker MW (2002) Anxiety over $GABA_A$ receptor structure relieved by AchBP. Trends Biochem Sci 27:180–287

Enna SJ, Möller H (1987) γ-aminobutyric acid (GABA) receptors and their association with benzodiazepine recognition sites. In: Meltzer HY (ed) Psychopharmacology: The Third Generation Schwartz RD, Mindlin MC (1988) Inhibition of the GABA receptor-gated chloride ion channel in brain by noncompetitive inhibitors of the nicotinic receptor-gated cation channel. J Pharmacol Exp Ther 244:963–970

Enna SJ, Snyder SH (1976) Influence of ions, enzymes, and detergents on γ-aminobutyric acid-receptor binding in synaptic membranes of rat brain. Mol Pharmacol 13:442–453

Gusti P, Ducic I, Puia G, Arban R, Walser A, Guidotti A, Costa E (1993) Imidazenil: A new partial positive allosteric modulator of γ-aminobutyric acid (GABA) action at $GABA_A$ receptors. J Pharmacol Exp Ther 266:1018–1028

Heaulme M, Chambon JP, Leyris R, Molimard JC, Wermuth CG, Biziere K (1986) Biochemical characterization of the interaction of three pyridazinyl-GABA derivatives with the $GABA_A$ receptor site. Brain Res 384:224–231

Heaulme M, Chambon JP, Leyris R, Wermuth CG, Biziere K (1987) Characterisation of the binding of [^{3}H]SR 95531, a $GABA_A$ antagonist, to rat brain membranes. J Neurochem 48:1677–1686

Johnston GAR (1996) $GABA_C$ receptors: relatively simple transmitter-gated ion channels? Trends Pharmacol Sci 17:319–323

Kittler JT, Moss SJ (2003) Modulation of $GABA_A$ receptor activity by phosphorylation and receptor trafficking: implications for the efficacy of synaptic inhibition. Curr Opin Neurobiol 13:341–347

Kleingoor C, Ewert M, von Blankenfeld G, Seeburg PH, Kettenmann H (1991) Inverse but not full benzodiazepine agonists modulate recombinant $\alpha_6\beta_2\gamma_2$ $GABA_A$ receptors in transfected human embryonic kidney cells. Neurosci Lett 130:169–172

Krogsgaard-Larsen P, Frølund B, Jørgensen FS, Schousboe A (1994) $GABA_A$ receptor agonists, partial agonists, and antagonists. Design and therapeutic prospects. J Med Chem 37:2489–2505

Krogsgaard-Larsen P, Frølund B, Liljefors T, Ebert B (2004) $GABA_A$ agonists and partial antagonists; THIP (Gaboxadol) as a non-opioid analgesic and a novel type of hypnotic. Biochem Pharmacol 68:1573–1580

Lambert JJ, Belelli D, Hill-Venning C, Peters JA (1995) Neurosteroids and $GABA_A$ receptor function. Trends Pharmacol Sci 16:295–303

Lambert JJ, Belelli D, Peden DR, Vardy AW, Peters JA (2003) Neurosteroid modulation of $GABA_A$ receptors. Prog Neurobiol 71:67–80

Lewin AH, de Costa BR, Rice KC, Solnick P (1989) *meta*- and *para*-Isothiocyanato-*t*-butylbicycloorthobenzoate: irreversible ligand of the γ-aminobutyric acid-regulated chloride ionophore. Mol Pharmacol 35:189–194

Lowry OH, Rosebrough NJ, Farr AL, Randall RJ (1951) Protein measurement with the Folin phenol reagent. J Biol Chem 193:265–275

Lüscher B, Keller CA (2004) Regulation of $GABA_A$ receptor trafficking, channel activity, and functional plasticity of inhibitory synapses. Pharmacol Ther 102:195–223
Macdonald RL, Gallagher MJ, Feng HJ, Kang J (2004) $GABA_A$ receptor epilepsy mutations. Biochem Pharmacol 68:1497–1506
Martini C, Rigacci T, Lucacchini A (1983) [^{3}H]muscimol binding site on purified benzodiazepine receptor. J Neurochem 41:1183–1185
Mody I, Pearce RA (2004) Diversity of inhibitory neurotransmission through $GABA_A$ receptors. Trends Neurosci 27:569–575
Mohler H, Malherbe P, Draguhn A, Richards JG (1990) $GABA_A$-receptors: structural requirements and sites of gene expression in mammalian brain. Neurochem Res 15:199–207
Rudolph U, Möhler H (2004) Analysis of $GABA_A$ receptor function and dissection of the pharmacology of benzodiazepines and general anesthetics through mouse genetics. Annu Rev Pharmacol Tocicol 44:475–498
Rudolph U, Crestani F, Möhler H (2001) $GABA_A$ receptor subtypes: dissecting their pharmacological functions. Trends Pharmacol Sci 22:188–194
Sieghart W (2000) Unraveling the function of $GABA_A$ receptor subtypes. Trends Pharmacol Sci 21:411–416
Smith GB, Olsen RW (1995) Functional domains and $GABA_A$ receptors. Trends Pharmacol Sci 16:162–168
Snodgrass SR (1978) Use of ^{3}H-muscimol for GABA receptor studies. Nature 273:392–394
Turner DM, Sapp DW, Olsen RW (1991) The benzodiazepine/alcohol antagonist Ro 15–4513: binding to a $GABA_A$ receptor subtype that is insensitive to diazepam. J Pharmacol Exp Ther 257:1236–1242
Vicini S (1991) Pharmacologic significance of the structural heterogeneity of the $GABA_A$ receptor-chloride ion channel complex. Neuropsychopharmacol 4:9–15
Williams M, Risley EA (1978) Characterization of the binding of [^{3}H]muscimol, a potent γ-aminobutyric acid antagonist, to rat synaptosomal membranes using a filtration assay. J Neurochem 32:713–718
Zhang D, Pan Z-H, Awobuluyi M, Lipton SA (2001) Structure and function of $GABA_C$ receptors: a comparison of native versus recombinant vectors. Trends Pharmacol Sci 22:121–132

E.2.1.1.4 $GABA_B$ Receptor Binding

PURPOSE AND RATIONALE

Baclofen, as an analogue of the inhibitory neurotransmitter γ-aminobutyric acid (GABA), binds as agonist to the subtype B of the GABA receptor. Baclofen is effective in the treatment of spasticity caused by multiple sclerosis or other diseases of the spinal cord, particularly traumatic lesions. Studies of similar compounds may lead to other effective antispasmodic drugs.

In rat cerebellar membranes, only the $GABA_B$ receptor is labeled in the given concentration range of the $GABA_B$ selective agonist ^{3}H-(–)baclofen. The assay allows specifically the estimation of the test drug's binding characteristics at the $GABA_B$ subtype receptor population.

The receptor on which baclofen acts is coupled via G_i/G_o proteins to Ca^{2+} and K^+ channels as well as adenyl cyclase in neurons and hence is classified as a metabotropic receptor.

As in other receptor families, heterogeneity of the $GABA_B$ receptor has been found (Scherer et al. 1988; Bittiger et al. 1992; Bonanno and Raiteri 1992, 1993a, b; Bowery 1993; Lanza et al. 1993). At least 3 distinct subtypes have be identified:

a) the postsynaptic receptor linked via a G-protein to a K^+ channel which upon stimulation by GABA hyperpolarizes the neuron,
b) the presynaptic autoreceptor at GABA nerve endings; blockade of this receptor augments the release of GABA in electrically stimulated rat cortical slices,
c) the presynaptic heteroreceptor at glutamate nerve endings; blockade with $GABA_B$ antagonists increases release of glutamate from K^+ stimulated cortical slices.

The structure of $GABA_B$ receptors was identified when isoforms were detected (Kaupmann et al. 1997). Potent $GABA_B$ antagonists were described (Bittiger et al. 1992, 1993; Froestl et al. 1996).

PROCEDURE

Materials

Radioligand: ^{3}H-(–)baclofen, specific activity 1.11–1.85 TBq/mmol (30–50 Ci/Mmol) New England Nuclear, Boston

Membrane Preparation

Rats are killed by decapitation, the cerebella quickly removed, and placed into ice-cold preparation buffer (50 mM Tris-HCl, pH 7.4). Approximately 5 g wet weight of the cerebella are homogenized using a glass Teflon potter, corresponding to 1 g cerebellum wet weight/50 ml buffer, and centrifuged at 48,000 *g* at 4°C for 10 min. The pellets are resuspended in approximately 270 ml preparation buffer, and centrifuged as before. The final pellets are dissolved in preparation buffer, corresponding to 1 g cerebellum wet weight/30 ml buffer. The membrane suspension is immediately stored in aliquots of 5–10 ml at –77°C. Protein content of the membrane suspension is determined according to the method of Lowry et al. with bovine serum albumin as a standard.

At the day of the experiment, the required volume of the membrane suspension is slowly thawed, and centrifuged at 50,000 *g* for 20 min. The pellets are resuspended in the same volume of incubation buffer, and stirred for 45 min at room temperature. The

suspension is recentrifuged as before. This washing step is repeated 3 times. The resulting pellets are resuspended in ice-cold incubation buffer in a volume, yielding a membrane suspension with a protein content of 1 mg/ml. The membrane suspension is stirred under cooling for 20–30 min until the start of the experiment.

Assay

For each concentration samples are used in triplicate. The total volume of each incubation sample is 200 µl (microtiter plates). The concentration of ^{3}H-(–)baclofen is constant in all samples ($1.8–2 \times 10^{-8}$ M).

Saturation Experiments

Total Binding

- 50 µl ^{3}H-(–)baclofen
- 50 µl non-radioactive racemic baclofen (15 concentrations, $0–1.2 \times 10^{-6}$ M)

Non-Specific Binding

The measurement of the non-specific binding is performed at the lowest concentration of the saturation range, i. e. 1.8×10^{-8} M of the ^{3}H-(–)baclofen without non-radioactive racemic baclofen.

- 50 µl ^{3}H-(–)baclofen
- 50 µl gamma-aminobutyric acid.

Competition Experiments

- 50 µl ^{3}H-(–)baclofen
- 50 µl incubation buffer without or with labeled test drug (15 concentrations, $10^{-10}–10^{-3}$ M)

The binding reaction is started by adding 100 µl membrane suspension per incubation sample (1 mg protein/1 ml). The samples are incubated for 60 min at 4°C. The reaction is stopped by subjecting the total incubation volume to rapid vacuum filtration over glass fiber filters. Thereby, the membrane bound is separated from the free radioactivity. The filters are washed with approximately 20 ml ice-cold buffer. The retained membrane bound radioactivity on the filter is measured after addition of 0.3 ml ethylene glycol monomethyl ether and 2 ml liquid scintillation cocktail per sample and an equilibration time of 1 h in a Packard liquid scintillation counter.

EVALUATION

The following parameters are calculated:

- total binding
- non-specific binding
- specific binding = total binding–non-specific binding.

The dissociation constant (K_i) of the test drug is determined from the competition experiment of ^{3}H-(–)baclofen versus non-labeled drug by a computer-supported analysis of the binding data.

$$K_i = \frac{K_D{}^3\mathrm{H} \times \mathrm{IC}_{50}}{K_D{}^3\mathrm{H} + [^3\mathrm{H}]}$$

IC_{50} = concentration of the test drug, which inhibits 50% of specifically bound ^{3}H-(–)baclofen in the competition experiment.

$[^3\mathrm{H}]$ = concentration of ^{3}H-(–)baclofen in the competition experiment

$K_D{}^3\mathrm{H}$ = dissociation constant of ^{3}H-(–)baclofen, determined from the saturation experiment.

The K_i-value of the test drug is the concentration, at which 50% of the receptors are occupied by the test drug.

MODIFICATIONS OF THE METHOD

Kaupmann et al. (1998) showed that $GABA_B$-receptor subtypes assemble into functional heteromeric complexes.

Bowery and Enna (2000) demonstrated that $GABA_B$ receptors are functional metabotropic heterodimers.

Molecular structure and physiological functions of $GABA_B$ receptors are reviewed by Bettler et al. (2003) and Bowery et al. (2003).

REFERENCES AND FURTHER READING

Bettler B, Kaupmann K, Mosbacher J, Gassmann M (2003) Molecular structure and physiological functions of $GABA_B$ receptors. Physiol Rev 84:835–867

Bittiger H, Bernasconi R, Froestl W, Hall R, Jaekel J, Klebs K, Krueger L, Mickel SJ, Mondadori C, Olpe HR, Pfannkuch F, Pozza M, Probst A, van Riezen H, Schmutz M, Schuetz H, Steinmann MW, Vassout A, Waldmeyer P, Bieck P, Farger G, Gleiter C, Schmidt EK, Marescuax C (1992) $GABA_B$ antagonists: potential new drugs. Pharmacol Commun 2:70–74

Bittiger H, Froestl W, Mickel SJ, Olpe HR (1993) $GABA_B$ receptor antagonists: From synthesis to therapeutic applications. Trends Pharmacol Sci 14:391–394

Bonanno G, Raiteri M (1992) Functional evidence for multiple γ-aminobutyric acid$_B$ receptor subtypes in the rat cerebral cortex. J Pharmacol Exp Ther 262:114–118
Bonanno G, Raiteri M (1993a) Multiple $GABA_B$ receptors. Trends Pharmacol Sci 14:259–261
Bonanno G, Raiteri M (1993b) γ-aminobutyric acid (GABA) autoreceptors in rat cerebral cortex and spinal cord represent pharmacologically distinct subtypes of the $GABA_B$ receptor. J Pharmacol Exp Ther 265:765–770
Bowery G, Hill DR, Hudson AL (1983) Characterization of $GABA_B$ receptor binding sites on rat whole brain synaptic membranes. Br J Pharmacol 78:191–206
Bowery NG (1993) $GABA_B$ receptor pharmacology. Annu Rev Pharmacol Toxicol 33:109–147
Bowery NG, Enna SJ (2000) γ-Aminobutyric acid$_B$ receptors: first of functional metabotropic heterodimers. J Pharmacol Exp Ther 292:2–7
Bowery NG, Hill DR, Hudson AL (1985) (^{3}H)(–)baclofen: An improved ligand for $GABA_B$ sites. Neuropharmacol 24:207–210
Bowery NG, Bettler B, Froestl W, Gallagher JP, Marshall F, Raiteri M, Bonner TI, Enna SJ (2003) International Union of Pharmacology. XXXIII. Mammalian γ-aminobutyric acid$_B$ receptors: structure and function. Pharmacol Rev 54:247–264
Cheng YC, Prusoff WH (1973) Relationship between the inhibition constant (K_i) and the concentration of inhibitor which causes 50 per cent inhibition (IC_{50}) of an enzymatic reaction. Biochem Pharmacol 22:3099–3108
Drew CA, Johnston GAR, Weatherby RP (1984) Bicuculline-insensitive GABA receptors: Studies on the binding of (–)-baclofen to rat cerebellar membranes. Neurosci Lett 52:317–321
Enna SJ, Möller H (1987) γ-aminobutyric acid (GABA) receptors and their association with benzodiazepine recognition sites. In: Meltzer HY (ed) Psychopharmacology: The Third Generation of Progress. Raven Press, New York, pp 265–272
Froestl W, Mickel SJ, Schmutz M, Bittiger H (1996) Potent, orally active $GABA_B$ receptor antagonists. Pharmacol Commun 8:127–133
Hill DR, Bowery NG (1981) ^{3}H-baclofen and ^{3}H-GABA bind to bicuculline-insensitive $GABA_B$ sites in rat brain. Nature 290:149–152
Kato K, Goto M, Fukuda H (1983) Regulation by divalent cations of ^{3}H-baclofen binding to $GABA_B$ sites in rat cerebellar membranes. Life Sci 32:879–887
Kaupmann K, Huggel K, Held J, Flor PJ, Bischoff S, Mickel SJ, McMaster G, Angst C, Bittiger H, Froesti W, Bettler B (1997) Expression cloning of $GABA_B$ receptors uncovers similarity to metabotropic receptors. Nature 386:239–246
Kaupmann K, Malitschek B, Schuler V, Heid J, Froestl J, Beck P, Mosbacher J, Bischoff S, Kulik A, Shigemoto R, Karschin AS, Bettler B (1998) $GABA_B$-receptor subtypes assemble into functional heteromeric complexes. Nature 396:683–687
Kerr DIB, Ong J, Prager RH, Gynther BD, Curtis DR (1987) Phaclofen: a peripheral and central baclofen antagonist. Brain Res 405:150–154
Kerr DIB, Ong J, Johnston GAR, Abbenante J, Prager RH (1988) 2-Hydroxy-saclofen: am improved antagonist at central and peripheral $GABA_B$ receptors. Neurosci Lett 92:92–96
Kerr DIB, Ong J, Johnston GAR, Abbenante J, Prager RH (1989) Antagonism of $GABA_B$ receptors by saclofen and related sulphonic analogues of baclofen and GABA. Neurosci Lett 107:239–244
Lanza M, Fassio A, Gemignani A, Bonanno G, Raiteri M (1993) CGP 52432: a novel potent and selective $GABA_B$ autoreceptor antagonist in rat cerebral cortex. Eur J Pharmacol 237:191–195
Lowry OH, Rosebrough NJ, Farr AL, Randall RJ (1951) Protein measurement with the Folin phenol reagent. J Biol Chem 193:265–275
Olpe HR, Karlsson G, Pozza MF, Brugger F, Steinman M, van Riezen H, Fagg G, Hall RG, Froestl W, Bittiger H (1990) CGP 35348: a centrally active blocker of $GABA_B$ receptors. Eur J Pharmacol 187:27–38
Paredes RG, Ågmo A (1992) GABA and behavior: The role of receptor subtypes. Neurosci Behav Rev 16:145–170
Robinson TM, Cross AJ, Green AR, Toczek JM, Boar BR (1989) Effects of the putative antagonists phaclofen and δ-aminovaleric acid on $GABA_B$ receptor biochemistry. Br J Pharmacol 98:833–840
Scherer RA, Ferkany JW, Enna SJ (1988) Evidence for pharmacologically distinct subsets of $GABA_B$ receptors. Brain Res Bull 21:439–443
Shank RP, Baldy WJ, Mattucci LC, Vilani FJ Jr (1990) Ion and temperature effects on the biding of γ-aminobutyrate to its receptors and the high-affinity transport system. J Neurochem 54:2007–2015
Shoulson I, Odoroff Ch, Oakes D, Behr J, Goldblatt D, Caine E, Kennedy J, Miller Ch, Bamford K, Rubin A, Plumb S, Kurlan R (1989) A controlled clinical trial of baclofen as protective therapy in early Huntington's disease. Ann Neurol 25:252–259
Wilkin GP, Hudson AL, Hill DR, Bowery NG (1981) Autoradiographic localisation of $GABA_B$ receptors in rat cerebellum. Nature 294:584–587

E.2.1.2 Benzodiazepine Receptor: [^{3}H]-Flunitrazepam Binding Assay

PURPOSE AND RATIONALE

Experiments using ^{3}H-diazepam or ^{3}H-flunitrazepam have demonstrated specific binding sites in CNS membrane preparations that satisfy the criteria for pharmacological receptors, e. g. saturability, reversibility, stereoselectivity and significant correlation with *in vivo* activities of the drugs in this class.

Heterogeneity of benzodiazepine receptors has been reported (Klepner et al. 1979; Supavilai and Karobath 1980; Hafely et al. 1993; Davies et al. 1994). There are four classes of benzodiazepine and non-benzodiazepine high affinity ligands for benzodiazepine recognition sites associated with $GABA_A$ receptors: The first class (e. g. diazepam, flunitrazepam, alprazolam) facilitates the action of GABA, increasing the opening frequency of Cl^- channels. These ligands are called full positive allosteric modulators, or full agonists. A second class of ligands, which includes the β-carbolines, can decrease the opening frequency of Cl^- channels. These ligands are known as full negative allosteric modulators, or full inverse agonists. A third class (e. g. flumazenil) binds with high affinity to ben-

zodiazepine recognition sites, but it can also prevent the GABA modulations elicited by positive or negative allosteric modulators; this class is called a modulator antagonist. A fourth class of ligands for benzodiazepine recognition sites is known to elicit either partial amplification or partial attenuation of GABA action at various $GABA_A$ receptors, and comprises the class called partial positive and partial negative allosteric modulators or partial agonists and partial inverse agonists, respectively.

The names **ω_1, ω_2, and ω_3-receptor subtypes** have been proposed to replace the nomenclature of benzodiazepine BZ_1, BZ_2, and BZ_p receptors (Langer and Arbilla 1988; Langer et al. 1990; Griebel et al. 1999a, b).

PROCEDURE

Reagents

- [Methyl-^{3}H]-Flunitrazepam (70–90 Ci/mmol) can be obtained from New England Nuclear.
- Clonazepam HCl can be obtained from Hoffmann La Roche

Tissue Preparation

Male Wistar rats are decapitated and the brains rapidly removed. The cerebral cortices are removed, weighed and homogenized with a Potter-Elvejhem homogenizer in 20 volumes of ice-cold 0.32 M sucrose. This homogenate is centrifuged at 1000 *g* for 10 min. the pellet is discarded and the supernatant is centrifuged at 30,000 *g* for 20 min. The resulting membrane pellet is resuspended in 40 volumes of 0.05 M Tris buffer, pH 6.9.

Assay

1 ml	0.05 Tris buffer, pH 6.9
560 µl	H_2O
70 µl	0.5 M Tris buffer, pH 6.9
50 µl	^{3}H-Flunitrazepam
20 µl	vehicle (for total binding) or 0.1 mM Clonazepam (for non-specific binding) or appropriate drug concentrations.
300 µl	tissue suspension.

The tubes containing ^{3}H-flunitrazepam, buffer, drugs and H_2O are incubated at 0–4°C in an ice bath. A 300 µl aliquot of the tissue suspension is added to the tubes at 10-s intervals. The timer is started with the addition of the mixture to the first tube. The tubes are then incubated at 0–4°C for 20 min and the assay stopped by vacuum filtration through Whatman GF/B filters. This step is performed at 10-s intervals. Each filter is immediately rinsed with three 5-ml washes of ice-cold buffer, pH 6.9. The filters are counted in 10 ml of liquid scintillation counting cocktail.

EVALUATION

Specific binding is defined as the difference between total binding and binding in the presence of clonazepam. Specific binding is approximately 97% of total ligand binding. The percent inhibition at each drug concentration is the mean of triplicate determinations. IC_{50} calculations are performed using log-probit analyses.

CRITICAL ASSESSMENT OF THE METHOD

Binding to the benzodiazepine receptor is not absolutely predictive for anxiolytic activity. A range of compounds have been discovered that do not have the benzodiazepine structure but that do interact with the benzodiazepine receptors (Gardner 1988; Byrnes et al. 1992). They may have a different pharmacological profile *in vivo*.

MODIFICATION OF THE METHOD

Takeuchi et al. (1992) developed a non-isotopic receptor assay for benzodiazepine drugs using the biotin-1012-S conjugate. The free conjugate in the supernatant was determined with a solid-phase avidin-biotin binding assay.

REFERENCES AND FURTHER READING

Byrnes JJ, Greenblatt DJ, Miller LG (1992) Benzodiazepine receptor binding of nonbenzodiazepines *in vivo*: Alpidem, Zolpidem and Zopiclone. Brain Res Bull 29:905–908

Chang RSL, Snyder SH (1978) Benzodiazepine receptors: labelling in intact animals with [^{3}H]-flunitrazepam. Eur J Pharmacol 48:213–218

Damm HW, Müller WE, Schläfer U, Wollert U (1978) [^{3}H]Flunitrazepam: its advantages as a ligand for the identification of benzodiazepine receptors in rat brain membranes. Res Commun Chem Pathol Pharmacol 22:597–600

Davies MF, Onaivi ES, Chen SW, Maguire PA, Tsai NF, Loew GH (1994) Evidence for central benzodiazepine receptor heterogeneity from behavior tests. Pharmacol Biochem Behav 49:47–56

Gardner CR (1988) Pharmacological profiles *in vivo* of benzodiazepine receptor ligands. Drug Dev Res 12:1–28

Griebel G, Perrault G, Letang V, Granger P, Avenet P, Schoemaker H, Sanger DJ (1999a) New evidence that the pharmacological effects of benzodiazepine receptor ligands can be associated with activities at different BZ (omega)

receptor subtypes. Psychopharmacology (Berl) 146:205–213
Griebel G, Perrault G, Tan S, Schoemaker H, Sanger DJ (1999b) Comparison of the pharmacological properties of classical and novel BZ-omega receptor ligands. Behav Pharmacol 10:483–495
Hafely WE, Martin JR, Richard JG, Schoch P (1993) The multiplicity of actions of benzodiazepine receptor ligands. Can J Psychiatry 38, Suppl 4:S102–S108
Iversen LL (1983) Biochemical characterisation of benzodiazepine receptors. In: Trimble MR (ed) Benzodiazepines Divided. John Wiley & Sons Ltd. pp 79–85
Jacqmin P, Wibo M, Lesne M (1986) Classification of benzodiazepine receptor agonists, inverse agonists and antagonists using bicuculline in an *in vitro* test. J Pharmacol (Paris) 17:139–145
Klepner CA, Lippa AS, Benson DI, Sano MC, Beer B (1979) Resolution in two biochemically and pharmacologically distinct benzodiazepine receptors. Pharmacol Biochem Behav 11:457–462
Langer SZ, Arbilla S (1988) Limitations of the benzodiazepine receptor nomenclature: a proposal for a pharmacological classification as omega receptor subtypes. Fundam Clin Pharmacol 2:159–170
Langer SZ, Arbilla S, Tan S, Lloyd KG, George P, Allen J, Wick AE (1990) Selectivity of omega-receptor subtypes as a strategy for the development of anxiolytic drugs. Pharmacopsychiatry 23:103–107
Lüddens H, Korpi ER, Seeburg PH (1995) $GABA_A$/benzodiazepine receptor heterogeneity: neurophysiological implications. Neuropharmacol 34:245–254
Mennini T, Garattini A (1982) Benzodiazepine receptors: Correlation with pharmacological responses in living animals. Life Sci 31:2025–2035
Möhler H, Okada T (1977a) Benzodiazepine receptor: Demonstration in the central nervous system. Science 198:849–851
Möhler H, Okada T (1977b) Properties of ^{3}H-diazepam binding to benzodiazepine receptors in rat cerebral cortex. Life Sci 20:2101–2110
Möhler H, Richards JG (1983) Benzodiazepine receptors in the central nervous system. In: Costa E (ed) The Benzodiazepines: From Molecular Biology to Clinical Practice. Raven Press, New York, pp 93–116
Olsen RW (1981) GABA-benzodiazepine-barbiturate receptor interactions. J Neurochem 37:1–13
Schacht U, Baecker G (1982) Effects of clobazam in benzodiazepine-receptor binding assays Drug Dev Res Suppl. 1:83–93
Sieghart W (1989) Multiplicity of $GABA_A$-benzodiazepine receptors. Trends Pharmacol Sci 10:407–410
Speth RC, Wastek GJ, Johnson PC, Yamamura HI (1978) Benzodiazepine binding in human brain: characterization using [^{3}H]flunitrazepam. Life Sci 22:859–866
Speth RC, Wastek GJ, Yamamura HI (1979) Benzodiazepine receptors: Temperature dependence of ^{3}H-diazepam binding. Life Sci 24:351–358
Squires RF, Braestrup C (1977) Benzodiazepine receptors in rat brain. Nature 266:732–734
Supavilai P, Karobath M (1980) Heterogeneity of benzodiazepine receptors in rat cerebellum and hippocampus. Eur J Pharmacol 64:91–93
Sweetnam PM, Tallman JF (1985) Regional difference in brain benzodiazepine receptor carbohydrates. Mol Pharmacol 29:299–306
Takeuchi T, Tanaka S, Rechnitz GA (1992) Biotinylated 1012–S conjugate as a probe ligand for benzodiazepine receptors: characterization of receptor binding sites and receptor assay for benzodiazepine drugs. Anal Biochem 203:158–162
Tallman JF (1980) Interaction between GABA and benzodiazepines. Brain Res Bull 5:829–832

E.2.1.3 Serotonin Receptor Binding

E.2.1.3.1 General Considerations

Several surveys on 5-HT receptors and their classification have been published, e. g., by Humphrey et al. (1993), Peroutka (1993), Boess and Martin (1994), Hoyer et al. (1994), Kebabian and Neumeyer (1994), Martin and Humphrey (1994), Saxena (1994), Brancheck (1995), Sleight et al. (1995), Bockaert et al. (1997), Branchek and Zgombick (1997), Briley et al. (1997), Costal and Naylor (1997), Glennon and Dukat (1997), Göthert and Schlicker (1997), Hamon (1997), Hartig (1997), Hoyer and Martin (1997), Jacobs and Fornal (1997), Roth and Hyde (1997), Uphouse (1997), Martin (1998), Martin and Eglen (1998), Saxena et al. (1998), Barnes and Sharp (1999), Pauwels (2000), and Gershon (2004).

The classification has evolved from a scheme recognizing three classes (5-HT_{1like}, 5-HT_2 and 5-HT_3) to one accepted by the NC-IUPHAR subcommittee for 5-hydroxytryptamine (serotonin) receptors in which seven classes embrace 14 distinct receptor subtypes (Martin 1988; Martin and Eglen 1998). Some revisions of the nomenclature were made:

Renaming the 5-HT_{1C} receptor to 5-HT_{2C} on the basis of recognitory, transductional and structural identity with the 5-HT_2 family.

Alignment of the classification scheme with the human genome, meaning that human receptors are given pre-eminence in the nomenclature.

Renaming the 5-$HT_{1D\alpha}$ and 5-$HT_{1D\beta}$ subtypes to 5-HT_{1D} and 5-HT_{1B}, respectively.

Recognition that the '5-HT_{1like}' positively coupled to adenylate cyclase and mediating smooth muscle relaxation, is the 5-HT_7 receptor.

Use of a lower-case notation to describe a putative receptor defined only by gene product, with 'promotion' to an upper-case notation when the receptor is fully defined in terms of operational, recognitory and structural properties.

Up to 7 functional isoforms of the 5-HT_{2C} receptor, two functional isoforms of the 5-HT_4 receptor and four isoforms of the 5-HT_7 receptor were recognized.

Murphy et al. (1999) reviewed molecular biology-based alterations in 5-HT receptors including al-

tered characteristics of mice lacking different 5-HT receptors, e. g., 5-HT_{1B}-receptor-deficient mice, 5-HT_{2C} receptor-deficient mice, 5-HT_{1A}-receptor-deficient mice, 5-HT cell-membrane-transporter deficient mice and vesicular monoamine-transporter-deficient mice.

The role of 5-HT_{1B}, 5-HT_{1D}, 5-HT_{1F}, 5-HT_{2B}, and 5-HT_7 receptors in cardiovascular physiology and pharmacology was discussed by Watts and Cohen (1999).

5-HT Receptor Types and Subtypes

5-HT_1 Subtypes. At least five *5-HT_1 subtypes* are described (5-HT_{1A}, 5-HT_{1B}, 5-HT_{1D}, 5-ht_{1E}, 5-ht_{1F}), which share 41–63% overall sequence identity and couple preferentially to $G_{i/o}$ to inhibit cAMP formation.

Hartig et al. (1996) suggested a revised nomenclature for 5-HT_{1B}, 5-$HT_{1D\alpha}$ and 5-$HT_{1D\beta}$ receptor subtypes.

5-HT_{1A} receptor agonists were described by Sills et al. (1984), Porsolt et al. (1992), Foreman et al. (1994), Wolff et al. (1997), Hamon (1997), 5-HT_{1A} receptor antagonists by Allen et al. (1997), 5-$HT_{1B/D}$ receptor antagonists by de Vries et al. (1997), 5-HT_{1D} receptor agonists by Macor et al. (1994), van Lommen et al. (1995), Valentin et al. (1996), 5-HT_{1D} receptor antagonists by Clitherow et al. (1994), de Vries et al. (1996), Rollema et al. (1996), Briley et al. (1997).

Ramboz et al. (1998) recommended serotonin receptor 1A knockout mice as an animal model of anxiety-related disorder.

Presynaptic receptors may be preferably involved in the anxiolytic effects of 5-HT_{1A} receptor agonists, whereas in the antidepressant effects postsynaptic receptors are strongly involved (De Vry 1991, 1995).

5-HT_1 receptors are involved in learning and memory processes (see F.3.3.7 and F.3.4.1).

An endogenous peptide interacting specifically with the serotonergic 1B receptor subtypes was identified (Rousselle et al. 1996).

5-HT autoreceptors, mainly of the 5-HT_{1D} subtype, were studied by Starke et al. (1989), Fink et al. (1995), Bühlen et al. (1996), Glennon et al. (1996), Roberts et al. (1996), Price et al. (1996).

Cushing et al. (1994) studied the role of a 5-HT_{1D}-like receptor in serotonin-induced contraction of canine coronary artery and saphenous vein.

Wainscott et al. (2005) and Lucaites et al. (2005) described [^{3}H]Y334370 as a radioligand for the 5-HT_{1F} receptor.

See E.2.1.3.2 and E.2.1.3.3 for binding assays of 5-HT_1 receptors.

5-HT_2 Receptors. *5-HT_2 receptors* have been subdivided into 5-HT_{2A}, 5-HT_{2B}, and 5-HT_{2C} receptors, which exhibit 46–50% overall sequence identity and couple preferentially to $G_{q/11}$ to increase the hydrolysis of inositol phosphates and elevate cytosolic [Ca^{2+}]. (Humphrey et al. 1993; Hoyer et al. 1994; Kebabian and Neumeyer 1994; Martin and Humphrey 1994; Saxena 1994; Shih et al. 1994; Tricklebank 1996; Martin 1998). The human 5-HT_2 receptors were cloned and characterized (Chen et al. 1992; Carey et al. 1996). Species differences in receptors were described (Johnson et al. 1995). 5-HT_2 receptors play a role in the action of antipsychotics and hallucinogens.

Saucler and Albert (1997) identified an endogenous 5-hydroxytryptamine$_{2A}$ receptor in NIH-3T3 cells.

Wolf and Schutz (1997) found that the serotonin 5-HT_{2C} receptor is a prominent serotonin receptor in basal ganglia.

Bonhaus et al. (1995) described the pharmacology and distribution of human 5-hydroxytryptamine$_{2B}$ (5-HT_{2B}) receptor gene products and compared this with 5-HT_{2A} and 5-HT_{2C} receptors.

Chagraoui et al. (2003) reported that agomelatine (S20088) antagonizes the penile erections induced by the stimulation of 5-HT_{2C} receptors in Wistar rats.

See E.5.1.9. and E.5.1.10 for binding assays to 5-HT_2 receptors.

5-HT_3 Receptor. The *5-HT_3 receptor* is a pentameric, ligand-gated ion channel, activation of which promotes entry of Na^+ and Ca^{2+}, egress of K^+ and hence neuronal depolarization. It belongs to the transmitter-gated cation super-family of receptors and appears to be located exclusively in neuronal tissue where it mediates fast depolarization (Malone et al. 1991). Responses are blocked by a wide range of potent antagonists, which are highly selective with respect to other 5-HT receptors (Silverstone and Greenshaw 1996). The Bezold-Jarisch reflex can be elicited by 5-HT_3 receptor agonists and be blocked by 5-HT_3 antagonists (see A.1.3.19). 5-HT_3 receptor antagonists are used as anti-migraine drugs. 5-HT_3 receptors are involved in feeding behavior (see L.3.1.1) Furthermore, gastric emptying (see J4.4.2) and emesis (see J.5.0.1, J.5.0.2, J.5.0.3 and J.5.0.4) can be influenced by 5-HT_3 antagonists.

5-HT_3 receptor antagonists, such as **ondansetron** (Koulu et al. 1990; Ishizuka et al. 1993; Miyata et al. 1995; Cappelli et al. 1996), **granisetron** (Sanger and Nelson 1989; Ito et al. 1995; Endo et al. 1999; Yan and White 2005), **tropisetron** (Macor et al. 2001; de la

Vega et al. 2005), **zacopride** (Waeber et al. 1990; Kidd et al. 1992), and **alosetron** (Clayton et al. 1999) are used clinically in the prevention of cisplatin-induced emesis (Karim et al. 1996; Roila et al. 1997).

The synthesis and pharmacological profile of several selective 5-HT_3 receptor antagonists have been reported (Fitzpatrick et al. 1990; Rosen et al. 1990; Swain et al. 1991; Ito et al. 1992; Bachy et al. 1993; Heidempergher et al. 1997; Rival et al. 1998; Modica et al. 2004).

Boess et al. (1997) analyzed the ligand binding site of the 5-KT_3 receptor using site direction mutagenesis.

See E.2.1.3.4 for binding assays to the 5-HT_3 receptor.

5-HT_4 Receptors. The *5-HT_4 receptors* couple preferentially to G_S protein and activate adenylate cyclase, thereby increasing intracellular cAMP levels (Martin 1998). This induces long-term modulation of ion-channel activity, which is fundamental in learning and memory (Eglen et al. 1995; Eglen and Hedge 1996). Excitatory responses were found in guinea pig ileum and colon, inhibitory responses in rat esophagus (Ford and Clarke 1993).

The tunica muscularis mucosae preparation of the rat esophagus has been recommended for evaluation of 5-HT_4 receptor ligands since it possesses a homogeneous population of 5-HT_4 receptors which mediates a well defined relaxant response to 5-HT (see J.2.0.1)

5-HT_4 receptors may mediate arrhythmias (Kaumann 1994). Two splice variants have been identified (Gerald et al. 1995). Several selective 5-HT_4 receptors agonists and antagonists were described (Gaster et al. 1995; Eglen and Hedge 1996; Eglen 1997).

Dumuis et al. (1992) characterized DAU 6285, a novel 5-HT_4 receptor antagonist of the azabicycloalkyl benzamidazolone class.

Wardle et al. (1994) described the effects of SB 204070, a highly potent and selective 5-HT_4 receptor antagonist on guinea pig distal colon.

The 5-HT_4 binding site in human brain was characterized by Arranz et al. (1998).

López-Rodríguez et al. (1999) reported the synthesis and structure–activity relationships of new benzimidazole-4-carboxamides and carboxylates as potent and selective 5-HT_4 receptor antagonists.

Radioligand binding assays for 5-HT_4 receptors using [^{3}H]-GR113808 have been described by Grossman et al. (1993), Domenech et al. (1994), Schiavi et al. (1994), Katayama et al. (1995), Ansanay et al. (1996).

Brattelid et al. (2004) reported cloning, the pharmacological characterization and tissue distribution of a novel 5-HT_4 receptor splice variant, 5-HT_{4i}.

A survey on molecular biology and potential functional role of **5-HT_5, 5-HT_6, and 5-HT_7receptors** was given by Branchek and Zoombick (1997).

A review on 5-HT_5 receptors was given by Nelson (2004).

5-HT_6. The rat *5-HT_6* receptor has been cloned by Ruat et al. (1993). The distinguishing features of this receptor are the high affinity for a series of antipsychotic compounds as well as affinity for a number of cyclic antidepressants (Branchek 1995).

Bourson et al. (1995) used antisense oligonucleotides to determine the role of the 5-HT_6 receptor in the rat brain.

Boess et al. (1998) reported labelling of 5-hydroxytryptamine binding sites in rat and porcine striatum by the 5-HT_6 receptor-selective ligand [^{3}H]Ro 63–0563.

Branchek and Blackburn (2000) reviewed 5-HT_6 receptors as emerging targets for drug discovery.

A review on 5-HT_6 receptors was given by Wooley et al. (2004).

Routledge et al. (2000) characterized SB-271046 as a potent, selective and orally active 5-HT_6 receptor antagonist.

Wooley et al. (2003) reported the reversal of cholinergic-induced deficit in a rodent model of recognition memory by the selective 5-HT_6 receptor antagonist Ro 04–6790.

5-HT_7. Lovenberg et al. (1993), Shen et al. (1993), Gobbi et al. (1996), Villalón et al. (1997) described an adenyl cyclase-activating serotonin receptor (*5-HT_7*) implicated in the regulation of mammalian circadian rhythms.

A receptor autoradiographic and hybridization analysis of the distribution of the 5-HT_7 receptor in rat brain was reported by Gustafson et al. (1996).

Stowe and Barnes (1998) used [^{3}H]5$^-$carboxamidotryptamine for selective recognition sites in rat brain.

Three different splice variants of the 5-HT_7 receptor have been described both in rat and human tissues (Vanhoenacker et al. 2000).

Roth et al. (1994) described the binding of typical and atypical antipsychotic agents to 5-hydroxytryptamine-6 and 5-hydroxytryptamine-7 receptors.

Hedlund and Sutcliffe (2004) reviewed the functional, molecular, and pharmacological advances in 5-HT_7 receptor research.

REFERENCES AND FURTHER READING

Allen AR, Singh A, Zhuang ZP, Kung MP, Kung HF, Lucki I (1997) The 5-HT_{1A} receptor antagonist p-MPPI blocks responses mediated by postsynaptic and presynaptic 5-HT_{1A} receptors

Ansanay H, Sebben M, Bockaert J, Dumuis A (1996) Pharmacological comparisons between [^{3}H]-GR113808 binding sites and functional 5-HT_4 receptors in neurons. Eur J Pharmacol 298:165–174

Arranz B, Rosel P, San L, Sarro S, Navarro MA, Marcusson J (1998) Characterization of the 5-HT_4 binding site in human brain. J Neural Transm 105:575–586

Bachy A, Héaulme M, Giudice A, Michaud JC, Lefevre IA, Souilhac J, Manara L, Emerit MB, Gozian H, Hamon M, Keane PE, Soubrié P, Le Fur G (1993) SR 57227A: a potent and selective agonist at central and peripheral 5-HT_3 receptors in vitro and in vivo. Eur J Pharmacol 237:299–309

Barnes NM, Sharp T (1999) A review of central 5-HT receptors and their function. Neuropharmacology 38:1083–1152

Bockaert J, Fagni L, Dumuis A (1997) 5-HT_4 receptors: An update. In: Baumgarten HG, Göthert M (eds) Handbook of Experimental Pharmacology, Vol 129, Serotoninergic Neurons and 5-HT Receptors in the CNS. Springer-Verlag Berlin Heidelberg, pp 439–474

Boess FG, Martin LL (1994) Molecular biology of 5-HT receptors. Neuropharmacol 33:275–317

Boess Fg, Steward LJ, Steele JA, Liu D, Reid J, Glencorse TA. Martin IL (1997) Analysis of the ligand binding site of the 5-KT_3 receptor using site direction mutagenesis: importance of glutamate 106. Neuropharmacology 36:637–647

Boess FG, Riemer C, Bos M, Bentley J, Bourson A, Sleight AJ (1998) The 5-hydroxytryptamine$_6$ receptor-selective radioligand [^{3}H]Ro 63–0563 labels 5-hydroxytryptamine receptor binding sites in rat and porcine striatum. Mol Pharmacol 54:577–583

Bonhaus DW, Bach C, DeSouza A, Salazar FH, Matsuoka DB, Zuppan P, Chan HW, Eglen RM (1995) The pharmacology and distribution of human 5-hydroxytryptamine$_{2B}$ (5-HT_{2B}) receptor gene products::comparison with 5-HT_{2A} and 5-HT_{2C} receptors. Br J Pharmacol 115:822–628

Bourson A, Borroni E, Austin RH, Monsma FJ Jr, Sleight AJ (1995) Determination of the role of the 5-ht$_6$ receptor in the rat brain: A study using antisense oligonucleotides. J Pharmacol Exp Ther 274:173–180

Branchek TA (1995) 5-HT_4, 5-HT_6, 5-HT_7; molecular pharmacology of adenylate cyclase stimulating receptors. Neurosci 7:375–382

Branchek TA, Blackburn TP (2000) 5-HT_6 receptors as emerging targets for drug discovery. Annu Rev Pharmacol Toxicol 40:119–134

Branchek TA, Zgombick (1997) Molecular biology and potential role of 5-HT_5, 5-HT_6, and 5-HT_7 receptors. In: Baumgarten HG, Göthert M (eds) Handbook of Experimental Pharmacology, Vol 129, Serotoninergic Neurons and 5-HT Receptors in the CNS. Springer-Verlag Berlin Heidelberg, pp 475–498

Brattelid T, Kvingedal AM, Krobert KA, Andressen KW, Bach T, Hystad ME, Kaumann AJ, Levy FO (2004) Cloning, pharmacological characterization and tissue distribution of an novel 5-HT_4 receptor splice variant, 5-HT_{4i}. Naunyn-Schmiedebergs Arch Pharmacol 369:616–628

Briley M, Chopin P, Marien M, Moret C (1997) Functional neuropharmacology of compounds acting on 5-$HT_{1B/1D}$ receptors. In: Baumgarten HG, Göthert M (eds) Handbook of Experimental Pharmacology, Vol 129, Serotoninergic Neurons and 5-HT Receptors in the CNS. Springer-Verlag Berlin Heidelberg, pp 269–306

Bühlen M, Fink K, Böing C, Göthert M (1996) Evidence for presynaptic localization of inhibitory 5-$HT_{1D\beta}$-like autoreceptors in the guinea-pig brain cortex. Naunyn-Schmiedeberg's Arch Pharmacol 353:281–289

Cappelli A, Donati A, Anzini M, Vomero S, de Benedetti PG, Menziani MC, Langer T (1996) Molecular structure and dynamics of some potent 5-HT_3 receptor antagonists. Insight into the interaction with the receptor. Bioorg Med Chem 4:1255–1269

Carey JE, Wood MD, Blackburn TP, Browne MJ, Gale DG, Glen A, Flanigan TP, Hastwell C, Muir A, Robinson JH, Wilson S (1996) Pharmacological characterization of a recombinant human 5HT_{2C} receptor expressed in HEK293 cells. Pharmacol Commun 7:165–173

Chagraoui A, Potais P, Fillpox T, Mocaer E (2003) Agomelatine (S20088) antagonizes the penile erections induced by the stimulation of 5-HT_{2C} receptors in Wistar rats. Psychopharmacology 170:17–22

Chen K, Yang W, Grimsby J, Shih JC (1992) The human 5-HT_2 receptor is encoded by a multiple intron-exon gene. Mol Brain Res 14:20–26

Clayton NM, Sargent R, Butler A, Gale J, Maxwell MP, Hunt AA, Barrett VJ, Cambridge D, Bountra C, Humphrey PP (1999) The pharmacological properties of the novel selective 5-HT_3 receptor antagonist, alsosetron, and its effects on normal and perturbed small intestinal transit in the fasted rat. Neurogastroenterol Motil 11:207–217

Clitherow JW, Scopes DIC, Skingle M, Jordan CC, Feniuk W, Campbell IB, Carter MC, Collington EW, Connor HE, Higgins GA, Beattie D, Kelly HA, Mitchell WL, Oxford AW, Wadsworth AH, Tyers MB (1994) Evolution of a new series of [(N,N-dimethylamino)propyl]- and piperazinylbenzanilides as the first selective 5-HT_{1D} antagonists. J Med Chem 37:2253–2257

Costal B, Naylor RJ (1997) Neuropharmacology of 5-HT_3 receptor ligands. In: Baumgarten HG, Göthert M (eds) Handbook of Experimental Pharmacology, Vol 129, Serotoninergic Neurons and 5-HT Receptors in the CNS. Springer-Verlag Berlin Heidelberg, pp 409–438

Cushing DJ, Baez M, Kursar JD, Schenk K, Cohen ML (1994) Serotonin-induced contraction in canine coronary artery and saphenous vein: role of a 5-HT_{1D}-like receptor. Life Sci 54:1671–1680

De la Vega L, Muñoz E, Calcado MA, Lieb K, Candelario-Jahil E, Gschaidmeier H, Färber L, Mueller W, Stratz T, Fiebich BL (2005) The 5-HT_3 receptor antagonist tropisetron inhibits T cell activation by targeting the calcineurin pathway. Biochem Pharmacol 70:369–380

De Vries P, Heilgers JPC, Villalón CM, Saxena PR (1996) Blockade of porcine carotid vascular responses to sumatripan by GR127935, a selective 5-HT_{1D} receptor antagonist. Br J Pharmacol 118:85–92

De Vries P, Apayadin S, Villalón CM, Heiligers JPC, Saxena PR (1997) Interactions of GR127935, a 5-$HT_{1B/D}$ receptor ligand, with functional 5-HT receptors. Naunyn-Schmiedeberg's Arch Pharmacol 355:423–430

de Vry J (1995) 5-HT_{1A} Receptor agonists: Recent developments and controversial issues. Psychopharmacology 121:1–26

de Vry J, Glaser T, Schuurman T, Schreiber R, Traber J (1991) 5-HT_{1A} receptors in anxiety. In: Briley M, File SE (eds)

New Concepts in Anxiety. McMillan Press Ltd., London, pp 94–129

Domenech T, Beleta J, Fernandez AG, Gristwood RW, Sanchez FC, Tolasa E, Palacios JM (1994) Identification and characterization of serotonin central 5-HT_4 receptor binding sites in human brain: Comparison with other mammalian species. Mol Brain Res 21:176–180

Dumuis A, Gozian H, Sebben M, Ansanay H, Rizzi CA, Turconi M, Monferini E, Giraldo E, Schiantarelli P, Ladinky H (1992) Characterization of a novel 5-HT_4 receptor antagonist of the azabicycloalkyl benzamidazolone class: DAU 6285. Naunyn-Schmiedebergs Arch Pharmacol 345:264–269

Eglen RM (1967) 5-Hydroxytryptamine (5-HT)$_4$ receptors and central nervous system function: an update. Prog Drug Res 49:9–24

Eglen RM, Hegde SS (1966) 5-Hydroxytryptamine (5-HT)$_4$ receptors: physiology, pharmacology and therapeutic potential. Exp Opin Invest Drugs 5:373–388

Eglen RM, Wong EHF, Dumuis A, Bockaert J (1995) Central 5-HT_4 receptors. Trends Pharmacol Sci 16:391–398

Endo T, Minami M, Kitamura N, Teramoto Y, Ogawa T, Nemoto M, Hamaue N, Hirafuji M, Yasuda E, Blower PR (1999) Effects of various 5-HT_3 receptor antagonists, granisetron, ondansetron, ramosetron and azasetron on serotonin (5-HT) release from the ferret isolated ileum. Res Commun Med Pathol Pharmacol 104:145–155

Fink K, Zentner J, Göthert M (1995) Subclassification of presynaptic 5-HT autoreceptors in the human cerebral cortex as 5-$HT_{1D\beta}$ receptors. Naunyn-Schmiedeberg's Arch Pharmacol 352:451–454

Fitzpatrick LR, Lambert RM, Pendley CE, Martin GE, Bostwick JF, Gessner GW, Airey JE, Youssefyeh RD, Pendleton RG, Decktor DL (1990) RG 12915: A potent 5-hydroxytryptamine-3 antagonist that is an orally effective inhibitor of cytotoxic drug-induced emesis in the ferret and dog. J Pharmacol Exp Ther 254:450–455

Ford APDW, Clarke DW (1993) The 5-HT_4 receptor. Med Res Rev 13:633–662

Foreman MM, Fuller RW, Rasmussen K, Nelson DL, Calligaro DO, Zhang L, Barrett JE, Booher RN, Paget CJ Jr, Flaugh ME (1994) Pharmacological characterization of LY293284: a 5-HT_{1A} receptor agonist with high potency and selectivity. J Pharmacol Exp Ther 270:1270–1291

Gaster LM, Joiner GF, King FD, Wyman PA, Sutton JM, Bingham S, Ellis ES, Sanger GJ, Wardle KA (1995) N-[(1-Butyl-4-piperidinyl)methyl]-3,4-dihydro-2H-[1,3]oxazino[3,2-α]-indole-10-carboxamide hydrochloride: the first potent and selective 5-HT_4 receptor antagonist amide with oral activity. J Med Chem 38:4760–4763

Gerald C, Adham N, Kao HT, Olsen MA, Laz TM, Schechter LE, Bard JA, Vaysse PJJ, Hartig PR, Branchek TA, Weinshank RL (1995) The 5-HT_4 receptor: molecular cloning and pharmacological characterization of two splice variants. EMBO J 14:2806–2815

Gershon MD (2004) Review article: serotonin receptors and transporters – roles in normal and abnormal gastrointestinal motility. Aliment Pharmacol Ther 20 [Suppl 7]:3–14

Glennon RA, Dukat M (1997) 5-HT_1 receptor ligands: Update 1997. Serotonin ID Research Alert 2:351–372

Glennon RA, Dukat M, Westkaemper RB, Ismaiel AM, Izzarelli DG, Parker EM (1996) The binding of propranolol at 5-hydroxytryptamine$_{1D\beta}$ T355N mutant receptors may involve formation of two hydrogen bonds to asparagine. Mol Pharmacol 49:198–206

Göthert M, Schlicker E (1997) Regulation of 5-HT release in the CNS by presynaptic 5-HT autoreceptors and by 5-HT heteroreceptors. In: Baumgarten HG, Göthert M (eds) Handbook of Experimental Pharmacology, Vol 129, Serotoninergic Neurons and 5-HT Receptors in the CNS. Springer-Verlag Berlin Heidelberg, pp 307–350

Gobbi M, Parotti L, Mennini T (1996) Are 5-hydroxytryptamine$_7$ receptors involved in [^{3}H]5-hydroxytryptamine binding to 5-hydroxytryptamine$_{1nonA\text{-}nonB}$ receptors in rat hypothalamus? Mol Pharmacol 49:556–559

Grossman CJ, Kilpatrick GJ, Bunce KT (1993) Development of a radioligand binding assay for 5-HT_4 receptors in guinea-pig and rat brain. Br J Pharmacol 109:618–624

Gustafson EL, Durkin MM, Bard JA, Zgombick J, Branchek TA (1996) A receptor autoradiographic and hybridization analysis of the distribution of the 5-HT_7 receptor in rat brain. Br J Pharmacol 117:657–666

Hamon M (1997) The main features of central 5-HT_{1A} receptor. In: Baumgarten HG, Göthert M (eds) Handbook of Experimental Pharmacology, Vol 129, Serotoninergic Neurons and 5-HT Receptors in the CNS. Springer-Verlag Berlin Heidelberg, pp 239–268

Hartig PR (1997) Molecular biology and transductional characteristics of 5-HT receptors. In: Baumgarten HG, Göthert M (eds) Handbook of Experimental Pharmacology, Vol 129, Serotoninergic Neurons and 5-HT Receptors in the CNS. Springer-Verlag Berlin Heidelberg, pp 175–212

Hartig PR, Hoyer D, Humphrey PPA, Martin GR (1996) Alignment of receptor nomenclature with the human genome: classification of 5-HT_{1B} and 5-HT_{1D} receptor subtypes. Trends Pharmacol Sci 17:103–105

Hedlund PB, Sutcliffe JG (2004) Functional, molecular and pharmacological advances in 5-HT_7 receptor research. Trends Pharmacol Sci 25:481–486

Heidempergher F, Pillan A, Pinciroli V, Vaghi F, Arrigoni C, Bolis G, Caccia C, Dho L, McArthur R, Varsi M (1997) Phenylimidazolin-2-one derivatives as selective 5-HT_3 receptor antagonists and refinement of the pharmacophore model for 5-HT_3 receptor binding. J Med Chem 40:3369–3380

Hoyer D, Martin GR (1997) 5-HT receptor classification and nomenclature: towards a harmonization with the human genome. Neuropharmacol 36:419–428

Hoyer D, Clarke DE, Fozard JR, Hartig PR, Martin GR, Mylecharane EJ, Saxena PR, Humphrey PP (1994) VII. International Union of Pharmacology Classification of Receptors for 5-Hydroxytryptamine (Serotonin). Pharmacol Rev 46:157–203

Humphrey PPA, Hartig P, Hoyer D (1993) A proposed new nomenclature for 5-HT receptors. Trends Pharmacol Sci 14:233–236

Ishizuka J, Hsieh AC, Townsend CM, Thompson JC (1993) The effect of 5-HT_3 receptor antagonist (ondansetron) on functioning human pancreatic carcinoids cells. Surg Oncol 2:221–225

Ito H, Hidaka K, Miyata K, Kamato T, Nishida A, Honda K (1992) Characterization of YM060, a potent and selective 5-hydroxytryptamine$_3$ receptor antagonist, in rabbit nodose ganglion and N1E-115 neuroblastoma cells. J Pharmacol Exp Ther 263:1127–1132

Ito H, Akuzawa SA, Tsutsumi R, Kiso T, Kamato T, Nishida A, Yamano M, Miyata K (1995) Comparative study of the 5-HT_3 receptor antagonists, YM060, YM114 (KAE-393) granisetron and ondansetron in rat vagus nerve and cerebral cortex. Neuropsychopharmacology 34:631–637

Jacobs BL, Fornal CA (1997) Physiology and pharmacology of brain serotoninergic neurons. In: Baumgarten HG,

Göthert M (eds) Handbook of Experimental Pharmacology, Vol 129, Serotoninergic Neurons and 5-HT Receptors in the CNS. Springer-Verlag Berlin Heidelberg, pp 91–116

Johnson MP, Baez M, Kursar JD, Nelson DL (1995) Species differences in 5-HT_{2A} receptors: cloned pig and monkey 5-HT_{2A} receptors reveal conserved transmembrane homology to the human rather than rat sequence. Biochem Biophys Acta 1236:201–206

Karim F, Roerig SC, Saphier D (1996) Role of 5-hydroxytryptamine$_3$ (5-HT_3) antagonists in the prevention of emesis caused by anticancer therapy. Biochem Pharmacol 52:685–692

Katayama K, Morio Y, Haga K, Fukuda T (1995) Cisapride, a gastroprokinetic agent, binds to 5-HT_4 receptors. Folia Pharmacol Jpn 105:461–468

Kaumann AJ (1994) Do human atrial 5-HT_4 receptors mediate arrhythmias? Trends Pharmacol Sci 15:451–455

Kebabian JW, Neumeyer JL (1994) The Handbook of Receptor Classification. Research Biochemicals International, Natick, MA, pp 58–61

Kidd E, Bouchelet de Vendegies I, Levy JC, Harmon M, Gozian H (1992) The potent 5-HT3 receptor antagonist (R)-zacopride labels an additional high affinity site in the central nervous system. Eur J Pharmacol 211:133–136

Koulu M, Lapppalainen J, Hietala J, Sjoholm B (1990) Effects of chronic administration of ondansetron (GR38032F), a selective 5-HT_3 receptor antagonist, on monoamine metabolism in mesolimbic and nigrostriatal dopaminergic neurons and on striatal D_2 receptor binding. Psychopharmacology (Berl) 101:166–171

López-Rodríguez ML, Benhamú B, Viso A, Morcollo MJ, Murcia M, Orensanz L, Alfaro MJ, Martín MI (1999) Benzimidazole derivatives. Part 1: Synthesis and structure-activity relationships of new benzimidazole-4-carboxamides and carboxylates as potent and selective 5-HT_4 receptor antagonists. Bioorg Med Chem 7:2271–2281

Lovenberg TW, Baron BM, de Lecea L, Miller JD, Prosser RA, Rea MA, Foye PE, Racke M, Slone AL, Siegel BW, Danielson PE, Sutcliffe JG, Erlander MG (1993) A novel adenyl cyclase-activating serotonin receptor (5-HT_7) implicated in the regulation of mammalian circadian rhythms. Neuron 11:449–458

Lucaites VL, Krushinski JH, Schaus JM, Audia JE, Nelson DE (2005) ^{3}H]Y334370, a novel radioligand for the 5-HT_{1F} receptor. II. Autoradiographic localization in rat, guinea pig, monkey and human brain. Naunyn-Schmiedebergs Arch Pharmacol 371:178–184

Macor JE, Blank DH, Fox CB, Lebel LA, Newman ME, Post RJ, Ryan K, Schmidt AW, Schulz DW, Koe BK (1994) 5-[(3-Nitropyrid-2-yl)amino]indoles: Novel serotonin antagonists with selectivity for the 5-HT_{1D} receptor. Variation of the C3 substituent on the indole template leads to increased 5-HT_{1D} receptor selectivity. J Med Chem 37:2509–2512

Macor JE, Gurley D, Lanthorn T, Loch J, Mack RA, Mullen G, Tran O, Wright N, Gordon JC (2001) The 5-HT_3 antagonist tropisetron (ICS 205–930) is a potent and selective α_7 nicotinic receptor partial agonist. Bioorg Med Chem Lett 11:319–321

Malone HM, Peters JA, Lambert JJ (1991) Physiological and pharmacological properties of 5-HT_3 receptors a patch-clamp study. Neuropeptides 19 (Suppl):S25–S30

Martin GR (1998) 5-Hydroxytryptamine receptors. NC-IUPHAR subcommittee for 5-hydroxytryptamine (serotonin) receptors. In Gridlestone D (ed) The IUPHAR Compendium of Receptor Characterization and Classification. IUPHAR Media, London, pp 167–184

Martin GR, Eglen RM (1998) 5-Hydroxytryptamine receptors. Trends Pharmacol Sci: Receptor and Ion Channel Nomenclature Supplement

Martin GR, Humphrey PPA (1994) Classification review. Receptors for 5-hydroxytryptamine: Current perspectives on classification and nomenclature. Neuropharmacol 33:261–273

Miyata K, Yamano M, Kamato T, Akuzawa S (1995) Effect of serotonin (5-HT)$_3$- receptor antagonists, YM060, YM114 (KAE-393), ondansetron and granisetron on 5-HT_4 receptors and gastric emptying in rodents. Jpn J Pharmacol 69:205–214

Modica M, Romeo G, Materia L, Russo F, Cagnotto A, Mennini T, Gáspár R, Falkay G, Fülöp F (2004) Synthesis and binding properties of several novel selective 5-HT_3 receptor ligands. Bioorg Med Chem 12:3891–3901

Murphy DL, Wichems C, Li Q, Heils A (1999) Molecular manipulations as tools for enhancing our understanding of 5-HT neurotransmission. Trends Pharmacol Sci 20:246–252

Nelson DL (2004) 5-HT_5 receptors. CNS Neurol Disord Drug Targets 3:53–58

Pauwels PJ (2000) Diverse signaling by 5-hydroxytryptamine (5-HT) receptors. Biochem Pharmacol 60:1743–1750

Peroutka SH (1993) 5-Hydroxytryptamine receptors. J Neurochem 60:408–418

Porsolt RD, Lenègre A, Caignard DH, Pfeiffer B, Mocaër E, Gardiola-Lemaître B (1992) Pharmacological profile of a new chroman derivative with 5-hydroxytryptamine$_{1A}$ agonist properties: S20499(+). Drug Dev Res 27:389–402

Price GW, Roberts C, Watson J, Burton M, Mulholland K, Middlemiss DN, Jones BJ (1996) Species differences in 5-HT autoreceptors. Behav Brain Res 73:79–82

Ramboz S, Oosting R, Amara DA, Kung HF, Blier P, Mendelson M, Mann JJ, Brunner D, Hen R (1998) Serotonin receptor 1A knockout: an animal model of anxiety-related disorder. Proc Natl Acad Sci US 95:14476–14481

Rival Y, Hoffmann R, Didier B, Rybaltchenko V, Bourguignon JJ, Wermuth CG (1998) 5-HT_3 antagonists derived from aminopyridazine-type muscarinic M_1 agonists. J Med Chem 41:311–317

Roberts C, Watson J, Burton M, Price GW, Jones BJ (1996) Functional characterization of the 5-HT terminal autoreceptor in the guinea-pig brain cortex. Br J Pharmacol 117:384–388

Roila F, Ballatori E, Tonato M, Del Favero (1997) 5-HT_3 Receptor antagonists: differences and similarities. Eur J Cancer 33:1364–1370

Rollema H, Clarke T, Sprouse JS, Schulz DW (1996) Combined administration of a 5-hydroxytryptamine (5-HT)$_{1D}$ antagonist and a 5-HT reuptake inhibitor synergistically increases 5-HT release in guinea pig hypothalamus *in vivo*. J Neurochem 67:2204–2207

Rosen T, Seeger TF, McLean S, Nagel AA, Ives JL, Guarino KJ, Bryce D, Furman J, Roth RW, Chalabi PM (1990) Synthesis, in vitro binding profile, and central nervous system penetrability of the highly potent 5-HT_3 receptor antagonist [^{3}H]-4-(2-methoxyphenly)-2-[4(5)-methyl-5(4)-imidazolylmethyl]thiazole. J Med Chem 33:3020–3023

Roth BL, Hyde EG (1997) Pharmacology of 5-HT_2 receptors. In: Baumgarten HG, Göthert M (eds) Handbook of Experimental Pharmacology, Vol 129, Serotoninergic Neurons and 5-HT Receptors in the CNS. Springer-Verlag Berlin Heidelberg, pp 367–394

Roth BL, Craigo SC, Choudhary MS, Uluer A, Monsma FJ, Shen YX, Meltzer HY, Sibley DR (1994) Binding of typical and atypical antipsychotic agents to 5-hydroxytryptamine-

6 and 5-hydroxytryptamine-7 receptors. J Pharmacol Exp Ther 268:1403–1410
Rousselle JC, Massot O, Delepierre M, Zifa M, Rousseau B, Fillion G (1996) Isolation and characterization of an endogenous peptide from rat brain interacting specifically with the serotonergic 1B receptor subtypes. J Biol Chem 271:726–735
Routledge C, Bromidge SM, Moss SF, Price GW, Hirst W, Newman H, Riley G, Gager T, Staen J, Upton N, Clarke SE, Brown AM, Middlemiss DM (2000) Characterization of SB-271046, a potent, selective and orally active 5-HT_6 receptor antagonist. Br J Pharmacol 130:1606–1612
Ruat M, Traiffort E, Arrang JM, Tradivel-Lacombe J, Diaz J, Leurs R, Schwartz CJ (1993) A novel rat serotonin (5-HT_6) receptor: Molecular cloning, localization and stimulation of cAMP accumulation. Biochem Biophys Res Commun 193:268–276
Sanger GJ, Nelson DR (1989) Selective and functional 5-hydroxytryptamine$_3$ receptor antagonism by BRL 43694 (granisetron). Eur J Pharmacol 159:113–124
Saucler C, Albert PE (1997) Identification of an endogenous 5-hydroxytryptamine$_{2A}$ receptor in NIH-3T3 cells: agonist-induced down-regulation involves decrease in receptor RNA and number. J Neurochem 68:1989–2011
Saxena PR (1994) Modern 5-HT receptor classification and 5-HT based drugs. Exp Opin Invest Drugs 3:513–523
Saxena PR, de Vries P, Villalón CM (1998) 5-HT_a-like receptors: a time to bid goodbye. Trends Pharmacol Sci 19:311–316
Schiavi GB, Brunet S, Rizzi CA, Ladinsky H (1994) Identification of serotonin 5-HT_4 recognition sites in the porcine caudate nucleus by radioligand binding. Neuropharmacol 33:543–549
Shen Y, Monsma FJ Jr, Metcalf MA, Jose PA, Hamblin MW, Sibley DR (1993) Molecular cloning and expression of a 5-hydroxytryptamine7 serotonin receptor subtype. J Biol Chem 268:18200–18204
Shi H, Chen K, Gallaher TK (1994) Structure and function of serotonin 5-HT_2 receptors. NIDA Res Monograph Series 146:284–297
Sills MA, Wolfe BB, Frazer A (1984) Determination of selective and nonselective compounds for the 5-HT_{1A} and 5-HT_{1B} receptor subtypes in rat frontal cortex. J Pharmacol Exp Ther 231:480–487
Silverstone PH, Greenshaw AJ (1996) 5-HT_3 receptor antagonists. Expert Opin Ther Pat 6:471–481
Sleight AJ, Boess FG, Bourson A, Sibley DR, Monsma FJ (1995) 5-HT_6 and 5-HT_7 serotonin receptors: Molecular biology and pharmacology. Neurotransmiss 11,(3):1–5
Starke K, Göthert M, Kilbinger H (1989) Modulation of neurotransmitter release by presynaptic autoreceptors. Physiol Rev 69:864–989
Stowe RL, Barnes NM (1998) Selective labelling of receptor recognition sites in rat brain using [^{3}H]5-carboxamidotryptamine. Neuropharmacol 37:1611–1619
Swain CJ, Baker K, Kneen C, Moseley J, Saunders J, Seward EM, Stevenson G, Beer M, Stanton J, Watling K (1991) Novel 5-HT_3 antagonists: indole oxadiazoles. J Med Chem 34:140–151
Tricklebank MD (1996) The antipsychotic potential of subtype-selective 5-HT-receptor ligands based on interactions with mesolimbic dopamine systems. Behav Brain Res 73:15–15
Uphouse L (1997) Multiple serotonin receptors: Too many, not enough, or just the right number? Neurosci Biobehav Rev 5:679–698
Valentin JP, Bonnafous R, John GW (1996) Influence of the endothelium and nitric oxide on the contractile response evoked by 5-HT_{1D} receptor agonists in the rabbit isolated saphenous vein. Br J Pharmacol 119:35–42
Vanhoenacker P, Haegeman G, Leysen JE (2000) The 5-HT_7 receptors: current knowledge and future prospects. Trends Pharmacol Sci 21:70–77
Van Lommen G, de Bruyn M, Schroven M, Verschueren W, Jansses W, Verrelst J, Leysen J (1995) The discovery of a series of new non-indole 5-HT_{1D} agonists. Bioorgan Med Chem Lett 5:2649–2654
Villalón CM, Centurión D, Luján-Estrada M, Terrón JA, Sánchez-López A (1997) Mediation of 5-HT-induced external carotid vasodilatation in GR 127935-pretreated vagosympathectomized dogs by the putative 5-HT_7 receptor. Br J Pharmacol 120:1319–1327
Waeber C, Pinkus LM, Palacios JM (1990) The (S) isomer of [^{3}H]zacopride labels 5-HT_3 receptors with high affinity in rat brain. Eur J Pharmacol 181:283–287
Wainscott DB, Krushinski JH, Audia JE, Schaus JM, Zgombick JM, Lucaites VL, Nelson DL (2005) ^{3}H]Y334370, a novel radioligand for the 5-HT_{1F} receptor. I. In vitro characterization of binding properties. Naunyn-Schmiedebergs Arch Pharmacol 371:169–177
Wardle KA, Ellis ES, Baxter GS, Kennett GA, Gaster LM, Sanger GJ (1994) The effects of SB 204070, a highly potent and selective 5-HT_4 receptor antagonist, on guinea-pig distal colon. Br J Pharmacol 112:789–794
Watts SW, Cohen ML (1999) Vascular 5-HT receptors: Pharmacology and pathophysiology of 5-HT_{1B}, 5-HT_{1D}, 5-HT_{1F}, 5-HT_{2B}, and 5-HT_7 receptors. Neurotransmiss 15:3–15
Wolf WA, Schutz LJ (1997) The serotonin 5-HT_{2C} receptor is a prominent serotonin receptor in basal ganglia. Evidence from functional studies on serotonin-mediated phosphoinositide hydrolysis. J Neurochem 69:1449–1458
Wolff MC, Benvenga MJ, Calligaro DO, Fuller RW, Gidda JS, Hemrick-Luecke S, Lucot JB, Nelson DL, Overshiner CD, Leander JD (1997) Pharmacological profile of LY301317, a potent and selective 5-HT_{1A} agonist. Drug Develop Res 40:17–34
Wooley ML, Marsden CA, Sleight AJ, Fone KCF (2003) Reversal of cholinergic-induced deficit in a rodent model of recognition memory by the selective 5-HT_6 receptor antagonist, Ro 04–6790. Psychopharmacology 170:358–367
Wooley ML, Marsden CA, Fone KCF (2004) 5-HT_6 receptors. CNS Neurol Disord Drug Targets 3:59–79
Yan D, White MM (2005) Spatial orientation of the antagonist granisetron in the ligand-binding site of the 5-HT_3 receptor. Mol Pharmacol 68:365–371

E.2.1.3.2
Serotonin (5-HT_{1A}) Receptor: Binding of [^{3}H]-8-Hydroxy-2-(di-n-Propylamino)-Tetralin ([^{3}H]-DPAT)

PURPOSE AND RATIONALE

Determination of the affinity of test compounds for the 5-HT_{1A} receptor in brain may be useful for predicting compounds with novel anxiolytic or atypical anti-psychotic profiles.

The existence of at least two populations of 5-HT_1 receptors in rat brain was shown by differential sensitivity to spiroperidol (Pedigo et al. 1981). The spiroperidol-sensitive receptors were designated

as the 5-HT_{1A} subtype and the insensitive receptors were referred to as the 5-HT_{1B} subtype (Middlemis and Fozard 1983). Other 5-HT binding sites (5-HT_{1C}, 5-HT_{1D}, 5-HT_3 and 5-HT_4) have subsequently been identified in various species, based on differential sensitivity to 5-HT antagonists (Peroutka 1988).

Schlegel and Peroutka (1986) identified [^{3}H]DPAT as a selective ligand for the 5-HT_{1A} receptor. These authors reported that [^{3}H]DPAT labeled an autoreceptor. Lesion studies suggest that [^{3}H]DPAT labeled receptors are not terminal autoreceptors, but may be somatodendritic autoreceptors (Gozlan et al. 1983). Although DPAT decreases the firing rate in the raphe nucleus and inhibits 5-HT release, the actual location and function is somewhat controversial (Verge et al. 1986). These studies and the sensitivity of [^{3}H]DPAT binding to guanine nucleotides and effects on adenylate cyclase suggest that DPAT acts as an agonist at the 5-HT_{1A} receptor (Schlegel and Peroutka 1986).

Serotonin may play a role in anxiety, since drugs which reduce serotoninergic function have anxiolytic effects in animal models (Dourish et al. 1986). Since buspirone and its analogs have relatively higher affinity for the 5-HT_{1A} receptor than other receptors and no effect on the benzodiazepine site, their anxiolytic properties are attributed to activity at the 5-HT_{1A} receptor (Verge et al. 1986; Iversen 1984; Traber and Glaser 1987).

Besides 5-HT_{1A} receptor agonists (Misslin et al. 1990; Griebel et al. 1992; Hascoet et al. 1994; Stanhope and Dourish 1996), 5-HT_{1A} receptor antagonists (Traber and Glaser 1987; Fletcher et al. 1996; Johansson et al. 1997; Cao and Rodgers 1998), 5-HT_{2A} receptor antagonists (Griebel 1996), 5-HT_{2C} receptor antagonists (Jenck et al. 1998), mixed receptor agonists/antagonists (Kleven et al. (1997), 5-HT_3 receptor antagonists (Artais et al. 1995; Roca et al. 1995) and 5-HT_4 receptor antagonists (Kennett et al. 1997) exhibit anxiolytic properties (Handley and McBlane 1993).

Fletcher et al. (1995) described visualization and characterization of 5-HT receptors and transporters *in vivo* and in man.

Several 5-HT_{1A} receptor antagonists were described in preclinical studies, such as **NAN-190** (Deans et al. 1989; Rydelek-Fitzgerald et al. 1990; Neckelmann et al. 1996), **(–)-alprenolol** (Bjorvatn et al. 1992), **pindolol** (Bel et al. 1994; Dreshfield et al. 1996; Seifritz et al. (1997), **BMY 7378** (Sharp et al. 1990; Grasby et al. 1992), **WAY 100635** (Fletcher et al. 1996; Trillat et al. 1998; Harder and Ridley 2000; Smart and Biello 2001), **(–)tertatolol** (Jolas et al. 2004).

Millan et al. (1999, 2001), Mattson et al. (2003), and Gilbert et al. (2004) described specific 5-HT_{1A} receptor antagonists.

PROCEDURE

Reagents

1. Tris buffers, pH 7.7
   a) 57.2 g Tris HCl
      16.2 g Tris base
      q.s. to 1 liter with distilled water (0.5 M Tris buffer, pH 7.7)
   b) Make a 1:10 dilution in deionized H_2O (0.05 M Tris buffer, pH 7.7)
   c) 0.05 M Tris buffer, pH 7.7 containing 10 µM pargyline, 4 mM $CaCl_2$ and 0.1% ascorbic acid.
      0.49 mg pargyline HCl
      111 mg $CaCl_2$
      250 mg ascorbic acid
      q.s. to 250 ml with 0.05 M Tris buffer, pH 7.7 (reagent 1b)
2. [^{3}H]-DPAT (2-(N,N-Di[2,3(n)$^{-3}$H]propylamino)-8-hydroxy-1,2,3,4-tetrahydronaphthalene) (160–206 Ci/mmol) was obtained from Amersham. For IC_{50} determinations: a 10 nM stock solution is made up and 50 µl are added to each tube (final concentration = 0.5 nM).
3. Serotonin creatinine sulfate. 0.5 mM stock solution is made up in 0.01 N HCl and 20 µl added to 3 tubes for determination of nonspecific binding (final concentration = 10 µM).
4. 4. Test compounds:
   For most assays, a 1 mM stock solution is made up in a suitable solvent and serially diluted, such that the final concentrations in the assay range from 2×10^{-5} to 2×10^{-8} M. Seven concentrations are used for each assay. Higher or lower concentrations may be used based on the potency of the drug.

Tissue Preparation

Male Wistar rats are sacrificed by decapitation. Hippocampi are removed, weighed and homogenized in 20 volumes of 0.05 M Tris buffer, pH 7.7. The homogenate is centrifuged at 48,000 *g* for 10 min and the supernatant is discarded. The pellet is resuspended in an equal volume of 0.05 M Tris buffer, incubated at 37°C for 10 min and recentrifuged at 48,000 *g* for 10 min. The final membrane pellet is resuspended in 0.05 M Tris buffer containing 4 mM $CaCl_2$, 0.1% ascorbic acid and 10 µM pargyline.

Assay

800 µl Tissue

130 µl 0.05 M Tris + $CaCl_2$ + pargyline + ascorbic acid

20 µl vehicle/5-HT/drug

50 µl [^{3}H]DPAT

Tubes are incubated for 15 min at 25°C. The assay is stopped by vacuum filtration through Whatman GF/B filters which are then washed 2 times with 5 ml of ice-cold 0.05 M Tris buffer. The filters are then placed into scintillation vials with 10 ml of Liquiscint scintillation cocktail and counted.

EVALUATION

Specific binding is defined as the difference between total binding and binding in the presence of 10 µM 5-HT. IC_{50} values are calculated from the percent specific binding at each drug concentration. The K_i value may then be calculated by the Cheng–Prusoff equation:

$$K_i = IC_{50}/1 + L/K_D$$

The K_D value for [^{3}H] DPAT binding was found to be 1.3 nM by Scatchard analysis in a receptor saturation experiment.

MODIFICATIONS OF THE METHOD

Yocca et al. (1987) described BMY 7378, a buspirone analog with high affinity, selectivity and low intrinsic activity at the 5-HT_{1A} receptor in rat and guinea pig hippocampal membranes.

Instead of the selective 5-HT_{1A} agonist 8-hydroxy-2-(di-n-propylamino)-tetralin (DPAT), selective antagonists to the 5-HT_{1A} receptor, 4-(methoxyphenyl)-1-[2′-(n-2″-pyridinyl)-p-iodobenzamido]-ethyl-piperazine ([^{125}I]p-MPPI), and [^{3}H]p-MPPF = 4-(2′-methoxy-)-phenyl-1-[2′-(*N*-2″-pyridyl)-*p*-fluorobenzamido] ethyl-piperazine have been recommended (Kung et al. 1994a, 1994b, 1995, 1996).

Several other selective 5-HT_{1A} receptor radioligands were recommended:

[^{3}H]lisuride (Sundaram et al. 1995); [^{3}H]WAY-100635 ([O-methyl-^{3}H]-N-(2-(4-(2-methoxyphenyl)-1-piperazinyl)ethyl)-N-(2-piridinyl)cyclohexane carboxamide trihydrochloride) (Laporte et al. 1994; Gozlan et al. 1995; Hume et al. 1995; Khawaja 1995; Khawaja et al. 1997); [^{3}H]Alnespirone (Fabre et al. 1997); [Carbonyl^{11}C]-Desmethyl-WAY 100635 (Pike et al. 1998); [^{3}H]S 15535 (4-(benzodioxan-5-yl)-1-(indan-2-yl)piperazine) (Newman-Tancredi et al. 1998a); NAD-299 (= (R)-3-N,N-dicyclobutylamino-8-fluoro-[6-^{3}H]-3,4-dihydro-2H-1-benzopyran-carboxamide) (Jerning et al. 1998; Sandell et al. 1999).

Newman-Tancredi et al. (1998b) performed autoradiographic studies with [^{35}S]-GTPγS and the selective radioligand [^{3}H]S 15535 for parallel evaluation of localization and functionality of the 5-HT_{1A} receptor.

Agonist-Stimulated [^{35}S]-GTPγS Binding

Agonist-stimulated [^{35}S]-GTPγS binding is the initial step in signal transduction following G protein activation (Elmendorf et al. 1998; Standaert et al. 1998; Lee et al. 1999). It can be used as an index of receptor stimulation, such as 5-HT_{1A} receptors (Alper and Nelson 1998, 2000; Hughes et al. 2005).

PROCEDURE

Sprague Dawley rats were killed by decapitation, the brains placed in ice-cold 0.9% NaCl for 1–3 min, the hippocampi dissected free-hand and placed in a vial on ice. The tissue was weighed and frozen at -70°C. Upon defrosting the tissue was homogenized using a Tekmar tissue homogenizer in cold Tris buffer (50 mM Tris base, pH 7.4). The homogenate was centrifuged (39,800 *g*, 4°C for 10 min), the supernatant decanted and the remaining pellet resuspended in the same Tris buffer. After homogenization the suspension was incubated at 37°C for 10 min in a shaking water bath. The suspension was then centrifuged, the supernatant decanted and the pellet again washed with cold Tris buffer. After one final centrifugation, the remaining pellet was homogenized in the same Tris buffer at a final concentration of approximately 100 mg tissue/ml. This suspension was frozen in aliquots at -70°C for later use. On the day of the assay, the frozen tissue suspension was defrosted, resuspended in approximately 35 ml Tris buffer and centrifuged as above. This final membrane pellet was suspended in assay buffer (4 mM $MgCl_2$, 160 mM NaCl, 0.267 mM EGTA, 67 mM Tris base, pH 7.4) to produce a protein concentration approximating 200 µg/ml.

GTPγS Binding Assay

To each assay tube was added 200 µl deionized water or drug, 200 µl [^{35}S]GTPγS (0.1 nM) in ligand buffer (assay buffer containing 1200 µM GDP to produce a final concentration of 300 µM), 200 µl assay buffer and 200 µl tissue homogenate (approximately 30–50 µg protein). The assay tubes were incubated for 30 min in a shaking water bath. All assays were conducted at 37°C. The reaction was terminated by rapid vacuum filtration through Whatman GF/B filters pre-

wet with 20 mM $Na_4P_2O_7 \cdot 10H_2O$ and pre-cooled with three washes of 2 ml cold 50 mM Tris buffer. After filtering the reaction mixture, the filters were washed 4 times with 1 ml cold 50 mM Tris buffer, placed into 7-ml scintillation vials and 5 ml Ready Protein scintillation cocktail added. The samples were shaken, allowed to sit for a minimum of 2 h, shaken again and counted (2 min/sample) in a Beckman scintillation counter. Non-specific binding was determined by the amount of [^{35}S]-GTPγS bound in the presence of 10 µM unlabeled GTPγS and was subtracted from all samples. Basal GTPγS binding is defined as the specific binding when 200 µl water containing no ligand was added to the assay tube. This is also referred to as agonist-independent binding.

REFERENCES AND FURTHER READING

Alper RH, Nelson DL (1998) Characterization of 5-HT$_{1A}$ receptor-mediated [^{35}S]-GTPγS binding in rat hippocampal membranes. Eur J Pharmacol 343:303–312

Alper RH, Nelson DL (2000) Inactivation of 5-HT$_{1A}$ receptors in hippocampal and cortical homogenates. Eur J Pharmacol 390:67–73

Artais I, Romero G, Zazpe A, Monge A, Caldero JM, Roca J, Lasheras B, del Rio J (1995) The pharmacology of VA21B7: An atypical 5-HT$_3$ receptor antagonist with anxiolytic-like properties in animal models. Psychopharmacology 117:137–148

Bel N, Romero L, Celada P, De Mantigny C, Blier P, Artigas F (1994) Neurobiological basis for the potentiation of the antidepressant effect of 5-HT reuptake inhibitors by the 5-HT$_{1A}$ antagonist pindolol. In: Durkin T, Spampinato U, Cador M (eds) Monitoring molecules in neuroscience. In: Proceedings of the 6th international conference on in vivo methods, 17–20 September, 1994, INSERM, Bordeaux, France, pp 209–210

Bjorvatn B, Neckelmann D, Ursin R (1992) The 5-HT$_{1A}$ antagonist (−)-alprenolol fails to modify sleep or zimeldine-induced sleep-waking effects in rats. Pharmacol Biochem Behav 42:49–56

Bradley PB (1991) Serotonin: Receptors and subtypes. In: Idzikowski C, Cowen PJ (eds) Serotonin, Sleep and Mental Disorder. Wrightson Biomedical Publishing Ltd., Petersfield, pp 9–22

Briley M, Chopin P, Moret C (1991) The role of serotonin in anxiety: Behavioural approaches. In: Briley M, File SE (eds) New Concepts in Anxiety. McMillan Press Ltd., London, pp 56–73

Cao BJ, Rodgers RJ (1998) Comparative effects of novel 5-HT$_{1A}$ receptor ligands, LY293284, LY315712 and LY297996 on plus-maze anxiety in mice. Psychopharmacology 139:185–194

Cowen PJ (1991) Serotonin receptor subtypes: Implications for psychopharmacology. Br J Psychiatry 159 (Suppl 12):7–14

Deakin JFW (1991) Serotonin subtypes and affective disorders. In: Idzikowski C, Cowen PJ (eds) Serotonin, Sleep and Mental Disorder. Wrightson Biomedical Publishing Ltd., Petersfield, pp 161–178

Deans C, Leathley M, Goudie A (1989) In vivo interactions of NAN-190, a putative selective 5-HT$_{1A}$ receptor antagonist with ipsapirone. Pharmacol Biochem Behav 34:927–929

Dourish CT, Hutson PH, Curzon G (1986) Putative anxiolytics 8-OH-DPAT, buspirone and TVX Q 7821 are agonists at 5-HT$_{1A}$ autoreceptors in the raphe nucleus. TIPS 7:212–214

Dreshfield LJ, Wong DT, Perry KW, Engelman EA (1996) Enhancement of fluoxetine-dependent increase of extracellular serotonin (5-HT) levels by (−)-pindolol, an antagonist at 5-HT$_{1A}$ receptors. Neurochem Res 21:557–562

Dugovic C, Leysen JE, Wauquier A (1991) Serotonin and sleep in the rat: the role of 5-HT$_2$ receptors. In: Idzikowski C, Cowen PJ (eds) Serotonin, Sleep and Mental Disorder. Wrightson Biomedical Publishing Ltd., Petersfield, pp 77–88

Elmendorf JS, Chen D, Pessin JE (1998) Guanosine 5′-O-(3-thiotriphosphate) (GPTγS) stimulation of GLUT4 translocation is tyrosine kinase-dependent. J Biol Chem 273:13289–13296

Fabre V, Boni C, Moçaer E, Lesourd M, Hamon M, Laporte AM (1997) [^{3}H]Alnespirone: a novel specific radioligand for 5-HT$_{1A}$ receptors in the rat brain. Eur J Pharmacol 337:297–308

Fletcher A, Pike VW, Cliffe IA (1995) Visualization and characterization of 5-HT receptors and transporters *in vivo* and in man. Semin Neurosci 7:421–431

Fletcher A, Forster EA, Bill DJ, Brown G, Cliffe IA, Hartley JE, Jones DE, McLenachen A, Stanhope KJ, Critchley DJP, Childs KJ, Middlefell VC, Lanfumey L, Corradetti R, Laporte AM, Gozian H, Hamon M, Dourish CT (1996) Electrophysiological, biochemical, neurohormonal and behavioural studies with WAY-100635, a potent, selective and silent 5-HT$_{1A}$ receptor antagonist. Behav Brain Res 73:337–353

Fozard JR (1984) MDL 72222: a potent and highly selective antagonist at neuronal 5-hydroxytryptamine receptors. Naunyn-Schmiedeberg's Arch Pharmacol 326:36–44

Frazer A, Maayani S, Wolfe BB (1990) Subtypes of receptors for serotonin. Annu Rev Pharmacol Toxicol 30:307–348

Fuller RW (1990) Serotonin receptors and neuroendocrine responses. Neuropsychopharmacol 3:495–502

Gilbert AM, Stack GP, Nilakantan R, Kodah J, Tran M, Scerni R, Shi X, Smith DL, Andree TH (2004) Modulation of selective serotonin uptake inhibitor and 5-HT$_{1A}$ antagonist activity in 8-aza-bicyclo 3.2.1]octane derivatives of 2,3-dihydro-1,4-benzodioxane. Bioorg Med Chem Lett 14:515–518

Glennon RA (1991) Serotonin receptors and site-selective agents. J Physiol Pharmacol 42:49–60

Göthert M (1990) Presynaptic serotonin receptors in the central nervous system. Ann NY Acad Sci 604:102–112

Gozlan H, El Mestikawy S, Pichat L, Glowinsky J, Hamon M (1983) Identification of presynaptic serotonin autoreceptors using a new ligand: ^{3}H-PAT. Nature 305:140–142

Gozlan H, Thibault S, Laporte AM, Lima L, Hamon M (1995) The selective 5-HT$_{1A}$ antagonist radioligand [^{3}H]WAY-100635 labels both G-protein-coupled and free 5-HT$_{1A}$ receptors in rat brain membranes. Eur J Pharmacol Mol Pharmacol Sect 288:173–186

Grahame-Smith DG (1991) The neuropharmacology of 5-HT in anxiety. In: Briley M, File SE (eds) New Concepts in Anxiety. McMillan Press Ltd., London, pp 46–55

Grasby PM, Sharp T, Allen T, Grahame-Smith DG (1992) The putative 5-HT$_{1A}$ antagonist BMY 7378 blocks 8-OH-DPAT-induced changes in local cerebral glucose utilization in the conscious rat. Neuropharmacology 31:547–551

Griebel G (1996) Variability in the effects of 5-HT-related compounds in experimental models of anxiety: Evidence for multiple mechanisms of 5-HT in anxiety or never ending story? Pol J Pharmacol 48:129–136

Griebel G, Misslin R, Pawlowski M, Lemaître BG, Guillaumet G, Bizot-Espiard J (1992) Anxiolytic-like effects of a selective 5-HT_{1A} agonist, S20244, and its enantiomers in mice. NeuroReport 3:84–86

Hall MD, El Mestikawy S, Emerit MB, Pichat L, Hamon M, Gozlan H (1985) [^{3}H]-8-Hydroxy-2-(di-n-propylamino)-tetralin binding to pre- and postsynaptic 5-hydroxytryptamine sites in various regions of rat brain. J Neurochem 44:1685–1696

Handley SL (1991) Serotonin in animal models of anxiety: The importance of stimulus and response. In: Idzikowski C, Cowen PJ (eds) Serotonin, Sleep and Mental Disorder. Wrightson Biomedical Publishing Ltd., Petersfield, pp 89–115

Handley SL, McBlane JM (1993) 5-HT drugs in animal models of anxiety. Psychopharmacology 112:13–20

Harder JA, Ridley RM (2000) The 5-HT_{1A} antagonist, WAY 100 635, alleviates cognitive impairments induced by dizocilpine (MK-801) in monkeys. Neuropharmacology 39:547–552

Hascoet M, Bourin M, Todd KG, Couetoux du Tertre A (1994) Anti-conflict effect of 5-HT_{1A} receptor agonists in rats: A new model for evaluating anxiolytic-like activity. J Psychopharmacol 8:227–237

Heuring RE, Peroutka SJ (1987) Characterization of a novel ^{3}H-5-hydroxytryptamine binding site subtype in bovine brain membranes. J Neurosci 7:894–903

Hughes ZA, Starr KR, Langmead CJ, Hill M, Bartoszyk GD, Hagan JJ, Middlemiss DN, Dawson LA (2005) Neurochemical evaluation of the novel 5-HT_{1A} receptor partial agonist/serotonin reuptake inhibitor, vilazodone. Eur J Pharmacol 510:49–57

Hume SP, Ashworth S, Opacka-Juffry J, Ahier RG, Lammertsma AA, Pike VW, Cliffe IA, Fletcher A, White AC (1995) Evaluation of [O-methyl-^{3}H]WAY-100635 as an *in vivo* radioligand for 5-HT_{1A} receptors in rat brain. Eur J Pharmacol 271:515–523

Iversen SD (1984) 5-HT and anxiety. Neuropharmacol 23:1553–1560

Jenck F, Bos M, Wichmann J, Stadler H, Martin JR, Moreau JL (1998) The role of 5-HT_{2C} receptors in affective disorders. Expert Opin Invest Drugs 7:1587–1599

Jerning E, Svantesson GT, Mohell N (1998) Receptor binding characteristics of [^{3}H]NAD-299, a new selective HT_{1A} receptor antagonist. Eur J Pharmacol 360:219–225

Johansson L, Sohn D, Thorberg SO, Jackson DM, Kelder D, Larsson LG, Renyi L, Ross SB, Wallsten C, Erikson H, Hu PS, Jerning E, Mohell N, Westlind-Danielsson A (1997) The pharmacological characterization of a novel selective 5-hydroxytryptamine$_{1A}$ receptor antagonist, NAD 299. J Pharmacol Exp Ther 283:216–225

Jolas T, Haj-Damane S, Lanfumey L, Fattaccini CM, Kidd EJ, Adrien J, Gozian H, Guardiola-Lemaitre B, Hamon M (2004) (–)Tertatolol is a potent antagonist at pre- and postsynaptic serotonin 5-HT_{1A} receptors in the rat brain. Naunyn-Schmiedebergs Arch Pharmacol 347:453–463

Khawaja X (1995) Quantitative autoradiographic characterization of the binding of [^{3}H]WAY-100635, a selective 5-HT_{1A} receptor antagonist. Brain Res 673:217–225

Khawaja X, Ennis C, Minchin MCW (1997) Pharmacological characterization of recombinant human 5-hydroxytryptamine$_{1A}$ receptors using a novel antagonist ligand [^{3}H]WAY-100635. Life Sci 60:653–665

Kennett GA, Bright F, Trail B, Blackburn TB, Sanger GJ (1997) Anxiolytic-like actions of the selective 5-HT_4 receptor antagonists SB204070A and SB207266A in rats. Neuropharmacol 36:707–712

Kleven MS, Assié MB, Koek W (1997) Pharmacological characterization of *in vivo* properties of putative mixed 5-HT_{1A} agonist/5-$HT_{2A/2C}$ antagonist anxiolytics. II. Drug discrimination and behavioral observation studies in rats. J Pharmacol Exp Ther 282:747–759

Kung HF, Kung MP, Clarke W, Maayani S, Zhuang ZP (1994a) A potential 5-HT_{1A} receptor antagonist: p-MPPI. Life Sci 55:1459–1462

Kung MP, Zhuang ZP, Frederick D, Kung HF (1994b) *In vivo* binding of [^{123}I]4-(2′-Methoxyphenyl)-1-[2′-(N-2′′-pyridinyl)-p-iodobenzamido]-ethyl-piperazine, p-MPPI, to 5-HT_{1A} receptors in rat brain. Synapse 18:359–366

Kung MP, Frederick D, Mu M, Zhuang ZP, Kung HF (1995) 4-(2′-Methoxyphenyl)-1-[2′-(n-2′′-pyridinyl)-*p*-iodobenzamido]-ethyl-piperazine ([^{125}I]p-MPPI) as a new selective radioligand on serotonin-1A sites in rat brain: *In vitro* binding and autoradiographic studies. J Pharmacol Exp Ther 272:429–437

Kung MP, Mu M, Zhuang ZP, Kung HF (1996) NCS-MPP (4-(2′-methoxy-phenyl)-1-[2′-(N-2′′-pyridinyl)-p-isothiocyanobenz amido]-ethyl-piperazine): a high affinity and irreversible 5-HT1A receptor ligand. Life Sci 58:179–186

Laporte AM, Lima L, Gozlan H, Hamon M (1994) Selective *in vivo* labelling of brain HT_{1A} receptors by [^{3}H]WAY-100635 in the mouse. Eur J Pharmacol 271:505–514

Larkman PM, Rainnie DG, Kelly JS (1991) Serotonin receptor electrophysiology and the role of potassium channels in neuronal excitability. In: Idzikowski C, Cowen PJ (eds) Serotonin, Sleep and Mental Disorder. Wrightson Biomedical Publishing Ltd., Petersfield, pp 41–64

Lee CH, Oh JI, Park HD, Kim HJ, Park TK, Kim JS, Hong CY, Lee SJ, Ahn KH, Kim YZ (1999) Pharmacological characterization of LB50016, N-(4-amino)butyl-3-phenylpyrrolidine derivative, as a new 5-HT1A receptor agonist. Arch Pharm Res 22:157–164

Mattson RJ, Catt JD, Sloan CP, Gao Q, Carter RB, Gentile A, Mahle CD, Matos FF, McGovern R, Vander Maelen CP, Yocca FD (2003) Development of a presynaptic 5-HT_{1A} antagonist. Bioorg Med Chem Lett 13:285–288

Meert TF, Awouters F (1991) Serotonin 5-HT_2 antagonists: a preclinical evaluation of possible therapeutic effects. In: Idzikowski C, Cowen PJ (eds) Serotonin, Sleep and Mental Disorder. Wrightson Biomedical Publishing Ltd., Petersfield, pp 65–76

Middlemiss DN, Fozard JR (1983) 8-Hydroxy-2-(di-n-propylamino)-tetralin discriminates between subtypes of the 5-HT_1 recognition site. Eur J Pharmacol 90:151–153

Millan MJ, Brocco M, Gobert A, Schreiber R, Dekeyne A (1999) S-16924 [(*R*)-2-1-2-(2,3-dihydro-benzo[1,4]dioxin-5-yloxy)-ethyl]-pyrrolidin-3yl-1-(4-fluorophenyl) ethanone], a novel, potential antipsychotic with marked serotonin$_{1A}$ agonist properties: III Anxiolytic actions in comparison with clozapine and haloperidol. J Pharmacol Exp Ther 288:1002–1014

Millan MJ, Gobert A, Lejeune F, Newman-Tancredi A, Rivet JM, Auclair A, Peglion JL (2001) S33005, a novel ligand of both serotonin and norepinephrine transporters: I Receptor binding, electrophysiological, and neurochemical profile in comparison with reboxetine, citalopraa, and clomipramine. J Pharmacol Exp Ther 298:565–580

Misslin R, Griebel G, Saffroy-Spittler M, Vogel E (1990) Anxiolytic and sedative effects of 5-HT_{1A} ligands, 8-OH-DPAT and MDL 73005EF, in mice. NeuroReport 1:267–270

Neckelmann D, Bjørkum AA, Bjorvatn B, Ursin R (1996) Sleep and EEG power spectrum of the 5-HT_{1A} receptor antagonist NAN-190 alone and in combination with citalopram. Behav Brain Res 75:159–168

New JS (1990) The discovery and development of buspirone: a new approach to the treatment of anxiety. Med Res Rev 10:283–326

Newman ME, Lerer B, Shapira B (1992) 5-HT-1A receptor-mediated effects of antidepressants. Progr Neuropsychopharmacol Biol Psychiat 17:1–19

Newman-Tancredi A, Verrièle L, Chaput C, Millan MJ (1998a) Labelling of recombinant human and native rat serotonin HT_{1A} receptors by a novel, selective radioligand, [^{3}H]S 15535: Definition of its binding profile using agonists, antagonists and inverse agonists. Naunyn-Schmiedeberg's Arch Pharmacol 357:205–217

Newman-Tancredi A, Chaput C, Touzart M, Verrièle L, Millan MJ (1998b) Parallel evaluation of 5-HT_{1A} receptor localization and functionality: autoradiographic studies with [^{35}S]-GTPγS and the novel, selective radioligand [^{3}H]S 15535. In: Martin GR, Eglen RM, Hoyer D, Hamblin MW, Yocca F (eds) Advances in Serotonin Research. Molecular Biology, Signal Transduction, and Therapeutics. Ann New York Acad Sci 861:263–264

Pazos A, Hoyer D, Palacios JM (1984) The binding of serotonergic ligands to the porcine choroid plexus: characterization of a new type of serotonin recognition site. Eur J Pharmacol 106:539–546

Pedigo NW, Yammamura HI, Nelson DL (1981) Discrimination of multiple [^{3}H]5-hydroxytryptamine binding sites by the neuroleptic spiperone in rat brain. J Neurochem 36:220–226

Peroutka SJ (1985) Selective interaction of novel anxiolytics with 5-hydroxytryptamine$_{1A}$ receptors. Biol Psychiatry 20:971–979

Peroutka SJ (1986) Pharmacological differentiation and characterization of 5-HT_{1A}, 5-HT_{1B} and 5-HT_{1C} binding sites in rat frontal cortex. J Neurochem 47:29–540

Peroutka SJ (1988) 5-Hydroxytryptamine receptor subtypes: molecular, biochemical and physiological characterization Trends Neurosci 11:496–500

Pike VW, Halldin C, McCarron JA, Lundkvist C, Hirani E, Olsson H, Hume SP, Karlsson P, Osman S, Swahn CG, Hall H, Wikstrom H, Mensonidas M, Poole KG, Farde L (1998) [Carbonyl^{11}C]-Desmethyl-WAY 100635 (DWAY) is a potent and selective radioligand for central 5-HT_{1A} receptors *in vitro* and *in vivo*. Eur J Nucl Med 25:338–346

Raymond JR, El Mestikawy S, Fargin A (1992) The 5-HT_{1A} receptor: from molecular characteristics to clinical correlates. In: Brann MR (ed) Molecular Biology of G-Protein-coupled receptors. Birkhäuser Boston Basel Berlin pp 113–141

Roca J, Artaiz I, del Rio J (1995) 5-HT_3 Receptor antagonists in development of anxiolytics. Expert Opin Invest Drugs 4:333–342

Rydelek-Fitzgerald, Tietler M, Fletcher PW, Ismaiel AM, Glennon RA (1990) NAN-190: agonist and antagonist interactions with brain 5-HT_{1A} receptors. Brain Res 532:191–196

Sanell J, Halldin C, Hall H, Thorberg SO, Werner T, Sohn D, Sedvall G, Farde L (1999) Radiosynthesis and autoradiographic evaluation of [^{11}C]NAD-299, a radioligand for visualisation of the 5-HT_{1A} receptor. Nucl Med Biol 26:159–164

Saxena PR, Lawang A (1985) A comparison of cardiovascular and smooth muscle effects of 5-hydroxytryptamine and 5-carboxamidotryptamine, a selective agonist of 5-HT_1 receptors. Arch Int Pharmacodyn 277:235–252

Schlegel JR, Peroutka SJ (1986) Nucleotide interactions with 5-HT_{1A} binding sites directly labeled by [^{3}H]-8-hydroxy-2-(di-n-propylamino)tetralin ([^{3}H] -8-OH-DPAT). Biochem Pharmacol 35:1943–1949

Seifritz E, Stahl SM, Gillin JC (1997) Human sleep EEG following the 5-HT_{1A} antagonist pindolol: possible disinhibition of raphe neuron activity. Brain Res 759:84–9p

Sharp T, Backus LI, Hjorth S, Bramwell SR, Grahame-Smith DG (1990) Further investigation of the in vivo pharmacological properties of the putative 5-HT_{1A} antagonist BMY 7378. Eur J Pharmacol 176:331–340

Smart CM, Biello SM (2001) WAY-100635, a specific 5-HT_{1A} antagonist, can increase the responsiveness of the mammalian circadian pacemaker to photic stimuli. Neurosci Lett 305:33–36

Standaert M, Bandyopadhyay G, Galloway L, Ono Y, Mukai H, Farese R (1998) Comparative effects of GPTγS and insulin of rho, phosphatidylinositol 3-kinase, and protein kinase N in rat adipocytes. J Biol Chem 273:7470–7447

Stanhope KJ, Dourish CT (1996) Effects of 5-HT_{1A} receptor agonists, partial agonists and a silent antagonists on the performance of the conditioned emotional response test in the rat. Psychopharmacology 128:293–303

Sundaram H, Turner JD, Strang PG (1995) Characterization of recombinant serotonin 5-HT_{1A} receptors expressed in Chinese hamster ovary cells: The agonist [^{3}H]lisuride labels free receptor and receptor coupled to G protein. J Neurochem 65:1909–1016

Traber J, Glaser T (1987) 5-HT_{1A} receptor-related anxiolytics. TIPS 8:432–437

Trillat AC, Malagié I, Allainmat MM, Anmela MC, Jacquot C, Langlois M, Gardier AM (1998) Effects of WAY 100635 and (−)-5-Me-8-OH-DPAT, a novel 5-HT_{1A} receptor antagonist on 8-OH-DPAT responses. Eur J Pharmacol 147:41–49

Verge D, Daval G, Marcinkiewicz M, Patey A, El Mestikawy H, Gozlan Hamon M (1986) Quantitative autoradiography of multiple 5-HT_1 receptor subtypes in the brain of control of 5,7-dihydroxytryptamine-treated rats. J Neurosci 6:3474–3482

Yocca FD, Hyslop DK, Smith DW, Maayani S (1987) BMY 7378, a buspirone analog with high affinity, selectivity and low intrinsic activity at the 5-HT_{1A} receptor in rat and guinea pig hippocampal membranes. Eur J Pharmacol 137:293–294

E.2.1.3.3 Serotonin (5-HT_{1B}) Receptors in Brain: Binding of [^{3}H]5-Hydroxytryptamine ([^{3}H]5-HT)

PURPOSE AND RATIONALE

The purpose of this assay is to determine the affinity of test compounds for the serotonin (5-HT_{1B}) receptor in brain.

The existence of two populations of 5-HT_1 receptors in rat brain was shown by differential sensitivity to spiroperidol (Pedigo et al. 1981). The spiroperidol-sensitive receptors were designated as the 5-HT_{1A} subtype and the insensitive receptors were referred to as the 5-HT_{1B} subtype (Middlemiss and Fozard 1983). The 5-HT_{1B} subtype has been identified in the brain of rats and mice (Peroutka 1986) and can be selectively labeled by 5-HT in rat striatum when spiroperidol is included to mask the 5-HT_{1A} and 5-HT_2 receptors. In contrast to the situation in rats and mice,

[^{3}H]5-HT binding in the basal ganglia of other mammals displays a pharmacological profile characteristic of 5-HT_{1D} sites. The distribution of 5-HT_{1B} sites in rat brain is similar to that of 5-HT_{1D} sites in human brain (Segu et al. 1991; Boulenguez et al. 1992; Palacios et al. 1992). Several 5-HT_{1B} antagonists have been described (Price et al. 1997; Selkirk et al. 1998).

By comparing the results in the 5-HT_{1B} assay with those in the 5-HT_{1A}, 5-HT_2 and the 5-HT_3 receptor binding assays the relative affinity of a test compound for the major subclasses of 5-HT receptors in the rat brain can be determined.

PROCEDURE

Reagents

1. Tris buffers, pH 7.7
   a) 57.2 g Tris HCl
      16.2 g Tris base
      q.s. to 1 liter with distilled water (0.5 M Tris buffer, pH 7.7)
   b) Make a 1:10 dilution in deionized H_2O (0.05 M Tris buffer, pH 7.7)
   c) 0.05 M Tris buffer, pH 7.7 containing 10 mM pargyline, 4 mM $CaCl_2$ and 0.1% ascorbic acid.
      0.49 mg pargyline HCl
      110.99 mg $CaCl_2$
      250 mg ascorbic acid
      q.s. to 250 ml with 0.5 M Tris buffer, pH 7.7.
2. 5-Hydroxy[G-^{3}H]tryptamine creatinine sulfate (17–20 Ci/mmol) (Amersham). For IC_{50} determinations: a 40 nM stock solution is made up and 50 ml added to each tube (final concentration = 2.0 nM).
3. Serotonin creatinine sulfate. A 0.5 mM stock solution is made up in 0.01 N HCl and 20 ml added to 3 tubes for determination of nonspecific binding (final concentration = 10 µM).
4. Spiroperidol is dissolved in dilute glacial acetic acid. A 20 µM stock solution is prepared and 50 µl added to each tube to prevent binding to 5-HT_{1A} and 5-HT_2 receptors (final concentration in the assay = 1 µM).
5. Test compounds:
   For most assays, a 1 mM stock solution is made up in a suitable solvent and serially diluted, such that the final concentration in the assay ranges from 2×10^{-5} to 2×10^{-8} M. Seven concentrations are used for each assay. Higher or lower concentrations may be used based on the potency of the drug.

Tissue Preparation

Male Wistar rats are sacrificed by decapitation. Striata are removed, weighed and homogenized in 20 volumes of 0.05 M Tris buffer, pH 7.7. The homogenate is centrifuged at 48,000 *g* for 10 min and the supernatant is discarded. The pellet is resuspended in an equal volume of 0.05 M Tris buffer, incubated at 37°C for 10 min and recentrifuged at 48,000 *g* for 10 min. The final membrane pellet is resuspended in 0.05 M Tris buffer containing 4 mM $CaCl_2$, 0.1% ascorbic acid and 10 mM pargyline.

Assay

800 µl	tissue
80 µl	0.05 M Tris + $CaCl_2$ + pargyline + ascorbic acid
20 µl	vehicle/ 5-HT/ drug
50 µl	[^{3}H]5-HT
50 µl	spiroperidol

Tubes are incubated for 15 min at 25°C. The assay is stopped by vacuum filtration through Whatman GF/B filters which are then washed 2 times with 5 ml of ice-cold 0.05 M Tris buffer. The filters are then placed into scintillation vials with 10 ml of Liquiscint scintillation cocktail and counted.

EVALUATION

Specific binding is defined as the difference between total binding and binding in the presence of 10 µM 5-HT. IC_{50} values are calculated from the percent specific binding at each drug concentration. The K_i value may then be calculated by the Cheng–Prusoff equation:

$$K_i = IC_{50}/1 + L/K_D$$

The K_D value for [^{3}H] 5-HT binding was found to be 16.5 nM by Scatchard analysis of a receptor saturation experiment.

MODIFICATIONS OF THE METHOD

[^{3}H]CP-96,501 = 3-(1,2,5,6-Tetrahydro-4-pyridyl-5-n-propoxyindole was recommended as a selective 5-HT_{1B} receptor radioligand (Koe et al. 1992; Lebel and Koe 1992).

Domenech et al. (1997) characterized human serotonin 1D and 1B receptors using [^{3}H]-GR-125743, a novel radiolabelled serotonin 5-$HT_{1D/1B}$ receptor antagonist.

[^{3}H]mesulergine has been used as radioligand for 5-HT_{1C} receptor binding (Jenck et al. 1993, 1994).

[^{3}H]-5-carboxytryptamine was recommended as label for 5-HT_{1D} binding sites (Mahle et al. 1991; Novak et al. 1993).

Massot et al. (1998) described molecular, cellular and physiological characteristics of 5-HT-moduline, a tetrapeptide (Leu-Ser-Ala-Leu), acting as endogenous modulator of the 5-HT_{1B} receptor subtype.

REFERENCES AND FURTHER READING

Boulenguez P, Chauveau J, Segu L, Morel A, Lanoir J, Delaage M (1992) Biochemical and pharmacological characterization of serotonin-O-carboxymethylglycyl-[^{125}I]iodotyrosinamide, a new radioligand probe for 5-HT_{1B} and 5-HT_{1D} binding sites. J Neurochem 58:951–959

Domenech T, Beleta J, Palacios JM (1997) Characterization of human serotonin 1D and 1B receptors using [^{3}H]-GR-125743, a novel radiolabelled serotonin 5-$HT_{1D/1B}$ receptor antagonist. Naunyn-Schmiedeberg's Arch Pharmacol 356:328–334

Hartig PR, Branchek TA, Weinshank RL (1992) A subfamily of 5-HT_{1D} receptor genes. Trends Pharmacol Sci 13:152–159

Hoyer D, Engel G, Kalkman HO (1985) Molecular pharmacology of 5-HT_1 and 5-HT_2 recognition sites in rat and pig brain membranes: radioligand binding studies with [^{3}H]5-HT, [^{3}H]8OH-DPAT, (–)I[^{125}I]iodocyanopindolol, [^{3}H]mesulergine and [^{3}H]ketanserin. Eur J Pharmacol 118:13–23

Hoyer D, Schoeffter P, Waeber C, Palacios JM (1990) Serotonin 5-HT_{1D} receptors. Ann NY Acad Sci 600:168–181

Humphrey PPA, Feniuk W, Marriott AS, Tanner RJN, Jackson MR, Tucker ML (1991) Preclinical studies on the antimigraine drug, Sumatriptan. Eur Neurol 31:282–290

Jenck F, Moreau JL, Mutel V, Martin JR, Haefely WE (1993) Evidence for a role of 5-HT_{1C} receptors in the antiserotoninergic properties of some antidepressant drugs. Eur J Pharmacol 231:223–229

Jenck F, Moreau JL, Mutel V, Martin JR (1994) Brain 5-HT_{1C} receptors and antidepressants. Progr Neuropsychopharmacol Biol Psychiat 18:563–574

Koe BK, Lebel LA, Fox CB, Macor JE (1992) Characterization of [^{3}H]CP-96,501 as a selective radioligand for the serotonin 5-HT_{1B} receptor: Binding studies in rat brain membranes. J Neurochem 58:1268–1276

Lebel LA, Koe BK (1992) Binding studies with the 5-HT_{1B} receptor agonist [^{3}H]CP-96,501 in brain tissues. Drug Dev Res 27:253–264

Mahle CD, Nowak HP, Mattson RJ, Hurt SD, Yocca FD (1991) [^{3}H]-carboxamidotryptamine labels multiple high affinity 5-HT_{1D}-like sites in guinea pig brain. Eur J Pharmacol 205:323–324

Massot O, Rousselle JC, Grimaldi B, Cloët-Tayarani I, Fillion MP, Plantefol M, Bonnin A, Prudhomme N, Fillion G (1998) Molecular, cellular and physiological characteristics of 5-HT-moduline, a novel endogenous modulator of 5-HT_{1B} receptor subtype. In: Martin GR, Eglen RM, Hoyer D, Hamblin MW, Yocca F (eds) Advances in Serotonin Research. Molecular Biology, Signal Transduction, and Therapeutics. Ann New York Acad Sci 861:174–182

Middlemiss DN (1984) Stereoselective blockade at [^{3}H]5-HT binding sites and at the 5-HT autoreceptor by propranolol. Eur J Pharmacol 101:289–293

Middlemiss DN, Fozard JR (1983) 8-Hydroxy-2-(di-n-propylamino)-tetralin discriminates between subtypes of the 5-HT_1 recognition site. Eur J Pharmacol 90:151–153

Nowak HP, Mahle CD, Yocca FD (1993) [^{3}H]-carboxamidotryptamine labels 5-HT_{1D} binding sites in bovine substantia nigra. Br J Pharmacol 109:1206–1211

Palacios JM, Waeber C, Bruinvels AT, Hoyer D (1992) Direct visualisation of serotonin$_{1D}$ receptors in the human brain using a new iodinated ligand. Mol Brain Res 346:175–179

Pedigo NW, Yammamura HI, Nelson DL (1981) Discrimination of multiple [^{3}H]5-hydroxytryptamine binding sites by the neuroleptic spiperone in rat brain. J Neurochem 36:220–226

Peroutka SJ (1986) Pharmacological differentiation and characterization of 5-HT_{1A}, 5-HT_{1B} and 5-HT_{1C} binding sites in rat frontal cortex. J Neurochem 47:529–540

Peroutka SJ (1988) 5-Hydroxytryptamine receptor subtypes: molecular, biochemical and physiological characterization. TINS 11:496–500

Peroutka S, Snyder SH (1979) Multiple serotonin receptors: differential binding of [^{3}H]5-hydroxytryptamine, [^{3}H]lysergic acid diethylamide and [^{3}H]spiroperidol. Mol Pharmacol 16:687–699

Price GW, Burton MJ, Collin LJ, Duckworth M, Gaster L, Göthert M, Jones BJ, Roberts C, Watson JM, Middlemiss DN (1997) SB-216641 and BL-15572 – compounds to pharmacologically discriminate h5-HT_{1B} and h5-HT_{1D} receptors. Naunyn-Schmiedebergs Arch Pharmacol 356:312–320

Schlicker E, Werner U, Hamon M, Gozlan H, Nickel B, Szelenyi I, Göthert M (1992) Anpirtoline, a novel highly potent 5-HT_{1B} receptor agonist with antinociceptive/antidepressant-like actions in rodents. Br J Pharmacol 105:732–738

Segu L, Chauveau J, Boulenguez P, Morel A, Lanoir J, Delaage M (1991) Synthesis and pharmacological study of radioiodinated serotonin derivative specific for 5-HT_{1B} and 5-HT_{1D} binding sites in the central nervous system. C R Acad Sci (Paris) 312:655–661

Selkirk JV, Scott C, Ho M, Burton MJ, Watson J, Gaster LM, Collin L, Jones BJ, Middlemiss DN, Price GW (1998) SB-224289 – a novel selective (human) 5-HT_{1B} receptor antagonist with negative intrinsic activity. Br J Pharmacol 125:202–208

E.2.1.3.4
5-HT_3 Receptor in Rat Entorhinal Cortex Membranes: Binding of [^{3}H]GR 65630

PURPOSE AND RATIONALE

The purpose of this assay is to determine the affinity of test compounds for the 5-HT_3 binding site in the brain. This assay may be useful for predicting the potential of compounds to exhibit anti-emetic, anxiolytic or atypical antipsychotic profiles.

The 5-HT_3 binding site has also been characterized on operational, transductional and structural characteristics. Originally it was believed that 5-HT_3 binding sites existed only in the periphery (Costall et al. 1988). However, with the introduction of potent and selective 5-HT_3 antagonists such as GR65630, zacopride, ICS 205 930 and MDL 72222, and agonists, data from binding studies have indicated that 5-HT_3 binding sites are also located in selected areas of the brain (Kilpatrick et al. 1987, 1989; Barnes et al. 1988, 1990, 1992; Watling et al. 1988; Miller et al. 1992).

The highest levels of 5-HT_3 binding sites have been detected in limbic and dopamine containing brain areas (entorhinal cortex, amygdala, nucleus accumbens and tuberculum olfactorium) (Costall et al. 1988). Besides possessing selective binding in dopamine rich areas, 5-HT_3 antagonists have been reported to block behavioral effects associated with certain drugs of abuse (nicotine and morphine) and to be active in behavioral tests predictive of anxiolytic activity. Based on these selective regional binding results and behavioral studies, it has been speculated that 5-HT_3 antagonists may have a therapeutic benefit in disease states believed to be associated with excessive dopaminergic activity; i. e., schizophrenia, anxiety and drug abuse.

Several authors described synthesis, pharmacology and therapeutic potential of H_3 receptor agonists and antagonists (Leurs et al. 1995, 1998; Stark et al. 1996).

PROCEDURE

Reagents

1. 0.05 M Krebs-HEPES buffer, pH 7.4
   11.92 g HEPES
   10.52 g NaCl
   0.373 g KCl
   0.277 g $CaCl_2$
   0.244 g $MgCl_2 \cdot 6H_2O$
   q.s. to 1 liter with distilled H_2O bring pH up to 7.4 (at 4°C) with 5N NaOH
2. [^{3}H]GR65630 (87.0 Ci/mmol) is obtained from New England Nuclear. For IC_{50} determinations: [^{3}H]GR65630 is made up to a concentration of 1.0 nM in Krebs-HEPES buffer such that when 100 µl is added to each tube a final concentration of 0.4 nM is attained in the 250 µl assay.
3. Ondansetron HCl (GR 38032F) is made up to a concentration of 500 µM in Krebs-HEPES buffer. 50 µl is added to each of 3 tubes for the determination of nonspecific binding (yielding a final concentration of 100 µM in the 250 µl assay.
4. Test compounds. For most assays, a 50 µM stock solution is made up in a suitable solvent and serially diluted with Krebs-HEPES buffer such that when 50 µl of drug is combined with the total 250 µl assay, a final concentration from 10^{-5} to 10^{-8} M is attained. Characteristically seven concentrations are studied for each assay; however, higher or lower concentrations may be used, depending on the potency of the drug.

Tissue Preparation

Male Wistar rats (150–200 g) are decapitated, the entorhinal cortex removed, weighed and homogenized in 10 volumes of ice-cold 0.05 M Krebs-HEPES buffer, pH 7.4. The homogenate is centrifuged at 48,000 *g* for 15 min at 4°C. The resulting pellet is rehomogenized in fresh Krebs-HEPES buffer and recentrifuged at 48,000 *g* for 15 min at 4°C. The final pellet is resuspended in the original volume of ice-cold Krebs-HEPES buffer. This yields a final tissue concentration of 1.2–1.6 mg/ml with the addition of 100 ml to the assay. Specific binding is approximately 55–65% of total bound ligand.

Assay

100 µl	Tissue suspension
100 µl	[^{3}H]GR65630
50 µl	Vehicle (for total binding) or 500 mM ondansetron HCl (for nonspecific binding) or appropriate drug concentration

Sample tubes are kept on ice for additions, then vortexed and incubated with continuous shaking for 30 min at 37°C. At the end of the incubation period, the incubate is diluted with 5 ml of ice-cold Krebs-HEPES buffer and immediately vacuum filtered through Whatman GF/B filters, followed by two 5-ml washes with ice-cold Krebs-HEPES buffer. The filters are dried and counted in 10 ml of liquid scintillation cocktail.

EVALUATION

Specific GR65630 binding is defined as the difference between the total binding and that bound in the presence of 100 µM Ondansetron HCl. IC_{50} calculations are performed using computer-derived log-probit analysis.

MODIFICATIONS OF THE METHOD

Dunn et al. (1991) found that preclinical data with 5-HT_3 antagonists predict anxiolytic rather than antipsychotic activity.

Davies et al. (1999) found that the 5-HT_{3B} subunit is a major determinant of serotonin receptor function.

Reiser and Hamprecht (1989) reported that substance P and serotonin (via 5-HT_3 receptors) act synergistically to activate the cation permeability as measured by [^{14}C]guanidinium uptake in neuroblastoma × glioma hybrid cells.

Bönisch et al. (1993) studied the 5-HT_3 receptor-mediated cation influx into N1E-115 mouse neuroblastoma cells by the use of the organic cation [^{14}C]-guanidinium.

Emerit et al. (1993) assessed the [^{14}C]guanidium accumulation in cells of the hybridoma (mouse neuroblastoma × rat glioma) clone NG 108–15 exposed to serotonin 5-HT$_3$ receptor ligands and substance P.

Bonhaus et al. (1993) characterized the binding of [^{3}H]endo-N-(8-methyl-8-azabicyclo[3.2.1.]oct-3-yl)-2,3-dihydro-3-ethyl-2-oxo-1H-benzimidazolone-1-carboxamide hydrochloride ([^{3}H]BIMU-1), a benzimidazolone with high affinity to 5-HT$_3$ and 5-HT$_4$ receptors in NG 108 cells and guinea pig hippocampus.

Kooyman et al. (1994) studied the specific binding of [^{3}H]GR65630 to 5-HT$_3$ recognition sites in cultured N1E-115 mouse neuroblastoma cells.

Several other selective 5-HT$_3$ receptor radioligands were recommended:

[^{3}H]Quipazine (Perry 1990); [^{3}H]GR67330 (Kilpatrick et al. 1990); tritium-labeled 1-methyl-N-[8-methyl-8-azabicyclo[3.2.1]oct-3-yl)-1H-indazole-3-carboxamide (Robertson et al. 1990); [^{125}I]-(S)-iodozacopride (Gehlert et al. 1993); [^{3}H]-BRL46470 (Steward et al. 1995); [^{3}H]YM060 (Azukawa et al. 1995); (^{125}I)iodophenpropit (Jansen et al. 1994), (^{125}I)iodoproxyfan (Ligenau et al 1994), (S)-Des-4-amino-3-[^{125}I]iodozacopride (Mason et al. 1996; Hewlett et al. 1998,1999).

Tairi et al. (1998) and Hovius et al. (1999) studied ligand binding to the serotonin 5-HT$_3$ receptor with a novel fluorescence ligand and developed a total internal reflection fluorescence assay which is suitable for high-through-put screening.

Thompson et al. (2005) reported locating an antagonist in the 5-HT$_3$ receptor binding site using modeling and radioligand binding.

REFERENCES AND FURTHER READING

Azukawa S, Miyata K, Fukutomi H (1995) Characterization of [^{3}H]YM060, a potent and selective 5-HT$_3$ receptor radioligand, in the cerebral cortex of rats. Eur J Pharmacol 281:37–42

Barnes JM, Barnes NM, Champaneria S, Costall B (1990) Characterization and autoradiographic localization of 5-HT$_3$ receptor recognition sites identified with [^{3}H]-(S)-zacopride in the forebrain of the rat. Neuropharmacol 29:1037–1045

Barnes JM, Barnes NM, Costall B, Jagger SM, Naylor RJ, Robertson DW, Roe SY (1992) Agonist interactions with 5-HT$_3$ receptor recognition sites in the rat entorhinal cortex labelled by structurally diverse radioligands. Br J Pharmacol 105:500–504

Barnes NM, Costall B, Naylor RJ (l988) [^{3}H]Zacopride: Ligand for the identification of 5-HT$_3$ recognition sites. J Pharm Pharmacol 40:548–551

Bonhaus DW, Loury DN, Jakeman LB, To Z, deSouza A, Eglen RM, Wong EHF (1993) [^{3}H]BIMU-1, a 5-hydroxytryptamine$_3$ receptor ligand in NG 108 cells, selectively labels sigma-2 binding sites in guinea pig hippocampus. J Pharmacol Exp Ther 267:961–970

Bönisch H, Barann M, Graupner J, Göthert M (1993) Characterization of 5-HT$_3$ receptors of N1E-115 mouse neuroblastoma cells by the use of the influx of the organic cation [^{14}C]-guanidinium. Br J Pharmacol 108:436–442

Butler A, Hill JM, Ireland SJ, Jordan CD, Tyres MB (1988) Pharmacological properties of GR38032F, a novel antagonist at 5-HT$_3$ receptors. Br J Pharmacol 94:397–412

Costall B, Naylor RJ, Tyers MB (1988) Recent advances in the neuropharmacology of 5-HT$_3$ agonists and antagonists. Rev Neuroscience 2:41–65

Costall B, Naylor RT, Tyers MB (1990) The psychopharmacology of 5-HT$_3$ receptors. Pharmac Ther 47:181–202

Davies PA, Pistis M, Hanna MC, Peters JA, Lambert JJ, Hales TG, Kirkness EF (1999) The 5-HT$_{3B}$ subunit is a major determinant of serotonin receptor function. Nature 397:359–363

Dunn RW, Carlezon WA Jr, Corbett R (1991) Preclinical anxiolytic versus antipsychotic profiles of the 5-HT$_3$ antagonists ondansetron, zacopride, 3α-tropanyl-1H-indole-3-carboxylic ester, and 1αH, 3αH, 5αH-tropan-3-yl-3,5-dihydrochlorobenzoate. Drug Dev Res 23:289–300

Emerit MB, Riad M, Fattacini CM, Hamon M (1993) Characteristics of [^{14}C]guanidium accumulation in NG 108–15 cells exposed to serotonin 5-HT$_3$ receptor ligands and substance P. J Neurochem 60:2059–2067

Gehlert DR, Schober DA, Gackenheimer SL, Mais DE, Ladouceur G, Robertson DW (1993) Synthesis and evaluation of [^{125}I]-(S)-iodozacopride, a high affinity radioligand for 5-HT$_3$ receptors. Neurochem Int 23:373–383

Hewlett WA, Fridman S, Trivedi BL, Schmidt DE, de Paulis T, Ebert MH (1998) Characterization of desamino-5-[^{125}I]iodo-3-methoxy-zacopride, ([^{125}I)MIZAK) binding to 5-HT$_3$ receptors in the rat brain. Prog Neuro-Psychopharmacol Biol Psychol 22:397–410

Hewlett WA, Trivedi BL, Zhang ZJ, de Paulis T, Schmidt DE, Lovinger DM, Sib Ansari M, Ebert MH (1999) Characterization of (S)-des-4-amino-3-[^{125}I]iodozacopride ([^{125}I]DAIZAC), a selective high affinity ligand for 5-hydroxytryptamine$_3$ receptors. J Pharmacol Exp Ther 288:221–231

Hovius R, Schmid EL, Tairi AP, Blasey H, Bernard AR, Lundstrom K, Vogel H (1999) Fluorescence techniques for fundamental and applied studies of membrane protein receptors: The serotonin 5-HT$_3$ receptor. J Recept Signal Transduction 19:533–545

Hoyer D (1990) Serotonin 5-HT$_3$, 5-HT$_4$ and 5-HT-M receptors. Neuropsychopharmacol 3:371–383

Hoyer D, Neijt HC (1988) Identification of serotonin 5-HT$_3$ recognition sites in membranes of N1E-115 neuroblastoma cells by radioligand binding. Mol Pharmacol 33:303–309

Hoyer D, Clarke DE, Fozard JR, Hartig PR, Martin GR, Mylecharane EJ, Saxena PR, Humphrey PP (1994) VII. International Union of Pharmacology Classification of Receptors for 5-Hydroxytryptamine (Serotonin). Pharmacol Rev 46:157–203

Jansen FP, Wu TS, Voss HP, Steinbusch HWM, Vollinga RC, Rademaker B, Bast A, Timmerman H (1994) Characterization of the binding of the first selective radiolabelled histamine H3 receptor antagonist, [^{125}I]iodophenpropit. Br J Pharmacol 113:355–362

Kilpatrick GJ, Jones BJ, Tyers MB (1987) Identification and distribution of 5-HT$_3$ receptors in rat brain using radioligand binding. Nature 330:746–748

Kilpatrick GJ, Jones BJ, Tyers MB (1989) Binding of the 5-HT$_3$ ligand, [^{3}H]-GR 65630, to rat area postrema, vagus nerve and the brains of several species. Eur J Pharmacol 159:157–164

Kilpatrick GJ, Bunce KT, Tyer MB (1990) 5-HT_3 Receptors. Med Res Rev 10:441–475
Kilpatrick GJ, Butler A, Hagan RM, Jones BJ, Tyers MB (1990) [^{3}H]GR67330, a very high affinity ligand for 5-HT_3 receptors. Naunyn-Schmiedeberg's Arch Pharmacol 342:22–30
Kooyman AR, Zwart R, Vanderheijden PML, van Hooft JA, Vijverberg HPM (1994) Interaction between enatiomers of mianserin and ORG3770 at 5-HT_3 receptors in cultured mouse neuroblastoma cells. Neuropharmacol 33:501–507
Leurs R, Vollinga RC, Timmerman H (1995) The medicinal chemistry and therapeutic potentials of ligands of the histamine H_3 receptor. Progr Drug Res 45:107–165
Leurs R, Blandina P, Tedford C, Timmerman H (1998) Therapeutic potentials of histamine H_3 receptor agonists and antagonists. Trends Pharmacol Sci 19:177–183
Ligneau X, Garbag M, Vizueta ML, Diaz J, Purand K, Stark H, Schunack W, Schwartz JC (1994) [^{125}I]Iodoproxyfan, a new antagonist to label and visualize cerebral histamine H_3 receptors. J Pharmacol Exp Ther 271:452–459
Martin GR, Humphrey PPA (1994) Classification review. Receptors for 5-hydroxytryptamine: Current perspectives on classification and nomenclature. Neuropharmacol 33:261–273
Mason NS, Hewlett WA, Ebert MH, Schmidt DE, de Paulis T (1996) Labeling of (S)-Des-4-amino-3-[^{125}I]iodozacopride (DAIZAC), a high affinity radioligand for the 5-HT_3 receptor. J Label Compd Radiopharm 38:955–961
Miller K, Weisberg E, Fletcher PW, Teitler M (1992) Membrane bound and solubilized 5-HT_3 receptors: Improved radioligand binding assays using bovine area postrema or rat cortex and the radioligands [^{3}H]-GR 65630, [^{3}H]-BRL43694, and [^{3}H]-Ly278584. Synapse 11:58–66
Peroutka SJ (1988) 5-Hydroxytryptamine receptor subtypes: Molecular, biochemical and physiological characterization. Trends Neuroscience 11:496–500
Peroutka SJ (1991) Serotonin receptor subtypes and neuropsychiatric diseases: Focus on 5-HT_{1D} and 5-HT_3 receptor agents. Pharmacol Rev 43:579–586
Perry DC (1990) Autoradiography of [^{3}H]quipazine in rat brain. Eur J Pharmacol 187:75–85
Pinkus LM, Sarbin NS, Barefoot DS, Gordon JC (1989) Association of [^{3}H]zacopride with 5-HT_3 binding sites. Eur J Pharmacol 168:355–362
Reiser G, Hamprecht B (1989) Substance P and serotonin act synergistically to activate a cation permeability in a neuronal cell line. Brain Res 479:40–48
Robertson DW, Bloomquist W, Cohen ML, Reid LR, Schenk K, Wong DT (1990) Synthesis and biochemical evaluation of tritium-labeled 1-methyl-N-[8-methyl-8-azabicyclo[3.2.1]oct-3-yl)-1H-indazole-3-carboxamide, a useful radioligand for 5-HT_3 receptors. J Med Chem 33:3176–3181
Saxena PR (1994) Modern 5-HT receptor classification and 5-HT based drugs. Exp Opin Invest Drugs 3:513–523
Stark H, Schlicker E, Schunack W (1996) Development of histamine H_3 receptor antagonists. Drugs Future 21:507–520
Steward LJ, Ge J, Bentley KR, Barber PC, Hope FG, Lambert FJ, Peters JA, Blackburn TP, Barnes NM (1995) Evidence that the atypical 5-HT_3 receptor ligand, [^{3}H]-BRL46470, labels additional 5-HT_3 binding sites compared to [^{3}H]-granisetron. Br J Pharmacol 116:1781–1788
Tairi AP, Hovius R, Pick H, Blasey H, Bernard A, Surprenant A, Lundstrom K, Vogel H (1998) Ligand binding to the serotonin 5-HT_3 receptor studied with a novel fluorescent ligand. Biochemistry 37:15850–15864
Thompson AJ, Price KL, Reeves DC, Chan SL, Chau PI, Lummis SCR (2005) Locating an antagonist in the 5-HT_3 receptor binding site using modeling and radioligand binding. J Biol Chem 280:20476–20482
Watling KJ (1989) 5-HT_3 Receptor agonists and antagonists. Neurotransmission 3:1–4
Watling KJ, Aspley S, Swain CJ, Saunders J (1988) [^{3}H]Quaternised ICS 205–930 labels 5-HT_3 receptor binding sites in rat brain. Eur J Pharmacol 149:397–39

E.2.1.4 Histamine H_3 Receptor Binding in Brain

PURPOSE AND RATIONALE

Histamine receptors have been classified on the basis of pharmacological analysis (Hill et al. 1997). Histamine exerts its action via at least four receptor subtypes. The H_1 receptor couples mainly to $G_{q/11}$, thereby stimulating phospholipase C, whereas the H_2 receptor interacts with G_s to activate adenylyl cyclase. The histamine H_3 and H_4 receptors couple to G_i proteins to inhibit adenylyl cyclase, and to stimulate MAPK. The histamine H_3 receptor is regarded as a therapeutic target for cognitive and sleep disorders (Leurs et al. 1991, 1998, 2005; Passani et al. 2004).

Histamine modulates its own synthesis and release from depolarized brain slices or synaptosomes by interacting with H_3 autoreceptors with a pharmacology distinct from that of H_1 and H_2 receptors (Arrang et al. 1985, 1987, 1990; Hill 1990, 1992; Hill et al. 1997; Leurs et al. 1991, 1998). The R-isomer of α-methylhistamine (α-MeHA) was identified as a highly selective H_3-receptor agonist active at nanomolar concentrations. Furthermore, this compound in ^{3}H-labeled form is a suitable probe for the H_3-receptor.

PROCEDURE

The cerebral cortex from guinea pigs is dissected and homogenized in 50 volumes ice-cold 50 mM KH_2PO_4/Na_2HPO_4 buffer, pH 7.5, in a Potter homogenizer. The homogenate is centrifuged for 15 min at 750 g. The pellet is discarded and the supernatant centrifuged at 42,000 *g* for 15 min. The supernatant is discarded and the pellet washed superficially with and then resuspended in fresh buffer. The protein concentration of the membrane suspension as determined according to Lowry et al. (1951) is about 0.3–0.4 mg/ml.

Aliquots of the membrane preparation are incubated for 60 min at 25°C with ^{3}H(R) α-MeHA and unlabeled substances in a final volume of 1 ml. The assay is stopped by dilution with 2 × 3 ml ice-cold medium, followed by rapid filtration under vacuum over Millipore AAWP filters which are then rinsed twice with 5 ml of ice-cold medium. Radioactivity retained on the filters is measured by liquid scintillation spectroscopy.

EVALUATION

Specific binding is defined as the difference between total binding and binding in the presence of 10 µM unlabeled α-MeHA. IC_{50} values are calculated from the percent specific binding at each drug concentration. The K_i value may then be calculated by the Cheng–Prusoff equation:

$$K_i = IC_{50}/1 + L/K_D$$

MODIFICATIONS OF THE METHOD

Jansen et al. (1992) described [^{125}I]iodophenpropit as a radiolabeled histamine H_3 receptor antagonist.

REFERENCES AND FURTHER READING

Arrang JM, Garbarg M, Schwartz JC (1985) Autoregulation of histamine release in brain by presynaptic H_3-receptors. Neurosci 15:533–562

Arrang JM, Garbarg M, Lancelot JC, Lecomte JM, Pollard H, Robba M, Schunack W, Schwartz JC (1987) Highly potent and selective ligands for histamine H_3-receptors. Nature 327:117–123

Arrang JM, Roy J, Morgat JL, Schunack W, Schwartz JC (1990) Histamine H_3-receptor binding sites in rat brain membranes: modulation by guanine nucleotides and divalent cations. Eur J Pharmacol 188:219–227

Haaksma EEJ, Leurs R, Timmerman H (1990) Histamine receptors: subclasses and specific ligands. Pharmac Ther 47:73–104

Hew KWS, Hodgkinson CR, Hill SJ (1990) Characterization of histamine H_3-receptors in guinea-pig ileum with H_3-selective ligands. Br J Pharmacol 101:621–624

Hill SJ (1990) Distribution, properties, and functional characteristics of three classes of histamine receptor. Pharmacol Rev 42:45–83

Hill SJ (1992) Histamine receptor agonists and antagonists. Neurotransmiss 8 (1):1–5

Hill SJ, Ganellin CR, Timmerman H, Schwartz JC, Shankley NP, Young JM, Schunack W, Levi R, Haas HL (1997) International Union of Pharmacology. XIII. Classification of histamine receptors. Pharmacol Rev 49:253–278

Jansen FP, Rademaker B, Bast A, Timmerman H (1992) The first radiolabeled histamine H_3 receptor antagonist, [^{125}I]iodophenpropit: saturable and reversible binding to rat cortex membranes. Eur J Pharmacol 217:203–205

Korte A, Myers J, Shih NY, Egan RW, Clark MA (1990) Characterization and tissue distribution of H_3 histamine receptors in guinea pigs by N^{α}-methylhistamine. Biochem Biophys Res Commun 168:979–986

Leurs R, van der Goot H, Timmerman H (1991) Histaminergic agonists and antagonists. Recent developments. Adv Drug Res 20:217–304

Leurs R, Blandina P, Tedford C, Timmerman H (1998) Therapeutic potential of histamine H_3 receptor agonists and antagonists. Trends Pharmacol Sci 19:177–183

Leurs R, Bakker RA, Timmerman H, de Esch IJP (2005) The histamine H_3 receptor: from gene cloning to H_3 receptor drugs. Nature Rev Drug Disc 4:107–120

Lowry OH, Rosebrough NJ, Farr AL, Randall RJ (1951) Protein measurement with the Folin phenol reagent. J Biol Chem 193:265–275

Passani MB, Lin JS, Hanccck A, Crochet S, Blandina P (2004) The histamine H_3 receptor as a novel therapeutic target for cognitive and sleep disorders. Trends Pharmacol Sci 25:618–625

Schlicker E, Betz R, Göthert M (1988) Histamine H_3-receptor-mediated inhibition of serotonin release in the rat brain cortex. Naunyn Schmiedeberg's Arch Pharmacol 337:588–590

Timmerman H (1990) Histamine H_3 ligands: just pharmacological tools or potential therapeutic agents? J Med Chem 33:4–11

Van der Goot H, Schepers MJP, Sterk GJ, Timmerman H (1992) Isothiourea analogues of histamine as potent agonists or antagonists of the histamine H_3-receptor. Eur J Med Chem 27:511–517

Van der Werf JF, Timmerman H (1989) The histamine H_3 receptor: a general presynaptic regulatory system? Trends Pharmacol Sci 10:159–162

West RE Jr, Zweig A, Shih NY, Siegel MI, Egan RW, Clark MA (1990) Identification of two H_3-histamine receptor subtypes. Mol Pharmacol 38:610–613

E.2.2 Anticonvulsant Activity

E.2.2.1 Pentylenetetrazole (Metrazol) Induced Convulsions

PURPOSE AND RATIONALE

This assay has been used primarily to evaluate antiepileptic drugs. However, it has been shown that most anxiolytic agents are also able to prevent or antagonize Metrazol-induced convulsions.

PROCEDURE

Mice of either sex with a body weight between 18 and 22 g are used. The test compound or the reference drug is injected sc. or i.p. or given orally to groups of 10 mice. Another group of 10 mice serves as control. Fifteen min after sc.-injection, 30 min after i.p.-injection, or 60 min after oral administration 60 mg/kg MTZ (Metrazol) are injected subcutaneously. Each animal is placed into an individual plastic cage for observation lasting 1 h. Seizures and tonic-clonic convulsions are recorded. At least 80% of the animals in the control group have to show convulsions.

EVALUATION

The number of protected animals in the treated groups is calculated as percentage of affected animals in the control group. ED_{50}-values can be calculated. Furthermore, the time interval between MTZ-injection and occurrence of seizures can be measured. The delay of onset is calculated in comparison with the control group.

CRITICAL ASSESSMENT OF THE METHOD

The method is widely accepted as a screening procedure and has been modified by many investigators. Chlordiazepoxide (20 mg/kg i.p.), diphenylhydantoin

(10 mg/kg i.p.) and phenobarbitone sodium (20 mg/kg i.p.) were found to be effective. Predominantly, the muscle relaxant and anticonvulsant effects of benzodiazepines are measured by this test. Stimulant, anti-depressant, neuroleptic and some anti-epileptic drugs do not show MTZ-antagonism at tolerable doses (Lippa et al. 1979). Nevertheless, the antagonism of MTZ-induced seizures appears to be a suitable procedure for detecting compounds with potential anxiolytic activity. Among a battery of tests, the MTZ-antagonism has been proposed to study centrally acting skeletal muscle relaxants (Bastian et al. 1959; Domino 1964).

MODIFICATIONS OF THE METHOD

Different routes of administration (i.p., i.v., s.c.) have been used by various investigators. Moreover, the dose of MTZ which causes seizures in 80 to 90% of the animals varies with the strain being used.

Bastian et al. (1959) published a modification, whereby mice are infused with a MTZ-solution through a small-diameter polyethylene tubing into the tail vein. In the same animal 3 end-points are registered: 1. Onset of persistent clonic convulsions, 2. beginning of the tonic flexor phase, and 3. time to death. The three endpoints are affected differently by various drugs providing the basis for the determination of drug specificity.

Löscher et al. (1991) tested 8 clinically established antiepileptic drugs in three pentylentetrazole seizure models: (1) the threshold for different types of pentylentetrazole seizures, i. e., initial myoclonus twitch, generalized clonus with loss of righting reflexes and tonic backward extension of forelimbs (forelimb tonus) in mice; (2) the traditional pentylentetrazole seizure test with s.c. injection of the CD97 for generalized clonic seizures in mice; and (3) the s.c. pentylentetrazole seizure test in rats. Various factors may cause misleading predictions from pentylentetrazole seizure models.

REFERENCES AND FURTHER READING

Bastian JW, Krause WE, Ridlon SA, Ercoli N (1959) CNS drug specificity as determined by the mouse intravenous pentylenetetrazole technique. J Pharmacol Exp Ther 127:75–80

Domino EF (1964) Centrally acting skeletal muscle relaxants. In: Laurence DR, Bacharach AL (eds) Evaluation of Drug Activities: Pharmacometrics. Academic Press, London and New York, pp 313–324

Lippa AS, Priscilla A, Nash BA, Greenblatt EN (1979) Preclinical neuropsychopharmacological testing procedures for anxiolytic drugs. In: Fielding St, Lal H (eds) Anxiolytics, Futura Publishing Comp. Inc., New York, pp 41–81

Löscher W, Hönack D, Fassbender CP, Nolting B (1991) The role of technical, biological and pharmacological factors in the laboratory evaluation of anticonvulsant drugs. III. Pentylentetrazole seizure models. Epilepsy Res 8:171–189

Starzl TE, Niemer WT, Dell M, Forgrave PR (1953) Cortical and subcortical electrical activity in experimental seizures induced by Metrazol. J Neuropath Exp Neurol 12:262–276

E.2.2.2 Strychnine-Induced Convulsions

PURPOSE AND RATIONALE

The convulsing action of strychnine is due to interference with postsynaptic inhibition mediated by glycine. Glycine is an important inhibitory transmitter to motoneurons and interneurons in the spinal cord, and strychnine acts as a selective, competitive antagonist to block the inhibitory effects of glycine at all glycine receptors. Strychnine-sensitive postsynaptic inhibition in higher centers of the CNS is also mediated by glycine. Compounds which reverse the action of strychnine have been shown to have anxiolytic properties.

PROCEDURE

Groups of 10 mice of either sex with a weight between 18 and 22 g are used. They are treated orally with the test compound or the standard (e. g. diazepam 5 mg/kg). One hour later the mice are injected with 2 mg/kg strychnine nitrate i.p. The time until occurrence of tonic extensor convulsions and death is noted during a 1 h period. With this dose of strychnine convulsions are observed in 80% of the controls.

EVALUATION

ED_{50}-values are calculated using various doses taking the percentage of the controls as 100%. For time-response curves the interval between treatment and strychnine injection varies from 30 to 120 min.

CRITICAL ASSESSMENT OF THE METHOD

The method has been proven to be useful in a battery of tests to characterize CNS-active drugs. (Costa et al. 1975).

MODIFICATIONS OF THE METHOD

McAllister (1992) induced spinal seizures in mice by rotating them along the body axis clockwise and anticlockwise alternatively three times following pretreatment with a subconvulsive dose of strychnine.

Lambert et al. (1994) tested the antagonism of a glycine derivative against seizures induced by 3-mercaptopropionic acid (3-MPA).

REFERENCES AND FURTHER READING

Bigler ED (1977) Comparison of effects of bicuculline, strychnine, and picrotoxin with those of pentylenetetrazol on photically evoked afterdischarges. Epilepsia 18:465–470

Costa E, Guidotti A, Mao CC (1975) New concepts in the mechanism of action of benzodiazepines. Life Sci. 17:167–186
Lambert DM, Poupaert JH, Maloteaux JM, Dumont P (1994) Anticonvulsant activities of *N*-benzyloxycarbonylglycine after parenteral administration. Neuro Report 5:777–780
McAllister KH (1992) N-Methyl-D-aspartate receptor antagonists and channel blockers have different effects upon a spinal seizure model in mice. Eur J Pharmacol 211:105–108

E.2.2.3 Picrotoxin-Induced Convulsions

PURPOSE AND RATIONALE

Picrotoxin induced convulsions are used to further evaluate CNS-active compounds. Picrotoxin is regarded as a $GABA_A$-antagonist modifying the function of the chloride ion channel of the $GABA_A$ receptor complex.

PROCEDURE

Groups of 10 mice of either sex with a weight between 18 and 22 g are treated either orally or i.p. with the test compound or the standard (e. g. 10 mg/kg diazepam i.p.). Thirty min after i.p. treatment or 60 min after oral administration the animals are injected with 3.5 mg/kg s.c. picrotoxin and are observed for the following symptoms during the next 30 min: clonic seizures, tonic seizures, death. Times of onset of seizures and time to death are recorded.

EVALUATION

For time-response curves the animals receive the drug 30, 60 or 120 min prior to picrotoxin. Protection is expressed as percent inhibition relative to vehicle control. The time period with the greatest percent inhibition is said to be the peak time of drug activity. ED_{50}-values are calculated taking the percentage of seizures in the control group as 100%.

CRITICAL ASSESSMENT OF THE METHOD

The method has been proven to be of value amongst a battery of tests for CNS-activity.

MODIFICATIONS OF THE METHOD

Buckett (1981) describes an intravenous bicuculline test in mice (see Sect. E.3.2.6). The compound bicuculline antagonizes the action of GABA by competition on postsynaptic receptors. In the whole animal bicuculline reproducibly induces myoclonic seizures. An intravenous dose of 0.55 mg/kg was found to induce myoclonic seizures in 90–100% of mice with less than 10% mortality. GABAergic compounds such as benzodiazepines at relatively low doses antagonize the bicuculline-induced myoclonic seizures.

REFERENCES AND FURTHER READING

Buckett WR (1981) Intravenous bicuculline test in mice: Characterisation with Gabaergic drugs. J Pharmacol Meth 5:35–41
Costa E, Guidotti A, Mao CC, Suria A (1975) New concepts in the mechanism of action of benzodiazepines. Life Sci 17:167–186
Enna SJ, Möhler H (1987) γ-aminobutyric acid (GABA) receptors and their association with benzodiazepine recognition sites. In: Meltzer HY (ed) Psychopharmacology: The Third Generation of Progress. Raven Press New York, pp 265–272
Usunoff G, Atsev E, Tchavdarov D (1969) On the mechanisms of picrotoxin epileptic seizure (macro- and microelectrode investigations). Electroencephalogr Clin Neurophysiol 27:444

E.2.2.4 Isoniazid-Induced Convulsions

PURPOSE AND RATIONALE

Isoniazid can precipitate convulsions in patients with seizure disorders. The compound is regarded as a GABA-synthesis inhibitor (Costa et al. 1975). Clonic-tonic seizures are elicited in mice which are antagonized by anxiolytic drugs.

PROCEDURE

Ten mice of either sex with a weight of 18 to 22 g are treated with the test compound or the standard (e. g. diazepam 10 mg/kg i.p.) by oral or intraperitoneal administration. Controls receive the vehicle only. 30 min after i.p. or 60 min after p.o. treatment the animals are injected with a subcutaneous dose of 300 mg/kg isoniazid (isonicotinic acid hydrazide). During the next 120 min the occurrence of clonic seizures, tonic seizures and death is recorded.

EVALUATION

The percentage of seizures or death occurring in the control group is taken as 100%. The suppression of these effects in the treated groups is calculated as percentage of controls. ED_{50}-values are calculated.

CRITICAL ASSESSMENT OF THE METHOD

The method has been proven to be of value amongst a battery of tests for CNS-activity.

REFERENCES AND FURTHER READING

Costa E, Guidotti A, Mao CC (1975) Evidence for involvement of GABA in the action of benzodiazepines: Studies on rat cerebellum. In: Costa E, Greengard P (eds) Mechanisms of Action of Benzodiazepines. Advances in Biochemical Psychopharmacology, Vol 14. Raven Press, New York,pp 113–151

E.2.2.5 Yohimbine-Induced Convulsions

PURPOSE AND RATIONALE

Antagonism against yohimbine-induced seizures in mice is considered to be a model predictive of potential anxiolytic and GABA-mimetic agents (Dunn and Fielding 1987).

PROCEDURE

Male Swiss-Webster mice (20–30 g) are individually placed in clear plastic cylinders and test compounds are administered i.p. 30 min prior to 45 mg/kg s.c. of yohimbine HCl. The animals are observed for the onset and number of clonic seizures for 60 min.

EVALUATION

ED_{50} values with 95% confidence limits are calculated for the antagonism of yohimbine-induced clonic seizures by means of the Lichtfield-Wilcoxon procedure.

CRITICAL ASSESSMENT OF THE METHOD

The antagonism against yohimbine-induced seizures can be regarded as an useful test amongst a battery of tests for anxiolytic activity.

REFERENCES AND FURTHER READING

Litchfield J, Wilcoxon F (1949) A simplified method of evaluating dose effect experiments. J Pharmacol Exp Ther 96:99–113

Dunn R, Fielding S (1987) Yohimbine-induced seizures in mice: A model predictive of potential anxiolytic and GABA-mimetic agents. Drug Dev Res 10:177–188

Dunn RW, Corbett R (1992) Yohimbine-induced convulsions involve NMDA and GABAergic transmission. Neuropharmacol 31:389–395

Dunn RW, Corbett R, Martin LL, Payack JF, Laws-Ricker L, Wilmot CA, Rush DK, Cornfeldt ML, Fielding S (1990) Preclinical anxiolytic profiles of 7189 and 8319, novel non-competitive NMDA antagonists. Current and Future Trends in Anticonvulsant, Anxiety, and Stroke Therapy, Wiley-Liss, Inc., pp 495–512

E.2.3 Anti-Aggressive Activity

E.2.3.1 Foot-Shock-Induced Aggression

PURPOSE AND RATIONALE

Since the discovery of the taming effects of benzodiazepines in vicious monkeys (Heise and Boff 1961; Randall et al. 1961) tests for agents with anti-aggressivity activity have been developed for various animal species. These tests include foot-shock induced aggression in mice and rats, fighting behavior of isolated mice and aggressiveness of rats which become extremely vicious after lesions in the septal area of the brain (Brady and Nauta 1953).

Foot-shock induced aggression is used for further characterization of centrally active drugs. Irwin et al. (1971) have attempted to compare drug classes with this method.

PROCEDURE

Male mice (NMRI, Ivanovas) with a weight between 20 and 30 g are used. Two mice are placed in a box with a grid floor consisting of steel rods with a distance of 6 mm. A constant current of 0.6 or 0.8 mA is supplied to the grid floor by a LVE constant current shocker with an associated scrambler. A 60-Hz current is delivered for 5 s followed by 5 s. intermission for 3 min. Each pair of mice is dosed and tested without previous exposure. The total number of fights are recorded for each pair during the 3-min period. The fighting behavior consists of vocalization, leaping, running, rearing and facing each other with some attempt to attack by hitting, biting or boxing. The test compound or the standard are applied either 30 min before the test i.p. or 60 min before the test orally. For a time response, the drug is given 30, 60 and 120 min prior to testing. Six pairs of drug-treated and two pairs of vehicle-treated animals are utilized for each time period. A dose range is tested at the peak of drug activity. A minimum of 3 doses (10 pairs of mice/dose) is administered for a range of doses. Control animals receive the vehicle.

EVALUATION

The percent inhibition of aggression is calculated from the vehicle control. ED_{50}-values are calculated.

CRITICAL ASSESSMENT OF THE METHOD

Not only anxiolytics but also other classes of drugs where found to be active in this test such as sedatives like meprobamate and phenobarbital, neuroleptics such as perphenazine, analgesics such as methadone, and ethyl alcohol.

MODIFICATIONS OF THE METHOD

A survey of aggressive behavior in the **rat** has been given by Blanchard and Blanchard (1977).

Induction of aggressive behavior by electrical stimulation in the hypothalamus of male rats was described by Kruk et al. (1979).

Mos and Olivier (1991) reviewed the concepts in animal models for pathological aggressive behavior in human.

Play fighting, a normal behavior in several species especially in young male rats (Pellis and McKenna 1995; Pellis et al. 1997; Pellis and Pellis 1998; Pellis 2002), has been used for evaluation of drugs by Siviy et al. (1995) and Hotchkiss et al. (2003). Schneider and Koch (2005) studied the effects of chronic pubertal treatment with cannabinoids on play behavior (pins, attacks, and defense) in rats.

REFERENCES AND FURTHER READING

Brady JV, Nauta WJH (1953) Subcortical mechanisms in emotional behavior: Affective changes following septal forebrain lesions in the albino rat. J Comp Physiol Psychol 46:339–346

Blanchard RJ, Blanchard DC (1977) Aggressive behavior in the rat. Behav Biol 21:197–224

Chen G, Bohner B, Bratten AC (1963) The influence of certain central depressants on fighting behavior of mice. Arch Int Pharmacodyn 142:30–34

Heise GA, Boff E (1961) Taming action of chlordiazepoxide. Fed Proc 20:393–397

Hotchkiss AK, Ostby JS, Vandenbergh JG, Gray LE Jr (2003) An environmental antiandrogen, vinclozolin, alters the organization of play behavior. Physiol Behav 79:151–156

Irwin S, Kinohi R, Van Sloten M, Workman MP (1971) Drug effects on distress-evoked behavior in mice: Methodology and drug class comparisons. Psychopharmacologia (Berl.) 20:172–185

Kruk MR, van der Poel AM, de Vos-Frerichs TP (1979) The induction of aggressive behaviour by electrical stimulation in the hypothalamus of male rats. Behaviour 70:292–322

Mos J, Olivier B (1991) Concepts in animal models for pathological aggressive behaviour in humans. In: Olivier B, Mos J, Slangen JL (eds) Animal Models in Psychopharmacology. Advances in Pharmacological Sciences. Birkhäuser Verlag, Basel, pp 297–316

Pellis SM (2002) Sex differences in play fighting revisited: traditional and nontraditional mechanisms of sexual differentiation in rats. Arch Sex Behav 31:17–26

Pellis SM, McKenna M (1995) What do rats find rewarding in play fighting? – an analysis using drug-induced non-playful partners. Behav Brain Res 68:65–73

Pellis SM, Pellis VC (1998) Play fighting in comparative perspective: a schema for neurobehavioral analyses. Neurosci Behav Rev 23:87–101

Pellis SM, Field EF, Smith LK, Pellis VC (1997) Multiple differences in the play fighting of male and female rats. Implications for the causes and functions pf play. Neurosci Neurobehav Rev 21:105–120

Randall LO, Heise GA, Schalleck W, Bagdon R.E, Banziger R, Boris A, Moe A, Abrams WB (1961) Pharmacological and clinical studies on Valium$^{(T.M.)}$. A new psychotherapeutic agent of the benzodiazepine class. Current Ther Res 9:405–425

Rudzik AD, Hester JB, Tang AH, Straw RN, Friis W (1973) Triazolobenzazepines, a new class of central nervous system-depressant compounds. In: Garattini S, Mussini E, Randall LO (eds) The Benzodiazepines, Raven Press New York, pp 285–297

Siviy SM, Line BS, Darcy EA (1995) Effects of MK-8o1 on rough-and-tumble play in juvenile rats. Physiol Behav 57:843–847

Schneider M, Koch M (2005) Deficient social and play behavior in juvenile and adult rats after neonatal cortical lesion: effects of chronic pubertal cannabinoid treatment. Neuropsychopharmacology 30:944–957

Tedeschi RE, Tedeschi DH, Mucha A, Cook L, Mattis PA, Fellows EJ (1959) Effects of various centrally acting drugs on fighting behavior of mice. J Pharmacol Exp Ther 125:28–34

Tedeschi DH, Fowler PJ, Miller RB, Macko E (1969) Pharmacological analysis of footshock-induced fighting behaviour. In: Garattini S, Sigg EB (eds) Aggressive behaviour. Excerpta Medica Foundation Amsterdam, pp 245–252

Ulrich R, Symannek B (1969) Pain as a stimulus for aggression In: Garattini S, Sigg EB (eds) Aggressive behaviour. Excerpta Medica Foundation Amsterdam, pp 59–69

E.2.3.2 Isolation-Induced Aggression

PURPOSE AND RATIONALE

Male mice, submitted to prolonged isolation, develop aggressive behavior against animals of the same sex. Compounds can be tested for their ability to suppress this isolation-induced aggression.

PROCEDURE

Male mice of NMRI-strain with an initial weight of 12 g are kept isolated in small Makrolon-cages for a period of 6 weeks. Prior to the administration of the test drug, the aggressive behavior of the animals is tested. A male mouse being accustomed to live together with other animals is placed into the cage of an isolated mouse for 5 min. Immediately, the isolated mouse will start to attack the "intruder". The aggressive behavior of the isolated mouse is characterized by hitting the tail on the bottom of the cage, screaming and biting. The reaction time until the first attack is less than 10 s for most of the isolated mice and relatively constant for one individual. After these initial tests, the isolated mice receive the test compound, the standard drug or the vehicle either orally or subcutaneously. The aggressive behavior is evaluated 60, 120 and 240 min after oral and 30, 60 and 120 min after sc. treatment. After treatment with certain centrally acting compounds the aggressive behavior of the isolated mice is changed. The reaction time until the first attack can be prolonged or shortened. The fighting reaction can be attenuated. Then, additional mechanical stimuli can be used to elicit the fighting behavior. With highly effective drugs the aggressive behavior is completely suppressed.

EVALUATION

The number of animals with complete suppression of the fighting behavior is calculated. In animals with

diminished aggressiveness the reaction time is registered. A gradual scale of inhibition of aggressiveness is established.

CRITICAL ASSESSMENT OF THE METHOD

The fighting behavior of isolated mice is not only altered by sedative and anxiolytic compounds but also by neuroleptics and antidepressants. For example, active doses are:

Lorazepam	2.5 mg/kg p.o.
Clonazepam	2.5 mg/kg sc.
Haloperidol	1.0 mg/kg p.o.
Chlorpromazine	10.0 mg/kg s.c.
Imipramine	25.0 mg/kg s.c.

In this way, anti-aggressive activity of several classes can be detected.

MODIFICATIONS OF THE METHOD

Krsiak (1974, 1979) described the effects of various drugs on behavior of aggressive **mice**.

Olivier and van Dalen (1982) discussed the social behavior in rats and mice as an ethologically based model for differentiating psychoactive drugs.

McMillen et al. (1987) tested the effects of drugs on aggressive behavior and brain monoaminergic neurotransmission.

Krsiak (1975) showed that about 45% of single-housed male mice showed timidity instead of aggression on interactions with group-housed male mice. Several drugs, such as benzodiazepines, chlorpromazine and barbitone inhibited the isolation induced timidity without reducing other motor activities in the timid mice.

Andrade et al. (1988) tested the effect of insulin-induced hypoglycemia on the aggressive behavior of isolated mice against intruders made anosmic by application of 25 µl of 4% zinc sulfate solution to the nasal tract 3 and 1 days before the encounters.

White et al. (1991) tested the effects of serotoninergic agents and other psychotropic compounds on isolation-induced aggression in mice at doses below those which produced debilitation in the rotarod performance. Guidotti et al. (2001) used the socially isolated mouse as a model to study the putative role of allopregnenolone and 5α-dihydroxyprogesterone in psychiatric disorders.

Francès (1988), Francès et al. (1990), Francès and Monier (1991) described an other phenomenon of isolation in rodents which can be used for evaluation of psychotropic drugs: the **isolation-induced behavioral deficit**. Male Swiss NMRI mice were either housed in groups of 6 in home cages or isolated at the age of 4–5 weeks for 7 days. Mice were tested in pairs (one isolated and one grouped mouse) under a transparent beaker. The number of escapes was counted for the first 2 min of observation. An attempt to escape was defined as one of the following: (1) the two forepaws were placed against the wall of the beaker, (2) the mouse was sniffing, its nose at the spout of the beaker, (3) the mouse was scratching at the glass floor. Behavioral observations were taped by an observer, blind to the treatment.

REFERENCES AND FURTHER READING

Anrade ML, Benton D, Brain PF, Ramirez JM, Walmsley SV (1988) A reexamination of the hypoglycemia-aggression hypothesis in laboratory mice. Intern J Neuroscience 41:179–186

Caharperntier J (1969) Analysis and measurement of aggressive behaviour in mice. In: Garattini S, Sigg EB (eds) Aggressive Behaviour. Excerpta Medica Foundation, Amsterdam, pp 86–100

Davbanzo JP (1969) Observations related to drug-induced alterations in aggressive behaviour. In: Garattini S, Sigg EB (eds) Aggressive Behaviour. Excerpta Medica Foundation, Amsterdam, pp 263–272

Francès H (1988) New animal model of social behavioral deficit: Reversal by drugs. Pharmacol Biochem Behav 29:467–470

Francès H, Monier C (1991) Tolerance to the behavioural effect of serotonergic (5-HT_{1B}) agonists in the isolation-induced social behavioural deficit test. Neuropharmacol 30:623–627

Francès H, Khidichian F, Monier C (1990) Increase in the isolation-induced social behavioural deficit by agonists at 5-HT_{1A} receptors. Neuropharmacol 29:103–107

Guidotti A, Dong E, Matsumoto K, Pinna G, Rasmusson AM, Costa E (2001) The socially-isolated mouse: a model to study the putative role of allopregnenolone and 5α-dihydroxyprogesterone in psychiatric disorders. Brain Res Rev 37:110–115

Hoffmeister F, Wuttke W (1969) On the actions of psychotropic drugs on the attack- and aggressive-defensive behaviour of mice and cats. In: Garattini S, Sigg EB (eds) Aggressive Behaviour. Excerpta Medica Foundation, Amsterdam, pp 273–280

Krsiak M (1974) Behavioral changes and aggressivity evoked by drugs in mice. Res Commun Chem Pathol Pharmacol 7:237–257

Krsiak M (1975) Timid singly-house mice: their value in prediction of psychotropic activity of drugs. Br J Pharmacol 55:141–150

Krsiak M (1979) Effects of drugs on behaviour of aggressive mice. Br J Pharmacol 65:525–533

Krsiak M, Janku I (1969) The development of aggressive behaviour in mice by isolation. In: Garattini S, Sigg EB (eds) Aggressive behaviour. Excerpta Medica Foundation, Amsterdam pp 101–105

Lagerspetz KMJ (1969) Aggression and aggressiveness in laboratory mice. In: Garattini S, Sigg EB (eds) Aggressive Behaviour. Excerpta Medica Foundation, Amsterdam, pp 77–85

Le Douarec JC, Broussy L (1969) Dissociation of the aggressive behaviour in mice produced by certain drugs. In: Garat-

tini S, Sigg EB (eds) Aggressive Behaviour. Excerpta Medica Foundation, Amsterdam, pp 281–295
McMillen BA, Scott SM, Williams HL, Sanghera MK (1987) Effects of gespirone, an aryl-piperazine anxiolytic drug, on aggressive behavior and brain monoaminergic neurotransmission. Naunyn Schmiedeberg's Arch Pharmacol 335:454–464
McMillen BA, Wooten MH, King SW, Scott SM, Williams HL (1992) Interaction between subchronic administration of alprazolam and aryl-piperazine anxiolytic drugs in aggressive mice. Biogenic Amines 9:131–140
Oliver B, Mos J (1992) Rodent models of aggressive behavior and serotonergic drugs. Progr Neuro-Psychopharm Biol Psychiat 16:847–870
Olivier B, van Dalen D (1982) Social behaviour in rats and mice: an ethologically based model for differentiating psychoactive drugs. Aggress Behav 8:163–168
Sánchez C, Arnt J, Moltzen EK (1996) The antiaggressive potency of (–)-penbutolol involves both 5-HT_{1A} and 5-HT_{1B} receptors and β-adrenoceptors. Eur J Pharmacol 297:1–8
Scriabine A, Blake M (1962) Evaluation of centrally acting drugs in mice with fighting behavior induced by isolation. Psychopharmacologia 3:224–226
Valzelli L (1967) Drugs and aggressiveness. In: Garratini S, Shore PA (eds) Advances in Pharmacology, Vol. 5, pp 79–108, Academic Press, New York
Valzelli L (1969) Aggressive behaviour induced by isolation. In: Garattini S, Sigg EB (eds) Aggressive Behaviour. Excerpta Medica Foundation, Amsterdam, pp 70–76
White SM, Kucharik RF, Moyer JA (1991) Effects of serotoninergic agents on isolation-induced aggression. Pharmacol Biochem Behav 39:729–736
Yen CY, Stanger RL, Millman N (1959) Ataractic suppression of isolation-induced aggressive behavior. Arch Int Pharmacodyn 123:179–185

E.2.3.3 Resident-Intruder Aggression Test

PURPOSE AND RATIONALE

Sijbesma et al. (1991), Mos et al. (1992), Muehlenkamp et al. (1995) studied the effects of drugs in a test for offensive aggression, the isolation-induced resident intruder aggression model (Flannelly and Lore 1975; Brain et al. 1979), in the rat.

PROCEDURE

Sprague-Dawley rats weighing 250 to 450 g are housed in a light-dark (12L:12D)-, temperature (ca. 22°C)- and humidity (ca. 55%)-controlled room.

Resident male rats (about 450 g) are tested in their home cages for aggression against a smaller (250 g) male intruder. They are treated by intraperitoneal injection of test drug or saline 15 min before the test. The resident female is removed from the cage 30 min prior to the start of the test period. After placing the intruder rat in the territorial cage, the behavior of the resident male is observed. The time until the first attack (in seconds), number of attacks, and duration of each attack (in seconds) are recorded for the next 15 min by a blind observer. Furthermore, a total of 49 different behavioral elements are scored and grouped into 7 behavioral categories: offensive, exploration, social interest, inactivity, avoidance, body care, defense.

EVALUATION

Paired and unpaired *t*-tests are used for comparisons of means of absolute values.

REFERENCES AND FURTHER READING

Brain PF, Howell PA, Benton D, Jones SE (1979) Studies on responses by "residents" rats housed in different ways to intruders of differing endocrine status. J Endocrinol 81:135–136
Flannelly K, Lore R (1975) Dominace-subordinance in cohabitating pairs of adult rats: Effects on aggressive behavior. Aggress Behav 1:331–340
Mos J, Olivier B, Poth M, van Aken H (1992) The effects of intraventricular administration of eltoprazine, 1-(3-trifluoromethylphenyl)piperazine hydrochloride and 8-hydroxy-2-(di-n-propylamino)tetralin on resident intruder aggression in the rat. Eur J Pharmacol 212:295–298
Muehlenkamp F, Lucion A, Vogel WH (1995) Effects of selective serotonergic agonists on aggressive behavior in rats. Pharmacol Biochem Behav 50:671–674
Sijbesma H, Schipper J, de Kloet ER, Mos J, van Aken H, Olivier B (1991) Postsynaptic 5-HT_1 receptors and offensive aggression in rats: A combined behavioural and autoradiographic study with eltoprazine. Pharmacol Biochem Behav 38:447–458

E.2.3.4 Water Competition Test

PURPOSE AND RATIONALE

The competitive water consumption test in rats (Baenninger 1970; Syme 1974) can be used to study the influence of drugs on defensive aggression and dominance (Muehlenkamp et al. 1995).

PROCEDURE

Male Sprague-Dawley rats weighing 250 to 400 g are kept in a light-dark (12L:12D)-, temperature (ca. 22°C)- and humidity (ca. 55%)-controlled room.

Animals of equal weight are paired and housed in one cage. After 6 days, the animals are deprived of water for 23 h. Then, one water bottle is introduced with a shielded spout so that only one animal of a pair can drink at a time. Time (in seconds) and frequency of spout possession and water consumption are recorded in numbers with a special computer program for 5 min. Animals are then allowed another 55 min for water consumption. This test is repeated on 3 subsequent days. Saline or test substances are injected intraperitoneally 15 min before tests 3 and 4. The animal with

the longest duration of water consumption and frequency of spout possession is considered to be the more aggressive and/or dominant animal.

EVALUATION

Paired and unpaired *t*-tests are used for comparisons of means of absolute values, as well as means of differences of the absolute value of the two rats.

REFERENCES AND FURTHER READING

Baenninger LP (1970) Social dominance orders in the rat: "Spontaneous" food and water competition. J Physiol Psychol 71:202–209

Muehlenkamp F, Lucion A, Vogel WH (1995) Effects of selective serotonergic agonists on aggressive behavior in rats. Pharmacol Biochem Behav 50:671–674

Syme GJ (1974) Competitive orders a measures of social dominance. Anim Behav 22:931–940

E.2.3.5 Maternal Aggression in Rats

PURPOSE AND RATIONALE

The model of 'maternal aggression' in rats was described by Olivier et al. (1985), Olivier and Mos (1986, 1992), Mos et al. (1987, 1989). Introduction of an intruder (male or female) in the cage of a parturient female rat, induces high levels of aggression against such intruders. Maternal aggression is characterized by short latency attacks of high intensity, mostly directed toward the head or neck of the intruder and is particularly pronounced during the first part of the lactating period. The behavior can be suppressed by several drugs, e. g., 5-HT_1 agonists (Mos et al. 1990; Olivier and Mos 1992).

PROCEDURE

Female rats weighing 250–350 g are placed with a breeding male in their home cages. On the bottom of each cage an iron gauze is placed which enables the collection of ejaculation plugs. After an ejaculation plug is detected the male is left for an other week with the female after which she is placed in the observation cage provided with nesting material where she stays for the rest of the experiment. These cages are situated in an observation room under a reversed day-night rhythm. The day of birth is marked as day 0. Every parturient female is tested each day against a naive male intruder which has about 25 g less body weight than the female. Tests are performed during the first part of the dark period under red light conditions. One male intruder is placed in the female's home cage for 5 min. The ongoing behavior is videotaped and analyzed later. Each intruder is used only once and sacrificed immediately afterwards with an i.p. overdose of pentobarbital, followed by shaving and describing the wounds on wound charts (Mos et al. 1984).

The aggressive behavior of the female is scored for:

- bite attack on the head (fierce biting on head and snout often causing severe wounds),
- bite attack on the body (mostly directed to the back),
- lateral threat (the animal kicks with a hindleg at the opponent),
- upright posture (accompanied by boxing),
- nipping (short and low intensity bite on the head of the opponent),
- pulling (the opponent is held by the teeth and drawn through the cage),
- lunge (very rapid movement toward the opponent, mostly followed by bite attacks),
- on top (the female holds down the opponent which lies on its back).

Besides the frequency and the duration of the elements, also the latency of the first attack and the number of attacks are recorded.

Drug experiments are performed on postpartum days 3, 5, 7, and 9 using a Latin-square design of dosage. Preceding days (day 1 and 2), intervening (4, 6 and 8) and following (10, 11, 12, and 13) days are used to establish an aggression base line and as washout days. Drugs are administered orally 60 min before testing.

EVALUATION

Analysis of variance is employed to detect overall significance, followed by Wilcoxon matched pairs comparison between dosages. Kruskal-Wallis analysis is used to test the differences in the bite target areas after drug treatment.

MODIFICATIONS OF THE METHOD

Postpartum aggression in rats did not influence threshold currents for electrical brain stimulation-induced aggression in rats (Mos et al. 1987).

Maternal aggression can be observed not only in rats but also in **mice** and **hamsters** (Mos et al. 1990).

Palanza et al. (1996) examined the effects of chlordiazepoxide on the differential response pattern in aggressive-naive and aggressive-experienced lactating female mice confronting intruders of either sex in a 10-min test.

Olivier et al. (1990) highlighted ethopharmacology as a creative approach to identification and characterization of novel psychotropics.

Olivier et al. (1995) gave a review on serotonin receptors and animal models of aggressive behavior.

REFERENCES AND FURTHER READING

Kruk MR, Zethof T (1987) Postpartum aggression in rats does not influence threshold currents for EBS-induced aggression. Brain Res 404:263–266

Mos J, Olivier B, Van Oorschot R (1984) Different test situations for measuring offensive aggression in male rats do not result in the same wound pattern. Physiol Behav 32:453–456

Mos J, Olivier B, Lammers JHCM, van der Poel AM, Kruk MR, Zethof T (1987a) Postpartum aggression in rats does not influence threshold currents for EBS-induced aggression. Brain Res 404:263–266

Mos J, Olivier B, van Oorschot R (1987b) Maternal aggression towards different sized male opponents: effect of chlordiazepoxide treatment of the mothers and d-amphetamine treatment of the intruders. Pharmacol Biochem Behav 26:577–584

Mos J, Olivier B, van Oorschot R, van Aken H, Zethof T (1989) Experimental and ethological aspect of maternal aggression in rats: five years of observations. In: Blanchard RJ, Brain PF, Blanchard DC, Parmigiani s (eds) Ethoexperimental Approaches to the Study of Behavior. Kluver Acad Publ, Dordrecht, Boston, London, pp 385–398

Mos J, Olivier B, van Oorschot R (1990) Behavioural and neuropharmacological aspects of maternal aggression in rodents. Aggress Behav 16:145–163

Olivier B (1981) Selective antiaggressive properties of DU27725: ethological analysis of intermale and territorial aggression in the male rat. Pharmacol Biochem Behav 14, Suppl 1:61–77

Olivier B, Mos J (1986) A female aggression paradigm for use in psychopharmacology: maternal agonistic behavior in rats. In: Brain PF, Ramirez JM (eds) Cross-Disciplinary Studies on Aggression. University of Seville Press, Seville, pp 73–111

Olivier B, Mos J (1992) Rodent models of aggressive behavior and serotonergic drugs. Progr Neuro-Psychopharm Biol Psychiat 16:847–870

Olivier B, Mos J, van Oorschot R (1985) Maternal aggression in rats: effects of chlordiazepoxide and fluprazine. Psychopharmacology 86:68–76

Olivier B, Rasmussen D, Raghoebar M, Mos J (1990) Ethopharmacology: A creative approach to identification and characterization of novel psychotropics. Drug Metabol Drug Interact 8:11–29

Olivier B, Mos J, van Oorschot R, Hen R (1995) Serotonin receptors and animal models of aggressive behavior. Pharmacopsychiat 28, Suppl.:80–90

Palanza P, Rodgers RJ, Ferrari PF, Parmigiani S (1996) Effects of chlordiazepoxide on maternal aggression in mice depend on experience of resident and sex of intruder. Pharmacol Biochem Behav 54:175–182

E.2.3.6 Rage Reaction in Cats

PURPOSE AND RATIONALE

An emotional aggressive behavior (rage reaction) can be elicited in unrestrained cats by high frequency electrical stimulation of the hypothalamus. Benzodiazepines have been reported (Malick 1970; Mursaki et al. 1976) to elevate the stimulus threshold for eliciting this rage reaction.

PROCEDURE

Emotional aggressive behavior is evoked by stimulation of the perifornical area of the lateral hypothalamus through chronically implanted stainless steel bipolar concentric electrodes by using threshold impulses of 1.0–2.6 mA, delivered at 50 Hz, to evoke a control attack response. Stimulation is discontinued immediately after the slowly rising current has reached threshold strength, and is performed once before drug administration as well as every 30 min thereafter. Drugs are injected by intraperitoneal route.

EVALUATION

Post-drug values are expressed as percentage of the pre-drug control value. Student's paired *t*-test is used for each time interval.

CRITICAL ASSESSMENT OF THE TEST

The method has been used for evaluation of new drugs. Most studies were devoted to the role of neurotransmitters regulating feline aggression (Siegel and Schubert 1995; Siegel et al. 1998) and the neural bases of aggression and rage in the cat (Siegel et al. 1997, 1999).

REFERENCES AND FURTHER READING

Glusman M (1974) The hypothalamic 'savage' syndrome. Res Publ Ass Nerv Ment Dis 52:52–92

Malick JB (1970) Effects of selected drugs on stimulus-bound emotional behaviour elicited by hypothalamic stimulation in the cat. Arch Int Pharmacodyn Ther 186:137–141

Murasaki M, Hara T, Oguchi T, Inami M, Ikeda Y (1976) Action of enpiprazole on emotional behaviour induced by hypothalamic stimulation in rats and cats. Psychopharmacologia 49:271–274

Pieri L (1983) Preclinical pharmacology of midazolam. Br J Clin Pharmacol 16:17S–27S

Siegel A, Schubert K (1995) Neurotransmitters regulating feline aggression. Rev Neurosci 6:47–61

Siegel A, Shaikh MB (1997) The neural bases of aggression and rage in the cat. Aggression Violent Behav 1:241–271

Siegel A, Schubert K, Shaikh MB (1997) Neurotransmitters regulating defensive rage behavior in the cat. Neurosci Biobeh Rev 21:733–742

Siegel A, Schubert KL, Shaikh MB (1998) Neurotransmitters regulating defensive rage behavior in the cat. Neurosci Biobehav Rev 21:733–742

Siegel A, Roeling TAP, Gregg TR, Kruk MR (1999) Neuropharmacology of brain-stimulation-evoked aggression. Neurosci Biobehav Rev 23:359–389

E.2.4
Effects on Behavior

E.2.4.1
Anti-Anxiety Test (Light-Dark Model)

PURPOSE AND RATIONALE

Crawley and Goodwin (1980) Crawley (1981) described a simple behavior model in mice to detect compounds with anxiolytic effects. Mice and rats tend to explore a novel environment, but to retreat from the aversive properties of a brightly-lit open field. In a two-chambered system, where the animals can freely move between a brightly-lit open field and a dark corner, they show more crossings between the two chambers and more locomotor activity after treatment with anxiolytics. The numbers of crossings between the light and dark sites are recorded.

PROCEDURE

The testing apparatus consists of a light and a dark chamber divided by a photocell-equipped zone. A polypropylene animal cage, 44 × 21 × 21 cm, is darkened with black spray over one-third of its surface. A partition containing a 13 cm long × 5 cm high opening separates the dark one third from the bright two thirds of the cage. The cage rests on an Animex activity monitor which counts total locomotor activity. An electronic system using four sets of photocells across the partition automatically counts movements through the partition and clocks the time spent in the light and dark compartments. Naive male mice or rats are placed into the cage. The animals are treated 30 min before the experiment with the test drugs or the vehicle intraperitoneally and are then observed for 10 min. Groups of 6–8 animals are used for each dose.

EVALUATION

Dose-response curves are obtained and the number of crossings through the partition between the light and the dark chamber are compared with total activity counts during the 10 min.

CRITICAL ASSESSMENT OF THE METHOD

It has been shown that a variety of anxiolytics, including diazepam, pentobarbital and meprobamate produce a dose-dependent increase in crossings, whereas non-anxiolytic agents do not have this facilitatory effect. Furthermore, the relative potency of anxiolytics in increasing exploratory behavior in the two-compartment chamber agrees well with the potency found in clinical trials.

The test has the advantage of being relatively simple with no painful stimuli to the animals. The specificity of the method remains open.

MODIFICATIONS OF THE METHOD

Using a similar method, called black and white test box, Costall et al. (1987, 1988, 1989) studied the effects of anxiolytic agents and reported an anxiolytic effect of dopamine receptor antagonists, such as sulpiride and buspirone.

Sanchez (1995) presented a fully automated version of the black and white two-compartment box for mice.

Barnes et al. (1992) used this model to study the interaction of optical isomers modifying rodent aversive behavior.

Kilfoil et al. (1989) used a similar apparatus to test compounds for anxiogenic and anxiolytic activity.

Animal models of anxiety and their relation to serotonin-interacting drugs have been reviewed by Broekkamp et al. (1989) and by Griebel (1995).

Laboratory rats prefer to dwell on a solid floor rather than an grid one, particularly when resting. Manser et al. (1996) described an operant test in rats to determine the strength of preference for flooring. The apparatus consisted of a grid-floored cage and a solid-floored cage, joined via a central box containing a barrier whose weight was adjustable. The rats had to lift the barrier in order to explore the whole apparatus or were confined on the grid floor and then had to lift the barrier in order to reach the solid floor.

Hascoët and Bourin (1998) tested anxiolytic and psychostimulant drugs in a fully automated and computer-integrated two-compartment light/dark box.

REFERENCES AND FURTHER READING

Barnes NM, Costall B, Domeney AM, Gerrard PA, Kelly ME, Krähling H, Naylor RJ, Tomkins DM, Williams TJ (1991) The effects of umespirone as a potential anxiolytic and antipsychotic agent. Pharmacol Biochem Behav 40:89–96

Barnes NM, Cheng CHK, Costall B, Ge J, Kelly ME, Naylor RJ (1992a) Profiles of R(+)/S(–)-Zacopride and anxiolytic agents in a mouse model. Eur J Pharmacol 218:91–100

Barnes NM, Costal B, Ge J, Kelly ME, Naylor RJ (1992b) The interaction of R(+)- and S(–)-zacopride with PCPA to modify rodent aversive behavior. Eur J Pharmacol 218:15–25

Blumstein LK, Crawley JN (1983) Further characterisation of a simple, automated exploratory model for the anxiolytic effects of benzodiazepines. Pharmacol Biochem Behav 18:37–40

Broekkamp CLE, Berendsen HHG, Jenk F, van Delft AML (1989) Animal models for anxiety and response to serotonergic drugs. Psychopathology 22(Suppl 1):2–12

Costall B, Hendrie CA, Kelly ME, Naylor RJ (1987) Actions of sulpiride and tiapride in a simple model of anxiety in mice. Neuropharmacol 26:195–200

Costall B, Kelley ME, Naylor RJ, Onaivi ES (1988) Actions of buspirone in a putative model of anxiety in the mouse. J Pharm Pharmacol 40:494–500
Costall B, Jones BJ, Kelly ME, Naylor RJ, Tomkins DM (1989) Exploration of mice in a black and white test box: validation as a model of anxiety. Pharmacol Biochem Behav 32:777–785
Crawley JN (1981) Neuropharmacologic specificity of a simple animal model for the behavioral actions of benzodiazepines. Pharmacol Biochem Behav 15:695–699
Crawley J, Goodwin KK (1980) Preliminary report of a simple animal behavior model for the anxiolytic effects of benzodiazepines. Pharmacol Biochem Behav 13:167–170
Griebel G (1995) 5-Hydroxytryptamine-interacting drugs in animal models of anxiety disorders: more than 30 years research. Pharmac Ther 65:319–395
Hascoët M, Bourin M (1998) A new approach to the light/dark test procedure in mice. Pharmacol Biochem Behav 60:645–653
Kilfoil T, Michel A, Montgomery D, Whithing RL (1989) Effects of anxiolytic and anxiogenic drugs on exploratory activity in a simple model of anxiety in mice. Neuropharmacol 28:901–905
Kauppila T, Tanila H, Carlson S, Taira T (1991) Effects of atipamezole, a novel α_2-adrenoreceptor antagonist, in open-field, plus-maze, two compartment exploratory, and forced swimming tests in rats. Eur J Pharmacol 205:177–182
Manser CE, Elliott H, Morriss TH, Broom DM (1996) The use of a novel operant test to determine the strength of preference for flooring in laboratory rats. Labor Animals 30:1–6
Sanchez C (1995) Serotonergic mechanisms involved in the exploratory behaviour of mice in a fully automated two-compartment black and white test box. Pharmacol Toxicol 77:71–78
Schipper J, Tulp MThM, Berkelmans B, Mos J, Van der Heijden JAM, Olivier B (1991) Preclinical pharmacology of Flesinoxan: A potential anxiolytic and antidepressant drug. Human Psychopharmacol 6:53–61
Treit D (1985) Animal models for the study of anti-anxiety agents: A review. Neurosci Biobehav Reviews 9:203–222

E.2.4.2 Anticipatory Anxiety in Mice

PURPOSE AND RATIONALE

When group-housed mice are removed one by one from their home cage, the last mice removed have always higher rectal temperatures than those removed first (Borsini et al. 1989; Lecci et al. 1990). This phenomenon is interpreted as being caused by anticipatory fear for an aversive event (handling causes stress-induced hyperthermia). Consequently, this test is thought to be a model of anticipatory anxiety. The anticipatory increase in temperature was prevented by prior treatment with diazepam and buspirone, whereas several other drugs did not affect this phenomenon (Lecci et al. 1990). The usefulness of this model for obsessive-compulsive disorder in man is discussed.

PROCEDURE

Groups of 18 male albino Swiss mice weighing 25–30 g are housed at constant room temperature and relative humidity for at least 7 days in Makrolon cages to adapt to the environment. Test drugs or standard (diazepam) or solvent are administered orally in various doses to groups of 18 mice prior to the test. Thirty min later, the first 3 mice are removed from the cage and the rectal temperature registered by inserting a silicone lubricated thermistor probe (2 mm diameter) for 2.5 cm into the rectum. The average temperature of these 3 mice is taken as basal value. Mice number 4 through 15 are simply removed and again returned to the cage, and thereafter body temperature is determined in the remaining three animals. The difference of the mean value of these mice and the basal values is calculated as increase. Vehicle treated test groups display increases of 1.1 to 1.3°C.

EVALUATION

The mean increase values of treated groups ± SEM are compared by ANOVA statistics with the controls.

MODIFICATIONS OF THE METHOD

Van der Heyden et al. (1997) adapted the group-housed stress-induced hyperthermia paradigm to single housed animals in order to drastically reduce the number of animals used. Repeated, but not single, disturbance of animals resulted in a strong hyperthermia (Δt) within 10 min. The final test paradigm chosen involved repeated temperature measurements at 10 min intervals, thus providing both information on basal temperature and Δt in each animal within a short time frame.

REFERENCES AND FURTHER READING

Borsini F, Lecci A, Volterra G, Meli A (1989) A model to measure anticipatory anxiety in mice? Psychopharmacology 98:207–211
Lecci A, Borsini F, Mancinelli A, D'Aranno V, Stasi MA, Volterra G, Meli A (1990a) Effects of serotoninergic drugs on stress-induced hyperthermia (SIH) in mice. J Neur Transmiss 82:219–230
Lecci A, Borsini F, Volterra G, Meli A (1990b) Pharmacological validation of a novel animal model of anticipatory anxiety in mice. Psychopharmacology 101:255–261
Tulp M, Olivier B, Schipper J, van der Pel G, Mos J, van der Heyden J (1991) Serotonin reuptake blockers: Is there preclinical evidence for their efficacy in obsessive-compulsive disorder? Human Psychopharmacol 6:S63–S71
Van der Heyden JASM, Zethof TKK, Olivier B (1997) Stress-induced hyperthermia in singly housed mice. Physiol Behav 62:463–470
Zelthof TJJ, van der Heyden JAM, Olivier B (1991) A new animal model for anticipatory anxiety? In: Olivier B, Mos J, Slangen JL (eds) Animal Models in Psychopharmacology.

Advances in Pharmacological Sciences. Birkhäuser Verlag, Basel, pp 65–68
Zelthof TJJ, van der Heyden JAM, Tolboom JTBM, Olivier B (1995) Stress-induced hyperthermia as a putative anxiety model. Eur J Pharmacol 294:125–135

E.2.4.3 Social Interaction in Rats

PURPOSE AND RATIONALE

In an unfamiliar and brightly lit environment, the normal social interaction of rats (e. g. sniffing, nipping, grooming) is suppressed. Anxiolytics counteract this suppression.

PROCEDURE

Male Sprague-Dawley rats (225–275 g body weight) are housed in groups of 5 animals The apparatus used for the detection of changes in social behavior and exploratory behavior consists of a Perspex open-topped box (51 × 51 cm and 20 cm high) with 17 × 17 cm marked areas on the floor. One hour prior to the test, two naive rats from separate housing cages are treated with the test compound orally. They are placed into the box (with 60 W bright illumination 17 cm above) and their behavior is observed over a 10-min period by remote video recording. Two types of behavior can be noted:

- social interaction between the animals is determined by timing the sniffing of partner, crawling under or climbing over the partner, genital investigation of partner, and following partner,
- exploratory motion is measured as the number of crossings of the lines marked on the floor of the test box.

Six pairs are used for each dose.

EVALUATION

The values of treated partners are compared with the data from 6 pairs of untreated animals using single factor analysis of variance followed by Dunnett's *t*-test.

CRITICAL ASSESSMENT OF THE METHOD

In spite of the fact that there may be some analogy between "social anxiety" in humans and the behavior of rats in the social interaction test, there appear some potential complications with this test, such as an increase of social interaction after anxiolytics independent from the environment, dependence on external variables such as time of the day, and the complicated nature of social interaction.

MODIFICATIONS OF THE TEST

Sams-Dodd (1995) described the automation of the social interaction test in rats by a commercially available video-tracking system.

Gheusi et al. (1994) studied the effects of tetrahydroaminoacridine (THA) on social recognition in rats indicating a dissociation of cognitive versus non-cognitive processes.

Doses of 1.0 to 4.0 mg/kg i.p. phencyclidine (PCP) reduce the social interaction time in rats in a dose-dependent fashion. Reversal of the PCP-induced social withdrawal has been used as an animal model for neuroleptic resistant schizophrenia (Carlsson and Carlsson 1990; Corbett et al. 1995).

Olfactory investigation of ovarectomized females by adult male mice decreases during repeated confrontations with the same female intruder, whereas aggressive behavior gradually increases (Winslow and Camacho 1995). Administration of scopolamine blocked decrements in olfactory investigation in repeated confrontations and significantly reduced aggression. Acetylcholinesterase inhibitors enhanced the rate of decrement of olfactory investigation, but had differential effects on aggression.

Wongwitdecha and Marsden (1996) investigated the effects of isolation rearing on anxiety using the social interaction paradigm and compared the effects of diazepam on social interactive behaviors in isolation and socially reared rats.

Sams-Dodd (1997) studied the effect of novel anti-psychotic drugs on phencyclidine-induced stereotyped behaviour and social isolation in the rat social interaction test.

The rat social interaction model has been used by various authors to characterize the potential anxiolytic effects of serotonin receptor antagonists, such as 5-HT_{1C} receptors antagonists (Kennett et al. 1989; Kennett 1992), 5-HT_2 receptor antagonists (Kennett et al. 1994, 1995, 1996a, b, 1997; Costall and Naylor 1995), 5-HT_3 receptor antagonists (Costall et al. 1990; Costall and Naylor 1992; Blackburn et al. 1993), 5-HT_4 receptor antagonists Kennett et al. (1997), cholestystokinin receptor antagonists (Hughes et al. 1990; Costall et al. 1991; Singh et al. 1991) and of nitric oxide synthase inhibitors (Volke et al. 1997).

File and Johnston (1989) reported a lack of effects of 5-HT_3 receptor antagonists in the social interaction test in the rat.

Woodall et al. (1996) described a **competition procedure** in rats. On the first week of experimentation groups of 3 rats (triads) are familiarized with the test box and sweetened milk from a drinking spout located

on the end wall. The drinking spout is surrounded by a Perspex tube (4.5 cm diameter) which ensures that only one animal is able to drink at a time. All animals are deprived of water overnight and on the following day placed into the testing box and given access to the sweetened milk for 15 min. On the second week of testing, the rats are not longer water deprived and are given access to the testing box and sweetened milk for 5 min. During the testing period, the rats are observed every 5 s, and a note is made which animal is drinking. This procedure is carried out twice a week for a period of 5 weeks. Drugs are administered to either the dominant or subordinate rat in each triad 15 min prior to testing. Following the drug study, all triads are tested for 2 trials to ensure that their rank orders return to baseline levels. The access of the subordinate member to sweetened milk is increased after administration of an anxiolytic drug.

REFERENCES AND FURTHER READING

Angelis L, File SE (1979) Acute and chronic effects of three benzodiazepines in the social interaction test in mice. Psychopharmacology (Berlin) 64:127–129

Barnes NM, Costall B, Domeney AM, Gerrard PA, Kelly ME, Krähling H, Naylor RJ, Tomkins DM, Williams TJ (1991) The effects of umespirone as a potential anxiolytic and antipsychotic agent. Pharmacol Biochem Behav 40:89–96

Blackburn TP, Baxter GS, Kennett GA, King FD, Piper DC, Sanger GJ, Thomas DR, Upton N, Wood MD (1993) BRL 46470A: A highly potent, selective and long acting 5-HT_3 receptor antagonist with anxiolytic-like properties. Psychopharmacology 110:257–264

Carlsson M, Carlsson A (1990) Interactions between glutaminergic and monoaminergic systems within the basal ganglia: implications for schizophrenia and Parkinson's disease. Trends Neural Sci 13:272–276

Corbett R, Dunn RW (1991) Effects of HA-966 on conflict, social interaction, and plus maze behaviors. Drug Dev Res 24:201–205

Corbett R, Fielding S, Cornfeldt M, Dunn RW (1991) GABAmimetic agents display anxiolytic-like effects in the social interaction and elevated plus maze procedures. Psychopharmacology 104:312–316

Corbett R, Hartman H, Kerman LL, Woods AT, Strupczewski JT, Helsley GC, Conway PC, Dunn RW (1993) Effects of atypical antipsychotic agents on social behavior in rodents. Pharmacol Biochem Behav 45:9–17

Corbett R, Camacho F, Woods AT, Kerman LL, Fishkin RJ, Brooks K, Dunn RW (1995) Antipsychotic agents antagonize non-competitive N-methyl-D-aspartate antagonist-induced behaviors. Psychopharmacology 120:67–74

Costall B, Naylor RJ (1992) Anxiolytic potential of 5-HT_3 receptor antagonists. Pharmacol Toxicol 70:157–162

Costall B, Naylor RJ (1995) Behavioural interactions between 5-hydroxytryptophan, neuroleptic agents and 5-HT receptor antagonists in modifying rodent response to adverse situations. Br J Pharmacol 116:2989–2999

Costall B, Kelly ME, Onaivi ES, Naylor RJ (1990) The effect of ketotifen in rodent models of anxiety and on the behavioural consequences of withdrawing from treatment with drugs of abuse. Naunyn-Schmiedeberg's Arch Pharmacol 341:547–551

Costall B, Domeney AM, Hughes J, Kelly ME, Naylor RJ, Woodruff GN (1991) Anxiolytic effects of CCK_B antagonists. Neuropeptides 19/ Suppl:65–73

Dunn RW, Corbett R, Martin LL, Payack JF, Laws-Ricker L, Wilmot CA, Rush DK, Cornfeldt ML, Fielding S (1990) Preclinical anxiolytic profiles of 7189 and 8319, novel non-competitive NMDA antagonists. Current and Future Trends in Anticonvulsant, Anxiety, and Stroke Therapy, Wiley-Liss, Inc., pp 495–512

File SE (1980) The use of social interactions as a method for detecting anxiolytic activity of chlordiazepoxide-like drugs. J Neurosci Meth 1:219–238

File SE, Hyde RJ (1979) A test of anxiety that distinguishes between the actions of benzodiazepines and those of other minor tranquilizers and stimulants. Pharmacol Biochem Behav 11:65–69

File SE, Johnston AL (1989) Lack of effects of 5-HT_3 receptor antagonists in the social interaction and elevated plus-maze tests in the rat. Psychopharmacology 99:248–251

Gardner C, Guy A (1984) A social interaction model of anxiety sensitive to acutely administered benzodiazepines. Drug Dev Res 4:207–216

Gheusi G, Bluthe RM, Goodall G, Dantzer R (1994) Ethological study of the effects of tetrahydroaminoacridine (THA) on social recognition in rats. Psychopharmacology 114:644–650

Hughes J, Boden P, Costall B, Domeney A, Kelly E, Horwell DC, Hunter JC, Pinnock RD, Woodruff GN (1990) Development of a class of selective cholecystokinin type B receptor antagonists having a potent anxiolytic activity. Proc Natl Acad Sci USA 87:6728–6732

Kennett GA (1992) 5-HT_{1C} Receptors antagonists have anxiolytic-like actions in the rat social interaction model. Psychopharmacology 107:379–384

Kennett GA, Whitton P, Shah K, Curzon G (1989) Anxiogenic-like effects of mCPP and TFMPP in animal models are opposed by 5-HT_{1C} receptor antagonists. Eur J Pharmacol 164:445–454

Kennett GA, Wood MD, Glen A, Grewal S, Forbes I, Gadre A, Blackburn TP (1994) *In vivo* properties of SB 200646A, a 5-$HT_{2C/2B}$ receptor antagonist. Br J Pharmacol 111:797–802

Kennett GA, Bailey F, Piper DC, Blackburn TP (1995) Effect of SB 200646A, a 5-HT_{2C}/5-HT_{2B} receptor antagonist, in two conflict models of anxiety. Psychopharmacology 118:178–182

Kennett GA, Bright F, Trail B, Baxter GS, Blackburn TP (1996a) Effects of the 5-HT_{2B} receptor antagonist, BW 723C86, on three rat models of anxiety. Br J Pharmacol 117:1443–1448

Kennett GA, Wood MD, Bright F, Cilia J, Piper DC, Gager T, Thomas D, Baxter GS, Forbes IT, Ham P, Blackburn TP (1996b) *In vitro* and *in vivo* profile of SE 206553, a potent 5-HT_{2C}/5-HT_{2B} receptor antagonist with anxiolytic-like properties. Br J Pharmacol 117:427–434

Kennett GA, Wood MD, Bright F, Trail B, Riley G, Holland V, Avenell KY, Stean TT, Upton N, Bromidge S, Forbes IT, Brown AM, Middlemiss DN, Blackburn TP (1997a) SE 242084, a selective and brain penetrant 5-HT_{2C} receptor antagonist. Neuropharmacol 36:609–620

Kennett GA, Bright F, Trail B, Blackburn TP, Sanger GJ (1997b) Anxiolytic-like actions of the 5-HT_4 receptor antagonists SB 204070A and SB 207266A in rats. Neuropharmacol 36:707–712

Sams-Dodd F (1995) Automation of the social interaction test by a video-tracking system: behavioural effects of re-

peated phencyclidine treatment. J Neurosci Meth 59:157–167
Sams-Dodd F (1997) Effect of novel antipsychotic drugs on phencyclidine-induced stereotyped behaviour and social isolation in the rat social interaction test. Behav Pharmacol 8:196–215
Singh L, Field MJ, Hughes J, Menzies R, Oles RJ, Vass CA, Woodruff GN (1991) The behavioural properties of CI-998, a selective cholecystokinin$_B$ receptor antagonist. Br J Pharmacol 104:239–245
Szewczak MR, Cornfeldt ML, Dunn RW, Wilker JC, Geyer HM, Glamkowski EJ, Chiang Y, Fielding S (1987) Pharmacological evaluation of HP 370, a potential atypical antipsychotic agent. 1. *In vivo* profile. Drug Dev Res 11:157–168
Treit D (1985) Animal models for the study of anti-anxiety agents: A review. Neurosci Biobehav Reviews 9:203–222
Volke V, Soosaar A, Koks S, Bourin M, Mannisto PT, Vasar E (1997) 7-Nitroindazole, a nitric oxide synthase inhibitor, has anxiolytic-like properties in exploratory models of anxiety. Psychopharmacology 131:399–405
Winslow JT, Camacho F (1995) Cholinergic modulation of a decrement in social investigation following repeated contacts between mice. Psychopharmacology 121:164–172
Wongwitdecha N, Marsden CA (1996) Social isolation increases aggressive behaviour and alters the effects of diazepam in the rat social interaction test. Behav Brain Res 75:27–32
Woodall KL, Domeney AM, Kelly ME (1996) Selective effects of 8-OH-DPAT on social competition in the rat. Pharmacol Biochem Behav 54:169–173

E.2.4.4 Elevated Plus Maze Test

PURPOSE AND RATIONALE

Out of many possibilities to modify maze tests (e. g. water maze (Danks et al. 1991), Y-maze, radial maze (Di Cicco 1991)) the **elevated plus maze** (Montgomery 1958; Pellow et al. 1985; Corbett et al. 1991) has found acceptance in many laboratories (Liebisch et al. 1998; Landgraf et al. 1999; Schwarzberg et al. 1999; Keck et al. 2001; Brakebusch et al. 2002). The test has been proposed for selective identification of anxiolytic and anxiogenic drugs. Anxiolytic compounds, by decreasing anxiety, increase the open arm exploration time; anxiogenic compounds have the opposite effect.

For effects on learning and memory see Sect. F.3.3.3.

PROCEDURE

The plus-maze consists of two open arms, 43 × 15 cm (L × W), and two enclosed arms, 43 × 1523 cm (L × W × H), open to the top, arranged so that the two open arms are opposite to each other. The maze is elevated to a height of 70 cm (TSE Systems, Bad Homburg, Germany). The rats (200–250 g body weight) are housed in pairs for 10 days prior to testing in the apparatus. During this time the rats are handled by the investigator on alternate days to reduce stress. Groups consist of 6 rats for each dose. Thirty min after i.p. administration of the test drug or the standard, the rat is placed in the center of the maze, facing one of the enclosed arms. During a 5 min test period the following measures are taken: the number of entries into and time spent in the open and enclosed arms; the total number of arm entries. The procedure is conducted preferably in a sound attenuated room, with observations made from an adjacent room via a remote control TV camera.

EVALUATION

Motor activity and open arm exploratory time are registered. The values of treated groups are expressed as percentage of controls. Benzodiazepines and valproate decrease motor activity and increase open arm exploratory time.

CRITICAL ASSESSMENT OF THE METHOD

The method is rather time consuming, but can be regarded as a reliable measure of anxiolytic activity. Computerized automatic elevated plus maze systems may help to overcome these difficulties (TSE Systems, Bad Homburg, Germany).

MODIFICATIONS OF THE METHOD

Latency to enter a mirrored chamber by mice has been described as a behavioral assay for anxiolytic agents (Toubas et al. 1990).

Handley and McBlane (1993) provided an assessment of the elevated X-maze for studying anxiety and anxiety-modulating drugs.

Lapin (1995) studied the effect of handling, sham injection, and intraperitoneal injection of saline on the behavior of mice in an elevated plus-maze. These procedures produce behavior considered to be typical for anxiety inducing drugs. Saline-treated groups taken as controls possess the behavioral profile of stressed and anxious animals.

Pokk et al. (1996) described a method of small platform-induced stress whereby mice were individually placed for 24 h on a small platform (3 cm high, 3.5 cm in diameter) which was fixed at the center of a plastic chamber (20 cm diameter, 40 cm high) and was surrounded by water (1 cm deep) at 22°C.

Shepherd et al. (1994) described the **elevated "zero-maze"** as a modification of the elevated plus-maze model of anxiety in rats which incorporates both traditional and novel ethological measures in the analysis of drug effects. The design comprises an elevated annular platform with two opposite enclosed quadrants

and two open, removing any ambiguity in interpretation of time spent in the central square of the traditional design and allowing uninterrupted exploration. A similar equipment, built for mice (TSE Systems, Bad Homburg, Germany), was used by Cryan et al. (2004) and Korsgaard et al. (2005).

Jardim et al. (1999) evaluated the elevated T-maze as an animal model of anxiety in the mouse and found important differences between mice and rats.

Based on their plus-maze behavior, that is the time spent in the open arms, Ho et al. (2002) divided male Wistar rats into two subgroups with either "low" or "high" anxiety.

Silva and Frussa-Filho (2000) recommended the plus-maze discriminative avoidance task as a model to study memory–anxiety interactions. Mice are conditioned to choose between two enclosed arms (in one of which light and noise are presented as aversive stimuli) while avoiding the two open arms of the apparatus. The test has the advantage of measuring, at the same time and in the same animals, learning/memory (by the percentage of time spent in aversive closed arm) and anxiety (by the percentage of time spent in the open arms).

Montag-Sallaz and Montag (2003) tested cognitive and motor coordination deficits in Tenascin-R-deficient mice on an elevated plus maze. For 5 min, the behavior was recorded on videotape and the numbers of entries into the central part, the closed or the open arms were counted and the time spent in these departments was determined using the VideoMot 2 system (TSE Systems, Bad Homburg, Germany).

The same system was used by Karl et al. (2003) to study behavioral effects of neuropeptide Y in F344 rat substrains with reduced dipeptidyl-peptidase IV activity.

Korte and De Boer (2003) recommended fear-potentiated behavior in the elevated plus-maze in rats as a robust animal model of state anxiety.

REFERENCES AND FURTHER READING

Brakebusch C, Seidenbecher CI, Asztely F, Rauch U, Matthies H, Meyer H, Krug M, Böckers TM, Zhou X, Kreutz MR, Montag D, Gundelfinger ED, Fässler R (2002) Brevican-deficient mice display impaired hippocampal CA1 long-term potentiation but show no obvious deficits in learning and memory. Mol Cell Biol 22:7417–7427

Brett RR, Pratt JA (1990) Chronic handling modifies the anxiolytic effect of diazepam in the elevated plus-maze. Eur J Pharmacol 178:135–138

Corbett R, Fielding St, Cornfeldt M, Dunn RW (1991) GABAmimetic agents display anxiolytic-like effects in the social interaction and elevated plus maze procedures. Psychopharmacology 104:312–316

Cryan JF, Kelly PH, Chaperon F, Gentsch C, Mombereau C, Lingenhoehl K, Froestl W, Bettler B, Kaupmann K, Spooren PJM (2004) Behavioral characterization of the novel $GABA_B$ receptor positive modulator GS39783 (*N,N′*-dicyclopentyl-2-methylsulfanyl-5-nitro-pyrimidine-4,6-diamine): anxiolytic-like activity without side effects associated with baclofen or benzodiazepines. J Pharmacol Exp Ther 310:952–963

Danks AM, Oestreicher AB, Spruijt Gispen WH, Isaakson RL (1991) Behavioral and anatomical consequences of unilateral fornix lesions and the administration of nimodipine. Brain Res 557:308–312

Di Cicco D, Antal S, Ammassari-Teule M (1991) Prenatal exposure to gamma/neutron irradiation: sensorimotor alterations and paradoxical effects on learning. Teratology 43:61–70

Dunn RW, Carlezon WA, Corbett R (1991) Preclinical anxiolytic versus antipsychotic profiles of the $5\text{-}HT_3$ antagonists ondansetron, zacopride, 3α-tropanyl-1H-indole-3-carboxylic acid ester, and 1αH, 3α, 5αH-Tropan-3-yl-3,5-dichlorobenzoate. Drug Dev Res 23:289–300

File SE, Mabbutt PS, Hitchcott PH (1990) Characterisation of the phenomenon of "one-trial tolerance" to the anxiolytic effect of chlordiazepoxide in the elevated plus-maze. Psychopharmacology 102:98–101

Handley SL, McBlane JW (1993) An assessment of the elevated X-maze for studying anxiety and anxiety-modulating drugs. J Pharm Toxicol Meth 29:129–138

Harro J, Pöld M, Vasar E (1990) Anxiogenic-like action of caerulein, a CCK-8 receptor agonist, in the mouse: influence of acute and subchronic diazepam treatment. Naunyn-Schmiedeberg's Arch Pharmacol 341:62–67

Ho YJ, Eichemdorff J, Schwarting RKW (2002) Individual response profiles of male Wistar rats in animal models for anxiety and depression. Behav Brain Res 136:1–12

Jardim MC, Nogueira RL, Graeff FG, Nunes-de-Souza RL (1999) Evaluation of the elevated T-maze as an animal model of anxiety in the mouse. Brain Res Bull 48:407–411

Karl T, Hoffmann T, Pabst R, von Hörsten S (2003) Behavioral effects of neuropeptide Y in F344 rat substrains with reduced dipeptidyl-peptidase IV activity. Pharmacol Biochem Behav 75:869–879

Kauppila T, Tanila H, Carlson S, Taira T (1991) Effects of atipamezole, a novel α_2-adrenoreceptor antagonist, in open-field, plus-maze, two compartment exploratory, and forced swimming tests in rats. Eur J Pharmacol 205:177–182

Keck ME, Welt T, Wigger A, Renner U, Engelmann M, Holsboer F, Landgraf R (2001) The anxiolytic effect of CRH_1 receptor antagonist R121919 depends on innate emotionality in rats. Eur J Neurosci 13 :373–380

Korsgaard MPG, Hartz BP, Brown WD, Ahring PK, Strøbæk D, Mirza NR (2005) Anxiolytic effects of Maxipost (BMS-204352) and Retigabine via activation of neuronal K_v7 channels. J Pharmacol Exp Ther 314:282–292

Korte SM, De Boer SF (2003) A robust animal model of state anxiety: fear-potentiated behaviour in the elevated plus-maze. Eur J Pharmacol 463:163–175

Landgraf R, Wigger A, Holsboer A, Neumann ID (1999) Hyperactive hypothalamo-pituitary-adrenocortical (HPA) axis in rats bred for high anxiety-related behavior. Neuroendocrinology 11:405–407

Lapin IP (1995) Only controls: effect of handling, sham injection, and intraperitoneal injection of saline on behavior of mice in an elevated plus-maze. J Pharmacol Toxicol Meth 34:73–77

Liebisch G, Montkowski A, Holsboer F, Landgraf R (1998) Behavioral profiles of two Wistar rat lines selectively bred

for high or low anxiety-related behavior. Behav Brain Res 94:301–310
Montag-Sallaz M, Montag D (2003) Severe cognitive and motor coordination deficits in Tenascin-R-deficient mice. Genes Brain Behav 2:20–31
Montgomery KC (1958) The relation between fear induced by novel stimulation and exploratory behaviour. J Comp Physiol Psychol 48:254–260
Munn NL (1950) The role of sensory processes in maze behavior. In: Handbook of Psychological Research in the Rat. Houghton Mifflin Comp., Boston, pp 181–225
Pellow S (1986) Anxiolytic and anxiogenic drug effects in a novel test of anxiety: Are exploratory models of anxiety in rodents valid? Meth and Find Exp Clin Pharmacol 8:557–565
Pellow S, File SE (1986) Anxiolytic and anxiogenic drug effects on exploratory activity in an elevated plus-maze: a novel test of anxiety in the rat. Pharmacol Biochem Behav 25:525–529
Pellow S, Chopin Ph, File SE, Briley M (1985) Validation of open:closed arm entries in an elevated plus-maze as a measure of anxiety in the rat. J Neurosci Meth 14:149–167
Pokk P, Liljequist S, Zharkovsky A (1996) Ro 15–4513 potentiates, instead of antagonizes, ethanol-induced sleep in mice exposed to small platform stress. Eur J Pharmacol 317:15–20
Schwarzberg H, Kalbacher H, Hoffmann W (1999) Differential behavioral effects of TFF peptides: injections of synthetic TFF3 into the rat amygdala. Pharmacol Biochem Behav 62:173–178
Shepherd JK, Grewal SS, Fletcher A, Bill DJ, Dourish CT (1994) Behavioral and pharmacologic characterization of the elevated "zero-maze" as an animal model of anxiety. Psychopharmacology (Berl) 116 :56–65
Silva RH, Frussa-Filho R (2000) The plus-maze discriminative avoidance task: a new model to study memory-anxiety interactions. Effects of chlordiazepoxide and caffeine. J Neurosci Meth 102 :117–125
Silverman P (1978) Approach to a conditioned stimulus: mazes. In: Animal behaviour in the laboratory. Chapman and Hall, London, pp 110–119
Toubas PL, Abla KA, Cao W, Logan LG, Seale TW (1990) Latency to enter a mirrored chamber: a novel behavioral assay for anxiolytic agents. Pharmacol Biochem Behav 35:121–126

E.2.4.5 Water Maze Test

PURPOSE AND RATIONALE

Spatial learning of rats can be tested in a water maze as described by Morris (1984) and McNaughton and Morris (1987).

For effects on learning and memory see Sect. F.3.3.5.

PROCEDURE

The water maze consists of a circular tank with 100 cm diameter and a wall 20 cm above the water level. A circular platform (9 cm diameter, covered with white linen material for grip) is hidden 2 cm below the water level. The water is made opaque using titanium dioxide suspension and is kept at about 23°C during the experiment. Training takes place on three consecutive days, with the rats receiving 4 consecutive trials per day with an inter-trial interval of 6–10 min. Each trial is started from one of four assigned polar positions with a different sequence each day. The latency to find the platform is measured as the time of placement of the rat in the water to the time it finds the platform. If the animal fails to find the platform in any trial within 3 min it is placed on it for 10 s.

EVALUATION

On day four a probe test is performed. The platform is removed and the time spent in the target quadrant (the quadrant in the center of which the platform has been located) and the number of annulus crossings (across the actual location where the platform has been located) in the first 60 s of exposure are measured. The time to the first annulus crossing is also taken as a measure of performance on the 13th (i. e. probe) trial.

Buspirone (Rowan et al. 1990) as well as benzodiazepines (McNaughton and Morris 1987) increase the latency to find the platform in the training period and impair the number and the time of annulus crossings.

CRITICAL ASSESSMENT OF THE METHOD

The water maze test measures learning and memory rather than the anxiolytic activity. If the test is used for memory, rats which have learned quickly and consistently to find the platform are kept in their cages for 2 weeks and then re-tested. Rats which solve the escape immediately, are considered to have retained memory (see also Sect. F.3.3.5).

MODIFICATIONS OF THE METHOD

Bane et al. (1996) used the Morris water maze to study the adverse effects of the non-competitive NMDA receptor antagonist dextromorphan on the spatial learning of rats.

Van der Staay (2000) studied the effects of the size of the Morris water tank on spatial discrimination learning in the CFW1 mouse. Mice can best be tested in a small pool, because the time and distance swam to find and escape onto the platform are decreased and the probability of success is increased.

Schmitt and Hiemke (2002) reported that a γ-aminobutyric acid transport inhibitor impairs spatial learning in the Morris water maze.

Winter et al. (2004) determined long-term functional outcome after mild focal cerebral ischemia by tracking swimming performance in a Morris water

maze with the computer-based VideoMot2 system (TSE Systems, Bad Homburg, Germany).

REFERENCES AND FURTHER READING

Bane A, Rojas D, Indermaur K, Bennett T, Avery D (1996) Adverse effects of dextromorphan on the spatial learning of rats in the Morris water maze. Eur J Pharmacol 302:7–12

Connor DJ, Langlais PJ, Thal LJ (1991) Behavioral impairments after lesions in the nucleus basalis by ibotenic acid and quisqualic acid. Brain Res 555:84–90

McNaughton N, Morris RGM (1987) Chlordiazepoxide, an anxiolytic benzodiazepine, impairs place navigation in rats. Behav Brain Res 24:39–46

Morris R (1984) Developments of a water-maze procedure for studying spatial learning in the rat. J Neurosci Meth 11:47–60

Morris RGM (1981) Spatial localization does not require the presence of local cues. Learn Motiv 12:239–260

Morris RGM, Anderson E, Lynch GS, Baudry M (1986) Selective impairment of learning and blockade of long-term potentiation by an *N*-methyl-D-aspartate receptor antagonist, AP5. Nature:319:774–776

Rowan MJ, Culle WK, Moulton B (1990) Buspirone impairment of performance of passive avoidance and spatial learning tasks in the rat. Psychopharmacology 100:393–398

Schmitt U, Hiemke C (2002) Tiagabine, a γ-amino-butyric acid transport inhibitor impairs spatial learning in the Morris water maze. Behav Brain Res 133:391–394

Van der Staay FJ (2000) Effects of the size of the Morris water tank on spatial discrimination learning in the CFW1 mouse. Physiol Behav 68:599–602

Winter B, Bert B, Fink H, Dirnagl U, Endres M (2004) Dysexecutive syndrome after mild cerebral ischemia? Mice learn normally but have deficits in strategic switching. Stroke 35:191–195

E.2.4.6 Staircase Test

PURPOSE AND RATIONALE

The staircase test for evaluating anxiolytic activity was originally described for rats by Thiebot et al. (1973). When introduced into a novel environment, rodents experience a conflict between anxiety and exploratory behavior manifested by increased vigilance and behavioral activity. In the staircase paradigm, step-climbing is purported to reflect exploratory or locomotor activity, while rearing behavior is an index of anxiety state. The number of rearings and steps climbed are recorded in a 5 min period. The dissociation of these parameters is considered to be characteristic for anxiolytic drugs. The test was modified for rapid screening of anxiolytic activity in mice (Simiand et al. 1984).

PROCEDURE

For experiments with mice the staircase is composed of five identical steps 2.5 cm high, 10 cm wide and 7.5 cm deep. The internal height of the walls is constant along the whole length of the staircase. Naive male mice (Charles River strain) with a weight between 18 and 24 g are used. Each animal is used only once. The drug or the standard is administered orally 1 h or 30 min subcutaneously before the test. The animal is placed on the floor of the box with its back to the staircase. The number of steps climbed and the number of rears are counted over a 3-min period. A step is considered to be climbed only if the mouse has placed all four paws on the step. In order to simplify the observation, the number of steps descended is not taken into account. After each test, the box has to be cleaned in order to eliminate any olfactory cues which might modify the behavior of the next animal.

EVALUATION

Twelve mice are used for the untreated control group, each drug group, and for the group receiving the standard. The average number of steps and rearings of the control group is taken as 100%. The values of treated animals are expressed as percentage of the controls.

CRITICAL ASSESSMENT OF THE METHOD

The staircase test has been proven as a simple and reliable method for screening of anxiolytics in several laboratories. Many applications and modifications have been described in the literature (Houri 1985; Steru et al. 1987; Keane et al. 1988; Emmannouil and Quock 1990; Simiand et al. 1993).

REFERENCES AND FURTHER READING

Emmanouil D, Quock RM (1990) Effects of benzodiazepine antagonist, inverse agonist and antagonist drugs in mouse staircase test. Psychopharmacology 102:95–97

Houri D (1985) Staircase test of central nervous system drugs. Pharmacometrics 30:467–479

Keane PE, Simiand J, Morre M, Biziere K (1988) Tetrazepam: A benzodiazepine which dissociates sedation from other benzodiazepine activities. I. Psychopharmacological profile in rodents. J Pharmacol Exper Ther 245:692–698

Porsolt RD, Lenègre A, Avril I, Doumont G (1988) Antagonism by exifone, a new cognitive enhancing agent, of the amnesias induced by four benzodiazepines in mice. Psychopharmacology 95:291–297

Simiand J, Keane PE, Morre M (1984) The staircase test in mice: A simple and efficient procedure for primary screening of anxiolytic agents. Psychopharmacology 84:48–53

Simiand J, Keane PE, Barnouin MC, Keane M, Soubrié P, Le Fur G (1993) Neurospychopharmacological profile in rodents of SR 57746A, a new, potent 5-HT_{1A} receptor agonist. Fundam Clin Pharmacol 7:413–427

Steru L, Thierry B, Chermat R, Millet B, Simon P, Porsolt RD (1987) Comparing benzodiazepines using the staircase test in mice. Psychopharmacology 92:106–109

Thiébot MH, Soubrié P, Simon P, Boissier JR (1973) Dissociation de deux composantes du comportement chez le Rat sous l'effet de psychotropes. Application à l'etude des anxiolytiques. Psychopharmacologia 31:77–90

E.2.4.7 Cork Gnawing Test in the Rat

PURPOSE AND RATIONALE

Cork gnawing behavior in the rat has been proposed as a screening method for buspirone-like anxiolytics by Pollard and Howard (1991).

PROCEDURE

Adult male Evans rats serve as subjects. They are housed 4 per cage on a regular light/dark cycle with free access to food and water except for the period between injection and the end of a test session. For the test session one animal is placed in a stainless steel cage with wire mesh bottom. A session consists of placing the subject in the test cage with a cork stopper weighing between 2–3 g for 30 min. Initially, the amount gnawed is relatively high and variable within and between subjects. After 30 training sessions, the amount is low and stabilized. The test compounds are injected 30 min before the test and food is withdrawn.

EVALUATION

Each cork is weighed to the nearest 0.01 g before and after the session. The average cork loss during the previous control days is taken as baseline and the amount after drug treatment is expressed as percentage of baseline. Buspirone-related compounds as well as benzodiazepines and meprobamate show a dose dependent increase of cork gnawing, but amphetamine, chlorpromazine, imipramine and morphine do not.

CRITICAL ASSESSMENT OF THE METHOD

The test is worthwhile to be mentioned, since buspirone – whose anxiolytic action was discovered during clinical trials to assess possible antipsychotic action and not by use of animal tests for anxiolysis – is active in this test but not in most other classical tests for anxiolytic activity.

REFERENCES AND FURTHER READING

Pollard GT, Howard JL (1991) Cork gnawing in the rat as a screening method for buspirone-like anxiolytics. Drug Dev Res 22:179–187

Pollard GT, Nanry KP, Howard JL (1992) Effects of tandospirone in three behavioral tests for anxiolytics. Eur J Pharmacol 221:297–305

E.2.4.8 Distress Vocalization in Rat Pups

PURPOSE AND RATIONALE

Measurement of ultrasonic vocalization induced by tail-holding in rat pups was proposed as a simple screening method for anxiolytic drugs by Gardner (1985).

PROCEDURE

Wistar rat pups are bred on site and left undisturbed with their mother, except for cage-bedding replacement, until the day of testing. The pups are tested at 9–12 days of age. On the day of testing the pups are separated from their mother and taken in their home cage to the quiet experimental room. In the morning all pups are subjected to handling stress and the magnitude of their ultrasound emission is observed. The stress consists of holding the pup by the base of the tail, between forefinger and thumb of the experimenter, and thus suspending it 5 cm above the bench for 30 s. A prior control recording (30 s) is taken when the pup is held gently in the experimenter's hand, whereby the pups emit only a few ultrasounds. Responses when held by the tail are more than 10 times higher. This entire hand-holding-tail-holding procedure is immediately repeated. Ultrasounds are recorded with suitable detectors with 42 kHz as the center of a 10 kHz recording range. The output of the detectors is fed into pen recorders. The total number of ultrasonic cries in the two sessions of hand holding and the two sessions of tail holding are calculated and used as the control activity of each pup. Any pup producing a total of less than 50 ultrasounds when held by the tail is excluded from the drug study. The pups are kept in the home cage in the test laboratory until the afternoon. Three to four hours after the first test the pups are randomly allocated to several equally seized groups, weighed, marked, and dosed intraperitoneally either with the vehicle or drug and placed back in the home cage. Thirty min after dosing, each pup is subjected to the same handling stress as that used in the morning session, and the total number of sounds produced is calculated in the same way.

EVALUATION

The afternoon response to tail holding is expressed as a factor of the morning response. The mean factor for the saline-treated animals is taken to be 100% in calculations of percentage changes in ultrasound emission by drugs.

CRITICAL ASSESSMENT OF THE METHOD

Anxiolytic benzodiazepines dose-dependent inhibit vocalization. Amitriptyline and haloperidol have no effect. Chlorpromazine, muscimol and prazosin reduce sound at doses which also induce overt sedation.

Therefore, the method can be regarded as relatively specific for anxiolytic activity.

MODIFICATIONS OF THE METHOD

Kehne et al. (2000) used the ULTRAVOX system (Noldus Information Technology, Wageningen, the Netherlands) to detect and quantify separation-induced ultrasonic vocalization in rat pups.

Using this equipment, Siemiatkowski et al. (2001) reported opposite effects of olanzapine and haloperidol in the rat ultrasonic vocalization test.

Molewijk et al. (1996), Griebel et al. (2002), and Steinberg et al. (2002) used maternal separation-induced distress vocalization in **guinea pig** pups to test anxiolytic and antidepressant drugs.

Rupniak et al. (2000) investigated the stress-induced vocalizations by central NK_1 receptors using pharmacological antagonists in guinea pigs, a species with human-like NK_1 receptors, and transgenic NK1R–/– mice.

REFERENCES AND FURTHER READING

Gardner CR (1985) Distress vocalisation in rat pups: A simple screening method for anxiolytic drugs. J Pharmacol Meth 14:181–187

Griebel G, Simiand J, Steinberg R, Jung M, Gully D, Roger P, Geslin M, Scatton B, Maffrand JP, Soubrié P (2002) 4-(2-Chloro-4-methoxy-5-methylphenyl)-*N*-[(1*S*)-2-cyclopropyl-1-(3-fluoro-4-methylphenyl)ethyl]5-methyl-*N*-(2-propynyl)1,3-thiazol-2-amine hydrochloride (SSR125543A), a potent and selective corticotrophin-releasing factor$_1$ receptor antagonist. II. Characterization in rodent models of stress-related disorders. J Pharmacol Exp Ther 301:332–345

Insel TR, Winslow JT (1991) Rat pup ultrasonic vocalizations: an ethologically relevant behaviour response to anxiolytics. In: Olivier B, Mos J, Slangen JL (eds) Animal Models in Psychopharmacology. Advances in Pharmacological Sciences. Birkhäuser Verlag Basel, pp 15–36

Kehne JH, Coverdale S, McCloskey TC, Hoffman DC, Cassella JV (2000) Effect of the CRF$_1$ receptor antagonist, CP 154,526, in the separation-induced vocalization anxiolytic test in rat pups. Neuropharmacology 39:1357–1367

Lister RG (1990) Ethologically-based animal models of anxiety disorders. Pharmac Ther 46:321–340

Molewijk HE, Hartog K, van der Poel AM, Mos J, Olivier B (1996) Reduction of guinea pig pup isolation calls by anxiolytic and antidepressant drugs. Psychopharmacology 128:31–38

Rupniak NMJ, Carlson EC, Harrison T, Oates B, Seward E, Owen S, de Felipe C, Hunt S, Wheeldon A (2000) Pharmacological blockade of substance P (NK_1) receptors attenuates neonatal vocalization in guinea-pigs and mice. Neuropharmacology 39:1413–1421

Schipper J, Tulp MThM, Berkelmans B, Mos J, Van der Heijden JAM, Olivier B (1991) Preclinical pharmacology of flesinoxan: A potential anxiolytic and antidepressant drug. Human Psychopharmacol 6:53–61

Siemiatkowski M, Maciejak P, Sienkiewicz-Jarosz, Czlonkowska AI, Szyndler J, Gryczyńska A, Plazńik A (2001) Opposite effects of olanzapine and haloperidol in rat ultrasonic vocalization test. Pol J Pharmacol 53:669–673

Steinberg R, Alonso R, Rouquier L, Desvignes C, Michaud JC, Cudennec A, Jung M, Simiand J, Griebel G, Emonds-Alt X, Le Fur G, Soubrie P (2002) SSR240600 [(R)-2-(1-[2-[4-[2-[3,5-bis(trifluoromethyl)phenyl]acetyl]-2-(3,4-dichlorophenyl)-2-morpholinyl]ethyl]-4-piperidinyl)-2-methylpropanamide], a centrally active nonpeptide antagonist of the tachykinin neurokinin 1 receptor: II. Neurochemical and behavioral characterization. J Pharmacol Exp Ther 303(3):1180–1188

Tulp M, Olivier B, Schipper J, van der Poel G, Mos J, van der Heyden J (1991) Serotonin reuptake blockers: Is there preclinical evidence for their efficacy in obsessive-compulsive disorder? Hum Psychopharmacol 6:S63–S71

van der Poel AM, Molewijk E, Mos J, Olivier B (1991) Is clonidine anxiogenic in rat pups? In: Olivier B, Mos J, Slangen JL (eds) Animal Models in Psychopharmacology. Advances in Pharmacological Sciences. Birkhäuser Verlag Basel, pp 107–116

E.2.4.9 Schedule Induced Polydipsia in Rats

PURPOSE AND RATIONALE

Food deprived rats exposed to a procedure in which food is delivered intermittently will drink large amounts of water if given the opportunity to do so. This behavioral phenomenon is termed schedule-induced polydipsia and is an example of a more general class of behaviors termed adjunctive behaviors (Falk 1971; Pellon and Blackman 1992). Adjunctive behaviors have been cited as potential animal models of human obsessive-compulsive disorders (Pitman 1989).

PROCEDURE

Male Wistar rats weighing 180–250 g are individually housed at a 12 h/12 h light/dark cycle for a 1 week acclimation period with free access to food and water. Then they are placed on a restricted diet which maintains 80% of their free feeding body weight. To induce polydipsia, rats are placed in test chambers housed in sound attenuated boxes where a pellet dispenser automatically dispenses two 45 mg pellets on a fixed time 60-s (FT-60s) feeding schedule over a 150 min test session. Water is available at all times in the test chambers. After 4 weeks exposure to the FT-60s feeding schedule, approximately 80% of the rats meet the predetermined criterion for water consumption (greater than 60 ml water per session) and are considered to have polydipsic behavior.

Rats receive the test compounds in various doses daily or the vehicle intraperitoneally 60 min prior to testing. They are tested once a week to assess schedule induced polydipsia. Water bottles are weighed before and after the 150-min test sessions.

EVALUATION

The experimental data comparing the effects of chronic administration of compounds on schedule-induced polydipsia are analyzed with the Mann Whitney *U*-test.

MODIFICATIONS OF THE METHOD

Yadin et al. (1991) proposed spontaneous alternation behavior in rats as an animal model for obsessive-compulsive disorder. Food-deprived rats were run on a T-maze in which both a white and a black goal box were equally baited with a small amount of chocolate milk. Each rat was given 7 trials every other day during which it was placed in the start box and allowed to make a choice. The mean number of choices until an alternation occurred was recorded. After a baseline of spontaneous alternation was achieved the rats were treated with the non-selective serotonin agonist 5-methoxy-N,N-dimethyltryptamine (5-MeODMT) (1.25 mg/kg i.p.) or the selective 5-HT_{1A} agonist 8-hydroxy-2-(di-n-propylamino)-tetralin hydrobromide (8-OH-DPAT) (2 mg/kg i.p.) which both disrupted the spontaneous alternation. A course of chronic treatment (2 × 5 mg/kg for 21 days) with the selective 5-HT uptake blocking agent fluoxetine had a protective effect on the 5-MeODMT-induced disruption of spontaneous alternation behavior. The authors speculated that serotonergic manipulations of spontaneous alternation may be a simple animal model for the perseverative symptoms or indecisiveness seen in patients with obsessive-compulsive disorder.

Bös et al. (1997) and Martin et al. (1998) tested agonists of $5HT_{2C}$ receptors in the schedule-induced polydipsia task in rats and proposed them as improved therapeutics for obsessive compulsive disorder.

REFERENCES AND FURTHER READING

Bös M, Jenck F, Martin JR, Moreau JL, Sleight AJ, Wichmann J, Widmer U (1997) Novel agonists of $5HT_{2C}$ receptors. Synthesis and biological evaluation of substituted 2-(indol-1-yl)-1-methylethylamines and 2-(indeno[1,2-*b*]pyrrol-1-yl)-1-methylethylamines. Improved therapeutics for obsessive compulsive disorder. J Med Chem 40:2762–2769

Didriksen M, Olsen GM, Christensen AV (1993) Effect of clozapine upon schedule-induced polydipsia (SIP) resembles neither the actions of dopamine D1 nor D2 receptor blockade. Psychopharmacol (Berlin) 113:28–34

Falk JL (1971) The nature and determinants of adjunctive behavior. Physiol Behav 6:577–588

Martin JR, Bös M, Jenck F, Moreau JL, Mutel V, Sleight AJ, Wichmann J, Andrews SJ Berendsen HHG, Broekkamp CLE, Ruigt GSF, Köhler C, van Delft AML (1998) 5-HT_{2C} receptor agonists: pharmacological characteristics and therapeutic potential. J Pharmacol Exp Ther 286:913–924

Pellon R, Blackman DE (1992) Effects of drugs on the temporal distribution of schedule-induced polydipsia in rats. Pharmacol Biochem Behav 43:689–695

Pitman RK (1989) Animal models of compulsive behavior. Biol Psychiatry 26:189–198

Woods A, Smith C, Szewczak M, Dunn RW, Cornfeldt M, Corbett R (1993) Selective re-uptake inhibitors decrease schedule-induced polydipsia in rats: a potential model for obsessive compulsive disorder. Psychopharmacology 112:195–198

Woods-Kettelberger AT, Smith CP, Corbett R, Szewczak MR, Roehr JE, Bores GM, Klein JT, Kongsamut S (1996) Besipirdine (HP 749) reduces schedule-induced polydipsia in rats. Brain Res Bull 41:125–130

Yadin E, Friedman E, Bridger WH (1991) Spontaneous alternation behavior: An animal model for obsessive-compulsive disorder? Pharmacol Biochem Behav 40:311–315

E.2.4.10 Four Plate Test in Mice

PURPOSE AND RATIONALE

The four plate test in mice has been described by Aron et al. (1971), Boissier et al. (1968) as a method for the rapid screening of minor tranquilizers.

PROCEDURE

The test box has the shape of a rectangle (25 × 18 × 16 cm). The floor is covered with 4 identical rectangular metal plates (8 × 11 cm) separated from one another by a gap of 4 mm. The plates are connected to a source of continuous current which applies to 2 adjacent plates a mild electrical shock of 0.35 mA for 0.5 s. This evokes a clear flight reaction of the animals.

Adult male Swiss albino mice, weighing 17 to 23 g, are randomly divided into different groups. Thirty min before the test the animals are injected intraperitoneally with the test drug or the vehicle.

At the beginning of the test, the mouse is gently dropped onto a plate and is allowed to explore the enclosure for 15 s. After this, every time the animal crosses from one plate to another, the experimenter electrifies the whole floor for 0.5 s, which evokes a clear flight-reaction of the mouse which often crosses 2 or 3 plates. If it continues running, no new shock is delivered during the following 3 min.

EVALUATION

The number of times the apparatus is electrified is counted each minute for 10 min. The delivery of shocks decreases dramatically the motor activity. The number of shocks received during the first min is taken as parameter. This number is increased by minor tranquilizers, such as benzodiazepines, but not by neuroleptics and psychoanaleptics.

CRITICAL ASSESSMENT OF THE METHOD

The test is of value to differentiate minor tranquilizers, such as benzodiazepine anxiolytics, from neuroleptics. However, some stimulants (e. g. amphetamine) produce an increase in punished plate crossings and some anxiolytics do not.

REFERENCES AND FURTHER READING

Aron C, Simon P, Larousse C, Boissier JR (1971) Evaluation of a rapid technique for detecting minor tranquilizers. Neuropharmacol 10:459–469

Boissier JR, Simon P, Aron C (1968) A new method for rapid screening of minor tranquilizers in mice. Eur J Pharmacol 4:145–151

Hascoe M, Bourin M, du Tertre C (1997) Influence of prior experience on mice behavior using the four-plate test. Pharmacol Biochem Behav 58:1131–1138

Lenègre A, Chermat R, Avril I, Stéru L, Porsolt RD (1988) Specificity of Piracetam's anti-amnesic activity in three models of amnesia in the mouse. Pharmacol Biochem Behav 29:625–629

Simon P (1970) Les Anxiolytiques. Possibilités d'étude chez l'animal. Actualités pharmacol. 23:47–78

Stephens DN, Schneider HH, Kehr W, Andrews JS, Rettig K-J, Turski L, Schmiechen R, Turner JD, Jensen LH, Petersen EN, Honore T, Bondo Jansen J (1990) Abecarnil, a metabolically stable, anxioselective β-carboline acting at benzodiazepine receptors. J Pharmacol Exper Ther 253:334–343

E.2.4.11 Foot-shock-Induced Freezing Behavior in Rats

PURPOSE AND RATIONALE

Footshock-induced freezing behavior in rats has been proposed as a model for anxiolytics by Conti et al. (1990).

PROCEDURE

Male Sprague-Dawley rats with a weight between 200 and 350 g are used. The animals receive a single i.p. injection of the test compound or the vehicle 30 min prior to being placed in a standard conditioning chamber (e. g., Coulborn Instruments) for a 6.5 min session. Two and 2.5 min after the start of the session, a scrambled footshock (0.5 mA, 0.5 s) is delivered through the grid floor of the chamber. Using an assembly of push buttons interfaced with a computer, an observer monitors the amount of time each animal spends engaged in the following mutually exclusive behaviors:

- Freezing: immobility with rigid body posture
- Sedated posture: sitting or sleeping
- Small exploratory movements: movements involving the torso or front paws only, vertical movements of the head, or sniffing.
- Locomotion: activity involving hind paws, grooming or rearing.

Frequency of rearing is also counted. All behaviors are monitored for the entire 6.5 min session.

EVALUATION

Duration of foot-shock induced freezing after the second shock is taken as the critical parameter. Time spent in freezing posture after administration of test compounds is compared with the controls. Anxiolytics like diazepam and buspirone show dose-dependent effects, but not haloperidol.

CRITICAL ASSESSMENT OF THE METHOD

The method seems to discriminate anxiolytics including buspirone from other centrally acting drugs.

MODIFICATIONS OF THE METHOD

Footshock-induced ultrasonic vocalization has been suggested as another model of anxiety (Tonoue et al. 1986; Kaltwasser 1990; Miczek et al. 1991; De Vry et al. 1993; Nielsen and Sánchez 1995; Schreiber et al. 1998). Test cages ($22 \times 22 \times 22$ cm) made of grey Perspex are equipped with a metal grid floor (distance between the bars = 1 cm). Electric footshocks are delivered from a 12 bit programmable shock source and ultrasounds are picked up by a microphone (range 18–26 Hz) placed in the center of the cage lid. The total vocalization time is measured. The rats are placed individually in the test cages and immediately receive a series of 0.5 mA inescapable footshocks each of 1 s duration with a shock interval of 5 s. The vocalization is measured for a 10 min period starting 1 min after the last shock. Drugs or saline are given subcutaneously 30 min before the test.

REFERENCES AND FURTHER READING

Conti LH, Maciver CR, Ferkany JW, Abreu ME (1990) Footshock-induced freezing behavior in rats as a model for assessing anxiolytics. Psychopharmacology 102:492–497

De Vry J, Benz U, Traber J (1993) Shock-induced ultrasonic vocalization in young adult rats: a model for testing putative anti-anxiety drugs. Eur J Pharmacol 249:331–339

Kaltwasser MT (1990) Startle-inducing stimuli evoke ultrasonic vocalization in the rat. Physiol Behav 48:13–17

Miczek KA, Tornatzky W, Vivian J (1991) Ethology and neuropharmacology: Rodent ultrasounds. In: Oliver B, Mos J, Sangar J (eds) Animal Models in Psychopharmacology. Birkhäuser Verlag Basel, pp 409–427

Nielsen CK, Sánchez C (1995) Effect of chronic diazepam treatment on footshock-induced ultrasonic vocalization in adult male rats. Pharmacol Toxicol 77:177–181

Schreiber R, Melon C, De Vry J (1998) The role of 5-HT receptor subtypes in the anxiolytic effects of selective serotonin

reuptake inhibitors in the rat ultrasonic vocalization test. Psychopharmacol 135:383–391
Tonoue T, Ashida A, Makino H, Hata H (1986) Inhibition of shock-elicited ultrasonic vocalization by opioid peptides in the rat: A psychotropic effect. Psychoneuroendocrinology 11:177–184

E.2.4.12 Experimental Anxiety in Mice

PURPOSE AND RATIONALE

Ogawa et al. (1966, 1990, 1993) designed a communication box to induce experimental anxiety in mice by employing intraspecies emotional communication. The inside of the communication box was divided into foot-shock and non-foot-shock compartments by transparent plastic boards. The animals, which were individually placed into each compartment, were unable to make physical contact with one another, but were able to receive other cues such as visual, auditory and olfactory sensations. During the foot shock period, the animals placed in the non-foot-shock compartments were exposed to the emotional cues from foot-shocked animals, such as shrieks, smell of feces or urine, and jumping response.

PROCEDURE

The floor of the communication box is equipped with grids for electric shock. The inside is divided into small compartments (10 × 10 cm), consisting of foot-shock compartments with a grid floor and non-foot-shock compartments with a grid floor covered by transparent plastic boards. The foot-shock compartments are arranged such as to surround the non-foot shock compartments.

The experimental groups consist of the following 3 groups: sender group, responder group, and food-yoked group to responder. Sender animals receive a foot shock of 10-s duration at intervals of 50 s for 3 h. The electric current for the shock is increased stepwise from 1.6 mA to 2.0 mA at a rate of 0.2 mA per 1 h. Responders are exposed daily to the emotional responses of sender animals, 3 h per day for 3 days. Sender animals are changed daily to naive mice to prevent a reduced emotional response to foot shock based on adaptation or learned helplessness due to repeated exposure. Both sender and responder animals are placed individually in each compartment of the communication box 15 min before beginning of the shock period. On day-1, responder animals are returned to their home cages after the 3-h foot shock period. On day-2, after completing the foot-shock period, they are transferred to metal cages and are housed in the cages with 4 animals per cage under food-deprivation condition. Food-yoked control animals are maintained to the metal cage during the foot-shock period under the aggregated housing condition (5 animals each) and then they are returned to the home cages after the foot shock period. From beginning of the day-2 experiment to completion of the day-3 experiment, they are maintained in the metal cages under aggregating housing. On day-3, just after completing the foot-shock period, the responders are sacrificed by chloroform, and their stomachs are removed. The stomachs are visually inspected for lesions.

Drugs are administered orally at different doses either with a single dose on day-3 or daily 30 min before the shock period.

EVALUATION

Data are reported as the incidence of mice with gastric lesions characterized by slight erosions or bleeding. Active anxiolytics reduce the incidence of gastric ulcers found in food-deprived animals. The incidence in food-yoked animals is much lower. The data are analyzed by Fisher's exact probability test.

REFERENCES AND FURTHER READING

Ogawa N, Kuwahara K (1966) Psychophysiology of emotion: communication of emotion. Japan J Psychosom Med 6:352–357
Ogawa N, Hara C, Ishikawa M (1990) Characteristic of sociopsychological stress induced by the communication box method in mice and rats. In: Manninen O (ed) Environmental Stress, ACES Publishing Ltd., Tampele, pp 417–427
Ogawa N, Hara C, Takaki S (1993) Anxiolytic activity of SC-48274 compared with those of buspirone and diazepam in experimental anxiety models. Japan J Pharmacol 61:115–121

E.2.4.13 mCPP-Induced Anxiety in Rats

PURPOSE AND RATIONALE

The metabolite of the antidepressant drug trazodone 1-(3-chlorphenyl)piperazine (= mCPP), classified as 5-HT_{1C} agonist (Rocha et al. 1993; Gibson et al. 1996) or 5-$HT_{1B/2C}$ agonist (Dryden et al. 1996), has been shown to be anxiogenic both in man and in rats (Curzon et al. 1991). The compound induces hypophagia (Samanin et al. 1979; Dryden et al. 1996; Yamada et al. 1996) and hypolocomotion (Kennett et al. 1996, 1997a), inhibits social interaction in rats, diminishes exploratory activity of rats in the open field test (Czyrak et al. 1994; Meert et al. 1997) and in the light-dark box test (Bilkei-Gorzo et al. 1998), induces hyperthermia (Aulakh et al. 1995; Kennett et al. 1997b)

and reduces ultrasound-induced defensive behavior in the rat (Beckett et al. (1996). Antagonism against these symptoms has been proposed as a screening model for anxiolytic drugs (Bilkei-Gorzo et al. 1996, 1998; Wallis and Lal 1998).

PROCEDURE

Male Sprague Dawley rats (220–250 g) are housed in groups of 6 under a 12 h light/dark cycle with free access to food and water.

mCPP-Induced Locomotion

Rats are placed in a room adjacent top the experimental room on the day of the procedure. They are dosed either orally 1 h, or i.p. 30 min before the locomotion test with test compound or vehicle, and injected 20 min before the test with 7 mg/kg mCPP i.p. or saline in groups of four. Rats are returned to their home cages after dosing. At 0 h they are each placed in automated locomotor activity cages made of black Perspex with a clear Perspex lid and sawdust covered floor under red light for 10 min. During this time, locomotion is recorded by means of alternately breaking two photocell beams traversing opposite ends of the box 3.9 cm above floor level.

mCPP-Induced Hypophagia

Rats are individually housed on day 1 and on day 3 they are deprived of food. Twenty-three hours later, the are orally treated with the test drug or vehicle and returned to their home cages. Forty min later, they are given 5 mg/kg mCPP or saline i.p. and again returned to their home cages. After a further 20 min, weighted amounts of their normal food pellets are placed in their food hoppers and the amount remaining after 1 h is measured.

EVALUATION

The effect of the test compound on mCPP-induced hypolocomotion is determined by one-way ANOVA and Newman-Keuls test. The dose producing 50% disinhibition of mCPP is also estimated. Feeding test data are subjected to one-way ANOVA and Dunnett's test.

MODIFICATIONS OF THE METHOD

Griebel et al. (1991) described neophobic and anxious behavior in mice induced by m-CPP.

Czyrak et al. (1994) measured the antagonism of anti-psychotics against the mCPP-induced hypothermia in mice.

REFERENCES AND FURTHER READING

Aulakh CS, Mazzola-Pomietto P, Murphy DL (1995) Long-term antidepressant treatments alter 5-HT_{2A} and 5-HT_{2C} receptor mediated hyperthermia in Fawn-Hooded rats. Eur J Pharmacol 282:65–70

Beckett SRG, Aspley S, Graham M, Marsden CA (1996) Pharmacological manipulation of ultrasound induced defense behaviour in the rat. Psychopharmacology 127:384–390

Bilkei-Gorzo A, Gyertyan I, Szabados T (1996) mCPP-induced anxiety – A potential new method for screening anxiolytic drugs. Neurobiology 4:253–255

Bilkei-Gorzo A, Gyertyan I, Levay G (1998) mCPP-induced anxiety in the light-dark box in rats – A new method for screening anxiolytic activity. Psychopharmacology 136:291–298

Curzon G, Gibson EL, Kennedy AJ, Kennett GA, Sarna GS, Whitton P (1991) Anxiogenic and other effects of mCPP, a 5-HT_{1C} agonist. In: Briley M, File SE (eds) New Concepts in Anxiety. McMillan Press Ltd., London, pp 154–167

Czyrak A, Skuza G, Rogóz Z, Frankiewicz T, Maij J (1994) Pharmacological action of zotepine and other antipsychotics on central 5-hydroxytryptamine receptor subtypes. Arzneim Forsch/Drug Res 44:113–118

Dryden S, Wang Q, Frankish HM, Williams G (1996) Differential effects of the 5-$HT_{1B/2C}$ receptor agonist mCPP and the 5-HT_{1A} agonist flexinoxan on neuropeptide Y in the rat: Evidence that NPY may mediate serotonin's effects on food intake. Peptides 17:943–949

Gibson EL, Barnfield AMC, Curzon G (1996) Dissociation of effects of chronic diazepam treatment and withdrawal on hippocampal dialysate 5-HT and mCPP-induced anxiety in rats. Behav Pharmacol 7:185–193

Griebel G, Misslin R, Pawloaski M, Vogel E (1991) m-Chlorophenylpiperazine enhances neophobic and anxious behaviour in mice. NeuroReport 2:627–629

Kennett GA, Whitton P, Shah K, Curzon G (1989) Anxiogenic-like effects of mCPP and TFMPP in animal models are opposed by 5-HT_{1C} receptor antagonists. Eur J Pharmacol 164:445–454

Kennett GA, Wood MD, Bright F, Cilia J, Piper DC, Gager T, Thomas D, Baxter GS, Forbes LT, Ham P, Blackburn TP (1996) *In vitro* and *in vivo* profile of SB 206553, a potent 5-HT_{2C}/5-HT_{2B} receptor antagonist with anxiolytic-like properties. Br J Pharmacol 117:427–434

Kennett GA, Wood MD, Bright F, Trail B, Riley G, Holland V, Avenell KY, Stean T, Upton N, Bromidge S, Forbes IT, Brown AM, Middlemiss DN, Blackburn TP (1997a) SB 242084, a selective and brain penetrant 5-HT_{2C} receptor antagonist. Neuropharmacol 36:609–620

Kennett GA, Ainsworth K, Trail B, Blackburn TP (1997b) BW 723C86, a 5-HT_{2B} receptor agonist, causes hyperphagia and reduced grooming in rats. Neuropharmacol 36:233–239

Meert TF, Melis W, Aerts N, Clinke G (1997) Antagonism of meta-chlorphenylpiperazine-induced inhibition of exploratory activity in an emergence procedure, the open field test, in rats. Behav Pharmacol 8:353–363

Robertson DW, Blooquist W, Wong DT, Cohen ML (1992) MCPP but not TFMPP is an antagonist at cardiac 5-HT_3 receptors. Life Sci 50:599–605

Rocha B, di Scala G, Jenk F, Moreau JL, Sandner G (1993) Conditioned place aversion induced by 5-HT_{1C} receptor antagonists. Behav Pharmacol 4:101–106

Samanin R, Mennini T, Ferraris A, Bendotti C, Borsini F, Garattini S (1979) m-Chlorophenylpiperazine: A central sero-

tonin agonist causing powerful anorexia in rats. Naunyn-Schmiedeberg's Arch Pharmacol 308:159–163
Wallis CJ, Lal H (1998) A discriminative stimulus produced by 1-(3-chlorophenyl)-piperazine (mCPP) as a putative animal model of anxiety. Progr Neuropsychopharmacol Biol Psychiatry 22:547–565
Yamada J, Sugimoto Y, Yoshikawa T, Horisaka K (1996) Effects of adrenomedullation and adrenalectomy on the 5-HT_2 receptor agonists DOI- and mCPP-induced hypophagia in rats. Neurosci Lett 209:113–116

E.2.4.14 Acoustic Startle Response in Rats

PURPOSE AND RATIONALE

The acoustic startle reflex is a relatively simple behavior that occurs naturally in mammals and is affected by a variety of treatments. It consists of a series of rapid movements beginning at the head and moving caudally involving contraction and extension of major muscle groups in response to auditory stimuli with a rapid onset, or rise time. Responses are graded in amplitude in relation to stimulus intensity, and may show habituation and sensitization. Startle response can be used to determine sites and mechanisms of drug action (Davis 1982).

PROCEDURE

Male Wistar rats weighing about 200 g are used. Acoustic startle reflexes are measured in a specially build apparatus, e. g., Coulborn Instruments Acoustic Response Test System or TSE Systems, Bad Homburg, Germany. The animals are individually placed in $8 \times 8 \times 16$ cm open air cages that restrict locomotion but do not immobilize the animal, and are placed on one of four platforms within a sound-attenuating acoustic chamber. A ventilating fan provides an ambient noise level. Acoustic stimuli consist of white noise bursts lasting 20 ms at 98 dB and 124 dB SPL. Simultaneously with the rapid onset of each stimulus, the animal's physical movement within the cage on the platform is measured for 200 ms as an electrical voltage change via a strain gauge which is converted to grams of weight change following analog to digital conversion. Data are recorded automatically by an interfaced microcomputer.

Pre-tests are performed with all animals to obtain control values. The animals are treated 2 h prior the experiment with test drugs or vehicle given orally or subcutaneously.

EVALUATION

The results are given as percentage of the change, related to the values obtained in the pre-test and assessed by a one-way ANOVA, followed by Dunnett's test when appropriate.

MODIFICATIONS OF THE METHOD

The test has been modified in various ways, e. g., inhibition by a prepulse (Keith et al. 1991; Rigdon and Viik 1991; Taylor et al. 1995) or fear-induced potentiation (Davis 1986, 1992).

Schulz et al. (1996) performed acoustic startle experiments in rats with a potent and selective nonpeptide antagonist of the corticotropin releasing factor receptors.

Walker and Davis (1997) found that the amplitude of acoustic startle response in rats was increased by high illumination levels.

Devices to register the intensity of fear-potentiated startle response in rats were described by Hijzen et al. (1995).Yilmazer-Hanke et al. (2002) studied fear-potentiated startle and exploration-related anxiety in inbred Roman high- and low-avoidance rats.

REFERENCES AND FURTHER READING

Acri JB, Grunberg NE, Morse DA (1991) Effects of nicotine on the acoustic startle reflex amplitude in rats. Psychopharmacology 104:244–248
Astrachan DI, Davis M (1981) Spinal modulation of the acoustic startle response: the role of norepinephrine, serotonin and dopamine. Brain Res 206:223–228
Cadet JL, Kuyatt B, Fahn S, De Souza EB (1987) Differential changes in ^{125}I-LSD-labeled 5-HT-2 serotonin receptors in discrete regions of brain in the rat model of persistent dyskinesias induced by iminodipropionitrile (IDPN): evidence from autoradiographic studies. Brain Res 437:383–386
Davis M (1980) Neurochemical modulation of sensory-motor reactivity: Acoustic and tactile startle reflexes. Neurosci Biobehav Rev 4:241–263
Davis M (1982) Agonist-induced changes in behavior as a measure of functional changes in receptor sensitivity following chronic antidepressant treatment. Science 18:137–147
Davis M (1986) Pharmacological and anatomical analysis of fear conditioning using the fear-potentiated startle paradigm. Behav Neurosci 100:814–824
Davis M (1992) The role of the amygdala in fear-potentiated startle: implications for animal models of anxiety. Trends Pharmacol Sci 13:35–41
Davis M, Astrachan DI, Kass E (1980) Excitatory and inhibitory effects of serotonin on sensomotoric reactivity measured with acoustic startle. Science 209:521–523Hijzen TH, Woudenberg F, Slangen JL (1990) The long-term effects of diazepam and pentylenetetrazol on the potentiated startle response. Pharmacol Biochem Behav 36:35–38
Hijzen TH, Houtzager SWJ, Joordens RJE, Olivier B, Slangen JL (1995) Predictive validity of the potentiated startle response as a behavioral model for anxiolytic drugs. Psychopharmacol 118:150–154
Keith VA, Mansbach RS, Geyer MA (1991) Failure of haloperidol to block the effects of phencyclidine and dizocilpine on prepulse inhibition of startle. Biol Psychiatry 30:557–566
Mansbach RS, Markou A, Patrick GA (1994) Lack of altered startle response in rats following termination of self-ad-

ministered or noncontingently infused cocaine. Pharmacol Biochem Behav 48:453–458
Rigdon GC, Viik K (1991) Prepulse inhibition as a screening test for potential antipsychotics. Drug Dev Res 23:91–99
Schulz DW, Mansbach RS, Sprouse J, Braselton JP, Collins J, Corman M, Dunaikis A, Faraci S, Schmidt AW, Seeger T, Seymour P, Tingley III FD, Winston EN, Chen YL, Heym J (1996) CP-154–526: A potent and selective nonpeptide antagonist of corticotropin releasing factor receptors. Proc Natl Acad Sci, USA 93:10477–10482
Taylor MK, Ison JR, Schwarzkopf SB (1995) Effects of single and repeated exposure to apomorphine on the acoustic startle reflex and its inhibition by a visual prepulse. Psychopharmacology 120:117–127
Vale AL, Green S (1996) Effects of chlordiazepoxide, nicotine and d-amphetamine in the rat potentiated startle model of anxiety. Behav Pharmacol 7:138–143
Varty GB, Higgins GA (1994) Differences between three rat strains in sensitivity to prepulse inhibition of an acoustic startle response: influence of apomorphine and phencyclidine pre-treatment. J Psychopharmacol 8:148–156
Vivian JA, Farrell WJ, Sapperstein SB, Miczek KA (1994) Diazepam withdrawal: effects of diazepam and gespirone on acoustic startle-induced 22 kHz ultrasonic vocalizations. Psychopharmacology 114:101–108
Walker DL, Davis M (1997) Anxiogenic effects of high illumination levels assessed with the acoustic startle response in rats. Biol Psychiatry 42:461–471
Weiss GT, Davis M (1976) Automated system for acquisition and reduction of startle response data. Pharmacol Biochem Behav 4:713–720
Yilmazer-Hanke DN, Faber-Zuschratter H, Linke R, Schwegler H (2002) Contribution of amygdala neurons containing peptides and calcium-binding proteins to fear-potentiated startle and exploration-related anxiety in inbred Roman high- and low-avoidance rats. Eur J Neurosci 15:1206–1218
Young BJ, Helmstetter FJ, Rabchenuk SA, Leaton RN (1991) Effects of systemic and intra-amygdaloid diazepam on long-term habituation of acoustic startle in rats. Pharmacol Biochem Behav 39:903–909
Zajaczkowski W, Górka Z (1993) The effects of single and repeated administration of MAO inhibitors on acoustic startle response in rats. Pol J Pharmacol 45:157–166

E.2.4.15 Unconditioned Conflict Procedure (Vogel Test)

PURPOSE AND RATIONALE

Vogel et al. (1971) described a simple and reliable conflict procedure for testing anti-anxiety agents. Thirsty, naive rats were administered shocks while licking water.

PROCEDURE

The apparatus is a clear Plexiglas box (38 × 38 cm) with a black Plexiglas compartment (10 × 10.5 cm) attached to one wall and an opening from the large box to the small compartment. The entire apparatus has a stainless-steel grid floor. A water bottle with a metal drinking tube is fitted to the outside of the small compartment, so that the tube extended into the box at a height 3 cm above the grid. Rats lick in bursts with a relatively constant rate of 7 licks per sec. A drinkometer circuit is connected between the drinking tube and the grid floor of the apparatus, so that the rat completes the circuit whenever it licks the tube. Shock is administered to the feet of the animal by switching the connections to the drinking tube and grids from the drinkometer to a shocker which applies an unscrambled shock between the drinking tube and the grid floor.

Naive adult male rats are used. Thirty min after intraperitoneal injection, the rat is placed in the apparatus and allowed to find the drinking tube and to complete 20 licks before shock (available at the tube for 2 s) is administered. The rat controls shock duration by withdrawing from the tube. A 3-min timer is automatically started after the termination of the first shock. During the 3-min period, shocks are delivered following each twentieth lick. The number of shocks delivered during the 3-min session is recorded for each animal.

EVALUATION

The number of shocks received after treatment is compared with untreated animals. Benzodiazepines increase dose-dependent the number of shocks. Barbiturates in low doses and meprobamate, but not d-amphetamine or scopolamine, are active in this test.

CRITICAL ASSESSMENT OF THE METHOD

The method is far more simple and less time consuming than the methods using conflict behavior after intensive training. The specificity may be less than that of the Geller paradigm.

MODIFICATIONS OF THE METHOD

The method and the apparatus have been modified by Patel and Malick (1982), Patel et al. (1983), Sanger et al. (1985), Langen et al. (2005), and Mathiasen and Mirza (2005).

Miklya and Knoll (1988) showed an increase of sensitivity of the method using rats deprived of food but supplied with tap water ad libitum for 96 h, than fed with dry pellets and punished for drinking during feeding. The punished drinking test has not only be used for identifying and studying anxiolytic agents, but also as a method for measuring anxiogenic activity (Uyeno et al. 1990).

La Marca and Dunn (1994) studied α_2-antagonists after intravenous administration in the Vogel lick-shock conflict paradigm.

REFERENCES AND FURTHER READING

La Marca S, Dunn RW (1994) The α_2 antagonists idazoxan and rauwolscine but not yohimbine or piperoxan are anxiolytic in the Vogel lick-shock paradigm following intravenous administration. Life Sci 54:179–184

Langen B, Egerland U, Bernöster K, Dost R, Unverferth K, Rundfeldt C (2005) Characterization in rats of the anxiolytic potential of ELB139 [1-(4-chlorphenyl)-4-piperidin-1-yl-1,5-dihydro-imidazol-2-on], a new agonist at the benzodiazepine binding site of the $GABA_A$ receptor. J Pharmacol Exp Ther 314:717–724

Mathiasen L, Mirza NR (2005) A comparison of chlordiazepoxide, bretazenil, L838,417 and zolpidem in a validated mouse Vogel conflict test. Psychopharmacology 182:475–484

Miklya I, Knoll J (1988) A new sensitive method which unlike the VOGEL test detects the anxiolytic effect of tofisopam. Pol J Pharmacol Pharm 40:561–572

Patel J, Malick JB (1982) Pharmacological properties of tracazolate: a new non-benzodiazepine anxiolytic agent. Eur J Pharmacol 78:323

Patel JB, Martin C, Malick JB (1983) Differential antagonism of the anticonflict effects of typical and atypical anxiolytics. Eur J Pharmacol 86:295–298

Przegalinski E, Chojnacka-Wojcik E, Filip M (1992) Stimulation of $5\text{-}HT_{1A}$ receptors is responsible for the anticonflict effect of ipsapirone in rats. J Pharm Pharmacol 44:780–782

Sanger DJ, Joly D, Zivkovic B (1985) Behavioral effects of non-benzodiazepine anxiolytic drugs: A comparison of CGS 9896 and zopiclone with chlordiazepoxide. J Pharm Exp Ther 232:831–837

Uyeno ET, Davies MF, Pryor GT, Loew GH (1990) Selective effect on punished versus unpunished responding in a conflict test as the criterion for anxiogenic activity. Life Sci 47:1375–1382

Vogel JR, Beer B, Clody DE (1971) A simple and reliable conflict procedure for testing anti-anxiety agents. Psychopharmacologia (Berl.) 21:1–7

E.2.4.16 Novelty-Suppressed Feeding

PURPOSE AND RATIONALE

Placing a hungry rat into an unfamiliar environment with access to food results in a suppression of feeding behavior relative to the condition when the test environment is familiar. This effect has been termed hyponeophagia (Shephard and Broadhurst 1982) and occurs because of the novelty of the test environment. The avoidance of novel foods is termed food neophobia. Both hyponeophagia and food neophobia have been assumed to measure emotionality or anxiety by eliciting a conflict situation arising from a fear of the novel setting and foods, and the drive to eat (Porschel 1971). A number of investigators have adopted these paradigms to explore the behavioral effects of anxiolytics (Soubrie et al. (1975;Cooper and Crummy 1978; Borsini et al. 1993).

PROCEDURE

The testing apparatus consists of individual Plexiglas open fields, $76 \times 76 \times 46$ cm. Thirty Purina lab chow pellets are placed in a pile directly in the center of the open field.

Animals are handled for 3 weeks prior the behavioral testing. Forty-eight hours prior to testing, all food is removed from the home cage, although water is still available ad lib. One h prior to testing, animals receive an intraperitoneal injection of test drugs or vehicle. At the time of testing, the animals are placed into individual open fields containing the food, and the latency to begin eating is measured. If the animal has not eaten within 720 s, the test is terminated and the animal is assigned a latency score of 720 s.

EVALUATION

The data are analyzed by a one-way analysis of variance followed by Fisher Last Significant Difference post hoc tests. An anxiolytic effect is defined as a significant decrease in mean latency to begin eating compared with vehicle controls.

CRITICAL ASSESSMENT OF THE METHOD

The test has the advantage of simplicity for screening procedures.

REFERENCES AND FURTHER READING

Bodnoff SR, Suranyi-Cadotte B, Aitken DH, Quirion R, Meaney MJ (1988) The effects of chronic antidepressant treatment in an animal model of anxiety. Psychopharmacology 95:298–302

Bodnoff SR, Suranyi-Cadotte B, Quirion R, Meaney MJ (1989) A comparison of the effects of diazepam versus typical and atypical anti-depressant drugs in an animal model of anxiety. Psychopharmacology 97:277–279

Borsini F, Brambilla A, Cesana R, Donetti A (1993) The effect of DAU 6215, a novel 5-HT-5 antagonist, in animal models of anxiety. Pharmacol Res 27:151–164

Cooper SJ, Crummy YMT (1978) Enhanced choice of familiar food in a food preference test after chlordiazepoxide administration. Psychopharmacology 59:51–56

Fletcher PJ, Davies M (1990) Effects of 8-OH-DPAT, buspirone and ICS 205–930 on feeding in a novel environment: comparison with chlordiazepoxide and FG 7142. Psychopharmacology 102:301–308

Porschel BPH (1971) A simple and specific screen for benzodiazepine-like drugs. Psychopharmacologia 19: 193–198

Shephard RA, Broadhurst PL (1982) Hyponeophagia and arousal in rats: effects of diazepam, 5-methoxy-N,N-dimethyltryptamine, d-amphetamine and food deprivation. Psychopharmacology 78:368–378

Soubrie P, Kulkarni S, Simon P, Boissier JR (1975) Effets des anxiolytiques sur la prise de norriture de rats et de souris places en situation nouvelle ou familière. Psychopharmacologia 45:203–210

E.2.4.17 Shock Probe Conflict Procedure

PURPOSE AND RATIONALE

The shock probe conflict procedure, an assay responsive to benzodiazepines, barbiturates and related compounds, was described by Meert and Colpaert (1986). Rats being placed in a novel test environment containing a probe, explore the environment and also the probe. The exploration of the probe, quantified as the number of times that the animal makes physical contact with it, is reduced when the probe is electrified. Rats treated with anxiolytics continue to touch the electrified probe.

PROCEDURE

Apparatus: The test environment consists of a Plexiglas chamber, measuring 40 × 40 × 40 cm, and having a metal grid floor. A Teflon probe (∅: 1 cm) with two uninsulated wires (∅: 0.5 mm) each independently wrapped 25 times around it, is inserted from the front panel protruding for a length of 6.5 cm into the test box, 3 cm above the floor of the chamber. The wires are connected to a shocker. Whenever the animal touches both wires simultaneously with some part of its body, a DC current flows through the animal. At the same time, a counter is triggered. Normally, a shock intensity of 0.9 mA is used.

Sixty min after treatment with saline or test substance, the animal is placed in a back corner of the testbox facing away from the probe. The test session starts from the moment makes the first contact and receives the first shock. The number of responses the animal makes during the subsequent 5-min episode is counted.

EVALUATION

Dose-response curves can be established for various drugs at different shock intensities. The Mann-Whitney *U*-test is used to evaluate differences between experimental conditions. To control whether a drug treatment increases responding above the saline control level, an one-tail *t*-test is used; a two-tail test in other cases.

CRITICAL ASSESSMENT OF THE METHOD

The procedure requires neither behavioral training nor expensive equipment and overcomes some of the limitations that are typical for other conflict procedures. However, the procedure still uses electric shock as inhibitory stimulus.

REFERENCES AND FURTHER READING

Meert TF, Colpaert FC (1986) The shock probe conflict procedure. A new assay responsive to benzodiazepines, barbiturates and related compounds. Psychopharmacol 88:445–450

E.2.4.18 Ultrasound Induced Defensive Behavior in Rats

PURPOSE AND RATIONALE

Rats exposed to aversive stimuli display specific defence behavior as a part of their natural survival strategy. One component of this behavior is the production of ultrasonic calls in the 20–27 kHz range, which are thought to serve a communication role. Artificially generated ultrasound produces intensity-related locomotion, characteristic of defensive behavior (Beckett et al. 1996).

PROCEDURE

The apparatus (Beckett and Marsden 1995) consists of a circular open field arena, 75 cm in diameter, 46 cm high walls, with a video camera suspended above. Locomotor behaviors are recorded and analyzed using a computer automated tracking system capable of following rapid movements (VideoTrack, CPL Systems, Cambridge, UK). This allows the ultrasound-induced change in locomotor behavior to be quantified in maximum speed, average speed and distance traveled by the animals. Data are expressed as 15 sequential 20-s bins over the duration of the experiment.

Ultrasound (continuous tone, square wave, 20 kHz) is produced using a multifunction signal generator at sound pressure intensities of 65, 72 and 75 dB, as measured from the arena, 20 cm horizontally from the speaker. Sound is delivered to the testing arena via a high frequency piezo electric speaker mounted at a height of 40 cm on the wall of the testing arena. The signal frequency and intensity delivered to the speaker are monitored using a digital oscilloscope. White noise is generated using a standard generator and the sound intensity measured as above.

Animals are placed in the test arena 20 min after intraperitoneal injection of drug or vehicle and locomotor activity is measured. After 2 min they are exposed to a 1-min, 20 kHz, square wave ultrasound tone (65, 72 or 75 dB sound pressure intensity, randomized) followed by a further 2 min without sound. This procedure is repeated for each intensity with a 1-min interprocedure interval. Locomotor activity values are then calculated for the maximum speed, average speed and total distance traveled throughout the 5-min test period and expressed as a series of 15–20-s time epochs.

EVALUATION

Maximum speed is analyzed using a two-way ANOVA. Significant interactions between treatment

and time are followed by one-way ANOVAs for individual time points with post-hoc Duncan's new multiple range test.

MODIFICATIONS OF THE METHOD

Moleweijk et al. (1995) evaluated ultrasound vocalizations of adult male rats in association with aversive stimulation as a screening method for anxiolytic drugs.

REFERENCES AND FURTHER READING

Beckett SRG, Marsden CA (1995) Computer analysis and quantification of periaqueductal grey-induced defence behavior. J Neurosci Meth 58:157–161

Beckett SRG, Aspley S, Graham M, Marsden CA (1996) Pharmacological manipulation of ultrasound induced defence behaviour in the rat. Psychopharmacol 127:384–390

Molewijk HE, van der Poel AM, van der Heyden JAM, Olivier B (1995) Conditioned ultrasonic distress vocalization in adult male rats as a behavioural paradigm for screening antipanic drugs. Psychopharmacology 117:32–40

E.2.4.19 Anxiety/Defense Test Battery in Rats

PURPOSE AND RATIONALE

Blanchard et al. (1989, 1990, 1992) described a set of procedures designed to assess the defensive reactions of rats to a natural predator, the cat. These tests involve a brief confrontation of laboratory rats with an unconditioned threat stimulus (cat) which, to preclude physical contact, is presented behind a wire mesh barrier. The primary measures, taken both during and after cat presentation, include movement arrest and risk assessment (proxemics/activity test) and the inhibition of non-defensive behaviors (eat/drink or freezing test).

PROCEDURE

The test apparatus for both the proxemics/activity and eat/drink procedures consists of two parallel subject chambers (53 × 20 × 25 cm). The inside walls of each chamber are constructed of opaque black Plexiglas, while outer walls and lids are clear Plexiglas to allow video recording from lateral and overhead views. The end wall of each chamber, constructed of wire mesh, adjoins a separate cat compartment. Subject movements are monitored by five photocells mounted at equal distances over the length of each chamber, and a food hopper and drinkometer are positioned 2.5 cm to each side of the central photocell. Access to the food hopper/drinkometer can be prevented by insertion of Plexiglas gates.

Each rat (Long-Evans strain, female or male, about 100 days old) receives the same injection (drug or saline) in each of the two successive paradigms. The initial study assesses the effects of cat exposure on proxemics/activity, followed 7 days later by analysis of eat/drink behavior during and after cat exposure. Both procedures are carried out under dim red light.

Proxemic/activity testing. Rats are individually placed in each compartment of the test apparatus. Following a 5-min pre-cat period, the cat is introduced to the cat compartment for 5 min. Following removal of the cat, behavior is recorded for a further 15 min post-cat period, for which measures are summed in three, 5-min blocks. The test session is video recorded for analysis of lying, crouching, rearing, locomotion and grooming. Proxemic location is measured by a digitizing system which divides the length of the subject compartment into thirds, indicating animal's location near the cat compartment, in the midsection of the box, or far from the cat compartment. Assessment of transits indicate movement from one section to another.

Eat/drink testing. Rats are individually given 2 g of finely crushed chocolate cereal on the 2 days after the proxemic/activity test, to familiarize them with this highly preferred food. In order to induce a mild water deprivation, water bottles are removed, 24 h prior to eat/drink testing. On the test day, animals are individually placed in the subject compartments for a 5-min pre-cat period, during which the food hopper and water dispenser are concealed with Plexiglas gates. At the beginning of the 5-min cat period, these gates are removed allowing free access to the crushed chocolate cereal and water. After removal of the cat, the rats are monitored for a further 15-min post-cat period. Measures of eating frequency and duration, and drinking frequency are taken for the cat and post-cat periods.

EVALUATION

The data are analyzed by analysis of variance (ANOVA). Subsequent comparisons between treatment groups and control are carried out using Newman-Keuls procedures.

MODIFICATIONS OF THE TEST

Farook et al. (2001, 2004a, 2004b) and Wang et al. (2003) described a **cat-freezing test apparatus**. The apparatus consisted of a completely enclosed, black, cat compartment (55 × 38 × 30 cm) with a wire mesh floor opening 42 × 19 cm, and an open-top rat compartment (38 × 24 × 19 cm) made of clear Plexiglas to allow observation. The cat compartment could be placed stably on the top of the rat compartment. Male PVG hooded rats weighing 210–260 g were used. Locomotor activity was monitored using an Opto-Varimex Mini (Columbus Instruments), which measured the in-

terruptions of optical beams that were placed 2.5 cm apart. The predator cat was a 4.3-kg male, which was selected for a total absence of aggressive behavior toward the rodents. During a 20-min test period, the duration of freezing, defined as the absence of all movements except movements related to breathing, was monitored. Freezing was expressed as the percentage of time the rat spent frozen during this 20-min session.

Blanchard et al. (1986a, b, 1989) developed a battery of tests designed to elicit a wide range of active and passive defensive activities in **wild rats**.

Griebel et al. (1997, 1998a, 1998b, 2001, 2002) designed a mouse defense test battery in which **Swiss mice** were confronted with a natural threat (a rat) and behaviors associated with this threat were recorded.

REFERENCES AND FURTHER READING

Blanchard DC, Hori K, Rodgers RJ, Hendrie CA, Blanchard RJ (1989) Differential effects of benzodiazepines and 5-HT_{1A} agonists on defensive patterns of wild rattus. In: Bean, Cools, Archer (eds) Behavioural Pharmacology of 5-HAT. Erlbaum, Hillsdale, pp 145–147

Blanchard RJ, Blanchard DC (1989) Antipredator defensive behaviors in a visible burrow system. J Comp Physiol 103:70–82

Blanchard RJ, Blanchard DC, Flannely KJ, Hori K (1986a) Ethanol changes patterns of defensive behaviour in wild rats. Physiol Behav 38:645–650

Blanchard RJ, Flannely HJ, Blanchard DC (1986b) Defensive behaviours of laboratory and wild Rattus norvegicus. J Comp Physiol 100:101–107

Blanchard DC, Blanchard RJ, Tom P, Rodgers RJ (1990) Diazepam changes risk assessment in an anxiety/defense test battery. Psychopharmacology 101:511–518

Blanchard DC, Shepherd JK, Rodgers RJ, Blanchard RJ (1992) Evidence for differential effects of 8-OH-DPAT on male and female rats in the anxiety/defense test battery. Psychopharmacology 106:531–539

Farook JM, Zhu YZ, Wang H, Moochhala S, Lee L, Wong PT (2001) Strain differences in freezing behavior of PVG hooded and Sprague Dawley rats: differential cortical expression of $cholecystokinin_2$ receptors. Neuroreport 12:2717–2720

Farook JM, Wang Q, Moochhala SM, Zhu ZY, Lee L, Wong PTH (2004a) Distinct regions of periaqueductal gray (PAG) are involved in freezing behavior in hooded PVG rats in the cat-freezing test apparatus. Neurosci Lett 354:139–142

Farook JM, McLachlan CS, Zhu YZ, Lee L, Moochhala SM, Wong PTH (2004b) The CCK_2 agonist BC264 reverses freezing behavior habituation in PVG hooded rats on repeated exposures to a cat. Neurosci Lett 355:205–208

Griebel G, Sanger DJ, Perrault G (1997) Genetic differences in the mouse defense battery. Aggress Behav 23:19–31

Griebel G, Curet O, Perrault G, Sanger DJ (1998a) Behavioral effects of phenelzine in an experimental model for screening anxiolytic and anti-panic drugs. Neuropharmacol 37:927–935

Griebel G, Perrault G, Sanger DJ (1998b) Characterization of the behavioral profile of the non-peptide CRF receptor antagonist CP-154,526 in anxiety models of rodents. Comparison with diazepam and buspirone. Psychopharmacology 138:55–66

Griebel G, Moindrot N, Aliaga C, Simiand J, Soubrié P (2001) Characterization of neurokinin-2 and neurotensin receptor antagonists in the mouse defense test battery. Neurosci Biobehav Rev 25:619–626

Griebel G, Simiand J, Steinberg R, Jung M, Gully D, Roger P, Geslin M, Scatton B, Maffrand JP, Soubrié P (2002) 4-(2-Chloro-4-methoxy-5-methylphenyl)-*N*-[(1*S*)-2-cyclopropyl-1-(3-fluoro-4-methylphenyl)ethyl]5-methyl-*N*-(2-propynyl)1,3-thiazol-2-amine hydrochloride (SSR125543A), a potent and selective corticotrophin-releasing $factor_1$ receptor antagonist. II. Characterization in rodent models of stress-related disorders. J Pharmacol Exp Ther 301:332–345

Wang H, Zhu YZ, Wong PTH, Farook JM, Teo AL, Lee LKH, Moochhala S (2003) cDNA microarray analysis of gene expression in anxious PVG and SD rats after cat-freezing test. Exp Brain Res 149:413–421

E.2.4.20 Repetitive Transcranial Magnetic Stimulation

PURPOSE AND RATIONALE

Transcranial magnetic stimulation was introduced by Barker et al. (1985). The regional electrical activity in the brain is influenced by a pulsed magnetic field. Repetitive transcranial magnetic stimulation can cause functional changes in the cortex. Effects have been demonstrated in humans as well as in animals (Weissman et al. 1992; Fleischmann et al. 1995; Zyss et al. 1997; Ji et al. 1998; Ben-Shachar et al. 1999; Hausmann et al. 2000; Luft et al. 2001). Most studies indicated an antidepressant or anxiolytic effect (Keck et al. 2000, 2001; Tsutsumi et al. 2002; Kanno et al. 2003); however, this effect is dependent on frequency of stimulation (Sachdev et al. 2002) and duration of treatment (Hedges et al. 2003, 2005; Isogawa et al. 2003). Isogawa et al. (2005) found that 10-day repetitive transcranial magnetic stimulation induced anxiety in normal rats, as evidenced by expression of anxiety behaviors in the elevated plus-maze.

PROCEDURE

Male Wistar rats were used. All animals received repetitive transcranial magnetic stimulation for 10 days. On day 10, groups of 5 rats were treated with saline i.p., or anxiolytics or antidepressants.

Magnetic stimulation was delivered via a high-frequency magnetic stimulator with a round coil (4 cm in diameter) positioned over the rat's head. The stimulator delivered a biphasic cosine current with a pulse width of 200 μs in duration. The switching elements transfer up to 250 J per pulse to the coil, depending on the intensity setting. The peak magnetic flux at the

center of the coil is approximately 2.2 T at maximal output. The stimulus amplitude was set at an intensity of 1.5 motor thresholds for motor-evoked potentials recorded from the gastrocnemius muscles.

To deliver the stimulation, awake animals were gently held by hand to minimize any discomfort. The coil was held tangentially in direct physical contact with the rat's head. To keep the same brain region stimulated, the center of the coil was set at the center of the vertex of the skull. All animals received one set of training stimuli daily between 13:00 and 18:00 hours for 10 days. To control for the auditory stimulation that accompanies high-frequency magnetic stimulation, sham stimulations were performed with the coil held far enough away (15 cm) from the induced magnetic field.

On the first day of testing, all rats were evaluated on the elevated plus-maze. This consisted of two opposite open arms (50×10 cm) without side walls and two opposite enclosed arms ($50 \times 8 \times 40$ cm), and was elevated 50 cm above the floor. At the beginning of the test, rats were placed in the middle of the maze facing one of the open arms, immediately left alone in the test room, and were observed for 300 s using a video camera. The following parameters were measured: (1) the time spent in the open arms, (2) total number of entries into the open arms, (3) total number of entries into the closed arms, (4) number of stretched-attend postures, and (5) number of head dips over the edge of the platform.

As a measure of exploratory activity, animals were placed in a standard apparatus. General motor activity was determined by the number of infrared photobeam breaks in a 2-h period. Rats were tested again after treatment with drugs on day 10.

EVALUATION

The results are presented as the means ± SEM of individual values from each group. Overall statistical significance was determined using one-way ANOVA with a post-hoc Dunnett test. For general motor activity, results were analyzed using two-way ANOVA.

REFERENCES AND FURTHER READING

Barker AT, Jalinous R, Freeston IL (1985) Non-invasive stimulation of the human motor cortex. Lancet 1:1106–1107

Ben-Shachar D, Gazawi H, Riboyad-Levin J, Klein E (1999) Chronic repetitive transcranial magnetic stimulation alters β-adrenergic and 5-HT_2 receptor characteristics in rat brain. Brain Res 816:78–83

Fleischmann, Prolov K, Abarbanel J, Belmaker RH (1995) The effect of transcranial magnetic stimulation of rat brain on behavioral models of depression. Brain Res 699:130–132

Hausmann A, Weis C, Marksteiner J, Humpel C (2000) Chronic repetitive transcranial magnetic stimulation enhances c-fos in the parietal cortex and hippocampus. Brain Res Mol Brain Res 76:355–362

Hedges DW, Massari C, Salyer DL, Lund TD, Hellewell JL, Johnson AC, Lephart ED (2003) Duration of transcranial magnetic stimulation effects on the neuroendocrine stress response and coping behavior of adult male rats. Prog Neuropsychopharm Biol Psychiatry 27:633–638

Hedges DW, Higginbotham BJ, Salyer DL, Lund TD (2005) Transcranial magnetic stimulation effects on one-trail learning and response to anxiogenic stimuli in adult male rats. J ECT 21:25–30

Isogawa K, Fujiki M, Akiyoshi J, Tsutsumi T, Horinouchi Y, Kodama K, Nagayama H (2003) Anxiety induced by repetitive transcranial magnetic stimulation is suppressed by chronic treatment of paroxtine in rats. Pharmacopsychiatry 36:7–11

Isogawa K, Fujiki M, Akiyoshi J, Tsutsumi T, Kodama K, Matsushita H, Tanaka Y, Kobayashi H (2005) Anxiolytic suppression of repetitive transcranial magnetic stimulation-induced anxiety in the rats. Progr Neuropsychopharm Biol Psychiatry 29:664–668

Ji RR, Schlaepfer TE, Aizenman CD, Epstein CM, Qiu D, Huang JC, Rupp F (1998) Repetitive transcranial magnetic stimulation activates specific regions in rat brain. Proc Natl Acad Sci USA 95:15635–15640

Kanno M, Matsumoto M, Togashi H, Yoshioka M, Mano Y (2003) Effects of repetitive transcranial magnetic stimulation on behavior and neurochemical changes in rats during an elevated plus-maze test. J Neurol Sci 211:5–14

Keck ME, Engelmann M, Müller MB, Henniger MSH, Hermann B, Rupprecht R, Neumann ID, Toschi N, Landgraf R, Post A (2000) Repetitive transcranial magnetic stimulation induces active coping strategies and attenuates the neuroendocrine stress response in rats. J Psych Res 14:265–276

Keck ME, Welt T, Post A, Müller MB, Toschi N, Wigger A, Landgraf R, Holsboer F, Engelmann M (2001) Neuroendocrine and behavioral effects of repetitive transcranial magnetic stimulation in a psychopathological animal model are suggestive of antidepressant-like effects. Neuropsychopharmacology 24:337–349

Luft AR, Kaelin-Lang A, Hauser TK, Cohen LG, Thakor NV, Hanley DF (2001) Transcranial magnetic stimulation in the rat. Exp Brain Res 140:112–121

Sachdev PS, McBride R, Loo C, Mitchell PM, Malhi GS, Crooker V (2002) Effect of different frequencies of transcranial magnetic stimulation (TMS) on the forced swim model of depression in rats. Biol Psychiatry 51:474–479

Tsutsumi T, Fujiki M, Akiyoshi J, Horinouchi Y, Isogawa K, Hori S, Nagayama H (2002) Effect of repetitive transcranial magnetic stimulation on forced swimming test. Progr Neuropsychopharm Biol Psychiatry 26:107–111

Weissman JD, Epstein CM, Davey KR (1992) Magnetic brain stimulation and brain size: relevance to animal studies. Electroencephalogr Clin Neurophysiol 85:215–219

Zyss T, Górka Z, Kowalska M, Vetulani J (1997) Preliminary comparison of behavioral and biochemical effects of chronic transcranial magnetic stimulation and electroconvulsive shock in the rat. Biol Psychiatry 42:920–924

E.2.4.21 Marmoset Human Threat Test

PURPOSE AND RATIONALE

The behavior of the common marmoset (*Callithrix jacchus*) as described by Stevenson and Poole (1976) can

be used for evaluation of potential anxiolytic drugs (Costall et al. 1988).

PROCEDURE

Male or female laboratory bred common marmosets weighing 350–400 g are housed in single sex pairs. Holding rooms are maintained at 25°C at a humidity of 55% on a 12 h light/dark cycle. Tests are conducted between 13:30 and 15:30 in the normal holding room. The holding cages are 75 cm high, 50 cm wide and 60 cm deep.

A behavioral change characterized by retreat from, and posturing toward a human threat is initiated by a human observer standing in close proximity in front of the holding cage. Changed behavior is recorded over a 2 min period by the observer. The behavioral measures selected are:

i. the % of time spent on the cage front in direct confrontation with the human threat,
ii. the number of body postures, primarily shown as raising the tail to expose the genital region with varying degrees of piloerection, anal scent marking and slit stare with flattened ear tufts.

The animals are used at 7 day intervals and are subject to a random cross-over of treatments.

Drugs are administered 45 min before exposure to the human threat situation.

EVALUATION

Statistical analysis is performed with one-way analysis of variance followed by Dunnett's *t*-test.

CRITICAL ASSESSMENT OF THE METHOD

The human threat test in marmosets has the advantage of using primates instead of rodents. However, it is subject to individual scoring of the observer.

MODIFICATIONS OF THE TEST

Cilia and Piper (1997) developed a method of measuring conspecific confrontation-induced behavioral changes in common marmosets together with automated monitoring of locomotor activity as a possible model of anxiety.

Barros et al. (2000) measured fear and anxiety in the marmoset (*Callithrix penicillata*) with a novel predator confrontation model. The wild cat (*Felis tigrina*) was chosen as taxidermized predator to induce anxiety-related behaviors.

Borsini et al. (1993) used female **cynomolgus monkeys** to test aggressiveness against the observer.

REFERENCES AND FURTHER READING

Barnes NM, Costall B, Domeney AM, Gerrard PA, Kelly ME, Krahling H, Naylor RJ, Tomkins DM, Williams TJ (1991) The effects of umespirone as a potential anxiolytic and antipsychotic agent. Pharmacol Biochem Behav 40:89–96

Barros M, Boere V, Huston JP, Tomaz C (2000) Measuring fear and anxiety in the marmoset (*Callithrix penicillata*) with a novel predator confrontation model: effects of diazepam. Behav Brain Res 108:205–211

Borsini F, Brambilla A, Cesana R, Donetti A (1993) The effect of DAU 6215, a novel 5HAT-3 antagonist in animal models of anxiety. Pharmacol Res 27:151–164

Cilia J, Piper DC (1997) Marmoset conspecific confrontation: an ethologically-based model of anxiety. Pharmacol Biochem Behav 58:85–91

Costall B, Domeney AM, Naylor RJ, Tyers MB (1987) Effects of the 5-HT_3 receptor antagonist, GR38032F, on raised dopaminergic activity in the mesolimbic system of the rat and marmoset brain. Br. J Pharmacol 92:881–894

Costall B, Domeney AM, Gerrard PA, Kelley ME, Naylor RJ (1988) Zacopride: Anxiolytic profile in rodent and primate models of anxiety. J Pharm Pharmacol 40:302–305

Costall B, Domeney AM, Farre AJ, Kelly ME, Martinez L, Naylor RJ (1992) Profile of action of a novel 5-hydroxytryptamine$_{1A}$ receptor ligand E-4424 to inhibit aversive behavior in the mouse, rat and marmoset. J Pharmacol Exp Ther 262:90–98

Jones BJ, Costall B, Domeney AM, Kelly ME, Naylor RJ, Oakley NR, Tyers MB (1988) The potential anxiolytic activity of GR38032F, a 5-HT_3 receptor antagonist. Br J Pharmacol 93:985–993

Stevenson MF, Poole TB (1976) An ethogram of the common marmoset (Callithrix jacchus): general behavioural repertoire. Anim Behav 24:428–451

E.2.4.22 Psychosocial Stress in Tree Shrews

PURPOSE AND RATIONALE

Male tree shrews (*Tupaia belangeri*) provide an animal model to study the neurobehavioral and endocrine consequences of chronic psychosocial stress (Fischer et al. 1985; Fuchs et al. 1993, 1996; Fuchs and Flügge 2002; Fuchs 2005). When living in visual and olfactory contact with a male conspecific by which it has been defeated, the subordinate tree shrew shows dramatic behavioral, physiological, and neuroendocrine changes. The pattern of these changes resembles a depression-like symptomatology.

PROCEDURE

Animals are subjected to a 10-day period of psychosocial conflict to elicit stress-induced behavioral and endocrine alterations before the onset of drug treatment. For a treatment period of 30 days, animals are given either saline or an oral dose of test compound.

EVALUATION

At the end of the test period, the following parameters are recorded: behavioral changes (marking, groom-

ing, locomotor activity) and endocrine changes (urinary cortisol and norepinephrine excretion).

MODIFICATIONS OF THE METHOD

Lucassen et al. (2004) found that treatment with an antidepressant reduces apoptosis in the hippocampal dentate gyrus and temporal cortex induced by a 7-day stress period in tree shrews.

Czéh et al. (2005) examined the effects of a NK_1 receptor antagonist in the chronic psychological stress model of adult male tree shrews.

Shively et al. (2005) described social stress-associated depression in adult female **cynomolgus monkeys**.

REFERENCES AND FURTHER READING

Czéh B, Pudovkina O, van der Hart MGC, Simon M, Heilbronner U, Michaelis T, Watanabe T, Frahm J, Fuchs E (2005) Examining SLV-323, a novel NK_1 receptor antagonist, in a chronic stress model for depression. Psychopharmacology 180:548–557

Fischer HD, Heinzeller T, Raab A (1985) Gonadal response to psychosocial stress in male tree shrews (*Tupaia belangeri*): morphometry of testis, epididymis and prostate. Andrologia 17:262–275

Fuchs E (2005) Social stress in tree shrews as an animal model of depression: an example of an behavioral model of a CNS disorder. CNS Spectr 10:182–190

Fuchs E, Flügge G (2002) Social stress in tree shrews. Effects on physiology, brain function, and behavior of subordinate individuals. Pharmacol Biochem Behav 73:247–258

Fuchs E, Jöhren O, Flügge G (1993) Psychosocial conflict in the tree shrew: effects on sympathoadrenal activity and blood pressure. Psychoneuroendocrinology 18:557–565

Fuchs E, Kramer M, Hermes B, Netter P, Hiemke C (1996) Psychological stress in tree shrews: clomipramine counteracts behavioral and endocrine changes. Pharmacol Biochem Behav 54:219–228

Lucassen PJ, Fuchs E, Czeh B (2004) Antidepressant treatment with tianeptine reduces apoptosis in the hippocampal dentate gyrus and temporal cortex. Biol Psychiatry 55:789–796

Shively CA, Register TC, Friedman PD, Morgan TM, Thompson J, Lanier T (2005) Social stress-associated depression in adult female cynomolgus monkeys (*Macaca fascicularis*). Biol Psychiatry 69:67–84

E.2.4.23 Aversive Brain Stimulation

PURPOSE AND RATIONALE

Electrical stimulation of brain aversive areas, in particular the midbrain central gray, induces defensive reaction and/or flight behavior in several species and, therefore, may be viewed as an animal model of anxiety or of panic attack. Most studies used intracerebral microinjections of neurotransmitters, their agonists and antagonists to elucidate the mechanisms of aversive or antiaversive effects (Schütz et al. 1985; Graeff et al. 1986, 1990, 1991 1993, 1997; Audi et al. 1988, 1991; Brandão et al. 1991, 1993; Broekkamp et al. 1991; Nogueira and Graeff 1991, 1995; Motta and Brandão 1993; Aguiar and Brandão 1994, 1996; Melo and Brandão 1995; Motta et al. 1995; De Araujo et al. 1998). Other groups evaluated the effect of drugs, e. g., serotonin receptor antagonists, on periaqueductal gray stimulation induced aversion after peripheral application (Bovier et al. 1982; Clarke and File 1982; Jenck et al. 1989, 1995, 1996, 1998, 1999; Beckett and Marsden 1997). Dorsal periaqueductal gray-induced aversion is considered as a model of panic anxiety.

PROCEDURE

Surgery. A stainless steel bipolar twisted electrode, insulated to the tip which is cut square to the shaft, is implanted to the dorsal part of the periaqueductal gray matter of male Wistar rats weighing 370–450 g under pentobarbital anesthesia. According to the atlas of Paxinos and Watson (1982), the coordinates for the electrode tip are 5.8 mm posterior to the bregma, 0.2 mm lateral to the midline and 5.0 mm ventral to the surface of the skull. The electrode is held in place with dental cement and five screws threaded into the skull.

Behavioral Procedure. Animals are placed in a rectangular cage ($20 \times 36 \times 20$ cm high) with a grid floor and a 2 cm high barrier dividing the cage in half. They are allowed to explore freely for 10–15 min before the stimulation begins.

Brain stimulation consists of constant current square wave, 0.1 ms duration, monophasic pulses conducted from the neurostimulator (Grass S88 + stimulus isolation unit SIU8) to the electrode by way of flexible wire leads. Pulse duration, pulse frequency and stimulation intensity are monitored by an oscilloscope. Animals are screened for stimulation-induced aversion using a fixed stimulation frequency of 50 Hz; current is raised slowly until aversive behavioral signs are observed. Aversive effects are first characterized by visible autonomic reactions (increase in respiratory rates, piloerection, eventually mydriasis) in animals which are behaviorally frozen. Increasing the intensity induces, following a freezing period, active behavioral signs, ranging from ear dressing and head weaving to sudden running and attempts to escape out of the cage.

With this fixed stimulation intensity, aversive behavior is shaped into an operant escape response: rats are trained to stop the stimulation by escaping from one compartment to the opposite compartment of the cage. Brain stimulation is switched off when the rat crosses the middle line separating the two compartments or after a maximal cut-off time of 20 s. A trial is

applied every min. Three to 10 daily sessions of 30 trials are required to obtain stable responses.

Self-Interruption Threshold Determination

Once an animal displays steady performances during 3 consecutive days on this task with fixed intensity and fixed stimulation frequency, it undergoes the next step of training aimed at determining its stimulation frequency threshold for escape reaction. This consists of testing the animals in a threshold procedure in which the frequency is varied while stimulation intensity is held constant. This procedure keeps the size of the stimulation field around the electrode tip constant.

A stimulation intensity is chosen and defined as the threshold intensity eliciting escape when the stimulation frequency is 50 Hz. With this intensity held fixed, a method of limits is employed to determine the frequency threshold for escape: the stimulation frequency is either decreased or increased depending on the response displayed by the animal on the previous trial. Starting from 50 Hz, stimulation frequency is decreased by 5 Hz steps following a trial in which the rat responds to the stimulation, and is increased by 5 Hz steps, in case the animal fails to respond to the stimulation. When a response is made, the time elapsing between the onset of the stimulation and the moment the animal crosses the midline barrier is also recorded as escape latency; no response is associated with the maximum cut-off time of 20 s.

Frequency threshold is calculated as the average frequency eliciting an escape reaction during a 20-min pre-injection session; an average escape latency is calculated the same way. Drugs are then injected intraperitoneally at various doses and 35 min following administration, frequency threshold is determined again over a 25–30 min post-injection session. Drug effects can be estimated by comparing thresholds and latencies for each animal before and after injection. Doses are injected at least 4 days in a counterbalanced order. Animals serve as their own controls and can undergo several treatments.

EVALUATION

Data are analyzed by means of analysis of variance, followed by paired *t*-tests. Dose-response curves are established for active drugs.

MODIFICATIONS OF THE METHOD

The group of Graeff and Brandão (1986) used an electrode-cannula, called chemitrode, for electrical stimulation and microinjection of drugs or neurotransmitters at the same place of the periaqueductal gray. This chemitrode was made of stainless steel cannula (outside diameter 0.6 mm, length 12.5 mm) glued to a brain electrode made of stainless steel (diameter 250 mm) enamel insulated except at the cross-section of the tip, reaching 1 mm below the lower end of the cannula (Nogueira and Graeff 1995).

Schenberg et al. (2001) appraised the isomorphism of dorsal periaqueductal gray-evoked defensive behaviors and panic attacks both in rats and humans.

REFERENCES AND FURTHER READING

Aguiar MS, Brandão ML (1994) Conditioned place aversion produced by microinjection of substance P into the periaqueductal gray of rats. Behav Pharmacol 5:369–373

Aguiar MS, Brandão ML (1996) Effects of microinjections of the neuropeptide substance P in the dorsal periaqueductal gray on the behavior of rats in the plus-maze test. Physiol Behav 60:1183–1186

Audi EA, de Aguiar JC, Graeff FG (1988) Mediation by serotonin of the antiaversive effect of zimelidine and propranolol injected into the dorsal midbrain central grey. J Psychopharmacol 2:26–32

Audi EA, de Oliveira RMW, Graeff FG (1991) Microinjection of propranolol into the dorsal periaqueductal gray causes an anxiolytic effect in the elevated plus-maze antagonized by ritanserin. Psychopharmacology 105:553–557

Beckett S, Marsden CA (1997) The effect of central and systemic injection of the 5-HT_{1A} receptor agonist 8-OHDPAT and the 5-HT_{1A} antagonist WAY100635 on periaqueductal grey-induced defensive behaviour. J Psychopharmacol 11:35–40

Brandão ML (1993) Involvement of opioid mechanisms in the dorsal periaqueductal gray in drug abuse. Rev Neurosci 4:397–405

Brandão ML, Lopez-Garcia JA, Roberts HMT (1991) Electrophysiological evidence for the involvement of 5-HT_2 receptors in the antiaversive action of 5-HT in the dorsal periaqueductal grey. In: Olivier B, Mos J, Slangen JL (eds) Animal Models in Psychopharmacology. Advances in Pharmacological Sciences. Birkhäuser Verlag, Basel, pp 75–79

Bovier P, Broekkamp CLE, Lloyd KG (1982) Enhancing GABAergic transmission reverses the aversive state in rats induced by electrical stimulation of the periaqueductal grey region. Brain Res 248:331–320

Broekkamp CL, Dortmans C, Berendsen HHG, Jenk F (1991) Pharmacology of fear, induced by periaqueductal gray stimulation in the rat. In: Olivier B, Mos J, Slangen JL (eds) Animal Models in Psychopharmacology. Advances in Pharmacological Sciences. Birkhäuser Verlag, Basel, pp 69–74

Clarke A, File SA (1982) Effects of ACTH, benzodiazepines and 5-HT antagonists on escape from periaqueductal grey stimulation in the rat. Progr Neuro-Psychopharmacol Biol Psychiat 6:27–35

De Araujo JE, Huston JP, Brandão ML (1998) Aversive effects of the C-fragment of substance P in the dorsal periaqueductal gray matter. Exp Brain Res 123:84–89

Graeff FG (1991) Neurotransmitters in the dorsal periaqueductal grey and animal models of panic anxiety. In: Briley M, File SE (eds) New Concepts in Anxiety. McMillan Press Ltd., London, pp 288–312

Graeff FG, Brandão ML, Audi EA, Schütz MTB (1986) Modulation of the brain aversive system by GABAergic and serotoninergic mechanisms. Behav Brain Res 21:65–72

Graeff FG, Audi EA, Almeida SS, Graeff EO, Hunziker MHL (1990) Behavioral effects of 5-HT receptor ligands in the aversive brain stimulation, elevated plus-maze and learned helplessness tests. Neurosci Biobehav Rev 14:501–506
Graeff FG, Silveira MCL, Nogueira RL, Audi EA, Oliveira RMW (1993) Role of the amygdala and periaqueductal gray in anxiety and panic. Behav Brain Res 58:123–131
Graeff FG, Viana MB, Mora PO (1997) Dual role of 5-HT in defense and anxiety. Neurosci Biobehav Rev 21:791–799
Jenck F, Broekkamp CLE, von Delft AML (1989) Effects of serotonin receptor antagonists on PAG stimulation induced aversion: different contribution of 5-HT_1, 5-HT_2 and 5-HT_3 receptors. Psychopharmacology 97:489–495
Jenck F, Moreau JL, Martin JR (1995) Dorsal periaqueductal gray-induced aversion as a simulation of panic anxiety: elements of face and predictive validity. Psychiatry Res 57:181–191
Jenck F, Martin JR, Moreau JL (1996) Behavioral effects of CCK_B receptor ligands in a validated simulation of panic anxiety in rats. Eur Neuropsychopharmacol 6:291–298
Jenck F, Moreau JL, Berendsen HHG, Boes M, Broekkamp CLE, Martin JR, Wichmann J, von Delft AML (1998) Antiaversive effects of 5-HT_{2c} receptor agonists and fluoxetine in a model of panic-like anxiety. Eur Neuropsychopharmacol 8:161–168
Jenck F, Martin JR, Moreau JL (1999) The 5-HT_{1A} receptor agonist flesinoxan increases aversion in a model of panic-like anxiety in rats. J Psychopharmacol 13:166–170
Melo LL, Brandão ML (1995) Involvement of 5-HT_{1A} and 5-HT_2 receptors of the inferior colliculus in aversive states induced by exposure of rats to the elevated plus-maze test. Behav Pharmacol 6:413–417
Motta V, Penha K, Brandão ML (1995) Effects of microinjections of m and k receptor agonists into the dorsal periaqueductal gray of rats submitted to the plus maze test. Psychopharmacology 120:470–474
Nogueira RL, Graeff FG (1991) 5-HT mediation of the antiaversive effect of isomoltane injected into the dorsal periaqueductal grey. Behav Pharmacol 2:73–77
Nogueira RL, Graeff FG (1995) Role of 5-HT receptor subtypes in the modulation of dorsal periaqueductal gray generated aversion. Pharmacol Biochem Behav 52:1–6
Paxinos G, Watson C (1982) The rat brain in stereotaxic coordinates. Academic Press, New York
Schenberg LC, Bittencourt AS, Sudré ECM, Vargas LC (2001) Modeling panic attacks. Neurosci Biobehav Rev 25:647–659
Schütz MTB, de Aguiar JC, Graeff FG (1985) Anti-aversive role of serotonin in dorsal periaqueductal grey matter. Psychopharmacology 85:340–345

E.2.5
Conditioned Behavioral Responses

E.2.5.1
Sidman Avoidance Paradigm

PURPOSE AND RATIONALE

Sidman (1953) described an apparatus for the evaluation of two temporal parameters (shock-shock interval and response-shock interval) of the maintenance of avoidance behavior by the white rat. The procedure has been widely used to evaluate CNS depressant compounds, neuroleptics, anxiolytics and sedatives.

PROCEDURE

The test cage is equipped with a single lever and a light. This cage is enclosed in a sound-attenuating chamber with a fan and with a speaker emitting a white-noise auditory background. The test cage has a grid floor of steel bars which are attached to a scrambled shock source. The data are recorded in an adjacent room. Male Sprague-Dawley rats with a starting weight of 250 to 300 g are housed in individual cages. They are trained to avoid an unsignalled shock by repetitive lever-pressing responses. A shock (1.5 mA for 0.5 s) is delivered to the grid floor every 15 s if no responses occur (shock-shock interval of 15 s = SS-15 s). A lever press (response) will delay the oncoming shock for 30 s (response-shock interval of 30 s = RS-30 s). The responses do not accumulate for delays of shock; a shock will be delivered 30 s after the last response is made even if 10 responses are made 31 s prior. Every 30 min, the total number of shocks received and the total number of responses made are accumulated and constitute the basic data. The animals are trained until they maintain a stable response rate and receive no more than 100 shocks/five hour test session. After reaching these criteria of performance, experimental compounds are administered and their effects on the performance of this learned avoidance behavior are evaluated. The experimental compounds or the standard are usually administered by i.p. injection immediately prior to testing in volumes of 1 ml/kg of body weight. Depressant drugs lower the rate of lever presses and increase the number of shocks received. Stimulant drugs increase the rate of lever pressing.

EVALUATION

The effect of a drug on the performance of an animal is compared to the data generated in the previous non-drug sessions. Each animal thereby serves as its own control. The basic measures of performance during a specific time interval, responses and shocks are used for evaluation. Responses are reported both as total and as percent of control responses. Shocks are reported as totals and as shock-avoided (SHA) as percent of control. This latter measure is computed by subtracting the number of shocks received from the total number of possible shocks if no responses had been made. In the initial screening of experimental compounds, the results are reported in terms of the total effect during a five-hour test. However, an ED_{50} is usually estimated during a representative time of peak activity.

CRITICAL ASSESSMENT OF THE METHOD

Anxiolytics show activity in this test, however, it has been proven to be more reliable for neuroleptic activity. Apparently, the present conditioned active avoidance paradigms do not constitute a reliable method for screening anxiolytic agents, in spite of their homologies with human anxiety.

MODIFICATIONS OF THE METHOD

Heise and Boff (1962) and Galizio et al. (1990) extended the method by using two levers, an "avoidance lever" and an "escape lever" for calculating ratios between shock rate, escape failure rate and avoidance rate.

Balfour (1990) described the effect of drugs on rat behavior in an unsignalled Sidman avoidance schedule.

Wadenberg et al. (1998) described and evaluated a newly designed apparatus for the assessment of conditioned avoidance response performance in rats.

Patel and Migler (1982) reported a sensitive and selective conflict test in **squirrel monkeys**.

Szewczak et al. (1995) tested antipsychotic agents using continuous avoidance behavior in adult male squirrel monkeys.

REFERENCES AND FURTHER READING

Balfour DJK (1990) A comparison of the effects of nicotine and(+)-amphetamine on rat behavior in an unsignalled Sidman avoidance schedule. J Pharm Pharmacol 42:257–260

Duffield PH, Jamieson DD, Duffield AM (1989) Effect of aqueous and lipid-soluble extracts of Kava on the conditioned avoidance in rats. Arch Int Pharmacodyn 301:81–90

Galizio M, Journey JW, Royal SA, Welker JA (1990) Variable-interval schedules of time-out from avoidance: Effects of anxiolytic and antipsychotic drugs in rats. Pharmacol Biochem Behav 37:235–238

Heise GA, Boff E (1962) Continuous avoidance as a base-line for measuring behavioral effects of drugs. Psychopharmacologia 3:264–282

Patel JB, Migler B (1982) A sensitive and selective monkey conflict test. Pharmacol Biochem Behav 17:645–549

Szewczak MR, Corbett R, Rush DK, Wilmot CA, Conway PG, Strupczewski JT, Cornfeldt M (1995) The pharmacological profile of iloperidone, a novel atypical antipsychotic agent. J Pharmacol Exp Ther 274:1404–1413

Shekar A, Hingtgen JN, DiMicco JA (1987) Selective enhancement of shock avoidance responding elicited by GABA blockade in the posterior hypothalamus of rats. Brain Res 420:118–128

Sidman M (1953a) Avoidance conditioning with brief shock and no enteroceptive warning signal. Science 118:157–158

Sidman M (1953b) Two temporal parameters of the maintenance of avoidance behavior by the white rat. J Comp Physiol Psychol 46:253–261

Wadenberg ML, Young KA, Trompler RA, Zavodny RA, Richter TJ, Hicks OB (1998) A novel computer-controlled conditioned avoidance apparatus for rats. J Pharmacol Toxicol Meth 38:211–215

E.2.5.2 Geller Conflict Paradigm

PURPOSE AND RATIONALE

Experimentally induced conflict by punishing food-rewarded behavior has been used to differentiate between various psychoactive drugs by Geller and Seifter (1960). The basic principle has been used and modified by many authors to reveal possible anti-anxiety effects of experimental compounds.

PROCEDURE

Male albino rats with a starting body weight of 300–400 g are housed individually. They are food deprived until the body weight is gradually reduced by approximately 20% of original and it is maintained at this level by restricted food diet. Conditioning is carried out in commercially available Skinner boxes (e. g. Campden Instruments, London, UK) equipped with a house light, a single lever, cue lights, a liquid dripper, and a grid-floor connected to a shocker. Sweetened condensed milk delivered by the liquid dipper serves as the positive reinforcer. The data are recorded on cumulative recorders.

The animals are trained to lever press for the milk reward in two distinct response-reward sections. In the anxiety or "conflict" segment (signalled by onset of both tone and cue lights), a dipper of milk is delivered in response to each lever press (continuos reinforcement schedule = CRF) However, lever presses during this period are also accompanied by a 40-ms pulse of aversive foot-shock through the grid floor. This creates a conflict between milk reward and the a painful foot shock. This conflict period is 3 min in duration.

During the other segment of this paradigm, the lever presses produce a drop of milk only at variable intervals of time from 60 to 210 s with an average reward of once per 2 min (variable interval = VI-2 min). No shocks are administered during this variable interval phase of testing which is 15 min in duration.

The test procedure consists of four 15 min non-shock variable interval segments where reinforcement is available on a restricted basis. Each variable interval period is followed by a three minute CRF-conflict period phase when reinforcement is constantly available but always accompanied by an aversive footshock. The shock level is adjusted for each subject to reduce the CRF responding to a total of less than 10 lever presses during the entire test. The rats are tested 2 to 4 days a week. Drugs are administered once per week and the performance is compared to the previous day's control trial. The VI responses are used to evaluate any general

debilitating drug effects while the CRF responses are used to evaluate any anti-anxiety effects as indicated by the increased responding during the CRF conflict period.

The test compounds are administered intraperitoneally 30 min or orally 60 min before the test period.

EVALUATION

The total number of lever presses during the conflict periods (CRF) and the non-conflict periods (VI) are counted. Values of treatment sessions are expressed as percentage of values of the preceding non-treatment day. An increase of lever presses in the conflict period is regarded as indication of an anti-anxiety effect, and a decrease of lever presses in the non-conflict period as an indication for a sedative effect. In this procedure linear dose-response curves are rarely found. Therefore, minimal effective doses (MED) are calculated.

CRITICAL ASSESSMENT OF THE METHOD

The method is suitable to distinguish anxiolytics from other centrally active drugs, such as sedatives and neuroleptics. The relative potency of various anxiolytic agents in a number of species compares favorably with their relative potency in humans. The negative aspects are the time consuming procedure, the high expenses for the apparatus and the difficulty to obtain ED_{50}-values.

The relevance of this test and other models has been challenged by Bignami (1988).

MODIFICATIONS OF THE METHOD

The method has been modified by many authors.

Davidson and Cook (1969), Cook and Davidson (1973) introduced a schedule of 10 lever presses for the delivery of one food pellet together with an electric foot-shock. In the variable interval reinforcement period, responses were reinforced by food delivery at varying intervals of time; the mean interval was 30 s. Also under these conditions differentiation of various psychotropic drugs could be achieved.

Iorio et al. (1986) and Chipkin et al. (1988) used a procedure during which a tone (5 s) preceded and then overlapped for 10 s with scrambled footshocks. After the start of the tone, the rat has the option to avoid (in the no shock period) or escape (in the shock period) the shock by jumping onto a platform located 17 cm above the grid floor.

Thiébot et al. (1991) developed the method further by introducing "safety signal withdrawal", a behavioral paradigm in rats sensitive to both anxiolytic and anxiogenic drugs.

Commissaris and Fontana (1991) published a potential animal model for the study of antipanic treatments. Rats were trained to drink their daily water ration during 10-minute sessions. These sessions were characterized by alterations of silence (unpunished periods) and the presence of a tone (punished periods). Tube contact during the tone periods resulted in a 0.25–0.5 mA shock delivered to the mouth of the animal for the duration of the tube contact. After 4 weeks of training, subjects received either chronic post-test treatment with an antidepressant or vehicle, twice daily, seven days per week. Acute pre-test administration of traditional anxiolytics (benzodiazepines, barbiturates) increased dramatically the number of punished contacts made in a dose-dependent manner. Typical antidepressants were not active after pre-test administration, however, active after chronic post-test treatment.

Beaufour et al. (1999) investigated the effects of chronic antidepressants in the conditioned suppression of operant behavior in rats. In daily 18-min sessions, three periods of non-punished lever pressing for food alternated with two 4-min periods signaled by a light-on conditioned stimulus during which 50% of the responses were randomly punished by electric foot shocks. Antidepressants were administered once daily for 7–8 weeks to trained, food-restricted rats.

The conflict test has also be adapted to the **mouse** (Prado de Carvalho et al. 1986).

The conflict behavior and anticonflict effect of anxiolytics has been demonstrated in a variety of species, including **pigeons** (Morse 1964; Wuttke and Kelleher 1970; McMillan 1973; Gleeson et al. 1989; Barrett et al. 1989; Barrett 1991; Schipper et al. 1991; Pollard et al. 1992; Barrett et al. 1994; Mos et al. 1997).

Patel and Migler (1982) described a sensitive and selective conflict model in male squirrel **monkeys** in which anti-anxiety agents exhibit pronounced anticonflict activity.

Ervin et al. (1987), Ervin and Cooper (1988), van Heest et al. 1991; Simiand et al. (1993) used **conditioned taste aversion** as a conflict model. Moderate taste aversions were induced by pairing the initial consumption of 0.25% sodium saccharin with either 25 mg/kg 5-hydroxytryptophan or 30 mg/kg i.p. LiCl. Antagonism was found with benzodiazepines and non-benzodiazepine-anxiolytic drugs.

REFERENCES AND FURTHER READING

Barrett JE (1991) Animal behavior models in the analysis and understanding of anxiolytic drugs acting on serotonin receptors. In: Olivier B, Mos J, Slangen JL (eds) Animal

Models in Psychopharmacology, Advances in Pharmacological Sciences, Birkhäuser Verlag Basel, pp 37–52

Barrett JE, Gleeson S, Nader MA, Hoffmann SM (1989) Anticonflict effects of the 5-HT_{1A} compound flesinoxan. J Psychopharmacol 3:64–69

Barrett JE, Gamble EH, Zhang L, Guardiola-Lemaître B (1994) Anticonflict and discriminative stimulus effect in the pigeon of a new methoxy-chroman 5-HT_{1A} agonist, (+)S 20244 and its enantiomers (+)S 20499 and (–)S 20500. Psychopharmacol 116:73–78

Beaufour CC, Ballon N, le Bihan C, Hamon M, Thiébot MH (1999) Effects of chronic antidepressants in an operant conflict procedure of anxiety in the rat. Pharmacol Biochem Behav 62:591–599

Bignami G (1988) Pharmacology and anxiety: Inadequacies of current experimental approaches and working models. Pharmacol Biochem Behav 29:771–774

Broersen LM, Woudenberg F, Slangen JL (1991) The lack of tolerance to the anxiolytic effects of benzodiazepines in the Geller/Seifter conflict test. In: Olivier B, Mos J, Slangen JL (eds) Animal Models in Psychopharmacology, Advances in Pharmacological Sciences, Birkhäuser Verlag Basel, pp 97–101

Chipkin RE, Iorio LC, Coffin VL, McQuade RD, Berger JG, Barnett A (1988) Pharmacological profile of SCH39166: A dopamine D1 selective benzonaphthazepine with potential antipsychotic activity. J Pharmacol Exper Ther 247:1093–1102

Commissaris RL, Fontana DJ (1991) A potential animal model for the study of antipanic treatments. In: Olivier B, Mos J, Slangen JL (eds) Animal Models in Psychopharmacology, Advances in Pharmacological Sciences, Birkhäuser Verlag Basel, pp 59–53

Cook L, Davidson AB (1973) Effects of behaviorally active drugs in a conflict-punishment procedure in rats. In: Garattini S, Mussini E, Randall LO (eds) The Benzodiazepines, Raven Press, New York, pp 327–345

Cook L, Sepinwall J (1975) Behavioral analysis of the effects and mechanisms of action of benzodiazepines. In: Costa E, Greengard P (eds) Mechanisms of Action of Benzodiazepines. Raven Press, New York, pp 1–28

Davidson AB, Cook L (1969) Effects of combined treatment with trifluoperazine-HCl and amobarbital on punished behavior in rats. Psychopharmacologia (Berl.) 15:159–168

Ervin GN, Cooper BR (1988) Use of conditioned taste aversion as a conflict model: Effects of anxiolytic drugs. J Pharmacol Exp Ther 245:137–146

Ervin GN, Soroko FS, Cooper BR (1987) Buspirone antagonizes the expression of conditioned taste aversion in rats. Drug Dev Res 11:87–95

Geller I, Seifter J (1960) The effects of meprobamate, barbiturates, d-amphetamine and promazine on experimentally induced conflict in the rat. Psychopharmacologia 1:482–492

Geller I, Kulak JT, Seifter J (1962) The effects of chlordiazepoxide and chlorpromazine on a punishment discrimination. Psychopharmacologia 3:374–385

Gleeson S, Ahlers ST, Mansbach RS, Foust JM, Barrett JE (1989) Behavioral studies with anxiolytic drugs: VI. Effects on punished responding of drugs interacting with serotonin receptor subtypes. J Pharmacol Exp Ther 250:809–817

Hanson HM, Stone CA (1964) Animal techniques for evaluating antianxiety drugs. In: Nodine JN, Siegler PE (eds) Animal and Clinical Pharmacologic Techniques in Drug Evaluation. Year Book Medical Publ., Chicago, pp 317–324

Howard JL, Pollard GT (1990) Effects of buspirone in the Geller-Seifter conflict test with incremental shock. Drug Dev Res 19:37–49

Iorio LC, Barnett A, Billard W, Gold EH (1986) Benzodiazepines: Structure-activity relationships between D_1 receptor blockade and selected pharmacological effects. In: Breese GR, Creese I (eds) Neurobiology of central D_1-dopamine receptors. pp 1–14, Plenum Press, New York

Iversen S (1983) Animal models of anxiety. In: Trimble RM (ed) Benzodiazepines Divided. John Wiley and Sons Ltd., pp 87–99

Koene P, Vossen JMH (1991) Drug effects on speed of conflict resolution in the Skinnerbox. In: Olivier B, Mos J, Slangen JL (eds) Animal Models in Psychopharmacology, Advances in Pharmacological Sciences, Birkhäuser Verlag Basel, pp 53–59

Keane PE, Siminand J, Morre M, Biziere K (1988) Tetrazepam: A benzodiazepine which dissociates sedation from other benzodiazepine activities. I. Psychopharmacological profile in rodents. J Pharmacol Exper Ther 245:692–698

Mc Millan DE (1973) Drugs and punished responding. I: Rate-dependent effects under multiple schedules. J Exp Anal Behav 19:133–145

Morse WH (1964) Effect of amobarbital and chlorpromazine on punished behavior in the pigeon. Psychopharmacologia 6:286–294

Mos J, van Hest A, van Drimmelen M, Herremans AHJ, Olivier B (1997) The putative 5-HT_{1A} receptor antagonist DU125530 blocks the discriminative stimulus of the5-HT_{1A} receptor agonist flesinoxan in pigeons. Eur J Pharmacol 325:145–153

Patel JB, Migler B (1982) A sensitive and selective monkey conflict test. Pharmacol Biochem Behav 17:645–649

Pollard GT, Nanry KP, Howard JL (1992) Effects of tandospirone in three behavioral tests for anxiolytics. Eur J Pharmacol 221:297–305

Prado de Carvalho L, Venault P, Potier MC, Dodd RH, Brown CL, Chapoutier G, Rossier RH (1986) 3-(Methoxycarbonyl)-amino-β-carboline, a selective antagonist of the sedative effects of benzodiazepines. Eur J Pharmacol 129:232–233

Schipper J, Tulp MThM, Berkelmans B, Mos J, Van der Heijden JAM, Olivier B (1991) Preclinical pharmacology of Flesinoxan: A potential anxiolytic and antidepressant drug. Human Psychopharmacol 6:53–61

Silverman P (1978) Operant conditioning. In: Animal behaviour in the laboratory. Chapman and Hall, London, pp 141–178

Simiand J, Keane PE, Barnouin MC, Keane M, Soubrié P, Le Fur G (1993) Neurospychopharmacological profile in rodents of SR 57746A, a new, potent 5-HT_{1A} receptor agonist. Fundam Clin Pharmacol 7:413–427

Slangen JL (1991) Drug discrimination and animal models. In: Olivier B, Mos J, Slangen JL (eds) Animal Models in Psychopharmacology. Advances in Pharmacological Sciences. Birkhäuser Verlag, Basel, pp 359–373

Thiébot MH, Dangoumau L, Richard G, Puech AJ (1991) Safety signal withdrawal: a behavioral paradigm sensitive to both "anxiolytic" and "anxiogenic" drugs under identical experimental conditions. Psychopharmacology 103:415–424

van Heest A, Slangen JL, Olivier B (1991) Is the conditioned taste aversion procedure a useful tool in the drug discrimination research? In: Olivier B, Mos J, Slangen JL (eds) Animal Models in Psychopharmacology. Advances in Pharmacological Sciences. Birkhäuser Verlag, Basel, pp 399–405

Wuttke W, Kelleher RT (1970) Effects of some benzodiazepines on punished and unpunished behavior in the pigeon. J Pharmacol Exper Ther 172:397–405

E.2.5.3 Progressive Ratio Procedure

PURPOSE AND RATIONALE

The progressive ratio schedule was introduced as a model for studying the psychomotor stimulant activity of drugs in the rat by Poncelet et al. (1983). Male Wistar rats were trained to press a lever with food reinforcement according to a continuously reinforced schedule (CRF). Afterwards, rats were subjected to three experimental sessions (30 min each) during which responding was rewarded according to a progressive ratio schedule (following an initial 2-min CRF period, the number of presses necessary for the pellet delivery was doubled every second minute). Responding during the first half of each session, i. e., pressing for food, was maintained at a significant level, whereas it was almost suppressed during the second part of the session. Animals treated with stimulants showed an increased rate of responding.

Several authors used the progressive ratio test (Richardson and Roberts 1991; McGregor et al. 1993; Bourland and Frenche 1995; Ferguson and Paule 1996; Pulvirenti et al. 1997, 1998; Duvauchelle et al. 1998; Grottick et al. 2000; Mobini et al. 2000; Wilcox et al. 2000; Woolverton et al. 2002; Schneider und Koch 2002,2003; Kozinowski et al. 2003; Solinas et al. 2004).

PROCEDURE

Drews et al. (2005) studied the effects of a cannabinoid agonist on operant behavior and locomotor activity in rats. The progressive ratio test was conducted in an operant chamber ($24 \times 28 \times 28$ cm) (Operant Behavior System, TSE Systems, Bad Homburg, Germany). First, male Wistar rats were habituated for 1 day to the test chamber, the palatable casein pellets and the noise of the magazine response. After shaping, rats were trained over 3 days at lever pressing in sessions of 30 min on a continuous reinforcement schedule until they reached a stable baseline. After lever pressing was completed, one progressive ratio test session (for 30 min) was conducted on the next day. The progressive ratio schedule (i. e., lever presses for one pellet) was changed every second minute according to the following exponential progression: 1, 2, 4, 6, 9, 12, 15,. . . , derived from the formula $5 \cdot e^{02\,n} - 5$, where n is the position in the sequence of ratios (Mobini et al. 2000). The so-called break point, the conventional index of performance on a progressive ratio schedule of reinforcement (Reilly 1999), was defined as the first progressive ratio sequence where lever pressing decreased $\leq 50\%$ relative to the previous phase without increasing $\geq 100\%$ in the following phase.

EVALUATION

Student's *t*-test was used to evaluate operant responding in the progressive ratio test.

MODIFICATIONS OF THE METHOD

Barr and Phillips (1999) found that withdrawal following exposure to d-amphetamine decreases responding for a sucrose solution as measured by a progressive ratio schedule of reinforcement. The authors concluded that the progressive ratio procedure may be a useful technique for evaluating changes in motivation to natural reinforcing stimuli following withdrawal from psychostimulant drugs.

For safety studies, the response requirement increases for every infusion or after a fixed period of time until the animal ceases to lever-press for a pre-determined interval, defined as the breaking point. The presumption of progressive ratio studies is that the higher the breaking point the greater the reinforcing effectiveness, although the same potential complications regarding pharmacokinetics that were noted above for a simple (FR) schedule of self administration also apply to progressive ratio schedules.

Weed et al. (1997) studied the relationship between reinforcing effects and *in vitro* effects of D1 agonists in **rhesus monkeys**.

REFERENCES AND FURTHER READING

Barr AM, Phillips AG (1999) Withdrawal following exposure to d-amphetamine decreases responding for a sucrose solution as measured by a progressive ratio schedule of reinforcement. Psychopharmacology (Berl) 141:99–106

Bourland JA, French ED (1995) Effects of remoxipride, an atypical antipsychotic, on cocaine self-administration in the rat using fixed- and progressive-ratio schedules of reinforcement. Drug Alcohol Depend 40:111–114

Drews E, Schneider M, Koch M (2005) Effects of the cannabinoid agonist win 55,212–2 on operant behavior and locomotor activity in rats. Pharmacol Biochem Behav 80:145–150

Duvauchelle CL, Sapoznik T, Kornetsky C (1998) The synergistic effects of combining cocaine and heroin ("Speedball") using a progressive-ratio schedule of drug reinforcement. Pharmacol Biochem Behav 61:297–302

Ferguson SA, Paule MG (1996) Effects of chlorpromazine and diazepam on time estimation behavior and motivation of rats. Pharmacol Biochem Behav 53:115–122

Grottnick AJ, Fletcher PJ, Higgins GA (2000) Studies to investigate the role of 5-HT_{2C1} receptors on cocaine- and food-maintained behavior. J Pharmacol Exp Ther 295:1183–1191

Kozinowski AP, Johnson KM, Deschaux O, Bandyopadhyay BD, Araldi GL, Carmona G, Munzar P, Smith MP, Balster RL, Beardsley PM, Tella SR (2003) Mixed

cocaine agonist/antagonist properties of (+).methyl-4β-(4-chlorophenyl)-1-methylpiperidine-3α-carboxylate, a piperidine-based analog of cocaine. J Pharmacol Exp Ther 305:143–150
McGregor A, Lacosta S, Roberts DC (1993) L-tryptophan decreases the breaking point under a progressive ratio schedule of intravenous cocaine reinforcement in the rat. Pharmacol Biochem Behav 44:651–655
Mobini S, Chiang TJ, Ho MY, Bradshaw CM, Szabadi E (2000) Comparison of the effects of clopazine, haloperidol, chlorpromazine and D-amphetamine on performance of a time-constrained progressive ratio schedule and on locomotor behavior in the rat. Psychopharmacology 152:47–54
Poncelet M, Chermat R, Soubrie P, Simon P (1983) The progressive ration schedule as a model for studying the psychomotor stimulant activity of drugs in the rat. Psychopharmacology (Berl) 80:184–189
Pulvirenti L, Balducci C, Koob GF (1997) Dextromorphan reduces intravenous cocaine self-administration in the rat. Eur J Pharmacol 321:279–281
Pulvirenti L, Balducci C, Pierci M, Koob GF (1998) Characterization of the effects of the partial dopamine agonist Terguride on cocaine self-administration in the rat. J Pharmacol Exp Ther 286:1231–1238
Reilly S (1999) Reinforcement value of gustatory stimuli determined by progressive ratio performance. Pharmacol Biochem Behav 63:301–311
Richardson NR, Roberts DC (1991) Fluoxetine pretreatment reduces breaking points on a progressive ratio schedule reinforced by intravenous cocaine self-administration in the rat. Life Sci 49:833–840
Schneider M, Koch M (2002) The cannabinoid agonist WIN 55–212–2 reduces sensorimotor gating and recognition memory in rats. Behav Pharmacol 13:29–37
Schneider M, Koch M (2003) Chronic pubertal, but not adult chronic cannabinoid treatment impairs sensorimotor gating, recognition memory, and the performance in a progressive ratio task in adult rats. Neuropsychopharmacology 28:1760–1769
Solinas M, Panililio LV, Goldberg SR (2004) Exposure to delta-9-tetrahydrocannabinol (THC) increases subsequent heroin taking but not heroin's reinforcing efficacy: a self-administration study in rats. Neuropsychopharmacology 29:1301–1311
Weed MR, Paul IA, Dwoskin LP, Moore SE, Woolverton WL (1997) The relationship between reinforcing effects and *in vitro* effects of D1 agonists in monkeys. J Pharmacol Exp Ther 283:29–38
Wilcox KM, Rowlett JK, Paul IA, Ordway GA, Woolverton WL (2000) On the relationship between the dopamine transporter and the reinforcing effects of local anesthetics: practical and theoretical concerns. Psychopharmacology 153:139–147
Woolverton WL, Ranaldi R, Wang Z, Ordway GA, Paul IA, Petukhov P, Kozinowski A (2002) Reinforcing strength of a novel dopamine transporter ligand: pharmacodynamic and pharmacokinetic properties. J Pharmacol Exp Ther 303:212–217

E.2.5.4 Conditioned Defensive Burying in Rats

PURPOSE AND RATIONALE

Besides the well known defensive reactions of animals in typical laboratory settings, like freezing, fleeing, and attacking, rats tested in the presence of bedding material develop a peculiar behavior when shocked through a stationary prod by burying the shock source. This behavior has been proposed as a new paradigm for the study of anxiolytic agents (Pinel and Treit 1978, 1983; Treit et al. 1981).

PROCEDURE

Male adult rats weighing 250–400 g are used. The testing is performed in $44 \times 30 \times 44$ cm Plexiglas test chambers, the floor of which is covered with 5 cm of a commercial bedding material. In the center of each of the four walls, 2 cm above the level of the bedding material, is a small hole though which a $6.5 \times 0.5 \times 0.5$ cm wire-wrapped wooden dowel (i. e., the shock prod) can be inserted. Electric current is administered through the two uninsulated wires wrapped around the prod. The behavior of each rat is monitored for 15 min from a separate room via closed circuit television.

Before each of the experiments, the rats are placed in the Plexiglas test chamber in groups of 5 or 6 for 30-min periods on each of 4 consecutive days. In the experiments, groups of 10 animals are used for each dose and control. The rat is injected intraperitoneally with the test drug or saline before being placed into the test chamber in which the shock prod is inserted. The animal is placed into the center of the chamber so that is faces away from the prod. When the rat first touches the prod with its forepaw, it receives a brief electric shock (1 mA) which typically elicits a flinch away from the prod and withdrawal towards the back of the chamber. Afterwards, the rat moves directly towards the prod, pushing and spraying a pile of bedding material ahead with rapid shoveling movements of its snout and alternating pushing movements of its forepaws. The prod is buried in a pile of bedding material. The duration of burying is recorded.

EVALUATION

The mean duration of burying in treated animals is compared with controls. Anxiolytics as well as neuroleptics shorten the burying behavior dose-dependent at low shock intensity (1 mA). A second measure is the height of the bedding material. At high shock intensity (10 mA) only neuroleptics but not benzodiazepines are active.

CRITICAL ASSESSMENT OF THE METHOD

The method of conditioned defensive behavior can be regarded as a simple and reliable method to detect anxiolytic activity of benzodiazepines and neuroleptics. However, using higher shock intensity – where only

chlorpromazine was found to be active – a separation between benzodiazepines and neuroleptics has been demonstrated.

The drug-class specificity of the test has been challenged by Craft et al. (1988).

MODIFICATIONS OF THE METHOD

Diamant et al. (1991) used telemetry to register autonomic and behavioral responses in the shock-prod burying test in rats.

Wiersma et al. (1996) reported that microinfusion of corticotropin-releasing hormone in the central amygdala of freely moving rats enhanced the active behavior responses in the conditioned defensive burying paradigm.

Fernandez-Guasti and Lopez-Rubalcava (1998) used the rat burying behavior test to study the effect of various potential anxiolytics.

Broekkamp et al. (1986), Njung'e and Handley (1991a, b; Gacsályi et al. 1997) described burying of marbles by *mice* as harmless objects without punishment by electrical shocks as a model for detection of anxiolytics. Thirty min after treatment with drugs, male Swiss mice, weighing 20–24 g, were individually placed in a 23 × 17 × 14 cm cage with 25 glass marbles, 1.5 cm in diameter. The glass marbles were placed in close contact in the middle of the cage on a 5 cm layer of sawdust. The mice were left in the cage with the marbles for 30 min after which the test was terminated by removing the mice and counting the number of marbles that were more than two thirds covered with sawdust.

DeBoer and Koolhaas (2003) reviewed the ethology, neurobiology and psychopharmacology of defensive burying in rodents.

REFERENCES AND FURTHER READING

Broekkamp CL, Rijk HW, Joly-Gelouin D, Lloyd KL (1986) Major tranquillizers can be distinguished from minor tranquillizers on the basis of effects on marble burying and swim-induced grooming in mice. Eur J Pharmacol 126:223–229

Craft RM, Howard JL, Pollard GT (1988) Conditioned defensive burying as a model for identifying anxiolytics. Pharmacol Biochem Behav 30:775–780

deBoer SF, Slangen JL, van der Gugten J (1990) Plasma catecholamine and corticosterone levels during active and passive shock-prod avoidance behavior in rats: Effects of chlordiazepoxide. Physiol Behav 47:1089–1098

deBoer SF van der Gugten J, Slangen Jl (1991) Behavioural and hormonal indices of anxiolytic and anxiogenic drug action in the shock prod defensive burying/avoidance paradigm. In: Olivier B, Mos J, Slangen JL (eds) Animal Models in Psychopharmacology, Birkhäuser Verlag Basel, pp 137–159

DeBoer SF, Koolhaas JM (2003) Defensive burying in rodents: ethology, neurobiology and psychopharmacology. Eur J Pharmacol 463:145–161

Diamant M, Croiset G, de Zwart N, de Wied D (1991) Shock-prod burying test in rats: autonomic and behavioral responses. Physiol Behav 50:23–31

Fernandez-Guasti A, Lopez-Rubalcava C (1998) Modification of the anxiolytic action of 5-HT_{1A} compounds by GABA-benzodiazepine agents in rats. Pharmacol Biochem Behav 60:27–32

Gacsályi I, Schmidt E, Gyertyán I, Vasar E, Lang A, Haapalinna A, Fekete M, Hietala J, Syvälahti E, Tuomainen P, Männistö P (1997) Receptor binding profile and anxiolytic-type activity of deramciclane (EGIS-3886) in animal models. Drug Dev Res 40:333–348

Njung'e K, Handley SL (1991a) Evaluation of marble-burying behavior as a model of anxiety. Pharmacol Biochem Behav 38:63–67

Njung'e K, Handley SL (1991b) Effects of 5-HT uptake inhibitors, agonists and antagonists on the burying of harmless objects by mice; a putative test for anxiolytic agents. Br J Pharmacol 104:105–112

Pinel JPJ, Treit D (1978) Burying as a defensive response in rats. J Compar Physiol Psychol 92:708–712

Pinel JPJ, Treit D (1983) The conditioned defensive burying paradigm and behavioral neuroscience. In: Robinson T (ed) Behavioral approaches to brain research. pp 212–234. Oxford Press

Treit D (1985) Animal models for the study of anti-anxiety agents. A review. Neurosci Biobehav Rev 9:203–222

Treit D, Pinel JPJ, Fibiger HC (1981) Conditioned defensive burying: A new paradigm for the study of anxiolytic agents. Pharmacol Biochem Behav 15:619–626

Wiersma A, Bohus B, Koolhaas JM, Nobel A, (1996) Corticotropin-releasing hormone microinfusion of in the central amygdala enhances active behavior responses in the conditioned defensive burying paradigm. Stress 1:113–122

E.2.5.5 Taste Aversion Paradigm

PURPOSE AND RATIONALE

When ingestion of a taste stimulus is paired with internal malaise the animal remembers the taste and rejects its ingestion thereafter. This phenomenon is called a conditioned taste aversion or taste aversion learning. In the classical experiment in rats, the conditioned stimulus is a 0.01 M drinking solution of saccharin paired with an intraperitoneal injection of 0.15 M LiCl solution as unconditioned stimulus. The underlying neural mechanisms (Yamamoto 1993; Agüero et al. 1993, 1996; Swank et al. 1995) as well as facilitating and inhibiting factors (Lipinski et al. 1995; Sobel et al. 1995) were investigated. Moreover, drugs by themselves can be studied. Rats are presented a fluid with palatable taste and immediately after consumption of this liquid injected with a drug, whose effect the animals have not experienced before. Subsequently, on a later occasion and under non-drug conditions, avoid-

ance of the taste associated with the drug is measured (De Beun et al. 1996).

PROCEDURE

Male Wistar rats weighing 220–250 g are housed in groups of four per cage under a normal 12L:12D regime at 22–23°C with free access to food and water. Twenty-four hours before the first conditioned taste aversion session, the animals are water deprived and fluid access is from then on restricted to daily experimental sessions of 15 min which takes place individually in a test cage. After each session, the animals are returned to their home cages. Food is freely available in the home cages throughout the procedure, but not available during the sessions. For a given subject, all six session required to complete a conditioned taste aversion experiment take place in the same test cage. Animals designated to the same experimental group are run in parallel. During the first four sessions (day 1 through day 4), both bottles contain plain tap water. During this phase of the procedure, the animal learns to drink a reasonable amount of fluid in a short period of time. For the 5th session (day 5, conditioning session), both bottles are filled with a 0.1% saccharin solution and immediately after completion of this session the animals are injected with either the vehicle or different doses of the test drug. Per animal, only one dose (or the vehicle) of a particular drug is tested. On days 6 and 7, no sessions are conducted (washout period) and the animals have free access to tap water in the home cages from the end of day 5 until the morning of day 7, when the animals are again deprived of water, 24 h prior to the final 6th session (day 8, test session). During this last session, one bottle contains the saccharin solution and the other bottle is filled with tap water. To control for location bias, the saccharin is presented in the left bottle for half of the animals in each group and in the right bottle for the other half. By measuring the amount of fluid consumed from both bottles separately, drug-induced conditioned taste aversion can be determined by comparison of the relative saccharin intake in the drug treated groups and their vehicle-treated controls.

EVALUATION

Data of test drugs are submitted separately to one-way analysis of variance, with the between-subjects factor DOSE. The dependent variable is the ratio of (saccharin solution/saccharin solution+tap water) intake. Fluid intake scores are calculated in grams. Post hoc analyses are used with Tukey HSD multiple comparisons. Results are considered significant when $p < 0.05$.

MODIFICATIONS OF THE METHOD

Besides LiCl, several other drugs were used to induce taste aversion, such as ethanol (Gauvin and Holloway 1992; June et al. 1992; Thiele et al. 1996; Bienkwoski et al. 1997), morphine (Miller et al. 1990; Bardo and Valone 1994), cocaine (Van Haaren and Highes 1990; Glowa et al. 1994), naloxone (Mucha 1997), apomorphine (McAllister and Pratt (1998), caffeine (Brockwell et al. 1991), d-amphetamine (Davies and Wellman 1990; Lin et al. 1994), nicotine (Shoaib and Stolermman 1996), quinine (Parker 1994), cisplatin (Mele et al. (1992), benzodiazepine and nonbenzodiazepine anxiolytics (Neisewander et al. 1990), 5-hydroxytryptamine (Rudd et al. 1998), dopamine D_3 agonists (Bevins et al. 1996), cyclosporine A (Exton et al. 1998), cholecystokinin (Ervin et al. 1995; Mosher et al. 1996) and Δ9-tetrahydrocannabinol (Parker and Gillies 1995).

Turenne et al. (1996) found individual differences in reactivity to the aversive properties of drugs. Rats were assigned to high conditioned taste avoidance and low conditioned taste avoidance groups on the basis of their intake of saccharin solution previously paired with morphine, amphetamine, lithium, or fenfluramine.

Willner et al. (1992) investigated the influence of drugs on taste-potentiated odor aversion learning in rats.

Rabin and Hunt (1992) studied taste aversion learning in **ferrets**.

REFERENCES AND FURTHER READING

Agüero A, Arnedo M, Gallo M, Puerto A (1993) The functional relevance of the lateral parabrachial nucleus in lithium chloride-induced aversion learning. Pharmacol Biochem Behav 45:973–978

Agüero A, Gallo M, Arnedo M, Molina F, Puerto A (1996) Effects of lesions of the medial parabrachial nucleus (PBNm): Taste discrimination and lithium-chloride-induced aversion learning after delayed and contiguous interstimulus intervals. Psychobiology 24:265–280

Bardo MT, Valone JM (1994) Morphine-conditioned analgesia using a taste cue: Dissociation of taste aversion and analgesia. Psychopharmacology 114:269–274

Bevins RA, Delzer TA, Bardo MT (1996) Characterization of the conditioned taste aversion produced by 7-OH-DPAT in rats. Pharmacol Biochem Behav 53:695–599

Bienkowski P, Kuca P, Piasecki J, Kostowski W (1997) 5-HT_3 receptor antagonist, tropisetron, does not influence ethanol-induced conditioned taste aversion and conditioned place aversion. Alcohol 14:63–69

Brockwell NT, Eikelboom R, Beninger RJ (1991) Caffeine-induced place and taste conditioning: Production of dose-dependent preference and aversion. Pharmacol Biochem Behav 38:513–517

Davies BT, Wellman PJ (1990) Conditioned taste reactivity in rats after phenylpropanolamine, d-amphetamine

or lithium chloride. Pharmacol Biochem Behav 36:973–977
De Beun R, Lohmann A, de Vry J (1996) Conditioned taste aversion and place preference induced by the calcium channel antagonist nimodipine in rats. Pharmacol Biochem Behav 54:657–663
Ervin GN, Birkemo LS, Johnson MF, Conger LK, Mosher JT, Menius JA Jr (1995) The effects of anorectic and aversive agents on deprivation-induced feeding and taste aversion conditioning in rats. J Pharmacol Exp Ther273:1203–1210
Exton MS, von Horsten S, Voge J, Westermann J, Schult M, Nagel E, Schedlowski M (1998) Conditioned taste aversion produced by cyclosporine A: concomitant reduction of lymphoid organ weight and splenocyte proliferation. Physiol Behav 63:241–247
Gauvin DV, Holloway FA (1992) Ethanol tolerance developed during intoxicated operant performance in rats prevents subsequent ethanol-induced conditioned taste aversion. Alcohol 9:167–170
Glowa JR, Shaw AE, Riley AL (1994) Cocaine-induced conditioned taste aversion: Comparisons between effects in LEW/N and F344/N rat strains. Psychopharmacology 114:229–232
June HL, June PL, Domangue KR, Hicks LH, Lummis GH, Lewis MJ (1992) Failure of Ro15–4513 to alter an ethanol-induced taste aversion. Pharmacol Biochem Behav 41:455–460
Land CL, Riccio DC (1997) D-Cycloserine, a positive modulator of the NMDA receptor, enhances acquisition of a conditioned taste aversion. Psychobiology 25:210–216
Lin HQ, McGregor IS, Atrens DM, Christie MJ, Jackson DM (1994) Contrasting effects of dopamine blockade on MDMA and d-amphetamine conditioned taste aversion. Pharmacol Biochem Behav 47:369–374
Lipinski WJ, Rusiniak KW, Hilliard M, Davis RE (1995) Nerve growth factor facilitates conditioned taste aversion learning in normal rats. Brain Res 692:143–153
McAllister KHM, Pratt JA (1998) GR205171 blocks apomorphine and amphetamine-induced conditioned taste aversions. Eur J Pharmacol 353:141–148
Mele PC, McDonough JR, McLean DB, O'Halloran KP (1992) Cisplatin-induced conditioned taste aversion: attenuation by dexamethasone but not by zacopride or GR38032F. Eur J Pharmacol 218:229–236
Miller JS, Kelly KS, Neisewander JL, McCoy DF, Bardo MT (1990) Conditioning of morphine-induced taste aversion and analgesia. Psychopharmacology 101:472–480
Mosher JT, Hohnson MF, Birkemo LS, Ervin GN (1996) Several roles of CCK_A and CCK_B receptor subtypes in CCK-8-induced and LiCl-induced taste aversion conditioning. Peptides 17:483–488
Mucha RF (1997) Preference for tastes paired with a nicotine antagonist in rats chronically treated with nicotine. Pharmacol Biochem Behav 56:175–179
Neisewander JL, McDougall SA, Bowling SL, Bardo MT (1990) Conditioned taste aversion and place preference with buspirone and gespirone. Psychopharmacology 100:485–490
Parker LA (1994) Aversive taste reactivity: Reactivity to quinine predicts aversive reactivity to lithium-paired sucrose solution. Pharmacol Biochem Behav 47:73–75
Parker LA, Gillies T (1995) THC-induced place and taste aversions in Lewis and Sprague-Dawley rats. Behav Neurosci 109:71–78
Rabin BM, Hunt WA (1992) Relationship between vomiting and taste aversion learning in ferrets: studies with ionizing radiation, lithium chloride, and amphetamine. Behav Neural Biol 58:83–93
Rudd JA, Ngan MP, Wai MK (1998) $5\text{-}HT_3$ receptors are not involved in conditioned taste aversions induced by 5-hydroxytryptamine, ipecacuanha or cisplatin. Eur J Pharmacol 352:143–149
Shoaib M, Stolerman IP (1996) The NMDA antagonist dizocilpine (MK801) attenuates tolerance to nicotine in rats. J Psychopharmacol 10:214–218
Sobel BFX, Wetherington CL, Riley AL (1995) The contribution of within-session averaging of drug- and vehicle-appropriate responding to the graded dose-response function in drug discriminating learning. Behav Pharmacol 6:348–358
Swank MW, Schafe GE, Bernstein IL (1995) c-Fos induction in response to taste stimuli previously paired with amphetamine or LiCl during taste aversion learning. Brain Res 673:251–261
Thiele TE, Roitman MF, Bernstein IL (1996) c-Fos induction in rat brainstem in response to ethanol- and lithium chloride-induced conditioned taste aversions. Alcohol Clin Exp Res 20:1023–1028
Turenne SD, Miles C, Parker LA, Siegel S (1996) Individual differences in reactivity to the rewarding/aversive properties of drugs: assessment by taste and place conditioning. Pharmacol Biochem Behav 53:511–516
Van Haaren F, Hughes CE (1990) Cocaine-induced conditioned taste aversions in male and female Wistar rats. Pharmacol Biochem Behav 37:693–696
Willner J, Gallagher M, Graham PW, Crooks GB Jr (1992) N-methyl-D-aspartate antagonist D-APV selectively disrupts taste-potentiated odor aversion learning. Behav Neurosci 106:315–323
Yamamoto T (1993) Neural mechanisms of taste aversion learning. Neurosci Res 16:181–185

E.2.5.6 Cued and Contextual Fear Conditioning

PURPOSE AND RATIONALE

Fear-conditioning is a form of Pavlovian conditioning where an animal is trained to associate a neural stimulus (e. g., a 10-s presentation of light) with an aversive, unconditioned stimulus (US), such as an electric foot shock. After such pairings, the light alone predicts the occurrence of the shock and acts as a conditioned stimulus (CS), eliciting a state of fear. Tones, lights, odors and tactile stimuli have been used as CS in fear-conditioning experiments (Anagnostaras et al. 1999; Fendt and Fanselow 1999). A startle response is elicited by a sudden acoustic, visual or tactile stimulus and is composed of a fast, sequential muscle contraction, with the most prominent reaction around the face, neck, and shoulders.

The **fear-potentiated startle paradigm** was initially described by Brown et al. (1951). Rats are given several pairings of light CS and foot shock. After this procedure, the mean amplitude of the acoustic startle response to a loud noise is usually 50%–100% higher in the presence of the light CS than to the noise alone. The difference between these two trial types represents

the fear potentiation of the startle response and acts as a measure of fear.

In the **cued and contextual fear conditioning paradigm,** animals learn to associate a novel environment (context) and a previously neutral stimulus (conditioned stimulus, a tone) with an aversive foot shock stimulus. Testing then occurs in the absence of the aversive stimulus. Conditioned animals, when exposed to the conditioned stimuli, tend to refrain from all but respiratory movement. Freezing responses can be triggered by exposure to either the context in which the shock was received (context test) or the conditioned stimulus.

Sullivan et al. (2003) determined the effects of doxapram for cue and contextual fear conditioning in rats.

PROCEDURE

Fear Conditioning Apparatus

Pavlovian fear conditioning was performed using a clear polycarbonate conditioning chamber encased by a sound-attenuating outer box and fitted with metal bars as a floor that can deliver current (context 1). For fear conditioning to cue, the context was changed between the conditioning and the testing day to enhance the specificity of the fear response to the tone cue on testing. For the testing day, striped walls were placed on the outer surface of the clear chamber walls, the floor was fitted with a black panel covering the bars, the ambient light was lower, and the floor had a peppermint odor from cleaning with a scented detergent (context 2). A microcamera on the ceiling of the chamber allowed observation during the experiments and a videotape record for scoring of behavior.

Cued fear conditioning behavioral procedure

On conditioning day 0, adult male Sprague Dawley rats were habituated to the conditioning chamber for 15 min. On conditioning day 1 the rats received an intraperitoneal injection of drug and were returned to the home cages. After 10 min each rat was placed in the conditioning chamber (context 1) and was trained with two trials of tone-shock pairings. The tone (10 kHz, 72 dB) lasted 20 s and co-terminated with a 0.5-s, 7-mA shock. The intertrial interval was variable (mean 120 s) and was generated by a computer program. Videotape of the conditioning allowed later scoring of the level of freezing during each tone. On test days 1, 2, and 3, rats were tested with the different contextual stimuli in the chamber (context 2). On each day they received ten presentations of the 20-s tone (no shocks) while being videotaped for later scoring of the time spent freezing during each tone. Rats were matched by weight for control and various doses of test drug.

Contextual fear-conditioning behavioral procedure

On conditioning day 0, the rats were habituated to the conditioning chamber (context 1) for 20 min. On conditioning day 1, the rats received an intraperitoneal injection of drug and were returned to their home cages. After 7 min, each rat was placed in the same chamber (context 1), and at 8 min after injection the computer program was initiated that trained with two shocks separated by a variable intertrial interval (mean 120 s). The shocks were 1.5 mA and lasted 0.5 s, and the total time in the chamber was 8 min for all subjects. On day 2, rats were tested in the same chamber (context 1) for 5 min while being videotaped for later scoring. The 30-s periods before and after shock 1, the 30-s period after shock 2, and the first 30 s of each minute during the 5 min of testing were scored for freezing. Rats were matched by weight for vehicle and drug-treated groups.

EVALUATION

Data were analyzed with a series of one-way analyses of variance with repeated measures or with Student's *t*-tests.

MODIFICATIONS OF THE METHOD

Several modifications of this procedure have been used for various purposes (Phillips and LeDoux 1992; Lu and Wehner 1997; Maren 1998; Laurent-Demir and Jaffard 2000; DeLorey et al. 2001; Gupta et al. 2001; Malkani and Rosen 2001; McKay et al. 2002; Riedel et al. 2002; Cambon et al. 2003; Fischer et al. 2003; Maciejak et al. 2003; Walker and Carrive 2003; Sienkiewicz-Jarosz et al. 2003; Célérier et al. 2004; Kudo et al. 2004; Mesches et al. 2004; Roberts et al. 2004; Takahashi 2004; Wehner et al. 2004).

Zhang et al. (2004) used a telemetric system for recording cardiovascular data and automated measurement of conditioned freezing behavior.

Contarino et al. (2002) described automated assessment of conditioning parameters for context and cued fear in mice.

Several authors (Radulovic et al. 1998; Stiedl et al. 1999, 2000; Kishimoto et al. 2000; Eckart et al. 2001; Maciejak et al. 2003; Tezval et al. 2004; Võikar et al. 2004; Radyushkin et al. 2005; Tovote et al. 2005) used a commercially available fear-conditioning system (TSE Systems, Bad Homburg, Germany) consist-

ing of the following components: up to four boxes with animal location sensors, shock grid and test arena; box housing with software-controlled loud speaker, software-controlled light and ventilator; control unit with integrated shocker/scrambler; fear-conditioning software; PC-interface.

Crestani et al. (2002) and Gould et al. (2004) distinguished between delay fear conditioning and trace fear conditioning. For delay fear conditioning, after 3 min exposure to the chamber mice received three successive tone-shock pairings with the shock delivered during the last 500 ms of the tone. Freezing was recorded 48 h later in a modified context (new olfactory, tactile, and visual cues) for 3 min and subsequently in the presence of the tone for 8 min. For trace fear conditioning, the procedure was similar to that for delay conditioning, except that an empty trace interval of 1 s was interposed between the tone and the foot shock in three learning trials.

REFERENCES AND FURTHER READING

Anagnostaras SG, Maren S, Sage JR, Goodrich S, Fanselow MS (1999) Scopolamine and Pavlovian fear conditioning in rats: dose-effect analysis. Neuropsychopharmacology 21:731–744

Brown JS, Kalish HI, Farber IE (1951) Conditioned fear as revealed by magnitude of startle response to an auditory stimulus. J Exp Psychol 41:317–328

Cambon K, Venero C, Berezin V, Bock E, Sandi C (2003) Post-training administration of a synthetic peptide ligand of the neural cell adhesion molecule, C3d, attenuates long-term expression of contextual fear conditioning. Neuroscience 122:183–191

Célérier A, Pierard C, Beracochea D (2004) Effect of ibotenic acid lesions of the dorsal hippocampus on contextual fear conditioning in mice: comparison with mammillary body lesions. Behav Brain Res 151:65–72

Contarino A, Baca L, Kennelly A, Gold LH (2002) Automated assessment of conditioning parameters for context and cued fear in mice. Learn Mem 9:89–96

Crestani F, Keist R, Fritschy JM, Benke D, Vogt K, Prut L, Blüthmann H, Möhler H, Rudolph U (2002) Trace fear conditioning involves hippocampal á$_5$ GABA$_A$ receptors. Proc Natl Acad Sci USA 99:8980–8985

DeLorey TM, Lin RC, McBrady B, He X, Cook JM, Lameh J, Loew GH (2001) Influence of benzodiazepine binding site ligands on fear-conditioned contextual memory. Eur J Pharmacol 426:45–54

Eckart K, Jahn O, Radulovic J, Tezval H, van Werven L, Spiess J (2001) A single amino acid serves as an affinity switch between the receptor and the binding protein of corticotrophin-releasing factor: Implications for the design of agonists and antagonists. Proc Natl Acad Sci USA 98:11142–11147

Fendt M, Fanselow MS (1999) The neuroanatomical and neurochemical basis of conditioned fear. Neurosci Biobehav Rev 23:743–70

Fischer A, Sananbenesi F, Schrick C, Spiess J, Radulovic J (2003) Regulation of contextual fear conditioning by baseline and inducible septo-hippocampal cyclin-dependent kinase 5. Neuropharmacology 44:1089–1099

Gould T, Feiro O, Moore D (2004) Nicotine enhances trace cued fear conditioning but not delay cued fear conditioning in C57BL/6 mice. Behav Brain Res 155:167–173

Gupta RR, Sen S, Diepenhorst LL, Rudick CN, Marebn S (2001) Estrogen modulates sexually dimorphic contextual fear conditioning and hippocampal long-term potentiation (LTP) in rats. Brain Res 888:336–365

Kishimoto J, Radulovic J, Radulovic M, Lin CR, Schrick C, Hooshmand F, Hermanson O, Rosenfeld MG, Spiess J (2000) Deletion of *Crhr2* reveals an anxiolytic role for corticotropin-releasing hormone receptor-2. Nature Genet 24:415–419

Kudo K, Qiao CX, Kanba S, Arita J (2004) A selective increase in phosphorylation of cyclic AMP response element-binding protein in hippocampal CA1 region of male, but not female, rats following contextual fear and passive avoidance conditioning. Brain Res 1024:233–243

Laurent-Demir C, Jaffard R (2000) Paradoxical facilitatory effect of fornix lesions on acquisition of contextual fear conditioning in mice. Behav Brain Res 107:85–91

Lu Y, Wehner JM (1997) Enhancement of contextual fear-conditioning by putative (±)-á-amino-3-hydroxy-5-methylisoxazole-4-propionic acid (AMPA) receptor modulators and *N*-methyl-D-aspartate (NMDA) receptor antagonists in DBA/2J mice. Brain Res 786:197–207

Maciejak P, Taracha E, Lehner M, Szyndler J, Bidzinski A, Skórzewska A, Wislowska A, Zienowicz M, Plaznik A (2003) Hippocampal mGluR1 and consolidation of contextual fear conditioning. Brain Res Bull 62:39–45

Malkani S, Rosen JB (2001) *N*-Methyl-D-aspartate receptor antagonism blocks contextual fear conditioning and differentially regulates early growth response-1 messenger RNA expression in the amygdala: implications for a functional amygdaloid circuit of fear. Neuroscience 102:853–861

Maren S (1998) Effects of 7-nitroindazole, a neuronal nitric oxide synthase (nNOS) inhibitor, on locomotor activity and contextual fear conditioning in rats. Brain Res 804:155–158

McKay BE, Lado WE, Martin LJ, Galic MA, Fournier NM (2002) Learning and memory in agmatine-treated rats. Pharmacol Biochem Behav 72:551–557

Mesches MH, Gemma C, Veng LM, Allgeier C, Young DA, Browning MD, Bickford PC (2004) Sulindac improves memory and increases NMDA receptor subunits in aged Fischer 344 rats. Neurobiol Aging 25:315–324

Phillips RG, LeDoux JE (1992) Differential contribution of amygdala and hippocampus to cued and contextual fear conditioning. Behav Neurosci 106:274–285

Radulovic J, Kammermeier J, Spiess J (1998) Generalization of fear responses in C57BL/6N mice subjected to one-trial foreground contextual fear conditioning. Behav Brain Res 95:179–189

Radyushkin K, Anokhin KL, Meyer BI, Jiang Q, Alvarez-Bolado G, Gruss P (2005) Genetic ablation of the mammillary bodies in the *Foxb1* mutant mouse leads to selective deficit of spatial working memory. Eur J Neurosci 21:219–229

Riedel G, Sandager-Nielsen K, Macphail EM (2002) Impairment of contextual fear conditioning in rats by Group I mGluRs: reversal by the nootropic nefiracetam. Pharmacol Biochem Behav 73:391–399

Roberts AJ, Krucker T, Levy CL, Slanina KA, Sutcliffe JG, Hedlund PB (2004) Mice lacking 5-HT$_7$ receptors show specific impairments in contextual learning. Eur J Neurosci 19:1913–1922

Sienkiewicz-Jarosz H, Maciajak P, Bidziński A, Szyndler J, Siemątkowski M, Czlonkowska A, Lehner M, Plaźnik A

(2003) Exploratory activity and a conditioned fear response: correlation with cortical and subcortical binding of the $\alpha 4\beta 2$ nicotinic receptor agonist [^{3}H]-epibatine. Pol J Pharmacol 55:17–23
Stiedl O, Radulovic J, Lohmann R, Birkenfeld K, Palve M, Kammermeier J, Sananbenesi F, Spiess J (1999) Strain and substrate differences in context- and tone-dependent fear conditioning of inbred mice. Behav Brain Res 104:1–12
Stiedl O, Misana I, Spiess J, Ögren SO (2000) Involvement of the 5-HT_{1A} receptors in classical fear conditioning in C57BL/6J mice. J Neurosci 20:8515–8527
Sullivan GM, Apergis J, Gorman JM, LeDoux JE (2003) Rodent Doxapram model of panic: behavioral effects and c-fos immunoreactivity in the amygdala. Biol Psychiatry 53:863–870
Takahashi H (2004) Automated measurement of freezing time to contextual and auditory cues in fear conditioning as a simple screening method to assess learning and memory in rats. J Toxicol Sci 29:53–61
Tezval H, Jahn O, Todorovic C, Sasse A, Eckart K, Spiess J (2004) Cortagine, a specific agonist of corticotrophin-releasing factor receptor subtype 1, is anxiogenic and antidepressive in the mouse model Proc Natl Acad Sci USA 101:9468–9473
Tovote P, Meyer M, Pilz PKD, Ronnenberg A, Ögren SO, Spiess J, Stiedl O (2005) Dissociation of temporal dynamics of heart rate and blood pressure responses elicited by conditioned fear but not acoustic startle. Behav Neurosci 119:55–65
Võikar V, Rossi J, Rauvala H, Airaksinen MS (2004) Impaired behavioural flexibility and memory in mice lacking GDNF family receptor $\alpha 2$. Eur J Neurosci 20:308–312
Walker P, Carrive P (2003) Role of ventrolateral periaqueductal gray neurons in the behavioral and cardiovascular responses to contextual conditioned fear and poststress recovery. Neuroscience 116:897–912
Wehner JM, Keller JJ, Keller AB, Piciotto MR. Paylor R, Booker TK, Beaudet A, Heinemann SF, Balogh SA (2004) Role of neuronal nicotinic receptors in the effects of nicotine and ethanol on contextual fear conditioning. Neuroscience 129:11–24
Zhang WN, Murphy CA, Feldon J (2004) Behavioral and cardiovascular responses during latent inhibition of conditioned fear measurement by telemetry and conditioned freezing. Behav Brain Res 154:199–209

E.2.6
Effects on the Endocrine System

E.2.6.1
Plasma Catecholamine Levels During and After Stress

PURPOSE AND RATIONALE

A wide variety of stressors causes significant biochemical, physiological, and behavioral changes. These changes include marked increases in plasma catecholamines, heart rate and blood pressure. Treatment with anxiolytic drugs can attenuate the stress induced increases of norepinephrine and epinephrine in plasma (Vogel et al. 1984; Livesey et al. 1985; Taylor et al. 1989; de Boer et al. 1990; Krieman et al. 1992).

PROCEDURE

Male Sprague-Dawley rats, 300–350 g, are individually housed and given food and water ad libitum. After 1 week of acclimatization, an aortic catheter is surgically implanted in each animal, running on top of the psoas muscle and brought out through an incision at the back of the neck. The catheters are flushed daily with heparinized saline. After a recovery period of 48 h baseline (time –15) blood samples are drawn and blood pressure recordings are taken using a Grass model 7 polygraph. The animals are then given an i.p injection of the test compound or the vehicle. 15 min after the injection (time 0), blood samples, and heart rate and blood pressure measurements are taken. Animals in control and treatment groups are then stressed by immobilization for 1 h and blood samples, heart rate and blood pressure recordings are taken at time 15, 30 and 60 min during stress. Immobilization is performed by taping the legs of the animals to the laboratory bench. After the stress period of 1 h, the animals are released, returned to the home cage for recovery and 1 h post-stress samples and recordings are taken. Non-stressed, compound or vehicle treated animals remain in the home cage for the entire test period and are sampled in the same manner as the stressed animals. Approximately 0.3 ml blood is withdrawn for each sample and an equal amount of 0.9% saline is reinfused to prevent changes in blood volume.

EVALUATION

Determinations of norepinephrine and epinephrine in plasma are made using an radio-enzymatic assay. Heart rate and systolic and diastolic blood pressure are determined directly from the polygraph tracings. The data are analyzed using a three-way analysis of variance (ANOVA) with repeated measures, two-way ANOVA, Students *t*-test, Student-Newman-Keuls and the trapezoidal rule for the area under the curve.

CRITICAL ASSESSMENT OF THE METHOD

Reduction of catecholamine levels but no changes of the cardiovascular parameters could be found after treatment with anxiolytics. The test can be used as a method for evaluation of the influence of psychoactive drugs on the endocrine system (Krieman et al. 1992).

REFERENCES AND FURTHER READING

deBoer SF, deBeun R, Slangen JL, van der Gugten J (1990a) Dynamics of plasma catecholamine and corticosterone concentrations during reinforced and extinguished operant behavior in rats. Physiol Behav 47:691–698

deBoer SF, Slangen JL, van der Gugten J (1990b) Plasma catecholamine and corticosterone levels during active and passive shock-prod avoidance behavior in rats: effects of chlordiazepoxide. Physiol Behav 47:1089–1098

Krieman MJ, Hershock DM, Greenberg IJ, Vogel WH (1992) Effects of adinazolam on plasma catecholamine, heart rate and blood pressure responses in stressed and non-stressed rats. Neuropharmacol 31:33–38

Livesey GT, Miller JM, Vogel WH (1985) Plasma norepinephrine, epinephrine and corticosterone stress responses to restraint in individual male and female rats. Neurosci Lett 62:51–56

Natelson BH, Creighton D, McCarty R, Tapp WN, Pittman D, Ottenweller JE (1987) Adrenal hormonal indices of stress in laboratory rats. Physiol Behav 39:117–125

Taylor J, Harris N, Krieman M, Vogel WH (1989) Effects of buspirone on plasma catecholamines, heart rate and blood pressure in stressed and non-stressed rats. Pharmacol Biochem Behav 34:349–353

Vogel WH, Miller J, DeTurck KH, Routzahn BK (1984) Effects of psychoactive drugs on plasma catecholamines during stress in rats. Neuropharmacology 23:1105–1109

E.2.6.2 Plasma Corticosterone Levels Influenced by Psychotropic Drugs

PURPOSE AND RATIONALE

Corticosterone levels in the blood of rats are elevated not only after stress but also after application of selective 5-HT receptor agonists (Koenig et al. 1987). This has been used to differentiate typical and atypical neuroleptics (Nash et al. 1988).

PROCEDURE

Male Sprague Dawley rats weighing 200–250 g are housed 6 per cage under temperature and light/dark controlled conditions with free access to food and water. On the day prior to an experiment, the animals are transferred to the experimental room. On the day of the experiment, various doses of test drugs or saline are injected intraperitoneally. After 60 min 2.5 mg/kg 6-chloro-2-(1-piperazinyl)pyrazine (MK-212) are injected intraperitoneally followed by decapitation after further 60 min. Trunk blood is collected and allowed to clot. Serum is obtained following centrifugation and stored at –20°C for the radioimmunoassay of corticosterone.

EVALUATION

Data are analyzed with a two-way analysis of variance. Differences between treatment groups are evaluated using the Student-Newman-Keuls test.

MODIFICATIONS OF THE METHOD

Korte et al. (1991) studied the effect of a 5-HT_{1A} agonist on behavior and plasma corticosterone levels in male Wistar rats before and after psychological stress of defeat.

Broqua et al. (1992) measured corticosterone and glucose levels in blood together with parameters of 5-HT metabolism in brain in stressed animals treated with the anti-depressant tianeptine.

Rittenhouse et al. (1992) measured plasma concentrations of renin, corticosterone, ACTH, and prolactin in rats after treatment with a 5-HT_{1A} agonist in three stress paradigms: immobilization, forced swim and conditioned fear.

Groenink et al. (1995) studied the corticosterone secretion in rats after application of 5-HT_{1A} receptor agonists and antagonists.

Aulakh et al. (1988, 1993) reported higher baseline levels of plasma corticosterone in fawn-hooded rats relative to Wistar and Sprague-Dawley strain rats. Long-term treatment (21 days) with antidepressant drugs significantly decreased plasma corticosterone in fawn-hooded rats. The authors recommended this strain as a genetic model of depression.

REFERENCES AND FURTHER READING

Aulakh CS, Wozniak KM, Hill JL, DeVane CL, Tolliver TJ, Murphy DL (1988) Differential neuroendocrine responses to the 5-HT agonist m-chlorophenylpiperazine in fawn-hooded rats relative to Wistar and Sprague-Dawley rats. Neuroendocrinol 48:401–406

Aulakh CS, Hill JL, Murphy DL (1993) Attenuation of hypercortisolemia in fawn-hooded rats by antidepressant drugs. Eur J Pharmacol 240:85–88

Broqua P, Baudrie V, Laude D, Chaouloff F (1992) Influence of the novel antidepressant tianeptine on neurochemical, neuroendocrinological, and behavioral effects of stress in rats. Biol Psychiatry 31:391–400

Groenink L, Van der Gugten J, Mos J, Maes RAA, Olivier B (1995) The corticosterone-enhancing effects of the 5-HT_{1A} receptor antagonist, (S)-UH301, are not mediated by the 5-HT_{1A} receptor. Eur J Pharmacol 272:177–183

Koenig JI, Gudelsky GA, Meltzer HY (1987) Stimulation of corticosterone and β-endorphin secretion in the rat by selective 5-HT receptor subtype activation. Eur J Pharmacol 137:1–8

Korte SM, Smit J, Bouws GAH, Koolhaas JM, Bohus B (1991) Neuroendocrine evidence for hypersensitivity in serotonergic neuronal system after psychological stress of defeat. In: Olivier B, Mos J, Slangen JL (eds) Animal Models in Psychopharmacology. Advances in Pharmacological Sciences. Birkhäuser Verlag, Basel, pp 199–203

Nash JF, Meltzer HY, Gudelsky GA (1988) Antagonism of serotonin receptor mediated neuroendocrine and temperature responses by atypical neuroleptics in the rat. Eur J Pharmacol 151:463–469

Rittenhouse PA, Bakkum EA, O'Connor PA, Carnes M, Bethea CL, van de Kar LD (1992) Comparison of neuroendocrine and behavioral effects of ipsapirone, a 5-HT_{1A} agonist, in three stress paradigms: immobilization, forced swim and conditioned fear. Brain Res 580:205–214

E.2.7
Benzodiazepine Dependence

E.2.7.1
General Considerations

Benzodiazepine dependence is a hypothetical construct for the adaptive changes that occur as a result of chronic drug exposure. Two measures are usually considered to reflect dependence: the development to a drug's effects, and the abstinence signs of drug withdrawal.

REFERENCES AND FURTHER READING

File SE, Hitcott PK (1991) Benzodiazepine dependence. In: Briley M, File SE (eds) New Concepts in Anxiety. McMillan Press Ltd., London, pp 237–255

E.2.7.2
Benzodiazepine Tolerance and Dependence in Rats

PURPOSE AND RATIONALE

Induction of benzodiazepine tolerance and physical dependence has been reported for several animal species, such as rats, mice, dogs and monkeys. Ryan and Boisse (1983) and Boisse et al. (1986) developed a reproducible model exemplified for chlordiazepoxide in rats.

PROCEDURE

Male Sprague Dawley rats weighing 350–575 g are used. Chordiazepoxide hydrochloride is administered as solution 75 mg/ml by gavage after an initial loading dose of 450 mg/kg given at 7:00 A.M. and 5:00 P.M. Impairment of motor function is evaluated by a neurological screen including five different ladder and open field tests.

Neurological Test	Maximum Depression Points
Ladder, head down	2
Ladder, head up	4
Ladder, grasp reflex	1
Motor activity	3
Walking	5
Maximum	15

The animals are rated by three independent observers. Once dependence is revealed, lower doses are used which are then increased in appropriate steps to induce an average depression rating of about five. Treatment is continued for 5 weeks during which time the dose has to be increased. The degree of increase (about 5-fold for in the case of chlordiazepoxide) reflects the **tolerance** of the test compound.

To test **dependence**, rats are challenged with the benzodiazepine receptor antagonist Ro 15–1788 (flumazenil; ethyl-8-fluoro-5,6-dihydro-5-methyl-6-oxo-4H-imidazo(1,5a)(1,4)benzodiazepine-3-carboxylate) at a dose of 25 mg/kg i.p. Withdrawal reactions are recorded just before, and 5, 15, 30 and 60 min after administration of the antagonist. Motor, autonomic and behavioral signs are monitored by operational defined criteria, such as position of the claws, salivation and diarrhea. The total withdrawal expression for each observation and each animal is estimated by summing the grades of all signs as recorded by three independent observers.

EVALUATION

For each animal and observation time, the scores are estimated by the average of all co-observers. From these estimates group means are computed and compared by *t*-test between control and test and by paired *t*-test for self-control comparisons before and after antagonist administration

MODIFICATIONS OF THE METHOD

Further studies in *rat* with benzodiazepines were preformed by Vellucci and File (1979), Treit (1985) and Nath et al. (1997).

File (1985) found very different rates at which tolerance develops to the sedative, anticonvulsive and anxiolytic actions of benzodiazepines.

Bonnafous et al. (1995) studied the increase of gastric emptying induced by benzodiazepine withdrawal in rats. Gastric emptying was measured with a test meal containing ^{51}Cr sodium chromate administered in rats, either previously receiving 15 mg/kg diazepam or DMSO i.p. for 7 days.

Benzodiazepine-like dependence potential of a putative 5-HT_{1A} agonist anxiolytic was assessed in rats by Goudie et al. (1994).

Studies in *mice* on tolerance and physical dependence with benzodiazepines were performed by Patel et al. (1988), Gallaher et al. (1986), Stephens and Schneider (1985), Nutt and Costello (1988) and Piot et al. (1990).

These phenomena were studied in *dogs* by McNicolas et al. (1988) and Löscher et al. (1989).

Studies in monkeys were performed by Lukas and Griffiths (1982), Yanagita (1983), Lamb and Griffiths 1984) and France and Gerak (1997).

REFERENCES AND FURTHER READING

Boisse NR, Periana RM, Guarino JJ, Kruger HS, Samorski GM (1986) Pharmacological characterization of acute chlordiazepoxide dependence in the rat. J Pharmacol Exp Ther 239:775–783

Bonnafous C, Lefevre P, Bueno L (1995) Benzodiazepine-withdrawal-induced gastric emptying disturbances in rats: Evidence for serotonin receptor involvement. J Pharmacol Exp Ther 273:995–1000

File SE (1985) Tolerance to the behavioral actions of benzodiazepines. Neurosci Biobehav Rev 9:113–121

France CP, Gerak LR (1997) Discriminative stimulus effects of flumazenil in Rhesus monkeys treated chronically with chlordiazepoxide. Pharmacol Biochem Behav 56:447–455

Gallaher EJ, Henauer SA, Jacques CJ, Hollister LE (1986) Benzodiazepine dependence in mice after ingestion of drug-containing food pellets. J Pharmacol Exp Ther 237:462–467

Goudie AJ, Leathley MJ, Cowgill J (1994) Assessment of the benzodiazepine-like dependence potential in rats of a putative 5-HT_{1A} agonist anxiolytic S-20499. Behav Pharmacol 5:131–140

Lamb RJ, Griffiths RR (1984) Precipitated and spontaneous withdrawal in baboons after chronic dosing with lorazepam and CGS 9896. Drug Alc Depend 14:11–17

Lukas SE, Griffiths RR (1982) Precipitated withdrawal by a benzodiazepine receptor antagonist (Ro 15–1788) after 7 days of diazepam. Science 217:1161–1163

Löscher W, Hönack D, Faßbender CP (1989) Physical dependence on diazepam in the dog: precipitation of different abstinence syndromes by the benzodiazepine receptor antagonists Ro 15–1788 and ZK 93426. Br J Pharmacol 97:843–852

McNicholas LF, Martin WR, Sloan JW, Wala E (1988) Precipitation of abstinence in nordiazepam- and diazepam-dependent dogs. J Pharmacol Exp Ther 245:221–224

Nath C, Patnaik GK, Saxena RC, Gupta MB (1997) Evaluation of inhibitory effect of diphenhydramine on benzodiazepine dependence in rats. Indian J Physiol Pharmacol 41:42–46

Nutt DJ, Costello MJ (1988) Rapid induction of lorazepam dependence with flumazenil. Life Sci 43:1045–1053

Patel JB, Rinarelli CA, Malick JB (1988) A simple and rapid method of inducing physical dependence with benzodiazepines in mice. Pharmacol Biochem Behav 29:753–754

Piot O, Betschart J, Stutzmann JM, Blanchard JC (1990) Cyclopyrrolones, unlike some benzodiazepines, do not induce physical dependence in mice. Neurosci Lett 117:140–143

Ryan GP, Boisse NR (1983) Experimental induction of benzodiazepine tolerance and physical dependence. J Pharmacol Exp Ther 226:100–107

Stephens DN, Schneider HH (1985) Tolerance to the benzodiazepine diazepam in an animal model of anxiolytic activity. Psychopharmacol 87:322–327

Treit D (1985) Evidence that tolerance develops to the anxiolytic effect of diazepam in rats. Pharmacol Biochem Behav 22:383–387

Vellucci SV, File SE (1979) Chordiazepoxide loses its anxiolytic action with long-term treatment. Psychopharmacology 62:61–65

Yanagita T (1983) Dependence potential of zopiclone studied in monkeys. Pharmacology 27, Suppl 2:216–227

E.2.8 Genetically Modified Animals in Psychopharmacology

E.2.8.1 General Considerations

The use of genetically altered animals in biological research has also affected psychopharmacology. Genetically engineered strains of mice, modified by transgenesis or gene targeting ("knockout") have been generated and are used as research tools for deciphering the genetic basis of behavior. These animals are designed to evaluate the efficacy of new pharmacological and gene therapy treatments in human hereditary diseases (Crnic 1996; Mayford et al. 1997; Costentin 1998; Picciotto and Wickmanm 1998; Anagnostopoulos et al. 2001).

REFERENCES AND FURTHER READING

Anagnostopoulos AV, Mobraaten LE, Sharp JJ, Davisson MT (2001) Transgenic and knockout databases: behavioral profiles of mouse mutants. Physiol Behav 73:675–689

Costentin J (1998) From gene to behavior, a new method for elaboration of new psychotropic agents. Ann Pharm Fr 56:60–67

Crnic LS (1996) Transgenic and null mutant animals for psychosomatic research. Psychosom Med 58:622–632

Mayford M, Mansuy IM, Müller RU, Kandel ER (1997) Memory and behavior: a second generation of genetically modified mice. Curr Biol 7:R580–R589

Picciotto MR, Wickmanm K (1998) Using knockout and transgenic mice to study neurophysiology and behavior. Physiol Rev 78:1131–1163

E.2.8.2 Special Reports on Genetically Altered Animals Useful for Evaluation of Drugs Against Anxiety

Wilson et al. (1996) reported that the **transgenic (mREN2) rat**, basically a model of genetically engineered hypertension, showed an anxiogenic profile in several tests, e. g., open field or elevated X-maze.

Saudou et al. (1994) found enhanced aggressive behavior in **mice lacking the 5-HT_{1B}receptor**. When confronted with an intruder, mutant mice attacked the intruder faster and more violently than did wild-type mice.

Trillat et al. (1998) studied the antidepressant effect of selective serotonin reuptake inhibitors (SSRIs) in homozygote mice deficient in the serotonin **5-HT_{1B}receptor**. The findings suggested that 5-HT_{1B} autoreceptors limit the effect of SSRIs particularly in the hippocampus while postsynaptic 5-HT_{1B} receptors are required for the antidepressant activity of SSRIs.

Parks et al. (1998) described increased anxiety in **mice lacking the serotonin 1A receptor**. Mice with an inactivated gene encoding the 5-HT_{1A} receptor have an increased tendency to avoid a novel and fearful environment and to escape a stressful situation.

Likewise, Heisler et al. (1998) found elevated anxiety and antidepressant-like responses in serotonin **5-HT_{1A} mutant mice**.

Ramboz et al. (1999) described **serotonin receptor 1A knockout mice** as an animal model of anxiety-related disorder. The authors demonstrated that mice without 5-HT_{1A} receptors display decreased exploratory activity and increased fear of aversive environments (open or elevated spaces). 5-HT_{1A} knockout mice also exhibited a decreased immobility in the forced swim test, an effect commonly associated with antidepressant treatment. These results showed that 5-HT_{1A} receptors are involved in the modulation of exploratory and fear-related behaviors and suggested that reductions in 5-HT_{1A} receptor density due to genetic defects or environmental stressors might result in heightened anxiety.

Gross et al. (2000) used genetically altered mice to determine the influence of different neurotransmitter receptors on fear and anxiety. **Mice with a genetic deletion of the 5-HT_{1A} receptor** were more fearful in a number of behavioral conflict tests, confirming the importance of this receptor in modulating anxiety.

Knapp et al. (2000) bred rats selectively for high or low hypothermic responses to the specific 5-HT_{1A} receptor agonist 8-hydroxy-2-di-n-propylamino tetralin (8-OH-DPAT). These rats differed in responses related to anxiety and depression.

Holmes (2001) reviewed targeted gene mutation approaches to the study of anxiety-like behavior in mice.

Schramm et al. (2001) found that the α_{2A}-adrenergic receptor plays a protective role in mice behavioral models of depression and anxiety. The genetic **knockout of the α_{2A}-adrenergic receptor** makes mice less active in a modified Porsolt's swim test and insensitive to the antidepressant effect of imipramine in this paradigm. Furthermore, α_{2A}-adrenergic receptor knockout mice appear more anxious than wild-type C57 Bl/6 mice in rearing and light/dark models of anxiety.

Quinlan et al. (2000) reported that **mice lacking the long splice variant of the gamma 2 subunit of the $GABA_A$ receptor** are more sensitive to benzodiazepines. Lack of the gamma 2L subunits may shift the $GABA_A$ receptor from an inverse-agonist-preferring toward an agonist-preferring configuration.

Yamada et al. (2000) described neurobehavioral alterations in mice with a targeted **deletion of the tumor necrosis factor-alpha gene** and the implications for emotional behavior.

Miyakawa et al. (2001) studied the behavior of **mice lacking the M_1 muscarinic acetylcholine receptor**. The animals exhibited a pronounced increase in locomotor activity in various tests, including open field, elevated plus maze, and light/dark transition tests. However, hippocampus-dependent learning was intact.

Picciotto et al. (2001) studied physiological and behavioral phenotypes of **neuronal nicotine acetylcholine receptor subunit knockout mice** and discussed possible implications for drug development.

Rupniak et al. (2001) used assays for antidepressant and anxiolytic drugs, such as resident-intruder or the forced swim test, to compare the phenotype of **NK1R–/– mice** with pharmacological blockade of the substance P (NK1) receptor.

Montag-Sallaz and Montag (2003) found severe cognitive and motor coordination deficits in **Tenascin-R-deficient mice**. The animals were tested for grip strength, open field behavior, elevated plus maze, light-dark avoidance, hole board examination, in the Morris water maze and in two-way active avoidance learning using several systems from TSE Systems, Bad Homburg, Germany).

Bilkei-Gorzo et al. (2004) studied behavioral and drug effects in **pre-proenkephalin-deficient mice** in the elevated zero-maze maze (using the VideoMot 2 system), the light-dark test using the animal activity monitor Actimot, and in the startle response test (all systems provided by TSE Systems, Bad Homburg, Germany)

REFERENCES AND FURTHER READING

Bilkei-Gorzo A, Racz H, Michel K, Zimmer A, Klingmüller D, Zimmer A (2004) Behavioral phenotype of pre-proenkephalin-deficient mice on diverse congenic backgrounds. Psychopharmacology 176:343–352

Gross C, Santarelli L, Brunner D, Zhuang X, Hen R (2000) Altered fear circuits in 5-HT_{1A} receptor KO mice. Biol Psychiatry 48:1157–1163

Heisler LK, Chu HM, Brennan JT, Danao JA, Bajwa P, Parsons LH, Tecott LH (1998) Elevated anxiety and antidepressant-like responses in serotonin 5-HT_{1A} mutant mice. Proc Natl Acad Sci USA 95:15049–15054

Holmes A (2001) Targeted gene mutation approaches to the study of anxiety-like behavior in mice. Neurosci Behav Rev 25:261–273

Knapp DJ, Sim-Selley LJ, Breese GR, Overstreet DH (2000) Selective breeding of 5-HT_{1A} receptor-mediated responses: application to emotion and receptor action. Pharmacol Biochem Behav 67:701–708

Miyakawa T, Yamada M, Duttaroy A, Wess J (2001) Hyperactivity and intact hippocampus-dependent learning in mice

lacking the M_1 muscarinic acetylcholine receptor. J Neurosci 21:5239–5250
Montag-Sallaz M, Montag D (2003) Severe cognitive and motor coordination deficits in Tenascin-R-deficient mice. Genes Brain Behav 2:20–31
Parks CL, Robinson PS, Sibille E, Shenk T, Toth M (1998) Increased anxiety in mice lacking the serotonin 1A receptor. Proc Natl Acad Sci USA 95:10734–10739
Picciotto MR, Caldarone BJ, Brunzell DH, Zachariou V, Stevens TR, King SL (2001) Neuronal nicotine acetylcholine receptor subunit knockout mice: physiological and behavioral phenotypes and possible clinical implications. Pharmacol Ther 92:89–108
Quinlan JJ, Firestone LL, Homanics GE (2000) Mice lacking the long splice variant of the gamma 2 subunit of the $GABA_A$ receptor are more sensitive to benzodiazepines. Pharmacol Biochem Behav 66:371–374
Ramboz S, Oosting R, Amara DA, Kung HF, Blier P, Mendelson M, Mann JJ, Brunner D, Hen R (1999) Serotonin receptor 1A knockout. An animal model of anxiety related disorder. Proc Natl Acad Sci USA 95:14476–14481
Rupniak NM, Carlson EJ, Webb JK, Harrison T, Porsolt RD, Roux S, d Felipe C, Hunt SP, Oates B, Wheeldon B (2001) Comparison of the phenotype of NK1R-/- mice with pharmacological blockade of the substance P (NK1) receptor in assays for antidepressant and anxiolytic drugs. Behav Pharmacol 12:497–508
Saudou F, Amara DA, Dierich A, LeMeur M, Ramboz S, Segu L, Buhot MC, Hen R (1994) Enhanced aggressive behavior in mice lacking $5\text{-}HT_{1B}$ receptor. Science 265:1875–1878
Schramm NL, McDonald MP, Limbird LE (2001) The á$_{2A}$-adrenergic receptor plays a protective role in mice behavioral models of depression and anxiety. J Neurosci 21:4875–4882
Trillat AC, Malagié I, Bourin M, Jacquot C, Hen R, Gardier AM (1998) Homozygote mice deficient in serotonin $5\text{-}HT_{1B}$ receptor and antidepressant effect of selective serotonin reuptake inhibitors. C R Sceances Biol Fil 192:1139–1147
Wilson W, Voigt P, Bader M, Marsden CA, Fink H (1996) Behavior of the transgenic (mREN2) rat. Brain Res 729:1–9
Yamada K, Iida R, Miyamoto Y, Saito K, Sekikawa K, Seishima M, Nabeshima T (2000) Neurobehavioral alterations in mice with a targeted deletion of the tumor necrosis factor-alpha gene: implications for emotional behavior. J Neuroimmunol 111:131–138

E.3 Anti-Epileptic Activity

E.3.0.1 General Considerations

Epilepsy is a disease of high prevalence, being well known since thousands of years as "morbus sacer". In spite of intensive investigations, the pathophysiology of epilepsy is still poorly understood. Studies with various animals models have provided ample evidence for heterogeneity in the mechanisms of epileptogenesis. New evidence derives from investigations of kindling, which involves the delivery of brief, initially subliminal, electrical or chemical stimuli to various areas of the brain. After 10 to 15 days of once-daily stimulation, the duration and intensity of after-discharges reach a stable maximum and a characteristic seizure is produced. Subsequent stimulation then regularly elicits seizures.

Surveys of methods being used to test compounds with anticonvulsant properties have been provided by Toman and Everett (1964), Woodbury (1972), Hout et al. (1973), Swinyard (1973), Koella (1985), Meldrum (1986), Rump and Kowalczyk 1987; Löscher and Schmidt (1988), Fisher (1989), Rogawski and Porter (1990), Porter and Rogawski (1992).

Epilepsy becomes drug resistant in 20%–30% of patients. Out of the animal models, the amygdala-kindled rat seems to be a suitable approach (Löscher 1997, 1998, 2002a, 2002b). Furthermore, the rat cortical dysplasia model is recommended (Smyth et al. 2002).

Several biochemical hypotheses have been advanced, involving the inhibitory GABAergic system and the system of the excitatory amino acids glutamate and aspartate. Excitatory receptors have been divided into subtypes according to the actions of specific agonists or antagonists. Agents which reduce $GABA_A$ synaptic function provoke convulsions. A convulsive state is induced by the direct blockade of $GABA_A$ receptors (e. g. to the action of bicuculline) or a reduction in the GABA-mediated opening of the chloride ion channel (e. g., by picrotoxin). One major factor in epileptogenesis seems to be a decreased function of $GABA_A$ synapses.

More recently, research has focused on the therapeutic potential of blocking excitatory amino acids – in particular glutamate. Of the three receptors of glutamate, the NMDA (N-methyl-D-aspartate)-receptor is considered the one of most interest in epilepsy and competitive NMDA receptor antagonists are proposed as potential anti-epileptic drugs. Excessive excitatory amino acid neurotransmission is thought to be associated with the neuropathologies of epilepsy, stroke and other neurodegenerative disorders. Antagonism of NMDA receptor function appears to be the mechanism of action of some novel anticonvulsant and neuroprotective agents. Excitatory amino acid receptors have been classified into at least three subtypes by electrophysiological criteria: NMDA, quisqualic acid (QA) and kainic acid (KA) (Cotman and Iversen 1987; Watkins and Olverman 1987).

Fabene and Sbarbati (2004) underlined the value of *in vivo* MRI in different models of experimental epilepsy.

REFERENCES AND FURTHER READING

Cotman CW, Iversen LL (1987) Excitatory amino acids in the brain-focus on NMDA receptors. Trends in Neurosci 10:263–265

Fabene PF, Sbarbati A (2004) In vivo MRI in different models of experimental epilepsy. Curr Drug Targets 5:629–636

Fisher RS (1989) Animal models of the epilepsies. Brain Res Rev 14:245–278

Gale K (1992) GABA and epilepsy: Basic concepts from preclinical research. Epilepsia 33 (Suppl. 5):S3–S12

Hout J, Raduoco-Thomas S, RaduocoThomas C (1973) Qualitative and quantitative evaluation of experimentally induced seizures. In: Anticonvulsant Drugs, Vol 1, Pergamon Press, Oxford, New York, pp 123–185

Koella WP (1985) Animal experimental methods in the study of antiepileptic drugs. In: Frey HH, Janz D (eds) Antiepileptic Drugs. Handbook of Experimental Pharmacology Vol 74, pp 283–339, Springer-Verlag, Berlin, Heidelberg

Löscher W (1997) Animal models of intractable epilepsy. Progr Neurobiol 53:239–258

Löscher W (1998) New visions in the pharmacology of anticonvulsion. Eur J Pharmacol 342:1–13

Löscher W (2002a) Animal models of drug-resistant epilepsy. Novartis Found Symp 243:149–159

Löscher W (2002b) Animal models of epilepsy for the development of antiepileptic and disease-modifying drugs. A comparison of the pharmacology of kindling and post-status epilepticus models of temporal epilepsy. Epilepsy Res 50:105–123

Löscher W, Schmidt D (1988) Which animal models should be used in the search for new antiepileptic drugs? A proposal based on experimental and clinical considerations. Epilepsy Res 2:145–181

MacDonald RL, McLean MJ (1986) Anticonvulsant drugs: Mechanisms of action. Adv Neurol 44:713–736

Meldrum BS (1986) Pharmacological approaches to the treatment of epilepsy. In: Meldrum BS, Porter RJ (eds) New Anticonvulsant Drugs. John Libbey, London Paris, pp 17–30

Meldrum BS (1989) GABAergic mechanisms in the pathogenesis and treatment of epilepsy. Br J Pharmacol 27:3S–11S

Porter RJ, Rogawski MA (1992) New antiepileptic drugs: From serendipity to rational discovery. Epilepsia 33, (Suppl. 1):S1–S6

Rogawski MA, Porter RJ (1990) Antiepileptic drugs: Pharmacological mechanisms and clinical efficacy with consideration of promising developmental stage compounds. Pharmacol Rev 42:223–286

Rump S, Kowalczyk M (1987) Effects of antiepileptic drugs in electrophysiological tests. Pol J Pharmacol Pharm 39:557–566

Smyth MD, Barbaro NM, Baraban SC (2002) Effects of antiepileptic drugs on induced epileptiform activity in a rat model of dysplasia. Epilepsy Res 50:251–264

Swinyard EA (1973) Assay of antiepileptic drug activity in experimental animals: standard tests. In: Anticonvulsant Drugs, Vol 1, Pergamon Press, Oxford, New York, pp 47–65

Toman JEP, Everett GM (1964) Anticonvulsants. In: Laurence DR, Bacharach AL (eds) Evaluation of Drug Activities: Pharmacometrics. pp 287–300. Academic Press, London and New York

Woodbury DM (1972) Applications to drug evaluations. In: Purpura DP, Penry JK, Tower DB, Woodbury DM, Walter RD (eds) Experimental Models of Epilepsy – A Manual for the Laboratory Worker. Raven Press, New York, pp 557–583

Watkins JC, Olverman HJ (1987) Agonists and antagonists for excitatory amino acid receptors. Trends Neurosci 10:265–272

E.3.1 In Vitro Methods

E.3.1.1 ^{3}H-GABA Receptor Binding

See Sect. E.2.1.1.

E.3.1.2 $GABA_A$ Receptor Binding

See Sect. E.2.1.2.

E.3.1.3 $GABA_B$ Receptor Binding

See Sect. E.2.1.3.

The *in vitro* assays for GABA-ergic compounds, described in the Sect. E.2 (anxiolytics) are similarly used for evaluation of anti-epileptic compounds.

REFERENCES AND FURTHER READING

Fonnum F (1987) Biochemistry, anatomy, and pharmacology of GABA neurons. In: Meltzer HY (ed) Psychopharmacology: The Third Generation of Progress. Raven Press, New York, pp 173–182

Lloyd KG, Morselli PL (1987) Psychopharmacology of GABAergic drugs. In: Meltzer HY (ed) Psychopharmacology: The Third Generation of Progress. Raven Press, New York pp 183–195

E.3.1.4 ^{3}H-GABA Uptake in Rat Cerebral Cortex Synaptosomes

PURPOSE AND RATIONALE

Roberts (1974) and others have proposed that the inhibitory action of the amino acid γ-aminobutyric acid (GABA) is the fine tuning control for pacemaker neurons. Disruption of this interplay due to inadequacies of the GABA system result in various disorders, in particular convulsive seizures (Roberts 1974; Korgsgaard-Larsen 1985). The nonspecific action of GABA-mimetics makes inhibition of the uptake mechanism, which terminates the neurotransmitters action, the ideal choice for increasing GABA's concentration at specific sites (Roberts 1974; Tapia 1975; Meldrum et al. 1982; Brehm et al. 1979). Demonstration of the high affinity mechanism that best reflects the *in vivo* condition utilizes GABA depleted cerebral cortex synaptosomes (Ryan and Roskoski 1977; Iversen and Bloom 1972; Roskoski 1978).

Although the physiological role of GABA transport systems is still unclear, uptake inhibitors such as THPO [4,5,6,7-tetrahydroisoxazolo-(4,5-C)pyrid-3-ol], nipecotic acid, cis-4-hydroxynipecotic acid, and guvacine exhibit anticonvulsant effects (Meldrum et al. 1982; Brehm et al. 1979). Furthermore, a number of neuroleptics have been shown to inhibit GABA uptake (Fjalland 1978). In particular, fluspirilene was found to be equivalent to the most potent uptake inhibitors known.

The assay is used as a biochemical screen for potential anticonvulsants or GABA (γ-aminobutyric acid) mimetic compounds that act by inhibiting GABA uptake.

PROCEDURE

Reagents

1. 0.5 M Tris buffer, pH 7.4
2. Ringer's solution+10 mM Tris buffer, pH 7.4 containing
   - glucose 10.0 mM,
   - NaCl 150.0 mM,
   - KCl 1.0 mM,
   - $MgSO_4$ 1.2 mM,
   - Na_2HPO_4 1.2 mM.
3. Depolarizing Ringer's solution, pH 7.4 reagent 2 containing
   - KCl 56 mM,
   - $CaCl_2$ 1 mM.
4. 0.32 M sucrose
5. ^{3}H-GABA is diluted to 2.5×10^{-4} M with distilled water. Forty µl of this solution in 1 ml of reaction mixture will yield a final concentration of 10^{-5} M.
1. Test compounds
   A 10 mM stock solution is made up in distilled water, ethanol, or DMSO and serially diluted, such that the final concentration in the assay ranges from 10^{-3} to 10^{-8} M. Total and nonspecific controls should use solvent of test compound.

Tissue Preparation

Male Wistar rats are decapitated and the brains rapidly removed. Cerebral cortex is weighed and homogenized in 9 volumes of ice-cold 0.32 M sucrose using a Potter-Elvejhem homogenizer. The homogenate is centrifuged at 1000 *g* for 10 min. The supernatant (S_1) is decanted and recentrifuged at 1000 *g* for 10 min. The pellet (P_2) is resuspended in 9 volumes of 0.32 M sucrose and centrifuged at 24,000 *g* for 10 min. The washed pellet is resuspended in15 volumes of depolarizing Ringer's solution, incubated at 25°C for 10 min and centrifuged at 3000 *g* for 10 min. The resulting pellet is resuspended in 15 volumes of Ringer's solution and is ready for use.

Assay

60 µl	Ringer's solution,
100 µl	vehicle or appropriate drug concentration,
800 µl	tissue suspension.

Microcentrifuge tubes are set up in triplicate. Nonspecific controls are incubated at 0°C and totals at 25°C for 10 min. Forty µl of ^{3}H-GABA are added and the tubes are reincubated for 10 min. All tubes are centrifuged at 13,000 *g* for 1 min. The supernatant is aspirated and 1 ml of solubilizer (Triton X-100 + 50% EtOH, 1:4, v/v) is added and mixed to dissolve pellets. Tubes are incubated at 90°C for 3 min, then centrifuged at 13,000 *g* for 15 min. 40 µl of supernatant is counted in 10 ml Liquiscint scintillation cocktail.

EVALUATION

Active uptake is the difference between cpm at 25°C and 0°C. The percent inhibition at each drug concentration is the mean of three determinations. IC_{50} values are derived from log-probit analysis.

REFERENCES AND FURTHER READING

Brehm L et al (1979) GABA uptake inhibitors and structurally related "pro-drugs". In: Krogsgaard-Larsen P et al (eds) GABA-Neurotransmitters. pp 247–261, Academic Press, New York

Fjalland B (1978) Inhibition by neuroleptics of uptake of ^{3}H GABA into rat brain synaptosomes. Acta Pharmacol et Toxicol 42:73–76 (1978)

Gray EG, Whittaker VP (1962) The isolation of nerve endings from brain: an electron microscopic study of cell fragments derived by homogenization and centrifugation. J Anat (Lond) 96:79–88

Iversen LL, Bloom FE (1972) Studies of the uptake of ^{3}H-GABA and ^{3}H-glycine in slices and homogenates of rat brain and spinal cord by electron microscopic autoradiography. Brain Res 41:131–143

Korgsgaard-Larsen P (1985) GABA agonist and uptake inhibitors. Research Biochemicals Incorporated – Neurotransmissions, Vol 1

Meldrum B et al (1982) GABA-uptake inhibitors as anticonvulsant agents. In: Okada Y, Roberts E (eds) Problems in GABA Research from Brain to Bacteria. pp 182–191, Excerpta Medica, Princeton

Roberts E (1974) γ-aminobutyric acid and nervous system function – a perspective. Biochem Pharmacol 23:2637–2649

Roskoski R (1978) Net uptake of L-glutamate and GABA by high affinity synaptosomal transport systems. J Neurochem 31:493–498

Ryan L, Roskoski R (1977) Net uptake of γ-aminobutyric acid by a high affinity synaptosomal transport system. J Pharm Exp Ther 200:285–291
Snodgrass SR (1990) GABA and GABA neurons: Controversies, problems, and prospects. In: Receptor Site Analysis, NEN, pp 23–33
Tapia R (1975) Blocking of GABA uptake. In: Iversen I, Iversen S, Snyder S (eds) Handbook of Psychopharmacology 4:33–34, Plenum Press, New York

E.3.1.5 GABA Uptake and Release in Rat Hippocampal Slices

PURPOSE AND RATIONALE

The GABA transporter, the subsynaptic $GABA_A$-receptor, and the $GABA_B$-autoreceptor are therapeutically the most relevant targets for drug actions influencing GABAergic synaptic transmission. Uptake inhibitors are potential anticonvulsants.

PROCEDURE

For measurement of GABA uptake, rat hippocampal slices are cut with a McIlwain tissue slicer (100 µm-thick prisms) and dispersed in ice-cold Krebs-Ringer solution with HEPES buffer (pH 7.4). Following two washes, slices (15 mg) are incubated at 37°C for 15 min in the presence or absence of test compound. [^{3}H]-GABA is added and samples are incubated for an additional 5 min before filtration through Whatman GF/F filters. Samples are then washed twice with 5 ml ice-chilled 0.9% saline. Distilled water is added and samples are allowed to sit at least 60 min before measured for radioactivity by liquid scintillation spectroscopy. Blanks are treated in an identical manner but are left on ice throughout the incubation.

For measurement of GABA release, rat hippocampal slices are prepared and dispersed in ice-cold HEPES-buffered (pH 7.2) Krebs Ringer solution and incubated with 0.05 µM [^{3}H]-GABA for 15 min at 37°C. Following two washes, the slices are incubated for an additional 15 min and finally resuspended in medium. Tissue (10 mg) is incubated at 37°C for a 15 min release period in the presence or absence of test compound. At the end of the release period, the medium is separated from tissue by centrifugation at 500 *g* for approximately 1 min and poured into 0.5 ml of perchloric acid (0.4 N). The tissue is homogenized in 0.13 N perchloric acid. Radioactivity in the samples is measured by using liquid scintillation spectroscopy.

EVALUATION

For GABA-uptake, IC_{50}-values (µM) are determined.

In GABA-release experiments, results are expressed as the amount of radioactivity released as a percent of the total radioactivity.

MODIFICATIONS OF THE METHOD

Roskoski (1978) studied the net uptake of GABA by high affinity synaptosomal transport systems.

Nilsson et al. (1990, 1992) tested GABA uptake in astroglial primary cultures.

The **isolated nerve-bouton preparation** was used to study GABA release (Jang et al. 2001; Kishimoto et al. 2001; Akaike et al. 2002; Akaike and Moorhouse 2003). The technique was developed by Drewe et al. (1988), Vorobjev (1991), Haage et al. (1998), Rhee et al. (1999), and Koyama et al. (1999).

The method is based on the local application of mechanical vibration directly to the chosen site of a brain slice and does not require the enzymatic pretreatment of the tissue. The mechanical vibration is applied via a glass rod (0.5 mm in diameter) mounted on a piezoelectric bimorph crystal at the site of the chosen brain tissue. The dissociated cells are allowed to settle at the bottom of a Petri dish for 20 min. The cell bodies are usually 10–15 µm at their longest axis, rounded or elongated in shape. Some cells had remaining neurites up to 100 µm long. The majority of cells had neurites less than 15 µm long.

In other studies (Koyama et al. 1999; Kishimoto et al. 2001), a custom-built vibrating stylus was placed in the appropriate region for mechanical dissociation. The glass capillary (1.5 mm o.d.) was pulled to a fine tip and fire-polished. The tip was placed within the appropriate region by a manipulator. The vibrating stylus was driven by an electronic relay and the tip was horizontally moved (excursions of 2–3 mm at 0.5–2 Hz) for 2 min.

Neurons with adherent functional synaptic terminals were investigated by tight-seal whole-cell recordings from the postsynaptic cells.

REFERENCES AND FURTHER READING

Akaike N, Moorhouse AJ (2003) Techniques: applications of the nerve-bouton preparation in neuropharmacolgy. Trends Pharmacol Sci 24:44–47
Akaike N, Muarkami N, Katsurabayashi S, Jin YH, Imazawa T (2002) Focal stimulation of single GABAergic presynaptic boutons on the rat hippocampus neuron. Neurosci Res 42:187–195
Drewe JA, Childs GV, Kunze DL (1988) Synaptic transmission between dissociated adult mammalian neurons and attached synaptic boutons. Science 241:1810–1813
Falch E, Larsson OM, Schousboe A, Krogsgard-Larsen P (1990) GABA-A agonists and GABA uptake inhibitors. Drug Dev Res 21:169–188

Haage D, Karlsson U, Johansson S (1998) Heterogeneous presynaptic Ca^{2+} channel types triggering GABA release onto medial preoptic neurons from rat. J Physiol (Lond) 507:77–91
Huger FP, Smith CP, Chiang Y, Glamkowski EJ, Ellis DB (1987) Pharmacological evaluation of HP 370, a potential atypical anti-psychotic agent. 2. *in vitro* profile. Drug Dev Res 11:169–175
Jang IS, Rhee JS, Watanabe T, Akaike N, Akaike N (2001) Histaminergic modulation of GABAergic transmission in rat ventromedial hypothalamic neurons. J Physiol (Lond) 534:791–803
Kishimoto K, Koyama S, Akaike N (2001) Synergistic μ-opioid and 5-HT_{1A} presynaptic inhibition of GABA release in rat periaqueductal gray neurons. Neuropharmacology 41:529–538
Koyama S, Kubo C, Rhee JS, Akaike N (1999) Presynaptic serotonergic inhibition of GABAergic synaptic transmission in mechanically dissociated rat basolateral amygdale neurons. J Physiol (Lond) 518:525–538
Lajtha A, Sershen H (1975) Inhibition of amino acid uptake by the absence of Na^+ in slices of brain. J Neurochem 24:667–672
Lüddens H, Korpi ER (1995) Biological function of $GABA_A$/benzodiazepine receptor heterogeneity. J Psychiat Res 29:77–94
Möhler H (1992) GABAergic synaptic transmission. Arzneim Forsch/Drug Res 42:211–214
Nilsson M, Hansson E, Rönnbäck L (1990) Transport of valproate and its effects on GABA uptake in astroglial primary culture. Neurochem Res 15:763–767
Nilsson M, Hansson E, Rönnbäck L (1992) Interactions between valproate, glutamate, aspartate, and GABA with respect to uptake in astroglial primary cultures. Neurochem Res 17:327–332
Rhee JS, Ishibashi H, Akaike N (1999) Calcium channels in the GABAergic presynaptic nerve terminals projecting to Meynert neurons of the rat. J Neurochem 72:800–806
Roskoski R (1978) Net uptake of L-glutamate and GABA by high affinity synaptosomal transport systems. J Neurochem 31:493–498
Suzdak PD, Jansen JA (1995) A review of the preclinical pharmacology of tiagabine: a potent and selective anticonvulsant GABA uptake inhibitor. Epilepsia 36:612–626
Taylor CP (1990) GABA receptors and GABAergic synapses as targets for drug development. Drug Dev Res 21:151–160
Taylor CP, Vartanian MG, Schwarz RD, Rock DM, Callahan MJ, Davis MD (1990) Pharmacology of CI-966:a potent GABA uptake inhibitor, *in vitro* and in experimental animals. Drug Dev Res 21:195–215
Vorobjev VS (1991) Vibrodissociation of sliced mammalian nervous tissue. J Neurosci Meth 38:145–150
Walton NY, Gunnawan S, Treiman DM (1994) Treatment of experimental status epilepticus with the GABA uptake inhibitor, tiagabine. Epilepsy Res 19:237–244

E.3.1.6 Glutamate Receptors: [^{3}H]CPP Binding

PURPOSE AND RATIONALE

The ionotropic glutamate receptors are ligand-gated ion channels that mediate the vast majority of excitatory neurotransmission in the brain. The family comprises three pharmacologically defined classes that were originally named after reasonably selective ligands: *N*-methyl-D-aspartate (NMDA), α-amino-3-hydroxy-5-methylisoxazole-4-propionic acid (AMPA), and kainate (Cotman and Iversen 1987; Watkins and Olverman 1987; Collingridge and Lester 1989; Monaghan et al. 1989; Carlsson and Carlsson 1990; Young and Fagg 1990; Nakanishi 1992; Cunningham et al. 1994; Herrling 1994; Iversen and Kemp 1994; Mayer et al. 1994; Meldrum and Chapman 1994; Monaghan and Buller 1994; Watkins 1994; Bettler and Mulle 1995; Fletcher and Lodge 1995; Becker et al. 1998; Danysz and Parsons 1998; Meldrum 1998; Chittajallu et al. 1999; Dingledine et al. 1999; Hatt 1999; Gallo and Ghiani 2000; Lees 2000; Meldrum 2000). It turned out that NMDA, AMPA and kainate receptor subunits are encoded by at least six gene families as defined by sequence homology: a single family of AMPA receptors, two for kainate, and three for NMDA (Dingledine et al. 1999; Mayer and Armstrong 2004).

The NMDA subtype is a hetero-oligomer consisting of an NR1 subunit combined with one or more NR2 subunits and a third subunit, NR3 (Loftis and Janowsky 2003). The receptor has two amino acid recognition sites, one for glutamate and one for glycine, both of which must be occupied to promote channel opening. A variety of drugs have been identified which block the channel selectively (Bräuner-Osborne et al. 2000; Kemp and McKernan 2002).

The AMPA subtype is a hetero-oligomer formed from combinations of iGluR1–4. Selective agonists and competitive antagonists acting at the glutamate recognition site have been useful for defining the physiological and pathophysiological roles played by the receptor. AMPA receptor modulators have been discussed as cognitive enhancers (Lynch 2004).

The kainate subtype consists of hetero-oligomers, comprising five subunits (Hollmann and Heinemann 1994; Huettner 2003).

Excessive excitatory amino acid neurotransmission has been associated with the neuropathologies of epilepsy, stroke and other neurodegenerative disorders (Cotman and Iversen 1987; Watkins and Olverman 1987; Parsons et al. 1998). Antagonism of NMDA receptor function appears to be the mechanism of action of some anticonvulsant and neuroprotective agents (Loscher 1998; Tauboll and Gjerstad 1998). The binding site for [^{3}H]2-amino-4-phosphonobutyric acid (AP4) may represent a fourth site which is less well characterized (Thomsen 1997). NMDA receptors are believed to be coupled to a cation channel

which converts to an open state with NMDA receptor activation (Kemp et al. 1987; Mukhin et al. 1997). The opening and closing of this cation channel are also modulated by glycine, Mg^{2+} and Zn^{2+}. Dissociative anesthetics, such as phencyclidine (PCP) and ketamine, and novel anticonvulsants, such as MK-801, block the ion channel and are noncompetitive NMDA receptor antagonists. Competitive NMDA receptor antagonists, such as CPP and the phosphono analogs of L-glutamate, AP7 and AP5 (2-amino-5-phosphonopentanoic acid), are inhibitors at the excitatory amino acid binding site (Olverman et al. 1986; Davies et al. 1986; Harris et al. 1986; Murphy et al. 1987; Lehmann et al. 1987).

The following assay is used to assess the affinity of compounds for the excitatory amino acid binding site of the NMDA receptor complex. [^{3}H]CPP 3-[(±)-2-carboxypiperazin-4-yl]-1-phosphonic acid is a structurally rigid analog of the selective NMDA receptor antagonist 2-AP7 (2-amino-7-phosphonoheptanoic acid).

PROCEDURE

Reagents

1. Buffer A: 0.5 M Tris HCl, pH 7.6
   60.0 g Tris HCl
   13.9 g Tris Base
   q.s. to 1 liter with distilled water
2. Buffer B: 50 mM Tris HCl, pH 7.6
   Dilute buffer A 1:10 with distilled water
3. L-Glutamic acid, 5×10^{-3} M
   Dissolve 7.36 mg of l-glutamic acid (Sigma G1251) with 10.0 ml distilled water. Aliquots of 20 µl to the assay tube will give a final concentration of 10^4M.
4. [^{3}H]CPP is obtained from New England Nuclear, specific activity 25–30 Ci/mmol. For IC_{50} determinations, a 200 nM stock solution is made with distilled water. Aliquots of 50 µl are added to each tube to yield a final concentration of 10 mM.
5. Test compounds. A stock solution of mM is made with a suitable solvent and serially diluted, such that the final concentration in the assay ranges from 10^{-5} to 10^{-8} M. Higher or lower concentrations may be used, depending on the potency of the drug.
6. Triton-X 100, 10% (v/v) (National Diagnostics, EC-606) A stock solution of Triton-X100, 10%, can be prepared and stored in the refrigerator. Dilute 1.0 ml of Triton-X100 to 10.0 ml with distilled water. On the day of the assay, the tissue homogenate (1:15 dilution) is preincubated with an aliquot of Triton-X 100, 10%, to give a final concentration of 0.05% (v/v).

Tissue Preparation

Cortices of male Wistar rats are dissected over ice and homogenized in ice-cold 0.32 M sucrose, 15 volumes of original wet weight of tissue, for 30 s with a Tissumizer setting at 70. The homogenate is centrifuged at 1000 *g* for 10 min. (SS34, 3000 rpm, 4°C). The supernatant is centrifuged at 20,000 *g* (SS34, 12,000 rpm, 4°C) for 20 min. Resuspend the pellet in 15 volumes of ice-cold distilled water (Tissumizer setting 60, 15 s) and spin at 7600 *g* (SS34, 8000 rpm, 4°C) for 20 min. Save the supernatant, swirl off the upper buffy layer of the pellet and add to the supernatant. Centrifuge the supernatant at 48,000 *g* (SS34, 20,000 rpm, 4°C) for 20 min. Resuspend the pellet with 15 volumes of cold distilled water and centrifuge. Discard the supernatant and store the pellet at –70°C.

On the day of the assay, resuspend the pellet in 15 volumes ice-cold 50 mM Tris buffer, pH 7.6. Preincubate the homogenate with Triton-X in a final concentration 0.05% (v/v) for 15 min at 37°C with agitation. Centrifuge the homogenate at 48,000 *g* (SS34, 20,000 rpm, 4°C for 20 min. Wash the pellet an additional 3 times by resuspension with cold buffer and centrifugation. The final pellet is resuspended in a volume 20 times the original wet weight.

Assay

1. Prepare assay tubes in triplicate.

380 µl	distilled water
50 µl	buffer A, 0.5 M Tris HCI, pH 7.6
20 µl	L-glutamic acid, 10^{-4} M, or destilled water, or appropriate concentration of inhibitor
50 µl	[^{3}H]CPP
500 µl	tissue homogenate

2. Following the addition of the tissue, the tubes are incubated for 20 min at 25°C with agitation. Place the tubes in an ice bath at the end of the incubation. Terminate the binding by centrifugation (HS4, 7000 rpm, 4°C) for 15 min. Return the tubes to ice. Aspirate the discard the supernatant. Carefully rinse the pellet three times with 1 ml ice-cold buffer, avoiding disruption of the pellet. Transfer the pellet to scintillation vials by vortexing the pellet with 2 ml scintillation fluid, rinse the tubes twice with 2 ml and add an additional 4 ml scintillation fluid.

EVALUATION

Specific binding is determined from the difference of binding in the absence of presence of 10^{-4} M L-

glutamic acid and is typically 60–70% of total binding. IC_{50} values for the competing drug are calculated by log-probit analysis of the data.

MODIFICATIONS OF THE ASSAY

Glutamate (Non Selective)

The assay measures the binding of glutamate, which binds non selectively to ionotropic glutamate receptors including the NMDA, AMPA, and kainate subtypes (Foster and Fagg 1987). In addition, glutamate binds to a family of metabotropic glutamate receptors.

Whole brains (except cerebellum) are obtained from male Wistar rats. A membrane fraction is prepared by standard techniques. Ten mg of membrane preparation is incubated with 1.6 nM [^{3}H]L-glutamate for 10 min at 37°C. Non-specific binding is estimated in the presence of 50 µM L-glutamate. Membranes are filtered and washed 3 times to separate bound from free ligand and filters are counted to determine [^{3}H]L-glutamate bound.

Convulsions induced in mice by intravenous injections of 2.0 mmol/kg L-glutamic acid can be inhibited by glutamate antagonists (Piotrovsky et al. 1991).

Glutamate AMPA

The assay measures the binding of [^{3}H]AMPA (α-amino-3-hydroxy-5-methyl-4-isoxazole propionic acid), a selective agonist which binds to the AMPA receptor subtype of glutamate-gated ion channels (Honore et al. 1982; Olsen et al. 1987; Fletcher and Lodge 1995).

Membranes are prepared from male rat brain cortices by standard techniques. Fifteen mg of membrane preparation is incubated with 5 nM [^{3}H]AMPA for 90 min at 4°C. Non-specific binding is estimated in the presence of 1 mM L-glutamate. Membranes are filtered and washed 3 times and the filters are counted to determine [^{3}H]AMP bound.

Mutel et al. (1998) recommended [^{3}H]Ro 48–8587 as specific for the AMPA receptor.

Fleck et al. (1996) described AMPA receptor heterogeneity in rat hippocampal neurons. AMPA receptor antagonists were described by Kohara et al. (1998), Wahl et al. (1998), Kodama et al. (1999), Nielsen et al. (1999) and reviewed by Chimirri et al. (1999).

Glutamate Kainate

The assay measures the binding of [^{3}H]kainate, a selective agonist that binds to the kainate subtype of the ionotropic glutamate receptors in rat brain (London and Coyle 1979; Clarke et al. 1997).

Whole brains (except cerebellum) are obtained from male Wistar rats. Fifteen mg of a membrane fraction prepared by standard techniques is incubated with 5.0 nM [^{3}H]kainate for 1 h at 4°C. Non-specific binding is estimated in the presence of 1 mM L-glutamate. Membranes are filtered and washed 3 times to separate free from bound ligand and filters are counted to determine [^{3}H]kainate bound.

Toms et al. (1997), Zhou et al. (1997) recommended [^{3}H]-(2S,4R)-4-methylglutamate as kainate-receptor selective ligand.

Irreversible inhibition of high affinity [^{3}H]kainate binding by a photoactivatable analogue was reported by Willis et al. (1997).

Worms et al. (1981) described the behavioral effects of systemically administered kainic acid.

Hu et al. (1998) described neuronal stress and seizure-induced injury in C57/BL mice after systemic kainate administration.

Glutamate NMDA-Agonist Site

The assay measures the binding of CGS 19755, a selective antagonist, to the agonist site of the NMDA receptor (Lehmann et al. 1988; Murphy et al. 1988; Jones et al. 1989)

REFERENCES AND FURTHER READING

Becker J, Li Z, Noe CR (1998) Molecular and pharmacological characterization of recombinant rat/mice N-methyl-D-aspartate receptor subtypes in the yeast Saccharomyces cerevisiae. Eur J Biochem 256:427–435

Bettler B, Mulle C (1995) Review: Neurotransmitter receptors. II. AMPA and kainate receptors. Neuropharmacol 34:123–139

Bräuner-Osboren H, Egebjerg J, Nielsen NØ, Madsen U, Krogsgaard-Larsen P (2000) Ligands for glutamate receptors: design and therapeutic properties. J Med Chem 43:2609–2645

Carlsson M, Carlsson A (1990) Interactions between glutaminergic and monoaminergic systems within the basal ganglia – implications for schizophrenia and Parkinson's disease. Trends Neurosci 13:272–276

Carter C, Rivy JP, Scatton B (1989) Ifenprodil and SL 82.0715 are antagonists at the polyamine site of the N-methyl-D-aspartate (NMDA) receptor. Eur J Pharmacol 164:611–612

Chimirri A, Gitto R, Zappala M (1999) AMPA receptor antagonists. Expert Opin Ther Pat 9:557–570

Chittajallu R, Braithwaite SP, Clarke VRJ, Henley JM (1999) Kainate receptors: subunits, synaptic localization and function. Trends Pharmacol Sci 20:26–35

Clarke VRJ, Ballyk BA, Hoo KH, Mandelzys A, Pellizari A, Bath CP, Thomas J, Sharpe EF, Davies CH, Ornstein PL, Schoepp DD, Kamboj RK, Collingridge GL, Lodges D, Bleakman D (1997) A hippocampal GluR5 kainate receptor regulating inhibitory synaptic transmission. Nature 389:599–603

Collingridge GL, Lester RAJ (1989) Excitatory amino acid receptors in the vertebrate central nervous system. Pharmacol Rev 40:143–210

Cotman CW, Iversen LL (1987) Excitatory amino acids in the brain-focus on NMDA receptors. Trends Neurosci 10:263–265

Cunningham MD, Ferkany JW, Enna SH (1994) Excitatory amino acid receptors: a gallery of new targets for pharmacological intervention. Life Sci 54:135–148

Danysz W, Parsons CG (1998) Glycine and N-methyl-D-aspartate receptors: Physiological significance and possible therapeutic applications. Pharmacol Rev 50:597–664

Davies J, Evans RH, Herrling PL, Jones AW, Olverman HJ, Pook P, Watkins JC (1986) CPP, a new potent and selective NMDA antagonist. Depression of central neuron responses, affinity for [^{3}H]D-AP5 binding sites on brain membranes and anticonvulsant activity. Brain Res 382:169–173

Dingledine R, Borges K, Bowie D, Traynelis SF (1999) The glutamate receptor ion channels. Pharmacol Rev 51:7–61

Dunn RW, Corbett R, Martin LL, Payack JF, Laws-Ricker L, Wilmot CA, Rush DK, Cornfeldt ML, Fielding S (1990) Preclinical anxiolytic profiles of 7189 and 8319, novel non-competitive NMDA antagonists. Current and Future Trends in Anticonvulsant, Anxiety, and Stroke Therapy, pp 495–512. Wiley-Liss, Inc.

Ferkany J, Coyle JT (1986) Heterogeneity of sodium-dependent excitatory amino acid uptake mechanisms in rat brain. J Neurosci Res 16:491–503

Fleck AW, Bahring R, Patneau DK, Mayer ML (1996) AMPA receptor heterogeneity in rat hippocampal neurons revealed by differential sensitivity to cyclothiazide. J Neurophysiol 75:2322–2333

Fletcher EJ, Lodge D (1995) New developments in the molecular pharmacology of α-amino-3-hydroxy-5-methyl-4-isoxazole propionate and kainate receptors. Pharmacol Ther 70:65–89

Foster AC, Fagg GE (1984) Acidic amino acid binding sites in mammalian neuronal membranes: Their characteristics and relationship to synaptic receptors. Brain Res Rev 7:103–164

Foster AC, Fagg GE (1987) Comparison of L-[^{3}H]glutamate, D-[^{3}H]aspartate, DL-[^{3}H]AP5 and [^{3}H]NMDA as ligands for NMDA receptors in crude postsynaptic densities from rat brain. Eur J Pharmacol 133:291–300

Gallo V, Ghiani CA (2000) Glutamate receptors in glia: new cells, new inputs and new functions. Trends Pharmacol Sci 21:252–258

Harris EW, Ganong AH, Monaghan DT, Watkins JC, Cotman CW (1986) Action of 3-((±)-2-carboxypiperazin-4-yl)-propyl-1-phosphonic acid (CPP): a new and highly potent antagonist of N-methyl-D-aspartate receptors in the hippocampus. Brain Res 382:174–177

Hatt H (1999) Modification of glutamate receptor channels: Molecular mechanisms and functional consequences. Naturwissensch 86:177–186

Herrling PL (1994) Clinical implications of NMDA receptors. In: Collingridge GL, Watkins JC (eds) The NMDA Receptor. 2nd edn. Oxford University Press, pp 376–394

Hollmann M, Heinemann S (1994) Cloned glutamate receptors. Annu Rev Neurosci 17:31–108

Honoré T, Lauridsen J, Krogsgaard-Larsen P (1982) The binding of [^{3}H]AMPA, a structural analogue of glutamic acid to rat brain membranes. J Neurochem 38:173–178

Honoré T, Davies SN, Drejer J, Fletchner EJ, Jacobsen P, Lodge D, Nielsen FE (1988) Quinoxalidinediones: Potent competitive non-NMDA glutamate receptor antagonists. Science 241:701–703

Hu RQ, Koh S, Togerson T, Cole AJ (1998) Neuronal stress and injury in C57/BL mice after systemic kainate administration. Brain Res 810:229–240

Huettner JE (2003) Kainate receptors and synaptic transmission. Progr Neurobiol 70:387–407

Iversen LL, Kemp JA (1994) Non-competitive NMDA antagonists as drugs. In: Collingridge GL, Watkins JC (eds) The NMDA Receptor. 2nd edn. Oxford University Press, pp 469–486

Jones SM, Snell LD, Johnson KM (1989) Characterization of the binding of radioligands to the N-methyl-D-aspartate, phenylcyclidine and glycine receptors in buffy coat membranes. J Pharmacol Meth 21:161–168

Kemp JA, Foster AC, Wong EHF (1987) Non-competitive antagonists of excitatory amino acid receptors. Trends Neurosci 10:294–298

Kemp JA, McKernan RM (2002) NMDA receptor pathways as drug targets. Nat Neurosci Suppl 5:1039–1042

Kohara A, Okada M, Tsutsumi R, Ohno K, Takahashi M, Shimizu-Sasamata M, Shishikura JI, Inami H, Sakamoto S, Yamaguchi T (1998) *In vitro* characterization of YM872, a selective, potent and highly water-soluble α-amino-3-hydroxy-5-methyl-isoxazole-4-propionate receptor antagonist. J Pharm Pharmacol 50:795–801

Kodama M, Yamada M, Sato K, Kitamura Y, Koyama F, Sato T, Morimoto K, Kuroda S (1999) Effects of YM90K, a selective AMP receptor antagonist, on amgdala-kindling and long-term hippocampal potentiation in rats. Eur J Pharmacol 374:11–19

Lees GJ (2000) Pharmacology of AMPA/kainate receptor ligands and their therapeutic potential in neurological and psychiatric disorders. Drug 59:33–78

Lehmann J, Schneider J, McPherson S, Murphy DE, Bernard P, Tsai C, Bennett DA, Pastor G, Steel DJ, Boehm C, Cheney DL, Liebman JM, Williams M, Wood PL (1987) CPP, a selective N-methyl-D-aspartate (NMDA)-type receptor antagonist: characterization *in vitro* and *in vivo*. J Pharmacol Exp Ther 240:737–746

Lehmann J, Hutchison AJ, McPherson SE, Mondadori C, Schmutz M, Sinton CM, Tsai C, Murphy DE, Steel DJ, Williams M, Cheney DL, Wood PL (1988) CGS 19755, a selective and competitive N-methyl-D-aspartate type excitatory amino acid receptor antagonist. J Pharmacol Exp Ther 246:65–75

Loftis JM, Janowsky A (2003) The *N*-methyl-D-aspartate receptor subunit NR2B: localization, functional properties, regulation, and clinical implications. Pharmacol Ther 97:55–85

London ED, Coyle JT (1979) Specific binding of [^{3}H]kainic acid to receptor sites in rat brain. Mol Pharmacol 15:492–505

Loscher W (1998) Pharmacology of glutamate receptor antagonists in the kindling model of epilepsy. Progr Neurobiol 54:721–741

Lynch G (2004) AMPA receptor modulators as cognitive enhancers. Curr Opin Pharmacol 4:4–11

Mayer ML, Westbrook GL (1987) The physiology of excitatory amino acids in the vertebrate central nervous system. Progr Neurobiol 28:197–276

Mayer ML, Benveniste M, Patneau DK (1994) NMDA receptor agonists and competitive antagonists. In: Collingridge GL, Watkins JC (eds) The NMDA Receptor. 2nd edn. Oxford University Press, pp 132–146

Mayer ML, Armstrong N (2004) Structure and function of glutamate receptor ion channels. Annu Rev Physiol 66:161–81

Meldrum BS (1998) The glutamate synapse as a therapeutic target: Perspectives for the future. Prog Brain Res 116:441–458

Meldrum BS (2000) Glutamate as a neurotransmitter in the brain: review of physiology and pathology. J Nutr 130, (4S Suppl):1007S–1015S

Meldrum BS, Chapman AG (1994) Competitive NMDA antagonists as drugs. In: Collingridge GL, Watkins JC (eds) The NMDA Receptor. 2nd edn. Oxford University Press, pp 457–468

Monaghan DT, Buller AL (1994) Anatomical, pharmacological, and molecular diversity of native NMDA receptor subtypes. In: Collingridge GL, Watkins JC (eds) The NMDA Receptor. 2nd edn. Oxford University Press, pp 158–176

Monaghan DT, Cotman CW (1982) The distribution of [^{3}H]kainic acid binding sites in rat CNS as determined by autoradiography. Brain Res 252:91–100

Monaghan DT, Bridges RJ, Cotman CW (1989) The excitatory amino acid receptors: Their classes, pharmacology, and distinct properties in the function of the central nervous system. Annu Rev Pharmacol Toxicol 29:365–402

Mukhin A, Kovaleva ES, London ED (1997) Two affinity states of N-methyl-D-aspartate recognition sites: Modulation by cations. J Pharmacol Exp Ther 282:945–954

Murphy DE, Schneider J, Boehm C, Lehmann J, Williams M (1987a) Binding of [^{3}H]3-(2-carboxypiperazin-4-yl)propyl-1-phosphonic acid to rat brain membranes: A selective, high-affinity ligand for N-methyl-D-aspartate receptors. J Pharmacol Exp Ther 240:778–784

Murphy DE, Snowhill EW, Williams M (1987b) Characterization of quisqualate recognition sites in rat brain tissue using DL-[^{3}H]α-amino-3-hydroxy-5-methylisoxazole-4-propionic acid (AMPA) and a filtration assay. Neurochem Res 12:775–782

Murphy DE, Hutchinson AJ, Hurt SD, Williams M, Sills MA (1988) Characterization of the binding of [^{3}H]-CGS 19755, a novel N-methyl-D-aspartate antagonist with nanomolar affinity in rat brain. Br J Pharmacol 95:932–938

Mutel V, Trube G, Klingelschmidt A, Messer J, Bleuel Z, Humbel U, Clifford MM, Ellis GJ, Richards JG (1998) Binding characteristics of a potent AMPA receptor antagonist [^{3}H]Ro 48–8587 in rat brain. J Neurochem 71:418–426

Nakanishi S (1992) Molecular diversity of glutamate receptors and implication for brain function. Science 258:593–603

Nielsen EO, Varming T, Mathiesen C, Jensen LH, Moller A, Gouliaev AH, Watjen F, Drejer J (1999) SPD 502: A water-soluble and *in vivo* long-lasting AMPA antagonist with neuroprotective activity. J Pharmacol Exp Ther 289:1492–1501

Olney JW (1990) Excitotoxic amino acids and neuropsychiatric disorders. Annu Rev Pharmacol Toxicol 30:47–71

Olsen RW, Szamraj O, Houser CR (1987) [^{3}H]AMPA binding to glutamate receptor subpopulations in rat brain. Brain Res 402:243–254

Olverman JH, Monaghan DT, Cotman CW, Watkins JC (1986) [^{3}H]CPP, a new competitive ligand for NMDA receptors. Eur J Pharmacol 131:161–162

Parsons CG, Danysz W, Quack G (1998) Glutamate in CNS disorders as a target for drug development. Drug News Perspect 11:523–569

Piotrovsky LB, Garyaev AP, Poznyakova LN (1991) Dipeptide analogues of *N*-acetylaspartylglutamate inhibit convulsive effects of excitatory amino acids in mice. Neurosci Lett 125:227–230

Rogawski MA, Porter RJ (1990) Antiepileptic drugs: Pharmacological mechanisms and clinical efficacy with considerations of promising developmental stage compounds. Pharmacol Rev 42:223–286

Tauboll E, Gjerstad L (1998) Effects of antiepileptic drugs on the activation of glutamate receptors. Prog Brain Res 116:385–393

Thomsen C (1997) The L-AP4 receptor. Gen Pharmacol 29:151–158

Toms NJ, Reid ME, Phillips W, Kemp MC, Roberts PJ (1997) A novel kainate receptor ligand [^{3}H]-(2S,4R)-4-methylglutamate. Pharmacological characterization in rabbit brain membranes. Neuropharmacology 36:1483–1488

Wahl P, Frandsen A, Madsen U, Schousboe A, Krogsgaard-Larsen P (1998) Pharmacology and toxicology of ATOA, an AMPA receptor antagonist and a partial agonist at GluR5 receptors. Neuropharmacology 37:1205–1210

Watkins JC (1994) The NMDA receptor concept: origins and development. In: Collingridge GL, Watkins JC (eds) The NMDA Receptor. 2nd edn. Oxford University Press, pp 1–30

Watkins JC, Olverman HJ (1987) Agonists and antagonists for excitatory amino acid receptors. Trends Neurosci 10:265–272

Worms P, Willigens MT, Lloyd KG (1981) The behavioral effects of systemically administered kainic acid: a pharmacological analysis. Life Sci 29:2215–2225

Willis CL, Wacker DA, Bartlett RD, Bleakman D, Lodge D, Chamberlin AR, Bridges RJ (1997) Irreversible inhibition of high affinity [^{3}H]kainate binding by a photoactivatable analogue: (2′S,3′S,4′R)-2′-carboxy-4′-(2-diazo-1-oxo-3,3,3-trifluoropropyl)-3′-pyrrolidinyl acetate. J Neurochem 68:1503–1510

Young AB, Fagg GE (1990) Excitatory amino acid receptors in the brain: membrane binding and receptor autoradiographic approaches. Trends Pharmacol Sci 11:126–133

Zeman S, Lodge D (1992) Pharmacological characterization of non-NMDA subtypes of glutamate receptor in the neonatal rat hemidissected spinal cord *in vitro*. Br J Pharmacol 106:367–372

Zhou L-L, Gu ZQ, Costa AM, Yamada KA, Mansson PE, Giordano T, Skolnick P, Jones KA (1997) (2S,4R)-4-methylglutamic acid (SYM 2081): A selective, high affinity ligand for kainate receptors. J Pharmacol Exp Ther 280:422–427

E.3.1.7 NMDA Receptor Complex: [^{3}H]TCP Binding

PURPOSE AND RATIONALE

The purpose of this assay is to determine the binding affinity of potential noncompetitive NMDA antagonists at the phencyclidine (PCP) binding site which is believed to be within or near the NMDA-regulated ion channel. TCP, 1-[1-(2-thienyl)cyclohexyl]-piperidine, is a thienyl derivative of PCP.

Excessive activity of excitatory amino acid neurotransmitters has been associated with the neuropathologies of epilepsy, stroke and other neurodegenerative disorders (Cotman and Iversen 1987; Watkins and Olverman 1987). Antagonism of NMDA receptor function appears to be the mechanism of action of some novel anticonvulsant and neuroprotective agents. Excitatory amino acid receptors have been classified into at least three subtypes by electrophysiological criteria: NMDA, quisqualic acid (QA) and kainic acid (KA) (Cotman and Iversen 1987; Watkins and Olverman 1987). The binding site for [^{3}H]2-

amino-4-phosphonobutyric acid (AP4) may represent a fourth site which is less well characterized. NMDA receptors are believed to be coupled to a cation channel which converts to an open state following activation (Kemp et al. 1987). The opening and closing of this cation channel are also modulated by glycine, Mg^{2+}, Zn^{2+} and polyamines (Loo et al. 1986; Snell et al. 1987; Reynolds et al. 1988; Thomson 1989; Snell et al. 1988; Sacaan and Johnson 1989; Thedinga et al. 1989; Williams et al. 1989). Dissociative anesthetics, such as phencyclidine (PCP) and ketamine, and the neuroprotective agent MK-801 block the ion channel and are noncompetitive NMDA receptor antagonists. Competitive NMDA receptor antagonists, such as 3-[(±)-2-carboxypiperazin-4-yl]-1-phosphonic acid (CPP), and the phosphono analogs of L-glutamate, 2-amino-7-phosphonoheptanoic acid (2-AP7) and 2-amino-5-phosphonopentanoic acid (2-AP5), are inhibitors at the excitatory amino acid recognition site.

Molecular cloning and functional expression of rat and mouse NMDA receptors (Moriyoshi et al. 1991; Meguro et al. 1992), a family of AMPA-selective glutamate receptors (Keinänen et al. 1990) and the metabotropic glutamate receptors mGluR1–mGluR6 (Schoepp et al. 1990; Masu et al. 1991; Abe et al. 1992; Bashir et al. 1993; Nakajima et al. 1993; Tanabe et al. 1993) have been reported.

PROCEDURE I

Reagents

1. Buffer A: 0.1 M HEPES, pH 7.5
   Weigh 23.83 g HEPES
   Add approximately 900 ml distilled water.
   Adjust pH to 7.5 with 10 N NaOH.
   q.s. to 1 liter with distilled water.
2. Buffer B: 10 mM HEPES, pH 7.5
   Dilute buffer A 1:10 with distilled water and adjust pH to 7.5.
3. L-Glutamic acid, 5×10^{-3} M
   Dissolve 7.36 mg with 10.0 ml distilled water.
   Aliquots of 20 µl to the assay tube will give a final concentration of 10^{-4} M.
4. Glycine, 5×10^{-4} M
   Dissolve 3.75 mg with 10.0 ml distilled water.
   Dilute 1:10 with distilled water.
   Aliquots of 20 µl to the assay tube will give a final concentration of 10^{-5} M.
5. Phencyclidine HCl (PCP) is used for nonspecific binding.
   Dissolve 0.7 mg in 0.5 ml distilled water.
   Aliquots of 20 µl to the assay tube will give a final concentration of 10^{-4} M.
6. [^{3}H]TCP is obtained from New England Nuclear, specific activity 42–60 Ci/mmole. For IC_{50} determinations, a 50 nM stock solution is made with distilled water. Aliquots of 50 µl are added to each tube to yield a final concentration of 2.5 nM.
7. Test compounds. A stock solution of 5 mM is made up with a suitable solvent and serially diluted, such that the final concentration in the assay ranges from 10^{-5} to 10^{-8} M. Higher or lower concentrations may be used, depending on the potency of the drug.

Tissue Preparation

Cerebral cortex of male Wistar rats, 7–10 weeks of age, is dissected over ice and homogenized in ice-cold 0.32 M sucrose, 30 volumes of original tissue weight, for 60 s with a Tissumizer setting at 70. The homogenate is centrifuged at 1000 *g* for 10 min. (SS34, 3000 rpm, 4°C). The supernatant is centrifuged at 20,000 *g* for 20 min. (SS34, 12,000 rpm, 4°C). The pellet is resuspended with cold distilled water, to 50 volumes of original tissue weight, using the Tissumizer, 60 s at setting of 70. The homogenate is incubated at 37°C for 30 min, transferred to centrifuge tubes, and centrifuged at 36,000 *g* for 20 min. (SS34, 16,500 rpm, 4°C). The pellet is again resuspended in 50 volumes distilled water, incubated and centrifuged. All resuspensions with the Tissumizer are for 60 s at a setting of 70. The resulting pellet is resuspended in 30 volumes of ice-cold 10 mM HEPES buffer, pH 7.5, centrifuged, and washed once again (resuspension and centrifugation) with buffer. Following resuspension in 30 volumes of buffer, the homogenate is frozen in the centrifuge tube and stored at –70°C until the day of the assay.

On the day of the assay, the homogenate is thawed and centrifuged at 36,000 *g* for 20 min. (SS34, 16,500 rpm, 4°C). The pellet is washed three times by resuspension with ice-cold 10 mM HEPES buffer, pH 7.5, centrifuged and finally resuspended in 30 volumes of buffer. Aliquots of 500 µl are used for each assay tube, final volume 1000 µl, and correspond to approximately 0.2 mg protein.

Assay

1. Prepare assay tubes in triplicate. For each test compound, inhibition of [^{3}H]TCP binding is measured both in the absence (basal) and presence (stimulated) of 100 µM L-glutamic acid and 10 mM glycine.

Basal	Stimulated	
380 µl	340 µl	Distilled water
50 µl	50 µl	Buffer A, 0.1 M HEPES, pH 7.5
20 µl	20 µl	PCP (reagent A5) or distilled water, or appropriate concentration of inhibitor
0 µl	20 µl	L-glutamic acid (reagent A3)
0 µl	20 µl	Glycine (reagent A4)
50 µ	50 µl	[^{3}H]TCP (reagent A6)
500 µl	500 µ	Tissue homogenate

2. Following the addition of the tissue, the tubes are incubated for 120 min at 25°C with agitation. The assay is terminated by separating the bound from nonbound radioligand by rapid filtration with reduced pressure over Whatman GF/B filters, pre-soaked in 0.05% polyethylene-imine, using the Brandell cell harvesters. The filters are rinsed once with buffer before filtering the tubes, and rinsed two times after filtration. The filters are counted with 10 ml Liquiscint.

EVALUATION

Specific binding is determined from the difference of binding in the absence or presence of 10^{-4} M PCP. Specific binding is typically 50% of total binding in basal conditions, and 90% of total binding when stimulated by L-glutamic acid and glycine. L-Glutamic acid and glycine typically increase specific binding to 300% and 200% of basal binding, respectively. The combination of L-glutamic acid and glycine typically produce a greater than additive effect, increasing specific binding to 700% of basal binding. IC_{50} values for the competing drug are calculated by log-probit analysis of the data.

Protocol Modification for Crude Membrane Homogenates

This modified procedure for the preparation of membrane homogenates does not use extensive lysing and washing of the tissue to remove endogenous L-glutamate, glycine and other endogenous compounds which enhance [^{3}H]TCP binding. This procedure may be used for rapid screening of compounds for inhibition of [^{3}H]TCP binding site without specifically defining an interaction at the ion channel or modulatory sites of the NMDA receptor complex.

PROCEDURE II

Reagents

1. Buffers A and B are prepared as described above.
2. Phencyclidine HCl is used for nonspecific binding and is prepared as described above.
3. [^{3}H]TCP is prepared as described above.
4. Test compounds are prepared as described above.

Tissue Preparation

Cortical tissue is dissected, homogenized in 30 volumes of 0.32 M sucrose and a crude P_2 pellet is prepared as described above. The pellet is resuspended in 30 volumes of 10 mM HEPES, pH 7.5, centrifuged at 36,000 *g* (SS34, 16,500 rpm, 4°C) for 20 min, and again resuspended in 100 volumes of buffer. This homogenate is used directly in the assay in aliquots of 500 µl.

Assay

1. Prepare assay tubes in triplicate.

Volume	Solution
380 µl	Distilled water
50 µl	Buffer A, 0.1 M HEPES, pH 7.5
20 µl	PCP (reagent IA5) or distilled water, appropriate concentration of inhibitor
50 µl	[^{3}H]TCP (reagent IA6)
500 µl	Tissue homogenate

2. Following the addition of the tissue, the tubes are incubated for 120 min at 25°C with agitation. The assay is terminated by rapid filtration as described above. The filters are rinsed and counted for bound radioactivity as above.

EVALUATION

Specific binding is determined from the difference of binding in the presence or absence of 10^{-4} M PCP. Specific binding is typically 90% of total binding. IC_{50} values for the competing drug are calculated by log-probit analysis.

MODIFICATIONS OF THE METHOD

Instead of [^{3}H]TCP, radiolabeled [^{3}H]MK-801 has been used as ligand (Wong et al. 1988; Javitt and Zukin 1989; Williams et al. 1989).

Sills et al. (1991) described [^{3}H]CGP 39653 as a N-methyl-D-aspartate antagonist radioligand with low nanomolar affinity in rat brain.

Nowak et al. (1995) reported that swim stress increases the potency of glycine to displace 5,7-[^{3}H[dichlorokynurenic acid from the strychnine-insensitive glycine recognition site of the *N*-methyl-D-aspartate receptor complex.

NMDA receptor cloning studies have shown that NMDA receptors contain at least one of seven different NMDAR1 subunits (NR1A–NR1G) (Sugihara

et al. 1992) and at least one of four NMDAR2 subunits (NR2A–NR2D) (Kutsuwada et al. 1992; Ishii et al. 1993). While the NR1 subunits are generated by alternative splicing of a single gene, the NR2 subunits are products of four highly homologous genes. Thus, there are thousands of potential subunit combinations yielding complexes of four or five subunits.

Grimwood et al. (1996) reported generation and expression of stable cell lines expressing recombinant human NMDA receptor subtypes, two cell lines expressing NR1a/NR2A receptors and one cell line expressing NR1a/NR2B receptors.

NR2B selective NMDA antagonists were described by Fischer et al. (1997), Kew et al. (1998), Reyes et al. (1998), Chenard and Menniti (1999).

For discovery of novel NMDA receptor antagonists, Bednar et al. (2004) developed a high-throughput functional assay based on fluorescence detection of intracellular calcium concentrations. Mouse fibroblasts L(tk-) cells expressing human NR1a/NR2B NMDA receptors were plated in 96-well plates and loaded with fluorescence calcium indicator fluo-3 AM. NR2B antagonists were added after stimulation of NMDA receptors with 10 µM glutamate and 10 µM glycine. Changes in fluorescence after addition of the antagonists were fitted with a single exponential equation providing k_{obs}.

REFERENCES AND FURTHER READING

Abe T, Sugihara H, Nawa H, Shigemoto R, Mizuno N, Nakanishi S (1992) Molecular characterization of a novel metabotropic glutamate receptor mGluR5 coupled to inositol phosphate/Ca^{2+} signal transduction. J Biol Chem 267:13361–13368

Bashir ZI, Bortolotto ZA, Davies CH, Berretta M, Irving AJ, Seal AJ, Henley AM, Jane DE, Watkins JC, Collingridge GL (1993) Induction of LTP in the hippocampus needs synaptic activation of glutamate metabotropic receptors. Nature 363:347–350

Bednar B, Cunningham ME, Kiss L, Cheng G, McCauley JA, Liverton NJ, Koblan KS (2004) Kinetic characterization of novel NR2B antagonists using fluorescence detection of calcium flux. J Neurosci Meth 137:247–255

Chenard BL, Menniti FS (1999) Antagonists selective for NMDA receptors containing the NR2B subunit. Curr Pharm Res 5:381–404

Cotman CW, Iversen LL (1987) Excitatory amino acids in the brain-focus on NMDA receptors. Trends Neurosci 10:263–265

Dannhardt G, von Gruchalla M, Elben U (1994) Tools for NMDA-receptor elucidation: Synthesis of spacer-coupled MK-801 derivatives. Pharm Pharmacol Lett 4:12–15

Dunn RW, Corbett R, Martin LL, Payack JF, Laws-Ricker L, Wilmot CA, Rush DK, Cornfeldt ML, Fielding S (1990) Preclinical anxiolytic profiles of 7189 and 8319, novel non-competitive NMDA antagonists. Current and Future Trends in Anticonvulsant, Anxiety, and Stroke Therapy, pp 495–512. Wiley-Liss, Inc

Ebert B, Madsen U, Lund TM, Lenz SM, Krogsgaard-Larsen P (1994) Molecular pharmacology of the AMPA agonist, (*S*)-2-amino-3-(3-hydroxy-5-phenyl-4-isoxazolyl)propionic acid [(*S*)-APPA] and the AMPA antagonist, (*R*)-APPA. Neurochem Int 24:507–515

Fischer G, Mutel V, Trube G, Malherbe P, Kew JNC, Mohacsi E, Heitz MP, Kemp JA (1997) Ro 25–6981, a highly potent and selective blocker of N-methyl-D-aspartate receptors containing the NRB2 subunit. J Pharmacol Exp Ther 283:1285–1292

Goldman ME, ME, Jacobson AE, Rice KC, Paul SM (1985) Differentiation of [^{3}H]phencyclidine and (+)-[^{3}H]SKF-10,047 binding sites in rat cerebral cortex. FEBS Lett 190:333–336

Grimwood S, lLe Bourdellès B, Atack JR, Barton C, Cockettt W, Cook SM, Gilbert E, Hutson PH, McKernan RM, Myers J, Ragan CI, Wingrove PB, Whiting PJ (1996) Generation and characterization of stable cell lines expressing recombinant human N-methyl-D-aspartate receptor subtypes. J Neurochem 66:2239–2247

Hansen JJ, Krogsgaard-Larsen P (1990) Structural, conformational, and stereochemical requirements of central excitatory amino acid receptors. Med Res Rev 10:55–94

Ishii T, Moriyoshi K, Sugihara H, Sakurada K, Kadotani H, Yokoi M, Akazawa C, Shigemoto R, Mizuno N, Masu M, Nakanishi S (1993) Molecular characterization of the family of N-methyl-D-aspartate receptor subunits. J Biol Chem 268:2836–2843

Iversen LL (1994) MK-801 (Dizocilpine maleate) – NMDA receptor antagonist. Neurotransmiss 10:1:1–4

Javitt DC, Zukin SR (1989) Biexponential kinetics of [^{3}H]MK-801 binding: Evidence for access to closed and open *N*-methyl-D-aspartate receptor channels. Mol Pharmacol 35:387–393

Johnson KM, Jones SM (1990) Neuropharmacol of phencyclidine: Basic mechanisms and therapeutic potential. Annu Rev Pharmacol Toxicol 30:707–750

Keinänen K, Wisden W, Sommer B, Werner P, Herb A, Verdoorn TA, Sakmann B, Seeburg PH (1990) A family of AMPA-selective glutamate receptors. Science 249:556–560

Kemp JA, Foster AC, Wong EHF (1987) Non-competitive antagonists of excitatory amino acid receptors. Trends Neurosci 10:294–298

Kew JNC, Trube G, Kemp JA (1998) State-dependent NMDA receptor antagonism by Ro 8–4304, a novel NR2B selective, non-competitive, voltage-independent antagonist. Br J Pharmacol 123:463–472

Kutsuwada T, Kashiwabuchi N, Mori H, Sakimura K, Kushyia E, Araki K, Meguro H, Masaki H, Kumanishi T, Arakawa M, Mishina M (1992) Molecular diversity of the NMDA receptor channel. Nature 358:36–41

Loo P, Braunwalder A, Lehmann J, Williams M (1986) Radioligand binding to central phencyclidine recognition sites is dependent on excitatory amino acid receptor agonists. Eur J Pharmacol 123:467–468

Loo PS, Braunwalder AF, Lehmann J, Williams M, Sills MA (1987) Interaction of L-glutamate and magnesium with phencyclidine recognition sites in rats brain: evidence for multiple affinity states of the phencyclidine/*N*-methyl-D-aspartate receptor complex. Mol Pharmacol 32:820–830

Maragos WF, Chu DCM, Greenamyre T, Penney JB, Young AB (1986) High correlation between the localization of [^{3}H]TCP binding and NMDA receptors. Eur J Pharmacol 123:173–174

Masu M, Tanabe Y, Tsuchida K, Shigemoto R, Nakanishi S (1991) Sequence and expression of a metabotropic glutamate receptor. Nature 349:760–765

Meguro H, Mori H, Araki K, Kushiya E, Katsuwada T, Yamazaki M, Kumanishi T, Arakawa M, Sakimura K, Mishina M (1992) Functional characterization of a heteromeric NMDA receptor channel expressed from cloned cDNAs. Nature 357:70–74
Monyer H, Sprengel R, Schoepfer R, Herb A, Higuchi M, Lomeli H, Burnashev N, Sakmann B, Seeburg PH (1992) Heteromeric NMDA receptors: Molecular and functional distinction of subtypes. Science 256:1217–1221
Moriyoshi K, Masu M, Ishii T, Shigemoto R, Mizuno N, Nakanishi S (1991) Molecular cloning and characterization of the rat NMDA receptor. Nature 354:31–37
Nakajima Y, Iwakabe H, Akazawa C, Nawa H, Shigemoto R, Mizuno N, Nakanishi N (1993) Molecular characterization of a novel retinal metabotropic glutamate receptor mGluR6 with a high agonist selectivity for L-2-amino-4-phosphonobutyrate. J Biol Chem 268:11868–11873
Nowak G, Remond A, McNamara M, Paul IA (1995) Swim stress increases the potency of glycine at the *N*-methyl-D-aspartate receptor complex. J Neurochem 64:925–927
Reyes M, Reyes A, Opitz T, Kapin MA, Stanton PK (1998) Eliprodil, a non-competitive, NR2B-selective NMDA antagonist, protects pyramidal neurons in hippocampal slides from hypoxic/ischemic damage. Brain Res 782:212–218
Reynolds IJ, Miller RJ (1988) Multiple sites for the regulation of the *N*-methyl-D-aspartate receptor. Mol Pharmacol 33:581–584
Rogawski MA, Porter RJ (1990) Antiepileptic drugs: Pharmacological mechanisms and clinical efficacy with considerations of promising developmental stage compounds. Pharmacol Reviews 42:223–286
Sacaan AI, Johnson KM (1989) Spermine enhances binding to the glycine site associated with the N-methyl-D-aspartate receptor complex. Mol Pharmacol 36:836–839
Schoepp D, Bockaert J, Sladeczek F (1990) Pharmacological and functional characteristics of metabotropic excitatory amino acid receptors. Trends Pharmacol Sci 11:508–515
Sills MA, Fagg G, Pozza M, Angst C, Brundish DE, Hurt SD, Wilusz EJ, Williams M (1991) [^{3}H]CGP 39653: a new N-methyl-D-aspartate antagonist radioligand with low nanomolar affinity in rat brain. Eur J Pharmacol 192:19–24
Simon RP, Swan JH, Griffiths T, Meldrum BS (1984) Blockade of *N*-methyl-D-aspartate receptors may protect against ischemic damage in the brain. Science 226:850–852
Snell LD, Morter RS, Johnson KM (1987) Glycine potentiates *N*-methyl-D-aspartate-induced [^{3}H]TCP binding to rat cortical membranes. Neurosci Lett 83:313–320
Snell LD, Morter RS, Johnson KD (1988) Structural requirements for activation of the glycine receptor that modulates the N-methyl-D-aspartate operated ion channel. Eur J Pharmacol 156:105–110
Sugihara H, Moriyoshi K, Ishii T, Masu M, Nakanishi S (1992) Structures and properties of seven isoforms of the NMDA receptor generated by alternative splicing. Biochem Biophys Res Commun 185:826–832
Tanabe Y, Nomura A, Masu M, Shigemoto R, Mizuno N, Nakanishi S (1993) Signal transduction, pharmacological properties, and expression patterns of two metabotropic glutamate receptors, mGluR3 and mGluR4. J Neurosci 13:1372–1378
Thedinga KH, Benedict MS, Fagg GE (1989) The N-methyl-D-aspartate (NMDA) receptor complex: a stoechiometric analysis of radioligand binding domains. Neurosci Lett 104:217–222
Thomson AM (1989) Glycine modulation of the NMDA receptor/channel complex. Trends in Neurosci 12:349–353
Vignon J, Chicheportiche R, Chicheportiche M, Kamenka JM, Geneste P, Lazdunski M (1983) [^{3}H]TPC: a new tool with high affinity to the PCP receptor in rat brain. Brain Res 280:194–197
Watkins JC, Olverman HJ (1987) Agonists and antagonists for excitatory amino acid receptors. Trends Neurosci 10:265–272
Watkins JC, Krogsgaard-Larsen P, Honoré T (1990) Structure-activity relationships in the development of excitatory amino acid receptor agonists and competitive antagonists. Trends Pharmacol Sci 11:25–33
Williams K, Romano C, Molinoff PB (1989) Effects of polyamines on the binding of [^{3}H]MK-801 to the *N*-methyl-D-aspartate receptor: pharmacological evidence for the existence of a polyamine recognition site. Mol Pharmacol 36:575–581
Wong EHF, Kemp JA (1991) Sites for antagonism on the *N*-methyl-D-aspartate receptor channel complex. Ann Rev Pharmac Toxic 31:401–425
Wong EHF, Knight AR, Woodruff GN (1988) [^{3}H]MK-801 labels a site on the *N*-methyl-D-aspartate receptor channel complex in rat brain membranes. J Neurochem 50:274–281
Yoneda Y, Ogita K (1991) Neurochemical aspects of the *N*-methyl-D-aspartate receptor complex. Neurosci Res 10:1–33

E.3.1.8 Metabotropic Glutamate Receptors

PURPOSE AND RATIONALE

In addition to ionotropic (AMPA, kainate and NMDA) receptors, glutamate interacts with a second family of receptors, metabotropic or mGlu receptors (Tanabe et al. 1992, 1993; Schoepp and Conn 1993; Hollmann and Heinemann 1994; Nakanishi and Masu 1994; Okamoto et al. 1994; Watkins and Collingridge 1994; Knöpfel et al. 1995, 1996; Pin and Duvoisin 1995; Conn and Pin 1997; Alexander et al. 2001; Skerry and Generver 2001; DeBlasi et al. 2001; Pin and Acher 2002; Conn 2003). Three groups of native receptors are distinguishable on the basis of similarities of agonist pharmacology, primary sequence, and G protein-effector coupling: Group I ($mglu_1$ and $mglu_5$ and splice variants) are coupled via $G_{q/11}$ to phosphoinositide hydrolysis. Group II ($mglu_2$ and $mglu_3$) are negatively coupled via G_i/G_o to adenylyl cyclase and inhibit the formation of cAMP following exposure of cells to forskolin or activation of an intrinsic G_s-coupled receptor (e. g. adenosine A_2 receptor). The group III receptors ($mglu_4$, $mglu_6$, $mglu_7$, and $mglu_8$) also inhibit forskolin-stimulated adenylyl cyclase.

Various agonists and antagonists for metabotropic glutamate receptors were described (Ishida et al. 1990, 1994; Porter et al. 1992; Jane et al. 1994; Watkins and Collingridge 1994; Knöpfel et al. 1995; Annoura et al. 1996; Bedingfield et al. 1996; Thomsen et al. 1996; Acher et al. 1997; Doherty et al. 1997; Brauner-Osborne et al. 1998; Kingston et al. 1998; Monn et al. 1999; Jane and Doherty 2000). Schoepp et al.

(1999) reviewed pharmacological agents acting at subtypes of metabotropic glutamate receptors. Gssparini et al. (2002) described allosteric modulators of group I metabotropic glutamate receptors as novel subtype-selective ligands and their therapeutic perspectives.

Several radioligands for metabotropic glutamate receptors were described:

- for subtype mGluR4a receptor by Eriksen and Thomsen (1995),
- for group II mGlu receptors by Cartmell et al. (1998), by Ornstein et al. (1998), and by Schaffhauser et al. (1998).

Riedel and Reymann (1996) discussed the role of metabotropic glutamate receptors in hippocampal long-term potentiation and long-term depression and their importance for learning and memory. Furthermore, possible roles in the treatment of neurodegenerative disorders (Nicoletti et al. 1996; Bruno et al. 1998), and of Parkinson's disease (Konieczny et al. 1998) were discussed. Anticonvulsive properties (Attwell et al. 1998; Thompson and Dalby 1998; Gasparini et al. 1999) as well as anxiolytic properties (Helton et al. 1998) of metabotropic glutamate receptor ligands were reported. Christoffersen et al. (1999) found a positive effect on short-term memory and a negative effect on long-term memory of the class I metabotropic glutamate receptor antagonist, AIDA, in rats.

PROCEDURE

Cultured cells are prepared from cerebral cortex of 17-day embryos of Wistar rats. Prior to the experiments, the culture is maintained for 8–12 days with minimum essential medium (MEM) containing 5% fetal calf serum and 5% horse serum.

For **cyclic AMP assays**, the cultured cells are preincubated with HEPES-buffered Krebs-Ringer solution containing 5.5 mM glucose (HKR) for 1–1.5 h, then exposed to various agonists for 15 min in the absence or presence of 10 μM forskolin. The content of cyclic AMP is measured using a radioimmuno-assay kit after homogenization with 0.1 M HCl.

For **phosphoinositide turnover assays**, the cultured cells are prelabeled with myo-1,2-[^{3}H]inositol in MEM for 8–10 h. The cells are washed twice with HKR containing 10 mM LiCl, and then exposed to various agonists in HKR containing 10 mM LiCl for 30 min. The reaction is terminated with 2% trichloroacetic acid, and the homogenized samples are analyzed for inositol constituents by anion exchange chromatography (Berridge et al. 1982). The extracts are applied to columns containing 1 ml of Dowex 1 in the formate form. The phosphate esters are then eluted by the step-wise addition of solutions containing increasing concentrations of formate. Glycerophosphoinositol and inositol 1:2-cyclic phosphate are eluted with 5 mM-sodium tetraborate plus 150 mM sodium formate. The penultimate solution contains 0.1 M-formic acid plus 0.3 M-ammonium formate, followed by 0.1 M-formic acid plus 0.75 M-ammonium formate, each of which removes more polar inositol phosphates.The 1 ml fractions eluted from the columns are counted for radioactivity after addition of 10 ml of Biofluor.

The percentage of radioactivity of inositol phosphates to the total applied to the column is calculated.

EVALUATION

Dose-response curves for inhibition of forskolin-stimulated cAMP formation and for percentage of phosphoinositide hydrolysis are established for each test compound.

MODIFICATIONS OF THE METHOD

Thomsen et al. (1993, 1994) used baby hamster kidney (BHK) cells stably expressing $mGluR_{1\alpha}$, $mGluR_2$ or $mGluR_4$ for measurements of phosphoinositol hydrolysis or cAMP formation.

Varney and Suto (2000) recommended functional high throughput screening assay for the discovery of subtype-selective metabotropic glutamate receptor ligands.

REFERENCES AND FURTHER READING

Acher FC, Tellier FJ, Azerad R, Brabet IN, Fagni L, Pin JPR (1997) Synthesis and pharmacological characterization of aminocyclopentanetricarboxylic acids: New tools to discriminate between metabotropic glutamate receptor subtypes. J Med Chem 40:3119–3129

Alexander S, Peters J, Mathie A, MacKenzie G, Smith A (2001) TiPS Nomenclature Supplement

Annoura H, Fukunaga A, Uesugi M, Tatsuoka T, Horikawa Y (1996) A novel class of antagonists for metabotropic glutamate receptors, 7-(hydroxyimino)-cyclopropa[*b*]chromen-1a-carboxylates. Bioorg Med Chem Lett 6:763–766

Attwell PJE, Singh-Kent N, Jane D, Croucher MJ, Bradford HF (1998) Anticonvulsant and glutamate release-inhibiting properties of the highly potent metabotropic glutamate receptor agonist (2S,2′R,3′R)-2-(2′3′-dicarboxycyclopropyl)-glycine (DCG-IV). Brain Res 805:138–143

Bedingfield JS, Jane DE, Kemp MC, Toms NJ, Roberts PJ (1996) Novel potent selective phenylglycine antagonists of metabotropic glutamate receptors. Eur J Pharmacol 309:71–78

Berridge MJ, Downes CP, Hanley MR (1982) Lithium amplifies agonist-dependent phosphatidylinositol responses in brain and salivary glands. Biochem J 206:587–595

Brauner-Osborne H, Nielsen B, Krogsgaard-Larsen P (1998) Molecular pharmacology of homologues of ibotenic acid at cloned metabotropic glutamic acid receptors. Eur J Pharmacol 350:311–316

Bruno V, Battaglia G, Copani A, Casabona G, Storto M, di Giorgi-Gerevini V, Ngomba R. Nicoletti F (1998) Metabotropic glutamate receptors and neurodegeneration. Prog Brain Res 116:209–221

Cartmell J, Adam G, Chaboz S, Henningsen R, Kemp JA, Klingelschmidt A, Metzler V, Monsma F, Schaffhauser H, Wichmann J, Mutel V (1998) Characterization of [^{3}H]-(2S,2′R,3′R)-2-(2′,3′-dicarboxycyclopropyl)glycine ([^{3}H]-DCG IV) binding to metabotropic $mGlu_2$ receptor transfected cell membranes. Br J Pharmacol 123:497–504

Christoffersen GRJ, Christensen LH, Hammer P, Vang M (1999) The class I metabotropic glutamate receptor antagonist, AIDA, improves short-term and impairs long-term memory in a spatial task for rats. Neuropharmacol 38:817–823

Conn PJ, Pin JP (1997) Pharmacology and function of metabotropic glutamate receptors. Ann Rev Pharmacol Toxicol 37:205–237

Conn PJ (2003) Physiological roles and therapeutic potential of metabotropic glutamate receptors. Ann NY Acad Sci 1003:12–21

DeBlasi A, Conn PJ, Pin JP, Nicolette F (2001) Molecular determinants of metabotropic glutamate signaling. Trends Pharmacol Sci 22:114–120

Doherty AJ, Palmer MJ, Henley JM, Collingridge GL, Jane DE (1997) (R,S)-2-chloro-5-hydroxyphenylglycine (CHPG) activates $mGlu_5$, but not $mGlu_1$, receptors expressed in CHO cells and potentiates NMDA responses in the hippocampus. Neuropharmacol 36:265–267

Eriksen L, Thomsen C (1995) [^{3}H]-L-2-amino-4-phosphonobutyrate labels a metabotropic glutamate receptor, mGluR4a. Br J Pharmacol 116:3279–3287

Gasparini F, Bruno V, Battaglia G, Lukic S, Leonhardt T, Inderbitzin W, Laurie D, Sommer B, Varney MA, Hess SD, Johnson EC, Kuhn R, Urwyler S, Sauer D, Portet C, Schmutz M, Nicoletti F, Flor PJ (1999) (R,S)-4-Phosphonophenylglycine, a potent and selective group III metabotropic glutamate receptor agonist, is anticonvulsive and neuroprotective *in vivo*. J Pharmacol Exp Ther 289:1678–1687

Gssparini F, Kuhn R, Pin JP (2002) Allosteric modulators of group I metabotropic glutamate receptors: novel subtype-selective ligands and therapeutic perspectives. Curr Opin Pharmacol 2:43–49

Helton DR, Tizzano JP, Monn JA, Schoepp DD, Kallman MJ (1998) Anxiolytic and side-effect profile of LY354740: A potent and highly selective, orally active agonist for group II metabotropic glutamate receptors. J Pharmacol Exp Ther 284:651–660

Hollmann M, Heinemann S (1994) Cloned glutamate receptors. Ann Rev Neurosci 17:31–108

Ishida M, Akagi H, Shimamoto K, Ohfune Y, Shinozaki H (1990) A potent metabotropic glutamate receptor agonist: electrophysiological actions of a conformationally restricted glutamate analogue in the rat spinal cord and *Xenopus oocytes*. Brain Res 537:311–314

Ishida M, Saitoh T, Nakamura Y, Kataoka K, Shinozaki H (1994) A novel metabotropic glutamate receptor agonist: (2S,1′S,2′R,3′R)-2-(carboxy-3-methoxymethylcyclopropyl)glycine (cis-MCG-I). Eur J Pharmacol Mol Pharmacol Sect 268:267–270

Jane D, Doherty A (2000) Muddling through the mGlu maze? Tocris Review No.13

Jane DE, Jones PLSJ, Pook PCK, Tse HW, Watkins JC (1994) Actions of two new antagonists showing selectivity for different subtypes of metabotropic glutamate receptor in the neonatal spinal cord. Br J Pharmacol 112:809–816

Kingston AE, Ornstein PL, Wright RA, Johnson BG, Mayne NG, Burnett JP, Belagaje R, Wu S, Schoepp DD (1998) LY341495 is a nanomolar potent and selective antagonist of group II metabotropic glutamate receptors. Neuropharmacol 37:1–12

Knöpfel T, Kuhn R, Allgeier H (1995) Metabotropic glutamate receptors: Novel targets for drug development. J Med Chem 38:1417–1425

Knöpfel T, Madge T, Nicoletti F (1996) Metabotropic glutamate receptors. Expert Opin Ther Pat 6:1061–1067

Konieczny J, Ossowska K, Wolfarth S, Pilc A (1998) LY354740, a group II metabotropic glutamate receptor agonist with potential antiparkinsonian properties in rats. Naunyn-Schmiedeberg's Arch Pharmacol 358:500–502

Monn JA, Valli MJ, Massey SM, Hansen MM, Kress TJ, Wepsiec JP, Harkness AR, Grutsch JL Jr, Wright PA, Johnson PG, Andis SL, Kingston A, Tomlinson R, Lewis R, Griffey KR, Tizzano JP, Schoepp DD (1999) Synthesis, pharmacological characterization, and molecular modeling of heterobicyclic amino acids related to (+)-2-aminobicyclo[3.1.0]-hexane-2,6-dicarboxylic acid (LY354740): Identification of two new potent, selective, and systemically active agonists for group II metabotropic glutamate receptors. J Med Chem 42:1027–1040

Nakanishi S, Masu M (1994) Molecular diversity and function of glutamate receptors. Ann Rev Biophys Biomol Struct 23:319–348

Nicoletti F, Bruno V, Copani A, Casabona G, Knöpfel T (1996) Metabotropic glutamate receptors: A new target for the treatment of neurodegenerative disorders? Trends Neurosci 19:267–271

Okamaoto N, Hori S, Akazawa C, Hayashi Y, Shigemoto R, Mizuno N, Nakanishi S (1994) Molecular characterization of a new metabotropic glutamate receptor $mGluR_7$ coupled to inhibitory cyclic AMP signal transduction. J Biol Chem 269:1231–1236

Ornstein PL, Arnold MB, Bleisch TJ, Wright RA, Wheeler WJ, Schoepp DD (1998) [^{3}H]LY341495, a highly potent, selective and novel radioligand for labeling group II metabotropic glutamate receptors. Bioorg Med Chem Lett 8:1919–1922

Pin JP, Duvoisin R (1995) The metabotropic glutamate receptors: Structure and functions. Neuropharmacol 34:1–26

Pin JP, Acher F (2002) The metabotropic glutamate receptors: structure, activation mechanism and pharmacology. Curr Drug Targets CNS Neurol Disord 1:297–317

Porter RHP, Briggs RSJ, Roberts PJ (1992) L-Aspartate-β-hydroxamate exhibits mixed agonist/antagonist activity at the glutamate metabotropic receptor in rat neonatal cerebrocortical slices. Neurosci Lett 144:87–89

Riedel G, Reymann KG (1996) Metabotropic glutamate receptors in hippocampal long-term potentiation and learning and memory. Acta Physiol Scand 157:1–19

Schaffhauser H, Richards JG, Cartmell J, Chaboz S, Kemp JA, Klingelschmidt A, Messer J, Stadler H, Woltering T, Mutel V (1998) *In vitro* binding characteristics of a new selective group II metabotropic glutamate receptor radioligand, [3H]LY354740, in rat brain. Mol Pharmacol 53:228–233

Schoepp DD, Conn PJ (1993) Metabotropic glutamate receptors in brain function and pathology. Trends Pharmacol Sci 14:13–20

Schoepp DD, Jane DE, Monn JA (1999) Pharmacological agents acting at subtypes of metabotropic glutamate receptors. Neuropharmacology 38:1431–1476
Skerry TM, Genever PG (2001) Glutamate signalling in non-neuronal tissues. Trends Pharmacol Sci 22:174–181
Tanabe Y, Masu M, Ishii T, Shigemoto R, Nakanishi S (1992) A family of metabotropic glutamate receptors. Neuron 8:169–179
Tanabe Y, Nomura A, Masu M, Shigemoto R, Mizuno N, Nakanishi S (1993) Signal transduction, pharmacological properties, and expression pattern of two rat metabotropic glutamate receptors, $mGluR_3$ and $mGluR_4$. J Neurosci 13:1372–1378
Thomsen C, Dalby NO (1998) Roles of metabotropic glutamate receptor subtypes in modulation of pentylenetetrazole-induced seizure activity in mice. Neuropharmacol 37:1465–1473
Thomsen C, Mulvihill ER, Haldeman B, Pickering DS, Hampson DR, Suzdak PD (1993) A pharmacological characterization of the mGluR1α subtype of the metabotropic glutamate receptor expressed in a cloned baby hamster kidney cell line. Brain Res 619:22
Thomsen C, Boel E, Suzdak PD (1994) Action of phenylglycine analogs at subtypes of the metabotropic glutamate receptor family. Eur J Pharmacol 267:77–84
Thomsen C, Bruno V, Nicoletti F, Marinozzi M, Pelliciari R (1996) (2S,1′S,2′S,3′R)-2-(2′-carboxy-3′-phenylcyclopropyl)glycine, a potent and selective antagonist of type 2 metabotropic glutamate receptors. Mol Pharmacol 50:6–9
Varney MA, Suto CM (2000) Discovery of subtype-selective metabotropic glutamate receptor ligands using functional HTS assays. Drug Disc Today: HTS Suppl 1:20–26
Watkins J, Collingridge G (1994) Phenylglycine derivatives as antagonists of metabotropic glutamate receptors. Trends Pharmacol Sci 15:333–342

E.3.1.9 Excitatory Amino Acid Transporters

PURPOSE AND RATIONALE

Glutamate is not only the predominant excitatory neurotransmitter in the brain but also a potent neurotoxin. Following release of glutamate from presynaptic vesicles into the synapse and activation of a variety of ionotropic and metabotropic glutamate receptors, glutamate is removed from the synapse. This is achieved through active uptake of glutamate by transporters located pre- but also post-synaptically, or glutamate can diffuse out of the synapse and be taken up by transporters located on the cell surface of glial cells. The excitatory amino acid transporters form a gene family out of which at least 5 subtypes were identified (Robinson et al. 1993; Seal and Amara 1999). A role for glutamate transporters has been postulated for acute conditions such as stroke, CNS ischemia, and seizure, as well as in chronic neurodegenerative diseases, such as Alzheimer's disease and amyotrophic lateral sclerosis. Glutamate transport is coupled to sodium, potassium and pH gradients across the cell membrane creating an electrogenic process. This allows transport to be measured using electrophysiological techniques (Vandenberg et al. 1997).

PROCEDURE

Complementary DNAs encoding the human glutamate transporters, EAAT1 and EAAT2, are subcloned into pOTV for expression in X. laevis oocytes (Arriza et al. 1994; Vandenberg et al. 1995). The plasmids are linearized with BAMHI and cRNA is transcribed from each of the cDNA constructs with T7 RNA polymerase and capped with 5′,7-methyl guanosine using the mMESSAGE mMACHINE (Ambion, Austin TX). cRNA (50 ng) encoding either EAAT1 or EAAT2 is injected into defolliculated Stage V X. laevis oocytes. Two to 7 days later, transport is measured by two-electrode voltage-clamp recording using a Geneclamp 500 amplifier (Axon Instruments, Foster City, CA) and a MacLab 2e recorder (ADI Instruments, Sydney, Australia) and controlled using a pCLAMP 6.01 interfaced to a Digidata 1200 (Axon Instruments). Oocytes are voltage-clamped at –60 mV and continuously superfused with ND96 buffer (96 mM NaCl, 2 mM KCl, 1.8 mM $CaCl_2$, 1 mM $MgCl_2$ and 5 mM HEPES, pH 7.5). For transport measurement, this buffer is changed to one containing the indicated concentration of substrate and/or blocker. The voltage dependence of block of glutamate transport is measured by clamping the membrane potential at –30 mV and then applying a series of 100 ms voltage pulses from –100 mV to 0 mV and measuring the steady state current at each membrane potential. This protocol is applied both before and during the application of the compound in question and then the base-line current at each membrane potential is subtracted from the current in the presence of the compounds to get a measure for the transport specific current at the various membrane potentials.

EVALUATION

Current (I) as a function of substrate concentration ([S]) is fitted by least squares to

$$I = I_{max}[S]/(K_m + [S])$$

where I_{max} is the maximal current and K_m is the Michaelis transport constant. The I_{max} values for the various substrates are expressed relative to the current generated by a maximal dose of L-glutamate in the same cell. I_{max} and K_m values are expressed as mean ± standard error and are determined by fitting data from individual oocytes. The potent competitive

blockers are characterized by Schild analysis (Arunlakshana and Schild 1959) and the K_b estimated from the regression plot. The less potent blockers are assumed to be competitive and K_i values calculated from IC_{50} values using the equation

$$K_i = IC_{50}/(1 + [\text{glutamate}]/K_m)$$

where K_i is the inhibition constant, IC_{50} is the concentration giving half maximum inhibition, K_m is the transport constant and [glutamate] is 30 µM. The fraction of the membrane electric field sensed by transport blockers when bound to the transporters is estimated using the Woodhull equation (Woodhull 1973),

$$K_i = K_i^0 \exp(-\zeta \delta FE/RT)$$

where K_i is the inhibition constant, $K_i{}^0$ is the inhibition constant at 0 mV, ζ is the charge on the blocker, δ is the fraction of the membrane field, F is Faraday's constant, E is the membrane potential, $R$is the gas constant and T is temperature in K.

REFERENCES AND FURTHER READING

Arriza JL, Fairman WA, Wadiche JI, Murdoch GH, Kavanaugh MP, Amara SG (1994) Functional comparisons of three glutamate transporter subtypes cloned from human motor cortex. J Neurosci 14:5559–5569

Arunlakshana O, Schild HO (1959) Some quantitative uses of drug antagonists. Br J Pharmacol 14:48–58

Robinson MB, Sinor JD, Dowd LA, Kerwin JF Jr (1993) Subtypes of sodium-dependent high-affinity L-[^{3}H]glutamate transport activity. Pharmacologic specificity and regulation by sodium and potassium. J Neurochem 60:1657–179

Seal RP, Amara SG (1999) Excitatory amino acid transporters: A family in Flux. Annu Rev Pharmacol Toxicol 39:431–456

Vandenberg RJ (1998) Molecular pharmacology and physiology of glutamate transporters in the central nervous system. Clin Exp Pharmacol Physiol 25:393–400

Vandenberg RJ, Arriza JL, Amara SG, Kavanaugh MP (1995) Constitutive ion fluxes and substrate binding domains of human glutamate transporters. J Biol Chem 270:17668–17671

Vandenberg RJ, Mitrovic AD, Chebib M, Balcar VJ, Johnston GAR (1997) Contrasting modes of action of methylglutamate derivatives on the excitatory amino acid transporters, EAAT1 and EAAT2. Molec Pharmacol 51:809–815

Woodhull AM (1973) Ion blockage of sodium channels in nerve. J Gen Physiol 61:667–708

E.3.1.10 [^{35}S]TBPS Binding in Rat Cortical Homogenates and Sections

PURPOSE AND RATIONALE

To screen potential anticonvulsant agents which interact at the convulsant binding site of the benzodiazepine/GABA/chloride ionophore complex by measuring the inhibition of binding of [^{35}S]TBPS to rat cortical membranes.

TBPS, t-butylbicyclophosphorothionate, is a potent convulsant which blocks GABA-ergic neurotransmission by interacting with the convulsant (or picrotoxin) site of the GABA/benzodiazepine/chloride ionophore receptor complex (Casida et al. 1985; Gee et al. 1986; Olsen et al. 1986; Squires et al. 1983; Supavilai and Karabath 1984). Picrotoxin, pentylenetetrazol and the so-called "cage convulsants" are believed to change the state of the chloride channel to a closed conformation, and thereby block GABA-induced increases in chloride permeability. Anticonvulsants such as the barbiturates and the pyrazolopyridines, cartazolate, etazolate and tracazolate, appear to interact at depressant sites allosterically coupled to the convulsant sites, and facilitate the effects of GABA on chloride permeability, by converting the ionophore to the open conformation. Benzodiazepines interact at a separate recognition site to modulate the actions of GABA. Convulsant compounds and some anticonvulsants can inhibit [^{35}S]TBPS binding. These two classes can be differentiated by their effects on dissociation kinetics (Macksay and Ticku 1985; Trifiletti et al. 1984, 1985). [^{35}S]TBPS dissociates slowly, half-life approximately 70 min, in a monophasic manner in the presence of convulsant compounds; anticonvulsants produce a biphasic dissociation, with rapid and slow phase components. It has been postulated that the rapid and slow phases of [^{35}S]TBPS dissociation may correspond to the open and closed conformation of the chloride ionophore.

PROCEDURE

Reagents

1. Buffer A 0.05 M Tris with 2 M KCl, pH 7.4

   6.61 g Tris HCl

   0.97 g Tris Base

   149.1 g KCl

   q.s. to 1 liter with distilled water
2. Buffer B
   a 1:10 dilution of buffer A in distilled water (5 mM Tris, 200 mM KCl, pH 7.4)
3. [^{35}S]TBPS is obtained from New England Nuclear with a high initial specific activity, 90–110 Ci/mmol. For an inhibition assay with a 2 nM final concentration of TBPS, a specific activity of 20–25 Ci/mmol will provide sufficient counts due to a high counting efficiency (87%)

for ^{35}S. The specific activity of [^{35}S]TBPS can be reduced with the addition of 3–5 volumes (accurate measurement with a Hamilton syringe) of an equimolar ethanolic solution of non-radiolabeled TBPS (7.9×10^{-6} M). The new specific activity (Ci/mmol) is calculated by dividing the number of Curies by the number of mmoles TBPS. Since [^{35}S]TBPS has a relatively short half-life, 87.1 days, the specific activity is calculated for each assay, based on the exponential rate of decay:

A_0 = initial specific activity
A = specific activity at time t
t = days from date of initial calibration of specific activity
$t_{1/2}$ = half-life of [^{35}S] in days (87.1)

For IC_{50} determinations, a 40 nM stock solution is made with distilled water and 25 µl is added to each tube to yield a final concentration of 2 nM in the assay.

4. Unlabeled TBPS is available from New England Nuclear. A stock dilution of 7.923×10^{-6} M is prepared in ethanol.
5. Picrotoxin, is obtained from Aldrich Chemical Company. A solution of 5×10^{-4} M is prepared with distilled water, with sonication if necessary. Aliquots of 10 µl are added to assay tubes to give a final concentration of 10^{-5} M.
6. Test compounds. A stock solution of 1 mM is made up with a suitable solvent and serially diluted, such that the final concentration in the assay ranges from 10^{-5} to 10^{-8} M. Higher or lower concentrations may be used, depending on the potency of the drug.

Tissue Preparation

Whole cerebral cortex of male Wistar rats is dissected over ice and homogenized with a Tekmar Tissumizer, 20 s at setting 40, in 20 volumes of 0.32 M sucrose, ice-cold. The homogenate is centrifuged at 1000 *g* for 10 min (SS34, 3000 rpm, 4°C). The supernatant is then centrifuged at 40,000 *g* for 30 min (SS34, 20,000 rpm, 4°C). The resulting pellet is resuspended in 20 volumes of ice-cold distilled water with two 6-s bursts of the Tissumizer, setting 40. The homogenate is centrifuged at 40,000 *g* for 30 min. The pellet is washed (resuspended and centrifuged) once with 20 volumes ice-cold buffer (Tris HCl 5 mM, KCl 200 mM, pH 7.4). The resulting pellet is resuspended with 20 volumes buffer and frozen at –70°C overnight. The following day, the tissue homogenate is thawed in a beaker of warm water, approximately 15 min, and then centrifuged at 40,000 *g* for 30 min (SS34, 20,000 rpm, 4°C). The pellet is washed twice with 20 volumes of ice-cold buffer, and then resuspended and frozen at –70°C for future use. On the day of the assay, the homogenate is thawed and centrifuged at 40,000 *g* for 30 min. The resulting pellet is washed once with 20 volumes ice-cold buffer and finally resuspended in 30 volumes buffer. Aliquots of 250 µl are used for each assay tube, final volume 500 µl, and correspond to 8.35 mg original wet weight tissue per tube, approximately 0.2 mg protein.

Assay

1. Prepare assay tubes in triplicate:

190 µl	distilled water
25 µl	Tris 0.05 M, KCl 2M, pH 7.4
10 µl	picrotoxin, 10^{-5} M final concentration or distilled water or inhibitor 25 µl [^{35}S]-TBPS, final concentration 2 nM
250 µl	tissue preparation, 1:30 homogenate

2. Following the addition of the tissue, the tubes are incubated at 25°C for 150 min with agitation. The assay is terminated by rapid filtration over Whatman GF/B filter circles, presoaked in buffer, with 5 × 4 ml rinses of ice-cold buffer. Vacuum filtration is performed with the 45-well filtration units to avoid contamination of the Brandell harvesters with [^{35}S]. The filters are counted with 10 ml Liquiscint.

EVALUATION

Specific binding is determined from the difference between binding in the absence or presence of 10 mM picrotoxin, and is typically 85–90% of total binding. The percent inhibition at each drug concentration is the mean of triplicate determinations. IC_{50} values for the competing drug are calculated by log-probit analysis of the data.

Modifications for Dissociation Experiments

1. Prepare assay tubes as follows:

185 µl	distilled water
25 µl	Tris 50 mM, KCl 2 M, pH 7.4
10 µl	test compound or vehicle

2. Add 250 ml tissue homogenate to tubes. Vortex. Pre-incubate 30 min at 25°C.
3. Add 25 ml [^{35}S]-TBPS. Vortex. Incubate 180 min at 25°C.
4. Add 5 ml picrotoxin (10^{-3} M) to give a final concentration of 10^{-5} M. Vortex.

5. At various times after the addition of picrotoxin (0–120 min) tubes are filtered and rinsed as described above.

Modification for [^{35}S]-TBPS Autoradiography

1. Sections of rat brain, 20 mm thickness, are collected onto gel-chrome alum subbed slides, freeze-dried for approximately 1 h and stored at –70°C until used.
2. After thawing and drying at room temperature, the sections are preincubated for 30 min in buffer B.
3. Preparation of slide mailers for incubation:
   a) for scintillation counting:
      2.47 ml distilled water
      0.325 ml buffer A
      3.25 ml buffer B
      0.13 ml picrotoxin, 10^{-5} M final concentration or distilled water or inhibitor
      0.325 ml [^{35}S]TBPS, final concentration 2 nM
      6.50 ml final volume
   b) for autoradiography:
      4.56 ml distilled water
      0.60 ml buffer A
      6.00 ml buffer B
      0.24 ml picrotoxin, 10^{-5} M final concentration or distilled water or inhibitor
      0.60 ml [^{35}S]TBPS, final concentration 2 nM
      12.0 ml final volume
4. Sections are incubated in slide mailers at room temperature with [^{35}S]TBPS in the absence or presence of appropriate inhibitors for 90 min.
5. Slides are transferred to vertical slide holders and rinsed in ice-cold solutions as follows: dip in buffer B, two 5 minute rinses in buffer A and a dip in distilled water.
6. Slides are dried under a stream of cool air and desiccated overnight at room temperature.
7. Slides are mounted onto boards with appropriate [^{35}S] brain mash standards.
8. In the dark room under safelight illumination (GBX filter), slides are opposed to Kodak X-OMAT AR film and stored in cassettes for 7–10 days.
9. Develop films as described in "X-OMAT AR Film Processing".

	[^{35}S]TBPS binding parameters	
	Slide-mounted sections	Cortical homogenates
Assay conditions		
Tissue	20 µ sections, rat freeze-dried, 1 h	Whole cortex, rat 1:30 homogenate prepared with 5 washes and 2 freeze-thaw cycles
	30 min preincubation	No preincubation
Buffer	5 mM Tris 200 mM KCl pH 7.4	5 mM Tris 200 mM KCl pH 7.4
Incubation time	90 min, 21–22°C	150 min, 25°C
Non specific	10^{-5} M picrotoxin	10^{-5} M picrotoxin
Tissue linearity	2.5–25 mg tissue per 0.5 ml assay tube	
Equilibrium constants		
KD (nM)	32.8	25.2
Bmax (fmol/mg prot)	1615	2020
Binding kinetics		
Association kobs (min^{-1})	0.0496	0.0138
k+1 (nM^{-min-1})	0.0164	0.0021
Dissociation k−1 (min^{-1})	0.017	0.001
Dissociation constant k+1/k−1 (nM)	1.03	4.73
IC_{50}M		
Picrotoxin	2.8×10^{-7}	3.4×10^{-7}
TBPS	8.7×10^{-8}	8.1×10^{-8}
GABA	1.7×10^{-6}	2.1×10^{-6}
Pentobarbital	1.2×10^{-4}	6.0×10^{-4}
Phenobarbital	None at 10^{-3}	None at 10^{-3}
Clonazepam	None at 10^{-6}	None at 10^{-6}

REFERENCES AND FURTHER READING

Casida JE, Palmer CJ, Cole LM (1985) Bicycloorthocarboxylate convulsants. Potent $GABA_A$ receptor antagonists. Mol Pharmacol 28:246–253

Gee KW, Lawrence LJ, Yamamura HI (1986) Modulation of the chloride ionophore by benzodiazepine receptor ligands: influence of gamma-aminobutyric acid and ligand efficacy. Mol Pharmacol 30:218–225

Macksay G, Ticku MK (1985a) Dissociation of [^{35}S]-*t*-butylbicyclophosphorothionate binding differentiates convulsant and depressant drugs that modulate GABAergic transmission. J Neurochem 44:480–486

Macksay G, Ticku MK (1985b) GABA, depressants and chloride ions affect the rate of dissociation of [^{35}S]-*t*-butylbicyclophosphorothionate binding. Life Sci 37:2173–2180

Olsen RW, Yang J, King RG, Dilber A, Stauber GB, Ransom RW (1986) Barbiturate and benzodiazepine modu-

lation of GABA receptor binding and function. Life Sci 39:1969–1976
Squires RF, Casida JE, Richardson M, Saederup E (1983) [^{35}S]*t*-Butylbicyclophosphorothionate binds with high affinity to brain specific sites coupled to γ-aminobutyric acid-A and ion recognition sites. Mol Pharmacol 23:326–336
Supavilai P, Karabath M (1984) [^{35}S]-t-Butylbicyclophosphorothionate binding sites are constituents of the γ-aminobutyric acid benzodiazepine receptor complex. J Neurosci 4:1193–1200
Trifiletti RR, Snowman AM, Snyder SH (1984) Anxiolytic cyclopyrrolone drugs allosterically modulate the binding of [^{35}S]t-butylbicyclophosphorothionate to the benzodiazepine/γ-aminobutyric acid-A receptor/chloride anionophore complex. Mol Pharmacol 26:470–476
Trifiletti RR, Snowman AM, Snyder SH (1985) Barbiturate recognition site on the GABA/Benzodiazepine receptor complex is distinct from the picrotoxin/TBPS recognition site. Eur J Pharmacol 106:441–447

E.3.1.11 [^{3}H]glycine Binding in Rat Cerebral Cortex

PURPOSE AND RATIONALE

The amino acid glycine is a major inhibitory transmitter in the vertebrate system. Glycinergic synapses are particularly abundant in spinal cord and brain stem, but are also found in higher regions, including the hippocampus. The inhibitory actions of glycine are potently blocked by strychnine. Glycine modulates and may activate the excitatory amino acid receptors of the NMDA-subtype (Thomson 1989; Laube et al. 2002).

The strychnine-sensitive, postsynaptic glycine receptor is a ligand-gated chloride channel protein that belongs to the nicotinic acetylcholine receptor family. It is a pentameric transmembrane protein composed of α and β subunits (Lynch 2004).

Glycine has been shown *in vitro* to potentiate the effects of l-glutamate or NMDA on the stimulation of [^{3}H]TCP binding (Snell et al. 1987, 1988; Bonhaus 1989) and [^{3}H]norepinephrine release (Ransom et al. 1988), and *in vivo* to act as a positive modulator of the glutamate-activated cGMP response in the cerebellum (Danysz et al. 1989; Rao et al. 1990). The activation of NMDA receptors requiring the presence of glycine is necessary for the induction of long-term potentiation (LTP), a type of synaptic plasticity which may be fundamental to learning processes (Oliver et al. 1990). A [^{3}H]glycine binding site in the brain has been identified and characterized as a strychnine-insensitive site associated with the NMDA receptor complex (Kessler et al. 1989; Monahan et al. 1989; Cotman et al. 1987). Autoradiographic studies have shown a similar distribution of [^{3}H]glycine and [^{3}H]TCP (NMDA ion channel radioligand) binding sites (Jansen et al. 1989). Compounds which interact with the glycine site offer a novel mechanism of action for intervention with NMDA receptor function.

Schmieden and Betz (1995) reviewed the pharmacology of the inhibitory glycine receptor, the agonist and antagonist actions of amino acids and piperidine carboxylic compounds.

Hyperekplexia is a hereditary neurological disorder in humans characterized by an excessive startle response which can be caused by mutations in the α_1-subunit of the heteropentameric inhibitory glycine receptor (Rees et al. 2002). Becker et al. (2002) generated transgenic mice resembling this disease.

The following assay is used to assess the affinity of compounds for the glycine binding site associated with the *N*-methyl-D-aspartate (NMDA) receptor complex using [^{3}H] glycine as the radioligand.

PROCEDURE

Reagents

1. Buffer A: 0.5M Tris maleate, pH 7.4
   59.3 g Tris maleate
   q.s. to 0.5l
   Adjust pH to 7.4 with 0.5M Tris base.
2. Buffer B: 50 mM Tris maleate, pH 7.4
   Dilute buffer A 1:10 with distilled water; adjust pH with 50 mM Tris maleate (acid) or 50 mM Tris base.
3. Glycine, 5×10^{-2} M
   Dissolve 3.755 mg of glycine (Sigma G7126) with 1.0 ml distilled water. Aliquots of 20 µl to the assay tube will give a final concentration of 10^{-3} M
4. [^{3}H]Glycine is obtained from New England Nuclear, specific activity 45–50 Ci mmol. For IC_{50} determinations, a 200 nM stock solution is made with distilled water. Aliquots of 50µl are added to yield a final assay concentration of 10 nM.
5. Test compounds. A stock solution of 5 mM is prepared with a suitable solvent and serially diluted, such that the final concentrations in the assay ranges from 10^{-4} to 10^{-7} M. Higher or lower concentrations may be used, depending on the potency of the compound.
6. Triton-X 100, 10% (v/v) (National Diagnostics, EC-606). A stock solution of Triton-X 100, 10% can be prepared and stored in the refrigerator. Dilute 1.0 ml of Triton-X 100 to 10.0 ml with distilled water. On the day of the assay, the tissue homogenate (1:15 dilution) is preincubated with an aliquot of the 10% solution to give a final concentration of 0.04% (v/v).

Tissue Preparation

Cortices of male Wistar rats are dissected over ice and homogenized in ice-cold 0.32 M sucrose, 15 volumes

of original wet weight of tissue, for 30 s with a Tissumizer setting at 70. Three cortices are pooled for one preparation. The homogenate is centrifuged at 1000 *g* for 10 min (SS34, 3000 rpm, 4°C). The supernatant is centrifuged at 20,000 *g* (SS34, 12,000 rpm, 4°C) for 20 min. Resuspend the pellet in 15 volumes of ice-cold distilled water (Tissumizer setting 70, 15 s) and spin at 7600 *g* (SS34, 8000 rpm 4°C) for 20 min. The pellet is resuspended with 15 volumes of cold distilled water and centrifuged. Discard the supernatant and store the pellet at –70°C.

On the day of the assay, the pellet is resuspended in 15 volumes ice-cold 50 mM Tris maleate, pH 7.4. Preincubate the homogenate with Triton-X in a final concentration of 0.04% (v/v) for 30 min at 37°C with agitation. Centrifuge the suspension at 48,000 *g* (SS34, 20,000 rpm, 4°C) for 20 min. Wash the pellet an additional 3 times by resuspension with cold buffer and centrifugation. The final pellet is resuspended in a volume 25 times the original wet weight.

Assay

1. Prepare assay tubes in quadruplicate.

380 µl	distilled water
50 µl	buffer A, 0.5 M Tris maleate, pH 7.4
20 µl	glycine, 10^{-3} M final concentration, or distilled water or appropriate concentration of inhibitor
50 µl	[^{3}H] glycine, final concentration 10 nM
500 µl	tissue homogenate.
1000 µl	final volume

2. Following the addition of the tissue, the tubes are incubated for 20 min in an ice-bath at 0–4°C. The binding is terminated by centrifugation (HS4, 7000 rpm, 4°C) for 20 min. Aspirate and discard the supernatant. Carefully rinse the pellet twice with 1 ml ice-cold buffer, avoiding disruption of the pellet. Transfer the pellet to scintillation vials by vortexing the pellet with 2 ml scintillation fluid, rinse the tubes twice with 2 ml and add an additional 4 ml scintillation fluid.

EVALUATION

Specific binding is determined from the difference of binding in the absence or in the presence of 10^{-4} M glycine and is typically 60–70% of total binding. IC_{50} values for the competing compound are calculated by log-probit analysis of the data.

MODIFICATIONS OF THE METHOD

Baron et al. (1996), Hofner and Wanner (1997), Chazot et al. (1998) described [^{3}H]MDL 105,519 as a high affinity ligand for the NMDA associated glycine recognition site.

REFERENCES AND FURTHER READING

Baron BM, Harrison BL, Miller FP, McDonald IA, Salituro FG, Schmidt CJ, Sorensen SM, White HS, Palfreyman MG (1990) Activity of 5,7-dichlorokynurenic acid, a potent antagonist at the *N*-methyl-D-aspartate receptor-associated glycine binding site. Mol Pharmacol 38:554–561

Baron BM, Siegel BW, Harrison BL, Gross RS, Hawes C, Towers P (1996) [^{3}H]MDL 105,519, a high affinity radioligand for the N-methyl-D-aspartate receptor-associated glycine recognition site. J Pharmacol Exp Ther 279:62–68

Becker L, von Wegener J, Schenkel J, Zeilhofer HU, Swandulla D, Weiher H (2002) Disease specific human glycine receptor α_1 subunit causes hyperekplexia phenotype and impaired glycine and $GABA_A$-receptor transmission in transgenic mice. J Neurosci 22:2505–2512

Bonhaus DW, Burge BC, McNamara JO (1978) Biochemical evidence that glycine allosterically regulates an NMDA receptor-coupled ion channel. Eur J Pharmacol 142:489–490

Bonhaus DW, Yeh G-C, Skaryak L, McNamara JO (1989) Glycine regulation of the *N*-methyl-D-aspartate receptor-gated ion channel in hippocampal membranes. Mol Pharmacol 36:273–279

Chazot PL, Reiss C, Chopra B, Stephenson FA (1998) [^{3}H]MDL 105,519 binds with equal high affinity to both assembled and unassembled NR1 subunits of the NMDA receptor. Eur J Pharmacol 353:137–140

Cotman CW, Monaghan DT, Ottersen OP, Storm-Mathisen J (1987) Anatomical organization of excitatory amino acid receptors and their pathways. Trends Neurosci 10:273–280

Danysz W, Wroblewski JT, Brooker G, Costa E (1989) Modulation of glutamate receptors by phencyclidine and glycine in the rat cerebellum: cGMP increase *in vivo*. Brain Res 479:270–276

Foster AC, Kemp JA, Leeson PD, Grimwood S, Donald AE, Marshall GR, Priestley T, Smith JD, Carling RW (1992) Kynurenic acid analogues with improved affinity and selectivity for the glycine site on the *N*-methyl-D-aspartate receptor from rat brain. Mol Pharmacol 41:914–922

Hargreaves RJ, Rigby M, Smith D, Hill RG (1993) Lack of effect of L-687,414 ((+)-*cis*-4-methyl-HA-966), an NMDA receptor antagonist acting at the glycine site, on cerebral glucose metabolism and cortical neuronal morphology. Br J Pharmacol 110:36–42

Hofner G, Wanner KT (1997) Characterization of the binding of [^{3}H]MDL 105,519, a radiolabelled antagonist for the N-methyl-D-aspartate receptor-associated glycine site to pig cortical brain membranes. Neurosci Lett 226:79–82

Jansen KLR, Dragunow M, Faull RLM (1989) [^{3}H]Glycine binding sites, NMDA and PCP receptors have similar distributions in the human hippocampus: an autoradiographic study. Brain Res 482:174–1178

Kessler M, Terramani T, Lynch B, Baudry M (1989) A glycine site associated with *N*-methyl-D-aspartic acid receptors: characterization and identification of a new class of antagonists. J Neurochem 52:1319–1328

Laube B, Maksay G, Schemm R, Betz H (2002) Modulation of glycine receptor function: a novel approach for therapeutic intervention at inhibitory synapses? Trends Pharmacol Sci 23:519–527

Lynch JW (2004) Molecular structure and function of the glycine receptor chloride channel. Physiol Rev 84:1051–1095
Monahan JB, Corpus VM, Hood WF, Thomas JW, Compton RP (1989) Characterization of a [^{3}H]glycine recognition site as a modulatory site of the *N*-Methyl-D-aspartate receptor complex. J Neurochem 53:370–375
Oliver MW, Kessler M, Larson J, Schottler F, Lynch G (1990) Glycine site associated with the NMDA receptor modulates long-term potentiation. Synapse 5:265–270
Ransom RW, Deschenes NL (1988) NMDA-induced hippocampal [^{3}H]norepinephrine release is modulated by glycine. Eur J Pharmacol 156:149–155
Rao TS, Cler JA, Emmet MR, Mick SJ, Iyengar S, Wood PL (1990) Glycine, glycinamide, and D-serine act as positive modulators of signal transduction at the N-methyl-D-aspartate (NMDA) receptor *in vivo*: differential effects on mouse cerebellar cyclic guanosine monophosphate levels. Neuropharmacol 29:1075–1080
Rees MI, Lewis TM, Kwok JBJ, Mortier GR, Govaert P, Snell RG, Schofield PR, Owen MJ (2002) Hyperekplexia associated with compound heterozygote mutations in the β-subunit of the human inhibitory glycine receptor. (*GLRB*). Hum Mol Genet 11:853–860
Reynolds IJ, Murphy SN, Miller RJ (1987) ^{3}H-labeled MK-801 binding to the excitatory amino acid receptor complex from rat brain is enhanced by glycine. Proc Natl Acad Sci USA 84:7744–7748
Sacaan AI, Johnson KM (1989) Spermine enhances binding to the glycine site associated with *N*-methyl-D-aspartate receptor complex. Mol Pharmacol 36:836–839
Schmieden V, Betz H (1995) Pharmacology of the inhibitory glycine receptor: agonist and antagonist actions of amino acids and piperidine carboxylic compounds. Mol Pharmacol 48:919–927
Snell LD, Morter RS, Johnson KM (1987) Glycine potentiates N-methyl-D-aspartate induced [^{3}H]TCP binding to rat cortical membranes. Neurosci Lett 83:313–317
Snell LD, Morter RS, Johnson KM (1988) Structural requirements for activation of the glycine receptor that modulates the N-methyl-D-aspartate operated ion channel. Eur J Pharmacol 156:105–110
Thomson AM (1989) Glycine modulation of the NMDA receptor/channel complex. Trends Neuroscience 12:349–353
White HS, Harmsworth WL, Sofia RD, Wof HH (1995) Felbamate modulates the strychnine-insensitive glycine receptor. Epilepsy Res 20:41–48

E.3.1.12 [^{3}H]strychnine-Sensitive Glycine Receptor

PURPOSE AND RATIONALE

The strychnine-sensitive glycine receptor is a member of the family of ligand-gated ion channel receptors. Within this family, the glycine receptor is most closely related to the GABA-receptor. Like the $GABA_A$-receptor, the glycine receptor has an inhibitory role, mediating an increase in chloride conductance. However, in contrast to the $GABA_A$-receptor, the glycine receptor is located mainly in the spinal cord and lower brainstem, where glycine appears to be the major inhibitory neurotransmitter. Purification and molecular cloning has shown that the glycine receptor is an oligomeric transmembrane protein complex composed of three α and two β subunits. The inhibitory actions of glycine are potently blocked by strychnine. In addition to strychnine, the steroid derivative RU5135 (Simmonds and Turner 1985), phenylbenzene-ω-phosphono-α-amino acid (Saitoh et al. 1996), and 5,7-dichloro-4-hydroxyquinoline-3-carboxylic acid (Schmieden et al. 1996) antagonize glycine responses in cultured neurons or cells expressing recombinant glycine receptors.

A glycine receptor agonist may be a potential antispastic agent.

PROCEDURE

Male Wistar rats weighing about 200 g are sacrificed. About 220 mg of frozen pons and medulla are homogenized in 2×10 ml ice-cold 50 mM potassium phosphate buffer, pH 7.1, by an Ultra-Turrax homogenizer. The homogenate is centrifuged for 10 min at 30,000 *g* at 0–4°C in a refrigerated centrifuge. The pellet is rehomogenized in another 2×10 ml portion of the same buffer and recentrifuged as before. This washing procedure is repeated a total of four times. The final pellet is resuspended in 200 vol/g original tissue in ice-cold 50 mM potassium phosphate buffer, pH 7.1, with or without 1000 mM NaCl, and used directly for binding assays.

Binding assays consist of 1 ml tissue homogenate, 50 µl test solution (water or 5% v/v ethanol/water is used for serial dilutions), 50 µl water, 5% ethanol/water or glycine solution (40 mM final concentration), and 25 µl [^{3}H]strychnine working solution, final concentration 2 nM. The samples are mixed well and incubated for 20 min in an ice bath. Free and bound radioactivity are separated by filtration through Whatman GF/C glass fiber filters followed by washing with 2×10 ml ice-cold 50 mM potassium phosphate buffer, pH 7.1. Tritium on the filters is monitored by convential scintillation counting in 3 ml Hydroluma. Nonspecific binding is binding in the presence of 40 mM glycine and is always subtracted from total binding to give specific binding.

EVALUATION

K_i values are calculated as

$$K_i = (IC_{50}/1 + [K_D]/[L])$$

whereby: IC_{50} are the concentrations that inhibit by 50% the specific binding of [^{3}H]strychnine determined

in two independent experiments using at least 3 concentrations of the agent in duplicate assays, [L] is the concentration of the radioligand, K_D is the affinity constant in the absence or the presence of 1000 mM NaCl.

NaCl shift used for differentiating glycine agonists from glycine antagonists is the ratio K_i 1000 mM NaCl versus K_i 0 mM NaCl.

REFERENCES AND FURTHER READING

Betz H, Kuhse J, Schmieden V, Laube B, Harvey R (1998) Structure, diversity and pathology of the inhibitory glycine receptor. Naunyn-Schmiedeberg's Arch Pharmacol 358, Suppl 2, R 570

Braestrup C, Nielsen M, Krogsgaard-Larsen P (1986) Glycine antagonists structurally related to 4,5,6,7-tetrahydroisoxazolo[5,4-*c*]pyridin-3-ol inhibit binding of [^{3}H]strychnine to rat brain membranes. J Neurochem 47:691–696

Bristow DR, Bowery NG, Woodruff GN (1986) Light microscopic autoradiographic localisation of [^{3}H]glycine and [^{3}H]strychnine binding sites in rat brain. Eur J Pharmacol 126:303–307

Bruns RF, Welbaum BEA (1985) A sodium chloride shift method to distinguish glycine agonists from antagonists in [^{3}H]strychnine binding. Fed Proc 44:1828

Graham D, Pfeiffer F, Simler R, Betz H (1985) Purification and characterization of the glycine receptor of pig spinal cord. Biochemistry 24:990–994

Johnson G, Nickell DG, Ortwine D, Drummond JT, Bruns RF, Welbaum BE (1989) Evaluation and synthesis of aminohydroxyisoxazoles and pyrazoles as potential glycine agonists. J Med Chem 32:2116–2128

Johnson G, Drummond JT, Boxer PA, Bruns RF (1992) Proline analogues as agonists at the strychnine-sensitive glycine receptor. J Med Chem 35:233–241

Kishimoto H, Simon JR, Aprison MH (1981) Determination of the equilibrium constants and number of glycine binding sites in several areas of the rat central nervous system, using a sodium-independent system. J Neurochem 37:1015–1024

Lambert DM, Poupaert JH, Maloteaux JM, Dumont P (1994) Anticonvulsant activities of *N*-benzyloxycarbonylglycine after parenteral administration. NeuroReport 5:777–780

Marvizón JCG, Vázquez J, Calvo MG, Mayor F Jr, Gómez AR, Valdivieso F, Benavides J (1986) The glycine receptor: Pharmacological studies and mathematical modeling of the allosteric interaction between the glycine- and strychnine-binding sites. Mol Pharmacol 30:590–597

Saitoh T, Ishida M, Maruyama M, Shinozaki H (1994) A novel antagonist, phenylbenzene-ω-phosphono-a-amino acid, for strychnine-sensitive glycine receptors in the rat spinal cord. Br J Pharmacol 113:165–170

Schmieden V, Jezequel S, Beth H (1996) Novel antagonists of the inhibitory glycine receptor derived from quinolinic acid compounds. Mol Pharmacol 48:919–927

Simmonds MA, Turner JP (1985) Antagonism of inhibitory amino acids by the steroid derivative RU5135. Br J Pharmacol 84:631–635

Young AB, Snyder SH (1974) Strychnine binding in rat spinal cord membranes associated with the synaptic glycine receptor: co-operativity of glycine interactions. Mol Pharmacol 10:790–809

E.3.1.13 Electrical Recordings from Hippocampal Slices in Vitro

PURPOSE AND RATIONALE

The transverse hippocampal slice has been described as a well-defined cortical structure maintained *in vitro* (Skrede and Westgard 1971). The hippocampus slice has the advantage that each slice may contain all hippocampal structures: The chain of neurons goes from the perforant path to granule cells of the dentate gyrus, through mossy fibres to CA-3 pyramidal cells and then through Schaffer collaterals to CA-1 cells with their axons leaving the hippocampus through the alveus. The pyramidal cells lie close together and can be easily seen and penetrated with fine microelectrodes.

PROCEDURE

Male guinea pigs weighing 300–400 g are anesthetized with ether, the brains removed and the hippocampi dissected. Transverse slices of the hippocampus (300–400 µm thick) are cut in parallel to the alvear fibres. After preparation, the slices are submerged in 28°C warm saline which is equilibrated with 95% O_2 and 5% CO_2. After a preincubation period of 2 h, slices are transferred in a Perspex chamber (1.5 × 4 cm) and attached to the bottom consisting of optically plain glass. The chamber is mounted on an inverted microscope allowing detailed inspection of the excised tissue. The slices are superfused by an approximately 3 mm thick layer of 32°C warm saline. Intracellular recordings are achieved by means of micropipettes with tip diameters of less than 0.5 µm which are filled with 3 mol/l potassium chloride. Under microscopic control the tips of the micropipettes are placed within the stratum pyramidale and moved by means of a step motor driven hydraulic microdrive. For intracellular injections of drugs, e. g., pentylenetetrazol, via the recording microelectrode, a passive bridge is used. Alternatively, drugs are added to the incubation bath.

EVALUATION

The resting membrane potential and paroxysmal depolarizations are recorded before and after application of drugs.

CRITICAL ASSESSMENT OF THE METHOD

The hippocampal slice has been one of the most useful models for the study of basic mechanisms underlying the epilepsies. The model has also been recommended for screening of putative anticonvulsant drugs.

MODIFICATIONS OF THE METHOD

Harrison and Simmonds (1985) performed quantitative studies on some antagonists of N-methyl-D-aspartate in slices of rat cerebral cortex consisting of cerebral cortex and corpus callosum.

Tissue culture models of epileptiform activity were described by Crain (1972).

Oh and Dichter (1994) studied the effect of a GABA uptake inhibitor on spontaneous postsynaptic currents in cultured rat hippocampal neurons by the whole cell patch clamp method.

Blanton et al. (1989) described whole cell recordings from neurons in slices of reptilian and mammalian cerebral cortex. Synaptic currents and membrane properties could be studied in voltage and current clamps in cells maintained within their endogenous synaptic currents.

Gähwiler (1988), Stoppini et al. (1991) described methods for organotypic cultures of nervous tissue. Hippocampal slices from 2–23-day old rats were maintained in culture at the interface between air and the culture medium. They were placed on a sterile, transparent and porous membrane and kept in Petri dishes in an incubator. This yielded thin slices which remained 1–4 layers thick and were characterized by a well preserved organotypic organization. Excitatory and inhibitory synaptic potentials could be analyzed using extra- or intracellular recording techniques. After a few days in culture, long-term potentiation of synaptic responses could reproducibly be induced.

Using this method, Liu et al. (1995) studied dopaminergic regulation of transcription factor expression in organotypic cultures of developing striatum of newborn rats.

Stuart et al. (1993) reported the implementation of infrared differential interference contrast video microscopy to an upright compound microscope and a procedure for making patch-pipette recordings from visually identified neuronal somata and dendrites in brain slices.

Bernard and Wheal (1995) described an *ex vivo* model of chronic epilepsy using slices of rat hippocampus previously lesioned by stereotactic injections of kainic acid. Extracellular population spikes were recorded from the stratum pyramidale of CA1 after stimulation by bipolar twisted wire electrodes placed in the stratum radiatum of CA1 area proximally to stratum pyramidale near the recording electrode.

Using hippocampal slices prepared from brain tissue of patients undergoing neurosurgery for epilepsy, Schlicker et al. (1996) showed that the serotoninergic neurons of the human hippocampus are endowed with presynaptic inhibitory autoreceptors.

REFERENCES AND FURTHER READING

Alger BE (1984) Hippocampus. Electrophysiological studies of epileptiform activity *in vitro*. In: Dingledine R (ed) Brain Slices. Plenum Press, New York, London, pp 155–199

Alger BE, Nicoll RA (1982) Pharmacological evidence of two kinds of GABA receptor on rat hippocampal pyramidal cells studied *in vitro*. J Physiol 328:125–141

Alger BE, Dhanjal SS, Dingledine R, Garthwaite J, Henderson G, King GL, Lipton P, North A, Schwartzkroin PA, Sears TA, Segal M, Whittingham TS, Williams J (1984) Brain Slice methods. In: Dingledine R (ed) Brain Slices. Plenum Press, New York, London, pp 381–437

Bernard C, Wheal HV (1995) Plasticity of AMP and NMDA receptor mediated epileptiform activity in a chronic model of temporal lobe epilepsy. Epilepsy Res 21:95–107

Bingmann D, Speckmann EJ (1986) Actions of pentylenetetrazol (PTZ) on CA3 neurons in hippocampal slices of guinea pigs. Exp Brain Res 64:94–104

Blanton MG, Turco JJL, Kriegstein AR (1989) Whole cell recording from neurons in slices of reptilian and mammalian cerebral cortex. J Neurosci Meth 30:203–210

Coan EJ, Saywood W, Collingridge GL (1987) MK-801 blocks NMDA receptor-mediated synaptic transmission and long term potentiation in rat hippocampal slices. Neurosci Lett 80:111–114

Crain SM (1972) Tissue culture models of epileptiform activity. In: Purpura DP, Penry JK, Tower DB, Woodbury DM, Walter RD (eds) Experimental Models of Epilepsy – A Manual for the Laboratory Worker. Raven Press, New York, pp 291–316

Dingledine R, Dodd J, Kelly JS (1980) The *in vitro* brain slice as a useful neurophysiological preparation for intracellular recording. J Neurosci Meth 2:323–362

Fisher RS (1987) The hippocampal slice. Am J EEG Technol 27:1–14

Fisher RS, Alger BE (1984) Electrophysiological mechanisms of kainic acid-induced epileptiform activity in the rat hippocampal slice. J Neurosci 4:1312–1323

Fredholm BB, Dunwiddie TV, Bergman B, Lindström K (1984) Levels of adenosine and adenine nucleotides in slices of rat hippocampus. Brain Res 295:127–136

Gähwiler BH (1988) Organotypic cultures of neuronal tissue. Trends Neurol Sci 11:484–490

Harrison NL, Simmonds MA (1985) Quantitative studies on some antagonists of N-methyl-D-aspartate in slices of rat cerebral cortex. Br J Pharmacol 84:381–391

Langmoe IA, Andersen P (1981) The hippocampal slice *in vitro*. A description of the technique and some examples of the opportunities it offers. In: Kerkut GA, Wheal HV (eds) Electrophysiology of Isolated Mammalian CNS Preparations. Academic Press, London, New York, pp 51–105

Liu FC, Takahashi H, Mc Kay RDG, Graybiel AM (1995) Dopaminergic regulation of transcription factor expression in organotypic cultures of developing striatum. J Neurosci 15:2367–2384

Misgeld U (1992) Hippocampal slices. In: Kettenmann H, Grantyn R (eds) Practical Electrophysiological Methods. John Wiley and Sons, New York, pp 41–44

Mosfeldt Laursen A (1984) The contribution of *in vitro* studies to the understanding of epilepsy. Acta Neurol Scand 69:367–375

Müller CM (1992) Extra- and intracellular voltage recording in the slice. In: Kettenmann H, Grantyn R (eds) Practical

Electrophysiological Methods. John Wiley and Sons, New York, pp 249–295
Oh DJ, Dichter MA (1994) Effect of a γ-aminobutyric acid uptake inhibitor, NNC-711, on spontaneous postsynaptic currents in cultured rat hippocampal neurons: implications for antiepileptic drug development. Epilepsia 35:426–430
Okada Y, Ozawa S (1980) Inhibitory action of adenosine on synaptic transmission in the hippocampus of the guinea pig *in vitro*. Eur J Pharmacol 68:483–492
Oliver AP, Hoffer BJ, Wyatt RJ (1977) The hippocampal slice: a model system for studying the pharmacology of seizures and for screening of anticonvulsant drugs. Epilepsia 18:543–548
Pandanaboina MM, Sastry BR (1984) Rat neocortical slice preparation for electrophysiological and pharmacological studies. J Pharmacol Meth 11:177–186
Saltarelli MD, Lowenstein PR, Coyle JT (1987) Rapid *in vitro* modulation of [^{3}H]hemicholinium-3 binding sites in rat striatal slices. Eur J Pharmacol 135:35–40
Schlicker E, Fink K, Zentner J, Göthert M (1996) Presynaptic inhibitory serotonin autoreceptors in the human hippocampus. Naunyn-Schmiedeberg's Arch Pharmacol 354:393–396
Schwartzkroin PA (1975) Characteristics of CA1 neurons recorded intracellularly in the hippocampal *in vitro* slice preparation. Brain Res 85:423–436
Siggins GR, Schubert P (1981) Adenosine depression of hippocampal neurons *in vitro*: an intracellular study of dose-dependent actions on synaptic and membrane potentials. Neurosci Lett 23:55–60
Skrede KK, Westgard RH (1971) The transverse hippocampal slice: A well-defined cortical structure maintained *in vitro*. Brain Res 35:589–659
Stoppini L, Buchs PA, Muller D (1991) A simple method for oganotypic cultures of nervous tissue. J Neurosci Meth 37:173–182
Stuart GJ, Dodt HU, Sakmann B (1993) Patch-clamp recordings from the soma and dendrites of neurons in brain slices using infrared video microscopy. Pflügers Arch 423:511–518
Teyler TT (1980) Brain slice preparation: Hippocampus. Brain Res Bull 5:391–40

E.3.1.14 Electrical Recordings from Isolated Nerve Cells

PURPOSE AND RATIONALE

The use of the cell-attached patch clamp configuration to record action potential currents has shown to have utility in the testing for drug actions on ion channels in excitable cell membranes (Kay and Wong 1986; McLarnon 1990, 1991).

PROCEDURE

Preparation of Cultured Cells

The cultured cells are obtained from the hippocampus or the hypothalamus of rat brain. The isolation of the hippocampal CA1 neurones is performed according the procedure of Banker and Cowan (1977). The dissociated hypothalamic neurons are prepared according to Jirikowski et al. (1981). The hippocampal and hypothalamic neurons that are selected for electrophysiological recording are bipolar in shape with the long axis dimension between 10–15 µm. The neurons are studied over a period of 5–10 days after isolation.

Electrophysiology

The cell-attached patch clamp configuration is used to record spontaneous action potentials in the cultured neurons. The bath solution contains 140 mM NaCl, 5 mM KCl, 0.5 mM $CaCl_2$, 1 mM $MgCl_2$, 5 mM HEPES, pH 7.3. The composition of the patch pipette solution is the same as the bath solution. The drugs used in the experiments are added to the bath solution.

The patch pipettes (Corning 7052 glass) are fabricated using a specific patch pipette puller (PP-83; Narishige, Tokyo) are fire-polished and filled immediately prior to use. The resistance of the pipettes is in the range 4–8 MΩ and the tip diameters are between 1 and 2 µm. An axopatch amplifier (Axon Instruments, Foster City, CA), with low-pass filter set at 5 kHz, is used to record the capacitative currents. After recording, at a sampling frequency of 5 kHz, the data are stored on hard disc or video tape for subsequent analysis. All data are obtained at room temperature (21–24°C).

EVALUATION

The capacitative component of current recorded by the patch pipettes is proportional to the rate of change of membrane potential and can be expressed as $I_C = C\mathrm{d}V/\mathrm{d}t$, where C is the specific membrane capacitance. Assuming a value of C of 1 µF/cm^2 and a tip diameter of the patch pipette of 2 µm, the membrane area isolated by the patch pipette is about 3×10^{-8} cm^2. Using a value of $\mathrm{d}V/\mathrm{d}t$ of 100 mV/ms gives an approximate expected magnitude of I_C near 3 pA. When a class III antiarrhythmic drug that blocks a delayed rectifier K^+ channel is added to the bath, the portion of I_C corresponding to the after-hyperpolarization component of the action potential is completely abolished. The Na^+ spike is not altered by the drug. The cell-attached recordings of I_C can also be used to determine effects on the Na^+ spike when tetrodotoxin is included in the bath solution. Thus, the spontaneous action potential can be used for evaluation of drug effects on both K^+ and Na^+ channels in excitable membrane.

MODIFICATIONS OF THE METHOD

Chen et al. (1990) measured current responses mediated by $GABA_A$ receptors in pyramidal cells acutely dissociated from the hippocampus of mature guinea pigs according to the procedure of Kay and Wong (1986) using whole-cell voltage-clamp recordings.

Caulfield and Brown (1992) studied inhibition of calcium current in NG108–15 neuroblastoma cells by cannabinoid receptor agonists using whole-cell voltage-clamp recordings.

Gola et al. (1992, 1993) performed voltage recordings on non-dissociated sympathetic neurones from rabbit coeliac ganglia using the whole-cell configuration of the patch clamp technique (Neher and Sakmann 1976; Sakmann and Neher 1983).

Stolc (1994) used the voltage-clamp technique in internally dialyzed single neurones isolated from young rat sensory ganglia to study the effects of pyridoindole stobadine on inward sodium and calcium currents and on slow non-inactivating components of potassium outward current.

McGivern et al. (1995) examined the actions of a neuroprotective agent on voltage dependent Na^+ currents in the neuroblastoma cell line, NIE-115, using the whole cell variant of the patch clamp technique.

Smith (1995) reviewed the use of patch- and voltage clamp procedures to study neurotransmitter transduction mechanisms.

Using whole-cell and perforated-patch recordings, Delmas et al. (1998) examined the part played by endogenous G-protein $\beta\gamma$ subunits in neurotransmitter-mediated inhibition of N-type Ca^{2+} channel current in dissociated rat superior cervical sympathetic neurones.

Gonzales et al. (1985) registered membrane potentials with intracellular electrodes in cultured olfactory chemoreceptor cells.

REFERENCES AND FURTHER READING

Banker GA, Cowan WM (1977) Rat hippocampal neurons in dispersed cell culture. Brain Res 126:397–425

Chen Q-X, Stelzer A, Kay AR, Wong RKS (1990) $GABA_A$ receptor function is regulated by phosphorylation in acutely dissociated guinea-pig hippocampal neurones. J Physiol 420:207–221

Caulfield MP, Brown DA (1992) Cannabinoid receptor agonists inhibit Ca current in NG108–15 neuroblastoma cells via a pertussis toxin-sensitive mechanism. Br J Pharmacol 106:231–232

Delmas P, Brown DA, Dayrell M, Abogadie FC, Caulfield MP, Buckley NJ (1998) On the role of endogenous G-protein $\beta\gamma$ subunits in N-type Ca^{2+} current inhibition by neurotransmitters in rat sympathetic neurones. J Physiol 506:319–329

Gola M, Niel JP (1993)Electrical and integrative properties of rabbit sympathetic neurons re-evaluated by patch-clamping non-dissociated cells. J Physiol 460:327–349

Gola M, Niel JP, Bessone R, Fayolle R (1992) Single channel and whole cell recordings from non dissociated sympathetic neurones in rabbit coeliac ganglia. J Neurosci Meth 43:13–22

Gonzales F, Farbman AI, Gesteland RC (1985) Cell and explant culture of olfactory chemoreceptor cells. J Neurosci Meth 14:77–90

Jirikowski G, Reisert I, Pilgrim C (1981) Neuropeptides in dissociated cultures of hypothalamus and septum; quantification of immunoreactive neurons. Neurosci 6:1953–1960

Kay AR, Wong RKS (1986) Isolation of neurons suitable for patch-clamping from adult mammalian central nervous systems. J Neurosci Meth 16:227–238

McGivern JG, Patmore L, Sheridan RD (1995) Actions of the novel neuroprotective agent, lifarizine (RS-87476), on voltage-dependent sodium currents in the neuroblastoma cell line, NIE-115. Br J Pharmacol114:1738–1744

McLarnon JG (1991) The recording of action potential currents as an assessment for drug actions on excitable cells. J Pharmacol Meth 26:105–111

McLarnon JG, Curry K (1990) Single channel properties of the N-methyl-D-aspartate receptor channel using NMDA and NMDA agonists: On-cell recordings. Exp Brain Res 82:82–88

Neher E, Sakmann B (1976) Single-channel currents recorded from membrane of denervated frog muscle fibres. Nature 260:799–802

Sakmann B, Neher E (1983) Single Channel Recording. Plenum Press, New York

Smith PA (1995) Methods for studying neurotransmitter transduction mechanisms. J Pharmacol Toxicol Meth 33:63–73

Stolc S (1994) Pyridoindole stobadine is a nonselective inhibitor of voltage-operated ion channels in rat sensory neurons. Gen Physiol Biophys 13:259–266

E.3.1.15 Isolated Neonatal Rat Spinal Cord

PURPOSE AND RATIONALE

The spinal cord of the neonatal rat is a useful *in vitro* preparation, originally proposed by Otsuka and Konishi (1974). In this preparation, ventral root potentials of ten seconds of duration can be recorded after supramaximal electrical stimulation of the lumbar dorsal root. Variously implicated in the generation of these slow ventral root potentials are tachykinins, such as substance P and neurokinin B (Yanagisawa et al. 1982; Akagi et al. 1985; Otsuka and Yanagisawa 1988; Guo et al. 1998) and agonists at the glutamate receptor sites (Evans et al. 1982; Ohino and Warnick 1988 1990; Shinozaki et al. 1989; Ishida et al. 1990, 1991, 1993; Woodley and Kendig 1991; Bleakman et al. 1992; King et al. 1992; Thompson et al. 1992; Zeman and Lodge 1992; Pook et al. 1993; Jane et al. 1994; Boxall et al. 1996). These long lasting reflexes are thought to reflect a nociceptive reflex for several reasons; the threshold of activation corresponds to that of C fibre primary afferents (Akagi et al. 1985); they can be depressed by opioids (Yanagisawa et al. 1985; Nussbaumer et al. 1989; Faber et al. 1997) and α_2-adrenoceptor agonists (Kendig et al. 1991) and a similar response can be evoked by peripheral noxious stimulation (Yanagisawa et al. 1995).

PROCEDURE

Preparation of Spinal Cord

Male Wistar rats aged 6–9 days are used. Under ether anesthesia the spinal column is quickly removed from the animal and placed in a Petri dish, filled with oxygenated physiological solution. A laminectomy is performed on the dorsal surface of the spinal column at room temperature. The spinal cord of the mid-thoracic to mid-sacral level is then carefully removed from the column and hemisected in the longitudinal plane under a dissecting microscope. After removal of the dura mater, the hemisected cord is completely submerged in the recording chamber (total volume: approximately 0.5 ml), which is perfused with physiological solution (124 mM NaCl, 5 mM KCl, 1.3 mM $MgSO_4$, 2.5 mM $CaCl_2$, 1.2 mM KH_2PO_4, 15 mM $NaHCO_3$, 11 mM glucose) at a flow rate of 1.5 to 2.5 ml/min. The perfusion medium is continuously bubbled with a gas mixture of 95% O_2 and 5% CO_2 and the temperature is kept at 25 ± 0.5°C. The cut ends of the corresponding dorsal and ventral roots in an $L_{3–5}$ segment are fixed to a pair of suction electrodes for stimulating and recording. The preparation is stabilized in the recording chamber for at least 90 min to allow recovery from the dissection and the sealing of the roots to suction electrodes.

Recording of Monosynaptic Reflexes

Test stimulations, composed of square wave pulses of 0.05–0.2 ms duration and 5–30 V, are applied to the dorsal root every 10 s. The discharges of the corresponding ventral root are recorded with a suction electrode, amplified and monitored on an oscilloscope and stored on an analog data recorder or computer discs for later analysis. The mean values for the waveform of the monosynaptic reflex (amplitude, area and latency) are obtained from 6–18 successive responses in each experiment before and during application of drugs.

Recording of Single Motoneuron Activity

Test pulses (0.01–0.1 ms duration and 5–15 V) are applied to the dorsal or ventral root every 2 s. The activity of single motoneurons is recorded extracellularly using glass microelectrodes (electrical resistance approximately 10–30 MΩ) filled with 3 M sodium chloride or 2 M sodium acetate. The microelectrode is inserted into the ventral part of the cord through the hemisected surface while monitoring the field potential. The motoneurons in the ventral horn are identified by the short and consistent latency of antidromic spikes (1.66 ± 0.46 ms, $n = 5$), following the stimulation of the ventral root. The motoneurons also produce transsynaptic spikes with orthodromic stimulation of the dorsal root, of which the latency is 10.26 ± 1.05 ms upon supramaximal stimulation. The spike generation of motoneurons is displayed on an oscilloscope and stored on magnetic tapes. The spontaneous firing of the motoneuron is also monitored on an oscilloscope and recorded through a window discriminator and spike counter. The mean number and latency of spikes and latency of the dorsal root-elicited spikes are obtained from 20–40 successive responses in each experiment. Comparisons are made before and 3–5 min after application of drugs.

EVALUATION

All data are expressed as the mean ± SEM. Statistical significance of the data is determined by repeated measures analysis of variance (ANOVA) and, when appropriate, Student's *t*-test. A P value of less than 0.05 is considered statistically significant.

MODIFICATIONS OF THE METHOD

Smith and Feldman (1987), Wong et al. (1996) described an *in vitro* neonatal rat brainstem/spinal cord preparation. The brainstem and cervical spinal cord were isolated from 0–4 days old ether anesthetized Sprague Dawley rats. The en bloc neuraxis was pinned down with ventral surface upward in a recording chamber and superfused continuously with artificial cerebrospinal fluid. Respiratory activity was recorded with suction electrodes from the C_4 ventral root.

REFERENCES AND FURTHER READING

Akagi H, Konishi S, Otsuka M, Yanagisawa M (1985) The role of substance P as a neurotransmitter in the reflexes of slow time courses in the neonatal rat spinal cord. Br J Pharmacol 84:663–673

Bleakman D, Rusin KI, Chard PS, Glaum SR, Miller RJ (1992) Metabotropic glutamate receptors potentiate ionotropic glutamate responses in the rat dorsal horn. Mol Pharmacol 42:192–196

Boxall SJ, Thompson SWN, Dray A, Dickenson AH, Urban L (1996) Metabotropic glutamate receptor activation contribute to nociceptive reflex activity in the rat spinal cord *in vitro*. Neurosci 74:13–20

Dong X-W, Morin D, Feldman JL (1996) Multiple actions of 1S, 3R-ACPD in modulating endogenous synaptic transmission to spinal respiratory motoneurons. J Neurosci 16:4971–4982

Evans RH, Francis AA, Jones AW, Smith DAS, Watkins JC (1982) The effects of a series of ω-phosphonic α-carboxylic amino acids on electrically evoked and excitant amino-acid-induced responses in isolated spinal cord preparations. Br J Pharmacol 75:65–75

Faber ESL, Chambers JP, Brugger F, Evans RH (1997) Depression of A and C fibre-evoked segmental reflexes by morphine and clonidine in the *in vitro* spinal cord of the neonatal rat. Br J Pharmacol 120:1390–1396

Guo JZ, Yoshioka K, Otsuka M (1998) Effects of a tachykinin NK_3 receptor antagonist, SR 142801, studied in isolated neonatal spinal cord. Neuropeptides 32:537–542
Ishida M, Shinozakai H (1991) Novel kainate derivatives: Potent depolarizing actions on spinal motoneurons and dorsal root fibres in newborn rats. Br J Pharmacol 104:873–878
Ishida M, Akagi H, Shimamoto K, Ohfune Y, Shinozaki H (1990) A potent metabotropic glutamate receptor agonist: electrophysiological actions of a conformationally restricted glutamate analogue in the rat spinal cord and *Xenopus oocytes*. Brain Res 537:311–314
Ishida M, Saitoh T, Shimamoto K, Ohfune Y, Shinozaki H (1993) A novel metabotropic glutamate receptor agonist: marked depression of monosynaptic excitation in the newborn rat isolated spinal cord. Br J Pharmacol 109:1169–1177
Jane DE, Jones PLSJ, Pook PCK, Tse HW, Watkins JC (1994) Actions of two new antagonists showing selectivity for different subtypes of metabotropic glutamate receptor in the neonatal rat spinal cord. Br J Pharmacol 112:809–816
Kendig JJ, Savola MKT, Woodley SJ, Maze M (1991) α_2-adrenoceptors inhibit a nociceptive response in neonatal rat spinal cord. Eur J Pharmacol 192:293–300
King AE, Lopez-Garcia JA, Cumberbatch M (1992) Antagonism of synaptic potentials in ventral horn neurons by 6-cyano-7-nitroquninoxaline-2,3-dione: a study in the rat spinal cord *in vitro*. Br J Pharmacol 107:375–381
Lev-Tov A, Pinco M (1992) *In vitro* studies of prolonged synaptic depression in the neonatal rat spinal cord. J Physiol 447:149–169
Nussbaumer JC, Yanagisawa M, Otsuka M (1989) Pharmacologic properties of a C fibre response evoked by saphenous nerve stimulation in an isolated spinal cord-nerve preparation of the newborn rat. Br J Pharmacol 98:373–382
Ohno Y, Warnick JE (1988) Effects of thyrotropin-releasing hormone on phencyclidine- and ketamine-induced spinal depression in neonatal rats. Neuropharmacol 27:1013–1018
Ohno Y, Warnick JE (1990) Selective depression of the segmental polysynaptic reflex by phencyclidine and its analogs in the rat *in vitro*: Interaction with N-methyl-D-aspartate receptors. J Pharmacol Exp Ther 252:246–252
Otsuka M, Konishi S (1974) Electrophysiology of mammalian spinal cord *in vitro*. Nature 252:733–734
Otsuka M, Yanagisawa M (1988) Effect of a tachykinin antagonist on a nociceptive reflex in the isolated spinal cord tail preparation of the newborn rat. J Physiol 395:255–270
Pook P, Brugger F, Hawkins NS, Clark KC, Watkins JC, Evans RH (1993) A comparison of action of agonists and antagonists at non-NMDA receptors of C fibres and motoneurons of the immature rat spinal cord *in vitro*. Br J Pharmacol 108:179–184
Shinozaki H, Ishida M, Shimamoto K, Ohfune Y (1989) Potent NMDA-like actions and potentiation of glutamate responses by conformational variants of a glutamate analogue in the rat spinal cord. Br J Pharmacol 98:1213–1224
Smith JC, Feldman JL (1987) *In vitro* brainstem-spinal cord preparations for study of motor systems for mammalian respiration and locomotion. J Neurosci Meth 21:321–333
Thompson SWN, Gerber G, Sivilotti LG, Woolf CJ (1992) Long duration of ventral root potentials in the neonatal spinal cord *in vitro*: the effects of ionotropic and metabotropic excitatory amino acid receptor antagonists. Brain Res 595:87–97
Woodley SJ, Kendig JJ (1991) Substance P and NMDA receptors mediate a slow nociceptive ventral root potential in neonatal rat spinal cord. Brain Res 559:17–22
Yanagisawa M, Otsuka M, Konishi S, Akagi H, Folkers K, Rosell S (1982) A substance P antagonist inhibits a slow reflex response in the spinal cord of the newborn rat. Acta Physiol Scand 116:109–112
Yanagisawa MT, Murakoshi T, Tamai S, Otsuka M (1985) Tail-pinch method *in vitro* and the effect of some antinociceptive compounds. Eur J Pharmacol 106:231–239
Zeman S, Lodge D (1992) Pharmacological characterization of non-NMDA subtypes of glutamate receptor in the neonatal rat hemisected spinal cord *in vitro*. Br J Pharmacol 106:367–372

E.3.1.16 Cell Culture of Neurons

PURPOSE AND RATIONALE

Cell culture of neurons, especially of hippocampal neurons, has become a widely used tool in pharmacological studies (Banker and Cowan 1977; Skaper et al. 1990, 1993, 2001; Araujo and Cotman 1993; Brewer 1997, 1999; Brewer et al. 1998; Li et al. 1998; Mitoma et al. 1998; Semkowa et al. 1998, 1999; Chaudieu and Privat 1999; May et al. 1999; Hampson et al. 2000; Novitskaya et al. 2000; Pickard et al. 2000; Vergun et al. 2001).

The basic information on methodology of cell culture of rat hippocampal neurones was given by Banker and Cowan (1977). One modification used by Skaper et al. (1990, 2001) studying the role of mast cells on potentiation by histamine of synaptically mediated excitotoxicity in cultured hippocampal neurones is described below.

PROCEDURE

Preparation of Hippocampus

Timed pregnancies are obtained in female Sprague Dawley rats by daily checking vaginal washings for sperm, the day on which sperm is found being regarded as day 0. At the appropriate stage of gestation the pregnant rats are anesthetized and the uterus removed to a sterile dish. The remainder of the cell preparations is performed in a sterile hood.

The brains are removed from the fetuses with a pair of fine scissors, and the cerebral hemispheres separated from the brain stem. When the hemisphere of an 18- to 19-day-old fetus in viewed in a dissecting microscope the hippocampus can be clearly seen on its medial surface. The hippocampal fissure, usually marked by a conspicuous group of blood vessels, indicates the approximate junction between the hippocampus and the adjoining subicular and entorhinal cortex. The developing fimbria is seen as a white translucent band along the free margin of the hippocampus. Before separating the hippocampus from the hemisphere, the meninges

and adherent chorioid plexus are carefully pulled off with fine forceps. At this stage the full depth of the hippocampal fissure can be seen. Then with iridectomy scissors the hippocampus is separated from the adjoining cortex by a cut parallel to the hippocampal fissure, and by transverse cuts at its rostral and caudal ends.

Cell Culture

Hippocampi isolated from embryonic rats (gestational age 17.5 days) are incubated with 0.08% trypsin, and dissociated in Neurobasal medium containing 10% heat-inactivated calf serum. Cells are pelleted by centrifugation (200 *g*, 5 min) and resuspended in Neurobasal medium containing B27 (Life Technologies, Inc.) supplements (with antioxidants), 25 µM glutamate, 1 mM sodium pyruvate, 2 mM L-glutamine, 50 U/ml penicillin, and 50 µg/ml streptomycin. The cell suspension is plated onto poly-D-lysine (10 µg/ml) coated 48-well culture plates at a density of 4.5×10^4 cells per cm^2. Cultures are maintained at 37°C in a humidified atmosphere of 5% CO_2-95% air. After 5 days, one-half of the medium is replaced with an equal volume of maintenance medium (plating medium but containing B27 supplements without antioxidants, and lacking glutamate). Additional medium exchanges (0.5 volume) are performed every 3–4 days thereafter. Cells are used between 14 and 16 days in culture. During this period, neurones develop extensive neuritic networks, and form functional synapses.

Mast cells are collected from the peritoneal lavage of male Sprague Dawley rats and isolated over a bovine serum albumin gradient to >90% purity, as judged by toluidine blue and safranin staining.

Neurotoxicity Assays

Cultures are washed once with Locke's solution (pH 7.0–7.4) with or without 1 mM $MgCl_2$. Drug treatments are carried out for 15–30 min (25°C) in a final volume of 0.5 ml. In the case of mast-cell-neurone co-cultures, transwell inserts (3-µm pore size, 9 mm diameter) are seeded with 5×10^4 mast cells in RPMI-1640 medium and placed in 24-well plates overnight. Inserts with mast cells are then placed into wells with hippocampal cells. Mast cells activation is achieved using an antigenic stimulus (0.3 µg/ml anti-DNP IgE/0.1 µg/ml DNP albumin). The mast cell containing inserts are removed at the end of the Mg^{2+}-free incubation. After this time all cell monolayers are washed with complete Locke's solution and returned to their original culture medium for 24 h. Cytotoxicity is evident during 24 h after the insult. Viable neurons have phase-bright somata of round-to-oval shape, with smooth, intact neurites. Neurones are considered nonviable when they exhibit neurite fragmentation and somatic swelling and vacuolation. Cell survival is quantified 24 h after the insult by a colorimetric reaction with 3-(4,5-dimethylthiazol-2-yl)-2,5-diphenyltetrazolium bromide (MTT).

EVALUATION

Data are analyzed by one-way ANOVA with Student-Newman-Keuls *post hoc* test for differences between groups.

MODIFICATIONS OF THE METHOD

Brewer (1997) reported the isolation and culture of adult rat hippocampal neurons. Using different proteases and special separation techniques, about 90000 viable neurons could be isolated from each hypothalamus at any age rat from birth to 24–36 months. Neurons were cultured for more than 3 weeks.

Flavin and Ho (1999) found that propentofylline protects hippocampal neurons in culture from death triggered by macrophage or microglia secretory products.

To study neurite outgrowth in cultured hippocampal cells from Wistar rat embryos, 5000 cells/well were seeded in 8-well LabTec tissue culture slides with a grown surface of permanox plastic and grown in Neurobasal medium supplemented with B27 (Life Technologies, Inc.), 20 mM HEPES, 0.4% bovine serum albumin, penicillin (100 IU/ml), and streptomycin (100 µg/ml). (Novitskaya et al. 2000). For image analysis, cells were fixed in 4% paraformaldehyde and stained for 20 min with Coomassie Blue R250. Cover slides were observed in an inverted microscope using phase contrast optics. To measure neurite outgrowth from hippocampal neurons, an unbiased counting frame containing a grid with a number of test lines was superimposed on the images of cells. The number of intersections of cellular processes with the test lines was counted and related to the number of cell bodies, thereby allowing quantification of neurite length per cell.

Cell culture experiments were also performed with **neuronal cells from other areas of the brain** besides the hippocampus.

Brain tissue samples of rat embryos containing either septum plus preoptic area or retrochiasmatic hypothalamus were dissociated and cultured for 14 and 21 days by Jirikowski et al. (1981). By means of immunofluorescence, LHRH, α-MSH, vasopressin and neurophysin-containing hormones could be identified.

Sinor et al. (2000) studied NMDA and glutamate evoked excitotoxicity at distinct cellular locations in rat cortical neurones *in vitro*.

Canals et al. (2001) examined neurotrophic and neurotoxic effects of nitric oxide on neuronal enriched fetal midbrain cultures from embryonic Sprague Dawley rats.

López et al. (2001) investigated the release of amino acid neurotransmitters in cultured cortical neurons obtained from gestation day 19 rats by nicotine stimulation.

Ehret et al. (2001) studied the modulation of electrically evoked acetylcholine release in cultured septal neurones from embryonic Wistar rats.

Tang et al. (2001) found a lack of replicative senescence in cultured rat oligodendrocyte precursor cells.

Yamagishi et al. (2001) used cultured rat cerebellar granule neurons as a model system for studying neuronal apoptosis.

Noh and Koh (2000) prepared mixed **mouse** cortical cultures containing both neurons and astrocytes, and pure astrocyte cultures, from fetal (15 d of gestation) and neonatal (1–3 postnatal days) mice.

Saluja et al. (2001) found that PPAR δ agonists stimulate oligodendrocyte differentiation in glial cell culture of mouse cerebra.

Ushida et al. (2000) succeeded to directly isolate clonogenic **human** central nervous system stem cells from fresh human brain tissue, using antibodies to cell surface markers and fluorescence-activated cell sorting.

For further studies with brain cell cultures see Sect. F.2.0.10.

REFERENCES AND FURTHER READING

Araujo DM, Cotman CW (1993) Trophic effects of interleukin-4, -7, and -8 on hippocampal neuronal cultures: potential involvement of glial-derived factors. Brain Res 600:49–55

Banker GA, Cowan WM (1977) Rat hippocampal neurons in dispersed cell culture. Brain Res 126:397–425

Brewer GJ (1997) Isolation and culture of adult hippocampal neurons. J Neurosci Meth 71:143–155

Brewer GJ (1999) Regeneration and proliferation of embryonic and adult rat hippocampal neurons in culture. Exp Neurol 159:237–247

Brewer GJ, Deshmane S, Ponnusamy E (1998) Precocious axons and improved survival of rat hippocampal neurons on lysine-alanine polymer substrate. J Neurosci Meth 85:13–20

Canals S, Casarejos MJ, Rodríguez-Martin E, de Bernardo S, Mena MA (2001) Neurotrophic and neurotoxic effects of nitric oxide on fetal midbrain cultures. J Neurochem 76:56–68

Chaudieu I, Privat A (1999) Neuroprotection of cultured foetal rat hippocampal cells against glucose deprivation: are GABAergic neurons less vulnerable or more sensitive to TCP protection? Eur J Neurosci 11:2413–2321

Ehret A, Haaf A, Jeltsch H, Heinrich B, Feuerstein TJ, Jakisch R (2001) Modulation of electrically evoked acetylcholine release in cultured septal neurones. J Neurochem 76:555–564

Flavin MP, Ho LT (1999) Propentofylline protects neurons in culture from death triggered by macrophage or microglia secretory products. J Neurosci Res 56:54–59

Hampson RE, Mu J, Deadwyler SA (2000) Cannabinoid and kappa opioid receptors reduced potassium K current via activation of G_s proteins in cultured hippocampal neurons. J Neurophysiol 84:2356–2364

Jirikowski G, Reisert I, Pilgrim Ch (1981) Neuropeptides in dissociated cultures of hypothalamus and septum: quantitation of immunoreactive neurons. Neuroscience 6:1953–1960

Li YX, Zhang Y, Lester HA, Schuman EM, Davidson N (1998) Enhancement of neurotransmitter release induced by brain-derived neurotrophic factor in cultured hippocampal neurons. J Neurosci 18:10231–10240

López E, Arce C, Vicente S, Oset-Gasque MJ, González MP (2001) Nicotinic receptors mediate the release of amino acid neurotransmitters in cultured cortical neurons. Cerebral Cortex 11:158–163

May PC, Robison PM, Fuson KS (1999) Stereoselective neuroprotection by a novel 2,3-benzodiazepine non-competitive AMPA antagonist against non-NMDA receptor mediated excitotoxicity in primary rat hippocampal culture. Neurosci Lett 262:219–221

Mitoma J, Ito M, Furuya S, Hirabayashi Y (1998) Bipotential roles of ceramide in the growth of hippocampal neurones: Promotion of cell survival and dendritic outgrowth in dose- and developmental stage-dependent manners. J Neurosci Res 51:712–722

Noh K-M, Koh J-Y (2000) Induction and activation by zinc of NADPH oxidase in cultured cortical neurons and astrocytes. J Neurosci 20: RC111:1–5

Novitskaya V, Grigorian M, Kriajevska M, Tarabykina S, Bronstein I, Berezin V, Bock E, Lukanidin E (2000) Oligomeric forms of the metastasis-related Mts1 (S100A4) protein stimulate neuronal differentiation in cultures of rat hippocampal neurons. J Biol Chem 275:41278–41286

Pickard L, Noël J, Henley JM, Collingridge GL, Molnar E (2000) Developmental changes in synaptic AMPA and NMDA receptor distribution and AMPA receptor subunit composition in living hippocampal neurons. J Neurosci 20:7922–7931

Saluja I, Granneman JG, Skoff RP (2001) PPAR δ agonists stimulate oligodendrocyte differentiation in tissue culture. Glia 33:191–204

Semkowa I, Wolz P, Krieglstein J (1998) Neuroprotective effect of 5-HT_{1A} receptor agonist, Bay X 3702, demonstrated *in vitro* and *in vivo*. Eur J Pharmacol 359:251–260

Semkowa I, Häberlein C, Krieglstein J (1999) Ciliary neurotrophic factor protects hippocampal neurons from excitotoxic damage. Neurochem Int 35:1–10

Sinor JD, Du S, Venneti S, Blitzblau RC, Leszkiewicz DN, Rosenberg PA, Aizenman E (2000) NMDA and glutamate evoke excitotoxicity at distinct cellular locations in rat cortical neurones *in vitro*. J Neurosci 20:8831–8837

Skaper SD, Facci L, Milani L, Leon A, Toffano G (1990) Culture and use of primary and clonal neural cells. In: Conn PM (ed) Methods in Neuroscience, Vol 2, Academic Press, San Diego, pp 17–33

Skaper SD, Leon A, Facci L (1993) Basic fibroblast growth factor modulates sensitivity of cultured hippocampal pyramidal neurones to glutamate cytotoxicity: interaction with ganglioside GM1. Brain Res Dev Brain Res 71:1–8

Skaper SD, Facci L, Kee WJ, Strijbos PJLM (2001) Potentiation by histamine of synaptically mediated excitotoxicity in cul-

tured hippocampal neurones: a possible role for mast cells. J Neurochem 76:47–55
Tang DG, Tokumoto YM, Apperly JA, Lloyd AC, Raff MC (2001) Lack of replicative senescence in cultured rat oligodendrocyte precursor cells. Science 291:868–871
Uchida N, Buck DW, He D, Reitsma MJ, Masek M, Phan TV, Tsukamoto AS, Gage FH, Weissman IL (2000) Direct isolation of human central nervous system stem cells. Proc Natl Acad Sci USA 97:14720–14725
Vergun O, Sobolevsky AI, Yelshansky MV, Keelan J, Khodorov BI, Duchen MR (2001) Exploration of the role of reactive oxygen species in glutamate neurotoxicity in rat hippocampal neurons in culture. J Physiol 531:147–163
Yamagishi S, Yamada M, Ishikawa Y, Matsumoto T, Ikeuchi T, Hatanaka H (2001) p38 Mitogen-activated protein kinase regulates low potassium-induced c-Jun phosphorylation and apoptosis in cultured cerebellar granule neurons. J Biol Chem 276:5129–5133

E.3.2
In Vivo Methods

E.3.2.1
Electroshock in Mice

PURPOSE AND RATIONALE

The electroshock assay in mice is used primarily as an indication for compounds which are effective in grand mal epilepsy. Tonic hindlimb extensions are evoked by electric stimuli which are suppressed by anti-epileptics but also by other centrally active drugs.

PROCEDURE

Groups of 6–10 male NMRI mice (18–30 g) are used. The test is started 30 min after i.p. injection or 60 min after oral treatment with the test compound or the vehicle. An apparatus with corneal or ear electrodes (Woodbury and Davenport 1952) is used to deliver the stimuli. The intensity of stimulus is dependent on the apparatus, e. g., 12 mA, 50 Hz for 0.2 s have been used. Under these conditions all vehicle treated mice show the characteristic extensor tonus.

EVALUATION

The animals are observed closely for 2 min. Disappearance of the hindleg extensor tonic convulsion is used as positive criterion. Percent of inhibition of seizures relative to controls is calculated. Using various doses, ED_{50}-values and 95% confidence interval are calculated by probit analysis.

ED_{50}-values after oral administration are:

- Diazepam 3.0 mg/kg
- Diphenylhydantoin 20.0 mg/kg

CRITICAL ASSESSMENT OF THE METHOD

The electroshock test in mice has been proven to be a useful tool to detect compounds with anticonvulsant activity.

MODIFICATIONS OF THE METHOD

Cashin and Jackson (1962) described a simple apparatus for assessing anticonvulsant drugs by the electroshock seizure test in mice.

Kitano et al. (1996) developed the increasing-current electroshock seizure test, a new method for assessment of anti- and pro-convulsant activities of drugs in mice. A single train of pulses (square wave, 5 ms, 20 Hz) of linearly increasing intensity from 5 to 30 mA was applied via ear electrodes. The current at which tonic hindlimb extension occurred was recorded as the seizure threshold. The method allows the determination of seizure threshold current for individual animals.

REFERENCES AND FURTHER READING

Cashin CH, Jackson H (1962) An apparatus for testing anticonvulsant drugs by electroshock seizures in mice. J Pharm Pharmacol 14:445–475
Kitano Y, Usui C, Takasuna K, Hirohashi M, Nomura M (1996) Increasing-current electroshock seizure test: a new method for assessment of anti- and pro-convulsant activities of drugs in mice. J Pharmacol Toxicol Meth 35:25–29
Löscher W, Stephens DN (1988) Chronic treatment with diazepam or the inverse benzodiazepine receptor agonist FG 7142 causes different changes in the effects of GABA receptor stimulation. Epilepsy Res 2:253–259
Rastogi SA, Ticku MK (1985) Involvement of a GABAergic mechanism in the anticonvulsant effect of phenobarbital against maximal electroshock-induced seizures in rats. Pharmacol Biochem Behav 222:141–146
Sohn YJ, Levitt B, Raines A (1970) Anticonvulsive properties of diphenylthiohydantoin. Arch. int. Pharmacodyn. 188:284–289
Swinyard EA (1972) Electrically induced convulsions. In: Purpura DP, Penry JK, Tower DB, Woodbury DM, Walter RD (eds) Experimental Models of Epilepsy – A Manual for the Laboratory Worker. Raven Press, New York, pp 433–458
Swinyard EA, Brown WC, Goodman LS (1952) Comparative assays of antiepileptic drugs in mice and rats. J Pharmacol Exp Ther 106:319–330
Toman JEP (1964) Animal techniques for evaluating anticonvulsants. In: Nodin JH and Siegler PE (eds) Animal and Clinical Techniques in Drug Evaluation. Year Book Med Publ, vol 1:348–352
Toman JEP, Everett GM (1964) Anticonvulsants. In: Laurence DR, Bacharach AL (eds) Evaluation of Drug Activities: Pharmacometrics. Academic Press, London, New York, pp 287–300
Turner RA (1965) Anticonvulsants. Academic Press, New York, London, pp 164–172
Woodbury LA, Davenport VO (1952) Design and use of a new electroshock seizure apparatus and analysis of factors altering seizure threshold and pattern. Arch int Pharmacodyn 92:97–107

E.3.2.2
Pentylenetetrazol Test in Mice and Rats

See Sect. E.2.2.1.

E.3.2.3
Strychnine-Induced Convulsions in Mice

See Sect. E.2.2.2.

E.3.2.4
Picrotoxin-Induced Convulsions in Mice

See Sect. E.2.2.3.

E.3.2.5
Isoniazid-Induced Convulsions in Mice

See Sect. E.2.2.4.

These tests, already described for evaluation of the anti-convulsive activity of anxiolytics, can be used and show activity for anti-epileptics.

Many other agents induce seizures in animals and have been used to test the anticonvulsant activity of drugs (Stone 1972), e. g., glutarimides (Hahn and Oberdorf 1960), pilocarpine (Tursky et al. 1987), methionine sulfoximine (Toussi et al. 1987), *N*-methyl-D-aspartic acid (Leander et al. (1988), γ-hydroxybutyrate (Snead 1988).

Shouse et al. (1989) described mechanisms of seizure suppression during rapid-eye-movement (REM) sleep in cats. Spike-wave paroxysms in the EEG accompanied by bilateral myoclonus of the head and the neck were induced by i.m. injection of 300000 to 400,000 IU/kg sodium penicillin G.

REFERENCES AND FURTHER READING

Hahn F, Oberdorf A (1960) Vergleichende Untersuchungen über die Krampfwirkung von Begrimid, Pentetrazol und Pikrotoxin. Arch Int Pharmacodyn 135:9–30

Leander JD, Lawson RR, Ornstein PL, Zimmerman DM (1988) *N*-methyl-D-aspartic acid induced lethality in mice: selective antagonism by phencyclidine-like drugs. Brain Res 448:115–120

Pollack GM, Shen DD (1985) A timed intravenous pentylenetetrazol infusion seizure model for quantitating the anticonvulsant effect of valproic acid in the rat. J Pharmacol Meth 13:135–146

Shouse MN, Siegel JM, Wu MF, Szymusiak R, Morrison AR (1989) Mechanism of seizure suppression during rapid-eye-movement (REM) sleep in cats. Brain Res 505:271–282

Snead III OC (1988) γ-Hydroxybutyrate model of generalized absence seizures: Further characterization and comparison with other absence models. Epilepsia 29:361–368

Stone WE (1972) Systemic chemical convulsants and metabolic derangements. In: Purpura DP, Penry JK, Tower DB, Woodbury DM, Walter RD (eds) Experimental Models of Epilepsy – A Manual for the Laboratory Worker. Raven Press, New York, pp 407–432

Testa R, Graziani L, Graziani G (1983) Do different anticonvulsant tests provide the same information concerning the profiles of antiepileptic activity? Pharmacol Res Commun 15:765–774

Toussi HR, Schatz RAS, Waszczak BL (1987) Suppression of methionine sulfoximine seizures by intranigral γ-vinyl GABA injection. Eur J Pharmacol 137:261–264

Tursky WA, Cavalheiro EA, Coimbra C, da Penha Berzaghi M, Ikonomidou-Turski C, Turski L (1987) Only certain antiepileptic drugs prevent seizures induced by pilocarpine. Brain Res Rev 12:281–305

E.3.2.6
Bicuculline Test in Rats

PURPOSE AND RATIONALE

Seizures can be induced by the $GAGA_A$-antagonist bicuculline and are antagonized by known anti-epileptics.

PROCEDURE

Female Sprague-Dawley rats are injected i.v. with 1 mg/kg bicuculline. At this dose, a tonic convulsion appears in all treated rats within 30 s after injection. Test compounds are administered orally 1 or 2 h before bicuculline injection. Dose-response curves can be obtained.

EVALUATION

Percentage of protected animals is evaluated. ED_{50}-values and 95% confidence limits are calculated by probit analysis.

CRITICAL ASSESSMENT OF THE METHOD

Like the electroshock test, the bicuculline test is considered to be relatively specific for anti-epileptic activity.

MODIFICATIONS OF THE METHOD

Czuczwar et al. (1985) studied the antagonism of N-methyl-D,L-aspartic acid-induced convulsions by antiepileptic drugs and other agents.

REFERENCES AND FURTHER READING

Buckett WR (1981) Intravenous bicuculline test in mice: Characterisation with GABAergig drugs. J Pharmacol Meth 5:35–41

Clineschmidt BV, Martin GE, Bunting PR (1982) Anticonvulsant activity of (+)-5-methyl-10,11-dihydro-5H-dibenzo[a,d]cyclohepten-5,10-imine (MK-801), a substance with potent anticonvulsant, central sympathomimetic, and apparent anxiolytic properties. Drug Dev Res 2:123–134

Czuczwar SJ, Frey HH, Löscher W (1985) Antagonism of N-methyl-D,L-aspartic acid-induced convulsions by

antiepileptic drugs and other agents. Eur J Pharmacol 108:273–280
Lloyd KG, Morselli PL (1987) Psychopharmacology of GABAergic drugs. In: Meltzer HY (ed) Psychopharmacology: The Third Generation of Progress. Raven Press, New York pp 183–195
Mecarelli O, de Feo MR, Rina MF, Ricci GF (1988) Effects of Progabide on bicuculline-induced epileptic seizures in developing rats. Clin Neuropharmacol 11:443–453

E.3.2.7 4-Aminopyridine-Induced Seizures in Mice

PURPOSE AND RATIONALE

The K^+ channel antagonist 4-aminopyridine is a powerful convulsant in animals and in man. The drug readily penetrates the blood-brain barrier and is believed to induce seizure activity by enhancing spontaneous and evoked neurotransmitter release. Although both excitatory and inhibitory synaptic transmission is facilitated by 4-aminopyridine, the epileptiform activity induced by the drug is predominantly mediated by non-NMDA type excitatory amino acid receptors. In mice, parenterally administered 4-aminopyridine induces clonic-tonic convulsions and lethality.

PROCEDURE

Male NIH Swiss mice weighing 25–30 g are allowed to acclimatize with free access to food and water for a 24-h period before testing. Test drugs are administered in various doses intraperitoneally 15 min prior to s.c. injection of 4-aminopyridine at a dose of 13.3 mg/kg which was found to be the LD_{97} in this strain of mice. Controls treated with 4-aminopyridine only exhibit characteristic behavioral signs, such as hyperreactivity, trembling, intermitted forelimb/hindlimb clonus followed by hindlimb extension, tonic seizures, opisthotonus and death. The mean latency to death at the LD_{97} is about 10 min. Groups of 8 mice are used for each dose.

EVALUATION

The percentage of protected animals at each dose is used to calculate ED_{50} values. Phenytoin-like anticonvulsants such as carbamazepine and broad spectrum anticonvulsants such as phenobarbital and valproate are effective whereas GABA-enhancers such as diazepam, several NMDA antagonists, and CA^{2+} channel antagonists such as nimodipine are not.

CRITICAL ASSESSMENT OF THE METHOD

The profile of drugs effective in this seizure model is distinct from other chemoconvulsant models and more similar to those that prevent tonic hindlimb extension in the maximal electroshock seizure test. The test is useful to differentiate the mode of action of anticonvulsant drugs.

MODIFICATIONS OF THE METHOD

Morales-Villagran et al. (1996) described protection against seizures induced by intracerebral or intra-cerebroventricular administration of 4-aminopyridine by NMDA receptor antagonists.

REFERENCES AND FURTHER READING

Morales-Villagran A, Urena-Guerrero ME, Tapia R (1996) Protection by NMDA receptor antagonists against seizures induced by intracerebral administration of 4-aminopyridine. Eur J Pharmacol 305:87–93
Rogawski MA, Porter RJ (1990) Antiepileptic drugs: pharmacological mechanisms and clinical efficacy with consideration of promising developmental stage compounds. Pharmacol Rev 42:223–286
Rutecki PA, Lebeda FJ, Johnston D (1987) 4-aminopyridine produces epileptiform activity in hippocampus and enhances synaptic excitation and inhibition. J Neurophysiol 57:1911–1924
Schaefer Jr EW, Brunton RB, Cunningham DJ (1973) A summary of the acute toxicity of 4-aminopyridine to birds and mammals. Toxicol Appl Pharmacol 26:532–538
Yamaguchi SI, Rogawski MA (1992) Effects of anticonvulsant drugs on 4-aminopyridine-induced seizures in mice. Epilepsy Res 11:9–16

E.3.2.8 3-Nitropropionic Acid-Induced Seizures in Mice

PURPOSE AND RATIONALE

3-Nitropropionic acid is a naturally occurring toxin demonstrated to impair energy metabolism via irreversible inhibition of a mitochondrial complex II component, succinate dehydrogenase (Alston et al. 1977; Ludolph et al. 1991). 3-Nitropropionic acid evokes seizures in mice after i.p. injection of 100–200 mg/kg (Urbańska et al. 1998, 1999). Urbańska et al. (1998) and Zuchora et al. (2005) evaluated anticonvulsants for their protective effect against 3-nitropropionic-acid-induced seizures.

PROCEDURE

Male albino Swiss mice weighing 20–25 g were injected i.p. with 210 mg/kg 3-nitropropionic acid, which is equal to the ED_{97} dose (i. e., the dose required to evoke seizures in 97% of the animals). Groups of eight mice received in addition various doses of the anticonvulsant drugs. Percentage of animals with seizures and latency until occurrence of seizures were determined. Mortality rate was determined 2 h after injection of 3-nitropropionic acid.

EVALUATION

ED_{50} and LD_{50} values together with their confidence limits were estimated by computerized fitting of the data by linear regression analysis according to Litchfield and Wilcoxon. Statistical comparisons of latency data were performed by means of one-way analysis of variance (ANOVA) followed by adjustment of *P* value by the Bonferroni method.

REFERENCES AND FURTHER READING

Alston TA, Mela L, Bright HL (1977) 3-Nitropropionate, the toxic substance of *Indigofera*, is a suicide inactivator of succinate dehydrogenase. Proc Natl Acad Sci USA 74:3767–3771

Ludolph AC, He F, Spencer PS, Hammerstad J, Sabri M (1991) 3-Nitropropionic acid – exogenous animal neurotoxin and possible human striatal toxin. Can J Neurol Sci 18:492–398

Urbańska EM, Blaszczak P, Saran T, Kleinrok Z, Turski WA (1998) Mitochondrial toxin 3-nitropropionic acid evokes seizures in mice. Eur J Pharmacol 359:55–58

Urbańska EM, Blaszczak P, Saran T, Kleinrok Z, Turski WA (1999) AMPA/kainate-related mechanisms contribute to convulsant and proconvulsant effects of 3-nitropropionic acid. Eur J Pharmacol 370:251–256

Zuchora B, Wielosz M, Urbańska EM (2005) Adenosine A1 receptors and the anticonvulsant potential of drugs effective in the model of 3-nitropropionic acid-induced seizures in mice. Eur Neuropsychopharmacol 15:85–93

E.3.2.9 Epilepsy Induced by Focal Lesions

PURPOSE AND RATIONALE

Intrahippocampal injections of noxious agents or certain cerebral lesions can induce seizures in animals. Cavalheiro et al. (1982) studied the long-term effects of intrahippocampal kainic acid injections in rats.

PROCEDURE

Adult male Wistar rats are anesthetized with a chloral hydrate/Nembutal mixture and placed in a stereotactic apparatus. For injections, a 0.3 mm cannula is inserted through a burr hole in the calvarium. The coordinates for hippocampal injections are based on a stereotactic atlas, e. g., Albe-Fessard et al. (1971). Kainic acid is dissolved in artificial serum and infused in various doses (0.1 to 3.0 µg) in a volume of 0.2 µl over a period of 3 min. For recording, bipolar twisted electrodes (100 µm) are positioned stereotaxically and fixed on the skull with dental acrylic cement. Depth recording sites include the dorsal hippocampus and amygdala ipsilateral to the injected side. Surface electrodes are guided from jeweler's screws over the occipital cortex. An additional screw in the frontal sinus serves as indifferent electrode for grounding. Signals are recorded by an EEG polygraph.

EVALUATION

EEG recordings and observations of convulsive seizures are performed during the acute phase and during the chronic phase (up to 2 months) with and without drug treatment.

MODIFICATIONS OF THE METHOD

Several agents have been used as convulsants after topical administration, e. g., application of alumina cream (Kopeloff et al. 1942, 1955; Ward 1972; Feria-Velasco et al. 1980), implantation of cobalt powder (Dow et al. 1962; Fischer et al. 1967), injection of a colloidal gel of tungstic acid (Blum and Liban 1960; Black et al. 1967), topical application of penicillin (Matsumoto and Marsan 1964), subpial injection of saturated $FeCl_3$ solution (Reid et al. 1979; Lange et al. 1980), intracerebral injections of zinc sulfate (Pei et al. 1983), intracerebral injection of antibodies to brain gangliosides (Karpiak et al. 1976, 1981), microinjections of cholinergic agonists (Ferguson and Jasper 1971; Turski et al. 1983), topical application of atropine (Daniels and Spehlman 1973), injection of tetanus toxin into the hippocampus (Mellanby et al. 1984; Hawkins and Mellanby 1987), injection of strychnine in the visual or somato-sensory cortex (Atsev and Yosiphov 1969), electrophoretic application of bicuculline from a fluid filled microelectrode (Campell and Holmes 1984).

Bernhard et al. (1955, 1956) evaluated the anticonvulsive effect of local anaesthetics in cats and monkeys. The head was fixed in light Nembutal anaesthesia, the parietal areas exposed and covered with paraffin oil. Stimulating electrodes were placed at the surface of the parietal region. The cortex was stimulated with repetitive square wave shocks (duration 1–3 ms) with a frequency of 25 per s for 5 s. In order to avoid muscular movements, d-tubocurarine was given. Cortical afterdischarge was registered before and after injection of local anaesthetics.

Cortical epileptic lesions were produced by local freezing (Stalmaster and Hanna 1972; Hanna and Stalmaster 1973; Loiseau et al. 1987).

Repetitive electrical stimulation of discrete regions of the central nervous system has been used as a convenient method for reproduction of the ictal phenomena of epilepsy (Marsan 1972; Racine 1972).

Remler and Marcussen (1986), Remler et al. (1986) studied the pharmacological response of systemically derived focal epileptic lesions. A defined area of left hemisphere of rats was radiated by α-particles from a cyclotron destroying the blood brain barrier. After a period of 150 days following irradiation, bicu-

culline was injected intraperitoneally resulting in focal lesions with EEG spikes and convulsions. Anticonvulsant drugs decreased these effects.

Walton and Treiman (1989) and Walton et al. (1994) described a model of cobalt-lesioned rats in which status epilepticus was induced by injection of homocysteine thiolactone.

Anderer et al. (1993) pointed out that restriction to a limited set of EEG-target variables may lead to misinterpretation of pharmaco-EEG results.

Krupp and Löscher (1998) developed a cortical ramp-stimulation model allowing repeated determinations of seizure threshold at short time intervals in individual rats without inducing postictal threshold increases.

REFERENCES AND FURTHER READING

Albe-Fessard D, Stutinsky F, Libouban S (1971) Atlas Stéréotaxique du Diencéphale du Rat Blanc. C.N.R.S., Paris

Anderer P, Barbanoj MJ, Saletu B, Semlitsch HV (1993) Restriction to a limited set of EEG-target variables may lead to misinterpretation of pharmaco-EEG results. Neuropsychobiology 27:112–116

Atsev E, Yosiphov T (1969) Changes in evoked perifocal electrical activity with an acute epileptogenic focus in cat's cortex. Electroencephalogr Clin Neurophysiol 27:444

Bernhard CG, Bohm E (1955) The action of local anaesthetics on experimental epilepsy in cats and monkeys. Br J Pharmacol 10:288–295

Bernhard CG, Bohm E, Wiesel T (1956) On the evaluation of the anticonvulsive effect of local anaesthetics. Arch Int Pharmacodyn 108:392–407

Black RG, Abraham J, Ward AA Jr (1967) The preparation of tungstic acid gel and its use in the production of experimental epilepsy. Epilepsia 8:58–63

Blum B, Liban E (1960) Experimental basotemporal epilepsy in the cat. Discrete epileptogenic lesions produced in the hippocampus or amygdaloid by tungstic acid. Neurology 10:546–554

Campell AM, Holmes O (1984) Bicuculline epileptogenesis in the rat. Brain Res 323:239–246

Cavalheiro EA, Riche DA, Le Gal la Salle G (1982) Long-term effects of intrahippocampal kainic acid injections in rats: a method for inducing spontaneous recurrent seizures. Electroencephalogr Clin Neurophysiol 53:581–589

Daniels JC, Spehlman R (1973) The convulsant effect of topically applied atropine. Electroencephalogr Clin Neurophysiol 34:83–87

Dow RS, Fernández-Guardiola A, Manni E (1962) The production of cobalt experimental epilepsy in the rat. Electroencephalogr Clin Neurophysiol 14:399–407

Ferguson JH, Jasper HH (1971) Laminar DC studies of acetylcholine-activated epileptiform discharge in cerebral cortex. Electroencephalogr Clin Neurophysiol 30:377–390

Feria-Velasco A, Olivares N, Rivas F, Velasco M, Velasco F (1980) Alumina cream-induced focal motor epilepsy in cats. Arch Neurol 37:287–290

Fischer J, Holubar J, Malik V (1967) A new method of producing chronic epileptogenic cortical foci in the rat. Physiol Bohemosclov 16:272–277

Hanna GR, Stalmaster RM (1973) Cortical epileptic lesions produced by freezing. Neurology 23:918–925

Hawkins CA, Mellanby JH (1987) Limbic epilepsy induced by tetanus toxin: a longitudinal electroencephalographic study. Epilepsia 28:431–444

Karpiak SE, Graf L, Rapport MM (1976) Antiserum to brain gangliosides produces recurrent epileptiform activity. Science 194:735–737

Karpiak SE, Mahadik SP, Graf L, Rapport MM (1981) An immunological model of epilepsy: seizures induced by antibodies to G_{M1} ganglioside. Epilepsia 22:189–196

Kopeloff LM, Barrera SE, Kopeloff N (1942) Recurrent convulsive seizures in animals produced by immunologic and chemical means. Am J Psychiatry 98:881–902

Kopeloff L, Chusid JG, Kopeloff N (1955) Epilepsy in Maccaca mulatta after cortical or intracerebral alumina. Arch Neurol Psychiatry 74:523–526

Krupp E, Löscher W (1998) Anticonvulsant drug effects in the direct cortical ramp-stimulation model in rats: comparison with convulsive seizure models. J Pharmacol Exp Ther 285:1137–1149

Lange SC, Neafsey EJ, Wyler AR (1980) Neuronal activity in chronic ferric chloride epileptic foci in cats and monkey. Epilepsia 21:251–254

Loiseau H, Avaret N, Arrigoni E, Cohadon F (1987) The early phase of cryogenic lesions: an experimental model of seizures updated. Epilepsia 28:251–258

Marsan CA (1972) Focal electrical stimulation. In: Purpura DP, Penry JK, Tower DB, Woodbury DM, Walter RD (eds) Experimental Models of Epilepsy – A Manual for the Laboratory Worker. Raven Press, New York, pp 147–172

Matsumoto H, Marsan CA (1964) Cortical cellular phenomena in experimental epilepsy: interictal manifestations. Exper Neurol 9:286–304

Mellanby J, Hawkins C, Mellanby H, Rawlins JNP, Impey ME (1984) Tetanus toxin as a tool for studying epilepsy. J Physiol, Paris 79:207–215

Pei Y, Zhao D, Huang J, Cao L (1983) Zinc-induced seizures: a new experimental model of epilepsy. Epilepsia 24:169–176

Racine RJ (1972) Modification of seizure activity by electrical stimulation: I. After-discharge threshold. Electroencephalogr Clin Neurophysiol 32:269–279

Reid SA, Sypert GW, Boggs WM, Wilmore LJ (1979) Histopathology of the ferric-induced chronic epileptic focus in cat: a Golgi study. Exper Neurol 66:205–219

Remler MP, Marcussen WH (1986) Systemic focal epileptogenesis. Epilepsia 27:35–42

Remler MP, Sigvardt K, Marcussen WH (1986) Pharmacological response of systemically derived focal epileptic lesions. Epilepsia 27:671–6777

Stalmaster RM, Hanna GR (1972) Epileptic phenomena of cortical freezing in the cat: Persistent multifocal effects of discrete superficial lesions. Epilepsia 13:313–324

Turski WA, Czuczwar SJ, Kleinrok Z, Turski L (1983) Cholinomimetics produce seizures and brain damage in rats. Experientia 39:1408–1411

Walton NY, Treiman DM (1989) Phenobarbital treatment of status epilepticus in a rodent model. Epilepsy Res 4:216–222

Walton NY, Gunnawan S, Treiman DM (1994) Treatment of experimental status epilepticus with the GABA uptake inhibitor, tiagabine. Epilepsy Res 19:237–244

Ward AA Jr (1972) Topical convulsant metals. In: Purpura DP, Penry JK, Tower DB, Woodbury DM, Walter RD (eds) Experimental Models of Epilepsy – A Manual for the Laboratory Worker. Raven Press, New York, pp 13–35

E.3.2.10 Kindled Rat Seizure Model

PURPOSE AND RATIONALE

Kindling, first described by Goddard et al. (1969), results from repetitive subconvulsive electrical stimulation of certain areas of the brain. Initially, local after-discharge is associated with mild behavioral signs; however, with continued stimulation electrical activity presumably spreads, and generalized convulsions occur. Although the pathogenesis of kindled seizures is not fully understood, it serves as a useful tool for investigating the efficacy of experimental anticonvulsant agents.

PROCEDURE

Adult female Sprague-Dawley rats (270–400 g) are used. The rats are implanted with an electrode in the right amygdala according to the coordinates of Pellegrino et al. (1979): frontal, 7.0; lateral, –4.7; horizontal, 2.5. At least 1 week has to elapse before electrical stimulation of the brain is started. After discharge threshold is determined for each rat. Duration and amplitude, behavioral seizure duration and seizure stage are recorded with increased stimuli afterdischarges. Seizure severity is classified into 5 stages (Racine 1972). Rats are considered to be kindled on the first stimulation causing a stage 5 seizure which is followed by at least 2 consecutive stage 5 seizures.

The animals are tested on the day before and after treatment with the test compound (i.p. or orally). Amygdala stimulation is applied at various time intervals.

EVALUATION

The occurrence and the degree of seizures are compared between control results and the those after administration of the test compound.

CRITICAL ASSESSMENT OF THE METHOD

The kindled seizure model offers an approach to study anticonvulsive drugs on the basis of a pathophysiological model. This method may give more relevant results than the simpler methods using maximal electroshock or chemically induced convulsions.

MODIFICATIONS OF THE METHOD

Generalized convulsive seizures have been induced by daily amygdaloid stimulation in **baboons** (Wada and Osawa 1976), and in **rhesus monkeys** (Wada et al. 1978).

The kindling effect can be produced by intermittent administration of small doses of pentylenetetrazol (Mason and Cooper 1972).

Dürmüller et al. (1994) tested a competitive (NBQX) and a non-competitive (GYKI 52446) AMPA antagonist, and a competitive NMDA antagonist (D-CPPene) against the development of kindling and against fully kindled seizures in amygdala-kindled rats.

Croucher et al. (1996) described a chemical kindling procedure in rats by daily focal microinjection of NMDA into the right basolateral amygdala and the inhibition of seizures by a NMDA receptor antagonist.

Suzuki et al. (1996) studied the anticonvulsant action of metabotropic glutamate receptor agonists in kindled amygdala of rats.

Löscher et al. (1993), Ebert et al. (1997), and Ebert and Löscher (1999) studied the effect of phenytoin on the spread of seizures in the amygdala kindling model in rats. Sprague Dawley rats implanted with a stimulation and recording electrode in the basolateral amygdala showed an increase in current intensity necessary for eliciting after-discharges of about 200% after administration of phenytoin, while seizure severity at threshold was increased compared to controls. Phenytoin-resistant kindled rats are considered as a model of drug-resistant epilepsy.

Löscher (1998) discussed the pharmacology of glutamate receptor antagonists in the kindling model of epilepsy.

The kindling procedure can also be used to evaluate antidepressant drugs (Babington 1975).

REFERENCES AND FURTHER READING

Babington RG (1975) Antidepressives and the kindling effect. In: Fielding S, Lal H (eds) Industrial Pharmacology, Vol II, Antidepressants, pp 113–124

Croucher MJ, Cotterell KL, Bradford HF (1996) Characterization of N-methyl-D-aspartate (NMDA)-induced kindling. Biochem Soc Transact 24:295S

Dürmüller N, Craggs M, Meldrum BS (1994) The effect of the non-NMDA receptor antagonists GYKI 52446 and NBQX and the competitive NMDA receptor antagonist D-CPPene on the development of amygdala kindling and on amygdala-kindled seizures. Epilepsy Res 17:167–174

Ebert U, Löscher W (1999) Characterization of phenytoin-resistant kindled rats, a new model of drug-resistant epilepsy: influence of genetic factors. Epilepsy Res 33:217–226

Ebert U, Cramer S, Löscher W (1997) Phenytoin's effect on the spread of seizures in the amygdala kindling model. Naunyn-Schmiedebergs Arch Pharmacol 356:341–347

Girgis M (1981) Kindling as a model for limbic epilepsy. Neurosci 6:1695–1706

Gilbert ME (1994) The phenomenology of limbic kindling. Toxicol Industr Health 10:4–5

Goddard GV (1967) Development of epileptic seizures through brain stimulation at low intensity. Nature 214:1020–1021

Goddard GV, McIntyre DC, Leech CK (1969) A permanent change in brain function resulting from daily electrical stimulation. Exp Neurol 25:295–330
Goddard GV, Dragunow M, Maru E, Macleod EK (1986) Kindling and the forces that oppose it. In: Doane BK, Livingston KE (eds) The Limbic System: Functional Organization and Clinical Disorders. Raven Press, New York, pp 95–108
Heit MC, Schwark WS (1987) An efficient method for time course studies of antiepileptic drugs using the kindled rat seizure model. J Pharmacol Meth. 18:319–325
Hoenack D, Loescher W (1989) Amygdala-kindling as a model for chronic efficacy studies on antiepileptic drugs: Experiments with carbamazepine. Neuropharmacol 28:599–610
Koella WP (1985) Animal experimental methods in the study of antiepileptic drugs. In: Frey HH, Danz D (eds) Antiepileptic Drugs, Chapter 12, 283–339. Springer-Verlag Heidelberg, New York, Tokyo
Le Gal la Salle G (1981) Amygdaloid kindling in the rat: regional differences and general properties. In: Wada JA (ed) Kindling 2, Raven Press, New York, pp 31–47
Löscher W (1998) Pharmacology of glutamate receptor antagonists in the kindling model of epilepsy. Prog Neurobiol 54:721–741
Löscher W, Nolting B, Hönack D (1988) Evaluation of CPP, a selective NMDA antagonist, in various rodent models of epilepsy. Comparison with other NMDA antagonists, and with diazepam and phenobarbital. Eur J Pharmacol 152:9–17
Löscher W, Rundfeldt C, Honack D (1993) Pharmacological characterization of phenytoin-resistant amygdala-kindled rats, a new model of drug-resistant partial epilepsy. Epilepsy Res 15:207–219
Lothman EW, Salerno RA, Perlin JB, Kaiser DL (1988) Screening and characterization of anti-epileptic drugs with rapidly recurring hippocampal seizures in rats. Epilepsy Res 2:367–379
Mason CR, Cooper RM (1972) A permanent change in convulsive threshold in normal and brain-damaged rats with repeated small doses of pentylenetetrazol. Epilepsia 13:663–674
McNamara JO (1984) Kindling: an animal model of complex partial epilepsy. Ann Neurol 16 (Suppl):S72–S76
McNamara JO (1986) Kindling model of epilepsy. In: Advances in Neurology. Basic Mechanisms of the Epilepsies. Molecular and Cellular Approaches. Delgado-Escueta AV, Ward AA, Woodbury DM, Porter RJ (eds) Vol 44, Chapter 14, 303–318. Raven Press; New York
Pellegrino LJ, Pellegrino AS, Cushman AJ (1979) A Stereotactic Atlas of the Brain. 2nd ed. New York: Plenum Press
Pinel JPJ, Rovner LI (1978) Experimental epileptogenesis: kindling-induced epilepsy in rats. Exper Neurol 58:190–202
Racine R (1978) Kindling: the first decade. Neurosurg 3:234–252
Racine RJ (1972) Modification of seizure activity by electrical stimulation. II. Motor seizure. Electroencephalogr. Clin Neurophysiol 32:281–294
Schmidt J (1990) Comparative studies on the anticonvulsant effectiveness of nootropic drugs in kindled rats. Biomed Biochim Acta 49:413–419
Suzuki K, Mori N, Kittaka H, Iwata Y, Osonoe K, Niwa SI (1996) Anticonvulsant action of metabotropic glutamate receptor agonists in kindled amygdala of rats. Neurosci Lett 204:41–44
Wada JA (1977) Pharmacological prophylaxis in the kindling model of epilepsy. Arch Neurol 34:387–395
Wada JKA, Osawa T (1976) Spontaneous recurrent seizure state induced by daily amygdaloid stimulation in Senegalese baboons (*Papio papio*). Neurol 22:273–286
Wada JA, Mizoguichi T, Osawa T (1978) Secondarily generalized convulsive seizures induced by daily amygdaloid stimulation in rhesus monkeys. Neurol 28:1026–1036
Wahnschaffe U, Loescher W (1990) Effect of selective bilateral destruction of the substantia nigra on antiepileptic drug actions in kindled rats. Eur J Pharmacol 186:157–167

E.3.2.11
Posthypoxic Myoclonus in Rats

PURPOSE AND RATIONALE

The syndrome of posthypoxic myoclonus in man was described by Lance and Adams (1963). Lance (1968), Fahn (1986). Troung et al. (1994), Jaw et al. (1994, 1995, 1996) reported on a model in rats resembling this human disorder.

PROCEDURE

Male Sprague Dawley rats fasted 12–24 h prior surgery are anesthetized with 100 mg/kg ketamine i.p., supplemented by 0.4 mg/kg atropine. The animal is placed on a circulating water pad and kept at a constant body temperature by a heating lamp. The rat is intubated and ventilated with 30% O_2 in N_2O. A femoral artery and vein are cannulated for monitoring blood pressure and delivery of drugs, respectively. Electrocardiogram and blood pressure are recorded with a polygraph. The rat is then paralyzed with 2 mg/kg succinylcholine i.v. and ventilator settings are adjusted to a rate of 60 strokes/min and a volume of 7.5 ml/kg, which yields blood gases of >150 mm Hg pO_2, 35–40 mm Hg pCO_2, and a pH of 7.35–7.40. N_2O is replaced with N_2 and an equilibrium period of 5 min is allowed.

Cardiac arrest is accomplished with a transthoracic intracardiac injection of KCl and cessation of the respiration. Resuscitation is begun 10 min after the arrest by turning on the ventilator (100% O_2), manual thoracic compressions, and i.v. injections of 20 µg/kg epinephrine hydrochloride and sodium bicarbonate (4 mEq/kg). The rat is then weaned from the ventilator over 2–4 h and extubated.

Auditory-induced myoclonus: Rats are presented with a series of 45 clicks from a metronome (1 Hz, 95 dB, 40 ms), and the response to each click is scored as follows: 0 = no response, 1 = ear twitch, 2 = ear and head jerk, 3 = ear, head, and shoulder jerk, 4 = whole body jerk, 6 = whole body jerk of such severity that it causes a jump. The total myoclonus score of each rat is determined by summing up the scores yielded over 45 clicks.

Since rats ranging from 3 to 14 days post cardiac arrest show similar susceptibility to audiogenic stimulation, animals within this period are used for pharmacological tests. Myoclonus scores are assessed 30 min before and 60 min after intraperitoneal drug application.

EVALUATION

Changes in myoclonus scores are analyzed by paired two-tailed Student's *t*-test.

CRITICAL ASSESSMENT OF THE TEST

Some anticonvulsant drugs, such as clonazepam and valproic acid were reported to be active in this test; however, phenytoin is not. Posthypoxic myoclonus may present a special pathological condition.

REFERENCES AND FURTHER READING

Fahn S (1986) Posthypoxic action myoclonus: literature review update. Adv Neurol 43:157–169

Jaw SP, Hussong MJ, Matsumoto RR, Truong DD (1994) Involvement of 5-HT_2 receptors in posthypoxic stimulus-sensitive myoclonus in rats. Pharmacol Biochem Behav 49:129–131

Jaw SP, Dang T, Truong DD (1995) Chronic treatments with 5-HT_{1A} agonists attenuate posthypoxic myoclonus in rats. Pharmacol Biochem Behav 52:577–580

Jaw SP, Nguyen B, Vuong QTV, Trinh TA, Nguyen M, Truong DD (1996) Effects of glutamate receptor antagonists in post-hypoxic myoclonus in rats. Brain Res Bull 40:163–166

Lance JW (1968) Myoclonic jerks and falls: aetiology, classification and treatment. Med J Aust 1:113–119

Lance W, Adams RD (1963) The syndrome of intention or action myoclonus as a sequel to hypoxic encephalopathy. Brain 86:111–136

Truong DD, Matsumoto RR, Schwartz PH, Hussong MJ, Wasterlain CG (1994) Novel cardiac arrest model of posthypoxic myoclonus. Movement Disorders 9:201–206

E.3.2.12 Rat Kainate Model of Epilepsy

PURPOSE AND RATIONALE

Temporal lobe epilepsy is characterized by complex partial seizures that involve and apparently originate in the mesial temporal structures of the limbic system. These complex partial seizures can evolve into secondarily generalized, tonic-clonic seizures. Patients become resistant to the treatment with the usual antiepileptic drugs. The kainate-treated rat is one of several models used to study temporal lobe epilepsy. Examination of the hippocampus and dentate gyrus from kainate-treated rats has revealed a similar pattern of neurodegeneration in the hippocampus and the presence of mossy fiber sprouting in the inner molecular level of the dentate gyrus. Several authors used this model to find drugs for treatment-resistant epilepsy (Bolanos et al. 1998; Hellier et al. 1998; Longo and Mello 1998; Maj et al. 1998; Bouilleret et al. 1999; Pitkänen et al. 1999; Cilio et al. 2001; Madsen et al. 2001; Ebert et al. 2002; Tamagami et al. 2004). Maj et al. (1998) tested the activity of several drugs against kainate-induced status epilepticus and hippocampal lesions in the rat.

PROCEDURE

Male Wistar rates weighing 225–250 g are anesthetized with sodium pentobarbital (50 mg/kg i.p.). The are implanted extradurally with electrodes over the frontal and parietal cortex and with a reference electrode on the cerebellum. Caution is taken not to break the inner table of the diploe. All the electrodes are connected to plugs and held to the skull with dental acrylic cement. At least 7 days after surgery, rats are treated with either saline or test drugs intraperitoneally. Then, 15 min later, the rats receive a single i.p. dose of kainic acid (10 mg/kg). EEG recordings and behavioral observations are performed up to 240 min after kainic acid administration. Status epilepticus is defined as a sustained ictal EEG pattern lasting 20 min or longer without any interruption longer than 1 min.

Seven days later, the rats are sacrificed, the brains removed and immersed for 48 h in 10% formalin. Coronal sections (4 μm) are stained with hematoxylin-eosin. Hippocampal injury is assessed by counting the number of histologically normal CA4 pyramidal neurons.

EVALUATION

The percentage of animals protected from status epilepticus is analyzed using Fisher's exact test. For calculation of the latency to status epilepticus (min) and duration of status epilepticus (min), all animals are included regardless of whether they showed status epilepticus or not. The data are evaluated by analysis of variance (ANOVA) followed by Dunnett's test. Neuronal counts are analyzed using the Mann-Whitney non-parametric test.

MODIFICATIONS OF THE METHOD

Cilio et al. (2001) used immature rats to test the anticonvulsant action and long-term effects of gabapentin.

Hellier et al. (1998) used repeated low-dose systemic treatment in order to reduce the mortality associated with single injections with kainate.

Since intracerebroventricular administration of kainic acid decreases hippocampal neuronal number

and increases dopamine receptor binding in the nucleus accumbens, kainic lesions have been discussed as an animal model of schizophrenia (Bardgett et al. 1995; Csernansky et al. 1998).

Humphrey et al. (2001) described methods for inducing neuronal loss in preweanling rats using an intracerebroventricular infusion of kainic acid.

Hu et al. (1998) investigated neuronal stress and injury in C57/BL **mice** after systemic kainic acid administration.

Bouilleret et al. (1999) tested recurrent seizures and hippocampal sclerosis following intrahippocampal kainate injection in adult **mice**.

REFERENCES AND FURTHER READING

Bardgett ME, Jackson JL, Taylor GT, Csernansky JG (1995) Kainic acid decreases hippocampal neuronal number and increases dopamine receptor binding in the nucleus accumbens: an animal model of schizophrenia. Behav Brain Res 70:153–164

Bolanos AR, Sarkisian M, Yang Y, Hori A, Helmers SL, Mikati M, Tandon P, Stafstrom CE, Holmes GL (1998) Comparison of alproate and phenobarbital treatment after status epilepticus in rats. Neurology 51:41–48

Bouilleret V, Ridoux V, Depaulis A, Marescaux C, Nehling A, LaSalles GLG (1999) Recurrent seizures and hippocampal sclerosis following intrahippocampal kainate injection in adult mice: electroencephalography, histopathology and synaptic reorganization similar to mesial temporal lobe epilepsy. Neuroscience 89:717–729

Cilio MR, Bolanos AR, Liu Z, Schmid R, Yang Y, Stafstrom CE, Mikati MA, Holmes GL (2001) Anticonvulsant action and long-term effects of gabapentin in the immature brain. Neuropharmacology 40:139–147

Csernansky JG, Csernansky CA, Kogelman L, Montgomery EM, Bardgett ME (1998) Progressive neurodegeneration after intracerebroventricular kainic acid administration in rats: implications for schizophrenia? Biol Psychiatry 44:1143–1150

Ebert U, Brandt C, Löscher W (2002) Delayed sclerosis, neuroprotection, and limbic epileptogenesis after status epilepticus in the rat. Epilepsia 43 [Suppl 5]:86–95

Hellier JL, Patrylo PR, Buckmaster PS, Dudek FE (1998) Recurrent spontaneous motor seizures after repeated low-dose systemic treatment with kainate: assessment of a rat model of temporal lobe epilepsy. Epilepsy Res 31:73–84

Hu RQ, Koh S, Torgerson T, Cole AJ (1998) Neuronal stress and injury in C57/BL mice after systemic kainic acid administration. Brain Res 810:229–240

Humphrey WM, Bardgett ME, Montgomery EM, Taylor GT, Csernanansky JG (2001) Methods for inducing neuronal loss in preweanling rats using intracerebroventricular infusion of kainic acid. Brain Res Prot 7:1–10

Longo BM, Mello LEAM (1998) Supragranular mossy fiber sprouting in rat is not necessary for spontaneous seizures in the intrahippocampal kainate model epilepsy in the rat. Epilepsy Res 32:172–182

Madsen U, Stensbol TB, Krogsgaard-Larsen P (2001) Inhibitors of AMPA and kainate receptors. Curr Med Chem 8:1291–1301

Maj R, Fariello RG, Ukmar G, Varasi M, Pevarello P, McArthur RA, Salvati P (1998) PNU-151774E protects against kainate-induced status epilepticus and hippocampal lesions in the rat. Eur J Pharmacol 359:27–32

Pitkänen A, Nissinen J, Jolkkonen E, Tuunanan J, Halonen T (1999) Effects of vigabatrin treatment on status epilepticus-induced neuronal damage and mossy fiber sprouting in the rat hippocampus. Epilepsy Res 33:67–85

Tamagami H, Morimoto K, Watanabe T, Ninomiya T, Hirao T, Tanaka A, Kakumoto M (2004) Quantitative evaluation of central-type benzodiazepine receptors with [^{125}I]Iomazenil in experimental epileptogenesis. I. The rat kainate model of temporal lobe epilepsy. Epilepsy Res 61:105–112

E.3.2.13 Pilocarpine Model of Epilepsy

PURPOSE AND RATIONALE

Several post-status models are described in which epilepsy develops after a chemically induced status epilepticus, such as the kainate, the pilocarpine and the pilocarpine-lithium model (Löscher 2002). Several modifications of the pilocarpine and the lithium-pilocarpine model are reported in the literature (Cavalheiro et al. 1991; Leite and Cavalheiro 1995; André et al. 2001; Biagini et al. 2001; Klitgaard et al. 2002; Leite et al. 2002; Wallace et al. 2003; Arida et al. 2004; Leroy et al. 2004; Lyon et al. 2004; Rigoulot et al. 2004; Setkowicz et al. 2004). When rats are pretreated with lithium chloride, status epilepticus can be produced with a substantially lower dose of pilocarpine, and rats display the same clinical and EEG features of status epilepticus as with pilocarpine alone (Honchar et al. 1983). André et al. (2001) and Rigoulot et al. (2004) tested antiepileptic drugs in the lithium-pilocarpine model of epilepsy.

PROCEDURE

Male Wistar rats weighing 225–250 g were anesthetized for electrode implantation by an i.p. injection of 2.5 mg/kg diazepam and 1 mg/kg ketamine chlorhydrate. Two single-contact recording electrodes were placed on the skull, one on each side of the parietal cortex, and one bipolar deep recording electrode was placed in the right hippocampus (Vergnes et al. 1982).

One week after surgery, rats received 3 mEq/kg lithium chloride i.p. On the following day, 1 mg/kg methylscopolamine bromide was administered s.c. to limit the peripheral effects of the convulsant. Status epilepticus was induced by injecting pilocarpine (25mg/kg s.c.) 30 min after methylscopolamine. Various doses of test drug (i.p.) or 2.5 mg/kg diazepam (i.m.) were injected at 1 h after the onset of status epilepticus. The onset of status epilepticus corresponds to the moment at which rats experience successive seizures without recovery. Continuous spiking of the

EEG occurs 30–60 min after pilocarpine administration. The bilateral EEG cortical activity and the unilateral EEG hippocampal activity were recorded during the whole duration of status epilepticus and concurrent behavioral changes were noted.

Quantification of neuronal damage was performed 14 days after status epilepticus. Brains of rats sacrificed in pentobarbital anesthesia were removed and coronal sections containing the hippocampus from the anterior to the posterior level were prepared. Quantification of cell density was performed with a microscopic grid. The numbers of cells obtained in 12 counted fields were averaged.

EVALUATION

Statistical analysis of neuronal damage and epilepsy between the different groups was performed by means of analysis of variance followed by a posthoc Dunnett's test for multiple comparisons.

MODIFICATIONS OF THE METHOD

Hort et al. (1999) studied the relation between spontaneous recurrent seizures and the derangement of cognitive function in pilocarpine-induced status epilepticus,

Tang et al. (2004) recorded EEG in freely moving mice after pilocarpine-induced status epilepticus. A transmitter (TSE Systems, Bad Homburg, Germany) was fixed on the electrode socket by plug connection with wires attached to the skull by two screws 3 days before pilocarpine induction. The EEG signals were telemetrically received via an HF receiver which passed the signals to the computer.

REFERENCES AND FURTHER READING

André V, Ferrandon A, Marescaux C, Nehlig A (2001) Vigabatrin protects against hippocampal damage but is not antiepileptogenic in the lithium-pilocarpine model of temporal lobe epilepsy. Epilepsy Res 47:99–117

Arida RM, Sanabria ERG, da Silva AC, Faria LC, Scorza FA, Cavalheiro EA (2004) Physical training reverts hippocampal electrophysiological changes in rats submitted to the pilocarpine model of epilepsy. Physiol Behav 83:165–171

Biagini G, Avoli M, Marcinkiewicz J, Marcinkiewicz M (2001) Brain-derived neurotrophic factor superinduction parallels anti-epileptic-neuroprotective treatment in the pilocarpine epilepsy model. J Neurochem 76:1814–1822

Cavalheiro EA, Leite JP, Bortolotto ZA, Turski WA, Ikonomidou C, Turski L (1991) Long-term effects of pilocarpin in rats: structural damages of the brain triggers kindling and spontaneous recurrent seizures. Epilepsia 32:778–782

Honchar MP, Olney JW, Sherman WR (1983) Systemic agents induce seizures and brain damage in lithium-treated rats. Science 220:323–325

Hort J, Brozek G, Mares P, Langmeier M, Komarek V (1999) Cognitive functions after pilocarpine-induced status epilepticus: changes during silent period precede appearance of spontaneous recurrent seizures. Epilpesia 40:1177–1183

Klitgaard H, Matagne A, Vanneste-Goemaere J, Margineanu G (2002) Pilocarpine-induced epileptogenesis in the rat: impact of initial duration of status epilepticus on electrophysiological and neuropathological alterations. Epilepsy Res 51:93–107

Leite JP, Cavalheiro EA (1995) Effect of conventional antiepileptic drugs in a model of spontaneous recurrent seizures in rats. Epilepsy Res 20:93–104

Leite JP, Garcia-Cairasco N, Cavalheiro EA (2002) New insights from the use of pilocarpine and kainate models. Epilepsy Res 50:93–103

Leroy C, Poisbeau P, Keller AF, Nehlig A (2004) Pharmacological plasticity of $GABA_A$ receptors at dentate gyrus synapses in a rat model of temporal lobe epilepsy. J Physiol (Lond) 557:473–487

Löscher W (2002) Animal models for the development of antiepileptogenic and disease-modifying drugs. A comparison of the pharmacology of kindling and post-status epilepticus models of temporal lobe epilepsy. Epilepsy Res 50:105–123

Lyon A, Marone S, Wainman D, Weaver DF (2004) Implementing a bioassay to screen molecules for antiepileptogenic activity. Chronic pilocarpine versus subdural haematoma models. Seizure 13:82–86

Rigoulot MA, Koning E, Ferrandon A, Nehlig A (2004) Neuroprotective properties of topiramate in the lithium-pilocarpine model of epilepsy. J Pharmacol Exp Ther 308:787–795

Setkowicz Z, Ciarach M, Guzik R, Janeczko K (2004) Different effects of neuroprotectants FK-506 and cyclosporine A on susceptibility to pilocarpine-induced seizures in rats with brain injured at different developmental stages. Epilepsy Res 61:63–72

Tang FR, Chia SC, Chen PM, Gao H, Lee WL, Yeo TS, Burgunder JM, Probst A, Sim MK, Ling EA (2004) Metabotropic glutamate receptor 2/3 in the hippocampus of patients with mesial temporal lobe epilepsy, and of rats and mice after pilocarpine-induced status epilepticus. Epilepsy Res 59:167–180

Vergnes M, Marescaux C, Micheletti G, Reis J, Depaulis A, Rumbach L, Warter SM (1982) Spontaneous paroxysmal electroclinical patterns in rat: a model of generalized nonconvulsive epilepsy. Neurosci Lett 33:97–101

Wallace MJ, Blair RE, Falenski KW, Martin BR, Delorenzo RJ (2003) The endogenous cannabinoid system regulates seizure frequency and duration in a model of temporal lobe epilepsy. J Pharmacol Exp Ther 307:129–137

E.3.2.14 Self-Sustained Status Epilepticus

PURPOSE AND RATIONALE

Status epilepticus causes neuronal damage that is associated with cognitive impairment. Self-sustained status epilepticus (SSSE) can be induced in rats by electrical stimulation of the perforant pathway (Halonen et al. 1996, 1999, 2001; Pitkänen et al. 1996; De Vasconcelos et al. 1999; Mazarati et al. 1999, 2004). This model is used to find antiepileptic drugs for patients with therapy-resistant epilepsy. Pitkänen et al. (1996), Halonen

et al. (1996, 1999, 2001), and Mazarati et al. (2004) studied the effect of drugs on status epilepticus in rats.

PROCEDURE

Under ketamine (60 mg/kg) and xylazine (15 mg/kg) anesthesia, male Wistar rats weighing 260–280 g were implanted with a bipolar stimulation electrode into the angular bundle of the perforant path (0.5 mm anterior and 4.5 mm left to lambda) and a bipolar recording electrode into the ipsilateral dentate gyrus (3 mm posterior and 2.5 mm left to bregma). The depth of the electrode was 3.5–4 mm from the brain surface and was optimized by finding the maximal population spike evoked from the dentate gyrus by stimuli applied to the perforant path.

For induction of self-sustained status epilepticus perforant path stimulation was delivered using a Grass stimulator model 8800, for 30 min with the following parameters: 10-s, 20-Hz trains for 1 ms, 30-V pulses delivered every minute, together with continuous 2 Hz stimulation using the same parameters.

Test drugs were injected i.v. into the tail vein either 20 min before perforant path stimulation, or 10 or 40 min after the end of perforant path stimulation. Control animals were treated with saline.

Electrographic activity was acquired and analyzed off-line using Harmonie software (Stellate Systems, Montreal), configured for automatic detection and saving spikes and seizures. Analysis of EEG was performed by a "blinded" unbiased investigator. All seizure EEGs were reviewed manually.

EVALUATION

The following indices were used to quantify seizure activity: duration of self-sustained status epilepticus (= time between the end of perforant path stimulation and the end of the last electrographic seizure); cumulative seizure time (the sum of the duration of all individual seizures); number of seizure episodes; average duration of individual seizures (cumulative seizure time divided by number of seizures); number of spikes per hour. Statistical analysis was carried out with one-way ANOVA followed by Newman-Keuls post hoc test, or, if the normality test failed, ANOVA on ranks followed by Mann-Whitney post hoc test.

MODIFICATIONS OF THE METHOD

Brown et al. (1953) and Barton et al. (2001) characterized the 6 Hz psychomotor seizure model of partial epilepsy in rats.

Nissinen et al. (2000) described a model of chronic temporal lobe epilepsy induced by electrical stimulation of the lateral nucleus of the amygdala in rats.

Walton et al. (1996) induced status epilepticus in rats with actively epileptogenic cortical cobalt lesions by administration of homocysteine thiolactone.

Laurén et al. (2003) described selective changes in gamma-aminobutyric acid type A receptor subunits in the hippocampus in spontaneously seizing rats with chronic temporal lobe epilepsy.

Brandt et al. (2003) studied epileptogenesis and neuropathology after different types of status epilepticus induced by prolonged electrical stimulation of the basolateral amygdala in rats.

REFERENCES AND FURTHER READING

Barton ME, Klein BD, Wolf HH, White HS (2001) Pharmacological characterization of the 6 Hz psychomotor seizure model of partial epilepsy. Epilepsy Res 47:217–227

Brandt C, Glien M, Potschka H, Volk H, Löscher W (2003) Epileptogenesis and neuropathology after different types of status epilepticus induced by prolonged electrical stimulation of the basolateral amygdala in rats. Epilepsy Res 55:83–103

Brown WC, Schiffman DO, Swinyard EA, Goodman LS (1953) Comparative assay of antiepileptic drugs by "psychomotor" seizure test and minimal electroshock threshold test. J Pharmacol Exp Ther 107:273–283

De Vasconcelos AP, Mazarati AM, Wasterlain CG, Nehlig A (1999) Self-sustaining status epilepticus after a brief electrical stimulation of the perforant path. A 2-deoxyglucose study. Brain Res 838:110–118

Halonen T, Nissinen J, Jansen JA, Pitkänen A (1996) Tiagabine prevents seizures, neuronal damage and memory impairment in experimental status epilepticus. Eur J Pharmacol 299:69–81

Halonen T, Nissinen J, Pitkänen A (1999) Neuroprotective effect of remacemide hydrochloride in a perforant pathway stimulation model of status epilepticus in the rat. Epilepsy Res 34:251–269

Halonen T, Nissinen J, Pitkänen A (2001) Effect of lamotrigine treatment on status epilepticus-induced neuronal damage and memory impairment of rats. Epilepsy Res 46:205–223

Laurén HB, Pitkänen A, Nissinen J, Soini SL, Korpi ER, Holopainen IE (2003) Selective changes in gamma-aminobutyric acid type A receptor subunits in the hippocampus in spontaneously seizing rats with chronic temporal lobe epilepsy. Neurosci Lett 349:58–62

Mazarati A, Liu H, Wasterlain C (1999) Opioid peptide pharmacology and immunocytochemistry in an animal model of self-sustaining status epilepticus. Neuroscience 89:167–173

Mazarati AM, Baldwin R, Klitgaard H, Matagne A, Wasterlain CG (2004) Anticonvulsant effects of levetiracetam and levetiracetam-diazepam combination in experimental status epilepticus. Epilepsy Res 58:167–174

Nissinen J, Halonen T, Koivisto E, Pitkänen A (2000) A new model of chronic temporal lobe epilepsy induced by electrical stimulation of the amygdala in rat. Epilepsy Res 38:177–205

Pitkänen A, Tuumanen J, Halonen T (1996) Vigabatrin and carbamazepine have different efficacies in the prevention

of status epilepticus induced neuronal damage in the hippocampus and amygdala. Epilepsy Res 24:29–45
Walton NY, Jaing Q, Hyun B, Treiman DM (1996) Lamotrigine vs. phenytoin for treatment of status epilepticus: comparison in an experimental model. Epilepsy Res 24:19–28

E.3.2.15 Rat Model of Cortical Dysplasia

PURPOSE AND RATIONALE

Epilepsy becomes drug resistant in 20%–30% of patients. Cortical dysplasia is implicated as a major contributing factor of many types of epileptic disorders that are resistant to pharmacological intervention (Becker 1991; Aicardi 1994). Several animal models of cortical dysplasia with specific clinical pathologies have been described (Amano et al. 1996; Jacobs 1996; Jacobs et al. 1999; Lee et al. 1997; Hirotsune et al. 1998; Chevassus au Louis et al. 1999; Zhu and Roper 2000; Wenzel et al. 2001; Benardete and Kriegstein 2002; Morimoto et al. 2004; Jacobs and Prince 2005).

Baraban and Schartzkroin (1995, 1996), Baraban et al. (2000), and Smyth et al. (2002) exposed rats *in utero* to methylazoxymethanol (MAM).

PROCEDURE

Dysplastic and control rats were generated by injecting pregnant Sprague Dawley rats on day 15 of gestation with 25 mg/kg i.p. MAM or vehicle (10% DMSO in 0.3 ml 0.9% saline).

For *in vitro* studies, recordings were performed using acute hippocampal slices from adult vehicle or MAM-treated rats. Hippocampi were not dissected out, and all slices included entorhinal cortex and other overlying cortical structures. After cutting, slices remained submerged in a holding chamber containing oxygenated recording medium (nACF) consisting of (in mM): 124 NaCl, 3 KCl, 1.25 NaH_2PO_4, 2 $MgSO_4$, 26 $NaHCO_3$, 2 $CaCl_2$ and 10 dextrose. A slice was then transferred to a gas-interface recording chamber and perfused with oxygenated nACF at a flow rate of 2.5 ml/min at 33.5°C. Borosilicate glass electrodes were pulled, filled with 2 M NaCl (2–8 MΩ) and placed in the CA1 region of stratum pyramidale and/or within neuronal heterotopias under visual microscopic control. A mono-polar stimulating electrode was placed in stratum radiatum. Voltage was recorded with a Neurodata IR-283 amplifier and monitored on a PC running pClamp software. Spontaneous field activity and evoked population spikes were stored on hard disk for later blinded analysis. Interictal epileptiform burst activity was initiated with perfusion of nACF containing 4-aminopyridine (100 µM), a potassium channel blocker known to cause seizures in humans and spontaneous epileptiform activity in hippocampal slice preparations. The 4-aminopyridine *in vitro* seizure model is based on blockade of A-type potassium channels leading to the appearance of giant excitatory postsynaptic potentials generated by the prolonged firing of pyramidal neurons in CA3 burst-generating regions of hippocampus. Burst frequency was determined by counting the number of interictal epileptiform events per second during a 3-min epoch before and after 60 min of antiepileptic drug co-perfusion, and was expressed as Hz. Burst amplitude (1.5–6 mV) was determined by measuring the average peak-to-peak interval for ten consecutive representative bursts during the same epoch. Evoked synaptic responses were analyzed by averaging the number of population spikes obtained on ten consecutive sweeps recorded after stratum radiatum stimulation (0.3- to 3-mA pulses 100 µs pulse-width). A downward voltage deflection ≥ 0.5 mV superimposed on the population excitatory post-synaptic potential (EPSP) was defined as a "population spike"; the number of population spikes was compared for each slice during perfusion with normal ACSF (baseline), ACSF plus 4-aminopyridine and ACSF plus 4-aminopyridine and antiepileptic drug. For each slice experiment, the population spike was monitored every 15 min.

For *in vivo* studies, control and MAM-exposed rats were administered 15 mg/kg kainic acid, a concentration that reliably produces acute seizure activity. Behavioral activity was scored on a 6-stage scale (Germano and Sperber 1997). Animals were treated with 400 mg/kg i.p. valproate 30 min before kainate injection. Latencies to the first sign of hyperexcitability and to the first tonic-clonic seizure were recorded.

EVALUATION

Date were plotted graphically as "survival" curves, and differences in mean latencies were ranked and analyzed using a non-parametric Kruskal-Wallis one-way ANOVA.

CRITICAL ASSESSMENT OF THE TEST

Since the MAM-exposed rats exhibit a dramatically reduced sensitivity to commonly prescribed antiepileptic drugs, this model is considered to be relevant for drug-resistant epilepsy.

MODIFICATIONS OF THE METHOD

Leré et al. (2002) described a model of "epileptic tolerance" for investigating neuroprotection, epileptic susceptibility and gene expression-related plastic changes. Expression of status epilepticus was triggered

by infusion of the excitotoxic agent kainate in the right hippocampus of adult rats. An appropriate dose of kainate was used to cause brain damage to the homolateral, but not contralateral, hippocampus. At various times following the preconditioning insult, kainite was then re-administered into the lateral ventricle and neuroprotection was observed in the contralateral side between 1 and 15 days later.

REFERENCES AND FURTHER READING

Aicardi J (1994) The place of neuronal migration abnormalities in child neurology. Can J Neurol Sci 21:185–193

Amano S, Ihara N, Umeura S (1996) Development of novel rat mutant with spontaneous limbic-like seizures. Am J Pathol 149:329–336

Baraban SC, Schwartzkroin PA (1995) Electrophysiology of CA1 pyramidal neurons in an animal model of neuronal migration disorders: prenatal methylazoxymethanol treatment. Epilepsy Res 22:145–156

Baraban SC, Schwartzkroin PA (1996) Flurothyl seizure susceptibility in rats following prenatal methylazoxymethanol treatment. Epilepsy Res 23:189–194

Baraban SC, Wenzel HJ, Hochman DW, Schwartzkroin PA (2000) Characterization of heterotopic cell clusters in the hippocampus of rats exposed to methylazoxymethanol in utero. Epilepsy Res 39:87–102

Becker LE (1991) Synaptic dysgenesis. Can J Neurol Sci 18:170–180

Benardete EA, Kriegstein AR (2002) Increased excitability and decreased sensitivity to GABA in an animal model of dysplastic cortex. Epilepsia 43:970–982

Chevassus au Louis N, Baraban SC, Gaiarsa JL, Ben-Ari Y (1999) Cortical malformations and epilepsy: new insight from animal models. Epilepsia 40:811–821

Germano IM, Sperber EF (1997) Increased seizure susceptibility in adult rats with neuronal migration disorders. Brain Res 777:219–222

Hirotsune S, Fleck MW, Gambello MJ, Bix GJ, Chen A, Clark GD, Ledbetter DH, McBain CJ, Wynshaw-Boris A (1998) Graded reduction of Pafah1b1 (Lis1) activity results in neuronal migration defects and early embryonic lethality. Nature Genet 19:333–339

Jacobs KM (1996) Hyperexcitability in a model of cortical maldevelopment. Cereb Cortex 6:514–523

Jacobs KM, Prince DA (2005) Excitatory and inhibitory polysynaptic currents in a rat model of epileptogenic microgyria. J Neurophysiol 93:687–696

Jacobs KM, Hwang BJ, Pronce DA (1999) Focal epileptogensis in a rat model of polymicrogyria. J Neurophysiol 81:159–173

Lee KS, Schottler F, Collins JL, Lanzino G, Couture D, Rao A, Hiramatsu KI, Goto Y, Hong SC, Caner H, Yamamoto H, Chen ZF, Bertram E, Berr S, Omary R, Scrable H, Jackson T, Goble J, Eisenman L (1997) A genetic animal model of human neocortical heterotypia associated with seizures. J Neurosci 17:6236–6242

Leré C, el Bahh B, La Salle GLG, Rougier A (2002) A model of "epileptic tolerance" for investigating neuroprotection, epileptic susceptibility and gene expression-related plastic changes. Brain Res Prot 9:49–56

Morimoto K, Watanabe T, Ninomiya T, Hirao T, Tanaka A, Onishi T, Tamagami H (2004) Quantitative evaluation of central-type benzodiazepine receptors with [^{125}I]Iomazenil in an experimental epileptogenesis: II. The rat cortical dysplasia model. Epilepsy Res 61:113–118

Smyth MD, Barbaro NM, Baraban SC (2002) Effects of antiepileptic drugs on induced epileptiform activity in a rat model of dysplasia. Epilepsy Res 50:251–264

Wenzel HJ, Robbins CA, Tsai LH, Schwartzkroin PA (2001) Abnormal morphological and functional organization of the hippocampus in a p35 mutant model of cortical dysplasia associated with spontaneous seizures. J Neurosci 21:983–998

Zhu WJ, Roper SN (2000) Reduced inhibition in an animal model of cortical dysplasia. J Neurosci 20:8925–8931

E.3.2.16 Genetic Animal Models of Epilepsy

PURPOSE AND RATIONALE

Several animal species exhibit epilepsy with spontaneous recurrent seizures such as dogs, rats, and mice (Löscher 1984). Serikawa and Yamada (1986) described spontaneous epileptic rats which are double mutants and exhibit both tonic and absence-like seizures.

PROCEDURE

Spontaneous epileptic rats are obtained by mating the tremor heterozygous rat (*tm/+*) with the zitter homozygous rat (*zi/zi*) found in a Sprague-Dawley colony. The behavior of the spontaneous epileptic rats is recorded weekly for 2 h on videotapes. The frequency of tonic convulsions and wild jumping occurring in the absence of external stimuli are recorded. Under anesthesia silver ball-tipped and monopolar stainless-steel electrodes are chronically implanted in the left frontal cortex and hippocampus. An indifferent electrode is placed on the frontal cranium. The frequency of absence-like seizures and tonic convulsions, as well as the duration of each seizure, are measured on the EEG. A mild tactile stimulus is given on the back of the animal every 2.5 min to induce consistent tonic convulsions. Compounds are given i.p. or orally.

EVALUATION

The number of seizures and the duration of each seizure are obtained and the total duration of the seizures (number × duration) is calculated every 5 min before and after injection of the drug. Percent changes between values before and after drug administration are calculated.

CRITICAL ASSESSMENT OF THE TEST

Studies in spontaneous epileptic rats and other genetic models are of value for an in depth investigation of a potential anti-epileptic drug.

MODIFICATIONS OF THE METHOD

The **tremor rat (*tm/tm*)** was described as a model of petit mal epilepsy (Serikawa and Yamada 1986;

Serikawa et al. 1987). Seki et al. (2002) attempted to determine whether gene transfer of aspartoacyclase inhibited absence-like seizures in tremor rats using recombinant adenovirus. Noda et al. (1998) and Iida et al. 1998) described the **NER rat strain** (Noda epileptic rat) as a genetic model in epilepsy research, which was developed by inbreeding rats with spontaneous tonic-clonic seizures in a stock of Crj:Wistar.

The **genetic epileptic WAG/RiJ rat** has been recommended as a useful model for general absence epilepsy in humans (Van Luijtelaar and Coenen 1986; Coenen et al. 1992; Budziszewska et al. 1999; Van Luijtelaar et al. 2003; Sarkisova et al. 2003; Bouwman and van Rijn 2004). Danober et al. (1995, 1998), Deransart et al. (2000), Lakaye et al. (2002), and Nehling and Boehrer (2003) studied the **GAERS rat**, the genetic absence epilepsy rat from Strasbourg, which shows generalized non-convulsive absence seizures characterized by the occurrence of synchronous and bilateral spike and wave discharges.

Amano et al. (1996) developed an **epileptic rat mutant with spontaneous limbic-like seizures** by successive mating and selection from an inherited cataract rat.

Racine et al. (1999) reported selective breeding of **kindling-prone** and kindling-resistant **rats**. The selection of these strains was based on their rates of amygdala kindling. From a parent population of Long Evans hooded and Wistar rats, the males and females that showed the fastest and slowest amygdala kindling rates were selected and bred.

Sarkisian et al. (1999) described seizures in the **Flathead (FH) rat** as a genetic model in early postnatal development.

Tsubota et al. (2003) identified the **Wakayama epileptic rat (WER)** in a colony of Wistar rats, a mutant exhibiting both tonic-clonic seizures and absence-like seizures

Several other genetic animal models have been described (Löscher and Frey 1984; Löscher and Meldrum 1984) showing epilepsy with spontaneous recurrent seizures, such as:

dogs (Cunningham 1971; Edmonds et al. 1979),

rats with petit mal epilepsy (Vergnes et al. 1982), rats with two mutations, zitter and tremor (Serikawa and Yamada 1986; Xie et al. 1990), rats with absence-like states and spontaneous tonic convulsions (Sasa et al. 1988),

tottering mice (Green and Sidman 1962; Noebels 1979; Noebels and Sidman 1979; Fletcher et al. 1966; Tehrani et al. 1997),

leaner mutant mice with severe ataxia and atrophic cerebellum (Herrup and Wilczynnski 1982; Heckroth and Abbott 1994),

the quaking mouse (Sidman et al. 1966; Chermat et al. 1981) having deficiencies in myelinization in the nervous system (Hogan 1977; Li et al. 1993; Bartoszewicz et al. 1995) and alterations in the dopaminergic (Nikulina et al. 1995) and α_2-adrenergic (Mitrovic et al. 1992) brain system,

the stargazer mutant mouse which shows generalized non-convulsive spike wave seizures with behavioral arrest that resembles the clinical phenotype of general absence epilepsy (Noebels et al. 1990; Di Pasquale et al. 1997) with a disrupted Cacng2 gene (Letts et al. 2005),

the lethargic (lh/lh) mouse as a model of absence seizures (Hosford et al. 1999).

There are models of **epilepsy with reflex seizures**, such as:

baboons with photomyoclonic seizures (Killam et al. 1966, 1967; Stark et al. 1970; Naquet and Meldrum 1972; Killam and Killam 1984; Smith et al. 1991; Chapman et al. 1995),

photosensitive fowls (Crawford 1969, 1970),

the Fayoumi strain of chickens (Fepi) (Batini et al. 2004),

audiogenic seizure susceptible mice (Collins 1972; Seyfried 1979; Chapman et al. 1984; Stenger et al. 1991),

mechanically stimulated mice (Imaizumi et al. 1959; Oguro et al. 1991),

the EL mouse which is a strain highly susceptible to convulsive seizures after repeated sensory stimulation (Seyfried et al. 1986; King and LaMotte 1989; Green and Seyfried 1991; Wang et al. 1997; Suzuki 2004),

audiogenic seizure susceptible rats (Wistar Audiogenic Rats WAR) (Consroe et al. 1979; Reigel et al. 1986; Smith et al. 1991; Patel et al. 1990; Scarlatelli-Lima et al. 2003; Galvis-Alonzo et al. 2004; Magalhães et al. 2004).

The genetically epilepsy-prone rat GEPR responding to acoustic stimulation has been described by Ko et al. (1982), Dailey and Jobe (1985), Dailey et al. (1989), Faingold et al. (1988), Faingold et al. (1992, 1994), Jobe et al. (1992, 1995) and Laird (1989). The inferior colliculus is strongly implicated as a critical initiation

site within the neuronal network for audiogenic seizures. Two strains were characterized: **GEPR-3** exhibiting moderate or clonic convulsions, and **GEPR-9** exhibiting more severe tonic extensor convulsions (Dailey et al. 1996; Kurtz et al. 2001; Moraes et al. 2005).

Gerbils with reflex seizures were described by Thiessen et al. (1968); Loskota et al. (1974); Majkowski and Kaplan (1983); Lee and Lomax (1984), Bartoszyk and Hamer (1987), and Lee et al. (1987).

Löscher et al. (1989) discussed **the sz mutant hamster** as a genetic model of epilepsy or of paroxysmal dystonia.

Quesney (1984) reported **generalized photosensitive epilepsy in cats** after long-term intramuscular administration of low-dose penicillin.

Famula et al. (1997) and Oberbauer et al. (2003) described the epidemiology of epilepsy in **tervurens** (**Belgian shepherd dogs**); Srenk et al. (1994) in **Golden Retrievers.**

Seizure susceptibility was described in ***Drosophila*** (Kuebler and Tanouye 2000; Kuebler et al. 2001; Zhang et al. 2002).

REFERENCES AND FURTHER READING

Amano S, Ihara N, Uemura S, Yokoyama M, Ikeda M, Serikawa T, Sasahara M, Kataoka H, Hayase Y, Hazama F (1996) Development of a novel rat mutant with spontaneous limbic-like seizures. Am J Pathol 149:329–336

Bartoszewicz ZP, Noronha AB, Fujita N, Sato S, Bo L, Trapp BD, Quarles RK (1995) Abnormal expression and glycosylation of the large and small isoforms of myelin-associated glycoprotein in dymyelinating quaking mutants. J Neurosci Res 41:27–38

Bartoszyk GD, Hamer M (1987) The genetic animal model of reflex epilepsy in the Mongolian gerbil: differential efficacy of new anticonvulsive drugs and prototype antiepileptics. Pharmacol Res Commun 19:429–440

Batini C, Teillet MA, Naquet R (2004) An avian model of genetic reflex epilepsy. Arch Ital Biol 142:297–312

Bouwman BM, van Rijn CM (2004) Effects of levetiracetam on spike and wave discharges in WAG/Rij rats. Seizure 13:591–594

Budziszewska B, Van Luijtelaar G, Coenen AML, Leźniewicz M, Lasoń W (1999) Effects of neurosteroids on spike-wave discharges in the genetic epileptic WAG/RiJ rat. Epilepsy Res 33:23–29

Chapman AG, Croucher MJ, Meldrum BS (1984) Evaluation of anticonvulsant drugs in DBA/2 mice with sound-induced seizures. Arzneim Forsch / Drug Res 34:1261–1264

Chapman AG, Dürmüller N, Harrison BL, Baron BM, Parvez N, Meldrum BS (1995) Anticonvulsant activity of a novel NMDA/glycine site antagonist, MDL 104,653, against kindled and sound-induced seizures. Eur J Pharmacol 274:83–88

Chermat R, Doaré L, Lachapelle F, Simon P (1981) Effects of drugs affecting the noradrenergic system on convulsions in the quaking mouse. Naunyn-Schmiedeberg's Arch Pharmacol 318:94–99

Coenen AML, Drinkenburg WHIM, Inoue M, Van Luijtelaar ELJM (1992) Genetic models of absence epilepsy, with emphasis on the WAG/RiJ strain of rats. Epilepsy Res 12:75–86

Collins RL (1972) Audiogenic seizures. In: Purpura DP, Penry JK, Tower DB, Woodbury DM, Walter RD (eds) Experimental Models of Epilepsy – A Manual for the Laboratory Worker. Raven Press, New York, pp 347–372

Consroe P, Picchioni A, Chin L (1979) Audiogenic seizure susceptible rats. Fed Proc 38:2411–2416

Crawford RD (1969) A new mutant causing epileptic seizures in domestic fowl. Poultry Sci 48:1799

Crawford RD (1970) Epileptic seizures in domestic fowl. J Hered 61:185–188

Cunningham JG (1971) Canine seizure disorders. J Am Vet Med Ass 158:589–598

Dailey JW, Jobe PC (1985) Anticonvulsant drugs and the genetically epilepsy-prone rat. Fed Proc 44:2640–2644

Dailey JW, Yan QS, Adams-Curtis LE, Ryu JR, Ko KH, Mishra PK, Jobe PC (1996) Neurochemical correlation of antiepikeptic drugs in the genetically epilepsy-prone rat. Life Sci 58:259–266

Danober L, Depaulis A, Vergnes M, Marescaux C (1995) Mesopontine cholinergic control over generalized non-convulsive seizures in a genetic model of absence epilepsy in the rat. Neuroscience 69:1183–1193

Danober L, Deransart C, Depaulis A, Vergnes M, Marescaux C (1998) Pathophysiological mechanisms of genetic absence epilepsy in the rat. Progr Neurobiol 55:27–57

Deransart C, Riban V, Lê BT, Marescaux C, Depaulis A (2000) Dopamine in the striatum modulates seizures in a genetic model of absence epilepsy in the rat. Neuroscience 100:335–344

Dailey JW, Reigel CE, Mishra PK, Jobe PC (1989) Neurobiology of seizure predisposition in the genetically epilepsy-prone rat. Epilepsy Res 3:3–17

Di Pasquale E, Keegan KD, Noebels JL (1997) Increase excitability and inward rectification in layer V cortical pyramidal neurons in the epileptic mouse *stargazer*. J Neurophysiol 77:621–631

Edmonds HL, Hegreberg GA, van Gelder NM, Sylvester DM, Clemmons RM, Chatburn CG (1979) Fed Proc 38:2424–2428

Faingold CL (1988) The genetically epilepsy-prone rat. Gen Pharmacol 19:331–338

Faingold CL, Naritoku DK (1992) The genetically epilepsy-prone rat: Neuronal networks and actions of amino acid neurotransmitters. In: Faingold CL, Fromm GH (eds) Drugs for Control of Epilepsy: Actions on Neuronal Networks Involved in Seizure Disorders. CRC Press, Boca Raton, Fl, pp 277–308

Faingold CL, Randall ME, Boersma Anderson CA (1994) Blockade of GABA uptake with tiagabine inhibits audiogenic seizures and reduces neuronal firing in the inferior colliculus of the genetically epilepsy-prone rat. Exp Neurol 126:225–232

Famula TR, Oberbauer AM, Brown KN (1997) Heritability of epileptic seizures in the Belgian tervueren. J Small Anim Pract 38:349–352

Fletcher CF, Lutz CM, O'Sullivan TM, Shaughnessy JD Jr, Hawkes R, Frankel WN, Copeland NG, Jenkins NA (1996) Absence epilepsy in tottering mutant mice is associated with calcium channel deficits. Cell 87:607–617

Green MC, Sidman RL (1962) Tottering – A neuromuscular mutation in the mouse. J Hered 53:233–237

Galvis-Alonzo OY, Cortes de Oliveira JA, Garcia-Cairasco N (2004) Limbic epileptogenicity, cell loss and axonal reorganization induced by audiogenic and amygdala kindling in Wistar audiogenic rats (WAR strain). Neuroscience 125:787–802

Green RC, Seyfried TN (1991) Kindling susceptibility and genetic seizure predisposition in inbred mice. Epilepsia 32:22–26

Heckroth JA, Abbott LC (1994) Purkinje cell loss from alternating sagittal zones in the cerebellum of leaner mutant mice. Brain Res 658:93–104

Herrup K, Wilczynsnki SL (1982) Cerebellar cell degeneration in the leaner mutant mouse. Neurosci 7:2185–2196

Hogan EL (1977) Animals models of genetic disorders of myelin. In: Morell P (ed) Myelin. Plenum Press, New York, pp 489–520

Hosford DA, Lin FH, Wang Y, Caddick SJ, Rees M, Parkinson NJ, Barclay J, Cox RD, Gardiner RM, Hosford DA, Denton P, Wang Y, Seldin MF, Chan B (1999) Studies of the lethargic (*lh/lh*) mouse model of absence seizures: regulatory mechanisms and identification of the gene. Adv Neurol 79:239–252

Iida K, Sasa M, Serikawa T, Noda A, Ishihara K, Akimitsu T, Hanaya R, Arita K, Kurisu K (1998) Induction of convulsive seizures by acoustic priming in a new genetically defined model of epilepsy (Noda epileptic rat: NER) Epilepsy Res 30:115–126

Imaizumi K, Ito S, Kutukake G, Takizawa T, Fujiwara K, Tutikawa K (1959) Epilepsy like anomaly of mice. Exp Anim (Tokyo) 8:6–10

Jobe PC, Mishira PK, Dailey JW (1992) Genetically epilepsy-prone rats: Actions of antiepileptic drugs and monoaminergic neurotransmitters. In: Faingold CL, Fromm GH (eds) Drugs for Control of Epilepsy: Actions on Neuronal Networks Involved in Seizure Disorders. CRC Press, Boca Raton, Fl, pp 253–275

Jobe PC, Mishra PK, Adams-Curtis LE, Deoskar VU, Ko KH, Browning RA, Dailey JW (1995) The genetically epiöepsy-prone rat (GEPR). Ital J Neurol Sci 16:91–99

Johnson DD, Davis HL, Crawford RD (1979) Pharmacological and biochemical studies in epileptic fowl. Fed Proc 38:2417–2423

Killam KF, Naquet R, Bert J (1966) Paroxysmal responses to intermittent light stimulation in a population of baboons (*Papio papio*). Epilepsia 7:215–219

Killam KF, Killam EK, Naquet R (1967) An animal model of light sensitivity epilepsy. Electroencephalogr Clin Neurophysiol 22:497–513

Killam EK, Killam KF Jr (1984) Evidence for neurotransmitter abnormalities related to seizure activity in the epileptic baboon. Fed Proc 43:2510–2515

King JT Jr, LaMotte CC (1989) El mouse as a model of focal epilepsy. Epilepsia 30:257–265

Ko KH, Dailey JW, Jobe PC (1982) Effect of increments of norepinephrine concentrations on seizure intensity in the genetically epilepsy-prone rat. J Pharmacol Exp Ther 222:662–669

Kuebler D, Tanouye MA (2000) Modification of seizure susceptibility in Drosophila. J Neurophysiol 83:998–1009

Kuebler D, Zhang H, Ren X, Tanouye MA (2001) Genetic suppression of seizure susceptibility in Drosophila. J Neurophysiol 86:1211–1225

Kurtz BS, Lehman J, Galick P, Amberg J, Mishra PK, Daikey JW, Weber R, Jobe PC (2001) Penetrance and expressivity of genes involved in the development of epilepsy in the genetically epilepsy-prone rat (GEPR). J Neurogenet 15:233–244

Laird HE 2nd (1989) The genetically epilepsy-prone rat. A valuable model for the study of epilepsies. Mol Chem Neuropathol 11:45–59

Lakaye B, Thomas E, Minet A, Grisar T (2002) The genetic absence epilepsy rat from Strasbourg (GAERS), a rat model of epilepsy: computer modeling and differential gen expression. Epilepsia 43, Suppl 5:123–129

Lee RJ, Lomax P (1984) The effect of spontaneous seizures on pentylenetrazole and maximum electroshock induced seizures in the Mongolian gerbil. Eur J Pharmacol 106:91–98

Lee RJ, Hong JS, McGinty JF, Lomax P (1987) Increased enkephalin and dynorphin immunoreactivity in the hippocampus of seizure sensitive Mongolian gerbils. Brain Res 401:353–358

Letts VA, Mahaffey CL, Beyer B, Frankel WN (2005) A targeted mutation in Cacng4 exacerbates spike-wave seizures in stargazer (Cacng2) mice. Proc Natl Acad Sci USA 102:2123–2128

Li W-X, Kuchler S, Zaepfel M, Badache A, Thomas D, Vincedon G, Baumann N, Zanetta JP (1993) Cerebellar soluble lectin and its glycoprotein ligands in the developing brain of control and dysmyelinating mutant mice. Neurochem Int 22:125–133

Löscher W (1984) Genetic animal models of epilepsy as a unique resource for the evaluation of anticonvulsant drugs. A review. Meth Find Exp Clin Pharmacol 6:531–547

Löscher W, Frey HH (1984) Evaluation of anticonvulsant drugs in gerbils with reflex epilepsy. Arzneim Forsch/Drug Res 34:1484–1488

Löscher W, Meldrum BS (1984) Evaluation of anticonvulsant drugs in genetic animal models of epilepsy. Fed Proc 43:276–284

Löscher W, Fisher JE Jr, Schmidt D, Fredow G, Honack D, Iturrian WB (1989) The sz mutant hamster: a genetic model of epilepsy or of paroxysmal dystonia? Mov Disord 4:219–232

Loskota WJ, Lomax P, Rich ST (1974) The gerbil as a model for the study of epilepsies. Epilepsia 15:109–119

Magalhães LHM, Garcia-Cairasco N, Massensini AR, Doretto MC, Moraes MFD (2004) Evidence for augmented brainstem activated forebrain seizures in Wistar Audiogenic rats subjected to transauricular electroshock. Neuroscience Lett 369:19–23

Majkowski J, Kaplan H (1983) Value of Mongolian gerbils in antiepileptic drug evaluation. Epilepsia 24:609–615

Mitrovic N, Le Saux R, Gioanni H, Gioanni Y, Besson MJ, Maurin Y (1992) Distribution of [^{3}H]clonidine binding sites in the brain of the convulsive mutant quaking mouse: A radioautographic analysis. Brain Res 578:26–32

Moraes MFD, Chavali M, Mishra PK, Jobe PC, Garcia-Cairasco N (2005) A comprehensive electrographic and behavioral analysis of generalized tonic-clonic seizures of GEPR-9s. Brain Res 1033:1–12

Naquet R, Meldrum BS (1972) Photogenic seizures in baboon. In: Purpura DP, Penry JK, Tower DB, Woodbury DM, Walter RD (eds) Experimental Models of Epilepsy – A Manual for the Laboratory Worker. Raven Press, New York, pp 373–406

Nehling A, Boehrer A (2003) Effects of remacemide in two models of genetically determined epilepsy, the GAERS and the audiogenic Wistar AS. Epilepsy Res 52:253–261

Nikulina EM, Skrinskaya JA, Avgustinovich DF, Popova NK (1995) Dopaminergic brain system in the quaking mutant mouse. Pharmacol Biochem Behav 50:333–337

Noda A, Hashizume R, Maihara T, Tomizawa Y, Ito Y, Inoue M, Kobayashi K, Asano Y, Sasa M, Serikawa T (1998) NER rat strain: a new type of genetic model in epilepsy research. Epilepsia 39:99–107

Noebels JL (1979) Analysis of inherited epilepsy using single locus mutations in mice. Fed Proc 38:2405–2410

Noebels JL, Sidman RL (1979)Inherited epilepsy: Spike-wave and focal motor seizures in the mutant mouse tottering. Science 204:1334–1336

Noeberls JL, Qiao X, Bronson RT, Spencer C, Davisson MT (1990) Stargazer, a new neurological muatant in chromosome 15 in the mouse with prolonged cortical seizures. Epilepsy Res 7:129–135

Oberbauer AM, Grossmann DI, Irion DN, Schaffer AL, Eggleston ML, Famula TR (2003) The genetics of epilepsy in the Belgian tervuren and sheepdog. J Herd 94:57–63

Oguro K, Ito M, Tsuda H, Mutoh K, Shiraishi H, Shirasaka Y, Mikawa H (1991) Association of NMDA receptor sites and seizures E1 mice. Epilepsy Res 9:225–230

Patel S, Chapman AG, Graham JL, Meldrum BS, Frey P (1990) Anticonvulsant activity of NMDA antagonists, D(–)4-(3-phosphonopropyl)piperazine-2-carboxylic acid (D-CPP) and D(–)(E)-4-(3-phosphonoprop-2-enyl)piperazine-2-carboxylic acid (D-CPPene) in a rodent and a primate model of reflex epilepsy. Epilepsy Res 7:3–10

Quesney LF (1984) Pathophysiology of generalized photosensitive epilepsy in the cat. Epilepsia 25:61–69

Racine RJ, Steingart M, McIntyre DC (1999) Development of kindling-prone and kindling resistant rats: selective breeding and electrophysiological studies. Epilepsy Res 35:183–195

Reigel CE, Dailey JW, Jobe PC (1986) The genetically epilepsy-prone rat: an overview of seizure-prone characteristics and responsiveness to anticonvulsant drugs. Life Sci 39:763–774

Sasa M, Ohno Y, Ujihara H, Fujita Y, Yoshimura M, Takaori S, Serikawa T, Yamada J (1988) Effects of antiepileptic drugs on absence-like and tonic seizures in the spontaneously epileptic rat, a double mutant rat. Epilepsia 29:505–513

Sarkisian MR, Rattan S, D'Mello SR, LoTurco LL (1999) Characterization of seizures in the flathead rat: a new genetic model in early postnatal development. Epilepsia 40:394–400

Sarkisova KY, Midzianovskaia IS, Kulikov MA (2003) Depressive-like behavioral alterations and c-fos expression in the dopaminergic brain regions in WAG/Rij rats with genetic absence epilepsy. Behav Brain Res 144:211–226

Scarlatelli-Lima AV, Magalhães LHM, Doretto MC, Moraes MFD (2003) Assessment of the seizure susceptibility of Wistar Audiogenic rat to electroshock, pentylenetetrazole and pilocarpine. Brain Res 960:184–189

Seki T, Matsubayashi H, Amano T, Kitada K, Serikawa T, Sakai N, Sasa M (2002) Adenoviral gene transfer of aspartoacyclase into the tremor rat, a genetic model of epilepsy, as a trial of gen therapy for inherited epileptic disorder. Neuroscience Lett 328:249–252

Serikawa T, Yamada J (1986) Epileptic seizures in rats homozygous for two mutations, zitter and tremor. J Hered 77:441–444

Serikawa T, Ohno Y, Sasa M, Yamada J, Takori S (1987) A new model of petit mal epilepsy: spontaneous spike and wave discharges in tremor rats. Lab Anim 21:68–71

Serikawa T, Kogishi K, Yamada J, Ohno Y, Ujihara H, Fujita Y, Sasa M, Takaori S (1990) Long-term effects of continual intake of phenobarbital on the spontaneously epileptic rat. Epilepsia 31:9–14

Seyfried TN (1979) Audiogenic seizures in mice. Fed Proc 38:2399–2404

Seyfried TN, Glaser GH, Yu RK, Palayoor ST (1986) Inherited convulsive disorders in mice. Adv Neurol 44:115–133

Sidman M, Ray BA, Sidman RL, Klinger JM (1966) Hearing and vision in neurological mutant mice: a method for their evaluation. Exp Neurol 16:377–402

Smith SE, Dürmüller N, Meldrum BS (1991) The non-N-methyl-D-aspartate receptor antagonists, GYKI 52466 and NBQX are anticonvulsant in two animal models of reflex epilepsy. Eur J Pharmacol 201:179–183

Srenk P, Jaggy A, Gaillard C, Busato A, Horlin P (1994) Genetische Grundlagen der idiopathischen Epilepsie beim Golden Retriever. Tierärztl Praxis 22 :574–578

Stark LG, Killam KF, Killam EK (1970) The anticonvulsant effects of phenobarbital, diphenylhydantoin and two benzodiazepines in the baboon, Papio papio. J Pharmacol Exp Ther 173:125–132

Stenger A, Boudou JL, Briley M (1991) Anticonvulsant effect of some anxiolytic drugs on two models of sound-induced seizures in mice. In: Briley M, File SE (eds) New Concepts in Anxiety. McMillan Press Ltd., London, pp 326–331

Suzuki J (2004) Investigations of epilepsy with a mutant animal (EL mouse) model. Epilepsia 45 [Suppl 8]:2–5

Tacke U, Björk E, Tuomisto J (1984) The effect of changes in sound pressure level and frequency on the seizure response of audiogenic seizure susceptible rats. J Pharmacol Meth 11:279–290

Tehrani MH, Baumgartner BJ, Liu SC, Barnes EM Jr (1997) Aberrant expression of $GABA_A$ receptor subunits in the tottering mouse: an animal model for absence seizures. Epilepsy Res 28:213–223

Thiessen DD, Lindzey G, Friend HC (1968) Spontaneous seizures in the Mongolian gerbil (Meriones unguiculatus) Psycho Sci 11:227–228

Tsubota Y, Miyashita E, Miyajima M, Owada-Makabe K, Yukawa K, Maeda M (2003) The Wakayama epileptic rat (WER), a new mutant exhibiting tonic-clonic seizures and absence-like seizures. Exp Anim 52:53–62

Ujihara H, Renming X, Sasa M, Ishihara K, Fujita Y, Yoshimura M, Kishimoto T, Serikawa T, Yamada J, Takaori S (1991) Inhibition by thyrotropin-releasing hormone of epileptic seizures in spontaneously epileptic rats. Eur J Pharmacol 196:15–19

Van Luijtelaar ELJM, Coenen AML (1986) Two types of electrocortical paroxysms in an inbred strain of rats. Neurosci Lett 70.393–397

Van Luijtelaar ELJM, Budziszewska B, Tetich M, Lasoń W (2003) Finasteride inhibits the progesterone-induced spike–wave discharges in a genetic model of absence epilepsy. Pharmacol Biochem Behav 75:889–894

Vergnes M, Marescaux C, Micheletti G, Reis J, Depaulis A, Rumbach L, Warter SM (1982) Spontaneous paroxysmal electroclincal patterns in the rat: A model of generalized non-convulsive epilepsy. Neurosci Lett 33:97–101

Wang H, Burdette LJ, Frankel WN, Masukawa LM (1997) Paroxysmal discharges in the EL mouse, a genetic model of epilepsy. Brain Res 760:266–271

Xie R, Fujita Y, Sasa M, Ishihara K, Ujihara H, Takaori S, Serikawa T, Jamada J (1990) Antiepileptic effect of CNK-602A, a TRH analogue, in the spontaneously epileptic rat (SER), a double mutant. Jap J Pharmacol 52 (Suppl 1):290P

Zhang HG, Tan J, Reynolds E, Kuebler D, Faulhaber S, Tanouye M (2002) The Drosophila *slamdance* gene: a mutation in an aminopeptidase can cause seizures, paralysis and neuronal failure. Genetics 162:1283–1299

E.3.2.17 Transgenic Animals as Models of Epilepsy

PURPOSE AND RATIONALE

The availability of transgenic animals has stimulated research on pathogenesis of epilepsy. Several surveys on this topic are available (Allen and Walsh 1999; Meldrum et al. 1999; Noebels 1999; Prasad et al. 1999; Toth and Tecott 1999; Schauwecker 2002; Weinshenker and Szot 2002; Upton and Stratton 2003; Giorgi et al. 2004; Yang and Frankel 2004). Several studies contribute to the understanding of pathology of epilepsy (Butler et al. 1995; Zeng et al. 1997; Campbell et al. 2000; Liang et al. 2000; Musumeci et al. 2000; Viswanath et al. 2000; Kearney et al. 2001; Knuesel et al. 2002; Potschka et al. 2002; Shimizu et al. 2002; Ludwig et al. 2003; Ferri et al. 2004; Diano et al. 2005; Peters et al. 2005).

Lüthi et al. (1997) found that mutant mice overexpressing protease nexin-1 (PN-1) in brain under the control of the Thy-1 promoter (Thy 1/PN-1) or lacking PN-1 (PN-1 –/–) develop epileptic activity *in vivo*. An endogenous serine protease inhibitor modulated epileptic activity and hippocampal long-term potentiation.

Kunieda et al. (2002) recommended mice with systemic overexpression of the alpha 1B-adrenergic receptor as an animal model of epilepsy.

Some of the studies gave hints for further development of antiepileptic drugs, such as the neuropeptide galanin (Kokaia et al. 2001; Mazarati et al. 2004) or the neuropeptide-Y (Shannon and Yang 2004). Several studies were devoted on the role of brain-derived neurotrophic factor (BDNF) (Lahteinen et al. 2002, 2003, 2004).

REFERENCES AND FURTHER READING

Allen KM, Walsh CA (1999) Genes that regulate neuronal migration in the cerebral cortex. Epilepsy Res 36:143–154

Butler LS, Silva AJ, Abeliovich A, Watanabe Y, Tonegawa S, McNamara JO (1995) Limbic epilepsy in transgenic mice carrying a Ca^{2+}/calmodulin-dependent kinase II α-subunit mutation. Proc Natl Acad Sci USA 92:6852–6855

Campbell KM, Veldman MB, McGrath M,J, Burton FJ (2000) TS+OCD-like neuropotentiated mice are supersensitive to seizure induction. Neuroreport 11:2335–2338

Diano S, Matthews RT, Patrylo P, Yang L, Beal MF, Barnstable CJ, Horvath TL (2005) Uncoupling protein 2 prevents neuronal death including that occurring during seizures: a mechanism for preconditioning. Endocrinology 144:5014–5021

Ferri AL, Cavallaro M, Braida D, Di-Christofano A, Canta A, Vezzani A, Ottolenghi S, Pandolfi PP, Sala M, DeBiasi S, Nicolis SK (2004) Sox2 deficiency causes neurodegeneration and impaired neurogenesis in the adult mouse brain. Development 131:3805–3819

Giorgi FS, Pizzanelli C, Biagioni F, Murri L, Fornai F (2004) The role of epinephrine ion epilepsy: from the bench to the bedside. Neurosci Behav Rev 28:507–524

Kearney JA, Plummer NW, Smith MR, Kapur J, Cummins TR, Waxman SG, Goldin AR, Meisler MH (2001) A gain-of-function mutation in the sodium channel gene Scn2a results in seizures and behavioral abnormalities. Neuroscience 102:307–317

Knuesel I, Riban V, Zuellig RA, Schaub MC, Grady RM, Sanes JR, Fritschy JM (2002) Increase vulnerability to kainate-induced seizures in utrophin-knockout mice. Eur J Neurosci 15:1474–1484

Kokaia M, Holmberg K, Nanobashvili A, Xu ZQD, Kokaia Z, Lendahl U, Hilke S, Theodorsson E, Kahl U, Bartfai T, Lindvall O, Hökfelt T (2001) Suppressed kindling epileptogenesis in mice with ectopic overexpression of galanin. Proc Natl Acad Sci USA 98:14006–14011

Kunieda T, Zuscik MJ, Boongird A, Perez DM, Luders HO, Najim IM (2002) Systemic overexpression of the alpha 1B-adrenergic receptor in mice: an animal model of epilepsy. Epilepsia 43:1324–1329

Lahteinen S, Pitkanen A, Saarelainen T, Nissinen J, Koponen E, Castren E (2002) Decreased BDNF signaling in transgenic mice reduces epileptogenesis. Eur J Neurosci 15:721–734

Lahteinen S, Pitkanen A, Koponen E, Saarelainen T, Castren E (2003) Exacerbated status epilepticus and acute cell loss, but no changes in epileptogenesis, in mice with increased brain-derived neurotrophic factor signaling. Neuroscience 122:1081–1092

Lahteinen S, Pitkanen A, Knuuttila J, Toronen P, Castren E (2004) Brain-derived beurotrophic factor signaling modifies hippocampal gene expression during epileptogenesis in transgenic mice. Eur J Neurosci 19:3245–3254

Liang LP, Ho YS, Patel M (2000) Mitochondrial superoxide production in kainate-induced hippocampal damage. Neuroscience 101:563–570

Ludwig A, Budde T, Stieber J, Moosmang S, Langebartels A, Wotjak C, Munsch T, Zong X, Feil S, Feil R, Lancel M, Chien KR, Konnerth A, Pape HC, Biel M, Hofmann F (2003) Absence epilepsy and sinus dysrhythmia in mice lacking the pacemaker channel HCN2. EMBO J 22:216–224

Lüthi A, van der Putten H, Botteri FM, Mansuy IM, Meins M, Frey U, Sansig G, Portet C, Schmutz M, Schröder M, Nitsch C, Laurent JP, Monard D (1997) Endogenous serine protease inhibitor modulates epileptic activity and hippocampal long-term potentiation. J Neurosci 17:34688–4699

Mazarati A, Lu X, Shinmei S, Badie-Mahdavi H, Bartfai T (2004) Patterns of seizures, hippocampal injury and neurogenesis in three models of status epilepticus in galanin receptor type 1 (GALR1) knockout mice. Neuroscience 128:431–441

Meldrum BS, Akbar MT, Chapman AG (1999) Glutamate receptors and transporters in genetic and acquired models of epilepsy. Epilepsy Res 36:189–204

Musumeci SA, Bosco B, Calabrese G, Bakker C, De-Sarro GB, Elia M, Ferri R, Oostra BA (2000) Audiogenic seizures susceptibility in transgenic mice with fragile X syndrome. Epilepsia 41:19–23

Noebels JL (1999) Single-gene models of epilepsy. Adv Neurol 79:227–238

Peters HC, Hu H, Pongs O, Storm JF, Isbrandt D (2005) Conditional transgenic suppression of M channels in mouse brain reveals functions in neuronal excitability, resonance and behavior. Nat Neurosci 8:51–60

Potschka H, Krupp E, Ebert U, Gumbel C, Leichtlein C, Lorch B, Pickert A, Kramps S, Young K, Grune U, Keller A, Welschof M, Vogt G, Xiao B, Worley PF, Löscher W, Hiemisch H (2002) Kindling-induced overexpression of Homer 1A and its functional implications for epileptogenesis. Eur J Neurosci 16:2157–2165

Prasad AN, Prasad C, Stafstrom CE (1999) Recent advances in the genetics of epilepsy: insights from human and animal studies. Epilepsia 40:1329–1352

Schauwecker PE (2002) Complications associated with genetic background effects in models of experimental epilepsy. Prog Brain Res 135:139–148

Shannon H, Yang L (2004) Seizure susceptibility of neuropeptide-Y null mutant mice in amygdale kindling and chemical-induced seizure models. Epilepsy Res 61:49–62

Shimizu T, Ikegami T, Ogawara M, Suzuki Y, Takahashi M, Morio H, Shirasawa T (2002) Transgenic expression of the protein-L-isoaspartyl methyltransferase (PIMT) gene in the brain rescues mice from the fatal epilepsy of PIMT deficiency. J Neurosci Res 69:341–352

Toth M, Tecott L (1999) Transgenic approaches to epilepsy. Adv Neurol 79:291–296

Upton N, Stratton S (2003) Recent developments from genetic mouse models of epilepsy. Curr Opin Pharmacol 3:19–26

Viswanath V, Wu Z, Fonck C, Wei Q, Boonplueang R, Andersen JK (2000) Transgenic mice neuronally expressing baculoviral p35 are resistant to diverse types of induced apoptosis, including seizure-associated neurodegeneration. Proc Natl Acad Sci USA 97:2270–2275

Weinshenker D, Szot P (2002) The role of catecholamines in seizure susceptibility: new results using genetically engineered mice. Pharmacol Ther 94:213–233

Yang Y, Frankel WN (2004) Genetic approaches to studying mouse model of human seizure disorders. Adv Exp Med Biol 548:1–11

Zeng Z, Kyaw H, Gakenheimer KR, Augustus M, Fan P, Zhang X, Su K, Carter KC, Li Y (1997) Cloning, mapping, and tissue distribution of a human homologue of the mouse jerky gene product. Biochem Biophys Res Commun 236:389–395

E.4 Hypnotic Activity

E.4.0.1 General Considerations

The term "hypnotic" has to be defined. In man, the purpose of taking hypnotics is to obtain a "normal" night's sleep from which the patient can be aroused without any subsequent hangover. In animal experiments, the term "hypnotic" has been applied to a much deeper stage of central depression of drug induced unconsciousness associated with loss of muscle tone and of righting reflexes. Therefore, most of the pharmacological models are questionable in regard to their predictivity to find an ideal hypnotic for human therapy. Many of the pharmacological tests are based on the potentiation of sleeping time induced by barbiturates or other sedative agents.

Since the biochemical events during sleep are rather unknown no *in vitro* method exists for testing compounds with potential hypnotic activity.

E.4.1 In Vivo Methods

E.4.1.1 Potentiation of Hexobarbital Sleeping Time

PURPOSE AND RATIONALE

The test is used to elucidate CNS-active properties of drugs. Not only hypnotics, sedatives, and tranquilizers but also antidepressants at high doses are known to prolong hexobarbital induced sleep after a single dose of hexobarbital. The loss of righting reflex is measured as criterion for the duration of hexobarbital-induced sleeping time. Mice are used in this test, since metabolic elimination of hexobarbital is rapid in this species.

PROCEDURE

Groups of 10 male NMRI-mice with an average weight of 18–22 g are used. They are dosed orally, i.p. or s.c. with the test compound or the reference standard (e. g., 3 mg/kg diazepam p.o.) or the vehicle. Thirty min after i.p. or s.c. injection or 60 min after oral dosing 60 mg/kg hexobarbital is injected intravenously. The animals are placed on their backs on a warmed (37°C) pad and the duration of loss of the righting reflex (starting at the time of hexobarbital injection) is measured until they regain their righting reflexes. Injection of 60 mg/kg hexobarbital usually causes anesthesia for about 15 min. If there is any doubt as to the reappearance of the righting reflex, the subject is placed gently on its back again and, if it rights itself within one minute, this time is considered as the endpoint.

EVALUATION

Mean values of duration of anesthesia (min) are recorded in control and experimental groups. The percent change in duration of anesthesia is calculated in the experimental groups as compared to those of the controls. ED_{50} values can be calculated. ED_{50} is defined as the dose of drug leading to a 100% prolongation in duration of anesthesia in 50% of the animals.

CRITICAL ASSESSMENT OF THE METHOD

The anxiolytic agents of the benzodiazepine type show an uniform pattern with oral ED_{50} values of less than 1 mg/kg. This is in agreement with the fact that barbiturates also show anxiolytic activity in anti-anxiety

tests with animals as well as in patients. Neuroleptics, such as chlorpromazine and haloperidol, also prolong hexobarbital sleeping time in low doses. The test is considered to be unspecific since compounds which inhibit liver metabolism of hexobarbital also prolong time of anesthesia. Balazs and Grice (1963) discussed the relationship between liver necrosis, induced by CCl_4 or nitrosamines, and pentobarbital sleeping time in rats.

OTHER USES OF THE TEST

Hexobarbital sleeping time is not only prolonged by the simultaneous administration of many compounds but also shortened under special conditions. Several CNS-active compounds (analeptics and stimulants like amphetamine and related compounds and methylxanthines) reduce hexobarbital sleeping time. Standard compounds for this kind of procedure are pentylenetetrazol, methamphetamine and aminophylline.

After repeated administrations, induction of metabolic enzymes in the liver is caused by many compounds and leads to an increased destruction of hexobarbital. Due to the accelerated metabolism of hexobarbital, sleeping time is reduced (Remmer 1972).

MODIFICATIONS OF THE TEST

Instead of hexobarbital, another barbiturate, thiopental can be used which has been proven in clinical use to be a short acting anesthetic. Test compounds or the standard are given 60 min before i.v. injection of 25 mg/kg thiopental to mice with a weight between 18 and 22 g. The animals are placed on their backs and the reappearance of the righting reflex is observed. The ED_{50} which results in a 100% prolongation in duration of anesthesia is between 2.5 and 4.0 mg/kg diazepam p.o.

Simon et al. (1982) tested the interaction of various psychotropic agents with sleep induced by barbital or pentobarbital in mice. Pentobarbital (50 mg/kg) or barbital (180 mg/kg) were injected i.p. and the latency and duration of sleep (loss of righting reflex) were recorded. The test compound was usually administered i.p. 30 min before the injection of the barbiturate. The test was recommended for detecting sedative or anti-sleep activity. Since pentobarbital is metabolized by the liver whereas barbital is not, a comparative study using the two compounds can be useful for determining whether an eventual potentiation or antagonism can be ascribed to enzymatic inhibition or induction.

Fujimori (1965) recommended the use of barbital-Na instead of hexobarbital for the sleeping time test since barbital is not biotransformed by the liver microsomal system.

REFERENCES AND FURTHER READING

Balazs T, Grice HC (1963) The relationship between liver necrosis and pentobarbital sleeping time in rats. Toxicol Appl Pharmacol 5:387–391

Harris LS, Uhle FC (1961) Enhancement of amphetamine stimulation and prolongation of barbiturate depression by a substituted pyrid[3,4-b]indole derivative. J Pharmacol Exp Ther 132:251–257

Fujimori H (1965) Potentiation of barbital hypnosis as an evaluation method for central nervous system depressants. Psychopharmacologia 7:374–378

Lim RKS (1964) Animal techniques for evaluating hypnotics. In: Nodine JH Siegler PE (eds) Animal and Clinical Pharmacologic Techniques in Drug Evaluation. Year Book Medical Publ., Inc., Chicago, pp 291–297

Mason DFJ (1964) Hypnotics and general anaesthetics. In: Laurence DR, Bacharach AL (eds) Evaluation of Drug Activities: Pharmacometrics. Academic Press, London and New York, pp 261–286

Remmer H (1972) Induction of drug metabolizing enzyme system in the liver. Eur J Clin Pharmacol 5:116–136

Simon P, Chermat R, Doaré L, Bourin M, Farinotti R (1982) Interactions imprévues de divers psychotropes avec les effets du barbital et du pentobarbital chez la souris. J Pharmacol (Paris) 13:241–252

E.4.1.2 Experimental Insomnia in Rats

PURPOSE AND RATIONALE

James and Piper (1978) described a method for evaluating potential hypnotic compounds in rats. Usually, the compounds are tested in normal animals where they do not significantly decrease wakefulness. Footshock induced "insomnia" in rats is proposed as suitable model for insomnia in patients.

PROCEDURE

Male Wistar rats (200–275 g) are prepared for chronic electroencephalographic and electromyographic recordings. Four silver/silver chloride epidural electrodes and two disc nuchal electrodes are implanted. A minimum of 10 days is allowed for recovery from surgery. The animals are placed into sound-attenuated recording chambers with grid floors. The frontal-occipital electroencephalogram and the electromyogram are recorded via nonrestraining recording leads on a polygraph and a tape recorder.

On the control day, the animals are dosed with the vehicle and a control nonstress recording is obtained for 8 h. On the next day, the animals are again injected with the vehicle and then exposed to electric footshocks for 8 h. The footshock is delivered through the grid floor of the recording chamber using the EMG

leads as indifferent electrodes, in the form of a 0.5 mA pulse of 15 ms width for 30 s at 1 Hz. During the footshock the EEG and EMG recording circuits are automatically interrupted. The delivery of electric footshock is triggered automatically by two adjustable timers. In this way, each shock period of 30 s is followed by an interval of 30 min. On the next day the rats are dosed with the test compound or the standard and recordings are obtained during a shock session of 8 h.

EVALUATION

The sleep-wake cycle is definitely altered by the stress procedure. The amounts of arousal and of slow wave sleep I are increased, whereas slow wave sleep II and paradoxical sleep are decreased. Phenobarbital and benzodiazepines antagonize these changes at least partially.

CRITICAL ASSESSMENT OF THE METHOD

For screening procedures, the method is too expensive and time-consuming. However, the EEG-parameters in a situation of insomnia similar to men can indicate the usefulness of a new compound.

MODIFICATIONS OF THE METHOD

Gardner and James (1987) described a modified shortened protocol in which a 2.5-h nonstressed control period is followed by drug or vehicle administration and a further 5.5-h recording of the electrocorticogram in the presence of intermittent footshock.

Laval et al. (1991) studied the effect of anxiolytic and hypnotic drugs on sleep circadian rhythms in the rat.

REFERENCES AND FURTHER READING

Gardner CR, James V (1987) Activity of some benzodiazepine receptor ligands with reduced sedative and muscle relaxant properties on stress-induced electrocorticogram arousal in sleeping rats. J Pharmacol Meth 18:47–54

James GWL, Piper DC (1978) A method for evaluating potential hypnotic compounds in rats. J Pharmacol Meth 1:145–154

Laval J, Stenger A, Briley M (1991) Effect of anxiolytic and hypnotic drugs on sleep circadian rhythms in the rat. In: Briley M, File SE (eds) New Concepts in Anxiety. McMillan Press Ltd., London, pp 338–346

E.4.1.3 EEG Registration in Conscious Cats

PURPOSE AND RATIONALE

The effect of hypnotics on sleep pattern of EEG tracings can be studied in conscious, freely moving cats with chronically implanted electrodes (Heinemann et al. 1970, 1973; Wallach et al. 1976; Hirotsu et al. 1988).

PROCEDURE

Female cats weighing 2.5–3.5 kg are anesthetized and prepared with bipolar subcortical electrodes in the reticular formation (A3, L3, H –1), dorsal hippocampus (A5, L –5, H8), and either amygdala (A12, L –9, H –5), or caudate nucleus (A11, L9.5, H –2). Cortical screw electrodes are placed over the anterior suprasylvian, lateral, medial suprasylvian and ectosylvian gyri. Two Teflon coated steel wires are placed in the cervical neck muscles. All wires are connected to a subminiature socket and implanted in dental acrylic. Cats of this chronic colony are then intermittently utilized for drug experiments at interdrug intervals of at least two weeks.

On experimental days, the cats are taken into an experimental chamber $70 \times 80 \times 80$ cm high. The box is lighted and ventilated with room air at 21°C. The cat is immediately connected to a cable which exits through the top center of the cage into a mercury swivel. This prevents the cable from becoming twisted and restricting the cat's movement. Recordings of the cortical EEG, cervical neck muscle tone and reticular formation multiple unit activity are obtained. Continuous recordings for up to 96 h are amplified and stored in a recorder. The recordings of cortical EEG, cervical neck muscle tone and reticular formation multiple unit activity are analyzed for REM sleep, slow wave sleep, and wakefulness. Undefined periods which can not be identified either as slow wave sleep or as wakefulness are included in the awake total. Since a first night effect was observed (Wallach et al. 1996) drugs are given at the third or fourth day.

EVALUATION

The data are analyzed by analysis of variance with subjects, days, and drug as factors.

MODIFICATIONS OF THE METHOD

Schallek and Kuehn (1965) measured the effects of benzodiazepines on spontaneous EEG and arousal responses in cats with implanted electrodes.

In addition to EEG and electromyogram, Holm et al. (1991) registered the electro-oculogram in conscious cats.

EEG studies in immobilized cats were performed by Ongini et al. (1982) for evaluation of a benzodiazepine hypnotic. Adult mongrel cats of both sexes were anesthetized with halothane. A tracheal cannula

was inserted and artificial respiration was maintained throughout the experiment. The spinal cord was transected at C_2 level (Encephalè isolè preparation). The femoral vein was cannulated for i.v. injection of drugs. Cortical electrodes were inserted into the skull in the frontal, parietal and occipital areas. All incisions were infiltrated with mepivacaine 1% to produce local anesthesia. The body temperature was maintained at 36.5–38.0°C by an electrical heat pad. After recovery from surgery and anesthesia, a continuous EEG recording of 2 h was taken prior to drug administration. Test drugs were injected intravenously at various doses. Electrocortical activity was recorded using a 8-channel electroencephalograph. In addition, two electrodes were connected with an EEG-analyzer for the on-line evaluation of the EEG power spectrum. This was computed by the Fast Fourier Transform at a frequency range of 0–32 Hz. Power spectral plots averaging 30 s of electrocortical activity were derived during the experiment.

Shibata et al. (1994) administered various local anesthetics intravenously with constant rates of equipotent doses to cats with implanted electrodes until EEG seizures appeared. During slow rates of infusion, a tetraphasic sequence of changes was found.

Wetzel (1985) evaluated EEG recordings in freely moving **rats** by visual analysis for wakefulness, slow wave sleep or paradoxical sleep.

Krijzer et al. (1991) presented a subclassification of antidepressants based on the quantitative analysis of the electrocorticogram in the rat.

Sarkadi and Inczeffy (1996) described an integrated quantitative electroencephalographic system for pharmacological and toxicological research in the rat. Peak latencies and amplitudes of visual-evoked potentials, occurrence, duration, and linear excursions of photically evoked afterdischarges, activity, mobility, complexity according to Hjorth (1970), and absolute spectral powers of delta, theta, alpha, and beta frequency bands of background activity of visual cortex and frontal-visual leads were measured in freely moving rats.

Rinaldi-Carmona et al. (1992) performed temporal EEG analysis of the sleep-waking cycle in rats with implanted electrodes after administration of a 5-hydroxytryptamine$_2$ receptor antagonist.

Lozito et al. (1994) compared loss of righting with EEG changes in rats with implanted electrodes after single and multiple infusions of fentanyl analogues.

Jones and Greufe (1994) described a quantitative electroencephalographic method in **dogs**.

REFERENCES AND FURTHER READING

Baust W, Heinemann H (1967) The role of the baroreceptors and of blood pressure in the regulation of sleep and wakefulness. Exp Brain Res 3:12–24

Jones RD, Greufe NP (1994) A quantitative electroencephalographic method for xenobiotic screening in the canine model. J Pharmacol Toxicol Meth 31:233–238

Hashimoto T, Hamada C, Wada T, Fukuda N (1992) Comparative study on the behavioral and EEG changes induced by diazepam. buspirone and a novel anxioselective anxiolytic, DN-2327, in the cat. Neuropsychobiol 26:89–99

Heinemann H, Stock G (1973) Chlordiazepoxide and its effect on sleep-wakefulness behavior in unrestrained cats. Arzneim Forsch/Drug Res 23:823–825

Heinemann H, Hartmann A, Sturm V (1968) Der Einfluß von Medazepam auf die Schlaf-Wach-Regulation von wachen, unnarkotisierten Katzen. Arzneim Forsch/Drug Res 18:1557–1559

Heinemann H, Hartmann A, Stock G, Sturm V (1970) Die Wirkungen von Medazepam auf Schwellen subcorticaler, limbischer Reizantworten gemessen an unnarkotisierten, frei beweglichen Katzen. Arzneim Forsch/Drug Res 20:413–415

Hirotsu I, Kihara T, Nakamura S, Hattori Y, Hatta M, Kitakaze Y, Takahama K, Hashimoto Y, Miyata T, Ishihara T, Satoh F (1988) General pharmacological studies on N-(2,6-dimethyl-phenyl)-8-pyrrolizidineacetamide hydrochloride hemihydrate. Arzneim Forsch/Drug Res 38:1398–1410

Holm E, Staedt U, Heep J, Kortsik C, Behne F, Kaske A, Mennicke I (1991) Untersuchungen zum Wirkungsprofil von D,L-Kavain. Zerebrale Angriffsorte und Schlaf-Wach-Rhythmus im Tierexperiment. Arzneim Forsch/Drug Res 41:673–683

Krijzer F, van der Molen R, Olivier B, Vollmer F (1991) Antidepressant subclassification based on the quantitatively analyzed electrocorticogram of the rat. In: Olivier B, Mos J, Slangen JL (eds) Animal Models in Psychopharmacology. Advances in Pharmacological Sciences. Birkhäuser Verlag, Basel, pp 237–241

Kuhn FJ, Schingnitz G, Lehr E, Montagna E, Hinzen HD, Giachetti A (1988) Pharmacology of WEB 1881-FU, a central cholinergic agent, which enhances cognition and cerebral metabolism. Arch Int Pharmacodyn 292:13–34

Lozito RJ, La Marca S, Dunn RW, Jerussi TP (1994) Single versus multiple infusions of fentanyl analogues in a rat EEG model. Life Sci 55:1337–1342

Moruzzi G, Magoun HW (1949) Brain stem reticular formation and activation of the EEG: Electroencephalogr Clin Neurophysiol 1:455–473

Ongini E, Parravicini L, Bamonte F, Guzzon V, Iorio LC, Barnett A (1982) Pharmacological studies with Quazepam, a new benzodiazepine hypnotic. Arzneim Forsch/Drug Res 32:1456–1462

Rinaldi-Carmona M, Congy C, Santucci V, Simiand J, Gautret B, Neliat G, Labeeuw B, Le Fur G, Soubrie P, Breliere JC (1929) Biochemical and pharmacological properties of SR 46349B, a new potent and selective 5-hydroxytryptamine$_2$ receptor antagonist. J Pharmacol Exp Ther 262:759–768

Ruckert RT, Johnson DN, Robins AH (1983) Effects of antihistaminic agents on sleep pattern in cats: a new method for detecting sedative potential. Pharmacologist 25:180

Sarkadi A, Inczeffy Z (1996) Simultaneous quantitative evaluation of visual-evoked responses and background EEG activity in rat: normative data. J Pharmacol Toxicol Meth 35:145–151

Schallek W, Kuehn A (1965) Effects of benzodiazepines on spontaneous EEG and arousal responses of cats. Progr Brain Res 18:231–236
Shibata M, Shingu K, Murakawa M, Adachi T, Osawa M, Nakao S, Mori K (1994) Tetraphasic actions of local anesthetics on central nervous system electrical activities in cats. Regional Anesth 19:255–263
Shouse MN, Siegel JM, Wu MF, Szymusiak R, Morrison AR (1989) Mechanisms of seizure suppression during rapid-eye-movement (REM) sleep in cats. Brain Res 505:271–282
Sommerfelt L, Ursin R (1991) Behavioral, sleep-waking and EEG power spectral effects following the two specific 5-HT uptake inhibitors zimeldine and alaproclate in cats. Behav Brain Res 45:105–115
Tobler I, Scherschlicht R (1990) Sleep and EEG slow-wave activity in the domestic cat: effect of sleep deprivation. Behav Brain Res 37:109–118
Wallach MB, Rogers C, Dawber M (1976) Cat sleep: A unique first night effect. Brain Res Bull 1:425–427
Wetzel W (1985) Effects of nootropic drugs on the sleep-waking pattern of the rat. Biomed Biochim Acta 44:1211–1217
Yamagushi N, Ling GM, Marczynski TJ (1964) Recruiting responses observed during wakefulness and sleep in unanesthetized chronic cats. Electroenceph Clin Neurophysiol 17:246–254

E.4.1.4 Automated Rat Sleep Analysis System

PURPOSE AND RATIONALE

Ruigt et al. (1988a, b, 1993) described an automated rat sleep classification system in rats which allows classification of psychotropic drugs such as potential antidepressants, antipsychotics and stimulants (Ruigt and von Proosdij 1990; de Boer and Ruigt 1995).

The system records and analyzes bioelectrical signals from several animals over extended periods of time. The analysis is based on 3 signals, the parieto-occipital EEG, nuchal EMG and a movement indicator signal.

PROCEDURE

Epidural screw electrodes are implanted over the parieto-occipital cortex of male rats weighing 250–300 g for the recording of EEG against a frontal electrode. Stainless-steel wire electrodes are inserted in the dorsal neck musculature for recording the electromyogram (EMG). After recovery from surgery animals are separately housed in a light- (12:12 h light-dark cycle) and temperature- (21°C) controlled room. Twenty-nine hour EEG and EMG recordings are made in sound-attenuated Faraday cages from 32 rats simultaneously. Movements of the rats are detected as capacitative artefacts generated in an open-ended wire of the non-restraining flat cable connecting the rats to a swivel commutator and to amplification and A/D conversion units, which are hooked up through a data controller to a dedicated PDP-11/83 minicomputer system for on-line spectral EEG analysis and data compression.

Off-line sleep staging on a micro VAX is done per 2-s epoch based on 5 spectral EEG band values (1.0–3.0, 3.0–6.0, 6.0–9.0, 9.5–20.0, 20.0–45.0 Hz), the integrated EMG level and the movement level. A first sleep stage assignment per epoch is done by application of a discriminant function to these epoch values. The discriminant function is derived from a discriminant analysis of visually classified representative recording segments from different sleep stages recorded during a separate calibration experiment for each rat. A moving average EEG smoothing procedure and a set of syntactic classification rules are then used to give a final sleep stage assignment to each specific EEG epoch.

Six sleep-wake stages are distinguished including 2 waking stages: (1) active waking characterized by movement, theta activity and high EMG, and (2) quiet waking without movement. Four sleep stages are discriminated: (3) quiet sleep, characterized by EEG spindles; (4) deep slow-wave sleep with prominent delta activity; (5) pre-REM sleep with spindles against a background of theta activity and low EMG, and (6) REM sleep with theta activity and low EMG.

Each experiment consists of 32 rats divided over maximally 4 groups, including various drug treatment groups (generally several doses of the same drug) and always one placebo group. Drug administration is done at the beginning of the light cycle of the rats. After each experiment 2–3 weeks are allowed for wash-out. Drug effects on sleep-waking behavior are assessed on several parameters extracted from the hypnogram, among which percentage time spent in each of the sleep stages per 30-min period and per rat. This gives for each compound a profile of changes over sleep stages and over time.

EVALUATION

Sleep stage-dependent and sleep-independent parts of the EEG power spectrum are defined by a procedure originally developed by Fairchild et al. (1969, 1971, 1975). First, a normal canonical discriminant analysis is done on 4 EEG frequency bands (1–3, 3–6, 6–9, 9.5–20 Hz) from representative segments of only 3 visually classified sleep stages (quiet waking, deep sleep and REM sleep), the sleep stage being the dependent variable. This results in 2 sleep stage-dependent canonical variables covering 100% of the variance in the data set and two residual canonical variables which are independent of sleep stage assignment. These 2 residual variables are subsequently used in

a second canonical discriminant analysis in which the presence or absence of the drug is used as the dependent variable, resulting in a single canonical variable (the drug score) associated with the drug effect on the sleep stage-independent variance of the EEG spectral parameters.

CRITICAL ASSESSMENT OF THE METHOD

According to the author's own judgment, antidepressants, antipsychotics and stimulants can be discriminated from each other and from placebo successfully from each other and from placebo by this method, whereas nootropics classified as placebo. Unfortunately, anxiolytics, hypnotics and anticonvulsants are classified poorly.

REFERENCES AND FURTHER READING

De Boer T, Ruigt GSF (1995) The selective α_2-adrenoceptor antagonist mirtazapine (Org 3770) enhances noradrenergic and 5-HT_{1A}-mediated serotonergic transmission. CNS Drugs 4, Suppl 1:29–38

Fairchild MD, Jenden DJ, Mickey MR (1969) Discrimination of behavioral state in the cat utilizing long-term EEG frequency analysis. Clin Neurophysiol 27:503–513

Fairchild MD, Jenden DJ, Mickey MR (1971) Quantitative analysis of some drug effects on the EEG by long-term frequency analysis. Proc West Pharmacol Soc 14:135–140

Fairchild MD, Jenden DJ, Mickey MR (1975) An application of long-term frequency analysis in measuring drug-specific alterations in the EEG of the cat. Electroenc Clin Neurophysiol 38:337–348

Ruigt GSF, van Proosdij JN (1990) Antidepressant characteristics of Org 3770, Org 4428 and Org 9768 on rat sleep. Eur J Pharmacol 183:1467–1468

Ruigt GSF, van Proosdij JN, van Delft AML (1989a) A large scale, high resolution, automated system for rat sleep staging. I. Methodology and technical aspects. Electroencephalogr Clin Neurophysiol 73:52–64

Ruigt GSF, van Proosdij JN, van Wezenbeek LACM (1989b) A large scale, high resolution, automated system for rat sleep staging. II. Validation and application. Electroencephalogr Clin Neurophysiol 73:64–71

Ruigt GSF, Engelen S, Gerrits A, Verbon F (1993) Computer-based prediction of psychotropic drug classes based on a discriminant analysis of drug effects on rat sleep. Neuropsychobiol 28:138–153

E.5 Neuroleptic Activity

E.5.0.1 General Considerations

Neuroleptics have been defined as therapeutics effective against schizophrenia. One has to bear in mind that the effect of certain drugs has not been predicted by pharmacological tests but has been found in clinical trials by serendipity. The clinical discoveries were followed by pharmacological studies in many laboratories (Courvoisier 1956).

Various studies have demonstrated the blockade of postsynaptic catecholamine receptors, especially D_2-receptors to be the main mode of action of most neuroleptics. Several *in vitro* methods measure the receptor blockade by neuroleptics.

Pharmacological models in the development of antipsychotic drugs were reviewed by Costall et al. (1991).

REFERENCES AND FURTHER READING

Costall B, Domeney AM, Kelly ME, Naylor RJ (1991) Pharmacological models in the development of antipsychotic drugs – new strategies. In: Olivier B, Mos J, Slangen JL (eds) Animal Models in Psychopharmacology. Advances in Pharmacological Sciences. Birkhäuser Verlag, Basel, pp 253–263

Courvoisier S (1956) Pharmacodynamic basis for the use of chlorpromazine in psychiatry. J Clin Exp Psychopathol 17:25–37

E.5.1 In Vitro Methods

E.5.1.1 D_1 Receptor Assay: [^{3}H]-SCH 23390 Binding to Rat Striatal Homogenates

PURPOSE AND RATIONALE

Dopamine receptors are the primary targets in the development of drugs for the treatment of schizophrenia, Parkinson's disease and Huntington's chorea (Seeman and Van Tol 1994).

Reviews on dopamine receptors and their subtypes were given by Baldessarini and Tarazi (1996, Missale et al. 1998), and by the NC-IUPHAR subcommittee on dopamine receptors (Schwartz et al. 1998).

Multiple dopamine receptors are known. Two groups are most studied, designated as D_1 and D_2. In the group of D_1-like dopamine receptors the subtypes D_{1A} and D_5/D_{1B} have been described. To D_2-like dopamine receptors belong the D_{2S}, the D_{2L}, the D_3, and the D_4 receptor (Sokoloff et al. 1990; Civelli et al. 1991; Grandy et al. 1991; Van Tol et al. 1991; Lévesque et al. 1992; Baldessarini et al. 1993; Ginrich and Caron 1993; Todd and O'Malley 1993; Waddington and Deveney 1996).

D_1 receptors are positively linked to adenylate cyclase and the D_2 receptor has been shown to be negatively linked to adenylate cyclase. For typical neuroleptic agents, like butyrophenones, a good correlation was found between D_2 receptor binding and clinically effective doses. Atypical neuroleptics, like cloza-

pine, were found to be potent inhibitors of D_1 and D_4 receptor binding, renewing interest in these receptor types. The compound SCH 23390 was found to be selective for the D_1 receptor.

PROCEDURE

Reagents

[N-Methyl-^{3}H] Sch 23390 (Amersham Lab., specific activity 67–73 Ci/mmol). For IC_{50} determinations, ^{3}H-Sch 23390 is made up to a concentration of 10 nM and 50 µl is added to each tube. This yields a final concentration of 0.5 nM in the assay.

d-Butaclamol (Ayerst Laboratories). A 1 mM stock solution is made and diluted 1:20.

20 µl are added to 3 tubes for the determination of nonspecific binding.

For the test compounds a 1 mM stock solution is made up in a suitable solvent and serially diluted, such that the final concentration in the assays ranges from 10^{-5} to 10^{-8} M.

Tissue Preparation

Male Wistar rats are decapitated, brains rapidly removed, striata dissected and weighed. The striata are homogenized in 100 volumes of 0.05 M Tris buffer, pH 7.7, using a Tekmar homogenizer. The homogenate is centrifuged at 40,000 *g* for 20 min and the final pellet is resuspended in the original volume of 0.05 Tris buffer, pH 7.7, containing physiological ions (NaCl 120 mM, KCl 5 mM, $MgCl_2$ 1 mM and $CaCl_2$ 2 mM).

Assay

50 µl	0.5 M Tris buffer, pH 7.7, containing physiological ions
380 µl	H_2O
20 µl	vehicle or butaclamol or appropriate concentration of test compound
50 µl	^{3}H-SCH 23390
500 µl	tissue suspension.

The tubes are incubated at 37°C for 30 min. The assay is stopped by rapid filtration through Whatman GF/B filters using a Brandell cell harvester. The filter strips are then washed 3 times with ice-cold 0.05 M Tris buffer, pH 7.7, and counted in 10 ml Liquiscint scintillation cocktail.

EVALUATION

Specific binding is defined as the difference between total binding and binding in the presence of 1 µM d-butaclamol. IC_{50} calculations are performed using log-probit analysis. The percent inhibition at each drug concentration is the average of duplicate determinations.

MODIFICATIONS OF THE METHOD

Wamsley et al. (1992) recommended the radioactive form of a dopamine antagonist, [^{3}H]SCH39166 as ligand for obtaining selective labeling of D_1 receptors.

Sugamori et al. (1998) characterized the compound NNC 01–0012 as a selective and potent D_{1C} receptor antagonist.

REFERENCES AND FURTHER READING

Anderson PH, Gronvald FC, Jansen JA (1985) A comparison between dopamine-stimulated adenylate cyclase and 3H-SCH 23390 binding in rat striatum. Life Sci 37:1971–1983

Anderson PH, Nielsen EB, Gronvald FC, Breastrup C (1986) Some atypical neuroleptics inhibit [^{3}H]SCH 23390 binding *in vivo*. Eur J Pharmacol 120:143–144

Anderson PH, Gingrich JA, Bates MD, Dearry AD, Falardeau P, Senogles SE, Caron MG (1990) Dopamine receptor subtypes: beyond the D_1/D_2 classification. Trends Pharmacol Sci 11:213–236

Baldessarini RJ, Kula NS, McGrath CR, Bakthavachalam V, Kebabian JW, Neumeyer JL (1993) Isomeric selectivity at dopamine D_3 receptors. Eur J Pharmacol 239:269–270

Baldessarini RJ, Tarazi FI (1996) Brain dopamine Receptors: A Primer on their current status, basic and clinical. Harvard Rev Psychiat 3:301–325

Billard W, Ruperto V, Crosby G, Iorio LC, Barnett A (1984) Characterisation of the binding of 3H-SCH 23390, a selective D-1 receptor antagonist ligand, in rat striatum. Life Sci 35:1885–1893

Chipkin RE, Iorio LC, Coffin VL, McQuade RD, Berger JG, Barnett A (1988) Pharmacological profile of SCH39166: a dopamine D1 selective benzonaphthazepine with potential antipsychotic activity. J Pharmacol Exp Ther 247:1093–1102

Civelli O, Bunzow JR, Grandy DK, Zhou QY, Van Tol HHM (1991) Molecular biology of the dopamine receptors. Eur H Pharmacol, Mol Pharmacol Sect 207:277–286

Clement-Cormier YC, Kebabian JW, Petzold GR, Greengard P (1974) Dopamine-sensitive adenylate cyclase in mammalian brain. A possible site of action of anti-psychotic drugs. Proc Natl Acad Sci USA 71:1113–1117

Creese I (1987) Biochemical properties of CNS dopamine receptors. In: Meltzer HY (ed) Psychopharmacology: The Third Generation of Progress. Raven Press, New York, pp 257–264

Dawson TM, Gehlert DR, Yamamura HI, Barnett A, Wamsley JK (1985) D-1 dopamine receptors in the rat brain: Autoradiographic localisation using [3H]SCH 23390. Eur J Pharmacol 108:323–325

Dearry A, Gingrich JA, Falardeau P, Fremeau RT, Bates MD, Caron MG (1990) Molecular cloning and expression of the gene for a human D_1 dopamine receptor. Nature 347:72–76

DeNinno MP, Schoenleber R, MacKenzie R, Britton DR, Asin KE, Briggs C, Trugman JM, Ackerman M, Artman L, Bednarz L, Bhatt R, Curzon P, Gomez E, Kang CH, Stittsworth J, Kebabian JW (1991) A68930: a potent agonist selective for the dopamine D_1 receptor: Eur J Pharmacol 199:209–219

Gerhardt S, Gerber R, Liebman JM (1985) SCH 23390 dissociated from conventional neuroleptics in apomorphine

climbing and primate acute dyskinesia models. Life Sci 37:2355–2363
Ginrich JA, Caron MC (1993) Recent advances in the molecular biology of dopamine receptors. Annu Rev Neurosci 16:299–321
Grandy DK, Zhang Y, Bouvier C, Zhou QY, Johnson RA, Allen L, Buck K, Bunzow JR, Salon J, Civelli O (1991) Multiple human dopamine receptor genes: a functional D_5 receptor and two pseudogenes. Proc Natl Acad Sci USA 88:9175–9179
Hess E, Battaglia G, Norman AB, Iorio LC, Creese I (1986) Guanine nucleotide regulation of agonist Robinson T (ed) Interactions at [^{3}H]SCH 23390-labelled D1 dopamine receptors in rat striatum. Eur J Pharmacol 121:31–38
Hyttel J (1983) SCH 23390 – the first selective dopamine D-1 antagonist. Eur J Pharmacol 91:153–154
Iorio LC, Barnett A, Leitz FH, Houser VP, Korduba CA (1983) SCH 23390, a potential benzazepine antipsychotic with unique interactions on dopamine systems. J Pharm Exper Ther 226:462–468
Kebabian JW, Calne DB (1979) Multiple receptors for dopamine. Nature 277:93–96
Kebabian JW, Britton DR, DeNinno MP, Perner R, Smith L, Jenner P, Schoenleber R, Williams M (1992) A-77363: a potent and selective D_1 receptor antagonist with antiparkinsonian activity in marmosets. Eur J Pharmacol 229:203–209
Kilpatrick GJ, Jenner P, Mardsen CD (1986) [^{3}H]SCH 23390 identifies D-1 binding sites in rat striatum and other brain areas. J Pharm Pharmacol 38:907–912
Lévesque D, Diaz J, Pilon C, Martres MP, Giros B, Souil E, Schott D, Morgat JL, Schwartz JC (1992) Identification, characterization, and localization of the dopamine D_3 receptor in rat brain using 7-[^{3}H]hydroxy-*N*,*N*-di-n-propyl-2-aminotetralin. Proc Natl Acad Sci USA 89:8155–8159
Missale C, Caron MG, Jaber M (1998) Dopamine receptors: From structure to function. Physiol Rev 78:189–225
Neumeyer JL, Kula NS, Baldessarini RJ, Baindur (1992) Stereoisomeric probes for the D_1 dopamine receptor: Synthesis and characterization of *R*-(+) and *S*-(–) enantiomers of 3-allyl-7,8-dihydroxy-1-phenyl-2,3,4,5-tetrahydro-1*H*-3-benzazepine and its 6-bromo analogue. J Med Chem 35:1466–1471
Niznik HB, Sunahara RK, van Tol HHM, Seeman P, Weiner DM, Stormann TM, Brann MR, O'Dowd BF (1992) The dopamine D_1 receptors. In: Brann MR (ed) Molecular Biology of G-Protein Coupled Receptors. Birkhäuser, Boston Basel Berlin, pp 142–159
O'Boyle KM, Waddington JL (1992) Agonist and antagonist interaction with D_1 dopamine receptors: agonist induced masking of D_1 receptors depends on intrinsic activity. Neuropharmacol 31:177–183
Schwartz JC, Carlsson A, Caron M, Scatton B, Civelli O, Kebabian JW, Langer SZ, Sedvall G, Seeman P, Spano PF, Sokoloff P, Van Tol H (1998) Dopamine receptors. NC-IUPHAR subcommittee for dopamine receptors. In Gridlestone D (ed) The IUPHAR Compendium of Receptor Characterization and Classification. IUPHAR Media, London, pp 141–151
Seeman P (1977) Anti-schizophrenic drugs. Membrane receptor sites of action. Biochem Pharmacol 26:1741–1748
Seeman P, Van Tol HHM (1994) Dopamine receptor pharmacology. Trends Pharmacol Sci 15:264–270
Seeman P, Chau-Wong C, Tedesco J, Wong K (1975) Binding receptors for antipsychotic drugs and dopamine: direct binding assays. Proc Natl Acad Sci USA 72:4376–4380
Snyder SH, Creese I, Burt DR (1975) The brain's dopamine receptor: labeling with [^{3}H]dopamine. Psychopharmacol Commun 1:663–673
Stoff JC, Kebabian JW (1982) Independent *in vitro* regulation by the D-2 dopamine receptor of dopamine-stimulated efflux of cyclic AMP and K^+-stimulated release of acetylcholine from rat neostriatum. Brain Res 250:263–270
Sugamori KS, Hamdanizadeh SA, Scheideler MA, Hohlweg R, Vernier P, Niznik HB (1998) Functional differentiation of multiple dopamine D_1-like receptors by NNC 01–0012. J Neurochem 71:1685–1693
Sunahara RK, Niznik HB, Weiner DM, Stormann TM, Brann MR, Kennedy JL, Gelernter JE, Rozmahel R, Yang Y, Israel Y, Seeman P, O'Dowd BF (1990) Human dopamine D_1 receptor encoded by an intronless gene on chromosome 5. Nature 347:80–83
Todd RD, O'Malley KL (1993) Family ties: The dopamine D_2-like receptor genes. Neurotransmiss 9(3):1–4
Trampus M, Ongini E, Borea PA (1991) The neutral endopeptidase-24.11 inhibitor SCH 34826 does not change opioid binding but reduces D_1 dopamine receptors in rat brain. Eur J Pharmacol 194:17–23
Tricklebank MD, Bristow LJ, Hutson PH (1992) Alternative approaches to the discovery of novel antipsychotic agents. Progr Drug Res 38:299–336
Van Tol HHM, Bunzow JR, Guan HC, Sunahara RK, Seeman P, Niznik HB, Civelli O (1991) Cloning of the gene of a human dopamine D_4 receptor with high affinity for the antipsychotic clozapine. Nature 350:610–614
Waddington JL, Deveney AM (1996) Dopamine receptor multiplicity: 'D_1-like'–'D_2-like' interactions and 'D_1-like' receptors not linked to adenylate cyclase. Biochem Soc Transact 24:177–182
Wamsley JK, Alburges ME, McQuade RD, Hunt M (1992) CNS distribution of D_1 receptors: use of a new specific D_1 receptor antagonist, [^{3}H]SCH39166. Neurochem Int 20 (Suppl):123S–128S
Weinshank RL, Adham N, Macchi M, Olsen MA, Branchek TA, Hartig PR (1991) Molecular cloning and characterization of a high affinity dopamine receptor ($D_{1\beta}$) and its pseudogene. J Biol Chem 266:22427–22435
Zhou QY, Grandy DK, Thambi L, Kusher JA, Van Tol HHM, Cone R, Pribnow D, Salon J, Bunzow JR, Civelli O (1990) Cloning and expression of human and rat dopamine D_1 receptors. Nature 347:76–80

E.5.1.2 D_2 Receptor Assay: [^{3}H]-Spiroperidol Binding

PURPOSE AND RATIONALE

The neuroleptic compound haloperidol has been used as binding ligand to study the activity of other neuroleptics. The use of haloperidol has been superseded by spiroperidol. Dopamine receptor binding assays employing dopaminergic antagonists in mammalian striatal tissue, a dopamine-enriched area of the brain, have been shown to be predictive of *in vivo* dopamine receptor antagonism and antipsychotic activity. Significant correlations exist between neuroleptic binding affinities and their molar potencies in antagonism of apomorphine- or amphetamine-induced stereotypy,

apomorphine-induced emesis in dogs, and antipsychotic activity in man. Spiroperidol is considered to be an antagonist specific for D_2 receptors.

PROCEDURE

Tissue Preparation

Male Wistar rats are decapitated, their corpora striata removed, weighed and homogenized in 50 volumes of ice-cold 0.05 M Tris buffer, pH 7.7. The homogenate is centrifuged at 40,000 *g* for 15 min. The pellet is rehomogenized in fresh buffer and recentrifuged at 40,000 *g*. The final pellet is then resuspended in Tris buffer containing physiological salts (120 mM NaCl, 5 mM KCl, 2 mM $CaCl_2$ and 1 mM $MgCl_2$) resulting in a concentration of 10 mg/ml.

Assay

The membrane preparations are incubated with ^{3}H-spiroperidol (0.25 nM) and various concentrations of test drug at 37°C for 20 min in a K/Na phosphate buffer (50 mM, pH 7.2), followed by cooling in an ice bath for 45 min. To determine non-specific binding, samples containing 10 mM (+)-butaclamol are incubated under identical conditions without the test compound.

Bound ligand is separated by rapid filtration through Whatman GF/B glass fiber filters. The filters are washed three times with ice-cold buffer, dried, and shaken thoroughly with 3.5 ml scintillation fluid. Radioactivity is determined in a liquid scintillation counter. Specific binding is defined as the difference between total binding and the binding in the presence of 2.0 mM (+)-butaclamol.

EVALUATION

The following parameters are determined:

- total binding of ^{3}H-spiroperidol
- non-specific binding: binding of samples containing 2 mM butaclamol
- specific binding = total binding – non-specific binding
- % inhibition: 100–specific binding as percentage of the control value.

IC_{50} values are determined using at least 3–4 different concentrations of the test compound in triplicate. Results are presented as mean ± standard deviation.

Dissociation constants (K_d) are determined, using ^{3}H-spiroperidol concentrations ranging between 0.1 and 1.0 nM. K_i values (inhibitory constants) are calculated using the following equation:

$$K_i = \frac{IC_{50}}{1 + c/K_d}$$

c = ^{3}H-spiroperidol concentrations used to determine IC_{50}.

Standard values: K_i of haloperidol = 6.0 ± 1.2 nM.

MODIFICATIONS OF THE METHOD

Two isoforms of the D_2 receptor were found by alternative splicing: the long (D_{2L}) and the short (D_{2S}) isoform (Dal Toso et al. 1988; Giros et al. 1989; Monsma et al. 1989; Itokawa et al. 1996).

Niznik et al. (1985) recommended [^{3}H]-YM-09151–2, a benzamide neuroleptic, as selective ligand for dopamine D_2 receptors.

Hall et al. (1985) used [^{3}H]-eticlopride, a substituted benzamide, selective for dopamine-D_2 receptors, for *in vitro* binding studies.

Radioactive ligands for the D_2 and the D_3 receptor were described by Seeman and Schaus (1991), Chumpradit et al. (1994), Booze and Wallace (1995), Gackenheimer et al. (1995), Seeman and van Tol (1995), Van Vliet et al. (1996).

Vessotskie et al. (1997) characterized binding of [^{125}I]S(–)5-OH-PIPAT to dopamine $D_{2\text{-like}}$ receptors.

Neve et al. (1992) used a special apparatus, the 'cytosensor microphysiometer' which measures the rate of proton excretion from cultured cells (McConnell et al. 1991, 1992; Owicki and Parce 1992). In C_6 glioma cells and L fibroblasts expressing recombinant dopamine D_2 receptors, the dopamine D_2 receptor agonist, quinpirole, accelerated the rate of acidification of the medium dose-dependent up to 100 nM quinpirole. The response was inhibited by the D_2 antagonist spiperone. The D_2 receptor stimulated acidification was due to transport of protons by a Na^+/H^+ antiporter which was verified by the inhibition with amiloride or methylisobutyl-amiloride.

The isolated rabbit ear artery was recommended as a useful model to characterize dopamine D_2 agonists and antagonists (Hieble et al. 1985).

Human Recombinant Dopamine D_{2A} and D_{2B} Receptors

Hayes et al. (1992) described functionally distinct human recombinant subtypes of the dopamine D_2 receptor, D_{2A} and D_{2B}.

D_{2A} Receptor Binding

In a radioligand binding assay the binding of [^{3}H]-spiperone to membranes prepared from COS cells

transiently expressing a recombinant human dopamine D_{2A} receptor is measured.

Twenty mg of membrane is incubated with [^{3}H]-spiperone at a concentration of 2.0 nM for 2 h at 25°C. Non-specific binding is estimated in the presence of 10 mM haloperidol. Membranes are filtered and washed 3 times with binding buffer, and filters are counted to determine [^{3}H]-spiperone bound.

D_{2B} Receptor Binding

In a radioligand binding assay the binding of [^{3}H]-spiperone to membranes prepared from COS cells transiently expressing a recombinant human dopamine D_{2B} receptor is measured.

Fifteen mg of membrane is incubated with [^{3}H]-spiperone at a concentration of 0.7 nM for 2 h at 37°C. Non-specific binding is estimated in the presence of 10 mM haloperidol. Membranes are filtered and washed 3 times with binding buffer, and filters are counted to determine [^{3}H]-spiperone bound.

REFERENCES AND FURTHER READING

Booze RM, Wallace DR (1995) Dopamine D_2 and D_3 receptors in the rat striatum and nucleus accumbens: Use of 7-OH-DPAT and [^{125}I]iodosulpiride. Synapse 19:1–13

Bunzow JR, Van Tol HHM, Grandy DK, Albert P, Salon J, Christie MD, Machida CA, Neve KA, Civelli O (1988) Cloning and expression of rat D_2 dopamine receptor cDNA. Nature 336:783–787

Chumpradit S, Kung MP, Vessotskie J, Foulon C, Mu M, Kung HF (1994) Iodinated 2-aminotetralins and 3-amino-1-benzopyrans: Ligands for D_2 and D_3 receptors. J Med Chem 37:4245–4250

Civelli O, Bunzow J, Albert P, van Tol HHM, Grandy D (1992) The dopamine D2 receptor. In: Brann MR (ed) Molecular Biology of G-Protein Coupled Receptors. Birkhäuser, Boston Basel Berlin, pp 160–169

Dal Toso R, Sommer B, Ewert M, Pritchett DB, Bach A, Chivers BD, Seeberg P (1989) The dopamine D_2 receptor: Two molecular forms generated by alternative splicing. EMBO J 8:4025–4034

Fields JZ, Reisine TD, Yamamura HI (1977) Biochemical demonstration of dopaminergic receptors in rat and human brain using [^{3}H]-spiroperidol. Brain Res 136:578–584

Gackenheimer SL, Schaus JM, Gehlert DE (1995) [^{3}H]quinelorane binds to D_2 and D_3 dopamine receptors in the rat brain. J Pharmacol Exper Ther 274:1558–1565

Giros B, Sokoloff P, Matres MP, Riou JF, Emorine LJ, Schwartz JC (1989) Alternative splicing directs the expression of two D_2 dopamine receptor isoforms. Nature 342:923–929

Grandy DK, Marchionni MA, Makam H, Stofko RE, Alfano M, Frothingham L, Fischer JB, Burke-Howie KJ, Bunzow JR, Server AC, Civelli O (1989) Cloning of the cDNA and gene for a human D_2 dopamine receptor. Proc Natl Acad Sci USA 86:9762–9766

Hall H, Köhler C, Gawell L (1985) Some *in vitro* receptor binding properties of [^{3}H]eticlopride, a novel substituted benzamide, selective for dopamine-D_2 receptors in the rat brain. Eur J Pharmacol 111:191–199

Hayes G, Biden TJ, Selbie LA, Shine J (1992) Structural subtypes of the dopamine D2 receptor are functionally distinct: Expression of the D_{2A} and D_{2B} subtypes in a heterologous cell line. Mol Endocrinol 6:920–926

Hieble JP, Nelson SH, Steinsland OS (1985) Neuronal dopamine receptors of the rabbit ear artery: pharmacological characterization of the receptor. J Auton Pharmacol 5:115–124

Itokawa M, Toru M, Ito K, Tsuga H, Kameyama K, Haga T, Arinami T, Hamaguchi H (1996) Sequestration of the short and long isoforms of dopamine D_2 receptors expressed in Chinese hamster ovary cells. Mol Pharmacol 49:560–566

Laduron PM, Janssen PFM, Leysen JE (1978) Spiperone: A ligand of choice for neuroleptic receptors. 2. Regional distribution and *in vivo* displacement of neuroleptic drugs. Biochem Pharmacol 27:317–328

Leysen JE, Gommeren W, Laduron PM (1978) Spiroperone: A ligand of choice for neuroleptic receptors. 1. Kinetics and characteristics of *in vitro* binding. Biochem Pharmacol 27:307–316

Locke KW, Dunn RW, Hubbard JW, Vanselous ChL, Cornfeldt M, Fielding St, Strupczewski JT (1990) HP 818: A centrally acting analgesic with neuroleptic properties. Drug Dev Res 19:239–256

Martres MP, Bouthenet ML, Sales N, Sokoloff P, Schwartz JC (1985) Widespread distribution of brain dopamine receptors evidenced with [^{125}I]iodosulpiride, a highly selective ligand. Science 228:752–755

McConnell HM, Rice P, Wada GH, Owicki JC, Parce JW (1991) The microphysiometer biosensor. Curr Opin Struct Biol 1:647–652

McConnell HM, Owicki JC, Parce JW, Miller DL, Baxter GT, Wada HG, Pitchford S (1992) The Cytosensor Microphysiometer: biological applications of silicon technology. Science 257:1906–1912

Monsma FJ, McVittie LD, Gerfen CR, Mahan LC, Sibley DR (1989) Multiple D_2 dopamine receptors produced by alternative RNA splicing. Nature 342:926–929

Neve KA, Kozlowski MR, Rosser MP (1992) Dopamine D2 receptor stimulation of Na^+/H^+ exchange assessed by quantification of extracellular acidification. J Biol Chem 267:25748–25753

Niznik HB, Grigoriadis DE, Pri-Bar I, Buchman O, Seeman P (1985) Dopamine D_2 receptors selectively labeled by a benzamide neuroleptic: [^{3}H]-YM-09151–2. Naunyn-Schmiedeberg's Arch Pharmacol 329:333–343

Owicki JC, Parce JW (1992) Biosensors based on the energy metabolism of living cells: The physical chemistry and cell biology of extracellular acidification. Biosensors Bioelectronics 7:255–272

Seeman P (1981) Brain dopamine receptors. Pharmacol Rev 32:229–313

Seeman P, Schaus JM (1991) Dopamine receptors labelled by [^{3}H]quinpirole. Eur J Pharmacol 203:105–109

Seeman P, van Tol HHM (1995) Deriving the therapeutic concentrations for clozapine and haloperidol: The apparent dissociation constant of a neuroleptic at the dopamine D_2 and D_4 receptors varies with the affinity of the competing radioligand. Eur J Pharmacol Mol Pharmacol Sect 291:59–66

Sibley DR, Monsma FJ Jr (1992) Molecular biology of dopamine receptors. Trends Pharmacol Sci 13:61–69

Strange PG (1992) Studies on the structure and function of D_2 dopamine receptors. Biochem Soc Transact 20:126–130

Terai M, Hidaka K, Nakamura Y (1989) Comparison of [^{3}H]YM-09151–2 with [^{3}H]spiperone and [^{3}H]raclopride for dopamine D-2 receptor binding to rat striatum. Eur J Pharmacol 173:177–182

Van Vliet LA, Tepper PG, Dijkstra D, Damstoa G, Wickstrom H, Pugsley DA, Akunne HC, Heffner TG, Glase SA, Wise LD (1996) Affinity for dopamine D_2, D_3, and D_4 receptors of 2-aminotetralins. Relevance of agonist binding for determination of receptor subtype selectivity. J Med Chem 39:4233–4237

Vessotskie JM, Kung MP, Chumpradit S, Kung HF (1997) Characterization of [^{125}]S(–)5-OH-PIPAT binding to dopamine D_2-like receptors expressed in cell lines. Neuropharmacol 36:999–1007

E.5.1.3 Dopamine D_2 Receptor Autoradiography (^{3}H-Spiperone Binding)

PURPOSE AND RATIONALE

Autoradiography of ^{3}H-spiperone binding sites using selective labeling conditions permits the visualization of the anatomical locations of D_2-dopamine receptors (Palacios et al. 1981). Quantitative measurements of the binding to receptors can be obtained with computer-assisted video analysis of the autoradiograms with a greater anatomical resolution and sensitivity than in membrane homogenates (Altar et al. 1984, 1985). Using autoradiographic techniques, it has been demonstrated that striatal D_2 receptors are present on intrinsic neurons (Trugman et al. 1986; Joyce and Marshall 1987) and that the distribution of D_2 receptors within the striatum is not homogeneous (Joyce et al. 1985). Anatomically discrete interactions of drugs with D_2 receptors can be examined *in vitro* with inhibition experiments and *ex vivo* following acute or chronic drug treatment of the whole animal.

Since ^{3}H-spiperone labels serotonin-2 (5-HT_2) sites in many brain regions, a masking concentration of a 5-HT_2 receptor blocker, e. g., ketanserin, is included to selectively define binding to D_2 receptors. This is necessary if the test compound inhibits 5-HT_2 binding, or if the brain region of interest has a low D_2 receptor density.

The assay is used to determine potential antipsychotic activity of compounds via direct interaction with the D_2 dopamine recognition site in discrete regions of the rat brain.

PROCEDURE

Reagents

1a. 0.5 M Tris+1.54 M NaCl, pH 7.4

1b. 0.05 M Tris+0.154 M NaCl, pH 7.4

2. ^{3}H-spiperone (specific activity 70–90 Ci/mmol) is obtained from Amersham (TRK.818).
   For IC_{50} determinations: ^{3}H-spiperone is prepared at a concentration of 8 nM and 0.55 ml is added to each slide mailer (yields a final concentration of 0.4 nM in the 11.0 ml assay volume).
   For saturation experiments: ^{3}H-spiperone is prepared at a concentration of 20 nM. The final concentrations should range from 0.2–1.0 nM. Typically, six concentrations are used by adding 0.55 ml or less to each mailer (for smaller volumes, add water to bring total addition of 0.55 ml).
3. Sulpiride is obtained from Sigma. A stock solution of 5×10^{-4} M is made by dissolving the sulpiride in 1.0 ml of 0.01 N acetic acid and bringing the final volume to 10 ml with distilled water. 0.22 ml of the stock solution is added to the nonspecific binding slide mailers (final concentration 10 µM). All other mailers receive 0.22 ml of vehicle (1 ml of 0.01 N acetic acid in a final volume of 10 ml with distilled water).
4. Ketanserin (free base or tartrate salt) is obtained from Janssen. A stock solution of 10^{-3} M is made by dissolving the ketanserin in 0.5 ml 1 N acetic acid and bringing the final volume to 10 ml with distilled water. The tartrate salt is water-soluble. This is further diluted to 5×10^{-6} M (50 µl q.s. to 10 ml). 0.22 ml is added to all mailers.
5. Test compounds (for IC_{50} determinations). For most assays, a 5×10^{-3} M stock solution is made up in a suitable solvent and serially diluted, such that the final concentrations in the assay range from 10^{-5} to 10^{-8} M. Seven concentrations are used for each assay. Higher or lower concentrations may be used depending on the potency of the drug.

Tissue Preparation

Rat brain sections are collected from plates 9 (rostral nucleus accumbens) through plate 17 (caudal striatum) of "The Rat Brain Atlas in Stereotaxic Coordinates" by Paxinos and Watson.

1. For *in vitro* inhibition experiments, 3–5 sets of 10 slides are collected with 3–4 sections per slide.
2. For saturation experiments, 3–5 sets of 12 slides are collected with 3–4 sections per slide.
3. For *ex vivo* inhibition experiments, a set of 8 slides is used, 4 for total binding and 4 for nonspecific binding.
4. For experiments in which the tissue sections will be swabbed and counted with scintillation fluid, 2 sections per slide are collected.

Assay

1. Preparation of slide mailers (11.0 ml volume/slide mailer):
   Note: If slides with sections are to be wiped for scintillation counting, a final volume of 6.5 ml is

sufficient to cover 2 sections. A proportional adjustment of the volumes to be pipetted is made.

a) *In vitro* inhibition experiments
Separate mailers are prepared for total binding, nonspecific binding and 7–8 concentrations of test compound. Ketanserin is included in all mailers to mask binding of [^{3}H]-spiperone to 5-HT_2 sites so that inhibition of binding is D_2-selective.

5.50 ml	buffer 1b
0.55 ml	buffer 1a
0.55 ml	[^{3}H]-spiperone, 0.4 nM final concentration
3.96 ml	distilled water
0.22 ml	ketanserin, 5×10^{-6} M, final concentration 100 nM or vehicle
0.22 ml	test compound, final concentration 10^{-8}–10^{-5} M or sulpiride 5×10^{-4}, final conc. 10 µM or vehicle

b) *Ex vivo* inhibition experiments
Separate mailers are prepared for total and nonspecific binding, as described above, including ketanserin to mask 5-HT_2 receptor binding.

c) Saturation experiments
Separate mailers are prepared for total and nonspecific binding at each radioligand concentration. Ketanserin is not included in the mailers, in saturation experiments, since specific binding is defined as sulpiride-displaceable.

5.50 ml	buffer 1b
0.55 ml	buffer 1a
0.55 ml	[^{3}H]-spiperone, final concentration 0.2–1.0 nM
4.18 ml	distilled water
0.22 ml	5×10^{-4} M sulpiride, final concentration 10 µM or vehicle

2. Slides are air-dried for 10–15 min at room temperature, preincubated in 0.05 M Tris+0.154 M NaCl, pH 7.4 for 5 min and further incubated for 60 min with [^{3}H]-spiperone. Slides are then rinsed with ice-cold solutions as follows: dipped in buffer 1b, rinsed in buffer 1b for 2 × 5 min, and dipped in distilled water.
Slides used for wipes: both sections are wiped with one Whatman GF/B filter and radioactivity is counted after addition of 10 ml of scintillation fluid.
Slides used for autoradiography: slides are dried under a stream of air at room temperature and are stored in a desiccator under vacuum at room temperature (usually over night). Slides are then mounted onto boards, along with ^{3}H-standards (Amersham RPA 506).
In the dark room under safelight illumination (Kodak GBX-2 filter), slides are exposed to Amersham Hyperfilm or LKB Ultrofilm for 14–17 days.

REFERENCES AND FURTHER READING

Altar CA et al (1984) Computer-assisted video analysis of [^{3}H]-spiroperidol binding autoradiographs. J Neurosci Meth 10:173–188

Altar CA et al (1985) Computer imaging and analysis of dopamine (D2) and serotonin (S2) binding sites in rat basal ganglia or neocortex labeled by [^{3}H]-spiroperidol. J Pharmacol Exp Ther 233:527–538

Joyce JN, Marshall JF (1987) Quantitative autoradiography of dopamine D2 sites in rat caudate-putamen: Localization to intrinsic neurons and not to neocortical afferents. Neurosci 20:773–795

Joyce JN, Loeschen SK, Marshall JF (1985) Dopamine D2 receptors in rat caudate-putamen: The lateral to medial gradient does not correspond to dopaminergic innervation. Brain Res 378:209–218

Kobayashi Y, Ricci A, Rossodivita I, Amenta F (1994) Autoradiographic localization of dopamine D_2-like receptors in the rabbit pulmonary vascular tree. Naunyn-Schmiedeberg's Arch Pharmacol 349:5598–564

Palacios JM, Niehoff DL, Kuhar MJ (1981) [^{3}H]Spiperone binding sites in brain: autoradiographic localization of multiple receptors. Brain Res 213:277–289

Tarazi FI, Campbell A, Yeghiayan SK, Balldessarini RJ (1998) Localization of dopamine receptor subtypes in corpus striatum and nucleus accumbens septi of rat brain. Comparison of D_1, D_2 and D_4-like receptors. Neurosci 83:169–176

Trugman JM et al (1986) Localization of D2 dopamine receptors to intrinsic striatal neurons by quantitative autoradiography. Nature 323:267–269

E.5.1.4 Binding to the D_3 Receptor

PURPOSE AND RATIONALE

Sokoloff et al. (1990) reported molecular cloning and characterization of a dopamine receptor (D_3) as a potential target for neuroleptics. The D_3 receptor is localized in limbic areas of the brain which are associated with cognitive, emotional and endocrine functions. Together with the D_{2S}, the D_{2L} and the D_4 receptor, the D_3 receptor belongs to the group of D_2-like dopamine receptors (Ginrich and Caron 1993). 7-[^{3}H]hydroxy-*N*,*N*-di-n-propyl-2-aminotetralin (Lévesque et al. 1992), R(+)-7-OH-DPAT (Baldessarini et al. 1993; and [^{125}I]trans-7-OH-PIPAT-A (Kung et al. 1993) have been recommended as ligands for receptor binding studies.

Chio et al. (1993) compared the heterologously in Chinese hamster ovary cells expressed D_3 dopamine receptors with D_2 receptors.

Damsma et al. (1993) described R-(+)-7-OH-DPAT (R-(+)-7-hydroxy-2-(N,N-di-n-propylamino)tetralin) as a putative dopamine D_3 receptor ligand.

Functional correlates of dopamine D_3 receptor activation in the rat *in vivo* and their modulation by the selective agonist, (+)-S 14297, have been described by Millan et al. (1995).

Isoforms of the D_3 receptor have been described (Pagliusi et al. 1993).

Akunne et al. (1995) described binding of the selective dopamine D_3 receptor agonist ligand [^{3}H]PD 128907=4aR,10bR-(+)-trans-3,4,4a,10b-tetrahydro-4-n-propyl-2H,5H-[1]benzopyrano[4,3-b]1,4-oxazin-9-ol.

PROCEDURE

Human dopamine D_3 receptor is expressed in Chinese hamster ovary cells. Cells are grown in Dulbecco's modified Eagle's medium containing 10% fetal bovine serum. Cells are harvested by trypsin treatment (0.25%) for 4–5 min and centrifugation at 2000 *g* for 5 min. They are homogenized with a Polytron in 10 mM Tris-HCl (pH 7.5) containing 1 mM EDTA and are centrifuged at 35,000 *g* for 15 min. The pellet is then resuspended by sonication in a buffer containing 50 mM NaHepes, 1 mM EDTA, 50 µM 8-hydroxyquinoline, 0.005% ascorbic acid, and 0.1% bovine serum albumin (pH 7.5) (incubation buffer). Membrane suspensions (15–25 µg protein) are added to polypropylene test tubes containing [^{3}H]7-OH-DPAT (7-[^{3}H]hydroxy-*N*,*N*-di-n-propyl-2-aminotetralin) for the D_3 receptor assay. Competing drugs are dissolved in incubation buffer, the final volume being 1 ml. Tubes are incubated in triplicate for 1 h at room temperature. The incubations are stopped by rapid filtration under reduced pressure through Whatman GF/C glass filters coated with 0.1% bovine serum albumin, followed by 3 rinses with 3–4 ml ice-cold buffer. Non-specific binding is measured in the presence of 1 µM dopamine.

EVALUATION

Saturation curves are analyzed by computer non-linear regression using a one-site cooperative model to obtain equilibrium dissociation constants (K_D) and maximal density of receptors (B_{max}). Inhibition constants (K_i) are estimated according to the equation

$$K_i = IC_{50}/1 + L/K_D$$

REFERENCES AND FURTHER READING

Akunne HC, Towers P, Ellis GJ, Dijkstra D, Wikstrom H, Heffner TG, Wise LD, Pugsley TA (1995) Characterization of binding of [^{3}H]PD 128907, a selective dopamine D_3 receptor agonist ligand to CHO-K1 cells. Life Sci 57:1401–1410

Baldessarini RJ, Kula NS, McGrath CR, Bakthavachalam V, Kebabian JW, Neumeyer JL (1993) Isomeric selectivity at dopamine D_3 receptors. Eur J Pharmacol 239:269–270

Brücke T, Wenger S, Podreka I, Asenbaum S (1991) Dopamine receptor classification, neuroanatomical distribution and *in vivo* imaging. Wien Klin Wochenschr 103:639–646

Chio CL, Lajiness ME, Huff RM (1993) Activation of heterologously expressed D3 dopamine receptors: Comparison with D2 dopamine receptors. Mol Pharmacol 45:51–60

Damsma G, Bottema T, Westerink BHC, Tepper PG, Dijkstra D, Pugsley TA, Mackenzie RG, Heffner TG, Wikstrom H (1993) Pharmacological aspects of R-(+)-7-OH-DPAT, a putative dopamine D_3 receptor ligand. J Pharmacol 249:R9–R10

Ginrich JA, Caron MC (1993) Recent advances in the molecular biology of dopamine receptors. Annu Rev Neurosci 16:299–321

Kung MP, Fung HF, Chumpradit S, Foulon C (1993) *In vitro* binding of a novel dopamine D_3 receptor ligand: [^{125}I]trans-7-OH-PIPAT-A. Eur J Pharmacol 235:165–166

Lévesque D, Diaz J, Pilon C, Martres MP, Giros B, Souil E, Schott D, Morgat JL, Schwartz JC (1992) Identification, characterization, and localization of the dopamine D_3 receptor in rat brain using 7-[^{3}H]hydroxy-*N*,*N*-di-n-propyl-2-aminotetralin. Proc Natl Acad Sci USA 89:8155–8159

MacKenzie RG, Van Leeuwen D, Pugsley TA, Shih YH, Demattos S, Tang L, Todd RD, O'Malley KL (1994) Characterization of the human dopamine D_3 receptor expressed in transfected cell lines. Eur J Pharmacol, Mol Pharmacol Sect 266:79–85

Millan MJ, Peglion JL, Vian J, Rivet JM, Brocco M, Gobert A, Newman-Tancredi A, Dacquet C, Bervoets K, Girardon S, Jacques V, Chaput C, Audinot V (1995) Functional correlates of dopamine D_3 receptor activation in the rat *in vivo* and their modulation by the selective agonist, (+)-S 14297: 1. Activation of postsynaptic D_3 receptors mediates hypothermia, whereas blockade of D_2 receptors elicits prolactin secretion and catalepsy. J Pharm Exp Ther 275:885–898

Pagliusi S, Chollet-Daemerius A, Losberger C, Mills A, Kawashima E (1993) Characterization of a novel exon within the D3 receptor gene giving rise to an mRNA isoform expressed in rat brain. Biochem Biophys Res Commun 194:465–471

Sibley DR (1991) Cloning of a 'D_3' receptor subtype expands dopamine receptor family. Trend Pharmacol Sci 12:7–9

Sokoloff P, Giros B, Martres MP, Bouthenet ML, Schwartz JC (1990) Molecular cloning and characterization of a novel dopamine receptor (D_3) as a target for neuroleptics. Nature 347:146–151

Todd RD, O'Malley KL (1993) Family ties: The dopamine D_2-like receptor genes. Neurotransmiss 9(3):1–4

E.5.1.5 Binding to D_4 Receptors

PURPOSE AND RATIONALE

Van Tol et al. (1991) reported cloning of the gene of a human dopamine D_4 receptor with high affinity for the antipsychotic clozapine. Together with the D_{2S}, the D_{2L} and the D_3 receptor, the D_4 receptor belongs to

the group of D_2-like dopamine receptors (Ginrich and Caron 1993). Recognition and characterization of this dopamine binding site may be useful in the design of new types of antipsychotic drugs.

Dopamine D_4 receptors have been localized in GABAergic neurons of the primate brain (Mrzljak et al. 1996).

PROCEDURE

A plasmid construct of a 3.9-kb gene-cDNA hybrid subcloned into the expression vector pCD-PS is introduced into COS-7 cells by calcium phosphate mediated transfection. Cells are cultivated and homogenized (Teflon pestle) in 50 mM Tris-HCl (pH 7.4 at 4°C) buffer containing 5 mM EDTA, 1.5 mM $CaCl_2$, 5 mM KCl, and 120 mM NaCl. Homogenates are centrifuged for 15 min at 39,000 *g*, and the resulting pellets resuspended in buffer at a concentration of 150–250 µg/ml. For saturation experiments, 0.25 ml of tissue homogenate are incubated in duplicate with increasing concentrations of [^{3}H]spiperone (70.3 Ci mmol^{-1}; 10–3000 pM final concentration) for 120 min at 22°C in a total volume of 1 ml. For competition binding experiments, assays are initiated by the addition of 0.25 ml membrane and incubated in duplicate with various concentrations of competing ligands (10^{-14}–10^{-3} M) and [^{3}H]spiperone (150–300 pM) either in the absence or the presence of 200 µM Gpp(NH)p for 120 min at 22°C. Assays are terminated by rapid filtration through a Titertek cell harvester and filters then monitored for tritium. For all experiments, specific binding is defined as that inhibited by 10 µM (–)sulpiride.

EVALUATION

Both saturation and competition binding data are analyzed by the non-linear least-square curve-fitting program LIGAND run on a suitable PC.

MODIFICATIONS OF THE METHOD

Human Recombinant Dopamine $D_{4,2}$, $D_{4,4}$, $D_{4,7}$ and D_5 Receptors

Van Tol et al. (1992) described multiple dopamine D_4 receptor variants in the human population.

Sunahara et al. (1991) reported the cloning of the gene for a human D_5 receptor.

Human Recombinant Dopamine $D_{4,2}$ Receptor Binding

In a radioligand binding assay the binding of [^{3}H]-spiperone to membranes prepared from COS cells transiently expressing a recombinant human dopamine $D_{4,2}$ receptor is measured.

Fifteen µg of membrane is incubated with [^{3}H]-spiperone at a concentration of 0.7 nM for 2 h at 25°C. Non-specific binding is estimated in the presence of 10 µM haloperidol. Membranes are filtered and washed 3 times with binding buffer, and filters are counted to determine [^{3}H]-spiperone bound.

Human Recombinant Dopamine $D_{4,4}$ Receptor Binding

In a radioligand binding assay the binding of [^{3}H]-spiperone to membranes prepared from COS cells transiently expressing a recombinant human dopamine $D_{4,4}$ receptor is measured.

Twenty-five µg of membrane are incubated with [^{3}H]-spiperone at a concentration of 1.0 nM for 2 h at 25°C. Nonspecific binding is estimated in the presence of 10 µM haloperidol. Membranes are filtered and washed 3 times with binding buffer, and filters are counted to determine [^{3}H]-spiperone bound.

Human Recombinant Dopamine $D_{4,7}$ Receptor Binding

In a radioligand binding assay the binding of [^{3}H]-spiperone to membranes prepared from COS cells transiently expressing a recombinant human dopamine $D_{4,7}$ receptor is measured.

Fifteen µg of membrane is incubated with[^{3}H]-spiperone at a concentration of 0.7 nM for 2 h at 25°C. Non-specific binding is estimated in the presence of 10 µM haloperidol. Membranes are filtered and washed 3 times with binding buffer, and filters are counted to determine [^{3}H]-spiperone bound.

Human Recombinant Dopamine D_5 Receptor

In a radioligand binding assay the binding of [^{3}H]SCH 23390 to membranes prepared from COS cells expressing a recombinant human dopamine D_5 receptor is measured.

First, 40 µg of membrane is incubated with [^{3}H]SCH 23390 at a concentration of 2 nM for 2 h at 25°C. Non-specific binding is estimated in the presence of 10 µM *cis*-flupentixol. Membranes are filtered and washed 3 times with binding buffer, and filters are counted to determine [^{3}H]SCH 23390 bound.

Several selective dopamine D_4 antagonists were described: Hikada et al. (1996), Merchant et al. (1996), Rowley et al. (1996), Bristow et al. (1997).

Some radioligands were proposed as being selective for dopamine D_4 receptors: [^{3}H]clozapine (Ricci et al. 1997a, b), [^{3}H]NGD 94–1 (Thurkauf 1997; Primus et al. 1997), RBI-257 (Kula et al. 1997).

REFERENCES AND FURTHER READING

Birstow LJ, Collinson N, Cook GP, Curtis N, Freedman SB, Kulagowski JJ, Leeson PD, Patel S, Ragan CI, Ridgill M, Saywell KL, Tricklebank MD (1997) L-745,870, a subtype selective dopamine D_4 receptor antagonist, does not exhibit a neuroleptic-like profile in rodent behavior tests. J Pharmacol Exp Ther 283:1256–1263

Ginrich JA, Caron MC (1993) Recent advances in the molecular biology of dopamine receptors. Annu Rev Neurosci 16:299–321

Hidaka K, Tada S, Matsumoto M, Ohmori J, Maeno K, Yamaguchi T (1996) YM-50001: a novel, potent and selective dopamine D_4 receptor antagonist. NeuroReport 7:2543–2546

Kula NS, Baldessarini RJ, Kebabian JW, Bakthavachalam V, Xu L (1997) RBI 257: A highly potent, dopamine D_4 receptor-selective ligand. Eur H Pharmacol 331:333–336

Merchant KM, Gill KS, Harris DW, Huff RM, Eaton MJ, Lookingland K, Lutzke BS, McCall RB, Piercey MF, Schreur PJKD, Sethy VH, Smith MW, Svensson KA, Tang AH, von Voigtlander PF, Tenbrink RE (1996) Pharmacological characterization of U-101387, a dopamine D_4 receptor selective antagonist. J Pharmacol Exp Ther 279:1392–1403

Mrzljak L, Bergson C, Pappy M, Huff R, Levenson R, Goldman-Rakic PS (1996) Localization of dopamine D_4 receptors in GABAergic neurons of the primate brain. Nature 381:245–248

Primus J, Thurkauf A, Xu J, Yevich E, McInerney S, Shaw K, Tallman JF, Gallager DW (1997) Localization and characterization of dopamine D_4 binding sites in rat and human brain by use of the novel D_4 receptor-selective ligand [^{3}H]NGD 94–1. J Pharmacol Exp Ther 282:1020–1027

Ricci A, Bronzetti E, Rossodivita I, Amenta F (1997a) Use of [^{3}H]clozapine as a ligand of the dopamine D_4 receptor subtype in peripheral tissues. J Auton Pharmacol 17:261–267

Ricci A, Bronzetti E, Felici L,Tayebati SK, Amenta F (1997b) Dopamine D_4 receptor in human peripheral blood lymphocytes: A radioligand binding assay study. Neurosci Lett 229:130–134

Rowley M, Broughton HB, Collins I, Baker R, Emms F, Marwood R, Patel S, Ragan CI, Freedman SB, Leeson PD (1996) 5-(4-Chlorophenyl)-4-methyl-3-(1-(2-phenylethyl)piperidin-4-yl)isoxazole: A potent, selective antagonist at cloned dopamine D_4 receptors. J Med Chem 39:1943–1945

Sunahara RK, Guan HC, O'Dowd BF, Seeman P, Laurier LG, Ng G, George SR, Torchia J, Van Tol HHM, Niznik HB (1991) Cloning of the gene for a human D_5 receptor with higher affinity for dopamine than D_1. Nature 350:614–619

Thurkauf A (1997) The synthesis of tritiated 2-phenyl-4-[4-(2-pyrimidyl)piperazinyl]methylimidazole ([^{3}H]NGD 94–1), a ligand selective for the dopamine D_4 receptor subtype. J Label Comp Radiopharm 39:123–128

Todd RD, O'Malley KL (1993) Family ties: The dopamine D_2-like receptor genes. Neurotransmiss 9(3):1–4

Van Tol HHM, Bunzow JR, Guan HC, Sunahara RK, Seeman P, Niznik HB, Civelli O (1991) Cloning of the gene for a human dopamine D_4 receptor with high affinity for the antipsychotic clozapine. Nature 350:610–614

Van Tol HHM, Wu CM, Guan HC, Ohara K, Bunzow JR, Civelli O, Kennedy J, Seeman P, Niznik HB, Jovanovic V (1992) Multiple dopamine D4 receptor variants in the human population. Nature 358:149–152

E.5.1.6 Determination of Dopamine Autoreceptor Activity

PURPOSE AND RATIONALE

The method describes the procedure to determine if a compound possesses autoreceptor blocking activity without the interference from postsynaptic effects. Striatal DOPA (3,4-dihydroxyphenylalanine), DOPAC (3,4-dihydroxyphenylacetic acid) and DA (dopamine) are quantitated following *in vivo* treatment with drug, apomorphine, gamma butyrolactone and NSD-1015. Antipsychotic compounds that block striatal dopaminergic presynaptic autoreceptors are believed to possess a greater liability for producing EPS.

PROCEDURE

Reagents

1. 0.1 M HCl
2. 1 N NaOH
3. 0.1 M perchloric acid (PCA) containing 4.3 mM EDTA
4. 2 mM solutions of DOPAC, DA and DOPA in 0.1 M HCl, 0.5 ml aliquots are stored at –60°C until use.
5. Preparation of 2° standard mixture
   10 µM solution of DOPAC, DA and DOPA diluted from reagent 4 with 0.1 M PCA/EDTA);
   The 2° standard solution is used for the preparation of standard curves.
6. Mobile phase/MeOH-buffer (4 : 96, v/v) buffer: 0.012 mM sodium acetate, 0.036 M citric acid and 152 µM sodium octane sulfonate, mobile phase: methanol/buffer (80 ml + 1920 ml) is filtered through a 0.2 µm nylon 66 filter.
7. Preparation of dosing solutions
   a) Apomorphine (2 mg/kg) is prepared in saline containing 1% Tween 80 + 0.1% ascorbic acid to prevent oxidation.
   b) GBL (750 mg/kg) is prepared as a solution in saline containing 1% Tween 80.
   c) NSD-1015 (100 mg/kg) is prepared as a solution in saline containing 1% Tween 80.

HPLC-Instrumentation

Consists of a

- pump, model SP8810 (Spectra Physics),
- injector, WISP 710B (Waters Associates),
- detector, 5100A electrochemical with a 5011 analytical cell and 5020 guard cell (ESA),

- integrator, D-2000 (Hitachi), used as a back-up for the data collection/integrator, CS 9000 (IBM) system
- analytical column: C18-ODS Hypersil, 3 µm, 100 × 4.6 mm (Shandon)

Tissue Preparation

Following treatment with test drug, rats are sacrificed by decapitation at the pre-determined time. The brain is rapidly removed, the striatum is dissected on ice and frozen on dry ice. The tissue is analyzed by HPLC the same day.

Tissue is homogenized in 500 µl 0.1 M PCA/EDTA. The homogenate is centrifuged for 6 min using a microcentrifuge (model 5413, Eppendorf). The supernatant is transferred to 0.2 µm microfilterfuge™ tubes and centrifuged for 6–8 min as before. The filtrate is transferred to WISP vials. Standards are included every 12–15 samples.

Five µl of the striatum homogenate is injected into the HPLC column.

HPLC flow rate is 1.5 ml/min, run time is 20 min. Helium flow is constant in mobile phase.

For protein analysis, 1.0 ml 1 N NaOH is added to the tissue pellet. The next day, the protein analysis is performed as described by Bradford (1976) using the BioRad assay kit.

EVALUATION

Peak area is used for quantitation. The mg of protein and pmoles of DOPAC, DA and DOPA are calculated from linear regression analyses using the corresponding standard curve. Final data are reported as pmoles/mg protein.

REFERENCES AND FURTHER READING

Bradford M (1976) A rapid and sensitive method for the quantitation of microgram quantities of protein utilizing the principle of protein-dye binding. Analyt Biochem 72:248–254

Magnusson O, Mohringe B, Fowler CJ (1987) Comparison of the effects of dopamine D1 and D2 receptor antagonists on rat striatal, limbic and nigral dopamine synthesis and utilization. J Neural Transm 69:163–177

Reinhard JF, Perry JA (1984) Fast analysis of tissue catechols using a short, high-efficiency (3 µM) LC column and amperometric detection. J Chromatography 7:1211–1220

Wagner J, et al (1979) Determination of DOPA, dopamine, DOPAC, epinephrine, norepinephrine, α-monofluoromethyldopa and α-difluoromethyldopa in various tissues of mice and rats using reversed-phase ion-pair liquid chromatography with electrochemical detection. J Chromatography 164:41–54

Walters JR, Roth RH (1976) Dopaminergic neurons: An *in vivo* system for measuring drug interactions with presynaptic receptors. Naunyn-Schmiedeberg's Arch. Pharmacol 296:5–14

E.5.1.7 Dopamine-Sensitive Adenylate Cyclase in Rat Striatum

PURPOSE AND RATIONALE

Agonist stimulation of dopamine D_1 receptors leads to increased cAMP formation mediated by a guanine nucleotide-binding regulatory protein. This effect is blocked by selective antagonists like SCH 23390.

Agonist stimulation of the dopamine D_2 receptor leads to a decreased cAMP formation mediated by a guanine nucleotide binding protein. Apomorphine is a potent agonist with full intrinsic activity at D_2 receptors. Phenothiazines block both D_1 and D_2 receptors, whereas butyrophenones and related drugs are very potent antagonists at D_2 receptors.

Studies on cAMP formation may be useful for differentiation of antipsychotic drugs.

PROCEDURE

Tissue Preparation

Male Wistar rats are sacrificed by decapitation, the brains removed, and the striata dissected out and weighed. Striatal tissue from 2 rats is homogenized in 25 volumes of ice-cold 0.08 M Tris-maleate buffer, pH 7.4, containing 2 mM EGTA. Protein content of an aliquot is determined. A 50 µl aliquot is used in the cyclase enzyme assay.

Enzyme Assay

The following volumes are placed in conical centrifuge tubes kept in an ice-water bath:

200 µl	incubation buffer (equal amounts of 0.8 mM Tris-maleate, pH 7.4; 60 mM $MgSO_4$; 100 mM theophylline and 4 mM EGTA)
50 µl	1 mM dopamine HCl or water
25 µl	test drug or water
125 µl	distilled water
50 µl	tissue homogenate

After incubation for 20 min at 0°C, the enzyme reaction is started by addition of 50 µl of 15 mM ATP solution. The tube rack is placed in a shaking water bath preset at 30°C for 2.5 min. The reaction is terminated by placing the tube rack in a boiling water bath for 4 min. Then, the tubes are centrifuged at 1000 *g* for 10 min.

A 25 µl aliquot of the supernatant in each tube is removed and the cAMP determined using a commercial RIA kit (Amersham).

EVALUATION

Results are expressed as pmoles cAMP/mg protein of dopamine stimulated vs. non dopamine stimulated level. Percentage inhibition of this dopamine stimulated level by test drugs is calculated and IC_{50} values determined by log-probit analysis.

REFERENCES AND FURTHER READING

Broaddus WC, Bennett JP Jr (1990) Postnatal development of striatal dopamine function. I. An examination of D_1 and D_2 receptors, adenylate cyclase regulation and presynaptic dopamine markers. Develop Brain Res 52:265–271

Clement-Cormier YC, Kebabian JW, Petzold GL, Greengard P (1974) Dopamine-sensitive adenylate cyclase in mammalian brain: a possible site of action of antipsychotic drugs. Proc Natl Acad Sci USA 71:1113–1117

Clement-Cormier YC, Parrish RG, Petzold GL, Kebabian JW, Greengard P (1975) Characterisation of a dopamine-sensitive adenylate cyclase in the rat caudate nucleus. J Neurochem 25:143–149

Creese I (1987) Biochemical properties of CNS dopamine receptors. In: Meltzer HY (ed) Psychopharmacology; The Third Generation of Progress. Raven Press New York, pp 257–264

Gale K, Giudotti A, Costa E (1977) Dopamine-sensitive adenylate cyclase: Location in substantia nigra. Science 195:503–505

Horn S, Cuello AC, Miller RJ (1974) Dopamine in the mesolimbic system of the rat brain: endogenous levels and the effect of drugs on the uptake mechanism and stimulation of adenylate cyclase activity. J Neurochem 22:265–270

Iversen LL (1975) Dopamine receptors in the brain. Science 188:1084–1089

Kebabian JW, Calne DB (1979) Multiple receptors for dopamine. Nature 277:93–96

Kebabian JW, Petzold GL, Greengard P (1972) Dopamine-sensitive adenylate cyclase in caudate nucleus of rat brain, and its similarity to the "dopamine receptor" Proc Nat Acad Sci USA 69:2145–2149

Magnusson O, Mohringe B, Fowler CJ (1987) Comparison of the effects of dopamine D1 and D2 receptor antagonists on rat striatal, limbic and nigral dopamine synthesis and utilisation. J Neural Transm 69:163–177

Setler PE, Rarau HM, Zirkle CL, Saunders HL (1978) The central effects of a novel dopamine agonist. Eur J Pharmacol 50:419–430

E.5.1.8 α_1-Adrenergic Receptor Binding in Brain

PURPOSE AND RATIONALE

The use of neuroleptic and antidepressant drugs is sometimes limited by their side effects, such as orthostatic hypotension and sedation. These side effects are attributed to blockade of central and peripheral adrenergic α-receptors. For neuroleptics the ratio between their dopamine antagonistic and their α-receptor antagonistic potencies should be taken into account rather than their absolute α-blocking effect. WB-4101 is a specific and potent antagonist of the α_1-adrenoreceptor, characterized *in vitro* in rat brain, heart, vascular smooth muscle and gastrointestinal smooth muscle.

The *in vitro* [^{3}H]-WB 4101 receptor binding assay quantitates the α-adrenergic blocking properties of psychoactive agents and is used to assess a compound's potential to cause orthostatic hypotension and sedation as well as primary blood pressure lowering effects through α_1-receptor blockade.

PROCEDURE

Reagents

[Phenoxy-3-^{3}H(N)]-WB 4101 = (2,6-dimethoxyphenoxyethyl)-aminomethyl-1,4-benzodioxane, New England Nuclear, (specific activity 20–35 Ci/mmol).

For IC_{50} determinations [^{3}H]-WB 4101 is made up to a concentration of 2 nM in Tris buffer and 500 µl is added to each tube (yields a final concentration of 0.5 nM in the 2 ml assay)

L-norepinephrine bitartrate (Sigma Chemical Company). A 800 µM solution is prepared in Tris buffer and 250 µl is added to each of 3 tubes to determine nonspecific binding. This yields a final concentration of 100 µM in the 2 ml assay.

Test compounds: A 80 µM stock solution is made up in a suitable solvent and serially diluted with Tris buffer, such that the final concentration in the assay ranges from 10^{-5} to 10^{-8} M. Usually, seven concentrations are studied for each assay.

Tissue Preparation

Male Wistar rats (100–150 g) are sacrificed by decapitation. The whole brain minus cerebellum is homogenized in 75 volumes of ice-cold 0.05 M Tris buffer, pH 7.7. The homogenate is centrifuged at 40,000 *g* at 4°C for 15 min. The supernatant is discarded and the pellet is rehomogenized in fresh Tris buffer and recentrifuged at 40,000 *g* at 4°C for 15 min. The final pellet is resuspended in the original volume of ice-cold 0.05 M Tris buffer. The final tissue concentration in the assay is 10 mg/ml. Specific binding is approximately 80% of total bound ligand.

Assay

1200 µl	tissue suspension
500 µl	^{3}H-WB 4101
250 µl	vehicle (for total binding) or
800 µM	L-norepinephrine bitartrate (for nonspecific binding) or appropriate drug concentration

Sample tubes are kept in ice for additions, then vortexed and incubated for 15 min at 25°C. The binding is terminated by rapid vacuum filtration through Whatman GF/B filters, followed by three 5 ml washes with ice-cold 0.05 M Tris buffer. The filters are counted in 10 ml of Liquiscint scintillation cocktail.

EVALUATION

Specific WB 4101 binding is defined as the difference between the total binding and that bound in the presence of 100 µM norepinephrine. IC_{50} calculations are performed using computer-derived log-probit analysis.

REFERENCES AND FURTHER READING

Creese I (1978) Receptor binding as a primary drug screening device. In: (HI Yamamura et al. eds) Neurotransmitter receptor binding pp 141–170, Raven Press, New York

Creese I, Burt DR, Snyder SH (1976) Dopamine receptor binding predicts clinical and pharmacological potencies of antischizophrenic drugs. Science 192:481–483

Greenberg DA, U'Prichard DC, Snyder SH (1976) Alpha-noradrenergic receptor binding in mammalian brain: Differential labelling of agonist and antagonist states. Life Sci 19:69–76

Huger FP, Smith CP, Chiang Y, Glamkowski EJ, Ellis DB (1987) Pharmacological evaluation of HP 370, a potential atypical antipsychotic agent. Drug Dev Res 11:169–175

Janowsky A, Sulser F (1987) Alpha and beta adrenoreceptors in brain. In: Meltzer HY (ed) Psychopharmacology: The Third Generation of Progress. pp 249–256, Raven Press, New York

Mottram DR, Kapur H (1975) The α-adrenoceptor blocking effects of a new benzodioxane. J Pharm Pharmacol 27:295–296

Peroutka SJ, U'Prichard DC, Greenberg DA, Snyder SH (1977) Neuroleptic drug interactions with norepinephrine alpha receptor binding sites in rat brain. Neuropharmacol 16:549–566

U'Prichard DC, Snyder SH (1979) Distinct α-noradrenergic receptors differentiated by binding and physiological relationships. Life Sci 24:79–88

U'Prichard DC, Greenberg DA, Shehan PP, Snyder SH (1978) Tricyclic antidepressants: Therapeutic properties and affinity for α-noradrenergic receptor binding sites in the brain. Science 199:197–198

Yamada S et al (1980) Characterisation of alpha-1 adrenergic receptors in the heart using [^{3}H]-WB 4101: Effect of 6-hydroxydopamine treatment. J Pharmacol Exper Ther 215:176–185

E.5.1.9 [^{3}H]Spiroperidol Binding to 5-HT$_2$ Receptors in Rat Cerebral Cortex

PURPOSE AND RATIONALE

The purpose of this assay is to determine the anti-serotonin activity of neuroleptics, antidepressants and antihypertensive compounds, by measuring the displacement of [^{3}H]spiroperidol from serotonergic antagonist binding sites in cerebral cortical membranes. The regulation of 5-HT$_2$ receptor density by chronic antidepressant treatment is discussed in a separate protocol (see Sect. E.6.1.6).

The receptor binding of serotoninergic sites in the CNS has been investigated using [^{3}H]serotonin (5-HT) (Bennett and Snyder 1976), [^{3}H]LSD (Peroutka and Snyder 1979) and [^{3}H]spiroperidol (Peroutka and Snyder 1979; List and Seeman 1981; Leysen et al. 1978) as the radioligand. Receptor sites have been defined kinetically and classified as 5-HT$_1$ sites (labeled by [^{3}H]5-HT, displaced by agonists) and 5-HT$_2$ sites (labeled by [^{3}H]-spiroperidol and displaced by antagonists). [^{3}H]LSD labels both 5-HT$_1$ and 5-HT$_2$ binding sites (Peroutka and Snyder 1979). Of the brain regions tested, the frontal cerebral cortex contained the greatest density of 5-HT$_2$ binding sites. Lesioning studies indicate that 5-HT$_2$ binding sites are post synaptic and not linked to adenylate cyclase (Peroutka et al. 1979).

The inhibition of 5-HT$_2$ binding correlates with the inhibition of quipazine-induced head twitch, which may reflect decreased behavioral excitation. The physiological and pharmacological role of these receptors is not clear. Although numerous neuroleptics and antidepressants of varying chemical structures are potent inhibitors of 5-HT$_2$ binding, there is no clear-cut relationship to the efficacy of these drugs. Methysergide and cyproheptadine are both potent inhibitors of 5-HT$_2$ binding without having neuroleptic or antidepressant effects. However, potent interaction with 5-HT$_2$ receptors may indicate a reduced potential for catalepsy, since methysergide blocks catalepsy induced by haloperidol (Rastogi et al. 1981). The interaction of serotonergic neurons with cholinergic neurons in the striatum (Samanin et al. 1978) may also be decreased by potent 5-HT$_2$ antagonists. In addition, the ratio of activity at D$_2$ and 5-HT$_2$ receptors may be useful in the screening of atypical antipsychotic agents (Meltzer et al. 1989). Furthermore, it has been shown that ketanserin, a selective 5-HT$_2$ antagonist, is an effective hypotensive agent which blocks peripheral vascular 5-HT receptors.

5-HT$_2$ receptors have been subdivided into 5-HT$_{2A}$, 5-HT$_{2B}$ and 5-HT$_{2C}$ receptors. The new 5-HT receptor classification has been published by the VII. International Union of Pharmacology Classification of Receptors for 5-Hydroxytryptamine (Serotonin) (Hoyer et al. 1994). Further comments were given by Humphrey et al. (1993), Martin and Humphrey (1994), Saxena (1994), Tricklebank (1996).

Several compounds with HT$_{2A}$ antagonistic activity are described, such as tradozone (Clements-Jewery

et al. 1980; Hingtgen et al. 1984; Stryjer et al. 2003), MDL 100,907 (Kehne et al. 1996; Moser et al. 1996), and sarpogrelate (Hayashi et al. 2003).

McCullough et al. (2006) described the 5-HT_{2B} antagonist and 5-HT_4 agonist activities of tegaserod in the anesthetized rat.

PROCEDURE

Reagents

1. 0.5 M Tris buffer, pH 7.7
   a) 57.2 g Tris HCl
      16.2 g Tris base
      q.s. to 1 liter (0.5 M Tris buffer, pH 7.7)
   b) Make a 1:10 dilution in distilled H_2O (0.05 M Tris buffer, pH 7.7)
2. Tris buffer containing physiological ions
   a) Stock buffer

      NaCl 7.014 g
      KCl 0.372 g
      $CaCl_2$ 0.222 g
      $MgCl_2$ 0.204 g

      q.s. to 100 ml in 0.5 M Tris buffer
   b) Dilute 1:10 in distilled H_2O
      This yields 0.05 M Tris HCl, pH 7.7; containing NaCl (120 mM), KCl (5 mM), $CaCl_2$ (2 mM) and $MgCl_2$ (1 mM)
3. [Benzene-^{3}H] spiroperidol (20–35 Ci/mmol) is obtained from New England Nuclear. For IC_{50} determinations: ^{3}H-spiroperidol is made up to a concentration of 30 nM in 0.01 N HCl and 50 µl added to each tube (yields a final concentration of 1.5 nM in the 1 ml assay).
4. Methysergide maleate is obtained from Sandoz. Methysergide maleate stock solution is made up to 0.25 mM for determination of nonspecific binding. The final concentration in the assay is 5 µM, when 20 µl of the stock solution is added to the reaction tube.
5. Test compounds. For most assays, a 1 mM stock solution is made up in a suitable solvent and serially diluted, such that the final concentration in the assay ranges from 10^{-5} to 10^{-8} M. Seven concentrations are used for each assay and higher or lower concentrations may be used, depending on the potency of the drug.

Tissue Preparation

Male Wistar rats are decapitated and the cerebral cortical tissue is dissected, weighed and homogenized in 50 volumes of 0.05 M Tris buffer, pH 7.7 (buffer 1b) with the Brinkman Polytron, then centrifuged at 40,000 *g* for 15 min. The supernatant is discarded and the pellet resuspended and recentrifuged as described above. This pellet is resuspended in 50 volumes of buffer 2b and stored in an ice bath. The final tissue concentration is 10 mg/ml. Specific binding is 7% of the total added ligand and 50% of total bound ligand.

Assay

50 µl	0.5 M Tris-physiological salts (buffer 2a)
380 µl	H_2O
20 µl	vehicle (for total binding) or 0.25 mM methysergide (for nonspecific binding) or appropriate drug concentration
50 µl	[^{3}H]spiroperidol
500 µl	tissue suspension

The samples are incubated for 10 min at 37°C, then immediately filtered under reduced pressure using Whatman GF/B filters. The filters are washed with three 5 ml volumes of ice-cold 0.05 M Tris buffer, pH 7.7 mM methysergide.

EVALUATION

IC_{50} calculations are performed using log-probit analysis. The percent inhibition at each drug concentration is the mean of triplicate determinations.

MODIFICATION OF THE METHOD

The receptor binding properties of the 5-HT_2 antagonist ritanserin were reported by Leysen et al. (1985).

Preclinical characterization of a putative antipsychotic as a potent 5-HT_{2A} antagonist was reported by Kehne et al. (1996).

Using [^{125}I]LSD and [^{3}H]5-HT binding assays Siegel et al. (1996) characterized a structural class of 5-HT_2 receptor ligands.

[^{3}H]Ketanserin has been described as a selective ^{3}H-ligand for 5-HT_2 receptor binding sites. (Leysen et al. 1981).

[^{3}H]RP 62203, a potent and selective 5-HT_2 antagonist was recommended for *in vivo* labeling of 5-HT_2 receptors (Fajolles et al. 1992).

Other selective 5-HT_2 receptor radioligands were recommended:

[^{125}I]-EIL (radioiodinated D-(+)-N1-ethyl-2-iodolysergic acid diethylamide) (Lever et al. 1991); [^{3}H]-MDL100,907 (Lopez-Gimenez et al. 1998).

REFERENCES AND FURTHER READING

Altar CA, Wasley AM, Neale RF, Stone GA (1986) Typical and atypical antipsychotic occupancy of D_2 and S_2 receptors: an autoradiographic analysis in rat brain. Brain Res Bull 16:517–525

Bennett JP Jr, Snyder SH (1976) Serotonin and lysergic acid diethylamide binding in rat brain membranes: Relationship to postsynaptic serotonin receptors. Mol Pharmacol 12:373–389

Clements-Jewery S, Robson PA, Chidley (1980) Biochemical investigations into the mode of action of trazodone. Neuropharmacology 19:1165–1173

Costall B, Fortune DH, Naylor RJ, Marsden CD, Pycock C (1975) Serotonergic involvement with neuroleptic catalepsy. Neuropharmacol 14:859–868

Dugovic C, Leysen JE, Wauquier A (1991) Serotonin and sleep in the rat: the role of 5-HT_2 receptors. In: Idzikowski C, Cowen PJ (eds) Serotonin, Sleep and Mental Disorder. Wrightson Biomedical Publishing Ltd., Petersfield, pp 77–88

Fajolles C, Boireau A, Pochant M, Laduron PM (1992) [^{3}H]RP 62203, a ligand of choice to label *in vivo* brain 5-HT_2 receptors. Eur J Pharmacol 216:53–57

Gelders YG, Heylen SLE (1991) Serotonin 5-HT_2 receptor antagonism in schizophrenia. In: Idzikowski C, Cowen PJ (eds) Serotonin, Sleep and Mental Disorder. Wrightson Biomedical Publishing Ltd., Petersfield, pp 179–192

Hayashi T, Sumi D, Matsui-Hirai H, Fukatsu A, Rani JA, Kano H, Tsunekawa T, Iguchi A (2003) Sarpogrelate HCl, a selective 5-HT_{2A} antagonist, retards the progression of atherosclerosis through a novel mechanism. Atherosclerosis 168:23–31

Hingtgen JN, Hendrie HC, Aprison MH (1984) Polysynaptic serotonergic blockade following chronic antidepressive treatment in an animal model of depression. Pharmacol Biochem Behav 20:425–428

Hoyer D, Clarke DE, Fozard JR, Hartig PR, Martin GR, Mylecharane EJ, Saxena PR, Humphrey PP (1994) VII. International Union of Pharmacology Classification of Receptors for 5-Hydroxytryptamine (Serotonin). Pharmacol Rev 46:157–203

Humphrey PPA, Hartig P, Hoyer D (1993) A proposed new nomenclature for 5-HT receptors. Trends Pharmacol Sci 14:233–236

Kehne JK, Baron BM, Carr AA, Chaney SF, Elands J, Feldman DJ, Frank RA, van Giersbergen PLM, McCloskey TC, Johnson MP, McCarty DR, Poirot M, Senyah Y, Siegel BW, Widmaier C (1996) Preclinical characterization of the potential of the putative atypical antipsychotic MDL 100,907 as a potent 5-HT_{2A} antagonist with a favorable CNS safety profile. J Pharmacol Exp Ther 277:968–981

Lever JR, Scheffel UA, Musachio JL, Stathis M, Wagner HN Jr (1991) Radioiodinated D-(+)-N1-ethyl-2-iodolysergic acid diethylamide: A ligand for *in vitro* and *in vivo* studies of serotonin receptors. Life Sci 48: PL-73–PL-78

Leysen JE, Niemegeers CJE, Tollenaere JP, Laduron PM (1978) Serotonergic component of neuroleptic receptors. Nature 272:168–171

Leysen JE, Niemegeers CJE, van Nueten JM, Laduron PM (1981) [^{3}H]Ketanserin (R 41 468), a selective ^{3}H-ligand for serotonin$_2$ receptor binding sites. Binding properties, brain distribution, and functional role. Mol Pharmacol 21:301–314

Leysen JE, Niemegeers CJE, Van Nueten JM, Laduron PM (1982) [^{3}H]Ketanserin (R41 468) a selective ^{3}H-ligand for serotonin$_2$ receptor binding sites. Mol Pharmacol 21:301–314

Leysen JE, de Chaffoy de Courcelles D, de Clerck F, Niemegeers CJE, van Nueten JM (1984) Serotonin-S2 receptor binding sites and functional correlates. Neuropharmacol 23:1493–1501

Leysen JE, Gommeren W, van Gompel P, Wynants J Janssen PFM, Laduron PM (1985) Receptor-binding properties *in vitro* and *in vivo* by ritanserin. A very potent and long acting serotonin-S_2 antagonist. Mol Pharmacol 27:600–611

List SJ, Seeman P (1981) Resolution of dopamine and serotonin receptor components of [^{3}H]spiperone binding of rat brain regions. Proc Natl Acad Sci USA 78:2620–2624

Lopez-Gimenez JF, Vilaro MT, Palacios JM, Mengod G (1998) [^{3}H]-MDL100,907 labels serotonin 5-HT_{2A} receptors selectively in primate brain. Neuropharmacology 37:1147–1158

Martin GR, Humphrey PPA (1994) Classification review. Receptors for 5-hydroxytryptamine: Current perspectives on classification and nomenclature. Neuropharmacol 33:261–273

McCullough JL, Armstrong SR, Hegde SS, Beattie DT (2006) The 5-HT_{2B} antagonist and 5-HT_4 agonist activities of tegaserod in the anaesthetized rat. Pharmacol Res 53:353–358

Meert TF, Awouters F (1991) Serotonin 5-HT_2 antagonists: a preclinical evaluation of possible therapeutic effects. In: Idzikowski C, Cowen PJ (eds) Serotonin, Sleep and Mental Disorder. Wrightson Biomedical Publishing Ltd., Petersfield, pp 65–76

Meltzer HV, Matsubara S, Lee JC (1989) Classification of typical and atypical antipsychotic drugs on the basis of dopamine D_1, D_2 and serotonin$_2$ pK_i values. J Pharmacol Exp Ther 251:238–246

Morgan DG, Marcusson JO, Finch CE (1984) Contamination of serotonin-2 binding sites with an alpha-1 adrenergic component in assays with (3H)spiperone. Life Sci 34:2507–2514

Moser PC, Moran PM, Frank RA, Kehne JH (1996) Reversal of amphetamine-induced behaviours by MDL 100.907, a selective 5-HT_{2A} antagonist. Behav Brain Res 73:163–167

Muramatsu M, Tamaki-Ohashi J, Usuki C, Araki H, Aihara H (1988) Serotonin-2 receptor mediated regulation of release of acetylcholine by minaprine in cholinergic nerve terminal of hippocampus of rat. Neuropharmacol 27:603–609

Palacios JM, Niehoff DL, Kuhar MJ (1981) [^{3}H]Spiperone binding sites in brain: autoradiographic localization of multiple receptors. Brain Res 213:277–289

Pazos A, Cortés R, Palacios JM (1985) Quantitative autoradiographic mapping of serotonin receptors in the rat brain. II. Serotonin-2 receptors. Brain Res 2346:231–249

Pedigo NW, Yamamura HI, Nelson DL (1981) Discrimination of multiple [^{3}H]5-hydroxytryptamine binding sites by the neuroleptic spiperone in rat brain. J Neurochem 36:220–226

Peroutka SJ, Snyder SH (1979) Multiple serotonin receptors: Differential binding of [^{3}H]5-hydroxytryptamine, [^{3}H]-lysergic acid diethylamide and [^{3}H]spiroperidol. Mol Pharmacol 16:687–699

Peroutka SJ, Lebovitz RM, Snyder SH (1979) Serotonin receptors binding sites affected differentially by guanine nucleotides. Mol Pharmacol 16:700–708

Rastogi RB, Singhal RL, Lapierre YD (1981) Effects of short- and long-term neuroleptic treatment on brain serotonin synthesis and turnover: Focus on the serotonin hypothesis of schizophrenia. Life Sci. 29:735–741

Samanin R, Quattrone A, Peri G, Ladinsky H, Consolo S (1978) Evidence of an interaction between serotonergic and cholinergic neurons in the corpus striatum and hippocampus of the rat brain. Brain Res 151:73–82

Saxena PR (1994) Modern 5-HT receptor classification and 5-HT based drugs. Exp Opin Invest Drugs 3:513–523

Siegel BW, Freedman J, Vaal MJ, Baron BM (1996) Activities of novel aryloxyalkylimidazolines on rat 5-HT_{2A} and 5-HT_{2C} receptors. Eur J Pharmacol 296:307–318

Stryjer R, Strous RD, Bar F, Poyurovsky M, Weizman A, Kotler M (2003) Treatment of neuroleptic-induced akathisia with the 5-HT_{2A} antagonist trazodone. Clin Neuropharmacol 26:137–141

Tricklebank MD (1996) The antipsychotic potential of subtype-selective 5-HT-receptor ligands based on interactions with mesolimbic dopamine systems. Behav Brain Res 73:15–15

E.5.1.10 Serotonin 5-HT_2 Receptor Autoradiography (^{3}H-Spiperone Binding)

PURPOSE AND RATIONALE

Autoradiography of ^{3}H-spiperone binding sites with selective labeling conditions permits the visualization of the anatomical locations of 5-HT_2 receptors (Palacios et al. 1981; Pazos et al. 1985; Altar et al. (1985). Quantitative measurements of the binding to receptors can be obtained with computer-assisted video analysis of the autoradiograms with a greater anatomical resolution and sensitivity than in membrane homogenates (Pazos et al. 1985; Altar et al. (1984). Using autoradiographic techniques, it has been demonstrated that there is a heterogeneous distribution of 5-HT_2 receptors, with much higher levels in telencephalic areas such as the neocortex and the claustrum than in meso- or metencephalic areas. Within the cortex, 5-HT_2 receptors are abundant in layers IV and V (Pazos et al. 1985). The high concentration of 5-HT_2 receptors in the frontoparietal motor area and the claustrum which connects to the motor cortex and other motor areas suggests a physiological role for 5-HT_2 receptors in some motor syndromes (Cadet et al. 1987; Costall et al. 1975; Kostowski et al. 1972). The high affinity of the atypical antipsychotic clozapine for 5-HT_2 receptors (Fink et al. 1984; Altar et al1986) and the down-regulation of 5-HT_2 receptors following chronic administration of clozapine (Reynolds et al. 1983; Lee and Tang 1984; Wilmot and Szczepanik 1989) suggests that 5-HT_2 receptor interaction may be a significant factor in the lack of extrapyramidal side effects and tardive dyskinesias with its clinical use.

Since ^{3}H-spiperone labels α_1-noradrenergic sites in the cerebral cortex, a masking concentration of the α_1-blocker prazosin is included to selectively define binding to 5-HT_2 receptors (Morgan et al. 1984). This is necessary if the test compound also inhibits α_1-receptors which may be present in the brain region of interest.

The assay is used to determine the direct interaction of potential antipsychotic compounds with the serotonin-5-HT_2 recognition site in discrete regions of the rat brain either *in vitro* or after *ex vivo* treatment of the whole animal.

PROCEDURE

Reagents

1a. 0.5 M Tris+1.54 M NaCl, pH 7.4

1b. 0.05 M Tris+0.154 M NaCl, pH 7.4

2. ^{3}H-spiperone (specific activity 70–90 Ci/mmol) is obtained from Amersham.
   - For IC_{50} determinations: ^{3}H-spiperone is made up to a concentration of 20 nM and 0.55 ml is added to each slide mailer (yields a final concentration of 1.0 nM in the 11.0 ml assay volume).
   - For saturation experiments: ^{3}H-spiperone is made up to a concentration of 20 nM. The final concentration should range from 0.5–2.5 nM. Typically, six concentrations are used by adding 0.55 ml or less to each mailer (for smaller volumes, add water to bring total addition of 0.55 ml).

3. Methysergide is used to determine nonspecific binding in brain sections of the frontal cortex.
   Methysergide maleate is obtained from Sandoz. A stock solution of 2.5×10^{-4} M is made by dissolving in distilled water. A volume of 0.22 ml of the stock solution is added to the nonspecific binding slide mailers (final concentration 5 µM). All other mailers receive 0.22 ml of vehicle (1 ml of 0.01 N acetic acid in a final volume of 10 ml with distilled water).

4. Ketanserin is used to determine nonspecific binding in those slide mailers containing sections with the nucleus accumbens and striatum.
   Ketanserin (free base or tartrate salt) is obtained from Janssen. A stock solution of 10^{-3} M is made by dissolving the ketanserin (free base) in 0.05 N acetic acid or the tartrate salt in distilled water. This is further diluted to 5×10^{-6} M (50 µM q.s 10 ml with distilled water). A volume of 0.22 ml is added to the slide mailers to give a final concentration of 100 nM.

5. Prazosin is used to mask α_1-receptors in cortical brain section.
   Prazosin HCl is obtained from Pfizer. A stock solution of 10^{-4} M is made by dissolving prazosin in 0.01 N acetic acid and bringing the final volume to 10 ml with distilled water. This is further diluted to 5×10^{-6} M (100 µM q.s 10 ml). A volume of 0.22 ml is added to those slide mailers to

be used for cortical brain sections to give a final concentration of 100 nM.

6. Sulpiride is used to mask D_2 receptor binding in brain sections from the nucleus accumbens and striatum.
   Sulpiride is obtained from Sigma. A stock solution of 10^{-4} M is made by dissolving sulpiride in 1.0 ml of 0.01 N acetic acid and bringing the final volume to 10 ml with distilled water. A volume of 0.22 ml is added to the appropriate slide mailers to give a final concentration of 10 µM.
7. Test compounds (for *in vitro* IC_{50} determinations). For most assays, a 5×10^{-3} M stock solution is made up in a suitable solvent and serially diluted, such that the final concentration in the assay ranges from 10^{-5} to 10^{-8} M. Seven concentrations are used for each assay. Higher or lower concentrations may be used depending on the potency of the drug.

Tissue Preparation

Frontal cortical brain sections are collected from plates 5 through 8 and nucleus accumbens/striatal sections are collected from plates 9 (rostral n. accumbens) through plate 17 (caudal striatum) of "The Rat Brain Atlas in Stereotaxic Coordinates" by Paxinos and Watson.

1. For *in vitro* inhibition experiments, 3–5 sets of 10 slides are collected with 4–5 sections per slide.
2. For saturation experiments, 3–5 sets of 12 slides are collected with 4–5 sections per slide.
3. For *ex vivo* inhibition experiments, a set of 8 slides is used, 4 for total binding and 4 for nonspecific binding.
4. For experiments in which the tissue sections will be swabbed and counted with scintillation fluid, two sections per slide are collected.

Assay

1. Preparation of slide mailers (11.0 ml volume/slide mailer):
   Note: If slides with sections are to be wiped for scintillation counting, a final volume of 6.5 ml is sufficient to cover 2 sections. A proportional adjustment of the volumes to be pipetted is made.
   a) *In vitro* inhibition experiments
      Separate mailers are prepared for total binding, nonspecific binding and 7–8 concentrations of test compound.
      1. For frontal cortical brain sections, prazosin is included in all mailers to mask the binding of [^{3}H]-spiperone to α_1-receptors and nonspecific binding is defined with 5 µM methysergide.
         5.50 ml buffer 1b
         0.55 ml buffer 1a
         0.55 ml [^{3}H]-spiperone, 1.0 nM final concentration
         3.96 ml distilled water
         0.22 ml prazosin 5×10^{-6} M, final concentration 100 nM or vehicle
         0.22 ml test compound, final concentration 10^{-8}–10^{-5} M or methysergide 2.5×10^{-4} M, final concentration 5 µM or vehicle
      2. For brain sections with the nucleus accumbens and striatum in which there is negligible binding of [^{3}H]-spiperone to α_1-receptors, prazosin is not included. Since levels of 5-HT_2 receptors in these brain areas are low, 10 µM sulpiride is included in all mailers to mask the binding of [^{3}H]-spiperone to D_2 receptors.
         Ketanserin, final concentration of 100 nM, is used to determine nonspecific binding since methysergide has a weak affinity for D_2 receptors (IC_{50} approximately 1–5 µM).
         5.50 ml buffer 1b
         0.55 ml buffer 1a
         0.55 ml [^{3}H]-spiperone, 1.0 nM final concentration
         3.96 ml distilled water
         0.22 ml sulpiride 5×10^{-4} M, final concentration 10 µM or vehicle
         0.22 ml test compound, final concentration 10^{-8}–10^{-5} M or ketanserin 5×10^{-5} M final concentration 100 nM or vehicle
   b) *Ex vivo* inhibition experiments
      Separate mailers are prepared for total and nonspecific binding, as described above, including sulpiride to mask D_2 receptor binding with brain sections through the nucleus accumbens and striatum and prazosin to mask α_1-receptors in cortical brain sections.
   c) Saturation experiments
      Separate mailers are prepared for total and nonspecific binding at each radioligand concentration. Prazosin is not included in the mailers in saturation experiments, since specific binding is defined by methysergide which has negligible affinity for α_1-receptors.

      5.50 ml buffer 1b

0.55 ml buffer 1a

0.55 ml [^{3}H]-spiperone, final concentrations 0.5–2.5 nM

4.18 ml distilled water

0.22 ml 2.5×10^{-4} M methysergide, final concentration 5 µM or vehicle

2. Slides are air-dried for 10–15 min at room temperature, preincubated in 0.05 M Tris+0.154 M NaCl, pH 7.4 for 5 min and further incubated for 60 min with [^{3}H]-spiperone. Slides are then rinsed with ice-cold solutions as follows: dipped in buffer 1b, 2 × 5 min rinsed in buffer 1b, dipped in distilled water.

   Slides used for wipes: both sections are wiped with one Whatman GF/B filter and radioactivity is counted after addition of 10 ml of scintillation fluid.

   Slides used for autoradiography: slides are dried under a stream of air at room temperature and are stored in a desiccator under vacuum at room temperature (usually overnight). Slides are then mounted onto boards, along with ^{3}H-standards (Amersham RPA 506).

   In the dark room under safelight illumination (Kodak GBX-2 filter), slides are exposed to Amersham Hyperfilm or LKB Ultrofilm for 14–17 days.

REFERENCES AND FURTHER READING

Altar CA et al (1984) Computer-assisted video analysis of [^{3}H]-spiroperidol binding autoradiographs. J Neurosci Meth 10:173–188

Altar CA et al (1985) Computer imaging and analysis of dopamine (D2) and serotonin (S2) binding sites in rat basal ganglia or neocortex labeled by [^{3}H]-spiroperidol. J Pharmacol Exp Ther 233:527–538

Altar CA, Wasley AM, Neale RF, Stone GA (1986) Typical and atypical antipsychotic occupancy of D_2 and S_2 receptors: an autoradiographic analysis in rat brain. Brain Res Bull 16:517–525

Cadet JL, Kuyatt B, Fahn S, De Souza EB (1987) Differential changes in ^{125}I-LSD-labeled 5-HT-2 serotonin receptors in discrete regions of brain in the rat model of persistent dyskinesias induced by iminodipropionitrile (IDPN): evidence from autoradiographic studies. Brain Res 437:383–386

Costall B, Fortune DH, Naylor RJ, Marsden CD, Pycock C (1975) Serotonergic involvement with neuroleptic catalepsy. Neuropharmacol 14:859–868

Fink H, Morgenstern R, Oelssner W (1984) Clozapine – a serotonin antagonist? Pharmacol Biochem Behav 20:513–517

Kostowski W, Gumulka W, Czlokowski A (1972) Reduced kataleptogenic effects of some neuroleptics in rats with lesioned midbrain raphe and treated with p-chlorophenylalanine. Brain Res 48:443–446

Lee T, Tang SW (1984) Loxapine and clozapine decrease serotonin (S_2) but do not elevate dopamine (D_2) receptor numbers in the rat brain. Psychiatry Res 12:277–285

Morgan DG, Marcusson JO, Finch CE (1984) Contamination of serotonin-2 binding sites with an alpha-1 adrenergic component in assays with (3H)spiperone. Life Sci 34:2507–2514

Pazos A, Cortés R, Palacios JM (1985) Quantitative autoradiographic mapping of serotonin receptors in the rat brain. II. Serotonin-2 receptors. Brain Res 346:231–249

Palacios JM, Niehoff DL, Kuhar MJ (1981) [^{3}H]Spiperone binding sites in brain: autoradiographic localization of multiple receptors. Brain Res 213:277–289

Reynolds CP, Garrett NJ, Rupniak N, Jenner P, Marsden CD (1983) Chronic clozapine treatment of rats down-regulates 5-HT_2 receptors. Eur J Pharmacol 89:325–326

Wilmot CA, Szczepanik AM (1989) Effects of acute and chronic treatment with clozapine and haloperidol on serotonin (5-HT_2) and dopamine (D_2) receptors in the rat brain. Brain Res 487:288–298

E.5.1.11 Binding to the Sigma Receptor

PURPOSE AND RATIONALE

Sigma receptors, as a class of binding sites in the brain, were originally described as a subtype of the opiate receptors. Efforts to develop less addicting opiate analgesics led to the study of several benzomorphan derivatives which produce analgesia without causing the classical morphine-induced euphoria. Unfortunately, these compounds, like N-allylnormetazocine (SKF 10,047) produced a variety of psychotic symptoms. This psychotomimetic effect is thought to be mediated by sigma receptors. This binding site is sensitive to many neuroleptics, most notably the typical antipsychotic haloperidol, leading to the hypothesis that drug interactions with the sigma site may be a new approach for the discovery of novel antipsychotics which are not dopamine receptor antagonists. D_2 receptor antagonism is thought to be linked with the occurrence of extrapyramidal symptoms in the form of hyperkinesia and Parkinson symptoms or tardive dyskinesia limiting the therapeutic use of traditional antipsychotic medication. It is hoped that ligands to the sigma receptor do not produce these adverse reactions. The sigma site is believed to be distinct from the binding site for the psychotomimetic drug phencyclidine.

PROCEDURE

Reagents

(+)-SKF 10,047 is prepared as a stock solution of 5×10^{-3} M with distilled water. 130 µl added to the 6.5 ml assay yields a final concentration of 10^{-4} M.

^{3}H-(+)-SKF 10,047 (specific activity 40 Ci/mmol) is obtained from New England Nuclear. A 200 nM stock solution is made up with distilled water for IC_{50} determinations. 325 µl added to each tube yields a final concentration of 10 nM in the 6.5 ml assay.

Test Compounds

A 5 mM stock solution is prepared in a suitable solvent and serially diluted, such that the final concentration in the assay ranges from 10^{-5} to 10^{-8} M.

Tissue Preparation

The assay utilizes slide-mounted cross-sections of brain tissue from male Hartley guinea pigs. Whole brain sections of 10 µm thickness are obtained from the hippocampus, thaw-mounted onto gel-chrome alum subbed slides, freeze-dried and stored at –70°C until use. On the day of the assay, the sections are thawed briefly at room temperature until the slides are dry and then used in the assay at a final volume of 6.5 ml.

Assay

Incubation solutions are prepared in plastic slide mailer containers as follows:

3.250 ml 0.05 M Tris buffer, pH 7.7

2.470 ml distilled water

0.325 ml 0.5 M Tris buffer, pH 7.7

0.130 ml (+)-SKF 10,047 or vehicle

0.325 ml [^{3}H](+)-SKF 10,047

Dried slides with tissue sections are added to the slide mailers and incubated at room temperature for 90 min. Non-bound radioligand is removed by rinsing the slides sequentially in two 5-min rinses in ice-cold 0.05 M Tris buffer and a dip in ice-cold distilled water. The sections are either swabbed with Whatman GF/B filters for scintillation counting of tissue-bound radioligand or exposed to tritium-sensitive film for autoradiography of the binding sites.

EVALUATION

Specific binding is determined from the difference of binding in the absence or presence of 10^{-4} M (+)-SKF 10,047 and is typically 60–70% of total binding. IC_{50} values for the competing drug are calculated by log-probit analysis of the data.

MODIFICATIONS OF THE METHOD

[^{3}H]-(+)-pentazocine has been recommended as a highly potent and selective radioligand for µ receptors (de Costa et al. 1989; DeHaven-Hudkins et al. 1992).

Classification of sigma binding sites into σ_1 and σ_2 receptors has been proposed (Walker et al. 1990; Quirion et al. 1992; Abou-Gharbia et al. 1993).

Hashimoto and London (1993) characterized [^{3}H]ifenprodil binding to σ_2 receptors in rat brain.

Ganapathy et al. (1999) provided evidence for the expression of the type 1 sigma receptor in the Jurkat human T lymphocyte cell line.

REFERENCES AND FURTHER READING

Abou-Gharbia M, Ablordeppey SY, Glennon RA (1993) Sigma receptors and their ligands: the sigma enigma. Ann Rep Med Chem 28:1–10

Angulo JA, Cadet JL, McEwen BS (1990) σ receptor blockade by BMY 14802 affects enkephalinergic and tachykinin cells differentially in the striatum of the rat. Eur J Pharmacol 175:225–228

de Costa BR, Bowen WD, Hellewell SB, Walker JM, Thurkauf A, Jacobson AE, Rice KC (1989) Synthesis and evaluation of optically pure [^{3}H]-(+)-pentazocine, a highly potent and selective radioligand for σ receptors. FEBS Lett 251:53–58

DeHaven-Hudkins DL, Fleissner LC, Ford-Rice FY (1992) Characterization of the binding of [^{3}H](+)-pentazocine to σ recognition sites in guinea pig brain. Eur J Pharmacol 227:371–378

Deutsch SI, Weizman A, Goldman ME, Morihisa JM (1988) The sigma receptor: A novel site implicated in psychosis and anti-psychotic drug efficacy. Clin Neuropharmacol 11:105–119

Ferris RM, Tang FLM, Chang KJ, Russell A (1986) Evidence that the potential antipsychotic agent rimcazole (BW 234U) is a specific, competitive antagonist of sigma sites in brain. Life Sci 38:2329–2339

Ganapathy ME, Prasad PD, Huang W, Seth P, Leibach FH, Ganapathy V (1999) Molecular and ligand-binding characterization of the sigma receptor in Jurkat human T lymphocyte cell line. J Pharmacol Exp Ther 289:251–260

Goldman ME, Jacobson AE, Rice KC, Paul SM (1985) Differentiation of [^{3}H]phencyclidine and (+)-[^{3}H]SKF-10,047 binding sites in rat cerebral cortex. FEBS Lett 190:333–336

Hashimoto K, London ED (1993) Further characterization of [^{3}H]ifenprodil binding to sigma receptors in rat brain. Eur J Pharmacol 236:159–163

Hoffman DW (1990) Neuroleptic drugs and the sigma receptor. Am J Psychiatry 147:1093–1094

Itzhak Y, Hiller JM, Simon EJ (1985) Characterisation of specific binding sites for [^{3}H](*d*)-*N*-allylnormetazocine in rat brain membranes. Mol Pharmacol 27:46–52

Kaiser C, Pontecorvo MJ, Mewshaw RE (1991) Sigma receptor ligands: Function and activity. Neurotransm 7:1–5

Khazan N, Young GA, El-Fakany EE, Hong O, Calligaro D (1984) *Sigma* receptors mediate the psychotomimetic effects of N-allylnormetazocine (SKF-0,047), but not its opioid agonistic-antagonistic properties. Neuropharmacol. 23:983–987

Largent BL, Gundlach AL, Snyder SH (1986) Pharmacological and autoradiographic discrimination of *sigma* and phencyclidine receptor binding sites in brain with (+)-[^{3}H]SKF 10,047, (+)-[^{3}H]-3-[3-hydroxyphenyl]-N-(1-propyl)piperidine and [^{3}H]-1-[1-(2-thienyl)cyclohexyl]piperidine. J Pharmacol Exp Ther 238:739–748

Quirion R, Chicheportiche R, Contreras PC, Johnson KM, Lodge D, Tam SW, Woods JH, Zukin SR (1987) Classification and nomenclature of phencyclidine and sigma receptor sites. Trends Neurosci 10:444–446

Quirion R, Bowen WD, Itzhak Y, Junien JL, Musacchio JM, Rothman RB, Su TP, Tam SW, Taylor DP (1992) A proposal for the classification of sigma binding sites. Trends Pharmacol Sci 13:85–86

Sircar R, Nichtenhauser R, Ieni JR, Zukin SR (1986) Characterisation and autoradiographic visualisation of (+)-[^{3}H]SKF 10,047 binding in rat and mouse brain: Further evidence for phencyclidine / "*sigma* opiate" receptor commonalty. J Pharmacol Exper Ther 237:681–688

Su TP (1982) Evidence for *sigma* opioid receptor: Binding of [^{3}H]-SKF 10047 to etorphine-inaccessible sites in guinea pig brain. J Pharmacol Exper Ther 223:284–290

Tam SW, Cook L (1984) σ-opiates and certain antipsychotic drugs mutually inhibit (+)-[^{3}H]-SKF 10,047 and [^{3}H]haloperidol binding in guinea pig membranes. Proc Natl Acad Sci USA 81:5618–5621

Taylor DP, Dekleva J (1987) Potential antipsychotic BMY 14802 selectively binds to sigma sites. Drug Dev Res 11:65–70

Vaupel DB (1983) Naltrexone fails to antagonize the σ effects of PCP and SKF 10.047 in the dog. Eur J Pharmacol 92:269–274

Walker JM, Bowen WD, Walker FO, Matsumoto RR, de Costa B, Rice KC (1990) Sigma receptors: Biology and function. Pharmacol Reviews 42:355–402

Weber E, Sonders M, Quarum M, McLean S, Pou S, Keana JFW (1986) 1,3-Di(2[5-^{3}H]tolyl)guanidine: A selective ligand that labels σ-type receptors. Proc Natl Acad Sci 83:8784–8788

Zukin SR, Tempel A, Gardner EL, Zukin RS (1986) Interaction for psychotomimetic opiates and antipsychotic drugs. Proc Natl Acad Sci 83:8784–8788

E.5.1.12 Simultaneous Determination of Norepinephrine, Dopamine, DOPAC, HVA, HIAA, and 5-HT from Rat Brain Areas

PURPOSE AND RATIONALE

To measure the effects of potential antipsychotic drugs on catecholamines and indols, a quantitative method for the determination of norepinephrine (NE), dopamine (DA), 3,4-dihydroxyphenylacetic acid (DOPAC), homovanillic acid (HVA), 5-hydroxyindolacetic acid (5HIAA) and 5-hydroxytryptamine (5-HT) from rat brain regions is used. These catecholamines and indols are measured in rat brain prefrontal cortex, nucleus accumbens and striatum.

PROCEDURE

Reagents

1. 0.1 M HCl
2. 1 N NaOH
3. 2 mM solutions of NE, DOPAC, DA, HVA, 5HIAA and 5-HT in 0.1 M HCl;
   0.5 ml aliquots are stored at –60°C until use.
4. Preparation of 2° Standard Mixture
   - 10 µM solution of NE, DOPAC, DA, HVA, 5HIAA and 5-HT (diluted from reagent 3) in mobile phase (reagent 5)
   - the 2° Standard solution is used for the preparation of standard curves.
5. Mobile phase/MeOH: buffer (7.5:92.5, v/v)
   - buffer: 0.07 M sodium acetate, 0.04 M citric acid, 130 µM EDTA and 230 µM sodium octane sulfonate
   - mobile phase: methanol/buffer (150 ml + 1850 ml) is filtered through a 0.2 µm nylon 66 filter

HPLC-Instrumentation

- pump, model SP8810 (Spectra Physics),
- injector, WISP 710B (Waters Associates),
- detector, 5100A electrochemical with a 5011 analytical cell and 5020 guard cell (ESA),
- integrator, D-2000 (Hitachi), used as a back-up for the data collection/integrator, CS 9000 (IBM) system,
- analytical column: C18-ODS Hypersil, 3 µm, 100 × 4.6 mm (Shandon)

Animal Treatment

Six rats per group (150–250 g) are dosed with 4–5 different concentrations of the putative antipsychotic drug; usual concentrations range from 0.03 to 30 mg/kg. At a predetermined time, usually 60 min, the rats are sacrificed.

Tissue Preparation

Following treatment with test drug, rats are sacrificed by decapitation. The brain is rapidly removed and placed on ice. The striatum, nucleus accumbens and/or prefrontal cortex are dissected and placed in 1.5 ml microcentrifuge tubes. The tubes are capped and immediately placed in dry ice. The frozen brain sections are stored at –60°C until HPLC analysis.

Tissue is homogenized in mobile phase (striatum: in 600 µl, nucleus accumbens and prefrontal cortex: in 300 µl). The homogenates are centrifuged for 6 min using a microcentrifuge (model 5413, Eppendorf). The supernatants are transferred to 0.2 µm microfilterfuge™ tubes and centrifuged for 6–8 min as before. The filtrate is transferred to WISP vials. Standards are included every 12–15 samples.

The following volumes are injected to the HPLC column:

- striatum: 5 µl; nucleus accumbens: 20 µl; prefrontal cortex: 50 µl.

- HPLC flow rate is 1.0 ml/min, run time is 25 min. Helium flow is constant in mobile phase.

For protein analysis, 1 N NaOH is added to the tissue pellets as follows:

- striatum: 1.0 ml;
- nucleus accumbens and prefrontal cortex: 0.5 ml.

The next day, the protein analysis is run in duplicate with 5 µl of striatum. 20 µl of nucleus accumbens and prefrontal cortex as described by Bradford (1976) using the BioRad assay kit.

EVALUATION

Peak area is used for quantitation. The mg of protein and pmoles of NE, DOPAC, DA, HVA, 5HIAA and 5-HT are calculated from linear regression analysis using the corresponding standard curve. Final data are reported as pmoles/mg protein.

REFERENCES AND FURTHER READING

Bradford M (1976) A rapid and sensitive method for the quantitation of microgram quantities of protein utilizing the principle of protein-dye binding. Analyt Biochem 72:248–254

Magnusson O, Nilsson LB, Westerlund D (1980) Simultaneous determination of dopamine, DOPAC and homovanillic acid. Direct injections of supernatants from brain tissue homogenates in a liquid chromatography-electrochemical detection system. J Chromatography 221:237–247

Magnusson O, Fowler CJ, Köhler C, Ögren SO (1986) Dopamine D2 receptors and dopamine metabolism. Relationship between biochemical and behavioural effects of substituted benzamide drugs. Neuropharmacol 25:187–197

Raiteri M, Marchi M, Maura G (1984) Release of catecholamines, serotonin, and acetylcholine from isolated brain tissue. In: Lajtha A (ed) Handbook of Neurochemistry, 2nd ed, Plenum Press New York, London, Vol 6, pp 431–462

Reinhard JF, Perry JA (1984) Fast analysis of tissue catechols using a short, high-efficiency (3 µM) LC column and amperometric detection. J Liquid Chromatography 7:1211–1220

Shibuya T, Sato K, Salafsky B (1982) Simultaneous measurement of biogenic amines and related compounds by high performance liquid chromatography. Int J Clin Pharmacol Toxicol 20:297–301

Wagner J, Palfreyman M, Zraika M (1979) Determination of DOPA, dopamine, DOPAC, epinephrine, norepinephrine, α-monofluoromethyldopa and α-difluoromethyldopa in various tissues of mice and rats using reversed-phase ion-pair liquid chromatography with electrochemical detection. J Chromatogr 164:41–54

Wagner J, Vitali P, Palfreyman MG, Zraika M, Hout S (1982) Simultaneous determination of 3,4-dihydroxyphenylalanine, 5-hydroxytryptophan, dopamine, 4-hydroxy-3-methoxyphenylalanine, norepinephrine, 3,4-dihydroxyphenylacetic acid, homovanillic acid, serotonin, and 5-hydroxyindolacetic acid in rat cerebrospinal fluid and brain by high-performance liquid chromatography with electrochemical detection. J Neurochem 38:1241–1254

E.5.1.13 Measurement of Neurotransmitters by Intracranial Microdialysis

PURPOSE AND RATIONALE

Methods to measure neurotransmitters and their metabolites in specific areas of the brain by microdialysis were introduced by Ungerstedt and his group (Ungerstedt et al. 1982; Zetterström et al. 1982, 1983; Zetterström and Ungerstedt 1983; Ungerstedt 1984; Stähle et al. 1991; Lindefors et al. 1989; Amberg and Lindefors (1989) and by Imperato and di Chiara 1984, 1985). In brain dialysis, a fine capillary fibre is implanted in a selected brain area. Low molecular weight compounds diffuse down their concentration gradients from the brain extracellular fluid into a physiological salt solution that flows through the capillary fibre at a constant rate. The fluid is collected and analyzed.

PROCEDURE

Several designs of dialysis probes have been used (Santiago and Westerink 1990; Kendrick 1991):

1. Horizontal Probe

A straight tube (Vita Fiber, 3 × 50 Amicon) with an outer diameter of 0.34 mm and a molecular weight cut-off of 50000 is used. The outer surface of the tube is porous and can easily be sealed by epoxy which is applied by passing the tube through a droplet of epoxy and then through a narrow hole corresponding to the outer diameter of the tube. The wall of the tube is sealed in this way except for the area where the dialysis is intended to take place. The length of this region can be varied from 2 to 8 mm depending upon which structure of the brain will be perfused. During the coating and all other handling of the tube it is supported by a thin tungsten or steel wire inserted into its lumen. One end of the tube is glued into a steel cannula (6 mm long, outer diameter 0.64 mm).

Male Sprague Dawley rats weighing 250–300 g are anesthetized with halothane and held in a stereotactic instrument. The animals are maintained under halothane anesthesia during the entire experiment.

Holes are drilled bilaterally (5.7 mm below and 1.5 mm in front of bregma) in the temporal bones after the temporal muscles have been retracted from the bones and folded away.

During the implantation, the cannula is held by the micromanipulator of the stereotactic instrument and the dialysis tube is passed horizontally through the brain through the holes drilled on both sides of the skull. A polyethylene tubing carrying the perfusion

fluid is connected to the steel cannula. The perfusate is collected at the other end.

2. Loop Probe

The probe is made of a flexible cellulosic tubing (Dow 50, outer diameter 0.25 mm). Both ends of the tube are inserted into 0.64 mm diameter steel tubes, one of which is bent in an angle. A very thin microsuture (0.1 mm in diameter) is inserted into the tube and positioned half between the steel tubes. Before implantation, the tube is moistened and bent in such a way that the two steel tubes are held closely together in the micromanipulator of the stereotactic instrument. A tungsten wire is inserted into the straight steel tube and passed down the lumen of the dialysis tube in order to stretch it and make it rigid enough to be implanted into the brain. The tube is implanted vertically and the steel cannulae are attached to the skull by dental cement. The tungsten wire is removed before starting the experiment. The cellulosic tube is flexible enough to withstand the bending at the lower end. The microsuture keeps the bend open.

Loop-shaped or U-shaped microdialysis probes have been used by several authors, e. g., Ichikawa and Meltzer (1990), Jordan et al. (1994), Westerink and Tuinte (1986), Auerbach et al. (1995).

3. Vertical Probe

The probe is sealed at one end by epoxy. The other end is glued into a 0.64-mm diameter steel tube. A thin inner cannula made of a steel tube or a glass capillary carries the fluid to the bottom of the dialysis tube where it leaves the inner capillary and flows upwards and leaves the probe by a lateral tube. This vertical probe can also be coated with epoxy. It is especially suited for reaching ventral parts of the brain and performing dialysis in small nuclei of the brain.

A similar device has been described for continuous plasma sampling in freely moving rats by Chen and Steger (1993).

Most of the commercially available microdialysis probes are based on this principle.

4. Commercially Available Microdialysis Probes

The microdialysis probes CMA/10, manufactured by Carnegie Medicine, Stockholm, Sweden, consist of a tubular membrane (polycarbonate; length: 3 mm; outside diameter: 0.50 mm; and inside diameter: 0.44 mm) glued to a cannula (outside diameter: 0.60 mm), and sealed with a glue at the tip (Stähle et al. 1991). The perfusion medium is carried to the dialyzing part of the probe by a thin cannula inside the probe. The medium leaves the inner cannula through two holes, flows back between the membrane and the inner cannula, and is collected at the outlet of the probe. The perfusion medium is delivered by means of a high precision micro-syringe pump.

This probe was used by several authors, e. g., Wood et al. (1988), Benveniste et al. (1989), Rollema et al. (1989), Scheller and Kolb (1991), Wang et al. (1993), Kreiss and Lucki (1995), Fink-Jensen et al. (1996).

CMA/11 probes were used by Boschi et al. (1995), Romero et al. (1996), Gobert et al. (1997).

Dialysis fibres with a semipermeable membrane AN 69-HF, Hospal-Dasco, Bologna, Italy, were used by de Boer et al. (1994), Rayevsky et al. (1995), Arborelius et al. (1996), Gainetdinov et al. (1996), Tanda et al. (1996).

EVALUATION

Samples of the dialysate are collected for different time intervals and analyzed for neurotransmitters. For the **evaluation of neuroleptics**, most authors measured dopamine, 3,4-dihydroxyphenyl acetic acid (DOPAC) and homovanillinic acid (HVA) by HPLC using appropriate detectors. See and Lynch (1996) analyzed dialysis samples for glutamate and GABA concentrations.

For the **evaluation of antidepressants** the concentrations of 5-hydroxytryptamine (5-HT), 5-hydroxy indole acetic acid (5-HIAA), dopamine (DA), dihydroxyphenylacetic acid (DOPAC), or noradrenaline (NA) were measured in the effluent by HPLC. Wood et al. (1988), Egan et al. (1996) used 3-methoxytyramine accumulation as an index of dopamine release.

CRITICAL ASSESSMENT OF THE METHOD

The results obtained from brain dialysis depend on at least three variables: type of probe, post-implantation interval, and whether anesthetized or freely moving animals are used (Di Chiara 1990).

Several authors analyzed the diffusion processes underlying the microdialysis technique and described the limitations of the experiments (Jacobson et al. 1985; Amberg and Lindefors 1989; Beneviste et al. 1989; Scheller and Kolb 1991; Le Quellec et al. 1995).

As a matter of fact, brain microdialysis has been used for the evaluation of many drugs in various indications, such as:

- for **neuroleptics** by Ichikawa and Meltzer 1990; Meil and See 1994; Hernandez and Hoebel 1994; See et al. 1995; Schmidt and Fadayel 1995; Semba et al. 1995; Rayevsky et al. 1995; Fink-Jensen et al.

1996; See and Lynch 1996; Gainetdinov et al. 1996; Egan et al. 1996; Klitenick et al. 1996,
- for **antidepressants** by de Boer et al. 1994; Jordan et al. 1994; Arborelius et al. 1995; Ascher et al. 1995; Auerbach et al. 1995; de Boer 1995, 1996; Casanovas and Artigas 1996; Gobert et al. 1995; Ichikawa and Meltzer 1995; Kreiss and Lucki 1996; Petty et al. 1996; Potter 1996; Romero et al. 1995; Sharp et al. 1996; Tanda et al. 1996a, b,
- for studies in **Parkinson** models by Rollema et al. 1989; Parsons et al. 1991.

MODIFICATIONS OF THE METHOD

Ferrara et al. (1990) continuously monitored ethanol levels in the brain by microdialysis.

Hernandez and Hoebel (1994) performed simultaneous cortical, accumbens, and striatal microdialysis in freely moving rats.

Hegarty and Vogel (1995) assayed dopamine, DOPAC and HVA in the brain of rats after acute and chronic diazepam treatment and immobilization stress.

Casanovas and Artigas (1996) implanted microdialysis probes simultaneously in six different brain areas of rats (frontal cortex, dorsal striatum, ventral hippocampus, dorsal hippocampus, dorsal raphe nucleus, median raphe nucleus).

Beneviste et al. (1984) determined extracellular concentrations of glutamate and aspartate in rat hippocampus during transient cerebral ischemia monitored by intracerebral microdialysis.

Boschi et al. (1995) showed that microdialysis of small brain areas in mice is feasible using the smallest commercially available probes.

REFERENCES AND FURTHER READING

Amberg G, Lindefors N (1989) Intracerebral microdialysis: II. Mathematical studies of diffusion kinetics. J Pharmacol Meth 22:157–183

Arborelius L, Nomikus GG, Hertel P, Salmi P, Grillner P, Hök BB, Hacksell U, Svensson TH (1996) The 5-HT_{1A} receptor antagonist (S)-UH-301 augments the increase in extracellular concentrations of 5-HT in the frontal cortex produced by both acute and chronic treatment with citalopram. Naunyn-Schmiedeberg's Arch Pharmacol 353:630–640

Ascher JA, Cole JO, Colin JN, Feighner JP, Ferris RM, Fibiger HC, Golden RN, Martin P, Zotter WZ, Richelson E, Sulser F (1995) Bupropion: A review of its mechanism of antidepressant activity. J Clin Psychiat 56:395–401

Ashby CR, Wang RY (1996) Pharmacological actions of the atypical antipsychotic drug clozapine: a review. Synapse 24:349–394

Auerbach SB, Lundberg JF, Hjorth S (1994) Differential inhibition of serotonin release by 5-HT and NA reuptake blockers after systemic administration. Neuropharmacol 34:89–96

Beneviste H, Drejer J, Schousboe A, Diemer NH (1984) Elevation of extracellular concentrations of glutamate and aspartate in rat hippocampus during transient cerebral ischemia monitored by intracerebral microdialysis. J Neurochem 43:1369–1374

Benveniste H, Hansen AJ, Ottosen NS (1989) Determination of brain interstitial concentrations by microdialysis. J Neurochem 52:1741–1750

Boschi G, Launay N, Rips R, Scherrmann JM (1995) Brain microdialysis in the mouse. J Pharmacol Toxicol Meth 33:29–33

Casanovas JM, Artigas F (1996) Differential effects of ipsapirone on 5-hydroxytryptamine release in the dorsal and median raphe neuronal pathways. J Neurochem 67:1945–1952

Chen Z, Steger RW (1993) Plasma microdialysis. A technique for continuous plasma sampling in freely moving rats. J Pharmacol Toxicol Meth 29:111–118

De Boer T (1995) The effects of mirtazepine on central noradrenergic and serotonergic neurotransmission. Intern Clin Psychopharmacol 10/Suppl 4:19–23

De Boer T (1996) The pharmacological profile of mirtazepine. J Clin Psychiat 57, Suppl 4:19–25

De Boer T, Nefkens F, van Helvoirt A (1994) The α_2-adrenenoceptor antagonist Org 3770 enhances serotonin transmission *in vivo*. Eur J Pharmacol 253:R5–R6

Di Chiara (1990) *In vivo* brain dialysis of neurotransmitters Trends Pharmacol Sci 11:116–121

Egan MF, Chrapusta S, Karoum F, Lipska BK, Wyatt RJ (1996) Effects of chronic neuroleptic treatment on dopamine release: insights from studies using 3-methoxytyramine. J Neural Transmiss 103:777–805

Ferraro TN, Weyers P, Carrozza DP, Vogel WH (1990) Continuous monitoring of brain ethanol levels be intracerebral microdialysis. Alcohol 7:129–132

Fink-Jensen A, Hansen L, Hansen JB, Nielsen EB (1996) Regional differences in the effect of haloperidol and atypical neuroleptics on interstitial levels of DOPAC in the rat forebrain: an *in vivo* microdialysis study. J Psychopharmacol 10:119–125

Gainetdinov RR, Sotnikova TD, Grekhova TV, Rayevsky KS (1996) Simultaneous monitoring of dopamine, its metabolites and trans-isomer of atypical neuroleptic drug carbidine concentrations in striatal dialysates of conscious rats. Progr Neuropharmacol Biol Psychiat 20:291–305

Gobert A, Rivet JM, Cistarelli L, Millan MJ (1997) Potentiation of fluoxetine-induced increase in dialysate levels of serotonin (5-HT) in the frontal cortex of freely moving rats by combined blockade of 5-HT_{1A} and 5-HT_{1B} receptors with WAY 100,635 and GR 127,935. J Neurochem 68:1159–1163

Hegarty AA, Vogel WH (1995) The effect of acute and chronic diazepam treatment on stress-induced changes in cortical dopamine in the rat. Pharmacol Biochem Behav 52:771–778

Hernandez L, Hoebel BG (1994) Chronic clozapine selectively decreases prefrontal cortex dopamine as shown by simultaneous cortical, accumbens, and striatal microdialysis in freely moving rats. Pharmacol Biochem Behav 52:581–589

Ichikawa J, Meltzer HY (1990) The effect of chronic clozapine and haloperidol on basal dopamine release and metabolism in rat striatum and nucleus accumbens studied by *in vivo* microdialysis. Eur J Pharmacol 176:371–374

Ichikawa J, Meltzer HY (1995) Effect of antidepressants on striatal and accumbens extracellular dopamine levels. Eur J Pharmacol 281:255–261

Imperato A, di Chiara G (1984) Trans-striatal dialysis coupled to reverse phase high performance liquid chromatography with electrochemical detection: A new method for the study

of the *in vivo* release of endogenous dopamine and metabolites. J Neurosci 4:966–977

Imperato A, di Chiara G (1985) Dopamine release and metabolism in awake rats after systemic neuroleptics studied by trans-striatal dialysis. J Neurosci 5:297–306

Imperato A, Tanda G, Frau R, di Chiara G (1988) Pharmacological profile of dopamine receptor agonists studied by brain dialysis in behaving rats. J Pharmacol Exp Ther 245:257–264

Jacobson I, Sandberg M, Hamberger A (1985) Mass transfer in brain dialysis devices – a new method for the estimation of extracellular amino acids concentration. J Neurosci Meth 15:263–268

Jordan S, Kramer GL, Zukas PK, Moeller M, Petty F (1994) *In vivo* biogenic amine efflux in medial prefrontal cortex with imipramine, fluoxetine, and fluvoxamine. Synapse 18:294–297

Kendrick KM (1991) *In vivo* measurement of amino acid, monoamine and neuropeptide release using microdialysis. In: Greenstein B (ed) Neuroendocrine Research Methods, Vol 1, Harwood Acad Publ, Chur, Chapter 12, pp 249–278

Klitenick MA, Taber MT, Fibiger HC (1996) Effects of chronic haloperidol on stress- and stimulation-induced increases in dopamine release: tests of the depolarization block hypothesis. Neuropsychopharmacol 15:424–428

Kreiss DS, Lucki I (1995) Effects of acute and repeated administration of antidepressant drugs on extracellular level of 5-hydroxytryptamine measured *in vivo*. J Pharmacol Exp Ther 274:866–876

Le Quellec A, Dupin S, Genissel P, Saivin S, Marchand B, Houin G (1995) Microdialysis probes calibration: gradient and tissue dependent changes in no net flux and reverse dialysis methods. J Pharmacol Toxicol Meth 33:11–16

Lindefors N, Amberg G, Ungerstedt U (1989) Intracerebral microdialysis: I. Experimental studies of diffusion kinetics. J Pharmacol Meth 22:141–156

Meil W, See RE (1994) Single pre-exposure to fluphenazine produces persisting behavioral sensitization accompanied by tolerance to fluphenazine-induced dopamine overflow in rats. Pharmacol Biochem Behav 48:605–612

Parsons LH, Smith AD, Justice JB Jr (1991) The *in vivo* microdialysis recovery of dopamine is altered independently of basal level by 6-hydroxydopamine lesions to the nucleus accumbens. J Neurosci Meth 40:139–147

Petty F, Davis LL, Kabel D, Kramer GL (1996) Serotonin dysfunction disorders: a behavioral neurochemistry prospective. J Clin Psychiat 57, Suppl 8:11–16

Potter WZ (1996) Adrenoreceptor and serotonin receptor function: relevance to antidepressant mechanisms of action. J Clin Psychiat 57, Suppl 4:4–8

Rayevsky KS, Gainetdinov RR, Grekhova TV, Sotnikova TD (1995) Regulation of dopamine release and metabolism in rat striatum *in vivo*: effects of dopamine receptor antagonists. Progr Neuro-Psychopharmacol Biol Psychiat 19:1285–1303

Rollema H, Alexander GM, Grothusen JR, Matos FF, Castagnoli N Jr (1989) Comparison of the effects of intracerebrally administered MPP^+ (1-methyl-4-phenylpyridinium) in three species: microdialysis of dopamine and metabolites in mouse, rat and monkey striatum. Neurosci Lett 106:275–281

Romero L, Hervás I, Artigas F (1996) The 5-HT_{1A} antagonist WAY-100635 selectively potentiates the effects of serotonergic antidepressants in rat brain. Neurosci Lett 219:123–126

Sandberg M, Butcher S, Hagberg H (1986) Extracellular overflow of neuroactive amino acids during severe insulin-induced hypoglycemia: *in vivo* dialysis of the rat hippocampus. J Neurochem 47:178–184

Santiago M, Westerink BHC (1990) Characterization of the *in vivo* release of dopamine as recorded by different types of intracerebral microdialysis probes. Naunyn Schmiedeberg's Arch Exp Pharmacol 342:407

Scheller D, Kolb J (1991) The internal reference technique in microdialysis: a practical approach to monitoring dialysis efficiency and to calculating tissue concentrations from dialysate samples. J Neurosci Meth 40:31–38

Schmidt CJ, Fadayel GM (1995) The selective 5-HT_{2A} receptor antagonist, MDL 100,907, increases dopamine efflux in the prefrontal cortex of the rat. Eur J Pharmacol 273:273–279

See RE, Lynch AM (1996) Duration-dependent increase in striatal glutamate following prolonged fluphenazine administration in rats. Eur J Pharmacol 308:279–282

See RE, Lynch AM, Aravagri M, Nemeroff CB, Owens MJ (1995) Chronic haloperidol-induced changes in regional dopamine release and metabolism and neurotensin content in rats. Brain Res 704:202–209

Semba J, Watanabe A, Kito S, Toru M (1995) Behavioural and neurochemical effects of OPC-14597, a novel antipsychotic drug, on dopamine mechanisms in rat brain. Neuropharmacol 34:785–791

Sharp T, Gartside SE, Umbers V (1996) Effects of co-administration of a monoamine oxidase inhibitor and a 5-HT_{1A} receptor antagonist on 5-hydroxytryptamine cell firing and release. Eur J Pharmacol 320:15–19

Stähle L, Segersvärd S, Ungerstedt (1991) A comparison between three methods for estimation of extracellular concentration of exogenous and endogenous compounds by microdialysis. J Pharmacol Meth 25:41–52

Tanda G, Bassareo V, di Chiara G (1996a) Mianserin markedly and selectively increases extracellular dopamine in the prefrontal cortex as compared to the nucleus accumbens in the rat. Psychopharmacology 123:127–130

Tanda G, Frau R, di Chiara G (1996b) Chronic desimipramine and fluoxetine differentially affect extracellular dopamine in the rat prefrontal cortex. Psychopharmacology 127:83–87

Ungerstedt U (1984) Measurement of neurotransmitter release by intracranial dialysis. In: Marsden CA (ed) Measurement of Neurotransmitter Release *in vivo*. John Wiley and Sons Ltd., New York, pp 81–105

Ungerstedt U (1986) Microdialysis – A new bioanalytical sampling technique. Curr Separat 7:43–46

Ungerstedt U, Herrera Marschitz M, Jungnelius U, Stähle L, Tossman U, Zetterström T (1982) Dopamine synaptic mechanisms reflected in studies combining behavioral recordings and brain dialysis. In: Kohsaka M (ed) Advances in Biosciences. Vol 37: Advances in Dopamine Research, pp 219–231. Pergamon Press, Oxford and New York

Wang Y, Wong SL, Sawchuk RJ (1993) Microdialysis calibration using retrodialysis and zero-net flux: application to a study of the distribution of zidovudine to rabbit cerebrospinal fluid and thalamus. Pharmac Res 10:1411–1419

Westerink BHC, Tuinte MHJ (1985) Chronic use of intracerebral dialysis for the *in vivo* measurement of 3,4-dihydroxyphenylethylamine and its metabolite 3,4-dihydroxyphenylacetic acid. J Neurochem 46:181–185

Wood PL, Kim HSD, Stocklin K, Rao TS (1988) Dynamics of the striatal 3-MT-pool in rat and mouse: species differences as assessed by steady-state measurements and intracerebral dialysis. Life Sci 42:2275–2281

Zetterström T, Ungerstedt U (1983) Effects of apomorphine on the *in vivo* release of dopamine and its metabolites, studied by brain dialysis. Eur J Pharmacol 97:29–36
Zetterström T, Vernet L, Ungerstedt U, Tossman U, Jonzon B, Fredholm BB (1982) Purine levels in the intact rat brain. Studies with an implanted perfused hollow fibre. Neurosci Lett 29:111–115
Zetterström T, Sharp T, Marsden CA, Ungerstedt U (1983) *In vivo* measurement of dopamine and its metabolites by intracerebral dialysis: changes after d-amphetamine. J Neurochem 41:1769–1773

E.5.1.14 Use of Push-Pull Cannulae to Determine the Release of Endogenous Neurotransmitters

PURPOSE AND RATIONALE

Originally reported by Gaddum (1961), the push-pull cannula has become recognized and utilized as a powerful tool in conjunction with sufficiently sensitive assays to measure low levels of neuroregulator release in distinct brain areas *in vivo*. (Philippu 1984).

This method has been used for various purposes, e. g.,

- to perfuse the ventricles of the brain with drugs, or to determine the release of labelled or endogenous compounds in the CSF (Bhattacharya and Feldberg 1958; Korf et al. 1976),
- to perfuse distinct brain areas with drugs and to study their effects on functions of the central nervous system (Myers et al. 1976; Bhargava et al. 1978; Ruwe and Myers 1978),
- to inject labelled monoamines or amino acids and to investigate the resting or induced release of radioactive compounds and their metabolites (Sulser et al. 1969; Strada and Sulser 1971; Kondo and Iwatsubo 1978),
- to perfuse distinct brain areas with labelled transmitter precursors and to determine the patterns of release of the newly synthesized transmitters (Philippu et al. 1974; Chéramy et al. 1977; Nieoullon et al. 1977; Gauchy et al. 1980),
- to perfuse distinct brain areas of anesthetized and conscious animals and to determine the release of endogenous neurotransmitters in the perfusate (Dluzen and Ramirez 1991).

PROCEDURE

The superfusion of the hypothalamus of the conscious, freely moving rabbit has been described by Philippu et al. (1981), Philippu (1984). Rabbits of both sexes are anesthetized with 40 mg/kg sodium pentobarbital i.p. Guide cannulae are mounted on a metal plate which is fixed on the skull with screws and dental cement. Some days after the operation, the guide cannulae are replaced with push-pull cannulae which are 4 mm longer than the guide cannulae, thus reaching the areas which are intended for superfusion. The push-pull cannulae are connected by tubing to two peristaltic pumps: one to push and another one to pull the fluid. The second pump is essential, because the superfusate is not directly collected from the side branch of the push-pull cannula, but from tubing which is connected to the side branch. The superfusate is automatically collected every 10 s in fraction collectors.

EVALUATION

The concentrations of neurotransmitters, e. g., epinephrine, norepinephrine, or dopamine are determined with appropriate analytical methods (Wolfensberger 1984) before and after stimulation.

MODIFICATIONS OF THE METHOD

Experiments in cats were described by Dietl et al. (1981), in rats by Tuomisto et al. (1983).

The cortical cup technique for collection of neurotransmitters has been described by Moroni and Pepeu (1984).

REFERENCES AND FURTHER READING

Bhargava KP, Jain IP, Saxena AK, Sinha NJ, Tangri KK (1978) Central adrenoceptors and cholinoceptors in cardiovascular control. Br J Pharmacol 63:7–15
Bhattacharya BK, Feldberg W (1958) Perfusion of cerebral ventricles: effects of drugs on outflow from the cisterna and the aqueduct. Br J Pharmacol 13:156–162
Chéramy A, Nieoullon A, Glowinski J (1977) Effects of peripheral and local administration of picrotoxin on the release of newly synthesized ^{3}H-dopamine in the caudate nucleus of the cat. Naunyn-Schmiedeberg's Arch Pharmacol 297:31–37
Dietl H, Sinha JN, Philippu A (1981) Presynaptic regulation of the release of catecholamines in the cat hypothalamus. Brain Res 208:143–147
Dluzen DE, Ramitez VD (1991) Push-pull cannula – construction, application and considerations for use in neuroendocrinology. In: Greenstein B (ed) Neuroendocrine Research Methods, Vol 1, Harwood Acad Publ, Chur, Chapter 8, pp 163–186
Gauchy C, Kemel ML, Glowinski J, Besson JM (1980) *In vivo* release of endogenously synthesized (^{3}H)GABA from the cat substantia nigra and the pallidoendopeduncular nuclei. Brain Res 193:129–141
Kondo A, Iwatsubo K (1978) Increased release of preloaded (^{3}H)GABA from substantia nigra *in vivo* following stimulation of caudate nucleus and globus pallidus. Brain Res 154:305–400
Korf J, Boer PH, Fekkes D (1976) Release of cyclic AMP into push-pull perfusates in freely moving rats. Brain Res 113:551–561
Moroni F, Pepeu G (1984) The cortical cup technique. In: Marsden CA (ed) Measurements of Neurotransmitter Release *in*

vivo. John Wiley and Sons, Ltd., Chichester, New York, pp 63–79

Myers RD, Simpson CW, Higgins D, Nattermann RA, Rice JC, Redgrave P, Metclaf G (1976) Hypothalamic Na^+ and Ca^{2+} ions and temperature set-point: New mechanisms of action of a central or peripheral thermal challenge and intrahypothalamic 5-HT, NE, PGE_1 and pyrogen. Brain Res Bull 1:301–327

Nieoullon A, Chéramy A, Glowinski J (1977) An adaptation of the push-pull cannula method to study the *in vivo* release of (^{3}H)dopamine synthesized from (^{3}H)tyrosine in the cat caudate nucleus: effects of various physical and pharmacological treatments. J Neurochem 28:819–828

Philippu A (1984) Use of push-pull cannulae to determine the release of endogenous transmitters in distinct brain areas of anesthetized and freely moving animals. In: Marsden CA (ed) Measurements of Neurotransmitter Release *in vivo*. John Wiley and Sons, Ltd., Chichester, New York, pp 3–37

Philippu A, Glowinski J, Besson JM (1974) *In vivo* release of newly synthesized catecholamines from the hypothalamus by amphetamine. Naunyn-Schmiedeberg's Arch Pharmacol 282:1–8

Philippu A, Dietl H, Eisert A (1981) Hypotension alters the release of catecholamines in the hypothalamus of the conscious rabbit. Eur J Pharmacol 69:519–523

Ruwe WD, Myers RD (1978) Dopamine in the hypothalamus of the cat: pharmacological characterization and push-pull perfusion analysis of sites mediating hypothermia. Pharmacol Biochem Behav 9:65–80

Strada SJ, Sulser F, (1971) Comparative effects of p-chloroamphetamine and amphetamine on metabolism and *in vivo* release of ^{3}H-norepinephrine in the hypothalamus of the rat *in vivo*. Eur J Pharmacol 15:45–51

Sulser F, Owens ML, Strada SJ, Dingell NJ (1969) Modification by desimipramine (DMI) of the availability of epinephrine released by reserpine in the hypothalamus of the rat *in vivo*. J Pharmacol Exp Ther 168:272–282

Tuomisto L, Yamatodani A, Dietl H, Waldmann U, Philippu A (1983) *In vivo* release of endogenous catecholamines, histamine and GABA in the hypothalamus of Wistar Kyoto and spontaneously hypertensive rats. Naunyn-Schmiedeberg's Arch Exp Pharm

Wolfensberger M (1984) Gaschromatographic and mass-fragmentographic measurement of amino acids released into brain perfusates collected *in vivo* by push-pull cannula techniques. In: Marsden CA (ed) Measurements of Neurotransmitter Release *in vivo*. John Wiley and Sons, Ltd., Chichester, New York, pp 39–61

E.5.1.15 Fos Protein Expression in Brain

PURPOSE AND RATIONALE

The proto-oncogene c-fos encodes a 55,000 mol wt, 380 amino-acid phosphoprotein (FOS), which after translation in the cytoplasm, re-enters the nucleus and binds to DNA (Morgan and Curran 1989). C-fos induction can occur as a consequence of synaptic activation. An increase in fos immunoreactivity is associated with an increased metabolic demand on a neuron, i. e., a marker for neurons that are metabolically activated. Intermediate early genes such as c-fos have been tentatively classified or linked to third messengers, whose function is to produce a long-term effect on the recipient neuron.

Acute administration of antipsychotics induces c-fos expression in several areas of the rat forebrain as was shown with immunocytochemical methods (Dragunow et al. 1990; Nguyen et al. 1992; Robertson and Fibiger 1992; MacGibbon et al. 1994). Fos protein is believed to act as an initiator of long-term cellular changes (neural plasticity) in response to a variety of extracellular stimuli, including drugs (Graybiel et al. 1990; Rogue and Vicendon 1992). Typical (e. g. haloperidol) and atypical (e. g. clozapine) neuroleptic drugs have different antipsychotic effects and side-effects. A differential FOS-protein induction in rat forebrain regions after haloperidol and clozapine treatment was found (Deutch et al. 1992; Fibiger 1994; Fink-Jensen and Kristensen 1994; Merchant et al. 1994; Sebens et al. 1995). The induction pattern of Fos-like immunoreactivity in the forebrain could serve as predictor of atypical antipsychotic drug activity (Robertson et al. 1994).

PROCEDURE

Groups of 4–6 male Wistar rats weighing 350–450 g are injected subcutaneously with saline (control) or with various doses of the standard drugs or compounds with putative antipsychotic activity. After two hours, the animals are deeply anesthetized by intraperitoneal injection of 100 mg/kg pentobarbital and perfused with 200 ml saline followed by 200 ml of 4% paraformaldehyde in phosphate buffer solution (PBS). Each brain is removed immediately after perfusion and placed in fresh fixative for at least 12 h.

After the postfixative period, 30-µm sections are cut from each brain using a vibratome. Several antisera to detect Fos can be used, such as a sheep polyclonal anti-body directed against residues 2 to 16 of the N-terminal region of the Fos molecule, or a polyclonal antiserum raised in rabbits against Fos peptide (4–17 amino acids of human Fos).

Sections are washed 3 times with 0.02 mM PBS and then incubated in PBS containing 0.3% hydrogen peroxide for 10 min to block endogenous peroxidase activity. Sections are then washed 3 times in PBS and incubated in PBS containing 0.3% Triton X-100, 0.02% azide and Fos primary antisera (diluted 1:200) for 48 h. The sections are then washed 3 times with PBS and incubated with a biotinylated rabbit antisheep secondary antibody (diluted 1:200) for 1 h. The sections are washed three times with PBS and incubated for 1 h with PBS containing 0.3% Triton X-100 and 0.5% avidin-biotinylated horseradish peroxidase com-

plex. After 3 washes in PBS the sections are rinsed in 0.1 M acetate buffer, pH 6.0. Fos immunoreactivity is revealed by placing the sections in a solution containing 0.05% 3,3′-diaminobenzidine, 0.2% ammonium nickel sulfate and 0.01% H_2O_2. The reaction is terminated with a washing in acetate buffer. The sections are mounted on chrome-alum-coated slides, dehydrated and prepared for microscopic observation.

Drug induced changes in Fos-like immunoreactivity are quantified by counting the number of immunoreactive nuclei in the medial prefrontal cortex, nucleus accumbens, medial and dorsolateral striatum and the lateral septal nucleus. The number of Fos-positive nuclei are counted with a 550 × 550 µm grid placed over each of these regions with a 100 × magnification.

Typical and atypical antipsychotics can be classified on the basis of difference between Fos-like immunoreactivity in the nucleus accumbens and lateral striatum. For this purpose, the data are corrected for the effects which are produced by the injection procedure itself. The injection corrected value for the dorsolateral striatum is subtracted from the corresponding accumbal value for each drug dose.

This manipulation yields a value termed the atypical index, i. e. number of Fos-positive neurons in the nucleus accumbens minus the number in the lateral striatum = atypical index. A negative index indicates the probability of side-effects, like extrapyramidal syndrome, exerted by the typical neuroleptics, a positive value to be devoid of it.

EVALUATION

A one-way analysis of variance is performed on the cell count data for each dose and the corresponding vehicle control. If the analysis of variance is significant, multiple comparisons are performed by using the Newman-Keuls test.

MODIFICATIONS OF THE METHOD

Graybiel et al. (1990) reported a drug-specific activation of c-fos gene in striosome-matrix compartments and limbic subdivisions of the striatum by amphetamine and cocaine.

Deutch et al. (1991) found that stress selectively increases Fos protein in dopamine neurons innervating the prefrontal cortex.

Gogusev et al. (1993) described modulation of C-fos and other proto-oncogene expression by phorbol diester in a human histiocytosis DEL cell.

Deutch et al. (1995) studied the induction of Fos protein in the thalamic paraventricular nucleus as locus of antipsychotic drug action.

REFERENCES AND FURTHER READING

Ashby CR, Wang RY (1996) Pharmacological actions of the atypical antipsychotic drug clozapine: a review. Synapse 24:349–394

Deutch AY (1994) Identification of the neural systems subserving the actions of clozapine: Clues from immediate early gene expression. J Clin Psychiatry 55, Suppl:37–42

Deutch AY, Lee MC, Gillham MH, Cameron DA, Goldstein M, Iadarola MJ (1991) Stress selectively increases Fos protein in dopamine neurons innervating the prefrontal cortex. Cerebr Cortex 1:273–292

Deutch AY, Lee M, Iadarola MJ (1992a) Regionally specific effects of atypical antipsychotic drugs on striatal Fos expression: The nucleus accumbens shell as a locus of antipsychotic action. Molec Cell Neurosci 3:332–341

Deutch AY, Lee MC, Iadorola MJ (1992b) Regionally specific effects of atypical antipsychotic drugs on striatal fos expression. The nucleus accumbens shell as a locus of antipsychotic action. Mol Cell Neurosci 3:332–341

Deutch AY, Öngür D, Duman RS (1995) Antipsychotic drugs induce Fos protein in the thalamic paraventricular nucleus: a novel locus of antipsychotic drug action. Neurosci 66:337–346

Dragunow M, Robertson GS, Faull RLM, Robertson HA, Jansen K (1990) D_2 Dopamine receptor antagonists induce FOS and related proteins in rat striatal neurons. Neurosci 37:287–294

Fibiger HC (1994) Neuroanatomical targets of neuroleptic drugs as revealed by Fos immunochemistry. J Clin Psychiatry 55, Suppl B:33–36

Fink-Jensen A, Kristensen P (1994) Effects of typical and atypical neuroleptics on Fos protein expression in the rat forebrain. Neurosci Lett 182:115–118

Gogusev J, Barbey S, Nezelof C (1993) Modulation of C-myc, C-myb, C-fos, C-sis and C-fms proto-oncogene expression and of CSF-1 transcripts and protein by phorbol diester in human histiocytosis DEL cell line with 5q 35 break point. Anticancer Res 13:1043–1048

Graybiel AM, Moratalla R, Robertson HA (1990) Amphetamine and cocaine induce drug-specific activation of the c-fos gene in striosome-matrix compartments and limbic subdivisions of the striatum. Proc Natl Acad Sci USA 87:6912–6916

MacGibbon GA, Lawlor PA, Bravo R, Dragunow M (1994) Clozapine and haloperidol produce a different pattern of immediate early gene expression in rat caudate-putamen, nucleus accumbens, lateral septum and islets of Calleja. Mol Brain Res 23:21–32

Merchant KM, Drosa DM (1993) Differential induction of neurotensin and c-fos gene expression by typical versus atypical antipsychotic drugs. Proc Natl Acad Sci USA 90:3447–3451

Merchant KM, Dobie DJ, Filloux FM, Totzke M, Aravagiri M, Dorsa DM (1994) Effects of chronic haloperidol and clozapine treatment on neurotensin and c-fos mRNA in rat neostriatal subregions. J Pharmacol Exp Ther 271:460–471

Morgan JI, Curran T (1989) Stimulus-transcription coupling in neurons: role of cellular immediate early genes. Trends Neurosci 12:459–462

Morgan JI, Curran T (1991) Stimulus-transcription coupling in the nervous system: Involvement of the inducible proto-oncogens fos and jun. Annu Rev Neurosci 14:421–451

Nguyen TV, Kosofsky BE, Birnbaum R, Cohen BM, Heyman SE (1992) Differential expression of c-Fos and Zif628 in rat striatum after haloperidol, clozapine and amphetamine. Proc Natl Acad Sci USA 89:4720–4724

Robertson GS, Fibiger HC (1992) Neuroleptics increase c-Fos expression in the forebrain. Contrasting effects of haloperidol and clozapine. Neuroscience 46:315–328

Robertson GS, Matsumara H, Fibiger HC (1994) Induction pattern of Fos-like immunoreactivity in the forebrain as predictors of atypical antipsychotic activity. J Pharmacol Exp Ther 271:1058–1066

Rogue P, Vincendon G (1992) Dopamine D_2 receptor antagonists induce immediate early genes in the rat striatum. Brain Res Bull 29:469–472

Sebens JB, Koch T, Ter Horst GJ, Korf J (1995) Differential Fos-protein induction in rat forebrain regions after acute and long-term haloperidol and clozapine treatment. Eur J Pharmacol 273:175–182

E.5.1.16 Neurotensin

E.5.1.16.1 General Considerations on Neurotensin and Neurotensin Receptors

Neurotensin is a 13-amino-acid peptide originally isolated from calf hypothalamus (Carraway and Leeman 1973). It is secreted by peripheral and neuronal tissues and produces numerous pharmacological effects in animals suggesting **analgesic** (Coguerel et al. 1988; Clineschmidt and McGuffin 1977; Smith et al. 1997), **wound healing** (Brun et al. 2005), **cardiovascular** (Carraway and Leeman 1973; Schaeffer et al. 1998; Seagard et al. 2000), **endocrine** (Rostene and Alexander 1997), **hypothermic** (Bissette et al. 1976; Benmoussa et al. 1996; Tyler-McMahon et al. 2000), and **antipsychotic** (Nemeroff 1986; Sarhan et al. 1997; Feifel et al. 1999; Kinkead et al. 1999; Cusack et al. 2000) actions. Neurotensin is even considered to be an endogenous neuroleptic (Ervin and Nemeroff 1988; Gully et al. 1995). Radke et al. (1998) studied synthesis and efflux of neurotensin in different brain areas after acute and chronic administration of typical and atypical antipsychotic drugs.

Neurotensin affects **gastrointestinal functions**, such as stimulating the growth of various gastrointestinal tissues (Feurle et al. 1987), modulating pre- and post-prandial intestinal motility (Pellissier et al. 1996), inhibiting gastric acid secretion (Zhang et al. 1989a), stimulating responses in rat stomach strips (Quirion et al. 1980), inducing contractile responses in intestinal smooth muscle (Unno et al. 1999), and maintaining gastric mucosal blood flow during cold water restraint (Zhang et al. 1989b; Xing et al. 1998).

Neurotensin acts as a **growth factor** on a variety of normal and cancer cells (Wang et al. 2000).

Like other neuropeptides, neurotensin is synthesized as part of a larger precursor which also contains neuromedin N, a six amino acid neurotensin-like peptide belonging to the gastrin-releasing peptide/bombesin family (see J.3.1.8).

Several peptidic and non-peptidic neurotensin agonists and antagonists have been synthesized and analyzed in pharmacological tests as potential drugs mainly in psychopharmacology (Gully et al. 1995, 1996, 1997; Azzi et al. 1996; Castagliuolo et al. 1996; Chapman and See 1996; Mule et al. 1996; Hong et al. 1997; Johnson et al. 1997; Sarhan et al. 1997; Betancur et al. 1998; Gudasheva et al. 1998; Schaeffer at al 1998; Kitabgi 2002). Furthermore, inhibitors of neurotensin-degrading enzymes were described (Bourdel et al. 1996). Binder et al. (2001) reviewed neurotensin and dopamine interactions.

REFERENCES AND FURTHER READING

Azzi M, Boudin H, Mahmudi N, Pelaprat D, Rostene W, Berod A (1996) *In vivo* regulation of neurotensin receptors following long-term pharmacological blockade with a specific receptor antagonist. Mol Brain Res 42:213–221

Benmoussa M, Chait A, Loric G, de Beaurepaire R (1996) Low doses of neurotensin in the preoptic area produce hypothermia. Comparison with other brain sites and with neurotensin-induced analgesia. Brain Res Bull 39:275–279

Betancur C, Canton M, Burgos A, Labeeuw B, Gully D, Rostene W, Pelaprat D (1998) Characterization of binding sites of a new neurotensin receptor antagonist, ^{3}H-SR 142948A, in the rat brain. Eur J Pharmacol 343:67–77

Binder EB, Kinkead B, Owens MJ, Nemeroff CB (2001) Neurotensin and dopamine interactions. Pharmacol Rev 53:453–486

Bissette G, Nemeroff CB, Loosen PT, Prange AJ Jr, Lipton MA (1976) Hypothermia and cold intolerance induced by the intracisternal administration of the hypothalamic peptide neurotensin. Nature 262:607–609

Bourdel E, Doulut S, Jarretou G, Labbé-Juilié C, Fehrentz JA, Doumbia O, Kitabgi P, Martinez J (1996) New hydroxamate inhibitors of neurotensin-degrading enzymes: Synthesis and enzyme active-site recognition. Int J Pept Protein Res 48:148–155

Brun P, Mastrotto C, Beggiao E, Stefani A, Barzon L, Sturniolo GC, Palù G, Castagliuolo I (2005) Neuropeptide neurotensin stimulates intestinal wound healing following chronic intestinal inflammation. Am J Physiol 288:G621–G629

Carraway R, Leeman SE (1973) The isolation of a new hypotensive peptide, neurotensin, from bovine hypothalami. J Biol Chem 248:6854–6861

Castagliuolo I, Leeman SE, Bartolak-Suki E, Nikulasson S, Quiu B, Carraway RE (1996) A neurotensin antagonist, SR 48692, inhibits colonic responses to immobilization stress in rats. Proc Natl Acad Sci USA 93:12611–12615

Chapman MA, See RE (1996) The neurotensin receptor antagonist SR 48692 decreases extracellular striatal GABA in rats

Clineschmidt R, McGuffin JC (1977) Neurotensin administered intracisternally inhibits responsiveness of mice to noxious stimuli. Eur J Pharmacol 49:395–396

Coguerel A, Dubuc I, Kitabgi P, Costentin J (1988) Potentiation by thiorphan and bestatin of the naloxon-insensitive analgesic effects of neurotensin and neuromedin N. Neurochem Int 12:361–366

Cusack B, Boules M, Tyler BM, Fauq A, McCormick DJ, Richelson E (2000) Effects of a novel neurotensin peptide

analog given extracranially on CNS behaviors mediated by apomorphine and haloperidol. Brain Res 856:48–54
Ervin GN, Nemeroff CB (1988) Interactions of neurotensin with dopamine-containing neurons in the central nervous system. Neuropsychopharmacol Biol Psychiatry 12:S53–S69
Feifel D, Reza TL, Wustrow DJ, Davis MD (1999) Novel antipsychotic-like effects on prepulse inhibition of startle produced by a neurotensin agonist. J Pharmacol Exp Ther 288:710–713
Feurle GE, Muller B, Rix E (1987) Neurotensin induces hyperplasia of the pancreas and growth of the gastric antrum in rats. Gut 28, Suppl 1:19–23
Gudasheva TA, Voronina TA, Ostrovskaya RU, Zaitseva NI, Bondarenko NA, Briling VK (1998) Design of N-acylprolyltyrosine 'tripeptoid' analogues of neurotensin as potential atypical antipsychotic agents. J Med Chem 41:284–290
Gully D, Jeanjean F, Poncelet M, Steinberg R, Soubrié P, Le Fur G, Maffrand JP (1995) Neuropharmacological profile of non-peptide neurotensin antagonists. Fundam Clin Pharmacol 9:513–521
Gully D, Lespy L, Canton M, Rostene W, Kitabgi P, le Fur G, Maffrand JP (1996) Effect of the neurotensin receptor antagonist SR 48692 on rat blood pressure modulation by neurotensin. Life Sci 58:665–674
Gully G, Labeeuw B, Boigegrain R, Oury-Donat F, Bachy A, Poncelet M, Steinberg R. Suaud-Chagny MF, Santucci V, Vita N, Pecceu F, Labbé-Jullié C, Kitabgi B, Soubriè P (1997) Biochemical and pharmacological activities of SR 142948A, a new potent neurotensin receptor antagonist. J Pharmacol Exp Ther 280:802–812
Hong F, Cusack B, Fauq A, Richelson E (1997) Peptidic and non-peptidic neurotensin analogs. Curr Med Chem 4:421–434
Johnson SJ, Akunne HC, Heffener TG, Kesten SR, Pugsley TA, Wise LD, Wustrow DJ (1997) Novel small molecule neurotensin antagonists: 3-(1,5-diaryl-1,5-dioxopentan-3-yl) benzoic acids. Bioorg Med Chem Lett 7:561–566
Kinkead B, Binder EB, Nemeroff CB (1999) Does neurotensin mediate the effects of antipsychotic drugs? Biol Psychiatry 46:340–351
Kitabgi P (2002) Targeting neurotensin receptors with agonists and antagonists for therapeutic purposes. Curr Opin Drug Discov Devel 5:764–776
Mule F, Serio R, Postorino A, Vetri T, Bonvissuto F (1996) Antagonism by SR 48692 on mechanical responses to neurotensin in rat intestine. Br J Pharmacol 117:488–492
Nemeroff CB (1986) The interaction of neurotensin with dopaminergic pathways in the central nervous system: Basic neurobiology and implications for the pathogenesis and treatment of schizophrenia. Psychoneuroendocrinology 11:15–37
Pellissier S, Eribon O, Chabert J, Gully D, Roche M (1996) Peripheral neurotensin participates in the modulation of pre- and postprandial intestinal motility in rats. Neuropeptides 30:412–419
Quirion R, Regoli D, Rioux F, St-Pierre S (1980) The stimulatory effect of neurotensin and related peptides in rat stomach strips and guinea pig atria. Br J Pharmacol 68:83–91
Radke JM, Owens MJ, Ritchie JC, Nemeroff CB (1998) Atypical antipsychotic drugs selectively increase neurotensin efflux in dopamine terminal regions. Proc Natl Acad Sci USA 95:11462–11464
Rostene W, Alexander MJ (1997) Neurotensin and neuroendocrine regulation. Front Neuroendocrinol 18:115–173
Sarhan S, Hitchcock JM, Grauffel CA, Wettstein JG (1997) Comparative antipsychotic profiles of neurotensin and a related systematically active peptide agonist. Peptides 18:1223–1227
Schaeffer P, Laplace MC, Bernat A, Prabonaud V, Gully D, Lespy L, Herbert JM (1998) SR142948A is a potent antagonist of the cardiovascular effects of neurotensin. J Cardiovasc Pharmacol 31:545–550
Saegard JL, Dean C, Hopp FA (2000) Neurochemical transmission of the baroreceptor input in the nucleus tractus solitarius. Brain Res Bull 51:111–118
Smith DJ, Hawranko AA, Monroe PJ, Gully D, Urban MO, Craig CR, Smith JP, Smith DI (1997) Dose-dependent pain-facilitatory and -inhibitory actions of neurotensin are revealed by SR 48692, a nonpeptide neurotensin antagonist: influence on the antinociceptive effect of morphine. J Pharmacol Exp Ther 282:899–908
Tyler-McMahon BM, Steward JA, Farinas F, McCormick DJ, Richelson E (2000) Highly potent neurotensin analog that causes hypothermia and antinociception. Eur J Pharmacol 390:107–111
Unno T, Komori S, Ohashi H (1999) Characterization of neurotensin receptors in intestinal smooth muscle using a non-peptide antagonist. Eur J Pharmacol, 369:73–80
Vincent JP, Mazella J, Kitagbi P (1999) Neurotensin and neurotensin receptors
Wang L, Friess H, Zhu Z, Graber H, Zimmermann A, Korc M, Reubi JC, Buchler MW (2000) Neurotensin receptor-1 mRNA analysis in normal pancreas and pancreatic disease. Clin Cancer Res 6:566–571
Xing L, Karinch AM, Kauffman GL Jr (1998) Mesolimbic expression of neurotensin and neurotensin receptor during stress-induced gastric mucosal injury. Am J Physiol 274, Regul Integr Comp Physiol:R38–R45
Zhang L, Xing L, Demers L, Washington J, Kauffman GL Jr (1989a) Central neurotensin inhibits gastric acid secretion: an adrenergic mechanism in rats. Gastroenterology 97:1130–1134
Zhang L, Colony PC, Washington JH, Seaton JF, Kauffman GL Jr (1989b) Central neurotensin affects rat gastric integrity, prostaglandin E2, and blood flow. Am J Physiol 256, Gastrointest Liver Physiol 19:G226–G232

E.5.1.16.2 Neurotensin Receptor Binding

PURPOSE AND RATIONALE

Neurotensin interacts with two cloned receptors that were originally differentiated on the basis of their affinity to the antihistaminic drug levocabastine (Schotte et al. 1986). The high sensitive, levocabastine-insensitive rat neurotensin receptor (*NTR1*) was cloned first (Tanaka et al. 1990) and shown to mediate a number of peripheral and central neurotensin responses, including the neuroleptic-like effects of the peptide (Labbé-Jullié et al. 1994). The human NTR1 has been cloned from the colonic adenocarcinoma cell line HT29 (Vita et al. 1993) and shown to consist of a 416 amino acid protein that shares 84% homology with rat NTR1. A second human NTR1 receptor differing only in one amino acid has been cloned from substantia nigra by Watson et al. (1993).

The lower-affinity, levocabastine-sensitive neurotensin receptor (*NTR2*) was cloned by Chalon et al. (1996), Mazella et al. (1996) and characterized by Yamada et al. (1998). Studies by Dubuc et al. (1999) indicate that NTR2 mediates neurotensin-induced analgesia.

A third neurotensin receptor (*NTR3*) was cloned from a human brain cDNA library (Mazella et al. 1998; Vincent et al. 1999; Mazella 2001; Mazella and Vincent 2006). It is identical with sortilin, a receptor-like protein, cloned from human brain (Petersen et al. 1997, 1999). The NT3/gp95/sortilin protein is a transmembrane neuropeptide receptor which does not belong to the superfamily of G-protein-coupled receptors.

Gully et al. (1997) described a binding assay for the neurotensin1 receptor.

PROCEDURE

Cell Culture

CHO cells transfected with cDNA of the human neurotensin receptor cloned from HT 29 cells (h-NTR1-CHO cells) are cultured at 37°C in modified Eagles medium without nucleosides, containing 10% fetal calf serum, 4 mM glutamine and 300 µg/ml geneticin (G418), in a humidified incubator under 5% CO_2 in O_2. The colonic adenocarcinoma HT 29 cell line (American Type Culture Collection, Rockville, MD) is cultured under similar conditions in Dulbecco's modified Eagle's medium/F-12 medium supplemented with 10% fetal calf serum, 4 mM glutamine, 200 IU/ml penicillin and 200 mg/ml streptomycin. One week after seeding, confluent monolayer cultures are washed three times with 3 ml PBS and harvested by enzymatic dissociation with trypsin. After dilution with PBS, cells are resuspended in the same culture medium at a density of 5×10^4 cells/ml and are plated into 35-mm-diameter, fibronectin-coated Petri culture dishes.

Membrane Homogenate Preparation and Binding Assay

Whole brains of male Sprague-Dawley rats albino guinea pigs or cell pellets are homogenized in 10 volumes of ice-cold 50 mM Tris-HCl buffer (pH 7.4) for 30 s, using a Polytron homogenizer (setting 5). After 20 min centrifugation at 30,000 *g*, the pellet is washed, centrifuged again under the same conditions, resuspended in a storage buffer containing 50 mM Tris-HCl (pH 7.4), 1 mM EDTA, 0.1% BSA, 40 mg/liter bacitracin, 1 mM 1,10-orthophenanthroline and 5 mM dithiothreitol and stored as aliquots in liquid nitrogen until used.

Aliquots of membranes (10, 50, 300 and 500 µg of protein for h-NTR1-CHO cells, HT 29 cells, rat and guinea pig brain, respectively) are incubated for 20 min at 20°C in the incubation buffer (0.5 ml final volume) containing appropriate concentrations of [^{125}I-Tyr^3]neurotensin (25–100 pM) and unlabeled drugs. After incubation, the assay medium is diluted with 4 ml of ice-cold 50 mM Tris-HCl buffer (pH 7.4) supplemented with 0.1% BSA and 1 mM EDTA, and the mixture is rapidly filtered under reduced vacuum through Whatman GF/B glass fibre filters that have been pretreated with 0.1% polyethyleneimine. The filters are washed under the same conditions three times and radioactivity is measured. Nonspecific binding is determined in the presence of 1 µM unlabeled neurotensin. All experiments are performed in triplicate, and data are expressed as the mean ± SEM of at least three separate determinations.

EVALUATION

The IC_{50} is the value of ligand that inhibits 50% of the specific binding and is determined using an iterative nonlinear regression program (Munson and Rodbard 1980).

MODIFICATIONS OF THE METHOD

Cusack et al. (1995) studied species selectivity of neurotensin analogs at the rat and two human NTR1 receptors.

Lugrin et al. (1991) produced a series of pseudopeptide analogs of neurotensin by systematically replacing peptide bonds in neurotensin with CH_2NH bonds. The compounds were screened *in vitro* for agonist or antagonist activity and for metabolic stability.

Le et al. (1997) cloned the human neurotensin receptor gene and determined the structure.

Labbé-Jullié et al. (1998) attempted to identify residues in the rat NTR1 that are involved in binding of a nonpeptide neurotensin antagonist.

Souazé et al. (1997), Najimi et al. (1998) studied the effects of a neurotensin agonist and showed in human colonic adenocarcinoma HT 29 cells after short incubation an increase, after prolonged exposure a decrease of mRNA levels and in the human neuroblastoma cell line CHP 212 a high affinity neurotensin receptor gene activation.

Ovigne et al. (1998) described a monoclonal antibody specific for the human NTR1.

Nouel et al. (1999) found that both NT2 and NT3 neurotensin receptor subtypes were expressed by cortical glial cells in culture.

Cusack et al. (2000) developed a neurotensin analog, NT34, that can distinguish between rat and human

neurotensin receptors, and exhibits more than a 100-fold difference in binding affinities.

Neuromedin N, a peptide belonging to the gastrin-releasing peptide/bombesin family (see J.3.1.7) shows a high affinity to brain neurotensin receptors and is rapidly inactivated by brain synaptic peptidases (Checler et al. 1990).

REFERENCES AND FURTHER READING

Chalon P, Vita N, Kaghad M, Guillemot M, Bonnin J, Delpech P, Le Fur G, Ferrara P, Caput D (1996) Molecular cloning of a levocabastine-sensitive binding site. FEBS Lett 400:211–214

Checler F, Vincent JP, Kitabgi P (1986) Neuromedin N: High affinity interaction with brain neurotensin receptors and rapid inactivation by brain synaptic peptidases. Eur J Pharmacol 126:239–244

Cusack B, McCormick DJ, Pang Y-P, Souder T, Garcia R, Fauq A, Richelson E (1995) Pharmacological and biochemical profiles of unique neurotensin 8–13 analogs exhibiting species selectivity, stereoselectivity, and superagonism. J Biol Chem 270:18359–18366

Cusack B, Chou T, Jansen K, McCormick DJ, Richelson E (2000) Analysis of binding sites and efficacy of a species-specific peptide at rat and human neurotensin receptors. J Pept Res 55:72–80

Dubuc I, Sarret P, Labbé-Jullié C, Botto JM, Honoré E, Bourdel E, Martinez J, Costentin J, Vincent JP, Kitabgi P, Mazella J (1999) Identification of the receptor subtype involved in the analgesic effect of neurotensin. J Neuroscience 19:503–510

Gully D, Labeeuw B, Boigegrain R, Oury-Donat F, Bachy B, Poncelet M, Steinberg R, Suaud-Chagny MF, Santucci V, Vita N, Pecceu F, Labbé-Jullié C, Kitabgi P, Soubrié P, Le Fur G, Maffrand JP (1997) Biochemical and pharmacological activities of SR 142948A, a new potent neurotensin receptor antagonist. J Pharmacol Exp Ther 280:802–812

Labbé-Jullié C, Dubuc I, Brouard A, Doulut S, Bourdel E, Pelaprat D, Mazella J, Martinez J, Rostène W, Costentin J, Kitabgi P (1994) *In vivo* and *in vitro* structure-activity studies with peptide and pseudopeptide neurotensin analogs suggest the existence of distinct central neurotensin receptor subtypes. J Pharmacol Exp Ther 268:328–336

Labbé-Jullié C, Barroso S, Nicolas-Etève D, Reversat JL, Botto JM, Mazella J, Barnassau JM, Kitabgi P (1998) Mutagenesis and modeling of the neurotensin receptor NTR1. Identification of residues that are critical for binding of SR 48692, a nonpeptide neurotensin. J Biol Chem 273:16351–16357

Le F, Groshan K, Zeng X-P, Richelson E (1997) Characterization of the genomic structure, promotor region, and a tetranucleotide repeat polymorphism of the human neurotensin receptor gene. J Biol Chem 272:1315–1322

Lugrin D, Vecchini F, Doulut S, Rodriguez M, Marinez J, Kitabgi P (1991) Reduced peptide bond pseudopeptide analogues of neurotensin: binding and biological activities, and *in vitro* metabolic stability. Eur J Pharmacol 205:191–198

Mazella J (2001) Sortilin/neurotensin receptor-3: a new tool to investigate neurotensin signaling and cellular trafficking? Cell Signal 13:1–6

Mazella J, Vincent JP (2006) Functional roles of the NTS2 and NTS3 receptors. Peptides 27:2469–2475

Mazella J, Botto JM, Guillemare E, Coppola T, Sarret P, Vincent JP (1996) Structure, functional expression, and cerebral localization of the levocabastine-sensitive neurotensin/neuromedin N receptor from mouse brain. J Neurosci 16:5613–5620

Mazella J, Zsürger N, Navarro V, Chabry J, Kaghad M, Caput D, Ferrara P, Vita N, Gully D, Maffrand JP, Vincent JP (1998) The 100-kDa neurotensin receptor is gp95/sortilin, a non-G-protein coupled receptor. J Biol Chem 273:26273–26276

Munson PJ, Rodbard D (1980) LIGAND: A versatile computerized approach for characterization of ligand-binding systems. Anal Biochem 107:220–239

Najimi M, Souzé F, Méndez M, Hermans E, Berbar T, Rostène W, Forgez P (1998) Activation of receptor gene transcription is required to maintain cell sensitization after agonist exposure. Studies on neurotensin receptor. J Biol Chem 273:21634–21641

Nouel D, Sarret P, Vincent JP, Mazella J, Beaudet A (1999) Pharmacological, molecular and functional characterization of glial neurotensin receptors. Neuroscience 94:1189–1197

Ovigne JM, Vermot-Desroches C, Lecron JC, Portier M, Lupker J, Pecceu F, Wijdenes J (1998) An antagonistic monoclonal antibody (B-N6) specific for the human neurotensin receptor-1. Neuropeptides 32:247–256

Petersen CM, Nielson MS, Nykjar A, Jacobsen L, Tommerup N, Rasmussen HH, Roigaard H, Gliemann J, Madsen P, Moestrup SK (1997) Molecular identification of a novel candidate sorting receptor purified from human brain by receptor-associated protein affinity chromatography. J Biol Chem 272:3599–3605

Petersen CM, Nielson MS, Jacobsen C, Tauris J, Jacobsen L, Gliemann J, Moestrup SK, Madsen P (1999) Propeptide cleavage conditions sortilin/neurotensin receptor-3 for ligand binding. EMBO J 18:595–604

Schotte A, Leysen JE, Laduron PM (1986) Evidence for a displaceable non-specific ^{3}H-neurotensin binding site in rat brain. Naunyn Schmiedeberg's Arch Pharmacol 333:400–405

Souazé F, Rostène W, Forgez P (1997) Neurotensin agonist induces differential regulation of neurotensin receptor mRNA. Identification of distinct transcriptional and post-transcriptional mechanisms. J Biol Chem 272:10087–10094

Tanaka K, Masu M, Nakanishi S (1990) Structure and functional expression of the cloned rat neurotensin receptor. Neuron 4:847–854

Vincent JP, Mazella J, Kitagbi P (1999) Neurotensin and neurotensin receptors

Vita N, Laurent P, Lefort S, Chalon P, Dumont X, Kaghad M, Gully D, Le Fur G, Ferrara P, Caput D (1993) Cloning and expression of a complementary DNA encoding a high affinity human neurotensin receptor. FEBS Lett 317:139–142

Watson M, Isackson PJ, Makker M, Yamada MS, Yamada M, Cusack B, Richelson E (1993) Identification of a polymorphism in the human neurotensin receptor gene. Mayo Clin Proc 68:1043–1048

Yamada M, Lombet A, Forgez P, Rostène W (1998) Distinct functional characteristics of levocabastine-sensitive rat neurotensin NT2 receptor expressed in Chinese hamster ovary cells. Life Sci 62: PL375–PL379

E.5.1.17
Genetically Altered Monoamine Transporters

Monoamine transporters, such as the dopamine transporter, 5-hydroxytryptamine transporter and noradrenaline transporter, in the plasma membrane pro-

vide effective control over the intensity of monoamine-mediated signaling by recapturing neurotransmitters released by presynaptic neurons (Gainetdinov et al. 2002). These transporters act also as molecular gateways for neurotoxins (Uhl and Kiayama 1993; Miller et al. 1999; Vincent et al. 1999).

Takahashi et al. (1997) found that heterozygote animals of VMAT2 knockout mice display reduced amphetamine-conditioned reward, enhanced amphetamine locomotion, and enhanced MPTP toxicity.

REFERENCES AND FURTHER READING

Gainetdinov RR, Sotnikova TD, Caron MG (2002) Monoamine transporter pharmacology and mutant mice. Trends Pharmacol Sci 23:367–373

Miller GW, Gainetdinov RR, Levey AI, Caron MG (1999) Dopamine transporters and neuronal injury. Trends Pharmacol Sci 20:424–429

Takahashi N, Miner LL, Sora I, Ujike H, Revay RS, Kostic V, Jackson-Lewis V, Przedborski S, Uhl GR (1997) VMAT2 knockout mice: heterozygotes display reduced amphetamine-conditioned reward, enhanced amphetamine locomotion, and enhanced MPTP toxicity. Proc Natl Acad Sci USA 94:9938–9943

Uhl GR, Kiayama S (1993) A cloned dopamine transporter. Potential insights into Parkinson's disease pathogenesis. Acta Neurol 60:321–324

Vincent JP, Mazella J, Kitabgi P (1999) Neurotensin and neurotensin receptors. Trends Pharmacol Sci 20:302–309

E.5.1.17.1 Dopamine Transporter Knockout Mice

Many drugs exert their psychotropic action via dopamine transporters (Amara and Kuhar 1993; Giros and Caron 1993).

Dopamine transporter knockout mice, which are generated by disruption of the gene encoding the dopamine transporter by homologous recombination (Giros et al. 1996; Sora et al. 1998), have a distinct biochemical and behavioral phenotype. At the neurochemical level, the homoeostasis of dopamine-containing neurons is altered markedly, including disrupted clearance of dopamine, an elevated extracellular concentration of dopamine and dramatically decreased intraneuronal storage of dopamine (Jones et al. 1998; Gainetdinov et al. 1998; Benoit-Marand et al. 2000).

In response to the elevated dopamine-mediated tone, both presynaptic and postsynaptic dopamine receptors are downregulated (Giros et al. 1996), but although autoreceptor functions are lost (Jones et al. 1999), some postsynaptic responses appear to be enhanced (Gainetdinov et al. 1999a; Fauchey et al. 2000).

Dopamine transporter knockout mice are hyperactive (Gainetdinov et al. 1999b; Spielewoy et al. 2000) and have a much reduced body size (Bossé et al. 1997). These animals have cognitive deficits (Gainetdinov et al. 1999a, 1999b), disrupted sensorimotor gating (Ralph et al. 2001) and sleep dysregulation (Wisor et al. 2001). Dopamine transporter knockout mice appear to provide a model of some aspects of manic behavior (Ralph-Williams et al. 2003).

Abnormalities in skeletal structure (Bliziotes et al. 2000) and altered regulation of gastrointestinal tract motility (Walker et al. 2000) are also observed.

REFERENCES AND FURTHER READING

Amara SG, Kuhar MJ (1993) Neurotransmitter transporters: recent progress. Ann Rev Neurosci 16:73–93

Benoit-Marand M, Jaber M, Gonon F (2000) Release and elimination of dopamine *in vivo* in mice lacking the dopamine transporter: functional consequences. Eur J Neurosci 12:2985–2992

Bliziotes M, McLoughlin S, Gunness M, Fumagalli F, Jones SR, Caron MG (2000) Bone histomorphometric and biochemical abnormalities in mice homozygous for deletion of the dopamine transporter gene. Bone 26:15–19

Bossé R, Fumagalli F, Jaber M, Giros B, Gainetdinov RR, Wetsel WC, Missale C, Caron MG (1997) Anterior pituitary hypoplasia and dwarfism in mice lacking the dopamine transporter. Neuron 19:127–138

Fauchey V, Jaber M, Caron MG, Bloch B, Le Moine C (2000) Differential regulation of the dopamine D1, D2 and D3 receptor gene expression and changes in the phenotype of the striatal neurons in mice lacking the dopamine receptor. Eur J Neurosci 12:19–26

Gainetdinov RR, Jones SR, Fumagalli F, Wightman RM, Caron MG (1998) Re-evaluation of the role of the dopamine transporter in dopamine homeostasis. Brain Res Brain Res Rev 26:148–153

Gainetdinov RR, Jones SR, Caron MG (1999a) Functional hyperdopaminergia in dopamine transporter knockout mice. Biol Psychiatry 46:303–311

Gainetdinov RR, Wetsel WC, Jones SR, Levin ED, Jaber M, Caron MG (1999b) Role of serotonin in the paradoxical calming effect of psychostimulants on hyperactivity. Science 283:397–401

Giros B, Caron MG (1993) Molecular characteristics of the dopamine transporter. Trends Pharmacol Sci 14:43–49

Giros B, Jaber M, Jones SR, Wightman RM, Caron MG (1996) Hyperlocomotion and indifference to cocaine and amphetamine in mice lacking the dopamine transporter. Nature 379:606–612

Jones SR, Gainetdinov RR, Jaber M, Giros B, Wightman RM, Caron MG (1998) Profound neuronal plasticity in response to inactivation of the dopamine transporter. Proc Natl Acad Sci USA 95:4029–4034

Jones SR, Gainetdinov RR, Hu XT, Cooper DC, Wightman RM, White FJ, Caron MG (1999) Loss of autoreceptor functions in mice lacking the dopamine transporter. Nat Neurosci 2:649–655

Ralph RJ, Paulus MP, Fumagalli F, Caron MG, Geyer MA (2001) Prepulse inhibition deficits and perseverative motor patterns in dopamine transporter knock-out mice: differential effects of D1 and D2 receptor antagonists. J Neurosci 21:305–313

Ralph-Williams RJ, Pauluis MP, Zhuang X, Hen R, Geyer MA (2003) Valproate attenuates hyperactive and perseverative behaviors in mutant mice with a dysregulated dopamine system. Biol Psychiatry 53:352–359
Sora I, Wichems C, Takahashi M, Li XF, Zeng Z, Revay R, Lesch KP, Murphy DL, Uhl GR (1998) Cocaine reward models: conditioned place preference can be established in dopamine- and serotonin-transporter knockout mice. Proc Natl Acad Sci USA 95:7699–7704
Spielewoy C, Roubert C, Hamon M, Nosten-Bertrand M, Betancur C, Giros B (2000) Behavioural disturbances associated with hyperdopaminergia in dopamine-transporter knockout mice. Behav Pharmacol 11:279–290
Walker JK, Gainetdinov RR, Mangel AW, Caron MG, Shetzline MA (2000) Mice lacking the dopamine transporter display altered regulation of distal colon motility. Am J Physiol 279:G311–G318
Wisor JP, Nishino S, Sora I, Uhl GH, Mignot R, Edgar M (2001) Dopaminergic role in stimulant-induced wakefulness. J Neurosci 21:1787–1794

E.5.1.17.2
Serotonin Transporter Knockout Mice

The serotonin transporter has a key role in regulating the intensity of 5-HT-mediated transmission and is the primary target for several antidepressants and psychostimulants (Amara and Kuhar 1993; Bengel et al. 1996).

Disruption of 5-HT uptake in serotonin transporter knockout mice increases the extracellular concentration of 5-HT sixfold and reduces intracellular concentration by 60%–80% (Fabre et al. 2000).

Holmes et al. (2003) found that mice lacking the serotonin transporter exhibit $5HT_{1A}$ receptor-mediated abnormalities in tests for anxiety-like behavior.

Lira et al. (2003) reported altered depression-related behaviors and functional changes in the dorsal raphe nucleus of serotonin-transporter-deficient mice.

Marked desensitization of both presynaptic and postsynaptic 5-HT_{1A} receptors is observed in electrophysiological studies (Gobbi et al. 2001).

There is a significant decrease in 5-HT_{1A} receptor binding sites, mRNA and protein in some, but not all, 5-HT-containing brain areas. Altered hypothermic and neuroendocrine responses to 8-hydroxy-2-(di-n-propylamino)-tetraline (8-OH-DPAT) are also reported (Li et al. 1999).

Thermal hyperalgesia in mice after chronic constrictive sciatic nerve injury was absent in serotonin-transporter-deficient mice (Vogel et al. 2003).

Decreases in 5-HT_{1A} and 5-HT_{1B} receptor coupling are observed, accompanied by disruption of the neurochemical responses to the 5-HT_{1A} receptor agonist ipsapirone and the 5-HT_{1A}/5-HT_{1D} receptor agonist GR127935 (Fabre et al. 2000).

The hyperlocomotor effect of MDMA, but not that of high doses of d-amphetamine, is disrupted in serotonin receptor knockout mice (Bengel et al. 1996).

In double knockout mice that lack the dopamine transporter and have no or one copy of the gene that encodes the serotonin transporter, no place preference for cocaine was observed (Sora et al. 2001).

REFERENCES AND FURTHER READING

Amara SG, Kuhar MJ (1993) Neurotransmitter transporters: recent progress. Ann Rev Neurosci 16:73–93
Bengel D, Murphy DL, Andrews AM, Wichems CH, Feltner D, Heils A, Mössner R, Westphal H, Lesch KP (1996) Altered brain homeostasis and locomotor insensitivity to 3,4-methylenedioxymethamphetamine ("Ecstasy") in serotonin transporter-deficient mice. Mol Pharmacol 53:649–655
Fabre V, Beaufour C, Evrad A, Rioux A, Hanoun N, Lesch KP, Murphy DL, Lanfumey L, Hamon M, Martres MP (2000) Altered expression and functions of serotonin 5-HT_{1A} and 5-HT_{1B} receptors in knock-out mice lacking the 5-HT transporter. Eur J Neurosci 12:2299–2310
Gobbi G, Murphy DL, Lesch K, Blier P (2001) Modifications of the serotonergic system in mice lacking serotonin transporters: an *in vivo* electrophysiological study. J Pharmacol Exp Ther 296:987–995
Holmes A, Yang RJ, Lesch KP, Crawley JN, Murphy DL (2003) Mice lacking the serotonin transporter exhibit $5HT_{1A}$ receptor-mediated abnormalities in tests for anxiety-like behavior. Neuropsychopharmacology 28:2077–2088
Li Q, Wichems C, Heils A, Van De Kar LD, Lasch KP, Murphy DL (1999) Reduction of 5-hydroxytryptamine (5-HT_{1A})-mediated temperature and neuroendocrine responses and 5-HT_{1A} binding sites in 5-HT transporter knockout mice. J Pharmacol Exp Ther 291:999–1007
Lira A, Zhou M, Castanon N, Ansorge MS, Gordon JA, Francis JH, Bradley-Moore M, Lira J, Underwood MD, Arango V, Kung HF, Hofer MA, Hen R, Gingrich JA (2003) Altered depression-related behaviors and functional changes in the dorsal raphe nucleus of serotonin transporter deficient mice. Biol Psychiatry 54:960–971
Sora I, Hall FS, Andrews AM, Itokawa M, Li XF, Wei HB, Wichems C, Lesch KP, Murphy DL, Uhl GR (2001) Molecular mechanisms of cocaine award: combined dopamine and serotonin transporter knockouts eliminate cocaine place preference. Proc Natl Acad Sci USA 98:5300–5305
Vogel C, Mössner R, Gerlach H, Heinemann T, Murphy DL, Riederer P, Lesch KP, Sommer C (2003) Absence of thermal hyperalgesia in serotonin transporter-deficient mice. J Neurosci 23:708–715

E.5.1.17.3
Noradrenaline Transporter Knockout Mice

The noradrenaline transporter has a role similar to that of the dopamine transporter and the serotonin transporter with respect to noradrenaline-mediated transmission (Blakely et al. 1994).

Noradrenaline-transporter knockout mice have been generated using homologous recombination (Xu et al. 2000).

Wang et al. (1999) reviewed genetic approaches to studying norepinephrine function using knockout of the mouse norepinephrine transporter gene.

The prolonged synaptic lifetime of noradrenaline in noradrenaline transporter knockout mice results in elevation of the extracellular concentration of noradrenaline and depletion of the intraneuronal stores. In addition, in noradrenaline transporter knockout mice, the α_1-adrenoceptor decreased in the hippocampus (Xu et al. 2000), although α_{2A}-adrenoceptor density did not change in the spinal cord (Bohn et al. 2000).

Noradrenaline-transporter knockout mice have a lower body weight and reduced locomotor responses to novelty. In the tail-suspension test used for screening antidepressant drugs, noradrenaline transporter knockout mice behaved like antidepressant-treated, wild-type animals and no additional effects of the antidepressants desimipramine, paroxetine and bupropion were observed in mutant mice in this test (Xu et al. 2000).

In the tail-flick assay, morphine induced greater analgesia in noradrenaline transporter knockout mice compared with wild-type mice (Bohn et al. 2000).

In synaptosomes from the frontal cortex of noradrenaline transporter knockout mice, cocaine and nisoxetine had no inhibitory effect on the uptake of dopamine, whereas in the nucleus accumbens the effectiveness of cocaine was somewhat reduced. Uptake of dopamine in brain regions that have low levels of dopamine transporter may depend primarily on the noradrenaline transporter (Morón et al. 2002).

Locomotor responses to cocaine and amphetamine are elevated in noradrenaline knockout mice and chronic administration of cocaine did not induce further sensitization. The enhanced responses to psychostimulants in noradrenaline transporter knockout mice correlate with the suppression of presynaptic dopamine function and supersensitivity to postsynaptic D2 and D3 receptors (Xu et al. 2000).

Haller et al. (2002) studied behavioral responses to social stress in noradrenaline transporter knockout mice.

REFERENCES AND FURTHER READING

Blakely RD, De Felice LJ, Hartzell HC (1994) Molecular physiology of norepinephrine and serotonin transporters. J Exp Biol 196:263–281

Bohn LM, Xu F, Gainetdinov RR, Caron MG (2000) Potentiated opioid analgesia in norepinephrine transporter knockout mice. J Neurosci 20:9040–9045

Haller J, Bakos N, Rodriguiz RM, Carin MG, Wetsel WC, Liposits Z (2002) Behavioral responses to social stress in noradrenaline transporter knockout mice: Effects on social behavior and depression. Brain Res Bull 58:279–284

Morón JA, Brockington A, Wise RA, Rocha BA, Hope BT (2002) Dopamine uptake through the norepinephrine transporter in brain regions with low levels of the dopamine transporter: evidence from knock-out mice lines. J Neurosci 22:389–395

Wang YM, Xu F, Gainetdinov RR, Caron MG (1999) Genetic approaches to studying norepinephrine function: knockout of the mouse norepinephrine transporter gene. Biol Psychiatry 46:1124–1130

Xu F, Gainetdinov RR, Wetsel WC, Jones SR, Bohn LM, Miller GW, Wang YM, Caron MG (2000) Mice lacking the norepinephrine transporter are supersensitive to psychostimulants. Nat Neurosci 3:465–471

E.5.2 In Vivo Tests

E.5.2.1 Golden Hamster Test

PURPOSE AND RATIONALE

"Innate behavior" of many species including man has been described by Lorenz (1943, 1966). The "Golden-hamster-test" (Ther, Vogel and Werner 1959) uses the innate behavior of this species (*Mesocricetus auratus*) for differentiation between neuroleptic and sedative – hypnotic activity. The aggressive behavior of male golden hamsters is suppressed by neuroleptics in doses which do not impair motor function.

PROCEDURE

Ten to 20 male golden hamsters with an average weight of 60 g are crowded together in Makrolon$^{(R)}$ cages for at least 2 weeks. During this time the animals develop a characteristic fighting behavior. For the test single animals are placed into glass jars of 2 liters. In this situation the hamsters assume a squatting and resting position during the day. If the animals are touched with a stick or a forceps they wake up from their daytime sleep and arouse immediately from the resting position. If one tries to hold the hamster with a blunted forceps, a characteristic behavior is elicited: The hamster throws himself onto his back, tries to bite and to push the forceps away with his legs, and utters angry shrieks. Touching the animals is repeated up to 6 times followed by punching with the forceps. Only animals responding to the stimulus with all three defense reactions (turning, vocalizing, biting) are included into the test.

The test compounds are applied either subcutaneously, intraperitoneally, or orally. Six animals are used for each dose.

EVALUATION

The stimuli are applied every 20 min for 3 h. The number of stimuli until response is recorded. Furthermore, the suppression of the defense reactions (turning, biting and vocalizing) is evaluated. An animal is regarded to be completely "tamed", if all defense reactions are suppressed even after punching with the forceps at least once during the test period.

After each stimulation the "tamed" animal is placed on an inclined board with 20 degree inclination. Normal hamsters and hamsters tamed by neuroleptics are able to support themselves or to climb on the board. Impaired motor function causes sliding down. This experiment is repeated three times after each testing of the defense reactions. An animal's coordination is considered to be disturbed if it falls three times during two tests of the experiments.

For each dose the number of tamed hamsters and the number of animals with impaired motor function is recorded. Using different doses, ED_{50} values can be calculated for the taming effect and for impairment of motor function.

The ED_{50} values of taming were 1.5 mg/kg for chlor-promazine s.c. and 0.2 mg/kg for reserpine s.c. Much higher doses (10 times of chlorpromazine and 5 times of reserpine) did not elicit motor disturbances. On the contrary, while ED_{50} values of 10 mg/kg phenobarbital s.c. and 180 mg/kg meprobamate p.o. for the taming effect were found, these doses already caused severe motor disturbances. The taming dose of diazepam was 10 mg/kg p.o. which already showed some muscle relaxing activity. The term "neuroleptic width" indicates the ratio between the ED_{50} for taming and the ED_{50} for motor disturbances. Only for neuroleptic drugs are ratios found between 1:5 and 1:30.

CRITICAL ASSESSMENT OF THE METHOD

The method has the advantage that neuroleptics can easily be differentiated from sedative and hypnotic drugs. Anxiolytics with pronounced muscle relaxing activity also show no significant differences between taming and impaired motor function. Moreover, the method has the advantage that no training of the animals and no expensive apparatus is needed.

REFERENCES AND FURTHER READING

Kreiskott H, Vater W (1959) Verhaltensstudien am Goldhamster unter dem Einfluß zentralwirksamer Substanzen. Naunyn-Schmiedeberg's Arch exp Path Pharm 236:100–105

Lorenz K (1943) Die angeborenen Formen möglicher Erfahrung. Zeitschr Tierpsychol 5:235–409

Lorenz K (1965) Evolution and modification of behavior. University of Chicago Press, Chicago

Lorenz K (1966) Evolution and modification of behavior. Methuen and Co Ltd., London

Ther L, Vogel G, Werner Ph (1959) Zur pharmakologischen Differenzierung und Bewertung von Neuroleptica. Arzneim Forsch/Drug Res 9:351–354

E.5.2.2 Influence on Behavior of the Cotton Rat

PURPOSE AND RATIONALE

The "cotton-rat test" is another attempt to use the innate behavior as described for several animal species by Lorenz (1943, 1966) for the differentiation of psychotropic drugs (Vogel and Ther 1960). The cotton rat (*Sigmodon hispidus*) is a very shy animal which conceals himself at any time. This innate flight reflex is suppressed by centrally active drugs. Simultaneous evaluation of motor function allows the differentiation between neuroleptic and sedative drugs.

PROCEDURE

Cotton rats are bred in cages equipped with a clay cylinder of 20 cm length and 10 cm diameter. This cylinder is used by the animals for hiding, sleeping and breeding. Moreover, the animals which bite easily can be transported from one cage to another just by closing the cylinder on both ends. For the test young animals with a body weight of 40 g are used. Young animals are as shy as old ones but less vicious. Nevertheless, leather gloves have to be used for handling of cotton rats. Normal cages ($25 \times 30 \times 20$ cm) with a wire lid are used. A tunnel of sheet metal (half of a cylinder) 20 cm long and 7 cm high is placed into the cage. The cotton rats hide immediately in this tunnel. If the tunnel is lifted and placed on another site of the cage, the cotton rats immediately hide again.

Three rats are placed in one cage and tested for their behavior. Selective shaving of the fur enables the observer to recognize each animal. If the rats behave as described, they are then treated with the test compound subcutaneously or orally. At least 6 animals divided in two cages are used for each dose of test compound or standard. Fifteen min after application of the drug the test period of three h is started. The tunnel is lifted and placed to another site. If the animals do not show the immediate flight reflex an airstream of short duration is blown through the wire lid. If the animal still does not respond with the flight reflex it is considered to be positively influenced. Afterwards, the animal is placed on an inclined board with 35 degree of inclination and tested for disturbance of motor coordination. A normal animal is able to climb upwards. If coordination is disturbed the rat slides down.

EVALUATION

The test procedure is repeated every 15 min over a period of 3 h. The animals which show at least one suppression of the flight reflex during the test period are counted as well as those who slide down on the inclined board. Using different doses ED_{50} values are calculated for both parameters. The ratio between these two ED_{50} values is regarded as "neuroleptic width" which is 1:20 for chlorpromazine and 1:30 for reserpine whereas ratios of 1:2 for phenobarbital and 1:1.5 for meprobamate indicate the absence of neuroleptic activity.

CRITICAL ASSESSMENT OF THE METHOD

The method allows the differentiation of drugs with neuroleptic activity against other centrally active drugs. No training of the animals and no expensive equipment are necessary.

REFERENCES AND FURTHER READING

Lorenz K (1943) Die angeborenen Formen möglicher Erfahrung. Zeitschr Tierpsychol 5:235–409

Lorenz K (1966) Evolution and modification of behavior. Methuen and Co Ltd., London

Vogel G, Ther L (1960) Das Verhalten der Baumwollratte zur Beurteilung der neuroleptischen Breite zentral-depressiver Stoffe. Arzneim Forsch/Drug Res 10:806–808

E.5.2.3 Artificial Hibernation in Rats

PURPOSE AND RATIONALE

Giaja (1938, 1940, 1953, 1954) studied the effects of reduced oxygen tension and cold environment on rats. The animals were placed in hermetically closed glass vessels which were submerged in ice-water. Due to the respiratory activity, the oxygen tension diminishes and the carbon dioxide content increases. Under the influence of cooling and of hypoxic hypercapnia, the rectal temperature falls to 15°C and the animal is completely anesthetized and immobilized. The rat can survive in this poikilothermic state for more than twenty hours. Complete recovery occurs after warming up. This kind of artificial hibernation was augmented by chlorpromazine (Courvoisier et al. 1953; Giaja and Markovic-Giaja 1954). Vogel (1959), Ther et al. (1959, 1963) used these observations for evaluation of neuroleptics and opioid analgesics.

PROCEDURE

Male Wistar rats weighing 100–150 g are deprived of food with free access to tap water overnight. The test compounds are injected subcutaneously 15 min prior to the start of the experiment. First, the rats are placed in ice-cold water to which surfactant is added in order to remove the air from the fur for 2 min. Then, the animals are placed into hermetically closed glass vessels of 750 ml volume which are placed into a refrigerator at 2°C temperature. During the following hour, the vessels are opened every 10 min for exactly 10 s allowing some exchange of air and reducing the carbon dioxide accumulation. At each time, animals are removed from the glass vessel and observed for signs of artificial hibernation which are not shown by control animals under these conditions. Treated animals, lying on the side, are placed on the back and further examined. An animal is considered positive, when it remains on the back, even if the extremities are stretched out. In this state, cardiac and respiration frequency are reduced and the rectal temperature has fallen to 12–15°C. The rigor of the musculature allows only slow movements of the extremities. The animals recover completely within a few hours if they are brought to their home cages at room temperature. Artificial hibernation is induced dose-dependent by neuroleptics of the phenothiazine type and by some opioid analgesics like meperidine and methadone. In contrast, morphine shows only slight activity.

EVALUATION

Various doses are applied to groups of 10 animals. Percentage of positive animals is calculated for each group and ED_{50} values with confidence limits are estimated according to Litchfield and Wilcoxon.

REFERENCES AND FURTHER READING

Courvoisier S, Fournel J, Ducrot R, Kolsky M, Koeschet P (1953) Propriétés pharmacodynamiques du chlorhydrate de chloro-3-(diméthylamino-3′-propyl)-10-phenothiazine (4.560 R.P.) Arch Int Pharmacodyn 92:305–361

Giaja J (1938) Sur l'analyse de la fonction de calorification de l'homéotherme par la dépression barométrique. C R Soc Biol 127:1355–1359

Giaja J (1940) Léthargie obtenue che le Rat par la dépression barométrique. C R Acad Sci 210:80–84

Giaja J (1953) Sur la physiologie de l'organisme refroidi. Press Medicale 61:128–129

Giaja J, Markovic-Giaja L (1954) L'hyperthermie produite par la chlorpromazine et la résistance a l'asphyxie. Bull Soc Chim Biol 36:1503–1506

Litchfield J, Wilcoxon F (1949) A simplified method of evaluating dose effect experiments. J Pharmacol Exp Ther 96:99–113

Ther L, Lindner E, Vogel G (1963) Zur pharmakologischen Wirkung der optischen Isomeren des Methadons. Dtsch Apoth Ztg 103:514–520

Ther L, Vogel G, Werner P (1959) Zur pharmakologischen Differenzierung und Bewertung der Neuroleptica. Arzneim Forsch/Drug Res 9:351–354

Vogel G (1959) Über die Wirkung von Dolantin und Polamidon im Vergleich zu anderen stark wirksamen Analgetica an der unterkühlten Ratte nach Giaja. Naunyn-Schmiedeberg's Arch exp Path Pharmak 236:214–215

E.5.2.4 Catalepsy in Rodents

PURPOSE AND RATIONALE

Catalepsy in rats is defined as a failure to correct an externally imposed, unusual posture over a prolonged period of time. Neuroleptics which have an inhibitory action on the nigrostriatal dopamine system induce catalepsy (Costall and Naylor 1974; Chermat and Simon 1975; Sanberg 1980) while neuroleptics with little or no nigrostriatal blockade produce relatively little or no cataleptic behavior (Honma and Fukushima 1976). Furthermore, cataleptic symptoms in rodents have been compared to the Parkinson-like extrapyramidal side effects seen clinically with administration of antipsychotic drugs (Duvoisin 1976).

PROCEDURE

Groups of 6 male Sprague-Dawley or Wistar rats with a body weight between 120 and 250 g are used. They are dosed intraperitoneally with the test drug or the standard. Then, they are placed individually into translucent plastic boxes with a wooden dowel mounted horizontally 10 cm from the floor and 4 cm from one end of the box. The floor of the box is covered with approximately 2 cm of bedding material. White noise is presented during the test. The animals are allowed to adapt to the box for 2 min. Then, each animal is grasped gently around the shoulders and under the forepaws and placed carefully on the dowel. The amount of time spent with at least one forepaw on the bar is determined. When the animal removes its paws, the time is recorded and the rat is repositioned on the bar. Three trials are conducted for each animal at 30, 60, 120 and 360 min.

EVALUATION

An animal is considered to be cataleptic if it remains on the bar for 60 s. Percentage of cataleptic animals is calculated. For dose-response curves, the test is repeated with various doses and more animals. ED_{50} values can be calculated. A dose of 1 mg/kg i.p. of haloperidol was found to be effective.

CRITICAL ASSESSMENT OF THE METHOD

The phenomenon of catalepsy can be used for measuring the efficacy and the potential side effects of neuroleptics.

MODIFICATIONS OF THE METHOD

Catalepsy induced by neuroleptic drugs can also be measured by the **PAW test**, which measures increase in forelimb and hindlimb retraction time in rats (Ellenbroek et al. 1987, 2001; Ellenbroek and Cools 1988, 2000; Prinssen et al. 1994, 1995).

The test is performed 30 min after intraperitoneal injection of test drug. Male Wistar rats weighing 220–300 g are placed on a Perspex platform (30 × 30 cm with a height of 20 cm) containing two holes for the forelimbs (40 mm) and two for the hindlimbs (50 mm), and a slit for the tail. The distance between the right and left forelimb holes is 15 mm, and the distance between forelimb and hindlimb holes is 55 mm. The rat is held behind the forelimbs, and the hindlimbs are gently placed in the holes. The forelimb retraction time and the hindlimb retraction time are defined as the time the animal needs to withdraw one forelimb and one hindlimb, respectively. The average forelimb retraction time and hindlimb retraction time (the mean of three measurements) is calculated for each rat.

Extrapyramidal syndromes after treatment with typical and atypical neuroleptics were measured in nonhuman primates (Cebus monkeys) by Casey (1989, 1991, 1993), Gerlach and Casey (1990).

REFERENCES AND FURTHER READING

Casey DE (1989) Serotoninergic aspects of acute extrapyramidal syndromes in nonhuman primates. Psychopharmacol Bull 25:457–459

Casey DE (1991) Extrapyramidal syndromes in nonhuman primates: Typical and atypical neuroleptics. Psychopharmacol Bull 27:47–50

Casey DE (1993) Serotonergic and dopaminergic aspects of neuroleptic-induced extrapyramidal syndromes in nonhuman primates. Psychopharmacology 112:S55–S59

Chermat R, Simon P (1975) Appréciation de la catalepsie chez le rat. J Pharmacol 6:493–496

Costall B, Naylor RJ (1973) Is there a relationship between the involvement of extrapyramidal and mesolimbic brain areas with the cataleptic action of neuroleptic agents and their clinical antipsychotic effects? Psychopharmacol (Berlin) 32:161–170

Costall B, Naylor RJ (1974) On catalepsy and catatonia and the predictability of the catalepsy test for neuroleptic activity. Psychopharmacol (Berl.) 34:233–241

Duvoisin R (1976) Parkinsonism: Animal analogues of the human disorder. In: Yahr M (ed) The Basal Ganglia. Raven Press, New York, pp 293–303

Ellenbroek B, Cools AR (1988) the PAW test: an animal model for neuroleptic drugs which fulfils the criteria for pharmacological isomorphism. Life Sci 42:1205–1213

Ellenbroek B, Cools AR (2000) Animal models for the negative symptoms of schizophrenia. Behav Pharmacol 11:223–233

Ellenbroek BA, Peeters BWE, Honig WM, Cools AR (1987) The paw test: a behavioural paradigm for differentiating be-

tween classical and atypical neuroleptic drugs. Psychopharmacology 93:343–345
Ellenbroek B, Liégeois JF, Bruhwyler J, Cools AR (2001) Effects of JL 13, a pyridobenzoxazepine with potential atypical antipsychotic activity, in animal models of schizophrenia. J Pharmacol Exp Ther 298:386–391
Gerlach J, Casey DE (1990) Remoxipride, a new selective D_2 antagonist, and haloperidol in Cebus monkeys. Progr Neuropsychopharmacol Biol Psychiatry 14:103–112
Honma T, Fukushima H (1976) Correlation between catalepsy and dopamine decrease in the rat striatum induced by neuroleptics. Neuropharmacol 15:601–607
Locke KW, Dunn RW, Hubbard JW, Vanselous CL, Cornfeldt M, Fielding S, Strupczewski JT (1990) HP 818:A centrally analgesic with neuroleptic properties. Drug Dev Res 19:239–256
Moore NA, Tye NC, Axton MS, Risius FC (1992) The behavioral pharmacology of olanzapine, a novel "atypical" antipsychotic agent. J Pharmacol Exp Ther 262:545–551
Prinssen EP, Ellenbroek BA, Cools AR (1994) Peripheral and central adrenoceptor modulation of the behavioural effects of clozapine in the paw test. Br J Pharmacol 112:769–774
Prinssen EPM, Ellenbroek BA, Stamatovic B, Cools AR (1995) Role of striatal dopamine D_2 receptors in the paw test, an animal model for the therapeutic efficacy and extrapyramidal side effects of neuroleptic drugs. Brain Res 673:283–289
Szewczak MR, Cornfeldt ML, Dunn RW, Wilker JC, Geyer HM, Glamkowski EJ, Chiang Y, Fielding S (1987) Pharmacological evaluation of HP 370, a potential atypical antipsychotic agent. 1. *In vivo* profile. Drug Dev Res 11:157–168

E.5.2.5 Pole Climb Avoidance in Rats

PURPOSE AND RATIONALE

The pole-climb avoidance paradigm is an avoidance-escape procedure used to separate neuroleptics from sedatives and anxiolytics. Whereas sedative compounds suppress both avoidance and escape responding at approximately the same doses, neuroleptic drugs reduce avoidance responding at lower doses than those affecting escape responding (Cook and Catania 1964).

PROCEDURE

Male rats of the Long-Evans strain with a starting body weight of 250 g are used. The training and testing of the rats is conducted in a $25 \times 25 \times 40$ cm chamber that is enclosed in a dimly lit, sound-attenuating box. Scrambled shock is delivered to the grid floor of the chamber. A 2.8-kHz speaker and a 28-V light are situated on top of the chamber. A smooth stainless-steel pole, 2.5 cm in diameter, is suspended by a counterbalance weight through a hole in the upper center of the chamber. A microswitch is activated when the pole is pulled down 3 mm by a weight greater than 200 g. A response is recorded when a rat jumps on the pole and activates the microswitch. The rat can not hold the pole down while standing on the grid floor because of the counterbalance tension and can not remain on the pole any length of time because of its smooth surface. The activation of the light and the speaker together are used as the conditioning stimulus. The conditioning stimulus is presented alone for 4 s and then is coincident with the unconditioned stimulus, a scrambled shock delivered to the grid floor, for 26 s. The shock current is maintained at 1.5 mA. A pole climb response during the conditioned stimulus period terminates the conditioned stimulus and the subsequent conditioned and unconditioned stimuli. This is considered an avoidance response. A response during the time when both the conditioned and unconditioned stimuli are present terminates both stimuli and is considered an escape response. Test sessions consist of 25 trials or 60 min, whichever comes first. There is a minimum intertrial interval of 90 s. Any time remaining in the 30 s allotted to make the pole climb is added to the 90 s intertrial interval. Responses during this time have no scheduled consequences; however, rats having greater than 10 intertrial interval responses should not be used in the experiment. Before testing experimental compounds, rats are required to make at least 80% avoidance responses without any escape failures.

EVALUATION

Data are expressed in terms of the number of avoidance and escape failures relative to the respective vehicle control data. ED_{50} values can be calculated using different doses.

REFERENCES AND FURTHER READING

Cook L, Catania AC (1964) Effects of drugs on avoidance and escape behavior. Fed Proc 23:818–835
Cook L, Weidley E (1957) Behavioral effects of some psychopharmacological agents. Ann NY Acad Sci 66:740–752
Dunn RW, Carlezon WA, Corbett R (1991) Preclinical anxiolytic versus antipsychotic profiles of the 5-HT_3-antagonists Ondansedron, Zacopride, 3α-tropanyl-1H-indole-3-carboxylic ester, and 1αH, 3α, 5αH-tropan-3-yl-3,5-dichlorobenzoate. Drug Dev Res 23:289–300
Locke KW, Dunn RW, Hubbard JW, Vanselous CL, Cornfeldt M, Fielding S, Strupczewski JT, (1990) HP 818:A centrally acting analgesic with neuroleptic properties. Drug Dev Res 19:239–256
Szewczak MR, Cornfeldt ML, Dunn RW, Wilker JC, Geyer HM, Glamkowski EJ, Chiang Y, Fielding S (1987) Pharmacological evaluation of HP 370, a potential atypical antipsychotic agent. 1. *In vivo* profile. Drug Dev Res 11:157–168

E.5.2.6 Foot-Shock Induced Aggression

PURPOSE AND RATIONALE

The test as described by Tedeschi et al. (1959) using mice which fight after foot-shock induced stimulation

is useful to detect neuroleptics but also shows positive effects with anxiolytics and other centrally effective drugs. The method has been used by several authors to test drugs with neuroleptic activity. The test is described in Sect. E.2.3.1.

REFERENCES AND FURTHER READING

Tedeschi RE, Tedeschi DH, Mucha A, Cook L, Mattis PA, Fellows EJ (1959) Effects of various centrally acting drugs on fighting behavior of mice. J Pharmacol Exp Ther 125:28–34

E.5.2.7 Brain Self Stimulation

PURPOSE AND RATIONALE

In several species, electrical stimulation of selected brain loci produces effects which are positively reinforcing and pleasurable (Olds and Milner 1954; Olds 1961, 1972). Most of the data available have been obtained from experiments using rats with electrodes chronically implanted in the median forebrain bundle at the level of hypothalamus. Minute electrical pulses sustain a variety of operant behaviors such as lever pressing. Neuroleptics have been shown to be potent blockers of self stimulation (Broekkamp and Van Rossum 1975; Koob et al. 1978; Gallistel and Freyd 1987). Conversely, compounds that facilitate catecholaminergic transmission such as d-amphetamine and methylphenidate, will increase responding for such stimulation.

PROCEDURE

Male Wistar rats (350–400 g) are anesthetized with 50 mg/kg pentobarbital i.p. and their heads placed on a level plane in a Kopf stereotactic instrument. A midline incision is made in the scalp and the skin held out of the way by muscle retractors. A small hole is drilled in the scull with a dental burr at the point indicated by the stereotactic instrument for the structure it is desired to stimulate. Using bregma as a reference point, the electrode (Plastic Products MS303/1) is aimed at the medium forebrain bundle according to the atlas of Paxinos and Watson (1986), using the coordinates of AP = –0.8 mm, Lat = +2.8 mm, and DV = –7.2 mm below dura. The assembly is then permanently affixed to the scull using stainless steel screws and bone cement.

After a minimum of 10 days for recovery, the animals are trained to bar press for electrical stimulation on a continuous reinforcement schedule in a standard operant box outfitted with a single lever. The reward stimulus is a train of biphasic square-wave pulses generated by a Haer stimulator (Pulsar 4i). The parameters are set at a pulse duration of 0.5 ms with 2.5 ms between each pulse pair. The train of pulses may vary between 16 and 30/s, and the intensity of the pulses that are delivered range from 0.1 to 0.5 mA using the lowest setting that will sustain maximal responding. After consistent baseline responding is obtained for 5 consecutive 30 min sessions, the animals are ready for testing with standard agents. Compounds are administered 60 min prior to testing. All data are collected on both cumulative recorders and counters.

EVALUATION

The number of drug responses are compared to the number of responses made during each animal's 30 min control session on the preceding day, which is considered to be equal to 100%. Testing various doses, ED_{50} values with 95% confidence limits can be calculated.

CRITICAL ASSESSMENT OF THE METHOD

Since there is sufficient evidence that self-stimulation behavior is maintained by catecholamines the method gives indirectly insight into the catecholaminergic facilitating or blocking properties of a compound. Active neuroleptic drugs inhibit the self-stimulation behavior in very small doses. The relative potency observed in this test of clinically efficacious drugs parallels their potency in the treatment of schizophrenia.

MODIFICATIONS OF THE METHOD

Reinforcing brain stimulation by electrodes placed in the medial forebrain bundle of rats is decreased after lesion of the internal capsule in the region of the diencephalic-telencephalic border. This decrement in rewarding processing can be reversed by antidepressant drugs (Cornfeldt et al. 1982).

Depoortere et al. (1996) used electrical self stimulation of the ventral tegmental area to study the behavioral effects of a putative dopamine D_3 agonist in the rat.

Anderson et al. (1995) examined the interaction of aversive and rewarding stimuli in self stimulating rats in terms of duration and direction. The rats were implanted with two moveable electrodes, one in a region supporting self-stimulation (the ventral tegmental area) and another in a region supporting escape (the nucleus reticularis gigantocellularis).

Kokkinidis et al. (1986) used amphetamine withdrawal for a behavioral evaluation. Mice implanted with stimulating electrodes in the lateral hypothalamus demonstrated stable and reliable rates of self-stimulation responding. After exposure to a chronic sched-

ule of amphetamine treatment response rates were severely depressed.

Post-amphetamine depression of self-stimulation from the substantia nigra can be reversed by cyclic antidepressants (Kokkinidis et al. 1980).

Moreau et al. (1992) reported that antidepressant treatment prevents chronic unpredictable mild stress-induced anhedonia as assessed by ventral tegmentum self-stimulation in rats.

REFERENCES AND FURTHER READING

Anderson R, Diotte M, Miliaressis E (1995) The bidirectional interaction between ventral tegmental rewarding and hindbrain aversive stimulation effects in rats. Brain Res 688:15–20

Brodie DA, Moreno OM, Malis JE, Boren JJ (1960) Rewarding properties of intracranial stimulation. Science 131:920–930

Broekkamp CLE, Van Rossum JM (1975) The effect of microinjections of morphine and haloperidol into the neostriatum and the nucleus accumbens on self-stimulation behavior. Arch Int Pharmacodyn 217:110–117

Corbett D, Laferriere A, Milner P (1982) Plasticity of the medial prefrontal cortex: Facilitated acquisition of intracranial self-stimulation by pretraining stimulation. Physiol Behav 28:531–543

Cornfeldt M, Fisher B, Fielding S (1982) Rat internal capsule lesion: a new test for detecting antidepressants. Fed Proc 41:1066

Depoortere R, Perrault Gh, Sanger DJ (1996) Behavioral effects in the rat of the putative dopamine D_3 receptor agonist 7-OH-DPAT: comparison with quinpirole and apomorphine. Psychopharmacology 124:231–240

Dunn RW, Carlezon WA, Corbett R (1991) Preclinical anxiolytic versus antipsychotic profiles of the 5-HT_3 antagonists ondansetron, zacopride, 3α-tropanyl-1H-indole-3-carboxylic acid ester, and 1αH, 3α, 5αH-tropan-3-yl-3,5-dichlorobenzoate. Drug Dev Res 23:289–300

Fielding S, Lal H (1978) Behavioral actions of neuroleptics. In: Iversen LL, Iversen SD, Snyder SH (eds) Neuroleptics and Schizophrenia, Vol 10, pp 91–128, Plenum Press, New York

Gallistel CR, Freyd G (1987) Quantitative determination of the effects of catecholaminergic agonists and antagonists on the rewarding efficacy of brain stimulation. Pharmacol Biochem Behav 26:731–741

Goldstein JM, Malick JB (1983) An automated descending rate-intensity self-stimulation paradigm: usefulness for distinguishing antidepressants from neuroleptics. Drug Dev Res 3:29–35

Kokkinidis L, Zacharko RM, Predy PA (1980) Post-amphetamine depression of self-stimulation from the substantia nigra: reversal by cyclic antidepressants. Pharmacol Biochem Behav 13:379–383

Kokkinidis L, Zacharko RM, Anisman H (1986) Amphetamine withdrawal: a behavioral evaluation. Life Sci 38:1617–1623

Koob GF, Fray PJ, Iversen SD (1978) Self-stimulation at the lateral hypothalamus and locus caeruleus after specific unilateral lesions of the dopamine system. Brain Res 146:123–140

Mekarski JE (1989) Main effects of current and pimozide on prepared and learned self-stimulation behaviors are on performance not reward. Pharmacol Biochem Behav 31:845–853

Mora F, Vives F, Alba F (1980) Evidence for an involvement of acetylcholine in self-stimulation of the prefrontal cortex in the rat. Experientia 36:1180–1181

Moreau JL, Jenck F, Martin JR, Mortas P, Haefely WE (1992) Antidepressant treatment prevents chronic unpredictable mild stress-induced anhedonia as assessed by ventral tegmentum self stimulation in rats. Eur Neuropsychopharmacol 2:43–49

Olds J (1961) Differential effects of drives and drugs on self-stimulation at different brain sites. In: Sheer DE (ed) Electrical Stimulation of the Brain. University of Texas Press, Austin TX, pp 350–366

Olds J, Milner P (1954) Positive reinforcement produced by electrical stimulation of septal area and other regions of rat brain. J Comp Physiol Psychol 47:419–427

Olds ME (1972) Alterations by centrally acting drugs of the suppression of self-stimulation behavior in the rat by tetrabenazine, physostigmine, chlorpromazine and pentobarbital. Psychopharmacology 25:299–314

Paxinos G, Watson C (1986) The rat brain in stereotaxic coordinates. 2nd edn. Academic Press, New York

Roberts DCS, Zito KA (1987) Interpretation of lesion effects on stimulant self-administration. In: Bozarth MA (ed) Methods for Assessing the Reinforcing Properties of Abused Drugs. Springer-Verlag New York, Berlin, Heidelberg, pp 87–103

Szewczak MR, Cornfeldt ML, Dunn RW, Wilker JC, Geyer HM, Glamkowski EJ, Chiang Y, Fielding S (1987) Pharmacological evaluation of HP 370, a potential atypical antipsychotic agent. 1. *In vivo* profile. Drug Dev Res 11:157–168

E.5.2.8 Prepulse Inhibition of Startle Response

PURPOSE AND RATIONALE

Prepulse inhibition is a model of sensorimotor gating which can be assessed in both animals and humans using the startle reflex response. When a fixed startle eliciting stimulus (i. e., the pulse) is preceded by 30–500 ms by a weak, non-startle-eliciting stimulus (i. e., the prepulse), the magnitude of the startle response is significantly reduced to the pulse alone. Schizophrenic patients have decreased prepulse inhibition relative to normal control subjects, and this is thought to reflect an impairment in their ability to filter irrelevant sensory stimuli (Braff and Geyer 1990; Geyer 1998). Similar reductions in prepulse inhibition are produced in rats by administration of psychotomimetic drugs such as the dopamine agonists amphetamine and apomorphine or the non-competitive NMDA antagonists phencyclidine and dizocilpine (MK801) (Mansbach and Geyer 1989; Swerlow et al. 1998; Geyer et al. 2001; Rowley et al. 2001; Weiss and Feldon 2001; Pouzet et al. 2002). Most antipsychotics tested are able to antagonize prepulse inhibition disruption produced by dopamine antagonists, whereas prepulse inhibition disruption by NMDA antagonists may be selectively sensitive to antipsychotics with atypical features (Bakshi and Geyer 1995; Bubenikova

et al. 2005; Fox et al. 2005). Haloperidol failed to block the effects of phencyclidine and dizocilpine prepulse inhibition of startle (Keith et al. 1991).

Feifel et al. (Feifel and Reza 1999; Feifel et al. 1999a, 1999b) tested the effects of a neurotensin agonist on prepulse inhibition of startle in rats.

PROCEDURE

Male Sprague Dawley rats were treated with various doses of test compound or saline s.c. Immediately afterwards, rats receive a second s.c. injection consisting of 2 mg/kg d-amphetamine, or 0.5 mg/kg apomorphine, or 0.1 mg/kg dizocilpine or saline. Then, 10 min later, animals were placed in special startle chambers (SR-LAB, San Diego Instruments, San Diego, Calif., USA). Startle chambers consist of a Plexiglas cylinder 8.2 cm in diameter resting on a 12.5 × 25.5 cm Plexiglas frame within a ventilated enclosure housed in a sound-attenuated room exposed to 70-dB background noise. After a 5-min acclimation period, acoustic stimuli were presented via a speaker mounted 24 cm above the animal. Acoustic stimuli consisted of a 120-dB pulse by itself (pulse alone) or a 120-dB pulse preceded by 100 ms by prepulses 3, 5, and 10 dB above background noise. There was an average of 15 s between stimuli. A piezoelectric accelerometer mounted below the Plexiglas frame detected and transduced the motion within the cylinder. Startle amplitude was defined as the degree of motion detected by this accelerometer. Each rat was tested on four separate occasions separated by 7 non-test days. On each test day, the dose of test compound was kept constant, but the specific psychotomimetic agent was alternated across test days in a counterbalanced fashion.

EVALUATION

Prepulse inhibition was calculated as the percentage of the pulse-alone startle amplitude using the following formula: [1 – (startle amplitude after prepulse–pulse pair/startle amplitude after pulse only)] × 100. Analysis of data was then carried out using a three-factor repeated-measures analysis of variance (ANOVA). Significant factor results from the ANOVA were followed up with separate one-way ANOVAs for each psychotomimetic agent and then, when indicated, with individual group mean comparisons using post hoc *t* tests for multiple comparisons using the Bonferroni method.

MODIFICATIONS OF THE METHOD

Sipes and Geyer (1995) studied the disruption of prepulse inhibition of the startle response in the rat by DOI [(2,5-dimethoxy-4-iodophenyl)-2-aminopropane hydrochloride], which is mediated by 5-HT_{2A} receptors. The authors suggested that studies of the serotonergic substrates of prepulse inhibition may provide a model of the possible serotonergic role in the sensorimotor gating abnormalities in patients with schizophrenia and with obsessive compulsive disorder.

Ellenbroeck et al. (1998) described the effects of an early stressful life event on sensorimotor gating in adult rats.

Andersen and Pouzet (2001) compared the effects of acute versus chronic treatment with typical or atypical antipsychotics on d-amphetamine-induced sensorimotor gating deficits in rats.

Heidbreder et al. (2000) used the prepulse inhibition of acoustic startle for behavioral, neurochemical and endocrinological characterization of the early social isolation syndrome.

Krebs-Thomson et al. (2001) reported that postweanling handling attenuates isolation-rearing disruption of prepulse inhibition in rats.

Weiss et al. (2001) studied the dissociation between the effects of pre-weaning and/or post-weaning social isolation on prepulse inhibition and latent inhibition in adult Sprague Dawley rats.

Dirks et al. (2003) reported reversal of startle gating deficits in transgenic **mice** overexpressing corticotropin-releasing factor by antipsychotic drugs.

Andreasen et al. (2006) studied the effect of nicotinic agents on prepulse inhibition (PPI) in mice using a startle response/PPI system from TSE Systems, Bad Homburg, Germany.

Lind et al. (2004) described prepulse inhibition of the acoustic startle reflex in **pigs** and its disruption by d-amphetamine.

REFERENCES AND FURTHER READING

Andersen PM, Pouzet B (2001) Effects of acute versus chronic treatment with typical or atypical antipsychotics on d-amphetamine-induced sensorimotor gating deficits in rats. Psychopharmacology 156:291–304

Andreasen JT, Andersen KK, Nielsen EØ, Mathiasen L, Mirza NR (2006) Nicotine and clozapine selectively reverse a PCP-induced deficit of PPI in BALB/cByJ but not in NMRI mice: comparison withe risperidine. Behav Brain Res 167:118–127

Bakshi VP, Geyer MA (1995) Antagonism of phencyclidine-induced deficits in prepulse inhibition by the putative "atypical" antipsychotic olanzapine. Psychopharmacology 122:198–201

Braff DL, Geyer MA (1990) Sensorimotor gating and schizophrenia: human and animal models. Arch Gen Psychiatry 47:181–188

Bubenikova V, Votava M, Horacek J, Palenicek T, Dockery C (2005) The effect of zotepine, risperidone, colzapine

and olanzapine on MK-801-disrupted sensorimotor gating. Pharmacol Biochem Behav 80:591–596
Dirks A, Groenink L, Westphal KGC, Olivier JDA, Verdouw PM, van der Gugten J, Geyer Ma, Olivier B (2003) Reversal of startle gating deficits in transgenic mice overexpressing corticotropin-releasing factor by antipsychotic drugs. Neuropsychopharmacol 28:1790–1798
Ellenbroeck BA, van den Kroonenberg PTJM, Cools AR (1998) The effects of an early stressful life event on sensorimotor gating in adult rats. Schizophrenia Res 30:251–260
Feifel D, Reza TL (1999) Effects of neurotensin administered into the tegmental area on prepulse inhibition of startle. Behav Brain Res 106:189–193
Feifel D, Reza TL, Wustro DJK, Davis D (1999a) Novel antipsychotic-like effects on prepulse inhibition of startle produced by a neurotensin agonist. J Pharmacol Exp Ther 288:710–713
Feifel D, Reza T, Robeck S (1999b) Antipsychotic potential of CCK-based treatments: an assessment using the prepulse inhibition model of psychosis. Neuropsychopharmacology 20:141–149
Fox GB, Esbenshade TA, Pan JB, Radek RJ, Krueger KM, Yao BB, Browman KE, Buckley MJ, Ballard ME, Komater VA, Miner H, Zhang M, Faghih R, Rueter LE, Bitner RS, Drescher KU, Wetter J, Marsh K, Lemaire M, Porsolt RD, Bennani YL, Sullivan JP, Cowart MD, Decker MW, Hancock AA (2005) Pharmacological properties of ABT-239 [4-(2-2-[(2*R*)-2-methylpyrrolidinyl]ethyl-benzofuran-5-yl)bezonitrile]: II. Neuropharmacological characterization and broad preclinical efficacy in cognition and schizophrenia of a potent and selective histamine H_3 receptor antagonist: J Pharmacol Exp Ther 313:176–190
Geyer MA (1998) Behavioural studies of hallucinogenic drugs in animals: implications for schizophrenia research. Pharmacopsychiatry 31:73–79
Geyer MA, Krebs-Thomsen K, Braff DL, Swerdlow NR (2001) Pharmacological studies of prepulse inhibition modlsl of sensorimotor gating deficits in schizophrenia: a decade in review. Psychopharmacology 156:117–154
Heidbreder CA, Weiss IC, Domeney AM, Pryce C, Homberg J, Hedou G, Feldon J, Moran MC, Nelson P (2000) Behavioral, neurochemical and endocrinological characterization of the early social isolation syndrome. Neuroscience 100:749–768
Keith VA, Mansbach RS, Geyer MA (1991) Failure of haloperidol to block the effects of phencyclidine and dizocilpine prepulse inhibition of startle. Biol Psychiatry 30:557–566
Krebs-Thomson K, Giracello D, Solis A, Geyer MA (2001) Post-weanling handling attenuates isolation-rearing disruption of prepulse inhibition in rats. Behav Brain Res 120:221–224
Lind NM, Arnfred SM, Hemmingsen RP, Hansen AK (2004) Prepulse inhibition of the acoustic startle reflex in pigs and its disruption by D-amphetamine. Behav Brain Res 155:217–222
Mansbach RS, Geyer MA (1989) Effects of phencyclidine and phencyclidine biologs on sensorimotor gating in the rat. Neuropsychopharmacology 2:299–306
Pouzet B, Didriksen M, Arnt J (2002) Effects of the 5-HT_6 receptor antagonist, SB-271046, in animal models of schizophrenia. Pharmacol Biochem Behav 71:635–643
Rowley M, Bristow LJ, Hutson PH (2001) Current and novel approaches to the drug treatment of schizophrenia. J Med Chem 44:477–501
Sipes TE, Geyer MA (1995) DOI disruption of prepulse inhibition of startle in the rat is mediated by 5-HT_{2A} and not by 5-HT_{2C} receptors. Behav Pharmacol 6:839–842
Swerdlow NR, Taaid N, Oostwegel JL, Randolph E, Geyer MA (1998) Towards a cross-species pharmacology of sensorimotor gating: effects of amantadine, bromocriptine, pergolide and ropinirole on prepulse inhibition of acoustic startle in rats. Behav Pharmacol 9:389–396
Weiss IC, Feldon J (2001) Environmental animal models for sensorimotor gating deficiencies in schizophrenia: a review. Psychopharmacology 156:305–326
Weiss IC, Domeney AM, Moreau JL, Russig H, Feldon J (2001) Dissociation between the effects of pre-weaning and/or post-weaning social isolation on prepulse inhibition and latent inhibition in adult Sprague-Dawley rats. Behav Brain Res 121:207–218

E.5.2.9 N40 Sensory Gating

PURPOSE AND RATIONALE

The N40 auditory-evoked potential has been used to develop an animal model for the study of sensory gating mechanisms (Boutros et al. 1997a; Boutros and Kwan 1998). The method has been applied to evaluation of psychotropic compounds (Adler et al. 1986; Boutros et al. 1994, 1997b). Bickford-Wimer et al. (1990) localized one possible source of the N40 waveform to the CA3 region of the hippocampus.

Fox et al. (2005) used the N40 sensory gating model in mice for evaluation of a potential antipsychotic drug.

PROCEDURE

Male DBA/2 mice were stereotaxically implanted with tripolar stainless steel wire head stages for EEG recordings in the CA3 region of the hippocampus. The mice were first anesthetized with a solution of 2.8% ketamine, 0.28% xylazine, and 0.05% acepromazine. Three access holes for the electrodes were made at AP –1.8 mm from the bregma, and in a plane perpendicular to the suture, ML 0.6 (cortical electrode), 1.6 (reference electrode), and 2.6 mm electrode directed at the hippocampus). The depth of the hippocampal electrode tip was DV 1.65–1.70 mm below the surface of the cortex. The depths of the cortical and reference electrodes were DV 0.5 mm from the surface of the skull, resulting in contact, but not penetration of the cortical tissue. The tripolar electrode was lowered into position with a stereotaxic electrode holder and affixed using cyanoacrylic gel and dental acrylic and two anchor screws. Mice were allowed to recover for 3 days before commencement of the experiments. Awake mice were recorded in acoustically isolated chambers. Flexible tethers and electrical swivels were used to convey EEG signals to differential AC EEG amplifiers and allowed the mice free movement within the chambers. The EEG was amplified 1000 × with

a 50- to 60-Hz notch filter engaged, and high- and low-pass filters were set at 1 and 100 Hz, respectively. Hippocampal auditory-evoked potentials were generated by presentation of 60 sets of 3 kHz paired tone bursts from a speaker within the recording chamber at a distance of 15–20 cm to the mouse. The first tone of the pair is referred to as the conditioning stimulus, and the second is referred to as the test stimulus. The duration of both the condition and test stimuli was 5 ms, with 0.5 s between the stimuli and 20 s between pairs. Data acquisition software recorded EEG signals 100 ms before and for 899 ms after the initial conditioning stimulus. The software averaged the 60 paired responses into one composite-evoked response. Various doses of test drug were administered i.p. 20–30 min before mice were placed into the recording chambers and initiation of auditory-evoked potential recording. Recording of paired auditory potentials continued for two 20-min sessions, each comprised of 60 paired stimuli. Each mouse was administered every treatment dose and a control vehicle treatment in a balanced order on separate days with at least 48 h between treatments. This within-subject design allowed each mouse to serve as its own control. The hippocampal response to auditory stimuli was identified as the highest positive peak deflection in the ongoing EEG at a latency of 10–20 ms after the stimulus (P20), followed by the lowest negative peak deflection in the ongoing EEG at 20–45 ms after the stimulus (N40). The difference in amplitude between P20 and N40 was defined as the N40 amplitude in microvolts.

EVALUATION

N40 amplitudes were determined for both the averaged conditioning and test-evoked potentials, and a ratio was derived between the two responses by dividing the test amplitude by the conditioning amplitude (T/C ratio).

MODIFICATIONS OF THE METHOD

Flack et al. (1996) studied sensory gating in a computer model of the CA3 neural network of the hippocampus.

Stevens et al. (1998) investigated changes in auditory information processing after kainic acid lesions in adult rats used as a model of schizophrenia.

REFERENCES AND FURTHER READING

Adler LE, Rose G, Freedman R (1986) Neurophysiological studies of sensory gating in rats: effects of amphetamine, phencyclidine, and haloperidol. Biol Psychiatry 21:787–798

Bickford-Wimer PC, Nagamoto H, Johnson R, Adler LE, Egan M, Rose GM, Freedman R (1990) Auditory sensory gating in hippocampal neurons: a model system in the rat. Biol Psychiatry 27:183–192

Boutros NN, Kwan SW (1998) Test-retest reliability of the rat N40 auditory evoked response: preliminary data. Psychiatry Res 81:269–276

Boutros NN, Uretsky N, Berntson G, Bornstein R (1994) Effects of cocaine on sensory inhibition in rats: preliminary data. Biol Psychiatry 36:242–248

Boutros NN, Bonnet KA, Millana R, Liu J (1997a) A parametric study of the N40 auditory evoked response in rats. Biol Psychiatry 42:1051–1059

Boutros NN, Uretsky NJ, Lui JJ, Millana RB (1997b) Effects of repeated cocaine administration on sensory inhibition in rats: preliminary data. Biol Psychiatry 41:461–466

Flack KA, Adler LE, Gerhardt GA, Miller C, Bickford P, MacGregor RJ (1996) Sensory gating in a computer model of the CA3 neural network of the hippocampus. Biol Psychiatry 40:1230–1245

Fox GB, Esbenshade TA, Pan JB, Radek RJ, Krueger KM, Yao BB, Browman KE, Buckley MJ, Ballard ME, Komater VA, Miner H, Zhang M, Faghih R, Rueter LE, Bitner RS, Drescher KU, Wetter J, Marsh K, Lemaire M, Porsolt RD, Bennani YL, Sullivan JP, Cowart MD, Decker MW, Hancock AA (2005) Pharmacological properties of ABT-239 [4-(2-2-[(2*R*)-2-methylpyrrolidinyl]ethyl-benzofuran-5-yl)bezonitrile]: II. Neuropharmacological characterization and broad preclinical efficacy in cognition and schizophrenia of a potent and selective histamine H_3 receptor antagonist. J Pharmacol Exp Ther 313:176–190

Stevens KE, Nagamoto H, Johnson RG, Adams CE, Rose GM (1998) Kainic acid lesions in adult rats as a model of schizophrenia: changes in auditory information processing. Neuroscience 82:701–708

E.5.2.10 Latent Inhibition

PURPOSE AND RATIONALE

Latent inhibition has been recommended as an animal model of schizophrenia (Feldon and Weiner 1992; Swerdlow et al. 1996; Vaitl and Lipp 1997; Moser et al. 2000; Bender et al. 2001). Latent inhibition refers to the retarded acquisition of a conditioned response that occurs if the subject being tested is first pre-exposed to the to-be-conditioned stimulus without the paired unconditioned stimulus. Because the "irrelevance" of the to-be-conditioned stimulus is established during non-contingent pre-exposure, the slowed acquisition of the conditioned stimulus–unconditioned stimulus association is thought to reflect the process of overcoming this learned irrelevance. Latent inhibition has been reported to be diminished in acutely hospitalized schizophrenia patients. Several authors used the latent inhibition model in rats to test psychotropic compounds (Solomon et al. 1981; Feldon and Weiner 1991; Moran and Moser 1992; De la Casa et al. 1993; Lacroix et al. 2000; Alves et al. 2002). Trimble et al. (2002) tested the effects of selective D_1 antagonists on latent inhibition in the rat.

PROCEDURE

Animals

Male Sprague Dawley rats weighing 300–400g were housed two to a cage under a 12-h reversed cycle lighting with food and water ad libitum. All experimental manipulations were carried out in the dark phase of the dark/light cycle.

Apparatus

Modified metal Skinner boxes (24.5 × 24.5 × 21 cm measured from a raised grid floor) were located in darkened, sound-insulated, ventilated outer boxes. A removable water bottle was located on one side of each Skinner box through a hole of 1.0 cm diameter, positioned 2 cm above the grid floor. When water was not required, the water bottle was removed. Licks at the spout of each water bottle were recorded using a lickometer (model 453, Campden Instruments, London, UK). The pre-exposed stimulus was a flashing light (10 s duration with three light flashes per second) situated in the middle of the roof of each Skinner box. The grid floor consisted of steel bars (0.5 cm in diameter) spaced 1 cm apart. Shock generators with scramblers were calibrated to produce 0.5-mA shocks via the grid floor.

Procedure

Rats were randomly assigned to experimental groups and were allocated to a particular Skinner box. They had experience of only that box for the duration of the experiment. After adaptation to the housing conditions for 1 week, rats were placed immediately on a 23-h water deprivation schedule that continued until the end of the experiments. Food remained freely available.

Baseline days (days 15–19)

After 7 days on the water deprivation period, 5 days of pre-training commenced. Each rat was placed in a Skinner box for 15 min. The water bottle was present and each rat could drink freely. After the baseline session was over, each rat was returned to its home cage and allowed access to water for 45 min.

Pre-exposure (day 20)

With the water bottle removed, each rat was placed in a Skinner box. Rats received ten stimulus (flashing house-light) presentations of 10 s duration (three light flashes per second) with a fixed stimulus interval of 50 s. Afterwards the rats were returned to their home cages and allowed access to water for 1 h.

Conditioning (day 21)

With the water bottle removed, each rat was placed in a Skinner box. Then, 5 min later, each rat received the first of two light foot-shock pairings. House-light parameters were identical to those of the pre-exposure period. The house-light was immediately followed by the footshock (0.5 mA, 1 s). The second light-shock pairing was given 5 min later. After the conditioning period had terminated, animals were returned to their home cages and allowed access to water for 1 h.

Re-baseline day (day 22)

With the water bottle present, each rat was placed in a Skinner box and allowed to drink as in the baseline sessions.

Test day (day 23)

With the water bottle present, each rat was placed in a Skinner box and allowed to drink. When each rat completed 75 licks, the flashing house-light was presented and continued until 5 min had elapsed from stimulus onset. Time bins of 30 s duration commenced from the time of stimulus presentation and the number of licks made by each rat within every time bin was recorded. This measure allowed the pattern of drinking over the course of stimulus presentation to be shown. The amount of suppression of licking for each rat was assessed using a suppression ratio calculated from the time (in seconds) to complete licks 51–75 (pre-stimulus) divided by the time (in seconds) to complete licks 51–100 (pre-stimulus + stimulus on). A suppression ratio of 0.01 indicates total suppression of licking (no latent inhibition), while a ratio of 0.5 indicates no change in licking rate from the pre-stimulus period to the stimulus-on period (latent inhibition).

DRUG Treatment

Test drugs or vehicle were administered by subcutaneous injection in various doses 30 min prior to pre-exposure and conditioning.

EVALUATION

Times to complete licks and the suppression ratios were analyzed independently using a 2 × 6 ANOVA with main factors of pre-exposure and drugs.

MODIFICATIONS OF THE METHOD

Lehmann et al. (1998) studied the long-term effects of repeated maternal separation on three different latent inhibition paradigms.

Pouzet et al. (2004) reported that latent inhibition is spared by NMDA-induced ventral hippocampal lesions, but is attenuated following local activation of the ventral hippocampus by intracerebral NMDA infusion.

Bethus et al. (2005) examined the effects of prenatal stress and gender in latent inhibition.

REFERENCES AND FURTHER READING

Alves CRR, Delucia R, Silva MTA (2002) Effects of fencamfamine on latent inhibition. Progr Neuropsychopharm Biol Psychiatry 26:1089–1093

Bender S, Müller B, Oades RD, Sartory G (2001) Conditioned blocking and schizophrenia: a replication and study of the role of symptoms, age, onset, onset-age of psychosis and illness-duration. Schizophrenia Res 49:157–170

Bethus I, Lemaire V, Lhomme M, Goodall G (2005) Does prenatal stress affect latent inhibition? It depends on the gender. Behav Brain Res 158:331–338

De la Casa LG, Ruiz G, Lubow RE (1993) Amphetamine-produced attenuation of latent inhibition is modulated by stimulus preexposure duration: implications for schizophrenia. Biol Psychiatry 15:707–711

Feldon J, Weiner I (1991) The latent inhibition model of schizophrenic attention disorder: haloperidol and sulpiride enhance rats' ability to ignore irrelevant stimuli. Biol Psychiatry 29:635–646

Feldon J, Weiner I (1992) From an animal model of an attentional deficit towards new insights into pathophysiology of schizophrenia. J Psychiatr Res 26:345–366

Lacroix L, Broersen LM, Feldon J, Weiner I (2000) Effect of local infusions of dopaminergic drugs into the medial prefrontal cortex of rats on latent inhibition, prepulse inhibition and amphetamine induced activity. Behav Brain Res 107:111–121

Lehmann J, Stöhr T, Schuller J, Domeney A, Heidbreder C, Feldon J (1998) Long-term effects of repeated maternal separation on three different latent inhibition paradigms. Pharmacol Biochem Behav 59:873–882

Moran PM, Moser PC (1992) MDL 73,147EF, a 5-HT_3 antagonist, facilitates latent inhibition in the rat. Pharmacol Biochem Behav 42:519–522

Moser PC, Hitchcock JM, Lister S, Moran PM (2000) The pharmacology of latent inhibition as an animal model of schizophrenia. Brain Res Rev 33:275–307

Pouzet B, Zhang WN, Weiner I, Feldon J, Yee BK (2004) Latent inhibition is spared by *N*-methyl-D-aspartate (NMDA)-induced ventral hippocampal lesions, but is attenuated following local activation of the ventral hippocampus by intracerebral NMDA infusion. Neuroscience 124:183–194

Solomon PR, Crider A, Winkelman JW, Turi A, Kamer RM, Kaplan LJ (1981) Disrupted latent inhibition in the rat with chronic amphetamine or haloperidol-induced hypersensitivity: relationship to schizophrenic attention disorder. Biol Pyschiatry 16:519–537

Swerdlow NR, Braff DL, Hartston H, Perry W, Geyer MA (1996) Latent inhibition in schizophrenia. Schizophrenia Res 20:91–103

Trimble KM, Bell R, King DJ (2002) Effects of the selective D_1 antagonists NNC 01–0112 and SCH 39166 on latent inhibition in the rat. Physiol Behav 77:115–123

Vaitl D, Lipp OV (1997) Latent inhibition and autonomic response: a psychophysiological approach. Behav Brain Res 88:85–93

E.5.3 Tests Based on the Mechanism of Action

E.5.3.1 Amphetamine Group Toxicity

PURPOSE AND RATIONALE

It is well known that aggregation of mice in small cages greatly enhances the toxicity of amphetamine. The death rate can be reduced by pretreatment with neuroleptics. This phenomenon is generally accepted as an indicator of neuroleptic activity. The increased toxicity results from increased behavioral activation due to aggregation inducing an increase of circulating catecholamines. The mechanism can be understood by the fact that amphetamine is an indirectly acting sympathomimetic amine that exerts its effects primarily by releasing norepinephrine from storage sites in the sympathetic nerves. After administration of high doses of amphetamine, mice exhibit an elevated motor activity which is highly increased by aggregation. This increased behavioral activation is followed by death within 24 h in 80–100% of control animals. Neuroleptics reduce this death rate. In contrast, non-neuroleptic sympatholytics and psychosedative agents like the barbiturates do not produce a dose-related protection. Moreover, anxiolytic agents like benzodiazepines are also found to be ineffective in the prevention of amphetamine group toxicity.

PROCEDURE

Ten male mice of the NMRI-strain are used for each group. They are dosed with the test compound or the standard either orally or intraperitoneally and all placed in glass jars of 18 cm diameter. Untreated animals serve as controls. The test has to be performed at room temperature of 24°C. Thirty min after i.p. or 1 h after oral administration the mice receive 20 mg/kg d-amphetamine subcutaneously. The mortality is assessed 1, 4 and 24 h after dosing.

EVALUATION

The mortality of amphetamine only treated animals is at least 80%. If less than 80% die due to low ambient temperature the test has to be repeated. The estimation of ED_{50} values for protection and their confidence limits are calculated by probit analysis of the data using the number of dosed vs. the number of surviving animals. Doses of 10 mg/kg chlorpromazine p.o. and 1 mg/kg haloperidol have been found to be effective.

CRITICAL ASSESSMENT OF THE METHOD

The amphetamine group toxicity test has been used by many investigators and has been found to be a reliable method for detecting neuroleptic activity.

REFERENCES AND FURTHER READING

Chance MRA (1946) Aggregation as a factor influencing the toxicity of sympathomimetic amines in mice. J Pharmacol 87:214–217

Derlet RW, Albertson TE, Rice P (1990) Protection against d-amphetamine toxicity. Am J Emerg Med 8:105–108

Locke KW, Dunn RW, Hubbard JW, Vanselous CL, Cornfeldt M, Fielding S, Strupczewski JT (1990) HP 818: A centrally acting analgesic with neuroleptic properties. Drug Dev Res 19:239–256

E.5.3.2 Inhibition of Amphetamine Stereotypy in Rats

PURPOSE AND RATIONALE

Amphetamine is an indirect acting sympathomimetic agent which releases catecholamines from its neuronal storage pools. In rats the drug induces a characteristic stereotypic behavior. This behavior can be prevented by neuroleptic agents.

PROCEDURE

Groups of 6 Wistar rats with a body weight between 120 and 200 g are used. They are injected simultaneously with d-amphetamine (10 mg/kg s.c.) and the test compound intraperitoneally and than placed individually in stainless-steel cages (40 × 20 × 18 cm). The control groups receive d-amphetamine and vehicle. Stereotypic behavior is characterized by continuous sniffing, licking or chewing and compulsive gnawing. The animals are observed 60 min after drug administration. An animal is considered to be protected, if the stereotypic behavior is reduced or abolished.

EVALUATION

The percent effectiveness of a drug is determined by the number of animals protected in each group. A dose response is obtained by using 10 animals per group at various doses. ED_{50} values can be calculated. The standard neuroleptic drugs have the following ED_{50} values: chlorpromazine 1.75 mg/kg i.p and haloperidol 0.2 mg/kg i.p.

CRITICAL ASSESSMENT OF THE METHOD

Inhibition of amphetamine-induced stereotypies in rats can be regarded as a simple method to detect neuroleptic activity. However, this may reflect the effects in the corpus striatum which are thought to be responsible for the Parkinsonism-like side effects of neuroleptics.

MODIFICATIONS OF THE METHOD

Ljungberg and Ungerstedt (1985) described a rapid and simple behavioral screening method for simultaneous assessment of limbic and striatal blocking effects of neuroleptic drugs. A low dose of 2 mg/kg d-amphetamine i.p. induces both increased locomotion, thought to reflect an increased dopamine transmission in the nucleus accumbens, and weak stereotypies, thought to reflect an increased dopamine transmission in the neostriatum. The behavior is measured in a combined open field apparatus with holes on the bottom to measure nose-pocking and registration of time spent in the corners. Neuroleptics with less propensity to induce unwanted extrapyramidal side effects can be differentiated from classical drugs with more extrapyramidal adverse reactions.

Segal and Kuczenski (1997) described an escalating dose "binge" model of amphetamine psychosis. Rats were exposed to escalating doses of amphetamine (1.0–8.0 mg/kg) before multiple daily injections of relatively high doses of the drug (8 mg/kg every 2 h × 4 injections).

Atkins et al. (2001) described stereotypic behaviors in mice selectively bred for high and low methamphetamine-induced stereotypic chewing.

Machiyama (1992) recommended chronic methylamphetamine intoxication in **Japanese monkeys** (*Macaca fuscata*) as a model of schizophrenia in animals.

Ellenbroek (1991) described the ethological analysis of **Java monkeys** (*Macaca fascicularis*) in a social setting as an animal model for schizophrenia.

Sams-Dodd and Newman (1997) described the effects of the administration regime on the psychotomimetic properties of d-amphetamine in the Squirrel monkey (*Saimiri sciureus*).

REFERENCES AND FURTHER READING

Atkins AL, Helms ML, O'Toole LA, Belknap JK (2001) Stereotypic behaviors in mice selectively bred for high and low methamphetamine-induced stereotypic chewing. Psychopharmacology (Berl) 157:96–104

Ellenbroek BA (1991) The ethological analysis of monkeys in a social setting as an animal model for schizophrenia. In: Olivier B, Mos J, Slangen JL (eds) Animal Models in Psychopharma-cology. Advances in Pharmacological Sciences. Birkhäuser Verlag, Basel, pp 265–284

Ljungberg T, Ungerstedt U (1985) A rapid and simple behavioral screening method for simultaneous assessment of limbic and striatal blocking effects of neuroleptic drugs. Pharmacol Bio-chem Behav 23:479–485

Locke KW, Dunn RW, Hubbard JW, Vanselous CL, Cornfeldt M, Fielding S, Strupczewski JT (1990) HP 818: A centrally acting analgesic with neuroleptic properties. Drug Dev Res 19:239–259

Machiyama Y (1992) Chronic methylamphetamine intoxication model of schizophrenia in animals. Schizophren Bull 18:107–113
Sams-Dodd F, Newman JD (1997) Effects of administration regime on the psychotomimetic properties of *d*-amphetamine in the Squirrel monkey (*Saimiri sciureus*). Pharmacol Biochem Behav 56:471–480
Segal DS, Kuczenski R, (1997) An escalating dose 'binge' model of amphetamine psychosis: behavioral and neurochemical characteristics. J Neurosci 17:2551–2566
Simon P, Chermat R (1972) Recherche d'une interaction avec les stéréotypies provoquées par l'amphétamine chez le rat. J Pharmacol 3:235–238

E.5.3.3 Inhibition of Apomorphine Climbing in Mice

PURPOSE AND RATIONALE

Administration of apomorphine to mice results in a peculiar climbing behavior characterized initially by rearing and then full-climbing activity, predominantly mediated by the mesolimbic dopamine system (Costall et al. 1978). The ability of a drug to antagonize apomorphine-induced climbing behavior in the mouse has been correlated with neuroleptic potential (Protais et al. 1976; Costall et al. 1978).

PROCEDURE

Groups of 10 male mice (20–22 g) are treated i.p. or orally with the test substance or the vehicle and placed individually in wire-mesh stick cages. Thirty min afterwards, they are injected s.c. with 3 mg/kg apomorphine. Ten, 20 and 30 min after apomorphine administration, they are observed for climbing behavior and scored as follows:

0 = four paws on the floor,
1 = fore feet holding the vertical bars,
2 = four feet holding the bars.

EVALUATION

The average values of the drug-treated animals are compared with those of the controls, the decrease is expressed as percent. The ED_{50}-values and confidence limits are calculated by probit analysis. Three dose levels are used for each compound and the standard with a minimum of 10 animals per dose level.

CRITICAL ASSESSMENT OF THE TEST

Similar to the enhancement of compulsive gnawing of mice after apomorphine by antidepressant drugs, the suppression of climbing behavior of mice after apomorphine can be used for testing neuroleptic drugs. The test has been modified by various authors.

In contrast to other strains of mice, apomorphine climbing is not induced in DBA2 mice unless subchronic manipulations of brain dopamine transmission are performed (Duterte-Boucher and Costentin 1989).

REFERENCES AND FURTHER READING

Bischoff S, Christen P, Vassout A (1988) Blockade of hippocampal dopamine (DA) receptors: A tool for antipsychotics with low extrapyramidal side effects. Prog Neuropsychopharmacol Biol Psychiat 12:455–467
Brown F, Campell W, Clark MSG, Graves DS, Hadley MS, Hatcher J, Mitchell P, Needham P, Riley G, Semple J (1988) The selective dopamine antagonist properties of BRL 34779: a novel substituted benzamide. Psychopharmacology 94:350–358
Cabib S, Puglisi-Allegra St (1988) A classical genetic analysis of two apomorphine-induced behaviors in the mouse. Pharmacol Biochem Behav 30:143–147
Corral C, Lissavetzky J, Valdeolmillos A, Bravo L, Darias V, Sánchez Mateo C (1992) Neuroleptic activity of 10-(4-methyl-1-piperazinyl)-thieno(3,2-b)(1,5)benzothiazepine derivatives. Arzneim Forsch/Drug Res 42:896–900
Costall B, Naylor RJ, Nohria V (1978) Climbing behavior induced by apomorphine in mice: A potent model for the detection of neuroleptic activity. Eur J Pharmacol 50:39–50
Duterte-Boucher D, Costentin J (1989) Appearance of a stereotyped apomorphine-induced climbing in unresponsive DBA2 mice after chronic manipulation of brain dopamine transmission. Psychopharmacology 98:56–60
Horváth K, Andrási P, Berzsenyi P, Pátfalusy M, Patthy M, Szabó G, Sebestyén L, Bagdy E, Körösi J, Botka P, Hamaori T, Láng T (1989) A new psychoactive 5H-2,3-benzodiazepine with an unique spectrum of activity. Arzneim Forsch/Drug Res 39:894–899
Moore NA, Axton MS (1988) Production of climbing behaviour in mice requires both D1 and D2 receptor activation. Psychopharmacology 94:263–266
Moore NA, Tye NC, Axton MS, Risius FC (1992) The behavioral pharmacology of olanzapine, a novel "atypical" antipsychotic agent. J Pharmacol Exp Ther 262:545–551
Protais P, Costentin J, Schwartz JC (1976) Climbing behavior induced by apomorphine in mice: A simple test for the study of dopamine receptors in the striatum. Psychopharmacology 50:1–6
Szewczak MR, Cornfeldt ML, Dunn RW, Wilker JC, Geyer HM, Glamkowski EJ, Chiang Y, Fielding S (1987) Pharmacological evaluation of HP 370, a potential atypical antipsychotic agent. 1. *In vivo* profile. Drug Dev Res 11:157–168
Vasse M, Chagraoui A, Protais P (1988) Climbing and stereotyped behaviors in mice require the stimulation of D-1 dopamine receptors. Eur J Pharmacol 148:221–229

E.5.3.4 Inhibition of Apomorphine Stereotypy in Rats

PURPOSE AND RATIONALE

Apomorphine induces a stereotyped behavior in rats, characterized by licking, sniffing and gnawing in a repetitive, compulsive manner, which is an indication of striatal dopaminergic stimulation (Anden et al. 1967; Ernst 1967; Costall and Naylor 1973). Compounds which prevent apomorphine-induced stereotypy antagonize dopamine receptors in the nigrostriatal system (Ljungberg and Ungerstedt 1978; Tarsy

and Baldessarini 1974). Furthermore, antagonism of this behavior is predictive of propensity for the development of extrapyramidal side effects and tardive dyskinesias (Klawans and Rubivits 1972; Tarsy and Baldessarini 1974; Christensen et al. 1976; Clow et al. 1980).

PROCEDURE

For screening, groups of 6 male Wistar rats with a body weight between 120 and 200 g are used. The test drug or the standard are administered i.p. 60 min prior apomorphine dosage. Apomorphine HCl is injected s.c. at a dose of 1.5 mg/kg. The animals are placed in individual plastic cages. A 10 s observation period is used to measure the presence of stereotypic activity such as sniffing, licking and chewing 10 min after apomorphine administration. An animal is considered protected if this behavior is reduced or abolished.

EVALUATION

The percent effectiveness of a drug is determined by the number of animals protected in each group. With a group size of 10 animals dose response curves are obtained and ED_{50} values calculated. ED_{50} values were found to be 0.2 mg/kg s.c. for haloperidol and 5.0 mg/kg for chlorpromazine, whereas clozapine was ineffective even at high doses.

MODIFICATIONS OF THE METHODS

Puech et al. (1978) studied the effects of several neuroleptic drugs on hyperactivity induced by a low dose of apomorphine in mice.

Apomorphine induces stereotypic behavior in a variety of species including pigeons. The symptoms in pigeons are manifested as pecking against the wall of the cage or on the floor. Aksas et al. (1984) described a method registering the pecking after apomorphine by a microphone, amplification through a pulse preamplifier and registration with a polygraph. The effect of apomorphine was dose-dependent decreased by yohimbine and neuroleptics.

Stereotyped behavior in guinea pigs induced by apomorphine or amphetamine consisting in continuous gnawing and sniffing of the cage floor was described by Klawans and Rubovits (1972) and used as an experimental model of tardive dyskinesia.

REFERENCES AND FURTHER READING

Akbas O, Verimer T, Onur R, Kayaalp SO (1984) The effects of yohimbine and neuroleptics on apomorphine-induced pecking behavior in the pigeon. Neuropharmacol 23:1261–1264

Andén NE, Rubenson A, Fuxe K, Hoekfelt T (1967) Evidence for dopamine receptor stimulation by apomorphine. J Pharm Pharmac 19:627–629

Christensen A, Fjalland B, Møller Nielsen I (1976) On the supersensitivity of dopamine receptors, induced by neuroleptics. Psychopharmacology 48:1–6

Clow A, Theodorou A, Jenner P, Marsden CD (1980) A comparison of striatal and mesolimbic dopamine function in the rat during a 6-month trifluoperazine administration. Psychopharmacology 69:227–233

Costall B, Naylor RJ (1973) On the mode of action of apomorphine. Eur J Pharmacol 21:350–361

Dall'Olio R, Gandolfi O (1993) The NMDA positive modulator D-cycloserine potentiates the neuroleptic activity of D_1 and D_2 dopamine receptor blockers in the rat. Psychopharmacology 110:165–168

Ernst AM (1967) Mode of action of apomorphine and dexamphetamine on gnawing compulsion in rats. Psychopharmacologia (Berlin) 10:316–323

Janssen PAJ, Niemegeers CJC, Jageneau AHM (1960) Apomorphine-antagonism in rats. Arzneim Forsch. 10:1003–1005

Jolicoeur FB, Gagne MA, Rivist R, Drumheller A, St Pierre S (1991) Neurotensin selectively antagonizes apomorphine-induced stereotypic climbing. Pharmacol Biochem Behav 38:463–465

Klawans HL, Rubovits R (1972) An experimental model of tardive dyskinesia. J Neural Transmiss 33:235–246

Kostowski W, Krzascik P (1989) Research for evaluating the role of dopaminergic mechanisms in the action of valproate. Biogen Amin 6:169–176

Ljungberg T, Ungerstedt U (1978) Classification of neuroleptic drugs according to their ability to inhibit apomorphine-induced locomotion and gnawing: evidence for two different mechanisms of action. Psychopharmacology 56:239–247

Locke KW, Dunn RW, Hubbard JW, Vanselous CL, Cornfeldt M, Fielding F, Strupczewski JT (1990) HP 818: A centrally acting analgesic with neuroleptic properties. Drug Dev Res 19:239–256

Puech AJ, Simon P, Boissier JR (1978) Benzamides and classical neuroleptics: comparison of their action using 6 apomorphine-induced effects. Eur J Pharmacol 50:291–300

Szewczak MR, Cornfeldt ML, Dunn RW, Wilker JC, Geyer HM, Glamkowski EJ, Chiang Y, Fielding S (1987) Pharmacological evaluation of HP 370, a potential atypical antipsychotic agent. 1. *In vivo* profile. Drug Dev Res 11:157–168

Tarsy D, Baldessarini RJ (1974) Behavioral supersensitivity to apomorphine following chronic treatment with drugs which interfere with the synaptic function of catecholamines. Neuropharmacol 13:927–940

E.5.3.5 Yawning/Penile Erection Syndrome in Rats

PURPOSE AND RATIONALE

Yawning is a phylogenetically old, stereotyped event that occurs alone or associated with stretching and/or penile erection in humans and in animals from reptiles to birds and mammals under different conditions (Argiolas and Melis 1998). The yawning-penile erection syndrome can be induced in rats by apomorphine and other dopamine autoreceptor stimulants (Ståhle

and Ungerstedt 1983; Gower et al. 1984) and can be antagonized by haloperidol and other dopamine antagonists. Antagonism against this syndrome can be regarded as indication of antipsychotic activity (Furukawa 1996).

Besides the **dopaminergic** system in this behavior (Mogilnicka and Klimek 1977; Baraldi et al. 1979; Benassi-Benelli et al. 1979; Nickolson and Berendsen 1980; Gower et al. 1984, 1986; Dourish et al. 1985; Doherty and Wisler 1994; Kurashima et al. 1995; Bristow et al. 1996; Fujikawa et al. 1996a; Asencio et al. 1999) also the **serotoninergic** (Baraldi et al. 1977; Berendsen and Broekkamp 1987; Berendsen et al. 1990; Protais et al. 1995; Millan et al. 1997), the **cholinergic** (Yamada and Furukawa 1980; Fujikawa et al. 1996b), the **GABAergic** (Zarrindast et al. 1995), the **NO system** (Melis et al. 1995, 1996, 1997a, b), and **steroid** as well as **peptide hormones** (Bertolini and Baldari 1975; Bertolini et al. 1978; Holmgren et al. 1980; Berendsen and Nickolson 1981; Berendsen and Gower 1986; Gully et al. 1995) are involved (Argiolas and Melis 1998).

PROCEDURE

Naive male Wistar rats, weighing 220–280 g, are housed under controlled 12 h light-dark cycle with free access to standard food pellets and tap water. Rats are pretreated with subcutaneous injection of the antagonist 30 min prior to injections of the agonist, such as apomorphine (0.02 to 0.25 mg/kg s.c.) or physostigmine (0.02 to 0.3 mg/kg s.c. or i.p.). After administration of the agonist, rats are placed in individual transparent Perspex cages. A mirror is placed behind the row of observation cages to facilitate observation of the animals for penile erections and yawns. Yawning is a fixed innate motor pattern characterized by a slow, wide opening of the mouth. A penile erection is considered to occur when the following behaviours are present: repeated pelvic thrusts immediately followed by an upright position, an emerging, engorged penis which the rats proceeds to lick while eating the ejaculate. The number of penile erections and yawns is counted for 30 min following the last injection.

EVALUATION

The results are expressed as the mean number of yawns and of penile erections per group ± SEM The statistical significance is determined by comparing the results of each group with the results of the relevant control group using a non-parametric rank sum test.

CRITICAL ASSESSMENT OF THE METHOD

Ferrari et al. (1993) published some evidence that yawning and penile erection in rats underlie different neurochemical mechanisms. Nevertheless, the procedure can be regarded as an useful behavioral tool to study putative antipsychotic activity of new compounds.

MODIFICATIONS OF THE METHOD

Two sublines of Sprague Dawley rats were bred for high- and low yawning frequency in males (Eguibar and Moyaho 1997).

Apomorphine produced more yawning in Sprague Dawley rats than in F344 rats (Tang and Himes 1995)

Sato-Suzuki et al. (1998) evoked yawning by electrical or chemical stimulation in the paraventricular nucleus of anesthetized rats.

The yawning – penile erection syndrome in rats can be elicited by injections of 50 ng NMDA or AMPA (Melis et al. 1994, 1997b) into the paraventricular nucleus of the hypothalamus or intracerebroventricular injection of 50 ng oxytocin (Melis et al. 1997a) or ACTH (Genedani et al. 1994; Poggioli et al. 1998) or α-MSH (Vergoni et al. 1998).

Champion et al. (1997), Bivalacqua et al. (1998) studied the effect of intracavernosal injections of adrenomedullin and other peptide hormones on penile erections in **cats**.

Dopaminergic influences on male sexual behavior of **rhesus monkeys** were studied by Pomerantz (1990, 1992).

REFERENCES AND FURTHER READING

Argiolas A, Melis MR (1998) The neuropharmacology of yawning. Eur J Pharmacol 343:1–16

Asencio M, Delaquerriere B, Cassels BK, Speisky H, Comoy E, Protais P (1999) Biochemical and behavioral effects of boldine and glaucine on dopaminergic systems. Pharmacol Biochem Behav 62:7–13

Baraldi M, Benassi-Benelli A, Lolli M (1977) Penile erections in rats after fenfluramine administration. Riv Farmacol Ter 8:375–379

Baraldi M, Benassi-Benelli A, Bernabei MT, Cameroni R, Ferrari F, Ferrari P (1979a) Apocodeine-induced stereotypies and penile erection in rats. Neuropharmacol 18:165–169

Benassi-Benelli A, Ferrari F, Pellegrini-Quarantotti B (1979b) Penile erection induced by apomorphine and N-n-propylnorapomorphine in rats. Arch Int Pharmacodyn 242:241–247

Berendsen HHG, Broekkamp CLE (1987) Drug-induced penile erections in rats: indication of serotonin$_{1B}$ receptor mediation. Eur J Pharmacol 135:279–287

Berendsen HHG, Gower AJ (1986) Opiate-androgen interaction in drug-induced yawning and penile erections in the rat. Neuroendocrinol 42:185–190

Berendsen HHG, Jenk F, Broekkamp CLE (1990) Involvement of 5-HT$_{1C}$-receptors in drug-induced penile erections in rats. Psychopharmacology 101:57–61

Bertolini A, Baraldi M (1975) Anabolic steroids: permissive agents of ACTH-induced penile erections in rats. Life Sci 17:263–266

Bertolini A, Genedani S, Castelli M (1978) Behavioural effects of naloxone in rats. Experientia 34:771–772

Bivalacqua TJ, Rajasekaran M, Champion HC, Wang R, Sikka SC, Kadowitz PJ, Hellstrom WJG (1998) The influence of castration of pharmacologically induced penile erection in the cat. J Androl 19:551–557

Bristow LJ, Cook GP, Gay JC, Kulagowski J, Landon L, Murray F, Saywell KL, Young L, Hutson PH (1996) The behavioral and neurochemical profile of the putative dopamine D_3 agonist, (+)-PD 128907, in the rat. Neuropharmacol 35:285–294

Champion HC, Wang R, Shenassa BB, Murphy WA, Coy DH, Hellstrom WJG, Kadowitz PJ (1997) Adrenomedullin induces penile erection in the cat. Eur J Pharmacol 319:71–75

Doherty PC, Wisler PA (1994) Stimulatory effects of quinelorane on yawning and penile erection in the rat. Life Sci 54:507–514

Dourish CT, Cooper SJ, Philips SR (1985) Yawning elicited by systemic and intrastriatal injection of piribedil and apomorphine in the rat. Psychopharmacology 86:175–181

Eguibar JR, Moyaho A (1997) Inhibition of grooming by pilocarpine differs in high- and low-yawning sublines of Sprague Dawley rats. Pharmacol Biochem Behav 58:317–322

Ferrari F, Pelloni F, Giuliani D (1993) Behavioural evidence that different neurochemical mechanisms underlie stretching-yawning and penile erection induced in male rats by SND 919, a new selective D_2 dopamine receptor agonist. Psychopharmacology 113:172–276

Fujikawa M, Nagashima M, Inuoe T, Yamada K, Furukawa T (1996a) Potential agonistic effects of OPC-14597, a potential antipsychotic agent, on yawning behavior in rats. Pharmacol Biochem Behav 53:903–909

Fujikawa M, Yamada K, Nagashima M, Domae M, Furukawa T (1996b) The new muscarinic M_1-receptor agonist YM796 evokes yawning and increases oxytocin secretion from the posterior pituitary in rats. Pharmacol Biochem Behav 55:55–60

Furukawa T (1996) Yawning behavior for preclinical drug evaluation. Meth Find Exp Clin Pharmacol 18:141–155

Genedani S, Bernardi M, Bertolini A (1994) Influence of ifenprodil on the ACTH-induced behavioral syndrome in rats. Eur J Pharmacol 252:77–80

Gower AJ, Berendsen HHG, Princen MM, Broekkamp CLE (1984) The yawning-penile erection syndrome as a model for putative dopamine autoreceptor activity. Eur J Pharmacol 103:81–89

Gower AJ, Berendsen HHG, Broekkamp CLE (1986) Antagonism of drug-induced yawning and penile erections in rats. Eur J Pharmacol 122:239–244

Gully D, Jeanjean F, Poncelet M, Steinberg R, Soubriè P, La Fur G, Maffrand JP (1995) Neuropharmacologic profile of nonpeptide neurotensin antagonists. Fundam Clin Pharmacol 9:513–521

Holmgren B, Urbá-Holmgren R, Aguiar M, Rodriguez R (1980) Sex hormone influences on yawning behavior. Acta Neurobiol Exp 40:515–519

Kurashima M, Katsushi Y, Nagashima M, Shirakawa K, Furukawa T (1995) Effects of putative D3 receptor agonists, 7-OH.DPAT, and quinpirole, on yawning, stereotypy, and body temperature in rats. Pharmacol Biochem Behav 52:503–508

Melis MR, Stancampiano R, Argiolas A (1994) Penile erection and yawning induced by paraventricular NMDA injection in male rats are mediated by oxytocin. Pharmacol Biochem Behav 48:203–207

Melis MR, Stancampiano R, Argiolas A (1995) Role of nitric oxide in penile erection and yawning induced by 5-HT_{1C} receptor agonists in male rats. Naunyn-Schmiedeberg's Arch Pharmacol 351:439–445

Melis MR, Succu S, Argiolas A (1996) Dopamine agonists increase nitric oxide production in the paraventricular nucleus of the hypothalamus: correlation with penile erection and yawning. Eur J Neurosci 8:2056–2063

Melis MR, Succu S, Iannucci U, Argiolas A (1997a) Oxytocin increases nitric oxide production in the paraventricular nucleus of the hypothalamus of male rats: correlation with penile erection and yawning. Regul Peptides 69:105–111

Melis MR, Succu S, Iannucci U, Argiolas A (1997b) N-Methyl-D-aspartic acid-induced penile erection and yawning: role of hypothalamic paraventricular nitric oxide. Eur J Pharmacol 328:115–123

Millan MJ, Peglion JL, Lavielle G, Perrin-Monneyron S (1997) 5-HT_{2C} receptors mediate penile erections in rats: actions of novel and selective agonists and antagonists. Eur J Pharmacol 325:9–12

Mogilnicka E, Klimek V (1977) Drugs affecting dopamine neurons and yawning behavior. Pharmacol Biochem Behav 7:303–305

Nickolson VJ, Berendsen HHG (1980) Effects of the potential neuroleptic peptide des-tyrosine$_1$-γ-endorphin and haloperidol on apomorphine-induced behavioural syndromes in rats and mice. Life Sci 27:1377–1385

Poggioli R, Arletti R, Benelli A, Cavazzuti E, Bertolini A (1998) Diabetic rats are unresponsive to the penile erection-inducing effect of intracerebroventricularly injected adrenocorticotropin. Neuropeptides 32:151–155

Pomerantz SM (1990) Apomorphine facilitates male sexual behavior of rhesus monkeys. Pharmacol Biochem Behav 35:659–664

Pomerantz SM (1992) Dopaminergic influences on male sexual behavior of rhesus monkeys: effects of dopamine agonists. Pharmacol Biochem Behav 41:511–517

Protais P, Windsor M, Mocaër E, Comoy E (1995) Post-synaptic 5-HT_{1A} receptor involvement in yawning and penile erections induced by apomorphine, physostigmine and mCCP in rats. Psychopharmacology 120:376–383

Sato-Suzuki I, Kita I, Oguri M, Arita H (1998) Stereotyped yawning responses induced by electrical and chemical stimulation of paraventricular nucleus of the rat. J Neurophysiol 80:2765–2775

Ståhle L, Ungerstedt U (1983) Assessment of dopamine autoreceptor properties of apomorphine, (+)-3-PPP and (–)-3-PPP by recording of yawning behaviour in rats. Eur J Pharmacol 98:307–310

Tang AH, Himes CS (1995) Apomorphine produced more yawning in Sprague Dawley rats than in F344 rats: a pharmacological study. Eur J Pharmacol 284:13–18

Vergoni AV, Bertoline A, Mutulis F, Wikberg JES, Schioth HB (1998) Differential influence of a selective melanocortin MC_4 receptor antagonist (HS014) on melanocortin-induced behavioral effects in rats. Eur J Pharmacol 362:95–101

Yamada K, Furukawa T (1980) Direct evidence for involvement of dopaminergic inhibition and cholinergic activation in yawning. Psychopharmacology 67:39–43

Zarrindast MR, Toloui V, Hashemi B (1995) Effects of GABAergic drugs on physostigmine-induced yawning in rats. Psychopharmacology 122:297–300

E.5.3.6 Inhibition of Mouse Jumping

PURPOSE AND RATIONALE

Lal et al. (1975) described a jumping response in mice after administration of L-dopa in amphetamine pretreated animals where the number of jumps can be objectively counted. The mouse jumping is due to dopaminergic overstimulation similar to that seen in rats when stereotypy is induced by higher doses of amphetamine. The phenomenon can be blocked by neuroleptics.

PROCEDURE

Male CD-1 mice weighing 22–25 g are injected with 4 mg/kg d-amphetamine sulfate, followed 15 min later by an i.p. injection of 400 mg/kg L-dopa. The mice spontaneously begin to jump at a high rate. A median of 175 jumps can be observed in these mice during 60 min. Since mice do not show any jumping after saline administration, the responses after drug administration are specific and can be measured automatically through a pressure-sensitive switch closure or properly positioned photoelectric beam disruptions. Test compounds are administered 60 min prior to L-dopa injection.

EVALUATION

Jumps of mice treated with test drugs or standard are counted and expressed as percentage of jumps in amphetamine/L-dopa treated animals. Using various doses, ED_{50} values with 95% confidence limits are calculated.

CRITICAL ASSESSMENT OF THE METHOD

The method has been found to be sensitive and rather specific for neuroleptic drugs.

REFERENCES AND FURTHER READING

Fielding S, Lal H (1978) Behavioral actions of neuroleptics. In: Iversen LL, Iversen SD, Snyder SH (eds) Neuroleptics and Schizophrenia Vol 10, pp 91–128, Plenum Press, New York

Fielding S, Marky M, Lal H (1975) Elicitation of mouse jumping by combined treatment with amphetamine and L-dopa: Blockade by known neuroleptics. Pharmacologist 17:210

Lal H, Colpaert F, Laduron P (1975) Narcotic withdrawal-like mouse jumping produced by amphetamine and L-dopa. Eur J Pharmacol 30:113–116

Lal H, Marky M, Fielding S (1976) Effect of neuroleptic drugs on mouse jumping induced by L-dopa in amphetamine treated mice. Neuropharmacol 15:669–671

E.5.3.7 Antagonism Against MK-801 Induced Behavior

PURPOSE AND RATIONALE

Dizocilpine (MK-801), a non-competitive NMDA antagonist, induces a characteristic behavior in rat and mice, which is regarded as a model of psychosis (Andiné et al. 1999). In mice MK-801 induces a characteristic stereotypy marked by locomotion and falling behavior through both dopamine dependent and dopamine independent mechanisms (Carlson and Carlson 1989; Verma and Kulkarni 1992). Antipsychotic agents dose-dependent antagonize this MK-801 induced behavior.

PROCEDURE

Male CD-1 mice (20–30 g) are individually placed in activity boxes lined with wire mesh flooring and allowed to acclimate for 60 min. The animals are then dosed with compounds 30 min prior to subcutaneous administration of MK-801 at 0.2 mg/kg. The mice are observed for locomotion and the presence of falling behavior 15 min following MK-801 administration.

EVALUATION

ED_{50} values and 95% confidence limits are calculated by the Litchfield and Wilcoxon method.

MODIFICATIONS OF THE METHOD

Deutsch and Hitri (1993), Rosse et al. (1995), Deutsch et al. (2002, 2003), and Mastropaolo et al. (2004) described methods to measure the MK-801-induced explosive behavior in mice, called “popping”.

Farber et al. (1996) showed that neuroleptic drugs can prevent neuronal vacuolization and necrosis induced by MK-801 (Fix et al. 1993).

REFERENCES AND FURTHER READING

Andiné P, Widermark N, Axelsson R, Nyberg G, Olafsson U, Marrtensson E, Sandberg M (1999) Characterization of MK-801-induced behavior as a putative rat model of psychosis. J Pharmacol Exp Ther 290:1393–1408

Carlson M, Carlson A (1989) The NMDA antagonist MK-801 causes marked locomotor stimulation in monoamine-depleted mice. J Neural Transm 75:221–226

Deutsch SI, Hitri A (1993) Measurement of an explosive behavior in the mouse, induced by MK-801, a PCP analogue. Clin Neuropharmacol 16:251–257

Deutsch SI, Rosse RB, Billingslea EN, Bellack AS, Mastropaolo J (2002) Topiramate antagonizes MK-801 in an animal model of schizophrenia. Eur J Pharmacol 449:121–125

Deutsch SI, Rosse RB, Billingslea EN, Bellack AS, Mastropaolo J (2003) Modulation of MK-801-elicited mouse popping behavior by galantamine is complex and dose-dependent. Life Sci 73:2355–2361

Farber NB, Foster J, Duhan NL, Olney JW (1996) Olanzepine and fluperlapine mimic clopazine in preventing MK-801 neurotoxicity. Schizophrenia Res 21:33–37
Fix AS, Horn JW, Wigtman KA, Johnson CA, Long GG, Storts RW, Farber N, Wozniak DF, Olney JW (1993) Neuronal vacuolization and necrosis induced by the noncompetitive N-methyl-D-aspartate (NMDA) antagonist MK(+)801 (dizocilpine maleate): a light and electron microscopic evaluation of the rat retrosplenial cortex. Exp Neurol 123:204–215
Litchfield J, Wilcoxon F (1949) A simplified method of evaluating dose effect experiments. J Pharmacol Exp Ther 96:99–113
Mastropaolo J, Rosse RB, Deutsch SI (2004) Anabasine, a selective nicotinic acetylcholine receptor agonist, antagonizes MK801-elicited mouse popping behavior, an animal model of schizophrenia. Behav Brain Res 153:419–422
Rosse RB, Mastropaolo J, Sussman DM, Koetzner L, Morn CB, Deutsch SI (1995) Computerized measurement of MK-801-elicited popping and hyperactivity in mice. Clin Neuropharmacol 18:448–457
Verma A, Kulkarni SK (1992) Modulation of MK-801 response by dopaminergic agents in mice. Psychopharmacol 107:431–436

E.5.3.8 Phencyclidine Model of Psychosis

PURPOSE AND RATIONALE

Phencyclidine- (PCP-) induced symptoms in rats are considered as a model of psychosis (Ogawa et al. 1994; Halberstadt 1995; Steinpreis 1996; Abi-Saab et al. 1998; Sams-Dodd 1998a; Jentsch and Roth 1999; Phillips et al. 2000; Farber 2003; Morris et al. 2005).

PCP-induced symptoms can be antagonized by neuroleptic drugs (Witkin et al. 1997; Sams-Dodd 1998b; Javitt et al. 2004).

Cartmell et al. (1999) found that metabotropic glutamate receptor agonists selectively attenuate phencyclidine versus d-amphetamine motor behaviors in rats.

PROCEDURE

Behavior of male Sprague Dawley rats weighing 250–300 g was monitored while in transparent, plastic shoebox cages of the dimensions 45 × 25 × 20 cm, with 1 cm depth of wood clips as bedding, and a metal grill on the top of the cage. Motor monitors consisted of a rectangular rack of 12 photobeams arranged in a 8 × 4 formation. Shoe boxes were placed inside these racks, enabling the activity of the rat to be monitored in a home-cage environment. The lower rack was positioned at a height of 5 cm, which allowed the detection of PCP-induced head movements in addition to movements of the body of the rat. Rearing activity was detected by a second rack placed 10 cm above the first. Rats were placed in the cage for an acclimation period of 30 min, then removed, administered the test compounds s.c. or sterile water and then returned to the same cages. After 30 min, the rats were given an s.c. injection of PCP or amphetamine or sterile water and once again returned to the cages. Motor activity was monitored for the following 60 min resulting in the measurement of three different parameters: ambulations (pattern of beam breaks indicating that the animal had relocated its entire body), fine movements (non-ambulatory beam breaks), and time at rest. An indication of rearing activity was detected in the upper rack of photobeams.

EVALUATION

Data were analyzed by a one-way ANOVA, and then post-hoc comparisons for each dose group versus control or PCP alone or PCP and test compound were made using Newman-Keuls Multiple Comparison test.

MODIFICATIONS OF THE METHOD

Furuya et al. (1998) investigated the effects of a strychnine-insensitive glycine site antagonist on the hyperactivity and the disruption of prepulse inhibition induced by phencyclidine (PCP) in rats.

Redmond et al. (1999) tested the effects of acute and chronic antidepressant administration on PCP-induced locomotor hyperactivity.

Boulay et al. (2004) tested a putative atypical antipsychotic for improvement of social interaction deficits induced by PCP in rats.

REFERENCES AND FURTHER READING

Abi-Saab WM, D'Souza DC, Moghaddam B, Krystal JH (1998) The NMDA antagonist model for schizophrenia: promise and pitfalls. Pharmacopsychiatry 31 [Suppl 2]:104–109
Boulay D, Depoortère R, Louis C, Perrault G, Griebel G, Soubrié P (2004) SSR181507, a putative atypical antipsychotic with dopamine D_2 agonist and 5-HT_{1A} agonist activities: improvement of social interaction deficits induced by phencyclidine in rats. Neuropharmacology 46:1121–1129
Cartmell J, Monn JA, Schopp DD (1999) The metabotropic glutamate 2/3 receptor agonists LY354740 and LY379268 selectively attenuate phencyclidine versus *d*-amphetamine motor behaviors in rats. J Pharmacol Exp Ther 291:161–170
Farber NB (2003) The NMDA receptor hypofunction model of psychosis. Ann N Y Acad Sci 2003:119–130
Furuya Y, Kagaya T, Nishizawa Y, Ogura H (1998) Differential effects of the strychnine-insensitive glycine site antagonist (+)-HA-966 on the hyperactivity and the disruption of prepulse inhibition induced by phencyclidine in rats. Brain Res 781:227–235
Halberstadt AL (1995) The phencyclidine-glutamate model of schizophrenia. Clin Neuropharmacol 18:237–249
Javitt DC, Balla A, Burch S, Suckow R, Xie S, Sershen H (2004) Reversal of phencyclidine-induced dopaminergic dysregulation by *N*-methyl-D-aspartae receptor/glycine-site agonists. Neuropsychopharmacology 29:300–307

Jentsch JD, Roth RH (1999) The neuropsychopharmacology of phencyclidine: from NMDA receptor hypofunction to the dopamine hypothesis of schizophrenia. Neuropsychopharmacology 20:201–225
Morris BJ, Cochran SM, Pratt JA (2005) PCP: from pharmacology to modeling schizophrenia. Curr Opin Pharmacol 5:101–106
Ogawa S, Okuyama S, Araki H, Nakazato A, Otomo S (1994) A rat model of phencyclidine psychosis. Life Sci 55:1605–1610
Phillips M, Wang C, Johnson KM (2000) Pharmacological characterization of locomotor sensitization induced by chronic phencyclidine administration.. J Pharmacol Exp Ther 296:905–913
Redmond AM, Harkin A, Kelly JP, Leonard BE (1999) Effects of acute and chronic antidepressant administration on phencyclidine (PCP) induced locomotor hyperactivity. Eur Neuropsychopharmacol 9:165–170
Sams-Dodd F (1998a) Effects of continuous D-amphetamine and phencyclidine administration on social behaviour, stereotyped behaviour, and locomotor activity in rats. Neuropsychopharmacology 19:18–25
Sams-Dodd F (1998b) Effects of diazepam, citaprolam, methadone and naloxone on PCP-induced stereotyped behavior and social isolation in the rat social interaction test. Neurosci Behav Rev 23:287–293
Steinpreis RE (1996) The behavioral and neurochemical effects of phencyclidine in humans and animals: some applications for modeling psychosis. Behav Brain Res 74:45–55
Witkin JM, Steele TD, Sharpe LG (1997) Effects of strychnine-insensitive glycine receptor ligands in rats discriminating dizocilpine or phencyclidine from saline. J Pharmacol Exp Ther 280:46–52

E.5.3.9 Inhibition of Apomorphine-Induced Emesis in the Dog

PURPOSE AND RATIONALE

The blockade of centrally acting dopaminergic mechanisms is considered to play a major role in suppression of psychotic reactions in schizophrenia. Apomorphine, regarded as a direct dopaminergic agonist, produces a pronounced emetic effect in dogs and the blockade of apomorphine emesis is used as an indication of dopaminergic blockade. However, although both antiemetic activity and antipsychotic activity are thought to be due to dopaminergic blockade, the sites of action are in different brain areas and there is a lack of complete correlation of these activities.

PROCEDURE

Adult beagle dogs of either sex are used in treatment groups of three to nine dogs/dose. The dogs are given the test compounds in a gelatin capsule; they are then dosed with 0.15 mg/kg apomorphine s.c. at various intervals after administration of the test compound. The dogs are first observed for overt behavioral effects, e. g., pupillary response to light, changes in salivation, sedation, tremors, etc; then, after the administration of apomorphine, the dogs are observed for stereotypic sniffing, gnawing and the emetic response. Emesis is defined as wretching movements followed by an opening of the mouth and either attempted or successful ejection of stomach content.

EVALUATION

If the experimental compound is anti-emetic in the primary screen, the dose is progressively lowered to obtain a minimal effective dose or an ED_{50} value. The ED_{50} values for haloperidol and chlorpromazine were found to be 0.06 mg/kg p.o. and 2.0 mg/kg p.o., respectively. Clozapine was not effective at doses between 2 and 10 mg/kg. p.o.

CRITICAL ASSESSMENT OF THE METHOD

The method has been extensively used by several laboratories. However, since non-classical neuroleptics like clozapine did not show pronounced activity the test has been abandoned. Moreover, tests in higher animals like dogs are limited due to regional regulations.

REFERENCES AND FURTHER READING

Chipkin RE, Iorio LC, Coffin VL, McQuade RD, Berger JG, Barnett A (1988) Pharmacological profile of SCH39166: A dopamine D1 selective benzonaphthazepine with potential antipsychotic activity. J Pharmacol Exp Ther 247:1093–1102
Janssen PAJ, Niemegeers CJE (1959) Chemistry and pharmacology of compounds related to 4-(4-hydroxy-4-phenylpiperidino)-butyrophenone. Part II – Inhibition of apomorphine vomiting in dogs. Arzneim Forsch 9:765–767
Janssen PA, Niemegeers CJE, Shellekens HL (1965) Is it possible to predict the clinical effects of neuroleptic drugs (major tranquilizers) from animal data? Arzneim Forsch 15:1196–1206
Rotrosen J, Wallach MB, Angrist B, Gershon S, (1972) Antagonism of apomorphine-induced stereotypy and emesis in dogs by thioridiazine, haloperidol and pimozide. Psychopharmacol (Berlin) 26:185–195

E.5.3.10 Purposeless Chewing in Rats

PURPOSE AND RATIONALE

Purposeless chewing can be induced in rats by directly acting cholinergic drugs or cholinesterase inhibitors (Rupniak et al. 1983), which can be blocked by anti-muscarinic agents. The chewing behavior has been proposed to be mediated through central M_2 receptors rather than via central M_1 sites (Stewart et al. 1989). Chewing can also be induced by chronic administration of neuroleptics in rats (Clow et al. 1979; Iversen et al. 1980). Purposeless chewing is mediated by dopaminergic and nicotinic mechanisms.

PROCEDURE

Male albino rats are housed 10 per cage at room temperature and kept on a 12 h light-dark cycle. For the experiments, rats are placed individually in a large glass cylinder (height 30 cm, diameter 20 cm) at 21 ± 1°C and allowed to habituate for 15 min before injection of drugs. The antagonists, e. g. sulpiride or mecamylamine as standards, are given at different doses 30 min before treatment either with 0.01 mg/kg nicotine or 1 mg/kg pilocarpine i.p. Number of chewings are counted by direct observation immediately after drug administration. The results are presented as number of chews in a 30 min period.

EVALUATION

Analysis of variance (ANOVA), followed by Newman-Keuls tests, are used to evaluate the significance of the results obtained. $P < 0.05$ is considered as significant.

MODIFICATIONS OF THE METHOD

Tremulous jaw movements induced by tacrine (Cousins et al. 1999) can be antagonized by antipsychotic drugs (Betz et al. 2005; Ishiwarii et al. 2005).

REFERENCES AND FURTHER READING

Betz A, Ishiwari K, Wisniecki A, Huyn N, Salamone JD (2005) Quetiapine (Seroquel) shows a pattern of behavioral effects similar to the atypical antipsychotics clozapine and olanzapine: studies with tremulous jaw movements in rats. Psychopharmacology 179:383–392

Clow A, Jenner P, Marsden CD (1979) Changes in dopamine-mediated behaviour during one year neuroleptic treatment. Eur J Pharmacol 57:365–375

Collins P, Broekkamp CLE, Jenner P, Marsden CD (1991) Drugs acting at D-1 and D-2 dopamine receptors induce identical purposeless chewing in rats which can be differentiated by cholinergic manipulation. Psychopharmacology 103:503–512

Cousins MS, Finn M, Trevitt J, Carriero DL, Conlan A, Salamone JD (1999) The role of ventrolateral striatal acetylcholine in the production of tacrine-induced jaw movements. Pharmacol Biochem Behav 62:439–447

Ishiwarii K, Betz A, Weber S, Felsted J, Salamone JD (2005) Validation of the tremulous jaw movement model for assessment of motor effects of typical and atypical antipsychotics: effects of pimozide (Orap) in rats. Pharmacol Biochem Behav 80:351–362

Iversen SD, Howells RB, Hughes RP (1980) Behavioural consequences of long-term treatment with neuroleptic drugs. Adv Biochem Psychopharmacol 24:305–313

Rupniak NMJ, Jenner P, Marsden CD (1983) Cholinergic manipulation of perioral behaviour induced by chronic neuroleptic administration to rats. Psychopharmacology 79:226–230

Stewart BR, Jenner P, Marsden CD (1989) Assessment of the muscarinic receptor subtype involved in the mediation of pilocarpine-induced purposeless chewing behaviour. Psychopharmacology 97:228–234

Samini M, Yekta FS, Zarrindast MR (1995) Nicotine-induced purposeless chewing in rats: possible dopamine receptor mediation. J Psychopharmacol 9:16–19

Zarrindast MR, Moini-Zanjani T, Manaheji H, Fathi F (1992) Influence of dopamine receptors on chewing behaviour in rats. Gen Pharmacol 23:915–919

E.5.3.11 Models of Tardive Dyskinesia

PURPOSE AND RATIONALE

Tardive dyskinesia is a severe side-effect of traditional neuroleptics affecting a considerable number of patients probably based on a genetic disposition, being characterized by involuntary movements of the oral region. Various authors used rats as animal model for tardive dyskinesia, either after treatment with reserpine (Waddington et al. 1990; Neisewander 1994; Bergamo et al. 1997; Quieroz and Frussa-Filho 1999; Andreassen 2000; Casey 2000; Van Kampen et al. 2000; Calvente et al. 2002; Abílio et al. 2003; Peixoto et al. 2003) or haloperidol (Takeuchi et al. 1998; Harvey and Nel 2003; Naidu et al. 2003; Burger et al. 2005). Several authors compared the effects of different neuroleptics (See and Ellison 1990; Tamminga et al. 1994) or studied potential antagonistic effects (Takeuchi et al. 1998; Quieroz and Frussa-Filho 1999; Abílio et al. 2003; Naidu et al. 2003; Peixoto et al. 2003).

Burger et al. (2005) found that ebselen attenuates haloperidol-induced orofacial dyskinesia and oxidative stress in rat brain.

PROCEDURE

Male Wistar rats weighing 270–320 g were injected sc. once a week with 12 mg/kg haloperidol decanoate for 4 weeks. Another group was pretreated with 30 mg/kg ebselen and received in addition to haloperidol every other day an ip. injection of 30 mg/kg ebselen.

The animals were observed for the quantification of orofacial dyskinesia just before haloperidol administration and on the 7th, 14th, 21st and 28th day after the first administration of haloperidol.

Rats were placed individually in cages (20 × 20 × 19 cm) containing mirrors under the floor and behind the back wall of the cage to allow behavioral quantification when the animal was faced away from the observer. To quantify the occurrence of oral dyskinesia, the incidence of tongue protrusions, vacuous chewing movements frequency, and the duration of facial twitching were recorded for 15 min. Observers were blind to drug treatment.

EVALUATION

Data were analyzed by a three-way ANOVA, followed, when appropriate, by univariate analysis and Duncan's Post Hoc test.

MODIFICATIONS OF THE METHOD

Several authors used monkeys (*Cebus apella* or *Macaca speciosa*) to evaluate the effect of neuroleptics to induce tardive dyskinesia-like symptoms (Gunne and Barany 1979; Domino 1985; Werge et al. 2003).

REFERENCES AND FURTHER READING

Abílio VC, Araujo CCS, Bergamo M, Calvente PRV, D'Almeida V, Ribeiro RA, Frussa-Filho R (2003) Vitamin E attenuates reserpine-induced oral dyskinesia and striatal oxidized glutathione/reduced glutathione ratio (GSSSG/GSH) enhancement in rats. Progr Neuropsychopharm Biol Psychiatry 27:109–114

Andreassen OA, Jorgensen HA (2000) Neurotoxicity associated with neuroleptic-induced oral dyskinesias in rats, implications for tardive dyskinesia. Progr Neurobiol 61:525–531

Bergamo M, Abílio VC, Queiroz MT, Barbosa-Júnior HN, Prussa-Filho R (1997) The effects of age on a new animal model of tardive dyskinesia. Neurobiol Aging 18:623–629

Burger ME, Fachinetto R, Zeni G, Rocha JBT (2005) Ebselen attenuates haloperidol-induced orofaccial dyskinesia and oxidative stress in rat brain. Pharmacol Biochem Behav 81:608–615

Calvente PRV, Araujo CCS, Bergamo M, Abílio VC, D'Almeida V, Riberiro RA, Frussa-Filho R (2002) The mitochondrial toxin 3-nitropropionic acid aggravates reserpine-induced oral dyskinesias in rats. Progr Neuropsychopharm Biol Psychiatry 26:401–405

Casey DE (2000) Tardive dyskinesia: pathophysiology and animal models. J Clin Psychiatry 61:5–9

Domino EF (1985) Induction of tardive dyskinesia in *Cebus apella* and *Macaca speciosa* monkeys. A review. Psychopharmacology Suppl 2:217–223

Gunne LM, Barany S (1979) A monitoring test for the liability of neuroleptic drugs to induce tardive dyskinesia. Psychopharmacology (Berl) 63:195–198

Harvey BH, Nel A (2003) Role of aging and striatal nitric oxide synthase activity in an animal model of tardive dyskinesia. Brain Res Bull 61:407–416

Naidu PS, Singh A, Kaur P, Sandhir R, Kulkarni SK (2003) Possible mechanism of action in melatonin attenuation of haloperidol-induced orofacial dyskinesia. Pharmacol Biochem Behav 74:641–648

Neisewander JL, Castañeda E, Davis DA, (1994) Dose-dependent differences in the development of reserpine-induced dyskinesia in rats: support for a model of tardive dyskinesia. Psychopharmacology 116:79–84

Peixoto MF, Abílio VC, Silva RH, Frussa-Filho R (2003) Effects of valproic acid on an animal model of tardive kinesia. Behav Brain Res 142:229–233

Queiroz CMT, Frussa-Filho R (1999) Effects of buspirone on a model of tardive dyskinesia. Progr Neuropsychopharm Biol Psychiatry 22:1405–1418

See RE, Ellison G (1990) Comparison of chronic administration of haloperidol and the atypical neuroleptics, clozapine and raclopride, in an animal model of tardive dyskinesia. Eur J Pharmacol 181:175–186

Takeuchi H, Ishigooka J, Kobayashi K, Watanabe S, Miura S (1998) Study on the suitability of a rat model for tardive dyskinesia and the preventive effects of various drugs. Progr Neuropsychopharm Biol Psychiatry 22:679–691

Tamminga CA, Thaker GK, Moran M, Kakigi T, Gao XM (1994) Clozapine in tardive dyskinesia: observations from human and animal studies. J Clin Psychiatry 55 [Suppl B]:102–106

Van Kampen JM, Stoessl AJ (2000) Dopamine D_{1A} receptor function in a rodent model of tardive dyskinesia. Neuroscience 101:629–635

Waddington JL (1990) Spontaneous orofacial movements induced in rodents by very long-term neuroleptic drug administration. Phenomenology, pathophysiology and putative relationship to tardive dyskinesia. Psychopharmacology 101:431–447

Werge T, Elbaek Z, Andersen MB, Lundbaek JA, Rasmussen HB (2003) *Cebus apella*, a nonhuman primate highly susceptible to neuroleptic side effects, carries the GLY9 dopamine reporter associated with tardive dyskinesia in humans. Pharmacogenomics J 3:97–100

E.5.3.12 Single Unit Recording of A9 and A10 Midbrain Dopaminergic Neurons

PURPOSE AND RATIONALE

Interactions with central nervous system dopamine pathways are crucial for the expression of antipsychotic effects seen with clinically effective neuroleptics. These interactions also have a role in the expression of several of the neurological side effects seen with these agents. Extracellular single unit recording techniques of rat A9 (substantia nigra) and A10 (ventral tegmental area) dopamine neurons show that after acute treatment with neuroleptics the number of spontaneously firing cells is increased in both areas. After repeated treatment (21 days) a decrease was found with all neuroleptics in the A10 neurons, whereas in the A9 cell only compounds with clinically evident extrapyramidal side effects induced a decrease. Clozapine which is believed not to produce extrapyramidal side effects resulted in the depolarization inactivation of A10 neurons but not A9 cells. The method provides a prediction of a compound's anti-psychotic potential as well as potential neurological side effects (Chiodo and Bunney 1983).

PROCEDURE

Male Wistar rats weighing 280–360 g are anesthetized with chloralhydrate intraperitoneally. The animal is mounted in a stereotaxic apparatus (Kopf, model 900). The cranium is exposed, cleaned of connective tissue and dried. The skull overlying both the substantia nigra (A9: anterior (A) 3000–3400 µm, lateral (L) 1800–2400 µm from lambda), and the ventral tegmental area (A10: A 3000–3400 µm, L 400–1000 µm from lambda) (Paxinos and Watson 1986) is removed. Using the dura as point of reference, a micropipette driven by a hydraulic microdrive is lowered through the opening of the skull at vertical 6000–8500 µm. Spontaneously firing dopamine neurons within both the substantia ni-

gra and the ventral tegmental area are counted by lowering the electrode into twelve separate tracks (each track separated from the other by 200 µm) in each region. The sequence of these tracks is kept constant, forming a block of tissue which can be reproducibly located from animal to animal.

Extracellular neuronal signals are sampled using a single barrel micropipette approximately one µm at its tip, and filled with 2 M NaCl saturated with 1% pontamine sky blue dye (*in vitro* impedance between 5 and 10 MΩ). Electrical potentials are passed through a high-impedance preamplifier and the signal is sent to a window discriminator which converts potentials above background noise levels to discrete pulses of fixed amplitude and duration. Only cell whose electrophysiological characteristics match those previously established for midbrain dopamine neurons are counted. In an anesthetized rat, a neuron is considered to be dopaminergic if it displays a triphasic positive-negative-positive spike profile of 0.4 to 1.5 mV amplitude and 2.5 ms duration, firing in an irregular pattern of 3 to 9 Hz with occasional bursts characterized by progressively decreasing spike amplitude and increasing spike duration.

At the end of each experiment, the location of the last recorded track tip is marked by passing 25 microampere cathodal current through the recording micropipet barrel for 15 min in order to deposit a spot of dye. The rat is sacrificed, the brain is then removed, dissected and frozen on a bed of dry ice. Frozen serial sections (20 µm in width) are cut, mounted and stained with cresyl violet and examined using a light microscope.

Animals pretreated with vehicle prior to neuronal sampling serve as controls. For animals that are used in an acute single-unit dopamine neuron sampling assay, test compounds are administered intraperitoneally one hour prior to the beginning of dopamine neuron sampling. For animals used in a chronic single-unit dopamine sampling assay, the compounds are administered once a day for 21 days, and dopamine neuron sampling is begun 2 h after the last dose on the 21st day.

EVALUATION

Drug treatment groups are compared to vehicle groups with a one-way ANOVA with a post hoc Neuman-Keuls analysis for significance.

MODIFICATIONS OF THE METHOD

Nybäck et al. (1975) tested the influence of tricyclic antidepressants on the spontaneous activity of norepinephrine-containing cells of the locus caeruleus in anesthetized rats.

Scuvée-Moreau and Dreese (1979) studied the effect of various antidepressant drugs on the firing rate of locus caeruleus and dorsal raphe neurons of the anesthetized rat with extracellular microelectrodes.

Using the method of single-unit recording of spontaneous firing of locus caeruleus neurons in rats, Cedarbaum and Aghajanian (1977) studied the inhibition by micro-iontophoretic application of catecholaminergic agonists.

Marwaha and Aghajanian (1982) examined in single unit studies the actions of adrenoceptor antagonists at *alpha*-1 adrenoceptors of the dorsal raphe nucleus and the dorsal lateral geniculate nucleus and *alpha*-2 adrenoceptors of the nucleus locus caeruleus.

Mooney et al. (1990) studied the organization and actions of the noradrenergic input to the superior colliculus of the hamster using micro-iontophoretic techniques together with extracellular single unit recording.

Bernardini et al. (1991) studied *in vitro* with brain slices of mice the amphetamine-induced and spontaneous release of dopamine from A9 and A10 cell dendrites.

Santucci et al. (1997) investigated the effects of synthetic neurotensin receptor antagonists on spontaneously active A9 and A10 neurones in rats.

REFERENCES AND FURTHER READING

Bernardini GL, Gu X, Viscard E, German DC (1991) Amphetamine-induced and spontaneous release of dopamine from A9 and A10 cell dendrites: an *in vitro* electrophysiological study in the mouse. J Neural Transm 84:183–193

Bowery B, Rothwell LA, Seabrock GR (1994) Comparison between the pharmacology of dopamine receptors mediating the inhibition of cell firing in rat brain slices through the substantia nigra pars compacta and ventral tegmental area. Br J Pharmacol 112:873–880

Bunney BS, Grace AA (1978) Acute and chronic haloperidol treatment: comparison of effects on nigral dopaminergic cell activity. Life Sci 23:1715–1728

Cedarbaum JM, Aghajanian GK (1977) Catecholamine receptors on locus caeruleus neurons: pharmacological characterization. Eur J Pharmacol 44:375–385

Chiodo LA, Bunney BS (1983) Typical and atypical neuroleptics: differential effect of chronic administration on the activity of A9 and A10 midbrain dopaminergic neurons. J Neurosci 3:1607–1619

Marwaha J, Aghajanian GK (1982) Relative potencies of *alpha*-1 and *alpha*-2 antagonists in the locus caeruleus, dorsal raphe and dorsal lateral geniculate nuclei: an electrophysiological study. J Pharmacol Exp Ther 222:287–293

Mooney RD, Bennett-Clarke C, Chiaia NL, Sahibzada N, Rhoades RW (1990) Organization and actions of the noradrenergic input to the hamster's superior colliculus. J Comp Neurol 292:214–230

Nybäck HV, Walters JR, Aghajanian GK, Roth RH (1975) Tricyclic antidepressants: effects on the firing rate of brain noradrenergic neurons. Eur J Pharmacol 32:302–312
Paxinos G, Watson C (1986) The Rat Brain in Stereotaxic Coordinates. 2nd ed, Academic Press, Sydney, Australia
Santucci V, Gueudet C, Steinberg R, Le Fur G, Soubrie P (1997) Involvement of cortical neurotensin in the regulation of rat mesocortico-limbic dopamine neurons: Evidence from changes in the number of spontaneously active A10 cells after neurotensin receptor blockade. Synapse 26:370–380
Schmidt CJ, Black CK, Taylor VL, Fadayel GM, Humphreys TM, Nieduzak TR, Sorensen SM (1992) The 5-HT_2 receptor antagonist, MDL 28,133A, disrupts the serotoninergic-dopaminergic interaction mediating the neurochemical effects of 3,4-methylenedioxymethylamphetamine. Eur J Pharmacol 220:151–159
Scuvée-Moreau JJ, Dreese AE (1979) Effect of various antidepressant drugs on the spontaneous firing rate of locus caeruleus and dorsal raphe neurons of the rat. Eur J Pharmacol 57:219–225
Todorova A, Dimpfel W (1994) Multiunit activity from the A9 and A10 areas in rats following chronic treatment with different neuroleptic drugs. Eur Neuropsychopharmacol 4:491–501
White FJ, Wang RY (1983a) Comparison of the effects of chronic haloperidol treatment on A9 and A10 dopamine neurons in the rat. Life Sci 32:983–993
White FJ, Wang RY (1983b) Differential effects of classical and atypical antipsychotic drugs on A9 and A10 dopamine neurons. Science 221:1054–1057

E.5.3.13 In Vivo Voltammetry

PURPOSE AND RATIONALE

Various groups (Lane et al. 1979, 1987, 1988; Blaha and Lane 1983, 1984, 1987; Crespi et al. 1984; Marsden et al. 1984; Maidment and Marsden 1987a, b; Armstrong-James and Millar 1979, 1984; Kawagoe et al. 1993) described *in vivo* voltammetry as an electrochemical technique that uses carbon fiber microelectrodes stereotactically implanted in brain areas to monitor monoamine metabolism and release. De Simoni et al. (1990) reported on a miniaturized optoelectronic system for telemetry of *in vivo* voltammetric signals in freely moving animals.

PROCEDURE

Carbon fibre working electrodes are made from pyrolytic carbon fibres supported in a pulled glass capillary (Armstrong-James and Millard 1979; Sharp et al. 1984) and electrically pretreated for simultaneous recording of ascorbic acid DOPAC and 5-HIAA (Crespi et al. 1984).

Male Sprague Dawley rats weighing 270–340 g are anesthetized with a 2–3% halothane O_2/NO_2 mixture (1:1) and held in a stereotactic frame. Reference and auxiliary electrodes are positioned on the surface of the dura through 1 mm holes drilled in the cranium and held in place with dental cement. Holes, approx. 2 mm in diameter, are drilled in the cranium above the left or right nucleus accumbens and contralateral anterior striatum, and the underlying dura is broken with a hypodermic needle. A working electrode is lowered in one of the above regions and cemented in place. A second electrode is then implanted in the remaining structure. The coordinates, measured from the bregma, are as follows: nucleus accumbens–rostro-caudal +3.4 mm; medio-lateral ± 1.4 mm; dorso-ventral –7 mm; striatum–rostro-caudal +2.8 mm; medio-lateral ± 2.6 mm; dorso-ventral –5.5 mm.

Drugs are injected subcutaneously. Voltammograms are recorded using a Princeton Applied Research 174A polarographic analyzer alternatively from each region every 5 min and after a 1 h stabilization period.

EVALUATION

Voltammetric data are expressed as percentage changes from pre-injection control values using the mean of the last 6 peak heights before administration of drug as the 100% value. However, statistical analysis of the data is carried out on the absolute peak heights using a paired Student's *t*-test to compare 6 pre-injection control peak heights with those after administration of drug at selected time points.

MODIFICATIONS OF THE METHOD

Swiergiel et al. (1997) constructed voltammetric probes from stainless steel and fused silica tubing sheathing carbon fibers and compared them with commercially available glass-sealed IVEV-5 electrodes. This type of electrodes can be easily manufactured and does not require any special equipment.

Parada et al. (1994, 1995) described a triple-channel swivel suitable for intracranial fluid delivery and microdialysis experiments which can be equipped with three electrical channels for *in vivo* voltammetry and measurement of intracranial temperature with a thermocouple.

Frazer and Daws (1998) used electrodes coated with a perfluorinated ion exchange resin (Nafion) to assess serotonin transporter function *in vivo* by **chrono-amperometry** whereby voltage is applied to the electrode in a pulsed manner and the current obtained measured as a function of time.

REFERENCES AND FURTHER READING

Armstrong-James M, Millar J (1979) Carbon fibre microelectrodes. J Neurosci Meth 1:279–287

Armstrong-James M, Millar J (1984) High-speed cyclic voltammetry and unit recording with carbon fibre microelectrodes. In: Marsden CA (ed) Measurement of Neurotransmitter Release *in vivo*. John Wiley and Sons Ltd., Chichester, New York, pp 209–224

Blaha CD, Lane RF (1983) Chemically modified electrode for *in vivo* monitoring of brain catecholamines. Brain Res Bull 10:861–864

Blaha CD, Lane RF (1984) Direct *in vivo* electrochemical monitoring of dopamine release in response to neuroleptic drugs. Eur J Pharmacol 98:113–117

Blaha CD, Lane RF (1987) Chronic treatment with classical and atypical antipsychotic drugs differentially decreases dopamine release in striatum and nucleus accumbens *in vivo*. Neurosci Lett 78:199–204

Buda M, Gonon FG (1987) Study of brain noradrenergic neurons by use of *in vivo* voltammetry. In: J.B. Justice Jr (ed) Voltammetry in the Neurosciences: Principles, Methods and Applications. Humana Press, Clifton, New Jersey, pp 239–272

Cespuglio R, Faradji H, Hahn Z, Jouvet M (1984) Voltammetric detection of brain 5-hydroxyindolamines by means of electrochemically treated carbon fibre electrodes: chronic recordings for up to one month with movable cerebral electrodes in the sleeping or waking rat. In: Marsden CA (ed) Measurement of Neurotransmitter Release *in vivo*. John Wiley and Sons Ltd., Chichester, New York, pp 173–191

Crespi F, Sharp T, Maidment NT, Marsden Ca (1984) Differential pulse voltammetry: simultaneous *in vivo* measurement of ascorbic acid, catechols and 5-hydroxyindoles in the rat striatum. Brain Res 322:135–138

de Simoni MG, de Luigi A, Imeri L, Algerin S (1990) Miniaturized optoelectronic system for telemetry of *in vivo* voltammetric signals. J Neurosci Meth 33:233–240

Frazer A, Daws LC (1998) Serotonin transporter function *in vivo*: Assessment by chronoamperometry. In: Martin GR, Eglen RM, Hoyer D, Hamblin MW, Yocca F (eds) Advances in Serotonin Research. Molecular Biology, Signal Transduction, and Therapeutics. Ann New York Acad Sci 861:217–229

Gonon F, Buda M, Oujol JF (1984) Treated carbon fibre electrodes for measuring catechols and ascorbic acid. In: Marsden CA (ed) Measurement of Neurotransmitter Release *in vivo*. John Wiley and Sons Ltd., Chichester, New York, pp 153–171

Gonon FG (1987) *In vivo* electrochemical monitoring of dopamine release. In: J.B. Justice Jr (ed) Voltammetry in the Neurosciences: Principles, Methods and Applications. Humana Press, Clifton, New Jersey, pp 163–183

Justice JB Jr (1987) Introduction to *in vivo* voltammetry. In: J.B. Justice Jr (ed) Voltammetry in the Neurosciences: Principles, Methods and Applications. Humana Press, Clifton, New Jersey, pp 3–102

Justice JB Jr, Michael AC (1987) Monitoring extracellular DOPAC following stimulated release of dopamine. In: J.B. Justice Jr (ed) Voltammetry in the Neurosciences: Principles, Methods and Applications. Humana Press, Clifton, New Jersey, pp 185–208

Kawagoe KT, Zimmerman JB, Wightman RM (1993) Principles of voltammetry and microelectrode surface states. J Neurosci Meth 48:225–240

Lane RF, Blaha CD (1986) Electrochemistry *in vivo*: Application to CNS pharmacology. Ann NY Acad Sci 473:50–69

Lane RF, Hubbard AT, Blaha CD (1979) Application of semidifferential electroanalysis to studies of neurotransmitters in the central nervous system. J Electroanalyt Chem 95:117–122

Lane RF, Blaha CD, Hari SP (1987) Electrochemistry *in vivo*: monitoring dopamine release in the brain of the conscious, freely moving rat. Brain Res Bull 19:19–27

Lane RF, Blaha CD, Rivet JM (1988) Selective inhibition of mesolimbic dopamine release following chronic administration of clozapine: Involvement of α_1-noradrenegic receptors demonstrated by *in vivo* voltammetry. Brain Res 460:389–401

Maidment NT, Marsden CA (1985) *In vivo* voltammetric and behavioral evidence for somatodendritic autoreceptor control of mesolimbic dopamine neurons. Brain Res 338:317–325

Maidment NT, Marsden CA (1987a) Acute administration of clozapine, thioridazine, and metoclopramide increases extracellular DOPAC and decreases extracellular 5-HIAA, measured in rat nucleus accumbens and striatum of the rat using *in vivo* voltammetry. Neuropharmacol 26:187–193

Maidment NT, Marsden CA (1987b) Repeated atypical neuroleptic administration: Effects on central dopamine metabolism monitored by *in vivo* voltammetry. Eur J Pharmacol 136:141–149

Marsden CA, Brazell MP, Maidment NT (1984) An introduction to *in vivo* electrochemistry. In: Marsden CA (ed) Measurement of Neurotransmitter Release *in vivo*. John Wiley and Sons Ltd., Chichester, New York, pp 127–151

Marsden CA, Martin KF, Brazell MP, Maidment NT (1987) *In vivo* voltammetry: Application to the identification of dopamine and 5-hydroxytryptamine receptors. In: J.B. Justice Jr (ed) Voltammetry in the Neurosciences: Principles, Methods and Applications. Humana Press, Clifton, New Jersey, pp 209–237

Nagatsu T, Ikeda M, Fujita K, Shinzato M, Takahashi H, Adachi T (1987) Application of *in vivo* voltammetry to behavioral pharmacology. In: J.B. Justice Jr (ed) Voltammetry in the Neurosciences: Principles, Methods and Applications. Humana Press, Clifton, New Jersey, pp 313–324

Parada MA, Puig de Parada M, Hoebel BG (1994) A new triple-channel swivel for fluid delivery in the range of intracranial (10 nl) and intravenous (100 µl) self-administration volumes and also suitable for microdialysis. J Neurosci Meth 54:1–8

Parada MA, Puig de Parada M, Hernandez L, Hoebel BG (1995) Triple electrical channels on a triple fluid swivel and its use to monitor intracranial temperature with a thermocouple. J Neurosci Meth 60:133–139

Plotsky PM (1987) Probing pathways of neuroendocrine regulation with voltammetric microelectrodes. In: J.B. Justice Jr (ed) Voltammetry in the Neurosciences: Principles, Methods and Applications. Humana Press, Clifton, New Jersey, pp 273–309

Schenk JO, Adams RN (1984) Chronoamperometric measurements in the central nervous system. In: Marsden CA (ed) Measurement of Neurotransmitter Release *in vivo*. John Wiley and Sons Ltd., Chichester, New York, pp 193–208

Sharp T, Maidment NT, Brazell MP, Zetterström T, Ungerstedt U, Bennett GW, Marsden CA (1984) Changes in monoamine metabolites measured by simultaneous *in vivo* pulse voltammetry and intracerebral dialysis. Neuroscience 12:1213–1221

Stamford JA, Kruk ZL, Millar J (1988) Actions of dopamine antagonists on stimulated striatal and limbic dopamine release: an *in vivo* voltammetric study. Br J Pharmacol 94:924–932

Swiergiel AH, Palamarchouk VS, Dunn AJ (1997) A new design of carbon fiber microelectrode for *in vivo* voltammetry using fused silica. J Neurosci Meth 73:29–33

E.5.4
Genetic Models of Psychosis

E.5.4.1
The Heterozygous Reeler Mouse

PURPOSE AND RATIONALE

Reelin is an extracellular matrix protein secreted by GABAergic interneurons that, acting through pyramidal neuron integrin receptors, provides a signal for dendritic spine plasticity. The gene responsible for a mouse mutant strain is called reeler (D'Arcangelo and Curran 1998; Lombroso and Goldowitz 1998; Fatemi 2001; Pappas et al. 2003). Heterozygous reeler mice that exhibit a 50% downregulation of reelin expression replicate the dendritic spine and GABAergig defects described in human schizophrenia (Larson et al. 2003). The heterozygote reeler mouse was recommended as a model for the development of a new generation of antipsychotics (Tueting et al. 1999; Rowley et al. 2001; Costa et al. 2002). This view has been challenged by Podhorna and Didriksen (2004).

Tomasiewicz et al. (1993) and Wood et al. (1998) proposed **NCAM-180 knockout mice** with a deletion of the neural cell adhesion molecule variant (N-CAM-180) displaying increased lateral ventricle size and a reduced prepulse inhibition of startle response as model for schizophrenia.

Dirks et al. (2003) reported reversal of startle gating deficits in **transgenic mice overexpressing corticotropin-releasing factor** by antipsychotic drugs.

Van den Buuse (2003) showed deficient prepulse inhibition of acoustic startle in **Hooded-Wistar** rats compared with Sprague Dawley rats suggesting that the Hooded-Wister line could be a useful genetic animal model to study the interaction of glutaminergic and dopaminergic mechanisms in anxiety and schizophrenia.

REFERENCES AND FURTHER READING

Costa E, Davis J, Pesold C, Tueting P, Guidotti A (2002) The heterozygote reeler mouse as a model for the development of a new generation of antipsychotics. Curr Opin Pharmacol 2:56–62

D'Arcangelo G, Curran T (1998) Reeler: new tales on an old mutant mouse. Bioassays 20:235–244

Dirks A, Groenink L, Westphal KGC, Olivier JDA, Verdouw PM, van der Gugten J, Geyer MA, Olivier B (2003) Reversal of startle gating deficits in transgenic mice overexpressing corticotropin-releasing factor by antipsychotic drugs. Neuropsychopharmacology 28:1790–1798

Fatemi SH (2001) Reelin mutations in mouse and man: from reeler mouse to schizophrenia, mood disorders, autism and lissencephaly. Mol Psychiatry 6:129–133

Larson J, Hoffman JS, Guidotti A, Costa E (2003) Olfactory discrimination learning deficit in heterozygous reeler mice. Brain Res 971:40–46

Lombroso PJ, Goldowitz D (1998) Brain development, VIII: the reeler mouse. Am J Psychiatry 155:1660

Pappas GD, Kriho V, Liu WS, Tremolizzo L, Lugli G, Larson J (2003) Immunocytochemical localization of reelin in the olfactory bulb of the heterozygous reeler mouse. An animal model for schizophrenia. Neurol Res 25:819–830

Podhorna J, Didriksen M (2004) The heterozygous reeler mouse: behavioural phenotype. Behav Brain Res 153:43–54

Rowley M, Bristow LJ, Hutson PH (2001) Current and novel approaches to the drug treatment of schizophrenia. J Med Chem 44:477–501

Tomasiewicz H, Ono K, Yee D, Thompson C, Goridis C, Rutishauser U, Magnuson T (1993) Genetic deletion of a neural cell adhesion molecule variant (N-CAM-180) produces defects in the central nervous system. Neuron 11:1163–1174

Tueting P, Costa E, Dwivedi Y, Guidotti A, Impagnatiello F, Manev R, Pesold C (1999) The phenotypic characterization of heterozygous reeler mouse. Neuroreport 10:1329–1334

van den Buuse M (2003) Deficient prepulse inhibition of acoustic startle in Hooded-Wistar rats compared with Sprague-Dawley rats. Clin Exp Pharmacol Physiol 30:254–61

Wood GK, Tomasiewicz H, Rutishauser U, Magnuson T, Quirion R, Rochford J, Srivasta LK (1998) NCAM-180 knockout mice display increased lateral ventricle size and reduced prepulse inhibition of startle. Neuroreport 16:461–466

E.5.4.2
The Hooded-Wistar Rat

PURPOSE AND RATIONALE

Van den Buuse (2003), Lodge et al. (2003), and Martin et al. (2004) suggested that the Hooded-Wistar line (fawn-hooded rats) could be a useful genetic animal model to study the interaction of glutamatergic and dopaminergic mechanisms in anxiety and schizophrenia.

Broderick (2002) compared hippocampal serotonin and norepinephrine release during open-field behavior in Sprague Dawley animals with the Fawn-Hooded animals model of depression.

REFERENCES AND FURTHER READING

Broderick PA (2002) Interleukin 1α alters hippocampal serotonin and norepinephrine release during open-field behavior in Sprague-Dawley animals: difference from the Fawn-Hooded animals model of depression. Progr Neuropsychopharmacolgy Biol Psychiatry 26:1355–1372

Lodge DJ, Roques BP, Lawrence AJ (2003) Atypical behavioural responses to CCK-B receptor ligands in Fawn-Hooded rats. Life Sci 74:1–12

Martin S, Lawrence AJ, van den Buuse M (2004) Prepulse inhibition in fawn-hooded rats: increased sensitivity to 5-HT_{1A} receptor stimulation. Eur Neuropsychopharmacology 14:373–379

Van den Buuse M (2003) Deficient prepulse inhibition of acoustic startle in Hooded-Wistar rats compared with Sprague-Dawley rats. Clin Exp Pharmacol Physiol 30:254–261

E.6 Antidepressant Activity

E.6.0.1 General Considerations

The first antidepressant drugs were detected by serendipity in clinical trials. Iproniazid was developed for the treatment of tuberculosis. The observation of mood-elevating effects was followed by the detection of the inhibition of the enzyme monoamine oxidase. During clinical investigation of phenothiazine analogs as neuroleptics, imipramine was found to be relatively ineffective in agitated psychotic patients but showed remarkable benefit in depressed patients. Later on, inhibition of uptake of biogenic amines was found to be the main mechanism of action resulting in downregulation of β-receptors (Vetulani et al. 1976). Influence on α_2-adrenoreceptors (Johnson et al. 1980) was discussed as well. Several lines of preclinical and clinical evidence indicate that an enhancement of 5-HT-mediated neurotransmission might underlie the therapeutic effect of most antidepressant treatments (Blier and de Montigny 1994).

Animal models of depression have been reviewed by Porsolt et al. (1991), Panksepp et al. (1991), Willner and Muscat (1991), and Cryan et al. (2002).

REFERENCES AND FURTHER READING

Blier P, de Montigny C (1994) Current advances and trends in the treatment of depression. Trends Pharmacol Sci 15:220–226

Chen G (1964) Antidepressives, analeptics and appetite suppressants. In: Laurence DR, Bacharach AL (eds) Evaluation of Drug Activities: Pharmacometrics. pp 239–260. Academic Press, London and New York

Cryan JF, Markou A, Lucki I (2002) Assessing antidepressant activity in rodents: recent developments and further needs. Trends Pharmacol Sci 23:238–245

Johnson RW, Reisine T, Spotnitz S, Weich N, Ursillo R, Yamamura HI (1980) Effects of desipramine and yohimbine on α_2- and β-adrenoreceptor sensitivity. Eur J Pharmacol 67:123–127

Kuhn R (1958) The treatment of depressive states with G22355 (imipramine hydrochloride) Am J Psychiatry 115:459–464

Panksepp J, Yates G, Ikemoto S, Nelson E (1991) Simple ethological models of depression: Socialisolation induced despair in chicks and mice. In: Olivier B, Mos J, Slangen JL (eds) Animal Models in Psychopharmacology. Advances in Pharmacological Sciences. Birkhäuser Verlag Basel, pp 161–181

Porsolt RD, Lenègre A, McArthur RA (1991) Pharmacological models of depression. In: Olivier B, Mos J, Slangen JL (eds) Animal Models in Psychopharmacology. Advances in Pharmacological Sciences. Birkhäuser Verlag Basel, pp 137–159

Vetulani J, Stawarz RJ, Dingell JV, Sulser F (1976) A possible common mechanism of action of antidepressant treatments: Reduction in the sensitivity of the noradrenergic cyclic AMP generating system in the rat limbic forebrain. Naunyn-Schmiedeberg's Arch. Pharmacol 293:109–114

Willner P, Muscat R (1991) Animals models for investigating the symptoms of depression and the mechanisms of action of anti-depressant drugs. In: Olivier B, Mos J, Slangen JL (eds) Animal Models in Psychopharmacology. Advances in Pharmacological Sciences. Birkhäuser Verlag Basel, pp 183–198

E.6.1 In Vitro Methods

E.6.1.1 Inhibition of [^{3}H]-Norepinephrine Uptake in Rat Brain Synaptosomes

PURPOSE AND RATIONALE

As shown by Hertting and Axelrod (1961) the neuronal re-uptake mechanism for norepinephrine is the most important physiological process for removing and inactivating norepinephrine in the synaptic cleft. This uptake is inhibited by cocaine, certain phenylethylamines and antidepressants. This mechanism is considered as one of the most important modes of action of anti-depressants leading to receptor down-regulation. In the brain, the hypothalamus shows the highest level and greatest uptake of noradrenaline. Therefore, this region is used for testing potential antidepressant drugs.

PROCEDURE

Tissue Preparation

Male Wistar rats are decapitated and the brains rapidly removed. The hypothalamic region is prepared, weighed, and homogenized in 9 volumes of ice-cold 0.32 M sucrose solution using a Potter-Elvejhem homogenizer. The homogenate is centrifuged at 1000 *g* at 0–4°C for 10 min. The supernatant is decanted and used for the uptake experiments.

Assay

200 µl of tissue suspension are incubated with 800 µl 62.5 nM ^{3}H-norepinephrine in Krebs-Henseleit bicarbonate buffer and 20 µl of the appropriate drug concentration (or the vehicle) at 37°C under a 95% O_2/5% CO_2 atmosphere for 5 min. For each assay, 3 tubes are incubated with 20 µl of vehicle at 0°C in an ice bath. After incubation all tubes are immediately centrifuged at 4000 *g* for 10 min. The supernatant fluid is aspirated and the pellets dissolved adding 1 ml of solubilizer (Triton X-100 + 50% ethanol, 1:4). The tubes are vigorously shaken, decanted into scintillation vials, and counted in 10 ml of liquid scintillation cock-

tail. Active uptake is the difference between cpm at 37°C and 0°C.

EVALUATION

The percent inhibition at each drug concentration is the mean of 3 determinations. IC_{50} values are derived from log-probit analysis. IC_{50} values for the standard drugs desipramine and nortriptyline are around 20 nM.

MODIFICATIONS OF THE METHOD

Pacholczyk et al. (1991) described the expression cloning of a cocaine- and antidepressant-sensitive human noradrenaline transporter.

Tejani-Butt (1992) recommended [3H]nisoxetine as radioligand for quantitation of norepinephrine uptake sites.

REFERENCES AND FURTHER READING

Coyle JT, Snyder SH (1969) Catecholamine uptake by synaptosomes in homogenates of rat brain: Stereospecificity in different areas. J Pharmacol Exper Ther 170:221–231

Hertting G, Axelrod J (1961) Fate of tritiated noradrenaline at the sympathetic nerve endings. Nature 192:172–173

Iversen LL (1975) Uptake mechanisms for neurotransmitter amines. Biochem Pharmacol 23:1927–1935

Lippmann W, Pugsley TA (1977) Effects of 3,4-dihydro-1H-1,4-oxazino[4,3-a]indoles, potential antidepressants, on biogenic amine uptake mechanisms and related activities. Arch Int Pharmacodyn 227:324–342

Morin D, Zini R, Urien S, Tillement JP (1989) Pharmacological profile of Binedaline, a new antidepressant drug. J Pharmacol Exp Ther 249:288–296

Pacholczyk T, Blakely RD, Amara SG (1991) Expression cloning of a cocaine- and antidepressant-sensitive human noradrenaline transporter. Nature 350:350–354

Schloss P, Mayser W, Betz H (1992) Neurotransmitter transporters. A novel family of integral plasma membrane proteins. FEBS Lett 307:76–80

Snyder SH, Coyle JT (1969) Regional differences in H^3-norepinephrine and H^3-dopamine uptake into rat brain homogenates. J Pharmacol Exper Ther 165:78–86

Tehani-Butt SM (1992) [^{3}H]Nisoxetine: a radioligand for quantitation of norepinephrine uptake sites by autoradiography or by homogenate binding. J Pharmacol Exp Ther 260:427–436

E.6.1.2 Inhibition of [^{3}H]-Dopamine Uptake in Rat Striatal Synaptosomes

PURPOSE AND RATIONALE

High affinity, saturable, temperature and sodium-dependent transport of ^{3}H-dopamine has been observed in various tissue preparations from different brain regions. The area striata has a high content of dopamine and is suitable for uptake experiments. The ^{3}H-dopamine uptake is inhibited by cocaine, certain phenylethylamines and antidepressants like nomifensine and bupropion, but not by tricyclic antidepressants. The test can be used to characterize the mode of action of antidepressant drugs.

PROCEDURE

Tissue Preparation

Male Wistar rats are decapitated and the brains rapidly removed. Corpora striata are prepared, weighed and homogenized in 9 volumes of ice cold 0.32 M sucrose solution using a Potter-Elvejhem homogenizer. The homogenate is centrifuged at 1000 *g* at 0–4°C for 10 min. The supernatant is decanted and used for the experiments.

Assay

100 µl of tissue suspension are mixed with 900 µl 55.5 nM ^{3}H-dopamine solution in Krebs-Henseleit bicarbonate buffer and 20 µl of drug solution in appropriate concentration (or the vehicle as control). The tubes are incubated at 37°C under a 95% O_2/5% CO_2 atmosphere for 5 min. For each assay, 3 tubes are incubated with 20 µl of vehicle at 0°C in an ice bath. After incubation all tubes are immediately centrifuged at 4000 *g* for 10 min. The supernatant fluid is aspirated and the pellets dissolved by adding 1 ml of solubilizer (Triton X-100 + 50% ethanol, 1:4). The tubes are vigorously shaken, decanted into scintillation vials, and counted in 10 ml liquid scintillation counting cocktail. Active uptake is the difference between cpm at 37°C and 0°C.

EVALUATION

The percent inhibition at each drug concentration is the mean of 3 determinations. IC_{50} values are derived from log-probit analyses. IC_{50} values for nomifensine are 460 nM, but >20,000 nM for tricyclic antidepressants.

MODIFICATIONS OF THE METHOD

Elsworth et al. (1993) differentiated between cocaine-sensitive and -insensitive dopamine uptake in various brain areas.

Cloning and pharmacological characterization of rat, bovine, and human dopamine transporters have been described (Giros et al. 1991; Kilty et al. 1991; Shimada et al. 1991; Usdin et al. 1991; Giros et al. 1992).

Binding characteristics of the dopamine transporter were studied (Reith et al. 1992; Rothman et al. 1992).

[^{3}H]-3β-(*p*-fluorophenyl)tropan-2β-carboxylic acid methyl ester ([^{3}H]WIN 35,428) is used as ligand

for the dopamine transporter (Carroll et al. 1992; Cline et al. 1992).

[^{3}H]GBR12935 (1-[2-(diphenylmethoxy)ethyl]-4-(3-phenylpropyl)piperazine) was used as labelled ligand by Richfield (1991), Nakachi et al. (1995).

Cocaine receptors are specifically labeled with [^{3}H]WIN 35,428 indicating the role of the dopamine transport system in mediating the behavioral effects and the abuse of cocaine (Madras et al. (1989).

Laruelle et al. (1993) reported **single photon emission computed tomography** (SPECT)} imaging of dopamine and serotonin transporters in nonhuman primates.

REFERENCES AND FURTHER READING

Altar CA, Marshall JF (1987) Neostriatal dopamine uptake and reversal of age-related movement disorders with dopamine-uptake inhibitors. Ann NY Acad Sci 515:343–353

Carroll FI, Gao Y, Abraham P, Lewin AH, Lew R, Patel A, Boja JW, Kuhar MJ (1992) Probes for the cocaine receptor. Potentially irreversible ligands for the dopamine transporter. J Med Chem 35:1814–1817

Cline EJ, Scheffel U, Boja JW, Carroll FI, Katz JL, Kuhar MJ (1992) Behavioral effects of novel cocaine analogs: a comparison with *in vivo* receptor binding potency. J Pharmacol Exp Ther 260:1174–1179

Cooper BR, Hester TJ, Maxwell RA (1980) Behavioral and biochemical effects of the antidepressant bupropion (Wellbutrin): Evidence of selective blockade of dopamine uptake *in vivo*. J Pharmacol Exper Ther 215:127–134

Elsworth JD, Taylor JR, Berger P, Roth RH (1993) Cocaine-sensitive and -insensitive dopamine uptake in prefrontal cortex, nucleus accumbens and striatum. Neurochem Int 23:61–69

Giros B, El Mestikawi S, Bertrand L, Caron MG (1991) Cloning and functional characterization of a cocaine-sensitive dopamine transporter. FEBS Lett 295:149–153

Giros B, El Mestikawi S, Godinot N, Zheng K, Han H, Yang-Feng T, Caron MG (1992) Cloning, pharmacological characterization, and chromosome assignment of the human dopamine transporter. Mol Pharmacol 42:383–390

Heikkila RE, Orlansky H, Cohen G (1975) Studies on the distinction between uptake inhibition and release of [^{3}H]dopamine in rat brain slices. Biochem Pharmacol 24:847–852

Horn AS, Coyle JT, Snyder SH (1970) Catecholamine uptake by synaptosomes from rat brain: Structure-activity relationships of drugs with different effects on dopamine and norepinephrine neurons. Mol. Pharmacol 7:66–80

Hunt P, Raynaud J-P, Leven M, Schacht U (1979) Dopamine uptake inhibitors and releasing agents differentiated by the use of synaptosomes and field-stimulated brain slices *in vitro*. Biochem Pharmacol 28:2011–2016

Kilty JE, Lorang D, Amara SG (1991) Cloning and expression of a cocaine-sensitive rat dopamine transporter. Science 254:578–579

Laruelle M, Baldwin RM, Malison RT, Zea-Ponce Y, Zoghbi SS, Al-Tikriti MS, Sybirska EH, Zimmermann RC, Wisniewski G, Neumeyer JL, Milius RA, Wang S, Smith EO, Roth RH, Charney DS, Hoffer PB, Innis RB (1993) SPECT imaging of dopamine and serotonin transporters with [^{123}I]β-CIT: Pharmacological characterization of brain uptake in nonhuman primates. Synapse 13:295–309

Madras BK, Spealman RD, Fahey MA, Neumeyer JL, Saha JK, Milius RA (1989) Cocaine receptors labeled by [^{3}H]2β-carbomethoxy-3β-(4-fluorophenyl)tropane. Mol Pharmacol 36:518–524

Michel MC, Rother A, Hiemke Ch, Ghraf R (1987) Inhibition of synaptosomal high-affinity uptake of dopamine and serotonin by estrogen agonists and antagonists. Biochem Pharmacol 36:3175–3180

Nakachi N, Kiuchi Y, Inagaki M, Inazu M, Yamazaki Y, Oguchi K (1995) Effects of various dopamine uptake inhibitors on striatal extracellular dopamine levels and behaviours in rats. Eur J Pharmacol 281:195–203

Reith MEA, de Costa B, Rice KC, Jacobson AE (1992) Evidence for mutually exclusive binding of cocaine, BTCP, GBR 12935, and dopamine to the dopamine transporter. Eur J Pharmacol 227:417–425

Richfield AK (1991) Quantitative autoradiography of the dopamine uptake complex in rats brain using [^{3}H]GBR 12935-binding characteristics. Brain Res 540:1–13

Rothman RB, Grieg N, Kim A, de Costa BR, Rice KC, Carroll FI, Pert A (1992) Cocaine and GBR 12909 produce equivalent motoric responses at different occupancy of the dopamine transporter. Pharmacol Biochem Behav 43:1135–1142

Saijoh K, Fujiwara H, Tanaka C (1985) Influence of hypoxia on release and uptake of neurotransmitters in guinea pig striatal slices: dopamine and acetylcholine. Japan J Pharmacol 39:529–539

Shimada S, Kitayama S, Lin CL, Patel A, Nanthakumar E, Gregor P, Kuhar M, Uhl G (1991) Cloning and expression of a cocaine-sensitive dopamine transporter complementary DNA. Science 254:576–578

Snyder SH, Coyle JT (1969) Regional differences in H^3-norepinephrine and H^3-dopamine uptake into rat brain homogenates. J Pharmacol Exper Ther 165:78–86

Tuomisto L, Tuomisto J (1974) Dopamine uptake in striatal and hypothalamic synaptosomes: conformational selectivity of the inhibition. Eur J Pharmacol 25:351–361

Usdin RB, Mezey E, Chen C, Brownstein MJ, Hoffman BJ (1991) Cloning of the cocaine-sensitive bovine dopamine transporter. Proc Natl Acad Sci USA 88:11168–11171

E.6.1.3 Inhibition of [^{3}H]-Serotonin Uptake

PURPOSE AND RATIONALE

Selective inhibitors of serotonin uptake (SSRIs) became the most powerful and widely used antidepressants (Pacher et al. 2001; Fray et al. 2006). These include citalopram (D'Amato et al. 1987; Brøsen and Narajo 2001), fluoxetine, sertraline, paroxetine (Pacher et al. 2001), and escitalopram (Sánchez et al. 2003; Murdoch and Keam 2005).

These antidepressants block the reuptake of 5-HT. ^{3}H-5-HT transport in brain has been found to be saturable, sodium- and temperature-dependent, to be inhibited by several agents, such as ouabain, tryptamine analogs, and tricyclic antidepressants. Apparently, the 5-HT uptake can be differentiated from catecholamine uptake. Therefore, the test can be used to detect com-

pounds that inhibit serotonin uptake into rat brain synaptosomes and may be potential antidepressants.

PROCEDURE

Tissue Preparation

Male Wistar rats are decapitated and the brains rapidly removed. Either the whole brain minus cerebellum or the hypothalamus is weighed and homogenized in 9 volumes of ice-cold 0.32 M sucrose solution using a Potter-Elvejhem homogenizer. The homogenate is centrifuged at 1000 *g* at 0–4°C for 10 min. The supernatant is decanted and used for further uptake experiments.

Assay

Two hundred µl of tissue suspension are mixed with 800 µl 62.5 nM ^{3}H-5-HT solution in Krebs-Henseleit bicarbonate buffer and 20 µl of drug solution in the appropriate concentration (or the vehicle as control). The tubes are incubated at 37°C under 95% O_2/5% CO_2 atmosphere for 5 min. For each assay, 3 tubes are incubated with 20 µl of the vehicle at 0°C in an ice bath. After incubation all tubes are immediately centrifuged at 4000 *g* for 10 min. The supernatant is aspirated and the pellets are dissolved by adding 1 ml of solubilizer (Triton X100+50% ethanol, 1+4). The tubes are vigorously shaken, decanted into scintillation vials, and counted in 10 ml of liquid scintillation counting cocktail. Active uptake is the difference between cpm at 37°C and 0°C.

EVALUATION

The percent inhibition of each drug concentration is the mean of 3 determinations. IC_{50} values are calculated from log-probit analyses. Standard drugs, such as chlorimipramine show IC_{50} values in the order of 10 nM for ^{3}H-5-HT uptake in rat synaptosomes from hypothalamus.

MODIFICATIONS OF THE METHOD

Similar methods were used by D'Amato et al. (1987), Weinshank et al. (1992), Cheng et al. (1993), Hatanaka et al. (1996), and Tordera et al. (2002).

Sánchez et al. (2003) and Chen et al. (2005) studied [^{3}H]-5-HT uptake inhibition in a COS-1 cell line stably transfected with h5-HTT.

Hallstrom et al. (1976) studied the platelet uptake of 5-hydroxytryptamine and dopamine in patients with depression.

Cloning of functional serotonin transporters has been described by Blakely et al. (1991) and by Hoffman et al. (1991).The role of serotonin in the mode of action of antidepressant drugs has been discussed by Hyttel and Larsen (1985), Åsberg and Mårtensson (1993), Hyttel (1994), Blier and de Montigny (1997), Keane and Soubrié (1997).

REFERENCES AND FURTHER READING

Åsberg M, Mårtensson B (1993) Serotonin selective antidepressant drugs: Past, present, future. Clin Neuropharmacol 16 (Suppl 3):S32–S44

Åsberg M, Thoren P, Traskman L, Bertillson L, Ringberger V (1975) "Serotonin depression" – A biochemical subgroup within the affective disorders. Science 191:478–480

Biegon A, Mathis C (1993) Evaluation of [^{3}H]paroxetine as an *in vivo* ligand for serotonin uptake sites: a quantitative autoradiographic study in the rat brain. Synapse 13:1–9

Blakely RD, Berson HE, Fremeau RT, Caron MG, Peek MM, Prince HK, Bradley CC (1991) Cloning and expression of a functional serotonin transporter from rat brain. Nature 354:66–70

Blier P, de Montigny C (1997) Current psychiatric uses of drugs acting on the serotonin system. In: Baumgarten HG, Göthert M (eds) Handbook of Experimental Pharmacology, Vol 129, Serotoninergic Neurons and 5-HT receptors in the CNS. Springer-Verlag Berlin Heidelberg, pp 727–750

Brøsen K, Narajo CA (2001) Review of pharmacokinetic and pharmacodynamic interaction studies with citalopram. Eur Neuropsychopharmacol 11:275–283

Chen F, Larsen MB, Sánchez C, Wiborg O (2005) The *S*-enatiomer of *R,S*-citalopram, increases inhibitor binding to the human serotonin transporter by an allosteric mechanism. Comparison with other serotonin transporter inhibitors. Eur Neuropsychopharmacol 15:193–198

Cheng CHK, Costall B, Naylor RJ, Rudd JA (1993) The effect of 5-HT receptor ligands on the uptake of [^{3}H]-5-HT into rat cortical synaptosomes. Eur J Pharmacol 239:211–214

D'Amato RJ, Largent BL, Snowman AM, Snyder SH (1987) Selective labeling of serotonin uptake sites in rat brain by [^{3}H]citalopram contrasted to labeling of multiple sites by [^{3}H]imipramine. J Pharmacol Exp Ther 242:364–371

de Montigy C (1980) Enhancement of 5-HT neurotransmission by antidepressant treatment. J Physiol (Paris) 77:455–461

Fray MJ, Bish G, Brown AD, Fish PV, Stobie A, Wakenhut F, Whitlok GA (2006) *N*-(1,2-Diphenylethyl)piperazines: a new class of dual serotonin/noradrenaline reuptake inhibitor. Bioorg Med Chem 16:4345–4348

Fuller RW (1990) Drugs affecting serotonin neurones. Progr Drug Res 35:85–108

Fuller RW (1993) Biogenic amine transporters Neurotransmissions 9/2:1–4

Fuller RW, Wong DT (1990) Serotonin uptake and serotonin uptake inhibition. Ann NY Acad Sci 600:68–80

Gershon MD, Miller Jonakait G (1979) Uptake and release of 5-hydroxytryptamine by enteric 5-hydroxytryptaminergic neurons: Effects of fluoxetine (Lilly 110140) and chlorimipramine. Br J Pharmacol 66:7–9

Grimsley SR, Jahn MW (1992) Paroxetine, sertaline, and fluvoxamine: new selective serotonin reuptake inhibitors. Clin Pharm 11:930–957

Hallstrom COS, Rees WL, Pare CMB, Trenchard A, Turner P (1976) Platelet uptake of 5-hydroxytryptamine and dopamine in depression. Postgrad Med J 52 (Suppl 3): 40–44

Hatanaka K, Nomura T, Hidaka K, Takeuchi H, Yatsugi S, Fujii M, Yamaguchi T (1996) Biochemical profile of YM992, a novel selective serotonin reuptake inhibitor with 5-HT_{2A} receptor antagonistic activity. Neuropharmacology 35:1621–1626

Hoffman BJ, Mezey E, Brownstein MJ (1991) Cloning of a serotonin transporter affected by antidepressants. Science 254:579–580

Horn AS (1973) Structure-activity relations for the inhibition of 5-HT uptake into rat hypothalamic homogenates by serotonin and tryptamine analogues, J Neurochem 21:883–888

Horn AS, Trace RCAM (1974) Structure-activity relations for the inhibition of 5-hydroxytryptamine uptake by tricyclic anti-depressants into synaptosomes from serotoninergic neurons in rat brain homogenates. Br J Pharmacol 51:399–403

Hyttel J (1994) Pharmacological characterization of selective serotonin reuptake inhibitors. Intern Clin Psychopharmacol 9 (Suppl 1):19–26

Hyttel J, Larsen JJ (1985) Serotonin-selective antidepressants. Acta Pharmacol Toxicol 56 (Suppl 1):146–153

Keane PE, Soubrié P (1997) Animal models of integrated serotoninergic functions: their predictive value for the clinical applicability of drugs interfering with serotoninergic transmission. In: Baumgarten HG, Göthert M (eds) Handbook of Experimental Pharmacology, Vol 129, Serotoninergic Neurons and 5-HT receptors in the CNS. Springer-Verlag Berlin Heidelberg, pp 709–725

Koe BK, Weissman A, Welch WM, Browne RG (1983) Sertaline, 1S,4S-N-methyl-4-(3,4-dichlorophenyl)-1,2,3,4-tetrahydro-1-naphthylamine, a new uptake inhibitor with selectivity for serotonin. J Pharmacol Exp Ther 226:686–700

Langer SZ, Moret C, Raisman R, Dubocovich ML, Briley M (1980) High-affinity [3H]imipramine binding in rat hypothalamus: association with uptake of serotonin but not of epinephrine. Science 210:1133–1135

Luo H, Richardson JS (1993) A pharmacological comparison of citalopram, a bicyclic serotonin selective uptake inhibitor, with traditional tricyclic antidepressants. Intern Clin Psychopharmacol 8:3–12

Marcusson JO, Norinder U, Högberg T, Ross SB (1992) Inhibition of [^{3}H]paroxetine binding by various serotonin uptake inhibitors: Eur J Pharmacol 215:191–198

Mennini T, Mocaer E, Garattini S (1987) Tianeptine, a selective enhancer of serotonin uptake in rat brain. Naunyn-Schmiedeberg's Arch Pharmacol 336:478–482

Murdoch D, Keam SJ (2005) Escitalopram. A review of its use in the management of major depressive disorder. Drugs 65:2379–2404

Ögren SO, Ross SB, Holm AC, Renyi AL (1981) The pharmacology of zimelidine: a 5-HT selective reuptake inhibitor. Acta Psychiat Scand 290:127–151

Pacher P, Kohegyi E, Kecskemeti V, Furst S (2001) Current trends in the development of new antidepressants. Curr Med Chem 8:89–100

Ross SB (1980) Neuronal transport of 5-hydroxytryptamine. Pharmacol 21:123–131

Sánchez C, Bergqvist PBF, Brennum LT, Gupta S, Hogg S, Larsen A, Wiborg O (2003) Escitalopram, the *S*-(+)-enantiomer of citalopram, is a selective serotonin reuptake inhibitor with potent effects in anima models predictive of antidepressant and anxiolytic activities. Psychopharmacology 167:353–362

Scatton B, Claustre Y, Graham D, Dennis T, Serrano A, Arbilla S, Pimoule C, Schoemaker H, Bigg D, Langer SZ (1988) SL 81.0385: a novel selective and potent serotonin uptake inhibitor. Drug Dev Res 12:29–40

Shank RP, Vaught JL, Pelley A, Setler PE, McComsey DF, Maryanoff BE (1988) McN-5652: a highly potent inhibitor of serotonin uptake. J Pharmacol Exp Ther 247:1032–1038

Shaskan EG, Snyder SH (1970) Kinetics of serotonin accumulation into slices from rat brain: relationship to catecholamine uptake. J Pharmacol Exp Ther 175:404–418

Tordera RM, Monge A, del Rio J, Lasheras B (2002) Antidepressant-like activity of VN2222. a serotonin reuptake inhibitor with high affinity at 5-HT_{1A} receptors. Eur J Pharmacol 442:63–71

Weinshank RL, Zgombick JM, Macchi MJ, Branchek TA, Hartig PR (1992) Human serotonin 1D receptor is encoded by a subfamily of two distinct genes: 5-$HT_{1D\alpha}$ and 5-$HT_{1D\beta}$. Proc Natl Acad Sci USA 89:3630–3634

Wong DT, Bymaster FP, Reid LR, Mayle DA, Krushiski JH, Robertson DW (1993) Norfluoxetine enantiomers as inhibitors of serotonin uptake in rat brain. Neuropsychopharmacology 8:337–344

E.6.1.4 Binding to Monoamine Transporters

PURPOSE AND RATIONALE

There is substantial clinical and experimental evidence that lesions in the serotonergic and noradrenergic systems are responsible for depression and that antidepressant treatment can reverse these alterations (Leonard 2000). Monoamine transporters are principle targets of widely used therapeutic drugs including antidepressants, psychostimulants and the addictive drug cocaine (Madras et al. 1996; Fleckenstein et al. 1999). The termination of neurotransmission is achieved by rapid uptake of the released neurotransmitter by high-affinity neurotransmitter transporters. Most of these transporters are encoded by a family of genes (Na^+/Cl^- transporters) having a similar membrane topography of 12 transmembrane helices. An evolutionary tree revealed five distinct subfamilies: GABA-transporters, monoamine transporters, amino acid transporters, "orphan" transporters and bacterial transporters (Nelson 1998).

Tatsumi et al. (1997) described the pharmacological profile of antidepressants at human monoamine transporters.

PROCEDURE

Expression of Human Transporters

The human serotonin transporter cDNA is directionally ligated into the expression vector pRc/CMV and transfected into HEK293 (human embryonic kidney) cells by the Ca^{2+} method. The human dopamine transporter cDNA is directionally ligated into the expression vector pcDNA3 and transfected into HEK293 cells, also by the Ca^{2+} method.

Cell Culture

The cell lines are grown, passaged, and harvested in 150 mm Petri dishes with 17.5 ml of Dulbecco's modified Eagle's medium containing 0.1 mM nonessential amino acid solution, 5% fetal clonebovine serum product and 1 U/µl penicillin and streptomycin solution. They are incubated in 10% CO_2, 90% air at 37°C and 100% humidity. The selecting antibiotic geneticin sulfate (250 µg/ml) is used continuously for culture of cells expressing the norepinephrine transporter.

Membrane Preparations

For the preparation of the homogenates, the medium is removed by aspiration. The cells are washed with 4 l modified Puck's D1 solution (solution 1) (Pfenning and Richelson 1990) and then incubated for 5 min at 37°C in 10 ml solution 1 and 100 mM EGTA. Afterwards cells are removed from the surface by scraping with a rubber spatula, placed in a centrifuge tube, and collected by centrifugation at 110 *g* for 5 min at 4°C. The supernatants are decanted. The pellets are resuspended in the respective binding assay buffer by use of a Polytron (Brinkman Instruments, Westbury, NY) for 10 s at setting 6. The mixture is then centrifuged at 35,600 *g* for 10 min at 4°C. The pellets are suspended in the same volume of the respective buffer and the centrifugation is repeated. The supernatants are decanted and the final pellets are suspended in the respective buffer and stored at –80°C until assayed. The final protein concentration is determined by the Lowry assay using bovine serum albumin as standard.

Radioligand Binding Assays

[^{3}H] imipramine Binding to Human Serotonin Transporter. Radioligand binding assays are performed by a modification of the method of O'Riordan et al. (1990) with a binding buffer containing 50 mM Tris, 120 mM NaCl, and 5 mM KCl (pH 7.4). Compounds to be tested are dissolved in 5 mM HCl and run in duplicate over at least 11 different concentrations against 1 nM [^{3}H]imipramine (specific activity 46.5 Ci/mmol) with 15 µg/tube membrane protein for 30 min at 22°C. Nonspecific binding is determined in the presence of 1 µM imipramine. With the use of a 48-well Brandel cell harvester, the assay is terminated by rapid filtration through a GF/B filter presoaked with 0.2% polyethylenimine. The filter strips are rinsed five times with ice-cold 0.9% NaCl. Finally, each filter is placed in a scintillation vial containing 6.5 ml of Redi-Safe (Beckman Instruments, Fullerton, CA) and counted in a liquid scintillation counter.

[^{3}H] Nisoxetine Binding to Human Norepinephrine Transporter. Radioligand binding assays are performed by a modification of the method of Jayanthi et al. (1993) in binding buffer containing 50 mM Tris, 300 mM NaCl and 5 mM KCl (pH 7.4). [^{3}H]nisoxetine (specific activity 85.0 Ci/mmol, from Amersham, Arlington Hts., IL) at 0.5 nM is incubated with competing drugs and 25 µg/tube membrane protein for 60 min at 22°C. Nonspecific binding is determined in the presence of 1 µM nisoxetine. The remainder of the assay is exactly as described above.

[^{3}H] WIN35428 Binding to Human Dopamine Transporter. Radioligand binding assays are performed using a modification of the method of Pristupa et al. (1994) in a binding buffer containing 50 mM Tris and 120 mM NaCl (pH 7.4). [^{3}H]WIN35428 (Dupont New England Nuclear, Boston MA, specific activity 83.5 Ci/mmol) at 1 nM is incubated with competing drugs and 30 µg/tube membrane protein for 120 min at 4°C. Nonspecific binding is determined in the presence of 10 µM WIN35428. The remainder of the assay is exactly as described above.

EVALUATION

The data are analyzed using the LIGAND program (Munson and Rodbard 1980) for calculation of K_D values and Hill coefficients.

MODIFICATIONS OF THE METHOD

Using the same methods, Tatsumi et al. (1999) described the pharmacological profile of several neuroleptics at human monoamine transporters.

Gu et al. (1994) constructed stable cell lines expressing transporters for dopamine, norepinephrine and serotonin using parental LLC-PK_1 cells which do not express any of these neurotransmitter transporters.

Meltzer et al. (1997) described inhibitors of monoamine transporters using dopamine- and serotonin-transporter assays. Membranes were prepared from coronal slices from caudate-putamen of brain from adult cynomolgus monkeys.

Owens et al. (1997) measured the affinity of several antidepressants and their metabolites for the rat and human serotonin and norepinephrine transporters.

Inazu et al. (1999) characterized dopamine transport in cultured rat astrocytes.

Siebert et al. (2000) used rat neuronal cultures and transfected COS-7 cells to characterize the interaction of haloperidol metabolites with neurotransmitter transporters.

Sato et al. (2000) studied the selective inhibition of monoamine neurotransmitter transporters by synthetic local anesthetics using cloned transporter cDNAs with transient functional expression in COS cells and stable expression in HeLa cells.

REFERENCES AND FURTHER READING

Fleckenstein AE, Haughey HM, Metzger RR, Kokoshka JM, Riddle EL, Hanson JE, Gibb JW, Hanson GR (1999) Differential effects of psychostimulants and related agents on dopaminergic and serotonergic transporter function. Eur J Pharmacol 382:45–49

Gu H, Wall SC, Rudnick G (1994) Stable expression of biogenic amine transporters reveals differences in inhibitor sensitivity, kinetics and ion dependence. J Biol Chem 269:7124–7130

Inazu M, Kubota N, Takeda H, Zhang J, Kiuchi Y, Oguchi K, Matsumiya T (1999) Pharmacological characterization of dopamine transport in cultured rat astrocytes. Life Sci 664:2239–2245

Jayanthi LD, Prasad PD, Ramamoorthy S, Mahesh VB, Leibach FH, Ganapahy V (1993) Sodium- and chloride-dependent, cocaine-sensitive, high-affinity binding of nisoxetine to the human placenta norepinephrine transporter. Biochemistry 32:12178–12185

Leonard BE (2000) Evidence for a biochemical lesion in depression. J Clin Psychiatry 61, Suppl 6:12–17

Madras BK, Pristupa ZB, Nizmik HB, Liang AY, Blundell P, Gonzalez MD, Meltzer PC (1996) Nitrogen-based drugs are not essential for blockade of monoamine transporters. Synapse 24:340–348

Meltzer PC, Liang AY, Blundell P, Gonzalez MD, Chen Z, George C, Madras BK (1997) 2-carbomethoxy-3-aryl-8-oxabicyclo[3.2.1]octanes: potent non-nitrogen inhibitors of monoamine transporters. J Med Chem 40:2661–2673

Munson PJ, Rodbard D (1980) LIGAND: A versatile computerized approach for characterization of ligand-binding systems. Analyt Biochem 107:220–239

Murphy DL, Wichems C, Li Q, Heils A (1999) Molecular manipulations as tools for enhancing our understanding of 5-HT neurotransmission. Trends Pharmacol Sci 20:246–252

Nelson N (1998) The family of Na^+/Cl^- neurotransmitter transporters. J Neurochem 71:1785–1803

O'Riordan C, Phillips OM, Williams DC (1990) Two affinity states for [^{3}H]imipramine binding to the human platelet 5-hydroxytryptamine carrier: an explanation for the allosteric interaction between hydroxytryptamine and imipramine. J Neurochem 54:1275–1280

Owens MJ, Morgan WN, Plott SJ, Nemeroff CB (1997) Neurotransmitter receptor and transporter binding profile of antidepressants and their metabolites. J Pharmacol Exp Ther 283:1305–1322

Pfenning MA, Richelson E (1990) Methods for studying receptors with cultured cells of nervous tissue origin. In: Yamamura HI, Enna SJ, Kuhar MJ (eds) Methods in Neurotransmitter Receptor Analysis. Raven Press, New York, pp 147–175

Pristupa ZB, Wilson JM, Hoffman BJ, Kish SJ, Niznik HB (1994) Pharmacological heterogeneity of the cloned an native human dopamine transporter: dissociation of [^{3}H]WIN 35,428 and [3H]GBR 12,935 binding. Mol Pharmacol 45:125–135

Sato T, Kitayama S, Mitsuhata C, Ikeda T, Morita K, Dohi T (2000) Selective inhibition of monoamine neurotransmitter transporters by synthetic local anesthetics. Naunyn-Schmiedeberg's Arch Pharmacol 361:214–220

Siebert GA, Pond SM, Bryan-Lluka LJ (2000) Further characterisation of the interaction of haloperidol metabolites with neurotransmitter transporters in rat neuronal cultures and in transfected COS-7 cells. Naunyn-Schmiedeberg's Arch Pharmacol 361:255–264

Tatsumi M, Groshan K, Blakely RD, Richelson E (1997) Pharmacological profile of antidepressants and related compounds at human monoamine transporters. Eur J Pharmacol 340:249–258

Tatsumi M, Jansen K, Blakely RD, Richelson E (1999) Pharmacological profile of neuroleptics at human monoamine transporters. Eur J Pharmacol 368:277–283

E.6.1.5 Antagonism of p-Chloramphetamine Toxicity by Inhibitors of Serotonin Uptake

PURPOSE AND RATIONALE

p-Chloramphetamine causes selective toxicity to serotonin neurons. At 10 mg/kg i.p. p-chloramphetamine (p-CA) causes long-term decreases in 5-HT, 5HIAA, [^{3}H]-5-HT-uptake and tryptophan hydroxylase. After acute administration of p-CA, serotonin uptake into synaptosomes isolated from whole brain is reduced for several hours and returns to control values between 1 and 2 days, after which there is a marked long-lasting decrease due to toxic destruction of 5-HT neurones. The initial behavioral effects of p-CA are due to release of dopamine and serotonin. The serotonergic toxicity of p-CA requires active transport into 5-HT neurones where a cytotoxic intermediate compound is formed. Therefore, compounds which block 5-HT uptake will prevent this toxicity. Antagonism of the long-term p-CA induced reduction of synaptosomal ^{3}H-5-HT *in vitro* uptake is a highly useful index of a compound's ability to inhibit 5-HT re-uptake *in vivo*.

PROCEDURE

Reagents

Two mg/ml dextrose and 0.30 mg/ml iproniazid phosphate are added to Krebs-Henseleit bicarbonate buffer. The mixture is aerated for 1 h with carbogen.

Serotonin creatinine sulfate (Sigma Chemical Co) as a 0.1 mM stock solution in 0.01 N HCl is used to dilute the specific activity of the radiolabeled 5-HT.

A solution of 62.5 nM ^{3}H-5-HT (5-[1,2-^{3}H(N)]-hydroxytryptamine creatinine sulfate, specific activity 20–30 Ci/mmol, New England Nuclear) is prepared in Krebs-Henseleit bicarbonate buffer.

(d,l)-p-Chloramphetamine (Regis Chemical Co) is dissolved in 0.9% NaCl at a concentration of 10 mg/ml.

Drug Treatment

Groups of 8 male Wistar rats, weighing 150–200 g are injected intraperitoneally with saline or molar equivalent doses of the test drug. For initial studies, the dose given is 37,5 µmol/kg (equivalent to 10 mg/kg desipramine base). After 30 min, 4 rats from each group are injected with saline or with p-CA 10 mg/kg i.p. Three days after treatment, the rats are sacrificed. For multiple dosing, the rats are pretreated with the test drug twice up to 4 times in 2 h intervals.

Tissue Preparation

The rats are decapitated and the brains rapidly removed. Whole brain minus cerebellum is weighed and homogenized in 9 volumes of ice-cold 0.32 M sucrose using a Potter-Elvejhem homogenizer. The homogenate is centrifuged at 1000 *g* at 0–4°C for 10 min. The crude synaptosomal supernatant is decanted and used for uptake experiments.

Assay

800 µl Krebs-Henseleit bicarbonate buffer+[^{3}H]-5-HT

200 µl Tissue suspension

Tubes are incubated at 37°C under a 95% O_2/5% CO_2 atmosphere for 5 min. For each assay, 3 tubes are incubated at 0°C in an ice bath. After incubation all tubes are immediately centrifuged at 4000 *g* at 0–4°C for 10 min. The supernatant fluid is aspirated and the pellets dissolved by adding 1 ml of solubilizer (Triton X-100 and 50% ethanol, 1:4, v/v). The tubes are vigorously vortexed, decanted into scintillation vials, and counted in 10 ml of aqueous (Liquiscint) scintillation counting cocktail. Active uptake is the difference between cpm at 37°C and 0°C.

EVALUATION

The percent protection is calculated according to the following formula:

$$\%\ \text{protection} = \frac{\text{cpm}[(\text{sal/sal}) - (\text{sal/pCA})]}{\text{cpm}[(\text{sal/sal}) - (\text{sal/pCA})]} - \frac{\text{cpm}[(\text{sal/sal}) - (\text{drug/pCA})]}{\text{cpm}[(\text{sal/sal}) - (\text{sal/pCA})]}$$

REFERENCES AND FURTHER READING

Fuller RW, Snoddy HD, Perry KW, Bymaster FP, Wong DT (1978) Importance of duration of drug action in the antagonism of *p*-chloroamphetamine depletion of brain serotonin – Comparison of fluoxetine and chlorimipramine. Biochem Pharmacol 27:193–198

Harvey JA, McMaster SE, Yunger LM (1975) p-Chloramphetamine: Selective neurotoxic action in brain. Science 187:841–843

Meek JL, Fuxe K, Carlsson A (1971) Blockade of p-chloromethamphetamine induced 5-hydroxytryptamine depletion by chlorimipramine, chlorpheniramine and meperidine. Biochem Pharmacol 20:707–709

Sekerke HJ, Smith HE, Bushing JA, Sanders-Busch E (1975) Correlation between brain levels and biochemical effects of the optical isomers of *p*-chloroamphetamine. J Pharmacol Exper Ther 193:835–844

Squires R (1972) Antagonism of p-chloramphetamine (PCA) induced depletion of 5-HT from rat brain by some thymoleptics and other psychotropic drugs. Acta Pharmacol Toxicol 31:35

E.6.1.6 Receptor Subsensitivity After Treatment with Antidepressants: Simultaneous Determination of the Effect of Chronic Anti-Depressant Treatment on β-Adrenergic and 5-HT_2 Receptor Densities in Rat Cerebral Cortex

PURPOSE AND RATIONALE

The catecholamine and indolamine systems are thought to be involved in affective disorders such as depression. The effect of antidepressants on biogenic amine re-uptake *in vitro* is immediate; whereas the onset of clinical activity is delayed and parallels more closely the time course of receptor changes measured in animal studies. Therefore, the experiment is designed to determine the *in vivo* effects of chronic (10 days) treatment with known and potential antidepressants on the β-receptor, as a measurement of noradrenergic interaction, and on the 5-HT_2 receptor as a measurement of serotoninergic interaction in the rat brain. Both receptor densities are measured in cortical tissue from the same animal and compared after treatment with test compounds at doses similar to those of standard drugs.

PROCEDURE

Drug Treatment

Groups of 4 male Wistar rats, receiving food and water at libitum are maintained on a 12-h diurnal light cycle and given i.p. injections twice daily for 10 days with saline or molar equivalent doses of the experimental drugs (equivalent to 10 mg/kg imipramine). Twenty-four hours after the last dose, the rats are decapitated and the cerebral cortices split along the mid-sagittal sinuses. One half is used for the (^{3}H)-DAH assay and the other half is used for the (^{3}H)-spiroperidol assay. This protocol allows the determination of effects of antidepressants on β-receptors and 5-HT_2-receptors in cerebral cortical tissue from the same animal.

Reagents

- (–)-[propyl-1,2,3-^{3}H]Dihydroalprenololol hydrochloride (45–52 Ci/mmol) is obtained from New England Nuclear.
- (±)-propranolol HCl is obtained from Ayerst.
- [Benzene-^{3}H]spiroperidol (20–35 Ci/mmol) is obtained from New England Nuclear.

Tissue Preparation

^{3}H-Dihydroalprenolol (^{3}H-DHA) Binding. The cerebral cortices are dissected free, weighed and homogenized in 50 vol of ice-cold 0.05 M Tris buffer, pH 8.0. This homogenate is centrifuged at 40,000 *g* and the supernatant decanted. The pellet is resuspended and again centrifuged at 40,000 *g*. The final pellet is resuspended in 0.05 M Tris buffer, pH 8.0. This tissue suspension is then stored on ice until use. The final tissue concentration is 10 mg/ml.

^{3}H-Spiroperidol Binding. The cerebral cortices are dissected, weighed and homogenized in 50 vol of 0.05 M Tris buffer, pH 7.7, and then centrifuged at 40000*g* for 15 min. The supernatant is discarded, the pellet resuspended and again centrifuged at 40,000 *g*. The final pellet is resuspended in 50 vol of 0.05 M Tris buffer, pH 7.7 and stored in an ice bath. The final concentration in the assay is 10 mg/ml.

Assay

^{3}H-DAH Binding

380 µl	H_2O
50 µl	0.5 M Tris buffer pH 8.0
20 µl	vehicle (for total binding) or 50 µM propranolol (for nonspecific binding)
50 µl	^{3}H-DAH stock solution
500 µl	tissue suspension

The tissue homogenates are incubated for 15 min at 25°C with varying concentrations of ^{3}H-DHA (0.25–4.0 nM). With each ligand concentration triplicate samples are incubated with 1 µM propranolol under identical conditions to determine nonspecific binding. The total added ligand is determined by counting 50 µl of each (^{3}H)-DHA concentration. The assay is stopped by vacuum filtration through Whatman GF/B filters which are washed 3 times with 5 ml of ice cold 0.05 M Tris buffer, pH 8.0. The filters are counted in 10 ml liquid scintillation cocktail.

^{3}H-Spiroperidol Binding

50 µl	0.5 M Tris-physiological salts
380 µl	H_2O
20 µl	H_2O (for total binding) or 0.25 mM methysergide (for nonspecific binding)
50 µl	^{3}H-spiroperidol stock solution
500 µl	tissue suspension

The tissue homogenates are incubated for 10 min at 37°C with varying concentrations of ^{3}H-spiroperidol (0.1–3.0 nM). With each ligand concentration, triplicate samples are incubated in the presence of 5 µM methysergide under identical conditions to determine nonspecific binding. The total added ligand is determined by counting 50 µl of each (^{3}H)-spiroperidol concentration. The assay is stopped by vacuum filtration through Whatman GF/B filters which are washed 3 times with 5 ml of ice cold 0.05 M Tris buffer, pH 7.7. The filters are transferred to scintillation vials and counted in 10 ml of liquid scintillation cocktail.

EVALUATION

Specific binding is defined as the difference in CPM in the presence or absence of excess "cold" ligand. The free ligand concentration is the difference between the total added and the specifically bound fraction at each concentration. The equilibrium binding constants (K_d and B_{max}) are determined by Scatchard analyses using least square regression analysis of the binding data. The Scatchard plot shows "bound/free" versus "bound". The K_d value is the reciprocal of the slope and B_{max} is the x-intercept. Significant differences of drug treatment are determined by either Dunnett's or Tukey's test after one way analysis of variance.

MODOFICATIONS OF THE METHOD

Buckett et al. (1988) found a rapid down-regulation of β-adrenoceptors in brains of rats after 3 days of oral treatment with sibutramine.

REFERENCES AND FURTHER READING

Banerjee SP, Kung SL, Riggi SJ, Chanda SK (1977) Development of β-adrenergic receptor subsensitivity by antidepressants. Nature 268:455–456

Bergstrom DA, Kellar KJ (1979) Adrenergic and serotoninergic receptor binding in rat brain after chronic desmethylimipramine treatment. J Pharmacol Exper Ther 209:256–261

Blackshear MA, Sanders-Bush E (1982) Serotonin receptor sensitivity after acute and chronic treatment with mianserin. J Pharmacol Exper Ther 221:303–308

Bucket WR, Thomas PC, Luscombe GP (1988) The pharmacology of sibutramine hydrochloride (BTS 54524), a new anti-depressant which induces rapid noradrenergic down-

regulation. Prog Neuro-Psychopharmacol Biol Psychiatry 12:575–584
Bylund DB, Snyder SH (1976) Beta adrenergic receptor binding in membrane preparations from mammalian brain. Mol Pharmacol 12:568–580
Charney DS, Menkes DB, Heninger GR (1981) Receptor sensitivity and the mechanism of action of antidepressant treatment. Arch Gen Psychiatry 38:1160–1180
Clements-Jewery S (1978) The development of cortical β-adrenoreceptor subsensitivity in the rat by chronic treatment with trazodone, doxepin and mianserin. Neuropharmacol 17:779–781
Enna SJ, Mann E, Kedall D, Stancel GM (1981) Effect of chronic antidepressant administration on brain neurotransmitter receptor binding. In: Enna SJ, Malick JB, Richelson E (eds) Antidepressants: Neurochemical, Behavioral, and Clinical Perspectives. pp 91–105, Raven Press New York
Lee T, Tang SW (1984) Loxapine and clozapine decrease serotonin (S_2) but do not elevate dopamine (D_2) receptor numbers in the rat brain. Psychiatry Res 12:277–285
Leysen JE, Niemegeers CJE, Van Nueten JM, Laduron PM (1982) [^{3}H]Ketanserin (R 41 468) a selective ^{3}H-ligand for serotonin$_2$ receptor binding sites. Mol Pharmacol 21:301–214
Maggi A, U'Prichard DC, Enna SJ (1980) Differential effects of antidepressant treatment on brain monoaminergic receptors. Eur J Pharmacol 61:91–98
Matsubara R, Matsubara S, Koyama T, Muraki A, Yamashita I (1993) Effect of chronic treatment with milnacipran (TN-912), a novel antidepressant, on β-adrenergic-receptor-adenylate cyclase system and serotonin$_2$ receptor in the rat cerebral cortex. Jpn J Neuropsychopharmacol 15:119–126
Meyerson LR, Ong HH, Martin LL, Ellis DB (1980) Effect of antidepressant agents on β-adrenergic receptor and neurotransmitter regulatory systems. Pharmacol Biochem Behav 12:943–948
Peroutka SJ, Snyder SH (1980) Regulation of serotonin$_2$ (5-HT_2) receptors labeled with [^{3}H]spiroperidol by chronic treatment with the antidepressant amitriptyline. J Pharmacol Exper Ther 215:582–587
Reynolds CP, Garrett NJ, Rupniak N, Jenner P, Marsden CD (1983) Chronic clozapine treatment of rats down-regulates 5-HT_2 receptors. Eur J Pharmacol 89:325–326
Savage DD, Frazer A, Mendels J (1979) Differential effects of monoamine oxidase inhibitors and serotonin reuptake inhibitors on ^{3}H-serotonin receptor binding in rat brain. Eur J Pharmacol 58:87–88
Scatchard G (1949) The attraction of proteins for small molecules and ions. Ann NY Acad Sci 51:660–672
Schmidt CJ, Black CK, Taylor VL, Fadayel GM, Humphreys TM, Nieduzak TR, Sorensen SM (1992) The 5-HT_2 receptor antagonist, MDL 28,133A, disrupts the serotonergic-dopaminergic interaction mediating the neurochemical effects of 3,4-methylenedioxymethamphetamine. Eur J Pharmacol 220:151–159
Scott JA, Crews FT (1983) Rapid decrease in rat brain beta adrenergic receptor binding during combined antidepressant alpha-2 antagonist treatment. J Pharmacol Exp Ther 224:640–646
Segawa T, Mizuta T, Nomura Y (1979) Modifications of central 5-hydroxytryptamine binding sites in synaptic membranes from rat brain after long-term administration of tricyclic antidepressants. Eur J Pharmacol 58:75–83
Sellinger-Barnette MM, Mendels J, Frazer A (1980) The effect of psychoactive drugs on beta-adrenergic receptor binding in rat brain. Neuropharmacol 19:447–454
Vetulani J, Stawarz RJ, Dingell JV, Sulser F (1976) A possible common mechanism of action of antidepressant treatments: Reduction in the sensitivity of the noradrenergic cyclic AMP generating system in the rat limbic forebrain. Naunyn-Schmiedeberg's Arch Pharmacol 293:109–114
Wilmot CA, Szczepanik AM (1989) Effects of acute and chronic treatment with clozapine and haloperidol on serotonin (5-HT_2) and dopamine (D_2) receptors in the rat brain. Brain Res 487:288–298

E.6.1.7 Measurement of β-Adrenoreceptor Stimulated Adenylate Cyclase

PURPOSE AND RATIONALE

Noradrenaline stimulates the β-adrenoreceptor linked adenylate cyclase in rat brain. Reduction of this stimulation after treatment with antidepressants is an indicator for receptor down-regulation.

PROCEDURE

Groups of male Sprague-Dawley rats are treated intraperitoneally twice daily for 14 days with saline, 10 mg/kg desimipramine or the test compound. The rats are decapitated and frontal cortices are removed, and placed into ice-cold Krebs physiological buffer (120 mM NaCl, 5 mM KCl, 2.5 mM $CaCl_2$, 2 mM KH_2PO_4, 2 mM $MgSO_4$, 25 mM $NaHCO_3$, 100 µM $Na_2S_2O_5$, 25 µM EDTA, and 10 mM glucose), pH 7.4. Cortices are cut 350 × 350 µ at right angles, added to 20 ml Krebs physiological buffer in 50 ml conical flasks, and separated by vortex mixing. The slices are incubated at 37°C for 1 h in a shaking water bath with the buffer replaced by freshly oxygenated medium every 15 min. After this step, 20 µl [^{3}H]adenine is added to each flask. The flasks are capped, and the slices are incubated for an additional 30 min at 37°C. This medium is then discarded and the slices are washed with 20 ml fresh buffer. Most of the medium is removed and 30 µl aliquots of the packed slices are pipetted into tubes containing 300 µM 3-isobutyl-1-methylxanthine in 270 µl Krebs physiological buffer. After incubation at 37°C for 15 min, 30 µl of noradrenaline (final concentration 100 µM) or 30 µl buffer are added to each tube and incubated for an additional 10 min. The reaction is stopped by addition of 0.5 ml 1 M HCl. The tubes are placed in ice for 10 min before addition of 0.5 ml NaOH and then centrifuged at 3000 *g* for 10 min at 4°C. The supernatants are transferred to tubes containing [^{14}C]-cyclic AMP (approximately 10,000 cpm) to monitor the recovery of [^{3}H]-cyclic AMP. The radio-labelled cyclic nucleotides are sep-

arated by two-stage column chromatography on alumina neutral WN-3 and Dowex AG 50W-X4 anion exchange resin.

EVALUATION

The activity of adenylate cyclase is calculated as the conversion of [^{3}H]-adenine to [^{3}H]-cyclic AMP. After treatment with antidepressants, this conversion rate is not altered without stimulation by noradrenaline, but significantly reduced in slices treated with the maximally stimulating concentration of 100 µM noradrenaline.

CRITICAL ASSESSMENT OF THE METHOD

Determination of β-adrenoreceptor stimulated adenylate cyclase is another parameter for measurement of down-regulation of adrenoreceptors by chronic treatment with antidepressants.

REFERENCES AND FURTHER READING

Banerjee SP, Kung SL, Riggi SJ, Chanda SK (1977) Development of β-adrenergic receptor subsensitivity by antidepressants. Nature 268:455–456

Clements-Jewery S (1978) The development of cortical β-adrenoreceptor subsensitivity in the rat by chronic treatment with trazodone, doxepin and mianserin. Neuropharmacol 17:779–781

Heal D, Cheetham SH, Martin K, Browning J, Luscombe G, Buckett R (1992) Comparative pharmacology of dothiepin, its metabolites, and other antidepressant drugs. Drug Dev Res 27:121–135

Lefkowitz RJ, Stadel JM, Caron MG (1983) Adenylate cyclase-coupled beta-adrenergic receptors. Structure and mechanisms of activation and desensitization. Ann Rev Biochem 52:159–186

Maggi A, U'Prichard DC, Enna SJ (1980) Differential effects of antidepressant treatment on brain monoaminergic receptors. Eur J Pharmacol 61:91–98

Meyerson LR, Ong HH, Martin LL, Ellis DB (1980) Effect of antidepressant agents on β-adrenergic receptor and neurotransmitter regulatory systems. Pharmacol Biochem Behav 12:943–948

Salomon Y (1979) Adenylate cyclase assay. In: Brooker G, Greengard P, Robinson GA (eds) Advances in Cyclic Nucleotide Research. Raven Press, New York, Vol 10, pp 35–55

Sulser F (1978) Functional aspects of the norepinephrine receptor coupled adenylate cyclase system in the limbic forebrain and its modification by drugs which precipitate or alleviate depression: molecular approaches to an understanding of affective disorders. Pharmacopsychiat 11:43–52

Vetulani J, Stawarz RJ, Dingell JV, Sulser F (1976) A possible common mechanism of action of antidepressant treatments: Reduction in the sensitivity of the noradrenergic cyclic AMP generating system in the rat limbic forebrain. Naunyn-Schmiedeberg's Arch Pharmacol 293:109–114

Wolfe BB, Harden TK, Sporn JR, Molinoff PB (1978) Presynaptic modulation of beta adrenergic receptors in rat cerebral cortex after treatment with antidepressants. J Pharmacol Exp Ther 207:446–457

E.6.1.8 [^{3}H]Yohimbine Binding to α_2-Adrenoceptors in Rat Cerebral Cortex

PURPOSE AND RATIONALE

This binding assay is used to investigate the interaction of compounds at central α_2 receptors and may indicate possible modes of action for antidepressant, anti-hypertensive and other classes of compounds.

[^{3}H]Yohimbine is a selective antagonist for α_2-receptors (Starke et al. 1975). The use of an antagonist radioligand avoids the complexity of saturation curves that can be observed with radio-labeled agonist ligands. Furthermore, a [^{3}H]antagonist label for the α_2 receptor permits a better evaluation of α_2/α_1 selectivity than a [^{3}H]agonist label, since α_1 affinities are measured with a [^{3}H]antagonist ([^{3}H]WB 4101).

Chronic treatment with desipramine has been shown to decrease the binding of [^{3}H]DHA to rat brain cortical β-receptors. Some investigators have reported that co-administration of yohimbine causes β-receptor down-regulation to occur after fewer antidepressant treatments (Johnson et al. 1980; Scott and Crews 1983). Therefore, it may be of interest to investigate compounds with yohimbine-like properties as antidepressant candidates themselves or in conjunction with antidepressant candidates.

PROCEDURE

Reagents

1. 20-fold concentrated buffer:

   2.36 M NaCl 137.92 g/liter

   100 mM KCl 7.45 g/liter

   200 mM glucose 36.03 g/liter in 0.5 M Tris, pH 7.4

2. 2-fold concentrated buffer:
   - fold dilution of reagent 1 in deionized water
3. Standard buffer:
   - 20-fold dilution of reagent 1 in deionized water
4. [Methyl-^{3}H] yohimbine (72–86 Ci/mmol) is obtained from New England Nuclear
   - For IC_{50} determinations: [^{3}H] Yohimbine is diluted to 40 nM in deionized H_2O
   - Fifty µl of this solution is a 2-ml reaction volume gives a final concentration of 1 nM
5. L-NE bitartrate is made up to 10 mM in 0.01 N HCl. 20 µl of this solution gives a final concentration of 100 µM in 2 ml of reaction mixture.

6. Test compounds. For most assays, a 10 mM stock solution is made up in a suitable solvent and serially diluted, such that the final concentration in the assay ranges from 10^{-4} to 10^{-7} M. Six or seven concentrations are used routinely.

Tissue Preparation

Male Wistar rats are decapitated and their brains rapidly removed. The cortices are weighed and homogenized in 9 volumes of ice-cold 0.32 M sucrose using a Potter-Elvehjem glass homogenizer fitted with a Teflon pestle (0.009–0.010 cm clearance). The homogenate is centrifuged at 1000 *g* for 10 min (approximately 3000 rpm using the Sorvall RC-5 centrifuge with heads SS-34 or SM-24). The supernatant is then recentrifuged at 17,000 *g* for 20 min (approximately 12,500 rpm using the Sorvall RC-5 centrifuge, and heads SS-34 or SM-24). The pellet (P_2) is resuspended in the original volume of 0.32 M sucrose and stored on ice.

Binding Assay

430 µl	H_2O
1000 µl	2-fold concentration buffer (reagent 2)
20 µl	drug or 10 mM L-NE bitartrate or vehicle
50 µl	^{3}H-yohimbine (reagent 4)
500 µl	tissue

Tubes are vortexed and incubated at 25°C for 10 min. Bound [^{3}H]yohimbine is captured via filtration under reduced pressure. The filters are washed three times with 5 ml aliquots of buffer (reagent 3). The filters are then counted in 10 ml of Liquiscint scintillation fluid.

EVALUATION

Specific binding of [^{3}H]yohimbine is the difference between total bound (in the presence of vehicle) and non-specifically bound (in the presence of 100 µM L-NE bitartrate). Percent inhibition of specific [^{3}H]yohimbine binding is calculated for each concentration of test drug and IC_{50} values determined by computer-derived log-probit analysis.

REFERENCES AND FURTHER READING

Johnson RW, Reisine T, Spotnitz S, Weich N, Ursillo R, Yamamura HI (1980) Effects of desipramine and yohimbine on α_2- and β-adrenoreceptor sensitivity. Eur J Pharmacol 67:123–127

Scott JA, Crews FT (1983) Rapid decrease in rat brain beta-adrenergic receptor binding during combined antidepressant-alpha-2 antagonist treatment. J Pharmacol Exp Ther 224:640–646

Starke K, Borowski E, Endo T (1975) Preferential blockade of presynaptic α-adrenoceptors by yohimbine. Eur J Pharmacol 34:385–388

E.6.1.9 Test for Anticholinergic Properties by [^{3}H]-QNB Binding to Muscarinic Cholinergic Receptors in Rat Brain

PURPOSE AND RATIONALE

Several tricyclic antidepressants exert considerable anti-cholinergic effects which limit the therapeutic use in some patients. Amitryptiline has the greatest incidence of these side effects and is the most potent in binding to muscarinic receptors. Desipramine, which exhibits less incidence of atropine like side effects shows a lower affinity for muscarinic receptors. Since there is no evidence that the anticholinergic effects contribute to the therapeutic efficacy, antidepressant drugs with low anti-cholinergic effects are desired.

Quinuclidinyl benzilate (QNB) is a specific muscarinic cholinergic antagonist in both peripheral and central tissues. The binding characteristics of ^{3}H-QNB were first described by Yamamura and Snyder (1974), who showed that this ligand was displaced by muscarinic antagonists, but not by nicotinic or non-cholinergic drugs. The levorotatory isomer being more potent than the racemate is used as the radioactive ligand.

PROCEDURE

Reagents

L-[Benzilic-4,4′-^{3}H]-quinuclidinyl benzilate (30–40 Ci/mmol) is obtained from New England Nuclear. For IC_{50} determinations [^{3}H]-QNB is made up to a concentration of 40 nM and 50 µl is added to each tube (yielding a final concentration of 1 nM in the assay).

Atropine sulfate is obtained from Sigma Chemical Co.

Test compounds: For most assays, a 1 mM stock solution is made up in a suitable solvent and serially diluted, so that the final concentration in the assay ranges from 10^{-5} to 10^{-8} M.

Tissue Preparation

Male Wistar rats are killed by decapitation and their brains rapidly removed. After removal of the cerebellum, each brain is homogenized in 10 volumes of ice-cold 0.32 M sucrose in a Potter-Elvejhem glass homogenizer. The homogenate is then centrifuged at

1000 *g* for 10 min and the pellet discarded. The resultant supernatant is further dispersed and used for [^{3}H]-QNB binding studies. Specific binding is 20% of the total added ligand and approximately 95% of the total bound ligand.

Assay

100 µl	0.5 M Na/K phosphate buffer, pH 7.4 (134 g $Na_2HPO_4 \cdot 7H_2O$+68 g KH_2PO_4)
780 µl	H_2O
50 µl	^{3}H-QNB stock solution
20 µl	vehicle (for total binding) or 2 mM atropine (for nonspecific binding)
1000 µl	0.05 M Na/K phosphate buffer (1:10 diluted) pH 7.4
50 µl	tissue suspension

Tissue homogenates are incubated for 60 min at 25°C with 1 nM ^{3}H-QNB and varying drug concentrations. With each binding assay, triplicate samples containing 2 µM atropine sulfate are incubated under identical conditions to determine nonspecific [^{3}H]-QNB binding. After incubation, the samples are cooled and then rapidly filtered through glass filters (Whatman GF/B) under reduced pressure. The filters are washed 3 times with 5 ml of ice-cold phosphate buffer and then placed in scintillation vials. After the addition of 10 ml of counting cocktail, radioactivity is assayed by liquid scintillation spectrophotometry.

EVALUATION

Specific [^{3}H]-QNB binding is determined by the difference between total [^{3}H]-QNB and bound radioactivity in the presence of 2 µM atropine sulfate. Data are converted to percent specific bound [^{3}H]-QNB displaced by test drugs and IC_{50} values obtained from computer derived log-probit analysis. The inhibition at each drug concentration is the mean of triplicate determinations.

REFERENCES AND FURTHER READING

Hollister LE (1964) Complications from psychotherapeutic drugs. Clin Pharmacol Ther 5:322–333

Marks MJ, Romm E, Collins AC (1987) Genetic influences on tolerance development with chronic oxotremorine infusion. Pharmacol Biochem Behav 27:723–732

Meyerhöffer A (1972) Absolute configuration of 3-quinuclidinyl benzilate and the behavioral effect in the dog of the optical isomers. J Med Chem. 15:994–995

Smith CP, Huger FP (1983) Effects of zinc on [^{3}H]-QNB displacement by cholinergic agonists and antagonists. Biochem Pharmacol 32:377–380

Snyder SH, Greenberg D, Yamamura HI (1974) Antischizophrenic drugs and brain cholinergic receptors. Arch Gen Psychiatry 31:58–61

Snyder SH, Yamamura HI (1977) Antidepressants and the muscarinic acetylcholine receptor. Arch Gen Psychiatry 34:236–239

Wamsley JK, Gehlert DL, Roeske WR, Yamamura HI (1984) Muscarinic antagonist binding site as evidenced by autoradiography after direct labeling with [^{3}H]-QNB and [^{3}H]-pirenzepine. Life Sci 34:1395–1402

Yamamura HI, Snyder SH (1974) Muscarinic cholinergic binding in rat brain (quinuclidinyl benzilate/receptors). Proc Nat Acad Sci USA 71:1725–1729

E.6.1.10 Monoamine Oxidase Inhibition: Inhibition of Type A and Type B Monoamine Oxidase Activities in Rat Brain Synaptosomes

PURPOSE AND RATIONALE

The mood-elevating effects of the antituberculosis drug iproniazid have been observed clinically. The mode of action was elucidated to be the inhibition of the enzyme monoamine oxidase. This was followed by wide use of monoamine oxidase inhibitors for the treatment of depression. However, side effects due to interaction with dietary amines have been observed. The biological role of monoamine oxidase is to regulate the levels of endogenous amines (norepinephrine, dopamine and serotonin) and exogenously administered amines. Based on different substrate and inhibitor specificities two forms of monoamine oxidase (A and B) were described. Dopamine and tyramine are substrates for both types, serotonin and epinephrine are substrates for type A, and β-phenylethylamine and benzylamine are substrates for type B. Iproniazid and tranylcypromine are nonselective inhibitors, clorgyline is a selective inhibitor of type A, deprenyl and pargyline are selective inhibitors of type B. It has been suggested that treatment with selective blockers of type B results in less detrimental food interactions.

PROCEDURE

Tissue Preparation

Male Wistar rats weighing 150–250 g are sacrificed and the brains rapidly removed. Whole brain minus cerebellum is homogenized in 9 volumes of ice-cold, phosphate-buffered 0.25 M sucrose, using a Potter-Elvejhem homogenizer. The homogenate is centrifuged at 1000 *g* for 10 min and the supernatant decanted and recentrifuged at 18,000 *g* for 20 min. The resulting pellet (P_2) is resuspended in fresh 0.25 M sucrose and recentrifuged at 18,000 *g* for 20 min. The washed pellet is resuspended in the original volume

of 0.25 M sucrose and serves as the tissue source for mitochondrial monoamine oxidase.

Assay

50 µl 0.5 M PO_4 buffer, pH 7.4

450 µl H_2O

100 µl H_2O or appropriate drug concentration

200 µl tissue suspension

The tubes are preincubated for 15 min at 37°C and the assay is started by adding 100 µl of substrate (^{14}C-5-HT or ^{14}C β-phenylethylamine) at 10 s intervals. The tubes are incubated for 30 min at 37°C and the reaction is stopped by the addition of 0.3 ml of 2 N HCl. Tissue blank values are determined by adding the acid before the substrate. Seven ml of diethylether are added, the tubes are capped and shaken vigorously for 10 min to extract the deaminated metabolites into the organic phase, which is separated from the aqueous phase by centrifugation at 1000 *g* for 5 min. A 4 ml aliquot of the ether layer is counted in 10 ml of liquid scintillation counting cocktail.

EVALUATION

The percent inhibition at each drug concentration is the mean of triplicate determinations. IC_{50} values are determined by log-probit analyses.

For example, deprenyl shows IC_{50}-values of 3.9×10^{-6} against MAO A and 3.0×10^{-8} against MAO B.

MODIFICATION OF THE METHOD

Colzi et al. (1992) measured dopamine and 3,4-dihydroxyphenylacetic acid (DOPAC) outflow after a reversible MAO-A inhibitor with a brain microdialysis technique in rats.

Frankhauser et al. (1994) tested the interaction of MAO inhibitors and dietary tyramine by measurement of peak systolic blood pressure in conscious rats. The increase of blood pressure after oral application of tyramine was potentiated by pretreatment with MAO inhibitors. Reversible MAO inhibitors could be differentiated from non-selective, irreversible MAO inhibitors.

REFERENCES AND FURTHER READING

Callingham BA (1989) Biochemical aspects of the pharmacology of moclobemide. The implications of animal studies. Br J Psychiatry 155 (Suppl 6):53–60

Cesura AM, Pletscher A (1992) The new generation of monoamine oxydase inhibitors. Progr Drug Res 38:171–297

Colzi A, d'Agostini F, Cesura AM, Da Prada M (1992) Brain microdialysis in rats: a technique to reveal competition between endogenous dopamine and moclobemide, a RIMA antidepressant. Psychopharmacology 106:S17–S20

Frankhauser C, Charieras T, Caille D, Rovei V (1994) Interaction of MAO inhibitors and dietary tyramine: a new experimental model in the conscious rat. J Pharmacol Toxicol Meth 32:219–224

Haefeli W, Burkard WP, Cesura AM, Kettler R, Lorez HP, Martin JR, Richards JG, Scherschlicht R, Da Prada M (1992) Biochemistry and pharmacology of moclobemide, a prototype RIMA. Psychopharmacol 106:S6–S14

Johnston JP (1968) Some observations upon a new inhibitor of monoamine oxidase in brain tissue. Biochem Pharmacol 17:1285–1297

Kettler R, Da Prada M, Burkard WP (1990) Comparison of monoamine oxydase-A inhibition by moclobemide *in vitro* and *ex vivo* in rats. Acta Psychiat Scand Suppl 82:101–102

Knoll J (1980) Monoamine oxidase inhibitors: Chemistry and pharmacology. In: Sandler M (ed) Enzyme inhibitors as drugs. pp 151–173. University Park Press

Ozaki M, Weissbach H, Ozaki A, Witkop B, Udenfriend S (1960) Monoamine oxidase inhibitors and procedures for their evaluation *in vivo* and *in vitro*. J Med Pharmac Chem 2:591–607

Rowler CJ, Ross SB (1984) Selective inhibitors of monoamine oxydase A and B: biochemical, pharmacological, and clinical parameters. Med Res Rev 4:323–358

Waldmeier PC (1993) Newer aspects of the reversible inhibitor of MAO-A and serotonin reuptake, Brofaromine. Progr Neuro-Psychopharmacol Biol Psychiat 17:183–198

Waldmeier PC, Stöcklin K (1990) Binding of [^{3}H]brofaromine to monoamine oxydase A *in vivo*: displacement by clorgyline and moclobemide. Eur J Pharmacol 180:297–304

White HL, Scates PW (1992) Mechanism of monoamine oxydase inhibition by BW 137U87. Drug Dev Res 25:185–193

Wurtman RJ, Axelrod J (1963) A sensitive and specific assay for the estimation of monoamine oxidase. Biochem Pharmacol 12:1439–1441

E.6.2 In Vivo Tests

E.6.2.1 Catalepsy Antagonism

PURPOSE AND RATIONALE

Observations about **cataleptic behavior in chicken** have first been described more than 300 years ago (Schwenter 1636; Kircher 1646), and again reported about 100 years ago (Czermak 1873; Heubel 1877; Verworn 1898). This phenomenon was used by Vogel and Ther (1963) as a simple method to detect antidepressants besides other central stimulants.

PROCEDURE

Adult white Leghorn chicken are used. The animal is grasped with both hands whereby the left hand pushes the chicken slightly down and the right hand supports the animal from the ventral side. Immediately, the chicken is turned on its back and hold with the

right hand for 1 min. Usually, cataleptic numbness occurs immediately. The cataleptic state can be sustained by slight pushing the head of the animal on the table. After 1 min the right hand is carefully withdrawn. The chicken remains in the cataleptic state for several min up to 1 h. The cataleptic rigor is interrupted by noise or fast movements of the observer. Clapping of the hands above the head arouses the chicken which jumps up and runs away. The chicken is always aroused by pulling on the wings. The animals are pretested in order to be sure about the cataleptic behavior of an individual chicken. As already found by previous investigators, the experiment can be repeated several times. Control studies showed that in untreated animals the phenomenon could be elicited 6 times every 30 min during a period 5 days. After the control experiments, the animals are injected i.p. with the test compound or the vehicle. The test is performed 4 times every 30 min during 2 h.

EVALUATION

The test is considered to be positive if the cataleptic rigor does not occur after treatment or is interrupted spontaneously within 1 min at least twice during the 2 h test period. The suppression of the cataleptic phenomenon is the criterion for a positive response. Furthermore, the arousal after hand-clapping or pulling on the wings is recorded in order to register central sedative effects. In order to obtain dose-response curves 12 animals per group are treated with various doses. ED_{50} values are calculated.

CRITICAL ASSESSMENT OF THE METHOD

The specificity of the method has been tested. Antidepressant agents like imipramine and ethyltryptamine-acetate or other monoamino-oxydase-inhibitors and d-desoxyephedrine show a dose dependent effect. Moreover, the effects were dependent on time. ED_{50} values decreased on consecutive days after imipramine and monoamino-oxydase inhibitors but not after d-desoxyephedrine. Therefore, the test can be considered as specific for central stimulants allowing the possibility to distinguish between antidepressants and central stimulants of the amphetamine type.

MODIFICATIONS OF THE METHOD

Simiand et al. (2003) and Gabriel et al. (2005) described **tonic immobility in gerbils** as a model for detecting antidepressant-like effects. When grasped by the skin of the nape and lifted into the air, the young of many altricial mammals exhibit an immobility response in which they tuck their limbs against their bodies and remain inert. Such a response can be induced also in adults of some species, such as Mongolian gerbils (De la Cruz and Junquera 1993). To test antidepressant-like effects in the tonic immobility paradigm in gerbils, animals (six to nine per group) were held on a flat surface and were firmly pinched for 15 s at the scruff of the neck using the thumb and the index finger. They were then placed on parallel bars (4 mm in diameter, 28 cm long, spaced 5 cm apart and having a 3-cm difference in height). The front paws were gently placed on the upper bar and the hind paws on the lower bar. The duration of tonic immobility was measured in five successive trials with a 30-s intertribal interval. Each trial ended when an animal started to move or after 90 s of immobility. Experiments were started 30 min after i.p. administration of test drug.

REFERENCES AND FURTHER READING

Czermak J (1873) Beobachtungen und Versuche über "hypnotische" Zustände bei Thieren. Pflüger's Arch ges Physiol 7:107–121

Danilewski B (1881) Über die Hemmungen der Reflex- und Willkürbewegungen. Beiträge zur Lehre vom thierischen Hypnotismus. Pflüger's Arch ges Physiol 24:489–525

De la Cruf F, Junquera J (1993) The immobility response elicited by clamping, bandaging and grasping in the Mongolian gerbil (*Meriones unguiculatus*). Behav Brain Res 54:165–169

Gabriel G, Stemmelin J, Scatton B (2005) Effects of the cannabinoid CB1 receptor antagonist rimonabant in models of emotional reactivity in rodents. Biol Psychiatry 57:261–267

Heubel E (1877) Über die Abhängigkeit des wachen Gehirnzustandes von äusseren Erregungen. Ein Beitrag zur Physiologie des Schlafes und zur Würdigung des Kircher'schen Experimentum mirabile. Pflüger's Arch ges Physiol 14:158–210

Kircher A (1646) Experimentum mirabile. De imaginatione gallinae. In: "Ars magna lucis et umbrae" Romae, Lib. II, pars I, 154

Schwenter D (1636) Deliciae physico-mathematicae oder Mathematische und Philosophische Erquickstunden. Nürnberg

Simiand J, Guitard J, Griebel G, Soubrié P (2003) Tonic immobility in gerbils. A new model for detecting antidepressant-like effects. Behav Pharmacol 14 [Suppl 1]:5–40

Verworn M (1898) Beitraege zur Physiologie des Centralnervensystems. Erster Theil. Die sogenannte Hypnose der Thiere. G Fischer Jena, pp 92

Vogel G, Ther L (1963) Zur Wirkung der optischen Isomeren von Aethyltryptaminacetat auf die Lagekatalepsie des Huhnes und auf die Motilitaet der Maus. Arzneim Forsch/Drug Res 13:779–783

E.6.2.2 Despair Swim Test

PURPOSE AND RATIONALE

Behavioral despair was proposed as a model to test for antidepressant activity by Porsolt et al. (1977, 1978). It was suggested that mice or rats forced to swim in a re-

stricted space from which they cannot escape are induced to a characteristic behavior of immobility. This behavior reflects a state of despair which can be reduced by several agents which are therapeutically effective in human depression.

PROCEDURE

Male Sprague-Dawley rats weighing 160–180 g are used. They are brought to the laboratory at least one day before the experiment and are housed separately in Makrolon cages with free access to food and water. Naive rats are individually forced to swim inside a vertical Plexiglas cylinder (height: 40 cm; diameter: 18 cm, containing 15 cm of water maintained at 25°C). Rats placed in the cylinders for the first time are initially highly active, vigorously swimming in circles, trying to climb the wall or diving to the bottom. After 2–3 min activity begins to subside and to be interspersed with phases of immobility or floating of increasing length. After 5–6 min immobility reaches a plateau where the rats remain immobile for approximately 80% of the time. After 15 min in the water the rats are removed and allowed to dry in a heated enclosure (32°C) before being returned to their home cages. They are again placed in the cylinder 24 h later and the total duration of immobility is measured during a 5 min test. Floating behavior during this 5 min period has been found to be reproducible in different groups of rats. An animal is judged to be immobile whenever it remains floating passively in the water in a slightly hunched but upright position, its nose just above the surface. Test drugs or standard are administered one hour prior to testing. Since experiments with the standard drug (imipramine) showed that injections 1, 5 and 24 h prior the test gave the most stable results in reducing floating these times are chosen for the experiment.

EVALUATION

Duration of immobility is measured in controls and animals treated with various doses of a test drug or standard. Antidepressant drugs, but also stimulants like amphetamine and caffeine, reduce duration of immobility. Dose-responses can be evaluated.

CRITICAL ASSESSMENT OF THE METHOD

The method, also called "forced swim test," has been used and modified by many authors, e. g. Kauppila et al. (1991, van der Heyden et al. 1991).

Advantages of the method are the relative simplicity and the fact that no interaction with other drugs is necessary. Like in other behavioral tests, e. g. the catalepsy test in chicken, not only antidepressants and monoamino-oxydase inhibitors but also central stimulants give positive results.

In a critical review of the forced swimming test, Borsini and Meli (1988) discussed the various modifications and proposed rats to be more suitable than mice for detecting antidepressant activity.

The model is purely behavioral without presuppositions concerning the mechanism of action of potential antidepressants. It is sensitive to a large number of atypical antidepressants otherwise inactive in the more classical tests. The rat version seems to be more selective (fewer false positives) and the mouse version more sensitive (fewer false negatives) (Porsolt et al. 1991).

Natoh et al. (1992) reviewed the theoretical background of the forced swimming test and the various factors which can possibly affect the results.

MODIFICATIONS OF THE METHOD

Wallach and Hedley (1979) reported positive results with antihistamines and Giardina and Ebert (1989) with an ACE-inhibitor. Differentiation is achieved by the simultaneous evaluation of motor activity.

Cervo and Samanin (1987) suggested potential antidepressant activities of a selective serotonin$_{1A}$ agonist based on anti-immobility activity in the forced swimming test in rats without effect on open-field activity.

Nishimura (1988, 1989, 1993) published a modification of the forced swim test using straw suspension in the water tank. The apparatus used was a vertical glass cylinder (height: 40 cm, diameter: 18 cm) equipped with 4 pieces of straw (length 24 cm, diameter: 0.4 cm) that were suspended from above. The cores of the straws were filled with cotton rope. The straws were painted black from the surface of the water to a height of 10 cm. The apparatus was filled with water to a height of 15 cm and maintained at 25°C. Thirty min after treatment with drugs or saline, the rats were placed in the apparatus without straw suspension and the total duration of immobility measured for a period of 5 min. Immediately thereafter, 4 pieces of straw were suspended and the total duration of immobility in the following 5-min observation period again measured.

In an effort to enhance the sensitivity of the traditional forced swim test in the rat so that it can be responsive to specific serotonin reuptake inhibitors, Lucki (1997) proposed several simple procedural modifications. These developments include increasing the water depth to 30 cm from the traditional 15–18 cm, and using a time sampling technique to rate the predominant behavior over a 5-s interval. Spe-

cific components of active behavior can be distinguished: (1) climbing behavior (also known as trashing), which is defined as upward-directed movements of the forepaws along the side of the swim chamber; (2) swimming behavior, the movement (usually horizontal) throughout the swim chamber that also includes crossing into another quadrant; and (3) immobility, which is defined as when no additional activity is observed other than that required to keep the rat's head above the water. As a result of the increase in water depth, there is considerably less immobility than in the traditional test because the animals cannot have contact with the cylinder bottom. The major advantage of this modified test is that it reveals that catecholaminergic agents decrease immobility with a corresponding increase in climbing behavior, whereas 5-HT-related compounds, such as specific serotonin reuptake inhibitors, also decrease immobility but increase swimming behavior.

López-Rubalcava and Lucki (2000) described strain differences in the behavioral effects of antidepressant drugs in the rat forced swim test when the noradrenergic antidepressant, desipramine, and the serotonergic antidepressants fluoxetine and 8-OH-DPAT were tested in Wistar–Kyoto rats and Sprague Dawley rats.

Sun and Alkon (2003, 2004) described the **open space swimming test** to index antidepressant activity. Rats were place individually in a round pool, with a diameter of 152 cm and a height of 60 cm and was filled with 40 cm water at 21°C. Rats were free to swim (or not to swim) for 15 min and then returned to their home cage. The same procedure was followed 24 h later for 3 days. The swimming/drifting path was recorded with a video tracking system. The measurement is considered to be more objective than the forced swimming test. The procedure induces depressive behavior and impairs learning and memory in the rats.

Galea et al. (2001) found that estradiol alleviates depressive-like symptoms in an animal model of post-partum depression. The effect of hormone withdrawal following hormone-simulated pregnancy on depressive-like behavior in the forced swim test was investigated in female Long-Evans rats.

Using the forced swim test or elevated plus-maze, Stoffel and Craft (2004) studied ovarian hormone withdrawal-induced "depression" in female rats.

Gregus et al. (2005) used the forced swim test to study the effect of repeated corticosterone injections and restraint stress on anxiety and depression-like behavior in male rats.

Buckett et al. (1982) described an automated apparatus for behavioral testing of typical and atypical antidepressants in **mice**. A multichannel system can test 10 mice simultaneously. Each mouse is placed in the beam of a Doppler radar head and horn assembly. The moving mouse causes reflections of a frequency differing from the transmitted signal. Within the Doppler head these reflected waves are mixed with a proportion of transmitted waves to produce a difference signal proportional to the activity of the mouse within the beam. The output of each Doppler head is fed to an amplifier whose gain has been calibrated to compensate for differences in sensitivity between individual heads. The method is claimed to eliminate human error and bias and to allow the testing of large numbers of compounds.

Alpermann et al. (1992) used a slightly modified behavioral despair test in mice. Sixty min after administration of the test compounds, the animals are placed in glass cylinders containing water up to a height of 10 cm (water temperature 22–24°C). From the second minute onward, immobility of each mouse is rated every 30 s. After 10 observations mean values and standard deviations in each treatment group are calculated. Compared with the immobility score of the control group percent reduction can be calculated.

Nomura et al. (1982) published a modification of the despair swim test in mice involving a small water wheel set in a water tank. Mice placed on this apparatus turned the wheel vigorously but, when they abandoned attempts to escape from the water, the wheel stopped turning. The number of rotations of the water wheel were counted.

Hata et al. (1995) studied the behavioral characteristics of SART (specific alterations of rhythm in temperature)-stressed mice in forced swimming tests and evaluated the effects of anxiolytics and antidepressants.

Weiss et al. (1998) reported selective breeding of rats for high and low motor activity in the swim test. Sprague Dawley rats were selectively bred for low motor activity (low struggling time/high floating time), while others were bred for high motor activity (high struggling time/low floating time).

Lucki et al. (2001) investigated the sensitivity to desipramine, a selective norepinephrine reuptake inhibitor, and fluoxetine, a selective serotonin reuptake inhibitor, in seven inbred and four outbred mouse strains. Considerable differences in the results of the forced swim test were found.

Sachdev et al. (2002) used the forced swim model of depression in rats to investigate the antidepressant effect of different frequencies of transcranial magnetic stimulation.

Krahe et al. (2002) tested the effects of rotational side preferences in immobile behavior of normal mice in the forced swimming test.

Buckley et al. (2004) used both the mouse forced swim test and the rat forced swim test to characterize a nicotinic agonist.

REFERENCES AND FURTHER READING

Alpermann HG, Schacht U, Usinger P, Hock FJ (1992) Pharmacological effects of Hoe 249: A new potential antidepressant. Drug Dev Res 25:267–282

Borsini F, Meli A (1988) Is the forced swimming test a suitable model for revealing antidepressant activity? Psychopharmacology 94:147 160

Buckett WR, Fletcher J, Hopcroft RH, Thomas PC (1982) Automated apparatus for behavioural testing of typical and atypical antidepressants in mice. Br J Pharmacol 75:170 P

Buckley MJ, Surowy C, Meyer M, Curzon P (2004) Mechanism of action of A-85380 in an animal model of depression. Progr Neuropsychopharmacol Biol Psychiatry 28:723–730

Cervo L, Samanin R (1987) Potential antidepressant properties of 8-hydroxy-2-(di-n-propylamino)tetralin, a selective serotonin$_{1A}$ agonist. Eur J Pharmacol 144:223–229

Giardina WJ, Ebert DM (1989) Positive effects of captopril in the behavioral despair swim test. Biol Psychiatry 25:697–702

Galea LAM, Wide JK, Barr AM (2001) Estradiol alleviates depressive-like symptoms in a novel animal model of postpartum depression. Behav Brain Res 122:1–9

Gregus A, Wintink AJ, Davis AC, Kalynchuk LE (2005) Effect of repeated corticosterone injections and restraint stress on anxiety and depression-like behavior in male rats. Behav Brain Res 156:105–114

Hata T, Itoh E, Nishikawa H (1995) Behavioral characteristics of SART-stressed mice in the forced swim test and drug action. Pharmacol Biochem Behav 51:849–853

Kauppila T, Tanila H, Carlson S, Taira T (1991) Effects of atipamezole, a novel α_2-adrenoreceptor antagonist, in open-field, plus-maze, two compartment exploratory, and forced swimming tests in the rat. Eur J Pharmacol 205:177–182

Krahe TE, Filgueiras CC, Schmidt SL (2002) Effects of rotational side preferences in immobile behavior of normal mice in the forced swimming test. Progr Neuropsychopharm Biol Psychiatry 26:169–176

López-Rubalcava C, Lucki I (2000) Strain differences in the behavioral effects of antidepressant drugs in the rat forced swim test. Neuropsychopharmacology 22:191–199

Lucki I (1997) The forced swimming test as a model for core and component behavioral effects of antidepressant drugs. Behav Pharmacol 8:523–532

Lucki I, Dalvi A, Mayorga AJ (2001) Sensitivity to the effects of psychopharmacologically selective antidepressants in different strains of mice. Psychopharmacology (Berl) 155:315–322

Naitoh H, Yamaoka K, Nomura S (1992) Behavioral assessment of antidepressants. 1. The forced swimming test: A review of its theory and practical application. Jpn J Psychopharmacol 12:105–111

Nishimura H, Tsuda A, Ida Y, Tanaka M (1988) The modified forced-swim test in rats: Influence of rope- or straw-suspension on climbing behavior. Physiol Behav 43:665–668

Nishimura H, Ida Y, Tsuda A, Tanaka M (1989) Opposite effects of diazepam and β-CCE on immobility and straw-climbing behavior of rats in a modified forced-swim test. Pharmacol Biochem Behav 33:227–231

Nishimura H, Tanaka M, Tsuda A, Gondoh Y (1993) Atypical anxiolytic profile of buspirone and a related drug, SM-3997, in a modified forced swim test employing straw suspension. Pharmacol Biochem Behav 46:647–651

Nomura S, Shimizu J, Kinjo M, Kametani H, Nakazawa T (1982) A new behavioral test for antidepressant drugs. Eur J Pharmacol 83:171–175

Porsolt RD, Anton G, Blavet N, Jalfre M (1978) Behavioural despair in rats: a new model sensitive to antidepressive treatments. Eur J Pharmacol 47:379–391

Porsolt RD, Bertin A, Jalfre M (1977a) Behavioural despair in mice: A primary screening test for antidepressants. Arch Int Pharmacodyn 229:327–336

Porsolt RD, Le Pichon M, Jalfre M (1977b) Depression: A new animal model sensitive to antidepressant treatments. Nature 266:730–732

Porsolt RD, Martin P, Lenègre, Fromage S, Drieu K (1990) Effects of an extract of Ginkgo biloba (EBG 761) on "learned helplessness" and other models of stress in rodents. Pharmacol Biochem Behav 36:963–971

Porsolt RD, Lenègre A, McArthur RA (1991) Pharmacological models of depression. In: Olivier B, Mos J, Slangen JL (eds) Animal Models in Psychopharmacology, Birkhäuser Verlag Basel, pp 137–159

Sachdev PS, McBride R, Loo C, Mitchell PM, Malhi GS, Crooker V (2002) Effect of different frequencies of transcranial magnetic stimulation (TMS) on the forced swim model of depression in rats. Biol Psychiatry 51:474–479

Stoffel EC, Craft RM (2004) Ovarian hormone withdrawal-induced "depression" in female rats. Physiol Behav 83:505–513

Sun MK, Alkon DL (2003) Open space swimming test to index antidepressant activity. J Neurosci Meth 126:35–40

Sun MK, Alkon DL (2004) Induced depressive behavior impairs learning and memory in rats. Neuroscience 129:129–139

van der Heyden JAM, Olivier B, Zethof TJJ (1991) The behavioral despair model as a prediction of antidepressant activity: effects of serotonergic drugs. In: Olivier B, Mos J, Slangen JL (eds) Animal Models in Psychopharmacology. Advances in Pharmacological Sciences. Birkhäuser Verlag, Basel, pp 211–215

Wallach MB, Hedley LR (1979) The effects of antihistamines in a modified behavioral despair test. Communic Psychopharmacol 3:35–39

Weiss JM, Cierpial MA, West CHK (1998) Selective breeding of rats for high and low motor activity in a swim test: toward as new animal model of depression. Pharmacol Biochem Behav 61:49–66

E.6.2.3 Tail Suspension Test in Mice

PURPOSE AND RATIONALE

The "tail suspension test" has been described by Steru et al. (1985) as a facile means of evaluating potential antidepressants. The immobility displayed by rodents when subjected to an unavoidable and inescapable stress has been hypothesized to reflect behavioral despair which in turn may reflect depressive disorders in humans. Clinically effective antidepressants reduce the immobility that mice display after active and unsuccessful attempts to escape when suspended by the tail.

PROCEDURE

Male Balb/cJ mice weighing 20–25 g are used preferentially. They are housed in plastic cages for at least 10 days prior to testing in a 12 h light cycle with food and water freely available. Animals are transported from the housing room to the testing area in their own cages and allowed to adapt to the new environment for 1 h before testing. Groups of 10 animals are treated with the test compounds or the vehicle by intraperitoneal injection 30 min prior to testing. For the test the mice are suspended on the edge of a shelf 58 cm above a table top by adhesive tape placed approximately 1 cm from the tip of the tail. The duration of immobility is recorded for a period of 5 min. Mice are considered immobile when they hang passively and completely motionless for at least 1 min.

EVALUATION

The percentage of animals showing the passive behavior is counted and compared with vehicle treated controls. Using various doses, ED_{50} values can be calculated.

CRITICAL ASSESSMENT OF THE METHOD

The tail suspension test has been found to be an easy method to test potential antidepressant compounds. However, it has been reported that several mouse strains are essentially resistant to tail-suspension induced immobility.

MODIFICATIONS OF THE METHOD

Chermat et al. (1986) adapted the tail suspension test to the rat.

Porsolt et al. (1987), Stéru et al. (1987) recommended the use of the automated tail suspension test for the primary screening of psychotropic agents. A specially developed computerized device automatically measures the duration of immobility of 6 mice at one time and at the same time provides a measure of the energy expended by each animal, the power of the movements.

Vaugeois et al. (1996) described a genetic mouse model of helplessness sensitive to imipramine. Lines of mice were selectively bred to diverge in their spontaneous helplessness in the tail-suspension test. By the second generation of selection, only mice of the helpless line were sensitive to the antidepressant imipramine.

Mayorga and Lucki (2001) demonstrated limitations on the use of the C57BL/6 mouse in the tail-suspension test. Under baseline conditions, the majority of C57BL/6 mice climbed up their tails during the 6-min test session. The occurrence of this behavior was not found in other strains of mice.

Liu and Gershenfeld (2001) found genetic differences in the tail-suspension test among 11 inbred strains of mice as far as basal immobility was concerned. Surprisingly, the reduction of immobility by imipramine was independent of basal immobility.

Ripoli et al. (2003) tested antidepressant-like effects in various mice strains in the tail-suspension test and found considerable differences depending on strain and test drug.

Shearman et al. (2003) tested antidepressant-like effects of a cannabinoid CB1 receptor inverse agonist in mice using an automated tail-suspension apparatus (TSE Systems, Bad Homburg, Germany) with a tail hanger connected to a precision load cell. Mice remained suspended by the tail, at a height of 35 cm from the tabletop, for 6 min. During this time the load cell recorded the mouse's movements and transmitted the information to a computer, which then recorded the rate of immobility within the course of the session, and calculated total duration of immobility.

REFERENCES AND FURTHER READING

Chermat R, Thierry B, Mico JA, Stéru L, Simon P (1986) Adaptation of the tail suspension test to the rat. J Pharmacol (Paris) 17:348–350

Liu X, Gershenfeld HK (2001) Genetic differences in the tail-suspension test and its relationship to imipramine response among 11 inbred strains of mice. Biol Psychiatry 49:575–581

Mayorga AJ, Lucki I (2001) Limitations on the use of the C57BL/6 mouse in the tail suspension test. Psychopharmacology (Berl) 155:110–112

Porsolt RD, Charmat R, Lenègre A, Avril I, Janvier S, Stéru L (1987) Use of the automated tail suspension test for the primary screening of psychotropic agents. Arch Int Pharmacodyn 288:11–30

Porsolt RD, Lenègre A, McArthur RA (1991) Pharmacological models of depression. In: Olivier B, Mos J, Slangen JL (eds) Animal Models in Psychopharmacology, Birkhäuser Verlag Basel, pp 137–159

Ripoli N, David DJP, Dailly E, Hascoët M, Bourin M (2003) Antidepressant-like effects in various mice strains in the tail suspension test. Behav Brain Res 143:193–200

Shearman LP, Rosko KM, Fleischer R, Wang J, Xu S, Tong XS, Rocha BA (2003) Antidepressant-like and anorectic effects of the cannabinoid CB1 receptor inverse agonist AM251 in mice. Behav Pharmacol 14:573–582

Steru L, Chermat R, Thierry B, Simon P (1985) Tail suspension test: A new method for screening antidepressants in mice. Psychopharmacology 85:367–370

Stéru L, Chermat R, Thierry B, Mico JA, Lenègre A, Stéru M, Simon P (1987) The automated tail suspension test: a computerized device which differentiates psychotropic drugs. Prog Neuro-Psychopharmacol Biol Psychiatry 11:659–671

Trullas R, Jackson B, Skolnick P (1989) Genetic differences in a tail suspension test for evaluating antidepressant activity. Psychopharmacology 99:287–288

van der Heyden J, Molewijk E, Olivier B (1987) Strain differences in response to drugs in the tail suspension test for antidepressant activity. Psychopharmacology 92:127–130
Vaugeois JM, Odèvre C, Loisel L, Costentin J (1996) A genetic mouse model of helplessness sensitive to imipramine. Eur J Pharmacol 316:R1–R2

E.6.2.4 Learned Helplessness in Rats

PURPOSE AND RATIONALE

Animals exposed to inescapable and unavoidable electric shocks in one situation later fail to escape shock in a different situation when escape is possible (Overmier and Seligman 1967; Maier and Seligman 1976). This phenomenon was evaluated as a potential animal model of depression (Sherman et al. 1979; Martin et al. (1986), Christensen and Geoffroy 1991; Tejedor del Real et al. 1991; Weiss and Kilts 1998).

PROCEDURE

Learned helplessness is produced in male Sprague-Dawley rats (300 g) by exposure to electric shock (0.7 mA) for 1 h on a schedule of 10 s of shock/min. The apparatus is a $30 \times 45 \times 30$ cm box with a grid floor. At a height of 20 cm above the floor, a platform (7.5×7.5 cm) can be inserted through one side wall to allow a jump-up escape response. The platform is not available during training. After the appropriate treatment, the animals are tested for acquisition of a jump-up escape in the same apparatus. At the beginning of a trial, the platform is pushed into the box and a 0.4 mA shock initiated. Shock is terminated in 10 s if the animal has not escaped onto the platform by this time. If an escape response occurred, the animal is allowed to remain on the platform for the duration of 10 s, then returned to the grid floor. Ten such trials with an intertrial interval of 20 s are given. In a naive control group of rats, this training resulted in 80% acquiring learned helplessness behavior. Drugs are given before the training and the test period.

EVALUATION

A drug is considered to be effective, if the learned helplessness is reduced and the number of failures to escape is decreased. Imipramine was found to be active only after repeated applications. A benzodiazepine was effective, whereas chlorpromazine was ineffective.

CRITICAL ASSESSMENT OF THE METHOD

The "learned helplessness" in the rat can be regarded as an additional measure for antidepressant activity in addition to other tests. The test is time consuming and its specificity is questionable. The major drawback of the model is that most of the depression-like symptomatology does not persist beyond 2–3 days following cessation of the uncontrollable shock.

MODIFICATIONS OF THE METHOD

Vaccheri et al. (1984) used an apparatus with an lever to be pressed to interrupt the shock. Giral et al. (1988), Porsolt et al. (1990) Simiand et al. (1992) used shuttle-boxes for escape.

Curzon et al. (1992) described a similar rat model of depression. Rats were tested in an open field after being restrained by taping them to wire grids for two h on the preceding day. The reduced activity is antagonized by antidepressant drugs.

A modification of the test incorporating aspects of chronic mild stress paradigm was described by Gambarana et al. (2001) A model of anhedonia is based on the finding that exposure to repeated unavoidable stress prevents the development of an appetitive behavior induced and maintained by a highly palatable food (vanilla sugar) in rats fed ad libitum (Ghiglieri et al. 1997).

The chronic stress procedure involves restraint and novel housing, and avoids the problems associated with food deprivation (Reid et al. 1997).

Vollmayr et al. (2001) studied brain-derived neurotrophic factor (BDNF) stress responses in rats bred for learned helplessness in a system provided by TSE Systems, Bad Homburg, Germany. Two strains of rats were bred, one which reacts with congenital helplessness to stress, and one which congenitally does not acquire helplessness when stressed. In rats with congenital helplessness, acute immobilization stress does not induce a reduction of BDNF expression in the hippocampus, which is observed in Sprague Dawley rats that do not acquire helplessness.

Vollmayr and Henn (2001) proposed key factors that can be manipulated to enhance both the usability and the reliability of the rat helplessness paradigm.

Rats bred for congenital learned helplessness (King et al. 1993; Shumake et al. 2000) responded less to sucrose but did not show deficits in activity or learning (Vollmayr et al. 2004).

REFERENCES AND FURTHER READING

Christensen AV, Geoffroy M (1991) The effect of different serotonergic drugs in the learned helplessness model of depression. In: Olivier B, Mos J, Slangen JL (eds) Animal Models in Psychopharmacology. Advances in Pharmacological Sciences. Birkhäuser Verlag, Basel, pp 205–209
Curzon G, Kennett GA, Sarna GS, Whitton PS (1992) The effects of tianeptine and other antidepressants on a rat model of depression. Br J Psychiatry 160 (Suppl 15):51–55

Gambarana C, Scheggi S, Tagliamonta A, Tolu P, DeMontis MG (2001) Animals models for the study of antidepressant activity. Brain Res Brain Res Protoc 7:11–20
Ghiglieri O, Gambarana C, Scheggi S, Tagliamonte A, Willner P, De Montis MG (1997) Palatable food induces an appetitive behaviour in satiated rats which can be inhibited by chronic stress. Behav Pharmacol 8:619–628
Giral P, Martin P, Soubrie P, Simon P (1988) Reversal of helpless behavior in rats by putative 5-HT_{1A} agonists. Biol Psychiat 23:237–242
King JA, Campell D, Edwards E (1993) Differential development of the stress response in congenital learned helplessness. Int J Dev Neurosci 11:435–442
Maier SF, Seligman MEP (1976) Learned helplessness: Theory and evidence. J Exp Psychol 105:3–46
Martin P, Soubrié P, Simon P (1986) Noradrenergic and opioid mediation of tricyclic-induced reversal of escape deficits caused by inescapable shock pretreatment in rats. Psychopharmacol 90:90–94
Overmier JB, Seligman MEP (1967) Effects of inescapable shock upon subsequent escape and avoidance learning. J comp Physiol Psychol 63:28–33
Porsolt RD, Martin P, Lenègre A, Fromage S, Drieu K (1990) Effects of an extract of Ginkgo biloba (EGB 761) on "learned helplessness" and other models of stress in rodents. Pharmacol Biochem Behav 36:963–971
Porsolt RD, Lenègre A, McArthur RA (1991) Pharmacological models of depression. In: Olivier B, Mos J, Slangen JL (eds) Animal Models in Psychopharmacology. Advances in Pharmacological Sciences, Birkhäuser Verlag Basel, pp 137–159
Reid I, Forbes N, Stewart C, Matthews K (1997) Chronic stress and depressive disorder: a useful new model. Psychopharmacology 134:365–367
Sherman AD, Allers GL, Petty F, Henn FA (1979) A neuropharmacologically-relevant animal model of depression. Neuropharmacol 18:891–893
Shumake J, Poremba A, Edwards E, Gonzalez-Lima F (2000) Congenital helpless rats as a genetic model for cortex metabolism in depression. Neuroreport 11:3793–3798
Simiand J, Keane PE, Guitard J, Langlois X, Gonalons N, Martin P, Bianchetti A, LeFur G, Soubrie P (1992) Antidepressive profile in rodents of SR 5811A, a new selective agonist for atypical β-adrenoreceptors. Eur J Pharmacol 219:193–201
Tejedor del Real P, Gilbert-Rahola J, Leonsegui I, Micó JA (1991) Relationship between emotivity level and susceptibility to the learned helplessness model of depression in the rat. In: Olivier B, Mos J, Slangen JL (eds) Animal Models in Psychopharmacology. Advances in Pharmacological Sciences. Birkhäuser Verlag, Basel, pp 217–224
Vaccheri A, Dall'Olio R, Gaggi R, Gandolfi O, Montanaro N (1984) Antidepressant versus neuroleptic activities of sulpiride isomers on four animal models of depression. Psychopharmacology 83:28–33
Vollmayr B, Henn FA (2001) Learned helplessness in the rat: improvements in validity and reliability. Brain Res Brain Res Protoc 8:1–7
Vollmayr B, Faust H, Lewicka S, Henn FA (2001) Brain-derived-neurotrophic-factor (BDNF) stress responses in rats bred for learned helplessness. Mol Psychiatry 6:471–474
Vollmayr B, Bachteler D, Vangelien V, Gass P, Spanagel R, Henn F (2004) Rats with congenital learned helplessness respond less to sucrose but show no deficits in activity or learning. Behav Brain Res 150:217–221
Weiss JMO, Kilts CD (1998) Animal models of depression and schizophrenia. In: Nemeroff CB, Schatzberg AF (eds) Textbook of psychopharmacology, 2nd edn. American Psychiatric Press, Bethesda, Md., pp 88–123

E.6.2.5 Muricide Behavior in Rats

PURPOSE AND RATIONALE

Horovitz et al. (1965) described a selective inhibition of mouse-killing behavior in rats (Karli 1956; Karli et al. 1969) by antidepressants. The test can be used to evaluate antidepressants such as tricyclics and MAO-inhibitors.

PROCEDURE

Male Sprague-Dawley rats (300–350 g) are isolated for 6 weeks in individual cages. They have access to food and water ad libitum. One mouse is placed into the rat's cage. About 10 to 30% of rats kill the mouse by biting the animal through the cervical cord. Only rats consistently killing mice within 5 min after presentation are used for the test. The mice are removed 15 to 45 s after they have been killed in order to prevent the rats from eating them. Drugs are injected i.p. to the rats before the test. Mice are presented 30, 60 and 120 min after drug administration.

EVALUATION

Failure to kill a mouse within 5 min is considered inhibition of muricidal behavior. Performing dose-response experiments, the ED_{50} is defined as the dose which inhibits mouse killing in 50% of the rats.

MODIFICATIONS OF THE METHOD

Injections of 5,7-dihydroxytryptamine into the lateral hypothalamus increased mouse-killing behavior in rats (Vergnes and Kempf 1982).

Molina et al. (1985) considered rats isolated for at least one month which do not kill mice in a 30 min test period as spontaneous non-killer rats. In these animals, mouse-killing behavior could be induced by i.p. injection of 150 mg/kg p-chlorophenylalanine daily for 2 days or by electrolytic lesions in the dorsal and median raphe.

McMillen et al. (1988) studied the effects of housing and muricidal behavior on serotonergic receptors and interactions with novel anxiolytic drugs.

CRITICAL ASSESSMENT OF THE METHOD

The mouse-killing behavior is inhibited not only by anti-depressants but also by central stimulants like d-amphetamine (Horovitz et al. 1966; Sofia 1969a, b), some antihistamines (Barnett et al. 1969), and some

cholinergic drugs (McCarthy 1966; Vogel and Leaf 1972; Wnek and Leaf 1972). Neuroleptics and benzodiazepines are active only in doses which impair motor performance.

REFERENCES AND FURTHER READING

Barnett A, Taber RI, Roth FE (1969) Activity of antihistamines in laboratory antidepressant tests. Int J Neuropharmacol 8:73–79

Horovitz ZP, Ragozzino PW, Leaf RC (1965) Selective block of rat mouse-killing by anti-depressants. Life Sci 4:1909–1912

Horovitz ZP, Piala JJ, High JP, Burke JC, Leaf RC (1966) Effects of drugs on the mouse-killing (muricide) test and its relationship to amygdaloid functions. Int J Neuropharmacol 5:405–411

Karli P (1956) The Norway rats's killing response to the white mouse: an experimental analysis. Behavior 10:81–103

Karli P, Vergnes M, Didiergeorges F (1969) Rat-mouse interspecific aggressive behaviour and its manipulation by brain ablation and by brain stimulation. In: Garattini S, Sigg EB (eds) Aggressive behaviour. Excerpta Medica Foundation, Amsterdam, pp 47–55

Kreiskott H (1969) Some comments on the killing response behaviour of the rat. In: Garattini S, Sigg EB (eds) Aggressive Behaviour. Excerpta Medica Foundation, Amsterdam, pp 56–58

Kulkarni AS (1068) Muricidal block produced by 5-hydroxytryptophan and various drugs. Life Sci 7:125–128

McCarthy D (1966) Mouse-killing induced in rats treated with pilocarpine. Fed Proc25:385, Abstract

McMillen BA, Chamberlain JK, DaVanzo JP (1988) Effects of housing and muricidal behavior on serotonergic receptors and interactions with novel anxiolytic drugs. J Neural Transm 71:123–132

Molina V, Ciesielski L, Gobaille S, Isel F, Mandel P (1985) Inhibition of mouse killing behavior by serotonin-mimetic drugs: effects of partial alterations of serotonin neurotransmission. Pharmacol Biochem Behav 27:123–131

Sofia RD (1969a) Effects of centrally active drugs on experimentally-induced aggression in rodents. Life Sci 8:705–716

Sofia RD (1969b) Structural relationship and potency of agents which selectively block mouse-killing (muricide) behavior in rats. Life Sci :1101–1210

Vergnes M, Kempf E (1982) Effect of hypothalamic injections of 5,7-dihydroxytryptamine on elicitation of mouse-killing in rats. Behav Brain Res 5:387–397

Vogel JR (1975) Antidepressant and mouse-killing (muricide) behavior. In: Fielding S, Lal H (eds) Industrial Pharmacology. Vol II: Antidepressants. Futura Publ Comp., pp 99–112

Vogel JR, Leaf RC (1972) Initiation of mouse-killing in non-killer rats by repeated pilocarpine treatment. Physiol Behav 8:421–424

Wnek DJ, Leaf RC (1973) Effects of cholinergic drugs on prey-killing in rodents. Physiol Behav 10:1107–1113

E.6.2.6 Behavioral Changes After Neonatal Clomipramine Treatment

PURPOSE AND RATIONALE

Vogel et al. (1988, 1990a), Hartley et al. (1990) reported that neonatally administered clomipramine produces changes in adult rats that resembles endogenous depression in man, based on earlier observations by Mirmiran et al. (1981), Rodriguez-Echandia and Broitman (1983). This phenomenon has been studied by several research groups in many respects (Neill et al. 1990; Vogel et al. 1990b–e, 1996a, b; Velazquez-Moctezuma and Diaz-Ruiz 1992; Yavari et al. 1993; Maudhuit et al. 1995, 1996; Prathiba et al. 1995, 1997, 1998, 1999; Feenstra et al. 1996; Kinney et al. 1997; Bonilla-Jaime et al. 1998; Dwyer and Rosenwasser 1998).

PROCEDURE

Three days after birth, all male pups of Sprague Dawley mother rats are cross-fostered and all female pups are killed. Cross-fostering consists of removing all pups from their biological mothers and placing them with another lactating female (the non-biological foster mother). Each litter is divided into two groups of approximately equal number. Each half of the litter is placed with a different lactating female (the foster mother), and each foster mother receives half the pups from two litters. All pups with each foster mother receive the same treatment (clomipramine or saline) and the two pup groups of each original litter are assigned to different treatments. Thus, each original pup litter contributes equally to experimental and control groups. Each pup is injected subcutaneously between the shoulder blades with 15 mg/kg clomipramine hydrochloride or saline vehicle twice daily on postnatal days 8 through 21. At one month of age the pups are weaned and housed as litters until approximately 3 weeks prior testing, at which time they are individually housed.

All testing is conducted in a Coulbourn operant conditioning chamber (Lehigh Valley, PA) placed in a quiet area. The floor rods are connected with a shock generator and a shock scrambler.

Behavioral testing is commenced at 3 months postnatally. Each test pair consists of one clomipramine-treated and one vehicle-treated rat. Prior to testing, all clomipramine- and saline-treated rats are paired by body weight (within 5 grams) to diminish size differences that could affect behavioral results. Pairs remain the same throughout the testing.

For evaluation of drugs, clomipramine-treated rats are administered subcutaneously for 4 days twice daily saline, or standard drug (10 mg/kg imipramine), or test drug.

Tests are done daily for 4 days. On the first day, the animals are placed in the chamber for 12 min habituation. On days 2–4, the sessions start with a 2 min

habituation period followed by 10 min of shock delivery. Shocks (1.33 mA, 0.5 s duration) are delivered on a variable schedule with a minimum of 5 and a maximum of 10 s shock intervals. This results in a total of 70–80 shocks within the 10-min session.

Two observers score simultaneously. Each watches one rat of the pair. The rats are identified by a red mark on the fur. The behaviors produced are almost totally in response to shock delivery; both animals are almost immobile between the shocks. Both observers are blind to the treatment conditions of the animals.

Offensive and defensive behaviors are scored including the following 4 behaviors:

1. An upright position which is part of a mutual upright posture in which the dominant rat towers over the submissive rat. The submissive rat rears on its hindlegs, with the head positioned at an upward angle, the forepaws extended toward the attacking animal, and the ventral surface of the body continually facing the opponent.
2. In the offensive crouch, the dominant animal turns its flank towards the subordinate; the submissive crouch is characterized by freezing in a motionless crouching position.
3. Mounting behavior is frequently seen and is the same as seen in the male prior to copulating with a female.
4. Leaps in response to the shock which are directed to the other rat are scored as aggressive responses.

Three defensive or submissive behaviors were observed:

1. Defensive upright posture;
2. submissive crouch;
3. a supine position in submission to the dominant rat.

In this system each offensive behavior by one rat is partly defined by a defensive behavior of the other rat and vice versa.

EVALUATION

The individual behaviors of the treatment and control groups are listed for offensive and defensive behavior on days 1, 2, and 3 and the total of scores calculated for each group. Analysis of variance is applied to offensive, defensive, difference (offensive minus defensive) and total (offensive plus defensive behavior scores. Rats treated postnatally with clomipramine have significantly fewer offensive and significantly more defensive behaviors. This effect is ameliorated by treatment with antidepressant drugs.

CRITICAL ASSESSMENT OF THE TEST

Not only clomipramine, but also other psychotropic drugs induce changes in behavior of adult rats after treatment in neonatal age (Drago et al. 1985; Frank and Heller 1997; Hansen et al. 1998), however, clomipramine induces the most pronounced effects (Velazquez-Moctezuma et al. 1993; Vogel and Hagler 1996; Hansen et al. 1997). Specificity of the procedure to evaluate potential antidepressant compounds remains to be established.

MODIFICATIONS OF THE METHOD

Neonatal treatment with clomipramine not only reduces shock induced aggression, but also induces REM sleep abnormalities (Mirmiran et al. 1981; Vogel et al. 1990b,c; Frank and Heller 1997), decreases intracranial self-stimulation (Vogel et al. 1990d), increases activity in open-field tests in adulthood (Hartley et al. (1990, Prathiba et al. 1997), increases immobility in the forced swim test (Velazquez-Moctezuma and Diaz-Ruiz 1992), reduces adult male rat sexual behavior (Neill et al. 1990; Velazquez-Moctezuma et al. 1993; Vogel et al. 1996; Bonilla-Jaime et al. 1998,), influences the hypothalamic-pituitary-adrenal axis in adult rats (Feenstra et al. 1996; Prathiba et al. 1998, 1999). Vázquez-Palacios et al. (2005) studied antidepressant effects of nicotine and fluoxetine in the animal model of depression induced by neonatal treatment with clomipramine.

REFERENCES AND FURTHER READING

Bonilla-Jaime H, Retana-Marquez S, Velasquez-Moctezuma J (1998) Pharmacological features of masculine sexual behavior in an animal model of depression. Pharmacol Biochem Behav 60:39–45

Drago F, Continella G, Alloro MC, Scapagnini U (1985) Behavioral effects of perinatal administration of antidepressant drugs in the rat. Neurobehav Toxicol Teratol 7:493–497

Dwyer SM, Rosenwasser AM (1998) Neonatal clomipramine treatment, alcohol intake and circadian rhythms in rats. Psychopharmacology 138:176–183

Feenstra MGP, van Galen H, Te Riele PJM, Botterblom MHA, Mirmiran M (1996) Decreased hypothalamic serotonin levels in adult rats treated neonatally with clomipramine. Pharmacol Biochem Behav 55:647–652

Frank MG, Heller HC (1997) Neonatal treatments with the serotonin uptake inhibitors clomipramine and zimelidine, but not the noradrenaline uptake inhibitor desipramine, disrupt sleep pattern in rats. Brain Res 768:287–293

Hansen HH, Mikkelsen JD (1998) Long-term effects on serotonin transporter mRNA expression of chronic neonatal exposure to a serotonin reuptake inhibitor. Eur J Pharmacol 253:307–315

Hansen HH, Sanchez C, Meier E (1997) Neonatal administration of the selective serotonin reuptake inhibitor Lu 10–134-C increases forced swimming-induced immobility in adult rats. A putative animal model of depression? J Pharmacol Exp Ther 283:133–1341

Hartley P, Neill D, Hagler M, Kors D, Vogel G (1990) Procedure- and age-dependent hyperactivity in a new animal model of endogenous depression. Neurosci Biobehav Rev 14:69–72
Kinney GG, Vogel GW, Feng P (1997) Decreased dorsal raphe nucleus neuronal activity in adult chloral hydrate anesthetized rats following neonatal clomipramine treatment: Implications for endogenous depression. Brain Res 756:68–75
Maudhuit C, Hamon M, Adrien J (1995) Electrophysiological activity of raphe dorsalis serotoninergic neurones in a possible model of endogenous depression. NeuroReport 6:681–684
Maudhuit C, Hamon M, Adrien J (1996) Effects of chronic treatment with zimelidine and REM sleep deprivation on the regulation of raphe neuronal activity in a rat model of depression. Psychopharmacology 124:267–274
Mirmiran M, van de Poll NE, Corner MA, van Oyen HG, Bour HL (1981) Suppression of active sleep by chronic treatment with chlorimipramine during early postnatal development: effects upon adult sleep and behavior in rats. Brain Res 204:129–146
Neill D, Vogel G, Hagler M, Kors D, Hennessy A (1990) Diminished sexual activity in a new animal model of endogenous depression. Neurosci Biobehav Rev 14:73–76
Prathiba J, Kumar KB, Karanth KS (1995) Effects of neonatal clomipramine on cholinergic receptor sensitivity and passive avoidance behavior in adult rats. J Neural Transm Gen Sect 100:93–99
Prathiba J, Kumar KB, Karanth KS (1997) Fear-potentiated post-startle activity in neonatal clomipramine treated rats. Indian J Pharmacol 29:201–203
Prathiba J, Kumar KB, Karanth KS (1998) Hyperactivity of hypothalamic pituitary axis in neonatal clomipramine model of depression. J Neural Transm 105:1335–1339
Prathiba J, Kumar KB, Karanth KS (1999) Effects of chronic administration of imipramine on the hyperactivity of hypothalamic-pituitary-adrenal axis in neonatal clomipramine treated rats. Indian J Pharmacol 31:225–228
Rodriguez-Echandia EL, Broitman ST (1983) Effect of prenatal and postnatal exposure to therapeutic doses of chlorimipramine to emotionality in the rat. Psychopharmacology, Berlin 79:236–241
Velazquez-Moctezuma J, Diaz-Ruiz O (1992) Neonatal treatment with clomipramine increased immobility in the forced swim test: An attribute of animal models of depression. Pharmacol Biochem Behav 42:737–739
Velazquez-Moctezuma J, Aguillar-Garcia A, Diaz-Ruiz O (1993) Behavioral effects of neonatal treatment of clomipramine, scopolamine, and idazoxan in male rats. Pharmacol Biochem Behav 46:215–217
Vázquez-Palacios G, Bonilla-Jaime H, Velázquez-Moctezuma J (2005) Antidepressant effects of nicotine and fluoxetine in an animal model of depression induced by neonatal treatment with clomipramine. Progr Neuropsychopharmacol Biol Psychiatry 29:39–46
Vogel G, Hagler M (1996) Effects of neonatally administered iprindole on adult behaviors of rats. Pharmacol Biochem Behav 55:157–161
Vogel G, Hartley P, Neill D, Hagler M, Kors D (1988) Animal depression model by neonatal clomipramine: Reduction of shock induced aggression. Pharmacol Biochem Behav 31:103–106
Vogel G, Neill D, Hagler M, Kors D (1990a) A new animal model of endogenous depression: A summary of present findings. Neurosci Biobehav Rev 14:85–91
Vogel G, Neill D, Kors D, Hagler M (1990b) REM sleep abnormalities in a new model of endogenous depression. Neurosci Biobehav Rev 14:77–83
Vogel GW, Buffenstein A, Minter K, Hennessey A (1990c) Drug effects on REM sleep and on endogenous depression. Neurosci Biobehav Rev 14:49–63
Vogel G, Neill D, Hagler M, Kors D, Hartley P (1990d) Decreased intracranial self-stimulation in a new animal model of endogenous depression. Neurosci Biobehav Rev 14:65–68
Vogel G, Hagler M, Hennessey A, Richard C (1996) Dose-dependent decrements in adult male sexual behavior after neonatal clomipramine treatment. Pharmacol Biochem Behav 54:605–609
Yavari P, Vogel GW, Neill DB (1993) Decreased raphe unit activity in a rat model of endogenous depression. Brain Res 611:31–36

E.6.2.7 Chronic Stress Model of Depression

PURPOSE AND RATIONALE

The chronic mild stress paradigm was developed in order to simulate in animals the symptom of anhedonia, a major feature of depression (Willner et al. 1987, 1992; Forbes et al. 1996; Willner 1997; Willner and Mitchell 2002; Grippo et al. 2003; Konkle et al. 2003; Pijlman et al. 2003; Strekalova et al. 2004). The model has been used to test compounds with antidepressant activity (Moreau et al. 1996; Kopp et al. 1999; Papp and Wieronska 2000; Harkin et al. 2002; Ducottet et al. 2003; Gabriel et al. 2005).

The stress regime was modified by several authors.

The stress regimen used by Moreau et al. (1996) consisted of exposing male Wistar rats each week to a variety of unpredictable, mild stressors such as repeated 1-h periods of confinement to small cages with bells ringing every 10 min, one period of overnight illumination, one overnight period of food and water deprivation immediately followed by 2 h of access to restricted food, one overnight period of water deprivation followed by 1 h exposure to an empty bottle, and one overnight period of group housing in a damp cage.

Grippo et al. (2003) exposed male Sprague Dawley rats to the following stressors in random order: continuous overnight illumination, 40° cage tilt along the vertical axis, paired housing, soiled cage, exposure to an empty water bottle immediately following a period of acute water deprivation, stroboscopic illumination, and white noise.

Ducottet et al. (2003) studied the effects of a selective non-peptide corticotropin-releasing factor receptor 1 antagonist in a mild stress model of depression in **mice**. The method is based on a regimen published by Kopp et al. (1999) and by Griebel et al. (2002a, 2002b).

PROCEDURE

Male BALB/cByJIco mice, aged 9 weeks at the beginning of chronic mild stress experiments, were housed for 1 week individually in small cages with food and water ad libitum at a 12/12 h light/dark cycle and 21°C. The chronic mild stress procedure consists of restraint in a small tube for 1 h, forced bath in water at 32°C for 30 min, water and food deprivation for 15 h, paired housing in damped sawdust for 18 h, food restriction for 3 h, access to an empty water bottle for 2 h, and inversion of the light/dark cycle. Over 3 weeks, four to six of these procedures were applied every day in random order. Physical state was controlled weekly using a scale from 1 to 3 using piloerection, dirty fur, and body weight as symptoms. At the end of the experiment, the mice were subjected to a light/dark test.

Treatment started at week 5, while the stress regimen was continuing. Mice were divided into three groups ($n = 20$) each subjected to a 5-week period of chronic mild stress before being administered during a 4-week period with one of the following treatments: vehicle, daily i.p. injections of 10 mg/kg fluoxetine as standard, or test drug.

EVALUATION

Data were analyzed using non-parametric exact analyses including the Monte Carlo correction. Data of physical state were analyzed with a Friedman test, followed by a Wilcoxon signed ranks test comparing initial week with chronic mild stress weeks and treatment weeks. Data of body weight were treated with a Kruskal-Wallis test for each week followed by a permutation test for two independent samples. The light/dark test was submitted to a Kruskal-Wallis test followed by an a posteriori permutation test.

MODIFICATIONS OF THE METHOD

Since the incidence of clinical depression is significantly higher in woman than in men, Konkle et al. (2003) compared the effects of 6 weeks of chronic mild stress administration among female and male rats of Sprague Dawley and of Long Evans strains.

Matthews and Robbins (2003) reported that a specific periodic neonatal maternal separation procedure leads to a robust constellation of behavioral changes in the adult rat that resembles core aspects of anhedonia in men.

Sammut et al. (2001, 2002) studied antidepressant reversal of interferon-α-induced anhedonia utilizing a three-bottle test (Muscat et al. 1991). A drinking and feeding monitoring system (TSE, Systems Bad Homburg, Germany) was used. In this test, three concentrations of sucrose (1%, 8%, and 32%) are simultaneously presented to each individually caged rat. The three-bottle test allows demonstration of the monotonic relationship between intake and hedonic value as is characteristic of human studies.

REFERENCES AND FURTHER READING

Ducottet C, Griebel G, Belzung C (2003) Effects of the selective nonpeptide corticotropin-releasing factor receptor 1 antagonist antalarmin in the mild stress model of depression in mice. Progr Neuropsychopharm Biol Psychiatry 27:625–631

Forbes NF, Stewart CA, Metthews K, Reid IC (1996) Chronic mild stress and sucrose consumption: validity as a model of depression. Physiol Behav 60:1481–1484

Gabriel G, Stemmelin J, Scatton B (2005) Effects of the cannabinoid CB1 receptor antagonist rimonabant in models of emotional reactivity in rodents. Biol Psychiatry 57:261–267

Griebel G, Simiand J, Serradeil-Le Gal C, Wagnon J, Pascal M, Scatton B, Maffrand JP, Soubrié P (2002a) Anxiolytic- and antidepressant-like effects of the non-peptide vasopressin V_{1b} receptor antagonist SSR149415, suggest an innovative approach for the treatment of stress-related disorders. Proc Natl Acad Sci USA 99:6370–6375

Griebel G, Simiand J, Steinberg R, Jung M, Gully D, Roger P, Geslin M, Scatton B, Maffrand JP, Soubrié P (2002b) 4-(2-Chloro-4-methoxy-5-methylphenyl)-*N*-[(1*S*)-2-cyclopropyl-1-(3-fluoro-4-methylphenyl)ethyl]5-methyl-*N*-(2-propynyl)1,3-thiazol-2-amine hydrochloride (SSR125543A), a potent and selective corticotrophin-releasing factor$_1$ receptor antagonist. II. Characterization in rodent models of stress-related disorders. J Pharmacol Exp Ther 301:332–345

Grippo AJ, Beltz TG, Johnson AK (2003) Behavioral and cardiovascular changes in the chronic mild stress model of depression. Physiol Behav 78:703–710

Harkin A, Houlihan DD, Kelly JP (2002) Reduction in preference for saccharin by repeated unpredictable stress in mice and its prevention by imipramine. J Psychopharmacol 16:115–123

Konkle ATM, Baker SL, Kentner AC, Barbagallo LSM, Merali Z, Bielajew C (2003) Evaluation of the effects of chronic mild stressors on hedonic and physiological responses: sex and strain compared. Brain Res 992:227–238

Kopp C, Vogel E, Rettori MC, Delagrange P, Misslin R (1999) The effects of melatonin on the behavioural disturbances induced by chronic mild stress in C3H/He mice. Behav Pharmacol 10:73–83

Matthews K, Robbins TW (2003) Early experience as a determinant of adult behavioural responses to reward: the effects of repeated maternal separation in the rat. Neurosci Biobehav Rev 27:45–55

Moreau JL, Bös M, Jenck F, Martin JR, Mortas P, Wichmann J (1996) $5HT_{2C}$ receptor antagonists exhibit antidepressant-like properties in the anhedonia model of depression in rats. Eur Neuropsychopharmacol 6:169–175

Muscat R, Kyprianou T, Osman M, Phillips G, Willner P (1991) Sweetness-dependent facilitation of sucrose drinking by raclopride is unrelated to caloric content. Pharmacol Biochem Behav 40:209–213

Papp M, Wieronska J (2000) Antidepressant-like activity of amisulpiride in two animal models of depression. J Psychopharmacol 14:46–52

Pijlman FTA, Wolterink G, van Ree JM (2003) Physical and emotional stress have differential effects on preference for saccharine and open field behavior in rats. Behav Brain Res 139:131–138
Sammut S, Goodall G, Muscat R (2001) Acute interferon-α administration sucrose consumption in the rat. Psychoendocrinology 26:261–272
Sammut S, Bethus I, Goodall G, Muscat R (2002) Antidepressant reversal of interferon-α-induced anhedonia. Physiol Behav 75:765–772
Strekalova T, Spanagel R, Bartsch D, Henn FA, Gass P (2004) Stress-induced anhedonia in mice is associated with deficits in forced swimming and exploration. Neuropsychopharmacology 29:2007–2017
Willner P (1997) Validity, reliability and utility of the chronic mild stress model of depression: a 10-year review and evaluation. Psychopharmacology 134:319–329
Willner P, Mitchell PJ (2002) The validity of animal models of predisposition to depression. Behav Pharmacol 13:169–188
Willner P, Towell A, Sampson D, Sophokleous S, Muscat R (1987) Reduction in sucrose preference by chronic unpredictable mild stress, and its restoration by a cyclic antidepressant. Psychopharmacology 93:358–364
Willner P, Muscat R, Papp M (1992) Chronic mild stress-induced anhedonia: a realistic animal model of depression. Neurosci Biobehav Rev 16:525–534

E.6.2.8 Novelty-Induced Hypophagia Test

PURPOSE AND RATIONALE

The onset of the therapeutic response to antidepressant treatment exhibits a characteristic delay. While acute antidepressant treatment increases synaptic monoamines within minutes to hours, weeks of sustained treatment are required to induce therapeutic effects (Blier 2003). Few models have been developed in which chronic, but not acute, antidepressant treatment alters behavior (Brodnoff et al. 1988, 1989; Borsini et al. 2002; Cyran et al. 2002; Cyran and Mombereau 2004). Dulawa et al. (2004) and Dulawa and Hen (2005) used the novelty-induced hypophagia test to study chronic antidepressant effects in mice.

PROCEDURE

For chronic testing, male Balb/cL mice were given various doses of test compound in the drinking water. On day 23 of treatment, mice were singly housed. They were trained to drink sweetened condensed milk for three consecutive days presented for 30 min each day in 10-ml serological pipettes with sippers attached with parafilm. Home cage testing occurred on day 28 when mice were briefly removed from their cages to position pipettes containing milk, and testing began when mice were returned to their home cages. The latency to drink and the volume consumed were recorded every 5 min for 30 min. Home cage testing occurred under dim lighting. Novel cage testing occurred on day 29, when mice were placed into new clean cages with the same dimensions but without shavings, with pipettes containing the milk positioned. Novel cage testing occurred under bright lighting with white paper under cages to enhance aversiveness. Again, the latency to drink and the volume consumed were recorded every 5 min for 30 min. For latency scores, a maximum cutoff of 600 s was used.

EVALUATION

Two-factor ANOVA with the home/novel cage condition as a within-subjects factor was applied to latency values. For consumption data, a three-factor ANOVA with block (5-min intervals) and the home/novel cage condition as within-subject factors and drug as a between-subject factor was used to assess whether the novel cage was sufficiently anxiogenic to reduce consumption.

REFERENCES AND FURTHER READING

Blier P (2003) The pharmacology of putative early-onset antidepressant strategies. Eur Neuropsychopharmacol 13:57–66
Borsini F, Podhorna J, Marazziti D (2002) Do animal models of anxiety predict anxiolytic-like effects of antidepressants? Psychopharmacology 163:121–141
Brodnoff SR, Suranyi-Cadotte B, Aitken DH, Quirion R, Meaney MJ (1988) Effects of chronic antidepressant treatment in an animal model of anxiety. Psychopharmacology 95:298–302
Brodnoff SR, Suranyi-Cadotte B, Quirion R, Meaney MJ (1989) A comparison of the effects of diazepam versus several typical and atypical antidepressant drugs in an animal model of anxiety. Psychopharmacology 97:277–279
Cyran JF, Mombereau C (2004) In search for a depressed mouse: utility of models for studying depression-related behavior in genetically modified mice. Mol Psychiatry 9:326–357
Cyran JF, Markou A, Lucki I (2002) Assessing antidepressant activity in rodents: recent developments and further needs. Trends Pharmacol Sci 23:238–245
Dulawa SC, Hen R (2005) Recent advances in animal models of chronic antidepressant effects: the novelty-induced hypophagia test. Neurosci Behav Rev 29:771–783
Dulawa SC, Holick KA, Gundersen B, Hen R (2004) Effects of chronic fluoxetine in animal models of anxiety and depression. Neuropsychopharmacology 29:1321–1330

E.6.2.9 Reduction of Submissive Behavior

PURPOSE AND RATIONALE

Pairs of rats competing for food develop a dominant/submissive behavior, which can be measured in a competition test as the relative success of two food-restricted rats to gain access to a sweetened milk supply. Submissive behavior for one subject can be objectively measured as the amount of time spent at the feeder relative to that by the paired dominant animal. Malatynska and Kostowski (1984), Malatynska et al.

(1995, 2002), and Knapp et al. (2002) described reduction of submissive behavior in rats as a test for antidepressant drug activity.

PROCEDURE

Drugs were given by i.p. injection once a day during the treatment period (including weekends). On weekdays, drugs were administered 1 h before behavioral testing. The testing apparatus and the reduction of submissive behavior model procedure are described by Malatynska et al. (2002).

The apparatus was constructed at OmniTech (Columbus, OH) according to a design by Malatynska and Kostowski (1984). The transparent Plexiglas apparatus consisted of two identical chambers ($24 \times 17 \times 14$ cm) connected by a $4.5 \times 4.5 \times 52$ cm passage. In the middle of the passage, a 10-ml glass beaker was placed into a hole cut in the floor of the passage. Prior to behavioral testing, the beaker was filled with sweetened milk (10 g sucrose/cup) through a hinged door in the ceiling of the passage.

The animals were randomly assigned to pairs prior to testing. They were group-housed four to a cage between testing sessions so that paired animals were always separated. Behavioral testing was performed once a day for a 5-min period on weekdays. During the testing period, an animal received one point when it was observed drinking milk during each 5-s interval of the 5-min period. Four different observers contributed to scoring different animal pairs and all were blinded to the treatment animals received. The design of the apparatus permits only one animal to drink at a time but it is possible for both animals to have consumed milk during an interval. At the end of the 5-min period, the animals were returned to their home cages and given free access to food for 1 h. The animals were also given free access to food from the Friday afternoon following testing to the Sunday afternoon when they were once again food-deprived. The animals showed normal weight gain during the course of the study.

EVALUATION

Each animal of the pair was scored on each testing day for 2 weeks. Week 2 data for the two animals of a pair were tested for significant differences using the two-tailed *t*-test assuming unequal variance. The member of a pair having a significantly lower drinking score ($p < 0.05$) was defined as "submissive" and the partner as "dominant." Any pairs not showing significant dominant–submissive relationship were dropped from the study. Submissive animals were treated with drugs or vehicle and dominant animals were treated with vehicle for the next 3–4 weeks.

The data used for subsequent analyses are referred to as dominance level values. They are calculated as the difference in daily drinking scores between paired rats. The daily dominance level values were averaged over each week starting with the 2nd week of testing for each pair selected. The *n* used for statistical purposes in the study was the averaged weekly dominance level value for a single pair of animals. The effect of treatment on dominance level values for animal pairs within a treatment group was tested for statistical significance by comparing dominance level values during the 2nd week of testing (control period) to values measured during subsequent weeks of testing (treatment period) by analysis of variance (ANOVA) followed by post hoc unpaired *t*-tests for significance between control and treatment data. A *p*-value of less than 0.05 was used as the cutoff for significance. This approach gives information for the time of effect onset and effect for a selected period. Effect onset is defined as the period (weeks) at which the drug-induced reduction of the dominance level becomes significant relative to the control value measured after the 2nd week before treatment is initiated. The relative effect of two treatments is determined for the same treatment period. This is done for the 3rd week of treatment after all drugs have passed the onset of activity.

MODIFICATIONS OF THE METHOD

Pinhasov et al. (2005) used automatic scoring by a multiple-subject video-tracking system for antidepressant activity testing of the reduction of submission behavior.

Leo et al. (2005) applied nuclear magnetic resonance-based metabonomics to the dominant-submissive rat behavioral model. Principal component analysis revealed a metabolite from milk sugar, galactose, as a discriminating factor between rats classified as dominant and those classified as submissive.

Malatynska et al. (2005) described submissive behavior in **mice** as a test for antidepressant drug activity.

REFERENCES AND FURTHER READING

Knapp RJ, Goldenberg R, Shuck C, Cecil A, Watkins J, Miller C, Crites G, Malatynska E (2002) Antidepressant activity of memory-enhancing drugs in the reduction of submissive behavior model. Eur J Pharmacol 440:27–35

Leo GC, Caldwell GW, Crooke J, Malatynska E, Cotto C, Hastings B, Scowcroft J, Hall J, Browne K, Hageman W (2005) The application of nuclear magnetic resonance-

based metabonomics to the dominant-submissive rat behavioral model. Anal Biochem 339:174–178
Malatynska E, Kostowski W (1984) The effect of antidepressant drugs on dominance behavior in rats competing for food. Pol J Pharmacol Pharm 36:531–540
Malatynska E, De Leon I, Allen D, Yamamura HI (1995) Effects of amitriptyline on GABA-stimulated 36Cl-uptake in relation to a behavioral model of depression. Brain Res Bull 37:53–59
Malatynska E, Goldenberg R, Shuck L, Haque A, Zamecki P, Crites G, Schindler N, Knapp RJ (2002) Reduction of submissive behavior in rats: a test for antidepressant drug activity. Pharmacology 54:8–17
Malatynska E, Rapp R, Harrawood D, Tunicliff G (2005) Submissive behavior in mice as a test for antidepressant drug activity. Pharmacol Biochem Behav 82:306–313
Pinhasov A, Crooke J, Rosenthal D, Brenneman D, Malatynska E (2005) Reduction of submission behavior for antidepressant activity testing: study using a video-tracking system. Behav Pharmacol 16:657–664

E.6.2.10 Animal Models of Bipolar Disorder

PURPOSE AND RATIONALE

Bipolar disorder is a psychiatric condition characterized by episodes of mania, depression, and underlying mood instability. The disease is distinguished by its cyclicity. Several attempts have been made to induce cyclic symptoms in animals. Preclinical studies with animal models of mania and depression have been developed to evaluate the potential efficacy of new psychotropic drugs. The main problem is to find a model that mimics mood cyclicity, which is a hallmark of bipolar disorder (Machado-Vieira et al. 2004). Antelman et al. (1995, 1998), Caggiula et al. (1998a, 1998b), and Kucinski et al. (1999) reported that repeated exposure to cocaine or other stressors can induce an oscillation or cycling in various physiological systems.

Cao and Peng (1993) and Arban et al. (2005) described a rodent model of mania, in which hyperactivity is induced by the combination of D-amphetamine and chlordiazepoxide.

PROCEDURE

Male CDI mice weighing 22–26 g were group housed at 21±2°C with 45%–70% humidity on a 12/12 h light/dark cycle. Test drugs were administered orally 60 min before the test. D-amphetamine sulfate (1.25 mg/kg i.p.) and chlordiazepoxide (6.25 mg/kg i.p.) were injected 30 min before the session. Locomotor activity was recorded using a Digiscan Analyzer (Model RXYZCM-8, Omnitech). Animals were individually placed in Plexiglas cages equipped with 48 photocells, and the total distance traveled (cm) by each mouse over a 30-min period was determined.

EVALUATION

Statistical analysis was carried out using an ANOVA followed by Dunnett's test. Results are expressed as mean ± SEM of the total distance traveled (in cm), with group size ranging from 9 to 12 mice.

MODIFICATIONS OF THE METHOD

Petty and Sherman (1981) proposed hyperactivity in rats induced by intraventricular injection of 6-hydroxydopamine as a pharmacological model of mania.

Gould et al. (2001) reported differential sensitivity to lithium's reversal of amphetamine-induced open-field activity in two inbred strains of mice.

Gessa et al. (1995) studied sleep deprivation in rats by the platform method as a possible animal model of mania.

Gambarana et al. (2000) found that long-term lithium administration abolishes the resistance to stress in rats sensitized to morphine and discussed this as a model of mania.

Shaldubina et al. (2002) induced a biphasic locomotor response starting with inhibition and followed by excitation by quinpirole, a D_2/D_3 agonist, and recommended this as a model of bipolar disorder.

D'Aquila et al. (2004) treated rats for 4 weeks with imipramine. After a withdrawal time of 40 days, the animals showed a depressive-like behavior indicated by an increase of immobility in the forced swimming test.

El Mallak et al. (1995, 2003) and Decker et al. (2000) administered intracerebroventricularly 5 µl of ouabain (10^{-3} M) to rats, which induced hyper- and hypoactivity and recommended this as a model of bipolar illness.

Wei et al. (2004) generated transgenic mice overexpressing the glucocorticoid receptor specifically in the forebrain. These mice display a significantly increased emotional lability and depressive-like behavior relative to wild type.

REFERENCES AND FURTHER READING

Antelmanm SM, Caggiula AR, Kiss S, Edwards DJ, Kocan D, Stiller R (1995) Neurochemical and physiological effects of cocaine oscillate with sequential drug treatment: possibly a major factor in drug variability. Neuropsychopharmacology 12:297–306
Antelman SM, Caggiula AR, Kucinski BJ, Fowler H, Gershon S, Edwards DJ, Austin MC, Stiller R, Kiss S, Kocan D (1998)

The effects of lithium on a potential cycling model of bipolar disorder. Progr Neuropsychopharmacol Biol Psychiatry 22:495–510
Arban R, Maraia G, Brackenborough K, Winyard L, Wilson A, Gerrard P, Large C (2005) Evaluation of lamotrigine, valproate and carbamazepine in a rodent model of mania. Behav Brain Res 158:123–132
Caggiula AR, Donny EC, Epstein LH, Sved AF, Knopf S, Rose C, McAllister CG, Antelman SM, Perkins KA (1998a) The role of corticosteroids in nicotine's physiological and behavioral effects. Psychoneuroendocrinology 23:143–159
Caggiula AR, Antelman S, Kucinski BJ, Fowler H, Edwards DJ, Austin MC, Gershon S, Stiller R (1998b) Oscillatory-sensitization model of repeated drug exposure: cocaine's effect on shock-induced hypoanalgesia. Progr Neuropsychopharmacol Biol Psychiatry 22:511–521
Cao BJ, Peng NA (1993) Magnesium valproate attenuates hyperactivity induced by dexamphetamine-chlordiazepoxide mixture in rodents. Eur J Pharmacol 237:177–181
D'Aquila PS, Panin F, Serra G (2004) Long-term imipramine withdrawal induces a depressive-like behavior in the forced swimming test. Eur J Pharmacol 492:61–63
Decker S, Grider G, Cobb M, Li XP, Huff MO, El Mallakk RS, Levy RS (2000) Open field is more sensitive than automated activity monitor in documenting ouabain-induced hyperlocomotion in the development of an animal model for bipolar illness. Prog Neuropsychopharmacol Biol Psychiatry 24:455–462
El Mallakh RS, Harrison LT, Changaris DG, Levy RS (1995) An animal model of mania: preliminary results. Prog Neuropsychopharmacol Biol Psychiatry 19:955–962
El Mallakh RS, El Masri MA, Huff MO, Li XP, Decker S, Levy RS (2003) Intracerebroventricular administration of ouabain as a model of mania in rats. Bipolar Disord 5:362–365
Gambarana C, Mangiavacchi S, Masi F, Scheggi S, Tagliamonte A, Tolu P, De Montis MG (2000) Long-term lithium administration abolishes the resistance to stress in rats sensitized to morphine. Brain Res 877:218–225
Gessa GL, Pani L, Fadda P, Fratta W (1995) Sleep deprivation in the rat: an animal model of mania. Eur Neuropsychopharmacol Suppl 5:879–893
Gould TJ, Keith RA, Bhat RV (2001) Differential sensitivity to lithium's reversal of amphetamine-induced open-field activity in two inbred strains of mice. Behav Brain Res 118:95–105
Kucinski BJ, Antelman SM, Caggiula AR, Fowler H, Gershon S, Edwards DJ (1999) Cocaine-induced oscillation is conditionable. Pharmacol Biochem Behav 63:449–455
Machado-Vieira R, Kapczinski F, Soares JC (2004) Perspectives for the development of animal models of bipolar disorder. Progr Neuropsychopharmacol Biol Psychiatry 28:209–224
Petty F, Sherman AD (1981) A pharmacologically pertinent animal model of mania. J Affect Disord 3:381–387
Shaldubina A, Einat H, Szechtman H, Shimon H, Belmaker RH (2002) Preliminary evaluation of oral anticonvulsant treatment in the quinpirole model of bipolar disorder. J Neural Transm 109:433–440
Wei Q, Lu XY, Liu L, Schafer G, Shieh KR, Burke S, Robinson TE, Watson SJ, Seasholtz AF, Akli H (2004) Glucocorticoid receptor overexpression in forebrain: a mouse model of increased emotional lability. Proc Natl Acad Sci USA 101:11851–11856

E.6.2.11
Animal Models of Obsessive-Compulsive Disorder

PURPOSE AND RATIONALE

Obsessive-compulsive disorder (OCD) is characterized by recurrent intrusive thoughts, feelings or ideas (obsessions) and ritualistic actions (compulsions) which cause significant distress and dysfunction. The disease has gained increasing attention (Stein 2000, 2002). The relevance of ethologic (naturally occurring) animal models (dogs: Stein et al. 1998; Overall 2000; birds: Woods-Kettelberger et al. 1997; horses: Nurnberg et al. 1997) has been discussed. Clinical studies and pharmacological experiments, mostly performed in rats (Joel et al. 2005; Tsaltas et al. 2005; Joel 2006), indicate the involvement of the serotoninergic system.

Deficits in spontaneous alterations produced by 8-OH-DPAT in rats were used as animal model of obsessive-compulsive behavior by Yadin et al. (1991), Fernández-Guasti et al. (2003), van Kuyck et al. (2003), Ulloa et al. (2004a, 2004b), and Agrati et al. (2005).

PROCEDURE

Apparatus

The testing apparatus for spontaneous alterations was a Plexiglas T maze with goal boxes characterized by distinctive cues. All arms (including the main arm and the two goal boxes) measured 50 × 10 cm. Guillotine doors separated the main arm and the goal boxes from the main body of the maze. Small plastic cups were placed in the corners of both goal boxes. The maze was covered with clear Plexiglas lids.

Experimental Procedure

Wistar rats weighing 250–300 g are exposed to three training sessions. On the first training day, animals were habituated to the maze for 20 min during which time they were allowed to explore the entire area. Thereafter, they were exposed to chocolate milk in their home cages, in order to acquaint them to the novel stimulus. On the second training day, animals were confined for 5 min to each goal arm, where chocolate milk was available. On the third training day, animals were placed in the main arm, the guillotine doors were lifted and rats were allowed to choose between the two goal arms, each one baited with chocolate milk. When the animal placed all four paws in a goal arm it was confined to it for 30 s and the entry was considered as a choice. Thereafter, the animals were removed and placed in a holding cage for 10 s. This procedure was repeated for a total nine runs.

Drug treatment (clomipramine or test drugs) was started on three consecutive days before the experimental sessions. One day before, the animals were deprived of food for 24 h.

Thereafter, they were injected i.p. with 1 mg/kg of the selective 5-HT_{1A} agonist 8-OH-DPAT and 15 min later they were placed in the main arm and allowed to choose between the two goal arms. The procedure was repeated up to seven runs or until they alternated their election. The choice made by the animal (right or left) was recorded. The number of repetitive choices until an alternation occurs indicates compulsive-like behavior. Additionally, the animals that chose the same alley in three consecutive occasions were defined as highly perseverative.

EVALUATION

The number of consecutive entries to the same alley of the T-maze is presented as the median and the number of highly perseverative per group is expressed as a percentage. Data were analyzed by means of nonparametric tests.

MODIFICATIONS OF THE METHOD

Joel and Avisar (2001) proposed excessive lever pressing following post-training signal attenuation in rats: a possible animal model of obsessive-compulsive disorder.

Szechtman et al. (2001) discussed compulsive checking behavior of quinpirole-sensitized rats as an animal model of obsessive-compulsive disorder.

Berridge et al. (2005) proposed sequential superstereotypy of an instinctive fixed action pattern in hyper-dopaminergic mutant **mice** as a model of obsessive-convulsive disorder.

REFERENCES AND FURTHER READING

Agrati D, Fernández-Guasti A, Zuluaga MJ, Uriarte N, Pereira M, Ferreira A (2005) Compulsive-like behavior according to the sex and the reproductive stage of female rats. Behav Brain Res 161:313–319

Berridge KC, Aldridge JW, Houchard KR, Zhuang X (2005) Sequential super-stereotypy of an instinctive fixed action pattern in hyper-dopaminergic mutant mice: a model of obsessive convulsive disorder and Tourette's. BMC Biology 3:1–16

Fernández-Guasti A, Ulloa RE, Nicolini H (2003) Age differences in the sensitivity to clomipramine in an animal model of obsessive compulsive disorder. Psychopharmacology 166:193–201

Joel D (2006) The signal attenuation rat model of obsessive-compulsive disorder. Psychopharmacology 186:487–503

Joel D, Avisar A (2001) Excessive lever pressing following post-training signal attenuation in rats: a possible animal model of obsessive compulsive disorder? Behav Brain Res 123:77–87

Joel D, Doljansky J, Roz N, Rehavi N (2005) Role of the orbital cortex and of the serotoninergic system in a rat model of obsessive compulsive disorder. Neuroscience 130:25–36

Nurnberg HG, Keith SJ, Paxton DM (1997) Consideration of the relevance of ethological animal models for human repetitive behavioral spectrum disorders. Biol Psychiatry 41:226–229

Overall KL (2000) Natural animal models of human psychiatric conditions: assessment of mechanism and validity. Prog Neuropsychopharmacol Biol Psychiatry 24:727–776

Stein DJ (2000) Neurobiology of the obsessive-compulsive spectrum disorders. Biol Psychiatry 47:296–304

Stein DJ (2002) Obsessive-compulsive disorder. Lancet 360:397–405

Stein DJ, Mendelson I, Potocnik F, Von Kradenberg J, Wessels C (1998) Use of the selective serotonin reuptake inhibitor citalopram in a possible animal analogue of obsessive-compulsive disorder. Depress Anxiety 8:39–42

Szechtman H, Eckert MJ, Tse WS, Boersma JT, Bonura CA, McClelland JZ, Culver KE, Eilam D (2001) Compulsive checking behavior of quinpirole-sensitized rats as an animal model of Obsessive-Compulsive Disorder (OCD): form and control. BMC Neuroscience 2:4

Tsaltas E, Kontis DK, Chrysikakou S, Giannou H, Biba A, Pallidi S, Christodoulou A, Maillis A, Rabavilas A (2005) Reinforced spatial alternation as an animal model of obsessive-compulsive disorder (OCD): investigation of 5-HT_{2C} and 5-HT_{1D} receptor involvement in OCD pathophysiology. Biol Psychiatry 57:1176–1185

Ulloa RE, Nicolini H, Fernández-Guasti A (2004a) Sex differences on spontaneous alteration in prepubertal rats: implications for an animal model of obsessive-compulsive disorder. Progr Neuropsychopharmacol Biol Psychiatry 28:687–692

Ulloa RE, Nicolini H, Fernández-Guasti A (2004b) Age differences in an animal model of obsessive-compulsive disorder: participation of dopamine. Dopamine in an animal model of OCD. Pharmacol Biochem Behav 78:661–666

Van Kuyck K, Demeulmeester H, Feys H, de Weerdt W, Dewil M, Tousseyn T, de Sutter P, Gybels J, Bogaerts K, Dom R, Nuttin B (2003) Effects of electrical stimulation or lesion in nucleus accumbens on the behaviour of rats after administration of 8-OH-DPAT or vehicle. Behav Brain Res 140:165–173

Woods-Kettelberger A, Kongsamut S, Smith CP, Winslow JT, Corbett R (1997) Animal models with potential applications for screening of compounds for the treatment of obsessive-compulsive disorder. Expert Opin Invest Drugs 6:1369–1381

Yadin E, Freidman E, Bridger WH (1991) Spontaneous alternation behavior: an animal model for obsessive-compulsive disorder? Pharmacol Biochem Behav 40:311–315

E.6.2.12 Antidepressant-Like Activity in Differential-Reinforcement of Low Rate 72-Second Schedule

PURPOSE AND RATIONALE

The differential-reinforcement of low-rate (DRL) 72-s schedule has been recommended for evaluation of antidepressant drugs (O'Donnell and Seiden 1983).

PROCEDURE

Male Sprague Dawley rats weighing 350–450 g are housed in suspended wire cages in rooms maintained at 21–23°C and 30% to 40% relative humidity having free access to laboratory chow except during experimental sessions. Water is provided after each daily session in order to maintain body weights.

Apparatus

Model C Gerbrand operant-conditioning chambers (O'Donnell and Seiden 1983) or Coulbourn operant chambers (Pollard and Howard 1986) are used. A lever that operates a microswitch is mounted on one wall 3 cm from the side, 2.5 cm above a grid floor and 6.5 cm from an access port for a dipper that provides 0.025 ml of water. A houselight is mounted on the opposite wall. A downwards force equivalent to approximately 15 g operates the lever, constituting a response. When the schedule requirements are met, the dipper is lifted from a water trough to an opening in the floor of the access port for 4 s, constituting a reinforcer.

Rats are water-deprived for 22 h before each session. Each rat is initially trained under an alternative fixed-ratio 1, fixed-time 1-min schedule for water reinforcement. Thus, each response is reinforced, and reinforcement is also provided every min if no responding occurs. All rats are then placed under a DRL (differential-reinforcement-of-low-rate) 18 s schedule for 3 weeks. The schedule requirement is then increased to 72 s (DRL 72-sec). When performances on the DRL 72-sec schedule are stabilized (approximately 6 weeks), drug treatments are initiated.

Each group of 6 to 10 rats is subjected to a dose-response determination for one ore more drugs. Drugs are administered one h before testing by intraperitoneal injection.

EVALUATION

Data are expressed as percentages of non-injected controls. The control values are the response and reinforcement rates on those days immediately preceding the test day. The number of responses and reinforcers per session at each drug dose are tested for statistically significant differences from control values with paired *t*-tests using a two tailed criterion of statistical significance.

CRITICAL ASSESSMENT OF THE TEST

The method is rather time consuming. Moreover, the specificity as screening method for antidepressants has been challenged (Pollard and Howard 1986).

REFERENCES AND FURTHER READING

Andrews JS, Jansen JHM, Linders S, Princen A, Drinkenburg WHIM, Coenders CJH, Vossen JHM (1994) Effects of imipramine and mirtazipine on operant performance in rats. Drug Dev Res 32:58–66

Marek GJ, Seiden LS (1988) Effects of selective 5-hydroxytryptamine-2 and nonselective 5-hydroxytryptamine antagonists on the differential-reinforcement-of-low-rate 72-second schedule. J Pharmacol Exp Ther 244:650–558

Marek GJ, Li AA, Seiden LS (1989) Selective 5-hydroxytryptamine$_2$ antagonists have antidepressant-like effects on differential-reinforcement-of-low-rate 72 second schedule. J Pharmacol Exp Ther 250:52–59

McGuire PS, Seiden LS (1980) The effects of tricyclic antidepressants on performance under a differential-reinforcement-of-low-rates schedule in rats. J Pharmacol Exp Ther 214:635–641

O'Donnell JM, Seiden LS (1983) Differential-reinforcement-of-low-rate 72-second schedule: selective effects of antidepressant drugs. J Pharmacol Exp Ther 224:80–88

Pollard GT, Howard JL (1986) Similar effects of antidepressant and non-antidepressant drugs on behavior under an interresponse-time >72-s schedule. Psychopharmacology 89:253–258

van Hest A, van Drimmelen M, Olivier B (1992) Flesinoxan shows antidepressant activity in a DRL 72-s screen. Psychopharmacology 107:474–479

E.6.3 Tests for Antidepressant Activity Based on the Mechanism of Action

E.6.3.1 Potentiation of Norepinephrine Toxicity

PURPOSE AND RATIONALE

Antidepressants block the re-uptake of biogenic amines into nervous tissue. In this way, the toxic effects of norepinephrine are potentiated.

PROCEDURE

Male NMRI mice (22–25 g) are randomly assigned to test groups of 10 subjects. The test drug, the standard or the vehicle are given orally 1 h prior to the s.c. injection of the sublethal dose of 3 mg/kg noradrenaline. The groups of 10 mice are placed into plastic cages with free access to food and water.

EVALUATION

The mortality rate is assessed 48 h post-dosing. ED_{50}, or dose which causes death of 50% of the treated subjects, is calculated by means of linear regression analysis.

CRITICAL ASSESSMENT OF THE METHOD

Several antidepressants block not only the uptake of noradrenaline, but also of dopamine and of serotonin.

By definition, this test can only measure the noradrenaline-uptake inhibition.

One of the earliest observations on the pharmacology of antidepressants was by Sigg (1959), who showed that imipramine, as distinguished from other tricyclic substances known at this time, produced a profound potentiation of the cardiovascular effects of exogenously administered catecholamines in animals.

REFERENCES AND FURTHER READING

Alpermann HG, Schacht U, Usinger P, Hock FJ (1992) Pharmacological effects of Hoe 249: A new potential antidepressant. Drug Dev Res 25:267–282

Sigg EB (1959) Pharmacological studies with Tofranil. Can Psych Assoc J 4:S75–S85

E.6.3.2 Compulsive Gnawing in Mice

PURPOSE AND RATIONALE

In man and in other species, like dogs, apomorphine induces emesis. Treatment of rodents with apomorphine causes compulsive gnawing instead of vomiting. The compulsive gnawing in mice induced by apomorphine is due to dopaminergic stimulation. Centrally acting anticholinergics shift the balance between acetylcholine and dopamine resulting in an enhancement of the apomorphine effect. Therefore, many compounds with psychotropic activity are known to have an apomorphine-synergistic effect. This enhancement is also found after administration of tricyclic antidepressants (Ther and Schremm 1962).

PROCEDURE

NMRI mice with a body weight between 18 and 20 g are injected s.c. with 10 mg/kg apomorphine. At the same time they are treated i.p. or s.c. with the test drug or the vehicle. For testing oral activity the animals are treated 30 min prior to apomorphine injection. Immediately after apomorphine injection 6 mice are placed into a cage $45 \times 45 \times 20$ cm with a wired lid. The bottom of the cage is covered with corrugated paper, the corrugation facing upwards. The mice start to bite into the paper causing fine holes or tear the paper. This behavior is enhanced by antidepressants. The mice remain 1 h in the cage.

EVALUATION

The number of bites into the corrugated paper is evaluated by placing a template upon the paper. The template has 10 rectangle windows divided into 10 areas of the same size. In a total of 100 areas the number of bites is checked. In this way percentage of damaged paper in calculated. Ten mg/kg apomorphine does not increase the biting rate of 5–10% which also occurs in normal animals. Likewise, atropine in doses of 40 and 80 mg/kg s.c. alone does not increase the biting behavior. In contrast, the combination of apomorphine and atropine greatly enhances the occurrence of gnawing. The same is true for antidepressants. For example, a dose of 25 mg/kg imipramine increases the damaged area by 40–70%. Percent gnawing of the test compound is compared with that of the standard.

CRITICAL ASSESSMENT OF THE TEST

Not only antidepressants, but also centrally acting anticholinergics and antihistaminics are active in this test. However, the test has the advantage of simplicity without any pretraining of the animals.

MODIFICATIONS OF THE METHOD

De Feo et al. (1983) reported on possible dopaminergic involvement in biting compulsion of mice induced by large doses of clonidine.

Stereotyped gnawing in mice is induced by methylphenidate (Pedersen and Christensen 1972). The phenomenon is potentiated by various drugs, such as benzodiazepines (Nielsen et al. 1991).

Stereotyped behavior in **guinea pigs** induced by apomorphine or amphetamine consisting in continuous gnawing and sniffing of the cage floor was described by Klawans and Rubovits (1972) and used as an experimental model of tardive dyskinesia.

Molander and Randrup (1974) investigated the mechanisms by which L-DOPA induces gnawing in mice.

REFERENCES AND FURTHER READING

De Feo G, Lisciani R, Pavan L, Samarelli M, Valeri P (1983) Possible dopaminergic involvement in biting compulsion induced by large doses of clonidine. Pharmacol Res Commun 15:613–619

Klawans HL, Rubovits R (1972) An experimental model of tardive dyskinesia. J Neural Transmiss 33:235–246

Molander L, Randrup A (1974) Investigation of the mechanism by which L-DOPA induces gnawing in mice. Acta Pharmacol Toxicol 34:312–324

Nielsen EB, Suzdak PD, Andersen KE, Knutsen LJS, Sonnewald U, Braestrup C (1991) Characterization of tiagabine (NO-328), a new potent and selective GABA uptake inhibitor. Eur J Pharmacol 196:257–266

Pedersen V, Christensen AV (1972) Antagonism of methylphenidate-induced stereotyped gnawing in mice. Acta Pharmacol Toxicol 31:488–496

Randall PK (1985) Quantification of dopaminergic supersensitization using apomorphine-induced behavior in the mouse. Life Sci 37:1419–1423

Ther L, Schramm H (1962) Apomorphin-Synergismus (Zwangsnagen bei Mäusen) als Test zur Differenzierung psychotroper Substanzen. Arch Int Pharmacodyn 138:302–310

E.6.3.3 Apomorphine-Induced Hypothermia in Mice

PURPOSE AND RATIONALE

Apomorphine induces hypothermia in mice which can be prevented by antidepressants.

PROCEDURE

Male NMRI mice (20–22 g) are used and randomly assigned to test groups of 6 subjects. One hour after oral administration of the test compounds or the vehicle a dose of 16 mg/kg apomorphine is injected s.c. The rectal temperature of each mouse is measured by an electronic thermometer immediately prior to apomorphine administration and 10, 20 and 30 min later. During the entire experiment, subjects are housed in groups of three in glass jars at room temperature.

EVALUATION

A time curve is constructed by plotting the temperature (mean of each group) against time in min. The AUC is calculated for all groups and converted into percent inhibition of apomorphine-induced hypothermia in the control group. An ED_{50} can be calculated by linear regression analysis.

CRITICAL ASSESSMENT OF THE METHOD

Antagonism against apomorphine-induced hypothermia can be regarded as a hint for antidepressant activity. Compounds with a marked noradrenergic or dopaminergic component are active against apomorphine-induced hypothermia but not antidepressants acting mainly through serotoninergic mechanisms.

MODIFICATIONS OF THE METHOD

Cox and Lee (1981) induced hypothermia in rats by intrahypothalamic injection of 5-hydroxytryptamine and recommended this as a model for the quantitative study of 5-hydroxytryptamine receptors.

REFERENCES AND FURTHER READING

Alpermann HG, Schacht U, Usinger P, Hock FJ (1992) Pharmacological effects of Hoe 249: A new potential antidepressant. Drug Dev Res 25:267–282

Cox B, Lee TF (1981) 5-Hydroxytryptamine-induced hypothermia in rats as an *in vivo* model for the quantitative study of 5-hydroxytryptamine receptors. J Pharmacol Meth 5:43–51

Porsolt RD, Lenègre A, McArthur RA (1991) Pharmacological models of depression. In: Olivier B, Mos J, Slangen JL (eds) Animal Models in Psychopharmacology, Birkhäuser Verlag Basel, pp 137–159

Puech AJ, Chermat R, Poncelet M, Doaré L, Simon P (1981) Antagonism of hypothermia and behavioural responses to apomorphine: a simple, rapid and discriminating test for screening anti-depressants and neuroleptics. Psychopharmacology 75:84–91

E.6.3.4 Tetrabenazine Antagonism in Mice

PURPOSE AND RATIONALE

Tetrabenazine (TBZ) induces a depletion of biogenic amines (e. g. noradrenaline, dopamine, serotonin) without affecting their de novo synthesis. TBZ depletes noradrenaline from nerve terminals and prolongs re-uptake into the granula. Noradrenaline is degraded by monoamino-oxydase. Antidepressants inhibit the re-uptake of noradrenaline into the nerve terminals and increase thereby the noradrenaline concentration at the receptor site. In this way, the effect of TBZ is antagonized. Therefore, both MAO-inhibitors and tricyclic antidepressants are known to prevent or to antagonize these effects. The prevention of TBZ induced ptosis and catalepsy can be used for evaluation of antidepressants.

PROCEDURE

Groups of 5–10 male NMRI mice (20–22 g) are used. Sixty min after oral or 30 min after i.p administration of the test compound or the vehicle 40 mg/kg i.p. TBZ are injected. The animals are placed into individual cages. The test is started 30 min after TBZ administration and repeated every 30 min up to 2 h. Catalepsy and ptosis are used as criteria. A stair is formed with 2 cork stoppers having 2 steps of 3 cm height. The animals are placed head downwards with their hindlegs upon the top cork. As long as TBZ exerts its cataleptic effect the animals remain in this catatonic state. If the cataleptic effect is not antagonized after a limit of 60 s the animals are placed into a normal position.

EVALUATION

Thirty days after replacement the degree of ptosis is scored: eyes closed = 4, eyes 3/4 closed = 3, eyes 1/2 closed = 2, eyes 1/4 closed = 1, eyes open = 0. (Rubin et al. 1957) Similarly, the cataleptic effect is scored according to the duration of catalepsy. Catalepsy more than 60 s = 5, between 30 and 60 s = 4, between 10 and 30 s = 3, between 5 and 10 s = 1, less than 5 s = 0. The scores of the TBZ controls are taken as 100% and the percentage is calculated for the treated animals.

Imipramine was found to be effective at a dose of 10 mg/kg s.c. or 20 mg/kg orally.

CRITICAL ASSESSMENT OF THE METHOD

The TBZ antagonism has been found to be a simple and reliable test for evaluation of classical antidepressants.

MODIFICATIONS OF THE METHOD

Ptosis in mice can be induced in a similar way by treatment with reserpine. Mice receive a single oral dose of the test compound followed by subcutaneous administration of 5 mg/kg reserpine 30 min later. Ptosis is observed for the next 1 or 2 h and scored in a similar way as in the TBZ test.

TBZ ptosis can also be elicited in rats. The test procedure and the evaluation is the same as in mice. Tetrabenazine-induced hyperthermia in mice has been proposed as test for antidepressant activity by Gylys et al. (1963).

REFERENCES AND FURTHER READING

Alpermann HG, Schacht U, Usinger P, Hock FJ (1992) Pharmacological effects of Hoe 249: A new potential antidepressant. Drug Dev Res 25:267–282

Benesová O, Náhunek K (1971) Correlation between the experimental data from animal studies and therapeutic effects of antidepressant drugs. Psychopharmacologia (Berlin) 20:337–347

Doble A, Girdlestone D, Piot O, Allam D, Betschart J, Boireau A, Dupuy A, Guérémy C, Ménager J, Zundel JL, Blanchard JC (1992) Pharmacological characterisation of RP 62203, a novel 5-hydroxytryptamine 5-HT_2 receptor antagonist. Br J Pharmacol 15:27–36

Gylys JA, Muccia PMR, Taylor MK (1963) Pharmacological and toxicological properties of 2-methyl-3-piperidinopyrazine, a new antidepressant. Ann NY Acad Sci 107:899–913

Jamieson DD, Duffield PH, Cheng D, Duffield AM (1989) Comparison of the central nervous system activity of the aqueous und lipid extract of kava (Piper methysticum) Arch Int Pharmacodyn 301:66–80

Nakagawa T, Ukai K, Kubo S (1993) Antidepressive effects of the stereoisomer cis-dosulepin hydrochloride. Arzneim Forsch/Drug Res 43:11–15

Rubin B, Malone MH, Waugh MH, Burke JC (1957) Bioassay of Rauwolfia roots and alkaloids. J Pharmacol Exp Ther 120:125–136

E.6.3.5 Reserpine-Induced Hypothermia

PURPOSE AND RATIONALE

Depletion of biogenic amines (noradrenaline, 5-hydroxytryptamine, dopamine) in the brain induces not only catalepsy and ptosis but also hypothermia in rodents. The decrease of body temperature induced by reserpine is antagonized by antidepressants, MAO-inhibitors and central stimulants. The subcutaneous administration of 2 mg/kg reserpine leads to a decrease of core temperature in mice to 20–23°C after 18 h. The fall in temperature can be antagonized by antidepressants, but also by amphetamine-like drugs. However, the time course is different: tricyclic antidepressants have a slow onset of action and a long lasting effect, whereas amphetamine-like drugs have a quick onset of action and a short-lasting effect.

PROCEDURE

Groups of 5 male NMRI mice (19–21 g body weight) are used. On the day before testing, they are dosed with 2 mg/kg reserpine s.c. They are housed in a climate-controlled animal colony and have free access to food and water. Eighteen hours after reserpine administration, the animals are placed into individual cages. The initial rectal temperature is determined by insertion of an electronic thermometer (e. g. Ellab T-3) to a constant depth of 2 cm. Following administration of the test compound (either i.p. or p.o.), the rectal temperature is measured again at 60 min intervals for 7 h.

EVALUATION

Rectal temperature is recorded every hour. The difference in temperature from vehicle controls is calculated for each time and the maximal difference is scored. The differences are then statistically compared using the *t*-test.

MODIFICATIONS OF THE METHOD

The time course and the administration route can be changed. Male mice are treated with the test drug or the standard 1 h prior to intravenous injection of 2 mg/kg reserpine. Rectal temperature is measured by a rectal thermometer prior and every 60 min up to 6 h The animals are kept in groups of 3 in glass jars at a controlled temperature of 20–21°C. Using a computer program the area under the curve is calculated by plotting the temperature (mean of each group) before and the decrease after reserpine against time in hours. Areas of treated groups are converted to percentage of controls.

Colpaert et al. (1975), Niemegeers (1975) described the antagonism of antidepressants and other drugs against Ro-4–1284, a benzoquinolizine derivative which by itself exhibits reserpine-like activities.

CRITICAL ASSESSMENT OF THE METHOD

The test has been proven as a simple and reliable method to detect antidepressant activity. However, the

reversal of hypothermia is not specific for antidepressants. The fall in body temperature can also be antagonized by amphetamines, and some antipsychotic agents (chlorpromazine). The different time course of antidepressants (slow onset of action, long-lasting effect) and amphetamine-like drugs (quick onset of action, short-lasting effect) allows differentiation between the two groups of drugs.

REFERENCES AND FURTHER READING

Alpermann HG, Schacht U, Usinger P, Hock FJ (1992) Pharmacological effects of Hoe 249: A new potential antidepressant. Drug Dev Res 25:267–282

Askew BM (1963) A simple screening procedure for imipramine-like antidepressant drugs. Life Sci 10:725–730

Bill DJ, Hughes IE, Stephens RJ (1989) The effects of acute and chronic desimipramine on the thermogenic and hypoactivity responses to α_2-agonists in reserpinized and normal mice. Br J Pharmacol 96:144–152

Bourin M (1990) Is it possible to predict the activity of a new antidepressant in animals with simple psychopharmacological tests? Fundam Clin Pharmacol 4:49–64

Bourin M, Poncelet M, Chermat R, Simon P (1983) The value of the reserpine test in psychopharmacology. Arzneim Forsch/Drug Res 33:1173–1176

Colpaert FC, Lenaerts FM, Niemegeers CJE, Janssen PAJ (1975) A critical study of Ro-4–1284 antagonism in mice. Arch Int Pharmacodyn 215:189–239

Koe BK, Lebel LA, Nielsen JA, Russo LL, Saccomano NA, Vinick FJ, Williams IA (1990) Effects of novel catechol ether imidazolidinones on calcium-dependent phosphodiesterase activity, (^{3}H)Rolipram binding, and reserpine-induced hypothermia in mice. Drug Dev Res 21:135–142

Niemegeers CJE (1975) Antagonism of reserpine-like activity. In: Fielding S, Lal H (eds) Industrial Pharmacology. Vol II: Antidepressants. Futura Publ Comp., pp 73–98

Muth EA, Moyer JA, Haskins JT, Andree TH, Husbands GEM (1991) Biochemical, neurophysiological, and behavioral effects of Wy-45,233 and other identified metabolites of the antidepressant Venlafaxine. Drug Dev Res 23:191–199

Pawlowski L, Nowak G (1987) Biochemical and pharmacological tests for the prediction of ability of monoamine uptake blockers to inhibit the uptake of noradrenaline *in vivo*: the effects of desimipramine, maprotiline, femoxitine and citalopram. J Pharm Pharmacol 39:1003–1009

Porsolt RD, Lenègre A, McArthur RA (1991) Pharmacological models of depression. In: Olivier B, Mos J, Slangen JL (eds) Animal Models in Psychopharmacology, Birkhäuser Verlag Basel, pp 137–159

E.6.3.6 5-Hydroxytryptophan Potentiation in Mice

PURPOSE AND RATIONALE

According to the monoamine hypothesis of depression compounds exert antidepressant activity because they are capable of enhancing central noradrenergic and/or serotoninergic functions. Several antidepressant agents potentiate serotonin effects by a block of the re-uptake of serotonin. DL-5-Hydroxytryptophan is used as the precursor of serotonin. Enzymatic breakdown is inhibited by the MAO-inhibitor pargyline. In mice the characteristic symptom of head-twitches is observed.

PROCEDURE

Groups of 6 male mice (18–30 g) are used. They are treated i.p with the test drug or the vehicle. Thirty min later, the mice receive 75 mg/kg pargyline HCl s.c. Ninety min after pargyline the animals are injected wit 10 mg/kg DL-5-hydroxytryptophan (5-HTP) i.v.

EVALUATION

Animals positively influenced show a characteristic behavior of head twitches. A animal is considered to be positive if it shows head twitches 15 min after 5-HTP injection. Enhancement is observed after treatment with serotonin uptake blockers relative to animals pretreated with pargyline only.

CRITICAL ASSESSMENT OF THE METHOD

The test can be considered as additional evidence for antidepressant activity based on uptake inhibition.

MODIFICATION OF THE METHOD

The head-twitch in mice can also be elicited without a MAO-inhibitor by using higher doses (200 mg/kg) of DL-5-hydroxytryptophan.

Moser and Redfern (1988) studied the effects of four benzodiazepines on the head-twitch response induced in mice by several 5-HT receptor agonists.

Meert et al. (1988) studied partial and complete blockade of 5-hydroxytryptophan (5-HTP)-induced head twitches in the *rat* by serotonin S_2 antagonists.

Niemegeers et al. (1983), Awouters et al. (1988) used *mescaline* induced head twitches in the rat as an *in vivo* method to evaluate serotonin S_2-antagonists. Head twitches were counted for 15 min after intravenous injection of 20 mg/kg mescaline. Twitch counts of less than 2 were considered as inhibition and of less than 2 as blockade of the mescaline response.

REFERENCES AND FURTHER READING

Ahtee L, Saarnivaara L (1971) The effect of drugs upon the uptake of 5-hydroxytryptamine and metaraminol by human platelets, J Pharm Pharmacol 23:495–501

Alpermann HG, Schacht U, Usinger P, Hock FJ (1992) Pharmacological effects of Hoe 249: A new potential antidepressant. Drug Dev Res 25:267–282

Awouters F, Niemegeers CJE, Megens AAHP, Meert TF, Janssen PAJ (1988) Pharmacological profile of ritanserin: a very specific central serotonin antagonist. Drug Dev Res 15:61–73

Chen G (1964) Antidepressives, analeptics and appetite suppressants. In: Laurence DR, Bacharach AL (eds) Evaluation of Drug Activities: Pharmacometrics. Academic Press, London and New York, pp 239–260

Corne SJ, Pickering RW, Warner BT (1963) A method for assessing the effects of drugs on the central actions of 5-hydroxytryptamine. Br J Pharmacol 20:106–120
Martin P, Frances H, Simon P (1985) Dissociation of head twitches and tremors during the study of interactions with 5-hydroxytryptophan in mice. J Pharmacol Meth 13:193–200
Meert TF, Niemegeers JE, Awouters F, Janssen PAJ (2003) Partial and complete blockade of 5-hydroxytryptophan (5-HTP)-induced head twitches in the rat: a study of ritanserin (R55667), risperidone (R64766), and related compounds. Drug Develop Res 13:237–244
Moore NA, Tye NC, Axton MS, Risius FC (1992) The behavioral pharmacology of olanzapine, a novel "atypical" antipsychotic agent. J Pharmacol Exp Ther 262:545–551
Moser PC, Redfern PH (1988) The effect of benzodiazepines on the 5-HT agonist-induced head-twitch response in mice. Eur J Pharmacol 151:223–231
Ortmann R, Martin S, Radeke E, Delini Stula A (1981) Interaction of beta-adrenoreceptor agonists with the serotonergic system in rat brain. A behavioural study using the L-5-HTP syndrome. Naunyn Schmiedeberg's Arch Pharmacol 316:225–230
Shank RP, Gardocki JF, Schneider CR, Vaught JL, Setler PE, Maryanoff BE, McComsey DF (1987) Preclinical evaluation of McN-5707 as a potential antidepressant. J Pharmacol Exp Ther 242:74–84
Shank RP, Vaught JL, Pelley KA, Setler PE, McComsey DF, Maryanoff BE (1988) McN-5652: A highly potent inhibitor of serotonin uptake. J Pharmacol Exp Ther 247:1032–1038

E.6.3.7
5-Hydroxytryptophan Potentiation in Rats

PURPOSE AND RATIONALE

The inhibition of serotonin re-uptake by some anti-depressants can be tested *in vivo* in rats by administration of the precursor 5-hydroxytryptophan and inhibition of its breakdown by the MAO-inhibitor pargyline. In contrast to mice exhibiting head twitches, rats show other symptoms such as continuous forelimb clonus.

PROCEDURE

Groups of 6 male Wistar rats weighing 150–200 g are used. Four hours prior to testing pargyline HCl is injected sc. at a dose of 75 mg/kg. Thirty min before i.p. injection of 1 mg/kg L-5-hydroxytryptophan, test compounds or standards are administered intraperitoneally. Fifteen min after the 5-hydroxytryptophan injection, the animals are observed for 15 min. An animal is considered to be positive if is exhibits continuous forelimb clonus.

EVALUATION

Enhancement is expressed as normalized percent increase relative to the vehicle control. Using various doses, ED_{50} values with 95% confidence limits can be determined by probit analysis.

MODIFICATIONS OF THE METHOD

Hallberg et al. (1985) developed a registration device based on accelerometry in order to accomplish an objective quantification of tremors in conscious unrestrained rats. Tremor intensity was continuously recorded by a small piecoresistive accelerometer mounted on the back of the freely moving rat. The accelerometer was connected to a Grass Polygraph. The integrated signals were further analyzed by a desk-top computer.

The behavior in rats induced by 10 mg/kg L-5-hydroxytryptophan i.p. can be antagonized by compounds having 5-HT_2 antagonist properties (Colpaert and Janssen 1983).

REFERENCES AND FURTHER READING

Ahtee L, Saarnivaara L (1971) The effect of drugs upon the uptake of 5-hydroxytryptamine and metaraminol by human platelets, J Pharm Pharmacol 23:495–501
Colpaert FC, Janssen PA (1983) The head-twitch response to intraperitoneal injection of 5-hydroxytryptophan in the rat: Antagonist effects of purported 5-hydroxytryptamine antagonists and of pirenperone, an LSD antagonist. Neuropharmacol 22:993–1000
Hallberg H, Carlson L, Elg R (1985) Objective quantification of tremor in conscious unrestrained rats, exemplified with 5-hydroxytryptamine-mediated tremor. J Pharmacol Meth 13:261–266
Matthews WD, Smith CD (1980) Pharmacological profile of a model for central serotonin receptor activation Life Sci 26:1397–1403
Shank RP, Gardocki JF, Schneider CR, Vaught JL, Setler PE, Maryanoff BE, McComsey DF (1987) Preclinical evaluation of McN-5707 as a potential antidepressant. J Pharmacol Exp Ther 242:74–84

E.6.3.8
Yohimbine Toxicity Enhancement

PURPOSE AND RATIONALE

Yohimbine occupies central α_2-receptors, and prevents noradrenaline from binding to these receptors. Compounds with antidepressant properties are known to inhibit physiological inactivation of noradrenaline and other biogenic amines by blocking the re-uptake at nerve terminals. Administration of a test compound with antidepressant properties leads to an increase in noradrenaline concentration. Following the simultaneous administration of yohimbine and antidepressants the animals die of noradrenaline poisoning.

PROCEDURE

Groups of 10 male NMRI mice (25–28 g) are used. Mice are placed in plastic cages and receive the test compound or the vehicle by oral or i.p. administration.

Thirty min later, a dose of 25 mg/kg yohimbine (a sublethal dose) is given s.c.

EVALUATION

Mortality rate is assessed 1 h, 2 h, 3 h, 4 h, 5 h, and 24 h after dosing. Lethality in the control group (Yohimbine only) is less than 10%, whereas 10 mg/kg desipramine-HCl causes death in about 90%. Using various doses ED_{50}-values can be calculated.

CRITICAL ASSESSMENT OF THE METHOD

The test has been proven as a simple method to detect antidepressants with monoamine uptake inhibiting properties.

REFERENCES AND FURTHER READING

Alpermann HG, Schacht U, Usinger P, Hock FJ (1992) Pharmacological effects of Hoe 249: A new potential antidepressant. Drug Dev Res 25:267–282

Bourin M, Malinge M, Colombel MC, Larousse C (1988) Influence of alpha stimulants and beta blockers on yohimbine toxicity. Prog Neuro-Psychopharmacol Biol Psychiat 12:569–574

Goldberg MR, Robertson D (1983) Yohimbine: A pharmacological probe for study the α_2-adrenoreceptor. Pharmacol Rev 35:143–180

Malick JP (1981) Yohimbine potentiation as a predictor of antidepressant action. In: Enna SJ, Malick JB, Richelson E (eds) Antidepressants: neurochemical, behavioral and clinical perspectives. Raven Press, New York, pp 141–156

Porsolt RD, Lenègre A, McArthur RA (1991) Pharmacological models of depression. In: Olivier B, Mos J, Slangen JL (eds) Animal Models in Psychopharmacology, Birkhäuser Verlag Basel, pp 137–159

Quinton RM (1963) The increase in the toxicity of yohimbine induced by imipramine and other drugs in mice. Br J Pharmacol 21:51–66

E.6.3.9 Tryptamine Seizure Potentiation in Rats

PURPOSE AND RATIONALE

Monoamine oxidase (MAO) inhibitors like iproniazid enhance seizures in rats caused by an intravenous infusion of tryptamine HCl. This procedure can be used to elucidate the *in vivo* MAO inhibiting properties of compounds.

PROCEDURE

Groups of 5 male Wistar rats weighing 150–200 g are used. Test compounds, standard or vehicle controls are administered intraperitoneally 0.5; 1; 2; and 4 h prior testing. At the time of testing 5 mg/kg tryptamine HCl freshly dissolved in saline are injected intravenously. Immediately after tryptamine HCl administration, the animals are observed individually for three min for the appearance of clonic "pedalling" movements of the forepaws which is considered a positive response. Frequently, these clonic seizures are preceded by a kyphotic curvature of the spine but this sign does not constitute a positive response.

In addition to the vehicle control group, a series of five positive control animals receiving tranylcypromine at 5 mg/kg i.p. with a 0.5 h pretreatment time are subjected to the test in order to check the effectiveness of the tryptamine HCl solution which is relatively unstable. A 100% response is expected. Fresh tryptamine HCl solution should be prepared hourly as needed.

EVALUATION

The normalized percent potentiation is calculated as follows:

$$100 \times \left[\frac{\%\ \text{animals potent. in drug group}}{1 - \%\ \text{animals potent. in vehicle group}} - \frac{\%\ \text{animals potent. in vehicle}}{1 - \%\ \text{animalspotent. in vehicle group}} \right]$$

A dose-response is obtained in the same manner at the peak time of drug effect except that a group size of 10 animals is used and four different doses are tested in addition to the vehicle and the tranylcypromine groups.

An ED_{50} is calculated using probit analysis.

MODIFICATIONS OF THE METHOD

Graham-Smith (1971) described the inhibitory effect of chlorpromazine on the syndrome of hyperactivity produced by L-tryptophan or 5-methoxy-N,N-dimethyltryptamine in rats treated with a monoamine oxidase inhibitor.

REFERENCES AND FURTHER READING

Graham-Smith DG (1971) Inhibitory effect of chlorpromazine on the syndrome of hyperactivity produced by L-tryptophan or 5-methoxy-N,N-dimethyltryptamine in rats treated with a monoamine oxidase inhibitor. Br J Pharmacol 43:856–864

Knoll J (1980) Monoamine oxidase inhibitors: Chemistry and pharmacology. In: Sandler M (ed) Enzyme Inhibitors as Drugs. pp 151–173. University Park Press

Ozaki M, Weissbach H, Ozaki A, Witkop B, Udenfriend S (1960) Monoamine oxidase inhibitors and procedures for their evaluation *in vivo* and *in vitro*. J Med Pharmac Chem 2:591–607

E.6.3.10 Serotonin Syndrome in Rats

PURPOSE AND RATIONALE

Compounds which stimulate serotonin receptors cause a series of behavioral changes in rats which is called the serotonin syndrome (Jacobs 1976; Green and Heal 1985; Tricklebank 1985) such as head weaving, increased locomotion, forepaw treading, flat posture and lower lip retraction. With increasing knowledge about the subtypes of serotonin receptors these symptoms were defined to be associated with 5-HT_{1A} receptors and their specific agonists (Smith and Peroutka (1986), Blanchard et al. 1993; Yu and Lewander 1997).

PROCEDURE

Time- and dose-dependence of **forepaw treading**, which is scored at 15, 30, 45, and 60 min according to a 3-point scale (0 = absent; 1 = periodic and weak; 2 = continuous) according to Arnt and Hyttel (1989) and Porsolt et al. (1992),

was measured by Deakin and Green (1978), Green et al. (1983), Goodwin and Green (1985), Goodwin et al. (1986), Berendsen and Broekkamp (1990), Schoeffter et al. (1993), Andersson and Larsson (1994), Forster et al. (1995), Kofman and Levin (1995), Lu and Nagayama (1996), O'Connell and Curzon (1966), Gaggi et al. (1997), Kleven et al. (1997), Yu and Lewander (1997),

of **flat body posture** by Deakin and Green (1978), Goodwin and Green (1985), Goodwin et al. (1986), Blanchard et al. (1993), Schoeffter et al. (1993), Andersson and Larsson (1994), Foreman et al. (1993, 1994, 1995), Forster et al. (1995), Kofman and Levin (1995), O'Connell and Curzon (1966), Gaggi et al. (1997), Kleven et al. (1997), Wolff et al. (1997), Yu and Lewander (1997),

of **hind limb abduction** by Deakin and Green (1978), Green et al. (1983), Goodwin and Green (1985), Goodwin et al. (1986), Kofman and Levin (1995),

of **increased motility** by Tricklebank (1985), Forster et al. (1995), Gaggi et al. (1997), O'Neill and Parameswaran (1997),

of **decreased body temperature** by Martin et al. (1992), Schoeffter et al. (1993), Simiand et al. (1993), Foreman et al. (1993, 1994, 1995), Forster et al. (1995), O'Connell and Curzon (1966), Bagdy and To (1997), Wolff et al. (1997), Yu and Lewander (1997),

of **head twitches** by Deakin and Green (1978), Green et al. (1983), Goodwin and Green (1985), Goodwin et al. (1986), Meert et al. (1988), Berendsen and Broekkamp (1990,) Kofman and Levin (1995), Gaggi et al. (1997), Kleven et al. (1997),

of **lower lip retraction**, which is scored according to Berendsen et al. (1989) after 15, 30, 45 min as follows: 0 = lower incisors not or hardly visible (not different from nontreated animals), 0.5 = partly visible, 1 = completely visible,

by Smith and Peroutka (1986), Berendsen et al. (1994, 1997), Porsolt et al. (1992), Blanchard et al. (1993), Andersson and Larsson (1994), Foreman et al. (1993, 1994, 1995), Moore et al. (1993), De Boer et al. (1995), Berendsen et al. (1966), Bagdy and To (1997), Groenink et al. 1997; Kleven et al. (1997), Wolff et al. (1997).

EVALUATION

Scores of each symptom are registered for each test animal. Average values of treated animals are compared with controls treated with vehicle alone. Dose-response and time response curves are evaluated.

CRITICAL ASSESSMENT OF THE TEST

Among the many symptoms of the serotonin syndrome in rats, forepaw treading, flat body posture and lower lip retraction were used by most authors to characterize agonists and antagonists of 5-HT_{1A} receptors.

MODIFICATIONS OF THE METHOD

Trulson et al. (1976) used the serotonin syndrome to test the supersensitivity after destruction of central serotonergic nerve terminals by intracerebral injection of 5,7-dihydroxytryptamine.

Blanchard et al. (1997) described the symptoms of selective activation of 5-HT_{1A} receptors in **mice**.

Locomotor activity of **guinea pigs** was increased in a dose-dependent manner by 5-HT_{1A} receptor agonists (Evenden 1994).

REFERENCES AND FURTHER READING

Andersson G, Larsson K (1994) Effects of FG 5893, a new compound with 5-HT_{1A} receptor agonistic and 5-HT_2 receptor antagonistic properties, on male rat sexual behavior. Eur J Pharmacol 255:131–137

Arnt J, Hyttel J (1989) Facilitation of 8-OH-DPAT-induced forepaw treading of rats by the 5-HT_2 agonist DOI. Eur J Pharmacol 161:45–51

Bagdy G, To CT (1997) Comparison of relative potencies of i.v. and i.c.v. administered 8-OH-DPAT gives evidence of different sites of action for hypothermia, lower lip retraction and tail flicks. Eur J Pharmacol 323:53–58

Berendsen HG, Broekkamp CLE (1990) Behavioural evidence for functional interactions between 5-HT-receptor subtypes in rats and mice. Br J Pharmacol 101:667–673

Berendsen HG, Broekkamp CLE (1997) Indirect *in vivo* 5-HT_{1A}-agonistic effects of the new antidepressant mirtazapine. Psychopharmacology 133:275–282

Berendsen HHG, Jenk F, Broekkamp CLE (1989) Selective activation of 5-HT_{1A} receptors induces lower lip retraction in the rat. Pharmacol Biochem Behav 33:821–827

Berendsen HHG, Bourgondien FGM, Broekkamp CLE (1994) Role of dorsal and median raphe nuclei in lower lip retraction in rats. Eur J Pharmacol 263:315–318

Berendsen HHG, Kester RCH, Peeters BWMM, Broekkamp CLE (1996) Modulation of 5-HT receptor subtype-mediated behaviours by corticosterone. Eur J Pharmacol 308:103–111

Blanchard RJ, Shepherd JK, Armstrong J, Tsuda SF, Blanchard DC (1993) An ethopharmacological analysis of the behavioral effects of 8-OH-DPAT. Psychopharmacology 112:55–65

Blanchard RJ, Griebel G, Guardiola-Lemaître B, Brush MM, Lee J, Blanchard DC (1997) An ethopharmacological analysis of selective activation of 5-HT_{1A} receptors: the mouse 5-HT_{1A} syndrome. Pharmacol Biochem Behav 57:897–908

Deakin JFW, Green AR (1978) The effects of putative 5-hydroxytryptamine antagonists on the behaviour produced by administration of tranylcypromine and L-Dopa in rats. Br J Pharmacol 64:201–209

De Boer T, Ruigt GSF, Berendsen HHG (1995) The alpha-2-selective adrenoceptor antagonist Org 3770 (mirtazapine, Remeron registered) enhances noradrenergic and serotonergic transmissions. Hum Psychopharmacol 10, Suppl2:S107–S118

Evenden JL (1994) The effect of 5-HT_{1A} receptor agonists on locomotor activity in the guinea pig. Br J Pharmacol 112:861–866

Foreman MM, Fuller RW, Leander JD, Benvenga MJ, Wong DT, Nelson DL, Calligaro DO, Swanson SP, Lucot JP, Flaugh ME (1993) Preclinical studies in LY228729: a potent and selective serotionin$_{1A}$ agonist. J Pharmacol Exp Ther 267:58–71

Foreman MM, Fuller RW, Rasmussen K, Nelson DL, Calligaro DO, Zhang L, Barrett JE, Booher RN, Paget CJ Jr, Flaugh ME (1994) Pharmacological characterization of LY293284: a 5-HT_{1A} receptor agonist with high potency and selectivity. J Pharmacol Exp Ther 270:1270–1291

Foreman MM, Fuller RW, Leander JD, Nelson DL, Calligaro DO, Lucaites VL, Wong DT, Zhang L, Barrett JE, Schaus HM (1995) Pharmacological characterization of enantiomers of 8-thiomethyl-2-(di-n-propylamino)tetralin, potent and selective 5-HT_{1A} receptor agonists. Drug Dev Res 34:66–85

Forster EA, Cliffed IA, Bill DJ, Dover GM, Jones D, Reilly Y, Fletcher A (1995) A pharmacological profile of the selective silent 5-HT_{1A} receptor antagonist, WAY-100635. Eur J Pharmacol 281:81–88

Gaggi R, Dall'Olio R, Roncada P (1997) Effects of the selective 5-HT receptor agonists 8-OHDPAT and DOI on behavior and brain biogenic amines of rats

Goodwin GM, Green AR (1985) A behavioural and biochemical study in mice and rats of putative selective agonists and antagonists for 5-HT_1 and 5-HT_2 receptors. Br J Pharmacol 84:743–753

Goodwin GM, De Souza RJ, Wood AJ, Green AR (1986) The enhancement by lithium of the 5-HT_{1A} mediated serotonin syndrome produced by 8-OH-DPAT in the rat: evidence for a postsynaptic mechanism. Psychopharmacology 90:488–493

Green AR, Heal DJ (1985) The effects of drugs on serotonin-mediated behavioural models. In Green A (ed) Neuropharmacol of Serotonin. Oxford University Press, pp 326–365

Green AR, O'Shaughnessy K, Hammond M, Schächter M, Grahame-Smith DG (1983) Inhibition of 5-hydroxytryptamine-mediated behaviour by the putative 5-HT_2 antagonist pirenperone. Neuropharmacol 22:573–578

Groenink L, Van der Gugten J, Compaan JC, Maes RAA, Olivier B (1997) Flesinoxan pretreatment differently affects corticosterone, prolactin and behavioural responses to a flesinoxan challenge. Psychopharmacology 131:93–100

Jacobs BL (1976) An animal behavior model for studying serotonergic synapses. Life Sci 19:777–786

Kleven MS, Assié MB, Koek W (1997) Pharmacological characterization of *in vivo* properties of putative mixed 5-HT_{1A} agonist/5-$HT_{1A/2C}$ antagonist anxiolytics. II. Drug discrimination and behavioral observation studies in rats. J Pharm Exp Ther 282:747–759

Kofman O, Levin U (1995) Myo-inositol attenuates the enhancement of the serotonin syndrome by lithium. Psychopharmacology 118:213–218

Lu JQ, Nagayama H (1996) Circadian rhythm in the response of central 5-HT_{1A} receptors to 8-OH-DPAT in rats. Psychopharmacology 123:42–45

Martin KF, Phillips I, Hearson M, Prow MR, Heal DJ (1992) Characterization of 8-OH-DPAT-induced hypothermia in mice as a 5-HT_{1A} autoreceptor response and its evaluation as a model to selectively identify antidepressants. Br J Pharmacol 107:15–21

Moore NA, Rees G, Sanger G, Perrett L (1993) 5-HT_{1A}-mediated lower lip retraction: effects of 5-HT_{1A} agonists and antagonists. Pharmacol Biochem Behav 46:141–143

O'Connell MT, Curzon G (1996) A comparison of the effects of 8-OH-DPAT pretreatment on different behavioural responses to 8-OH-DPAT. Eur J Pharmacol 312:137–143

O'Neill MF, Parameswaran T (1997) RU24699-induced behavioural syndrome requires activation of both 5-HT_{1A} and 5-HT_{1B} receptors. Psychopharmacology 132:255–260

Porsolt RD, Lenègre A, Caignard DH, Pfeiffer B, Mocaër E, Guardiola-Lemaître B (1992) Psychopharmacological profile of a new chroman derivative with 5-hydroxytryptamine$_{1A}$ agonist properties: S20499(+). Drug Develop Res 27:389–402

Schoeffter P, Fozard JR, Stoll A, Siegl H, Seiler MP, Hoyer D (1993) SDZ 216–525, a selective and potent 5-HT_{1A} receptor antagonist. Eur J Pharmacol 244:251–257

Simiand J, Keane PE, Barnouin MC, Keane M, Soubrié P, Le Fur G (1993) Neuropsychopharmacological profile in rodents of SR 57746A, a new, potent 5-HT_{1A} receptor agonist. Fundam Clin Pharmacol 7:413–427

Smith LM, Peroutka SJ (1986) Differential effects of 5-hydroxytrytamine$_{1A}$ selective drugs on the 5-HT behavioral syndrome. Pharmacol Biochem Behav 24:1513–1519

Tricklebank MD (1985) The behavioural response to 5-HT receptor agonists and subtypes of the central 5-HT receptor. Trends Pharmacol Sci 14:403–407

Trulson ME, Eubanks EE, Jacobs BL (1976) Behavioral evidence for supersensitivity following destruction of central serotonergic nerve terminals by 5,7-dihydroxytryptamine. J Pharmacol Exp Ther 198:23–32

Wolff MC, Benvenga MJ, Calligaro DO, Fuller RW, Gidda JS, Hemrick-Luecke S, Lucot JB, Nelson DL, Overshiner CD, Leander JD (1997) Pharmacological profile of LY301317, a potent and selective 5-HT_{1A} agonist. Drug Develop Res 40:17–34

Yu H, Lewander T (1997) Pharmacokinetic and pharmacodynamic studies of (R)-8-hydroxy-2-(di-n-propylamino)tetralin in the rat. Eur Neuropsychopharmacol 7:165–172

E.6.3.11 Hypermotility in Olfactory-Bulbectomized Rats

PURPOSE AND RATIONALE

Bilateral olfactory bulbectomy in the rat is associated with changes in exploratory behavior that are reversed by chronic, but not acute treatment with antidepressant drugs (Cairncross et al. 1978, 1979; Leonard and Tuite 1981; Janscár and Leonard 1981). The olfactory bulbectomized rat is used as an animal model of depression. Several behavioral changes have been observed following bilateral olfactory bulbectomy: hyperactivity in a closed arena, such as the open field; enhanced nocturnal activity; deficits in memory as shown by passive avoidance behavior and in the Morris water maze and the radial maze; increased open-arm entries in the elevated-plus maze, and changes in food-motivated and conditioned taste aversion behavior. Alteration in the noradrenergic, serotonergic, cholinergic, GABAergic, and glutamatergic neurotransmitter systems are also associated with olfactory bulbectomy (Wren et al. 1977; Van Riezen and Leonard 1990; Kelly et al. 1997).

PROCEDURE

Male Sprague Dawley rats are anesthetized with intraperitoneal injection of 2.5% tribromo-ethanol solution (Cairncross et al. 1977). Following exposure of the skull, a burr hole is drilled at points 7 mm anterior to the bregma and 2 mm either side of the midline at a point corresponding to the posterior margin of the orbit of the eye. The olfactory bulbs are removed by suction and the burr holes filled with hemostatic sponge. Tetramycin powder is then applied to the wound and the skin closed by surgical clips. Sham-operated animals are treated in the same way but although the dura above the bulbs is cut, the bulbs are left intact. The animals are allowed to recover for 14 days after surgery.

For drug evaluation the animals are treated subcutaneously with the test drug or the standard or the vehicle once daily at 09:00 for 14 days. In each experiment sham-operated controls treated with test drug, standard and vehicle are included.

The behavior of the animals is tested from the 12th day onwards. The rats are placed singly in the center of an open field apparatus. Ambulation (no. of squares crossed), rearing (forepaws raised from the floor), grooming and defecation (no. of fecal boli) scores are recorded for an 3 min period of observation.

EVALUATION

The results are analyzed statistically using Student's *t*-test (2 tail test), the significance being set at $P < 0.05$.

CRITICAL ASSESSMENT OF THE METHOD

The bulbectomized rat model has been shown to be highly selective for both typical and atypical antidepressants, however, the procedure is quite time consuming.

MODIFICATIONS OF THE METHOD

Various authors used this model to demonstrate antidepressant-like activity: such as Briley et al. (1996) for milnacipran, a serotonin and noradrenaline uptake inhibitor, Hancock et al. (1995) for A-80426, an α_2-adrenoceptor antagonist with serotonin uptake blocking activity, McNamara et al. (1995) for the centrally active serotonin agonist 8-hydroxy-2-(di-n-propylamino) tetralin (8-OH-DPAT), Redmont et al. (1997) for dizocilpine (MK-801), Song and Leonard (1994) for the serotonin reuptake inhibitors fluvoxamine and sertraline, Song et al. (1996a) for centrally administered neuropeptide Y, Song et al. (1996b) for the H_1 receptor antagonist terfenadine.

Kelly and Leonard (1994, 1995) studied the effects of potential antidepressants, such as selective serotonin reuptake inhibitors, in olfactory bulbectomized rats. Kelly et al. (1997) anesthetized male Sprague Dawley rats weighing 230–280 g with 375 mg/kg i.p. chloral hydrate. The surgical procedure involves drilling two burr holes (2 mm diameter, 8 mm anterior to bregma) either side, 2 mm from the midline of the frontal bone overlying the olfactory bulbs. The olfactory bulbs can be visualized through these burr holes and can be aspirated by means of a blunt hypodermic needle attached to a water pump, taking care not to cause damage to the frontal cortex. Prevention of blood loss from the burr holes is achieved by filling them with hemostatic sponge. Antibiotic powder is applied to the wound, prior to closing with 7.5-mm surgical clips. A period of 2 weeks allows for the recovery from the surgical procedure and is optimal for the development of the bulbectomy syndrome.

Potential antidepressant drugs are preferably administered for a period of 2 weeks. Various procedures can be used to test the drug's effect in olfactory bulbectomized rats, such as open field (Cryan et al. 1999; Slotkin et al. 1999), home cage activity (Redmont et al.

1997), forced swim test (Kelly and Leonard 1999), elevated plus maze (McGrath and Norman 1999), passive avoidance (Martin et al. 1998; Nowak et al. 2003), and olfactory bulbectomy-induced hyperemotionality (Chaki et al. 2004).

Redmont et al. (1995) studied the effect of chronic antidepressant administration on the conditioned taste aversion to 8-OHDPAT in the olfactory bulbectomized rat.

Kelly et al. (1997) gave an update of the olfactory bulbectomized rat as a model of depression. Tricyclic antidepressants (amitryptiline, desimipramine), atypical agents (mianserin), selective serotonin reuptake inhibitors (paroxetine, sertraline, fluvoxamine), reversible inhibitors of monoamine oxidase A (moclobemide), as well as putative antidepressants, such as 5-HT_{1A} agonists (zalospirone, ipsapirone), noncompetitive NMDA antagonists (MK-801) and triazolobenzazepines (alprazolam, adinazolam), have demonstrated antidepressant-like activity in this model.

Zhou et al. (1998) found serotoninergic hyperinnervation of the frontal cortex in the bulbectomized rat.

Increases in the concentrations of the neuropeptides corticotropin-releasing factor, thyrotropin-releasing factor, somatostatin (Bissette 2001), and neuropeptide Y (Holmes et al. 1998), which may play a role in mediating the antidepressant-sensitive behaviors, have been demonstrated.

Comparing the behavioral and biochemical effects of bulbectomy in young versus aged rats, Slotkin et al. (1999) suggested that this test might provide a useful animal model with which to test therapeutic intervention for geriatric depression.

Ho et al. (2000) demonstrated increased striatal glutamate release during novelty exposure-induced hyperactivity in olfactory bulbectomized rats that may have a modulatory role in the antidepressant-sensitive response.

Wrynn et al. (2000) performed an *in vivo* magnetic resonance imaging study in olfactory bulbectomized rats and demonstrated alterations in signal intensities in cortical, hippocampal, caudate and amygdaloid regions.

Holmes et al. (1998) studied the effects of olfactory bulbectomy on neuropeptide gene expression in the rat olfactory system.

Bilkei-Gorzo et al. (2002) and Zueger et al. (2005) tested alterations in locomotor activity and exploratory behavior after olfactory bulbectomy in **mice** (using systems provided by TSE Systems, Bad Homburg, Germany).

REFERENCES AND FURTHER READING

Bilkei-Gorzo A, Racz I, Michel K, Zimmer A (2002) Diminished anxiety- and depression-related behaviors in mice with selective deletion of the *Tac1* gene. J Neurosci 22:10046–10052

Bissette G (2001) Effects of sertraline on regional neuropeptide concentrations in olfactory bulbectomized rats. Pharmacol Biochem Behav 69:269–281

Briley M, Prost JF, Moret C (1996) Preclinical pharmacology of milnacipran. Int Clin Psychopharmacol 11/Suppl 4:9–14

Cairncross KD, Wren A, Cox B, Schieden H (1977) Effects of olfactory bulbectomy and domicile on stress-induced corticosterone release in the rat. Physiol Behav 19:405–487

Cairncross KD, Cox B, Forster C, Wren AF (1978) A new model for the detection of antidepressant drugs: olfactory bulbectomy in the rat compared with existing models. J Pharmacol Meth 1:131–143

Cairncross KD, Cox B, Forster C, Wren AF (1979) Olfactory projection system, drugs and behaviour: a review. Psychoneuroendocrinology 4:253–272

Chaki S, Nakazato A, Kennis L, Nakamura M, Mackie C, Sugiura M, Vinken P, Ashton D, Langlois X, Steckler T (2004) Anxiolytic- and antidepressant-like profile of a new CRF_1 receptor antagonist, R278955/CRA0450. Eur J Pharmacol 485:145–158

Cryan JF, McGrath C, Leonard BE, Norman TR (1999) Onset of the effects of the 5-HT_{1A} antagonist, WAY-100635, alone, and in combination with paroxetine, on olfactory bulbectomy and 8-OH-DPAT-induced changes in the rat. Pharmacol Biochem Behav 63:333–338

Hancock AA, Buckner SA, Oheim KW, Morse PA, Brune ME, Meyer MD, Williams M, Kervin LF Jr (1995) A-80426, a potent α_2-adrenoceptor antagonist with serotonin uptake blocking activity and putative antidepressant-like effects: I. Biochemical profile. Drug Dev Res 35:237–245

Ho YJ, Chang YC, Liu TM, Tai MY, Wong CS, Tsai YF (2000) Striatal glutamate release during novelty exposure-induced hyperactivity in olfactory bulbectomized rats. Neurosci Lett 287:117–120

Holmes PV, Davis RC, Masini CV, Primeaux SD (1998) Effects of olfactory bulbectomy on neuropeptide gene expression in the rat olfactory/limbic system. Neuroscience 86:587–596

Janscár SM, Leonard BE (1984) The effect of (±)mianserin and its enantiomers on the behavioural hyperactivity of the olfactory bulbectomized rat. Neuropharmacol 23:1065–1070

Kelly JP, Leonard BE (1994) The effects of tianeptine and sertraline in three animal models of depression. Neuropharmacol 33:1011–1016

Kelly JP, Leonard BE (1995) The contribution of pre-clinical drug evaluation in predicting the clinical profile of the selective serotonin reuptake inhibitor paroxetine. J Serotonin Res 1:27–46

Kelly JP, Leonard BE (1999) An investigation of the antidepressant properties of lofepramine and its desmethylated metabolites in the forced swim and olfactory bulbectomized rat model of depression. Eur Neuropsychopharmacol 9:101–105

Kelly JP, Wrynn AS, Leonard BE (1997) The olfactory bulbectomized rat as a model of depression: an update. Pharmacol Ther 74:299–316

Leonard BE, O'Connor WJ (1984) Effect of isomers of the 6-aza derivative of mianserin on behaviour and noradrenaline metabolism in bulbectomized rats. Br J Pharmacol 82:246P

Leonard BE, Tuite M (1981) Anatomical, physiological and behavioral aspects of olfactory bulbectomy in the rat. Int Rev Neurobiol 22:251–286

Martin JR, Bös M, Jenck F, Moreau JL, Mutel V, Sleight AJ, Wichmann J, Andrews JS, Berendsen HHG, Broekkamp CLE, Ruigt GSF, Köhler C, van Delft AML (1998) 5-HT_{2C} receptor antagonists: pharmacological characteristics and therapeutic potential. J Pharmacol Exp Ther 286:913–924

McGrath C, Norman TR (1999) (+)-S-20499 – a potential antidepressant? A behavioural and neurochemical investigation in the olfactory bulbectomized rat. Eur Neuropsychopharmacol 9:21–27

McNamara MG, Kelly JP, Leonard BE (1995) Effect of 8-OH-DPAT in the olfactory bulbectomized rat model of depression. J Serotonin Res 2:91–99

Nowak G, Szewczyk B, Wieronska JM, Branski P, Palucha A, Pilc A, Sadlik K, Piekoszewski W (2003) Antidepressant-like effects of acute and chronic treatment with zinc in forced swim test and olfactory bulbectomy model in rats. Brain Res Bull 61:159–164

O'Connor WT, Leonard BE (1986) Effect of chronic administration of the 6-aza analogue of mianserin (ORG 3770) and its enantiomers on behaviour and changes in noradrenaline metabolism of olfactory-bulbectomized rats in the "open field" apparatus. Neuropharmacol 25:267–270

Porsolt RD, Lenègre A, McArthur RA (1991) Pharmacological models of depression. In: Olivier B, Mos J, Slangen JL (eds) Animal Models in Psychopharmacology, Birkhäuser Verlag Basel, pp 137–159

Redmont AM, Kelly JP, Leonard BE (1995) Effect of chronic antidepressant administration on the conditioned taste aversion to 8-OHDPAT in the olfactory bulbectomized rat model of depression. Med Sci Res 23:487–488

Redmont AM, Kelly JP, Leonard BE (1997) Behavioral and neurochemical effects of dizocilpine in the olfactory bulbectomized rat model of depression. Pharmacol Biochem Behav 58:355–359

Slotkin TA, Miller DB, Fumagalli F, McCook EC, Zhang J, Bissette G, Seidler FJ (1999) Modeling geriatric depression in animals: biochemical and behavioral effects of olfactory bulbectomy in young versus old rats. J Pharmacol Exp Ther 289:334–345

Song C, Leonard BE (1994) Serotonin reuptake inhibitors reverse the impairments in behaviour neurotransmitter and immune functions in the olfactory bulbectomized rat. Hum Psychopharmacol 9:135–146

Song C, Early B, Leonard BE (1966a) The effects of central administration of neuropeptide Y on behavior, neurotransmitter, and immune functions in the olfactory bulbectomized rat model of depression. Brain Behav Immun 10:1–16

Song C, Early B, Leonard BE (1966b) Behavioural and immunological effects of the antihistamine terfenadine in olfactory bulbectomized rats. Eur Neuropsychopharmacol 6:157–162

Van Riezen H, Leonard BE (1990) Effects of psychotropic drugs on the behavior and neurochemistry of olfactory bulbectomized rats. Pharmacol Ther 47:21–34

Wren A, van Riezen H, Rigter H (1977) A new animal model for the prediction of antidepressant activity. Pharmakopsychiatrie Neuropsychopharmakologie 10:96–100

Wrynn AS, MacSweeney CP, Franconi F, Lemaire L, Pouliquen D, Herlidou S, Leonard BA, Ganton J, de Certaines JD (2000) An *in-vivo* magnetic resonance imaging study on the olfactory bulbectomized rat model of depression. Brain Res 879:193–199

Zhou D, Greksch G,Becker A, Frank C, Pilz J, Hueter G (1998) Serotoninergic hyperinnervation of the frontal cortex in an animal model of depression, the bulbectomized rat. J Neurosci Res 54:109–116

Zueger M, Urani A, Chourbaji S, Zacher C, Roche M, Hrkin A, Gass P (2005) Olfactory bulbectomy in mice induces alterations in exploratory behavior. Neurosci Lett 374:142–146

E.6.3.12 Sexual Behavior in Male Rats

PURPOSE AND RATIONALE

Sexual behavior in male rats is stimulated by 5-HT_{1A} receptors agonists (Ahlenius et al. 1981; Gorzalka et al. (1990), Foreman et al. 1993, 1994, 1995; Anderson and Larsson 1994; Tallentire et al. 1996; Ahlenius and Larsson 1997; Fernández-Guasti and Rodriguez-Manzo 1997) and inhibited by serotonin receptor antagonists (Mendelson and Gorzalka 1981) and by 5-HT_{1B} receptors antagonists (Fernández-Guasti et al. 1989). The test procedure was described in detail by Arnone et al. (1995).

PROCEDURE

Adult male and ovarectomized female Sprague Dawley rats are housed in sex-separated rooms at 21 ± 1°C in a reversed light-dark cycle with free access to food and water.

Mating Behavior

Male rats of two levels of sexual performance are selected for drug testing: sexually naive and sexually experienced. The latter are given 4 mating pretests, twice a week. Only sexually active males that achieve at least two ejaculations per test, are included in the experiments.

The mating tests are performed between 12:30 and 17:00, during the dark phase of the lighting cycle. Drug is administered orally 1 h before the test to the male rat. The animal is allowed to adapt to the test area (60 cm diameter, 50 cm high) illuminated with a dim red light. Each behavioral test starts with the introduction of a stimulus female brought into sexual receptivity by s.c. treatment with estradiol benzoate (10 µg/rat), followed 48 h later by progesterone (500 µg/rat), 4–5 h before testing. The tests end either 20 min later or after the first post-ejaculatory mount (or 2 h later for sexual satiation).

The following behavioral parameters are recorded:

- **Mount and intromission latencies:** time interval from the first introduction of the female to the first mount or intromission, respectively. Mounts are accompanied by an average of three or four brief shallow thrusts, while the intromission, which succeeds

this event, is marked by a single deep thrust indicative of penile insertion.
- **Mount frequency:** total number of pre-ejaculatory mounts with and without intromission.
- **Intromission frequency:** total number of pre-ejaculatory intromissions.
- **Ejaculatory latency:** time interval from the first intromission to ejaculation. A total of 1200 s is scored for the latencies of rats failing to mount, intromit or ejaculate.

Sexual Satiation

The mating pattern of the male rat consists of repeated mounts and intromissions, culminating in an ejaculation. The ejaculation is followed by a period of 4–5 min during which time the male remains refractory to sexual stimulation by the female. The sexual activity is thereafter resumed with a new series of mounts and intromissions followed by ejaculation. If uninterrupted, the rat may achieve five to six ejaculations before sexual satiation sets in. Sexually experienced male rats are allowed to copulated with a receptive female for 2 h. The behaviors are recorded on a videotape. The criterion for satiation is that the male fails to mount within 20 min post ejaculation. The latency to satiation and the number ejaculations are recorded.

Finally, for each ejaculatory series, the following parameters are recorded:

- **Copulation duration:** time interval between the first mount and the ejaculation.
- **Post ejaculatory interval:** time interval from the ejaculation to the first mount of the next series.

Penile Erections

One hour before the experiment, male rats are allowed to adapt to the quiet observation room. One hour after oral drug administration, rats are placed in individual plastic cages ($10.5 \times 24 \times 16$ cm). Series of nine rats comprising, at random, control and drug-treated animals, are observed simultaneously for 45 min and the number of penile erections is counted. Penile erection is defined as a period of pelvic thrusting followed by an upright position with genital grooming and the display of the engorged penis. Animals are used only once.

EVALUATION

Data are analyzed using non-parametric statistics. The Fisher test is used for percentage responding. For quantified behavioral parameters, the Kruskal-Wallis test, followed by the Mann-Whitney *U*-test corrected by Holm's method is used for comparisons versus the control group. The Mann-Whitney *U*-test is used for comparison of a single treated group versus its own control group.

MODIFICATIONS OF THE METHOD

Barr et al. (1999) subjected male rats to a 4-day escalating dose schedule of d-amphetamine. Twelve hours after the final dose the rats were tested for sexual behavior. Withdrawal from the amphetamine was associated with decrements in several motivational components of sexual behavior. The procedure was recommended as a rodent model of depression.

Pomerantz et al. (1993) studied the influence of 5-HT receptor agonists on male sexual behavior of **rhesus monkeys**.

REFERENCES AND FURTHER READING

Ahlenius S, Larsson K (1997) Specific involvement of central 5-HT_{1A} receptors in the mediation of male rat ejaculatory behavior. Neurochem Res 22:1965–1070

Ahlenius S, Larsson K, Svensson L, Hjorth S, Carlsson A, Lindberg P, Wikström H, Sanchez D, Arvidsson LE, Hacksell U, Nilsson JLG (1981) Effects of a new type of 5-HT receptor agonist on male rat sexual behavior. Pharmacol Biochem Behav 15:785–792

Andersson G, Larsson K (1994) Effects of FG 5893, a new compound with 5-HT_{1A} receptor agonistic and 5-HT_2 receptor antagonistic properties, on male rat sexual behavior. Eur J Pharmacol 255:131–137

Arnone M, Baroni M, Gai J, Guzzi U, Desclaux MF, Keane PE, Le Fur G, Soubrié P (1995) Effect of ST 59026A, a new 5-HT_{1A} receptor agonist, on sexual activity in male rats. Behav Pharmacol 6:276–282

Barr AM, Florino DF, Phillips AG (1999) Effects of withdrawal from an escalating dose schedule of d-amphetamine on sexual behavior in the male rat. Pharmacol Biochem Behav 64:597–604

Fernández-Guasti A, Escalante A, Ågmo A (1989) Inhibitory actions of various HT_{1B} receptor agonists on rat masculine sexual behaviour. Pharmacol Biochem Behav 34:811–816

Fernández-Guasti A, Rodriguez-Manzo G (1997) OH-DPAT and male rat sexual behavior: Partial blockade by noradrenergic lesion and sexual exhaustion. Pharmacol Biochem Behav 56:111–116

Foreman MM, Fuller RW, Leander JD, Benvenga MJ, Wong DT, Nelson DL, Calligaro DO, Swanson SP, Lucot JP, Flaugh ME (1993) Preclinical studies in LY228729: a potent and selective serotonin$_{1A}$ agonist. J Pharmacol Exp Ther 267:58–71

Foreman MM, Fuller RW, Rasmussen K, Nelson DL, Calligaro DO, Zhang L, Barrett JE, Booher RN, Paget CJ Jr, Flaugh ME (1994) Pharmacological characterization of LY293284: a 5-HT_{1A} receptor agonist with high potency and selectivity. J Pharmacol Exp Ther 270:1270–1291

Foreman MM, Fuller RW, Leander JD, Nelson DL, Calligaro DO, Lucaites VL, Wong DT, Zhang L, Barrett JE, Schaus HM (1995) Pharmacological characterization of enantiomers of 8-thiomethyl-2-(di-n-propylamino)tetralin,

potent and selective 5-HT_{1A} receptor agonists. Drug Dev Res 34:66–85
Gorzalka BB, Mendelson SD, Watson NV (1990) Serotonin receptor subtypes and sexual behavior. Ann NY Acad Sci 600:435–446
Mendelson SD, Gorzalka BB (1981) Serotonin antagonist pirenperone inhibits sexual behavior in the male rat: attenuation by quipazine. Pharmacol Biochem Behav 22:565–571
Pomerantz SM, Hepner BC, Wertz JM (1993) 5-HT_{1A} and 5-$HT_{1C/1D}$ receptor agonists produce reciprocal effects on male sexual behavior of rhesus monkeys. Eur J Pharmacol 243:227–234
Tallentire D, McRae G, Spedding M, Clark R, Vickery B (1996) Modulation of sexual behaviour in the rat by a potent and selective α_2-adrenoceptor agonist, delequamine (RS-15835–197) Br J Pharmacol 118:63–72

E.6.4 Genetic Models of Depression

E.6.4.1 Flinders Sensitive Line of Rats

The **Flinders Sensitive Line of rats** was established by genetically selecting (breeding) Sprague Dawley rats for a behavioral trait, supersensitivity to cholinergic agents (Overstreet and Russell 1982; Overstreet 1986; Overstreet et al. 1986, 1990, 1992; Daws and Overstreet 1999). The name Flinders refers to University of Flinders, Australia, where the line was first selected. The usefulness of the Flinders Sensitive Line of rats as an animal model for depression is evident because it exhibits behavioral features characteristic of depression in humans and responds to chronic, but not acute, treatment with antidepressants (Overstreet 1993; Overstreet et al. 1995; Yadid et al. 2000; Overstreet and Griebel 2004; Overstreet et al. 2004; Dremencov et al. 2005).

Vasquez et al. (2000) tested the effects of electroconvulsive stimuli and d-amphetamine on neuropeptide Y concentrations in brain and on locomotion in the Flinders Sensitive Line rat.

Ferreira-Nuño et al. (2002) studied masculine sexual behavior features in Flinders sensitive and resistant line rats.

Shayit et al. (2003) demonstrated 5-HT_{1A} receptor subsensitivity in infancy and supersensitivity in adulthood in the Flinders Sensitive Line rat.

Dremencov et al. (2004) showed in the Flinders Sensitive Line of rats that the serotonin–dopamine interaction is critical for the fast-onset action of antidepressant treatment. Seven-day treatment with nefazodone (a putative fast-onset antidepressant) but not with desipramine (a classical antidepressant) normalized immobility time in the swim test in Flinders Sensitive Line rats. Serotonin-induced dopamine release but not basal dopamine levels correlated with the improvement of depressive-like behavior.

Lavi-Avnon et al. (2005) showed an abnormal pattern of maternal behavior in the Flinders Sensitive Line of rats.

Maayan et al. (2005) demonstrated the involvement of dehydroepiandrosterone and its sulfate ester in blocking the therapeutic effect of electroconvulsive shocks in the Flinders Sensitive Line of rats.

King and Edwards (1999), King et al. (2001), and Shumake et al. (2003) bred **congenital learned helpless rats**, which exhibit physiological symptoms of analgesia, cognitive deficits and hyporesponsivity of the hypothalamic–pituitary–adrenal axis similar to those observed in human subjects with post-traumatic stress disorder.

Will et al. (2003) described **selectively bred Wistar–Kyoto rats** as an animal model of depression and hyper-responsiveness to antidepressants. Based on the significant decrease in investigative behavior of male rats towards a female intruder, reflecting the presence of anhedonia, Paré (2000) concluded that the Wistar–Kyoto rat strain represents a useful animal model of depressive behavior.

REFERENCES AND FURTHER READING

Daws LC, Overstreet DH (1999) Ontogeny of muscarinic cholinergic supersensitivity in the Flinders sensitive line rat. Physiol Biochem Behav 62:367–380
Dremencov E, Gispan-Herman I, Rosenstein M, Mendelman A, Overstrett DH, Zohar J, Yadid G (2004) The serotonin-dopamine interaction is critical for fast-onset action of antidepressant treatment: in vivo studies in an animal model of depression. Prog Neuropsychopharmacol Biol Psychiatry 28:141–147
Dremencov E, Newman ME, Kinor N, Blatman-Jan G, Schindler CJ, Overstreet DH, Yadid G (2005) Hyperfunctionality of serotonin-2C receptor mediated inhibition of accumbal dopamine release in an animal model of depression is reversed by antidepressant treatment. Neuropharmacology 48:34–42
Ferreira-Nuño A, Overstreet DH, Morales Otat A, Velázques-Moctezuma J (2002) Masculine sexual behavior features in the Flinders sensitive and resistant line rats. Behav Brain Res 128:113–119
King JA, Edwards E (1999) Early stress and genetic influences on hypothalamic-pituitary-adrenal axis functioning in adulthood. Horm Behav 36:79–85
King JA, Abend S, Edwards E (2001) Genetic predisposition and the development of posttraumatic stress disorder in an animal model. Biol Psychiatry 50:231–237
Lavi-Avnon Y, Yadid G, Overstreet DH, Weller A (2005) Abnormal patterns of maternal behavior in a genetic animal model of depression. Physiol Behav 84:607–615
Maayan R, Morad O, Dorfamn P, Overstreet DH, Weizman A, Yadid G (2005) The involvement of dehydroepiandrosterone (DHEA) and its sulfate ester (DHEAS) in blocking the therapeutic effect of electroconvulsive shocks in an an-

imal model of depression. Eur Neuropsychopharmacology 15:253–262
Overstreet DH (1986) Selective breeding for increases cholinergic function: Development of a new animal model of depression. Biol Psychiatry 21:49–58
Overstreet DH (1993) The Flinders sensitive line rats: a genetic animal model of depression. Neurosci Biobehav Rev 17:51–68
Overstreet DH, Griebel G (2004) Antidepressant-like effects of CRF1 receptor antagonist SSR125543 in an animal model of depression. Eur J Pharmacol 497:49–51
Overstreet DH, Russell RW (1982) Selective breeding for diisopropyl fluorophosphates-sensitivity: behavioural effects of cholinergic agonists and antagonists. Psychopharmacology 78:150–155
Overstreet DH, Janowsky DS, Gillin JC, Shiromani PJ, Sutin EL (1986) Stress-induced immobility in rats with cholinergic hypersensitivity. Biol Psychiatry 21:657–664
Overstreet DH, Rezvani AH, Janowsky DS (1990) Impaired active avoidance responding in rats selectively bred for increased cholinergic function. Physiol Behav 47:787–788
Overstreet DH, Russell RW, Hay DA, Crocker AD (1992) Selective breeding for increased cholinergic function: biometrical genetic analysis of muscarinic responses. Neuropsychopharmacology 7:197–204
Overstreet DH, Pucilowski O, Rezvani AH, Janowsky DS (1995) Administration of antidepressants, diazepam and psychomotor stimulants further confirm the utility of Flinders Sensitive Line rats as an animal model of depression. Psychopharmacology 121:27–37
Overstreet DH, Keeney A, Hogg S (2004) Antidepressant effects of citalopram and CRF receptor antagonist CP-154,526 in a rat model of depression. Eur J Pharmacol 492:195–201
Paré WP (2000) Investigatory behavior of a novel conspecific by Wistar Kyoto, Wistar and Sprague-Dawley rats. Brain Res Bull 53:759–765
Shayit M, Yadid G, Overstreet DH, Weller A (2003) 5-HT_{1A} receptor subsensitivity in infancy and supersensitivity in adulthood in an animal model of depression. Brain Res 980:100–108
Shumake J, Edwards E, Gonzalez-Lima F (2003) Opposite metabolic changes in the habenula and ventral tegmental area of a genetic model of helpless behavior. Brain Res 963:274–281
Vasquez PAJ, Salmi P, Ahlenius S, Mathé AA (2000) Neuropeptide Y in brains of the Flinders Sensitive Line rat, a model of depression. Effects of electroconvulsive stimuli and *d*-amphetamine on peptide concentrations and locomotion. Behav Brain Res 111:115–123
Will CC, Aird F, Redel EE (2003) Selectively bred Wistar–Kyoto rats: an animal model of depression and hyper-responsiveness to antidepressants. Mol Psychiatry 8:925–932
Yadid G, Nakash R, Deri I, Tamar G, Kinor N, Gispan I, Zangen A (2000) Elucidation of the neurobiology of depression: insight from a novel genetic animal model. Prog Neurobiol 62:353–378

E.6.4.2 Genetically Altered Mice as Models of Depression

Cryan et al. (2002) published a survey on the use of genetically altered mice to assess antidepressant-related phenotypes. Cyran and Mombereau (2004) discussed the utility of models for studying depression-related behavior in genetically modified mice.

Cases et al. (1995) found aggressive behavior and altered amounts of brain serotonin and epinephrine in mice lacking **MAO_A**. Pup behavioral alterations including trembling, difficulties in righting, and fearfulness were reversed by the serotonin inhibitor parachlorophenylalanine. Adults manifested a distinct behavioral syndrome, including enhanced aggression in males.

Lijam et al. (1997) created mice deficient in *Dvl1*, one of the three mouse homologs of the *Drosophila* polarity gene *Dishevelled*, by gene targeting. These mice exhibited reduced social interaction and sensorimotor gating abnormalities.

Grimsby et al. (1997) reported an increased stress response and increased levels of α-phenylethylamine in **MAO_B**-deficient mice. In addition, mutant mice were resistant to the neurodegenerative effects of 1-methyl 4-phenyl 1,2,3,6-tetrahydropyridine (MPTP), a toxin that induces a condition reminiscent of Parkinson's disease.

Sallinen et al. (1999) reported that general alteration of the **α_2-adrenoceptor subtype c** in mice affects the development of behavioral despair and stress-induced increases in plasma corticosterone levels. α_{2c}-Adrenoceptor overexpression increased, and the lack of α_{2c}-adrenoceptors, decreased the immobility of mice in the forced swimming test.

Cyran et al. (2001) used **dopamine-beta-hydroxylase-deficient** mice to determine the role of norepinephrine in the mechanisms of action of antidepressant drugs. The dopamine-beta-hydroxylase-deficient mice failed to demonstrate antidepressant-like behavioral effects following the administration of several classes of antidepressants.

Mayorga et al. (2001) studied antidepressant-like behavioral effects in **5-hydroxytryptamine$_{1A}$and 5-hydroxytryptamine$_{1B}$receptor mutant mice**. The results suggested, that 5-HT_{1A} and 5-HT_{1B} receptors have different roles in the response to antidepressant drugs in the tail-suspension test.

Froger et al. (2001) found that 5-hydroxytryptamine$_{1A}$ autoreceptor adaptive changes in **substance P (neurokinin 1) receptor knockout mice** mimic antidepressant-induced desensitization. The constitutive lack of NK_1 receptors appeared to be associated with a downregulation/functional desensitization of 5-HT_{1A} autoreceptors resembling that induced by chronic treatment with antidepressants.

Jaber et al. (1997) inactivated the expression of the **dopamine transporter** in mice. The authors claimed that these genetically altered mice offer a unique model to test the specificity and selectivity

of dopamine-transporter-acting drugs and provide new concepts related to clinical conditions such as Parkinson's disease, schizophrenia, and drug addiction.

Xu et al. (2000) reported that mice lacking the **norepinephrine transporter** are supersensitive to psychostimulants. Disruption of the norepinephrine transporter (NET) gene prolonged the clearance of norepinephrine and elevated extracellular levels of this catecholamine. In a classical test for antidepressant drugs, the NET-gene-deficient mice behaved like antidepressant-treated wild-type mice.

Holmes et al. (2001) characterized the **dopamine receptor D_5null mutant** of mice in behavioral tests.

Based on pharmacology of adenosine A_{2A} receptor antagonists and results with **A_{2A}receptor knockout mice**, El Yacoubi et al. (2001) claimed that adenosine A_{2A} receptor antagonists are potential depressants.

MacQueen et al. (2001) investigated the performance of heterozygous **brain-derived neurotrophic factor knockout mice** on behavioral analogs of anxiety, nociception, and depression.

Conti et al. (2002) reported that cAMP-response-element-binding protein is essential for the upregulation of **brain-derived neurotrophic factor** transcription, but not the behavioral or endocrine responses to antidepressant drugs. cAMP-response-element-binding-protein-deficient mice were used to study the effects of desipramine and fluoxetine in behavioral, endocrine and molecular analyses.

Stork et al. (2000) studied postnatal development of a GABA deficit and disturbance of neural functions in mice lacking GAD65. Adult **GAD65(–/–) mice** showed a largely abnormal neural activity with frequent paroxysmal discharges and spontaneous seizures. They furthermore displayed increased anxiety-like behavior in a light/dark avoidance test and reduced inter-male aggression, as well as reduced forced-swimming-induced immobility indicative of an antidepressant-like behavior.

Svenningsson et al. (2002) studied the involvement of striatal and extrastriatal DARPP-32, a cAMP-regulated phosphoprotein, in biochemical and behavioral effects of fluoxetine using **DARPP-32 knockout mice**.

Calapai et al. (2001) used **interleukin-6 knockout mice** to characterize the antidepressant action of *Hypericum perforatum*.

Porsolt (2000) reviewed the utility of animal models of depression for transgenic research.

El Yacoubi et al. (2003) published the behavioral, neurochemical, and electrophysiological characterization of a genetic mouse model of depression.

Wei et al. (2004) generated mice overexpressing glucocorticoid receptor specifically in forebrain. These mice display a significant increase in anxiety-like and depression-like behaviors relative to wild type.

REFERENCES AND FURTHER READING

Calapai G, Crupi A, Firenzuoli F, Inferrera G, Ciliberto G, Parisi A, De Sarro G, Caputi AP (2001) Interleukin-6 involvement in antidepressant action of *Hypericum perforatum*. Pharmacopsychiatry 34 [Suppl 1]: S8–10

Cases O, Seif I, Grimsby J, Gaspar P, Chen K, Pournin S, Müller U, Aguet M, Babinet C, Shih JC (1995) Aggressive behavior and altered amounts of brain serotonin and epinephrine in mice lacking MAO_A. Science 268:1763–1766

Conti AC, Cryan JF, Dalvi A, Lucki I, Blendy JA (2002) cAMP response element-binding protein is essential for the upregulation of brain-derived neurotrophic factor transcription, but not the behavioral or endocrine responses to antidepressant drugs. J Neurosci 22:3262–3268

Cyran JF, Mombereau C (2004) In search of a depressed mouse: utility of models for studying depression-related behavior in genetically modified mice. Mol Psychiatry 9 :326–357

Cyran JF, Dalvi A, Jin SH, Hirsch BR, Lucki I, Thomas SA (2001) Use of dopamine-beta-hydroxylase-deficient mice to determine the role of norepinephrine in the mechanisms of action of antidepressant drugs. J Pharmacol Exp Ther 298:651–657

Cryan JF, Markou A, Lucki I (2002) Assessing antidepressant activity in rodents: recent developments and future needs. Trends Pharmacol Sci 23:238–245

El Yacoubi M, Ledent C, Parmentier M, Bertorelli R, Ongini E, Costentin J, Vaugeous JM (2001) Adenosine A_{2A} receptor antagonists are potential depressants: evidence based on pharmacology and A_{2A} receptor knockout mice. Br J Pharmacol 134:68–77

El Yacoubi M, Bouali S, Popa D, Naudon L, Leroux-Nicollet I, Hamon M, Costentin J, Adrien J, Vaugeois JM (2003) Behavioral, neurochemical, and electrophysiological characterization of a genetic mouse model of depression. Proc Natl Acad Sci USA 100:6227–6232

Froger N, Gardier AM, Moratalla R, Alberti I, Lena I, Boni C, De Felipe C, Rupniak NM, Hunt SP, Jacquot C, Hamon M, Lanfumey L (2001) 5-Hydroxytryptamine$_{1A}$ autoreceptor adaptive changes in substance P (neurokinin 1) receptor knock-out mice mimic antidepressant-induced desensitization. J Neurosci 21:8188–8197

Grimsby J, Toth M, Chen K, Kumatawa T, Klaidman L, Adams JD, Karoum F, Gal J, Shih JC (1997) Increased stress response and β-phenylethylamine in MAO_B deficient mice. Nat Genet 17:206–210

Holmes A, Hollon TR, Gleason TC, Liu Z, Dreiling J, Sibley DR, Crawley JN (2001) Behavioral characterization of dopamine receptor D_5 null mutant mice. Behav Neurosci 115:1129–1144

Jaber M, Jones S, Giros B, Caron MG (1997) The dopamine transporter: a crucial component regulating dopamine transmission. Mov Disord 12:629–633

Lijam N, Paylor R, McDonald MP, Crawley JN, Deng CX, Herrup K, Stevens KE, Maccaferri G, McBain CJ, Sussman DJ, Wynshaw-Boris A (1997) Social interaction and sensorimotor gating abnormalities in mice lacking *Dvl1*. Cell 90:895–905

MacQueen GM, Ramakrishnan K, Croll SD, Siuciak JA, Yu G, Young LT, Fahnestock M (2001) Performance of heterozy-

gous brain-derived neurotrophic factor knockout mice on behavioral analogues of anxiety, nociception, and depression. Behav Neurosci 2001:1145–1153
Mayorga AJ, Dalvi A, Page ME, Zimov-Levinson S, Hen R, Lucki I (2001) Antidepressant-like behavioral effects in 5-hydroxytryptamine$_{1A}$ and 5-hydroxytryptamine$_{1B}$ receptor mutant mice. J Pharmacol Exp Ther 298:1101–1107
Porsolt RD (2000) Animal models of depression: utility for transgenic research. Rev Neurosci 11:53–58
Sallinen J, Haapalinna A, MacDonald E, Viitamaa T, Lähdesmäki J, Rybnikova A, Pelto-Huikko M, Kobilka BK, Scheinin M (1999) General alteration of the á$_2$-adrenoceptor subtype c in mice affects the development of behavioral despair and stress-induced increases in plasma corticosterone levels. Mol Psychiatry 4:443–452
Stork O, Ji FY, Kaneko K, Stork S, Yoshinobu Y, Moriya T, Shibata S, Obata K (2000) Postnatal development of a GABA deficit and disturbance of neural functions in mice lacking GAD65. Brain Res 865:45–58
Svenningsson P, Tzavara ET, Witkin JM, Flenberg AA, Nomikos GG, Greengard P (2002) Involvement of striatal and extrastriatal DARPP-32 in biochemical and behavioral effects of fluoxetine (Prozac) Proc Natl Acad Sci USA 99:3182–3187
Wei Q, Lu XY, Liu L, Schafer G, Shieh KR, Burke S, Robinson TE, Watson SJ, Seasholtz AF, Akil H (2004) Glucocorticoid receptor overexpression in forebrain: a mouse model of increased emotional lability. Proc Natl Acad Sci USA 101:11851–11856
Xu F, Gainetdinov RR, Wetsel WC, Jones SR, Bohn LM, Miller GW, Wang YM, Caron MG (2000) Mice lacking the norepinephrine transporter are supersensitive to psychostimulants. Nat Neurosci 3:465–471

E.7 Anti-Parkinsonism Activity

E.7.0.1 General Considerations

A fundamental lesion in Parkinson's disease is a marked deficiency in the dopaminergic innervation of the basal ganglia owing to degeneration of neurons in the substantia nigra. Enhancement of dopaminergic transmission restores motor function at least partially. The decrease in dopaminergic activity in the basal ganglia results in a relative excess of cholinergic influence. Therefore, dopaminergic agonists, such as levodopa a precursor of dopamine, and cholinergic (muscarinic) antagonists can be combined in the treatment of Parkinson's disease. Parkinson-like syndromes also occur after depletion of central stores by reserpine and after treatment with phenothiazines and other antipsychotic drugs blocking dopamine receptors. (Vernier 1964; Marsden et al. 1975; Duvoisin 1976; Hornykiewicz 1975; Miller and Hiley 1975). The pathology of Parkinson's disease is typified by the presence of cytoplasmic inclusions (Lewy bodies). The formation of these proteinaceous inclusions involves the interaction of several proteins, including α-synuclein, synphilin, parkin and ubiquitin carboxyl-terminal hydrolases (Goldberg and Lansbury 2000; Shimohama et al. 2003; Le and Appel 2004; Meredith et al. 2004; Snyder and Wolozin 2004; von Bohlen und Halbach et al. 2004). Orr et al. (2002) gave a review on inflammatory aspects of Parkinson's disease and highlighted the cell-to-cell interactions and immune regulations critical for neuronal homeostasis and survival. Parkinson's disease and related synucleinopathies are considered as a new class of nervous system amyloidoses (Trojanowski and Lee 2002; Dev et al. 2004; Liu et al. 2005).

REFERENCES AND FURTHER READING

Dev KK, Hofele K, Barbien S, Buchman VL, van der Putten H (2004) Part II: α-synuclein and its molecular pathophysiological role in neurodegenerative disorders. Neuropharmacology 45:14–44
Duvoisin RC (1976) Parkinsonism: Animal analogues of the human disorder. In: Yahr MD (ed) The basal ganglia. Raven, New York, pp 293–303
Goldberg MS, Lansbury PT Jr (2000) Is there a cause-and-effect relationship between α-synuclein fibrillization and Parkinson's disease? Nat Cell Biol 2:E115–E119
Hornykiewicz O (1975) Parkinsonism induced by dopaminergic antagonists. In: Caine DB, Chase TN, Barbeau A (eds) Advances in neurology. Raven, New York, pp 155–164
Le W, Appel SH (2004) Mutant genes responsible for Parkinson's disease. Curr Opin Pharmacol 4:79–84
Liu CW, Giasson BI, Lewis KA, Lee VM, DeMartino GN, Thomas PJ (2005) A precipitating role for truncated α-synuclein and the proteasome in α-synuclein aggregation. J Biol Chem 280:22670–22678
Marsden CD, Duvoisin RC, Jenner P, Parkes JD, Pycock C, Tarsy D (1975) Relationship between animal models and clinical parkinsonism. In: Caine DB, Chase TN, Barbeau A (eds) Advances in neurology. Raven, New York, pp 165–175
Meredith GE, Halliday GM, Totterdell S (2004) A critical review of the development and importance of proteinaceous aggregates in animal models of Parkinson's disease: new insights into Lewy body formation. Parkinsonism Relat Disord 10:191–2002
Miller R, Hiley R (1975) Antimuscarinic actions of neuroleptic drugs. In: Caine DB, Chase TN, Barbeau A (eds) Advances in neurology. Raven, New York, pp 141–154
Orr CF, Rowe DB, Halliday GM (2002) An inflammatory review of Parkinson's disease. Prog Neurobiol 68:325–340
Shimohama S, Sawada H, Kitamura Y, Taniguchi T (2003) Disease model: Parkinson's disease. Trends Mol Med 9:360–305
Snyder H, Wolozin B (2004) Pathological proteins in Parkinson's disease: focus on the proteasome. J Mol Neurosci 24:425–442
Trojanowski JQ, Lee VMY (2002) Parkinson's disease and related synucleinopathies are a new class of nervous system amyloidoses. Neurotoxicol 23:457–460
Vernier VG (1964) Anti-Parkinsonian agents. In: Laurence DR, Bacharach AL (eds) Evaluation of drug activities: pharmacometrics. Academic, London, pp 301–311

Von Bohlen und Halbach O, Schober A, Krieglstein K (2004) Genes, proteins, and neurotoxins involved in Parkinson's disease. Prog Neurobiol 73:151–177

E.7.1 In Vitro Methods

E.7.1.1 Culture of Substantia Nigra

PURPOSE AND RATIONALE

Although *in vivo* animal studies have been used to examine the effects of a number of Parkinson-inducing compounds, there is little information on reliable *in vitro* methodologies that can recapitulate the previously observed in *vivo* results. Cardozo (1993) and Smeyne and Smeyne (2002) described details of a method for generating mixed and chimeric neuron/glial cultures of postnatal substantia nigra (SN), independent of other monoaminergic nuclei in the ventral midbrain. Since many toxins do not affect regions of the midbrain except the SN, use of whole ventral midbrain from embryos can dilute any measurement of cell death. By specifically culturing ventrolateral midbrain containing the SN, one can more directly target the effects of dopaminergic toxins. In addition, this method can be used to test potential therapies for amelioration of Parkinson's disease.

PROCEDURE

Generation of SN Cultures

1. Postnatal day 2–5 C57Bl/6 mice and/or Swiss-Webster (SWR) mice (Harlan) are placed on ice for 2–3 min to achieve an appropriate plane of anesthesia.
2. Animals are quickly decapitated and ≈ 8–10 brains from P2–P5 C57BL/6 or SWR matings are removed and placed in a freshly prepared dissociation media (= DM containing 12.8 g sodium sulfate; 5.2 g potassium sulfate; 0.036 g calcium chloride· $2H_2O$; 1.18 g magnesium chloride· $6H_2O$; 1.8 g glucose anhydrous; 0.238 g HEPES in 1 l deionized water, adjusted to pH 7.4 with NaOH).
3. Brains are placed on their ventral surface and a slice of midbrain rostral to the cerebellum and caudal to the hippocampus is isolated. This removed brain slab is placed flat in DM and either the entire midbrain or the ventrolateral midbrain containing the SN is dissected and minced into small pieces.
4. The minced SN or midbrain is then incubated in papain and DNAase (Dissociation Kit, Worthington Biochemical, Freehold, N.J., USA, follow kit instructions) for 30 min at 37°C. A second incubation with fresh papain solution (30 min, 37°C) is followed by three rinses in DM, and one rinse in plating media (PM).
5. Tissue is triturated in 5 ml PM and the cell suspension is added to 2 ml (1 ml of BSA stock and 1 ml ovalbumin stock).
6. The cell suspension is spun 1400 rev/min for 8 min and the pellet is then resuspended in 1.0 ml plating media containing 2% rat serum.
7. Once resuspended, cells are counted using trypan blue (0.4%) to determine cell viability.
8. Cells are adjusted to 1.2×10^6 cells/ml and plated at ≈ 200,000 cells/cm^2 in Lab-Tek 4-well Permanox™ chamber slides that were previously coated with laminin (200 mg/ml, Collaborative Biomedical Products) and poly-D-lysine (200 mg/ml, Collaborative Biomedical Products) 1:1 (v:v) and rinsed once with deionized water. Cells are maintained in an incubator at 37°C, 5% CO_2, and fed 2–3 times per week with feeding media complete with 2% rat serum (RS) by exchanging approximately one-fifth of the media (100 µl).

Chimeric Neuron/Glial Cultures

1. SNpc cells plated on pre-plated SNpc glia are produced using a variation of the previously described methods. SNpc glial feeder layers from P2–5 C57BL/6 or SWR mice are produced using the above described method, but cells are plated at 20,000–50,000 cells/cm^2 and fed with plating media containing 2% rat serum and 8% fetal bovine serum to promote glial proliferation and neuronal death.
2. For astrocyte cultures, this is the final step.
3. To generate mixed neuron/glial cultures, 3–4 weeks after the initial SNpc cells are plated, the glial feeder layers are rinsed once with plating media without serum, and 0.5 ml of plating media with 2% rat serum (RS) are added.
4. SNpc cells from C57BL/6 or SWR mice are isolated (as above) and plated at 250,000 cells/well on the previously generated glial feeding layers.
5. Twenty-four hours after plating of neurons onto the glial feeder layers, the cultures are fed with feeding media complete with 2% RS by an exchange of approximately one-fifth of the medium (100 µl) and cytosine β-D-arabinofuranoside (Ara-C, 2 µM) to prevent glial proliferation of the freshly plated cells. Thereafter, Ara-C (10 µM, final concentration) is added at each feeding.

MPTP Treatment

1. 1-Methyl-4-phenyl-1,2,3,6-tetrahydropyridine (MPTP) is added to cultures 7–10 days after the neurons are plated onto glia. The MPTP is prepared by dissolving MPTP in feeding media for a 1-mM stock, then diluting to a 1-μM stock with feeding media complete with 2% rat serum and adding this directly to the cultures. The final concentration of the MPTP in media is 50 nM. Two feedings of MPTP, in 2 days, are necessary to achieve the desired toxic effect.
2. Seven days after MPTP is added, the cultures are rinsed 3× with TBS, fixed in 4% buffered paraformaldehyde for 10 min, and rinsed 3× with TBS.

EVALUATION

Identification of SN Cells

1. To determine the number of SN cells, cultures are immunostained for expression of tyrosine hydroxylase. First, endogenous peroxidase activity is quenched by rinsing with 0.3% hydrogen peroxide in methanol in 1 × TBS for 2 × 15 min. Cells are permeabilized with 0.1% Triton X-100, 5% goat serum in TBS for 2 × 15 min. Cultures are covered in 400 μl of a polyclonal antibody directed against tyrosine hydroxylase (Eugene Tech International, Ramsey, N.J., USA or Pel-Freeze, Burlingame, Calif., USA: each 1:500) and incubated in this solution overnight at 4°C. The next day, cultures are rinsed three times with TBS followed by application of secondary antibody (goat α-rabbit) and amplification with Avidin–Biotin (ABC Elite Peroxidase kit, Vector Labs, Burlingame, Calif., USA). Final visualization of the immunopositive neurons is made using diaminobenzidine (DAB kit, Vector Labs) as a chromagen.
2. All TH-positive cells having the previously described characteristics of SNpc neurons (TH-positive cytoplasm surrounding a pale unstained nucleus, Hamre et al. 1999) from each culture are counted at a magnification of 200×. Note: to control for variability between cultures, all MPTP treatments are performed on matched cultures present on one single slide. Once cells are counted in each well, the number of TH-positive cells in the MPTP-treated cultures from each genotype is compared to the adjacent non-treated culture. Since an identical number of cells generated from the same brains was plated on a single slide, these cultures are directly compared to determine the percentage cell loss following MPTP. The percentage cell loss data following MPTP are then pooled from all C57Bl/6, SWR or mixed cultures.

REFERENCES AND FURTHER READING

Cardozo DL (1993) Midbrain dopaminergic neurons from postnatal rat in long-term primary culture. Neuroscience 56:409–421

Hamre R, Tharp K, Poon X, Xiong, Smeyne RJ (1999) Differential strain susceptibility following 1-methyl-4-phenyl-1,2,3,6-tetrahydropyridine (MPTP) administration acts in an autosomal dominant fashion: quantitative analysis in seven strains of *Mus musculus*. Brain Res 828:91–103

Smeyne M, Smeyne RJ (2002) Method for culturing postnatal substantia nigra in an in vitro model of experimental Parkinson's disease. Brain Res Protocols 9:105–111

E.7.1.2 Inhibition of Apoptosis in Neuroblastoma SH-SY5Y Cells

PURPOSE AND RATIONALE

A dopamine-derived neurotoxin, 1(*R*), 2(*N*)-dimethyl-6,7-dihydroxy-1,2,3,4-tetrahydroisoquinoline [*N*-methyl(*R*)salsolinol] was found to cause parkinsonism in rats and to deplete selectively dopamine neurons in the substantia nigra after infusion in the striatum. This isoquinoline occurs enantio-specifically in the nigra-striatum of human brains. The biosynthesis from dopamine is catalyzed by two enzymes, (*R*)salsolinol synthase and (*R*)salsolinol *N*-methyltransferase. The isoquinoline increases in the cerebrospinal fluid from parkinsonian patients, and the increase is ascribed to high activity of its synthesizing neutral (*R*)salsolinol *N*-methyltransferase, as shown by analyses in lymphocytes. The cell death caused by this neurotoxin in dopaminergic human neuroblastoma SH-SY5Y cells proved to be apoptotic. Apoptosis by this neurotoxin is mediated by intracellular sequential process, loss of mitochondrial membrane potential, activation of caspases and DNA fragmentation (Maruyama et al. 1997; Naoi et al. 1996, 1997, 2000, 2002).

Neuroprotection to halt progressive cell death of neurons has been proposed as a future therapy for neurodegenerative disorders. In these disorders, such as Parkinson's disease and Alzheimer's disease, apoptosis contributes to neuronal death in most cases (Tatton 2000). The well-regulated and relatively slow apoptotic process was proposed as a target of neuroprotection (Thompson 1995; Naoi and Maruyama 2001). Apoptosis is induced in neurons by various insults: oxidative stress, metabolic compromise, excitotoxicity, and neurotoxins. Apoptotic signaling is a multi-step pathway induced by opening a mitochondrial mega-channel called permeability transition (PT) pore, followed by decline in membrane potential, $\Delta\Psi m$, re-

lease of apoptosis-inducing factors, activation of caspases and fragmentation of nuclear DNA. Mitochondrial PT pore is regulated by Bcl-2 protein family, preventively by Bcl-2 and Bcl-xL and in a promotive way by BAX and BAD. Several papers describe the neuroprotective-antiapoptotic action of the anti-Parkinson drug rasagiline (Akao et al. 2002a, 2002b; Youdim et al. 2003; Maruyama et al. 2002, 2004b).

Maruyama et al. (2004a) described the neuroprotective function of *R*-(–)-1-(benzofuran-2-yl)-2-propylaminopentane, [*R*-(–)-BPAP], against apoptosis induced by *N*-methyl(*R*)salsolinol, an endogenous dopaminergic neurotoxin, in human dopaminergic neuroblastoma SH-SY5Y cells.

PROCEDURE

SH-SY5Y cells were cultured in Cosmedium-001 tissue culture medium (CosmoBio, Tokyo, Japan), supplemented by 5% fetal calf serum in an atmosphere of 95% air /5% CO_2.

Assessment of Apoptosis Induced by NM(R)Sal and the Protection by BPAP Derivatives

Apoptosis was quantitatively measured by fluorescence-augmented flow cytometry (FACS) with FACScan and CellQuest software (Becton Dickinson, San Jose, Calif., USA). Cells cultured in a 6-well poly-L-lysine-coated culture flask were incubated with or without 1 μM to 1 nM (−)-BPAP analogs at 37°C for 30 min, and then for 24 h with 250 μM *N*M(*R*)Sal in Cosmedium-001 culture medium supplemented with fetal calf serum. The cells were treated with trypsin, gathered, washed with the culture medium and twice with phosphate-buffered saline (PBS). The cells were incubated with 100 nM test drugs solution in an ice-bath for 30 min, washed and suspended in PBS, then subjected to FACS analysis.

Measurement of Changes in $\Delta\Psi$m

Decline in $\Delta\Psi$m induced by *N*M(*R*)Sal was quantified by measuring the reduction of Rhodamine 123 fluorescence pre-loaded in the cells (Patarino et al. 1996), as reported by Akao et al. (2002b). To examine the effects of (−)-BPAP analogs, the cells cultured in 6-well poly-L-lysine-coated tissue culture flasks were stained with 5 μM Rhodamine 123 in DMEM for 30 min at 37°C. After being washed twice with PBS, the cells were suspended in DMEM, incubated with 1 μM to 1 nM BPAP derivatives for 30 min, then with 250 μM *N*M(*R*)Sal for 1 h. After being washed and gathered by treatment with trypsin, the cells were suspended in PBS and the fluorescence at 535 nm was measured with excitation at 505 nm in a Shimadzu spectrofluorophotometer, RF-5000 (Kyoto, Japan).

Measurement of bcl-2 mRNA Level in the Cells Treated with BPAP Derivatives

SH-SY5Y cells were cultured in the presence of various concentrations (100 nM to 10 pM) of (−)-BPAP analogs for 24 h, and mRNA levels of bcl-2 were quantitatively assessed by RT-PCR (Akao et al. 2002a, 2002b). The cells were gathered and washed with PBS, and the total RNA was extracted by the phenol/guanidinium thiocyanate method. cDNA was generated by reverse transcription of 2 μg of the total RNA, and the cDNA fragments were amplified using the PCR primers. The linearity of the relationship of the amount of PCR product to the time of PCR amplification was confirmed under the conditions used in this study. PCR products were analyzed by electrophoresis on 3% agarose gels, and α-actin was used as an internal standard. The amounts of mRNA were quantified using NIH imaging software (version 1.62, developed at the U.S. National Institute for Health).

Measurement of Bcl-2 Levels in the Cells Treated with (–)-BPAP Derivatives

SH-SY5Y cells treated with 1 μM to 1 pM (–)-BPAP analogs for 24 h, and the cells were gathered, washed with PBS and suspended in RIPA buffer (10 mM Tris-HCl buffer, pH 7.5, containing 1% NP-40, 0.1% sodium deoxycholate, 0.1% sodium dodecylsulfate, 150 mM NaCl and 1 mM EDTA 2Na). The lyzed protein (5 μg) was separated by SDS-PAGE using a 10%–20% gradient polyacrylamide gel (Bio-Rad, Hercules, Calif., USA) and electroblotted onto PVDF membranes (Du Pont, Boston, Mass., USA). After blockage with 5% nonfat milk in PBS containing 0.1% Tween 20, the membrane was incubated overnight at 4°C with anti-human Bcl-2 (100) antibody (Santa Cruz Biotechnology, Santa Cruz, Calif., USA), or anti-β-actin antibody as control (Sigma, St. Louis, Mo., USA). The membranes were incubated further with alkaline phosphatase-conjugated goat anti-mouse antibody (Promega, Madison, Wis., USA) at room temperature. The immunoblots were visualized by use of an enhanced chemiluminescence detection kit (New England Biolabs, Beverly, Mass., USA), and quantified by computer-assisted image analysis with the NIH imaging software.

EVALUATION

Experiments were repeated four to eight times, and the results were expressed as the mean and SD. Differences were statistically evaluated by analysis of variance (ANOVA) followed by Sheffe's *F*-test. A p value less than 0.05 was considered to be statistically significant.

MODIFICATIONS OF THE METHOD

Maruyama et al. (2000) found that dopaminergic neurotoxins, 6,7-dihydroy-1-(3′,4′-dihydroxybenzyl)-isoquinolines, cause different cell death in SH-SY5Y cells: apoptosis was induced by oxidized papaverolines and necrosis by reduced tetrahydropapaverolines.

Maruyama et al. (2003) described the anti-apoptotic action of an anti-Alzheimer drug, TV3326 [(N-propargyl)-(3R)-aminoindan-5-yl)-ethyl methyl carbamate], a novel cholinesterase-monoamine oxidase inhibitor.

REFERENCES AND FURTHER READING

Akao Y, Maruyama W, Yi H, Shamoto-Nagai M, Youdim MBH, Naoi M (2002a) An anti-Parkinson's disease drug, *N*-propargyl-1(*R*)-aminoindan (rasagiline), enhances expression of anti-apoptotic bcl-2 in human dopaminergic SH-SY5Y cells. Neurosci Lett 326:105–108

Akao Y, Maruyama W, Shimizu S, Yi H, Nakagawa Y, Shamoto-Nagai M, Youdim MBH, Tsujimoto Y, Naoi M (2002b) Mitochondrial permeability transition mediates apoptosis induced by *N*-methyl(*R*)salsolinol, an endogenous neurotoxin, and is inhibited by Bcl-2 and rasagiline, *N*-propargyl-1(*R*)-aminoindan. J Neurochem 82:913–923

Maruyama W, Sobue G, Matsubara K, Hashizume Y, Dostert P, Naoi M (1997) A dopaminergic neurotoxin, 1(*R*), 2(*N*)-dimethyl-6,7-dihydroxy-1,2,3,4-tetrahydroisochinoline, *N*-methyl-(*R*)-salsolinol, and its oxidation product, 1,2(*N*)-dimethyl-6,7-dihydroxyisoquinolinium ion, accumulate in the nigro-striatal system of the human brain. Neurosci Lett 223:61–64

Maruyama W, Sango K, Iwasa K, Minami C, Dostert P, Kawai M, Moriyasu M, Naoi M (2000) Dopaminergic neurotoxins, 6,7-dihydroy-1-(3′,4′-dihydroxybenzyl)-isoquinolines, cause different cell death in SH-SY5Y cells: apoptosis was induced by oxidized papaverolines and necrosis by reduced tetrahydropapaverolines. Neurosci Lett 291:89–92

Maruyama W, Akao Y, Carrillo MC, Kitani KI, Youdium MBH, Naoi M (2002) Neuroprotection by propargylamines in Parkinson's disease. Suppression of apoptosis and induction of prosurvival genes. Neurotoxicol Teratol 24:675–682

Maruyama W, Weinstock M, Youdin MBH, Nagai M, Naoi M (2003) Anti-apoptotic action of anti-Alzheimer drug, TV3326 [(N-propargyl)-(3R)-aminoindan-5-yl)-ethyl methyl carbamate, a novel cholinesterase-monoamine oxidase inhibitor. Neurosci Lett 341:233–236

Maruyama W, Yi H, Takahashi T, Shimazu S, Ohde H, Yoneda F, Iwasa K, Naoi M (2004a) Neuroprotective function of *R*-(–)-1-(benzofuran-2-yl)-2-propylaminopentane, [*R*-(–)-BPAP], against apoptosis induced by *N*-methyl(*R*)salsolinol, an endogenous dopaminergic neurotoxin, in human dopaminergic neuroblastoma SH-SY5Y cells. Life Sci 75:107–117

Maruyama W, Nitta A, Shamoto-Nagai M, Hirata Y, Akao Y, Yodim M, Furukawa S, Nabeshima T, Naoi M (2004b) *N*-Propargyl-1 (*R*)-aminoindan, rasagiline, increases glial cell line-derived neurotrophic factor (GDNF) in neuroblastoma SH-SY5Y cells through activation of NF-κB transcription factor. Neuro chem Int 44:393–400

Naoi M, Maruyama W (2001) Future of neuroprotection in Parkinson's disease. Parkinsonism Relat Disord 8:139–145

Naoi M, Maruyama W, Dostert P, Hashizume Y, Nakahara D, Takahashi T, Ota M (1996) Dopamine-derived endogenous 1(*R*), 2(*N*)-dimethyl-6,7-dihydroxy-1,2,3,4-tetrahydroisochinoline, *N*-methyl-(*R*)-salsolinol, induced parkinsonism in rat: biochemical, pathological and behavioral studies. Brain Res 709:285–295

Naoi M, Maruyama W, Dostert P, Hashizume Y (1997) *N*-methyl-(*R*)-salsolinol as a dopaminergic neurotoxin: from an animal model to an early marker of Parkinson's disease. J Neural Transm Suppl 50:89–105

Naoi M, Maruyama W, Akao Y, Zhang J, Parvez H (2000) Apoptosis induced by an endogenous neurotoxin, *N*-methyl(*R*)salsolinol, in dopamine neurons. Toxicology 153:123–141

Naoi M, Maruyama W, Akao Y, Yi H (2002) Dopamine-derived endogenous *N*-methyl-(*R*)-salsolinol. Its role in Parkinson's disease. Neurotoxicol Teratol 24:579–591

Patorino JG, Simbula G, Yamamoto K Jr, Glascott PA, Rothman RJ, Farber G (1996) The cytotoxicity of tumor necrosis factor depends on induction of the mitochondrial permeability transition. J Biol Chem 271:27792–27798

Tatton NA (2000) Increased caspase 3 and Bax immunoreactivity accompany nuclear GAPDH translocation and neuronal apoptosis in Parkinson's disease. Exp Neurol 166:29–43

Thompson CB (1995) Apoptosis in the pathogenesis and treatment of disease. Science 267:1456–1462

Youdim MBH, Amit T, Falach-Yogev M, Am OB, Maruyama W, Naoi M (2003) The essentiality of Bcl-2, PKC and proteasome-ubiquitin complex activations in the neuroprotective-antiapoptotic action of the anti-Parkinson drug, rasagiline. Biochem Pharmacol 66:1635–1641

E.7.2 In Vivo Methods

E.7.2.1 Tremorine and Oxotremorine Antagonism

PURPOSE AND RATIONALE

The muscarinic agonists tremorine and oxotremorine induce parkinsonism-like signs such as tremor, ataxia, spasticity, salivation, lacrimation and hypothermia. These signs are antagonized by anticholinergic drugs.

PROCEDURE

Groups of six to ten male NMRI mice weighing 18–22 g are used. They are dosed orally with the test compound or the standard (5 mg/kg benzatropine mesilate) 1 h prior to the administration of 0.5 mg/kg oxotremorine s.c. Rectal temperature is measured before administration of the compound (basal value) and 1, 2 and 3 h after oxotremorine injection. Tremor is scored after oxotremorine dosage in 10-s observation periods every 15 min for 1 h.

Tremor	Score
absent	0
slight	1
medium	2
severe	3

Salivation and lacrimation are scored 15 and 30 min after oxotremorine injection.

absent	0
slight	1
medium	2
severe	3

EVALUATION

Hypothermia

The differences of body temperature after 1, 2 and 3 h versus basal values are summarized for each animal in the control group and the test groups. The average values are compared statistically.

Tremor

The scores for all animals in each group at the three observation periods are summarized. The numbers in the treated groups are expressed as percentage of the number of the control group.

Salivation and Lacrimation

The scores for both symptoms for all animals in each group are summarized at the two observation periods. The numbers in the treated groups are expressed as a percentage of the number of the control group.

CRITICAL ASSESSMENT OF THE METHOD

The oxotremorine antagonism has been proven to be a reliable method for testing central anticholinergic activity. The overt isomorphism between the animal model and the symptoms of Parkinson's disease recommend this test for screening of anti-Parkinson drugs (Cho et al. 1962; Vernier 1964; Everett 1964; Turner 1965; Bebbington et al. 1996; Frances et al. 1980; Ringdahl and Jenden 1983). However, the model measures only central anticholinergic activity (Duvoisin 1976).

MODIFICATIONS OF THE METHOD

Matthews and Chiou (1979) developed a method for quantifying resting tremors in a rat model of limb dyskinesias. The model involved permanent cannulation of the caudate nucleus for the introduction of carbachol. Tremors were quantified with a small transducer and an electronic data collecting system. The system allows the construction of dose–response curves for tremor inhibition by potential antiparkinsonism drugs.

Johnson et al. (1986) developed a procedure for quantifying whole-body tremors in mice. Displacement of a free floating platform by animal movement created a change in resistance across a strain gauge. Administration of oxotremorine, 2.5 mg/kg, i.p, produced numerous high-frequency, high-intensity peaks within 5 min.

Clement and Dyck (1989) constructed and tested a tremor monitor that quantitates soman- and oxotremorine-induced tremors. The device consisted of a force transducer, from which a plastic beaker was suspended containing a mouse. The signal from the force transducer was fed into a tremor monitor and quantitated using the Applecounter from Columbus Instruments.

Coward et al. (1977) recommended *N*-carbamoyl-2-(2,6-dichlorophenyl)acetamidine hydrochloride (LON-954), a tremorigenic agent, as an alternative to oxotremorine for the detection of anti-Parkinson drugs.

Rats treated with 3-acetylpyridine show a selective degeneration of neurons in the inferior olive nucleus and the olivo-cerebellar tract with characteristic motor inco-ordination and ataxia (Denk et al. 1968; Watanabe et al. 1997; Kinoshita et al. 1998). Similar motor dysfunction is seen in patients with olivo-ponto-cerebellar atrophy. To measure the effect of 3-acetylpyridine and the ameliorating effect of TRH agonists in rats the maximal height of vertical jump after stimulation by a foot shock was measured.

Stanford and Fowler (1997) used a special technique for measuring forelimb tremor in rats induced by low doses of physostigmine. The rats pressed a force-sensing operandum while a computer measured force output and performed Fourier analyses on resulting force–time waveforms.

Several studies indicate that the exposure to the pesticide **rotenone** causes highly selective dopaminergic degeneration and α-synuclein aggregation in rats (Betarbet et al. 2000; Sherer et al. 2003a, 2003b).

Tremulous jaw movements in rats induced by tacrine (Mayorga et al. 1997; Cousins et al. 1999) are considered to reflect symptoms in Parkinson's disease. The are suppressed by dopamine agonists (Salamone et al. 2005).

REFERENCES AND FURTHER READING

Agarwal JC, Chandishwar N, Sharma M, Gupta GP, Bhargava KP, Shanker K (1983) Some new piperazino deriva-

tives as antiparkinson and anticonvulsant agents. Arch Pharm (Weinheim) 316:690–694
Bebbington A, Brimblecombe RW, Shakeshaft D (1966) The central and peripheral activity of acetylenic amines related to oxotremorine. Br J Pharmacol 26:56–67
Betarbet R, Sherer TB, MacKenzie G, Garcia-Osuma M, Panov AV, Greenamyre JT (2000) Chronic systemic pesticide exposure reproduces features of Parkinson':s disease. Nat Neuroscio 3:1301–1306
Cho AK, Haslett WL, Jenden DJ (1962) The peripheral actions of oxotremorine, a metabolite of tremorine. J Pharmacol Exp Ther 138:249–257
Clement JG, Dyck WR (1989) Device for quantitating tremor activity in mice: antitremor activity of atropine versus soman- and oxotremorine-induced tremors. J Pharmacol Meth 22:25–36
Cousins MS, Finn M, Trevitt J, Carriero DL, Conlan A, Salamone JD (1999) The role of ventrolateral striatal acetylcholine in the production of tacrine-induced jaw movements. Pharmacol Biochem Behav 62:439–447
Coward DM, Doggett NS, Sayers AC (1977) The pharmacology of N-carbamoyl-2-(2,6-dichlorophenyl)acetamidine hydrochloride (LON-954) a new tremorigenic agent. Arzneim Forsch/Drug Res 27:2326–2332
Denk H, Haider M, Kovac W, Studynka G (1968) Behavioral changes and neuropathological feature in rats intoxicated with 3-acetylpyridine. Acta Neuropathol 10:34–44
Duvoisin RC (1976) Parkinsonism: Animal analogues of the human disorder. In: Yahr MD (ed) The basal ganglia. Raven, New York, pp 293–303
Everett GM (1964) Animal and clinical techniques for evaluating anti-Parkinson agents. In Nodin JH, Siegler PE (eds) Animal and clinical pharmacologic techniques in drug evaluation. Year Book Medical, Chicago, Ill., pp 359–368
Frances H, Chermat R, Simon P (1980) Oxotremorine behavioural effects as a screening test in mice. Prog Neuropsychopharmacol Biol Psychiatry 4:241–245
Johnson JD, Meisenheimer TL, Isom GE (1986) A new method for quantification of tremors in mice. J Pharmacol Meth 16:329–337
Kinoshita K, Watanabe Y, Yamamura M, Matsuoka Y (1998) TRH receptor agonists ameliorate 3-acetylpyridine-induced ataxia through NMDA receptors in rats. Eur J Pharmacol 343:129–133
Matthews RT, Chiou CY (1979) A rat model for resting tremor. J Pharmacol Meth 2:193–201
Mayorga AJ, Carriero MS, Cousins MS, Gianutsos G, Salamone JD (1997) Tremulous jaw movements produced by acute tacrine administration: possible relation to Parkinsonian side effects. Physiol Biochem Behav 56:273–279
Ringdahl B, Jenden DJ (1983) Pharmacological properties of oxotremorine and its analogs. Life Sci 32:2401–2413
Salamone JD, Carlson BB, Rios C, Lentini E, Correa M, Wisniecki A, Betz A (2005) Dopamine agonists suppress cholinomimetic-induced tremulous jaw movements in an animal model of Parkinsonism: tremorolytic effects of pergolide, ropinirole and CY 208–243. Behav Brain Res 156:173–179
Sherer TB, Betarbet R, Testa CM, Seo BB, Richardson JR, Kim JH, Miller GW, Yagi T, Matsuno-.Yagi A, Greenamyre JZ (2003a) Mechanism of toxicity in rotenone models of Parkinson's disease. J Neurosci 23:10756–10764
Sherer TB, Kim JH, Betarbet R, Greenamyre JT (2003b) Subcutaneous rotenone exposure causes highly selective dopaminergic degeneration and α-synuclein aggregation. Exp Neurol 1789:9–16
Stanford JA, Fowler SC (1997) Scopolamine reversal of tremor produced by low doses of physostigmine in rats: evidence for a cholinergic mechanism. Neurosci Lett 225:157–160
Turner RA (1965) Anticonvulsants. Academic Press, New York, pp 164–172
Vernier VG (1964) Anti-Parkinsonian agents. In: Laurence DR, Bacharach AL (eds) Evaluation of drug activities: pharmacometrics. Academic Press, London, pp 301–311
Watanabe Y, Kinoshita K, Koguchi A, Yamamura M (1997) A new method for evaluating motor deficits in 3-acetylpyridine-treated rats. J Neurosci Meth 77:25–29

E.7.2.2 MPTP Model of Parkinson's Disease

PURPOSE AND RATIONALE

MPTP (*N*-methyl-4-phenyl-1,2,3,6-tetrahydropyridine) has been shown to cause symptoms of Parkinson's disease in exposed individuals. The first observation was made in a relatively young, drug-abusing population. This initiated many clinical and experimental studies (Chiba et al. 1984; Heikkila et al. 1984; Kindt et al. 1988; Review by Special 2002). When administered to primates this compound causes a partial destruction of basal ganglia and a syndrome that resembles Parkinson's disease.

PROCEDURE

Burns et al. (1983) treated eight adult rhesus monkeys weighing 5–8 kg over a period of 5–8 days with cumulative intravenous doses of *N*-methyl-4-phenyl-1,2,3,6-tetrahydropyridine (N-MPTP) up to 10–18 mg/kg. These animals showed a parkinsonism-like disorder (akinesia, rigidity, postural tremor, flexed posture, eyelid closure, drooling) which was reversed by the administration of L-dopa. The pathological and biochemical changes produced by N-MPTP are similar to the well established changes in patients with Parkinsonism.

The N-MPTP intoxication was applied using marmosets by Nomoto et al. (1985, 1988), Temlett et al. (1989) and by Kebabian et al. (1992) to evaluate potential antiparkinson drugs.

EVALUATION

The severity of parkinsonian symptoms is rated by trained observers using a scale of 0 (normal) to 17 (maximum severity) that assesses movement (0: normal; 1: reduced; 2: sleepy), checking movements (0: present; 1: reduced; 2: absent), attention and blinking (0: normal; 1: abnormal), posture (0: normal; 1: abnormal trunk; 2: abnormal trunk and tail; 3: abnormal trunk, tail, and limbs; 4: flexed posture), balance and coordination (0: normal; 1: impaired; 2: unstable;

4: falls), reactions (0: normal; 1: reduced; 2: slow; 3: absent) and vocalizations (0: normal; 1: reduced; 2: absent).

MODIFICATIONS OF THE METHOD

Close and Elliott (1991) studied the behavioral effects of anti-Parkinsonian drugs in normal and MPTP-treated marmosets following central microinfusions.

Kebabian et al. (1992) tested a selective D_1 receptor agonist with antiparkinsonian activity in MTPT-treated marmosets.

Domino and Sheng (1993) studied the relative potency of some dopamine agonists with varying selectivities for D_1 and D_2 receptors in MPTP-induced hemi-parkinsonian monkeys.

Gnanalingham et al. (1995) used MTPT-treated marmosets and found differential effects with D_1 dopamine antagonists as compared with the effects in rats with unilateral 6-OGDA-induced lesions, where 6-OGDA is 6-hydroxydopamine.

Doudet et al. (1993) used intravenous administration of ^{15}O-labeled water and 6-(^{18}F)-L-fluorodopa to assess abnormal striatal activity in monkeys after long-term recovery of unilateral lesions of the dopaminergic nigro-striatal system induced by MPTP. Positron emission tomography (PET) data were examined in relation to behavioral and biological parameters, such as cerebral blood flow.

Belluzzi et al. (1994) induced a hemiparkinsonian syndrome in *Macaca nemestrina* **monkeys** by unilateral infusion of MPTP into the right coronary artery.

Raz et al. (2000) recorded hand tremor and simultaneous activity of several neurons in the external and internal segments of the globus pallidus in **vervet monkeys** before and after treatment with MPTP.

Rollema et al. (1989) compared the effects of intracerebrally administered MPP^+ (1-methyl-4-phenylpyridinium) in three species (**mouse, rat** and **monkey**) by microdialysis determinations of dopamine and metabolites in the striatum.

Asin et al. (1997) tested a selective D_1 receptor agonist in **rats** previously given unilateral 6-hydroxydopamine injections and in **macaques** previously given unilateral, intracarotid infusions of MPTP.

Lange (1989, 1990) described circling behavior in old **rats** after unilateral intranigral injection of MPTP.

Fuxe et al. (1992) studied the protection against MPTP-induced degeneration of the nigrostriatal dopamine neurons in the **black mouse**.

There are marked species differences in susceptibility to the neurotoxic effects of MTPT (Giovanni et al. 1994; Schober 2005).

Grünblatt et al. (2001) described gene expression analysis of mice in the MPTP model of Parkinson's disease using cDNA microarray.

Mandel et al. (2003) reviewed the use of cDNA microarrays to assess Parkinson's disease models and the effects of neuroprotective drugs.

Hamre et al. (1999) performed a quantitative analysis in seven strains of **mice** and found that differential strain susceptibility following MPTP administration acts in an autosomal fashion.

Sedelis et al. (2001) described behavioral phenotyping of the MPTP mouse model on Parkinson's disease.

Muramatu et al. (2003) published an immunocytochemical study on cerebral alterations in an MPTP mouse model of Parkinson's disease.

REFERENCES AND FURTHER READING

Asin KE, Domino EF, Nikkel A, Shiosaki K (1997) The selective dopamine D_1 receptor agonist A-86929 maintains efficacy with repeated treatment in rodent and primate models of Parkinson's disease. J Pharmacol Exp Ther 281:454–459

Belluzzi JD, Domino EF, May JM, Bankiewicz KS, McAfee DA (1994) N-0923, a selective dopamine D_2 receptor agonist, is efficacious in rat and monkey models of Parkinson's disease. Mov Disord 9:147–154

Bernardini GL, Speciale SG, German DC (1990) Increased midbrain dopaminergic activity following 2′CH_3-MPTP-induced dopaminergic cell loss: an *in vitro* electrophysiological study. Brain Res 527:123–129

Burns RS, Chiueh CC, Markey SP, Ebert MH, Jacobowitz DM, Kopin IJ (1983) A primate model of parkinsonism: selective destruction of dopaminergic neurones in the pars compacta of the substantia nigra by *N*-methyl-4-phenyl-1,2,3,6-tetrahydropyridine. Proc Natl Acad Sci USA 80:4546–4550

Chiba K, Trevor A, Castagnoli N (1984) Metabolism of the neurotoxic tertiary amine, MPTP, by brain monoamine oxidase. Biochem Biophys Res Commun 120:574–578

Close SP, Elliott PJ (1991) Procedure for assessing the behavioral effects of novel anti-Parkinsonian drugs in normal and MPTP-treated marmosets following central microinfusions. J Pharmacol Meth 25:123–131

Domino EF, Sheng J (1993) Relative potency of some dopamine agonists with varying selectivities for D_1 and D_2 receptors in MPTP-induced hemiparkinsonian monkeys. J Pharmacol Exp Ther 265:1387–1391

Doudet DJ, Wyatt RJ, Cannon-Spoor E, Suddath R, McLellan CA, Cohen RM (1993) 6-(^{18}F)-Fluoro-L-DOPA and cerebral blood flow in unilaterally MPTP-treated monkeys. J Neural Transplant Plast 4:27–38

Fuxe K, Janson AM, Rosén L, Finnman UB, Tanganelli S, Morari M, Goldstein M, Agnati LF (1992) Evidence for a protective action of the vigilance promoting drug Modafinil on the MPTP-induced degeneration of the nigrostriatal dopamine neurons in the black mouse: an immunocytochemical and biochemical analysis. Exp Brain Res 88:117–130

Giovanni A, Sonsalla PK, Heikkila RF (1994) Studies on species sensitivity to the dopmainergic neurotoxin 1-methyl-4-phenyl-1,2,3,6-tetrahydropyridine. Part 2: Central administration of 1-methyl-4-phenylpyridinium. J Pharmacol Exp Ther 270:1008–1014

Gnanalingham KK, Hunter AJ, Jenner P, Marsden CD (1995) Selective dopamine antagonist pretreatment on the antiparkinsonian effects of benzazepine D_1 dopamine agonists in rodent and primate models of Parkinson's disease – the differential effects of D_1 dopamine antagonists in the primate. Psychopharmacology 117:403–412

Grünblatt E, Mandel S, Maor G, Youdim MBH (2001) Gene expression analysis of *N*-methyl-4-phenyl-1,2,3,6-tetrahydropyridine mice model of Parkinson's disease using cDNA microarray: effect of *R*-apomorphine. J Neurochem 78:1–12

Hamre K, Tharp R, Poon K, Xiong X, Smeyna RJ (1999) Differential strain susceptibility following 1-methy-4-phenyl-1,2,3,6-tetrahydropyridine (MPTP) administration acts in an autosomal fashion: quantitative analysis in seven strains of *Mus musculus*. Brain Res 828:91–103

Heikkila RE, Manzino L, Cabbat FS, Duvoisin RC (1984) Protection against dopaminergic neurotoxicity of 1-methyl-4-phenyl-1,2,5,6-tetrahydropyridine by monoamine oxidase inhibitors. Nature 311:467–469

Kebabian JW, Britton DR, DeNinno MP, Perner R, Smith L, Jenner P, Schoenleber R, Williams M (1992) A-77363: a potent and selective D_1 receptor antagonist with antiparkinsonian activity in marmosets. Eur J Pharmacol 229:203–209

Kindt MV, Youngster SK, Sonsalla PK, Duvoisin RC, Heikkila RE (1988) Role for monoamine oxidase-A (MAO-A) in the bioactivation and nigrostriatal dopaminergic neurotoxicity of the MPTP analog, 2′Me-MTPT. Eur J Pharmacol 146:313–318

Lange KW (1989) Circling behavior in old rats after unilateral intranigral injection of 1-methyl-4-phenyl-1,2,3,6-tetrahydropyridine (MPTP). Life Sci 45:1709–1714

Lange KE (1990) Behavioural effects and supersensitivity in the rat following intranigral MPTP and MPP^+ administration. Eur J Pharmacol 175:57–61

Mandel S, Weinreb O, Youdim MBH (2003) Using cDNA microarray to assess Parkinson's disease models and the effects of neuroprotective drugs. Trends Pharmacol Sci23:184–191

Muramatu Y, Kurosaki R, Watanabe H, Michimata M, Matsubara M, Imai Y, Araki T (2003) Cerebral alterations in a MPTP-mouse model of Parkinson's disease – an immunocytochemical study. J Neural Transmission 110:1129–1144

Nomoto M, Jenner P, Marsden CD (1985) The dopamine D_2 agonist LY 141865, but not the D_1 agonist SKF 38393, reverses parkinsonism induced by 1-methyl-4-phenyl-1,2,3,6-tetrahydropyridine (MPTP) in the common marmoset. Neurosci Lett 57:37–41

Nomoto M, Jenner P, Marsden CD (1988) The D_1 agonist SKF 38393 inhibits the anti-parkinsonian activity of the D_2 agonist LY 141555 in the MPTP-treated marmoset. Neurosci Lett 93:275–280

Raz A, Vaadia E, Bergman H (2000) Firing pattern and correlations of spontaneous discharge of pallidal neurons in the normal and the tremulous 1-methyl-4-phenyl-1,2,3,6-tetrahydropyridine vervet model of parkinsonism. J Neurosci 20:8559–8571

Rollema H, Alexander GM, Grothusen JR, Matos FF, Castagnoli N Jr (1989) Comparison of the effects of intracerebrally administered MPP^+ (1-methyl-4-phenylpyridinium) in three species: microdialysis of dopamine and metabolites in mouse, rat and monkey striatum. Neurosci Lett 106:275–281

Schober A (2005) Classic toxin-induced animal models of Parkinson's disease: 6-OHDA and MPTP. Cell Tissue Res 318:215–224

Sedelis M, Schwarting RKW, Huston JP (2001) Behavioral phenotyping of the MPTP mouse model on Parkinson's disease. Behav Brain Res 125:109–122

Special SG (2002) MPTP: Insights into parkinsonian neurodegeneration. Neurotoxicol Teratol 24:607–620

Temlett JA, Quinn NP, Jenner PG, Marsden CD, Pourcher E, Bonnet AM, Agid Y, Markstein R, Lataste X (1989) Antiparkinsonian activity of CY 208–243, a partial D-1 dopamine receptor agonist, in MTPT-treated marmosets and patients with Parkinson's disease. Movement Disord 4:261–265

E.7.2.3 Reserpine Antagonism

PURPOSE AND RATIONALE

Reserpine induces depletion of central catecholamine stores. The sedative effect can be observed in mice shortly after injection, followed by signs of eyelid ptosis, hypokinesia, rigidity, catatonia, and immobility. These phenomena can be antagonized by dopamine agonists.

PROCEDURE

Male NMRI mice of either sex weighing 20–25 g are used. They are injected intraperitoneally with 5 mg/kg reserpine and tested 24 h later. The test compounds are injected 30 min prior to observation. The animals are placed singly onto the floor of a Perspex container (30 × 26 cm, 20 cm high), situated on a Panlab proximity sensor unit. Horizontal movements are recorded for 10 min. Moreover, rearings and grooming episodes are recorded by an experienced observer.

EVALUATION

Locomotor activity and grooming scores of drug-treated animals are compared with controls treated with reserpine and vehicle only by analysis of variance.

MODIFICATIONS OF THE METHOD

Rats treated with reserpine develop spontaneous orofacial dyskinesia that has features similar to tardive dyskinesia in humans (Abbot et al. 1991; Nisewander et al. 1994). The incidence of tongue protrusions was recorded to quantify the occurrence of oral dyskinesia.

REFERENCES AND FURTHER READING

Abbott B, Starr BS, Starr MS (1991) CY 208–243 behaves as a typical D-1 agonist in the reserpine-treated mouse. Pharmacol Biochem Behav 38:259–263

Agarwal JC, Chandishwar N, Sharma M, Gupta GP, Bhargava KP, Shanker K (1983) Some new piperazine derivatives as antiparkinson and anticonvulsant agents. Arch Pharm (Weinheim) 316:690–694

Amt J (1985) Behavioral stimulation is induced by separate dopamine D_1 and D_2 receptor sites in reserpine pretreated but not in normal rats. Eur J Pharmacol 113:79–88
Duvoisin RC (1976) Parkinsonism: animal analogues of the human disorder. In: Yahr MD (ed) The basal ganglia. Raven, New York, pp 293–303
Nisewander JL, Castañeda E, Davis DA (1994) Dose-dependent differences in the development of reserpine-induced oral dyskinesias in rats: support of a model of tardive dyskinesia. Psychopharmacology 116:79–84

E.7.2.4 Circling Behavior in Nigrostriatal Lesioned Rats

PURPOSE AND RATIONALE

Unilateral lesion of the dopaminergic nigrostriatal pathway in the rat by the neurotoxin 6-hydroxydopamine (6-OHDA) induces hypersensitivity of the postsynaptic dopaminergic receptors in the striatum of the lesioned side (Ungerstedt 1971). The rats rotate in a direction towards the lesioned side (ipsilateral) when an indirect acting compound such as amphetamine is administered, but to the opposite direction (contralateral) when a directly acting dopamine agonist, e. g., apomorphine, or the dopamine precursor L-dopa is given. Therefore, this test can be used for the study of central dopamine function and the evaluation of dopamine antagonists and agonists, particularly the activity of novel antiparkinsonian drugs.

PROCEDURE

Male Wistar rats weighing 200–250 g at the time of surgery are used. The are housed individually in a controlled environment with free access to food and water.

The animals are anesthetized with sodium pentobarbital. The head is placed in a stereotaxic device (DKI 900) and positioned according to the atlas of König and Klippel (1963). After a sagittal cut is made in the skin of the skull, a 2-mm-wide hole is drilled with an electrical trepan drill. Care is taken not to lesion the meninges. A 30-gauge stainless-steel cannula connected to a Hamilton syringe is aimed at the anterior zona compacta of the substantia nigra (coordinates anterior 4.1, lateral 1.0 and dorso-ventral –2.5 from instrument zero). A total of 8 µg of 6-OHDA in 4 γ/l of saline is injected at a rate of 1 γ/4 min. After the intracranial injection the wound is closed. The animal is allowed several weeks for recovery and for development of the lesion.

Specially constructed opaque plastic spheres attached to solid-state programming equipment serve as test chambers. The number of full turns, either ipsilateral or contralateral to the lesion, is recorded on an automatic printout counter every 15 min for 1- or 2-h test sessions.

To determine the control values for ipsilateral turning, each subject is administered 2.5 mg/kg of d-amphetamine and immediately placed in the circling chamber for 2 h. Control values for contralateral circling are determined by injecting apomorphine at 1 mg/kg s.c. and recording the rat's circling for 1 h.

Test compounds are given i.p or s.c. and the animals placed into the circling chambers. Circling is recorded over a 1-h period.

EVALUATION

Percent change of drug turns from control turns is recorded. Using various doses ED_{50} values can be calculated.

MODIFICATIONS OF THE METHOD

Etemadzadeh et al. (1989) described a computerized rotometer apparatus for recording circling behavior. The digital pulses derived from the infrared photocell detector induced by the animal rotations were fed directly to a 20-megabyte microcomputer for online recording and were processed further to the Digital Equipment Corporation's VAX computer with the SAS software system for statistical and graphical analysis.

Hudson et al. (1993) described a 16-channel automated rotometer system for reliable measurement of turning behavior in 6-hydroxydopamine-lesioned and transplanted rats. The system is preferable to more tedious methods such as videotaping and subsequent manual analysis or various other mechanical systems.

A rotometer differentiating between clockwise and counter-clockwise rotations with computerized evaluation is available from Technical and Scientific Equipment (Bad Homburg, Germany; Schwarz et al. 1978).

Carey (1989) tested stimulant drugs as conditioned and unconditioned stimuli in a classical conditioning paradigm using drug-induced rotational behavior in rats with unilateral lesions of dopamine neurons.

The production of asymmetry and circling behavior following unilateral, intrastriatal administration of neuroleptics was discussed by Costall et al. (1983).

Rotational behavior produced by intranigral injections of bovine and human β-casomorphins in rats was described by Herrera-Marschitz et al. (1989).

Perese et al. (1989) created a hemiparkinsonian model in rats in which there is 6-OHDA-induced destruction of the dopaminergic nigrostriatal pathway but sparing of the dopaminergic mesolimbic pathway.

Sauer and Oertel (1994) published a retrograde tracing and immunocytochemical study on the pro-

gressive degeneration of nigrostriatal dopamine neurons following intrastriatal terminal lesions with 6-hydroxydopamine in the rat.

Garrett and Holtzman (1996) compared the effects of apomorphine, d-amphetamine, cocaine and caffeine on locomotor activity and rotational behavior in rats with unilateral 6-OHDA-induced lesions of the nigrostriatal tract.

McElroy and Ward (1995) reported that the high-affinity and selective dopamine D_3 receptor ligand, 7-OH-DPAT, caused 6-OHDA-lesioned rats to rotate in a direction contralateral to the lesioned side similarly to the direct-acting dopamine agonist apomorphine.

Haque et al. (1996) directly infused the neurotrophins NT3 and NT4/5 intraparenchymally in close proximity to transplanted nigral tissue placed in the dopamine-depleted striatum of 6-hydroxydopamine-lesioned rats.

A survey on the unilateral 6-hydroxydopamine lesion model in behavioral brain research was prepared by Schwarting and Huston (1996).

DSP-4 [*N*-(2-chloroethyl)-*N*-ethyl-2-bromobenzylamine] is highly toxic to noradrenergic neurons (Finnegan et al. 1999). Srinivasan and Schmidt (2003, 2004) showed that parkinsonian symptoms in 6-hydroxydopamine-induced partial degeneration of substantia nigra in rats are potentiated after depletion of nucleus coeruleus noradrenaline by intraperitoneal treatment with DPS-4.

Harro et al. (2003) studied the effect of denervation of the locus coeruleus projections by DSP-4 treatment on [^{3}H]-raclopride binding to dopamine D_2 receptors and D_2 receptor–G protein interaction in rat striatum.

Löscher et al. (1996) described a mutant rat strain (*CI*) with abnormal circling behavior reminiscent of 6-hydroxydopamine-lesioned rats.

Mele et al. (1997) studied alterations in striatal dopamine overflow by *in vivo* microdialysis during rotational behavior of rats induced by amphetamine, phencyclidine and MK 801.

Smith et al. (1996) reported contralateral turning in chronically cannulated rats after stimulation of glutamate receptors by unilateral intrastriatal injections of glutamate receptor agonists, such as kainate or AMPA.

Spooren et al. (2000) tested the effects of a prototypical $mGlu_5$ receptor antagonist on rotarod locomotor activity and rotational responses in unilateral 6-OHDA-lesioned rats using an accelerated rotarod and automated rotameter cylinders (TSE Systems, Bad Homburg, Germany).

Using the same equipment, Breysse et al. (2002) reported that chronic but not acute treatment with a metabotropic glutamate 5 receptor antagonist reverses the akinetic deficits in rats with 6-hydroxydopamine lesions.

Using automated rotameter bowls (TSE Systems, Bad Homburg, Germany), Meissner et al. (2002) found that deep brain stimulation of subthalamic neurons induces contralateral circling in freely moving 6-hydroxydopamine-lesioned rats.

With this equipment, Lebsanft et al. (2005) found, that 3,4-methylenedioxymethylamphetamine counteracts akinesia enantioselectively in rat rotational behavior.

O'Neill et al. (2004) described neurotrophic actions of an AMPA receptor potentiator, which may increase brain-derived neurotrophic factor expression, in rodent models of Parkinson's disease.

Inhibition of sinistrotorsion induced in **guinea pigs** by injection of physostigmine into the right carotid artery was proposed as a method of screening central anticholinergic activity by De Jonge and Funcke (1962).

Behavioral quantification of striatal dopaminergic supersensitivity after bilateral 6-hydroxydopamine lesions in the **mouse** was reported by Mandel et al. (1992).

Worms et al. (1986) and Poncelet et al. (1993) studied turning behavior in mice induced by intrastriatal injection of neuropeptides.

Fitzgerald et al. (1992) recommended the **chakragati mouse (ckr)**, a transgenic insertional mutant which displays lateral circling, locomotor hyperactivity and hyperreactivity, as a model to study aspects of neuropsychiatric disorders associated with dopaminergic abnormalities.

Emonds-Alt et al. (1995) injected 0.3 pg senktide into the striatum of **gerbils** inducing contralateral rotations which were antagonized by intraperitoneal or oral administration of a tachykinin NK_3 receptor antagonist.

Vernier and Unna (1963) tested drugs against the tremor induced by stereotactically oriented electric lesions in the region of the subthalamus or the mesencephalic reticular formation in **monkeys**.

REFERENCES AND FURTHER READING

Agarwal JC, Chandishwar N, Sharma M, Gupta GP, Bhargava KP, Shanker K (1983) Some new piperazine derivatives as antiparkinson and anticonvulsant agents. Arch Pharm (Weinheim) 316:690–694

Agid Y, Javoy F, Glowinski J, Bouvet D, Sotelo C (1973) Injection of 6-hydroxydopamine into the substantia nigra of the rat. II. Diffusion and specificity. Brain Res 58:291–301

Breysse N, Baunez C, Spooren W, Gasparini F, Amalric M (2002) Chronic but not acute treatment with a metabotropic

glutamate 5 receptor antagonist reverses the akinetic deficits in a rat model of Parkinsonism. J Neurosci 22:5669–5678

Carey RJ (1989) Stimulant drugs as conditioned and unconditioned stimuli in a classical conditioning paradigm. Drug Dev Res 16:305–315

Carpenter MB, McMasters RE (1964) Lesions of the substantia nigra in the rhesus monkey. Efferent fiber degeneration and behavioral observations. Am J Anat 114:293–319

Clineschmidt BV, Martin GE, Bunting PR (1982) Central sympathomimetic activity of (+)-5-methyl-10,11-dihydro-5H-dibenzo[a,d]cyclohepten-5,10-imine (MK-801), a substance with potent anticonvulsant, central sympathomimetic, and apparent anxiolytic properties. Drug Dev Res 2:135–145

Costall B, Kelly ME, Naylor RJ (1983) The production of asymmetry and circling behavior following unilateral, intrastriatal administration of neuroleptic agents: a comparison of abilities to antagonise striatal function. Eur J Pharmacol 96:79–86

De Jonge MC, Funcke ABH (1962) Sinistrotorsion in guinea pigs as a method of screening central anticholinergic activity. Arch Int Pharmacodyn 137:375–382

Emonds-Alt X, Bichon D, Ducoux JP, Heaulme M, Miloux B, Poncelet M, Proietto V, Van Broeck D, Vilain P, Neliat G, Soubrié P, Le Fur G, Brelière JC (1995) SR 142801, the first potent non-peptide antagonist of the tachykinin NK_3 receptor. Life Sci 56:27–32

Engber TM, Susel Z, Juncos JL, Chase TN (1989) Continuous and intermittent levodopa differentially affect rotation induced by D-1 and D-2 dopamine agonists. Eur J Pharmacol 168:291–298

Etemadzadeh E, Koskinen L, Kaakola S (1989) Computerized rotometer apparatus for recording circling behavior. Meth Find Exp Clin Pharmacol 11:399–407

Finnegan KT, Skratt JJ, Irwin I, De Lanney LE, Langston JW (1990) Protection against DSP-4-induced neurotoxicity by deprenyl is not related to its inhibition of MAK B. Eur J Pharmacol 184:119–126

Fitzgerald LW, Miller KJ, Ratty AK, Glick SD, Teitler M, Gross KWl (1992) Asymmetric evaluation of striatal dopamine D_2 receptors in the chakragati mouse: Neurobehavioral dysfunction in a transgenic insertional mutant. Brain Res 580:18–26

Fuxe K, Agnati LF, Corrodi H, Everitt BJ, Hökfelt T, Löfström A, Ungerstedt U (1975) Action of dopamine receptor agonists in forebrain and hypothalamus: rotational behavior, ovulation, and dopamine turnover. In: Caine DB, Chase TN, Barbeau A (eds) Advances in neurology. Raven, New York, pp 223–242

Garrett BE, Holtzman SG (1995) The effects of dopamine agonists on rotational behavior in non-tolerant and caffeine-tolerant rats. Behav Pharmacol 6:843–851

Garrett BE, Holtzman SG (1996) Comparison of the effects of prototypical behavioral stimulants on locomotor activity and rotational behavior in rats. Pharmacol Biochem Behav 54:469–477

Haque NSK, Hlavin ML, Fawcell JW, Dunnett SB (1996) The neurotrophin NT4/5, but not NT3, enhances the efficacy of nigral grafts in a rat model of Parkinson's disease. Brain Res 712:45–52

Harro J, Terasmaa A, Eller M, Rinken A (2003) Effect of denervation of the locus coeruleus projections by DSP-4 treatment on [^{3}H]-raclopride binding to dopamine D_2 receptors and D_2 receptor-G protein interaction in rat striatum. Brain Res 976:209–215

Herrera-Marschitz M, Terenius L, Grehn L, Ungerstedt U (1989) Rotational behaviour produced by intranigral injections of bovine and human β-casomorphins in rats. Psychopharmacology 99:357–361

Hudson JL, Levin DR, Hoffer BJ (1993) A 16-channel automated rotometer system for reliable measurement of turning behavior in 6-hydroxydopamine lesioned and transplanted rats. Cell Transplant 2:507–514

Kebabian JW, Britton DR, DeNinno MP, Perner R, Smith L, Jenner P, Schoenleber R, Williams M (1992) A-77363: a potent and selective D_1 receptor antagonist with antiparkinsonian activity in marmosets. Eur J Pharmacol 229:203–209

König JFR, Klippel RA (1963) The rat brain – a stereotaxic atlas. Williams and Wilkins, Baltimore, Md.

Lebsanft HB, Kohler T, Kovar KA, Schmidt WJ (2005) 3,4-Methylenedioxymethylamphetamine counteracts akinesia enantioselectively in rat rotational behavior and catalepsy. Synapse 55:148–155

Löscher W, Richter A, Nikkhah G, Rosenthal C, Ebert U, Hedrich HJ (1996) Behavioral and neurochemical dysfunction in the circling (*CI*) rat: a novel genetic animal of a movement disorder. Neuroscience 74:1135–1142

Mandel RJ, Wilcox RE, Randall PK (1992) Behavioral quantification of striatal dopaminergic supersensitivity after bilateral 6-hydroxydopamine lesions in the mouse. Pharmacol Biochem Behav 41:343–347

McElroy JF, Ward KA (1995) 7-OH-DPAT, a dopamine D_3-selective receptor agonist, produces contralateral rotation in 6-hydroxydopamine-lesioned rats. Drug Dev Res 34:329–335

Meissner W, Harnack D, Paul G, Reum T, Sohr R, Morgenstern R, Kupsch A (2002) Deep brain stimulation of subthalamic neurons increases dopamine metabolism and induces contralateral circling in freely moving 6-hydroxydopamine-lesioned rats. Neurosci Lett 328:105–108

Mele A, Fontana D, Pert A (1997) Alterations in striatal dopamine overflow during rotational behavior induced by amphetamine, phencyclidine and MK 801. Synapse 26:218–244

Morelli M (1990) Blockade of NMDA transmission potentiates dopaminergic D-1 while reduces D-2 responses in the 6-OHDA model of Parkinson. Pharmacol Res 22 [Suppl 2]:343

O'Neill MJ, Murray TK, Whalley K, Ward MA, Hicks CA, Woodhouse S, Osborne DJ, Skolnick P (2004) Neurotrophic actions of the novel AMPA receptor potentiator, LY404187 in rodent models of Parkinson's disease. Eur J Pharmacol 486 :163–174

Perese DA, Ulman J, Viola J, Ewing SE, Bankiewicz KS (1989) A 6-hydroxydopamine-induced selective parkinsonian rat model. Brain Res 494:285–293

Poncelet M, Gueudet C, Emonds-Alt X, Belière JC, Le Fur G, Soubrié PH (1993) Turning behavior induced in mice by a neurokinin A receptor antagonist: selective blockade by SR 48968, a non-peptide receptor antagonist. Neurosci Lett 149:40–42

Sauer H, Oertel WH (1994) Progressive degeneration of nigrostriatal dopamine neurons following intrastriatal terminal lesions with 6-hydroxydopamine: a combined retrograde tracing and immunocytochemical study in the rat. Neuroscience 59:401–415

Schwarting RKW, Huston JP (1996) The unilateral 6-hydroxydopamine lesion model in behavioral brain research. Analysis of functional deficits, recovery and treatments. Prog Neurobiol 50:275–331

Schwarz RD, Stein JW, Bernard P (1978) Rotometer for recording rotation in chemically or electrically stimulated rats. Physiol Behav 20:351–354
Smith ID, Todd MJ, Beninger RJ (1996) Glutamate receptor agonist injections into the dorsal striatum cause contralateral turning in the rat: involvement of kainate and AMPA receptors. Eur J Pharmacol 301:7–17
Spooren WPJM, Gasparini F, Bergmann R, Kuhn R (2000) Effects of the prototypical $mGlu_5$ receptor antagonist 2-methyl-6-(phenylethynyl)-pyridine on rotarod, locomotor activity and rotational responses in unilateral 6-OHDA-lesioned rats. Eur J Pharmacol 406:403–410
Srinivasan J, Schmidt WJ (2003) Potentiation of parkinsonian symptoms by depletion of locus coeruleus noradrenaline in 6-hydroxydopamine-induced partial degeneration of substantia nigra in rats. Eur J Neurosci 17:2586–2592
Srinivasan J, Schmidt WJ (2004) Behavioral and neurochemical effects of noradrenergic depletion with *N*-(2-chloroethyl)-*N*-ethyl-2-bromobenzylamine in 6-hydroxydopamine-induced rat model of Parkinson's disease. Behav Brain Res 151:191–199
Ungerstedt U (1971) Postsynaptic hypersensitivity after 6-hydroxydopamine induced degeneration of the nigro-striatal dopamine system. Acta Physiol Scand Suppl 367:69–93
Vernier VG, Unna KR (1963) The central nervous system effects of drugs in monkeys with surgically-induced tremor: atropine and other antitremor agents. Arch Int Pharmacodyn 141:30–53
Worms P, Martinez J, Briet C, Castro B, Bizière K (1986) Evidence for dopaminomimetic effect of intrastriatally injected cholecystokinin octapeptide in mice. Eur J Pharmacol 121:395–401

E.7.2.5 Elevated Body Swing Test

PURPOSE AND RATIONALE

Borlongan and Sanberg (1995); Borlongan et al. (1995) proposed the elevated body swing test as a measure of asymmetrical motor behavior of hemiparkinsonian animals in a drug-free state.

PROCEDURE

Male, 8-week-old Sprague Dawley rats are anesthetized with sodium pentobarbital (60 mg/kg i.p.) and mounted in a Kopf stereotaxic frame. They are lesioned by injection of 8 µg 6-hydroxydopamine in 4 µl saline containing 0.02% ascorbic acid in the left substantia nigra (AP – 5.0, ML+1.5, DV – 8.0). The solution is injected over a 4-min period and the needle left in place for an additional 5 min before retraction.

Seven days after the lesion, behavioral testing is performed. The animal is allowed to habituate in a Plexiglas box and attain a neutral position having all four paws on ground. The rat is held about 2.5 cm from the base of its tail and elevated 2.5 cm above the surface on which it has been resting. A swing is recorded whenever the animal moves its head out of the vertical axis to either side. Before attempting another swing, the animal must return to the vertical position for the next swing to be counted. Swings are counted for 60 s over four consecutive 15-s segments. The total number of swings made to each side is divided by the overall total number of swings made to both sides to get percentages of left and right swings. The criterion of biased swing is set at 70% or higher. At 30 and 45 s, 6-OHDA-lesioned rats exhibit right-biased swings of 70% or higher compared to normal rats.

EVALUATION

A two-way ANOVA is used to analyze swing behavior data across the 15-s segments.

REFERENCES AND FURTHER READING

Borlongan CV, Sanberg PR (1995) Elevated body swing test: a new behavioral parameter for rats with 6-hydroxydopamine-induced hemiparkinsonism. J Neurosci 15:5372–5378
Borlongan CV, Randall TS, Cahill DW, Sanberg PR (1995) Asymmetrical motor behavior in rats with unilateral excitotoxic lesions as revealed by the elevated body swing test. Brain Res 676:231–234

E.7.2.6 Skilled Paw Reaching in Rats

PURPOSE AND RATIONALE

Montoya et al. (1990, 1991), Abrous et al. (1993), Abrous and Dunnett (1994), Nikkhah et al. (1993), and Barnéoud et al. (1996) used the skilled paw reaching test as a model of Parkinson's disease in the rat. The term "staircase test" mentioned in this context has nothing to do with the staircase test described by Thiebot et al. (1973) for evaluating anxiolytic activity in rats (see E.2.4.6).

Unilateral injection of 6-OHDA into the medial forebrain bundle results in an impairment of paw reaching on both sides which can be ameliorated by drug treatment or transplantation of a nigral cell suspension.

The apparatus has been developed after earlier studies by Whishaw et al. (1986) who investigated the contributions of motor cortex, nigrostriatal dopamine and caudate-putamen to skilled forelimb use in the rat.

PROCEDURE

Apparatus

The apparatus consists of a clear Perspex chamber with a hinged lid. A narrower compartment with a central platform running along its length, creating a trough

on either side, is connected to the chamber. The narrowness of the side compartment prevents rats from turning around, so they can use only their left paw for reaching into the left trough and their right paw for reaching into the right trough. A removable double staircase is inserted into the end of the box, sliding into the troughs on either side of the central platform. Each of the steps of the staircase contains a small well, and two 45-mg saccharin-flavored pellets are placed in each well.

Learning Procedure

The week before the start of the training period, the rats are deprived of food and their body weight is stabilized at 85% of the weight of non-deprived rats. At the same time, they are gently manipulated and familiarized with the appetitive saccharin-flavored pellets.

The animals then begin to learn the paw reaching task. For 4 weeks they are placed in the test boxes once per day for 10–15 min. The number of pellets eaten during the test period indicates the rat's success in grasping and retrieving the pellets; the number of steps from which pellets have been removed provides an index of the attempts to reach the food and how far the rat can reach; the number of missed pellets remaining at the end of the test on the floor of the side compartment indicates a lack of sensorimotor coordination in grasping and retrieving the pellets. In addition to these three parameters, it is noted which forepaw the rat used for the first movement to reach the pellet on each test day. A first choice score of +1 corresponds to the paw contralateral to the lesion, a score of –1, to the paw ipsilateral to the lesion. Because rodents exhibit a "pawedness," it must be noted whether there is a preference for one paw.

Lesions

The mesotelencephalic system is lesioned by a stereotaxic unilateral injection of 6-OHDA into the medial forebrain bundle under equithesin anesthesia. 6-OHDA is injected in a volume of 1.5 µl and at a concentration of 4 µg/µl of 0.9% saline and 0.01% ascorbic acid twice over 3 min via a 30-gauge stainless steel cannula at the stereotaxic coordinates: $L = 1.6$ mm, $AP = 0$ mm, $V = -7.6$ mm and $L = 1.6$ mm, $AP = -1$ mm, $V = -8$ mm. The coordinates AP and L are estimated relative to the bregma, and V is measured from the level of the dura, with the incisor bar set 5 mm above the interaural line. Following each injection, the cannula is left in place for an additional 4 min to allow the diffusion of the neurotoxin away from the injection site. The sham-operated group receives sham lesions by identical injection of ascorbate-saline solution alone.

Drug Treatment

The animals are injected i.p. with the test drug or saline 30 min before the unilateral 6-OHDA lesion and 24 h thereafter.

EVALUATION

Test sessions are performed 4, 5, 7, and 8 weeks after 6-OHDA lesion. The parameters success, attempts and sensorimotor coordination are subjected to a two-way ANOVA with group as the independent measure and weeks as the dependent measure.

MODIFICATIONS OF THE METHOD

Fricker et al. (1996) investigated the effect of unilateral ibotenic acid lesions in the dorsal striatum, placed at anterior, posterior, medial, or lateral loci, in the staircase test of skilled forelimb use.

Nakao et al. (1996) studied paw reaching ability in rats with unilateral quinolinic acid lesions of the striatum as an animal model for Huntington's disease.

Barnéoud et al. (1996) evaluated the neuroprotective effects of riluzole using impaired skilled forelimb use, circling behavior, and altered dopaminergic metabolism of the mesotelencephalic system in unilaterally 6-OHDA-lesioned rats.

Fricker et al. (1997) studied the correlation between positron emission tomography, using ligands to the D_1 and D_2 receptors, and reaching behavior in rats with ibotenic acid lesions and embryonic striatal grafts.

Grabowski et al. (1993), Marston et al. (1995), and Sharkey et al. (1996) tested drug effects on skilled motor deficits produced by middle cerebral artery occlusion in rats using the paw reaching test.

Meyer et al. (1997) described a revolving food pellet test for measuring sensorimotor performance in rats.

REFERENCES AND FURTHER READING

Abrous DN, Dunnett SB (1994) Paw reaching test in rats: the staircase test. Neurosci Protocols 10:1–11

Abrous DN, Shaltot ARA, Torres EM, Dunnett SB (1993) Dopamine-rich grafts in the neostriatum and/or nucleus accumbens: effects on drug-induced behaviours and skilled paw-reaching. Neuroscience 53:187–197

Barnéoud P, Parmentier S, Mazadier M, Miquet JM, Boireau A, Dubedat P, Blanchard JC (1995) Effects of complete and partial lesions of the dopaminergic mesotelenephalic system of skilled forelimb use in rats. Neuroscience 67:837–846

Barnéoud P, Mazadier M, Miquet JM, Parmentier S, Dubédat P, Doble A, Boireau A (1996) Neuroprotective effects of rilu-

zole on a model of Parkinson's disease in the rat. Neuroscience 74:971–983
Fricker RA, Annett LE, Torres EM, Dunnett SB (1996) The placement of a striatal ibotenic acid lesion affects skilled forelimb use and the direction of drug-induced rotation. Brain Res Bull 41:409–416
Fricker RA, Torres EM, Hume SP, Myers R, Opacka-Juffrey J, Ashworth S, Brooks DJ, Dunnett SB (1997) The effects of donor stage on the survival and function of embryonic grafts in the adult rat brain. II. Correlation between positron emission tomography and reaching behaviour. Neurosci 79:711–721
Grabowski M, Brundin P, Johansson BB, Kontos HA (1993) Paw reaching, sensorimotor, and rotational behavior after brain infarction in rats. Stroke 24:889–895
Marston HM, Faber ESL, Crawford JH, Butcher SP, Sharkey J (1995) Behavioural assessment of endothelin-1 induced middle cerebral artery occlusion in rats. Neuroreport 6/7:1067–1071
Meyer C, Jacquart G, Joyal CC, Mahler P, Lalonde R (1997) A revolving food pellet test for measuring sensorimotor performance in rats. J Neurosci Meth 72:117–122
Montoya CP, Astell S, Dunnett SB (1990) Effects of nigral and striatal grafts on skilled forelimb use in the rat. In: SB Dunnett, SJ Richards (eds) Progress in brain research, Vol 82. Elsevier, Amsterdam, pp 459–466
Montoya CP, Campell-Hope LJ, Pemberton KD, Dunnett SB (1991) The staircase test: a measure of independent forelimb reaching and grasping abilities in the rat. J Neurosci Meth 36:219–228
Nakao N, Grasbon-Frodl EM, Widner H, Brundin P (1996) DARPP-32-rich zones in grafts of lateral ganglionic eminence govern the extent of functional recovery in skilled paw reaching in an animal model of Huntington' disease. Neuroscience 74:959–970
Nikkhah G, Duan WM, Knappe U, Jödicke A, Björklund A (1993) Restoration of complex sensorimotor behavior and skilled forelimb use by a modified nigral cell suspension transplantation approach in the rat Parkinson model. Neuroscience 56:33–43
Olsson M, Nikkhah G, Bentlage C, Björklund A (1995) Forelimb akinesia in the rat Parkinson model: differential effects of dopamine agonists and nigral transplants as assessed by a new stepping test. J Neurosci 15:3863–3875
Sharkey J, Crawford JH, Butcher SP, Marston HM, Hayes RL (1996) Tacrolimus (FK506) ameliorates skilled motor deficits produced by middle artery occlusion in rats. Stroke 27:2282–2286
Whishaw IQ, O'Connor WT, Dunnett SB (1986) The contributions of motor cortex, nigrostriatal dopamine and caudate-putamen to skilled forelimb use in the rat. Brain 109:805–843

E.7.2.7 Stepping Test in Rats

PURPOSE AND RATIONALE

Schallert et al. (1992),Olsson et al. (1995) and Rosenblad et al. (1997) introduced the stepping test as a clinically relevant unilateral model of Parkinsonian akinesia. The 6-OHDA lesion induced marked and long-lasting impairments in the initiation of stepping movements with the contralateral paw which can be ameliorated by the systemic application of drugs.

PROCEDURE

6-OHDA Lesion Surgery

Female Sprague Dawley rats receive two stereotaxic injections of 6-OHDA (3.6 µg/µl in 0.2 µg/ml ascorbate-saline) into the right ascending mesostriatal dopamine pathway using a 10-µl Hamilton syringe at the following coordinates (in mm, with reference to bregma and dura):

1. 2.5 µl at AP –4.4, L 1.2, V 7.8, tooth bar –2.4;
2. 3.0 µl at AP –4.0, L 0.8, V 8.0, tooth bar +3.4 at an injection rate of 1 µl/min.

The cannula is left in place for an additional 5 min before slowly retracted.

Experimental Setup for Stepping Test

The tests monitoring initiation time, stepping time and step length are performed using a wooden ramp with a length of 1 m connected to the rat's home cage. A smooth-surfaced table is used for measuring adjusted steps.

During the first 3 days the rats are handled by the experimenter to familiarize them with the experimenter's grip. During the subsequent 1–2 days the rats are trained to run spontaneously up the ramp to the home cage.

The stepping test comprises two parts: first, the time to initiation of a movement of each forelimb, the step length, and the time required for the rat to cover a set distance along the ramp with each forelimb; and second the initiation of adjusting steps by each forelimb when the animal was moved sideways along the bench surface. Each test consists of two tests per day for three consecutive days and the mean of six subtests is calculated.

Initiation Time, Stepping Time, and Step Length

The rat is held by the experimenter with one hand fixing the hindlimbs and slightly raising the hind part above the surface. The other hand fixes the forelimb not to be monitored. Time is measured until the rat initiates movement with the forelimb not fixed by the experimenter, using 180 s as break-off point. Stepping time is measured from initiation of movement until the rat reaches the home cage. Step length is calculated by dividing the length of the ramp by the number of steps required for the rat to run up the ramp. The sequence of testing is right paw testing followed by left paw testing, repeated twice.

Adjusting Steps

The rat is held in the same position as described above with one paw touching the table, and is then moved

slowly sideways (5 s for 0.9 m) by the experimenter, first in the forehand and then in the backhand direction. The number of adjusting steps is counted for both paws in the backhand and forehand directions of movement. The sequence of testing is right paw forehand and backhand adjusting stepping, followed by left paw forehand and backhand directions. The test is repeated twice each day.

The paw contralateral to the lesion is passively dragging when the rat is moved in the forehand direction, while the ipsilateral paw performs frequent stepping movements.

Drug Application

Stepping tests are repeated to determine the baseline weekly after the 6-OHDA lesion. The drug tests are administered for 1 day only. Various drugs can be evaluated in weekly intervals.

EVALUATION

Results are expressed as means ± SEM. For statistical evaluation, the data are subjected to one-factor analysis of variance (ANOVA) and Fisher post hoc test.

MODIFICATIONS OF THE METHOD

Schallert et al. (2000), Picconi et al. (2003, 2004), and Centonze et al. (2005) described the limb-use asymmetry test to measure motor performance in rats with 6-OHDA-induced lesions. Forelimb use during exploratory activity was analyzed in a transparent cylinder (20 cm diameter and 30 cm height) for 3–10 min depending on the degree of movement maintained during the trial. The number of supporting wall contacts executed independently with the right of the left forelimb was counted. The percentage of wall contacts executed by the impaired forelimb (contralateral to the lesion) was then subtracted from the percentage of contacts with the non-impaired forelimb to obtain a limb-use asymmetry score.

REFERENCES AND FURTHER READING

Centonze D, Gubellini P, Rossi S, Picconi B, Pisani A, Bernardi G, Calabrese P, Baunez C (2005) Subthalamic nucleus lesion reverses motor abnormalities and striatal glutamatergic overactivity in experimental parkinsonism. Neuroscience 133:831–840

Olsson M, Nikkhah G, Bentlage C, Björklund A (1995) Forelimb akinesia in the rat Parkinson model: differential effects of dopamine agonists and nigral transplants as assessed by a new stepping test. J Neurosci 15:3863–3875

Picconi B, Centonze D, Hakansson K, Bernardi G, Greengard P, Fisone G, Cenci MA, Calabrese P (2003) Loss of bidirectional striatal synaptic plasticity in L-DOPA induced dyskinesia. Nat Neurosci 6:501–506

Picconi B, Centonze D, Rossi S, Bernardi G, Calabresi P (2004) Therapeutic doses of L-dopa reverse hypersensitivity of cortical D2-dopamine receptors and glutamatergic overactivity in experimental parkinsonism. Brain 127:1661–1669

Rosenblad C, Martinez-Serrano A, Björklund A (1997) Intrastriatal cell line-derived neurotrophic factor promotes sprouting of spared nigrostriatal dopaminergic afferents and induces recovery of function in a rat model of Parkinson's disease. Neuroscience 82:129–137

Schallert T, Norton D, Jones TA (1992) A clinically relevant unilateral model of Parkinsonian akinesia. J Neur Transplant Plast 3:332–333

Schallert T, Fleming M, Leasure JL, Tillerson JL, Balnd STR (2000) CNS plasticity and assessment of forelimb sensorimotor outcome in unilateral rat models of stroke, cortical ablation, parkinsonism and spinal cord injury. Neuropharmacology 39:777–787

E.7.2.8 Transgenic Animal Models of Parkinson's Disease

PURPOSE AND RATIONALE

New insight in the pathobiology of Parkinson's disease has led to the development of transgenic animal models (Gonzalez-de Aguilar et al. 2003; Kirik and Björklund 2003; Levine et al. 2004).

The most prominent models are related to **α-synuclein**. The first transgenic mice that express human α-synuclein were generated by Masliah et al. (2000). These mice displayed a progressive accumulation of α-synuclein and ubiquitin-immunoreactive inclusions in neurons of the neocortex, hippocampus, and substantia nigra. These alterations were associated with a loss of dopaminergic terminals in the basal ganglia and with motor impairments. Since then, several studies on transgenic α-synuclein mice have been performed (van der Putten et al. 2000; Masliah et al. 2001; Giasson et al. 2002; Kirik et al. 2002; Gispert et al. 2003; Hashimoto et al. 2003; Fernagut and Chesselet 2004; Martin-Clemente et al. 2004; Cabin et al. 2005; Frasier et al. 2005; Poon et al. 2005). Masliah and Hashimoto (2002) discussed the possible role of **β-synuclein** for development of new treatments for Parkinson's disease using transgenic animal models.

Ubiquitin carboxyl-terminal hydrolase L1 (**UCH-L1**) is a neuron-specific ubiquitin recycling enzyme, which may be implicated in the pathogenesis of Parkinson's disease (Leroy et al. 1998). Lindsten et al. (2003) developed a model for *in vivo* analysis of the ubiquitin/proteasome system by generating mouse strains transgenic for a green fluorescence protein reporter carrying a constitutively active degradation signal.

Loss-of-function mutations in **parkin** are the major cause of early-onset familial Parkinson's disease. To investigate the pathogenic mechanism by which loss

of parkin function causes Parkinson's disease, Goldberg et al. (2003) generated a mouse model bearing a germline disruption in parkin. In addition to PARK1 (representing the α-synuclein gene) and PARK2 (representing the UCH-L1 gene), other monogenic forms of Parkinson's disease have been described (Lansbury and Brice 2002; von Bohlen und Halbach et al. 2004).

The ***weaver*** **mutant mouse** has been proposed as another model of Parkinson's disease (Bankiewicz et al. 1993; Bandmann et al. 1996; Cheng et al. 1997; Ebadi et al. 2005).

MODIFICATIONS OF THE METHOD

Lo Bianco et al. (2002) studied α-synucleinopathy and selective dopaminergic neuron loss in a **rat** lentiviral-based model of Parkinson's disease.

Kirik et al. (2003) described nigrostriatal α-synucleinopathy induced by viral vector-mediated overexpression of human α-synuclein using a primate (adult **marmosets**) model of Parkinson's disease.

Transgenic **Drosophila** models expressing human α-synuclein were described by Feany and Bender (2000), Pendleton et al. (2002), and Scherzer et al. (2003).

Brown et al. (2002) published multiplex three-dimensional brain gene expression mapping in a mouse model of Parkinson's disease.

Son et al. (2003) described cloning and expression analysis of the Parkinson's disease gene, **UCH-L1**, and its promoter in **zebrafish**.

REFERENCES AND FURTHER READING

Bandmann O, Davis MB, Marsden CD, Wood NW (1996) The human homologue of the weaver mouse gene in familial and sporadic Parkinson's disease. Neuroscience 72:877–879

Bankiewicz K, Mandel RJ, Sofroniew MV (1993) Trophism, transplantation, and animal models of Parkinson's disease. Exp Neurol 124:140–149

Brown VM, Ossadtchi A, Khan AH, Yee S, Lacan G, Melega WP, Cherry SR, Leahy RM, Smith DJ (2002) Multiplex three-dimensional brain gene expression mapping in a mouse model of Parkinson's disease. Genome Res 12:868–884

Cabin DE, Gispert-Sanchez S, Murphy D, Asuburger G, Myers RR, Nussbaum RL (2005) Exacerbated synucleinopathy in mice expressing A53T SNCA on a Snca null background. Neurobiol Aging 26:25–35

Cheng SC, Ehrhard P, Goldowitz D, Smeyne RJ (1997) Developmental expression of the GIRK family of inward rectifying potassium channels: implications for abnormalities in the *weaver* mutant mouse. Brain Res 778:251–264

Ebadi M, Brown-Borg H, El Rafaey H, Singh BB, Garrett S, Shavali S, Sharma SK (2005) Metallothionein-mediated neuroprotection in genetically engineered mouse models of Parkinson's disease. Brain Res Mol Brain Res 134:67–75

Feany MB, Bender WW (2000) A *Drosophila* model of Parkinson's disease. Nature 404:394–398

Fernagut PO, Chesselet MF (2004) α-Synuclein and transgenic mouse models. Neurobiol Dis 17:123–130

Frasier M, Walzer M, McCarthy L, Magnuson D, Lee JM, Haas C, Kahle P, Wolozin B (2005) Tau phosphorylation increases in symptomatic mice overexpressing A30P α-synuclein. Exp Neurol 192:274–287

Giasson BI, Duda JE, Quinn SM, Zhang B, Trojanowski JQ, Lee VM (2002) Neuronal α-synucleinopathy with severe movement disorder in mice expressing A53T human α-synuclein. Neuron 34:521–533

Gispert S, Del Turco D, Garrett L, Chen AS, Bernard DJ, Hamm-Clement J, Korf HW, Deller T, Braak, Auburger G, Nussbaum RL (2003) Transgenic mice expressing mutant A53T human α-synuclein show neuronal dysfunction in the absence of aggregate formation. Mol Cell Neurosci 24:419–429

Goldberg MS, Fleming SM, Palacino JJ, Cepeda C, Lam HA, Bhatnagar A, Meloni EG, Wu N, Ackerson LC, Klapstein GJ, Gajendiran M, Roth BL, Chesselet MF, Maidment NT, Levine MS, Shen J (2003) Parkin-deficient mice exhibit nigrostriatal deficits but not loss of dopaminergic neurons. J Biol Chem 278:43628–42635

Gonzalez-De-Aguilar JL, Rene F, Dupuis L, Loefflöer JP (2003) Neuroendocrinology of neurodegenerative diseases: insights from transgenic mouse models. Neuroendocrinology 78:244–252

Hashimoto M, Rockenstein E, Masliah E (2003) Transgenic models of α-synuclein pathology: past, present and future. Ann NY Acad Sc 991:171–188

Kirik D, Björklund A (2003) Modeling CNS neurodegneration by overexpressing of disease-causing proteins using viral vectors. Trends Neurosci 26:386–392

Kirik D, Rosenblad C, Burger C, Lundberg C, Johansen TE, Muzyczka N, Mandel RJ, Björklund A (2002) Parkinson-like neurodegeneration induced by targeted overexpression of α-synuclein in the nigrostriatal system. J Neurosci 22:2780–2791

Kirik D, Annett LE, Burger C, Muzyczka N, Mandel RJ, Björklund A (2003) Nigrostriatal α-synucleinopathy induced by viral vector-mediated overexpression of human α-synuclein: a new primate model of Parkinson's disease. Proc Natl Acad Sci USA 100:2884–2889

Lansbury PT Jr, Brice A (2002) Genetics of Parkinson's disease and biochemical studies of implicated gene products. Curr Opin Cell Biol 14:653–660

Leroy E, Boyer R, Auburger G, Leube B, Ulm G, Mezey E, Harta G, Brownstein MJ, Jonnalagada S, Chernova T, Dhejia A, Lavedan C, Gasser T, Steinbach PJ, Wlkinson KD, Polymeropoulos MH (1998) The ubiquitin pathway in Parkinson's disease. Nature 395:451–452

Levine MS, Cepeda C, Hickey MA, Fleming SM, Chesselet MF (2004) Genetic mouse models of Huntington's and Parkinson's disease: illuminating but imperfect. Trends Neurosci 27:691–697

Lindsten K, Menéndez-Benito V, Masucci MG, Danuma NP (2003) A transgene mouse model of the ubiquitin/proteasome system. Nature Biotech 21:897–902

Lo Bianco C, Ridet JL, Schneider BL, Déglon N, Aebischer P (2002) α-Synucleinopathy and selective dopaminergic neuron loss in a rat lentiviral-based model of Parkinson's disease. Proc Natl Acad Scvi USA 99:10812–10818

Martín-Clemente B, Alvarez-Castelao B, Mayo I, Sierra AB, Díaz V, Milán M, Fariñas I, Gómez-Isla T, Ferrer I, Castaño JG (2004) α-Synuclein expression levels do not significantly affect proteasome function and expression in

mice and stably transfected PC12 cell lines. J Biol Chem 279:52984–52990
Masliah E, Hashimoto M (2002) Development of new treatments for Parkinson's disease in transgenic animal models: a role for β-synuclein. NeuroToxicol 23:461–468
Masliah E, Rockenstein E, Veinbergs I, Mallory M, Hashimoto M, Takeda A, Sagara Y, Sisk A, Mucke L (2000) Dopaminergic loss and inclusion body formation in α-synuclein mice: implications for neurodegenerative disorders. Science 287:1265–1269
Masliah E, Rockenstein E, Veinbergs I, Sagara Y, Mallory M, Hashimoto M, Mucke L (2001) β-Amyloid peptides enhance α-synuclein accumulation and neuronal deficits in a transgenic mouse model linking Alzheimer's disease and Parkinson's disease. Proc Natl Acad Sci USA 98:12245–12250
Pendleton RG, Parvez F, Sayed M, Hilman R (2002) Effects of pharmacological agents upon transgenic model of Parkinson's disease in *Drosophila melanogaster*. J Pharmacol Exp Ther 300:91–96
Poon HF, Frasier M, Shreve N, Calabrese V, Wolozin B, Butterfield DA (2005) Mitochondrial associated metabolic proteins are selectively oxidized in A30P α-synuclein transgenic mice – a model of familial Parkinson's disease. Neurobiol Dis 18:492–498
Scherzer CR, Jensen RV, Gullans SR, Feany MB (2003) Gene expression changes presage neurodegeneration in a *Drosophila* model of Parkinson's disease. Hum Mol Genet 12:2457–2466
Son OL, Kim HT, Ji MH, Yoo KW, Rhee M, Kim CH (2003) Cloning and expression analysis of a Parkinson's disease gene, *uch-L1*, and its promoter in zebrafish. Biochem Biophys Res Commun 312:601–607
Van der Putten H, Wiederhold KH, Probst A, Barbieri S, Mistl C, Danner S, Kauffmann S, Hofele K, Spooren WPJM, Ruegg MA, Lin S, Caroni P, Sommer B, Tolnay M, Bilbe G (2000) Neuropathology in mice overexpressing human α-synuclein. J Neurosci 20:6021–6029
Von Bohlen und Halbach O, Schober A, Krieglstein K (2004) Genes, proteins, and neurotoxins involved in Parkinson's disease. Progr Neurobiol 73:151–177

E.7.2.9 Cell Transplantations into Lesioned Animals

PURPOSE AND RATIONALE

Human embryonic stem cells may potentially serve as a renewable source of cells for transplantation. In Parkinson's disease, embryonic stem-cell-derived dopaminergic neurons may replace the degenerated neurons in the brain. To substantiate this goal, numerous animal experiments were performed. Most authors used rats rendered hemi-Parkinsonian by injection of 6-OHDA into the substantia nigra as recipients (Zawada et al. 1998; Mendez et al. 2000; Sawamoto et al. 2001; Björklund et al. 2002; Hao et al. 2002; Kim et al. 2002; Ben-Hur et al. 2004; Burnstein et al. 2004; Jollivet et al. 2004; Levy et al. 2004; Yoshizaki et al. 2004; Rafuse et al. 2005; Richardson et al. 2005).

Takagi et al. (2005) reported that dopaminergic neurons generated from cynomolgus monkey embryonic stem cells functioned in the MPTP primate model of Parkinson's disease. However, complications were reported by Blanchet et al. (2003) using a similar approach.

In spite of almost 20 years of experimental experience, clinical trials with cell transplantation for Parkinson's disease have had disappointing results (Drucker-Colin and Verdugo-Diaz 2004; Linazaroso 2004; Roitberg et al. 2004).

REFERENCES AND FURTHER READING

Ben-Hur T, Idelson M, Khaner H, Pera M, Reinhartz E, Itzik H, Reubinoff BE (2004) Transplantation of human embryonic stem cell-derived neural progenitors improves behavioral deficits in Parkinsonian rats. Stem Cells 22:1246–1255
Björklund LM, Sánchez-Pernaute R, Chung S, Andersson T, Chen IYC, McNaught KSP, Brownell AL, Jenkins BG, Wahlestedt C, Kim KS, Isacson O (2002) Embryonic stem cells develop into functional dopaminergic neurons after transplantation in a Parkinson rat model. Proc Natl Acad Sci USA 99:2344–2349
Blanchet PJ, Konitsiotis S, Mochzuki H, Pluta R, Emerich DF, Chase TN, Mouradian MM (2003) Complications of a trophic xenotransplant approach in parkinsonian monkeys. Progr Neuropsychopharm Biol Psychiatry 27:607–612
Burnstein RM, Foltynie T, He X, Menon DK, Svendsen CN, Caldwell MA (2004) Differentiation and migration of long term expanded human neural progenitors in a partial lesion model of Parkinson's disease. Int J Biochem Cell Biol 16:702–713
Drucker-Colin R, Verdugo-Diaz L (2004) Cell transplantation for Parkinson's disease: present status. Cell Mol Neurobiol 24:301–316
Hao G, Yao Y, Wang J, Zhang L, Viroonchaptapan N, Wang ZZ (2002) Intrastriatal grafting of glomus cells ameliorates behavioral defects of Parkinsonian rats. Physiol Behav 77:519–525
Jollivet C, Aubert-Pouessel A, Clavreul A, Venier-Julienne MC, Montero-Menei CN, Benoit JP, Menei P (2004) Long-term effect of intra-striatal glial cell line-derived neurotrophic factor-releasing microspheres in a partial rat model of Parkinson's disease. Neurosci Lett 356:207–210
Kim JH, Auerbach JM, Rodriguez-Gómez JA, Velasco I, Gavin D, Lumelsky N, Lee SH, Nguyen J, Sánchez-Pernaute R, Banklewicz K, McKay R (2002) Dopamine neurons derived from embryonic stem cells function in an animal model of Parkinson's disease. Nature 418:50–56
Levy YS, Sroomza M, Melamed E, Offen D (2004) Embryonic and adult stem cells as a source for cell therapy in Parkinson's disease. J Mol Neurosci 24:353–386
Linazaroso G (2004) Recent failures of new potential symptomatic treatments for Parkinson's disease: causes and solutions. Mov Disord 19:743–754
Mendez I, Baker KA, Hong M (2000) Simultaneous intrastriatal and intranigral grafting (double grafts) in the rat model of Parkinson's disease. Brain Res Rev 32:328–338
Rafuse VF, Soundararajan P, Leopold C, Robertson HA (2005) Neuroprotective properties of cultured neural progenitor cells are associated with the production of sonic hedgehog. Neuroscience 131:899–916
Richardson RM, Broaddus WC, Holloway KL, Fillmore HL (2005) Grafts of adult subependymal zone neuronal pro-

genitor cells rescue hemiparkinsonian behavioral decline. Brain Res 1032:11–23
Roitberg B, Urbaniak K, Emborg M (2004) Cell transplantation for Parkinson's disease. Neurol Res 26:355–362
Sawamoto K, Nakao N, Kobayashi K, Matsushita N, Takahashi H, Kakishita K, Yamamoto A, Yoshizaki T, Terashima T, Murakami F, Itakura T, Okano H (2001) Visualization, direct isolation, and transplantation of midbrain dopaminergic neurons. Proc Natl Acad Sci USA 98:6423–6428
Takagi Y, Takahashi J, Saiki H, Morizane A, Hayashi T, Kishi Y, Fukuda H, Okamoto Y, Koyanagi M, Ideguchi M, Hayashi H, Imazato T, Kawasaki H, Suemori H, Omachi S, Iida H, Itoh N, Nakatsuji N, Sasai Y, Hashimoto N (2005) Dopaminergic neurons generated from monkey embryonic stem cells function in a Parkinson primate model. J Clin Invest 115:102–109
Yoshizaki T, Inaji M, Kouike H, Shimazaki T, Sawamoto K, Ando K, Date I, Kobayashi K, Suhara T, Uchiyama Y, Okano H (2004) Isolation and transplantation of dopaminergic neurons generated from mouse embryonic stem cells. Neurosci Lett 363:33–37
Zawada WM, Cibelli JB, Choi PK, Clarkson ED, Golueke PJ, Witta SE, Bell KP, Kane J, de Leon FAP, Jerry DJ, Robl JM, Freed CR, Stice SL (1998) Somatic cell cloned transgenic bovine neurons for transplantation in parkinsonian rats. Nature Med 4:569–574

E.7.2.10 Transfer of Glial Cell Line-Derived Neurotrophic Factor (GDNF)

PURPOSE AND RATIONALE

Recombinant viral vectors derived from adenovirus, adeno-associated virus or lentivirus have been developed into highly effective vehicles for gene transfer to the adult central nervous system. These vectors have been shown to be effective for long-term delivery of glial cell-line derived neurotrophic factor (GDNF) in the nigrostriatal system. GDNF is a strong candidate agent in the neuroprotective treatment of Parkinson's disease. The injection of adeno-associated virus encoding rat glial cell line-derived neurotrophic factor protected nigral neurons in the 6-OHDA-induced degeneration model of Parkinson's disease in rats (Yoshimoto et al. 1995; Bilang-Bleuel et al. 1997; Lapchak et al. 1997; Mandel et al. 1997; Björklund et al. 2000; Chen et al. 2003; Wang et al. 2002; Thi et al. 2004). Jollivet et al. (2004) used intra-striatal glial cell line-derived neurotrophic-factor-releasing microspheres. Yasuhara et al. (2005) reported the use of glial cell line-derived neurotrophin-factor-producing cells encapsulated into hollow fibers. Kojima et al. (1997) and Cheng et al. (1998) found that glial cell-line-derived neurotrophic factor protects against MPTP-induced neurotoxicity in **mice**. Kordower et al. (2000) reported that neurodegeneration was prevented by lentiviral vector delivery of GDNF in primate models (**rhesus monkeys** treated with MPTP) of Parkinson's disease.

REFERENCES AND FURTHER READING

Bilang-Bleuel A, Revah F, Colin P, Locquet I, Robert JJ, Mallet J, Horellou P (1997) Intrastriatal injection of an adenoviral vector expressing glial-cell-line-derived neurotrophic factor prevents dopaminergic neuron degeneration and behavioral impairment in a rat model of Parkinson disease. Proc Natl Acad Sci USA 94:8818–8823
Björklund A, Kirik D, Rosenblad C, Georgievska B, Lundberg C, Mandel RJ (2000) Towards a neuroprotective gene therapy for Parkinson's disease: use of adenovirus, AAV and lentivirus vectors for gene transfer of GDNF to the nigrostriatal system in the rat Parkinson model. Brain Res 886:82–98
Chen X, Liu W, Guoyuan Y, Liu Z, Smith S, Calne DB, Chen S (2003) Protective effects of intracerebral adenoviral-mediated GDNF gene transfer in a rat model of Parkinson's disease. Parkinsonism Relat Disord 10:1–7
Cheng FC, Ni DR, Wu MC, Kuo JS, Chia LG (1998) Glial cell line-derived neurotrophic factor protects against 1-methyl-4,4-phenyl-1,2,3,6-tetrahydopyridine (MPTP)-induced neurotoxicity in C57BL/6 mice. Neurosci Lett 252:87–90
Jollivet C, Aubert-Pouessel A, Clavreul A, Venier-Julienne MC, Montero-Menei CN, Benoit JP, Menei P (2004) Long-term effect of intra-striatal glial cell line-derived neurotrophic factor-releasing microspheres in a partial rat model of Parkinson's disease. Neurosci Lett 356:207–210
Kojima H, Abiru Y, Sakajiri K, Watanabe K, Ohishi N, Takamori M, Hatanaka H, Yagi K (1997) Adenovirus-mediated transduction with human glial cell line-derived neurotrophic factor gene prevents 1-methyl-4-phenyl-1,2,3,6-tetrahydropyridine-induced dopamine depletion in striatum of mouse brain. Biochem Biophys Res Commun 238:569–573
Kordower JH, Emborg ME, Bloch J, Ma SY, Chu Y, Leventhal L, McBride J, Chen EY, Palfi S, Roitberg BZ, Brown WD, Holden JE, Pyzalski R, Taylor MD, Carvey P, Ling ZD, Trono D, Hantraye P, Déglon N, Aebischer P (2000) Neurodegeneration prevented by lentiviral vector delivery of GDNF in primate models of Parkinson's disease. Science 290:767–773
Lapchak PA, Araujo DM, Hilt DC, Sheng J, Jiao S (1997) Adenoviral vector-mediated GDNF gene therapy in a rodent lesion model of late stage Parkinson's disease. Brain Res 777:153:160
Mandel RJ, Spratt Sk, Snyder RO, Leff SE (1997) Midbrain injection of recombinant adeno-associated virus encoding rat glial cell line-derived neurotrophic factor protects nigral neurons in a progressive 6-hydroxydopamine-induced degeneration model of Parkinson's disease in rats. Proc Natl Acad Sci USA 94:14083–14088
Thi NAD, Saillour P, Ferrero L, Dedieu JF, Mallet J, Paunio T (2004) Delivery of GDNF by an E1,E3/E4 deleted adenoviral vector and driven by a GFAP promoter prevents dopminergic neuron degeneration in a rat model of Parkinson's disease. Gene Ther 11:746–756
Wang L, Muaramatsu S, Lu Y, Ikeguchi K, Fujimoto K, Okada T, Mizukami H, Hanazono Y, Kume A, Urano F, Ichinose H, Nagatsu T, Nakano I, Ozawa K (2002) Delayed delivery of AAV-GDNF prevents nigral neurodegenration and promotes functional recovery in a rat model of Parkinson's disease. Gene Ther 9:381–389
Yasuhara T, Shingo T, Muraoka K, Kobayashi K, Takeuchi A, Yano A, Wenji Y, Kameda M, Matsui T, Miyoshi Y,

Date I (2005) Early transplantation of an encapsulated glial cell line-derived neurotrophin factor-producing cell demonstrating strong neuroprotective effects in a rat model of Parkinson disease. J Neurosurg 102:80–89
Yoshimoto Y, Lin Q, Collier TJ, Frim DM, Breakefield XO, Bohn MC (1995) Astrocytes retrovirally transduced with BDNF elicit behavioral improvement in a rat model of Parkinson's disease. Brain Res 691:25–36

E.8
Animal Models of Neurological Disorders

E.8.1
Huntington's Disease

E.8.1.1
General Considerations

PURPOSE AND RATIONALE

Huntington's disease is a neurological disorder characterized by loss of striatal neurons and the motor signs of dyskinesia, dystonia and chorea, as well as complex neuropsychiatric changes (Hayden 1981). Brouillet et al. (1999) reviewed the different aspects of the replicating Huntington's disease phenotype in experimental animals. There is at present no effective therapy against this disorder. The gene responsible for the disease has been cloned and the molecular defect identified as an expanded polyglutamine tract in the N-terminal region of a protein, named huntingtin (Landles and Bates 2004; Li and Li 2004). Huntingtin interacts with a number of proteins and it has been suggested that alterations in glycolysis, vesicle trafficking or apoptosis play a role in the pathophysiology of Huntington's disease.

REFERENCES AND FURTHER READING

Brouillet E, Condé F, Beal MF, Hantraye P (1999) Replicating Huntington's disease phenotype in experimental animals. Prog Neurobiol 59:427–468
Hayden MR (1981) Huntington's chorea. Springer, Berlin Heidelberg New York
Landles C, Bates GP (2004) Huntingtin and the molecular pathogenesis of Huntington's disease. EMBO Rep 5:958–963
Li SH, Li XJ (2004) Huntingtin and its role in neuronal degeneration. Neuroscientist 10:467–475

E.8.1.2
3-Nitropropionic Acid Animal Model of Huntington's Disease

PURPOSE AND RATIONALE

An animal model of **Huntington's disease** was recommended by Beal et al. (1993), Brouillet et al. (1993), and Borlongan et al. (1995, 1997a, 1997b). Administration of 3-nitropropionic acid, an inhibitor of the mitochondrial citric acid cycle, produces a very selective striatal degeneration and results in a progressive locomotor deterioration in rodents resembling that of Huntington's disease.

PROCEDURE

Borlongan et al. (1995) injected male Sprague Dawley rats i.p. with 10 mg/kg of 3-nitropropionic acid once every 4 days for 28 days and measured passive avoidance in a step-down apparatus and locomotor activity using the Digiscan Animal Activity Monitor System. Using the same system, Borlongan et al. (1997b) found hyperactivity after two injections, whereas four injections or more lead to hypoactivity.

Lee et al. (2000) evaluated the neuroprotective effect of lamotrigine and MK-801 on rat brain lesions induced by 3-nitropropionic acid by magnetic resonance imaging and *in vivo* proton magnetic resonance spectroscopy.

Male Sprague Dawley rats received daily i.p. injections of 15 mg/kg of 3-nitropropionic acid for five consecutive days. Test drugs were injected daily before 3-nitropropionic acid injections.

Behavioral changes were recorded daily, and immediately before sacrifice, graded according to the neurological scale described by Guyot et al. (1997). A total of 6 grades included: Grade 0, normal behavior; grade 1, general slowness in movement due to mild hind-limb impairment; grade 2, prominent gait abnormality with poor coordination; grade 3, nearly complete hind-limb paralysis; grade 4, incapability to move due to four-limb impairment; and grade 5, recumbency.

Magnetic resonance measurements were performed on the sixth day under anesthesia with 60 mg/kg i.p. pentobarbital. An endotracheal tube was set for artificial ventilation with an animal ventilator. The expiratory CO_2 concentration was maintained between 3.5% and 4.5% by adjusting the ventilator. Magnetic resonance measurements were performed on a Biospec 4.7 T spectrometer with an active shielding gradient at 6.9 Gy/cm in 500 µs. The rats were placed in a prone position with a custom-designed head-holder. A 20-cm birdcage coil was used for RF excitation, and a 2-cm-diameter surface coil placed directly over the head was used for signal receiving. After magnetic field optimization, a multi-slice multi-echo image was obtained with the following parameters: field of view = 5 cm, four slices (2 mm thick with a 1-mm gap), matrix 256 × 128, TR = 4,000 ms, and initial TE = 20 ms with an echo spacing of 20 ms for six echos. Pixel-by-pixel T2 maps were obtained

with commercial analysis software. The average of T2 values of bilateral hippocampus or striatum calculated from multi-echo images was applied for statistical analysis.

The point-resolved spectroscopy (PRESS) sequence preceded by three consecutive chemical shift selective saturation (CHESS) pulses for water suppression was used to acquire the localized proton spectra over the striatum. After manually adjusting the transmitter and receiver, magnetic field shimming of the striata and maximizing the suppression of the water signal, spectral data were obtained with the following parameters: TR = 2000 ms, TE = 136 ms, scan no. = 256, spectral width = 4000 Hz. The peak areas of *N*-acetyl-aspartate, choline, creatine, succinate, and lactate were recognized. The ratios of cerebral metabolites relative to creatine were used for statistical analysis.

EVALUATION

The data were expressed as means ± SD. One-way ANOVA followed by a Tukey test was used for evaluating significant difference among sham controls and various treatment groups.

MODIFICATIONS OF THE METHOD

Matthews et al. (1998) found neuroprotective effects of creatine and cyclocreatine against lesions induced by malonate or 3-nitropropionic acid.

Quary et al. (2000) demonstrated major strain differences in response to chronic systemic administration of the mitochondrial toxin 3-nitropropionic acid in rats.

Pubill et al. (2001) reported that orphenadrine (an anticholinergic drug with NMDA receptor antagonist properties) prevented 3-nitropropionic-acid-induced neurotoxicity *in vitro* and *in vivo*.

Lastres-Becker et al. (2003) found that compounds acting on the endocannabinoid and/or endovanilloid systems reduce hyperkinesia in rats induced by bilateral intrastriatal injection of 3-nitropropionic acid.

Lee and Chang (2004) used magnetic resonance imaging and spectroscopy to assess 3-nitropropionic-acid-induced brain lesions in rats.

Tunez et al. (2004) described a protective effect of melatonin on 3-nitropropionic-acid-induced oxidative stress in synaptosomes in rats.

Hantraye et al. (1992) reported that intrastriatal transplantation of cross-species fetal striatal cells reduced abnormal movements in **baboons** injected with the neurotoxin ibotenic acid.

Palfi et al. (1996) showed that chronic 3-nitropropionic acid treatment replicates the cognitive and motor deficits in Huntington's disease also in **baboons.**

Mittoux et al. (2000) reported restoration of cognitive and motor function by ciliary neurotrophic factor in a primate model (***Macaca fascicularis***) of Huntington's disease.

REFERENCES AND FURTHER READING

Beal MF, Brouillet E, Jenkins BG, Ferrante RJ, Kowall NW, Miller JM, Storey E, Srivastava R, Rosen BR, Hyman BT (1993) Neurochemical and histologic characterization of striatal excitotoxic lesions produced by the mitochondrial toxin 3-nitropropionic acid. J Neurosci 13:4181–4192

Borlongan CV, Koutouzis TK, Randall TS, Freeman TB, Cahill DW, Sanberg PR (1995) Systemic 3-nitropropionic acid: behavioral deficits and striatal damage in adult rats. Brain Res Bull 36:549–556

Borlongan CV, Koutouzis TK, Sanberg PR (1997a) 3-Nitropropionic acid animal model and Huntington's disease. Neurosci Biobehav Rev 21:289–293

Borlongan CV, Koutouzis TK, Freeman TB, Hauser RA, Cahill DW, Sanberg PR (1997b) Hyperactivity and hypoactivity in a rat model of Huntington's disease: the systemic 3-nitropropionic acid model. Brain Res Prot 1:253–257

Brouillet E, Jenkins BG, Hyman BT, Ferrante RJ, Kowall MW, Srivastava R, Roy DS, Rosen BR, Beal MF (1993) Age-dependent vulnerability of the striatum to the mitochondrial toxin 3-nitropropionoic acid. J Neurochem 60:356–359

Guyot MC, Hantraye P, Dolan R, Palfi S, Maziére M, Brouillet E (1997) Quantificable bradykinesia gait abnormalities and Huntington's disease-like striatal lesionsa in rats chronically treated with 3-nitropropionic acid. Neuroscience 79:45–56

Hantraye P, Riche D, Maziere M, Isacson O (1992) Intrastriatal transplantation of cross-species fetal striatal cells reduces abnormal movements in a primate model of Huntington's disease. Proc Natl Acad Sci USA 89:4187–4191

Lastres-Becker I, de Miguel R, de Petrocellis L, Makriyannis A, di Marzo V, Fernandez-Ruiz J (2003) Compounds acting on the endocannabinoid and/or endovanilloid systems reduce hyperkinesia in a rat model of Huntington's disease. J Neurochem 84:1097–1109

Lee WT, Chang C (2004) Magnetic resonance imaging and spectroscopy in assessing 3-nitrpropionic acid-induced brain lesions. an animal model of Huntington's disease. Prog Neurobiol 72:87–110

Lee WT, Shen YZ, Chang C (2000) Neuroprotective effect of lamotrigine and MK-801 on rat brain lesions induced by 3-nitropropionic acid: evaluation by magnetic resonance imaging and *in vivo* proton magnetic resonance spectroscopy. Neuroscience 95:89–95

Matthews RT, Yang L, Jenkins BC, Ferrante RJ, Rosen BR, Kaddurah-Daouk R, Beal MF (1998) Neuroprotective effects of creatine and cyclocreatine in animal models of Huntington's disease. J Neurosci 1 8:156–153

Mittoux V, Joseph JM, Conde F, Palfi S, Dautry C, Poyot T, Bloch J, Deglon N, Ouary S, Nimchinsky EA, Brouillet E, Hof PR, Peschanski M, Aebischer P, Hantraye P (2000) Restoration of cognitive and motor function by ciliary neurotrophic factor in a primate model of Huntington's disease. Hum Gene Ther 11:1177–1187

Palfi S, Ferrante RJ, Brouillet E, Beal MF, Dolan R, Guyot MC, Peschanski M, Hantraye P (1996) Chronic 3-nitropropionic acid treatment in baboons replicates the cognitive and motor deficits in Huntington's disease. J Neurosci 16:3019–3025

Pubill D, Verdaguer E, Canudas AM, Sureda FX, Escubedo E, Camrasa J, Pallas M, Camis A (2001) Orphenadrine prevents 3-nitropropionic acid-induced neurotoxicity *in vitro* and *in vivo*. Br J Pharmacol 132:693–702

Quary S, Bizat N, Altairac S, Ménétrat N, Mittoux V, Condé F, Hantraye P, Brouillet E (2000) Major strain differences in response to chronic systemic administration of the mitochondrial toxin 3-nitropropionic acid in rats: implications for neuroprotection studies. Neuroscience 97:521–530

Tunez I, Montilla P, del Carmen-Munoz M, Feijoo M, Salcedo M (2004) Protective effect of melatonin on 3-nitropropionic acid-induced oxidative stress in synaptosomes in an animal model of Huntington's disease. J Pineal Res 37:252–256

E.8.1.3 Quinolinic Acid Rat Model of Huntington's Disease

PURPOSE AND RATIONALE

Intrastriatal injection of quinolate, an NMDA receptor agonist, replicates many neurochemical, histological, and behavioral features of Huntington's disease (Beal et al. 1986, 1988, 1991; DiFigla 1990; Burns et al. 1995; Pérez-Navarro et al. 2000a).

Araujo and Hilt (1997) found that the glial cell-line-derived neurotrophic factor attenuates the behavioral and neurochemical deficits induced by quinolinic acid in rats.

PROCEDURE

Female Sprague Dawley rats were anesthetized with pentobarbital (50 mg/kg) before being placed in a stereotaxic apparatus (Kopf). A small hole was made on the left side of the skull 3.0 mm lateral to the midline, through which a hypodermic needle attached to a Hamilton syringe was lowered 5 mm below the dura into the striatum. For each lesioned rat, 200 nmol of quinolinic acid dissolved in 2 µl of phosphate-buffered saline was injected over a 1-min interval through the needle into two sites (0.7 and 1.4 mm anterior to the bregma) in the left striatum, while the contralateral striatum was left intact.

Neurotrophic factors were given 30 min prior to the toxin injections. Recombinant glia-cell-derived neurotrophic factor (Lin et al. 1993; Lapchak et al. 1997), brain-derived neurotrophic factor or neurotrophin-3 was administered intraventricularly. For i.c.v. treatment, a Hamilton syringe or an infusion cannula was lowered through a hole drilled in the skull of anesthetized rats at the following coordinates: 1.4 mm posterior to the bregma, 2 mm lateral to the midline, and 3.5 mm below the dura.

Rotational Behavior

The effects of quinolinic acid lesions and neurotrophic factor treatment on rotational behavior were assessed using a Rota-Count 8 automated rotor system (Columbus Instruments), which monitors both clockwise and counterclockwise turning behavior. One week following surgery, rats were given 5 mg/kg amphetamine i.p. 15 min prior to placement into the apparatus. The total number of turns in successive 10-min intervals was measured in a 1-h period.

Histology

The extent of the lesion produced by quinolinic acid was illustrated using Nissl-stained coronal sections.

D_1 and D_2 dopamine receptor binding was evaluated in homogenized lesioned and unlesioned striata.

Striatonigral [^{3}H]neurotransmitter uptake was measured in synaptosomes from striatal tissue containing putamen-pallidum as well as a portion of the globus pallidus.

Striatal choline acetyltransferase activity was determined in striatal homogenates using a radiochemical assay.

Neuropeptide levels in tissue homogenates were measured using commercial radioimmunoassay kits.

EVALUATION

Results are expressed as mean ± SEM of the number of rats, where each sample was the average of duplicate or triplicate measures. Statistical significance was assessed using a one-way ANOVA, followed by post hoc Bonferroni or Dunnett's Multiple Comparisons analysis.

MODIFICATIONS OF THE METHOD

Anderson et al. (1996) reported that the ciliary neurotrophic factor protects striatal output neurons in the quinolinic acid rat model.

Nakao et al. (1996) studied paw reaching ability in rats with unilateral quinolinic acid lesions of the striatum.

Shear et al. (1998) compared intrastriatal injections of quinolinic acid and 3-nitropropionic acid for use in animal models of Huntington's disease.

Hughes et al. (1999) found that administration of recombinant human activin-A has powerful neurotrophic effects on selected striatal phenotypes in the quinolinic acid lesion model.

Pérez-Navarro et al. (1999) reported that intrastriatal grafting of a glia cell-line-derived neurotrophic-factor-producing cell line protects striatonigral neurons from quinolinic acid excitotoxicity *in vivo*.

Reggio et al. (1999) found that the intrastriatal injection of an adenosine A_2 receptor antagonist prevents frontal cortex EEG abnormalities in the quinolinic acid rat model.

Nakao et al. (1999) reported that embryonic striatal grafts restore neuronal activity of the globus pallidus in the quinolinic acid rat model.

Pérez-Navarro et al. (2000b) found that neurturin protects striatal neurons but not interneurons in the quinolinic acid rat model.

Bensadoun et al. (2001) found a neuroprotective effect of interleukin-6 and IL6/IL6R chimera in the quinolinic acid rat model.

Gianfriddo et al. (2003) found that adenosine A_{2A} antagonism increases striatal glutamate outflow in the quinolinic acid rat model.

Ryu et al. (2003) described neuroprotective effects of pyruvate in the quinolinic acid rat model.

Scattoni et al. (2004) reported progressive behavioral changes in the spatial open-field in the quinolinic acid rat model.

REFERENCES AND FURTHER READING

Anderson KD, Panayotatos N, Corcoran TL, Lindsay RM, Wiegand SJ (1996) Ciliary neurotrophic factor protects striatal output neurons in an animal model of Huntington's disease. Proc Natl Acad Sci USA 93:7346–7351

Araujo DM, Hilt DC (1997) Glial cell line-derived neurotrophic factor attenuates the excitotoxin-induced behavioral and neurochemical deficits in a rodent model of Huntington's disease. Neuroscience 81:1099–1110

Beal MF, Kowall NW, Ellison DW, Mazurek MF, Swarz KJ, Martin JB (1986) Replication of the neurochemical characteristics of Huntington's disease by quinolinic acid. Nature 321:168–171

Beal MF, Kowall NW, Swartz KJ, Ferrante RJ, Martin JB (1988) Systemic approaches to modifying quinolinic acid striatal lesions in rats. J Neurosci 8:3901–3906

Beal MF, Ferrante RJ, Swartz KJ, Kowall NW (1991) Chronic quinolinic acid lesions in rats closely resemble Huntington's disease. J Neurosci 11:1649–1659

Bensadoun JC, de Almeida LP, Dreano M, Aebischer P, Deglon N (2001) Neuroprotective effect of interleukin-6 and IL6/IL6R chimera in the quinolinic acid rat model of Huntington's disease. Eur J Neurosci 14:1753–1761

Burns LH, Pakzaban P, Deacon TW, Brownell AW, Tatter SB, Jenkins GB, Isacson O (1995) Selective putaminal Excitotoxic lesions in non-human primates model the movement disorders of Huntington's disease. Neuroscience 64:1007–1017

DiFiglia M (1990) Excitotoxic injury of the neostriatum: a model for Huntington's disease. Trends Neurosci 13:286–289

Gianfriddo M, Corsi C, Melani A, Pèzzola A, Reggio R, Popoli P, Pedata F (2003) Adenosine A_{2A} antagonism increases striatal glutamate outflow in the quinolinic acid rat model of Huntington's disease. Brain Res 979:225–229

Hughes PE, Alexi T, Williams CE, Clark RG, Gluckman PD (1999) Administration of recombinant human activin-A has powerful neurotrophic effects on selected striatal phenotypes in the quinolinic acid lesion model of Huntington's disease. Neuroscience 92:197–209

Lapchak PA, Jiao SJ, Collins F, Miller PJ (1997) Glial cell line-derived neurotrophic factor: distribution and pharmacology in the rat following a bolus intraventricular injection. Brain Res 747:92–102

Lin LF, Doherty DH, Lile JD, Bektesch S, Collins P (1993) GDNF: a glial cell line-derived neurotrophic factor for midbrain dopaminergic neurons. Science 260:1130–1132

Nakao N, Grasbon-Frodl EM, Widner H, Brundin P (1996) DARPP-32-rich zones in grafts of lateral ganglionic eminence govern the extent of functional recovery in skilled paw reaching in an animal model of Huntington' disease. Neuroscience 74:959–970

Nakao N, Ogura M, Nakai K, Itakura T (1999) Embryonic striatal grafts restore neuronal activity of the globus pallidus in a rodent model of Huntington's disease. Neuroscience 88:469–477

Pérez-Navarro E, Arenas E, Marco S, Alberch J (1999) Intrastriatal grafting of GDNF-producing cell line protects striatonigral neurons from quinolinic acid excitotoxicity in vivo. Eur J Neurosci 11:241–249

Pérez-Navarro E, Canudas AM, Akerud P, Alberch J, Arenas E (2000a) Brain-derived neurotrophic factor, neurotrophin-3 and neurotrophin 4/5 prevent the death of striatal projection neurons in a rodent model of Huntington's disease. J Neurochem 75:2190–2199

Pérez-Navarro E, Ãkerud P, Marco S, Canals JM, Tolosa E, Arenas E, Alberch J (2000b) Neurturin protects striatal neurons but not interneurons in a rat model of Huntington's disease. Neuroscience 98:89–96

Reggio R, Pèzzzola A, Popoli P (1999) The intrastriatal injection of an adenosine A_2 receptor antagonist prevents frontal cortex EEG abnormalities in a rat model of Huntington's disease. Brain Res 831:315–318

Ryu JK, Kim SU, McLarnon JG (2003) Neuroprotective effects of pyruvate in the quinolinic acid rat model of Huntington's disease. Exp Neurol 183:700–704

Scattoni ML, Valanzano A, Popoli P, Pezzola A, Reggio R, Calamandrei G (2004) Progressive behavioral changes in the spatial open-field in the quinolinic acid rat model of Huntington's disease. Behav Brain Res 152:375–383

Shear DA, Dong J, Gundy CD, Haik-Creguer KL, Dunbar GL (1998) Comparison of intrastriatal injections of quinolinic acid and 3-nitropropionic acid for use in animal models of Huntington's disease. Prog Neuropsychopharmacol Biol Psychiatry 22:1217–1240

E.8.1.4 Transgenic Animal Models of Huntington's Disease

PURPOSE AND RATIONALE

Several **transgenic models** of Huntington's disease are described, among them:

The **R6/2 HD mouse model** (Ona et al. 1999; Hickey and Morton 2000; Hemlinger et al. 2002; Keene et al. 2002; Hockly et al. 2003a, 2003b; Zucker et al. 2004; Chou et al. 2005);

the **yeast artificial chromosome (YAC) mouse** (Ainscough et al. 2001; Slow et al. 2003; Al Mahdawi et al. 2004);

the **TgCAG100 mouse** (Laforet et al. 2001; Ariano et al. 2005);

the **Hdh^{Q111}mouse** (Gines et al. 2003).

A **transgenic rat model** of Huntington's disease was described by Von Hörsten et al. (2003). Behavioral phenotyping was performed using computerized systems from TSE Systems (Bad Homburg, Germany).

Segalat and Neri (2003) recommended *Caenorhabditis elegans* as a model for human inherited degenerative disorders, such as Duchenne's muscular dystrophy and Huntington's disease.

A **transgenic *Drosophila* model** of Huntington's disease was recommended by Lee et al. (2004) and Agrawal et al. (2005).

REFERENCES AND FURTHER READING

Agrawal N, Pallos J, Slöepko N, Apostol BL, Bodai L, Chang LW, Chiang AS, Thompson LM, Marsh JL (2005) Identification of combinatorial drug regimens for treatment of Huntington's disease using *Drosophila*. Proc Natl Acad Sci USA 102:3777–3781

Ainscough JF, John RM, Barton SC (2001) Production of YAC transgenic mice by pronuclear injection. Methods Mol Biol 181:55–65

Al Mahdawi S, Pinto RM, Ruddle P, Carroll C, Webster Z, Pook M (2004) GAA repeat instability in Friedreich ataxia YAC transgenic mice. Genomics 84:301–310

Ariano MA, Cepeda C, Calvert CE, Flores-Hernández J, Hernández-Echeagaray E, Klapstein GJ, Chandler SH, Aronin N, DiFiglia M, Levine MS (2005) Striatal potassium channel dysfunction in Huntington's disease transgenic mice. J Neurophysiol 93:2565–2574

Chou SY, Lee YC, Chen HM, Chiang MC, Lai HL, Chang HH, Wu YC, Sun CN, Chien CL, Lin YS, Wang SC, Tung YY, Chang C, Chern Y (2005) CGS21680 attenuates symptoms of Huntington's disease in a transgenic mouse model. J Neurochem 93:310–320

Gines S, Seong IS, Fossale E, Ivanova E, Trettel F, Gusella JF, Wheeler VC, Persichetti F, MacDonald ME (2003) Specific progressive cAMP reduction implicates energy deficit in presymptomatic Huntington's disease knock-in mice. Human Mol Genet 12:497–508

Helmlinger D, Yvert G, Picaud S, Marienne K, Sahel J, Mandel JL, Devys D (2002) Progressive retinal degeneration and dysfunction in R6 Huntington's disease mice. Human Mol Genet 11:3351–3359

Hickey MA, Morton AJ (2000) Mice transgenic for the Huntington's disease mutation are resistant to chronic 3-nitropropionic acid-induced striatal toxicity. J Neurochem 75:2163–2171

Hockly E, Woodman B, Mahal A, Lewis CM, Bates G (2003a) Standardization and statistical approaches to therpeutic trials in the R6/2 mouse. Brain Res Bull 61:469–479

Hockly E, Richon VM, Woodman B, Smith D, Zhou X, Rosa E, Sathasivam K, Ghazi-Noori S, Mahal A, Lowden PAS, Steffan JS, Marsh JL, Thompson LM, Lewis CXM, Marks PA, Bates GP (2003b) Suberoylanilide hydroxamic acid, a histone deacetylase inhibitor, ameliorates motor deficits in a mouse model of Huntington's disease. Proc Natl Acad Sci USA 100:2041–2046

Keene CD, Rodrigues CMP, Eich T, Chhabra MS, Steer CJ, Low WC (2002) Tauroursodeoxycholic acid, a bile acid, is neuroprotective in a transgenic animal model of Huntington's disease. Proc Natl Acad Sci USA 99:10671–10676

Laforet GA, Sapp E, Chase K, McIntyre C, Boyce FM, Campbell M, Cadigan BA, Warzecki L, Tagle DA, Reddy PH, Cepeda C, Calvert CR, Jokel ES, Klapstein GJ, Ariano MA, Levine MS, DiFiglia M, Aronin N (2001) Changes in cortical and striatal neurons predict behavioral and electrophysiological abnormalities in a transgenic murine model of Huntington's disease. J Neurosci 21:9112–9123

Lee WCM, Yoshihara M, Littleton JT (2004) Cytoplasmatic aggregates trap polyglutamine-containing proteins and block axonal transport in a *Drosophila* model of Huntington's disease. Proc Natl Acad Sci USA 101:3224–3229

Ona VO, Li M, Vonsattel JPG, Andrews LJ, Khan SQ, Chung WM, Frey AS, Menon AS, Li XJ, Stieg PE, Yuan J, Penney JB, Young AB, Cha JHJ, Friedlander RM (1999) Inhibition of caspase-1 slows disease progression in a mouse model of Huntington's disease. Nature 399:264–267

Segalat L, Neri C (2003) C. elegans comme modele pour les maladies degeneratives hereditaires humaines. Med Sci (Paris) 19:1218–1225

Slow EJ, van Raamsdonk J, Rogers D, Coleman SH, Graham RK, Deng Y, Oh R, Bissada N, Hossain SM, Yang YZ, Li XJ, Simpson EM, Gutekunst CA, Leavitt BR, Hayden MR (2003) Selective striatal neuronal loss in a YAC128 mouse model of Huntington disease. Human Mol Genet 12:1555–1567

Von Hörsten S, Schmitt I, Nguyen HP, Holzmann C, Schmidt T, Walther T, Bader M, Pabst R, Kobbe P, Krotova J, Stiller D, Kask A, Vaarmann A, Rathke-Hartlieb S, Schulz JB, Grasshoff U, Bauer I, Menezes AM, Vieira-Saeker AMM, Paul M, Jones L, Lindenberg KS, Landwehrmeyer B, Bauer A, Li XJ, Riess O (2003) Transgenic rat model of Huntington's disease. Human Mol Genet 12:617–624

Zucker B, Ludin DE, Gerds TA, Lücking CH, Landwehrmeyer GB, Feuerstein TJ (2004) Gabapentin-lactam, but not gabapentin, reduces protein aggregates and improves motor performance in a transgenic mouse model of Huntington's disease. Naunyn Schmiedebergs Arch Pharmacol 370:131–139

E.8.2 Amyotrophic Lateral Sclerosis

E.8.2.1 General Considerations

PURPOSE AND RATIONALE

Amyotrophic lateral sclerosis is an adult-onset neurological disease characterized by the selective loss of motor neurons. The early symptoms, principally limb and bulbar muscle weakness, begin in middle life and progress usually rapidly to death within 2 or 3 years. Clinical subtypes of the disease are defined according to the predominant site of weakness and whether upper or lower motor neurons are primarily involved (Rowland and Shneider 2001; Morrison 2002; Waldmeier 2003). Several experimental models for amyotrophic lateral sclerosis have been developed (Kaal et al. 1999; Anger 1991; Senior 2002).

REFERENCES AND FURTHER READING

Anger WK (1991) Animal test systems to study behavioral dysfunctions of neurodegenerative disorders. Neurotoxicology 12:403–413

Kaal ECA, Dijkstra S, van Wasterlaak MGH, Joosten EAJ, Bar PR (1999) Experimental models for ALS – A short review. Neurosci Res Commun 25:1–11

Morrison KE (2002) Therpies in amyotrophic lateral sclerosis – beyond riluzole. Curr Opin Pharmacol 2:302–309

Rowland LP, Shneider NA (2001) Amyotrophic lateral sclerosis. N Engl J Med 344:1688–1700

Senior K (2002) New rodent models gnawing at the black box of ALS. Drug Disc Today 7:1070–1071

Waldmeier PC (2003) Prospects for antiapoptotic drug therapy in neurodegenerative diseases. Prog Neuropsychopharmacol Biol Psychiatry 27:303–321

E.8.2.2 Transgenic Animal Models of Amyotrophic Lateral Sclerosis

PURPOSE AND RATIONALE

Most of the transgenic mouse models are based on familial superoxide dismutase 1 (SOD1) mutations. Of these, the **G93A** mouse is the most investigated (Gurney et al. 1994; Kostic et al. 1997; Trieu and Uckun 1999; Vukosavic et al. 1999, 2000; Azzouz et al. 2000; Li et al. 2000; Spooren and Hengerer 2000; Andreassen et al. 2001; Canton et al. 2001; Jung et al. 2001; Wendt et al. 2002; Azari et al. 2003; Copray et al. 2003; Maragakis et al. 2003; Snow et al. 2003; van Damme et al. 2003; Raiteri et al. 2004; Raman et al. 2004; Waibel et al. 2004). These mice express mutant human SOD1 with a substitution of glycine to alanine in position 93, which induces a severe, progressive motoneuron disease. Several studies were performed with **G37R** (Nguyen et al. 2001; Farah et al. 2003; Robertson et al. 2003, 2003), **H46R** (Nagai et al. 2001), and **G85R** (Bruijn et al. 1998; Amedola et al. 2004) mutant mice. Pasinelli et al. (1998) reported cleavage and activation of caspase-1 in these animals, and Lee et al. (2001) found increased vulnerability of cells transfected with these mutant forms of SOD1 to apoptotic stimuli and protection by overexpression of Bcl-2.

Van Damme et al. (2003) tested the AMPA receptor antagonist NBXQ for survival in a transgenic mouse model of amyotrophic lateral sclerosis. Canton et al. (2001) described the pharmacological properties and activity in the SOD1-G53A animal model of amyotrophic lateral sclerosis of a synthetic AMPA antagonist.

PROCEDURE

Transgenic mice [B6SJL-TgN(SOD1-G93A)G1H] heterozygous for the deficient SOD1 gene and wild-type littermates were identified by polymerase chain reaction. Animals were treated starting on the 50th day of life, until their death with various subcutaneous doses of the test compound.

The following parameters were examined:

Muscle strength: Animals were tested for muscle strength at intervals using a muscle strength meter. Each mouse was held by the tail and pulled steadily over a metal grill three times in rapid succession. The force was recorded on a force meter. The highest score for muscle strength was taken.

Glutamate uptake: Animals were sacrificed at 150 days and spinal cord rapidly dissected for synaptosomal preparations and high-affinity Na^+-dependent glutamate uptake was measured. Spinal cords were homogenized in 20 volumes of sucrose (0.32M) and the homogenate centrifuged at 800 *g* for 10 min. After centrifugation of the supernatant at 20,000 *g* for 20 min, the pellet was resuspended and washed in 50 volumes of sucrose buffer. Transport assays were performed in Krebs-HEPES buffer. Duplicate samples, with or without sodium chloride, were incubated at 37°C for 3 min in the presence of [^{3}H]L-glutamate after appropriate isotopic dilution. The reaction was stopped by addition of ice-cold buffer containing choline and followed by filtration and scintillation counting of the radioactivity retained on filters. High-affinity Na^+-dependent uptake was calculated by subtracting results obtained in choline buffer from that obtained with Na^+ buffer.

Life expectancy: Remaining mice were treated until day of death, which was noted.

EVALUATION

Statistical significance of the biochemical and behavioral data was assessed using Kruskal-Wallis non-parametric analysis of variance followed by Dunn's multiple comparison test.

MODIFICATIONS OF THE METHOD

Haase et al. (1998) described therapeutic effects and mechanism of action of adenovirus-mediated transfer of the neurotrophin-3 gene into skeletal muscle of pmn (progressive motor neuropathy) mice.

Schmalbruch et al. (1991) described an autosomal-recessive mouse mutant with progressive motor neuropathy. Homozygotes develop paralysis of the hindlimbs during the third week of life. Soon thereafter the forelimbs also become weak, and all mice die 6–7 weeks after birth.

Zhu et al. (2002) reported that minocycline inhibits cytochrome c release and delays progression of amyotrophic lateral sclerosis in transgenic mice.

Howland et al. (2002) described focal loss of the glutamate transporter EAAT2 in a transgenic **rat** model of SOD1 mutant-mediated amyotrophic lateral sclerosis.

Bordet et al. (1999, 2001) reported protective effects of cardiotrophin-1 adenoviral gene transfer on neuromuscular degeneration in transgenic amyotrophic lateral sclerosis mice overexpressing a mutated form of human superoxide dismutase-1 with a $Gly^{93}Ala$ substitution.

Ralph et al. (2005a, 2005b) reported that a silencing mutant SOD1 using interfering RNA protects against neurodegeneration and extends survival in the G93A model of amyotrophic lateral sclerosis.

Pharmacology and mechanism of action of riluzole, which has demonstrated beneficial effects in amyotrophic lateral sclerosis in clinical studies, have been investigated in several preclinical studies (Doble 1996; Gurney et al. 1998; Jimonet et al. 1999; Snow et al. 2003).

REFERENCES AND FURTHER READING

Amedola J, Verrier B, Roubertoux P, Durand J (2004) Altered sensorimotor development in a transgenic mouse model of amyotrophic lateral sclerosis. Eur J Neurosci 20:2822–2826

Andreassen OA, Dedeoglu A, Friedlich A, Ferrante KL, Hughes DS, Szabo C, Beal MF (2001) Effects of an inhibitor of poly(ADP-ribose) polymerase, desmethylselegiline, trientine, and lipoic acid in transgenic ALS mice. Exp Neurol 168:419–424

Azari MF, Lopes EC, Stubna C, Turner BJ, Zang D, Nicola NA, Kurek JB, Cheema SS (2003) Behavioral and anatomical effects of systematically administered leukemia inhibitory factor in the $SOD1_{G93A\ GIH}$ mouse model of familial amyotrophic lateral sclerosis. Brain Res 982:92–97

Azzouz M, Hottinger A, Paterna JC, Zurn AD, Aebischer P, Büeler H (2000) Increased motoneuron survival and improved neuromuscular function in transgenic ALS mice after intraspinal injection of an adeno-associated virus encoding Bcl-2. Human Mol Genet 9:803–811

Bordet T, Schmalbruch H, Pettmann B, Hagege A, Castelnau-Ptakhine L, Kahn A, Haase G (1999) Adenoviral cardiotrophin-1 gene transfer protects *pmn* mice from progressive neuronopathy. J Clin Invest 104:1077–1085

Bordet T, Lesbordes JC, Rouhani S, Castelnau-Ptakhine L, Schmalbruch H, Haase G, Kahn A (2001) Protective effects of cardiotrophin-1 adenoviral gene transfer on neuromuscular degeneration in transgenic ALS mice. Hum Mol Genet 10:1925–1933

Bruijn LI, Houseweart MK, Kato S, Anderson KL, Andersson SD, Omaha E, Reaume AG, Scott RW, Cleveland DW (1998) Aggregation and motor neuron toxicity of an ALS-linked SOD1 mutant independent from wild-type SOD1. Science 281:1851–1854

Canton T, Böhme GA, Boireau A, Bordier F, Mignani S, Jimonet P, Jahn G, Alavijeh M, Stygall J, Roberts S, Brealey C, Vulhorgne M, Debono MW, le Guern S, Laville M, Briet D, Roux M, Stutzmann JM, Pratt J (2001) RPR 119990, a novel α-amino-3-hydroxy-5-methyl-4-isoxazolepropionic acid antagonist: synthesis, pharmacological properties, and activity in an animal model of amyotrophic lateral sclerosis. J Pharmacol Exp Ther 299:314–322

Copray JCVM, Jaarsma D, Küst BM, Bruggeman RWG, Mantingh I, Brouwer N, Boddek HWGM (2003) Expression of the low affinity neurotropin receptor p75 in spinal motoneurons in a transgenic mouse model for amyotrophic lateral sclerosis. Neuroscience 116:685–694

Doble A (1996) The pharmacology and mechanism of action of riluzole. Neurology 466 [Suppl4]:S233–241

Farah CA, Nguyen MD, Julien CP, Leclerc N (2003) Altered levels and distribution of microtubule-associated proteins before disease onset in a mouse model of amyotrophic lateral sclerosis. J Neurochem 84:77–86

Gurney ME, Pu H, Chiu AY, dal Canto MC, Polchow CY, Alexander DD, Caliendo J, Hentati A, Known YW, Deng HX (1994) Motor neuron degeneration in mice that express a human Cu, Zn superoxide dismutase mutation. Science 264:1772–1775

Gurney ME, Fleck TJ, Himes CS, Hall ED (1998) Riluzole preserves motor function in a transgenic model of familial amyotrophic lateral sclerosis. Neurology 50:62–66

Haase G, Pettmann B, Vigne E, Castelnau-Ptakhine L, Schmalbruch H, Kahn A (1998) Adenovirus-mediated transfer of the neurotrophin-3 gene into skeletal muscle of pmn mice: therapeutic effects and mechanism of action. J Neurol Sci 160 [Suppl 1]:S97–S105

Howland DS, Liu J, She Y, Goad B, Maragakis NJ, Kim B, Erickson J, Kulik J, DeVito L, Psaltis G, DeGennaro LJ, Cleveland DW, Rothstein JD (2002) Focal loss of the glutamate transporter EAAT2 in a transgenic rat model of SOD1 mutant-mediated amyotrophic lateral sclerosis (ALS). Proc Natl Acad Sci USA 99:1604–1609

Jimonet P, Audiau F, Barreau M, Blanchard JC, Boireau A, Bour Y, Coleno MA, Doble A, Doerfliner G, Huu CD, Donat MH, Duchesne JM, Ganil P, Gueremy C, Honor E, Just P, Kerphirique R, Gontier S, Huberet P, Laduron PM, Le-Blevec J, Meunier M, Miquet JM, Nemecek C, Mignani S (1999) Riluzole series. Synthesis and in vivo "antiglutamate" activity of 6-substituted-2-benzothiazolamines and 3-substituted-2-imino-benzothiazolines. J Med Chem 42:2828–2843

Jung C, Rong Y, Doctrow S, Baudry M, Malfroy B, Xu Z (2001) Synthetic superoxide dismutase/catalase mimetics reduce oxidative stress and prolong survival in a mose amyotrophic lateral sclerosis model. Neurosci Lett 304:157–160

Kostic V, Jackson-Lewis V, de Bilbao F, Dubois-Dauphin M, Przedborski S (1997) Bcl-2: prolonging life in a transgenic mouse model of familial amyotrophic lateral sclerosis. Science 2277:559–562

Lee M, Hyun DH, Halliwell B, Jenner P (2001) Effect of overexpression of wild-type and mutant Cu/ZN-superoxide dismutases on oxidative stress and cell death induced by hydrogen peroxide, 4-hydroxynonenal or serum deprivation: potentiation of injury by ALS-related mutant superoxide dismutases and protection by Bcl-2. J Neurochem 78:209–220

Li M, Ona VO, Guégan C, Chen M, Jackson-Lewis V, Andrews LJ, Olszewski AJ, Stieg PE, Lee JP, Przedborski S, Friedlander RM (2000) Functional role of caspase-1 and caspase-3 in an ALS transgenic mouse model. Science 288:335–339

Maragakis NJ, Jackson M, Ganel R, Rothstein JD (2003) Topiramate protects against motor neuron degeneration in organotypic spinal cord cultures but not in G93A SOD1 transgenic mice. Neurosci Lett 338:107–110

Nagai M, Aoki M, Miyoshi I, Kato M, Pasinelli P, Kasai N, Brown RH Jr, Itoyama Y (2001) Rats expressing human cytosolic copper-zinc superoxide dismutase transgenes with amyotrophic lateral sclerosis: associated mutations develop motor neuron diseases. J Neurosci 21:9246–9254
Nguyen MD, Lariviere RC, Julien JP (2001) Deregulation of Cdk5 in a mouse model of ALS: toxicity alleviated by perikaryal neurofilament inclusions. Neuron 30:135–147
Pasinelli P, Borchelt DR, Houseweart MK, Cleveland DW, Brown HR Jr (1998) Caspase-1 is activated in neural cells and tissue with amyotrophic lateral sclerosis-associated mutations in copper-zinc dismutase. Proc Natl Acad Sci USA 95:15763–15768
Raiteri L, Stigliani S, Zappettini S, Mercuri NB, Raiteri M, Bonanno G (2004) Excessive and precocious glutamate release in a mouse model of amyotrophic lateral sclerosis. Neuropharmacology 46:782–792
Ralph GS, Radcliffe PA, Day DM, Carthy JM, Leroux MA, Lee DCP, Wong LF, Bilsland LG, Greensmith L, Kingsman SM, Mitrophanous KA, Mazarakis ND, Azzouz M (2005a) Silencing mutant SOD1 using RNAi protects against neurodegeneration and extends survival in an ALS model. Nature Med 11:429–433
Ralph GS, Mazarakis ND, Azzouz M (2005b) Therapeutic gene silencing in neurological disorders, using interfering RNA. J Mol Med 83:413–419
Raman C, McAllister SD, Rizvi G, Patel SG, Moore DH, Abood ME (2004) Amyotrophic lateral sclerosis: delayed disease progression in mice by treatment with a cannabinoid. Amyotroph Lateral Scler Other Motor Neuron Disord 5:33–39
Robertson J, Doroudchi MM, Nguyen MD, Durham HD, Strong MJ, Shaw G, Julien JP, Mushynski WE (2003) A neurotoxic peripherin splice variant in a mouse model of ALS. J Cell Biol 160:939–949
Schmalbruch H, Jensen HJ, Bjaerg M, Kamieniecka Z, Kurland R (1991) A new mouse mutant with progressive motor neuropathy. J Neuropath Exp Neurol 50:192–204
Snow RJ, Turnbull J, da Silva S, Jinang F, Tzarnopolsky MA (2003) Creatine supplementation and riluzole treatment provide similar beneficial effects in copper, zinc superoxide dismutase (G93A) transgenic mice. Neurosci 119:661–667
Spooren WP, Hengerer B (2000) DNA laddering and caspase 3-like activity in the spinal cord of a mouse model of familial amyotrophic lateral sclerosis. Cell Mol Biol 46:63–69
Trieu VN, Uckun FM (1999) Genistein is neuroprotective in murine models of female amyotrophic lateral sclerosis and stroke. Biochem Biophys Res Commun 258:685–688
Van Damme P, Leyssen M, Callewaen G, Robberecht W, van den Bosch L (2003) The AMPA receptor antagonist NBQX prolongs survival in a transgenic mouse model of amyotrophic lateral sclerosis. Neurosci Lett 343:81–84
Vukosavic S, Dubois-Dauphin M, Romero N, Przedborski S (1999) Bax and Bcl-2 interaction in a transgenic mouse model of familial amyotrophic lateral sclerosis. J Neurochem 73:2460–2468
Vukosavic S, Stefanis L, Jackson-Lewis V, Guégan C, Romero N, Chen C, Dubois-Dauphin M, Przedborski S (2000) Delaying caspase activation by Bcl-2: a clue to disease retardation in a transgenic mouse model of amyotrophic lateral sclerosis. J Neurosci 20:9119–9125
Waibel S, Reuter A, Malessa S, Blaugrund E, Ludolph AG (2004) Rasagiline alone and in combination with riluzole prolongs survival in an ALS mouse model. J Neurol 251:1080–1084
Wendt S, Dedeoglu A, Speer O, Wallimann T, Beal MF, Andreassen OA (2002) Reduced creatine kinase activity in transgenic amyotrophic lateral sclerosis mice. Free Radical Biol Med 32:920–926
Zhu S, Stavrovskaya IG, Drozda M, Kim BYS, Ona V, Li M, Sarang S, Liu AS, Hartley DM, Wu DC, Gullans S, Ferrante RJ, Przedborski S, Kristal BS, Friedlander RM (2002) Minocycline inhibits cytochrome c release and delays progression of amyotrophic lateral sclerosis in mice. Nature 417:74–78

E.8.3 Spinal Muscular Atrophy

E.8.3.1 General Considerations

PURPOSE AND RATIONALE

Spinal muscular atrophy is a common genetic disease of the motor neuron with a high mortality during infancy (Strober and Tennekoon 1999; Iannaccone et al. 2004; Ogino and Wilson 2004). Among the group of clinically and genetically heterogeneous spinal muscular atrophies, the autosomal recessive proximal types I–III are the most frequent (Schara and Mortier 2004). They are caused by mutations of the telemetric copy of the survival motor neuron gene (SMN1) on chromosome sq while loss of the centromeric copy (SMN2) does not lead to spinal muscular atrophy (Talbot and Davis 2001; Frugier et al. 2002; Wirth 2002; Nicole et al. 2002).

Transgenic mouse models have been developed for these types of disease.

REFERENCES AND FURTHER READING

Frugier T, Nicole S, Cifuentes-Diaz C, Melki J (2002) The molecular bases of spinal muscular atrophy. Curr Opin Genet Devel 12:294–298
Iannnaccone ST, Smith SA, Simard LR (2004) Spinal muscular atrophy. Curr Neurol Neurosci Rep 4:74–80
Nicole S, Diaz CC, Frugier T, Melki J (2002) Spinal muscular atrophy: recent advances and future perspectives. Muscle Nerve 26:4–13
Ogino S, Wilson RB (2004) Spinal muscular atrophy: molecular genetics and diagnostics. Expert Rev Mol Diagn 4:15–29
Schara U, Mortier W (2004) Neuromuskuläre Erkrankungen. Teil 1: Spinale Muskelatrophien, periphere Nervenerkrankungen, kongenitale myasthenische Syndrome. Nervenarzt 75:1231–1245
Strober JB, Rennekoon GI (1999) Progressive spinal muscular atrophies. J Child Neurol 14:691–695
Talbot K, Davies KE (2001) Spinal muscular atrophy. Semin Neurol 21:189–197
Witrth B (2002) Spinal muscular atrophy: state-of-the-art and therapeutic perspectives. Amyotroph Lateral Scler Other Motor Neuron Disord 3:87–95

E.8.3.2 Transgenic Animal Models of Spinal Muscular Atrophy

PURPOSE AND RATIONALE

Several mouse models of spinal muscular atrophy are described (Bergin et al. 1997; Deniselle et al. 1997;

DiDonato et al. 1997, 2001; Schrank et al. 1997; Fricker 2000; Frugier et al. 2000; Hsieh-Li et al. 2000; Jablonka et al. 2000, 2001; Monani et al. 2000a, 2000b, 2003; Cifuentes-Diaz et al. 2001, 2002; Melki 2001; Tucker et al. 2001; Ferri et al. 2003, 2004; Rossoll et al. 2003; Azzouz et al. 2004; Grohmann et al. 2004; Le et al. 2005). These studies are intended to mimic spinal muscular atrophy in humans resulting from loss-of-function mutations in the survival motor neuron gene (Smn). Mice carrying a homozygous deletion of Smn exon 7 display a dramatic and progressive loss of motor axons involving both proximal and terminal regions. The human centromeric survival motor neuron gene (*SMN2*) rescues embryonic lethality in $Smn^{-/-}$ mice. SMNDelta7, the major product of the centromeric survival motor neuron (SMN2) gene, extends survival in mice with spinal muscular atrophy.

Chang et al. (2001) reported treatment of spinal muscular atrophy in transgenic mice by sodium butyrate.

PROCEDURE

Cell Culture

Epstein-Barr-virus-transformed lymphoid cell lines from different SMA-type patients with deleted *SMN1* genes were established. Lymphocytes were collected from the whole blood of patients by Ficoll hypaque separation. The buffy coat was collected and washed twice with 5 ml PBS. The pellet was resuspended in 5 ml RPMI medium containing 0.5 ml Epstein-Barr virus, 50 µl phytohemagglutinin (0.5 mg/ml), and 50 µl ciclosporin (0.2 mg/ml). Cells were incubated at 37°C with 5% CO_2 until they became viable.

Mice

Five independent human *SMN2* gene transgenic mice were generated and crossed with mice heterozygous for the *Smn* locus knockout. Transgenic mice that were also homozygous for the knockout alleles ($Smn^{-/-}SMN2$) were then generated by crossing with the above mice. These knockout transgenic mice developed progressive motor neuron disease similar to that in human SMA patients. The SMA-like mice were classified into three groups based on their phenotypes, which were judged by three independent observers. Mice with the most severe pathological form (type 1) did not develop furry hair and died before postnatal day 10; mice with intermediate severity (type 2) showed poor activity and variable symptoms and died at 2–4 weeks; the type 3 mice survived and bred normally, but had short and enlarged tails (Hsieh-Li et al. 2000). SMA-like mice (non-pregnant and pregnant) were supplied with sterile water ad libitum and rodent pellets. The sodium butyrate-treated group received sodium butyrate at a concentration of 0.8 mg/ml or 8 mg/ml in distilled water, beginning immediately after diagnosis or after 15 days gestation in SMA-like pregnant mice. Both groups consumed about 5–10 ml per day per mouse. After 1–12 weeks of treatment, the mice were sacrificed, and their organs or tissues were quickly removed and frozen in liquid nitrogen.

Reverse Transcriptase-PCR Analysis

Reverse transcriptase-PCR analysis was performed according to Hsieh-Li et al. (2000) and Jong et al. (2000).

Subcellular Fractionation

Fresh frozen spinal cord, brain, and skeletal muscle samples (500 mg) from different types of SMA mice were fractionated. Tissues were homogenized with a tight-fitting glass pestle in ice-cold buffer. The nuclei were pelleted by centrifugation at 800 *g* for 3 min. The nuclear pellet was resupended by trituration in 100 µl of buffer and kept on ice for 15 min followed by centrifugation at 15,000 *g* for 10 min ar 4°C. The supernatant (soluble nuclear extract) was removed, and the insoluble nuclear pellet was further sonicated in sonication buffer.

Western Blot Analysis

Synthetic peptides containing part of human SMN exon 7 (amino acids 279–288) and exon 2 (amino acids 72–84) were used to immunize rabbits and to purify specific antibodies(H2 and H7) from rabbit crude sera with an EAH Sepharose 4B column. Two mouse anti-SR protein antibodies (anti-SRp20 and 16H3) were used to detect the human SR proteins. Proteins were loaded on a 5% polyacrylamide stacking gel above a 12% separating gel, and the the gel was run with a discontinuous buffer using Laemmli's method. After electrophoresis, proteins were transferred electrophoretically to poly-(vinylidene difluoride) membranes. After the transfer, the membranes were blocked with TBST containing 4% BSA for 2 h at room temperature. The blots were washed for three 20-mim periods in TBST and then incubated with a 1:32,000 dilution of an anti-rabbit IgG alkaline phosphatase conjugate in TBST for 1 h at room temperature. The reaction was detected by adding 1.5% 5-bromo-4-chloro-3-indolyl phosphate and 3% nitro blue tetrazolium in a developing buffer.

Histopathological Analysis

Histopathological analysis was performed according to Hsieh-Li et al. (2000).

EVALUATION

Results from multiple experiments were expressed as mean ± standard error. Survival data of treated and untreated mice are presented as a Kaplan-Meier plot using the log rank test. A standard χ_2 test was used to assess differences in the frequency of mild or severe phenotype in the SMA-like mice born from treated and untreated mothers, which analyzed the percentage of type 1 (or 2+3) newborn mice as a fraction of the total number of pups.

MODIFICATIONS OF THE METHOD

Lesbordes et al. (2003) reported therapeutic benefits of cardiotrophin-1 gene transfer in a mouse model of spinal molecular atrophy.

Andreassi et al. (2001) found that aclarubicin treatment restored SMH levels to cells derived from type I spinal muscular atrophy patients.

Haddad et al. (2003) reported that riluzole attenuates spinal muscular atrophy disease progression in a mouse model.

He et al. (2005) described an inherited motor neuron disease in domestic cats as a model of spinal muscular atrophy.

REFERENCES AND FURTHER READING

Andreassi C, Jarecki J, Zhou J, Coovert DD, Monani UR, Chen X, Whitney M, Pollok B, Zhang M, Androphy E, Burghes AHM (2001) Aclarubicin treatment restored SMH levels to cells derived from type I spinal muscular atrophy patients. Hum Mol Genet 10:2841–2849

Azzouz M, Le T, Ralph S, Walmsley L, Monani UR, Lee DCP, Wilkes F, Mitrophanous KA, Kinsman SM, Burghes AHM, Mazarakis ND (2004) Lentivector-mediated *SMN* replacement in a mouse model of spinal muscular atrophy. J Clin Invest 114:1726–1731

Bergin A, Kim G, Price DL, Sisodia SS, Lee MK, Rabin BA (1997) Identification and characterization of a mouse homologue of Spinal Muscular Atrophy-determining gene, survival motor neuron. Gene 204:47–53

Chang JG, Hsieh-Li HM, Jong YJ, Wang NM, Tsai CH, Li H (2001) Treatment of spinal muscular atrophy by sodium butyrate. Proc Natl Acad Sci USA 989808–9813

Cifuentes-Diaz C, Frugier T, Tiziano FD, Lacène E, Roblot N, Joshi V, Moreau MH, Melki J (2001) Deletion of murine *SMN* exon 7 directed to skeletal muscle leads to severe muscular dystrophy. J Cell Biol 152:1107–1114

Cifuentes-Diaz C, Nicole S, Velasco ME, Borra-Cebrian C, Panozzo C, Frugier T, Millet G, Roblot N, Joshi V, Melki J (2002) Neurofilament accumulation at the motor endplate and lack of axonal sprouting in the spinal muscular atrophy model. Hum Mol Genet 11:1439–1447

Deniselle MCG, González S, Piroli G, Ferrini M, Lima AE, de Nicola AF (1997) Glucocorticoid receptors and actions in the spinal cord of the Wobbler mouse, a model of neurodegenerative diseases. J Steroid Biochem Mol Biol 60:205–213

DiDonato CJ, Chen XN, Noya D, Korenberg JR, Nadeau JH, Simard LR (1997) Cloning, characterization, and copy number of the murine survival motor neuron gene: homolog of the spinal muscular atrophy-determining gene. Genome Res 7:339–352

DiDonato C, Lorson CL, de Repentigny Y, Simard L, Chartrand C, Androphy EJ, Kothary R (2001) Regulation of murine survival motor neuron (*Smn*) protein levels by modifying *Smn* exon 7 splicing. Hum Mol Genet 10:2727–2736

Ferri A, Sanes JR, Coleman MP, Cunningham JM, Kato AC (2003) Inhibiting axon degeneration and synapse loss attenuates apoptosis and disease progression in a mouse model of motoneuron disease. Curr Biol 13:669–673

Ferri A, Melki J, Kato AC (2004) Progressive and selective degeneration of motoneurons in a model of SMA. Neuroreport 15:275–280

Fricker J (2000) Mouse model of spinal muscular atrophy. Drug Disc Today 5:220–221

Frugier T, Tiziano FD, Cifuentes-Diaz C, Miniou P, Roblot N, Dierich A, le Meur M, Melki J (2000) Nuclear targeting defect of SMN lacking the C-terminus in a mouse model of spinal muscular atrophy. Hum Mol Genet 9:849–858

Grohmann K, Rossoll W, Kobsar I, Holtmann B, Jablonka S, Wessig C, Stoltenburg-Didinger G, Fischer U, Hübner C, Martini R, Sendtner M (2004) Characterization of Ighmbp2 in motor neurons and implications for the pathomechanism in a mouse model of human spinal muscular atrophy with respiratory distress type I (SMARD1). Hum Mol Genet 13:2031–2042

Haddad H, Cifuentes-Diaz C, Miroglio A, Roblot N, Joshi V, Melki J (2003) Riluzole attenuates spinal muscular atrophy disease progression in a mouse model. Muscle Nerve 28:432–437

He Q, Lowrie C, Shelton GD, Castellani RJ, Menotti-Raymond M, Murphy W, O'Brien SJ, Swanson WF, Fyfe JC (2005) Inherited motor neuron disease in domestic cats: a model of spinal muscular atrophy. Pediatr Res 57:324–330

Hsieh-Li JHM, Chang JG, Jong YJ, Wu MH, Wang NM, Tsai CH, Li H (2000) A mouse model for spinal muscular atrophy. Nat Genet 24:66–69

Jablonka S, Schrank B, Kralewski M, Rossoll W, Sendtner M (2000) Reduced survival motor neuron (*Smn*) gene dose in mice leads to motor neuron degeneration: an animal model for spinal muscular atrophy type III. Human Mol Genet 9:341–346

Jablonka S, Bandilla M, Wiese S, Bühler D, Wirth B, Sendtner M, Fischer U (2001) Co-regulation of survival of motor neuron (SMN) protein and its interactor SIP1 during development and in spinal muscular atrophy. Hum Mol Genet 10:497–505

Jong YJ, Chang JG, Lin SP, Yang TY, Wang JC, Chang CP, Lee CC, Li H, Hsieh-Li HM, Tsai CH (2000) Analysis of the mRNA transcripts of the survival motor neuron (SMN) gene in the tissue of an SMA fetus and the peripheral blood mononuclear cells of normal carriers and SMA patients. J Neurol Sci 173:147–153

Le TT, Pham LT, Butchbach ME, Zhang HL, Monani UR, Coovert DD, Gavrilina TO, Xing L, Bassell GJ, Burghes AH (2005) SMNDelta7, the major product of the centromeric survival motor neuron (SMN2) gene, extends survival in mce with spinal muscular atrophy and associates with full-length SMN. Hum Mol Genet 14:845–857

Lesbordes JC, Cifuentes-Diaz C, Miroglio A, Joshi V, Bordet T, Melki J (2003) Therapeutic benefits of cardiotrophin-1 gene transfer in a mouse model of spinal molecular atrophy. Hum Mol Genet 12:1233–1239

Melki J (2001) Mouse models of spinal muscular atrophy. Acta Myologica 20:159–161

Monani UR, Sendtner M, Coovert DD, Parsons DW, Andeasst C, Le TT, Jablonka S, Schrank B, Rossol W, Prior TW, Morris GE, Burghes AHM (2000a) The human centromeric survival motor neuron gene (*SMN2*) rescues embryonic lethality in $Smn^{-/-}$ mice and results in a mouse with spinal muscular atrophy. Hum Mol Genet 9:333–339

Monani UR, Coovert DD, Burghes AHM (2000b) Animal models of spinal muscular atrophy Hum Mol Genet 9:2451–2457

Monani UR et al (2003) A transgene carrying an A2G missense mutation in the SMN gene modulates phenotypic severity in mice with severe (type I) spinal muscular atrophy. J Cell Biol 160:41–52

Rossoll W, Jablonka S, Andreassi C, Kröning AK, Karle K, Monani UR, Sendtner M (2003) SMN, the spinal muscular atrophy-determining gene product, modulates axon growth and location of β-actin mRNA in growth cones of motoneurons, J Cell Biol 163:801–812

Schrank B, Götz R, Gunnersen J, Ure JM, Toyka KV, Smith AG, Sendtner M (1997) Inactivation of the survival motor gene, a candidate gene for human spinal muscular atrophy, leads to massive cell death in early mouse embryos. Proc Natl Acad Sci USA 94:9920–9925

Tucker KE, Berciano MT, Jacobs EY, LePage DF, Shpargel KB, Rossire JJ, Chan EKL, Lafarga M, Conlon RA, Matera AG (2001) Residual Cajal bodies in coilin knockout mice fail to recruit SM snRNPs and SMN, the spinal muscular atrophy gene product. J Cell Biol 154:293–307

E.8.4
Spinal and Bulbar Muscular Atrophy

E.8.4.1
General Considerations

PURPOSE AND RATIONALE

Spinal and bulbar muscular atrophy is a late-onset motor neuron disease characterized by proximal muscle atrophy, weakness, contraction fasciculations, and bulbar involvement. The disease exclusively affect males, while females are usually asymptomatic (Katsuno et al. 2003, 2004).

REFERENCES AND FURTHER READING

Katsuno M, Adachi H, Inukai A, Subue G (2003)Transgenic mouse models of spinal and bulbar muscular atrophy (SBMA) Cytogenet Genome Res 100:243–251

Katsuno M, Adachi H, Tnaka F, Sobue G (2004) Spinal and bulbar muscular atrophy: ligand-dependent pathogenesis and therapeutic perspectives. J Mol Med 82:298–307

E.8.4.2
Transgenic Animal Models of Spinal and Bulbar Muscular Atrophy

PURPOSE AND RATIONALE

Spinal and bulbar muscular atrophy is a polyglutamine disease caused by expansion of a CAG repeat in the androgen receptor gene (Adachi et al. 2001; Katsuno et al. 2002; Walcott and Merry 2002). Several transgenic mouse models were developed (Bates and Davies 1997; Abel et al. 2001; MacManamny et al. 2002).

Katsuno et al. (2003) reported that leuprolin rescues polyglutamine-dependent phenotypes in a transgenic mouse model of spinal and bulbar muscular atrophy.

PROCEDURE

Animals

Transgenic mice were generated carrying a full-length androgen receptor containing 97 CAGs (Katsuno et al. 2002). A full-length human androgen receptor fragment was subcloned containing 24 or 97 CAG repeats (Kobayashi et al. 1998) into a pCAGGS vector (Niwa et al. 1991) digested with *Hind*III. The result was microinjected into fertilized eggs of BDF1 mice. Five founders with AR-97Q were obtained. These mouse lines were maintained by back-crossing with CS7B1/6 mice.

Neurological status was measured with the Rotarod test (Columbus Instruments) and cage activity with the AB system (Neuroscience, Tokyo).

Hormonal Treatment

Leuprolin acetate was injected subcutaneously at a dose of 25, 50 or 100 µg per mouse every 2 weeks from 5 weeks of age. Control mice were treated with vehicle. Leuprolin-treated AR-97Q mice were given either leuprolin only or leuprolin plus 20 µg testosterone enanthate dissolved in sesame oil s.c. weekly from the age of 13 weeks. Flutamide was injected at a dose of 1.8 mg per mouse once every second day.

Serum testosterone was assayed with a radioimmunoassay.

Protein Expression Analysis

Mice were sacrificed by anesthesia and exsanguination and their tissues snap-frozen with powdered CO_2 in acetone. Tissues were homogenized in 50 mM TRIS, pH 8.0, 150 mM NaCl, 1% Nonidet-P40, 0.5% deoxycholate, 0.1% SDS and 1 mM 2-mercaptoethanol with 1 mM PMSF and 6 µg/ml aprotinine and centrifuged at 2,500 *g* for 15 min at 4°C. Each lane of a 5%–20% SDS-PAGE gel was loaded with 160 µg protein from nerve tissue and 80 µg for muscle from the respective supernatant fraction. This was transferred on Hybond-P membranes in a transfer buffer of 25 mM TRIS, 192 mM glycine, 0.1% SDS and 10% methanol. After immuno-probing with a rabbit antibody to the androgen receptor, a secondary antibody probing and detection with the ECL Plus kit (Amersham) was performed. The signal intensity of the bands was quantified using the NIH Image program. The quantita-

tive data of three independent Western blots were expressed as mean ± SD.

Immunohistochemistry and Histology

Deeply anesthetized mice were perfused through the left cardiac ventricle with 20 ml of a 4% paraformaldehyde fixative in phosphate buffer. The tissues were post-fixed overnight in 10% phosphate-buffered formalin and processed for paraffin embedding. De-paraffinized tissue sections 4 µm in thickness were dehydrated in alcohol, treated with formic acid for 5 min at room temperature and stained with the polyglutamine-specific antibody 1C2 (1:10,000 dilution) (Holmberg et al. 1998). After formalin fixation, tail specimens were washed with 70% alcohol and decalcified with 7% formic acid and 70% ethanol for 7 days followed by paraffin embedding. To assess 1C2-positive cells in muscle, the number of 1C2-positive cells in more than 500 fibers in the entire area was calculated and expressed as the number per 100 muscle fibers. The air-dried cryostat sections (6 µm in thickness) of gastrocnemius muscles were stained with hematoxylin-eosin.

EVALUATION

Data were analyzed using the unpaired *t*-test.

MODIFICATIONS OF THE METHOD

Adachi et al. (2003) reported that heat shock protein 70 chaperone overexpression ameliorates phenotypes of the spinal and bulbar muscular transgenic mouse model by reducing nuclear localized mutant androgen receptor protein.

Chevalier-Larsen et al. (2004) found that castration restores the function and neurofilament alterations of aged symptomatic males in a transgenic mouse model of spinal and bulbar muscular atrophy.

Minamiyama et al. (2004) reported that sodium butyrate ameliorates phenotypic expression in a transgenic mouse model of spinal and bulbar muscular atrophy.

REFERENCES AND FURTHER READING

Abel A, Walcott J, Woods JA, Duda J, Merry DE (2001) Expression of expandet repeat androgen receptor produces neurological disease in transgenic mice. Hum Mol Genet 10:107–116

Adachi H, Kume A, Li M, Nakagomi Y, Niwa H, Do J, Sang C, Kobayashi Y, Doyu M, Sobue G (2001) Transgenic mice with an expanded CAG repeat controlled by the human AR promotor show polyglutamine nuclear inclusions and neuronal dysfunction without neuronal cell death. Hum Mol Genet 10:1039–1048

Adachi H, Katsuno M, Minamiyama M, Sang C, Pagoulatos G, Angelidis C, Kusakabe M, Yoshiki A, Kobayashi Y, Duyu M, Sobue G (2003) Heat shock protein 70 chaperone overexpression ameliorates phenotypes of the spinal and bulbar muscular transgenic mouse model by reducing nuclear localized mutant androgen receptor protein. J Neurosci 23:2203–2211

Bates GP, Davies SW (1997) Transgenic mouse models of neurodegenerative sisease caused by CAG/polyglutamine expansions. Mol Med Today 3:508–515

Chevalier-Larsen ES, O'Brien CJ, Wang H, Jenkins SC, Holder L, Lieberman AP, Merry DE (2004) Castration restores function and neurofilament alterations of aged symptomatic males in a transgenic mouse model of spinal and bulbar muscular atrophy. J Neurosci 24:4778–4786

Holmberg M, Duyckaerts C, Dürr A, Cancel G, Gourfinkel-An I, Damier P, Faucheux B, Trottier Y, Hirsch EC, Agid Y, Brice A (1998) Spinocerebellar ataxia type 7 (SCAT7): a neurodegenerative disorder with neuronal intranuclear inclusions. Hum Mol Genet 7:913–918

Katsuno M, Adachi H, Kume A, Li M, Nakagomi Y, Niwa H, Sang C, Kobayashi Y, Doyu M, Subue G (2002) Testosterone reduction prevents phenotypic expression in a transgenic mouse model of spinal and bulbar muscular atrophy. Neuron 35:843–854

Katsuno M, Adachi H, Doyu M, Minamiyama M, Sang C, Kobayashi Y, Inukai A, Sobue G (2003) Leuprolin rescues polyglutamine-dependent phenotypes in a transgenic mouse model of spinal and bulbar muscular atrophy. Nature Med 9:768–773

Kobayashi Y, Miwa S, Merry DE, Kume A, Mei L, Doyu M, Sobue G (1998) Caspase-3 cleaves the expanded androgen receptor protein of spinal and bulbar muscular atrophy in a polyglutamine repeat length-dependent manner. Biochem Biophys Res Commun 252:145–150

MacManamny P, Chy HS, Finkelstein DI, Craithorn RG, Crack PJ, Kola I, Cheema SS, Horne MK, Wreford NG, O'Bryan MK, de Ketser DM, Morrison JR (2002) A mouse model of spinal and bulbar muscular atrophy. Hum Mol Genet 11:2103–2111

Minamiyama M, Katsuno M, Adachi H, Waza M, Sang C, Kobayashi Y, Tanaka F, Doyu M, Inukai A, Subue G (2004) Sodium butyrate ameliorates phenotypic expression in a transgenic mouse model of spinal and bulbar muscular atrophy. Hum Mol Genet 13:1183–1192

Niwa H, Yamamura K, Miyazaki J (1991) Efficient selection of high-expression trasnfectants with a novel eukaryotic vector. Gene 108:193–199

Walcott JL, Merry DE (2002) Trinucleotide repeat disaese: the androgen receptor in spinal and bulbar muscular atrophy. Vitam Horm 65:127–147

E.8.5 Models of Down Syndrome

PURPOSE AND RATIONALE

Down syndrome, the most common known genetic cause of mental retardation, is the result of trisomy of chromosome 21. Although the degree of cognitive impairment in Down syndrome can be quite variable, individuals with Down syndrome have significantly lower IQs with impaired speech and language skills as well as specific difficulties in auditory and visual memory, in spatial memory and in the acquisition of conditioned and operant responses. Down syndrome is considered to be caused by trisomy of the human chromosome 21.

Several attempts have been made to find animal models for Down disease. Since the mouse chromosome 16 is homologous to the human chromosome 21, mice with trisomy of chromosome 16 were created. Cox et al. (1984) reported production of a viable trisomy 16 diploid mouse chimera as a model of human trisomy 21 (Down syndrome). This model has been extensively used (Epstein et al. 1985; Sweeney et al. 1989; Holtzman et al. 1992; Shetty et al. 1996). However, the value of this model is limited to some extent because trisomy 16 mouse fetuses do not survive as live-born animals.

The **Ts65Dn mouse** carries only a partial trisomy for mouse chromosome 16 in a region that has highly homology to the Down syndrome region of human chromosome 21. These mice survive until adulthood and have therefore been used as animal model for Down syndrome in more recent studies (Davisson et al. 1993; Coussons-Read and Crnic 1996; Klein et al. 1996; Kola and Hertzog 1997; Costa et al. 1999; Cooper et al. 2001; Galdzicki et al. 2001; Granholm et al. 2002; Bimonte-Nelson et al. 2003; Stasko and Costa 2004).

Ema et al. (1999) described an animal model of Down syndrome in mice overexpressing the *mSim2* gene located on chromosome 16. Borella et al. (2003) characterized social behaviors and oxytoninergic neurons in the S-100β overexpressing mouse model of Down syndrome originally described by Friend et al. (1992).

A number of experimental compounds have been developed that result in improved cognitive performance in animal models. Moran et al. (2002) described the effects of piracetam on cognitive performance in a mouse model of Down syndrome.

PROCEDURE

Male 5-week-old Ts65Dn and euploid littermate control mice received daily injection of one of three dose of piracetam (75, 150, and 300 mg/kg) or saline vehicle. Piracetam treatment continued for 4 weeks prior to and throughout the 4-week testing period. Testing consisted of assessments of performance on the visible- and hidden-platform components of the Morris maze task and assessment of spontaneous activity within computerized activity chambers.

EVALUATION

Significant effects were explored with two-way ANOVA, analysis of main effects, and paired *t* comparisons.

MODIFICATIONS OF THE METHOD

Cardenas et al. (2002) established and characterized immortal neuronal cell lines derived from the spinal cord of normal and trisomy 16 fetal mice.

REFERENCES AND FURTHER READING

Bimonte-Nelson H, Hunter CL, Nelson ME, Granholm ACE (2003) Frontal cortex BDNF levels correlate with working memory in an animal model of Down syndrome. Behav Brain Res 139:47–57

Borella A, Sumangali R, Ko J, Whitaker-Azmitia PM (2003) Characterization of social behaviors and oxytoninergic neurons in the S-100β overexpressing mouse model of Down syndrome. Behav Brain Res 141:229–236

Cardenas AM, Allen DD, Arriagada C, Olivares A, Bennett LB, Caviedes R, Dagnino-Subriabre A, Mendoza IE, Segura-Aguilar J, Rapoport SI, Caviedes P (2002) Establishment and characterization of immortal neuronal cell lines derived from the spinal cord of normal and trisomy 16 fetal mice, an animal model of Down syndrome. J Neurosci Res 68:46–58

Cooper JD, Salehi A, Delcroix JD, Howe CL, Belichenko PV, Chua-Couzens J, Kilbridge JF, Carlson EJ, Epstein CJ, Mobley WC (2001) Failed retrograde transport of NGF in a mouse model of Down's syndrome: reversal of cholinergic neurodegenerative phenotypes following NGF infusion. Proc Natl Acad Sci USA 98:10439–10444

Costa ACS, Walsh K, Davisson MT (1999) Motor dysfunction in a mouse model for Down syndrome. Physiol Behav 68:211–220

Coussons-Read ME, Crnic LS (1996) Behavioral assessment of the Ts65Dn mouse, a model for Down syndrome: altered behavior in the elevated plus maze and open field. Behav Genet 26:7–13

Cox DR, Smith SA, Epstein LB, Epstein CJ (1984) Mouse trisomy 16 as a model of human trisomy 21 (Down syndrome): production of a viable trisomy 16 diploid mouse chimera. Dev Biol 101:416–424

Davisson MT, Schmidt C, Reeves RH, Irving NG, Akeson EC, Harris BS, Bronson RT (1993) Segmental trisomy as a mouse model for Down syndrome. Prog Clin Biol Res 384:117–133

Ema M, Ikegami S, Hosoya T, Mimura J, Ohtani H, Nakao K, Inokuchi K, Katsuki M, Fujii-Kuriyama Y (1999) Mild impairment of learning and memory in mice overexpressing the *mSim2* gene located on chromosome 16: an animal model of Down's syndrome. Human Mol Genet 8:1409–1415

Epstein CJ, Cox DR, Epstein LB (1985) Mouse trisomy 16: an animal model for human trisomy 21 (Down syndrome) Ann N Y Acad Sci 450:157–168

Friend WC, Clapoff S, Landry C, Becker LE, O'Hanlon D, Allore RJ (1992) Cell-specific expression of high levels of human S100 beta in transgenic mouse brain is dependent on gene dosage. J Neurosci 12:4337–4346

Galdzicki Z, Siarey R, Pearce R, Stoll J, Rapoport SI (2001) On the cause of mental retardation in Down syndrome: extrapolation from full and segmental trisomy 16 mouse models. Brain Res Rev 35:115–145

Granholm ACE, Ford KA, Hyde LA, Bimonta HA, Hunter CL, Nelson M, Albeck D, Sanders LA, Mufson EJ, Cmic LS (2002) Estrogen restores cognition and cholinergic phenotype in an animal model of Down syndrome. Physiol Behav 77:371–385

Holtzman DM, Bayney RM, Li Y, Khosrovi H, Berger CN, Epstein CJ, Mobley MC (1992) Dysregulation of gene expres-

sion in mouse trisomy 16, an animal model of Down syndrome. EMBO J 11:619–627
Klein SL, Kriegsfeld LJ, Hairston JE, Rau V, Nelson RJ, Yarowsky PJ (1996) Characterization of sensomotor performance, reproductive and aggressive behaviors in segmental trisomic 16 (Ts65Dn) mice. Physiol Behav 60:1159–1164
Kola I, Hertzog PJ (1997) Animal models in the study of the biological function of human chromosome 21 and their role in the pathology of Down syndrome. Human Mol Genet 6:1713–1727
Moran TH, Capone GT, Knipp S, Davisson MT, Reeves RH, Gearhart JD (2002) The effects of piracetam on cognitive performance in a mouse model of Down's syndrome. Physiol Behav 77:403–409
Shetty HU, Holloway HW, Acevedo LD, Galdzicki Z (1996) Brain accumulation of myo-inositol in the trisomy 16 mouse, an animal model of Downs's syndrome. Biochem J 313(pt 1):31–33
Stasko MR, Costa AC (2004) Experimental parameters affecting the Morris water maze performance of a mouse model of Down syndrome. Behav Brain Res 154:1–17
Sweeney JE, Hohmann CF, Oster-Granite ML, Coyle JT (1989) Neurogenesis of the basal forebrain in euploid and trisomy 16 mice: an animal model for developmental disorders in Down syndrome. Neuroscience 31:413–425

E.8.6 Models of Wilson's Disease

PURPOSE AND RATIONALE

Wilson disease is an **inherited disorder of copper metabolism** caused by autosomal recessive mutations of the *ATP7B* gene. The mutant ATP7B proteins lead to an impaired copper efflux, a decreased copper incorporation into ceruloplasmin and to hepatic copper accumulation, resulting in hepatocellular injury and deposition of copper in extra-hepatic tissues. Patients suffer from chronic or acute liver disease, psychiatric symptoms and neurological abnormalities with extrapyramidal symptoms, such as tremor and ataxia. D-penicillamine has been used for treatment of patients with Wilson disease, but more recently ammonium tetrathiomolybdate has been recommended (Stremmel et al. 1991; Silva et al. 1996; Brewer et al. 2003).

The **Long-Evans Cinnamon rat** has a mutation homologous to the human Wilson disease gene, leading to gross copper accumulation and development of hepatitis. This rat strain has ben extensively used as animal model for Wilson disease (Yamaguchi et al. 1994; Suzuki 1995; Adachi et al. 1997; Kodama et al. 1998; Nagano et al. 1998; Nomiyana et al. 1999; Terada and Sugiyama 1999; Klein et al. 1998, 2000, 2004; Komatsu et al. 2000, 2002; Meng et al. 2004).

Klein et al. (2004) reported the effects of tetrathiomolybdate in the treatment of acute hepatitis in Long-Evans Cinnamon rats.

PROCEDURE

Female Long-Evans Cinnamon rats (Charles River, Japan) at an age of between 60 and 100 days were used, whereas female Long-Evans Aguti rats served as controls. Long-Evans Cinnamon (LEC) rats were randomly divided in different groups:

LEC rats without any treatment and without signs of liver disease,

jaundiced LEC rats without any treatment,

jaundiced LEC rats treated once intraperitoneally with 10 mg/kg tetrathiomolybdate.

The tetrathiomolybdate-treated rats were sacrificed either 1 or 4 days after treatment.

Tissue Preparation and Subcellular Fractionation

Livers were flushed *in situ* with ice-cold 0.9% NaCl in order to remove the blood. A part of the liver was fixed in 4% neutral formalin, embedded in paraffin, and sections were stained for light microscopy. From homogenates lysosomal and mitochondrial fractions were prepared (Klein et al. 1998, 2000). Electron microscopy and X-ray microanalysis were performed. Metals and metallothionein were quantified.

EVALUATION

Student's *t*-test was used for statistical evaluation.

OTHER DISORDERS OF COPPEER METABOLISM

Besides Wilson's syndrome, other inherited diseases of cellular copper metabolism are known, such as Menkes disease and the toxic milk syndrome in mice (Palida and Ettinger 1991; La Fontaine et al. 2001).

Menkes' syndrome is an X-linked recessive disorder associated with copper deficiency, lethal in early childhood. Menkes' children show impaired synthesis of collagen and elastin. Furthermore, they are severely mentally retarded. Diffuse atrophy, focal degeneration of gray matter and prominent neuronal loss have been detected in the cerebellum. The molecular basis of this syndrome has been identified as a mutated gene (*ATP7A*) encoding for a P-type cation-transporting ATPase (Kodama and Murata 1999; Tumer et al. 1999; Rossi et al. 2001).

The mutant **macular** mouse has been used as animal model for Menkes' disease (Tanaka et al. 1990; Murata et al. 1997, 1998; Suzuki-Kurasaki et al. 1997). The **brindled mouse mutant** (Mo^{br}) is considered to be the closest model to Menkes' disease (Grimes et al. 1997; Rossi et al. 2001). The mutant mice are hypopigmented and die at around 15 days after birth, but can be saved by treatment with copper before the 10th postnatal day.

REFERENCES AND FURTHER READING

Adachi Y, Okyama Y, Miya H, Toshinori K (1997) Presence of ATP-dependent copper transport in the hepatocyte canalicular membrane of the Long-Evans Cinnamon rat, an animal of Wilson disease. J Hepatol 26:216–217

Brewer GJ, Hedera P, Kluin KJ, Carlson M, Askari F, Dick RB, Sitterly J, Fink JK (2003) Treatment of Wilson disease with ammonium tetrathiomolybdate: III. Initial therapy in a total of 55 neurologically affected patients and follow-up with zinc therapy. Arch Neurol 60:379–385

Grimes A, Hearn CJ, Lockhart P, Newgreen DF, Mercer JFB (1997) Molecular basis of the brindled mouse mutant (Mo^{br}): a murine model of Menkes disease. Hum Mol Genet 6:1037–1042

Klein D, Lichtmannegger J, Heinzmann U, Müller-Höcker J, Micaelsen S, Summer KH (1998) Association of copper to metallothionein in hepatic lysosomes of Long-Evans Cinnamon (LEC) rats during the development of hepatitis. Eur J Clin Invest 28:302–310

Klein D, Lichtmannegger J, Heinzmann U, Summer KH (2000) Dissolution of copper-rich granules in hepatic lysosomes by D-penicillamine prevents the development of fulminant hepatitis in Long-Evans cinnamon rats. J Hepatol 32:193–201

Klein D, Arora U, Lichtmannegger J, Finckh M, Heinzann U, Summer KH (2004) Tetrathiomolybdate in the treatment of acute hepatitis in an animal model of Wilson disease. J Hepatol 40:409–416

Kodama H, Murata Y (1999) Molecular genetics and pathophysiology of Menkes disease. Pedriatr Int 41:430–435

Kodama H, Murata Y, Mochizuki D, Abe T (1998) Copper and ceruloplasmin metabolism in the LEC rat, an animal model of Wilson disease. J Inherit Metab Dis 21:203–206

Komatsu Y, Sadakata I, Ogra Y, Suzuki KT (2000) Excretion of copper complexed with thiomolybdate into the bile and blood in LEC rats. Chem Biol Interact 124:217–231

Komatsu Y, Ogra Y, Suzuki KT (2002) Copper balance and ceruloplasmin in chronic hepatitis in a Wilson disease animal model, LEC rats. Arch Toxicol 76:502–508

La Fontaine S, Theophilos MB, Firth SD, Gould R, Parton RG, Mercer JFB (2001) Effect of the toxic milk mutation (*tx*) on the function and intracellular location of Mnd, the murine homologue of the Wilson copper ATPase. Hum Mol Genet 10:361–370

Meng Y, Miyoshi I, Hirabayashi M, Su M, Mototani Y, Okamura T, Terada K, Ueda M, Enomoto K, Sugiyama T, Kasai N (2004) Restoration of copper metabolism and rescue of hepatic abnormalities in LEC rats, an animal model of Wilson disease, by expression of human ATP7B gene. Biochim Biophys Acta 1690:208–219

Murata Y, Kodama H, Abe T, Ishida N, Nishimura M, Levinson B, Gitschier J, Packman S (1997) Mutation analysis and expression of the mottled gene in the macular mouse model of Menkes disease. Pediatr Res 42:436–442

Murata Y, Kodama H, Mori Y, Kobayashi M, Abe T (1998) Mottled gene expression and copper distribution in the macular mouse, an animal model for Menkes disease. J Inherit Metab Dis 21:199–202

Nagano K, Nakamura K, Urakami KI, Umeyama K, Uchiyama H, Koiwai K, Hattori S, Yamamoto T, Matsuda I, Endo F (1998) Intracellular distribution of the Wilson's disease gene product (ATPase7B) after in vitro and in vivo exogenous expression in hepatocytes from the LEC rat, an animal model of Wilson's disease. Hepatology 27:799–807

Nomiyama K, Nomiyama H, Kameda N, Tsuji A, Sakuari H (1999) Mechanism of hepatorenal syndrome in rats of Long-Evans Cinnamon strain, an animal model of fulminant Wilson's disease. Toxicology 132:201–214

Palida FA, Ettinger MJ (1991) Identification of proteins involved in intracellular copper metabolism. J Biol Chem 266:4586–4592

Rossi L, de Martino A, Marchese E, Piccirilli S, Rotilio G, Ciriolo MR (2001) Neurodegeneration in the animal model of Menkes' disease involves Bcl-2-linked apoptosis. Neurosci 103:181–188

Silva EES, Sarles J, Buts JP, Sokal EM (1996) Successful treatment of severely decompensated Wilson disease. J Pediatr 128:285–287

Stremmel W, Meyerrose KW, Niederau C, Hefter H, Kreuzpainter G, Strohmeyer G (1991) Wilson disease: clinical presentation, treatment, and survival. Ann Int Med 115:720–726

Suzuki KT (1995) Disordered copper metabolism in LEC rats, an animal model or Wilson disease. Role of metallothionein. Res Commun Mol Pathol Pharmacol 89:221–240

Suzuki-Kurasaki M, Okabe M, Kurasaki M (1997) Copper-metallothionein in the kidney of macular mice: a model for Menkes disease. J Histochem Cytochem 45:1493–1501

Tanaka K, Kobayashi K, Fujita Y, Fukuhara C, Onosaka S, Min K (1990) Effects of chelators on copper therpy of macular mouse, a model of Menkes' kinky disease. Res Commun Chem Pathol Pharmacol 69:217–227

Terada K, Sugiyama T (1999) The Long-Evans Cinnamon rat. An animal model for Wilson's disease. Pediatr Int 41:414–418

Tumer Z, Moller LB, Horn N (1999) Mutation spectrum of ATP7A, the gene defective in Menkes disease. Adv Exp Med Biol 448:83–95

Yamaguchi Y, Heiny ME, Shimizu N, Aoki T, Gitlin JD (1994) Expression of the Wilson disease gene is deficient in the Long-Evans Cinnamon rat. Biochem J 301 (Pt 1):1–4

E.8.7
Models of Cerebellar Ataxia

The pathology mechanisms underlying the signs of hereditary cerebellar ataxia in humans are not well understood (Harding 1984).

Kato et al. (1982) and Yamaguchi et al. (1992) regarded the rolling mouse Nagoya as an animal model of hereditary cerebellar ataxia.

Niimi et al. (1982) made an animal model of cerebellar ataxia by injections of kainic acid into both sides of the cerebellar hemispheres of male rats.

Grüsser-Cornehls et al. (1999) recommended Weaver mutant mice as an animal model of cerebellar ataxia.

Fernandez et al. (1998) induced ataxia in adult rats either with intraperitoneal injection of 50–65 mg/kg 3-acetylpyridine or by bilateral electrocoagulation of the inferior olive. Insulin-like growth factor 1 restored motor coordination in this rat model of cerebellar ataxia.

Ataxia-telangiectasia is a complex multiparametric disease associated with oculocutaneous telangiectasias, cerebellar ataxia, elevated chromosomal aberration frequency, and varied degrees of immunodefi-

ciency. Kaiserlian et al. (1986) described the wasted mouse as a model of this disease.

Clark et al. (2000) reported X-linked transmission of the *shake*r mutation in rats with hereditary Purkinje cell degeneration and ataxia.

Sausbier et al. (2004) described cerebellar ataxia and Purkinje cell dysfunction in mice caused by Ca^{2+}-activated K^+ channel deficiency

REFERENCES AND FURTHER READING

Clark BR, LaRegina M, Tolbert DL (2000) X-linked transmission of the *shake*r mutation in rats with hereditary Purkinje cell degeneration and ataxia. Brain Res 858:264–273

Fernandez AM, de la Vega AG, Torres-Aleman L (1998) Insulin-like growth factor 1 restored motor coordination in a rat model of cerebellar ataxia. Proc Natl Acad Sci USA 95:1253–1258

Grüsser-Cornehls U, Grüsser C, Bäurle J (1999) Vermectomy enhances ovalbumin expression and improves motor performance in Weaver mutant mice, an animal model of cerebellar ataxia. Neuroscience 91:315–326

Harding HE (1984) The hereditary ataxias and related disorders. Churchill Livingstone, Edinburgh

Kaiserlian D, Savino W, Uriel J, Hassid J, Dardenne M, Bach JF (1986) The wasted mutant mouse. II Immunological abnormalities in a mouse model of ataxia-telangiectasia. Clin Exp Immunol 63:562–569

Kato M, Hosokawa S, Tobimatsu S, Kuriowa Y (1982) Increased local cerebral glucose utilization in the basal ganglia of the rolling mouse Nagoya. J Cereb Blood Flow Metab 2:385–393

Niimi M, Takahara J, Aoki Y, Fujino H, Ofuji T (1982) A cerebellar ataxic rat produced by kainic acid and changes in concentrations and turnover rates of catecholamines in discrete brain regions. Acta Med Okayama 36:223–227

Sausbier M, Hu H, Arntz C, Feil S, Kamm S, Adelsberger H, Sausbier U, Sailer CA, Feil R, Hofmann F, Korth M, Shipston MJ, Knaus HG, Wolfer DP, Pedroarena CM, Storm JF, Ruth P (2004) Cerebellar ataxia and Purkinje cell dysfunction caused by Ca^{2+}-activated K^+ channel deficiency. Proc Natl Acad Sci USA 101:9474–9478

Yamaguchi T, Kato M, Fukui M, Akazawa K (1992) Rolling mouse Nagoya as a mutant animal model of basal ganglia dysfunction: determination of absolute rates of local cerebral glucose utilization. Brain Res 598:38–44

E.8.8 Models of Niemann-Pick Syndrome

PURPOSE AND RATIONALE

Niemann-Pick disease type C is a progressive neurodegenerative disorder caused by mutations in the *NPC1* gene and characterized by intracellular accumulation of cholesterol and sphingolipids.

Pentchev et al. (1980, 1984) described a genetic storage disorder in BALB/C mice with metabolic block in esterification of exogenous cholesterol. The murine model of Niemann-Pick C disease with mutation in a cholesterol homeostasis gene (**npc1^{-}/$^{-}$mutant mice**) has been used in several studies (Weintraub et al. 1985, 1987; Higashi et al. 1993; Loftus et al. 1997; Erickson et al. 2000; Bascunan-Castillo et al. 2004). Some attempts have been made to improve the clinical course of the Niemann-Pick C disease mouse (Liu et al. 2000). Treatment with cyclodextrins had variable effects in delaying neurological symptoms and in decreasing liver cholesterol storage (Camargo et al. 2001). Zhan et al. (2004) showed that cyclin-dependent kinase inhibitors attenuate protein hyperphosphorylation, cytoskeletal lesion formation, and motor defects in Niemann-Pick type C mice.

MODIFICATIONS OF THE METHOD

Sym et al. (2000) described a model for Niemann-Pick type C disease in the nematode *Caenorhabditis elegans*.

REFERENCES AND FURTHER READING

Bascunan-Castillo EC, Erickson RP, Howison CM, Hunter RJ, Heidenreich RH, Hicks C, Trouard TP, Gillies RJ (2004) Tamoxifen and vitamin E treatments delay symptoms in the mouse model of Niemann-Pick C. J Appl Genet 45:461–467

Camargo FC, Erickson RP, Garver WS, Hossain GS, Carbone PN, Heidenreich RA, Blanchard J (2001) Cyclodextrins in the treatment of a mouse model of Niemann-Pick C disease. Life Sci 70:131–142

Erickson RP, Garver WS, Camargo F, Hossain GS, Heidenreich RA (2000) Pharmacological and genetic modifications of somatic cholesterol do not substantially alter the course of CNS disease in Niemann-Pick C mice. J Inherit Metab Dis 23:54–62

Higashi Y, Murayama S, Pentchev PG, Suzuki K (1993) Cerebellar degeneration in the Niemann-Pick type C mouse. Acta Neuropathol (Berl) 85:175–184

Liu Y, Wu YP, Wada R, Neufeld EB, Mullin KA, Howard AC, Pentchev PG, Vanier MT, Suzuki K, Proia RL (2000) Alleviation of neuronal ganglioside storage does not improve the clinical course of the Niemann-Pick C disease mouse. Human Mol Genet 9:1087–1093

Loftus SK, Morris JA, Carstena ED, Gu JZ, Cummings C, Brown A, Ellison J, Ohno K, Rosenfeld MA, Tagle DA, Pentchev PG, Pavan WJ (1997) Murine model of Niemann-Pick C disease: mutation in a cholesterol homeostasis gene. Science 277:232–235

Pentchev PG, Gal AE, Booth AD, Omodeo-Sale F, Fouks J, Neumeyer BA, Quirk JM, Dawson G, Brady RO (1980) A lysosomal storage disorder in mice characterized by a dual deficiency of sphingomyelinase and glucocerebrosidase. Biochim Biophys Acta 619:669–679

Pentchev PG, Boothe AD, Kruth HS, Weintroub H, Stivers J, Brady RO (1984) A genetic storage disorder in BALB/C mice with a metabolic block in esterification of exogenous cholesterol. J Biol Chem 259:5784–5791

Sym M, Basson M, Johnson C (2000) A model for Niemann-Pick type C disease in the nematode *Caenorhabditis elegans*. Curr Biol 10:527–530

Weintraub H, Abramovici A, Sandbank U, Pentchev PG, Brady RO, Sekine M, Suzuki A, Sela B (1985) Neurological mutation characterized by demyelination in NCTR-

Balb/C mouse with lysosomal lipid storage disease. J Neurochem 45:665–672
Weintraub H, Abramovici A, Sandbank U, Booth AD, Pentchev PG, Sela B (1987) Demyelination on NCTR-Balb/C mouse mutant with a lysosomal storage disorder. Morphological survey. Acta Neuropathol 74:374–381
Zhang M, Chakrabarty P, Bu B, Vincent I (2004) Cyclin-dependent kinase inhibitors attenuate protein hyperphosphorylation, cytoskeletal lesion formation, and motor defects in Niemann-Pick type C mice. Am J Pathol 165:843–853

E.8.9 Models of Gangliosidosis

PURPOSE AND RATIONALE

The glycosphingolipid lysosomal storage diseases are inherited metabolic diseases in which a gene encoding a lysosomal hydrolase or one of their co-factors is mutated. Two classes of glycosphingolipid storage diseases are known, those in which the storage glycosphingolipid is neutral (**Gaucher** and **Fabry** disease) and the gangliosidoses in which the storage lipid is a ganglioside (glycosphingolipid containing one or more sialic acid residues). The gangliosidoses include the G_{M2} storage disorders, **Tay-Sachs** and **Sandhoff disease** (O'Dowd et al. 1986; Paw et al. 1989; Koller and Sandhoff 1998; Schröder et al. 1991; Glaros et al. 2005), and the G_{M1} storage disorder termed G_{M1} gangliosidosis or **Morquio** B disease (Matsuda et al. 2003).

Spontaneous gangliosidosis has been described in several animal species, such as **dogs** (Singer and Cork 1989; Kaye et al. 1992; Wang et al. 2000; Yamato et al. 2003, 2004b; Kreutzer et al. 2005), **cats** (Cork et al. 1977; Neuwelt et al. 1985; Muldoon et al. 1994; Kroll et al. 1995; Yamato et al. 2004a; Martin et al. 2005), **sheep** (Skelly et al. 1995; Ryder and Simmons 2001), **deer** (Fox et al. 1999), and **pigs** (Kosanke et al. 1978).

***β*-Galactosidase-deficient mice** were described as an animal model for G_{M1}-gangliosidoses (Hahn et al. 1997; Matsuda et al. 1997a, 1997b; Oshima 1998; Callahan 1999; Itoh et al. 2001). Mouse models of G_{M2} gangliosidosis are reported by Huang et al. (1997) and Jeyakumar et al. (2003).

No effective treatment of patients is known as yet, but Jeyakumar et al. (1999) found delayed symptom onset and increased life expectancy in Sandhoff disease mice treated with *N*-butyldeoxynojirimycin. Yamaguchi et al. (2003) reported that plasmid-based gene transfer ameliorates visceral storage in a mouse model of Sandhoff disease. Martino et al. (2002) described restoration of the G_{M2} ganglioside metabolism in bone-marrow-derived stromal cells from a Tay–Sachs disease mouse model. Furthermore, Martino et al. (2005) reported that a direct gene strategy via brain internal capsule reverses the biochemical defect in Tay–Sachs disease.

REFERENCES AND FURTHER READING

Callahan JW (1999) Molecular basis of G_{M1} gangliosidosis and Morquio disease, type B. Structure-function studies of lysosomal β-galactosidase and the non-lysosomal β-galactosidase-like protein. Biochim Biophys Acta 1455:85–103
Cork LC, Munnell JF, Lorenz MD, Murphy JV, Baker HJ, Rattazzi MG (1977) G_{M2} ganglioside lysosomal storage disease in cats with β-hesosaminidase deficiency. Science 196:1014–1017
Fox J, Li YT, Dawson G, Alleman A, Johnsrude J, Schumacher J, Homer B (1999) Naturally occurring G_{M2} gangliosidosis in two Muntjak deer with pathological and biochemical features of human classical Tay-Sachs disease (type B G_{M2} gangliosidosis). Acta Neuropathol (Berl) 97:57–62
Glaros EN, Kim WS, Quinn CM, Wong J, Gelissen I, Jessup W, Garner B (2005) Glycosphingolipid accumulation inhibits cholesterol efflux via the ABCA1/apolipoprotein A-I pathway. 1-Phenyl-decanoylamino-3-morpholino-1-propanol is a novel cholesterol efflux accelerator. J Biol Chem 280:24515–24523
Hahn CN, del Pilar Martin M, Schröder M, Vanier MT, Hara Y, Suzuki K, Suzuki K, d'Azzo A (1997) Generalized CND disease and massive G_{M1}-ganglioside accumulation in mice defective in lysosomal acid β-galactosidase. Human Mol Genet 6:205–211
Huang JQ, Trasler JM, Igdoura S, Michaud J, Hanai N, Gravel RA (1997) Apoptotic cell death in mouse models of G_{M2} gangliosidosis and observations in human Tay-Sachs and Sandhoff disease. Human Mol Genet 6:1879–1885
Itoh M, Matsuda J, Suzuki O, Ogura A, Oshima A, Tai T, Suzuki Y, Takashima S (2001) Development of lysosomal storage in mice with targeted disruption of the β-galactosidase gene: a model of G_{M1}-gangliosidossi. Brain Dev 23:379–384
Jeyakumar M, Butters TD, Cortina-Borja M, Hunnam V, Proia RL, Perry VH, Dwek RA, Platt FM (1999) Delayed symptom onset and increased life expectancy in Sandhoff disease mice treated with *N*-butyldeoxynojirimycin. Proc Natl Acad Sci USA 96:6388–6393
Jeyakumar M, Thomas R, Elliot-Smith E, Smith SA, van der Spoel AC, d'Azzo A, Perry HV, Butters TD, Dwek RA, Platt FM (2003) Central nervous system inflammation is a hallmark of pathogenesis in mouse models of GM1 and GM2 gangliosidosis. Brain 126:974–987
Kaye EM, Alroy J, Raghavan SS, Schwarting GA, Adelman LS, Runge V, Geblum D, Thalhammer JG, Zuniga G (1992) Dysmyelinogenesis in animal model of gangliosidosis. Pediatr Neurol 8:255–261
Kolter T, Sandhoff K (1998) Recent advances in the biochemistry of sphingolipidoses. Brain Pathol 8:79–100
Kosanke SD, Pierce KR, Bay WW (1978) Clinical and biochemical markers in porcine G_{M2}-gangliosodosis. Vet Pathol 15:685–699
Kreutzer R, Leeb T, Muller G, Moritz A, Baumgartnet W (2005) A duplication of the canine β-galactosidase gene GLB1 causes exon skipping and G_{M1}-gangliosodosis in Alaskan huskies. Genetics 170:1857–1861

Kroll RA, Pagel Ma, Roman-Goldstein S, Barkovich J, D'Agostino AN, Neuwelt EA (1995) White matter changes associated with feline G_{M2} gangliosidosis (Sandhoff disease): correlation of MR findings with pathologic and ultrastructural abnormalities. Am J Neuroradiol 16:1219–1226

Martin DR, Cox NR, Morrison NE, Kennamer DM, Peck SL, Dodson AN, Gentry AS, Griffin B, Rolsma MD, Baker HJ (2005) Mutation of the G_{M2} activator protein in a feline model of G_{M2} gangliosidosis. Acta Neuropathol (Berl) 110:443–450

Martino S, Cavalieri C, Emiliani C, Dolcetta D, Cusella de Angelis MG, Chigorni V, Severini GM, Sandhoff K, Bordignon C, Sonnino S, Orlacchio A (2002) Restoration of the G_{M2} ganglioside metabolism in bone-marrow-derived stromal cells from Tay-Sachs disease animal model. Neurochem Res 27:793–800

Martino S, Marconi P, Tancini B, Dolcetta D, de Angelis MG, Montanucci P, Bregola G, Sandhoff K, Bordignon C, Emiliani C, Manservigi R, Orlacchio A (2005) A direct gene strategy via brain internal capsule reverses the biochemical defect in Tay-Sachs disease. Hum Mol Genet 14:2113–2123

Matsuda J, Suzuki O, Oshima A, Ogura A, Noguchi Y, Yamamoto Y, Asano T, Takimoto K, Sukegawa K, Suzuki Y, Naiki M (1997a) β-Galactosidase-deficient mouse as an animal model for G_{M1}-gangliosidoses. Glycoconj J 14:729–738

Matsuda J, Suzuki O, Oshima A, Ogura A, Naiki M, Suzuki Y (1997b) Neurological manifestations of knockout mice with β-galactosidase deficiency. Brain Dev 19:19–20

Matsuda J, Suzuki O, Oshima A, Yamamoto Y, Noguchi A, Takimoto K, Itoh M, Matsuzaki Y, Yasuda Y, Ogawa S, Sakata Y, Nanba E, Higaki K, Ogawa Y, Tominaga L, Ohno K, Iwasaki H, Watanabe H, Brady RO, Suzuki Y (2003) Chemical chaperone therapy for brain pathology in G_{M1}-gangliosidosis. Proc Natl Acad Sci USA 100:15912–15917

Muldoon LL, Neuwelt EA, Pagel MA, Weiss DL (1994) Characterization of the molecular defect in a feline model for type II G_{M2}-gangliosidosis (Sandhoff disease). Am J Pathol 144:1109–1118

Neuwelt EA, Johnson WG, Blank NK, Pagel MA, Maslen-McClure C, McClure MJ, Wu PM (1985) Characterization of a new model of G_{M2}-gangliosidosis (Sandhoff's disease) in Korat cats. J Clin Invest 76:482–490

O'Dowd BF, Klavins MH, Willard HF, Gravel R, Lowden JA, Mahuran DJ (1986) Molecular heterogeneity in the infantile and juvenile form of Sandhoff disease (O-variant G_{M2} gangliosidosis). J Biol Chem 261:12680–12685

Oshima A (1998) G_{M1}-ganglioside knockout mouse. No To Hattatsu 30:148–151

Paw BH, Kaback MM, Neufeld EF (1989) Molecular basis of adult-onset and chronic GM2 gangliosidoses in patients of Askenazi Jewish origin: substitution of serine for glycine at position 269 of the α-subunit of β-hexosaminidase. Proc Natl Acad Sci USA 86:2413–2417

Ryder SJ, Simmons MM (2001) A lysosomal storage disease of Rommey sheep that resembles human type 3 G_{M1} gangliosidosis. Acta Neuropathol (Berl) 101:225–228

Schröder M, Schnabel D, Suzuki K, Sandhoff K (1991) A mutation in the gene of a glycolipid-binding protein (GM2 activator) that causes GM2-gangluiosidosis variant AB. FEBS Lett 290:1–3

Singer HS, Cork LC (1989) Canine G_{M2} gangliosidosis: morphological and biochemical analysis. Vet Pathol 26:114–120

Skelly BJ, Jeffrey M, Franklin RJ, Winchester BG (1995) A new form of G_{M1}-gangliosidosis. Acta Neuropathol (Berl) 89:374–379

Wang ZH, Zeng B, Shibuya H, Johnson GS, Alroy J, Pastores GM, Raghavan S, Kolodny EH (2000) Isolation and characterization of the normal canine β-galactosidase gene and its mutation in a dog model of G_{M1}-gangliosidosis. J Inherit Metab Dis 12:593–606

Yamaguchi A, Katsuyama K, Suzuki K, Kosaka K, Aoki I, Yamanak S (2003) Plasmid-based gene transfer ameliorates visceral storage in a mouse model of Sandhoff disease. J Mol Med 81:185–193

Yamato O, Masuoka Y, Yonemura M, Hatakeyama A, Satoh H, Kobayashi A, Nakayama M, Asano T, Shoda T, Yamasaki M, Ochiai K, Umemura T, Maede Y (2003) Clinical and clinico-pathologic characteristics of Shiba dogs with a deficiency of lysosomal β-galactosidase: a canine model of human G_{M1} gangliosidosis. J Vet Med Sci 65:213–217

Yamato O, Matsunaga S, Takeda K, Uetsuka K, Satoh H, Shoda T, Baba Y, Yasoshima A, Kato K, Takahashi K, Yamasaki M, Nakayama H, Doi K, Maede Y, Ogawa H (2004a) G_{M2}-gangliosidosis variant 0 (Sandhoff-like disease) in a family of Japanese domestic cats. Vet Rec 155:739–744

Yamato O, Jo EO, Shoda T, Yamsaki M, Maede Y (2004b) Rapid and simple mutation screening of G_{M1} gangliosidosis in Shiba dogs by direct amplification of deoxyribonucleic acid from various forms of canine whole-blood species. J Vet Diagn Invest 16:469–472

E.8.10 Models of Mucopolysaccharidosis

PURPOSE AND RATIONALE

Mucopolysaccharidosis type IIIA or **Sanfilippo syndrome** is a lysosomal storage disorder characterized by progressive neurological pathology. Patients exhibit aggression, disturbed sleep, hyperactivity and mental decline ultimately resulting in inanition and death. Four mucopolysaccharidosis subtypes result from deficiencies in different lysosomal enzymes that sequentially degrade heparin sulfate: sulfamidase (MPS IIIA), α-*N*-acetylglucosaminidase (MPS IIIB), acetyl-CoA:α-glucosamidine *N*-acetyltransferase (MPS IIIC), and glucosamine-6-sulfatase (MPS IIID).

Mucopolysaccharidosis III has been described in several animal species, such as mice (Li et al. 1999, 2002; Yu et al. 2000; Gografe et al. 2003; Garbuzova-Davis et al. 2005), dogs (Fischer et al. 1998; Aronovich et al. 2000; Ellinwood et al. 2003), emus (Giger et al. 1997; Aronovich et al. 2001), and goats (Thompson et al. 1992).

A naturally occurring mouse model of MPS-IIIA has been discovered (Bhaumik et al. 1999; Bhattacharyya et al. 2001), with pathophysiology and symptoms that resemble the human conditions (Glid-

don and Hopwood 2004; Hemsley and Hopwood 2005).

No effective drug treatment for patients with Sanfilippo disease is available; however, experiments in mice showed beneficial effects after transplantation of human umbilical cord blood cells (Garbuzova-Davis et al. 2005), or treatment with lentiviral NAGLU vector (Di Natale et al. 2005) or enzyme replacement (Yu et al. 2000; Gliddon and Hopwood 2004).

REFERENCES AND FURTHER READING

Aronovich EL, Carmichael KP, Morizono H, Koutlas IG, Deanching M, Hoganson G, Fischer A, Whitley CB (2000) Canine heparin sulfate sulfamidase and the molecular pathology underlying Sanfilippo syndrome type A in Dachshunds. Genomics 68:80–84

Aronovich EL, Johnston JM, Wang P, Giger U, Whitley CB (2001) Molecular basis for mucopolysaccharidosis type IIIB in emu (*Dromaius novaehollandiae*): an avian model of Sanfilippo syndrome type B. Genomics 74:299–305

Bhattacharyya R, Gliddon B, Beccarai T, Hopwood JJ, Stamley P (2001) A novel missense mutation in lysosomal sulfamidase is the basis of MPS III A in a spontaneous mouse mutant. Glycobiology 11:99–103

Bhaumik M, Muller VJ, Rozaklis T, Johnson L, Dobrenis K, Bhattacharyya R, Wurzelmann S, Finamore P, Hopwood JJ, Walkley SU, Stanley P (1999) A mouse model for mucopolysaccharidosis type III A (Sanfilippo syndrome). Glycobiology 9:1389–1396

Di Natale P, Di Domenico C, Gargiulo N, Castaldo S, Gonzalez Y, Reyero E, Mithbaokar P, de Felice M, Follenzi A, Naldini L, Villani GR (2005) Treatment of the mouse model of mucopolysaccharidosis type IIIB with lentiviral NAGLU vector. Biochem J 388:639–646

Ellinwood NM, Wang P, Skeen T, Sharp NJ, Cesta M, Decker S, Edwards NJ, Bublot I, Thompson JN, Bush W, Hardam E, Haskins ME, Giger U (2003) A model of mucopolysaccharidosis IIIB (Sanfilippo syndrome IIIB): N-acetyl-α-D-glucosaminidase deficiency in Schipperke dogs. J Inherit Metab Dis 26:489–504

Fischer A, Carmichael KP, Munnell JF, Jhabvala P, Thompson JN, Matalon R, Jezyl PF, Wang P, Giger U (1998) Sulfamidase deficiency in a family of Dachshunds: a canine model of mucopolysaccharidosis IIIA (Sanfilippo A). Pediatr Res 44:74–82

Garbuzova-Davis S, Willing AE, Desjarlais T, Davis-Sanberg C, Sanberg PR (2005) Transplantation of human umbilical cord blood cells benefits an animal model of Sanfilippo syndrome type B. Stem Cells Dev 14:384–394

Giger U, Shivaprasad H, Wang P, Jezyk P, Pazzerson D, Bradley G (1997) Mucopolysaccharidosis type III B (Sanfilippo B syndrome) in emus. Vet Pathol 34:473

Gliddon BL, Hopwood JJ (2004) Enzyme-replacement therapy from birth delays the development of behavior and learning problems in mucopolysaccharidosis type IIIA mice. Pediatr Res 56:65–72

Gografe SI, Garbuzova-Davis S, Willing AE, Haas K, Chamizo W, Sanberg PR (2003) Mouse model of Sanfilippo syndrome type B: relation of phenotypic features to background strain. Comp Med 53:622–632

Hemsley KM, Hopwood JJ (2005) Development of motor deficits in a murine model of mucopolysaccharidosis type IIIA (MPS-IIIA). Behav Brain Res 158:191–199

Li HH, Yu WH, Rozengurt N, Zhao HZ, Lyons KM, Anagnostaras S, Fanselow MS, Suzuki K, Vanier MT, Neufeld EF (1999) Mouse model of Sanfilippo syndrome type B produced by targeted disruption of the gene encoding α-*N* acetylglucosaminidase. Proc Natl Acad Sci USA 96:14505–14510

Li HH, Zhao HZ, Neufeld EF, Cai Y, Gomez-Pinilla F (2002) Attenuated plasticity in neurons and astrocytes in the mouse model of Sanfilippo syndrome type B. J Neurosci Res 69:30–38

Thompson JN, Jones MZ, Dawson G, Huffman PS (1992) N-acetylglucosamine 6-sulphatase deficiency in a Nubian goat: a model of Sanfilippo syndrome type D (mucopolysaccharidosis IIID). J Inherit Metab Dis 15:760–766

Yu WH, Zhao KW, Ryaznatsev S, Rosengurt N, Neufeld EF (2000) Short-term enzyme replacement in the mouse model of Sanfilippo syndrome B. Mol Genet Metab 71:573–580

E.9 General Anesthesia

E.9.1 Intravenous Anesthesia

E.9.1.1 General Considerations

PURPOSE AND RATIONALE

The first agents which could be used as intravenous anesthetics were **barbiturates**. Barbiturates with a duration of action appropriate to the requirements of surgery became available with the introduction of hexobarbital and thiopental (Volwiler and Tabern 1930; Miller et al. 1936). The studies with barbiturates were extended (Butler and Bush 1942; Christensen and Lee 1973). Intravenous anesthetics from other chemical groups were developed, such as **acetamidoeugenol** (Estil, Domenjoz 1959), steroid derivatives (Presuren = **hydroxydione sodium**, Laubach et al. 1955; **alfaxolone**, CT1341, Child et al. 1971), **propanidid** (Epontol, Goldenthal 1971), **ketamine** (CI-581, Chen et al. 1966; Reich and Silvay 1989), **etomidate** (Janssen et al. 1975), **propofol** (ICI 35868, Glen 1980), **midazolam** (Pieri 1983; Reilly and Nimmo 1987).

REFERENCES AND FURTHER READING

Büch H, Butello W, Neurohr O, Rummel W (1968) Vergleich von Verteilung, narkotischer Wirksamkeit und metabolischer Elimination der optischen Antipoden von Methylphenobarbital. Biochem Pharmacol 17:2391–2398

Büch H, Grund W, Buzello W, Rummel W (1969) Narkotische Wirksamkeit und Gewebsverteilung der optischen Antipoden des Pentobarbitals bei der Ratte. Biochem Pharmacol 18:1995–1009

Butler TC, Bush MT (1942) Anesthetic potency of some new derivatives of barbituric acid. Proc Soc Exp Biol Med 50:232–243

Chen G, Ensor CR, Bohner B (1966) The Neuropharmacol of 2-(o-chlorophenyl)-2-methylaminocyclohexanone hydrochloride. J Pharm Exp Ther 152:332–339
Child KJ, Currie JP, Davis B, Dodds MG, Pearce DR, Twissell DJ (1971) The pharmacological properties in animals of CT1341 – a new steroid anaesthetic agent. Br J Anaesth 43:2–24
Christensen HD, Lee IS (1973) Anesthetic potency and acute toxicity of optically active disubstituted barbituric acids. Toxicol Appl Pharmacol 26:495–503
Domenjoz R (1959) Anaesthesist 8:16
Glen JB (1980) Animal studies of the anesthetic activity of ICI 35868. Br J Anaesth 52:731–742
Goldenthal EI (1971) A compilation of LD50 values in newborn and adult animals. Toxicol Appl Pharmacol 18:185–207
Janssen PAJ, Niemegeers CJE, Marsboom RPH (1975) Etomidate, a potent non-barbiturate hypnotic. Intravenous etomidate in mice, rats, guinea pigs, rabbits and dogs. Arch Int Pharmacodyn 214:92–132
Laubach GD, Pan SY, Rudel HW (1955) Steroid anesthetic agent. Science 122:78
Miller E, Munch JC, Crossley FS, Hartung WH (1936) J Am Chem Soc 58:1090
Pieri L (1984) Preclinical pharmacology of midazolam. Br J Clin Pharmacol 16:17S–27S
Reich DL, Silvay G (1989) Ketamine: an update on the first twenty-five years of clinical experience. Can J Anaesth 36:186–197
Reilly CS, Nimmo WS (1987) New intravenous anaesthetics and neuromuscular blocking drugs. Drugs 34:98–135
Volwiler EH, Tabern DL (1930) J Am Chem Soc 52:1676

E.9.1.2
Screening of Intravenous Anesthetics

PURPOSE AND RATIONALE

Screening of intravenous anesthetics or hypnotics is performed mostly in mice or rats. Doses for loss of righting reflex and lethal doses are determined. Onset of action and duration of action are the secondary parameters.

PROCEDURE

Male mice weighing 18–22 g are injected intravenously via the tail vein. The anesthetic activity is estimated from the number of animals that loose their righting reflex. The righting reflex is considered lost when the mouse, placed on its back, fails to recover from this position within 1 min. The acute toxicity is based on lethality within a 24-h observation period.

To determine onset and duration of action groups of 20 mice are used. They are placed in individual observation cages maintained at room temperature (24 ± 1°C). They are not stimulated during the interval between loss and recovery of the righting reflex. The onset is defined as the complete loss of the righting reflex, i. e., no attempt to move the head or body. Recovery is considered to have occurred when the animal after spontaneous righting would re-right itself within 15 s when placed on its back.

EVALUATION

The median anesthetic dose (AD_{50}) and the median lethal dose (LD_{50}) are determined from dose-response curves with at least 4 doses by the method of Litchfield and Wilcoxon (1949).

The data for onset and duration of action are analyzed statistically by Student's *t*-test.

MODIFICATIONS OF THE METHOD

Volwiler and Tabern (1930) determined the minimum effective dose in rats after subcutaneous injection of various barbiturates not being awakened when outer ear passage was tickled with a straw.

Büch et al. (1968) studied the distribution, anaesthetic potency and metabolic elimination of the optical isomers of methylphenobarbital in rats.

Glen (1977) described a method for the laboratory evaluation of the speed of onset of i.v. anesthesia in **mice**. Various clinically used intravenous anesthetics were compared. The technique involves a) determination of the medium hypnotic dose (HD_{50}) by plotting the probit value of the mice sleeping against dose on a logarithmic scale, b) plotting mean induction time over a range of doses against the logarithm of the dose and c) comparison of induction times at 1.25 HD_{50}. All doses were given over 1 s or 10 s. A 1-s injection was thought to be of most value in the of structure activity effects.

Chen et al. (1966) tested the anesthetic activity and the neuropharmacological spectrum of ketamine (CI-581) in mice, pigeons and monkeys.

Child et al. (1971) tested the anesthetic activity of alfaxolone (CT1341) in **mice, rats, rabbits, cats, dogs** and **monkeys**.

Janssen et al. (1975) tested onset and duration of anesthesia after etomidate in mice, rats, guinea pigs and dogs.

New intravenous anesthetics were reviewed by Reilly and Nimmo (1987).

The anesthetic potency of remifentanil in dogs in terms of reduction of enflurane *MAC* was tested by Michelsen et al. (1996).

Dingwall et al. (1993) described the tolerometer as a fast, automated method for the measurement of righting reflex latency.

REFERENCES AND FURTHER READING

Büch H, Buzello W, Neurohr O, Rummel W (1968) Vergleich von Verteilung, narkotischer Wirksamkeit und metabolis-

cher Elimination der optischen Antipoden von Methylphenobarbital. Biochem Pharmacol 17:2391–2398
Chen G, Ensor CR, Bohner B (1966) The Neuropharmacol of 2-(o-chlorophenyl)-2-methylaminocyclohexanone hydrochloride. J Pharm Exp Ther 152:332–339
Child KJ, Currie JP, Davis B, Dodds MG, Pearce DR, Twissell DJ (1971) The pharmacological properties in animals of CT1341 – a new steroid anaesthetic agent. Br J Anaesth 43:2–24
Christensen HD, Lee IS (1973) Anesthetic potency and acute toxicity of optically active disubstituted barbituric acids. Toxicol Appl Pharmacol 26:495–503
Dingwall B, Reeve B, Hutchinson M, Smith PF, Darlington CL (1993) The tolerometer: a fast, automated method for the measurement of righting reflex latency in chronic drug studies. J Neurosci Meth 48:11–114
Glen JB (1977) A technique for the laboratory evaluation of the speed of onset of i.v. anesthesia. Br J Anaesth 49:545–549
Janssen PAJ, Niemegeers CJE, Marsboom RPH (1975) Etomidate, a potent non-barbiturate hypnotic. Intravenous etomidate in mice, rats, guinea pigs, rabbits and dogs. Arch Int Pharmacodyn 214:92–132
Litchfield JT Jr, Wilcoxon FA (1949) Simplified method of evaluating dose-effect experiments. J Pharm Exp Ther 96:99–113
Michelsen LG, Salmenperä M, Hug CC, Sziam F, van der Meer D (1996) Anesthetic potency of remifentanil in dogs. Anesthesiol 84:865–872
Reilly CS, Nimmo WS (1987) New intravenous anaesthetics and neuromuscular blocking drugs. Drugs 34:98–135
Volwiler EH, Tabern DL (1930) 5,5-Substituted barbituric acids. J Am Chem Soc 52:1676–1679

E.9.1.3 EEG Threshold Test in Rats

PURPOSE AND RATIONALE

The electroencephalographic (EEG) threshold test has been used to determine and compare the potency of several CNS depressant agents (Bolander et al. 1984; Koskela and Wahlström 1989; Norberg and Wahlström 1988; Norberg et al. 1987). Korkmaz and Wahlström (1997) described in detail the protocol of the EEG burst suppression threshold test for the determination of CNS sensitivity to intravenous anesthetics in rats.

PROCEDURE

Adult Sprague-Dawley rats are housed at a reversed light/dark cycle and an ambient temperature of 23 ± 1°C. Twenty four hours prior to the EEG threshold test, the rats are placed in a tube restrainer. Twisted stainless steel wire and suitable surgical needles are used to sew the electrodes to the scalp above the frontal cortex. Since generalized changes in EEG recordings are used, this stainless steel material is adequate for recording purposes. Care is taken to prevent irritation of periosteal tissue. Since this procedure causes little discomfort, the use of local anesthetics and general anesthesia can be avoided.

For EEG threshold testing, the rat is placed on a warm cloth and held gently by the assistant. A needle is placed on one lateral tail vein and connected with an infusion pump. Crocodile clips are used to connect the electrodes to the EEG recorder and a crocodile clip is attached to one of the ears of the rats as a signal ground.

The EEG recording is closely observed by the technician. The changes in the EEG induced by the anesthetic agent are used to measure drug effects on the CNS. The normal EEG in an awake rat has a low amplitude and a frequency of approx. 30 cycles/s. During the first part of infusion, an increase in amplitude and a slight decrease in frequency are observed. At this stage of infusion, dependent on the anesthetic agent, jerks or sometimes convulsive episodes may occur. As the infusion continues, the frequency decreases and burst suppression periods appear. The loss of righting reflex occurs at this stage. When a burst suppression lasts one second or, the threshold criterion which is called ‘silent second’ is reached and the time is recorded. After the threshold determination, the rats are placed in the recovery room.

EVALUATION

The threshold dose is calculated by multiplying the time required to reach the threshold criterion with the dose administration rate. Threshold doses are determined for each anesthetic at various dose administration rates indicating the optimal dose administration rate.

MODIFICATIONS OF THE METHOD

Wauquier et al. (1988) studied relationships between quantitative EEG measures and pharmacodynamics of alfentanil in dogs. Before, during and up to 3 h after infusion, the effects of 3 doses on 6 quantitative EEG measures (zero-crossing frequency, root mean square amplitude, spectral edge, relative delta, alpha and beta power) were assessed.

REFERENCES AND FURTHER READING

Bolander HG, Wahlström G, Norberg L (1984) Reevaluation of potency and pharmacokinetic properties of some lipid-soluble barbiturates with an EEG-threshold method. Acta Pharmacol Toxicol 54:33–40
Korkmaz S, Wahlström G (1997) The EEG burst suppression threshold test for the determination of CNS sensitivity to intravenous anesthetics in rats. Brain Res Protocols 1:378–384
Koskela T, Wahlström G (1989) Comparison of anaesthetic and kinetic properties of thiobutabarbital, butabarbital and hexobarbital after intravenous threshold doses in the male rat. Pharmacol Toxicol 64:308–313

Norberg L, Wahlström G (1988) Anaesthetic effects of flurazepam alone and in combination with thiopental or hexobarbital evaluated with an EEG-threshold method in male rats. Arch Int Pharmacodyn Ther 292:45–57

Norberg L, Wahlström G, Bäckström T (1987) The anaesthetic potency of 3α-hydroxy-5α-pregnan-20-one and 3α-hydroxy-5β-pregnan-20-one determined with an intravenous EEG threshold method in male rats. Pharmacol Toxicol 61:42–47

Wauquier A, De Ryck M, Van den Broeck W, Van Loon J, Melis W, Janssen P (1988) Relationships between quantitative EEG measures and pharmacodynamics of alfentanil in dogs. Electroencephalogr Clin Neurophysiol 69:550–560

E.9.1.4 Efficacy and Safety of Intravenous Anesthetics

PURPOSE AND RATIONALE

Besides determination of the ratio between anesthetic and lethal dose, intravenous anesthetics have to be tested for their influence on the cardiovascular and pulmonary system. Borkowski et al. (1990 described a method to compare intravenous anesthetics in rabbits.

PROCEDURE

Adult New Zealand White rabbits with a mean weight of 4.5 kg are used. To provide access for direct blood pressure measurement and arterial blood samples, an 18-gauge catheter is implanted into the left carotid artery under halothane anesthesia. Following a minimum 24-h recovery period, the rabbit is placed in a sling and a pneumograph is fitted around the rabbit's caudal thorax at the level of 10th to 12th ribs to monitor respiratory rate and pattern. From the arterial catheter blood is withdrawn for blood gas analysis. Then the catheter is connected to a blood-pressure transducer. A 10-min acclimatization period is allowed before control measurements are recorded. Each rabbit serves as its own control in that cardiopulmonary parameters and responses to noxious stimuli are determined before anesthesia is induced. The right marginal ear vein is catheterized with a 22-gauge catheter, which is secured with adhesive tape, flushed with physiologic sterile saline and used for the administration of the anesthetic agents.

One third of the dose of the anesthetic to be tested is injected manually over a 1-min period. When the rabbit is relaxed it is removed from the sling and is placed in left lateral recumbence on a heating blanket. The degree of muscle tension and reaction to noxious stimuli are determined while the rabbit is in the sling and at 15 min intervals following anesthesia. The assessments performed include those of jaw tone, leg muscle tone, palpebral reflex, corneal reflex, ear pinch reflex and pedal withdrawal reflex. Jaw tone is evaluated subjectively by pulling the lower jaw open by an index finger. Leg muscle tone is evaluated by flexion and extension of the right rear leg according to subjective scores. The corneal reflex is tested by placing a moistened cotton swab on the cornea. The palpebral reflex is tested by touching the medial canthus with a dry cotton swab. Assessment of the ear pinch reflex is performed by applying a compression force with an alligator clip. The pedal withdrawal reflex is determined by applying the same clip on the right rear fifth digit at the distal phalanx.

Cardiopulmonary parameters and rectal body temperature are determined while the rabbit is in the sling and also at 15 min intervals following induction of anesthesia with the rabbit in lateral recumbency. Heart rate, mean arterial blood pressure, respiratory rate and respiratory pattern are calculated from tracings from the physiological recorder. Arterial blood pH, partial pressure of oxygen (PaO_2), and partial pressure of carbon dioxide ($PaCO_2$) are determined from arterial blood samples.

EVALUATION

The heart rate, mean arterial blood pressure, respiratory rate, pH, PaO_2 and $PaCO_2$ are analyzed using a two-factor analysis on repeated measures. The control values are treated as covariate to allow standardization of the inherent variation between rabbits. The single *t*-test for paired differences is used to compare control values to data obtained during the later testing intervals. The standard error of the mean (SEM) is calculated for each variable at each time interval. Data for muscle tone and responses to noxious stimuli are calculated as frequency percentages. The Fisher's Exact test is used to compare between treatments. For all of the statistical analyses, a *p*-value of less than 0.05 is considered significant.

MODIFICATIONS OF THE METHOD

Details of anesthesia in the rabbit were also described by Murdock (1969).

Peeters et al. (1988) performed a comparative study of four methods for general anesthesia in rabbits.

Glenn (1980) examined the anesthetic activity of propofol (ICI 35868) in mice, rats, rabbits, cats pigs and monkeys including cardiovascular and respiratory parameters and EEG studies.

REFERENCES AND FURTHER READING

Borkowski GL, Dannemann PJ, Russel GB, Lang CM (1990) An evaluation of three intravenous regimens in New Zealand rabbits. Lab Anim Sci 40:270–276

Glen JB (1980) Animal studies of the anesthetic activity of ICI 35868. Br J Anaesth 52:731–742
Murdock HR (1969) Anesthesia in the rabbit. Fed Proc 28:1510–1516
Peeters ME, Gil D, Teske E, Eyzenbach V, v.d. Brom WE, Lumeij JT, de Vries HW (1988) Four methods for general anesthesia in rabbits: a comparative study. Lab Animals 22:355–360

E.9.2 Inhalation Anesthesia

E.9.2.1 General Considerations

PURPOSE AND RATIONALE

The efficacy and safety of new inhalation anesthetics has to be evaluated in pharmacological experiments. Robbins (1946) defined the anesthetic AD_{50} as the concentration of anesthetic at which 50% of mice failed to right themselves for 15 s when placed in a rotating bottle with a known concentration of anesthetic. The concentration of the anesthetic that caused apnea in 50% of the mice in 10 min was defined as the LD_{50} and the ratio LD_{50}/AD_{50} as and an index of safety.

Wolfson et al. (1972) recommended brain anesthetic concentration for construction of anesthetic indices.

REFERENCES AND FURTHER READING

Fang Z, Gong D, Ionescu P, Laster MJ, Eger II EI, Kendig J (1997) Maturation decreases ethanol minimum alveolar anesthetic concentration (*MAC*) more than desflurane *MAC* in rats. Anaesth Analg 84:852–858
Robbins BH (1946) Preliminary studies of the anesthetic activity of fluorinated hydrocarbons. J Pharmacol Exp Ther 86:197–204
Wolfson B, Dorsch SE, Kuo TS, Siker ES (1972) Brain anesthetic concentration – a new concept. Anesthesiol 36:176–179

E.9.2.2 Screening of Volatile Anesthetics

PURPOSE AND RATIONALE

A simple technique for preliminary testing of anesthetic agents is the introduction of a measured amount of volatile liquid into a covered glass container of known volume. If the density and molecular weight of the liquid are known, the volume % concentration of the anesthetic mixture can be calculated (assuming 1 mol of vapor = 22.4 l). Mice or rats are introduced into the chamber and the quality of anesthesia is noted. Conditions are then adjusted until the anesthetic concentration has been established.

PROCEDURE

Male NMRI mice weighing 20–25 g or male Wistar rats weighing 250–300 g are used. A wide-mouth, screw-cap glass jar of 3 Liter volume is flushed with oxygen for 1 min and a measured amount of the volatile substance is placed on the bottom through a suitable syringe. The amount is calculated to give 1.25 vol% concentration of vapor in the jar (or a logarithmic multiple of 1.25%, i. e., 0.63, 2.5, 5.0, 10.0). The jar is closed and evaporation of the substance is facilitated by gentle rotation of the jar. One rat or 5 mice are quickly placed from a beaker into the jar, and the jar is immediately closed. Every 15 s the jar is gently rotated and the time noted for each animal to become anesthetized (loss of righting reflexes). The procedure is repeated until all animals are anesthetized. Induction should occur not sooner than 30 s and not later than 5 min. The animals are allowed to remain in the anesthesia jar for 10 min, with testing of righting reflexes until they are quickly removed into room air. The time of recovery to righting or walking is recorded for each animal. Postanesthetic analgesia is tested by gently pressing the base of the tail every min until recovery has occurred. Recovery time is defined as the time in min until the mouse spontaneously moves in upright position. If induction time is shorter than 30 s or longer than 10 min, the concentration of anesthetic is decreased or increased until the proper concentrations is found.

EVALUATION

The results are reported as mean induction time and mean recovery time. Twenty-four-hour survival rate is recorded for latent toxicity.

MODIFICATIONS OF THE METHOD

Burns et al. (1961) used a simplified mouse test apparatus with a small container and an open circuit technique.

Raventós (1956) used cats, dogs and monkeys to evaluate the cardiovascular effects of fluothane.

REFERENCES AND FURTHER READING

Burgison RM (1964) Animal techniques for evaluating anesthetic drugs. In: Nodine JH, Siegler PE (eds) Animal and Clinical Techniques in Drug Evaluation. Year Book Med. Publ., Inc., Chicago, pp 369–372
Burns THS, Hall JM, Bracken A, Gouldstone G (1961) Investigation of new fluorine compounds in anaesthesia (3): The anaesthetic properties of hexafluorobenzene. Anaesthesia 16:333–339
Raventós J (1956) Action of fluothane – A new volatile anaesthetic. Br J Pharmacol 11:394

Ravento J, Spinks A (1958) Development of halothane. Methods of screening volatile anaesthetics. Manchester Univ Med School Gaz 37:55

Van Poznak A, Artusio JF Jr (1960) Anesthetic properties of a series of fluorinated compounds: II. Fluorinated ethers. Toxicol Appl Pharmacol 2:374

E.9.2.3 Determination of Minimal Alveolar Anesthetic Concentration (MAC)

PURPOSE AND RATIONALE

The term **"minimum alveolar anesthetic concentration" (MAC)** was coined by Merkel and Eger (1963) as an index to compare various anesthetic agents.

The use of *MAC* which represents the partial anesthetic pressure in the brain has gained wide acceptance (Eger et al. 1965; Quasha et al. 1980).

For **man**, Saidman and Eger (1964) defined *MAC* as the point at which 50% of the patients moved in response to a surgical incision.

A method for determining minimum alveolar concentration of anesthetic in the **rat** was published by Waizer et al. (1973). Kashimoto et al. (1997) determined the minimum alveolar concentration of sevoflurane in rats. Eger et al. (1999) studied maximum alveolar anesthetic concentration of fluorinated alkanols in rats and dicussed the relevance to theories of narcosis. Eger et al. (2003) studied additive minimum alveolar concentration (MAC) effects o halothane and isofluroane in rats.

Issues in the design and interpretation of minimum alveolar anesthetic concentration (MAC) studies were discussed by Sonner (2002).

PROCEDURE

Minimum alveolar anesthetic concentrations (MAC) are determined in Sprague Dawley rats weighing 300–450 g. Each rat is placed in an individual gas tight plastic cylinder closed at both ends by rubber stoppers. The stoppers are pierced with holes for various purposes. A rectal temperature probe (temperature maintained between 36°C and 38.5°C) and the rat's tail are drawn separately through holes in the rubber stopper closing the distal end of the cylinder. Delivered gases at an average inflow rate of 1L/min to each rat enter through ports at at the head (proximal) end of the cylinder and exit at the tail (distal end), a flow to minimize rebreathing (inspired $CO_2 < 10$ mm Hg). Exiting gases are scavenged.

The anesthetics are introduced from conventional vaporizers. For the determination of MAC, an initial concentration is used that permits movement of the rats in response to noxious stimulation. A tail clamp is applied for 1 minor until the animal moves, and the anesthetic partial pressure is measured by gas chromatography. If the animal moves, the partial pressure is increased by 0.2% or 0.3% atmospheres. After equilibration for 30 min, the tail clamp is appliedagaion and the anesthetic partial pressure measured by gas chromatography. This procedure is repeated until the partial pressures bracketing movement-nonmovement are determined for each rat.

EVALUATION

MAC is defined as the average of the partial pressures that just prevented movement in response to clamping of the tail. Differences between anesthetics are accepted at $P < 0.05$.

MODIFICATIONS OF THE METHOD

Fang et al. (1997) found that maturation decreases ethanol minimum alveolar anesthetic concentration (*MAC*) more than desflurane *MAC* in **rats**.

Gong et al. (1998) assessed the effect of rat strain on susceptibility to anesthesia and convulsions produced by inhaled compounds.in five different rat strains. Strain minimally influenced anesthetic and convulsant requirements of inhaled compounds in rats.

Doquier et al. (2003) studied the minimum alveolar anesthetic concentration of volatile anesthetics in rats as tools to assess antinociception in animals.

Determination of the minimal alveolar concentration (*MAC*) of halothane in the white New Zealand **rabbit** was published by Davis et al. (1975).

Determination of an anesthetic index (Apnea/*MAC*) in experiments in **dogs** has been proposed by Regan and Eger (1967).

Murphy and Hug (1982), Hall et al. (1987) used the reduction of enflurane *MAC* values in **dogs** as parameter for the anesthetic potency of fentanyl or sufentanyl, respectively.

Seifen et al. (1987) used *MAC* values for comparison of cardiac effects of enflurane, isoflurane, and halothane in the **dog heart-lung preparation**.

Ide et al. (1998) used airway occlusion in **cats** as a noxious respiratory stimulus that induces a visceral sensation of choking for determination of minimum alveolar anesthetic concentrations during halothane, isoflurane, and sevoflurane anesthesia. These values were compared with *MAC* values for somatic noxious stimuli such as toe pinch or tetanic stimulus. The authors recommended this method as a new concept for *MAC* determination.

Eger et al. (1988) determined minimum alveolar concentration of fluorinated anesthetics in **pigs**.

REFERENCES AND FURTHER READING

Davis NL, Nunnally RL, Malinin TI (1975) Determination of the minimal alveolar concentration (*MAC*) of halothane in the white New Zealand rabbit. Br J Anesthesiol 47:341–345

Doquier MA, Lavand'homme P, Ledermann C, Collet V, de Kock M (2003) Can determining the minimum alveolar anesthetic concentration of volatile anesthetic be used as an objective tool to assess antinociception in animals? Anesth Analg 97:1033–1039

Eger EI II, Saidman LJ, Brandstater B (1965) Minimum alveolar anesthetic concentration: a standard of anesthetic potency. Anesthesiol 26:756–763

Eger EI II, Johnson BH, Weiskopf RB, Holmes MA, Yasuda N, Targ A, Rampil IJ (1988) Minimum alveolar concentration of I-653 and isoflurane in pigs. Anaesth Analg 67:1174–1176

Eger EI II, Ionescu P, Laster MJ, Gong D, Hudlicky T, Kendig JJ, Harrius RA, Trudell JR, Pohorille A (1999) Maximum alveolar anesthetic concentration of fluorinated alkanols in rats: relevance to theories of narcosis. Anesth Analg 88:867–876

Eger EI II, Xing Y, Laster M, Sonner J, Antognini JF, Carstens E (2003) Halothane and isofluroane have additive minimum alveolar concentration (MAC) effects in rats. Anesth Analg 96:1350–1353

Fang Z, Gong D, Ionescu P, Laster MJ, Eger II EI, Kendig J (1997) Maturation decreases ethanol minimum alveolar anesthetic concentration (*MAC*) more than desflurane *MAC* in rats. Anaesth Analg 84:852–858

Gong D, Fang Z, Ionescu P, Laster M, Terrell RC, Eger EI II (1998) Strain minimally influences anesthetic and convulsant requirements of inhaled compounds in rats. Anesth Analg 87:963–966 Eger EI II

Hall RI, Murphy MR, Hug CC (1987) The enfluorane sparing effect in dogs. Anesthesiol 67:518–525

Ide T, Sakurai Y, Aono M, Nishino T (1998) Minimum alveolar anesthetic concentrations for airway occlusion in cats: A new concept of minimum alveolar anesthetic concentration-airway occlusion response. Anaesth Analg 86:191–197

Kashimoto S, Furuya A, Nonoka A, Oguchi T,Koshimizu M, Kumazawa T (1997) The minimum alveolar concentration of sevoflurane in rats. Eur J Anesthesiol 14:395–361

Merkel G, Eger EI II (1963) A comparative study of halothane and halopropane anesthesia. Anesthesiol 24:346–357

Murphy MR, Hug CC (1982) The anesthetic potency of fentanyl in terms of its reduction of enflurane *MAC*. Anesthesiol:485–488

Quasha AL, Eger EI II, Tinker JH (1980) Determination and applications of *MAC*. Anesthesiol 53:315–334

Regan MJ, Eger EI II (1967) Effect of hypothermia in dogs on anesthetizing and apneic doses of inhalation agents. Determination of the anesthetic index (Apnea/*MAC*). Anesthesiol 28:689–700

Saidman LJ, Eger EI II (1964) Effect of nitrous oxide and narcotic premedication on the alveolar concentration of halothane required for anesthesia. Anesthesiol 25:302–306

Seifen E, Seifen AB, Kennedy RH, Bushman GA, Loss GE, Williams TG (1987) Comparison of cardiac effects of enflurane, isoflurane, and halothane in the dog heart-lung preparation. J Cardiothor Anesth 1:543–553

Sonner JM (2002) Issues in the design and interpretation of minimum alveolar anesthetic concentration (MAC) studies. Anesth Analg 95:609–614

Waizer PR, Baez S, Orkin LR (1973) A method for determining minimum alveolar concentration of anesthetic in the rat. Anesthesiol 39:394–397

E.9.2.4 Efficacy and Safety of Inhalation Anesthetics

PURPOSE AND RATIONALE

To assess the safety margin of a inhalation anesthetic not only the ED_{50} values but also the maximally effective dose and the dose with a minimal danger of fatal outcome should be determined. In particular, *cardiovascular parameters* are observed (Kissin et al. 1983).

PROCEDURE

Male Sprague Dawley rats weighing 300–350 g are placed into a clear chamber with the tail protruding from a special opening. An anesthetic-oxygen non-humidified mixture is directed into the chamber at a rate of 4 l/min. The inhalation anesthetics, e. g., halothane or isoflurane, are vaporized in Draeger vaporizers and the level in the chamber is monitored with a gas analyzer which is calibrated with a mass spectrometer. Rectal temperature is monitored and maintained at 37°C with a heating pad. Each rat is exposed to only one pre-determined concentration of anesthetic for 30 min, at which time the presence or absence of the end point of anesthesia is determined. For the lethal end point, rats are tracheotomized and ventilated at 60 strokes/min through an endotracheal catheter. Tidal volume is adjusted to maintain Pa_{CO2} at 40 ± 5 mm Hg.

As endpoints of anesthesia are used:

- Loss of righting reflex. The test is regarded as positive if the animal fails to right itself with all four feet on the floor within 15 s after being placed in a side position.
- Prevention of purposeful movements response to a noxious stimulus. The animals are stimulated for 60 s by placement of a 1-kg weight on the middle of the tail. Only the purposeful movement of the head or legs is considered to be a response.
- Prevention of the heart rate increase to a noxious stimulus (ECG signals). An increase in heart rate of greater than 1% is regarded as a positive response.
- The end point for the lethal effect is 7 mm Hg in the femoral artery with artificial respiration.

With each of the anesthetics, four series of experiments are performed: to determine the righting reflex, purposeful movement response, heart rate response,

and lethal effect. The concentrations of the test compounds and the standard are spaced equally between the above-mentioned doses.

After determination of the heart rate effect and the lethal effect, the rats are sacrificed for determinations of brain tissue concentrations. The whole brain is removed and tissue anesthetic concentration is determined by gas chromatography.

EVALUATION

For calculation of the dose-effect curves, the probit method of statistical analysis is used.

For the assessment of anesthetic safety, not only the therapeutic ratio (LD_{50}/ED_{50}) but also the standard safety margin

$$SSM = (LD_5 - ED_{95})/ED_{95} \times 100$$

is used. This represents the percentage by which the ED_{95} has to be increased before LD_5 is reached.

CRITICAL ASSESSMENT OF THE METHOD

The standard safety margin has definitive advantages over therapeutic ratio. In contrast to the LD_{50}/ED_{50} index, the standard safety margin is influenced not only by the distance between central points of the anesthetic and lethal dose-effect curves, but also by the slope of these curves.

MODIFICATIONS OF THE METHOD

A similar concept, based on response to tail clamping, respiratory arrest and cardiovascular failure in the **rat** was published as anesthetic index by Wolfson et al. (1973).

An other attempt to determine anesthetic requirements in rats was published by White et al. (1974).

Kissin et al. (1984) studied the morphine-halothane interaction in rats.

Fukuda et al. (1996) investigated the effects of sevoflurane and isoflurane on bupivacaine-induced arrhythmias and seizures in rats.

Kanaya et al. (1998) Compared myocardial depression by sevoflurane, isofluorane, or halothane in **cultured neonatal rat ventricular myocytes**. Changes in beating rate and amplitude during exposure to the anesthetics were measured.

Chaves et al. (2003) used non-invasive electrocardiography in **mice** to study the effects of intravenous and inhalation anesthetics and of age.

Krantz et al. (1941, 1953) described an anesthetic index between surgical anesthesia (cornea and wink reflexes abolished) and respiratory failure in **dogs**.

Van Poznak and Artusio (1960a, b) determined the anesthetic properties of fluorinated compounds in dogs using a face mask for the induction of anesthesia and a cuffed endotracheal tube later on. ECG (lead II) and EEG were monitored.

Steffey and Howland (1978) determined the potency of enflurane in dogs in comparison with halothane and isoflurane.

Johnson et al. (1998) compared isoflurane with sevoflurane for anesthesia induction and recovery in adult dogs.

Salmempera et al. (1992) studied in dogs the potency of remifentanil, a short acting opioid analgesic, which is used as anesthetic adjunct by variable-rate infusion. Enfluorane minimal alveolar concentration was measured by the tail-clamp method in dogs before and after sequential infusion of various doses of remifentanil. The plasma concentration causing a 50% reduction of enfluorane minimal alveolar concentration was determined.

Kataoka et al. (1994) studied the negative inotropic effects of sevoflurane, isoflurane, enflurane and halothane in canine blood-perfused papillary muscles.

Hirano et al. (1995) compared the coronary hemodynamics during isoflurane and sevoflurane anesthesia in dogs.

Mutoh et al. (1997) compared the cardiopulmonary effects of sevoflurane with those of halothane, enflurane, and isoflurane, in dogs.

Hashimoto et al. (1994) examined the effects of sevoflurane and halothane on the effective refractory period and ventricular activation in a canine myocardial infarction model.

The effects of desflurane, sevoflurane and halothane on postinfarction spontaneous dysrhythmias in dogs were examined by Novalija et al. (1998).

Cardiopulmonary effects in **cats** were studied for desflurane by McMurphy and Hodgson (1996), for sevoflurane by Hisaka et al. (1997).

Saeki et al. (1996) determined the effects of sevoflurane, enflurane, and isoflurane on baroreceptor-sympathetic reflex in **rabbits**.

Hanagata et al. (1995) found that isoflurane and sevoflurane produce a dose-dependent reduction in the shivering threshold in rabbits.

Antognini and Eisele (1993) determined anesthetic potency and cardiopulmonary effects of enfluorane, halothane, and isofluorane in **goats.**

The effects of multiple administrations of sevoflurane to cynomolgus **monkeys** were evaluated by Soma et al. (1995).

The effect of inhalation anesthetics on the **respiratory system** was investigated in several studies:

Mazzeo et al. (1996) compared the relaxing effects of desflurane and halothane at various *MAC*s on isolated proximal and distal airways of dogs precontracted with acetylcholine.

Hashimoto et al. (1996) compared the bronchodilating effect of sevoflurane, enflurane and halothane in dogs using a superfine fiberoptic bronchoscope. The dogs were anesthetized with pentobarbital, paralyzed with pancuronium, and the lungs were mechanically ventilated. The endotracheal tube had an additional lumen to insert the superfine fiberoptic bronchoscope (outer diameter 2.2 mm) which was located between a second and third bronchial bifurcation to continuously monitor the bronchial cross-sectional area of third or forth generation bronchi. Bronchoconstriction was produced by histamine injection and infusion. The bronchial cross-sectional area was printed out by a video-printer at the end of expiration and was calculated on a computer using an image program after various *MAC*s of the different inhalation anesthetics.

Mitsuhata et al. (1994) induced systemic anaphylaxis in dogs sensitized to Ascaris suum by intravenous injection of the antigen and measured pulmonary resistance and dynamic pulmonary compliance. Sevoflurane was as effective as isoflurane in attenuating bronchoconstriction associated with anaphylaxis in dogs.

Cervin and Lindberg (1998) examined the short-term effects of halothane, isoflurane and desflurane on mucociliary activity in the rabbit maxillary sinus *in vivo*.

REFERENCES AND FURTHER READING

Antognini JF, Eisele PH (1993) Anesthetic potency and cardiopulmonary effects of enfluorane, halothane, and isofluorane in goats. Lab Anim Sci 43:607–610

Cervin A, Lindberg S (1998) Changes in mucociliary activity may be used to investigate the airway-irritating potency of volatile anaesthetics. Br J Anaesth 80:475–480

Chaves AA, Dech SJ, Nakayama T, Hamlin RL, Bauer JA, Carnes CA (2003) Age and anesthetic effects on murine electrocardiography. Life Sci 72:2401–2412

Fukuda H, Hirabayashi Y, Shimizu R, Saitoh K, Mitsuhata H (1996) Sevoflurane is equivalent to isoflurane for attenuating bupivacaine-induced arrhythmias and seizures in rats. Anesth Analg 83:570–573

Hanagata K, Matsukawa T, Sessler DI, Miyaji T, Funayama T, Koshimizu M, Kashimoto S, Kumazawa T (1995) Isoflurane and sevoflurane produce a dose-dependent reduction in the shivering threshold in rabbits. Anesth Analg 81:581–584

Hashimoto H, Imamura S, Ikeda K, Nakashima M (1994) Electrophysiological effects of volatile anesthetics, sevoflurane and halothane, in a canine myocardial infarction model. J Anesth 8:93–100

Hashimoto Y, Hirota K, Ohtomo N, Ishihara H, Matsuki A (1996) *In vivo* direct measurement of the bronchodilating effect of sevoflurane using a superfine fiberoptic bronchoscope: Comparison with enflurane and halothane. J Cardiothorac Vasc Anesth 10:213–216

Hirano M, Fujigaki T, Shibata O, Sumikawa K (1995) A comparison of coronary hemodynamics during isoflurane and sevoflurane anesthesia in dogs. Anesth Analg 80:651–656

Hisaka Y, Ohe N, Takase K, Ogasawara S (1997) Cardiopulmonary effects of sevoflurane in cats: Comparison with isoflurane, halothane, and enflurane. Res Vet Sci 63:205–210

Johnson RA, Striler E, Sawyer DC, Brunson DB (1998) Comparison of isoflurane with sevoflurane for anesthesia induction and recovery in adult dogs. Am J Vet Res 59:487–481

Kanaya N, Kawana S, Tsuchida H, Miyamoto A, Ohshika H, Namiki A (1998) Comparative myocardial depression of sevoflurane, isofluorane, and halothane in cultured neonatal rat ventricular myocytes. Anesth Analg 67:1041–1047

Kataoka Y, Manabe M, Takimoto E, Tokai H, Aono J, Hishiyama K, Ueda W (1994) Negative inotropic effects of sevoflurane, isoflurane, enflurane and halothane in canine blood-perfused papillary muscles. Anesth Resusc 30:73–76

Kissin I, Morgan PL, Smith LR (1983) Comparison of isoflurane and halothane safety margins in rats. Anesthesiol 58:556–561

Kissin I, Kerr CR, Smith LR (1984) Morphine-halothane interaction in rats. Anesthesiol 60:553–561

Krantz JC Jr, Carr CJ, Forman SE, Evans WE Jr, Wollenweber H (1941) Anesthesia. IV. The anesthetic action of cyclopropylethyl ether. J Pharmacol Exp Ther 72:233–244

Krantz JC Jr, Carr CJ, Lu G, Bell FK (1953) Anesthesia. XL. The anesthetic action of trifluoroethyl vinyl ether. J Pharm Exp Ther 108:488–495

McMurphy RM, Hodgson DS (1996) Cardiopulmonary effects of desflurane in cats. Am J Vet Res 57:367–370

Mazzeo AJ, Cheng EY, Bosnjak ZJ, Coon RL, Kampine JP (1996) Differential effects of desflurane and halothane on peripheral airway smooth muscle. Br J Anaesth 76:841–846

Mitsuhata H, Saitoh J, Shimizu R, Takeuchi H, Hasome N, Horiguchi Y (1994) Sevoflurane and isoflurane protect against bronchospasm in dogs. Anesthesiol 81:1230–1234

Mutoh T, Nishimura R, Kim HY, Matsunage S, Sasaki N (1997) Cardiopulmonary effects of sevoflurane, compared with halothane, enflurane, and isoflurane, in dogs. Am J Vet Res 58:885–890

Novalija E, Hogan QH, Kulier AH, Turner LH, Bosnjak ZJ (1998) Effects of desflurane, sevoflurane and halothane on postinfarction spontaneous dysrhythmias in dogs. Acta Anaesthesiol Scand 42:353–357

Saeki Y, Hasegawa Y, Shibamoto T, Yamaguchi Y, Hayashi T, Tanaka S, Wang GH, Koyama S (1996) The effects of sevoflurane, enflurane, and isoflurane on baroreceptor-sympathetic reflex in rabbits. Anesth Analg 82:342–348

Soma LR, Terney WJ, Hogan GK, Satoh N (1995) The effects of multiple administrations of sevoflurane to cynomolgus monkeys: Clinical pathologic, hematologic and pathologic study. Anesth Analg 81:347–352

Van Poznak A, Artusio F Jr (1960a) Anesthetic properties of a series of fluorinated compounds. I. Fluorinated hydrocarbons. Toxicol Appl Pharmacol 2:363–373

Van Poznak A, Artusio F Jr (1960b) Anesthetic properties of a series of fluorinated compounds. II. Fluorinated ethers. Toxicol Appl Pharmacol 2:363–373

Wolfson B, Kielar CM, Lake C, Hetrick WD, Siker ES (1973) Anesthetic index – a new approach. Anesthesiol 38:583–586
White PF, Johnston RR, Eger EI II (1974) Determination of anesthetic requirement in rats. Anesthesiol 40:52–57
Salmempera M, Wilson D, Szlam F, Hugg CC Jr (1992) Anesthetic potency of the opioid GI 87084B in dogs. Anesthesiology 77:A368
Steffey EP, Howland D (1978) Potency of enflurane in dogs: comparison with halothane and isoflurane. Am J Vet Res 39:573–577

E.10 NMRI Methods in Psychoneuropharmacology

E.10.1 General Considerations

PURPOSE AND RATIONALE

Magnetic resonance imaging (MRI) is the preferred technique for the visualization of lesions in the brain and spinal cord of patients with MS. It visualizes the resonance signals of tissue protons when they are placed in a time-varying strong magnetic field. The most frequently used parameters measured in MS are the spin-lattice relaxation time (T_1) and the spin-spin relaxation time (T_2). MRI is routinely used as a tomographic imaging technique, where anatomical pictures are created of 1-mm-thick tissue sections. The contrast differences between brain structures in most MRI techniques are determined by the different densities and diffusion of protons, as well as differences in relaxation times. T_2 images are sensitive to water and, because all pathological alterations in MS brains are associated with altered distribution of tissue water (edema), this technique is highly useful for visualization of the spatial distribution of lesions. Contrast in T_1 images is determined mainly by different lattice densities. Dense structures, such as compact white matter, have low T_1 values, whereas relatively loose structures, such as gray matter or lesions, have higher T_1 values.

To distinguish inflammatory active from inactive lesions, the paramagnetic dye gadolinium-DTPA is intravenously injected (0.1–0.3 mmol/kg) and, in areas of increased blood–brain barrier permeability, leaks into the brain parenchyma, causing local enhancement of the T_1-weighted signal intensity.

A third important MRI technique in MS is magnetization transfer ratio (MTR) imaging. The MTR of a given tissue is defined as the ratio of free protons versus protons bound to tissue macromolecules.

Besides general applications to body composition in animals (Mitchell et al. 2001; Changani et al. 2003; Mirsattari et al. 2005) NMR studies contributed to evaluation of drugs in psychoneuropharmacology.

REFERENCES AND FURTHER READING

Changani KK, Nicholson A, White A, Latcham JK, Reid DG, Clapham JC (2003) A longitudinal magnetic resonance imaging (MRI) study of differences in abdominal fat distribution between normal mice, and lean overexpressors of mitochondrial uncoupling protein-3 (UCP-3). Diabet Obes Metab 5:99–105
Mirsattari SM, Bihari F, Leung S, Menon RS, Wang Z, Ives JR, Bartha R (2005) Physiological monitoring of small animals during magnetic resonance imaging. J Neurosci Method 144:207–213
Mitchell AD, Scholz AM, Wang PC, Song H (2001) Body composition of the pig by magnetic resonance imaging. J Anim Sci 79:1800–1813

E.10.2 NMRI Psychopharmacological Studies in Rats

E.10.2.1 NMRI Study of Experimental Allergic Encephalomyelitis in Rats

PURPOSE AND RATIONALE

Duckers et al. (1997) studied the effect of a neurotropic treatment on cortical lesion development in experimental allergic encephalomyelitis in rats by longitudinal *in vivo* magnetic resonance imaging methods.

PROCEDURE

Animals

Female Lewis rats weighing approximately 190 g were used for*in vivo* proton MRI. The rats were housed individually in Macrolon cages and had free access to rat chow and water during the 5-month study. The rats were divided at random into three groups. In two groups of rats chronic experimental allergic encephalomyelitis was induced by s.c. injection of myelin/adjuvant. The third group was injected with vehicle.

Immunization of Animals

Two hours before inoculation, spinal cords from Duncan Hartley guinea pigs were dissected and homogenized in an equal volume of phosphate-buffered saline (PBS) (pH 7.3; 1 g spinal cord in 1 ml PBS). Equal parts of guinea pig spinal cord homogenate in PBS and complete Freund's adjuvant (CFA) were mixed as described by Lassmann (1983) and Wisniewski and Keith (1977).

Anesthetized rats were sensitized by injecting 0.3 ml of the CNS emulsion in the dorsum pedis of the hindlimbs. Age-matched controls were challenged

similarly except that the emulsion solely contained PBS in CFA. The day of inoculation was designated day 0 post-inoculation (dpi 0).

Peptide Treatment

For the neurotrophic treatment, an $ACTH_{4–9}$ analog devoid of corticotrophic activity [Org2766, H-Met(O_2)-Glu-His-Phe-D-Lys-Phe-OH] was used. The heptapeptide has well-documented neurotrophic properties, as demonstrated previously in different animal models for peripheral and central nerve damage (Bär et al. 1990; Stand et al. 1991). The rats with chronic experimental allergic encephalomyelitis were given s.c. injections, in the neck, of either the $ACTH_{4–9}$ analog (75 µg/kg in 0.5 ml saline) or 0.5 ml saline every 48 h. Age-matched control animals received saline injections every 48 h. Treatment was started on the day of inoculation and continued until the experiment ended 21 weeks after inoculation.

Neurological Status of the Rats

The clinical status of the rats was evaluated every 48 h by weighing the rats and scoring their neurological status on a 0–9 ordinal scale. The scores represent the following neurological symptoms: grade 0, no visible neurological symptoms; grade 1, loss of tail tip reflex; grade 2, flaccid tail; grade 3, moderate paraparesis, manifested as minor locomotion disturbances; grade 4, severe paraparesis accompanied by lordosis, severe disturbed locomotion and severe weight loss; grade 5, one paralysed hindlimb; grade 6, complete paralysis; grade 7, paralysis from diaphragm upwards; grade 8, tetraplegia, only head movements possible; grade 9, death due to chronic experimental allergic encephalomyelitis.

T2-Weighted and Short Tau Inversion Recovery Magnetic Resonance Imaging

Animals were examined by using MRI at 5, 10, and 20 weeks post-inoculation. The rats were anesthetized with Hypnorm (containing 10 mg/ml fluanisone and 0.315 mg/ml fentanyl citrate, dose 0.6 ml/kg s.c.) and Stesolid (diazepam). After intubation, the rats were mechanically ventilated with 70% oxygen and 30% N_2O with 0.5% v/v halothane.

The ^{1}H-MRI experiments were performed with a SISCO 200/400 system (SISCO, Palo Alto, Calif., USA) operating at 4.7 T and equipped with actively shielded gradients (max. gradient 18 Mt/m). In all experiments, an Alderman-Grant type radio frequency coil with an inner diameter of 5 cm was used. For accurate and reproducible positioning, animals were mounted in a stereotaxic holder positioned on the coil support. For each animal, a sagittal T1W scout image [echo time (TE) 20 ms, repetition time (TR) 600 ms] outlined the start (border of frontal lobe and olfactory bulb) and endpoint (border of cerebellum–spinal cord) for subsequent coronal multislice experiments used to quantify the extent of tissue damage.

All MRI experiments were based on a spin-echo sequence with 5-ms sinc-modulated radiofrequency pulses. A total of 11 T2W coronal multislice images per animal was obtained (slice thickness 1.1 mm, interslice gap 0.7 mm), using a TR of 2 s and a TE of 60 ms; two transients were averaged. The field of view was $5 \times 5\,cm^2$; 128 points were acquired in the phase encoding direction and 512 points in the read-out direction. After processing, these were presented in a square matrix of 512×512 pixels.

Subsequently, multislice coronal short tau inversion recovery (STIR) images were recorded as described above (TR/TE 2000/60, number of transients 2), except that the spin echo sequence was preceded by a 180° inversion pulse followed by an inversion time of 250 ms. In pilot experiments, this inversion time was found to yield optimal contrast between compromised and healthy brain tissue.

In order to measure the coronal relaxation time T2 on a pixel-by-pixel basis, six rats (two age-matched control rats and four rats with chronic experimental allergic encephalomyelitis) were used in a series of T2W imaging experiments with a TE of 20 ms, 40 ms, 60 ms, and 80 ms and a TR of 6 s. In this experiment, which was performed at week 21 post-inoculation, all other parameters were identical to those of the above-mentioned T2W imaging experiment. The series of T2W images at a given slice position were used to reconstruct a two-dimensional map of T2 by fitting the data on a pixel-by-pixel basis to monoexponential decay functions. T2 values of cortex tissue, thalamus and ventricles were read from the T2 map and averaged among animals. T2 values of lesioned tissue were calculated for lesions which extended throughout the thickness of the MRI slice.

All MRI data were analysed using MRI specific software (Image Browser, SISCO, Sunnyvale, Calif., USA) by two different investigators who were blind to the treatment given to the animals. A filter was positioned over the region of interest (cortex and subcortical regions) in MRI slices. The filters were preset at fixed values, which appeared to yield an optimal differentiation between areas of relatively low and high signal intensity in pilot experiments. Pixels with relatively high signal intensities (e. g., higher than the fil-

ter setting) were added to obtain the total surface area of the brain regions with high signal intensities in that given slice. These surface areas with high signal intensity were summed for all slices for each animal and converted to total lesion volume (in µl). In the analysis, interslice gaps were not included in the calculation of the total lesion volume.

EVALUATION

Application of the drugs, evaluation of the clinical status and the MRI were all performed by different investigators who were blind to the treatment given to the animals. Treatment codes were broken at the end of the experiment after data analysis had been completed. The distribution of clinical scores in the different treatment groups was analyzed using a nonparametric Wilcoxon Rank Sum test. Treatment effects on lesion volume measured by MRI were tested by an analysis of variance for repeated measurements (MANOVA) followed by additional Student's *t*-tests (two-paired). $P < 0.05$ was considered to be significantly different.

REFERENCES AND FURTHER READING

Bär PR, Schrama LH, Gispen WH (1990) Neurotrophic effects of ACTH/MSH-like peptides in the peripheral nervous system. In De Wied D (ed) Neuropeptides, basics and perspectives. Elsevier, Amsterdam, pp 175–211

Duckers HJ, Muller HJ, Verhaagen J, Nicolay K, Gispen WH (1997) Longitudinal *in vivo* magnetic resonance imaging studies in experimental allergic encephalomyelitis : effect of a neurotropic treatment on cortical lesion development. Neuroscience 77:1163–1173

Lassmann H (1983) Comparative neuropathology of chronic experimental allergic encephalomyelitis and multiple sclerosis. Springer, Berlin Heidelberg New York

Strand FL, Rose KJL, Zuccarelli A, Kume J, Alves SE, Antonawich FJ, Garrett LY (1991) Neuropeptide hormones as neurotrophic factors. Physiol Rev 71:1017–1046

Wisniewski HM, Keith AB (1977) Chronic relapsing experimental allergic encephalomyelitis: an experimental model of multiple sclerosis. Ann Neurol 1:144

E.10.2.2 NMRI Study of 3-Nitropropionic Acid-Induced Neurodegeneration in Rats

PURPOSE AND RATIONALE

Effective clinical therapies for neurodegenerative diseases are currently lacking because the precise mechanisms underlying cell death are still obscure. It is hypothesized that a defect in mitochondrial energy metabolism may be the basis of secondary excitotoxic neuronal death in neurodegenerative diseases. 3-Nitropropionic acid is an irreversible succinate dehydrogenase inhibitor which blocks both the Krebs' cycle and mitochondrial electron transport. 3-Nitropropionic-acid-intoxicated rats serve as the animal model for one neurodegenerative disease, Huntington's disease. Chyi and Chang (1999) applied noninvasive diffusion- and T_2-weighted magnetic resonance imaging to study the temporal evolution and spatial distribution of brain lesions which were produced by intravenous injection of 3-nitropropionic acid in rats.

PROCEDURE

Animal Preparation

Male Sprague Dawley rats were anesthetized intraperitoneally with sodium pentobarbital (60 mg/kg). Anesthesia was maintained by serial supplement of pentobarbital (5 mg/50 min, i.v.) 2 h after the initial injection. One femoral vein was cannulated for chemical administration, and an endotracheal tube was set for artificial ventilation with an animal ventilator. A muscle relaxant, gallamine was injected intravenously to avoid spontaneous ventilation and movement during the image-acquisition period. The initial dose of gallamine was 12 mg and the maintaining dose was 6 mg/h. A bolus injection of 3-nitropropionic acid was intravenously administered.

Image Acquisition

Experiments were performed on a 4.7 T spectrometer (Spectrospin, Biospec 4.7 T, Fällanden, Switzerland) with an active shielding gradient at 5.6 G/cm in 500 µs. A 70-mm birdcage RF coil was used, and rats were placed in a prone position with a custom-designed head-holder. Four transverse images (2-mm-thick) along anterior–posterior direction were obtained using a 5-cm field of view and 128×256 matrix. The offsets were set corresponding to the sections −4.3, −1.8, +0.7, and +3.2 mm to the bregma. A fast spin-echo sequence was applied for T_2-weighted images (T_2WIs) with relaxation TIME = 4000 ms, effective echo TIME = 80 ms, and echo train LENGTH = 8. For diffusion-weighted images (DWIs), the pulsed field gradient method was employed with a relaxation time of 2000 ms, echo time of 59 ms, δ of 20 ms, Δ of 27 ms, and b-value of 1300 s/mm^2. The diffusion-sensitive gradients were applied in the read (x) direction before and after the 180° pulse. The controlled T_2WIs and DWIs were acquired prior to 3-nitropropionic administration. Then 2.5 min after the injection of 3-nitropropionic, sequential T_2WIs and DWIs were continuously performed for 8 h.

In a separate preparation, DSC MRI was performed immediately after diffusion-weighted MRI at 5 min be-

fore and 4 h after 3-nitropropionic acid administration. A 2-mm-thick transverse single-slice was chosen and centered at 0.5 mm anterior to the bregma where the striatal lesion sites were easily observed on the DWIs. A series of 30 gradient-echo images with a 64×256 matrix size, relaxation TIME = 30 ms, echo TIME = 10 ms, and $\alpha = 15°$ were acquired. The acquiring time for each gradient echo image was 1.92 s. The bolus of susceptibility contrast agent, gadopentic acid (0.3 mmol/kg, Schering, Berlin, Germany), was injected intravenously 10 s after the start of image acquisition.

EVALUATION

Data processing was performed using a commercially available image analysis software (MRVision, MRVision, Menlo Park, Calif., USA). According to Paxinos and Watson (1986), selected regions of interest (ROIs) in the striatum, hippocampus, cortex, and corpus callosum were defined. A signal-to-noise ratio (SNR) of a ROI was defined as the ratio of the mean signal intensity (SI) in this ROI to the mean SI in an adjacent background area. The relative contrast of a ROI was calculated according to the following formula: $|SI_A - SI_C| / SI_C$, where SI_A is the mean SI in this ROI and SI_C is the mean SI in the cortical ROI on the same image (Knowles and Markisz 1988). The SI_C was selected as reference because its SNR remained constant throughout the experimental period. The rCBV maps were generated by the integral under the ΔR_2^* transit curves on a pixel-by-pixel basis. The SNR, relative contrast, and regional rCBV determined from the rCBV map were all unit-less ratios.

Results were presented as means ± SEM. Statistical analyses were performed using paired Student's *t*-test to compare controlled and 3-nitropropionic-acid-treated data. $P < 0.01$ was considered statistically significant.

MODIFICATIONS OF THE METHOD

Using magnetic resonance imaging and *in vivo* proton magnetic resonance spectroscopy, Lee et al. (2000) evaluated the neuroprotective effect of lamotrigine and MK-801 on rat brain lesions induced by 3-nitropropionic acid.

REFERENCES AND FURTHER READING

Chyi T, Chang C (1999) Temporal evolution of 3-nitropropionic acid-induced neurodegeneration in the rat brain by T_2-weighted, diffusion-weighted, and perfusion magnetic resonance imaging. Neuroscience 92:1035–1041

Knowles RJ, Markisz JA (1988) General imaging measurement. In: Quality assurance and images artifacts in magnetic resonance image, Brown Press, Boston, Mass., p 35

Lee WT, Shen YZ, Chang C (2000) Neuroprotective effect of lamotrigine and MK-801 on rat brain lesions induced by 3-nitropropionic acid: evaluation by magnetic resonance imaging and *in vivo* proton magnetic resonance spectroscopy. Neuroscience 95:89–95

Paxinos G, Watson C (1986) The rat brain in stereotaxic coordinates. Academic Press, San Diego, Calif.

E.10.2.3 NMRI Studies of Brain Activation in Rats

PURPOSE AND RATIONALE

Brain functional magnetic resonance imaging (fMRI) is capable of revealing *in vivo* biochemical, structural, and functional information that reflects the physiological integrity of the brain (Jenkins et al. 1996). In general, brain fMRI includes four different aspects of MR methods including tissue water movement (diffusion-weighted MRI) (Le Bihan et al. 1986), capillary flow (perfusion-weighted MRI) (Williams et al. 1992; Kim 1995), neuronal activation (blood oxygenation level-dependent, BOLD, MRI) (Ogawa et al. 1992), and cerebral metabolites (magnetic resonance spectroscopy) (Brown et al. 1982). In all of these methods, the BOLD effect, based on the difference in magnetic susceptibility between paramagnetic blood deoxyhemoglobin and surrounding tissues, is frequently employed to *in vivo* map functional changes during brain activation (McCarthy et al. 1993; Turner et al. 1993).

Chang and Shyu (2001) described a functional magnetic resonance imaging (fMRI) study of brain activations during non-noxious and noxious electrical stimulation of the sciatic nerve of rats.

PROCEDURE

Male Sprague Dawley rats were initially treated with atropine (6 mg/kg, i.p.), and then anesthetized with methohexital sodium, 65 mg/kg, i.p. A PE-240 tube was inserted via tracheotomy for artificial ventilation. A PE-50 catheter was placed in the femoral vein for the administration of drug. α-Chloralose (50 mg/kg) was given intravenously. After the sciatic nerve was exposed and isolated, a cuff electrode made from silicon tube and stainless steel wires was placed around the nerve. The surrounding muscle and skin were carefully sutured, and paraffin oil was filled around the electrode to prevent short-circuiting. Artificial ventilation was applied and CO_2 concentration was monitored and controlled within the range of 3.5%–4.5%. Rectal temperature was measured and maintained at about 37°C by a feedback-controlled warm-air system. After the

head-holder was in place, muscle relaxant (gallamine triethiodide, 50 mg/kg, i.v.) was given for muscle relaxation.

Electrophysiological Experiment

Laminectomy was performed between T12 and L5. Dorsal roots at L4 and L5 level were carefully isolated and cut. Each of the peripheral ends of the roots was ligated with a cotton thread previously soaked with normal saline. A silver–silver chloride electrode hooked on the end of the root was used to record the evoked field potentials extracellularly ipsilateral to the stimulating sites. The extracellular field potentials were amplified by a high-input impedance amplifier. All analog signals were displayed on either an analog or digital storage oscilloscope. Twenty sweeps of evoked compound potentials were averaged for each stimulus intensity. The threshold current for inducing minimal muscle twitch was tested before applying the muscle relaxant. The electrical current was delivered by a constant current pulse generator. The electrical pulse was a square wave, 0.5 ms duration, 2 Hz. This muscle twitch threshold current was used to compare with the threshold for inducing the minimal compound action potentials. The intensity was increased as a multiple of the threshold current value.

Imaging Acquisition in fMRI Experiments

MR experiments were performed on a Biospec BMT 47/40 4.7 T system equipped with an actively shielded gradient system (up to 5.9 G/cm in 500 μs). A 70-mm birdcage RF coil was used, and rats were placed in a prone position with a custom-designed head-holder. T1-weighted spin-echo images were scanned in transverse and sagittal planes to position the animal properly so that images were centered 1 mm posterior to the bregma. For identifying anatomical location, T_2-weighted spin-echo images with four slices in the transverse plane were acquired using a repetition time (TR) of 4 s, an echo time (TE) of 80 ms, a field of view (FOV) of 5 cm, and a slice thickness (SLTH) of 2 mm. The acquisition matrix was 256×128 with a matrix of 256×256 after zero-filling. Thus, the images covered the rat brain from 3 mm anterior to the bregma to 5 mm posterior to the bregma. At the same locations of T_2-weighted spin-echo images, a series of 40 gradient-echo images per slice for four slices in the transverse plane were collected for baseline and stimulation sets with a TR of 180 ms, an TE of 20 ms, a flip angle of 22.5°, a FOV of 5 cm and a SLTH of 2 mm. The acquisition matrix was 256×64 with a matrix of 256×256 after zero-filling. The total scanning time for each image was 23 s. In the baseline set, the stimulation was turned off during the first eight image acquisitions. The electrical stimulation was switched on in two stimulation sets during acquisition of images 9–16 and 25–32. The stimulator was switched off for the rest of the period. The stimulation consisted of rectangular pulses of 0.5 ms duration and a 2 Hz frequency current. The same muscle twitch measurement as described in the electrophysiological study session was conducted to determine the intensity of the threshold current. In each image acquisition session, only one stimulation intensity was used. Stimuli with varied threshold-multiplied intensities were applied randomly in three different sessions in each rat. At least 30 min waiting time was allowed between each acquisition session.

Physiological Data Acquisition System in fMRI Experiments

Inside the magnet, animals were placed in an acrylic head-holder for accurate positioning of the location of brain structures. The integrated physiological data acquisition system we used was processed and controlled by a program written in Microsoft BASIC language on an IBM personal computer (Shyu et al. 1996). The data acquisition and control signals were channeled through serial ports and a PCL-818 (Advantech, A/D converter and digital input/output) interface card. All digitized physiological data, timing events and trigger pulses from each image acquisition were displayed in real time to view the animal's condition. The same data were placed in a data array and stored on a hard disk for off-line analyses, plotting, and printing.

EVALUATION

Image data processing and analyses of significance of signal changes were performed using MRVision (MRVision, USA) running on a Silicon Graphics INDY workstation. The series of multi-sliced images were realigned in the vertical and horizontal direction related to the first image in the series. The analyses of the aligned data were based on the cross-correlation processing strategy (Bandettini et al. 1993). The correlation coefficient between each pixel of the series of images and a model of a square wave (whose OFF–ON–OFF–ON–OFF period was the same as the stimulation pattern) was calculated. An associated *t*-statistic image was generated by the fitting function. The *t*-statistic image was used to determine whether the correlation coefficient for each pixel was significantly different from zero. The same analysis procedure was carried out in each slice of the four slices. A critical *t*-value for each pixel for the desired level

of significance (e. g., $P < 0.01$) and degrees of freedom (total images-2) was calculated and an output image, an activated map consisting of clusters of pixels whose values exceeded the level of significance, was generated. This image, white color in appearance, was then overlaid with a high-resolution T_2-weighted image, resulting in an image showing the significantly activated region in white overlapping the anatomical image. The region of interest (ROI) from the *t*-statistic image was selected according to its corresponding location in the T_2-weighted image. The stereotaxic atlas of the rat (Paxinos and Watson 1998) was used as the reference for determining the corresponding anatomical structures in T_2-weighted images. The time course of signal intensities of 40 images of each of the four slices was obtained in the selected ROI. The extent of the functional activation was obtained by calculating the percentage change of averaged signals between the OFF period and the first and the second ON periods. Each chosen ROI corresponded to an anatomical structure that appeared in different slices, thus the signal intensity changes of each ROI in different slices could be averaged. The area of each ROI as depicted by pixel numbers appearing in different slices was summed. The mean percent signal increases and total area of each ROI activated by different intensities were compared using one-way ANOVA with $P < 0.05$ or < 0.001 considered to be significant. Post-hoc examination of the difference between groups was performed by the Student–Newman–Keuls test.

MODIFICATIONS OF THE METHOD

Kerskens et al. (1996) compared ultrafast perfusion-weighted MRI of functional brain activation in rats during forepaw stimulation with $T2^*$-weighted MRI.

Several other studies using MRI were performed in rats:

Wrynn et al. (2000) reported an *in vivo* magnetic resonance imaging study of the olfactory bulbectomized rat model of depression. The magnetic resonance imaging (MRI) investigation demonstrated alterations in signal intensities in cortical, hippocampal, caudate and amygdaloid regions in olfactory bulbectomized animals, but not in sham-operated controls. Ventricular enlargement was also evident in olfactory bulbectomized animals.

Itoh et al. (2004) described magnetic resonance and biochemical studies during pentylenetetrazole-kindling development and the relationship between nitric oxide, neuronal nitric oxide synthase and seizures. The daily administration of pentylenetetrazole was associated with an increase in the amount of neuronal nitric oxide synthase (nNOS). NO generation was measured directly by *in vivo* and *ex vivo* electron paramagnetic resonance on rats undergoing progressive convulsions. Morphological changes in the brain structure of rats were measured by magnetic resonance imaging during epileptic convulsions induced by repetitive administration of pentylenetetrazole.

Watanabe et al. (2006) described mapping of the habenulo-interpeduncular pathway in living **mice** using manganese-enhanced 3D MRI. Six hours after intracerebroventricular microinjection of $MnCl_2$, T1-weighted 3D MRI (2.35 T) at 117 µm isotropic resolution revealed a continuous pattern of anterograde labeling from the habenula via the fasciculus retroflexus to the interpeduncular nucleus.

Hasegawa et al. (2003) described diffusion-weighted imaging in kainic-acid-induced complex partial status epilepticus in **dogs**. A cannula was stereotactically inserted into the left amygdala. One week after surgery, all dogs were imaged using MRI. Pre-injection imaging consisted of T2-weighted (T2W) imaging, fluid attenuated inversion recovery (FLAIR), and DWI. Two weeks after surgery, five dogs received intra-amygdaloid KA microinjections. MRI was carried out at 3, 6, 12, 24, and 48 h after onset of complex partial status epilepticus.

REFERENCES AND FURTHER READING

Bandettini PA, Jesmanowicz A, Wong EC, Hyde JS (1993) Processing strategies for time-course data sets in functional MRI of the human brain. Magn Reson Med 30:161–173

Brown TR, Kincaid BM, Ugurbil K (1982) NMR chemical shift imaging in three dimensions. Proc Natl Acad Sci USA 79:3523–3526

Chang C, Shyu BC (2001) A fMRI study of brain activations during non-noxious and noxious electrical stimulation of the sciatic nerve of rats. Brain Res 897:71–81

Hasegawa D, Orima H, Fujita M, Nakamura S, Takahashi K, Ohkibo S, Igarashi H, Hashizume K (2003) Diffusion-weighted imaging in kainic acid-induced complex partial status epilepticus in dogs. Brain Res 983:115–127

Itoh K, Watanabe M, Yoshikawa K, Kanaho Y, Berliner LJ, Fujii H (2004) Magnetic resonance and biochemical studies during pentylenetetrazole-kindling development: the relationship between nitric oxide, neuronal nitric oxide synthase and seizures. Neuroscience 129:757–766

Jenkins BG, Brouillet E, Chen YI, Storey JB, Schulz JB, Kirschner P, Beal MF, Rosen BR (1996) Non-invasive neurochemical analysis of focal excitotoxic lesions in models of neurodegenerative illness using spectroscopic imaging. J Cereb Blood Flow Metab 16:.450–461

Kerskens CM, Hoehn-Berlage M, Schmitz B, Busch E, Bock C, Gyngell ML, Hossmann KA (1996) Ultrafast perfusion-weighted MRI of functional brain activation in rats during forepaw stimulation: comparison with $T2^*$-weighted MRI. NMR Biomed 8:20–23

Kim SG (1995) Quantification of relative cerebral blood flow change by flow-sensitive alternating inversion recov-

ery (FAIR) technique: application to functional mapping. Magn Reson Med 34:293–301
Le Bihan D, Breton E, Lallemand D, Grenier P, Cabanis E, Laval-Jeantet M (1986) MR imaging of intravoxel incoherent motions: application to diffusion and perfusion in neurologic disorders. Radiology 161:401–403
McCarthy G, Blamire AM, Rothman DL, Gruetter R, Shulman RG (1993) Echo-planar magnetic resonance imaging studies of frontal cortex activation during word generation in humans. Proc Natl Acad Sci USA 90:4952–4956
Ogawa S, Tank DW, Menon R, Ellermann JM, Kim SG, Merkle H, Ugurbil K (1992) Intrinsic signal changes accompanying sensory stimulation: functional brain mapping with magnetic resonance imaging. Proc Natl Acad Sci USA 89:5951–5955
Paxinos G, Watson C (1998) The rat brain in stereotaxic coordinates, 4th edn. Academic Press, New York
Shyu BC, Hsieh KC, Yen CFC, Liu CP, Chang C (1996) An integrated physiological data acquisition and control system for fMRI study in rats. Proc ISMRM 4:1836
Turner R, Jezzard P, Wen H, Kwong KK, Le Bihan D, Zeffiro T, Balaban RS (1993) Functional mapping of the human visual cortex at 4 and 1.5 tesla using deoxygenation contrast EPI. Magn Reson Med 29:277–279
Watanabe T, Radulovic J, Boretius S, Frahm J, Michaelis T (2006) Mapping of the habenulo-interpeduncular pathway in living mice using manganese-enhanced 3D MRI. Magn Reson Imaging 24:209–215
Williams DS, Detre JA, Leigh JS, Koretsky AP (1992) Magnetic resonance imaging of perfusion using spin inversion of arterial water. Proc Natl Acad Sci USA 89:212–216
Wrynn AS, MacSweeney CP, Franconi F, Lemaire L, Pouliquen D, Herlidou S, Leonard BE, Gandon JM, de Cartaines JD (2000) An in-vivo magnetic resonance imaging study of the olfactory bulbectomized rat model of depression. Brain Res 879:193–199

E.10.3 NMRI Psychoneuropharmacological Studies in Primates

E.10.3.1 Functional NMRI Studies in the Brain of Rhesus Monkeys

PURPOSE AND RATIONALE

Zhang et al. (2000) and Andersen et al. (2002) published methodological details for functional MRI studies in awake rhesus monkeys.

PROCEDURE

Adult female rhesus monkeys (*Macaca mulatta*) were maintained on a 12-h light:12-h dark cycle in individual cages with water available ad libitum. They had to be adapted to an MRI environment.

The goal was to elicit cooperative involvement of the rhesus monkeys through positive reinforcement. The animals were first acclimated to working with the trainers in their home cage room. Visual contact, vocal familiarity and positive reinforcements (juice rewards and preferred foods) were used to promote bonding and establish a working relationship between subject and trainer. A pole-and-collar system was used to handle and train monkeys. The monkeys were trained to voluntarily exit their home cages with use of positive reinforcements and the pole-and-collar system. After subjects were sufficiently trained, they were introduced to the primate-training chair. Food was removed from the subject's home cage approximately 20 h prior to a training session. Training sessions lasted 45–75 min and were conducted at least twice a week per subject until no major movements were observed.

Apparatus

The animals were adapted to the MRI-compatible chair constructed from non-ferromagnetic materials and designed to comfortably position an adult rhesus monkey in a prone, sphinx-like position within the magnet bore. The head-holder was designed to restrict head motion without having to surgically attach a head-holder to the skull. The head frame was placed over the monkey's head and secured to the training chair using four nylon screws. The monkey's head rested comfortably on a padded chin support that acted as a stabilizer and cushion. Its nose and mouth were positioned outside the head-holder for comfort and ease of breathing. Under local anesthesia (1% lidocaine, 2.0 ml on each side), two MRI-compatible pins were inserted through the overlying skin and connective tissue to contact the bony cranium. Earbars/earplugs were constructed that followed the natural angle of the rhesus ear canal and secured firmly to the chair-mounted head-holder. Earbars/earplugs were used both for MRI and training sessions to reduce head movement and protect the animals from the high ambient MRI noise levels. Two separate boxes in front of the MRI-compatible chair accommodated the front limbs of the monkey.

fMRI Procedures

The scans were conducted on a Siemens VISION (VB33A) 1.5T MRI scanner using the body coil to transmit radio frequency and an 8-cm surface coil placed above the monkey's head for RF signal reception. The anatomic structures of interest were visualized using a 3D FLASH sequence with 1 mm isotropic resolution (TR/TE = 21/6 ms, flip ANGLE = 30°, image matrix SIZE = 128 × 128 × 90, field of VIEW = 128 mm, BANDWIDTH = 195 Hz per pixel). No correction was made for the fall-off in signal intensity with distance from the surface coil in the anatomic images, but sufficient sensitivity was

available to accurately visualize anatomic structures throughout the entire slice.

Functional MR images were acquired continuously using a FLASH 2D multiple gradient-recalled-echo (MGRE) navigator sequence. Slices were acquired interleaved for three non-contiguous positions in the coronal plane: the first slice covering the area of the putamen and the caudate, the second one covering globus pallidus, and the last one included the substantia nigra (Zhang et al. 2000). An 11-echo MGRE sequence was used to map on a pixel-by-pixel basis the local transverse relaxation rate R_2^* Menon; Andersen; Chen and Chen). R_2^* is the local transverse relaxation rate for the measured MR signal intensity, $S(\mathrm{TE}) = S_0 \exp(-R_2^* \mathrm{TE})$, where TE is the echo delay time. It is the parameter that affects contrast in a T_2^*-weighted image sensitized to local susceptibility effects such as those caused by changes in the blood oxygenation level. Darker regions in T_2^*-weighted images have larger baseline R_2^* values reflecting a more rapid MR signal decay rate ($R_2^* = 1/T_2^*$). The increase in blood oxygenation level associated with brain "activation" causes a decrease in the value of the R_2^* parameter. There are several advantages of using R_2^*. As an intrinsic MR parameter, its value is not affected by the non-uniform sensitivity pattern of the surface coil used for signal reception, provided the images at all echo times TE have sufficient signal level, well above the intrinsic noise floor. Also, R_2^* is insensitive to changes in the absolute image intensity, S_0, that may occur over the duration of a long scan. A disadvantage is that the rate of acquisition is slower, although a single-shot multi-echo EPI method was recently developed for quantitative R_2^* mapping in functional MR imaging (Posse et al. 1999).

The last TE images were acquired without phase encoding gradients to serve as a navigator echo for detection of head motion occurring during the acquisition of data for reconstruction of single R_2^* images. The FLASH 2D acquisition parameters were: TR = 250 ms, TE = 7–75 ms, image acquisition matrix SIZE = 112 × 128, rectangular field of VIEW = 112 × 128 mm, slice THICKNESS = 3 mm, flip ANGLE = 40°, BANDWIDTH = 156 Hz per pixel. Local shimming of the static magnetic field B_0 in the basal ganglia was used to optimize sensitivity to the BOLD effect. For each animal, 20 min of baseline fMRI data were collected, after which 0.1 mg/kg apomorphine was injected subcutaneously. Data collection then resumed for another 20 min. In cases where replicate scans were obtained in the same animal, there was at least a 1-week interval between scans.

EVALUATION

The calculation of R_2^* values was carried out on a pixel-by-pixel basis by fitting the gradient echo signal decay to a first-order model $\ln(S) = \ln(S_0) - R_2^* \mathrm{TE}$. The corresponding percentage signal changes, $\Delta S/S$, reported in our activation studies are determined from ΔR_2^* as the values that would have been observed at a representative single echo time of TE = 45 ms (Blamire et al. 1992; Menon et al. 1993). The latter time is chosen to match the relaxation time T_2^* in brain tissue for maximum contrast [assuming the signal intensity S is maintained constant across studies ($\Delta S/S \approx -\Delta R_2^* \mathrm{TE}$)]. While R_2^* itself does not report on the BOLD effect directly (only the temporal contrast due to changes ΔR_2^* does), repeatability in the measurement of baseline R_2^* values in specific brain regions of a given animal helps ensure consistency during replicate scans over a period of months. However, the baseline R_2^* in some tissues, such as the globus pallidus, does change slowly over a period of years due to metal deposition (e. g., iron) with aging. While there are differences between brain areas in their baseline R_2^* value, we have not seen a significant correlation between baseline and drug-evoked changes (ΔR_2^*). Thus, quantitative measures of changes in R_2^* can be detected regardless of baseline values. Additionally, any departure from a log-linear signal decay behavior can be mapped to help yield information about the intra- or extra-vascular origin of the signal (Chen et al. 1996). All of the analyses have been conducted using MAT:LAB software on Unix/Linux workstations (Mathworks, Natick, Mass., USA).

The fMRI data needed for computation of the R_2^* maps were acquired at a rate of one set consisting of three image slices every 30 s. Rigid-body motion between successive time points was not corrected since most effects were in the through-slice direction. Prior to administration of any drug, a total of 40 time frames were collected over 20 min for the baseline state. Following the injection of drug, an additional 40 images were collected to track the dynamic response. First, the time-course data for each pixel were adjusted by centering so as to have a zero mean during the baseline period comprising the first 40 time frames. The sample covariance matrix of dimension 80 × 80 was then computed from the measured R_2^* response for all image voxels in the brain, and the principal component time-course profiles were determined as the eigenvectors. The associated pixel-wise scores across the slice images represented the spatial modes/patterns.

Information in the navigator echo data from all three slices was used to detect line-to-line changes and sub-

sequently discard image time frames where motion had occurred during the acquisition. Additionally, formal statistical methods of influence analysis for PCA were used to flag and subsequently remove outlying observations that exerted undue influence and contributed disproportionately in the partitioning of variance (Andersen et al. 2002). These observations typically corresponded to spikes at points in the time series data and present as artifacts in the corresponding R_2^* maps. In a typical fMRI study of an awake rhesus monkey, on the order of 5–10 time frame observations out of a total of 80 would be detected by the navigator echo and 10–20 would be flagged as statistical outliers in the influence analysis for PCA. From the trimmed data set, the sample covariance matrix and principal component time course profiles were then recomputed yielding a far more robust representation.

The first principal component, which also represents the largest source of variance in the data, was then used to model the temporal response in each voxel across the brain image slices. This approach of filtering and fitting enables both an analysis of the dynamic nature of the temporal response to administration of a drug in a single animal and the development of an unbiased measure of activation that can be used in the analysis of data combined across multiple animals. From the filtered data, the change ΔR_2^* representing the fMRI activation response to a drug was determined as the difference between the mean R_2^* value across 20 images post drug administration during the period of peak response and the mean value within the 40 images acquired as baseline prior to administration.

MODIFICATIONS OF THE METHOD

Stefanacci et al. (1998) and Dubowitz et al. (2001) reported MRI studies in conscious monkeys.

Howell et al. (2001) described an apparatus and behavioral training protocol to conduct positron emission tomography (PET) neuroimaging in conscious rhesus monkeys reporting the development and standardization of PET neuroimaging protocols in conscious rhesus monkeys and their application to the characterization of the acute effects of cocaine on cerebral blood flow. Specific attention was devoted to the development of an effective and comfortable head restraint device to be used in the imaging of conscious monkeys. The restraint device was designed to attach to a standard primate chair to facilitate frequent immobilization. Subjects received extensive behavioral training prior to neuroimaging in order to ensure their comfort and minimize potential stress associated with the imaging protocols. Functional changes in cerebral blood flow were characterized in three subjects with the positron-emitting tracer ^{15}O water following acute i.v. administration of cocaine. Regions of interest were defined on MRI scans with a high degree of accuracy.

REFERENCES AND FURTHER READING

Andersen AH, Zhang Z, Barber T, Ryens WS, Zhang J, Grondin R, Hardy P, Gerhardt GA, Gash DM (2002) Functional MRI studies in awake rhesus monkeys: methodological and analytical strategies. J Neurosci Meth 118:141–152

Blamire AM, Ogawa S, Ugurbil K, Rothman D, McCarthy G, Ellerman JM, Hyder F, Rattner Z, Shulman RG (1992) Dynamic mapping of the human visual cortex by high-speed magnetic resonance imaging. Proc Natl Acad Sci USA 89:11069–11073

Dubowitz DJ, Chen DY, Atkinson DJ, Scadeng M, Martinex A, Andersen MB, Andersen RA, Bradley WG (2001) Direct comparison of visual cortex in human and non-human primates using functional magnetic resonance imaging. J Neurosci Methods 107:71–80

Howell LL, Hoffman JM, Votaw JR, Landrum AM, Jordan JF (2001) An apparatus and behavioral training protocol to conduct positron emission tomography (PET) neuroimaging in conscious rhesus monkeys. J Neurosci Methods 106:161–169

Menon RS, Ogawa S, Tank DW, Ugurbil K (1993) 4 Tesla gradient recalled echo characteristics of photic stimulation-induced signal changes in the human primary visual system. Magn Reson Med 30:380–386

Posse S, Wiese S, Gembris D, Mathiak K, Kessler C, Grosse-Ruyken ML, Elghahwagi B, Richards T, Dager SR, Kiselev VG (1999) Enhancement of BOLD-contrast Sensitivity By Single-shot Multi-echo Functional MR Imaging. Magnetic Resonance in Medicine 42:87–97

Stefanacci L, Reber P, Costanza J, Wong E, Buxton R, Zola S, Squire L, Albright T (1998) FMRI of monkey visual cortex. Neuron 20:1051–1057

Zhang Z, Andersen AH, Avison MJ, Gerhardt GA, Gash DM (2000) Functional MRI of apomorphine activation of the basal ganglia in awake rhesus monkeys. Brain Res 852:290–296

E.10.3.2 Functional NMRI Studies in the Brain of Common Marmosets

PURPOSE AND RATIONALE

Massacesi et al. (1995) and Genain and Hauser (1997) described actively and passively induced experimental autoimmune encephalomyelitis in common marmosets as a model of multiple sclerosis. ‘t Hart et al. (1998, 2004) used this model for detailed MRI studies with histopathological characterization of MRI-detectable white matter lesions.

PROCEDURE

Eleven marmosets (*Callithrix jacchus*) were used for this study. The body weight of the monkeys at the start

of the experiment ranged between 295 and 320 g. During the experiments, the monkeys were individually housed in spacious cages with padded shelter on the bottom. The daily diet consisted of commercial food pellets for non-human primates, supplemented with rice and fresh fruit. Drinking water was provided ad libitum

Induction of Experimental Autoimmune Encephalomyelitis (EAE)

Myelin was isolated from human brain white matter, which was kindly provided by Dr. Rivka Ravid of the Dutch Brain Bank (Amsterdam, The Netherlands). The myelin concentration in the stock solution was 30 mg/ml on a dry-weight basis and 1.3 mg/ml protein on a protein basis as measured according to Bradford (1976).

In a first group of five monkeys the myelin stock solution was emulsified in an equal volume of enriched complete adjuvant. Enriched complete adjuvant was prepared by mixing incomplete adjuvant (DIFCO Laboratories, Detroit, Mich., USA) with 6 mg/ml desiccated mycobacteria (*Mycobacterium tuberculosis*, H37A, DIFCO) followed by brief sonication. Under ketamine anesthesia, each monkey was injected intradermally on the back with 600 µl of emulsion divided over four spots, two in the inguinal and two in the axillary region. In addition, 1 ml phosphate-buffered saline (pH 7.4) containing 1010 heat-inactivated *Bordatella pertussis* particles was injected immediately after immunization and 48 h later.

In a second group of six monkeys, the original immunization protocol was modified in two respects. First, the *Mycobacterium* concentration in the antigen-adjuvant emulsion was reduced from 1.5 to 0.5 mg/ml to diminish the severity of ulceration around the injection sites. Secondly, *B. pertussis* administration as second adjuvant was omitted to obtain a milder EAE in which patterns of EAE reactivity can be associated with the presence of certain mhc alleles and cytokine profiles.

Clinical Diagnosis

The clinical course of EAE was recorded daily by a trained observer using semiquantitative scoring: 0 = no clinical signs; 0.5 = apathy, loss of appetite, altered walking pattern without ataxia; 1 = lethargy and/or anorexia; 2 = ataxia; 2.5 = para- or monoparesis and/or sensory loss and/or brainstem syndrome; 3 = para- or hemiplegia; 4 = quadriplegia; 5 = spontaneous death attributable to EAE. The highest per-day scores were averaged over 1 week. Moreover, each monkey was weighed at least three times per week to obtain a more objective score of the clinical wellbeing.

MRI

MRI was performed at the Bijvoet Center of Utrecht University, the Netherlands. For each monkey, T2- and T1-weighted magnetic resonance (MR) images were recorded, the latter also with contrast enhancement after intravenous injection of gadolinium-diethylenetriamine-penta-acetic acid (DTPA) (triple dose). The time points for performing MRI after immunization were chosen during periods of clinically active EAE

In Vivo MRI

In preparation for the experiment, the monkeys were anesthetized with ketamine/Vetranquil (9/1 v/v). During scanning, each monkey was placed on a 37°C water-filled heating pad to prevent hypothermia. The head of the monkey was fixed in a custom-built stereotaxic apparatus made of metal-free plastics to ensure reproducible positioning in the magnetic field and to minimize movement artifacts. The stereotaxic apparatus was placed inside a saddle-type radiofrequency coil.

MRI was performed on a SISCO 200-MHz spectrometer (Varian, Palo Alto, Calif., USA) equipped with an actively shielded gradient (maximum gradient 3.2 G/cm, 33 cm inner diameter).

Postmortem MRI

T2-weighted MR images were recorded from formalin-fixed brains to enable the determination of the exact localization of the lesions that were detected *in vivo*. In both scannings the same orientation points were chosen for slice localization. Because movement artifacts were absent and long acquisition times can be used, images of very high contrast can be obtained.

Slice Orientation and Scanning Procedure

First, a sagittal scout scan was made. The posterior and anterior positions of the corpus callosum were chosen as orientation markers for precise localization of the slices for the *in vivo* and postmortem MRI. A T2-[echo time (TE)/repetition time (TR), 60/2500 ms-] weighted multislice scan (20 slices of 1 mm thickness) was obtained followed by a T1-weighted scan (TE/TR, 25/1000 ms) with the same spatial prescription. Gadolinium-DTPA (Magnevist; Schering, Berlin, Germany) was injected intravenously (0.3 mmol/kg)

and allowed to circulate for 10 min to ensure adequate distribution. Next, the T1-weighted MRI was repeated to attain a post-contrast data set. Each slice was recorded with a matrix of 256 × 128 data points and a field of view of 5 × 5 cm. The data set was analyzed on an Apple Macintosh Performa 630 using the public domain NIH Image program.

The T1-weighted MR images had an unexpected gray-white matter contrast. In images recorded with the NMR machines that are now used in clinical settings, which are 1.5 T or less, a contrast conversion of the white and gray matter is normally seen on T1-weighted versus T2-weighted images. In T1-weighted images the NMR signal of the white matter is hyperintense in comparison with that of the gray matter, whereas in T2-weighted images the white matter signal is hypointense compared with that of the gray matter.

In both the T1- and T2-weighted images recorded on our 4.7-T machine, white matter is hypointense as compared with gray matter, and lesions are visible as hyperintensities. This is not a unique feature of the marmoset brain, given that it was also observed in cat brains. The most likely explanation for this discrepancy is that with the high magnetic field used, T1 values of gray and white matter converge, whereas T2 values are unaffected by the strength of the field. In our T1-weighted images, the intensities of white and gray matter are most likely determined by the longer T2 value of gray matter and the different proton densities of both tissues. This phenomenon did not affect the detection of gadolinium enhancement, because even in long TR/short TE images ("proton-density" weighted) contrast enhancement can be observed.

REFERENCES AND FURTHER READING

Bradford M (1976) A rapid and sensitive method for the quantitation of microgram quantities of protein utilizing the principle of protein-dye binding. Anal Biochem 72:248–254

Genain CP, Hauser SL (1997) Creation of a model for multiple sclerosis in *Callithrix jacchus* marmosets. J Mol Med 75:187–197

Massacesi L, Genain CP, Lee-Parritz D, Letvin NL, Canfield D, Hauser SL (1995) Active and passively induced experimental autoimmune encephalomyelitis in common marmosets: A new model of multiple sclerosis. Ann Neurol 37:519–530

't Hart BA, Bauer J, Muller HJ, Melchers B, Nicolay K, Brok H, Bontrop RE Lassmann H, Massacesi L (1998) Histopathological characterization of magnetic resonance imaging-detectable white matter lesions in a primate model of multiple sclerosis. A correlative study in the experimental autoimmune encephalomyelitis model in common marmosets (*Callithrix jacchus*). Am J Pathol 153:649–663

't Hart BA, Vogels J, Bauer J, Brok HPM, Blezer E (2004) Noninvasive measurement of brain damage in a primate model of multiple scerosis. Trends Mol Med 10:85–91

Chapter F
Drug Effects on Learning and Memory[1]

[1] With contributions by F.J. Hock, F.P. Huger, W.H. Vogel, J.D. Brioni, J.L. McGaugh and E. Dere

F.1 Introduction

It is easily understood that behavioral psychopharmacologies faced with the task of dealing with extremely complex behavioral disturbances. This holds true for both patient groups: young people with learning and memory problems and elderly patients with memory deficits. For the elderly, difficulties arise in designing appropriate animal models of human aging or the deficits occurring during human aging. One of the major problems for experimental behavioral pharmacology is whether or not old animals are the appropriate models. At the first view it seems obvious that the study of potential geronto-psychopharmacologic drugs should be performed in old animals. However, the problem is much more complicated. Laboratory animals are not a homogenous population, especially when old. Most of these old animals, which are one-third survivors of a population, have an individually different pathological history that is mostly unknown to the investigators. Some animals may be arthritic others may have bronchitis or cardiac deficiencies. If, for example, an arthritic rat is given a performance task associated with lever pressing, the animals may fail because of his rigid and painful joints and not because of a brain deficit or of the ineffectiveness of the test compound. Similar effects can be observed with old animals having a cataract in a visual discrimination task. Failure to perform a task may even be the result of both central and peripheral disturbances. Consequently it is impossible to describe the failure of one animal to perform the task to deficits in some parts of the brain or to pathological changes in the body.

Considerable evidence indicates that there are age-related changes in learning and memory (Gold and McGaugh 1975; Gold et al. 1975). Myslivecek (1997) described ontogeny of memory and learning in rats. For certain kinds of learning, there are specific developmental periods at which acquisition and retention are optimal; for example, imprinting in animals (Hess 1972; Scheich 1987) and language acquisition in humans (Lennenberg 1967). For other forms of learning and memory, acquisition and long-term retention in animals mature gradually with development (Campbell and Spear 1972). There is some evidence that aged organisms have impaired memory function. For example, in humans, performance on recent memory tasks appears to decay at shorter training-test intervals and is more susceptible to retroactive interference in elderly subjects than in young adult subjects (Craik 1977; Kubanis and Zornetzer 1971). Recent memory also appears to be deficient in aged non-human primates (Bartus et al. 1980).

Although drug discovery is based upon many factors, animal models provide a crucial part in identifying chemical compounds with potential for clinical efficacy. A number of important animal models of human disease have come into existence based upon "serendipitous" discoveries of their ability to identify chemicals with a particular set of therapeutic actions. However, in the absence of truly effective therapeutic agents for age-associated dementia to serve as standards, the development of appropriate animal models for dementia represents a serious challenge. In the case of Alzheimer's disease or age-associated memory impairment, successful development of animal models may well depend upon our ability to accurately reproduce specific pathophysiological or etiologic factors.

It is generally agreed that an ideal animal model of human dementia would exhibit some or all the behavioral and neurological dysfunctions known to be associated with the clinical disorder, as well as the pathological processes leading to the demented condition. An early approach was the measurement of the spinal cord fixation time in rats as described by Giurgea and Mouravieff-Lesiusse (1971), Giurgea and Salama (1977).

McDonald and Overmier (1998) presented a critical review of animal models of the mnemonic impairments in Alzheimer's disease. Socci et al. (1995) could show that chronic antioxidant treatment improves cognitive performance of aged rats. Several authors discussed chronic alcohol intoxication in rats and mice as a model for neurodegeneration (Ahrendt et al. 1988; Fadda and Rossetti 1998; Raghavendra and Kulkarni 2001; Wozniak et al. 2004).

Miller et al. (1999) and McClearn (1999) discussed the use of inbred strains for gerontological research. There are limitations on research with uniform genotypes and advantages of heterogeneous populations. However, for specific purposes, the uniformity and stability of inbred strains are extremely valuable attributes.

Since cholinesterase inhibitors, such as physostigmine (Christie et al. 1981; David and Mohs 1982; Thal et al. 1983) and tacrine (Summers et al. 1986) have been shown to improve cognitive function in

patients with Alzheimer's type dementive disorders and based on analytical data in brains of aged subjects, the cholinergic hypothesis of geriatric memory dysfunction has been established. Numerous attempts have been made to study the influence of potential drugs on the central cholinergic system, e. g., inhibition of acetylcholinesterase activity in rat striatum *in vitro*, differentiation of this activity versus the inhibition of butyrylcholinesterase activity, *ex vivo* cholinesterase inhibition in rat striatum, release of acetylcholine from rat brain slices after electrical stimulation, binding to muscarinic cholinergic receptors in rat forebrain, stimulation of phosphatidyl-inositol turnover via muscarinic receptors, binding to nicotinic cholinergic receptors in rat frontal cortex. Presynaptic cholinergic markers include choline acetyl-transferase and acetylcholinesterase activities, high-affinity transport of choline, acetylcholine synthesis, and muscarinic receptor binding. The high-affinity transport of choline is influenced by a cholinotoxin, ethylcholine aziridinium (AF64A) that induces *in vivo* a persistent central cholinergic hypofunction of presynaptic origin (Fisher and Hanin 1986).

Changeux et al. (1998) discussed the role of nicotinic acetylcholine receptors in the brain in learning and reinforcement.

These approaches may give hints for the discovery of new antidementic drugs. The "cholinergic hypothesis" (Bartus et al. 1982, 1987) is not unequivocal in the pathophysiology of Alzheimer's disease (Francis et al. 2005). The role of other transmitters has to be studied (Nordberg 1990). *In vitro* and *in vivo* studies have to be performed in parallel in order to find new approaches to treat Alzheimer's disease or Alzheimer's type dementia.

The **amyloid cascade hypothesis** has gained much interest (Thorsett and Latimer 2000; Yamada and Nabeshima 2000; Emre and Qizilbash 2001; Sommer 2002; Lichtenthaler and Haass 2004).

As early as 1907, Alzheimer described the appearance of plaques and neurofibrillary tangles (Alzheimer 1907). Senile plaques are extracellular insoluble, congophilic protein aggregates composed of amyloid β, a 39- to 43-amino-acid peptide. Neurofibrillary tangles are intracellular lesions consisting of paired helical filaments from the hyperphosphorylated cytoskeletal protein τ, which is a microtubule-associated protein that is involved in microtubule assembly and stabilization. In Alzheimer's disease, τ is abnormally phosphorylated, aggregates into paired helical filaments, and loses its ability to stabilize axonal microtubules (Mandelkow and Mandelkow 1998).

Goedert and Hasegawa (1999) discussed the tauopathies as an experimental animal model for Alzheimer's disease and other dementing disorders.

The discovery of autosomal dominant mutations in the gene encoding the amyloid precursor protein that were causal for early-onset familial Alzheimer's disease strongly suggested amyloid β to be the prime suspect in the pathogenesis of Alzheimer's disease, resulting in the formulation of the amyloid cascade hypothesis (Hardy and Higgins 1992).

In line with the amyloid cascade hypothesis, a strategy for disease-modifying pharmacological intervention would be the selective inhibition of β- and γ-secretase, the proteases that process amyloid precursor protein to amyloid β.

Bartzokis (2004) presented age-related myelin breakdown as a hypothetical model of cognitive decline and Alzheimer's disease.

REFERENCES AND FURTHER READING

Alzheimer A (1907) Über eine eigenartige Erkrankung der Hirnrinde. Allg Z Psychiatr 64:146–148

Arendt T, Henning D, Gray JA, Marchbanks R (1988) Loss of neurons in the rat forebrain cholinergic projection system after prolonged intake of ethanol. Brain Res Bull 21:563–5659

Bartus RT, Dean RL, Beer B (1980) Memory deficits in aged Cebus monkeys and facilitation with central cholinomimetics. Neurobiol Aging 1:145–152

Bartus RT, Dean RL, Beer B, Lippa AS (1982) The cholinergic hypothesis of geriatric memory dysfunction. Science 217:408–417

Bartus RT, Dean RL, Flicker C (1987) Cholinergic psychopharmacology: an integration of human and animal research on memory. In: Meltzer HY (ed) Psychopharmacology: The Third Generation of Progress. Raven Press, New York, pp 219–232

Bartzokis G (2004) Age-related myelin breakdown: a developmental model of cognitive decline and Alzheimer's disease. Neurobiol Aging 25:5–18

Campbell BA, Spear NE (1972) Ontogeny of memory. Psychol Rev 79:215–236

Changeux JP, Bertrand D, Corringer PJ, Dehaene S, Edelstein S, Léna C, LeNovère N, Marubio L, Picciotto M, Zoli M (1998) Brain nicotinic receptors: structure and regulation, role in learning and reinforcement. Brain Res Rev 26:198–216

Christie JE, Shering A, Ferguson J, Glen AIM (1981) Physostigmine and arecoline: Effects of intravenous infusions in Alzheimer presenile dementia. Br J Psychiatry 138:46–50

Craik FJM (1977) Age differences in human memory. In: Birren JE, Schaie KW (eds) Handbook of the Psychobiology of Aging, Von Nostrand Reinhold Co., New York, NY, pp 384–420

Davis KL, Mohs RC (1982) Enhancement of memory processes in Alzheimer's disease with multiple dose intravenous physostigmine. Am J Psychiatry 139:1421–1424

Emre E, Qizilbash N (2001) Experimental approaches and drugs in development for the treatment of dementia. Expert Opin Invest Drugs 10:607–617

Fadda F, Rossetti ZL (1998) Chronic ethanol consumption: from neuroadaptation to neurodegeneration. Prog Neurobiol 15:385–431
Francis PT, Nordber A, Arnold SE (2005) A preclinical view of cholinesterase inhibitors in neuroprotection: do they provide more than symptomatic benefits in Alzheimer's disease? Trends Pharmacol Sci 26:104–111
Goedert M, Hasegawa M (1999) The Tauopathies. Toward an experimental animal model. Am J Pathol 154:1–6
Hardy JA, Higgins GA (1992) Alzheimer's disease: the amyloid cascade. Science 256:184–185
Hess EH (1972) "Imprinting" in a natural laboratory. Scientific American 227:24–31
Kubanis P, Zornetzer SF (1981) Age-related behavioral and neurobiological changes: A review with emphasis on memory. Behav neural Biol 31:115–172
Lennenberg E (1967) The Biological Foundations of Language. Wiley & Sons, New York, NY
Lichtenthaler SF, Haass C (2004) Amyloid at the cutting edge: activation of α-secretase prevents amyloidogenesis in an Alzheimer disease mouse model. J Clin Invest 113:1384–1387
Mandelkow EM, Mandelkow E (1998) Tau in Alzheimer's disease. Trends Cell Biol 8:425–427
McClearn GE (1999) Commentary: Exotic mice as models for aging research: polemic and prospectus by R. Miller et al. Neurobiol Aging 20:233–236
McDonald MP, Overmier JB (1998) Present imperfect: a critical review of animal models of the mnemonic impairments in Alzheimer's disease. Neuroscience Behav Rev 22:99–120
Miller RA, Austad S, Burke D, Chrisp C, Dysko R, Galecki A, Jackson A, Monnier V (1999) Exotic mice as models for aging research: polemic ads prospectus. Neurobiol Aging 20:217–231
Myslivecek J (1997) Inhibitory learning and memory in newborn rats. Progr Neurobiol 53:399–430
Nordberg A (1990) Pharmacological modulation of transmitter activity in Alzheimer brains – an experimental model. In: Novel Therapeutic Strategies for Dementia Diseases. Acta Neur Scand, Suppl 129:17–20
Raghavendra V, Kulkarni SK (2001) Possible antioxidant mechanism in melatonin reversal of aging and chronic ethanol-induced amnesia in plus-maze and passive avoidance memory tasks. Free Radical Biol Med 30:595–603
Scheich H (1987) Neural correlates of auditory filial imprinting. J Comp Physiol A 161:605–619
Socci DJ, Crandall BM, Arendash GW (1995) Chronic antioxidant treatment improves cognitive performance of aged rats. Brain Res 693:88–94
Sommer B (2002) Alzheimer's disease and the amyloid cascade hypothesis. Curr Opin Pharmacol 2:87–92
Summers WE, Viesselman JO, March GM, Candelora K (1981) Use of THA in treatment of Alzheimer-like dementia. Pilot study in twelve patients. Biol Psychiatry 16:145–153
Thal LJ, Fuld PA, Masur DM, Sharpless NS (1983) Oral physostigmine and lecithin improve memory in Alzheimer's disease. Ann Neurology 13:491–496
Thorsett ED, Latimer LH (2000) Therapeutic approaches to Alzheimer's disease. Curr Opin Chem Biol 4:377–382
Wozniak DF, Hartman RE, Boyle MP, Vogt SK, Brooks AR, Tenkova T, Young C, Olney JW, Muglia LJ (2004) Apoptotic neurodegeneration induced by ethanol in neonatal mice with profound learning/memory deficits in juveniles followed by progressive functional recovery in adults. Neurobiol Dis 17:403–414
Yamada K, Nabeshima T (2000) Animal models of Alzheimer's disease and evaluation of anti-dementia drugs. Pharmacol Ther 88:93–113

F.2 In Vitro Methods

F.2.0.1 In Vitro Inhibition of Acetylcholine-Esterase Activity in Rat Striatum

PURPOSE AND RATIONALE

The purpose of this assay is to screen drugs for inhibition of acetylcholine-esterase activity. Inhibitors of this enzyme may be useful for the treatment of Alzheimer's disease.

Acetylcholinesterase (AChE), which is sometimes called true or specific cholinesterase, is found in nerve cells, skeletal muscle, smooth muscle, various glands and red blood cells (Nachmansohn and Rothenberg 1945; Koelle et al. 1950; Ellman et al. 1961). AChE may be distinguished from other cholinesterases by substrate and inhibitor specificities and by regional distribution. Its distribution in brain roughly correlates with cholinergic innervation and subfractionation shows the highest level in nerve terminals.

It is generally accepted that the physiological role of AChE is the rapid hydrolysis and inactivation of acetylcholine. Inhibitors of AChE show marked cholinomimetic effects in cholinergically-innervated effector organs (Taylor 1996) and have been used therapeutically in the treatment of glaucoma, myasthenia gravis and paralytic ileus. However, recent studies (Christie et al. 1981; Summers et al. 1981; Davies and Mohs 1982; Atak et al. 1983) have suggested that AChE inhibitors may also be beneficial in the treatment of Alzheimer's dementia.

Augustinsson (1971) reviewed a number of methods for assaying cholinesterase activity and concluded that the method described by Ellman et al. (1961) was one of the best. The method described is a modification of Ellman's procedure.

PROCEDURE

Reagents

1. 0.05 M Phosphate buffer, pH 7.2
   a) 6.85 g $NaH_2PO_4 \cdot H_2O$/100 ml distilled H_2O
   b) 13.40 g $Na_2HPO_4 \cdot 7H_2O$/100 ml distilled H_2O
   c) add a) to b) until pH reaches 7.2
   d) Dilute 1:10
2. Substrate in buffer
   a) 198 mg acetylthiocholine chloride (10 mM)

b) q.s. explain to 100 ml with 0.05 M NaH_2PO_4, pH 7.2 (reagent 1)

3. DTNB in buffer
   a) 19.8 mg 5,5-dithiobisnitrobenzoic acid (DTNB) (0.5 mM)
   b) q.s. to 100 ml with 0.05 M NaH_2PO_4, pH 7.2 (reagent 1)
4. A 2 mM stock solution of the test drug is made up in a suitable solvent and q.s. to volume with 0.5 mM DTNB (reagent 3). Drugs are serially diluted (1:10) such that the final concentration (in cuvette) is 10^{-4} M and screened for activity. If active, IC_{50} values are determined from the inhibitory activity of subsequent concentrations.

Tissue Preparation

Male Wistar rats are decapitated, brains rapidly removed, corpora striata dissected free, weighed and homogenized in 19 volumes (approximately 7 mg protein/ml) of 0.05 M NaH_2PO_4, pH 7.2 using a Potter-Elvejhem homogenizer (Kontes, Vineland, NJ). A 25 µl aliquot of this suspension is added to 1 ml of the vehicle or various concentrations of the test drug and reincubated for 10 min at 37°C.

Assay

Enzyme activity is measured with the Beckman DU-50 spectrophotometer. This method can be used for IC_{50} determinations and for measuring kinetic constants.

Reagents are added to the blank and sample cuvettes as follows:

Blank: 0.8 ml PO_4 buffer/DTNB
0.8 ml buffer/Substrate

Control: 0.8 ml PO_4 buffer/DTNB/Enzyme
0.8 ml PO_4 buffer/Substrate

Drug: 0.8 ml PO_4 buffer/DTNB/Drug/Enzyme
0.8 ml PO_4 buffer/Substrate

Blank values are determined for each run to control for non-enzymatic hydrolysis of substrate and these values are automatically subtracted by the kin-data program available on kinetics soft-pac module. This program (Beckman DU-50 series spectrophotometer, kinetics Soft-Pac™ module operation instructions: 1–7 also calculates the rate of absorbance change for each cuvette.

EVALUATION

For IC_{50} determinations: Substrate concentration is 10 mM diluted 1:2 in an assay yielding a final concentration of 5 mM. DTNB concentration is 0.5 mM yielding 0.25 mM final concentration

$$\% \text{ Inhibition} = \frac{\text{slope control} - \text{slope drug}}{\text{slope control}} \times 100$$

IC_{50} values are calculated from log-probit analysis.

REFERENCES AND FURTHER READING

Atak JR, Perry EK, Bonham JR, Perry RH, Tomlinson BE, Blessed G, Fairbairn A (1983) Molecular forms of acetylcholinesterase in senile dementia of Alzheimer type: selective loss of the intermediate (10S) form. Neurosci Lett 40:199–204

Augustinsson KB (1971) Determination of activity of cholinesterases. In: Glick D (ed) Methods of Biochemical Analysis, John Wiley & Sons, New York, pp 217–273

Chan SL, Shirachi DY, Bhargava HN, Gardner E, Trevor AJ (1972) Purification and properties of multiple forms of brain acetylcholinesterase. J Neurochem 19:2747–2758

Cheng Y, Prusoff WH (1973) Relationship between the inhibition constant (K_i) and the concentration of inhibitor which causes 50 percent inhibition (IC_{50}) of an enzymatic reaction. Biochem Pharmacol 22:3099–3108

Christie JE, Shering A, Ferguson J, Glen AIM (1981) Physostigmine and arecoline: Effects of intravenous infusions in Alzheimer presenile dementia. Br J Psychiatry 138:46–50

Davis KL, Mohs RC (1982) Enhancement of memory processes in Alzheimer's disease with multiple dose intravenous physostigmine. Am J Psychiatry 139:1421–1424

Ellman GL, Courtney KD, Andres V, Featherstone RM (1961) A new and rapid colorimetric determination of acetylcholinesterase activity. Biochem Pharmacol 7:88–95

Grassi J, Vigny M, Massoulié J (1982) Molecular forms of acetylcholinesterase in bovine caudate nucleus and superior cervical ganglion: solubility properties and hydrophobic character. J Neurochem 38:457–469

Koelle GB, Koelle FS, Friedenwald JS (1950) The effect of inhibition of specific and non-specific cholinesterases. J Pharmacol Exp Ther 100:180–191

McIntosh CHS, Plummer DT (1973) Multiple forms of acetylcholinesterase from pig brain. Biochem J 133:655–665

Nachmansohn D, Rothenberg MA (1945) Studies on cholinesterase 1. On the specificity of the enzyme in nerve tissue. J Biol Chem 158:653–666

Rieger F, Vigny M (1976) Solubilization and physicochemical characterization of rat brain acetylcholinesterase: development and maturation of its molecular forms. J Neurochem 27:121–129

Summers WE, Viesselman JO, March GM, Candelora K (1981) Use of THA in treatment of Alzheimer-like dementia. Pilot study in twelve patients. Biol Psychiatry 16:145–153

Taylor P (1996) Anticholinesterase agents. In: Goodman and Gilman's The Pharmacological Basis of Therapeutics, 9thed. McGraw-Hill, New York, pp 161–176

Thal LJ, Fuld PA, Masur DM, Sharpless NS (1983) Oral physostigmine and lecithin improve memory in Alzheimer's disease. Ann Neurology 13:491–496

Trevor AJ, Gordon MA, Parker KK, Chan SL (1978) Acetylcholinesterases. Life Sci 23:1209–1220

F.2.0.2 In Vitro Inhibition of Butyrylcholine-Esterase Activity in Human Serum

PURPOSE AND RATIONALE

This assay can be used in conjunction with the acetylcholine-esterase assay to determine the enzyme selectivity of various cholinesterase inhibitors.

Butyrylcholine-esterase (BChE), which is sometimes called pseudocholinesterase, preferentially hydrolyzes butyrylcholine. This enzyme is found in the highest amounts in serum, but its physiological role is not known (Chemnitius et al. 1983; Walker and Mackness 1983). Ethopropazine and tetra-isopropyl pyrophosphoramide (ISO-OMPA) are selective inhibitors of butyrylcholinesterase. In an *ex vivo* experiment with the selective BChE inhibitor, ISO-OMPA, it was shown that inhibition of butyrylcholinesterase was not correlated with any significant acute cholinomimetic effects.

PROCEDURE

Reagents

1. 0.05 M phosphate buffer, pH 7.2
   a) 6.85 g $NaH_2PO_4 \cdot H_2O$/100 ml distilled H_2O
   b) 13.40 g $Na_2HPO_4 \cdot H_2O$/100 ml distilled H_2O
   c) Add (a) to (b) until pH reaches 7.2
   d) Dilute 1:10
2. Substrate in buffer
   a) 225.8 mg s-butyrylthiocholine chloride
   b) q.s. to 100 ml with 0.05 M phosphate buffer, pH 7.2 (reagent 1)
3. DTNB in buffer
   a) 19.8 mg 5,5-dithiobisnitrobenzoic acid (DTNB) (0.5 mM)
   b) q.s. to 100 ml with 0.05 M phosphate buffer, pH 7.2 (reagent 1)
4. A 2 mM stock solution of the test drug is made up in a suitable solvent and q.s. to volume with 0.5 mM DTNB (reagent 3). Drugs are serially diluted (1:10) such that determined from the inhibitory activity of subsequent concentrations.

Enzyme Preparation

A vial of lyophilized human serum (Precilip, Biodynamics, Houston, Texas) is reconstituted in 3 ml of distilled water. A 25 ml aliquot of this suspension is added to 1 ml of the vehicle or various concentrations of the test drug and pre-incubated for 10 min at 37°C.

Assay

Enzyme activity is measured with the Beckman DU-50 spectrophotometer. This method can be used for IC_{50} determinations and for measuring kinetic constants.

Reagents are added to the blank and sample cuvettes as follows:

Blank: 0.8 ml PO_4 buffer/DTNB
0.8 ml buffer/Substrate

Control: 0.8 ml PO_4 buffer/DTNB/Enzyme
0.8 ml PO_4 buffer/Substrate

Drug: 0.8 ml PO_4 buffer/DTNB/Drug/Enzyme
0.8 ml PO_4 buffer/Substrate

Blank values are determined for each run to control for non-enzymatic hydrolysis of substrate and these values are automatically subtracted by the kindata program available on kinetics soft-pac module. This program also calculates the rate of absorbance change for each cuvette.

EVALUATION

For IC_{50} determinations: Substrate concentration is 10 mM diluted 1:2 in assay yielding final concentration of 5 mM. DTNB concentration is 0.5 mM yielding 0.25 mM final concentration

$$\% \text{ Inhibition} = \frac{\text{slope control} - \text{slope drug}}{\text{slope control}} \times 100$$

IC_{50} values are calculated from log-probit analysis.

REFERENCES AND FURTHER READING

Chemnitius J-M, Haselmeyer K-H, Zech R (1983) Brain cholinesterases: Differentiation of target enzymes for toxic organophosphorus compounds. Biochem Pharmacol 32:1693–1699

Ellman GL, Courtney KD, Andres V, Featherstone RM (1961) A new and rapid colorimetric determination of acetylcholinesterase activity. Biochem Pharmacol 7:88–95

Walker CH, Mackness MI (1983) Esterases: Problems of identification and classification. Biochem Pharmacol 32:3265–3269

F.2.0.3 Ex Vivo Cholinesterase Inhibition

PURPOSE AND RATIONALE

This assay is used to determine the dose-response relationship and duration of action of cholinesterase inhibitors *in vivo*.

Cholinesterase inhibitors, including physostigmine (Christie et al. 1981; David and Mohs 1982; Thal et al. 1983) and tacrine (Summers et al. 1986) have been shown to improve cognitive functions in Alzheimer's disease. Physostigmine is a potent, but nonselec-

tive inhibitor of cholinesterase (Taylor 1996) and has a short duration of action. Tacrine also inhibits both acetylcholine-esterase (true) and butyrylcholine-esterase (pseudo), but is more potent as an inhibitor of the pseudo-enzyme (Heilbronn 1961).

The mechanism of inhibition of these two drugs is quite different. Physostigmine is a competitive inhibitor and blocks the active site of the enzyme by carbamylation of a serine hydroxyl group at the esteratic site of the enzyme (Taylor 1996; O'Brien 1969). This covalently bound carbamyl group then dissociates from the enzyme much more slowly than the acetyl group left by the natural substrate, but the inhibition is not irreversible like that of the organophosphates. The inhibition characteristics of physostigmine, i. e., submicromolar affinity for the enzyme and covalent binding of the inhibiting group, are ideal for *ex vivo* studies. Tacrine, however, is a mixed competitive inhibitor of cholinesterase (Heilbronn 1961), with lower apparent affinity than physostigmine for the enzyme (based on IC_{50} values at saturated substrate concentrations). Tacrine binds to the anionic site of cholinesterase through weak hydrophobic interactions (Steinberg et al. 1975).

Ideally, a dose-response for cholinesterase inhibition is determined first. Then a dose which gives a reasonable effect (> 50% inhibition if possible) is chosen to do the time-course experiment. The effects on brain acetylcholinesterase activity are examined in striatal tissue, using 5 mM acetylthiocholine as a substrate (Ellman et al. 1961). Effects on butyrylcholine-esterase activity may be determined in plasma samples, with 5 mM butylthiocholine used as a substrate.

PROCEDURE

Reagents

1. 0.05 M Phosphate buffer, pH 7.2
   a) 6.85 g $NaH_2PO_4 \cdot H_2O$/100 ml distilled H_2O
   b) 13.40 g $Na_2HPO_4 \cdot 7H_2O$/100 ml distilled H_2O
   c) add a) to b) until pH reaches 7.2
   d) Dilute 1:10
2. DTNB in buffer
   a) 19.8 mg 5,5-dithiobisnitrobenzoic acid (DTNB) (0.5 mM)
   b) q.s. to 100 ml with 0.05 M phosphate buffer, pH 7.2 (reagent 1)
3. Substrate in buffer
   a) 198 mg acetylthiocholine chloride (10 mM)
   b) q.s. to 100 ml with 0.05 M phosphate buffer, pH 7.2 (reagent 1)

Drug Treatment

Groups of four male Wistar rats are dosed i.p. or p.o. with vehicle or the test drug. For the initial dose response study, the rats are given varying doses of drug based on toxicity reported in primary overt effects testing and sacrificed at either 30 min or 1 h after dosing. The animals are observed and the occurrence of cholinergic signs is noted (piloerection, tremors, convulsions, salivation, diarrhea and chromodacryorrhea). For the time-course study, a dose of the test drug is given which gave significant inhibition of cholinesterase activity.

Tissue Preparation

Male Wistar rats are decapitated, brains rapidly removed, corpora striata dissected free, weighed and homogenized in 4 volumes of 0.05 M phosphate buffer, pH 7.2 using a Potter-Elvehjem homogenizer (Kontes, Vineland, NJ). A 12.5 ml aliquot of the homogenate is added to 1 ml 0.05 M phosphate buffer, pH 7.2/DTNB (reagent 2).

Assay

1. Enzyme activity is measured with the Beckman DU-50 spectrophotometer.
   Reagents are added to the blank and sample cuvettes as follows:

   Blank: 0.8 ml PO_4 buffer/DTNB (reagent 2)
   0.8 ml PO_4 buffer/Substrate (reagent 3)

   Control: 0.8 ml PO_4 buffer/DTNB/Enzyme from control animal
   0.8 ml PO_4 buffer/Substrate

   Drug: 0.8 ml PO_4 buffer/DTNB/Enzyme from treated animal
   0.8 ml PO_4 buffer/Substrate

   Blank values are determined for each run to control for non-enzymatic hydrolysis of substrate and these values are automatically subtracted by the kin-data program available on kinetics soft-pac module. This program also calculates the rate of absorbance change for each cuvette.
2. Substrate concentration is 10 mM diluted 1:2 in the assay yielding final concentration of 5 mM. DTNB concentration is 0.5 mM yielding 0.25 mM final concentration.

EVALUATION

The percent inhibition at each dose or time is calculated by comparison with the enzyme activity of the

vehicle control group.

$$\% \text{ Inhibition} = \frac{\text{slope control} - \text{slope drug}}{\text{slope control}} \times 100$$

Ex vivo time course experiments for physostigmine

	Physostigmine, 0.3 mg/kg, i.p.	
Time (h)	% Inhibition striatum	Cholinergic signs
0.25	48.6	P,T,D
0.5	28.5	P,T,D
1.0	27.0	P,T
2.0	7.6	P,T
4.0	1.4	P,T

P = piloerection, T = tremors, D = diarrhea.

MODIFICATIONS OF THE METHOD

Antagonism of physostigmine-induced lethality in mice has been used by Gouret (1973) as a general indicator of central or peripheral anticholinergic activity. A low dose of physostigmine can be used for detecting procholinergic activity.

REFERENCES AND FURTHER READING

Christie JE, Shering A, Ferguson J, Glen AIM (1981) Physostigmine and arecoline: Effects of intravenous infusions in Alzheimer presenile dementia. Br J Psychiatry 138:46–50

Davis KL, Mohs RC (1982) Enhancement of memory process in Alzheimer's disease with multiple dose intravenous physostigmine. Am J Psychiatry 139:1421–1424

Ellman GL, Courtney KD, Andres V, Featherstone RM (1961) A new and rapid colorimetric determination of acetylcholinesterase activity. Biochem Pharmacol 7:88–95

Gouret C (1973) Etude de cinq tests rapides de sélection d'une activité anticholinergique chez la souris. J Pharmacol (Paris) 4:105–128

Heilbronn E (1961) Inhibition of cholinesterase by tetrahydroaminacrin. A Chem Scand 15:1386–1390

Muller F, Dumez Y, Massoulié J (1985) Molecular forms and solubility of acetylcholinesterase during the embryonic development of rat and human brain. Brain Res 331:295–302

O'Brien RD (1969) Phosphorylation and carbamylation of cholinesterase. Ann NY Acad Sci 160:204–214

Sivam SP, Norris JC, Lim DK, Hoskins B, Ho IK (1983) Effect of acute and chronic cholinesterase inhibition with diisopropylfluorophosphate on muscarinic, dopamine, and GABA receptors in the rat striatum. J Neurochem 40:1414–1422

Steinberg GM, Mednick ML, Maddox J, Rice R, Cramer J (1975) A hydrophobic binding site in acetylcholinesterase. J Med Chem 18:1056–1061

Summers WK, Majovski LV, Marsh GM, Tachiki K, Kling A (1986) Oral tetrahydroaminoacridine in long-term treatment of senile dementia, Alzheimer type. New Eng J Med 315:1241–1245

Taylor P (1996) Anticholinesterase agents. In: Goodman and Gilman's The Pharmacological Basis of Therapeutics, 9thed. McGraw-Hill, New York, pp 161–176

Thal LJ, Fuld PA, Masur DM, Sharpless NS (1983) Oral physostigmine and lecithin improve memory in Alzheimer's disease. Ann Neurology 13:491–496

Yamada S, Isogai M, Okudaira H, Hayashi R (1983) Correlation between cholinesterase inhibition and reduction in muscarinic receptors and choline uptake by repeated diisopropylfluorophosphate administration: antagonism by physostigmine and atropine. J Pharmacol Exp Ther 226:519–525

F.2.0.4 Molecular Forms of Acetylcholinesterase from Rat Frontal Cortex and Striatum

PURPOSE AND RATIONALE

Different molecular forms of acetylcholinesterase can be isolated from animal tissues after solubilization in buffers containing various detergent and salt concentrations. The number of forms isolated, their relative amounts and molecular characteristics depend on the tissue source and the conditions used for solubilization of the membrane bound enzyme (McIntosh and Plummer 1973; Reiger and Vigny 1976; Trevor et al. (1976). Bon et al. (1979) have classified these forms as globular (G_1, G_2 and G_4) and asymmetric (A_4, A_8 and A_{12}), where the subscripts indicate the number of catalytic subunits. The G_1 and G_4 forms, having sedimentation coefficients of approximately 4S and 10S, respectively, are the major forms contained in bovine caudate nucleus (Grassi et al. 1982). Under conditions of high salt concentrations and detergent, AChE is quantitatively extracted from rat brain, with 10S form being the predominant component (Reiger and Vigny 1976). After solubilization, the molecular forms may be separated according to sedimentation properties by density gradient centrifugation, molecular weight by gel filtration or by electrophoretic mobility.

Although most of these studies on molecular forms of AChE have focused on the physical differences, Chan et al. (1972) reported some difference in sensitivity of the low molecular weight form to physostigmine and fluoride ion, while Lenz and Maxwell (1981) showed differential sensitivity to soman of forms separated by isoelectric focusing. Studies showing selective increases in the 10S form during development (Muller et al. 1985) and selective loss in Alzheimer's disease (Atack et al. 1983) suggest that this form of the enzyme may be developmentally and functionally more important. Cortical and striatal areas show different patterns of cholinergic innervation; the cortex having primarily extrinsic innervation, while the striatal cholinergic pathways are predominantly intrinsic (Ceullo and Sofroniew 1984).

The purpose of this procedure is to determine the effects of various cholinesterase inhibitors on the two major molecular forms of acetylcholinesterase isolated from rat striatum and cerebral cortex.

PROCEDURE

The procedure is divided into three main parts:

I. Preparation and isolation of molecular forms of AChE,

II. Assays for the marker enzymes,

III. Enzyme inhibition studies.

I.a Preparation of molecular forms of AChE

Male Wistar rats (200–250 g) are sacrificed, their brains rapidly removed and frontal cortices or corpora striata removed. The brain areas are weighed and homogenized in 5 volumes (wt/vol) of 10 mM phosphate buffer, pH 7.1, containing 1 M NaCl and 1% Triton X-100, except were indicated. The homogenates are centrifuged at 20,000 *g* for 20 min at 4°C. The supernatant is aspirated and marker enzymes for 16S (*E. coli* β-galactosidase), 11.3S (bovine catalase) and 4.8S (horse liver alcohol dehydrogenase) fractions are added. The supernatant is then centrifuged at 37,000 rpm (140,000 *g* max) for 17.5 h in a Beckman L5–65 ultracentrifuge with a SW-60 rotor. 15-drop fractions are collected for each centrifuge tube and assayed for protein, β-galactosidase, catalase, alcohol dehydrogenase and acetylcholinesterase activity. In addition, butyrylcholinesterase can be measured.

A 400 µl sample of the 20,000 *g*-supernatant is carefully layered on top of a 5–20% continuous sucrose gradient. This gradient is made up in a centrifuge tube from 1.65 ml of 20% sucrose and 1.65 ml of 5% sucrose in homogenizing buffer by means of a gradient maker. A 50% sucrose cushion (0.5 ml) is placed at the bottom of the tube.

Fractions are collected from the bottom of the tube, i.e, the densest fractions are collected first. Each fraction is 15 drops or approximately 24 fractions are collected per centrifuge tube.

I.b Analysis of fractions

β-Galactosidase, catalase and alcohol dehydrogenase are determined by enzymic activity (Hestrin et al. 1955; Chance and Maehly 1955; Bonnichsen and Brink 1955). Protein concentrations are determined by the method of Lowry et al. (1951). Acetylcholinesterase activity or butyrylcholinesterase activity are determined by a modification of the method of Ellman et al. (1961). Briefly, 10 µl aliquots of the fractions are added to 0.25 mM dithionitrobenzoic acid (DTNB) and 5 mM acetylthiocholine or 5 mM butyrylthiocholine in 0.05 M phosphate buffer, pH 7.2 and the absorbance is measured at 412 nm. Fractions of peak acetylcholinesterase activity are characterized by their sedimentation characteristics relative to the marker enzymes and peak fractions are pooled for enzyme inhibition studies or determination of kinetic constants.

II. Assays for marker enzymes

A Equine liver alcohol dehydrogenase (ADH), sedimentation coefficient 4.8 S

1. Enzyme: alcohol dehydrogenase from equine liver, crystallized and lyophilized (Sigma Chem. Co.)
2. Reagents:
   a) β-nicotinamide adenine dinucleotide (NAD) (Sigma Chem. Co.)
   b) 0.1 M glycine-NaOH buffer, pH 9.6
   c) absolute ethanol
   d) buffer-substrate-NAD mixture:
   875 µl NAD+875 µl ethanol+18.75 ml
   0.1 M glycine-NaOH buffer, pH 9.6
3. Assay
   10 µl enzyme fraction and
   850 µl mixture (reagent 2d)
   are incubated for 5 min at room temperature. The reaction is stopped by adding:
   300 µl 1.5 M $ZnSO_4$
   Absorbance is read at 340 nm and enzyme units are determined from a standard curve using values of 1.25, 2.5, 5, 10 and 20 mU of ADH.

B Bovine liver catalase, sedimentation coefficient 11.3 S

1. Enzyme: catalase from bovine liver, purified powder (Sigma Chem. Co., C-10)
2. Reagents:
   a) 30% hydrogen peroxide
   b) 0.05 M sodium phosphate buffer, pH 7.0
   c) mixture: 111 µl 30% hydrogen peroxide + 100 ml buffer, yielding 0.033% peroxide.
3. Assay
   10 µl enzyme fraction
   2990 µl peroxide-buffer mixture (reagent 2c)

Wavelength is set to 240 nm, absorbance is adjusted to 0.480 units. The amount of time is recorded for absorbance to decrease from 0.450 to 0.400. This corresponds to 3.45 µmol of hydrogen peroxide in 3 ml solution. Total catalase activity in 3 ml is 3.45 µMol/min.

C *E. coli* β-galactosidase, sedimentation coefficient 16.0 S

1. Enzyme: β-galactosidase from *E. coli*, grade VI, partially purified, lyophilized (Sigma Chem. Co)
2. Reagents:
   a) substrate: 15 mg/ml O-nitrophenyl-β-D-galacto-pyranoside (Sigma Chem. Co.) in water
   b) 0.6 M Na_2CO_3, pH 7.25
   c) 1 M $NaCO_3$
3. Assay
   10 µl enzyme fraction,
   150 µl 0.6 M phosphate buffer, pH 7.25, and
   50 µl O-Nitrophenyl-β-D-galactopyranoside
   (12 mM in assay) are incubated for 25 min at 30°C. The reaction is stopped by adding:
   500 µl 1 M Na_2CO_3, 1.75 ml water.
   Absorbance is read at 420 nm and enzyme units are determined from a standard curve using values of 0.015, 0.030, 0.525, 0.125 and 0.250 U of β-galactosidase.

III. Enzyme inhibition studies

For the enzyme inhibition studies, 25 µl aliquots of the enzyme preparation are preincubated with varying concentrations of the inhibitor for 10 min at 25°C and acetylcholinesterase activity is determined as previously described.

EVALUATION

Values for the IC_{50} are determined by log-probit analysis of the inhibition data using six to seven concentrations of the inhibitor and represent the means of 3 separate experiments.

REFERENCES AND FURTHER READING

Atack JR, Perry EK, Bonham JR, Perry RH, Tomlinson BE, Blessed G, Fairbairn A (1983) Molecular forms of acetylcholinesterase in senile dementia of the Alzheimer type: Selective loss of the intermediate (10S) form. Neurosci Lett 40:199–204

Bon S, Vigny M, Massoulié J (1979) Asymmetric and globular forms of acetylcholinesterase in mammals and birds. Proc Natl Acad Sci. USA 76:2546–2550

Bonnichsen RK, Brink NG (1955) Liver alcohol dehydrogenase. In: Colowick SP, Kaplan NO (eds) Methods of Enzymology, Vol. I, p. 241, Academic Press, New York

Ceullo AC, Sofroniew MV (1984) The anatomy of the CNS cholinergic neurons. TINS 7:74–78

Chan SL, Shirachi DY, Bhargava HN, Gardner E, Trevor AJ (1972) Purification and properties of multiple forms of brain acetylcholinesterase. J Neurochem 19:2747–2758

Chance B, Maehly AC (1955)Catalase assay by the disappearance of peroxide. In: Colowick SP, Kaplan NO (eds) Methods of Enzymology, Vol. II, pp 764–768, Academic Press, New York

Ellman GL, Courtney KD, Andres V, Featherstone RM (1961) A new and rapid colorimetric determination of acetylcholinesterase activity. Biochem Pharmacol 7:88–95

Grassi J, Vigny M, Massoulié J (1982) Molecular forms of acetylcholinesterase in bovine caudate nucleus and superior cervical ganglion: solubility properties and hydrophobic character. J Neurochem 38:457–469

Hestrin S, Feigold DS, Schramm M (1955) Hexose hydrolases. In: Colowick SP, Kaplan NO (eds) Methods of Enzymology, Vol. I, pp 231–257, Academic Press, New York

Lenz DE, Maxwell DM (1981) Inhibition of rat cerebrum acetylcholinesterase isozymes after acute administration of soman. Biochem Pharmacol 30:1369–1371

Lowry OH, Rosebrough NJ, Farr AL, Randall RJ (1951) Protein measurement with the Folin phenol reagent. J Biol Chem 193:265–275

McIntosh CHS, Plummer DT (1973) Multiple forms of acetylcholinesterase from pig brain. Biochem J 133:655–665

Muller F, Dumez Y, Massoulié J (1985) Molecular forms and solubility of acetylcholinesterase during the embryonic development of rat and human brain. Brain Res 331:295–302

Reiger F, Vigny M (1976) Solubilization and physicochemical characterization of rat brain acetylcholinesterase: Development and maturation of its molecular forms. J Neurochem 27:121–129

Trevor AJ, Gordon MA, Parker KK, Chan SL (1978) Acetylcholinesterases. Life Sci 23:1209–1220

F.2.0.5 Release of [^{3}H]ACh and Other Transmitters from Rat Brain Slices

PURPOSE AND RATIONALE

Electrically stimulated release of [^{3}H]ACh is used as a biochemical screen for agents which may possibly enhance or inhibit release of [^{3}H]ACh through a direct muscarinic interaction or other indirect interactions.

Muscarinic autoreceptors have been shown to have a role in the regulation of ACh release in several areas of the CNS (Hadhazy and Szerb 1977; DeBelleroche and Gardiner 1982; Strittmatter et al. 1982; James and Cubeddu 1984). Direct stimulation of muscarinic receptors with muscarinic agonists or indirect stimulation with acetylcholinesterase inhibitors decreases ACh release evoked by either increased potassium concentration or electrical stimulation. Muscarinic antagonists can either block their inhibition, or, under certain conditions, enhance ACh release (James and Cubeddu 1987; Sethy et al. 1988). Furthermore, other

neurotransmitters, most notably 5-HT and DA, can also inhibit [^{3}H]ACh release via interaction with 5-T_2 and D_2 heteroreceptors (Robinson 1983; Jackson et al. 1988; Muramatsu et al. 1988; Drukarch et al. 1989) and this inhibition can be reversed by the appropriate receptor antagonists. A compound's effect on [^{3}H]ACh release may provide evidence for a wide variety of releasing activities.

The advantages of using the electrically stimulated release technique on tissue slices have been described by Zahniser et al. (1986). This technique measures only presynaptic effects of test compounds.

PROCEDURE

This assay is based on the methods described by James and Cubeddu (1984, 1987).

Reagents

1. Krebs-Henseleit bicarbonate buffer, pH 7.4 (KHBB)
   Make a 2 liter batch, containing the following salts:

NaCl	13.84 g	118.4 mM
KCl	0.70 g	4.7 mM
$MgSO_4 \cdot 7H_2O$	0.58 g	1.2 mM
KH_2PO_4	0.32 g	2.2 mM
$NaHCO_3$	4.20 g	24.9 mM
$CaCl_2$	0.28 g	1.3 mM
Prior to use, add:		
Dextrose	4.00 g	11.1 mM

   Aerate for 60 min with 95% O_2/5% CO_2 on ice and check pH.
2. [Methyl-^{3}H]-choline chloride (80–90 Ci/mmol) is obtained from New England Nuclear. The final desired concentration of [^{3}H]choline is 100 nM. Add 0.25 nmol of [^{3}H]choline to 2.5 ml KHBB.
3. For most assays, a 10 mM stock solution of the test compound is prepared in a suitable solvent and diluted such that the final concentration in the assay is 10 µM. Higher or lower concentrations may be used depending on the potency of the test compound.
4. Hemicholinium-3 or HC-3 (Sigma): Make a 10 mM stock solution in H_2O. Two milliliters of this stock are then diluted to one liter in KHBB to give a final concentration of 20 µM.

Tissue Preparation

Male Wistar rats (100–150 g) are decapitated, and cortical, striatal, or hippocampal tissue removed on ice and 0.4 mm slices are prepared with a McIlwain tissue slicer. The slices are made individually, placed in cold, oxygenated buffer (10–20 ml) and incubated at 35°C for 30 min under oxygen. After this incubation, the buffer is decanted, leaving the slices behind. Then 2.5 ml of cold oxygenated buffer is added, and enough [^{3}H]choline to bring the final concentration to 100 nM. This is then incubated and shaken for 60 min at 35°C under oxygen. After this step, the buffer is decanted and the "loaded" slices are immediately placed on nylon mesh in the stimulation chambers.

Assay

Control buffer is pumped through the chamber for 42 min at a flow rate of 0.7 ml/min, to establish a stable baseline. Under these conditions released [^{3}H]ACh is subject to hydrolysis by acetylcholinesterase. The perfusion buffer is changed to fresh KHBB containing 20 µM HC-3. The potent choline uptake inhibitor HC-3 is included to prevent the re-uptake of any [^{3}H]choline formed from the hydrolysis of released [^{3}H]ACh. This maintains the stoichiometry of the stimulated release. The evoked release has been shown to be mostly [^{3}H]ACh rather than [^{3}H]choline, whereas spontaneous release under control, drug-free conditions is mostly [^{3}H]choline (Richardson and Szerb 1974; Szerb et al. 1977; Supavilai and Karobath 1985; Saijoh et al. 1985; Nishino et al. 1987).

SPECIAL CONDITIONS

1. Stimulation parameters are set at 2 Hz (2 ms duration) for 120 s, with 1 ms delay and voltage setting of 750 SIU (250 Ω). Agonists are more potent modulators of [^{3}H]ACh release at low stimulation frequencies (5).
2. For striatal slices, 2 µM sulpiride is present in the buffer to prevent DA inhibition of ACh release.
3. In some experiments, 5 µM methysergide is present in the buffer to prevent the serotonergic inhibition of ACh release mediated by 5-HT_2 receptors.
4. In order to determine the muscarinic regulation of [^{3}H]ACh release, 10 µM atropine can be included in some experiments.
5. In some experiments, physostigmine is added to the perfusion buffer. This causes a marked inhibition of stimulated release via feedback at pre-synaptic receptors. Under these conditions, receptor antagonists enhance [^{3}H]ACh release.

After the experiment is completed, the chambers are washed with distilled water for at least 20 min, 200 ml of 20% methanol in distilled water and again with distilled water for at least 20 min.

EVALUATION

After conversion of dpm, percent fractional release is calculated for each fraction, using a Lotus program.

Percent fractional release is defined as the amount of radiolabeled compound released divided by the amount present in the tissue. "Spontaneous Release" (SP) values are the average of the two fractions preceding and the first fraction in that range after the stimulation period. "Stimulated" (S) values are the summed differences between the percent fractional release during stimulation and the appropriate SP value.

The effects of drugs can be reported as S_2/S_1 ratios. To normalize the data, drug effects can be estimated by first calculating S_2/S_1 values for control and drug-treated slices and then expressing the S_2/S_1 value for the drug-treated slices as a percentage of the S_2/S_1 value for the control slices for each experiment. Each condition should be tested in slices from the same animal.

MODIFICATIONS OF THE METHOD

Release of Other Neurotransmitters From Brain Tissue in Vitro

Several authors (Harms et al. 1979; de Belleroche and Gardiner 1982; James and Cubeddu 1984; Raiteri et al. 1984; Zahniser et al. 1986; Smith et al. 1984, 1994) studied the release of neurotransmitters from brain tissue *in vitro*.

Raiteri et al. (1974) described a simple apparatus for studying the release of neurotransmitters from synaptosomes.

De Boer et al. (1988) determined the release of noradrenaline and serotonin in synaptosomes from rat cerebral cortex.

Saijoh et al. (1985) studied the influence of hypoxia on release and uptake of the neurotransmitters dopamine and acetylcholine in guinea pig striatal slices.

PROCEDURE

[^{3}H] Norepinephrine Release from Cortical Slices

Cortical slices (0.4 mm) from male Wistar rats are preincubated in Krebs buffer saturated with 95% O_2/5% CO_2, pH 7.4 for 30 min at 35°C, and then incubated in fresh buffer containing 25 nM [^{3}H]NE (35 Ci/mmol) for 30 min at 35°C. The slices are then placed in glass superfusion chambers containing platinum electrodes and perfused at 0.75 ml/min. Fractions are collected at 7 min intervals. Slices are electrically stimulated with unipolar pulses (15–30 mA) of 2 ms duration at 5 Hz for 60 s. Two rounds of stimuli are applied, separated by 10 fractions. Test compound is applied at fraction 14 (28 min after the first stimulation).

The fractions collected are counted for tritium in 10 ml of Liqiscint scintillation fluid and corrected for quench. For measurement of remaining tritium, slices are dissolved overnight in 0.5 ml of Protosol, buffered with 1 ml of Tris HCl, and counted. Percent fractional release is defined as the ratio of tritium released versus the amount present in the tissue.

[^{3}H] Norepinephrine Release from Cortical Synaptosomes

Cortices from male Wistar rats are homogenized in 9 volumes of 0.32 M sucrose in a Potter-Elvejhem homogenizer and then centrifuged at 1000 *g* for 10 min at 4°C. The supernatant is recentrifuged at 17000*g* for 20 min, and the pellet is resuspended in 0.32 M sucrose at the original volume.

The freshly prepared synaptosomes are incubated with 50 nM [^{3}H]NE in Krebs buffer containing 10 mM pargyline for 10 min at 37°C. The ratio of buffer to tissue suspension is 80:20. The [^{3}H]NE-loaded synaptosomes are then separated by centrifugation (17000 *g* for 20 min), washed with buffer containing pargyline, recentrifuged, and then finally resuspended in 0.32 M sucrose at their original volume. The assay mixture consists of 900 ml Krebs buffer containing 10 mM pargyline, 100 ml of [^{3}H]NE-loaded synaptosomes, and 10 ml of vehicle or drug. This mixture is then vortexed and incubated for 5 min at either 37°C or 0°C (to define total versus non-specific release). After a 10 min centrifugation (3000 *g*), the pellets are solubilized in a Triton X-100/ethanol mixture and transferred to scintillation vials, and counted in 10 ml of Liquiscint.

The net disintegrations for the 37°C and 0°C incubations are calculated, and % increase values determined as [(control–drug)/control] × 100.

Several chemical methods to measure acetylcholine (Israël and Lesbats 1982; Damsa et al. 1985; Stadler and Nesselhut 1986), or catecholamines and serotonin (Wagner et al. 1979; Magnusson et al. 1980; Nielsen and Johnston 1982; Wagner et al. 1982) are available.

REFERENCES AND FURTHER READING

Damsa G, Westerink GHC, Horn AS (1985) A simple, sensitive, and economic assay for choline and acetylcholine using HPLC, an enzyme reactor, and an electrochemical detector. J Neurochem 45:1649–1652

DeBelleroche JS, Gardiner IM (1982) Cholinergic action in the nucleus accumbens: Modulation of dopamine and acetylcholine release. Br J Pharmacol 75:359–365

De Boer T, Maura G, Raiteri M, de Vos CJ, Wieringa J, Pinder RM (1988) Neurochemical and autonomic pharmacological profiles of the 6-aza-analogue of mianserin, ORG 3770 and its enantiomers. Neuropharmacology 27:399–408

Drukarch B, Schepens E, Schoffelmeer ANM, Stoof JC (1989) Stimulation of D-2 dopamine receptors decreases the evoked *in vitro* release of [^{3}H]-acetylcholine from rat neostriatum: Role of K^+ and Ca^{2+}. J Neurochem 52:1680–1685

Gibson GE, Peterson C (1981) Aging decreases oxidative metabolism and the release and synthesis of acetylcholine. J Neurochem 37:978–984

Hadhazy P, Szerb JC (1977) The effect of cholinergic drugs on [^{3}H] acetylcholine release from slices of rat hippocampus, striatum and cortex. Brain Res 123:311–322

Harms HH, Wardeh G, Mulder AH (1979) Effects of adenosine on depolarization-induced release of various radiolabelled neurotransmitters from slices of rat corpus striatum. Neuropharmacol 18:577–580

Israël M, Lesbats B (1982) Application to mammalian tissue of the chemoluminescent method for detecting acetylcholine. J Neurochem 39:248–250

Jackson D, Stachowiak MK, Bruno JP, Zigmond MJ (1988) Inhibition of striatal acetylcholine release by endogenous serotonin. Brain Res 457:259–266

James MK, Cubeddu LX (1984) Frequency-dependent muscarinic receptor modulation of acetylcholine and dopamine release from rabbit striatum. J Pharmacol Exp Ther 229:98–104

James MK, Cubeddu LX (1987) Pharmacological characterization and functional role of muscarinic autoreceptors in the rabbit striatum. J Pharmacol Exp Ther 240:203–214

Magnusson O, Nilsson LB, Westerlund D (1980) Simultaneous determination of dopamine, DOPC and homovanillic acid. Direct injections of supernatants from brain tissue homogenates in a liquid chromatography-electrochemical detection system. J Chromatogr 221:237–247

Muramatsu M, Tamaki-Ohashi J, Usuki C, Araki H, Aihara H (1988) Serotonin-2 receptor-mediated regulation of release of acetylcholine by minaprine in cholinergic nerve terminal of hippocampus of rat. Neuropharmacol 27:603–609

Nielsen JA, Johnston CA (1982) Rapid, concurrent analysis of dopamine, 5-hydroxytryptamine, their precursors and metabolites utilizing high performance liquid chromatography with electrochemical detection: analysis of brain tissue and cerebrospinal fluid. Life Sci 31:2847–2856

Nishino N, Fuji Y, Kondo M, Shuntoh H, Fujiwara H, Tanaka C (1987) Effects of L-*Threo*-3,4,-dihydroxyphenylserine on efflux of monoamines and acetylcholine in guinea pig brain. J Pharmacol Exp Ther 242:621–628

Parker EM, Cubeddu LX (1986) Effects of *d*-amphetamine and dopamine synthesis inhibitors on dopamine and acetylcholine neurotransmission in the striatum. I. Release in the absence of vesicular transmitter stores. J Pharmacol Exp Ther 237:179–192

Raiteri M, Angelini F, Levi G (1974) A simple apparatus for studying the release of neurotransmitters from synaptosomes. Eur J Pharmacol 25:411–414

Raiteri M, Marchi M, Maura G (1984) Release of catecholamines, serotonin, and acetylcholine from isolated brain tissue. In: Lajtha A (ed) Handbook of Neurochemistry, 2nd ed, Plenum Press New York, London, pp 431–462

Richardson IW, Szerb JC (1974) The release of labelled acetylcholine and choline from cerebral cortical slices stimulated electrically. Br J Pharmacol 52:499–507

Robinson S (1983) Effect of 5-HT-lesions on cholinergic neurons in the hippocampus, cortex and striatum. Life Sci 32:345–353

Saijoh K, Fujiwara H, Tanaka C (1985a) Influence of hypoxia on release and uptake of neurotransmitters in guinea pig striatal slices: Dopamine and acetylcholine. Jpn J Pharmacol 39:529–539

Saijoh K, Fujiwara H, Tanaka C (1985b) Influence of hypoxia on release and acetylation of [^{3}H]choline in brain slices from adult and newborn guinea pigs. Neurosci Lett 58:371–374

Schacht U, Leven M, Bäcker G (1977) Studies on brain metabolism of biogenic amines. Br J Clin Pharmacol 4:77S–87S

Sethy VH, Francis JW, Russell RR, Ruppel PL (1988) Dual effect of N-methyl-N-(1-methyl-4-pyrrolidino)-2-butyl) acetamide on release of (^{3}H) acetylcholine from the rat hippocampal slices. Neuropharmacol 27:1191–1195

Smith CP, Petko WW, Kongsamut S, Roehr JE, Effland RC, Klein HT, Huger FP (1984) Mechanisms for the increase in electrically-stimulated norepinephrine (NE) release from cortical slices by HP 749 [N-(n-propyl)-N-(4-pyridinyl)-1H-indol-1-amine]. Drug Dev Res 32:13–18

Smith CP, Huger FP, Petko W, Kongsamut S (1994a) HP 749 enhances calcium-dependent release of [^{3}H]norepinephrine from rat cortical slices and synaptosomes. Neurochem Res 19:1265–1270

Smith CP, Petko WW, Kongsamut S, Roehr JE, Effland RC, Klein JT, Huger FP (1994b) Mechanisms for the increase in electrically stimulated [^{3}H]norepinephrine release from rat cortical slices by N-(n-propyl)-N-(4-pyridinyl)-1H-indol-1-amine. Drug Dev Res 32:13–18

Spignoli G, Pedata F, Giovannelli L, Banfi S, Moroni F, Pepeu G (1986) Effect of oxiracetam and piracetam on central cholinergic mechanisms and active-avoidance acquisition. Clin Neuropharmacol 9:S39–S47

Stadler S, Nesselhut T (1986) Simple and rapid measurement of acetylcholine and choline by HPLC and enzymatic-electrochemical detection. Neurochem Int 9:127–129

Strittmatter H, Jackisch R, Hertting G (1982) Role of dopamine receptors in the modulation of acetylcholine release in the rabbit hippocampus. Naunyn-Schmiedeberg's Arch Pharmacol 321:195–200

Supavilai P, Karobath M (1985) Modulation of acetylcholine release from rat striatal slices by the GABA/benzodiazepine receptor complex. Life Sci 36:417–426

Szerb JC, Hadhazy P, Dudar JC (1977) Release of [^{3}H]-acetylcholine from rat hippocampal slices: Effect of septal lesion and of graded concentrations of muscarinic agonists and antagonists. Brain Res 128:285–291

Wagner J, Palfreyman M, Zraika M (1979) Determination of DOPA, dopamine, DOPAC, epinephrine, norepinephrine, α-fluoromethylDOPA, and α-difluoromethylDOPA in various tissues of mice and rats using reversed-phase ion-pair liquid chromatography with electrochemical detection. J Chromatogr 221:237–247

Wagner J, Vitali P, Palfreyman MG, Zraika M, Huot S (1982) Simultaneous determination of 3,4-dihydroxyphenylalanine, 5-hydroxytryptophan, dopamine, 4-hydroxy-3-methoxyphenylalanine, norepinephrine, 3,4-dihydroxyphenylacetic acid, homovanillic acid, serotonin, and 5-hydroxyindoleacetic acid in rat cerebrospinal fluid and brain by high-performance liquid chromatography with electrochemical detection. J Neurochem 38:1241–1254

Zahniser NR, Peris J, Dwoskin LP (1986) Modulation of neurotransmitter release: an assay for receptor function. In: Chemical and functional assay of receptor binding. Soc Neurosci, Short Course 1, Syllabus, Washington, DC, pp 73–81

F.2.0.6 [^{3}H]Oxotremorine-M Binding to Muscarinic Cholinergic Receptors in Rat Forebrain

PURPOSE AND RATIONALE

The muscarinic receptors are members of the superfamily of G-protein-coupled receptors. They are relatively abundant and mediate the diverse action of acetylcholine in the CNS, as well as throughout nonnervous tissues innervated by the parasympathetic nervous system. Five separate genes (m1–m5) encode muscarinic receptor proteins exhibiting the rhodopsin-like structural motif containing seven transmembrane domains. They show strong sequence homology with each other and with related G-protein-coupled receptors within the transmembrane spanning domains, but each receptor has unique amino acid sequences located at the extracellular amino end and in the third intracellular loop (Caulfield 1993; Jones 1993; McKinney 1993; Wess 1996).

The purpose of this assay is to determine the binding affinity of potential cholinomimetic drugs for muscarinic receptors in brain, using an agonist ligand.

Oxotremorine is a potent centrally and peripherally acting muscarinic cholinergic agonist (Chao et al. 1962; Bebbington et al. 1966), which has been shown to be active in isolated tissue preparations as well as *in vivo* (Rindahl and Jenden 1983). Both central and peripheral effects of oxotremorine are blocked by anti-muscarinic drugs such as atropine (Chao et al. 1962; Bebbington et al. 1966). Structural modification of the oxotremorine molecular yields compounds which are full agonists, partial agonists and antagonists at muscarinic receptors (Rindahl and Jenden 1983). Oxotremorine-M (oxo-M), a quaternary nitrogen analog of oxotremorine, is a full agonist for the phosphatidyl-inositol response, while oxotremorine is a partial agonist (Fisher et al. 1984). Both oxotremorine and oxo-M are full agonists for inhibition of adenylate cyclase (Ehlert 1985; Olianas et al. 1983; Brown and Brown 1984). Of the muscarinic agonists, oxotremorine is the most potent inhibitor of [^{3}H]QNB binding, however, the IC_{50} is still only in the micromolar range. The apparent low affinity of agonist competition for [^{3}H]-antagonist binding sites is a common phenomena and is due to the existence of multiple agonist affinity states of the receptor, as described by Birdsall et al. (1978). For this reason, it is desirable to use an agonist ligand to measure the binding affinities of potential agonists.

Molecular methods have disclosed the existence of five muscarinic receptors which are coupled to different second messenger systems. At least four of them are expressed as functional receptor proteins in the neocortex and hippocampus formation (McKinney and Coyle 1991).

PROCEDURE

Reagents

1. 0.5 M Tris buffer, pH 7.4
   66.1 g of Tris HCl
   9.7 g of Tris base
   q.s. to 1 liter with deionized water
2. 0.05 M Tris buffer, pH 7.4
   (10-fold dilution of reagent 1)
3. [Methyl-^{3}H]-oxotremorine acetate (specific activity 83–85 Ci/mmol) is obtained from New England Nuclear.
   For IC_{50} determinations: [^{3}H]Oxotremorine-M is made up to a concentration of 100 nM. Fifty µl of this solution is added to each assay tube (yields a final concentration of 5 nM).
4. Atropine sulfate is obtained from Sigma Chemical Company. A 2 mM stock solution is made up in distilled water. Twenty µl is added to 3 tubes for determination of non-specific binding (yields a final concentration of 40 µM).
5. A 0.5% (w/v) solution of polyethylene-imine is prepared in distilled water. GF/C filters are soaked in this solution for at least three hours at room temperature. This is done to reduce the binding of the ligand to the filter strips.
6. Test compounds: For most assays, a 10 mM stock solution is made up in a suitable solvent and serially diluted, such that the final concentration in the assay ranges from 2×10^{-4} to 2×10^{-7} M.

Tissue Preparation

Male Wistar rats are decapitated and their brains rapidly removed. The forebrains (all tissue forward of a vertical cut in front of the hypothalamus) are weighed (400–500 mg each) and homogenized in 10 volumes of 0.05 M Tris buffer, pH 7.4 (reagent 2) using a Potter-Elvehjem glass homogenizer fitted with a Teflon pestle. The homogenate is centrifuged at 1000 *g* for 10 min. The supernatant is then centrifuged at 50,000 *g* for 60 min. The supernatant from this centrifugation is discarded and the pellet resuspended in the original volume of 0.05 M Tris buffer, pH 7.4, on the Polytron to 100 mg/ml (wet weight). Specific binding is roughly 1% of total added and 50% of total bound.

Binding Assay

50 µl	0.5 M Tris buffer, pH 7.4 (reagent 1)
380 µl	H_2O
20 µl	drug or 2 mM atropine
50 µl	^{3}H-oxotremorine-M (reagent 3)
500 µl	tissue

Tubes are vortexed and incubated at 30°C for 45 min (2). Bound [^{3}H]-oxotremorine-M is captured by filtration under reduced pressure. The incubation mixture is diluted with approximately 4 ml ice-cold 0.05 M Tris buffer, pH 7.4 (reagent 2), then exposed to vacuum, and tubes washed once more with approximately 5 ml of reagent 2. The filters (GFC in 0.5% polyethylene-imine for more than 3 h, reagent 5) are then counted in 10 ml Liquiscint scintillation fluid.

EVALUATION

Specific binding is the difference between total bound (in presence of vehicle) and that bound in the presence of 40 µM atropine. Percent inhibition of specific [^{3}H]-oxotremorine-M is calculated for each concentration of test drug and IC_{50} values determined by computer-derived log probit analysis. The percent inhibition at each drug concentration is the mean of duplicate or triplicate determinations. Some day-to day variability is present in this assay, and IC_{50} values should be confirmed by repeat analysis.

MODIFICATION OF THE METHOD

[^{3}H]Pirenzepine has been used to identify muscarinic receptor subtypes in the brain (Watson et al. 1983a, b).

REFERENCES AND FURTHER READING

Aronstam RS, Narayanan TK (1988) Temperature effect on the detection of muscarinic receptor-G protein interactions in ligand binding assays. Biochem Pharmacol 37:1045–1049

Aronstam RS, Abood LG, Hoss W (1978) Influence of sulfhydryl reagents and heavy metals on the functional state of the muscarinic acetylcholine receptor in rat brain. Mol Pharmacol 14:575–586

Bebbington A, Brimblecombe RW, Shakeshaft D (1966) The central and peripheral activity of acetylenic amines related to oxotremorine. Br J Pharmacol 26:56–57

Birdsall NJM, Burgen ASV, Hulme EC (1978) The binding of agonists to brain muscarinic receptors. Mol Pharmacol 14:723–736

Brown JH, Brown SL (1984) Agonists differentiate muscarinic receptors that inhibit cyclic AMP formation from those that stimulate phosphoinositide metabolism. J Biol Chem 259:3777–3781

Caulfield MP (1993) Muscarinic receptors – characterization, coupling and function. Pharmacol Ther 58:319–379

Cho AK, Haslett WL, Jenden DJ (1962) The peripheral actions of oxotremorine, a metabolite of tremorine. J Pharmacol Exp Ther 138:249–257

Ehlert FJ (1985) The relationship between muscarinic receptor occupancy and adenylate cyclase inhibitor in the rabbit myocardium. Mol Pharmacol 28:410–421

El-Fakahani EE, Ramkumar V, Lai WS (1986) Multiple binding affinities of N-methylscopolamine to brain muscarinic acetylcholine receptors: differentiation from M_1 and M_2 subtypes. J Pharmacol Exp Ther 238:554–563

Fisher SK, Figueirdo JC, Bartus RJ (1984) Differential stimulation of inositol phospholipid turnover in brain by analogs of oxotremorine. J Neurochem 43:1171–1179

Hulme EC, Birdsall NJM, Burger ASV, Mehta P (1978) The binding of antagonists to muscarinic receptors. Mol Pharmacol 14:737–750

Jones SVP (1993) Muscarinic receptor subtypes: Modulation of ion channels. Life Sci 52:457–464

Luthin GR, Wolfe BB (1984) Comparison of [^{3}H]pirenzepine and [^{3}H]quinuclidinylbenzilate binding to muscarinic cholinergic receptors in rat brain. J Pharmacol Exp Ther 228:648–655

Marks MJ, O'Connor MF, Artman LD, Burch JB, Collins AC (1984) Chronic scopolamine treatment and brain cholinergic function. Pharmacol Biochem Behav 20:771–777

McKinney M (1993) Muscarinic receptor subtype-specific coupling to second messengers in neuronal systems. Progr Brain Res 98:333–340

McKinney M, Coyle JT (1991) The potential for muscarinic receptor subtype-specific pharmacotherapy for Alzheimer's disease. Mayo Clinic Proc 66:1225–1237

Narahashi T (1992) Overview of toxins and drugs as tools to study excitable membrane ion channels: II. Transmitter activated channels. Meth Enzymol 207:643–658Sokolovsky M, Gurwitz D, Galron R (1980) Muscarinic receptor binding in mouse brain: regulation by guanine nucleotides. Biochem Biophys Res Commun 94:487–492

Nonaka R, Moroji T (1984) Quantitative autoradiography of muscarinic cholinergic receptors in the rat brain. Brain Res 296:295–303

Olianas MC, Onali P, Neff NH, Costa E (1983) Adenylate cyclase activity of synaptic membranes from rat striatum: inhibition by muscarinic receptor agonists. Mol Pharmacol 23:393–398

Ringdahl B, Jenden DJ (1983) Minireview: Pharmacological properties of oxotremorine and its analogs. Life Sci 32:2401–2413

Smith CP, Huger FP (1983) Effect of zinc on [^{3}H]-QNB displacement by cholinergic agonists and antagonists. Biochem Pharmacol 32:377–380

Watson M, Roeske WR, Yamamura HI (1982) [^{3}H]Pirenzepine selectively identifies a high affinity population of muscarinic cholinergic receptors in the rat cerebral cortex. Life Sci 31:2019–2023

Watson M, Yamamura HI, Roeske WR (1983b) A unique regulatory profile and regional distribution of [^{3}H]pirenzepine in the rat provide evidence for distinct M_1 and M_2 muscarinic receptor subtypes. Life Sci 32:3001–3011

Wess J (1996) Molecular biology of muscarinic acetylcholine receptors. Crit Rev Neurobiol 10:69–99

F.2.0.7 [^{3}H]N-Methylscopolamine Binding in the Presence and Absence of Gpp(NH)p

PURPOSE AND RATIONALE

G-protein-linked muscarinic receptors are converted by guanine nucleotides from a high-affinity bind-

ing state to a low-affinity binding state for muscarinic agonists (Gilman 1986), while the binding of muscarinic antagonists to the receptor is not affected. The effects of guanine nucleotides on muscarinic agonist affinity are brain region- and temperature-dependent (Aronstram and Narayanan 1988). Therefore, incubation of cerebellar membranes with 50 µM 5′-guanylylimidophosphate (Gpp(NH)p), the non-hydrolyzable analog of GTP, causes a shift to the right (decreased affinity) of the muscarinic agonist inhibition curves when ^{3}H-NMS is used as the ligand.

The assay differentiates the interaction of muscarinic agonists and muscarinic antagonists with ^{3}H-N-me-thylscopolamine (^{3}H-NMS)-labeled receptors in cerebellar tissue based on the selective effect of guanine nucleotides on the affinity of muscarinic agonists for the receptor.

PROCEDURE

The procedure is based on ^{3}H-NMS rat brain binding assay described by Aronstram and Narayanan (1988).

Reagents

1. 0.5 M Tris-HCl buffer, pH 7.4
2. 0.05 M Tris-HCl buffer, pH 7.4
3. 0.05 M Tris-HCl buffer, pH 7.4 + 2 mM $MgCl_2$
4. 0.05 M Tris-HCl buffer, pH 7.4 + 2 mM $MgCl_2$ + 100 µM phenylmethylsulfonyl fluoride
5. Atropine sulfate is made up to 1 mM in distilled water and 20 µl is added to a 2 ml reaction mixture. This yields a final concentration of 10 µM. Atropine is used for nonspecific binding.
6. 5′-Guanylylimidodiphosphate (Gpp(NH)p) is made up to 2 mM in distilled water. The final concentration in the reaction mixture is 50 µM.
7. ^{3}H-N-Methylscopolamine (NMS) is obtained from Amersham and diluted to 4 nM in distilled water. The final concentration in the reaction mixture is 0.1 nM.
8. Test compounds
   For most assays, a 10 mM stock solution is made up in a suitable solvent and serially diluted, such that the final concentration in the assay ranges from 10^{-4} to 10^{-7} M. Seven concentrations are used for each assay. Higher or lower concentrations may be used depending on the potency of the drug.

Tissue Preparation

Male Wistar rats are decapitated and their brains rapidly removed. The cerebella are dissected, weighed and homogenized in 10 volumes of 0.05 M Tris-HCl buffer, pH 7.4 + 2 mM $MgCl_2$+100 µM phenylmethylsulfonyl fluoride (buffer 4), using a Potter-Elvehjem glass homogenizer fitted with a Teflon pestle. The homogenate is centrifuged at 20,000 *g* for 20 min. The pellet is resuspended in 10 volumes of 0.05 M Tris-HCl buffer+2 mM $MgCl_2$ (buffer 3).

Binding Assay

1000 µl	0.05 M Tris buffer + 2 mM $MgCl_2$
780 µl	H_2O
20 µl	vehicle or 1 mM atropine or appropriate drug concentration
50 µl	H_2O or Gpp(NH)p
50 µl	[^{3}H]NMS
100 µl	tissue suspension

Tubes are incubated at 20°C for 90 min. Bound [^{3}H]NMS is captured by vacuum filtration. The filters are washed three times with 5 ml aliquots of 0.05 M Tris buffer, pH 7.4. Filters are counted in 10 ml Liquiscint scintillation fluid.

EVALUATION

Specific binding of [^{3}H]NMS is the difference between total bound (in the presence of vehicle) and that bound in the presence of 1 mM atropine. Percent inhibition of specific [^{3}H]NMS binding is calculated for each concentration of test drug and IC_{50} values are determined by computer-derived log-probit analysis. The percent inhibition at each drug concentration is the mean of triplicate determinations.

REFERENCES AND FURTHER READING

Aronstam RS, Narayanan TK (1988) Temperature effect on the determination of muscarinic receptor-G protein interactions in ligand binding assays. Biochem Pharmacol 37:1045–1049

Gilman AG (1986) Receptor-regulated G proteins. TINS 9:460

F.2.0.8 Stimulation of Phosphatidylinositol Turnover in Rat Brain Slices

PURPOSE AND RATIONALE

The purpose of this assay is to determine the ability of test compounds to stimulate the turnover of phosphatidylinositol (PI) in brain tissue. This assay can be used to determine agonist activity at a number of CNS receptors known to be linked to the PI response. A major interest is the evaluation of muscarinic cholinergic receptors.

Receptor-activated hydrolysis of inositol phospholipids is now recognized as an important second messenger system for muscarinic, alpha-adrenergic, histaminergic, serotonergic, excitatory amino acid and various neuropeptide receptors (Berridge and Irvine 1984; Nahorski et al. 1986; Fisher and Agranoff 1987). Furthermore, the hydrolysis of phosphatidylinositol 4,5-bisphosphate (PIP_2) yields at least two important biologically-active intermediates (Hirasawa and Nishizuka 1985; Berridge 1987). These include 1,4,5-inositol trisphosphate (IP_3), which acts to mobilize Ca^{2+} from the endoplasmic reticulum and diacylglycerol, which activates protein kinase C (PKC). These responses are associated with many cellular responses such as stimulus-secretion coupling, stimulus-contraction coupling and cell proliferation. The exact mechanism for receptor-mediated turnover of cell membrane PI is not well understood, but it seems to involve coupling through a G-protein (Cockcroft and Gomperts 1985) and requires extracellular Ca^{2+} to activate phospholipase C (Fisher et al. 1989).

Although the muscarinic receptor-PI link has been known for some time (Hokin and Hokin 1955), recent advances in knowledge of receptor mechanisms and increased interest in the muscarinic receptor have stimulated considerable research in this area. Even though muscarinic agonists can be shown to be weak partial agonists or full agonists for this response (Fisher et al. 1983) and there are brain regional differences in sensitivity (Fisher and Bartus 1985); attempts to show receptor subtype selectivity for stimulation of PI turnover in either heart (Brown et al. 1985) or brain tissue (Fisher and Bartus 1985) have been disappointing. However, recent experiments using cells transfected with genomic clones for the various muscarinic receptors have had more success (Shapiro et al. 1988; Conklin et al. 1988). These studies show that the m_1, m_3 and the m_5 receptor subtypes are linked to PI turnover.

Stimulation of PI turnover by agents such as veratridine, batrachotoxin and ouabain (Gusovsky et al. 1986) show that there are also non-receptor mechanisms that can cause the stimulation of PI turnover.

PROCEDURE

Equipment and Materials

1. McIlwain tissue slicer
2. Disposable columns (Kontes, 200 mm)
3. Column rack (Kontes)
4. Disposable screw-cap tubes (Pyrex, 16 × 100 mm)
5. Disposable culture tubes (Fisher, 16 × 125 mm)

Reagents

1. Modified Krebs bicarbonate buffer

	g/l	mM
NaCl	8.30	142.0
KCl	0.42	5.6
$CaCl_2$	0.24	2.2
$NaHCO_3$	0.30	3.6
$MgCl_2 \cdot 6H_2O$	0.20	1.0
HEPES	7.15	30.0
Adjust pH to 7.4 with NaOH		
d-Glucose[a]	1.01	5.6

[a]Glucose added just before incubation.

2. Concentrated Krebs buffer+LiCl (9-fold concentrated ions, 10-fold concentrated Li^+), stock solution contains no glucose or Ca^{2+}.

	g/100 ml
NaCl	6.88 (amount adjusted to correct for Li^+)
KCl	0.38
$NaHCO_3$	0.27
$MgCl_2 \cdot 6H_2O$	0.18
HEPES	6.44
LiCl	0.42

$CaCl_2$ (11 mg) and d-glucose (45 mg) are added to 5 ml of concentrated buffer before incubation.

3. Dowex AG-1-X8 (100–200 mesh) formate form (Biorad)
4. [^{3}H]Inositol (spec. act. 15 Ci/mmol) is obtained from American Radiolabeled Chemicals, Inc.
5. Myo-inositol (M.Wt. 180.2) is obtained from Sigma Chemical Co. A 5 mM solution is made (0.9 g/l).
6. 1 M Ammonium formate/0.1 M formic acid. Ammonium formate is obtained from Sigma Chemical Co.: 3.85 ml 99% formic acid + 63.1 g ammonium formate to 1 liter in H_2O.
7. $CHCl_3$/methanol (1:2, v/v).

Tissue Preparation

Male Wistar rats, approximately 6/assay.

1. Remove surface blood vessels by rolling brain on filter paper.
2. Remove cerebral cortex and gently scrape myelin layer off.
3. Prepare 350 × 350 micron tissue slices with the McIlwain tissue chopper and place slices in buffer at 37°C.
   Incubate for 10 min.

4. Disperse slices by aspirating into 1-ml pipet (cut off tip).
5. Allow slices to settle, aspirate supernatant, add buffer and repeat until the supernatant is clear.

Assay: Prelabeled Method

1. Add to screw-cap tubes:

   50 µl tissue slices
   350 µl [^{3}H]inositol

2. Incubate for 90 min at 37°C under O_2
3. Add:

   50 µl drug
   H_2O to a final volume of 500 µl

4. Incubate for 30 min at 37°C under O_2.
5. Stop the reaction by the addition of 1.5 ml of $CHCl_3$: MeOH. Place in ice bath.

Assay: Continuous Labeling Method

1. Add to screw-cap tubes:

   50 µl tissue slices
   350 µl [^{3}H]inositol
   50 µl drug
   H_2O to a final volume of 500 µl

2. Incubate for 120 min. at 37°C under O_2.
3. Stop the reaction by the addition of 1.5 ml of $CHCl_3$: MeOH. Place in ice bath.

For antagonist inhibition studies, the antagonist is usually preincubated with the slices before the agonist is added.

Extraction of Total [^{3}H] Inositol Phosphates

1. Add 1 ml of $CHCl_3$ and 0.5 ml of H_2O to each tube. Cap and vortex.
2. Centrifuge at 3000 rpm for 10 min.
3. Aspirate the aqueous phase and place in culture tubes.
4. Add 1.7 ml of H_2O and heat in water bath at 55°C for 20 min.
5. Place samples in cold room overnight.
6. Add 0.5 ml of Dowex 50% slurry to each tube. Vortex 4 times.
7. Centrifuge at 3000 rpm for 10 min.
8. Aspirate.
9. Add 2.5 ml of 5 mM myo-inositol, let the resin settle and aspirate. Repeat 5 times.
10. Centrifuge at 3000 rpm for 10 min.
11. Add 1 ml of ammonium formate/formic acid, pH 4.8.
12. Put 0.7 ml of supernatant into scintillation vial, add 10 ml cocktail and count.

EVALUATION

The stimulation phosphatidylinositol turnover for each test compound is calculated as percent increase in total [^{3}H] inositol phosphates relative to the basal turnover rate of non-treated control brain slices. The EC_{50} values for agonists are determined by log-probit analysis of these data. IC_{50} values for antagonists are determined by log-probit analysis of the percent inhibition of stimulation by a full agonist.

REFERENCES AND FURTHER READING

Berridge MJ (1987) Inositol trisphosphate and diacylglycerol: two interacting second messengers. Ann Rev Biochem 56:159–193

Berridge MJ, Irvine RF (1984) Inositol trisphosphate, a novel second messenger in cellular signal transduction. Nature 312:315–321

Cockcroft S, Gomperts BD (1985) Role of guanine nucleotide binding protein in the activation of polyphosphoinositide phosphodiesterase. Nature 313:534–536

Conklin BR, Brann MR, Ma AL, Buckley NJ, Bonner TI, Axelrod J (1988) Stimulation of arachidonic acid release in transfected cells expressing cloned muscarinic receptors. Soc Neurosci Abst 14:600

Fisher SK, Agranoff BW (1987) Receptor activation and inositol lipid hydrolysis in neural tissues. J Neurochem 48:999–1017

Fisher SK, Bartus RT (1985) Regional differences in the coupling of muscarinic receptors to inositol phospholipid hydrolysis in guinea pig brain. J Neurochem 45:1085–1095

Fisher SK, Klinger PD, Agranoff BW (1983) Muscarinic agonist binding and phospholipid turnover in brain. J Biol Chem 258:7358–7363

Fisher SK, Figueiredo JC, Bartus RT (1984) Differential stimulation of inositol phospholipid turnover in brain by analogs of oxotremorine. J Neurochem 43:1171–1179

Fisher SK, Domask LM, Roland RM (1989) Muscarinic receptor regulation of cytoplasmic Ca^{2+} concentrations in human SK-N-SH neuroblastoma cells: Ca^{2+} requirements for phospholipase C activation. Mol Pharmacol 35:195–204

Gusovsky F, Daly JW (1988) Formation of inositol phosphates in synaptoneurosomes of guinea pig brain: stimulatory effects of receptor agonists, sodium channel agents and sodium and calcium ionophores. Neuropharmacol 27:95–105

Gusovsky F, Hollingsworth EB, Daly JW (1986) Regulation of phosphatidylinositol turnover in brain synaptoneurosomes: Stimulatory effects of agents that enhance influx of sodium ions. Proc Natl Acad Sci USA 83:3003–3007

Gusovsky F, McNeal EZ, Daly JW (1987) Stimulation of phosphoinositide breakdown in brain synaptoneurosomes by agents that activate sodium influx: antagonism by tetrodotoxin, saxitoxin, and cadmium. Mol Pharmacol 32:479–487

Heller Brown J, Brown SL (1984) Agonists differentiate muscarinic receptors that inhibit cyclic AMP formation from those that stimulate phosphoinositide metabolism. J Biol Chem 259:3777–3788

Heller Brown J, Goldstein D, Masters SB (1985) The putative M_1 muscarinic receptor does not regulate phosphoinositide hydrolysis. Mol Pharmacol 27:525–531
Hirasawa K (1985) Phospatidylinositol turnover in receptor mechanisms and signal transduction. Ann Rev Pharmacol Toxicol 25:147–170
Hirasawa K, Nishizuka Y (1985) Phosphatidylinositol turnover in receptor mechanism and signal transduction. Ann Rev Pharmacol Toxicol 25:147–170
Hokin LE, Hokin MR (1955) Effects of acetylcholine on the turnover of phosphoryl units in individual phospholipids of pancreas slices and brain cortex slices. Biochem Biophys Acta 18:102–110
McKinney M (1993) Muscarinic receptor subtype-specific coupling to second messengers in neuronal systems. In: Cuello AC (ed) Progress in Brain Research, Vol 98, Chapter 40, pp 333–340
Nahorski SR, Kendall DA, Batty I (1986) Receptors and phosphoinositide metabolism in the central nervous system. Biochem Pharmacol 35:2447–2453
Shapiro RA, Scherer NM, Habecker BA, Subers EM, Nathanson NM (1988) Isolation, sequence and functional expression of the mouse M_1 muscarinic acetylcholine receptor gene. J Biol Chem 263:18397–18403

F.2.0.9 [^{3}H]N-Methylcarbamylcholine Binding to Nicotinic Cholinergic Receptors in Rat Frontal Cortex

PURPOSE AND RATIONALE

Nicotinic acetylcholine receptors are a family of ligand-gated ion channels that are classified on the basis of their activation by nicotine, although acetylcholine is the endogenous ligand. These conductance channels for Ca^{2+}, K^+ and Na^+ are pentameric in structure. They are members of a supergene family that also includes glycine, $GABA_A$, and 5-HT3 receptors. α, β, γ, and δ subunits constitute a pentameric neuronal receptor resulting in various receptor subtypes (Alkondon and Albuquerque 1993; Sargent 1993). Ten α (α 1–α10) and four β (β 1–β 4) subunits have been cloned from mammalian and avian sources, each of which has a structural motif of four transmembrane spanning domains M1–M4 of which M2 lines the channel (Gotti et al. 1997; Jensen et al. 2005).

Nicotinic cholinergic receptors are classified as ligand-gated ion channels (Le Novere et al. 2002; Jensen et al. 2005), and are found in skeletal muscle, autonomic ganglia and brain tissue. Nicotine itself has a variety of behavioral effects. Due to its rapid desensitization of the receptor, both stimulatory and depressant effects may result. Also, many of nicotine's effects are thought to be associated with release of neurotransmitter substances (Balfour 1982). Nicotine functions as a nicotinic cholinergic receptor agonist in the CNS and is thought to play a role in learning and memory (Clarke 1987; Levey 1996; Dajas-Bailador and Wonnacott 2004). Reductions in nicotinic binding sites were found in post-mortem tissues from Alzheimer's patients by four separate groups of investigators (Whitehouse et al. 1988; Nordberg and Winblack 1986; Araujo et al. 1988; Shimohama et al. 1986). Neuronal nicotinic acetylcholine receptors play a role in acute and chronic neurodegeneration (O'Neill et al. 2002).

Unconventional ligands and modulation of nicotinic receptors are discussed by Pereira et al. (2002).

The structure and function of the acetylcholine-binding protein (ACHB), a homolog of the ligand-binding domain of the nicotinic acetylcholine receptor, are described by Smit et al. (2003).

Unwin (2003) explored structure and action of the nicotinic acetylcholine receptor by electron microscopy.

Cognitive improvement in Alzheimer patients 30 min after a nicotine infusion was reported (Sunderland et al. 1988). Therefore nicotinic agonists may prove beneficial (Hogg and Bertrand 2004), however, clinical data are still quite limited. N-Methylcarbamylcholine (NMCC) is a nicotinic agonist which binds specifically and with high affinity to central nicotinic receptors and, like nicotine, causes an increase of acetylcholine release from certain cholinergic nerve terminals (Araujo et al. 1988; Lapchak et al. 1989). In addition, chronic nicotine treatment increases [^{3}H] NMCC binding sites in several rat brain regions, as it does with [^{3}H]nicotine and [^{3}H]ACh labeled sites (Lapchak et al. 1989). This is due to the loss of presynaptic nicotinic autoreceptor function (Lapchak et al. 1989). Pharmacological results reveal that along with its specificity and high affinity, [^{3}H]NMCC is selectively displaced by agonists (Araujo et al. 1988; Lapchak et al. 1989), making it a desirable ligand to screen for potential agonistic compounds.

The purpose of the following assay is to determine the binding affinity of potential nicotinic cholinergic agonists in brain, using an agonist ligand.

PROCEDURE

Reagents

1. 0.5 M Tris buffer, pH 7.7
   a) 57.2 g Tris HCl
      16.2 g Tris Base
      q.s. to 1 liter with distilled water
   b) Make a 1:10 dilution in distilled H_20 (0.05 M Tris buffer, pH 7.7 at 25°C)
2. Tris buffer containing physiological ions
   a) Stock buffer
      NaCl 7.014 g

KCl 0.372 g
$CaCl_2$ 0.222 g
$MgCl_2$ 0.204 g q.s. to 100 ml with
0.5 M Tris buffer

b) Dilute 1:10 in distilled H_20
This yields 0.05 M Tris HCl, pH 7.7, containing NaCl (120 mM), KCl (5 mM), $CaCl_2$ (2 mM) and $MgCl_2$ (1 mM).

3. Methylcarbamoylcholine iodide, [N-Methyl-^{3}H]- is obtained from New England Nuclear
For IC_{50} determinations [^{3}H]-NMCC is made up to a concentration of 100 nM in distilled H_2O and 50 µl added to each tube (yields a final concentration of 5 nM in the 1 ml assay).
4. (–)Nicotine ditartrate is obtained from Research Biochemicals Incorporated.
A stock solution of (–)nicotine ditartrate is made up to a concentration of 0.5 mM in distilled H_2O. Twenty µl of stock is added to 3 tubes for the determination of nonspecific binding (yields a final concentration of 10 µM in the assay).
5. Test compounds. For most assays in 1 mM stock solution is made up in a suitable solvent and serially diluted, such that the final concentration in the assay ranges from 2×10^{-5} to 2×10^{-8} M. Seven concentrations are used for each assay and higher or lower concentrations may be used depending on the potency of the drug.
6. A 0.5% (w/v) solution of polyethyleneimine is prepared in distilled H_2O. GF/B filters are soaked in this solution for at least four hours at 4°C. This is done to reduce binding of the ligand to the filter strips.

Tissue Preparation

Male Wistar rats are decapitated, their frontal cortices removed, weighed and homogenized in 40 volumes of ice-cold 0.05 M Tris buffer, pH 7.7 (1 b). The homogenate is centrifuged at 48,000 *g* for 10 min. The pellet is rehomogenized in fresh buffer and recentrifuged at 48000*g* for 10 min two more times. The final pellet is resuspended in the original volume of buffer, but with physiological salts (2b). This yields a final tissue concentration of 20 mg/ml in the assay.

Assay

130 µl	0.05 M Tris pH 7.7-physiological salts (2 b).
20 µl	Vehicle (for total binding) or 0.5 mM (–)nicotine ditartrate (for nonspecific binding) or appropriate drug concentration.
50 µl	N-[^{3}H]Methylcarbamylcholine stock solution
800 µl	tissue.

The tubes are incubated at 0°C for 60 min. The assay is stopped by rapid filtration through Whatman GF/B filters which are then washed 4 times with 3 ml of ice-cold 0.05 M Tris buffer, pH 7.7. The filters are then counted in 10 ml of Liquiscint scintillation cocktail.

EVALUATION

Specific binding is defined as the difference between total binding and binding in the presence of the 10 µM (–)nicotine ditartrate. Specific binding is about 1% of the total added ligand and 60–70% of the total bound ligand. IC_{50} calculations are performed using log-probit analysis. The percent inhibition at each drug concentration is the mean of triplicate determinations.

MODIFICATION OF THE METHOD

Pabreza et al. (1991) recommended [^{3}H]cytisine as a useful ligand for studying neuronal nicotinic receptors because of its high affinity and low nonspecific binding.

Badio and Daly (1994) determined [^{3}H]nicotine receptor binding in rat cerebral cortex membrane preparations. The authors concluded that the analgesic activity of epibatidine, an alkaloid originally characterized from frog skin, is due to its activity as nicotinic agonist.

REFERENCES AND FURTHER READING

Alkondon M, Albuquerque EX (1993) Diversity of nicotinic acetylcholine receptors in rat hippocampal neurons. I. Pharmacological and functional evidence for distinct structural subtypes. J Pharmacol Exp Ther 265:1455–1473

Araujo DM, Lapchak PA, Collier B, Quirion R (1988a) Characterization of *N*-[^{3}H]methylcarbamylcholine on acetylcholine release in rat brain J. Neurochem 51:292–299

Araujo DM, Lapchat PA, Robitaille Y, Gauthier S, Quirion R (1988b) Differential alteration of various cholinergic markers in cortical and subcortical regions of human brain in Alzheimer's disease. J Neurochem 50:1914–1923

Badio B, Daly JW (1994) Epibatidine, a potent analgesic and nicotinic agonist. Mol Pharmacol 45:563–569

Balfour DJK (1982) The effects of nicotine on brain neurotransmitter systems. Pharmacol Ther 16:269–282

Clarke PBS (1987) Nicotine and smoking: A perspective from animal studies. Psychopharmacology 92:135–143

Connolly J, Boulter J, Heinemann SF (1992) α4-β2 and other nicotinic acetylcholine receptor subtypes as targets of psychoactive and addictive drugs. Br J Pharmacol 105:657–666

Dajas-Bailador F, Wonnacott S (2004) Nicotine acetylcholine receptors and the regulation of neuronal signaling. Trends Pharmacol Sci 25:317–324

Drasdo A, Caulfield M, Bertrand D, Bertrand S, Wonnacott (1992) Methyllycaconitine: a novel nicotinic antagonist. Mol Cell Neurosci 3:237–243

Gotti C, Fornasaru D, Clementi F (1997) Human neuronal nicotinic receptors. Progr Neurobiol 53:199–237

Hogg RC, Bertrand D (2004) Nicotine acetylcholine receptors as drug targets. Curr Drug Targets CNS Neurol Disord 3:123–130
Jensen AA, Frølund B, Liljefors T, Krogsgaard-Larsen P (2005) Neuronal nicotinic acetylcholine receptors: structural relations, target identification, and therapeutic inspirations. J Med Chem 48:4705–4745
Karlin A (1991) Explorations of the nicotinic acetylcholine receptor. Harvey Lect 85:71–107
Lapchak PA, Araujo DM, Quirion R, Collier B (1989) Effect of chronic nicotine treatment on nicotinic autoreceptor function and *N*-[^{3}H]methylcarbamylcholine binding sites in the rat brain. J Neurochem 52:483–491
Le Novere N, Corringer PJ, Changeux JP (2002) The diversity of subunit composition in nAChRs: evolutionary origins, physiologic and pharmacologic consequences. J Neurobiol 53:447–456
Levey AI (1996) Muscarinic acetylcholine receptor expression in memory circuits: implications for treatment of Alzheimer disease. Proc Natl Acad Sci USA 93:13541–13456
Luetje CW, Patrick J (1991) Both α- and β-subunits contribute to the agonist sensitivity of neuronal nicotinic acetylcholine receptors. J Neurosci 11:837–845
Luetje CW, Wada K, Rogers S, Abramson SN, Tsuji K, Heinemann S, Patrick J (1990) Neurotoxins distinguish between different neuronal nicotinic acetylcholine receptor subunit combinations. J Neurochem 55:632–640
Mulle C, Vidal C, Benoit P, Changeux JP (1991) Existence of different subtypes of nicotinic acetylcholine receptors in the rat habenulo-interpeduncular system. J Neurosci 11:2588–2597
Nordberg A, Winblad B (1986) Reduced number of [^{3}H]nicotine and [^{3}H]-acetylcholine binding sites in the frontal cortex of Alzheimer brains. Neurosci Lett 72:115–119
O'Neill MJ. Murray TK, Lakics V, Visanji NP, Duty S (2002) The role of neuronal nicotinic acetylcholine receptors in acute and chronic neurodegeneration. Curr Drug Targets CNS Neurol Disord 1:399–411
Pabreza LA, Dhawan S, Kellar KJ (1991) [^{3}H]Cytisine binding to nicotinic cholinergic receptors in brain. Mol Pharmacol 39:9–12
Pereira EP, Hilmas C, Santos MD, Alkondon M, Maelicke A, Albuquerque EX (2002) Unconventional ligands and modulation of nicotinic receptors. J Neurobiol 53:479–500
Role LW (1992) Diversity in primary structure and function of neuronal nicotinic acetylcholine receptor channels. Curr Opin Neurobiol 2:254.262
Sargent PB (1993) The diversity of neuronal nicotinic acetylcholine receptors. Annu Rev Neurosci 16:403–443
Shimohama S, Taniguchi T, Fujiwara M, Kameyama M (1986) Changes in nicotinic and muscarinic cholinergic receptors in Alzheimer-type dementia. J Neurochem 46:288–293
Smit AB, Brejc K, Syed N, Sixma TK (2003) Structure and function of ACHBP, homologue of the ligand-binding domain of the nicotinic acetylcholine receptor. Ann NY Acad Sci 998:81–92
Sunderland T, Tariot PN, Newhouse PA (1988) Differential responsivity of mood, behavior and cognition to cholinergic agents in elderly neuropsychiatric populations. Brain Res Rev 13:371–389
Unwin N (2003) Structure and action of the nicotinic acetylcholine receptor explored by electron microscopy. FEBS Lett 555:91–95
Vernalllis AB, Conroy WG, Berg DK (1993) Neurons assemble acetylcholine receptors with as many as three kinds of subunits while maintaining subunit segregation among receptor subtypes. Neuron 10:451–464
Whitehouse PJ, Martino AM, Wagster MV, Price DL, Mayeux R, Atack JR, Kellar KJ (1988) Reductions in [^{3}H]nicotinic acetylcholine binding in Alzheimer's disease and Parkinson's disease: an autoradiographic study. Neurology 38:720–723

F.2.0.10 Uncompetitive NMDA Receptor Antagonism

PURPOSE AND RATIONALE

The uncompetitive NMDA antagonist memantine with moderate affinity to the (+)MK801-binding site has shown positive effects in the treatment of dementia (Möbius et al. 2004; Sonkusare et al. 2005). Several studies were performed to elucidate the mode of action (Frankiewicz and Parsons 1999; Parsons et al. 1999, 2004; Ikonomidou et al. 2000; Linden et al. 2001; Blanpied et al. 2005; Chen and Lipton 2005; Losi et al. 2006; Volbracht et al. 2006; Zoladz et al. 2006).

Sobolevsky and Koshelev (1998) and Sobolevsky et al. (1998, 1999) studied the blocking effects of memantine in open *N*-methyl-D-aspartate channels.

PROCEDURE

Pyramidal neurons were acutely isolated from the CA-1 region of rat hippocampus using "vibrodissociation techniques" (Vorobjev 1991). The experiments began after 3 h of incubation of the hippocampal slices in a solution containing (in mM): NaCl, 124; KCl, 3; $CaCl_2$, 1.4; $MgCl_2$, 2; glucose, 10; and $NaHCO_3$, 26. The solution was bubbled with carbogen at 32°C. During the whole period of isolation and current recording, nerve cells were washed with a Mg^{2+}-free solution containing 3 µM glycine (in mM: NaCl, 140; KCl, 5; $CaCl_2$, 2; glucose, 15; and HEPES, 10, pH 7.3). Fast replacement of superfusion solutions was achieved by using the concentration jump technique (Benveniste et al. 1990; Vorobjev 1991) with one application tube. This technique allows substitution of the tubular solution for the flowing solution with a time constant <30 ms but backward with the time constant of 30–100 ms (Sobolevsky 1999). Therefore, except where noted, the rate of the solution exchange was fast at the beginning of any application and slightly slower at its termination. The currents were recorded at 18°C in the whole-cell configuration using micropipettes made from Pyrex tubes and filled with an "intracellular" solution (in mM: CsF, 140; NaCl, 4; and HEPES, 10; pH 7.2). Electrical resistance of the filled micropipettes was 3–7 MΩ Analog current signals were digitized at 1 kHz frequency.

EVALUATION

Statistical analysis was performed using the scientific and technical graphics computer program Microcal Origin (version 4.1 for Windows). The data presented are mean ± SE; comparison of the means was done by ANOVA, with $p < 0.05$ taken as significant.

MODIFICATIONS OF THE METHOD

Maskell et al. (2003) reported inhibition of human $\alpha 7$ nicotine acetylcholine receptors by open channel blockers of *N*-methy-D-aspartate receptors. Human $\alpha 7$ nicotine acetylcholine receptors were expressed in *Xenopus* oocytes and the effects of the NMDA receptor open channel blockers memantine and cerestat on this receptor were examined using two-electrode voltage-clamp recordings and the ^{125}I-labeled α-bungarotoxin binding.

Aracava et al. (2005) found that memantine blocks $\alpha 7$* nicotinic acetylcholine receptors more potently than *N*-methyl-D-aspartate receptors in rat hippocampal neurons. Primary hippocampal cultures were from 16- to 29-day-old fetal rats. Electrophysiological recordings were obtained from cultured neurons by means of the whole-cell mode of the patch-clamp technique. Atropine (1 µM) and tetrodotoxin (0.1–0.3 µM) were added to the external solution to block muscarinic receptors and voltage-gated Na^+ channels, respectively. The agonist solutions, with or without memantine, were applied to the neurons through a glass U-tube. Memantine was added at various concentrations to the bathing solution.

REFERENCES AND FURTHER READING

Aracava Y, Pereira EFR, Maelicke A, Albuquerque EX (2005) Memantine blocks $\alpha 7$* nicotinic acetylcholine receptors more potently than *N*-methyl-D-aspartate receptors in rat hippocampal neurones. J Pharmacol Exp Ther 312:1195–1205

Benveniste M, Mienville J-M, Sernagor E, Mayer ML (1990) Concentration-jump experiments with NMDA antagonists in mouse cultured hippocampal neurons. J Neurophysiol 63:1373–1384

Blanpied TA, Clarke RJ, Johnson JW (2005) Amantadine inhibits NMDA receptors by accelerating channel closure during channel block. J Neurosci 25:3312–3322

Chen HSV, Lipton SA (2005) Pharmacological implications of two distinct mechanisms of interaction on memantine with *N*-methyl-D-aspartate-gated channels. J Pharmacol Exp Ther 31:961–971

Frankiewicz T, Parsons CG (1999) Memantine restores long term potentiation impaired by tonic *N*-methyl-D- aspartate (NMDA) receptor activation following reduction of Mg^{2+} in hippocampal slices. Neuropharmacology 38:1253–1259

Ikonomidou C, Stefanovska V, Turki L (2000) Neuronal death enhanced by *N*-methyl-D-aspartate antagonists. Proc Natl Acad Sci USA 97:12885–12890

Linden AM, Vasanen J, Storvik M, Lakso M, Korpi ER, Wong G, Casttren E (2001) Uncompetitive antagonists of the N-methyl-D-aspartate (NMDA) receptors alter the mRNA expression of proteins associated with the NMDA receptor complex. Pharmacol Toxicol 88:98–105

Losi G, Lanza M, Makovec F, Artusi R, Caselli G, Puia G (2006) Functional in vitro characterization of CR 3394: a novel voltage dependent N-methyl-D-aspartate (NMDA) receptor antagonist. Neuropharmacology 50:277–285

Maskell PD, Speder P, Newberry NR, Bermudez I (2003) Inhibition of human $\alpha 7$ nicotine acetylcholine receptors by open channel blockers of *N*-methy-D-aspartate receptors. Br J Pharmacol 140:1313–1319

Möbius HJ, Stöffler A, Graham SM (2004) Memantine hydrochloride. Pharmacological and clinical profile. Drugs Today 40:685–695

Parsons CG, Quack G, Bresink I, Baran L, Przegalinski E, Kostowski W, Krzascik P, Hartmann S, Danysz W (1999) Comparison of the potency, kinetics and voltage-dependency of a series of uncompetitive NMDA receptor antagonists *in vitro* with anticonvulsant and motor impairment activity *in vivo*. Neuropharmacology 34:1239–1258

Parsons CG, Danysz W, Quack G (2000) Memantine and the amino-alkyl-cyclohexane MRZ 2/579 are moderate affinity uncompetitive NMDA receptor antagonists – in vitro characterization. Amino Acids 19:157–166

Sobolevsky A, Koshelev S (1998) Two blocking sites of amino-adamantane derivatives in open *N*-methyl-D-aspartate channels. Biophys J 74:1305–1319

Sobolevsky AI (1999) Two-component blocking kinetics of open NMDA channels by organic cations. Biochim Biophys Acta 1416:69–91

Sobolevsky AI, Koshelev SD, Khodorov BI (1998) Interaction of memantine and adamantine with agonist-unbound NMDA-receptor channels in acutely isolated rat hippocampal neurons. J Physiol (Lond) 512:47–60

Sobolevsky AI, Koshelev SG, Khodorov BI (1999) Probing of NMDA channels with fast blockers. J Neurosci 19:10611–1626

Sonkusare SK, Kaul CL, Ramarao P (2005) Dementia of Alzheimer's disease and other neurodegenerative disorders – memantine, a new hope. Pharmacol Res 51:1–7

Volbracht C, van Beek J, Zhu C, Blomgren K, Leist M (2006) Neuroprotective properties of memantine in different *in vitro* and *in vivo* models of excitotoxicity. Eur J Neurosci 23:2611–2622

Vorobjev VS (1991) Vibrodissociation of sliced mammalian nervous tissue. J Neurosci Methods 38:145–150

Zoladz PR, Campbell AM, Park CR, Schaefer D, Danysz W, Diamond DM (2006) Enhancement of long-term spatial memory in adult rats by the noncompetitive NMDA receptor antagonists, memantine and neramexane. Pharmacol Biochem Behav 85:298–306

F.2.0.11 Secretion of Nerve Growth Factor by Cultured Neurons/Astroglial Cells

PURPOSE AND RATIONALE

Cultured brain cells can be used for many purposes such as investigation of synthesis and secretion of nerve growth factor or for testing neuroprotective drugs (Peruche and Krieglstein 1991). Nerve growth factor is required for the development and maintenance

of peripheral and sensory neurons (Thoenen and Barde 1980). Nerve growth factor (NGF) prevents neuronal death after brain injury (Hefti 1986; Williams et al. 1986; Kromer 1987), especially in basal forebrain nuclei involved in memory processes. Drug induced increase in nerve growth factor secretion may be beneficial in primary degenerative dementia.

NGF belongs to the family of neurotrophins which includes besides of the nerve growth factor, the neurotrophin 3 (NT3), neurotrophin 4/5 (NT 4/5) and brain-derived neurotrophic factor (BDNF). Two types of neurotrophin transmembrane receptors are known: (1) a receptor termed p75, which is common to all neurotrophins and (2) a family of neurotrophin receptor tyrosine kinases trkA, trkB and trkC (Saragovi and Gehring 2000). TrkA is the receptor tyrosine kinase for NGF (Huang and Reichardt 2003).

NGF has a crucial role in the generation of pain and hyperalgesia in several acute and chronic pain states (Hefti et al. 2006).

PROCEDURE

Whole brains of 8-day-old mice (ICR) are dissected out and cut into small pieces. The pieces are washed with calcium- and magnesium-free phosphate-buffered saline, treated with 0.25% trypsin at 37°C for 30 min, and triturated with a Pasteur pipette. The excess trypsin is removed by centrifugation at 200 *g* for 5 min. The cells or cell clumps from one brain are cultured in a culture bottle with Dulbecco's modified Eagle's minimum essential medium (DMEM) containing 10% fetal calf serum (FCS), 50 milliunits/ml penicillin, and 50 mg/ml of streptomycin at 37°C in a humid atmosphere of 5% CO_2 for 1–2 weeks with medium changes every 3 days. After confluence is reached, the cells in each bottle are dissociated by trypsin treatment and recultured in new bottles. This procedure is repeated 3 times. The culture becomes composed of morphologically uniform cells.

Preparation of quiescent cells is performed by inoculating into 96-well plates and culture in FCS-containing DMEM until confluence is reached. Then, the cells are cultured for an additional week in FCS-free DMEM containing 0.5% BSA, with medium changes every 3 days. Because the cells never proliferate in FCS-free medium, most of the cells are arrested in the quiescent phase. Then, the medium is changed to DMEM containing 0.5% BSA with or without drugs, and the cells are cultured for 24 h.

Nerve growth factor (NGF) content in the culture medium is determined by a two-site enzyme immunoassay (Furukawa et al. 1983; Lärkfors and Ebendal 1987). Mouse βNGF isolated from male mouse submaxillary glands is purified by CM-Sephadex C-50 chromatography. Antiserum to this mouse βNGF is produced in New Zealand White rabbits by repeated subcutaneous injections of an emulsion in complete Freund's adjuvant over 18 months. Immunoglobin G is prepared from Anti-mouse βNGF antiserum by Sepharose chromatography. Antibody IgG is incubated with pepsin and chromatographed. Fab' fragments are coupled to β-D-galactosidase. IgG-coated solid phase is prepared in polystyrene tubes. The IgG-coated polystyrene tubes are incubated with 0.25 ml buffer containing various amounts of NGF with gentle shaking. After incubation for 18–24 h at 4°C, each tube is washed twice with 1 ml of buffer and 0.13 milliunits of the Fab'-β-D-galactosidase complex in 0.25 ml buffer is added. After incubation for 18–24 h at 4°C with gentle shaking each tube is washed as described above and β-D-galactosidase activity bound to the tube is assayed. The enzyme reaction is started by addition of 60 mM 4-methylumbelliferyl-β-D-galactoside and 0.1% Triton X-100 in 0.25 ml buffer. After 1-h incubation at room temperature, the enzyme reaction is stopped by the addition of 1.25 ml 0.1 M glycine-NaOH buffer (pH 10.3). The amounts of 4-methylumbelliferone formed are measured by fluorometry (Excitation wavelength 360 nm, emission wavelength 450 nm).

EVALUATION

Time-response curves of release of NGF into the medium are established after addition of drug and compared with controls. Dose-response curves can be prepared after addition of various amounts of test drug.

MODIFICATIONS OF THE METHOD

Cultured neurons from chick embryo hemispheres were used for testing cerebroprotective drug effects *in vitro* and for testing antihypoxic drug effects by Krieglstein et al. (1988), Peruche et al. (1990), Oberpichler-Schwenk and Krieglstein (1994).

Semkowa et al. (1996) found that clenbuterol protects mouse cerebral cortex and rat hippocampus from ischemic damage and attenuates glutamate neurotoxicity in cultured hippocampal neurons by induction of nerve growth factor.

Prehn et al. (1993, 1995) tested the prevention of glutamate neurotoxicity in neocortical cultures from rats. Mixed neuronal/glial primary cultures were derived from the cerebral cortices of neonatal Fischer 344 rats. Excitotoxic injury was induced after 14 days

by L-glutamate following a procedure described by Choi et al. (1988), Koh and Choi (1988).

Kinoshita et al. (1991) used primary cultured neurons from 17-day-old rat fetuses.

Qi et al. (1997), Horton et al. (2001) described a novel catecholaminergic CAD CNS neuronal cell line in which neurotrophin-3 mediates the autocrine survival.

Shinpo et al. (1999) used cultured mesencephalic neurons from embryonic Sprague Dawley rats to study the protective effects of the TNF-ceramide pathway against glutamate neurotoxicity.

Matsumoto et al. (1990) described a method for quantifying the effects of neurotrophic factors on the number of surviving neurons and the total length of neurites in primary cultures from cerebral cortex and hippocampus of the brains from two-week old rats by using digital image processing techniques. Binary images of neuronal neurites were extracted from gray images of cultured neurons stained with Coomassie brilliant blue.

White et al. (1995) measured calcium transients in mouse cerebellar granule cells with the Ca^{2+}-sensitive probe indo-1/AM.

Beresini et al. (1997) developed two types of high throughput assays to identify small molecules that interact with neurotrophin receptors. The first, the receptor binding assay, is a competitive binding assay that uses a recombinant receptor fusion protein and biotinylated neurotrophin. This assay detects compounds that inhibit neurotrophin binding to the receptor; these compounds may be either agonistic or antagonistic. The second assay, the kinase receptor activation ELISA, detects receptor autophosphorylation in response to sample- or neurotrophin-stimulation of receptor transfected cells. Receptor autophosphorylation is evaluated by analyzing lysates of the stimulated cells in a receptor-specific ELISA for phosphotyrosine residues. This assay is bioactivity based, and consequently, has the power of detecting as well as distinguishing receptor agonists and antagonists.

Höglinger et al. (1998) used free-floating roller tube cultures prepared from embryonic-day-14 rat ventral mesencephalon to study the influence of brain-derived neurotrophic factor treatment on dopamine neuron survival and function.

Nerve growth factor is crucial for survival of nociceptive neurons during development. Shu and Mendell (1999) investigated the acute effects of NGF on capsaicin responses of small-diameter dorsal root ganglion cells in culture.

For further studies with brain cell cultures see E.3.1.16.

REFERENCES AND FURTHER READING

Beresini MH, Sadick MD, Galloway AL, Yen R, Yeh SH, Chang AC, Shelton DL, Wong WLT (1997) Assays for small molecule agonists and agonists of the neurotrophin receptors. In: Devlin JP (ed) High Throughput Screening. The Discovery of Bioactive Substances. Marcel Dekker Inc., New York, Basel, pp 329–343

Choi DW, Koh JY, Peters S (1988) Pharmacology of glutamate neurotoxicity in cortical cell culture: attenuation by NMDA antagonists. J Neurosci 8:185–195

Dichter MA (1986) The pharmacology of cortical neurons in tissue culture. In: Electrophysiological Techniques in Pharmacology, Alan R. Liss, Inc., pp 121–147

Furukawa S, Furukawa Y, Akazawa S, Satoyoshi E, Itoh K, Hayashi K (1983) A highly sensitive enzyme immunoassay for mouse β nerve growth factor. J Neurochem 40:734–744

Furukawa S, Furukawa Y, Satoyoshi E, Hayashi K (1986) Synthesis and secretion of nerve growth factor by mouse astroglial cells in culture. Biochem Biophys Res Commun 136:57–63

Furukawa S, Furukawa Y, Satoyoshi E, Hayashi K (1987) Regulation of nerve growth factor synthesis/secretion by catecholamine in cultured mouse astroglial cells. Biochem Biophys Res Commun 147:1048–1054

Graeber MB, Kreutzberg GW (1986) Astrocytes increase in glial fibrillary acidic protein during retrograde changes of facial motor neurons. J Neurocytol 15:363–373

Hefti F (1986) Nerve growth factor promotes survival of septal cholinergic neurons after fibrial transsections. J Neurosci 6:2155–2162

Hefti FF, Rosenthal A, Walicke PA, Wyatt S, Vergara G, Shelton DL, Davies AM (2006) Novel class of pain drugs based on antagonism of NGF. Trends Pharmacol Sci 27:85–91

Höglinger GU, Sautter J, Meyer M, Spengler C, Seiler RW, Oertel WH, Widmer HR (1998) Rat fetal ventral mesencephalon grown as a solid tissue culture: influence of culture time and BDNF treatment on dopamine neuron survival and function. Brain Res 813:313–322

Horton CD, Qi Y, Chikaraishi D, Wang JKT (2001) Neurotrophin-3 mediates the autocrine survival of the catecholaminergic CAD CNS neuronal cell line. J Neurochem 76:201–209

Huang EJ, Reichardt LF (2003) trk receptors: roles in neuronal signal transmission. Annu Rev Biochem 72:609–642

Kinoshita A, Yamada K, Hayakawa T (1991) Human recombinant superoxide dismutase protects primary cultured neurons against hypoxic injury. Pathobiol 59:340–344

Koh JY, Choi DW (1988) Vulnerability of cultured cortical neurons to damage by excitotoxins: Differential susceptibility of neurons containing NADPH-diaphorase. J Neurosci 8:2153–2163

Krieglstein J, Brungs H, Peruche B (1988) Cultured neurons for testing cerebroprotective drug effects *in vitro*. J Pharmacol Meth 20:39–46

Kromer LF (1987) Nerve growth factor treatment after brain injury prevents neuronal death. Science 235:214–216

Lärkfors L, Ebendal T (1987) Highly sensitive immunoassays for β-nerve growth factor. J Immunol Meth 97:41–47

Matsumoto T, Oshima K, Miyamoto A, Sakurai M, Goto M, Hayashi S (1990) Image analysis of CNS neurotrophic factor effects on neuronal survival and neurite outgrowth. J Neurosci Meth 31:153–162

Oberpichler-Schwenk H, Krieglstein J (1994) Primary cultures of neurons for testing neuroprotective drug effects. J Neural Transm (Suppl) 44:1–20

Ogura A, Miyamoto M, Kudo Y (1988) Neuronal death *in vitro*: parallelism between survivability of hippocampal neurons and sustained elevation of cytosolic Ca^{2+} after exposure to glutamate receptor agonist. Exp Brain Res 73:447–458

Peruche B, Krieglstein J (1991) Neuroblastoma cells for testing neuroprotective drug effects. J Pharmacol Meth 26:139–148

Peruche B, Ahlemeyer B, Brungs H, Krieglstein J (1990) Cultured neurons for testing antihypoxic drug effects. J Pharmacol Meth 23:63–77

Prehn JHM, Backhauß C, Krieglstein J (1993) Transforming growth factor-β_1 prevents glutamate neurotoxicity in rat neocortical cultures and protects mouse neocortex from ischemic injury *in vivo*. J Cerebr Blood Flow Metab 13:521–525

Prehn JHM, Lippert K, Krieglstein J (1995) Are NMDA or AMPA/kainate receptor antagonists more efficacious in the delayed treatment of excitotoxic neuronal injury? Eur J Pharmacol 292:179–189

Qi Y, Wang J, McMillan M, Chikaraishi D (1997) Characterization of a CNS cell line CAD, in which morphological differentiation is initiated by serum deprivation. J Neurosci 17:1217–1225

Saragovi HU, Gehring K (2000) Development of pharmacological agents for targeting neurotrophins and their receptors. Trends Pharmacol Sci 21:93–98

Semkowa I, Schilling M, Heinrich-Noak P, Rami A, Krieglstein J (1996) Clenbuterol protects mouse cerebral cortex and rat hippocampus from ischemic damage and attenuates glutamate neurotoxicity in cultured hippocampal neurons by induction of NGF. Brain Res 711:44–54

Shinoda I, Furukawa Y, Furukawa S (1990) Stimulation of nerve growth factor synthesis/secretion by propentofylline in cultured mouse astroglial cells. Biochem Pharmacol 39:1813–1816

Shinpo K, Kikuchi S, Morikawa F, Tashiro K (1999) Protective effects of the TNF-ceramide pathway against glutamate neurotoxicity on cultured mesencephalic neurons. Brain Res 819:170–173

Shu X-Q; Mendell M (1999) Neurotrophins and hyperalgesia. Proc Natl Acad Sci 96:7693–7696

Thoenen H, Barde YA (1980) Physiology of nerve growth factor. Physiol Rev 60:1284–1355

White HS, Harmsworth WL, Sofia RD, Wof HH (1995) Felbamate modulates the strychnine-insensitive receptor. Epilepsy Res 20:41–48

Williams LR, Varon S, Peterson GM, Wictorin K, Fischer W, Bjorklund A, Gage FH (1986) Continuous infusion of nerve growth factor prevents basal forebrain neuronal death after fimbria fornix transsection. Proc Natl Acad Sci USA 83:9231–9235

Yankner BA, Shooter EM (1982) The biology and mechanism of action of nerve growth factor. Ann Rev Biochem 51:845–968

Yu ACH, Hertz E, Hertz L (1984) Alterations in uptake and release rates for GABA, glutamate, and glutamine during biochemical maturation of highly purified cultures of cerebral neurons, a GABAergic preparation. J Neurochem 42:951–960

F.2.0.12 Inhibition of Respiratory Burst in Microglial Cells/Macrophages

PURPOSE AND RATIONALE

Activated phagocytes can produce large amounts of oxygen intermediates that result from a process during which NADPH oxidase reduces O_2 to the superoxide anion (O_2^-), which subsequently dismutates together with H^+ to H_2O_2 and O_2. H_2O_2 is then reduced to hypochlorous acid by myeloperoxidase (Bellavite 1988). The cascade of metabolic steps is known as respiratory bursts. The intracellular formation of reactive oxygen intermediates can be determined by measuring the oxidation of the membrane permeable and non-fluorescent dihydrorhodamine 123 to the cationic and intracellularly trapped, green fluorescent rhodamine 123 in single viable cells. Microglial/brain macrophage-mediated damage in the central nervous system is accompanied by an increased production of free radicals, which also seems important in primary degenerative dementia (Alzheimer's disease) (Banati et al. (1993). Inhibition of this process by drugs may indicate therapeutic value in Alzheimer's disease.

PROCEDURE

Cell Culture

Cultures of new-born rat brain are prepared as described by Guilian and Baker (1986); Frei et al. (1987). Isolated cerebral cortices from new-born albino rats are stripped of the meninges, minced in culture medium and dissociated by trituration for 2 h in 0.25% trypsin solution. Cells are plated in 75 cm^2 plastic culture flasks containing 10 ml medium with 10% fetal bovine serum at a density of 85,000 cells/ml. After 7 days, confluent cultures are vigorously agitated on a rotary shaker at 37°C for 15 h. Glial fibrillary acid protein positive astroglia remain adherent to the flasks. The resulting cell suspension, rich in amoeboid microglia and oligodendroglia, is placed in plastic flasks and allowed to adhere at 37°C. After a 1–3 h adhering interval, loosely adhering and suspended cells (most of which are oligodendroglia) are removed by gently shaking the flasks at room temperature. The strongly adherent microglia cells are then released by vigorous shaking in medium with 0.2% trypsin. Once the majority of microglia is suspended, fetal bovine serum is added (15% final volume), and the cell suspension added to new flasks. After a second 1–3 h interval to allow adhesion, the medium is removed, and adhering microglia are suspended using trypsin. Final prepara-

tion show a nearly homogeneous population of nonspecific esterase positive cells.

Peritoneal macrophages are obtained from 12-week-old male Wistar rats.

For flow cytometric measurement, cells are suspended ($3–4 \times 10^6$ cells/ml) in Hank's buffered saline (HBS; Sigma Chemie, Deisenhofen, Germany) supplemented with N-2-hydroxyethylpiperazine-N′-2-ethane-sulfonic acid (HEPES; 5 mM, pH 7.35; Serva Feinbiochemica, Heidelberg, Germany) (HBS-HEPES) and stored at 4°C for a maximum of 2 h.

Flow Cytometric Measurement of Respiratory Burst

Dihydrorhodamine 123 (DHR) is obtained from Molecular Probes (Eugene, OR, USA) and dissolved to obtain a 1 mM stock solution in N,N-dimethylformamide (DMF; Merck, Darmstadt, Germany).

The cellular suspensions of peritoneal macrophages and microglial cells (10 µl) are each further diluted with 1 ml HBS-HEPES and stained for 5 min at 37°C with 10 µl of a 100 µM DHR solution in HBS (1 mM stock solution in DMF). The DHR-loaded cells are incubated with the test drug at various concentrations for 15, 25, 35, 45, and 60 min with and without Con A (100 µg/ml; Sigma Chemie) stimulation. The DNA of dead cells is counter stained with 10 µl of 3 mM propidium iodide (Serva Feinbiochemica) solution in HBS 3 min before the flow cytometric measurement. To exclude effects from a possible release of endogenous adenosine, control experiments with incubation medium containing adenosine deaminase (200 U/mg, 5 µg/ml Sigma Chemie) are performed.

The forward scatter, side scatter and two fluorescences of at least 10,000 cells/sample are measured simultaneously on a FACScan flow cytometer (Becton Dickinson, San Jose, CA, USA). Rhodamine 123 green fluorescence (515–545 nm) and propidium iodide red fluorescence (> 650 nm) are measured with the light from an argon laser of 488-nm excitation wavelength.

EVALUATION

The differences in respiratory burst activities caused by Con A stimulation and treatment with test drug are tested for significance by unpaired *t*-test. The *t*-test is performed for each time point including the data of at least four independent experiments. Each single fluorescence value of each experiment is based on the measurement of at least 10,000 cells. Before each experiment the flow cytometer is calibrated with standardized yellow-green fluorescent microspheres of 4.3-µm diameter (Polysciences, St. Goar, Germany), thus ensuring the compatibility of the fluorescence values from different experimental series.

REFERENCES AND FURTHER READING

Banati RB, Rothe G, Valet G, Kreutzberg GW (1991) Respiratory burst in brain macrophages: a flow cytometric study on cultured brain macrophages. Neuropath Appl Neurobiol 17:223–230

Banati RB, Schubert P, Rothe G, Rudolphi K, Valet G, Kreutzberg GW (1994) Modulation of intracellular formation of reactive oxygen intermediates in peritoneal macrophages and microglial/brain macrophages by propentofylline. J Cerebr Blood Flow Metab 14:145–149

Bellavite P (1988) The superoxide-forming enzymatic system of phagocytes. Free Rad Biol Med 4:255–261

Frei K, Siepl C, Groscurth P, Bodmer S, Schwerdel C, Fontana A (1987) Antigen presentation and tumor cytotoxicity by interferon-γ-treated microglial cells. Eur J Immunol 17:1271–1278

Giulian D, Baker TJ (1986) Characterization of ameboid microglia isolated from developing mammalian brain. J Neurosci 6:2163–2178

Rothe G, Valet G (1994) Flow cytometric assays of oxidative burst activity in phagocytes. Meth Enzymol 233:539–548

Rothe G, Oser A, Valet G (1988) Dihydrorhodamine 123: a new flow cytometric indicator for respiratory burst activity in neutrophil granulocytes. Naturwissensch 75:354–355

F.3 In Vivo Methods

F.3.1 Inhibitory (Passive) Avoidance

One of the most common animal tests in memory research is the inhibition to imitate activities or learned habits. The term "passive avoidance" is usually employed to describe experiments in which the animal learns to avoid a noxious event by suppressing a particular behavior. Netto and Izquierdo (1985) have discussed this term in a brief paper. The term "inhibitory avoidance" is used more often in later publications.

REFERENCES AND FURTHER READING

Netto CA, Izquierdo I (1985) On how passive is inhibitory avoidance. Behav Neural Biol 43:327–330

F.3.1.1 Step-down

PURPOSE AND RATIONALE

An animal (mouse or rat) in an open field spends most of the time close to the walls and in the corners. When placed on an elevated platform in the center of a rectangular compartment, it steps down almost immediately to the floor to explore the enclosure and to approach the wall. The technique is employed in different mod-

ifications, which are described by Jarvik and Essmann (1960), Hudspeht et al. (1964), Chorover and Schiller (1965), Kubanis and Zornetzer (1981), Zornetzer et al. (1982), Abdel-Hafez et al. 1998).

PROCEDURE

Mice or rats of either sex are used. A rectangular box (50 × 50 cm) with electrifiable grid floor and 35 cm fits over the block. The grid floor is connected to a shock device, which delivers scrambled foot shocks. The actual experiments can be performed in different ways. A typical paradigm consists of three phases: (1) Familiarization: The animal is placed on the platform, released after raising the cylinder, and the latency to descend is measured. After 10 s of exploration, it is returned to the home cage. (2) Learning: Immediately after the animal has descended from the platform an unavoidable footshock is applied (Footshock: 50 Hz; 1.5 mA; 1 s) and the animal is returned to the home cage, (3) Retention Test: 24 h after the learning trial the animal is again placed on the platform and the step-down latency is measured. The test is finished when the animal steps down or remains on the platform (cut-off time: 60 s).

EVALUATION

The time of descent during the learning phase and the time during the retention test is measured. A prolongation of the step-down latency is defined as learning.

MODIFICATIONS OF THE TEST

This test procedure is employed in different modifications. One of the most common modifications is to induce amnesia in animals. There are different methods to do so including (i) electroconvulsive shock, (ii) scopolamine, (iii) alcohol, (iv) CO_2.

Ricceri et al. (1996) studied the effect of nerve growth factor on passive avoidance learning and retention in developing mice. At the beginning of each trial 11- or 15-day-old pups were placed on the central platform. Immediately thereafter, the platform began vibrating and a timer was simultaneously activated. A trial was ended when the pup gave a step-down response, or after 120 s without descent from the platform. Each step-down response was followed by a 3-s 0.3-mA foot shock.

CRITICAL ASSESSMENT OF THE METHOD

The variability of this method is relative high; therefore, it is necessary to test large groups of animals (minimum 10 animals per group). There are some critical parts in the experimental procedure: (i) Placing the animal on the platform, since the tendency of the animal to escape the contact with the human hand may shorten the step-down latencies. (ii) Another important point is the timing of the electric shock. It must not be applied at the first contact of the animal with the floor, since the light touch with the forelimbs does not cause the required shock intensity. The duration and intensity of the shock should be constant. (iii) It is also necessary to keep the room sound-proof, and this can be done by using a white noise generator (60–70 dB). Due to all these critical variables the results of different authors are difficult to compare.

REFERENCES AND FURTHER READING

Abdel-Hafez AA, Meselhy MR, Nakamura N, Hattori M, Watanabe H, Murakami Y, El-Gendy MA, Mahfouz NM, Mohamed TA (1998) Effects of paeoniflorin derivates on scopolamine-induced amnesia using a passive avoidance task in mice. Biol Pharm Bull 21:1174–1179

Chorover SL, Schiller PH (1965) Short-term retrograde amnesia in rats. J Comp Physiol Psychol 59:73–78

Dilts SL, Berry CA (1967) Effect of cholinergic drugs on passive avoidance in the mouse. J Pharmacol Exp Ther 158:279–285

Dunn RW, Flanagan DM, Martin LL, Kerman LL, Woods AT, Camacho F, Wilmot CA, Cornfeldt ML, Effland RC, Wood PL, Corbett R (1992) Stereoselective R-(+) enantiomer of HA-966 displays anxiolytic effects in rodents. Eur J Pharmacol 214:207–214

Hudspeth WJ, McGaugh JL, Thomson CW (1964) Aversive and amnesic effects of electroconvulsive shock. J Comp Physiol Psychol 57:61–64

Jarvik ME, Essmann WB (1960) A simple one-trial learning situation in mice. Psychol Rep 6:290

Kubanis P, Zornetzer SF (1981) Age-related behavioral and neurobiological changes: A review with emphasis on memory. Behav neural Biol 31:115–172

Lien EJ (1993) Design and discovery of new drugs by stepping-up and stepping-down approaches. Progr Drug Res 40:63–189

Ricceri L, Alleva E, Chiarotti F, Calamandrei G (1996) Nerve growth factor affects passive avoidance learning and retention in developing mice. Brain Res Bull 39:219–226

Zornetzer SF, Thompson R, Rogers J (1982) Rapid forgetting in aged rats. Behav Neural Biol 36:49–60

F.3.1.2 Step-through

PURPOSE AND RATIONALE

This test uses normal behavior of mice and rats. These animals avoid bright light and prefer dim illumination. When placed into a brightly illuminated space connected to a dark enclosure, they rapidly enter the dark compartment and remain there. The standard technique was developed for mice by Jarvik and Kopp (1967) and modified for rats by King and Glasser (1970). It is widely used in testing the effects of mem-

ory active compounds (Fekete and de Wied 1982; Hock and McGaugh 1985; Hock et al. 1989; Hock 1994).

PROCEDURE

Mice and rats of either sex are used. The test apparatus consists of a small chamber connected to a larger dark chamber via a guillotine door. The small chamber is illuminated with a 7 W/12 V bulb. The test animals are given an acquisition trial followed by a retention trial 24 h later. In the acquisition trial the animal is placed in the illuminated compartment at a maximal distance from the guillotine door, and the latency to enter the dark compartment is measured. Animals that do not step through the door within a cut-off time: 90 s (mice) or 180 s (rats) are not used. Immediately after the animal enters the dark compartment, the door is shut automatically and an unavoidable footshock (Footshock: 1 mA; 1 s – mice; 1.5 mA; 2 s – rat) is delivered. The animal is then quickly removed (within 10 s) from the apparatus and put back into its home cage. The test procedure is repeated with or without drug. The cut-off time on day 2 is 300 s (mice) or 600 s (rats), respectively.

EVALUATION

The time to step-through during the learning phase is measured and the time during the retention test is measured. In this test a prolongation of the step-through latencies is specific to the experimental situation. An increase of the step-through latency is defined as learning.

CRITICAL ASSESSMENT OF THE METHOD

Same as in step-down method

MODIFICATIONS OF THE TEST

This test procedure is employed in different modifications. To test drugs usually several test-groups can be tested. (i) CXC-group: vehicle – without amnesia – vehicle; (ii) DXD-group: drug – without amnesia – drug; (iii) CAC-group: vehicle – amnesia – vehicle; (iv) DAD-group: drug – amnesia – drug; (v) CAD-group: vehicle – amnesia – drug; (vi) DAC-group: drug – amnesia – vehicle. (The first figure means treatment on day 1; the third figure means treatment on day 2). There are different methods to induce amnesia: (i) electroconvulsive shock, (ii) scopolamine, (iii) alcohol, (iv) CO_2 etc.

Step-through experiments were performed after unilateral ibotenic acid lesions in the right nucleus basalis magnacellularis as a rat model of Alzheimer disease by Fine et al. (1985).

Wan et al. (1990) recorded changes in heart rate and body temperature via a telemetry system during step through passive avoidance behavior in rats.

Picciotto et al. (1995) used gene targeting to mutate $\beta 2$, the most widely expressed neuronal nicotinic acetylcholine receptor in the central nervous system for pharmacological and behavioral studies. Retention of the inhibitory avoidance response was better in mutant mice than in their non-mutant siblings.

Galeotti et al. (1997) modified the step-through method. After entry to the dark compartment, mice received a non-painful punishment consisting of a fall into a cold water bath (10°C). For this purpose the dark chamber was constructed with a pitfall floor. The memory degree of received punishment (fall into cold water) was expressed as the increase (in seconds) in the retention latency in comparison with the training latency.

Itokazu et al. (2001) showed that L-DOPA caused memory deficits in mice in a step-through passive avoidance test and recommended this as a model for human dementia.

REFERENCES AND FURTHER READING

Banfi S, Cornelli U, Fonio W, Dorigotti L (1982) A screening method for substances potentially active on learning and memory. J Pharmacol Meth 8:255–263

Fekete M, deWied D (1982) Potency and duration of action of the $ACTH_{4–9}$ analog (ORG 2766) as compared to $ACTH_{4–10}$ and [D-Phe^7]$ACTH_{4–10}$ on active and passive avoidance behavior of rats. Pharmacol Biochem Behav 16:387–392

Fine A, Dunnett SB, Björklund A, Iversen SD (1985) Cholinergic ventral forebrain grafts into the neocortex improve passive avoidance memory in a rat model of Alzheimer disease. Proc Natl Acad Sci USA 82:5227–5230

Fisher A, Brandeis R, Karton I, Pittel Z, Gurwitz D, Haring R, Sapir M, Levy A, Heldman E (1991) (±)-cis-2-Methylspiro(1,3-oxathiolane-5,3′)quinuclidine, an M_1 selective cholinergic agonist, attenuates cognitive dysfunctions in an animal model of Alzheimer's disease. J Pharmacol Exp Ther 257:392–403

Galeotti N, Ghelardini C, Teodori E, Gualtieri F, Bartolini A (1997) Antiamnesic activity of metoclopramide, cisapride and SR-17 in the mouse passive avoidance test. Pharmacol Res 36:59–67

Hock FJ (1994) Involvement of nitric oxide-formation in the action of losartan (DUP 753): effects in an inhibitory avoidance model. Behav Brain Res 61:163–167

Hock FJ, McGaugh JL (1985) Enhancing effects of Hoe 175 on memory in mice. Psychopharmacology 86:114–117

Hock FJ, Gerhards HJ, Wiemer G, Stechl J, Rüger W, Urbach H (1989) Effects of the novel compound, Hoe 065, upon impaired learning and memory in rodents. Eur J Pharmacol 171:79–85

Itokazu N, Yamamoto K, Ouchi Y, Cyong JC (2001) Establishment of L-3,4-dihydroxyphenilalaninde-induced pharmacological dementia model mouse. Neurosci Lett 305:123–126

Jarvik ME, Kopp R (1967) An improved one-trial learning situation in mice. Psychol Rep 21:221–224
King RA, Glasser RL (1970) Duration of electroconvulsive shock-induced retrograde amnesia in rats. Physiol Behav 5:335–339
Picciotto MR, Zoli M, Léna C, Bessis A, Lallemand Y, Le Novère N, Vincent P, Pich EM, Brûlet P, Changeux JP (1995) Abnormal avoidance learning in mice lacking functional high-affinity nicotine receptor in the brain. Nature 374:65–67
Rush DK, Streit K (1992) Memory modulation with peripherally acting cholinergic drugs. Psychopharmacology 106:375–382
Wan R, Diamant A, de Jong W, de Wied D (1990) Changes in heart rate and body temperature during passive avoidance behavior in rats. Physiol Behav 47:493–499

F.3.1.3 Two Compartment Test

PURPOSE AND RATIONALE

A rodent in an open field tends to enter any recesses in the walls and to hide there. When placed into a large box, connected through a narrow opening with a small dark compartment, the animal rapidly finds the entrance into the small chamber, enters it and spends most of its time there. The times spent in the large and small compartments are measured. The latency of the first entrance into the dark chamber and the number of crossings from one compartment into the other can be used as auxiliary criteria. The technique described was developed by Kurtz and Pearl (1960) and modified by Bures and Buresova (1963).

PROCEDURE

Mice and rats of either sex and a rectangular box with a 50 × 50 cm grid floor and 35 cm high walls are used. In the centre of one wall is a 6 × 6 cm opening connecting the large compartment to a small 15 × 15 cm box with dark walls, electrifiable grid floor and removable ceiling. The connection between the two compartments can be closed with a transparent sliding door. Illumination is provided with a 100 W bulb placed 150 cm above the centre of the large compartment.

EVALUATION

The times the animal spends in the large and the small compartment are measured.

CRITICAL ASSESSMENT OF THE METHOD

Same as in step-down method.

REFERENCES AND FURTHER READING

Banfi S, Cornelli U, Fonio W, Dorigotti L (1982) A screening method for substances potentially active on learning and memory. J Pharmacol Meth 8:255–263
Bures J, Buresova O (1963) Cortical spreading depression as a memory disturbing factor. J Comp Physiol Psychol 56:268–272
Gouret C, Raynaud G (1976) Utilisation du test de la boite a deux compartiments pour la recherche de substances protégeant le rat contre l'amnésie par hypoxie: Intérèt at limites de la méthode. J Pharmacol (Paris) 7:161–175
Kurtz KH, Pearl J (1960) The effect of prior fear experience on acquired-drive learning. J Comp Physiol Psychol 53:201–206

F.3.1.4 Up-Hill Avoidance

PURPOSE AND RATIONALE

Many animal species exhibit a negative geotaxis, i. e. the tendency to orient and move towards the top when placed on a slanted surface. When placed on a tilted platform with head facing down-hill, rats and mice invariably turn around and move rapidly up the incline (Staubli and Huston 1978).

PROCEDURE

Rats of both sex were used and maintained under standard conditions. The experimental apparatus is a 50 × 50 cm box with 35 cm high opaque plastic walls. The box can be inclined at different angles. The floor consists of 10 mm diameter stainless steel grid bars placed 13 mm apart. To deliver the tail-shock, a tail-electrode is constructed, consisting of a wire clip connected to a constant current shock source. The animal is first fitted with the tail-electrode and then placed onto the grid with its nose facing down. During baseline-trials the animal's latency to make a 180° turn and initiate the first climbing response is measured. Thereafter the animal is returned to its home cage. During the experimental trials the latencies are measured and additionally a tail-shock (1.5 or 2 mA) was administered contingent on the first climbing response after the 180° turn. Immediately after the shock the animal is placed in its home cage. Retest is performed 24 h later.

EVALUATION

The latencies are measured.

CRITICAL ASSESSMENT OF THE METHOD

The up-hill avoidance technique promises to provide a useful addition to the existing arsenal of inhibitory (passive) avoidance methods. Its most obvious advantage is that it can be administered to animals debilitated in sensory-motor coordination by pharmacological or surgical treatments that would preclude use of other inhibitory (passive) avoidance tasks.

REFERENCES AND FURTHER READING

Staubli U, Huston JP (1978) Up-hill avoidance: A new passive avoidance task. Physiol Behav 21:775–776

F.3.1.5 Trial-to-criteria inhibitory avoidance

PURPOSE AND RATIONALE

As animals experience different sensitivity to the footshock punishment applied in the dark area, immediately after the first trial the animal is returned to the lighted area to evaluate if the task has been acquired. A criteria is established to determine the learning of the test, usually requiring the animal to remain in the lighted area for a period of 30–60 s. (Decker et al. 1990). In this way, all the animals have a similar degree of learning independently of the amount of trials needed to attain it.

PROCEDURE

Mice or rats are generally used. The animals are trained in the same way as in the step-through version. They are placed in the lighted compartment and after they entered with the four paws into the dark area, the door is closed and a mild footshock is delivered. Immediately after the shock they are placed back in the lighted area for another trial. Training would continue this way until the animal remains in the lighted area for a certain period of time (30 or 60 s), a time at which the training is considered to be acquired by all the animals. The number of trials to attain criteria are counted as an indication of the speed of acquisition.

EVALUATION

Retention of the test is measured 24 or 48 Hs later. The animals are placed in the lighted area, the door opened and the latency to step with the four paws into the dark area is recorded. A cut-off latency of 180 or 300 s is usually imposed.

CRITICAL ASSESSMENT OF THE TEST

This modification of the classical inhibitory avoidance procedure is useful to determine the effect of drugs on acquisition as amnesic drugs significantly increase the number of trials to reach the criterion. Saline-treated animals generally need 1–2 trials to reach criterion while animals under diazepam or scopolamine need 3–6 trials. Once the animals have been trained to a predetermined criteria (i. e., 30 s. avoidance) any effect of the drug on the retention trial can be associated to drug effects on consolidation rather on the acquisition process (Brioni 1993; Decker et al. 1990). Alternatively, drugs could be administered before the test session in order to determine the effect of the drug on retrieval processes. Brain lesions differentially affect acquisition or retention (Hepler et al. 1985; Tomaz et al. 1992), and this task has also been used to demonstrate the effect of grafts on recovery of function (Fine et al. 1985).

MODIFICATIONS OF THE TEST

This test can also be performed as a continuous trial-to-criterion. In this procedure the door is not closed after the animal enters the dark area and upon delivery of the shock the animal can escape to the lighted area. The experimenter does not have to touch the animal to placed it in the lighted area for the next trial.

Kameyama et al. (1986) described a similar model for the study of learning and memory in mice using a step-down-type passive avoidance- and escape-learning method.

REFERENCES AND FURTHER READING

Brioni JD (1993) Role of GABA during the multiple consolidation of memory. Drug Dev Res 28:3–27

Decker MW, Tran T, McGaugh JL (1990) A comparison of the effects of scopolamine and diazepam on acquisition and retention of inhibitory avoidance in mice. Psychopharmacology 100:515–521

Fine A, Dunnett SB, Bjorklund A, Iversen SD (1985) Cholinergic ventral forebrain grafts into the neocortex improve passive avoidance memory in a rat model of Alzheimer's disease. Proc Natl Acad Sci, USA 82:5227–5230

Hepler DJ, Wenk G, Cribbs BL, Olton DS, Coyle JT (1985) Memory impairments following basal forebrain lesions. Brain Res 346:8–14

Kameyama T, Nabeshima T, Kozawa T (1986) Step-down-type passive avoidance- and escape-learning method. J Pharmacol Meth 16:39–52

Tomaz C, Dickinson-Anson H, McGaugh JL (1992) Basolateral amygdala lesions block diazepam-induced anterograde amnesia in an inhibitory avoidance task. Proc Natl Acad Sci USA 89:3615–3619

F.3.1.6 Scopolamine-Induced Amnesia in Mice

PURPOSE AND RATIONALE

The administration of the antimuscarinic agent scopolamine to young human volunteers produces transient memory deficits (Drachman and Leavitt 1974). Analogously, scopolamine has been shown to impair memory retention when given to mice shortly before training in a dark avoidance task (Dilts and Berry 1967; Glick and Zimmerberg 1972; Schindler et al. 1984). The ability of a range of different cholinergic agonist drugs to reverse the amnesic effects of scopolamine is now well documented in animals and human volun-

teers. However, the neuropathology of dementia of the Alzheimer type is not confined to the cholinergic system (Iversen 1998).

PROCEDURE

The scopolamine test is performed in groups of 10 male NMRI mice weighing 26–32 g in a one-trial, passive avoidance paradigm. Five min after i.p. administration of 3 mg/kg scopolamine hydrobromide, each mouse is individually placed in the bright part of a two-chambered apparatus for training. After a brief orientation period, the mouse enters the second, darker chamber. Once inside the second chamber, the door is closed which prevents the mouse from escaping, and a 1 mA, 1-s foot shock is applied through the grid floor. The mouse is then returned to the home cage. Twenty-four hours later, testing is performed by placing the animal again in the bright chamber. The latency in entering the second darker chamber within a 5 min test session is measured electronically. Whereas untreated control animals enter the darker chamber in the second trial with a latency of about 250 s, treatment with scopolamine reduces the latency to 50 s. The test compounds are administered 90 min before training. A prolonged latency indicates that the animal remembers that it has been punished and, therefore, does avoid the darker chamber.

EVALUATION

Using various doses latencies after treatment with test compounds are expressed as percentage of latencies in mice treated with scopolamine only. In some cases, straight dose-response curves can be established whereas with other drugs inverse U-shaped dose-responses are observed (Schindler et al. 1984).

CRITICAL ASSESSMENT OF THE METHOD

In spite of the fact that the pathogenesis of primary degenerative dementia (Alzheimer's disease) in man has been only partially elucidated, the scopolamine-amnesia test is widely used as primary screening test for so-called anti-Alzheimer drugs.

MODIFICATIONS OF THE METHOD

Lenègre et al. (1988) investigated the effects of piracetam on amnesias induced by scopolamine, diazepam and electroconvulsive shock.

Yamaoto et al. (1990) studied the effect of drugs on the impairment of working memory produced by scopolamine, ethylcholine aziridinium (AF64A) or cerebral ischemia using a repeated acquisition procedure in a three-panel runway apparatus.

Hiramatsu and Inoue (2000) demonstrated improvement by low doses of nociceptin on scopolamine-induced impairment of learning and/or memory in mice.

Martin et al. (1995) studied reversal of scopolamine-induced memory impairment by aniracetam in **rats** in an experiment conducted over a 1-year period.

Braida et al. (1998) investigated the short (120 min) and long-lasting (360 min) antagonism of scopolamine-induced amnesia in rats in an eight-arm radial maze by a cholinesterase inhibitor.

Giovannini et al. (1999) investigated the effects of histamine H_3 receptor agonists and antagonists on cognitive performance and scopolamine-induced amnesia.

Several **other drugs** have been shown to induce memory impairment.

Amnesia can also be induced by pretreatment with **benzodiazepines** (Porsolt et al. 1988).

Nabeshima et al. (1986) studied the antagonism against **phencyclidine**-induced retrograde amnesia in mice.

Maurice and Privat (1997) examined learning impairment induced by the non-competitive NMDA receptor agonist **dizocilpine** in mice.

Pitts et al. (2006) showed that **chlordiazepoxide** and **dizocilpine**, but not morphine, selectively impair acquisition under a novel repeated-acquisition and performance task in rats.

Ellison (1995) reported that the ***N*-methyl-D-aspartate antagonists** phencyclidine, ketamine, and dizocilpine provide behavioral and anatomical models of dementia.

Tanaka et al. (1998) studied learning and memory deficits induced by **β-amyloid** protein in rats.

Anandatheerthavarada et al. (2003) reported that mitochondrial targeting and a transmembrane arrest of Alzheimer's **amyloid precursor protein** impairs mitochondrial function in neuronal cells.

Ukai et al. (2001) showed that **endorphins** 1 and 2, endogenous μ-opioid receptor agonists, impair passive avoidance learning in rats.

Patil et al. (2002) used **lipopolysaccharide**-intoxicated mice as a model for Alzheimer's disease.

Yang et al. (2004) induced learning and memory impairment in mice by treatment with 1-methyl-4-phenyl-1,2,3,6-tetrahydropyridine (**MPTP**).

Sparks and Schreurs (2003) reported that trace amounts of **copper** in water induce β-amyloid plaques and learning deficits in a **rabbit model** of Alzheimer's disease using the nictitating membrane response (Buck et al. 2001).

REFERENCES AND FURTHER READING

Anandatheerthavarada HK, Biswas G, Robin MA, Avadhani NG (2003) Mitochondrial targeting and a novel transmembrane arrest of Alzheimer's amyloid precursor protein impairs mitochondrial function in neuronal cells. J Cell Biol 161:41–54

Braida D, Paladini E, Griffini P, Lamperti M, Colibretti L, Sala M (1998) Long-lasting antiamnesic effect of a novel anticholinesterase inhibitor (MF268). Pharmacol Biochem Behav 59:897–901

Buck DL, Seager MA, Schreurs BG (2001) Conditioning-specific reflex modification of the rabbit (*Oryctolagus cuniculus*) nictitating membrane response: generality and nature of the phenomenon. Behav Neurosci 115:1039–1047

Dilts SL, Berry CA (1976) Effects of cholinergic drugs on passive avoidance in the mouse. J Pharmacol Exper Ther 158:279–285

Drachman DA, Leavitt J (1974) Human memory and the cholinergic system. Arch Neurol 30:113–121

Ellison G (1995) The *N*-methyl-D-aspartate antagonists phencyclidine, ketamine and dizocilpine as both behavioral and anatomical models of dementia. Brain Res Rev 20:250–267

Giovannini MG, Bartolini L, Bacciottini L, Greco L, Blandina P (1999) Effects of histamine H_3 receptor agonists and antagonists on cognitive performance and scopolamine-induced amnesia. Behav Brain Res 104:147–155

Glick SD, Zimmerberg B (1972) Amnesic effects of scopolamine. Behav Biol 7:245–254

Hiramatsu M, Inoue K (2000) Improvement by low doses of nociceptin on scopolamine-induced impairment of learning and/or memory. Eur J Pharmacol 395:149–156

Iversen SD (1998) Behavioural Pharmacology of Dementia. Naunyn Schmiedeberg's Arch Pharmacol 358, Suppl 2, R 371

Lenègre A, Chermat R, Avril I, Stéru L, Porsolt RD (1988) Specificity of piracetam's anti-amnesic activity in three models of amnesia in the mouse. Pharmacol Biochem Behav 29:625–629

Martin JR, Moreau JL, Jenck F (1995) Amiracetam reverses memory impairment in rats. Pharmacol Res 31:133–136

Maurice T, Privat A (1997) SA4503, a novel cognitive enhancer with σ_1 receptor agonist properties, facilitates NMDA receptor-dependent learning in mice. Eur J Pharmacol 328:9–18

Nabeshima T, Kozawa T, Furukawa H, Kameyama T (1986) Phencyclidine-induced retrograde amnesia in mice. Psychopharmacology 89:334–337

Patil C, Singh VP, Satyanarayan PSV, Jain NK, Singh A, Kulkarni SK (2002) Protective effect of flavonoids against aging- and lipopolysaccharide-induced impairment in mice. Pharmacology 69:59–67

Pitts RC, Buda DR, Keith LR, Cerutti DT, Galizio M (2006) Chlordiazepoxide and dizocilpine, but not morphine, selectively impair acquisition under a novel repeated-acquisition and performance task in rats. Psychopharmacology 189:135–143

Porsolt RD, Lenègre A, Avril I, Doumont G (1988) Antagonism by exifone, a new cognitive enhancing agent, of the amnesias induced by four benzodiazepines in mice. Psychopharmacology 95:291–297

Schindler U, Rush DK, Fielding S (1984) Nootropic drugs: Animal models for studying effects on cognition. Drug Devel Res 4:567–576

Sparks L, Schreurs BG (2003) Trace amounts of copper in water induce β-amyloid plaques and learning deficits in a rabbit model of Alzheimer's disease. Proc Natl Acad Sci USA 100:11065–11069

Tanaka T, Yamada K, Senzaki K, Narimatsu H, Nishimura K, Kameyama T, Nabeshima T (1998) NC-1900, an active fragment analog of arginine vasopressin, improves learning and memory deficits induced by β-amyloid protein in rats. Eur J Pharmacol 352:135–142

Ukai M, Watanabe Y, Kameyana T (2001) Endorphins 1 and 2, endogenous μ-opioid receptor agonists, impair passive avoidance learning in rats. Eur J Pharmacol 421:115–119

Yamaoto T, Yatsugi SI, Ohno M, Furuya Y, Kitajima I, Ueki S (1990) Minaprine improves impairment of working memory induced by scopolamine and cerebral ischemia in rats. Psychopharmacology 100:316–322

Yang J, He, L, Wang J, Adams JD Jr (2004) Early administration of nicotinamide prevents learning and memory impairment in mice induced by 1-methyl-4-phenyl-1,2,3,6-tetrahydropyridine. Pharmacol Biochem Behav 78:179–183

F.3.1.7 Cognitive Deficits on Chronic Low Dose MPTP-Treated Monkeys

PURPOSE AND RATIONALE

Röltgen and Schneider (1994), Schneider et al. (1990, 1993, 1994a, b) described the effect of chronic low-dose 1-methyl-4-phenyl-1,2,3,6-tetrahydropyridine (MPTP) exposure on cognitive functions in monkeys. These animals develop cognitive deficits and difficulties in performing previously learned tasks, such as delayed response, delayed matching-to-sample, delayed alternation, visual discrimination reversal, and object retrieval, as well as dopamine depletions in several brain areas without severe Parkinsonian signs as found after high MPZP doses (Burns et al. 1983), see E.7.1.2. In addition, these animals exhibit other behavioral changes such as decreased task persistence, increased restlessness and decreased attention.

PROCEDURE

Adult Macaca monkeys are trained to perform a delayed response task while seated in a restraining chair placed inside a sound attenuating modified Wisconsin General Test apparatus. The monkey sits behind an opaque screen that when raised allows access to a sliding tray that contains recessed food wells with identical sliding white Plexiglas covers that serve as stimulus plaques that can be displaced by the animal to obtain rewards (raisins). Monkeys are trained to retrieve a raisin from one of the food wells after observing the experimenter baits the well. Right and left wells are baited in a randomized, balanced order. Animals are maintained on a restricted diet during the week and tested while food deprived. Training is accomplished with a non-correction procedure with 0 s delay and progressing to 5 s delay. Animals are trained until performance with a 5 s delay is 90% correct or

better for at least 5 consecutive days. Each daily session consists of 25 trials. A response is scored a 'mistake' if the monkey makes its response choice to a well that is not baited with reward. A 'no response' error is scored if the monkey fails to respond to a trail within 30 s.

Once the animals are performing at criterion level, MPTP is administered intravenously in doses ranging from 0.05 mg/kg at the start of the study to 0.20 mg/kg. Animals receive cumulative doses up to 60 mg over periods up to one year.

Pharmacological data are obtained after animals consistently show at least a 15% performance deficit on delayed response. Drugs are administered subcutaneously. Delayed response testing begins 8 min after dug administration. On drug testing days, animals receive drug or saline and are tested for delayed response performance, administered drug (or saline), and retested on the delayed response task.

EVALUATION

Delayed response performance after drug administration is compared with matched control performance obtained on the same day prior to drug administration. The total number of correct responses as well as the number of mistakes and 'no response' errors are tabulated for each session. Date are then expressed as mean (± standard deviation) performance. All animals serve as their own controls. Statistical analysis consists of analysis of variance, repeated measures design, with post hoc comparisons (Bonferroni *t*-test).

REFERENCES AND FURTHER READING

Burns RS, Chiueh CC, Markey SP, Ebert MH, Jacobowitz DM, Kopin IJ (1983) A primate model of Parkinsonism: Selective destruction of dopaminergic neurones in the pars compacta of the substantia nigra by N-methyl-4-phenyl-1, 2,3,6-tetrahydropyridine. Proc Natl Acad Sci, USA, 80:4546–4550

Röltgen DP, Schneider JS (1994) Task persistence and learning ability in normal and chronic low dose MPTP-treated monkeys. Behav Brain Res 60:115–124

Schneider JS, Kovelowski CJ (1990) Chronic exposure to low doses of MPTP. Cognitive deficits in motor asymptomatic monkeys. Brain Res 519:122–128

Schneider JS, Sun ZQ, Röltgen DP (1993) Delayed matching-to-sample, object retrieval, and discrimination reversal deficits in chronic low-dose MPTP-treated monkeys. Brain Res 615:351–354

Schneider JS, Sun ZQ, Röltgen DP (1994a) Effects of dopamine agonists on delayed response performance in chronic low-dose MPTP-treated monkeys. Pharmacol Biochem Behav 48:235–240

Schneider JS, Sun ZQ, Röltgen DP (1994b) Effects of dihydrexidine, a full dopamine D-1 receptor agonist on delayed response performance in chronic low dose MPTP-treated monkeys. Brain Res 663:140–144

F.3.2 Active Avoidance

Active avoidance learning is a fundamental behavioral phenomenon (Herrnstein 1969; Brush 1971; Campbell and Church 1969; D'Amato 1970). As in other instrumental conditioning paradigms the animal learns to control the administration of the unconditioned stimulus by appropriate reactions to the conditioned stimulus preceding the noxious stimulus. The first stage of avoidance learning is usually escape, whereby a reaction terminates the unconditioned stimulus.

REFERENCES AND FURTHER READING

Brush FR (1971) Aversive Conditioning and Learning. Academic Press, New York and London

Campbell BA, Church RM (1969) Punishment and Aversive Behavior. Appleton-Century-Crofts, New York

D'Amato MR (1970) Experimental Psychology: Methodology, Psychophysics and Learning. McGraw-Hill, New York, pp 381–416

Herrnstein RJ (1969) Method and theory in the study of avoidance. Psychol Rev 76:49–69

F.3.2.1 Runway Avoidance

PURPOSE AND RATIONALE

A straightforward avoidance situation features a fixed aversive gradient which can be traversed by the animal. The shock can be avoided when the safe area is reached within the time allocated (Munn 1950; Capaldi and Capaldi 1972; Hock and McGaugh 1985).

PROCEDURE

Mice or rats of either sex are used and maintained under standard conditions and handled for several days before the experiment. The same box as used in the step-through model can be used in this experiment. The apparatus is uniformly illuminated by an overhead light source. A loudspeaker, mounted 50 cm above the start-box, serves for presenting the acoustic conditioned stimulus (CS; an 80 dB, 2000 Hz tone from an audiogenerator). The footshock is employed by the same source as in the step-through avoidance. The animal is allowed to explore the whole apparatus for 5 min. The guillotine door is then closed and the animal is placed into the light starting area. After 10 s the acoustic CS is applied and the door is simultaneously opened. Shock is turned on after 5 s. The CS continuous until the animal reaches the safe area. It is left there for 50–70 s (intertrial interval, ITI) before returned to the same area again. The procedure starts again. The training is continued until the animal attains the criterion of 9 avoidances in 10 consecutive trials. On the

next day the procedure is repeated until the same learning criterion is reached. The time needed to reach the safe area is measured.

EVALUATION

The time the animal needs to reach the safe area on both days is measured. In addition, the number of errors (not reaching the safe area) is recorded.

MODIFICATIONS OF THE TEST

Several modifications are described in the literature. The CS also can be a light signal. The number of trials and the criterion can be changed.

CRITICAL ASSESSMENT OF THE METHOD

Same as in step-down method.

REFERENCES AND FURTHER READING

Capaldi EJ, Capaldi ED (1972) Aversive learning situations: apparatus and procedures. In: Myers RD (ed) Methods in Psychobiology, Vol. 2, Academic Press, London and New York, NY, pp 59–81

Hock FJ, McGaugh JL (1985) Enhancing effects of Hoe 175 on memory in mice. Psychopharmacology 86:114–117

Munn NL (1950) Handbook of Psychological Research on the Rat. Houghton Mifflin, Boston, MA

Silverman P (1978) Conditioned avoidance of aversive stimuli. In: Animal behaviour in the laboratory. Chapman and Hall, London, pp 204–219

F.3.2.2 Shuttle Box Avoidance (Two-Way Shuttle Box)

PURPOSE AND RATIONALE

Compared to runway avoidance, shuttle box avoidance (two-way-shuttle-box) is a more difficult task. Since the animal is not handled between trials, the shuttle-box can be easily automated (Capaldi and Capaldi 1972).

PROCEDURE

Rats of both sex are used and maintained under standard conditions. The apparatus used consists of a rectangular box 50 × 15 cm with 40 cm high metal walls, and an electrifiable grid floor. The box is divided by a wall with a manually or solenoid-operated guillotine door (10 × 10 cm). into two 25 × 15 cm compartments. Each compartment can be illuminated by a 20 W bulb mounted in the hinged Plexiglas lids. A fixed resistance shock source with an automatic switch (0.5 s on 1.5 s off) is used. Simple programming equipment provides for automatic delivery of the conditioned stimulus (CS) and the unconditioned stimulus (US). The apparatus is placed in a dimly lit room with a masking noise background (white noise) of 60 dB. The animal is allowed to explore the apparatus for 5 min with the connecting door open and the compartment lights switched off. The guillotine door is then closed. After 20 s the light is switched on in the compartment containing the animal, and the door is opened. A tone (CS) is presented and 5 s later the floor shock is applied in the illuminated compartment and continued until the animal escapes to the dark side of the compartment, the connecting door is closed and the shock discontinued. After a variable intertrial interval (ITI; 30–90 s) the light is switched on in the previous dark compartment, the door is opened and the animal is required to cross to the other side. The training is continued until the animal reaches the criterion of 9 avoidances in 10 consecutive trials. Retention is tested at different intervals after the original training by retraining the animal to the same criterion again.

EVALUATION

The time the animal needs to reach the safe area on both days is measured. In addition, the number of errors (not reaching the safe area) are recorded.

CRITICAL ASSESSMENT OF THE METHOD

The task is rather difficult due to the lack of a permanent safe area, lack of a simple instrumental response, presence of a variable aversive gradient and increased weight of emotional factor.

MODIFICATIONS OF THE METHOD

Salmi et al. (1994) described a computer-assisted two-way avoidance conditioning equipment for rats.

REFERENCES AND FURTHER READING

Capaldi EJ, Capaldi ED (1972) Aversive learning situations: apparatus and procedures. In: RD. Myers (ed), Methods in Psychobiology, Vol. 2, Academic Press, London and New York, NY, pp 59–81

Netto CA, Valente JT, Borges-Sobrinho JB, Lasevitz J, Tomaz CA (1991) Reversal of retrieval impairment caused by retroactive interference in a two-way active avoidance task in rats. Behav Neur Biol 55:114–122

Salmi P, Samualsson J, Ahlenius S (1994) A new computer-assisted two-way avoidance conditioning equipment for rats: behavioral and pharmacological validation. J Pharmacol Toxicol Meth 32:155–159

F.3.2.3 Jumping Avoidance (One-Way Shuttle Box)

PURPOSE AND RATIONALE

Since a high degree of automation and minimum handling are additional requirements for this model, the obvious solution is a simplified one-way avoidance, allowing for the spontaneous or forced return of the animal to the start. In order to enhance the start-goal

distinction a vertical gradient is introduced which requires the animal to perform a discrete response of an all-or-none character, such as the jump, which clearly differs from the more continuous translational movements required in the usual avoidance tasks (Tenen 1966; McKean and Pearl 1968).

PROCEDURE

Rats of both sex are used and maintained under standard conditions. The apparatus used consists of a rectangular box 40 × 25 cm with 40 cm high metal walls, an electrifiable grid floor and a Plexiglas ceiling. A 12 × 12 × 25 cm opaque plastic pedestrial, mounted onto one of the narrow walls of the box provides the isolated goal area. Flush with the horizontal surface of the pedestal moves a vertical barrier, which can either be retracted to the rear wall of the apparatus to expose the goal area or pushed forward to block access to the goal completely. The animal is placed into the apparatus for 5 min with the goal area exposed (barrier retracted). The barrier is then moved forwards and the goal is blocked for 2 s. The first trial starts by exposing the goal area and applying an acoustic CS (1000 Hz, 85 dB). Electric shocks – US (1.0 mA; 50 Hz; 0.5 s) – are applied 5 s later (once per 2 s), and continued together with the CS until the animal jumps onto the platform. After 30 s the barrier pushes the animal off the platform onto the grid floor. The sequence is repeated until the criterion of 10 consecutive avoidances is reached. Retention is tested on the next day until the animal reaches criterion.

EVALUATION

The time the animal needs to reach the safe area on both days is measured. In addition, the number of errors (not reaching the safe area) is recorded.

CRITICAL ASSESSMENT OF THE METHOD

In automated procedures extinction is more rapid, especially when short inter test intervals are used.

REFERENCES AND FURTHER READING

McKean DB, Pearl J (1968) Avoidance box for mice. Physiol Behav 3:795–796

Tenen SS (1966) An automated one-way avoidance box for the rat. Psychosom Sci 6:407–408

F.3.3 Discrimination Learning

In the experiments described above the animals have no choice between the conditioned stimuli. They have only one conditioned stimulus. The following examples illustrate the special techniques employed for discrimination among different stimulus modalities. The experiments can be classified either as simultaneous or successive discrimination paradigms. An exhaustive survey of discrimination studies can be found in Gilbert and Sutherland (1969).

REFERENCES AND FURTHER READING

Gilbert RM (1969) Discrimination learning? In: Gilbert RM, Sutherland NS (eds) Animal Discrimination Learning. Academic Press, New York, NY and London, pp 455–498

Hurwitz HMB (1969) Discrimination learning under avoidance schedules. In: Gilbert RM, Sutherland NS (eds) Animal Discrimination Learning. Academic Press, New York, NY and London, pp 413–454

Siegel S (1969) Discrimination overtraining and shift behavior. In: Gilbert RM, Sutherland NS (eds) Animal Discrimination Learning. Academic Press, New York, NY and London, pp 187–213

Sutherland NS (1969) Outlines of a theory of visual pattern recognition in animals and man. In: Gilbert RM, Sutherland NS (eds) Animal Discrimination Learning. Academic Press, New York, NY and London, pp 385–411

F.3.3.1 Spatial Habituation Learning[2]

PURPOSE AND RATIONALE

The open-field test utilizes the natural tendency of rodents to explore novel environments in order to open up new nutrition, reproduction and lodging resources (Birke and Archer 1983; Cerbone and Sadile 1994). The rate of exploratory behaviors exhibited in an unfamiliar environment is limited through the inherent necessity to avoid potential dangers. The observed behavior therefore is always a compromise between these conflicting interests and is regulated in part by the momentary physiological needs (Gerlai 1999; Groves and Thompson 1970). Spatial habituation learning is defined as a decrement in reactivity to a novel environment after repeated exposure to that now familiar environment. This reduction in exploratory behaviors during re-exposures is interpreted in terms of remembering or recognition of the specific physical characteristics of the environment. The test can be used to examine short-term spatial memory (within-trial reductions in exploratory activity) and/or long-term spatial memory (between-trial reductions in exploratory activity after a retention interval of 24, 48 or 96 h after the initial exposure) (Lát 1973).

PROCEDURE

The open-field apparatus is a rectangular chamber (rats: 60 × 60 × 40 cm, mice: 26 × 26 × 40) made of painted wood or grey PVC. A 25 W red or green

[2] Contribution by E. Dere.

light bulb is placed either directly above or beneath the maze to achieve an illumination density at the centre of approximately 0.3 lx. Masking noise is provided by a broad spectrum noise generator (60 dB). Prior to each trial, the apparatus is swept out with water containing 0.1% acetic acid. Housing room and the testing location are separated and animals are transported to the testing room 30 min before testing. The digitized image of the path taken by each animal is stored and analyzed post hoc with a semi-automated analysis system (e. g. Ethovision, Noldus, The Netherlands or Truscan, Coulbourn Instruments, Allentown, PA). In aged or hypoactive rodents testing is performed during the animals dark phase of day. The rodent is placed on the center or in a corner of the open-field for 5–10 minute sessions (mice: up to 20 min, because of the high basal activity level). The animals are re-exposed to the open-field 24 and 96 h after the initial trial (Thiel et al. 1999; Schwarting et al. 1999).

EVALUATION

The exploratory behaviours registered are: (1) Rearings or vertical activity: the number of times an animal was standing on its hind legs with forelegs in the air or against the wall. (2) The duration of single rearings as a measure of non-selective attention (Aspide et al. 2000) (3) Locomotion or horizontal activity: the distance in centimeters an animal moved.

MODIFICATIONS OF THE TEST

In order to assess emotionality parameters either in interaction with spatial novelty (a single exposure) or in interaction with spatial habituation learning (repeated exposures), the aversivity of the open-field can be varied by increasing the size (inducing agoraphobia) and/or the illumination density (inhibits exploration) of the apparatus (File 1980). Rodents exposed to a big sized brightly lit open field tend to spent more time in the corners or close to the wall and avoid the central part of the apparatus. The emotional behaviors registered are: (1) Corner time: the time spent in the 4 corner squares (rats: 15 × 15 cm; mice: 6.5 × 6.5 cm). (2) Wall time: the time an animal spent close to the wall as a measure for thigmotaxis (scanning the walls of the apparatus with the vibrissae). (3) Center time: the time spent in the center of the open field (rats: 20 × 20 cm; mice: 10 × 10 cm). (4) Defecation: number of boli deposited. (5) Freezing: the time the animal stays completely immobile except for movements associated with respiratory activity (Hall 1936; Frisch et al. 2000). To assess habituation learning not only by decrements in exploratory behaviors but also via increments, one can place an object in the center of the open-field. The number of entries into and the time spent in the center increases from exposure one to exposure two without affecting other indices of spatial habituation (Dai et al. 1995).

CRITICAL ASSESSMENT OF THE TEST

The open-field paradigm is a well validated, simple and time economical test, which has been widely used to examine the neurobiological foundations subserving spatial memory, general activity and emotionality in rodents with different approaches including: lesions, drugs, electrophysiology, neuroanatomy, and neurogenetics.

REFERENCES AND FURTHER READING

Aspide R, Fresiello A, de Filippis G, Carnevale UA, Sadile AG (2000) Non-selective attention in a rat model of hyperactivity and attention deficit: subchronic methylphenidate and nitric oxide synthesis. Neurosci Biobehav Rev 24:59–71

Birke LIA, Archer J (1983) Some issues and problems in the study of animal exploration. In: Archer J, Birke L (eds) Exploration in animals and humans, Van Nostrand Reinhold, Berkshire, UK

Cerbone A, Sadile AG (1994) Behavioral habituation to spatial novelty in rats: interference and non-interference studies. Neurosci Biobehav Rev 18:497–518

Dai H, Krost M, Carey RJ (1995) A new methodological approach to the study of habituation: the use of positive and negative behavioral indices of habituation. J Neurosci Meth 62:169–174

File SE (1980) The use of social interaction as a method for detecting anxiolytic activity in chlordiazepoxide-like drugs. J Neurosci Meth 2:219–238

Frisch C, Dere E, de Souza Silva MA, Gödecke A, Schrader J, Huston JP (2000) Superior water maze performance and increase in fear-related behavior in the endothelial nitric oxide synthase-deficient mouse together with monoamine changes in cerebellum and ventral striatum. J Neurosci 20:6694–6700

Gerlai R (1999) Ethological approaches in behavioral neurogenetic research. In: Crusio WE, Gerlai RT (eds) Handbook of Molecular-Genetic Techniques for Brain and Behavior Research (Techniques in the Behavioral and Neural Sciences, Vol. 13). Elsevier Science B.V. New York, pp 605–613

Groves PM, Thompson RI (1970) Habituation: a dual-process theory. Psychol Rev 77:419–450

Hall CS (1936) Emotional behavior in the rat. III. The relationship between emotionality and ambulatory activity. J Comp Physiol Psychol 22:345–352

Lát J (1973) The analysis of habituation. Acta Neurobiol Exp 33:771–789

Schwarting RKW, Sedelis M, Hofele K, Auburger GW, Huston JP (1999) Strain-dependent recovery of open-field behavior and striatal dopamine deficiency in the mouse MPTP model of Parkinson's disease. Neurotox Res 1:41–56

Thiel CM, Müller CP, Huston JP, Schwarting RKW (1999) High vs low reactivity to a novel environment: Behavioral, pharmacological and neurochemical measures. Neuroscience 93:959–962

F.3.3.2 Spatial Discrimination

PURPOSE AND RATIONALE

In the simplest case of discrimination learning the animal distinguishes between two symmetric stimulus-response sets, the equal probability of which has been changes by differential reinforcement events. Position of the cues with respect to the animal's body defines the CS^+ and CS^-. Usually left-right discrimination is employed, while axial orientation of the body is ensured by the construction of the apparatus (Siegel 1969).

PROCEDURE

Rats and mice of both sex are used and maintained under standard conditions. The apparatus used is usually a simple T- or Y-maze, with an electrifiable grid floor. The last 10 cm of each arm are separated from the rest of the apparatus by a swing-door which prevent the animal from seeing the food cup or the plastic sheet covering the grid in the goal area. A fixed resistance shock source is connected to an automatically operated switch. In an aversively motivated spatial discrimination learning the animal is trained to escape and/or to avoid foot shocks by always going to the right. Training starts by allowing the animal to explore the apparatus. Then the animal is placed on the start and after 5 s electric shocks (0.5 s, 50 Hz, 1.0 mA) are applied at 3 s intervals. The animals are trained to a criterion. On the following day the animal is retrained to the same criterion. After a 60 min interval the safe goal area is shifted to the other arm of the maze and the discrimination is reversed.

EVALUATION

Errors are scored. An error means that the animal enters the wrong arm with all four legs. During retention the number of trials until the animal makes correct choices are counted.

CRITICAL ASSESSMENT OF THE METHOD

The ecology of rodents makes these animals specially proficient in spatial discrimination learning, which is usually mastered in a few trials. Most of the initial errors are not due to the inability of the animal to remember the correct solution, but rather to its tendency to explore alternative pathways.

MODIFICATIONS OF THE TEST

Barnes (1979) and others introduced the radial maze as a modification of spatial discrimination. This method is now well established and widely used.

Ingram et al. (1994a, b) recommended the Stone 14-unit T-maze to find new pharmacological approaches for cognitive enhancement.

REFERENCES AND FURTHER READING

Barnes CA (1979) Memory deficits associated with senescence: a neurophysiological and behavioral study in rat. J Comp Physiol Psychol 93:74–104

Ingram KD, Spangler EL, Iijima S, Kuo H, Bresnahan EL, Greig NH, London ED (1994a) New pharmacological strategies for cognitive enhancement using a rat model of age-related impairment. Ann NY Acad Sci 717:16–32

Ingram KD, Spangler EL, Iijima S, Ikari H, Kuo H, Greig NH, London ED (1994b) Rodent models in memory dysfunction in Alzheimer's disease and normal aging: moving beyond the cholinergic hypothesis. Life Sci 55:2037–2049

Lamberty Y, Gower AJ (1990) Age-related changes in spontaneous behavior and learning in NMRI mice from maturity to middle age. Physiol Behav 47:1137–1144

Sara SJ, Devauges V (1989) Idazoxan, an α-2 antagonist, facilitates memory retrieval in the rat. Behav Neural Biol 51:401–411

Siegel S (1969) Discrimination overtraining and shift behavior. In: Gilbert RM, Sutherland NS (eds) Animal Discrimination Learning, Academic Press, New York, NY, pp 187–213

F.3.3.3 Spatial Learning in the Radial Arm Maze

PURPOSE AND RATIONALE

Olton and co-workers have developed a spatial discrimination task for rodents that has been extensively used in learning and memory studies, and that has served as the basic task for one of the most important theories on the role of the hippocampus (Olton et al. 1979; Olton and Samuelson 1976). The rat uses spatial information provided by the distal cues in the room to efficiently locate the baited arms. The radial arm-maze allows the study of spatial reference and working memory processes in the rat. In reference memory procedures, information is useful for many sessions/days and may usually be needed during the entire experiment. On the contrary, working memory procedures have a major temporal component as the information presented in the maze (arms baited) is useful for one session but not for subsequent ones; the rat has to remember the information during a delay interval (min to h). Correct choices in the radial arm-maze are rewarded by food.

PROCEDURE

The apparatus is a wooden elevated eight-arm radial maze with the arms extending from a central platform 26 cm in diameter. Each arm is 56 cm long and 5 cm wide with 2 cm high rails along the length of the arm. The maze is well illuminated and numerous cues are

present. Food pellets (reward) are placed at the end of the arms. During the test, rats are fed once a day and their body weights maintained at 85% of their free-feeding weight to motivate the rat to run the maze. Animals are trained on a daily basis in the maze to collect the food pellets. The session is terminated after 8 choices and the rat has to obtain the maximum number of rewards with a minimum number of errors.

EVALUATION

The number of errors (entries to non-baited arms) are counted during the session.

MODIFICATIONS OF THE TEST

Depending on the hypothesis being tested in the radial arm-maze (1) animals can be trained extensively and then receive specific brain lesions (hippocampus, septum or fimbria-fornix); after recovery from the surgery the rats are re-trained to determine the cognitive ability or the speed of recovery as these lesions severely disrupt processing of spatial information (Olton et al. 1978). (2) In working memory studies animals are forced to obtain reward in specific arms (4 arms), and after a time delay they have to either return to the same arms (win-stay) or to avoid these arms and obtain the food in the rest of the arms (win-shift). (3) Animals are trained to find food in only one arm, and after a delay they are required to return to the same arm. Many versions of the maze exist with differences in the shape, arm-length or the number of arms (12 or 24 arm-mazes), but all of them are appetitively-motivated. An aversively-motivated maze was developed by locating an 8-arm maze in a water tank (Buresova et al. 1985). Extensive modifications on the arm-maze were also developed by Kesner and co-workers and are the basis of the multidimensional attribute theory that characterize mnemonic functions (Kesner 1980, 1986).

CRITICAL ASSESSMENT OF THE TEST

The radial arm-maze has been widely used to determine the neurobiological mechanisms underlying spatial learning in rodents and to evaluate the effect of drugs. The deleterious effects of scopolamine, atropine, ethanol, benzodiazepines, haloperidol, ketamine, PCP, as well as the facilitatory effects of physostigmine, nicotine, pramiracetam, picrotoxin, naloxone have been reported in the literature (Levin 1988). One of the disadvantages of the test is that hypothalamic lesions or the anorectic effect of certain drugs (amphetamine) affect the appetitive nature of the maze and animals do not master the maze for this reason.

REFERENCES AND FURTHER READING

Buresova O, Bures J, Oitzl M, Zahalka A (1985) Radial maze in the water tank: an aversively motivated spatial working memory task. Physiol Behav 34:1003–1005

Kesner R (1980) An attribute analysis of memory: the role of the hippocampus. Physiol Psychol 8:189–197

Kesner R (1986) Neurobiological views of memory, In: Martinez J, Kesner R (eds) Learning and Memory, Academic Press, Inc.: Orlando, pp 399–438

Levin ED (1988) Psychopharmacological effects in the radial-arm maze. Neurosci Biobehav Rev 12:169–175

Olton DS (1983) Memory functions and the hippocampus. In: Seifert W (ed) Neurobiology of the Hippocampus. Academic Press, London, New York, pp 335–373

Olton DS, Samuelson RJ (1976) Remembrance of places passed: spatial memory in rats. J Exp Psychol An Behav Proc 2:97–116

Olton D, Walker J, Gage F (1978) Hippocampal connections and spatial discrimination. Brain Res 139:295–308

Olton DS, Becker J, Handelman G (1979) Hippocampus, space and memory. The Behavioral and Brain Sciences 2:313–365

Willig F, Palacios A, Monmaur P, Mhrazi M, Laurent J, Delacour J (1987) Short-term memory, exploration and locomotor activity in aged rats. Neurobiol Aging 8:393–403

F.3.3.4 Visual Discrimination

PURPOSE AND RATIONALE

Vision is better than any other sensory system for the analysis of spatial relationships in the environment of the animal. From the retina to the cerebral cortex, the organization of the visual system ensures processing of visual information according to simple principles, i. e. by fitting the distribution of light over the receptive surface to elementary geometrical concepts and by comparing these patterns with images stored in the memory. Visual pattern recognition is one of the most challenging problems of contemporary neurophysiology and experimental psychology, with significant implications for mathematical and technical modeling of perceptual phenomena (artificial intelligence). For review and details see Grüsser and Klinke (1971) and Sutherland (1969). Experimental studies of pattern discrimination must take into account the visual capability of the given species and present the discriminanda under conditions compatible with light sensitivity and acuity of the eye. The constructions of the apparatus should ensure that the discriminanda are viewed from one optimum distance and for a sufficient period of time. A thorough discussion of the pattern discrimination technique is to be found in Munn (1950).

PROCEDURE

Rats and mice of both sexes are used and maintained under standard conditions. The apparatus consists of a square 10×10 cm start area separated by a Plexi-

glas sliding door from the choice area, which is connected by swing doors to the goal compartment. The grid floor in the starting and the choice areas is electrifiable. The stimulus (mostly plastic cards 8 × 8 cm) can be attached to the swing doors. The patterns are black on a white background and have different forms. The apparatus is illuminated by a dim light. The animal is placed into the apparatus with all doors open and allowed to explore it. Then it is placed in the start and after 5 s released by raising the Plexiglas door. After another 5 s, electric shocks (1 mA, 50 Hz, 0.5 s, 1/3 s) are applied until the animal escapes through either of the open doors to the safe goal compartment where it is left for some seconds. As soon as this preliminary step is mastered, the stimulus cards are inserted, the negative door is locked and the grid section in front of this door is electrified. The animal is trained to a criterion. On the next day the animal is retrained to the same criterion and retention is expressed in savings. Another parameter which can be used to evaluate the savings is the cumulative number of errors until the criterion is reached (Thompson 1969).

EVALUATION

The number of correct answers as well as the number of trials until the criterion is reached are counted.

CRITICAL ASSESSMENT OF THE METHOD

The method is time consuming and only useful to address a specific hypothesis.

MODIFICATIONS OF THE TEST

Steckler et al. (2000) and Van Gaalen et al. (2003) tested mice for their ability to learn and perform a series of simultaneous visual discriminations, which allowed a dissociation between accuracy of discrimination from those of motivation and behavioral disinhibition. Five operant chambers (20 × 15 cm) with curved rear walls (developed with TSE, Bad Homburg, Germany) were used. Set in the curved wall of each box was an array of five circular holes, 2 cm in diameter, 3 cm deep and 1.5 cm above floor level. Each hole was equipped with an infrared photocell beam crossing the entrance vertically, a yellow LED at the rear end of the hole, providing 5 lux illumination at the hole's entrance, and a food pellet dispenser which allowed delivery of a 20-mg dustless food pellet directly into the hole where a correct response has been made. Presentation of the light stimulus, the operandum and the food reward all in the same location was chosen to enhance stimulus–response–reward contiguity. Each hole could be closed separately by a metal sheet to prevent access for the animal, if required. In addition, the chamber could be illuminated by a white house light (30 lux) mounted in the center of the roof. The boxes were housed in dark, sound-attenuating compartments. On-line control of the apparatus and data collection were performed using a special computer system. After habituation and autoshaping, the program was switched to five-choice discrimination and then to two-choice discrimination with increasing and decreasing response requirement.

REFERENCES AND FURTHER READING

Grüsser OJ, Klinke R (eds) Pattern Recognition in Biological and Technical Systems. Springer-Verlag, Berlin (1971)

Munn NL (1950) Handbook of Psychological Research on the Rat. Houghton Mifflin, Boston, MA

Steckler T, Sauvage M, Holsboer F (2000) Glucocorticoid receptor impairment enhances impulsive responding in transgenic mice performing on a simultaneous visual discrimination task. Eur J Neurosci 2559–2569

Sutherland NS (1969) Outlines of a theory of visual pattern recognition in animals and man. In: Gilbert RM, Sutherland NS (eds) Animal Discrimination Learning. Academic Press, New York, NY, pp 385–411

Thompson R (1969) Localization of the 'visual memory system' in the white rat. J Comp Physiol Psychol 69:1–29

Thompson R, Huestis PW, Crinella FM, Yu J (1987) Further lesion studies on the neuroanatomy of mental retardation in the white rat. Neurosci Biobehav Rev 11:415–440

Van Gaalen MM, Stenzel-Poore M, Holsboer F, Steckler T (2003) Reduced attention in mice overproducing corticotrophin-releasing hormone. Behav Brain Res 142:69–79

F.3.3.5 Spatial Learning in the Water Maze

PURPOSE AND RATIONALE

A task was developed where rats learn to swim in a water tank to find an escape platform hidden under the water (Morris 1984). As there are no proximal cues to mark the position of the platform, the ability to locate it efficiently will depend on the use of a configuration of the cues outside the tank. Learning is reflected on the shorter latencies to escape and the decrease on the length of the path to find the platform. Although rodents can find the platform by using non-spatial strategies, the use of a spatial strategy is the most efficient way to escape and young animals develop the spatial strategy after a small number of trials.

PROCEDURE

Different strains of rats are generally used (Long Evans, Wistar, Sprague-Dawley). The apparatus is a circular water tank filled to a depth of 20 cm with 25°C water (Brioni et al. 1990; Morris 1984). Four points equally distributed along the perimeter of the

tank serve as starting locations. The tank is divided in four equal quadrants and a small platform (19 cm height) is located in the centre of one of the quadrants. The platform remains in the same position during the training days (reference memory procedure). The rat is released into the water and allowed 60–90 s. to find the platform. Animals usually receive 2–4 trials per day for 4–5 days until they escape onto the platform. Well-trained rats escape in less than 10 s.

EVALUATION

The latency to reach the escape platform is measured during the training days. A free-swim trial is generally performed after the training days where the escape platform is removed and the animal is allowed to swim for 30 s. With the help of a video system, the latency to reach the previous position of the platform, the number of annulus crossings as well as the time the rat spent in the training quadrant are measured. Well-trained rats show short latencies, a large number of annulus crossings and bias to the quadrant where the escape platform was located during the training sessions.

MODIFICATIONS OF THE TEST

In the "cue" version of the water maze, the platform is clearly visible over the water and allows the evaluation of the motor and motivational aspects of the rat under study, as the animals should easily find the visible platform in 10–15 s. As circling or other non-spatial strategies can be used to find the platform, alternative measures of learning were developed (Gallagher et al. 1993), like the use of brief probe trials during training (rather than at the end), the use of proximity measures (an index of search error or deviations from the optimal path), and the learning index (proximity measures during weighted probe trials). Buresova and co-workers have developed the use of a collapsible platform to improve the accuracy of the water maze (Buresova et al. 1985). To evaluate working memory processes in the water maze, the rat can be trained to find a new platform position and later its performance is tested after a short delay (2–4 h). A spatial discrimination version of the water maze was also developed (Decker et al. 1992; Morris 1984), where the rat has to discriminate between two similar platforms based on spatial differences (one platform provides a mean to escape while the other sinks upon contact).

CRITICAL ASSESSMENT OF THE TEST

This test allows the researcher to study working and reference memory processes, and to dissociate the memory deficits induced by brain lesions or drug injections from the motor, motivational or sensory deficits. This test has been used to study the effect of drugs on memory (Brioni et al. 1991; Brioni et al. 1990. Decker et al. 1992), the participation of the hippocampus, septum, amygdala and nucleus basalis magnocellularis (Morris et al. 1986; Morris 1989), catecholamine depletions, as well as recovery of function (McNamara and Skelton 1993). It has been particularly sensitive to demonstrate that aged rats exhibit deficits in the acquisition of spatial information when compared to young or middle age controls (Rapp et al. 1987). The major advantages of the water maze over the radial arm-maze are: (1) that animals can be trained in a significantly shorter period of time (one week) while the arm-maze studies require several weeks of training; (2) intramaze cues like odor trails are eliminated in the pool; (3) large dose-response studies can be conducted in a week's time; (4) the motor or motivational problems in the rat can be detected in a cue trial; and (5) that the animals are not food-deprived during the test. From a theoretical point of view, the water maze is an aversively-motivated task while the arm-maze is appetitively-motivated.

MODIFICATIONS OF THE METHOD

Nitta et al. (1994, 1996; Nabeshima 1995) found an impairment of the performance of the water maze task in rats treated by infusion into the cerebral ventricle for 14 days with β-amyloid protein which consisted of senile plaques of Alzheimer's disease. The authors recommended that β-amyloid protein-treated rats as an animal model for Alzheimer's disease.

Song et al. (1997) reported that thymectomized rats, 5 weeks after surgery, showed a significant impairment of learning and memory as shown in deficits in passive avoidance and in the Morris water maze test.

Sun and Alkon (2004) found that induced depressive behavior impairs learning and memory in rats using an open space swim test. The model indexes searching activity of the animals, with the induced depressive immobility behavior showing specific sensitivity to three major prototypic classes of antidepressants and a selective serotonin reuptake inhibitor.

Zoladz et al. (2006) reported enhancement of long-term spatial memory in adult rats by the non-competitive NMDA receptor antagonists memantine and neramexane.

REFERENCES AND FURTHER READING

Brandeis R, Dachir S, Sapir M, Levy A, Fisher A (1990) Reversal of age-related cognitive impairments by an M1 cholinergic agent, AF102B. Pharmacol Biochem Behav 36:89–95

Brioni JD, Decker MW, Gamboa LP, Izquierdo I, McGaugh JL (1990) Muscimol injections in the medial septum impair spatial learning. Brain Res 522:227–234
Brioni JD, Arolfo MP, Jerusalinski D, Medina JH, Izquierdo I (1991) The effect of flumazenil on acquisition, retention and retrieval of spatial information. Behav Neural Biol 56:329–335
Buresova O, Krekule I, Zahalka A, Bures J (1985) On-demand platform improves accuracy of the Morris water maze. J Neurosci Meth 15:63–72
Decker MW, Majchrzak MJ, Anderson DJ (1992) Effects of nicotine on spatial memory deficits in rats with spatial lesions. Brain Res 572:281–285
Gallagher M, Burwell R, Burchinal M (1993) Severity of spatial learning impairment in aging: development of a learning index for performance in the Morris water maze. Behav Neurosci 107:618–626
Nabeshima T (1995) Trial to produce animal model of Alzheimer's disease by continuous infusion of β-amyloid protein into the rat cerebral ventricle. Jpn J Psychopharmacol 15:411–418
McNamara R, Skelton R (1993) The neuropharmacological and neurochemical basis of place learning in the Morris water maze. Brain Res Rev 18:33–49
Nitta A, Nabeshima T (1996) Experimental techniques for developing new drugs acting on dementia. Alzheimer's disease animal model induced by β-amyloid protein. Jpn J Psychopharmacol 16:85–90
Nitta A, Itoh A, Hasegawa T, Nabeshima T (1994) β-Amyloid protein-induced Alzheimer's disease animal model. Neurosci Lett 170:63–66
Morris R (1984) Developments of a water-maze procedure for studying spatial learning in the rat. J Neurosci Meth 11:47–60
Morris R, Anderson E, Lynch G, Baudry M (1986) Selective impairment of learning and blockade of long-term potentiation by an N-methyl-D-aspartate receptor antagonist. Nature 319:774–776
Morris RGM (1981) Spatial localization does not require the presence of local cues. Learn Motitiv 12:239–260
Morris RGM (1989) Synaptic plasticity and learning: Selective impairment in rats and blockade of long-term potentiation *in vivo* by the N-methyl-D-aspartate receptor antagonist AP5. J Neurosci 9:3040–3057
Rapp PR, Rosenberg RA, Gallagher M (1987) An evaluation of spatial information processing in aged rats. Behav Neurosci 101:3–12
Song C, Earley B, Leonard BE (1997) Effect of chronic treatment with piracetam and tacrine on some changes caused by thymectomy in the rat brain. Pharmacol Biochem Behav 56:697–704
Sun MK, Alkon DL (2004) Induced depressive behavior impairs learning an memory in rats. Neuroscience 129:129–139
Zoladz PR, Campbell AM, Park CR, Schaefer D, Danysz W, Diamond DM (2006) Enhancement of long-term spatial memory in adult rats by the noncompetitive NMDA receptor antagonists, menantine and neramexane. Pharmacol Biochem Behav 85:298–306

F.3.3.6 Active Allothetic Place Avoidance Task

PURPOSE AND RATIONALE

Bures et al. (1997), Fenton et al. (1998), Cimadevilla et al. (2000, 2001a, 2001b), Stuchlik and Bures (2002), Stuchlik et al. (2004), and Stuchlik and Vales (2005) designed a pharmacological mode, which they called the active allothetic place avoidance (AAPA) task, a cognitive task which requires rats to separate two conflicting spatial reference frames (room and arena frames), when only the room frame is relevant for solution of the task. Stuchlik and Vales (2005) showed that systemic administration of MK-801 elicits a behavioral deficit in rats in the AAPA task irrespective of their intact spatial pretraining.

PROCEDURE

Male Long-Evans starin rats weighing 350–450 g were housed under constant temperature at a 12:12 light:dark cycle. Under light ether anesthesia, animals were implanted with a low-impedance connector made from a hypodermic needle, which pierced the rat's skin between the shoulders. The sharp end of the needle was then cut off and bent with tweezers to form a small loop, which prevented the connector from slipping out and provided anchor for an alligator clip, which was connected to a shock-delivering wire.

MK-801 was injected i.p. in doses of 0.15 or 0.2 mg/kg 30 min before each training session.

The AAPA task apparatus consists of a smooth metallic circular arena (80 cm in diameter) enclosed within a 30-cm-high transparent Plexiglas wall and elevated 1 cm above the floor. There were two arenas located in two different rooms. The upstairs room (4 m × 5 m) contained various extramaze landmarks. The downstairs room (5 m × 5 m) contained different visual cues organized in a different layout. At the beginning of each training session, a rat was placed on the rotating arena (1 rpm), where a directly imperceptible 60° to-be-avoided sector (shock sector) was defined by the computer-based tracking system, located in an adjacent room. The location of the shock sector could be determined exclusively by its spatial relation to distal orienting cues in the room. The rat wore an infrared light-emitting diode fixed between the shoulders with a light latex harness, and its position was tracked every 40 ms and recorded onto a computer track file, allowing subsequent reconstruction of the track with an off-line analysis program.

Whenever a rat entered the shock sector for more than 0.5 s, mild electric shocks (50 Hz, 0.5 s) were delivered in intervals of 1.5 s until the rat left the shock sector for at least 0.5 s. The shocks were delivered through a thin low-impedance wire implant on the back of the rat standing on the grounded floor. The appropriate shock current (ranging between 0.2 and 0.7 mA) was individualized for each rat to elicit a rapid

escape reaction but to prevent freezing. Since the arena was rotating, the rat had to move actively away from the shock in the direction opposite to the arena rotation, otherwise it was passively transported to the shock sector. Experimental sessions in AAPA lasted 20 min and each rat had one session every day, carried out during daylight hours.

Initially, non-injected rats were trained for four consecutive daily sessions to avoid a sector located in the north of the upstairs room to learn the task without any drug administration. Subsequently, in session 5 they were injected with either saline or MK-801 and tested for the effect of the drug on the well-pretrained place avoidance (reinforced retention). After a weekend break rats were trained daily under saline or MK-801 in the downstairs arena in order to test reacquisition of AAPA in a new environment, when they were already familiar with the procedural component of the AAPA task (sessions 6–10). The shock sector was defined in the south of the room in the downstairs arena.

Rats were divided in three experimental groups: controls, MK-801 0.15 or 0.2 mg/kg i.p., respectively.

EVALUATION

The following parameters were recorded and analyzed in order to assess rats' behavior in the AAPA: the total distance traveled in a session (DISTANCE) measured in the arena frame (which only takes into account active locomotion) reflected the locomotor activity of the rats, and the number of entrances in the shock sector (ERRORS) reflected the efficiency of spatial performance in the AAPA task. The maximum time a rat spent in the safe part of the arena between two ERRORS in a particular session was also recorded. It reflected the ability to remember the shock sector location and to avoid it. Data from the initial 4 days of intact pretraining in the upstairs room were analyzed using a two-way ANOVA (groups × sessions) with repeated measures on sessions, data from the fifth day (retention session) were compared in a between-group fashion using one-way ANOVA, and data from the reacquisition training in the downstairs room were analyzed with a two-way ANOVA (groups × session) with repeated measures on sessions. Tukey's HSD test was used when appropriate.

CRITICAL ASSESSMENT OF THE METHOD

The AAPA task has been used for various pharmacological studies. In this paper, the authors claim that testing the effect of various substances using the AAPA task may be a promising way to predict their influence on cognitive symptoms.

REFERENCES AND FURTHER READING

Bures J, Fentom AA, Kaminsky Y, Zinyuk L (1997) Place cells and place navigation. Proc Natl Acad Sci USA 94:343–350

Cimadevilla JM, Kaminsky Y, Fenton A, Bures J (2000) Passive and active place avoidance as a tool of spatial memory research in rats. J Neurosci Meth 102:155–164

Cimadevilla JM, Wesierska M, Fenton AA, Bures J (2001a) Inactivating one hippocampus impairs avoidance of a stable room-defined place during dissociation of arena cues from room cues by rotation of the arena. Proc Natl Acad Sci USA 98:3531–3536

Cimadevilla JM, Fenton AA, Bures J (2001b) New spatial recognition tests for mice: passive place avoidance and active place avoidance on rotating arenas. Brain Res Bull 54:559–563

Fenton AA, Wesierska M, Kaminsky Y, Bures J (1998) Both here and there: simultaneous expression of autonomous spatial memories in rats. Proc Natl Acad Sci USA 95:11493–11498

Stuchlik A, Bures J (2002) Relative contribution of allothetic and idiothetic navigation to place avoidance on stable and rotating arenas in darkness. Behav Brain Res 128:179–188

Stuchlik A, Rezacova L, Vales K, Bubenikova V, Kubik S (2004) Application of a novel active allothetic place avoidance task (AAPA) in testing a pharmacological model of psychosis in rats: comparison with the Morris water maze. Neurosci Lett 366:162–166

Stuchlik A, Vales K (2005) Systemic administration of MK-801, a non-competitive NMDA-receptor antagonist, elicits a behavioral deficit in rats in the Active Allothetic Place Avoidance (AAPA) task irrespectively of their intact spatial pretraining. Behav Brain Res 159:163–171

F.3.3.7 Olfactory Learning

PURPOSE AND RATIONALE

Odors provide rodents with important information on the environment and the learning of successive olfactory discrimination problems in rats is closely related to the acquisition rules of higher primates. Odor-reward associations are learned in few trials as odors exert more discriminative control over other sensory modalities like tones or lights (Nigrosh et al. 1957). Animals have to learn to discriminate an arbitrary designated positive odor (i. e., banana) from a negative one (i. e., orange) to receive a reward.

PROCEDURE

Rats (Sprague-Dawley or Long Evans) are generally used. In procedures described in the literature (Eichenbaum et al. 1992; Roman et al. 1993), animals are deprived of water for 48 h before the training and during the test they receive ad libitum water for only 30 min. The olfactory apparatus is a rectangular box (30 × 30 × 55 cm) with a photosensitive cell mounted

on top of the water spout/odor outlet. Rats are trained to approach the water spout and to brake the light beam. Responses to the positive odor are rewarded with water while responses to the negative odor results in the presentation of a light flash. The intertrial interval before the presentation of a new odor is usually 15 s. and the sessions last 30 min. per day. Sessions are terminated when the rat makes 90% correct choices or after 400 trials.

EVALUATION

The animal is rewarded with 0.05 ml of water when it brakes the beam to the positive odor or when it does not respond to the negative odor. Incorrect responses ("no go" to the positive odor or "go" to the negative odor are followed by a flash and a longer intertrial interval). Results are reported as the % correct responses or as a logit transformation of the % correct/incorrect response ratio.

CRITICAL ASSESSMENT OF THE TEST

The anatomical connections from the olfactory bulbs to cortical as well as subcortical areas are fairly well known, and brain lesions that impair olfactory discrimination learning (Otto et al. 1991; Roman et al. 1993; Stäubli et al. 1984) could be used as models of amnesia. Systemic injections of scopolamine disrupts the performance of rats during long delays with no effect on immediate recall, data that are consistent with the effect of scopolamine in humans (Ravel et al. 1992). Antagonists of the NMDA receptor impair acquisition of odor discriminations and block LTP, an electrophysiological correlate of memory (Lynch and Stäubli 1991). The test can also be used to evaluate the cognitive effects of drugs such as ACTH analogs that facilitate the storage of olfactory information (Roman et al. 1989).

MODIFICATIONS OF THE TEST

A T-maze with controlled access to the reward compartment was developed (Ravel et al. 1992), that allows the test to evaluate working memory processes after time delays (1–3 min.).

Willer et al. (1992) examined the effects of a competitive NMDA agonist on the ability of rats to acquire potentiated aversions to the odor element of a taste-odor compound.

Larson et al. (1995) studied in rats the facilitation of olfactory learning by a modulator of AMPA receptors.

REFERENCES AND FURTHER READING

Eichenbaum H, Otto T, Cohen NJ (1992) The hippocampus – what does it do? Behav Neural Biol 57:2–36

Larson J, Lieu T, Petchpradub V, LeDuc B, NgoH, Rogers GA, Lynch G (1995) Facilitation of olfactory learning by a modulator of AMPA receptors. J Neurosci 15:8023–8030

Lynch G, Stäubli U (1991) Possible contributions of long-term potentiation to the encoding and organization of memory. Brain Res Rev 16:204–206

Nigrosh BJ, Slotnik BM, Nevin JA (1957) Olfactory discrimination, reversal learning and stimulus control in rats. J Comp Physiol Psychol 89:285–194

Otto T, Schottler F, Stäubli U, Eichenbaum H, Lynch G (1991) Hippocampus and olfactory discrimination learning: effects of entorhinal cortex lesions on olfactory learning and memory in a successive-cue go-no-go task. Behav Neurosci 105:111–119

Ravel N, Vigouroux M, Elaagouby A, Gervais R (1992) Scopolamine impairs delayed matching in an olfactory task in rats. Psychopharmacology 109:439–443

Roman F, Han D, Baudry M (1989) Effects of two ACTH analogs on successive odor discrimination learning in rats. Peptides 10:303–307

Roman FS, Simonetto I, Soumireu-Mourat B (1993) Learning and memory of odor-reward association: selective impairment following horizontal diagonal band lesions. Behav Neurosci 107:72–81

Stäubli U, Ivy G, Lynch G (1984) Hippocampal denervation causes rapid forgetting of olfactory information in rats. Proc Natl Acad Sci, USA 81:5885–5887

Willer J, Gallagher M, Graham PW, Crooks GB Jr (1992) N-methyl-D-aspartate agonist D-AVP selectively disrupts taste-potentiated odor aversion learning. Behav Neurosci 106:315–323

F.3.3.8 Aversive Discrimination in Chickens

PURPOSE AND RATIONALE

One to 2-days old chicks have been extensively used to study learning and memory. The chicks are trained to discriminate between an aversive and a non-aversive stimulus (colored glass beads) in a single 10–15 s learning trial. Following this learning trial, retention is monitored over a comprehensive range of learning-retention intervals to chart the course and to differentiate possible stages of memory formation. Three behaviorally sequentially dependent stages have been identified: a short-term memory stage, lasting approximately 10 min after learning; an intermediate-memory stage, available between 20 and 50 min post-learning, and a long-term memory stage available from 60 min after learning. The three stages are behaviorally separated by transient retention deficits occurring at around 15 and 55 min post-training. Gibbs and Barnett (1976), Gibbs and Ng (1976, 1979), Rickard et al. (1994, 2001), Bennett et al. (1996), Ng et al. (1997) used a three-stage model to test the influence of drugs on memory formation.

PROCEDURE

Day-old, male, White-leghorn black-Australop chickens are housed at an ambient temperature of 28°C. In

a single passive avoidance learning trial, chicks are pre-trained to peck at a 4 mm chromed bead, dipped in water and presented for 10 s. A similar bead, dipped in the chemical aversant methyl anthranilate, is the presented for 10 s. Data from chicks failing to peck the bead on this trial or not showing characteristic disgust responses after pecking are eliminated from subsequent data analysis. Retention is tested by presenting for 10 s a dry bead similar to that used for the pretraining trail.

In a discrimination paradigm, chicks are trained to avoid a red bead and are tested on red and blue beads successively and discrimination ratios registered.

In an additional discrimination paradigm, chicks are given two aversive beads – a chrome and a red bead. They are trained on one of the aversive beads sometime before drug treatment. The other aversive bead is associated with drug treatment and the chicks are subsequently tested with all three beads.

Twenty different chicks are used for each data point. Retention in both paradigms is indexed by the proportion of chicks avoiding the aversive bead, with the proviso that in the discrimination paradigm is indicated by the avoidance of the red bead and pecking on the blue bead. Retention is tested at various times between 5 and 180 min after learning or at 24 h.

Drugs are administered in 0.1 ml volumes subcutaneously into a fold of skin on the ventral side of the rib cage.

EVALUATION

Discrimination ratios of treated animals after various time intervals following administration of drugs are statistically compared with saline treated controls.

CRITICAL ASSESSMENT OF THE METHOD

The test has been used with slight modifications successfully by many authors in several research groups (e. g., Hölscher and Rose 1992; Sandi and Rose 1994; Stephenson and Andrew 1994; Zhao et al. 1994; Deyo and Hittner 1995; Crowe and Shaw 1997; Venero and Sandi 1997; Bennett et al. 1998; Tiunova et al. 1998; Rose and Stewart 1999)

MODIFICATIONS OF THE TEST

Bourne et al. (1991) compared the taste and odor aversant methyl anthranilate with the odorless quinine as averants.

Clements and Bourne (1996) and Stamatakis et al. (1998) injected drugs, e. g., GABA agonists or α_2-noradrenergic agonists and antagonists, directly into the intermediate median hyperstriatum ventrale of day-old chicks, prior to training on a chrome bead dipped in either methyl anthranilate or quinine.

Colombo et al. (1997) injected enkephalins into 2 regions of the 2-day-old chick brain: the intermediate medial hyperstriatum and the lobus parolfactorius.

Tiunova et al. (1996) trained chicks to discriminate between edible chick crumbs and arrays of colored bead glued to the floor of their cage.

Gilbert et al. (1989) reported a simple, one-trial, learning paradigm in young chicks. Chicks were separated from their brood mates and placed in a small isolation chamber. A T-maze connected the isolation chamber to the brood space, allowing the chick to escape isolation stress and rejoin the brood. When the chick successfully negotiated the corridor, the latency to perform this task was recorded. On a subsequent trial, any improvement in the speed of performance was recorded to reflect the chick's memory of the task.

REFERENCES AND FURTHER READING

Bennett PC, Zhao W, Lawen A, Ng KT (1996) Cyclosporin A, an inhibitor of calcineurin, impairs memory formation in day-old chicks. Brain Res 730:107–117

Bennett PC, Singaretnam LL, Zhao L-Q, Lawen A, Ng KT (1998) Peptidyl-prolyl-cis/trans-isomerase activity may be necessary for memory formation. FEBS Lett 431:386–390

Bourne RC, Davies DC, Stewart MG, Csillag A, Cooper M (1991) Cerebral glycoprotein synthesis and long-term memory formation in the chick (Gallus domesticus) following passive avoidance training depends on the nature of the aversive stimulus. Eur J Neurosci 3:243–248

Clements MP, Bourne RC (1996) Passive avoidance learning in the day-old chick is modulated by GABAergic agents. Pharmacol Biochem Behav 53:629–634

Colombo PJ, Rivera DT, Martinez JL Jr, Bennett EL, Rosenzweig MR (1997) Evidence for localized and discrete roles for enkephalins during memory function in the chick. Behav Neurosci 111:114–122

Crowe SF, Shaw S (1997) Salbutamol overcomes the effect of the noradrenergic neurotoxin DSP-4 on memory function in the day-old chick. Behav Pharmacol 8:216–222

Deyo RA, Hittner JM (1995) Effects of the Ca^{2+} channel antagonist flunarizine on visual discrimination learning. Neurobiol Lear Memory 64:10–16

Gibbs ME, Barnett JM (1976) Drug effects on successive discrimination learning in young chickens. Brain Res Bull 1:295–299

Gibbs ME, Ng KT (1976) Psychobiology of memory: Towards a model of memory formation. Biobehav Res 1:113–136

Gibbs ME, Ng KT (1979) Neuronal depolarization and the inhibition of short-term memory formation. Physiol Behav 23:369–375

Gilbert DB, Patterson TA, Rose SPR (1989) Midazolam induces amnesia in a simple, one-trial, maze-learning task in young chicks. Pharmacol Biochem Behav 34:439–442

Hölscher Ch, Rose SPR (1992) In inhibitor of nitric oxide synthesis prevents memory formation in the chick. Neurosci Lett 145:165–167

Ng KT, O'Dowd BS, Rickard NS, Robinson SR, Gibbs ME, Rainey C, Zhao W-Q, Sedman GL, Hertz L (1997) Com-

plex roles of glutamate in the Gibbs-Ng model of one-trial aversive learning in the new-born chick. Neurosci Behav Rev 21:45–54
Rickard NS, Ng KT, Gibbs ME (1994) A nitric oxide agonist stimulates consolidation of long-term memory in 1-day old chick. Behav Neurosci 108:640–644
Rickard NS, Kowadlo N, Gibbs ME (2001) Effect of *Ginkgo biloba* extract, EGb 761, on memory formation in day-old chicks. Pharmacol Biochem Behav 69:351–358
Rose SPR, Stewart MG (1999) Cellular correlates of stages of memory formation in the chick following passive avoidance training. Behav Brain Res 98:237–243
Sandi C, Rose SPR (1994)Corticosteroid receptor antagonists are amnesic for passive avoidance learning in day-old chicks. Eur J Neurosci 6:1292–1297
Stamatakis A, Stewart MG, Dermon CR (1998) Passive avoidance learning involves α_2-noradrenergic receptors in a day old chick. NeuroReport 9:1679–1683
Stephenson RM, Andrew RJ (1994) The effects of 5-HT receptor blockade on memory formation in the chick: Possible interactions between β-adrenergic and serotoninergic systems. Pharmacol Biochem Behav 48:971–975
Tiunova A, Anokhin K, Rose SPR, Mileusnic R (1996) Involvement of glutamate receptors, protein kinases, and protein synthesis in memory for visual discrimination in the young chick. Neurobiol Learn Memory 65:233–243
Tiunova A, Anokhin K, Rose SPR (1998) Two critical periods of protein and glycoprotein synthesis in memory consolidation for visual categorization learning in chicks. Learn Memory 2:401–410
Venero C, Sandi C (1997) Effects of NMDA and AMPA receptor antagonists on corticosterone facilitation of long-term memory in the chick. Eur J Neurosci 9:1923–1928
Zhao W, Sedman GL, Gibbs ME, Ng KT (1994) Effect of PKC inhibitors and activators on memory. Behav Brain Res 60:151–160

F.3.4
Conditioned Responses

F.3.4.1
Conditioned Nictitating Membrane Response in Rabbits

PURPOSE AND RATIONALE

The rabbit's classically conditioned eyeblink response has become a widely used model system for studying associative learning in mammals (Gormezano et al. 1987) and to find drugs potentially useful in the treatment of age-related memory disorders (Ghoneim et al. 1994; Woodruff-Pak et al. 1994a, b, 1997; Solomon et al. 1988, 1995a, b).

PROCEDURE

Animals

New Zealand white albino rabbits weighing 2.0 kg are housed individually under consistent light with free access to food and water.

Apparatus and General Procedure

A small loop of surgical nylon is sutured into the right nictitating membrane, and the surrounding hair is removed. One day later, the rabbit is placed in a Plexiglas restrainer, and two stainless-steel wound clips are applied to the skin over the parietal region. The rabbit is fit with a headmount that supports a photoresistive assembly for recording the nictitating membrane response by physical coupling with a length of thread to the nylon loop in the nictitating membrane. The transducer assembly converts nictitating membrane movements into electrical signals that are subjected to an analog-to-digital conversion using a 5-ms sampling rate and a resolution of 0.06 mm actual membrane extension. The animal is then positioned in a ventilated, sound-attenuated chamber facing a stimulus panel containing an 11.4-cm speaker and two 6-W, 24-V DC house lights, one mounted at each side of the speaker. During the course of the experiment, two stimuli are employed as conditioned stimulus: a) a 1000-ms, 1-kHz, 84-dB tone; b) a 1000-ms, intermittently presented light produced by interruption of the house lights at 10 Hz to yield a change in illumination, measured at the eye level of the rabbit from 32.11 to 8.01. The unconditioned stimulus is a 100-ms, 3-mA, 60Hz shock delivered to the wound clips by a constant current shock generator.

Drugs

Drug solutions or saline are injected subcutaneously into the cervical area of the rabbit via an infusion pump at a rate of 3 ml/min, 30 min before behavioral testing.

Procedure

Experimentally naive rabbits are randomly assigned in equal numbers to each of the treatments ($n = 10$ per treatment). The experiment consists of two phases: Phase 1 is an adaptation day followed by 9 days of acquisition training. No stimuli are presented during the 60-min adaptation session. Subjects are injected with their assigned treatment 30 min before each acquisition session. Each acquisition session consists of 30 tone-shock and 30 light-shock trials presented in a randomized sequence within 10 trial blocks, with the restriction that no more than three consecutive tone or light trials can occur. On each conditioned stimulus – unconditioned stimulus trial, the offset of the 1000-ms tone or light conditioned stimulus occurs simultaneously with the onset of the 100-ms unconditioned stimulus. The inter-trial interval is about 60 s. A response is defined as at least a 0.5-mm extension of the nictitating membrane. Responses occurring during the tone or light conditioned stimulus, but before the unconditioned stimulus are recorded as conditioned response;

those occurring after the unconditioned stimulus onset are recorded as unconditioned response.

EVALUATION

The data are analyzed by repeated measures analyses of variance and Tukey tests. The significance level is set at $p < 0.05$.

CRITICAL ASSESSMENT OF THE METHOD

The rabbit nictitating membrane response has been used widely to study the effects of drugs on learning (Schindler and Harvey 1990).

MODIFICATIONS OF THE TEST

Several authors used a corneal air puff as unconditioned stimulus (Robinson et al. 1993; Solomon et al. 1995, 1996).

Scavio et al. (1992) studied post-training effects of several drugs, such as amphetamine, chlorpromazine, ketamine, and scopolamine, on the acquisition and extinction of the rabbit's conditioned membrane response.

The effects of modulating tone frequency, intensity, and duration on the classically conditioned rabbit nictitating membrane response were studied by Kehoe et al. (1995).

Solomon et al. (1996) described behavioral paradigms for delay, trace, and long-delay conditioning.

Various drugs influence the nictitating membrane response in rabbits, such as morphine (McEchron and Gormezano 1991), cocaine (Marshall-Goodell and Gormezano 1991), sodium pentobarbital (Chen et al. 1992), haloperidol (Sears and Steinmetz 1990), MDA (3,4-methylenedioyamphetamine) (Kirkpatrick-Steger et al. 1991; Romano and Harvey 1993), harmaline (Harvey and Romano 1993; Du and Harvey 1997), ketamine (Ghoneim et al. (1994), isoflurane (El-Zahaby et al. 1994), L-NAME (nitric oxide synthesis inhibitor, Du and Harvey 1996), serotonin antagonists and agonists (Welsh et al. 1998a, b), calcium antagonists (Woodruff-Pak et al. 1997), nitrous oxide (Ghoneim et al. 1999).

REFERENCES AND FURTHER READING

Chen P, Ghoneim PP, Gormezano I (1992) Sodium pentobarbital: Sensory and associative effects in classical conditioning of the rabbit nictitating membrane response. Psychopharmacology 107:365–372

Du W, Harvey JA (1996) The nitric oxide synthesis inhibitor L-name facilitates associative learning. Prog Neuro-Psychopharmacol Biol Psychiatry 20:1183–1195

Du W, Harvey JA (1997) Harmaline-induced tremor and impairment of learning are both blocked by dizocilpine in the rabbit. Brain Res 745:183–188

El-Zahaby HM, Ghoneim MM, Johnson GM, Gormezano I (1994) Effects of subanesthetic concentrations of isoflurane and their interactions with epinephrine on acquisition and retention of the rabbit nictitating membrane response. Anesthesiology 81:229–237

Ghoneim MM, Chen P, El-Zahaby HM, Block RI (1994) Ketamine: Acquisition and retention of classically conditioned responses during treatment with large doses. Pharmacol Biochem Behav 49:1961–1066

Ghoneim MM, El-Zahaby HM, Block RI (1999) Classical conditioning during nitrous oxide treatment: influence of varying the interstimulus interval. Pharmacol Biochem Behav 63:449–455

Gormezano I, Prokasy WF, Thompson RF (eds) (1987) Classical Conditioning: III. Behavioral, Physiological and Neurochemical Studies in the Rabbit. Hillsday NJ: Erlbaum

Harvey JA, Romano AG (1993) Harmaline-induced impairment of Pavlovian conditioning in the rabbit. J Neurosci 13:1616–1623

Kehoe EJ, Schreurs BG, Macrae M, Gormezano I (1995) Effects of modulating tone frequency, intensity, and duration on the classically conditioned rabbit nictitating membrane response. Psychobiology 23:103–115

Kirkpatrick-Steger K, Vander Linden S, Gormezano I (1991) Effects of MDA on classical conditioning of the rabbit nictitating membrane response. Pharmacol Biochem Behav 39:183–189

McEchron MD, Gormezano I (1991) Morphine's effect on differential serial compound conditioning and reflex modification of the rabbit's (Oryctolagus cuniculus) nictitating membrane response. Behav Neurosci 105:510–520

Marshall-Goodell B, Gormezano I (1991) Effects of cocaine on conditioning of the rabbit nictitating membrane response. Pharmacol Biochem Behav 39:503–507

Robinson GB, Port RL, Stillwell EJ (1993) Latent inhibition of the classically conditioned rabbit nictitating membrane response is unaffected by the NMDA antagonist MK801. Psychobiology 21:120–124

Romano AG, Harvey JA (1993) Enhanced learning following a single, acute dose of MDA. Pharmacol Biochem Behav 44:965–969

Scavio MJ, Scavio Clift P, Wills JC (1992) Post-training effects of amphetamine, chlorpromazine, ketamine, and scopolamine on the acquisition and extinction of the rabbit's conditioned membrane response. Behav Neurosci 106:900–908

Schindler CW, Harvey JA (1990) Use of classical conditioning procedures in behavioral pharmacology. Drug Dev Res 20:169–187

Sears LL, Steinmetz JE (1990) Haloperidol impairs classically conditioned nictitating membrane responses and conditioning-related cerebellar interpositus nucleus activity in rabbits. Pharmacol Biochem Behav 36:821–830

Solomon PR, Beal MF, Pendlebury WW (1988) Age-related disruption of classical conditioning: A model systems approach to age-related memory disorders. Neurobiol Aging 9:935–946

Solomon PR, Barth CL, Wood MS, Velazquez E, Groccia-Ellison ME, Yang B-Y (1995a) Age-related deficits in retention of classically conditioned nictitating membrane responses in rabbits. Behav Neurosci 109:18–23

Solomon PR, Wood MS, Groccia-Ellison ME, Yang B-Y, Fanelli RJ, Mervis RF (1995b) Nimodipine facilitates retention of the classically conditioned nictitating membrane

response in aged rabbits over long retention intervals. Neurobiol Aging 16:791–796
Solomon PR, Groccia-Ellison ME (1996) Classic conditioning in aged rabbits: delay, trace, and long delay conditioning. Behav Neurosci 110:427–435
Welsh SE, Romano AG, Harvey JA (1998a) Effects of 5-HT (2A/2C) antagonists on associative learning in the rabbit. Psychopharmacology 137:157–163
Welsh SE, Kachelries WJ, Romano AG, Simansky KJ, Harvey JA (1998b) Effects of LSD, ritanserin, 8-OH-DPAT, and lisuride on classical conditioning in the rabbit. Pharmacol Biochem Behav 59:469–475
Woodruff-Pak DS, Coffin JM, Papka M (1994a) A substituted pyrrolidinone, BMY 21502, and classical conditioning of the nictitating membrane response in young and older rabbits. Psychobiology 22:312–319
Woodruff-Pak DS, Li Y-T, Kem WR (1994b) A nicotinic agonist (GTS-21), eyeblink classical conditioning, and nicotine receptor binding in rabbit brain. Brain Res 645:309–317
Woodruff-Pak DS, Chi J, Li Y-T, Pak MH, Fanelli RJ (1997) Nimodipine ameliorates impaired eyeblink classical conditioning in older rabbits in the long-delay paradigm. Neurobiol Aging 18:641–649

F.3.4.2 Automated Learning and Memory Model in Mice

PURPOSE AND RATIONALE

Vanover and Barrett (1998) developed and validated pharmacologically an automated, relatively rapid, and reproducible behavioral model of learning and memory using an autoshaped procedure in mice. Autoshaping procedures were first described for pigeons by Brown and Jenkins (1968) and have been used subsequently as a means to assess learning and memory in monkeys (Sidman and Fletcher (1968), in rats (Steckler et al. 1993; Oscos et al. 1998), and in mice (O'Connell 1980).

PROCEDURE

Naive male mice weighing 25–35 g are randomly assigned to experimental groups. They are housed at approximately 22°C at a 12:12 light/dark cycle with food and water continuously available. Twenty-four hours before each test, mice are isolated into individual cages and all food is removed. Water remains continuously available. Tests are conducted on two consecutive days. Mice are fed 1.5 g food immediately after the first session (day 1).

For experimental sessions, mice are placed in sound-attenuating enclosures containing specially designed operant chambers ($12.5 \times 11 \times 12.5$ cm) equipped with a recess (dipper well; 2.2 cm diameter, 1.3 cm deep) for dipper accessibility on one wall of the chamber and two additional smaller holes (1.3 cm diameter, 0.9 cm deep) on either side of the dipper well. The dipper can be raised into the dipper well for a sucrose solution (110 g/1.01 water) reinforcer presentation. Each recess has a photocell monitoring nose-poke responses. In addition, a speaker capable of sounding a stimulus tone is located on the wall opposite to the dipper and a house-light is on the ceiling. A computer and associated interface controls stimulus events and records nose-poke responses.

Five to 9 mice per group are tested in a 2-day procedure designed to measure acquisition and retention of nose-poke response under an autoshaping schedule of reinforcement. Experimental sessions are conducted at the same time each day for 2 consecutive days. Both the acquisition session (day 1) and the retention session (day 2) are identical.

During the autoshaping procedure which is used to measure acquisition and retention of the response reinforcement for nose-poking a tone is added. This tone sounds on a variable-interval schedule of presentation (mean of 45 s, range 4–132) and stays for either 6 s or until a nose-poke in the dipper well is made before the end of the 6 s period, at which time the tone is turned off and a dipper with sucrose solution is presented. If a mouse fails to make a dipper well nose-poke during the tone, the dipper is automatically presented at the termination of the tone. A dipper well nose-poke response made during the presence of the tone is counted as reinforced response. Dipper well nose-poke responses made while the tone is off are counted but have no consequence. Each sessions lasts for 2 h or until 20 reinforcers have been earned, whichever comes first. In addition to dipper well nose-poke responses, nose-pokes in the smaller holes to the left and right of the dipper are counted but have no consequence.

Drugs in various doses or vehicle are administered i.p. immediately before the session.

Rates of nose-poke responses made in the small holes on either side of the dipper well serve as a measure of general activity. The computer presents tones on a variable interval with a mean of 45 s and 10 possible intervals (4, 10, 15, 22, 29, 38, 49, 64, 87, 132 s) chosen randomly without replacement until all intervals have been used.

The latency of the response to the 10th reinforcer is considered as a measure of acquisition and retention, because all mice have been exposed to all possible intervals (in random order) by the 10th tone. In order to eliminate the variance due to the variability of the first reinforcer, it is necessary to adjust any measure of acquisition and retention according to the response latency to the first reinforcer. The 10th response latency measure is thus adjusted by subtracting the response latency to the first reinforcer (L-10-1) in order to en-

sure all mice have been exposed to the reinforcement contingency.

An other measure of acquisition and retention consists of the rate of nose-poke responding in the dipper well during the total session.

EVALUATION

The mean and standard error of the mean are calculated for every group. Two-tailed Student *t*-tests are used to compare two independent groups on any one dependent variable. In addition, two-tailed paired *t*-tests are conducted to compare data from day 1 to data from day 2 for any one group. One-way analyses of variance (ANOVA) are conducted across groups for effects of dose on acquisition (day 1 performance). One-way analyses of covariance (ANCOVA) are conducted across groups for effects of dose for retention (day 2 of performance) with the performance on day 1 as the covariate. When an ANOVA or ANCOVA shows statistical significance, post-hoc Duncan's multiple range tests are conducted with every group compared with vehicle. *P* values less or equal to 0.05 are considered statistically significant.

REFERENCES AND FURTHER READING

Brown PL, Jenkins HM (1968) Autoshaping of the pigeons key-peck. J Exp Anal Behav 11:1–8

O'Connell MF (1980) Autoshaping and food acquisition in mice: a genetic analysis. J Comp Physiol Psychol 94:1149–1159

Oscos A, Martinez JL, McGaugh JL (1988) Effects of post-training d-amphetamine on acquisition of an appetitive autoshaped lever press response in rats. Psychopharmacology 95:132–134

Sidman M, Fletcher FG (1968) A demonstration of autoshaping in monkeys. J Exp Anal Behav 11:307–309

Steckler T, Andrews JS, Marten P, Turner JD (1993) Effects of NBM lesions with two neurotoxins on spatial memory and autoshaping. Pharmacol Biochem Behav 44:877–889

Vanover KE, Barrett JE (1998) An automated learning and memory model in mice: pharmacological and behavioral evaluation of an autoshaped response. Behav Pharmacol 9:273–283

F.3.4.3 Learning Deficits after Postnatal Anoxia in Rats

PURPOSE AND RATIONALE

Oxygen deprivation causes irreversible damage to the adult mammalian brain, but during perinatal development the nervous systems appears to be more tolerant to hypoxic events. Several animal models have been developed to study in detail the pathophysiology of perinatal hypoxia and its behavioral consequences (Speiser et al. 1988; Dell'Anna et al. 1991; Speiser et al. 1991; Raju 1992; Buwalda et al. 1995; Roohey et al. 1997; Lebedev et al. 2003; Zhuravin et al. 2004). Speiser et al. (1998) tested the effect of a monoamine oxidase B inhibitor on cholinergic functions and behavior in rats submitted to postnatal anoxia.

PROCEDURE

Wistar rats were kept at 24 ± 2°C and a 12:12 h light:dark cycle with free access to food and water. For breeding, a male 4- to 8-month-old was kept with a pair of females, 2- to 5-months-old, for 10 days. The male was withdrawn, and the females were kept together for an additional 10-day period, and then housed in individual cages where they had a litter of about 9–12 pups. Mother and five to seven male offspring were kept together until weaning (21 days), then separated and housed five to seven to a cage.

Only male pups were used for anoxia. On the second postnatal day, five to six pups were placed in a glass container equipped with an inlet and outlet for the displacement with 100% nitrogen at near atmospheric pressure. After a stay of 30 min, the pups were removed to room air and resuscitated by soft intermittent massage to the chest, then returned to their mothers.

To avoid handling which could affect behavior, the test drug was administered in drinking water to the nursing mothers starting on the first day of delivery. Controls received tap water. After weaning and to completion of the study, the young rats were given access to drug in drinking water.

For evaluation, motor behavior was recorded at ages of 14, 21, 28, and 35 days. Retention of one-trial step-through passive avoidance was determined at the age of 45 days. Water-maze tests were performed at the age of 50–60 days.

EVALUATION

Data were analyzed by either ANOVA or the unpaired or paired two-tailed Student's *t*-test.

REFERENCES AND FURTHER READING

Buwalda B, Nyakas C, Vosselman HJ, Luiten PGM (1995) Effects of postnatal anoxia on adult learning and emotion in rats. Behav Brain Res 67:83–90

Dell'Anna ME, Calzolari S, Molinari M, Iuvone L, Calimici R (1991) Neonatal anoxia induces transitory hyperactivity, permanent spatial memory deficits and CA1 cell density reduction in developing rats. Behav Brain Res 45:125–134

Lebedev SV, Volodin NN, Blinov DV, Lazarenko IP, Rogatkin SO, Chekhonin VP (2003) Neurological deficit and disturbances in higher nervous activity during modeling of perinatal hypoxic-ischemic damage to the central nervous system in rat pups. Bull Exp Biol Med 136:242–245

Raju TNK (1992) Some animal models for the study of perinatal asphyxia. Biol Neonate 62:202–214
Roohey T, Raju TN, Moustogiannis AN (1997) Animal models for the study of perinatal hypoxic-ischemic encephalopathy: a critical analysis. Early Hum Dev 47:115–146
Speiser Z, Amitzi-Sonder J, Gitter S, Cohen S (1988) Behavioral differences in the developing rat following postnatal anoxia or postnatally injected AF-64A, a cholinergic neurotoxin. Behav Brain Res 30:89–94
Speiser Z, Uziel J, Defrin-Assa R, Gitter S, Urca G (1991) Different behavioral deficits are induced by anoxia/hypoxia in neonatal and senescent rats: blockade by MK-801. Behav Brain Res 42:181–186
Speiser Z, Katzir O, Rehavi M, Zabarski T, Cohen S (1998) Sparing of Rasagiline (TVP-1012) of cholinergic functions and behavior in the postnatal anoxia rat. Pharmacol Biochem Behav 60:387–393
Zhuravin IA, Dubrovskaya NM, Tumanova NL (2004) Postnatal physiological development of rats after acute prenatal hypoxia. Neurosci Behav Physiol 34:809–816

F.3.5 Studies in Monkeys

PURPOSE AND RATIONALE

Nonhuman primates have the closest taxonomic relationship to humans, sharing many morphologic and physiologic similarities in the central nervous system. These similarities increase the likelihood that studies in aged nonhuman primates will provide information about drugs that is relevant to humans. Nonhuman primates offer additional advantages for neurobehavioral animal models of aging in that many of the behavioral processes thought to be affected by aging (e. g. reaction time, attention, learning and memory) can be studied easily in nonhuman primates. Evidence is beginning to accumulate suggesting that certain neurological and behavioral deficits are observed in aged human and in nonhuman primates (Bartus 1979; Struble et al. 1982; Wisniewski et al. 1973).

PROCEDURE

The apparatus developed specifically for the series of studies used to develop the primate model was the Automated General Experimental Device (AGED), the rationale upon which its development was based and its application to geriatric research have been discussed in detail elsewhere (Bartus 1979; Bartus and Dean 1981; Dean et al. 1983). The AGED is a totally automated, computer-controlled testing system, whose prominent feature consists of a 3×3 matrix of stimulus response (SR) panels. Each SR panel is hinge-mounted directly in front of the reinforcement well so that when a panel is pushed, a red switch is magnetically activated and a reinforcement well is exposed. Both colored and patterned stimuli can be projected onto the SR panels. A plastic partition with a stimulus window and armholes separates the monkey from the SR matrix. The stimulus observation window is equipped with a photocell and an infrared light source to detect when the monkey's head is oriented toward the stimuli.

EVALUATION

The monkey must remember the stimulus location to get a reinforcement. Number of correct answers will be counted as well as the time until the monkey answers correctly.

CRITICAL ASSESSMENT OF THE METHOD

This system provides an accurate and objective means of collecting data under a number of behavioral paradigms. Further, this system provides experimental control over a number of variables that might confound behavioral measures (especially in drugged or aged subjects), thus simplifying the interpretation of differences observed and increasing the likelihood that these interpretations are accurate.

MODIFICATIONS OF THE METHOD

Cai and Arnstein (1997) described dose-dependent effects of Dopamine D1 receptor agonists on spatial working memory in aged monkeys.

Gandy and Walker (2004) proposed non-human primates for modeling hemorrhagic and encephalitic complications of Alzheimer amyloid-β vaccination and for assessing the efficacy and safety of immunotherapeutics in Alzheimer's disease.

Taffe et al. (2004) reported the development of a visuo-spatial paired-associate learning task in rhesus monkeys for early detection of symptoms of Alzheimer's type dementia.

REFERENCES AND FURTHER READING

Bartus RT (1979a) Physostigmine and recent memory: Effects in young and aged non-human primates. Science 206:1087–1089
Bartus RT(1979b) Effects of aging on visual memory, sensory processing and discrimination learning in the non-human primate. In: Ordy JM, Brizzee K (eds) Aging. Vol. 10. Raven Press, New York, NY, pp 85–114
Bartus RT, Dean RL (1981) Age-related memory loss and drug therapy: Possible directions based on animal models. In: Enna SJ, Samorajski T, Beer B (eds) Aging Vol. 17. Raven Press New York, NY, pp 209–223
Cai J-X, Arnstein AFT (1997) Dose-dependent effects of the dopamine receptor agonists A77636 and SKF81297 on spatial working memory in aged monkeys. J Pharmacol Exp Ther 283:183–189
Dean RL, Loullis C, Bartus RT (1983) Drug effects in an animal model of memory deficits in the aged: implications

for future clinical trials. In: Walker RF, Cooper RL (eds) Experimental and Clinical Interventions in Aging. Marcel Dekker, New York, NY, pp 279–303
Gandy S, Walker L (2004) Toward modeling hemorrhagic and encephalitic complications of Alzheimer amyloid-β vaccination in nonhuman primates. Curr Opin Immunol 16:607–615
Struble RG, Cork LC, Whitehouse PJ, Price DL (1982) Cholinergic innervation in neuritic plaques. Science 216:413–414
Taffe MA, Weed MR, Gutierrez T, Davis SA, Gold LH (2004) Modeling a task that is sensitive to dementia of the Alzheimer's type: individual differences in acquisition of a visuo-spatial paired-associate learning task in rhesus monkeys. Behav Brain Res 149:123–133
Wisniewski HM, Ghetti T, Terry RD (1973) Neuritic (senile) plaques and filamentous changes in aged Rhesus monkeys. J Neuropathol Exp Neurol 32:566–584

F.3.6 Electrophysiological Methods

F.3.6.1 Long-Term Potentiation in Hippocampal Slices

PURPOSE AND RATIONALE

Long-term potentiation (LTP) in the hippocampus is perhaps the most dramatic example of activity-dependent synaptic plasticity that has yet been identified in the mammalian brain (Landfield and Deadwyler 1988; Bashir et al. 1994). A brief tetanus to any one of a number of monosynaptic excitatory pathways in the hippocampus can enhance the amplitude of evoked responses in the tetanized pathway for h or days thereafter. The fact that it occurs in the hippocampus has done much to stimulate interest in LTP as a synaptic model of memory, since the importance of the hippocampus for memory processing has been evident ever since the discovery that its bilateral removal in man causes a profound impairment in the ability to lay down new memories (Scoville and Milner 1957; Milner 1972). The particular popularity of the slice preparation prepared from the rodent hippocampus rests on its lamellar and laminar organization (Teyler 1980).

PROCEDURE

Transverse slices, 400 mm thick, are cut from the hippocampus of male albino guinea pigs weighing 250–300 g and prepared for electrophysiological recordings (Teyler 1980; Tanaka et al. 1989, 1990). Slices are incubated for 90–120 min in the recording chamber to allow equilibration with artificial cerebrospinal fluid. They are submerged, placed on a nylon mesh and perfused at a flow rate of 2–2.5 ml/min with oxygenated (95% O_2/5% CO_2) cerebrospinal fluid having the following composition (in mM): NaCl 124, KCl 3.3, $CaCl_2$ 2.5, KH_2PO_4 1.25, $MgSO_4$ 2, $NaHCO_3$ 25,7, glucose 10. The recording chamber is maintained at 33 ±2°C. The extracellular population spike is obtained using glass microelectrodes filled with 2 M NaCl, which have resistances of 2–5 MΩ. The electrodes are placed into the stratum pyramidale of CA1 or CA3. The signal is amplified and stored on magnetic discs for later analysis. The evoked responses are averaged and analyzed off-line using a personal computer. The magnitude of the population spike is evaluated by taking the voltage difference between the negative peak and the following positive peak. Either mossy fibers in the hilus fasciae or commissural/associational fibers in the stratum radiatum are activated via bipolar, sharpened silver wire electrodes insulated except for the tips. Constant current pulses (100 ms) are delivered with a frequency of 0.2 Hz, only during the test intervals. The stimulation intensity is adjusted to elicit the population spike of about 40% and 80% of its maximal amplitude in CA1 and CA3, respectively. After the baseline is recorded for 10–20 min, LTP is induced by repetitive stimulation of 100 pulses at 20 Hz for 5 s in CA1 and at 50 Hz for 2 s in CA3 at the same strength as for the test pulses. Responses by test pulses are recorded 0, 10, 20 and 30 min after repetitive stimulation. The test drugs are dissolved in the artificial cerebrospinal fluid and applied extracellularly at various concentrations by switching perfusion reservoirs.

EVALUATION

The time course of LTP is registered for CA1 and CA3. The mean percent increase in the amplitude of the population spike from baseline responses after drug application is compared with controls.

MODIFICATIONS OF THE METHOD

Fujii et al. (1997) studied the effects of an adenosine A_1 receptor antagonist, 8-cyclopentyltheophylline, on the reduction of long-term potentiation in CA1 neurons of **guinea pig** hippocampal slices. Reduction of long-term potentiation (depotentiation) was achieved by delivering a train of low-frequency afferent stimuli 20 min after the tetanus.

Behnisch and Reymann (1993) employed slices of hippocampal area CA1 in the **rat** to test the hypothesis that the activation of metabotropic glutamate receptors during tetanization is necessary for the maintenance of long-term potentiation.

Akhondzadeh and Stone (1995) studied the phenomenon of hippocampal long-term depression. Extracellular recordings were made in the CA1 pyramidal cell layer of **rat** hippocampal slices following ortho-

dromic stimulation of Schaffer collateral fibres in stratum radiatum.

Oomura et al. (1996) measured long-term potentiation in hippocampal slice preparations after a brief tetanic stimulation at the Schaffer collateral/-commissural afferents of senescence-accelerated **mice** which were treated from 3 weeks of age up to 10 months either with subcutaneous injections of acidic fibroblast growth factor or saline.

REFERENCES AND FURTHER READING

Akhondzadeh S, Stone TW (1995) Induction of a novel form of hippocampal long-term depression by muscimol: Involvement of $GABA_A$ but not glutamate receptors. Br J Pharmacol 115:527–533

Alger BE, Dhanjal SS, Dingledine R, Garthwaite J, Henderson G, King GL, Lipton P, North A, Schwartzkroin PA, Sears TA, Segal M, Whittingham TS, Williams J (1984) Brain slice methods. In: R. Dingledine (ed) Brain Slices, Plenum Press. New York, NY pp 381–437

Bashir ZI, Berreta N, Bortolotto ZA, Clark K, Davies CH, Frenguelli BG, Harvey J, Potier B, Collingridge GL (1994) NMDA receptors and long-term potentiation in the hippocampus. In: Collingridge GL, Watkins JC (eds) The NMDA Receptor. Second Ed. Oxford University Press, Oxford, New York, Tokyo, pp 294–312

Behnisch T, Reymann KG (1993) Co-activation of metabotropic glutamate and N-methyl-D-aspartate receptors is involved in mechanisms of long-term potentiation maintenance in rat hippocampal CA1 neurons. Neurosci 54:37–47

Bliss TVP, Lømo T (1973) Long-lasting potentiation of synaptic transmission in the dentate area of the anaesthetized rabbit following stimulation of the perforant path. J Physiol 232:331–356

Dingledine RY, Dodd Y, Kelly JS (1980) The *in vitro* brain slice as a useful neurophysiological preparation for intracellular recording. J Neurosci Methods 2:323–362

Fujii S, Sekino Y, Kuroda Y, Sasaki H, Ito KI, Kato H (1997) 8-Cyclopentyltheophylline, an adenosine A_1 receptor antagonist, inhibits the reversal of long-term potentiation in hippocampal CA1 neurons. Eur J Pharmacol 33:9–14

Kettenmann H, Grantyn R (eds) Practical electrophysiological methods. Wiley-Liss, New York, NY (1992)

Landfield PW, Deadwyler SA (eds) (1988) Long-term Potentiation: From Biophysics to Behavior. Alan R. Liss, Inc., New York, NY

McIlwain H, Rodnight R (1962) Preparing neural tissues for metabolic study *in vitro*. In: McIlwain H, Rodnight R (eds) Practical neurochemistry. Churchill Ltd. London, pp 109–133

Milner B (1972) Disorders of learning and memory after temporal lobe lesions in man. Clin Neurosurg 19:421–446

Misgeld U (1992) Hippocampal Slices. In: Kettenmann H, Grantyn R (eds) Practical electrophysiological methods. Wiley-Liss, New York, NY, pp 41–44

Oomura Y, Sasaki K, Li A, Yoshii H, Yago H, Kimura H, Tooyama I, Hanai K, Nomura Y, Yanaihara N (1996) Protection against impairment of memory and immunoreactivity in senescence-accelerated mice by acidic fibroblast growth factor. Ann New York Acad Sci 786:337–347

Scoville WB, Milner B (1957) Loss of recent memory after bilateral hippocampal lesions. J Neurol Neurosurg Psychiatry 20:11–21

Tanaka Y, Sakurai M, Hayashi S (1989) Effect of scopolamine and HP 029, a cholinesterase inhibitor, on long term potentiation in hippocampal slices of the guinea pig. Neurosci Lett 98:179–183

Teyler TJ (1980) Brain slice preparations: Hippocampus. Brain Res Bull 5:391–403

F.3.6.2 Long Term Potentiation in Vivo

PURPOSE AND RATIONALE

Placing recording and bipolar stimulating electrodes in the granule cell layer of the dentate gyrus and angular bundle allows the evaluation of long-term-potentiation *in vivo*, even in freely moving animals, and the comparison with effects on learning.

PROCEDURE

Female Sprague Dawley rats weighing 225–250 g are anesthetized with 1.5 g/kg urethane (i.p.) and placed in a Kopf stereotaxic instrument. The recording and bipolar stimulating electrodes are placed in the granule cell layer of the dentate gyrus and angular bundle, respectively (from bregma and cortical surface: Dentate: A.P. −4.0 mm, M.L. +2.4 mm, D.V. 3.0 mm. Angular bundle: A.P. −7.9 mm, M.L. +4.0 mm, D.V. −3.0 mm, incisor bar −5.0 mm). The recording electrodes are pulled from thin-walled glass capillary tubes, filled with 150 mM NaCl, and adjusted to resistances ranging from 2.0 to 4.0 MΩ. Stimulating electrodes are made from twisted nichrome wire with Teflon insulation, and approximately 0.75 mm separated each tip. The recording electrode is first lowered into area CA1 of the dorsal hippocampus. The stimulating electrode is then placed into the ipsilateral angular bundle. As the recording electrode is lowered further, field potentials are evoked to determine when the recording electrode enters the dentate granule cell layer.

All rats are maintained at 37°C. Responses are evoked using a Grass S-88 stimulator and a Microprobe System M-7070A amplifier, and are recorded on a Nicolet 310 oscilloscope.

Once the electrodes are appropriately placed, field potentials are generated over a range of stimulus intensities to generate an input/output (I/O) curve (pulse duration = 1 ms). The field potentials are quantified in two ways: The population spike (PS) is expressed as the distance from the deepest point (in mV) of negativity to the preceding highest positivity on the left and right side of the response, and then averaged. The slope of the rising phase of the population excitatory postsynaptic potential (pESP) is measured in mV/ms. The amplitude of the test pulse is based is based on the I/O

curve being 25% of the current intensity which evokes the maximal population spike. Long-term-potentiation is induced using three theta-burst stimulus trains, each delivered 1 min apart. Each train consists of five groups of four pulses at 100 Hz, separated by an interval of 150 ms. Each train is delivered at the stimulus intensity which evokes the maximal population spike at the I/O curve.

At the end of the experiment, the electrode placements are verified using standard histological techniques.

EVALUATION

Student's *t*-tests are used to assess the significance of differences between the means of both the population spike amplitudes and the pESP slopes.

CRITICAL ASSESSMENT OF THE METHOD

Hölscher et al. (1997a, 1997b, 2002) argued that high-frequency stimulation-induced long-term potentiation and low-frequency stimulation-induced depotentiation in area CA1 of the hippocampus are not good models for learning.

MODIFICATIONS OF THE METHOD

Errington et al. (1987) perfused a NMDA receptor antagonist through a push-pull cannula into the dentate gyrus of anesthetized **rats** in order to observe its effect on the induction and maintenance of long-term potentiation and on the increase in release of endogenous glutamate associated with long-term potentiation.

Bennett et al. (1992) recommended cytochrome oxidase inhibition as an animal model of Alzheimer's disease. Rats were infused chronically with the selective inhibitor of cytochrome oxidase, sodium azide, delivered via subcutaneously implanted minipumps. The azide treatment impaired both spatial and non-spatial learning. Further, the azide treatment inhibited a low-threshold form of hippocampal long-term potentiation, primed burst potentiation.

Croll et al. (1997) used this model to study time course and corresponding pathology of learning deficits in rats.

Brakebusch et al. (2002) found that mice deficient in brevican (a brain-specific proteoglycan) displayed impaired hippocampal CA1 long-term potentiation but showed no obvious deficits in learning and memory.

Namgung et al. (1995) described the characteristics of long-term potentiation in the intact **mouse**. Perforant path stimulation evoked both a population excitatory postsynaptic potential and a population spike potential from the hippocampal dentate gyrus in urethane anesthetized animals. Long-term potentiation, as measured by increased population-spike amplitude and population excitatory postsynaptic potential slope, was successfully induced and reliably maintained at a stable level for at least 12 h.

Davis et al. (1997) described a simple method for inducing and monitoring long-term potentiation at perforant path-granule cell synapses in the dentate gyrus of freely moving mice using readily available miniaturized components. Tetanic stimulation induced long-term potentiation of the field excitatory postsynaptic potential and the population spike which persisted for more than 24 h but was not present 10 days after the tetanus.

Jibiki et al. (1993) and Kubota et al. (1994) studied the drug-induced blockade of induction of long-term potentiation in perforant path-dentate gyrus pathway in chronically prepared **rabbits**.

Gutnikov and Gaffan (1996) studied the effects of a NMDA receptor antagonist on memory acquisition and retrieval of visual-reward associations in the object-in-place memory task and on NMDA neurotoxicity in **rhesus monkeys**.

REFERENCES AND FURTHER READING

Bennett MC, Diamond DM, Stryker SL, Parks JK, Parker WD Jr (1992) Cytochrome oxidase inhibition: A novel animal model of Alzheimer's disease. J Geriatr Psychiatry Neurol 5:93–101

Beukers M, Boddeke EWGM (1991) Pharmacology of long-term potentiation. A model for learning reviewed. Pharm Weekbl Sci Ed 13:7–12

Brakebusch C, Seidenbecher C, Asztely F, Rauch U, Matthies H, Meyer H, Krug M, Böckers TM, Zhou X, Kreutz MR, Montag D, Gundelfinger ED, Fässler R (2002) Brevican-deficient mice display impaired hippocampal CA1 long-term potentiation but show no obvious deficits in learning and memory. Mol Cell Biol 22:7417–7427

Brioni JD (1993) Role of GABA during the multiple consolidation of memory. Drug Dev Res 28:3–27

Brucato FH, Levin ED, Mott DD, Lewis DV, Wilson WA, Swartzwelder HS (1996) Hippocampal long-term potentiation and spatial learning in the rat: effects of $GABA_B$ receptor blockade. Neurosci 74:331–339

Croll SD, Greene NA, Lindsay RM, Wiegand SJ (1997) Sodium azide-induced learning deficits in rats: Time course and corresponding pathology. Psychobiology 25:34–47

Davis S, Bliss TVP, Dutrieux G, Laroche S, Errington ML (1997) Induction and duration of long-term potentiation in the hippocampus of the freely moving mouse. J Neurosci Methods 75:75–80

Errington ML, Lynch MA, Bliss TVP (1987) Long-term potentiation in the dentate gyrus: induction and increased glutamate release are blocked by D(–)aminophosphonovalerate. Neurosci 20:279–284

Gutnikov SA, Gaffan D (1996) Systemic NMDA receptor antagonist CGP-40116 does not impair memory acquisition but

protects against NMDA neurotoxicity in rhesus monkeys. J Neurosci 16:4041–4050
Hölscher Ch, McGlinchey L, Anwyl R, Rowan MJ (1997a) HFS-induced long-term potentiation and LSF-induced depotentiation in area CA1 of the hippocampus are not good models for learning. Psychopharmacology 130:174–182
Hölscher Ch, Anwyl R, Rowan M (1997b) Block of HFS-induced LTP in the dentate gyrus by 1S,3S-ACPD. Further evidence against LTP as a model of learning. NeuroReport 8:451–454
Hölscher C (2002) Metabotropic glutamate receptors control gating of spike transmission in the hippocampus area CA1. Pharmacol Biochem Behav 73:307–316
Jibiki I, Wakita S, Kubota T, Kurokawa F, Fukushima T, Yamaguchi N (1993) Haloperidol-induced blockade of induction of long-term potentiation in perforant path-dentate gyrus pathway in chronically prepared rabbits. Pharmacol Biochem Behav 46:847–852
Kubota T, Jibiki I, Fukushima T, Kurokawa K, Yamaguchi N (1994) Carbamazepine-induced blockade of induction of long-term potentiation in the perforant path-dentate gyrus pathway in chronically prepared rabbits. Neurosci Lett 170:171–174
Namgung U, Valcourt E, Routtenberg A (1995) Long-term potentiation in the intact mouse hippocampus. Brain Res 689:85–92

F.3.6.3 Long Latency Averaged Potentials

PURPOSE AND RATIONALE

Wirtz-Brugger et al. (1986, 1987) studied long latency averaged evoked potentials (P300) in anesthetized rats as a possible model for detecting memory-enhancing drugs. The P300 waveform is described as a positive long-latency (∼ 300 ms) potential believed to reflect endogenous cognitive processes rather than exogenous physical parameters of the stimulus. Compounds that have been shown clinically to enhance cognitive ability also significantly increase the integrated area under the P300 wave.

PROCEDURE

Male Wistar rats weighing 300–500 g are anesthetized with 120 mg/kg i.p. Inactin. Stainless steel screws serve as recording electrodes located at the surface of the cortex of seven distinct brain areas: posterior: Pz (midline), P3, P4 (lateral); central: Cz (midline); and frontal: Fz (midline, F3, F4 (lateral). A linked reference is provided with platinum needle electrodes behind the ears. All leads are fed into a digital averaging computer. Event-related potentials are elicited in response to an oddball paradigm of two tones (500 Hz frequent and 3 KHz rare) randomly presented with a probability of 10% for the rare tone. The intensity of the tones is 95 bB, pulse duration 100 ms, rise/fall 9.9 ms. The auditory stimuli are delivered bilaterally at a rate of 0.3/s through special Nicolet tubal tip inserts into the ear of each subject. One repetition of the paradigm consists of 300 tones. It is presented twice, before and after drug application. Evaluation of the rare responses consists of defining and comparing the P300 in terms of integrated area before and after drug. P300 area is calculated by integration of area under the curve.

EVALUATION

Values are expressed as means and standard error per group and percent changes from control. Statistical evaluation consists of paired *t*-tests to demonstrate significant differences.

MODIFICATIONS OF THE METHOD

Caudle (1993) demonstrated long latency potentials in the CA1 regions of the rat hippocampal slice suggesting that the *in vitro* P3 is an *in vitro* version of the long latency evoked potential known as the P300 in electroencephalogram studies.

Ikeda et al. (1995) studied the effect on a nootropic compound on event-related potential P300 in rats with lesions of the nucleus basalis magnocellularis.

Antal et al. (1994) studied the influence of cholinergic agents on visual discrimination and P300 in the behaving **monkey**. P300 latency was increased following scopolamine administration. Acetyl-L-carnitine increased P300 amplitude and decreased its latency.

In **squirrel monkeys**, clonidine significantly decreased the area and increased the latency of P300-like potential (Swick et al. 1993).

Kaga et al. (1992) studied P300 and choline acetyltransferase immunohistochemistry in septohippocampal neurons of **cats**.

Wang et al. (1999) reported that P300-like potential depends on muscarinic receptor activation in **rabbits**.

REFERENCES AND FURTHER READING

Antal A, Kovanecz I, Bodis-Wollner I (1994) Visual discrimination and P300 are affected in parallel by cholinergic agents in the behaving monkey. Physiol Behav 56:161–166
Caudle RM (1993) The demonstration of long latency potentials in the CA1 region of the rat hippocampal slice. Brain Res 613:247–250
Ikeda K, Egashira T, Yamashita J, Okoyama S (1995) Effect of vagal autotransplantation and bifemelane hydrochloride on cholinergic markers and event-related potential in rats with lesions of the nucleus basalis magnocellularis. Brain Res 688:171–183
Kaga K, Harrison JB, Butcher LL, Woolf NJ, Buchwald JS (1992) Cat 'P300' and cholinergic septohippocampal neurons: Depth recordings, lesions, and choline acetyltransferase immunohistochemistry. Neurosci Res 13:53–71

Swick D, Pineda JA, Foote SL (1993) Effects of systemic clonidine on auditory event-related potentials in squirrel monkeys. Brain Res Bull 33:79–86
Wang YP, Kawai Y, Nakashima K (1999) Rabbit P300-like potential depends on cortical muscarinic receptor activation. Neuroscience 89:423–427
Wirtz-Brugger F, McCormack K, Szewczak M, Fielding S, Connfeldt M (1986) P300 in anesthetized rat: possible model for detecting memory-enhancing drugs. Neurosci Abstr 193.4
Wirtz-Brugger F, Cornfeldt M, McCormack K, Szewczak M Fielding S (1987) Effect of several CNS agents on P300 in rats. Neurosci Abstr 475.13

F.3.7
Metabolic Influence

F.3.7.1
Sodium Nitrite Intoxication ($NaNO_2$)

PURPOSE AND RATIONALE

The manipulation of brain metabolism was used to show the beneficial effects of substances which influence learning and memory. Gibson et al. (1976, 1978), during investigations of sodium-nitrite ($NaNO_2$) on brain metabolism, demonstrated a close relationship between oxidative metabolism and cholinergic function. From the results of their studies, the possibility cannot be excluded that an induction of impairment of the cholinergic transmission in addition to a deficiency in brain metabolisms was induced (Schindler et al. 1984).

PROCEDURE

Male or female mice are used and maintained under standard conditions. Chemical hypoxia is induced by the injection of sodium nitrite ($NaNO_2$: 250 mg/kg s.c.), which reduces the oxygen-carrying capacity of the blood by converting hemoglobin to methemoglobin. This lethal dose (lethality 100% of controls) is injected 60 min after drug treatment. Immediately after the $NaNO_2$-injection the animals are placed in small Makrolon cages and the time between injection of $NaNO_2$ and cessation of respiration is recorded (Hock 1993).

EVALUATION

The time between injection of $NaNO_2$ and cessation of respiration is recorded. The prolongation of survival time is expressed in percent.

MODIFICATIONS OF THE METHOD

Using lower doses of $NaNO_2$ mice are submitted to a positive reinforcement paradigm (Schindler et al. 1984). Groups of 10 mice are water deprived for 24 h. The mice are treated with the test compound 45 min before they are placed individually in a large chamber. On one wall of the chamber, there is a small compartment that contains a water bottle. The mouse easily finds the bottle and is allowed to drink for 30 s. Each mouse then receives a subcutaneous injection of 75 mg/kg $NaNO_2$ before being returned to the home cage. Twenty-four hours later, retention testing is performed by placing the mouse in the large chamber, but at this time, the small compartment is kept empty. The duration and frequency of the mouse's exploration of the small compartment while searching for water is evaluated over a period of 3 min. An increase in duration and frequency correlates with improved learning.

The tight rope test (Barclay et al. 1981) was used to test the effect of $NaNO_2$ with and without treatment on performance in mice (Peterson and Gibson 1982; Gibson et al. 1983).

REFERENCES AND FURTHER READING

Barclay LL, Gibson GE, Blass PJ (1981) The string test: An early behavioral change in thiamine deficiency. Pharmacol Biochem Behav 14:153–157
Gibson GE, Blass JP (1976) Impaired synthesis of acetylcholine in brain accompanying mild hypoxia and hypoglycemia. J Neurochem 27:37–42
Gibson GE, Shimada M, Blass JP (1978) Alterations in acetylcholine synthesis and cyclic nucleotides in mild cerebral hypoxia. J Neurochem 31:757–760
Gibson GE, Pulsinelli W, Blass JP, Duffy TE (1981) Brain dysfunction in mild to moderate hypoxia. Am J Med 70:1247–1254
Gibson GE, Pelmas CJ, Peterson C (1983) Cholinergic drugs and 4-aminopyridine alter hypoxic-induced behavioral deficits. Pharmacol Biochem Behav 18:909–916
Hock FJ (1993) Effects of cromakalim on sodium nitrite intoxication. In: Elsner N, Heisenberg M (eds) Gene, Brain and Behaviour. Proceedings of the 21st Göttingen Neurobiology Conference. Georg Thieme Verlag, Stuttgart, 681
Peterson C, Gibson GE (1982) 3,4-Diaminopyridine alters acetylcholine metabolism and behavior during hypoxia. J Pharmacol Exp Ther 222:576–582
Schindler U, Rush DK, Fielding S (1984) Nootropic drugs: Animal models for studying effects on cognition. Drug Develop Res 4:567–576

F.4
Animals with Memory Deficits

F.4.1
Memory Deficits After Cerebral Lesions

PURPOSE AND RATIONALE

Cerebral lesions have been used as a method of determining the involvement of a particular brain area in performing a particular function. By training an animal to perform a certain task, then lesioning a specific brain area, one can determine whether that area of the brain

is necessary or sufficient to perform that function; alternatively one can lesion before training and measure the rate of acquisition to determine the involvement of a brain area in learning a particular task.

Memory impairment has been produced by lesions caused by bilateral injections of ibotenic acid into the basal forebrain of rats. Water-maze tasks, habituation tasks, passive avoidance tasks with a light/dark compartment apparatus, and inhibition of the decrease of choline acetyltransferase activity in the cortex can be used to evaluate the effect of drugs (Fuji et al. 1993a).

PROCEDURE

Male Wistar rats weighing 270–310 g are anesthetized with sodium pentobarbital (45 mg/kg i.p.) and placed in a stereotaxic apparatus. Neurotoxic lesions of the basal forebrain are produced by injection of ibotenic acid. An injection needle connected to a 5-µl microsyringe is inserted into the basal forebrain, identified according to the Paxinos and Watson (1986) atlas of rat brain (1.5 mm posterior, 2.8 mm bilateral to the bregma, 7.3 mm below the dura). Ibotenic acid is dissolved in 50 mM Na phosphate buffer at a concentration of 12 µg/ml, and then 0.5 ml (6 µg per side) is infused for 5 min. The injection needle is left in place for an additional 5 min to allow the toxin to diffuse away from the needle tip. One week later, the contralateral side is treated in the same manner. The same procedure is used to administer microinjections of 50 mM Na phosphate buffer into the basal forebrain of sham-operated rats. The lesion sites are mainly distributed in the ventromedial globus pallidus.

Then, 3–5 weeks after the first lesion, the animals are tested on the acquisition of a task in a Morris water maze (Morris 1981), on a habituation task in a novel situation, and on a passive avoidance task with light and dark compartments. The rats are treated once a day during the experiment.

After the behavioral experiments, the animals are sacrificed for determination of choline acetyltransferase activity in the brain according to Fonnum (1975). The tissue is homogenized (4% w/v) in cold 50 mM Na phosphate buffer (pH 7.4), and Triton X-100 (0.55, v/v) is added to homogenates to ensure enzyme release. To 75 µl of enzyme solution, 125 µl of substrate mixture {0.4 mM [^{14}C]acetyl-Co A (50.6 mCi/mmol or 1.87 GBq/mmol), 300 mM NaCl, 50 mM Na phosphate buffer (pH 7.4), 8 mM choline chloride, 20 mM EDTA-2Na, and 0.1 mM physostigmine} is added in a scintillation vial and the mixture is incubated at 37°C for 30 min. After the incubation, 0.8 ml of cold 50 mM phosphate buffer, 0.5 ml of acetonitrile containing 2.5 mg of tetraphenylborate and 2.0 ml toluene are added to the scintillation vial. The vials are shaken lightly and allowed to stand overnight before radioactivity is determined.

EVALUATION

Data are evaluated by usual statistical means. All analyses are followed by a Bonferroni's test.

MODIFICATIONS OF THE METHOD

Although usually permanent, temporary lesions can be made by cooling the tissue of interest or by injecting a local anesthetic. Permanent lesions are of three primary types: **aspirative, electrical, and chemical** (McDonald and Overmier 1998).

Aspirative lesions are made by sucking out the tissue of interest. Lesions of this type are not selective with respect to tissue type. Neurons, support cells, and fibers coursing through the area are all eliminated.

Electrical lesions are also non-selective, i. e., they destroy all tissue types in the lesion area, including cell bodies, support cells, and fibers of passage. Harder et al. (1996) performed bilateral transection of the fornix in young adult **marmosets** producing a specific pattern of cognitive deficits, notably a lack of ability to recall visuospatial tasks learnt preoperatively, and a deficit in acquiring new visuospatial tasks following transection. This impairment could be ameliorated by cholinergic agonists and 5-HT_{1A} antagonists.

Ennaceur (1998) studied the effects of electrolytic lesions of the Medial Septum/Vertical Diagonal Band of Broca, the Globus Pallidus and the Substantia Innominata/Ventral Pallidum on the performance of **rats** in object-recognition memory and radial-maze learning tasks.

Chambers et al. (1996) proposed lesioning of the ventral hypothalamus in neonatal rats as an experimental model of schizophrenia with learning deficits.

Chen et al. (1997) observed a remarkable impairment of passive avoidance response by bilateral dorsal hippocampal lesions in rats.

In several studies **monkeys** were used:

Gaffan (1994) described a model of episodic memory impairment in monkeys with fornix transection.

Alvarez et al. (1994) studied memory functions in monkeys with lesions of the hippocampal formation and adjacent cortex.

Chemical lesions are induced by injecting chemical agents into specific brain sites. Chemical agents induce a more selective lesion, typically destroying cell bodies and dendrites while sparing axons (Coyle et al. 1981; Coyle 1983; Choi 1992).

The most commonly used neurotoxins in memory research are **excitatory amino acid neurotransmitters**, such as glutamate, and glutamate analogs such as ibotenate, NMDA, kainate, quisqualate and AMPA (Dunnet et al. 1989; Connor et al. 1991). These excitotoxins vary in their selectivity for the types of tissue damaged. For example, glutaminergic receptors in the hippocampal CA3 pyramidal cell layer are predominantly of the kainate subtype (Monaghan et al. 1983), and thus kainate administration induces more damage at this site than in areas of the hippocampus, in which kainate receptor density is not as great. In contrast, glutamate receptors in the dentate granule cells are primarily of the quisqualate and NMDA subtypes. As a result, they are relatively insensitive to damage by kainate administration, but highly vulnerable to ibotenate insult (Köhler and Schwarcz 1983).

Ishikawa et al. (1997) reported hippocampal-degeneration-inducing impairment of learning in rats after neonatal administration of monosodium glutamate or oral administration of trimethylin.

Misztal et al. (1996) produced a short-term working memory deficit in rats by intraventricular infusion of quinolinic acid via ALZET osmotic minipumps for 2 weeks.

Zalewska-Wiñska and Wísniewski (2000) tested the influence of (S)-3,5-DHPG, a selective agonist of group 1 metabotropic glutamate receptors, on the activity of the central nervous system in rats.

Zajaczkowski and Danysz (1997) induced deficits of spatial learning in rats by entorhinal cortex lesions with quinolinic acid.

Yamamoto et al. (2003) and Ahmed et al. (2004) infused ibotenic acid into the nucleus basalis magnocellularis of rats in order to establish a model of Alzheimer's disease.

Spowart-Manning and van der Staay (2005) found spatial discrimination deficits in the Morris water escape task in rats after bilateral lesions of the entorhinal cortex by injections of ibotenic acid.

Car and Wiśniewski (1998) evaluated the effect of intracerebroventricular injection of baclofen and AP-7 on behavior in rats.

Two types of chemical lesions are used to examine the role of the cholinergic system in learning and memory. Ethylcholine mustard aziridinium ion, or **AF64A**, is a neurotoxin that is specific to cholinergic cells (Mantione et al. 1981). However, some noncholinergic cells may also be destroyed. A neurotoxin more specific to cholinergic cells in the basal forebrain was described by Wiley et al. (1991). The compound, ^{192}IgG-saporin, is a monoclonal antibody to the low-affinity nerve growth factor receptor (^{192}IgG) conjugated to saporin, a ribosome-inactivating protein. It specifically destroys cholinergic cell bodies in the nucleus basalis Meynert and the medial septal area. Cholinergic cells in the striatum, ventral pallidum, and thalamus are spared, as are non-cholinergic cells.

Fuji et al. (1993b) studied autoradiographically the influence of drugs on alterations in muscarinic cholinergic receptor [^{3}H]QNB binding induced by basal forebrain lesion in rats.

In order to confirm the antisense effects of sigma$_1$ (σ_1) receptor agonists on memory, Maurice et al. (2001) administered a phosphorothioate-modified antisense oligonucleotide and a mismatched analog intracerebroventricularly to mice.

Brandeis et al. (1995) induced deficits in cognitive functioning by stereotaxic application of AF64A (3 nmol/2 µl per side) in both lateral cerebral ventricles in rats.

Carli et al. (1997) caused impairment of spatial learning in rats by intrahippocampal administration of scopolamine or 7-chloro-kynurenic acid.

Abe et al. (1998) investigated the effect of a benzodiazepine receptor partial inverse agonist on the impairment of spatial memory in basal forebrain-lesioned rats.

Stancheva et al. (1993) studied in rats the effect of neonatal 6-hydroxydopamine treatment on learning and retention and on the level of biogenic monoamines in some brain structures as well as the influence of nootropic drugs.

Nitta et al. (1997) reported that the continuous infusion of anti-nerve growth factor monoclonal antibody into the septum of rats produces an impairment of memory.

Inagawa (1994) reported impairment of spatial working memory in rats induced by intracerebroventricular injection of the cholinergic neurotoxin, ethylcholine mustard aziridinium picrylsulfonate.

Bjugstad et al. (1998) gave chronic intraventricular infusions of tumor necrosis factor alpha to rats and found symptoms resembling the AIDS dementia complex in humans, including learning and memory impairment.

Beers et al. (1995) described spatial recognition memory deficits in Lewis rats following encephalitis after intranasal inoculation with herpes simplex virus type 1.

Harkany et al. (1998) showed that bilateral injection of β-amyloid [Phe(SO$_3$H)^{24}]25–35 in rat nucleus basalis magnocellularis induces behavioral dysfunc-

tions, impairs learning and memory, and disrupts cortical cholinergic innervation.

Miguel-Hidalgo et al. (1998) induced specific degeneration of a large part of neurons in the lateral blade of the gyrus dentatus by small intrahippocampal injections of water with or without **β-amyloid 1–28** fragment.

Ogasawara et al. (1999) studied the effects of NS-105, a cognition enhancer, on memory disruption by scopolamine, electrolytic lesion of the nucleus basalis magnocellularis, as well as by AF64A-, baclofen-, cerebral ischemia- and electroconvulsive shock-induced memory disruption in rats.

Baldi et al. (1999) studied the effects of combined medial septal area, fimbria-fornix and entorhinal cortex **tetrodotoxin** inactivations on passive avoidance response consolidation in the rat. Functional inactivation of these brain areas was induced by administration of 5 ng tetrodotoxin dissolved in 0.5 µl saline according to the respective stereotaxic coordinates.

Intracerebroventicular injection of **streptozotocin**, in a subdiabetic dose to rats, causes prolonged impairment of brain glucose and energy metabolism. This is accompanied by impairment in learning and memory (Lannert and Hoyer 1998; Sharma and Gupta 2000, 2002).

Razani et al. (2001) reported that intracerebroventricular infusion of the 5-hydroxytryptamine$_{1A}$ receptor agonist 8-hydroxy-2-(di-*N*-propylamino)tetraline (8-OH-DPAT) in rats induced a deficit in passive avoidance retention, which was attenuated by intraventricular galanin infusion.

Tchekalarova et al. (2003) showed that intracerebroventricular infusion of sarmesin, an angiotensin II analog, decreased seizure susceptibility, memory retention, and nociception in rats.

Rall et al. (2003) demonstrated that infusion of a **cyclooxygenase-2 inhibitor** into the dorsal hippocampus attenuates memory acquisition in rats.

Yu et al. (1997) reported significant impairment of learning and memory ability in **mice** after hippocampal microinfusion with colchicine.

Chapman et al. (1998) observed spatial working memory impairment in apolipoprotein E-deficient mice.

English et al. (1998) showed that infection with the LP-BM5 murine leukemia virus causes an AIDS-like syndrome – murine acquired immunodeficiency syndrome – in C57B1/6 mice and impairs spatial learning without gross motor impairment.

Hiramatsu and Inoue (1999) studied the effects of nocistatin on nociceptin-induced impairment of learning and memory in mice. The drugs were injected into the lateral ventricle of the mouse brain in a volume of 5 µl/mouse under brief ether anesthesia.

Fernandez-Ruiz et al. (1995) studied the long-term cognitive impairment in MPTP-treated **rhesus monkeys**.

Ye et al. (1999) evaluated a reversible acetylcholinesterase inhibitor for its ability to reverse the deficits in spatial memory produced by scopolamine in young adult monkeys and those that are naturally occurring in aged monkeys in a delayed-response task.

Yoneoka et al. (1999) established an adult rat model for the late onset of **radiation-induced cognitive dysfunctio**n in adult rats. Rats were irradiated with a total dose of 40 Gy, given as eight fractions in 24 days. At 12 months after irradiation, the passive avoidance task revealed a deterioration of the cognitive function.

REFERENCES AND FURTHER READING

Abe K, Takeyama C, Yoshimura K (1998) Effects of S-8510, a novel benzodiazepine receptor partial inverse agonist, on basal forebrain lesioning-induced dysfunction in rats. Eur J Pharmacol 347:145–152

Ahmed MM, Hoshino H, Chikuma T, Yamada M, Kato T (2004) Effect of memantine on the levels of glia cells, neuropeptides, and peptide-degrading enzymes in rat brain regions of ibotenic acid-treated Alzheimer's disease model. Neuroscience 126:639–649

Alvarez P, Zola-Morgan S, Squire LR (1994) The animal model of human amnesia: Long-term memory impaired and short-term memory intact. Proc Natl Acad Sci USA 91:5637–5641

Baldi E, Lorenzini CA, Sacchetti B, Tassoni G, Bucherelli C (1999) Effects of combined medial septal area, fimbria-fornix and entorhinal cortex tetrodotoxin inactivations on passive avoidance response consolidation in the rat. Brain Res 821:503–510

Beers DR, Henkel JS, Kesner RP, Stroop WG (1995) Spatial recognition memory deficits without notable CNS pathology in rats following herpes simplex encephalitis. J Neurol Sci 131:119–127

Bjugstad KB, Flitter WD, Garland WA, Su GC, Arendash GW (1998) Preventive actions of a synthetic antioxidant in a novel animal model of AIDS dementia. Brain Res 795:349–357

Brandeis R, Saphir M, Hafif N, Abraham S, Oz N, Stein E, Fisher A (1995) AF150(S): a new functionally selective M_1 agonist improves cognitive performance in rats. Pharmacol Biochem Behav 51:667–674

Car H, Wiśniewski K (1998) The effect of baclofen and AP-7 on selected behavior in rats. Pharmacol Biochem Behav 59:685–689

Carli M, Bonalumi P, Samanin R (1997) Way 100635, a 5-HT_{1A} receptor antagonist, prevents the impairment of spatial learning caused by intrahippocampal administration of scopolamine or 7-chloro-kynurenic acid. Brain Res 774:167–174

Chambers RA, Moore J, McEnvoy JP, Levin ED (1996) Cognitive effects of neonatal hippocampal lesions in a rat model of schizophrenia. Neuropsychopharmacology 15:587–594

Chapman S, Fisher A, Weinstock M, Brandies R, Shohami E, Michaelson DM (1998) The effects of the acetylcholinesterase inhibitor ENA713 and the M1 agonist AF 150(S) on apolipoprotein E deficient mice. J Physiol (Paris) 92:34

Chen Z, Sugimoto Y, Kamei C (1997) Effects of histamine and its related compounds on impairment of passive avoidance response following hippocampal lesions in rats. J Brain Sci 23:225–240

Choi DW (1992) Excitotoxic cell death. J Neurobiol 23:1261–1276

Connor DJ, Langlais PJ, Thal LJ (1991) Behavioral impairment after lesions of the nucleus basalis by ibotenic acid and quisqualic acid. Brain Res 555:84

Coyle JT (1983) Neurotoxic action of kainic acid. J Neurochem 41:1–11

Coyle JT, Bird SJ, Evans RH, Gulley RL, Nadler JV, Nicklas WJ, Oley JW (1981) Excitatory amino acid neurotoxins: selectivity and mechanism of action. Neurosci Res Progr Bull 19:331–427

Dunnett SB, Whishaw IQ, Jones GH, Bunch ST (1989) Behavioral, biochemical and histochemical effects of different neurotoxic amino acids injected into nucleus basalis magnocellularis of rats. Neuroscience 20:653–669

English JA, Hemphill KM, Paul IA (1998) LP-BM5 infection impairs acquisition, but not performance, of active avoidance responding in C57B1/6 mice. FASEB J 12:175–179

Ennaceur A (1998) Effects of lesions of the Substantia Innominata/Ventral Pallidum, Globus Pallidus and Medial Septum on rat's performance in object-recognition and radial-maze tasks: Physostigmine and amphetamine. Pharmacol Res 38:251–263

Enz A, Boddeke H, Sauter A, Rudin M, Shapiro G (1993) SDZ ENS 163 a novel pilocarpin like drug: pharmacological *in vitro* and *in vivo* profile. Life Sci 52:513–520

Fernandez-Ruiz J, Doudet DJ, Aigner TG (1995) Long-term cognitive impairment in MPTP-treated rhesus monkeys. Neuro-Report 7:102–104

Fisher A, Hanin I (1986) Potential animal models for senile dementia of Alzheimer's type, with emphasis on AF64A-induced cholinotoxicity. Ann Rev Pharmacol Toxicol 26:161–181

Fonnum F (1975) A rapid radiochemical method for the determination of choline acetyltransferase. J Neurochem 24:407–409

Fuji K, Hiramatsu M, Kameyama T, Nabeshima T (1993a) Effects of repeated administration of propentofylline on memory impairment produced by basal forebrain lesion in rats. Eur J Pharmacol 236:411–417

Fuji K, Hiramatsu M, Hayashi S, Kameyama T, Nabeshima T (1993b) Effects of propentofylline, a NGF stimulator, on alterations in muscarinic cholinergic receptors induced by basal forebrain lesion in rats. Neurosci Lett 150:99–102

Gaffan D (1994) Scene-specific memory for objects: A model of episodic memory impairment in monkeys with fornix transection. J Cogn Neurosci 6:305–320

Harder JA, Maclean CJ, Alder JT, Francis PT, Ridley RM (1996) The 5-HT_{1A} antagonist, Way 100635, ameliorates the cognitive impairment induced by fornix transection in the marmoset. Psychopharmacology 127:245–254

Harkany T, O'Mahony S, Kelly JP, Soós K, Törö I, Penke B, Luíten PGM, Nyakas C, Gulya K, Leonard BE (1998) β-Amyloid(Phe(SO_3H)^{24}) 25–35 in rat nucleus basalis induces behavioral dysfunctions, impairs learning and memory and disrupts cortical cholinergic innervation. Behav Brain Res 90:133–145

Hiramatsu M, Inoue K (1999) Effects of nocistatin on nociceptin-induced impairment of learning and memory in mice. Eur J Pharmacol 367:151–155

Hock FJ (1987) Drug influences on learning and memory in aged animals and humans. Neuropsychobiol 17:145–160

Inagawa K (1994) Impairment of spatial working memory of rats in radial maze performance induced by ethylcholine mustard aziridinium picrylsulfonate (AF6P-P): Retention curve analysis. Jpn J Psychopharmacol 14:9–17

Ishikawa K, Kubo T, Shibanoki S, Matsumoto A, Hata H, Asai S (1997) Hippocampal degeneration inducing impairment of learning in rats: Model of dementia? Behav Brain Res 83:39–44

Jarvik ME (1964) Techniques for evaluating the effects of drugs on memory. In: Nodin JH, Siegler PE (eds) Animal and Clinical Pharmacologic Techniques in Drug Evaluation. Year Book Medical Publ. Inc.; Chicago, pp 339–347

Köhler C, Schwarcz R (1983) Comparison of ibotenate and kainate neurotoxicity in rat brain: a histological study. Neuroscience 8:819–835

Lannert H, Hoyer S (1998) Intracerebroventricular injection of streptozotocin causes long-term diminutions on learning and memory abilities and cerebral energy metabolism in adult rats. Behav Neurosci 112:1199–1208

Mantione CR, Fisher A, Hanin I (1981) The AF64A-treated mouse: possible model for central cholinergic hypofunction. Science 213:579–580

Maurice T, Phan VL, Privat A (2001) The antisense effects of sigma$_1$ (σ_1) receptor agonists confirmed by in vivo antisense strategy in the mouse. Brain Res 898:113–121

McDonald MP, Overmier JB (1998) Present imperfect: a critical review of animal models of the mnemonic impairments in Alzheimer's disease. Neuroscience Behav Rev 22:99–120

Miguel-Hidalgo JJ, Vecino B, Fernández-Novoa L, Álvarez A, Cacabelos R (1998) Neuroprotective role of S12024 against neurodegeneration in the rat dentate gyrus. Eur Neuropsychopharmacol 8:203–208

Misztal M, Skangiel-Kramska J, Niewiadomska G, Danysz W (1996) Subchronic intraventricular infusion of quinolinic acid produces working memory impairment. A model of progressive excitotoxicity. Neuropharmacology 35:449–458

Monaghan DT, Holets VR, Toy DW, Cotman DW (1983) Anatomical distributions of four pharmacologically distinct ^{3}H-L-glutamate binding sites. Nature 306:176–179

Morris RGM (1981) Spatial localization does not require the presence of local cues. Learn Motiv 12:239–260

Nitta A, Ogihara Y, Onishi J, Hasegawa T, Furukawa S, Nabeshima T (1997) Oral administration of propentofylline, a stimulator of nerve growth factor (NGF) synthesis, recovers cholinergic neuronal dysfunction induced by the infusion of anti-NGF antibody into the rat septum. Behav Brain Res 83:201–204

Ogasawara T, Itoh Y, Tamura M, Mushiroi T, Ukai Y, Kise M, Kimura K (1999) Involvement of cholinergic and GABAergic systems in the reversal of memory disruption by NS-105, a cognition enhancer. Pharmacol Biochem Behav 64:41–52

Paxinos G, Watson C (1986) The rat brain in stereotaxic coordinates. 2nd Edition, Academic Press, New York

Rall JM, Mach SA, Dash PK (2003) Intrahippocampal infusion of a cyclooxygenase-2 inhibitor attenuates memory acquisition in rats. Brain Res 968:273–276

Razani H, Díaz-Cabiale Z, Misane I, Wang FH, Fuxe K, Ögren SO (2001) Prolonged effects of intraventricular galanin in

a 5-hydroxytryptamine$_{1A}$ receptor mediated function in the rat. Neuroscience Lett 299:145–149
Schindler U, Rush DK, Fielding S (1984) Nootropic drugs: Animal models for studying effects on cognition. Drug Devel Res 4:567–576
Sharma M, Gupta YK (2000) Intracerebroventricular injection of streptozotocin in rats produces both oxidative stress and cognitive impairment. Life Si 68:1021–1029
Sharma M, Gupta YK (2002) Chronic treatment with trans resveratrol prevents intracerebroventicular streptozotocin induced cognitive impairment and oxidative stress in rats. Life Sci 71:2487–2498
Spowart-Manning L, van der Staay FJ (2005) Spatial discrimination deficits by excitotoxic lesions in the Morris water escape task. Behav Brain Res 156:269–276
Stancheva S, Papazova M, Alova L, Lazarova-Bakarova M (1993) Impairment of learning and memory in shuttle-box trained rats neonatally injected with 6-hydroxydopamine. Effect of nootropic drugs. Acta Physiol Pharmacol Bulg 19:77–82
Sunderland T, Tariot PN, Newhouse PA (1988) Differential responsitivity of mood, behavior, and cognition to cholinergic agents in elderly, neuropsychiatric populations. Brain Res Rev 13:371–389
Tchekalarova J, Pechlivanova D, Kambourova T, Matsoukas J, Georgiev V (2003) The effects of sarmesin, an angiotensin II analogue on seizure susceptibility, memory retention and nociception. Regul Pept 11:191–197
Thompson G (1983) Rodent models of learning and memory in aging research. In Walker RF, Cooper RL (eds) Experimental and Clinical Interventions in Aging. Marcel Dekker, Inc., New York and Basel, pp 261–278
Tienari PJ, de Strooper B, Ikonen E, Ida N, Simons M, Masters CL, Dotti CG, Bayreuther K (1996) Neuronal sorting and processing of amyloid precursor protein: Implications for Alzheimer's disease. Cold Spring Harbor Symposia on Quantitative Biology 61:575–585
Weidemann A, König G, Bunke D, Fischer P, Salbaum JM, Masters CL, Beyreuther K (1989) Identification, biogenesis, and localization of precursors of Alzheimer's disease A4 amyloid protein. Cell 57:115–126
Wiley RG, Oeltmann TN, Lappi DA (1991) Immunolesioning: selective destruction of neurons using immunotoxin to rat NGF receptor. Brain Res 562:149–153
Yamamoto M, Chikuma T, Kato T (2003) Changes in the levels of neuropeptides and their metabolic enzymes in the brain regions of nucleus basalis magnocellularis-lesioned rats. J Pharmacol Sci 92:400–410
Ye W-Y,Cai J-X, Wang L-M, Tang X-C (1999) Improving effects of huperizine A on spatial working memory in aged monkeys and in young adult monkeys with experimental cognitive impairment. J Pharmacol Exp Ther 288:814–819
Yoneoka Y, Satoh M, Akiyama K, Sano K, Fujii Y, Tanaka R (1999) An experimental study of radiation-induced cognitive dysfunction in an adult rat model. Br J Radiol 72:1196–1201
Yu Z, Cheng G, Hu B (1997) Mechanism of colchicine impairment of learning and memory, and protective effect of CGP-36742 in mice. Brain Res 750:53–58
Zajaczkowski W, Danysz W (1997) Effects of D-cycloserine and aniracetam on spatial learning in rats with entorhinal cortex lesions. Pharmacol Biochem Behav 56:21–29
Zalewska-Wiñska A, Wísniewski K (2000) Behavioural activity of (S)-3,5-DHPG, a selective agonist of group 1 metabotropic glutamate receptors. Pharmacol Res 42:239–245

F.4.2
Cognitive Deficits After Cerebral Ischemia

PURPOSE AND RATIONALE

Cerebral vessel occlusion has been used as a model for stroke and multi-infarct cerebral dysfunction (see A.8.1).

Impairment of cerebral metabolism induced by reduced blood supply is known to induce cognitive deficits (Gibson et al. 1981). Because of the absence of posterior communicating arteries in the brain of **Mongolian gerbils**, complete forebrain ischemia can be produced by occluding both common carotid arteries resulting in amnesia (Levine and Sohn 1969; Schindler 1983; Schindler et al. 1984; Chandler et al. 1985; Lundy et al. 1986).

PROCEDURE

Male Mongolian gerbils (strain Hoe:Gerk) weighing 50–70 g are anesthetized by i.p. pentobarbital injection. Both common carotid arteries are exposed through a ventral neck incision and occluded for 5 or 10 min with miniature aneurysm clips. In sham-operated controls, the common carotid arteries are exposed but not occluded. Then, 24 h after occlusion, each animal is placed in the bright part of a light/dark-chambered apparatus for training. After a brief orientation period, the gerbil enters the second, dark chamber. Once inside the second chamber, the door is closed which prevents the animal from escaping, and a 100-V, 2-s foot shock is applied through the grid floor. The gerbil is then returned to the home cage. Testing is repeated 24 h later by placing the animal again in the bright chamber. The latency in entering the second dark chamber within a 5-min test session is measured electronically. The latency compared with sham-operated controls is decreased depending on the duration of ischemia. After drug treatment, an increase of latency before entering the dark compartment indicates good acquisition.

EVALUATION

Using various doses a dose-dependent increase of latency can be found after active drugs, sometimes resulting in inverse U-shaped dose–response curves.

Tamura et al. (2001) described the effect of permanent middle cerebral artery occlusion on cognitive impairments in **rats**.

PROCEDURE

Rats are anesthetized with 2% halothane in a gas mixture of 30% O_2 and 70% N_2O, then maintained with

1% halothane. Under anesthesia, the head is placed in a stereotaxic apparatus and the skin is incised between the external foramen and external canthus. A small hole is bored in the cranial bone under a surgical microscope. The dura is dissected and the middle cerebral artery exposed. The middle cerebral artery is electrically coagulated from its origin using a bipolar forceps. In sham-operated rats, the dura is exposed but the middle cerebral artery is not occluded.

MODIFICATIONS OF THE METHOD

Using a similar method, Yamaguchi et al. (1995) found that a muscarinic agonist improves the impairment of learning behavior in rats. Yonemori et al. (1996) tested spatial memory disturbances after focal cerebral ischemia in rats.

Noda et al. (1995) used a somewhat modified technique of permanent occlusion of the middle cerebral artery. Rats were anesthetized with halothane 2%. After the temporal muscle was retracted via a transretroorbital approach without removal of the temporalis muscle and zygomatic arch, the animals underwent a left subtemporal craniotomy. The stem of the middle cerebral artery was electrocauterized just medial to the olfactory tract and waa cut to ensure the completeness of the vascular occlusion.

Another technique was described by Borlongan et al. (1995). Rats were anesthetized with 60 mg/kg pentobarbital, then shaved on the ventral portion of the neck. A V-shaped incision was made beginning at the caudal end of the sternomastoid and sternothyroid muscles, cutting towards the ears. After dissection, the right common carotid artery was exposed and carefully separated from the vagus nerve. The external carotid artery was then tied off tightly with two 5.0 silk sutures. The internal carotid artery was tied loosely and a small clamp was placed distal to the tie. Upon clamping off the common carotid artery, a small cut was made in the external carotid artery just above the bifurcation. The embolus was then introduced through the external carotid artery and guided into the internal carotid artery until resistance was felt. Mean length of the embolus inserted was 18–22 mm. The embolus, which was made by coating a 30-mm piece of 4.0 silk suture with silicone mixed with hardener, blocked the origin of the right middle cerebral artery. The embolus was left in place for 1 h. After removal of the embolus, the entry point of the embolus was cauterized, and the skin sutured.

Plaschke et al. (1999) used a model of permanent brain vessel occlusion originally described by Pulsinelli and Brierley (1979) to study the interrelation between cerebral energy metabolism and behavior in rats.

Kimura et al. (2000) investigated the pathogenesis of vascular dementia in stroke-prone spontaneously hypertensive rats.

Hattori et al. (2000) tested cognitive deficits after focal cerebral ischemia in **mice**. Adult male C57/BL6 mice were anesthetized with 1%–1.5% halothane in oxygen-enriched air delivered by a face mask, then subjected to 60 or 90 min of intraluminal middle coronary artery occlusion or sham surgery. Unilateral middle coronary artery occlusion was achieved by introducing a 6–0 nylon monofilament into the right internal carotid artery through the external carotid artery, then positioning the filament tip for occlusion at a distance of 6 mm beyond the internal artery-pterygopalatine artery bifurcation. Then, the wound was closed and the animal was allowed to emerge from anesthesia in its home cage. After 60 or 90 min of occlusion, the animals were briefly re-anesthetized with halothane, and the monofilament was removed. Cognitive deficits were evaluated by several behavioral tests and in the elevated plus-maze test.

REFERENCES AND FURTHER READING

Borlongan CV, Cahill DW, Sanberg PR (1995) Locomotor and passive avoidance deficits following occlusion of the middle cerebral artery. Physiol Behav 58:909–917

Chandler MJ, DeLeo JA, Carney JM (1985) An unanesthetized-gerbil model of cerebral ischemia-induced behavioral changes. J Pharmacol Meth 14:137–146

Gibson GE, Pulsinelli W, Blass JP, Duffy TE (1981) Brain dysfunction in mild to moderate hypoxia. Am J Med 70:1247–1254

Hattori K, Lee H, Hurn PD, Crain BJ, Traystman RJ, DeVries AC (2000) Cognitive deficits after focal cerebral ischemia in mice. Stroke 31:1939–1944

Kimura S, Saito H, Minami M, Togashi H, Nakamura N, Nemoto M, Parvez HS (2000) Pathogenesis of vascular dementia in stroke-prone spontaneously hypertensive rats. Toxicology 153:167–178

Levine S, Sohn D (1969) Cerebral ischemia in infant and adult gerbils. Arch Pathol 87:315–317

Lundy EF, Solik BS, Frank RS, Lacy PS, Combs DJ, Zelenok GB, D'Alecy LG (1986) Morphometric evaluation of brain infarcts in rats and gerbils. J Pharmacol Meth 16:201–214

Noda Y, Furukawa K, Kohayakawa H, Oka M (1995) Effects of RGH-2202 on behavioral deficits after focal cerebral ischemia in rats. Pharmacol Biochem Behav 52:695–699

Plaschke K, Yun SW, Martin E, Hoyer S, Bardenheuer HJ (1999) Interrelation between cerebral energy metabolism and behaviour in a rat model of permanent brain vessel occlusion. Brain Res 830:320–329

Pulsinelli WA, Brierley JB (1979) A new model of bilateral hemispheric ischemia in the unanesthetized rat. Stroke 10:267–272

Schindler U (1983) The effect of graded cerebral ischemia on brain water content and learning ability in the Mongolian gerbil. J Cerebr Blood Flow Metab 3:S335–S336

Schindler U, Rush DK, Fielding S (1984) Nootropic drugs: animal models for studying effects on cognition. Drug Dev Res 4:567–576

Tamura M, Aoki Y, Seto T, Itoh Y, Ukai Y (2001) Cerebroprotective action of Na^+/Ca^{2+} channel blocker NS-7. II Effect on the cerebral infarction, behavioral and cognitive impairments at the chronic stage of permanent middle cerebral artery occlusion in rats. Brain Res 890:170–176

Yamaguchi T, Suzuki M, Yamamoto M (1995) YM796, a novel muscarinic agonist, improves the impairment of learning behavior in a rat model of chronic cerebral ischemia. Brain Res 669:107–114

Yonemori F, Yamada H, Yamaguchi T, Uemura A, Tamura A (1996) Spatial memory disturbances after focal cerebral ischemia in rats. J Cerebr Blood Flow Metab 16:973–980

F.4.3
Strains with Hereditary Memory Deficits

Several animal strains have been recommended to study age-dependent memory deficits, such as the **senescence-accelerated mouse (SAM)** (Takeda et al. 1981, 1994, 1996, 1997; Fujibayashi et al. 1994; Maurice et al. 1996; Nishiyama et al. 1997; Flood and Morley 1998; Markowska et al. 1998). SAM includes accelerated senescence prone SAMP (SAMP1, P2, P3, P6; P7, P8, P9 and P10) and accelerated senescence-resistant mouse SAMR (SAMR1, R2 and R4) (Hosokawa et al. 1984; Yagi et al. 1998). SAMP is associated with signs of advanced senescence, such as reduced activity, hair loss, lack of hair glossiness, skin coarseness, periophthalmic lesions, increased lordokyphosis of the spine, and a shortened life span. In the SAMP series, SAMP8 showed more spontaneous age-related detoriation of memory and learning abilities in passive avoidance response tests (Miyamoto et al. 1986), especially in the acquisition stage (Yagi et al. 1988), than did control SAMR1 mice.

Shimada (1999) reviewed age-dependent cerebral atrophy and cognitive dysfunction in SAMP10 mice.

Banks et al. (2003) found an impairment of efflux of human and mouse amyloid β proteins 1–40 and 1–42 from brain in SAMP8 mice.

Farr et al. (2004) reported that dehydroepiandrosterone sulfate improved learning and memory in aged SAMP8 mice.

Epileptic fowl having a hereditary form of primary generalized epilepsy are characterized by tonic-clonic seizures (Gervais-Fagnou and Tuckek 1996).

REFERENCES AND FURTHER READING

Banks WA, Robinson SM, Verma S, Morley JE (2003) Efflux of human and mouse amyloid β proteins 1–40 and 1–42 from brain: impairment in a mouse model of Alzheimer's disease. Neuroscience 121:487–492

Farr SA, Banks WA, Uezu K, Gaskin FS, Morley JE (2004) DHEAS improves learning and memory in aged SAMP8 mice but not in diabetic mice. Life Sci 75:2775–2785

Flood JF, Morley JE (1998) Learning and memory in the SAMP8 mouse. Neurosci Biobehav Rev 22:1–20

Fujibayashi Y, Waki A, Wada K, Ueno M, Magata Y, Yonekura Y, Konishi J, Takedaa T, Yokoyama A (1994) Differential aging pattern of cerebral accumulation of radiolabeled glucose and amino acid in the senescence accelerated mouse (SAM), a new model for the study of memory impairment. Biol Pharm Bull 17:102–105

Gervais-Fagnou DD, Tuchek JM (1996) Learning impairment in 1–2 day-old chicks. Epilepsia 37:322–327

Hosokawa H, Kasai R, Higuchi K, Takeshita S, Shimizu K, Hamamoto H, Honma A, Irino M, Toda K, Matsumara A, Matsushida M, Takeda T (1984) Grading score system; a method for evaluation of the degree of senescence in senescence-accelerated mouse (SAM). Mech Ageing Dev 26:91–102

Markowska AL, Spangler EL, Ingram DK (1998) Behavioral assessment of the senescence-accelerated mouse (SAM P8 and R1) Physiol Behav 64:15–26

Maurice T, Roman FJ, Su T-P, Privat A (1996) Beneficial effects of sigma agonists on the age-related learning impairment in the senescence-accelerated mouse (SAM). Brain Res 733:219–230

Miyamoto M, Kiyota Y, Yamazaki N, Nagaoka A, Matsuo T, Nagawa Y, Takeda T (1986) Age-related changes in learning and memory in the senescence accelerated mouse (SAM). Physiol Behav 38:399–406

Nishiyama N, Moriguchi T, Saito H (1997) Beneficial effects of aged garlic extract on learning and memory impairment in the senescence-accelerated mouse. Exp Gerontol 32:149–160

Shimada A (1999) Age-dependent cerebral atrophy and cognitive dysfunction in SAMP10 mice. Neurobiol Aging 20:125–136

Takeda T (1996) Senescence-accelerated mouse (SAM): With special reference to age-associated pathologies and their modulation. Jpn J Hyg 51:569–578

Takeda T, Hosokawa M, Takeshida M, Irino K, Higuchi K, Matsushita T, Tomita Y, Yasuhira K, Hamamoto H, Shimizu K, Ishii M, Yamamuro T (1981) A new murine model of accelerated senescence. Mech Ageing Dev 17:183–194

Takeda T, Hosokawa M, Higuchi K, Hosono M, Akiguchi I, Katoh H (1994) A murine model of aging, Senescence-Accelerated Mouse. Arch Gerontol Geriatr 19:185–192

Takeda T, Matsushita T, Kurozumi M, Takemura K, Higuchi K, Hosokawa M (1997) Pathobiology of the senescence-accelerated mouse (SAM). Exp Gerontol 32:117–127

Yagi H, Katoh S, Akiguchi I, Takeda T (1988) Age-related deterioration of ability of acquisition in memory and learning in senescence accelerated mouse: SAM-P/8 as an animal model of disturbance in recent memory. Brain Res 474:86–93

Yagi H, Akiguchi I, Ohta A, Yagi N, Hosokawa M, Takeda T (1998) Spontaneous and artificial lesions of magnocellular reticular formation of brainstem deteriorate avoidance learning in senescence-accelerated mouse (SAM). Brain Res 791:90–98

F.4.4
Genetically Modified Animals

The use of genetically altered animals in biological research has also affected research in learning

and memory. Genetically engineered strains of mice, modified by transgenesis or gene targeting ("knockout") have been generated and are used as research tools for deciphering the genetic basis of behavior. These animals may be helpful to evaluate the efficacy of new pharmacological treatments (Mayford et al. 1997; Costentin 1998; Anagnostopoulos et al. 2001; Higgins and Jacobsen 2003). Various authors described transgenic mouse models of Alzheimer's disease (van Leuven 2000; Götz 2001; Janus and Westaway 2001).

Several strains were described, such as:

Transgenic mice, which **overexpress S100β**, a calcium binding astrocytic protein influencing hippocampal long-term potentiation (LTP) and depression (LTD) (Roder et al. 1996),

Transgenic **Cu/Zn-SOD mice overexpressing the gene encoding copper/zinc superoxide dismutase** which is also overexpressed in human Down syndrome (Gahtan et al. 1998),

a mutant mice strain exhibiting delayed Wallerian degeneration (Fox and Faden 1998),

Mice with a **modified β-amyloid precursor protein gene** (Tremml et al. 1998; Kim et al. 2004),

Gozes et al. (1993) reported learning impairment and prolonged retardation in memory acquisition in transgenic mice carrying a chimeric gene for the vasoactive intestinal peptide (VIP).

Franowicz et al. (2002) compared mice with a point mutation of the α_{2A}-adrenoceptor, which serves a functional knockout with wild mice. Working memory performance was impaired and the cognitive enhancement by guanfacine was lost.

Silva et al. (1992) studied memory mechanisms in mutant mice that do not express the alpha-calcium-calmodulin kinase II. These mice are deficient to produce hippocampal long-term potentiation and were recommended as a suitable model for studying the relation between long-term potentiation and the learning process.

Moechars et al. (1999) reported early phenotypic changes in transgenic mice cloned by cDNA coding of human wild-type **APP (695 isoform**), the Swedish (K670N,M671L) mutant (770 isoform) and the London (V642I) mutant (695 isoform) in the pTSC vector in the mouse *thy-1* gene (Moechars et al. 1996).

Strazielle et al. (2003) investigated regional brain cytochrome oxidase activity in β-amyloid precursor protein transgenic mice with the Swedish mutation. **APP23 mice** were generated under the control of the murine Thy-1 gene promoter and were backcrossed by several generations to the C57BL6J background (Sturchler Pierrat et al. 1997; Phinney et al. 1999; Boncristiano et al. 2002).

Using this model, Kelley et al. (2003) reported progressive age-related impairment of cognitive behavior in APP23 transgenic mice.

Van Dam et al. (2005) described the symptomatic effects of donepezil, rivastigmine, galantamine and memantine of cognitive deficits in the APP23 model.

Johnson-Wood et al. (1997) studied amyloid precursor protein processing and Aβ_{42} deposition in the PDAPP transgenic mouse model of Alzheimer's disease.

Touma et al. (2004) investigated the TgCRND8 line, a double mutant (Swedish and Indiana) human APP_{695} model of Alzheimer's disease, generated by Chishti et al. (2001).

Steiner et al. (2001) found that **galanin transgenic mice** display cognitive and neurochemical deficits characteristic of Alzheimer's disease. The mouse galanin gene was coupled to the human dopamine β-hydoxylase reporter (Mazarati et al. 2000; Cadd et al. 1992).

Huber et al. (2002) and Qin et al. (2002) described a **fragile X knockout mouse** (*fmr1*KO) mouse, which resembles the fragile X mental retardation syndrome in humans.

Richardson et al. (2003) described a transgenic mouse line overexpressing the 695-amino-acid isoforms of human amyloid precursor protein harboring the Swedish double familial Alzheimer's disease mutation. This line, referred as **TAS10**, exhibits neuropathological features and cognitive deficits that are closely related to the accumulation of Aβ in their brain and that are reminiscent to those observed in Alzheimer's disease.

Oddo et al. (2003) generated a triple transgenic model of Alzheimer's disease harboring three mutant genes: **β-amyloid precursor protein (βAPP_{Swe})**, **presenilin-1 ($PS1_{M146V}$)**, and **tau P_{301L}**. The mice progressively develop Aβ and tau pathology, with a temporal- and regional-specific profile that closely mimics their development in the human Alzheimer's disease brain.

The **Tg2576 transgenic model** of Alzheimer's disease was studied by several authors (Hsiao et al. 1996; Haugabook et al. 2001; King and Arendash 2002; Lehman et al. 2003; Li et al. 2003; Parvathenani et al. 2003; Quinn et al. 2003; Zong et al. 2003; Middei et al. 2004; Rodrigo et al. 2004). Tg2576 transgenic mice overexpressing a mutant gene for β-amyloid precursor protein develop Aβ deposits at the age of 9–11 months. At this time, the animals are impaired in Y-maze spon-

taneous alteration, visible platform recognition, and several sensorimotor tasks. Gong et al. (2004) tested immunization of Alzheimer model (Tg2576) mice with adenovirus vectors encoding amyloid β-protein and granulocyte-macrophage colony-stimulating factor (GM-CSF) and found a reduction of amyloid load in the brain.

Skovronsky et al. (2000) synthesized a fluorescent ligand, [(*trans,trans*)-1-bromo-2,5-bis-(3-hydroxycarbonyl-4-hydroxy)-styrylbenzene (BSB)] which allows *in vivo* detection of amyloid plaques in the Tg2576 transgenic mouse model of Alzheimer's disease.

Tanemura et al. (2001, 2002) and Tatebayashi et al. (2002) generated **Tg mouse lines expressing R406W human tau**.

Reilly et al. (2003) analyzed amyloid deposition in the hippocampus and entorhinal cortex in a transgenic mouse model. Heterozygous **PDAPP transgenic mice** carrying the APPV717F familial AD mutation (Murrell et al. 1991) were bred from the established line PDAPP-109 over several generations on hybrid background representing combinations of C57BL/6. DBNA, and Swiss-Webster strains (Games et al. 1995).

Using these mice strains, Rockenstein et al. (1995) investigated levels and alternative splicing of amyloid β protein precursor (APP) transcripts in brains of APP transgenic mice.

Postina et al. (2004) generated transgenic **mice overexpressing either ADAM10** or a catalytically inactive mutant. ADAM (adisintegrin and metalloprotease) 10 has many properties of a physiologically relevant α-secretase: it cleaves APP-derived peptides at the main α-secretase cleavage site between positions 16 and 17 of the Aβ region and is expressed in mouse and human brain (Hartmann et al. 2002). A disintegrin-metalloproteinase prevents amyloid plaque formation and hippocampal defects in an Alzheimer's disease mouse model.

Apolipoprotein E plays a major role in the amyloid cascade. Xu et al. (1999), Levi et al. (2003), Ophir et al. (2003) and Dolev and Michaelson (2004) used **apoE3- and apoE4-transgenic mice** for their studies.

Oike et al. (1999) generated a mouse model of the **Rubinstein-Taybi syndrome** by an insertional mutation into the cyclic AMP response element-binding protein gene. These mice showed deficiencies in long-term memory and other clinical features of the Rubinstein-Taybi syndrome, such as growth retardation, retarded osseous maturation, hypoplastic maxilla, cardiac anomalies, and skeletal abnormalities.

Impairment of the ubiquitin/proteasome system has been proposed to play a role in neurodegenerative disorders such as Alzheimer's and Parkinson's diseases. Lindsten et al. (2003) developed a model for *in vivo* analysis of the **ubiquitin/proteasome system** by generating mouse strains transgenic for a green fluorescent protein reporter carrying a constitutively active degradation signal.

Higuchi et al. (2005) generated transgenic **mice that overexpress human calplastatin**, a specific and the only natural inhibitor of calpains. Distinct mechanistic roles of calpain and caspase activation in neurodegeneration were revealed in these mice.

Hoyle et al. (2006) reported impaired performance of **alpha7 nicotinic receptor knockout mice** in the five-choice serial reaction time task.

Doubly transgenic mice have been used by several authors to analyze Alzheimer-like pathology (Arendash et al. 2001; Battaglia et al. 2003; Gong et al. 2004; Trinchese et al. 2004).

REFERENCES AND FURTHER READING

Anagnostopoulos AV, Mobraaten LE. Sharp JJ, Davisson MT (2001) Transgenic and knockout database: behavioral profiles of mouse mutants. Physiol Behav 73:675–689

Arendash GW, King DL, Gordon MC, Morgan D, Hatcher JM, Hope CE, Diamond DM (2001) Progressive, age-related behavioral impairments in transgenic mice carrying both mutant amyloid precursor protein and presenilin-1 transgenes. Brain Res 891:42–53

Battaglia F, Trinchese F, Liu S, Walter S, Nixob RA, Arancio O (2003) Calpain inhibitors, a treatment for Alzheimer's disease: position paper. J Mol Neurosci 20:357–362

Boncristiano S, Calhoun ME, Kelly PH, Pfeifer M, Bondolfi L, Stalder M, Phinney AL, Abramowski D, Sturchler-Pierat C, Enz A, Sommer B, Staufenbiel M, Jucker M (2002) Cholinergic changes in the APP23 transgenic mouse model of cerebral amyloidosis. J Neurosci 22:3234–3243

Cadd GG, Hoyle GW, Quaife CJ, Marck B, Matsumoto AM, Brinster RL, Palmiter RD (1992) Alteration of neurotransmitter phenotype in noradrenergic neurons of transgenic mice. Mol Endocrinol 6:1951–1960

Chishti AM, Yang DS, Janus C, Phinney AL, Horne P, Pearson J, Strome R, Zuker N, Loukides J, French J, Turner S, Lozza G, Grilli M, Kunicki S, Morisette C, Paquette J, Gervais F, Bergeron C, Fraser PE, Carlson GA, St. George-Hyslop P, Westaway D (2001) Early-onset amyloid deposition and cognitive deficits in transgenic mice expressing a double mutant for of amyloid precursor protein 695. J Biol Chem 276:21562–21570

Costentin J (1998) From gene to behavior, a new method for elaboration of new psychotropic agents. Ann Pharm Fr 56:60–67

Dovel I, Michaelson M (2004) A nontransgenic mouse model shows inducible amyloid-β (Aβ) peptide deposition and elucidates the role of apolipoprotein E in the amyloid cascade. Proc Natl Acad Sci USA 101:13909–13914

Fox GB, Faden AI (1998) Traumatic brain injury causes delayed motor and cognitive impairment in a mutant mouse strain known to exhibit delayed Wallerian degeneration. J Neurosci Res 53:718–727

Franowicz JS, Kessler LE, Borja CM, Kobilka BK, Limbird LE, Arnsten AF (2002) Mutation of the α_{2A}-adrenoceptor impairs working memory performance and annuls cognitive enhancement by guanfacine. J Neurosci 22:8771–8777

Gahtan E, Auerbach JM, Groner Y, Segal M (1998) Reversible impairment of long-term potentiation in transgenic Cu/Zn-SOD mice. Eur J Neurosci 10:538–544

Games D, Adams D, Alessandrini R, Barbour R, Berthelette P, Blackwell C, Carr T, Clemens J, Donaldson T, Gillespie (1995) Alzheimer-type neuropathology in transgenic mice overexpressing V717F β-amyloid precursor protein. Nature 373:523–527

Gong B, Vitolo OV, Trinchese F, Liu S, Shelanski M, Arancio O (2004) Persistent improvement in synaptic and cognitive functions in an Alzheimer mouse model after rolipram treatment. J Clin Invest 114:1624–1634

Götz J (2001) Tau and transgenic animal models. Brain Res Rev 35:266–286

Gozes I, Glowa J, Brenneman DE, McCune SK, Lee E, Westphal H (1993) Learning and sexual deficiencies in transgenic mice carrying a chimeric vasoactive intestinal peptide gene. J Mol Neurosci 4:185–193

Hartmann D, de Strooper B, Serneels L, Craessaerts K, Herreman A, Anaert W, Umans L, Lübke T, Illert AL, von Figura K, Saftig P (2002) The disintegrin/metalloprotease ADAM 10 is essential for Notch signalling but not for α-secretase activity in fibroblasts. Human Mol Genet 11:2615–2624

Haugabook SJ, Le T, Yager D, Zenk B, Healy BM, Eckman EA, Prada C, Younkin L, Murphy P, Pinnix I, Onstead L, Sambamurti K, Golde TE, Dickson D, Younkin SG, Eckman CB (2001) Reduction of Aβ accumulation in the Tg2576 animal model of Alzheimer's disease after oral administration of the phosphatidyl-inositol kinase inhibitor wortmannin. FASEB J 15:16–18

Higgins GA, Jacobsen H (2003) Transgenic mouse models of Alzheimer's disease: phenotype and application. Behav Pharmacol 14:419–436

Higuchi M, Tomioka M, Takano J, Shirotani K, Iwata N, Masumoto H, Maki M, Itohara S, Saido TC (2005) Distinct mechanistic roles of calpain and caspases activation in neurodegeneration as revealed in mice overexpressing their specific inhibitors. J Biol Chem 280:15229–15237

Hoyle E, Genn RF, Fernandes C, Stolerman IP (2006) Impaired performance of alpha7 nicotinic receptor knockout mice in the five-choice serial reaction time task. Psychopharmacology 189:211–223

Hsiao K, Chapman P, Nilsen S, Eckman C, Harigaya Y, Younkin S, Yang F, Cole G (1996) Correlative memory deficits, Abeta elevation, and amyloid plaques in transgenic mice. Science 274:99–102

Huber KM, Gallgher SM, Warren ST, Bear MF (2002) Altered syanptoc plasticity in a mouse model of fragile X mental retardation. Proc Natl Acad Sci USA 99:7746–7750

Janus C, Westaway D (2001) Transgenic mouse models of Alzheimer's disease. Physiol Behav 73:873–886

Johnson-Wood K, Lee M, Motter R, Hu K, Gordon G, Barbour R, Khan K, Gordon M, Tan H, Games D, Lieberburg I, Schenk D, Seubert P, McConlogue L (1997) Amyloid precursor protein processing and Aβ_{42} deposition in a transgenic mouse model of Alzheimer disease. Proc Natl Acad Sci USA 94:1550–1555

Kelly PH, Bondolfi L, Hunziker D, Schlecht HP, Carver K, Maguire E, Abramowski D, Wiederhold KH, Sturchler-Pierrat C, Jucker M, Bergmann R, Staufenbiel M, Sommer B (2003) Progressive age-related impairment of cognitive behavior in APP23 transgenic mice. Neurobiol Aging 24:365–378

Kim HD, Kong FK, Cao Y, Lewis TL, Kim H, Tang DC, Fukuchi KI (2004) Immunization of Alzheimer model mice with adenovirus vectors encoding amyloid β-protein and GM-CSF reduces amyloid load in the brain. Neurosci Lett 370:218–223

King DL, Arendask GW (2002) Behavioral characterization of the TG2576 transgenic model of Alzheimer's disease through 19 months. Physiol Behav 75:627–642

Lehman JH, Kulnane LS, Lamb BT (2003) Alterations in b-amyloid production and deposition in brain regions of two transgenic models. Neurobiol Aging 24:645–653

Levi O, Jongen-Rtelo AL, Feldon J, Roses AD, Michaelson DM (2003) ApoE4 impairs hippocampal plasticity isoform-specifically and blocks environmental stimulation of synaptogenesis and memory. Neurobiol Dis 13:273–282

Li L, Cao D, Garber DW, Kim H, Fukuchi KI (2003) Association of aortic atherosclerosis with cerebral β-amyloidosis and learning deficits in a mouse model of Alzheimer's disease. Am J Pathol 163:2155–2164

Lindsten K, Menéndez-Benito V, Masucci MG, Dantuma NP (2003) A transgenic mouse model of the ubiquitin/proteasome system. Nature Biotechnol 21:897–902

Mayford M, Mansuy IM, Müller RU, Kandel ER (1997) Memory and behavior: a second generation of genetically modified mice. Curr Biol 7:R580–589

Mazarati AM, Hohmann JG, Bacon A, Lu H, Sankar R, Steiner RA, Wynick D, Westerlain CG (2000) Modulation and hippocampal excitability and seizures by galanin. J Neurosci 20:6276–6281

Middei S, Geracitano R, Caprioli A, Mercuri N, Ammassari-Teule M (2004) Preserved fronto-striatal plasticity and enhanced procedural learning in a transgenic mouse model of Alzheimer's disease overexpressing mutant hAPPswe. Learn Mem 11:447–452

Moechars D, Lorent K, de Strooper B, Dewachter I, van Leuwen F (1996) Expression in brain of amyloid precursor protein mutated in the a-secretase site causes disturbed behavior, neuronal degeneration and premature death in transgenic mice. EMBO J 15:1265–1274

Moechars D, Dewachter I, Lorent K, Reversé D, Baekelandt V, Naidu A, Tesseur I, Spittaels K, van den Haute C, Checler F, Godaux E, Cordell B, van Leuwen F (1999) Early phenotypic changes in transgenic mice that overexpress different mutants of amyloid precursor protein in brain. J Biol Chem 274:6483–6492

Murrell J, Farlow M, Ghetti B, Benson MD (1991) A mutation in the amyloid precursor protein associated with hereditary Alzheimer's disease. Science 254:97–99

Oddo S, Caccamo A, Kitazawa M, Tseng B, LaFerla FM (2003) Amyloid deposition precedes tangle formation in a triple transgenic model of Alzheimer's disease. Neurobiol Aging 24:1063–1070

Oike Y, Hata A, Mamiya T, Kaname T, Noda Y, Suzuki M, Yasue H, Nabeshima T, Araki K, Yamamura K (1999) Truncated CBP protein leads to classical Rubinstein-Taybi syndrome phenotypes in mice: implications for a dominant-negative mechanism. Human Mol Gen 8:387–396

Ophir G, Meilin S, Efrati M, Chapman J, Karussis D, Roses A, Michaelson DM (2003) Human apoE3 but not apoE4 rescues impaired astrocyte activation in apoE null mice. Neurobiol Dis 12:56–64

Parvathenani LK, Tertyshnikova S, Greco CR, Roberts Sb, Robertson B, Posmantur R (2003) $P2X_7$ mediates superoxide production in primary microglia and is up-regulated

in a transgenic mouse model of Alzheimer's disease. J Biol Chem 278:13309–13317
Phinney AL, Deller T, Stalder M, Calhoun ME, Frotscher M, Sommer B, Staufenbiel M, Jucker M (1999) Cerebral amyloid induces aberrant axonal sprouting and ectopic terminal formation in amyloid precursor protein transgenic mice. J Neurosci 19:8552–8559
Postina R, Schroeder A, Dewachter I, Bohl J, Schmitt U, Kojro E, Prinzen C, Endres K, Hiemke C, Blessing M, Flamez P, Dequenne A, Godaux E, van Leuwen F, Fahrenholz F (2004) A disintegrin-metalloproteinase prevents amyloid plaque formation and hippocampal defects in an Alzheimer disease mouse model. J Clin Invest 113:1456–1464
Qin M, Kang J, Smith CB (2002) Increased rates of cerebral glucose metabolism in a mouse model of fragile X mental retardation. Proc Natl Acad Sci USA 99:15738–15763
Quinn J, Montine T, Morrow J, Woodward WR, Kulhanek D, Eckenstein F (2003) Inflammation and cerebral amyloidosis are disconnected in an animal model of Alzheimer's disease. J Neuroimmunol 137:33–41
Reilly JF, Games D, Rydel RE, Freedman S, Schenk D, Young WG, Morrison JH, Bloom FE (2003) Amyloid deposition in the hippocampus and entorhinal cortex: quantitative analysis in a transgenic mouse model. Proc Natl Acad Sci USA 100:4837–4842
Richardson JC, Kendal CE, Anderson R, Priest F, Gower E, Soden P, Gray R, Topps S, Howlett DR, Lavender D, Clarke NJ, Barnes JC, Haworth R, Stewart MG, Rupniak HT (2003) Ultrastructural and behavioural changes precede amyloid deposition in a transgenic model of Alzheimer's disease. Neuroscience 122:213–228
Rockenstein EM, McConlogue L, Tan H, Power M, Masliah E, Mucke L (1995) Levels and alternative splicing of amyloid β protein precursor (APP) transcripts in brains of APP transgenic mice and humans with Alzheimer's disease. J Biol Chem 270:28257–28267
Roder JK, Roder JC, Gerlai R (1996) Memory and the effect of cold shock in the water maze in S100β transgenic mice. Physiol Behav 60:611–615
Rodrigo J, Fernández-Vizarra P, Castro-Blanco S, Bentura ML, Nieto M, Gómmez-Isla T, Martínez-Murillo R, Martínez A, Serrano J, Fernández AP (2004) Nitric oxide in the cerebral cortex of amyloid-precursor protein (SW) Tg2576 transgenic mice. Neuroscience 128:73–89
Silva AJ, Stevens CF, Tonegawa S, Wang Y (1992) Deficient hippocampal long-term potentiation in alpha-calcium-calmodulin kinase II mutant mice. Science 257:201–206
Skovronsky DM, Zhang B, Kung MP, Kung HF, Trojanowski JQ, Lee VMY (2000) *In vivo* detection of amyloid plaques in a mouse model of Alzheimer's disease. Proc Natl Acad Sci USA 97:7609–7614
Steiner RA, Hohmann JG, Holmes A, Wrenn CC, Cadd G, Juréus A, Clifton DK, Luo M, Gutshall M, Ma SY, Mufson EJ, Crawley JN (2001) Galanin transgenic mice display cognitive and neurochemical deficits characteristic of Alzheimer's disease. Proc Natl Acad Sci USA 98:4184–4189
Strazielle C, Sturchler-Pierrat C, Staufenbiel M, Lalonde R (2003) Regional brain cytochrome oxidase activity in β-amyloid precursor protein transgenic mice with the Swedish mutation. Neuroscience 118:1151–1163
Sturchler-Pierrat C, Abramowski D, Duke M, Wiederhold KH, Mistl C, Rothacher S, Ledermann B, Bürki K, Frey P, Paganetti PA, Waridel C, Calhoun ME, Jucker M, Probst A, Staufenbiel M, Sommer B (1997) Two amyloid precursor protein transgenic mouse models with Alzheimer disease-like pathology. Proc Natl Acad Sci USA 84:13287–13292
Tanemura K, Akagi T, Murayama M, Kikuchi N, Murayama O, Hashikawa T, Yoshiike Y, Park JM, Matsuda K, Nakao S, Sun Y, Sato S, Yamaguchi H, Takashima A (2001) Formation of filamentous tau aggregations in transgenic mice expressing V337M human tau. Neurobiol Dis 8:1036–1045
Tanemura K, Murayama M, Akagi T, Hasikawa T, Tominaga T, Ichikawa M,Yamaguchi H, Takashima A (2002) Neurodegeneration with tau accumulation in a transgenic mouse expressing V337M human tau. J Neurosci 22:133–141
Tatebayashi Y, Miyasaka T, Chui DH, Akagi T, Mishima KI, Iwasaki K, Fujiwara M, Tanemura K, Murayama M, Ishiguro K, Planel E, Sato S, Hashikawa T, Takashima A (2002) Tau filament formation and associative memory deficit in aged mice expressing human mutant (R406W) human tau. Proc Natl Acad Sci USA 99:13896–13901
Touma C, Ambrée O, Görtz N, Keyvani K, Lewejohann L, Palme R, Paulus W, Schwarze-Eicker K, Sachser N (2004) Age- and sex-dependent development of adrenocortical hyperactivity in a transgenic mouse model of Alzheimer's disease. Neurobiol Aging 25:893–904
Tremml P, Lipp HP, Müller U, Ricceri L, Wolfer DP (1998) Neurobehavioral development, adult open field exploration and swimming navigation learning in mice with a modified β-amyloid precursor protein gene. Behav Brain Res 95:65–76
Trinchese F, Liu S, Battaglia F, Walter S, Matthews PM, Arancio O (2004) Progressive age-related development of Alzheimer-like pathology in APP/PS1 mice. Ann Neurol 55:801–813
Van Dam D, Abramowski D, Staufenbiel M, de Deyn PP (2005) Symptomatic effect of donepezil, rivastigmine, galantamine and memantine of cognitive deficits in the APP23 model. Psychopharmacology 180:177–190
Van Leuwen F (2000) Single and multiple transgenic mice as models for Alzheimer's disease. Prog Neurobiol 61:305–312
Xu PT, Schmechel D, Qiu HL, Herbstreith M, Rothrock-Christian T, Eyster M, Roses AD, Gilbert JR (1999) Sialylated human apolipoprotein E (apoEs) is preferentially associated with neuron-enriched cultures from APOE transgenic mice. Neurobiol Dis 6:63–75
Zong P, Gu Z, Wang X, Jiang H, Feng J, Yan Z (2003) Impaired modulation of GABAergic transmission by muscarinic receptors in a mouse transgenic model of Alzheimer's disease. J Biol Chem 278:26888–2696

F.4.5 Studies in Invertebrate Animals

F.4.5.1 Studies in Caenorhabditis Elegans

The worm *Caenorhabditis elegans* has been recommended as a model of human disease (Baumeister 2002). Link (2001, 2005) reviewed invertebrate models of Alzheimer's disease with special emphasis on *Caenorhabditis elegans.*

Link et al. (2001) reported visualization of fibrillar amyloid deposits in living, transgenic *Caenorhabditis elegans* animals using the sensitive amyloid dye X-34.

Drake et al. (2003) found that oxidative stress precedes fibrillar deposition of Alzheimer's disease amyloid β-peptide (1–42) in a transgenic *Caenorhabditis elegans* model.

Link et al. (2003) described gene expression analysis in a transgenic *Caenorhabditis elegans* Alzheimer's disease model. Transgenic *Caenorhabditis elegans* animals were engineered to inducibly express the human beta amyloid peptide.

Strayer et al. (2003) reported that expression of the small heat-shock protein Hsp16–2 in *Caenorhabditis elegans* is suppressed by *Ginkgo biloba* extract EGb 761.

REFERENCES AND FURTHER READING

Baumeister R (2002) The worm in us – *Caenorhabditis elegans* as a model of human disease. Trends Biotechnol 20:147–148

Drake J, Link CD, Butterfield DA (2003) Oxidative stress precedes fibrillar deposition of Alzheimer's disease amyloid β-peptide (1–42) in a transgenic *Caenorhabditis elegans* model. Neurobiol Aging 24:415–420

Link CD (2001) Transgenic invertebrate models of age-associated neurodegenerative diseases. Mech Ageing Dev 122:1639–1649

Link CD (2005) Invertebrate models of Alzheimer's disease. Genes Brain Behav 4:147–156

Link CD, Jahnson CJ, Fonte V, Paupard MC, Hall DH, Styren S, Mathis CA, Klunk WE (2001) Visualization of fibrillar amyloid deposits in living, transgenic *Caenorhabditis elegans* animals using the sensitive amyloid dye, X-34. Neurobiol Aging 22:217–226

Link CD, Taft A, Kapulkin V, Duke K, Kim S, Fei Q, Wood DE, Sahagan BG (2003) Gene expression analysis in a transgenic *Caenorhabditis elegans* Alzheimer's disease model. Neurobiol Aging 24:397–413

Strayer A, Wu Z, Christen Y, Link CD, Luo Y (2003) Expression of the small heat-shock protein Hsp16–2 in *Caenorhabditis elegans* is suppressed by *Ginkgo biloba* extract EGb 761. FASEB J 17:2305–2307

F.4.5.2 Studies in Drosophila

Götz et al. (2004) reviewed transgenic animal models of Alzheimer's disease and related disorders mentioning mice, fish (*Petromyzon marinus*, the sea lamprey), worms (*Caenorhabditis elegans*), and flies (*Drosophila melanogaster*).

Ferber (2001) recommended using the fruit fly to model tau malfunction.

Shulman and Feany (2003) conducted a genetic modifier screen in a *Drosophila* model of taupathy to investigate the molecular mechanisms responsible for Tau-induced neurodegeneration.

Finelli et al. (2004) showed that overexpression of Aβ42 peptides in the nervous system of *Drosophila melanogaster* results in phenotypes associated with neuronal degeneration in a dose- and age-dependent manner.

Crowther et al. (2004) reported that transgenic flies expressing the toxic β-amyloid develop neurodegeneration. The flies exhibit a clear phenotype from a few days of age, including reduced locomotor function, impaired olfactory memory and shortened lifespan. Therapeutic agents that interfere with the generation of toxic aggregates of β-amyloid peptides have been shown to rescue the flies. *Drosophila* is recommended as a model of Alzheimer's disease.

Iijima et al. (2004) used the *Drosophila* model to compare the specific pathological roles of human Aβ40 and Aβ42 in Alzheimer's disease.

Nichols (2006) published a survey on *Drosophila melanogaster* neurobiology, neuropharmacology, and how the fly can inform central nervous system drug discovery.

REFERENCES AND FURTHER READING

Crowther DC, Kinghorn KJ, Page R, Lomas DA (2004) Therapeutic targets from a *Drosophila* model of Alzheimer's disease. Curr Opin Pharmacol 4:513–516

Ferber D (2001) Neurodegenerative disease: using the fruit fly to model tau malfunction. Science 292:1983–1984

Finelli A, Kelkar A, Song HJ, Yang H, Konsolaki M (2004) A model for studying Alzheimer's Aβ42-induced toxicity in *Drosophila melanogaster*. Mol Cell Neurosci 26:365–375

Götz J, Streffer JR, David D, Schild A, Hoerndli F, Pennanen L, Kurosinski P, Chen F (2004) Transgenic animal models of Alzheimer's disease and related disorders: histopathology, behavior and therapy. Mol Psychiatry 9:664–683

Iijima K, Liu HP, Chiang AS, Hearn SA, Konsolaki M, Zhong Y (2004) Dissecting the pathological effects of human Aβ40 and Aβ42 in *Drosophila*: a potential model for Alzheimer's disease. Proc Natl Acad Sci USA 101:6623–6628

Nichols CD (2006) *Drosophila melanogaster* neurobiology, neuropharmacology, and how the fly can inform central nervous system drug discovery. Pharmacol Ther 112:677–700

Shulman JM, Feany MB (2003) Genetic modifiers of taupathy in *Drosophila*. Genetics 165:1233–1242

Chapter G
Effects On Peripheral Nerve Function

G.1 Local Anesthetic Activity

G.1.0.1 General Considerations

One 1′ has to generally distinguish between conduction anesthesia, infiltration anesthesia, and surface anesthesia (Fromherz 1922; Schaumann 1938), and special pharmacological tests have been developed for each of these.

The mode of action of local anesthetics has been reviewed by Ritchie and Greengard (1966), Ritchie (1971), Borchard (1977), Steiner (1978), Butterworth and Strichartz (1990).

REFERENCES AND FURTHER READING

Borchard U (1979) Studies on the action mechanism and pharmacological characterization of local anesthetics. Habilitation Thesis of the High Faculty of Medicine of the University of Duesseldorf for Attainment of venia legendi. (Untersuchungen zum Wirkungsmechanismus und zur pharmakologischen Charakterisierung von Lokalanaesthetika. Habilitationsschrift Universität Düsseldorf)

Butterworth JF, Strichartz GR (1990) Molecular mechanisms of local anesthesia. Anesthesiol 72:711–734

Camougis G, Takman BH (1971) Nerve and nerve-muscle preparations (as applied to local anesthetics) In: Schwartz A (ed) Methods in Pharmacology, Vol 1, Appleton-Cen-

tury-Crofts, Educational Division, Meredith Corp., New York. pp 1–40
Fromherz K (1922) Über die Wirkung verschiedener Gruppen der Lokalanästhetika im Lichte verschiedener Untersuchungsmethoden. Naunyn-Schmiedeberg's Arch exp Path Pharmakol 93:72–91
Ritchie JM (1971) The mechanism of action of local anesthetic agents. In: Radouco-Thomas C (ed) International Encyclopedia of Pharmacology and Therapeutics. Section 8: Local Anesthetics. (P Lechat, Section editor), Vol 1, pp 131–166, Pergamon Press, Oxford New York
Ritchie JM, Greengard P (1966) On the mode of action of local anesthetics. Ann Rev Pharmacol 6:405–430
Schaumann O (1938) Chemie und Pharmakologie der Lokalanaesthetica. Naunyn-Schmiedeberg's Arch exp Path Pharmakol 190:30–51
Steiner R (1978) Zur Pharmakodynamik der Lokalanästhetika. In: Lokalanästhesie (Ahnefeld FW, Bergmann H, Burri C, Dick W, Halm\'agyi M, Hossli G, Rügheimer R, eds) Springer-Verlag Berlin Heidelberg New York, pp 17–23

G.1.1
Conduction Anesthesia

G.1.1.1
Conduction Anesthesia in the Sciatic Nerve of the Frog

PURPOSE AND RATIONALE

Based on earlier studies by Sollmann (1918), Fromherz (1922), Fußgänger and Schaumann (1931), and Bülbring and Wajda (1945) on plexus anesthesia in frogs, Ther (1953a, b, 1958) described a method for conduction anesthesia of the sciatic nerve in frogs.

PROCEDURE

Frogs (*Rana temporaria*) of either sex are used and are kept at 4°C. The frog is decapitated with a pair of scissors. The skin is incised in the thigh region at both sides and the sciatic nerves are carefully exposed in the thigh, avoiding any stretching and injury of the nerve. The frog is suspended on a vertical board. Small pieces of white cotton are soaked with different concentrations of the test preparations (between 0.05% and 1%) or the standard and placed gently around the sciatic nerve for 1 min. Then the cotton swab is removed and the frog is placed with its extremities into a bath with 0.65% NaCl solution. This allows testing for duration and reversibility of the local anesthetic effect. One side is used for the test preparation and the other for the standard (e. g., 0.25% butanilicaine). Every 3 min the frog is removed from the bath and the toes of the legs or the ankle joint are pinched three times with a small forceps. The reflex contraction is abolished when conduction anesthesia is effective. The stimuli are repeated every 3 min until anesthesia vanishes. Two to 5 frogs are used for each concentration.

EVALUATION

Time of onset and duration of anesthesia are recorded for each concentration. Time-response and dose-response curves can be established.

MODIFICATIONS OF THE METHOD

In the original method by Bülbring and Wajda (1945) the frogs were decapitated and the upper part of the spinal cord was destroyed down to the level of the third vertebra. The viscera are removed exposing the lumbar plexus without damaging it. The frog was pinned to a vertical board and the solution of the local anesthetic dissolved in 0.7% saline is put into the pocket formed by the lower abdomen. Different concentrations of HCl are used as stimuli into which the feet of the frog were immersed every min.

Idänpään-Heikkilä and Guilbaud (1999) used a **rat** model of trigeminal neuropathic pain where the neuropathy is produced by a chronic constriction injury of the infra-orbital branch of the trigeminal nerve, and studied the effects of various drugs on this purely sensory model of neuropathic pain (see H.1.2.11)

For mechanical stimulation, a graded series of ten of von Frey filaments with a bending force between 0.217 and 12.5 g was used. The stimuli were applied within the infra-orbital nerve territory, near the center of the vibrissal pad, on the hairy skin surrounding the mystacial vibrissae. Local injection of an local anesthetic (articaine) into the rostral orbital cavity of the lesioned side, into the close proximity of the ligated infra-orbital nerve increased the mechanical threshold to the upper level. The duration of the effect was dose-dependent.

REFERENCES AND FURTHER READING

Bülbring E, Wajda I (1945) Biological comparison of local anesthetics. J Pharmacol Exp Ther 85:78–84
Camougis G, Takman BH (1971) Nerve and nerve-muscle preparations (as applied to local anesthetics) In: Schwartz A (ed) Methods in Pharmacology, Vol 1, pp 1–40. Appleton-Century-Crofts, Educational Division, Meredith Corp., New York
Fromherz K (1922) Über die Wirkung verschiedener Gruppen der Lokalanästhetika im Lichte verschiedener Untersuchungsmethoden. Naunyn-Schmiedeberg's Arch exp Path Pharmakol 93:72–91
Fußgänger R, Schaumann O (1931) Über ein neues Lokalanästhetikum der Novokainreihe (Pantokain). Naunyn-Schmiedeberg's Arch exp Path Pharmakol 160:53–65
Idänpään-Heikkilä JJ, Guilbaud G (1999) Pharmacological studies on a rat model of trigeminal neuropathic pain: baclofen, but not carbamazepine, morphine or tricyclic antidepressants, attenuates the allodynia-like behaviour. Pain 79:281–290
Muschaweck R, Rippel R (1974) Ein neues Lokalanästhetikum (Carticain) aus der Thiophenreihe. Prakt Anästh 9:135–146

Muschaweck R, Habicht R, Rippel R (1986) Lokalanaesthetica. In: Ehrhart G, Ruschig H (eds) Arzneimittel. Entwicklung – Wirkung – Darstellung. Verlag Chemie GmbH, Weinheim. pp 1–44

Sollmann T (1918) Comparative activity of local anesthetics. II. Paralysis of sensory fibres. J Pharmacol Exp Ther 11:1–7

Ther L (1953a) Zur Prüfung der lokalanästhetischen Wirkung des Pantocain und des 4-n-Butylaminosalicylsäuredimethylaminoaethylesters im Tierversuch. Arzneim Forsch 3:345–348

Ther L (1953b) Über ein neues Leitungsanaesthetikum der "Nirvanin"-Reihe mit großer Entgiftungsgeschwindigkeit (Hostacain). Naunyn Schmiedeberg's Arch exper Path Pharmakol 220:300–316

Ther L (1958) Zur pharmakologischen Beurteilung von lokalanaesthetisch wirksamen Substanzen unter besonderer Berücksichtigung ihrer Entgiftung. Medizin und Chemie 6:399–410

G.1.1.2 Conduction Anesthesia in the Sciatic Nerve of the Rat

PURPOSE AND RATIONALE

Based on earlier studies (Truant 1958; Truant and Wiedling 1958/59, Åström and Persson 1961) Camougis and Takman (1971) have written a detailed description for testing conduction anesthesia of the sciatic nerve in the rat.

PROCEDURE

Male Wistar or Sprague Dawley rats weighing 125 to 175 g are used. The animal is suspended in a prone position by grasping the base of the tail and thoracic cage. A hind limb is extended to its full length and the depression for needle insertion is located by palpation with the left index finger. The site of injection is the area under the skin at the junction of the biceps femoris and the gluteus maximus muscles. The sciatic nerve is blocked in the midthigh region with 0.2 ml of the drug solution administered by a 24- to 25-gauge needle attached to a 0.25 ml tuberculin syringe. Usually a 1% solution of the test drug in 0.9% NaCl is used as a test solution. The other leg is used for a control drug (e. g., procaine or lidocaine). Immediately after the injection, repeated checks of the digit of the foot and the walking behavior are performed. In the normal foot, the digits are wide apart, while in the blocked leg the digits of the foot are close together. Also the successful block is evidenced by dragging of the leg and an inability of the animal to use the leg in walking up the inclined wire mesh cover of the cage. After the time of block for each leg is noted, each animal is examined every 5 to 10 min in order to note the time of recovery.

EVALUATION

From the data, averages for onset and duration of action are calculated, plus the frequency of blocks are noted. Using various doses of test compound and standard, dose-response curves can be established and potency ratios calculated.

MODIFICATIONS OF THE METHOD

With a similar technique Lembeck (1953) tested the effect of the added vasoconstringent agents adrenaline, noradrenaline and Corbasil to procaine.

Sciatic nerve blockade in the **rat** was used by Feldman and Covino (1988) to study comparative motor-blocking effects of bupivacaine and ropivacaine.

Grant et al. (1992) used a **rat** sciatic nerve model for independent assessment of sensory and motor block induced by local anesthetics. Motor block was assessed by measuring hind paw grip strength with a dynamometer. Sensory block was determined by measuring hind paw withdrawal latency from radiant heat.

Kohane et al. (1998) studied sciatic nerve blockade with ropivacaine and bupivacaine in infant, adolescent, and adult **rats**. Rats were anesthetized briefly with halothane by face mask. The sciatic block was conducted by introducing a 30-gauge needle posteromedially to the greater trochanter, pointing in an anteromedial direction. Once bone was contacted, the needle was withdrawn 1 mm and drug was injected. Nerve blockade was assessed by withdrawal of the hind leg after pinching the lateral aspect of the plantar surface, by a modified hot-plate test, by the positional placing response as a test of proprioception, by extensor postural thrust as a measure of motor strength, and by ability to hop. Thermal latency in the contralateral (uninjected) limb was determined as a measure of systemic toxicity.

Grant et al. (2001) tested perineural antinociceptive effects of opioids in a **rat** model. Analgesia was assessed using the hind paw latency response to radiant heat.

Luduena and Hoppe (1952) used **guinea pigs** to test sciatic nerve block by local anesthetics. The anesthetic solutions were injected close to the sciatic nerve. Sensory paralysis was determined by pricking the posterior site of the thigh with a needle. The effect on motor nerve fibers was determined by observing the abnormal position of the injected leg in locomotion.

Siems and Soehring (1952) described a model in **guinea pigs** resembling peridural and paravertebal anesthesia in man.

Åkerman et al. (1988) used **guinea pigs** to determine brachial plexus block. The syringe was directed towards a line between the head of the humerus and the manubrium of the sternum and the first ribs. The

needle was inserted about 1.5 cm into the pocket felt as a depression by palpation between the head of the humerus and sternum and associated structures. Following retraction of the needle by a few millimeters, 0.2 ml of the solution was injected. The orientation of the needle was changed 3–4 times during the injection to enable all branches of the plexus to be reached. Assessment was made of motor and sensory blockade.

Leszczynska and Kau (1992) used a sciatic nerve blockade method in **mice** to differentiate drug-induced local anesthesia from neuromuscular blockade. The drugs were injected into the popliteal space of the right hind-limb. A positive local anesthetic activity was recorded when a mouse was only able to walk using three limbs on an inverted wire mesh screen and the injected limb was hanging in the air. A positive neuromuscular blockade was recorded when a mouse could walk normally on the top of the wire mesh screen but was unable to stay on the inverted screen.

Thut et al. (1995) used the **rabbit** tooth-pulp assay (see H.1.2.8) to quantify efficacy and duration of antinociception by local anesthetics infiltrated into maxillary tissues.

Rosenberg and Heinonen (1983) found a differential sensitivity of A and C nerve fibers to long-acting local anesthetics.

The Local Anesthetics for Neuralgia Study Group (1994) designed a surgically implantable nerve irrigation system for intermittent delivery of local anesthetics and evaluated long-term performance and histocompatibility in rats.

REFERENCES AND FURTHER READING

Åkerman B, Hellberg IB, Trossvik C (1988) Primary evaluation of the local anesthetic properties of the amino amide agent ropivacaine (LEA 103). Acta Anesthesiol Scand 32:571–578

Åström A, Persson NH (1961) Some pharmacological properties of o-methyl-α-propyl-amino-propionanilide, a new local anesthetic. Br J Pharmacol 16:32–44

Camougis G, Takman BH (1971) Nerve and nerve-muscle preparations (as applied to local anesthetics) In: Schwartz A (ed) Methods in Pharmacology, Vol 1, pp 1–40. Appleton-Century-Crofts, Educational Division, Meredith Corp., New York

Feldman HS, Covino BG (1988) Comparative motor-blocking effects of bupivacaine and ropivacaine, a new amino amide local anesthetic, in the rat and dog. Anesth Analg 67:1047–1052

Grant GJ, Vermeulen K, Zakowski MI, Sutin KM, Ramanathan S, Langerman L, Weisman TE, Turndorf H (1992) A rat sciatic nerve model for independent assessment of sensory and motor block induced by local anesthetics. Anesth Analg 75:889–894

Grant GJ, Vermeulen K, Zakowski MI, Langerman L (2001) Perineural antinociceptive effects of opioids in a rat model. Acta Anaesthesiol Scand 45:906–910

Kohane DS, Sankar WN, Shubina M, Hu D, Rital N, Berde CB (1998) Sciatic nerve blockade in infant, adolescent, and adult rats. A comparison of ropivacaine with bupivacaine. Anesthesiology 89:1199–1208

Lembeck F (1953) Adrenalin, Noradrenalin und Corbasil als Zusatz zu Novocain. Arch exp Path Pharmacol 217:274–279

Leszczynska K, Kau ST (1992) A sciatic nerve blockade method to differentiate drug-induced local anesthesia from neuromuscular blockade in mice. J Pharm Toxicol Meth 27:85–93

Luduena FP, Hoppe JO (1952) Local anaesthetic activity, toxicity and irritancy of 2-alkoxy analogs of procaine and tetracaine. J Pharm Exp Ther 104:40–53

Markham A, Faulds D (1996) Ropivacaine. A review of its pharmacology and therapeutic use in regional anaesthesia. Drugs 52:429–449

Rosenberg PH, Heinonen E (1983) Differential sensitivity of A and C nerve fibres to long-acting local anaesthetics. Br J Anaesth 55:163–167

Siems KJ, Soehring K (1952) Die Ausschaltung sensibler Nerven durch peridurale und paravertebrale Injektion von Alkylpolyäthylenoxyd-äthern bei Meerschweinchen. Arzneim Forsch 2:109–111

The Local Anesthetics for Neuralgia Study Group (Riopelle JM, Coordinator) (1994) A surgically implantable nerve irrigation system for intermittent delivery of dissolved drugs: evaluation of long-term performance and histocompatibility in rats. J Pharmacol Toxicol Meth 31:221–232

Thut PD, Turner MD, Cordes CT, Wynn RL (1995) A rabbit tooth-pulp assay to quantify efficacy and duration of antinociception by local anesthetics infiltrated into maxillary tissues. J Pharmacol Toxicol Meth 33:231–236

Truant AP (1958) Studies on the pharmacology of meprylcaine (Oracaine), a local anesthetic. Arch Int Pharmacodyn 115:483–497

Truant AP, Wiedling S (1958/59) A contribution to the pharmacological and toxicological evaluation of a new local anaesthetic, dl-N-methylpipecolyl-2,6-xylidide. Acta Chir Scand 116:351–361

G.1.1.3 Conduction Anesthesia on the Mouse Tail

PURPOSE AND RATIONALE

The radiant heat method as being used for evaluation of systemic analgesic activity (D'Armour et al. 1941; Ther et al. 1963; Grant et al. 1993) can also be used for determination of conduction anesthesia by injecting the local anesthetic into the root of the tail.

PROCEDURE

Groups of 10 mice (NMRI-strain) of both sexes with a weight between 18 and 22 g are used for each dose. Before administration of the test compound or the standard the normal reaction time is determined. The animal is placed into a small cage with an opening for the tail at the rear wall. The tail is hold gently by the investigator. By opening of a shutter, a light beam exerting radiant heat is directed to the proximal third of the tail. After about 6 s, the reaction of the animal is

observed by the investigator. The mouse tries to pull the tail away and turns the head. The shutter is closed with a switch when the investigator notices this reaction. Mice with a reaction time of more than 6 s are not used in the test.

The test compounds and the standard are injected in a volume of 0.1 ml on both sides in the area of the tail root. The animals are submitted to the radiant heat again after 10 min. The area of heating is about 1.5 cm distal to the injection site. For each individual animal the reaction time is noted.

EVALUATION

There are two possibilities for evaluation:

1. The average values of reaction time after each time interval are calculated and compared with the pretest value by analysis of significance.
2. At each time interval only those animals which show a reaction time twice as high or higher as the pretest value are regarded as positive. Percentages of positive animals are counted for each time interval and each dose and ED_{50} values are calculated according to LITCHFIELD and WILCOXON.

MODIFICATIONS OF THE METHOD

Bianchi (1956) used the tail-clip method of Haffner (1929) as a simple quantitative method for testing local anesthetics. Fully grown albino **mice** of either sex were used. A small artery clip with its blades covered by thin rubber tube was applied to the root of the tail. Those animals that did not show the pain reflex (the mice turn again and again trying to remove the clip) within 30 s were eliminated. The remainder received subcutaneously, about 1 cm from the root of the tail, 0.1 ml of the solution of drug. The pain reflex is tested 15 min after injection, applying the stimulus to the zone where the compound was injected. The proportion of animals that proved to be anesthetized was noted for each dose.

Saxen et al. (1993) and Smith (1997) described the mouse paw withdrawal assay: a method for determining the potency and duration of the effect of local anesthetics in mice. A standard rodent tail-flick apparatus was used to stimulate the dorsal skin of each hind paw in the mouse. The radiant heat intensity of the lamp was adjusted to yield hind paw withdrawal latencies of 6–8 s, with a 20-s cut-off time to prevent tissue damage. Testing was performed by gently restraining the animal in a small towel and passively placing one hind paw on the stage so that the animal was free to withdraw its paw from the stimulus without restriction. Paws were tested in alternative order (right, then left; left, the right, etc.) to minimize procedural bias. The individual left and right paw withdrawal latency times were determined in each mouse and the difference between left and right latencies were calculated. Paw withdrawal time difference was calculated by subtracting the experimentally modified paw withdrawal latency from the control paw latency.

Grant et al. (1993) quantified the duration of the local anesthetic-induced conduction block in the mouse using the tail flick test.

Grant et al. (1994) studied prolonged analgesia with liposomal bupivacaine in mice using the tail flick test.

The tail flick procedure using **rats** as test animals has been proposed by Herr et al. (1953).

Madan et al. (1970) determined conduction anesthesia by a tail-pinch technique in rats. The local anesthetic was injected subcutaneously bilaterally at the root of the tail. The test for local anesthesia was begun 15 min after injection by pinching with a polyethylene sheathed artery forceps and repeated every 15 min. The number of animals failing to remove the forceps by biting was recorded.

Kamerling et al. (1985) described a method for studying cutaneous pain perception and analgesia in **horses**. This method was used by Harkins et al. (1996, 1997) for determination of highest no effect dose (HNED) for local anesthetic responses to procaine, cocaine, bupivacaine, benzocaine and of a plant extract. A heat projection lamp was used as noxious stimulus directed onto the pastern to elicit a flexion-withdrawal reflex. Hoof withdrawal latency was defined as the time between lamp illumination and withdrawal of the hoof. The local anesthetic drugs were injected into the area of the palmar nerve where it passes lateral to the sesamoid bone.

REFERENCES AND FURTHER READING

Bianchi C (1956) A simple new quantitative method for testing local anaesthetics. Br J Pharmacol 11:104–106

D'Amour FE, Smith DL (1941) A method for determining loss of pain sensation. J Pharmacol Exp Ther 72:74–79

Grant GJ, Zakowski MI, Vermeulen K, Langerman L, Ramanathan S, Turndorf H (1993) Assessing local anesthetic effect using the mouse tail flick test. J Pharm Toxicol Meth 29:223–226

Grant GJ, Vermeulen K, Langerman L, Zakowski M, Turndorf H (1994) Prolonged analgesia with liposomal bupivacaine in a mouse model. Reg Anesth 19:264–269

Haffner F (1929) Experimentelle Prüfung schmerzstillender Mittel. Dtsch Med Wschr 55:731–733

Harkins JD, Mundy GD, Stanley S, Woods WE, Rees WA, Thompson KN, Tobin T (1996) Determination of highest no effect dose (HNED) for local anaesthetic responses to procaine, cocaine, bupivacaine and benzocaine. Equine Vet J 28:30–37

Harkins JD, Mundy GD, Stanley S, Sams RA, Tobin T (1997) Lack of local anaesthetic efficacy of Sarapin in the abaxial sesamoid block. J Vet Pharmacol Ther 20:229–232
Herr F, Nyiri M, Pataky G (1953) Messung der Leitungs- und Infiltrationsanästhesie an Ratten mit einer neuen Methode. Naunyn-Schmiedeberg's Arch exp Path Pharmakol 217:207–216
Kamerling SG, Weckman TJ, Dequick DJ,Tobin T (1985) A method for studying cutaneous pain perception and analgesia in horses. J Pharmacol Meth 13:267–274
Madan BR, Madan V, Pendse VK, Gupta RS (1970) A study of the antiarrhythmic and local anaesthetic actions of phencarbamide. Arch Int Pharmacodyn 185:53–65
Saxen MA, Welch SP, Dewey WL (1993) The mouse paw withdrawal assay: a method for determining the effect of calcitonin gene-related peptide on cutaneous heat nociception latency time. Life Sci 53:397–405
Smith FL (1997) Regional cutaneous differences of bupivacaine local anesthesia in mice. Life Sci 60:1613–1621
Ther L (1953a) Zur Prüfung der lokalanästhetischen Wirkung des Pantocain und des 4-n-Butylaminosalicylsäuredimethylaminoaethylesters im Tierversuch. Arzneim Forsch 3:345–348
Ther L (1953b) Über ein neues Leitungsanaesthetikum der "Nirvanin"-Reihe mit großer Entgiftungsgeschwindigkeit (Hostacain). Naunyn Schmiedeberg's Arch exper Path Pharmakol 220:300–316
Ther L, Lindner E, Vogel G (1963) Zur pharmakodynamischen Wirkung der optischen Isomeren des Methadons. Dtsch Apoth Ztg 103:514–520
Wiedling S (1964) Xylocaine. The pharmacological basis of its clinical use. Almqvist & Wiksell, Stockholm, Göteborg, Uppsala. pp 27–46

G.1.1.4 Rabbit Tooth Pulp Assay

PURPOSE AND RATIONALE

The rabbit tooth-pulp assay (see H.1.2.8) has been used successfully to evaluate the potency, efficacy, and duration of antinociception of analgesics (Yim et al. 1955; Piercey and Schroeder 1980; Wynn et al. 1984). Thut et al. (1995) described a method for administration of local anesthetic drugs to the maxillary arch of rabbits and subsequent measurement of antinociceptive action.

PROCEDURE

Pulp chambers are exposed close to the facial gingival line of the two central incisors in New Zealand White male rabbits (1.5–2.0 kg) using a high-speed dental drill and 0.5-mm round burr immediately after the i.v. administration of 30 mg/kg ketamine. All experiments are conducted 48 h or more after pulp exposure. A linear ramp function stimulator is used as the direct current voltage source. The rabbit is slightly restrained, and the current is applied to the pulp via fine-wire platinum electrodes held in each of the cavities. Linearly rising voltage is applied at a rate of 0.33 V/s until a patterned lick-chew response occurs. Mean threshold voltages are established for controls using an average of 3 determinations, and then obtained after treatment using a single determination up to a maximum of 10 V. Rabbits having control values greater than 3 V are excluded from the study. The injection site of the test drug is 1.5 cm posterior to the central incisors and 4 mm below the roof of the maxillary buccal vestibule. The buccal vestibule is the area where the cheek and the top of the maxillary tissue join. The tip of a 27-Ga × 1/2″ syringe needle is inserted until it contacts the cancellous bone. The volume of injection is 0.4 ml. Injections are made bilaterally so that the total volume injected is 0.8 ml. The animals can be used chronically, but no rabbit should be exposed to the same drug or the same dose more than once, and non should be injected more frequently than very third day. One animal is used per dosage when analgesia is observed to be either 0% or 100%. Two or 3 animals are used for dosages with effects between 0% and 100%. When more than one animal is used, data are averaged and treated as a single observation. Pulp chambers have to be re-exposed when the drilled openings disappear because of incisor growth (approximately after 3 weeks).

EVALUATION

The percentage of maximum effect (*MPE*) for each observation time is calculated from the following equation:

$$MPE = (TV - CV)/(10V - CV) \times 100$$

TV is the voltage after treatment, *CV* is the control voltage, and *10V* are the maximum volts applied. The voltage that elicits the response is recorded at zero time and 5, 10, 15, 30, 60, 120, and 180 min after injection. The *MPE* is calculated for each observation time. Graphs of the *MPE* values versus time are constructed, and the maximal effect and time of the maximal effect are recorded. Further, the duration of each dosage is defined as the length of time that that dose achieved a *MPE* greater than 25%. Data are regressed between observed time points to provide estimates of the time when 25% *MPE* is first achieved and also the time when 25% *MPE* is no longer observed. A computer program or the standard method of Litchfield and Wilcoxon (1949) can be used to calculate ED_{50}, ED_{90}, and ED_{95} values with 95% confidence limits.

REFERENCES AND FURTHER READING

Litchfield JT Jr, Wilcoxon F (1949) A simplified method of evaluating dose-effect experiments. J Pharmacol Exp Ther 96:99–113

Piercey MF, Schroeder LA (1980) A quantitative analgesic assay in the rabbit based on response to tooth pulp stimulation. Arch Int Pharmacodyn Ther 248:294–304
Thut PD, Turner MD, Cordes CT, Wynn RL (1995) A rabbit tooth-pulp assay to quantify efficacy and duration of antinociception by local anesthetics infiltrated into maxillary tissue. J Pharmacol Toxicol Meth 33:231–236
Wynn RL, El'Baghdady YM, Ford RD, Thut PD, Rudo FG (1984) A rabbit tooth-pulp assay to determine ED_{50} values and duration of action of analgesics. J Pharmacol Meth 11:109–117
Yim GKW, Keasling HH, Gross EG, Mitchell CW (1955) Simultaneous respiratory minute volume and tooth pulp threshold changes following levorphan, morphine and levorphan-levallorphan mixtures in rabbits. J Pharmacol Exp Ther 115:96–105

G.1.1.5 Infraorbital Nerve Block in the Rat

PURPOSE AND RATIONALE

Several authors have used the infraorbital nerve block in the rat to study the potency and duration of action of local anesthetics (Fink et al. 1975, 1978; Ready and Fink 1980; Buckley and Fink 1981; Buckley et al. 1985; Renck et al. 1988; Hassan et al. 1989, 1993).

PROCEDURE

Male Sprague-Dawley rats weighing 500–600 g are used. The infraorbital nerve of the rat is 2–3 mm in diameter and supplies the upper lip and whisker area. It is homologous with the infraorbital nerve in humans. Since the rat lacks a closed orbit, the nerve runs forward beneath the eye and emerges from the maxilla through a deep notch rather than a foramen. The animals are lightly anesthetized with intraperitoneal phenobarbitone 25 mg/kg. This degree of sedation abolishes the righting reflex but does not interfere with the generalized aversive response to pinching the upper lip with an artery forceps. Test solution (0.2 ml) is injected unilaterally on the right side. The intact left side serves as control for comparing the responses on the two sides. Only animals whose aversive response is abolished within 60 s of the time of injection are included in the study. The animals are tested at 5-min intervals thereafter until the first sign of return of the aversive response on the injected side. Ten animals are used for each concentration of each test compound.

EVALUATION

The incidence of blocks at each concentration is recorded. The duration of the analgesic block (± SD) is calculated for each concentration and each test compound.

MODIFICATIONS OF THE METHOD

Renck and Hassan (1992) tested analgesia of the upper lip by electrical stimulation using externally applied bipolar stimulatory electrodes (blunted 27-gauge hypodermic needles) connected to a constant current stimulator delivering one impulse per second of 0.24 ms duration.

REFERENCES AND FURTHER READING

Buckley FP, Fink BR (1981) Duration of action of nerve blocks produced by mixtures of local anesthetics and low molecular weight dextran: studies in rat infraorbital nerve blocks. Anesth Analg 60:142–145
Buckley FP, Duval Neto G, Fink BR (1985) Acid and alkaline solutions of local anesthetics: duration of nerve block and tissue pH. Anesth Analg 64:477–482
Fink BR, Aasheim G, Kish SJ, Croley TS (1975) Neurokinetics of lidocaine in the infraorbital nerve of the rat *in vivo*. Relation to sensory block. Anesthesiology 42:731–736
Fink BR, Aasheim G, Levy BA (1978) Neural pharmacokinetics of epinephrine. Anesthesiology 48:263–266
Hassan HG, Pilcher CW, Akerman B, Renck H (1989) Antinociceptive effects of localized administration of opioids compared with lidocaine. Reg Anesth 14:138–144
Hassan HG, Youssef H, Renck H (1993) Duration of experimental nerve block by combination of local anesthetic agents. Acta Anaesthesiol Scand 37:70–74
Ready LB, Fink BR (1980) Experimental evaluation of local anaesthetic solutions using rat infraorbital nerve block. Canad Anaesth Soc 27:58–61
Renck H, Hassan HG, Lindberg G, Akerman B (1988) Effects of macromolecular adjuvants on the duration of prilocaine. Experimental studies on the effect of variations of viscosity and sodium content and of inclusion of adrenaline. Acta Anaesthesiol Scand 32:355–364
Renck H, Hassan HG (1992) Epinephrine as an adjuvant to amino-amid local anesthetics does not prolong the duration of action in infraorbital nerve block in the rat. Acta Anaesthesiol Scand 36:387–392

G.1.1.6 Retrobulbar Block in Dogs

PURPOSE AND RATIONALE

Defalque and Stoelting (1976) published a method to determine latency and duration of action of local anesthetics after retrobulbar injection in dogs.

PROCEDURE

Young female mongrel dogs weighing 13–15 kg are used. Twenty-four h before the test, 0.25% eserine ointment is placed in each conjunctival sac of the dog. Pentobarbital (25 mg/kg) is administered intravenously, then repeated with 10 mg/kg at hourly intervals, thus maintaining the animal in light anesthesia (corneal reflex present). Ten min after induction, the dog is put into 30-degree head-down position, and 20 ml of 0.05% tetracaine is forced into the epidural

space through the interarcuate ligament. Horner's syndrome occurs within 5 min.

A 150-watt surgical lamp is now focused upon the eye from an 1 meter distance. Fifteen min later, a retrobulbar block is performed: The sclera is seized with an ophthalmic forceps and the eyeball is pulled downward and medially; a 23-gauge needle is then introduced through the superior rectus muscle, tangentially to the globe, and is immobilized as soon as a click indicates penetration of the retrobulbar space; correct placement is confirmed by free motion of the needle tip and protrusion-rotation of the eyeball upon injection of 1 ml of air.

After aspiration, 2 ml of the tested anesthetic is then injected at a rate of 0.5 ml per second. The pupil dilates and reaches its maximal diameter (6 mm) within a few minutes. This apparent diameter is estimated with a 2-cm long ruler calibrated in millimeters, whose center is gently applied to the corneal center. The pupil is measured every 15 s for 5 min, then every 5 min until reappearance of maximal miosis (pinpoint and asymmetrical), a precise endpoint which generally coincides with corneal reflex and lacrimation.

EVALUATION

Drug latency (in min) and duration (in 5-min units) are averaged for both eyes of each animal, and the mean and standard deviation then calculated for all test animals. Analysis of variance is performed to find significant differences between various local anesthetics.

REFERENCES AND FURTHER READING

Defalque RJ, Stoelting VK (1967) Latency and duration of action of common local anesthetics: an experimental evaluation. Anesth Analg 46:311–314

G.1.1.7 Isolated Sciatic Nerve Preparation of the Frog

PURPOSE AND RATIONALE

Isolated nerves are immersed between stimulating and recording electrodes in solutions containing local anesthetics which allows electrophysiological measurements (Paterson and Hamilton 1970).

PROCEDURE

A large frog is sacrificed by decapitation with a pair of scissors, and the spinal cord severed. The skin around the entire body in the region immediately posterior to the forelimbs is cut, and the abdomen and hind legs are skinned by peeling the skin in a posterior direction. The fat, muscles, and other tissues are cut at the posterior end of the body so as to expose the nerves extending posteriorly from the cord. The muscles of the thigh are cut and retracted so as to expose the sciatic nerve. Finally, the gastrocnemius muscle is removed and the peroneus muscle is extended laterally from the tibiofibula. The entire sciatic nerve with branches should now be exposed. A thread with a loop next to the nerve is tied around the nerve in the region of the sacral vertebra. The nerve is then cut anterior to the thread. During the isolation procedure the nerve is kept moist with frog Ringer solution. The connective tissue and the nerve branches are cut carefully. The nerve is finally cut near the distal end of the tibiofibula and extended on a filter paper previously soaked with Ringer solution. With the nerve anchored by the thread, the remaining connective tissue is peeled back toward the distal end of the nerve. Any remaining branches are cut at the point of their bifurcation. The distal end of the nerve is tied with a length of thread. The sciatic-peroneal nerve preparation is mounted in a nerve chamber for recording.

Electrodes for stimulation are placed on the proximal end of the nerve while recording electrodes are placed at the distal end. The nerve is immersed in a trough containing frog Ringer solution as bathing fluid. The stimuli are applied with a commercial stimulator (e. g., Grass Model S4) with a duration of 5 ms, a frequency between 30/s, and 1.5 to 15 mV. The recording electrodes are connected with an amplification and display system. Stimulation of the nerve produces a display on the oscilloscope. Adjusting the voltage setting on the stimulator will cause the action potential to increase and decrease correspondingly on the scope. After pinching the nerve between the last two recording sites, the action potential should be monophasic and appear entirely above the base line. The spike is observed periodically for several min to ascertain its stability.

The bathing trough is changed to a trough containing the local anesthetic dissolved in Ringer solution. At one or 2 min intervals the amplitude of the spike is read and recorded on a polygraph. After 5 min treatment, the drug trough is removed and the nerve is immersed in the Ringer solution of the bathing trough. Amplitudes are measured in periodic intervals and thus the recovery process is recorded.

EVALUATION

Block and recovery curves are achieved with various concentrations of the test compound and the standard. Dose-response curves can be obtained.

MODIFICATIONS OF THE METHOD

Specialized techniques with isolated nerves (desheathed nerves, equilibrium blocks, single nerve fibers) have been described by Camougis and Takman (1971).

Den Hertog (1974) used the **desheathed cervical vagus of the rabbit** mounted in a single sucrose gap apparatus and measured changes in the membrane potential and compound action potential. The ratio of the distance between stimulation and recording electrode (15 mm) and the time between stimulation of the nerve and the top of the action potential was taken as an index for the mean conduction velocity.

Salako et al. (1976) tested a new anti-arrhythmic drug as a local anesthetic on desheathed **frog** nerve.

Lee-Son et al. (1992) used the sucrose-gap method on desheathed isolated frog peripheral nerves to study the stereoselective inhibition of neuronal sodium channels by local anesthetics.

Lambert et al. (1994) studied the reversibility of conduction blockade in desheathed bullfrog sciatic nerves, using the sucrose gap method for recording compound action potentials, before and during exposure to local anesthetics and during drug washout.

Isolated nerves from other species have been used for the study of local anesthetics, such as those from rabbits by Ritchie et al. (1965a, b), or from rats by Condouris and Lagomarsino (1966), Štolc and Mai (1993).

Gissen et al. (1980) observed differential sensitivities of mammalian nerve fibers to local anesthetic agents in rabbits. A fibers were blocked at the lowest drug concentrations, the intermediate B fibers were blocked at a higher drug concentration, and the smallest, slowest-conducting C fibers required the highest drug concentration for conduction blockade.

Fink and Cairns (1984) showed differential slowing and block of conduction by lidocaine in individual afferent myelinated and unmyelinated axons in rabbits.

Åkerman et al. (1988) studied the block of evoked action potential in the isolated sheathed sciatic nerve of the frog for primary evaluation of a local anesthetic compound.

REFERENCES AND FURTHER READING

Åkerman B, Hellberg IB, Trossvik C (1988) Primary evaluation of the local anesthetic properties of the amino amide agent ropivacaine (LEA 103). Acta Anesthesiol Scand 32:571–578

Camougis G, Takman BH (1971) Nerve and nerve-muscle preparations (as applied to local anesthetics) In: Schwartz A (ed) Methods in Pharmacology, Vol 1, pp 1–40. Appleton-Century-Crofts, Educational Division, Meredith Corp., New York

Condouris GA, Lagomarsino WE (1966) Adrenalectomy in rats and its influence on local anesthesia of peripheral nerves. J Pharmacol Exp Ther 152:417–424

Den Hertog (1974) The effect of carticain on mammalian nonmyelinated nerve fibres. Eur J Pharmacol 26:175–178

Fink BR, Cairns AM (1984) Differential slowing and block of conduction by lidocaine in individual afferent myelinated and unmyelinated axons. Anesthesiology 60:111–120

Gissen AJ, Covino BG, Gregus J (1980) Differential sensitivities of mammalian nerve fibers to local anesthetic agents. Anesthesiology 53:467–474

Lambert LA, Lambert DH, Strichartz GR (1994) Irreversible conduction block in isolated nerve by high concentrations of local anesthetics. Anesthesiology 80:1082–1093

Lee-Son S, Wang HK, Concus A, Crill E, Strichartz G (1992) Stereoselective inhibition of neuronal sodium channels by local anesthetics. Anesthesiology 77:324–335

Paterson JG, Hamilton JT (1970) A nerve chamber bioassay of local anesthetic activity. Arch Int Pharmacodyn 183:360–390

Ritchie JM, Ritchie B, Greengard P (1965a) The active structure of local anesthetics. J Pharmacol Exp Ther 150:152–159

Ritchie JM, Ritchie B, Greengard P (1965b) The effect of the nerve sheath on the action of local anesthetics. J Pharmacol Exp Ther 150:160–164

Rud J (1961) Local anesthetics. An electrophysiological investigation of local anesthesia of peripheral nerves with special reference to xylocaine. Acta Physiol Scand 51, Suppl 178:1–169

Salako LA, Vaughan Williams EM, Wittig JH (1976) Investigations to characterize a new anti-arrhythmic drug, ORG 6001, including a simple test for calcium antagonism. Br J Pharmacol 57:251–262

Stämpfli R (1968) Voltage-Clamp-Analyse lokalanästhetischer Wirkungen am Ranvier'schen Schürring des Frosches. Naunyn-Schmiedeberg's Arch Pharmacol 260:P203–P204

Stämpfli R, Hille B (1976) Electrophysiology of the peripheral myelinated nerve. In: Llinás R, Precht W (eds) Frog Neurobiology. A Handbook. Springer Berlin, Heidelberg, New York. pp 3–32

Štolc S, Mai PM (1993) Comparison of local anesthetic activity of pentacaine (trapencaine) and some of its derivatives by three different techniques. Pharmazie 48:210–212

Truant AP (1965) Local anesthetic and toxicological properties of Citanest. Acta Anesth Scand Suppl XVI:19–22

Truant AP, Wiedling S (1958/59) A contribution to the pharmacological and toxicological evaluation of a new local anesthetic, dl-N-methylpipecolyl-2,6-xylidide. Acta Chir Scand 116:351–361

Weatherby JH (1964) Local anesthetics. In: Laurence DR, Bacharach AL (eds) Evaluation of Drug Activities: Pharmacometrics. Academic Press, London, New York, pp 205–214

G.1.1.8 Isolated Mammalian Sciatic Nerve Preparation

PURPOSE AND RATIONALE

Karlsson et al. (1994) tested the local anesthetic-like effects of an NK_1 receptor antagonist in a mammalian sciatic nerve preparation using guinea pigs.

PROCEDURE

Male guinea pigs weighing 250–400 are sacrificed and the sciatic-tibial nerves immediately excised and cleaned in buffer equilibrated with 95% O_2 + 5% CO_2 under a dissecting microscope. The nerve is mounted in a Plexiglas chamber consisting of three connecting wells. The central well is perfused with buffer at a rate of 5 ml/min and contained the grounding electrode (Ag/AgCl), the in- and outlet of the peristaltic pump driven perfusion system and a thermistor probe. The two lateral wells (one for stimulating, the other for recording) are filled with mineral oil. Stimulating and recording electrodes are made from bare platinum-iridium wire. The passages between the central and lateral wells are sealed with petroleum jelly. The length of the nerve exposed to the drug in the central well is 8 mm. The nerve chamber is kept at a temperature of 27.0 ± 0.5°C.

A constant current supramaximal stimulus of 50 µs duration is used throughout the experiment. The intensity of the stimulus is ten times greater than the threshold intensity required to elicit a compound action potential. Throughout the experiment the nerve is stimulated at the low frequency of 1/min to determine basal compound action potential amplitude. Once the response has stabilized, a single burst of pulses (pulse train duration 250 ms, at 40 Hz) is applied approximately 5 min before drug application (control train) and again after drug application to determine the extent of frequency dependent block. The compound action potentials are digitized with a computer interface and a software program and recorded on a PC. A two channel storage oscilloscope is used to follow the experiment and to automatically sample and calculate the amplitudes of the compound action potentials.

The drugs are dissolved in buffer and applied approximately 5 min after the control train. The development of basal block following drug application is followed with 0.0167 Hz stimulation. In the case of lidocaine, the maximal inhibition is reached 20–30 min after application. The basal block is allowed to reach equilibrium, which is defined as the condition in which the difference in amplitude between the first and the last of five consecutive responses is less than 1% of the control compound action potential amplitude obtained prior to drug application. To assess frequency dependent block, a second stimulus is given after equilibrium is reached. Once basal and frequency dependent block has been determined, the nerves are washed with fresh buffer.

EVALUATION

The magnitude of the basal block (%) is calculated by comparing the average peak amplitude of the last three compound action potentials with the average peak amplitude of the last three compound action potentials prior to drug application. Similarly, frequency dependent block is expressed in percent of the control train, and is effectively the basal block plus the additional decrease in compound action potential amplitude. Dose-response curves for the standard and the test drugs are constructed by plotting basal block and frequency dependent block against drug concentration. The pIC_{50} values (the negative logarithm of the molar concentration of the drug producing 50% inhibition of the compound action potential amplitude) are estimated by linear regression analysis of the results in the 10–90% interval of the dose-response curves.

The dose-response data obtained with the standard and the test drugs and the effect of a single concentration (0.5 mM) of all compounds on basal block and frequency dependent block are analyzed by ANOVA. The values of latency to the peak of compound action potential are analyzed by paired *t*-test.

MODIFICATIONS OF THE METHOD

Fink and Cairns (1984) studied differential slowing and block of conduction by lidocaine in individual afferent myelinated and unmyelinated axons.

REFERENCES AND FURTHER READING

Butterworth IVJF, Strichartz GR, (1990) Molecular mechanisms of local anesthesia: a review. Anesthesiology 72:711–734

Courtney KR, Kendig JJ, Cohen EN (1978) Frequency-dependent conduction block: the role of nerve impulse pattern in local anesthetic potency. Anesthesiology 48:11–117

Fink BR, Cairns AM (1984) Differential slowing and block of conduction by lidocaine in individual afferent myelinated and unmyelinated axons. Anesthesiology 60:11–120

Gissen AJ, Covine BG, Gregus J (1980) Differential sensitivities of mammalian nerves to local anesthetic agents. Anesthesiology 53:467–474

Karlsson U, Näsström J, Berge OG (1994) (±)-CP-96,345, an NK_1 receptor antagonist, has localanesthetic-like effects in a mammalian sciatic nerve preparation. Regulatory Peptides 52:39–46

Wildsmith JAW, Gissen AJ, Gregus J, Covino BG (1985) Differential nerve blocking activity of amino-ester local anaesthetics. Br J Anaesth 57:612–620

G.1.1.9 Effect of Local Anesthetics on Different Nerve Fibers

PURPOSE AND RATIONALE

Wildsmith et al. (1989) examined the *in vitro* sensitivities of different types of fibers in rabbit vagus nerves to

local anesthetic block with a range of local anesthetic drugs at high and low frequency stimulation. Rapidly conducting, myelinated (A) fibers are more sensitive than more slowly conducting, unmyelinated (C) fibers.

PROCEDURE

The cervical portions of the vagus nerves of rabbits weighing 2.5 kg are removed, desheathed and mounted in an airtight chamber which is maintained at 37°C by a water jacket. A central 1-cm section of the nerve chamber is perfused at 0.5 ml/min with carbonated Liley solution (pH 7.4 ± 0.02 after equilibration with 5% carbon dioxide in oxygen). A tap system allows the perfusate to be changed to test solution without admission of air.

A square wave generator is used to apply supramaximal electrical stimuli (10–15 V for 1 ms) at a rate of 0.0167 Hz during a 30-min period of stabilization. Two trains of stimuli (duration 0.25 s) are applied, one at 20 Hz and the other at 40 Hz. The preparation is considered valid only if there is less than 5% decrement in height of the action potential during stimulation at 40 Hz. The signals from the nerve are amplified, digitized (Unilab 532.001 interface sampling at 40 µs intervals for 8 ms, then at 200 µs intervals for 50 ms) and recorded with a microcomputer based system. The numeric derivative of the signal can be printed out immediately or stored on disc for subsequent processing. Signals are monitored also on a storage oscilloscope.

A submaximal blocking concentration of the hydrochloride salt of a test drug dissolved in carbonated Liley solution is applied. Only one concentration of one drug is applied to each nerve. The stimulation rate remains at 0.0167 Hz until any changes in the compound action potential are complete (minimum period 30 min), when the trains of high frequency stimulation are repeated. Drug effect is measured as the percent decreases in the height of the three components (A, B and C fibers) of the compound action at each frequency of stimulation. At 20 and 40 Hz, the last signal produced by each train of stimulation is used for analysis. An experiment is considered valid only if the action potentials recover to more than 90% of control height on washing the drug from the nerve.

EVALUATION

From the data obtained, the ED_{50} (and its SE) for the effect of each drug on each fiber type at each rate of stimulation is determined by log-probit analysis. Plots of the development of block while the nerves are being stimulated at 0.0167 Hz are also made. From these an index of the rate of development of A and C fiber block is derived ($T_{1/2B}$). This is defined as the time taken to develop 50% of the eventual maximum degree of block for the particular fiber type in each experiment.

MODIFICATIONS OF THE METHOD

Scurlock et al. (1975) examined the relative sensitivity of sympathetic preganglionic and postganglionic axons, B and C fibers, respectively, to structurally dissimilar local anesthetics. Cervical sympathetic trunks from adult rabbits were submerged in Krebs-Henseleit solution except during the brief recording periods, when they were stimulated electrically with twice maximal square-wave pulses of 0.15 ms (B fibers) or 0.5 ms (C fibers) duration. After control records, the bath chambers were filled with various concentrations of local anesthetics and the action potentials recorded at 5-min intervals. The decrease of action potentials of the B- and C-fibers was recorded separately.

REFERENCES AND FURTHER READING

De Jong RH (1980) Editorial views: differential nerve block by local anaesthetics. Anesthesiology 53:443–444

Gissen AJ, Covino BG, Gregus J (1980) Differential sensitivity of mammalian nerves to local anesthetic drugs. Anesthesiology 53:467–474

Scurlock JE, Heavener JE, de Jong RH (1975) Differential B and C fibre block by an amide- and an ester-linked local anaesthetic. Br J Anaesth 47:1135–1139

Wildsmith JAW, Gissen AJ, Gregus J, Covino BG (1985) Differential nerve blocking activity of amino-ester local anaesthetics. Br J Anaesth 57:612–620

Wildsmith JAW, Gissen AJ, Takman B, Covino BG (1987) Differential nerve blockade: esters v. amides and the influence of pK_a. Br J Anaesth 59:379–384

Wildsmith JAW, Brown DT, Paul D, Johnson S (1989) Structure-activity relationships in differential nerve block at high and low frequency stimulation. Br J Anaesth 63:444–452

G.1.1.10 Measurement of Sodium and Potassium Conductance in Voltage Clamp Experiments

PURPOSE AND RATIONALE

Voltage clamp experiments on single nodes of Ranvier can be performed with single myelinated nerve fibers from the sciatic nerve of the frog (Stämpfli 1954, 1968; Nonner 1969; Nonner et al. 1975; Stämpfli and Hille 1976; Borchard and Drouin 1978). Sodium, potassium and leakage currents (I_{Na}, I_K, I_L) can be measured.

Descriptions of structure and function of voltage-gated sodium channels were given by Catterall (1988, 1992), Stühmer (1991), Narahashi and Herman (1992), Cohen and Barchi (1993).

PROCEDURE

Single myelinated nerve fibers are dissected from the sciatic nerve of the frog (*Rana esculenta*). The fibers

are bathed in a Ringer solution containing 110 mM NaCl, 2.5 mM KCl, 1.8 mM $CaCl_2$, 5.0 mM Tris, pH 7.3, at 15°C. For measurement of sodium, potassium and leakage currents (I_{Na}, I_K, I_L), the nodal membrane is clamped to a holding potential of –30 mV (relative to the resting potential of –70 mV). Hyperpolarizing prepulses (–40 mV, 50 ms) followed by 2 ms test pulses (60 mV) are applied every 5 s to record peak sodium currents, I_{Na}, and to avoid the influence of accumulation of frequency-dependent block. Every second pulse is followed by an afterpulse (120 mV, 20 ms) to measure steady state I_K. The leakage current, I_L, is measured at the end of the hyperpolarizing prepulse and recorded every 10 s.

After superfusion of the nodal membrane with a local anesthetic, a quick and then a slow decrease of the peak sodium current (I_{Na}) occurs. When the application of the local anesthetic is stopped, I_{Na} increases quickly and then slowly within min indicating a reversible action of the local anesthetic on the nerve fiber. With local anesthetics, the potassium current (I_K) behaves similarly, whereas the leakage current (I_L) remains unchanged.

Dose Dependent Action of Local Anesthetics on I_{Na}-V Relations

The holding potential is set at –30 mV. A hyperpolarizing prepulse (–40 mV, 50 ms) is followed by a depolarizing test pulse (30 ms) with varying amplitudes. Local anesthetics induce a dose-dependent reduction of sodium-inward and -outward currents over the whole range of voltage clamp steps. The measurements are performed at extracellular pH 7.3.

Dose Dependent Action of Local Anesthetics on I_K-V Relations

Potassium currents, I_K, are measured at the end of depolarizing test pulses of 30 ms duration. Local anesthetics induce a dose-dependent decrease of potassium currents at extracellular pH 7.3.

EVALUATION

The effects on sodium, potassium and leakage currents (I_{Na}, I_K, I_L), the dose dependence of action on I_{Na}-V relations, and the dose dependence of action on I_K-V relations of various local anesthetics are compared.

MODIFICATIONS OF THE METHOD

Bräu et al. (1998) determined half-maximal blocking concentrations of local anesthetics for tonic block of Na^+ and K^+ channels by using the axonal patch clamp method (Vogel and Schwarz 1995) to study potencies of clinically used local anesthetics in suppressing Na^+ and delayed rectifier K^+ channels of peripheral nerve.

Sciatic nerves of the clawed **toad** *Xenopus laevis* were enzymatically prepared (Jonas et al. 1989). The nerves were dissected, desheathed, and treated with collagenase and protease to obtain single, partially demyelinated fibers. For recording axonal ionic currents, the outside-out configuration of the patch clamp method (Hamill et al. 1981) was applied to partially demyelinated axons. Patch pipettes were pulled from borosilicate glass (Clark Electromedical Instruments, Pangbourne, UK) and coated with Sylgard 184 (Dow Corning, Seneffe, Belgium) and were fire-polished at the tip before use. The resistance of the pipettes after filling with internal solution was 15–25 MΩ. The bath solution contained (in mM): NaCl 115; KCl 2.5; $CaCl_2$ 2, HEPES 10; adjusted to pH 7.4 with TRIS. For Na^+ current recording, 10 mM tetraethylammoniumchloride was added to suppress K^+ currents; for K^+ recording, 100 nM tetrodotoxin was added to suppress Na^+ currents. The pipette solution for Na^+ current recording contained (in mM): CsCl 110; NaCl 13; EGTA 2; HEPES 10, pH adjusted to 7.2 with TRIS. For the investigation of K^+ channels, CsCl was replaced by KCl.

Different concentrations of local anesthetics were applied to the patches using a multi-barrel perfusion system that allowed solution changes within 1 s.

After forming an outside-out patch from the nodal membrane, the holding potential was adjusted to –90 mV in the voltage clamp mode using an EPC7 patch clamp amplifier (List, Darmstadt, Germany). The pulse protocol used to elicit Na^+ currents comprised a 50-ms prepulse to –130 mV to remove fast inactivation, followed by a 50-ms test pulse to –40 mV to activate Na^+ currents. Steady-state K^+ currents were activated by a 50-ms potential step to 60 mV and were measured as the mean current during the last 20 ms of the pulse. For analysis, currents were filtered with a four-pole Bessel filter, digitized with a Labmaster TM-40 AD/DA board (Scientific Solutions, Solon, Ohio, USA), and stored in the hard disk of a computer. To reduce the noise of single current traces that originated from individual channel openings, 20 successive traces, elicited every 5 s, were averaged to measure the peak Na^+ current or steady-state K^+ current. Blocking potencies of the local anesthetics were determined by analyzing concentration–inhibition curves, which were constructed by measuring the inhibition of the peak Na^+ current or steady-state K^+ current amplitude at different concentrations normalized to control.

Half-maximal inhibiting concentrations (IC_{50}) were obtained from non-linear least-square fits of the function $F_1 = b_{max}/(1+[IC_{50}/c]^p)$ to the data points. As first-order binding kinetics of the drug with the channel were assumed, the Hill coefficient (p) was set to 1 during fitting; b_{max} is the maximal achievable block. Data acquisition and evaluation were performed with pClamp 5.5.1 (Axon Instruments, Burlingame, Calif., USA); Fig.P 5.0 software (Biosoft, Cambridge, UK) was used for fitting procedures.

Olschewski et al. (1998) applied the patch clamp technique to intact lateral horn neurons from laminae I-III identified in 200-µm slices of spinal cord from newborn rats. Under voltage clamp conditions, the whole-cell Na^+ and K^+ currents activated by depolarization were recorded in the presence of different concentrations of anesthetics.

Olschewski et al. (2002) combined the patch clamp recordings in spinal cord slices of the rat with the "entire soma isolation" method, as described by Safronov et al. (1997) and Safronov (1999). In the whole-cell recording mode, the entire soma of the neuron was isolated from the slice by slow withdrawal of the recording pipette, leaving all or nearly all of its processes in the slice. The isolated structure was classified as *soma* if it had lost all its processes during isolation and preserved only 10%–20% of the original Na^+ current recorded from the neuron in the slice before its isolation. The isolated structure was considered as *soma + axon* complex if it contained one 10- to 100-µm process and preserved > 85% of the original Na^+ current recorded from the neuron in the slice before isolation. The structure was considered as *axon + dendrite* if it preserved one adjacent process but the amplitude of the Na^+ current was in the range of those typically seen in isolated *somata*. A successful isolation was usually accompanied by a considerable decrease in membrane leakage currents due probably to the loss of the large area of the dendritic membrane. The good physiological state of the isolated structures was confirmed by a considerable increase in their output resistances (reflecting a decrease in membrane leakage conductance), and by stable and even improved membrane resting potentials. Three types of tetrodotoxin-sensitive voltage-gated Na^+ channels on soma and processes of dorsal horn neurons of rat spinal cord were identified. Bupivacaine, lidocaine and mepivacaine at low concentrations (1–100 µM) enhanced delayed-rectifier potassium current in intact neurons within the spinal cord slice, while exhibiting a partial blocking effect at higher concentrations (> 100 µM).

REFERENCES AND FURTHER READING

Århem P, Frankenhaeuser B (1974) Local anesthetics: effects on permeability properties of nodal membrane in myelinated nerve fibres from Xenopus. Potential clamp experiments. Acta Physiol Scand 91:11–21

Borchard U (1978) Untersuchungen zum Wirkungsmechanismus und zur pharmakologischen Charakterisierung von Lokalanästhetika. Habilitationsschrift. Medizinische Fakultät, Universität Düsseldorf

Borchard U, Drouin H (1978) Effects of the antituberculous agent ethambutol on myelinated nerve. Eur J Pharmacol 50:307–316

Borchard U, Drouin H (1980) Carticaine: action of the local anesthetic on myelinated nerve fibres. Eur J Pharmacol 62:73–79

Bräu ME, Vogel W, Hempelmann G (1998) Fundamental properties of local anesthetics: half-maximal blocking concentrations for tonic block of Na^+ and K^+ channels in peripheral nerve. Anesth Analg 87:885–889

Catterall WA (1988) Structure and function of voltage-sensitive ion channels. Science 242:50–61

Catterall WA (1992) Cellular and molecular biology of voltage-gated sodium channels. Physiol Rev 72:S15–S48

Cohen SA, Barchi RL (1993) Voltage-dependent sodium channels. Int Rev Cytol 137C:55–103

Courtney KR (1975) Mechanism of frequency-dependent inhibition of sodium currents in frog myelinated nerve by the lidocaine derivative GEA 968. J Pharm Exp Ther 195:225–236

Drouin H (1976) Surface charges at nerve membranes. Bioelectrochem Bioenerget 3:222–229

Drouin H, Neumcke (1974) Specific and unspecific charges at the sodium channels of the nerve membrane. Pflügers Arch 351:207–229

Hamill OP, Marty A, Neher E, Sakmann B, Sigworth FJ (1981) Improved patch-clamp techniques for high-resolution current recording from cells and cell-free membrane patches. Pflüger's Arch 391:85–100

Hille B (1977a) The pH-dependent rate of action of local anesthetics on the node of Ranvier. J Gen Physiol 69:475–496

Hille B (1977b) Local anesthetics: Hydrophilic and hydrophobic pathways for the drug-receptor reaction. J Gen Physiol 69:497–515

Jonas P, Bräu ME, Hermsteiner M, Vogel W (1989) Single-channel recording in myelinated nerve fibers reveals one type of Na channel but different K channels. Proc Natl Acad Sci USA 86:7238–7242

Narahashi T, Herman MD (1992) Overview of toxins and drugs to study excitable membrane ion channels: I. Voltage-activated channels. Meth Enzymol 207:620–643

Nonner W (1969) A new voltage clamp method for Ranvier nodes. Pflügers Arch 309:176–192

Nonner W, Rojas E, Stämpfli R (1974) Displacement currents in the node of Ranvier. Voltage and time dependence. Pflügers Arch 354:1–18

Olschewski A, Hempelmann G, Vogel W, Safronow BV (1998) Blockade of Na^+ and K^+ currents by local anesthetics in the dorsal horn neurones of the spinal cord. Anesthesiology 88:172–179

Olschewski A, Wolff M, Bräu ME, Hempelmann G, Vogel W, Safranow BV (2002) Enhancement of delayed-rectifier potassium conductance by low concentrations of local anesthetics in spinal sensory neurons. Br J Pharmacol 136:540–549

Safronov BV (1999) Spatial distribution of Na^+ and K^+ channels in spinal horn neurones. Role of the soma, axon and dendrites in spike generation. Prog Neurobiol 59:217–241

Safronov BV, Wolff M, Vogel W (1997) Functional distribution of three types of Na^+ channel on soma and processes of dorsal horn neurones of spinal cord. J Physiol (Lond) 503:371–385
Stämpfli R (1954) A new method for measuring membrane potentials with external electrodes. Experientia 10:508–509
Stämpfli R (1968) Voltage-Clamp-Analyse lokalanästhetischer Wirkungen am Ranvier'schen Schürring des Frosches. Naunyn-Schmiedeberg's Arch Pharmacol 260:P203–P204
Stämpfli R, Hille B (1976) Electrophysiology of the peripheral myelinated nerve. In: Llinás R, Precht W (eds) Frog Neurobiology. A Handbook. Springer Berlin, Heidelberg, New York. pp 3–32
Straub R (1956) Effects of local anesthetics on resting potential of myelinated nerve fibres. Experientia 12:182–184
Stühmer W (1991) Structure-function studies of voltage-gated ion channels. Annu Rev Biophys Chem 20:65–78
Vogel W, Schwarz JR (1995) Voltage clamp studies in axons: macroscopic and single-channel currents. In: Waxman SC, Kocsis JD, Stys PK (eds) The axon. Oxford University Press, Oxford, pp 257–280

G.1.1.11 Inhibition of Fast Axonal Transport

PURPOSE AND RATIONALE

Local anesthetics block not only nerve conduction but also fast axonal transport (Aasheim et al. 1974; Lavoie 1983; Lavoie et al. 1989). This mechanism may also be the way in which local anesthetics cause injury to nerve and spinal cord (Kalichman 1993).

PROCEDURE

The biological material consists of the eighth and ninth dorsal root ganglia of the bullfrog (*Rana catesbeiana*) and their respective spinal nerves. Each side of the animal provides one such set of ganglia and associated structures. The dissection is performed at room temperature with the preparation in an oxygenated medium with a pH of 7.1 and of the following composition (in mM): NaCl, 114; KCl, 2.0; $CaCl_2$, 1.8; dextrose; 5.5; HEPES 20. Once the dissection is completed, each spinal nerve is ligated at approximately 24 mm from the ganglion.

The ganglia are pulse-labeled with [^{3}H]leucine for 1 h. After the pulse-labeling, the preparations are incubated for 16–17 h at 18°C in medium free of radioactivity; the two ganglia and spinal nerves from one side of the animal serve as control preparations and those from the other side as experimental preparations. The preparations are placed in a Lucite incubation chamber. The ganglion and the first 10 mm of the nerve trunk occupy one compartment, the next 3 mm is in the groove between two communicating compartments, and the rest of the nerve trunk (including the point of ligature) is placed in the second compartment. The two communicating compartments are then sealed from one another by filling the rest of each groove with silicone grease. The compartment containing the control ganglia and that containing the experimental ganglia are filled with medium for all experiments. A local anesthetic agent is added to the medium bathing the distal half of the experimental nerve trunks whereas the same area of the control nerve trunks is in the corresponding medium without local anesthetic.

At the end of the incubation, the nerves are cut into 2-mm segments, and the protein-bound radioactivity of each ganglion and nerve segment is determined by liquid scintillation counting (Lavoie 1981). For each preparation, the total quantity of transported radioactivity is calculated by summing up the radioactivity present in the individual segments of the nerve starting at 6 mm from the ganglion and extending up to the point of ligature. The total quantity of [^{3}H]leucine incorporated into protein is calculated for each preparation as the sum of transported radioactivity and radioactivity remaining in the ganglion.

EVALUATION

Mean values ± SEM for the ratio of radioactivity in the experimental preparation to radioactivity in the control preparation are computed in each pair of preparations for the total incorporated radioactivity, the total transported radioactivity, and the radioactivity at the ligature. The difference in the absolute amount of radioactivity at the ligature, the difference in total transported radioactivity, and the difference in total incorporated radioactivity are calculated for each pair of preparations. A Student's *t*-test for paired samples is performed on the mean differences between control and experimental preparations. Using the individual ratios of radioactivity in experimental preparation to control preparation, an analysis of variance on parallel groups is done to compare the drugs; pairwise comparisons are obtained using Scheffé's critical *F* value.

MODIFICATIONS OF THE METHOD

Anderson and Edström (1973) and Lavoie (1982) used frog sciatic nerves *in vitro* to study the effect of local anesthetics on fast axonal transport of proteins. Rabbit vagus nerves were used by Fink et al. (1972) and Aasheim et al. (1974).

Factors, such as kinesin and dynein, influencing fast axonal transport have been identified (Shea and Flanagan 2001).

REFERENCES AND FURTHER READING

Aasheim G, Fink BR, Middaugh M (1974) Inhibition of rapid axoplasmatic transport by procaine hydrochloride. Anesthesiology 41:549–553

Anderson KE, Edström A (1973) Effect of nerve blocking agents on fast axonal transport of proteins in frog sciatic nerves *in vitro*. Brain Res 50:125–134
Fink BR, Kennedy RD, Hendrickson AE, Middaugh ME (1972) Lidocaine inhibition of rapid axonal transport. Anesthesiology 36:422–432
Kalichman MW (1993) Physiologic mechanisms by which local anesthetics may cause injury to nerve and spinal cord. Reg Anesth 18:448–452
Lavoie PA (1981) Importance of monovalent ions for the fast axonal transport of proteins. Can J Physiol Pharmacol 59:31–36
Lavoie PA (1982) Block of fast axonal transport *in vitro* by the local anesthetics dibucaine and etidocaine. J Pharmacol Exp Ther 223:251–256
Lavoie PA (1983) Inhibition of fast axonal transport *in vitro* by the local anesthetics prilocaine, mepivacaine, and bupivacaine. Can J Physiol Pharmacol 61:1478–1482
Lavoie PA, Khaten T, Filion PR (1989) Mechanisms of the inhibition of fast axonal transport by local anesthetics. Neuropharmacology 28:175–181
Shea TB, Flanagan LA (2001) Kinesin, dynein, and neurofilament transport. Trends Neurosci 24:644–648

G.1.2 Infiltration Anesthesia

G.1.2.1 Infiltration Anesthesia in Guinea Pig's Wheals

PURPOSE AND RATIONALE

Based on earlier work by McIntyre and Sievers (1937) and Sievers and McIntyre AR (1938), the use of intracutaneous wheals in guinea pigs was recommended by Bülbring and Wajda (1945). This method has become a standard operating procedure for testing local anesthetics.

PROCEDURE

Adult guinea pigs of either sex weighing 250–300 g are chosen. On the day preceding the experiment the hair on the back is clipped and two areas of 4–5 cm diameter are shaved. This produces a certain amount of irritation which disappears overnight. The sensitivity of the skin is greatest in the midline and slightly more so in the front than in the back area. For this reason each concentration of a local anesthetic must be tested in both areas. Six tests using three guinea pigs can be performed simultaneously. The doses of local anesthetics are always injected intracutaneously in 0.1 ml saline. Three guinea pigs receive one dose in the front area and another dose in the back area; the size of the wheal is marked with ink. One side is used for the test preparation, the other side for the standard (e. g., 1% butanilicaine). The reaction to pin prick is tested 5 min after injection in the following way. After observing the animal's normal reaction to a prick applied outside the wheal, six pricks are applied inside the wheal and the number of pricks is counted to which the guinea pig fails to react. The pricks are applied at intervals of about 3–5 s. Six pricks are applied every 5 min for 30 min. Having completed the test on 3 guinea pigs, the same solutions are injected into 3 other guinea pigs, but the solution which was used for the front is now used for the back area and vice versa.

EVALUATION

The number of times the prick fails to elicit a response during the 30 min period is added up, and the sum, out of possible 36, gives an indication of the degree of anesthesia. Using various doses, dose-response curves can be established. For time-response curves, the prick tests are repeated every 10 min. Half-life times are calculated as the time, when after complete anesthesia 3 out of 6 pricks elicit again a response (Ther 1953a, b).

MODIFICATIONS OF THE METHOD

The test can also be used to study the influence of vasoconstrictors, such as adrenaline.

REFERENCES AND FURTHER READING

Bülbring E, Wajda I (1945) Biological comparison of local anesthetics. J Pharmacol Exp Ther 85:78–84
Camougis G, Takman BH (1971) Nerve and nerve-muscle preparations (as applied to local anesthetics) In: Schwartz A (ed) Methods in Pharmacology, Vol 1, pp 1–40. Appleton-Century-Crofts, Educational Division, Meredith Corp., New York
McIntyre AR, Sievers RF (1937) The toxicity and anaesthetic potency of some alkoxy benzoates and related compounds. J Pharmacol Exp Ther 61:107–120
Muschaweck R, Rippel R (1974) Ein neues Lokalanästhetikum (Carticain) aus der Thiophenreihe. Prakt Anästh 9:135–146
Muschaweck R, Habicht R, Rippel R (1986) Lokalanaesthetica. In: Ehrhart G, Ruschig H (eds) Arzneimittel. Entwicklung – Wirkung – Darstellung. Verlag Chemie GmbH, Weinheim. pp 1–44
Sievers RF, McIntyre AR (1938) The toxicity and anesthetic potency of some new benzoyl derivatives. J Pharmacol Exp Ther 62:252–262
Ther L (1953a) Zur Prüfung der lokalanästhetischen Wirkung des Pantocain und des 4-n-Butylaminosalicylsäuredimethylaminoaethylesters im Tierversuch. Arzneim Forsch 3:345–348
Ther L (1953b) Über ein neues Leitungsanaesthetikum der "Nirvanin"-Reihe mit großer Entgiftungsgeschwindigkeit (Hostacain). Naunyn Schmiedeberg's Arch exper Path Pharmakol 220:300–316
Wiedling S (1964) Xylocaine. The pharmacological basis of its clinical use. Almqvist & Wiksell, Stockholm, Göteborg, Uppsala. pp 27–46

G.1.2.2 Infiltration Anesthesia in Mice

PURPOSE AND RATIONALE

Grant et al. (2000) described a mouse model for evaluation of skin anesthesia after infiltration of local anesthetics.

PROCEDURE

Male Swiss Webster mice weighing 23±3 g are used. On the day preceding the experiment, the abdominal hair is shaved using electric clippers. On the day of the experiment, on either side of the abdomen (∼0.5 cm lateral to the midline and ∼1.0 cm below the thoracic cage) circular areas of ∼0.7 cm diameter are marked with indelible ink for subcutaneous injections. For the generation of nociceptive electrical stimuli, a square wave general purpose generator (model S48, Grass Instruments) coupled to an isolator unit (Model PSIU6 F, Grass Instruments) is used. The stimuli are delivered to the skin via blunt electrodes fashioned from 25-gauge needles. A thin layer of electrically conductive gel is applied to the area to be tested with a cotton-tipped applicator.

Mice are screened to determine their vocalization threshold, the current required to produce a vocalization (squeak).While nociceptive stimulus is applied, animals are restrained gently in the experimenter's palm by grasping the nape of their neck and their tail. The output of the stimulator is initially set at 5 mA, and is progressively increased in steps of 1 mA. Mice are screened once, and those animals that vocalized at ≤8 mA are included in the study.

The local anesthetics are injected in various concentration subcutaneously in a volume of 0.15 ml in the marked area of one side. After fixed time intervals (5, 10, 20, 30, 40, 50, 60, and 70 min) the skin overlying the injection sire and the corresponding "control" side are stimulated using the threshold stimulus. If the animal does not vocalize after the threshold stimulus was applied to the test site, the intensity of the stimulus is increased twice in 1-mA increments, to deliver a "maximal" stimulus 2 mA above the threshold. This is done to ensure lack of vocalization response.

To assess the duration analgesia is tested at 15-min intervals.

EVALUATION

The all-or-none response data are subjected to statistical analysis using the survival curves procedure. The curves are generated using the method of Kaplan and Meier, and the 95% confidence interval for fractional survival at any particular time is calculated using the Prism program (GraphPad Software). The curves are compared using the log rank test. In this method of statistical analysis, the term "survival" refers to any well-defined end-point and in the present study it is lack of analgesia. The two-tailed p value of $< 0{,}05$ is considered significant.

REFERENCES AND FURTHER READING

Grant GJ, Piskoun B, Lin A, Bansinath M (2000) An in vivo method for the quantitative evaluation of local anesthetics. J Pharmacol Toxicol Meth 43:69–72

G.1.3 Surface Anesthesia

G.1.3.1 Surface Anesthesia on the Cornea of Rabbits

PURPOSE AND RATIONALE

Following the pioneering work of Sollmann (1918), block of the rabbit corneal reflex as described by Régnier (1923) has become a standard test method for evaluating local anesthetics (Quevauviller 1971).

PROCEDURE

Albino rabbits of either sex weighing 2.5–3 kg are placed into rabbit holding cages. The upper and lower eyelashes are carefully clipped. The conjunctival sac of one eye is held open, thus forming a pocket. From a 1 ml syringe with a 22-gauge needle, 0.5 ml of a solution of the anesthetic is applied into the conjunctival sac for 30 s. Then the procedure is repeated, so that 1.0 ml is applied within 1 min. One ml of the standard (0.1% solution of tetracaine hydrochloride) is applied to the other eye. Effective local anesthetics extinguish the corneal reflex (blinking) elicited by any touch of the cornea. For quantitative purposes, the irritation with a bristle according to von Frey (1894, 1896, 1922) has been recommended. An equine hair bending at a load of 230 mg is attached perpendicularly to a glass rod. Within 25 s, the cornea is touched 100 times. The summation of many stimuli applied this way gives better results than a single touch with a glass rod (Ther and Mügge 1953). The test is started 5 min after application of the drug and repeated every 5 min until anesthesia vanishes and blinking occurs again. The time between disappearance and reappearance of the corneal reflex is registered.

EVALUATION

Using the time of loss of the corneal reflex as parameter after application of different doses, dose-response curves can be established and potency ratios versus the standard calculated.

MODIFICATIONS OF THE METHOD

Chance and Lobstein (1944) used **guinea pigs** for testing surface anesthesia by the corneal reflex.

Bartsch and Knopf (1970) described an electrically operated stimulator with a bristle allowing variable frequencies to evaluate surface anesthesia on rabbit cornea.

Hotovy (1956) investigated the synergism between the local anesthetic compound dibucaine hydrochloride applied to the conjunctival sac of rabbits and intravenously administered analgesics using Régnier's method

REFERENCES AND FURTHER READING

Bartsch W, Knopf KW (1970) Eine modifizierte Methode zur Prüfung der Oberflächenanästhesie an der Kaninchen-Cornea. Arzneim Forsch/Drug Res 20:1140–1143

Camougis G, Takman BH (1971) Nerve and nerve-muscle preparations (as applied to local anesthetics) In: Schwartz A (ed) Methods in Pharmacology, Vol 1, pp 1–40. Appleton-Century-Crofts, Educational Division, Meredith Corp., New York

Chance MRA, Lobstein H (1944) The value of the guinea pig corneal reflex for tests of surface anaesthesia. J Pharm Exp Ther 82:203–210

Gerlough TD (1931) The influence of pH on the activity of certain local anesthetics as measured by the rabbit's cornea method. J Pharmacol Exp Ther 41:307–316

Geßner O, Klenke J, Wurbs FR (1932) Die Lokalanästhetika Pantokain (I.G. Farben) und Larokain (Roche) im Vergleich zu Novokain. Naunyn-Schmiedeberg's Arch exp Path Pharmakol 168:447–472

Hotovy R (1956) Messung zentralanalgetischer Wirkungen mit der Régnierschen Methode. Arch Exp Path Pharmakol 228:387–402

Muschaweck R, Habicht R, Rippel R (1986) Lokalanaesthetica. In: Ehrhart G, Ruschig H (eds) Arzneimittel. Entwicklung – Wirkung – Darstellung. Verlag Chemie GmbH, Weinheim. pp 1–44

Nieschulz O, Hoffmann I, Popendiker K (1958) Zur Pharmakologie des N-[4-(Phenoxy-methyl)-γ-phenyl-propyl]-morpholin, eines Aminoäthers mit lokalanaesthetischer Wirkung. Arzneim Forsch 8:539–544

Quevauviller A (1971) Experimental methods for comparing local anesthetic activity. In: Radouco-Thomas (ed) International Encyclopedia of Pharmacology and Therapeutics. Section 8: Local Anesthetics (Lechat P, Section editor) Vol*I*, Pergamon Press, Oxford New York, pp 291–318

Régnier MJ (1923) Essai de mesure de l'anesthésie produite sur les terminaisons nerveuses de la cornée par les anesthésiques locaux. Comparaison des pouvoirs anesthésiques de la cocaïne, de la novocaïne et de la stovaïne. C R hebd Scéances Acad Sci 177:558–560

Sollmann T (1918) Comparison of activity of local anesthetics. IV. Anesthesia of rabbit's cornea. J Pharmacol Exp Ther 11:17–25

Štolc S, Mai PM (1993) Comparison of local anesthetic activity of pentacaine (trapencaine) and some of its derivatives by three different techniques. Pharmazie 48:210–212

Ther L (1953a) Zur Prüfung der lokalanästhetischen Wirkung des Pantocain und des 4-n-Butylaminosalicylsäuredimethylaminoaethylesters im Tierversuch. Arzneim Forsch 3:345–348

Ther L (1953b) Über ein neues Leitungsanaesthetikum der "Nirvanin"-Reihe mit großer Entgiftungsgeschwindigkeit (Hostacain). Naunyn Schmiedeberg's Arch exper Path Pharmakol 220:300–316

Ther L, Mügge F (1953) Über ein neues Oberflächenanaesthetikum in der Augenheilkunde (Cornecain). v. Graefes Arch Ophthalmol 154:244–252

von Frey M (1894) Beiträge zur Physiologie des Schmerzsinns. Ber Sächs Gesellsch Wiss, Leipzig, Math Phys Kl 46:185–195

von Frey M (1896) Untersuchungen über die Sinnesfunctionen der menschlichen Haut. Erste Abhandlung: Druckempfindung und Schmerz. Abhandlungen der Mathematisch-physischen Classe der Königl. Sächsischen Gesellschaft der Wissenschaften 23:173–266

von Frey M (1922) Versuche über schmerzerzeugende Reize. Z Biologie 76:1–24

Wiedling S (1960) Studies on α-n-propylamino-2-methylpropionanilide – a new local anaesthetic. Acta Pharmacol Toxicol 17:233–244

G.1.3.2 Suppression of Sneezing Reflex in Rabbits

PURPOSE AND RATIONALE

Nieschultz et al. (1958), Åström und Persson (1960) used the sneezing reflex in rabbits to test local anesthetic activity.

PROCEDURE

Groups of male rabbits weighing 3 kg are used. Using a cotton tampon, the test solution is applied to the mucous membrane of one nostril. The solution of a standard local anesthetic is administered to the nasal mucosa of the other nostril. After 2 min the mucous membrane is stimulated by a fine pencil. Loss of the sneezing reflex is regarded as sign of complete anesthesia. The stimulation is repeated after 3, 6, 10 and 15 min and continued every 5 min until the sneezing reflex reappears. Various concentrations of test compound and standard are applied.

EVALUATION

Using the loss of the sneezing reflex as parameter after application of different doses, dose-response curves can be established and potency ratios versus the standard calculated. Furthermore, the duration of activity can be evaluated.

REFERENCES AND FURTHER READING

Åström A, Persson NH (1960) The toxicity of some local anesthetics after application on different mucous membranes and its relation to anesthetic action on the nasal mucosa of the rabbit. J Pharmacol Exp Ther 132:87–90

Nieschultz O, Hoffmann I, Popendiker K (1958) Zur Pharmakologie des N-[4-[Phenoxy-methyl)-γ-phenyl-propyl]-morpholin, eines Aminoäthers mit lokalanaesthetischer Wirkung. Arzneim Forsch 8:539–544

G.1.4 Epidural Anesthesia

G.1.4.1 Epidural Anesthesia in Various Species

PURPOSE AND RATIONALE

Activity and tolerability of new local anesthetics after epidural injection have to be studied in various animal species in order to predict both parameters in patients.

PROCEDURE

Studies in Rats

Blomberg and Rickstein (1988) described a simple technique for cannulation of the thoracic epidural space in conscious and anesthetized rats. Male Wistar rats weighing 300–400 g were anesthetized with methohexital sodium 100 mg/kg intraperitoneally for insertion of PE-50 catheters into the tail artery and right jugular vein. Supplementary doses of methohexital were given during the cannulation of the epidural space. The catheters were exteriorized in the neck and the animals were placed in a lucite restraining cylinder where they were left to recover for 1–2 h from methohexital anesthesia and cannulation procedures. Arterial pressure, heart rate, and body temperature were recorded. A PE-50 catheter was inserted into the right common carotid artery for measurement of cardiac output with the cardiogreen dye-dilution technique and measurement of left ventricular end-diastolic pressure.

For cannulation of the thoracic epidural space, the skin of the upper part of the back of the animal was shaved and a 3-mm-long midline incision was made over the spinous process from a point between the two scapulae. The fascia covering the superficial muscles of the back was opened and the muscles were dissected from the thoracic vertebrae and retracted laterally. The thick and protruding spinous process of the second thoracic vertebra was localized. The identification of the spinous process of Th3 to Th7 was easily made by the nail of the index finger. The interspinal muscles and ligaments between the spinous processes of Th6 to Th7 were cut and the spinous process of Th7 was removed. The distance between Th6 and Th7 was then maximized by a rostral traction of Th6 with a forceps attached to spinous process of Th6. The yellow ligament between Th6 and Th7 was identified by a dissecting microscope at ×16 magnification and cut open to visualize the dura and the spinal cord. A PE-10 catheter, filled with the local anesthetic, was introduced cranially to a length of 1 cm. The area between Th6 and Th7 was covered and the catheter was firmly attached with cyanoacrylate, which completely prevented extradural leakage of the local anesthetic. The catheter tip was now located at the Th4–5 level. The superficial muscles were then sutured and the catheter was brought through the closed skin incisions. Incremental doses of 10 µl of bupivacaine were administered epidurally and the amount of the anesthetic bupivacaine (5 mg/ml) that caused no further heart rate decrease was assessed. The spread of the analgesia was assessed by a modified pin-prick technique. All hemodynamic measurements were made before, and then 10–15 min and 45–55 min after the induction of thoracic epidural anesthesia.

Studies in Guinea Pigs

A method to test epidural anesthesia in guinea pigs was described by Åkerman et al. (1988).

Male guinea pigs weighing 300–500 g are anesthetized by means of an intraperitoneal injection of an aqueous solution of chloral hydrate 42.5 g/l; ethanol 90 g/l; propylene glycol 428 g/l; sodium pentobarbitone 9.75 g/l; and magnesium chloride 21 g/l. A skin incision is made from the level of the lumbosacral fossa and approximately 1.5 cm down in order to expose the sacral area in the mid-line. With the vertebral column flexed, the lumbosacral intervertebral ligament is carefully incised. Through this small opening a polyethylene catheter (PE 10) is inserted maximally 1.5 cm along the roof of the vertebral canal to the L4–L5 region. The catheter is sutured to the overlying lumbar fascia which is then closed. The catheter is tunneled under the skin and exteriorized through an incision in the neck region. After fixation of the catheter to the fascia of the neck muscles and suturations of the incisions, the catheter is filled with saline and sealed.

After a recovery period of at least 1 day, 0.1 ml of 2.0% lidocaine is injected over a period of 1 min, and the motor and sensory blocks are assessed. The injection of lidocaine which results in a bilateral, reversible blockade indicates a successful preparation. A minimum of 8 animals are used in the further experiments for each test solution.

Mean time to onset of block and mean duration of block are calculated from number of legs blocked.

Siems and Soehring (1952) described a model in **guinea pigs** resembling peridural and paravertebal anesthesia in man.

Studies in Rabbits

Chernyakova et al. (1994) studied the effects of azacaine during epidural anesthesia in **rabbits**.

Hughes et al. (1993) described a rabbit model for the evaluation of epidurally administered local anesthetics. A "loss of resistance technique" similar to that employed in caudal epidural injection in humans was used. The rabbit was carefully restrained by an assistant. The readily palpable cranial dorso-iliac spines, lying on either side of the prominent spinous process of the seventh lumbar vertebra, served as landmarks.

The thumb and the middle finger of the left hand were placed on the two crests and the left index finger used to palpate the midline, L7 spine and the depression over the lumbosacral fossa. With the index finger in position on the L7 spine to serve as a guide, a short bevel 1.5 cm 20 gauge spinal needle was introduced a right angles to the skin in the midline with the bevel aligned longitudinally. After passage through the skin, only minor resistance was felt until the ligamentum flavum was reached. When passing through the ligament, a definite "pop" was felt and resistance to advancement of the needle was lost. When correctly placed, the needle was at a depth of approximately 0.75 to 1.0 cm and firmly held by the ligament. The stylet was then withdrawn and the hub inspected for the presence of blood or cerebrospinal fluid. If absent, the needle was rotated through 90° to direct the bevel caudally, a 1.0 ml syringe was attached and 0.1 ml of air injected. Accurate placement was indicated by the absence of resistance to injection and lack of subcutaneous crepitus. A syringe containing the desired dose of the local anesthetic was attached and the solution injected over a 5–10 s period. The pharmacodynamic responses were assessed by (1) sensory loss, (2) loss of weight-bearing ability, and (3) flaccid paresis.

Studies in Dogs

Kief and Bähr (1970) studied the epidural tolerance of artecaine with and without addition of Suprarenin in Beagle dogs weighing 9–12 kg. For pre-operative sedation, the dogs received 0.03 ml/kg Combelen (= propionylpromazine) intravenously. The fur of the lumbosacral area was shaved and the skin disinfected. A single dose of 5 ml of a 2% articaine solution was administered epidurally under sterile conditions. All dogs showed the typical symptoms of spinal anesthesia, which subsided after a few hours. The dogs were sacrificed after 1 or 3 days. The portion of the vertebral column with the site of injection in the middle was removed and placed in 8% buffered formalin. When semifixed, the vertebral arches were opened and the spinal cord as well as the roots of the spinal nerves with the adipose tissue of the epidural space were removed. After embedding in gelatin and Paraplast, the serial sections from the area of injection were stained with fast red 7B, hematoxylin-eosin and myelin sheath staining after Olivecrona was performed. Furthermore, the PAS and iron reaction were performed on one section. The presence or absence of nerve damage and of inflammation was noted.

A technique for epidural administration in the **dog** was described by Feldman and Covino (1988).

Defalque and Stoelting (1966) used a standard veterinary epidural technique to study latency and duration of action of some local anesthetic mixtures in **dogs**. The animals, prone and with their spread-out extremities attached to the table, were placed in 40-degree Trendelenburg position. Under sterile conditions, the epidural space was penetrated through the interarcual ligament with a short-beveled No. 22 spinal needle. After identification of the epidural space (aspiration, air injection), 4 ml of the investigated solution were injected with a constant injection rate of 2 ml per sec. Absence to skin-twitch response to pinching with an Allis clamp was considered analgesia. This was tested on both flanks, along a line 2 cm off the spine. Disappearance of contraction of the anal sphincter in response to stroking all quadrants of the anal margin closely correspond to complete analgesia at the level of the interarcual ligament; since this was an easily measurable parameter, disappearance and recurrence of this reflex was chosen as endpoint of latency and duration of action, respectively.

Raner et al. (1994) performed thoracic epidural anesthesia in **dogs** after general anesthesia with thiopental/chloralose and under artificial respiration. A thoracic epidural catheter (18G, Braun-Melsungen, Germany) was inserted percutaneously via the Th7–8 or Th8–9 interspace. Thoracic epidural anesthesia was established with a bolus injection of 10 mg/kg mepivacaine followed by a continuous infusion of 5 mg/kg per hour.

Kamibayachi et al. (1995) studied the halothane-induced myocardial sensitization to the dysrhythmogenic effect of epinephrine after thoracic epidural anesthesia in **dogs**. An epidural catheter was inserted under halothane anesthesia. The vertebral arches of T8 and T9 were surgically exposed and the catheter was introduced, via the T8–9 interspace, to the epidural space, which was identified by the loss-of-resistance technique. The catheter was advanced 5 cm in the cephalad direction and secured to the back. After the experiment, the position of the catheter was confirmed radiographically by injection of iopamidol (0.2 ml/kg).

Studies in Other Species

Ide et al. (2001) studied the effect of epidural anesthesia on respiratory distress induced by airway occlusion in isoflurane-anesthetized **cats**. The authors developed an animal model for the study of airway occlusion and proposed new concepts of minimum alveolar anesthetic concentration for airway occlusion, and the duration from the start of airway occlusion to the onset of the positive motor response. Adult cats were anesthetized with isoflurane and an epidural catheter was placed after L5 laminectomy.

Richer et al. (1998) described sacrococcygeal and trans-sacral epidural aesthesia in the laboratory **pig**. The aim of the study was to assess epidural accessibility in 30- to 50-kg piglets, not in adult hogs. Each animal received general anesthesia combined with epidural anesthesia. The level of catheter insertion was the sacrococcygeal interspinous space or the adjacent space (S4-S5). Localization of the injection site was simple. The sacrococcygeal junction corresponds to the junction between the fixed portion (sacrum) and the mobile portion (coccyx) of the animal's tail. The catheter was inserted along the median line at this level or the level above. The bony structures were palpable beneath the superficial planes. The animals were placed on their sides under general anesthesia and disinfected under surgical conditions. Epidural space injection was performed using a 16-gauge needle, traversing the sacrococcygeal or trans-sacral interspinous space. Entry to the epidural space was detected by a loss of resistance to puncture with absence of blood or cerebrospinal fluid on aspiration and by the ease of cephalic catheter progression within this space. A first injection of local anesthetic was performed 10 min prior to laparotomy. Epidural analgesia was maintained after this first injection by continuous administration of the same agent with a syringe. It was discontinued on awaking for a brief period in order to confirm functional recovery of the lower limbs.

Lebeaux (1975) recommended the **sheep** as a model for testing spinal and epidural anesthetic agents. To ensure accurate and reproducible administration of drugs into these restricted anatomical regions, a wooden stock was built to restrain the sheep without stress but allow arching of the lumbosacral spine in order to open the inter vertebral space. The stock consisted of a table with holes for the front feet, hinged at one end to a fixed stanchion. The hinges permitted tilt of the table. The sheep was placed prone on the table, the head secured in the stanchion and the front feet passed through the holes and tied. The lumbosacral interspace used for both spinal and epidural tap was separated by positioning and tying the rear limbs cephalad beside the abdomen, thereby extending the knee and flexing the hip. The wool was clipped from the sheep's back, the skin of the lumbosacacral area was washed and swabbed with iodine, and the vertebral spines and interspaces identified by palpation, marked, and numbered with a felt pen.

Epidural block was performed with a 19-gauge Crawford-point needle, using the loss-of-resistance method, with a syringe containing saline to identify the epidural space. After withdrawal of the stylet, a Luer-Lok syringe containing 10 ml of sterile saline solution with a final concentration of 1:200,000 epinephrine and 25.0 mg (0.25%) bupivacaine was attached to the needle. After careful aspiration of blood or spinal fluid, the local anesthetic solution was injected within 30 s. The needle was withdrawn and the table kept horizontal.

Immediately after injection, the rear feet were untied and allowed to hang free on either side of the table for evaluation of sensation and/or reflexes in the rear limbs. Then, 20 min after injection the sheep was removed from the table and positioned in a sling fashioned from a heavy duty 50-gallon plastic barrel split in half longitudinally and mounted on a metal support. Holes cut in the barrel allowed the feet to drop through so that comfortable sternal recumbency was maintained while permitting anesthetic evaluation to continue. When complete sensation returned in the skin of the dorsum, the sheep was removed from the sling and placed on a straw-bedded floor so that weight support and full recovery could be assessed.

Feldman et al. (1997) compared anesthetic efficacy and pharmacokinetics of epidurally administered ropivacaine and bupivacaine in the **sheep**.

REFERENCES AND FURTHER READING

Åkerman B, Hellberg IB, Trossvik C (1988) Primary evaluation of the local anesthetic properties of the amino amide agent ropivacaine (LEA 103). Acta Anesthesiol Scand 32:571–578

Blomberg S, Rickstein SE (1988) Thoracic epidural anesthesia in conscious and anesthetized rats. Effects on central haemodynamics compared to cardiac beta adrenoceptor and ganglionic blockade. Acta Anaesthesiol Scand 32:166–172

Chernyakova IV, Zhukov VN, Osipov SA, Shadiev AS, Skovpen TV (1994) Epidural and conduction anesthesia with azacaine in the experiment. Exp Clin Pharmacol 57:13–15

Defalque RJ, Stoelting VK (1966) Latency and duration of action of some local anesthetic mixtures. Anesth Analg 45:106–116

Feldman HS, Covino BG (1988) Comparative motor-blocking effects of bupivacaine and ropivacaine, a new amino

amide local anesthetic, in the rat and dog. Anesth Analg 67:1047–1052
Feldman HS, Dvoskin S, Halldin MH, Ask AL, Doucette AM (1997) Comparative anesthetic efficacy and pharmacokinetics of epidurally administered ropivacaine and bupivacaine in the sheep. Regional Anesthesia 22:451–460
Hughes PJ, Doherty MM, Charman WN (1993) A rabbit model for the evaluation of epidurally administered local anaesthetics. Anaesth Intens Care 21:298–303
Ide T, Okitsu Y, Nehashi S, Yamamoto F, Nishino T (2001) The effect of epidural anesthesia on respiratory distress induced by airway occlusion in isofluorane anesthetized cats. Anesth Analg 92:749–754
Kamibayachi T, Hayashi Y, Mammoto T, Yamatodani A, Taenaka N, Yoshiya I (1995) Thoracic epidural anesthesia attenuates halothane-induced myocardial sensitization to dysrhythmogenic effect of epinephrine in dogs. Anesthesiology 82:129–134
Kief H, Bähr H (1970) Epidural tolerance of artecaine in dogs. Personal communication
Lebeaux M (1975) Sheep: a model for testing spinal and epidural anesthetic agents. Lab Anim Sci 25:629–633
Raner C, Biber B, Lundberg J, Martiner J, Winsö O (1994) Cardiovascular depression by isofluorane and concomitant thoracic epidural anesthesia is reversed by dopamine. Acta Anesthesiol Scand 36:136–143
Richer JP, Lacoste L, Faure JP, Hauet T, Ferrié JC, Carretier M (1998) Sacrococcygeal and transsacral epidural aesthesia in the laboratory pig: a model for experimental surgery. Surg Radiol Anat 20:431–435
Siems KJ, Soehring K (1952) Die Ausschaltung sensibler Nerven durch peridurale und paravertebrale Injektion von Alkyl-polyäthylenoxyd-äthern bei Meerschweinchen. Arzneim Forsch 2:109–111

G.1.5 Intrathecal (Spinal) Anesthesia

G.1.5.1 Spinal Anesthesia in Various Species

PURPOSE AND RATIONALE

Transient neurological symptoms have been observed in patients after spinal anesthesia (Hampl et al. 1995). Myers and Sommer (1993) published a survey on methodology for spinal neurotoxicity studies.

Activity and tolerability of new local anesthetics after intrathecal injection were studied in various animal species in order to predict both parameters for spinal (subarachnoid) anesthesia in patients.

PROCEDURE

Studies in Rats

Intrathecal injections to **rats** are performed according to the method of Hylden and Wilcox (1980) or Åkerman (1985) as being used by Ossipov et al. (1988). Male Sprague-Dawley rats weighing 50–75 g are used. The rat is held firmly by the pelvic girdle. A 30-gauge needle is attached to a 25-µl Hamilton syringe is inserted into the tissue on one side of the L5 or L6 spinous process at an angle of about 20°. The needle is advanced to the groove between the spinous and transverse processes and then moved forward the intervertebral space at an angle of about 10°. About 0.5 cm of the needle is then in the vertebral column. Correct placement of the needle is indicated by an arching of the tail. Drugs are dissolved in saline or water and administered in a volume of 5 µl. Antinociception is determined in a modification of tail flick assay in rats by placing the tail of the rat under a focused radiant heat source. The degree of antinociception is defined as the percentage of maximum possible effect. This percentage is determined for each dose at each time measured allowing to calculate ED_{50}values.

Omote et al. (1995) studied the effects of verapamil on spinal anesthesia induced by local anesthetics administered via a chronic intrathecal polyethylene catheter in **rats**. The catheter was inserted 15 mm cephalad into the lumbar subarachnoid space at the L4–5 vertebrae with the tip located near the lumbar enlargement of the spinal cord. The catheter was tunneled subcutaneously and externalized through the skin in the neck region. At least 6 days of postsurgical recovery was allowed before animals were used in experiments. The tail-flick and the mechanical paw pressure tests were used to assess thermal and mechanical nociceptive thresholds.

Mestre et al. (1994) described a method for performing direct intrathecal injections in **rats** without introducing a spinal catheter.

Wang et al. (1991) described lumbar subarachnoid catheterization in rats. Male Wistar rats weighing 500–600 g were anesthetized with intraperitoneal ketamine 75–100 mg/kg. Following a midline skin incision, the paravertebral muscles were detached from the spinous processes and retracted laterally. The intervertebral ligament between Th13 and L1 or between L1 and L2 was removed. After dissection, the inferior border of T13 or L1 was retracted cephalad, facilitating the application of rongeurs for partial laminectomy at the cephalic border of L1 or L2. This exposed the dura and the underlying spinal cord, which was easily identified by a mid-line blood vessel. Lidocaine (1.5%) was applied topically to the dura to prevent movement of the animal when the dura was picked up with fine forceps. The dura was perforated with a short-bevel No. 20-gauge needle, resulting in some leakage of cerebrospinal fluid. Under magnification, a PE10 catheter was immediately inserted tangentially through the dural opening. It was directed caudally and maintained dorsal to the spinal cord. The catheter, 10 cm in length and containing a volume of 0.02 ml was advanced

slowly in the subarachnoid space to a mark 1.5 cm from the tip, while 0.01–0.02 ml of normal saline was simultaneously injected to open the way. Leakage of fluid through the dural opening during injection confirmed the patency of the catheter and also indicated that the catheter was properly placed in the subarachnoid space.

For fixation of the catheter, the spinous process rostral to the laminectomy was denuded and perforated with a No. 18-gauge needle. The free end of the catheter was threaded through this lumen. On retraction of the needle, the PE10 catheter was left in the perforation of the spinous process, and anchored with cyanoacrylate glue. A connector was attached to the free end of the catheter for injection.

The wound was irrigated with saline and closed in layers leaving the catheter buried in the subcutaneous tissue. The hub of the connector was sutured to the skin with fine stainless steel wire. The injection port, covered by a removable metal cap, was brought out of the skin via a separate small opening lateral to the main skin incision.

One week after surgery, 0.03–0.05 ml of 1.5% lidocaine was injected through the subarachnoid catheter. Correct positioning of the catheter was evidenced by prompt sensory and motor block of the hind limbs, developing in 1–5 min, and exhibiting motor blockade for 20–30 min.

Dirksen et al. (1992) studied the dose–response and time–effect relationships of intrathecal bupivacaine in rats. The effect was a quantified drug-induced and graded reduction in the magnitude of the withdrawal reflexes elicited by transcutaneous stimulation.

Sakura et al. (1996) described an improved technique for morphological analysis of drug-induced injury after intrathecal catheterization in the rat. Male Sprague Dawley rats weighing 200–300 g were anesthetized by intraperitoneal injection of methohexital (40–60 mg/kg). Catheters were composed of 28-gauge polyurethane, 32-gauge polyimide, 32-gauge polyurethane, PE10 polyethylene, or PE-10 polyethylene that has been stretched to twice its original length. They were passed through a slit in the atlanto-occipital membrane and advanced 11 cm, to lie with the tip caudal to the conus medullaris. Animals were allowed to recover for 24 h before the study was started. The animals were placed in a horizontal acrylic restraint, and baseline tail-flick latency was assessed immediately before infusion. Infusions were administered via a mechanical infusion pump at a rate of 1 µl/min for 4 h. Animals were evaluated for alteration in tail-flick latency 7 days after infusion.

Animals were sacrificed by injecting an overdose of pentobarbital 7 days after infusion. They were perfused intracardially with a phosphate-buffered glutaraldehyde-paraformaldehyde fixative. The spinal cord and nerve roots were dissected out, immersed in the same glutaraldehyde solution for infusion fixation and embedded in glycol methacrylate. The embedded tissue was sectioned at the conus medullaris, 6 mm rostral, and 6 and 12 mm caudal, using a Sorvall JB-4 microtome. The tissue was stained with hematoxylin-eosin or was treated with 4% osmium tetroxide and stained with toluidine blue. Histologic evaluation was performed with light microscopy. Specimens obtained 12 mm caudal to the conus were used for quantitative comparison of catheter-induced damage. This region was chosen because cross sections obtained below the conus have a greater number of fascicles. Each fascicle present in the cross-section was assigned to injury scores of 1 to 3, where 0 = normal, 1 = mild, 2 = moderate, and 3 = severe injury. The injury score of each cross-section was then calculated as the average score of all fascicles present in the cross-section. The data were compared using the Kruskal-Wallis test and Dunnett's test. For all comparisons, $P < 0.05$ was considered significant.

Grouls et al. (1997) compared the effects of *n*-butyl-*p*-aminobenzoate and bupivacaine after epidural and intrathecal solution in the **rat**. Anesthesia was measured by the latency of tail withdrawal from warm water (55°C).

Kirihara et al. (2003) compared the **neurotoxicity** of intrathecal and epidural lidocaine in **rats**. Male Sprague Dawley rats were anesthetized with sodium pentobarbital (30 mg/kg i.p.) and 1.5% halothane. A catheter of stretched polyethylene tubing PE10 was introduced into the subarachnoid or epidural space using an aseptic technique. Catheters were passed via the L4–L5 intervertebral space and advanced 1.3 cm in the caudal direction. Rats were allowed 4 days to rest for recovery from the operation.

To measure the response to noxious heat stimulus, a tail-flick test was performed. A 100-W projector lamp was focused on the distal segment of the tail approximately 5 cm from the tip. The time at which rats withdrew the tail was defined as the tail-flick latency. A cutoff time of 10 s was used to avoid damaging the tail.

To measure the response of legs to a noxious mechanical stimulus, a paw pressure test was applied to the dorsal surface of both hind paws using a device capable of progressively increasing the pressure at a rate of 15 g/s. The pressure at which the rat withdrew the

paw from the device was defined as the paw pressure threshold, and the mean for both paws was used for analysis. A cutoff pressure of 400 g was used to prevent damage to the paws.

Motor function in the lower limbs was assessed by grading: 0 = none, 1 = partially blocked, and 2 = completely blocked.

Various concentrations of local anesthetic or saline were injected intrathecally in a volume of 20 µl or epidurally in a volume of 100 µl followed by 10 µl saline to flush the catheter. Tail-flick test, paw pressure test and motor function assessment were performed 10, 20. 30. 60. 120, 180, and 240 min after injection and continued daily for 4 days.

After the last experiments, the rats were euthanized by injection of an overdose of pentobarbital and then perfused intracardially with a phosphate-buffered 2.0% paraformadehyde/2.5% glutaraldehyde fixative. Methyl green solution was injected to confirm the location of the catheter after the perfusion. The spinal cord and nerve roots were dissected out and immersed in the same fixative for 4 h. Two specimens (10 mm rostral and caudal to the conus medullaris from each rat) were postfixed with cacodylate-buffered 1% osmium tetroxide, dehydrated in a series of graded alcohol solutions, and embedded in epoxy resin. From the embedded tissue, 1- µm transverse sections were obtained and stained with toluidine blue dyes. Sections obtained from 10 mm rostral to the conus (caudal spinal cord) were used for qualitative evaluation. Quantitative analysis of nerve injury was performed using the sections obtained from 10 mm caudal to the conus. Each fascicle present in the cross-section was assigned an injury score of 0 to 3. The injury score for each cross-section was then calculated as the average score of all fascicles present in the cross-section.

Data are presented as mean ± SEM. Tail-flick latencies and paw pressure thresholds were converted to the percentage of the maximal possible effect. The area under the time–effect curve was calculated by accumulating the effect measured at discrete time intervals using the trapezoidal integration method. The results were analyzed by ANOVA with repeated measures followed by Scheffe and Dunnett tests. The injury score for each technique and each solution was compared using two-way ANOVA followed by the Scheffe test. The frequency (i. e., the number of rats with lesions) in each group was analyzed by the chi-square test.

De la Calle and Paíno (2002) described a procedure for direct **lumbar puncture in rats**. Female Sprague Dawley rats weighing 180–250 g were used. The rats were placed in a transparent plastic box and anesthetized with a mixture of 4% isoflurane in O_2:N_2O (30:70 v:v). Then, a mask was placed over the rat's nose and mouth, and the isoflurane concentration was lowered to 1.5%–2% for the remainder of the procedure. The lower half of the animal's back was shaved and scrubbed with povidone-iodine. The animals were then placed in a prone position on a Styrofoam board (25 cm ×13 cm ×6 cm), with the mask opening fixed 12 cm from the end of the board. The rat's forelimbs were extended to the front and fixed to the board with tape, taking care not to force the neck. The hind limbs were left to hang off the board, lying on the table. In that way, the animal's vertebral column was flexed around the L3–L5 level, widening these intervertebral spaces. Using the anterior part of the iliac crest as a tactile landmark for the L5–L6 intervertebral level, a 2-cm longitudinal incision was made with a scalpel rostral to this point. The fascia of the paravertebral muscles was excised and withdrawn to the sides with the help of sterile cotton plugs. A neonatal lumbar puncture needle (25 G × 1 TW) was introduced perpendicular to the surface through the widest intervertebral space and lowered until it came into contact with the vertebral body. Occasionally, a short flicking of the tail or of a limb was observed. The moment of penetration into the intrathecal space could be detected by a change of resistance to the introduction of the needle. Normally, the bevel of the needle was oriented rostrally although, if the puncture was not initially successful, the needle was tentatively rotated. A few seconds after withdrawal of the inner needle filament, the cerebrospinal fluid (CSF) could be observed to spontaneously flow into the needle cup. Triggering or accelerating liquid flow could be achieved by: (1) pressing the neck of the animal with a finger (thereby increasing the intrathecal pressure), (2) holding the head of the rat secure with one hand and pulling its tail with the other (the mechanical traction accommodates the needle tip in the intrathecal space), and (3) changing the inclination of the board to about 45° (also increases intrathecal pressure).

The procedure can also be used for the delivery of chemical products or cell suspensions to the intrathecal space. After collecting 20–50 µl CSF, 50 µl of 2% mepivacaine was injected. Hind limb paresis and anesthesia were produced that lasted for 30 min.

Bahar et al. (1984a) described chronic cannulation of the intradural and extradural space in the **rat**. Under anesthesia a hole was drilled in the penultimate lumbar vertebra of male rats and the appropriate space can-

nulated. The catheter was tunneled subcutaneously to emerge at the neck.

Using this technique, Chanimov et al. (1997) studied neurotoxicity after spinal anesthesia induced by serial intrathecal injections of magnesium sulfate. Male Wistar rats were given intrathecal injections of 0.02 ml of 6.3% or 12.6% magnesium sulfate or 2% lignocaine or 0.9% sodium chloride as a series of 15 injections on alternate days for a period of 1 month.

Yaksh and Rudy (1976) described a procedure of chronic catheterization of the spinal subarachnoid space in **rats** and **rabbits**. A polyethylene catheter (PE-10) was inserted through a puncture of the atlanto-occipital membrane into the spinal channel in anesthesia and secured to the skull. In this way, drugs could be administrated into the spinal subarachnoidal space of unanesthetized animals.

Cole et al. (1990) used this model to determine the influence of spinal tetracaine on central nervous system metabolism during nociceptive stimulation in **rats**.

Studies in Mice

Åkerman et al. (1988a, b) used **mice** to study spinal morphine antinociception potentiation by local anesthetics.

A simple technique for intrathecal injections by lumbar puncture in unanesthetized **mice** was described by Hylden and Wilcox (1980).

This model has been used by Langerman et al. (1994) to evaluate the potency of various local anesthetics. Adult Swiss Webster male mice were slightly anesthetized with halothane and the skin overlying the dorsal lumbar spine was opened using a transverse incision 8–10 mm. Animals were allowed to recover for 1 h before the evaluation of the baseline nociceptive response latency. Thirty min after baseline testing, intrathecal local injections were performed with an automatic syringe fitted with a 30-gauge needle. Fourth spinal space was identified and the needle was inserted between the two spinal processes in a cephalad direction at a 20° angle. Resistance encountered at approximately 5–6 mm from the skin indicated proper location of the needle in the spinal canal. A fixed 10 µl volume of injectate was used. Analgesia was measured using the tail-flick test based on tail withdrawal in response to heat generated by a light beam focused on the ventral tail surface.

Using this model, Åkerman (1985) obtained dose–response curves for lignocaine, mepivacaine, bupivacaine, amethocaine and cinchocaine after a single intrathecal injection in **mice**.

Studies in Rabbits

Bieter et al. (1936a) described a method of inducing spinal anesthesia in the **rabbit** and determined threshold anesthetic and lethal concentrations. Injections were performed at the lumbo-sacral union between the spinous process of the last lumbar vertebra and the first sacral spinous process. A dose of 0.02 ml per centimeter of spinal length was chosen as standard volume for determining minimal anesthetic and minimal lethal doses. These authors (Bieter et al. 1936b) determined the duration of spinal anesthesia in the rabbit after applying an electrical stimulus to the skin of the animal and observing the changes in respiration.

This method was also used by Luduena et al. (1960).

Langerman et al. (1991) studied the duration of anesthesia after a single subarachnoid injection of a local anesthetic in **rabbits**. Tetracaine 1% 0.5 mg/kg was administered in 10% glucose or in lipid solution via catheters chronically implanted in the subarachnoid space. The pharmacologic effect was assessed by evaluating the intensity and duration of motor blockade according to a three-stage scale.

Wakamatsu et al. (1999), Ohtake et al. (2000), and Oka et al. (2001) studied the effects of intrathecally administered local anesthetics on glutamate release and neuronal injury in **rabbits**. New Zealand white rabbits were anesthetized with isoflurane. With the rabbits in prone position, midline skin and subcutaneous fascia were incised between the third lumbar and the first sacral spinous process after infiltration with 0.25% bupivacaine. Muscles were dissected; the third to seventh processes, ligamentum flavum and epidural fat were sequentially removed; and the underlying dura was exposed. Using an operating microscope, a small slit was made in the dura and arachnoid membrane at the L3–L4 interlaminar space. A loop-type dialysis probe was then implanted. A PE10 catheter for the administration of saline or the local anesthetic to be tested was implanted intrathecally through the slit made at the L6–7 interlaminar space so that the tip of the catheter was located at the level of the cauda equina. The implanted dialysis probe was perfused with artificial cerebrospinal fluid bubbled with 95% oxygen and 5% CO_2 at pH 7.2. Samples were collected before and after administration of test substance and analyzed for glutamate.

After collecting the last sample (90 min after intrathecal administration of test substance) the catheters were removed, and all incisions were sutured. Isoflurane was discontinued, and the lungs were ventilated with 100% oxygen. Extubation of the trachea was

performed when adequate spontaneous ventilation occurred. The animals were allowed to recover with infusion of Ringer's solution and antibiotic treatment.

The animals were neurologically assessed daily until 1 week after test drug administration by an observer unaware of the treatment group. Sensory function was evaluated by seeking an aversive response to pinprick stimulation with a 23-gauge needle, progressing from sacral to thoracic dermatomes. The score of the sensory function was assessed by a three-point grading scale. The hind limb motor function was assessed by a five-point grading scale.

After completion of the neurologic function scoring at 1 week, the animals were re-anesthetized, and transcardiac perfusion and fixation were performed. The spinal cord was removed and refrigerated in phosphate-buffered formalin 10% for 48 h. After dehydration in graded concentrations of ethanol and butanol, the spinal cord was embedded in paraffin. The coronal sections of the spinal cord at L3, L4, and L5 levels were cut at a thickness of 8 μm and stained with hematoxylin and eosin. The degree of spinal cord damage was assessed in terms of vacuolation of the dorsal funiculus with a four-point grading scale and chromatolytic changes in the motor neuron. The neurons with chromatolytic appearance were identified by round-shaped cytoplasm with the loss of Nissl substance from the central part of the cell and eccentric nuclei. The number of motor neurons with a chromatolytic appearance was counted in two sections for each animal and averaged.

Parametric data were presented as mean ± SD. To determine differences in glutamate concentrations, a repeated-measures analysis of variance was performed. The cutaneous sensation, hind limb motor function, and morphological changes of the spinal cord were analyzed with a non-parametric method (Kruskal-Wallis test) followed by the Mann–Whitney *U*-test

Studies in Dogs

Wagner et al. (1940) performed spinal anesthesia in anesthetized **dogs** by puncture at the fourth lumbar interspace and measured the duration of anesthesia after the application of various local anesthetics.

Muschaweck et al. (1971) performed comparative intrathecal tolerance studies in dogs. **Beagle dogs** weighing 8–12 kg were anesthetized with 30 mg/kg sodium pentobarbital intravenously. The animals were intubated and submitted to artificial respiration. The fur on the neck was shaved and the skin disinfected. All further procedures were carried out under sterile conditions. The spinal canal was punctured through the foramen magnum at the atlanto-occipital joint. Successful entry of the spinal cervical canal was checked by withdrawal of cerebrospinal fluid. Then 5 ml of cerebrospinal fluid was withdrawn and used as the solvent for the tested local anesthetics. The same volume was injected intrathecally either as a solution of local anesthetics in concentrations used in therapy or as control (saline solution). Artificial respiration was continued until spontaneous breathing resumed. Motor performance was checked for 24 h. Two days later, the animals were sacrificed under anesthesia. Dissection included the cerebellum, medulla oblongata, and sections from the cervical, thoracic and lumbar cord, carefully observing that the same segments were always taken, including the injection site. Segments were semi-fixed in 8% buffered formaldehyde for 2 days. When semi-fixed, the vertebral arches were opened, and the spinal cord as well as the roots of the spinal nerves were removed and completely fixed. After embedding in gelatin and Paraplast, a fast red 7B and myelin sheath staining according to Olivecrona were performed on serial sections from the site of injection as well as from cervical, thoracic and lumbar marrow. Hematoxylin–eosin staining as well as periodic acid-Schiff (PAS) staining and the iron reaction were all performed in one section. The presence or absence of nerve damage and of inflammation was noted.

A chronic model for investigation of experimental spinal anesthesia in the **dog** was described by Feldman and Covino (1981).

Dohi et al. (1987) inserted a polyethylene catheter into the lumbar subarachnoid space in **dogs** through a small hole in the dura for administration of drugs. The tip of the catheter was placed approximately 2–3 cm cephalad to the lumbar electrode introduced for recording of hydrogen clearance to measure spinal cord blood flow.

Kozody et al. (1985) measured spinal cord and spinal dural blood flow in the cervical, thoracic and lumbosacral regions in **dogs** using the microsphere technique. Measurements were taken 20 and 40 min after lumbar subarachnoidal injection through the L5-L6 or L6-L7 interspace.

Yaksh et al. (1995) studied the safety of chronically administered neostigmine methylsulfate in rats and **dogs**. Adult beagle dogs weighing 13–17 kg were adapted for 5 days to experimental protocols and placement of a nylon vest. For placement of the spinal catheter, the dogs were sedated (atropine 0.04 mg/kg and xylazine-Rompun 1–2 mg/kg i.m.) given an i.m. injection of penicillin G and procaine. Anesthesia

was induced by mask administration of halothane (3%–5%) and then the trachea was intubated. The dog was maintained under spontaneous ventilation with 1%–2% halothane and 50% N_2/50%O_2. Surgical areas on the back of the neck and head were shaved and prepared with alcohol and a povidone-iodine scrub, and the dog was placed in a stereotaxic head holder. After draping and using sterile technique, the cisterna magna was exposed, and a small incision (1–2 mm) was made. The intrathecal catheter (polyethylene rubbing PE-50 stretched by 30%, making the nominal diameter 0.6 mm) was inserted and passed caudally at a distance of 40 cm, to a level corresponding approximately to the L3–L4 segment. The presence of the catheter in the intrathecal space was confirmed by free withdrawal of cerebrospinal fluid. A small stainless steel screw was placed in the skull and the catheter fixed to the screw. The catheter was tunneled subcutaneously and caudally to exit on the upper left back at the level of the scapula. The incision was closed by sutures, the halothane turned off and the animal allowed to recover. An analgesic was administered for postoperative pain medication. At this time, the catheter was connected to the infusion pump placed into a vest side pocket, and an infusion of sterile saline (2 ml/day) was started.

For a 28-day infusion study, dogs were randomly assigned to receive saline or neostigmine (4 mg/4 ml). After 28 days of infusion, the dogs were sacrificed. After induction of deep anesthesia, the animal was manually ventilated to maintain adequate oxygenation. A percutaneous puncture of the cisterna magna was performed and cerebrospinal fluid withdrawn for analysis. The chest was opened and a large-bore cannula placed in the aortic arch through which was perfused saline followed by 10% formalin. After fixation, the dura was exposed by an extensive laminectomy of the spinal canal and the lower brainstem, being careful to leave the catheter and the dura undisturbed. Dye was injected through the catheter to determine its integrity, visualize the position of the intrathecal catheter, and determine the spread of dye around the catheter. The spinal cord was removed in four blocks (cervical, thoracic, caudal, and rostral from the catheter tip), taking care to keep the dura intact, and placed in formalin. After fixation, tissue blocks were embedded in paraffin and then decalcified overnight, embedded in paraffin, sectioned at a thickness of 6–7 µm and stained with hematoxylin and eosin. Particular attention was given to the presence or absence of fibrosis and other reactions around the catheter, dural thickening or other reaction, such as inflammation in the epidural space, leptomeninges/subarachnoid space, or spinal cord parenchyma, microglial nodules, demyelinization, or gliosis. The degree of chronic and/or acute inflammation was graded as normal, mild, moderate or severe.

Studies in Other Species

Bahar et al. (1984b) performed chronic implantations of nylon catheters into the subarachnoid space of Wistar **rats** and **marmosets** and tested the effects of local anesthetics.

The technique of evaluation of spinal anesthesia by a local anesthetic in the **Rhesus monkey** was described by Denson et al. (1981).

Lebeaux (1975) recommended the **sheep** as a model for testing spinal and epidural anesthetic agents. To ensure accurate and reproducible administration of drugs into these restricted anatomical regions, a wooden stock was built to restrain the sheep without stress but to allow arching of the lumbosacral spine in order to open the inter vertebral space. The stock consisted of a table with holes for the front feet, hinged at one end to a fixed stanchion. The hinges permitted tilt of the table. The sheep was placed prone on the table, the head secured in the stanchion and the front feet passed through the holes and tied. The lumbosacral interspace used for both spinal and epidural tap was separated by positioning and tying the rear limbs cephalad beside the abdomen, thereby extending the knee and flexing the hip. The wool was clipped from the sheep's back, the skin of the lumbosacacral area was washed and swabbed with iodine, and the vertebral spines and interspaces identified by palpation, marked, and numbered with a felt pen.

Spinal block was performed using either the midline or lateral approach for tapping the subarachnoid space. A 22-gauge disposable spinal needle was inserted subarachnoidally, and proper position was verified by spontaneous flow of cerebrospinal fluid upon removal of the stylet. With the table top and sheep parallel to the floor, the Luer-Lok syringe holding 1 ml of sterile 5.0% dextrose solution containing 2.5 mg (0.25%) tetracaine was attached to the needle. After aspiration of spinal fluid, the solution was injected within 5 s. At completion of the injection, spinal fluid was again aspirated to confirm injection into the subarachnoid space. The needle was withdrawn and the table tilted 10° caudally to restrict the spread of the hyperbaric solution to the lumbosacral area. The sheep was held in this position for 20 min.

Immediately after injection, the rear feet were untied and allowed to hang free on either side of the table

for evaluation of sensation and/or reflexes in the rear limbs. Then, 20 min after injection the sheep was removed from the table and positioned in a sling fashioned from a heavy duty 50-gallon plastic barrel split in half longitudinally and mounted on a metal support. Holes cut in the barrel allowed the feet to drop through so that comfortable sternal recumbency was maintained while permitting anesthetic evaluation to continue. When complete sensation returned in the skin of the dorsum, the sheep was removed from the sling and placed on a straw-bedded floor so that weight support and full recovery could be assessed.

Kyles et al. (1992) described a simple and noninvasive method for the chronic implantation of intrathecal catheters in the **sheep**.

REFERENCES AND FURTHER READING

Åkerman B (1985) A methodological study of spinal (subarachnoid) anesthesia in the rat and mouse. Br J Anesth 57:29–332

Åkerman B, Hellberg IB, Trossvik C (1988a) Primary evaluation of the local anesthetic properties of the amino amide agent ropivacaine (LEA 103). Acta Anesthesiol Scand 32:571–578

Åkerman B, Arweström E, Post C (1988b) Local anesthetics potentiate spinal morphine antinociception. Anesth Analg 67:943–948

Bahar M, Rosen M, Vickers MD (1984a) Chronic cannulation of the intradural and extradural space in the rat. Br J Anaesth 56:405–410

Bahar M, Nunn JF, Rosen M, Flecknell P (1984b) Differential sensory and motor blockade after spinal cocaine in the rat and marmoset. Eur J Anaesthesiol 1:31–36

Bieter RN, Cunningham RW, Lenz OA, McNearney JJ (1936a) Threshold anesthetic and lethal concentrations of certain spinal anesthetics in the rabbit. J Pharm Exper Ther 57:221–244

Bieter RN, McNearney JJ, Cunningham RW, Lenz OA (1936b) On the duration of spinal anesthesia in the rabbit. Pharmacol Exp Ther 57:264–273

Chanimov M, Cohen ML, Grinspun Y, Herbert M, Reif R, Kaufman I (1997) Neurotoxicity after spinal anaesthesia induced by serial intrathecal injections of magnesium sulphate. Anaesthesia 52:223–228

Cole DJ, Lin DM, Drummond JC, Shapiro HM (1990) Spinal tetracaine decreases central nervous system metabolisms during somatosensory stimulation in the rat. Can J Anesth 37:231–237

De la Calle JL, Paíno CL (2002) A procedure for direct lumbar puncture in rats. Brain Res Bull 59:245–250

Denson DD, Bridenbaugh PO, Phero JC, Raj PP, Turner PA, Ohlweiler DF (1981) Evaluation of lidocaine spinal anesthesia in the Rhesus monkey. Anesth Analg 10:756–759

Dirksen R, Lerou J, Bakker H, van Luijtelaar E, Nijhuis G, Gielen M, Booij L (1992) The dose-response and time-effect relationships of intrathecal bupivacaine in rats. The influence of epinephrine and pH. Acat Anaesth Scand 36:153–158

Dohi S, Takeshima R, Naito H (1987) Spinal cord blood flow during spinal anesthesia in dogs: the effects of tetracaine, epinephrine, acute blood loss, and hypercapnia. Anesth Analg 66:599–606

Feldman HS, Covino BG (1981) A chronic model for investigation of experimental spinal anesthesia in the dog. Anesthesiology 54:148–152

Grouls RJE, Meert TF, Korsten HHM, Hellebrekers LJ, Breimer DD (1997) Epidural and intrathecal n-butyl-p-aminobenzoate solution in the rat: comparison with bupivacaine. Anesthesiology 86:181–187

Hampl KF, Schneider MC, Ummenhofer W, Drews J (1995) Transient neurological symptoms after spinal anesthesia Anesth Analg 81:1148–1153

Hylden JLK, Wilcox GL (1980) Intrathecal morphine in mice: a new technique. Eur J Pharmacol 67:313–316

Kirihara Y, Saito Y, Sakura S, Hashimoto K, Kishimoto T, Yasui Y (2003) Comparative neurotoxicity of intrathecal and epidural lidocaine in rats. Anesthesiology 99:961–968

Kozody R, Palahniuk RJ, Cumming RO (1985) Spinal cord flow following subarachnoid tetracaine. Can Anesth Soc J 32:23–29

Kyles AE, Waterman A, Livingston A (1992) Chronic intrathecal catheterization in the sheep. J Pharmacol Toxicol Meth 27:177–183

Langerman L, Golomb E, Benita S (1991) Spinal anesthesia: Significant prolongation of the pharmacologic effect of tetracaine with lipid solution of the agent. Anesthesiology 74:105–107

Langerman L, Bansinath M, Grant GJ (1994) The partition coefficient as a predictor of local anesthetic potency for spinal anesthesia: Evaluation of five local anesthetics in a mouse model. Anesth Analg 79:490–494

Lebeaux M (1975) Sheep: a model for testing spinal and epidural anesthetic agents. Lab Anim Sci 25:629–633

Luduena FP, Hoppe JO, Coulston F, Drobeck HP (1960) The pharmacology and toxicology of mepivacaine, a new local anesthetic. Toxicol Appl Pharmacol 2:295–315

Mestre C, Pélissier T, Fialip J, Wilcox G, Eschalier A (1994) A method to perform direct transcutaneous intrathecal injections in rats. J Pharmacol Toxicol Meth 32: 197–200

Muschaweck R, Kief H, Baehr H (1971) Comparative intrathecal tolerance of artcaine in dogs. Personal communication

Myers RR, Sommer C (1993) Methodology for spinal neurotoxicity studies. Reg Anaesth 18:439–447

Ohtake K, Matsumoto A, Wakamatsu H, Kawai K, Nakakimura S, Sakabe T (2000) Glutamate release and neuronal injury after intrathecal injection of local anesthetics. Neuroreport 11:1105–1109

Oka S, Matsumoto M, Ohtake K, Kiyoshima T, Nakakimura K, Sakabe T (2001) The addition of epinephrine to tetracaine injected intrathecally sustains an increase in glutamate concentrations in the cerebrospinal fluid and worsens neuronal injury. Anesth Analg 93:1050–1057

Omote K, Iwasaki H, Kawamata M, Satoh O, Namiki A (1995) Effects of verapamil on spinal anesthesia with local anesthetics. Anesth Analg 80:444–448

Ossipov MH, Suarez LJ, Spaulding TC (1988) A comparison of antinociceptive and behavioral effects of intrathecally administered opiates, α-2-adrenergic agonists, and local anesthetics in mice and rats. Anesth Analg 67:616–624

Sakura S, Hashimoto K, Bollen AW, Ciriales R, Drasner K (1996) Intrathecal catheterization in the rat: improved technique for morphological analysis of drug-induced injury. Anesthesiology 85:1184–1189

Wagner JC, Sievers RF, Bennett AL, McIntyre AR (1940) Spinal anaesthesia in dogs. J Pharmacol Exp Ther 68:437

Wakamatsu H, Matsumoto M, Nakakimura K, Sakabe T (1999) The effects of moderate hypothermia and intrathecal tetracaine on glutamate concentrations of intrathecal dialysate

and neurologic outcome in transient spinal cord ischemia in rabbits. Anesth Analg 88:56–62
Wang BC, Hillman DE, Li D, Turndorf H (1991) Lumbar subarachnoid catheterization in rats. Pharmacol Biochem Behav 38:685–688
Yaksh TL, Rudy TA (1976) Chronic catheterization of the spinal subarachnoid space. Physiol Behav 17:1031–1036
Yaksh TL, Grafe MR, Malkmus SAHT, Rathbun ML, Eisenach JC (1995) Studies on the safety of chronically administered neostigmine methylsulfate in rats and dogs. Anesthesiology 82:412–427

G.1.5.2 Blockade of Urethral Reflex in Rabbits

PURPOSE AND RATIONALE

For evaluation of spinal anesthetics the test substance has to be injected into the spine. For the study of local anesthetics for which conduction anesthesia has been verified, intraspinal injection provides more complete information. Spinal anesthesia has been studied in rabbits (Bieter et al. 1936a, 1936b; Luduena and Hoppe 1951; Luduena 1957; Gonzalez and Luduena 1961; Turner RA 1965), cats (Sechzer 1965), and dogs (Dvorak and Manson 1930). If the solution of test substance is injected intrathecally to male rabbits, the presence of anesthesia may be determined by the urethral reflex (Luduena 1957).

PROCEDURE

Male Chinchilla rabbits weighing 3.0–3.5 kg are used. The volume administered intrathecally is 0.02 ml per centimeter of spinal length. It is injected at a rate of 1 ml per min with a 22-gauge needle that is 3.8 cm long. The needle is introduced between the sixth and seventh lumbar vertebrae, and not through the lumbosacral space. The needle, held as lightly as possible between the thumb and forefinger, is introduced slowly until a typical sharp and sudden twitch occurs. This indicates penetration into the subarachnoidal space. A one ml tuberculin syringe is then attached to the needle. It is not possible to aspirate fluid after insertion of the needle. However, it is possible to aspirate a portion of the injected solution. Very little pressure is required for injection of 0.4 to 0.6 ml of anesthetic solution while the animal is restrained in a canvas hammock. A catheter is inserted into the urethra, where it is kept without digital pressure. At 15- or 20-s intervals, 2 to 3 ml of water, at room temperature, are injected rapidly into the catheter. This causes the "urethral reflex", consisting of retraction of the penis and contraction of the anal sphincter. The water runs out of the urethra around the catheter. Without medium or high concentrations of the anesthetics the reflex is absent on the first reading. After loss of the urethral reflex, the test is repeated every minute or two for 15 min, and thereafter at longer intervals. The duration of urethral areflexia is taken as the time of the first positive reading (reflex absent) to the middle of the interval between the last positive and the first negative reading. This duration varies linearly with the logarithm of concentration.

EVALUATION

The threshold anesthetic concentration in grams per 100 ml for abolition of the urethral reflex for 5 min, the TAC_5, is a standard for comparison. There is a correlation between activity and systemic toxicity. The ratio of the activity to the irritancy is the most important parameter.

MODIFICATIONS OF THE METHOD

Burdyga and Magura (1986) studied the effects of local anesthetics on the electrical and mechanical activity of the guinea-pig ureter.

REFERENCES AND FURTHER READING

Bieter RN, Cunningham RW, Lenz OA, McNearney JJ (1936a) Threshold anesthetic and lethal concentrations of certain spinal anesthetics in the rabbit. J Pharmacol Exp Ther 57:221–244
Bieter RN, McNearney JJ, Cunningham RW, Lenz OA (1936b) On the duration of spinal anesthesia in the rabbit. J Pharmacol Exp Ther 57:264–273
Burdyga TV, Magura IS (1986) The effects of local anaesthetics on the electrical and mechanical activity of the guinea-pig ureter. Br J Pharmacol 88:523–530
Dvorak H, Manson MH (1930) Technique of spinal anesthesia in the dog. Proc Soc Exp Biol Med 28:344–347
Gonzales E, Luduena FP (1961) Experimental spinal anaesthesia produced by members of a homologous series. J Med Pharm Chem 3:555–560
Luduena FP (1957) Experimental spinal anesthesia. Arch Int Pharmacodyn 109:143–156
Luduena FP, Hoppe JO (1951) 2-Phenyl-4-thiazolidone derivatives as local anesthetics. J Am Pharm Ass 40:132–137
Sechzer PH (1965) The effect of organophosphates on nerve conduction. Arch Int Pharmacodyn 157:432–441
Turner RA (1965) Local and spinal anesthetics. In: Turner RA (ed) Screening Methods in Pharmacology. Academic Press, New York and London, pp 268–269

G.1.6 Endoanesthetic Effect

PURPOSE AND RATIONALE

Endoanesthesia has been described as the effect of local anesthetics on viscero-afferent receptors, located predominantly in the lung as distension receptors (Meier and Bein 1950; Zipf 1953, 1957, 1959, 1966.

1968; Zipf et al. 1955; Zipf and Oehler 1955; Reichertz et al. 1957; Zipf and Reichertz 1957; Zipf et al. 1963; Wellhöner and Conrad 1965; Siemoneit et al. 1966; Dittmann and Zipf 1973; Borchard 1979). The endoanesthetic effect has been claimed to be the basis of an antitussive action of local anesthetics (Bucher 1956; Bein and Bucher 1957; Kraushaar et al. 1964).

PROCEDURE

Male guinea pigs weighing 300–400 g are anesthetized by intraperitoneal injection of 1.25 g/kg urethane. The studies are carried out on spontaneously breathing or artificially respirated monovagotomized or bivagotomized animals. Intravenous injections are given via a catheter into the jugular vein. The flow rate of the respiratory air is measured with a Fleisch tube connected to a pneumotachograph. In experiments with positive pressure respiration, the open end of the Fleisch tube is attached to a respiratory pump (40 strokes per min). A cannula is inserted into the carotid artery and connected to a pressure transducer.

The left nervus vagus is exposed from the thorax aperture until his entry into the foramen jugulare and cut in the middle of the distance. Both ends are placed over 3 wires of Ag/AgCl 6-way electrodes. The edges of the skin wound are pulled upwards with clamps and the space around the trachea is filled with paraffin to prevent the nerve from drying out. The afferent and efferent vagus potentials and also their integration curve (Zipf and Reichertz 1957) are recorded on a direct recorder. In addition, the ECG in the second lead is recorded continuously. The animal is shielded electrically with the aid of a Faraday cage.

The nervus vagus conducts not only afferences from the lung but also from other organs to the brain. The base points of the integral curve, which correspond to the vagus action potentials being synchronous with inspiration and issued by the pulmonary distension receptors, therefore lie above the baseline of the recorder tracing. The vagus afferences which remain after subtraction of the vagus activity synchronous with respiration ("inspiratorial activity") are called "residual activity". The level of inspiratorial activity depends both on the bronchial width (degree of inflation of the lungs) and on the functional state of the pulmonary receptors and of the afferent pathway. The occurrence of a bronchospasm is detectable from the decrease in the pneumotachogram, if the respiratory rate is not reduced at the same time.

EVALUATION

The following parameters are evaluated:

Afferent and efferent inspiratorial vagal activity, maximum flow rate of the respiratory air during inspiration and expiration, tidal volume, duration of the respiratory phases (inspiration = t_i, expiration = t_e, respiratory pause = t_p), heart rate and blood pressure.

The decrease of electrical activity after various doses of standard and test drugs is calculated at different time intervals after drug administration. Maximum of activity and decay with time are registered.

Statistical analysis is performed using the paired and non-paired *t*-test, after the applicability has been first checked with the F-test.

CRITICAL ASSESSMENT OF THE METHOD

The correlation between antitussive and local anesthetic activity has been challenged by Sell et al. (1958) and by Ther and Lindner(1961).

MODIFICATIONS OF THE METHOD

Bein and Bucher (1967), Wellhöner and Conrad (1955) tested various compounds for their anesthetic effect on pulmonary stretch receptors of **rabbits**.

REFERENCES AND FURTHER READING

Bein HJ, Bucher K (1957) Anästhetische Wirkung an Lungendehnungsrezeptoren und anderen nervösen Substraten. (Zur Pharmakologie des Tessalon). Helv Physiol Acta 15:55–62

Borchard U (1979) Studies on the action mechanism and pharmacological characterization of local anesthetics. Habilitation Thesis of the High Faculty of Medicine of the University of Duesseldorf for Attainment of venia legendi

Bucher K (1956) Tessalon, ein hustenstillendes Mittel von neuartigem Wirkungsmechanismus. Schweiz Med Wschr 86:94–96

Dittmann EC, Zipf HF (1973) Schmerzauslösung und Pharmakologie der Lokalanästhetika. In: Kilian H. (Hgb.) Lokalanästhesie und Lokalanästhetika. Thieme Verlag Stuttgart, pp 76–144

Kraushaar AE, Schunk RW, Thym HF (1964) Ein neues Antitussivum: 2-(β-Hexamethyleniminoäthyl)-cyclo-hexanon-2-carbonsäure-benzylester HCl. Arzneim Forsch 14:986–995

Meier R, Bein HJ (1950) Neuere Befunde über die organisationsspezifischen Wirkungen am autonomen Nervensystem. Bull schweiz Akad med Wiss 6:209–233

Reichertz P, Zipf HF, Hansen K (1957) Vergleichende Prüfung verschiedener Endoanaesthetica an den Lungendehnungsrezeptoren des Meerschweinchens. Arzneim Forsch 7:739–742

Sell R, Lindner E, Jahn H (1958) Untersuchungen über die Anästhesie der Dehnungs- und Berührungsrezeptoren durch einige Lokalanästhetika im Vergleich zur hustenstillenden Wirkung. Naunyn Schmiedeberg's Arch exp Path Pharmak 234:164–178

Siemoneit KD, Zipf HF, Dittmann EC (1966) Untersuchungen zur endoanästhetischen und hypnotisch/narkotischen Wirkung von 2-Methoxy-4-allyl-phenoxyessigsäure-N,N′-diäthylamid (G29505) und verwandten Phenolderivaten. Arch Int Pharmacodyn 164:30–46

Ther L, Lindner E (1961) Über die hustenstillende Wirkung von Lokalanästhetika. Medizin und Chemie (Weinheim), pp 351–357
Wellhöner HH, Conrad B (1965) Über die Wirkung von Aconitin auf die Impulstätigkeit in afferenten Fasern aus Lungendehnungsrezeptoren. Naunyn Schmiedeberg's Arch Exp Path Pharmak 252:269–285
Zipf HF (1953) Die Endoanästhesie, ein pharmakologischer Weg zur Ausschaltung innerer sensibler Rezeptoren. Dtsch Med Wschr 78:1587–1589
Zipf HF (1957) Lungensensibilität und ihre Ausschaltung durch Endoanästhesie. Klin Wschr 35:1031–1037
Zipf HF (1959) Die Allgemeinwirkungen der Lokalanästhetika. In: Kilian H. (Hgb.) Lokalanästhesie und Lokalanästhetika. Thieme Verlag Stuttgart, pp 111–189
Zipf HF (1966) The pharmacology of viscero-afferent receptors with special reference to endoanesthesia. Acta neuroveg (Wien) 28:169–196
Zipf HF (1968) New light on the properties of local anaesthetics. Germ Med Mth 13:238–247
Zipf HF, Oehler H (1955) Die Trachealverschlußreaktion nach HEAD, eine Hilfsmethode zum Nachweis endeoanästhetischer Wirkungen. Naunyn Schmiedeberg's Arch exp Path Pharmak 226:363–376
Zipf HF, Reichertz P (1957) Darstellung der totalen und reversiblen Endoanästhesie der Lungendehungsrezeptoren durch Zeit/Wirkungskurven. Naunyn Schmiedeberg's Arch exp Path Pharmak 231:96–110
Zipf HF, Kreppel E, Wetzels E (1955) Untersuchungen zur Definition einer katelektrotonischen Form der Endoanaesthesie. Arch Exper Path Pharmakol 226:348–362
Zipf HF, Dittmann EC, Marquardt H (1963) Lokalanästhetische und endoanästhetische Wirkungen von Tropeinen. Arzneim Forsch 13:1097–1100

G.1.7 Effect on Electroretinogram

PURPOSE AND RATIONALE

The retina, which belongs in ontogenesis to the central nervous system, can be prepared without damaging the parenchyma. The transretinal potential which can be induced by a light flash can be used as an objective criterion for the functional state (Sickel et al. 1960). The multi-phase potential path of the electroretinogram consists of an initial a-wave, a subsequent b-wave and an e-wave which starts with a delay after the end of the stimulus. While the amplitudes of the a- and e-wave are in the order of 50 µV, the amplitude of the b-wave (Φ_b) is 500–1000 µV. The electroretinogram can be used for various purposes, such as the evaluation of local anesthetics (Borchard 1979).

PROCEDURE

Frogs (*Rana esculenta*) are kept in dark for 1 h before beginning of the preparation. The frog is sacrificed by decapitation, the eyeball excised in dim red light and cut into two halves with the aid of a rotating blade. The retina together with the pigmented epithelium and choroid is removed from the rear half of the eye and transferred to a dish with Tyrode solution. The retina is then detached from the pigmented epithelium by careful shaking and spread out on a Monodur net. The net is fixed to a round carrier with a narrow ring and the chamber is transferred to a flow-through apparatus. An electrical pump is used for superfusion of the retina with Tyrode solution.

In order to apply the local anesthetic only to the receptor or vitreous body side of the retina, an apparatus is used in which the tissue on a silk net is stretched as the partition between two chamber halves which can perfused separately (Borchard and Erasmi 1974).

The electroretinogram is recorded with Ag/AgCl electrodes. After amplification, the signal is registered on a recorder or an oscillograph. Light stimuli of 10 ms are generated. The light from a low-voltage light source is focused on a electromagnetic shutter with a stimulus frequency of 0.1 Hz. Light stimuli of 1 s duration are used at intervals of 3 min to measure the influence of the local anesthetics on the electroretinogram as a function of light intensity.

All experiments are performed after adaptation to darkness and at room temperature. The amplitude of the b-waves (Φ_b) which is measured from the lowest point of the a-wave to the maximum of the b-wave is used for evaluation. In order to obtain stationary test conditions, the experiment is started after a 45 min adaptation period. The stimulus signal is recorded by means of a photocell inserted in the light path.

Various concentrations of the local anesthetics are applied and various light intensities are used. The decrease of the b-wave starts immediately and then progresses slowly and continuously. After changing over to Tyrode solution, the decrease in the exposure potential is completely reversible.

EVALUATION

After various doses, time-response curves can be drawn and for a given time interval ED_{50} values can be calculated. Moreover, the influence of local anesthetics on the b-wave at various light intensities can be estimated.

MODIFICATIONS OF THE METHOD

Isolated retina for electroretinogram has been used not only from **frogs** but also from **rats** (Huang et al. 1991; Doly et al. 1993), **rabbits** (Mochizuki et al. 1992; Maynard et al. 1998) and from **beef** (Gosbell et al. 1996; Walter et al. 1999).

Moreover, the electroretinogram has been used as parameter for many *in vivo* studies with different purposes, e. g., on the effect of drugs after retinal ischemia, in various animal species, such as **rats** (Sugimoto et al. 1994; Hotta et al. 1997; Biró et al. 1998; Block and Schwarz 1998; Estrade et al. 1998; Ettaiche et al. 1999; Li et al. 1999), **rabbits** (Takei et al. 1993; Zemel et al. 1995; Horiguchi et al. 1998; Jarkman et al. 1998; Liang et al. 1998), **cats** (Imai et al. 1991; Ostwald et al. 1997; Kim et al. 1998), **dogs** (Jones et al. 1995; Yanase and Ogawa 1997) or **monkeys** (Tagliati et al. 1994).

REFERENCES AND FURTHER READING

Ames III A, Gurian BS (1960) Measurement of function in an *in vitro* preparation of mammalian central nervous tissue. J Neurophysiol 23:676–691

Biró K, Pálhalmi J, Tóth AJ, Kukorelli T, Juhász G (1998) Bimoclomol improves early electrophysiological signs of retinopathy in diabetic rats. NeuroReport 9:2029–2033

Block F, Schwarz M (1998) The b-wave of the electroretinogram as an index of retinal ischemia. Gen Pharmac 30:281–287

Borchard U (1975) The effect of dimethylsulfoxide (DMSO) on the bioelectric activity of the isolated retina. Pflügers Arch Suppl 355:R111

Borchard U (1979) Studies on the action mechanism and pharmacological characterization of local anesthetics. Habilitation Thesis of the High Faculty of Medicine of the University of Duesseldorf for Attainment of venia legendi

Borchard U, Erasmi W (1974) Na^+ diffusion in the retinal tissue of the frog. Vision Res 14:17–22

Doly M, Cluzel J, Millerin M, Bonhomme B, Braquet P (1993) Prevention of chloroquine-induced electroretinographic damage by a new platelet-activating factor antagonist, BN 50730. Ophthalmic Res 25:314–318

Estrade M, Grondin P, Cluzel J, Bonhomme B, Doly M (1998) Effect of a cGMP-specific phosphodiesterase inhibitor on retinal function. Eur J Pharmacol 352:157–163

Ettaiche M, Fillacier K, Widmann C, Heurteaux C, Lazdunski M (1999) Riluzole improves functional recovery after ischemia in the rat retina. Invest Ophthalmol Vis Sci 40:729–736

Furukawa T, Hanawa I (1955) Effects of some common cations on electroretinogram of the toad. Jap J Physiol 5:289–300

Gosbell A, Favilla I, Jablonski P (1996) The effects of insulin on the electroretinogram of bovine retina *in vitro*. Curr Eye Res 15:1132–1137

Horiguchi M, Suzuki S, Kondo M, Tanikawa A, Miyake Y (1998) Effect of glutamate analogues and inhibitory neurotransmitters on the electroretinograms elicited by random sequence stimuli in rabbits. Invest Ophthalmol Vis Sci 39:2171–2176

Hotta N, Nakamura J, Sakakibara F, Hamada Y, Hara T, Mori K, Nakashima E, Sasaki H, Kasama N, Inukai S, Koh N (1997) Electroretinogram in sucrose-fed diabetic rats treated with an aldose reductase inhibitor or an anticoagulant. Am J Physiol 273 (Endocrinol Metab 36) E965–E971

Huang JC, Salt TE, Voaden J, Marshall J (1991) Non-competitive NMDA-receptor antagonists and anoxic degeneration of the ERG B-wave *in vitro*. Eye 5:467–480

Imai R, Sugimoto S, Ando T, Sato S (1991) A procedure for recording electroretinogram and visual evoked potential in freely moving cats. J Toxicol Sci 15:263–274

Jarkman S, Kato M, Bragadottir R (1998) Effects of pituitary adenylate-cyclase-activating polypeptide on the direct-current electroretinogram of the rabbit eye. Ophthalmic Res 30:199–206

Jones RD, Hamilton BF, Dass PD (1995) The effects of physostigmine on the electroretinogram in the Beagle dog. Vet Res Commun 19:135–147

Kim S-Y, Kwak J-S, Shin J-P, Lee S-H (1998) The protection of the retina from ischemic injury by the free radical scavenger Egb 761 and zinc in the cat retina. Ophthalmologica 212:268–274

Li S, Mizota A, Adachi-Usami E (1999) Effects of intravitreal injection of botulinum toxin on the electroretinogram of rats. Ophthalmic Res 31:392–298

Liang C, Peyman GA, Sun G (1998) Toxicity of intraocular lidocaine and bupivacaine. Am J Ophthalmol 125:191–196

Maynard KI, Arango PM, Chen D, Ogilvy CS (1998) Acetylsalicylate administered during simulated ischemia reduces the recovery of neuronal function in the *in vitro* rabbit retina. Neurosci Lett 249:159–162

Mochizuki K, Yamashita Y, Torisaki T, Komatsu K, Tanahashi T, Sakai H (1992) Intraocular penetration and effect on the retina of fluconazole. Les-Eye-Toxic-Res 9:537–546

Ostwald P, Park SS, Toledano AY, Roth S (1997) Adenosine receptor blockade and nitric oxide synthase inhibition in the retina: Impact upon post-ischemic hyperemia and the electroretinogram. Vis Res 37:3453–3461

Sickel W, Lippmann HG, Haschke W, Baumann C (1960) Elektrogramm der umströmten menschlichen Retina. Ber Dtsch Ophthalm Ges 63:316–318

Sugimoto S, Imawaka M, Ozaki H, Ito T, Ando T, Sato S (1994) A procedure for recording electroretinogram (ERG) with a contact lens-type electrode, and effects of sodium iodate on ERG in rats. J Pharmacol Toxicol Sci 19: Suppl 3:531–542

Tagliati M, Bodis-Wollner I, Kovanecz I, Stanzione P (1994) Spatial frequency tuning of the monkey pattern ERG depends on D2 receptor-linked action of dopamine. Vis Res 34:2051–2057

Takei K, Sato T, Nonoyama T, Miyauchi T, Goto K, Hommura S (1993) A new model for transient complete obstruction of retinal vessels induced by endothelin-1 injection into the posterior vitreous body in rabbits. Graefe's Arch Clin Exp Ophthalmol 231:476–481

Walter P, Luke C, Sickel W (1999) Antibiotics and light responses in superfused bovine retina. Cell Mol Neurobiol 19:87–92

Yanase J, Ogawa H (1997) Effects of halothane and sevoflurane on the electroretinogram of dogs. Am J Vet Res 58:904–909

Zemel E, Loewenstein A, Lazar M, Perlman I (1995) The effects of lidocaine and bupivacaine on the rabbit retina. Docum Ophthalm 90:189–199

G.2 Neuromuscular Blocking Activity

G.2.0.1 General Considerations

Neuromuscular transmission is mediated by mediated by nicotinic acetylcholine receptors for which various

subtypes are described (Sargent 1993; McGehee and Role 1995; Karlin and Akabas 1995; Alexander et al. 2001).

Neuromuscular blocking agents are distinguished by whether or not they cause depolarization of the motor end plate. They are classified either as competitive (stabilizing) agents, of which d-tubocurarine is the classical example, or as depolarizing, desensitizing agents such as succinylcholine.

The **rabbit head-drop method** was described by Varney et al. (1948, 1949), Burn et al. (1952), Levis et al. (1953). Rabbits were given an interrupted intravenous injection at a rate of 0.1 ml every 15 s until the muscles supporting the head become sufficiently relaxed to prevent the head to be raised when the back is stimulated. This method has been replaced by the rabbit sciatic nerve-gastrocnemius muscle preparation, the isolated phrenic nerve diaphragm preparation of the rat, and the chick sciatic nerve-tibialis anticus muscle preparation.

The method described by Allmark and Bachinski (1949) used an inclined screen for testing curare-like activity in **rats**.

Skinner and Young (1947) placed **mice** weighing 15–17 g in sloping rotating cylinders. Mice falling away during 20 min after subcutaneous injection were considered as reactors. Dose response-curves and potency ratios could be calculated from the logarithmic dose-response curves using different doses of test compound and the standard tubocurarine chloride.

Collier et al. (1949) used a rotating drum to assess the activities of paralysant, convulsant and anesthetic drugs in mice.

Fatt and Katz (1951) performed an extensive study on neuromuscular junction by recording end-plate potentials from curarized frog sartorius motor end-plates, using a KCl-filled microelectrode inserted into the muscle fiber in the region of the motor end-plate.

Electrophysiological analysis of transmission at the skeletal neuromuscular junction was reviewed by Prior et al. (1993).

A review on new neuromuscular blocking drugs was given by Hunter (1995).

Savarese et al. (1975) discussed the potential uses of short-acting non-depolarizing neuromuscular-blocking agents as predicted from animal experiments.

REFERENCES AND FURTHER READING

Alexander S, Peters J, Mathie A, MacKenzie G, Smith A (2001) TiPS nomenclature Supplement 2001

Allmark MG, Bachinski WM (1949) A method of assay for curare using rats. J Am Pharm Ass 38:43–45

Burn JH, Finney DJ, Goodwin LG (1952) Biological Standardization. Chapter XX, Curare-like compounds. Oxford University Press, London, New York, Toronto, pp 345–354

Collier HOJ, Hall RA, Fieller EC (1949) Use of a rotating drum in assessing the activities of paralysant, convulsant and anaesthetic drugs. Analyst 74:592–596

Fatt P, Katz B (1951) An analysis of the end-plate potential recorded with an intra-cellular electrode. J Physiol 115:320–370

Hoppe JO (1955) Observations on the potency of neuromuscular blocking agents with particular reference to succinylcholine. Anaesthesiology 16:91–124

Hunter JM (1995) New neuromuscular blocking drugs. New Engl J Med 332:1691–1699

Karlin A, Akabas MH (1995) Toward a structural basis for the function of nicotinic acetylcholine receptors and their cousins. Neuron 15:1231–1244

Levis S, Preat S, Dauby J (1953) Étude pharmacodynamique de deux séries de curarisants de synthèse. Arch Int Pharmacodyn 93:46–54

McGehee DS, Role LW (1995) Physiological diversity of nicotinic acetylcholine receptors expressed by vertebrate neurons. Annu Rev Physiol 57:521–546

Prior C, Dempster J, Marshall IG (1993) Electrophysiological analysis of transmission at the skeletal neuromuscular junction. J Pharm Toxicol Meth 30:1–17

Sargent PB (1995) The diversity of neuronal nicotinic acetylcholine receptors. Annu Rev Neurosci 16:403–443

Savarese JJ, Antonio RP, Ginsburg S (1975) Potential uses of short-acting nondepolarizing neuromuscular-blocking agents as predicted from animal experiments. Anesth Analg 54:669–678

Skinner HG, Young DM (1947) A mouse assay for curare. J Pharm Exper Ther 91:144–146

Varney RF, Linegar CR, Holaday HA (1948) The rabbit 'head-drop' method for the biological assay of curare and its alkaloids. Fed Proc 7:261–262

Varney RF, Linegar CR, Holaday HA (1949) The assay of curare by the rabbit 'head-drop' method. J Pharmacol Exp Ther 97:72–83

Zaimis E, Head S (1976) Depolarizing neuromuscular blocking drugs. In: Zaimis E (ed) Neuromuscular Junction. Handbook of Experimental Pharmacology, Vol 42, Springer-Verlag, Berlin, Heidelberg, New York, pp 365–419

G.2.0.2 Isolated Phrenic Nerve Diaphragm Preparation of the Rat

PURPOSE AND RATIONALE

The isolated phrenic nerve diaphragm preparation of the rat was originally described by Bülbring (1946) to study the influence of adrenaline on tissue functions normally elicited by acetylcholine. The method has been modified and is widely used by many investigators for studying drugs affecting the neuromuscular transmission.

PROCEDURE

Adult male Wistar rats are used. The animal is sacrificed and the blood is drained. The skin is removed from the middle of the chest. The thorax is opened and the front part of the left thoracic wall is removed.

The phrenic nerve can bee seen quite distinctly. The nerve is cut just below the thymus and a thread is attached to the cut end. The nerve is than freed carefully from the attached tissue. However, no attempt is made to clean the nerve completely from all attached tissue. An incision is made in the left abdominal wall just below the diaphragm. Two converging cuts are made through the diaphragm and the ribs towards the tendinous part of the diaphragm with the phrenic nerve attached to the center of the diaphragm. The fan-like preparation is about 3 mm wide at the tendinous end and is about 15 mm wide at the costal margin. A thread is attached to the tendinous part of the diaphragm.

The preparation is fixed by a stainless steel rod with a pair of pins hooked to the rib. It is lowered into an organ bath and the thread from the muscle is attached to a force transducer. The nerve is stimulated with a pair of electrodes with a hole about 1 mm wide. The right phrenic nerve-diaphragm preparation is isolated in the same manner. The organ bath containing Tyrode solution with 2.0 g/l glucose is oxygenated at 37°C with 95% O_2 and 5% CO_2. The nerve is stimulated 12 times per min by rectangular-wave pulses of 0.5 ms duration at 3–5 V. Contractions are isometrically recorded through a transducer on a polygraph. The test drugs are left in the organ bath either for short periods of time (3–8 min) or for as long as the maximum effect can be observed. After a wash-out period of 3–5 min, the next dose can be added.

EVALUATION

The force of contractions after addition of various doses of the test drug is compared with the effect seen prior to drug application. Dose-response curves can be established.

CRITICAL ASSESSMENT OF THE METHOD

The isolated phrenic nerve diaphragm preparation of the rat is an excellent method for determining the potency of a drug to block or facilitate neuromuscular transmission. However, it is not a good preparation for differentiating between depolarizing and non-depolarizing neuromuscular blocking agents because, in many cases, depolarizing blocking agents fail to demonstrate initial facilitation and fail to reverse the effect of non-depolarizing blocking agents. For differentiating between depolarizing and non-depolarizing blocking agents the chick sciatic nerve-tibialis anticus muscle preparation is preferred. In this preparation, the curare-like drugs produce a neuromuscular blockade whereas the decamethonium-like drugs induce a contracture of the slow fiber when the neuromuscular transmission is blocked.

MODIFICATIONS OF THE METHOD

Colbert et al. (1990) studied the effects of temperature on the experimental reliability of the isolated rat phrenic nerve/diaphragm preparation.

Vizi et al. (2003) used *in vitro* isolated phrenic nerve-hemidiaphragm preparations of mice, rats and guinea pigs and *in vivo* sciatic nerve-anterior tibialis muscle preparations from anesthetized rats, guinea pigs and cats to characterize a new short-acting non-depolarizing muscle relaxant.

Van Riezen (1968a, b) described the sciatic nerve-tibialis anticus muscle preparation in **chicks**. Three to 8 day old chicks are decapitated and the skin of the legs is rapidly removed. The leg is separated from the body by cutting through the hip joint. The muscles of the thigh are dissected and the sciatic nerve with the superficial peroneal branch is freed from the upper leg tissue. The fascia is removed from the lower leg and the tibialis anticus tendon identified. A thread is attached to the tendon of the muscle and the tibialis anticus muscle is freed towards but not up to the knee joint attachment where the nerve enters into this region. The upper and lower leg bones are then cut off leaving the muscle with its nerve attached to the knee joint. The tendon is fasted by a hook to a ring in the bottom of the organ bath. A thin steel rod is attached to the knee joint. The contractions of the muscle are recorded isometrically. The nerve is passed through an electrode similar to that used in the rat phrenic nerve-diaphragm method. The nerve is stimulated six times per min for 0.5 ms duration at supramaximal voltage.

Jenden et al. (1954) described the isolated lumbrical muscle of the **rabbit** as a preparation which is sensitive to competitive (*d*-tubocurarine-like) and depolarizing (decamethonium-like) blocking agents. This muscle is cylindrical in shape, about 18 mm long and 1 mm in diameter and has a wet weight of about 15 mg.

Jenden (1955) used the isolated diaphragm of **guinea pigs** to study the effect of drugs upon neuromuscular transmission.

Hoppe (1955) reviewed the potency of neuromuscular blocking agents in various species.

Birmingham and Hussain (1980) used the phrenic nerve-diaphragm and the hypogastric nerve-vas deferens preparation of the guinea pig for comparison of the skeletal neuromuscular and autonomic ganglion-blocking potencies of non-depolarizing relaxants.

Wessler and Kilbinger (1986), Wessler and Steinlein (1987), Wessler et al. (1992) described a modi-

fied **rat** phrenic nerve-hemidiaphragm preparation whereby most of the muscle was cut off (end-plate preparation).

Muir et al. (1989) used biventer cervicis nerve-muscle preparations from **young chickens** and phrenic nerve-hemidiaphragm preparations from **rats** to evaluate neuromuscular blocking agents. Microelectrode recordings were obtained from the nerve-hemidiaphragm preparation of the rat and from the costocutaneous nerve-muscle preparation of the North American **garter snake** (*Thamnophis sirtalis*). The later preparation is particularly suitable for voltage clamp recording from the neuromuscular junction because it possesses large diameter fibers which aid visualization and penetration of endplates. This, coupled with compact endplates, allows good control of membrane voltage over the entire endplate region when using the two-microelectrode voltage clamp technique.

In order to record evoked endplate currents without accompanying muscle contraction, cut fiber preparations were used. Dissection and cutting of muscle fibers was performed at low K^+ (2 mmol/L) physiological solution perfused for approximately 30 min. Snake nerve-muscle preparations were mounted in a physiological salt solution of pH 7.1–7.2 containing (mmol/l) NaCl 159, KCl 4.2, $CaCl_2$ 1.5, $MgCl_2$ 4.2, HEPES 10. Rat nerve-muscle preparations were mounted in Krebs solution of the same composition as that used for tension experiments. The muscles were mounted in a Sylgard-coated Perspex dish and endplates were voltage clamped using glass capillary microelectrodes (resistance 2–10 MΩ). Voltage recording electrodes were filled with potassium chloride 3 mol/l and current passing electrodes were filled with potassium sulfate 0.6 mol/l.

The nerves were stimulated through platinum electrodes at a frequency of 0.5 Hz with rectangular pulses of 0.05 ms duration and of strength sufficient to produce evoked endplate currents. The evoked endplate currents were filtered by a 5-kHz low pass filter and recorded on magnetic tape. The currents were amplified and digitized by a laboratory interface connected to a computer at a digitization rate of 25 kHz. Ten to 20 evoked endplate currents were collected and averaged after alignment at the middle of their rising phase. Evoked endplate currents decayed as a single exponential function according to the following relationship:

$$I(t) = I(0)\exp^{-t/\tau}$$

where I(t) is the current amplitude at time t after the peak, $I(0)$ is the peak current amplitude and τ is the decay constant.

Experiments were carried out at room temperature. Drug solutions were perfused through the tissue bath for 10 min by peristaltic pump, ensuring a complete exchange of solution.

REFERENCES AND FURTHER READING

Beani L, Bianchi C, Ledda F (1964) The effect of tubocurarine on acetylcholine release from motor nerve terminals. J Physiol 174:172–183

Birmingham AT, Hussain SZ (1980) A comparison of the skeletal neuromuscular and autonomic ganglion-blocking potencies of five non-depolarizing relaxants. Br J Pharmacol 70:501–506

Bülbring E (1946) Observations on the isolated phrenic nerve diaphragm preparation of the rat. Br J Pharmacol 1:38–61

Bülbring E, Chou TC (1947) The relative activity of prostigmine homologues and other substances as antagonists to tubocurarine. Br J Pharmacol 2:8–22

Chang CC, Chuang ST, Lee CY, Weio JW (1972) Role of cardiotoxin and phospholipase A in the blockade of nerve conduction and depolarization of skeletal muscle induced by cobra venom. Br J Pharmac 44:752–764

Colbert WE, Wilson BF, Williams PD (1990) The effects of temperature on the experimental reliability of the isolated rat phrenic nerve/diaphragm preparation. J Pharmacol Meth 24:53–57

Hoppe JO (1955) Observations on the potency of neuromuscular blocking agents with particular reference to succinylcholine. Anesthesiol 16:91–124

Jenden DJ (1955) The effect of drugs upon neuromuscular transmission in the isolated guinea pig diaphragm. J Pharmacol Exper Ther 114:398–408

Jenden DJ, Kamijo K, Taylor DB (1994) The action of decamethonium on the isolated rabbit lumbrical muscle. J Pharmacol Exper Ther 111:229–240

Kojima M, Takagi H (1969) Effects of some anticholinergic drugs on antidromic activity in the rat phrenic nerve-diaphragm preparation. Eur Pharmacol 5:161–167

Long JP, Chiou CY (1970) Pharmacological testing methods for drugs acting on the peripheral nervous system. J Pharmaceut Sci 59:133–148

Muarata T, Murai T, Kanai T, Ogaki Y, Sanai K, Kanda H, Sato S, Kajikawa N, Umetsu T, Matsuura H, Fukatsu Y, Isogaya M, Yamada N, Nishio S (1989) General pharmacology of beraprost sodium. 2nd Communication: Effects on the autonomic, cardiovascular and gastrointestinal systems, and other effects. Arzneim Forsch/Drug Res 39:867–876

Muir AW, Houston J, Green KL, Marshall RJ, Bowman WC, Marshall IG (1989) Effects of a new neuromuscular blocking agent (ORG 9426) in anaesthetized cats and pigs and in isolated nerve-muscle preparations. Br J Anaesth 63:400–410

Randic M, Straughan DM (1964) Antidromic activity in the rat phrenic nerve-diaphragm preparation. J Physiol 173:130–148

Thesleff S (1958) A study on the interaction between neuromuscular blocking agents and acetylcholine at the mammalian motor end-plate. Acta Anaesth Scand 2:69–79

Van Riezen H (1968a) Classification of neuromuscular blocking agents in a new neuromuscular preparation of the chick *in vitro*. Eur J Pharmacol 5:29–36

Van Riezen H (1968b) Effect of cholinergic and anticholinergic drugs on a new neuromuscular preparation of the chick. Eur J Pharmacol 5:37–48

Vizi ES, Tuba Z, Maho S, Foldes FF, Nagano O, Doda M, Takagi S, Chaudhry IA, Saubermann AJ, Nagashima H (2003) A new short-acting non-depolarizing muscle relaxant (SZ1677) without cardiovascular side effects. Acta Anaesthesiol Scand 47:291–300

Wessler I, Kilbinger H (1986) Release of [^{3}H]acetylcholine from a modified rat phrenic nerve-hemidiaphragm preparation. Naunyn-Schmiedeberg's Arch Pharmacol 334:357–364

Wessler I, Steinlein O (1987) Differential release of [^{3}H]acetylcholine from the rat phrenic nerve-hemidiaphragm preparation by electrical nerve stimulation and by high potassium. Neurosci 22:289–299

Wessler I, Wagner G, Walczok A (1992) Suppression by cholinesterase inhibition of a Ca^{2+}-independent efflux of [^{3}H]acetylcholine from the neuromuscular junction of the isolated rat diaphragm. Eur J Pharmacol 221:371–376

West GB (1947) Note on the biological assay of tubocurarine. Quart J Pharm Pharmacol 20:518–527

G.2.0.3 Sciatic Nerve-Gastrocnemius Muscle Preparation in the Rabbit

PURPOSE AND RATIONALE

Levis et al. (1953), Long and coworkers (1959, 1967, 1969) described the sciatic nerve-gastrocnemius muscle preparation in the rabbit as an *in vivo* model for testing neuromuscular blocking agents.

PROCEDURE

Dutch rabbits, weighing 1–2 kg, are anesthetized with 200 mg/kg of phenobarbital administered slowly into the marginal ear vein. The sciatic nerve is ligated and cut, and a shielded electrode is placed on the peripheral portion of the nerve. The gastrocnemius muscle is freed as completely as possible from surrounding muscles and a thread is attached to the tendon of the muscle. The twitches of the muscle are elicited by supramaximal stimulation and are recorded through a force transducer. The parameters for interrupted tetanic stimulation are 250 c.p.s. with pulse durations of 1 ms at 15 V applied for 0.2 s every 10 s. The test drugs are administered intravenously into the marginal ear vein.

EVALUATION

The force of contraction after injection of various doses of the test drug is compared to the values obtained prior drug administration.

CRITICAL ASSESSMENT OF THE METHOD

The preparation has the advantage of studying the drug effects under conditions similar to clinical use.

MODIFICATIONS OF THE METHOD

There are two other preparations, the **cat soleus muscle** preparation and the **cat tibialis anticus muscle** preparation that very useful. They can be prepared in a method similar to that described for gastrocnemius muscle except that close arterial injection can be made using the tibialis anticus preparation. Also, soleus muscle consists primarily of slow muscle, whereas tibialis anticus is fast muscle. The experimental procedures for these two preparations are described in detail by Brown (1938), Bowman et al. (1962), Salafsky (1968).

REFERENCES AND FURTHER READING

Benz FW, Long JP (1969) Investigations on a series of heterocyclic hemicholinium-3 analogs. J Pharm Exp Ther 166:225–236

Bowman WC, Goldberg AAJ, Raper C (1962) A comparison between the effects of a tetanus and the effects of sympathomimetic amines on the fast- and slow-contracting mammalian muscles. Br J Pharmacol 19:464–484

Bülbring E, Chou TC (1947) The relative activity of prostigmine homologues and other substances as antagonists to tubocurarine. Br J Pharmacol 2:8–22

Chiou CY, Long JP (1969) Effects of α,α'-bis-(dimethylammoniumacetaldehyde diethylacetal)-*p*,*p*'-diacetylbiphenyl bromide (DMAE) on neuromuscular transmission. J Pharm Exp Ther 167:344–350

Durant NN, Bowman WC, Marshall IG (1977) A comparison of the neuromuscular and autonomic blocking activities of (+)-tubocurarine and its N-methyl and O,O,N-trimethyl analogues. Eur J Pharmacol 46:297–302

Levis S, Preat S, Dauby J (1953) Étude pharmacodynamique de deux séries de curarisants de synthèse. Arch Int Pharmacodyn 93:46–54

Long JP, Evans CT, Wong S (1967) A pharmacological evaluation of hemicholinium analogs. J Pharm Exp Ther 155:223–230

MacIntosh (1938) The effect of preganglionic section on acetylcholine in the ganglion. J Physiol 92:22P

Paton WDM, Zaimis EJ (1948) Clinical potentialities of certain bisquarternary salts causing neuromuscular and ganglionic block. Nature 20:810

Paton WDM, Zaimis EJ (1951) The action of D-tubocurarine and of decamethonium on respiratory and other muscles in the cat. J Physiol 112:311–331

Reitzel NL, Long JP (1959) The neuromuscular properties of α,α'-dimethylamino-4,4′-biacetophenone (hemicholinium). Arch Int Pharmacodyn 119:20–30

Salafsky B (1968) The effect of succinylcholine on denervated fast and slow skeletal muscle. Arch Intern Pharmacodyn 174:294–303

Wilson H, Long JP (1959) Effect of hemicholinium (HC-3) at various peripheral cholinergic transmitting sites. Arch Int Pharmacodyn 120:343–352

G.2.0.4 Evaluation of Neuromuscular Blockade in Cats, Pigs, Dogs and Monkeys

PURPOSE AND RATIONALE

Neuromuscular blocking drugs have been evaluated in various animal species. Muir et al. (1991) studied the effects of an analog of vecuronium in anesthetized cats, pigs, dogs and monkeys.

PROCEDURE

Anesthetized Cats

Experiments were carried out on cats of either sex anesthetized with a mixture of α-chloralose (80 mg/kg) and pentobarbitone (5 mg/kg) injected intraperitoneally. Animals were ventilated with air at a rate of 26 breaths per minute using a tidal volume of 13 ml/kg. The right hind limb was immobilized and the contractile responses of the tibialis anterior and soleus muscles to single shock stimulation of the sciatic nerve were recorded. The sciatic nerve was stimulated at a rate of 0.1 Hz using rectangular pulses of 0.2 ms duration and of a strength greater than that required to produce a maximal twitch. Contractions of the nictitating membrane were evoked in response to preganglionic stimulation of the cervical sympathetic nerve with 10-s-duration trains at a frequency of 5 Hz and a strength sufficient to produce maximal contractions of the nictitating membrane. Arterial blood pressure was recorded from the carotid artery using a Statham PC45 pressure transducer. The blood pressure pulse triggered a cardiotachograph to display the heart rate. Both vagus nerves were ligated and, at 100-s intervals, the right vagus nerve was stimulated with 10-s-duration trains at a frequency of 2–5 Hz and with pulses of 0.5 ms duration and strength greater than that required to produce a maximal reduction of heart rate. Contractile responses of muscles were recorded using Grass FTO3C and FT10C force displacement transducers. All responses were displayed on a Grass model 5 ink writing oscillograph.

Savarese (1979) determined not only the potencies of metocurine and d-tubocurarine but also the autonomic margins of safety in anesthetized cats.

PROCEDURE

Adult cats of either sex are anesthetized with α-chloralose, 80 mg/kg, and pentobarbital 7 mg/kg, given intraperitoneally. Cannulas were placed in the left femoral vein and artery for drug injection and recording blood pressure and heart rate. The lungs were mechanically ventilated through a tracheostomy and a small animal ventilator set to deliver 15 ml/kg tidal volume and 20 breaths/min.

The right vagus nerve and the right sympathetic trunk were exposed and divided in the neck. The distal ends were placed on the same shielded platinum wire electrode to permit preganglionic stimulation of both nerve trunks. The left sympathetic trunk was also dissected along its postganglionic portion at the base of the skull, and cut distal to the superior cervical ganglion to permit postganglionic stimulation through another electrode. Trains of square wave pulses (20 Hz for 10 s) were delivered at supramaximal voltage every 4 min simultaneously to all three autonomic nerve trunks. The resulting bradycardia and hypotension (the vagal response) were measured. Contractions of both nictitating membranes, one (the right) elicited preganglionically and the other (the left) elicited postganglionically, were recorded. The maximal vagal response (i. e., cardiac arrest for 10 s) was achieved by stimulation of the right vagus nerve or of both vagus nerves.

Twitches of the right tibialis anterior muscle were elicited at 0.15 Hz via the peroneal branch of the right sciatic nerve, to which square-wave shocks of 0.2 ms were applied at supramaximal voltage. Twitch recording was done via a transducer. All nerves and tendons were kept moist in small pools of mineral oil or in cotton pledges soaked in mineral oil. Tibialis anterior and esophageal muscle temperatures were monitored and kept between 35°C and 38°C by heat lamps.

Simultaneous recordings of heart rate, arterial pressure, pre- and postganglionic elicited contractions of the nictitating membrane, and twitches of the tibialis anterior muscle were made on a polygraph. Cumulative dose–response curves for inhibition of neuromuscular, vagal (parasympathetic) and sympathetic functions were determined simultaneously for each animal. The mechanism of vagal inhibition was localized at parasympathetic ganglia or cardiac muscarinic receptors by determining whether the bradycardic response to methacholine (20 µg/kg) was blocked as well as the neurally elicited bradycardia.

A single-bolus dose of the neuromuscular relaxants producing the delayed depressor response plus tachycardia (Paton 1957) was determined in each animal. This response, being pathognomonic for histamine release, is defined as sudden hypotension to less than 80% of the control arterial pressure within 2 min of relaxant injection and with tachycardia to more than 25% above the baseline value.

Test drugs were given intravenously.

EVALUATION

Data analysis was done by the method of Litchfield and Wilcoxon. Mean dose–response curves were plotted on log-probit paper. Best fit to straight lines on these scales was determined by computerized regression. The cumulative ED_{50} values for vagal and sympathetic inhibition and the cumulative ED_{95} values for neuromuscular blockade were determined from the lines and 95% confidence limits were calculated. Dif-

ferences in potency were considered significant when $P < 0.05$.

The occurrence of histamine release was also treated as an all-or-none response to permit log-probit plotting. The delayed depressor response plus tachycardia was judged to have or have not occurred after each single bolus injection of the drugs. The percentage of animals responding at each dose level was then determined and the data handled by the Litchfield–Wilcoxon method.

The autonomic margins of safety of the test drugs were calculated as the ratios of cumulative doses producing 50% block (ED_{50}) of vagal (parasympathetic) and sympathetic transmission and the ED_{50} for histamine release, each divided by the ED_{50} of neuromuscular blockade.

Anesthetized Dogs

Anesthesia was induced in beagle dogs using intravenous pentobarbitone sodium (3 mg/kg). Animals were intubated, without the use of a muscle relaxant, and artificially ventilated. Anesthesia was maintained with halothane (1.2% inspired concentration) and oxygen. The electrocardiogram was recorded continuously and the signal used to integrate heart rate throughout the experiment. Catheters were inserted percutaneously into the right femoral artery and vein for the recording of arterial blood pressure and the injection of drugs respectively.

A "boomerang" type transducer, originally constructed for recording adductor human pollicis tension (Walts 1973), was fitted to the lower left leg for recording muscle contractions. Submaximal rectangular pulses of 0.1 ms duration at a frequency of 0.1 Hz were delivered to the sciatic nerve through electrodes inserted percutaneously, and the resultant twitches of the foot recorded.

Clutton et al. (1992) studied the autonomic and cardiovascular effects of neuromuscular blockade antagonism in the **dog**. Neuromuscular blockade was antagonized with various anticholinesterase-antimuscarinic drug combinations including atropine, neostigmine, and glycopyrrolate.

Anesthetized Pigs

Domestic pigs of either sex (10–15 kg) were administered a tranquillizing dose (approximately 2 mg/kg) of azaperone about 20 min before induction of anesthesia with 3%–4% halothane in oxygen. Following induction, anesthesia was maintained with α-chloralose (200 mg/kg) dissolved in polyethylene glycol 300 given slowly into a jugular vein. Approximately 1 h later, anesthesia was supplemented with additional chloralose given by slow intravenous infusion which was continued throughout the investigation. The lungs were mechanically ventilated with room air via a tracheal cannula at a rate of 28 breaths per minute and a tidal volume of 12–14 ml/kg. Arterial pressure was recorded through a polyethylene catheter placed in the right carotid artery and connected to a Gould-Statham pressure transducer. Heart rate was monitored continuously by using the arterial pulse pressure to trigger a Grass 7P4F cardiotachometer. Drugs were administered through a catheter in the contralateral vein. Contractions of the tibialis anterior and soleus muscle were recorded by force displacement transducers. A resting tension of 30 g was applied to each muscle. Twitches were evoked every 10 s by stimulation the two branches of the sciatic nerve supplying the lower leg, immediately distal to the point where the nerve divides, using square wave pulses of 0.25 ms duration and at twice the voltage required to produce maximum contraction.

Anesthetized Rhesus Monkeys

Rhesus monkeys were anesthetized with intramuscular ketamine (10 mg/kg). Endotracheal intubation was performed without the use of muscle relaxants. Anesthesia was maintained using a single bolus of pentobarbitone sodium (4 mg/kg) given intravenously followed by infusion, which was adjusted to maintain a steady state of anesthesia. Heart rate was measured continuously by integration of the electrocardiogram. Atropine sulfate (0.25–0.5 mg) was administered i.m. to prevent excessive salivation. Artificial ventilation was supplied and blood pressure recorded continuously. The ulnar nerve was stimulated with rectangular electrical pulses via bipolar subcutaneous needle electrodes. The twitch response of the adductor pollicis muscle were recorded via a Statham transducer attached by a wire to a small U-clamp, which was fixed firmly to the basal phalanx of the thumb.

EVALUATION

Experiments were performed in the various animal species by injecting different doses at hourly intervals to obtain a range of neuromuscular paralysis, i. e., between 10 and 95% inhibition of single-twitch tension. From the data, dose-inhibition lines were constructed using the Levenberg-Marquardt non-linear interactive curve-fitting routine (Brown and Dennis 1972). From these data, doses producing 50% inhibition of induced contractions of the tibialis anterior muscle (cat and pig), hind limb (dog) and adductor pollicis muscle

(monkey) were calculated. Time course measurements were made with doses which produced between 85% and 95% neuromuscular block. Onset time was measured as the time from injection to the first maximally depressed contraction. The recovery time was the time from 75% block to 25% block and the duration of action was the time elapsing from injection to 90% spontaneous recovery compared to pre-drug control twitch tension.

MODIFICATIONS OF THE METHOD

Bowman et al. (1988) investigated structure:action relationships among some desacetoxy analogues of pancuronium and vecuronium in the anesthetized **cat**. Blockade of sciatic nerve-induced contraction of the tibialis and soleus muscles, as well as the effects on vagal-induced bradycardia and on sympathetically induced contractions of the nictitating membrane, were studied.

Khuenl-Brady et al. (1990) used anesthetized **cats** to study the effects of two new nondepolarizing neuromuscular blocking drugs. The indirectly evoked twitch tension of the anterior tibialis muscle elicited by supramaximal square-wave stimuli applied to the peroneal nerve was continuously quantitated by means of a force-displacement transducer and recorded. Onset time (from injection of muscle relaxant to maximum depression of twitch tension), duration of action and recovery index were determined.

Muir et al. (1989) used tibialis anterior and soleus muscle/sciatic nerve preparations in anesthetized **cats** and **pigs** to evaluate neuromuscular blocking agents.

Hoppe (1950) used a nerve-muscle preparation in **dogs** to evaluate curarimimetic drugs. Diaphragmatic respiration was recorded directly by means of a light thread from a suture imbedded in the peritoneal aspect of the right hemi-diaphragm. Stimulation of the peripheral end of the sectioned tibial nerve was accomplished by an induced current once every ten seconds. Muscle contraction was recorded from the Achilles tendon being severed just proximal to the calcaneus.

Hughes and Chapple (1976a, b, 1981; Hughes 1984) used nerve-muscle preparations of **cats**, **dogs** and **rhesus monkeys**.

Ono et al. (1990) recorded the twitch tension of the gastrocnemius-soleus muscle in **rats** after stimulation of the distal stump of the tibial nerve under the influence of a centrally acting muscle relaxant.

Cullen et al. (1980) described two mechanical techniques to measure neuromuscular activity in the intact, anesthetized **dog**. Simultaneous stimulation of the dorsal buccal branch of the facial nerve and ulnar nerve was performed and the evoked mechanical muscle responses measured.

Keesey (1988) discussed the use of single-fiber electromyography (SFEMG) by the AAEE minimonograph 33 as an electrodiagnostic approach to defects of neuromuscular transmission.

Marshall et al. (1994) gave an overview of the pharmacology of rocuronmium bromide in experimental animals.

REFERENCES AND FURTHER READING

Bowman WC, Rodger IW, Houston J, Marshall RJ, McIndewar I (1988) Structure: action relationships among some desacetoxy analogues of pancuronium and vecuronium in the anesthetized cat. Anesthesiology 69:57–62

Brown KM, Dennis JS (1972) Derivative free analogs of the Levenberg-Marquardt and Gauss algorithms for non-linear least square approximation. Numer Math 18:288–297

Clutton RE, Boyd C, Flora R, Payne J, McGrath CJ (1992) Autonomic and cardiovascular effects of neuromuscular blockade antagonism in the dog. Vet Surg 21:68–75

Cullen LK, Jones RS, Snowdon SL (1980) Neuromuscular activity in the intact dog: techniques for recording evoked mechanical responses. Br Vet J 136:154–159

Hoppe JO (1950) A pharmacological investigation of 2,5-bis-(3-diethylaminopropylamino) benzoquinone-bis-benzylchloride (WIN 2747) A new curarimimetic drug. J Pharmacol Exper Ther 100:333–345

Hughes R (1984) Experimental and clinical evaluation of neuromuscular blocking agents. J Pharmacol Meth 12:1–27

Hughes R, Chapple DJ (1976a) Effects of non-depolarizing neuromuscular blocking agents on peripheral autonomic mechanisms in cats. Br J Anaesth 48:59–68

Hughes R, Chapple DJ (1976b) Cardiovascular and neuromuscular effects of dimethyl tubocurarine in anaesthetized cats and rhesus monkeys. Br J Anaesth 48:847–852

Hughes R, Chapple DJ (1981) The pharmacology of atracurium: a new competitive neuromuscular blocking agent. Br J Pharmacol 53:31–44

Keesey JC (1988) AAEE minimonograph33: electrodiagnostic approach to defects of neuromuscular transmission. Muscle & Nerve 12:613–626

Khuenl-Brady K, Castagnoli KP, Canfell PC, Caldwell JE, Agoston S, Miller RD (1990) The neuromuscular blocking effects and pharmacokinetics of ORG 9426 and ORG 9616 in the cat. Anesthesiology 72:669–674

Marshall RJ, Muir AW, Sleigh T, Savage DS (1994) An overview of the pharmacology of rocuronmium bromide in experimental animals. Eur J Anaesthesiol 11 [Suppl 9]:9–15

Muir AW, Houston J, Green KL, Marshall RJ, Bowman WC, Marshall IG (1989) Effects of a new neuromuscular blocking agent (ORG 9426) in anaesthetized cats and pigs and in isolated nerve-muscle preparations. Br J Anaesth 63:400–410

Muir AW, Anderson K, Marshall RJ, Booij LHDJ, Crul FJ, Prior C, Bowman WC, Marshall IG (1991) The effects of a 16-N-homopyridine analogue of vecuronium in anesthetized cats, pigs, dogs and monkeys, and in isolated preparations.. Acta Anaesthesiol Scand 35:85–90

Ono H, Saito KI, Kondo M, Morishita SI, Kato K, Hasebe Y, Nakayama M, Kato F, Nakamura T, Satoh M, Oka JI, Goto M, Fukuda H (1990) Effects of the new centrally acting muscle relaxant 7-chloro-N,N,3-trimethylbenzo[b]furan-2-

carboxamide on motor and central nervous systems in rats. Arzneim Forsch/Drug Res 40:730–735
Paton WDM (1957) Histamine release by compounds of simple chemical structure. Pharmacol Rev 9:269–328
Savarese JJ (1979) The autonomic margins of safety of metocurine and d-tubocurarine in the cat. Anesthesiology 50:40–46
Walts LF (1973) The "Boomerang" – a method for recording adductor pollicis tension. Can Anaesth Soc J 20:706–708

G.2.0.5 Evaluation of Neuromuscular Blockade in Anesthetized Mice

PURPOSE AND RATIONALE

Electromyographic investigations of the neuromuscular junction are relatively easy to perform in large animal species such as the dog (Cullen et al. 1980). A simple *in vivo* method for the quantitative evaluation of neuromuscular blockade in anesthetized mice has been described by Lefebvre et al. (1992).

PROCEDURE

Female BALB/c mice, 7–9 weeks old, are anesthetized by intraperitoneal administration of 50 mg/kg etomidate or 250 mg/kg mephenesin. Hair is removed from the sciatic area and hind leg by application of a depilatory cream. A lamp is placed 30 cm above the anesthetized animal to maintain a constant body temperature. Two monopolar needle-stimulating electrodes are subcutaneously inserted into the sciatic notch area and two monopolar recording electrodes subcutaneously over the gastrocnemicus belly and in the vicinity of the tendo calcaneus communis, respectively. A ground electrode is inserted under the skin between recording and stimulating electrodes. Stimulation is carried out using a square signal of 0.2-ms duration. The supramaximal stimulation of the sciatic nerve consists of a train of 10 stimuli, lasting 3.3 s with a frequency of 3 Hz. Stimulation intensity is fixed to a value 50% higher than that required to attain the maximal evoked potential response. Two control trains of stimulation are applied before test-drugs administration and then repeated at 1-min intervals until the end of anesthesia which is assessed by reflex movement after pinching the toes or the tail.

Muscle action potentials are recorded using an electromyograph. The low and high cut-off frequencies are set to 16 Hz and 10 kHz, respectively. The electromyogram signal is amplified and plotted on an oscilloscope screen and printed. Evoked active potentials are analyzed using an 8 bits digitizer and the area under the response wave is evaluated for each stimulus (S).

The neuromuscular blocking agents are administered by intraperitoneal route.

EVALUATION

The effects of the test drugs are quantified by measuring the ratio of the fifth response (S5) to the first one (S1) in a given train (S5/S1 response) according to Keesey (1989). These values are almost not influenced by etomidate anesthesia. Neuroblocking agents of competitive type, such as alcuronium, or depolarizing type, such as suxamethonium, decrease this ratio significantly. These effects can be blocked by neostigmine, but not the effect of the snake venom alpha-bungarotoxin.

REFERENCES AND FURTHER READING

Cullen LK, Jones RS, Snowdon DL (1980) Neuromuscular activity in the intact dog: Techniques for recording evoked mechanical responses. Br Vet J 136:154–159
Keesey JC (1989) AAEE Minimonograph 33: Electrodiagnosis approach to defects of neuromuscular transmission. Muscle Nerve 12:613–626
Lefebvre HP, Cardona A, Toutain PL, Morel E, Bach JF, Vernetder-Garabedian B (1992) A simple method for the quantitative evaluation of neuromuscular blockade in mice. J Pharm Toxicol Meth 27:129–133

G.3 Safety Pharmacology

See Vogel (2006).

REFERENCES AND FURTHER READING

H.G Vogel (2006) Peripheral Nervous System In: Drug Discovery and Evaluation Safety and Pharmacokinetic Assays, Chapter I.H, pp-195-209 H. G. Vogel (ed) F.J. Hock, J. Maas, D. Mayer (Co-eds) Springer-Verlag Berlin Heidelberg New York

Chapter H
Analgesic, Anti-inflammatory, and Anti-pyretic Activity[1]

[1] Contributions to earlier editions by R. Schleyerbach, K.U. Weithmann and R.R. Bartlett.

H.1 Central Analgesic Activity

H.1.0.1 General Considerations

Pain is a symptom of many diseases requiring treatment with analgesics. Severe pain due to cancer metastases needs the use of strong analgesics, that means opioid drugs. The addiction liability of opioids led to intensive research for compounds without this side effect. Many approaches have been used to differentiate the various actions of strong analgesics by developing animal models not only for analgesic activity but also

for addiction liability. Several types of opioid receptors have been identified in the brain allowing *in vitro* binding tests. However, the *in vitro* tests can only partially substitute for animal experiments involving pain. Pain is a common phenomenon in all animals, at least in vertebral animals, similar to that felt by man. Analgesic effects in animals are comparable with the therapeutic effects in man. Needless to say, that in every instance painful stimuli to animals must be restricted as much as possible. Painful stimuli can consist of direct stimulation of the efferent sensory nerves or stimulation of pain receptors by various means such as heat or pressure. The role of endogenous peptides such as enkephalins and endorphins gives more insight into brain processes and the action of central analgesics.

Pain can also be elicited by inflammation. Progress has been made in elucidating the role of various endogenous substances such as prostaglandins and peptides in the inflammatory process. Most of the so called non-steroidal anti-inflammatory agents have also analgesic activity. Lim and Guzman (1968) differentiated between antipyretic analgesics causing analgesia by blocking impulse generation at pain receptors in the periphery while the narcotic analgesics block synaptic transmission of impulses signaling pain in the central nervous system. An old but excellent survey on methods being used to test compounds for analgesic activity has been provided by Collier (1964). Today, the classification into central and peripheral analgesics is definitively too simplified (Bannwarth et al. 1993) but provides a guide for differentiation by pharmacological methods.

REFERENCES AND FURTHER READING

Bannwarth B, Demotes-Mainard F, Schæverbeke T, Dahais J (1993) Where are peripheral analgesics acting? Ann Rheum Dis 52:1–4

Besson JM, Chaouch A (1987) Peripheral and spinal mechanisms of nociception. Physiol Rev 67:67–186

Collier HOJ (1964) Analgesics. In: Laurence DR, Bacharach AL (eds) Evaluation of Drug Activities: Pharmacometrics. pp 183–203. Academic Press London, New York

Lim RKS, Guzman F (1968) Manifestations of pain in analgesic evaluation in animals and man. In: Soulairac A, Cahn J, Charpentier J (eds) Pain. Academic Press, London, New York, pp 119–152

H.1.1 In Vitro Methods for Central Analgesic Activity

H.1.1.1 Survey

In 1973, high-affinity stereospecific binding of radiolabeled opiate compounds by CNS membrane preparations was reported (Pert and Snyder 1973; Simon et al. 1973; Terenius 1973). The *in vivo* pharmacological potency of opiate agonists and antagonists parallels the *in vitro* displacement of ^{3}H-naloxone, a potent narcotic antagonist. Based on these findings, the ^{3}H-naloxone binding assay was introduced for evaluation of potential analgesics with opiate-like properties. According to different pharmacological profiles of opiates, several receptor types have been identified designated as μ, κ, δ, and σ receptor (μ for morphine = MOP receptor, κ for ketocyclazocine = KOP receptor, δ for deferens because it was first identified in mouse vas deferens = DOP receptor). The σ receptor (σ for SKF10047) was only initially classified as an opioid receptor (see below). Several reviews on opioid receptors have been published: Knappe et al. (1995), Mansour et al. (1995), Satoh and Minami (1995), Dhawan et al. (1996), Singh et al. (1997), Standifer and Pasternak (1997), Law et al. (2000), Snyder and Pasternak (2003), Janecka et al. (2004), Eguchi (2004), and Waldhoer et al. (2004).

The opioid receptors were reclassified according to recommendations of the International Union of Physiological Sciences, the International Union of Pharmacology (IUPHAR; Dhawan et al. 1996, 1998; Alexander and Peters 2000). This nomenclature applies an abbreviation of the generic term for the family (OP for opioid) and a subscript number. **OP_1 stands for δ, OP_2 for κ**, and **OP_3 for μ receptor.**

For the **μ receptor, subtypes named μ_1 and μ_2** have been described (Fowler and Fraser 1994; Traynor 1994; Pasternak 2001). Analgesia is thought to involve activation of μ receptors (largely at supraspinal sites) and κ receptors (principally within the spinal cord); δ receptors may also be involved at the spinal and supraspinal level. Other consequences of μ activation include respiratory depression, miosis, reduced gastrointestinal motility, and euphoria. The μ_1 receptors are postulated to mediate the supraspinal analgesic action and the μ_2 receptors to mediate respiratory depression and suppression of gastrointestinal motility. Moreover, different effects on heart rate were described (Paakkari et al. 1992). Two endogenous peptides were described, named **endomorphins**, as agonists with high specific affinity for the μ-receptor (Hackler et al. 1997; Zadina et al. 1997, 1999; Horvath 2000).

Several studies provide evidence for the existence of **δ-opioid receptor subtypes** (Sofuoglu et al. 1991; Porreca et al. 1992; Horan et al. 1993; Miyamoto et al. 1993; Tiseo and Yaksh 1993; Burkey et al. 1998).

Binding studies with δ opioid receptors have been performed by Mosberg et al. (1983). Simonin et al. (1994) reported the genomic organization, cDNA cloning, the functional expression in COS cells, and the distribution in human brain of the human δ-opioid receptor.

Endogenous ligands for δ receptors are **enkephalins**.

A rat **κ opioid receptor** has been cloned (Meng et al. 1993). Evidence for different subtypes of the κ-opioid receptor is available (Zukin et al. 1988; Clark et al. 1989; Rothman et al. 1989, 1992, 1993; Wollemann et al. 1993). Simonin et al. (1995) described cDNA and genomic cloning, chromosomal assignment, functional expression, pharmacology, and expression pattern in the central nervous system of the δ-opioid receptor in humans.

Salvinorin A – derived from *Salvia divinorum*, a hallucinogenic plant used by Mazatec Indians of Mexico for traditional spiritual ceremonies – is a highly selective κ-opioid receptor agonist with antinociceptive effects (Yan and Roth 2004; John et al. 2006; Rothman et al. 2006; Stewart et al. 2006; Vortherms and Roth 2006).

Endogenous ligands for κ receptors are **dynorphins**.

With the development of highly selective ligands it has become possible to label selectively each of the μ-, δ-, and κ-opioid binding sites.

The **μ-binding sites** are labeled with [^{3}H]-[Tyr-D-Ala^2,MePhe^4,Gly-ol^5]enkephalin (Kosterlitz and Paterson 1981), ^{125}I-FK 33–824 (Moyse et al. 1986), [^{3}H]-Tyr-Pro-MePhe-D-Pro-NH_2 (PL O17; Hawkins et al. 1987), or [^{3}H]-[H-D-Phe-Cys-Tyr-D-Trp-Orn-Thr-Pen-Thr-NH_2] (CTOP); Hawkins et al. 1989), the **δ-binding sites** with [^{3}H]-[D-Pen^2,D-Pen^5]enkephalin (Akiyama et al. 1985; Cotton et al. 1985; Mosberg et al. 1987); [^{3}H]-D-Ser^2 (O-*tert*-butyl),Leu^5]enkephalyl-Thr^6 (Delay-Goyet et al. 1988) or [^{3}H]-[D-Pen^2-pClPhe^4,D-Pen^5]enkephalin (Vaughan et al. 1989); [^{3}H]TIPP (Nevin et al. 1993), and the **κ-sites** with [^{3}H]-U-69593 (Lahti et al. 1985; Maguire et al. 1992), [^{3}H]-PD117302 (Clark et al. 1988), or [^{3}H]-CI-977 (Boyle et al. 1990) or [^{3}H]norBNI (Marki et al. 1995).

Cloning and molecular biology of opioid receptors has been reviewed (Reisine and Bell 1993).

Advances in research on non-peptide opioid receptor ligands were published by Kaczor and Matusiuk (2002).

Exploring the opioid system by gene knockout was described by Kieffer and Gaveriaux-Ruff (2002).

Oligomerization of opioid receptors and the generation of novel signaling units was discussed by Levac et al. (2003).

OTHER RECEPTORS

There is some evidence that other opioid receptors may exist, such as a β-endorphin-sensitive **ε receptor** (Wüster et al. 1981). The **ζ receptor** (Zagon et al. 1991) and a high affinity binding site referred to as the **λ site** (Grevel et al. 1985) may also be part of the opioid receptor system.

The existence of a **σ receptor** was first postulated by Martin et al. (1976) to account for the psychotomimetic effects of N-allylnormetazocine (SKF 10,047) in the chronic spinal dog. σ Binding sites were proposed to be identical to phencyclidine binding sites based on the finding that phencyclidine generalized to (+)-SKF 10,047 in drug discrimination tests. Further work led to the application of the **term σ to an unique class of non-opiate, non-phencyclidine sites** that may serve as receptors for an as yet unidentified neuromodulator or neurotransmitter (Monnet et al. 1994). At least two subtypes of binding sites, σ_1 and σ_2, are proposed (Bowen et al. 1989; Itzhak and Stein 1991; Karbon et al. 1991; Knight et al. 1991; Connick et al. 1992; Quirion et al. 1992; Leitner et al. 1994). Radioligands for σ receptors (Weber et al. 1986; de Costa et al. 1989) and for subtype σ_1 (Matsuno et al. 1996) and subtype σ_2 (Mach et al. 1999) were described. Pharmacological studies indicate a role of σ receptors not only in analgesia (Mach et al. 1999), but also in motor function (Walker et al. 1993), schizophrenia (Debonnel and de Montigny 1996; Guitard et al. 1998; Takahashi et al. 1999) and learning and memory (Maurice et al. 1999).

The heterogeneity of opioid receptors has been studied in **isolated tissue preparations** in which neurotransmission is sensitive to inhibition by opioids. The relative potencies of opioid agonists are assessed by their ability to inhibit the electrically evoked contractions of isolated tissue preparations from five different species: the contractions of the mouse **vas deferens** are inhibited by μ-, δ-, and κ-agonists (Maguire et al. 1992), those of **the guinea-pig myenteric plexus-longitudinal muscle** preparation by μ- and κ-agonists (Berzetei-Gurske 1992), those of the **rabbit vas deferens** by κ-agonists, and those of the **hamster vas deferens** by δ-agonists (Sheehan et al. 1986). The contractions of the **rat vas deferens** are inhibited mainly, but not exclusively, by δ-agonists. The actions of β-endorphin in the rat vas deferens are mediated by a further type of opioid receptors, termed **ε-receptor**

(Wüster et al. 1981; Corbett et al. 1992; Smith and Leslie 1992).

REFERENCES AND FURTHER READING

Akiyama K, Gee KW, Mosberg HI, Hruby VJ, Yamamura HI (1985) Characterization of [^{3}H][2-D-penicillamine,5-D-penicillamine]-enkephalin binding to δ-opiate receptors in the rat brain and neuroblastoma-glioma hybrid cell line (NG 108–15). Proc Natl Acad Sci USA 82:2543–2547

Alexander SPH, Peters JA (2000) 2000 Receptor and Ion Channel Nomenclature Supplement. Trends Pharmacol Sci pp 70–71

Berzetei-Gurske IP, Troll L (1992) The μ-opioid activity of κ-opioid receptor agonist compounds in the guinea pig ileum. Eur J Pharmacol 212:283–286

Bowen WD, Hellewell SB, McGarry KA (1989) Evidence for a multi-site model of the rat brain σ receptor. Eur J Pharmacol 163:309–318

Boyle SJ, Meecham KG, Hunter JC, Hughes J (1990) [^{3}H]-CI-977: a highly selective ligand for the k-opioid receptor in both guinea-pig and rat forebrain. Mol Neuropharmacol 1:23–29

Burkey TH, Ehlert FJ, Hososhata Y, Quok RM, Cowell S, Hosohata K, Stropova VD, Li X, Slate C, Nagase H, Porreca F, Hruby VJ, Roeske WR, Yamamura HI (1998) The efficacy of opioid receptor-selective drugs. Life Sci 62:1531–1536

Clark CR, Birchmore B, Sharif NA, Hunter JC, Hill RG, Hughes J (1988) PD117302: a selective agonist for the κ-opioid receptor. Br J Pharmacol 93:618–626

Clark JA, Liu L, Price M, Hersh B, Edelson M, Pasternak GW (1989) Kappa opiate receptor multiplicity: Evidence for two U50,488 sensitive k_1 subtypes and a novel κ_3 subtype. J Pharmacol Exp Ther 251:461–468

Corbett AD, Paterson SJ, Kosterlitz HW (1992) Selectivity of ligands for opioid receptors. In: Herz A, Akil H, Simon EJ (eds) Opioids I, Handbook of Experimental Pharmacology Vol 104/I, Chapter 26, pp 645–679. Springer Berlin, Heidelberg, New York

Connick JH, Hanlon G, Roberts J, France L, Fox PK, Nicholson CD (1992) Multiple σ binding sites in guinea-pig and rat brain membranes: G-protein interactions. Br J Pharmacol 107:726–731

Cotton R, Kosterlitz HW, Paterson SJ, Rance MJ, Traynor JR (1985) The use of [^{3}H]-[D-Pen^2,D-Pen^5]enkephalin as a highly selective ligand for the δ-binding site. Br J Pharmacol 84:927–932

Bebonnel G, de Montigny C (1996) Modulation of NMDA and dopaminergic neurotransmissions by sigma ligands: possible implications for the treatment of psychiatric disorders. Life Sci 58:721–733

de Costa BR, Bowen WD, Hellewell, Walker JM, Thurkauf A, Jacobson AE, Rice KC (1989) Synthesis and evaluation of optically pure [^{3}H]-(+)-pentazocine, a highly potent and selective ligand for σ receptors. FEBS Lett 251:53–58

Delay-Goyet P, Seguin C, Gacel G, Roques BP (1988) [^{3}H]-[-D-Ser^2 (*O-tert*-butyl),Leu^5]enkephalyl-Thr^6 and [D-Ser^2(O-*tert*-butyl),Leu^5]enkephalyl-Thr^6(*O-tert*-butyl). Two new enkephalin analogs with both a good selectivity and high affinity towards δ-opioid binding sites. J Biol Chem 263:4124–4130

Dhawan BN, Cesselin F, Rhaghubir R, Reisine T, Bradley PB, Portoghese PS, Hamon M (1996) International Union of Pharmacology. XII. Classification of opioid receptors. Pharmacol Rev 48:567–592

Dhawan BN, Raghubir R, Hamon M, NC-IUPHAR Subcommittee on Opioid Receptors (1998) Opioid receptors. The IUPHAR Compendium of Receptor Characterization and Classification. IUPHAR Media, London, UK, pp 218–226

Eguchi M (2004) Recent advances in selective opiod agonists and antagonists. Med Res Rev 24:182–212

Fowler CJ, Fraser GL (1994) μ-, δ-, κ-Opiod receptors and their subtypes: a critical review with emphasis on radioligand binding experiments. Neurochem Int 24:401–426

Goldstein A, Naidu A (1989) Multiple opioid receptors: ligand selectivity profiles and binding site signatures. Mol Pharmacol 36:265–272

Grevel J, Yu V, Sadee W (1985) Characterization of a labile naloxone binding site in rat brain. J Neurochem 44:1647–1656

Guitard X, Codony X, Ballarin N, Dordal A, Farre AJ (1998) E-5842: A new potent and preferential sigma ligand. Preclinical pharmacological profile. CNS Drug Rev 4:201–224

Hackler L, Zadina JE, Ge L-G, Kastin AJ (1997) Isolation of relatively large amounts of endomorphin-1 and endomorphin-2 from human brain cortex. Peptides 18:1635–1639

Hawkins KN, Morelli M, Gulya K, Chang KJ, Yamamura HI (1987) Autoradiographic localization of [^{3}H][MePhe^3,D-Pro^4] morphiceptin ([^{3}H]PL O17) to μ-opioid receptors in rat brain. Eur J Pharmacol 133:351–352

Hawkins KN, Knapp RJ, Lui GK, Gulya K, Kazmierski W, Wan YP, Pelton JT, Hruby VJ, Yamamura HI (1989) [^{3}H]-[H-D-Phe-Cys-Tyr-D-Trp-Orn-Thr-Pen-Thr-NH_2] ([^{3}H]CTOP), a potent and highly selective peptide for μ-opioid receptors in rat brain. J Pharmacol Exp Ther 248:73–80

Horan PJ, Wild KD, Misicka A, Lipkowski A, Haaseth RC, Hruby VJ, Weber SJ, Davis TP, Yamamura HI, Porreca F (1993) Agonist and antagonist profiles of [D-Ala^2,Glu^4]deltorphin and its [Cys^4]- and [Ser^4]-substituted derivatives: further evidence for opioid delta receptor multiplicity. J Pharmacol Exp Ther 265:896–902

Horvath G (2000) Endomorphin-1 and endomorphin-2: pharmacology of the selective endogenous μ-opioid receptor agonists. Pharmacol Ther 88:437–463

Itzhak Y, Stein I (1991) Regulation of σ receptors and responsiveness to guanine nucleotides following repeated exposure of rats to haloperidol: further evidence of multiple σ binding sites. Brain Res 566:166–172

Janecka A, Fichna J, Janecki T (2004) Opioid receptors and their ligands. Curr Top Med Chem 4:1–17

John TF, Fench LG, Erlichman JS (2006) The antinociceptive effect of Salvinorin A in mice. Eur J Pharmacol 545:129–153

Kaczor A, Matusiuk D (2002) Non-peptide opioid receptor ligands – recent advances. Part II Antagonists. Curr Med Chem 9:1591–1603

Karbon EW, Naper K, Pontecorvo MJ (1991) [^{3}H]DTG and [^{3}H](+)-3-PPP label pharmacologically distinct σ binding sites in guinea pig membranes. Eur J Pharmacol 193:21–27

Kieffer BL, Gaveriaux-Ruff C (2002) Exploring the opioid system by gene knockout. Prog Neurobiol 66:285–306

Knappe RJ, Malatynska E, Collins N, Fang L, Wang JY, Hruby VJ, Roeske WB, Yamamura HI (1995) Molecular biology and pharmacology of cloned opioid receptors. FASEB J 9:516–525

Knight AR, Gillard J, Wong EHF, Middlemiss DN (1991) The human σ site, which resembles that in NCB20 cells, may correspond to a low-affinity site in guinea pig brain. Neurosci Lett 131:233–236

Kosterlitz HW, Paterson SJ (1981) Tyr-D-Ala Gly-MePhe-$NH(CH_2)_2OH$ is a selective ligand for the μ-opiate binding site. Br J Pharmacol 73:299P

Lahti RA, Mickelson MM, McCall JM, von Voigtlander PF (1985) [^{3}H]-U-69593, a highly selective ligand for the opioid κ-receptor. Eur J Pharmacol 109:281–284

Law PY, Wong YH, Loh HH (2000) Molecular mechanisms and regulation of opioid receptor signaling. Annu Rev Pharmacol Toxicol 40:389–430

Leitner ML, Hohmann AG, Patrick SL, Walker JM (1994) Regional variation in the ratio σ_1 to σ_2 binding in rat brain. Eur J Pharmacol 259:65–69

Levac BAR, O'Dowd BF, George SR (2003) Oligomerization of opioid receptors: generation of novel signaling units. Curr Opin Pharmacol 2:76–81

Loh HH, Smith AP (1990) Molecular characterization of opioid receptors. Annu Rev Pharmacol Toxicol 30:123–147

Mach RH, Wu L, West T, Whirrett BR, Childers SR (1999) The analgesic tropane analogue [±]-SM 21 has a high affinity for σ_2 receptors. Life Sci 64: PL131–137

Maguire P, Tsai N, Kamal J, Cometta-Morini C, Upton C, Loew G (1992) Pharmacological profiles of fentanyl analogs at μ, δ and κ opiate receptors. Eur J Pharmacol 213:219–225

Mansour A, Fox CA, Akil H, Watson SJ (1995) Opioid-receptor mRNA expression in the rat CNS: anatomical and functional implications. Trends Neurosci 18:22–29

Marki A, Otvos F, Toth G, Hoszafi S, Borsodi A (1995) Characterization of kappa opioid receptor with tritiated norBNI. Analgesia 1:557–560

Martin WR (1967) Opioid antagonists. Pharmacol Rev 19:463–521

Martin WR, Eades CG, Thompson JA, Huppler RE, Gilbert PE (1976) The effects of morphine- and morphine-like drugs in the nondependent and morphine-dependent chronic spinal dog. J Pharmacol Exp Ther 197:517–532

Matsuno K, Nakazawa M, Okamoto K, Kawashima Y, Mita S (1996) Binding properties of SA4503, a novel and selective σ_1 receptor agonist. Eur J Pharmacol 306:271–279

Maurice T, Phan V-L, Noda Y, Yamada K, Privat A, Nabeshima K (1999) The attenuation of learning impairment induced after exposure to CO or trimethylin in mice by sigma (σ) receptor ligands involves both σ_1 and σ_2 sites. Br J Pharmacol 127:335–342

McKnight AT, Rees DC (1991) Opioid receptors and their ligands. Neurotransm 7 (2):1–6

Meng F, Xie G-X, Thompson RC, Mansour A, Goldstein A, Watson SJ, Akil H (1993) Cloning and pharmacological characterization of rat κ opioid receptor. Proc Natl Acad Sci USA 90:9954–9958

Miyamoto Y, Portoghese PS, Takemori AE (1993) Involvement of *delta*$_2$ opioid receptors in the development of morphine dependence in mice. J Pharmacol Exp Ther 264:1141–1145

Moyse SE, Pasquini F, Quirion R, Beaudet A (1986) ^{125}I-FK 33–824: a selective probe for autoradiographic labeling of μ opioid receptors in the brain. Peptides 7:351–355

Monnet FP, Debonnel G, Bergeron R, Gronier B, de Montigny C (1994) The effects of sigma ligands and neuropeptide Y on N-methyl-D-aspartate-induced neuronal activation of CA_3 dorsal hippocampus neurones are differentially affected by pertussis toxin. Br J Pharmacol 112:709–715

Mosberg HI, Hurst R, Hruby VJ, Gee K, Yamamura HI, Galligan JJ, Burks TF (1983) Bis-penicillamine enkephalins possess highly improved specificity toward δ opioid receptors. Proc Natl Acad Sci USA, 80:5871–5874

Mosberg HI, Omnaas JR, Goldstein A (1987) Structural requirements for δ opioid receptor binding. Mol Pharmacol 31:599–602

Nevin ST, Toth G, Nguyen TDM, Schiller PW, Borsodi A (1993) Synthesis and binding characteristics of the highly specific tritiated opioid antagonist [^{3}H]TIPP. Life Sci 53:57–62

Paakkari P, Paakkari I, Feuerstein G, Sirén AL (1992) Evidence for differential opioid μ_1- and μ_2-receptor-mediated regulation of heart rate in the conscious rat. Neuropharmacol 31:777–782

Pasternak GW (1987) Opioid receptors. In: Psychopharmacology: The Third Generation of Progress. ed. by HY Meltzer, Raven Press New York, pp 281–288

Pasternak GW (1988) Multiple morphine and enkephalin receptors and the relief of pain. JAMA. 259:1362–1367

Pasternak GW (2001) Insights into mu opioid pharmacology: the role of mu opioid receptor subtypes. Life Sci 68:2213–2219

Patricia M, et al (1992) Pharmacological profiles of fentanyl analogs at μ, δ, and κ opiate receptors. Eur J Pharmacol 213:219–225

Pert CB, Snyder SH (1973) Opiate receptor: Demonstration in nervous tissue. Science 179:1011–1014

Porreca F, Takemori AE, Sultana M, Portoghese PS, Bowen WD, Mosberg HI (1992) Modulation of *mu*-mediated antinociception in the mouse involves opioid *delta*-2 receptors. J Pharmacol Exp Ther 263:147–152

Quirion R, Bowen WD, Itzhak Y, Junien JL, Musacchio JM, Rothman RB, Su T-P, Tam SW, Taylor DP (1992)A proposal for the classification of sigma binding sites. Trends Pharmacol Sci 13:85–86

Reisine T, Bell GI (1993) Molecular biology of opioid receptors. Trends Neurosci 16:506–510

Rothman RB, France CP, Bykov V, de Costa BR, Jacobson AE, Woods JH, Rice KC (1989) Pharmacological activities of optically pure enantiomers of the κ opioid agonist, U50,488, and its cis diastereomer: evidence for three κ receptor subtypes. Eur J Pharmacol 167:345–353

Rothman RB, Bykov V, Xue BG, Xu H, de Costa BR, Jacobson AE, Rice KC, Kleinman JE, Brady LS (1992) Interaction of opioid peptides and other drugs with multiple kappa receptors in rat and human brain. Evidence for species differences. Peptides 13:977–987

Rothman RB, Xu H, Char GU, Kim A, de Costa BR, Rice KC, Zimmerman DM (1993) Phenylpiperidine opioid antagonists that promote weight loss in rats have high affinity to the κ_{2B} (enkephalin-sensitive) binding site. Peptides 14:17–20

Rothman RB, Murphy DL, Xu H, Godin JA, Dersch CM, Partilla JS, Tidgewell K, Schmidt M, Prisinzano TE (2006) Salvinorin A: allosteric interaction with the mu opioid receptor. J Pharmacol Exp Ther 320:801–810

Satoh M, Minami M (1995) Molecular pharmacology of the opioid receptors. Pharmacol Ther 68:343–364

Sheehan MJ, Hayes AG, Tyers MB (1986) Pharmacology of δ-opioid receptors in the hamster vas deferens. Eur J Pharmacol 130:57–64

Simon EJ, Hiller JM, Edelman I (1973) Stereospecific binding of the potent narcotic analgesic [^{3}H]etorphine to rat-brain homogenate. Proc. Natl Acad Sci USA 70:1947–1949

Simonin F, Befort K, Gavériaux-Ruff C, Matthes H, Nappey V, Lannes B, Micheletti G, Kieffer B (1994) The human δ-opioid receptor: genomic organization, cDNA cloning, functional expression, and distribution in human brain. Mol Pharmacol 46:1015–1021

Simonin F, Gavériaux-Ruff C, Befort K, Matthes H, Lannes B, Micheletti G, Mattéi MG, Charron N, Bloch B, Kieffer B (1995) κ-Opioid receptor in humans: cDNA and genomic cloning, chromosomal assignment, functional expression, pharmacology, and expression pattern in the central nervous system. Proc Natl Acad Sci USA 92:7006–7010

Singh VK, Bajpai K, Biswas S, Haq W, Khan MY, Mathur KB (1997) Molecular biology of opioid receptors: recent advances. Neuroimmunomodulation 4:285–297
Smith JAM, Leslie FM (1992) Use of organ systems for opioid bioassay. In: Herz A, Akil H, Simon EJ (eds) Opioids I, Handbook of Experimental Pharmacology Vol 104/I, Chapter 4, pp 53–78. Springer Berlin, Heidelberg, New York
Snyder SH, Pasternak GW (2003) Historical review: opioid receptors. Trends Pharmacol Sci 24:198–205
Sofuoglu M, Portoghese PS, Takemori AE (1991) Differential antagonism of delta opioid agonists by naltrindole and its benzofuran analog (NTB) in mice: evidence for delta opioid receptor subtypes. J Pharmacol Exp Ther 257:676–680
Standifer KM, Pasternak GW (1997) G proteins and opioid receptor-mediated signaling. Cell Signal 9:237–248
Stewart DJ, Fahmy H, Roth BL, Yan F, Zjawiony JK (2006) Biosteric modifications of salvinorin A, a potent and selective kappa-opioid receptor agonist. Arzneimittelforsch 56:269–275
Takahashi S, Sonehara K, Takagi K, Miwa T, Horikomi K, Mita N, Nagase H, Iizuka K, Sakai K (1999) Pharmacological profile of MS-377, a novel antipsychotic agent with selective affinity for sigma receptors. Psychopharmacology 145:295–302
Terenius L (1973) Stereospecific interaction between narcotic analgesics in synaptic plasma membrane of rat cerebral cortex. Acta Pharmacol Toxicol 32:317–320
Tiseo PJ, Yaksh TL (1993) Dose-dependent antagonism of spinal opioid receptor agonists by naloxone and naltrindole: additional evidence for δ-opioid receptor subtypes in the rat. Eur J Pharmacol 236:89–96
Traynor JR (1994) Opiod receptors and their subtypes: Focus on peripheral isolated tissue preparations. Neurochem Int 24:427–432
Uphouse LA, Welch SP, Ward CR, Ellis EF, Embrey JP (1993) Antinociceptive activity of intrathecal ketorolac is blocked by the κ-opioid receptor antagonist, nor-binaltorphimine. Eur J Pharmacol 242:53–58
Vaughn LK, Knapp RJ, Toth G, Wan Y-P, Ruby VJ, Yamamura HI (1989) A high affinity, highly selective ligand for the delta opioid receptor: [^{3}H]-[D-Pen^2,*p*Cl-Phe^4,D-Pen^5]enkephalin. Life Sci 45:1001–1008
Vortherms TA, Roth BL (2006) Salvinorin A: from natural product to human therapeutics. Mol Interv 6:257–265
Waldhoer M, Bertlett SE, Whistler JL (2004) Opioid receptors. Annu Rev Biochem 73:953–990
Walker JM, Bowen WD, Patrick SL, Williams WE, Mascarella SW, Bai X, Carroll FI (1993) A comparison of (–)-deoxybenzomorphanes devoid of opioid activity with their dextrorotatory phenolic counterparts suggests role of σ_2 receptors in motor function. Eur J Pharmacol 231:61–68
Weber E, Sonders M, Quarum M, McLean S, Pou S, Keana JFW (1986) 1,3-Di(2-[5-^{3}H]tolyl)guanidine: A selective ligand that labels σ-type receptors for psychotomimetic opiates and anti-psychotic drugs. Proc Natl Acad Sci USA 83:8783–8788
Wollemann M, Benyhe S, Simon (1993) The kappa-opioid receptor: evidence of different subtypes. Life Sci 52:599–611
Wüster M, Schulz R, Herz A (1981) Multiple opiate receptors in peripheral tissue preparations. Biochem Pharmacol 30:1883–1887
Yan F, Roth BL (2004) Salvinorin A: a novel and highly selective κ-opioid receptor agonist. Life Sci 75:2615–2619
Zadina JE, Hackler L, Ge L-G, Kastin AJ (1997) A potent and selective endogenous agonist for the mu opiate receptor. Nature 386:499–502
Zadina JE, Schild SM, Gerall AE, Kastin AJ, Hackler L, Ge L-J, Zhang X (1999) Endomorphins: Novel endogenous μ-receptor agonists in regions of high μ-opiate receptor density. In: Sandman CA, Chronwall BM, Strand FL, Flynn FW, Beckwith B, Nachman RJ (eds) Neuropeptides. Structure and Function in Biology and Behavior. Ann New York Acad Sci 897:136–144
Zagon IS, Gibo DM, McLaughlin PJ (1991) Zeta, a growth related opioid receptor in developing rat cerebellum: identification and characterization. Brain Res 551:28–35
Zamanillo D, Andreu Fovalle S, Perez MP, Romero G, Farre AJ, Guitart X (2000) Up-regulation of σ_1 receptor mRNA in rat brain by a putative atypical antipsychotic and sigma receptor ligand. Neurosci Lett 282:169–1723
Zukin RS, Eghbali M, Olive D, Unterwald EM, Tempel A (1988) Characterization and visualization of rat and guinea pig brain κ opioid receptors: evidence for κ_1 and κ_2 opioid receptors. Proc Natl Acad Sci USA 85:4061–4065

H.1.1.2 ^{3}H-Naloxone Binding Assay

PURPOSE AND RATIONALE

A good correlation between the *in vivo* pharmacological potency of opiate agonists and antagonists with their ability to displace radiolabeled naloxone has been reported. The later discovery that Na^+ (100 mM) enhances the binding of antagonists and reduces the binding of agonists has led to the development of an assay which is used to classify compounds as opiate agonists, mixed agonist-antagonists and antagonists by determining the IC_{50} values for ^{3}H-Naloxone in the presence or absence of Na^+.

PROCEDURE

Reagents

[N-allyl-2,3-^{3}H] Naloxone (38–58 Ci/mmol) is obtained from New England Nuclear.

For IC_{50} determinations ^{3}H-naloxone is made up to a concentration of 100 nM and 50 µl is added to each tube yielding a final concentration 5 nM in the assay.

Levorphanol tartrate is obtained from Hoffmann LaRoche. A stock solution of 1 mM levorphanol is made up in distilled water. This stock is diluted 1:200 in distilled water and 20 µl is added to 3 tubes to determine stereospecific binding yielding a final concentration of 0.1 µM in the assay.

Dextrorphan tartrate is obtained from Hoffmann LaRoche. A stock solution of 1 mM dextrophan is made up in distilled water. This stock is diluted 1:200 in distilled water and 20 µl is added to the tubes containing the various concentrations of test drug and the tubes for total binding.

Test compounds: For most assays, a 1 mM stock solution is made up in a suitable solvent and serially diluted, such that the final concentration in the assay

ranges from 10^{-5} to 10^{-8} M. At least 7 concentrations are used for each assay. Higher or lower concentrations may be used, depending on the potency of the drug.

Tissue Preparation

Male Wistar rats are decapitated and their brains rapidly removed. Whole brains minus cerebella are weighed and homogenized in 50 volumes of ice-cold 0.05 M Tris buffer with a Tekmar tissue homogenizer. The homogenate is centrifuged at 40,000 *g* for 15 min, the supernatant is decanted and the pellet resuspended in fresh buffer and recentrifuged at 40,000 *g*. The final pellet is resuspended in the original volume of fresh 0.05 M Tris buffer. This yields a tissue concentration in the assay of 10 mg/ml.

Assay

310 µl	H_2O
20 µl	5 µM dextrorphan (total binding) or
	5 µM levorphanol (non-specific binding)
50 µl	2 M NaCl or H_2O
50 µl	0.5 M Tris buffer, pH 7.7
20 µl	drug or vehicle
50 µl	^{3}H-naloxone
500 µl	tissue suspension.

The tubes are incubated for 30 min at 37°C. The assay is stopped by vacuum filtration through Whatman GF/B filters which are then washed 3 times with ice-cold 0.05 M Tris buffer, pH 7,7. The filters are then counted in 10 ml of Liquiscint liquid scintillation cocktail. Stereospecific binding is defined as the difference between binding in the presence of 0.1 µM dextrorphan and 0.1 µM levorphanol. Specific binding is roughly 1% of the total added ligand and 50% of the total bound in the absence of Na^+ and 2% of the total added ligand and 65% of the total bound ligand in the presence of Na^+ (100 mM). The increase in binding is due to an increase in specific binding.

EVALUATION

Data are converted into % stereospecific ^{3}H-naloxone binding displaced by the test drug. IC_{50} values are determined from computer-derived log-probit analysis. The sodium shift is calculated from IC_{50} values with and without NaCl. High sodium shifts are found with agonists, low values with antagonists and medium values with mixed agonists-antagonists.

Data can be analyzed using a computer program as described by McPherson (1985).

REFERENCES AND FURTHER READING

Hubbard JW, Locke KW, Forster HV, Brice AG, Pan LG, Lowry TF, Forster AML, Forster MA, Cornfeldt M, Vanselous CL, Hamer RRL, Glamkowski EJ, Fielding S (1992) Cardiorespiratory effects of the novel opioid analgesic HP 736 in the anesthetized dog and conscious goat. J Pharmacol Exp Ther 260:1268–1277

McPherson GA (1985) Analysis of radioligand binding experiments. A collection of computer programs for the IBM PC. J Pharmacol Meth 14:213–228

Mini-Symposium (1981) The *in vivo* differentiation of opiate receptors. Life Sci 28:1543–1584

Pert CB, Snyder SH (1973) Properties of opiate-receptor binding in rat brain. Proc. Natl. Acad. Sci, USA 70:2243–2247

Pert CB, Snyder SH (1974) Opiate receptor binding of agonists and antagonists affected differentially by sodium. Molec Pharmacol 10:868–879

Pert CB, Snyder SH (1975) Differential interactions of agonists and antagonists with the opiate receptor. In: Snyder and Watthysse (eds) Opiate Receptor Mechanisms. MIT Press Cambridge. pp 73–79

Pert CB, Pasternak G, Snyder SH (1973) Opiate agonists and antagonists discriminated by receptor binding in brain. Science 182:1359–1361

Wolozin BL, Nishimura S, Pasternak GW (1982) The binding of κ- and σ-opiates in rat brain. J Neurosci 2:708–713

H.1.1.3 ^{3}H-Dihydromorphine Binding to μ Opiate Receptors in Rat Brain

PURPOSE AND RATIONALE

μ Receptors are considered to mediate the supraspinal activity of opioids. ^{3}H-Dihydromorphine (^{3}H-DHM) exhibits some selectivity for the μ receptor, a high affinity opiate binding site. The test is used to detect compounds that inhibit binding of ^{3}H-DHM in a synaptic membrane preparation obtained from rat brain.

PROCEDURE

Reagents

[1,7,8-^{3}H]Dihydromorphine (^{3}H-DHM) (specific activity 69 Ci/mmol) is obtained from Amersham.

For IC_{50} determinations a 20 nM stock solution is made up. Fifty µl are added to each test tube to yield a final concentration of 0.5 nM in the 2 ml assay.

Levallorphan tartrate is used for the determination of nonspecific binding. A 0.1 mM stock solution is prepared in deionized water. Twenty µl added to each of 3 tubes yields a final concentration of 0.1 µM in the 2 ml assay.

A 1 mM stock solution is made up of the test compounds in a suitable solvent and serially diluted, such that the final concentrations in the assay range from 10^{-6} to 10^{-9} M. At least 7 concentrations are used for each assay.

Tissue Preparation

Male Wistar rats are sacrificed by decapitation. Whole brains minus cerebella are removed, weighed and homogenized in 30 volumes of ice-cold 0.05 M Tris buffer, pH 7.7. The homogenate is centrifuged at 48,000 *g* for 15 min, the supernatant is decanted and the pellet resuspended in the same volume of buffer. This homogenate is then incubated for 30 min at 37°C to remove the endogenous opiate peptides and centrifuged again as before. The final pellet is resuspended in 50 volumes of 0.05 M Tris buffer, pH 7.7.

Assay

1850 µl	tissue suspension
80 µl	distilled water
20 µl	vehicle, or levallorphan, or appropriate concentration of drug
50 µl	[^{3}H]DHM.

Tubes are incubated for 30 min at 25°C. The assay is stopped by vacuum filtration through Whatman GF/B filters which are washed twice with 5 ml of 0.05 M Tris buffer. The filters are then placed into scintillation vials with 10 ml Liquiscint scintillation cocktail and counted.

EVALUATION

Specific binding is defined as the difference between total binding and binding in the presence of 0.1 mM levallorphan. IC_{50} values are calculated from the percent specific binding at each drug concentration.

The K_D value for [^{3}H]DHM binding was found to be 0.38 nM by Scatchard analysis of a receptor saturation experiment. The K_i value may be calculated from the IC_{50} by the Cheng–Prusoff equation:

$$K_i = IC_{50}/1 + L/K_D\,.$$

REFERENCES AND FURTHER READING

Adler MW (1981) Mini-Symposium on Opiate Receptors. Life Sci 28:1543–1584

Cheng YC, Prusoff WH (1973) Relationship between the inhibition constant (K_i) and the concentration of inhibitor which causes 50 percent inhibition (I_{50}) of an enzymatic reaction. Biochem Pharmacol 22:3099–3108

Childers S, Creese I, Snowman AM, Snyder SH (1979) Opiate receptor binding affected differentially by opiates and opioid peptides. Eur J Pharmacol 55:11–18

Goldstein A (1987) Binding selectivity profiles for ligands of multiple receptor types: Focus on opioid receptors. TIPS 8:456–459

Hubbard JW, Locke KW, Forster HV, Brice AG, Pan LG, Lowry TF, Forster AML, Forster MA, Cornfeldt M, Vanselous CL, Hamer RRL, Glamkowski EJ, Fielding S (1992) Cardiorespiratory effects of the novel opioid analgesic HP 736 in the anesthetized dog and conscious goat. J Pharmacol Exp Ther 260:1268–1277

Laugwitz KL, Offermanns S, Spicher K, Schulz G (1993) μ and δ opioid receptors differentially couple to G protein subtypes in membranes of human neuroblastoma SH-SY5Y cells. Neuron 5:233–242

Locke KW, Dunn RW, Hubbard JW, Vanselous ChL, Cornfeldt M, Fielding St, Strupczewski JT (1990) HP 818: A centrally acting analgesic with neuroleptic properties. Drug Dev Res 19:239–256

Mansour A, Lewis ME, Khachaturian H, Akil H, Watson SJ (1986) Pharmacological and anatomical evidence of selective μ, δ and κ opioid receptor binding in rat brain. Brain Res 399:69–79

Pasternak GW (1987) Opioid receptors. In: Meltzer HY (ed) Psychopharmacology: The Third Generation of Progress. Raven Press, New York pp 281–288

Pasternak GW, Wilson HA, Snyder SH (1975) Differential effects of protein-modifying reagents on the receptor binding of opiate agonists and antagonists. Mol Pharmacol 11:340–351

Robson LE, Foote RW, Maurer R, Kosterlitz HW (1984) Opioid binding sites of the κ-type in guinea pig cerebellum. Neurosci 12:621–627

Snyder SH (1984) Drug and neurotransmitter receptors in the brain. Science 224:22–31

Wolozin BL, Nishimura S, Pasternak GW (1982) The binding of κ and σ opiates in rat brain. J Neurosci 2:708–713

Zukin RS, Zukin SR (1981) Multiple opiate receptors: Emerging concepts. Life Sci 29:2681–2690

H.1.1.4 ^{3}H-Bremazocine Binding to κ Opiate Receptors in Guinea Pig Cerebellum

PURPOSE AND RATIONALE

κ Receptors are thought to be involved in the analgesic activity of opiates mainly within the spinal cord, whereas μ receptors are predominately located at supraspinal sites. The pharmacological effects of κ agonists differ from the μ agonists in various analgesic tests, effects on diuresis, sensitivity to naloxone and propensity to cause respiratory depression. κ Agonists may induce water diuresis (Salas et al. 1992). The receptor subtype selectivity can be determined by testing the affinity of new compounds for the κ opiate receptor and comparing these results with the data from the μ receptor assay.

Although the benzomorphanes, such as ethylketocyclazocine and bremazocine, are potent κ agonists, they are not selective for this receptor subtype. To demonstrate specific binding of these ligands to κ receptors, the assay must be done in a tissue where the κ subtype predominates, such as the guinea pig cerebellum. Moreover, binding to μ and δ receptors is prevented by inclusion of the peptide DAGO (Tyr-D-Ala-Gly-N-Me-Phe-Gly-ol) to mask the μ receptor and of

[D-Pen^{2,5}]-enkephalin (Tyr-D-Pen-Gly-Phe-D-Pen) to mask the δ receptor.

PROCEDURE

Reagents

Bremazocine(–)-[9-^{3}H] (specific activity 21–28 Ci/mmol), is obtained from, New England Nuclear. For IC_{50} determinations a 24 nM stock solution is made up. Fifty µl are added to each tube to yield a final concentration of 0.6 nM in the 2 ml assay.

U50,488H is made up to a 500 µM stock solution in deionized water. Twenty ml are added to each of the 3 tubes for determination of unspecific binding yielding a final concentration of 5.0 µM in the 2 ml assay.

Opiate peptides of the μ- and δ-type are included in the assay to prevent binding of the radioligand and the test drug to these receptors. DAGO and [D-Pen^{2,5}]-enkephalin are obtained from Penninsula Laboratories. Concentrated stock solutions of 10^{-3} M are made up in deionized water and further diluted to 10^{-5} M. Twenty µl of this solution are added to each tube to result in a final concentration of 100 nM of each in the 2 ml assay.

For the assays a 1 mM stock solution of test compounds is made up in a suitable solvent and serially diluted, such that the final concentration in the assay ranges from 10^{-5} to 10^{-8} M. At least 7 concentrations are used for each assay.

Tissue Preparation

Male guinea pigs are sacrificed and cerebella are removed, weighed and homogenized in 10 volumes of ice-cold 0.05 M Tris-buffer, pH 7.4. The homogenate is centrifuged at 48,000 *g* for 10 min, the supernatant decanted and the pellet resuspended in 20 volumes of buffer. This homogenate is then incubated for 45 min at 37°C to remove endogenous opiate peptides and centrifuged again as before. This pellet is resuspended in 200 volumes of 0.05 M Tris buffer, pH 7.4.

Assay

1850 µl	tissue suspension
60 µl	distilled water
20 µl	peptide solution
20 µl	vehicle, or U50,488H, or test drug
50 µl	[^{3}H]bremazocine

Tubes are incubated for 40 min at 25°C. The assay is stopped by vacuum filtration through Whatman GF/B filters which are then washed 3 times with 5 ml of 0.05 M Tris buffer. The filters are then placed in scintillation vials with 10 ml Liquiscint scintillation cocktail and counted.

EVALUATION

Specific binding is defined as the difference between total binding and binding in the presence of 5.0 µM U50,488H. IC_{50} values are calculated from the percent specific binding at each drug concentration.

The K_D value for [^{3}H]bremazocine binding was found to be 0.14 nM by Scatchard analysis of a receptor saturation experiment. The K_i value may be calculated from IC_{50} by the Cheng–Prusoff equation:

$$K_i = IC_{50}/1 + L/K_D\,.$$

REFERENCES AND FURTHER READING

Abbott FV et al (1986) A dose-ratio comparison of μ and κ agonists in formalin and thermal pain. Life Sci 39:2017–2024

Cheng YC, Prusoff WH (1973) Relationship between the inhibition constant (K_i) and the concentration of inhibitor which causes 50 percent inhibition (I_{50}) of an enzymatic reaction. Biochem Pharmacol 22:3099–3108

Goodman RR, Snyder SH (1982) Autoradiographic localization of kappa opiate receptors to deep layers of the cerebral cortex may explain unique sedative and analgesic effects. Life Sci 31:1291–1294

Higginbottom M, Nolan W, O'Toole J, Ratcliffe GS, Rees DC, Roberts E (1993) The design and synthesis of kappa opioid ligands based on a binding model for kappa agonists. Bioorg Med Chem Lett 3:841–846

Hubbard JW, Locke KW, Forster HV, Brice AG, Pan LG, Lowry TF, Forster AML, Forster MA, Cornfeldt M, Vanselous CL, Hamer RRL, Glamkowski EJ, Fielding S (1992) Cardiorespiratory effects of the novel opioid analgesic HP 736 in the anesthetized dog and conscious goat. J Pharmacol Exp Ther 260:1268–1277

Inenaga K, Nagamoto T, Nakao K, Yanaihara N, Yamashita HY (1994) Kappa-selective agonists decrease postsynaptic potentials and calcium components of action potentials in the supraoptic nucleus of rat hypothalamus *in vitro*. Neurosci 58:331–340

Kosterlitz HW, Paterson SJ, Robson LE (1981) Characterization of the κ-subtype of the opiate receptor in the guinea pig brain. Br J Pharmacol 73:939–949

Mansour A, Lewis ME, Khachaturian H, Akil H, Watson SJ (1986) Pharmacological and anatomical evidence of selective μ, δ and κ opioid receptors in brain. Brain Res 399:69–79

Peter GR et al (1987) Diuretic actions in man of a selective kappa opioid agonist: U-62,066E. J Pharmacol Exper Ther 240:128–131

Robson LE, Foote RW, Maurer R, Kosterlitz HW (1984) Opioid binding sites of the κ-type in guinea pig cerebellum. Neurosci 12:621–627

Salas SP, Roblero JS, López LF, Tachibana S, Huidobro-Toro JP (1992) [N-Methyl-Tyr^1,N-methyl-Arg^7-D-Leu^8]-dynorphin-A-(1–8) ethylamide, a stable dynorphin analog, produces diuresis by kappa-opiate receptor activation in the rat. J Pharmacol Exp Ther 262:979–986

Snyder SH (1984) Drug and neurotransmitter receptors in the brain. Science 224:22–31
Steinfels GF, Cook L (1986) Antinociceptive profiles of μ and κ opioid agonists in a rat tooth pulp stimulation procedure. J Pharmacol Exper Ther 236:111–117
Tyers MB (1982) Studies on the antinociceptive activities of mixtures of μ- and κ-opiate agonists and antagonists. Life Sci 31:1233–1236
Wolozin BL, Nishimura S, Pasternak GW (1982) The binding of κ- and σ-opiates in rat brain. J Neurosci 2:708–713
Zukin RS, Zukin SR (1981) Multiple opiate receptors: Emerging concepts. Life Sci 29:2681–2690

H.1.1.5 Inhibition of Enkephalinase

PURPOSE AND RATIONALE

Since the discovery of brain peptides with pharmacological properties similar to morphine (Hughes 1975), the metabolic breakdown of enkephalins has been studied (Malfroy et al. 1978; Llorens and Schwartz 1981; Mumford et al. 1981; Malfroy and Schwartz 1982; Roques 1982; Schwartz 1983). Roques BP et al. (1980), Costentin et al. (1986) found that the enkephalinase inhibitor thiorphan shows antinociceptive activity in mice. A highly sensitive fluorometric assay for "enkephalinase", a neutral metalloendopeptidase that releases tyrosine-glycine-glycine from enkephalins has been developed by Florentin et al. (1984). A fluorogenic peptide, dansyl-D-Ala-Gly-Phe(pNO$_2$)-Gly (DAGNPG) was synthesized as a selective substrate for the neutral metalloendopeptidase involved in enkephalin metabolism. This enzyme, designated "enkephalinase" cleaves the Gly-Phe(pNO$_2$) peptide bond of DAGNPG leading to a fluorescence increase related to the disappearance of intramolecular quenching of the dansyl fluorescence by the nitrophenyl residue.

Enkephalinase induces inactivation of atrial natriuretic factor (ANF). The protection of endogenous ANF against inactivation may result in therapeutic applications (Schwartz et al. 1990).

PROCEDURE

Fresh rat kidney is homogenized in 10 vol of cold 0.05 M Tris-HCl buffer, pH 7.4, using a Polytron homogenizer. The homogenate is centrifuged for 5 min at 1000 g. The pellet is discarded and the supernatant centrifuged at 60,000 g for 60 min. The resulting pellet is resuspended in 50 mM Tris-HCl buffer, pH 7.4, and used as the enzyme source.

Standard assays for "enkephalinase" activity using DAGNPG are carried out at 37°C in hemolysis tubes. A 0.1-ml amount of 50 mM Tris-HCl buffer, pH 7.4, containing 50 µM DAGNPG is preincubated 15 min at 37°C. The reaction is initiated by addition of 50 µl of the enzyme preparation together with 0.5 µM Captopril. The tubes are incubated for 30 min in a water bath with constant shaking. The enzymatic reaction is stopped by boiling at 100°C for 5 min. The samples are then diluted with 1.35 ml of Tris HCl buffer and centrifuged at 500 g for 30 min. An aliquot of 1 ml of the supernatant is transferred to thermostated cells of a spectrofluorometer. Readings are performed at 562 nm with an excitation wavelength of 342 nm. A calibration curve is prepared by adding increasing concentrations of DNS-D-Ala-Gly and decreasing concentrations of the substrate in Tris-HCl buffer containing the denaturated enzymatic preparation. For the assay of "enkephalinase" inhibition, the test compound or the standard thiorphan = [(R-,S-)-3-mercapto-2-benzylpropanoyl]glycine is added in various concentrations.

EVALUATION

The inhibitory potencies of test compounds are compared with the standard.

MODIFICATIONS OF THE METHOD

Ksander et al. (1989) incubated synaptic membranes from rat striatum with ^{3}H-Tyr-Leu-enkephalin for 15 min at 30°C, pH 6.5, in the presence of 10^{-6} M bestatin. The reaction was stopped by the addition of 30% acetic acid and the reaction product ^{3}H-Tyr-Gly-Gly was separated from unreacted ^{3}H-Tyr-Leu-enkephalin on a Porapak Q column followed by a Cu^{2+} chelex column. The ^{3}H-Tyr-Gly-Gly was counted by liquid scintillation.

The antinociceptive effects of intrathecally administered SCH32615, an enkephalinase inhibitor were studied in the rat by Oshita et al. (1990).

REFERENCES AND FURTHER READING

Chipkin RE (1986) Inhibition of enkephalinase: The next generation of analgesics. Drugs Future 11:593–606
Chipkin RE, Berger JG, Billard W, Iorio LC, Chapman R, Barnett A (1988) Pharmacology of SCH 34826, an orally active enkephalinase inhibitor analgesic. J Pharm Exp Ther 245:829–838
Costentin J, Vlaiculescu A, Chaillet P, Natan B, Aveaux D, Schwartz JC (1986) Dissociated effects of inhibitors of enkephalin-metabolizing peptidases or naloxone on various nociceptive responses. Eur J Pharmacol 123:37–44
Florentin D, Sassi A, Roques BP (1984) A highly sensitive fluorimetric assay for "enkephalinase", a neutral metalloendopeptidase that releases tyrosine-glycine-glycine from enkephalins. Anal Biochem 141:62–69

Hughes J (1975) Isolation of an endogenous compound from the brain with pharmacologic properties similar to morphine. Brain Res 88:295–308
Ksander GM, Diefenbacher CG, Yuan AM, Clark F, Sakane Y, Ghai RD (1989) Enkephalinase inhibitors. I. 2,4-Dibenzylglutaric acid derivatives. J Med Chem 32:2519–2526
Llorens C, Schwartz JC (1981) Enkephalinase activity in rat peripheral organs. Eur J Pharmacol 69:113–116
Malfroy B, Schwartz JC (1982) Properties of "enkephalinase" from rat kidney: comparison of dipeptidyl-carboxypeptidase and endopeptidase activities. Biochem Biophys Res Commun 106:276–285
Malfroy B, Swerts JP, Guyon A, Roques BP, Schwartz JC (1978) High-affinity enkephalin-degrading peptidase in brain is increased after morphine. Nature 276:523–526
Mumford RA, Pierzchala PA, Strauss AW, Zimmerman M (1981) Purification of a membrane bound metalloendopeptidase from porcine kidney that degrades peptide hormones. Proc Natl Acad Sci USA 78:6623–6627
Oshita S, Yaksh TL, Chipkin R (1990) The antinociceptive effects of intrathecally administered SCH32615, an enkephalinase inhibitor in the rat. Brain Res 515:143–148
Roques BP, Fournié-Zaluski MC, Soroca E, Lecomte LM, Malfroy B, Llorens C, Schwartz JC (1980) The enkephalinase inhibitor thiorphan shows antinociceptive activity in mice. Nature 288:286–288
Roques BP, Fournié-Zaluski MC, Florentin D, Waksman G, Sassi A, Chaillet P, Collado H, Ciostentin J (1982) New enkephalinase inhibitors as probes to differentiate "enkephalinase" and angiotensin-converting-enzyme active sites. Life Sci 31:1749–1752
Schwartz JC (1983) Metabolism of enkephalins and the inactivating neuropeptidase concept. TINS 1983:45–48
Schwartz JC, Gros C, Lecomte JM, Bralet J (1990) Enkephalinase (EC 3.4.24.11) inhibitors: protection of endogenous ANF against inactivation and potential therapeutic applications. Life Sci 47:1279–1297

H.1.1.6 Nociceptin

H.1.1.6.1 General Considerations on Nociceptin

PURPOSE AND RATIONALE

A heptadekapeptide (nociceptin or orphanin FQ) has been isolated as endogenous agonist of the **opioid receptor-like ORL_1 receptor** (Reinscheid et al. 1995; Meunier et al. 1995; Barlocco et al. 2000; Mollereau and Mouledous 2000; Mogil and Pasternak 2001; Witta et al. 2004) which shows high structural homology with opioid peptides, especially dynorphin A (Calò et al. 2000). Nociceptin activates a specific receptor, which has been cloned in man and animals and has been shown to be structurally similar to opioid receptors (Mollereau et al. 1994; Calò et al. 2000; Hawkinson et al. 2000). At the cellular level, the nociceptin receptor has been shown to act through the same mechanisms as classical opioid receptors, namely the inhibition of adenylyl cyclase, the activation of potassium channels and inhibition of calcium channels (Connor et al. 1996a, b). *In vitro* and *in vivo* studies have demonstrated that nociceptin mediates a variety of biological actions (Civelli et al. 1998; Darland et al. 1998). Nociceptin induces analgesia when administered intrathecally (Stanfa et al. 1996; Xu et al. 1996), while it causes hyperalgesia and reversal of opioid induced analgesia when given intracerebroventricularly; nociceptin stimulates food intake (Polidori et al. 2000) and produces anxiolysis. Depending on the dose, nociceptin stimulates or inhibits locomotor activity. Nociceptin inhibits long-term potentiation, memory processes, induces bradycardia, hypotension and diuresis. In addition, nociceptin inhibits neurotransmitter release both at central and peripheral sites. Intracavernosal injection of nociceptin induces a potent and relatively long-lasting erectile response in the cat (Champion et al. 1997, 1998). Intrathecal injection of nociceptin elicits scratching, licking and biting in mice (Sakurada et al. 1999, 2000). Synthetic agonists and antagonists of the nociceptin receptor have been reported (Guerrini et al. 1998; Salvadori et al. 1999; Calò et al. 2000; Hashimoto et al. 2000; Meunier 2000; Ozaki et al. 2000).

REFERENCES AND FURTHER READING

Barlocco D, Cignarella G, Giardina GAM, Toma L (2000) The opioid-receptor-lie 1 (ORL-1) as a potential target for new analgesics. Eur J Med Chem 35:275–282
Calò G, Guerrini R, Bigoni R, Rizzi A, Marzola G, Okawa H, Bianchi C, Lambert DG, Salvadori S, Regoli D (2000) Characterization of [Nph^1]nociceptin(1–13)NH_2, a new selective nociceptin receptor antagonist. Br J Pharmacol 129:1183–1193
Champion HC, Wang R, Hellstrom WJG, Kadowitz PJ (1997) Nociceptin, a novel endogenous ligand for the ORL_1 receptor, has potent erectile activity in the cat. Am J Physiol 273 (Endocrinol Metab 36):E214–E219
Champion HC, Bivalacqua TJ, Wang R, Hellstrom WJG, Kadowitz PJ (1998) [Tyr^1]nociceptin and nociceptin have similar naloxoneinsensitive erectile activity in the cat. J Androl 19:747–753
Civelli O, Nothacker HP, Reinscheid R (1998) Reverse physiology: discovery of the novel neuropeptide, orphanin FQ/nociceptin. Crit Rev Neurobiol 12:163–176
Connor M, Vaughan CW, Chieng B, Christie MJ (1996a) Nociceptin receptor coupling to a potassium conductance in rat locus coeruleus neurones *in vitro*. Br J Pharmacol 119:1614–1618
Connor M, Yeo A, Henderson G (1996b) Effect of nociceptin on Ca^{2+} channel current and intracellular Ca^{2+} in the SH-SY5Y human neuroblastoma cell line. Br J Pharmacol 118:205–207
Darland T, Heinricher MM, Grandy DK (1998) OrphaninFQ/nociceptin: a role in pain and analgesia, but so much more. Trends Neurosci 21:215–221
Guerrini R, Calò G, Rizzi A, Bigoni R, Bianchi C, Salvadori S, Regoli D (1998) A new selective antagonist of the nociceptin receptor. Br J Pharmacol 123:163–165

Hashimoto Y, Calò G, Guerrini R, Smith G, Lambert DG (2000) Antagonistic effects of [Nphe^1]nociceptin(1–13)NH_2 on nociceptin mediated inhibition of cAMP formation in Chinese hamster ovary cells stably expressing the recombinant human nociceptin receptor. Neurosci Lett 278:109–112
Hawkinson JE, Acosta-Burruel M, Espitia SE (2000) Opioid activity profiles indicate similarities between nociceptin/orphanin FQ and opioid receptors. Eur J Pharmacol 389:107–114
Meunier JC (2000) The therapeutic value of nociceptin agonists and antagonists. Expert Opin Ther Pat 10:371–388
Meunier JC, Mollereau C, Toll L, Suaudeau C, Moisand C, Alvinerie P, Butour JL, Guillemot JC, Ferrara P, Monserrat B, Mazarguil H, Vassart G, Parmentier M, Costentin J (1995) Isolation and structure of the endogenous agonist of opioid receptor-like ORL_1 receptor. Nature 377:532–535
Mogil JS, Pasternak (2001) The molecular and behavioral pharmacology of the orphanin FQ/nociception peptide and receptor family. Pharmacol Rev 53:381–415
Mollereau C, Mouledous L (2000) Tissue distribution of the opioid receptor-like (ORL1) receptor. Peptides 21:907–917
Mollereau C, Parmentier M, Mailleux P, Butour JL, Moisand C, Chalon P, Caput D, Vassart G, Meunier JC (1994) ORL1, a novel member of the opioid receptor family: cloning, functional expression and localization. FEBS Lett 341:33–38
Ozaki S, Kawamoto H, Itoh Y, Miyaji M, Iwasawa Y, Ohta H (2000) A potent and highly selective nonpeptidyl nociceptin/orphanin FQ receptor (ORL1) antagonist: J-113397. Eur J Pharmacol 387:R17–R18
Polidori C, Calò G, Ciccocioppo R, Geurrini R, Regoli D, Massi M (2000) Pharmacological characterization of the nociceptin receptor mediating hyperphagia: Identification of a selective antagonist. Psychopharmacology 148:430–437
Reinscheid RK, Nothacker HP, Bourson A, Ardati A, Henningsen RA, Bunzow JR, Grandy DK, Langen H, Monsma FJ, Civelli O (1995) Orphanin FQ: a neuropeptide that activates an opioidlike G protein-coupled receptor. Science 270:792–794
Sakurada T, Katsuyama S, Sakurada S, Inoue M, Tan No-K, Kisara K, Sakurada C, Ueda M, Sasaki J (1999) Nociceptin-induced scratching, biting and licking in mice: Involvement of spinal NK_1 receptors. Br J Pharmacol 127:1712–1718
Sakurada T, Sakurada S, Katsuyama S, Hayashi T, Sakurada C, Tan No-K, Johansson H, Sandin J, Terenius L (2000) Evidence that N-terminal fragments of nociceptin modulate nociceptin-induced scratching, biting and licking in mice. Neurosci Lett 279:61–64
Salvadori S, Guerrini R, Calò G, Regoli D (1999) Structure-activity studies on nociceptin/orphanin FQ: From full agonist to partial agonist, to pure antagonist. Farmaco 54:810–825
Stanfa LC, Chapman V, Kerr N, Dickenson AH (1996) Inhibitory action of nociceptin on spinal dorsal horn neurones of the rat, *in vivo*. Br J Pharmacol 118:1875–1877
Varani K, Rizzi A, Calò G, Bigoni R, Toth G, Guerrini R, Gessi S, Salvadori S, Borea PA, Regoli D (2000) Pharmacology of [Tyr^1]nociceptin analogs: receptor binding and bioassay studies. Naunyn-Schmiedeberg's Arch Pharmacol 360:270–277
Witta J, Palkovits M, Rosenberger J, Cox BM (2004) Distribution of nociception/orphanin FQ in adult human brain. Brain Res 30:24–29
Xu X-J, Hao J-X, Wiesenfeld-Hallin Z (1996) Nociceptin or anti-nociceptin: potent spinal antinociceptive effect of orphanin FQ/nociceptin in the rat. NeuroReport 7:2092–2094

H.1.1.6.2 Receptor Binding of Nociceptin

PURPOSE AND RATIONALE

The nociceptin receptor has been termed by different groups of investigators as ORL1, LC132, ROR (see Meunier 1997). Based on the structural and transductional similarities between receptors for nociceptin and those for opioids, Hamon (1998) proposed to include the nociceptin receptor in the opioid receptor family with the name OP_4.

Varani et al. (1999) tested synthetic nociceptin analogs for their displacement at the nociceptin- and at classical opioid receptors. The displacement of [^{3}H]$NCNH_2$ ([^{3}H]nociceptin amide, ORL1 site), and of the selective opioid receptor ligands [^{3}H]DAMGO (μ site), [^{3}H]deltorphin II (δ site), and [^{3}H]U69593 (κ site) was studied.

Wisner et al. (2006) described human opiorphin, a natural antinociceptive modulator of opioid-dependent pathways inhibiting enkephalin-inactivating zinc ectopeptidases.

PROCEDURE

Membrane Preparation

Guinea pigs are decapitated and the whole brain (without cerebellum) rapidly removed. The tissue is disrupted in a Polytron homogenizer (setting 5) in 50 mM Tris HCl, pH 7.4, to prepare membranes for the classic opioid receptor studies. The homogenate is centrifuged at 4000 *g* for 10 min and the pellet is resuspended with a Polytron PTA 10 probe (setting 5) in the same ice-cold buffer. To study the binding to ORL1 receptor, the tissue is homogenized in 50 mM Tris HCl, 2 mM EDTA and 100 µM phenylmethylsulphonylfluoride HCl (PMSF) at pH 7.4. The suspension is centrifuged at 40,000 *g* for 10 min and the pellet is resuspended in the same buffer. After 30 min of incubation at 37°C the membranes are centrifuged at 40,000 *g* for 10 min and the pellets are stored at –70°C. The protein concentration is determined with bovine albumin as standard.

Binding Assays

Classic opioid receptors, μ, δ and κ, are studied according to Bhargava and Zhao (1996). Saturation binding experiment are carried out using 8–10 different concentrations of [^{3}H]DAMGO ranging from 0.15 nM to 15 nM, [^{3}H]deltorphin II from 0.1 nM to 10 nM, and [^{3}H]U69593 from 0.15 nM to 15 nM, respectively. Inhibition experiments are carried out in duplicate in a final volume of 250 µl in test tubes containing ei-

ther 1.5 nM [^{3}H]DAMGO or 1.0 nM [^{3}H]deltorphin II or 1.5 nM [^{3}H]U69593, 50 mM Tris HCl at pH 7.4, guinea pig brain membranes (150–200 µg of protein/assay) and at least 8–10 different concentrations of the ligands under study. Binding assays to the ORL1 receptor are carried out according to Varani et al. (1998). In saturation studies, membranes are incubated with 8–10 different concentrations of [^{3}H]$NCNH_2$ ([^{3}H]nociceptin amide) ranging from 0.1 mM to 10 mM. Inhibition experiments are carried out in duplicate in a final volume of 250 µl in test tubes containing 1 mM [^{3}H]$NCNH_2$, 50 mM Tris HCl, 2 mM EDTA, 100 µM phenylmethylsulphonylfluoride HCl (PMSF) at pH 7.4, guinea pig membranes, and at least 8–10 different concentration of the compound under examination. The incubation time is 1 h for [^{3}H]DAMGO and [^{3}H]U69593 and 2 h for [^{3}H]deltorphin II and [^{3}H]$NCNH_2$. Nonspecific binding is defined as the binding measured in the presence of 100 µM bremazocine for classic opioid receptors and 10 µM $NCNH_2$ for ORL1 receptors.

Bound and free radioactivity are separated by filtering the assay mixture through Whatman GF/B glass-fibre filters, previously treated with PEI 0.1%; the incubation mixture is diluted with 3 ml of ice-cold incubation buffer, rapidly filtered by vacuum, and the filter washed three times with 3 ml of incubation buffer. The filter-bound radioactivity is measured in a Beckman LS-1800 Spectrometer.

EVALUATION

The inhibitory binding constant (K_i) values are calculated from the IC_{50} values according to the Cheng and Prusoff equation. The weighted non-linear last-squares curved fitting program LIGAND (Munson and Rodbard 1980) is used for computer analysis of saturation and inhibition experiments.

MODIFICATIONS OF THE METHOD

Ardati et al. (1997) developed two radioligands for the orphanin FQ receptor: a tritiated OFQ peptide ([^{3}H]orphanin FQ) and radioiodinated form in which Leu^{14} is substituted by tyrosine (^{125}I-Tyr^{14}-orphanin FQ). Both exhibit virtually identical characteristics.

Seki et al. (1999) analyzed the pharmacological properties of κ-opioid receptor-selective agonist TRK-820 using Chinese hamster ovary cells expressing cloned rat μ-, δ- and κ-opioid receptors and human nociceptin receptor.

Mouledous et al. (2000) reported a site-directed mutagenesis study of the ORL1 receptor transmembrane-binding domain.

REFERENCES AND FURTHER READING

Ardati A, Henningsen RA, Higelin J, Reinscheid RK, Cinelli O, Monsma FJ (1997) Interaction of [^{3}H]orphanin FQ and ^{125}I-Tyr^{14}-orphanin FQ with the orphanin FQ receptor: kinetics and modulation by cations and guanine nucleotides. Mol Pharmacol 51:816–824

Bhargava HN, Zhao GM (1996) Effects of competitive and non-competitive antagonists of the N-methyl-D-aspartate receptor on the analgesic action of δ1 and δ2 opioid receptors in mice. Br J Pharmacol 119:1586–1590

Calò G, Rizzi A, Bodin M, Neugebauer W, Salvadori S, Guerrini R, Bianchi C, Regoli D (1997) Pharmacological characterization of nociceptin receptor: an *in vitro* study. Can J Physiol Pharmacol 75:713–718

Hamon M (1998) The new approach to opioid receptors. Naunyn-Schmiedeberg's Arch Pharmacol 358 (Suppl 2):SA 5.3

Meunier JC (1997) Nociceptin/orphanin FQ and the opioid receptor-like ORL1 receptor. Eur J Pharmacol 340:1–15

Mouledous L, Topham CM, Moisand C, Mollereau C, Meunier JC (2000) Functional investigation of the nociceptin receptor by alanine substitution of glutamine 286 at the C terminus of the transmembrane segment VI: Evidence from a site-directed mutagenesis study of the ORL1 receptor transmembrane binding domain. Mol Pharmacol 57:495–502

Munson PJ, Rodbard D (1980) LIGAND; a versatile computerized approach for the characterization of ligand binding systems. Anal Biochem 107:220–239

Seki T, Awamura S, Kimura C, Ide S, Sakano K, Minami M, Nagase H, Satoh M (1999) Pharmacological properties of TRK-820 on cloned μ-, δ- and κ-opioid receptors and nociceptin receptor. Eur J Pharmacol 376:159–167

Varani K, Calò G, Rizzi A, Merighi S, Toth G, Guerrini R, Salvadori S, Borea PA, Regoli D (1998) Nociceptin receptor binding in mice forebrain membranes: thermodynamic characteristics and structure-activity relationships. Br J Pharmacol 125:1485–1490

Varani K, Rizzi A, Calò G, Bigoni R, Toth G, Guerrini R, Gessi S, Salvadori S, Borea PA, Regoli D (1999) Pharmacology of [Tyr1]nociceptin analogs: receptor binding and bioassay studies. Naunyn-Schmiedeberg's Arch Pharmacol 360:270–277

Wisner A, Dufour E, Messaoudi M, Nejdi A, Marcel A, Ungeheuer MN, Rougeot C (2006) Human opiorphin, a natural antinociceptive modulator of opioid-dependent pathways. Proc Natl Acad Sci USA 193:17979–17984

H.1.1.6.3 Bioassays for Nociceptin

PURPOSE AND RATIONALE

Nociceptin receptors in the periphery can be characterized by studies in isolated organs (Guerrini et al. 1998; Bigoni et al. 1999): the guinea pig ileum according to Paton (1957) (see J.4.3.1), the mouse vas deferens according to Hughes et al. (1975), the rabbit vas deferens according to Oka et al. (1980) (see A.1.2.3), the guinea pig renal pelvis (Giuliani and Maggi 1996) (see C.4.2.1).

PROCEDURE

Tissues are taken from male Swiss mice (25–30 g), guinea pigs (300–350 g) Sprague Dawley rats (300–350 g) and New Zealand albino rabbits (1.5–1.8 kg). They are suspended in 10 ml organ baths containing Krebs solution oxygenated with 95% O_2 and 5% CO_2. The temperature is set at 33°C for the mouse vas deferens and at 37°C for the other tissues. A resting tension of 0.3 g is applied to the mouse deferens, 1 g to the guinea pig ileum, rats vas deferens, and rabbit vas deferens and 0.15 g to the guinea pig renal pelvis. For experiments at the mouse vas deferens a Mg^{2+}-free Krebs solution is used and for rat vas deferens experiments a Krebs solution containing 1.8 mM $CaCl_2$. Guinea pig renal pelvis experiments are performed in the presence of indomethacin (3 μM).

The mouse vas deferens, guinea pig ileum, rat vas deferens, and rabbit vas deferens are continuously stimulated through two platinum ring electrodes with supramaximal voltage rectangular pulses of 1 ms duration and 0.1 Hz frequency. The electrically evoked contractions are measured isotonically with a strain gauge transducer and recorded on a multichannel chart recorder. After an equilibration period of about 60 min the contractions induced by electrical field stimulation are stable; at this time, cumulative concentration response curves to nociceptin or opioid peptides are performed (0.5 log unit steps).

The guinea pig renal pelvis is stimulated through two platinum ring electrodes with 100 V square wave pulses of 1 ms duration at a frequency of 5 Hz for 10 s. The spontaneous activity and the positive inotropic responses to electrical field stimulation are measured by an isotonic transducer and recorded by a two channel recorder. The experiments are started following a 60 min equilibration period. Four electrical field stimulation are performed with each tissue at 30 min intervals. Agonists are added to the bath 5 min, and antagonists 15 min before the next stimulus. The contractile responses to electrical field stimulation are expressed as % increment the spontaneous activity of the tissue; the biological effects of the application of agonists or antagonists are expressed as % inhibition of electrical filed stimulation-induced contraction.

EVALUATION

Data are expressed as means ±SEM of *n* experiments and statistically analyzed with Student two-tailed *t*-test of one way ANOVA plus Dunnett test. The agonist potencies are given as pE_{50}, which is the negative logarithm to base 10 of the agonist molar concentration that produces 50% of the maximal possible effect of that agonist. The E_{max} is the maximal effect that an agonist can elicit in a given preparation. Antagonist potencies are expressed in terms of pA_2, which is the negative logarithm to base 10 of the antagonist molar concentration that makes it necessary to double the agonist concentration to elicit the original submaximal response.

MODIFICATIONS OF THE METHOD

Rizzi et al. (1999) studied nociceptin and nociceptin analogs in the isolated mouse colon.

Bigoni et al. (1999) used nociceptin, a series of nociceptin fragments, naloxone as well as [$Phe^1\Psi$ (CH_2-NH)Gly^2]nociceptin(1–13)NH_2 and [$Nphe^1$]nociceptin(1–13)NH_2 to characterize nociceptin receptors in peripheral organs, such as mouse and rat vas deferens (noradrenergic nerve terminals), in the guinea pig ileum (cholinergic nerves) and renal pelvis (sensory nerves) and *in vivo* by measuring the blood pressure and heart rate in anesthetized rats.

Menzies et al. (1999) described the agonist effects of nociceptin and [$Phe^1\Psi$ (CH_2-NH)Gly^2] nociceptin(1–13)NH_2 in the mouse and rat colon and in the mouse vas deferens.

Kolesnikov and Pasternak (1999) found an ED_{50} of 16.3 μg after peripheral administration of nociceptin in the tail flick test in mice.

Bertorelli et al. (1999) found anti-opioid effects of nociceptin and the ORL1 ligand [$Phe^1\Psi$ (CH_2-NH)Gly^2]nociceptin(1–13)NH_2 in the Freund's adjuvant-induced arthritic rat model of chronic pain.

Yamamoto and Sakashita (1999) studied the effect of nocistatin, a 17 amino acid peptide which is processed from prepronociceptin and its interaction with nociceptin in the rat formalin test.

Hashiba et al. (2003) measured the effects of nociceptin/orphanin FQ receptor ligands on blood pressure, heart rate, and plasma catecholamine concentrations in guinea pigs.

Using the forced swimming test and the tail suspension test in rats and mice, Gavioli et al. (2004) demonstrated antidepressant-like effects of the nociceptin/orphanin FQ receptor antagonist UFP-101.

Varty et al. (2005) characterized a nociceptin receptor (ORL-1) agonist in tests of anxiety across three species: rat, guinea pig, and mouse.

REFERENCES AND FURTHER READING

Bertorelli R, Corradini L, Rafiq K, Tupper J, Calò G, Ongini E (1999) Nociceptin and the ORL1 ligand [Phe$^1\Psi$ (CH_2-NH)Gly^2]nociceptin(1–13)NH_2 exert anti-opioid effects in the Freund's adjuvant-induced arthritic rat model of chronic pain. Br J Pharmacol 128:1252–1258

Bigoni R, Giuliani S, Calò G, Rizzi A, Guerrini R, Salvadori S, Regoli D, Maggi CA (1999) Characterization of nociceptin receptors in the periphery: *in vitro* and *in vivo* studies. Naunyn-Schmiedeberg's Arch Pharmacol 359:160–167

Calò G, Guerrini R, Bigoni R, Rizzi A, Marzola G, Okawa H, Bianchi C, Lambert DG, Salvadori S, Regoli D (2000) Characterization of [Nph^1]nociceptin(1–13)NH_2, a new selective nociceptin receptor antagonist. Br J Pharmacol 129:1183–1193

Gavioli EC, Vaughan CW, Marzola G, Guerrini R, Mitchell VA, Zucchini S, De Lima TC, Rae GA, Salvadori S, Regoli D, Calo G (2004) Antidepressant-like effects of the nociceptin/orphanin FQ receptor antagonist UFP-101: new evidence from rats and mice. Naunyn-Schmiedebergs Arch Pharmacol 369:547–553

Giuliani S, Maggi CA (1996) Inhibition of tachykinin release from peripheral endings of sensory nerves by nociceptin, a novel opioid peptide. Br J Pharmacol 118:1567–1569

Guerrini R, Calò G, Rizzi A, Bigoni R, Bianchi C, Salvadori S, Regoli D (1998) A new selective antagonist of the nociceptin receptor. Br J Pharmacol 123:163–165

Hashiba E, Hirota K, Kudo T, Calo G, Guerrini R, Matsuki A (2003) Effects of nociceptin/orphanin FQ receptor ligands on blood pressure, heart rate, and plasma catecholamine concentrations in guinea pigs. Naunyn-Schmiedebergs Arch Pharmacol 367:342–347

Hughes J, Kosterlitz HW, Leslie FM (1974) Assessment of the agonistic and antagonistic activities of narcotic analgesic drugs by means of the mouse vas deferens. Br J Pharmacol 51:139P–140P

Kolesnikov YA, Pasternak GW (1999) Peripheral orphanin FQ/nociceptin analgesia in the mouse. Life Sci 64:2021–2028

Menzies JRW, Glen T, Davies MRP, Paterson SJ, Corbett AD (1999) *In vitro* agonist effects of nociceptin and [Phe$^1\Psi$ (CH_2-NH)Gly^2]nociceptin(1–13)NH_2 in the mouse and rat colon and the mouse vas deferens. Eur J Pharmacol 385:217–223

Oka T, Negishi K, Suda M, Matsumiya T, Inazu T, Ueki M (1980) Rabbits vas deferens: a specific bioassay for opioid κ-receptor agonists. Eur J Pharmacol 73:235–236

Paton WDM (1957) The action of morphine and related substances on contraction and on acetylcholine output of coaxially stimulated guinea-pig ileum. Br J Pharmacol 12:119–127

Rizzi A, Bigoni R, Calò G, Guerrini R, Salvadori S, Regoli D (1999) [Nphe^1]nociceptin(1–13)NH_2 antagonizes nociceptin effects in the mouse colon. Eur J Pharmacol 385:2–3

Varty GB, Hyde LA, Hodgson RA, Lu SX, McCool MF, Kazdoba TM, DelVecchio RA, Guthrie DH, Pond AJ, Grzelak ME, Xu X, Korfmacher WA, Tulshian D, Parker EM, Higgins GA (2005) Characterization of the nociceptin receptor (ORL-1) agonist, Ro64–6198, in tests of anxiety across multiple species. Psychopharmacology 182:132–143

Yamamoto T, Sakashita Y (1999) Effect of nocistatin and its interaction with nociceptin/orphanin FQ on the rat formalin test. Neurosci Lett 262:179–182

H.1.1.7 Vasoactive Intestinal Polypeptide (VIP) and Pituitary Adenylate Cyclase-Activating Peptide (PACAP)

PURPOSE AND RATIONALE

Several peptides are considered to play a role in the altered transmission of sensory information in neuropathic conditions, such as neuropathic pain arising from trauma or compression injury of peripheral nerves (Zhang et al. 1998).

Vasoactive intestinal polypeptide (VIP), isolated by Nakajima et (1970), is a neuropeptide of 28 amino acids with widespread distribution in both the central and peripheral nervous system (Fahrenkrug 1979; Gafvelin 1990).

Together with the structurally related pituitary adenylate cyclase-activating peptide (PACAP) this peptide is considered to play an important role in the somatosensory processing of pain (Dickinson and Fleetwood-Walker 1999). PACAP-38 (a 38 amino-acid polypeptide) and the C-terminally truncated form PACAP-37 share 68% amino acid homology at their N-terminal domain with VIP. A shorter peptide with 27 amino acids, named as PACAP27 was described by Miyata et al. (1990). These peptides are members of a superfamily of hormones that includes glucagon, glucagon-like peptide, secretin and growth hormone releasing factor.

Three G-protein-coupled receptors are described: the $VPAC_1$ receptor, originally described as the VIP receptor and subsequently designated as VIP_1 receptor; the $VPAC_2$ receptor, previously designated VIP_2; and the PAC_1 receptor, previously known as PACAP type I receptor (Buscail et al. 1990; Guijarro et al. 1991; Felley et al. 1992; Calvo et al. 1994; Van Rampelbergh et al. 1996; Harmar et al. 1998; Robberecht et al. 1999).

Many peripheral activities of VIP/PACAP are described, such as stimulation of pancreatic secretion (Onaga et al. 1997; Ito et al. 1998; Soo Tek Lee et al. 1998); stimulation of duodenal bicarbonate secretion (Takeuchi et al. 1998); relaxation of smooth muscle cells in the intestinal tract, e. g., gall bladder (Pang and Kline 1998), cecal circular smooth muscle (Motomura et al. 1998), internal anal sphincter (Rattan and Chakder 1997); on duodenal motility (Onaga et al. 1998); enhancement of insulin secretion (Yada et al. 1997; Filipsson et al. 1998); bronchodilation (Linden et al. 1998; Shigyo et al. 1998; Okazawa et al. 1998). Centrally administered PACAP showed an anorectic effect (Mizuno et al. 1998).

Agonists (Gourlet et al. 1997a, b) and antagonists (Gozes et al. 1991; Gourlet et al. 1997c) for VIP were described. Further studies are aimed to development of drugs for neuropathic analgesia, ultimately of non-peptide nature, using $VPAC_1$, $VPAC_2$, and PAC_1, receptors as drug targets (Dickinson and Fleetwood-Walker 1999).

PROCEDURE

CHO cell lines expressing the rat VIP_1 receptor (Ciccarelli et al. 1994), the human VIP_2 receptor (Sreedharan et al. 1993), the rat PACAP I receptor (Ciccarelli et al. 1995), and the rat secretin receptor (Ishihara et al. 1991) are used.

Transfected CHO cells are harvested with a rubber policeman and pelleted by low speed centrifugation. The supernatant is discarded and the cell lysed in mM $NaHCO_3$ solution and immediate freezing in liquid nitrogen. After thawing, the lysate is first centrifuged at 4°C for 10 min at 400 *g* and the supernatant is further centrifuged at 20,000 *g* for 10 min. The pellet, resuspended in 1 mM $NaHCO_3$ is used immediately as a crude membrane fraction.

Binding is performed using [^{125}I]VIP (specific radioactivity of 0.5 Ci/nmol), [^{125}I]Tyr^{25} secretin (specific radioactivity of 1.0 Ci/nmol) and [^{125}I-Ac-His^{1}]PACAP-27 (specific radioactivity of 0.7 Ci/nmol) as tracers. In all cases, non-specific binding is defined as the residual binding in the presence of 1 μM of the unlabeled peptide corresponding to the tracer. Binding is performed at 37°C in a 20 mM Tris-maleate, 2 mM $MgCl_2$, 0.1 mg/ml bacitracin, 1% bovine serum albumin (pH 7.4) buffer. Bound radioactivity is separated from free by filtration through glass-fibre GF/C filters presoaked for 24 h in 0.1% polyethyleneimine and rinsed three times with a 20 mM (pH 7.4) sodium phosphate buffer containing 1% bovine serum albumin.

EVALUATION

The IC_{50} values (in mM) for each peptide on each receptor are calculated from complete dose-effect curves performed on three different membrane preparations using the LIGAND program.

MODIFICATIONS OF THE METHOD

Schmidt et al. (1993) studied the binding of PAPAC, VIP and analogues of VIP and PAPAC in rat AR 4–2J pancreatic carcinoma cells and isolated pancreatic acini to the PAPAC-1 receptor, abundantly expressed in AR 4–2J pancreatic carcinoma cells, and to the VIP/PAPAC-2 receptor. Simultaneously, biological effects (lipase secretion and cAMP production) in pancreatic acini were determined. PAPAC was regarded as a potent ligand for both receptor types and as a potent VIP-like secretagogue.

REFERENCES AND FURTHER READING

Buscail L, Gourlet P, Cauvin A, de Neef P, Gossen D, Arimura A, Miyata A, Coy DH (1990) Presence of highly selective receptors for PACAP (pituitary adenylate cyclase activating peptide) in membranes from the rat pancreatic acinar cell line AR 4-J. FEBS Lett 262:77–81

Calvo JR, Montilla ML, Guerrero JM, Segura JJ (1994) Expression of VIP receptors in mouse peritoneal macrophages: Functional and molecular characterization. J Neuroimmunol 50:85–93

Ciccarelli E, Vilardaga JP, de Neef P, di PaoloE, Warelbroeck M, Bollen A, Robberecht P (1994) Properties of the VIP-PACAP type II receptor stably expressed in CHO cells. Regul Pept 54:397–407

Ciccarelli E, Svoboda M, de Neef P, di Paolo E, Bollen A, Dubeaux C, Vilardage JP, Waelbroeck M, Robberecht P (1995) Pharmacological properties of two recombinant splice variants of the PACAP type I receptor transferred and stably expressed in CHO cells. Eur J Pharmacol 288:259–267

Couvineau A, Rousset M, Laburthe M (1985) Molecular identification and structural requirement of vasoactive intestinal peptide (VIP) receptors in the human colon adenocarcinoma cell line, HT-29. Biochem J 213:139–143

Dickinson T, Fleetwood-Walker SM (1999) VIP and PACAP: very important in pain? Trends Pharmacol Sci 20:324–329

Fahrenkrug J (1979) Vasoactive intestinal peptide: Measurement, distribution and putative neurotransmitter function. Digestion 19:149–169

Felley CP, Qian JM, Mantey S, Pradhan T, Jensen RT (1992) Chief cells possess a receptor with high affinity for PACAP and VIP that stimulates pepsinogen release. Am J Physiol 263 (Gastrointest Liver Physiol 26):G901–G907

Filipsson K, Pacine G, Scheurink AJW, Ahren B (1998) PACAP stimulates insulin secretion but inhibits insulin sensitivity in mice. Am J Physiol 274; Endocrinol Metab 37:E834–E842

Gafvelin (1990) Isolation and primary structure of VIP from sheep brain. Peptides 11:703–706

Gourlet P, Vertongen P, Vandermeers A, Vandermeers-Piret MC, Rathe J, de Neef P, Waelbroeck M, Robberecht P (1997) The long-acting vasoactive intestinal polypeptide agonist RO 25–1553 ins highly selective of the VIP_2 receptor subclass. Peptides 18:403–408

Gourlet P, Vandermeers A, Vertongen P, Rathe J, de Neef P, Cnudde J, Waelbroeck M, Robberecht P (1997b) Development of high affinity selective VIP_1 receptor agonists. Peptides 18:1539–1545

Gourlet P, de Neef P, Cnudde J, Waelbroeck M, Robberecht P (1997c) *In vitro* properties of a high affinity selective antagonist of the VIP_1 receptor. Peptides 18:1555–1560

Gozes I, McCune SK, Jacobson L, Warren D, Moody TW, Fridkin M, Brenneman DE (1991) An antagonist to vasoactive intestinal peptide affects cellular functions in the central nervous system. J Pharmacol Exp Ther 257:959–966

Guijarro LG, Rodriguez-Pena MS, Prieto JC (1991) Characterization of vasoactive intestinal peptide receptors in rat seminal vesicle. Am J Physiol 260 (Endocrinol Metab 23):E286–E291

Harmar AJ, Arimura A, Gozes I, Journot L, Laburthe M, Pisegna JR, Rawlings SR, Robberecht P, Said SI, Sreedha-

ran SP, Wank SA, Wascheck JA (1998) International Union of Pharmacology. XVIII. Nomenclature of receptors for vasoactive intestinal peptide and pituitary adenylate cyclase-activating polypeptide. Pharmacol Rev 50:265–270
Ishihara T, Nakamura S, Kaziro Y, Takahashi T, Takahashi K, Nagata S (1991) Molecular cloning and expression of a cDNA encoding the secretion receptor. EMBO J 10:1635–1641
Ito O, Naruse S, Kitagawa M, Ishiguro H, Ko S, Nakajima M, Hayakawa t (1998) The effect of VIP/PACAP family of peptides on pancreatic blood flow and secretion in conscious dogs. Regul Pept 78:105–112
Linden A, Cardell LO, Yoshihara S, Stjarne P, Nadel JA (1998) PACAP 1–38 as an inhaled bronchodilator in guinea pigs *in vivo*. Peptides 19:93–98
Miyata A, Jiang L, Dahl RD, Kitada C, Kubo K, Fujino M, Minamino N, Arimura A (1990) Isolation of a neuropeptide corresponding to the N-terminal 27 residues of the pituitary adenylate cyclase-activating polypeptide with 38 residues (PACAP38). Biochem Biophys Res Commun 170:643–648
Mizuno Y, Kondo K, Terashima Y, Arima H, Murase T, Oiso Y (1998) Anorectic effect of pituitary adenylate cyclase activating polypeptide (PACAP) in rats: Lack of evidence for involvement of hypothalamic neuropeptide gene expression. J Neuroendocrinol 10:611–616
Motomura Y, Chijiiwa Y, Iwakiri Y, Ochiai T, Nawata H (1998) Interactive mechanisms among pituitary adenylate cyclase-activating peptide, vasoactive intestinal peptide, and parathyroid receptors in guinea pig cecal circular smooth muscle cells. Endocrinology 139:2869–2878
Nakajima T, Tanimura T, Pisano JJ (1970) Isolation and structure of a new vasoactive peptide Fed Proc 29:282
Okazawa A, Cui ZH, Lotvall J, Yoshihara S, Skoogh BE, Kashimoto K, Linden A (1998) Effect of a novel PACAP-27 analogue on muscarinic airway responsiveness in guinea pigs *in vivo*. Eur Respir J 12:1062–1066
Onaga T, Okamoto K, Harada Y, Mineo H, Kato S (1997) PACAP stimulates pancreatic exocrine secretion via the vagal cholinergic nerves in sheep. Regul Pept 72:1147–153
Onaga T, Harada Y, Okamoto K (1998) Pituitary adenylate cyclase-activating polypeptide (PACAP) induces duodenal phasic contractions via the vagal cholinergic nerves in sheep. Regul Pept 77:69–76
Robberecht P, Vertongen P, Perret J, van Rampelbergh J, Juarranz MG, Waelbroeck M (1999) Receptors for VIP and PACAP. Trends Pharmacol Sci; Receptor and Ion Channel Nomenclature Supplement
Schmidt WE, Seebeck J, Höcker M, Schwarzhoff R, Schäfer H, Fornefeld H, Morys-Wortmann C, Fölsch UR, Creutzfeldt W (1993) PAPAC and VIP stimulate enzyme secretion in rat pancreatic acini via interaction with VIP/PACAP-2 receptors: additive augmentation of CCK/carbachol-induced enzyme release. Pancreas 8:476–487
Shigyo M, Aizawa H, Inoue H, Matsumoto K, Takada S, Hara N (1998) Pituitary adenylate cyclase activating peptide regulates neurally mediated airway responses. Eur Resp J 12:64–70
Soo Tek Lee, Kae Yol Lee, Li P, Coy D, Chang TM, Chey WY (1998) Pituitary adenylate cyclase-activating peptide stimulates rat pancreatic secretion via secretin and cholecystokinin releases. Gastroenterology 114:1054–1060
Sreedharan SP, Patel DR, Huang j-X, Goetzl EJ (1993) Cloning and functional expression of a human neuroendocrine vasoactive intestinal peptide receptor. Biochem Biophys Res Commun 193:546–553
Takeuchi K, Yagi K, Sugamoto S, Furukawa O, Kawauchi S, (1998) Involvement of PACAP in acid-induced HCO_3^- response in rat duodenum. Pharmacol Res 38:475–480
Van Rampelbergh J, Gourlet P, de Neef P, Robberecht P, Waelbrouck M (1996) Properties of the pituitary adenylate cyclase-activating polypeptide I and II receptors, vasoactive intestinal peptide$_1$, and chimeric amino-terminal pituitary adenylate cyclase-activating polypeptide/vasoactive intestinal peptide$_1$ receptors: Evidence for multiple receptor states. Mol Pharmacol 50:1596–1604
Yada T, Sakurada M, Ishihara A, Nakata M, Shioda S, Yaekura K, Hamakawa N, Yanagida K, Kikuchi M, Oka Y (1997) Pituitary adenylate cyclase-activating polypeptide (PACAP) is an islet substance serving as an intra-islet amplifier of glucose-induced insulin secretion in rats. J Physiol 505:319–328
Zhang Y, Danielson N, Sundler F, Mulder H (1998) Pituitary adenylate cyclase-activating peptide in upregulated in sensory neurons by inflammation. NeuroReport 9:2833–2836

H.1.1.8 Cannabinoid Activity

H.1.1.8.1 General Considerations on Cannabinoids

In the centuries since hashish and marijuana (*Cannabis sativa*) were used as psychoactive drugs the most significant discoveries in regard to the mechanism of action were made with the isolation of (–)-trans-Δ^9-tetrahydrocannabinol (Δ^9-THC) as the principal active ingredient (Mechoulam et al. 1970), the characterization and localization of the cannabinoid receptor in the brain (Devane et al. 1988), the cloning of its gene (Matsuda et al. 1990), and the identification of an endogenous ligand (Devane et al. 1992). Most cannabinoid effects occur receptor mediated in the CNS (Martin 1986; Herkenham et al. 1990; Porter and Felder 2001; Howlett et al. 2002). The recognized CNS responses to cannabinoids include alterations in cognition and memory, euphoria and sedation (Howlett 1995). Ranganathan and D'Souza (2006) reviewed the acute effects of cannabinoids on memory in humans.

Cannabinoids have been shown to produce analgesia without the respiratory problems associated with opioid analgesics (Buxbaum 1972; Martin 1985; Dewey 1986; Razdan 1986; Compton et al. 1992; Meng et al. 1998; Strangman et al. 1998) which may be of value for therapeutic applications (Hollister 1986; Izzo et al. 2000a; Pertwee 2000). Simultaneous administration of cannabinoid receptor agonists and μ- or κ-receptor agonists indicate a cannabinoid-opioid interaction in anti-nociception (Manzanares et al. 2000). Baker et al. (1990, 2000) described experimental allergic encephalomyelitis with relapsing-remitting episodes, spasticity and tremor similar to multiple scle-

rosis in human beings in Biozzi AB/H mice. These symptoms could be antagonized by cannabinoids.

A multiple-evaluation paradigm of *in vivo* mouse assays is employed to test for cannabimimetic effects. This paradigm includes assays for reduction in spontaneous activity, and the production of hypothermia, catalepsy, and antinociception measured by tail-flick assay (Compton et al. 1992; Welch et al. 1998). The behavioral effects of Δ^9-THC and related cannabinoids in mice have been termed the "popcorn" effect. That is, groups of mice are in a sedated state with little or no movement until a stimulus causes one mouse to jump (hyper-reflexia). This animal falls on another mouse which in turn jumps so that this repeated hyper-reflexic jumping looks like corn popping in a machine. Subsequently, all mice will be sedated until another stimulus reinitiates the process (Dewey 1986). Like the opioids, cannabinoids inhibit electrically evoked contractions of the mouse vas deferens and the guinea pig ileum, but unlike the opioids, these effects are not antagonized by naloxone (Pertwee et al. 1992; Hillard et al. 1999).

In addition to the effects in the CNS (Chaperon and Thiebot 1999), peripheral effects of cannabinoids are known (Lynn and Herkenham 1994) including actions on the **endocrine system** (Patra and Wadsworth 1990, (Block et al. 1991; Wenger et al. 2000), on the **digestive tract** (Rosell and Agurell 1975; Izzo et al. 1990a, b, 2000; Coutts et al. 2000; Massa et al. 2005), on **ingestive behavior** (Giuliani et al. 2000), on the **pulmonary and cardiovascular system** (Stengel et al. 1998; White and Hiley 1998; Niederhoffer and Szabo 1999; Liu et al. 2000; Niederhoffer et al. 2003), and on **immune modulation** (Kaminski et al. 1992; Lynn and Herkenham 1994; Achiron et al. 2000).

An endogenous cannabinoid was isolated from porcine brain by Devane et al. (1992) and found to be an unsaturated fatty acid ethanolamide, arachidonylethanolamide, also called **anandamide**, which activates CB1 receptors (Devane et al. 1992; Hillard and Jarrahian 2005) and produces similar effects as Δ^9-tetrahydrocannabinol including anti-nociception, hypothermia, hypomotility and catalepsy in mice (Smith et al. 1994). The brain enzyme hydrolyzing and synthesizing anandamide has been characterized by Ueda et al. (1995). The human brain fatty-acid amide hydrolase was characterized by Maccarrone et al. (1998) as a single protein, which hydrolyses anandamide to arachidonate and ethanolamine.

Similar effects are produced by other polyunsaturated N-acetylethanolamines, such as N-palmitoylethanolamine, which activates the CB-2-like receptor subtype (Hanu et al. 1993; Facci et al. 1995). Both endogenous cannabinoids (called endocannabinoids) derive from cleavage of a precursor phospholipid, N-acylphosphatidylethanolamine, catalyzed by Ca^{2+}-activated D-type phosphodiesterase activity (Cadas et al. 1996). 2-Arachidonylglycerol was described as a further endogenous ligand for cannabinoid receptors (Ameri and Simmet 2000; Sigiura et al. 2000)

Numerous synthetic analogs and cannabimimetic compounds have been evaluated as agonists and antagonists by *in vitro* and *in vivo* pharmacological methods (Martin et al. 1991; D'Ambra et al. 1992; Melvin et al. 1993; Barth and Rinaldi-Carmona 1999; Hillard et al. 1999; Palmer et al. 2000; Piomelli et al. 2000; De Petrocellis et al. 2004; Costa et al. 2005; Griebel et al. 2005; Lange et al. 2005; Makriyannis et al. 2005; Pertwee 2006).

Costa et al. (2004) described oral anti-inflammatory activity of cannabidiol, a non-psychoactive constituent of cannabis, in acute carrageenan-induced inflammation in the rat paw.

For studies on the effects of cannabinoids and cannabinoid antagonists on digestive system and obesity see L.3.1.3.

REFERENCES AND FURTHER READING

Achiron A, Miron S, Lavie V, Margali R, Biegon A (2000) Dexanabinol (HU-211) effect on experimental autoimmune encephalomyelitis. J Neuroimmunol 102:26–31

Ameri A, Simmet T (2000) Effects of 2-arachidonylglycerol, an endogenous cannabinoid, on neuronal activity in rat hippocampal slices. Naunyn-Schmiedeberg's Arch Pharmacol 361:265–272

Baker D, O'Neill JK, Gschmeissner SE, Wilcox CE, Butter C, Turk JL (1990) Induction of chronic relapsing experimental allergic encephalomyelitis in Biozzi mice. J Neuroimmunol 28:261–270

Baker D, Pryce G, Croxford JL, Brown P, Pertwee RG, Huffman HW, Layward L (2000) Cannabinoids control spasticity and tremor in a multiple sclerosis model. Nature 202:84–87

Barth F, Rinaldi-Carmona M (1999) The development of cannabinoid antagonists. Curr Med Chem 6:745–755

Block RI, Farinpour R, Schlechte JA (1991) Effects of chronic marijuana use on testosterone, luteinizing hormone, follicle stimulating hormone, prolactin and cortisol in men and women. Drug Alcohol Depend 28:121–128

Buxbaum DM (1972) Analgesic activity of Δ^9-tetrahydrocannabinol in the rat and mouse. Psychopharmacology 25:275–280

Cadas H, Gaillet S, Beltramo M, Venance L, Piomelli D (1996) Biosynthesis of an endogenous cannabinoid precursor in neurons and its control by calcium and cAMP. J Neurosci 16:3934–3942

Chaperon F, Thiebot MH (1999) Behavioral effects of cannabinoid agents in animals. Crit Rev Neurobiol 13:243–281

Compton DR, Johnson MR, Melvin LS, Martin BR (1992) Pharmacological evaluation of a series of bicyclic cannabinoid

analogs: Classification as cannabimimetic agents. J Pharmacol Exp Ther 260:201–209

Costa B, Colleoni M, Conti S, Parolaro D, Franke C, Trovato AE, Giagnoni G (2004) Oral anti-inflammatory activity of cannabidiol, a non-psychoactive constituent of cannabis, in acute carrageenan-induced inflammation in the rat paw. Naunyn-Schmiedebergs Arch Pharmacol 369:294–299

Costa B, Trovato AE, Colleoni M, Giagnoni G, Zarini E, Croci T (2005) Effect of the cannabinoid CB1 receptor antagonist, SR141716, on nociceptive response and nerve demyelination in rodents with chronic constriction injury of the sciatic nerve. Pain 116:52–61

Coutts AA, Brewster M, Ingram T, Razdan RK, Pertwee RG (2000) Comparison of novel cannabinoid partial agonist and SR 141716A in the guinea pig small intestine. Br J Pharmacol 129:645–652

D'Ambra TE, Estep KG, Bell MR, Eissenstat MA, Josef KA, Ward SJ, Haycock DA, Baizman ER, Casiano FM, Beglin NC, Chippari SM, Grego JD, Kullnig RK, Daley GT (1992) Conformationally restrained analogues of pravadoline: nanomolar potent, enatioselective, (aminoalkyl)indole agonists on the cannabinoid receptor. J Med Chem 35:124–135

De Petrocellis L, Cascio MG, Di Marzo V (2004) The endocannabinoid system: a general view and latest additions. Br J Pharmacol 141:765–774

Devane WA, Dysarz FAI, Johnson MR, Melvin LS, Howlett AC (1988) Determination and characterization of a cannabinoid receptor in rat brain. Mol Pharmacol 34:605–613

Devane WA, Hanus L, Breuer A, Pertwee RG, Stevenson LA, Griffin G, Gibson D, Mandelbaum A, Etinger A, Mechoulam R (1992) Isolation and structure of a brain constituent that binds to the cannabinoid receptor. Science 258:1946–1949

Dewey WL (1986) Cannabinoid pharmacology. Pharmacol Rev 38:151–178

Facci L, Dal Torso R, Romanello S, Buriani A, Skaper SD, Leon A (1995) Mast cells express a peripheral cannabinoid receptor with differential sensitivity to anandamide and palmitoyletholamine. Proc Natl Acad Sci USA 92:3376–3380

Giuliani D, Ottani A, Ferrari F (2000) Effects of the cannabinoid receptor agonist, HU 210, on ingestive behavior and body weight in rats. Eur J Pharmacol 391:275–279

Griebel G, Stemmelin J, Scatton B (2005) Effects of the cannabinoid CB1 receptor antagonist rimonabant in models of emotional reactivity in rodents. Biol Psychiatry 57:261–267

Hanu L, Gopher A, Almog S, Mechoulam R (1993) Two new unsaturated fatty acid ethanolamines in brain bind to the cannabinoid receptor. J Med Chem 36:3032–3034

Herkenham M, Lynn AB, Little MD, Johnson MR, Melvin LS, de Costa BR, Rice KC (1990) Cannabinoid receptor localization in brain. Proc Natl Acad Sci USA 87:1932–1936

Hillard CJ, Manna S, Greenberg MJ, DiCamelli R, Ross RA, Stevenson LA, Murphy V, Pertwee RG, Campbell WB (1999) Synthesis and characterization of potent and selective agonists of the neuronal cannabinoid receptor (CB1). J Pharmacol Exp Ther 289:1427–1433

Hillard CJ, Jarrahian A (2005) Accumulation of anandamide: evidence for cellular diversity. Neuropharmacology 48:1072–1078

Hollister LE (1986) Health aspects of cannabis. Pharmacol Rev 38:1–20

Howlett AC (1995) Pharmacology of cannabinoid receptors. Annu Rev Pharmacol Toxicol 35:607–634

Howlett AC, Barth F, Bonner TI, Cabral G, Casellas P, Devane WA, Felder CC, Herkenham M, Mackie K, Martin BR, Mechoulam R, Pertwee RG (2002) International Union of Pharmacology XXVII. Classification of cannabinoid receptors. Pharmacol Rev 54:161–202

Izzo AA, Mascolo N, Capasso R, Germano MP, DePasquale R, Capasso F (1999a) Inhibitory effects of cannabinoid agonists on gastric emptying in rats. Naunyn-Schmiedeberg's Arch Pharmacol 360:221–223

Izzo AA, Mascolo N, Pinto N, Capasso R, Capasso F (1999b) The role of cannabinoid receptors in intestinal motility, defaecation and diarrhoea in rats. Eur J Pharmacol 384:37–42

Izzo AA, Mascolo N, Capasso F (2000a) Marijuana in the new millenium: perspectives for cannabinoid research. Trends Pharmacol Sci 21:281–282

Izzo AA, Mascolo N, Tonini M, Capasso F (2000b) Modulation of peristalsis by cannabinoid CB-1 ligands in the isolated guinea pig ileum. Br J Pharmacol 129:984–990

Kaminski NE, Abood ME, Kessler FK, Martin BR, Schatz AR (1992) Identification of a functionally relevant cannabinoid receptor on mouse spleen cells that is involved in cannabinoid-mediated immune modulation. Mol Pharmacol 42:736–742

Lange JHM, van Stuivenberg HH, Veerman W, Wals HC, Stork B, Coolen HKAC, McCreary AC, Adolfs TJP, Kruse CG (2005) Novel 3,4-diarylpyrazolines as potent cannabinoid CB1 receptor antagonists with lower lipophilicity. Bioorg Med Chem Lett 15:4794–4798

Liu J, Gao B, Mirshahi F, Sanyal AJ, Khanolkar AD, Makriyanniss A, Kumos G (2000) Functional CB1 cannabinoid receptors in human endothelial cells. Biochem J 346:835–840

Lynn AB, Herkenham M (1994) Localization of cannabinoid receptors and nonsaturable high-density cannabinoid receptor sites in peripheral tissues of the rat: implications for receptor-mediated immune modulation by cannabinoids. J Pharmacol Exp Ther 268:1612–1623

Maccarrone M, van der Stelt M, Rossi A, Veldink GA, Vliegenthart JF, Agrò AF (1998) Anandamide hydrolysis by human cells in culture and brain. J Biol Chem 273:32332–32339

Makriyannis A, Mechoulam R, Piomelli D (2005) Therapeutic opportunities through modulation of the endocannabinoid system. Neuropharmacology 48:1068–1071

Manzanares J, Corchero J, Romero J, Fernández-Ruiz JJ, Ramos JA, Fuentes JA (2000) Pharmacological and biochemical interactions between opioids and cannabinoids. Trends Pharmacol Sci 20:287–294

Martin BR (1985) Characterization of the antinociceptive activity of intravenously administered Δ^9-tetrahydrocannabinol in mice. In: Harvey DJ (ed) Marihuana '84. IRL Press, Oxford, pp 685–692

Martin BR (1986) Cellular effects of cannabinoids. Pharmacol Rev 38:45–74

Martin Br, Compton DR, Thomas BF, Prescott WR, Little PJ, Razdan RK, Johnson MR, Melvin LS, Mechoulam R, Ward SJ (1991) Behavioral, biochemical, and molecular modeling evaluations of cannabinoid analogs. Pharmacol Biochem Behav 40:471–478

Massa F, Storr M, Lutz B (2005) The endocannabinoid system in the physiology and pathophysiology of the gastrointestinal tract. J Mol Med 83:1432–1440

Matsuda LA, Lolait SJ, Brownstein MJ, Young AC, Bonner TI (1990) Structure of a cannabinoid receptor and functional expression of the cloned cDNA. Nature (Lond.) 346:561–564

Mechoulam R, Shani A, Elderly H, Grunfeld Y (1970) Chemical basis of hashish activity. Science 169:611–612
Mechoulam R, Hanu L, Martin B (1994)Search for endogenous ligands of the cannabinoid receptor. Biochem Pharmacol 48:1537–1544
Melvin LS, Milne GM, Johnson MR, Subramaniam B, Wilken GH, Howlett AC (1993) Structure-activity relationships for cannabinoid receptor-binding and analgesic activity: studies of bicyclic cannabinoid analogs. Mol Pharmacol 44:1998–1015
Meng ID, Manning BH, Martin MJ, Fields HL (1998) An analgesia circuit activated by cannabinoids. Nature 395:381–383
Niederhoffer N, Szabo B (1999) Effect of the cannabinoid receptor agonist WIN55212–2 on sympathetic cardiovascular regulation. Br J Pharmacol 126:457–466
Niederhoffer N, Schmid K, Szabo B (2003) The peripheral sympathetic nervous system is the major target of cannabinoids in eliciting cardiovascular depression. Naunyn-Schmiedebergs Arch Pharmacol 367:434–443
Palmer SL, Khanolkar AD, Makriyannis A (2000) Natural and synthetic endocannabinoids and their structure-activity relationships. Curr Pharm Design 6:1381–1397
Patra PB, Wadsworth RM (1990) Effect of the synthetic cannabinoid nabilone on spermatogenesis in mice. Experientia 46:852–854
Pertwee RG (2000) Neuropharmacology and therapeutic potential of cannabinoids. Addict Biol 5:37–46
Pertwee RG (2006) The pharmacology of cannabinoid receptors and their ligands: an overview. Int J Obes 30:513–518
Pertwee RG, Stevenson LA, Elrick DB, Mechoulam R, Corbett AD (1992) Inhibitory effects of certain enantiomeric cannabinoids in the mouse deferens and the myenteric plexus preparation of guinea pig small intestine. Br. J Pharmacol 105:980–984
Piomelli D, Giuffrida A, Calignano A, de Fonseca FR (2000) The endocannabinoids system as a target for therapeutic drugs. Trend Pharmacol Sci 21:218–224
Porter AC, Felder CC (2001) The endocannabinoids nervous system: unique opportunities for therapeutic intervention. Pharmacol Ther 90:45–60
Ranganathan M, D'Souza DC (2006) The acute effects of cannabinoids on memory in humans: a review. Psychopharmacology (Berl) 188:425–444
Razdan RK (1986) Structure-activity relationships in cannabinoids. Pharmacol Rev 38:75–149
Reggio PH (1999) Cannabinoid receptors. Tocris Reviews No. 10
Rosell A, Agurell S (1975) Effects of 7-hydroxy-Δ^6-tetrahydrocannabinol and some related cannabinoids on the guinea pig isolated ileum. Acta Physiol Scand 94:142–144
Sigiura T, Kondo S, Kishimoto S, Miyashita T, Nakane S, Kodaka T, Suhara Y, Takayama H, Waku K (2000) Evidence that 2-arachidonoylglycerol but not N-palmitoylethanolamine or amandamine is the physiological ligand for the cannabinoid CB2 receptor. Comparison of various cannabinoid receptor ligands in HL-60 cells. J Biol Chem 275:605–612
Smith PB, Compton DR, Welch SP, Razdan RK, Mechoulam R, Martin BR (1994) The pharmacology of anandamide, a putative endogenous cannabinoid in mice. J Pharmacol Exp Ther 270:219–227
Stengel PW, Rippy MK, Cockerham SL, Devane WA, Silbaugh SA (1998) Pulmonary actions of anandamide, an endogenous cannabinoid receptor agonist, in guinea pigs. Eur J Pharmacol 355:57–66
Strangman NM, Patrick SL, Hohmann AG, Tsou K, Walker JM (1998) Evidence for a role of endogenous cannabinoids in the modulation of acute and tonic pain sensitivity. Brain Res 813:323–328
Ueda N, Kurahashi Y, Yamamoto S, Tokunaga T (1995) Partial purification and characterization of the porcine brain enzyme hydrolyzing and synthesizing anandamide. J Biol Chem 270:23823–23827
Welch SP, Huffman JW, Lowe J (1998) Differential blockade of the antinociceptive effects of centrally administered cannabinoids by SR141716A. J Pharmacol Exp Ther 286:1301–1308
Wenger T, Jamali KA, Juaneda C, Bacsy E, Tramu G (2000) The endogenous cannabinoid, anandamide, regulates anterior pituitary secretion *in vitro*. Addict Biol 5:59–64
White R, Hiley CR (1998) The actions of some cannabinoid receptor ligands in the rat isolated mesenteric artery. Br. J Pharmacol 125:533–541

H.1.1.8.2 Receptor Binding of Cannabinoids

PURPOSE AND RATIONALE

After the discovery of cannabinoid receptors in brain (Howlett et al. 1988; Devane et al. 1988; Pertwee 1993), two cannabinoid receptor subtypes were identified: CB1 and CB2. Cannabinoid receptors and were reviewed by Felder and Glass (1998), Pertwee (1999, 2001).

CB1 has an amino acid sequence consistent with a tertiary structure typical of the seven transmembrane-spanning proteins that are coupled to G proteins (Gerard et al. 1990, 1991; Howlett et al. 1990; Matsuda et al. 1990). The CNS responses to cannabinoid compounds are apparently mediated exclusively by CB1, since CB2 transcripts could not be found in brain tissue. CB1 transduces signals in response to CNS active constituents of *Cannabis sativa*, as well as synthetic bicyclic and tricyclic analogs, aminoalkylindole, and eicosanoid cannabi-mimetic compounds. CB1 is coupled to G_1 to inhibit adenylate cyclase activity and to a pertussis-sensitive G protein to regulate Ca^{2+} currents. Zimmer et al. (1999) produced a mouse strain with a disrupted CB1 gene. These CB1 knockout mice had a significantly increased mortality rat and displayed reduced locomotor activity, increased ring catalepsy, and hypoalgesia in hot plate and formalin tests.

CB2, the second cannabinoid-binding seven-transmembrane spanning receptor, exhibits 68% identity to CB1 within the helical regions, and 44% identity throughout the total protein. The CB2 clone was derived from a human promyelocytic leukemia cell lin HL60 cDNA library (Munro et al. 1993), also expressed in human leukocytes (Bouaboula et al. 1993). The gene for the rat CB2 receptor was cloned,

expressed, and its properties compared with those of mouse and human CB2 receptors (Griffin et al. 2000).

Receptor binding of cannabinoids in correlation to *in vivo* activities was described by Compton et al. (1993).

PROCEDURE

Membrane Preparation

Male Sprague Dawley rats weighing 150–200 g are decapitated and the brain rapidly removed. The cortex is dissected free using visual landmarks following reflection of cortical material from the midline and immersed in 30 ml of ice-cold centrifugation solution (320 mM sucrose, 2 mM Tris-EDTA, 5 mM $MgCl_2$). The process is repeated until the cortices of five rats are combined. The cortical material is homogenized with a Potter-Elvehjem glass-Teflon grinding system. The homogenate is centrifuged at 1600 *g* for 15 min, the supernatant saved and combined with the two subsequent supernatants obtained from washing and 1600 *g* centrifugation of the P_1 pellet. The combined supernatant fractions are centrifuged at 39,000 *g* for 15 min. The P_2 pellet is resuspended in 50 ml buffer (50 mM Tris-HCl, 2 mM Tris EDTA, 5 mM $MgCl_2$, pH 7.0), incubated for 10 min at 37°C, then centrifuged at 23,000 *g* for 10 min. The P_2 membrane is resuspended in 50 ml of buffer A, incubated again except at 30°C for 40 min, then centrifuged at 11,000 *g* for 15 min. The final wash-treated P_2 pellet is resuspended in assay buffer B (50 mM Tris-HCl, 1 mM Tris EDTA, 3 mM $MgCl_2$, pH 7.4) to a protein concentration of approximately 2 mg/ml. The membrane preparation is divided into 4 aliquots and quickly frozen in a bath solution of dry ice and 2-methylbutane and then stored at −80°C.

Binding Assay

Binding is initiated by the addition of 150 mg of P_2 membrane to test tubes containing [^{3}H]CP-55,940 (79 Ci/mmol), a cannabinoid analog, (for displacement studies) and a sufficient quantity of buffer C (50 mM Tris-HCl, 1 mM Tris EDTA, 3 mM $MgCl_2$, 5 mg/ml BSA) to bring the total incubation volume to 1 ml. The concentration of [^{3}H]CP-55,940 in displacement studies is 400 pM, whereas that in saturation studies varies from 25 to 2500 pM. Nonspecific binding is determined by the addition of 1 mM unlabeled CP-55,940. The standard CP-55,940 and other cannabinoid analogs are prepared in suspension buffer C from a 1 mg/ml ethanolic stock without evaporation of the alcohol.

After incubation at 30°C for 1 h, binding is terminated by addition of 2 ml ice-cold buffer D (50 mM Tris-HCl, 1 mg/ml BSA) and vacuum filtration through pretreated filters in a 12-well sampling manifold. Reaction vessels are washed once with 2 ml of ice-cold buffer D, and the filters washed twice with 4 ml of ice-cold buffer D. Filters are placed into 20-ml plastic scintillation vials with 1 ml of distilled water and 10 ml of Budget-Solve (RPI Corp., Mount Prospect, IL). After shaking for 1 h, the radioactivity present is determined by liquid scintillation photometry.

EVALUATION

The B_{max} and K_d values obtained from Scatchard analysis are determined via a suitable computer program. Displacement IC_{50} values are determined by unweighted least squares linear regression of log concentration-percent displacement data and then converted to K_I values.

MODIFICATIONS OF THE METHOD

To further characterize neuronal cannabinoid receptors, Thomas et al. (1998) compared the ability of cannabinoid analogs to compete for receptor sites labeled either with [^{3}H]SR141716A or[^{3}H]CP-55940.

Herkenham et al. (1991) characterized and localized cannabinoid receptors in rat brain by a quantitative autoradiographic study.

Felder et al. (1995) compared the pharmacology and signal transduction of the human cannabinoid CB1 and CB2 receptors.

Ross et al. (1998) compared cannabinoid binding sites in guinea pig forebrain and small intestine.

Rinaldi-Camora et al. (1998) tested the affinity of an antagonist of the CB2 cannabinoid receptor for rat spleen and cloned human CB2 receptors.

Bilkei-Gorzo et al. (2005) described early age-related cognitive impairment in mice lacking cannabinoid CB1 receptors.

REFERENCES AND FURTHER READING

Bilkei-Gorzo A, Racz I, Valverde O, Otto M, Michel K, Sarstre M, Zimmer A (2005) Early age-related cognitive impairment in mice lacking cannabinoid CB1 receptors. Proc Natl Acad Sci USA 102:15670–15675

Bouaboula M, Rinaldi M, Carayon P, Carillon C, Delpech B, Shire D, Le Fur G, Casellas P (1993) Cannabinoid-receptor expression in human leukocytes. Eur J Biochem 214:173–180

Compton DR, Rice KC, de Costa BR, Razdan RK, Melvin LS, Johnson MR, Martin BR (1993) Cannabinoid structure-activity relationships: Correlation of receptor binding and *in vivo* activities. J Pharmacol Exp Ther 265:218–226

Devane WA, Dysarz FA, Johnson MR, Melvin LS, Howlett CA (1988) Determination and characterization of a cannabinoid receptor in rat brain. Mol Pharmacol 34:605–613

Felder CC, Joyce KE, Briley EM, Mansouri J, Mackie K, Blond O, Lay Y, Ma AL, Mitchell RL (1995) Comparison of the pharmacology and signal transduction of the human cannabinoid CB1 and CB2 receptors. Mol Pharmacol 48:443–450
Felder CC, Glass M (1998) Cannabinoid receptors and their endogenous agonists. Ann Rev Pharmacol Toxicol 38:179–200
Gerard C, Mollereau C, Vassart G, Parmentier M (1990) Nucleotide sequence of a human cannabinoid receptor cDNA. Nucleic Acids Res 18:7142
Gerard CM, Mollereau C, Vassart G, Parmentier M (1991) Molecular cloning of a human cannabinoid receptor which is also expressed in testis. Biochem J 279:129–134
Griffin G, Tao Q, Abood ME (2000) Cloning and pharmacological characterization of the rat CB2 cannabinoid receptor. J Pharmacol Exp Ther 292:886–894
Herkenham M, Lynn AB, Johnson MR, Melvin LS, de Costa BR, Rice KC (1991) Characterization and localization of cannabinoid receptors in rat brain: a quantitative autoradiographic study. J Neurosci 11:563–583
Howlett AC (1995) Pharmacology of cannabinoid receptors. Annu Rev Pharmacol Toxicol 35:607–634
Howlett AC, Johnson MR, Melvin LS, Milne GM (1988) Nonclassical cannabinoid analgesics inhibit adenylate cyclase: development of a cannabinoid receptor model. Mol Pharmacol 33:297–302
Howlett AC, Bidaut-Russell M, Devane WA, Melvin LS, Johnson MR, Herkenham M (1990) The cannabinoid receptor: biochemical, anatomical and behavioral characterization. Trends Neurosci 13:420–423Matsuda LA, Lolait SJ, Young AC, Bonner TI (1990)Structure of a cannabinoid receptor and functional expression of the cloned cDNA, Nature 346:561–564
Munro S, Thomas KL, Abu-Shaar M (1993) Molecular characterization of a peripheral receptor for cannabinoids. Nature 365:61–65
Pertwee RG (1993) The evidence of the existence of cannabinoid receptors. Gen Pharmac 24:811–824
Pertwee RG (1999) Pharmacology of cannabinoid receptor ligands. Curr Med Chem 6:635–664
Pertwee RG (2001) Cannabinoid receptors and pain. Progr Neurobiol 63:569–611
Rinaldi-Carmora M, Barth F, Millan J, Derocq JM, Casellas P, Congy C, Oustric D, Sarran M, Bouaboula M, Calandra B, Portier M, Shire D,. Brelière JC, Le Fur G (1998) SR 144528, the first potent and selective antagonist of the CB2 cannabinoid receptor. J Pharmacol Exp Ther 284:644–650
Ross RA, Brockie HC, Fernando SR, Sha B, Razdan RK, Pertwee RG (1998) Comparison of cannabinoid binding sites in guinea pig forebrain and small intestine. Br J Pharmacol 125:1345–1351
Zimmer A, Zimmer AM, Hohmann AG, Herkenham M, Bonner TI (1999) Increased mortality, hypoactivity, and hypoalgesia in cannabinoid CB1 receptor knockout mice. Proc Natl Acad Sci USA 96:5780–5785

H.1.1.9 Vanilloid (Capsaicin) Activity

H.1.1.9.1 General Considerations on Vanilloids

PURPOSE AND RATIONALE

Several authors reviewed the recent development of capsaicin and vanilloid receptors (Holzer P 1991; Bíró et al. 1997; Sterner and Szallasi 1999; Szallasi and Blumberg 1999; Caterina and Julius 2001; Piomelli 2001; Gunthorpe et al. 2002). Capsaicin was isolated by Thresh (1846). The chemical structure was determined by Nelson (1919). The analgesic use of capsaicin was reviewed by Lembeck (1987). Capsaicin excites a subset of primary sensory neurons with somata in the dorsal root ganglion or trigeminal ganglion. As a general rule, these vanilloid-sensitive neurons are peptidergic, small diameter (50 µm) neurons, giving rise to thin, unmyelinated C fibers. Among sensory neuropeptides, the tachykinin Substance P shows the best correlation with vanilloid sensitivity. Vanilloid-sensitive neurons transmit noxious information (usually perceived as itching or pain) to the CNS, whereas peripheral terminals rare sites of release of a variety of pro-inflammatory neuropeptides. Among irritant compounds acting on primary sensory neurons, capsaicin and related vanilloids are unique in that the initial stimulation by vanilloids is followed by a long lasting refractory state. Neurotoxicity has been observed when capsaicin as given to newborn rats (Jancsó et al. 1977; Nagy and van der Kooy 1983).

Besides capsaicin, several natural vanilloid agonists were described (Jonassohn and Sterner 1997; Liu et al. 1997; Sterner and Szallasi 1999; Mendes et al. 2000). The irritant principle from *Euphorbia resinifera*, named resiniferatoxin, was isolated by Hergenhahn et al. (1975). In several assays, resiniferatoxin and its derivatives are several thousand-fold more potent than capsaicin (Szolcsanyi et al. 1990; Ács et al. 1995), which is explained by specific receptor binding (Szallasi and Blumberg 1990; Ács et al. 1994). Lee et al. (2001) described simplified resiniferatoxin derivatives as potent vanilloid receptor agonists with potent analgesic activity and reduced pungency.

The high affinity of vanilloid receptors argues for the existence of endogenous vanilloids. Hwang et al. (2000), Piomelli (2001) reported a direct activation of capsaicin receptors by products of lipogenases. Pain-inducing substances, such as bradykinin, may activate phospholipase-linked receptors in sensory neurons, mobilizing arachidonic acid from phospholipids and generating 12-HPETE. This lipid second messenger interacts in turn with a cytosolic domain of the VR1 receptor channel, increasing its opening probability and causing the sensory neuron to become depolarized.

The endogenous ligand of CB_1 cannabinoid receptors, anandamide, is also a full agonist at vanilloid VR1 receptors (Zygmunt et al. 1999; Maccarrone et al. 2000; Smart et al. 2000; DePetrocellis et al. 2001).

Premkumar and Ahern (2000) showed that activation of protein kinase C activates VR1 channel activity.

The first capsaicin or vanilloid receptor, termed VR1, was cloned by Caterina et al. (1997). Hayes et al. (2000) reported the cloning and functional expression of a human orthologue of rat vanilloid receptor 1. Pharmacological differences between the human and rat vanilloid receptor 1 were observed (McIntyre et al. 2001). VR1 functions as a molecular integrator of painful chemical and physical stimuli including capsaicin, noxious heat and low pH (Tominaga et al. 1998; Michael and Priestley 1999; Davis et al. 2000; Welch et al. 2000). In mice lacking the capsaicin receptor impaired nociception and pain sensation was observed (Caterina et al. 2000).

Vanilloid receptors are differently distributed in the central and peripheral nervous system (Szallasi 1995; Szallasi et al. 1995; Mezey et al. 2000; Ichikawa and Sugimoto 2001). Bíró et al. (1998) reported characterization of functional vanilloid receptors expressed by mast cells. Biological and electrophysiological data indicate heterogeneity within the vanilloid receptors. Caterina et al. (1999) described a capsaicin-receptor homologue, named vanilloid-receptor-like protein (VRL-1) with a high threshold for noxious heat. A novel human vanilloid receptor-like protein, named VRL-2 was identified and characterized by Delany et al. (2001).

Price et al. (2004) repoted modulation of trigeminal sensory neuron activity by the dual cannabinoid-vanilloid agonists anandamide, *N*-arachidonoyl-dopamine and arachidonyl-2-chloroethylamide.

Several vanilloid antagonists were described, such as capsazepine (Bevan et al. 1992; Walpole et al. 1994) or iodo-resiniferatoxin (Wahl et al. 2001).

REFERENCES AND FURTHER READING

Ács G, Palkovits M, Blumberg PM (1994) [^{3}H]resiniferatoxin binding by the human vanilloid (capsaicin) receptor. Brain Res Mol Brain Res 23:185–190

Ács G, Lee J, Marquez VE, Wang S, Milne GW, Du L, Lewin NE, Blumberg PM (1995) Resiniferatoxin-amide and analogues as ligands for protein kinase C and vanilloid receptors and determination of their biological activities as vanilloids. J Neurochem 65:301–318

Bevan S, Hothi S, Hughes G, James IF, Rang HP, Shah K, Walpole CJS, Yeats JC (1992) Capsazepine: A competitive antagonist of the sensory neuron excitant capsaicin. Br J Pharmacol 107:544–552

Bíró T, Ács G, Ács P, Modarres S, Bluber PM (1997) Recent advances in understanding of vanilloid receptors: a therapeutic target for treatment of pain and inflammation in skin. J Invest Dermatol Symp Proc 2:56–60

Bíró T, Maurer M, Modarres S, Lewin NE, Brodie C, Ács G, Ács P, Paus R, Blumberg PM (1998) Characterization of functional vanilloid receptors expressed by mast cells. Blood 91:1332–1340

Caterina MJ, Julius D (2001) The vanilloid receptor: A molecular gateway to the pain pathway. Ann Rev Neurosci 24:487–517

Caterina MJ, Schumacher MA, Tominaga M, Rosen TA, Levine JD, Julius D (1997) The capsaicin receptor: a heat-activated ion channel in the pain pathway. Nature 389:816–824

Caterina MJ, Rosen TA, Tomigaga M, Brake AJ, Julius D (1999) A capsaicin-receptor homologue with a high threshold for noxious heat. Nature 398:436–441

Caterina MJ, Leffler A, Malmberg AB, Martin WJ, Trafton J, Petersen-Zeitz KR, Koltzenburg M, Basbaum AI, Julius D (2000) Impaired nociception and pain sensation in mice lacking the capsaicin receptor. Science 288:306–313

Davis JB, Gray J, Gunthorpe MJ, Hatcher JP, Davey PT, Overend P, Harries MH, Latcham J, Clapham C, Atkinson K, Hughes SA, Rances K, Grau E, Harper AJ, Pugh PL, Rogers DC, Bingham S, Randall A, Sheardown SA (2000) Vanilloid receptor-1 is essential for inflammatory thermal hyperalgesia. Nature 405:183–187

Delany NS, Hurle M, Facer P, Alnadaf T, Plumpton C, Kinghorn I, See C-G, Costinan M, Anand P, Woolf CJ, Crowther D, Sanseau P, Tate SN (2001) Identification and characterization of a novel human vanilloid receptor-like protein, VRL-2. Physiol Genomics 4:165–174

DePetrocellis L, Bisogno T, Maccarrone M, Davis JB, Finazzi-Agrò A, di Marczo V (2001) The activity of anandamide at vanilloid VR1 receptors requires facilitated transport across the cell membrane and is limited by intracellular metabolism. J Biol Chem

Gunthorpe MJ, Benham CD, Randall A, Davis JB (2002) The diversity in the vanilloid (TRPV) receptor family of ion channels. Trends Pharmacol Sci 23:183–191

Hayes P, Meadows HJ, Gunthorpe MJ, Harries MH, Duckworth DM, Cairns W, Harrison DC, Clarke CA, Ellington K, Prinja RK, Barton AJL, Medhurst AD, Smith GD, Topp S, Murdock P, Sanger GJ, Terrett J, Jenkins O, Benham CD, Randall AD, Gloger IS, Davis BJ (2000) Cloning and functional expression of a human orthologue of rat vanilloid receptor-1. Pain 88:205–215

Hergenhahn M, Adolf W, Hecker E (1975) Resiniferatoxin and other esters of novel polyfunctional diterpenes from Euphorbia resinifera and unispina. Tetrahedron Lett 19:1595–1598

Holzer P (1991) Capsaicin: Cellular targets, mechanism of action, and selectivity for thin sensory neurons. Pharmacol Rev 43: mechanism for action, and selectivity of thin sensory neurons. Pharmacol Rev 43:143–201

Hwang SW, Cho H, Kwak J, Lee S-Y, Kang C-J, Jung J, Cho S, Min KH, Suh Y-G, Kim D, Oh U (2000) Direct activation of capsaicin receptors by products of lipogenases: Endogenous capsaicin-like substances. Proc Natl Acad Sci USA 97:6155–6159

Ichikawa H, Sugimoto T (2001) VR1-immunoreactive primary sensory neurons in the rat trigeminal ganglion. Brain Res 890:184–188

Janscó G, Király E, Janscó-Gábor A (1977) Pharmacologically induced selective degeneration of chemosensitive primary sensory neurones. Nature 270:741–743

Jonassohn M, Sterner O (1997) Terpenoid unsaturated 1,4-dialdehydes, occurrence and biological activities. Trends Org Chem 6:23–43

Lee J, Kim J, Kim SY, Chun MW, Cho H, Hwang SW, Oh U, Park YH, Marquez VE, Behesthi M, Szabo T, Blumberg PM (2001) N-(3-acyloxy-2-benzylpropyl)-N′-

(4-hydroxy-3-methoxybenzyl)-thiourea derivatives as potent vanilloid receptor agonists and analgesics. Bioorg Med Chem 9:19–32
Lembeck F (1987) Columbus, capsicum and capsaicin. Past, present and future. Acta Physiol Hung 69:265–273
Liu L, Lo Y-C, Chen I-J, Simon SA (1997) Responses of rat trigeminal ganglion neurons to capsaicin and two nonpungent vanilloid receptor agonists, olvanil and glyceryl nonamide. J Neurosci 17:41001–4111
Maccarrone M, Lorenzon T, Bari M, Melino G, Finazzi-Agrò A (2000) Anandamide induces apoptosis in human cells via vanilloid receptors. Evidence for a protective role of cannabinoid receptors. J Biol Chem 275:31938–31945
McIntyre P, McLatchie LM, Chambers A, Phillips E, Clarke M, Savidge J, Toms C, Peacocl M, Shah K, Winter J, Weerasakera N, Webb M, Rang HP, Bevan S, James IF (2001) Pharmacological differences between the human and rat vanilloid receptor 1 (VR1). Br J Pharmacol 132:1084–1094
Mendes GL, Santos ARS, Malheiros A, Filho AC, Yunes RA, Calixto JB (2000) Assessment of mechanisms involved in anti-nociception caused by sesquiterpene polygodial. J Pharmacol Exp Ther 292:164–172
Mezey E, Tóth ZE, Cortright DN, Arzubi MK, Krause JE, Elde R, Guo A, Blumberg PM, Szallasi A (2000) Distribution of mRNA for vanilloid subtype 1 (VR1), and VR1-like immunoreactivity, in the central nervous system of the rat and human. Proc Natl Acad Sci USA 97:3655–3660
Michael GJ, Priestley JV (1999) Differential expression of the mRNA for the vanilloid receptor subtype 1 in cells of the adult rat dorsal root and nodose ganglia and its downregulation by axotomy. J Neurosci 19:1844–1854
Nagy JI, van der Kooy D (1983) Effect of neonatal capsaicin treatment on nociceptive thresholds in the rat. J Neurosci 3:1145–1150
Nelson EK (1919) The constitution of capsaicin – the pungent principle of capsicum. J Am Chem Soc 41:1115–1117
Piomelli D (2001) The ligand that came from within. Trends Pharmacol Sci 22:17–19
Prekumar LS, Ahern GP (2000) Induction of vanilloid receptor channel activity by protein kinase C. Nature 408:985–900
Price TJ, Patwardhan A, Akopian AN, Hargreaves KM, Flores CM (2004) Modulation of trigeminal sensory neuron activity by the dual cannabinoid-vanilloid agonists anandamide, *N*-arachidonoyl-dopamine and arachidonyl-2-chloroethylamide. Br J Pharmacol 141:1118–1130
Smart D, Gunthorpe MJ, Jerman JC, Nasir S, Gray J, Muir AI, Chambers JK, Randall AD, Davis JB (2000) The endogenous lipid anadamide is a full agonist at the human vanilloid receptor (jVR1). Br J Pharmacol 129:227–230
Sterner O, Szallasi A (1999) Novel natural vanilloid receptor agonists: new therapeutic targets for drug development. Trends Pharmacol Sci 20:459–465
Szallasi A (1995) Autoradiographic visualization and pharmacological characterization of vanilloid (capsaicin) receptors in several species, including man. Acta Physiol Scand Suppl 629:1–68
Szallasi A, Blumberg PM (1990) Specific binding of resiniferatoxin, an ultrapotent capsaicin analog, by dorsal root membranes. Brain Res 524:106–111
Szallasi A, Blumberg PM (1999) Vanilloid (capsaicin) receptors and mechanisms. Pharmacol Rev 51:159–212
Szallasi A, Nilsson S, Farkas-Szallasi T, Blumberg PM, Höckfelt T, Lundberg M (1995) Vanilloid (capsaicin) receptors in the rat: distribution, regional differences in the spinal cord, axonal transport to the periphery, and depletion by systemic vanilloid treatment. Brain Res 703:175–183
Szolcsanyi J, Szallasi A, Szallasi Z, Joo F, Blumberg PM (1990) Resiniferatoxin: an ultrapotent selective modulator of capsaicin-sensitive afferent neurons. J Pharmacol Exp Ther 255:923–928
Thresh LT (1846) Isolation of capsaicin. Pharm J 6:941
Tominaga M, Caterina MJ, Malmberg AB, Rosen TA, Gilbert H, Skinner K, Raumann BE, Basbaum AI, Julius D (1998) The cloned capsaicin receptor integrates multiple pain-producing stimuli. Neuron 21:531–543
Wahl P, Foged C, Tullin S, Thomsen C (2001) Iodo-resiniferatoxin, a new potent vanilloid receptor antagonist. Mol Pharmacol 59:9–15
Walpole CS, Bevan S, Boverman G, Boelsterli JJ, Breckenridge R, Davies JW, Hughes GA, James I, Oberer L, Winter J (1994) The discovery of capsazepine, the first competitive antagonist of the sensory neuron excitants capsaicin and resiniferatoxin. J Med Chem 37:1942–1954
Welch JM, Simon SA, Reinhart PH (2000) The activation mechanism of rat vanilloid receptor 1 by capsaicin involves the pore domain and differs from the activation by either acid or heat. Proc Natl Acad Sci 97:13889–13894
Zygmunt PM, Petersson J, Andersson DA, Chuang H-H, Sørgård M, DiMarzo V, Julius D, Högestätt ED (1999) Vanilloid receptors on sensory nerves mediate the vasodilator action of anadamide. Nature 400:452–457

H.1.1.9.2 Vanilloid Receptor Binding

PURPOSE AND RATIONALE

Ács et al. (1994) described [^{3}H]resiniferatoxin binding by the human vanilloid (capsaicin) receptor. Receptor types and species differences of the vanilloid receptor were described by Szallasi et al. (1994, 1996). The rat vanilloid receptor (rVR1) was cloned and stably expressed in HEK293 cells by Jerman et al. (2000). A detailed pharmacological characterization was conducted using the Ca^{2+}-sensitive dye, Fluo3AM in a fluorimetric imaging plate reader (FLIPR). Ross et al. (2001) studied structure-activity relationship for the endogenous cannabinoid, anadamide, and certain of its analogues at vanilloid receptors in transfected CHO cells.

PROCEDURE

Cell Culture

Rat vanilloid receptor (rVR1) transfected CHO cells are maintained in MEM Alpha minus media containing 2 mM L-glutamine supplemented with 10% hyclone fetal bovine serum, 350 µg/ml G418 (Sigma-Aldrich), 100 units/ml penicillin and 100 µg/ml streptomycin. Cells are maintained in 5% CO_2 at 37°C and passed twice a week using non-enzymatic cell dissociation solution. For the radioligand binding assay, cells are removed from flasks by scraping and then frozen as a pellet at –20°C for up to one month.

Radioligand Binding Experiments

Assays are performed in DMEM containing HEPES (25 mM) and BSA (0.25 mg/ml). Total assay volume is 500 µl containing 20 µg of cell membranes. Binding is initiated by addition of [^{3}H]resiniferatoxin ([^{3}H]-RTX). Assays are carried out at 37°C for 1 h, before termination by addition of ice-cold wash buffer (50 mM Tris-buffer, 1 mg/ml BSA, pH 7.4) and vacuum filtration using a 12-well sampling manifold (Brandell cell harvester) and Whatman GF/B filters that have been soaked in wash buffer at 4°C for at least 24 h. Each reaction is washed 9 times with a 1.5 ml aliquot of wash buffer. The filters are oven-dried and then placed in 5 ml scintillation fluid. Radioactivity is quantified by liquid scintillation spectrometry. Specific binding is determined in the presence of 1 µM unlabelled RTX. Protein assays are performed using a Bio-Rad De Kit. Unlabelled compounds are added in a volume of 50 µl after serial dilution using assay buffer from a 10 mM stock in ethanol or DMSO. [^{3}H]-RTX is also added in a 50 µl volume following dilution in assay buffer.

EVALUATION

The K_D value and B_{max} for [^{3}H]-RTX and the concentration of competing ligands to produce 50% displacement of the radioligand (IC_{50}) from specific binding sites are calculated using GraphPad Prism (GraphPad Software, San Diego). Dissociation constant (K_i) values are calculated using the Cheng and Prussoff equation.

MODIFICATIONS OF THE METHOD

Wardle et al. (1997) used a 96-well plate assay system to characterize pharmacologically the vanilloid receptor in the dorsal spinal cord of the rat.

Hayes et al. (2000) described the cloning and functional expression of a human orthologue of rat vanilloid receptor-1.

REFERENCES AND FURTHER READING

Ács G, Palkovits M, Blumberg PM (1994) [^{3}H]resiniferatoxin binding by the human vanilloid (capsaicin) receptor. Brain Res Mol Brain Res 23:185–190

Hayes P, Meadows HJ, Gunthorpe MJ, Harries MH, Duckworth DM, Cairns W, Harrison DC, Clarke CE, Ellington K, Prinja RK, Barton AGL, Medhurst AD, Smith GD, Topp S, Murdock P, Sanger GJ, Terrett J, Jenkins O, Benham CD, Randall AD, Gloger IS, Davis JB (2000) Cloning and functional expression of a human orthologue of rat vanilloid receptor-1. Pain 88:205–215

Jerman JC, Brough SJ, Prinjha R, Harries MH, Davis JB, Smart D (2000) Characterization using FLIPR of rat vanilloid receptor (rVR1) pharmacology. Br J Pharmacol 130:916–922

Ross RA, Gibson TM, Brockie HC, Leslie M, Pashmi G, Craib SJ, DiMarzo V, Pertwee RC (2001) Structure-activity relationship for the endogenous cannabinoid, anadamide, and certain of its analogues at vanilloid receptors in transfected cells and vas deferens. Br J Pharmacol 132:631–640

Szallasi A (1994) The vanilloid (capsaicin) receptor: receptor types and species differences. Gen Pharmacol 25:223–243

Szallasi A, Blumberg PM (1996) Vanilloid receptors: new insights enhance potential as a therapeutic target. Pain 68:195–208

Wardle KA, Ranson J, Sanger GJ (1997) Pharmacological characterization of the vanilloid receptor in the rat dorsal spinal cord. Br J Pharmacol 121:1012–1016

H.1.1.9.3 Evaluation of Vanilloid Receptor Antagonists

PURPOSE AND RATIONALE

Several vanilloid receptor antagonists were described, such as capsazepine (Bevan et al. 1992; Walpole et al. 1994) or iodo-resiniferatoxin (Wahl et al. 2001). Kirschstein et al. (1999) described the inhibition of rapid heat responses in nociceptive primary sensory neurons of rats by vanilloid receptor antagonists.

PROCEDURE

Adult Sprague Dawley rats of both sexes are deeply anesthetized with diethyl ether and rapidly decapitated. The spine is chilled at 4°C in F12 Dulbecco's modified Eagle's medium saturated with carbogen gas and additionally containing 30 mM $NaHCO_3$, 100,000 units/l penicillin and 100 mg/l streptomycin. Thoracic and lumbar dorsal root ganglions are quickly dissected and freed from connective tissue. Neurons are dissociated in an incubation chamber enriched with carbogen gas at 37°C using collagenase CLS II (5–10 mg/ml, 10–12 min) and trypsin (0.2–1 mg/ml, 10–12 min) dissolved in F12 medium. After trituration (4–6 times with a Pasteur pipette) neurons are plated in 35-mm culture dishes, which also serve as recording chambers, and stored at 37°C in a humidified 5% CO_2 atmosphere before used for electrophysiological recordings.

Only round or oval-shaped neurons without any processes are included in the study. The average of the major and the minor diameter is used to measure the size of oval shaped neurons. Whole cell patch-clamp experiments are performed in carbogen gas saturated F12 medium (pH 7.4) at room temperature using an Axo-patch 200A amplifier (Axon Instruments) in voltage-clamp mode at a holding potential of –80 mV controlled by pCLAMP6 software. Data are also registered on a chart recorder. Patch pipettes are fabricated from borosilicate glass using a horizontal micropipette puller and filled with a solution contain-

ing (in mM) 160 KCl, 8.13 EGTA, 10 HEPES (pH 7.2, $R_{Tip} = 5.3 \pm 0.2$ MΩ, mean ±SE). Cell diameter, cross sectional area, and membrane capacitance are measured, and excitability is tested by depolarizing voltage steps for each neuron. Cells lacking a fast inward current with a reversal potential close to the equilibrium potential of sodium followed by a prolonged outward current are excluded from further investigation. Experiments in current-clamp mode are performed to measure the resting membrane potential of each neuron and to investigate single action potentials elicited by short (3 ms) depolarizing current pulses in neurons that are hyperpolarized by constant current injection resulting in membrane potentials between –70 and –80 mV. Inflections in the repolarizing phase are qualitatively detected as second negative peak in the first derivative (dV/dt) of each action potential; the duration of repolarization is quantitatively assessed by the 10–90% decay time.

Applications of ~50 µl of heated extracellular solution through a puffing system fixed on a micromanipulator is used to elicit heat-evoked currents. Control measurements with a fast temperature sensor (BAT-12, Physitemp; $\tau = 5$ ms) in place of the neurons are made revealing an effective temperature of ~53°C, a rise time of ~250 ms, and a decay with a time constant of ~20 s. Effects are compared with those of application of the same amount of medium at room temperature. Heat stimuli with or without vanilloid receptor antagonists and control applications at room temperature are repeated 2–10 times, and the elicited currents are averaged. A neuron is considered as heat sensitive when the heat-evoked inward current is significantly greater than any fluctuations caused by superfusion of solution at room temperature. Heating the buffered solution may change its pH, and acid solution of pH 6.2 are known to activate nociceptive dorsal root ganglion neurons (Bevan and Yeats 1991). The pH of a HEPES-buffered solution decreases while heating (e. g., pH 7.1 at 50°C). In contrast, higher temperatures increase the pH of a $NaHCO_3/CO_2$ buffer, because the solubility of CO_2 is reduced and thus reverses the HEPES effect. The pH of the F12 medium maximally changes in a range of 7.28–7.52 while heating to 50°C and cooling down to room temperature. The membrane conductance is measured in voltage-clamp mode by hyperpolarizing pulses (5 mV, 10 ms, 50 s^{-1}), and conductance changes are determined at the maximum amplitude of heat evoked currents.

Reversal potentials of heat- and capsaicin-induced currents are measured as described by Liu et al. (1997) using fast depolarizing ramps (–80 to +30 mV in 22 ms every 550 ms). Patch pipettes are filled with a potassium-free solution containing (in mM) 140 CsCl, 10 HEPES, 10 EGTA, and 4 $MgCl_2$ (adjusted to pH 7.2). Tetrodotoxin (100 µM) and nifedipine (1 µM) are added to the extracellular solution to block voltage gated Na^+ and Ca^{2+} channels. Capsaicin is dissolved in ethanol, diluted to its final concentration with F12 medium, and applied through the puffing system. Capsazepine (dissolved in DMSO) and ruthenium red are prepared as concentrated stock solutions, diluted to final concentration in F12 medium, and applied either at room temperature or at ~53°C. Reversibility of antagonist action is tested by reapplication of heated extracellular solution without any agents.

EVALUATION

Off-line measurements and statistical analysis is done using pCLAMP6 (Axon Instruments) and EXCEL 5.0 (Microsoft). Data are presented as means ± SE. Treatment effects are statistically analyzed by Student's t-test for paired data and χ^2 test for analysis of incidences.

MODIFICATIONS OF THE METHOD

Nagy et al. (1983) described dose-dependent effects of capsaicin on primary sensory neurons in the neonatal rat.

Lopshire and Nicol (1998) performed whole-cell and single-channel studies in rat sensory neurons and found a prostaglandin E_2 induced enhancement of the capsaicin elicited current.

Jung et al. (1999) performed patch-clamp experiments in dorsal root ganglion neurons of neonatal rats and concluded that capsaicin binds to the intracellular domain of the capsaicin-activated ion channel.

Nagy and Humphrey (1999) compared the membrane responses of rat sensory neurons to noxious heat and capsaicin, using electrophysiological and ion flux measurements.

Baumann and Martenson (2000) found that extracellular protons both increase the activity and reduce the conductance of capsaicin-gated channels.

Liu et al. (2001) investigated mechanisms underlying capsaicin-mediated inhibition of action potentials and modulation of voltage-gated sodium channels in cultured trigeminal ganglion neurons.

Gunthorpe et al. (2004) identified and characterized a potent and selective vanilloid receptor antagonist isolated via high-throughput screening of a large chemical library in an FLPR-based C^{2+} assay.

For further information on the vanilloid receptor see A.1.1.32.5.

REFERENCES AND FURTHER READING

Baumann TK, Martenson ME (2000) Extracellular protons both increase the activity and reduce the conductance of capsaicin-gated channels. J Neurosci 20: RC80 (1–5)

Bevan S, Yeats JC (1991) Protons activate a cation conductance in a subpopulation of rat dorsal root ganglion neurons. J Physiol (Lon.) 433:145–161

Bevan S, Hothi S, Hughes G, James IF, Rang HP, Shah K, Walpole CJS, Yeats JC (1992) Capsazepine: A competitive antagonist of the sensory neuron excitant capsaicin. Br J Pharmacol 107:544–552

Gunthorpe MJ, Rami HK, Jerman JC, Smart D, Gill CH, Soffin EM, Luis Hannan S, Lappin SC, Egerton J, Smith GD, Worby A, Howett L, Owen D, Nasir S, Davies CH, Thompson M, Wyman PA, Randall AD, Davis JB (2004) Identification and characterization of SB-366791, a potent and selective vanilloid receptor (VR1/TRPV1) antagonist. Neuropharmacology 46:133–149

Jung J, Hwang SW, Kwak J, Lee S-Y, Kang C-J, Kim W-B, Kim D, Oh U (1999) Capsaicin binds to the intracellular domain of the capsaicin-activated ion channel. J Neurosci 19:529–538

Kirschstein T, Greefrath W, Büsselberg D, Treede RD (1999) Inhibition of rapid heat responses in nociceptive primary sensory neurons of rats by vanilloid receptor antagonists. J Neurophysiol 82:2853–2860

Liu L, Lo Y-C, Chen I-J, Simon SA (1997) The response or rat trigeminal ganglion neurons to capsaicin and two nonpungent vanilloid receptor agonists, olvanil and glyceryl nonamide. J Neurosci 17:4101–4111

Liu L, Oortgiesen M, Li L, Simon SA (2001) Capsaicin inhibits activation of voltage-gated sodium currents in capsaicin-sensitive trigeminal ganglion nerves. J Neurophysiol 85:745–758

Lopshire JC, Nicol GD (1998) The cAMP transduction cascade mediates the prostaglandin E_2 enhancement of the capsaicin elicited current in rat sensory neurons: whole-cell and single-channel studies. J Neurosci 18:6081–6092

Nagy I, Humphrey PR (1999) Similarities and differences between the responses of rat sensory neurons to noxious heat and capsaicin. J Neurosci 19:10647–10655

Nagy JI, Iversen LL, Goedert M, Chapman D, Hunt SP (1983) Dose-dependent effects of capsaicin on primary sensory neurons in the neonatal rat. J Neurosci 3:399–406

Walpole CS, Bevan S, Boverman G, Boelsterli JJ, Breckenridge R, Davies JW, Hughes GA, James I, Oberer L, Winter J (1994) The discovery of capsazepine, the first competitive antagonist of the sensory neuron excitants capsaicin and resiniferatoxin. J Med Chem 37:1942–1954

H.1.2 In Vivo Methods for Testing Central Analgesic Activity

H.1.2.1 General Considerations

Although the *in vivo* methods have been used more extensively in the past, they are still necessary in present research analgesic tests in animals before a compound can be given to man. Mostly, rodents, such as mice or rats, are used for analgesic tests, but in some instances experiments in higher animals such as monkeys are necessary.

Several methods are available for testing central analgesic activity, such as

- Haffner's tail clip method in mice,
- tail flick or other radiant heat methods,
- tail immersion tests,
- hot plate methods in mice or rats,
- electrical stimulation (grid shock, stimulation of tooth pulp or tail),
- monkey shock titration,
- formalin test in rats.

REFERENCES AND FURTHER READING

Von Voigtlander PF (1982) Pharmacological alteration of pain: The discovery and evaluation of analgesics in animals. In: Lednicer D (ed) Central Analgesics. John Wiley and Sons, New York, pp 51–79

H.1.2.2 Haffner's Tail Clip Method

PURPOSE AND RATIONALE

The method was described as early as 1929 by Haffner who observed the raised tail (Straub phenomenon) in mice treated with morphine or similar opioid drugs and found the tail after drug treatment to be less sensitive to noxious stimuli. He already described the high sensitivity of this method to morphine. Since then, the method has been used and modified by many authors.

PROCEDURE

An artery clip is applied to the root of the tail of mice and the reaction time is noted. Male mice (Charles River strain or other strains) with a weight between 18 and 25 g are used. The control group consists of 10 mice. The test compounds are administered subcutaneously to fed mice or orally to fasted animals. The test groups and the control group consist of 7–10 mice. The drug is administered 15, 30 or 60 min prior testing. An artery clip is applied to the root of the tail (approximately 1 cm from the body) to induce pain. The animal quickly responds to this noxious stimuli by biting the clip or the tail near the location of the clip. The time between stimulation onset and response is measured by a stopwatch in 1/10 seconds increments.

EVALUATION

A cut-off time is determined by taking the average reaction time plus 3 times the standard deviation of

the combined latencies of the control mice at all time periods. Any reaction time of the test animals which is greater than the cut-off time is called a positive response indicative of analgesic activity. The length of time until response indicates the period of greatest activity after dosing. An ED_{50} value is calculated at the peak time of drug activity. ED_{50} values found by this method were 1.5 mg/kg s.c. for morphine and 7,5 mg/kg for codeine s.c.

CRITICAL ASSESSMENT OF THE TEST

The test does not need any sophisticated equipment but a skilled, preferably "blind", observer. Peripheral analgesics of the salicylate type are not detected by this test.

MODIFICATIONS OF THE METHOD

Bartoszyk and Wild (1989) described a modification of the original Haffner clip test using pressure on the tail of rats instead of mice. Additionally hyperalgesia was induced by injection of carrageenan suspension into the tail. In this case not only an effect of a nonsteroidal anti-inflammatory agent but also a potentiation by B-vitamins could be shown.

Takagi et al. (1966) published a modification of HAFFNER's method for testing analgesics.

Ossipov et al. (1988) used the Haffner test to compare the antinociceptive effects of intrathecally administered opiates, α_2-adrenergic agonists, and local anesthetics.

Yanagisawa et al. (1984) described a tail pinch method *in vitro* for testing antinociceptive drugs consisting of an isolated spinal cord, spinal nerve roots and the functionally connected tail of a new-born rat. Changes of electric potential in the ventral root are induced by noxious pressure on the tail. In addition, responses after electric stimulation of the dorsal root were recorded. The authors recommend the method for studying actions of analgesic drugs.

Pinch of the toes of guinea pigs was recommended as a test for opioid analgesics by Collier (1965).

Tail-pinch feeding in rats after intracerebroventricular injection of various opioid antagonists has been used to differentiate opioid receptor subtypes (Koch and Bodnar 1993).

Person et al. (1985) used three different techniques of mechanical tail stimulation (reaction threshold determined with an Analgesymeter at two different cut-off values and HAFFNER's tail clip) to study morphine-caffeine analgesic interaction in rats.

Arndt et al. (1984) studied pain responses (increase of heart rate and arterial pressure, respiratory effects) to tail clamping in trained unanesthetized spontaneously breathing dogs after administration of fentanyl.

REFERENCES AND FURTHER READING

Arndt JO, Mikat M, Parasher C (1984) Fentanyl's analgesic, respiratory, and cardiovascular actions in relation to dose and plasma concentrations in unanesthetized dogs. J Anesth 61:355–361

Bartoszyk GD, Wild A (1989) B-vitamins potentiate the antinociceptive effect of diclofenac in carrageenin-induced hyperalgesia in the rat tail pressure test. Neurosci Lett 101:95–100

Bianchi C, Franceschini J (1954) Experimental observations on Haffner's method for testing analgesic drugs. Br J Pharmacol 9:280–284

Collier HOJ (1965) Multiple toe-pinch test for potential analgesic drugs. In: Keele, Smith (eds) Assessment of Pain in Man and Animals. Livingston, London, pp 262–270

Fleisch A, Dolivo M (1953) Auswertung der Analgetica im Tierversuch. Helv Physiol Acta 11:305–322

Haffner F (1929) Experimentelle Prüfung schmerzstillender Mittel. Dtsch Med Wschr 55:731–733

Koch JKE, Bodnar RJ (1993) Involvement of mu_1 and mu_2 opioid receptor subtypes in tail-pinch feeding in rats. Physiol Behav 53:603–605

Ossipov MH, Suarez LJ, Spaulding TC (1988) A comparison of the antinociceptive and behavioral effects of intrathecally administered opiates, α 2-adrenergic agonists, and local anesthetics in mice and rats. Anesth Analg 67:616–624

Person DL, Kissin I, Brown PT, Xavier AV, Vinik HR, Bradley EL (1985) Morphine-caffeine analgesic interaction in rats. Anesth Analg 64:851–856

Takagi H, Inukai T, Nakam M (1966) A modification of Haffner's method for testing analgesics. Jpn J Pharmacol 16:287–295

Vanderwende C, Spoerlein M (1972) Antagonism by DOPA of morphine analgesia. A hypothesis for morphine tolerance. Res Comm Chem Pathol Pharmacol 3:37–45

Yanagisawa M, Murakoshi T, Tamai S, Otsuka M (1984) Tail-pinch method *in vitro* and the effects of some antinociceptive compounds. Eur J Pharmacol 106:231–239

H.1.2.3 Radiant Heat Method

PURPOSE AND RATIONALE

Originally, the method was developed by Schumacher et al. (1940), Wolff et al. (1940) for quantitative measurements of pain threshold in man against thermal radiation and for evaluation of analgesic activity of opiates. Later on, the procedure has been used by many authors to evaluate analgesic activity in animal experiments by measuring drug-induced changes in the sensitivity of mice or rats to heat stress applied to their tails. The test is very useful for discriminating between centrally acting morphine-like analgesics and non-opiate analgesics.

Mice are placed into cages leaving the tail exposed. A light beam is focused to the proximal third of the tail.

Within a few seconds the animal flicks the tail aside or tries to escape. The time until this reaction occurs is measured.

PROCEDURE

The method was described by Ther, Lindner and Vogel (1963) as a modification of earlier publications (D'Armour and Smith 1941). Groups of 10 mice (NMRI-strain) of both sexes with a weight between 18 and 22 g are used for each dose. Before administration of the test compound or the standard the normal reaction time is determined. The animal is put into a small cage with an opening for the tail at the rear wall. The tail is held gently by the investigator. By opening of a shutter, a light beam exerting radiant heat is directed to the proximal third of the tail. For about 6 s the reaction of the animal is observed by the investigator. The mouse tries to pull the tail away and turns the head. With a switch the shutter is closed as soon as the investigator notices this reaction. Mice with a reaction time of more than 6 s are not used in the test. The escape reaction which is the endpoint of this test can be regarded as a complex phenomenon mediated by the brain. In contrast, the simple tail flick as an endpoint of this test may be mediated as a spinal reflex. Therefore the observation of the escape reaction can be regarded as a true assessment of the influence of the drug on the brain.

The test compounds and the standard are administered either orally or subcutaneously. The animals are submitted to the same testing procedure after 30, 60 and eventually 120 min. For each individual animal the reaction time is noted. Other time intervals can be used according to the question to be investigated.

EVALUATION

There are two possibilities for evaluation:

- The average values of reaction time after each time interval are calculated and compared with the pretest value by analysis of significance.
- At each time interval only those animals which show a reaction time twice as high or higher as the pretest value are regarded as positive. Percentages of positive animals are counted for each time interval and each dose and ED_{50} values are calculated according to LITCHFIELD and WILCOXON.

As standards codeine, pethidine and morphine can be used. The ED_{50} values of these drugs are:

- Codeine 12 mg/kg s.c.
- Pethidine 12 mg/kg s.c.
- Morphine 2 mg/kg s.c.

CRITICAL ASSESSMENT OF THE TEST

The radiant heat test on the tail of mice is very effective to estimate the efficacy and potency of central acting analgesic drugs. With pyrazolones ED_{50} values still can be calculated but these are achieved only with relatively high doses. Compounds like acetylsalicylic acid and phenyl-acetic acids show only slight effects making it impossible to calculate ED_{50} values.

MODIFICATIONS OF THE METHOD

Originally, the method has been described for testing analgesic properties in the rat (D'Armour and Smith 1941, Winter et al. 1954, Harris and Pierson 1964). Goldstein and Malseed (1979) adapted the procedure for utilization in **cats**. The effect of morphine could be antagonized by naloxone in this test. No response to sodium salicylate or pentobarbital was observed. Lutz et al. (1994) used a modification of the rat tail withdrawal test to investigate the structure-activity profile of a series of opioid analgesics. One day before testing, polyethylene tubings were implanted in the femoral vein and externalized behind the neck for intravenous application of test substances.

Various instruments have been described for measuring tail flick latencies by several authors, e. g., Davies et al. 1946; Owen et al. (1981), Isabel et al. (1981), Walker and Dixon (1983), Yoburn et al. (1984), Harris et al. (1988).

Tail flick analgesy meters are commercially available (e. g., IITC Life Science, Woodland Hills, CA, USA).

Green and Young (1951) compared the heat and pressure analgesiometric methods in rats. Mohrland et al. (1983) described an ultrasound-induced tail-flick procedure.

Hargreaves et al. (1988), Costello and Hargreaves (1989), Hylden et al. (1991) exposed the plantar surface of hindpaws of unrestrained rats to a beam of radiant heat applied through the glass floor of a testing chamber. Paw withdrawal latency was automatically recorded by a photocell.

This method was also used by Schuligoi et al. (1994).

Taylor et al. (1997) used this method to investigate the brief (phase 1) and persistent (phase 2) nociceptive responses of rats after injection of dilute formalin into the hindpaw.

Carmon and Frostig (1981) used brief laser induced heat applied to the rat ear for pharmacological testing of analgesics.

Perkins et al. (1993), Perkins and Kelly (1993) used ultra-violet-induced hyperalgesia in rat paw. Female

Sprague-Dawley rats weighing about 100 g were exposed on the plantar surface of one hind paw to UV light (intensity maximum 365 nm, 69 mW/cm^2) for 90 s and this was repeated 18 h later. On the following days, each group of rats was placed in a transparent Perspex box and the withdrawal threshold to a focused beam of radiant heat applied to the underside of each hind paw was measured.

McCallister et al. (1986) directed radiant heat to the **ears of rabbits** and measured ear-withdrawal time.

REFERENCES AND FURTHER READING

Carmon A, Frostig R (1981) Noxious stimulation of animals by brief laser induced heat: advantages to pharmacological testing of analgesics. Life Sci 29:11–16

Costello AH, Hargreaves KM (1989) Suppression of carrageenan-induced hyperalgesia, hyperthermia and edema by a bradykinin antagonist. Eur J Pharmacol 171:259–263

D'Armour FE, Smith DL (1941) A method for determining loss of pain sensation. J Pharmacol Exp Ther 72:74–79

Davies OL, Raventós J, Walpole AL (1946) A method for the evaluation of analgesic activity using rats. Br J Pharmacol 1:255–264

Dewey WL, Harris LS, Howes JF, Nuite JA (1970) The effect of various neurohumoral modulators on the activity of morphine and the narcotic antagonists in the tail-flick and the phenylquinone tests. J Pharmacol Exp Ther 175:435–442

Geller I, Axelrod LR (1968) Methods for evaluating analgesics in laboratory animals. In: Soulairac A, Cahn J, Charpentier J (eds) Pain. Acad Press, London New York, pp 153–163

Goldstein FJ, Malseed RT (1979) Evaluation of narcotic analgesic activity using a cat tail-flick procedure. J Pharmacol Meth 2:333–338

Gray WD, Osterberg A, Scuto TJ (1970) Measurement of the analgesic efficacy and potency of pentazocine by the D'Armour and Smith method. J Pharmacol Exp Ther 172:154–162

Green AF, Young PA (1951) A comparison of heat and pressure analgesiometric methods in rats. Br J Pharmacol 6:572–585

Hargreaves KM, Dubner R, Brown F, Flores C, Joris J (1988) A new and sensitive method for measuring thermal nociception in cutaneous hyperalgesia. Pain 32:77–82

Harris DP, Burton R, Sinclair G (1988) A simple microcomputer interface for tail-flick determination. J Pharmacol Meth 20:103–108

Harris LS, Pierson AK (1964) Some narcotic antagonists in the benzomorphan series. J Pharmacol Exp Ther 143:141–148

Howes JF, Harris LS, Dewey WL, Voyda CA (1969) Brain acetylcholine levels and inhibition of the tail-flick reflex in mice. J Pharmacol Exp Ther 169:23–28

Hylden JLK, Thomas DA, Iadarola MJ, Nahin RL, Dubner R (1991) Spinal opioid analgesic effects are enhanced in a model of unilateral inflammation/hyperalgesia: possible involvement of noradrenergic mechanisms. Eur J Pharmacol 194:135–143

Isabel G, Wright DM, Henry JL (1981) Design of an inexpensive unit for measuring tail flick latencies. J Pharmacol Meth 5:241–247

Litchfield JT, Wilcoxon F (1949) A simplified method for evaluating dose-effect experiments. J Pharmacol Exp Ther 96:99

Lutz MW, Morgan OH, James MK, Feldman OL, Brackeen MF, Lahey AP, James SV, Bilotta JM, Pressley JC (1994) A pharmacodynamic model to investigate the structure-activity profile of a series of novel opioid analgesics. J Pharmacol Exp Ther 271:795–803

McCallister LW, Lipton JM, Giesecke AH Jr, Clark WG (1986) The rabbit ear-withdrawal test: A new analgesiometric procedure. Pharmacol Biochem Behav 25:481–482

Mohrland JS, Johnson EE, von Voigtlander PF (1983) An ultrasound-induced tail-flick procedure: evaluation of nonsteroidal antiinflammatory analgesics. J Pharmacol Meth 9:297–282

Owen JA, Milne B, Jhamandas K, Nakatsu K (1981) Assembly of an inexpensive tail flick analgesia meter. J Pharmacol Meth 6:33–37

Perkins MN, Kelly D (1993) Induction of bradykinin B_1 receptors *in vivo* in a model of ultra-violet irradiation-induced thermal hyperalgesia in the rat. Br J Pharmacol 110:1441–1444

Perkins MN, Campell E, Dray A (1993) Antinociceptive activity of the bradykinin B_1 and B_2 receptor antagonists, des-Arg^9,[Leu^8]-BK and Hoe 140, in two models of persistent hyperalgesia in rats. Pain 53:191–197

Schuligoi R, Donnerer J, Amann R (1994) Bradykinin-induced sensitization of afferent neurons in the rat. Neurosci 59:211–215

Schumacher GA, Goodell H, Hardy JD, Wolff HG (1940) Uniformity of the pain threshold in man. Science 92:110–112

Taylor BK, Peterson MA, Basbaum AI (1997) Early nociceptive events influence the temporal profile, but not the magnitude, of the tonic response to subcutaneous formalin: effects with remifentanil. J Pharmacol Exp Ther 280:876–883

Ther L, Lindner E, Vogel G (1963) Zur pharmakodynamischen Wirkung der optischen Isomeren des Methadons. Dtsch Apoth Ztg 103:514–520

Tulunay FC, Takemori AE (1974) The increased efficacy of narcotic antagonists induced by various narcotic analgesics. J Pharmacol Exp Ther 190:395–400

Walker JM, Dixon WC (1983) A solid state device for measuring sensitivity to thermal pain. Physiol Behav 30:481–483

Winter CA, Orahovats PD, Flataker L, Lehman EG, Lehman JT (1954) Studies on the pharmacology of N-allylnormorphine. J Pharmacol Exp Ther 112:152–160

Wolff HG, Hardy JD, Goodell H (1940) Studies on pain. Measurement of the effect of morphine, codeine, and other opiates on the pain threshold and an analysis of their relation to the pain experience. J Clin Invest 19:659–680

Yoburn BC, Morales R, Kelly DD, Inturrisi CE (1984) Constrains on the tail flick assay: morphine analgesia and tolerance are dependent upon locus of tail stimulation. Life Sci 34:1755–1762

H.1.2.4 Hot Plate Method

PURPOSE AND RATIONALE

The paws of mice and rats are very sensitive to heat at temperatures which are not damaging the skin. The responses are jumping, withdrawal of the paws and licking of the paws. The time until these responses occur is prolonged after administration of centrally acting analgesics, whereas peripheral analgesics of the acetylsalicylic acid or phenyl-acetic acid type do not generally affect these responses.

PROCEDURE

The method originally described by Woolfe and Mac Donald (1944) has been modified by several investigators. The following modification has been proven to be suitable:

Groups of 10 mice of either sex with an initial weight of 18 to 22 g are used for each dose. The hot plate, which is commercially available, consists of a electrically heated surface. The temperature is controlled for 55° to 56°C. This can be a copper plate or a heated glass surface. The animals are placed on the hot plate and the time until either licking or jumping occurs is recorded by a stop-watch. The latency is recorded before and after 20, 60 and 90 min following oral or subcutaneous administration of the standard or the test compound.

EVALUATION

The prolongation of the latency times comparing the values before and after administration of the test compounds or the values of the control with the experimental groups can be used for statistical comparison using the *t*-test. Alternatively, the values which exceed the value before administration for 50% or 100% can be regarded as positive and ED_{50} values can be calculated.

Doses of 7.5 mg/kg s.c. morphine hydrochloride, 30 mg/kg s.c. codeine hydrochloride, 30 mg/kg s.c. pethidine hydrochloride and 400 mg/kg s.c. phenazone were found to be effective, whereas aspirin showed no effect even at high doses.

CRITICAL ASSESSMENT OF THE TEST

The hot plate test has been used by many investigators and has been found to be suitable for evaluation of centrally but not of peripherally acting analgesics. Mice as well as rats have been used. The method has the drawback that sedatives and muscle relaxants (Woolfe and MacDonald 1944) or psychotomimetics (Knoll 1967) cause false positives, while mixed opiate agonists-antagonists provide unreliable results. The validity of the test has been shown even in the presence of substantial impairment of motor performance (Plummer et al. 1991). Mixed opiate agonists-antagonists can be evaluated if the temperature of the hot plate is lowered to 49.5°C (O'Callaghan and Holtzman 1975; Zimer et al. 1986).

MODIFICATIONS OF THE METHOD

O'Neill et al. (1983) described an automated, high-capacity method for measuring jump latencies on a hot plate. A hot-plate test with increasing temperature was recommended by Tjølsen et al. (1991).

Hot plate analgesy meters are commercially available (e. g., IITC Life Science, Woodland Hills, CA, USA).

REFERENCES AND FURTHER READING

Eddy NB, Leimbach D (1953) Synthetic analgesics: II. Dithienylbutenyl- and dithienylbutylamines. J Pharmacol Exp Ther 107:385–393

Jacob J, Blozovski M (1961) Action des divers analgésiques sur le comportement de souris exposées a un stimulus thermoalgésique. Arch Int Pharmacodyn 138:296–309

Jacob J, Loiseau G, Echinard-Garin P, Barthelemy C, Lafille C (1964) Caractérisation et détection pharmacologiques des substances hallucinogènes. II.-antagonismes vis-a-vis de la morphine chez la souris. Arch Int Pharmacodyn 148:14–30

Kitchen I, Crowder M (1985) Assessment of the hot-plate antinociceptive test in mice. A new method for the statistical treatment of graded data. J Pharmacol Meth 13:1–7

Knoll J (1967) Screening and grouping of psychopharmacological agents. In: Siegler PE, Moyer HJ (eds) Animal and Clinical Pharmacologic Techniques in Drug Evaluation. Yearbook Med Publ. Inc., Chicago, pp 305–321

O'Neill KA, Courtney C, Rankin R, Weissman A (1983) An automated, high-capacity method for measuring jump latencies on a hot plate. J Pharmacol Meth 10:13–18

O'Callaghan JP, Holtzman SG (1975) Quantification of the analgesic activity of the narcotic antagonists by a modified hot plate procedure. J Pharm Exp Ther 192:497–505

Plummer JL, Cmielewski PL, Gourlay GK, Owen H, Cousins MJ (1991) Assessment of antinociceptive drug effects in the presence of impaired motor performance. J Pharmacol Meth 26:79–87

Tjølsen A, Rosland JH, Berge OG, Hole K (1991) The increasing temperature hot-plate test: an improved test of nociception in mice and rats. J Pharmacol Meth 25:241–250

Witkin LB, Heubner CF, Galgi F, O'Keefe E, Spitaletta P, Plummer AJ (1961) Pharmacology of 2-aminino-indane hydrochloride (SU 8629): a potent non-narcotic analgesic. J Pharmacol Exp Ther 133:400–408

Woolfe G, MacDonald AD (1944) The evaluation of the analgesic action of pethidine hydrochloride (DEMEROL) J Pharmacol Exper Ther 80:300–307

Zimer PO, Wynn RL, Ford RD, Rudo FG (1986) Effect of hot plate temperature on the antinociceptive activity of mixed opioid agonist antagonist compounds. Drug Dev Res 7:277–280

H.1.2.5 Tail Immersion Test

PURPOSE AND RATIONALE

The method has been developed to be selective for morphine-like compounds. The procedure is based on the observation that morphine-like drugs are selectively capable of prolonging the reaction time of the typical tail-withdrawal reflex in rats induced by immersing the end of the tail in warm water of 55°C.

PROCEDURE

Young female Wistar rats (170–210 g body weight) are used. They are placed into individual restraining cages

leaving the tail hanging out freely. The animals are allowed to adapt to the cages for 30 min before testing. The lower 5 cm portion of the tail is marked. This part of the tail is immersed in a cup of freshly filled water of exactly 55°C. Within a few seconds the rat reacts by withdrawing the tail. The reaction time is recorded in 0.5 s units by a stopwatch. After each determination the tail is carefully dried. The reaction time is determined before and periodically after either oral or subcutaneous administration of the test substance, e. g., after 0.5, 1, 2, 3, 4 and 6 h. The cut off time of the immersion is 15 s. The withdrawal time of untreated animals is between 1 and 5.5 s. A withdrawal time of more than 6 s therefore is regarded as a positive response.

EVALUATION

ED_{50} values can be calculated for each compound and time response curves (onset, peak and duration of the effect) be measured. All the morphine-like analgesics have been shown to be active at doses which do not produce gross behavioral changes. For example, an ED_{50} of 3.5 mg/kg s.c. for morphine and an ED_{50} of 1.7 mg/kg s.c. methadone was found. Acetylsalicylic acid at a dose of 640 mg/kg p.o., phenylbutazone at a dose of 160 mg/kg s.c. as well as nalorphine at a dose of 40 mg/kg s.c. were inactive.

CRITICAL ASSESSMENT OF THE TEST

The test is useful to differentiate central opioid like analgesics from peripheral analgesics.

MODIFICATIONS OF THE METHOD

Ben-Bassat et al. (1959) described the receptacle method in mice. Each mouse was inserted in a conoid paper receptacle with its tail protruding, the cone being closed by a stapler. The protruding tail was entirely immersed in a water bath (58°C) and the time until withdrawal of the tail was measured by a stop watch.

Pizziketti et al. (1985) modified the tail immersion test in rats in this way that they used a 1:1 mixture of ethylene-glycol and water **cooled** to a temperature of minus 10°C as noxious stimulus. Linear dose-response curves were found with levo-methadone and morphine. Low ceiling effects or curvilinear dose-response curves were obtained with narcotic agonist-antagonist analgesics such as pentazocine. Diazepam and aspirin were inactive.

Tiseo et al. (1988) could show that the endogenous kappa agonist dynorphin A was inactive in the rat tail immersion test at 55°C, but gave dose-response curves in the cold water version of the test.

Abbott and Melzack (1982) examined the effects of brainstem lesions on morphine analgesia using the formalin test which produced moderate pain that lasted about 2 h, and the tail-flick hot water-immersion test which measured brief threshold-level pain.

Abbott and Franklin (1986) used two forms of the rat tail flick test: In the restrained form of the test rats were placed in wire restraining tubes from 10 min before drug injection till the end of the test. In the unrestrained form of the test rats were left free in their home cages and handheld during each test for approximately 30 s. Responses to the thermal pain stimulus were assessed by the latency with which the rat removed its tail from 55°C water. Two types of morphine analgesia have been postulated in animals: One type, exemplified in rats that are restrained during tail flick testing, is sensitive to an interaction between morphine and brain 5-HT, the level of which is elevated by restrained stress (Kelly and Franklin 1984).

Luttinger (1985) determined the antinociceptive activity of drugs using different water temperatures in a tail-immersion test in mice. The results roughly paralleled the differences in the severity of pain for which various analgesics are effective.

Dykstra et al. (1986, 1987) described a tail withdrawal procedure for assessing analgesic activity in **Rhesus monkeys** by immersion of the tail into water of 55°C. This procedure was used by Rothman et al. (1989) to determine the pharmacological activities of optically pure enantiomers of the κ opioid agonist, U50,488, and its cis diastereomer.

Using this method, Ko et al. (1999) found that activation of peripheral κ opioid receptors inhibits capsaicin-induced nociception in Rhesus monkeys.

REFERENCES AND FURTHER READING

Abbott FV, Melzack R (1982) Brainstem lesions dissociate neural mechanisms of morphine analgesia in different kinds of pain. Brain Res 251:149–155

Abbott FV, Franklin KBJ (1986) Noncompetitive antagonism of morphine analgesia by diazepam in the formalin test. Pharmacol Biochem Behav 24:319–321

Ben-Bassat J, Peretz E, Sulman FG (1959) Analgesimetry and ranking of analgesic drugs by the receptacle method. Arch Int Pharmacodyn 122:434–447

Cowan A (1990) Recent approaches in the testing of analgesics in animals. In: Modern Methods in Pharmacology, Vol. 6, Testing and Evaluation of Drugs of Abuse, pp 33–42, Wiley-Liss Inc

Dykstra LA, Woods JH (1986) A tail withdrawal procedure for assessing analgesic activity in Rhesus monkeys. J Pharmacol Meth 15:263–269

Dykstra LA, Gmerek DE, Winger G, Woods JH (1987) Kappa opioids in rhesus monkeys. Diuresis, sedation, analgesia and discriminative stimulus effects. J Pharm Exp Ther 242:413–420

Evangelista S, Pirisino R, Perretti F, Fantozzi R, Brunelleschi S, Malmberg-Aiello P, Bartolini A (1987) The pharmacological properties of 1,4-dihydro-1-ethyl-7-phenylpyrrol- (1,2-a)-pyrimidine-4-one, a new antipyretic and analgesic drug. Drugs Exp Clin Res 13:501–510
Grotto M, Sulman FG (1967) Modified receptacle method for animal analgesimetry. Arch Int Pharmacodyn 165:152–159
Janssen P, Niemegeers CJE, Dony JGH (1963) The inhibitory effect of Fentanyl and other morphine-like analgesics on the warm water induced tail withdrawal reflex in rats. Arzneim-Forsch 13:502–507
Kelly SJ, Franklin KBJ (1984) Evidence that stress augments morphine analgesia by increasing brain tryptophan. Neurosci Lett 44:305–310
Ko M-C, Butelman ER, Woods JH (1999) Activation of peripheral κ opioid receptors inhibits capsaicin-induced nociception in Rhesus monkeys. J Pharmacol Exp Ther 287:378–385
Luttinger D (1985) Determination of antinociceptive activity of drugs in mice using different water temperatures in a tail-immersion test. J Pharmacol Meth 13:351–357
Ono M, Satoh T (1988) Pharmacological studies of Lappaconitine. Analgesic studies. Arzneim Forsch/Drug Res 38:892–895
Pizziketti RJ, Pressman NS, Geller EB, Cowan A, Adler MW (1985) Rat cold water tail-flick: A novel analgesic test that distinguishes opioid agonists from mixed agonists-antagonists. Eur J Pharmacol 119:23–29
Ramabadran K, Bansinath M, Turndorf H, Puig MM (1989) Tail immersion test for the evaluation of a nociceptive reaction in mice. J Pharmacol Meth 21:21–31
Rothman RB, France CP, Bykov V, de Costa BR, Jacobson AE, Woods JH, Rice KC (1989) Pharmacological activities of optically pure enantiomers of the κ opioid agonist, U50,488, and its cis diastereomer: evidence for three κ receptor subtypes. Eur J Pharmacol 167:345–353
Sewell RDE, Spencer PSJ (1976) Antinociceptive activity of narcotic agonist and partial agonist analgesics and other agents in the tail-immersion test in mice and rats. Neuropharmacol 15:683–688
Tiseo PJ, Geller EB, Adler MW (1988) Antinociceptive action of intracerebroventricularly administered dynorphin and other opioid peptides in the rat. J Pharm Exp Ther 246:449–453

H.1.2.6 Electrical Stimulation of the Tail

PURPOSE AND RATIONALE

Since the tail of mice is known to be sensitive to any stimulus, a method of electrical stimulation has been described as early as 1950 by Burn et al. The stimulus can be varied either by the duration of the electric shock or by an increase in the electric current.

PROCEDURE

As described by Kakunaga et al. (1966), male mice with a weight of 20 g are placed into special cages. A pair of alligator clips is attached to the tail whereby the positive electrode is placed at the proximal end of the tail. Rectangular wave pulses from a constant voltage stimulator at an intensity of 40–50 V are applied. The frequency of the stimulation is 1 shock/s, and the pulse duration 2.5 ms. The normal response time range of the stimuli is 3–4 s. Following administration of the drug, the response time is registered at 15 min intervals until the reaction time returns to control levels.

EVALUATION

The data for each animal are plotted with reaction times on the ordinate and time intervals following administration on the abscissa. The area under the time response curve is calculated. In control animals the reaction time remains fairly constant and the area under the curve is approximately zero. Effects of morphine at 5 mg/kg s.c. and meperidine 30 mg/kg s.c. could easily be demonstrated.

CRITICAL ASSESSMENT OF THE TEST

The effect of central analgesics can be clearly demonstrated, however also the activity of peripheral analgesics given at higher doses can be detected.

MODIFICATIONS OF THE METHOD

Vidal et al. (1982) measured the thresholds of 3 nociceptive reactions (tail withdrawal, vocalization, vocalization afterdischarge) following electrical stimulation of the tail.

A variation of the test has been introduced by Yanaura et al. (1976), using ultrasonic stimulation instead of electric stimulation. The method is considered to be fast, simple, and precise. The stimulus can be applied repeatedly without causing injury to the tissue. A vocalization test in rats with electrical stimulation of the tail has been described by Hoffmeister (1968).

Ludbrook et al. (1995) described a method for frequent measurement of sedation and analgesia in sheep using the response to a ramped electrical stimulus. Sheep were placed in a canvas sling in their metabolic crates to allow their limbs to partially bear weight in order to minimize spontaneous limb movements. Two needles were placed subcutaneously 0.5 cm apart in the anterior aspect of the lower third of the sheep's hind and connected to the nerve stimulator. The current ramp rate was set at one mA per sec. As soon as limb withdrawal was observed, the stimulus was switched off and the highest current and ramp duration were recorded.

REFERENCES AND FURTHER READING

Burn JH, Finney DJ, Goodwin LG (1950) Chapter XIV: Antipyretics and analgesics. In: Biological Standardization. Oxford University Press, London, New York, pp 312–319
Carroll MN, Lim RKS (1960) Observations on the neuropharmacology of morphine and morphinelike analgesia. Arch Int Pharmacodyn 125:383–403

Charpentier J (1968) Analysis and measurement of pain in animals. A new conception of pain. In: Soulairac A, Cahn J, Charpentier J (eds) Pain. Acad Press, London New York, pp 171–200
Hoffmeister F (1968) Tierexperimentelle Untersuchungen über den Schmerz und seine pharmakologische Beeinflussung. Arzneim Forsch 16. Beiheft:5–116
Kakunaga T, Kaneto H, Hano K (1966) Pharmacological studies on analgesics. VII. Significance of the calcium ion in morphine analgesia. J Pharm Exp Ther 153:134–141
Ludbrook G, Grant C, Upton R, Penhall C (1995) A method for frequent measurement of sedation and analgesia in sheep using the response to a ramped electrical stimulus. J Pharmacol Toxicol Meth 33:17–22
Nilsen PL (1961) Studies on algesimetry by electrical stimulation of the mouse tail. Acta Pharmacol Toxicol 18:10–22
Paalzow G, Paalzow L (1973) The effect of caffeine and theophylline on nociceptive stimulation in the rat. Acta Pharmacol Toxicol 32:22–32
Vidal C, Girault JM, Jacob J (1982) The effect of pituitary removal on pain reaction in the rat. Brain Res 233:53–64
Yanaura S, Yamatake Y, Ouchi T (1976) A new analgesic testing method using ultrasonic stimulation. Effects of narcotic and non-narcotic analgesics. Jpn J Pharmacol 26:301–308

H.1.2.7 Grid Shock Test

PURPOSE AND RATIONALE

The electric grid shock test in mice has been described by Blake et al. (1963) as a modification of an earlier approach (Evans 1962) to measure the analgesic properties by the "Flinch-jump" procedure in rats.

PROCEDURE

Male mice with a weight between 18 and 20 g are individually placed into clear plastic chambers. The floor of the box is wired with tightly strung stainless steel wire, spaced about 1 mm apart. The stimulus is given in the form of square wave pulses, 30 cycles per second with a duration of 2 ms per pulse. The output of the stimulator has to be connected to alternate wires of the grid. A fixed resistance is placed in series with the grid and in parallel to an oscilloscope to allow calibration in milliamperes. With increasing shock intensities the mice flinch, exhibit a startling reaction, increase locomotion or attempt to jump. The behavior is accurately reflected on the oscilloscope by marked fluctuations of the displayed pulse and defined as pain threshold response. Pain thresholds are determined in each individual mouse twice before administration of the test drug and 15, 30, 60, 90 and 120 min after dosing. Groups of 10 animals are used for control and for the test drugs.

EVALUATION

The current as measured in milliamperes is recorded for each animal before and after administration of the drug. The average values for each group at each time interval are calculated and statistically compared with the control values. Placebo treated controls show a slight increase of threshold over time. Morphine sulfate in a dose of 10 mg/kg p.o. but also acetylsalicylic acid in a dose of 200 mg/kg p.o. definitely increase the threshold.

CRITICAL EVALUATION OF THE METHOD

The modification of the method as described by Blake et al. (1963) showed an effect not only of morphine but also of acetylsalicylic acid which is not easily picked up by other tests based on stimulation by physical means.

MODIFICATIONS OF THE TEST

Weiss and Laties (1961) in a "fractional escape" procedure trained animals to press a lever to reduce the intensity of shock delivered continuously through the floor grids of the experimental chamber. Each time, the rat depresses the lever, it reduces the intensity of the shock. An external timer is programmed to increase the intensity of the shock every few seconds. If the animal fails to press the lever, the shock continues to increase in intensity until lever-pressing behavior drives it down. Thus, the level of shock fluctuates depending on the rat's lever pressing. The action of an analgesic in altering the level of shock which the rat will "tolerate" can than be measured by comparing the average level at which the rat maintains the shock under control conditions with the average level at which the rat maintains the shock during treatment.

Painful stimulation of the paws of mice placed into cages equipped with metal bands for electrical stimulation was described by Charlier et al. (1961) as "pododolorimetry".

A modification of the jump-flinch technique for measuring pain sensitivity in rats based on four categories of responses was described by Bonnet and Peterson (1975).

Eschalier et al. (1988) described an automated method to analyze vocalization of unrestrained rats submitted to noxious stimuli.

REFERENCES AND FURTHER READING

Banzinger R (1964) Animal techniques for evaluating narcotic and non-narcotic analgesics. In: Nodine JH and Siegler PE (eds) Animal and Clinical Pharmacologic Techniques in Drug Evaluation. Year Book Medical Publ, Inc., pp 392–396
Blake L, Graeme ML, Sigg EB (1963) Grid shock test for analgesic assay in mice. Med exp 9:146–150

Bonnet KA, Peterson KE (1975) A modification of the jump-flinch technique for measuring pain sensitivity in rats. Pharmacol Biochem Behav 3:47–55
Charlier R, Prost M, Binon F, Deltour G (1961) Étude pharmacologique d'un antitussif, le fumarate acide de phénéthyl-1 (propyne-2 yl)-4-propionoxy-4 pipéridine. Arch Int Pharmacodyn 134:306–327
Eschalier A, Montastruc JL, Devoice JL, Rigal F, Gaillard-Plaza G, Péchadre JC (1981) Influence of naloxone and methysergide on the analgesic effect of clomipramine in rats. Eur J Pharmacol 74:1–7
Eschalier A, Marty H, Trolese JF, Moncharmont L, Fialip J (1988) An automated method to analyze vocalization of unrestrained rats submitted to noxious stimuli. J Pharmacol Meth 19:175–184
Evans WO (1961) A new technique for the investigation of some analgesic drugs on a reflexive behavior in the rat. Psychopharmacologia 2:318–325
Evans WO (1962) A comparison of the analgesic potency of some analgesics as measured by the "Flinch-jump" procedure. Psychopharmacol 3:51–54
Evans WO, Bergner DP (1964) A comparison of the analgesic potencies of morphine, pentazocine, and a mixture of methamphetamine and pentazocine in the rat. J New Drugs 4:82–85
Jokovlev V, Sofia RD, Achterrath-Tuckermann U, von Schlichtegroll A, Thiemer K (1985) Untersuchungen zur pharmakologischen Wirkung von Flupirtin, einem strukturell neuartigen Analgeticum. Arzneim Forsch/Drug Res 35:30–43
Weiss B, Laties VG (1961) Changes in pain tolerance and other behavior produced by salicylates. J Pharm Exp Ther 131:120

H.1.2.8 Tooth Pulp Stimulation

PURPOSE AND RATIONALE

The method has been first described by Kohl and Reffert (1938) and by Ruckstuhl and Gordanoff (1939) for testing central analgesic activity in rabbits and has since applied by several authors to various animal species. Stimulation of the tooth pulp induces characteristic reactions, such as licking, biting, chewing and head flick which can be observed easily.

PROCEDURE

Rabbits of either sex with an weight between 2 and 3 kg are anaesthetized with 15 mg/kg thiopental or 0.2 mg/kg fentanyl-citrate intravenously. Pulp chambers are exposed close to the gingival line in the lateral margins of the two front upper incisors with a high-speed dental drill. On the day of the experiment, clamping electrodes are placed into the drilled holes. After an accommodation period of 30 min stimulation is started to determine the threshold value. The stimulus is applied by rectangular current with a frequency of 50 Hz and a duration of the stimulus of 1 s. The electrical current is started with 0.2 mA and increased until the phenomenon of licking occurs. In some cases, the current has to be increased and than to be decreased again in order to find the appropriate threshold. For assessing the basic value, the threshold is determined 3 times in each animal. Each animal serves as its own control. For testing analgesic activity of a new drug and determination of an ED_{50} 8 to 10 animals are used for each dose of the analgesic. The test substance is either injected intravenously or given orally by gavage. The threshold as the indicator of the antinociceptive effect is determined again after 15, 30, 60 and 120 min. The animals serve as their own controls. Threshold current is determined again 5, 15, 30, 45 and 60 min after intravenous application and 15, 30, 60 and 120 min after oral application.

EVALUATION

For screening procedures the increase of threshold, expressed in mV, is the indicator of intensity and duration of the analgesic effect. For determination of the ED_{50}, 8 to 10 rabbits are used for each dose, using 3 doses, which provided effects between 10 and 90%. An antinociceptive effect is defined as an increase of the threshold versus the initial control by a factor of 2 or more.

CRITICAL ASSESSMENT OF THE METHOD

Central analgesics, especially opioid agonists, have been found to be very active in this test. Compared with other tests for central analgesic activity, like the hot plate test in mice, the tests result in lower ED_{50}-values indicating a high sensitivity of the method. In addition, non-opiate analgesics like ketamine and peripheral analgesics like pyrazolone derivatives gave a positive response.

MODIFICATIONS OF THE METHOD

The method has been performed primarily in rabbits (Hertle et al. 1957; Hoffmeister 1962, 1968; Piercey and Schröder 1980), but also **dogs** (Koll and Fleischmann 1941; Skinkle and Tyers 1979) and **cats** (Mitchell 1964) have been used.

Among several methods in different species, Fleisch and Dolivo (1953) found the electrical stimulation of the tooth pulp in the rabbit as the only satisfactory method to test the efficacy of different analgesic drugs.

The effects of tooth pulp stimulation in the thalamus and hypothalamus of the **rat** have been investigated by Shigena et al. (1973).

The method has been adapted for freely moving rats (Steinfels and Cook 1986). Medium effective doses could be determined for ì and ê agonists. Non-steroidal

anti-inflammatory drugs were also effective in this test procedure, but the slopes of the dose-response curves for these compounds were lower than for the opioid analgesics. Microinfusion of bradykinin solution onto the tooth pulp of unrestrained rats was described by Foong et al. (1982) as a reliable method for evaluating analgesic potencies of drugs on trigeminal pain.

Kidder and Wynn (1983) described an automatic electronic apparatus for generating and recording a ramp stimulus for analgesia testing.

Thut et al. (1995) used the rabbit tooth-pulp assay to quantify efficacy and duration of antinociception by local anesthetics infiltrated into maxillary tissues.

Shyu et al. (1984) studied the role of central serotoninergic neurons in the development of dental pain in the **monkey**.

REFERENCES AND FURTHER READING

Chau TT (1989) Analgesic testing in animal models. In: Pharmacological Methods in the Control of Inflammation. Alan R Liss, Inc. pp 196–212

Chin JH, Domino EF (1961) Effects of morphine on brain potentials evoked by stimulation of the tooth pulp of the dog. J Pharmacol Exp Ther 132:74–86

Fleisch A, Dolivo M (1953) Auswertung der Analgetica im Tierversuch. Helv Physiol Acta 11:305–322

Foong FW, Satoh M, Takagi H (1982) A newly devised reliable method for evaluating analgesic potencies of drugs on trigeminal pain. J Pharmacol Meth 7:271–278

Hertle F, Schanne O, Staib I (1957) Zur Methodik der Prüfung der Analgesie am Kaninchen. Arzneim Forsch 7:311–314

Hoffmeister F (1962) Über cerebrale polysynaptische Reflexe des Kaninchens und ihre Beeinflussbarkeit durch Pharmaka. Arch Int Pharmacodyn 139:512–527

Hoffmeister F (1968) Tierexperimentelle Untersuchungen über den Schmerz und seine pharmakologische Beeinflussung. Arzneim Forsch 16. Beiheft:5–116

Kidder GW, Wynn RL (1983) An automatic electronic apparatus for generating and recording a ramp stimulus for analgesia testing. J Pharmacol Meth 10:137–142

Koll W, Fleischmann G (1941) Messungen der analgetischen Wirksamkeit einiger Antipyretica am Hund. Naunyn-Schmiedeberg's Arch Exp Path Pharmakol 198:390–406

Koll W, Reffert H (1938) Eine neue Methode zur Messung analgetischer Wirkungen im Tierversuch. Versuche mit Morphin und einigen Morphinderivaten am Hund. Arch exp Path Pharmakol 190:67–87

Matthews B, Searle BN (1976) Electrical stimulation of teeth. Pain 2:245–251

Mitchell CL (1964) A comparison of drug effects upon the jaw jerk response to electrical stimulation of the tooth pulp in dogs and cats. J Pharmacol Exp Ther 146:1–6

Piercey MF, Schroeder LA (1980) A quantitative analgesic assay in the rabbit based on response to tooth pulp stimulation. Arch Int Pharmacodyn Ther 248:294–304

Ruckstuhl K (1939) Beitrag zur pharmakodynamischen Prüfung der Analgetica. Inaug.-Dissertation, Bern

Shigena Y, Marao S, Okada K, Sakai A (1973) The effects of tooth pulp stimulation in the thalamus and hypothalamus of the rat. Brain Res 63:402–407

Shyu KW, Lin MT, Wu TC (1984) Possible role of central serotoninergic neurons in the development of dental pain and aspirin-induced analgesia in the monkey. Exp Neurol 84:179–187

Skingle M, Tyers MB (1979) Evaluation of antinociceptive activity using electrical stimulation of the tooth pulp in the conscious dog. J Pharmacol Meth 2:71–80

Steinfels GF, Cook L (1986) Antinociceptive profiles of μ and κ opioid agonists in a rat tooth pulp stimulation procedure. J Pharm Exp Ther 236:111–117

Thut PD, Turner MD, Cordes CT, Wynn RL (1995) A rabbit tooth-pulp assay to quantify efficacy and duration of antinociception by local anesthetics infiltrated into maxillary tissues. J Pharmacol Toxicol Meth 33:231–236

Wilhelmi G (1949) Über die pharmakologischen Eigenschaften von Irgapyrin, einem neuen Präparat aus der Pyrazolonreihe. Schweiz Med Wschr 25:577–582

Wirth W, Hoffmeister F (1967) Zur Wirkung von Kombinationen aus Phenothiazin-Derivaten mit Analgetika-Antipyretika. Wien Med Wschr 117:973–978

Wynn RL, El'Baghdady YM, Ford RD, Thut PD, Rudo FG (1984) A rabbit tooth-pulp assay to determine ED_{50} values and duration of action of analgesics. J Pharmacol Meth 11:109–117

Wynn RL, Ford RD, McCourt PJ, Ramkumar V, Bergman SA, Rudo FG (1986) Rabbit tooth pulp compared to 55°C mouse hot plate assay for detection of antinociceptive activity of opiate and nonopiate central analgesics. Drug Dev Res 9:233–239

Yim GKW, Keasling HH, Gross EG, Mitchell CW (1955) Simultaneous respiratory minute volume and tooth pulp threshold changes following levorphan, morphine and levorphan-levallorphan mixtures in rabbits. J Pharmacol Exp Ther 115:96–105

H.1.2.9 Monkey Shock Titration Test

PURPOSE AND RATIONALE

Generally, analgesic tests in rats and mice result in correlation with the analgesic activity of a drug in man. To clarify the mode of action in more detail and to find a suitable dose for therapy in man, experiments in monkeys may be necessary.

PROCEDURE

This test has been recommended by Weiss and Laties (1958) and later developed further by several authors. The monkeys are seated in restraining chairs. Electrical current is delivered by a Coulbourn Instrument Programmable Shocker through electrodes coupled to two test tube clamps which are attached to a shaved portion of the tail. The current ranges from 0 to 4 mA through 29 progressive steps. The monkey presses a bar to interrupt the shock. A stable baseline shock level is established for each monkey on the day prior to drug administration. After drug administration shock titration activity is rated according to the change in maximum level of median shock intensity attained for drug as compared to control levels. Doses of 3.0 mg/kg i.m.

morphine, 1.7 mg/kg i.m. methadone and 10 mg/kg i.m. pentazocine were found to be effective.

CRITICAL ASSESSMENT

The monkey shock titration test may be used for final evaluation of a new compound before administration to man. For screening activities the procedure can not be recommended since the test is too time consuming and the apparatus too complicated. Furthermore, higher animals such as monkeys should only be used if absolutely necessary.

REFERENCES AND FURTHER READING

Bloss JL, Hammond DL (1985) Shock titration in the rhesus monkey: effects of opiate and nonopiate analgesics. J Pharmacol Exp Ther 235:423–430

Campell ND, Geller I (1968) Comparison of analgesic effects of O-(4-methoxy phenyl carbamoyl)-3-diethylaminopropiophenone oxime HCl (USVP E-142), pentazocine and morphine in cynomolgus monkeys. Fed Proc FASEB 27:653 (2465)

Dykstra LA (1979) Effects of morphine, pentazocine and cyclazocine alone and in combination with naloxone on electric shock titration in the squirrel monkey. J Pharm Exp Ther 211:722–732

Dykstra LA (1980) Nalorphine's effect under several schedules of electric shock titration. Psychopharmacology 70:69–72

Dykstra LA, Macmillan DE (1977) Electric shock titration: Effects of morphine, methadone, pentazocine, nalorphine, naloxone, diazepam and amphetamine. J Pharm Exp Ther 202:660–669

Römer D (1968) A sensitive method for measuring analgesic effects in the monkey. In: Soulairac A, Cahn J, Charpentier J (eds) Pain. Acad Press London, New York, pp 165–170

Weiss B, Laties VG (1964) Analgesic effects in monkeys of morphine, nalorphine, and a benzomorphan narcotic antagonist. J Pharm Exp Ther 143:169–173

H.1.2.10 Formalin Test in Rats

PURPOSE AND RATIONALE

The formalin test in rats has been proposed as a chronic pain model which is sensitive to centrally active analgesic agents by Dubuisson and Dennis (1977).

PROCEDURE

Male Wistar rats weighing 180–300 g are administered 0.05 ml of 10% formalin into the dorsal portion of the front paw. The test drug is administered simultaneously either sc. or orally. Each individual rat is placed into a clear plastic cage for observation. Readings are taken at 30 and 60 min and scored according to a pain scale. Pain responses are indicated by elevation or favoring of the paw or excessive licking and biting of the paw. Analgesic response or protection is indicated if both paws are resting on the floor with no obvious favoring of the injected paw.

EVALUATION

Using various doses, ED_{50} values for protection can be calculated. Doses of 1.7 mg/kg morphine s.c. and 15 mg/kg s.c. pethidine were found to be effective.

CRITICAL ASSESSMENT

The formalin test identifies mainly centrally active drugs, whereas peripherally acting analgesics are almost ineffective. Therefore, the formalin test may allow a dissociation between inflammatory and non-inflammatory pain, a rough classification of analgesics according to their site and their mechanism of action (Chau 1989). Cowan (1990) underlined the aspect that the formalin-test is a model of chronic pain whereas most other methods measure only the effect on acute pain.

MODIFICATIONS OF THE METHOD

Murray et al. (1988) used **mice** instead of rats. They injected 0.020 ml of 5% formalin solution into the subplantar region of the hind paw. Morphine at a dose of 2.1 mg/kg s.c. and pentazocine at a dose of 23.8 mg/kg s.c. were active whereas the cyclooxygenase inhibitor zomepirac was inactive even at a dose of 100 mg/kg s.c.

Hunskaar et al. (1986), Hunskaar and Hole (1987) injected a small amount of formalin (20 µl of 1% solution) under the skin of the dorsal surface of the right hind paw of mice. A biphasisic response with an early (0–5 min) and a late (20–30 min) phase with high licking activity was observed. Central acting analgesics were active in both phases, whereas non-steroidal anti-inflammatory drugs and corticosteroids inhibited only the late phase. Acetylsalicylic acid and paracetamol were antinociceptive in both phases.

Shibata et al. (1989) again used lower concentrations of formalin (0.025 ml of 0.5% formalin solution) and also mice instead of rats. They found a characteristic biphasic pain response. Centrally acting drugs such as morphine inhibited both phases, whereas according to their data peripherally acting drugs such as acetylsalicylic acid, oxyphenylbutazone and corticosteroids inhibited only the second phase.

Abbott et al. (1995) used the formalin test for scoring properties of the first and second phases of the pain response in rats.

Abbadie et al. (1997) determined the pattern of c-fos expression in the rat spinal cord to study the two phases of the formalin test.

Clavelou et al. (1989), Dallel et al. (1995). Gilbert et al. (2001) used a modification of the formalin test for assessing pain and analgesia in the **orofacial region of the rat**. After injection into the upper lip, pain intensity was evaluated by the animal's behavior of rubbing of the injected area. A subcutaneous injection of 0.05 ml of 0.92% formaldehyde solution was made into the upper lip, just lateral to the nose. Following injection, the rat was immediately brought back in a test box equipped with a videocamera for a 45 min observation period. The recording time was divided into 15 blocks of 5 min and a pain score was determined for each block, by measuring the number of seconds that the animals spent rubbing the injected area with the ipsilateral fore- or hindpaw. The animals were sacrificed after the end of the experiment to avoid unnecessary suffering.

Tjølsen et al. (1992) attributed the early phase to C-fibre activation, whereas the late phase appeared to be dependent on the combination of an inflammatory reaction in the peripheral tissue and functional changes in the dorsal horn of the spinal cord.

Alreja et al. (1984) used the formalin test for assessing pain in **monkeys** after volunteering of one of the authors to carry out the same procedure on himself.

Corrêa and Calixto (1993) studied the participation of B_1 and B_2 kinin receptors in the formalin-induced nociceptive response in the **mouse**. Pain response was increased after ACE-inhibition and decreased by bradykinin receptor antagonists.

Herman and Felinska (1979) proposed a rapid test for screening of narcotic analgesics in mice by evaluation of behavioral symptoms after subcutaneous injection of EDTA.

Legat et al. (1994), Dumas et al. (1997) induced hyperalgesia in rats by subplantar injection of collagenase (100 µg in 100 µl saline) and rated the behavioral reactions after treatment with analgesics according to a modified formalin-test.

REFERENCES AND FURTHER READING

Abbadie C, Taylor BK, Peterson MA, Basbaum AI (1997) Differential contribution of the two phases of the formalin test to the pattern of c-fos expression in the rat spinal cord: studies with remifentanile and lidocaine. Pain 69:101–110

Abbott FV, Franklin KBJ, Ludwick RJ, Melzack R (1981) Apparent lack of tolerance in the Formalin test suggests different mechanisms for morphine analgesia in different types of pain. Pharmacol Biochem Behav 15:637–640

Abbott FV, Melzack R, Samuel C (1982) Morphine analgesia in the tail-flick and Formalin pain tests is mediated by different neural systems. Exp Neurol 75:644–651

Abbott FV, Franklin KBJ, Westbrook RF (1995) The formalin test: scoring properties of the first and second phases of the pain response in rats. Pain 60:91–102

Alreja M, Mutalik P, Nayar U, Machanda SK (1984) The formalin test: a tonic pain model in the primate. Pain 20:97–105

Chau TT (1989) Analgesic testing in animal models. In: Pharmacological Methods in the Control of Inflammation. Alan R. Liss, Inc., pp 195–212

Clavelou P, Pajot J, Dallel R, Raboisson P (1989) Application of the formalin test to the study of orofacial pain in the rat. Neurosci Lett 103:349–353

Corrêa CR, Calixto JB (1993) Evidence for participation of B_1 and B_2 kinin receptors in formalin-induced nociceptive response in the mouse. Br J Pharmacol 110:193–198

Cowan A (1990) Recent approaches in the testing of analgesics in animals. In: Modern Methods in Pharmacology, Vol 6, Testing and Evaluation of Drugs of Abuse. Wiley-Liss, Inc. pp 33–42

Dallel R, Raboisson P, Clavelou P, Saade M, Woda A (1995) Evidence for a peripheral origin of the tonic nociceptive response to subcutaneous formalin. Pain 61:11–16

Dubuisson D, Dennis SG (1977) The Formalin test: A quantitative study of the analgesic effects of morphine, meperidine and brain stem stimulation in rats and cats. Pain 4:161–174

Dumas J, Liégeois JF, Bourdon V (1997) Involvement of 5-hydroxytryptamine and bradykinin in the hyperalgesia induced in rats by collagenase from clostridium histolyticum. Naunyn-Schmiedeberg's Arch Pharmacol 355:566–570

Gilbert SD, Clatk TC, Flores CM (2001) Antihyperalgesic activity of epibatidine in the formalin model of facial pain. Pain 89:159–165

Herman ZS, Felinska W (1979) Rapid test for screening of narcotic analgesics in mice. Pol J Pharmacol Pharm 31:605–608

Hunskaar S, Berge OG, Hole K (1986) Dissociation between antinociceptive and anti-inflammatory effects of acetylsalicylic acid and indomethacin in the formalin test. Pain 25:125–132

Hunskaar S, Hole K (1987) The formalin test in mice: dissociation between inflammatory and non-inflammatory pain. Pain 30:103–114

Legat FJ, Griesbacher T, Lembeck F (1994) Mediation of bradykinin of the rat paw oedema induced by collagenase from Clostridium histolyticum. Br J Pharmacol 112:453–460

Malmberg AB, Yaksh TL (1992) Antinociceptive actions of spinal nonsteroidal anti-inflammatory agents on the formalin test in the rat. J Pharm Exp Ther 263:136–146

Murray CW, Porreca F, Cowan A (1988) Methodological refinements to the mouse paw formalin test. J Pharmacol Meth 20:175–186

North MA (1977) Naloxone reversal of morphine analgesia but failure to alter reactivity to pain in the formalin test. Life Sci 22:295–302

Shibata M, Ohkubo T, Takahashi H, Inoki R (1989) Modified formalin test: characteristic biphasic pain response. Pain 38:347–352

Theobald W (1955) Vergleichende Untersuchung anti-inflammatorischer Wirkstoffe am Formalinoedem. Arch Int Pharmacodyn 103:17–26

Tjølsen A, Berge OG, Hunskaar S, Rosland JH, Hole K (1992) The formalin test: an evaluation of the method. Pain 51:5–17

Wheeler H, Porreca F, Cowan A (1989) Formalin is unique among potential noxious agents for the intensity of its behavioral response in rats. FASEB J 3:A278 (310)

H.1.2.11 Neuropathic Pain

H.1.2.11.1 General Considerations

Partial injury to somatosensory nerves sometimes causes causalgia in humans. Causalgia is characterized by spontaneous burning pain combined with hyperalgesia and allodynia and usually follows an incomplete peripheral nerve injury. Allodynia, a pain sensation due to normally innocuous stimulation, is a particularly troublesome symptom in patients. Neuropathic pains are classified according to either the etiological diagnosis of the neuropathy (e. g., painful diabetic neuropathy, post-herpetic neuralgia, post-traumatic neuralgia, etc.), or the anatomical lesion (e. g., central pain, peripheral neuralgia). See Hansson and Dickenson (2005). Various animal models are described to study neuropathic pain. See below.

REFERENCES AND FURTHER READING

Hansson PT, Dickenson AH (2005) Pharmacological treatment of peripheral neuropathic pain conditions based on shared commonalities despites multiple etiologies. Pain 113:251–254

H.1.2.11.2 Chronic Nerve Constriction Injury

PURPOSE AND RATIONALE

Bennet and Xie (1988) described a peripheral neuropathy due to nerve constriction in the rat that produces disorders of pain sensation like those seen in man. This method with slight modifications was used by Davar et al. (1991), Mao et al. (1992), Munger et al. (1992), Yamamoto and Yaksh (1992), Tal and Bennet (1993) and reviewed by Bennett (1993).

PROCEDURE

Anesthesia is induced in male Sprague-Dawley rats by inhalation with halothane 4% and maintained at a concentration of 2–3% as needed. After a local incision, the biceps femoralis of each leg is bluntly dissected at midtigh to expose the sciatic nerve. Each nerve is then mobilized with care taken to avoid undue stretching. Four 4–0 chromic gut sutures are each tied loosely with a square knot around the right sciatic nerve. The left sciatic nerve is only mobilized. Both incisions are closed layer to layer with silk sutures and the rats allowed to recover. During the next days, the animals show a mild eversion of the affected paw and a mild-to-moderate degree of foot drop.

The thermal nociceptive threshold is measured according to the method of Hargreaves et al. (1988), (see H.1.2.3). The rats are placed beneath a clear plastic cage ($10 \times 20 \times 24$ cm) upon an elevated floor of clear glass. A radiant heat source (halogen projector lamp) is placed beneath the glass floor on a movable holder and positioned such that is focuses at the plantar area of one hind paw. The time interval between the application of the light beam and the brisk hind paw withdrawal response is measured to the nearest 01. sec.

The maximum hyperesthesia occurs between 7 and 14 days after nerve ligation. Before intrathecal injection of the drug or vehicle, the hind paws are tested 3 times alternatively with 5-min intervals as the baseline data. The left and right test sequence is carried out at 5, 15, 30, 60 and 90 min after injection.

EVALUATION

The mean ±SEM of the paw withdrawal latency (PWL) is plotted. To analyze the magnitude of hyperesthesia, the difference score (DS) is calculated by subtraction the maximum PWL of the control side (left side) from the maximum PWL of the affected side (right side). Maximum PWL is defined as the PWL that was the maximum during the first 30 min after injection. To analyze the drug effects in hyperesthetic rats, the dose is plotted against the change in DS (post-drug difference score minus pre-drug difference score).

MODIFICATIONS OF THE METHOD

The chronic constriction injury (CCI) model according to Bennett and Xie (1988) has been used by several authors: Sotgiu and Biella (1998), Toda et al. (1998), Blackburn-Munro and Jensen (2003), Keay et al. (2004), Bingham et al. (2005), Bomholt et al. (2005), Costa et al. (2005), and Howard et al. (2005).

Sotgiu et al. (1996) performed laminectomy from L1 to S2 in anesthetized rats with sciatic chronic constriction injury. For extracellular recording, two tungsten microelectrodes were positioned under a dissecting microscope on the surface of the spinal cord at L2 and L5–L6 level ipsilaterally to the injured nerve, and were advanced at steps of 2 μm. Neuronal activity was conventionally recorded and then digitized; frequency histograms were constructed by computer programs. The search stimulus for dorsal horn neurons at L2 and L5–L6 segments was the electrical stimulation of saphenous and sciatic nerve peripheral territories. Nat-

ural stimuli (brushing of the skin) and noxious stimuli (calibrated pinching) were defined. After the responses to saphenous stimuli in the neurons were recorded, a small pad of gel-foam soaked with 0.5 ml lidocaine was placed around the intact epineurium proximally to the ligatures on the sciatic nerve. The saphenous stimulation was repeated during the block and after complete recovery of the preblock baseline activity. In this way, the effect of the local anesthetic on the spontaneous activity and on the response to a noxious stimulus could be evaluated.

The first animal model of painful neuropathy was reported by Wall et al. (1979a, b). The sciatic nerve of rats or mice was sectioned and either tied or implanted in a polyethylene tube sealed at its far end. Moreover, in one modification also the saphenous nerve was cut, such that the hind paw was completely denervated. This procedure, which is known as the neuroma model, is believed to replicate the human syndromes seen after amputation (phantom pain) or after nerve transection in an intact limb (anesthesia dolorosa). Within several days, the animals begin to self-mutilate the hindpaw on the side of the nerve transection: a behavior named 'autotomy'.

Seltzer et al. (1990) ligated only one-half of the sciatic nerve in rats unilaterally. The withdrawal thresholds to repetitive von Frey hair stimulation at the plantar side were decreased bilaterally as were the withdrawal thresholds to CO_2 laser heat pulses. The contralateral phenomena resemble the "mirror image" pains in humans with causalgia.

This "partial sciatic nerve injury model" has been used by several authors (Malmberg and Basbaum 1998; Lindenlaub and Sommer 2000; Bingham et al. 2005). Patel et al. (2001) studied the effects of $GABA_B$ agonists and gabapentin on mechanical hyperalgesia in models of neuropathic (partial sciatic ligation) and inflammatory (Freund's complete adjuvant) pain in the rat and the inhibitory action on spinal transmission *in vitro*.

Hofmann et al. (2003) described the tibial nerve injury model in rats as a surgically uncomplicated model of neuropathic pain based on unilateral transection (neurotomy) of the tibial branch of the sciatic nerve.

Walczak et al. (2005) characterized the saphenous nerve partial ligation in rats as a model of neuropathic pain.

Kim and Chung (1992) described an experimental model for peripheral neuropathy produced by segmental spinal nerve ligation in the rat. Either both the L_5 and L_6 spinal nerves or the L_5 spinal nerve alone on one side of the rat were tightly ligated. A modified version of this technique was used by LaBuda and Little (2005) and by Bertorelli et al. (2005).

DeLeo et al. (1994) performed cryoneurolysis of the sciatic nerve in the rat using a cryoprobe cooled to –60°C in a 30/5/30 s freeze-thaw-freeze sequence. Autotomy was observed after 4–14 days.

Coderre et al. (2004) produced a neuropathic-like pain syndrome in rats following prolonged hind paw ischemia and reperfusion, creating an animal model of complex regional pain syndrome-type I (CRPS-I; reflex sympathetic dystrophy), called **chronic post-ischemia pain**. A tourniquet ring was placed on one hindlimb of an anesthetized rat just proximal to the ankle joint for 3 h, which was removed prior to termination of anesthesia to allow reperfusion. Rats exhibited hyperemia and edema/plasma extravasation of the ischemic hind paw for a period of 2–4 h after reperfusion. Hyperalgesia to noxious mechanical stimulation (pin prick) and cold (acetone exposure), as well as mechanical allodynia to innocuous mechanical stimulation (von Frey hairs) are evident in the affected hindpaw as early as 8 h after reperfusion, and extend for at least 4 weeks.

Mice that lack protein kinase C gamma (PKCγ) displayed normal response to acute pain stimuli, but they almost completely failed to develop a neuropathic pain syndrome after partial sciatic nerve section, and the neurochemical changes that occurred in the spinal cord after nerve injury were blunted (Malmberg et al. 1997).

Shimoyama et al. (2002) developed a **mouse model of neuropathic cancer pain** by inoculating Meth A sarcoma cells in the immediate proximity of the sciatic nerve in BALB/c mice. The tumor grows predictably with time and gradually compresses the nerve, thereby causing nerve injury. Time courses of thermal hypersensitivity and mechanical sensitivity to von Frey hairs were determined and signs of spontaneous pain were evaluated. The authors compared this model with the chronic constriction model.

Panesar et al. (1997) and Campbell et al. (1998) studied mechanical hyperalgesia associated with partial peripheral ligation in the **guinea pig**.

REFERENCES AND FURTHER READING

Bennett GJ (1993) An animal model of neuropathic pain: a review. Muscle Nerve 16:1040–1048

Bennet GJ, Xie YK (1988) A peripheral mononeuropathy in the rat that produces disorders of pain sensation like those seen in man. Pain 33:87–108

Bertorelli R, Fredduzzi S, Tarozzo G, Campanella M, Grundy R, Beltramo M, Reggiani A (2005) Endogenous and exogenous melanocortin antagonists induce anti-allodynic ef-

fects in a model of rat neuropathic pain. Behav Brain Res 157:55–62
Bingham S, Beswick PJ, Bountra C, Brown T, Campbell JP, Chessell IP, Clayton N, Collins SD, Davey PT, Goodland H, Gray N, Haslam C, Hatcher JP, Hunter AJ, Lucas F, Murkitt G, Naylor A, Pickup E, Sargent P, Summerfield SG, Stevens A, Stratton SC, Wiseman J (2005) The cyclooxygenase-2 inhibitor GW406381X [2-(4-ethoxyphenyl)-3-[4-(methylsulfonyl)phenyl]pyrazol[1,5-*b*]pyridazine] is effective in animal models of neuropathic pain and central sensitization. J Pharmacol Exp Ther 312:1161–1169
Blackburn-Munro G, Jensen BS (2003) The anticonvulsant retigabine attenuates nociceptive behavior in rat models of persistent and neuropathic pain. Eur J Pharmacol 460:109–116
Bomholt SF, Mikkelsen JD, Blackburn-Munro G (2005) Antinociceptive effects of the antidepressants amitriptyline, duloxetine, mirtazepine and citalopram in animal models of acute, resistant and neuropathic pain. Neuropharmacology 48:252–261
Campbell EA, Gentry CT, Patel S, Panesar MS, Walpole CJS, Urban L (1998) Selective neurokinin-1 receptor antagonists are anti-hyperalgesic in a model of neuropathic pain in the guinea pig. Neuroscience 87:527–532
Coderre TJ, Xanthos DN, Francis L, Bennett GJ (2004) Chronic post-ischemia pain (CPIP): a novel animal model of complex regional pain syndrome-Type I (CRPS-I; reflex sympathetic dystrophy) produced by prolonged hindpaw ischemia and reperfusion in the rat. Pain 112:94–105
Costa B, Trovato AE, Colleoni M, Giagnoni G, Zarini E, Croci T (2005) Effect of the cannabinoid CB1 receptor antagonist, SR141716, on nociceptive response and demyelination in rodents with chronic injury of the sciatic nerve. Pain 116:52–61
Davar G, Hama A, Deykin A, Vos B, Maciewicz R (1991) MK-801 blocks the development of thermal hyperalgesia in a rat model of experimental painful neuropathy. Brain Res 553:327–330
DeLeo JA, Coombs DW, Willenbring S, Colburn RW, Fromm C, Wagner R, Twitchell BB (1994) Characterization of a neuropathic pain model: sciatic cryoneurolysis in the rat. Pain 56:9–16
Hofmann HA, de Vry J, Siegling A, Spreyer P, Denzer D (2003) Pharmacological sensitivity and gene expression analysis of the tibial nerve injury model of neuropathic pain. Eur J Pharmacol 470:17–23
Howard RF, Walker SM, Mota PM, Fitzgerald M (2005) The ontogeny of neuropathic pain: postnatal onset of mechanical allodynia in rat spared nerve injury (SNI) and chronic constriction injury (CCI) models. Pain 115:382–389
Keay KA, Monassi CR, Levinson DB, Bandler R (2004) Peripheral nerve injury evokes disabilities and sensory dysfunction in a subpopulation of rats: a closer model to human chronic neuropathy pain? Neurosci Lett 361:188–191
Kim SH, Chung JM (1992) An experimental model for peripheral neuropathy produced by segmental spinal nerve ligation in the rat. Pain 50:355–363
LaBuda CJ, Little PJ (2005) Pharmacological evaluation of the selective nerve ligation model of neuropathic pain in the rat. J Neurosci Methods 144:175–181
Lindenlaub T, Sommer C (2000) Partial sciatic nerve transection as a model of neuropathic pain: a qualitative and quantitative neuropathological study. Pain 89:97–106
Malmberg A, Basbaum AI (1998) Partial sciatic nerve injury in the mouse as a model of neuropathic pain: behavioral and neuroanatomical correlation. Pain 76:215–222
Mao J, Price DD, Mayer DJ, Lu J, Hayes RL (1992) Intrathecal MK-801 and local anesthesia synergistically reduce nociceptive behaviors in rats with experimental peripheral neuropathy. Brain Res 576:254–262
Munger BL, Bennett GJ, Kajander KC (1992) An experimental painful peripheral neuropathy due to nerve constriction. Exper Neurol 118:204–214
Panesar MS, Patel S, Gentry CT, Campbell EA (1997) A novel model of neuropathic pain in the guinea pig. Comparative analgesic activity in a model of inflammatory pain. Br J Pharmacol 120:230P
Patel S, Naeem S, Kesingland A, Froestl W, Capogna M, Urban L, Fox A (2001) The effects of $GABA_B$ agonists and gabapentin on mechanical hyperalgesia in models of neuropathic and inflammatory pain. Pain 90:217–226
Seltzer Z, Dubner R, Shir Y (1990) A novel behavioral model of neuropathic pain disorders produced in rats by partial sciatic nerve injury. Pain 43:205–218
Shimoyama M, Tanaka K, Hasue F, Shimoyama N (2002) A mouse model of neuropathic cancer pain. Pain 99:167–174
Sotgiu ML, Biella G (1998) Contralateral inhibitory control of spinal nociceptive transmission in rats with chronic peripheral nerve injury. Neurosci Lett 253:21–24
Sotgiu ML, Biella G, Lacerenza M (1996) Injured nerve block alters adjacent nerves spinal interaction in neuropathic rats. NeuroReport 7:1385–1388
Tal M, Bennet GJ (1993) Dextrorphan relieves neuropathic heat-evoked hyperalgesia in the rat. Neurosci Lett 151:107–110
Toda K, Muneshige H, Ikuta Y (1998) Antinociceptive effects of neurotropin in a rat model of painful peripheral mononeuropathy. Life Sci 62:913–921
Walczak JS, Pichette V, Leblond F, Desbiens K, Beaulieu P (2005) Behavioral, pharmacological and molecular characterization of the saphenous nerve partial ligation: a new model of neuropathic pain. Neuroscience 132:1093–1102
Wall PD, Devor M, Inbal R, Scadding JW, Schonfeld D, Seltzer Z, Tomkiewicz MM (1979a) Autotomy following peripheral nerve lesions: experimental anesthesia dolorosa. Pain 7:103–113
Wall PD, Scadding JW, Tomkiewicz MM (1979b) The production and prevention of experimental anesthesia dolorosa. Pain 6:175–182
Yamamoto T, Yaksh TL (1992) Spinal pharmacology of thermal hyperesthesia induced by constriction injury of sciatic nerve. Excitatory amino acid antagonists. Pain 49:121–128

H.1.2.11.3 Peripheral Nerve Injury Model

PURPOSE AND RATIONALE

In addition to chronic ligation techniques, nerve dissection and nerve crush models have been used to study neuropathic pain. Nerve crush injury was described by Decosterd et al. (2002).

PROCEDURE

Male Sprague Dawley rats weighing 200–250 g were anesthetized with halothane (1.5%–3%). The left sciatic nerve was exposed at the mid-thigh level and crushed by a pair of hemostat forceps with smooth protective pads that were placed perpendicularly to the

sciatic trunk for 30 s (Bester et al. 2000). Muscle and skin were closed in two layers.

Animals were habituated to the tester, the environment and the handling procedures prior to commencement of the testing. A calibrated von Frey monofilament was applied five times until it bent on the lateral dorsal side of the hindpaw that is in crushed nerve territory or the intact sural nerve, ipsilateral to the nerve lesion. A series of monofilaments (1.0–200.0 g) were applied and the test started with the lowest force filament. The mechanical withdrawal threshold corresponds to the minimum force required to elicit a reproducible flexor withdrawal movement after application of the von Frey hairs. Once baseline threshold was determined, eight light strokes were applied manually at 1 Hz to the dorsum of the paw at 5-min intervals, for 2 h. The mechanical withdrawal threshold was recorded immediately after the application of the light touch, at the same interval of 5 min during the whole test period.

EVALUATION

Data are expressed as mean ±SEM of the recorded mechanical withdrawal threshold in grams, or as a percentage of the baseline value. The differences between groups were analyzed with analysis of variance (ANOVA) two-way repeated measures.

MODIFICATIONS OF THE METHOD

Vogelaar et al. (2004) described sciatic nerve regeneration in mice and rats. Under anesthesia, the sciatic nerve was carefully exposed. At a point immediately distal from the gluteus maximus muscle, the nerve was crushed for 30 s using a hemostatic forceps. The animals were followed for 70 (rats) and 32 (mice) days and functional recovery of sciatic nerve function was monitored by the foot reflex withdrawal test, locomotor pattern, and mechanical withdrawal thresholds.

Rodrigues-Filho et al. (2003, 2004) published the technique of avulsion injury of the rat brachial plexus that triggers hyperalgesia and allodynia in the hindpaws. Male Wistar rats weighing 250–300 g were anesthetized by chloralose i.p. The brachial plexus was approached through a horizontal incision parallel to the clavicle, running from the sternum to the axillary region. The pectoralis major muscle was displaced, leaving the cephalic vein intact. The subclavian vessels were located and the lower trunk dissected and crushed three times for 5 s using microsurgical forceps. At the end of this procedure, the nerve was completely flattened and transparent. The tissue layers were then brought together and the skin closed with silk sutures.

For assessment of mechanical hyperalgesia, mechanical thresholds were measured in the hindpaws with an analgesymeter (Ugo Basile, Italy) according to the method of Randall and Sellitto (1957). Furthermore, thermal hyperalgesia, mechanical allodynia, and cold allodynia were measured in the hindpaws, as well as grasping force in the forepaws.

Sweitzer et al. (2001) studied prevention of allodynia induced by transection of the L5 spinal nerve in rats.

Devor et al. (2005) studied heritability of symptoms in the neuroma model of neuropathic pain.

REFERENCES AND FURTHER READING

Bester H, Beggs S, Woolf CJ (2000) Changes in tactile stimuli-induced behavior and c-Fos expression in the superficial dorsal horn and in parabrachial nuclei after sciatic nerve crush. J Comp Neurol 428:45–61

Decosterd I, Allchorne A, Woolf CJ (2002) Progressive tactile hypersensitivity after peripheral nerve crush: non-noxious mechanical stimulus-induced neuropathic pain. Pain 100:155–162

Devor M, del Canho S, Raber P (2005) Heritability of symptoms in the neuroma model of neuropathic pain: replication and complementation analysis. Pain 116:294–301

Randall LO, Selitto JJ (1957) A method for measurement analgesic activity in inflamed tissue. Arch Int Pharmacodyn 111:409–419

Rodrigues-Filho R, Santos ARS, Bertelli JA, Calixto JB (2003) Avulsion injury of the rat brachial plexus triggers hyperalgesia and allodynia in the hindpaws: a new model of neuropathic pain. Brain Res 982:186–194

Rodrigues-Filho R, Campos MM, Ferreira J, Santos ARS, Bertelli JA, Calixto JB (2004) Pharmacological characterization of the rat brachial plexus avulsion model of neuropathic pain. Brain Res 1018:159–170

Sweitzer SM, Schubert P, DeLeo JA (2001) Propentofylline, a glial modulating agent, exhibits antiallodynic properties in a rat model of neuropathic pain. J Pharmacol Exp Ther 297:1210–1217

Vogelaar CF, Vrinten DH, Hoekman MFM, Brakkee JH, Burbach JPH, Hamers FPT (2004) Sciatic nerve regeneration in mice and rats: recovery and sensory innervation is followed by a slowly retreating neuropathic pain-like syndrome. Brain Res 1027:67–72

H.1.2.11.4 Spared Nerve Injury Model

PURPOSE AND RATIONALE

In addition to the above-described models of peripheral neuropathic pain [chronic constriction injury model according to Bennett and Xie (1988), partial ligation according to Seltzer et al. (1990), segmental spinal nerve ligation according to Kim and Chung (1992)], Decosterd and Woolf (2000) described **spared nerve injury** as an animal model of persistent peripheral neuropathic pain.

PROCEDURE

Adult male Sprague Dawley rats were used. Under halothane (2%) anesthesia the skin on the lateral surface of the thigh was incised and a section made directly through the biceps femoris muscle exposing the sciatic nerve and its three terminal branches: the sural, common peroneal and tibial nerves. The procedure comprises an axotomy and ligation of the tibial and common peroneal nerves leaving the sural nerve intact. The common peroneal and the tibial nerves were tightly ligated with 5.0 silk and sectioned distal to the ligation, removing 2–4 mm of the distal nerve stump. Care was taken to avoid any contact with or stretching of the intact sural nerve. Muscle and skin were closed in two layers. Behavior testing was performed only after a period of at least 1 week.

For testing mechanical allodynia, animals were placed on an elevated wire grid and the plantar surface of the paw stimulated with a series of ascending force von Frey filaments. The threshold was taken as the lowest force that evoked a brisk withdrawal response to one of five repetitive stimuli. The lateral and medial plantar surface of the paw as well as its dorsal surface were tested.

For testing mechanical hyperalgesia, a pin prick test was performed using a safety pin. The lateral part of the plantar surface of the paw was briefly stimulated at an intensity to indent but not penetrate the skin. The duration of paw withdrawal was recorded.

For testing cold allodynia, a drop of acetone solution was delicately dropped onto the lateral plantar surface of the paw, using a blunt needle connected to a syringe without touching the skin. The duration of the withdrawal response was recorded.

The lateral plantar surface was exposed to a beam of radiant heat through a transparent Perspex surface (Hargreaves et al. 1988). The withdrawal latency and duration were recorded. The heat stimulation was repeated 3 times at an interval of 5–10 min for each paw and the mean calculated.

EVALUATION

Results were presented as mean ±SEM. The data were analyzed by one-way ANOVA and the non-parametric Wilcoxon matched-pairs signed-rank tests.

MODIFICATIONS OF THE METHOD

The rat spared nerve injury model has been used by several authors: Blackburn-Munro and Jensen (2003), Rode et al. (2005), and Howard et al. (2005).

REFERENCES AND FURTHER READING

Bennett GJ, Xie YK (1988) A peripheral mononeuropathy in the rat that produces disorders of pain sensation like those seen in man. Pain 33:87–108

Blackburn-Munro G, Jensen BS (2003) The anticonvulsant retigabine attenuates nociceptive behavior in rat models of persistent and neuropathic pain. Eur J Pharmacol 460:109–116

Decosterd I, Woolf CJ (2000) Spared nerve injury: an animal model of persistent peripheral neuropathic pain. Pain 87:149–158

Hargreaves K, Dubner R, Brown F, Flores C, Joris J (1988) A new and sensitive method for measuring thermal nociception in cutaneous hyperalgesia. Pain 32:77–88

Howard RF, Walker SM, Mota PM, Fitzgerald M (2005) The ontogeny of neuropathic pain: postnatal onset of mechanical allodynia in rat spared nerve injury (SNI) and chronic constriction injury (CCI) models. Pain 115:382–389

Kim SH, Chung JM (1992) An experimental model for peripheral neuropathy produced by segmental spinal nerve ligation in the rat. Pain 50:355–363

Rode F, Jensen DG, Blackburn-Munro G, Bjerrum OJ (2005) Centrally-mediated antinociceptive actions of $GABA_A$ receptor agonists in the rat spared nerve injury model of neuropathic pain. Eur J Pharmacol 516:131–138

Seltzer Z, Dubner R, Shir Y (1990) A novel behavioral model of neuropathic pain disorders produced in rats by partial sciatic nerve injury. Pain 43:205–218

H.1.2.11.5 Spinal Cord Injury

PURPOSE AND RATIONALE

Spinal cord injuries result in a devastating loss of function. Chronic central pain syndromes frequently develop in the majority of affected patients. Several attempts have been made to find animal models of this situation. Xu et al. (1992), Hao and Xu (1996), Hao et al. (1998a, 1998b, 2000), Wu et al. (2003), and Colpaert et al. (2004) performed studies in rats after ischemic spinal cord injury photochemically induced by laser irradiation.

PROCEDURE

Female Sprague Dawley rats were anesthetized with 300 mg/kg chloral hydrate i.p. and one jugular vein was cannulated. Vertebrae T11–L2 were exposed after a midline incision of the skin on the back. The animals were positioned beneath a tuneable argon ion laser (Innova, Model 70, Coherent Laser Production Division) and irradiated with a knife edge beam, which was used to cover the single T13 vertebra with an average power of 0.16 W for 10 min. No laminectomy was performed. Immediately before the irradiation, erythrosine B (Red No. 3, Aldrich-Chemie) was injected intravenously in 0.9% saline at a dose of 32.5 mg/kg. Since erythrosine B is rapidly metabolized, the injection at this dose was repeated at 5-min intervals during the irradiation in order to maintain an adequate blood concentration.

Erythrosine B has an optimal absorption wavelength similar to that of the laser light. When it receives this light, a photochemical reaction occurs inside the spinal cord blood vessel where the laser is aimed. One of the reaction products accumulates in the vessel, injuring the endothelial layer and causing platelet release and coagulation and, thus, ischemia. After irradiation the incision was closed and the animals were kept warm for 2 h. The bladders were emptied manually 2–3 times a day until normal function was regained.

A set of calibrated von Frey hairs was used to test the vocalization threshold in response to graded mechanical pressure ranging from 0.021 to 410.0 g. During the test the rats were gently restrained in a standing position by the experimenter and the von Frey hair was pushed onto the skin until the filament became bent. The frequency of the stimulation was about every 3–4 s per stimulus and at each intensity. The stimuli were applied 5–10 times. The pressure which induced consistent vocalization (>75% response rate) over a relatively large skin area was considered to be the pain threshold.

EVALUATION

Rats were randomized for different treatment groups. The data are expressed as medians and variability as mean ±SEM. Data were analyzed with Kruskal-Wallis one-way ANOVA followed by Wilcoxon signed ranks test or by Mann-Whitney *U*-test.

MODIFICATIONS OF THE METHOD

Christensen et al. (1996), Christensen and Hulsebosch (1997a, 1007b), and Bennett et al. (2000a, 2000b) used a rodent spinal hemisection model of spinal cord injury in which mechanical and thermal allodynia develop by 24 days after injury.

Male Sprague Dawley rats (175–200 g) were deeply anesthetized by i.p. injection of 75 mg/kg ketamine and 15 mg/kg xylazine. The spinal cord was hemidissected at T13 on the left side by the following procedure: after palpation of the dorsal surface to locate the cranial borders of the sacrum and the dorsal spinous processes of the lower thoracic and lumbar vertebrae, the T11, T12, and T13 laminae were determined by locating the last rib, which attaches the cranial end of the T13 vertebrae. The surgical field was shaved and prepared with povidone-iodine, and a longitudinal incision was made exposing several segments. A laminectomy was performed at vertebral level T11, the lumbar spinal cord was identified with the accompanying dorsal vessel, and the spinal cord was hemisected at T13, cranial to the L1 dorsal root entry zone, with a scalpel blade without damage to the major dorsal vessel or vascular branches. The musculature and the fascia were then sutured and the skin was apposed by autoclips.

Siddall et al. (1995) and Drew et al. (2004) described mechanical allodynia following contusion injury of the rat spinal cord. Contusive spinal cord injury was produced in anesthetized Wistar rats weighing 200–300 g. Laminectomy was performed at the vertebral thoracic T10 level to expose a 3-mm window over the dorsal spinal cord and adjacent rostral and caudal spinous processes were clamped to stabilize the spine. A brass guide tube 15 cm in length was positioned perpendicularly above the exposed cord and a cylindrical 10 g steel weight (2 mm in diameter) with a rounded tip was suspended within the tube 2 cm above the cord surface. The weight was held within the tube by a metal pin. Removing the pin and allowing the weight to drop onto the exposed cord produced spinal cord injury at the T12–T13 segmental level. The wound was closed in layers and antibiotics were administered.

Abraham et al. (2001) and Caudle et al. (2003) described excitotoxic spinal cord injury induced by intraspinal injection of quisqualic acid.

Zochodne et al. (1994) induced a segmental chronic pain syndrome by lumbar intrathecal NMDA infusion.

Malmberg and Yaksh (1992) reported that hyperalgesia mediated by spinal glutamate or substance P receptor is blocked by spinal cyclooxygenase inhibition.

REFERENCES AND FURTHER READING

Abraham KE, McGinty JF, Brewer KL (2001) The role of kainic acid/AMPA and metabotropic glutamate receptors in the regulation of mRNA expression and the onset of pain-related behavior following excitotoxic spinal cord injury. Neuroscience 104:863–874

Bennett AD, Everhart AW, Hulsebosch CE (2000a) Intrathecal administration of an NMDA or a non-NMDA receptor antagonist reduces mechanical but not thermal allodynia in a rodent model of chronic pain after spinal cord injury. Brain Res 859:72–82

Bennett AD, Chastain KM, Hulseboscj CE (2000b) Alleviation of mechanical and thermal allodynia by $CGRP_{8–37}$ in a rodent model of chronic central pain. Pain 86:163–175

Caudle RM, Perez FM, King C, Yu CG, Yezierski RP (2003) *N*-Methyl-D-aspartate subunit expression and phosphorylation following excitotoxic spinal cord injury in rats. Neurosci Lett 349:37–40

Christensen MD, Hulsebosch CE (1997a) Spinal cord injury and anti-NGF treatment results in changes in CGRP density and distribution in the dorsal horn in the rat. Exp Neurol 147:463–475

Christensen MD, Hulsebosch CE (1997b) Chronic central pain after spinal cord injury. J Neurotrauma 14:517–537

Christensen MD, Everhart AW, Pickelman JT, Hulsebosch CE (1996) Mechanical and thermal allodynia in chronic central pain following spinal cord injury. Pain 68:97–107

Colpaert FC, Wu WP, Hao JX, Royer I, Sautel F, Wiesenfeld-Hallin Z, Xu XJ (2004) High-efficacy 5-HT1A receptor activation causes a curative-like action on allodynia in rats with spinal cord injury. Eur J Pharmacol 497:29–33

Drew GM, Siddall PJ, Duggan AW (2004) Mechanical allodynia following contusion injury of the rat spinal cord is associated with loss of GABAergic inhibition in the dorsal horn. Pain 109:379–388

Hao JX, Xu XJ (1996) Treatment of a chronic allodynia-like response in spinally injured rats: effects of systemically administered excitatory amino acid receptor antagonists. Pain 66:279–285

Hao JX, Yo W, Wiesenfeld-Hallin Z, Xu XJ (1998a) Treatment of chronic allodynia in spinally injured rats: effects of intrathecal selective opioid receptor agonists. Pain 75:209–217

Hao JX, Xu IS, Wiesenfeld-Hallin Z, Xu XJ (1998b) Antihyperalgesic and anti-allodynic effects of intrathecal nociceptin/orphanin FQ in rats after spinal cord injury, peripheral nerve injury and inflammation. Pain 76:385–393

Hao JX, Xu JX, Urban L, Wiesenfeld-Hallin Z (2000) Repeated administration of systemic gabapentin alleviates allodynia-like behaviors in spinally injured rats. Neurosci Lett 280:211–214

Malmberg AB, Yaksh TL (1992) Hyperalgesia mediated by spinal glutamate or substance P receptor is blocked by spinal cyclooxygenase inhibition. Science 257:1276–1279

Malmberg AB, Chen C, Tonegawa S, Basbaum AI (1997) Preserved acute pain and reduced neuropathic pain in mice lacking PKCγ. Science 278:279–283

Siddall PJ, Xu CL, Cousins MJ (1995) Allodynia following traumatic spinal cord injury in the rat. NeuroReport 6:1241–1244

Wu WP, Hao JX, Xu XJ, Wiesenfeld-Hallin Z, Koek W, Colpaert FC (2003) The very-high-efficacy 5-HT_{1A} receptor agonist, F 13640, preempts the development of allodynia-like behaviors in rats with spinal cord injury. Eur J Pharmacol 478:131–137

Xu XJ, Hao JX, Aldskogius H, Seiger A, Wiesenfeld-Hallin Z (1992) Chronic pain-related syndrome in rats after ischemic spinal cord lesion: a possible animal model for pain in patients with spinal cord injury. Pain 48:279–290

Zochodne DW, Murray M, Nag S, Riopelle RJ (1994) A segmental chronic pain syndrome in rats associated with intrathecal infusion of NMDA: evidence for selective action in the dorsal horn. Can J Neurol Sci 21:24–28

H.1.2.11.6 Chemotherapy-Induced Pain

PURPOSE AND RATIONALE

Within the numerous adverse effects associated with antineoplastic drugs, painful peripheral neuropathy is frequent. Vincristine, an antineoplastic agent widely used in cancer therapy, was found to be neurotoxic for all treated patients and can induce peripheral neuropathy (Windebank 1999). Aley et al. (1996), Authier et al. (1999, 2003) and Marchand et al. (2003) developed an animal model of nociceptive neuropathy using repeated injections of vincristine.

PROCEDURE

Male Sprague Dawley rats weighing 180–200 g received five intravenous injections of 150 µg/kg vincristine every 2 days until a cumulative dose of 750 µg/kg was reached. Thresholds to paw pressure were determined before and 14 days after vincristine treatment. Test drug was then applied and the vocalization thresholds were determined 15, 30, 45, 60, 90, and 120 min after this injection.

The C-fiber-evoked flexor reflex elicited in the right hind limb (Falinower et al. 1994; Mestre et al. 1997) was recorded from halothane-anesthetized rats. Rectangular electric pulses of 6–7 mA strength and 2 ms duration were applied every 10 s to the sural nerve receptive field by means of two stainless steel needles inserted into the skin of toes 4 and 5. The C-fiber-evoked reflex response (electromyographic responses) was recorded from the ipsilateral biceps muscle by utilizing another pair of stainless steel needles. Once a stable threshold C reflex response was obtained, the stimulus strength was increased by a factor of threefold. Test drug was then injected in various doses and the mean C-fiber reflex (mean of the 12 C-fiber reflexes recorded during the 2-min period) was calculated every 2 min between 25 and 35 min.

EVALUATION

The data analysis was performed by a two-way analysis of variance (ANOVA) followed by a Student-Newman-Keuls test for the time course of the effect of drug on mechanical nociceptive thresholds. For the C reflex, results were expressed as mean percentage inhibition of the integrated C reflex responses obtained between 25 and 35 min after drug injection and plotted against log dose, allowing ED_{50} calculation.

MODIFICATIONS OF THE METHOD

Lynch et al. (2005) tested the effect of a nicotinic acetylcholine agonist against allodynia in rats in the vincristine-induced pain model.

Polomano et al. (2001) described painful peripheral neuropathy in the rat produced by the chemotherapeutic drug, paclitaxel.

Dalziel et al. (2004) described allodynia in rats infected with varicella zoster virus as an animal model for **post-herpetic neuralgia**.

REFERENCES AND FURTHER READING

Aley KO, Reichling DB, Levine JD (1996) Vincristine hyperalgesia in the rat: a model of painful vincristine neuropathy in humans. Neuroscience 73:259–265

Authier N, Coudore F, Eschalier A, Fialip J (1999) Pain related behavior during vincristine-induced neuropathy in rats. NeuroReport 10:965–968
Authier N, Gillet JP, Fialip J, Eschalier A, Coudore F (2003) A new animal model of vincristine-induced nociceptive peripheral neuropathy. NeuroToxicology 24:797–805
Dalziel RG, Bingham S, Sutton D, Grant D, Champion JM, Dennis SA, Quinn JP, Bountra C, Mark MA (2004) Allodynia in rats infected with varicella zoster virus – a small animal model for post-herpetic neuralgia. Brain Res Rev 46:234–242
Falinower S, Willer JC, Junien JL, Le Bars D (1994) A C-fiber reflex modulated by heterotopic noxious somatic stimuli in the rat. J Neurophysiol 72:194–213
Lynch III JJ, Wade CL, Mikusa JP, Decker MW, Honore P (2005) ABT-594 (a nicotinic acetylcholine agonist): antiallodynia in a rat chemotherapy-induced pain model. Eur J Pharmacol 509:43–48
Marchand F, Alloui A, Pelissier T, Hernández A, Authier N, Alvarez P, Eschalier A, Ardid D (2003) Evidence of an antihyperalgesic effect of venlafaxine in vincristine-induced neuropathy in rats. Brain Res 980:117–120
Mestre C, Hernandez A, Eschalier A, Pelissier T (1997) Effects of clomipramine and desimipramine on a C-fiber reflex in rats. Eur J Pharmacol 335:1–8
Polomano RC, Mannes AJ, Clark US, Bennett GJ (2001) A painful peripheral neuropathy in the rat produced by the chemotherapeutic drug, paclitaxel. Pain 94:293–304
Windebank AJ (1999) Chemotherapeutic neuropathy. Curr Opin Neurol 12:565–571

H.1.2.11.7 Trigeminal Neuropathic Pain Model

PURPOSE AND RATIONALE

Trigeminal neuralgia is an extreme form of neuropathic pain. Although the pathophysiology of the disorder is uncertain, vascular compression of the trigeminal root resulting in damage to primary afferent neurons is thought to play a major role in the generation of pain. Idänpään-Heikkilä and Guilbaud (1999) used a rat model of **trigeminal neuropathic pain**, developed by Gregg (1973), Jacquin and Zeigler (1983), Vos and Maciewicz (1991), Vos et al. (1994), and Vos and Strassman (1995), where the neuropathy is produced by a chronic constriction injury of the infra-orbital branch of the trigeminal nerve, and studied the effects of various drugs on this purely sensory model of neuropathic pain.

PROCEDURE

Male Sprague Dawley rats weighing 175–200 g were used. The head of the rat, which was anesthetized with sodium pentobarbital 50 mg/kg i.p. and treated with 0.4 mg/kg atropine i.p., was fixed in a stereotaxic frame. A mid-line scalp incision was made exposing skull and nasal bone. To expose the intra-orbital part of the left infra-orbital nerve, the edge of the orbit, formed by the maxillary, frontal, lacrimal and zygomatic bones, was dissected free. To give access to the infra-orbital nerve, the orbital contents were gently deflected with a cotton-tipped wooden rod. The infra-orbital nerve was dissected free at its most rostral extent of the orbital cavity, just caudal to the infra-orbital foramen. Two chromic catgut (5–0) ligatures (2 mm apart) were loosely tied around the infra-orbital nerve. The ligatures reduced the diameter of the nerve by just a noticeable amount and retarded, but did not interrupt, the epineural circulation. The scalp incision was closed with silk sutures.

Before the first actual stimulation session, the rats were allowed to adapt to the observation cage and to the testing environment. During this period, the experimenter reached slowly into the cage to touch the walls with a plastic rod, similar to the ones on which the von Frey filaments were mounted.

For mechanical stimulation, a graded series of ten von Frey filaments with a bending force of between 0.217 and 12.5 g was used. The stimuli were applied within the infra-orbital nerve territory, near the center of the vibrissal pad, on the hairy skin surrounding the mystacial vibrissae. The complete series of von Frey hair intensities was presented in an ascending series and either a brisk withdrawal of the head or an attack/escape reaction was considered as the mechanical threshold. Local injection of a local anesthetic (articaine) into the rostral orbital cavity of the lesioned side, in close proximity to the ligated infra-orbital nerve, increased the mechanical threshold to the upper level. The duration of the effect was dose-dependent.

EVALUATION

Data are expressed as means ±SEM. The non-parametric Kruskal–Wallis one-way ANOVA was used and comparisons between the groups were performed using the Mann-Whitney *U*-test.

MODIFICATIONS OF THE METHOD

Christensen et al. (2001) studied the effect of gabapentin and lamotrigine on mechanical allodynia-like behavior in the rat model of trigeminal neuropathic pain.

Deseure et al. (2002) studied the effects of acute i.p. injections of 5-HT_{1A} receptor agonists on mechanical allodynia in a rat model of trigeminal pain.

Cutrer and Moskowitz (1996) studied the actions of valproate and neurosteroids in a **guinea pig model** of trigeminal pain. Hartley guinea pigs were pretreated with valproate or allopregnanolone 30 min prior to activation of trigeminal afferent fibers via intracisternal

injection of capsaicin. The effects were examined on c-fos expression within the trigeminal nucleus caudalis.

REFERENCES AND FURTHER READING

Christensen D, Gautron M, Guilbaud G, Kayser V (2001) Effect of gabapentin and lamotrigine on mechanical allodynia-like behavior in a rat model of trigeminal neuropathic pain. Pain 93:147–153

Cutrer FM, Moskowitz MA (1996) The actions of valproate and neurosteroids in a model of trigeminal pain. Headache 36:579–585

Deseure K, Koek W, Colpaerte FC, Adriansen H (2002) The 5-HT_{1A} receptor agonist F 13640 attenuates mechanical allodynia in a rat model of trigeminal pain. Eur J Pharmacol 456:51–57

Gregg JM (1973) A surgical approach to the ophthalmic-maxillary nerve trunks in the rat. J Dent Res 52:392–395

Idänpään-Heikkilä JJ, Guilbaud G (1999) Pharmacological studies on a rat model of trigeminal neuropathic pain: baclofen, but not carbamazepine, morphine or tricyclic antidepressants, attenuates the allodynia-like behaviour. Pain 79:281–290

Jacquin MF, Zeigler HP (1983) Trigeminal orosensation and ingestive behavior in the rat. Behav Neurosci 97:62–97

Vos B, Maciewicz R (1991) Behavioral changes following ligation of the infraorbital nerve in rat: an animal model of trigeminal neuropathic pain. In: JM Besso, Giulbaud G (eds) Lesions of primary afferent fibers as a tool for the study of clinical pain. Elsevier, Amsterdam, pp 147–158

Vos BP, Strassman AM (1995) Fos expression in the medullary dorsal horn of the rat after chronic constriction injury to the infraorbital nerve. J Comp Neurol 357:362–375

Vos BP, Strassman AM, Maciewicz RJ (1994) Behavioral evidence of trigeminal neuropathic pain following chronic constriction injury to the rat's infraorbital nerve. J Neurosci 14:2708–2723

H.1.2.11.8 Migraine Model in Cats

PURPOSE AND RATIONALE

In order to simulate pain experienced by humans in migraine attacks, Storer and Goadsby (1997) developed a model of **craniovascular pain in cats** by stimulating the superior sagittal sinus and monitoring trigeminal neuronal activity using electrophysiological techniques.

PROCEDURE

Adult cats were anesthetized with α-chloralose (60 mg/kg i.p.), paralyzed (gallamine 6 mg/kg i.v.) and ventilated. The superior sagittal sinus was accessed and isolated for electrical stimulation by a mid-line circular craniotomy. The region of the dorsal surface of C_2 spinal cord was exposed by a laminectomy and an electrode placed for recording evoked activity by sinus stimulation and spontaneous activity of the same cells. Signals were amplified and monitored on-line. Cells were recorded that were activated by stimulation of the sinus and were also spontaneously activated. Cells fired with latencies consistent with Aδ and C fibers, generally firing three or four times per stimulus (0.3 Hz, 250 µs duration, 100 V) delivered to the sinus. Both evoked and spontaneous firing could be inhibited by iontophoretic application of serotonin (5-$HT)_{1B/1D}$ agonists.

EVALUATION

The suppression or activation of cell firing was determined from both peri-stimulus and post-stimulus histograms using the criteria of a shift of >30% from baseline. Drug comparisons were made using the Kruskal-Wallis one-way analysis of variance assessing significance at the $P < 0.05$ level.

MODIFICATIONS OF THE METHOD

Using the same method, Goadsby et al. (2002) studied the inhibition of trigeminovascular nociceptive transmission by adenosine A_1 receptor agonists.

REFERENCES AND FURTHER READING

Goadsby PJ, Hoskin KL, Storer RJ, Edvinsson L, Connor HE (2002) Adenosine A_1 receptor agonists inhibit trigeminovascular nociceptive transmission. Brain 125:1392–1401

Storer RJ, Goadsby PJ (1997) Microiontophoretic application of serotonin (5-$HT)_{1B/1D}$ agonists inhibits trigeminal cell firing in the cat. Brain 120:2171–2177

H.1.3 Side Effects of Central Analgesic Drugs

See Chap. I.J.

H.2 Peripheral Analgesic Activity

H.2.0.1 General Considerations

The differentiation between central and peripheral analgesic drugs is nowadays of more or less historical value. Most of the so called peripheral analgesics possess anti-inflammatory properties and in some cases also antipyretic activity besides analgesia. For many of them the mode of action has been elucidated as an inhibition of cyclooxygenase in the prostaglandin pathway. Nevertheless, new peripheral analgesics have to be tested not only for their *in vitro* activity on cyclooxygenase but also for their *in vivo* activity.

The most commonly used methods for measuring peripheral analgesic activity are the writhing tests

in mice (various modifications) and the RANDALL-SELITTO-test in rats.

H.2.0.2 Writhing Tests

PURPOSE AND RATIONALE

Pain is induced by injection of irritants into the peritoneal cavity of mice. The animals react with a characteristic stretching behavior which is called writhing. The test is suitable to detect analgesic activity although some psychoactive agents also show activity. An irritating agent such as phenylquinone or acetic acid is injected intraperitoneally to mice and the stretching reaction is evaluated. The reaction is not specific for the irritant.

PROCEDURE

Mice of either sex with a weight between 20 and 25 g are used. Phenylquinone in a concentration of 0.02% is suspended in a 1% suspension of carboxymethylcellulose. An aliquot of 0.25 ml of this suspension is injected intraperitoneally. Groups of 6 animals are used for controls and treated mice. Preferably, two groups of 6 mice are used as controls. Test animals are administered the drug or the standard at various pretreatment times prior to phenylquinone administration. The mice are placed individually into glass beakers and five min are allowed to elapse. The mice are then observed for a period of ten min and the number of writhes is recorded for each animal. For scoring purposes, a writhe is indicated by stretching of the abdomen with simultaneous stretching of at least one hind limb. The formula for computing percent inhibition is: average writhes in the control group minus writhes in the drug group divided by writhes in the control group times 100%. The time period with the greatest percent of inhibition is considered the peak time. A dose range is reserved for interesting compounds or those which inhibit writhing more than 70%. Compounds with less than 70% inhibition are considered to have minimal activity.

EVALUATION

A dose range is run in the same fashion as the time response except 8 animals/ group are tested at the peak time of drug activity. Four drug groups and a vehicle control group are employed. Animals are dosed and tested in a randomized manner. An estimated ED_{50} is calculated. Doses of 1.0 mg/kg p.o. indomethacin, 30 mg/kg p.o. acetylsalicylic acid, 40 mg/kg p.o. amidopyrine and 80 mg/kg p.o. phenacetin have been found to be ED_{50} values.

CRITICAL ASSESSMENT OF THE TEST

In this test both central and peripheral analgesics are detected. The test, therefore, has been used by many investigators and can be recommended as a simple screening method. However, it has to be mentioned that other drugs such as clonidine and haloperidol also show a pronounced activity in this test. Because of the lack of specificity, caution is required in interpreting the results, until other tests have been performed. Nevertheless, a good relationship exists between the potencies of analgesics in writhing assays and their clinical potencies.

MODIFICATIONS OF THE METHOD

Instead of a phenylquinone suspension, 0.1 ml of a 0.6% solution of acetic acid is injected intraperitoneally to mice with an weight between 18 and 25 g (Koster et al. 1959; Taber et al. 1969). The response is similar to that after phenylquinone. Some authors have used this method together with observation of changes in capillary permeability in order to distinguish between narcotic and non-narcotic analgesics (Whittle 1964).

Eckhardt et al. (1958), Collier et al. (1968), Loux et al. (1978) showed that several substances are able to elicit the writhing response. For example, Amanuma et al. (1984) as well as Nolan et al. (1990) used as irritant intraperitoneal injections of acetylcholine.

Emele and Shanaman (1963), Burns et al. (1968) proposed bradykinin being a endogenous transmitter of pain as irritant.

Sancillo et al. (1987) induced abdominal constriction in mice by intraperitoneal injection of 31.6 µg/kg of prostaglandin E_1.

Bhalla and Bhargava (1980) described a method for assessing aspirin-like activity using aconitine to induce writhing.

Adachi (1994) described a device for automatic measurement of writhing in mice.

Analgesic effects of non-acidic non-steroidal anti-inflammatory drugs in the acetic acid writhing test after intracisternal administration have been found by Nakamura et al. (1986).

The writhing phenomenon can also be observed in **rats** (Fukawa et al. 1980). The writhing responses were induced by intraperitoneal injection of 4% sodium chloride solution. Narcotic and non-narcotic analgesics, antipyretic and nonsteroidal anti-inflammatory drugs were effectively evaluated at relatively low doses. Methamphetamine also showed an analgesic action. VonVoigtlander and Lewis (1982, 1983) induced writhing in rats by injection of

7 ml air or 6% aqueous saline into the peritoneal cavity.

Ethacrinic acid-induced writhing response in rats was used by Björkman et al. (1992).

Schweizer et al. (1988) described a photoelectronic motility monitoring apparatus to measure automatically the writhing movements. A good correlation was found between ED_{50} values after oral administration in mice and the clinically effective oral doses in man.

Heapy et al. (1993) induced the abdominal constriction response in mice by intraperitoneally injecting 0.4 ml of either 0.25% acetic acid, 7.5 mg/ml kaolin suspension, 2.4 mg/ml zymosan solution, or 25 µg/ml bradykinin solution.

REFERENCES AND FURTHER READING

Adachi KI (1994) A device for automatic measurement of writhing and its application to the assessment of analgesic agents. J Pharmacol Toxicol Meth 32:79–84

Amanuma F, Wakaumi C, Tanaka M, Muramatsu M, Aihara H (1984) The analgesic effects of non-steroidal anti-inflammatory drugs on acetylcholine-induced writhing in mice. Folia Pharmacol Japon 84:543–551

Bhalla TN, Bhargava KP (1980) Aconitine-induced writhing as a method for assessing Aspirin-like analgesic activity. J Pharmacol Meth 3:9–14

Björkman RL, Hedner T, Hallman KM, Henning M, Hedner J (1992) Localization of central antinociceptive effects of diclofenac in the rat. Brain Res 590:66–73

Blumberg H, Wolf PS, Dayton HB (1965) Use of writhing test for evaluating activity of narcotic antagonists. Proc Soc Exp Biol Med 118:763–766

Burns RBP, Alioto NJ, Hurley KE (1968) Modification of the bradykinin-induced writhing test for analgesia. Arch Int Pharmacodyn 175:41–55

Carey F, Haworth D, Edmonds AE, Forder RA (1988) Simple procedure for measuring the pharmacodynamics and analgesic potential of lipoxygenase inhibitors. J Pharmacol Meth 20:347–356

Chernov HI, Wilson DE, Fowler F, Plummer AJ (1967) Non-specificity of the mouse writhing test. Arch Int Pharmacodyn 167:171–178

Collier HOJ, Dinneen LC, Johnson CA, Schneider C (1968) The abdominal constriction response and its suppression by analgesic drugs in the mouse. Br J Pharmac Chemother 32:295–310

Eckhardt ET, Cheplovitz F, Lipo M, Govier WM (1958) Etiology of chemically induced writhing in mouse and rat. Proc Soc Exp Biol Med 98:186–188

Emele JF, Shanaman J (1963) Bradykinin writhing: A method for measuring analgesia. Proc Soc Exp Biol Med 114:680–682

Fukawa K, Kawano O, Hibi M, Misaki M, Ohba S, Hatanaka Y (1980) A method for evaluating analgesic agents in rats. J Pharmacol Meth 4:251–259

Heapy CG, Shaw JS, Farmer SC (1993) Differential sensitivity of antinociceptive assays to the bradykinin antagonist Hoe 140. Br J Pharmacol 108:209–213

Hendershot LC, Forsaith J (1959) Antagonism of the frequency of phenylquinone-induced writhing in the mouse by weak analgesics and non-analgesics. J Pharmacol Exp Ther 125:237–240

Kokka N, Fairhurst AS (1977) Naloxone enhancement of acetic acid-induced writhing in rats. Life Sci 21:975–980

Koster R, Anderson M, de Beer EJ (1959) Acetic acid for analgesic screening. Fed Proc 18:412

Loux JJ, Smith S, Salem H (1978) Comparative analgesic testing of various compounds in mice using writhing techniques. Arzneim Forsch/Drug Res 28:1644–1677

Nakamura H, Shimoda A, Ishii K, Kadokawa T (1986) Central and peripheral analgesic action of non-acidic non-steroidal anti-inflammatory drugs in mice and rats. Arch Int Pharmacodyn 282:16–25

Nolan JC, Osman MA, Cheng LK, Sancilio LF (1990) Bromfenac, a new nonsteroidal anti-inflammatory drug: Relationship between the anti-inflammatory and analgesic activity and plasma drug levels in rodents. J Pharm Exp Ther 254:104–108

Okun R, Liddon SC, Lasagna L (1963) The effects of aggregation, electric shock, and adrenergic blocking drugs on inhibition of the "writhing syndrome". J Pharm Exp Ther 139:107–109

Rae GA, Souza RLN, Takahashi RN (1986) Methylnalorphinium fails to reverse naloxone-sensitive stress-induced analgesia in mice. Pharmacol Biochem Behav 24:829–832

Sancillo LF, Nolan JC, Wagner LE, Ward JW (1987) The analgesic and antiinflammatory activity and pharmacologic properties of Bromfenac. Arzneim Forsch/Drug Res 37:513–519

Schweizer A, Brom R, Scherrer H (1988) Combined automatic writhing/motility test for testing analgesics. Agents Actions 23:29–31

Siegmund E, Cadmus R, Lu G (1957) A method for evaluating both non-narcotic and narcotic analgesics. Proc Soc Exp Biol Med 95:729

Taber RI, Greenhouse DD, Rendell JK, Irwin S (1969) Agonist and antagonist interactions of opioids on acetic acid-induced abdominal stretching in mice. J Pharm Exp Ther 169:29–38

VonVoigtlander PF, Lewis RA (1982) Air-induced writhing: a rapid broad spectrum assay for analgesics. Drug Dev Res 2:577–581

VonVoigtlander PF, Lewis RA (1983) A withdrawal hyperalgesia test for physical dependence: evaluation of μ and mixed partial opioid agonists. J Pharmacol Meth 10:277–282

Whittle BA (1964) The use of changes in capillary permeability in mice to distinguish between narcotic and non narcotic analgesics. Br J Pharmacol 22:246–253

H.2.0.3 Pain in Inflamed Tissue (RANDALL-SELITTO-Test)

PURPOSE AND RATIONALE

This method for measuring analgesic activity is based on the principle that inflammation increases the sensitivity to pain and that this sensitivity is susceptible to modification by analgesics. Inflammation decreases the pain reaction threshold and this low pain reaction threshold is readily elevated by non-narcotic analgesics of the salicylate-amidopyrine type as well as by the narcotic analgesics. Brewers yeast has been used as an inducer for inflammation which increases pain after pressure.

PROCEDURE

Groups of male Wistar rats (130 to 175 g) are used. Only for oral testing the animals are starved 18 to 24 h prior to administration. Otherwise, the route of administration can be intraperitoneal or subcutaneous. To induce inflammation, 0.1 ml of a 20% suspension of Brewer's yeast in distilled water is injected subcutaneously into the plantar surface of the left hind paw of the rat. Three hours later, pressure is applied through a tip to the plantar surface of the rat's foot at a constant rate by a special apparatus to the point at which the animal struggles, squeals or attempts to bite. The apparatus being used has been modified by various authors such as using the Analgy Meter (Ugo Basile, Apparatus for Biological Research, Milan, Italy). Each animal is tested for its control pain threshold. Any animal with a control pain threshold greater than 80 g is eliminated and replaced.

For a time response, groups of at least 7 animals are used, four groups for the agent to be tested and one for the vehicle control. The tests are done at 15 min intervals after subcutaneous administration and at 30 min intervals after oral administration for any change in pain threshold. The interval of time which indicates the greatest increase in pain threshold is regarded as the peak time.

A dose range is obtained in the same manner as the time response. The drug to be tested is administered in a randomized manner. The pain threshold is recorded at time zero and again at the determined peak time.

EVALUATION

The mean applied force is determined for each time interval tested. The percentage increase in pain threshold is calculated by subtracting the applied force of the vehicle control from the applied force of the drug group which is divided by the applied force of the vehicle control in order to give the percentage of increase in pain threshold of the drug group. Doses of 50 mg/kg s.c. Na salicylate, 50 mg/kg amidopyrine, 3 mg/ kg s.c. morphine, 12.5 mg/kg s.c. codeine or pethidine have been found to be effective.

CRITICAL ASSESSMENT OF THE METHOD

The method originally described by RANDALL and SELITTO has been used by many investigators and has been proven to detect central analgesics as well as peripheral analgesics. Peripherally acting analgesics such as the nonsteroidal anti-inflammatory drugs increase only the threshold of the inflamed paw, whereas opiate analgesics increase also the threshold of the intact paw (Dubinsky et al. 1987). In most modifications, the assay has a shallow dose-response curve. Nevertheless, the ED_{50} values of nonsteroidal anti-inflammatory drugs in this test showed a good correlation with human doses (Romer 1980).

MODIFICATIONS OF THE METHOD

The test has been modified by various authors. In some instances the pressure on the inflamed paw has been omitted. Instead the animals were allowed to walk on a metal grid. The gait of the animals is assessed by an observer using a scoring system:

- 0 = three-legged gait
- 0.5 = marked limping
- 1 = normal gait.

The scores are transformed into percent analgesia.

Other noxious stimuli were used to induce inflammation and hyperalgesia, such as carrageenin (Winter et al. 1962), Freund's adjuvant or prostaglandin E_2 (Ferreira et al. 1978a).

Vinegar et al. (1990) injected 0.1 ml of 0.25% solution of trypsin into the subplantar region and applied the load force 60 min later. They found a biphasic hyperalgesia and relatively low ED_{50} values for central and peripheral analgesics.

Technically, the method has been improved by several authors, such as Takesue et al. (1969).

Chipkin et al. (1983) modified the test by decreasing the rate of acceleration of the noxious stimulus (mechanical pressure) on the inflamed paw from 20 to 12.5 mm Hg/s and an extension of the cut-off time from 15 to 60 s. This modification is claimed to discriminate analgesics active against mild to severe clinical pain (narcotic-like) from those only useful against mild to moderate pain (non-narcotic-like).

Randall-Selitto analgesy meters are commercially available (e. g., IITC Life Science, Woodland Hills, CA, USA).

Central and peripheral analgesic action of aspirin-like drugs has been studied with a modification of the Randall-Selitto method applying constant pressure to the rat's paw by Ferreira et al. (1978b).

A modification of an analgesia meter for paw pressure antinociceptive testing in neonatal rats was described by Kitchen (1984).

Learning and retention has been tested in rats by Greindl and Preat (1976) inducing pain by a light quantifiable pressure applied to the normal hind paw.

Hargreaves et al. (1988) described a sensitive method for measuring thermal nociception in cutaneous hyperalgesia in rats. One paw was injected with

0.1 ml carrageenan solution, the other paw with saline. The rats were placed in chambers with glass floor and radiant heat was directed to the paws. A photoelectric cell detected the light reflected from the paw and turned off the radiant heat when paw movement interrupted the reflected light.

Perkins et al. (1993) described hyperalgesia after injection of 100 µl of Freund's adjuvant into the knee of anesthetized rats. After 64–70 h the animal was placed with each hind paw on a pressure transducer and a downward force was exerted until the uninjected leg was bearing 100 g. At this point animals were less tolerant to a load on the injected leg, indicating a hyperalgesic response.

Davis et al. (1996) induced mechanical hyperalgesia by injection of substance P and capsaicin in the rat knee joint and measured the download force tolerated by the injected leg.

Ferreira et al. (1993a, b) induced hyperalgesia by intraplantar injection in the hindpaw of rats of various agents, e. g., bradykinin, carrageenin, LPS, PGE_2, dopamine, TNFα, IL-1β, IL-6 and IL-8. A constant pressure of 20 mm Hg was applied to the hind paws and discontinued when the rats presented a typical freezing reaction.

Subplantar injection of 0.1 µg of serotonin in the rat results in a brief period (up to 20 min) of increased pain sensitivity to an applied force (hyperalgesia) which precedes a longer period of decreased pain sensitivity (hypoalgesia). Vinegar et al. (1989) used this phenomenon for pharmacologic characterization of the algesic response.

Similarly, a biphasic algesic behavior after subplantar injection of 250 µg of trypsin was described by Vinegar et al. (1990)

Courteix et al. (1994) proposed the Randall-Selitto paw pressure test in rats with streptozocin-induced diabetes as a model of chronic pain with signs of hyperalgesia and allodynia that may reflect signs observed in diabetic humans.

Amann et al. (1955, 1996) evaluated local edema and effects on thermal nociceptive threshold after intraplantar injection of nerve growth factor into the rat hind paw and studied the effect of a 5-lipoxygenase inhibitor in this test.

Zhou et al. (1996) tested the effects of peripheral administration of NMDA, AMPA or KA on pain behavior in rats. A 28-gauge needle was inserted in the skin of rats proximal to the footpads and advanced about 1 cm so that the tip reached the base of the third toe. A bolus of 20 µl containing concentrations between 1 and 10,000 µM of KA, NMDA or AMPA. For behavioral testing, each animal was placed in a Plexiglas box on a wire mesh screen. Mechanical stimuli were applied using four von Frey filaments with different bending forces. Each von Frey filament was applied 10 times to the skin on the base of the third toe. The paw withdrawal was rated as scores allowing dose-response curves for the hyperalgesic effects of excitatory amino acids. Furthermore, using the highest concentration of the stimulant, effects of antagonists were tested.

REFERENCES AND FURTHER READING

Amann R, Schuligoi R, Herzeg G, Donnerer J (1955) Intraplantar injection of nerve growth factor into the rat hind paw: local edema and effects on thermal nociceptive threshold. Pain 64:323–329

Amann R, Schuligoi R, Lanz I, Peskar BA (1996) Effect of a 5-lipoxygenase inhibitor on nerve growth factor-induced thermal hyperalgesia in the rat. Eur J Pharmacol 306:89–91

Chipkin RE, Latranyi MB, Iorio LC, Barnett A (1983) Determination of analgesic drug efficacies by modification of the Randall and Selitto rat yeast paw test. J Pharmacol Meth 10:223–229

Courteix C, Bardin M, Chantelauze C, Lavarenne L, Eschalier A (1994) Study of the sensitivity of the diabetes-induced pain model in rats to a range of analgesics. Pain 57:153–160

Davis AJ, Perkins MN (1996) Substance P and capsaicin-induced mechanical hyperalgesia in the rat knee joint; the involvement of bradykinin B_1 and B_2 receptors. Br J Pharmacol 118:2206–2212

Dubinsky B, Gebre-Mariam S, Capetola RJ, Rosenthale ME (1987) The analgesic drugs: Human therapeutic correlates of their potency in laboratory animals of hyperalgesia. Agents Actions 20:50–60

Ferreira SH, Nakamura M, DeAbreu Castro MS (1978a) The hyperalgesic effects of prostacyclin and prostaglandin E_2. Prostaglandins 16:31–37

Ferreira SH, Lorenzetti BB, Corrêa FMA (1978b) Central and peripheral antialgesic action of aspirin-like drugs. Eur J Pharmacol 53:39–48

Ferreira SH, Lorenzetti BB, Poole S (1993a) Bradykinin initiates cytokine-mediated inflammatory hyperalgesia. Br J Pharmacol 110:1227–1231

Ferreira SH, Lorenzetti BB, Cunha FQ, Poole S (1993b) Bradykinin release of TNF-α plays a key role in the development of inflammatory hyperalgesia. Agents Actions 38:C7–C9

Greindl MG, Preat S (1976) A new model of active avoidance conditioning adequate for pharmacological studies. Arch Int Pharmacodyn 223:168–170

Hargreaves K, Dubner R, Brown F, Flores C, Joris J (1988) A new and sensitive method for measuring thermal nociception in cutaneous hyperalgesia. Pain 32:77–88

Kitchen I (1984) Modification of an analgesy meter for paw-pressure antinociceptive testing in neonatal rats. J Pharmacol Meth 12:255–258

Perkins MN, Campell E, Dray A (1993) Antinociceptive activity of the bradykinin B_1 and B_2 receptor antagonists, des-Arg^9, [Leu^8]-BK and Hoe 140, in two models of persistent hyperalgesia in rats. Pain 53:191–197

Randall LO, Selitto JJ (1957) A method for measurement of analgesic activity on inflamed tissue. Arch Int Pharmacodyn 111:409–419

Rios L, Jacob JJC (1982) Inhibition of inflammatory pain by naloxone and its N-methyl quaternary analogue. Life Sci 31:1209–1212
Romer D (1980) Pharmacological evaluation of mild analgesics. Br J Clin Pharmacol 10:247S–251S
Takesue EI, Schaefer W, Jukniewicz E (1969) Modification of the Randall-Selitto analgesic apparatus. J Pharm Pharmacol 21:788–789
Tanaka K, Shimotori T, Makino S, Aikawa Y, Inaba T, Yoshida C, Takano S (1992) Pharmacological studies of the new anti-inflammatory agent 3-formylamino-7-methylsulfonyl-amino-6-phenoxy-4H-1-benzopyran-4-one. 1st Communication: anti-inflammatory, analgesic and other related properties. Arzneim Forsch/Drug Res 42:935–944
Vinegar R, Truax JF, Selph JL, Johnston PR (1989) Pharmacologic characterization of the algesic response to the subplantar injection of serotonin in the rat. Eur J Pharmacol 164:497–505
Vinegar R, Truax JF, Selph JL, Johnston PR (1990) New analgesic assay utilizing trypsin-induced hyperalgesia in the hind limb of the rat. J Pharmacol Meth 23:51–61
Winter CA, Flakater L (1965) Reaction thresholds to pressure in edematous hindpaws of rats and response to analgesic drugs. J Pharm Exp Ther 150:165–171
Winter CW, Risley EA, Nuss GW (1962) Carrageenin-induced edema in hind paw of the rat as an assay for antiinflammatory drugs. Proc Soc Exp Biol Med 111:544–547
Zhou S, Bonasera L, Carlton SM (1996) Peripheral administration of NMDA, AMPA, or KA results in pain behaviors of rats. NeuroReport 7:895–900

H.2.0.4 Mechanical Visceral Pain Model in the Rat

PURPOSE AND RATIONALE

Animal models designed to test the effectiveness of analgesic agents against visceral pain typically rely on noxious chemical irritation of the peritoneum, e. g., acetic acid and phenylquinone induced writhing tests based on acute inflammation. Ethical constraints prevent repeated assessments in a single animal, thereby compounding the difficulty of assessing development of tolerance to analgesic agents. To overcome these constraints, a model for mechanical visceral pain was developed based on repeatable and reversible distension of duodenum in the rat (Coburn et al. 1989; deLeo et al. 1989).

PROCEDURE

A one-piece balloon catheter is prepared composed of PE 50 tubing with a terminal latex rubber balloon which is 7.5 mm long and distensable to hold more than 1.5 ml fluid. Male Sprague Dawley rats weighing 175–200 g are anesthetized with N_2O and halothane. The abdomen is shaved and an 2.5 cm incision is made transversely just below the left costal margin. On the greater curvature of the stomach an incision is made 10 to 20 mm above the pylorus and a purse string is accomplished with 4–0 silk prior to gastrostomy. Through a 2 mm gastrostomy the catheter is introduced and advanced through the pylorus to the first portion of the duodenum (approximately 15–20 mm from the pylorus). The purse string is tied snugly closing the gastrostomy around the catheter. The catheter is tunneled to the base of the scull, externalized and anchored to the dermis with a silicon sleeve and suture. The animals recover from anesthesia within 5 min. Following a 4–5 days recovery period, the duodenal distension volume is determined by the mean threshold that produces writhing (usually 0.5 to 0.7 ml). For the test, the animals are randomized and administered either saline, the standard (0.1, 0.25, 1, and 10 mg/kg indomethacin i.p.) or the test drug in various doses prior to challenging. The animals are placed in a polypropylene box and challenged by inflating the balloon with saline, using a 1 ml calibrated syringe, pulsed 5 times over 30 s and then distended for 1 min. Behavioral responses are scored:

- 0 = Normal behavior defined as exploration, escape attempts and resting
- 1 = Slightly modified behavior defined as cessation of exploration, focusing, wet-dog shake, excessive facial grooming, teeth chattering and deep breathing
- 2 = Mildly to moderately modified behavior defined as retching-like activity, hunching, abdominal grooming or nipping and immobility of the hind limbs (disappears with removal of the stimulus).
- 3 = Severely modified behavior defined as stretch ing of the hindlimbs, arching and dorsoflection of the hind paws.
- 4 = Intensive visceromotor activity defined as repetitive stretching of the body, extension of the hind limbs, and pelvis, frequent rotating sideward, i. e., writhing.

EVALUATION

The average scores of the groups are plotted on semi log paper and ED_{50} values are determined by best line fit.

CRITICAL ASSESSMENT OF THE METHOD

In the mechanical visceral pain model in the rat, morphine and indomethacin have been found to be active but not other agents involved in prostaglandin inhibition, like acetylsalicylic acid and mefenamic acid. Other mechanisms besides those involving the arachidonic acid cascade have to be investigated.

MODIFICATIONS OF THE METHOD

Ness and Gebhart (1988) used colorectal distension as a noxious visceral stimulus in awake, unanesthetized, unrestrained rats. A 7–8 cm flexible latex balloon was inserted intra-anally under ether anesthesia and kept in position by taping to the base of the tail. Opening a solenoid gate to a constant pressure air reservoir initiated a 20 s, constant pressure stimulus in the descending colon and rectum. Femoral arterial and venous catheters were tunneled subcutaneously and exteriorized at the back of the neck. Teflon-coated stain-less steel wire electrodes were stitched into the external oblique musculature immediately superior to the inguinal ligament for electromyographic recordings. Blood pressure and heart frequency increase were proportional to the degree of colorectal distension. These effects could be dose-dependently antagonized by morphine and clonidine.

Renal pelvis distension with a pressure of 80 cm H_2O causes a decline in mean arterial blood pressure in pentobarbital-anesthetized rats. Brasch and Zetler (1982) used this blood pressure response, which disappears rapidly after cessation of the distension, to study the effects of analgesic drugs known to be effective in renal colic pain in man.

Moss and Sanger (1990) measured falls in diastolic blood pressure and intragastric pressure after distension of the duodenum by rapid application of intraluminal pressure (10–75 cm H_2O) in anesthetized rats. The distension-induced responses were blocked by pretreatment with morphine, an action reversible by injection of naloxone. Bilateral cervical vagotomy reduced the distension-evoked fall in intragastric pressure but had no effect on the corresponding fall in blood pressure.

REFERENCES AND FURTHER READING

Brasch H, Zetler G (1982) Caerulein and morphine in a model of visceral pain. Effects on the hypotensive response to renal pelvis distension in the rat. Naunyn-Schmiedeberg's Arch Pharmacol 319:161–167

Colburn RW, Coombs DW, Degnan CC, Rogers LL (1989) Mechanical visceral pain model: chronic intermittent intestinal distension in the rat. Physiol Behav 45:191–197

deLeo JA, Colburn RW, Coombs DW, Ellis MA (1989) The differentiation of NSAIDs and prostaglandin action using a mechanical visceral pain model in the rat. Pharmacol Biochem Behav 33:253–255

Moss HE, Sanger GJ (1990) Effects of granisetron, ICS 205–930 and ondansetron on the visceral pain reflex induced by duodenal extension. Br J Pharmacol 100:497–501

Ness TJ, Gebhart FG (1988) colorectal distension as a noxious visceral stimulus: physiologic and pharmacologic characterization of pseudoaffective reflexes in the rat. Brain Res 450:153–169

H.2.0.5 Antagonism Against Local Effects of Bradykinin

PURPOSE AND RATIONALE

Guzman et al. (1962) and Lim et al. (1964) described the responses (vocalization, respiratory and blood pressure changes) to intra-arterial injection of bradykinin and other algesic agents in cats and dogs. Deffenu et al. (1966) and Blane (1968) used the bradykinin-induced effects after intra-arterial injection in rats as an assay for analgesic drugs. Paravascular sensory nerves which accompany blood vessels throughout the body to end in unmyelinated free-branching terminals close to the capillaries and venules most likely carry the chemoreceptors of pain (Lim 1970). Due to rapid enzymatic degradation, bradykinin is ineffective as noxious stimulus after intravenous or oral administration.

PROCEDURE

Male Wistar rats weighing 280–320 g are lightly anesthetized with ether. A polyethylene catheter with an internal diameter of 0.5 mm is inserted centripetally into the right carotid artery. The catheter is passed through the subcutaneous tissues to protrude from the back of the animal. One hour after recovery from anesthesia, the first dose of bradykinin is injected into the catheter producing dextro-rotation of the head, flexing of the forelimb and occasionally squeaking. For each rat the minimum dose of bradykinin is determined necessary to provoke these effects. The test compounds are applied subcutaneously or intraperitoneally 15 min prior to injection of the threshold dose of bradykinin. The bradykinin injections are repeated in 5 min intervals until the bradykinin effect reappears. Each rat receives one drug at one dose level.

EVALUATION

The criterion for protection is the disappearance of the bradykinin effect after at least 2 consecutive doses of bradykinin. Using groups of 10 rats for various dose levels, ED_{50} values are calculated.

CRITICAL ASSESSMENT OF THE METHOD

Not only narcotic analgesics, but also pyrazolones and phenacetin or acetylsalicylic acid are active in this test. In some animals, the bradykinin-induced response can be diminished after repeated injections, classified as the noxious-adaptable group (Satoh et al. 1979).

MODIFICATIONS OF THE METHOD

Haubrich et al. (1990) tested analgesic activity by the intracarotid bradykinin-induced head/forepaw flexion in the rat. Male Charles River rats (280–320 g) fasted overnight were prepared surgically under light ether anesthesia by insertion of a capped polyethylene cannula (PE-60) centripetally into the right carotid artery and then exteriorizing the cannula to a harness on the back, to permit repeated i.a. injections. The rats were allowed to recover at least 2 h from the surgery, and then given single i.a. injections of bradykinin (triacetate salt in 0.2 ml 0.9% NaCl per injection) at 10-min intervals to determine the threshold dose which produced marked dextrorotation of the head and flexion of the right forepaw of each rat. This response was elicited by threshold doses of bradykinin ranging from 0.1 to 0.5 µg/injection. After administration of the test drugs, the response of the threshold dose of bradykinin was determined at 10-min intervals for 1 h and then at 20-min intervals during the second hour. ED_{50} values were determined by probit analysis of the maximum percentage of rats that failed to respond to bradykinin at each dose of test drug any time within the 2-h test period.

Collier and Lee (1963) described nociceptive responses of **guinea pigs** to intradermal injections of bradykinin and kallidin-10.

Vargaftig (1966) measured the effect of nonnarcotic analgesics on the hypotension induced by intra-arterial injection of bradykinin in **rabbits**.

Adachi and Ishii (1979) used the response to injection of bradykinin into the femoral artery of guinea pigs for quantitative assessment of analgesic agents.

Griesbacher and Lembeck (1987) and Lembeck et al. (1991) used the reflex hypotensive response as an indicator of nociception after injection of bradykinin into the ear artery of anesthetized rabbits. Rabbits were anesthetized and the blood pressure was recorded from the carotid artery. The central artery of one ear was cannulated and the ear was separated from the head with the exception of the auricular nerve, which remained connected to the head. The ear was perfused with Tyrode solution to which acetylcholine and bradykinin were added. The reflex fall in blood pressure induced by bradykinin and acetylcholine were monitored. The effect could be inhibited by bradykinin antagonists.

Heapy et al. (1993) tested the effects of the bradykinin antagonist HOE140 on the abdominal constriction response after intraperitoneal injection of bradykinin to **mice**.

Further Methods Used to Study the Role of Bradykinin and Bradykinin Antagonists in Inflammation and Algesia

Teixeira et al. (1993) investigated the mechanisms of inflammatory response induced by extracts of *Schistosoma mansoni* larvae in guinea pig skin. *Biomphalaria glabrata* snails with patent *Schistosoma mansoni* infections were induced to shed cercariae by exposure to light and water with a temperature of 31°C. The cercariae were concentrated, homogenized and extracts prepared. Purified eosinophils or neutrophils obtained from peritoneal exudates were radiolabeled by incubation with ^{111}In chelated to 2-mercaptopyridine-*N*-oxide. Radiolabeled leukocyte infiltration and edema formation were measured simultaneously at injected skin sites. [^{125}I]Human serum albumin was added to the labeled leukocytes and these were injected i.v. into anesthetized guinea pigs. After 15 min the extracts of cercariae were locally injected with/or without the inhibitors. After 2 h, the animals were sacrificed and the injected sites were punched out with a 17-mm punch. Serum exudation and leukocyte infiltration were measured by counting the two isotopes. The bradykinin antagonist HOE 140 reduced substantially the extract-induced inflammation.

Ahluwalia et al. (1994) induced plasma protein extravasation in the rat urinary bladder by i.p. injection of cyclophosphamide mediated by capsaicin-sensitive primary afferent neurons which could be significantly inhibited by the bradykinin B_2 receptor antagonist HOE140 and the tachykinin NK_1 receptor antagonist RP67,580.

Davis and Perkins (1994a, b) described a model of persistent inflammatory mechanical hyperalgesia using intra-articular injections of bradykinin or cytokines into the knee joint of rats.

Lecci et al. (1995) analyzed the local and reflex responses to bradykinin on rat urinary bladder motility *in vivo*.

REFERENCES AND FURTHER READING

Adachi KI, Ishii Y (1979) Vocalization response to close-arterial injection of bradykinin and other algesic agents in guinea pigs and its application to quantitative assessment of analgesic agents. J Pharm Exp Ther 209:117–124

Ahluwalia A, Maggi CA, Santicioli P, Lecci A, Giuliani S (1994) Characterization of the capsaicin-sensitive component of cyclophosphamide-induced inflammation in the rat urinary bladder. Br J Pharmacol 111:1017–1022

Beck PW, Handwerker HO (1974) Bradykinin and serotonin effects on various types of cutaneous nerve fibres. Pflügers Arch 347:209–222

Blane GF (1968) A new laboratory model for evaluating analgesic and analgesic-antagonist drugs. In: Soulairac A,

Cahn J, Charpentier J (eds) Pain. Academic Press, London, New York, pp 218–222
Collier HOJ, Lee IR (1963) Nociceptive responses of guinea-pigs to intradermal injections of bradykinin and kallidin-10. Br J Pharmacol 21:155–164
Davis AJ, Perkins MN (1994a) Induction of B1 receptors *in vivo* in a model of persistent mechanical hyperalgesia in the rat. Neuropharm 33:127–133
Davis AJ, Perkins MN (1994b) Involvement of bradykinin B_1 and B_2 receptor mechanisms in cytokine-induced mechanical hyperalgesia in rats. Br J Pharmacol 113:63–68
Deffenu G, Pegrasso L, Lumachi B (1966) The use of bradykinin-induced effects in rats as an assay for analgesic drugs. J Pharm Pharmac 18:135
Griesbacher T, Lembeck F (1987) Effect of bradykinin antagonists on bradykinin-induced plasma extravasation, venoconstriction, prostaglandin E_2 release, nociceptor stimulation and contraction of the iris sphincter muscle in the rabbit. Br J Pharmacol 92:333–340
Guzman F, Braun C, Lim RKS (1962) Visceral pain and the pseudoaffective response to intra-arterial injection of bradykinin and other algesic agents. Arch Int Pharmacodyn 136:353–384
Heapy CG, Shaw JS, Farmer SC (1993) Differential sensitivity of antinociceptive assays to the bradykinin antagonist Hoe 140. Br J Pharmacol 108:209–213
Haubrich DR, Ward SJ, Baizman E, Bell MR, Bradford J, Ferrari R, Miller M, Perrone M, Pierson AK, Saelens JK, Luttinger D (1990) Pharmacology of pravodoline: a new analgesic agent. J Pharmacol Exp Ther 255:511–521
Lecci A, Giuliani S, Meine S, Maggi CA (1995) Pharmacological analysis of the local and reflex responses to bradykinin on rat urinary bladder motility *in vivo*. Br J Pharmacol 114:708–714
Lembeck F, Griesbacher T, Eckhardt M, Henke S, Breipohl G, Knolle J (1991) New, long acting, potent bradykinin antagonists. Br J Pharmacol 102:297–304
Lim RKS (1970) Pain. Annu Rev Physiol 32:269–288
Lim RKS, Guzman F (1968) Manifestations of pain in analgesic evaluation in animals and man. In: Soulairac A, Cahn J, Charpentier J (eds) Pain. Academic Press, London, New York, pp 119–152
Lim RKS, Guzman F, Rodgers DW, Goto K, Braun C, Dickerson GD, Engle RJ (1964) Site of action of narcotic and non-narcotic analgesics determined by blocking bradykinin-evoked visceral pain. Arch Int Pharmacodyn 152:25–58
Satoh M, Kawajiri SI, Yamamoto M, Makino H, Takagi H (1979) Reversal by naloxone of adaptation of rats to noxious stimuli. Life Sci 24:685–690
Teixeira MM, Doenhoff MJ, McNeice C, Williams TJ, Hellewell G (1993) Mechanisms of the inflammatory response induced by extracts of *Schistosoma mansoni* larvae in guinea pig skin. J Immunol 151:5525–5534
Vargaftig B (1966) Effet des Analgésiques non narcotiques sur l'hypotension due à la Bradykinine. Experientia 22:182–183

H.2.0.6 Effect of Analgesics on Spinal Neurons

PURPOSE AND RATIONALE

The mode of action of peripheral analgesics is still a matter of debate. Besides inhibition of the arachidonic acid derived pathway, activities on the spinal and central level have been discussed. Schaible and Schmidt (1983a, b, 1985, 1987, 1988) performed electrophysiological experiments in anesthetized cats and rats after local mechanical stimulation and after induction of acute arthritis of the knee joint. With this method Xe et al. (1990a, b), Neugebauer et al. (1994) found evidence for a spinal antinociceptive action of antipyretic analgesics, such as dipyrone.

PROCEDURE

In cats weighing 2.0–4.0 kg anesthesia is induced by i.m. injection of 15–30 mg/kg ketamine hydrochloride followed by i.v. injection of 60 mg/kg α-chloralose. After immobilization with i.v. pancuronium bromide the cats are artificially ventilated. The skin of the right thigh is incised from rostral of the inguinal fossa to a point below the medial condyle of the tibia. The tendon of the sartorius muscle is cut close to its insertion at the capsule of the knee joint. The muscle is removed to expose the medial aspects of the joint and the medial articular nerve (MAN). The thigh is rigidly fixed to the mounting table by a threaded bolt fitted through the femur so that the lower leg can be flexed and extended in the horizontal plane. The saphenous nerve is cut in the inguinal fossa for recording. Bipolar electrodes are inserted at the MAN near the knee for en passent stimulation of articular afferents. **Extracellular recordings from single MAN units** in the saphenous nerve are performed using platinum wire electrodes. According to their conduction velocities units are classed as group IV afferents (<2.5 m/s, unmyelinated axons) or group III afferents (2.5–20 m/s, thinly myelinated axons).

For **recordings from spinal cord neurons** the spinal segments T12–L7 are exposed by laminectomy. The spinal cord is transected at the lower thoracic region after injection of 0.1 ml of 1% procaine hydrochloride solution to prevent mechanical activation of axons in the long spinal tracts. The animals are fixed to a rigid frame with spinal and pelvic clamps. A pool is formed by skin flaps and filled with warm paraffin oil. The upper lumbar spinal cord is mounted on a pair of platinum wire stimulating electrodes surrounding the whole cord. Ascending tract neurons are identified by electrical stimulation (Neugebauer and Schaible 1990). Single spinal neurons that can be excited by mechanical stimulation of the knee joint tissue are recorded extracellularly using glass-insulated carbon filament electrodes. The neurons are either nociceptive specific neurons responding only to noxious mechanical stimuli or wide dynamic range neurons re-

sponding to innocuous stimuli but showing strongest responses to stimuli of noxious intensity.

Acute arthritis in the right knee joint is induced several hours before recordings are started by injecting 0.3–0.5 ml of 4% kaolin suspension and 15–20 min later 0.3 ml of 2% carrageenan solution. Acute arthritis develops within 1–3 h.

Action potentials are displayed on a storage oscilloscope, amplified, filtered, fed to a window discriminator and processed using an interface and a personal computer for construction of peristimulus time histograms. After a control period of at least 40 min during which a stable discharge rate of the afferent or spinal cord unit is obtained, the test substances are administered i.v. in various doses. Effects of the test substance on ongoing and mechanically evoked activity (by movements, pressure stimuli) are determined.

EVALUATION

Ongoing activity is counted every min. The means and standard deviations in 10 min periods are calculated before and after drug application. The values after drug injection are calculated as percentage of control values. To calculate the net effects of the different mechanical stimuli, the number of impulses in the preceding 30 s is subtracted from the total discharges during the stimulus. The responses to at least 4 stimuli before drug application are averaged and set to 100%. The responses to the different mechanical stimuli after drug administration are expressed as a percentage of the controls. Statistical significance is evaluated using the *t*-test for unpaired samples.

MODIFICATIONS OF THE METHOD

Using the model of kaolin-induced arthritis in the knee of rats, Han and Neugebauer (2005) and Han et al. (2005) developed a computerized analysis of audible and ultrasonic vocalizations of rats as a standardized measure of pain-related behavior.

Several other electrophysiological methods have been applied to elucidate the mode of action of non-opioid analgesic agents. Carlsson et al. (1986, 1988), Jurna and Brune (1990) recorded the activity from single neurons in the dorsomedial part of the ventral nucleus of the thalamus in rats. Activity was elicited by supramaximal stimulation of nociceptive afferents in the sural nerve. In addition, activity was recorded in ascending axons of the spinal cord.

Chapman and Dickenson (1992) studied the spinal and peripheral roles of bradykinin and prostaglandins in nociceptive processing in the rat by recording C-fibre activity in the dorsal spinal horn after injection of formalin into the center of the respective field of the toe of the hind paw.

Dray et al. (1992) described a preparation of the neonatal rat spinal cord with functionally connected tail maintained *in vitro*. The preparation was placed in a chamber and the spinal-cord and tail were separately superfused with a physiological salt solution. Peripheral nociceptive fibers were activated by superfusion of the tail with bradykinin, capsaicin or by a superfusate heated to 48–50°C (noxious heat). The activation of peripheral fibres was assessed by measuring the depolarization produced in a spinal ventral root.

Malmberg and Yaksh (1992) described a direct analgesic action of NSAIDs through spinal cyclooxygenase inhibition by blocking the thermal hyperalgesia in rats induced after intrathecal administration of excitatory amino acids or substance P.

A simple technique for intrathecal injections by lumbar puncture in unanesthetized mice was described by Hylden and Wilcox (1980).

Mestre et al. (1994) described a method for performing direct intrathecal injections in rats without introducing a spinal catheter.

Bahar et al. (1984) performed chronic implantations of nylon catheters into the subarachnoid space of Wistar rats and marmosets and tested the effects of local anesthetics.

McQueen et al. (1991) investigated the effects of paracetamol and lysine acetylsalicylate on high-threshold mechano-nociceptors by recording neural activity from the inflamed ankle joint in anesthetized rats with mild adjuvant-induced mono-arthritis.

Yamamoto and Yaksh (1992) studied the effects of excitatory amino acid antagonists administered through chronically implanted lumbar intrathecal catheters on the thermal hyperesthetic state induced by unilateral partial ligation of the sciatic nerve in rats.

Hashimoto and Fukuda (1990) described a spinal cord injury model produced by spinal cord compression in the rat.

Aanonsen and Wilcox (1987) tested effects of spinally administered opioids, phencyclidine and sigma agonists on the action of intrathecally administered NMDA in the tail-flick, hot-plate and biting and scratching nociceptive tests in **mice**.

Brambilla et al. (1996) demonstrated that intrathecal administration of AMPA produced a dose-dependent behavioral syndrome in mice characterized by caudally directed biting, which could be antagonized by peripheral administration of AMPA-receptor and NMDA-receptor antagonists.

Aanonsen et al. (1990) tested the effect of iontophoretically applied excitatory amino acid agonists, such as NMDA, AMPA, quisqualate and kainate, on the firing rate of rat spinal neurons after peripheral noxious stimulation.

Cumberbatch et al. (1994) studied the roles of receptors for AMPA in spinal nociceptive and non-nociceptive transmission on dorsal horn wide dynamic range neurones in anesthetized spinalized rats. The effects of systemically administered competitive and non-competitive AMPA antagonists were examined on responses to peripheral noxious heat and non-noxious tap stimuli as well as to iontophoretic AMPA and NMDA.

With this technique, Chizh et al. (1994) studied the effects of intravenous administration of AMPA antagonists to iontophoretically applied excitatory amino acids.

Watkins et al. (1994) induced hyperalgesia in rats by intraperitoneally administered lipopolysaccharides as measured by radiation heat tail flick in rats. Intrathecal catheters were implanted into the subdural space surrounding the spinal cord to test the involvement of excitatory amino acids, substance P, CCK and opioids assessing the effects of antagonists.

Mjellem et al. (1993) produced a behavioural syndrome of caudally directed biting in mice by intrathecal injection of either NMDA or AMPA.

REFERENCES AND FURTHER READING

Aanonsen LM, Wilcox GL (1987) Nociceptive action of excitatory amino acids in the mouse: effects of spinally administered opioids, phencyclidine and sigma agonists. J Pharmacol Exp Ther 243:9–19

Aanonsen LM, Lei S, Wilcox GL (1990) Excitatory amino acid receptors and nociceptive neurotransmission in rat spinal cord. Pain 41:309–321

Bahar M, Nunn JF, Rosen M, Flecknell P (1984) Differential sensory and motor blockade after spinal cocaine in the rat and marmoset. Eur J Anaesthesiol 1:31–36

Brambilla A, Prudentio A, Grippa N, Borsini F (1996) Pharmacological characterization of AMPA-induced biting behavior in mice. Eur J Pharmacol 305:115–117

Carlsson KH, Helmreich J, Jurna I (1986) Comparison of central antinociceptive and analgesic effects of the pyrazolone derivatives, metamizol (Dipyrone) and aminophenzone ("Pyramidon"). Schmerz – Pain – Douleur 3:93–100

Carlsson KH, Monzel W, Jurna I (1988) Depression of morphine and the non-opioid analgesic agents, metamizol (dipyrone), lysine acetyl salicylate, and paracetamol, of activity in rat thalamus neurons evoked by electrical stimulation of nociceptive afferents. Pain 32:313–326

Chapman V, Dickenson AH (1992) The spinal and peripheral roles of bradykinin and prostaglandins in nociceptive processing in the rat. Eur J Pharmacol 219:427–433

Chizh BA, Cumberbatch MJ, Headley PM (1994) A comparison of intravenous NBQX and GYKI 53655 as AMPA antagonists in the rat spinal cord. Br J Pharmacol 112:843–846

Cumberbatch MJ, Chizh BA, Headley PM (1994) AMPA receptors have an equal role in spinal nociceptive and non-nociceptive transmission. NeuroReport 5:877–880

Dray A, Patel IA, Perkin MN, Rueff A (1992) Bradykinin-induced activation of nociceptors: receptor and mechanistic studies on the neonatal rat spinal cord-tail preparation *in vitro*. Br J Pharmacol 107:1129–1134

Han JS, Neugebauer V (2005) mGluR1 and mGluR5 antagonists in the amygdala inhibit different components of audible and ultrasonic vocalization in a model of arthritic pain. Pain 113:211–222

Han JS, Bird GC, Li W, Jones J, Neugebauer V (2005) Computerized analysis of audible and ultrasonic vocalizations of rats as a standardized measure of pain-related behavior. J Neurosci Methods 141:261–269

Hashimoto T, Fukuda N (1990) New spinal cord injury model produced by spinal cord compression in the rat. J Pharmacol Meth 23:203–212

He X, Neugebauer V, Schaible HG, Schmidt RF (1990a) Effects of antipyretic analgesics on pain-related neurons of the spinal cord. In: Brune K, Santoso B (eds) Antipyretic Analgesics: New Insights. Birkhäuser Verlag, Basel, pp 13–23

He X, Neugebauer V, Schaible HG, Schmidt RF (1990b) New aspects of the mode of action of dipyrone. In: Brune K (ed) New Pharmacological and Epidemiological Data in Analgesics Research. Birkhäuser Verlag, Basel, pp 9–18

Hylden JLK, Wilcox GL (1980) Intrathecal morphine in mice: a new technique. Eur J Pharmacol 67:313–316

Jurna I, Brune K (1990) Central effect of the non-steroid anti-inflammatory agents, indomethacin, ibuprofen, and diclofenac, determined in C fibre-evoked activity in single neurons of rat thalamus. Pain 41:71–80

Malmberg AB, Yaksh TL (1992) Hyperalgesia mediated by spinal glutamate or substance P receptor blocked by spinal cyclo-oxygenase inhibition. Science 257:1276–1279

McQueen DS, Iggo A, Birrell GJ, Grubb BD (1991) Effects of paracetamol and aspirin on neural activity of joint mechanoceptors in adjuvant arthritis. Br J Pharmacol 104:178–182

Mestre C, Pélissier T, Fialip J, Wilcox G, Eschalier A (1994) A method to perform direct transcutaneous intrathecal injections in rats. J Pharmacol Toxicol Meth 32:197–200

Mjellem N, Lund A, Hole K (1993) Different functions of spinal 5-HT_{1A} and 5-HT_2 receptor subtypes in modulating behaviour induced by excitatory amino acid receptor agonists in mice. Brain Res 626:78–82

Neugebauer V, Schaible HG (1990) Evidence for a central component in the sensitization of spinal neurons with joint input during development of acute arthritis in cat's knee. J Neurophysiol 64:299–311

Neugebauer V, Schaible HG, He X, Lücke T, Gündlich P, Schmidt RF (1994) Electrophysiological evidence for a spinal anti-nociceptive action of dipyrone. Agents Actions 41:62–70

Schaible HG, Schmidt RF (1983a) Responses of fine medial articular nerve afferents to passive movements of knee joint. J Neurophysiol 49:1118–1126

Schaible HG, Schmidt RF (1983b) Activation of groups III and IV sensory units in medial articular nerve by local mechanical stimulation of knee joint. J Neurophysiol 49:35–44

Schaible HG, Schmidt RF (1985) Effects of an experimental arthritis on the sensory properties of fine articular afferent units. J Neurophysiol 54:1109–1122

Schaible HG, Schmidt RF (1988) Time course of mechanosensitivity changes in articular afferents during a developing experimental arthritis. J Neurophysiol 60:2180–2195

Schaible HG, Schmidt RF, Willis WD (1987) Enhancement of the responses of ascending tract cells in the cat spinal cord by acute inflammation of the knee joint. Exp Brain Res 66:489–499
Szolcsányi J (1996) Capsaicin-sensitive sensory nerve terminals with local and systemic efferent functions: facts and scopes of an unorthodox neuroregulatory mechanism. Progr Brain Res 113:343–359
Watkins LR, Wiertelak EP, Furness LE, Maier SF (1994) Illness-induced hyperalgesia is mediated by spinal neuropeptides and excitatory amino acids. Brain Res 664:17–24
Yamamoto T, Yaksh TL (1992) Spinal pharmacology of thermal hyperesthesia induced by constriction injury of sciatic nerve. Excitatory amino acid antagonists. Pain 49:121–128

H.2.0.7
Antagonism to Nerve Growth Factor

H.2.0.7.1
General Considerations on Nerve Growth Factor

Nerve growth factor (NGF) is a member of the neurotrophin family of structurally related secreted proteins that includes brain-derived neurotrophic factor (BDNF), neurotrophin 3 (NT-3) and NT-4. Mature neurotrophins are homodimers that are derived by proteolytic cleavage from precursor proteins encoded by separate genes. They bind to two types of receptor: a common receptor, $p75^{NTR}$, which binds all neurotrophins with a similar affinity; and members of the trk family of receptor tyrosine kinases, trkA, trkB and trkC, which bind different neurotrophins.

NGF and BDNF have a crucial role in the generation of pain and hyperalgesia in several acute and chronic pain states (Woolf et al. 1994; McMahon 1996; Mannion et al. 1999; Thompson et al. 1999; Pezet et al. 2002; Allen and Dawbarn 2006). The expression of NGF is high in injured and inflamed tissues, and activation of the receptor tyrosine kinase trkA in nociceptive neurons triggers and potentiates pain signaling by multiple mechanisms (McMahon et al. 1995; Huang and Reichardt 2003; Hefti et al. 2006) (see also F.2.0.10).

An effective pain therapeutic needs to prevent the activation of trkA by NGF. This may be achieved by agents that remove free NGF, by molecules that prevent binding to trkA, and by molecules that prevent activation of trkA.

REFERENCES AND FURTHER READING

Allen SJ, Dawbarn D (2006) Clinical relevance of the neurotrophins and their receptors. Clin Sci 110:175–191
Hefti FF, Rosenthal A, Walicke PA, Wyatt S, Vergara G, Shelton DL, Davies AM (2006) Novel class of pain drugs based on antagonism of NGF. Trends Pharmacol Sci 27:85–91
Huang EJ, Reichardt LF (2003) trk receptors: roles in neuronal signal transmission. Annu Rev Biochem 72:609–642
Mannion RJ, Costigan M, Decosterd I, Amaya F, Ma PQ, Holstege JC, Ji RR, Acheson A, Lindsay RM, Wilkinson GA, Woolf CJ (1999) Neurotrophins: peripherally and centrally acting modulators of tactile stimulus-induced inflammatory pain hypersensitivity. Proc Natl Acad Sci USA 96:9385–9390
McMahon SB (1996) NGF as a mediator of inflammatory pain. Philos Trans R Soc Lond B Biol Sci 351:431–440
McMahon SB, Bennett DL, Priestley JV, Shelton DL (1995) The biological effects of endogenous nerve growth factor on adult sensory neurons revealed by a trkA-IgG fusion molecule. Nat Med 1:774–780
Pezet S, Malcangio M, McMahon SB (2002) BDNF: a neuromodulator in nociceptive pathways? Brain Res Rev 40:240–249
Thompson SWN, Bennett DLH, Kerr BJ, Bradbury EJ, McMahon SB (1999) Brain-derived neurotrophic factor is an endogenous modulator of nociceptive responses in the spinal cord. Proc Natl Acad Sci USA 96:7714–7718
Woolf CJ, Safieh-Garabedian B, Ma PQ, Crilly P, Winter J (1994) Nerve growth factor contributes to the generation of inflammatory hypersensitivity. Neuroscience 62:327–331

H.2.0.7.2
In Vitro Assays of Nerve Growth Factor

PURPOSE AND RATIONALE

The neurotrophin nerve growth factor (NGF) binds to two receptor types: the tyrosine kinase receptor TrkA and the common neurotrophin receptor $p75^{NTR}$. Although many of the biological effects of NGF (such as neuronal growth and survival) are associated with TrkA activation, $p75^{NTR}$ also contributes to these activities by enhancing the action of TrkA when receptors are coexpressed (Verdi et al. 1994; Kaplan and Miller 1997). Colquhoun et al. (2004) studied the NGF antagonist PD90780 (Spiegel et al. 1995), which interacts with NGF, preventing its binding to $p75^{NTR}$. In this study, the actions of this compound were further explored, and it was found that PD90780 is not able to inhibit the binding of either brain-derived neurotrophic factor or neurotrophin-3 to $p75^{NTR}$, consistent with the direct interactions of the antagonist with NGF. In addition, it was demonstrated that the ability of PD90780 to inhibit NGF-$p75^{NTR}$ interactions is lower when receptors are coexpressed, compared with when $p75^{NTR}$ is the only neurotrophin receptor expressed.

PROCEDURE

Radiolabeled Neurotrophin and Receptor Preparation

The iodination of NGF (mouse 2.5s; Cedarlane Labs, Toronto, ON) and rhBDNF (Alomone Labs, Jerusalem, Israel) was performed as described by Sutter et al. (1979) with modification (Ross et al. 1997). The ability of PD90780 to block neurotrophin binding to the $p75^{NTR}$ receptor was evaluated under various receptor conditions. This was accomplished with

the use of PC12 cells (TrkA and $p75^{NTR}$), $PC12^{nnr5}$ cells ($p75^{NTR}$ only), and truncated $p75^{NTR}$. The two cell types were cultured in RPMI 1640 medium with 10% fetal calf serum. Recovery of the cells was permitted with the replacement of the medium with calcium/magnesium-free balanced salt solution followed by a 15-min incubation at 37°C. Cells were centrifuged, and pellets were suspended in HKR buffer (10 mM HEPES, pH 7.35 containing 125 mM NaCl, 4.8 mM KCl, 1.3 mM $CaCl_2$, 1.2 mM $MgSO_4$, 1.2 mM KH_2PO_4, 1 g/l glucose, and 1 g/l bovine serum albumin). In the case of truncated $p75^{NTR}$, the culture medium used to grow PC12 cells was removed and centrifuged to ensure it was free of cells. This medium contained $p75^{NTR}$ extracellular domains previously sloughed by the cells (molecular weight approximately 50 kDa) (DiStefano and Johnson 1988).

Chemical Cross-Linking of ^{125}I-NGF to TrkA and/or $p75^{NTR}$ in the Presence of Antagonists and Immunoprecipitation

^{125}I-NGF (0.1 nM) alone or in combination with NGF (100 nM), BDNF (10 nM), or PD90780 (100 μM) was incubated with PC12 cells at a concentration of 10^6 cells/ml in HKR buffer in a volume of 1 ml for 2 h at 4°C with rocking. After binding, 20 μl of the cross-linker bis-(sulfosuccinimidyl)suberate (BS^3) was added (final concentration of 0.4 mM) to each sample and incubated at room temperature for 30 min. The cells were washed three times with TBS, after which reducing SDS sample buffer was added to the pelleted cells to dissolve the proteins, or in the case of immunoprecipitations prepared as described below. Cell samples undergoing immunoprecipitations for TrkA or $p75^{NTR}$ were solubilized in lysis buffer (TBS containing 10% glycerol, 1% Triton X-100, 1 mM phenylmethylsulfonyl fluoride, 10 μg/ml aprotinin, and 1 μg/ml leupeptin) and incubated for 40 min at 4°C. After centrifugation, the lysates were removed to a new tube, and either rabbit polyclonal anti-Trk cytoplasmic domain antibody or rabbit polyclonal anti-$p75^{NTR}$ antibody (9992) (antisera against glutathione *S*-transferase-fusion protein containing the cytoplasmic domain of $p75^{NTR}$) was added to the soluble proteins to isolate the respective receptors. The samples were left to incubate at 4°C overnight. Antibody complexes were removed through application and incubation with 70 μl of a 50% slurry of immobilized Protein G (Pierce Chemical, Rockford, Ill., USA) for 2 h at 4°C. The solid phase was washed with lysis buffer three times, with distilled water once, and then the proteins were dissolved in SDS sample buffer. Proteins from cross-linking and immunoprecipitation experiments were separated via 6% SDS-polyacrylamide gel electrophoresis (PAGE).

Chemical Cross-Linking of ^{125}I-NGF to $p75^{NTR}$ and Concentration Effect Assays

^{125}I-NGF was incubated at 4°C for 2 h with or without PD90780. PC12 or $PC12^{nnr5}$ cells were added at 10^6 cells/ml, and samples were incubated at 4°C for 2 h with rocking. Bound ^{125}I-NGF and $p75^{NTR}$ proteins were cross-linked with final concentrations of 5 mM 1-ethyl-3-(3-dimethylaminopropyl)carbodiimide (EDC) and 2 mM sulfo-*N*-hydroxy-sulfosuccinimide (SNHS) (20 μl of each) and incubated with rocking at room temperature for 30 min. Samples were washed with TBS [10 mM Tris(hydroxymethyl)-aminomethane, pH 8.0, and 150 mM NaCl] three times before the addition of reducing SDS sample buffer to dissolve the proteins. The proteins were then separated on a 6% SDS-PAGE gel. In the experiments involving truncated $p75^{NTR}$, ^{125}I-NGF or ^{125}I-BDNF was exposed to the same concentrations of PD90780 and incubated with medium containing truncated $p75^{NTR}$ before cross-linking with EDC/SNHS. The reaction was quenched by adding 15 μl of 1 M glycine followed by 10 min of mixing. The samples were then immunoprecipitated using 192 IgG, which recognizes the extracellular domain of $p75^{NTR}$ (Calbiochem, San Diego, Calif., USA).

Neurotrophin Receptor Binding

Neurotrophins NGF, BDNF, and NT-3 were iodinated, and PC12 and $PC12^{nnr5}$ cells were cultivated and recovered as previously described. Tubes were set up containing single data points that held iodinated neurotrophin (0.5 nM), PD90780 (10 μM), a final concentration of 10^6 cells/ml and NGF (at 50 nM for nonspecific binding) as required, and were then incubated at 4°C for 2 h. Aliquots (100 μl) were layered on top of 200 μl of 10% glycerol in HKR buffer in 0.4-ml tubes. Samples were then centrifuged at 5000 rpm for 2 min, after which the tip containing the cell pellet was cut off and radioactivity present was determined.

TrkA Phosphorylation Assay

Modification of the methods described permitted determination of TrkA phosphorylation (Ross et al. 1998). NGF (40 pM) was incubated with varying concentrations of PD90780 (3, 30, or 300 μM) for 2 h in HKR buffer. PC12 cells used at 10^6 cells/ml were incubated with NGF and PD90780 solutions for 15 min at 37°C. Samples were washed once with cold PBS and once with cold TBS and then lysed with solutions

containing 500 μM orthovanadate and immunoprecipitated with anti-Trk antibody as previously described. An SDS-PAGE run on 6% gel followed by Western blot analysis performed with antiphosphotyrosine antibody (4G10; UBI, Lake Placid, N.Y., USA) and visualized with ECL (Amersham) permitted the resolution of isolated phosphoproteins. The resulting bands were quantified via densitometry analysis.

NGF Protomer Cross-Linking

^{125}I-NGF (0.1 nM) was incubated for 2 h at 4°C with $ZnCl_2$ (100 μM), PD90780 (30 μM), or $ZnCl_2$ and PD90780 (100 and 30 μ M, respectively), along with HKR buffer, for a total volume of 0.1 ml. After incubation, BS^3 was added (final concentration of 0.4 mM) in 5 μl volume and set at room temperature for 30 min. Proteins were dissolved with the addition of 50 μl of SDS sample buffer and heating to 95°C for 10 min. Separation of ^{125}I-NGF dimers and ^{125}I-NGF monomers was completed using a 15% acrylamide gel SDS-PAGE.

EVALUATION

Following SDS-PAGE, gels were fixed and dried, and the radio-iodinated ligands cross-linked to receptors were detected via autoradiography. Receptor ligand bands within SDS-PAGE gels were excised, and radioactivity within each band was detected with a Beckman gamma counter. The concentration–effect curves, SEM, IC_{50} values, and 95% confidence intervals (CIs) described in the concentration–effect studies were determined by non-linear regression analyses and carried out by the program GraphPad Prism, version 3.00 (GraphPad Software, San Diego, Calif., USA).

MODIFICATIONS OF THE METHOD

Debeir et al. (1999) described a nerve growth factor mimetic TrkA antagonist that causes withdrawal of cortical cholinergic boutons in the adult rat. A small peptide, C(92–96), which blocks NGF–TrkA interactions, was delivered stereotactically into the rat cortex over a 2-week period, and its effect and potency were compared with those of an anti-NGF monoclonal antibody (mAb NGF30). Two presynaptic antigenic sites were studied by immunoreactivity, and the number of presynaptic sites was counted by using an image analysis system. Synaptophysin was used as a marker for overall cortical synapses, and the vesicular acetylcholine transporter was used as a marker for cortical cholinergic presynaptic sites.

Owolabi et al. (1999) characterized the antiallodynic actions of ALE-0540, a novel nerve growth factor receptor antagonist that inhibits the binding of NGF to tyrosine kinase (Trk) A or both p75 and TrkA (IC_{50} 5.88± 1.87 μM, 3.72±1.3 μM, respectively), as well as signal transduction and the biological responses mediated by TrkA receptors.

REFERENCES AND FURTHER READING

Colquhoun A, Lawrence GM, Shamovsky IL, Riopelle RJ, Ross GM (2004) Differential activity of the Nerve Growth Factor (NGF) antagonist PD90780 [7-(Benzolylamino)-4,9-dihydro-4-methyl-9-oxo-pyrazolo[5,1-*b*]quinazoline-2-carboxylic Acid] suggests altered NGF-$p75^{NTR}$ interactions in the presence of TrkA. J Pharmacol Exp Ther 310:505–511

Debeir T, Sargovi HU, Cuello AC (1999) A nerve growth factor mimetic TrkA antagonist causes withdrawal of cortical cholinergic boutons in the adult rat. Proc Natl Acad Sci USA 96:4067–4072

DiStefano PS, Johnson EM Jr (1988) Identification of a truncated form of the nerve growth factor receptor. Proc Natl Acad Sci USA 85**:**270–274

Kaplan DR, Miller FD (1997) Signal transduction by the neurotrophin receptors. Curr Opin Cell Biol 9:213–221

Owolabi JB, Rizkalla G, Tehim A, Ross GM, Riopelle RJ, Kamboj R, Ossipov M, Bian D, Wegert S, Porreca F, Lee DKH (1999) Characterization of antiallodynic actions of ALE-0540, a novel nerve growth factor receptor antagonist, in the rat. J Pharmacol Exp Ther 289:1271–1276

Ross GM, Shamovsky IL, Lawrance G, Solc M, Dostaler SM, Jimmo SL, Weaver DF, Riopelle RJ (1997) Zinc alters conformation and inhibits biological activities of nerve growth factor and related neurotrophins. Nat Med 3:872–878

Ross GM, Shamovsky IL, Lawrance G, Solc M, Dostaler SM, Weaver DF, Riopelle RJ (1998) Reciprocal modulation of TrkA and $p75^{NTR}$ affinity states is mediated by direct receptor interactions. Eur J Neurosci 10:890–898

Spiegel K, Agrafiotis D, Caprathe B, Davis RE, Dickerson MR, Fergus JH, Hepburn TW, Marks JS, Van Dorf M, Wieland DM, Jae JC (1995) PD 90780, a nonpeptide inhibitor of nerve growth factor's binding to the p75 NGF receptor. Biochem Biophys Res Commun 217:488–494

Sutter A, Riopelle RJ, Harris-Warrick RM, Shooter EM (1979) Nerve growth factor receptors. Characterization of two distinct classes of binding sites on chick embryo sensory ganglia cells. J Biol Chem 254:5972–5982

Verdi JM, Birren SJ, Ibáñez CF, Persson H, Kaplan DR, Benedetti M, Chao MV, Anderson DJ (1994) $p75^{LNGFR}$ regulates Trk signal transduction and NGF-induced neuronal differentiation in MAH cells. Neuron 12:733–745

H.2.0.7.3 In Vivo Assays of Nerve Growth Factor Antagonism

PURPOSE AND RATIONALE

Many studies indicate the role of NGF in pain perception.

Herzberg et al. (1997) reported NGF involvement in pain induced by chronic constriction injury of the rat sciatic nerve.

Ma and Woolf (1997) reported that the progressive tactile hyperalgesia induced by peripheral inflammation is nerve growth factor dependent. An i.p. injection

of anti-NGF antiserum (5 µl/g) 1 h before induction of inflammation by intraplantar complete Freund's adjuvant (CFA) injection and 24 h after reduced the basal inflammatory hypersensitivity and significantly attenuated the progressive increase of spontaneous activity, touch-, pinch- and Aβ-afferent-evoked responses, as well as the progressive reduction of the mechanical threshold of biceps femoris/semitendinosus alpha motoneurons normally evoked by repeated (every 5 min) tactile stimulation of the inflamed hindpaw, in decerebrate-spinal rats.

Ro et al. (1999) described the effect of NGF and anti-NGF on neuropathic pain in rats following chronic constriction injury of the sciatic nerve.

Theodosiou et al. (1999) studied the role of nerve growth factor in hyperalgesia due to nerve damage.

Gwak et al. (2003) found attenuation of mechanical hyperalgesia following spinal cord injury by administration of antibodies to nerve growth factor in the rat.

PROCEDURE

Adult Sprague Dawley rats (200–250 g) were spinally hemisected at T13 (Christensen et al. 1996). Under enflurane anesthesia (induction 3% and maintenance 2%) the T11–12 laminae were determined by counting the dorsal spinous processes from the sacrum. The surgical field was then shaved, a longitudinal incision made exposing several segments, and a laminectomy performed at two vertebral segments, T11–T12. The spinal cord was hemisected just cranial to the L1 dorsal root entry zone with a micro-dissecting knife without damaging the major dorsal vessel or vascular branches. An insulin syringe with a 28-gauge needle was placed dorsal-ventrally at the midline of the cord, and pulled laterally to ensure the completeness of the hemisection. The incised skin was sutured, and postoperative care was done. After the hemisection, animals were either treated once a day for 10 days with anti-NGF (anti-nerve growth factor-2.5S, Sigma, i.p., 2 µg, 0.2 ml), or with saline (0.2 ml), or were untreated.

In the behavioral experiments, rats were housed in clear plastic boxes ($8 \times 8 \times 24$ cm) above a metal mesh (0.5×0.5 cm) and acclimatized for 30 min to avoid the stress associated with environmental change. Mechanical paw withdrawal threshold to the application of a von Frey filament was measured by using the up-down testing paradigm (Ro et al. 1999). An ascending series of von Frey filaments of incremental force (0.35, 0.53, 0.78, 2.5, 3.7, 5.2, 6.0, and 12.5 g) was applied for 3 s to the middle of the plantar surface of the hind paw, starting with the 2.5 g stimulus (Chaplan et al. 1994).

For electrophysiology experiments, rats were anesthetized with sodium pentobarbital (40–50 mg/kg), with supplementary pancuronium bromide (2–4 mg/kg per h), and artificially ventilated. Extracellular recordings of neuronal activity were made from the dorsal horn neurons in the lumbar spinal cord (L4–L5), using a recording glass microelectrode with a carbon filament (3–5 MΩ) while mechanical stimuli were applied onto the receptive fields. The single unit responses of the dorsal horn neurons, characterized as wide dynamic range (WDR) neurons by their graded responses to increased intensities of mechanical stimuli, were amplified, filtered, and displayed on an oscilloscope. The output signals were also fed into a data acquisition system (CED 1401 plus) via a window discriminator for the construction of real-time recordings of peristimulus time histograms, which were displayed as the number of spikes per second.

The mechanical stimuli were applied for 10 s and included: (1) brushing the skin with a camel hair brush in a stereotypic manner (brush); (2) sustained application of a large clamp that produced a sense of firm pressure when placed on human skin (pressure); and (3) sustained application of a small clamp that produced a distinctly painful sensation (pinch).

EVALUATION

Statistical analysis was performed using Mann–Whitney's unmatched pairs rank-sum test to evaluate the differences between the scores in two groups. All data are displayed as means ±standard error.

MODIFICATIONS OF THE METHOD

Spinal cord injury often leads to central pain syndrome including hyperalgesia to mechanical stimulation. Several authors studied the influence of nerve growth factor in **models of neuropathic pain** (Ramer and Bisby 1999; Li et al. 2002, 2003; Cahill et al. 2003; Ruiz et al. 2004).

Nerve Ligation Injury

Nerve ligation injury was performed according to the method described previously (Kim and Chung 1992). This technique produces signs of tactile allodynia and thermal hyperalgesia. Rats were anesthetized with halothane and the L5 and L6 spinal nerves were exposed, carefully isolated, and tightly ligated with 4–0 silk suture distal to the dorsal root ganglion (DRG). After ensuring homeostatic stability, the wounds were sutured, and the animals were allowed to recover in individual cages. Sham-operated

rats were prepared in an identical fashion except that the L5 and L6 spinal nerves were not ligated.

Intrathecal Catheter Placement

Two routes of administration, a systemic i.p. and a spinal intrathecal (i.th.) route, were used explore the activity of compounds. For the spinal route, test compounds were injected through indwelling i.th. catheters in the manner described by Yaksh and Rudy (1976). While under anesthesia, polyethylene tubing 10 tubing (8 cm) was inserted through an incision made in the atlanto-occipital membrane to the level of the lumbar enlargement of the rat and secured. Drug injections were made in a volume of 5 µl followed by a 9-µl saline flush.

Thermal Sensitization

Rats were lightly anesthetized with ether. The left hindpaw was placed in a water bath maintained at 50°C for 1 min. Inflammation suggested by rubor of the paw developed immediately. The rats were allowed to recover from anesthesia and tactile testing was begun 2 h after thermal sensitization. This procedure has produced signs of thermal hyperalgesia and tactile allodynia that persisted for over 12 h.

Evaluation of Tactile Allodynia

Mechanical allodynia was determined in the manner described previously (Chaplan et al. 1994). The paw withdrawal threshold was determined in response to probing with calibrated von Frey filaments. The rats were kept in suspended cages with wire mesh floors and the von Frey filaments were applied perpendicularly to the planar surface of the paw of the rat until it bent slightly, and was held for 3–6 s, or until the paw was withdrawn. A positive response was indicated by a sharp withdrawal of the paw. The 50% paw withdrawal threshold was determined by the nonparametric method (Dixon 1980).

Shelton et al. (2005) found that nerve growth factor mediates **hyperalgesia and cachexia in autoimmune arthritis**. Function-blocking antibodies to NGF completely reverse established pain in rats with fully developed arthritis despite continuing joint destruction and inflammation. Likewise, these antibodies reverse weight loss while not having any effect on levels of the pro-cachectic agent tumor necrosis factor (TNF).

Banik et al. (2005) reported that increased nerve growth factor after rat plantar incision contributes to **guarding behavior and heat hyperalgesia**. The therapeutic effect of a monoclonal antibody against endogenous NGF was evaluated by intraperitoneal administration of a single preoperative dose of anti-NGF.

Adult male, 225–275 g, Sprague-Dawley rats were used in a plantar incision animal model. The animals were anesthetized with 1.5%–2% halothane and the surgical field was prepared in a sterile manner. A 1-cm longitudinal incision was made in the plantar aspect of the hind paw beginning 0.5 cm from the end of heel; skin, fascia and muscle were incised and the skin was closed with 5–0 nylon suture. Topical antibiotics were administered. On the second postoperative day, sutures were removed under brief anesthesia.

For measuring guarding behaviors, unrestrained rats were placed on a small plastic mesh floor (grid 8 × 8 mm). Using an angled magnifying mirror, the incised and non-incised paws were viewed. Both paws of each animal were closely observed over a 1-min period repeated every 5 min for 1 h. Depending on the position in which each paw was found during the majority of the 1-min scoring period, a 0, 1 or 2 was given. A score of 0 was given for full weight bearing with the area of the wound blanched or distorted by the mesh; 1 for the wound area just touching the mesh without blanching or distortion; and 2 for the wound area completely off the mesh. The sum of the 12 scores (0–24) obtained during 1-h session for each paw was obtained.

For measuring heat sensitivity rats were placed individually on a glass floor covered with a clear plastic cage and allowed to acclimate. Withdrawal latencies to radiant heat were assessed by applying a focused radiant heat source underneath a glass floor on the middle of the incision. The latency time to evoke a withdrawal was determined with a cut-off value of 30 s. The intensity of the heat was adjusted to produce a withdrawal latency in normal rats of 25–30 s. Each rat was tested at least three times, at an interval of 10 min. The average of at least three trials was used to obtain paw withdrawal latency.

For measuring mechanosensitivity, rats were placed individually on a plastic mesh floor covered with a clear plastic cage and allowed to acclimate. The withdrawal response to punctate mechanical stimulation was determined using calibrated von Frey hairs applied underneath the cage to an area adjacent to the incision. Each filament was applied once starting with 10 mN and continuing until a withdrawal response occurred or 250 mN was reached. If a rat did not respond to the 250-mN filaments (522 mN), the next filament was recorded. This was repeated a total of three times with at least a 5- to 10-min test-free period between withdrawal responses. The lowest force from the three

tests producing a response was considered the withdrawal threshold.

Zahn et al. (2004) described the effect of blockade of nerve growth factor and tumor necrosis factor on pain behaviors after plantar incision.

Obata et al. (2002) described the expression of neurotrophic factors in the dorsal root ganglion in a **rat model of lumbar disc herniation**. The left L4/5 nerve roots were exposed after hemilaminectomies and autologous intervertebral discs, which were obtained from coccygeal intervertebral discs, were implanted on each of the exposed nerve roots without mechanical compression.

Lamb et al. (2003) studied nerve growth factor (NGF) and **gastric hyperalgesia** in the rat. Male Sprague Dawley rats (300–400 g) were anesthetized and the stomach exposed and placed in a circular clamp. Acetic acid (60%) or saline was injected into this area and aspirated 45 s later, resulting in kissing ulcers. A balloon was surgically placed into the stomach and electromyographic responses to gastric distension recorded from the acromiotrapezius muscle. Animals received a daily injection of neutralizing NGF antibody or control serum for 5 days; NGF in the stomach was measured with an ELISA. The severity of gastric injury was assessed microscopically and by determination of myeloperoxidase activity.

Winston et al. (2003) investigated molecular and behavioral changes in nociception in a novel **rat model of chronic pancreatitis** induced by pancreatic infusion of trinitrobenzene sulfonic acid as a model of painful pancreatitis. Nociception was assessed by measuring mechanical sensitivity of the abdomen and by recording the number of nocifensive behaviors in response to electrical stimulation of the pancreas. Expression of neuropeptides calcitonin gene-related peptide (CGRP) and substance P (SP) in the thoracic dorsal root ganglia receiving input from the pancreas and nerve growth factor in the pancreas were measured.

Guerios et al. (2006) reported that nerve growth factor (NGF) mediates peripheral mechanical hypersensitivity that accompanies **experimental cystitis in mice**. Cystitis was induced by intraperitoneal injection of cyclophosphamide (CYP) in female mice. Sensitivity of hind paws to mechanical stimuli was determined prior to and 4, 9, and 24 h after CYP, and the sensitivity of the tail to thermal stimuli was determined prior to, and 4 and 24 h after CYP treatment. To investigate the role of NGF in these processes, other groups of mice received NGF antiserum or normal serum intravenously 30 min after CYP administration. CYP induced bladder inflammation that was not ablated by treatment with NGF antiserum. Sensitivity to mechanical stimuli was increased 4 and 9 h after CYP administration. This was reversed by NGF antiserum but not by normal serum.

Cyclophosphamide-induced cystitis was also used as a model for visceral pain by Lanteri-Minet et al. (1995), Boucher et al. (2000), and Bon et al. (2003).

Jaggar et al. (1999) studied hyperalgesia to thermal stimulation of the hind limb of rats after inflammation of the urinary bladder by instillation of 0.5 ml of 50% turpentine in olive oil.

Dmitrieva and McMahon (1996) and Dmitrieva et al. (1997) reported sensitization of visceral afferents by NGF in the adult rat.

Delafoy et al. (2003) studied the role of NGF in **trinitrobenzene sulfonic acid-induced colonic hypersensitivity**. The function of NGF as a mediator of persistent pain states was tested in a model of colonic hypersensitivity measured by isobaric distension in conscious rats. The effects of exogenous NGF on colonic pain threshold, the involvement of NGF in trinitrobenzene sulfonic acid-induced colonic hypersensitivity, and the involvement of sensory nerves in the effects of NGF and trinitrobenzene sulfonic acid using rats treated neonatally with capsaicin were studied.

Sevcik et al. (2005) found that anti-NGF therapy profoundly reduced **bone cancer pain** and the accompanying increase of markers of peripheral and central sensitization. Osteolytic murine sarcoma cells were injected into the intramedullary space of the mouse femur. Administrations of a NGF-sequestering antibody produced a profound reduction in cancer pain-related behavior that was greater than that achieved with administration of morphine.

REFERENCES AND FURTHER READING

Banik RK, Subieta AR, Wu C, Brennan TJ (2005) Increased nerve growth factor after rat plantar incision contributes to guarding behavior and heat hyperalgesia. Pain 117:68–76

Bon K, Lichtensteiger CA, Wilson SG, Mogli JS (2003) Characterization of cycophosphamide cystitis, a model of visceral and referred pain, in the mouse: species and strain differences. J Urol 170:1008–1012

Boucher M, Meen M, Codron JP, Coudore F, Kemeny JL, Eschalier A (2000) Cyclophosphamide-induced cystitis in freely moving conscious rats: behavioural approach to a new model of visceral pain. J Urol 164:203–208

Cahill CM, Dray A, Coderre TJ (2003) Intrathecal nerve growth factor restores opioid effectiveness in an animal model of neuropathic pain. Neuropharmacology 45:543–552

Chaplan SR, Bach FW, Pogrel JW, Chung JM, Yaksh TL (1994) Quantitative measurement of tactile allodynia in the rat paw. J Neurosci Methods 53:55–63

Christensen MD, Evertart AW, Pickelman JT, Hulsebosch CE (1996) Mechanical and thermal allodynia in chronic central pain following spinal cord injury. Pain 68:97–107
Delafoy L, Raymond F, Doherty AM, Eschalier A, Diop L (2003) Role of nerve growth factor in the trinitrobenzene sulfonic acid-induced colonic hypersensitivity. Pain 105:489–497
Dixon WJ (1980) Efficient analysis of experimental observations. Annu Rev Pharmacol Toxicol 20:441–462
Dmitrieva N, McMahon SB (1996) Sensitization of visceral afferents by nerve growth factor in the adult rat. Pain 66:87–97
Dmitrieva N, Shelton D, Rice ASC, McMahon SB (1997) The role of nerve growth factor in a model of visceral inflammation. Neuroscience 78:449–459
Guerios S, Wang ZY, Bjorling DE (2006) Nerve growth factor mediates peripheral mechanical hypersensitivity that accompanies experimental cystitis in mice. Neurosci Lett 392:193–197
Gwak YS, Nam TS, Paik KS, Hulsebosch CE, Leem JW (2003) Attenuation of mechanical hyperalgesia following spinal cord injury by administration of antibodies to nerve growth factor in the rat. Neurosci Lett 336:117–120
Herzberg U, Eliav E, Dorsey JM, Gracely RH, Kopin IJ (1997) NGF involvement in pain induced by chronic constriction injury of the rat sciatic nerve. NeuroReport 8:1613–1618
Jaggar SI, Scott HCF, Rice ASC (1999) Inflammation of the rat urinary bladder is associated with a referred thermal hyperalgesia which is nerve growth factor dependent. Br J Anaesth 83:442–448
Kim SH, Chung JM (1992) An experimental model for peripheral neuropathy produced by segmental spinal nerve ligation in the rat. Pain 50:355–363
Lamb K, Kang YM, Gebhart GF, Bielefeldt K (2003) Nerve growth factor and gastric hyperalgesia in the rat. Neurogastroenterol Mot 15:355–361
Lanteri-Minet M, Bon K, de Pommery J, Michiels JF, Menetrey D (1995) Cyclophosphamide cystitis as a model of visceral pain in rats: model elaboration and spinal structures involved as revealed by the expression of c-Fos and Krox-24 proteins. Exp Brain Res 105:220–232
Li L, Xian CJ, Zhong JH, Zhou XF (2002) Effect of lumbar 5 ventral root transection on pain behaviours: a novel model for neuropathic pain without axotomy of primary sensory neurons. Exp Neurol 175:23–34
Li L, Xian CJ, Zhong JH, Zhou XF (2003) Lumbar 5 ventral root dissection-induced upregulation of nerve growth factor in sensory neurons and their target tissues: a mechanism of neuropathic pain. Mol Cell Neurosci 23:232–250
Ma QP, Woolf CJ (1997) The progressive tactile hyperalgesia induced by peripheral inflammation is nerve growth factor dependent. NeuroReport 8:807–810
Obata K, Tsujino H, Yamanka H, Yi D, Fukuoka T, Hashimoto N, Yomenobu K, Yoshikawa H, Noguchi K (2002) Expression of neurotrophic factors in the dorsal root ganglion in a rat model of lumbar disc herniation. Pain 99:121–132
Ramer MS, Bisby MA (1999) Adrenergic innervation of rat sensory ganglia following proximal or distal painful sciatic neuropathy: distinct mechanisms revealed by anti-NGF treatment. Eur J Neurosci 11:837–846
Ro LS, Chen ST, Tang LM, Jacobs JM (1999) Effect of NGF and anti-NGF on neuropathic pain in rats following chronic constriction injury of the sciatic nerve. Pain 79:265–274
Ruiz G, Ceballos D, Baños JE (2004) Behavioral and histological effects of endoneurial administration of nerve growth factor: possible implications in neuropathic pain. Brain Res 1011:1–6
Sevcik MA, Ghilardi JR, Peters CM, Lindsay TH, Halvorson KG, Jonas BM, Kubota K, Kuskowski MA, Boustany L, Shelton DL, Mantyh PW (2005) Anti-NGF therapy profoundly reduced bone cancer pain and the accompanying increase of markers of peripheral and central sensitization. Pain 115:128–141
Shelton DL, Zeller J, Ho WH, Pons J, Rosenthal A (2005) Nerve growth factor mediates hyperalgesia and cachexia in autoimmune arthritis. Pain 116:8–16
Theodosiou M, Rush RA, Zhou XF, Hu D, Walker JS, Tracey DJ (1999) Hyperalgesia due to nerve damage: role of nerve growth factor. Pain 81:245–255
Winston JH, He ZJ, Shenoy M, Xiao SY, Pasricha PJ (2003) Molecular and behavioural changes in nociception in a novel rat model of chronic pancreatitis for the study of pain. Pain 117:214–222
Yaksh TL, Rudy TA (1976) Chronic catheterization of the spinal subarachnoid space. Physiol Behav 17:1031–1036
Zahn PK, Subieta A, Park SS, Brennan TJ (2004) Effect of blockade of nerve growth factor and tumor necrosis factor on pain behaviours after plantar incision. J Pain 5:157–163

H.3 Anti-Inflammatory Activity

H.3.0.1 General Considerations

Inflammation was characterized two thousand years ago by Celsus by the four Latin words: Rubor, calor, tumor and dolor. Inflammation has different phases: the first phase is caused by an increase of vascular permeability resulting in exudation of fluid from the blood into the interstitial space, the second one by infiltration of leukocytes from the blood into the tissues and the third one by granuloma formation. Accordingly, anti-inflammatory tests have to be divided into those measuring acute inflammation, subacute inflammation and chronic repair processes. In some cases, the screening is directed to test compounds for local application. Predominantly, however, these studies are aimed to find new drugs against polyarthritis and other rheumatic diseases. Since the etiology of polyarthritis is considered to be largely immunologically, special tests have been developed to investigate various immunological and allergic factors (see Chapter I).

H.3.1 In Vitro Methods for Anti-Inflammatory Activity

H.3.1.1 General Considerations

An array of physiological substances, sometimes called autacoids, are involved in the process of inflammation and repair. These include histamine, serotonin,

bradykinin, substance P, and the group of eicosanoids (prostaglandins, thromboxanes and leucotrienes), the platelet-activating factor (PAF) as well as cytokines and lymphokines. Their discovery makes the use of *in vitro* studies possible. The influence of non-steroidal anti-inflammatory agents on the eicosanoid pathway gave rise to numerous studies.

H.3.1.2 ^{3}H-Bradykinin Receptor Binding

PURPOSE AND RATIONALE

Tissue injury or trauma initiates a cascade of reactions which results in the proteolytic generation of bradykinin and kallidin from high-molecular-weight precursors, kininogens, found in blood and tissue. The rapid enzymatic cleavage of kininogens is accomplished by the kallikreins, a group of proteolytic enzymes which are present in most tissues and body fluids. Bradykinin produces pain by stimulating A and C fibers in the peripheral nerves, participates in the inflammatory reaction and lowers blood pressure by vasodilatation. Since its breakdown occurs via the same enzyme responsible for converting angiotensin I into angiotensin II some of the effects of converting enzyme inhibitors may be due to presence of bradykinin. The ^{3}H-bradykinin receptor binding is used to detect compounds that inhibit binding of ^{3}H-bradykinin in membrane preparations obtained from guinea-pig ileum. Two types of bradykinin receptors (B_1 and B_2 receptors) are known (Feres et al. 1992; Bascands et al. 1993; Tropea et al. 1994; Marceau et al. 1998; Calixto et al. 2004; Leeb-Lundberg et al. 2005). The existence of a pulmonary BK_3 receptor has been proposed by Farmer et al. (1989) and Meini et al. (2004). Evidence was obtained for the existence of three subtypes of B_2 receptors, B_{2a}, B_{2b}, and B_{2c} (Seguin et al. 1992; Seguin and Widdowson 1993).

PROCEDURE

Ileum from guinea pigs is cleaned from its content and cut into pieces of 2 cm length. They are homogenized for 30 s in ice-cold TES buffer, pH 6.8, containing 1 mM 1,10-phenanthroline, in a Potter homogenizer. The homogenates are filtered through 3 layers of gauze and centrifuged twice at 50,000 *g* for 10 min with an intermediate rehomogenization in buffer.

For routine studies the final pellets are resuspended in 40 vol of incubation buffer (25 mM TES buffer, pH 6.8, containing 1 mM 1,10-phenanthroline, 0.1% bovine serum albumin, 140 µg/ml bacitracin, 1 mM dithiothreitol, 0.1 µM captopril). In the competition experiment, 50 µl ^{3}H-bradykinin (one constant concentration of $0.5–2 \times 10^{-9}$ M), 50 µl test compound (6 concentrations, $10^{-5}–10^{-10}$ M) and 150 µl membrane suspension from guinea pig ileum (approx. 6.6 mg wet weight/ml) per sample are incubated in a shaker bath at 25°C for 90 min.

Saturation experiments are performed with 12 concentrations of ^{3}H-bradykinin ($14.2–0.007 \times 10^{-9}$ M). Total binding is determined in the presence of incubation buffer, non-specific binding is determined in the presence of non-labeled bradykinin (10^{-6} M).

The reaction is stopped by rapid vacuum filtration through glass fibre filters. Thereby the membrane-bound radioactivity is separated from the free one. The retained membrane-bound radioactivity on the filter is measured after addition of 3 ml liquid scintillation cocktail per sample in a liquid scintillation counter.

EVALUATION

The following parameters are calculated:

- total binding of ^{3}H-bradykinin
- non-specific binding in the presence of 10 µM bradykinin
- specific binding = total binding–non-specific binding
- % inhibition: 100–specific binding as percentage of control value

Compounds are first tested at a single high concentration (10,000 nM) in triplicate. For those showing more than 50% inhibition a displacement curve is constructed using 7 different concentrations of test compound. Binding potency of compounds is expressed either as a relative binding affinity (*RBA*) with respect to the standard compound (bradykinin) which is tested in parallel or as an IC_{50}.

$$RBA = \frac{IC_{50}\ \text{standard compound}}{IC_{50}\ \text{compound}} \times 100\%$$

The dissociation constant (K_i) and the IC_{50} value of the test drug are determined from the competition experiment of ^{3}H-bradykinin versus non-labeled drug by a computer-supported analysis of the binding data (McPherson 1985).

Tests for Bradykinin Receptor Types and Subtypes

Prado et al. (2002) described mechanisms regulating the expression, self-maintenance, and signaling function of the bradykinin B_2 and B_1 receptors.

Cloning and pharmacological characterization of a human bradykinin (BK-2) receptor was reported by Hess et al. (1992).

Menke et al. (1994) reported the expression cloning of a human bradykinin B_1 receptor.

Bradykinin B_1 receptors have been studied in the isolated rabbit aorta (Bouthillier et al. 1987), in the isolated rabbit carotid artery (Pruneau and Bélichard 1993) and in the rabbit urinary bladder (Butt et al. 1955).

A potent bradykinin B_1 receptor antagonist has been described by Wirth et al. (1991).

Heterogeneity of B_1 receptors has been suggested by Wirth et al. (1992).

Heitsch (2002) reviewed non-peptide antagonists and agonists of the bradykinin B_2 receptor.

Bradykinin receptor ligands were described by Marceau and Regoli (2004) and Fortin and Marceau (2006).

Drummond and Cocks (1995) used rings of bovine left anterior descending coronary artery to study endothelium-dependent relaxations mediated by inducible B_1 and constitutive B_2 kinin receptors.

The production of cyclic GMP via activation of B_1 and B_2 kinin receptors in cultured bovine aortic endothelial cells was described by Wiemer and Wirth (1992).

Pharmacological characterization of bradykinin receptors in canine cultured tracheal smooth muscle cells has been reported by Yang et al. (1995).

Bradykinin B_2 receptors and their antagonists have been studied in human fibroblasts by Alla et al. (1993), with the high affinity radioligand [^{125}I]PIP HOE 140 by Brenner et al. (1993), in guinea pig gall bladder by Falcone et al. (1993), in the smooth muscle of guinea-pig taenia caeci by Field et al. (1994), in guinea pig ileum membranes by Graneß and Liebmann (1994), Liebmann et al. (1994a), in isolated blood vessels from different species by Félétou et al. (1994), in endothelial cells by Wirth et al. (1994).

Hallé et al. (2000) described *in vitro* and *in vivo* effects of kinin B_1 and B_2 receptor agonists and antagonists in inbred control and cardiomyopathic hamsters.

The role of B_1 and B_2 receptors and of nitric oxide in bradykinin-induced relaxation and contraction of isolated rat duodenum was studied by Rhaleb and Carretero (1994).

Campos et al. (1996) investigated the effect of pretreatment with bacterial endotoxin on the bradykinin B_1 and B_2 receptor-induced edema in the rat paw and the interaction of B_1-mediated responses with other inflammatory mediators.

Characterization of kinin receptors by bioassays was described by Gobeil and Regoli (1994). Molecular cloning, functional expression and pharmacological characterization of a human bradykinin B_2 receptor gene was performed by Eggerickx et al. (1992).

Simpson et al. (2000) characterized bradykinin analogues on recombinant human bradykinin B_1 and B_2 receptors using a high throughput functional assay which measures intracellular Ca^{2+} responses.

Bradykinin B_2 receptor subtypes were discussed by Liebmann et al. (1994b) and Regoli et al. (1994).

Evidence for a pulmonary B_3 bradykinin receptor has been given by Farmer et al., (1989) and Meini et al. (2004).

Bradykinin B_3 receptors have been described by Field et al. (1992) in the smooth muscle of the guinea-pig *taenia caeci* and trachea.

REFERENCES AND FURTHER READING

Alla SA, Buschko J, Quitterer U, Maidhof A, Haasemann M, Breipohl G, Knolle J, Müller-Esterl W (1993) Structural features of human bradykinin B_2 receptor probed by agonists, antagonists, and anti-idiotypic antibodies. J Biol Chem 268:17277–17285

Bascands JL, Pecher C, Rounaud S, Emond C, Tack JL, Bastie MJ, Burch R, Regoli D, Girolami JP (1993) Evidence for existence of two distinct bradykinin receptors on rat mesangial cells. Am J Physiol 264:F548–F556

Bouthillier J, Deblois D, Marceau F (1987) Studies on the induction of pharmacological responses to des-Arg^9-bradykinin *in vitro* and *in vivo*. Br J Pharmacol 92:257–264

Brenner NJ, Stonesifer GY, Schneck KA, Burns HD, Ransom RW (1993) [^{125}I]PIP HOE 140, a high affinity radioligand for bradykinin B_2 receptors. Life Sci 53:1879–1886

Burch RM, Kyle DJ (1992) Minireview: Recent developments in the understanding of bradykinin receptors. Life Sci 50:829–838

Burch RM, Farmer SG, Steranka LR (1990) Bradykinin receptor antagonists. Medicin Res Rev 10:237–239

Burch RM, Kyle DJ, Stormann TM (1993) Molecular Biology and Pharmacology of Bradykinin Receptors: The Pharmacological Classification of Kinins. RG Landes Comp., Austin, pp 6–18

Butt SK, Dawson LG, Hall JM (1995) Bradykinin B_1 receptors in the rabbit urinary bladder: induction of responses, smooth muscle contraction, and phopshatidylinositol hydrolysis. Br J Pharmacol 114:612–617

Calixto JB, Medeiros R, Fernandes ES, Ferreira J, Caprini DA, Campos MM (2004) Kinin B1 receptors: key G-protein-coupled receptors and their role in inflammatory and painful processes. Br J Pharmacol 143:803–818

Campos MM, Souza GEP, Calixto JB (1996) Upregulation of B_1 receptor mediating des-Arg^9-BK-induced rat paw edema by systemic treatment with bacterial endotoxin. Br J Pharmacol 117:793–798

Drummond GR, Cocks TM (1995) Endothelium-dependent relaxations mediated by inducible B_1 and constitutive B_2 kinin receptors in the bovine coronary artery. Br J Pharmacol 116:2473–2481

Eggerickx D, Raspe E, Bertrand D, Vassart G, Parmentier M (1992) Molecular cloning, functional expres-

sion and pharmacological characterization of a human bradykinin B_2 receptor gene. Biochem Biophys Res Commun 187:1306–1313

Emond C, Bascands JL, Pecher C, Cabos-Boutot G, Pradelles P, Regoli D, Girolami JP (1990) Characterization of a B_2-bradykinin receptor in rat mesangial cells. Eur J Pharmacol 190:381–392

Falcone RC, Hubbs SJ, Vanderloo JD, Prosser JC, Little J, Gomes B, Aharony D, Krell RD (1993) Characterization of bradykinin receptors in guinea pig gall bladder. J Pharm Exp Ther 266:1291–1299

Farmer SG, Burch RM, Meeker SA, Wilkins DE (1989) Evidence for a pulmonary B_3 bradykinin receptor. Mol Pharmacol 36:1–8

Félétou M, Germain M, Thurieau C, Fauchère JL, Canet E (1994) Agonistic and antagonistic properties of the bradykinin B2 receptor antagonist, Hoe 140, in isolated blood vessels from different species. Br J Pharmacol 112:683–689

Feres T, Paiva ACM, Paiva TB (1992) BK_1 and BK_2 bradykinin receptors in the rat duodenum smooth muscle. Br J Pharmacol 107:991–995

Field JL, Hall JM, Morton IKM (1992) Putative novel bradykinin B_3 receptors in the smooth muscle of the guinea-pig taenia caeci and trachea. Recent Progress on Kinins, Birkhäuser Basel, pp 540–545

Field JL, Butt SK, Morton IKM, Hall JM (1994) Bradykinin B_2 receptors and coupling mechanisms in the smooth muscle of guinea-pig taenia caeci. Br J Pharmacol 113:607–613

Fortin JP, Marceau F (2006) Advances in the development of bradykinin receptor ligands. Curr Topics Med Chem 6:1353–1363

Galizzi JP, Bodinier MC, Chapelain B, Ly SM, Coussy L, Giraud S, Neliat G, Jean T (1994) Up-regulation of [^{3}H]-des-arg^{10}-kallidin binding to the bradykinin B_1 receptor by interleukin-1β in isolated smooth muscle cells: correlation with B_1 agonist-induced PGI_2 production. Br J Pharmacol 113:389–394

Gobeil F, Regoli D (1994) Characterization of kinin receptors by bioassays. Braz J Med Biol Res 27:1781–1791

Graneß A, Liebmann C (1994) Affinity cross-linking of bradykinin B_2 receptors in guinea pig ileum membranes. Eur J Pharmacol 268:271–274

Hallé S, Gobeil F Jr, Ouelette J, Lambert C, Regoli D (2000) *In vitro* and *in vivo* effects of kinin B1 and B2 receptor agonists and antagonists in inbred control and cardiomyopathic hamsters. Br J Pharmacol 129:1641–2648

Heitsch H (2002) Non-peptide antagonists and agonists of the bradykinin B_2 receptor. Curr Med Chem 9:913–928

Hess JKF, Borkowski JA, Young GS, Strader CD, Ramson RW (1992) Cloning and pharmacological characterization of a human bradykinin (BK-2) receptor. Biochem Biophys Res Commun 184:260–268

Hock FJ, Wirth K, Albus U, Linz W, Gerhards HJ, Wiemer G, Henke S, Breipohl G, König W, Knolle J, Schölkens BA (1991) Hoe 140 a new potent and long acting bradykinin antagonist: *in vitro* studies. Br J Pharmacol 102:769–773

Innis RB, Manning DC, Stewart JM, Snyder SH (1981) [^{3}H]Bradykinin receptor binding in mammalian tissue membranes. Proc Natl Acad Sci USA., 78:2630–2634

Kachur JF, Allbee W, Danjo W, Gaginella TS (1987) Bradykinin receptors: functional similarities in guinea pig gut muscle and mucosa. Regul Peptides 17:63–70

Leeb-Lundberg LMF, Marceau F, Müller-Esterl W, Pettibone DJ, Zuraw BL (2005) International Union of Pharmacology. XLV. Classification of the kinin receptor family: from molecular mechanisms to pathophysiological consequences. Pharmacol Rev 57:27–77

Liebmann C, Bossé R, Escher E (1994b) Discrimination between putative bradykinin B_2 receptor subtypes in guinea pig ileum smooth muscle membranes with a selective, iodinatable, bradykinin analogue. Molec Pharmacol 46:949–956

Liebmann C, Mammery K, Graneß A (1994a) Bradykinin inhibits adenylate cyclase activity in guinea pig membranes via a separate high-affinity bradykinin B_2 receptor. Eur J Pharmacol 288:35–43

Manning DC, Vavrek R, Stewart JM, Snyder SH (1986) Two bradykinin binding sites with picomolar affinities. J Pharmacol Exp Ther 237:504–512

Marceau F, Regoli D (2004) Bradykinin receptor ligands: therapeutic perspectives. Nature Rev Drug Disc 3:845–852

Marceau F, Hess JF, Bachvarov DR (1998) The B_1 receptors for kinins. Pharmacol Rev 50:357–386

McEachern AE, Shelton ER, Bhakta S, Obernolte R, Bach C, Zuppan P, Fujisaki J, Aldrich RW, Jarnagin K (1991) Proc Natl Acad Sci USA 88:7724–7728

McPherson GA (1985) Analysis of radioligand binding experiments. A collection of computer programs for the IBM PC. J Pharmacol Meth 14:213–228

Meini S, Bellucci F, Cucchi P, Giuliani S, Quartara L, Giolitti A, Zappitelli S, Rotondaro L, Boels K, Maggi CA (2004) Bradykinin B2 and GPR100 receptors: a paradigm for receptor signal transduction pharmacology. Br J Pharmacol 143:938–941

Menke JG, Borkowski JA, Bierilo KK, MacNeill T, Derrick AW, Schneck KA, Ransom RW, Strader CD, Linemeyer DL, Hess JF (1994) Expression cloning of a human bradykinin B_1 receptor. J Biol Chem 269:21583–21586

Prado GN, Taylor L, Zhou X, Ricupero D, Mierke DF, Polgar P (2002) Mechanisms regulating the expression, self-maintenance, and signaling-function of the bradykinin B2 and B1 receptors. J Cell Physiol 193:275–286

Pruneau D, Bélichard P (1993) Induction of bradykinin B_1 receptor-mediated relaxation in the isolated rabbit carotid artery. Eur J Pharmacol 239:63–67

Regoli D, Gobeil F, Nguyen QT, Jukic D, Seoane PR, Salvino JM, Sawutz DG (1994) Bradykinin receptor types and B_2 subtypes. Life Sci 55:735–749

Rhaleb NE, Carretero OA (1994) The role of B_1 and B_2 receptors and of nitric oxide in bradykinin-induced relaxation and contraction of isolated rat duodenum. Life Sci 55:1351–1363

Rhaleb NE, Rouissi N, Jukic D, Regoli D, Henke S, Breipohl G, Knolle J (1992) Pharmacological characterization of a new highly potent B_2 receptor antagonist (HOE 140: D-arg-[hyp^3,thi^5,D-tic^7,oic^8]bradykinin. Eur J Pharmacol 210:115–120

Schneck KA, Hess JF, Stonisifer GY, Ransom RW (1994) Bradykinin B_1 receptors in rabbit aorta smooth muscle in culture. Eur J Pharmacol, Mol Pharmacol Sect 266:277–282

Seguin L, Widdowson PS (1993) Effects of nucleotides on [^{3}H]bradykinin binding in guinea pig: further evidence for multiple B_2 receptor subtypes. J Neurochem 60:652–757

Seguin L, Widdowson PS, Giesen-Crouse E (1992) Existence of three subtypes of bradykinin B_2 receptors in guinea pig. J Neurochem 59:2125–2133

Simpson PB, Woollacott AJ, Hill RG, Seabrook GR (2000) Functional characterization of bradykinin analogues on recombinant human bradykinin B_1 and B_2 receptors. Eur J Pharmacol 392:1–9

Tropea MM, Gummelt D, Herzig MS, Leeb-Lundberg LMF (1994) B1 and B2 kinin receptors on cultured rabbit superior mesenteric artery smooth muscle cells: receptor specific stimulation of inositol phosphate formation and arachidonic acid release by des-arg^9-bradykinin and bradykinin. J Pharmacol Exp Ther 264:930–937

Wiemer G, Wirth K (1992) Production of cyclic GMP via activation of B_1 and B_2 kinin receptors in cultured bovine aortic endothelial cells. J Pharm Exp Ther 262:729–733

Wirth K, Breipohl G, Stechl J, Knolle J, Henke S, Schölkens B (1991) DesArg^9-D-Arg[Hyp^3,Thi^5,D-Tic^7, Oic^8]bradykinin (desArg^{10}-[Hoe140]) is a potent bradykinin B_1 receptor antagonist. Eur J Pharmacol 205:217–218

Wirth KJ, Schölkens BA, Wiemer G (1994) The bradykinin B_2 receptor antagonist WIN 64338 inhibits the effect of des-arg^9-bradykinin in endothelial cells. Eur J Pharmacol 288:R1–R2

Wirth KJ, Wiemer G, Schölkens BA (1992) Des-Arg^{10}[HOE 140] is a potent B_1 bradykinin antagonist. Recent Progress on Kinins. Birkhäuser, Basel, pp 406–413

Yang CM, Luo SF, Hsia HC (1995) Pharmacological characterization of bradykinin receptors in canine cultured tracheal smooth muscle cells. Br J Pharmacol 144:67–72

H.3.1.3 Substance P and the Tachykinin Family

H.3.1.3.1 General Considerations

Substance P belongs to the tachykinin family of peptides that share a common carboxy-terminal sequence (Phe-X-Gly-Leu-Met-NH_2). It was first described by von Euler and Gaddum (1931) as a brain and gut extract that stimulates smooth muscle contraction. Bioassay extracts from spinal dorsal roots implicated substance P as a pain neurotransmitter (Lembeck 1953; Lembeck and Holzer 1979). After determination of the amino acid sequence (Chang et al. 1971) the distribution of substance P in the CNS could be studied (Hökfelt et al. 1975). Neurokinins belong like substance P to a group of neuropeptides named tachykinins. Following the discovery of neurokinin A and neurokinin B, three distinct G protein-coupled receptors, NK_1, NK_2 and NK_3, were described (Maggi et al. 1993; Mussap et al. 1993; Patacchini and Maggi 1995). Neurokinin A and substance P are preferred agonists of the tachykinin NK_1 and NK_2 receptors, whereas neurokinin B preferentially interacts with the tachykinin NK_3 receptor. The receptor sensitivity of these peptides is relatively poor, and it is possible that their actions could be mediated by interactions with their less preferred receptors.

Nomenclature of tachykinins and tachykinin receptors has been discussed repeatedly (Henry 1987; Maggi 2000).

Tachykinin NK_1 antagonists are potent antiemetics, however other possible therapeutic uses, including rheumatoid arthritis, asthma, migraine, pain and psychiatric disorders, were suggested (Longmore et al. 1995). The P-preferring NK_1 receptor has attracted most interest as a CNS target because it is the predominant tachykinin receptor expressed in the human brain, while NK_2 and NK_3 receptor expression is in extremely low abundance or absent. Several NK_1 receptor agonists antagonists were synthesized and evaluated (Snider et al. 1991; Emonds-Alt et al. 1993; Cascieri et al. 1992; Sakurada et al. 1993; Bristow and Young 1994; Jung et al. 1994; Rupniak and Williams 1994; Smith et al. 1994; Vassout et al. 1994; Patacchini and Maggi 1995; Bonnet et al. 1996; Chapman et al. 1996; Herbert and Bernat 1996; Palframan et al. 1996; Ren et al. 1996). Moreover, agonists and antagonists at the NK_2 receptor (Hagan et al. 1991, 1993; Beresford et al. 1995; Robineau et al. 1995; Kudlacz et al. 1997; Lecci et al. 1997) and at the NK_3 receptor (Guard et al. 1990; Edmonds-Alt et al. 1995; Patacchini et al. 1995; Nguyen-Le et al. 1996; Beaujouan et al. 1997; Sarau et al. 1997) were reported (Longmore et al. 1995; Rupniak 1999).

Understanding the role of substance P in the brain has been complicated by marked species differences in the distribution of the tachykinin receptor types. There appears to be a relative increase in NK_1 receptor density during evolution, such that NK_3 receptors ara abundant in lower vertebrates and mammals but, like NK_2 receptors, are apparently absent in human brain. Preclinical studies with substance P receptor antagonists have been hindered not only by phylogenetic differences in tachykinin receptor expression, but also by pharmacological heterogeneity of the NK_1 receptor and the NK_2 receptor. An other confounding feature of neurokinin receptor antagonist is the blockade of Na^+ and Ca^{2+} channels at high doses which produces effects in various assays that are independent of receptor antagonism (Patacchini and Maggi 1995; Rupniak 1999). Most developments were guided by the effects of substance P as a pain neurotransmitter. Surprisingly, most clinical studies of analgesic activity of NK_1 receptor antagonists were negative (Rupniak and Kramer 1999). However, clinical findings indicated that substance P receptor antagonists ara able to alleviate depression and anxiety in patients suffering from major depressive disorder (Kramer et al. 1998).

REFERENCES AND FURTHER READING

Beaujouan JC, Saffroy M, Torrens Y, Glowinski J (1997) Potency and selectivity of the tachykinin NK_3 receptor antagonist SR 14801. Eur J Pharmacol 319:307–316

Beresford IJM, Sheldrick RLG, Ball DI, Turpin MP, Walsh DM, Hawcock AB, Coleman RA, Hagan RM, Tyers MB (1995) GR159897, a potent non-peptide antagonist at tachykinin NK_2 receptors. Eur J Pharmacol 272:241–248

Bonnet J, Kucharczyk N, Robineau P, Lonchampt M, Dacquet C, Regoli D, Fauchère JL, Canet E (1996) A water soluble, stable dipeptide NK_1 receptor-selective neurokinin receptor antagonist with potent *in vivo* pharmacological effects: S18523. Eur J Pharmacol 310:37–46

Bristow LJ, Young L (1994) Chromodacryorrhea and repetitive hind paw tapping. Models of peripheral and central tachykinin NK_1 receptor activation in gerbils. Eur J Pharmacol 253:245–252

Cascieri MA, Ber E, Fong TM, Sadowski S, Bansal A, Swain C, Seward E, Frances B, Burns D, Strader CD (1992) Characterization of the binding of a potent, selective, radioiodinated antagonist to the human neurokinin-1 receptor. Mol Pharmacol 42:458–463

Chang MM, Leeman SE, Niahl HD (1971) Amino acid sequence of substance P. Nature 232:86–88

Chapman V, Buritova J, Honoré P, Besson JM (1996) Physiological contribution of neurokinin 1 receptor activation, and interactions with NMDA receptors, to inflammatory-evoked spinal c-Fos expression. J Neurophysiol 76:1817–1827

Emonds-Alt X, Doutremepuich JD, Heaulme M, Neliat G, Santucci V, Steinberg R, Vilain P, Bichon D, Ducoux JP, Proietto V, van Broeck D, Soubrié P, le Fur G, Brelière JC (1993) *In vitro* and *in vivo* biological activities of SR140333, a novel potent non-peptide tachykinin NK_1 receptor antagonist. Eur J Pharmacol 250:403–413

Edmonds-Alt X, Bichon D, Ducoux JP, Heaulme M, Miloux B, Poncelet M, Proietto V, van Broeck D, Vilain P, Soubrié P, le Fur G, Brelière JC (1995) SR 142801, the first potent non-peptide antagonist of the tachykinin NK_3 receptor. Life Sci 56:PL 27–32

Guard S, Watson S, Maggio JE, Too HP, Waitling KJ (1990) Pharmacological analysis of [^{3}H]-senktide binding to NK_3 tachykinin receptors in guinea-pig ileum longitudinal muscle-myenteric plexus and cerebral cortex membranes. Br J Pharmacol 99:767–773

Hagan RM, Ireland SJ, Jordan CC, Beresford IJM, Deal MJ, Ward P (1991) Receptor-selective, peptidase resistant agonists at neurokinin NK-1 and NK-2 receptors: new tools for investigating neurokinin function. Neuropeptides 19:127–135

Hagan RM, Beresford IJM, Stables J, Dupere J, Stubbs CM, Elliott PJ, Sheldrick RLG, Chollet A, Kawashima E, McElroy AB, Ward P (1993) Characterization, CNS distribution and function of NK_2 receptors studied using potent NK_2 receptor antagonists. Regul Pept 46:9–19

Henry JL (1987) Discussion of nomenclature for tachykinins and tachykinin receptors. In: Henry JL et al (eds) Substance P and Neurokinins. Springer-Verlag, Heidelberg, p XVII

Herbert JM, Bernat A (1996) Effect of SR 140333, a selective NK_1 antagonist, on antigen-induced oedema formation in rat skin. J Lipid Mediat Cell Signal 13:223–232

Hökfelt T, Kellerth JO, Nilsson G, Pernow B (1975) Substance P: Localization in the central nervous system and in some primary sensory neurons. Science 190:889–890

Jung M, Calassi R, Maruani J, Barnouin MC, Souilhac J, Poncelet M, Gueudet C, Edmonds-Alt X, Soubriè P, Brelière JC, le Fur G (1994) Neuropharmacological characterization of SR 140333, a non peptide antagonist of NK_1 receptors. Neuropharmacol 33:167–179

Kramer MS, Cutler N, Feighner J, Shrivastava R, Carman J, Sramek JJ, Reines SA, Lui G, Snavely D, Wyatt-Knowles E, Hale JJ, Mills SG, MacCoss M, Swain CJ, Harrison T, Hill RG, Hefti F, Scolnik EM, Cascieri MA, Chicchi GG, Sadowski S, Williams AR, Hewson L, Smith D, Carlson EJ, Hargreaves J, Rupniak NMJ (1998) Distinct mechanism for antidepressant activity by blockade of central substance P receptors. Science 281:1640–1645

Kudlacz EM, Knippenberg RW, Shatzer SA, Kehne JH, McCloskey TC, Burkholder TP (1997) The peripheral NK-1/NK-2 receptor antagonist MDL 105,172A inhibits tachykinin-mediated respiratory effects in guinea-pigs. J Autonom Pharmacol 17:109–119

Lecci A, Giulani S, Tramontana M, Criscuoli M, Maggi CA (1997) MEN 11,420, a peptide tachykinin NK_2 receptor antagonist, reduces motor responses induced by intravesical administration of capsaicin *in vivo*. Naunyn Schmiedeberg's Arch Pharmacol 356:182–188

Lembeck F (1953) Zur Frage der zentralen Übertragung afferenter Impulse. III. Mitteilung. Das Vorkommen und die Bedeutung der Substanz P in den dorsalen Wurzeln des Rückenmarks. Arch Exp Path Pharmakol 219:197–213

Lembeck F, Holzer P (1979) Substance P as neurogenic mediator of antidromic vasodilation and neurogenic plasma extravasation. Naunyn Schmiedeberg's Arch Pharmacol 310:175–183

Longmore J, Swain CJ, Hill RG (1995) Neurokinin receptors. Drug News Perspect 8:5–12

Maggi CA (2000) The troubled story of tachykinins and neurokinins. Trends Pharmacol Sci 21:173–175

Maggi CA, Patacchini R, Rovero P, Giachetti A (1993) Tachykinin receptors and tachykinin receptor antagonists. J Autonom Pharmacol 13:23–93

Mussap CJ, Geraghty DP, Burcher E (1993) Tachykinin receptors. A radioligand binding perspective. J Neurochem 6:1987–2009

Nguyen-Le XK, Nguyen QT, Gobeil F, Pheng LH, Emonds-Alt X, Brelière JC, Regoli D (1996) Pharmacological characterization of SR 142801: a new non-peptide antagonist of the neurokinin NK-3 receptor. Pharmacology 52:283–291

Palframan RT, Costa SKP, Wilsoncroft P, Antunes E, de Nucci G, Brain SD (1996) The effect of a tachykinin NK_1 receptor antagonist, SR 14033, on oedema formation induced in rat skin by venom from the *Phoneutria nigriventer* spider. Br J Pharmacol 118:295–298

Patacchini R, Maggi CA (1995) Tachykinin receptors and receptor subtypes. Arch Int Pharmacodyn 329:161–184

Patacchini R, Barthò L, Holzer P, Maggi CA (1995) Activity of SR 142801 at peripheral tachykinin receptors. Eur J Pharmacol 278:17–25

Ren K, Iadarola MJ, Dubner R (1996) An isobolographic analysis of the effects of N-methyl-D-aspartate and tachykinin NK_1 receptor antagonists on inflammatory hyperalgesia in rats. Br J Pharmacol 117:196–202

Robineau P, Lonchampt M, Kucharczyk N, Krause JE, Regoli D, Fauchère JL, Prost JF, Canet E (1995) *In vitro* and *in vivo* pharmacology of S 16474, a novel dual tachykinin NK_1 and NK_2 receptor antagonist. Eur J Pharmacol 294:677–684

Rupniak MNJ (1999) Use of substance P receptor antagonists as a research tool in psychopharmacology. Neurotransmission 15/3:3–11

Rupniak NMJ, Kramer MS (1999) Discovery of the antidepressant and anti-emetic efficacy of substance P receptor (NK_1) antagonists. Trends Pharmacol Sci 20:484–490

Rupniak MNJ, Williams AR (1994) Differential inhibition of foot tapping and chromodacryorrhoea in gerbils by CNS penetrant and non-penetrant NK_1 receptor antagonists. Eur J Pharmacol 265:179–183

Sakurada T, Katsumata K, Yogo H, Tan-No K, Sakurada S, Kisara K (1993) Antinociception induced by CP 96,345, a non-peptide NK-1 receptor antagonist, in the mouse formalin and capsaicin tests. Neurosci Lett 151:142–145

Sarau HM, Griswold DE, Potts W, Foley JJ, Schmidt DB, Webb EF, Martin LD, Brawner ME, Elshourbagy NA, Medhurst AD, Giardina GAM, Hay DWP (1997) Nonpeptide tachykinin receptor antagonists: I. Pharmacological and pharmacokinetic characterization of SB 223412, a novel, potent and selective neurokinin-3 receptor antagonist. J Pharmacol Exp Ther 281:1303–1311

Smith G, Harrison S, Bowers J, Wiseman J, Birch P (1994) Nonspecific effects of the tachykinin NK_1 receptor antagonist, CP-99,994, in antinociceptive tests in rat, mouse and gerbil. Eur J Pharmacol 271:481–487

Snider RM, Constantine JW, Lowe JA III, Longo KP, Lebel WS, Woody HA, Drozda SE, Desai MC, Vinick FJ, Spencer RW, Hess HJ (1991) A potent nonpeptide antagonist of the substance P (NK_1) receptor. Science 251:435–437

Vassout A, Schaub M, Gentsch C, Ofner S, Schilling W, Veenstra S (1994) P7/CGP 49823, a novel NK_1 receptor antagonist: behavioural effects. Neuropeptides 26, Suppl 1:38

Von Euler US, Gaddum JH (1931) An unidentified depressor substance in certain tissue extracts. J Physiol 72:74–89

H.3.1.3.2 ^{3}H-Substance P Receptor Binding

PURPOSE AND RATIONALE

Substance P is an undekapeptide which is widely distributed in the central and peripheral nervous systems and functions as a neurotransmitter/neuromodulator in a variety of physiological processes. Substance P is released from neurons in the midbrain in response to stress where it facilitates dopaminergic neurotransmission and from sensory neurons in the spinal cord in the response to noxious stimuli, where it excites dorsal neurons. In the periphery, release of substance P from sensory neurons causes vasodilatation and plasma extravasation, suggesting a role in neurogenic inflammation. Selective antagonists to substance P found in receptor binding studies may elucidate the physiological role of substance P and may be candidates for anti-inflammatory and analgesic drugs.

PROCEDURE

Fresh porcine brains are obtained from the slaughterhouse. Striata are dissected and homogenized (Ultraturrax) in 50 mM ice-cold Tris-HCl buffer, pH 7.4) containing 150 mM NaCl, 150 mM KCl, 12 mM EDTA, 200 µM phenylmethylsulfonylfluoride, 40 µg/ml bacitracin, 4 µ g/ml leupeptin, and 2 µg/ml chymostatin. These homogenates are then incubated for 30 min at 4°C before being centrifuged at 30,000 *g* for 20 min at 4°C and washed twice with 50 mM Tris-HCl (pH 7.4) buffer. Pellets are resuspended in 0.32 M sucrose containing 200 µM phenylmethyl sulfonylfluoride and 40 µg/ml bacitracin before storage at –80°C until use.

Sixty-minute incubations are carried out at room temperature in 50 mM Tris-HCl buffer, pH 7.4, containing various concentrations of [^{3}H]substance P ([^{3}H]SP) (0.05–20 nM), 5 mM $MgSO_4$, 40 mg/ml bacitracin, 4 mg/ml leupeptin, and 2 mg/ml chymostatin in the presence of 0.8–1 mg of membrane protein in a final volume of 1 ml. Total binding and nonspecific binding are determined in triplicate in the absence or presence of 1 mM unlabeled substance P. Incubations are terminated by adding 4 ml of ice-cold Tris-HCl buffer (pH 7.4) and membranes are filtered on Whatman glass fiber filters that are presoaked in 0.5% polyethylenimine for a minimum of 3 h to reduce absorption. Filters are then washed three times (5 ml each) using ice-cold Tris-HCl buffer (pH 7.4). Bound radioactivities are determined using a liquid scintillation counter.

EVALUATION

Saturation and competition data are analyzed using a computer program as described by McPherson (1985).

REFERENCES AND FURTHER READING

Iversen LL, Jessell T, Kanazawa I (1976) Release and metabolism of substance P in rat hypothalamus. Nature 264:81–83

Lee CM, Javitch JA, Snyder SH (1983) ^{3}H-Substance P binding to salivary gland membranes. Mol Pharmacol 23:563–569

Liu YF, Quirion R (1991) Presence of various carbohydrate moieties including β-galactose and *N*-acetylglucosamine residues on solubilized porcine brain neurokinin-1/substance P receptors. J Neurochem 57:1944–1950

McLean S, Ganong AH, Seeger TF, Bryce DK, Pratt KG, Reynolds LS, Siok CJ, Lowe III JA, Heym J (1991) Activity of binding sites in brain of a nonpeptide substance P (NK_1) receptor antagonist. Science 251:437–439

McPherson GA (1985) Analysis of radioligand binding experiments. A collection of computer programs for the IBM PC. J Pharmacol Meth 14:213–228

Mizrahi J, D'Orléans-Juste P, Drapeau G, Escher E, Regoli D (1983) Partial agonists and antagonists for substance P. Eur J Pharmacol 91:139–140

Perrone MH, Diehl RE, Haubrich DR (1983) Binding of [^{3}H]substance P to putative substance P receptors in rat brain membranes. Eur J Pharmacol 95:131–133

H.3.1.3.3 Neurokinin Receptor Binding

PURPOSE AND RATIONALE

The actions of tachykinins are mediated through three subtypes of neurokinin receptors belonging to the G protein-linked receptor family, namely, NK_1, NK_2 and NK_3. Substance P displays highest affinity to NK_1

receptors, whereas neurokinin A and neurokinin B preferably bind to NK_2 and NK_3 receptors, respectively. NK_1 receptors are expressed in a wide variety of peripheral tissues and in the CNS. NK_2 receptors are expressed primarily in the periphery, while NK_3 receptors are primarily expressed in the CNS.

PROCEDURE

Tachykinin NK_1 receptor binding assay is performed in intact Chinese hamster ovary (CHO) cells expressing the human tachykinin NK_1 receptor (Cascieri et al. 1992). The receptor is expressed at a level of 3×10^5 receptors per cell. Cells are grown in a monolayer culture, detached from the plate with enzyme-free cell dissociation solution (Specialty Media), and washed prior to use in the assay. ^{125}I[Tyr^8]substance P (0.1 nM, 2000 Ci/mmol; New England Nuclear) is incubated in the presence or absence of test compounds (dissolved on 5 µl DMSO) with 5×10^4 CHO cells. Ligand binding is performed in 0.25 ml of 50 mM Tris-HCl, pH 7.5, containing 5 mM $MnCl_2$, 150 mM NaCl, 0.02% bovine serum albumin, 40 µg/ml bacitracin, 0.01 mM phosphoramidon and 4 µg/ml leupeptin. The incubation proceeds at room temperature until equilibrium is achieved (>40 min) and the receptor ligand complex is harvested by filtration over GF/C filters presoaked in 0.1% polyethylenimine using a Tomtek 96-well harvester. Nonspecific binding is determined using excess substance P (1 µM) representing <10% of total binding.

For **NK_2 receptor binding assays** membranes of CHO cells transfected with human ileum NK_2 receptor are used (Hagan et al. 1993; Beresford et al. 1995). The membrane suspensions (5 µg protein) in assay buffer (Tris base (50 mM), $MnCl_2$ (3 mM), bovine serum albumin (0.05%), chymostatin (2 µg/ml) and leupeptin 4 µg/ml, pH 7.4) are incubated for 90 min at room temperature with wash buffer (Tris base (50 mM), $MnCl_2$ (3 mM), lauryl sulphate (0.01%), pH 7.4) or test compound, and [^{3}H]-GR100679 (0.5 nM final concentration). Non-specific binding is defined by use of GR159897 (1 µM).

For **NK_3 receptor binding assays** guinea pig cortical membranes (Guard et al. 1990) are incubated at room temperature for 60 min with HEPES wash buffer or test compound and [^{3}H]-senktide (final concentration 0.8–1.0 nM). Non-specific binding is defined by addition of eledoisin (10 µM).

EVALUATION

Inhibition curves are analyzed and pIC_{50} values calculated by use of a curve fitting program. pIC_{50} values are converted to inhibition constants (pK_i values) using the Cheng Prussoff equation

$$K_i = IC_{50}/(1 + L/K_D)$$

where L is the ligand concentration and K_D is the dissociation constant. The K_D and B_{max} (maximum number of binding site per mg of tissue) are determined from saturation curves and analyzed by a curve fitting program. Values are expressed as means ±SEM.

MODIFICATIONS OF THE METHOD

Watson et al. (1955) performed substance P binding assays in **ferret brain membranes** and assessed neurokinin NK_1 receptor binding using human lymphoblasts (IM-9 cells).

Rupniak et al. (1997) studied displacement of ^{125}I-[Tyr^8]substance P binding to cloned human tachykinin NK_1 receptors and to ferret brain membranes *in vitro*.

Beattie et al. (1995) used U373 MG cell membranes and cerebral cortical membranes from rat, ferret and gerbil and [^{3}H]substance P for NK_1 receptor binding assays.

Bonnet et al. (1996), McLean et al. (1996) used the IM9 lymphoblastoma cell line expressing the human NK_1 receptor.

Emonds-Alt et al. (1995) studied binding of [^{125}I] Bolton-Hunter labelled substance P to **NK_1 receptors** of rat brain cortex, human lymphoblast cells (IM9), and human astrocytoma cells (U373MG, STTG1), binding of [^{125}I]iodohistidyl-NKA (or [^{125}I]neuropeptide γ) to **NK_2 receptors** of rat or hamster urinary bladder or guinea pig ileum, binding of [^{125}I]iodohistidyl-[Me-Phe^7]NKB (or [^{125}I]Eledoisin) to tachykinin **NK_3 receptors** of rat, guinea pig and gerbil brain cortex., and of [^{125}I]iodohistidyl-[Me-Phe^7]NKB to the human NK_3 receptor, cloned and expressed in CHO cells (Buell et al. 1992).

Cascieri et al. (1992) described the binding of a potent, selective, radioiodinated antagonist to the human neurokinin-1 receptor.

A radioligand of the tachykinin NK_2 receptor was described by Renzetti et al. (1998).

Jordan et al. (1998) evaluated the Cytosensor microphysiometer, a system that measures the extracellular acidification rate as an index of the integrated functional response to receptor activation, as a method to study NK_3 receptor pharmacology and used this system to assess the functional activity of novel compounds at this receptor.

Appell et al. (1998) reported biological characterization of neurokinin antagonists discovered through

screening of a combinatorial library. Using stably transfected CHO-K1 cell lines expressing human NK-1, NK-2 and NK-3 receptor subtypes and europium time-resolved fluorescence, primary receptor binding assays were designed to define active compounds. In addition, a secondary, functional assay measuring intracellular calcium flux with the calcium-sensitive fluorophore, fluo-3, in CHO cells transfected with the human NK-1 or NK-2 receptor was used to determine agonist or antagonist activities.

REFERENCES AND FURTHER READING

Appell KC, Chung TDY, Solly KJ, Chelsky D (1998) Biological characterization of neurokinin antagonists discovered through screening of a combinatorial library. J Biomol Screening 3:19–27

Beattie DT, Beresford IJM, Connor HE, Marshall FH, Hawcock AB, Hagen RM, Bowers J, Birch PJ, Ward P (1995) The pharmacology of GR203040, a novel, potent and selective tachykinin NK_1 receptor antagonist. Br J Pharmacol 116:3149–3157

Beresford IJM, Ball DI, Sheldrick RGL, Turpin MP, Walsh DM, Hawcock AB, Coleman RM, Tyers MB (1995) GR 159897, a potent, non-peptide antagonist at NK_2 receptors. Eur J Pharmacol 272:241–248

Bonnet J, Kucharczyk N, Robineau P, Lonchampt M, Dacquet C, Regoli D, Fauchère JL, Canet E (1996) A water soluble, stable dipeptide NK_1 receptor-selective neurokinin receptor antagonist with potent *in vivo* pharmacological effects: S18523. Eur J Pharmacol 310:37–46

Buell G, Schulz MF, Arkinstall SJ, Maury K, Missotten M, Adami N, Talabot F, Kawashima E (1992) Molecular characterization, expression and localization of human neurokinin-3 receptor. FEBS Lett 299:90–95

Cascieri MA, Ber E, Fong TM, Sadowski S, Bansal A, Swain C, Seward E, Frances B, Burns D, Strader CD (1992) Characterization of the binding of a potent, selective, radioiodinated antagonist to the human neurokinin-1 receptor. Mol Pharmacol 42:458–463

Cascieri MA, Fong TM, Strader CD (1995) Molecular characterization of a common binding site for small molecules within the transmembrane domain of G-protein coupled receptors. J Pharmacol Toxicol Meth 33:179–185

Emonds-Alt X, Doutremepuich JD, Heaulme M, Neliat G, Santucci V, Steinberg R, Vilain P, Bichon D, Ducoux JP, Proietto V, Van Brock D, Soubrie P, Le Fur G, Breliere JC (1993) *In vitro* and *in vivo* biological activities of SR140333, a novel potent non-peptide tachykinin NK_1 receptor antagonist. Eur J Pharmacol 250:403–413

Emonds-Alt X, Bichon D, Ducoux JP, Heaulme M, Miloux B, Poncelet M, Proietto V, Van Broeck D, Vilain P, Neliat G, Soubrié P, Le Fur G, Brelière JC (1995) SR 142801, the first potent non-peptide antagonist of the tachykinin NK_3 receptor. Life Sci 56:27–32

Guard S, Watson SP, Maggio JE, Phon Too H, Watling KJ (1990) Pharmacological analysis of [^{3}H]-senktide binding to NK_3 tachykinin receptors in guinea pig ileum longitudinal muscle-myenteric plexus and cerebral cortex membranes. Br J Pharmacol 99:767–773

Hagan RM, Beresford IJ, Stables J, Dupere J, Stubbs CM, Elliott PJ, Sheldrick RL, Chollet A, Kawashima E, McElroy AB, Ward P (1993) Characterization, CNS distribution and function of NK_2 receptors studied using potent NK_2 receptor antagonists. Regul Peptides 46:9–19

Jordan RE, Smart D, Grimson P, Suman-Chauhan N, McKnight AT (1998) Activation of the cloned human NK_3 receptor in Chinese hamster ovary cells characterized by the cellular acidification using the Cytosensor microphysiometer. Br J Pharmacol 125:761–766

Longmore J, Swain CJ, Hill RG (1995) Neurokinin receptors. Drug News Perspect 8:5–12

Maggi CA, Patacchini R, Rovero P, Giachetti A (1993) Tachykinin receptors and tachykinin receptor antagonists. J Autonom Pharmacol 13:23–93

Matuszek MA, Zeng XP, Strigas J, Burcher E (1998) An investigation of tachykinin NK_2 receptor subtypes in the rat. Eur J Pharmacol 352:103–109

McLean S, Ganong A, Seymour PA, Bryce DK, Crawford RT, Morrone J, Reynolds LS, Schmidt AW, Zorn S, Watson J, Fossa A, DePasquale M, Rosen T, Nagahisa A, Tsuchiya M, Heym J (1996) Characterization of CP-122,721, a nonpeptide antagonist of the neurokinin NK-1 receptor. J Pharmacol Exp Ther 277:900–908

Mussap CJ, Geraghty DP, Burcher E (1993) Tachykinin receptors: a radioligand perspective. J Neurochem 60:1987–2009

Nakanishi S (1991) Mammalian tachykinin receptors. Annu Rev Neurosci 14:123–136

Otsuka M, Yoshioka K (1939) Neurotransmitter functions of mammalian tachykinins. Phys Rev 73:229–308

Quartara L, Maggi CA (1998) The tachykinin receptor. Part II: Distribution and pathophysiological roles. Neuropeptides 32:1–49

Regoli D, Boudon A, Fachere JL (1994) Receptors and antagonists for substance P and related peptides. Pharmacol Rev 46:551–559

Renzetti AR, Catalioto RM, Criscuoli M, Cucchi P, Lippi AS, Guelfi M, Quartara L, Maggi CA (1998) Characterization of [^{3}H]MEN 11420, a novel glycosylated peptide antagonist of the tachykinin NK_2 receptor. Biochem Biophys Res Commun 248:78–82

Rupniak NMJ, Tattersall FD, Williams AR, Rycroft W, Carlson EJ, Cascieri MA, Sadowski S, Ber E, Hale JJ, Mills SG, McCoss M, Seward E, Huscroft I, Owen S, Swain CJ, Hill RG, Hargreaves RJ (1997) *In vitro* and *in vivo* predictors of the anti-emetic activity of tachykinin NK_1 receptor antagonists. Eur J Pharmacol 326:201–209

Snider RM, Constantine SJW, Lowe JA III, Longo KP, Lebel WS, Woody HA, Drozda SE, Desai MC, Vinick FJ, Spencer RW, Hess HJ (1991) A potent nonpeptide antagonist of the substance P (NK_1) receptor. Science 251:435–437

Watson JW, Gonsalves SF, Fossa AA, McLean S, Seeger T, Obach S, Andrews PLR (1995) The anti-emetic effects of CP-99,994 in the ferret and the dog: Role of the NK_1 receptor. Br J Pharmacol 115:84–94

H.3.1.3.4 Characterization of Neurokinin Agonists and Antagonists by Biological Assays

PURPOSE AND RATIONALE

Several biological assays have been used to characterize neurokinin agonists and antagonists on their receptors (Review by Regoli et al. 1994).

The following functional assays are recommended for evaluation of antagonists:

For NK_1 Receptors

- Inhibition of [Sar^9,$Met(O_2)^{11}$]substance P-induced endothelium-dependent **relaxation of rabbit pulmonary artery**, previously contracted with 0.1 µM noradrenaline (D'Orléans-Juste et al. 1986; Rubino et al. 1992; Emonds-Alt et al. 1993),
- inhibition of [Sar^9,$Met(O_2)^{11}$]substance P or [Sar^9]substance P sulfone-induced contractions of **guinea pig ileum** in the presence of 3 µM atropine and 3 µM mepyramine and indomethacin (Dion et al. 1987; Emonds-Alt et al. 1993; Patacchini et al. 1995; Hosoki et al. 1998; Walpole et al. 1998),
- **rabbit vena cava** stimulated by substance P or [Sar^9,$Met(O_2)^{11}$]substance P (Nantel et al. 1991; Regoli et al. 1994; Gitter et al. 1995; Robineau et al. 1995; Bonnet et al. 1996; Nguyen-Le et al. 1996),
- inhibition of substance P-induced **relaxation of the isolated dog carotid artery** previously contracted with norepinephrine (Snider et al. 1991),
- **rat urinary bladder**, stimulated by the selective agonist [Sar^9,$Met(O_2)^{11}$]substance P and treated with SR 48986 (1.7×10^{-7} mol/l) to eliminate NK-2 functional sites (Rouissi et al. 1993; Nguyen-Le et al. 1996),
- Ca^{2+} mobilization in **rat vas deferens** (Nagata et al. 1991),
- inhibition of **substance P-induced plasma extravasation in the bladder and bronchi** of the guinea pig (Bonnet et al. 1996),
- inhibition of **substance P-induced vasodilation in the nasal mucosa of pigs** using an acoustic rhinometer (Rinder and Lundberg 1996),
- inhibition of **[Sar^9,$Met(O_2)^{11}$]substance P-induced plasma extravasation in guinea-pig bronchi** (Cirillo et al. 1998),
- inhibition of **methacholine-induced contractions of isolated rat tracheal strips** (Tian et al. 1997),
- inhibition of **cyclophosphamide- and radiation-induced damage in the rat and ferret organs** (Alfieri and Gardner 1997, 1998),
- inhibition of **edema formation induced by substance P and antigen in rat skin** (Herbert and Bernat 1996),
- inhibition of **reciprocal hindlimb scratching after intracerebroventricular injection of substance P, [Sar^9, $Met(O_2)^{11}$]substance P or septide in mice (Jung et al. 1994) or gerbils** (Smith et al. 1994),
- inhibition of **turning behavior after intracerebroventricular injection of substance P, [Sar^9,$Met(O_2)^{11}$] substance P or septide in mice** (Jung et al. 1994),
- inhibition of **hind paw tapping and chromodacryorrhea after intracerebroventricular injection of tachykinin agonists in gerbils** (Graham et al. 1993; Bristow and Young 1994; Rupniak and Williams 1994; Rupniak et al. 1995, 1997; Vassout et al. 1994),
- inhibition of **cis-platin-induced emesis in ferrets** (Rupniak et al. 1997; Singh et al. 1997; Minami et al. 1998).

For NK_2 Receptors

- Inhibition of neurokinin A-induced contraction of **isolated rabbit aorta** (Snider et al. 1991),
- inhibition of neurokinin A-induced contraction of **isolated endothelium-deprived rabbit pulmonary artery or hamster trachea** (D'Orléans-Juste et al. 1986; Emonds-Alt et al. 1993; Patacchini et al. 1995),
- the **hamster urinary bladder** (Dion et al. 1987; Maggi et al. 1990; Regoli et al. 1994; Emonds-Alt et al. 1997; Tramontana et al. 1998),
- inhibition of **motor responses induced by intravesival administration of capsaicin** in rats *in vivo* (Lecci et al. 1997),
- **rat esophageal tunica muscularis** (Croci et al. 1995),
- inhibition of **turning behavior induced by intrastriatal injection of Nle^{10}-neurokinin A in mice** (Emonds-Alt et al. 1997).

For NK_3 Receptors

- Inhibition of **senktide- or neurokinin B-induced contractions of the rat portal vein** (Mastrangelo et al. 1987; Snider et al. 1991; Emonds-Alt et al. 1993; Patacchini et al. 1995),
- antagonism against **senktide-induced contractions in the isolated rabbit iris sphincter muscle** (Medhurst et al. 1997; Sarau et al. 1997),
- inhibition of**colonic propulsion in rats** (Broccardo et al. 1999)
- inhibition of **turning behavior induced by intrastriatal injection of senktide in gerbils** (Emonds-Alt et al. 1994),
- inhibition of **citric acid-induced cough in guinea pigs** (Daoui et al. 1998).
- The failure of NK_1 receptor antagonists in most clinical tests for analgesia in spite of clear preclinical data is a matter of discussion (Hill R 2000a, b; Urban and Fox 2000).

REFERENCES AND FURTHER READING

Alfieri A, Gardner C (1997) The NK-1 antagonist GR203040 inhibits cyclophosphamide-induced damage in the rat and ferret bladder. Gen Pharmacol 29:245–250

Alfieri A, Gardner C (1998) Effects of GR203940, an NK-1 antagonist, on radiation- and cisplatin-induced tissue damage in the ferret. Gen Pharmacol 31:741–746

Bonnet J, Kucharczyk N, Robineau P, Lonchampt M, Dacquet C, Regoli D, Fauchère JL, Canet E (1996) A water soluble, stable dipeptide NK_1 receptor-selective neurokinin receptor antagonist with potent *in vivo* pharmacological effects: S18523. Eur J Pharmacol 310:37–46

Bristow LJ, Young L (1994) Chromodacryorrhea and repetitive hind paw tapping: models of peripheral and central tachykinin NK_1 receptor activation in gerbils. Eur J Pharmacol 253:245–252

Broccardo M, Improta G, Tabacco A (1999) Central tachykinin NK_3 receptors in the inhibitory action on rat colonic propulsion of a new tachykinin, PG-KII. Eur J Pharmacol 376:67–71

Cirillo R, Astolfi M, Conte B, Lopez G, Parlani M, Terracciano R, Fincham CI, Manzini S (1998) Pharmacology of the peptidomimetic, MEN 11149, a new potent, selective and orally effective tachykinin NK_1 receptor antagonist. Eur J Pharmacol 341:201–209

Croci T, Emonds-Alt X, Le Fur G, Manara L (1995) *In vitro* characterization of the non-peptide tachykinin NK-1 and NK-2-receptor antagonists, SR 140333 and SR 48968 in different rat and guinea-pig intestinal segments. Life Sci 56:267–275

Daoui S, Cognon C, Naline E, Emonds-Alt X, Advenier C (1998) Involvement of tachykinin NK_3 receptors in citric-acid-induced cough and bronchial responses in guinea pigs. Am J Respir Crit Care Med 158:42–48

Dion S, D'Orléans-Juste P, Drapeau G, Rhaleb NE, Rouissi N, Tousignant C, Regoli D (1987) Characterization of neurokinin receptors in various isolated organs by use of selective agonists. Life Sci 14:2269–2278

D'Orléans-Juste P, Dion S, Drapeau G, Regoli d (1986) Different receptors are involved in the endothelium-mediated relaxation and the smooth muscle contraction of rabbit pulmonary artery in response to substance P and related neurokines. Eur J Pharmacol 125:37–44

Emonds-Alt X, Doutremepuich JD, Heaulme M, Neliat G, Santucci V, Steinberg R, Vilain P, Bichon D, Ducoux JP, Proietto V, Van Brock D, Soubrie P, Le Fur G, Breliere JC (1993) *In vitro* and *in vivo* biological activities of SR140333, a novel potent non-peptide tachykinin NK_1 receptor antagonist. Eur J Pharmacol 250:403–413

Emonds-Alt X, Bichon D, Ducoux JP, Heaulme M, Miloux B, Poncelet M, Proietto V, van Broeck D, Vilain P, Neliat G, Soubrié P, Le Fur G, Brelière JC (1995) SR 142801, the first potent non-peptide antagonist of the tachykinin NK_3 receptor. Life Sci 56: PL 27–32

Emonds-Alt X, Advenier C, Cognon C, Croci T, Daoul S, Ducoux JP, Landl M, Maline E, Nellat G, Poncelet M, Proletto V, Von Broeck D, Vilain P, Soubrié P, Le Fur G, Maffrand JP, Brelière JC (1997) Biochemical and pharmacological activities of SR 144190, a new potent non-peptide tachykinin NK_2 receptor antagonist. Neuropeptides 31:449–458

Gitter BD, Bruns RF, Howbert JJ, Waters DC, Threlkeld PG, Cox LM, Nixon JA, Lobb KL, Mason NR, Stengel PW, Cockerham SL, Silbaugh SA, Gehlert DL, Schober DA, Iyengar S, Calligaro DO, Regoli D, Hipskind PA (1995) Pharmacological characterization of LY303870: A novel, potent and selective nonpeptide substance P (neurokinin-1) receptor antagonist. J Pharmacol Exp Ther 275:737–744

Graham EA, Turpin MP, Stubbs CM (1993) P100 characterization of the tachykinin-induced hindlimb thumping response in gerbils. Neuropeptides 4:228–229

Herbert JM, Bernat A (1996) Effect of SR 140333, a selective NK_1 antagonist, on antigen-induced oedema formation in rat skin. J Lipid Mediat Cell Signal 13:223–232

Hill R (2000a) NK_1 (substance P) receptor antagonists – why are they not analgesic in humans? Trends Pharmacol Sci 21:244–246

Hill R (2000b) Reply: will changing the testing paradigms show that NK_1 receptor antagonists are analgesic in humans? Trends Pharmacol Sci 21:265

Hosoki R, Yanagisawa M, Onishi Y, Yoshioka K, Otska M (1998) Pharmacological profiles of new orally active non-peptide tachykinin NK_1 receptor antagonists. Eur J Pharmacol 341:235–241

Jung M, Calassi R, Maruani J, Barnouin MC, Souilhac J, Poncelet M, Gueudet C, Edmonds-Alt X, Soubriè P, Brelière JC, le Fur G (1994) Neuropharmacological characterization of SR 140333, a non peptide antagonist of NK_1 receptors. Neuropharmacol 33:167–179

Lecci A, Giulani S, Tramontana M, Criscuoli M, Maggi CA (1997) MEN 11,420, a peptide tachykinin NK_2 receptor antagonist, reduces motor responses induced by intravesical administration of capsaicin *in vivo*. Naunyn Schmiedeberg's Arch Pharmacol 356:182–188

Maggi CA, Patacchini R, Giulani S, Rovero P, Dion S, Regoli D, Giachetti A, Meli A (1990) Competitive antagonists discriminate between NK-2 tachykinin receptor subtypes. Br J Pharmacol 100:588–592

Mastrangelo D, Mathison R, Huggel HJ, Dion S, D'Orléans-Juste P, Rhaleb NE, Drapeau G, Rovero P, Regoli D (1987) The rat isolated portal vein: A preparation sensitive to neurokinins, particularly to neurokinin B. Eur J Pharmacol 134:321–326

Medhurst AD, Parson AA, Roberts JC, Hay DWP (1997) Characterization of NK_3 receptors in rabbit isolated iris sphincter muscle. Br J Pharmacol 120:93–101

Minami N, Endo T, Kikuchi K, Ihira E, Hirafuji M, Hamaue N, Monma Y, Sakurada T, Tanno K, Kisara K (1998) Antiemetic effects of sendide, a peptide tachykinin NK_1 receptor antagonist, in the ferret. Eur J Pharmacol 363:49–55

Nagata K, Saito H, Matsuki N (1991) Efficient Ca^{2+} mobilization induced by neurokinin A in rat vas deferens. Eur J Pharmacol 204:295–300

Nantel F, Roussi N, Rhaleb D, Jukic D, Regoli D (1991) Pharmacological evaluation of the angiotensin, kinin and neurokinin receptors on the rabbit vena cava. J Cardiovasc Pharmacol 18:398–405

Nguyen-Le XK, Nguyen QT, Gobeil F, Pheng LH, Emonds-Alt X, Brelière JC, Regoli D (1996) Pharmacological characterization of SR 142801: a new non-peptide antagonist of the neurokinin NK-3 receptor. Pharmacology 52:283–291

Patacchini R, Barthò L, Holzer P, Maggi CA (1995) Activity of SR 142801 at peripheral tachykinin receptors. Eur J Pharmacol 278:17–25

Regoli D, Nguyen QT, Jukic D (1994) Neurokinin receptor subtypes characterized by biological assays. Life Sci 54:2035–2047

Rinder J, Lundberg JM (1996) Effects of hCGRP 8–37 and the NK_1-receptor antagonist SR 140.333 on capsaicin-evoked vasodilation in the pig nasal mucosa *in vivo*. Acta Physiol Scand 156:115–122

Robineau P, Lonchampt M, Kucharczyk N, Krause JE, Regoli D, Fauchère JL, Prost JF, Canet E (1995) *In vitro* and *in vivo* pharmacology of S 16474, a novel dual tachykinin NK_1 and NK_2 receptor antagonist. Eur J Pharmacol 294:677–684

Rouissi N, Claing A, Nicolau M, Jukic D, D'Orléans-Juste P, Regoli D (1993) Substance P (NK-1 receptor) antagonists: *In vivo* and *in vitro* activities in rats and guinea pigs. Life Sci 52:1141–1147

Rubino A, Thomann H, Henlin JM, Schilling W, Criscione L (1992) Endothelium-dependent relaxant effect of neurokinins on rabbit aorta is mediated by the NK_1 receptor. Eur J Pharmacol 212:237–243

Rupniak NMJ, Williams AR (1994) Differential inhibition of foot tapping and chromodacryorrhoea in gerbils by CNS penetrant and non penetrant tachykinin NK_1 receptor antagonists. Eur J Pharmacol 265:179–183

Rupniak NMJ, Webb JK, Williams AR, Carlson E, Boyce S, Hill HG (1995) Antinociceptive activity of the tachykinin NK_1 receptor antagonist, CP-99994, in conscious gerbils. Br J Pharmacol 116:1937–1943

Rupniak NMJ, Tattersall FD, Williams AR, Rycroft W, Carlson EJ, Cascieri MA, Sadowski S, Ber E, Hale JJ, Mills SG, MacCoss M, Seward E, Huscroft I, Owen S, Swain CJ, Hill RG, Hargreaves RJ (1997) *In vitro* and *in vivo* predictors of the anti-emetic activity of tachykinin NK_1 receptor antagonists. Eur J Pharmacol 326:201–209

Sarau HM, Griswold DE, Potts W, Foley JJ, Schmidt DB, Webb EF, Martin LD, Brawner ME, Elshourbagy NA, Medhurst AD, Giardina GAM, Hay DWP (1997) Nonpeptide tachykinin receptor antagonists: I. Pharmacological and pharmacokinetic characterization of SB 223412, a novel, potent and selective neurokinin-3 receptor antagonist. J Pharmacol Exp Ther 281:1303–1311

Singh L, Field MJ, Hughes J, Kuo BS, Suman-Chauhan N, Tuladhar BR, Wright DS, Naylor RJ (1997) The tachykinin NK_1 receptor antagonist PD 154075 blocks cisplatin-induced delayed emesis in the ferret. Eur J Pharmacol 321:209–216

Snider RM, Constantine JW, Lowe JA III, Longo KP, Lebel WS, Woody HA, Drozda SE, Desai MC, Vinick FJ, Spencer RW, Hess HJ (1991) A potent nonpeptide antagonist of the substance P (NK_1) receptor. Science 251:435–437

Smith G, Harrison S, Bowers J, Wiseman J, Birch P (1994) Nonspecific effects of the tachykinin NK_1 receptor antagonist, CP-99,994, in antinociceptive tests in rat, mouse and gerbil. Eur J Pharmacol 271:481–487

Tian J, Wei EQ, Chen JS, Zhang WP (1997) Effect of SR 140333, a neurokinin NK_1 receptor antagonist, on airway reactivity to methacholine in sedated rats. Acta Pharmacol Sin 18:485–488

Tramontana M, Patacchini R, Lecci A, Giuliani S, Maggi CA (1998) Tachykinin NK_2 receptors in the hamster urinary bladder: *In vitro* and *in vivo* characterization. Naunyn-Schmiedeberg's Arch Pharmacol 358:293–300

Urban LA, Fox A (2000) NK_1 receptor antagonists – are they really without effects in the pain clinic? Trends Pharmacol Sci 21:462–464

Vassout A, Schaub M, Gentsch C, Ofner S, Schilling W, Veenstra S (1994) P7/CGP 49823, a novel NK_1 receptor antagonist: behavioural effects. Neuropeptides 26, Suppl 1:38

Walpole CSJ, Brown MCS, James IF, Campbell EA, McIntyre P, Docherty R, Ko S, Hedley L, Ewan S, Buchheit KH, Urban LA (1998) Comparative, general pharmacology of SDZ NKT 343, a novel, selective NK_1 receptor antagonist. Br J Pharmacol 124:83–92

H.3.1.4 Assay of Polymorphonuclear Leukocyte Chemotaxis In Vitro

PURPOSE AND RATIONALE

Leukocyte accumulation is an important aspect of host defense mechanisms. Chemotactic factors attract leukocytes to an infected or inflamed site. The method of Boyden (1962) has been widely employed to measure the chemotactic effects on polymorphonuclear leukocytes. Watanabe et al. (1989) described a rapid assay of polymorphonuclear leukocyte chemotaxis *in vitro*.

PROCEDURE

Two 96-well tissue-culture plates are utilized as one set of multiple Boyden chambers. One plate as multiple lower compartments and the other plate upside down as multiple upper compartments can be tightly sandwiched with the aid of 12 sets of bolts. The holes, into which bolts are set and polymorphonuclear leukocytes (PMN) suspensions are introduced, are opened by a heated stick. Eight sets of 6 holes are made on the bottom of the upper plate to serve as multiple upper compartments for introducing PMN suspensions. Eight sets of polycarbonate filter (approximately 3.2 × 2.2 cm), cut from a round filter (Nuclepore Co.) with pores of 2 μm in diameter, are sandwiched between the upper and lower plates. One sheet of the filter can separate six sets of the upper compartments from the lower ones. Silicon grease is spread on all the plate surfaces that attach to the filters. The lower compartments are filled with a chemoattractant (400 μ l/well) diluted in RPMI-1640 medium. The eight sheets of filter paper are carefully placed on each set of the lower compartments to avoid air bubbles. The upper plate is positioned over the lower plate and fastened with bolts. The upper compartments are filled with 0.3 ml of PMN suspension (at 10^7 cells/ml). The assembly is incubated at 37°C for 60 min in a humidified atmosphere containing 5% CO_2. Then the fluid in the upper compartment is decanted and the upper compartments are completely washed with a jet of water. The lower plate is centrifuged at 2400 rpm for 5 min at room temperature and the supernatant in the well is decanted. The pellet of PMNs is dispersed in 200 μl of phosphate buffered saline containing 0.1% EDTA. Absorbance at 660 nm of each well containing PMN suspension is determined with a 96-well microplate reader. The number of PMNs in the lower compartments is further determined by a Coulter counter.

EVALUATION

The migration rate is calculated as percentage from the number of PMNs in the lower compartment/number of PMNs applied in the upper compartment. The migration rate is dependent on the concentration of the chemoattractant (e. g., zymosan-activated serum). Moreover, a dose dependent decrease of migration rate is achieved by chemotaxis inhibitors.

MODIFICATIONS OF THE METHOD

Nelson et al. (1975) described chemotaxis under agarose as a simple method for measuring chemotaxis and spontaneous migration of human polymorphonuclear leukocytes and monocytes.

Migration of PMNs in agarose gel was measured after fixation with glutaraldehyde and staining with Giemsa by Shalaby et al. (1987).

Optimal conditions for simultaneous purification of mononuclear and polymorphonuclear leukocytes from human blood were described by Ferrante and Thong (1980).

PMN chemotaxis was measured in multiwell microchemotaxis chambers separated by 5-µm pore size polyvinylpyrrolidone-free polycarbonate membranes by Harvath et al. (1980), Figari et al. (1987).

REFERENCES AND FURTHER READING

Atkins PC, Norman ME, Zweiman B (1978) Antigen-induced neutrophil chemotactic activity in man. J Allergy Clin Immunol 62:149–155

Boyden S (1962) The chemotactic effects of mixtures of antibody and antigen on polymorphonuclear leukocytes. J Exp Med 115:453–466

Bray MA, Ford-Hutchinson AW, Shipley ME, Smith MJH (1980) Calcium ionophore A23187 induces release of chemokinetic and aggregating factors from polymorphonuclear leukocytes. Br J Pharmacol 71:507–512

Camussi G, Tetta C, Bussolino F, Baglioni C (1990) Antiinflammatory peptides (antiflammins) inhibit synthesis of platelet-activating factor, neutrophil aggregation and chemotaxis, and intradermal inflammatory reactions. J Exp Med 171:913–927

Ferrante A, Thong YH (1980) Optimal conditions for simultaneous purification of mononuclear and polymorphonuclear leukocytes from human blood by the Hypaque-Ficoll method. J Immunol Meth 36:109–117

Figari IS, Mori NA, Palladino MA (1987) Regulation of neutrophil migration and superoxide production by recombinant tumor necrosis factors-α and -β: Comparison to recombinant interferon-γ and interleukin-1α. Blood 70:979–984

Harvath L, Falk W, Leonard EJ (1980) Rapid quantitation of neutrophil chemotaxis: Use of a polyvinylpyrrolidone-free polycarbonate membrane in a multiwell assembly. J Immunol Meth 37:39–45

Issekutz AC, Issekutz TB (1989) Quantitation of blood cell accumulation and vascular responses in inflammatory reactions. In: Pharmacological Methods in the Control of Inflammation. Alan R. Liss, Inc., pp 129–150

Matzner Y, Drexler R, Levy M (1984) Effect of dipyrone, acetylsalicylic acid and acetaminophen on human neutrophil chemotaxis. Eur J Clin Invest 14:440–443

Nelson RD, Quie PG, Simmons RL (1975) Chemotaxis under agarose: a new and simple method for measuring chemotaxis and spontaneous migration of human polymorphonuclear leukocytes and monocytes. J Immunol 115:1650–1656

Roch-Arveiller M, Roblin G, Allain M, Giroud JP (1985) A visual technique of chemotactic assessment for pharmacological studies. J Pharmacol Meth 14:313–321

Shalaby MR, Palladino MA, Hirabayashi SE, Eessalu TE, Lewis GT, Shepard HM, Aggarwal BB (1987) Receptor binding and activation of polymorphonuclear neutrophils by tumor necrosis factor-alpha. J Leukoc Biol 41:196–204

Watanabe K, Kinoshita S, Nakagawa H (1989) Very rapid assay of polymorphonuclear leukocyte chemotaxis *in vitro*. J Pharmacol Meth 22:13–18

H.3.1.5 Polymorphonuclear Leukocytes Aggregation Induced by FMLP

PURPOSE AND RATIONALE

Aggregation of polymorphonuclear leukocytes (PMNs) can be induced by FMLP (formyl-L-methionyl-L-leucyl-L-phenylalanine). The aggregation can be inhibited by xanthine derivatives.

PROCEDURE

PMNs cell suspensions are prepared from peritoneal exudates obtained 17 h after intraperitoneal injection of 10 ml 6% sodium caseinate into Sprague Dawley rats. The cells are washed twice in Geys-balanced-salt-solution (Gibco GBSS) and resuspended to a final concentration of 15×10^6 cells/ml. The test compounds and the standard (pentoxiphylline) are dissolved in GBSS. FMLP (formyl-L-methionyl-L-leucyl-L-phenylalanine) is dissolved in DMSO. The further dilutions are made up to a final concentration of 10^{-7} mol FMLP in GBSS. Before addition of FMLP, the cell suspensions are pre-incubated for 10 min with the drugs. PMNs aggregation is carried out in a Born aggregometer.

EVALUATION

The results are expressed as change in transmittance, measured in mm on the recorder. The mean peak of the untreated cells is set 100%.

MODIFICATIONS OF THE METHOD

Moqbel et al. (1986) measured the activation of human leukocytes after FMLP in a rosette assay by the change in the expression of complement (C3b) and IgG (Fc)

receptors and in a cytotoxic assay by the *in vitro* capacity to adhere to and kill the complement-coated larvae (schistosomula) of Schistosoma mansoni.

Bradford and Rubin (1986) determined the effect of various drugs on IP_3 accumulation evoked by FMLP in neutrophils from New Zealand white rabbits.

Bourgoin et al. (1991) studied the influence of granulocyte-macrophage colony-stimulating factor (GM-CSF) on phosphatidylcholine breakdown by phospholipase D in human neutrophils.

REFERENCES AND FURTHER READING

Bradford PG, Rubin RP (1986) The differential effects of nedocromil sodium and sodium cromoglycate on the secretory response of rabbit peritoneal neutrophils. Eur J Respir Dis 69 (Suppl 147):238–240

Bray MA, Ford-Hutchinson AW, Shipley ME, Smith MJH (1980) Calcium ionophore A23187 induces release of chemokinetic and aggregating factors from polymorphonuclear leucocytes. Br J Pharmacol 71:507–512

Bourgoin S, Borgeat P, Poubelle PE (1991) Granulocyte-macrophage colony-stimulating factor (GM-CSF) primes human neutrophils for enhanced phosphatidylcholine breakdown by phospholipase D. Agents Actions 34:32–34

Moqbel R, Walsh GM, Kay AB (1986) Inhibition of human granulocyte activation by nedocromil sodium. Eur J Respir Dis 69 (Suppl 147):227–229

H.3.1.6 Constitutive and Inducible Cellular Arachidonic Acid Metabolism In Vitro

PURPOSE AND RATIONALE

The various metabolites of arachidonic acid are involved in many inflammatory processes. Arachidonic acid is released from the cellular phospholipid fraction by the action of phospholipase A_2, and subsequently metabolized via two major routes: the cyclooxygenase pathway yielding the primary prostaglandins and thromboxane, and the 5-lipoxygenase pathway yielding the leukotrienes. Thromboxanes, prostaglandins, and leukotrienes play a pathophysiological role in many diseases. Receptor assays for these autocoids were developed (Haluska et al. 1989). Murata et al. (1997) produced mice lacking the prostaglandin receptor which showed increased susceptibility to thrombosis and altered pain reception and inflammatory response.

The therapeutic mode of action of the classical non-steroidal anti-inflammatory drugs (NSAID), such as aspirin or indomethacin, is primarily explained by their inhibitory effect on cyclooxygenase, the key enzyme of the prostaglandin pathway. Inhibitors of the 5-lipoxygenase pathway have attracted considerable attention as potential anti-inflammatories with high potency. Appropriate assay systems for the determination of the different eicosanoids allow to study the influence of drugs towards the specific pathways of the arachidonic acid cascade in various cellular systems (Samuelsson 1986; Vane and Botting 1987).

According to recent discoveries there are two forms of cyclooxygenase (Xie et al. 1992; Lee et al. 1992; Gierse et al. 1996). Cyclooxygenase-1 (COX-1) is found as a constitutive enzyme in most tissues including blood platelets. Prostaglandins generated by constitutive pathways may exert cytoprotective effects, and are involved in maintaining vital functions in vascular hemostasis, gastric mucosa and kidney.

Chandrasekharan et al. (2002) described the cloning, structure and expression COX-3, a cyclooxygenase-1 variant, which is selectively inhibited by analgesic/antipyretic drugs, such as acetaminophen, phenacetin, antipyrine, and dipyrone.

The inhibition of these prostaglandins by the classical cyclooxygenase inhibitors is now generally accepted as an explanation of their adverse side effects.

COX-2 which shares about 62% amino acid homology with COX-1, is only expressed after cell activation, especially by mitogenic or inflammatory stimuli (Herrmann et al. 1990; Funk et al. 1991; Crofford 1997). Thus, specific suppression of the COX-2-pathway may represent a superior target for the evaluation of new antiinflammatory drugs. Drugs which have a high potency on COX-2 and a favorable COX-2/COX-1 ratio have potent anti-inflammatory activity with fewer side effects (Riendeau et al. 1997; Vane 1998; Hawkey 1999; Song et al. 1999; Chan et al. 1999). Shigeta et al. (1998) described the role of cyclooxygenase-2 (COX-2) in the healing of gastric ulcers in rats. Hull et al. (2005) investigated the expression of cyclooxygenase-1 and -2 by human gastric endothelial cells.

The cardiovascular value of selective COX-2 inhibitors has been questioned because they selectively reduce prostacyclin production, thus disrupting the hormonal balance and promoting a prothrombotic state (Hankey and Eikelboom 2003).

These theoretical concerns were supported by the results of clinical trials demonstrating an increased risk of myocardial infarction with COX-2 inhibitors compared with conventional non-steroidal anti-inflammatory drugs (NSAIDs) (Bombadier et al. 2000). The debate on benefit-risk assessment of COX-2 inhibitors is ongoing (Bing 2003; Schmidt et al. 2004).

H.3.1.6.1 Formation of Leukotriene B_4 in Human White Blood Cells In Vitro

PROCEDURE

Human white blood cells are prepared according to the standard procedure published by Salari et al. (1984): 40 ml freshly drawn citrated blood are admixed with 8 ml of PM16-buffer, containing 6% (v/v) dextran (MW = 480,000), and incubated at room temperature for one hour. The supernatant containing the white blood cell fraction is removed, diluted 1:1 (v/v) with PM16 and centrifuged for 15 min at 300 *g*. The precipitate is resuspended in PM16 and adjusted to 10^{10} cells/l (Counter HT, Coulter Electronics, Krefeld, FRG).

The metabolism of endogenously bound arachidonic acid to LTB_4 is measured in a total volume of 0.3 ml of the cell suspension at 37°C. The reaction tube contains 2 mmol/l $CaCl_2$, 0.5 mmol/l $MgCl_2$ and the investigational drug. After 15 min pre-incubation the reaction is started by addition of 12.5 µg of the Ca-ionophore A 23187 and 2 µg glutathione. After 5 min the reaction is stopped with 30 µl 0.1 M HCl at 0°C. After centrifugation for 2 min at 0°C, aliquots of the supernatant are subjected to HPLC, similarly as described by Veenstra et al. (1988), using a C-18 Nucleosil column (5 µm, 100 × 3 mm, Chrompack GmbH, Frankfurt, FRG) and, at a flow rate of 0.7 ml/min, a solvent mixture consisting of 725 ml methanol, 275 ml water and 0.1 ml acetic acid. Authentic standard drugs are used to identify cis-, trans- and epi-LTB_4. The separation of the three isomers can be followed photometrically at the UV-maximum of 278 nm.

EVALUATION

The peak areas of cis-, trans- and epi-LTB_4 are measured as a function of drug concentration, and related to a control experiment without drug.

CRITICAL ASSESSMENT

The tested pathway involves the enzymatic steps of phospholipase A_2 and the 5-lipoxygenase. Thus inhibitors of these enzymes are to decrease formation of the three isomers of LTB_4. The step of phospholipase A_2 can be circumvented by the addition of exogenous arachidonic acid (1 µmol/l).

Inhibitors of LTA_4-hydrolase which catalyzes the intermediary conversion of LTA_4 to the biologically active cis-LTB_4, can also be identified by this assay. Such drugs are to exhibit an increased formation of the non-enzymatic hydrolysis products trans- and epi-LTB_4 at the expense of decreased cis-LTB_4.

MODIFICATIONS OF THE METHOD

Winkler et al. (1988) used differentiated U-937 cells expressing LTB_4 receptors to study Ca^{2+} mobilization in response to LTB_4.

Jones et al. (1995) tested inhibition of [^{3}H]leukotriene D_4 specific binding in guinea pig lung, sheep lung, and dimethylsulfoxide-differentiated U837 cell plasma membrane preparations.

H.3.1.6.2 Formation of Lipoxygenase Products from ^{14}C-Arachidonic Acid in Human Polymorphonuclear Neutrophils (PMN) In Vitro

PROCEDURE

PMN are prepared by the standard procedure of Böyum (1976). The first steps are carried out at room temperature: 50 ml citrated human blood are centrifuged at 130 *g* for 15 min. The pellet is resuspended in 20 ml Dulbecco's minimal essential medium, and subsequently underlayered with 15 ml lymphoprep. After centrifugation at 400 *g* for 25 min the pellet is resuspended in 28 ml Dulbecco's HBSS containing 3% dextran. After incubation at 0°C for 120 min the decanted supernatant is centrifuged at 400 *g* for 15 min. The pellet is resuspended in 1 ml Dulbecco's PBS, containing 11 µmol/l glucose, to a leukocyte count of 2×10^{10}/l.

The method of HPLC determination of cellular metabolites of exogenous 1-C-14-arachidonic acid, as published by Borgeat and Samuelsson (1979), is modified as briefly described:

0.1 ml of the leukocyte suspension are incubated in Dulbecco's phosphate buffered saline (DPBS) at 37°C with the test drugs for 15 min. The incubation is then interrupted by cooling in an ice bath. Calcium ionophore A 23187 (final concentration 7×10^{-5} mol/l) and 1-C-14-arachidonic acid (final concentration 8.4×10^{-5} mol/l, 0.5 µCi) are added, and, after a second incubation period of 15 min at 37°C, terminated by the addition of 0.4 ml methanol. The assay mixture is then extracted with chloroform. The chloroform is evaporated, and, after redissolving the residue in a minor amount of methanol/water, analyzed by HPLC and radiomonitoring for the C-14-eicosanoids.

HPLC-conditions are as follows: Column: Nucleosil C-18, 5 µm; organic phase: 700 ml methanol, 300 ml water, 0.1 ml acetic acid; after 35 min change to pure methanol. Flow: 1 ml/min, 2000 psi. Radiomonitor: LB 507 (Berthold, Wildbad, FRG).

A viability assay (trypan blue exclusion) ascertains that cells remain intact during incubation periods.

EVALUATION

The radioactivity of the separated 5-HETE and LTB_4 is measured as a function of drug concentration, and related to a control experiment without drug. Two further lipoxygenase products, 12-HETE and 15-HETE, which are additionally generated under the test conditions, can be quantified in a similar way.

CRITICAL ASSESSMENT

The measured reaction sequence starts with arachidonic acid, and involves its transformation to 5-HETE by 5-lipoxygenase, as well as the subsequent enzymatic hydrolysis to LTB_4. Inhibitors of 5-lipoxygenase exhibit a decreased formation of 5-HETE and LTB_4. Effects of drugs on the side products 12-HETE and 15-HETE can also be studied in this test system.

H.3.1.6.3 Formation of Eicosanoids from ^{14}C-Arachidonic Acid in Human Platelets In Vitro

PROCEDURE

Blood is drawn from the vena brachialis of healthy volunteers and collected into plastic tubes containing sodium citrate (0.38% final concentration (w/v)). After centrifugation at 100 *g* for 15 min the platelet rich plasma (PRP) containing about $2{,}5 \times 10^{11}$ platelets/l (Counter HT, Coulter Electronics, Krefeld, FRG) is saved, and kept at 20°C no longer than one hour until the experiment is started. Metabolism of ^{14}C-arachidonic acid is followed by the HPLC procedures published by Weithmann et al. (1994), modifying the method of Powell (1985). PRP is mixed with the same volume of a citrate/D-glucose solution (27.35 g trisodium citrate· $2H_2O$, 1.47 g citric acid and 27.74 g D(+)-glucose· H_2O ad 1 l water) and centrifuged at 1000 *g* for 20 min (4°C). The saved precipitate is resuspended in Dulbecco's solution (DPBS, Serva, Heidelberg, FRG) in the original volume. 0.495 ml of this platelet suspension is incubated at 37°C for 15 min with the test compound. Subsequently eicosanoid formation is started by the addition of 5 µl of 1-^{14}C-arachidonic acid solution (50 Ci/mol, 9×10^{-4} Ci/l, NEN, Dreieich, FRG). After 5 min (37°C) the reaction is stopped by adding 0.5 ml of chilled acetone/0.1 ml 1n HCl, cooled to 0°C, and extracted two times with 3 ml ethylacetate. The combined organic extracts are evaporated and the residue redissolved in 0.2 ml methanol. Aliquots are separated by HPLC at a flow rate of 1.5 ml/min, using a C-18 Nucleosil column (5 µm, 125 × 4.6 mm, Bischoff, Leongang, FRG) connected with a pre-column C-18 Nucleosil (5 µm, 20 × 4.6 mm) of the same type. The formed ^{14}C-eicosanoids are analyzed using a liquid scintillation flow detector LB 507 (Berthold, Wildbad, FRG). The radiochromatogram is analyzed by comparison with tritiated authentic eicosanoids (NEN, Dreieich, FRG). The elution system consists of the following solvent mixtures (elution time in parenthesis): I 725 ml water/275 ml acetonitrile/1 ml acetic acid (40 min), II 700 ml methanol/300 ml H_2O/1 ml acetic acid (40 min), III pure methanol (20 min).

EVALUATION

The radioactivity of the separated TXB_2 and PGE_2 is measured as a function of drug concentration, and related to a control experiment without drug addition.

A further lipoxygenase product, 12-HETE, which is additionally generated under the test conditions, can be quantified in a similar way.

Lasché and Larson determined PGI_2 by a bioassay based on its generation by aortic rings and assay by its ability to inhibit platelet aggregation.

CRITICAL ASSESSMENT

The measured reaction sequence starts with arachidonic acid, and involves its transformation to prostaglandin endoperoxides, which is catalyzed by cyclooxygenase. The unstable and short-living endoperoxides transform immediately into thromboxane A_2 by the action of thromboxane isomerase. TXA_2 is unstable, too, and yields the stable non-enzymatic hydrolysis product TXB_2.

Inhibitors of cyclooxygenase exhibit a decreased formation of TXB_2. Specific inhibition of the thromboxane isomerase step results in an accumulation of the mentioned endoperoxide intermediates, which due to their chemical instability are non-enzymatically transformed to the primary PGE_2. Thus, inhibitors of the TXA_2-isomerase lead to a significant increase of the PGE_2-peak at the expense of the TXB_2-peak. Effects of drugs on the side product 12-HETE can also be studied in this test system.

H.3.1.6.4 Stimulation of Inducible Prostaglandin Pathway in Human PMNL

PROCEDURE

The procedure of Herrmann et al. (1990) with the modification of Weithmann et al. (1994), is used to stimu-

late cyclohexamide-inhibitable generation of PGE_2 in human PMNL by LPS.

H.2.5×10^9 PMNL/l culture medium (RPMI 1640, completed with 1 mmol/l sodium pyruvate, 5% FCS (w/v), 2 mmol/l glutamine and each 100 U/ml penicillin/streptomycin) are incubated with 100 µmol/l acetylsalicylic acid for 60 min (37°C, 5% CO_2), and the latter subsequently removed by four times washing with medium. 0.25 ml-aliquots (containing 2.5×10^9 PMNL/l medium) are incubated with 0.1 mg/ml LPS (lipopolysaccharide from Salmonella abortus equii, Sigma GmbH, Deisenhofen, FRG) along with the test compound for 18 h (96-well plates, 37°C, 5% CO_2). The generation of eicosanoids is induced by the administration of 7×10^{-5} mol/l of the calcium ionophore A 23187. After incubation for 30 min at 37°C the plates are centrifuged at 400 *g* for 15 min. PGE_2 is determined in the supernatant, using an ELISA-kit commercially available from several distributors. Alternatively the test compound is added along with the calcium ionophore. At least 90% of the cells remain intact during incubation times (trypan blue exclusion assay).

EVALUATION

The PGE_2-concentration in the sample is determined from appropriate calibration curves. The PGE_2-concentration is measured as a function of drug concentration, and related to a control experiment without drug.

CRITICAL ASSESSMENT

Long term activation with LPS or other inflammatory effectors leads in human polymorphonuclear neutrophils to the stimulation of a prostaglandin synthesizing capacity, which under normal conditions is not present in this system. The described assay system detects compounds which interfere with this activation process.

Incubation of drugs with already activated cells allows to search for drugs that directly influence the enzyme activity.

H.3.1.6.5 COX-1 and COX-2 Inhibition

PURPOSE AND RATIONALE

Several assays were described to characterize COX-1 and COX-2-inhibitors, such as *in vitro* COX enzyme assay (Seibert et al. 1994), COX-2 protein extraction and analysis (Anderson et al. 1996), a human whole blood assay using LPS-induced PGE_2 production as an index for cellular COX-2 activity (Riendeau et al. 1997) or whole-cell assays with transfected Chinese hamster ovary cells expressing COX-1 and COX-2 or COX-2 specific (osteosarcoma cells) and COX-1 specific (U937 cells) making use of PGE_2 production after arachidonic challenge as an index of cellular potency and selectivity of cyclooxygenase inhibitors (Chan et al. 1999; FitzGerald and Loll 2001; Rao et al. 2003).

PROCEDURE

In Vitro Cyclooxygenase Inhibition

The ability of test compounds to inhibit COX-1 and COX-2 (IC_{50} values, µM) is determined using an enzyme immunoassay kit (Cyman Chemical, Ann Arbor, Mich., USA, no. 560101) (Uddin et al. 2004). This COX (ovine) inhibitor screening assay directly measures the amount of the prostaglandin $PGF_{2\alpha}$ produced in the cyclooxygenase reaction. The prostanoid product is quantified via enzyme immunoassay (EIA) using a broadly specific antibody that binds to all the major prostaglandin compounds. Thus, this COX assay is more accurate and reliable than an assay based on peroxidase inhibition. The COX (ovine) inhibitor screening assay includes both ovine COX-1 and COX-2 enzymes in order to screen isozyme-specific inhibitors. This assay is an excellent tool, which can be used for general inhibitor screening, or to eliminate false-positive leads generated by less specific methods.

Cyclooxygenase catalyzes the first step in the biosynthesis of arachidonic acid to PGH_2. $PGF_{2\alpha}$ produced from PGH_2 by reduction with stannous chloride is measured by enzyme immunoassay. This assay is based on the competition between PGs and a PG-acetylcholinesterase conjugate (PG tracer) for a limited amount of PG antiserum. The amount of PG tracer that is able to bind to the PG antiserum is inversely proportional to the concentration of PGs in the wells since the concentration of PG tracer is held constant while the concentration of PGs varies. This antibody–PG complex binds to a mouse anti-rabbit monoclonal antibody that was previously attached to the well. The plate is washed to remove any unbound reagents and then Ellman's reagent, which contains the substrate for acetylcholinesterase, is added to the well. The product of this enzymatic reaction produces a distinct yellow color that absorbs at 405 nm. The intensity of this color, determined spectrophotometrically, is proportional to the tracer bound to the well, which is inversely proportional to the amount of PGs present in the well during the incubation. Percent inhibition is calculated by the comparison of compound treated to various control incubations. The concentration of the

test compound causing 50% inhibition (IC_{50}, μM) is calculated from the concentration–inhibition response curve.

Inhibition Studies with Recombinant Human COX-1 and COX-2

Microsomal preparations of recombinant human COX-1 and COX-2 are prepared from a vaccine virus-COS-7 cell expression system (O'Neill et al. 1994). Recombinant human COX-1 and COX-2 are expressed in baculovirus-Sf9 cells, and enzymes are purified (Ouellet and Percival 1995; Cromlish and Kennedy 1996). Enzymatic activity is monitored continuously by either a fluorescence assay measuring the appearance of the oxidized form of the reducing agent cosubstrate homovanillic acid or by oxygen consumption (Ouellet and Percival 1995).

Classical non-steroidal anti-inflammatory drugs (NSAIDs) and COX-2 inhibitors are time-dependent, irreversible inhibitors of hCOX-2, which is consistent with a two-step process involving an initial rapid equilibrium binding of enzyme and inhibitor, followed by the slow formation of a tightly bound enzyme–inhibitor complex. COX-2 inhibitors show a time-independent inhibition of hCOX-1, consistent with the formation of a reversible enzyme–inhibitor complex (Ouellet and Percival 1995; Riendeau et al. 2001).

HPLC Assay for Oxygenation of Radiolabeled Arachidonic Acid by COX-1

Purified recombinant human COX-1 (50 μl of 1 μg/ml in 100 mM Tris-HCl, pH 8.0, 5 mM EDTA, 1 mM phenol, 1 μM hematin) is preincubated with 2 μl of the inhibitor solution (50 fold concentrated stock in DMSO, 0–2.5 mM) for 15 min. The reaction is then initiated by the addition of 5 μl of 1 μM [^{14}C]-arachidonic acid (0.005 μCi) to obtain a final concentration of 0.1 μM. After 7 min incubation at room temperature, the reaction is stopped by the addition of 5 μl 1 M HCl and 50 μl acetonitrile. Aliquots of 50 μl of each reaction mixture are analyzed for substrate conversion by reverse phase HPLC onto a C-18 Nova-Pak column (3.9 × 150 mm) which is developed with acetonitrile/water/acetic acid (85:15:0.1) at 2 ml/min. Arachidonic acid metabolites and arachidonic acid eluted at 0.6–1 min and 2.2–2.5 min, respectively, are quantitated by a Packard radiochromatography detector. Percentages of inhibition are calculated from the difference in conversion of arachidonic acid to prostaglandin metabolites between inhibitor-treated samples and controls exposed to DMSO vehicle.

Determination of the Stoichiometry of Inhibitor Binding

Aliquots of purified COX-2 (0.25 mg/ml, concentration of subunit of 3.4 mM) are incubated in buffer (100 mM Tris-HCl, pH 8.0, 5 mM EDTA, 1 mM phenol) in the presence of various inhibitors (0–8 μM) for 15 or 30 min. An aliquot (20 μl) is then removed for determination of the cyclo-oxygenase activity which is monitored continuously by oxygen consumption by a Clark-type polarographic oxygen probe. The oxygen chamber is filled with 0.6 ml of reaction buffer (100 mM Tris-HCl, pH 8.0, 5 mM EDTA, 1 μM hematin,1 mM phenol, 100 μM arachidonic acid at 30° or 37°C) and the reaction is initiated by the addition of 20 μl of a solution of 4 mM hydrogen peroxide and 0.5 mM N,N,N′,N′-tetramethyl-p-phenylenediamine (TMPD) in assay buffer. Enzyme concentration is determined by amino acid concentration following acid hydrolysis.

Determination of the Dissociation Rate Constant of the Enzyme-Inhibitor Complex

Purified COX-2 (2.0 nmol, 2 ml) in 20 mM Tris-HCl, pH 8.0, 0.1 mM EDTA, 2 μM hematin, 0.1% β-octylglucoside is treated with 2.0 nmol [^{14}C]-DFU (18 Ci/mol) and incubated at 20°C for 3 h. A control (0.7 ml) is removed and 13 nmol unlabelled DFU is added to the remaining 1.3 ml of the mixture containing COX-2 and [^{14}C]-DFU. At timed intervals, 0.1 ml (in duplicate) is transferred to a Microcon-30 micro concentration device (Amicon) and the free inhibitor is separated from enzyme-bound inhibitor by centrifugation at 14,000 *g* for 6 min at 4°C. Buffer (0.1 ml) is added to the retentate and the centrifugation repeated. The filtrate and retentate are then removed and mixed with 10 ml scintillation fluid and counted in a liquid scintillation counter.

An aliquot of purified COX-2 (1.0 nmol) is treated with 1.25 mol equivalents of inhibitor or with DMSO vehicle control and incubated at 20°C for 1 h. The enzyme-inhibitor mixture is then transferred to a Pierce Microdialyzer 100 apparatus and dialyzed continuously against 2 l of buffer (20 mM Tris-HCl, pH 8.0, 0.1 mM EDTA, 0.1 mM phenol, 0.1% octylglucoside) for 5 h at 22°C during which aliquots are moved and frozen at –70°C until assayed for cyclyo-oxygenase activity by oxygen uptake as described above.

Recovery of Inhibitor from the COX-2-Inhibitor Complex

Purified COX-2 (0.79 nmol) is treated with 1.0 mol equivalent of inhibitor and the mixture is incubated for 60 min at room temperature. The remaining activity at this time is 4% that of a vehicle-treated con-

trol. The sample is then divided in two and the protein denaturated by treatment with four volumes of ethyl acetate/methanol/1 M citric acid (30:4:1). After extraction and centrifugation (10,000 *g* for 5 min), the organic layer is removed and the extraction repeated. The two organic layers are combined and dried under N_2. The extract is dissolved in 10 µl of HPLC solvent mixture consisting of water/acetonitrile/acetic acid (50:41:0.1) and 50 µl are injected onto a Novapak C-18 column (3.9 × 150 mm) and developed at 1 ml/min. The inhibitor is detected by absorption at 260 nm and eluted with a retention time of 6.6 min in this system. Control experiments for inhibitor recovery are performed with incubation of the inhibitor in the absence of enzyme and processing of the samples in an identical fashion before quantitation by HPLC.

Spectrophotometric Assay of Recombinant Human COX-2

Enzymatic activity of the purified COX-2 is measured using a chromogenic assay based on the oxidation of N,N,N′,N′-tetramethyl-p-phenylenediamine (TMPD) during the reduction of PGG_2 to PGH_2 (Copeland et al. 1994). The assay mixture (180 µl) contains 100 mM sodium phosphate, pH 6.5, 1 µM hematin, 1 mg/ml gelatin, 2 to 5 µg/ml of purified COX-2, and 4 µl of the test compound in DMSO. The assay is also performed in the presence of the detergent Genapol X-100 at a final concentration of 2 mM. The mixture is preincubated at room temperature (22°C) for 15 min before the initiation of the enzymatic reaction by the addition of 20 µl of a solution of 1 mM arachidonic acid and 1 mM TMPD in assay buffer (without enzyme or hematin). For assays in the presence of Genapol, the arachidonic acid and TMPD solution is prepared in 50% aqueous ethanol. The enzyme activity is measured by estimation of the initial velocity of TMPD oxidation over the first 36 s of the reaction as followed from the increase in absorbancy at 610 nm. A low rate of non-enzymatic oxidation is observed in the absence of COX-2 and is subtracted before the calculation of the percentage of inhibition.

Whole-Cell Assays with Transfected Chinese Hamster (CHO) Cells Expressing COX-1 and COX-2

Stably transfected CHO cells expressing human COX-1 and COX-2 are cultured and assayed for the production of PGE2 after stimulation with arachidonic acid (Kargman et al. 1996). Cells (0.3×10^6 cells in 200 µ l) are pre-incubated in HBSS containing 15 mM HEPES, pH 7.4, with 3 µl of the test drug or DMSO vehicle for 15 min at 37°C before challenge with arachidonic acid. Cells are challenged for 15 min with an arachidonic acid solution (10% ethanol in HBSS) to yield final concentrations of 10 µM arachidonic acid in the CHO[COX-2] assay and 0.5 µM arachidonic acid in the CHO[COX-1] assay. In the absence of addition of exogenous arachidonic acid, levels of PGE_2 in samples from CHO[COX-1] are <30 pg $PGE_2/10^6$ cells. In the presence of 0.5 µM exogenous arachidonic acid, levels of PGE_2 in samples from CHO[COX-1] cells increase to 260 to 1500 pg $PGE_2/10^6$ cells. After stimulation with 10 µM exogenous arachidonic acid, levels of PGE_2 in samples from CHO[COX-2] cells increase from <120 to 700 to 1600 pg $PGE_2/10^6$ cells. Compounds are tested in eight concentrations in duplicate using 3-fold serial dilutions in DMSO. COX activity in the absence of test compounds is determined as the difference in PGE_2 levels of cells challenged with arachidonic acid versus PGE_2 levels in cells mock-challenged with ethanol vehicle.

Arachidonic acid-dependent production of PGE_2 is measured in both cell lines after addition of test drugs. Indomethacin shows similar IC_{50} values in both CHO[COX-1] and CHO[COX-2] cells, whereas specific COX-2 inhibitors show a 1,000-fold specificity.

Assays with Murine Macrophages

Mitchell et al. (1994), Hu et al. (2003), and Joo et al. (2004) used mouse peritoneal macrophages for evaluation of COX-2 inhibitors.

Adherent peritoneal macrophages were harvested from the peritoneal cells of male C5BL-6J mice after intraperitoneal injection of brewer thioglycollate medium (5 ml/100 g body weight) for 3 days. The peritoneal cells obtained from three to four mice were mixed and seeded in 48-well culture cluster at a cell density of 1 × 109 cell/l in RPMI-1640 supplemented with 5% newborn calf serum, penicillin, and streptomycin. After settlement for 2–3 h, non-adherent cells were washed by D-Hanks' balanced salt solution. Then macrophages were cultured in RPMI-1640 without serum. Almost all of the adherent cells were macrophages as assessed by Giemsa staining. Cell viability was examined by trypan blue dye exclusion. All incubation procedures were performed with 5% CO_2 in humidified air at 37°C.

COX-1 Assay

Macrophages were incubated with test compound at different concentrations or solvent (Me_2SO) for 1 h and were stimulated with calcimycin 1 µmol/l for 1 h. The amount of 6-keto-$PGF_{1\alpha}$ (a stable metabolite of PGI_2) in supernatants was measured by RIA according to manufacturer's guide. The inhibitory ratio was

calculated as

$$IR = \frac{(C_s - C_t)}{(C_s - C_c)}.$$

C_s, C_t, C_c refer to 6-keto-PGFα concentration in supernatants of calcimycin, test compound, and control groups, respectively.

COX-2 Assay

Macrophages were incubated with test compound at different concentrations or solvent (Me_2SO) for 1 h and were stimulated with lipopolysaccharide (LPS) 1 mg/l for 9 h. The amount of PGE_2 in supernatants was measured by RIA. The inhibitory ratio was calculated using the same formula as in COX-1 assay section. C_s, C_t, C_c refer to PGE_2 concentration in supernatants of LPS, test compound, and control groups, respectively.

Statistical analysis data were expressed as the mean ±SD of more than three independent experiments. Dose–inhibitory effect curves were fit through "uphill dose–response curves, variable slope" using Prism, GraphPad version3.00:

$$Y = \frac{1}{1 + 10^{[(\log IC_{50} - X) \times \text{Hillslope}]}}.$$

Whole-Cell Assays with Osteosarcoma Cells (COX-2) and U937 Cells (COX-1)

The human osteosarcoma cell line has been shown to selectively express COX-2 by reverse transcription-polymerase chain reaction and immunoblot analysis, whereas undifferentiated human lymphoma U937 cells selectively express COX-1. The production of PGE_2 by these cells after arachidonic acid challenge is used as an index of cellular COX-2 and COX-1 activity, respectively. Test substances are preincubated for 5 to 15 min with the cells under serum-free conditions (HBSS) before a 10-min stimulation with 10 µM arachidonic acid and measurement of PGE_2 production (Wong et al. 1997). COX activity in each cell line is defined as the difference in PGE_2 concentrations in samples incubated in the presence or absence of arachidonic acid.

Human Whole Blood Assay

For the COX-2 assay, fresh heparinized human whole blood is incubated with lipopolysaccharide from *E. coli* at 100 µg/ml and with 2 µl of vehicle or a test compound for 24 h at 37°C (Brideau et al. 1996). PGE_2 levels in the plasma are measured using radioimmunoassay after deproteination. For the COX-1 assay, an aliquot of fresh blood is mixed with either DMSO or test compound and is allowed to clot for 1 h at 37°C. TBX_2 levels in the serum are measured using an enzyme immunoassay after deproteination.

MODIFICATIONS OF THE METHOD

Young et al. (1996) and Khanapure et al. (2003) used a similar assay to determine COX-1 and COX-2 enzyme activity in human whole blood. Human blood from non-fasted donors, who had not taken any aspirin or NSAIDs for 14 days, was collected in sodium heparin and distributed in 1-ml aliquots per well in a 24-well tissue culture plate. The plate was placed on a gently rotating platform shaker in a 5% CO_2 incubator at 37°C for 15 min. Test compounds were dissolved and diluted in dimethylsulfoxide (DMSO) and 1 µl of each dilution of test compound was added per well in duplicate wells. To induce COX-2, lipopolysaccharide (LPS) from *E. coli* was added at 10 µg/ml to appropriate wells 15 min after addition of the test compounds. For the stimulation of COX-1, the calcium ionophore A23187 was added to a final concentration of 25 µM to separate wells 4.5 h after the addition of the test compounds. At 30 min after addition of A23187 or 5 h after LPS addition, all incubations were terminated by cooling on ice and adding EGTA to a final concentration of 2 mM. The blood samples were then transferred to 15 ml polypropylene centrifuge tubes and centrifuged at 1200 *g* for 10 min at 4°C. Then, 100 µl of plasma was removed from each blood sample and added to 1 ml of methanol in a 15 ml polypropylene centrifuge tube, mixed vigorously, and stored overnight at –20°C. The next day, the samples were centrifuged at 2000 *g* for 10 min at 4°C, and the supernatants were transferred to glass tubes and evaporated to dryness. After reconstitution with EIA buffer, and appropriate dilution (2000-fold for COX-1 and 500-fold for COX-2), the samples were assayed for thromboxane B2 using EIA kits (Cayman, Ann Arbor, Mich., USA) in duplicate wells.

Kalajdzic et al. (2002) showed that a preferential COX-2 inhibitor suppresses peroxisome proliferator-activated receptor induction of COX-2 gene expression in human synovial fibroblasts.

Berg et al. (1997) developed a cell assay system using the human erythroleukemic cell line HEL as a source for COX-1 and the human monocytic cell line Mono Mac 6 as a source for COX-2.

Kalgutkar et al. (2000) exploited biochemical differences between the COX isoforms to improve upon the selectivity of carboxylate-containing NSAIDs as COX-2 inhibitors.

Faust et al. (2003) recommended human peritoneal macrophages in culture as a model for studying inflammatory disorders *in vitro*.

Krause et al. (2003) reported that the NSAIDs indomethacin and diclofenac and a selective COX-2 inhibitor uncouple mitochondria in intact cells. To analyze the effects on energy metabolism of rat thymocytes, top-down elasticity analysis (Brand 1996, 1998; Ainscow and Brand 1999) was applied. Energy metabolism was conceptually divided into three blocks of reactions that generated and consumed the central intermediate mitochondrial membrane potential (ψ_m). The substrate oxidation subsystem encompassed all cellular catabolic reactions that provide the respiratory chain with its substrates NADH and succinate (e. g., glucose, fatty acid, and amino acid metabolism) and the electron transport chain itself, which together generate ψ_m. The ψ_m -consuming reactions were further divided into the subsystems proton leak and ATP turnover. The ATP turnover subsystem encompassed ATP synthesis by ATP synthase and subsequent ATP consumption by cellular pathways (e. g., ion pumps or protein synthesis). Manipulation of the biochemical properties of one block of reactions prompted a change of the intermediate ψ_m. The whole system evolved into a new steady state, which was determined by the kinetic responses of the other blocks to changes of ψ_m. Successive inhibition of one block of reactions permitted determination of these kinetic responses of the other blocks to changes of ψ_m. A comparison of the kinetic responses in the presence and absence of effectors (e. g., drugs) allowed for the identification of sites of actions.

REFERENCES AND FURTHER READING

Ainscow EK, Brand MD (1999) Top-down control analysis of ATP turnover, glycolysis and oxidative phosphorylation in rat hepatocytes. Eur J Biochem 263:671–685

Anderson GD, Hauser SD, McGarity KL, Bremer ME, Isakson PC, Gregory SA (1996) Selective inhibition of cyclooxygenase (COX)-2 reverses inflammation and expression of COX-2 and interleukin 6 in rat adjuvant arthritis. J Clin Invest 97:2672–2679

Berg J, Christoph T, Widerna M, Bodenteich A (1997) Isoenzyme-specific cyclooxygenase inhibitors: A whole cell assay system using the human erythroleukemic cell line HEL and the human monocytic cell line Mono Mac 6. J Pharmacol Toxicol Meth 37:179–186

Bing JR (2003) Cyclooxygenase-2 inhibitors. Is there an association with coronary or renal events? Curr Atheroscler Rep 5:114–117

Bombardier C, Leine L, Reich A, Shapiro D, Burgos-Vargas R, Davis B, Day R, Ferraz MB, Hawkey CJ, Hochberg MC, Kvien TK, Schnitzer TJ, for the VIGOR Study Group (2000) Comparison of upper gastrointestinal toxicity of rofecoxib and naproxen in patients with rheumatic arthritis. New Engl J Med 343:1520–1528

Boopathy R, Balasubramanian AS (1988) Purification and characterization of sheep platelet cyclooxygenase. Biochem J 239:371–377

Borgeat P, Samuelsson B (1979), Arachidonic acid metabolism in polymorphonuclear leukocytes: Effect of ionophore A 23187. Proc Natl Acad Sci USA 76:2148–2152

Boyum A (1976) Isolation of lymphocytes, granulocytes and macrophages. Scand J Immunol 5 (Suppl 5)9–15

Brand MD (1996) Top down metabolic control analysis. J Theor Biol 182:351–360

Brand MD (1998) Top-down elasticity analysis and its application to energy metabolism in isolated mitochondria and intact cells. Mol Cell Biochem 184:13–20

Brideau C, Kargman S, Liu S, Dallob AL, Ehich EW, Rodger IW, Chan C-C (1996) A human whole blood assay for clinical evaluation of biochemical efficacy of cyclooxygenase inhibitors. Inflamm Res 45:68–74

Bruns RF, Thomsen WJ, Pugsley TA (1983) Binding of leukotrienes C_4 and D_4 to membranes from guinea pig lung: regulation by ions and guanine nucleotides. Life Sci 33:645–653

Chan CC, Boyce S, Brideau C, Charleson S, Cromlish W, Ethier D, Evans J, Ford-Hutchinson AW, Forrest MJ, Gauthier JY, Gordon R, Gresser M, Guay J, Kargman S, Kennedy B, Leblanc Y, Léger S, Mancini J, O'Neill GP, Ouellet M, Patrick D, Percival H, Perrier H, Prasit P, Rodger I, Tagari P, Thérien M, Vickers P, Visco D, Wang Z, Webb J, Wong E, Xu LJ, Young RN, Zamboni R, Riendeau D (1999) Rofecoxib [Vioxx, MK-0966; 4-(4′-Methylsulfonylphenyl)-3-phenyl-2-(5H)-furanone]: A potent and orally active cyclogenase-2 inhibitor. Pharmacological biochemical profiles. J Pharmacol Ex Ther 290:551–560

Chandrasekharan NV, Dai H, Roos KLT, Evanson NK, Tomsik J, Elton TS (2002) COX-3, a cyclooxygenase-1 variant inhibited by acetaminophen and other analgesic/antipyretic drugs: cloning, structure and expression. Proc Natl Acad Sci USA 99:13926–13931

Cheng JB, Cheng EIP, Kohi F, Townley RG (1986) [^{3}H]Leukotriene B_4 binding to the guinea-pig spleen membrane preparation: a rich tissue source for a high-affinity leukotriene B_4 receptor site. J Pharmacol Exp Ther 236:126–132

Cochran FR, Finch-Arietta MB (1989) Optimization of cofactors which regulate RBL-1 arachidonate 5-lipoxygenase. Biochem Biophys Res Comm 161:1327–1332

Coleman RA, Smith WL, Narumiya S (1994) VIII. International union of pharmacology classification of prostanoid receptors: Properties, distribution, and structure of the receptors and their subtypes. Pharmacol Rev 46:205–229

Copeland RA, Williams JM, Giannaras J, Nurnberg S, Covington M, Pinto D, Pick S, Trzaskos JM (1994) Mechanism of selective inhibition of the inducible isoform of prostaglandin G/H synthase. Proc Natl Acad Sci USA 91:11202–11206

Crofford LJ (1997) COX-1 and COX-2 tissue expression: implications and predictions. J Rheumatol 24, Suppl 49:15–19

Cromlish WA, Kennedy BP (1996) Selective inhibition of cyclogenase-1 and -2 using intact insect cell assays. Biochem Pharmacol 52:1777–1785

Evans AT, Formukong EA, Evans FJ (1987) Actions of cannabis constituents on enzymes of arachidonate metabolism: anti-inflammatory potential. Biochem Pharmacol 36:2035–2037

Faust D, Akoglu B, Faust AC, Milovic V (2003) Human peritoneal macrophages in culture: a model for studying inflammatory disorders in vitro. Clin Exp Med 3:15–19

FitzGerald GA, Loll P (2001) COX in a crystal ball: current status and future promise of prostaglandin research. J Clin Invest 107:1335–1337

Funk CD, Funk LB, Kennedy ME, Pong AS, Fitzgerald GA (1991) Human platelet/erythroleukemia cell prostaglandin G/H synthase: cDNA cloning, expression, and gene chromosomal assignment, FASEB J 5:2304–2312

Gierse JK, McDonald JJ, Hauser SD, Rangwala SH, Koboldt CM, Seibert K (1996) A single amino acid difference between cyclogenase-1 (COX-1) and -2 /COX-2) reverses the selectivity of COX-2 specific inhibitors. J Biol Chem 271:15810–15814

Halushka PV, Mais DE, Mayeux PR, Morinelli TA (1989) Thromboxane, prostaglandin and leukotriene receptors. Annu Rev Pharm Tox 10:213–239

Hankey GJ, Eikelboom JW (2003) Cyclogenase-2 inhibitors. Are they really atherothrombotic, and if not, why not? Stroke 34:2736–2740

Harvey J, Osborne DJ (1983) A rapid method for detecting inhibitors of both cyclooxygenase and lipoxygenase metabolites of arachidonic acid. J Pharmacol Meth 9:147–155

Hawkey CJ (1999) COX-2 inhibitors. Lancet 353:307–314

Hedberg A, Hall SE, Ogletree ML, Harris DN, Liu ECK (1988) Characterization of [5,6-^{3}H]SQ 29,548 as a high affinity radioligand, binding to thromboxane A_2/prostaglandin H_2-receptors in human platelets. J Pharmacol Exp Ther 245:786–792

Herrmann F, Lindemann A, Gauss J, Mertelsmann R (1990) Cytokine-stimulation of prostaglandin synthesis from endogenous and exogenous arachidonic acids in polymorphonuclear leukocytes involving activation and new synthesis of cyclooxygenase. Eur J Immunol 20:2513–2516

Hock FJ, Wirth K, Albus U, Linz W, Gerhards HJ, Wiemer G, Henke S, Breipohl G, König W, Knolle J, Schölkens BA (1991) Hoe 140 a new potent and long acting bradykinin antagonist: *in vitro* studies. Br J Pharmacol 102:769–773

Hu W, Guo Z, Chu F, Bai A, Yi X, Cheng G, Li J (2003) Synthesis and biological evaluation of substituted 2-sulfonylphenyl-3–3-phenyl-indoles: a new series of selective COX-2 inhibitors. Bioorg Med Chem 11:1153–1160

Hull MA, Thomson JL, Hawkey CJ (2005) Expression of cyclooxygenase 1 and 2 by human gastric endothelial cells. Gut 45:529–536

Irvine RF (1982) Review article: How is the level of free arachidonic acid controlled in mammalian cells? Biochem J 204:3–16

Izumi T, Shimizu T, Seyama Y, Ohishi N, Takaku F (1986) Tissue distribution of leukotriene A_4 hydrolase activity in guinea pig. Biochem Biophys Res Commun 135:139–145

Jakschik BA, Kuo CG (1983) Characterization of leukotriene A_4 and B_4 biosynthesis. Prostaglandins 25:767–781

Jones TR, Labelle M, Belley M, Champion E, Charette L, Evans J, Ford-Hutchinson AW, Gauthier JY, Lord A, Masson P, McAuliffe M, McFarlane CS, Metters KM, Pickett C, Piechuta H, Rochette C, Rodger IW, Sawyer N, Young RN, Zamboni R, Abraham WM (1995) Pharmacology of montelucast sodium (Singular™), a potent and selective leukotriene D_4 receptor antagonist. Can J Physiol Pharmacol 73:191–201

Joo YH, Kim JK, Kang SH, Noh MS, Ha JY, Choi JK, Lim KM, Chung S (2004) 2,3-Diarylpyranon-4-ones: a new series of selective cyclogenase-2 inhibitors. Bioorg Med Chem Lett 14:2195–2198

Kalajdzic T, Faour WH, He QW, Fahmi H, Martel-Pelletier J, Pelletier JP, di Battista JA (2002) Nimesulide, a preferential cylooxoxygenase 2 inhibitor suppresses peroxisome proliferator-activated receptor induction of cyclooxygenase 2 gene expression in human synovial fibroblasts. Arthritis Rheum 46:494–506

Kalgutkar AS, Crews BC, Rowlinson SW, Marnett AB, Kozak KR, Remmel RP, Marnett LJ (2000) Biochemically based design of cyclooxygenase-2 (COX-2) inhibitors: facile conversion of nonsteroidal antiinflammatory drugs into potent and highly selective COX-2 inhibitors. Proc Natl Acad Sci USA 97:925–930

Kargman S, Wong E, Greig GM, Falgueyret JP, Cromlish W, Ethier D, Yergey JA, Riendeau D, Evans JF, Kennedy B, Tagari P, Francis DA, O'Neill GP (1996) Mechanism of selective inhibition of human prostaglandin G/H synthase-1 and -2 in intact cells. Biochem Pharmacol 52:1113–1125

Katsumata M, Gupta C, Goldman AS (1986) A rapid assay for activity of phospholipase A_2 using radioactive substrate. Anal Biochem 154:676–681

Kemal C, Louis-Flamberg P, Krupinski-Olsen R, Shorter AL (1987) Reductive inactivation of soybean lipoxygenase 1 by catechols: a possible mechanism for regulation of lipoxygenase activity. Biochemistry 26:7064–7072

Khanapure SP, Garvey DS, Young DV, Ezawa M, Earl EA, Gaston RD, Fang X, Murty M, Martino A, Shumway M, Trocha M, Marek P, Tam SW, Janero DR, Letts LG (2003) Synthesis and structure-activity relationship of novel, highly potent metharyl and methcycloalkyl cyclooxygenase-2 (COX-2) selective inhibitors. J Med Chem 46:5484–5504

Klein T, Nüsing RM, Pfeilschifter J, Ullrich V (1994) Selective inhibition of cyclooxygenase 2. Biochem Pharmacol 48:1605–1610

Krause MM, Brand MD, Krauss S, Meisel C, Vergin H, Burmester RG, Buttgereit F (2003) Nonsteroidal antiinflammatory drugs and a selective cyclooxygenase 2 inhibitor uncouple mitochondria in intact cells. Arthritis Rheum 48:1438–1444

Kuhl P, Borbe HO, Fischer H, Römer A, Safayhi H (1986) Ebselen reduces the formation of LTB_4 in human and porcine leukocytes by isomerisation to its 5S,12R-6-trans-isomer. Prostaglandins 31:1029–1048

Lasché EM, Larson RE (1982) Interaction of insulin and prostacyclin production in the rat. Diabetes 31:454–458

Lee SH, Soyoola E, Chanmugam P, Hart S, Sun W, Zhong H, Liou S, Simmons D, Hwang D, (1992) Selective expression of mitogen-inducible cyclooxygenase in macrophages stimulated with lipopolysaccharide. J Biol Chem 267:25934–25938

Lewis R, Austen KF (1981) Mediation of local homeostasis and inflammation by leukotrienes and other mast cell-dependent compounds. Nature 293:103–108

Mitchell JA, Akarasereenont P, Thiemermann C, Flower RJ, Vane JR (1994) Selectivity of nonsteroidal antiinflammatory drugs as inhibitors of constitutive and inducible cyclooxygenase. Proc Natl Acad Sci 90:11693–11697

Mong S, Wu HL, Hogaboom GK, Clark MA, Crooke ST (1984) Characterization of the leukotriene D_4 receptor in guinea-pig lung. Eur J Pharmacol 102:1–11

Murata T, Ushikubi F, Matsuoka T, Hirata M, Yamasaki A, Sugimoto Y, Ichikawa A, Aze Y, Tanaka T, Yoshida N, Ueno A, Oh-Ishi S, Narumiya S (1997) Altered pain reception and inflammatory response in mice lacking prostaglandin receptor. Nature 388:678–682

Noushargh S, Hoult JRS (1986) Inhibition of human neutrophil degranulation by forskolin in the presence of phosphodiesterase inhibitors. Eur J Pharmacol 122:205–212

O'Neill GP, Mancini JA, Kargman S, Yergey J, Kwan MY, Falgueyret JP, Abramovitz M, Kennedy PP, Ouellet M, Cromlish W, Colp S, Evans JP, Ford-Hutchinson AW, Vickers PJ (1994) Overexpression of human prostaglandin G/H

synthase-1 and -2 by recombinant vaccinia virus: Inhibition by nonsteroidal anti-inflammatory drugs and biosynthesis of 15-hydroxyeicosatetranoic acid. Mol Pharmacol 45:245–254
O'Sullivan MG, Huggins EM Jr, Meade EA, DeWitt DL, McCall CE (1992) Lipopolysaccharide induces prostaglandin H synthase-2 in alveolar macrophages. Biochem Biophys Res Commun 187:1123–1127
Ouellet M, Percival MD (1995) Effect of inhibitor time-dependency on selectivity towards cyclooxygenase isoforms. Biochem J 306:247–251
Powell WS (1987) Reversed-phase high-pressure liquid chromatography of arachidonic acid metabolites formed by cyclooxygenasem & lipoxygenases. Analyt Biochem 148:59–69
Pugsley TA, Spencer C, Boctor AM, Gluckman MI (1985) Selective inhibition of the cyclooxygenase pathway of the arachidonic acid cascade by the nonsteroidal antiinflammatory drug isoxicam. Drug Dev Res 5:171–178
Rådmark O, Shimizu T, Jörnvall H, Samuelsson B (1984) Leukotriene A_4 hydrolase in human leukocytes. J Biol Chem 259:12339–12345
Rao PN, Amini M, Li H, Habeeb AG, Knaus EE (2003) Design, synthesis, and biological evaluation of 6-substituted-3-(4-methanesulfonylphenyl) -4-phenylpyran-2-ones: a novel class of diarylheterocyclic selective cyclooxygenase-2 inhibitors. J Med Chem 46:4872–4882
Riendeau D, Percival MD, Brideau C, Charleson S, Dubé D, Ethier D, Falgueyret JP, Friesen RW, Gordon R, Greig G, Guay J, Mancini J, Ouellet M, Wong E, Xu L, Boyce S, Visco D, Girard Y, Prasit P, Zamboni R, Rodger IW, Gresser M, Ford-Hutchinson AW, Young RN, Chan CC (2001) Etoricoxib (MK-0663): preclinical profile and comparison with other agents that selectively inhibit cyclooxygenase-2. J Pharmacol Exp Ther 296:558–566
Riendeau D, Percival MD, Boyce S, Brideau C, Charleson S, Cromlish W, Ethier D, Evans J,Falgueyret JP, Ford-Hutchinson AW, Gordon R, Greig G, Gresser G, Guay J, Kargman S, Léger S, Mancini JA, O'Neill G, Ouellet M, Rodger IW, Thérien M, Wang Z, Webb JK, Wong E, Xu L, Young RN, Zamboni R, Prasit P, Chan C C (1997) Biochemical and pharmacological profile of a tetrasubstituted furanone as a highly selective COX-2 inhibitor. Br J Pharmacol 121:105–117
Safayhi H, Mack T, Sabieraj J, Anazodo MI, Subramanian LR, Ammon HPT (1992) Boswellic acids: Novel, specific, nonredox inhibitors of 5-lipoxygenase. J Pharmacol Exp Ther 261:1143–1146
Salari H, Braquet P, Borgeat P (1984) Comparative effects of indomethacin, acetylenic acids, 15-HETE, nordihydroguajaretic acid and BW 755c on the metabolism of arachidonic acid in human leukocytes and platelets. Prostagl Leukotr Med 13:53–60
Samuelsson B (1986) Leukotrienes and other lipoxygenase products. Prog Lipid Res 25:13–18
Saussy DL Jr, Mais DE, Burch RM, Halushka PV (1986) Identification of a putative thromboxane A_2/prostaglandin H_2 receptor in human platelet membranes. J Biol Chem 261:3025–3029
Schmidt H, Woodcock BC, Geisslinger G (2004) Benefit-risk assessment of rofecoxib in the treatment of osteoarthritis. Drug Safety 27:185–196
Seibert K, Zhang Y, Leahy K, Hauser S, Masferrer J, Perkins W, Lee L, Isakson P (1994) Pharmacological and biochemical demonstration of the role of cyclooxygenase 2 in inflammation and pain. Proc Natl Acad Sci USA 91:12013–12017
Seibert K, Masferrer J, Zhang Y, Gregory S, Olson G, Hauser S, Leahy K, Perkins W, Isakson P (1995) Mediation of inflammation by cyclooxygenase-2. Agents Actions 46:41–50
Shigeta JI, Takahashi S, Okabe S (1998) Role of cyclogenase-2 in the healing of gastric ulcers in rats. J Pharmacol Exp Ther 186:1383–1390
Shimizu T, Rådmark O, Samuelsson B (1984) Enzyme with dual lipoxygenase activities catalyzes leukotriene A_4 synthesis from arachidonic acid. Proc Natl Acad Sci USA 81:689–693
Smith WL, Meade EA, DeWitt DL (1994) Pharmacology of prostaglandin endoperoxide synthase isoenzymes-1 and-2. Ann New York Acad Sci 71:136–142
Takeguchi C, Kohno E, Sih CJ (1971) Mechanism of prostaglandin biosynthesis. I. Characterization and assay of bovine prostaglandin synthetase. Biochemistry 10:2372–2377
Uddin MJ, Rao PNP, Knaus EE (2004) Design and synthesis of acyclic triaryl (Z)-olefins: a novel class of cyclooxygenase-2 (COX-2) inhibitors. Bioorg Med Chem 12:5929–5940
Vane J (1987) The evolution of non-steroidal anti-inflammatory drugs and their mechanisms of action. Drugs 33 (Suppl 1):18–27
Vane J (1998) The mechanism of action of anti-inflammatory drugs. Naunyn-Schmiedeberg's Arch Pharmacol 358, Suppl 1, R 8
Vane J, Botting R (1987) Inflammation and the mechanism of action of anti-inflammatory drugs. FASEB J 1:89–96
Vane JR, Bakhle YS, Botting RM (1998) Cyclooxygenases 1 and 2. Ann Rev Pharmacol Toxicol 38:97–120
Veenstra J, van de Pol H, van der Torre H, Schaafsma G, Ockhuizen T (1988) Rapid and simple methods for the investigation of lipoxygenase pathways in human granulocytes. J Chromatogr 431:413–417
Weithmann KU, Schlotte V, Seiffge D, Jeske S (1993) Concerted action of pentoxifylline in conjunction with acetylsalicylic acid on platelet cyclic AMP and aggregation. Thromb Haemorrh Dis 8:1–8
Weithmann KU, Jeske S, Schlotte V (1994) Effect of leflunomide on constitutive and inducible pathways of cellular eicosanoid generation. Agents Actions 41:164–170
Winkler JD, Sarau HM, Foley JJ, Mong S, Crooke ST (1988) Leukotriene B_4-induced homologous desensitization of calcium mobilization and phosphoinositide metabolism in U-937 cells. J Pharmacol Exp Ther 246:204–210
Wong E, DeLucca C, Boily C, Charleson S, Cromlish W, Denis D, Kargman S, Kennedy BP, Ouellet M, Skorey K, O'Neill GP, Vickers PJ, Riendeau D (1997) Characterization of autocrine inducible prostaglandin H synthase-2 (PGHS-2) in human osteosarcoma cells. Inflamm Res 46:51–59
Xie W, Robertson DL, Simmons DL (1992) Mitogen-inducible prostaglandin G/H synthase: A new target for nonsteroidal antiinflammatory drugs. Drug Dev Res 25:249–265
Young JM, Panah S, Satchawatcharaphong C, Cheung PS (1996) Human white blood assays for inhibition of prostaglandin G/H synthase-1 and -2 using A23187 and lipopolysaccharide stimulation of thromboxane B_2 production. Inflamm Res 45:245–253

H.3.1.7 Influence of Cytokines

H.3.1.7.1 Induced Release of Cytokines (Interleukin-1α, IL-1β, IL-6, IL-8 and TNFα) from Human White Blood Cells In Vitro

PURPOSE AND RATIONALE

Cytokines represent a class of different, biologically highly potent peptides, that are endogenously syn-

thesized upon stimulation. They are involved in numerous cellular processes, such as inflammation, immunological responses and many others. Their broad pleiotrophic biological activities are best characterized by their former classification as

- B-cell activating and differentiating factor, endogenous pyrogen, osteoclast activating factor, thymocyte proliferation factor, monocyte cell factor, leukocyte endogenous factor (IL-1);
- hepatocyte stimulatory factor, hybridoma growth factor, haematopoietic cell stimulatory factor (IL-6);
- neutrophil chemotactic factor and adhesion inhibitor (IL-8);
- tumor necrosis factor (TNFalpha).

There are presently 18 cytokines with the name interleukin (IL) (Dinarello 2000). The concept of proinflammatory cytokines and antiinflammatory cytokines (IL-4, IL-10, IL-13) is fundamental to cytokine biology and novel drug discovery strategies.

Blocking IL-1 or TNF has been highly successful in patients with rheumatoid arthritis, inflammatory bowel disease, or graft-vs.-host disease.

The following procedure is used to detect compounds that interact with the lipopolysaccharide in ced cytokine release from human mononuclear blood cells. The cytokines measured are interleukines 1alpha, 1beta, 6 and 8, as well as TNFalpha.

PROCEDURE

According to Böyum (1976)10 ml of freshly prepared human citrated blood is diluted 1:1 with PM 16-buffer (Serva, Heidelberg, FRG), and underlayered with 15 ml Lymphoprep (Molter GmbH, Heidelberg, FRG), and subsequently centrifuged at 20°C with 400 *g* (Minifuge, Heraeus, Hanau, FRG) for 30 min. The cell fraction appearing as a white ring between the two phases is carefully removed by means of a syringe, diluted 1:1 (v/v) with PM 16 and again centrifuged for 15 min. The pellet is washed with 10 ml of RPMI 1640 (Gibco, Berlin, FRG), containing in addition 300 mg/l L-glutamine. The washed cell fraction is taken up in 1 ml RPMI 1640, containing in addition 300 mg/l L-glutamine, 25 mmol/l HEPES, 5% FCS and 100 IU/ml penicillin/streptomycin (Gibco). Using a cell counter (type IT, Coulter Diagnostics, Krefeld, FRG) the cell suspension which consists of about 90% lymphocytes and 10% monocytes is adjusted to approx. 5×10^9 cells/ml.

Synthesis and release of cytokines according to Tiku et al. (1986) is performed in 96 wells microtiter plates. To 0.23 ml of the cell fraction 500 ng LPS (lipopolysaccharide from Salmonella abortus equii, Sigma GmbH, Deisenhofen, FRG), dissolved in 0.01 ml dimethylsulfoxide/water (1:10, v/v), and the investigational drug, dissolved in 0.01 ml, are added. The cell suspension is now kept at 37°C/5% CO_2 in a common incubator. Incubation time is usually 20 h (for Il-6 and Il-8 only four or one hour, respectively). The reaction is stopped by placing the microtiter plate into an ice bath. The plate is then centrifuged at 2000 rpm for 2 min. The cytokine levels are determined in various aliquots of the supernatant using the appropriate ELISA-kit, which is commercially available from several distributors.

EVALUATION

The cytokine-concentration in the sample is determined from appropriate calibration curves. The cytokine-concentration is measured as a function of drug concentration, and related to a control experiment without drug. In general, Hostacortin (10 to 0,1 µmol/l) is used as the standard compound.

CRITICAL ASSESSMENT

Drugs interfering with LPS-activation, biosynthesis and cellular release of cytokines are to exhibit activity in these assay systems. Usually cell viability is not altered, as assessed by the lactate-dehydrogenase test.

MODIFICATIONS OF THE METHOD

Van der Pouw-Kraan et al. (1992) examined the regulation of interleukin (IL)-4 production by human peripheral blood T cells. Production of IL-4 as measured by ELISA was shown to be regulated differently from IL-2 and INF-γ (also measured by ELISA).

A proinflammatory role for interleukin-18 (IL-18) in rheumatoid arthritis was attributed by Gracie et al. (1999).

The role of the interleukin-6 family of cytokines in inflammatory arthritis and bone turnover was reviewed by Wong et al. (2003).

Kim et al. (2005) reported an inhibitory effect of luteolin, a flavonoid from *Lonicera japonica*, on tumor-necrosis-factor-α-induced IL-8 production in human colon epithelia cells.

REFERENCES AND FURTHER READING

Bird TA, Saklatvala J (1986) Identification of a common class of high-affinity receptors for both types of porcine interleukin-1 on connective tissue cells. Nature 324:263–266

Boyum A (1976) Isolation of lymphocytes, granulocytes and macrophages. Scand J Immunol 5 (Suppl 5):9–15

Chin J, et al (1987) Identification of a high affinity receptor for native interleukin-1α and interleukin-1β on normal human lung fibroblasts. J Exp Med 165:70–86
Dinarello CA (1991) Interleukin-1 and interleukin-1 antagonism. Blood 77:1627–1652
Dinarello CA (2000) Proinflammatory cytokines. Chest 118:503–508
Eugui EM, Delustro B, Rouhafza S, Wilhelm R, Allison AC (1993) Coordinate inhibition by some antioxidants of TNFα, IL-1β and IL-6 production by human peripheral blood mononuclear cells. Ann NY Acad Sci 696:171–184
Gracie JA, Forsey RJ, Chan WL, Gilmour A, Leung BP, Greer MR, Kennedy K, Carter R, Wei XQ, Xu D, Filed M, Foulis A, Liew FY, McInnes IB (1999) A proinflammatory role for IL-18 in rheumatoid arthritis. J Clin Invest 104:1393–1401
Grob PM, David E, Warren TC, DeLeon RP, Farina PR, Homon CA (1990) Characterization of a receptor for human monocyte-derived neutrophil chemotactic factor intereukin-8. J Biol Chem 265:8311–8316
Ibelgaufts H (ed) (1992) Lexikon Zytokine, München
Killian PL (1986) Interleukin-1α and interleukin-1β bind to the same receptor on T cells. J Immunol 136:4509–4514
Kim JA, Kim DK, Kang OH, Choi YA, Park HJ, Choi SC, Kim TH, Yun KJ, Nah YH, Lee YM (2005) Inhibitory effect of luteolin on TNF-α-induced IL-8 production in human colon epithelia cells. Int Immunopharmacol 5:209–217
Lewis GP, Barrett ML (1986) Immunosuppressive actions of prostaglandins and the possible increase in chronic inflammation after cyclooxygenase inhibitors. Agents Actions 19:59–65
Maloff BL, Shaw JE, Di Meo TM, Fox D, Bruin EM (1989) Development of a RIA-based primary screen for IL-1 antagonists. Clin Chim Acta 180:73–78
Moser B, Schumacher C, von Tscharner V, Clark-Lewis I, Baggiolini M (1990) Neutrophil-activating peptide 2 and *gro*/melanoma growth-stimulatory activity interact with neutrophil-activating peptide-1/interleukin-8 receptors on human neutrophils. J Biol Chem 266:10666–10671
Tiku K, Tiku ML, Skosey JL (1986) Interleukin-1 production by human polymorphonuclear neutrophils. J Immunol 136:3677–3685
Van der Pouw-Kraan T, Van Kooten C, Rensink I, Aarden L (1992) Interleukin (IL)-4 production by human T cells: differential regulation of IL-4 *vs*. IL-2 production. Eur J Immunol 22:1237–1241
Warren JS (1993) Inflammation. DN&P (Drugs, News and Perspectives) 6:450–459
Whicher JT, Thompson D, Billingham MEJ, Kitchen EA (1989) Acute phase proteins. In: Pharmacological Methods in the Control of Inflammation. Alan R. Liss, Inc., pp 101–128
Wong PKK, Campbell IK, Egan PJ, Ernst M, Wicks IP (2003) The role of the interleukin-6 family of cytokines in inflammatory arthritis and bone turnover. Arthritis Rheum 48:1177–1189

H.3.1.7.2 Flow Cytometric Analysis of Intracellular Cytokines

PURPOSE AND RATIONALE

Flow cytometry is a powerful analytical technique in which individual cells can be simultaneously analyzed for several parameters, including size an granularity, as well as the expression of surface and intracellular markers defined by fluorescent antibodies. Fluorescent anti-cytokine and anti-chemokine monoclonal antibodies are very useful for the intracellular staining and multiparameter flow cytometric analysis of individual cytokine-producing cells within mixed populations. Multicolor immunofluorescent staining with antibodies against intracellular cytokines and cell surface markers provides a high resolution method to identify the nature and frequency of cells which express particular cytokines (Sander et al. 1991, 1993; Jung 1993).

PROCEDURE

Cells and Cell Culture

Peripheral blood is obtained from healthy human volunteers. Mononuclear cells are isolated by Ficoll gradient centrifugation. For purification of T cells or further cell sorting, mononuclear cells are incubated with neuraminidase treated sheep red blood cells and centrifuged over Ficoll. Erythrocytes are eliminated by ammonium chloride lysis. For isolation of memory cells or naive cells, T cells are incubated with a cocktail of antibodies containing anti-CD16, anti-CD56, anti-CD20, anti-CD14, (anti-CD8), and anti-CD45RA or anti-CD45R0. Cell sorting is done with the magnetic cell sorter (MACS) according to Abts et al. (1989), Miltenyi et al. (1990) using rat anti-mouse IgG1 or Ig2a antibodies labeled with superparamagnetic beads (Miltenyi, Bergisch Gladbach, Germany). Depleted cells are highly enriched with $CD4^+(CD3^+)CD45R0^+$ or $CD4^+(CD3^+)CD45R0^-CD45RA^+$ cells (>95%) and are referred to as memory cells and naive cells ($CD4^+CD45R0^-CD45RA^+$) respectively. Only depleted cells are used for experiments.

Cells (2×10^5/100 ml) are cultured in 96 well flat bottom plates for various periods of time at 37°C and 8% CO_2 in RPMI 1640 supplemented with 2 mM glutamine, 1 mM sodium pyruvate, 100 IU/ml penicillin, 100 µg/ml streptomycin, 2×10^{-5} M mercaptoethanol and 10% AB serum. Cells are stimulated with phorbol 12-myristate 13-acetate 1–10 ng/ml+1 µM ionomycin, phytohemagglutinin 2.4 µg/ml or phytohemagglutinin 2.4 µg/ml+phorbol 12-myristate 13-acetate 1 ng/ml in the presence or absence of 3 µM monensin (Sigma).

Staining

Cultured cells are washed twice in Hanks' balanced solution (HBSS) and then fixed in ice-cold HBSS containing 4% paraformaldehyde for 10 min. After two further washes in HBSS the cells are resuspended to 2×10^5 in 300 µl HBSS containing 0.1% saponin, 10% AB serum, 100 µ g/ml goat IgG and 0.01 M HEPES buffer. After 10 min, the cells are spun

down and cytokine specific antibodies diluted in HBSS with 0.1% saponin and 0.1 M HEPES buffer (saponin buffer) are added at a concentration of 1 µg/ml for 30 min at room temperature. Cells are washed twice in saponin buffer and subsequently incubated with isotype-specific second step antibodies in a concentration ranging from 0.5 to 5 µg/ml for 20 min in the dark. Cells are washed in saponin buffer and stained with streptavidin conjugates or in the case of surface staining incubated with 200 µg/ml mouse IgG diluted in saponin buffer for 15 min. After subsequent washing in saponin buffer cells are washed twice in HBSS and stained for 20 min with different antibodies in order to determine their surface phenotype. As a last step, cells are washed in HBSS.

Flow Cytometry

A FACScan flow cytometer (Becton Dickinson, Mountain View, USA) equipped with a 15 mW argon ion laser and filter settings for fluorescein-isothiocyanate (530 nm), phycoerythrin (585 nm) and TRI-Color (Medac, Hamburg, Germany) or PerCP (Becton Dickinson, USA) emitting in the deep red (>650 nm) is used.

EVALUATION

5000–10000 cells are computed in list mode and analyzed using the FACScan research software (Becton Dickinson)

MODIFICATIONS OF THE METHOD

Slauson et al. (1999) combined the analytical power of flow cytometry with mitogen-driven, whole blood lymphocyte activation and proliferation assays to investigate the *in vitro* mechanism of action of malononitrilamides.

Protocols for immunofluorescent staining of intracellular cytokines for flow cytometric analysis are provided by BD Phar Mingen, Life Science Research Europe, Heidelberg, Germany.

Ashcroft and Lopez (2000) highlighted the opportunities in high throughput flow cytometry (HTFC) which are opened by commercial high speed machines. The specifications of these machines are cell analysis rates over 100,000 cells/s and cell sorting rates of 55,000 cells/s with high purity.

REFERENCES AND FURTHER READING

Abt H, Emmerich M, Miltenyi S, Radbruch A, Tesch H (1989) CD20 positive human B lymphocytes separated with the magnetic cell sorter (MACS) can be induced to proliferation and antibody secretion *in vitro*. J Immunol Meth 125:19–28

Ashcroft RG, Lopez PA (2000) Commercial high speed machines open new opportunities in high throughput flow cytometry. J Immunol Meth 243:13–24

Jung T, Schauer U, Heusser C, Neumann C, Rieger C (1993) Detection of intracellular cytokines by flow cytometry. J Immunol Meth 159:197–207

Miltenyi S, Möller W, Weichel W, Radbruch A (1990) High gradient magnetic cell separation with MACS. Cytometry 11:231

Sander B, Andersson J, Andersson U (1991) Assessment of cytokines by immunofluorescence and the paraformaldehyde-saponin procedure. Immun Rev 119:65–93

Sander B, Hoiden I, Andersson U, Moller E, Abrams JS (1993) Similar frequencies and kinetics of cytokine producing cells in murine peripheral blood and spleen. Cytokine detection by immunoassay and intracellular immunostaining. J Immunol Meth 166:201–214

Slauson SD, Silva HT, Sherwood SW, Morris RE (1999) Flow cytometric analysis of the molecular mechanisms of immunosuppressive action of the active metabolite of leflunomide and its malononitrilamide analogues in a novel whole blood assay. Immunol Lett 67:179–183

H.3.1.7.3 Screening for Interleukin-1 Antagonists

PURPOSE AND RATIONALE

Interleukin-1α and -1β are potent regulators of inflammatory processes. The naturally occurring IL-1 receptor antagonist (IL-1ra) is effective *in vitro* and *in vivo* in modulating biological responses to IL-1 (Carter et al. 1990; Hannum et al. 1990; Schreuder et al. 1995). Using a combination of anion exchange, gel filtration, and reverse-phase HPLC, three species of native IL-1ra were identified. An unglycosylated, intracellular isoform is designated as icIL-1ra (Lennard 1995; Arend et al. 1991, 1998).

A cell-free, non-isotopic assay has been developed to discover molecules that compete with the natural ligands for binding to the active sites of the type-I IL-1 receptor. The key reagents are the IL-1 receptor antagonist, a recombinant soluble form of the receptor (sIL-1R), and a specific anti-sIL-1R non-neutralizing monoclonal antibody (Sarrubi et al. 1996).

PROCEDURE

Proteins

The extracellular portion of the type-I IL-1 receptor (sIL-1R) is expressed on the membrane of Chinese hamster ovary cells using a phosphatidinyl-inositol-glycan linkage (PIG-tail). Its expression, cleavage with phosphoinositol-specific phospholipase C, and purification are performed according to Whitehorn et al. (1995).

The three IL-1 ligands are expressed in *Escherichia coli* using synthetic genes (Dower et al. 1989; Yanofsky and Zurawski 1990). The purification of IL-1ra

and IL-β is accomplished according to Schreuder et al. (1995) and Yem et al. (1988).

IL-1α is purified as follows: *E. coli* cell sonicates are precipitated with 2 M ammonium sulfate, and the pellet is resuspended in TE (25 mM Tris/HCl, pH 8.9, 1 mM EDTA), dialyzed against the same buffer and loaded on a DEAE-Sepharose column equilibrated with TE. The protein is eluted with a linear NaCl gradient to 300 mM. Ammonium sulfate to 0.8 M is added to the IL-1α-containing fractions which are loaded onto a phenyl-Sepharose column equilibrated with TE containing 0.8 M ammonium sulfate. The elution is performed with a linear gradient to TE with no salt. IL-1α-containing fractions are concentrated and chromatographed on a Sephacryl S-200 column in PBS (phosphate-buffered saline: 20 mM sodium phosphate, pH 7.3, 150 mM sodium chloride).

Fluorescein-labeled IL-1α is obtained by incubating 1 mg/ml IL-1α with 1 mg/ml fluorescein isothiocyanate in PBS for 2 h at room temperature in the dark. The reaction solution is passed directly over a G-25 column (Pharmacia) equilibrated with PBS to remove unreacted fluorescein isothiocyanate.

The monoclonal antibody Mab79 is used as direct dilutions ($1{:}10^5$–10^6) of ascitic fluid in PBSA (PBS containing 0.3% bovine serum albumin). Horseradish-peroxidase-linked anti-mouse IgG polyclonal antibody is used.

Protein concentrations are determined using the Bio-Rad protein assay kit, based on the dye-binding procedure according to Bradford (1976). BSA is used as reference protein.

Immobilized-Ligand IL-1 Receptor Binding Assay

Essentially the same procedure can be used for both manual and automated versions of the assay, with all steps and incubations performed at room temperature. In the automated assay a Beckman Biomek 1000 Work-Station was used for all steps, from coating to spectrophotometric measurements.

Ligand immobilization is obtained by incubation of 3.6 µg/ml IL-1ra in 50 µl PBS in flat-bottomed culture-treated microplate wells, equivalent to 10 pmol/well of IL-1ra. After overnight incubation microplates are emptied and 250 µl/well of 3% BSA in PBS is added to block unreacted sites. After 2 h of incubation and three washes with an excess of PBS, the ligand-coated microplates are ready for the receptor binding reaction.

In separate microplates with U-shaped wells, 12 µl of samples (containing up to 50% DMSO or DMF) or controls (the same solution without compound) is mixed with 48 µl of 150 pM sIL-1R in PBSA. Then 50 µl of these mixtures is transferred to the IL-1ra-coated plates (equivalent to 6 fmol/well of sIL-1R) and incubated for 2 h. Microplates are then washed twice with PBS and 50 µl of 1:500,000 dilution of Mab79 ascitic fluid in PBSA is added to each well. After 1 h of incubation, 25 µl of 1:100 dilution of HRP-labeled anti-mouse IgG in PBSA is added and the incubation prolonged for an additional hour. Plates are finally washed four times with PBS and bound peroxidase activity is measured spectrophotometrically, using either *o*-phenylenediamine (OPD) or tetramethylbenzidine (TMB) as substrate. In the first case, 150 µl of 1 mg/ml OPD in 0.1 M citric acid, pH 5.0, containing 0.03% of a 35% solution of hydroperoxide is added and, after color development, the reaction is stopped with 50 µl of 4.5 M sulfuric acid. Alternatively, 100 µl of 0.1 mg/ml TMB in 25 mM citric acid and 50 mM sodium phosphate, containing 0.02% hydrogen peroxide (35% solution), is added and the reaction is stopped with 50 ml of 2.5 M sulfuric acid.

EVALUATION

Absorbance (at 492 nm for OPD and 450 nm for TMB) is measured using either a Titertek microplate reader (for the manual procedure) or directly by the Biomek 1000 WorkStation (in the automated version). IC_{50} values can be calculated from dose–response curves.

CRITICAL ASSESSMENT OF THE METHOD

Since no cells or cell membranes are used, the assay is very robust, with no interference from membrane-perturbing agents, and has high resistance to the organic solvent normally used to resuspend compounds of chemical libraries.

MODIFICATIONS OF THE METHOD

High-affinity type I interleukin-1 receptor antagonists were discovered by screening recombinant peptide libraries (Yanosfky et al. 1996).

Akeson et al. (1996a) developed an *ex vivo* method for studying inflammation in cynomolgus monkeys using whole blood for analysis of IL-1 antagonists administered *in vivo*. Animals were given an i.v. infusion of IL-1ra, and blood samples were taken pre-infusion and during the infusion. The samples were incubated with or without IL-1β and the subsequent *ex vivo* induction of IL-6 determined. This allows the analysis of the *in vivo* efficacy of antagonists without exposing the animals to IL-1.

A novel low-molecular-weight antagonist, selectively binding the type I IL-1 receptor and blocking the *in vivo* responses to IL-1 was described by Akeson et al. (1996b).

Evaluation of the IL-1 receptor antagonist IL-1ra in a rodent abscess model of host resistance was published by Colagiovanni and Shopp (1996).

Blocking monoclonal antibodies (mAbs) specific to mouse IL-1 receptor antagonist (IL-1ra) were prepared by immunizing Armenian hamsters with recombinant mouse IL-1ra by Fujioka et al. (1995). A sensitive and specific ELISA against mouse IL-1ra was established.

Miesel et al. (1995) tested the anti-arthritic reactivity of the IL-1 receptor antagonist IL-1ra in male DBA/1xB10A(4R) mice with arthritis induced by intraplantar injection of potassium peroxochromate. Then 3 µ mol/kg K_3CrO_8 was administered topically into the left hind paws and 1 h after the induction of arthritis, 2 mg/kg IL-1ra was administered intraperitoneally, which was repeated on day 2. An arthritis index was determined daily.

Nakae et al. (2003) found that IL-17 production from activated T cells is required for the spontaneous development of destructive arthritis in mice deficient in IL-1 receptor antagonist.

Redlich et al. (2003) reviewed rheumatoid arthritis therapy after tumor necrosis factor and interleukin-1 blockade.

REFERENCES AND FURTHER READING

Akeson A, Bohnke R, Schroeder K, Kastner P, Seligmann B, Robinson J (1996a) An *ex vivo* method for studying inflammation in cynomolgus monkeys: analysis of interleukin-1 receptor antagonist. J Pharmacol Toxicol Meth 36:155–161

Akeson AL, Woods CW, Hsieh LC, Bohnke RA, Ackermann BL, Chan KY, Robinson JL, Yanofsky SD, Jacobs JW, Barrett RW, Bowlin TL (1996b) AF12198, a novel low molecular weight antagonist, selectively binds type I interleukin (IL)-1 receptor and blocks *in vivo* responses to IL-1. J Biol Chem 271:30517–30523

Arend WP (1991) Interleukin 1 receptor antagonist. A new member of the interleukin 1 family. J Clin Invest 88:1445–1451

Arend WP, Malyak M, Guthridge CJ, Gabay C (1998) Interleukin-1 receptor antagonist: role in biology. Annu Rev Immunol 16:27–55

Bradford M (1976) A rapid and sensitive method for the quantitation of microgram quantities of protein utilizing the principle of protein-dye binding. Anal Biochem 72:248–252

Carter DB, Deibel MR Jr, Dunn CJ, Tomich CSC, Laborde AL, Slightom JL, Berger AE, Bienkowski MJ, Sun FF, McEwan RN (1990) Purification, cloning, expression and biological characterization of an interleukin-1 receptor antagonist protein. Nature (Lond) 344:633–638

Colagiovanni DB, Shopp GM (1996) Evaluation of the interleukin-1 receptor antagonist (IL-1ra) and tumor necrosis factor binding protein (TNF-BP) in a rodent abscess model of host resistance. Immunopharmacol Immuntoxicol 18:397–419

Dower SK, Wignall JM, Schooley K, McMahan CJ, Jackson JL, Prickett KS, Lupton S, Cosman D, Sims JE (1989) J Immunol 142:4314–4320

Fujioka N, Mukaida N, Harada A, Akiyama M, Kasahara T, Kuno K, Ooi A, Mai M, Matsushima K (1995) Preparation of specific antibodies against murine IL-1ra and the establishment of IL-1ra as an endogenous regulator of bacteria-induced fulminant hepatitis in mice. J Leukocyte Biol 58:90–98

Hannum CH, Wilcox CJ, Arend WP, Joslin FG, Dripps DJ, Heimdal PL, Armes LG, Sommer A, Eisenberg SP, Thompson RC (1990) Interleukin-1 receptor antagonist activity of a human interleukin-1 inhibitor. Nature (Lond) 343:336–340

Lennard AC (1995) Interleukin-1 receptor antagonist. Critical Rev Immunol 15:77–105

Miesel R, Ehrlich W, Wohlert H, Kurpisz M, Kröger H (1995) The effects of interleukin-1 receptor antagonist on oxidant-induced arthritis in mice. Clin Exper Rheumatol 13:595–610

Nakae S, Saijo S, Horai R, Sudo K, Mori S, Iwakura Y (2003) IL-17 production from activated T cells is required for the spontaneous development of destructive arthritis in mice deficient in IL-1 receptor antagonist. Proc Natl Acad Sci USA 1000:5986–5990

Redlich K, Schett G, Steiner G, Hayer S, Wagner EF, Smolen JS (2003) Rheumatoid arthritis therapy after tumor necrosis factor and interleukin-1 blockade. Arthritis Rheum 48:3308–3319

Sarrubi E, Yanofsky SD, Barrett RW, Denaro M (1996) A cell-free, nonisotopic, high-throughput assay for inhibitors of type-I interleukin-1 receptor. Anal Biochem 237:70–75

Schreuder HA, Rondeau JM, Tardif C, Soffientini A, Sarubbi E, Akeson A, Bowlin TL, Yanofsky S, Barrett RW (1995) Refined crystal structure of the interleukin-1 receptor antagonist. Presence of a disulfide link and a cis-proline. Eur J Biochem 227:838–847

Whitehorn E, Tate E, Yanofsky SD, Kochersperger L, Davis A, Mortensen RB, Yonkivich S, Bell K, Dover WJ, Barrett RW (1995) Biotechnology 13:1215–1219

Yanosfky SD, Zurawski G (1990) Identification of key residues in the amino-terminal third of human interleukin-1α. J Biol Chem 265:13000–13006

Yanosfky SD, Baldwin DN, Butler JH, Holden FR, Jacobs JW, Balasubramanian P, Chinn JP, Cwirla SE, Peters-Bhatt E, Whitehorn EA, Tate EH, Akeson A, Bowlin TL, Dower WJ, Barrett RW (1996) High affinity type I interleukin 1 receptor antagonists discovered by screening recombinant peptide libraries. Proc Natl Acad Sci USA 93:7381–7386

Yem AW, Richard KA, Staite ND, Deibel MR (1988) Resolution and biological properties of three N-terminal analogues of recombinant human interleukin-1 beta. Lymphokine Res 7:85–92

H.3.1.7.4 Inhibition of Interleukin-1β Converting Enzyme (ICE)

PURPOSE AND RATIONALE

Programmed cell death (apoptosis) is effected through a cascade of intracellular proteases known as caspases (Alnemri et al. 1996). The interleukin-1β-converting enzyme (ICE), alternatively known as capsase-1, was

the first such protein identified on the basis of its sequence homology to the pro-apoptotic *Caenorhabditis elegans* gene product, ced-3 (Yuan et al. 1993). The caspase family includes 10 reported human homologs of ICE. By sequence homology comparisons between three caspase subfamilies have been identified. The ICE subfamily includes three caspases: ICE, TX (caspase-4), and TY (caspase-5). The CPP32 subfamily includes CPP32 (caspase-3), CMH-1 (caspase-7), and MCH-2 (caspase-6). A third caspase subfamily includes ICH-1 (caspase-2), FLICE (caspase-8) and caspases-9 and -10.

ICE processes pro-IL-1β to yield active IL-1β, which plays a pivotal role in inflammatory cell activation (Dinarello 1996) and is known to inhibit the expression of apoptosis (Tatsuda et al. 1996). Inhibition of IL-1β formation is an approach for the treatment of inflammatory disorders such as rheumatoid arthritis. Livingstone (1997) presented a review on *in vitro* and *in vivo* studies of peptidyl ICE inhibitors.

PROCEDURE

Neutrophil Isolation

Neutrophils are isolated from healthy volunteers by dextran sedimentation and centrifugation through a discontinuous Ficoll gradient (Lee et al. 1993). Isolated neutrophils are resupended in polypropylene tubes at a concentration of 1×10^6 cells/ml in DMEM supplemented with 10% FCS, 1% glutamine, and 1% penicillin/streptomycin solution. Neutrophil purity is assessed by size and granularity on flow cytometry.

Quantification of Apoptosis

Neutrophil apoptosis is quantified by flow cytometry as the percentage of cells with hypodiploid DNA (Nicoletti et al. 1991). Cells are centrifuged at 200 *g* for 10 min, gently resuspended in 500 µl of hypotonic fluorochrome solution (50 µg/ml propidium iodide, 3.4 mM sodium citrate, 1 mM Tris, 0.1 mM EDTA, and 0.1% Triton X-100) and stored in the dark at 4°C for 3–4 h before analysis using a Coulter Epics XL-MCL cytofluorometer. A minimum of 5000 events are collected and analyzed. Apoptotic nuclei are distinguished from normal neutrophil nuclei by their hypodiploid DNA; neutrophil debris is excluded from analysis by raising the forward threshold. Apoptotic nuclei appear as a broad hypodiploid DNA peak which is easily discernible from the narrow peak of cells with normal diploid DNA content. Apoptosis is assessed at 24 h after treatment.

Assay of Caspase-1 Activity

Cell lysates are prepared from the membrane fraction of 20×10^6 neutrophils following experimental manipulation. Aliquots of the lysates (10 µl) are diluted in assay buffer 100 mM HEPES (pH 7.4), 10% sucrose, and 0.1% 3-([[3-cholamidopropyl]dimethylammonio]-1-propanesulfonate) containing 20 µM Ac-Tyr-Val-Ala-Asp-7-amino-4-methylcoumarin (Calbiochem) and then incubated for 45 min at room temperature. The release of 7-amino-4-methylcoumarin is detected by continuous measurement using a Perkin-Elmer LS50 luminescence spectrometer with an excitation of 380 nm and an emission slit at 460 nm. Specific ICE (caspase-1) activity is measured as pmol/s per milligram of protein.

EVALUATION

Individual experiments are repeated a minimum of four times; results are expressed as the mean ±SD. Analysis is performed using the Student's *t*-test or ANOVA with Scheffè's correction.

MODIFICATIONS OF THE METHOD

Norman et al. (1997) found that the severity and mortality of experimental pancreatitis are dependent on interleukin-1 converting enzyme.

REFERENCES AND FURTHER READING

Alnemri ES, Livingston DJ, Nicholson DW, Salvesen G, Thornberry NA, Wong WW, Yuan JY (1996) Human ICE/CED3 nomenclature. Cell 87:171

Dinarello CA (1996) Biological basis for interleukin-1 in disease. Blood 87:2095–2147

Lee A, Whyte MKB, Haslett C (1993) Inhibition of apoptosis and prolongation of neutrophil functional longevity by inflammatory mediators. J Leukocyte Biol 54:283–288

Livingstone DJ (1997) *In vitro* and *in vivo* studies of ICE inhibitors. J Cell Biochem:19–26

Nicoletti I, Migliorati G, Pagliacci MC, Grignani F, Riccardi C (1991) A rapid and simple method for measuring thymocyte apoptosis by propidium iodide staining and flow cytometry. J Immunol Methods 139:271–279

Norman J, Yang J, Fink G, Carter G, Ku G, Denham W, Livingston D (1997) Severity and mortality of experimental pancreatitis are dependent on interleukin-1 converting enzyme (ICE). J Interferon Cytokine Res 17:113–118

Tatsuda T, Cheng J, Mountz JD (1996) Intracellular IL-1β is an inhibitor of Fas-mediated apoptosis. J Immunol 157:3949–3957

William R, Watson G, Rotstein OD, Parodo J, Bitar R, Marshall JC (1998) The IL-1β-converting enzyme (caspase-1) inhibits apoptosis on inflammatory neurophils through activation of IL-1β. J Immunol 161:957–962

Yuan JS, Shaham S, Ledoux S, Ellis HM, Horvitz HR (1993) The C. elegans cell death gene ced-3 encodes a protein similar to mammalian interleukin 1β-converting enzyme. Cell 75:641

H.3.1.7.5
Nuclear Factor-κB

H.3.1.7.5.1
General Considerations

Nuclear factor kappa B (NF-κB) is an inducible transcription factor of the Rel family, sequestered in the cytoplasm by the IκB family of proteins. NF-κB exists in several dimeric forms, but the p50/p65 heterodimer is the predominant one. Activation of NF-κB by a range of physical, chemical, and biological stimuli leads to phosphorylation and proteasome dependent degradation of IκB, leading to the release of free NF-κB. This free NF-κB then binds to its target site (κB sites in the DNA), to initiate transcription. This transcription is involved in a number of diseases including cancer, AIDS, autoimmune diseases, and inflammatory disorders. The nuclear factor κB is essential for the transcriptional regulation of the proinflammatory cytokines IL-1, IL-6, IL-8 and tumor necrosis factor α. NF-κ B is also the target for glucocorticoid–mediated IL-8 repression. Reduction-oxidation (redox) regulation is implicated in the activation of NF-κB. (Mukaida et al. 1994, Aupperle et al. 1999, Christman et al. 2000a, 2000b, Nichols et al. 2001, D'Acquisto et al. 2002, Nishi et al. 2002, Palanki 2002, Tian et al. 2002, Heynink et al. 2003, Aggarwal et al. 2004, Pande and Ramos 2003, 2005, Kaltschmidt et al. 2005). The IKK complex, as a critical activator of NF-κB function, consists of a core of three subunits, two of which, namely IKKα and IKKβ contain functional kinase domains and are capable of phosphorylating IκB at specific N-terminal residues to initiate its ubiquitination. In contrast, the third core subunit of the IKK complex, called NEMO (also known as IKKγ or IKKAP) is a non-catalytic component that functions as a key regulator of IKK activity (Gosh and Karin 2002, Karin et al. 2004).

Studying joint erosion in rheumatoid arthritis O'Gradaigh et al. (2003) found that interactions between tumor necrosis factor α, interleukin, and receptor activator of nuclear factor κB ligand (RANKL) regulate osteoclasts

REFERENCES AND FURTHER READING

Aggarwal BB, Takada Y, Shishodia S, Gutierrrez AM, Oommen OV, Ichikawa H, Baba Y, Kumar A (2004) Nuclear transcription factor NF-kappa B. Role in biology and medicine. Indian J Exp Biol 42:341–353

Aupperle KR, Bennett BL, Boyle DL, Tak PP, Manning AM, Firestein GS (1999) NF-κB regulation by IκB kinase in primary fibroblast-like synoviocytes. J Immunol 163:427–433

Christman JW, Blackwell TS, Juurlink BH (2000a) Redox regulation of nuclear factor kappa B: therapeutic potential for attenuating inflammatory responses. Brain Pathol 10:153–162

Christman JW, Sadikot RT, Blackwell TS (2000b) The role of nuclear factor κB in pulmonary diseases. Chest 117:1482–1487

D'Acquisto F, May MJ, Gosh S (2002) Inhibition of nuclear factor kappa B (NF-κB): An emerging ther in antiinflammatory therapies. Mol Interventions 2:22–35

Gosh S, KarinM (2002) Missing pieces in the NF-κB puzzle. Cell 109:S81-S96

Heynink K, Wullaert A, Beyaert R (2003) Nuclear factor-kappa B plays a central role in tumor necrosis factor-mediated liver disease. Biochem Pharmacol 66:1409–1415

Kaltschmidt B, Widera D, Kaltschmidt C (2005) Signaling via NF-kappa B in the nervous system. Biochim Biophys Acta 1745:287–299

Katin M, Yamamoto Y, Wang QM (2004) The IKK NF-κB system: a treasure trove for drug development. Nature Rev 3:17–26

Mukaida N, Morita M, Ishikawa Y, Rice N, Okamoto SI, Kasahara T, Matsushima K (1994) Novel mechanism of glucocorticoid-mediated gene repression. J Biol Chem 269:13289–13295

Nichols TC, Fischer TH, Deliagyris EN, Baldwin AS Jr (2001) Role of nuclear factor kappa B (NF-κB) in inflammation, periodontitis, and atherogenesis. Ann Periodontol 6:20–29

Nishi T, Shimizu N, Hiramoto M, Sato I, Yamaguchi Y, Hasegawa M, Aizawa S, Tanak H, Kataoka K, Watanabe H, Handa H (2002) Spatial redox regulation of a critical cysteine residue of NF-κB *in vivo*. J Biol Chem 277:44548–44556

O'Gradaigh D, Ireland D, Bord S, Compston JE (2003) Joint erosion in rheumatoid arthritis: interactions between tumor necrosis factor α, interleukin, and receptor activator of nuclear factor κB ligand (RANKL) regulate osteoclasts. Ann Rheum Dis 63:354–359

Palanki MSS (2002) Inhibitors of AP-1 and NF-κB mediated transcriptional activation: therapeutic potential in autoimmune diseases and structural diversity. Curr Medicinal Chem 9:219–227

Pande Y, Ramos MJ (2003) Nuclear factor kappa B: a potential target for anti-HIV chemotherapy. Curr Med Chem 10:1603–1615

Pande Y, Ramos MJ (2005) NF-κB in human disease: Current inhibitors and prospects for *de novo* structure based design of inhibitors. Curr Med Chem 12:357–373

Tian Y, Rabson AB, Gallo MA (2002) Ah receptor and NF-κB interactions: mechanisms and physiological implications. Chem Biol Interact 141:97–115

H.3.1.7.5.2
Inhibition of Nuclear Factor-κB

PURPOSE AND RATIONALE

Several authors studied the inhibition of NF-κB by compounds.

Staal et al. (1990) found that intracelluar thiols regulate activation of nuclear factor κB and transcription of human immunodeficiency virus. Schrenk et al. (1992) reported dithiocarbamates as potent inhibitors of nuclear factor κB activation in intact cells. Natara-

jan et al. (1996) described caffeic acid phenyl ester as a potent and specific inhibitor of activation of nuclear transcription factor NF-κB. Geng et al. (1997) reported that S-allyl cysteine inhibits activation of nuclear factor κB in human T cells. Hiramoto et al. (1998) described nuclear-targeted suppression of NF-κB by a quinone derivative. Ichiyama et al. (1999) found inhibition of peripheral NF-κB activation by a central action of α-melanocyte-stimulating hormone. Castrillo et al. (2001) described inhibition of the nuclear factor κ B pathway by tetracyclic kaurene diterpenes in macrophages with specific effects on NF-κB-inducing kinase activity and on the coordinated activation of ERK and p38 MAPK. Kang et al. (2001) reported that genistein prevents nuclear factor kappa B activation and acute lung injury induced by intratracheal treatment of rats with lipopolysaccaride. Lee et al. (2002) found that kamebakaurin, a kaurane diterpene, inhibits NF-κB by directly targeting the DNA-binding activity of p50 and blocks the expression of antiapoptotic NF-κB target genes. Palanki et al. (2002) reported structure–activity relationship studies of ethyl 2-[3-methyl-2,5-dioxo(3-pyrrolinyl) amino]-4-(trifluoromethyl)pyrimidine-5-carboxylate, an inhibitor or AP-1 and NF-κB mediated gene expression. Kim et al. (2004) found that tripolide, a natural compound extracted from the Chinese herb *Tripterygium wilfordii*, inhibits murine-inducible nitric synthase expression by down-regulating lipopolysaccharide-induced activity of nuclear factor κB and c-Jun NH_2-terminal kinase. Jancso et al. (2005) studied the effect of acetylsalicylic acid on nuclear factor-κB activation and on late preconditioning against infarction of the myocardium. Kunsch et al. (2005) described redox-sensitive inflammatory gene expression of AGIX-4207, an antioxidant and anti-inflammatory compound.

Tse et al. (2005) found that honokiol, a small m olecular weight lignan isolated from *Magnolia officinalis*, inhibits tumor-necrosis-factor-α-stimulated NF-κB activation and NF-κB-regulated gene expression through suppression of inhibitor κB kinase (IKK) activation.

PROCEDURE

Honokiol was dissolved in DMSO as a 100 mM stock solution and stored at -20°C.

Cell Culture

The cell lines used in this experiment were obtained from American Type Culture Collection (Manassas, Va., USA). U937 and HL-60 cells were grown in RPMI-1640 medium containing 10% fetal bovine serum, 100 U/ml penicillin, and 100 µg/ml streptomycin (Gibco, NY, USA) at 37°C in humidified 5% CO_2 atmosphere. MCF-7 and HeLa cells were cultured in Eagles' minimum essential medium containing 10% fetal bovine serum under the same condition.

Electrophoretic Mobility Shift Assay (EMSA)

For the electrophoretic mobility shift assay according to Chaturvedi et al. (2000), equal quantities of nuclear protein (5 µg) from each sample was incubated with radiolabeled gel shift oligonucleotides for 15 min at 37°C and then resolved on a non-denaturing 5% (w/v) polyacrylamide gel. The gel was dried onto 3 MM blotting paper and used to expose X-ray film for overnight at −70°C. For supershift assays, 1 µl of antiserum recognizing each of the NF-κB subunits was added to the EMSA reaction 30 min before electrophoresis.

Western Blot Analysis

To obtain the whole-cell lysates, samples containing 1×10^7 cells were pelleted, washed twice with ice-cold PBS, then lysed in 150 µ l of modified RIPA buffer [50 mM Tris–Cl, 1% (v/v) NP-40, 0.35% (w/v) sodium-deoxycholate, 150 mM NaCl, 1 mM EDTA, 1 mM EGTA, pH 7.4] supplemented with 1 mM phenylmethylsulfonyl fluoride (PMSF), 1 mM NaF, 1 mM Na_3VO_4, 10 µg/ml each of aprotinin, leupeptin and pepstatin A for 20 min at 4°C. Supernatants after centrifugation at 14,000 *g* for 15 min at 4°C were collected. Alternatively, cytoplasmic extracts were prepared. Samples containing 30–50 µg of protein were separated on SDS-polyacrylamide gel and then transferred onto nitrocellulose membrane (0.45 µm, Bio-Rad). Membranes were immunoblotted with primary antibodies and followed by horseradish-peroxidase-conjugated secondary antibodies (1:5000) and visualized by ECL (Amersham Biosciences) according to manufacturer's instructions.

IKK Assay

Whole-cell lysates (500 mg) were collected in modified RIPA buffer without sodium deoxycholate, and cellular debris was removed by high-speed centrifugation. Lysates were pre-cleared by incubation with 0.25 µg of the appropriate control IgG together with 20 µl of protein A/G plus (25%, v/v) agarose conjugate for 30 min at 4°C, followed by centrifugation. Supernatants were then incubated with 1 µg of anti-IKKα/β for 2 h at 4°C, and then 20 µl of protein A/G plus agarose was added and incubated at 4°C on a rocker platform

overnight. After several washes with IP buffer and PBS, beads containing IKKα/β were incubated with 0.5 µg GST- Iκ *B*α substrate, 200 µM ATP in 20 µl kinase buffer (50 mM Tris–Cl pH 7.4, 20 mM $MgCl_2$, 20 mM β-glycerophosphate, 1 mM NaF, 1 mM Na_3VO_4, 1 mM PMSF, 0.5 mM DTT, 1 mM benzamidine, 10 µg/ml aprotinin and 1 µg/ml leupeptin) at 30°C for 30 min. Kinase reactions were stopped by the addition of 5 µl 5 × Laemmli's loading buffer and heated at 100°C for 5 min. The samples were resolved by 8% SDS-PAGE, electro-transferred to nitrocellulose membrane and probed with anti-phosphor-Iκ *B*α (Ser^{32}) antibody (1:1000). Membranes were re-probed with anti-IKK to ensure equal loading and the presence of total IKK protein.

Plasmids, Transfection and NF-κB-Dependent-Luciferase Reporter Assay

To measure the effect of honokiol on TNF-α-induced NF-κ B-dependent gene reporter transcription, HeLa cells were seeded into 24-well plates at a density 1.6×10^5 cells/well for 24 h. Subsequently, cells were transiently transfected with p3EnhConA-Luc or pControl-Luc (0.75 µg) using LipofectAMINE 2000 (Invitrogen). To normalize the transfection efficiency, cells were co-transfected with 0.25 µg of β-galactosidase control vector. After overnight incubation, cells were pre-treated with honokiol for 12 h following by 5 ng/ml TNF-α for 15 h and then harvested with 1 × reporter lysis buffer (Promega, Madison, Wis., USA). Relative luciferase activity was measured with a Bright-GLO luciferase assay system using POLARStar OPTIMA luminometer (BMG Labtechnologies). Luciferase activity was normalized with β-galactosidase activity, as measured by the Beta-GLO luciferase assay system according to the manufacturer's instructions.

To measure the effect of honokiol on NF-κB-dependent gene reporter transcription induced by various kinases, HeLa cells were transfected with p3EnhConA-Luc and β-galactosidase control vector together with 0.2 µg of expression vectors. After 5 h of incubation, cells were treated with honokiol for 24 h and then harvested and assayed as described above.

EVALUATION

Statistical analyses were performed using an unpaired two-tailed Student's *t*-test. Two compounds (A and B) were considered enhancing each other's actions if the effect of combined treatment (AB) was larger then the sum of their individual effects (AB > A + B) after subtraction of the respective background control values.

MODIFICATIONS OF THE METHOD

Mortellaro et al. (1999) reported that the immunosuppressive drug PNU156804 blocks IL-2-dependent proliferation and NF-κB and AP-1 activation in human primary T lymphocytes.

Spencer et al. (1999) found in murine NIH3T3 fibroblasts and primate COS-7 cells that taxol selectively blocks microtubule-dependent NF-κB activation by phorbol ester via inhibition of Iκ *B*α phosphorylation and degradation.

Yan and Polk (1999) reported that aminosalicylic acid inhibits IκB kinase α phosphorylation of Iκ *B*α in mouse intestinal epithelial cells.

Acarin et al. (2000) found that oral administration of the anti-inflammatory substance triflusal results in the downregulation of constitutive transcription factor NF-κB in the postnatal rat brain.

Eberhardt et al. (2002) studied involvement of nuclear factor κB and Ets transcription factors in glucocorticoid-mediated suppression of cytokine-induced matrix metalloprotease-9 expression in rat mesangial cells.

Kang et al. (2002) showed that inhaled nitric oxide attenuated acute lipopolysaccharide-induced lung injury in rabbits via inhibition of nuclear factor-κB.

Macotela et al. (2002) found on rat pulmonary fibroblasts that 16K prolactin induces NF-κB activation.

Roshak et al. (2002) reported small-molecule inhibitors of NF-κB for the treatment of inflammatory joint disease.

Burke et al. (2003) found that BMS-345541 is a highly selective inhibitor of IκB kinase that binds at an allosteric site of the enzyme and blocks NF-κB–dependent transcription in mice.

Castro et al. (2003) described β-carbolines as inhibitors of the NF-κB kinase.

Clarke et al. (2003) reported that two distinct phases of virus-induced nuclear factor κB regulation enhance tumor necrosis factor-related apoptosis-inducing ligand-mediated apoptosis in virus-infected cells.

Murata et al. (2003) described discovery of selective IKK-β serine-threonin protein kinase inhibitors.

Yadav et al. (2003) reported that a diarylheptanoid from lesser galangal (*Alpinia officinarum*) inhibits proinflammatory mediators via inhibition of mitogen-activated protein kinase, P44/42, and transcription factor nuclear factor-κB.

HMG-CoA reductase inhibitors (statins) inhibited the binding of nuclear proteins to both NF-κB and AP-1 DNA consensus oligonucleotides in human endothelial and vascular smooth muscle cells as assed by EMSA (Dichtl et al. 2003).

Gupta et al. (2004) discussed the essential role of caspases in epigallocatechin-3-gallate-mediated inhibition of nuclear factor *kappa*B and induction of apoptosis.

Mühlbauer et al. (2004) studied differential effects of deoxycholic acid and taurodeoxycholic acid on NF-κB signal transduction and IL-8 gene expression in human colonic epithelial cells.

Syrovets et al. (2005) found that acetyl-boswellic acids inhibit lipopolysaccaride-mediated TNF-α induction by direct interaction with IκB kinases.

Eberhardt et al. (2005) found that dissociated glucocorticoids equipotently inhibit cytokine- and cAMP-induced matrix degrading proteases in rat mesangial cells.

Matsubara et al. (2005) found that a histamine H1 receptor antagonist blocks histamine-induced proinflammatory cytokine production through inhibition of Ca^{2+}-dependent protein kinase C, Raf/MEK/ERK and IKK/ Iκ B/NF-κB signal cascades.

Mendoza-Milla et al. (2005) reported that NF-κB activation but not PIK/Akt is required for dexamethasone-dependent protection against TNF-α cytotoxicity in L929 cells.

APPENDIX

Electrophoretic Mobility Shift Assay (EMSA)

Most papers mentioned above used the electrophoretic mobility shift assay (EMSA) for determination of nuclear factor κB. This method is one of the most sensitive ones for studying the DNA-binding properties of a protein. It can be used to deduce the binding parameters and relative affinities of a protein for one or more DNA sites or for comparing the affinities of different proteins to the same sites (Fried 1989). It is also useful for studying higher-order complexes containing several proteins, observed as a "supershift assay." EMSA can also be used to study protein- or sequence-dependent DNA bending (Crothers et al. 1991).

In an EMSA, or simple "gel shift," a ^{32}P-labeled DNA fragment containing a specific DNA site is incubated with a candidate DNA-binding protein. The protein–DNA complexes are separated from free (unbound) DNA by electrophoresis through a nondenaturing polyacrylamide gel. The protein retards the mobility of the DNA fragments to which it binds; thus, the free DNA migrates faster through the gel than does the DNA–protein complex. An image of the gel reveals the positions of the free and bound ^{32}P-labeled DNA.

A protocol of the detailed procedure was described by Carey and Smale (2000).

PROCEDURE

1. Prepare a 40-ml 4.5% native acrylamide gel (using 1- to 1.5-mm spacers)

Acrylamide mix (30%:29:1 acrylamide:bisacrylamide)	6 ml
5 × Tris-borate/EDTA (TBE) buffer	4 ml
Glycerol (20% vol/vol)	2 ml
Water	28 ml
Ammonium persulfate (10% solution in water)	300 µl
N,N,N,N-tetramethylenediamine (add just before pouring the gel)	30 µl

Pre-run the gel for 2 h at 10 mA.

2. Set up binding reactions in 0.5-ml siliconized microcentrifuge tubse

Recombinant protein (0.5–100 ng)	1.00 µl
^{32}P-labeled DNA template (ideally 1 fmol)	1.00 µl
Poly(dl:dC) (1 µg/µl)	0.20 µl
Dimethylsulfoxide (0.1 M)	0.10 µl
$MgCl_2$ (0.1 M)	0.75 µl
Buffer D	6.70 µl
Water	to 10 µl

Buffer D is 20 mM HEPES-KOH (pH 7.9), 20% glycerol (vol/vol), 0.2 mM EDTA, 0.1 M KCl, 0.5 mM phenylmethylsulfonyl fluoride (PMSF), 1 mM DTT. Add PMSF and DTT just before use.

3. Incubate the reaction at 30°C (incubate at 15°C–25°C or on ice for crude extracts) for 1 h.
4. Load the samples directly (with no dye) onto gel. Carefully layer the mix onto the bottom of the well and observe the schlieren line form at the glycerol–buffer interface.
5. Rune the gel for desired time at 10 mA; for a 30-bp fragment, allow the bromophenol blue dye to migrate about two-thirds of the way down the gel.
6. When the electrophoresis run is complete, carefully pour out the buffer into the sink and remove the gel from the apparatus. Remove the comb and split the plates, leaving the gel attached to one plate.
7. (Optional) Fix the gel in gel fixing solution (200 ml methanol, 100 ml acetic acid, 700 ml water) at 15°C–25°C for 15 min.
8. Place the gel on two sheets of Whatman 3MM paper. Cover the other side of the gel with Saran Wrap and dry on a gel dryer at 70°C for 1 h.
9. Expose the gel to autoradiography film or to phosphorimager screen overnight.

REFERENCES AND FURTHER READING

Acarin L, González B, Castellano B (2000) Oral administration of the anti-inflammatory substance triflusal results in the downregulation of constitutive transcription factor NF-κB in the postnatal rat brain. Neurosci Lett 288:41–44

Burke JR, Pattoli MA, Gregor KR, Brassil PJ, MacMaster JF, McIntyre KW, Yang X, Iotzova VS, Clarke W, Strnad J, Qiu Y, Zusi FC (2003) BMS-345541 is a highly selective inhibitor of IκB kinase that binds at an allosteric site of the enzyme and blocks NF-κB–dependent transcription in mice. J Biol Chem 278:1450–1456

Carey M, Smale ST (2000) Electrophoretic mobility shift assays. In: Transcriptional regulation in eukaryotes: concepts, strategies, and techniques. Chap 13, Protocol 13.5:493–496 (Cold Spring Harbor Laboratory Press, Cold Spring Harbor, New York, USA, 2000). Nature Methods 2:557–558

Castrillo A, de las Heras B, Hortelano S, Rodríguez B, Villar A, Boscá L (2001) Inhibition of the nuclear factor κB (NF-κ B) pathway by tetracyclic kaurene diterpenes in macrophages. J Biol Chem 276:15854–15860

Castro AC, Dang LC, Soucy F, Grenier L, Mazdiyasni H, Hottelet M, Parent L, Pien C, Palombella V, Adams J (2003) Novel IKK inhibitors: β-carbolines. Bioorg Med Chem Lett 13:2419–2422

Chaturvedi MM, Mukhopadhyay A, Aggarwal BB (2000) Assay for redox-sensitive transcription factor. Methods Enzymol 319:585–602

Clarke P, Meintzer SM, Moffitt LA, Tyler KL (2003) Two distinct phases of virus-induced nuclear factor κB regulation enhance tumor necrosis factor-related apoptosis-inducing ligand-mediated apoptosis in virus-infected cells. J Biol Chem 278:18092–18100

Crothers DM, Gartenberg MR, Shrader TE (1991) DNA bending in protein-DNA complexes. Methods Enzymol 208:118–146

Dichtl W, Dulak J, Frick M, Alber HF, Schwarzacher SP, Ares MPS, Nilsson J, Pachinger O, Weidinger F (2003) HMG-CoA reductase inhibitors regulate inflammatory transcription factors in human endothelial and vascular smooth muscle cells. Arterioscler Thromb Vasc Biol 23:58–63

Eberhardt W, Schulze M, Engels C, Klasmeier E, Pfeilschifter J (2002) Glucocorticoid-mediated suppression of cytokine-induced matrix metalloprotease-9 expression in rat mesangial cells. Involvement of nuclear factor κB and Ets transcription factors. Mol Endocrinol 16:1752–1766

Eberhardt W, Kilz T, Akool ES, Müller R, Pfeilschifter J (2005) Dissociated glucocorticoids equipotently inhibit cytokine- and cAMP-induced matrix degrading proteases in rat mesangial cells. Biochem Pharmacol 70:433–445

Fried MG (1989) Measurement of protein-DNA interaction parameters by electrophoretic mobility shift assay. Electrophoresis 10:366–376

Geng Z, Rong Y, Lau BHS (1997) S-allyl cysteine inhibits activation of nuclear factor kappa B in human T cells. Free Radical Biol Med 23:345–350

Gupta S, Hastak K, Afaq F, Ahmad N, Mukhtar H (2004) Essential role of caspases in epigallocatechin-3-gallate-mediated inhibition of nuclear factor *kappa*B and induction of apoptosis. Oncogene 23:2507–2522

Hiramoto M, Shimizu N, Sugimoto K, Tang J, Kawakami Y, Ito M, Aizawa S, Tanaka H, Makino I, Handa H (1998) Nuclear targeted suppression of NF-κB by the novel quinone derivative E3330. J Immunol 160:810–819

Ichiyama T, Sakai T, Catania A, Barsh GS, Furukawa S, Lipton JM (1999) Inhibition of peripheral NF-κB activation by central action of α-melanocyte-stimulating hormone. J Neuroimmunol 99:211–217

Jancso G, Cseperes B, Gasz B, Benkö L, Ferencz A, Borsiczki B, Lantos J, Dureja A, Kiss K, Szeberényi J, Röth E (2005) Effect of acetylsalicylic acid on nuclear factor-κB activation and on late preconditioning against infarction of the myocardium. J Cardiovasc Pharmacol 46:295–301

Kang JL, Lee HW, Pack IS, Chong Y, Castranova V, Koh Y (2001) Genistein prevents nuclear factor kappa B activation and acute lung injury induced by lipopolysaccaride. Am J Respir Crit Care Med 164:2206–2212

Kang JL, Park W, Pack IS, Lee HS, Kim MJ, Lim CM, Koh Y (2002) Inhaled nitric oxide attenuated acute lung injury via inhibition of nuclear factor-κB and inflammation. J Appl Physiol 92:75–801

Kim YH, Lee SH, Lee JY, Choi SW, Park JW, Kwon TK (2004) Tripolide inhibits murine-inducible nitric synthase expression by down-regulating lipopolysaccharide-induced activity of nuclear factor κB and c-Jun NH_2-terminal kinase. Eur J Pharmacol 494:1–9

Kunsch C, Luchoomun J, Chen XI, Dodd GL, Karu KS, Meng CQ, Marino EM, Olliff LK, Piper D, Qiu FH, Sikorski JA, Somers PK, Suen KL, Thomas S, Whalen AM, Wasserman MA, Sundell CL (2005) AGIX-4207 [2-[4-[[1-[[3,5-bis(1,1-dimethylethyl)-4-hydroxyphenyl]thio]-1-methylethyl]thio]-2,6-bis(1,1-dimethylethyl)phenoxy]acetic acid], a novel antioxidant and anti-inflammatory compound: cellular and biochemical characterization of antioxidant activity and inhibition of redox-sensitive inflammatory gene expression.J Pharm Exp Ther 313:492–501

Lee JH, Koo TH, Hwang BY, Lee JJ (2002) Kaurane diterpene, kamebakaurin, inhibits NF-κB by directly targeting the DNA-binding activity of p50 and blocks the expression of antiapoptotic NF-κB target genes. J Biol Chem 277:18411–18420

Macotela Y, Mendoza C, Corbacho AM, Cosío G, Eiserich JP, Zentella A, de la Escalera GM, Clapp C (2002) 16K Prolactin induces NF-κB activation in pulmonary fibroblasts. J Endocrinol 175:R13–R18

Matsubara M, Tamura T, Ohmori K, Hasegawa K (2005) Histamine H1 receptor antagonist blocks histamine-induced proinflammatory cytokine production through inhibition of Ca^{2+}-dependent protein kinase C, Raf/MEK/ERK and IKK/ IκB/NF-κB signal cascades. Biochem Pharmacol 69:433–449

Mendoza-Milla C, Rodríguez CM, Alarcón EC, Bernal AE, Toledo-Cuevas EM, Martínez EM, Dehesa AZ (2005) NF-κB activation but not PIK/Akt is required for dexamethasone dependent protection against TNF-α cytotoxicity in L929 cells. FEBS Lett 579:3947–3952

Mortellaro A, Sangia S, Gnocchi P, Ferrari M, Fornasiero C, D'Alessio R, Isetta A, Colotta F, Golay J (1999) New immunosuppressive drug PNU156804 blocks IL-2-dependent proliferation and NF-κB and AP-1 activation. J Immunol 162:7102–7109

Mühlbauer M, Allard B, Bosserhoff AK, Kiessling S, Herfarth H, Rogler G, Schölmerich J, Jobin C, Hellerbrand C (2004) Differential effects of deoxycholic acid and taurodeoxycholic acid on NF-κB signal transduction and IL-8 gene expression in colonic epithelial cells. Am J Physiol 286:G1000–G1008

Murata T, Shimada M, Sakakibara S, Yoshino T, Kadono H, Masuda T, Shimazaki M, Shintani T, Fuchikami K, Sakai K, Inbe H, Takeshita K, Niki T, Umeda M, Bacon KB, Ziegelbauer KB, Lowinger TB (2003) Discovery of novel and selective IKK-β serine-threonin protein kinase inhibitors. Part I. Bioorg Med Chem Lett 13:913–918

Natarajan K, Singh S, Burke TR, Grunberger D (1996) Caffeic acid phenyl ester is a potent and specific inhibitor of activation of nuclear transcription factor NF-κB. Proc Natl Acad Sci USA 93:9090–9095

Palanki MSS, Gayo-Fung LM, Shevlin GI, Erdman P, Sato M, Goldman M, Ransone LJ, Spooner C (2002) Structure-activity relationship studies of ethyl 2-[(3-methyl-2,5-dioxo(3-pyrrolinyl)amino]-4-(trifluoromethyl)pyrimidine-5-carboxylate: an inhibitor or AP-1 and NF-κB mediated gene expression. Bioorg Med Chem Lett 12:2573–2577

Roshak AK, Callahan JF, Blake SM (2002) Small-molecule inhibitors of NF-κB for the treatment of inflammatory joint disease. Curr Opin Pharmacol 2:316–321

Schrenk R, Meier B, Männel DN, Dröge W, Baeuerle PA (1992) Dithiocarbamates as potent inhibitors of nuclear factor κB activation in intact cells. J Exp Med 175:1181–1194

Spencer W, Kwon H, Crépieux P, Leclerc N, Lin R, Hiscott J (1999) Taxol selectively blocks microtubule dependent NF-κB activation by phorbol ester via inhibition of Iκ *Bα* phosphorylation and degradation. Oncogene 18:495–505

Staal FJT, Roederer M, Hertenberg LA, Hertenberg LA (1990) Intracelluar thiols regulate activation of nuclear factor κB and transcription of human immunodeficiency virus. Proc Natl Acad Sci USA 87:9943–9947

Syrovets T, Büchele B, Krauss C, Laumonnier Y, Simmet T (2005) Acetyl-boswellic acids inhibit lipopolysaccaride-mediated TNF-α induction by direct interaction with IκB kinases. J Immunol 174:498–506

Tse AKW, Wan CK, Shen XL, Yang M, Fong WF (2005) Honokiol inhibits TNF-α-stimulated NF-κB activation and NF-κ B-regulated gene expression through suppression of IKK activation. Biochem Pharmacol 70:1443–1457

Yadav PN, Liu Z, Rafi MM (2003) A diarylheptanoid from lesser galangal (*Alpinia officinarum*) inhibits proinflammatory mediators via inhibition of mitogen-activated protein kinase, P44/42, and transcription factor nuclear factor- κB. J Pharmacol Exp Ther 305:925–931

Yan F, Polk DB (1999) Aminosalicylic acid inhibits Iκ B kinase α phosphorylation of Iκ *Bα* in mouse intestinal epithelial cells. J Biol Chem 274:36631–36636

H.3.1.8 TNF-α Antagonism

H.3.1.8.1 General Considerations

TNF-α has been cloned and identified by Beutler et al. (1985). It is primarily produced in macrophages, lymphocytes, neutrophils, endothelial cells, keratinocytes and fibroblasts during acute inflammatory reactions. TNF-α is a member of a large family of proteins and receptors that are involved in immune regulation such as kinases, including nuclear factor kappa B (NF-κ B), p38 MAP kinase, JUN kinases and others. Therefore, it is a therapeutic target for immune-mediated inflammatory diseases (Pfizenmaier et al. 1996; Van Deventer 1997; Rath and Aggarwal 1999; Feldmann et al. 2001; Furst et al. 2001; Taylor 2001; Doggrell 2002; Braun et al. 2003; Sharma and Anker 2003; Louie et al. 2003; Nanes 2003; Peng et al. 2003; Chen et al. 2003; Taylor et al. 2004; Gupta et al. 2005; Pfeifer et al. 2006; Reber et al. 2006; Wagner and Laufer 2006). This may be achieved by small molecular anti-cytokine agents inhibiting cytokine production, which target p38 mitogen activated protein (MAP) kinase, TNF-α converting enzyme (TACE), or IL-1β converting enzyme (ICE).

Several so-called "biologicals" are in clinical use:

Etanercept (Enbrel), a fully human soluble TNF receptor fusion protein consisting of the extracellular ligand-binding domain of the 75-kDa receptor for human tumor necrosis factor-α and and the constant portion of human IgG1 (Jarvis and Faulds 1999; Pugsley 2001; Scallon et al. 2002; Agnholt et al. 2003; Cole and Rabasseda 2004; Goffe 2004; Moe et al. 2004; Vallejo et al. 2005). The compound has been approved for treatment of psoriasis, psoriatic arthritis, ankylosing spondylitis and rheumatoid arthritis.

Infliximab (Remicade), a chimeric anti human TNF-α monoclonal antibody (Scallon et al. 2002; Agnholt et al. 2003; Di Sabatino et al. 2004; Wagner et al. 2004; Panaccione et al. 2005; Shen et al. 2005; Pfeifer et al. 2006). The compound is used for treatment of rheumatoid arthritis and Crohn's disease.

Adalimumab (HUMIRA), a recombinant human anti-human TNF-α monoclonal antibody (Gordon et al. 2005; Aggarwal et al. 2006; Scheinfeld 2006; Shen et al. 2006). The compound is used for treatment of rheumatoid arthritis and psoriatic arthritis.

Imatinib mesylate (STI571, Gleevec), a kinase inhibitor of TNF-α production (Kilic et al. 2000; Traxler et al. 2001; Dietz et al. 2004; Kaelin 2004; Lassila et al. 2005; Wolf et al. 2005; Adcock et al. 2006). The compound has been found to be active in the treatment of chronic myelogenous leukemia, gastrointestinal stromal tumors, eosinophilic disorders, and systemic mast cell disease.

Omalizumab (Xolair), a recombinant humanized monoclonal antibody which specifically binds the Cε3 domain of IgE, the site of high-affinity IgE receptor binding (Easthope and Jarvis 2001; Anonymous 2002; Johansson et al. 2002; Davis 2004; Richards et al. 2004; Belliveau 2005; D'Amato 2006). The compound is used for treatment of bronchial asthma and allergic rhinitis.

Anakinra (Kineret) is a specific recombinant human interleukim-1 receptor antagonist that differs from naturally occurring IL-1 receptor antagonist by the presence of a methionine group (Cvetkovic and Keating 2002; Fleischmann et al. 2004; Le and Abbenante 2005; Waugh and Perry 2005). The compound is effective in patients with active rheumatoid

arthritis, either when given alone or in combination with methotrexate.

REFERENCES AND FURTHER READING

Adcock IM, Chung KF, Karamori G, Ito K (2006) Kinase inhibitors and airway inflammation. Eur J Pharmacol 533:118–132

Aggarwal BB, Shishodia S, Takada Y, Jackson-Bernitsas D, Ahn KS, Sethi G, Ichikawa H (2006) TNF blockade: an inflammatory issue. Ernst Schering Res Found Workshop 56:161–186

Agnholt J, Dahlerup JF, Kaltoft K (2003) The effect of etanercept and infliximab on the production of tumor necrosis factor α, interferon-γ and GM-CSF in in vivo activated intestinal T lymphocyte cultures. Cytokine 23:76–85

Anonymous (2002) Omalizumab: anti-IgE antibody E25, E25, humanized anti-IgE MAb, IGE 025, monoclonal antibody E25, Olizumab, Xolair, rhuMAb-E25. BioDrugs 16:380–386

Belliveau PP (2005) Omaizumab: a monoclonal anti-IgE antibody. Med Gen Med 7:27

Beutler B, Greenwald D, Hulmes JD, Chang M, Pan YC, Mathison J, Ulevitch R, Cerami A (1985) Identity of tumor necrosis factor and the macrophage-secreted factor catechin. Nature 316:552–554

Braun J, Brandt J, Listing J, Rudwaleit M, Sieper J (2003) Biologic therapies in the spondyloarthritis: new opportunities, new challenges. Curr Opin Rheumatol 15:394–407

Chen JJ, Dewdney N, Lin X, Martin RL, Walker KAM, Huang J, Chu F, Eugui E, Mirkovich A, Kim Y, Sarma K, Arzeno H, van Wart HE (2003) Design and synthesis of orally active inhibitors of TNF synthesis as anti-rheumatoid arthritis drugs. Bioorg Med Chem Lett 13:3951–3954

Cole P, Rabasseda X (2004) The soluble tumor necrosis factor receptor Etanercept: a new strategy in the treatment of autoimmune rheumatic disease. Drugs Today 40:281–324

Cvetkovic RS, Keating G (2002) Anakinra. BioDrugs 16:303–311

D'Amato (2006) Role of anti-IgE monoclonal antibody (omalizumab) in the treatment of bronchial asthma and allergic respiratory diseases. Eur J Pharmacol 533:302–307

Davis LA (2004) Omalizumab: a novel therapy for allergic asthma. Ann Pharmacother 38:1236–1242

Di Sabatino A, Ciccocioppo R, Cinque B, Millimaggi D, Morera R, Ricevuti L, Cifone MG, Corazza GR (2004) Defective mucosal T cell death is sustainably reverted by infliximab in a capsase dependent pathway in Crohn's disease. Gut 53:70–77

Dietz AB, Souan L, Knutson GJ, Bulur PA, Litzow MR, Vuk-Pavloviæ S (2004) Imatinib mesylate inhibits T-cell proliferation in vitro and delayed-type hypersensitivity in vivo. Blood 104:1094–1099

Doggrell SA (2002) TACE inhibition: a new approach in treating inflammation. Expert Opin Invest Drugs 11:1003–1006

Easthope S, Jarvis B (2001) Omalizumab. Drugs 61:353–260

Feldmann M, Brennan FM, Foxwell BMJ, Maini RN (2001) The role of TNF-α and IL-1 in rheumatoid arthritis. Curr Dir Autoimmun 3:188–199

Fleischmann R, Stern R, Iqbal I (2004) Anakinra. An inhibitor of IL-1 for the treatment of rheumatoid arthritis. Expert Opin Biol Ther 4:1333–1344

Furst DE, Keystone EC, Breedveld FC, Kalden JR, Smolen JS, Antoni CE, Burmester GR, Crofford LJ, Kavanaugh A (2001) Updated consensus statement on tumor necrosis factor blocking agents for the treatment of rheumatoid arthritis and other rheumatic disorders.. Ann Rheum Dis 60:2–5

Goffe B (2004) Etanercept (Enbrel) – an update. Skin Ther Lett 9:1–4

Gordon KB, Bonish BK, Patel T, Leonardi CL, Nickoloff BJ (2005) The tumor necrosis factor-α inhibitor adalimumab rapidly reverses the decrease in epidermal Langerhans cell density in psoriatic plaques. Br J Dermatol 153:945–953

Gupta S, Gollapudi S (2005) Molecular mechanisms of TNF-α-induced apoptosis in aging human T cell subsets. Int J Biochem Cell Biol 37:1934–1042

Jarvis B, Faulds D (1999) Etanercept. A review on its use in rheumatoid arthritis. Drugs 57:945–966

Johansson SGO, Haahtela T, O'Byrne PM (2002) Omalizumab and the immune system: an overview of preclinical and clinical data. Ann Allergy Asthma Immunol 89:132–138

Kaelin WG Jr (2004) Gleevec: prototype or outlier? SciSTKE 225:12

Kilic T, Alberta JA, Zdunek PR, Acar M, Iannarelli P, O'Reilly T, Buchdunger E, Black PM, Stiles CD (2000) Intracranial inhibition of platelet-derived growth factor-mediated glioblastoma cell growth by an orally active kinase inhibitor of the 2-phenylaminopyrimidine class. Cancer Res 60.5143–5150

Lassila M, Jandeleit-Dahm K, Seah KK, Smith CM, Calkin AC, Allen ZJ, Cooper ME (2005) Imatinib attenuates diabetic nephropathy in apolipoprotein E-knockout mice. J Am Soc Nephrol 16:363–373

Le GT, Abbenante G (2005) Inhibitors of TACE and caspase-1 as anti-inflammatory drugs. Curr Med Chem 12:2963–2977

Louie SG, Park B, Yoon H (2003) Biological response modifiers in the management of rheumatoid arthritis. Am J Health Syst Pharm 60:346–355

Moe GW, Marin-Garcia J, Konig A, Goldenthal M, Lu X, Feng Q (2004) In vivo TNF-α inhibition ameliorates cardiac mitochondrial dysfunction, oxidative stress, and apoptosis in experimental heart failure. Am J Physiol 287:H1813–H1820

Nanes MS (2003) Tumor necrosis factor-α: molecular and cellular mechanisms in skeletal pathology. Gene 432:1–15

Panaccione R, Ferraz JG, Beck P (2005) Advances in medical therapy of inflammatory bowel disease. Curr Opin Pharmacol 5:566–572

Peng T, Lu X, Lei M, Moe GW, Feng Q (2003) Inhibition of p38 MAPK decreases myocardial TNF-alpha expression and improves myocardial function and survival in endotoxemia. Cardiovasc Res 59:893–900

Pfeifer C, Wagner G, Laufer S (2006) New approaches to the treatment of inflammatory disorders small molecule inhibitors of p38 MAP kinase. Curr Top Med Chem 6:113–149

Pfizenmaier K, Wajant H, Grell M (1996) Tumor necrosis factors in 1996. Cytokine Growth Factor Rev 7:271–277

Pugsley MK (2001) Etanercept: Immunex. Curr Opin Invest Drugs 2:1725–1731

Rath PC, Aggarwal BB (1999) TNF-induced signaling in apoptosis. J Clin Immunol 19:350–364

Reber L, da Silva CA, Frossard N (2006) Stem cell factor and its receptor c-Kit as targets for inflammatory diseases. Eur J Pharmacol 533:327–340

Richards ML, Lio SC, Sinha A, Tieu KK, Sircar JC (2004) Novel 2-(substituted phenyl)benzimidazole derivatives with potent activity against IgE, cytokines, and CD23 for the treatment of allergy and asthma. J Med Chem 47:6451–6454

Scallon B, Cai A, Solowski N, Rosenberg A, Song XY, Shealy D, Wagner C (2002) Binding and functional comparisons of two types of tumor necrosis factor antagonists. J Pharmacol Exp Ther 301:418–426

Scheinfeld N (2006) Adalimumab (HUMIRA): a review. J Drugs Dermatol 2:375–377
Sharma R, Anker SD (2002) Cytokines, apoptosis and cachexia: the potential for TNF antagonism. Int J Cardiol 85:161–171
Shen C, Maerten P, Geboes K, van Assche G, Rutgeers P, Ceuppens JL (2005) Inflixemab induces apoptosis of human monocytes and T lymphocytes in a human-mouse chimeric model. Clin Immunol 115:250–259
Shen C, Van Assche G, Rutgeerts P, Cauppens JL (2006) Caspase activation and apoptosis induction by Adalimumab: demonstration in vitro and in vivo in a chimeric mouse model. Inflamm Bowel Dis 12:22–28
Taylor PC (2001) Anti-tumor necrosis factor therapies, Curr Opin Rheumatol 13:164–169
Taylor PC, Williams RO, Feldmann M (2004) Tumor necrosis factor α as a therapeutic target for immune-mediated inflammatory diseases. Curr Opin Biotechnol 15:557–563
Traxler P, Bold G, Buchdunger E, Caravatti G, Furet P, Manley P, O'Reilly T, Wood J, Zimmermann J (2001) Tyrosine kinase inhibitors: from rational design to clinical trials. Med Res Rev 21:499–512
Vallejo JG, Nemoto S, Ishiyama M, Yu B, Knuefermann P, Diwan A, Baker JS, Defreitas G, Tweardy DJ, Mann DL (2005) Functional significance of inflammatory mediators in a murine model of resuscitated hemorrhagic shock. Am J Physiol 288:H1272–H1277
Van Deventer SJH (1997) Tumor necrosis factor and Crohn's disease. Gut 40:443–448
Wagner G, Laufer S (2006) Small molecular anti-cytokine agents. Med Res Rev 26:1–62
Wagner U, Pierer M, Wahle M, Moritz F, Kaltenhäuser S, Häntschel H (2004) Ex vivo homeostatic proliferation of $CD4^+$ T cells in rheumatoid arthritis is dysregulated and driven by membrane-anchored TNFα. J Immunol 173:2825–2833
Waugh J, Perry CM (2005) Anakinra: a review of its use in the management of rheumatoid arthritis. BioDrugs 19:189–202
Wolf AM, Wolf D, Rumpold H, Ludwiczek S, Enrich B, Gastl G, Weiss G, Tilg H (2005) The kinase inhibitor imatinib mesylate inhibits TNF-α production *in vitro* and prevents TNF-dependent acute hepatic inflammation. Proc Natl Acad Sci USA 102:13622–13627

H.3.1.8.2 Inhibition of TNF-α Release

PURPOSE AND RATIONALE

There are two distinct types of tumor necrosis factors, TNF-alpha (cachectin) and TNF-beta (lymphotoxin), with biological activities going beyond the necrosis of tumor cells. Some of the known activities include the induction of interleukin 1, activation of PMNs, modulation of endothelial cell functions, and augmentation of specific immune functions. The complex sequence of hemodynamic and metabolic collapse, which leads to shock and death during lethal endotoxinemia, appear to represent the response of the infected host to the acute, systemic release of TNF-alpha. Thus, drugs that antagonize the activity of this mediator could be of clinical value in combating its fatal effects.

PROCEDURE

Twenty hours before the initiation of the experiments, L 929 cells are harvested from stock cultures and are plated in 96 well culture plates (2×10^4 cells/well) and incubated at 37°C and 5% CO_2 in air. For each group 6 wells are set up. The cells are then preincubated for 30 min with test substances or solvent before TNF-alpha is added (between 1 and 10 IU/well). After an additional incubation time of 20 h, the culture plates are flicked out and the remaining living cells are lysed by the addition of bidistilled water (100 µl). After 30 min incubation at room temperature, 100 µl of LDH reagent are given to each culture well. After 15 min, the enzyme activity is determined photometrically at 490 nm.

EVALUATION

The percent inhibition is calculated according to the formula:

$$\% \text{ inhibition} = 100\% - \frac{\text{ext. test group} - \text{ext. spontaneous lysis}}{\text{ext.positive control} - \text{ext. spontaneous lysis}} .$$

The positive control is the group which receives vehicle and TNF-alpha. The spontaneous lysis is based on cultures which receive vehicle without TNF-alpha.

MODIFICATIONS OF THE METHOD

Maloff and Delmendo (1991) measured the binding of tumor necrosis factor (TNF-α) to the human TNF receptor. Membranes were prepared from HeLa S3 human cervical epithelioid carcinoma cells. An aliquot of 0.2 mg of membrane preparation was incubated with 62 pM [^{125}I]TNF-α for 3 h at 4°C. Nonspecific binding was measured in the presence of 50 nM TNF-α. Membranes were filtered and washed 3 times and the filters were counted to determine the bound [^{125}I]TNF-α.

Golebiowski et al. (2005) tested pyrazolone-based cytokine synthesis inhibitors for the inhibition of TNF-α production using lipopolysaccharide-stimulated monocytic cells. Duplicate cultures of human monocytic cells (2.0×10^6/well) were incubated for 15 min in the presence or absence of various concentrations of inhibitor before the stimulation of cytokine release by the addition of lipopolysaccharide (1 µg/ml). The amount of TNF-α released was measured 4 h later using an ELISA system.

Kumar et al. (1997) described homologs of CSBP/p38 MAP kinase, their activation, as well as substrate specificity and sensitivity to inhibition by pyridyl imidazoles.

McLay et al. (2001) reported the discovery of a p38 MAP kinase inhibitor displaying a good oral anti-arthritic efficacy.

Ignar et al. (2003) described the regulation of TNF-α secretion by a specific melanocortin-1 receptor peptide agonist.

Kinases Assay

The p38 enzyme assay is carried out at room temperature for 1 h, using 40 ng/well of the mouse enzyme. The substrate, 50 µg/ml ATF-2 transformation factor, is coated onto 96-well plates, and the assay is carried out in 25 mM Hepes buffer, pH 7.7 containing 25 mM magnesium chloride, 2 mM dithiothreitol, 1 mM sodium orthovanadate and 100 µM ATP. Phosphorylated ATF-2 is quantitated using a phospho-specific ATF-2 primary antibody (rabbit anti-human) followed by a europium-labeled secondary antibody (sheep anti-rabbit IgG) with addition of the DELFIA enhancement solution resulting in fluorescence. ERK was measured using a [^{33}P]ATP filtration assay format using for substrates myelin basic protein. ZAP-70, Syk and Lck kinase activities were measured using the homogeneous time-resolved fluorescence methodology (HTRF) with the catalytic domains of each of the tyrosine kinases, biotinylated, specific peptide substrates, streptavidin-linked APC and europium cryptate-conjugated anti-phosphotyrosine antibody.

Monocyte TNF-α Release Assay

Adherent human monocytes (100,000 cells/well) were incubated with LPS (10 ng/ml) in the absence and presence of compound for 18 h. Individual experiments were carried out in quadruplicate samples. TNF-α was measured by sandwich ELISA and IC_{50} values calculated for the activity of individual compounds. IC_{50} values shown from repeat experiments are means ±SEM.

Mouse TNF-α Release Assay

Compound was administered orally to BALB/c mice 30 min prior to LPS (0.1 mg/kg i.p.) challenge. Serum TNF-α levels were determined 90 min after LPS insult. Results represent means ±SEM.

REFERENCES AND FURTHER READING

Flick DA, Gifford GE (1984) Comparison of *in vitro* cell cytotoxic assays for tumor necrosis factor. J Immunol Meth 68:167–175

Golebiowski A, Towner J, Laufersweiler MJ, Brugel TA, Clark MP, Clark CM, Djung JF, Laughlin SK, Sabat MP, Bookland RG, VanRens JC, De B, Hsieh LC, Janusz MJ, Walter RL, Webster ME, Mekel MJ (2005) The development of monocyclic pyrazolone based cytokine synthesis inhibitors. Bioorg Med Chem Lett 15:2285–3389

Ignar D, Andrews JL, Jansen M, Eilert MM, Pink HM, Lin P, Sherrill RG, Szewczyk JR, Conway JG (2003) Regulation of TNF-α secretion by a specific melanocortin-1 receptor peptide agonist. Peptides 24:709–716

Kumar S, McDonnell PC, Gum RJ, Hand AT, Lee JC, Young PR (1997) Novel homologues of CSBP/p38 MAP kinase: activation, substrate specificity and sensitivity to inhibition by pyridyl imidazoles. Biochem Biophys Res Commun 235:533–538

McLay IM, Halley F, Souness JE, McKenna J, Benning V, Birrell M, Burton B, Belvisi M, Collis A, Constan A, Foster M, Hele D, Jayyosi Z, Kelley M, Maslen C, Miller G, Ouldelhkim MC, Page K, Phipps S, Pollock K, Porter B, Ratcliffe AJ, Redford EJ, Webber S, Slater B, Thybaud V, Wilsher N (2001) The discovery of RPR 200765A, a p38 MAP kinase inhibitor displaying a good oral anti-arthritic efficacy. Bioorg Med Chem 9:537–554

Maloff BL, Delmendo RE (1991) Development of high throughput for interleukin-1α (IL-1α) and tumor necrosis factor (TNF-α) in isolated membrane preparations. Agents Actions 34:32–34

H.3.1.8.3 Effect of TNF-α Binding

PURPOSE AND RATIONALE

Several authors compared the effects of the prototypes of the tumor necrosis factor (TNF) antagonists infliximab or adalimumab and etanercept (Vuolteenaho et al. 2002; Kirchner et al. 2004; Shen et al. 2005).

Scallon et al. (2002) compared the binding and functional properties of the two prototypes of the TNF antagonists infliximab and etanercept-

Although both infliximab and etanercept are potent neutralizers of TNF bioactivity, there are fundamental differences in their molecular structures, their binding specificities, and the manner in which they neutralize TNF. Infliximab is a chimeric monoclonal antibody (mAb) with murine variable regions and human IgG1 and κ constant regions (Knight et al. 1993). The size (149 kDa) and structure of infliximab are therefore similar to those of naturally occurring antibodies. Etanercept is a fusion protein made up of the extracellular domain of the p75 TNF receptor (CD120b) and the hinge and Fc domains of human IgG1 (Mohler et al. 1993), a structure distinct from any known naturally occurring molecule. Importantly, infliximab is not known to bind to any antigen other than TNF, whereas etanercept binds equally well to both TNF and lymphotoxin α (LT α), consistent with observations reported for the cellular p75 TNF receptor (Schall et al. 1990; Smith et al. 1990). Each infliximab molecule is capable of binding to two TNF molecules, and up to three infliximab molecules can bind to each TNF ho-

motrimer, thereby blocking all receptor binding sites on TNF. In contrast, it is believed that the bivalent etanercept molecule forms a 1:1 complex with the TNF trimer in which two of the three receptor binding sites on TNF are occupied by etanercept, and the third receptor binding site is open. In addition, the p75 TNF receptor is known to have fast rates of association and dissociation with TNF (Evans et al. 1994), which suggests that etanercept may only transiently neutralize the activity of an individual TNF molecule.

PROCEDURE

Cell Culture

KYM-1D4 cells that endogenously express TNF receptors (Butler et al. 1994) were maintained in RPMI-1640 medium supplemented with 2 mM L-glutamine and 10% FBS. Human umbilical vein endothelial (HUVE) cells from Cell Systems (Seattle, Wash., USA) were maintained in HUVE cell medium supplied by Cell Systems. K2 cells were maintained in Iscove's modified Dulbecco's medium (IMDM) supplemented with 5% FBS, 2 mM L-glutamine, 0.5 µg/ml mycophenolic acid, 2.5 µg/ml hypoxanthine, and 50 µg/ml xanthine. All cells were cultured in a humidified incubator maintained at 37°C and 5% CO_2.

Binding to Monomer Subunits of TNF

Dimethylsulfoxide (DMSO) was added to ^{125}I-TNF (40–60 µCi/µ g; 1.48–2.2 MBq/µg) to a final concentration of 10% DMSO and incubated at 20°C for 30 min to allow dissociation of TNF trimers. The mixture was passed over a 10 × 300-mm Superose 12 column equilibrated with PBS, and ^{125}I-TNF trimer and monomer were collected separately. Polystyrene 96-well microtiter plates were coated by incubating 50 µl of 1 µg/ml of infliximab, etanercept, or an isotype-matched, negative control antibody (cM-T412) in the wells overnight at 4°C. After washing with PBS-0.05% Tween 20 (PBS-T), all wells were blocked for 1 h at 37°C with PBS-1% bovine serum albumin and washed three times with PBS-T. Triplicate wells were then incubated with ^{125}I-TNF trimer [0.4 µCi (14.8 kBq), 10 ng/ml] or ^{125}I-TNF monomer [0.1 µCi (3.7 kBq), 2.5 ng/ml] alone or with 5 µg/ml unlabeled TNF. After 1 h at 37°C, the wells were washed with PBS-T and counted for ^{125}I.

Binding Assay to Measure Stability of Complexes with Soluble TNF

Each well of a 96-well enzyme immunoassay plate was incubated overnight at 4°C with 100 µl of 0.1 M carbonate, pH 9.6, containing 10 µ g/ml goat anti-human γ Fc antibody. Plates were washed three times with PBS-T and then incubated for 1 h at 37°C in blocking buffer (10 mM HEPES, pH 7.5, containing 0.1% porcine gelatin, 150 µl/well). Wells were incubated for 1 h at 37°C with 100 µl/well of blocking buffer containing 1 µg/ml infliximab or etanercept. Plates were washed three times with PBS-T, and then all TNF binding sites were saturated by incubating the wells for 1 h at 37°C in 100 µl/well of blocking buffer containing 10 ng/ml ^{125}I-TNF (40–60 µCi/µg). Wells were washed three times with PBS-T and then filled with 100 µl/well of blocking buffer alone or containing an excess of soluble, unlabeled competitor such as infliximab, etanercept, or human TNF, and subsequently incubated at 37°C. At the indicated time points, triplicate wells were washed three times with PBS-T to remove free ^{125}I-labeled TNF. The last wash was aspirated and replaced with 50 µl of scintillation fluid and the entire plate counted in a Packard TopCount gamma counter.

Assay for Bioactivity of Dissociated Soluble TNF

Microtiter plates were coated with goat anti-human γ Fc antibody and used to capture etanercept as described above. Wells were washed three times with PBS-T and incubated with 100 µl of 10 ng/ml unlabeled human TNF in 100 µl/well of blocking buffer for 1 h at 37°C. Wells were washed three times with KYM media, filled with 100 µl of KYM media, and 500 ng/ml mouse TNF was added to each well as a competitor. After a 1-h incubation at 37°C, the soluble fraction was removed and pre-incubated for 1 h in fresh wells with either no mAb, 10 µg/ml anti-human TNF mAb (infliximab), 85 µg/ml anti-mouse TNF mAb (cV1q huG3), or a combination of 10 µg/ml anti-human TNF and 85 µg/ml anti-mouse TNF mAb. After the pre-incubation, the soluble fractions were added to cultures of KYM-1D4 cells (50,000 cells/well in a 96-well plate) and the cells incubated for 16 h at 37°C in the presence of 0.5 µg/ml actinomycin D. To quantitate cell viability, MTT dye was added to a final concentration 0.5 mg/ml and the cells incubated at 37°C for 4 h. The medium was aspirated and 100 µl of 100% DMSO was added to the cells. The difference between the absorbance at 550 and 650 nm was then determined.

HUVE Cell Assay to Measure Stability of Complexes with Soluble TNF

Infliximab or etanercept was mixed with 1 µg/ml human TNF at 10:1 or 30:1 M ratios in HUVE cell medium and incubated for 30 min at 37°C. Serial di-

lutions of the preformed complexes were then added to confluent HUVE cells cultured in 96-well plates. Cells were incubated with the preformed complexes in 100 µl of HUVE cell medium for 4 h at 37°C and then washed three times with HBSS. The cells were then incubated for 1 h at 37°C in HBSS containing 1 µg/ml ^{125}I-labeled anti-E-selectin (20 µCi/µg). Cells were washed three times with HBSS, the last wash was aspirated and replaced with 30 µl of scintillation fluid, and the entire plate was counted in a Packard TopCount gamma counter.

Binding Assay to Measure Stability of Complexes with Transmembrane TNF

K2 cells, which stably express an uncleavable and thus permanently transmembrane (tm) form of TNF, were seeded at a density of 5×10^4 cells/well in a 96-well round-bottom plate in 100 µl of IMDM, 5% FBS. Subsequently, ^{125}I-labeled infliximab or ^{125}I-labeled etanercept (both at 8.5 µCi/µg) was added to a final concentration of 0.5 µg/ml (enough to saturate all TNF binding sites on the cells). After a 1-h incubation at 25°C, unbound infliximab and etanercept were removed by washing three times with IMDM medium. Fresh IMDM, 5% FBS medium (100 µl) alone, or containing 50 µg/ml of an unlabeled soluble competitor, was added to the cells. Soluble competitors were either infliximab or etanercept for samples treated with radiolabeled infliximab and one of infliximab, etanercept, or human LTα for samples treated with radiolabeled etanercept. The cells were then incubated at 37°C in 5% CO_2. At different time points, cells in selected wells were washed with PBS, and the number of counts bound to the cells determined using a gamma counter (PerkinElmer Wallac, Wellesley, Mass., USA).

Characterization of Infliximab and Etanercept Binding to tmTNF

K2 cells or TNF-negative Sp2/0 control cells were seeded in 96-well round-bottom plates at a density of 5×10^4 cells/well in IMDM, 5% FBS. Varying amounts of ^{125}I-labeled infliximab (23.4 µ Ci/µg) or ^{125}I-labeled etanercept (22.4 µCi/µg) were added to the cells. After a 16-h incubation at 4°C, cells were washed four times with culture medium (IMDM, 5% FBS), the last wash was aspirated, and 50 µl of culture medium was added to each well. The cells were then removed with cotton swabs and the number of counts per well was determined using a gamma counter (PerkinElmer Wallac). The resulting binding data were analyzed by non-linear regression using Prism software (GraphPad Software, San Diego, Calif., USA).

HUVE Cell Assay to Compare Ability to Inhibit tmTNF Bioactivity

K2 cells or Sp2/0 control cells were seeded in 96-well round-bottom plates at a density of 1×10^5 cells/well in IMDM, 5% FBS. Varying amounts of infliximab or etanercept in IMDM, 5% FBS were added and the mixture incubated for 1 h at 37°C. This mixture was then added to confluent cultures of HUVE cells in 96-well plates. The resulting cell-cell mixture was incubated for an additional 4 h at 37°C in a 5% CO_2 incubator. Cells were then washed three times with HBSS and incubated for 1 h with 1 µg/ml ^{125}I-anti-E-selectin (20 µCi/µg). Cells were washed three times with HBSS, the last wash was aspirated and replaced with 30 µl of scintillation fluid, and the plate counted in a Packard TopCount gamma counter.

EVALUATION

Data were analyzed using a paired Student's *t*-test to determine whether there was a statistically significant difference between the capacities of infliximab and etanercept to block the bioactivity of tmTNF.

MODIFICATIONS OF THE METHOD

Maloff and Delmendo (1991) developed high-throughput radioligand binding assays for interleukin 1-α (IL-1-α) and tumor necrosis factor (TNF-α) in isolated membrane preparations.

Zhang et al. (2002) described identification and characterization of a dual tumor necrosis factor converting enzyme/matrix metalloprotease inhibitor for the treatment of rheumatoid arthritis.

Transgenic mice expressing human tumor necrosis factor develop severe polyarthritis (Keffer et al. 1991; Kollias et al. 1999; Kontoyiannis et al. 1999; Mijatovic et al. 2000; Akassoglou et al. 2003; Li and Schwarz 2003). A targeting vector containing a genomic fragment encoding the entire TNF-α with the ARE-containing 3′ UTR was replaced with the 3′ UTR from the β-globin gene. This mutation increases the stability and translational efficiency of TNF-α mRNA and thus results in chronic TNF-α over-expression that leads to severe erosive polyarthritis. Administration of anti- TNF-α antibodies completely prevents the disease.

REFERENCES AND FURTHER READING

Akassoglou K, Douni E, Bauer J, Lassmann H, Kollias G, Probert L (2003) Exclusive tumor necrosis factor (TNF) signaling by the p75TNF receptor triggers inflammatory ischemia in the CNS of transgenic mice. Proc Natl Acad Sci USA 100:709–714

Butler DM, Scallon B, Meager A, Kissonerghis M, Corcoran A, Chernajovsky Y, Feldmann M, Ghrayeb J, Brennan FM (1994) TNF receptor fusion proteins are effective inhibitors of TNF-mediated cytotoxicity on human KYM-1D4 rhabdomyosarcoma cells. Cytokine 6:616–623

Evans TJ, Moyes D, Carpenter A, Martin R, Loetscher H, Lesslauer W, Cohen J (1994) Protective effect of 55- but not 75-kD soluble tumor necrosis factor receptor-immunoglobulin G fusion proteins in an animal model of gram-negative sepsis. J Exp Med 180:2173–2179

Keffer J, Probert L, Cazlaris H, Georgopoulos S, Kaslaris E, Kioussis D, Kollias G (1991) Transgenic mice expressing human tumour necrosis factor: a predictive model of arthritis. EMBO J 10:4025–4031

Kirchner S, Holler E, Haffner S, Andreesen R, Eissner G (2004) Effect of different tumor necrosis factor (TNF) reactive agents on reverse signaling of membrane integrated TNF in monocytes. Cytokine 28:67–74

Knight DM, Trinh H, Le J, Siegel S, Shealy D, McDonough M, Scallon B, Moore MA, Vilcek J, Daddona P (1993) Construction and initial characterization of a mouse-human chimeric anti-TNF antibody. Mol Immunol 30:1443–1453

Kollias D, Douni E, Kassiotis G, Kontoyannis D (1999) The function of tumour necrosis factor and receptors in models of multi-organ inflammation, rheumatoid arthritis, multiple sclerosis and inflammatory bowel disease. Ann Rheum Dis 58 [Suppl 1]:I32–I39

Kontoyiannis D, Pasparakis M, Pizarro TT, Cominelle F, Kollias G (1999) Impaired on/off regulation of TNF biosynthesis in mice lacking TNF AU-rich elements: implications for joint and gut-associated immunopathologies. Immunity 10:387–398

Li P, Schwarz EM (2003) The TNF-α transgenic mouse model in inflammatory arthritis. Springer Semin Immonopathol 25:19–33

Maloff BL, Delmendo RE (1991) Development of high-throughput radioligand binding assays for interleukin 1-α (IL-1-α) and tumor necrosis factor (TNF-α) in isolated membrane preparations. Agents Actions 34:132–134

Mijatovic T, Houzet L, Defence P, Droogmans L, Huez G, Kruys V (2000) Tumor necrosis factor-α mRNA remains unstable and hypoadenylated upon stimulation of macrophages by lipopolysaccharides. Eur J Biochem 267:6004–6011

Mohler KM, Torrance DS, Smith CA, Goodwin RG, Stremler KE, Fung VP, Madani H, Widmer MB (1993) Soluble tumor necrosis factor (TNF) receptors are effective therapeutic agents in lethal endotoxemia and function simultaneously as both TNF carriers and TNF antagonists. J Immunol 151:1548–1561

Scallon B, Cai A, Solowski N, Rosenberg A, Song XY, Shealy D, Wagner C (2002) Binding and functional comparisons of two types of tumor necrosis factor antagonists. J Pharmacol Exp Ther 301:418–426

Schall TJ, Lewis M, Koller KJ, Lee A, Rice GC, Wong GH, Gatanaga T, Granger GA, Lentz R, Raab H (1990) Molecular cloning and expression of a receptor for human tumor necrosis factor. Cell 61:361–370

Shen C, Assche GV, Colpaert S, Maerten P, Geboes K, Rutgeerts P, Ceuppens JL (2005) Adalimumab induces apoptosis of human monocytes: a comparative study with infliximab and etanercept. Aliment Pharmacol Ther 21:251–258

Smith CA, Davis T, Anderson D, Solam L, Beckmann MP, Jerzy R, Dower SK, Cosman D, Goodwin RG (1990) A receptor for tumor necrosis factor defines an unusual family of cellular and viral proteins. Science 248:1019–1023

Vuoltteenaho K, Moilanen T, Hämäläinen M, Moilanen T (2002) Effects of TNF-α antagonists on nitric oxide production in human cartilage. Osteoarthr Cartil 10:327–332

Zhang Y, Xu J, Levin J, Hegen M, Li G, Robertshaw H, Brennan F, Cummons T, Clarke D, Vansell N, Nickerson-Nutter C, Barone D, Mohler K, Black R, Skotnicki J, Gibbons J, Feldmann M, Frost P, Larsen G, Lin LL (2002) Identification and characterization of 4-[[4-(2-butynyloxy]phenyl]sulfonyl)-*N*-hydroxy-2,2-dimethyl-(3S)-thiomorpholinecarboxamide (TMI-1), a novel dual tumor necrosis factor converting enzyme/matrix metalloprotease inhibitor for the treatment of rheumatoid arthritis. J Pharmacol Exp Ther 309:348–355

H.3.1.9 Binding to Interferon Receptors

PURPOSE AND RATIONALE

The interferons (IFNs) were discovered in 1957 as biological agents interfering with virus replication. They are a family of secreted proteins occurring in vertebrates and can be classified as cytokines. The IFNs are multifunctional and are components of the host defense against viral and parasitic infections and certain tumors. They affect the functioning of the immune system in various ways and also affect cell proliferation and differentiation.

IFNs were initially classified by their sources as leukocyte, fibroblast, and immune IFNs. Leukocyte and fibroblast IFNs, together, were also designated as Type 1 IFNs and immune IFN as Type 2 IFN. The recent nomenclature designates leukocyte IFNs as IFN-α and IFN-ω (earlier α-1 and α-2, respectively) fibroblast IFN as IFN-β, and immune IFN as IFN-γ.

Interferons bind to receptors on the cell surface and induce the synthesis of specific proteins. Littman et al. (1985) found that recombinant IFN-γ produced in bacteria, which is not glycosylated, binds to cellular receptors with an affinity similar to that of natural IFN-γ.

PROCEDURE

Human lymphoblastoid cells (Daudi, MOLT-4 and Raji) are grown in stationary cultures in Dulbecco's medium with 10% heat-inactivated horse serum. HeLa cells are grown in Eagle's medium with 7% horse serum.

The following interferons are used: Purified recombinant interferon-γ (rIFN-γ) (Genentech, antiviral activity 1.2×10^7 units/mg); natural human INF-β (Interferon Working Group of the NCI, antiviral activity 2×10^5 roentgen units/mg); rIFN-2α (Schering, antiviral activity 2×10^8 reference units/mg); rIFN-β (Cetus Corp., antiviral activity 2.6×10^8 reference units/mg).

Fifty micrograms of rIFN-γ are reacted for 2 h at 0°C with 1 mCi of ^{125}I-Bolton-Hunter reagent

(2000 Ci/mmol) in 0.25 ml of sodium borate buffer, pH 8.0. The reaction is stopped by the addition of glycine to a final concentration of 0.2 M and applied to a 26×0.7 cm column of Sephadex G-75 equilibrated with phosphate-buffered saline, pH 7.4, containing 0.25% gelatin. The reaction vial is washed with 20-µl aliquots of this buffer containing 40% ethylene glycol and then with buffer alone. The washes are added to the column and 0.32 ml fractions are collected. The fractions containing ^{125}I-rIFN-γ are pooled and diluted with 1/10 volume of 10-fold concentrated Eagle's medium containing 10 mg/ml bovine serum albumin and 0.1 mM dithiothreitol.

Cells harvested from exponentially growing cultures are centrifuged and resuspended at 8×10^6/ml in their own medium supplemented with 10 mM HEPES buffer, pH 7.4. Standard binding assays contain 3 to 5×10^6 cells and 0.46 nM ^{125}I-rIFN-γ. At the end of the reaction, the cells are centrifuged through 10% sucrose at 10,000 rpm in Microfuge tubes and the cell pellet is counted. A blank value is determined by incubating and processing in the same way an equal amount of ^{125}I-rIFN-γ in the absence of cells; this blank is subtracted from the cpm bound.

EVALUATION

The binding data are analyzed using the LIGAND program developed by Munson and Rodbard (1980).

MODIFICATIONS OF THE METHOD

Blatt et al. (1996) described the biological activity of consensus interferon, a wholly synthetic type I interferon, developed by scanning several interferon-alpha nonallelic subtypes and assigning the most frequently observed amino acid in each position.

IFN-τ, a new class of type I interferon was described by Pontzer et al. (1994), Alexenko et al. (1997, 1999), Martal et al. (1998), Swann et al. (1999).

Thiam et al. (1998) reported the agonist activities of a lipopeptide derived from INF-γ on murine and human cells by analysis and quantification of cell surface markers using flow cytometry and cell-ELISA.

Bosio et al. (1999) reported efficacy of type I interferon in cytomegalovirus infections *in vivo*. Oral administration of type I interferons (murine INF-α and INF-β) reduced early replication of murine cytomegalovirus in both the spleen and liver of infected BLB/c mice.

Tovey and Maury (1999) found a marked antiviral activity of murine interferon-α/β or individual recombinant species of murine INF-α, INF-β, or INF-γ or recombinant human INF-α1–8 in mice challenged systemically with a lethal dose of encephalomyocarditis virus, vesicular stomatitis virus, or varicella zoster virus. Oromucosal administration of INF-α also exerted a marked antitumor activity in mice injected i.v. with highly malignant Friend erythroleukemia cells or other transplantable tumors, such as L1210 leukemia, the EL4 tumor, or the highly metastatic B16 melanoma.

To gain more insight into similarities of different INF-α species, Viscomi et al. (1999) evaluated neutralization and immunoactivity of a variety of INF preparations with various monoclonal antibodies obtained through immunization with recombinant, lymphoblastoid, and leukocyte INF-α.

Reporter transgenic mice expressing the luciferase gene under the control of separate TCR-response elements from the INF-γ promoter or expressing the green fluorescent protein gene under the control of an INF-γ minigene were employed by Zhang et al. (1999) to explore the basis for IL-12 regulation of INF-γ gene transcription.

Poynter and Daynes (1999) studied the influence of constitutively expressed INF-γ on age-associated alterations in inducible nitric oxide synthase regulation using cell cultures from mouse spleen for nitrite and cytokine analysis.

REFERENCES AND FURTHER READING

Alexenko AP, Leaman DW, Li J, Roberts RM (1997) The antiproliferative and antiviral activities of IFN-τ variants in human cells. J Interferone Cytokine Res 17:769–779

Alexenko AP, Ealy AD, Roberts RM (1999) The cross-species antiviral activities of different IFN-τ subtypes on bovine, murine, and human cells: contradictory evidence for therapeutic potential. J Interferon Cytokine Res 19:1335–1341

Blatt LM, Davis JM, Klein SB, Taylor MW (1996) The biological activity and molecular characterization of a novel synthetic interferon-alpha species, consensus interferon. J Interferon Cytokine Res 16:488–499

Bosio E, Beilharz MW, Watson MW, Lawson CM (1999) Efficacy of low-dose oral use of type I interferon in cytomegalovirus infections *in vivo*. J Interferon Cytokine Res 19:869–876

Littman SJ, Faltynek CR, Baglioni C (1985) Binding of human recombinant ^{125}I-interferon to receptors on human cells. J Biol Chem 260:1191–1195

Martal JL, Chene NM, Huynh LP, L'Haridon RM, Reinaud PB, Guillomot MW, Charlier MA, Charpigny SY (1998) IFN-τ: A novel subtype I IFN1. Structural characteristics, non-ubiquitous expression, structure-function relationships, a pregnancy hormonal embryonic signal and cross-species therapeutic potentialities. Biochemie 80:755–777

Munson PJ, Rodbard D (1980) LIGAND, a versatile computerized approach for characterization of ligand binding systems. Anal Biochem 107:220–239

Pontzer CH, Ott TL, Bazer FW, Johnson HM (1994) Structure/function studies with interferon τ : evidence for multiple active sites. J Interferon Res 14:133–141
Poynter ME, Daynes RA (1999) Age-associated alterations in splenic iNOS regulation: influence of constitutively expressed INF-γ and correction following supplementation with PPARα activators of vitamin E. Cell Immunol 195:127–136
Sen GC, Lengyel P (1992) The interferon system. A bird's eye view of its biochemistry. J Biol Chem 267:5017–5020
Swann SL, Bazer FW, Villarete LH, Chung A, Pontzer CH (1999) Functional characterization of monoclonal antibodies to interferon-τ. Hybridoma 18:399–405
Thiam K, Loing E, Delanoye A, Diesis E, Gras-Masse H, Auriault C, Verwaerde C (1998) Unrestricted agonist activity on murine and human cells of a lipopeptide derived from INF-γ. Biochem Biophys Res Commun 253:639–647
Tovey MG, Maury C (1999) Oromucosal interferon therapy: marked antiviral and antitumor activity. J Interferon Cytokine Res 19:145–155
Viscomi GC, Antonelli G, Bruno C, Scapol L, Malavasi F, Funaro A, Simeoni E, Pestka S, de Pisa F, Dianzani F (1999) Antigenic characterization of recombinant, lymphoblastoid, and leukocyte INF-α by monoclonal antibodies. J Interferon Cytokine Res 19:319–326
Zhang F, Nakamura T, Aune TM (1999) TCR and IL-12 receptor signals cooperate to activate an individual response element in the INF-γ promoter on Th cells. J Immunol 163:728–735

H.3.1.10 Chemokine Antagonism

PURPOSE AND RATIONALE

The human chemokine system comprises about 50 distinct chemokines and 20 G-protein-coupled chemokine receptors (Rossi and Zlotnik 2000; Sallusto et al. 2000; Zlotnik and Yoshie 2000; Fernandez and Lolis 2002; D'Ambrosio et al. 2003; Houshmand and Zlotnik 2003; Ono et al. 2003; Proudfoot et al. 2003; Chen et al. 2004; Haringman and Tak 2004; Cunha et al. 2005). The biological activities of chemokines range from the control of leukocyte trafficking in basal and inflammatory conditions to regulation of hematopoiesis, angiogenesis, tissue architecture and organogenesis. Grainger and Reckless (2005) studied the anti-inflammatory effects of broad-spectrum chemokine inhibitors. Several groups described CC chemokine receptor-1 antagonists (Liang et al. 2000a, 2000b; Naya et al. 2001; Eltayeb et al. 2003; Gladue et al. 2006). CC chemokine receptor-3 (CCR3) antagonists were reported by De Lucca et al. (2005) and Fryer et al. (2006). CC chemokine receptor-5 (CCR5) antagonists were described by Rosi et al. (2005) and Saita et al. (2005).

De Lucca et al. (2005) described the discovery of CC chemokine receptor-3 (CCR3) antagonists with picomolar potency.

PROCEDURE

Biological Assays

CCR3-Receptor Binding

Millipore filter plates (no. MABVN1250) are treated with 5 µg/ml protamine in phosphate-buffered saline, pH 7.2, for 10 min at room temperature. Plates are washed three times with phosphate-buffered saline and incubated with phosphate-buffered saline for 30 min at room temperature. For binding, 50 µl of binding buffer (0.5% bovine serum albumen, 20 mM HEPES buffer, and 5 mM magnesium chloride in RPMI 1640 media) with or without a test concentration of a compound present at a known concentration is combined with 50 µl of ^{125}I-labeled human eotaxin (to give a final concentration of 150 pM radioligand) and 50 µl of cell suspension in binding buffer containing 5×10^5 total cells. Cells used for the binding assay are CHO cell lines transfected with a gene expressing human CCR3 (Daugherty et al. 1996). The mixture of compound, cells, and radioligand is incubated at room temperature for 30 min. Plates are placed onto a vacuum manifold, vacuum is applied, and the plates are washed three times with binding buffer with 0.5 M NaCl added. The plastic skirt is removed from the plate, and the plate is allowed to air-dry; the wells are punched out, and the radioactivity counted (cpm).

EVALUATION

The percent inhibition of binding is calculated using the total count obtained in the absence of any competing compound or chemokine ligand and the background binding determined by addition of 100 nM eotaxin in place of the test compound.

Human Eosinophil Chemotaxis Assay

Neuroprobe MBA96 96-well chemotaxis chambers with Neuroprobe poly(vinylpyrrolidone)-free polycarbonate PFD5 5-µm filters in place are warmed in a 37°C incubator prior to the assay. Freshly isolated human eosinophils are suspended in RPMI 1640 with 0.1% bovine serum albumin at 1×10^6 cells/ml and warmed in a 37°C incubator prior to the assay. A 20 nM solution of human eotaxin in RPMI 1640 with 0.1% bovine serum albumin is warmed in a 37°C incubator prior to the assay. The eosinophil suspension and the 20 nM eotaxin solution are each mixed 1:1 with prewarmed RPMI 1640 with 0.1% bovine serum albumin with or without a dilution of a test compound that is at twofold the desired final concentration. The filter is separated, and the eotaxin/compound mixture is

placed into the bottom part of the chemotaxis chamber. The filter and upper chamber are assembled, and 200 µL of the cell suspension/compound mixture is added to the appropriate wells of the upper chamber. The upper chamber is covered with a plate sealer, and the assembled unit is placed in a 37°C incubator for 45 min. After incubation, the plate sealer is removed and all remaining cell suspension is aspirated off. The chamber is disassembled, and unmigrated cells are washed away with phosphate-buffered saline and then the filter is wiped with a rubber-tipped squeegee. The filter is allowed to completely dry and stained with Wright Giemsa. Migrated cells are enumerated by microscopy.

Calcium Mobilization Assay

Intracellular calcium flux was measured as the increase in fluorescence emitted by the calcium-binding fluorophore, fluo-3, when preloaded cells were stimulated with CCR3 ligand. Freshly isolated eosinophils were loaded with fluorophore by resuspending them in a HEPES-buffered PBS solution containing 5 µM fluo-3 and incubating for 60 min at 37°C. After being washed twice to remove excess fluorophore, cells were resuspended in binding buffer (without phenol red) and plated into 96-well plates at 2×10^5/well. Plates were placed individually in a FLIPR-1 (Molecular Devices) that uses an argon-ion laser to excite the cells and robotically adds reagents while monitoring changes in fluorescence in all wells simultaneously. To determine the IC_{50}, compound or buffer alone was added and cells were incubated for 5 min; eotaxin was then added to a final concentration of 10 nM. The fluorescence shift was monitored, and the base-to-peak excursion was computed automatically. All conditions were tested in duplicate, and the mean shift per condition was determined. The inhibition achieved by graded concentrations of compound was calculated as a percentage of the compound-free eotaxin control.

MODIFICATIONS OF THE METHOD

Chen et al. (1998) reported *in vivo* inhibition of CC and CX_3C chemokine-induced leukocyte infiltration and attenuation of glomerulonephritis in Wistar–Kyoto (WKY) rats by the viral protein vMIP-II.

Ruth et al. (2001) investigated fractalkine, a chemokine, in rheumatoid arthritis and in rat adjuvant-induced arthritis. Fractaline in vascular biology was discussed by Umehara et al. (2004).

Laudanna and Constanin (2003) described new models of intravital microscopy for analysis of chemokine receptor-mediated leukocyte vascular recognition.

REFERENCES AND FURTHER READING

Chen L, Pei G, Zhang W (2004) An overall picture of chemokine receptors: basic research and drug development. Curr Pharm Design 10:1045–1055

Chen S, Bacon KB, Li L, Garcia GE, Xia Y, Lo D, Thompson DA, Siani MA, Yamamoto T, Harrison Jk, Feng L (1998) In vivo inhibition of CC and CX_3C chemokine-induced leukocyte infiltration and attenuation of glomerulonephritis in Wistar–Kyoto (WKY) rats by vMIP-II. J Exp Med 188:193–198

Cunha TM, Verri WA Jr, Silva JS, Poole S, Cunha FQ, Ferreira SH (2005) A cascade of cytokines mediates mechanical inflammatory hypernociception in mice. Proc Natl Acad Sci USA 102:1755–1760

D'Ambrosio D, Panina-Bordignon P, Sinigaglia F (2003) Chemokine receptors in inflammation: an overview. J Immunol Meth 273:3–13

Daugherty BL, Siciliano SJ, DeMartino JA, Malkowitz L, Sirotina A, Springer MS (1996) Cloning, expression, and characterization of the human eosinophil eotaxin receptor. J Exp Med 183:2349–2354

De Lucca GV, Kim UT, Vargo BJ, Duncia JV, Santella JB, Gardener DS, Zheng C, Liauw A, Wang Z, Emmett G, Wacker DA, Welch PK, Covington M, Stowell NC, Wadman EA, Das AM, Davies P, Yeleswaram S, Graden DM, Solomon KA, Newton RC, Trainor GL, Decicco CP, Ko SS (2005) Discovery of CC chemokine receptor-3 (CCR3) antagonists with picomolar potency. J Med Chem 48:2194–2211

Eltayeb S, Sunnemark D, Berg AL, Nordvall G, Malmberg Å, Lassmann H, Wallström E, Olsson T, Ericsson-Dahlstrand A (2003) Effector stage CC chemokine receptor-1 selective antagonism reduces multiple sclerosis-like rat disease. J Neuroimmunol 142:75–85

Fernandez EJ, Lolis E (2002) Structure, function, and inhibition of chemokines. Annu Rev Pharmacol Toxicol 42:469–499

Fryer AD, Stein LH, Nie Z, Curtis DE, Evans CM, Hodgson ST, Jose PJ, Belmonte KE, Titch E, Jacoby DB (2006) Neuronal eotaxin and the effects of CCR3 antagonist on airway hyperreactivity and M2 receptor dysfunction. J Clin Invest 116:228–236

Gladue RP, Cole SH, Roach ML, Tylaska LA, Nelson RT, Shepard RM, McNelsh JD, Ogborne KT, Neote KS (2006). The human specific CCR1 antagonist CP-481,715 inhibits cell infiltration and inflammatory responses in human DDR1 transgenic mice. J Immunol 176:3141–3138

Grainger DJ, Reckless J (2005) Broad-spectrum chemokine inhibitors (BSCIs) and their anti-inflammatory effects *in vivo*. Biochem Pharmacol 65:1027–1034

Haringman JJ, Tak PP (2004) Chemokine blockade: a new area in the treatment of rheumatoid arthritis? Arthritis Res Ther 6:93–97

Houshmand P, Zlotnik A (2003) Therapeutic applications in the chemokine superfamily. Curr Opin Chem Biol 7:457–460

Laudanna C, Constanin G (2003) New models of intravital microscopy for analysis of chemokine receptor-mediated leukocyte vascular recognition. J Immunol Methods 273:115–124

Liang M, Mallari C, Rosser M, Ng HP, May K, Monahan S, Bauman JG, Islam I, Ghannam A, Buckman B, Shaw K, Wei GP, Xu W, Zhao Z, Ho E, Shen J, Oanh H, Subramanyam B, Vergona R, Taub D, Dunning L, Harvey S, Snider RM, Hesselgesser J, Morrissey MM, Perez HD

(2000a) Identification and characterization of a potent, selective, and orally active antagonist of the CC chemokine receptor-1. J Biol Chem 275:19000–19008
Liang M, Rosser M, NG HP, May K, Bauman JG, Islam I, Ghannam A, Kretschmer PJ, Pu H, Dunning L, Snider RM, Morrissey MM, Hesselgesser J, Perez HD, Horuk R (2000b) Species selectivity of a small molecule antagonist for the CCR1 chemokine receptor. Eur J Pharmacol 389:41–49
Naya A, Sagara Y, Ohwaki K, Saeki T, Ichikawa D, Iwasawa Y, Noguchi K, Ohtake N (2001) Design, synthesis and discovery of a novel CCR1 antagonist. J Med Chem 44:1429–1435
Ono SJ, Nakamura T, Miyazaki D, Ohbayashi M, Dawson M, Toda M (2003) Chemokines: roles in leukocyte development, trafficking, and effector function. J Allergy Clin Immunol 111:1185–1199
Proudfoot AEI, Power CA, Rommel C, Wells TNC (2003) Strategies for chemokine antagonists as therapeutics. Seminars Immunol 15:57–65
Rosi S, Pert CB, Ruff MR, McGann-Gramling K, Wenk GL (2005) Chemokine recptor 5 antagonist D-ala-peptide T-amide reduces microglia and astrocyte activation within the hippocampus in a neuroinflammatory rat model of Alzheimer's disease. Neuroscience 134:671–676
Rossi D, Zlotnik A (2000) The biology of chemokines and their receptors. Ann Rev Immunol 18:217–242
Ruth JH, Volin MV, Haines GK, Woodruff DC, Katsche KJ Jr, Woods JM, Park CC, Morel JCM, Koch AE (2001) Fractalkine, a novel chemokine in rheumatoid arthritis and in rat adjuvant-induced arthritis. Arthritis Rheum 44:1568–1581
Saita Y, Kondao M, Miyazaki T, Yamji N, Shimizu Y (2005) Transgenic mouse expressing human CCR5 as a model for in vivo assessments of human selective CCR5 antagonists. Eur J Pharmacol 518:227–233
Sallusto F, Mackay CR, Lanzvecchia A (2000) The role of chemokine receptors in primary, effector, and memory immune responses. Annu Rev Immunol 18:593–620
Umehara H, Bloom ET, Okazaki T, Nagano Y, Yoshie O, Imai T (2004) Fractaline in vascular biology. From basic research to clinical disease. Arterioscler Thromb Vasc Biol 24:34–40
Zlotnik A, Yoshie O (2000) Chemokines: a new classification system and their role in immunity. Immunity 12:121–127

H.3.1.11 Influence of Peroxisome Proliferator-Activated Receptors (PPARs) on Inflammation

PURPOSE AND RATIONALE

Peroxisome proliferator-activated receptors (PPARs) play an important role not only in lipid metabolism and diabetes but also in the inflammation process (Devchand et al. 1996; Delerive et al. 2001; Cabrero et al. 2002; Clark 2002; Blanquart et al. 2003; Moller and Berger 2003; Nencioni et al. 2003; Tai et al. 2003; Woerly et al. 2003; Diep et al. 2004).

Jiang et al. (1998) reported that PPAR-γ antagonists inhibit production of monocyte inflammatory cytokines.

PROCEDURE

Monocyte Preparation

Human monocytes are isolated from freshly collected buffy-coat preparations of whole human blood. The mononuclear cell fraction is prepared by dilution with an equal volume of phosphate-buffered saline (PBS) at room temperature and layered over a solution containing 3 ml Ficoll-Hypaque per 10 ml blood and PBS and centrifuged for 10 min at 900 *g*. The mononuclear cell layer is transferred to a fresh tube, mixed with 3 vols of PBS, and centrifuged for 10 min at 400 g. The supernatant is removed and the dilution and centrifugation are repeated three times. Mononuclear cells are resuspended in RPMI medium 1640, counted and diluted to 5×10^6 cell per ml, after which 1 ml is transferred to each well of a 24-well tissue culture plate and incubated for 37°C in a 5% CO_2 humidified incubator. The non-adherent cells are removed and the monocytes washed once with PBS before adding 1 ml of fresh RPMI medium 1640 with 10% fetal bovine serum. Experiments are initiated on the day blood is collected, and all manipulations are carried out under endotoxin-free conditions.

Cytokine Assay

Monocytes in fresh medium are treated with inducers and candidate induction inhibitors at the time of culture initiation. Medium is collected from triplicate wells 18–20 h after the test compounds are added. Supernatant concentrations of TNF-α, IL-6 and IL-1β are measured by ELISA.

RNA Blot

Total RNA of human monocyte cultures is isolated 15 h after stimulation with 25 nM PMA in the absence or presence of PPARγ agonists. RNA blot analyses are performed with standard procedures and labeled probes prepared from human TNF-α and GAPDH cDNA with the Megaprime DNA labeling Kit (Amersham Life Science).

Luciferase Assay

U937 cells (2×10^7) are transfected with 10–20 µg luciferase reporter DNA by electrophoresis at 875 V cm^{-1}, 960 µF (Bio-Rad Laboratories). Transfected cells are allowed to recover for 1 h and triplicate samples are either untreated or treated with 25 nM PMA in the absence or presence of indicated drugs. Luciferase activity is measured 18–36 h later using the Dual-luciferase reporter assay system (Promega) with the pRL-TK vector as an internal reporter control.

EVALUATION

To obtain IC_{50} values, data are fitted to a four-parameter exponential and the derived parameters used to calculate the concentration at which 50% of the maximal activity is observed.

MODIFICATIONS OF THE METHOD

Kojo et al. (2003) evaluated human PPAR subtype selectivity of a variety of anti-inflammatory drugs based on a novel assay for PPARδ (β).

PROCEDURE

Plasmids

The cDNAs for human PPAR α, δ, and γ were synthesized using the polymerase chain reaction (PCR) with human liver cDNA for human PPARα, human heart cDNA for human PPARδ (β), and human fat cell cDNA for human PPARγ 1 as templates. Retinoid X receptor (RXR)α expression plasmids were constructed by inserting a coding sequence of RXRα into the expression vector pcDNA3.1(+) (Invitrogen, Carlsbad, Calif., USA). The cDNA for human RXRα was synthesized with human kidney cDNA as a template. The template cDNAs used were purchased from Clontech Laboratories (Palo Alto, Calif., USA). The amplified cDNA fragments were cloned into pCRII (Invitrogen) and the nucleotide sequences of the cDNAs were determined by the dideoxy chain termination method using an automated laser fluorescent DNA sequencer. Multiple clones of each cDNA were sequenced and artifacts generated by the *Taq* polymerase used in the PCR were revised by replacement of the specified region among the clones. The PPAR and RXRα expression plasmids were constructed by inserting each full-length cDNA at a multiple cloning site of the mammalian expression vector pCDM8, pcDNAI, or pcDNA3.1 (+) (Invitrogen). Coactivator expression plasmids pcDNA3.1-CBP and pcDNA3.1-SRC-1 were provided by Fujimura and Aramori of the Pharmacological Research Laboratories of Fujisawa Pharm. The human RXRγ expression plasmid was purchased from Invitrogen.

The reporter gene plasmid pGVPPREluc-1 was constructed as follows. Three copies of a 33-bp PPRE identical to that of acyl CoA oxidase were first cloned at the *Sal*I site of pBLCAT-2 to generate pBLPPRECAT-1. The luciferase reporter plasmid pGVPPRELuc was constructed by inserting the PPRE-containing fragment of pBLPPRECAT-1 at a multiple cloning site of PGV-P2 (Wako Pure Chemical, Osaka).

Gal4-PPARδ (β) fusion expression plasmid for one-hybrid assay was constructed as follows: full-length PPARδ (β) cDNA and PPARδ (β)-LBD cDNA were prepared by PCR amplification using pCDM8-hPPARδ as a template, and the amplified cDNA was cloned into a multiple cloning site of the pBIND vector (Promega, Madison, Wis., USA). The nucleotide sequence of each fusion expression plasmid was checked with an automated DNA sequencer. Reporter plasmid pG5luc for the one-hybrid assay was purchased from Promega.

Transient Transfection Assay

The African green monkey fibroblast cell line CV-1 was obtained from ATCC (Manassas, Va., USA) and maintained in Dulbecco's modified Eagle's medium (DMEM) (Gibco-BRL, Gaithersburg, Md., USA) supplemented with penicillin, streptomycin, and 10% heat-inactivated fetal calf serum. Cells were seeded at 2×10^5 per well of 6-well culture dishes and after overnight culture transiently transfected with 1 µg each of pGVPPRELuc luciferase reporter plasmid, PPAR expression plasmid, and RXRα expression plasmid together with the control *Renilla* luciferase expression plasmid RL-TK (Promega) using Lipofectamine 2000 (Gibco-BRL). Coactivator expression plasmid was also included when a transfection was performed for the PPARδ assay. For the one-hybrid assay, cells were transfected with 1 µg each of pG5luc reporter plasmid and Gal4-PPARδ fusion expression plasmid with RL-TK control plasmid. Cells were harvested 4 h after transfection and plated again at 1.6×10^4 per well onto 96-well plates. The drugs dissolved in dimethyl sulfoxide were added to the culture and the cells were incubated at 37°C for 24 h. After being washed with PBS(-), cells were lysed with PLB (passive lysis buffer) (Promega) and the lysates were used for reporter assays. Expression of the reporter was measured by the activity of firefly luciferase using the dual luciferase reporter assay system (Promega) and ARVO HTS 1420 multilabel counter (Amersham Biosciences) as a luminometer. Firefly luciferase activity was corrected for transfection efficiency based on the activity of internal control *Renilla* luciferase.

Bishop-Bailey and Warner (2003) found that PPARγ ligands induce prostaglandin production in vascular smooth muscle cells and concluded that indomethacin acts as a peroxisome proliferator-activated receptor-γ antagonist.

Fahmi et al. (2001) reported that peroxisome proliferator-activated receptor γ activators, such as 15-deoxy-$\Delta^{12,14}$-PGJ_2, inhibit interleukin-1β-induced nitric oxide and metalloproteinase 13 production in human chondrocytes.

Cheng et al. (2004) found that peroxisome proliferator-activated receptor γ, which is activated by ligands such as troglitazone or 15-deoxy-$\Delta^{12,14}$-PGJ_2, inhibits interleukin-1β-induced membrane-associated prostaglandin E_2 synthase-1 expression in human synovial fibroblasts by interfering with the early growth response protein Egr-1.

REFERENCES AND FURTHER READING

Bishop-Bailey D, Warner TD (2003) PPARγ ligands induce prostaglandin production in vascular smooth muscle cells: indomethacin acts as a peroxisome proliferator-activated receptor-γ antagonist. FASEB J 17:1925–1927

Blanquart C, Barbier O, Fruchart JC, Staels B, Glineur C (2003) Peroxisome proliferators-activated receptors: regulation of transcriptional activities and roles in inflammation. J Steroid Biochem Mol Biol 85:267–273

Cabrero A, Laguna JC, Vázquez M (2002) Peroxisome proliferator-activated receptors and the control of inflammation. Curr Drug Targets Inflamm Allergy 1:243–248

Cheng S, Afif H, Martel-Pelletier J, Pelletier, Li X, Farrajota K, Lavigne M, Fahmi H (2004) Activation of peroxisome proliferator-activated receptor γ inhibits interleukin-1β induced membrane-associated prostaglandin E_2 synthase-1 expression in human synovial fibroblasts by interfering with Egr-1. J Biol Chem 279:22057–22065

Clark RB (2002) The role of PPARs in inflammation and immunity. J Leukoc Biol 71:388–400

Delerive P, Fruchart JC, Staels B (2001) Peroxisome proliferators-activated receptors in inflammation control. J Endocrinol 169:453–459

Devchand PR, Keller H, Peters JM, Vasquez M, Gonzales FJ, Wahli W (1996) The PPARα-leukotriene B_4 pathway in inflammatory control. Nature 384:39–43

Diep QN, Benkirane K, Amiri F, Cohn JS, Endemann D, Schiffrin EL (2004) PPARγ activator fenofibrate inhibits myocardial inflammation and fibrosis in angiotensin II-infused rats. J Mol Cell Biol 36:295–304

Fahmi H, di Battista JA, Pelletier JP, Mineau F, Ranger P, Martell-Peletier J (2001) Peroxisome proliferator-activated receptor γ activators inhibit interleukin-1β induced nitric oxide and metalloproteinase 13 production in human chondrocytes. Arthritis Rheum 44:595–607

Jiang C, Ting AT, Seed B (1998) PPAR-γ antagonists inhibit production of monocytes inflammatory cytokines. Nature 391:82–86

Kojo H, Fukagawa M, Tajima K, Suzuki A, Fujimura T, Aramori I, Hayashi KI Nishimura S (2003) Evaluation of human peroxisome-activated receptor (PPAR) subtype selectivity of a variety of anti-inflammatory drugs based on an novel assay for PPARδ (β). J Pharmacol Sci 93:347–355

Moller DE, Berger JP (2004) Role of PPARs in the regulation of obesity-related insulin sensitivity and inflammation. Int J Obes 27:517–521

Nencioni A, Wesselborg S, Brossart P (2003) Role of peroxisome proliferator-activated receptor γ and its ligands in the control of immune responses. Crit Rev Immunol 23:1–13

Tai ES, Ali AB, Zhang Q, Loh LM, Tan CE, Retnam L, Oakley RME, Lim SK (2003) Hepatic expression of PPARγ, a molecular target of fibrates, is regulated during inflammation in a gender-specific manner. FEBS Lett 546:237–240

Woerly G, Honda K, Loyens M, Papin JP, Auwerx J, Staels B, Capron M, Dombrowicz D (2003) Peroxisome proliferator-activated receptors α and γ downregulate allergic inflammation and eosinophil activation. J Exp Med 198:411–421

H.3.1.12 Binding to Histamine H_4 Receptor

PURPOSE AND RATIONALE

Histamine receptors have been classified on the basis of pharmacological analysis (Hill et al. 1997). Histamine exerts its action via at least four receptor subtypes. The H_1 receptor couples mainly to $G_{q/11}$, thereby stimulating phospholipase C, whereas the H_2 receptor interacts with G_s to activate adenylyl cyclase. The histamine H_3 and H_4 receptors couple to G_i proteins to inhibit adenylyl cyclase, and to stimulate MAPK (Hough 2001).

The H_4 receptor is highly expressed in peripheral leukocytes and intestinal tissue, making this receptor an interesting target in inflammatory diseases (Fung-Leung et al. 2004; De Esch et al. 2005; Lim et al. 2006; Zhang et al. 2006). The new receptor was cloned and characterized by Oda et al. (2000). Liu et al. (2001b) reported comparison of histamine H_4 receptors in several species. Gbahou et al. (2006) compared the pharmacology of human histamine H_3 and H_4 receptors and described structure–activity relationships of histamine derivatives. Thurmond et al. (2004) described a potent and selective histamine H_4 antagonist with anti-inflammatory properties. Lim et al. (2005) evaluated histamine H_1-, H_2-, and H_3-receptor ligands at the human H_4 receptor and identified 4-methylhistamine as the first potent and selective H_4 receptor agonist.

PROCEDURE

Cell Culture

SK-N-MC cell lines, which stably express either the human H_3R (SK-N-MC/hH_3) or H_4R (SK-N-MC/hH_4) as well as a cAMP-responsive-element-(CRE-) driven β-galactosidase reporter gene SK-N-MC/hH_3 or SK-N-MC/hH_4 cells (Lovenberg et al. 1999; Liu et al. 2001a), were cultured in Eagle's minimum essential medium supplemented with 5% fetal calf serum, 0.1 mg/ml streptomycin, 100 U/ml penicillin, and 600 µg/ml G418 at 37°C in 5% CO_2 and 95% humidity.

Radioligand Binding Assays

The SK-N-MC/hH_3 cell homogenates were incubated for 40 min at 25°C with approximately 1 nM [^{3}H]*N*-methylhistamine in 25 mM KPO_4 buffer and 140 mM NaCl (pH 7.4 at 25°C), with or without competing ligands, whereas the SK-N-MC/hH_4 cell homogenates were incubated 1 h at 37°C in 10 nM [^{3}H]histamine and 50 mM Tris-HCl (pH 7.4 at 37°C), with or without competing ligands. Bound radioligands were col-

lected on 0.3% polyethyleneimine-pretreated Whatman GF/C, and washed three times with 3 ml of ice-cold washing buffer (4°C) containing 25 mM Tris-HCl and 140 mM NaCl (pH 7.4 at 4°C) for the hH_3R and 50 mM Tris-HCl (pH 7.4 at 4°C) for the hH_4R).

EVALUATION

Binding analysis of 10 nM [^{3}H]JNJ 7777120 (test compound) and 0.1 nM [^{125}I]iodophenpropit to the hH_4R was performed with the same conditions as described for [^{3}H]histamine. In saturation binding analysis, the non-specific binding of [^{3}H]histamine or [^{3}H]JNJ 7777120 was determined with 1 μM clobenpropit. The binding analysis of [^{3}H]mepyramine and [^{125}I]iodoaminopotentidine binding to human H_1R and human H_2R, respectively, was performed according to Bakker et al. (2004). The binding data were analyzed with Prism 4.0 (GraphPad Software, San Diego, Calif., USA), and data are presented as mean ±SEM. Mouse and rat H_4R radioligand binding assays were performed according to Liu et al. (2001b).

REFERENCES AND FURTHER READING

Bakker RA, Weiner DM, ter Laak T, Beuming T, Zuiderveld OP, Edelbroek M, Hacksell U, Timmerman H, Brann MR, Leurs R (2004) 8*R*-lisuride is a potent stereospecific histamine H_1-receptor partial agonist. Mol Pharmacol 65**:**538–549

De Esch IJ Thurmond RL, Jongejan A, Leurs R (2005) The histamine H4 receptor as a new therapeutic target for inflammation. Trends Pharmacol Sci 26:462–469

Fung-Leung WP, Thurmond RL, Ling P, Karlsson L (2004) Histamine H4 receptor antagonists: the new antihistamines? Curr Opin Invest Drugs 5:1174–1183

Gbahou F, Vincent L, Humbert-Claude M, Tardivel-Lacombe J, Chabret C, Arrang JM (2006) Compared pharmacology of human histamine H_3 and H_4 receptors: structure-activity relationships of histamine derivatives. Br J Pharmacol 147:744–754

Hill SJ, Ganellin CR, Timmerman H, Schwartz JC, Shankley NP, Young JM, Schunack W, Levi R, Haas HL (1997) International Union of Pharmacology. XIII. Classification of histamine receptors. Pharmacol Rev 49:253–278

Hough LB (2001) Genomics meets histamine receptors: new subtype, new receptor. Mol Pharmacol 59:415–419

Lim HD, van Rijn RM, Ling P, Bakker RA, Thurmond RL, Leurs R (2005) Evaluation of histamine H_1-, H_2-, and H_3-receptor ligands at the human H_4 receptor: identification of 4-methylhistamine as the first potent and selective H_4 receptor agonist. J Pharmacol Exp Ther 314:1310–1321

Lim HD, Smits RA, Leurs R, de Esch IJP (2006) The emerging role of the histamine H4 receptor in anti-inflammatory therapy. Curr Topics Med Chem 6:1365–1373

Liu C, Ma X-J, Jiang X, Wilson SJ, Hofstra CL, Blevitt J, Pyati J, Li X, Chai W, Carruthers N, Lovenberg TW (2001a) Cloning and pharmacological characterization of a fourth histamine receptor (H_4) expressed in bone marrow. Mol Pharmacol 59**:**420–426

Liu C, Wilson SJ, Kuei C, Lovenberg TW (2001b) Comparison of human, mouse, rat, and guinea pig histamine H_4 receptors reveals substantial pharmacological species variation. J Pharmacol Exp Ther 299:121–130

Lovenberg TW, Roland BL, Wilson SJ, Jiang X, Pyati J, Huvar A, Jackson MR, Erlander MG (1999) Cloning and functional expression of the human histamine H_3 receptor. Mol Pharmacol 55**:**1101–1107

Oda T, Morikawa N, Saito Y, Masuho Y, Matsumoto SI (2000) Molecular cloning and characterization of a novel type of histamine receptor preferentially expressed in leukocytes. J Biol Chem 275:36781–36786

Thurmond RL, Desai PJ, Dunford PJ, Fung-Leung WP, Hofstra CL, Jiang W, Nguyen S, Riley JP, Sun S, Williams KN, Edwards JP, Karlsson L (2004) A potent and selective histamine H_4 antagonist with anti-inflammatory properties. J Pharmacol Exp Ther 309:404–413

Zhang M, Venable JD, Thurmond RI (2006) The histamine H4 receptor in autoimmune disease. Expert Opin Invest drugs 15:1443–1452

H.3.2 In Vivo Methods for Anti-inflammatory Activity

H.3.2.1 General considerations

The inflammatory process involves a series of events that can be elicited by numerous stimuli, e. g., infectious agents, ischemia, antigen-antibody interactions, chemical, thermal or mechanical injury. The response is accompanied by the clinical signs of erythema, edema, hyperalgesia and pain. Inflammatory responses occur in three distinct phases, each apparently mediated by different mechanisms:

- an acute, transient phase, characterized by local vasodilatation and increased capillary permeability,
- a subacute phase, characterized by infiltration of leukocytes and phagocytic cells,
- and a chronic proliferative phase, in which tissue degeneration and fibrosis occur.

According to these phases, pharmacological methods have been developed.

Methods for testing acute and subacute inflammation are:

- UV-erythema in guinea pigs
- Vascular permeability
- Oxazolone-induced ear edema in mice
- Croton-oil ear edema in rats and mice
- Paw edema in rats (various modifications and various irritants)
- Pleurisy tests
- Granuloma pouch technique (various modifications and various irritants)

The proliferative phase is measured by methods for testing granuloma formation, such as:

- Cotton wool granuloma
- Glass rod granuloma
- PVC sponge granuloma.

Furthermore, methods for testing immunological factors have been developed, such as:

- Adjuvant arthritis in rats (various modifications)
- Experimental allergic encephalomyelitis
- Schultz-Dale-reaction
- Passive cutaneous anaphylaxis
- Arthus type immediate hypersensitivity
- Delayed type hypersensitivity

(see Chapter I).

H.3.2.2 Methods for Testing Acute and Subacute Inflammation

H.3.2.2.1 Ultraviolet Erythema in Guinea Pigs

PURPOSE AND RATIONALE

The test was first described by Wilhelmi (1949) who was able to delay the development of ultraviolet erythema on albino guinea pig skin by systemic pretreatment with clinically equivalent doses of phenylbutazone and other nonsteroidal anti-inflammatory agents. The test procedure was further developed by Winder et al. (1958) and since that time modified by various investigators.

PROCEDURE

Albino guinea pigs (Pirbright white strain) of both sexes with an average weight of 350 g are used. Eighteen h prior testing, the animals are shaved on both flanks and on the back. Then they are chemically depilated by a commercial depilation product or by a suspension of barium sulfide. Twenty minutes later, the depilation paste and the fur are rinsed off in running warm water. On the next day, the test compound is dissolved (or suspended) in the vehicle and half the dose of the test compound is administered by gavage (at 10 ml/kg) 30 min before ultraviolet exposure. Control animals are treated with the vehicle alone. Four animals are used for each treatment group and control. The guinea pigs are placed in a leather cuff with a hole of 1.5 × 2.5 cm size punched in it, allowing the ultraviolet radiation to reach only this area. An original Hanau ultraviolet burner Q 600 is warmed up for about 30 min prior to use and placed at a constant distance (20 cm) above the animal. Following a 2 min ultraviolet exposure, the remaining half of the test compound is administered. The investigator has to protect himself/herself by gloves and ultraviolet glasses. The erythema is scored 2 and 4 h after exposure.

EVALUATION

The degree of erythema is evaluated visually by 2 different investigators in a double-blinded manner. The followings scores are given:

- 0 = no erythema,
- 1 = weak erythema,
- 2 = strong erythema,
- 4 = very strong erythema.

Animals with a score of 0 or 1 are considered to be protected. The scoring after 2 and after 4 h gives some indication of the duration of the effect. ED_{50} values can be calculated. Doses of 1.5 mg/kg indomethacin p.o., 4 mg/kg phenylbutazone p.o. and 60 mg/kg acetylsalicylic acid p.o. have been found to be effective.

CRITICAL ASSESSMENT

The test has the advantage of simplicity but needs training of the investigators. Attempts to use reflection photometers in order to eliminate subjective scoring were unsuccessful. Corticosteroids after systemic application are rather ineffective in this test, however, can be evaluated after topical administration. The test is not particularly useful to study the duration of the anti-inflammatory effect.

MODIFICATIONS OF THE TEST

Yawalkar et al. (1991) tested several steroids after local application in the ultraviolet-induced dermatitis inhibition in guinea pigs. Clobetasol propionate was more effective than hydrocortisone, halobetasol propionate was superior to both corticosteroids.

Woodward and Owen (1979) used the albino guinea-pig ear as the site of inflammation produced by UV radiation. Ear temperature, water content of the ear and vascular permeability were measured. Indomethacin, phenylbutazone and aspirin given subcutaneously were active but paracetamol was not.

Warren et al. (1993) studied the role of nitric oxide synthase and cyclo-oxygenase in the skin blood flow to UVB irradiation in the shaved dorsal skin of anesthetized male **Sprague Dawley rats** with a laser Doppler flow probe. Topical application of clobetasol-

17-propionate immediately after irradiation inhibited the 18 h UVB response in a dose-dependent manner.

Gloxhuber (1976) measured skin thickness using calipers in **hairless mice** after UV-irradiation of the back and treatment with anti-inflammatory drugs.

Woodbury et al. (1994), Kligman (1994) described a rapid assay of the anti-inflammatory activity of topical corticosteroids by inhibition of a UVA-induced neutrophil infiltration in hairless mouse skin. Skh-hairless mice were irradiated with UVA light on an area of 2 × 2 cm square on the dorsal trunk fore 200 min in anesthesia. Steroid treatment was once daily for 7 days. Irradiation was on the 8th day. Neutrophils were counted microscopically in punch biopsies.

REFERENCES AND FURTHER READING

Gloxhuber Ch (1976) A new inflammation model. Arzneim Forsch/Drug Res 26:43–45

Kligman LH (1994) Rapid assay of the anti-inflammatory activity of topical corticosteroids by inhibition of a UVA-induced neutrophil infiltration in hairless mouse skin. II. Assessment of name brand versus generic potency. Acta Derm Venereol (Stockh) 74:18–19

Selve N (1991) EM 405: a new substance with an uncommon profile of anti-inflammatory activity. Agents Actions 32:59–61

Warren JB, Loi RK, Coughlan ML (1993) Involvement of nitric oxide synthase in delayed response to ultraviolet light irradiation of rat skin *in vitro*. Br J Pharmacol 109:802–806

Wilhelmi G (1949) Ueber die pharmakologischen Eigenschaften von Irgapyrin, einem neuen Präparat aus der Pyrazolreihe. Schweiz Med Wschr 79:577–582

Wilhelmi G, Domenjoz H (1951) Vergleichende Untersuchungen über die Wirkung von Pyrazolen und Antihistaminen bei verschiedenen Arten der experimentellen Entzündung. Arch Int Pharmacodyn 85:129–143

Winder CV, Wax J, Burr V, Been M, Rosiere CE (1958) A study of pharmacological influences on ultraviolet erythema in guinea pigs. Arch Int Pharmacodyn 116:261–292

Woodbury RA, Kligman LH, Woodbury MJ, Kligman AM (1994) Rapid assay of the anti-inflammatory activity of topical corticosteroids by inhibition of a UVA-induced neutrophil infiltration in hairless mouse skin. I. The assay and its sensitivity. Acta Derm Venereol (Stockh) 74:15–17

Woodward DF, Owen DAA (1979) Quantitative measurement of the vascular changes produced by UV radiation and carrageenin using the guinea-pig ear as the site of inflammation. J Pharmacol Meth 2:5–42

Yawalkar S, Wiesenberg-Boettcher I, Gibson JR, Siskin SB, Pignat W (1991) Dermatopharmacologic investigations of halobetasol propionate in comparison with clobetasol 17-propionate. Am Acad Dermatol 25:1137–1144

H.3.2.2.2 Vascular Permeability

PURPOSE AND RATIONALE

The test is used to evaluate the inhibitory activity of drugs against increased vascular permeability which is induced by a phlogistic substance (Miles and Miles 1992). Mediators of inflammation, such as histamine, prostaglandins and leucotrienes are released following stimulation e. g. of mast cells. This leads to a dilation of arterioles and venules and to an increased vascular permeability. As a consequence, fluid and plasma proteins are extravasated and edemas are formed. These effects are counteracted by H_1-antihistaminics, inhibitors of arachidonic acid metabolism and by leucotriene receptor antagonists. In addition, membrane-stabilizing drugs are able to reduce capillary permeability. Vascular permeability is increased by intracutaneous injection of the mast cell-degranulating compound 48/80. The increase of permeability can be recognized by the infiltration of the injected sites of the skin with the vital dye Evan's blue.

PROCEDURE

Male Sprague-Dawley rats with a body weight between 160 and 200 g are used. The ventral sides of the animal are shaved. Five ml/kg of an 1% solution of Evan's blue are injected intravenously. One hour later the animals are dosed with the test compound orally or intraperitoneally or with the vehicle. Ten animals are used for each test group and the control. Thirty minutes later, the animals are briefly anaesthetized with ether and 0.05 ml of an 0.01% solution of compound 48/80 are injected intracutaneously at 3 sites both at the left and ventral side. Ninety minutes after the injection of compound 48/80 the animals are sacrificed by ether anesthesia. The abdominal skin is removed and the dye-infiltrated areas of the skin are measured.

EVALUATION

The diameter of the dye-infiltrated areas is measured in millimeters in two perpendicular directions and the mean values of all injection sites in one animal are calculated. The percent inhibition in the treated animals as compared to the control group is calculated. A treated animal which shows values less than 50% of controls can be considered as positive. ED_{50} values can be calculated in this way. Phenylephrine at a dose of 15 mg/kg has been found to be effective.

CRITICAL ASSESSMENT OF THE METHOD

The test for vascular permeability is useful for characterization of a new anti-inflammatory compound.

Since compounds with sympathomimetic activity have a pronounced effect this test cannot be regarded as a primary screening test for anti-inflammatory products. Together with an observation of writhing or

"squirming" of mice, Whittle (1964) has proposed to be able to distinguish between narcotic and non narcotic analgesics.

MODIFICATIONS OF THE METHOD

Shionoya and Ohtake (1975) described a simple method for extraction of extravasated dye (Evan's blue) in the skin.

Frimmer and Müller (1962) presented a critical survey on the use of dye methods for quantitative determination of increased capillary permeability following intracutaneous injection of active substances.

McClure et al. (1992) used the Olympus CUE-2 Image Analyzer to quantify vascular permeability in the Miles assay in guinea pigs.

Zentel and Töpert (1994) used oxazolone-induced Evans blue extravasation for preclinical evaluation of topical corticosteroids. Female**NMRI-mice** were sensitized by topical application of 50 µl of 40% oxazolone in ethanol to 4 cm^2 of the left flank. After 13 days the animals were injected intravenously with 0.2 ml of 0.5% Evan's blue in water and 20 µl of 4% oxazolone in ethanol were topically applied to 6 cm^2 of the right flank immediately after injection. Three h later the challenged skin was treated with various corticosteroids in ointment. The animals were sacrificed 24 h after treatment and the challenged skin removed. Evans blue extravasation was measured spectrophotometrically at 623 nm.

Teixeira et al. (1993) studied acute inflammatory reactions in **guinea pig skin** measuring infiltration of ^{111}In-labelled eosinophils and neutrophils and edema formation by extravasation of ^{125}I-human serum albumin.

Fujii et al. (1996) quantified vascular permeability by the extravasation of pontamine sky blue in the skin of male ddY mice after subcutaneous injection of lipopolysaccharides.

Blackham and Woods (1986) measured extravasation of pontamine sky blue in the **mouse** peritoneal cavity.

Cambridge et al. (1996) investigated 6-hydroxydopamine-induced plasma extravasation in **rat skin** after intravenous injection of ^{125}I-human serum albumin and Evan's blue.

Rouleau et al. (1997) measured the inhibition of capsaicin-induced plasma extravasation by a histamine H_3 receptor agonist prodrug by analysis of extravasated Evan's blue in skin, eye conjunctiva, nasal mucosa, trachea, main bronchi, esophagus and urinary bladder of rats.

Watanabe et al. (1984) used fluorescein isothiocyanate-labeled bovine serum albumin as tracer to measure vascular permeability in the **carrageenin air pouch of rats**.

Collins et al. (1993) studied the pro-inflammatory properties of the human recombinant vascular permeability factor containing 165 amino acids in **rabbits**.

Urinary bladder cystitis induced by cyclophosphamide was used as model of intestinal inflammation and pain by several authors (Ahluwahlia et al. 1994; Bon et al. 1996; Boucher et al. 1997; Alfieri and Gardner 1997). Male Wistar rats weighing 300–400 g were treated first with test drug or saline subcutaneously or intraperitoneally and then injected 5 min later with 150 mg/kg i.p. cyclophosphamide. One h later, anaesthesia was induced by 40 mg/kg i.p. pentobarbitone and 50 mg/kg Evans blue were injected into the jugular vein. Fifteen min later, the rat was exsanguinated by infusion of 50 ml saline into the left cardiac ventricle. The urinary bladder, the left kidney, the superior lobe of the left lung and approximately 1-cm portions of the duodenum and jejunum were removed and blotted before dry weighing. The content of Evens blue dye was determined by spectrophotometry at 620 nm after extraction in known volumes of formamide at 60°C for 60 h.

Ferrets were treated in the same way, but the dose of cyclophosphamide was 125 mg/kg and the volume of exsanguination was 300 ml.

Hirota et al. (1995) induced **chemical peritonitis in rats** by applying 0.02 M HCl on the surface of the cecum or appendix and quantified the inflammation by measuring the extravasation of intravenously injected Evan's blue bound to albumin extracted from those tissues.

REFERENCES AND FURTHER READING

Ahluwalia A, Maggi C, Santiccioli P, Lecci A, Giulani S (1994) Characterisation of the capsaicin-sensitive component of cyclophosphamide-induced inflammation in the rat urinary bladder. Br J Pharmacol 111:1017–1022

Alfieri A, Gardner C (1997) The NK_1 antagonist GR203040 inhibits cyclophosphamide-induced damage in the rat and ferret bladder. Gen Pharmacol 29:245–250

Bennett AJ, West GB (1978) Measurement of the changes in vascular permeability in rat skin. J Pharmacol Meth 1:105–108

Blackham A, Woods FAM (1986) Immune complex mediated inflammation in the mouse peritoneal cavity. J Pharmacol Meth 15:77–85

Bon K, Lantéri-Minet M, de Pommery J, Michiels JF, Menétrey D (1996) Cyclophosphamide cystitis as a model of visceral pain in rats. A survey of hindbrain structures involved in visceroception and nociception using the expression of c-Fos and Krox-24 proteins. Exp Brain Res 108:404–416

Boucher M, Meen M, Codron JP, Coudoré F, Kémény JL, Eschalier A (1997) Cyclophosphamide cystitis in rats: A new behavioral model of visceral pain. Fund Clin Pharmacol 11:160

Cambridge H, Ajuebor MN, Brain SD (1996) Investigation of 6-hydroxydopamine-induced plasma extravasation in rat skin. Eur J Pharmacol 301:151–157

Collins PD, Connolly DT, Williams TJ (1993) Characterization of the increase in vascular permeability induced by vascular permeability factor *in vivo*. Br J Pharmacol 109:195–199

Feldberg W, Miles A (1953) Regional variations of increased permeability of skin capillaries induced by a histamine liberator and their relation to the histamine content in skin. J Physiol 120:205–213

Frimmer M, Müller FW (1962) Brauchbarkeit und Grenzen der Farbstoffmethoden zur Bestimmung vermehrter Durchlässigkeit der Haut-Capillaren. Med Exp 6:327–330

Fujii E, Irie K, Ogawa A, Ohba K, Muraki T (1996) Role of nitric oxide and prostaglandins in lipopolysaccharide-induced increase in vascular permeability in mouse skin. Eur J Pharmacol 297:257–263

Hirota K, Zsigmond EK, Matsuki A, Rabito SF (1995) Topical ketamine inhibits albumin extravasation in chemical peritonitis in rats. Acta Anaesthesiol Scand 39:174–178

Lembeck F, Holzer P (1979) Substance P as neurogenic mediator of antidromic vasodilation and neurogenic plasma extravasation. Naunyn Schmiedeberg's Arch Pharmacol 310:175–183

McClure N, Robertson DM, Heyward P, Healy DL (1994) Image analysis quantification of the Miles assay. J Pharmacol Toxicol Meth 32:49–52

Miles AA, Miles EM (1952) Vascular reactions to histamine, histamine-liberator and leukotaxine in the skin of guinea-pigs. J Physiol 118:228–257

Nagahisa A, Kanai Y, Suga O, Taniguchi K, Tsuchiya M, Lowe III JA, Hess HJ (1992) Antiinflammatory and analgesic activity of a non-peptide substance P receptor antagonist. Eur J Pharmacol 217:191–195

Pouleau A, Garbag M, Ligneau X, Mantion C, Lavie P, Advenier C, Lecomte JM, Krause M, Stark H, Schunack W, Schwartz JC (1997) Bioavailability, antinociceptive and antiinflammatory properties of BP 2–94, a histamine H_3 receptor agonist prodrug. J Pharmacol Exp Ther 281:1985–1094

Saria A, Lundberg JM, Skofitsch G, Lembeck F (1983) Vascular protein leakage in various tissues induced by substance P, capsaicin, bradykinin, serotonin, histamine and by antigen challenge. Naunyn-Schmiedeberg's Arch Pharmacol 324:212–218

Sensch KH, Zeiller P, Raake W (1979) Zur antiexsudativen und antioedematösen Wirkung von Sympathikomimetika. Arzneim Forsch/Drug Res 29:116–121

Shionoya H, Ohtake S (1975) A new simple method for extraction of extravasated dye in the skin. Japan J Pharmacol 103, Suppl 25:103

Teixeira MM, Williams TJ, Hellewell PG (1993) Role of prostaglandins and nitric oxide in acute inflammatory reactions in guinea-pig skin. Br J Pharmacol 110:1515–1521

Watanabe K, Nakagawa H, Tsurufuji S (1984) A new sensitive fluorometric method for measurement of vascular permeability. J Pharmacol Meth 11:167–176

Whittle BA (1964) The use of changes in capillary permeability in mice to distinguish between narcotic and non narcotic analgesics. Br J Pharmacol 22:246–253

Zentel HJ, Töpert M (1994) Preclinical evaluation of a new topical corticosteroid methylprednisolone aceponate. J Eur Acad Dermatol Venereol 3, Suppl 1:S32–S38

H.3.2.2.3 Inhibition of Leukocyte Adhesion to Rat Mesenteric Venules In Vivo

PURPOSE AND RATIONALE

Reversible adherence of leukocytes to endothelium, basement membranes and other surfaces is an essential event in the establishment of inflammation. Their entry into tissues is controlled by the dynamic interaction between adhesion molecules expressed by these cells and the endothelium. White cells circulating in the blood have the tendency to adhere to the walls of blood vessels and this tendency is greatly increased in states of inflammation. Normally, when leukocytes collide with the vessel wall, the collision behaves elastically and the cells bounce off and back into the lumen. However, biochemical changes in inflamed tissues results in inelastic collisions of cells and an increase in their adhesion, thus initiating rolling of leukocytes along the endothelial surface. As adhesion further increases, rolling is slowed and may be followed by the cells coming to a complete stop and their migration out of the vessel. This can be observed by preparing a mesenteric venule of an anesthetized rat and following the flow and rolling of leukocytes by means of a microscope, thus allowing in-vivo studies. In this test procedure, adhesion of leukocytes, to the vessel wall, is artificially induced by the application of the formyl-methionyl peptide fMet-Leu-Phe (FMLP). Formyl peptides are released from bacteria and mitochondria of damaged tissue, so these peptides provide a specific signal marking the presence of invading bacteria or tissue damage. The density of FMLP receptors ranges from 10^4 to 10^5 per cell, depending on the cell type. Activation of leukocytes through this receptor results in rapid expression of preformed L-selectin (LECAM-1) on the cell surface which causes the cells to roll along the endothelial surface. LECAM-1 are very rapidly shed from the surface of leukocytes, however, and integrins take over to maintain further adhesion and migration into the tissue.

PROCEDURE

Sprague-Dawley rats are anesthetized by administration of Nembutal. The trachea, jugular vein and carotid artery are prepared free, the abdominal cavity is opened and a section of ileum is pulled out and draped over a heated microscope table. Prior to test compound administration, the number of spontaneous adhering leukocytes is counted, every 5 min, in a defined section of a venule (covered with paraffin oil) during a 30-min period (control). Blood pressure, body

temperature and velocity of blood flow are also registered. The test compound is administered via continuous infusion during the entire test procedure beginning at $t = -30$ min. Following the determination of control values for spontaneous adhesion, FMLP (f-Met-Leu-Phe, 10^{-4} M) is dripped twice ($t = -30$ min and $t = 0$ min) on the preparation and the number of adhering leukocytes is determined every 5 min over a 90 min period, beginning with the second application of FMLP ($t = 0$ min). Each test group consists of at least 10 animals. The mean leukocyte count of every rat prior to FMLP and/or test substance application is taken as the 100% value to obtain the baseline for further comparisons. The test compounds are dissolved in 0.9% NaCl shortly before application.

EVALUATION

Following the second topical application of FMLP (10^{-4} M), the number of adhering leukocytes in the mesenteric venule section is counted 30 min after the stimulus is given, and again at the end of the observation period of 2 h. The influence of a continuous i.v. infusion of the test drug is compared with the positive control group (FMLP stimulation, without drug).

MODIFICATIONS OF THE METHOD

A simple, rapid, *in vitro* assay for granulocyte adherence was developed by MacGregor et al. (1974). Heparinized whole blood is filtered through nylon fibers packed in Pasteur pipettes, and the percentage of granulocytes adhering was calculated.

Neutrophil adherence was tested *in vitro* by Burch et al. (1992). Human umbilical vein endothelial cells were plated at 5×10^4 cells/well into collagen coated culture plates and grown to confluence. Neutrophils were labeled with ^{51}Cr. Experimental agents were added to the neutrophils before their activation with FMLP. After 15 min incubation at 37°C, the non-adherent leukocytes were removed by gentle aspiration followed by a wash with saline. The adherent neutrophils were lysed by 1 N NaOH and the radioactivity was quantitated.

REFERENCES AND FURTHER READING

Burch RM, Connor JR, Bator JM, Weitzberg M, Laemont K, Noronha-Blob L, Sullivan JP, Steranka LR (1992) NPC 15669 inhibits the reverse passive Arthus reaction in rats by blocking neutrophil recruitment. J Pharm Exp Ther 263:933–937

Lawrence MB, Springer TA (1991) Leukocytes roll on a selectin at physiologic flow rates: Distinction from and prerequisite for adhesion through integrins. Cell 65:859–873

MacGregor RR, Spagnuolo PJ, Lentnek AL (1974) Inhibition of granulocyte adherence by ethanol, prednisone, and aspirin, measured with an assay system. New Engl J Med 291:642–646

Stecher VJ, Chinea GL (1978) The neutrophil adherence assay as a method for detecting unique anti-inflammatory agents. Agents Actions 8:258 262

Zielinski T, Müller HJ, Schleyerbach R, Bartlett RR (1994) Differential effects of leflunomide on leukocytes: Inhibition of rat *in vivo* adhesion and human *in vitro* oxidative burst without affecting surface marker modulation. Agents Actions 41 Spec Conf Issue: C276–278

H.3.2.2.4 Oxazolone-Induced Ear Edema in Mice

PURPOSE AND RATIONALE

The oxazolone-induced ear edema model as first described by Evans (1971) in mice is a model of delayed contact hypersensitivity that permits the quantitative evaluation of the topical and systemic anti-inflammatory activity of a compound following topical administration.

PROCEDURE

Mice of either sex with a weight of 25 g are used. Before each use a fresh 2% solution of oxazolone (4-ethoxymethylene-2-phenyl-2-oxazolin-5-one) in acetone is prepared. The mice are sensitized by application of 0.1 ml on the shaved abdominal skin or 0.01 ml on the inside of both ears under halothane anesthesia. The mice are challenged 8 days later again under anesthesia by applying 0.01 ml 2% oxazolone solution to the inside of the right ear (control) or 0.01 ml of oxazolone solution, in which the test compound or the standard is solved. Special pipettes of 0.1 ml or 0.01 ml are used. Groups of 10 to 15 animals are treated with the irritant alone or with the solution of the test compound. The left ear remains untreated. The maximum of inflammation occurs 24 h later. At this time the animals are sacrificed under anesthesia and a disc of 8 mm diameter is punched from both sides. The discs are immediately weighed on a balance. The weight difference is an indicator of the inflammatory edema.

EVALUATION

Average values of the increase of weight are calculated for each treated group and compared statistically with the control group. A 0.003% solution of hydrocortisone and a 1% solution of indomethacin were found to be active.

CRITICAL ASSESSMENT OF THE METHOD

The method is suitable for both steroidal and non-steroidal compounds as well as for the evaluation of various topical formulations.

MODIFICATIONS OF THE METHOD

Griswold et al. (1974) applied a 3% solution of oxazolone to the left paw of mice. The edema was assessed plethysmographically.

Various cutaneous models of inflammation for the evaluation of topical and systemic pharmacological agents have been discussed by Young and Young (1989).

Bailey et al. (1995) described a contact hypersensitivity model in mice for rank-ordering formulated corticosteroids. Male Swiss Webster mice were sensitized with 20 µl of 2% oxazolone on the inner and outer aspects of each ear (10 µl each side). Mice were challenged 7 days later with 2% oxazolone in acetone:olive oil (4:1) on both sides of the right ear. Animals were topically treated with corticosteroids or non-steroidal antiinflammatory drugs or 20 mg formulated corticosteroids immediately after challenge. The mice were sacrificed after 24 h and edema and myeloperoxidase activity were determined. Edema was measured by taking the weight of 6 mm trephine punch biopsies of the right and left ears. Inhibition was calculated from change in ear weight of control or drug treated ears versus placebo treated ears. Myeloperoxidase activity was assessed spectrophotometrically (Williams et al. 1983) on tissue homogenates. In a delayed-type hypersensitivity model animals were treated as in the contact hypersensitivity model, except the mice were sensitized with 40 µl of 2% oxazolone in acetone:olive oil (4:1) on the unshaved inguinal areas.

Meingassner et al. (1997) studied anti-inflammatory activity using allergic contact dermatitis im **mice, rats** and **pigs**. Mice were sensitized on the shaved abdomen with 50 µl of 2% oxazolone solution in acetone. After 7 days, they were challenged with 10 µl of 2% (for topical testing) or 0.5% (for systemic testing) oxazolone on the inner surface of the right ears. Pinnal weight was taken as a measure of inflammatory edema 24 h after challenge. Female Sprague Dawley *rats* were sensitized by application of 80 µl of 2,4-dinitrofluorobenzene solution applied in 20 µl volumes to the inner surface of both ear lobes and to both shaved inguinal regions on day 1. Allergic contact dermatitis was elicited with 30 µl of 0.5% 2,4-dinitrofluorobenzene applied to the test sites of ≈15 mm in diameter on both shaved flanks on day 12. Animals were treated by gavage 2 h before and immediately after challenge. Dermatitis was evaluated by measuring the thickness of the lifted skin fold at the test sites with a spring-loaded micrometer. Domestic **pigs** were sensitized wit 400 µl of 10% 2,4-dinitrofluorobenzene applied to four areas on both ears and groins. Challenge reactions were elicited 12 days later with 15 µl of 2,4-dinitrofluorobenzene (1%) applied topically to test sites arranged in four craniocaudal lines on the dorsolateral shaved back (24 or 32 per pig). Test sites were treated twice either with 20 µl solution of test compound or with ≈50 mg of a cream formulation applied topically 30 min and 6 h after challenge. One day after challenge the test sites were visually evaluated for intensity and extent of erythema and induration.

REFERENCES AND FURTHER READING

Alpermann HG, Sandow J, Vogel HG (1982) Tierexperimentelle Untersuchungen zur topischen und systemischen Wirksamkeit von Prednisolon-17-ethylcarbonat-21-propionat. Arzneim Forsch/Drug Res 32:633–638

Bailey SC, Asghar F, Przekop PA, Kurtz ES (1995) A novel contact hypersensitivity model for rank-ordering formulated corticosteroids. Inflamm Res 44, Suppl 2:S162–163

Evans PD, Hossack M, Thomson DS (1971) Inhibition of contact sensitivity in the mouse by topical application of corticosteroids. Br J Pharmacol 43:403

Griswold DE, DiLorenzo JA, Calabresi P (1974) Quantification and pharmacological dissection of oxazolone-induced contact sensitivity in the mouse. Cell Immunol 11:198–204

Meingassner JG, Grassberger M, Fahrngruber H, Moore HD, Schuurman H, Stütz A (1997) A novel anti-inflammatory drug, SDZ ASM 981, for the topical and oral treatment of skin diseases. *In vivo* pharmacology. Br J Dermatol 137:568–576

Williams RN, Paterson CA, Eakins KE, Bhattacherjee P (1983) Quantification of ocular inflammation: Evaluation of polymorphonuclear leukocyte infiltration by measuring myeloperoxidase activity. Current Eye Res 2:465–470

Young JM, Young LM (1989) Cutaneous models of inflammation for the evaluation of topical and systemic pharmacological agents. In: Pharmacological Models in the Control of Inflammation. Alan R. Liss, Inc., pp 215–231

H.3.2.2.5 Croton-oil Ear Edema in Rats and Mice

PURPOSE AND RATIONALE

The method has been developed primarily as a bioassay for the concomitant assessment of the antiphlogistic and thymolytic activities of topically applied steroids by Tonelli et al. (1965)

PROCEDURE

For tests in mice the irritant is composed as follows (v/v): 1 part Croton oil, 10 parts ethanol, 20 parts pyridine, 69 parts ethyl ether. For tests in rats the following mixture is prepared (v/v): 4 parts Croton oil, 10 parts ethanol, 20 parts pyridine, 66 parts ethyl ether. The standards and the test compounds are dissolved in this solution. For tests in mice male NMRI-mice with an weight of 22 g, for tests in rats male

Sprague-Dawley rats with a weight of 70 g are used. Ten animals are used for controls and each test group. The test compounds are dissolved in a concentration of 0.03 mg/ml to 1 mg/ml for mice and in a 3 to 10 times higher concentration for rats in the irritant solution. On both sides of the right ear 0.01 ml in mice or 0.02 ml in rats are applied. Controls receive only the irritant solvent. The left ear remains untreated. The irritant is applied under ether anesthesia. Four hours after application the animals are sacrificed under anesthesia. Both ears are removed and discs of 8 mm diameter are punched. The discs are weighed immediately and the weight difference between the treated and untreated ear is recorded indicating the degree of inflammatory edema. In the originally described method the ears are removed by sharp, straight scissors 6 h after application and weighed as total. The animals were sacrificed 48 h after topical administration and the thymus glands were removed, weighed and expressed as mg thymus/100 g body weight.

EVALUATION

The antiphlogistic effect can be determined by expressing the increase in weight of the treated ear as percentage of the weight of the contralateral control ear. The difference of both weights is divided by the weight of the contralateral ear times 100. Otherwise, the difference between both ears or excised discs is calculated as the average values for treated and control groups and the effect is evaluated by statistical methods. Concentration of 0.5 to 1 mg/ml hydrocortisone have been proven to be effective.

CRITICAL ASSESSMENT OF THE METHOD

The method is useful for evaluation of anti-inflammatory topical steroids especially in the modification when thymus weight is determined simultaneously. The method also can be used for topically applied nonsteroidal antiphlogistics.

MODIFICATIONS OF THE METHOD

Wilhelmi and Domenjoz (1951) tested various drugs using Croton oil induced ear edema in mice and rabbits.

Tubaro et al. (1985) tested various anti-inflammatory drugs in the Croton oil test in mice. Granulocyte infiltration in plugs taken from the inflamed ears was assessed by measuring peroxidase activity.

Zentel and Töpert (1994) used Croton oil-induced ear edema in rats to evaluate topical corticosteroids. A plastic collar was fixed around the neck of Wistar rats of either sex (160–200 g body weight) to exclude oral uptake of the compounds. Fifty µl of 5% Croton oil in ethanol or ethanol alone were topically applied to both ears. In the treatment groups drugs were coapplied with Croton oil. Five h after treatment the animals were sacrificed by CO_2 gas and the ears removed. Edema formation was measured by the increase in wet weight.

Iwasaki et al. (1995) measured the inhibition of Croton oil-induced ear edema in Wistar rats by locally applied clobetasol-17-propionate, a synthetic glucocorticoid, and the influence of simultaneously applied RU 486.

Weirich et al. (1977) measured skin temperature, ear thickness and weight of excised punches after Croton oil induced edema in the ears of **white rabbits** and calculated phlogostasis values as the products of the percent reduction in skin temperature, auricular thickness and tissue weight in relation to controls. The authors recommended this model for the primary evaluation of topical anti-inflammatory agents.

Colorado et al. (1991) described an apparatus to measure Croton oil induced ear edema in mice using precisely reproducible pressure on the ear. The device allows to follow the time course of inflammation by repeated measurements.

Akiyama et al. (1994) studied staphylococcus aureus infection on experimental Croton oil-inflamed skin in mice. Staphylococcus aureus cells were inoculated on the surface of skin inflamed by application of Croton oil in cyclophosphamide-treated mice. Skin specimens were taken at 1, 3, 6, 12, and 24 h after inoculation and examined by microscopy. The staphylococcus aureus cells which attached to the surface of the skin immediately after inoculation had invaded the horny layer within 1 h. The cells gradually penetrated deeper into the epidermis. Application of corticosteroid ointments decreased the number of staphylococcus aureus cells in the lesions.

Anderson and Groth (1984) induced **toxic contact reactions** to Croton oil or dinitrochlorobenzene (DNCB), or **allergic contact reactions** to DNCB or oxazolone in guinea pig skin and tested the effect of various locally applied corticosteroids by macroscopic assessment and microscopic evaluation of cellular infiltrates.

Tarayre et al. (1984) used a 0.25% solution of **cantharidin** in acetone and applied 0.025 ml to one mouse ear. Two phases of inflammation were observed. After local application nonsteroidal drugs showed effects in the first phase only, whereas steroids influenced both phases.

De Young et al. (1987) induced ear inflammation in rats by intradermal injection of 10 ng **recombinant human interleukin-1β** in 10 µl of saline.

Maloff et al. (1989) injected 20 µl of interleukin-1 solution into the left ear of mice and found a dose-dependent increase of ear thickness and myeloperoxidase activity which reached the maximum after 24 h. These effects were reduced by high doses of glucocorticoids but not by nonsteroidal anti-inflammatory drugs.

Chang et al. (1987) applied 4 µg **tetradecanoyl phorbol acetate** and test drugs dissolved in acetone to the right ear of mice. Ear edema was calculated by subtracting the thickness of the left ear (vehicle control) from the right ear (treated ear).

De Young et al. (1989) examined the temporal patterns of edema and accumulation of the polymorphic nuclear cell marker enzyme myeloperoxidase following application of tetradecanoyl phorbol acetate to mouse ears. Topical and oral corticosteroids inhibited both edema and myeloperoxidase accumulation, whereby clobetasol propionate was more effective than fluocinolone and dexamethasone. Cyclo-oxygenase and lipoxygenase inhibitors were very effective against myeloperoxidase accumulation but were inactive or moderately active vs. edema.

Murakawa et al. (2006) studied the involvement of tumor necrosis factor-α in phorbol ester 12-*O*-tetradecynoylphorbol-13-acetate- (TPA-) induced skin edema in mice.

Topical application of arachidonic acid to mouse ear has become a widely used test (Young et al. 1983, 1984; Opas et al. 1985; Crummey et al. 1987; Hensby et al. 1987; Tomchek et al. 1991) One mg arachidonic acid is applied to the right ear of mice and vehicle to the left ear of each animal. Drugs are topically applied in acetone to the ear 30 min prior to the arachidonic acid application. Ear swelling was measured using a caliper one hour after arachidonic acid.

Griswold et al. (1995) induced inflammation in mice by local application of arachidonic acid or phorbol ester. Besides ear thickness, myeloperoxidase and DNA content was measured.

REFERENCES AND FURTHER READING

Akiyama H, Kanzaki H, Abe Y, Tada H, Arata J (1994) Staphylococcus aureus infection on experimental croton oil-inflamed skin in mice. J Dermatol Sci 8:1–10

Anderson CD, Groth O (1984) The influence on the dermal cellular infiltrate of topical steroid applications and vehicles in guinea pig skin: normal skin, allergic and toxic reactions. Contact Dermatitis 10:193–200

Alpermann HG, Sandow J, Vogel HG (1982) Tierexperimentelle Untersuchungen zur topischen und systemischen Wirksamkeit von Prednisolon-17-ethylcarbonat-21-propionat. Arzneim Forsch / Drug Res 32:633–638

Chang J, Blazek E, Skowronek M, Marinari L, Carlson RP (1987) The antiinflammatory action of guanabenz is mediated through 5-lipoxygenase and cyclooxygenase inhibition. Eur J Pharm 142:197–205

Colorado A, Slama JT, Stavinoha WB (1991) A new method for measuring auricular inflammation in the mouse. J Pharmacol Meth 26:73–77

Crummey A, Harper GP, Boyle EA, Mangan FR (1987) Inhibition of arachidonic acid-induced ear oedema as a model for assessing topical anti-inflammatory compounds. Agents Actions 20:69–72

De Young LM, Spires DA, Kheifets J, Terrell TG (1987) Biology and pharmacology of recombinant interleukin-1β-induced rat ear inflammation. Agents Actions 21:325–327

De Young LM, Kheifets JB, Ballaron SJ, Young JM (1989) Edema and cell infiltration in the phorbol ester-treated mouse ear are temporally separate and can be differentially modulated by pharmacologic agents. Agents Actions 26:335–341

Griswold DE, Chabot-Fletcher M, Webb EF, Martin L, Hillegass L (1995) Antiinflammatory activity of topical auranofin in arachidonic acid- and phorbol ester-induced inflammation in mice. Drug Dev Res 34:369–375

Hensby CN, Eustache J, Shroot B, Bouclier M, Chatelus A, Luginbuhl B (1987) Antiinflammatory aspects of systemic and topically applied retinoids. Agents Actions 21:238–240

Iwasaki K, Mishima E, Miura M, Sakai N, Shimao S (1995) Effect of RU 486 on the atrophogenic and antiinflammatory effects of glucocorticoids in skin. J Dermatol Sci 10:151–158

Maloff BL, Shaw JE, DiMeo TM (1989) IL-1 dependent model of inflammation mediated by neutrophils. J Pharmacol Meth 22:133–140

Murakawa M, Yamaoka K, Tanaba Y, Fukuda Y (2006) Involvement of tumor necrosis factor (TNF)-α in phorbol ester 12-*O*-tetradecynoylphorbol-13-acetate (TPA)-induced skin edema in mice. Biochem Pharmacol 71:1331–1336

Opas EE, Bonney RJ, Humes JL (1985) Prostaglandin and leukotriene synthesis in mouse ears inflamed by arachidonic acid. J Invest Dermatol 84:253–256

Tarayre JP, Aliaga M, Barbara M, Villanova G, Caillol V, Lauressergues H (1984) Pharmacological study of cantharidin-induced ear inflammation in mice. J Pharmacol Meth 11:271–277

Tomchek LA, Hartman DA, Lewin AC, Calhoun W, Chau TT, Carlson RP (1991) Role of corticosterone in modulation of eicosanoid biosynthesis and antiinflammatory activity by 5-lipoxygenase (5-LO) and cyclooxygenase (CO) inhibitors. Agents Actions 34:20–24

Tonelli G, Thibault L, Ringler I (1965) A bioassay for the concomitant assessment of the antiphlogistic and thymolytic activities of topically applied steroids. Endocrinology 77:625–630

Tubaro A, Dri P, Delbello G, Zilli C, Della Loggia R (1985) The Croton oil ear test revisited. Agents Actions 17:347–349

Ueno H, Maruyama A, Miyake M, Nakao E, Nakao K, Umezu K, Nitta I (1991) Synthesis and evaluation of antiinflammatory activities of a series of corticosteroid 17α-esters containing a functional group. J Med Chem 34:2468–2473

Weirich EG, Longauer JK, Kirkwood AH (1977) New experimental model for the primary evaluation of topical contrainflammatory agents. Arch Derm Res 259:141–149

Wilhelmi G, Domenjoz H (1951) Vergleichende Untersuchungen über die Wirkung von Pyrazolen und Antihistaminen bei verschiedenen Arten der experimentellen Entzündung. Arch Int Pharmacodyn 85:129–143

Young JM, Wagner M, Spires DA (1983) Tachyphylaxis in 12-O-tetradecanoylphorbol acetate- and arachidonic acid-induced ear edema. J Invest Dermatol 80:48–52

Young JJ, Spires DA, Bedord CJ, Wagner B, Ballaron SJ, DeYoung LM (1984) The mouse ear inflammatory response to topical arachidonic acid. J Invest Dermatol 82:367–371

Zentel HJ, Töpert M (1994) Preclinical evaluation of a new topical corticosteroid methylprednisolone aceponate. J Eur Acad Dermatol Venereol 3, Suppl 1:S32–S38

H.3.2.2.6 Paw Edema

PURPOSE AND RATIONALE

Among the many methods used for screening of anti-inflammatory drugs, one of the most commonly employed techniques is based upon the ability of such agents to inhibit the edema produced in the hind paw of the rat after injection of a phlogistic agent. Many phlogistic agents (irritants) have been used, such as brewer's yeast, formaldehyde, dextran, egg albumin, kaolin, Aerosil, sulfated polysaccharides like carrageenin or naphthoylheparamine. The effect can be measured in several ways. The hind limb can be dissected at the talocrural joint and weighed. Usually, the volume of the injected paw is measured before and after application of the irritant and the paw volume of the treated animals is compared to the controls. Many methods have been described how to measure the paw volume by simple and less accurate and by more sophisticated electronically devised methods. The value of the assessment is less dependent on the apparatus but much more on the irritant being chosen. Some irritants induce only a short lasting inflammation whereas other irritants cause the paw edema to continue over more than 24 h.

PROCEDURE

Male or female Sprague-Dawley rats with a body weight between 100 and 150 g are used. The animals are starved overnight. To insure uniform hydration, the rats receive 5 ml of water by stomach tube (controls) or the test drug dissolved or suspended in the same volume. Thirty minutes later, the rats are challenged by a subcutaneous injection of 0.05 ml of 1% solution of carrageenan into the plantar side of the left hind paw. The paw is marked with ink at the level of the lateral malleolus and immersed in mercury up to this mark. The paw volume is measured plethysmographically immediately after injection, again 3 and 6 h, and eventually 24 h after challenge.

Apparatus

Various devices have been developed for plethysmography of the paw. Winter et al. (1963) used mercury for immersion of the paw. A more sophisticated apparatus has been described by Hofrichter et al. (1969). Alpermann and Magerkurth (1972) described an apparatus based on the principle of transforming the volume being increased by immersion of the paw into a proportional voltage using a pressure transducer. Webb and Griswold (1984) reported a sensitive method of measuring mouse paw volume by interfacing a Mettler DeltaRange top-loading balance with a microcomputer. Several authors used a commercially available plethysmometer from Ugo Basile, Varese, Italy (Damas and Remacle-Volon 1992; Braga da Motta et al. 1994; Legat et al. 1994; Griesbacher et al. 1994).

EVALUATION

The increase of paw volume after 3 or 6 h is calculated as percentage compared with the volume measured immediately after injection of the irritant for each animal. Effectively treated animals show much less edema. The difference of average values between treated animals and control groups is calculated for each time interval and statistically evaluated. The difference at the various time intervals give some hints for the duration of the anti-inflammatory effect. A dose-response curve is run for active drugs and ED_{50} values can be determined.

MODIFICATIONS

Many agents can be used as irritants to induce paw edema in rats or mice. These are:

- 0.05 ml undiluted fresh egg white (Randall and Baruth 1976)
- 0.1 ml of 1% ovalbumin solution (Turner 1965)
- 0.1 ml of 1% formalin (Turner 1965)
- 0.1 ml of 0.2% carrageenan solution (Schönhöfer 1967) Introduction
- 0.1 ml of 1% carrageenan solution plus 100 ng PGE_2 or PGI_2 (Higgs et al. 1978; Portanova et al. 1996)
- 0.1 ml of 1 to 3% dextran solution (Turner 1965)
- 0.1 ml of 2.5% brewer's yeast powder suspension (Tsumuri et al. 1986)
- 0.1 ml of 0.5% β-naphthoylheparamine solution (Peterfalvi et al. 1966)
- 0.1 ml of 0.1% trypsin solution (Kalbhen and Smalla 1977)

0.1 ml of 0.1% collagenase solution (Souza Pinto et al. 1995)

0.1 ml of 0.1% solution of collagenase from *Clostridium histolyticum* (Legat et al. 1994)

0.1 ml of solution of 100 IU hyaluronidase (Dewes 1955, Kalbhen and Smalla 1977)

0.1 ml of complete Freund's adjuvant

0.05 ml of 0.02% serotonin solution (Kalbhen and Smalla 1977)

0.1 ml of 0.005% bradykinin solution (Damas and Remacle-Volon 1992)

0.1 ml of 0.1 mg/ml prostaglandin E2 (Nikolov et al. 1978)

0.1 ml of 2.0 µg/ml prostaglandin E2 (repeated injections, Willis and Cornelsen 1973)

0.1 ml of 1% concanavalin A solution (Lewis et al. 1976)

0.1 ml of 2.5% suspension of Aerosil

0.1 ml of 5% suspension of kaolin (Lorenz 1961; Wagner-Jauregg et al. 1962)

0.05 ml of bentonite gel (Marek 1980)

0.1 ml of nystatin 15000 units (Schiatti et al. 1970, Arrigoni-Martelli et al. 1971)

0.1 ml of 1% phytohaemagglutinin-P solution (Lewis et al. 1976)

0.01 ml of 0.5% adriamycin (mouse paw) (Siegel et al. 1980)

0.1 ml of 0.001–0.1% solutions of various phospholipases A2 (Cirino et al. 1989)

0.1 ml of 0.1% Zymosan solution (Gemmell et al. 1979)

0.1 ml of 0.05% anti^{-}IgG solution (Gemmell et al. 1979)

0.1 ml of 2.5% mustard powder suspension (Tsumuri et al. 1986)

0.1 ml of solution containing 1 unit of cobra venom factor(Leyck and Parnham 1990)

0.05 ml of 0.02–0.2% sonic extract from *Porphyromonas gingivalis* (Griesbacher et al. 1994)

0.1 ml of 0.25% suspension of papaya latex (Gupta et al. 1994)

The edema induced by the various irritants lasts for different times such as a few hours after serotonin and up to 2 days after Aerosil or after kaolin. These irritants therefore are suitable to study not only the degree but also the duration of the anti-inflammatory action.

Standards

Depending on the irritant steroidal and nonsteroidal anti-inflammatory drugs have a pronounced effect in the paw edema test. With carrageenan as irritant doses of 50 to 100 mg/kg phenylbutazone p.o. have been found to be effective.

CRITICAL ASSESSMENT OF THE METHOD

The paw edema method has been used by many investigators and has been proven to be suitable for screening purposes as well as for more in depth evaluations. Dependent on the irritant steroidal and nonsteroidal anti-inflammatory drugs, antihistaminics and also, to a lesser degree, serotonin antagonists are active in the paw edema tests. Since so many different irritants have been used by the various investigators the results are often difficult to compare.

FURTHER MODIFICATIONS OF THE METHOD

Besides paw volume Shirota et al. (1984) determined the surface temperature of the inflamed paw in rats using a special cage with rolling rods.

Kunz et al. (2004) assessed protein patterns in lumbar cord during a zymosan-induced paw inflammation in rats employing a two-dimensional gel electrophoresis revealing a time-dependent breakdown of scaffolding proteins such as neurofilament light chain protein. A calpain inhibitor prevented inflammation-induced neurofilament light chain breakdown in the spinal cord and reduced hyperalgesia.

Brooks et al. (1991) used anesthetized **dogs** and demonstrated that a significant inflammatory response can be elicited in the dog paw by subcutaneous injection of carrageenan. The increase in paw volume can be quantitatively measured as a pressure change recorded via a water-filled balloon fixed against the paw with nonexpandable tape. Effective doses of nonsteroidal antiinflammatory drugs were closer to human therapeutic doses in dogs than in rats.

Oyanagui and Sato (1991) described an **ischemic paw assay in mice**. A commercial rubber ring (1×1 mm, $d = 42$ mm) was bound 14 times to the right hind leg of mice just above the articulation. After 20 min of ischemia, the rubber was cut off with scissors. Paw swelling was measured after an other 20 min of natural blood recirculation.

Wirth et al. (1992) described a **thermic edema** which was induced in anesthetized Sprague-Dawley rats by immersing paws of the right and left hindlimb into water of 55°C. Immediately thereafter, the rats received the test drug (the bradykinin antag-

onist Hoe 140) intravenously. Paw volume was measured at regular intervals by plethysmography.

Braga da Motta et al. (1994) described drug modulation of **antigen-induced paw edema in guinea-pigs**. Male short-haired guinea pigs weighing 250–350 g received on day 0 a single dorsal s.c. injection of 1 ml of phosphate buffered saline containing 20 µg of ovalbumin, dispersed in 1 mg $Al(OH)_3$. The animals were boosted with a similar injection of antigen on days 14, 21, and 28. Thirty five days after the first injection of antigen or $Al(OH)_3$, the animals received an intraplantar injection of 0.5, 5, 50, or 200 µg ovalbumin, diluted in 100 µl of phosphate buffered saline. Edema was measured 2, 4, 6, 8, 24, and 48 h after the challenge.

REFERENCES AND FURTHER READING

Alpermann HG, Magerkurth KO (1972) Messanordnung zur Bestimmung der Wirkung von Antiphlogistika. Arzneim Forsch/Drug Res 22:1078–1088

Alpermann HG, Sandow J, Vogel HG (1982) Tierexperimentelle Untersuchungen zur topischen und systemischen Wirksamkeit von Prednisolon-17-ethylcarbonat-21-propionat. Arzneim Forsch/Drug Res 32:633–638

Arrigoni-Martelli E, Schatti P, Selva D (1971) The influence of anti-inflammatory and immunosuppressant drugs on nystatin induced oedema. Pharmacology 5:215–224

Braga da Motta JI, Cinha FQ, Vargaftig BB, Ferreira SH (1994) Drug modulation of antigen-induced paw oedema in guinea-pigs: effects of lipopolysaccharide, tumor necrosis factor and leucocyte depletion. Br J Pharmacol 112:111–116

Branceni D, Azadian-Boulanger A, Jequier R (1964) L'inflammation expérimentale par un analogue de l'héparine. Un test d'activité antiinflammatoire. Arch Int Pharmacodyn 152:15–24

Brooks RR, Carpenter JF, Jones SM, Ziegler TC, Pong SF (1991) Canine carrageenin-induced acute paw inflammation model and its response to nonsteroidal antiinflammatory drugs. J Pharmacol Meth 25:275–283

Burch RM, DeHaas Ch (1990) A bradykinin antagonist inhibits carrageenan edema in rats. Naunyn-Schmiedeberg's Arch Pharmacol 342:189–193

Cirino G, Peers SH, Wallace JL, Flower RJ (1989) A study of phospholipase A2-induced oedema in rat paw. Eur J Pharmacol 166:505–510

Damas J, Remacle-Volon G (1992) Influence of a long-acting bradykinin antagonist, Hoe 140, on some acute inflammatory reactions in the rat. Eur J Pharmacol 211:81–86

Dewes R (1955) Auswertung antiphlogistischer Substanzen mit Hilfe des Hyaluronidase-Ödems. Arch Int Pharmacodyn 104:19–28

Gemmel DK, Cottney J, Lewis AJ (1979) Comparative effects of drugs on four paw oedema models. Agents and Actions 9:107–116

Griesbacher T, Sutliff RL, Lembeck F (1994) Anti-inflammatory and analgesic activity of the bradykinin antagonist, icatibant (Hoe 140), against an extract from Porphyromonas gingivalis. Br J Pharmacol 112:1004–1006

Gupta OP, Sharma N, Chand D (1994) Application of papaya-latex-induced rat paw inflammation: model for evaluation of slowly acting antiarthritic drugs. J Pharmacol Toxicol Meth 31:95–98

Higgs EA, Moncada S, Vane JR (1978) Inflammatory effects of prostacyclin (PGI_2) and 6-oxo-$PGF_{1\alpha}$ in the rat paw. Prostaglandins 16:153–161

Hofrichter G, Liehn HD, Hampel H (1969) Eine plethysmometrische Messanordnung zur Bestimmung des Rattenpfotenvolumens. Arzneim Forsch / Drug Res 19:2016–2017

Kalbhen DA, Smalla HD (1977) Pharmakologische Studien zur antiphlogistischen Wirkung von Pentosanpolysulfat in Kombination mit Metamizol. Arzneim Forsch/Drug Res 27:1050–1057

Kunz S, Niederberger E, Ehnert C, Coste O, Pfenninger A, Kruip J, Wendrich TM, Schmidtko A, Tegeder I, Geisslinger G (2004) The calpain inhibitor MDL 28170 prevents inflammation-induced neurofilament light chain breakdown in the spinal cord and reduces hyperalgesia. Pain 110:409–418

Legat FJ, Griesbacher T, Lembeck F (1994) Mediation by bradykinin of rat paw oedema induced by collagenase from Clostridium histolyticum. Br J Pharmacol 112:433–460

Lewis AJ, Cottney J, Nelson DJ (1976) Mechanisms of phytohaemagglutinin-P, concanavalin-A and kaolin-induced oedemas in the rat. Eur J Pharmacol 40:1–8

Leyck S, Parnham MJ (1990) Acute antiinflammatory and gastric effects of the seleno-organic compound ebselen. Agents Actions 30:426–431

Lorenz D (1961) Die Wirkung von Phenylbutazon auf das Pfotenoedem der Ratte nach oraler Applikation. Naunyn-Schmiedeberg's Arch exp Path Pharm 241:516–517

Marek J (1980) Bentonite-induced paw edema as a tool for simultaneous testing of prophylactic and therapeutic effects of anti-inflammatory and other drugs. Pharmazie 36:46–49

Moore E, Trottier RW (1974) Comparison of various types of carrageenin in promoting pedal edema in the rat. Res Commun Chem Pathol Pharmacol 7:625–628

Nikolov R, Nikolova M, Peneva M (1978) Study of dipyrone (Analgin) antagonism toward certain pharmacological effects of prostaglandins E2 and F2a. In: Ovtcharov R, Pola W (eds) Proceedings Dipyrone. Moscow Symposium, Schattauer-Verlag, Stuttgart New York, pp 81–89

Oyanagui Y, Sato S (1991) Inhibition by nilvadipine of ischemic and carrageenan paw edema as well as of superoxide radical production from neutrophils and xanthine oxidase. Arzneim Forsch / Drug Res 41:469–474

Peterfalvi M, Branceni D, Azadian-Boulanger G, Chiflot L, Jequier R (1966) Etude pharmacologique d'un nouveau composé analgésique antiiflammatoire, la Glaphénine. Med Pharmacol Exp 15:254–266

Portanova JP, Zhang Y, Anderson GD, Hauser SD, Masferrer JL, Seibert K, Gregory SA, Isakson PC (1996) Selective neutralization of prostaglandin E_2 blocks inflammation, hyperalgesia, and interleukin 6 production *in vivo*. J Exp Med 184:883–891

Randall LO, Baruth H (1976) Analgesic and anti-inflammatory activity of 6-chloro-alpha-methyl-carbazole-2-acetic acid (C-5720). Arch Int Pharmacodyn 220:94–114

Schiatti P, Selva D, Arrigoni-Martelli E (1970) L'edema localizzato da nystatin come modello di inflammazione sperimetale. Boll Chim Farm 109:33–38

Schönhöfer P (1967) Eine kritische Bemerkung zur Vergleichbarkeit der Wirkung entzündungshemmender Pharmaka auf die Glucosamin-6-phosphat-Synthese *in vitro* und am Rattenpfotenödem *in vivo*. Med Pharmacol Exp 16:66–74

Shirota H, Kobayashi S, Shiojiri H, Igarashi T (1984) Determination of inflamed paw surface temperature in rats. J Pharmacol Meth 12:35–43

Siegel DM, Giri SN, Scheinholtz RM, Schwartz LW (1980) Characteristics and effect of antiinflammatory drugs on adriamycin-induced inflammation in the mouse paw. Inflammation 4:233–248

Souza Pinto JC, Remacle-Volon G, Sampaio CAM, Damas J (1995) Collagenase-induced oedema in the rat paw and the kinin system. Eur J Pharmacol 274:101–107

Tsumuri K, Kyuki K, Niwa M, Kokuba S, Fujimura H (1986) Pharmacological investigations of the new antiinflammatory agent 2-(10,11-dihydro-10-oxodibenzo(b,f)thiepin-2-yl) propionic acid. Arzneim Forsch/Drug Res 36:1796–1800

Wagner-Jauregg Th, Jahn U, Buech O (1962) Die antiphlogistische Prüfung bekannter Antirheumatika am Rattenpfoten-Kaolinödem. Arzneim Forsch / Drug Res 12:1160–1162

Webb EF, Griswold DE (1984) Microprocessor-assisted plethysmograph for the measurement of mouse paw volume. J Pharmacol Meth 12:149–153

Willis AL, Cornelsen M (1973) Repeated injection of prostaglandin E2 in rat paws induces chronic swelling and a marked decrease in pain threshold. Prostaglandins 3:353–357

Winter CA, Risley EA, Nuss GW (1962) Carrageenin-induced oedema in hind paw of the rat as an assay for antiinflammatory drugs. Proc Soc Exp Biol Med 111:544–547

Winter CA, Risley EA, Nuss GW (1963) Antiinflammatory and antipyretic activities of indomethacin, (1-(p-chlorobenzoyl)-5-methoxy-2-methyl-indole-3-acetic acid. J Pharmacol Exp Ther 141:369–376

Wirth KJ, Alpermann HG, Satoh R, Inazu M (1992) The bradykinin antagonist HOE 140 inhibits carrageenan- and thermically induced paw edema in rats. Recent Progress on Kinins, Birkhäuser, Basel, pp 428–431

H.3.2.2.7 Pleurisy Test

PURPOSE AND RATIONALE

Pleurisy is a well known phenomenon of exudative inflammation in man. In experimental animals pleurisy can be induced by several irritants, such as histamine, bradykinin, prostaglandins, mast cell degranulators, dextran, enzymes, antigens, microbes, and nonspecific irritants, like turpentine and carrageenan (Survey by DeBrito 1989). Carrageenan-induced pleurisy in rats is considered to be an excellent acute inflammatory model in which fluid extravasation, leukocyte migration and the various biochemical parameters involved in the inflammatory response can be measured easily in the exudate.

PROCEDURE

Male Sprague-Dawley rats weighing 220–260 g are used. The animal is lightly anaesthetized with ether, placed on its back and the hair from skin over the ribs of the right side is removed using animal clippers. The region is swabbed with alcohol. A small incision is made into the skin under the right arm between the seventh and eighth rib. The wound is opened and a further shallow incision is made into the exposed intercostal muscle. 0.1 ml of 2% carrageenin solution is injected into the pleural cavity through this incision. The injection needs to be made swiftly to avoid the risk of injuring the lung. The wound is closed with a Michel clip.

One hour before carrageenan injection and 24 and 48 h thereafter, groups of 10 rats are treated with the standard or the test compound subcutaneously or orally. A control group receives only the vehicle of medication. The animals are sacrificed 72 h after carrageenin injection by ether inhalation. The animal is pinned on a dissection board with the forelimbs fully extended. An incision in the skin over the xiphosternal cartilage is made to free the cartilage from overlying connective tissue. The cartilage is lifted with a forceps and a small cut is made with scissors in the body wall below to gain access into the pleural cavity. One ml of heparinized Hank's solution is injected into the pleural cavity through this cut. The cavity is gently massaged to mix its contents. The fluid is aspirated out of the cavity using a pipette. This is made easier if the dissection board is raised to an angle of 45–60°; the contents then pool in the corners of the cavity. The aspirated exudate is collected in a graduated plastic tube.

EVALUATION

One ml (the added Hank's solution) is subtracted from the measured volume. The values of each experimental group are averaged and compared with the control group. ED_{50} values can be calculated using various doses. Several other parameters can be used:

- Measuring the white blood cell number in the exudate using a Coulter counter or a hematocytometer,
- Determination of lysosomal enzyme activities,
- Determination of fibronectin,
- Determination of PgE_2.

CRITICAL ASSESSMENT OF THE METHOD

The pleurisy model has been accepted as a reliable method to study acute and subacute inflammation allowing the determination of several parameters simultaneously or successively. The activity of steroids as well as of non-steroidal drugs can be measured (Tomlinson et al. 1994; Harada et al. 1996).

MODIFICATIONS OF THE METHOD

The Evans blue-carrageenan-induced pleural effusion model has been proposed by Sancilio (1969, 1973) for screening of compounds with anti-inflammatory activity.

Meyers et al. (1993) tested the effect of treatment with interleukin-1 receptor antagonist on the development of carrageenan-induced pleurisy in intact and adrenalectomized rats.

Fröde et al. (2001, 2002) tested the effects of TNF-α and IL-1β, IL-6, and IL-10 and their specific antibodies in the acute inflammatory response induced by carrageenan in a **mouse** model of pleurisy. Adult Swiss mice received a single intrapleural injection of 0.1 ml of sterile saline containing 1% carrageenan. As the inflammatory response caused by carrageenan in the pleural space of the mice exhibits a biphasic response, peaking at 4 h, characterized primarily by neutrophils, and at 48 h due mainly to mononuclear cells, both interval points were studied. On the day of the experiment, different doses of TNF-α, IL-1β, IL-6 or IL-10 and their antibodies were injected into the pleural cavity of anesthetized mice. After 4 h or 48 h, the animals were sacrificed, the thorax was opened and the pleural cavity was washed with 1 ml of sterile PBS containing 20 IU/ml heparin. All animals had been injected 60 min previously with a solution of Evans blue dye (25 mg/kg, 0.2 ml, i.v.) in order to evaluate the degree of exudation into the pleural space. Leukocytes were counted and evaluated microscopically. The amount of dye was estimated by colorimetry.

REFERENCES AND FURTHER READING

Ackerman N, Tomolonis A, Miram L, Kheifets J, Martinez S, Carter A (1980) Three day pleural inflammation: A new model to detect drug effects on macrophage accumulation. J Pharmacol Exp Ther 215:588–595

De Brito FB (1989) Pleurisy and pouch models of acute inflammation. In: Pharmacological Methods in the Control of Inflammation. Alan R. Liss, Inc. pp 173–194

Dunn CJ, Doyle DV, Willoughby DA (1993) Investigation of the acute and chronic anti-inflammatory properties of diphosphonates using a broad spectrum of immune and non-immune inflammatory reactions. Drug Dev Res 28:47–55

Fröde TS, Souza GEP, Calixto JB (2001) The modulatory role played by TNF-α and IL-1β in the inflammation responses induced by carrageenan in the mouse model of pleurisy. Cytokine 13:162–168

Fröde TS, Souza GEP, Calixto JB (2002) The effects of IL-6 and IL-10 and their specific antibodies in the acute inflammatory response induced by carrageenan in the mouse model of pleurisy. Cytokine 17:149–156

Harada Y, Hatanaka K, Kawamura M, Saito M, Ogino M, Majima M, Ohno T, Ogino K, Yamamoto K, Taketani Y, Yamamoto S, Katori M (1996) Role of prostaglandin synthase-2 in prostaglandin E_2 formation in rat carrageenin-induced pleurisy. Prostaglandins 51:19–33

Meyers KP, Czachowski CL, Coffey JW (1993) Effect of treatment with interleukin-1 receptor antagonist on the development of carrageenan-induced pleurisy in the rat. Inflammation 17:121–134

Mielens ZE, Connolly K, Stecher VJ (1985) Effects of disease modifying antirheumatic drugs and nonsteroidal anti-inflammatory drugs upon cellular and fibronectin responses in a pleurisy model. J Rheumatol 12:1083–1087

Mikami T, Miyasaka K (1983) Effects of several anti-inflammatory drugs on the various parameters involved in the inflammation response in rat carrageenin-induced pleurisy. Eur J Pharmacol 95:1–12

Sancilio L (1969) Evans blue-carrageenan pleural effusion as a model for the assay of nonsteroidal antirheumatic drugs. J Pharmacol Exp Ther 168:199–204

Sancilio LF, Fishman A (1973) Application of sequential analysis to Evans blue-carrageenan-induced pleural effusion for screening of compounds for anti-inflammatory activity. Toxicol Appl Pharmacol 26:575–584

Tomlinson A, Appleton I, Moore AR, Gilroy DW, Willis D, Mitchell JA, Willoughby DA (1994) Cyclo-oxygenase and nitric oxide synthase isoforms in rat carrageenin-induced pleurisy. Br J Pharmacol 113:693–698

Tsurumi K, Mibu H, Okada K, Hasegawa J, Fujimura H (1986) Pharmacological investigations of the new antiinflammatory agent 2-(10,11-dihydro-10-oxodibenzo[b,f]thiepin-2-yl) propionic acid. Arzneim Forsch/Drug Res 36:1806–1809

Ushida Y, Oh-Ishi S, Tanaka K, Harada Y, Ueno A, Katori M (1982) Activation of plasma kallikrein-kinin system and its significant role in the pleural fluid accumulation of rat carrageenin-induced pleurisy. In: Fritz H (ed) Recent Progress on Kinins. Agents and Actions Suppl Vol 9:379–383

H.3.2.2.8 Granuloma Pouch Technique

PURPOSE AND RATIONALE

The method originally invented by Selye has been developed for screening by Robert and Nezamis (1957) using croton oil as irritant. An aseptic inflammation resulting in large volumes of hemorrhage exudate is elicited which resembles the subacute type of inflammation. Instead of croton oil carrageenan can be used as irritant.

PROCEDURE

Male or female Sprague-Dawley rats with a body weight between 150 and 200 g are used. Ten animals are taken for controls and for test groups. The back of the animals is shaved and disinfected. With a very thin needle a pneumoderma is made in the middle of the dorsal skin by injection of 20 ml of air under ether anesthesia. Into the resulting oval airpouch 0.5 ml of a 1% solution of Croton oil in sesame oil is injected avoiding any leakage of air. Forty-eight hours later the air is withdrawn from the pouch and 72 h later any resulting adhesions are broken. Instead of croton oil 1 ml of a 20% suspension of carrageenan in sesame oil can be used as irritant. Starting with the formation of the pouch, the animals are treated every day either orally or subcutaneously with the test compound or the standard. For testing local activity, the test compound is injected directly into the air sac at the same time as the

irritant. On the 4th or the 5th day the animals are sacrificed under anesthesia. The pouch is opened and the exudate is collected in glass cylinders. Controls have an exudate volume between 6 and 12 ml, which is reduced dose dependent in the treated animals.

EVALUATION

The average value of the exudate of the controls and the test groups is calculated. Comparison is made by statistical means. A clear dose response curve could be found by s.c. injection of 0.5, 1.0 and 2.0 mg hydrocortisone acetate/rat. Also doses of 1.5 mg/kg indomethacin were found to be active.

CRITICAL ASSESSMENT OF THE METHOD

The method has been very useful to estimate the potency of anti-inflammatory corticosteroids both after local and after systemic application. By injection of a depot-preparation and induction of the granuloma pouch after various time intervals up to 4 weeks the duration of action can also be determined (Vogel 1963, 1965).

MODIFICATIONS OF THE METHOD

Carrageenin was used to induce exudate formation (Boris and Stevenson 1965).

Bobalik and Bastian (1967) developed a modified granuloma pouch technique in which *Mycobacterium butyricum* (adjuvant) was used as phlogistic agent.

Moreno (1993) sensitized rats by subcutaneous injection of methylated bovine serum albumin emulsified in complete Freund's adjuvant one week prior to the preparation of air pouches which were reinflated 4 days later. Seven days after formation of the air pouches inflammation was induced in the pouches by injection of 1 mg methylated bovine serum albumin.

Martin et al. (1994) described an air pouch model in the 6-day-old rat by injection of carrageenan. Besides the usual parameters, leukocyte influx and the level of prostaglandin E_2 in the pouch exudate were measured.

In order to measure the effects of different classes of proteinase inhibitors, Karran and Harper (1995) studied collagen degradation in subcutaneous air pouches in rats. The air pouches were formed in the dorsal region and were inflamed 6 to 8 days later by injecting λ-type carrageenan. Degradation of ^{14}C-collagen was followed in the inflammatory exudate fluid of the air pouches.

Sugio and Tsurufuji S (1981) re-evaluated the vascular constriction hypothesis as the mechanism of anti-inflammatory action of glucocorticoids. Rats were injected with 8 ml of air subcutaneously on the dorsal surface under light ether anesthesia to make an oval air sac. After 24 h, 4.0 ml of 2% heat-sterilized solution of carrageenin in 0.9% NaCl solution was injected into the air sac (day 0). Drug effects were tested on day 7. Vascular permeability in the granuloma pouch was measured using ^{125}I-HSA and ^{131}I-HSA. About 1 μCi of purified ^{125}I-HSA in 0.2 ml saline was injected into the femoral vein. After 30 min, 1.0 ml of the pouch fluid was withdrawn to measure the leakage of ^{125}I-HSA into the pouch fluid. After administration of the drug, about 1 μCi of purified ^{131}I-HSA was injected into the femoral vein. After 30 min, 1.0 ml of the pouch fluid was again withdrawn to measure the concentration of ^{131}I-HSA. The ratio of ^{125}I-HSA/^{131}I-HSA was taken as an index of vascular permeability change induced by drug treatment.

Atkinson et al. (1962) implanted compressed pellets of carrageenin subcutaneously to rats and measured the effects of some anti-inflammatory substances on wet weight of the pellets.

Bowers et al. (1985) described a method to induced a **granuloma in the rat lung** by instillation of a 2% carrageenan solution into one lower lobe of the lung via the trachea. No respiratory impairment was noticed during this procedure.

Further phlogistic agents inducing specific inflammatory cascades such as zymosan (complement activation) or lipopolysaccharide (cytokine release) have been used for pharmacological evaluation of anti-inflammatory agents (Erdö 1994; Miller 1997).

REFERENCES AND FURTHER READING

Atkinson RM, Jenkins L, Tomich EG, Woollett EA (1962) The effects of some anti-inflammatory substances on carrageenin-induced granulomata. J Endocrinol 25:87–93

Bobalik GR, Bastian JW (1967) Effects of various antiphlogistic agents on adjuvant-induced exudate formation in rats. Arch Int Pharmacodyn 166:466–472

Boris A, Stevenson RH (1965) The effects of some non-steroidal anti-inflammatory agents on carrageenin-induced exudate formation. Arch Int Pharmacodyn 153:205–210

Bowers RR, Birch ML, Thomas DW (1985) A biochemical study of the carrageenan-induced granuloma in the rat lung. Conn Tiss Res 13:191–206

De Brito FB (1989) Pleurisy and pouch models of acute inflammation. In: Pharmacological Methods in the Control of Inflammation. Alan R. Liss, Inc. pp 173–194

Erdö F, Török K, Szekely JI (1994) Measurement of interleukin-1 in zymosan air-pouch exudate in mice. Agents and Actions 41:93–95

Karran EH, Harper GP (1995) Collagen degradation within subcutaneous air pouches *in vivo*: the effects proteinase inhibitors. J Pharmacol Toxicol Meth 34:97–102

Martin SW, Stevens AJ, Brennan BS, Davies D, Rowdland M, Houston JB (1994) The six-day-old rat air pouch model of inflammation: characterization of the inflammatory response to carrageenan. J Pharmacol Toxicol Meth 32:139–147

Miller AJ, Hopkins SJ, Luheshi GN (1997) Sites of action of IL-1 in the development of fever and cytokine response to tissue inflammation in the rat. Br J Pharmacol 120:1274–1279
Moreno JJ (1993) Time course of phopsholipase A_2, eikosanoid release and cellular accumulation in rat immunological air pouch inflammation. Int J Immunopharmacol 15:597–603
Robert A, Nezamis JE (1957) The granuloma pouch as a routine assay for antiphlogistic compounds. Acta Endocr (Kbh) 25:105–112
Selye H (1953) On the mechanism through which hydrocortisone affects the resistance of tissues to injury. An experimental study with the granuloma pouch technique. J Am Med Ass 152:1207–1213
Ueno H, Maruyama A, Miyake M, Nakao E, Nakao K, Umezu K, Nitta I (1991) Synthesis and evaluation of antiinflammatory activities of a series of corticosteroid 17α-esters containing a functional group. J Med Chem 34:2468–2473
Sugio K, Tsurufuji S (1981) Mechanisms of anti-inflammatory action of glucocorticoids: re-evaluation of vascular constriction hypothesis. Br J Pharmacol 73:605–608
Vogel HG (1963) Intensität und Dauer der antiinflammatorischen und glykoneogenetischen Wirkung von Prednisolon und Prednisolonazetat nach oraler und subcutaner Applikation an der Ratte. Acta Endocr (Kbh) 42:85–96
Vogel HG (1965) Intensität und Dauer der Wirkung von 6-Methylprednisolon und seinen Estern an der Ratte. Acta Endocr (Kbh.) 50:621–642

H.3.2.2.9 Urate-Induced Synovitis

PURPOSE AND RATIONALE

The importance of urate in gout and the deposition of sodium urate in gouty tophi is well known. Faires and McCarty (1962) reported that they themselves were the subjects for a study injecting 20 mg sodium urate crystal suspension in their own knee-joint. They experienced severe pain and prostration which resembled an acute gouty attack. Based on this experience they developed an experimental model in dogs for testing anti-inflammatory compounds (McCarty et al. 1963, 1966).

PROCEDURE

Preparation of Sodium Urate Crystals

0.4 g (0.01 Mol) sodium hydroxide pellets are dissolved in 400 ml distilled water in a glass beaker; 1.68 g (0.01 Mol) uric acid is added. The resultant opaque preparation is allowed to remain overnight at room temperature. The next morning, the crystals are harvested by decanting the supernatant solution and are then washed 3 times in cold saline, resuspended in saline and sterilized in an autoclave. Suspensions for injections are kept in rubber-stoppered, multi-dose vials containing 15 to 24 mg of urate per ml.

Unanesthetized healthy dogs weighing between 18 and 25 kg are used. They are trained to lie quietly on their backs in a dog cradle under light restraint. The skin above one knee is shaved, disinfected and a sterile 21-gauge needle inserted into the joint. Slight aspiration produces a small amount of clear, viscous synovial fluid, indicating entry into the joint. The needle is left in place, a syringe containing the urate suspension is attached and volumes from 0.1 to 0.5 ml are injected into the joint (approximately 2–10 mg urate).

One hour before the injection of urate crystals the animals are treated with the test compound or the standard. Experiments are designed so that a pair of dogs is tested on each of 2 days. On the first day, only one dog receives the drug. One week later the opposite knee of each dog is injected, but the other dog is treated.

EVALUATION

A scoring system is adopted in which inflammatory symptoms ranging from tenderness, limping, occasional 3-legged gait to complete 3-legged gait are scored from 1+ to 4+.

CRITICAL ASSESSMENT OF THE METHOD

In spite of the fact that the experiment originally has been performed in human volunteers and that the method closely resembles pathological conditions in man, due to animal protection law conditions the method can be recommended only for special investigations.

MODIFICATIONS OF THE METHOD

Carlson et al. (1986) developed an automated microcomputer-based system for determining canine paw pressure quantitatively in the dog synovitis model.

According to Phelps et al. (1967) dogs are anesthetized and placed on their sides with the hind leg firmly fixed with tape so that the femur and tibia form a 90-degree angle. The knee is punctured with a needle. When a few drops of synovial fluid can be withdrawn indicating a correct puncture of the joint, 6–10 ml of saline are injected to distend the joint and a polyethylene catheter is inserted through the needle, which is then withdrawn. 0.5 ml of a 0.02% sodium urate suspension are injected into the joint. The catheter is attached to a pressure transducer. Constant pressure recordings can be taken during the acute phase of inflammation. Pressure changes are plotted against time, whereby each dog is compared with his own control. Treatment with nonsteroidal anti-inflammatory drugs, such as indomethacin, show a considerable reduction of intraarticular pressure.

Fujihira et al. (1971) injected the urate suspension into the knee joint of a hind leg of well trained Beagle dogs. They were placed on three weighing ma-

chines whereby both forelegs rested on one balance, and the hindlegs individually on other balances. In this way, the relative change of weight on each hindleg after intra-articular injection of urate suspension can be measured, indicating a decrease of weight in the injected leg, counterbalanced to the other leg. Time response curves could be found after non-steroidal anti-inflammatory drugs.

Rosenthale et al. (1972) found a long-lasting inflammatory effect of prostaglandins PGE_1 and PGE_2 after injection in the knee joint of dogs.

Schaible and Schmidt (1985) induced an acute experimental arthritis in the knee joint of anesthetized **cats** by intraarticular injection of a 4% kaolin suspension and recorded the activity of single fine afferent units from filaments of the saphenous nerve.

Perkins and Campell (1992) injected either sodium urate crystals or Freund's complete adjuvant into one knee of **rats**. The maximum tolerated pressure was determined with or without treatment by analgesic drugs after 18–24 h (urate injections) or 64–70 h (Freund's complete adjuvant).

Daniel and Jouvin (1984) induced inflammation of the **guinea pig palatal mucosa** by injection of a microcrystalline suspension of monosodium urate.

Botrel et al. (1994) induced chronic inflammation in the knee joint of Beagle dogs by intra-articular injection of Freund's complete adjuvant. Besides body temperature, differences in skin temperature, difference in stifle diameter, the vertical force exerted by the arthritic hind limb measured by a force plate was chosen as parameter.

Schött et al. (1994) induced monoarthritis in rats by injection of 300 µg carrageenan in 50 µl saline into the right tibio-tarsal joint. Weight bearing was found to be an objective measure of arthritic pain.

Carleson et al. (1996) induced acute inflammation in the temporomandibular joint of rats by intraarticular injection of substance P and measured neurokinin A, calcitonin gene-related peptide and neuropeptide Y in the perfusate.

REFERENCES AND FURTHER READING

Botrel MA, Haak T, Legrand C, Concordet D, Chevalier R, Toutain PL (1994) Quantitative evaluation of an experimental inflammation induced with Freund's complete adjuvant in dogs. J Pharmacol Toxicol Meth 32:63–71

Carleson J, Alstergren P, Appelgren A, Appelgren B, Kopp S, Theodorsson E, Lundeberg T (1996) A model for experimental induction of acute temporomandibular joint inflammation in rats: Effects of substance P (SP) in neuropeptide-like immunoreactivity. Life Sci 59:1193–1201

Carlson RP, Datko LJ, Welch TM, Purvis WF, Shaw GW, Thompson JL, Brunner TR (1986) An automated microcomputer-based system for determining canine paw pressure quantitatively in the dog synovitis model. J Pharmacol Meth 15:95–104

Chau TT (1989) Analgesic testing in animal models. In: Pharmacological models in the control of inflammation. Alan R. Liss, Inc., pp 195–212

Daniel A, Jouvin JL (1984) Experimentally induced inflammation of the guinea pig palatal mucosa by injection of a microcrystalline suspension of monosodium urate. J Pharmacol Meth 12:155–166

Dubinsky B, Gebre-Mariam S, Capetola RJ, Rosenthale ME (1987) The antialgesic drugs: Human therapeutic correlates of their potency in laboratory animal models of hyperalgesia. Agents and Actions 20:50–60

Faires JS, McCarty DJ (1962) Acute arthritis in man and dog after intrasynovial injection of sodium urate crystals. Lancet 2:682–685

Fujihira E, Mori T, Nakazawa M, Ozawa H (1971) A simple method for evaluating analgesic efficacy of non-steroidal anti-inflammatory drugs. Chem Pharm Bull 19:1506–1508

McCarty DJ, Faires JS (1963) A comparison of the duration of local anti-inflammatory effects of several adrenocorticosteroid esters – a bioassay technique. Curr Ther Res 5:284–290

McCarty DJ, Phelps P, Pyenson J (1966) Crystal-induced inflammation in canine joints. I. An experimental model with quantification of the host response. J Exp Med 124:99–114

Perkins MN, Campell EA (1992) Capsazepine reversal of the antinociceptive action of capsaicin *in vivo*. Br J Pharmacol 107:329–333

Phelps P, McCarty DJ (1967) Animal techniques for evaluating anti-inflammatory drugs. In: Siegler PE. Moyer JH (eds) Animal and pharmacological techniques in drug evaluation. Vol 2. Year Book Medical Publishers, Inc., Chicago, pp 742–747

Rosenthale ME, Kassarich J, Schneider F (1966) Effect of anti-inflammatory agents on acute experimental synovitis in dogs. Proc Soc Exp Biol Med 122:693–696

Rosenthale ME, Dervinis A, Kassarich J, Singer S (1972) Prostaglandins and anti-inflammatory drugs in the dog knee joint. J Pharm Pharmacol 24:149–150

Schaible HG, Schmidt RF (1985) Effects of an experimental arthritis on the sensory properties of fine articular afferent units. J Neurophysiol 54:1109–1122

Schött E, Berge OG, Ängeby-Möller K, Hammerström G, Dalsgaard CJ, Brodin E (1994) Weight bearing as an objective measure of arthritic pain in the rat. J Pharmacol Toxicol Meth 31:79–83

Tanaka K, Shimotori T, Makino S, Aikawa Y, Inaba T, Yoshida C, Takano S (1992) Pharmacological studies of the new anti-inflammatory agent 3-formylamino-7-methylsulfonylamino-6-phenoxy-4H-1-benzopyran-4-one. 1st Communication: anti-inflammatory, analgesic and other related properties. Arzneim Forsch/Drug Res 42:935–944

H.3.2.3 Methods for Testing the Proliferative Phase (Granuloma Formation)

H.3.2.3.1 Cotton Wool Granuloma

PURPOSE AND RATIONALE

The method has been described first by Meier et al. (1950) who showed that foreign body granulomas

were provoked in rats by subcutaneous implantation of pellets of compressed cotton. After several days, histologically giant cells and undifferentiated connective tissue can be observed besides the fluid infiltration. The amount of newly formed connective tissue can be measured by weighing the dried pellets after removal. More intensive granuloma formation has been observed if the cotton pellets have been impregnated with carrageenin.

PROCEDURE

Male Wistar rats with an average weight of 200 g are anaesthetized with ether. The back skin is shaved and disinfected with 70% ethanol. An incision is made in the lumbar region. By a blunted forceps subcutaneous tunnels are formed and a sterilized cotton pellet is placed on both sides in the scapular region. The pellets are either standardized for use in dentistry weighing 20 mg or pellets formed from raw cotton which produce a more pronounced inflammation than bleached cotton. The animals are treated for 7 days subcutaneously or orally. Than, the animals are sacrificed, the pellets prepared and dried until the weight remains constant. The net dry weight, i. e. after subtracting the weight of the cotton pellet is determined.

EVALUATION

The average weight of the pellets of the control group as well as of the test group is calculated. The percent change of granuloma weight relative to vehicle control group is determined.

CRITICAL ASSESSMENT OF THE METHOD

The method has been useful for evaluation of steroidal and nonsteroidal anti-inflammatory drugs. For testing corticosteroids, the test can be performed in adrenalectomized rats.

MODIFICATIONS OF THE METHOD

Bush and Alexander (1960) produced granulomata in rats by means of cotton-wool pellets which have been impregnated with carrageenin.

Tanaka et al. (1960) implanted filter paper pellets soaked with 7% formalin solution in rats.

Hicks (1969) implanted pellets impregnated with irritant substances, such as capsicum oleoresin.

Instead of cotton pellets, paper disks have been implanted (Tsurumi et al. 1986).

Roszkowski et al. (1971) immersed the cotton pellets in a 1% carrageenan solution, dried overnight and soaked in a 0.25 oxytetracycline solution before implantation.

D'Arcy and Howard (1967) induced a localized inflammatory reaction in the chorio-allantoic membrane of the chick embryo by the implantation of a sterile filter paper disc, followed by re-incubation *in situ* for 4 days.

Rudas (1960) described a method for quantitative evaluation of the granulation tissue formed in experimental wounds. Plastic rings were incorporated into the wounds on the back of rats inhibiting contraction of the wound edges and epithelialization of the wound. The growth of granulation tissue inside the rings was measured.

REFERENCES AND FURTHER READING

Alpermann HG, Sandow J, Vogel HG (1982) Tierexperimentelle Untersuchungen zur topischen und systemischen Wirksamkeit von Prednisolon-17-ethylcarbonat-21-propionat. Arzneim Forsch/Drug Res 32:633–638

Bush IE, Alexander RW (1960) An improved method for the assay of antiinflammatory substances in rats. Acta Endocr (Kbh) 35:268–276

Hicks R (1969) The evaluation of inflammation induced by material implanted subcutaneously in the rat. J Pharm Pharmacol 21:581–588

Meier R, Schuler W, Desaulles P (1950) Zur Frage des Mechanismus der Hemmung des Bindegewebswachstums durch Cortisone. Experientia 6:469–471

Penn GB, Ashford A (1963) The inflammatory response to implantation of cotton pellets in the rat. J Pharm Pharmacol 15:798–803

Roszkowski AP, Rooks WH, Tomolonis AJ, Miller LM (1971) Anti-inflammatory and analgesic properties of *d*-2-(6′-methoxy-2′-naphthyl)-propionic acid (NAPROXEN). J Pharmacol Exper Ther 179:114–123

Rudas B (1960) Zur quantitativen Bestimmung von Granulationsgewebe in experimentell erzeugten Wunden. Arzneim Forsch 10:226–229

Tanaka A, Kobayashi F, Miyake T (1960) A new antiinflammatory activity test for corticosteroids. The formalin-filter paper pellet method. Endocrinol Japon 7:357–364

Tsurumi K, Mibu H, Okada K, Hasegawa J, Fujimura H (1986) Pharmacological investigations of the new antiinflammatory agent 2-(10,11-dihydro-10-oxodibenzo[b,f]thiepin-2-yl) propionic acid. Arzneim Forsch/Drug Res 36:1806–1809

H.3.2.3.2 Sponge Implantation Technique

PURPOSE AND RATIONALE

The sponge implantation technique was described first by Saxena (1960) for short term experiments but was used subsequently to study the formation of granulomata using long-term implantation.

PROCEDURE

Sponges used for implantation are prepared from polyvinyl foam sheets (thickness 5 mm). Discs are punched out to a standard size and weight (10.0 ±

0.02 mg) using a 13 mm cork borer. The sponges are then soaked in 70% v/v ethanol for 30 min, rinsed four times with distilled water and heated at 80°C for 2 h. Prior to implantation in the animal, the sponges are soaked in sterile 0.9% saline in which either drugs, antigens or irritants have been suspended. Typical examples include 1% carrageenan, 1% yeast, 1% Zymosan A, 6% dextran, heat killed *Bordetella pertussis* (4×10^9 to 5×10^{10} organisms/ml) or 0.5% heat killed mycobacterium tuberculosis.

Sponges are implanted in female Wistar rats weighing 150–200 g under ether anesthesia. A 20 mm dorsal incision is made and the dermis separated from the underlying muscle layer by insertion of blunt forceps to form separate cavities into which sponges are inserted. Up to 8 sponges may be implanted per rat. The dorsal incision is closed with Michel clips and the animals are maintained at a constant temperature of 24°C.

For short term experiments, the animals are treated with test drug or standard once before implantation orally or subcutaneously. For long term experiments, the rats are treated daily up to 3 weeks.

EVALUATION

For estimation of the fluid phase of sponge exudates, e. g. protein content, enzyme levels and biological mediators such as prostaglandins as well as for leukocyte migration, the sponges are removed already after 9 h.

For studying the chronic phase of inflammation besides dry weight DNA, indicating cell content, hexosamine, indicating glycosaminoglycane content, and hydroxyproline, indicating collagen content, can be determined.

CRITICAL ASSESSMENT OF THE METHOD

The sponge implantation technique has been proven to be a versatile method which was used and modified by many investigators.

MODIFICATIONS OF THE METHOD

Boucek and Noble (1955) implanted polyvinyl sponges in rats, hamsters, rabbits and humans.

Holm-Pedersen and Zederfeldt (1971) implanted 2 cubes $10 \times 10 \times 10$ mm of cellulose sponge connected with a silk suture. After various implantation periods, the sponges were dissected free and the strength of the connection between the two parts of the sponge was determined after removal of the connecting suture.

Paulini et al. (1974, 1976) implanted polyester-polyurethane sponges which were inserted at both ends of a 15 mm long PVC tube separated by a cotton wool plug.

Bonta et al. (1979) used polyether sponges measuring $4 \times 1.5 \times 0.5$ cm. A thin polyethylene cannula is inserted into a hole of the sponge and fixed with two stitches. After implantation of the sponge the cannula is pulled through a subdermal tunnel to a neck incision where about 1.5 cm is exteriorized and closed with a tube sealer. One ml of a 2% carrageenin solution is injected into the sponge via the cannula. To study the local effect of drugs, the test compounds can be injected together with the carrageenin. The drugs can be administered repeatedly at any time.

The cannulated sponge method was further modified by Bragt et al. (1980) using a subdermally implanted Teflon cylinder. This cylinder is provided with holes to ensure contact and exchange between the inner chamber and the surrounding tissue and with two cannulae allowing injection of material and withdrawal of exudate at any given stage of granuloma development.

Damas and Remacle-Volon (1992) implanted in rats sterilized polyester sponges which were removed after 4 h and weighed.

REFERENCES AND FURTHER READING

Bonta IL, Adolfs MJP, Parnham MJ (1979) Cannulated sponge implants in rats for the study of time-dependent pharmacological influences on inflammatory granulomata. J Pharmacol Meth 2:1–11

Boucek RJ, Noble NL (1955) Connective tissue. A technique for its isolation and study. AMA Arch Pathol 59:553–558

Bragt PC, Bonta IL, Adolfs MJP (1980) Cannulated Teflon chamber implant in the rat: A new model for continuous studies on granulomatous inflammation. J Pharmacol Meth. 3:51–61

Damas J, Remacle-Volon G (1992) Influence of a long-acting bradykinin antagonist, Hoe 140, on some acute inflammatory reactions in the rat. Eur J Pharmacol 211:81–86

Ford-Hutchinson AW, Walker JR, Smith MJH (1978) Assessment of anti-inflammatory activity by sponge implantation techniques. J Pharmacol Meth 1:3–7

Higgs GA (1989) Use of implanted sponges to study the acute inflammatory response. In: Pharmacological Methods in the Control of Inflammation. Alan R. Liss, Inc., pp 151–171

Holm-Pedersen P, Zederfeldt B (1971) Granulation tissue formation in subcutaneously implanted cellulose sponges in young and adult rats. Scand J Plast Reconstr Surg 5:13–16

Paulini K, Körner B, Beneke G, Endres R (1974) A quantitative study of the growth of connective tissue: Investigation on implanted polyester-polyurethane sponges. Conn Tiss Res 2:257–264

Paulini K, Körner B, Mohr W, Sonntag W (1976) The effect of complete Freund – adjuvant on chronic proliferating inflammation in an experimental granuloma model. Z Rheumatol 35:123–131

Saxena PN (1960) Effects of drugs on early inflammation reaction. Arch Int Pharmacodyn Ther 126:228–237

H.3.2.3.3 Glass Rod Granuloma

PURPOSE AND RATIONALE

The glass rod granuloma as first described by Vogel (1970) reflects the chronic proliferative inflammation. Of the newly formed connective tissue not only wet and dry weight, but also chemical composition and mechanical properties can be measured.

PROCEDURE

Glass rods with a diameter of 6 mm are cut to a length of 40 mm and the ends rounded off by flame melting. They are sterilized before implantation by boiling in water. Male Sprague-Dawley rats with an initial weight of 130 g are anaesthetized with ether, the back skin shaved and disinfected. From an incision in the caudal region a subcutaneous tunnel is formed in cranial direction with a closed blunted forceps. One glass rod is introduced into this tunnel finally lying on the back of the animal. The incision wound is closed by sutures. The animals are kept in separate cages. The rods remain *in situ* for 20 or 40 days. Treatment with drugs is either during the whole period or only during the last 10 or 2 days. At the end the animals are sacrificed under CO_2 anesthesia. The glass rods are prepared together with the surrounding connective tissue which forms a tube around the glass rod. By incision at one end the glass rod is extracted and the granuloma sac inverted forming a plain piece of pure connective tissue. Wet weight of the granuloma tissue is recorded. The specimens are kept in a humid chamber until further analysis. For measurement of the mechanical properties the specimens are fixed into the clamps of the Instron$^{(R)}$ instrument allowing a gauge length of 30 mm. The load until break is recorded with a crosshead speed of 50 mm/min. In order to calculate tensile strength (N/mm^2), the value of load at rupture (N) is divided by cross sectional area (measured as volume = wet weight divided by length). Finally, the granuloma tissue is dried and the dry weight is recorded. In addition, biochemical analyses, such as determination of collagen and glycosaminoglycans, can be performed.

EVALUATION

Several parameters can be determined by this method. Granuloma weight was reduced by corticosteroids depending on dose and time of administration and was also diminished after treatment with nonsteroidal anti-inflammatory agents and lathyrogenic compounds. Furthermore, antiproliferative terpenoids reduced the granuloma weight. The mechanical parameters showed different results after these drugs indicating a different mode of action. Treatment with corticosteroids increased tensile strength. Only after long term treatment with toxic doses a decrease was found. Anti-inflammatory compounds, such as acetylsalicylic acid or indomethacin and antiproliferative terpenoids showed an increase of strength at medium and high doses.

CRITICAL ASSESSMENT OF THE METHOD

In contrast to most other granuloma methods, the glass rod granuloma measures the late proliferative phase of inflammation. Since the newly formed connective tissue is not contaminated with the irritant biochemical analyses can be performed. The peculiar feature is the possibility to study the mechanical properties of newly formed proliferative connective tissue.

REFERENCES AND FURTHER READING

Vogel HG (1970) Das Glasstabgranulom, eine Methode zur Untersuchung der Wirkung von Corticosteroiden auf Gewicht, Festigkeit und chemische Zusammensetzung des Granulationsgewebes an Ratten. Arzneim Forsch/Drug Res 20:1911–1918

Vogel HG (1975) Collagen and mechanical strength in various organs of rats treated with d-penicillamine or amino-acetonitrile. Conn Tiss Res 3:237–244

Vogel HG (1977) Mechanical and chemical properties of connective tissue organs in rats as influenced by non-steroidal anti-rheumatic drugs. Conn Tiss Res 5:91–95

Vogel HG, De Souza NJ, D's A (1990) Effect of terpenoids isolated from Centella asiatica on granuloma tissue. Acta therapeut 16:285–298

H.3.3 Side Effects of Anti-inflammatory Compounds

See Vogel (2006).

REFERENCES AND FURTHER READING

Vogel SM (2006) Safety Pharmacology of Antiinflammatory Drugs. In: Vogel HG, Hock FJ, Maas J, Mayer D (eds) Drug Discovery and Evaluation – Safety and Pharmacokinetic Assays, Chapter I.K. Springer-Verlag, Berlin Heidelberg New York

H.4 Antipyretic Activity

H.4.0.1 General Considerations

Treatment with antipyretics has been very important in the pre-antibiotic era. Nevertheless, for treatment of acute viral diseases and for treatment of protozoal infections like malaria reduction of elevated body temperature by antipyretics is still necessary. For anti-

inflammatory compounds, an antipyretic activity is regarded as a positive side effect. To evaluate these properties, fever is induced in rabbits or rats by injection of lipopolysaccharides or Brewer's yeast.

H.4.0.2 Antipyretic Testing in Rats

PURPOSE AND RATIONALE

The subcutaneous injection of Brewer's yeast suspension is known to produce fever in rats. A decrease in temperature can be achieved by administration of compounds with antipyretic activity.

PROCEDURE

A 15% suspension of Brewer's yeast in 0.9% saline is prepared. Groups of 6 male or female Wistar rats with a body weight of 150 g are used. By insertion of a thermocouple to a depth of 2 cm into the rectum the initial rectal temperatures are recorded. The animals are fevered by injection of 10 ml/kg of Brewer's yeast suspension subcutaneously in the back below the nape of the neck. The site of injection is massaged in order to spread the suspension beneath the skin. The room temperature is kept at 22–24°C. Immediately after yeast administration, food is withdrawn. 18 h post challenge, the rise in rectal temperature is recorded. The measurement is repeated after 30 min. Only animals with a body temperature of at least 38°C are taken into the test. The animals receive the test compound or the standard drug by oral administration. Rectal temperatures are recorded again 30, 60, 120 and 180 min post dosing.

EVALUATION

The differences between the actual values and the starting values are registered for each time interval. The maximum reduction in rectal temperature in comparison to the control group is calculated. The results are compared with the effect of standard drugs, e. g. aminophenazone 100 mg/kg p.o. or phenacetin 100 mg/kg p.o.

CRITICAL ASSESSMENT OF THE METHOD

The antipyresis test in rats in can be regarded as a classical method in pharmacology.

MODIFICATIONS OF THE METHOD

Stitt and Shimada (1991), Shimada et al. (1994) induced fever in rats by microinjecting 20 ng PGE_1 directly into one of the brain's circumventricular organs of the rat known as the organum vasculosum laminae terminalis.

Luheshi et al. (1996) induced fever by intraperitoneal injection of 100 µ g/kg lipopolysaccharide into rats and measured the inhibition of fever by interleukin-1 receptor antagonist.

Telemetry has been used to record body temperature in animals (Riley et al. 1978; Gallaher et al. 1985; Clement et al. 1989; Guillet et al. 1990; Kluger et al. 1990; Bejanian 1991; Watkinson et al. 1996; Miller et al. 1997).

REFERENCES AND FURTHER READING

Bejanian M, Jones BL, Syapin PJ, Finn DA, Alkana RJ (1991) Brain temperature and ethanol sensitivity in mice: A radiotelemetric study. Pharmacol Biochem Behav 39:457–463

Brune K, Alpermann H (1983) Non-acidic pyrazoles: inhibition of prostaglandin production, carrageenan oedema and yeast fever. Agents Actions 13:360–363

Burn JH, Finney DJ, Goodwin LG (1950) Chapter XIV: Antipyretics and analgesics. In: Biological Standardisation, Oxford University Press, London, New York, pp 312–319

Clement JG, Mills P, Brockway B (1989) Use of telemetry to record body temperature and activity in mice. J Pharmacol Meth 21:129–140

Gallaher EJ, Egner DA, Swen J (1985) Automated remote temperature measurement in small animals using a telemetry/microcomputer interface. Comput Biol Med 15:103–110

Guillet MC, Molinié B, Laduron PM, Terlain B (1990) Effects of ketoprofen in adjuvant-induced arthritis measured in a new telemetric model test. Eur J Pharmacol 183:2266–2267

Inoue K, Fujisawa H, Sasaki Y, Nishimura T, Nishimura I, Inoue Y, Yokota M, Masuda T, Ueda F, Shibata Y, Kimura K, Inoue K, Komiya Y, Nishioka J (1991) Pharmacological properties of the new non-steroidal anti-inflammatory agent Etodolac. Arzneim Forsch/Drug Res 41:228–235

Kluger MJ, Carole AC, Franklin B, Freter R, Abrams BD (1990) Effect of gastrointestinal flora on body temperature of rats and mice. Am J Physiol 258:R552–R557

Loux JJ, DePalma PD, Yankell SL (1972) Antipyretic testing of aspirin in rats. Toxicol Appl Pharmacol 22:672–675Riley JL, Thursten JR, Egemo CL, Elliot HL (1978) A radiotelemetry transmitter for transmitting temperatures from small animals. J Appl Physiol 45:1016–1018

Luheshi G, Miller AJ, Brouwer S, Dascombe MJ, Rothwell NJ, Hopkins SJ (1996) Interleukin-1 receptor antagonist inhibits endotoxin fever and systemic interleukin-6 induction in the rat. Am J Physiol, Endocrinol Metab 270/1 33–1:E91–E95

Miller AJ, Hopkins SJ, Luheshi GN (1997) Sites of action of IL-1 in the development of fever and cytokine response to tissue inflammation in the rat. Br J Pharmacol 120:1274–1279

Roszkowski AP, Rooks WH, Tomolonis AJ, Miller LM (1971) Anti-inflammatory and analgesic properties of *d*-2-(6′-methoxy-2′-naphthyl)-propionic acid (NAPROXEN). J Pharmacol Exper Ther 179:114–123

Shimada SG, Otterness IG, Stitt JT (1994) A study of the mechanism of action of the mild analgesic dipyrone. Agents Actions 41:188–192

Smith PK, Hambourger WE (1935) The ratio of the toxicity of acetanilide to its antipyretic activity in rats. J Pharmacol Exp Ther 54:346–351

Stitt JT, Shimada SG (1991) Calcium channel blockers inhibit endogenous pyrogen fever in rats and rabbits. J Appl Physiol 71:951–955

Tanaka K, Shimotori T, Makino S, Aikawa Y, Inaba T, Yoshida C, Takano S (1992) Pharmacological studies of the new anti-inflammatory agent 3-formylamino-7-methylsulfonylamino-6-phenoxy-4H-1-benzopyran-4-one. 1st Communication: anti-inflammatory, analgesic and other related properties. Arzneim Forsch/Drug Res 42:935–944

Watkinson WP, Highfill JW, Slade R, Hatch GE (1996) Ozone toxicity in the mouse: comparison and modeling of responses in susceptible and resistant strains. J Appl Physiol 80:2134–2142

H.4.0.3 Antipyretic Testing in Rabbits

PURPOSE AND RATIONALE

Lipopolysaccharides from Gram-negative bacteria, e. g. *E. coli*, induce fever in rabbits after intravenous injection. Only lipopolysaccharide fractions are suitable, which cause after 60 min an increase of body temperature of 1°C or more at a dose between 0.1 and 0.2 µg/kg. In the rabbit, two maxima of temperature increases are observed. The first maximum occurs after 70 min, the second after 3 h.

PROCEDURE

Rabbits of both sexes and of various strains with a body weight between 3 and 5 kg can be used. The animals are placed into suitable cages and thermocouples connected with an automatic recorder are introduced into the rectum. The animals are allowed to adapt to the cages for 60 min. Then 0.2 ml/kg containing 0.2 µg lipopolysaccharide are injected intravenously into the rabbit ear. Sixty min later the test compound is administered either subcutaneously or orally. Body temperature is monitored for at least 3 h.

EVALUATION

A decrease of body temperature for at least 0.5°C for more than 30 min as compared with the temperature value before administration of the test compound is regarded as positive effect. This result has been found after 45 mg/kg phenylbutazone s.c. or 2.5 mg/kg indomethacin s.c.

CRITICAL ASSESSMENT OF THE METHOD

Measurement of body temperature in rabbits with polysaccharide induced fever is a more sensitive test than the yeast fever in rats. Furthermore, the method is used as a decisive test for the absence of pyrogens in parenteral drugs by several pharmacopoeias such as USP 23 (1955).

MODIFICATIONS OF THE METHOD

Cashin and Heading (1968) described a simple and reliable assay for antipyretic drugs in **mice**, using intracerebral injection of pyrogens.

Davidson et al. (1991) tested the effect of human recombinant lipocortin on the pyrogenic action of the synthetic polyribonucleotide polyinosini:polycytidylic acid in rabbits.

Yeast-induced pyrexia in **rats** has been used for antipyretic efficacy testing by Loux et al. (1982) and Cashin et al. (1977).

van Miert et al. (1977) studied the effects of antipyretic agents on fever and ruminal stasis induced by endotoxins in **conscious goats**.

Petrova et al. (1978) used turpentine-induced fever in rabbits to study antipyretic effects of dipyrone and acetylsalicylic acid.

Lee et al. (1985) studied the antipyretic effect of dipyrone on endotoxin fever of **macaque monkeys**.

Loza Garcia et al. (1993) studied the potentiation of chlorpromazine-induced hypothermia by the antipyretic drug dipyrone in anesthetized rats.

Shimada et al. (1994) studied the mechanism of action of the mild analgesic dipyrone preventing fever induced by injection of prostaglandin E_1 or interleukin-1β into the organum vasculosum terminalis of rat brain.

REFERENCES AND FURTHER READING

Cashin CH, Heading CE (1968) The assay for anti-pyretic drugs in mice, using intracerebral injection of pyretogenins. Br J Pharmacol 34:148–158

Cashin CH, Dawson W, Kitchen EA (1977) The pharmacology of benoxaprofen (2-[4-chlorophenyl]-α-methyl-5-benzoxazole acetic acid), LRCL 3794, a new compound with anti-inflammatory activity apparently unrelated to prostaglandin synthesis. J Pharm Pharmacol 29:330–336

Davidson J, Flower RJ, Milton AS, Peers SH, Rotondo D (1991) Antipyretic actions of human recombinant lipocortin-1. Br J Pharmacol 102:7–9

Deeter LB, Martin LW, Lipton JM (1989) Antipyretic effect of central α-MSH summates with that of acetaminophen or ibuprofen. Brain Res Bull 23:573–575

Lee TF, Mora F, Myers RD (1985) Effect of intracerebroventricular vasopressin on body temperature and endotoxin fever of macaque monkey. Am J Physiol 248:R674–R678

Loza Garcia MI, Baamonde Arbaiza A, Hidalgo Balsera A, Andres-Trelles F (1993) Potenciación por dipirona (metamizol) magnésica y dipirona sódica de la hipotermia producida por chlorpromazina en rata anestesiada. An Real Acad Farm 59:181–190

Matuszek M, Szreder Z, Korolkiewicz Z (1990) The antipyretic effect of some newer alpha-1 antagonists. Eur J Pharmacol 183:2279–2280

Petrova L, Nikolova M, Nikolov R, Stefanova D (1978) Dipyrone and acetylsalicylic acid comparative pharmacological research. Antipyretic, anti-inflammatory and analgesic

action. In: Ovtcharov R, Pola W (eds) Proceedings Dipyrone. Moscow Symposium, Schattauer-Verlag, Stuttgart New York, pp 99–107

Shimada SG, Otterness IG, Stitt JT (1994) A study of the mechanism of action of the mild analgesic dipyrone. Agents Actions 41:188–192

Szeder Z (1990) Comparison of the effect of prazosin with that of dihydrobenzperidol and nifedipine on thermoregulatory responses produced by pyrogen in rabbits. Gen Pharmacol 21:833–838

Szreder Z, Korolkiewicz Z (1991) Inhibition of pyrogen *Escherichia coli* fever with intracerebral administration of prazosin, dihydrobenzperidol and nifedipin in the rabbits. Gen Pharmacol 22:381–388

USP 23 (1995) Pyrogen test. The United States Pharmacopeia 23, p 1718

van Miert ASJPAM, van Essen JA, Tromp GA (1972) The antipyretic effect of pyrazolone derivates and salicylates on fever induced with leukocytic or bacterial pyrogen. Arch int Pharmacodyn 197:388–391

van Miert ASJPAM, van der Wal-Komproe, van Duin CTM (1977) Effects of antipyretic agents on fever and ruminal stasis induced by endotoxins in conscious goats. Arch Int Pharmacodyn 225:39–50

Zimecki M, Schnaper HW, Wieczorek Z, Webb DR, Pierce CW (1990) Inhibition of interleukin 1 (IL-1)-elicited leukocytosis and LPS-induced fever by soluble immune response suppressor (SIRS). Immunopharmacol 19:39–46

Chapter I
Antiarthrotic and Immunomodulatory Activity[1]

[1] With contributions to this and former editions by A. Huwiler, R.X. Raiss, R.R. Bartlett, and R. Schleyerbach.

I.1 Anti-Arthrotic Activity

I.1.0.1 General Considerations

Multifactorial causes can lead to osteoarthritis (OA), and its pathogenesis is not clearly understood as yet. The main characteristics of OA are the slowly progressing deterioration of the articular cartilage, accompanied by intermitted painful inflammatory episodes, and a continuous subchondral bone remodeling, often resulting in osteophyte formation in non-weight-bearing joint areas. Because of the lack of innervation and vascularization of cartilage, the destruction of this specific tissue remains unnoticed until other joint compartments are involved such as synovial membranes, answering with reactive synovitis to cartilage debris, or mechanoreception changes in the underlying bone, or until the diminution of articular cartilage results in a radiographically detectable joint space narrowing.

Therefore, analgesic and anti-inflammatory therapy has been the major treatment for OA in the past, and NSAIDs still constitute 92% of the drugs used against OA. Intraarticular injections of corticosteroids are also applied, although with geographically variable emphasis. Nevertheless they are still considered a useful tool in severe cases. Both classes of drugs are now reviewed more carefully with regard to their potentially harmful effects on cartilage maintenance and chondrocyte function – which leads to a more critical approach in drug selection. So-called 'chondroprotective' drugs, mainly sulfated polysaccharides, played a certain role in the pharmacotherapy of OA in Central Europe and some Eastern countries, but failed to demonstrate clinical efficacy, and now have lost significance.

Anti-oxidative enzymes or drugs such as superoxide dismutase or diacerein are also considered to influence osteoarthritic conditions. Recently, matrix metalloprotease-inhibitors (MMP-I), originally designed to inhibit tumor cell invasion, have shown promising results in counteracting the progressive enzymatic cartilage degradation, and some compounds are being developed for this indication. A further treatment gaining interest are derivatives of hyaluronic acid, which are applied intra-articularly in a series of injections. Their mechanism, however, is not clear yet, and most preparations have been filed as 'devices' rather than 'drugs', claiming a viscosupplementation with anti-inflammatory, analgesic, and chondroprotective properties.

I.1.1 In Vitro Methods for Anti-Osteoarthritic Activity

I.1.1.1 General Considerations

Since most of the drugs in use for OA were originally selected for other (e. g. arthritic) indications and only subsequently claimed to be effective in OA, they have not been primarily selected and optimized by *in vitro* assays specific for this condition. Thus, the indication lacks commonly agreed upon *in vitro* assays as well as clearly defined standard drugs to evaluate such models. Correspondingly, the variety of assay systems used to test compounds for their effect on cartilage maintenance and/or degradation is large, and the list below reflects this multitude.

The *in vitro* systems applied to assess drug effects upon chondrocytes range from homogenates of cartilage (Yu et al. 1991; Vignon et al. 1991; Zafarullah et al. 1992) over chondrocyte monolayers at different culture conditions and passages, suspensions of aggregated chondrocytes or clusters, cells cultured in or over an artificial matrix like agarose to cartilage explants and even organ cultures (Korver et al. 1989) like mouse patellas (Verschure et al. 1994). The species used in these studies vary over an equally wide range from mouse (Mohamed-Ali 1992), rat (Ismaiel et al. 1991; Seed et al. 1993; Seong et al. 1994; Srinivas et al. 1994), rabbit (Akatsuka et al. 1993; Collier, Ghosh 1991; Shimazu et al. 1993), dog (Venn et al. 1990), cattle, to human tissues (Bulstra et al. 1992; Green et al. 1995) derived from normal as well as osteoarthritic conditions. The chondrocyte and cartilage explant culture systems used for several years are described in more detail below with special emphasis on comparability and standardization.

PURPOSE AND RATIONALE

Articular chondrocytes not only control the regular balance of matrix synthesis and degradation in healthy cartilage turnover, but are also regarded as key players in the enhanced degradation and finally reduced synthesis of matrix components in pathological conditions like OA. The two main cartilage constituents are col-

lagen type II fibrillar network, and proteoglycans attached to hyaluronic acid filaments, also termed aggrecans. The latter are the more sensitive and the first ones to change in cartilage degradation. Therefore, the *in vitro* assays are performed mainly with chondrocytes, and the parameters measured focus on proteogly can synthesis and/or degradation.

The exact mechanisms of cartilage pathophysiology are not yet elucidated, but enzymatic degradation involving metallo-proteinases are considered the main events. *In vitro*, interleukin-1 and retinoic acid induce enhanced matrix degradation as well as reduced matrix synthesis, as observed in OA. Their role in the actual disease process *in vivo*, however, remains obscure. They therefore are used rather as tools to induce a disease-relevant condition *in vitro* than being subject of direct pharmacological intervention. Thus, the *in vitro* assays described here are suitable to compare and select a variety of drugs for their effect upon the main biological activity of articular chondrocytes. To address the respective mechanisms of drug action, more specific follow-up assays like enzyme inhibition or cytokine release or inhibition tests should be applied.

REFERENCES AND FURTHER READING

Akatsuka M, Yamamoto Y, Tobetto K, Yasui T, Ando T (1993) *In vitro* effects of hyalurononan on prostaglandin E_2 induction by interleukin-1 in rabbit articular chondrocytes. Agents Actions 38:122–125

Bulstra SK, Kuijer R, Buurman WA, Terwindt-Rouwenhorst E, Guelen PJM, van der Linden AJ (1992) The effect of piroxicam on the metabolism of isolated human chondrocytes. Clin Orthop 277:289–296

Collier S, Ghosh P (1991) Comparison of the effects of nonsteroidal anti-inflammatory drugs (NSAIDs) on proteoglycan synthesis by articular cartilage explant and chondrocyte monolayer cultures. Biochem Pharmacol 41:1375–1384

Green GD, Chipman SD, Birkhead JR, Troubetskoy OV, Goldring MB (1995) Interleukin-1 modulation of matrix metalloprotease and proteoglycan expression in human chondrocytes immortalized by simian virus 40. Trans Orthop Res Soc 20:334

Ismaiel S, Hollander AP, Atkins RM, Elson CJ (1991) Differential responses of human and rat cartilage to degrading stimuli *in vitro*. J Pharm Pharmacol 43:207–209

Korver GHV, van de Stadt RJ, van Kampen GPJ, Kiljan E, van der Korst JK (1989) Bovine sesamoid bones: a culture system for anatomically intact articular cartilage. *In vitro* Cell Dev Biol 25:1099–1106

Mohamed-Ali H (1992) Influence of synovial cells on cartilage *in vitro*: induction of breakdown and inhibition of synthesis. Virchows Archiv B Cell Pathol 62:227–236

Seed MP, Ismaiel S, Cheung CY, Thomson TA, Gardner CR, Atkins RM, Elson CJ (1993) Inhibition of interleukin 1β induced rat and human cartilage degradation *in vitro* by the metalloproteinase inhibitor U27391. Ann Rheum Dis 52:37–43

Seong SC, Matsumura T, Lee FY, Whelan MC, Li XQ, Trippel SB (1994) Insulin-like growth factor I regulation of swarm rat chondrosarcoma chondrocytes in culture. Exp Cell Res 211:238–244

Shimazu A, Jikko A, Iwamoto M et al (1993) Effects of hyaluronic acid on the release of proteoglycan from the cell matrix in rabbit chondrocyte cultures in the presence and absence of cytokines. Arthr Rheum 36:247–253

Srinivas GR, Chichester CO, Barrach HJ, Matoney AL (1994) Effects of certain antiarthritic agents on the synthesis of type II collagen and glycosaminoglycans in rat chondrosarcoma cultures. Agents and Actions 41:193–199

Venn G, Lauder RM, Hardingham TE, Muir H (1990) Effects of catabolic and anabolic cytokines on proteoglycan biosynthesis in young, old and osteoarthritic canine cartilage. Biochem Soc Trans 18:973–974

Verschure PJ, van der Kraan PM, Vitters EL, van den Berg WB (1994) Stimulation of proteoglycan synthesis by triamcinolone acetonide and insulin-like growth factor 1 in normal and arthritic murine articular cartilage. J Rheumatol 21:920–926

Vignon E, Mathieu P, Louisot P, Richard M (1991) *In vitro* effect of nonsteroidal antiinflammatory drugs on proteoglycanase and collagenase activity in human osteoarthritic cartilage. Arthr and Rheum 34:1332–1335

Yu LP Jr, Smith GN Jr, Hasty KA, Brandt KD (1991) Doxycycline inhibits type XI collagenolytic activity of extracts from human osteoarthritic cartilage and of gelatinase. J Rheumatol 18:1450–1452

Zafarullah M, Martel-Pelletier J, Cloutier JM, Gedamu L, Pelletier JP (1992) Expression of c-fos, c-jun, jun-B, metallothionein and metalloproteinase genes in human chondrocyte. FEBS 306:169–172

I.1.1.2 Modulation of Cellular Proteoglycan Metabolism

PURPOSE AND RATIONALE

In primary cultures, articular chondrocytes grown in an artificial matrix after digestion of the original bone, maintain their characteristic synthesis and turnover rate of cartilage matrix macromolecules for a long time. These metabolic processes can be influenced pharmacologically. In the following assay, compounds are tested for their effect upon the normal turnover of cartilage matrix by chondrocytes. The test is used to detect stimulation of matrix formation, but also to check for potential impairment of cartilage function. Specific matrix staining reveals the amount of newly formed matrix remaining around the cells at the end of treatment. Alternatively, incorporation of radiolabeled sulfate into the newly formed proteoglycans allows to quantitate the anabolic activity at the end of the experiment.

PROCEDURE

Reagents

A 1% (w/v) solution of Pronase from Boehringer in Ham's F12 is prepared, filtered under sterile conditions, and supplemented with 10% FCS.

A 0.025% (w/v) solution of Collagenase type II, activity 242 U/mg, from Worthington, corresponding to an activity of 6 U/ml in Ham's F12 is prepared, filtered under sterile conditions, and supplemented with 10% FCS.

Hank's balanced salt solution (HBSS) is obtained from Biochrome.

Ham's F12 is supplemented with 50 µg/ml gentamycine and 2.5 µg/ml amphotericin B.

A sterile stock solution of 5 mg/ml ascorbic acid in Ham's F12 is prepared, and aliquots are stored at –20°C.

A 2% solution of low melting agarose from Seaplaque in 0.9% NaCl is prepared by heating in a microwave, and stored in a water bath at about 50°C.

A buffer of 25 mM sodium-acetate (2.051 g/l) with 0.4 M magnesium-chloride 6-hydrate (81.32 g/l) is prepared, and adjusted with acetic acid to pH 5.6.

A staining solution is prepared with 0.1 g of alcian-blue, obtained from Sigma, in 67.5 ml buffer, filtered, and supplemented with 10 ml of a 25% solution of glutaraldehyde.

An 8 M guanidinium-hydrochloride solution is prepared.

Tissue and Cell Preparation

Fetlocks of freshly slaughtered steers (age 18 to 20 months) are skinned and the metacarpo-phalangeal joint opened under semi-sterile conditions. With a sterile scalpel, articular cartilage is then carefully removed from the underlying bone from all accessible cartilaginous regions and transferred into a sterile Ham's F12 solution at +4°C. The tissue is washed with Ham's F12 to remove adherent synovial fluid. The pieces are then transferred into a 150 ml trypsinizing flask, containing the pronase solution including the added serum, and incubated with gentle stirring for 1 h at 37°C and 95% humidity. The fluid is then removed, and the collagenase solution including the added serum is incubated with gentle stirring overnight. The resulting cell suspension is first filtered through a 90 µm and then a 50 µm Nylon filter and then centrifuged at 800 rpm for 10 min. Resuspension and washing is performed with HBSS and cells are counted and checked for vitality under the microscope using the Eosin staining. The vitality level should reach at least 95%. A cell suspension is prepared of 4×10^6 cells/ml Ham's F12 supplemented with 20% FCS.

To prepare the agarose cell cultures, 24 well plates are coated with 0.2 ml/well of a 1:1 mixture of the 2% agarose solution with preheated Ham's F12 and left at room temperature to gel. Then 0.1 ml/well (0.2 ml/well for radiolabeling) of a 1:1 mixture of the above described cell suspension with the 2% agarose solution is added. Care has to be taken to maintain an even cell suspension, and not to overheat the cells during this procedure. After gel formation at room temperature, the multiwell plates are placed in the incubator, and 0.5 ml/well medium is added either 4 h later or the following day. The medium consists of Ham's F12 supplemented with 5% FCS and 25 µg/ml ascorbic acid, and is changed every second day.

Assay

The assay starts 5 days after cell preparation. Compounds are added to the medium in a final concentration of 10 µM with 6 to 8 replicae per compound, and added anew with each change of medium over a total period of 8 days. The concentration can be varied according to the expected potency of the drug studied. An untreated control group as well as standard compound groups are always included. As standard compound, pentosane polysulfate to check for matrix increase, or retinoic acid to cause matrix decrease, can be applied.

At the end of treatment, the medium is removed, the wells washed 3× with 500 µl of medium without supplements, and 1 ml/well of the staining solution is added for 48 h. After removal of the supernatant, the following washing steps are performed for 10 min each:

- 3 × 500 µl/well 3% acetic acid,
- 1 × 500 µl/well 3% acetic acid in 25% ethanol,
- 2 × 500 µl/well 50% ethanol,
- 1 × 500 µl/well 70% ethanol.

With 500 µl/well of 8 M guanidinium hydrochloride solution, the bound stain is then extracted for 24 h at +4°C. After shaking the plates gently for 10 min, 100 µl/well of each supernatant is then transferred to round-bottom microtiter-plates, and the extinction photometrically assessed in the plate-reader at a wavelength of 610 nm.

EVALUATION

The extinction is expressed in percentage as staining density with the control values defined as 100%. Values $\geqslant 110\%$ are interpreted as stimulation of matrix formation, values lower than 80% as inhibition of matrix formation. Experiments with 8 wells/treatment usually exhibit a standard deviation below 7%.

CRITICAL ASSESSMENT OF THE TEST

The described method is suitable to compare up to 50 drugs in one experiment. The price for this is the limited quantification, as the staining is not strictly stoichiometric, and does not allow the distinction between matrix synthesis and degradation. For more detailed assessment, radiolabeling is the better choice. The limitation of these primary culture assays lies in the elaborate preparation and isolation of the chondrocytes. Several attempts to immortalize this differentiated mesenchymal cell type have resulted in the loss of cartilage-specific properties. A new cell line developed by MB Goldring (Green et al. 1995) might overcome this difficulty, but has not yet been reported to be modified pharmacologically.

MODIFICATIONS OF THE TEST

The agarose culture system for chondrocytes, originally described by Benya and Schaffer (1982), has been well characterized by Aydelotte et al. (1988, 1992), and the effects of different agarose densities have been studied by Verbruggen et al. (1990).

Instead of agarose gel cultures, some authors use 3D chondrocyte clusters in suspension (Bassleer et al. 1990, 1992; Henrotin et al. 1992), or suspensions over agarose (Archer et al. 1990), or embedded in collagen gels (Malemud et al. 1994).

Alternatively, encapsulation in alginate beads, either directly after isolation (Guo et al. 1989), even as primary culture for several months (Häuselmann et al. 1994), or after expansion in monolayers (Bonaventure et al. 1994), offers the opportunity to recover the chondrocytes later by depolymerization of the alginate.

Monolayers of articular chondrocytes can be used as well, but preferentially short-term (up to three days of culture), as under this culture condition chondrocytes tend to dedifferentiate to a fibroblast-like appearance and metabolic program. Authors using this modification are e. g. Kolibas, Goldberg (1989), Lane et al. (1992), and McCollum et al. (1991). The importance of culture conditions is addressed in the study by Seid et al. (1993), and that of culture duration in the paper by van der Kraan et al. (1992).

A dot blot assay by cuprolinic blue precipitation has been described by Jortikka et al. (1993), which is restricted to serum free conditions. Instead of matrix staining, radiolabeling can be applied as described in the next assay. In this case, the amount of cells should be doubled per well to assure sufficient label incorporation.

REFERENCES AND FURTHER READING

Archer CW, McDowell J, Bayliss MT, Stephens MD, Bentley G (1990) Phenotypic modulation in sub-populations of human articular chondrocytes *in vitro*. J Cell Sci 97:361–371

Aydelotte MB, Kuettner KE (1988) Differences between subpopulations of cultured bovine articular chondrocytes. I. Morphology and cartilage matrix production. Conn Tiss Res 18:205–222

Aydelotte MB, Greenhill RR, Kuettner KE (1988) Differences between sub-populations of cultured bovine articular chondrocytes. II. Proteoglycan metabolism. Conn Tiss Res 18:223–234

Aydelotte MB, Raiss RX, Caterson B, Kuettner KE (1992) Influence of interleukin-1 on the morphology and proteoglycan metabolism of cultured bovine articular chondrocytes. Conn Tiss Res 28:143–159

Bassleer C, Henrotin Y, Franchimont P (1990) *In vitro* assays of chondrocyte functions: the influence of drugs and hormones. Scand J Rheumatology (Suppl 81):13–20

Bassleer CT, Henrotin YE, Reginster JYL, Franchimont PP (1992) Effects of tiaprofenic acid and acetylsalicylic acid on human articular chondrocytes in 3-dimensional culture. J Rheumatol 19:1433–1438

Benya PD, Schaffer JD (1982) Dedifferentiated chondrocytes reexpress the differentiated collagen phenotype when cultured in agarose gels. Cell 30:215–224

Bonaventure J, Kadhom N, Cohen-Solal L, Ng KH, Bourguignon J, Lasselin C, Freisinger P (1994) Reexpression of cartilage-specific genes by dedifferentiated human articular chondrocytes cultured in alginate beads. Exp Cell Res 212:97–104

Greiling H, Gressner AM, Stuhlsatz HW (1977) Influence of anti-inflammatory drugs on connective tissue metabolism. In: Glynn LE, Schlumberger HD (eds) Experimental Models of Chronic Inflammatory Diseases. Springer-Verlag, Berlin Heidelberg New York, pp 406–420

Guo J, Jourdian GW, MacCallum DK (1989) Culture and growth characteristics of chondrocytes encapsulated in alginate beads. Conn Tiss Res 19:277–297

Häuselmann HJ, Fernandes RJ, Mok SS, Schmid TM, Block JA, Aydelotte MB, Kuettner KE, Thonar EJMA (1994) Phenotypic stability of bovine articular chondrocytes after long-term culture in alginate beads. J Cell Sci 107:17–27

Henrotin Y, Bassleer C, Franchimont P (1992) *In vitro* effects of etodolac and acetylsalicylic acid on human chondrocyte metabolism. Agents and Actions 36:317–323

Jortikka M, Lammi MJ, Parkkinen JJ, Lahtinen R, Tammi MI (1993) A high sensitivity dot-blot assay for proteoglycans by cuprolinic blue precipitation. Conn Tiss Res 29:263–272

Kolibas LM, Goldberg RL (1989) Effect of cytokines and antiarthritic drugs on glycosaminoglycan synthesis by bovine articular chondrocytes. Agents and Actions 27:245–249

Lane NE, Williams III RJ, Schurman DJ, Smith RL (1992) Inhibition of interleukin 1 induced chondrocyte protease activity by a corticosteroid and a nonsteroidal antiinflammatory drug. J Rheumatol 19:135–139

Malemud CJ, Stevenson S, Mehraban F, Papay RS, Purchio AF, Goldberg VM (1994) The proteoglycan synthesis repertoire of rabbit chondrocytes maintained in type II collagen gels. Osteoarthritis and Cartilage 2:29–42

McCollum R, Martel-Pelletier J, DiBattista J, Pelletier JP (1991) Regulation of interleukin 1 receptors in human articular chondrocytes. J Rheumatol (Suppl 27) 18:85–88

Seid JM, Rahman S, Graveley R, Bunning RAD, Nordmann R, Wishart W, Russel RG (1993) The effect of interleukin-1 on cytokine gene expression in cultured human articular chon-

drocytes analyzed by messenger RNA phenotyping. Arthritis and Rheumatism 36:35–43
van der Kraan P, Vitters E, van den Berg W (1992) Differential effect of transforming growth factor β on freshly isolated and cultured articular chondrocytes. J Rheumatol 19:140–145
Verbruggen G, Veys EM, Wieme N, Malfait AM, Gijselbrecht L, Nimmegeers J, Almquist KF, Broddelez C (1990) The synthesis and immobilisation of cartilage-specific proteoglycan by human chondrocytes in different concentrations of agarose. Clin Exp Rheumatol 8:371–378

I.1.1.3 Cellular Chondrocytic Chondrolysis

PURPOSE AND RATIONALE

In this assay a disease-relevant situation is achieved by adding interleukin-1 (IL-1) to articular chondrocytes grown in agarose gel. IL-1 suppresses proteoglycan (PG) synthesis as well as increases their degradation, and thus results in a process which is also observed in degradative joint diseases *in vivo*. This process is termed chondrocytic chondrolysis. The test is used to detect the potential interference of a drug with this pathological process. Effect upon PG synthesis is studied by radiolabeling at the end of the experiment, and measuring the amount of incorporated sulfate. The effect upon PG degradation, and its release from the cellular environment, can be examined by prelabeling with $Na_2{}^{35}SO_4$, and following the amount of released incorporated sulfate over time from the supernatant with each or every second medium change.

PROCEDURE

Reagents

A 1% (w/v) solution of Pronase from Boehringer in Ham's F12 is prepared, filtered under sterile conditions, and supplemented with 10% FCS.

A 0.025% (w/v) solution of Collagenase type II, activity 242U/mg, from Worthington, corresponding to an activity of 6 U/ml in Ham's F12 is prepared, filtered under sterile conditions, and supplemented with 10% FCS.

Hank's balanced salt solution (HBSS) is obtained from Biochrome.

Ham's F12 is supplemented with 50 µg/ml gentamycin and 2.5 µg/ml amphotericin B.

A sterile stock solution of 5 mg/ml ascorbic acid in Ham's F12 is prepared, and aliquots are stored at –20°C.

A 2% solution of low melting Agarose from Seaplaque in 0.9% NaCl is prepared under heating and microwave application, and stored in a water bath at about 50°C.

Human recombinant interleukin-1 (IL-1)α or β from Genzyme is stored in aliquots at –20°C.

For radiolabeling, $Na_2{}^{35}SO_4$is purchased from Amersham.

A 4 M and 8 M guanidinium-hydrochloride (GuHCl) solution is prepared.

Tissue and Cell Preparation

Tissue and cell preparations are performed as for the previous assay, except the initial number of cells/well should be 400000, corresponding to a cell-containing gel volume of 0.2 ml/well, and the medium added is supplemented with 10% FCS and 25 µg/ml ascorbic acid. It is changed every second day.

Assay

The assay starts 6 days after cell preparation. Except for a control group, interleukin-1α is added in a concentration of 3 U/well, and added anew with each consecutive medium change. Except for the IL-1-control group, compounds are added to the medium in a final concentration of 10 µM with 4 replicae per compound, and with the subsequent medium changes. The concentration can be varied according to the expected potency of the drug studied. At the end of an 8 day treatment, the medium is replaced by medium containing 1 µCi $Na_2{}^{35}SO_4$/well and incubated for 24 h. The supernatant is then removed, mixed 1:1 with 8 M GuHCl, and separated with a PD10-Sephadex column into free versus incorporated sulfate. The multiwell plates with the remaining gels are deep frozen for at least 24 h to facilitate solubilization, thawed and then extracted with 500 µl/well 8 M GuHCl supplemented with inhibitors. The content of each well is then centrifuged at 13,000 rpm for 30 min. After this step, the supernatant contains the matrix trapped around the cells. This is equally separated by a PD10 Sephadex column into free versus incorporated radiolabel. The probes containing the incorporated sulfate and derived from both fractions (medium and gel) are then mixed with scintillating fluid and assessed in a β-scintillation counter.

EVALUATION

Counts per minute (cpm) from medium and gel fraction are calculated and related to the total well content. They are added if total incorporation is measured, or left separately, in case the ratio between released versus retained label is of interest. The data are converted into percent incorporation, with the values of the untreated control group or those of the IL-1 control group serving as 100%.

CRITICAL ASSESSMENT OF THE TEST

This is a sensitive test, in which an adequate labeling protocol can provide detailed information. The time- and material-consuming separation of free from incorporated radiolabel at the end, however, limits the size of the experiments and number of compounds to be studied.

In both cellular tests drug effects should be checked for (anti)proliferative activity in a separate proliferation test.

MODIFICATIONS OF THE TEST

If the catabolic response to a drug is of more interest than the anabolic one, the radiolabeling can be shifted to a time point prior to treatment, and the release of incorporated sulfate into the supernatant will allow to follow the time course and amount of PG degradation. This prelabeling should not start earlier than 4 days after plating to assure a comparable matrix synthesis rate. Because IL-1 suppresses PG synthesis at a lower concentration than it stimulates its degradation, a double to triple amount of IL-1 should be used in this modification.

Instead of bovine, human chondrocytes can be used (Raiss et al. 1992). One should allow 4 days of adjustment in the agarose system before starting treatment with human cells. If available, human serum gives a higher PG synthesis rate than fetal calf serum (Oestensen et al. 1991). The heterogeneity of responses depends on the individual source and should be considered (Verbruggen et al. 1989).

When using human instead of bovine cells, the stimulation of degradation and inhibition of synthesis is more effective with IL-1β than IL-1α: a concentration of 0.1 U/ml results in a reduction of PG synthesis of ca 50% (Raiss et al. 1995). When incubating with radiolabeled sulfate, the exposure time should be doubled to 48 h to yield sufficient incorporation.

To exclude direct interference of a drug with interleukin-1, all-trans retinoic acid can be used instead of this cytokine.

REFERENCES AND FURTHER READING

Aydelotte MB, Schleyerbach R, Zeck BJ, Kuettner KE (1986) Articular chondrocytes cultured in agarose gel for study of chondrocytic chondrolysis. In: Kuettner (ed) Articular Cartilage Biochemistry. Raven Press, New York, pp 235–256

Oestensen M, Veiby OP, Raiss R, Hagen A, Pahle J (1991) Responses of normal and rheumatic human articular chondrocytes cultured under various experimental conditions in agarose. Scand J Rheumatol 20:172–182

Raiss RX, Oestensen M, Aydelotte MB (1992) Drug evaluation on isolated articular chondrocytes. In: Kuettner K et al (eds) Articular Cartilage and Osteoarthritis, Raven Press Ltd., New York, pp 569–582

Raiss RX, Karbowski A, Aigner T, Schleyerbach R (1995) Chondrocytes and antirheumatic drugs. J Rheumatol (Suppl 43) 22:152–154

Verbruggen G, Veys EM, Malfait AM, Schatteman L, Wieme N, Heynen G, Vanhoutte V, Broddelez C (1989) Proteoglycan metabolism in isolated chondrocytes from human cartilage and in short-term tissue-cultured human articular cartilage. Clin Exp Rheumatol 7:13–17

I.1.1.4 Cartilage Explant Chondrolysis

PURPOSE AND RATIONALE

Chondrocytes vary in their metabolic activity and cytokine response depends on the relative location within the joint (surfacial vs deep, weight-bearing vs non-weight-bearing, etc). Therefore, the cellular assays are a homogeneous mixture of an otherwise heterogeneous cell population. Two reasons suggest a verification of the cellular results obtained in tissue culture assays: First, chondrocytes are more reactive after isolation compared to those in tissue culture, which may lead to false positive results. Second, intact cartilage matrix acts as barrier for certain compounds of high molecular size and fixed charge, so that they may not reach their target cells. Therefore, explant assays are recommended as a follow-up to the cellular tests.

PROCEDURE

Reagents

Ham's F12 medium is supplemented with 50 µg/ml gentamycin and 2.5 μ g/ml amphotericin B.

A sterile stock solution of 5 mg/ml ascorbic acid in Ham's F12 is prepared, and aliquots are stored at –20°C.

Human recombinant interleukin-1 (IL-1)α or β from Genzyme is stored in aliquots at –20°C.

For radiolabeling, $Na_2{}^{35}SO_4$ is purchased from Amersham.

A 4 M and 8 M guanidinium-hydrochloride (GuHCl) solution is prepared.

Tissue Preparation

Fetlocks of freshly slaughtered steers (age 18 to 20 months) are skinned and the metacarpo-phalangeal joint opened under semi-sterile conditions. With a sterile punch (as used for obtaining skin biopsies) full thickness disks of cartilage are obtained from all accessible cartilaginous areas and their wet weight is assessed. In each well, 1 ml of medium is added, consisting of Ham's F12 supplemented with 10% FCS and 25 µg/ml ascorbic acid, and approximately 30 mg wet

weight of cartilage are transferred corresponding to 3 discs of 4 mm diameter.

Assay

The assay is started 1 to 2 days after tissue preparation. Except for a control group, interleukin-1α is added in a concentration of 8 U/well, and with each of the following medium changes (every second day). Except for an IL-1-control group, compounds are added to the medium in a final concentration of 10 µM with 6 to 8 replicae per compound, which are also added with each medium change. The concentration can be varied according to the expected potency of the drug studied. At the end of an 8 day treatment, the medium is replaced by a medium containing 15 µCi $Na_2{}^{35}SO_4$/well and incubated for 24 h. The supernatant is removed, mixed 1:1 with 8 M GuHCl, and separated with a PD10-Sephadex column into free versus incorporated sulfate. The explants are washed three times with Ham's F12 at +4°C, and extracted with 1 ml/well 4 M GuHCl supplemented with inhibitors for 48 h, and then a second time with 0.5 ml/well for 24 h. Both fractions are mixed, and separated with a PD10 Sephadex column into free versus incorporated sulfate. The samples containing the incorporated sulfate derived from medium as well as explant extraction are then mixed with scintillating fluid and assessed in a β-scintillation counter.

EVALUATION

Counts per minute (cpm) from medium and explant fractions are calculated related to mg wet weight of cartilage of the respective wells. They are either added if total incorporation is measured, or left separately, in case the ratio between released versus retained matrix is of interest. The data are converted into percent incorporation in comparison with the values of the untreated control or of the IL-1 control group serving as 100%.

CRITICAL ASSESSMENT OF THE TEST

Punched discs of similar size standardize the surface/volume ratio, and give more reproducible results than chips of cartilage obtained by scalpel dissection. A disadvantage is the greater amount of cartilage needed, which makes it unsuitable for human tissue obtained from joint replacement surgery. When using human tissue, interpretation and comparison of results should be restricted to the same source: striking differences occur between specimens from surgery or postmortem, between different joints (hip vs knee), and different ages of the donor (young or adolescent vs 35 years and older), as well as different stages of severity and the duration of degenerative joint diseases in cases of surgical specimens.

MODIFICATIONS OF THE TEST

The effect of serum concentrations on proteoglycan synthesis has been studied by McQuillen et al. (1986), and the effect of different concentrations of DMSO and glycerol, of importance for cryopreservation, has been examined on human fetal hip cartilage by Yang and Zhang (1991).

Some authors (Nixon et al. 1991) use bovine nasal septum as cartilage source, but the convenient homogeneity and mass of this tissue is outweighed by a matrix composition and biomechanical properties clearly distinct from articular cartilage.

Several authors use human cartilage from joint replacement surgery (e. g. Pelletier et al. 1989; Pelletier, Martel-Pelletier 1989), and some compare drug effects upon visually normal cartilage to those with fibrillated or osteoarthritic cartilage (Lafeber et al. 1992, 1993; Verbruggen et al. 1989, 1990).

A step towards organ culture represents the culture of full thickness cartilage with subchondral bone, cultured for 24 h on moist lens tissue (Chayen et al. 1994).

Bordji et al. (2000) published evidence for the presence of peroxisome proliferator-activated receptor (PPAR) α and γ and retinoid Z receptor in cartilage.

Bondeson et al. (2006) established a model of cultures of synovial cells from digested osteoarthritis synovium derived from patients undergoing knee or hip arthroplasties.

REFERENCES AND FURTHER READING

Bondeson J, Wainwright SD, Lauder S, Amos N, Hughes CE (2006) The role of synovial macrophages and macrophage-produced cytokines in driving aggrecanases, matrix metalloproteinases, and other destructive and inflammatory responses in osteoarthritis. Arthritis Res Ther 8:R187

Bordji K, Grillasca JP, Gouze JN, Magdalou J, Schohn H, Keller JM, Bianchi A, Dauça M, Netter P, Terlain B (2000) Evidence for the presence of peroxisome proliferator-activated receptor (PPAR) α and γ and retinoid Z receptor in cartilage. J Biol Chem 275:12243–12250

Chayen J, Bitensky L, Mehdizadeh S, Dunham J, Older J (1994) Testing drugs on human osteoarthritic articular cartilage. Cell Biochem Funct 12:63–68

Lafeber FPG, van Roy H, Wilbrink B, Huber-Bruning O, Bijlsma JWJ (1992) Human osteoarthritic cartilage is synthetically more active but in culture less vital than normal cartilage. J Rheumatol 19:123–129

Lafeber FPJG, van der Kraan PM, van Roy JLAM, Huber-Bruning O, Bijlsma JWJ (1993) Articular cartilage explant culture; an appropriate *in vitro* system to compare osteoarthritic and normal human cartilage. Conn Tiss Res 29:287–299

McQuillan DJ, Handley CJ, Robinson HC (1986) Control of proteoglycan biosynthesis. Biochem J 237:741–747
Nixon JS, Bottomley KMK, Broadhust MJ et al (1991) Potent collagenase inhibitors prevent interleukin-1-induced cartilage degradation *in vitro*. Int J Tiss Reac 13:237–243
Pelletier JP, Martel-Pelletier J (1989) Evidence for the involvement of interleukin 1 in human osteoarthritic cartilage degradation: protective effect of NSAID. J Rheumatol (Suppl 18) 16:19–27
Pelletier JP, Cloutier JM, Martel-Pelletier J (1989) *In vitro* effects of tiaprofenic acid, sodium salicylate and hydrocortisone on the proteoglycan metabolism of human osteoarthritic cartilage. J Rheumatol 16:646–655
Sabatini M, Bardiot A, Lesur C, Moulharat N, Thomas M, Richard I, Fradin A (2002) Effects of agonists of peroxisome proliferator-activated receptor γ on proteoglycan degradation and matrix metalloproteinase production in rat cartilage *in vitro*. Osteoarthr Cart 10:673–679
Verbruggen G, Veys EM, Malfait AM et al (1989) Proteoglycan metabolism in tissue cultured human articular cartilage. Influence of piroxicam. J Rheumatol 16:355–362
Verbruggen G, Veys EM, Malfait AM et al (1990) Proteoglycan metabolism in tissue-cultured human articular cartilage. Scand J Rheumatology 19:257–268
Yang XH, Zhang ZX (1991) Effects of DMSO and glycerol in ^{35}S incorporation of articular cartilage. Cryo-Letters 12:53–58

I.1.1.5 Influence on Matrix Metalloproteases

PURPOSE AND RATIONALE

Matrix metalloproteases (MMPs) form a multigene family of more than 20 secreted and membrane-tethered zinc-dependent endopeptidases, which are classified according to their structures and substrate specificities (Nicholson et al. 2005). Members of the family include: collagenases (MMP-1, -8, -13), gelatinases (MMP-2, -9), stromelysins (MMP-3, -7, -10, -11, -12) and membrane-type matrix metalloproteases (MT1-MMP to MT6-MMP). They are regulated by natural inhibitors, such as α_2-macroglobulin and the tissue inhibitors of metalloproteases (TIMPs). The catalytic domains of the MMPs have an ellipsoid shape with a small active cleft. This cleft contains the catalytic zinc ion, which is essential for catalysis. MMPs can degrade all components of the extracellular matrix and have been implicated in a number of pathological conditions. They are produced in response to the pro-inflammatory cytokines tumor necrosis factor (TNF) and interleukin-1 (IL-1) and are found in excess in the arthritic joint (Borkakoti 1998, 2004; Close 2001; Rosenblum et al. 2003; Mott and Werb 2004). MMPs belong to the metzincin superfamily of metalloproteinases, which also includes astacins, ADAMs (proteins with a disintegrin and metalloprotease domain) and ADAM-TS (an ADAM with a thrombospondin-like motif). Several trials are ongoing to find inhibitors of MMPs for treatment of rheumatism and osteoarthritis (Levin et al. 1998; Bigg and Rowan 2001; Martel-Pelletier et al. 2001; Matter et al. 2002; Nelson et al. 2002; Aranapakam et al. 2003; Skotnicki et al. 2003; Zask et al. 2003; Matter and Schudok 2004; Skiles et al. 2004). Besides these indications, metalloprotease inhibitors may be useful in treatment of other diseases, such as chronic obstructive bronchitis, atherosclerosis, inflammatory bowel disease, and cancer (Chang and Werb 2001; Whelan 2004).

Cauchard et al. (2004) tested the activation of latent transforming growth factor 1 and inhibition of matrix metalloproteinase activity by a thrombospondin-like tripeptide linked to elaidic acid.

PROCEDURE

In Vitro Assays

The influence of test substances on recombinant MMP-2, MMP-3, and MMP-9 activity was determined using the fluorescent quenched substrate Mca-Pro-Leu-Gly-LeuDpa-Leu-Ala-Arg [where Mca = (7-methoxy-coumarin-4-yl) acetyl and Dpa = 3-(2′,4′-dinitrophenyl)-L-2,3-diaminopropionyl].

Each enzyme was active site-titrated using a standard preparation of human recombinant TIMP-1 for MMP-1, and TIMP-2 for MMP-2 and TIMP-9 for MMP-9. Then, 200 pM MMP-2 or MMP-9, 400 pM of MMP-3 or 3 nM of MMP-1 was mixed with increasing concentrations of test substances in a 50 mM HEPES buffer, pH 7.6, containing 150 mM NaCl and 5 mM $CaCl_2$ and the assay was initiated by adding 2 µM of substrate. The rate of substrate hydrolysis was linear up to 30 min at 22°C. The reaction was stopped by adding 10 mM EDTA. The rate of the reaction was measured in triplicate for each test drug concentration examined using Perkin-Elmer LS50B spectrofluorometer with excitation and emission wavelength of 325 and 375 nm, respectively. Less than 5% of the substrate was hydrolyzed during the rate measurements.

EVALUATION

IC50 (µM) values were determined by plotting V_i/V_0, where V_i is the rate of substrate hydrolysis in the presence of inhibitor, V_0 is the rate in its absence, as a function of test drug concentrations and non-linear regression analysis.

MODIFICATIONS OF THE METHOD

Similar procedures were used in the following studies:

Lewis et al. (1997) to study an orally active collagenase inhibitor;

Billinghorst et al. (2000) and Dahlberg et al. (2000) to compare the degradation of type II collagen and proteoglycan in nasal and articular cartilages induced by interleukin-1;

Berton et al. (2001) to study the inhibition of matrix metalloproteinase activities by long-chain fatty acids; and

Matter et al. (2002) to investigate structure–activity relationship of tetrahydroisoquinoline-3-carboxylate-based matrix-metalloprotease inhibitors.

Bottomley et al. (1997) studied the inhibition of bovine nasal cartilage degradation by selective matrix metalloprotease inhibitors.

The potency of the inhibitors against human collagenase 1 (MMP-1), stromelysin (MMP-3), gelatinase B (MMP-9), and aggrecan metabolism was tested. Medium from human dermal fibroblasts (CCD45) cultured in the presence of recombinant human IL-1α (25 ng/ml) was used as source of collagenase. Collagenase activity was determined by measuring the degradation of ^{14}C-labeled collagen fibrils. Human prostromelysin-1 was antibody-affinity purified from conditioned human fibroblast culture medium. Progelatinase B was purified by gelatin-agarose affinity chromatography from human neutrophils. Both prostromelysin and procollagenase B were activated by treatment with trypsin. Stromelysin and gelatinase B activities were determined by measuring the cleavage of the fluorogenic substrate Mca-Pro-Lys-Pro-Leu-Gly-Leu-Dpa-NH_2; assays were performed using 50 mM borate buffer/1 mM $CaCl_2$ containing 0.05% Brij-35, at a substrate concentration of 2 µM. Assays were started by the addition of enzyme to a mixture of substrate and an inhibitor, and incubated for 4 h at 37°C; the assay was stopped by addition of acetic acid to a final concentration of 0.17 mM. The fluorescence of the product Mca-Pro-Lys-Pro-Leu-Gly (λ_{ex} 325 nm; λ_{em} 395 nm) was measured with a Hitatchi F-4500 fluorescence spectrophotometer.

A similar method was used by Reichelt et al. (2002) for design, synthesis, and evaluation of matrix metalloprotease inhibitors bearing cyclopentane-derived peptidomimetics as P1′ and P2′ replacements.

Perlman et al. (2003) found that IL-6 and matrix metalloproteinase-1 are regulated by the cyclin-dependent kinase inhibitor p21 in human synovial fibroblasts.

A fluorescent screening assay for collagenase using collagen labeled with 2-methoxy-2,4-diphenyl-3(2*H*)-furanone was recommended by O'Grady et al. (1984).

Zhang et al. (2004) identified and characterized a dual tumor necrosis factor-α-converting enzyme (**TACE**)/matrix metalloprotease inhibitor for the treatment of rheumatoid arthritis.

Assay of TNF-α Converting Enzyme (TACE)

A synthetic peptide of pro-TNF-α containing the minimal TACE cleavage sequence, Abz-LAQAVRSSSR-Dpa, was used as substrate. A segment of the extracellular portion of the human TACE that comprises the catalytic domain, the disintegin domain, the epidermal growth factor-like domain, and the Crambin-like domain was used. The protein was expressed in Chinese hamster ovary (CHO) cells and purified by nickel-nitrilotriacetic acid and preparative size exclusion chromatography to near homogeneity. Compounds were tested for their ability to inhibit the cleavage of the substrate by the purified enzyme in a fluorescence-based fluorescence resonance energy transfer (FRTE) assay. The human TACE protein (1 µg/ml) was pretreated with the inhibitors at various concentrations for 10 min at room temperature. The reaction was initiated by the addition of pro-TNF-α peptide to the TACE protein, and the increase in fluorescence was monitored at an excitation wavelength of 320 nm and emission wavelength of 420 nm over a period of 10 min (Jin et al. 2002).

MMP Enzymatic Assays

A continuous assay was used in which the substrate is a synthetic peptide containing a fluorescent group (7-methoxycoumarin), which is quenched by energy transfer to a 2,4-dinitrophenyl group. When the peptide was cleaved by MMPs, an increase in fluorescence was observed. The substrate used was 7-methoxycoumarine-PQGL-(3-[2,4-dinitrophenyl]-L-2,3-diaminopropionyl)-AR-OH. The assays were carried out at room temperature in a buffer containing 50 mM HEPES, pH 7.4; 100 mM NaCl, 5 mM $CaCl_2$, and 0.005% Brij-35 (Knight et al. 1992). The enzyme reaction was initiated by adding the substrate to a final concentration of 20 µM. The initial rate of the cleavage reaction was determined immediately after substrate addition.

Sadowski and Steinmeyer (2001) studied the effects of non-steroidal anti-inflammatory drugs and dexamethasone on the activity and expression of MMP-1, MMP-3 and tissue inhibitor of metalloproteinases-1. Bovine chondrocytes were cultured in alginate gel beads. Cells were treated with IL-interleukin 1α in the presence of vehicle or drugs at various concentrations. After 48 h mRNA expression of MMP-1, MMP-3, and the tissue inhibitor of metalloproteinases (TIMP-1) was analyzed by RT-PCR-ELISA. The protein synthe-

sis of TIMP-1 and MMP-3 was determined by immunoprecipitation. The activity of enzymes and inhibitors was measured by functional assays (Yoshioka et al. 1987; Steinmeyer et al. 1998).

The synthesis and biological activity of **TACE-inhibitors** are described by Beck et al. (2002), by Letavic et al. (2002, 2003) and by Tsukida et al. (2004).

Downs et al. (2001) used an **ELISA** for analysis of collagenase-cleavage of type II collagen to the C-terminal neoepitope. Valleala et al. (2003) described an ELISA assay for MMP-9 (gelatinase B).

Microtiter plates were coated with 100 µl of 5 µg/ml MMP-9-specific monoclonal antibody (TNO-S22.2) in PBS overnight at 4°C. After three washes in PBS containing 0.05% Tween 20 (PBS-T), 100 µl of purified MMP-9 or cell supernatant was added. After overnight incubation at 4°C, the plates were washed and incubated for 1 h at 37°C with 100 µl of biotin-labeled anti-MMP-9 polyclonal antibody (TNO-B21) diluted in PBS-T/EDTA + 0.1% casein (PBS-T/DTA/C) (0.8 µg/ml). After washing, bound polyclonal antibody was assessed by incubation with 100 μl of avidin/HRP at 1:10,000 in PBS-T/EDTA/C. Non-bound conjugate was washed away after 1 h at 37°C, and the chromogene 3,3′ 5,5′-tetramethyl benzidine in the presence of H_2O_2 was added. The reaction was stopped after 20 min with 2M H_2SO_4 and the absorption was measured at 450 nm in a Titertek Multiscan spectrophotometer.

Peppard et al. (2003) developed an assay suitable for high-throughput screening to measure matrix metalloprotease activity.

Sabatini et al. (2005) studied the effect of inhibition of matrix metalloproteinases on cartilage loss *in vitro* and in a guinea pig model of osteoarthritis.

Zymography was used by several authors to measure the activity of metalloproteases (Maquoi et al. 1998, 2002; Hattori et al. 2002; Sartor et al. 2002; Sato et al. 2002; Kaji et al. 2003; Kerkvliet et al. 2003; Kim and Kim 2004; Liu et al. 2004; Martin-Chouly et al. 2004; Naqvi et al. 2005).

Samples were subjected to electrophoresis on a 4.5% acrylamide stacking gel/7% acrylamide separating gel containing 1 mg/ml gelatin, in the presence of sodium dodecyl sulfate, under non-reducing conditions. After electrophoresis, gels were washed twice with 2.5% Triton X-100, rinsed with water, and incubated at 37°C overnight in 50 mM Tris, 5 mM $CaCl_2$, 2 mM $ZnCl_2$, pH 8.0. The gels were stained with Coomassie brilliant blue and destained in a solution of 25% ethanol and 10% acetic acid. Gelatinase activities appeared as clear bands against a blue background. To determine the inhibition profile of the enzyme activities, gels were incubated in the presence of one of the following inhibitors in the activation buffer: 10 mM EDTA as an inhibitor of MMPs, or 10 mM PMSF (phenylmethylsulfonyl fluoride) as an inhibitor of serine proteases. The molecular weight of gelatinolytic bands was estimated using recombinant protein molecular weight markers. Images of zymograms were acquired with the Gel Doc 1000 Gel Documentation System. The amount of enzyme was quantified by measuring the intensity of the negative bands using a densitometer analyzer with Quantity one software. Results were expressed as arbitrary units of relative intensity.

REFERENCES AND FURTHER READING

Aranapakam V, Grosu GT, Davis JM, Hu B, Ellingboe J, Baker JL, Skotnitcki JS, Zask A, DiJoseph JF, Sung A, Sharr MA, Killar LM, Walter T, Jin G, Cowling R (2003) Synthesis and structure-activity relationship of α-sulfonylhydroxamic acids as novel, orally active matrix metalloprotease inhibitors for the treatment of osteoarthritis. J Med Chem 46:2361–2375

Beck G, Bottomley G, Bradshaw D, Brewster M, Broadhurst M, Devos R, Hill C, Johnson W, Kim HJ, Kirtland S, Kneer J, Lad N, Mackenzie R, Martin R, Nixon J, Price G, Rodwell A, Rose F, Tang JP, Walter DS, Wilson K, Worth E (2002) (*E*)-2(*R*-[1(*S*)-(hydroxycarbamoyl)-4-phenyl-3-butenyl]-2′-isobutyl-2′-(methanesulfonyl)-4-methylvalerohydrazide (Ro 32–7315), a selective and orally active inhibitor of tumor necrosis factor-α convertase. J Pharmacol Exp Ther 302:390–396

Berton A, Rigot V, Huett E, Decarme M, Eeckhout Y, Patthy L, Godeau G, Hornebeck W, Bellon G, Emonard H (2001) Involvement of fibronectin type II repeats in the efficient inhibition of gelatinases A and B by long-chained unsaturated fatty acids. J Biol Chem 276:20458–20465

Bigg HF, Rowan AD (2001) Inhibition of metalloproteinases as a therapeutic target in rheumatoid arthritis and osteoarthritis. Curr Opin Pharmacol 1:314–320

Billinghorst RC, Wu W, Ionescu M, Reiner A, Dahlberg L, Chen J, van Wart H, Poole AR (2000) Comparison of the degradation of type II collagen and proteoglycan in nasal and articular cartilages induced by interleukin-1 and selective inhibition of type II collagen cleavage by collagenase. Arthritis Rheum 43:664–672

Borkakoti N (1998) Matrix metalloproteases: variations on a theme. Prog Biophys Mol Biol 70:73–94

Borkakoti N (2004) Matrix metalloprotease inhibitors: design from structure. Biochem Soc Trans 32:17–20

Bottomley KM, Borkakoti N, Bradshaw D, Brown PA, Broadhurst MJ, Budd JM, Elliott L, Eyers P, Hallam TJ, Handa BK, Hill CH, James M, Lahm HW, Lawton G, Merritt JE, Nixon JS, Röthlisberger U, Whittle A, Johnson WH (1997) Inhibition of bovine nasal cartilage degradation by selective matrix metalloprotease inhibitors. Biochem J 323:483–488

Cauchard JH, Berton A, Godeau G, Hornebeck W, Bellon G (2004) Activation of latent transforming growth factor 1 and inhibition of matrix metalloproteinase activity by

a thrombospondin-like tripeptide linked to elaidic acid. Biochem Pharmacol 67:2013–2022

Chang C, Werb Z (2001) The many faces of metalloproteases: cell growth, invasion and metastasis. Trends Cell Biol 11:S37–S34

Close DR (2001) Matrix metalloproteinase inhibitors in rheumatic diseases. Ann Rheum Dis 60:iii62–iii67

Dahlberg L, Billinghurst RC, Manner P, Nelson F, Webb G, Ionescu M, Reiner A, Tanzer M, Zukor D, Chen J, van Wart HE, Poole AR (2000) Selective enhancement of collagenase-mediated cleavage of resident type II collagen in cultured osteoarthritic cartilage and arrest with a synthetic inhibitor that spares collagenase 1 (matrix metalloproteinase 1). Arthritis Rheum 43:673–682

Downs JT, Lane CL, Nestor NB, McLellan TJ, Kelly MA, Karam GA, Mezes PS, Pelletier JP, Otterness IG (2001) Analysis of collagenase-cleavage of type II collagen using a neoepitope ELISA. J Immunol Meth 247:25–34

Hattori S, Fujisaki H, Kiriyama T, Yokoyama T, Irie S (2002) Real-time zymography and reverse zymography: a method for detecting activities of metalloproteinases and their inhibitors using FITC-labeled collagen and casein as substrates. Anal Biochem 301:27–34

Jin G, Huang X, Black R, Wolfson M, Rauch C, McGregor H, Ellestad G, Cowling R (2002) A continuous fluorometric assay for tumor necrosis factor-alpha converting enzyme. Anal Biochem 302:269–275

Kaji M, Moriyama S, Sasaki H, Saitoh Y, Kiriyama M, Fukai I, Yamakawa Y, Mitsui A, Toyama T, Nemori R, Fujii Y (2003) Gelatinolytic activity of matrix metalloproteinase in lung cancer studied using film in situ zymography stamp method. Lung Cancer 39:125–130

Kerkvliet EHM, Jansen IDC, Schoenmaker TAM, Docherty AJP, Beertsen W, Everts V (2003) Low molecular weight inhibitors of matrix metalloproteinases can enhance the expression of matrix metalloproteinase-2 (gelatinase A) without inhibiting its activation. Cancer 97:1582–1588

Kim JR, Kim CH (2004) Association of a high activity of matrix metalloproteinase-9 to low levels of tissue inhibitors of metalloproteinase-1 and -3 in human hepatitis B-viral hepatoma cells. Int J Biochem Cell Biol 36:2293–2306

Knight CG, Willenbrock F, Murphy G (1992) A novel coumarin-labeled peptide for sensitive continuous assays of the matrix metalloproteinases. FEBS Lett 296:263–266

Letavic MA, Axt MZ, Barberia JT, Carty TJ, Danley DE, Geoghegan KF, Halim NS, Hoth LR, Kamath AV, Laird ER, Lopresti-Morrow LL, McClure KF, Mitchell PG, Natarajan V, Noe MC, Pandit J, Reeves L, Schulte GK, Snow SL, Sweeney FJ, Tan DH, Yu CH (2002) Synthesis and biological activity of selective pipecolic acid-based TNF-α converting enzyme (TACE) inhibitors. Bioorg Med Chem Lett 12:1378–1390

Letavic MA, Barberia JT, Carty TJ, Hardink JR, Liras J, Lopresti-Morrow LL, Mitchell PG, Noe MC, Reeves LM, Snow SL, Stam EJ, Sweeney FJ, Vaughn ML, Yu CH (2003) Synthesis and biological activity of piperazine-based dual MMP-13 and TNF-α converting enzyme inhibitors. Bioorg Med Chem Lett 13:3243–3246

Levin JI, DiJoseph JF, Killar LM, Sharr MA, Skotnicki JS, Patel DV, Xiao XY, Shi L, Navre M, Campbell DA (1998) The asymmetric synthesis and in vivo characterization of succinyl mercaptoalcohol and mercaptoketone inhibitors of metalloproteinases. Bioorg Med Chem Lett 8:1163–1168

Lewis EJ, Bishop J, Bottomley KMK, Bradshaw D, Brewster M, Broadhurst MJ, Brown PA, Budd JM, Elliott L, Greenham AK, Johnson WH, Nixon JS, Rose F, Sutton B, Wilson K (1997) Ro 32–3555, an orally active collagenase inhibitor, prevents cartilage breakdown *in vitro* and *in vivo*. Br J Pharmacol 121:540–546

Liu JR, Yang BF, Chen BQ, Yng YM, Dong HW, Song YQ (2004) Inhibition of α-ionone on SGC-7901 cell proliferation and upregulation of metalloproteinases-1 and -2 expression. World J Gastroenterol 10:167–171

Maquoi E, Noël A, Frankenne F, Angliker H, Murphy G, Foidart JM (1998) Inhibition of matrix metalloprotease 2 maturation and HT1089 invasiveness by a synthetic furin factor. FEBS Lett 424:262–266

Maquoi E, Munaut C, Colige A, Lambert C, Frankenne F, Noël A, Grams F, Krell HW, Foidart JM (2002) Stimulation of matrix metalloproteinase-9 expression in human fibrosarcoma cells by synthetic matrix metalloproteinase inhibitors. Exp Cell Res 275:110–121

Marle-Pelletier J, Welsch DJ, Pelletier JP (2001) Metalloproteases and inhibitors of arthritic diseases. Best Pract Res Clin Rheum 15:805–829

Martin-Chouly CAE, Astier A, Jacob C, Prunaux MP, Bertrand C, Lagente V (2004) Modulation of matrix metalloproteinase production by type 4 phosphodiesterase inhibitors. Life Sci 75:823–840

Matter H, Schudok M (2004) Recent advances in the design of metalloprotease inhibitors. Curr Opin Drug Disc Dev 7:513–535

Matter H, Schudok M, Schwab W, Thorwart W, Barbier D, Billen G, Haase B, Neises B, Weithmann KU, Wollmann T (2002) Tetrahydroisoquinoline-3-carboxylate based matrix-metalloprotease inhibitors: design, synthesis and structure-activity relationship. Bioorg Med Chem 10:3529–3544

Mott JD, Werb Z (2004) Regulation of matrix biology by matrix metalloproteinases. Curr Opin Cell Biol 16:558–564

Naqvi T, Duong TT, Hashem G, Shiga M, Zhang Q, Kapila S (2005) Relaxin's induction of metalloproteinases is associated with the loss of collagen and glycosaminoglycans in synovial joint fibrocartilaginous explants. Arthritis Res Ther 7:R1–R11

Nelson FC, Santos ED, Levin JI, Chen JM, Skotnicki JS, DiJoseph JF, Sharr MA, Sung A, Killar LM, Cowling R, Jin G, Roth CE, Albright JD (2002) Benzodiazepine inhibitors of MMPs and TACE. Bioorg Med Chem Lett 12:2867–2870

Nicholson AC, Malik SB, Logsdon JM Jr, van Meir EG (2005) Functional evolution oif ADAMTS genes: evidence from analyses of phylogeny and gene organization. BMC Evolut Biol 5:11–24

O'Grady RL, Nethery A, Hunter N (1984) A fluorescent screening assay for collagenase using collagen labeled with 2-methoxy-2,4.diphenyl-3(2H)-furanone. Anal Biochem 140:490–494

Peppard J, Pham Q, Clark A, Farley D, Sakane Y, Graves R, George J, Norey C (2003) Development of an assay suitable for high-throughput screening to measure matrix metalloprotease activity. Assay Drug Dev Technol 1:425–433

Perlman H, Bradley K, Liu H, Cole S, Shamiyeh E, Smith RC, Walsh K, Fiore S, Koch AE, Firestein GS, Haines III GK, Pope RM (2003) IL-6 and matrix metalloproteinase-1 are regulated by the cyclin-dependent kinase inhibitor p21 in synovial fibroblasts. J Immunol 170:838–845

Reichelt A, Gaul C, Frey RR, Kennedy A, Martin SF (2002) Design, synthesis, and evaluation of matrix metalloprotease inhibitors bearing cyclopentane-derived peptidomimetics as P1′ and P2′ replacements. J Org Chem 76:4062–4075

Rosenblum G, Meroueh SO, Kleifeld O, Brown S, Singson SP, Fridman R, Mobashery S, Sagi I (2003) Structural basis for potent slow binding inhibition of human matrix metalloprotease-1 (MMP-2). J Biol Chem 278:27009–27015

Sabatini M, Lesur C, Thomas M, Chomel A, Anract P, de Nanteuil G, Pastoureau P (2005) Effect of inhibition of matrix metalloproteinases on cartilage loss in vitro and in a guinea pig model of osteoarthritis. Arthritis Rheum 52:171–180

Sadowski T, Steinmeyer J (2001) Effects of non-steroidal antiinflammatory drugs and dexamethasone on the activity and expression of matrix metalloproteinase-1, matrix metalloproteinase-3 and tissue inhibitor of metalloproteinases-1 by bovine articular chondrocytes. Osteoarthritis Cartilage 9:407–415

Sartor L, Pezzato E, Dell'Aica I, Caniato R, Biggin S, Garbisa S (2002) Inhibition of matrix-proteinases by polyphenols: chemical insights for anti-inflammatory and anti-invasion drug design. Biochem Pharmacol 64:229–237

Sato T, Koike L, Miyata Y, Hirata M, Mimaki Y, Sashida Y, Yano M, Ito A (2002) Inhibition of activator protein-1 binding activity and phosphatidylinositol 3-kinase pathway by nobiletin, a polymethoxy flavonoid, results in augmentation of metalloproteinases-1 production and suppression of production of matrix metalloproteinases-1 and –9 in human fibrosarcoma HT-1080 cells. Cancer Res 62:1025–1029

Skiles JW, Gonnella NC, Jeng AY (2004) The design, structure and clinical update of small molecular weight matrix metalloproteinase inhibitors. Curr Med Chem 11:2911–2977

Skotnicki JS, DiGrandi MJ, Levin JI (2003) Design strategies for the identification of MMP-13 and TACE-inhibitors. Curr Opin Drug Disc Dev 6:742–759

Steinmeyer J, Daufeldt S, Taiwo YO (1998) Pharmacological effect of tetracyclines on proteoglycans from interleukin-1 treated articular cartilage. Biochem Pharmacol 55:93–100

Tsukida T, Moriyama H, Inoue Y, Kondo H, Yoshino K, Nishimura SI (2004) Synthesis and biological activity of selective azasugar-based TACE inhibitors. Bioorg Med Chem Lett 14:1569–1572

Valleala H, Hanemaaijer R, Mandelin J, Salminen A, Teronen O, Mönkkönen J, Konttinen YT (2003) Regulation of MMP-9 (gelatinase B) in activated human monocytes/macrophages by two different types of biphosphonates. Life Sci 73:2413–2420

Whelan CJ (2004) Metalloprotease inhibitors as anti-inflammatory agents: an evolving target? Curr Opin Invest Drugs 5:511–516

Yoshioka H, Oyamada I, Usuku G (1987) An assay of collagenase activity using enzyme-linked immunosorbent assay for mammalian collagenase. Anal Biochem 166:22–26

Zask A, Gu Y, Albright JD, Du X, Hogan M, Levin JI, Chen JM, Killar LM, Sung A, DiJoseph JF, Sharr MA, Roth CE, Skala S, Jin G, Cowling R, Mohler KM, Barone D, Black R, March C, Skotnicki JS (2003) Synthesis and SAR of bicyclic heteroaryl hydroxamic acid MMP and TACE inhibitors. Bioorg Med Chem Lett 13:1487–1490

Zhang Y, Xu J, Levin J, Hegen M, Li G, Robertshaw H, Brennan F, Cummons T, Clarke D, Vansell N, Nickerson-Nutter C, Barone D, Mohler K, Black R, Skotnicki J, Gibbons J, Feldmann M, Frost P, Larsen G, Lin LL (2004) Identification and characterization of 4-[[4-(2-butynyloxy)phenyl]sulfonyl]-*N*-hydroxy-2,2-dimethyl-(3-*S*)-thiomorpholinecarboxamide (TMI 1), a novel dual tumor necrosis factor-a-converting enzyme/matrix metalloprotease inhibitor for the treatment of rheumatoid arthritis. J Pharmacol Exp Ther 309:348–355

I.1.1.6 Aggrecanase Inhibition

PURPOSE AND RATIONALE

Degenerative joint diseases are characterized by cartilage extracellular matrix degeneration, where loss of aggrecan, an aggregating proteoglycan, is an early event in the destruction of articular cartilage. Aggrecan, a multidomain proteoglycan, is a major component of cartilage and provides compressive resistance to articular cartilage. During the early stages of osteoarthritis, and then throughout the disease, there is increased loss of glycosaminoglycan-rich aggrecan fragments via proteolysis attributable to "aggrecanase" activity.

Aggrecanase-1 and -2 are members of the ADAMTS (a disintegrin and metalloprotease possessing thrombospondin domain) family of zinc-containing metalloproteases, responsible for the cleavage of the aggrecan interglobular domain (IGD) at the Glu^{373}-Ala^{374} peptide bond, a unique site untouched by any previously identified enzyme (Arner et al. 1998; Abbaszade et al. 1999; Arner et al. 2002; Little et al. 1999; Tortorella et al. 1999, 2001; Arner 2002; Patwari et al. 2005; Stanton et al. 2005; Wight 2005; Song et al. 2007).

Inhibition of aggrecanase may impart overall cartilage protection and offer a potential therapy to alter the progression of osteoarthritis. Besides of endogenous inhibitors of aggrecanase (Bonassar et al. 1997; Sandy et al. 1998; Hashimoto et al. 2001, 2004; Little et al. 2002a; Malfait et al. 2002; Munteanu et al. 2002; Gendron et al. 2003; Pratta et al. 2003; Tortorella et al. 2004); also synthetic inhibitors are described (Bottomley et al. 1997; Munteanu et al. 2000; Little et al. 2002b; Sabatini et al. 2002, 2005; Sawa et al. 2002; Wada et al. 2002; Cherney et al. 2003; Vankemmelbeke et al. 2003; Noe et al. 2004; Liacini et al. 2005).

Xiang et al. (2006) described the synthesis and biological evaluation of biphenylsulfonamide carboxylate aggrecanase-1 inhibitors.

PROCEDURE

Bovine carpal joints were obtained from young (1- to 2-week-old) animals. Full-depth articular cartilage plugs were harvested using a cork borer and then sliced on a custom dice to generate individual disks 6 mm wide, 1 mm thick, and 30 mg in weight.

Cartilage explants were cultured at 37°C for 5 days in a humidified atmosphere of 5% CO_2 in air in cartilage explant media (CEM) consisting of Dulbecco's modified Eagle's medium containing 1% an-

timycotic/antibiotic, 2 mM glutamine, 10 mM HEPES, and 50 µg/ml of ascorbate (all from Sigma, St. Louis, Mo., USA). The explants were washed with CEM and one weighed disk per well was placed in a 96-well culture dish with 0.2 ml medium and six to eight replicates per treatment and cultured for 3 days in the presence or absence of recombinant human IL-1α (rhIL-1, 5 ng/ml, Sigma) and the presence or absence of small molecule compound. Media were replaced every day. The proteoglycan content in the medium was measured as sulfated glycosaminoglycan (GAG) by a colorimetric assay (Farndale et al. 1982) using dimethylmethylene blue (DMMB) and chondroitin sulfate C from shark cartilage (Sigma) as a standard. Treatment of cartilage with IL-1 results in the induction of catabolic enzymes including aggrecanases that degrade cartilage matrix proteoglycan. The cleaved proteoglycan is released from the matrix into the media. Addition of the compound together with IL-1 to the cartilage results in a decrease of proteoglycan release, indicating the inhibition of proteoglycan degradation. During this early phase of proteoglycan degradation, aggrecanases are the predominant catabolic enzymes that cleave aggrecan with no significant role of other MMPs (Pratta et al. 2003).

EVALUATION

Measured proteoglycan was expressed per weight of cartilage. IC_{50} values were calculated.

MODIFICATIONS OF THE METHOD

Miller et al. (2003) reported a microplate assay specific for the enzyme aggrecanase. Peppard et al. (2003) developed a high-throughput screening assay for inhibitors of aggrecan cleavage using luminescent oxygen channeling (AlphaScreen).

A simplified assay was reported by Kashiwagi et al. (2001).

Activities of ADAM-TS4 and ADAM-TS5 were measured by incubating enzyme with purified bovine aggrecan (500 nM) in 100 µl of 50 mM Tris-HCl buffer, pH 7.5, containing 0.1 M NaCl and 10 mM $CaCl_2$, for 2 h at 37 °C and terminating the reaction with 10 mM EDTA. The digestion products were then deglycosylated with chondroitinase ABC (0.1 units/10 µg aggrecan) and then with keratinase (0.1 units/10 µg aggrecan) and keratinase II (0.002 units/10 µg aggrecan) for 2 h at 37 °C in 0.1 M Tris-HCl, pH 6.5, containing 50 mM sodium acetate. The enzymatically treated products were analyzed by Western blotting using BC-3 antibody or an antibody against the GELE^{1480} neoepitope (Tortorella et al. 2000). To determine apparent inhibition constant $K_{i(app)}$ values for inhibitors against the aggrecanases, ADAM-TS4 or ADAM-TS5 (at a final concentration of 50 pM) was incubated with various concentrations of the inhibitor in 44 µl of the above buffer at room temperature for 30 min and then a solution of bovine aggrecan (5.5 µl) was added. The reaction products were detected with anti-GELE^{1480} antibody. The concentrations of ADAM-TS4 and ADAM-TS5 were confirmed by titration with recombinant N-TIMP-3.

REFERENCES AND FURTHER READING

Abbaszade I, Liu RQ, Yang F, Rosenfeld SA, Ross OH, Link JR, Ellis DM, Tortorella MD, Pratta MA, Hollis JM, Wynn R, Duke JL, George HJ, Hillman MC, Jr, Murphy K, Wiswall BH, Copeland RA, Decicco CP, Bruckner R, Nagase H, Itoh Y, Newton R.C, Magolda RL, Trzaskos JM, Hollis GF, Arner EC, Burn TC (1999) Cloning and characterization of ADAMTS11, an aggrecanase from the ADAMTS family. J Biol Chem. 274:23443–23450

Arner EC (2002) Aggrecanase-mediated cartilage degradation. Curr Opin Pharmacol 2:322–329

Arner EC, Hughes CE, Dicicco CP, Caterson B, Tortorella MD (1998) Cytokine-induced cartilage proteoglycan degradation is mediated by aggrecanase. Osteoarthr Cart 6:214–228

Bonassar LJ, Sandy JD, Lark MW, Plaas AKH, Frank EH, Grodzinsky AJ (1997) Inhibition of cartilage degradation and changes in physical properties induced by IL-1β and retinoic acid using matrix metalloproteinase inhibitors. Arch Biochem Biophys 344:404–412

Bottomley KM, Borkakoti N, Bradshaw D, Brown PA, Broadhorst MJ, Budd JM, Elliott L, Eyers P, Hallam TJ, Handa BK, Hill CH, James M, Lahm HW, Lawton G, Merritt JE, Nixon JS, Röthlisberger U, Whittle A, Johnson WH (1997) Inhibition of bovine nasal cartilage degradation by selective matrix metalloproteinase inhibitors. Biochem J 323:483–488

Cherney RJ, Mo RT, Meyer DT, Wang L, Yao W, Wasserman ZL, Liu RQ, Covington MB, Tortorella MD, Arner EC, Qian M, Christ DD, Trzaskos JM, Newton RC, Magolda RL, Decicco CP (2003) Potent and selective aggrecanase inhibitors containing cyclic P1 substituents. Bioorg Med Chem Lett 13:1297–1300

Farndale RW, Sayers CA, Barrett AJ (1982) A direct spectrophotometric microassay for sulfated glycosaminoglycans in cartilage cultures. Connect Tissue Res 9:247–248

Gendron C, Kashiwagi M, Hughes C, Caterson B, Nagase H (2003) TIMP-3 inhibits aggrecanase-mediated glycosaminoglycan release from cartilage explants stimulated by catabolic factors. FEBS Lett 555:431–436

Hashimoto G, Aoki T, Nakamura N, Tanzawa K, Okada Y (2001) Inhibition of ADAMTS4 (aggrecanase-1) by tissue inhibitors of metalloproteinases (TIMP-1, 2, 3 and 4). FEBS Lett 494:192–195

Hashimoto G, Shimoda M, Okada Y (2004) ADAMTS4 (aggrecanase-1) interaction with the C-terminal domain of fibronectin inhibits proteolysis of aggrecan. J Biol Chem 279:33483–33491

Kashiwagi M, Tortorella M, Nagase H, Brew K (2001) TIMP-3 is a potent inhibitor of aggrecanase 1 (ADAM-TS4) and aggrecanase 2 (ADAM-TS5). J Biol Chem 276:12501–12504

Liacini A, Sylvester J, Zafarullah M (2005) Tripolide suppresses proinflammatory cytokine-induced matrix metalloproteinase and aggrecanase-1 gene expression in chondrocytes. Biochem Biophys Res Commun 327:320–227

Little CB, Flannery CR, Hughes CE, Mort SJ, Roughley PJ Dent C, Caterson B (1999) Aggrecanase versus metalloproteases in the catabolism of the interglobular domain of aggrecan in vitro. Biochem J 344:61–68

Little C, Hughes C, Curtis C, Janusz M, Bohme R, Wang-Weigand S, Taiwo Y, Mitchell P, Otterness I, Flannery C, Caterson B (2002a) Matrix metalloproteinases are involved in C-terminal and interglobolar domain processing of cartilage aggrecan in late stage of cartilage degradation. Matrix Biol 21:271–288

Little CB, Hughes CE, Curtis CL, Jones SA, Caterson B, Flannery CR (2002b) Cyclosporin A inhibition of aggrecanase-mediated proteoglycan catabolism in articular cartilage. Arthritis Rheum 46:124–129

Malfait AM, Liu RQ, Ijiri K, Komiya S, Tortorella MC (2002) Inhibition of ADAM-TS4 and ADAM-TS5 prevents aggrecan degradation in osteoarthritic cartilage. J Biol Chem 277:22201–22208

Miller JA, Liu RQ, Davis GL, Pratta MA, Trzaskos JM, Copeland RA (2003) A microplate assay specific for the enzyme aggrecanase. Anal Biochem 314:260–265

Munteanu SE, Ilic MZ, Handley CJ (2000) Calcium pentosan polysulfate inhibits the catabolism of aggrecan in articular cartilage explant cultures. Arthritis Rheum 43:2211–2218

Munteanu SE, Ilic MZ, Handley CJ (2002) Highly sulphated glycosaminoglycans inhibit aggrecanase degradation of aggrecan by bovine articular cartilage explant cultures. Matrix Biol 21:429–440

Noe MC, Snow SL, Wolf-Gouveia LA, Mitchell PG, Lopresti-Morrow L, Reeves LM, Yocum SA, Liras JL, Vaughn M (2004) 3-Hydroxy-4-arylsulfonyltetrahydropyranyl-3-hydroxamic acids are novel inhibitors of MMP-13 and aggrecanase. Bioorg Med Chem Lett 14:4727–4730

Patwari P, Gao G, Lee JH, Grodzinsky AJ, Sandy JD (2005) Analysis of ADAMTS4 and MT4-MMP indicates that both are involved in aggrecanolysis in interleukin-1-treated bovine cartilage. Osteoarthr Cart 13:269–227

Peppard J, Glickman F, He Y, Si H, Doughty J, Goldberg R (2003) Development of a high-throughput screening assay for inhibitors of aggrecan cleavage using luminescent oxygen channelling (AlphaScreen). J Biomol Screen 8:149–156

Pratta MA, Yao W, Decicco C, Tortorella MD, Liu RQ, Copeland RA, Magolda R, Newton RC, Trzaskos JM, Arner EC (2003) Aggrecan protects cartilage collagen from proteolytic cleavage. J Biol Chem 278 45539–45545

Sabatini M, Bardiot A, Lesur C, Moulharat N, Thomas M, Richard I, Fradin A (2002) Effects of peroxisome proliferator-activated receptor γ on proteoglycan degradation and matrix metalloproteinase production in rat cartilage *in vitro*. Osteoarthr Cart 10:673–679

Sabatini M, Lesur C, Thomas M, Chomel A, Anract P, de Nateuil G, Pastoureau P (2005) Effect of inhibition of matrix metalloproteases on cartilage loss in vitro and in a guinea pig model of osteoarthritis. Arthritis Rheum 52:171–180

Sandy JD, Gamett D, Verscharen C (1998) Chondrocyte-mediated catabolism of aggrecan: aggrecanase-dependent cleavage induced by interleukin-1 or retinoic aced can be inhibited by glucosamine. Biochem J 355:59–66

Sawa M, Kiyoi T, Kurokawa K, Kumihara H, Yamamoto M, Miyasaka T, Ito Y, Hirayama R, Inoue T, Kirii Y, Nishiwaki E, Ohmoto H, Maeda Y, Ishibushi E, Inoue Y, Yoshino K Kondo H (2002) New type of metalloprotease inhibitor: design and synthesis of new phosphonamide-based hydroxamic acids. J Med Chem 45:919–929

Song RH, Tortorella H, Malfait AM, Alston JT, Yang Z, Arner EC, Griggs DW (2007) Aggrecan degradation in human articular cartilage explants is mediated by both ADAMTS-4 and ADAMTS-5. Arthritis Rheum 56:575–585

Stanton H, Rogerson FM, East CJ, Golub SB, Lawlor KE, Meeker CT, Little CB, Last K, Farmer PJ, Campbell JK, Fourle AM, Fosang AJ (2005) ADAMTS5 is the major aggrecanase in mouse cartilage *in vivo* and *in vitro*. Nature 434:648–652

Tortorella MD, Burn TC, Pratta MA, Abbaszade I, Hollis JM, Liu R, Rosenfeld SA, Copeland RA, Decicco CP, Wynn R, Rockwell A, Yang F, Duke JL, Solomon K, George H, Bruckner R, Nagase H, Itoh Y, Ellis DM, Ross H, Wiswall BH, Murphy K, Hillman MC, Jr, Hollis GF, Arner EC (1999) Purification and cloning of aggrecanase-1: a member of the ADAMSTS family of proteins. Science 284**:**1664–1666

Tortorella MD, Pratta M, Liu RQ, Austin J, Ross OH, Abbaszade I, Burn T, Arner E (2000) Sites of aggrecan cleavage by recombinant aggrecanase-1 (ADAMTS-4). J Biol Chem 275:18566–18573

Tortorella MD, Malfait AM, Deciccio C, Arner E (2001) The role of ADAM-TS4 (aggrecanase-1) and ADAM-TS5 (aggrecanase-2) in a model of cartilage degradation. Osteoarthr Cart 9:539–552

Tortorella MD, Arner EC, Hills R, Easton A, Korte-Sarfaty J, Fok K, Wittwer AJ, Liu RQ, Malfait AM (2004) α_2-Macroglobulin is a novel substrate for ADAMTS-4 and ADAMTS-5 and represents an endogenous inhibitor of these enzymes. J Biol Chem 279:17553–17561

Vankemmelbeke MN, Jones GC, Fowles C, Ilic MZ, Handley CJ, Day AJ, Knight CG, Mort JS, Buttle DJ (2003) Selective inhibition of ADAMTS-1, -4 and -5 by catechin gallate esters. Eur J Biochem 270:2394–2403

Wada CK, Holms JH, Curtin ML, Dai Y, Florjancic AS, Garland RB, Guo Y, Heyman HR, Stacey JR, Steinman DH, Albert DH, Bouska JJ, Elmore HN, Goodfellow CL, Marcotte PA, Tapang M, Morgan DW, Michaelides MR, Davidsen SK (2002) Phenoxyphenyl sulfone *N*-formylhydroxylamines (retrohydroxyamates) as potent, selective, orally bioavailable matrix metalloproteinase inhibitors. J Med Chem 45:219–232

Wight TN (2005) The ADAMTS proteases, extracellular matrix, and vascular disease. Arterioscler Thromb Vasc Biol 25:12–14

Xiang-JS, Hu Y, Rush TS, Thomason JR, Ipek M, Sum PE, Abrous L, Sabatini JJ, Georgiadis K, Reifenberg E, Majumdar M, Morris EA, Tam S (2006) Synthesis and biological evaluation of biphenylsulfonamide carboxylate aggrecanase-1 inhibitors. Bioorg Med Chem Lett 16:311–316

I.1.2
In Vivo Methods for Anti-Osteoarthritic Activity

I.1.2.1
General Considerations

The current availability of animal models of osteoarthritis (OA) for pharmacological assessment is impeded in several aspects: Firstly, the difficulty to address a generally slow progression of cartilage destruc-

tion and deterioration of joint function as encountered in human OA with an animal model achieving sufficient similarity to human pathology in an acceptable time frame. Secondly, the discrepancy between the need of mild, reversible pathological changes, which can be modified therapeutically, and the paucity of reliable parameters with which to determine normal versus disease stages with a gradable range large enough to assess drug effects. This includes also the lack of validation (clinically as well as in animal models) of noninvasive methods to assess disease progression. Thirdly, the lack of a true disease-modifying standard drug with which to validate the pharmacological effects in respect to the predicted clinical outcome.

This results in a situation that animal models closer to human pathology like the spontaneous OA in the Hartley strain of guinea pigs or the surgically inflicted joint instability in the Pond-Nuki dog model are too elaborate to be used routinely for drug selection. On the other hand, models like the chymopapain-induced cartilage degradation in rabbits, are suitable to study drugs, but are limited in their predictive value.

Some progress can be expected from the use of genetically modified animals (Rintala et al. 1997; Serra et al. 1997; Ameye and Young 2002; Han et al. 2002; van Lent et al. 2002; Johnson and Terkeltaub 2003; Scharstuhl et al. 2003; Glasson et al. 2004, 2005; Ueblacker et al. 2004; Ford-Hutchinson et al. 2005; Wadhwa et al. 2005; Xu et al. 2005; Zaka and Williams 2005; Zhang et al. 2005).

It should be noted that differences exist in the pathomechanisms of cartilage destruction between rheumatoid arthritis (RA) and OA. The destruction occurring in RA is closely linked to the inflammatory process, synovial tissue proliferation and transgression across the cartilage surface, degrading cartilage proteoglycans and collagens simultaneously. In OA inflammation is only an intermitted event, not instrumental in the degenerative cartilage destruction, in which proteoglycan degradation is the early event, and collagen loss occurs at a distinctly later stage. Therefore, animal models with a predominant inflammatory component as the air pouch model or other arthritis models, even those focusing on cartilage destruction, are not discussed in this chapter (see Sect. H.3). They are described in detail by Greenwald and Diamond (1988) and recently reviewed by Greenwald (1991, 1993).

PURPOSE AND RATIONALE

As a multitude of different events can lead to OA, equally different techniques have been used to initiate osteoarthritic conditions in animal models: Surgical methods are used to either stiffen the joint in a defined position (Palmoski, Brandt 1982; Konttinen et al. 1990; Meyer-Carrive and Ghosh 1992; Torelli et al. 2005) or inflict joint instability by partial meniscectomy or anterior crucial ligament (ACL) dissection. They are performed mainly in dogs, rabbits (Colombo et al. 1983; Moskowitz et al. 1973, 1979), and guinea pigs (Schwartz 1985; Meacock et al. 1990). Chemical modifications like intraarticular injections of iodoacetate, cytokines like IL-1, or enzymes like chymopapain or stromelysin, are carried out mainly in rabbits (Williams et al. 1992; Reglin et al. 1989), in chicken (Kalbhen 1983, 1987), and in rats (Combe et al. 2004). Mechanical forces are applied on bent or opened joints like impulse loading on sheep (Lindenhayn et al. 1984) or rabbit (Farkas et al. 1987; Mazière et al. 1984) knees, resulting in trauma models of OA. Spontaneously occurring OA is described in horses (Todhunter and Lust 1992; Haakenstad 1969), some breeds of dogs (Lust et al. 1985), rhesus macaques (Pritzker et al. 1989), guinea pigs (Bendele, Hulman 1988) and several strains of mice. For pharmacological purposes only guinea pigs and STR/1N (Walton 1965; Raiss et al. 1992), STR/ORT (Dunham et al. 1989), and C57 black (Pataki et al. 1990) mice have been adapted. In all models mentioned (except horses), the relevant joint is the knee.

Since there exist recent extensive and critical reviews of OA models (Burton-Wurster et al. 1993; Pritzker 1994; Moskowitz 1990, 1992; Adams and Billingham 1982; Oegema et al. 1999; Bendele 2001, 2002; Bonnet and Walsh 2005), also with respect to reversibility (Pita et al. 1986), with special emphasis on drug testing (Hess & Herman 1986; Hinz and Brune 2004; Wieland et al. 2005), and in perspective to cartilage research and markers (Malemud 1993; Carney 1991), only some representative models of each category are described here.

REFERENCES AND FURTHER READING

Adams ME, Billingham MFJ (1982) Animal models of degenerative joint disease. Current Topics in Pathology 71:265–297

Ameye L, Young MF (2002) Mice deficient in small leucin-rich proteoglycans. novel *in vivo* models for osteoporosis, osteoarthritis, Ehlers-Danlos syndrome, muscular dystrophy, and corneal diseases. Glycobiology 12:107R–116R

Bendele AM (2001) Animal models of osteoarthritis. J Musculoskelet Neuronal Interact 1:363–376

Bendele AM (2002) Animal models of osteoarthritis in an era of molecular biology. J Musculoskelet Neuronal Interact 2:501–503

Bendele AM, Hulman JF (1988) Spontaneous cartilage degeneration in guinea pigs. Arthr Rheum 31:561–565

Bonnet CS, Walsh DA (2005) Osteoarthritis, angiogenesis and inflammation. Rheumatology (Oxford) 44:7–16

Burton-Wurster N, Todhunter RJ, Lust G (1993) Animal models of osteoarthritis. In: Woessner JF, Howell DS (eds) Joint cartilage degradation. Basic and clinical aspects. New York, Marcel Dekker Inc., pp 347–384

Carney SL (1991) Cartilage research, biochemical, histologic, and immunohistochemical markers in cartilage, and animal models of osteoarthritis. Current Opinion Rheumatol 3:669–675

Colombo C, Butler M, O'Byrne E, Hickman L (1983) A new model of osteoarthritis in rabbits. I: Development of knee joint pathology following lateral meniscectomy and section of the fibular collateral and sesamoid ligaments. Arthr Rheum 26:875–886

Combe R, Bramwell S, Field MJ (2004) The monosodium iodoacetate model of osteoarthritis: a model of chronic nociceptive pain in rats? Neurosci Lett 370:236–240

Farkas T, Boyd RD, Schaffler MB, Radin EL, Burr DB (1987) Early vascular changes in rabbit subchondral bone after repetitive impulsive loading. Clin Orthop 30:259–267

Ford-Hutchinson AF, Ali Z, Seerattan RA, Cooper DML, Hallgrímsson B, Salo PT, Jirik FR (2005) Degenerative knee joint disease in mice lacking 3′-phosphoadenosine 5′-phosphosulfate synthetase 2 (Papss2) activity: a putative model of human *PAPSS2* deficiency-associated arthrosis. Osteoarthritis Cart 13:418–425

Glasson SS, Askew R, Sheppard B, Carito BA, Blanchet T, Ma HL, Flannery CR, Kanki K, Wang E, Peluso D, Yang Z, Majumdar MK, Morris EA (2004) Characterization and osteoarthritis susceptibility in ADAMTS-4-knockout mice. Arthritis Rheum 50:2547–2558

Glasson SS, Askew R, Sheppard B, Carito B, Blanchet T, Ma HL, Flannery CR, Peluso D, Kanki K, Yang Z, Majumdar MK, Morris EA (2005) Deletion of active ADAMTS5 prevents cartilage degeneration in a murine model of osteoarthritis. Nature 434:644–648

Greenwald RA (1991) Animal models for evaluation of arthritis drugs. Meth Find Clin Pharmacol 13:75–83

Greenwald RA (1993) Cartilage degradation in animal models of inflammatory joint disease. In: Woessner JF, Howell DS (eds) Joint cartilage degradation. Basic and clinical aspects. New York, Marcel Dekker Inc., pp 385–408

Greenwald RA, Diamond HS (eds) (1988) CRC Handbook of animal models for the rheumatic diseases. CRC press, Boca Raton, Vol 1

Haakenstad LH (1969) Chronic bone and joint diseases in relation to conformation in the horse. Eq Vet J 1:248

Han F, Kipnes JR, Li Y, Tuan RS, Hall DJ (2002) The murine COMP (cartilage oligomeric matrix protein) promoter contains a potent transcriptional repressor region. Osteoarthritis Cartil 10:638–645

Hess EV, Herman JH (1986) Cartilage metabolism and antiinflammatory drugs in osteoarthritis. Am J Med 81:36–43

Hinz B, Brune K (2004) Pain and osteoarthritis: new drugs and mechanisms. Curr Opin Rheumatol 16:628–633

Johnson K, Terkeltaub R (2003) Upregulated ank expression in osteoarthritis can promote both chondrocyte MMP-13 expression and calcification via chondrocyte extracellular PP_i excess. Osteoarthritis Cartil 12:321–335

Kalbhen DA (1983) Pharmakologische Beurteilung von Möglichkeiten einer Knorpelschutztherapie bei degenerativen Gelenkerkrankungen (Arthrose). Z Rheumatol 42:187–194

Kalbhen DA (1987) Chemical model of osteoarthritis – a pharmacological evaluation. J Rheumatol 14:130–131

Konttinen YT, Michelsson JE, Tolvanen E, Bergroth V (1990) Primary inflammatory reaction in synovial fluid and tissue in rabbit immobilization osteoarthritis. Clin Orthop Rel Res 260:280–286

Lindenhayn K, Haupt R, Kristan J, Regling G (1984) Proteinase activity in the joint cartilage of sheep following mechanical arthrosis induction using an impulse stress instrument. Beitr Orthop Traumatol 31:507–511

Lust G, Rendano VT, Summers BA (1985) Canine hip dysplasia: concepts and diagnosis. J Am Vet Med Assoc 187:638–640

Malemud CJ (1993) Markers of osteoarthritis and cartilage research in animal models. Current Opinion in Rheumatology 5:494–502

Mazières B, Herou P, Dambreville JM, Thiechart H (1984) Die Wirkung eines Glykosaminoglykan-Peptid-Komplexes (GAG-Peptid-Komplex) bei experimenteller Arthrose am Kaninchen. Akt Rheumatol 9:133–138

Meacock SCR, Bodmer JL, Billingham MFJ (1990) Experimental osteoarthritis in guinea pigs. J Exp Pathol 71:279–293

Meyer-Carrive I, Ghosh P (1992) Effects of tiaprofenic acid (Surgam) on cartilage proteoglycans in the rabbit joint immobilization model. Ann Rheum Dis 51:448–455

Moskowitz RW (1990) The relevance of animal models in osteoarthritis. Scand J Rheum 81 (Suppl):21–23

Moskowitz RW (1992) Experimental models of osteoarthritis. In: Moskowitz RW, Howell DS, Goldberg VM, Mankin HJ (eds) Osteoarthritis: Diagnosis and medical/surgical management. 2nd ed. Philadelphia: W.B. Saunders, pp 213–232

Moskowitz RW, Davis W, Sammarco J, Martens M, Baker J, Mayor M, Burstein AH, Frankel BH (1973) Experimentally induced degenerative joint lesions following partial menisectomy in the rabbit. Arthr Rheum 16:397–405

Moskowitz RW, Howell DS, Goldberg VM, Muniz O, Pita JC (1979) Cartilage proteoglycan alterations in an experimentally induced model of rabbit osteoarthritis. Arthr Rheum 22:155–163

Oegema TR, Visco D (1999) Animal models of osteoarthritis. In: An YH, Friedman RJ (eds) Animal models in orthopaedic research. CRC Press LLC Boca Raton, pp 349–367

Palmoski MJ, Brandt KD (1982) Aspirin aggravates the degeneration of canine joint cartilage caused by immobilization. Arthritis Rheum 25:1333–1342

Pita JC, Manicourt DH, Muller FJ, Howell DS (1986) Studies on the potential reversibility of osteoarthritis in some experimental animal models. In Kuettner KE, Schleyerbach R, Hascall VC (eds) Articular cartilage biochemistry. Raven Press New York, pp 349–363

Pritzker KPH (1994) Animal models for Osteoarthritis: Processes, problems, and prospects. Ann Rheum Dis 53:406–420

Pritzker KPH, Chateauvert JM, Grynpas MD, Renlund RC, Turnquist J, Kessler MJ (1989) Rhesus macaques as an experimental model for degenerative arthritis. P R Health Sci J 8:99–102

Regling G, Buntrock P, Geiss W (1989) Monoiodoacetic acid-induced arthropathy of the rabbit knee – a contribution to the pathogenesis of arthrosis. Beitr Orthop Traumatol 36:193–203

Rintala M, Metsaranta M, Saamanen AM, Vuorio E, Ronning O (1997) Abnormal craniofacial growth and early mandibular osteoarthritis in mice harbouring a mutant type II collagen transgene. J Anat 190 (Pt 2):201–208

Scharstuhl A, Diepens R, Lensen J, Vitters E, van Beuningen H, van der Kraan P, van den Berg W (2003) Adenoviral overexpression of Smad-7 and Smad-6 differentially regulates TGF-β-mediated chondrocyte proliferation and proteoglycan synthesis. Osteoarthritis Cartil 11:773–382

Schwartz ER (1985) Surgically induced osteoarthritis in guinea pigs: studies of proteoglycans, collagens, and non-collagen proteins. In: Peyron JG (ed) Osteoarthritis: current clinical and fundamental problems. Proc of a Workshop held in Paris April 9–11, 1984. Rueil-Malmaison: Geigy: 273–288

Serra R, Johnson M, Filvaroff EH, LaBorde J, Sheehan DM, Derynck R, Moses HL (1997) Expression of a truncated, kinase-defective TGF-β type II receptor in mouse skeletal tissue promotes terminal chondrocyte differentiation and osteoarthritis. J Cell Biol 139:541–552

Todhunter RJ, Lust G (1992) Synovial joint anatomy, biology and pathobiology. In: Auer J (ed) Equine Surgery Philadelphia, Saunders, pp 844–866

Torelli SR, Rahal Sc. Volpi RS, Sequeira JL, Grassioto IQ (2005) Histopathological evaluation of treatment with chondroitin sulphate for osteoarthritis induced by continuous immobilization in rabbits. J Vet Med A Physiol Pathol Clin Med 52:45–51

Ueblacker P, Wagner B, Krüger A, Voigt S, DeSantis G, Kennerknecht E, Brill T, Hillemanns M, Salzmann GM, Imhoff AB, Plank C, Gänsbacher B, Martinek V (2004) Inducible nonviral gene expression in the treatment of osteochondral defects. Osteoarthritis Cartil 12:711–719

Van Lent PLEM, Holthuysen AEM, Slöetjes A, Lubberts E, van den Berg WB (2002) Local overexpression of adeno-viral IL-4 protects cartilage from metalloproteinase-induced destruction during immune complex-mediated arthritis by preventing activation of pro-MMPs. Osteoarthritis Cartil 10:234–243

Wadhwa S, Embree MC, Kilts T, Young MF, Ameye LG (2005) Accelerated osteoarthritis in the temporomandibular joint of biglycan/fibromodulin double-deficient mice. Osteoarthritis Cartil 13:817–827

Wieland HA, Michaelis M, Kirschbaum BJ, Rudolphi KA (2005) Osteoarthritis – an untreatable disease? Nature Rev 4:331–343

Williams JM, Uebelhart D, Ongchi DR, Kuettner KE, Thonar EJMA (1992) Animal models of articular cartilage repair. In: Kuettner KE, Schleyerbach R, Pyron JG, Hascall VC (eds) Articular cartilage and osteoarthritis. New York Raven Press, pp 511–525

Xu L, Peng H, Wu D, Hu K, Goldring MB, Olsen BR, Li Y (2005) Activation of the discoidin domain receptor 2 induces expression of matrix metalloproteinase 13 associated with osteoarthritis in mice. J Biol Chem 280:548–555

Zaka R, Williams CJ (2005) Genetics of chondrocalcinosis. Osteoarthritis Cartil 13:745–740

Zhang YW, Su Y, Lanning N, Swiatek PJ, Bronson RT, Sigler R, Marin RW, Woude GFV (2005) Targeted disruption of *Mig-6* in the mouse genome leads to early onset degenerative joint disease. Proc Natl Acad Sci USA 102:11740–11745

I.1.2.2 Canine Anterior Cruciate Ligament (ACL) Transection Model

PURPOSE AND RATIONALE

Similar to human ACL ruptures, ACL transection in the dog knee and the subsequent joint instability results in progressive cartilage erosion, fibrillation, and formation of osteophytes. This elaborate model is well characterized, and regarded of high predictive value. It is mostly known as the "Pond-Nuki dog model". These authors achieved the ACL transection originally through a lateral stab incision, whereas others also performed the ligament transection after opening the joint. Both versions lead to similar morphological and biochemical changes, and are described and illustrated in detail by Adams and Pelletier (1988).

PROCEDURE

Animals

Mongrels, beagles, greyhounds, and foxhounds are reported to be suitable, provided purebred strains are used. In general, younger animals display more repair phenomena, whereas older ones seem to show more rapid degeneration. As the epiphyses fuse at the age of 13 months, and as pronounced changes require up to 4 months to fully develop, careful planning ahead is essential.

Operation

The dogs are initially anesthetized with 30 mg/kg sodium pentobarbital i.v., followed by a continuous inhalation of 1% halothane with 1 l/min N_2O and 2 l/min O_2. After shaving and sterilizing the knee joint externally, it is fixed in a bent position at 90°, and a scalpel blade is inserted medially deep into the joint space diagonally posterior to the ACL, and parallel to the lateral border of the patellar ligament. By rotation of the blade, the ACL is then dissected, the blade withdrawn, and the wound closed. In the contralateral knee, a sham operation is performed to inflict similar disturbance to the joint tissue, but without harming the ACL. The ACL dissection results after 8 to 12 weeks, in contrast to the sham-operated contralateral knee, in fibrillation and erosion of the cartilage, more pronounced on the tibial plateau than on the femoral condyles. Also observed histologically is a loss of metachromatic staining, and a fissured surface with cell clones appears. A marked osteophytosis and subchondral sclerosis has also developed at that time. Proteoglycan content and overall cartilage thickness, however, seems to remain stable (Pelletier and Martel-Pelletier 1985) or even increase not only for several months (McDevitt et al. 1977; Vignon et al. 1983; Brandt and Adams 1989), but for up to 3 years after transection, as Brandt, Myers et al. (1991) could show. At later stages, however, severe cartilage thinning and loss is recorded (Brandt, Braunstein et al. 1991).

EVALUATION

Macroscopic inspection of cartilage and osteophytes are recorded. Histological grading based on the Mankin score has been reported to be modified by drug

treatment over 7 weeks (Abatangelo et al. 1989; Schiavinato et al. 1989). As levels and activity of neutral matrix metalloproteases are elevated in cartilage and synovium (Pelletier, Martel-Pelletier 1985), they might be additional parameters of interest to profile the test compounds.

CRITICAL ASSESSMENT OF THE TEST

In this instability model, a polysulfated glycosaminoglycan preparation (Arteparon), as well as intra-articular injections of a hyaluronic acid preparation induced some morphological and biochemical changes, whereas low-dose prednisone had no effect. As there seems to prevail an anabolic response to the instability in the articular cartilage for quite a long time, the selected time points and parameters to assess disease progression and therapeutic success require careful consideration.

MODIFICATIONS OF THE TEST

Caron et al. (1996) and Pelletier et al. (1997) investigated the *in vivo* effect of the recombinant human interleukin-1 receptor antagonist on the development of lesions in the anterior cruciate ligament transection model in dogs.

Wenz et al. (1998) used the Pond-Nuki model in dogs to evaluate the effectiveness of intra-articular application of hyaluronic acid on early forms of femoropatellar arthrosis. Transection of the anterior cruciate ligament in dogs was also used in studies by Myers et al. (1999), Boileau et al. (2002, 2005), Smith et al. (1999, 2002), Behets et al. (2004), and Matyas et al. (2004).

Pelletier et al. (2005) studied the effects of licofelone, a 5-lipoxygenase/cycloogygenase inhibitor, in the experimental anterior cruciate ligament dog model of osteoarthritis.

ACL transection can be performed also in an arthrotomy operation as described by Adams and Pelletier (1988), and an instability can be achieved equally by meniscectomy (Hannan et al. 1987).

The **rabbit** is the main other species used for instability models, as described in detail for partial medial meniscectomy by DiPasquale et al. (1988), and for partial lateral meniscectomy in connection with ligament transection by Colombo (1988).

Obara et al. (1993) induced osteoarthritis by surgical dissection of the anterior cruciate ligament in rabbits and investigated fluorescence distribution after intra-articular administration of fluorescein-labeled sodium hyaluronate.

Anterior cruciate ligament transection in rabbits was used in several studies (Amiel et al. 2003; Kawano et al. 2003; Doschak et al. 2004; Zhang et al. 2004; Diaz-Gallego et al. 2005; Tiraloche et al. 2005).

Kobayashi et al. (2005) studied a vitamin B1 derivate, and its ability to enhance the chondroprotective effects of glucosamine hydrochloride and chondroitin sulfate in osteoarthritis created by partial medial meniscectomy of the knee joint in rabbits.

A partial medial meniscectomy with ligament transection is described for the **guinea pig** by Bendele (1987) and Schwartz (1988). This method has been used by Bendele et al. (1999) and by Sabatini et al. (2005).

Layton et al. (1987) produced biomechanical stress-induced hip osteoarthritis in guinea pigs by extra-articular myectomy and tendotomy.

The Hartley guinea pig strain spontaneously develops knee osteoarthritis whose manifestations are markedly similar to those of spontaneous knee osteoarthritis in humans (Bendele et al. 1989; Kraus et al. 2004).

Janusz et al. (2002) described a model of osteoarthritis in **rats** induced by surgically transecting the medial collateral ligament and meniscus and evaluated the effectiveness of a matrix metalloproteinase inhibitor in this model. Using this model, Moore et al. (2005) found that fibroblast growth factor-18 stimulates chondrogenesis and cartilage repair.

Machner et al. (1999) investigated the influence of an altered sensible joint innervation on the development of knee osteoarthritis in Wistar rats. Partial sensible joint denervation was performed by injection of 100 µg capsaicin into a sponge placed on the sensible nerve trunk. Half of the rats underwent strenuous running exercises (20 km in a running wheel by intracranial self-stimulation). Under these conditions, severe osteoarthritis changes were observed, which were only mild without exercise.

Hayamai et al. (2004) studied cartilage degeneration and osteophyte formation in the anterior cruciate ligament transection model in rats**.**

Wancket et al. (2005) used the medial meniscotomy model in Lewis rats to study the anatomical localization of cartilage degradation markers.

Ghosh et al. (1993), Appleyard et al. (1999), and Burkhart et al. (2001) used an osteoarthritis model induced by lateral meniscectomy in **sheep**.

REFERENCES AND FURTHER READING

Abatangelo G, Botti P, Del Bue M, Gei G, Samson JC, Cortivo R, DeGalateo A, Martelli M (1989) Intra-articular

sodium hyaluronate injections in the Pond-Nuki experimental model of osteoarthritis in dogs. I. Biochemical results. Clin Orthop Rel Res 241:278–285

Adams ME, Pelletier JP (1988) Canine anterior cruciate ligament transection model of osteoarthritis. In Greenwald RA, Diamond HS (eds) CRC handbook of animal models for the rheumatic diseases CRC press Boca Raton Vol 2:57–81

Amiel D, Toyoguchi T, Kobayashi K, Bowden K, Amiel ME, Healey M (2003) Long-term effect of sodium hyaluronate (Hyalgan) on osteoarthritis progression in a rabbit model. Osteoarthr Cartil 11:636–643

Appleyard RC, Gosh P, Swain MV (1999) Biomechanical, histological and immunohistological studies of patella cartilage in an ovine model of osteoarthritis induced by lateral meniscectomy. Osteoarthr Cartil 7:281–294

Behets C, Williams JM, Chappard D, Devogelaer JP, Manicourt DH (2004) Effects of calcitonin on subchondral trabecular bone changes and on osteoarthrotic cartilage lesions after acute cruciate ligament deficiency. J Bone Miner Res 19:1821–1826

Bendele AM (1987) Progressive chronic osteoarthritis in femorotibial joints of partial medial meniscectomized guinea pigs. Vet Pathol 24:444–448

Bendele AM, White SL, Hulman JF (1989) Osteoarthritis in guinea pigs. Histopathologic and scanning electron microscope features. Lab Anim Sci 39:115–121

Bendele A, McComb J, Gould T, McAbee T, Sennelo G, Chlipala E, Guy M (1999) Animal models of arthritis: relevance to human disease. Toxicol Pathol 27:134–142

Boileau C, Martel-Pelletier J, Jouzeau JY, Netter P, Moldovan F, Laufer S, Ries S, Pelletier JP (2002) Licofelone (ML-3000), a dual inhibitor of 5-lipoxygenase and cyclooxygenase, reduces the level of cartilage chondrocyte death in vivo in experimental dog osteoarthritis: inhibition of pro-apoptotic factors. J Rheumatol 29:1446–1453

Boileau C, Martel-Pelletier J, Brunet J, Tardif G, Schrier D, Flory C, El-Kattan A, Boily M, Pelletier JP (2005) Oral treatment with PD-0200347, an oral $\alpha_2\delta$ ligand, reduces the development of experimental osteoarthritis by inhibiting metalloproteinases and inducible oxide synthase gene expression and synthesis of cartilage chondrocytes. Arthritis Rheum 52:488–500

Brandt KD, Adams ME (1989) Exuberant repair of articular cartilage damage. Effect of anterior cruciate ligament transection in the dog. Trans Orthop Res Soc 14:584

Brandt KD, Braunstein EM, Visco DM, O'Connor B, Heck D, Albrecht M (1991a) Anterior (cranial) cruciate ligament transection in the dog: A bona fide model of osteoarthritis, not merely of cartilage injury and repair. J Rheumatol 18:436–446

Brandt KD, Myers SL, Burr D, Albrecht M (1991b) Osteoarthritic changes in canine articular cartilage, subchondral bone and synovium 54 months after transection of the anterior cruciate ligament. Arthritis Rheum 34:1560–1570

Burkhardt D, Hwa SY, Ghosh P (2001) A novel microassay for the quantitation of sulfated glycosaminoglycan content of histological sections: its application to determine the effects of Diacerhein on cartilage in an ovine model of osteoarthritis. Arthritis Cartil 9:238–247

Caron JP, Fernandes JC, Martel-Pelletier J, Tardif G, Mineau F, Geng C, Pelletier JP (1996) Chondroprotective effect of intraarticular injections of interleukin-1 antagonist in experimental arthritis: Suppression of collagenase-1 expression. Arthritis Rheum 39:1535–1544

Colombo C (1988) Partial lateral meniscectomy with section of fibular collateral and sesamoid ligaments in the rabbit. In: Greenwald RA, Diamond HS (eds) CRC handbook of animal models for the rheumatic diseases CRC press Boca Raton Vol 2:27–55

Diaz-Gallego L, Prieto JG, Coronel P, Gamazo LE, Gimeno M, Alvarez AI (2005) Apoptosis and nitric oxide in an experimental model of osteoarthritis in rabbit after hyaluronic acid treatment. J Orthop Res 23:1370–1376

DiPasquale G, Caputo CB, Crissman JW (1988) Rabbit partial medial meniscectomy. In: Greenwald RA, Diamond HS (eds) CRC handbook of animal models for the rheumatic diseases. CRC, Boca Raton, Fla., Vol 2:19–25

Doschak MR, Wohl GR, Hanley DA, Bray RC, Zernicke RF (2004) Antiresorptive therapy conserves some periarticular bone and ligament mechanical properties after anterior cruciate ligament disruption in the rabbit knee. J Orthop Res 22:942–948

Ghosh P, Read R, Armstrong S, Wilson D, Marshall R, McNair P (1993) The effects of intra-articular administration of hyaluran in a model of early osteoarthritis in sheep. I. Gait analysis, radiological and morphological studies. Semin Arthritis Rheum 6 [Suppl 1]:31–42

Hannan H, Ghosh P, Bellenger C, Taylor T (1987) Systemic administration of glycosaminoglycan polysulfate (Arteparon) provides partial protection of articular cartilage from damage produced by meniscectomy in the canine. J Orthop Res 5:47–59

Hayamai T, Pickarski M, Wesolowski GA, Mclane J, Bone, Destefano J, Rodan GA, Duong LT (2004) The role of subchondral bone remodeling in osteoarthritis. Reduction of cartilage degeneration and prevention of osteophyte formation by alendronate in the rat anterior cruciate ligament transection model. Arthritis Rheum 50:1193–1206

Janusz MJ, Bendele AM, Brown KK, Taiwo YO, Hsieh L, Heitmeyer SA (2002) Induction of osteoarthritis in the rat by surgical tear of the meniscus: inhibition of joint damage by a matrix metalloproteinase inhibitor. Osteoarthr Cartil 10:785–791

Johnson RG (1986) Transection of the canine anterior cruciate ligament: a concise review of experience with this model of degenerative joint disease. Exp Pathol 30:209–213

Kawano T, Miura H, Mawatari T, Moro-Oka T, Nakanishi Y, Higaki H, Iwamoto Y (2003) Mechanical effects of the intraarticular administration of high molecular weight hyaluronic acid plus phospholipid on synovial joint lubrication and prevention of articular cartilage degeneration in experimental osteoarthritis. Arthritis Rheum 48:1923–1929

Kobayashi T, Notoya K, Nakamura A, Akimoto K (2005) Fursultimine, a vitamin B1 derivate, enhances chondroprotective effects of glucosamine hydrochloride and chondroitin sulfate in rabbit experimental osteoarthritis. Inflamm Res 54:249–255

Kraus VB, Huebner JL, Stabler T, Flahiff CM, Setton LA, Fink C, Vilim V, Clark AG (2004) Ascorbic acid increases the severity of spontaneous osteoarthritis in a guinea pig model. Arthritis Rheum 50:1822–1831

Layton MW, Arsever C, Bole GG (1987) Use of guinea pig myectomy osteoarthritis model in the examination of cartilage-synovium interactions. J Rheumatol 14/Spec No:125–126

Machner A, Pap G, Schwarzberg H, Eberhardt R, Roessner A, Neumann W (1999) Störung sensibler Gelenkinnervation als begünstigender Faktor für die Arthroseentstehung. Eine tierexperimentelle Untersuchung am Rattenmodel. (Deterioration in sensible joint innervation as a possible cause for the development of osteoarthritis. An animal study in rats.) Z Rheumatol 58:148–154

Matyas JR, Atley L, Ionescu M, Eyre DR, Poole AR (2004) Analysis of cartilage biomarkers in the early phases

of canine experimental osteoarthritis. Arthritis Rheum 50:543–552
McDevitt C, Gilbertson E, Muir H (1977) An experimental model of osteoarthritis; early morphological and biochemical changes. J Bone Joint Surg 59B:24–35
Moore EE, Bendele AM, Thompson DL, Littau A, Waggie KS, Reardon B, Ellsworth JL (2005) Fibroblast growth factor-18 stimulates chondrogenesis and cartilage repair in a rat model of injury-induced osteoarthritis. Osteoarthr Cartil 13:623–631
Myers SL, Brandt KD, O'Connor BL (1991) Low dose prednisone treatment does not reduce the severity of osteoarthritis in dogs after cruciate ligament transection. J Rheum 18:1856–1862
Myers SL, Brandt KD, Burr DB, O'Connor BL, Albrecht M (1999) Effects of a biphosphonate on bone histomorphometry and dynamics in the canine cruciate deficiency model of osteoarthritis. J Rheumatol 26:2845–2853
Newton CH, Fetter DA, Bashey RI, Jimenez SA (1984) Clinical studies and pathological changes in articular cartilage in experimental canine osteoarthrosis and effects of the *in vivo* administration of a glycosaminoglycan peptide (GAG-Peptide-complex) from bone marrow and cartilage. Akt Rheumatol 9:128–132
Obara T, Yamaguchi T, Moriya Y, Namba K (1993) Tissue distribution of fluorescein-labeled sodium hyaluronate in experimentally-induced osteoarthritis. Jpn Pharmacol Ther 21/Suppl 2:193–200
Pelletier JP, Martel-Pelletier J (1985) Cartilage degradation by neutral proteoglycanases in experimental osteoarthritis: suppression by steroids. Arthritis Rheum 28:1393
Pelletier JP, Martel-Pelletier J (1991) *In vivo* protective effects of prophylactic treatment with tiaprofenic acid or intraarticular corticosteroids on osteoarthritic lesions in the experimental dog model. J Rheumatol 18 (Suppl 27):127–130
Pelletier JP, Caron JP, Evans C, Robbins PD, Georgescu HI, Javanovic D, Fernandes JC (1997) *In vivo* suppression of early experimental osteoarthritis by interleukin-1 receptor antagonist using gene therapy. Arthritis Rheum 40:1012–1019
Pelletier JP, Boileau C, Boily M, Brunet j, Mineau F, Geng C, Reboul P, Laufer S, Lajeunesse D, Martel-Pelletier J (2005) The protective effect of licofelone on experimental osteoarthritis is correlated with the downregulation of gene expression and protein synthesis of several major catabolic factors: MMP-13, cathepsin K and aggrecanases. Arthritis Res Ther 7:R1091–R1102
Pond MJ, Nuki G (1973) Experimentally-induced osteoarthritis in the dog. Ann Rheum Dis 32:387
Sabatini M, Lesur C, Thomas M, Chomel A, de Nanteuil G, Pastoureau P (2005) Effect of inhibition of matrix metalloproteinase on cartilage loss in vitro and in a guinea pig model of osteoarthritis. Arthritis Rheum 52:171–180
Schiavinato A, Lini E, Guidolin D, Pezzoli G, Botti P, Martelli M, Cortivo R, DeGalateo A, Abatangelo G (1989) Intra-articular sodium hyaluronate injections in the Pond-Nuki experimental model of osteoarthritis in dogs. II. Morphological findings. Clin Orthop Rel Res 241:286–299
Schwartz E (1988) Surgically induced osteoarthritis in guinea pigs. In: Greenwald RA, Diamond HS (eds) CRC handbook of animal models for the rheumatic diseases CRC press, Boca Raton, Vol 2:89–95
Smith GN, Myers SL, Brandt KD, Mickler EA, Albrecht ME (1999) Diacerhein treatment reduces the severity of osteoarthritis in the canine cruciate-deficiency model of osteoarthritis. Arthritis Rheum 42:545–554
Smith GN, Mickler EA, Albrecht ME, Myers SL, Brandt KD (2002) Severity of medial meniscus damage in the canine knee after anterior cruciate ligament transection. Osteoarthr Cartil 10:321–326
Tiraloche G, Girard C, Chouinard L, Sampalis J, Moquin L, Ionescu M, Reiner A, Pole AR, Laverty S (2005) Effect of oral glucosamine on cartilage degradation in a rabbit model of osteoarthritis. Arthritis Rheum 52:1118–1128
Vignon E, Arlot M, Hartman D, Moyer B, Ville G (1983) Hypertrophic repair of articular cartilage in experimental osteoarthrosis. Ann Rheum Dis 42:82–88
Wancket LM, Baragi V, Bove S, Kilgore K, Korytko PJ, Guzman RE (2005) Anatomical localization of cartilage degradation markers in a surgically induced osteoarthritis model. Toxicol Pathol 33:484–489
Wenz W, Graf J, Brocai DR, Breusch SJ, Mittacht M, Thomas O, Niethard FU (1998) Wirksamkeit von intraartikulär applizierter Hyaluronsäure auf Frühformend der Femoropatellararthrose. Eine experimentelle Untersuchung an Hunden. Effectiveness of intra-articular application of hyaluronic acid on early forms of femeropatellar arthrosis. An experimental study in dogs. Z Orthop Grenzgebiete 136:298–3003
Zhang X, Mao Z, Yu C (2004) Suppression of early experimental osteoarthritis by gene transfer of interleukin-1 receptor antagonist and interleukin-10. J Orthop Res 22:742–750

I.1.2.3 Chymopapain-Induced Cartilage Degeneration in the Rabbit

PURPOSE AND RATIONALE

Intraarticular injection of chymopapain into the rabbit knee joint results in cartilage degradation with rapid loss of proteoglycans. A transient inflammation shortly after injection normally subsides after 1–2 days. Severity and reversibility of the cartilage damage can be altered using different protocols (Williams et al. 1992).

PROCEDURE

Most authors use New Zealand White rabbits at the age of 2 to 4 months. Male Chinchilla and Chinchilla Bastard rabbits are preferred, as they display a thicker cartilage than the New Zealand strain. The animals with an initial body weight of ca 2.5 kg are anesthetized with a continuous inhalation of 4% halothane – 3 l/min N_2O – 1.8 l/min O_2. Both knee joints are carefully shaved and moisturized with 70% alcohol. With a sterile syringe a volume of 0.1 ml of the following solution is injected laterally into the joint space: eighteen mg chymopapain (Sigma) are dissolved in 1 ml 0.9% NaCl, and 50 mg l-cysteine-HCl is added for activation. The preparation is then passed under sterile conditions through a 0.22 µm Millipore filter, and tested for activity prior to each operation. (Potential direct interference of the therapeutic agent to be tested with the chymopapain can also be addressed at that point). One injection of 1.8 mg chymopapain in 0.1 ml per joint usually results in a proteoglycan loss/cartilage

dry weight of ca 40% after 10 to 12 days. Two to 4 animals per experiment receive chymopapain in 0.9% NaCl in one joint, and 0.9% NaCl into the contralateral knee to assess the proteoglycan loss caused by the enzyme. Care is taken with all injections to apply the same volume to both joints, as the contralateral serves as internal control. If the drug is given orally, only one knee receives chymopapain treatment, whereas if the drug is applied intraarticularly into one knee (1 to 5 injections of 0.1 ml volume each, vehicle into contralateral joint, in a period of 5 to 10 days), both knees are treated with chymopapain. The animals are sacrificed after 10 to 14 days, and from defined regions of weight-bearing areas in the joint full thickness samples are obtained for histology and assessment of proteoglycan content.

Histology is performed on full thickness sections of the articular cartilage, fixed with 3% formalin, embedded in paraffin, and stained routinely with safranin-O/fast green, or with toluidin-blue (Romeis 1989).

The proteoglycan content is determined with the dimethyl-methylen blue (DMB) method modified after Farndale et al. (1986) and Chandrasekhar et al. (1987). The wet weight of the cartilage samples is determined immediately after preparation, and their dry weight is recorded after 3 day drying at 60°C. Samples are then soaked overnight in 1 ml buffer (containing 20 mM disodiumhydrogenphosphate, 1 mM EDTA, and 2 mM dithiothreitol in 500 ml aqua bidest at pH 6.8). Ten µl of papain, suspended in 0.05 M sodiumacetate (Sigma 9001–73-4), are then added, and incubated at 60°C for 6 h. Ten µl of standard (shark chondroitinsulfate C (Sigma C4384) in a concentration range from 10–200 µg/ml buffer) and of each probe are then transferred into a 96 well microtiter-plate. Two hundred µl of DMB is added, and, after 1 min, the extinction recorded photometrically at 690/540 nm. The DMB solution is prepared by dissolving 16 mg DMB (Serva 20335) in 2 ml methanol, adding 400 ml aqua bidest, 9.6 ml 1N HCl-solution, 3.04 g glycine, and 2.36 g NaCl, stirred and warmed until dissolved, and then diluted to a final volume of 1000 ml with aqua dest (pH 3.0). The results are recorded as µg chondroitinsulfate equivalents/mg cartilage dry weight.

EVALUATION

The histological appearance of the articular cartilage is assessed with a modified Mankin score, emphasizing more earlier changes, and separating degradative aspects, (e. g. loss of safranin staining), from repair aspects, (e. g. the occurrence of pericellular staining). The proteoglycan content is expressed as % change to the contralateral knee, or, comparing groups, to chymopapain-treated or. untreated control groups. To relate the proteoglycan content to cartilage dry weight has been found to be more reliable than choosing wet weight as baseline, as the cartilage water content is known to change in this model according to matrix composition.

CRITICAL ASSESSMENT OF THE TEST

In this model, hyaluronic acid preparations and some MMP inhibitors can be detected, NSAIDs do not change the parameters tested. The protocol can be modified to emphasize repair phenomena, or to assure a more severe course of cartilage loss (Williams et al. 1993).

MODIFICATIONS OF THE MODEL

Muehleman et al. (2002) investigated bone remodeling inhibition by a biphosphonate in the rabbit model of cartilage matrix damage by chymopapain injection.

To avoid interaction of a drug with the enzymatic nature of the chymopapain, other degradation mediators can be applied instead, as e. g. fibronectin fragments (Williams et al. 1988).

To ensure continuous synovial levels of a given drug, an osmotic minipump containing the drug can be implanted into the femoral muscles with a prolonged fine tube to insert into the patellar groove (Karbowski et al. in prep). This is an elaborate procedure in which a Ketavet/Rampun anesthesia is needed, and postoperative plastic collars to prevent the rabbits to interfere with the operated region for the first three days. This results in highly consistent data compared to repeated injections.

Kikuchi et al. (1998) induced experimental osteoarthritis in mature rabbits by intra-articular injection of collagenase.

Pomonis et al. (2005) developed a **rat model of osteoarthritis pain.** Male Sprague Dawley rats were anesthetized with isoflurane and received a single injection of iodoacetate (0.3, 1, or 3 mg), papain (0.5, 1, 2, or 3%) or saline in a 50 µl volume into the left knee joint using a 27-gauge needle inserted through the patella tendon. Assessment of pain-related behaviors was performed using a hind limb weight-bearing apparatus (Linton Incapacitance Tester Stoelting, Wood Dale, Ill., USA). Animals treated with intra-articular iodoacetate were evaluated for alterations in weight bearing after the acute and chronic administration of various drugs.

Osteoarthritic lesions in the knee joints of male C57bl10 mice were induced by a single intra-articular

injection of bacterial collagenase (Van der Kraan et al. 1990; Van den Berg et al. 1993).

Van der Kraan et al. (1989) and Scharstuhl et al. (2002) induced arthritis in mice by a single intra-articular injection of papain in their knee joints.

Van Osch et al. (1995) developed a device to measure laxity of knee joints in mice. Reproducible, non-linear S-shaped load displacement curves were determined from knee joints of normal mice. Parameters of anterior-posterior translation, varus-valgus rotation, and compliance were calculated from the curves. Laxity was marked increased in animals with osteoarthritis induced by intra-articular injection of collagenase.

Saez-Llorens et al. (1991) and Cohen et al. (2004) described a model of **septic arthrosis** in rabbits.

Four-month-old female New Zealand rabbits were anesthetized with an intramuscular injection of 60 mg/kg ketamine and 6 mg/kg xylazine. The skin overlying the knees was shaved and cleansed with povidone-iodine and 70% ethanol. The right knee was injected with 10^5–10^6 colony forming units of *Staphylococcus aureus*, while the left knees were injected with sterile saline. Following injection, all rabbits were allowed normal cage activity. The rabbits were left either untreated, or were treated with antibiotic (40 mg/kg ceftriaxone) alone or additionally with different doses of test drug. Animals were anesthetized at 1, 4, and 7 days following initiation of treatment. Prior to aspiration of synovial fluid, the knee joint was inspected for evidence of effusion and range of motion testing. Following an arthrotomy, the gross appearance of the joint was examined for joint degradation and the fluid grossly inspected for purulence. Prior to sacrifice, an arterial blood sample was plated on agar plates, incubated for 48 h at 37°C, and analyzed for colony growth. In the synovial fluid the number of white blood cells was determined and bacterial growth examined in serial dilutions. Histology was performed in synovial tissue from the pre-patellar fat pad and the medial femoral condyle.

REFERENCES AND FURTHER READING

Chandrasekhar S, Esterman MA, Hoffman HA (1987) Microdetermination of proteoglycans and glycosaminoglycans in the presence of guanidine hydrochloride. Anal Biochem 161:103–108

Cohen SB, Gill SS, Baer GS, Leo BM, Scheld WM, Diduch DR (2004) Reducing joint destruction due to septic arthrosis using an adenosine$_{2A}$ receptor agonist. J Orthop Res 22:427–435

Farndale RW, Buttle DJ, Barrett AJ (1986) Improved quantitation and discrimination of sulphated glycosaminoglycans by use of dimethyl-methylene blue. Biochim Biophys Acta 883:173–177

Karbowski A, Raiss RX, Schneider EJ (in prep) Continuous intraarticular therapy using an osmotic minipump

Kikuchi T, Sakuta T, Yamaguchi T (1998) Intra-articular injection of collagenase induces experimental osteoarthritis in mature rabbits. Osteoarthr Cartil 6:177–186

Mankin HJ, Dorfman H, Lipiello L (1971) Biochemical and metabolic abnormalities in articular cartilage from osteoarthritic human hips. J Bone Joint Surgery 53A:523–537

Muehleman C, Green J, Williams JM, Kuettner KE, Thonart EJMA, Sumner DR (2002) The effect of bone remodeling inhibition by zoledronic acid in an animal model of cartilage matrix damage. Osteoarthr Cartil 10:226–233

Pomonis JD, Boulet JM, Gottshall SL, Phillips S, Sellers R, Bunton T, Walker K (2005) Development and pharmacological characterization of a rat model of osteoarthritis pain. Pain 114:339–346

Romeis B (1989) Mikroskopische Technik. 17th ed., Urban & Schwarzenberg München

Rosenberg L (1971) Chemical basis for the histological use of safranin-O in the study of articular cartilage. J Bone Joint Surgery 53A:69–82

Saez-Llorens X, Jafari HS, Olsen KD, Nariuchi H, Hansen EJ, McCracken GH Jr (1991) Induction of suppurative arthritis in rabbits by Haemophilus endotoxin, tumor necrosis factor-alpha, and interleukin-1 beta. J Infect Dis 163:1267–1273

Scharstuhl A, Glansbeek HL, van Beuningen HM, Vitters EL, van der Kraan PM, van den Berg WB (2002) Inhibition of endogenous TGF-β during experimental osteoarthritis prevents osteophyte formation and impairs cartilage repair. J Immunol 169:507–514

Van den Berg WB, van Osch GJM, van der Kraan PM, van Beuningen HM (1993) Cartilage destruction and osteophytes in instability-induced murine osteoarthritis: Role of TGFβ in osteophyte formation? Agents Actions 40:215–219

Van der Kraan PM, Vitters EL, van de Putte LB, van den Berg (1989) Development of osteoarthritic lesions in mice by "metabolic" and "mechanical" alterations in the knee joints. Am J Pathol 135:1001–1014

Van der Kraan PM, Vitters EL, van Beuningen HM, van de Putte LBA, van den Berg WB (1990) Degenerative knee joint lesions in mice after a single intra-articular collagenase injection. A new model of osteoarthritis. J Exp Pathol GBR 71:19–31

Van der Sluijs JA (1992) The reliability of the Mankin score for osteoarthritis. J Orthop Res 10:58–61

Van Osch GJVM, Blankevoort L, van der Kraan PM, Janssen B, Hekman E, Huiskes R (1995) Laxicity characteristics of normal and pathological murine knee joints *in vitro*. J Orthop Res 13:783–791

Williams JM, Downey C, Thonar EJMA (1988) Increase in levels of serum keratan sulfate following cartilage proteoglycan degradation in the rabbit knee joint. Arthr Rheum 31:557–560

Williams JM, Ongchi DR, Thonar EJMA (1993) Repair of articular cartilage injury following intra-articular chymopapain-induced matrix proteoglycan loss. J Orthop Res 11:705–716

I.1.2.4 Spontaneous OA Model in STR/1N Mice

PURPOSE AND RATIONALE

This spontaneous model has the advantage of a gradually developing OA starting with cartilage surface ero-

sion and fibrillation to osteophyte formation, subchondral bone remodeling, and finally eburnation, in a moderate time frame. All these steps, with only intermittent inflammatory flares, are similar to human pathology, and develop without any interference. The disadvantages are, however, the restriction to systemic drug application, due to the relative small animal size, and the variance in onset and severity of the disease among the animals.

PROCEDURE

The STR/1N mouse strain, characterized extensively by Walton (1977–1979) can be obtained from the National Institute of Health, Bethesda MA, USA. It is not identical to the STR/ORT strain as described by Benjamin et al. (1995), since it displays, in contrast to the ORT, no calcification in ligaments or tendons. Male mice develop OA earlier and more consistently than females, and, without dietary restriction, develop additionally obesity.

Beginning at the age of 10 weeks, male mice are trained to walk on a slowly rotating cylinder (or treadmill, manufactured by Ugo Basili, Italy) recording the mean walking time of each mouse. Mice with a moderate activity (neither dropping off too soon, nor staying on for hours) are then selected to enter the experiment. In groups of 8 to 10 animals, the drug is applied systemically for 8 weeks, and the mobility of each animal is recorded once or twice a week on the rotating cylinder. The body weight is recorded regularly as well. At the end of the experiment, the animals are sacrificed, both knee joints dissected, fixed, decalcified, and embedded in defined orientation for histology.

EVALUATION

The mean walking time decreases with age and disease progression, and is recorded in a time-dependent graph over the treatment period. The medial tibial plateau of the knee joints exhibits the most pronounced cartilage fibrillation and loss, and is, therefore, selected for histological evaluation, based on a modified Mankin grade.

CRITICAL ASSESSMENT OF THE TEST

Since this model is best suitable for oral drug application, experience with disease-modifying drugs for osteoarthritis is limited. Drugs with anti-inflammatory properties increase walking time, but do not alter the morphological aspects of cartilage degradation in the joint. Analgesic drugs have no effect on either.

MODIFICATIONS OF THE TEST

Rudolphi et al. (2003) studied an inhibitor of interleukin-1β converting enzyme in STR/1N mice and in a collagenase-induced osteoarthritis model in Balb/c mice. Weakening of knee joint ligaments was achieved by intra-articular injection of highly purified bacterial collagenase leading to increased joint laxity which resulted in osteoarthritic lesions preferentially in the medial compartments of the injected knee joint (Van der Kraan et al. 1990).

Several authors (Nakamura 1990; Pataki and Witzemann 1990; Wilhelmi and Meyer 1983) have used the C57black mouse which, however, is reported to vary considerably in the incidence and severity of the disease, and also to develop the osteoarthritis only at older ages.

The STR/ORT strain differs in its calcification of fibrous cartilage (Benjamin et al. 1995), and seems to change the orientation of the proteoglycans in the hyaline cartilage (Dunham et al. 1989).

Gaffen et al. (1997) found elevated aggrecan mRNA in STR/ort mice. Brewster et al. (1998) tested an orally active collagenase inhibitor in STR/ORT mice. Microfocal X-ray-generated images of the hind limbs as well as histologic sections of the knees were scored for degradative changes and drug effects. Chambers et al. (2001) reported that matrix metalloproteinases and aggrecanases cleave aggrecan in different zones of normal cartilage but co-localize in the development of osteoarthritis lesions on STR/ort mice. Mason et al. (2001) reviewed the use of the STR/ort mouse as a model of osteoarthritis. Flannelly et al. (2002) studied the temporal expression of matrix metalloproteinases and tissue inhibitors in the murine STR/ort model of osteoarthritis. Price et al. (2002) compared collagenase-cleaved articular cartilage collagen in mice in the naturally occurring STR/ort model of osteoarthritis and in collagen-induced arthritis.

Glant et al. (1998) reported progressive polyarthritis induced in BALB/c mice by aggrecan from normal and osteoarthritic human cartilage.

REFERENCES AND FURTHER READING

Benjamin M, Ralphs JR, Archer CW, Mason RM, Chambers M, Dowthwaite GP (1995) Cytoskeletal changes in articular fibrocartilage are an early indicator of osteoarthritis in STR/ORT mice. Orthop Res Soc 20:246

Brewster M, Lewis EJ, Wilson KL, Greenham AK, Bottomley KM (1998) Ro 32–3555, an orally active collagenase selective inhibitor, prevents structural damage in the STR/ORT mouse model of osteoarthritis. Arthritis Rheum 41:1639–1644

Chambers MG, Cox L, Chong L, Suri N, Cover P, Bayliss MT, Mason RM (2001) Matrix metalloproteinases and aggrecanases cleave aggrecan in different zones of normal cartilage but colocalize in the development of osteoarthritis lesions on STR/ort mice. Arthritis Rheum 44:1455–1465
Dunham J, Chambers MG, Jasani MK, Bitenski L, Chayen J (1989) Quantitative criteria for evaluating the early development of osteoarthritis and the effect of diclofenac sodium. Agents Actions 28:93–97
Flannelly J, Chambers MG, Dudhia J, Hembry RM, Murphy G, Mason RM, Bayliss MT (2002) Metalloproteinase and tissue inhibitor of metalloproteinase expression in the murine STR/ort model of osteoarthritis. Osteoarthr Cartil 10:722–733
Gaffen JD, Bayliss MT, Mason RM (1997) Elevated aggrecan mRNA in an early murine osteoarthritis. Osteoarthr Cartil 5:227–233
Glant TT, Szabo G, Nagase H, Jacobs JJ, Ikecz K (1998) Progressive polyarthritis induced in BALB/c mice by aggrecan from normal and osteoarthritic human cartilage. Arthritis Rheum 41:1007–1018
Mason RM, Chambers MG, Flanelly J, Gaffen DJ, Didhia J, Bayliss MT (2001) The STR/ort mouse and its use as a model of osteoarthritis. Osteoarthr Cartil 9:85–91
Nakamura Y (1990) Histochemical and immunohistochemical studies on knee joint cartilage in spontaneous osteoarthritis in C57 black mice. J Tokyo Med Coll 48:308–319
Pataki A, Graf HP, Witzemann E (1990) Spontaneous osteoarthritis of the knee-joint in C57BL mice receiving chronic oral treatment with NSAID's or prednisone. Agents Actions 29:210–217
Price JS, Chambers MG, Poole AR, Fradin A, Mason RM (2002) Comparison of collagenase-cleaved articular cartilage collagen in mice in the naturally occurring STR/ort model of osteoarthritis and in collagen-induced arthritis. Osteoarthr Cartil 10:172–179
Raiss RX, Caterson B (1992) Immunohistochemical localization of chondroitin sulfate isomers in the knee joint of osteoarthritic mice. In: Kuettner KE, Schleyerbach R, Pyron JG, Hascall VC (eds) Articular cartilage and osteoarthritis. New York Raven Press, pp 714–715
Raiss RX, Bartlett RR, Schleyerbach R (1992) Genetically Induced Mouse Models of Rheumatic Diseases. Effects of Leflunomide on Articular Manifestations. In: Kuettner KE, Schleyerbach R, Pyron JG, Hascall VC (eds) Articular cartilage and osteoarthritis. NewYork Raven Press, pp 712–713
Rudolphi K, Gerwin N, Verziji N, van der Kraan P, van den Berg W (2003) Pralnacasan, an inhibitor of interleukin-1â converting enzyme, reduces joint damage in two murine models of osteoarthritis. Osteoarthr Cartil 11:738–746
Schünke M, Tillmann B, Brück M, Müller-Ruchholtz W (1988) Morphologic characteristics of developing osteoarthrotic lesions in the knee cartilage of STR/1N mice. Arthr Rheum 31:898–905
Sokoloff L, Crittenden LB, Yamamoto RS, Jay GE (1962) The genetics of degenerative joint disease in mice. Arthr Rheum 5:531–545
Van der Kraan PM, Vitters EL, van Beuningen HM, van de Putte LB, van den Berg WB (1990) Degenerative joint lesions in mice after a single intra-articular collagenase injection. J Exp Pathol 71:19–31
Walton M (1977a) Degenerative joint disease in the mouse knee; histological observations. J Pathol 123:109–122
Walton M (1977b) Degenerative joint disease in the mouse knee; radiological and morphological observations. J Pathol 123:97–107
Walton M (1977c) Studies of degenerative joint disease in the mouse knee joint; scanning electron microscopy. J Pathol 123:211–217
Walton M (1979) Patella displacement and osteoarthrosis of the knee joint in mice. J Pathol 127:165–172
Wilhelmi G, Maier R (1983) Zur Prüfung potentieller Antiarthrotika an der spontanen Arthrose der Maus. Z Rheumatol 42:203–205

I.1.2.5 Transgenic Mice as Models of Osteoarthritis

PURPOSE AND RATIONALE

Osteoarthritis comprises a group of diseases characterized by gradual degeneration of articular cartilage and a number of associated processes within the joint. Consequently, no single animal model based on one genetic alteration is likely to fulfill all the criteria of human osteoarthritis (Helminen et al. 2002; Säämänen and Vuorio 2004). Transgenic mice with **collagen mutations** include different types of collagen.

Several lines of transgenic mice have been produced harboring mutations in the type II collagen gene. These include a line expressing a human *COL2A1* transgene with a large internal deletion (Vandenberg et al. 1991), and another expressing a murine *Col2a1* transgene with a Gly58Cys substitution in the helical domain (Garofalo et al. 1991). An osteoarthritis phenotype can also be produced by increasing the expression rate of the normal *Col2a1* gene, which leads to disruption of the regulation of type II collagen fibril assembly (Garofalo et al. 1993). The transgenic mouse line Del1 harbors six copies of a *Col2a1* transgene with a 150-bp deletion of exon 7 and introns 7, removing sequences coding for the 15 amino acids at the amino-terminal end of the triple helical domain (Metsäranta et al. 1992). Homozygous Del1 mice die at birth due to respiratory distress. Heterozygous Del1 mice develop early-onset human osteoarthritis-like lesions, usually confined to the knee joint (Säämänen et al. 2000).

Mice transgenic for type IX collagen mutations carrying a central in-frame deletion mutation that codes for truncated α1(IX) chains develop mild chondrodysplasia and progressive osteoarthritis with ocular involvement (Nakata et al. 1993). Fässler et al. (1994) reported non-inflammatory degenerative joint disease in mice lacking α1(IX) collagen.

Xu et al. (2003) demonstrated osteoarthritis-like changes and decreased mechanical function of articular cartilage in the joints of mice with the chondrodysplasia gene (*cho*). A mutation in the gene encoding the α1 chain of type XI collagen (*Col11a1)* was identified as the genetic cause of chondrodysplasia in mice.

Several transgenic models of osteoarthritis with mutations in non-collagenous molecules were described. Ameye et al. (2002) reported that abnormal collagen fibrils in tendons of biglycan/fibromodulin-deficient mice lead to gait impairment, ectopic ossification, and osteoarthritis. Ameye and Young (2002) recommended mice deficient in small leucine-rich proteoglycans as novel *in vivo* models of osteoporosis, osteoarthritis, Ehlers-Danlos syndrome, muscular dystrophy, and corneal diseases.

Zemmyo et al. (2003) described accelerated, aging-dependent development of osteoarthritis in $\alpha 1$ integrin-deficient mice. Morko et al. (2004) reported upregulation of cathepsin K expression in articular chondrocytes in a transgenic mouse model of osteoarthritis.

Involvement of **matrix metalloproteinases** has been demonstrated in the degradation of cartilage and the development of human osteoarthritis lesions. Holmbeck et al. (1999) reported that MT1-MMP-deficient mice develop dwarfism, osteopenia, arthritis, and connective tissue disease due to inadequate collagen turnover. Neuhold et al. (2001) found that postnatal expression in hyaline cartilage of constitutively active human collagenase-3 (MMP-13) induces osteoarthritis in mice. These mice develop cartilage lesions with histological similarities to human osteoarthritis. Salminen et al. (2002) reported differential expression patterns of matrix metalloproteinases and their inhibitors during development of osteoarthritis in the transgenic Del1 mouse model. Glasson et al. (2005) reported that deletion of active ADAMTS5 prevents cartilage degradation in a murine model of osteoarthritis.

REFERENCES AND FURTHER READING

Ameye L, Young MF (2002) Mice deficient in small leucin-rich proteoglycans: novel *in vivo* models of osteoporosis, osteoarthritis, Ehlers-Danlos syndrome, muscular dystrophy, and corneal diseases. Glycobiology 12:107R–116R

Ameye L, Aria D, Jepsen K, Oldberg A, Xu T, Young MF (2002) Abnormal collagen fibrils in tendons of biglycan/fibromodulin-deficient mice lead to gait impairment, ectopic ossification, and osteoarthritis. FASEB J 16:673–680

Fässler R, Schnegelsberg PNJ, Dausman J, Shinya T, Muatgaki Y, McCarthy MT, Olsen BR, Jaenisch R (1994) Mice lacking $\alpha 1$(IX) collagen develop noninflammatory degenerative joint disease. Proc Natl Acad Sci USA 91:5070–5074

Garofalo S, Vuorio E, Metsäranta M, Rosati R, Toman D, Vaughan J, Lozano G, Mayne R, Ellard J, Horton W, de Crombrugghe B (1991) Reduced amounts of cartilage collagen fibrils and growth plate anomalies in transgenic mice harboring a glycine-to-cysteine mutation in the mouse type II procollagen α_1-chain gene. Proc Natl Acad Sci USA 88:9648–9652

Garofalo S, Metsäranta M, Ellard J, Smith C, Horton W, Vuorio E, de Crombrugghe B (1993) Assembly of cartilage collagen fibrils is disrupted by overexpression of normal type II collagen in transgenic mice. Proc Natl Acad Sci USA 90:3825–3829

Glasson SS, Askew R, Sheppard B, Carito B, Blanchet T, Ma HL, Flannery CL, Peluso D, Kanki K, Yang Z, Majumdar M, Morris EA (2005) Deletion of active ADAMTS5 prevents cartilage degradation in a murine model of osteoarthritis. Nature 434:644–648

Helminen HJ, Säämänen AM, Salminen H, Hyttinen MM (2002) Transgenic mouse models for studying the role of cartilage macromolecules in osteoarthritis. Rheumatology 41:848–856

Holmbeck K, Bianco P, Caterina J, Yamada S, Kromer M, Kuznetsov SA, Mankani M, Robey PG, Poole AR, Pidoux I, Ward JM, Birkedal-Hansen H (1999) MT1-MMP-deficient mice develop dwarfism, osteopenia, arthritis, and connective tissue disease due to inadequate collagen turnover. Cell 99:81–92

Metsäranta M, Garolfo S, Decker G, Rintala M, de Crombrugghe B, Vuorio E (1992) Chondrodysplasia in transgenic mice harboring a 15 amino acid deletion in triple helical domain of pro $\alpha 1$(II) collagen chain. J Cell Biol 118:203–212

Morko JP, Söderström M, Säämänen AMK, Salminen HJ, Vuorio EI (2004) Upregulation of cathepsin K expression in articular chondrocytes in a transgenic mouse model of osteoarthritis. Ann Rheum Dis 63:649–655

Nakata K, Ono K, Miyazaki J, Olson BR, Muragaki Y, Adachi E, Yamamura KI, Kimura T (1993) Osteoarthritis associated with mild chondrodysplasia in transgenic mice expressing $\alpha 1$(IX) collagen chains with a central deletion. Proc Natl Acad Sci USA 90:2870–2874

Neuhold LA, Killar L, Zhao W, Sung MLA, Warner L, Kulik J, Turner J, Wu W, Billinghurst C, Meijers T, Poole AR, Babij P, DeGennaro LJ (2001) Postnatal expression in hyaline cartilage of constitutively active human collagenase-3 (MMP-13) induces osteoarthritis in mice. J Clin Invest 107:35–44

Säämänen AM, Vuorio E (2004) Generation and use of transgenic mice as models for osteoarthritis. Method Mol Med 101:1–23

Säämänen AMK, Salminen HJ, Dean PB, de Crombrugghe B, Vuorio EI, Metsäranta MPH (2000) Osteoarthritis-like lesions in transgenic mice harboring a small deletion mutation in type II collagen gene. Osteoarthr Cartil 8:248–257

Salminen HJ, Säämänen AMK, Vankemmelbeke MN, Auho PK, Perälä MP, Vuorio EI (2002) Differential expression patterns of matrix metalloproteinases and their inhibitors during development of osteoarthritis in a transgenic mouse model Ann Rheum Dis 61:591–597

Vandenberg P, Khillan JS, Prockop DJ, Helminen A, Kontusaari S, Ala-Kokko L (1991) Expression of a partially deleted gene of human type II procollagen (*COL2A1*) in transgenic mice produces chondrodysplasia. Proc Natl Acad Sci USA 88:7640–7644

Xu L, Flahiff CM, Waldman BA, Wu D, Olsen BR, Setton LA, Li Y (2003) Osteoarthritis-like changes and decreased mechanical function of articular cartilage in the joints of mice with the chondrodysplasia gene (*cho*). Arthritis Rheum 48:2509–2518

Zemmyo M, Meharra EJ, Kühn K, Creighton-Achermann L, Lotz M (2003) Accelerated, aging-dependent development of osteoarthritis in $\alpha 1$ integrin-deficient mice. Arthritis Rheum 48:2873–2880

I.2
Methods for Testing Immunological Factors

I.2.1
In Vitro Methods

I.2.1.1
Inhibition Of Histamine Release from Mast Cells

PURPOSE AND RATIONALE

Hypersensitivity reactions can be elicited by various factors: either immunologically induced, i. e. allergic reactions to natural or synthetic compounds mediated by IgE, or non-immunologically induced, i. e. activation of mediator release from cells through direct contact, without the induction of, or the mediation through immune responses. Mediators responsible for hypersensitivity reactions are released from mast cells. An important preformed mediator of allergic reactions found in these cells is histamine. Specific allergens or the calcium ionophore 48/80 induce release of histamine from mast cells. The histamine concentration can be determined with the *o*-phthalaldehyde reaction.

PROCEDURE

Preparation of Mast Cell Suspension

Wistar rats are decapitated and exsanguinated. Fifty ml of Hank's balanced salt solution (HBSS) are injected into the peritoneal cavity and following massage of the body, the abdominal wall is opened. The fluid containing peritoneal cells is collected in a centrifuge tube and centrifuged at 2000 rpm. The cells are resuspended in HBSS. Then the cell suspension is brought to a final concentration of 10^5 mast cells/100 µl.

Test Compound Administration and Induction of Histamine Release

1 ml test drug (concentration range between 10^{-4} and 10^{-8} Mol) is added to the mast cell suspension (10^5 cells/100 ml) and the mixture is incubated at 37°C for 15 min. The cells are made up to a volume of 3 ml with HBSS, an equal volume of calcium-ionophore (10^{-6} g/ml), compound 48/80 or specific allergen is added. The suspension is incubated at 37°C for 30 min followed by centrifugation at 2500 rpm.

The Following Control Solutions are Needed

- *Spontaneous histamine release:* contains only mast cells and solutions used to determine baseline.
- *Histamine release:* contains mast cells and solutions and calcium-ionophore (10^{-6} g/ml).
- *Test compound control:* contains solutions and test compound to test the compound for native fluorescence.
- *Solution control:* contains only solutions used in the test to determine baseline.

Extraction of Histamine

One ml of the top layer is transferred to a tube containing 300 mg NaCl and 1.25 ml butanol. The sample is alkalized to extract the histamine into butanol by adding 1 ml 3 N NaOH. Following mechanical shaking, the sample is centrifuged for 5 min. One ml of the top layer (butanol) is pipetted into a 5 ml tube containing 2 ml of n-heptane and 0.4 ml of 0.12 N HCl. The tube is mixed by inverting it several times. Following separation into aqueous and organic phases, 0.5 ml of the aqueous phase is transferred to another tube.

Induction of o-Phthaladehyde Complexing Reaction

To each sample 100 µl 1 N NaOH is added under constant stirring immediately followed by administration of 100 µl 0.2% *o*-phthalaldehyde solution. After 2 min, the *o*-phthalaldehyde complexing reaction is stopped by addition of 50 µl 3 N HCl.

Determination of Histamine Release

The total sample is transferred to an autosampler vial and the histamine concentration is determined by a fluorescence detector (using excitation and emission wave lengths of 350 and 450 nm respectively).

EVALUATION

Percent histamine release (hist. rel.) can be expressed by the following formula:

$$\frac{\text{sample hist. rel.} - \text{spontaneous hist. rel.}}{100\%\ \text{hist. rel.} - \text{spontaneous hist. rel.}} \times 100$$

The statistical evaluation is carried out using the Student's *t*-test (comparison of 100% control to experimental group)

CRITICAL ASSESSMENT OF THE METHOD

Disodium cromoglycate has been reported to inhibit the release of histamine and the degranulation of rat mast cells (Orr and Cox 1969; Orr et al. 1971; Johnson and Bach 1975; Church and Young 1983). However, this effect of disodium cromoglycate and its analogues does not parallel the clinical efficacy (Kay et al. 1987).

MODIFICATIONS OF THE METHOD

Johnston et al. (1978) studied the increased superoxide anion production by immunologically activated and chemically elicited macrophages.

Flint et al. (1985) found a significant inhibition of histamine release by disodium cromoglycate in human mast cells recovered by bronchoalveolar lavage.

Ali et al. (1985) investigated the histamine release from rat peritoneal mast cells, human basophil and neutrophil leukocytes, mast cells from mesentery lung and heart of rats and guinea pigs by the skin irritating constituents thapsigargin and thapsigargicin from the resin of the umbelliferous plant *Thapsia gargania.*

Eady (1986) studied the reactivity of mast cells in bronchoalveolar lavage fluid of macaques repeatedly infected with *Ascaris suum*.

Wells et al. (1986) compared release of histamine, LTC_4, and PGD_2 from primate bronchoalveolar mast cells with that of rat peritoneal mast cells.

The release of β-hexosaminidase from mouse or rat bone marrow derived mast cells and from rat peritoneal mast cells was studied by Broide et al. (1986).

Peretti et al. (1990) recommended flow cytometry to investigate mast cell degranulation. Peptides, including substance P and bradykinin analogs release histamine from human skin mast cells (Lawrence et al. 1989).

Williams et al. (1991) studied the vancomycin-induced release of histamine from rat peritoneal mast cells and a rat basophil cell line (RBL-1).

A sensitive colorimetric assay for the release of tryptase from human lung mast cells *in vitro* has been described by Lavens et al. (1993).

REFERENCES AND FURTHER READING

Ali H, Brøgger Christensen S, Foreman JC, Pearce FL, Piotrowski W, Thastrup O (1985) The ability of thapsigargin and thapsigargicin to activate cells involved in the inflammatory response. Br J Pharmacol 85:705–712

Bartlett RR, Dimitrijevic M, Mattar T, Zielinski T, Germann T, Rüde E, Thoenes GH, Küchle CCA, Schorlemmer HU, Bremer E, Finnegan A, Schleyerbach R (1991) Leflunomide (HWA 486), a novel immunomodulating compound for the treatment of auto-immune disorders and reactions leading to transplantation rejection. Agents and Actions 32:11–21

Broide D, Marquardt D, Wasserman S (1986) Effect of nedocromil sodium and sodium cromoglycate on connective tissue and bone marrow derived mast cells: acute and chronic studies. Eur J Respir Dis 69: (Suppl 147):196–198

Church MK, Young KD (1983) The characteristics of inhibition of histamine release from human lung fragments by sodium cromoglycate, salbutamol and chlorpromazine. Br J Pharmacol 78:671–679

Eady RP (1986) The pharmacology of nedocromil sodium. Eur J Respir Dis 69: (Suppl 147):112–119

Flint KC, Leung KBP, Oearce FL, Hudspith BN, Brostoff J, Johnson N (1985) Human mast cells recovered by bronchoalveolar lavage: their morphology, histamine release and the effects of disodium cromoglycate. Clin Sci 68:427–432

Johnson HG, Bach MK (1975) Prevention of calcium ionophore-induced release of histamine in rat mast cells by disodium cromoglycate. J Immunol 114:514–516

Johnston RB, Godzik CA, Cohn ZA (1978) Increased superoxide anion production by immunologically activated and chemically elicited macrophages. J Exp Med 148;115–127

Kay AB, Walsh GM, Moqbel R, MacDonald AJ, Nagakura T, Carroll MP, Richerson HB (1987) Disodium cromoglycate inhibits activation of human inflammatory cells *in vitro*. J Allergy Clin Immunol 80:1–8

Lavens SE, Proud D, Warner JA (1993) A sensitive colorimetric assay for the release of tryptase from human lung mast cells *in vitro*. J Immunol Meth 166:93–102

Lawrence ID, Warner JA, Cohan VL, Lichtenstein LM, Kagey-Sobotka A, Vavrek JR, Stewart JM, Proud D (1989) Induction of histamine release from human skin mast cells by bradykinin analogs. Biochem Pharmacol 38:227–233

Orr TSC, Cox JSG (1969) Disodium cromoglycate, an inhibitor of mast cell degranulation and histamine release induced by phospholipase A. Nature 223:197–198

Orr TSC, Hall DE, Gwilliam JM, Cox JSG (1971) The effect of sodium cromoglycate on the release of histamine and degranulation of rat mast cells induced by compound 48/80. Life Sci 10:805–812

Peretti M, Nuti S, Parente L (1990) Investigation of rat mast cell degranulation using flow cytometry. J Pharmacol Meth 23:187–194

Riley PA, Mather ME, Keogh RW, Eady RP (1987) Activity of nedocromil sodium in mast-cell-dependent reactions in the rat. Int Arch Allergy Appl Immun 82:108–110

Siriganian RP (1976) Histamine release and assay methods for the study of human allergy. In: Rose NR, Friedman H (eds) Manual of Clinical Immunology, American Society of Microbiology, Washington. pp 603–615

Skolfitsch G, Saria A, Holzer P, Lembeck F (1981) Histamine in tissue: Determination by high-performance liquid chromatography PLC condensation with *o*-phthalaldehyde. J Chromatogr 226:53–59

Wells E, Jackson CG, Harper ST, Mann J, Eady RP (1986) Characterization of primate bronchoalveolar mast cells. II. Inhibition of histamine, LTC_4, and PGD_2 release from primate bronchoalveolar mast cells and a comparison with rat peritoneal mast cells. J Immunol 137:3941–3945

Williams PD, Laska DA, Shetler TJ, McGrath JP, White SL, Hoover DM (1991) Vancomycin-induced release of histamine from rat peritoneal mast cells and a rat basophil cell line (RBL-1). Agents Actions 32:217–223

I.2.1.2 Mitogen Induced Lymphocyte Proliferation

PURPOSE AND RATIONALE

Cultured lymphocytes can be stimulated to a proliferative response and to DNA synthesis by various mitogens. Measurement of DNA synthesis can be accomplished by pulse-labeling the culture with tritiated thymidine (^{3}H-thymidine), a nucleoside which is incorporated into the newly synthesized DNA. Immunmodulating properties can be detected either by pre-

treatment of the animals *in vivo* or by adding the test drug to the cultured lymphocytes.

PROCEDURE

Mice of NMRI strain weighing 18–20 g or rats of Lewis strain weighing 180–200 g are used.

Materials

Sheep red blood cell (SRBC) specific antigen and/or the following mitogens:

- Lipopolysaccharide 10–0.1 µg/ml
- Dextran sulfate 30–7.5 µg/ml
- Phytohaemagglutinin 0.5–0.12 % stock solution
- Concanavallin A 0.5–0.12 µg/ml
- As standards levamisole, cyclosporine A, prednisolone or leflunomide are used.

Ex Vivo

Animals receive the test compound once a day for 5 days. Thereafter, they are sacrificed, spleens are removed and a single cell suspension of 5×10^6 cells/ml is prepared. Mitogens are titrated (4 replicates/group) in 0.1 ml/well and 0.1 ml of the cell suspension is added. Plates are incubated at 37°C in 5% CO_2 in air for 48–60 h and for another 8 h after addition of 0.25 µC ^{3}H-thymidine per well. Cells are harvested on glass fiber filters and after drying the degree of radioactivity is determined using a β-counter.

In Vitro

Animals are sacrificed and their spleens removed. A single cell suspension of 10^7 cells/ ml is prepared and 0.05 ml placed in each microtiter well (4 replicates/group). Then the test compound (4 times concentrated) is added in 0.05 ml. At last 0.1 ml of the double concentrated mitogen is added. Plates are incubated and processed as described above.

EVALUATION

Stimulation index = proliferation ratio according to positive control, either with or without mean spleen weight. Statistical evaluation is carried out using the Student's *t*-test (comparison of positive and/or negative control to experimental group).

REFERENCES AND FURTHER READING

Bartlett RR (1986) Immunopharmacological profile of HWA 486, a novel isoxazol derivative-II. *in vivo* immunomodulating effects differ from those of cyclophosphamide, prednisolone, or cyclosporin A. Int J Immunpharmacol 8:199–204

di Padova FE (1989) Pharmacology of cyclosporine (Sandimmune) V. Pharmacological effects on immune function: *in vitro* studies. Pharmacol Rev 41:373–405

Elves MW (1972) The Lymphocytes, Chapter 7, *In vitro* lymphocyte transformation and antibody formation. Lloyd Luke Ltd. 2nd ed, pp 381–457

Sensi M, di Mario U, Pozzilli P (1984) Lymphocyte populations. Evaluation of T and B populations, T cell subpopulations and K cells. In: Larner J, Pohl SL (eds) Methods in Diabetes Research, Vol I: Laboratory Methods, Part B, John Wiley & Sons, New York, pp 77–97

Yamamura M, Nikbin B, Hobbs JR (1976) Standardisation of the mixed lymphocyte reaction. J Immunol Meth 10:367–378

Zan-Bar I (1983) Modulation of B and T cell subsets in mice treated with fractionated total lymphoid irradiation. I. Blockade of differentiating B cell pathways. Eur J Immunol 13:35–40

I.2.1.3 Inhibition of T Cell Proliferation

PURPOSE AND RATIONALE

Activation and/or proliferation of clonal populations of T cells are critical for the initiation of an antigen-specific immune response. Thus, inhibition of T cell activation provides a potent means for suppressing specific immune response. A number of immunosuppressive agents exhibit the ability to suppress T cell activation.

PROCEDURE

Purification of Peripheral Blood Leukocytes and T Cells

Peripheral blood leukocytes from normal donors are separated on Ficoll-Hypaque (Pharmacia, Piscataway, NJ). Leukocyte suspensions are washed in HBSS and are resuspended in RPMI 1664 medium (Gibco, Grand Island, NY) containing 10% heat-inactivated fetal bovine serum and 100 U/ml penicillin/streptomycin. Leukocyte suspensions are resuspended in RPMI 1664 containing 10% heat-inactivated pooled human serum. Highly enriched T cells are obtained by passing leukocytes through a nylon wool column to remove macrophages and B cells and then depleted of NK and monocytes with anti-Leu 11 b (Becton Dickinson, Mountain View, CA) plus complement (Pel-Freeze, Brown Deer, WI). These highly enriched T cells are approximately 95% CD3+ cells, the remaining cells being B lymphocytes.

Mixed Lymphocyte Reaction

Peripheral blood leukocytes are incubated at 2×10^5/well with equal numbers of gamma-irradiated (3000 rads) allogenic peripheral blood leukocytes and various concentrations of test compounds. Assays are performed in triplicate in 96-well, U-bottom plates. After 6 days of coculture, the cells are pulsed for 6 h with 1 µC of [^{3}H]thymidine per well. [^{3}H]Thymidine incorporation is then measured by scintillation

counting. Data are presented as:

$$\% \text{ inhibition} = \frac{CPM_{expt} - CPM_{bckgrd}}{CPM_{ctrl} - CPM_{bckgrd}} \times 100$$

where CPM_{expt} is mean counts per min of experimental cultures, CPM_{bckgrd} is mean counts per min of background well, unstimulated cultures, and CPM_{ctrl} is mean counts per min of uninhibited, stimulated cultures.

Lymphocyte Stimulation and Proliferation

Peripheral blood leukocytes and isolated T cells are cultured with anti-CD3 (5 ng/ml) plus PMA (5 ng/ml), anti-CD28 (1:5000 dilution) plus PMA (5 ng/ml), or 100 U/ml rhuIL-2 in RPMI 1644 containing 10% fetal bovine serum. Peripheral blood leukocytes or T cells are cultured at 2×10^5 cell per well in a total volume of 200 µl/well. Assays are performed in quadruplicate in 96-well, U-bottom plates. [^{3}H]Thymidine (1 µC) is added to each well after 48 h of coculture and after a 20 h pulse of [^{3}H]thymidine, the cells are harvested and the amount of [^{3}H]thymidine uptake is quantitated on a scintillation counter.

ELISA Assays

Supernatants/well (100 ml) are harvested 24 h after initiation of cultures of peripheral blood leukocytes or T cells stimulated with anti-CD3 or anti-CD28 plus PMA. IL-2 in the coculture supernatant is quantitated using a commercially available IL-2 ELISA kit. All experiments are performed in duplicate.

IL-2R Assays

The expression of IL-2R on T cells stimulated for 48 h with anti-CD3 or anti-CD28 plus PMA is determined using FITC-conjugated anti-CD25 mABs (Becton Dickinson, Mountain View, CA). T cells are washed in HBSS and then stained with phycoerythrin-conjugated anti-CD3 mAB and fluorescein-conjugated antiCD25 mAB. The percent of cells coexpressing CD3+ and CD25+ are determined from 2000 cells using an EPICS C flow cytometer (Coulter, Hialeah, FL).

EVALUATION

Dose response curves of inhibition of one-way mixed lymphocyte reaction and of IL-2 in the supernatant after stimulation with antiCD3 or anti-CD28 are established.

MODIFICATIONS OF THE METHOD

Zielinski et al. (1993, 1994) studied the influence of leflunomide on expression of lymphocyte activation expression markers (IL-2 and transferrin receptors) as well as on cell cycle and on IL-2 receptor gene expression.

Calcineurin was found to be a key signaling enzyme in T lymphocyte activation and the target of immunosuppressive drugs (Clipstone and Crabtree 1993).

REFERENCES AND FURTHER READING

Chong ASF, Finnegan A, Jiang XL, Gebel H, Sankary HN, Foster P, Williams JW (1993a) Leflunomide, a novel immunosuppressive agent. Transplantation 55:1361–1366

Chong ASF, Gebel H, Finnegan A, Petraitis EE, Jiang XL, Sankary HN, Foster P, Williams JW (1993b) Leflunomide, a novel immunomodulatory agent: *In vitro* analyses of the mechanism of immuno-suppression. Transplant Proc 25:747–749

Clipstone NA, Crabtree GR (1993) Calcineurin is a key signaling enzyme in T lymphocyte activation and the target of the immunosuppressive drugs cyclosporin A and FK506. Ann NY Acad Sci 696:20–30

Dayton JS, Turka LA, Thompson CB, Mitchell BS (1992) Comparison of the effects of mizoribine with those of azathioprine, 6-mercaptopurine, and mycophenolic acid on T lymphocyte proliferation and purine ribonucleotide metabolism. Mol Pharmacol 41:671–676

di Padova FE (1989) Pharmacology of cyclosporine (Sandimmune) V. Pharmacological effects on immune function: *in vitro* studies. Pharmacol Rev 41:373–405

Yamamura M, Nikbin B, Hobbs JR (1976) Standardisation of the mixed lymphocyte reaction. J Immunol Meth 10:367–378

Zielinski T, Herrmann M, Müller HJ, Riedel N, Bartlett RR (1994) The influence of leflunomide on cell cycle, IL-2-receptor (IL-2-R) and its gene expression. Agents Actions 41, Spec Conf Issue:C204–C205

Zielinski T, Müller HJ, Bartlett RR (1993) Effects of leflunomide (HWA 486) on expression of lymphocyte activation markers. Agents Actions 38, Spec Conf Issue: C80–C83

I.2.1.4 Chemiluminescence in Macrophages

PURPOSE AND RATIONALE

The stimulation of macrophages by antigen, complement, phorbol-esters, ect. leads to elaboration of O_2^- and other oxygen metabolites. Superoxide ion (O_2^-) and other highly reactive oxygen metabolites (radicals) form the basis for an efficient microbicidal system *in vivo*. Yet, when these radicals are released in response to self-antigens, tissue damage is often the result. Inhibition of this process can be regarded as a measure for immun-modulating effects of compounds. The oxygen metabolites can produce light-emitting reactions (chemiluminescence), which is measurable if amplified with suitable agents, such as the cyclic hydrazide luminol.

PROCEDURE

NMRI mice weighing 30 g or Sprague-Dawley rats weighing 250–300 g of either sex are used.

Positive Control

1. Sensitized mice, receiving vehicle
2. Mice, developing an autoimmune disease, receiving vehicle
3. Rats, developing adjuvant arthritis, receiving vehicle

Negative Control

1. Mice not sensitized, receiving vehicle
2. Mice, not developing an autoimmune disease, receiving vehicle
3. Rats without adjuvant arthritis.

Materials

- 5×10^8 SRBC (sheep red blood cells)/0.5 ml 0.9% NaCl solution (for sensitization)
- *Phorbolester:* Stock solution of 1 mg/ml phorbolmyristenacetate. This stock solution is diluted with Hank's balanced salt solution to a final concentration of 3.5 µM (working solution). For the induction of chemiluminescence, the working solution is diluted in the test tube 1:4, resulting in a final phorbolester concentration of 0.875 µM.
- Luminol (5-amino-2,3-dihydro-1,4-phthalazinedione, Sigma) final concentration 25 µg /ml

Ex Vivo Experiment

Groups of 6 animals are treated for 6 days orally or subcutaneously with test compound or the standard (prednisolone acetate or leflunomide). They are decapitated and exsanguinated. Macrophages are obtained by flushing the peritoneal cavity with 10 ml saline, containing 250 IU heparin. The cells are pooled, washed several times and suspended again at a final concentration of 2×10^6/200 µl.

For measurement in the luminometer the following mixture is prepared:

200 µl macrophages (2×10^6)
100 µl luminol solution (100 µg/ml)
100 µl phorbolmyristenacetate solution (3.5 µM)

Each sample is mixed thoroughly without the phorbolmyristenacetate solution, put into the luminometer and counted at 2 min intervals for 10 s. The addition of the phorbolester induces the reaction.

In Vitro Experiment

To 100 µl of macrophage suspension (2×10^6 cells) are 100 µl of the solution of the test compound added and incubated for 15 min at 37°C.

Then, 100 µl of luminol solution (100 µg/ml) and 100 µl of the 3.5 µM phorbolester solution are added and the luminescence measured in the luminometer.

EVALUATION

The time of maximal counts for the positive control is recorded. For all groups the ratio of counts per 10 s is determined at that time, compared to the positive control counts per 10 s and the percent change is calculated. For statistical evaluation the experimental group is compared with the positive control group using Student's *t*-test.

MODIFICATIONS OF THE METHOD

Bird and Giroud (1985) described a technique of polymorphonuclear leukocyte chemiluminescence as a means to detect compounds with anti-inflammatory activity. Inflammatory polymorphonuclear leukocytes were obtained by injecting rats intrapleurally with 1 ml of a 1% solution of calcium pyrophosphate and collection of the pleural exudate 4 h later. Chemoluminescence responses were measured using a Packard Picolite chemoluminometer and opsonized zymosan as the stimulus.

Seeds et al. (1985) found an independent stimulation of membrane potential changes and the oxidative metabolic burst in polymorphonuclear leukocytes.

A microtechnique for studying chemiluminescence response of phagocytes using whole blood was described by Selvaraj et al. (1982).

REFERENCES AND FURTHER READING

Bartlett RR (1986) Immunopharmacological profile of HWA 486, a novel isoxazol derivative-II. *in vivo* immunomodulating effects differ from those of cyclophosphamide, prednisolone, or cyclosporin A. Int J Immunpharmacol 8:199–204

Bird J, Giroud JP (1985) An appraisal of the technique of polymorphonuclear leukocyte chemiluminescence as a means to detect compounds with antiinflammatory activity. J Pharmacol Meth 14:305–312

Johnson Jr RB, Codzik CA, Cohn ZA (1978) Increased superoxide anion production by immunologically activated and chemically elicited macrophages. J Exper Med 148:115–120

Kurosawa M, Hanawa K, Kobayashi S, Nakano M (1990) Inhibitory effects of azelastine on superoxide anion generation from activated inflammatory cells measured by a simple chemiluminescence method. Arzneim Forsch/ Drug Res 40:767–770

Merétey K, Boehm U, Falus A (1983) Chemiluminescence response of human blood mononuclear cells to PAH and histamine. Agents Actions 13:237–240

Seeds MC, Parce JW, Szeijda P, Bass DA (1985) Independent stimulation of membrane potential changes and the oxidative metabolic burst in polymorphonuclear leukocytes. Blood 65:233–240

Selvaraj R, Sbarra AJ, Thomas GB, Cetrulo CL, Mitchell GW (1982) A microtechnique for studying chemiluminescence response of phagocytes using whole blood and its application to the evaluation of phagocytes in pregnancy. J Reticuloend Soc 31:3–16

Weidemann MJ, Smith R, Heaney T, Alaudeen S (1980) On the mechanism of the generation of chemiluminescence by macrophages. Behring Inst. Mitt. 65:42–54
Weinberg JB, Misokonis MA (1983) Phorbol diester-induced H_2O_2 production by peritoneal macrophages. Cell Immun 80:405–415

I.2.1.5 PFC (Plaque Forming Colony) Test In Vitro

PURPOSE AND RATIONALE

Identification of antibody producing cells is based on the ability of the secreted IgM antibody to fix complement and thereby lyse the indicator erythrocytes. Spleen cells or peripheral blood lymphocytes, previously incubated with antigen, are mixed with sheep red blood cells (SRBC). After addition of compliment and incubation, plaques (clear areas) caused by the lysis of SRBC appear in the otherwise cloudy layer. Antibody forming cells can be detected by the appearance of plaques. The number of plaques obtained is proportional to the number of antibody producing lymphocytes in the cell population.

PROCEDURE

NMRI mice weighing 16–18 g or Lewis rats weighing 180–200 g of either sex are used.

Materials

- absorbed guinea pig complement
- SRBC stored in Alsever's solution

Positive Control

Spleen cells incubated with antigen and medium

Negative Control

Spleen cells incubated with medium alone. The animals are decapitated and the spleens are removed from the peritoneal cavity. A single cell suspension of 15×10^6 cells/ml is prepared. For the induction of PFC, a 0.5 ml splenocyte suspension is added to 0.5 ml of a suspension of SRBC, previously washed in medium and diluted to 8×10^6 cells/ml. Thereafter, 1 ml of the solution of the test compound is added and the limbrowells are incubated at 37°C in a CO_2 incubator for 5 days. Per group 3 limbrowells are set up. On day 5, the 3 wells of each group are pooled, washed in medium and the number of cells is determined. For each cell pellet, 875 µl of washed SRBC and 125 µl absorbed guinea pig compliment are added. The suspension is mixed thoroughly and filled in chambers constructed of microslides. The chambers are placed in the incubator at 37°C for 90–120 min. The plaque forming colonies are counted immediately after incubation.

EVALUATION

The activity of test compounds can be determined using the following formula:

1. 1. PFC/3 wells:

$$x = \frac{\text{plaques} \times 100}{\mu\text{l}}$$

2. % change in the number of plaques:

$$x = \frac{\text{plaques} \times 100}{\text{plaquespos. control}}$$

$$d\% = x - 100$$

3. % change in number of cells:

$$x = \frac{\text{number of cells} \times 100}{\text{number of cells pos. control}}$$

$$d\% = x - 100$$

REFERENCES AND FURTHER READING

Bartlett RR (1986) Immunopharmacological profile of HWA 486, a novel isoxazol derivative – II. *in vivo* immunomodulating effects differ from those of cyclophosphamide, prednisolone, or cyclosporin A. Int J Immunpharmacol 8:199–204
Borel JF, Feurer C, Gubler HU, Stähelin H (1976) Biological effects of cyclosporin A: a new antilymphocytic agent. Agents Actions 6:468–475
Cunningham AJ, Szenberg A (1968) Further improvements in the plaque technique for detecting single antibody forming cells. Immunology 14:599–608
Stockinger (1978) Negative Rückkoppelungsmechanismen des Immunsystems. Johannes Gutenberg Universität Mainz
Zaalberg (1964) A simple method for detecting single antibody-forming cells. Nature 202:1231

I.2.1.6 Inhibition of Dihydro-Orotate Dehydrogenase

PURPOSE AND RATIONALE

Dihydro-orotate dehydrogenase catalyzes the fourth committed step in the de novo biosynthesis of pyrimidines. As rapidly proliferating human T cells have an exceptional requirement for de novo pyrimidine biosynthesis, small molecule dihydro-orotate dehydrogenase inhibitors constitute an attractive therapeutic approach to autoimmune diseases, immunosuppression, and cancer. The main mode of action of the immuno-suppressive compound leflunomide and its active metabolites is considered to be the inhibition of the enzyme dihydro-orotate dihydrogenase (Bruneau et al. 1998; Graul and Castañer 1998; Knecht and Löffler 1998; Rückemann et al. 1998; Schorlemmer et al. 1998; Herrmann et al. 2000; Liu et al. 2000).

PROCEDURE

A fragment of human dihydro-orotate dehydrogenase is expressed by means of the baculovirus expression vector system and purified to a specific activity greater than 50 U/mg (Knecht et al. 1996, 1997). Enzyme assays are performed with purified recombinant dihydro-orotate dehydrogenase at 30°C. The oxidation of the substrate dihydro-orotate and the reduction of the co-substrate quinone is coupled to the reduction of the chromogen 2,6-dichlorophenolindophenol (DCIP). The reaction mixture contains 0.1 mM Q_D or 0.1 M Q_{10}, 1 mM L-dihydro-orotate, 0.06 mM DCIP, 0.1% Triton X-100 in 50 mM Tris-HCl buffer, 150 mM KCl, pH 8.0. The reaction is started by addition of the enzyme. The loss of absorbance of the blue DCIP is monitored at 600 nm; $\in = 18.800\,l\,mol^{-1}cm^{-1}$. The enzyme activity in control assays without Q_D or Q_{10} which is approximately 1% of maximum enzyme activity is subtracted from the activity values measured. Stock solutions of the test compounds are prepared in dimethylsulfoxide with further dilutions in the buffer taken for the assays.

EVALUATION

To determine the inhibitory potency of the agents, the initial velocity of dihydro-orotate dehydrogenase reaction is measured at saturating substrate concentrations, 1 mM dihydro-orotate and 100 µM Q_D and varying concentrations of the drugs (1 nM through 100 µM). The equation is fitted to the initial velocities:

$$v = V/\{1 + [I]/IC_{50}\}$$

([I] is the inhibitor concentration) in order to find the concentration causing 50% inhibition of the enzyme activity (IC_{50}).

REFERENCES AND FURTHER READING

Bruneau JM, Yea CM, Spinella-Jaegle S, Fudali C, Woodward K, Robson PA, Sautès C, Westwood R, Kuo EA, Williamson RA, Ruuth E (1998) Purification of human dihydro-orotate dehydrogenase and its inhibition by A77 1726, the active metabolite of leflunomide. Biochem J 336:299–303

Graul A, Castañer J (1998) Leflunomide. Drugs Future 23:827–837

Herrmann ML, Schleyerbach R, Kirschbaum BJ (2000) Leflunomide: an immunomodulatory drug for the treatment of rheumatoid arthritis and other autoimmune diseases. Immunopharmacol 47:273–289

Knecht W, Löffler M (1998) Species-related inhibition of human and rat dihydroorotate dehydrogenase by immunosuppressive isoxazol and cinchoninic acid derivatives. Biochem Pharmacol 56:1259–1264

Knecht W, Bergjohann U, Gonski S, Kirschbaum B, Löffler M (1996) Functional expression of a fragment of human dihydro-oratate dehydrogenase by means of the baculovirus vector system, and kinetic investigation of the purified enzyme. Eur J Biochem 240:292–301

Knecht W, Altekruse D, Rotgeri A, Gonski S, Löffler M (1997) Rat dihydroorotate dehydrogenase: isolation of the recombinant enzyme from mitochondria of insect cells. Protein Exp Purif 10:89–99

Liu S, Neidhardt EA, Grossman TH, Ocain T, Clardy J (2000) Structures of human dihydroorotate dehydrogenase in complex with antiproliferative agents. Structure Fold Des 8:25–33

Rückemann K, Fairbanks LD, Carrey EA, Hawrylowicz CM, Richards DF, Kirschbaum B, Simmonds HA (1998) Leflunomide inhibits pyrimidine de novo synthesis in mitogen-stimulated T-lymphocytes from healthy humans. J Biol Chem 273:21682–21691

Schorlemmer HU, Milbert U, Haun G, Wunschel M, Zeitter D, Schleyerbach R (1998) De novo pyrimidine biosynthesis in Jurkat T cells is inhibited by leflunomide's primary metabolite A77–1726 at the level of dihydroorotate dehydrogenase. Int J Immunother 14:193–204

I.2.1.7 Sphingosine 1-Phosphate

I.2.1.7.1 General Considerations

Sphingolipids have emerged as molecules whose metabolism is regulated to generation of bioactive products including ceramide, sphingosine, and sphingosine-1-phosphate. The balance between cellular levels of these bioactive products is recognized to be critical to cell regulation and may be a promising approach to tumor therapy (Huwiler and Pfeilschifter 2006); whereby ceramide and sphingosine cause apoptosis and growth arrest phenotypes, and sphingosine-1-phosphate mediates proliferative and angiogenic responses. Sphingosine kinase is a key enzyme in modulating the levels of these lipids (Hannun and Obeid 1995; Hofmann and Dixit 1998; Mathias et al. 1998; Prieschl et al. 1999; Pyne and Pyne 2000; Cummings et al. 2002; MacKinnon et al. 2002; Rosen and Liao 2003; Chen et al. 2004; Deguchi et al. 2004; Lee et al. 2004; Peng et al. 2004; Cyster 2005; Kee et al. 2005; Watterson et al. 2005; Gardell et al. 2006; Taha et al. 2006). Ceramide formation and degradation are influenced by nitric oxide (NO) (Huwiler et al. 1999a, 1999b; Franzen et al. 2002a, 2002b).

REFERENCES AND FURTHER READING

Chen XL, Grey JY, Thomas S, Qiu FH, Medford RM, Wasserman MA, Kunsch C (2004) Sphingosine kinase-1 mediates TNF-α induced MCP-1 gene expression in endothelial cells: upregulation by oscillatory flow. Am J Physiol 287:H1452–H1458

Chun J, Rosen H (2006) Lysophospholipid receptors as potential drug targets in tissue transplantation and autoimmune diseases. Curr Pharm Des 12:161–171

Cummings RJ, Parinandi NL, Zaiman A, Wang L, Usatyuk PV, Garcia JGN, Natarajan V (2002) Phospholipase D activation by sphingosine 1-phosphate regulates interleukin-8 secretion in human bronchial epithelial cells. J Biol Chem 277:30227–30235

Cyster JG (2005) Chemokines, sphingosine-1-phosphate, and cell migration in secondary lymphoid organs. Annu Rev Immunol 23:127–159

Deguchi H, Yegneswaran S, Griffin JH (2004) Sphingolipids as bioactive regulators of thrombin generation. J Biol Chem 279:12036–12042

Franzen R, Fabbro D, Aschrafi A, Pfeilschifter J, Huwiler A (2002a) Nitric oxide induces degradation of the neutral ceramidase in rat mesangial cells and is counterregulated by protein kinase C. J Biol Chem 277:46184–46190

Franzen R, Pfeilschifter J, Huwiler A (2002b) Nitric oxide induces neutral ceramidase degradation by the ubiquitin/proteasome complex in renal mesangial cell cultures. FEBS Lett 552:441–444

Gardell SE, Dubin AE, Chun J (2006) Emerging medical roles for lysophospholipid signaling. Trends Mol Med 12:65–75

Hannun YA, Obeid LM (1995) Ceramide: an intracellular signal for apoptosis. Trends Biol Sci 20:73–77

Hofmann K, Dixit VM (1998) Ceramide in apoptosis – does it really matter? Trends Biol Sci 23:374–377

Huwiler A, Pfeilschifter J, van den Bosch (1999a) Nitric oxide donors induce stress signaling via ceramide formation in rat renal mesangial cells. J Biol Chem 274:7190–7195

Huwiler A, Dorsch S, Briner V, van den Bosch H, Pfeilschifter J (1999b) Nitric oxide stimulates ceramide formation in glomerular endothelial cells. Biochem Biophys Res Commun 258:60–65

Huwiler A, Pfeilschifter J (2006) Altering the sphingosine-1-phosphate/ceramide balance: a promising approach to tumor therapy. Curr Pharm Design 12:4625–4635

Kee TH, Vit P, Melendez AJ (2005) Sphingosine kinase signaling in immune cells. Clin Exp Pharmacol Physiol 32:153–161

Lee H, Lin CI, Liao JJ, Lee YW, Yang HY, Lee CY, Hsu HY, Wu HL (2004) Lysophospholipids increase ICAM-1 expression in HUVEC through a G_i- und NF-κB-dependent mechanism. Am J Physiol 287:C1657–C1666

MacKinnon AC, Buckley A, Chilvers ER, Rossi AG, Haslett C, Sethi T (2002) Sphingosine kinase: a point of convergence in the action of diverse neutrophil priming agents. J Immunol 169:6394–6400

Mathias S, Pena LA, Kolesnick RN (1998) Signal transduction of stress via ceramide. Biochem J 335:465–480

Peng X, Hassoun PM, Sammani S, McVerry BJ, Burne MJ, Rabb H, Pearse D, Tuder RM, Garcia JGN (2004) Protective effects of sphingosine 1-phsophate in murine endotoxin-induced inflammatory lung injury. Am J Resp Crit Care Med 169:1245–1251

Prieschl EE, Csonga R, Novotny V, Kikuchi GE, Baumruker T (1999) The balance between sphingosine and sphingosine-1-phosphate is decisive for mast cell activation after Fcε receptor I triggering. J Exp Med 190:1–8

Pyne S, Pyne NJ (2000) Sphingosine 1-phosphate signaling in mammalian cells. Biochem J 349:385–402

Rosen H, Liao J (2003) Sphingosine 1-phosphate pathway therapeutics: a lipid ligand-receptor paradigm. Curr Opin Chem Biol 7:461–468

Taha TA, Hannun YA, Obeid LM (2006) Sphingosine kinase: biochemical and cellular regulation and role in disease. J Biochem Mol Biol 39:113–131

Watterson KR, Ratz PH, Spiegel S (2005) The role of sphingosine-1-phosphate in smooth muscle contraction. Cell Signal 17:289–298

I.2.1.7.2 Binding to Sphingosine 1-Phosphate Receptors

PURPOSE AND RATIONALE

At least five subtypes of the sphingosine 1-phosphate receptor with tissue specificity are known (Meyer zu Heringdorf et al. 1998; Kon et al. 1999; Im et al. 2000, 2001; Forrest et al. 2004; Hale et al. 2004a; Sanna et al. 2004; Zhou and Murthy 2004; Xin et al. 2004; Lepley et al. 2005; Kimura et al. 2006; Kitano et al. 2006).

The immunomodulator FTY720 is an agonist to sphingosine 1-phosphate receptors (Brinkmann et al. 2002; Gräler and Goetzl 2004; Kunzendorf et al. 2004; Xin et al. 2004; Albert et al. 2005; Bandhuvula et al. 2005; Chiba 2005; Sawicka et al. 2003, 2005; Habicht et al. 2005; Xin et al. 2006; Zhou et al. 2006). FTY720 is derived from ISP-1 (myriomycin), a fungal metabolite that is an eternal youth nostrum in traditional Chinese herbal medicine (Fujita et al. 1994). The compound {2-amino-2-[2-(4-octophenyl)ethyl]propane-1,3-diol} is a highly potent immune modulating agent.

Further derivates such as sphingosine 1-phosphate receptor agonists (Hale et al. 2004b, 2004c; Clemens et al. 2005; Foss et al. 2005; Kiuchi et al. 2005; Jo et al. 2005; Li et al. 2005; Colandrea et al. 2006) and antagonists (Davis et al. 2005) have been described. Brinkmann et al. (2002) used the [γ-^{35}S]GTPS binding assay to study the binding of the immune modulator FTY720 to sphingosine 1-phosphate receptors.

Forrest et al. (2004) studied the binding of sphingosine 1-phosphate agonists on distinct receptor subtypes.

PROCEDURE

Receptors and Cell Lines

CHO cells stably expressing human $S1P_{1,2,3,4,5}$ were used (Mandala et al. 2002). cDNA sequences encoding rodent S1P receptors were cloned from genomic DNA by polymerase chain reaction using the following primers for each respective receptor:
5′-GAACCCGGGTGTCCACTAGCATCCCGG and 5′CCCGAATTCTTAGGAAGAAGAATTGACGTTTCC (mouse $S1P_1$), 5′-GAACCCGGGCGGCTTATACTCAGAGTACC and 5′-GGCGAATTCTCAGACCACTGTGTTACCCTC (mouse $S1P_2$), 5′-GAACCCGGGCAACCACGCATGCGCAGG and 5′-GTCGAATTCTCACTTGCAGAGGACCCCG (mouse $S1P_3$), 5′-GA

ACCCGGGAACATCAGTACCTGGTCCACGC and GCGGAATTCTAGGTGCTGCGGACGCTGG (mouse $S1P_4$), 5′-GAACCCGGGCTGCTGCGGCC GG and 5′-CGCGAATTCAGTCTGTAGCAGTAGG CACC (mouse $S1P_5$), 5′-GTAGGATCCGTGTCCTC CACCAGCATC and 5′GGCCGAATTCTTAAGAAG AAGAATTGACGTTTC (rat $S1P_1$), 5′-GAACCCGG GCATCCACGCATGCGCAG and 5′-GCCGAATTC TCACTTGCAGAGGACCCCATTCTG (rat $S1P_3$).

The polymerase chain reaction products were inserted in-frame after a FLAG tag using vector pCMV-Tag2 (Stratagene, La Jolla, Calif., USA). Stable lines were established by transfecting plasmids into CHO cells using lipofectamine reagent, selecting for neomycin resistance, and screening single cell cultures for increased [^{33}P]S1P-specific binding. Membranes were prepared from positive clones and confirmed in [^{33}P]S1P and [^{35}S]GTPγS binding assays.

S1P Receptor Assays

Binding assays were conducted as described by Mandala et al. (2002). [^{33}P]S1P was sonicated with fatty-acid-free bovine serum albumin, added to test compounds diluted in dimethylsulfoxide (DMSO), and mixed with membranes in 200 µl in 96-well plates with assay concentrations of 0.1 nM [^{33}P]S1P (22,000 dpm), 0.5% bovine serum albumin, 50 mM HEPES-Na (pH 7.5), 5 mM $MgCl_2$, 1 mM $CaCl_2$, and 0.3 to 0.7 µg of membrane protein. Binding was performed for 60 min at room temperature and terminated by collecting the membranes onto GF/B filter plates with a Packard Filtermate Universal Harvester. Filter bound radionuclide was measured on a Perkin Elmer 1450 MicroBeta. Specific binding was calculated by subtracting radioactivity that remained in the presence of 1000-fold excess of unlabeled S1P.

To measure functional activation of the S1P receptors, [^{35}S]GTPγS binding was measured. Membranes (1–4 µg of protein) were incubated in 96-well plates with test compounds diluted in DMSO in 100 µl of buffer containing 20 mM HEPES (pH 7.4), 100 mM NaCl, 10 mM $MgCl_2$, and 2–10 µM GDP, depending on the expressed receptor. The assay was initiated with the addition of 100 µl of [^{35}S]GTPγS (1200 Ci/mmol or 44,400 BGq/mmol; Perkin Elmer Life and Analytical Sciences, Boston, Mass., USA) for an assay concentration of 125 pM. After 60 min of incubation at room temperature, membranes were harvested onto GF/B filter plates and bound radionuclides were measured.

MODIFICATIONS OF THE METHOD

Murata et al. (2000) described a radioreceptor-binding assay for quantitative measurement of sphingosine 1-phosphate.

REFERENCES AND FURTHER READING

Albert R, Hinterding K, Brinkmann V, Guerini D, Müller-Hartwieg C, Knecht H, Simeon C, Streiff M, Wagner T, Welzenbach K, Zecri F, Zollinger M, Cooke N, Francotte E (2005) The novel immunomodulator FTY720 is phosphorylated in rats and humans to form a single stereoisomer. Identification, chemical proof, and biological characterization of the biologically active species and its enantiomer. J Med Chem 48:5373–5377

Bandhuvula P, Tam YY, Oskoulan B, Saba JD (2005) The immune modulator FTY720 inhibits sphingosine-1-phosphate lyase activity. J Biol Chem 280:33697–33700

Brinkmann V, Davis MD, Heise CE, Albert R, Cottens S, Hof R, Bruns C, Prieschl E, Baumruker T, Hiestand P, Foster CA, Zollinger M, Lynch KR (2002) The immune modulator FTY720 targets sphingosine 1-phosphate receptors. J Biol Chem 277:21453–21457

Chiba K (2005) FTY720, a new class of immunomodulators, inhibits lymphocyte egress from secondary lymphoid tissues and thymus by agonistic activity at sphingosine 1-phosphate receptors. Pharmacol Ther 108:308–319

Clemens JJ, Davis MD, Lynch KR, Macdonald TL (2005) Synthesis of 4(5)-phenylimidazole-based analogues of sphingosine 1-phosphate and FTY720: discovery of potent $S1P_1$ receptor agonists. Bioorg Med Chem Lett 15:3568–3572

Colandrea VJ, Legiec IE, Huo P, Yan L, Hale JJ, Mills SG, Bergstrom J, Card D, Chebret G, Hajdu R, Keohane CA, Milligan JA, Rosenbach MJ, Shei GJ, Mandala SM (2006) 2,5-Disubstituted pyrrolidines carboxylates as potent, orally active sphingosine-1-phosphate (S1P) receptor agonists. Bioorg Med Chem Lett 16:2905–2908

Davis MD, Clemens JJ, Macdonald TL, Lynch KR (2005) Sphingosine 1-phosphate analogs as receptor antagonists. J Biol Chem 280:9833–9844

Forrest M, Sun SY, Hajdu R, Bergstrom J, Card D, Doherty G, Hale J, Keohane C, Meyers C, Milligan J, Mills S, Nomura H, Rosen H, Rosenbach M, Shei GJ, Singer II, Tian M, West S, White V, Xie J, Proia RL, Mandala S (2004) Immune cell regulation and cardiovascular effects of sphingosine 1-phosphate agonists in rodents are mediated via distinct receptor subtypes. J Pharmacol Exp Ther 309:758–768

Foss FW, Jr, Clemens JJ, Davis MD, Snyder AH, Zigler MA, Lynch KR, Macdonald TL (2005) Synthesis, stability, and implications of phosphothionate agonists of sphingosine-1-phosphate receptors. Bioorg Med Chem Lett 15:4470–4474

Fujita T, Inoue K, Yamamoto S, Ikumoto T, Sasaki S, Toyama R, Chiba K, Hoshima Y, Okumato T (1994) Fungal metabolites. Part II. A potent immunosuppressive activity found in *Isaria sinclairii* metabolite. J Antibiot 47:208–215

Gräler MH, Goetzl EJ (2004) The immunosuppressant FTY720 down-regulates sphingosine 1-phosphate G-protein-coupled receptors. FASEB J 18:551–553

Habicht A, Clarkson MR, Yang J, Henderson J, Brinkmann V, Fernandes S, Jurewicz M, Yuan X, Sayegh MH (2005) Novel insights into the mechanism of action of FTY720 in a transgenic model of allograft rejection: implications for therapy of chronic rejection. J Immunol 176:36–42

Hale JJ, Doherty G, Toth L, Li Z, Mills SG, Hajdu R, Keohane CA, Rosenbach M, Milligan J, Shei GJ, Chrebet G,

Bergstrom J, Card D, Rosen H, Mandala S (2004a) The discovery of 3-(N-alkyl)aminopropylphosphonic acids as potent S1P receptor agonists. Bioorg Med Chem Lett 14:3495–3499

Hale JJ, Yan L, Neway WE, Hajdu R, Bergstrom JD, Milligan JA, Shei GJ, Chrebet GL, Thornton RA, Card D, Rosenbach E, Rosen H, Mandala S (2004b) Synthesis, stereochemical determination and biochemical characterization of the enantiomeric phosphate esters of the novel immunosuppressive agent FTY720. Bioorg Med Chem 12:4803–4807

Hale JJ, Neway W, Mills SG, Hajdu R, Keohane CA, Rosenbach M, Milligan J, Shei GJ, Chrebet G, Bergstrom J, Card D, Koo GC, Koprak SL, Jackson JJ Rosen H, Mandala S (2004c) Potent S1P receptor agonists replicate the pharmacologic actions of the novel immune modulator FTY720. Bioorg Med Chem Lett 14:3351–3355

Im DS, Heise CE, Ancellin N, O'Dowd BF, Shei GJ, Heavens RP, Rigby MR, Hla T, Mandala S, McAllister G, George SR, Lynch KR (2000) Characterization of a novel sphingosine 1-phosphate receptor, Edg-8. J Biol Chem 275:14281–14286

Im DS, Clemens J, Macdonald T, Lynch KR (2001) Characterization of the human and mouse sphingosine 1-phosphate receptor, $S1P_5$ (Edg-8): structure-activity relationship of sphingosine 1-phosphate receptors. Biochemistry 40:14053–14060

Jo E, Sanna MG, Gonzalez-Cabrera PJ, Thangada S, Tigyl G, Osborne DA, Hla T, Parill ASL, Rosen H (2005) $S1P_1$-selective in vivo-active agonists from high-throughput screening:off-the-shelf chemical probes of receptor interactions, signaling and fate. Chem Biol 12:703–715

Kimura T, Tomura H, Mogi C, Kuwabara A, Ishiwara M, Shibasawa K, Sato K, Ohwada S, Im DS, Kurose H, Ishizuka T, Murakami M, Okajima F (2006) Sphingosine 1-phosphate receptors mediate stimulatory and inhibitory signalings for expression of adhesion molecules in endothelial cells. Cell Signal 18:841–850

Kitano M, Hla T, Sekiguchi M, Kawahito Y, Yoshimura R, Miyazawa K, Iwasaki T, Sano H (2006) Sphingosine 1-phosphate/sphingosine 1-phosphate receptor 1 signaling in rheumatoid synovium. Regulation of synovial proliferation and inflammatory gene expression. Arthritis Rheum 54:742–753

Kiuchi M, Adachi K, Tomatsu A, Chino M, Takeda S, Tanaka Y, Maeda Y, Sato N, Mitsutomi N, Sugahara K, Chiba K (2005) Asymmetric synthesis and biological evaluation of the enantiomeric isomers of the immunosuppressive FTY720-phosphate. Bioorg Med Chem 13:425–432

Kon J, Sato K, Watanabe T, Tomura H, Kuwabara A, Kimura T, Taman KI, Ishizuka T, Murata Nkanda T, Kobayashi I, Ohta H, Ui M, Okajima F (1999) Comparison of intrinsic activities of the putative sphingosine 1-phosphate receptor subtypes to regulate several signaling pathways in their transfected Chinese hamster ovary cells. J Biol Chem 274:23940–23947

Kunzendorf U, Ziegler E, Kabelitz D (2004) FTY720-the first compound of a new promising class of immunosuppressive drugs. Nephrol Dial Transplant 19:1677–1681

Lepley D, Paik JH, Hla T, Ferrer F (2005) The G protein-coupled receptor $S1P_2$ regulates Rho/Rho kinase pathway to inhibit tumor cell migration. Cancer Res 65:3788–3795

Li Z, Chen W, Hale JJ, Lynch CL, Mills SG, Hajdu R, Keohans CA, Rosenbach MJ, Milligan JA, Shei GJ, Chrebet G, Parent SA, Bergstrom J, Card D, Forrest M, Quackenbush EJ, Wickham LA, Vargas H, Evans TRM, Rosen H, Mandala S (2005) Discovery of potent 3,5-diphenyl-1,2,4-oxadiazole sphingosine 1-phosphate ($S1P_1$) receptor agonists with exceptional selectivity against $S1P_2$ and $S1P_3$. J Med Chem 48:6169–6173

Mandala S, Hajdu R, Bergstrom J, Quackenbush E, Xie J, Milligan J, Thronton R, Shei GJ, Card D, Keohane CA, Rosenbach M, Hale J, Lynch CL, Rupprecht K, Parsons W, Rosen H (2002) Alteration of lymphocyte trafficking by sphingosine receptor agonists. Science 296:346–349

Meyer zu Heringdorf D, Lass H, Alemany R, Laser KT, Neumann E, Zhang C, Schmidt M, Rauen U, Jakobs KH, van Koppen CJ (1998) Sphingosine kinase-mediated Ca^{2+} signalling by G-protein-coupled receptors. EMBO J 17:2830–2837

Murata N, Sato K, Kon J, Tomura H, Okajima F (2000) Quantitative measurement of sphingosine 1-phosphate by radioreceptor-binding assay. Anal Biochem 282:115–120

Sanna MG, Liao J, Jo E, Alfonso C, Ahn MY, Peterson MS, Webb B, Lefebvre S, Chun J, Gray N, Rosen H (2004) Sphingosine 1-phosphate (S1P) receptor subtypes $S1P_1$ and $S1P_3$, respectively, regulate lymphocyte recirculation and heart rate. J Biol Chem 279:13839–13848

Sawicka E, Zuany-Amorim C, Manlius C, Trifilieff A, Brinkmann V, Kemeny DM, Walker C (2003) Inhibition of Th1- and Th2-mediated airway inflammation by the sphingosine 1-phopsphate receptor agonist FTY720. J Immunol 171:6206–6214

Sawicka E, Dubois G, Jarai G, Edwards M, Thomas M, Nicholls A, Albert R, Newson C, Brinkmann V, Walker C (2005) The sphingosine 1-phosphate receptor agonist FTY720 differentially affects the sequestration of $CD4^+/CD25^+$ T-regulatory cells and enhances their functional activity. J Immunol 175:7973–7980

Xin C, Ren S, Pfeilschifter J, Huwiler A (2004) Heterologous desensitization of the sphingosine 1-phosphate receptors by purinoceptor activation in renal mesangial cells. Br J Pharmacol 143:581–589

Xin C, Ren S, Eberhardt W, Pfeilschifter J, Huwiler A (2006) The immunomodulators FTY720 and its phosphorylated derivative activate the Smad signaling cascade and upregulate connective tissue growth factor and collagen IV expression in renal mesangial cells. Br J Pharmacol 147:164–174

Zhou C, Ling MT, Lee TKW, Man K, Wang X, Wong YC (2006) FTY720, a fungus metabolite, inhibits invasion ability of androgen-independent prostate cancer cells through inactivation of RhoA-GTPase. Cancer Lett 223:36–47

Zhou H, Murthy K (2004) Distinctive G protein-dependent signaling in smooth muscle by sphingosine 1-phosphate receptors $S1P_1$ and $S1P_2$. Am J Physiol 286:C1130–C1138

I.2.1.7.3 Sphingosine Kinase Activation Assay

PURPOSE AND RATIONALE

Sphingosine 1-phosphate produced by two sphingosine kinase isoenzymes, denoted SphK1 and SphK2, is the ligand for a family of specific G-protein-coupled receptors that regulate cytoskeletal re-arrangements and cell motility. Unlike the proliferative action of SphK1, the isoenzyme SphK2 has been shown to possess anti-proliferative and pro-apoptotic action. Both kinases have been cloned and functionally characterized (Kohama et al. 1998; Liu et al. 2000, 2003; Nava et al. 2000; Olivera 2000; Igarashi et al. 2003; Paugh et

al. 2003; Sanchez et al. 2003; Billich et al. 2005; Döll et al. 2005; Hait et al. 2005; Kharel et al. 2005; Okada et al. 2005; De Palma et al. 2006; Zemann et al. 2006).

Sphingosine kinase activity assays were performed in a similar way by Paugh et al. (2003) and by Huwiler et al. (2006).

PROCEDURE

Sphingosine Kinase Activity Assay

In vitro kinase reactions were performed according to Olivera et al. (2000). In brief, 30 µg of protein lysates was incubated with 50 µmol/l of sphingosine (dissolved as 1 mmol/l stock solution in 4 mg/ml of BSA in PBS) and 10 µCi (370 kBq) of [γ-^{32}P]ATP for 15 min at 37°C. For SK-2 activity assay, the same buffer including 1 M KCl was used to inhibit SK-1 activity (Liu et al. 2000). Reactions were terminated by addition of 20 µl of 1N HCl followed by 800 µl of chloroform/methanol/HCl (100:200:1, v/v), 240 µl of chloroform and 240 µl of 2 mol/l KCl. After vigorous vortexing and phase separation, 50 µl of the lower organic phase was loaded onto TLC plates and run in 1-butanol/ethanol/acetic acid/water (80:20:10:20, v/v).

EVALUATION

Spots corresponding to S1P were analyzed and quantified using an Imaging System (Fuji).

REFERENCES AND FURTHER READING

Billich A, Bornancin F, Mechtcheriakova D, Natt F, Huesken D, Baumruker T (2005) Basal and induced sphingosine kinase 1 activity in A549 carcinoma cells: function in cell survival and IL-1β and TNF-α induced production of inflammatory mediators. Cell Signal 17:1203–1217

De Palma C, Meacci E, Perrotta C, Bruni P, Clementi E (2006) Endothelial nitric oxide synthase activation by tumor necrosis factor a through neutral sphinomyelinase 2, sphingosine kinase 1, and sphingosine 1 receptors. Arterioscler Thromb Vasc Biol 26:99–105

Döll F, Pfeilschifter J, Huwiler A (2005) The epidermal growth factor stimulates sphingokinase-1 expression and activity in the human mammary carcinoma cell line MCF7. Biochim Biophys Acta 1738:72–81

Hait NC, Sarkar S, Le Stunff H, Mikami A, Maceyka M, Milstien S, Spiegel S (2005) Role of sphingosine kinase 2 in cell migration toward epidermal growth factor. J Biol Chem 280:29462–29469

Huwiler A, Döll F, Ren S, Klawitter S, Greening A, Römer I, Bubnova S, Reinsberg L, Pfeilschifter J (2006) Histamine increases sphingosine kinase-1 expression and activity in the human endothelial cell line E.A.hy926 by a PCK-α-dependent mechanism. Biochim Biophys Acta 1761:367–376

Igarashi N, Okada T, Hayashi S, Fujita T, Jahangeer S, Nakamura SI (2003) Sphingosine kinase 2 is a nuclear protein and inhibits DNA synthesis. J Biol Chem 278:46832–46839

Kharel Y, Lee S, Snyder AH, Sheasley-O'Neill SL, Morris MA, Setiady Y, Zhu R, Zigler MA, Burcin TL, Ley K, Tung KSK, Engelhard VH, Macdonald TL, Pearson-White S, Lynch KR (2005) Sphingosine kinase 2 is required for modulation of lymphocyte traffic by FTY720. J Biol Chem 280:36856–36872

Kohama T, Olivera A, Edsall L, Nagiec MM, Dickson R, Spiegel S (1998) Molecular cloning and functional characterization of murine sphingosine kinase. J Biol Chem 273:23722–23728

Liu H, Sugiura M, Nava VE, Edsall LC, Kono K, Poultoni S, Milstien S, Kohama T, Spiegel S (2000) Molecular cloning and functional characterization of a novel mammalian sphingosine kinase type 2 isoform. J Biol Chem 275:19513–19520

Liu H, Toman RE, Goparaju SK, Maceyka M, Nava VE, Sankala H, Payne SG, Bektas M, Ishii I, Chun J, Milstien S, Spiegel S (2003) Sphingosine kinase 2 is a putative BH3-only protein that induces apoptosis. J Biol Chem 278:40330–40336

Nava VE, Lacana E, Poulton S, Liu H, Sugiura M, Kono K, Milstien S, Kohama T, Spiegel S (2000) Functional characterization of human sphingosine kinase-1. FEBBS Lett 473:81–84

Okada T, Ding G, Sonoda H, Kajimoto T, Haga Y, Khosrowbeygi A, Goa S, Miwa N, Jahangeer S, Nakamura SI (2005) Involvement of N-terminal-extended form of sphingosine kinase 2 in serum-dependent regulation of cell proliferation and apoptosis. J Biol Chem 280:36318–36325

Olivera A, Barlow KD, Spiegel S (2000) Assaying sphingosinekinase activity. Methods Enzymol 311:215–223

Paugh SW, Payne SG, Barbour SE, Milstien S, Spiegel S (2003) The immunosuppressant FTY720 is phosphorylated by sphingosine kinase type 2. FEBS Lett 554:189–193

Sanchez T, Estrada-Hernandez T, Paik JH, Wu MT, Venkataraman K, Brinkmann V, Claffey K, Hla T (2003) Phosphorylation and action of the immunomodulator FTY720 inhibits vascular endothelial cell growth factor-induced vascular permeability. J Biol Chem 278:27281–27290

Zemann B, Kinzel B, Müller M, Reuschel R, Mechtcheriakowa D, Urtz N, Bomancin F, Baumruker T, Billich A (2006) Sphingosine kinase type 2 is essential for lymphopenia induced by the immunomodulatory drug FTY720. Blood 107:1454–1458

I.2.1.7.4 Lymphocyte Trafficking After Sphingosine 1-Phosphate Receptor Agonists

PURPOSE AND RATIONALE

Adaptive immunity depends on T-cell exit from the thymus and T and B cells traveling between secondary lymphoid organs to survey for antigen. After activation in lymphoid organs, T cells must again return to circulation to reach sites of infection. The immunomodulatory drug FTY720 induces sequestration of circulating mature lymphocytes by acceleration of lymphocyte homing via the S1P receptor 1 (Chiba et al. 1998; Yanagawa et al. 1998a, 1998b; Henning et al. 2001; Forrest et al. 2004; Matloubian et al. 2004; Hait et al. 2005; Kharel et al. 2005; Huwiler et al. 2006). Mandala et al. (2000) described alteration of lymphocyte

trafficking by sphingosine 1-phosphate receptor agonists.

PROCEDURE

Induction of Lymphopenia and Reduction of Thoracic Duct (TD) Lymphocytes by S1P and Analogs in Rats

Blood or thoracic duct lymph lymphocyte counts were determined by autoanalyzer (H2000, CARESIDE, Culver City, Calif., USA) and normalized to counts in vehicle controls after administration of FTY720 (2.5 mg/kg p.o.), or test compound. S1P was administered by continuous infusion beginning at 8 mg/kg per hour for 20 min followed by 2 mg/kg per hour for a further 220 min. The measured physiological S1P concentration in rat plasma by LC-MS was 0.5 µg/ml. This rose to a C_{max} of 2.5 µg/ml at 30 min and was maintained at 1.5 µg/ml for the remainder of the experiment. Studies on the effect on lymphocyte numbers in thoracic-duct-cannulated rats were performed after administration of FTY720 or test compound. Lymph flow remained constant for the duration of the experiment and numbers are shown as the average cell concentration maintained over the preceding 30 min.

FACS Measurement of Peripheral Blood Lymphocyte Depletion in Cannulated Rats:

Percentage depletion by FTY720 compared to vehicle control was measured. Similar nadir lymphopenia was produced by FTY720 or non-metabolizable phosphonates. Peripheral blood samples were diluted 1:1 with phosphate-buffered saline (PBS), layered on the same volume of Lymphocyte Separation Medium (ICN Biomedicals, Aurora, Ohio, USA) and centrifuged at 400 *g* for 30 min. Peripheral blood mononuclear cells (PBMC) were resuspended in PBS and counted using a hemocytometer. PBMC were then stained with FITC-labeled anti-CD8, PE-labeled anti-CD45RA, and Cy-Chrome-labeled anti-CD4 antibodies. Numbers of CD4-, CD8- and CD45RA-positive cells were calculated by multiplying total PBMC count with the percentages of $CD4^+$, $CD8^+$ and $CD45RA^+$ generated from flow cytometry.

Quantitation of Lymph Node Cells

Single-cell suspensions were prepared by passage of tissues through a 40-µm sieve. Peripheral blood lymphocytes were further isolated from spleens by ammonium chloride lysis of red blood cells. Cells were subsequently washed in UltraCULTURE medium (Biowhittaker, Walkersville, Md., USA) and all samples were adjusted to the same volume with PBS. An equal volume of 4% paraformaldehyde was added while gently vortexing the samples. The total number of viable, unstained lymphocytes per sample was determined by flow cytometry (FACScan; Becton Dickinson) using CELLquest software (Becton Dickinson), based upon forward and side scatter characteristics. Beads (Sigma; P7458) were used as an internal standard.

EVALUATION

Data were calculated as cell number per node by dividing the total number of lymphocytes quantitated by the number of nodes harvested per site (i. e., the number of Peyer's patches, mesenteric or peripheral lymph nodes collected).

MODIFICATIONS OF THE METHOD

Kawa et al. (1997) reported inhibition of chemotactic motility and trans-endothelial migration of human neutrophils by sphingosine 1-phosphate.

Fueller et al. (2003) described activation of human monocytic cells by lysophosphatidic acid and sphingosine-1-phosphate.

Roviezzo et al. (2004) studied human eosinophil chemotaxis and selective *in vivo* recruitment by sphingosine 1-phosphate.

REFERENCES AND FURTHER READING

Brinkmann V, Davis MD, Heise CE, Albert R, Cottens S, Hof R, Bruns C, Prieschl E, Baumruker T, Hiestand P, Foster CA, Zollinger M, Lynch KR (2002) The immune modulator FTY720 targets sphingosine 1-phosphate receptors. J Biol Chem 277:21453–21457

Chiba K, Yanagawa Y, Masubuchi Y, Karaoka H, Kawaguchi T, Ohtsuki M, Hoshino Y (1998) FTY720, a novel immunosuppressant, induces sequestration of circulating mature lymphocytes by acceleration of lymphocyte homing in rats. I. FTY720 selectively decreases the number of circulating mature lymphocytes by acceleration of lymphocyte homing. J Immunol 160:5037–5044

Forrest M, Sun SY, Hajdu R, Bergstrom J, Card D, Doherty G, Hale J, Keohane C, Meyers C, Milligan J, Mills S, Nomura H, Rosen H, Rosenbach M, Shei GJ, Singer II, Tian M, West S, White V, Xie J, Proia RL, Mandala S (2004) Immune cell regulation and cardiovascular effects of sphingosine 1-phosphate agonists in rodents are mediated via distinct receptor subtypes. J Pharmacol Exp Ther 309:758–768

Fueller M, Wang DA, Tigyi G, Siess W (2003) Activation of human monocytic cells by lysophosphatidic acid and sphingosine-1-phosphate. Cell Signal 15:367–375

Hait NC, Sarkar S, Le Stunff H, Mikami A, Maceyka M, Milstien S, Spiegel S (2005) Role of sphingosine kinase 2 in cell migration toward epidermal growth factor. J Biol Chem 280:29462–29469

Henning G, Ohl L, Junt T, Reiterer P, Brinkmann V, Nakano H, Hohenberger W, Lipp M, Förster R (2001) CC chemokine receptor 7-dependent and -independent pathways for lymphocyte homing: Modulation by FTY720. J Exp Med 194:1875–1881

Huwiler A, Döll F, Ren S, Klawitter S, Greening A, Römer I, Bubnova S, Reinsberg L, Pfeilschifter J (2006) Histamine increases sphingosine kinase-1 expression and activity in the human endothelial cell line E.A.hy926 by a PCK-α-dependent mechanism. Biochim Biophys Acta 1761:367–376

Kawa S, Kimura S, Hakomori SI, Igarashi Y (1997) Inhibition of chemotactic motility and trans-endothelial migration of human neutrophils by sphingosine 1-phosphate. FEBS Lett 420:196–200

Kharel Y, Lee S, Snyder AH, Sheasley-O'Neill SL, Morris MA, Setiady Y, Zhu R, Zigler MA, Burcin TL, Ley K, Tung KSK, Engelhard VH, Macdonald TL, Pearson-White S, Lynch KR (2005) Sphingosine kinase 2 is required for modulation of lymphocyte traffic by FTY720. J Biol Chem 280:36856–36872

Kimura T, Boehmler AM, Seitz G, Kuçi S, Wiesner T, Brinkmann V, Kanz L, Möhle R (2004) The sphingosine 1-phosphate receptor agonist FTY720 supports CXCR4-dependent migration and bone marrow homing of human $CD34^+$ progenitor cells. Blood 103:4478–4486

Mandala S, Hajdu R, Bergstrom J, Quackenbush E, Xie J, Milligan J, Thronton R, Shei GJ, Card D, Keohane CA, Rosenbach M, Hale J, Lynch CL, Rupprecht K, Parsons W, Rosen H (2000) Alteration of lymphocyte trafficking by sphingosine receptor agonists. Science 296:346–349

Matloubian M, Lo CG, Cinamom G, Lesneski MJ, Xu Y, Brinkmann V, Allende ML, Proia RL, Cyster JG (2004) Lymphocyte egress from thymus and peripheral lymphoid organs is dependent on S1P receptor 1. Nature 427:355–360

Roviezzo F, del Galdo F, Abbate G, Bucci M, D'Agostino B, Antunes E, de Dominicis G, Parente L, Rossi F, Cirino G, de Palma R (2004) Human eosinophil chemotaxis and selective in vivo recruitment by sphingosine 1-phosphate. Proc Natl Acad Sci USA 101:11170–11175

Yanagawa Y, Sugahara K, Kataoka H, Kawaguchi T, Masubuchi Y, Chiba K (1998a) FTY720, a novel immunosuppressant, induces sequestration of circulating mature lymphocytes by acceleration of lymphocyte homing in rats. II. FTY720 prolongs allograft survival by decreasing T cell infiltration into grafts but not cytokine production in vivo. J Immunol 160:5493–5499

Yanagawa Y, Masubuchi Y, Chiba K (1998b) FTY720, a novel immunosuppressant, induces sequestration of circulating mature lymphocytes by acceleration of lymphocyte homing in rats. Immunology 95:591–594

Zemann B, Kinzel B, Müller M, Reuschel R, Mechtcheriakowa D, Urtz N, Bomancin F, Baumruker T, Billich A (2006) Sphingosine kinase type 2 is essential for lymphopenia induced by the immunomodulatory drug FTY720. Blood 107:1454–1458

I.2.2 In Vivo Methods for Testing Immunological Factors

I.2.2.1 Spontaneous Autoimmune Diseases in Animals

Several spontaneous autoimmune diseases have been reported in several inbred animal strains:

New Zealand black mouse (NZB mouse) (Bielschowski et al. 1959; Howie and Helyer 1968; Barthold et al. 1974; Blanchard and Bach 1980). The NZB mouse develops a spontaneous autoimmune disease with autoimmune hemolytic anemia, splenomegaly, glomerulonephritis, lymphoproliferative disorders and peptic ulcerations.

New Zealand black/white F1 (B/W) mouse (Helyer and Howie 1963; Kessler 1968): These animals develop nephritis similar to that in human systemic lupus erythematosus and show mononuclear cell infiltration in salivary and lachrymal glands such as in human Sjögren's syndrome.

A substrain of the autoimmune-prone mouse, NZB/kl, was found to show spontaneous elevation of the auditory brainstem response threshold with age (Sone et al. 1995).

Immunodeficient alymphoplasia mice were recommended as a spontaneous model for Sjøgren's syndrome (Tsubata et al. 1996). Mice homozygous for an autosomal recessive mutation aly (alymphoplasia) lack both lymph nodes an Peyer's patches and show defects in both humoral and cellular immunity. Histopathological analyses revealed chronic inflammatory changes in exocrine organs such as the salivary gland, lacrimal gland and the pancreas.

The **Palmerston North autoimmune mouse strain** which exhibits both spontaneous systemic autoimmune disease and otic capsule bone formation has been proposed as a model for otic capsule osteogenesis and otosclerosis (Hertler and Trune 1990; Traynor et al. 1992).

In aging **BDF1 mice**, Hayashi et al. (1988) described spontaneous development of autoimmune sialadenitis.

Robison et al. (1994) examined the relationship between orchitits and aspermatogenesis in various strains of H_2 congenic mice and defined a genetic predisposition to spontaneous aspermatogenesis.

Motheaten mice. Mice homozygous for the autosomal recessive motheaten (me) or the allelic viable motheaten (me^v) mutations develop severe and early-age onset of systemic autoimmune and inflammatory disease (Green and Shultz 1975; Shultz et al. 1984; Shultz 1988; Su et al. 1998).

The genetic, hormonal and behavioural influence on spontaneously developing arthritis in normal mice has been reviewed by Holmdahl et al. (1992).

Non-obese diabetic mouse (NOD mouse) (Makino et al. 1980; Miyazaki et al. 1985; Leiter et al. 1987). The inbred NOD mouse is considered a good model for type I diabetes mellitus. Mononuclear cells infiltrate the pancreatic islets of Langerhans from 6–8 weeks of age, followed by a progressive and

selective destruction of insulin-producing β-cells and the onset of IDDM from the 12th week of age onwards.

Itoh et al. (1997) studied the requirement of Fas for the development of autoimmune diabetes in nonobese diabetic mice.

Quartey-Papafio et al. (1995) showed that aspartate at position 57 of nonobese diabetic I-A(g7) β-chain diminishes the spontaneous incidence of insulin-dependent diabetes mellitus in the NOD mouse.

The NOD mouse was also recommended to study the pathogenesis of autoimmune thyroiditis (Many et al. 1996).

Bio-breeding rat (BB rat) (Like et al. 1982; Field 1983; Yale and Marliss 1984). On the basis of clinical and histopathological parameters, the BB rat is considered a useful model for human IDDM. The disease in the BB Rat is characterized by infiltration of lymphocytes and macrophages into the islets of Langerhans.

Allen and Thupari (1995) described spontaneous autoimmune lymphocytic thyroiditis in*BB/Wor rats.*

Obese strain chicken (OS chicken) (van Tienhoven and Cole 1962; Cole 1966; Cole et al. 1968, 1970; Wick et al. 1974). The OS chicken is perhaps the best studied model for an organ-specific, spontaneously occurring autoimmune disease, viz. spontaneous autoimmune thyroiditis, which closely resembles human Hashimoto thyroiditis. The spontaneous autoimmune thyroiditis in obese chicken was further studied by Neu et al. 1986; Kroemer et al. 1989; Cihak et al. 1995; Hala et al. 1996; Dietrich et al. 1997.

Chickens of the University of California line 200 **(UCD-200 chickens)** develop an inherited inflammatory fibrotic disease that closely resembles human progressive systemic sclerosis (scleroderma) (Gershwin et al. 1981; Van de Water et al. 1984; Brezinscheck et al. 1993).

Schumm-Draeger and Fortmeyer (1996) described **autoimmune thyroiditis in the cat** as a spontaneous disease model.

Spontaneous autoimmune thyroiditis was found in **Mastomys** (*Praeomys coucha*) by Solleveld et al. (1985) and recommended as an animal model of human disease.

REFERENCES AND FURTHER READING

Allen EM, Thupari JN (1995) Thyroglobin-reactive T lymphocytes in thyroiditis-prone BB/Wor rats. J Endocrinol Invest 18:45–49

Barthold DR, Kysela S, Steinberg AD (1974) Decline in suppressor T cell function with age in female NZB mice. J Immunol 112:9

Bielschowski M, Helyer BJ, Howie JB (1959) Spontaneous anemia in mice of the NZB/BL strain. Proc Univ Otago Med School 37:9–11

Blanchard D, Bach MA (1980) Thymic function in NZB mice. Clin Exp Immunol 42:1–9

Brezinscheck HP, Gruschwitz M, Sgone R, Moormann S, Herold M, Gershwin ME, Wick G (1993) Effects of cytokine application on glucocorticoid secretion in an animal model for systemic scleroderma. J Autoimmun 6:719–733

Cihak J, Hoffmann-Fezer G, Koller A, Kaspers B, Merkle H, Hala K, Wick G, Losch U (1995) Preferential TCR Vβ1 gene usage by autoreactive T cells in spontaneous autoimmune thyroiditis of the obese strain of chickens. J Autoimmun 8:507–520

Cole RK (1966) Hereditary hypothyroidism in domestic fowl. Genetics 13:1021–1033

Cole RK, Kite JH, Witebsky E (1968) Hereditary autoimmune thyroiditis in the fowl. Science 160:1357–1358

Cole RK, Kite JH, Wick G, Witebsky E (1970) Inherited autoimmune thyroiditis in the fowl. Poultry Sci 49:480–488

Del Prete GF, Tiri A, Parronchi P, Pinchera A, Romagnani S, Ricci M, Mariotti S (1989) Thyroiditis as a model of organ specific autoimmune disease. Clin Exper Rheumatol 7, Suppl 3:S41–S46

Dietrich HM, Oliveira Dos Santos AJ, Wick G (1997) Development of spontaneous autoimmune thyroiditis in Obese strain (OS) chickens. Vet Immunol Immunopathol 57:141–146

Field JB (ed) (1983) The juvenile diabetes foundation workshop on the spontaneously diabetic BB rat: its potential for insight into human juvenile diabetes. Metabolism 32 (Suppl 1)

Gershwin ME, Abplanalp JJ, Castles RM, Ikeda J, van de Water J, Eklund J, Haynes D (1981) Characterization of a spontaneous disease of white leghorn chickens resembling progressive systemic sclerosis (scleroderma). J Exp Med 153:1640–1659

Green MC, Shultz LD (1975) Motheaten, an immunodeficient mutant of the mouse. I. Genetics and pathology. J Hered 66:250–258

Hala K, Malin G, Dietrich H, Loesch U, Boeck G, Wolf H, Kaspers B, Geryk J, Falk M, Boyd RL (1996) Analysis of the initiation period of spontaneous autoimmune thyroiditis (SAT) in the obese strain (OS) of chickens. J Autoimmun 9:129–138

Hayashi Y, Kurashima C, Utsuyama M, Hirokawa K (1988) Spontaneous development of autoimmune sialadenitis in aging BDF1 mice. AM J Pathol 132:173–179

Helyer BW, Howie JB (1963) Renal disease associated with positive lupus erythematosus test in a cross-bred strain of mice. Nature 197:197

Hertler CK, Trune DR (1990) Otic capsule bony lesions in the Palmerston North autoimmune mouse. Otolaryngol Head Neck Surg 103:713–718

Holmdahl R, Jansson L, Andersson M, Jonsson R (1992) Genetic, hormonal and behavioural influence on spontaneously developing arthritis in normal mice. Clin Exp Immunol 88:467–472

Howie JB, Helyer BJ (1968) The immunology and pathology of NZB mice. In: Advances in Immunology. New York, Academic Press, 9:215–266

Itoh N, Imagawa M, Hanafusa T, Waguri M, Yamamoto K, Iwahshi A, Morikawi M, Nakajima H, Miyagawa J, Namba M, Makino S, Nagata S, Kono N, Matsuzawa Y (1997) Requirement of Fas for the development of autoimmune diabetes in nonobese diabetic mice. J Exp Med 186:613–618

Kessler HS (1968) A laboratory model for Sjögren's syndrome. Am J Pathol 52:671–685
Kroemer G, Neu N, Kuehr T, Dietrich F, Fassler R, Hala K, Wick G (1989) Immunogenetic analysis of spontaneous autoimmune thyroiditis of obese strain of chickens. Clin Immunol Immunopathol 52:202–213
Leiter EH, Prochazka M, Coleman DL (1987) Animal model of human disease. The non-obese diabetic (NOD) mouse. Am J Pathol 128:380–383
Like AA, Butler L, Williams RM, Appel MC, Weringer EJ, Rossini AA (1982) Spontaneous autoimmune diabetes mellitus in the BB rat. Diabetes 31 (Suppl) 7–13
Makino S, Kunimoto K, Muraoka Y, Mizushima Y, Katagiri K, Tochino Y (1980) Breeding of a non-obese, diabetic strain of mice. Exp Anim 29:1–13
Many MC, Maniratunga S, Denef JF (1996) The non-obese diabetic (NOD) mouse: an animal model for autoimmune thyroiditis. Exp Clin Endocrinol Diabetes 104/Suppl 3:17–20
Miyazaki A, Hanafusa T, Yamada K, Miyagawa J, Fujino-Kurihara H, Nagajima H, Nonaka K, Tarui S (1985) Predominance of T lymphocytes in pancreatic islets and spleen of pre-diabetic non-obese diabetic (NOD) mice: a longitudinal study. Clin Exp Immunol 60:622–630
Neu N, Hala K, Dietrich H, Wick G (1986) Genetic background of spontaneous autoimmune thyroiditis in the obese strain of chickens studied in hybrids with an inbred line. Int Arch Allergy Appl Immunol 80:168–173
Quartey-Papafio R, Lund T, Chandler P, Picard J, Ozegbe P, Hutchings PR, O'Reilly L, Kioussis D, Simpson E, Cooke A (1995) Aspartate at position 57 of nonobese diabetic I-A(g7) β-chain diminishes the spontaneous incidence of insulin-dependent diabetes mellitus. J Immunol 154:5567–5575
Robison R, Tung KSK, Meeker ND, Monson FG, Teuscher C (1994) A murine model of spontaneous aspermatogenesis: Linkage to H_2. J Reprod Immunol 26:251–260
Schumm-Draeger PM, Fortmeyer HP (1996) Autoimmune thyroiditis – Spontaneous disease models – Cat. Exp Clin Endocrinol Diabetes 104/Suppl 3:12–13
Schuurs AHWM, Verheul HAM, Wick G (1989) Spontaneous autoimmune models. Pharmacological Methods in the Control of Inflammation. pp 449–485, Alan R. Liss, Inc
Shultz LD (1988) Pleiotropic effects of deleterious alleles in the "motheaten" locus. Curr Top Microbiol Immunol 137:216–222
Shultz LD, Coman DR, Bailey CL, Beamer WG, Sidman CL (1984) "Viable motheaten", a new allele in the motheaten locus. Am J Pathol 116:179–192
Solleveld HA, Coolen J, Haajiman JJ (1985) Animal model of human disease: Autoimmune thyroiditis. Spontaneous autoimmune thyroiditis in praomys (mastomys) coucha. Am J Pathol 119:345–349
Sone M, Nariuchi H, Saito K, Yanagita M (1995) A substrain of NZB mouse as an animal model of autoimmune inner ear disease. Hear Res 83:26–26
Su X, Zhou T, Yang P, Edwards CK III, Mountz JD (1998) Reduction of arthritis and pneumonitis in motheaten mice by soluble tumor necrosis factor receptor. Arthr Rheum 41:139–149
Traynor SJ, Cohen JI, Morton JI, Trune DR (1992) Immunohistochemical analysis of otic capsule osteogenesis in the Palmerston North autoimmune mouse. Otolaryngol Head Neck Surg 106:196–201
Tsubata R, Tsubata T, Hiai H, Shinkura R, Matsumura R, Sumida T, Miyawaki S, Ishida H, Kumagai S, Nakao I, Honjo T (1996) Autoimmune disease of exocrine organs in immunodeficient alymphoplasia mice: A spontaneous model for Sjøgren's syndrome. Eur J Immunol 26:2742–2748
Van de Water J, Gershwin ME, Aplanalp H, Wick G, van der Mark K (1984) Serial observations and definition of mononuclear cell infiltrates in avian scleroderma, an inherited fibrotic disease of chickens. Arthr Rheum 27:807–815
van Tienhoven A, Cole RK (1962) Endocrine disturbance in obese chickens. Anat Rev 142:111–122
Wick G, Sundick RS, Albini B (1974) The obese strain (OS) of chickens: an animal model with spontaneous autoimmune thyroiditis. Clin Immunol Immunopathol 3:272–300
Yale JF, Marliss EB (1984) Altered immunity and diabetes in the BB rat. Clin Exp Immunol 57:1–11

I.2.2.2 Acute Systemic Anaphylaxis in Rats

PURPOSE AND RATIONALE

Rats are immunized with ovalbumin and *Bordetella pertussis* suspension as adjuvant. After 11 days the animals are challenged by intravenous injection of ovalbumin. The shock symptoms can by inhibited by corticosteroids and intravenous disodium cromoglycate.

PROCEDURE

Female Sprague-Dawley rats weighing 120 g are immunized by i.m. injection of 10 mg/kg highly purified ovalbumin. Simultaneously 1 ml of *Bordetella pertussis* suspension (2×10^{10} organisms) is injected intraperitoneally. IgE antibodies are induced and attached to the surface of mast cells and basophilic granulocytes. Eleven days later the animals are challenged by intravenous injection of 25 mg/kg highly purified ovalbumin. This results in formation of antigen-antibody-complexes on the surface of mast cells and basophilic granulocytes in blood and in all organs with immediate release of various mediators of anaphylaxis, such as histamine, serotonin, SRS-A, prostaglandins; in shock symptoms and 80% lethality. Corticosteroids, e. g. dexamethasone 1–10 mg/kg s.c. are given 18 h prior to challenge, or 30 mg/kg disodium cromoglycate i.v. before injection of ovalbumin. Ten–20 animals are used for each group.

EVALUATION

The shock symptoms are scored and mortality counted. Results after treatment are compared with untreated controls. Pretreatment with corticosteroids or disodium cromoglycate can inhibit death and ameliorate shock symptoms. Statistical calculation is performed using the χ^2-test.

MODIFICATIONS OF THE METHOD

Desensitization by repeated 'microshocks' of constant strength in guinea pigs has been reported by Herxheimer (1952).

Acute systemic anaphylaxis experiments have also been performed in guinea pigs and in mice. In guinea pigs anaphylactic bronchospasm can be measured with the Konzett and Rössler method (see D.2.2.1) (Davies and Evans 1973).

Moreover, anaphylactic bronchospasm can be measured in isolated guinea pig lungs according to the method of Bhattacharya and Delaunois (1955).

Anaphylaxis can be measured in the chopped guinea pig lung by assay of the supernatant in the isolated guinea pig ileum in the presence of 2×10^{-7} M atropine (Austen and Brocklehurst (1961).

Ufkes and Ottenhof (1984) sensitized Brown-Norway rats with a suspension of trinitrophenyl haptenized ovalbumin together with $AlPO_4$ as adjuvant. Bronchial and cardiovascular function were studied after treatment with anti-allergic agents and antigen challenge.

Elwood et al. (1992) studied the effect of dexamethasone and cyclosporin A on allergen-induced airway hyperresponsiveness and inflammatory cell responses in sensitized Brown-Norway rats.

REFERENCES AND FURTHER READING

Austen KF, Brocklehurst WE (1961) Anaphylaxis in chopped guinea pig lung. J Exp Med 113:521–537

Bhattacharya BK, Delaunois AL (1955) An improved method for the perfusion of isolated lung of guinea pig. Arch Int Pharmacodyn 101:495–510

Davies GE, Evans (1973) Studies with two new phosphodiesterase inhibitors (ICI 58,301 and ICI 63,197) on anaphylaxis in guinea pigs, mice and rats. Int Arch Allergy 45:467–478

Elwood W, Lötvall JO, Barnes PJ, Chung KF (1992) Effect of dexamethasone and cyclosporin A on allergen-induced airway hyperresponsiveness and inflammatory cell responses in sensitized Brown-Norway rats. Am Rev Resp Dis 145:1289–1294

Herxheimer H (1952) Repeatable 'microshocks' of constant strength in guinea pig anaphylaxis. J Physiol 117:251–255

Omote M, Sakai K, Mizusawa H (1994) Acute effects of deflazacort and its metabolite 21-desacetyl-deflezacort on allergic reactions. Arzneim Forsch/Drug Res 44:149–153

Ufkes JGR, Ottenhof M (1984) Characterization of various anti-allergic agents using a new method for inducing systemic anaphylaxis in the rat. J Pharmacol Meth 11:219–226

I.2.2.3 Anti-Anaphylactic Activity (Schultz–Dale Reaction)

PURPOSE AND RATIONALE

Guinea pigs are sensitized against egg albumin. Challenge after 3 weeks causes in isolated organs release of mediators, e. g. histamine, which induce contraction in isolated ileum.

PROCEDURE

Guinea pigs of either sex weighing 300–350 g are sensitized with alum precipitated egg albumin. Alum egg albumin is prepared by dissolving egg albumin (1 mg/ml) in six percent aluminum hydroxide gel, suspended in saline. The mixture is stirred and kept at room temperature. Each animal receives at the same time injections of 0.125 ml of this mixture in each foot pad and 0.5 ml subcutaneously. After 4 weeks the animals are killed and the ileum is dissected out. Cleaned pieces, about 2–3 cm long, are mounted in an organ bath containing Tyrode solution at 37°C. The strips are allowed to equilibrate for 15 min. The contractility of the ileum strips is tested by adding 10^{-4} g/ml $BaCl_2$ solution. To one organ bath the standard (2×10^{-6} g/ml final concentration of Tribenosid = 1-O-ethyl-3,5,6-tri-O-benzyl-D-glucofuranoside = Glyvenol CIBA) and to other vials the test compounds (final concentration up to 10^{-5} g/ml) are added. One organ bath serves as control. After 3 min ovalbumin in a final concentration of 2×10^{-6} g/ml is added. The contractions are recorded with strain gauges by a polygraph.

EVALUATION

The results are expressed as presence or absence of blocking activity (percentage inhibition). If anti-anaphylactic activity is observed, ED_{50} values using different doses are calculated.

CRITICAL ASSESSMENT OF THE METHOD

Positive results can also be achieved with spasmolytics, local anesthetics, antihistaminics, and sympathicomimetics.

MODIFICATIONS OF THE METHOD

The method has been modified by testing histamine release in the lung after challenging with egg albumin. Either lung strips from sensitized guinea pigs are suspended in an organ bath and their contractions are measured after addition of egg albumin or the entire lung tissue is dissected out and washed free from blood by perfusing with warm oxygenated Tyrode solution via the pulmonary artery. The lung tissue is chopped and washed with Tyrode solution in order to remove the remaining blood. The chopped lung tissue is divided into 24 samples, each of approximately 100 mg wet weight. These are incubated at 37°C in Tyrode solution for 15 min with continuous agitation by rocking, after which, 1 mg/ml of egg albumin is added to

the reaction mixture. After shaking for 10 min at 37°C, the supernatant is collected and assayed for histamine with guinea pig ileum. Atropine sulfate 2 mg/ml is added in Tyrode solution. The residual histamine is obtained by boiling the tissue in 5 ml Tyrode solution for 10 min. The tubes are then placed on ice for 1 h to allow complete diffusion. Released histamine is expressed as a percentage of total histamine content.

Koppel et al. (1981) developed a method to induce contraction of immunologically sensitized mouse trachea by antigen (Schultz–Dale reaction).

The trachea of sensitized guinea pigs was used by Omote et al. (1994).

REFERENCES AND FURTHER READING

Anderson P, Brattsand R (1982) Protective effects of the glucocorticoid, budesonide, on lung anaphylaxis in actively sensitized guinea pigs: Inhibition of the IgE – but not of the IgG – mediated anaphylaxis. Br J Pharmacol 76:139–147

Austen KF, Brocklehurst WE (1961) Anaphylaxis in chopped guinea pig lung. I. Effect of peptidase substrates and inhibitors. J Exper Med 113:521–537

Dale HH (1913) The anaphylactic reaction of plain muscle in the guinea-pig. J Pharmacol Exper Ther 4:167–223

Koppel GA, Haisch KD, Spaethe SM, Schmidtke JR, Fleisch JH (1981) Schultz–Dale reaction in mouse trachea. J Pharmacol Meth 6:39–43

Laekeman GM, Herman AG, van Nueten JM (1977) Influence of different drugs on the slow response of the intestine during the Schultz–Dale reaction. Arch Int Pharmacodyn 230:335

Omote M, Sakai K, Mizusawa H (1994) Acute effects of deflazacort and its metabolite 21-desacetyl-deflezacort on allergic reactions. Arzneim Forsch/Drug Res 44:149–153

Schultz WH (1910) Physiological studies in anaphylaxis. 1. The reaction of smooth muscle of the guinea-pig sensitized with horse serum. J Pharmacol Exper Ther 1:549–567

I.2.2.4 Passive Cutaneous Anaphylaxis

PURPOSE AND RATIONALE

Passive cutaneous anaphylaxis is a immune reaction of the immediate type. By passive immunization of rats in the skin with rat anti-ovalbumin serum and a challenge 2 days later with ovalbumin at the same skin area antigen-antibody complexes are formed in the mast cells inducing release of mediators. This results in vasodilatation, increase in permeability of the vessel walls and leakage of plasma. To make the allergic reaction visible, Evan's blue dye is administered along with the antigen. Evan's blue dye is attached to the albumin fraction of plasma, producing a blue spot. This blue spot indicates that an anaphylactic reaction has taken place in the skin.

PROCEDURE

For preparation of antiserum male rats weighing 200–250 g are adrenalectomized and are allowed to recover for 3 days. Thereafter, animals are sensitized with egg albumin (1 mg/animal) using aluminium hydroxide gel (200 mg) as adjuvant. Alum egg albumin is prepared by dissolving 1 mg/ml of egg albumin in 20% aluminium hydroxide gel, suspended in saline. Each animal simultaneously receives 0.125 ml of the above solution in each foot pad and 0.5 ml subcutaneously. After 8 days, the animals are bled and antiserum is collected.

For the test, the antiserum is diluted in such a manner as to give a wheal of 15–20 mm diameter in a preliminary titration. Aliquots of 100 µl of appropriate dilution of antiserum are injected intradermally into the shaved dorsal skin of normal male rats weighing about 100 g. After 24 h of latent period each animal is challenged with the intravenous administration of 0.1 ml of 2.5% Evans blue dye containing 25 mg/ml of egg albumin. In the case of intravenous administration, the test compound is administered simultaneously with the antigen and the dye. In case of oral testing, the compound is given orally 1 h prior to challenge. The animals are sacrificed 30 min after the challenge. The amount of Evans blue dye leaked at the site of passive cutaneous anaphylactic reaction is extracted and determined colorimetrically at 620 µm wavelength.

EVALUATION

The amount of Evans blue extracted from passive cutaneous anaphylactic reaction is taken as 100 percent. Percent inhibition of passive cutaneous anaphylactic reaction in the rats treated with the test compound is calculated. The standard disodium cromoglycate at a dose of 3 mg/kg i.v. or 30 mg/kg orally results in 80–100% inhibition. Using different doses, ED_{50} values can be calculated.

MODIFICATIONS OF THE METHOD

Goose and Blair (1969) used *Bordetella pertussis* and extracts of the worm *Nippostrongylus brasiliensis* as antigens in passive cutaneous anaphylaxis experiments in the rat.

Patterson et al. (1971) tested passive cutaneous reactivity to antihuman IgE in rhesus monkeys.

Without immunization, plasma extravasation after bradykinin injection can be tested in anesthetized Sprague-Dawley rats (Lembeck et al. 1991). Evans blue dye is injected to stain plasma proteins. After injection of bradykinin antagonists followed by bradykinin injection, the rats are perfused with phys-

iological saline. The trachea, the urinary bladder, and the duodenum are resected, weighed and incubated for 48 h in formamide at 50°C (Saria et al. 1983). The amount of Evans blue extracted is measured photometrically at 620 nm.

Vascular reactions to histamine, histamine-liberator and leukotaxine in the skin of guinea pigs using pontamine sky blue 6X as indicator were studied by Miles and Miles (1952).

REFERENCES AND FURTHER READING

Goose J, Blair AMJN (1969) Passive cutaneous anaphylaxis in the rat, induced with two homologous reagin-like antibodies and its specific inhibition with disodium cromoglycate. Immunology 16:749–760

Griesbacher T, Lembeck F (1987) Actions of bradykinin antagonists on bradykinin-induced plasma extravasation, venoconstriction, prostaglandin E_2 release, nociceptor stimulation and contraction of the iris sphincter muscle of the rabbit. Br J Pharmacol 92:333–340

Katayama S, Shionoya H, Ohtake S (1975) A new simple method for extraction of extravasated dye in the skin. Japan J Pharmacol Suppl 25:103P

Miles AA, Miles EM (1952) Vascular reactions to histamine, histamine-liberator and leukotaxine in the skin of guinea pigs. J Physiol 118:228–257

Patterson R, Talbot CH, Brandfonbrener M (1971) The use of IgE mediated responses as a pharmacologic test system. The effect of disodium cromoglycate in respiratory and cutaneous reactions and in the electrocardiograms of rhesus monkeys. Int Arch Allergy 41:592–603

Saria A, Lundberg JM, Skofitsch G, Lembeck F (1983) Vascular protein leakage in various tissues induced by substance P, capsaicin, bradykinin, histamine and by antigen challenge. Naunyn Schmiedeberg's Arch Pharmacol 324:212–218

Watanabe N, Ovary Z (1977) Antigen and antibody detection by *in vivo* methods: a reevaluation of passive cutaneous anaphylactic reactions. J Immunol Meth 14:381–390

I.2.2.5 Arthus Type Immediate Hypersensitivity

PURPOSE AND RATIONALE

The immune complex induced Arthus reaction comprises inflammatory factors that have been implicated in the acute responses in joints of rheumatic patients. Complement and polymorphonuclear neutrophiles are activated via precipitating antigen-antibody complexes leading to an inflammatory focus characterized by edema, hemorrhage and vasculitis. Arthus reaction of the immediate type becomes maximal 2–8 h after challenge.

PROCEDURE

Ovalbumin Suspension

1700 mg ovalbumin are suspended in 100 ml paraffin oil. 4.38 ml pertussis vaccine are suspended in 70 ml 0.9% NaCl-solution. Both suspensions are mixed to form an emulsion.

Wistar or Sprague-Dawley rats of either sex weighing 220–280 g can be used. Seven days prior to start of the experiment rats are sensitized by i.m. administration of 0.5 ml of the ovalbumin suspension. They are housed in groups of eight with standard food and water ad libitum.

Twenty-four hours and one hour prior to induction of the Arthus reaction, test compounds are administered to groups of 8 animals. The rats are challenged by injection of 0.1 ml of 0.04% solution of highly purified ovalbumin in the left hind paw. Swelling of the paw occurs which reaches a maximum after a few hours. The footpad thickness can be measured by calipers. One group of sensitized animals treated with solvent alone serves as positive control, one group of non-sensitized animals treated with solvent alone serves as negative control. Standard doses are 30 mg/kg cortisone or 10 mg/kg prednisolone p.o.

EVALUATION

The change in footpad thickness is expressed as the percent change from the vehicle control group. Comparison of experimental group to positive control is evaluated statistically using Student's *t*-test.

MODIFICATIONS OF THE METHOD

Instead of ovalbumin, sheep red blood cell suspensions can be used for immunization and for challenge in mice (Omote et al. 1994).

Nagakawa et al. (1990) sensitized mice by s.c. injection of bovine serum albumin in complete Freund's adjuvant and boosted on day 21 by an intradermal injection of BSA. On day 28, the Arthus reaction was elicited by intradermal injection of BSA. Four hours later, an erythematous skin reaction over an area of more than 8 mm^2 was regarded as positive.

Kamei et al. (1991) immunized guinea pigs by injection of a mixture of egg albumin and Freund's complete adjuvant subcutaneously into the food pad or i.m. into the hind leg. The injection was repeated 4 times at 7 day intervals. Ten days after the last immunization, 0.2 ml of 2.5% egg albumin was injected sc. into the dorsal skin of the animals. The intensity of the Arthus reaction was evaluated by measuring the inflamed area according to scores.

REFERENCES AND FURTHER READING

Bartlett RR, Gebert U, v. Kerékjártó B, Schleyerbach R, Thorwart W, Weitmann KU (1989) Substituted 3-phenyl-7*H*-thiazolo(3,2-b)(1,2,4)triazin-7-ones as antiinflammatory agents with immunomodulating properties. Drugs Exp Clin Res 15:521–526

Horvat J, Vidic B, Kosec D, Stojic Z, Jankovic BD (1990) Suppression of Arthus and delayed hypersensitivity reactions to bovine serum albumin by dopaminergic antagonists. Period Biol 92:81–82
Kamei C, Izushi K, Adachi Y, Shimazawa M, Tasaka K (1991) Inhibitory effect of epinastine on the type II–IV allergic reactions in mice, rats and guinea pigs. Arzneim Forsch/Drug Res 41:1150–1153
Nagakawa Y, Ogawa T, Kobayashi M, Wagatsuma K, Munakata H, Umezu K, Sato S, Shibata Y, Inoue K, Ishida N (1990) Immunopharmacological studies of 4-acetylaminophenylacetic acid. (MS-932). Int J Immunother 6:131–140
Omote M, Sakai K, Mizusawa H (1994) Acute effects of deflazacort and its metabolite 21-desacetyl-deflezacort on allergic reactions. Arzneim Forsch/Drug Res 44:149–153

I.2.2.6 Delayed Type Hypersensitivity

PURPOSE AND RATIONALE

Delayed type hypersensitivity is a reaction of cell mediated immunity and becomes visible only after 16–24 h. The same methods as for testing immediate type hypersensitivity can be used.

PROCEDURE

Rats are sensitized in the same way by i.m. administration of 0.5 ml ovalbumin suspension 7 days prior to the start of the experiment as described for testing immediate type hypersensitivity. They are challenged by injection of 0.1 ml of 0.04% solution of highly purified ovalbumin in the left hind paw. Footpad thickness is measured immediately and 24 h after ovalbumin administration.

MODIFICATIONS OF THE METHOD

Mizukoshi et al. (1994) injected female CDF1 mice intradermally with a suspension of 2×10^8 sheep red blood cells/50 µl into the left foot pad. A second booster of the same dose was given to the right foot pad on day 4. The thickness of the foot pads was measured on the following day, and the difference in the thickness between the right and the left food pads was taken as the degree of swelling.

Kamei et al. (1991) immunized mice by applying 0.15 ml of 7% picryl chloride/ethanol solution to the skin of the shaved abdomen. The second immunization was performed 6 days later. One week after the second immunization, 1 drop of 1% picryl chloride olive oil solution was applied to the ear and the thickness of the ear was measured by a thickness gauge 24 h later.

REFERENCES AND FURTHER READING

Borel JF (1989) Pharmacology of cyclosporine (Sandimmune). IV. Pharmacological properties *in vivo*. Pharmacol Rev 41:259–371
Borel JF, Feurer C, Magnée C, Stähelin H (1977) Effects of the new anti-lymphocytic peptide cyclosporin A in animals. Immunology 32:1017–1025
Herrmann P, Schreier MH, Borel JF, Feurer C (1988) Mast cell degranulation as a major event in the effector phase of delayed-type hypersensitivity induced by cloned helper cells. Int Arch Allergy Appl Immunol 86:102–105
Kamei C, Izushi K, Adachi Y, Shimazawa M, Tasaka K (1991) Inhibitory effect of epinastine on the type II–IV allergic reactions in mice, rats and guinea pigs. Arzneim Forsch/Drug Res 41:1150–1153
Mizukoshi S, Tsukamoto M, Tanaka H, Nakamura K, Kato F (1994) Antiinflammatory and immunosuppressive effects of 1,6-anhydro-3,4-dideoxy-2-furfuryl-β-D-*threo*-3-enopyranose (MT 2221), a novel anhydro-enopyranose derivative, on experimental animal models. Biol Pharm Bull 17:1070–1074
Nagakawa Y, Ogawa T, Kobayashi M, Wagatsuma K, Munakata H, Umezu K, Sato S, Shibata Y, Inoue K, Ishida N (1990) Immunopharmacological studies of 4-acetylaminophenyl-acetic acid. (MS-932). Int J Immunother 6:131–140
Titus RG, Chiller JM (1981) A simple and effective method to assess murine delayed type hypersensitivity to proteins. J Immunol Meth 45:65–78

I.2.2.7 Reversed Passive Arthus Reaction

PURPOSE AND RATIONALE

In the reversed passive Arthus reaction the antigen is injected intravenously followed by a local injection – either intradermally or into the pleural space – of the respective antibody. Generation of an immune-mediated reverse passive Arthus reaction in the rat pleural cavity results in a classic acute inflammatory response. The methods are used to evaluate new anti-inflammatory agents.

PROCEDURE

Male Lewis rats weighing 200–250 g are fasted overnight prior to use with free access to water. The animals receive 5 mg bovine serum albumin in 0.2 ml sterile saline intravenously, followed 30 min later by injection of 1 mg rabbit anti-BSA in 0.2 ml sterile saline into the right pleural cavity under light halothane anesthesia. Drugs or vehicle controls are administered by gastric gavage in 1 ml/100 g body weight at different times prior to the anti-BSA. The animals are sacrificed at various intervals after anti-BSA injections by CO_2 inhalation (after 5 min for thromboxane B_2 determination, after 10 min for leukotriene B_4 determination, and after 4 h at the peak time of neutrophil infiltration). The fluid exudate is removed from the pleural cavity by gentle vacuum aspiration and the volume is recorded. Eikosanoids in the pleural exudate are quantitated by commercial RIA kits.

EVALUATION

The values after treatment with various doses of test compounds are compared with those of vehicle controls.

MODIFICATIONS OF THE METHOD

The antibody can be injected intradermally into the shaved skin of rats after intravenous injection of the antigen (e. g., human albumin) together with Evans blue dye solution. Extravasated dye is determined in skin punches (Camussi et al. 1990; Burch et al. 1992; Okamoto et al. 1992).

Bailey and Sturm (1983) induced the reverse passive Arthus reaction in rats using bovine serum albumin as antigen into the tail vein and rabbit anti-bovine serum albumin into the skin site. One hour after oral dosing with vehicle or drug, animals were lightly anesthetized and their hair was shaved from the mid-dorsal region with electric clippers. Each animal was injected intradermally with 40 µl on the left side of the mid-dorsal line and with 40 µl of rabbit anti-bovine serum albumin (5.0 mg/ml antibody protein), diluted 1:4 with phosphate-buffered saline on the right side of the dorsal midline. Immediately following the intradermal challenge, each rat received 0.5 ml phosphate-buffered saline containing 1.0 mg bovine serum albumin injected in the tail vein. Four hours after intradermal challenge, the animals were sacrificed. The full thickness skin was removed from the back and discs 8 mm in diameter were punched out with a metal punch. Wet weight of the samples from the phosphate-buffered saline- and antibody-injected site was determined and the edema induced by the reverse passive Arthus reaction calculated as the difference between both weights.

REFERENCES AND FURTHER READING

Bailey PJ, Sturm A (1983) Immune complexes and inflammation. A study of the activity of anti-inflammatory drugs in the reverse passive Arthus reaction in the rat. Biochem Pharmacol 32:475–481

Berkenkopf JW, Weichman BM (1991) Comparison of several new 5-lipoxygenase inhibitors in a rat Arthus pleurisy model. Eur J Pharmacol 193:29–34

Berkenkopf JW, Marinari LR, Weichman BM (1991) Phospholipase A_2 acyl-hydrolytic activity in rat RPAR-induced pleurisy. Agents Actions 34:93–96

Burch RM, Connor JR, Bator JM, Weitzberg M, Laemont K, Noronha-Blob L, Sullivan JP, Steranka LR (1992) NPC 15669 inhibits the reverse passive Arthus reaction in rats by blocking neutrophil recruitment. J Pharm Exp Ther 263:933–937

Camussi G, Tetta C, Bussolino F, Baglioni C (1990) Antiinflammatory peptides (antiflammins) inhibit synthesis of platelet-activating factor, neutrophil aggregation and chemotaxis, and intradermal inflammatory reactions. J Exp Med 171:913–927

Carter GW, Young PR, Albert DH, Bouska J, Dyer R, Bell RL, Summers JB, Brooks DW (1991) 5-Lipoxygenase inhibitory activity of Zileuton. J Pharm Exp Ther 256:929–937

Chang YH, Otterness IG (1981) Effects of pharmacologic agents on the reversed passive Arthus reaction in the rat. Eur J Pharmacol 69:155–164

Humphrey JH (1955a) The mechanism of Arthus reactions. I. The role of polymorphonuclear leukocytes and other factors in reversed passive Arthus reactions in rabbits. Br J Exp Pathol 36:268–282

Humphrey JH (1955b) The mechanism of Arthus reactions. II. The role of polymorphonuclear leukocytes and platelets in reversed passive Arthus reactions in the guinea-pig. Br J Exp Pathol 36:283–289

Kim KH, Martin IC, Young PR, Carter GW, Haviv F (1990) Inhibitors of immune complex-induced inflammation: 5-substituted 3-[1-(2-benzoxazolyl)hydrazino]propanenitrile derivatives. J Pharm Sci 79:682–684

Okamoto H, Iwahisa Y, Terawasa M (1992) Suppression of the Arthus reaction by Y-24180, a potent and specific antagonist of platelet-activating factor. Agents Actions 35:149–158

Ting PC, Kaminski JJ, Sherlok MH, Tom WC, Lee JF, Bryant RW, Watnick AD, McPhail AT (1990) Substituted 1,3-dihydro-2*H*-pyrrolo[2,3-*b*]pyridin-2-ones as potential antiinflammatory agents. J Med Chem 33:2697–2706

Yamamoto S, Dunn CD, Deporter DA, Capasso F, Willoughby DA, Huskisson EC (1975) A model for the quantitative study of Arthus (immunologic) hypersensitivity in rats. Agents Actions 5:374–377

I.2.2.8 Adjuvant Arthritis in Rats

PURPOSE AND RATIONALE

Adjuvant arthritis in rats has been described by Pearson and Wood (1959) exhibiting many similarities to human rheumatoid arthritis. Injections of complete Freund's adjuvant into the rat paw induces inflammation as primary lesion with a maximum after 3 to 5 days. Secondary lesions occur after a delay of approximately 11 to 12 days which are characterized by inflammation of non-injected sites (hindleg, forepaws, ears, nose and tail), a decrease of weight and immune responses. The procedure has been modified by several authors in order to differentiate between anti-inflammatory and immunosuppressive activity (e. g. Perper et al. 1971). Anti-inflammatory compounds do not inhibit secondary lesions, which are prevented or diminished by immunosuppressive agents. Two protocols, termed "preventative" (or "prophylactic") and "therapeutic" (or "established") adjuvant arthritis, have gained wide usage for assessing a drug's potential anti-arthritic activity (Schorlemmer et al. 1999).

PROCEDURE

The choice of the animal strain has been found to be very important for the performance of this test.

Wistar–Lewis rats have been proven to be very suitable in contrast to other sub strains. Male rats with an initial body weight of 130 to 200 g are used. On day 1, they are injected into the sub plantar region of the left hind paw with 0.1 ml of complete Freund's adjuvant. This consists of 6 mg mycobacterium butyricum (Difco) being suspended in heavy paraffin oil (Merck) by thoroughly grinding with mortar and pestle to give a concentration of 6 mg/ml. Dosing with the test compounds or the standard is started on the same day and continued for 12 days. Paw volumes of both sides and body weight are recorded on the day of injection, whereby paw volume is measured plethysmographically with equipment as described in the paw edema tests. On day 5, the volume of the injected paw is measured again, indicating the primary lesion and the influence of therapeutic agents on this phase. The severity of the induced adjuvant disease is followed by measurement of the non-injected paw (secondary lesions) with a plethysmometer. Purposely, from day 13 to 21, the animals are not dosed with the test compound or the standard. On day 21, the body weight is determined again and the severity of the secondary lesions is evaluated visually and graded according the following scheme:

		score
ears:	absence of nodules and redness	0
	presence of nodules and redness	1
nose:	no swelling of connective tissue	0
	intensive swelling of connective tissue	1
tail:	absence of nodules	0
	presence of nodules	1
forepaws:	absence of inflammation	0
	inflammation of at least 1 joint	1
hind paws:	absence of inflammation	0
	slight inflammation	1
	moderate inflammation	2
	marked inflammation	3

EVALUATION

a) For primary lesions: The percent inhibition of paw volume of the injected left paw over vehicle control is measured at day 5.
b) For secondary lesions: The percentage inhibition of paw volume of the non-injected right paw over controls is measured at day 21.
c) An arthritic index is calculated as the sum of the scores as indicated above for each animal. The average of the treated animals is compared with the control group.
d) The total percentage change is calculated as follows by addition of:
   percent inhibition of the injected paw on day 5 + percent inhibition of the non-injected paw on day 21 + percent change of the arthritic index.

Doses of 0.3 mg/kg indomethacin p.o. and 20–50 mg/kg phenylbutazone p.o. are effective on the primary lesions when dosage is started at the day of injection of the irritant. They are not effective on the secondary lesions.

In contrast, immunosuppressants like cyclophosphamide at a dose of 7 mg/kg inhibited the secondary lesions even when started at day 9 or later.

CRITICAL ASSESSMENT OF THE METHOD

Evidence was given that adjuvant arthritis in the rat is associated with chronic pain (Colpaert 1987) The measure of pain in this model still presents some technical problems since the evaluation is based on the somewhat biased observation of the behavioral responses.

MODIFICATIONS OF THE METHOD

A review was given by Gardner (1960) on the experimental production of arthritis.

Moran et al. (1999) compared adjuvant arthritis and selected animal models of arthritis to rheumatoid arthritis with special emphasis on the mechanism of joint destruction.

Kazuna and Kawai (1975) and Rooks et al. (1982) used rats with established lesions to test analgesics in the arthritic flexion pain test. The method is claimed to be specific by detecting only central analgesics and nonsteroidal anti-inflammatory drugs but not other classes such as CNS-depressant or antihistaminic drugs.

Brackertz et al. (1977) established antigen-induced arthritis in the mouse by immunization with methylated bovine serum albumin in complete Freund's adjuvant with B pertussis vaccine.

A streptococcal cell wall-induced arthritis in rats has been described by Wilder et al. (1982, 1987) and Yocum et al. (1986).

Lewis et al. (1997) studied degradation of articular cartilage in a rat monoarthritis model induced by an intra-articular injection of *Propionibacterium acnes*.

Crossley et al. (1989) reported on a monoarticular antigen-induced arthritis in rabbits and mice.

α-2-Glycoprotein levels have been recommended as parameter for severity and inhibition of experimental immunoarthritis in the rat by Sandow et al. (1971).

Pircio et al. (1975) recommended a method for the evaluation of analgesic activity using adjuvant-induced arthritis in rats. The degree of vocalization

was recorded from 5 rats placed together in a counting chamber.

Cruwys et al. (1994) sensitized rats on day 0 and 7 with multiple intradermal injections of methylated bovine serum albumin emulsified in Freund's complete adjuvant. On day 21, the animals were challenged by the intra-articular injection of 100 µl 0.5% solution of methylated bovine serum albumin into the right knee. The progress of the monoarticular arthritis was monitored by daily measurement of joint diameter.

Butler et al. (1991) described a limited arthritic pain model for chronic pain and inflammation studies using injections of 0.05 ml of complete Freund adjuvant into the left tibio-tarsal joint of Sprague-Dawley rats.

Issekutz et al. (1994) studied the role of tumor necrosis factor-alpha and IL-1 in polymorphonuclear leukocyte and T lymphocyte recruitment to joint inflammation in adjuvant arthritis.

Esser et al. (1995) measured radiographic changes in adjuvant-induced arthritis in rats by quantitative image analysis. Digitized radiographs of the calcaneus were examined for changes in the mean and in the distribution of gray values. Periostal new bone formation was measured as an increase in image area of the calcaneus.

Mercuric chloride ($HgCl_2$) induces a syndrome of autoimmunity in Brown-Norway rats characterized by a variety of IgG antibodies, very high concentrations of serum IgE, proteinuria, leukocytoclastic vasculitis which predominantly affects the caecum, and an inflammatory polyarthropathy (Kiely et al. 1995, 1996).

Kawahito et al. (2000) reported that 15-deoxy-$\Delta^{12,14}$-PGJ_2 which activates PPAR-α, induces synoviocyte apoptosis and suppresses adjuvant-induced arthritis in rats. Cuzzocrea et al. (2002) found that prostaglandin 15-deoxy-$\Delta^{12,14}$-prostaglandin J_2 attenuates the development of acute and chronic inflammation.

Bolon et al. (2004) described a method for rapid quantification of intralesional osteoclasts in the hind paws of Lewis rats with adjuvant-induced arthritis. A 4-µm-thick section of the decalcified hind paw was stained to demonstrate osteoclasts using an indirect immunoperoxidase method and a rabbit anti-human monoclonal antibody directed against the osteoclast marker cathepsin K, which is an osteoclast protease primarily responsible for the resorption of bone. The sections were evaluated using tiered, semi-quantitative criteria to grade bone erosions and intralesional osteoclasts.

Kong et al. (1999), Campagnuolo et al. (2002), and Bolon et al. (2002a, 2002b) used Lewis rats with adjuvant arthritis to describe the effects of osteoprotegerin, an endogenous antiosteoclast factor for protecting bone in rheumatoid arthritis.

Francischi et al. (2000) described anti-inflammatory and analgesic effects of the phosphodiesterase 4 inhibitor rolipram in the rat model of adjuvant-induced arthritis.

Boyle et al. (2001) reported anti-inflammatory effects of a non-nucleoside adenosine kinase inhibitor in rat adjuvant arthritis.

Fujisawa et al. (2002) demonstrated the effects of highly water-soluble matrix metalloproteinase inhibitors in a rat adjuvant-induced arthritis model.

Wei et al. (2004) described effects and mechanisms of a dual inhibitor of interleukin-1 and tumor necrosis factor on adjuvant arthritis in rats.

Boe et al. (1999) reported that interleukin 6 knockout **mice** are resistant to antigen-induced experimental arthritis.

Gauldie et al. (2004) described a robust model of adjuvant-induced chronic unilateral arthritis in two mouse strains. DBA/1 and C57BL/6 male mice were injected intra-articularly into a stifle joint with FCA (5 µg in 5 µl) once per week for 4 weeks. Measurement of joint diameter and joint histopathology were used to monitor the course of arthritis. Inflammatory hyperalgesia was assessed as the pressure causing a limb withdrawal. Standard drugs, such as indomethacin or prednisolone, caused a decrease in joint inflammation and associated hyperalgesia.

Consden et al. (1971), Cook and Jasin (1972), Cook et al. (1972), Jasin and Cook (1977) produced a chronic experimental monoarthritis by intra-articular injection of antigens into previously immunized **rabbits**.

Henderson et al. (1990) induced monoarticular arthritis in ovalbumin-sensitized rabbits by intraarticular injection of ovalbumin (antigen-induced arthritis) or in naive rabbits by injecting hyaluronic acid mixed with the polycation poly-D-lysine (polycation-induced arthritis).

Arner et al. (1995) compared the alterations in proteoglycan metabolism in antigen-induced arthritis and polycation-induced arthritis in rabbits and determined the involvement of interleukin-1 in the cartilage degradation that occurs in these models of rheumatoid arthritis.

Lewthwaite et al. (1995) studied the antifibrotic action of interleukin-1 receptor antagonist in antigen-induced monoarticular arthritis in New Zealand White rabbits.

Arthritis occurs in **pigs** due to infection with *Erysipelothrix rhusiopathiae* (Ajmal 1969). Experimental erysipelothrix infection in pigs can be used as a model for rheumatism research (Schulz et al. 1975a, b, 1977). Infections are established by oral or parenteral administration of standardized serotype B erysipelas strains.

Erysipelothrix arthritis could also produced in rats and **rabbits** (White et al. 1975; Glynn 1977).

Arthritis due to infection with *Mycoplasma synoviae* occurs naturally among domestic poultry (Olson et al. 1954, 1964). Arthritis in **chickens** after mycoplasma infection has been used as experimental model (Kerr and Olson 1970; Cullen 1977).

Experimental models of arthritis due to streptococcal infections have been proposed for various species: **mice** (Cayeux et al. 1966; Hook et al. 1960; Ohanian et al. 1969), **rats** (Jasmin 1967; Koga et al. 1973), **rabbits** (Cecil et al. 1939; Cook and Fincham 1966; Ginsburg et al. 1968, 1977; Norlin 1960; Shimizu et al. 1958; Stein et al. 1973), **pigs** (Roberts et al. 1968, 1969).

Avridine-Induced Arthritis

The injection of avridine [*N*,*N*-dioctadecyl-N′,N′-bis (2-hydroxyethyl) propanediamine / CP-20961], emulsified in Freund's adjuvant, at the base of the tail is arthritogenic in susceptible rat strains (Meacock et al. 1994; Brun et al. 1995; Vingsbo et al. 1995; Lorentzen and Klareskog 1997; Joe and Wilder 1999; Van Bilsen et al. 2004).

REFERENCES AND FURTHER READING

Ajmal M (1969) Erysipelothrix rhusiopathiae and spontaneous arthritis in pigs. Res Vet Sci 10:579

Arner EC, Harris RR, DiMeo TM, Collins RC, Galbraith W (1995) Interleukin-1 receptor antagonist inhibits proteoglycan breakdown in antigen induced but not in polycation induced arthritis in the rabbit. J Rheumatol 22:1338–1346

Bartlett RR, Schleyerbach R (1985) Immunopharmacological profile of a novel isoxazol derivative, HWA 486, with potential antirheumatic activity. I. Disease modifying action on adjuvant arthritis of the rat. Int J Immunopharmacol 7:7–18

Beck FWJ, Whitehouse MW, Pearson CM (1974) Drug sensitivity of rat adjuvant arthritis, induced with 'adjuvants' containing no mineral oil components. Proc Soc Exp Biol Med 146:665–669

Boe A, Baiocchi M, Carbonatto M, Papoian R, Serlupi-Crescenzi O (1999) Interleukin 6 knock-out mice are resistant to antigen-induced experimental arthritis. Cytokine 11:1057–1064

Bolon B, Shalhoub V, Kostenuik PJ, Campagnuolo G, Morony S, Boyle WJ, Zack D, Feige U (2002a) Osteoprotegerin, an endogenous antiosteoclast factor for protecting bone in rheumatoid arthritis. Arthritis Rheum 46:3121–3135

Bolon B, Campagnuolo G, Feige U (2002b) Duration of bone protection by a single osteoprotegerin injection in rats with adjuvant-induced arthritis. Cell Mol Life Sci 59:1569–1576

Bolon B, Morony S, Cheng Y, Hu YL, Feige U (2004) Osteoclast numbers in Lewis rats with adjuvant-induced arthritis: identification of preferred sites and parameters for rapid quantititive analysis. Vet Pathol 41:30–36

Boyle DL, Kowaluk EA, Jarvis MF, Lee CH, Bhagwat SS, Williams W, Firestein GS (2001) Anti-inflammatory effects of ABT-702, a novel non-nucleoside adenosine kinase inhibitor, in rat adjuvant arthritis. J Pharmacol Exp Ther 296:495–500

Brackertz D, Mitchell GF, MacKay IR (1977) Antigen-induced arthritis in mice. Arthr Rheum 20:841–850

Brun JG, Haland G, Haga HJ, Fagerhol MK, Jonsson R (1995) Effect of calprotectin in avridine-induced arthritis. APMIS 103:233–240

Butler SH, Godefroy F, Besson JM, Weil-Fugazza J (1991) Increase in "pain sensitivity" induced by exercise applied during the onset of arthritis in a model of monoarthritis in the rat. Int J Tiss Reac 13:299–304

Campagnuolo G, Bolon B, Feige U (2002) Kinetics of bone protection by recombinant osteoprotegerin therapy in Lewis rats with adjuvant arthritis. Arthritis Rheum 46:1926–1936

Cayeux P, Panijel J, Cluzan R, Levillain R (1966) Streptococcal arthritis and cardiomyopathy experimentally induced in white mice. Nature 212:688–691

Cecil RL, Angevine DM, Rothbard S (1939) Experimental arthritis in rabbits produced by streptococci and other organisms. Am J Med Sci 198:463–475

Colpaert FC (1987) Evidence that adjuvant arthritis in the rat is associated with chronic pain. Pain 28:201–222

Connolly KM, Stecher VJ, Danis E, Pruden DJ, LaBrie T (1988) Alteration of interleukin-1 production and the acute phase response following medication of adjuvant arthritic rats with cyclosporin-A or methotrexate. Int J Immunopharmac 10:717–728

Consden R, Doble A, Glynn LE, Nind AP (1971) Production of a chronic arthritis with albumin. Its retention in rabbit knee joints. Ann Rheum Dis 30:307–315

Cook J, Fincham WJ (1966) Arthritis produced by intra-articular injection of streptolysin S in rabbits. J Path Bact 99:283–297

Cooke TD, Jasin HE (1972) The pathogenesis of chronic inflammation in experimental antigen-induced arthritis. I. The role of antigen on the local immune response. Arthr Rheum 15:327–337

Cooke TD, Hurd ER, Ziff M, Jasin HE (1972) The pathogenesis of chronic inflammation in experimental antigen-induced arthritis. II Preferential localization of antigen-antibody complexes to collagenous tissues. J Exp Med 135:323–338

Crossley MJ, Holland T, Spowage M, Hunneyball IM (1989) Monarticular antigen-induced arthritis in rabbits and mice. In: Pharmacological Methods in the Control of Inflammation. Alan R Liss, Inc., pp 415–439

Cruwys SC, Garrett NE, Perkins MN, Blake DR, Kidd BL (1994) The role of bradykinin B_1 receptors in the maintenance of intra-articular plasma extravasation in chronic antigen-induced arthritis. Br J Pharmacol 113:940–944

Cullen GA (1977) Mycoplasma infection and arthritis in chickens. In: Glynn LE, Schlumberger HD (eds) Experimental Models of Chronic Inflammatory Diseases. Springer-Verlag, Berlin Heidelberg New York, pp 240–255

Cuzzocrea S, Wayman NS, Mazzon E, Dugo L, di Paola R, Serraino I, Britti D, Chatterjee PK, Caputi AP, Thiemermann C (2002) The cyclopentone prostaglandin 15-deoxy-$\Delta^{12,14}$-

prostaglandin J_2 attenuates the development of acute and chronic inflammation. Mol Pharmacol 61:997–1007
del Pozo E, Graeber M, Payne T (1990) Regression of bone and cartilage loss in adjuvant arthritic rats after treatment with cyclosporin A. Arthr Rheum 33:247–252
Esser RE, Hildebrand AR, Angelo RA, Watts AM, Murphey MD, Baugh LE (1995) Measurement of radiographic changes in adjuvant-induced arthritis in rats by quantitative image analysis. Arthr Rheum 38:129–138
Francischi JN, Yokoro CM, Poole S, Tafuri WL, Cunha FQ, Teixeira MM (2000) Anti-inflammatory and analgesic effects of the phosphodiesterase 4 inhibitor rolipram in a rat model of arthritis. Eur J Pharmacol 399:243–249
Fujisawa T, Igeta K, Odake S, Morita Y, Yasuda J, Morikawa T (2002) Highly-water soluble matrix metalloproteineases inhibitors and their effects in a rat adjuvant-induced arthritis model. Bioorg Med Chem 10:2569–2581
Gardner DL (1960) The experimental production of arthritis. A review. Ann rheum Dis 19:297–317
Gauldie SD, McQueen DS, Clarke CJ, Chessell (2004) A robust model of adjuvant-induced chronic unilateral arthritis in two mouse strains. J Neurosci Methods 139:281–291
Ginsburg I, Silberstein Z, Spira G, Bentwich Z, Boss JH (1968) Experimental arthritis in rabbits induced by group A streptococcal products. Experientia (Basel) 24:256–257
Ginsburg I, Zor U, Floman Y (1977) Experimental models of streptococcal arthritis: Pathogenic role of streptococcal products and prostaglandins and their modification by anti-inflammatory agents. In: Glynn LE, Schlumberger HD (eds) Experimental Models of Chronic Inflammatory Diseases. Springer-Verlag, Berlin Heidelberg New York, pp 256–299
Glynn LE (1977) Erysipelothrix arthritis in rabbits. In: Glynn LE, Schlumberger HD (eds) Experimental Models of Chronic Inflammatory Diseases. Springer-Verlag, Berlin Heidelberg New York, pp 238–239
Hook EW, Wagner RR, Lancefield RC (1960) An epizootic in Swiss mice caused by a group A streptococcus, newly designed type 50. Am J Hyg 72:11–119
Issekutz AC, Meager A, Otterness I, Issekutz TB (1994) The role of tumor necrosis factor-alpha and IL-1 in polymorphonuclear leukocyte and T lymphocyte recruitment to joint inflammation in adjuvant arthritis. Clin Exp Immunol 97:26–32
Jasin HE, Cooke TD (1977) Persistence of antigen in experimental allergic monoarthritis. In: Glynn LE, Schlumberger HD (eds) Experimental Models of Chronic Inflammatory Diseases. Springer-Verlag, Berlin Heidelberg New York, pp 28–32
Jasmin G (1967) Experimental arthritis in rats. A comprehensive review with specific reference to mycoplasma. In: Rohstein J (ed) Rheumatology Vol 1, Karger, Basel, pp 107–131
Joe B, Wilder RL (1999) Animal models of rhematoid arthritis. Mol Med Today 5:367–369
Kawahito Y, Kondo M, Tsubouchi Y, Hashiramoto A, Bishop-Bailey D, Inoue KI, Kohno M, Yamada R, Hla T, Sano H (2000) 15-deoxy-$\Delta^{12,14}$-PGJ_2 induces synoviocyte apoptosis and suppresses adjuvant-induced arthritis in rats. J Clin Invest 106:189–197
Kazuna S, Kawai K (1975) Evaluation of analgesic agents in rats with adjuvant arthritis. Chem Pharm Bull (Tokyo) 23:1184–1191
Kerr KM, Olson NO (1970) Pathology of chickens inoculated experimentally or contact-infected with Mycoplasma synoviae. Avian Dis 14:291–320
Kiely PDW, Thiru S, Oliveira DGB (1995) Inflammatory polyarthritis by mercuric chloride in the Brown Norway rat. Lab Invest 73:284–293
Kiely PDW, O'Brien D, Oliveira DGB (1996) Anti-CD8 treatment reduces the severity of inflammatory arthritis, but not vasculitis, in mercuric chloride-induced autoimmunity. Clin Exp Immunol 106:280–285
Koga T, Pearson CM, Narita T, Kotani S (1973) Polyarthritis induced in the rat by cell walls from several bacteria and two Streptomyces species. Proc Soc Exp Biol NY 143:824–827
Kong YY, Feige U, Sarosi I, Bolon B, Tafuri A, Morony S, Capparelli C, Li JI, Elliott R, McCabe S, Wong T, Campagnuolo G, Moran E, Bogoch ER, Van G, Nguyen LT, Ohashi PS, Lacey DL, Fish E, Boyle WJ, Penninger JM (1999) Activated T cells regulate bone loss and joint destruction in adjuvant arthritis through osteoprotegerin ligand. Nature 402:304–309
Leisten JC, Gaarde WA, Scholz W (1990) Interleukin-6 serum levels correlate with footpad swelling in adjuvant-induced arthritic Lewis rats treated with cyclosporin A or indomethacin. Clin Immunol Immunopathol 56:108–115
Lewis EJ, Bishop J, Bottomley KM, Bradshaw D, Brewster M, Broadhurst MJ, Brown PA, Budd JM, Elliott L, Greenham AK, Johnson WH, Nixon JS, Rose F, Sutton B, Wilson K (1997) Ro 32–3555, an orally active collagenase inhibitor, prevents cartilage breakdown *in vitro* and *in vivo*. Br J Pharmacol 121:540–546
Lewthwaite J, Blake S, Thompson RC, Hardingham TE, Henderson B (1995) Antifibrotic action of interleukin-1 receptor antagonist in lapine monoarticular arthritis. Ann Rheum Dis 54:591–596
Lorentzen JC, Klareskog L (1997) Comparative susceptibility of DA, LEW, and LEW.1AV1 rats to arthritis induced by different arthritogens: mineral oil, mycobacteria, muramyl dipeptide avridine and rat collagen II. Transplant Proc 29:1692–1693
Meacock SC, Brandon DR, Billigham ME (1994) Arthritis in Lewis rats induced by the non-immunogenic adjuvant CP20961: an immunohistochemical analysis of the developing disease. Ann Rheum Dis 53:653–658
Mohr W, Wild A (1976) Adjuvant arthritis. Arzneim Forsch/Drug Res 26:1860–1866
Moran EL, Bogoch ER (1999) Animal models of rheumatoid arthritis. In: An YH, Friedman RJ (eds) Animal models in orthopaedic research. CRC Press LLC Boca Raton, pp 369–390
Norlin G (1960) Experimental rheumatoid arthritis in rabbits. Acta Rheum Scand 6:309–319
Ohanian SH, Schwab JH, Cromartie WJ, (1969) Relation to rheumatic-like lesions of the mouse to localization of group A streptococci cell walls. J Exp Med 129:37–49
Olson NO, Bletner JK, Shelton DC, Munro DA, Anderson GC (1954) Enlarged joint condition in poultry caused by an infectious agent. Poultry Sci 33:1075–1080
Olson NO, Kerr KM, Cambell A (1964) Control of infectious synovitis. The antigen study of three strains. Avian Dis 8:209–215
Pearson CM (1956) Development of arthritis, periarthritis and periostitis in rats given adjuvants. Proc Soc Exper Biol Med 91:95–101
Pearson CM (1963) Experimental joint disease. Observations on adjuvant-induced arthritis. J Chron Dis 16:863–874
Pearson CM, Wood FD (1959) Studies on polyarthritis and other lesions induced in rats by injection of mycobacterium adjuvant. I. General clinic and pathological characteristics and some modifying factors. Arthr Rheum 2:440–459
Perper RJ, Alvarez B, Colombo C, Schroder H (1971) The use of a standardized adjuvant arthritis assay to differentiate between anti-inflammatory and immunosuppressive agents. Proc Soc Exp Biol Med 137:506–512

Pircio AW, Fedele CT, Bierwagen ME (1975) A new method for the evaluation of analgesic activity using adjuvant-induced arthritis in the rat. Eur J Pharmacol 31:207–215
Roberts ED, Ramsey KF, Switzer WP, Layton JM (1968) Pathologic changes of porcine suppurative arthritis produced by *streptococcus equisimilis*. Am J Vet Res 29:253–262
Roberts ED, Ramsey KF, Switzer WP, Layton JM (1969) Electron microscopy of porcine synovial membrane cell layer in streptococcus equisimilis arthritis. J Comp Path 79:47–51
Rooks WH, Tomolonis AJ, Maloney PJ, Wallach MB, Schuler ME (1982) The analgesic and anti-inflammatory profile of (±-5-benzoyl-1,2-dihydro-3H-pyrrolo[1,2a]pyrrole-1-carboxylic acid (RS-37619). Agents Actions 12:684–690
Sandow J, Alpermann H, Metzger H, Vogel HG (1971) α-2-Glycoprotein levels in the experimental immunoarthritis of the rat. Naunyn-Schmiedeberg's Arch Pharmacol 269:483
Schorlemmer HU, Dickneite G (1992) Preclinical studies with 15-deoxyspergualin in various animal models for autoimmune diseases. Ann NY Acad Sci 685:155–174
Schorlemmer HU, Kurrle R, Schleyerbach R, Bartlett RR (1999) Disease-modifying activity of malononinitrilamides, derivates of leflunomide's active metabolite, on models of rheumatoid arthritis. Inflamm Res 48, Suppl 2:S113–S114
Schulz LC, Drommer W, Seidler D, Ehard H, v. Mickwitz G, Hertrampf B, Böhm KH (1975a) Experimenteller Rotlauf bei verschiedenen Spezies als Ursache einer systemischen Bindegewebskrankheit. I. Systemische vaskuläre Prozesse bei der Organmanifestation. Beitr Path 154:1–20
Schulz LC, Drommer W, Seidler D, Ehard H, Leimbeck R, Weiss R (1975b) Experimenteller Rotlauf bei verschiedenen Spezies als Modell einer systemischen Bindegewebskrankheit. II. Chronische Phase mit besonderer Berücksichtigung der Polyarthritis. Beitr Pathol 154:27–51
Schulz LC, Ehard H, Hertrampf B, Drommer W, Seidler D, Böhm KH (1977) Hemostasis, fibrin incorporation and local mesenchymal reaction in erysipelothrix infection as a model for rheumatism research. In: Glynn LE, Schlumberger HD (eds) Experimental Models of Chronic Inflammatory Diseases. Springer-Verlag, Berlin Heidelberg New York, pp 215–237
Shimizu G, Shichikawa K, Takiuchi K (1958) Studies on the etiology of rheumatic arthritis. III. Experimental production of arthritis in rabbits following focal infection of paranasal sinus with hemolytic streptococcus. Med J Osaka Univ 9:447–468
Stein H, Yarom R, Levine S, Dishon T, Ginsburg I (1973) Chronic self-perpetuating arthritis induced in rabbits by a cell-free extract of group A streptococci. Proc Soc Exp Biol (NY) 143:1106–1112
Tsurumi K, Kokuba S, Okada K, Yanagihara M, Fujimura H (1986) Pharmacological investigations of the new antiinflammatory agent 2-(10,11-dihydro-10-oxodibenzo[b,f]thiepin-2-yl) propionic acid. 4th Communication: Inhibitory effects on rat adjuvant arthritis. Arzneim-Forsch/Drug Res 36:1810–1817
Van Bilsen JHM, Wagenaar-Hilbers JPA, Grosfeld-Stulemeijer MCJT, van der Cammen MJF, van Dijk MEA, van Eden E, Wauben MHM (2004) Matrix metalloproteinases as targets for the immune system during experimental arthritis. J Immunol 172:5063–5068
Vingsbo C, Jonsson R, Holmdahl R (1995) Avridine-induced arthritis in rats: a T cell-dependent chronic disease influenced both by MHC genes and by non-MHC genes. Clin Exp Immunol 99:359–363
Wei YH, Li Y, Qiang CJ (2004) Effects and mechanisms of FR167653, a dual inhibitor of interleukin-1 and tumor necrosis factor, on adjuvant arthritis in rats. Int Immunopharm 4:1625–1632
Walz DT, DiMartino MJ, Kuch JH, Zuccarello W (1969) Adjuvant-induced arthritis in rats – Temporal relationship of drug effects on physiological, biochemical, and haematological parameters. Pharmacologist 11:266
Weichman BM (1989) Rat adjuvant arthritis: A model of chronic inflammation. In: Pharmacological Methods in the Control of Inflammation. Alan R Liss, Inc., pp 363–380
White TG, Puls Jl, Hargrave P (1975) Production of synovitis in rabbits by fractions of a cell-free extract of Erysipelothrix rhusiopathiae. Clin Immunol Immunopath 3:531–540
Wilder RL, Calandra GB, Garvin AJ, Wright KD, Hansen CT (1982) Strain and sex variation in the susceptibility to streptococcal wall-induced polyarthritis in the rat. Arthritis Rheum 25:1064–1072
Wilder RL, Allen JB, Hansen C (1987) Thymus-dependent and -independent regulation of Ia antigen expression *in situ* by cells in the synovium of rats with streptococcal cell wall-induced arthritis, J Clin Invest 79:1160–1171
Yocum DE, Allen JB, Wahl SM, Calandra GB, Wilder RL (1986) Inhibition by cyclosporin A of streptococcal wall-induced arthritis and hepatic granulomas in rats. Arthritis Rheum 29:262–273

I.2.2.9 Collagen Type II Induced Arthritis in Rats

PURPOSE AND RATIONALE

As reported by Trentham et al. (1977) intradermal injection of homologous or heterologous type II collagen in incomplete Freund's adjuvant results in an inflammatory polyarthritis in rats. The demonstration of antibodies to collagen in patients with rheumatic polyarthritis suggests that autoimmunity may contribute to the pathophysiology of synovitis and joint destruction. Because of the similarities of the symptoms in rats to human disease the test is considered to be useful to detect anti-inflammatory and immunosuppressive properties of test compounds.

PROCEDURE

Bovine type II collagen is prepared from nasal septum cartilage, which is cut into small fragments, frozen in liquid nitrogen, and pulverized in a freezer mill. Proteoglycans are extracted overnight by stirring 25 g of pulverized cartilage in 1 liter of 0.2 N NaOH. Following centrifugation at 20,000 *g* for 30 min, the residue is washed with 250 ml of absolute ethanol, the supernatant aspirated, and the residue vacuum dried. Hundred mg pepsin are added to 150 ml of 0.5 M acetic acid, after which 1.0 g of cartilage is added to reach a cartilage to pepsin ratio of 10:1 (w/w). The mixture is stirred 18 h at room temperature and centrifuged at 20,000 *g* for 1 h. Acid soluble collagen present in the supernatant is precipitated by adding NaCl to reach a final concentration of 0.9 M, followed by centrifugation at 20,000 *g* for 1 h. The precipitate from 1.0 g car-

tilage is dissolved in 100 ml 1.0 N NaCl/0.005 M Tris-HCl, pH 7.5, and stirred for 3 days. Then, the solution is dialyzed against 0.02 M Na_2HPO_4, pH 9.4, and the precipitate collected by centrifugation at 30,000 *g* for 1 h. The pellet is dissolved in 0.5 M acetic acid, dialyzed against 6 liters of 0.01 M acetic acid, and lyophilized. All procedures, unless otherwise stated are performed at 4°C.

Test procedure. Collagen is dissolved in a concentration of 2.0 mg/ml in 0.1 M acetic acid overnight at 4°C. This solution is added dropwise to an equal volume of chilled incomplete Freund's adjuvant. Six to 12 male Wistar rats with an initial weight of about 120 g are used for each group. On day 1, each rat receives a total of 0.5 mg collagen in 0.5 ml, equally divided, in 5 sites. All injections are intradermal, one at the base of each appendage and one in the nape of the neck. Seven days post-immunization, the animals receive identical booster injections. Control animals receive only the incomplete Freund's adjuvant diluted with 0.1 M acetic acid.

The volume of both hind paws is measured plethysmographically on day 20. To minimize the possibility of including animals with minimal transient disease, only animals with a paw volume of 1.8 ml or greater are used for further testing. From days 20–40, the animals receive the test compounds p.o. once a day. On day 41, the paw volumes are recorded again.

EVALUATION

The paw volumes of treated animals are recorded plethysmographically. The increase versus day 20 is calculated. The increase is compared with that of controls or animals treated with a standard drug. Otherwise, arthritic scores can be determined. Nonsteroidal anti-inflammatory drugs such as indomethacin in a dose of 2 mg/kg p.o. or phenylbutazone in a dose of 150 mg/kg p.o., but not acetylsalicylic acid in a dose of 50 mg/kg p.o. have been found to be active. Likewise, corticosteroids and immunosuppressives, but not D-penicillamine, were active.

CRITICAL ASSESSMENT OF THE METHOD

Non-steroidal and steroidal anti-inflammatory compounds are detected by this method which, however, does not allow a separation between this two groups.

MODIFICATIONS OF THE METHOD

From studies with a neutrophil elastase inhibitor Janusz and Durham (1997) concluded that of the destruction of the joints in rat collagen-induced arthritis is at least partially due to neutrophil elastase.

Romas et al. (2002) reported that osteoprotegerin reduces osteoclast numbers and prevents bone erosion in collagen-induced arthritis in Dark Aguti rats.

Studies in Mice

Hom et al. (1988), Takagishi et al. (1986, 1992), Cannon et al. (1990), Nemoto et al. (1992) and Carlson et al. (1992) described the effects of immunomodulating agents in collagen-induced arthritis in mice.

Wooley et al. (1993) investigated the anti-arthritic effect of recombinant human interleukin-1 receptor antagonist protein on type II collagen-induced arthritis and antigen-induced arthritis in mice.

Joosten et al. (1994) found an accelerated onset of collagen-induced arthritis in DBA_1 lac/J mice by remote inflammation.

Miesel et al. (1993, 1994a, b) studied the effects of an active center analogue of Cu_2Zn_2-superoxide dismutase in collagen type II-induced arthritis. Furthermore, the authors described a model potassium peroxochromate-induced inflammation in rats and mice. One to 3 µmol/kg K_3CrO_8 was administered by intraplantar application into the left hind-paws of anesthetized rats or mice. Arthritis index was assessed by a score system or the inflammatory response was quantified scintigraphically under a gamma camera by intravenous injection of 500 µCi $Na^{99m}TcO_4$.

Kumar et al. (1997) compared the cellular mechanisms involved in the control of collagen II-induced arthritis and experimental autoimmune encephalomyelitis in mice.

Ruchatz et al. (1998) studied the role of IL-15 in development of antigen-induced immunopathology in collagen-induced arthritis in DBA/1 mice. A soluble fragment of IL-15 receptor profoundly suppressed the symptoms of collagen-induced arthritis.

Joosten et al. (1999) immunized male DBA-1 mice with 100 µg bovine type II collagen in CFA enriched with *Mycobacterium tuberculosis* H37Ra (4 mg/ml) at the base of the tail. The mice were boosted i.p. with 100 µg collagen dissolved in saline. After disease onset on day 28, the mice were treated either with dimerically linked PEGylated soluble p55 TNFR1 receptor or with purified rabbit anti-murine IL-1α and anti IL-1β. IL-1$\alpha\beta$ blockade prevented cartilage and bone destruction, whereas TNF-α blockade only ameliorated joint inflammation.

Using a similar protocol, Plater-Zyberg et al. (2001) found a therapeutic effect of neutralizing endogenous IL-18 activity in the collagen-induced model of arthritis and Lubberts et al. (2004) after treatment with a neutralizing anti-murine interleukin-17 antibody.

Cuzzocrea et al. (2003) found a reduction in the evolution of murine type II collagen-induced arthritis by treatment with rosiglitazone, a ligand of PPARγ.

McIntyre et al. (2003) reported that a highly selective inhibitor of IκB kinase blocked both inflammation and destruction in collagen-induced arthritis in mice.

Chen et al. (2003) tested orally active inhibitors of TNF synthesis as anti-rheumatoid arthritis drugs using collagen-induced arthritis in male DBA/1J mice.

Nakae et al. (2002, 2003) generated IL-17-deficient mice and found a suppression of collagen-induced arthritis.

Podolin et al. (2005) described attenuation of murine collagen-induced arthritis by a selective small molecule inhibitor of IκB kinase 2, occurring via reduction of proinflammatory cytokines and antigen-induced T cell proliferation.

Kuno et al. (2006) reported anti-inflammatory activity of a non-nucleoside adenosine deaminase inhibitor in mice.

REFERENCES AND FURTHER READING

Cannon GW, McCall S, Cole BC, Griffiths MM, Radov LA, Ward JR (1990) Effects of indomethacin, cyclosporin, cyclophosphamide, and placebo on collagen-induced arthritis of mice. Agents Actions 29:315–323

Carlson RP, Baeder WL, Caccese RG, Warner LM, Sehgal SN (1992) Effects of orally administered rapamycin in animal models of arthritis and other autoimmune diseases. Ann NY Acad Sci 685:86–113

Chen JJ, Dewdney N, Lin X, Martin RL, Walker KAM, Huang J, Chu F, Eugui E, Mirkovich A, Kim Y, Sarma K, Arzeno H, van Wart HE (2003) Design and synthesis of orally active inhibitors of TNF synthesis as anti-rheumatoid arthritis drugs. Bioorg Med Chem Lett 13:3951–3954

Cuzzocrea S, Mazzon E, Dugo L, Patel NSA, Seraino I, di Paola R, Genovese T, Britti D, de Maio M, Caputi AP, Theimermann C (2003) Reduction in the evolution of murine type II collagen-induced arthritis by treatment with rosiglitazone, a ligand of the peroxisome proliferator-activated receptor γ. Arthritis Rheum 48:3544–3556

Henderson H, Staines NA, Burrai I, Cox JH (1984) The anti-arthritic and immunosuppressive effects of cyclosporine on arthritis induced in the rat by type II collagen. Clin Exp Immunol 57:51–56

Hom JT, Butler LD, Riedl PE, Bendele AM (1988) The progression of the inflammation in established collagen-induced arthritis can be altered by treatments with immunological or pharmacological agents which inhibit T cell activities. Eur J Immunol 18:881–888

Janusz MJ, Durham SL (1997) Inhibition of cartilage degradation in rat collagen-induced arthritis but not adjuvant arthritis by the neutrophil elastase inhibitor MDL 101,146. Inflamm Res 46:503–508

Joosten LAB, Helsen MMA, Van den Berg WB (1994) Accelerated onset of collagen-induced arthritis by remote inflammation. Clin Exp Immunol 97:204–211

Joosten LAB, Helsen MMA, Saxne T, van de Loo FAJ, Heinegård D, van den Berg WB (1999) IL-1$\alpha\beta$ blockade prevents cartilage and bone destruction in murine type II collagen-induced arthritis, whereas TNF-α blockade only ameliorates joint inflammation. J Immunol 163:5049–5055

Kaibara N, Hotokebuchi T, Takagishi K, Katsuki I (1983) Paradoxical effects of cyclosporin A on collagen arthritis in rats. J Exp Med 158:2007–2015

Kumar V, Aziz F, Sercarz E, Miller A (1997) Regulatory T cells specific for the same framework 3 region of the Vβ8.2 chain are involved in the control of collagen II-induced arthritis and experimental autoimmune encephalomyelitis. J Exp Med 185:1725–1733

Kuno M, Seki N, Tsujimoto S, Nakanishi I, Kinoshita T, Nakamura K, Terasaka T, Nishio N, Sato A, Fujii T (2006) Anti-inflammatory activity of non-nucleoside adenosine deaminase inhibitor FR234938. Eur J Pharmacol 534:241–249

Lubberts E, Koenders MI, Oppers-Walgreen B, van den Bersselaar, Coenen-de Roo CJJ, Joosten LAB, van den Berg WB (2004) Treatment with a neutralizing anti-murine interleukin-17 antibody after the onset of collagen-induced arthritis reduces joint inflammation, cartilage destruction, and bone erosion. Arthritis Rheum 50:650–659

McIntyre KW, Shuster DJ, Gillooly KM, Dambach DM, Pattoli MA, Lu P, Zhou XD, Zusi FC, Burke JR (2003) A highly selective inhibitor of IκB kinase, BMS-.345541, blocks both inflammation and destruction in collagen-induced arthritis in mice. Arthritis Rheum 48:2652–2659

Miesel R, Haas R (1993) Reactivity of an active center analog of Cu_2Zn_2-superoxide dismutase in murine model of acute and chronic inflammation. Inflammation 17:595–611

Miesel R, Dietrich A, Brandl B, Ulbrich N, Kurpisz M, Kröger H (1994a) Suppression of arthritis by an active center analogue of Cu_2Zn_2-superoxide dismutase. Rheumatol Int 14:119–126

Miesel R, Kröerg H, Ulbrich N, Kurpisz M (1994b) Arthritogenic reactivity of chromium(V). Z Rheumatol 53:59

Nakae S, Komiyama Y, Nambu A, Sudo K, Iwase M, Homma I, Sekikawa K, Asano M, Iwakura Y (2002) Antigen-specific T cell sensitization in impaired in IL-17-deficient mice, causing suppression of allergic cellular and humoral responses. Immunity 17:375–378

Nakae S, Nambu A, Sudo K, Iwakura Y (2003) Suppression of immune induction of collagen-induced arthritis in IL-17-deficient mice. J Immunol 171:6173–6177

Nemoto K, Mae T, Abe F, Takeuchi T (1992) Successful treatment with a novel immunosuppressive agent, deoxyspergualin, in type II collagen-induced arthritis in mice. Ann NY Acad Sci 685:148–154

Phadke K, Carroll J, Nanda S (1982) Effects of various anti-inflammatory drugs on type II collagen-induced arthritis in rats. Clin Exp Immunol 47:579–586

Plater-Zyberg C, Joosten LAB, Helsen MMA, Sattonnet-Roche P, Siegfried C, Alouani S, van de Loo FAJ, Graber P, Aloni S, Cirillo R, Lubberts E, Dinarello CA, van den Berg WB, Chvatchko Y (2001) Therapeutic effect of neutralizing endogenous IL-18 activity in the collagen-induced model of arthritis. J Clin Invest 108:1825–1832

Podolin PL, Callahan JF, Bolognese BJ, Li YH, Carlson K, Davis TG, Mellor GF, Evans C, Roshak AK (2005) Attenuation of murine collagen-induced arthritis by a novel, potent, selective small molecule inhibitor of IκB kinase 2, TPCA-1 (2[(aminocarbonyl)amino]-5-(4-fluorophenyl)-3-thiophenecarboxamide), occurs via reduction of proinflammatory cytokines and antigen-induced T cell proliferation. J Pharmacol Exp Ther 312:373–381

Romas E, Sims NA, Hards DK, Lindsay M, Quinn JWM, Ryan OFJ, Dunstan CR, Martin TJ, Gillespie MT (2002) Osteoprotegerin reduces osteoclast numbers and prevents

bone erosion in collagen-induced arthritis. Am J Pathol 161:1419–1427
Ruchatz H, Leung BP, Wi XQ, McInnes IB, Liew FY (1998) Soluble IL-15 receptor α-chain administration prevents murine collagen-induced arthritis: A role for IL-15 in development of antigen-induced immunopathology. J Immunol 160:5654–5660
Probeert AW, Schrier DJ, Gilbertsen RB (1984) Effects of antiarthritic compounds on type II collagen-induced arthritis in rats. Arch Int Pharmacodyn 269:167–176
Takagishi K, Kaibara N, Hotokebuchi T, Arita C, Morinaga M, Arai K (1986) Effects of cyclosporin on collagen induced arthritis in mice. Ann Rheum Dis 45:339–344
Takagishi K, Yamamoto M, Miyahara H, Hotokebuchi T, Kaibara N (1992) Comparative study of effects of cyclosporins A and G on collagen arthritis in mice. Agents Actions 37:284–289
Tanaka K, Shimotori T, Makino S, Aikawa Y, Inaba T, Yoshida C, Takano S (1992) Pharmacological studies of the new anti-inflammatory agent 3-formylamino-7-methylsulfonylamino-6-phenoxy-4H-1-benzopyran-4-one. 1st Communication: anti-inflammatory, analgesic and other related properties. Arzneim Forsch/Drug Res 42:935–944
Trentham DE, Dynesius-Trentham RA (1989) Type II collagen-induced arthritis in the rat. In: Pharmacological Methods in the Control of Inflammation. Alan R. Liss, Inc., pp 395–413
Trentham DE, Townes AS, Kang AH (1977) Autoimmunity to type II collagen: an experimental model of arthritis. J Exper Med 146:857–868
Wooley PH, Whalen JD, Chapman DL, Berger AE, Richard KA, Aspar DG, Staite ND (1993) The effect of an interleukin-1 receptor antagonist protein on type II collagen-induced arthritis and antigen-induced arthritis in mice. Arthritis Rheum 36:1305–1314

I.2.2.10 Proteoglycan-Induced Progressive Polyarthritis in Mice

PURPOSE AND RATIONALE

Glant et al. (1987, 1992), Mikecz et al. (1987, 1990), Poole (1989) described a proteoglycan-induced progressive arthritis and spondylitis in BALB/c mice as an animal model displaying similarities to human rheumatoid arthritis and ankylosing spondylitis as indicated by clinical assessments, immunological parameters and histopathological studies of diarthrodial joints and spine.

PROCEDURE

High buoyant density cartilage proteoglycans are prepared from fetal and adult human, canine or bovine articular cartilages as well as from 1-week-old mouse epiphyseal cartilage. Fetal human articular cartilage proteoglycan digested with chondroitinase ABC (Hascall and Heinegård 1974) is used to induce arthritis in female BALB/c mice. The mice are sensitized by intraperitoneal injection of 100 µg of chrondroitinase ABC-treated proteoglycan in 100 µl of phosphate buffered saline, pH 7.2, and in Freund's complete adjuvant in a 1:1 emulsion. They are re-injected twice more with the antigen in incomplete Freund's adjuvant after one and three weeks. All BALB/c mice immunized with human articular cartilage proteoglycan develop arthritis in diarthrodial joints after the third antigen injection. Sera from mice with progressive polyarthritis are tested for antibodies to arthritogenic proteoglycans during weeks 12–18 of immunization. The limbs of all mice are examined daily to record clinical arthritic changes. Swelling and redness, as the first symptoms of arthritis, and the thickness (diameter) of the knee, ankle (intermalleolar diameter), wrist and the dorsovolar thickness of the paw are recorded three times a week. The most objective joint diameter is the intermalleolar one. The animals are treated with test drug or vehicle for 12 weeks and serum samples taken by retroorbital puncture for determination of antibodies to proteoglycans. Seven weeks later, the mice are sacrificed, limbs, tails and lumbar spine are fixed, decalcified and embedded in paraffin for histological examination.

EVALUATION

Mean values of intermalleolar diameter and antibody titers of treated and non-treated animals are compared by non-parametric statistics.

MODIFICATIONS OF THE METHOD

Stimpson and Schwab (1989) described a chronic remittent erosive arthritis in rats induced by bacterial peptidoglycan-polysaccharide structures.

REFERENCES AND FURTHER READING

Glant TT, Mikecz K, Arzoumanian A, Poole AR (1987) Proteoglycan-induced arthritis in BALB/c mice: Clinical features and histopathology. Arthritis Rheum 30:201–212
Glant TT, Mikecz K, Bartlett RR, Deák F, Thonar EJMA, Williams JM, Mattar T, Kuettner KE, Schleyerbach R (1992) Immunomodulation of proteoglycan-induced progressive polyarthritis by leflunomide. Immunopharmacology 23:105–116
Hascall VC, Heinegård D (1974) Aggregation of proteoglycans. I. The role of hyaluronic acid. J Biol Chem 249:4232–4241
Heinegård D (1972) Extraction, fractionation and characterization of proteoglycans from bovine tracheal cartilage. Biochim Biophys Acta 285:181–192
Mikecz K, Glant TT, Poole AR (1987) Immunity to cartilage proteoglycans in BALB/c mice with progressive polyarthritis and ankylosing spondylitis induced by injection of human cartilage proteoglycan. Arthritis Rheum 30:306–318
Mikecz K, Glant TT, Bukás E, Poole AR (1990) Proteoglycan-induced polyarthritis and spondylitis adoptively transferred to naive (nonimmunized) BALB/c mice. Arthritis Rheum 33:866–876
Poole AR (1989) Cartilage proteoglycan-induced arthritis: a combined model for rheumatoid arthritis and ankylosing spondylitis. In: Pharmacological Methods in the Control of Inflammation. pp 441–447, Alan R. Liss, Inc

Stimpson AS, Schwab JH (1989) Chronic remittent erosive arthritis induced by bacterial peptidoglycan-polysaccharide structures. In: Pharmacological Methods in the Control of Inflammation. pp 381–394, Alan R. Liss, Inc

I.2.2.11 Pristane-Induced Arthritis in Mice

PURPOSE AND RATIONALE

The mineral oil 2,6,10,14-tetramethylpentadecne (known as **pristane**) induces a chronic inflammatory arthritis in **mice** after intraperitoneal injection (Potter and Wax 1981; Hopkins et al. 1984; Wooley et al. 1989; Chapdelaine et al. 1991; Wooley and Whalen 1991; Levitt et al. 1992; Abe et al. 1995; Thompson et al. 1998; Wooley et al. 1998; Vigar et al. 2000). The immunological involvement in the pathogenesis of pristane-induced arthritis was studied by several authors (Bedwell et al. 1987; Thompson et al. 1990; Ghoraishian et al. 1993; Nishikaku et al. 1994; Vingsbo et al. 1996; Stasiuk et al. 1997; Morgan et al. 2004). Moreover, the genetic basis for the susceptibility to pristane-induced arthritis was studied (Lu et al. 2002; Olofsson et al. 2003; Brenner et al. 2005; Jensen et al. 2006). Not only in mice, but also in **rats**, arthritis could be induced by pristane injections (Vingsbo et al. 1996; Zheng et al. 2002, 2003; Wester et al. 2003; Holmberg et al. 2006).

Patten et al. (2004) characterized the model of pristine-induced arthritis (PIA) in mice by studying the response to antirheumatic agents, expression of joint cytokines, and immunopathology.

PROCEDURE

Induction and Characterization of PIA

Male DBA/101aHsd mice were placed under isoflurane anesthesia and injected intraperitoneally with 0.5 ml of pristane (Sigma-Aldrich, Poole, UK), and an identical booster injection was given 7 weeks thereafter. The severity of arthritis was graded visually by assessing the level of swelling in each paw, including the tarsus (ankle) or carpus (wrist) joints. The following scoring system was used: 0.5 = swelling of toes only or very slight ankle/wrist swelling; 1 = slight swelling of paw; 2 = moderate swelling of paw; 3 = marked swelling of paw; and 4 = substantial swelling of paw. Thus, the maximum total score per animal was 16. All batches also contained animals that were not treated with pristane, and these served as comparators for all studies undertaken.

Mice were observed for paw or toe swelling in a time-course study lasting up to 180 days after the first pristane injection. After study termination, the initially swollen hind paws were obtained for histologic assessment and allocated to different study groups according to the duration of swelling. The remaining three paws of each animal were used in cytokine studies.

Drug preparation and Administration Schedules

The effects of administration of established and novel antirheumatic compounds were assessed using a therapeutic dosing schedule. Separate batches of mice for each drug study were monitored weekly for the development of swollen paws from day 80 after the first injection of pristane. Mice were included in the drug studies only if they developed a score of $\geqslant 1$ in a hind paw on two consecutive weekly observations between day 120 and day 134 after the first injection of pristane ($n = 7$–13 per treatment group). At study termination, paws were obtained for histologic and cytokine assessments, normally at 1 h after the final drug administration.

All orally administered treatments were undertaken by gavage. Prednisolone was suspended in 0.5% methylcellulose and administered orally once daily at a dose of 2 mg/kg. Methotrexate was dissolved in physiologic saline and administered intraperitoneally 3 times per week at a dose of 9 mg/kg. Indomethacin and diclofenac were suspended in 1% methylcellulose and given orally once daily at doses of 3 mg/kg and 2 mg/kg, respectively. Celecoxib was suspended in a solution of 66% polyethylene glycol, 33% water, and 1% dimethylsulfoxide, and was administered orally twice daily at a dose of 30 mg/kg. Etanercept was dissolved in the supplied vehicle according to the instructions of the manufacturer and diluted using physiologic saline, and was administered intraperitoneally 3 times per week at doses of 300 µg and 100 µg per mouse. Murine sTNFR, consisting of two murine p75 receptors fused to murine IgG2a, was dissolved in physiologic saline and administered intraperitoneally 3 times per week at doses of 300 µg and 100 µg per mouse. The selective p38 MAPK inhibitor SB242235 (synthesized at the US GSK Research Center) was suspended in 0.5% tragacanth and 0.03M hydrochloric acid and given orally twice daily at doses of 30 mg/kg and 15 mg/kg.

Joint Cytokine Messenger RNA (mRNA) and Protein Assays

The levels of mRNA and protein for the pro-inflammatory cytokines TNFα, IL-1β, and IL-6 were measured in disaggregated joints by TaqMan real-time reverse transcription-polymerase chain reaction (PCR) and enzyme-linked immunosorbent assays (ELISAs),

respectively. At study termination and, in the drug studies, 1 h after the final drug treatment administration, the primary ankle joint was removed for histology and the remaining paws were removed and snap-frozen in liquid nitrogen (six to eight mice per group). For cytokine assessment, the paw showing the highest score for swelling was selected with the proviso that it had also been swollen at the start of the drug study. If the remaining three paws exhibited no swelling at study termination, then the remaining ankle was selected for assay. Whole paws were frozen and pulverized using a mortar and pestle filled with liquid nitrogen.

For the mRNA studies, total RNA was isolated from homogenized paws using RNeasy Mini-kits (Qiagen, Crawley, UK). Samples were treated with 10 units of RNase-free DNase (Qiagen) for 15 min during the RNA isolation process. Reverse transcription of mRNA was carried out using TaqMan reverse transcription reagents in an MJ Research PTC-200 PCR Peltier Thermal Cycler. TaqMan probes and forward and reverse primers for the genes of interest (TNFα, IL-1β, and IL-6) and for housekeeping genes (GAPDH and cyclophilin) were designed with Primer Express TM software (PE Applied Biosystems). Cytokine mRNA expression levels were quantified by TaqMan real-time PCR using the ABI Prism 7900 Sequence Detector System (PE Applied Biosystems).

Measurement of Serum Antibody Levels

Blood was withdrawn from all mice before pristane injection and monthly thereafter. Levels of antibodies were determined by ELISA. Plates were coated with 100 µl of coating buffer (0.4 M phosphate buffer, pH 7.6) containing 5 µg of each antigen, at 4°C overnight. The antigens assessed were bovine aggrecan, bovine biglycan, human endoplasmic reticulum molecular chaperone protein, bovine chondroitin sulfate A, bovine chondroitin sulfate B, bovine type I collagen, chick type II collagen, murine type II collagen peptide, bovine decorin, bovine double-stranded DNA, human fibronectin, lupine glucose-6-phosphate isomerase, mycobacterial 65-kDa heat-shock protein, murine aggregated IgG, joint extract from normal mice, and joint extract from arthritic mice. Plates were washed 3 times with 0.05% Tween 20 in PBS and nonspecific binding was blocked by 5% non-fat milk in PBS overnight at 4°C. Serum samples from at least six individual mice per time point were used. Since 1:100 was the dilution determined to produce the optimal response to high-density proteoglycans, mouse serum diluted 1:100 in 5% milk/PBS was added to each well and incubated overnight at 4°C. Subsequently, the plates were washed 6 times with 0.05% Tween 20 in PBS and incubated with alkaline phosphatase-conjugated goat anti-mouse IgG (Southern Biotechnology Associates, Birmingham, Ala., USA) at 37°C for 1 h. Plates were again washed 6 times and developed for 40 min in the dark, using *p*-nitrophenyl phosphate as a chromatogen substrate. The optical density was measured at 405 nm ($OD_{405\,nm}$) using an ultraviolet max spectrophotometer (Molecular Devices, Sunnyvale, Calif., USA). To ensure uniformity of the assay, negative control sera obtained prior to blood withdrawal and a standard mouse anti-type II collagen antiserum were titered on each plate. Antibody binding was expressed as the $OD_{405\,nm}$ in units-blank.

Isolation of Splenocytes and Cell Proliferation Assays.

Spleens were excised and immediately immersed in PBS. Tissue was mechanically disrupted to release cells, which were suspended in 10 ml of sterile PBS and centrifuged for 10 min at 1,500 rpm. Prior to resuspension in medium, red blood cells were removed from the spleen preparations by adding distilled water for 10 s and then adding PBS. Spleen cells were then counted using a hemocytometer, and washed and resuspended in RPMI at a final concentration of 2.5×10^6/ml.

Next, 100 µl of spleen cell aliquots (2.5×10^6/ml) were transferred to 96-well plates with 50 µg/ml of each antigen (aggrecan, biglycan, chondroitin sulfate A, chondroitin sulfate B, type I collagen, type II collagen, type II collagen peptide, decorin, fibronectin, and heat-shock protein; all were derived from the same species as described for the serum antibody studies) in complete RPMI 1640 medium. Cells were incubated for 72 h at 37°C in the presence of antigen. Then 20 µl of MTT solution (a mitochondrial enzyme substrate) was added to each well (5 mg/ml). After a 6-h incubation, the culture supernatant was discarded and 200 µl of 10% sodium dodecyl sulfate solution was added to each well. After incubation at 37°C overnight, the $OD_{590\,nm}$ was read by microplate photospectrometer (Molecular Devices). The mean OD values were recorded for each cell sample as a measure of antigen stimulation. Antigen-specific responses were calculated as follows: ($OD_{590\,nm}$ [stimulated culture]) – ($OD_{590\,nm}$ [spontaneous proliferation culture]).

Histopathologic Evaluation

In all studies, the primary ankle joint that was swollen at the beginning of the time-course study or drug study was excised and fixed in 10% neutral buffered formalin. The tissues were decalcified with formic acid and

embedded in paraffin blocks. Sections (4–7 μm) were cut along a longitudinal axis, mounted, and stained with hematoxylin and eosin or toluidine blue, and representative slides for each animal were assessed. The following features were scored in six to ten animals per group: inflammatory exudate, neutrophil and mononuclear cell infiltration, bone resorption, and synovial hyperplasia. For drug studies, the effects of the agents on the pristane-induced pathologic condition were scored as follows: + = mild inhibition of pathologic features, ++ = moderate inhibition of pathologic features, +++ = marked inhibition of pathologic features.

EVALUATION

Graphic and tabular data are expressed as the mean ± SEM. Statistical significance was tested by application of the Kruskal-Wallis test for clinical scores, and by analysis of variance followed by Dunnett's test for the cytokine mRNA and protein time-course results. Antibody and cell proliferation studies were analyzed using the least-squares significant difference post hoc test.

MODIFICATIONS OF THE METHOD

Brenner et al. (2006) published thermal signature analysis as a novel method for evaluating inflammatory arthritis activity using rats with Freund's adjuvant-induced monoarthritis and pristane-induced arthritis. The thermal imaging system employs a platinum silicide 256 × 256 pixel detector array filtered to be sensitive to infrared radiation at a wavelength of 3–5 μm.

Lange et al. (2005) investigated the mode of action of methotrexate in different models for rheumatic arthritis, such as fibroblast-induced arthritis in SCID mice, collagen-induced arthritis and anticollagen-II-antibody-induced arthritis in rats, pristane-induced arthritis in DA rats, and models of multiple sclerosis, such as experimental autoimmune encephalomyelitis in (Balb/c x B10.Q)F1 and B10.Q mice.

Pristane induces lupus-like kidney and pulmonary disease in mice (Satoh et al. 1995; Richards et al. 1998; Lin et al. 2004; Chae et al. 2006).

REFERENCES AND FURTHER READING

Abe C, Hirano S, Wakazono K, Mase T, Yamamoto R, Matsufuji M, Sakata N, Agata N, Iguchi H, Ishizuka M (1995) Effects of cytogenin on spontaneous arthritis in MRL/1 mice and on pristane-induced arthritis (PIA) in DBA/1J mice. Int J Tissue React 17:175–180

Bedwell AE, Elson CJ, Hinton CE (1987) The immunological involvement in the pathogenesis of pristane-induced arthritis. Scand J Immunol 25:393–398

Brenner M, Meng HC, Yarlett NC, Joe B, Griffiths MM, Remmers EF, Wilder RL, Gulko PS (2005) The non-MHC quantitative trait locus *Cia5* contains three major arthritis genes that differentially regulate disease severity, pannus formation, and joint damage in collagen- and pristane-induced arthritis. J Immunol 174:7894–7903

Brenner M, Braun C, Oster M, Gulka PS (2006) Thermal signature analysis as a novel method for evaluating inflammatory arthritis activity. Ann Rheum Dis 65:306–311

Chae BS, Park JS, Shin TY (2006) Endotoxin induces late increase un the production of pulmonary proinflammatory cytokines in murine lupus-like pristane-primed models. Arch Pharm Res 29:302–309

Chapdelaine JM, Whalen JD, Wooley PH (1991) Pristane-induced arthritis. II. Genetic regulation in F1 hybrid mice and cellular abnormalities following pristane injection. Autoimmunity 8:215–220

Ghoraishian M, Elson CJ, Thompson SJ (1993) Comparison between the protective effects of mycobacterial 65-kD heat shock protein and ovomucoid in pristane-induced arthritis. relationship with agalactosyl IgG. Clin Exp Immunol 94:247–251

Holmberg J, Tuncel J, Yamada H, Lu S, Olofsson P, Holmdahl R (2006) Pristane, a non-antigenic adjuvant induces MHC class II-restricted, arthritogenic T cells in the rat. J Immunol 176:1172–1179

Hopkins SJ, Freemont AJ, Jayson MI (1984) Pristane-induced arthritis in BALB/c mice. I. Clinical and histological features of the arthropathy. Rheumatol Int 5:21–28

Jensen JR, Peters LC, Borrego A, Ribeiro OG, Cabrera WHK, Starobinas M, Siqueira M, Ibañez OCM, de Franco M (2006) Involvement of antibody trait loci in the susceptibility to pristane-induced arthritis in the mouse. Genes Immunity 7:44–50

Lange F, Bajtner E, Rintisch C, Nandakumar KS, Sack U, Holmdahl R (2005) Methotrexate ameliorates T cell dependent autoimmune arthritis and encephalomyelitis but not antibody induced or fibroblast induced arthritis. Ann Rheum Dis 64:599–605

Levitt NG, Fernandez-Madrid F, Wooley PH (1992) Pristane induced arthritis in mice. IV. Immunotherapy with mononuclear antibodies directed against lymphocyte subsets. J Rheumatol 19:1342–1347

Lin L, Gerth AJ, Peng SL (2004) Susceptibility of mast cell-deficient W/Wv mice to pristane-induced experimental lupus nephritis. Immunol Lett 91:93–97

Lu S, Nordquist N, Holmberg J, Olofsson P, Pettersson U, Holmdahl R (2002) Both common and unique susceptibility genes in different rat strains with pristane-induced arthritis. Eur J Hum Genet 10:475–483

Morgan R, Wu B, Song Z, Wooley PH (2004) Immune reactivity to connective tissue antigens in pristane-induced arthritis. J Rheumatol 31:1497–1505

Nishikaku F, Aono S, Koga Y (1994) Protective effects of D-penicillamine and a thiazole derivative, SM-8849, on pristane-induced arthritis in mice. Int J Immunopharmacol 16:91–100

Olofsson P, Holmberg J, Pettersson U, Holmdahl R (2003) Identification and isolation of dominant susceptibility loci for pristane-induced arthritis. J Immunol 171:407–416

Patten C, Bush K, Rioja I, Morgan R, Wooley P, Trill J, Life P (2004) Characterization of pristine-induced arthritis, a murine model of chronic disease. Response to antirheumatic agents, expression of joint cytokines, and immunopathology. Arthritis Rheum 50:3334–3345

Potter M, Wax JS (1981) Genetics of susceptibility of pristine-induced plasmacytomas in BALB/sAn: reduced suscep-

tibility in BALB/cJ with a brief description of pristine-induced arthritis. J Immunol 127:1591–1595
Richards HB, Satoh M, Shaw M, Libert C, Poli V, Reeves WH (1998) Interleukin 6 dependence of anti-DNA antibody production: evidence for two pathways of autoantibody formation in pristane-induced lupus. J Exp Med 188:985–990
Satoh M, Kumar A, Kanwar YS, Reeves WH (1995) Anti-nuclear antibody production and immune-complex glomerulonephritis in BALB/c mice treated with pristane. Proc Natl Acad Sci USA 92:10934–10938
Stasiuk LM, Ghoraishian M, Elson CJ, Thompson SJ (1997) Pristane-induced arthritis is $CD4^+$ T cell dependent. Immunology 90:81–86
Thompson SJ, Rook GA, Brealey TJ, van der Zee R, Elson CJ (1990) Autoimmune reactions to heat-shock proteins in pristane-induced arthritis. Eur J Immunol 20:2479–2484
Thompson SJ, Francis JN, Siew LK, Webb GR, Jenner PJ, Colston MJ, Elson CJ (1998) An immunodominant epitope from mycobacterial 65-kDa heat shock protein protects against pristane-induced arthritis. J Immunol 160:4628–4634
Vigar ND, Cabrera WH, Araujo LM, Ribeiro OG, Ogata TR, Siqueira M, Ibanez OM, de Franco M (2000) Pristane-induced arthritis in mice selected for maximal or minimal acute inflammatory reaction. Eur J Immunol 30:431–437
Vingsbo C, Sahlstrand P, Brun JG, Jonsson R, Saxne T, Holmdahl R (1996) Pristane-induced arthritis in rats:: a new model for rheumatoid arthritis with a chronic disease course influenced by major histocompatibility complex and non-major histocompatibility complex genes. Am J Pathol 149:1675–1683
Webster L, Olofsson P, Ibrahim SM, Holmdahl R (2003) Chronicity of pristane-induced arthritis in rats is controlled by genes on chromosome 14. J Autoimmun 21:305–313
Wooley PH, Whalen JD (1991) Pristane-induced arthritis in mice. III Lymphocyte phenotypic and functional abnormalities precede the development of pristine-induced arthritis. Cell Immunol 138:251–259
Wooley PH, Seibold JR, Whalen JD, Chapedelaine JM (1989) Pristane-induced arthritis: the immunological and genetic features of an experimental murine model of autoimmune disease. Arthritis Rheum 32:1022–1030
Wooley PH, Sud S, Whalen JD, Nasser S (1998) Pristane-induced arthritis in mice. V. Susceptibility to pristine-induced arthritis is determined by the genetic regulation of the T cell repertoire. Arthritis Rheum 41:2022–2031
Zheng CL, Hossain MA, Kukita A, Ohki K, Satoh T, Kohashi O (2002) Complete Freund's adjuvant suppresses the development and progression of pristane-induced arthritis in rats. Clin Immunol 103:204–208
Zheng CL, Ohki K, Hossain MA. Kukita A, Satoh T, Kohashi O (2003) Complete Freund's adjuvant promotes the increase of IFN-γ and nitric oxide in suppressing chronic arthritis induced by pristane. Inflammation 27:247–255

I.2.2.12 Experimental Autoimmune Thyroiditis

PURPOSE AND RATIONALE

Immunization of rats or mice with porcine thyroglobulin results in thyroiditis (Vladutiu 1971, 1983; McGregor et al. 1983; Hassman et al. 1985; Salamero et al. 1987; Fournier et al. 1990).

PROCEDURE

Crude porcine thyroglobulin (PTg) solution is emulsified in complete Freund's adjuvant in a 1:1 ratio. Female mice (6–8 weeks old) are primed with 50 µg PTg given s.c. into four or five sites of injection and are boosted 14 days later with the same dose of PTg (s.c.) emulsified in incomplete Freund's adjutant. The test compounds are administered from day 0 (at priming) until day 21. Mice are bled on day 21 and on day 28 after priming. The sera are tested for the levels of anti-PTg antibodies using an enzyme-linked immunosorbent assay (ELISA). On day 28, the animals are sacrificed and the thyroid glands prepared. Five-micrometer thick sections are stained with Masson-Goldner's trichrome solution.

EVALUATION

The histological severity of experimental autoimmune thyroiditis is graded as a function of mononuclear cell thyroid infiltration indices:

1. interstitial accumulation of inflammatory cells distributed between two ore more follicles.
2. one or two foci of inflammatory cells reaching at least the size of one follicle
3. 10 to 40% of the thyroid replaced by inflammatory cells.
4. more than 40% of the thyroid replaced by inflammatory cells.

Mean values of treated animals are compared with controls.

MODIFICATIONS OF THE METHOD

Castagliola et al. (1994) induced autoimmune thyroid disease in BALB/c mice by immunizing with the extracellular domain of the human TSH receptor expressed as a maltose-binding protein fusion in bacteria. This type of thyroiditis could be transferred to naive BALB/c and NOD mice (Castagliola et al. 1996).

Green et al. (1995) described a spontaneous model of autoimmune thyroiditis in MRL-lpr/lpr mice.

Furthermore, Green et al. (1996) induced thyroiditis in Lewis rats by immunization with thyroid extract and thyroglobulin. A reduction of the gap junction proteins connexin 43, connexin 32 and connexin 26 was found in diseased thyroid tissue.

REFERENCES AND FURTHER READING

Castagliola S, Many MC, Stalmans-Falys M, Tonacchera M, Vassart G, Ludgate M (1994) Recombinant thyrotropin receptor and the induction of autoimmune thyroid disease in BALB/c mice: A new animal model. Endocrinology 135:2150–2159

Castagliola S, Many MC, Stalmans-Falys M, Vassart G, Ludgate (1996) Transfer of thyroiditis, with syngeneic spleen cells sensitized with the human thyrotropin receptor, to naive BALB/c and NOD mice. Endocrinology 137:4637–4643
Fournier C, Gepner P, Saouk M, Charreire J (1990) *In vivo* beneficial effects of cyclosporin A and 1,25-dihydroxyvitamin D_3 on the induction of experimental autoimmune thyroiditis. Clin Immunol Immunopathol 54:53–63
Green LM, LaBue M, Lazarus JP, Colburn KK (1995) Characterization of autoimmune thyroiditis in MRL-lpr/lpr mice. Lupus 4:187–196
Green LM, LaBue M, Lazarus JP, Jennings JC (1996) Reduced cell-cell communication in experimentally induced autoimmune thyroid disease. Endocrinology 137:2823–2832
Hassman RA, Dieguez C, Rennie DP, Weetman AP, Hall R, McGregor AM (1985) The influence of cyclosporin A on the induction of experimental autoimmune thyroid disease in the PVG/c rat. Clin Exp Immunol 59:10–16
McGregor AM, Rennie PD, Weetman AP, Hassman RA, Foord SM, Dieguez C, Hall R (1983) The influence of cyclosporin A on experimental autoimmune thyroid disease in the rat. Life Sci 32:97–108
Penhale WJ, Farmer A, Irvine WJ (1975) Thyroiditis in T cell-depleted rats: influence of strain, radiation dose, adjuvants and antilymphocyte serum. Clin Exp Immunol 21:362–375
Salamero J, Remy JJ, Michel-Béchet M, Chareire J (1987) Experimental autoimmune thyroiditis induced by a 5–10 kDa tryptic fragment from porcine thyroglobin. Eur J Immunol 17:843–848
Tamura K, Woo J, Murase N, Nalesnik M, Thomson AW (1993) Inhibitory effect of FK 506 on autoimmune thyroid disease in the PVG rat. Ann NY Acad Sci 696:257–262
Vladutiu AO (1983) Effect of cyclosporine on experimental autoimmune thyroiditis in mice. Transplantation 35:518–520
Vladutiu AO, Rose NR (1971) Autoimmune murine thyroiditis relation to histocompatibility (H-2) type. Science 174:1137–1139

I.2.2.13 Coxsackievirus B3-Induced Myocarditis

PURPOSE AND RATIONALE

The effects of immunosuppressant drugs can be studied in the murine model of Coxsackie virus B-3 myocarditis.

PROCEDURE

Three week old male BALB/c mice are kept for 7 days before the experiment in a single, self-contained animal isolation unit to exclude pre-diseased animals. They are maintained in disposable, filter-topped cages and handled with gloves by gowned and masked personnel. The intraperitoneal route is used for injection of virus in a 0.5 ml volume.

The CVB3 virus strain is grown on either Hep-2 or VERO cells, aliquotted, and maintained at –70°C until use. At the time of infection, seed virus is grown on either VERO or LLC-MK-2 cells with Dulbecco's modified Eagle medium, 12% fetal calf serum and gentamycin. Virus is harvested and adjusted to an inoculum of 1.75×10^7 plaque forming units/0.5 ml RPMI-1640. The test drugs are given subcutaneously daily for 8 days. On day 8, the animals are sacrificed, the hearts rapidly removed and divided into two equal cross sections. The basal portion is snap frozen for isolation of virus and determination of drug level. The apical portion is fixed in 10% formalin, dehydrated and embedded in paraffin. Five mm sections are stained with hematoxylin-eosin and Masson's trichrome stains. The bases of the individual hearts are minced with a sterile scalpel, suspended in 1 ml RPMI-1640, and homogenized in a glass tissue grinder. The suspension is centrifuged at 8000 *g* for 10 min at 4°C. Supernatants are harvested and frozen at –70°C until assay. Serial 10-fold dilutions of heart homogenates in minimum essential medium are layered on confluent, 72-h-old VERO cells, that had been grown in 96-well microtiter plates. Monolayers are checked daily for 7 days for presence or absence of virus and rate of cell destruction.

EVALUATION

The slides are examined by two observers blinded to the slide code, and inflammation and necrosis are quantitated.

MODIFICATIONS OF THE METHOD

Lane et al. (1991) showed that lipopolysaccharides promote CB3-induced myocarditis in otherwise resistant B10.A mice.

Beisel et al. (1991) identified a putative shared epitope between Cocksackie virus B4 and mouse alpha cardiac myosin heavy chain.

Gauntt et al. (1993) found that epitopes shared between Coxsackie virus B3 and normal heart tissue contribute to CVB3-induced myocarditis in mice.

Instead of Coxsackie virus B-3, Monrad et al. (1986) used encephalomyocarditis virus to induce experimental myocarditis in mice.

REFERENCES AND FURTHER READING

Beisel KW, Srinivasappa J, Prabhakar BS (1991) Identification of a putative shared epitope between Coxsackie virus B4 and alpha cardiac myosin heavy chain. Clin Exp Immunol 86:49–55
Estrin M, Huber SA (1987) Coxsackie virus B3-induced myocarditis. Autoimmunity is $L3T4^+$ T helper cell and IL-2 independent in Balb/c mice. Am J Pathol 127:337–341
Estrin M, Smith C, Huber S (1986) Coxsackie virus B-3 myocarditis. T-cell autoimmunity to heart antigens is resistant to cyclosporin-A treatment. Am J Pathol 125:244–251
Estrin M, Herzum M, Buie C, Huber SA (1987) Immunosuppressives in murine myocarditis. Eur Heart J 8 (Suppl J):259–262
Gauntt CJ, Higdon HL, Arizpe HM, Tamayo MR, Crawley R, Henkel RD, Pereira MEA, Tracy SM, Cunningham MW (1993) Epitopes shared between Cocksackie virus B3

(CVB3) and normal heart tissue contribute to CVB3-induced murine myocarditis. Clin Immunol Immunopathol 68:129–134
Huber SA, Lodge PA (1984) Coxsackie virus B-3 myocarditis in Balb/c mice. Evidence for autoimmunity to myocyte antigens. Am J Pathol 116:21–29
Huber SA, Lodge PA (1986) Coxsackie virus B-3 myocarditis. Identification of different pathogenic mechanisms in DBA/2 and Balb/c mice. Am J Pathol 122:284–291
Lane JR, Neumann DA, Lafond-Walker A, Herskowitz A, Rose NR (1991) LPS promotes CB3-induced myocarditis in B10.A mice. Cell Immunol 136:219–233
Monrad ES, Matsumori A, Murphy JC, Fox JG, Crumpacker CS, Abelmann WH (1986) Therapy with cyclosporine in experimental murine myocarditis with encephalomyocarditis virus. Circulation 7:1058–1064
O'Connell JB, Reap EA, Robinson JA (1986) The effects of cyclosporine on acute murine Coxsackie B-3 myocarditis. Circulation 73:353–359
Rose NR, Herskowitz A, Neumann DA (1993) Autoimmunity in myocarditis: Models and mechanisms. Clin Immunol Immunopathol 68:95–99

I.2.2.14 Porcine Cardiac Myosin-Induced Autoimmune Myocarditis in Rats

PURPOSE AND RATIONALE

Pummerer et al. (1991), Inomata et al. (1995), Suzuki 1995; Dimitrijevic et al. (1998) described autoimmune myocarditis in rats induced by porcine cardiac myosin.

PROCEDURE

Male Sprague Dawley or Lewis rats at the age of 8 to 10 weeks are immunized with porcine cardiac myosin either purchased from Sigma (St. Louis, MO, USA) or prepared from the ventricular muscle of porcine hearts according to Murakami et al. (1976). The cardiac myosin fraction is dissolved in phosphate buffer at a concentration of 10 mg/ml. The antigen solution is emulsified with equal volume of complete Freund's adjuvant supplemented with heat-killed mycobacterium tuberculosis. Rats are injected subcutaneously into the foot pad with an immunizing dose of 5 mg of antigen in complete Freund's adjuvant/kg of body weight. Rats are injected intraperitoneally with test compounds either from day 0 to 6 (early treatment group) or from day 14 to 20 (late treatment group).

Immunized rats are sacrificed on days 8, 16, 21, and 34, respectively. Disease course and severity are analyzed by macroscopic findings of the hearts, heart weight/bodyweight ratio, as well as by histological and immunohistochemical analysis. Macroscopic findings are scored as follows: 0: normal finding; 1: presence of focal discolored area on the surface; 2: presence of diffuse discolored areas (Kodama et al. 1995).

The hearts are removed and weighted immediately after the rats are sacrificed, fixed in 10% buffered formalin and embedded in paraffin. Serial section (5 µm in thickness) are stained with hematoxylin-eosin. The severity of myocarditis is determined according the following scoring system: 0, no inflammation; 1: histological cross section infiltrated up to 5%; 2: 5–10% infiltrates/section; 3: 10–20% infiltrates/section; more than 20% infiltrates/section.

For immunohistochemical staining, heart samples are embedded in OCT compound (Miles, Elkhart, IN) and rapidly frozen. Cryostat sections are cut sequentially at 7 µm in thickness, mounted on glass slides and prepared for immunoperoxidase staining. Sections are fixed in cold acetone for 10 min and extensively washed in 0.1 M Tris buffer solution, pH 7.6. Murine monoclonal antibodies specific for different rat molecules are added at appropriate concentrations. After incubation at 4°C over night and further buffer washes, the sections are incubated with peroxidase-conjugated anti-mouse immunoglobulins for 60 min. Peroxidase reaction is visualized with 0.05% diaminobenzidine in 0.01% H_2O_2 for 7–8 min. The color development is stopped by washing slides in running water. All samples are lightly counterstained with hematoxylin, mounted in gelatin/glycerol medium and assessed by light microscopy.

EVALUATION

Macroscopic and microscopic scores are expressed as mean values. Body weights, heart weights and heart weight/body weight ratio are expressed as mean ± SD. Student's *t*-test for paired samples is used for comparison data within groups in reference to time, while two-sample *t*-test is used for comparison data between groups.

MODIFICATIONS OF THE METHOD

Koyama et al. (1995) immunized Lewis rats with human cardiac myosin suspended in complete Freund's adjuvant and induced severe active myocarditis with acute and chronic heart failure. The baseline left ventricular pressure was significantly lower in the chronic phase group and peak dP/dt was significantly lower in both the acute phase group and the chronic phase group than in the respective controls. The animal model was recommended to study both acute heart failure related to acute myocarditis and chronic heart failure due to diffuse myocardial fibrosis.

Neu et al. (1990, 1991ab; Penninger et al. 1993) induced severe autoimmune myocarditis in some mouse

strains by immunization with cardiac myosin in complete Freund's adjuvant.

Wahed et al. (2005) used the method of immunization with porcine cardiac myosin to test the effects of eplerenone, a selective aldosterone blocker, on the progression of left ventricular dysfunction and remodeling in rats with dilated cardiomyopathy.

REFERENCES AND FURTHER READING

Dimitrijevic M, Milenkovic M, Milosavljevic P, Stojic-Vukanic Z, Colic M, Bartlett R (1998) Beneficial effects of leflunomide on cardiac myosin-induced experimental autoimmune myocarditis in rats. Int J Immunother 14:9–21

Inomata T, Hanawa H, Miyanishi T, Yajima E, Nakayama S, Maita T, Kodama M, Izumi T, Shibata A, Abo T (1995) Localization of porcine cardiac myosin epitopes that induce experimental autoimmune myocarditis. Circ Res 76:726–733

Kodama M, Zhang S, Hanawa H, Saeki M, Inomata T, Suzuki K, Koyama S, Shibata A (1995a) Effects of 15-deoxyspergualin on experimental autoimmune giant cell myocarditis of the rat. Circulation 91:1116–1122

Koyama S, Kodama M, Izumi T, Shibata A (1995b) Experimental rat model representing both acute and chronic failure related to autoimmune myocarditis. Cardiovasc Drugs Ther 9:701–707

Murakami U, Uchida K, Hiratsuka T (1976) Cardiac myosin from pig heart ventricle: purification and enzymatic properties. J Biochem 80:611

Neu N, Ploier B (1991a) Experimentally induced autoimmune myocarditis: Production of heart myosin-specific antibodies. Autoimmunity 8:317–322

Neu N, Ploier B, Ofner C (1990) Cardiac myosin-induced myocarditis. Heart autoantibodies are not involved in the induction of the disease. J Immunol 145:4094–4100

Neu N, Klieber R, Frühwirth M, Berger P (1991b) Cardiac myosin-induced myocarditis as a model of postinfectious autoimmunity. Eur Heart J 12, Suppl D:117–120

Penninger JM, Neu N, Timms E, Wallace VA, Koh D R. Kishihara K, Pummerer C, Mak TW (1993) Induction of experimental autoimmune myocarditis in mice lacking CD3 or CD8 molecules. J Exp Med 178:1837–1842

Pummerer C, Berger P, Frühwirth M, Ofner C, Neu N (1991) Cellular infiltrate, major histocompatibility antigen expression and immunopathogenic mechanisms in cardiac myosin-induced myocarditis. Lab Invest 65:538

Suzuki K (1995) A histological study on experimental autoimmune myocarditis with special reference to initiation of the disease and cardiac dendritic cells. Virchows Arch 426:493–500

Wahed MII, Watanabe K, Ma M, Yamaguchi K, Takahashi T, Tachikawa H, Kodame M, Aizawa Y (2005) Effects of eplerenone, a selective aldosterone blocker, on the progression of left ventricular dysfunction and remodeling in rats with dilated cardiomyopathy. Pharmacology 73:81–88

I.2.2.15 Experimental Allergic Encephalomyelitis

PURPOSE AND RATIONALE

Experimental allergic encephalomyelitis was first produced in laboratory animals by Rivers et al. in 1933. This pathological model is an immunologic disease arising from a delayed hypersensitivity reaction to nervous tissue. In many respects, the model resembles autoimmune diseases, especially demyelinating diseases, in man. The method is used for evaluation of immunosuppressive properties of drugs.

PROCEDURE

Preparation of the encephalitogen: 3 g of spinal cord from guinea pigs or rats are homogenized with 7.5 ml bidistilled water, 3.8 ml phenol and 7.5 ml complete Freund's adjuvant under cooling.

Groups of 6–12 male Wistar–Lewis rats with an initial body weight of 130–200 g are used. On day 0, experimental allergic encephalomyelitis is induced by subplantar injection of 0.1 ml of the encephalitogen into the left hind paw. An equal volume of *Bordetella pertussis* vaccine concentrate (200×10^9 organisms/ml) is injected into the same foot. From days 1–2, the animals receive the test compound or vehicle only or the standard drug by oral administration once a day. Body weights of the animals are recorded every second day. The clinical signs of experimental allergic encephalomyelitis consist of ataxia or paresis, i. e., grossly irregular gait and weakness of one or both hind legs followed by flaccid paralysis of the hindquarters, urinary incontinence, fecal impaction and abdominal wall flaccidity. Animals showing one of these clinical signs are considered positive for the purpose of evaluation.

EVALUATION

Starting from day 7, the severity of clinical signs and mortality are determined daily and scored according to the following scheme:

	score
per 20 g loss of weight	1
paralysis of the tail	1
paralysis of the hind paw	3
complete paralysis	5
death	6

Calculation of the Results

The delay of onset of the paralytic symptoms is determined. The total score per day is recorded for treated and control groups. On the day of maximal clinical symptoms occurring among control animals, the total scores of the treated groups is compared to the total score of the control group. The percentage change is evaluated.

Doses of 0.5 mg/kg p.o. methotrexate, 1 mg/kg p.o. hydrocortisone, 2.5 mg/kg p.o. cyclophosphamide were found to be active, whereas non-steroidal anti-inflammatory compounds were inactive.

CRITICAL ASSESSMENT OF THE METHOD

The model of experimental allergic encephalomyelitis in rats is suitable to distinguish between immunosuppressive and anti-inflammatory drugs. Experimental autoimmune encephalomyelitis is considered as a rodent model of the autoimmune disease multiple sclerosis (Pearson et al. 1997; Deng et al. 2002).

MODIFICATIONS OF THE METHOD

The phosphodiesterase inhibitor pentoxifylline was found to prevent induction of experimental autoimmune encephalomyelitis in Lewis rats (Rott et al. 1993).

Martin and Near (1995) studied the protective effect of the interleukin-1 antagonist IL-1ra on experimental allergic encephalomyelitis in Lewis rats.

Experimental autoimmune encephalomyelitis in different strains of mice was described by Heremans et al. (1996), Glabinski et al. (1997), Liblau et al. (1997).

Baker et al. (1990, 1991, 2000) induced experimental allergic encephalomyelitis in Biozzi AB/H mice by sensitization with 1 mg of mouse spinal cord homogenate emulsified in Freund's complete adjuvant on days 0 and 7. The disease is characterized by relapsing-remitting episodes similar to multiple sclerosis in human beings. Biozzi AB/H mice also develop spasticity and tremor which can be antagonized by cannabinoids.

A chronic relapsing-remitting form of experimental autoimmune encephalomyelitis was induced in the common marmoset Callithrix jacchus following a single immunization with human white matter by Massacesi et al. (1995), Genain and Hauser (1997) and recommended as a new model for multiple sclerosis. This model has been used for histopathological characterization of magnetic resonance imaging-detectable white matter lesions in a primate model of multiple sclerosis by 't Hart et al. (1998, 2004) (see E.10.3.2).

Experimental allergic neuritis in several animal species has been described by Waksman and Adams 1955, 1956; King et al. 1983; McCombe et al. 1990; Nakayasu et al. 1990). This disorder has been considered to show similarities to the Guillain-Barré syndrome in man. The demyelating process initiated by the injected antigens is a lymphocyte-mediated reaction in which activated macrophages strip myelin off the axons. Hartung et al. (1987) described the adoptive transfer experimental autoimmune neuritis in Lewis rats by injection of P2-reactive T lymphocyte cell lines.

Mix et al. (1992) studied the effect of stilbene-type anion channel blockers on the immune response during experimental allergic neuritis induced by bovine peripheral myelin.

Kojima et al. (1994) investigated the pathogenic potential of autoimmune T cell responses to nonmyelin autoantigens in the Lewis rat using the astrocyte-derived calcium-binding protein S100β, as a model non-myelin autoantigen. In contrast to the experimental autoimmune encephalomyelitis induced by the adoptive transfer of myelin basic protein-specific T line cells, S100β-specific T cell transfer induced intense inflammation not only in the spinal cord but also throughout the entire CNS and also in the uvea and retina of the eye.

Gautam et al. (1992) reported that a polyalanine peptide with only five native basic protein residues induces autoimmune encephalomyelitis in mice. This peptide, called myelin basic protein (MBP) Ac1–11, has been used by several authors for further studies on experimental autoimmune encephalomyelitis (Ratts et al. 1999; Matejuk et al. 2003).

Pearson et al. (1997) reported the induction of a heterogeneous T-cell receptor repertoire in (PL/JXSJL/J)F2 mice by myelin basic protein peptide Ac1–11 and its analog Ac1–11[4A].

Deng et al. (2002) found that expression of the tyrosine phosphatase Src homology 2 domain-containing protein tyrosine phosphatase 1 determines the T cell activation threshold and severity of experimental autoimmune encephalomyelitis.

Maron et al. (2002) investigated the immunological properties of Cop1 (glatiramer acetate) to determine the degree to which its effects were antigen specific using myelin basic protein T-cell receptor transgenic mice. Immunization of these mice fed glatiramer acetate, myelin basic protein or MBP Ac1–11 resulted in decreased proliferation, and IL-2, IL-6, and IFN-γ production, and increased secretion of IL-10 and TGF-β in glatiramer acetate-fed animals.

Gilgun-Sherki et al. (2003) reported that riluzole suppresses myelin oligodendrocyte glycoprotein-induced experimental autoimmune encephalomyelitis in mice.

Pollak et al. (2003) studied the experimental allergic encephalitis-associated behavioral syndrome and the modulation by anti-inflammatory treatments.

Diab et al. (2004) found that ligands for the PPAR-γ and the retinoid X receptor exert additive anti-inflammatory effects on experimental autoimmune encephalomyelitis. Duckers et al. (1997) studied the effect of a neurotropic treatment on cortical lesion development in experimental allergic encephalomyelitis in rats by longitudinal *in vivo* magnetic resonance imaging methods.

REFERENCES AND FURTHER READING

Alvord EC (1984) The challenge: how good a model of MS is EAE today? In: Alvord EC, Kies MW, Suckling AJ (eds) Experimental allergic encephalomyelitis: a useful model for multiple sclerosis. Alan R Liss, New York, pp 3–5

Arnon R (1981) Experimental allergic encephalomyelitis – Susceptibility and suppression. Immunol Rev 55:5–30

Baker D, O'Neill JK, Gschmeissner SE, Wilcox CE, Butter C, Turk JL (1990) Induction of chronic relapsing experimental allergic encephalomyelitis in Biozzi mice. J Neuroimmunol 28:261–270

Baker D, O'Neill JK, Turk JL (1991) Cytokines in the nervous system of mice during chronic relapsing experimental allergic encephalomyelitis. Cell Immunol 134:505–510

Baker D, Pryce G, Croxford JL, Brown P, Pertwee RG, Huffman HW, Layward L (2000) Cannabinoids control spasticity and tremor in a multiple sclerosis model. Nature 202:84–87

Ben-Nun A, Cohen IR (1982) Experimental autoimmune encephalomyelitis (EAE) mediated by T cell lines: process of selection of lines and characterization of the cells. J Immunol 129:303–308

Bolton C, Borel JF, Cuzner ML, Davison AN, Turner AM (1982) Immunosuppression by cyclosporin A of experimental allergic encephalomyelitis. J Neur Sci 56:147–153

Carlson RP, Baeder WL, Caccese RG, Warner LM, Sehgal SN (1992) Effects of orally administered rapamycin in animal models of arthritis and other autoimmune diseases. Ann NY Acad Sci 685:86–113

Carlson RP, Hartman DA, Tomchek LA, Walter TL, Lugay JR, Calhoun W, Sehgal SN, Chang JY (1993) Rapamycin, a potential disease-modifying antiarthritic drug. J Pharmacol Exp Ther 266:1125–1138

Chabannes D, Ryffel B, Borel JF (1992) SRI 62–834, a cyclic ether analogue of the phospholipid ET-18-OCH_3, displays long-lasting beneficial effects in chronic relapsing encephalomyelitis in the Lewis rat. Comparison with cyclosporin and (Val^2)-dihydrocyclosporin effects in clinical, functional and histological studies. J Autoimmun 5:199–211

Deng C, Minguela A, Hussain RZ, Lovett-Racke AE, Radu C, Ward ES, Racke MK (2002) Expression of the tyrosine phosphatase Src homology 2 domain-containing protein tyrosine phosphatase 1 determines T cell activation threshold and severity of experimental autoimmune encephalomyelitis. J Immunol 168:4511–4518

Diab A, Hussain RZ, Lovett-Racke AE, Chavis JA, Drew PD, Racke MK (2004) Ligands for the peroxisome proliferator-activated receptor-γ and the retinoid X receptor exert additive anti-inflammatory effects on experimental autoimmune encephalomyelitis. J Neuroimmun148:116–126

Duckers HJ, Muller HJ, Verhaagen J, Nicolay K, Gispen WH (1997) Longitudinal *in vivo* magnetic resonance imaging studies in experimental allergic encephalomyelitis : effect of a neurotropic treatment on cortical lesion development. Neuroscience 77:1163–1173

Feurer C, Chow LH, Borel JF (1988) Preventive and therapeutic effects of cyclosporin and valine^2-dihydro-cyclosporin in chronic relapsing experimental allergic encephalomyelitis in the Lewis rat. Immunol 63:219–223

Gautam AM, Pearson CI, Smilek DE, Steinman L, McDevitt HO (1992) A polyalanine peptide with only five native basic protein residues induces autoimmune encephalomyelitis. J Exp Med 176:605–609

Genain CP, Hauser SL (1997) Creation of a model for multiple sclerosis in Callithrix jacchus marmosets. J Mol Med 75:187–197

Gilgun-Sherki Y, Panet H, Melamed E, Offen D (2003) Riluzole suppresses experimental autoimmune encephalomyelitis: implications for the treatment of multiple sclerosis. Brain Res 989:196–204

Glabinski AR, Tani M, Strieter RM, Tuohy VK, Ransohoff RM (1997) Synchronous synthesis of α- and β-chemokines by cells of diverse lineage in the central nervous system of mice with relapses of chronic experimental autoimmune encephalomyelitis. Am J Pathol 150:617–630

Hartung HP, Schäfer B, Fierz W, Heininger K, Toyka KV (1987) Cyclosporin A prevents P2 T cell line-mediated experimental autoimmune neuritis (AT-EAN) in rat. Neurosci Lett 83:195–200

Heremans H, Dillen C, Groenen M, Martens E, Billiau A (1996) Chronic relapsing experimental autoimmune encephalomyelitis in mice: Enhancement by monoclonal antibodies against interferon-gamma. Eur J Immunol 26:2393–2398

Hinrichs DJ, Wegmann KW, Peters BA (1983) The influence of cyclosporin A on the development of actively induced and passively transferred experimental allergic encephalomyelitis. Cell Immunol 77:202–209

King RHM, Craggs RI, Gross MLP, Tompkins C, Thomas PK (1983) Suppression of experimental allergic neuritis by cyclosporin A. Acta Neuropathol (Berl) 59:262–268

Koshima K, Berger T, Lassmann H, Hinze-Selch D, Zhang Y, Gehrmann J, Reske K, Wekerle H, Linington C (1994) Experimental autoimmune panencephalitis and uveoretinitis transferred to the Lewis rat by T lymphocytes specific for the S100β molecule, a calcium binding protein of astroglia. J Exp Med 180:817–829

Levine S, Sowinski R (1977) Suppression of the hyperacute form of experimental allergic encephalomyelitis by drugs. Arch Int Pharmacodyn 230:309–318

Liblau R, Steinman L, Brocke S (1997) Experimental autoimmune encephalomyelitis in IL-4 deficient mice. Int Immunol 9:799–803

Maron R, Slavin Aj, Hoffmann E, Komagata Y, Weiner HL (2002) Oral tolerance to copolymer 1 in myelin basic protein (MBP) TCR transgenic mice: cross-reactivity with MBP-specific TCR and differential induction of anti-inflammatory cytokines. Int Immunol 14:131–138

Martin D, Near SL (1995) Protective effect of the interleukin-1 antagonist (IL-1ra) on experimental allergic encephalomyelitis in rats. J Neuroimmunol 61:241–245

Massacesi L, Genain CP, Lee-Parritz D, Letvin NL, Canfield D, Hauser SL (1995) Active and passively induced experimental autoimmune encephalomyelitis in common marmosets: A new model of multiple sclerosis. Ann Neurol 37:519–530

Matejuk A, Hopke C, Dwyer J, Subramanian S, Jones RE, Bourdette DN, Vandenbark AA, Offner H (2003) CNS gene expression pattern associated with spontaneous experimental autoimmune encephalomyelitis. J Neurosci Res 73:667–678

McCombe PA, van der Kreek SA, Pender MP (1990) The effects of prophylactic cyclosporin A on experimental allergic neuritis (EAN) in the Lewis rat. Induction of relapsing EAN using low dose of cyclosporin A. J Neuroimmunol 28:131–140
McFarlin DF, Blank SE, Kibler RF, McKneally S, Shapira R (1973) Experimental allergic encephalomyelitis in the rat: response to encephalitogenic proteins and peptides. Science 179:478–483
Mix E, Correale J, Olsson T, Solders G, Link H (1992) Effect of stilbene-type anion channel blockers on the immune response during experimental allergic neuritis. Immunpharmacol Immuntoxicol 14:579–609
Nakayasu H, Ota K, Tanaka H, Irie H, Takahashi H (1990) Suppression of actively induced and passively transferred experimental allergic neuritis by cyclosporin A. J Neuroimmunol 26:219–227
Pearson CI, Smilek DE, Danska JS, McDevitt HO (1997) Induction of a heterogeneous TCR repertoire in (PL/JXSJL/J)F2 mice by myelin basic protein peptide Ac1–11 and its analog Ac1–11[4A]. Mol Immunol 14:781–792
Pollak Y, Ovadia H, Orion E, Yimiya R (2003) The EAE-associated behavioral syndrome: II. Modulation by anti-inflammatory treatments. J Neuroimmunol 137:100–108
Polman CH, Matthaei I, de Groot CJA, Koetsier JC, Sminia T, Dijkstra CD (1988) Low-dose cyclosporin A induces relapsing remitting experimental allergic encephalomyelitis in the Lewis rat. J Neuroimmunol 17:209–216
Ratts RB, Arredono LR, Bittner P, Perrin PJ, Lovett-Racke AE, Racke MK (1999) The role of CTLA-4 in tolerance induction and T cell differentiation in experimental autoimmune encephalomyelitis.: i.p. antigen administration. Int Immunol 11:1881–1888
Rivers TM, Sprunt DH, Berry GP (1933) Observations on attempts to produce acute disseminated encephalomyelitis in monkeys. J Exper Med 58:39–53
Rosenthale ME, Datko LJ, Kassarich J, Schneider F (1969) Chemotherapy of experimental allergic encephalomyelitis (EAE) Arch Int Pharmacodyn 179:251–275
Rott O, Cash E, Fleischer B (1993) Phosphodiesterase inhibitor pentoxifylline, a selective suppressor of T helper type 1- but not type 2-associated lymphokine production, prevents induction of experimental autoimmune encephalomyelitis in Lewis rats. Eur J Immunol 23:1745–1751
Schuller-Levis GB, Kozlowski PB, Wisniewski HM (1986) Cyclosporin A treatment of an induced attack in a chronic relapsing model of experimental allergic encephalomyelitis. Clin Immunol Immunopathol 40:244–252
't Hart BA, Bauer J, Muller HJ, Melchers B, Nicolay K, Brok H, Bontrop RE Lassmann H, Massacesi L (1998) Histopathological characterization of magnetic resonance imaging-detectable white matter lesions in a primate model of multiple sclerosis. A correlative study in the experimental autoimmune encephalomyelítis model in common marmosets (*Callithrix jacchus*). Am J Pathol 153:649–663
't Hart BA, Vogel J, Bauer J, Brok HPM, Blezer E (2004) Non-invasive measurement of brain damage in a primate model of multiple scerosis. Trends Mol Med 10:85–91
Waksman BH, Adams RD (1955) Allergic neuritis: an experimental disease of rabbits induced by the injection of peripheral nervous tissue and adjuvants. J Exp Med 102:213–234
Waksman BH, Adams RD (1956) A comparative study of experimental allergic neuritis in rabbit, guinea-pig and mouse. J Neuropathol Exp Neurol 15:293–374

I.2.2.16
Acute Graft Versus Host Disease (GVHD) in Rats

PURPOSE AND RATIONALE

The intravenous injection of a mixture of parental splenocytes into healthy inbred F_1-rats results in graft-versus-host (GVH) induced immune abnormalities. This is due to T-lymphocytes in the donor inoculum that recognize the major histocompatibility alloantigens expressed by the F_1-animals. The host F_1 T-cells are genetically unable to recognize antigens of the parental donor as foreign, thus the response involves only donor recognition of host and not host recognition of donor. The ensuing immune abnormalities lead to clinical symptoms of an acute, lethal GVH-disease (GVHD), i. e. profound immunodeficiency, anemia, hypogamma-globulinemia and runting.

PROCEDURE

Three to 4 month old, male F_1-hybrid rats of the inbred strains Lewis (Rt-1 l) and Brown Norway (BN, Rt-1n) (Zentralinstitut für Versuchstierkunde Hannover Germany) are used as hosts for cell grafts from the Lewis parental strain. The bone marrow cells are obtained by flushing hind femur bone shafts with culture medium. These cells are then pooled together with spleen cells (ratio 2 bones: 1 spleen). The cell viability, determined by trypan exclusion, has to be more than 90%. Each recipient is injected with about 40×10^7 cells in a 1.5 ml-suspension volume. The route of injection is the penis vein, allowing an optimal control of correct intravenous application.

Prophylactic Drug Application

For this experiment, 2 groups of 6 F_1-hybrids each are injected with the above mentioned bone marrow/spleen cell suspension. One group receives the test drug orally and daily until the end of the experiment, homogeneously suspended in 1% carboxymethylcellulose (CMC) solution. The other group receives CMC alone and, thus, serving as the GVHD control group. The experiment is terminated two weeks after disease induction i. e. 1 week after the first appearance of GVHD-symptoms. All animals are sacrificed and clinical aspects documented, spleens weighed, histology of the skin, liver, spleen and lymph-nodes performed and organs photographed.

Therapeutic Drug Application

In this experiment, rats are separated into four groups treatment begins with the first sign of GVHD-symptoms (beginning of the second week). Because of

the expected, greater therapeutic difficulty, the daily dose of the test drug has to be doubled, again for 2 weeks duration.

The experiment is terminated either by sacrificing those rats that are too sick to be able to move around the cage, or at the end of the 4 week observation period, regardless of the clinical condition of the animals. The clinical-chemical parameters are determined by routine procedures conducted with a HITACHI autotechnicon.

EVALUATION

The tested parameters of therapeutic success or disease, respectively, are survival rate (%), spleen weight (g), and body weight (g) as well as clinical-chemical parameters (bilirubin, alkaline phosphatase, creatinine, white cell count) after 2 and 3 weeks.

MODIFICATIONS OF THE METHOD

Gelpi et al. (1994) established a chronic graft vs host disease in (C5BL/10 x DBA/2)F_1 mice with an injection of lymphoid cells from the parent DBA/2 strain. Most of the animals developed antibodies against transfer RNA/protein particles.

Mosier et al. (1988) reported transplantation of human peripheral blood lymphocytes (PBL) into severe combined immunodeficient (scid) mice to construct hu-PBL-scid mice. Kim et al. (1997) suggested these mice for routine immunotoxicity investigations using lymph nodes of intestines as the lymphocyte sources.

Ford et al. (1970), Schorlemmer et al. (1997, 1998) used the popliteal lymph node assay to study the local graft vs. host reaction. The test is based on the enlargement of the draining popliteal lymph nodes as a result of injecting immuno-competent cells (1×10^8 parental Lewis spleen cells) into the hind foot pad of Lewis × Brown-Norway F1 recipients. The reaction is measured at day 6 after challenge as a gain in lymph node weights.

REFERENCES AND FURTHER READING

Bartlett RR, Dimitrijevic M, Mattar T, Zielinski T, Germann T, Rüde E, Thoenes GH, Küchle CCA, Schorlemmer HU, Bremer E, Finnegan A, Schleyerbach R (1991) Leflunomide (HWA 486), a novel immunomodulating compound for the treatment of auto-immune disorders and reactions leading to transplantation rejection. Agents and Actions 32:11–21

Bartlett RR, Anagnostopulos H, Zielinski T, Mattar T, Schleyerbach R (1993) Effects of leflunomide on immune responses and models of inflammation. Springer Semin Immunopathol 14:381–394

Ford WL, Burr W, Simonsen G (1970) A lymph node weight assay for the graft-versus-host activity of rat lymphoid cells. Transplantation 10:258

Gelpi C, Martinez MA, Vidal S, Targoff IN, Rodriguez-Sanchez JL (1994) Antibodies to a transfer RNA-associated protein in a murine model of chronic graft versus host disease. J Immunol 152:1989–1999

Kim HM, Han SB, Hong DH, Yoo BS, Oh GT (1977) Limitation of Hu-PBL-scid mouse model in direct application to immunotoxicity assessment. J Pharmacol Toxicol Meth 37:83–89

Küchle CCA, Thoenes GH, Langer KH, Schorlemmer HU, Bartlett RR, Schleyerbach R (1991) Prevention of kidney and skin graft rejection in rats by leflunomide, a new immunomodulating agent. Transplant Proc 23:1083–1086

Mosier DE, Gulizia RJ, Baird SM, Wilson DB (1988) Transfer of a functional human immune system to mice with severe combined immunodeficiency. Nature 335:256–259

Mrowka C, Thoenes GH, Langer KH, Bartlett RR (1994) Prevention of acute graft versus host disease (GVHD) in rats by the immunomodulating drug leflunomide. Ann Hematology 68:195–199

Murase N, Demetris AJ, Woo J, Tanabe M, Furuya T, Todo S, Starzl TE (1993) Graft-versus-host disease after Brown Norway-to-Lewis and Lewis-to-Brown Norway rat intestinal transplantation under FK 506. Transplantation 55:1–7

Renkonen R, Häyry P (1984) Bone marrow transplantation in the rat. I. Histologic correlation and quantification of cellular infiltrates in acute graft-versus-host disease. Am J Pathol 117:462–470

Schorlemmer HU, Seiler FR, Bartlett RR (1993) Prolongation of allogenetic transplanted skin grafts and induction of tolerance by leflunomide, a new immunosuppressive isoxazol derivative. Transplant Proc 25:763–767

Schorlemmer HU, Kurrle R, Bartlett R (1997) The new immunosuppressants, the malononitrilamides MNA 279 and MNA 715, inhibit various graft-vs.-host diseases (GvHD) in rodents. Drugs Exp Clin Res 23:167–173

Schorlemmer HU, Kurrle R, Schleyerbach R (1998) A77–1726, leflunomide's active metabolite, inhibits *in vivo* lymphoproliferation in the popliteal lymph node assay. Int J Immunotherapy 14:205–211

Shaffer D, Muanza T, Blakely ML, Simpson MA, Monaco AP (1993) Prevention of graft-versus-host-disease by RS-61443 in two different rodent models. Transplantation 55:221–223

Thoenes GH, Sitter T, Langer KH, Bartlett RR, Schleyerbach R (1989) Leflunomide (HWA 486) inhibits experimental autoimmune tubulointerstitial nephritis in rats. Int J Immunopharmacol 11:921–929

Wakely E, Oberholser JH, Corry RJ (1990) Elimination of acute GVHD and prolongation of rat pancreas allograft survival with DST, cyclosporine, and spleen transplantation. Transplantation 49:241–245

I.2.2.17 Influence on SLE-Like Disorder in MRL/lpr Mice

PURPOSE AND RATIONALE

Systemic lupus erythematosus (SLE) is an autoimmune disease in man that affects multiple body organs and is characterized by the development of certain types of self antigens. Primarily, the antibodies formed against double-stranded DNA (dsDNA), the most prevalent in this ailment, complex together and, with complement, deposit in the small blood vessels, leading to widespread vasculitis. MRL Mpf lpr/lpr

(MRL/lpr)-mice spontaneously develop a severe disease with many symptoms very similar to human SLE, i. e. hypergamma-globulinemia, and glomerulonephritis (Theofilopoulos and Dixon 1981).

PROCEDURE

Female MRL/lpr-mice (originally from Jackson Laboratories, USA), displaying distinct symptoms of SLE (between 12 and 13 weeks of age) are randomized and divided into groups of 12 animals each. At this age, the animals have already clinical manifestations of the SLE-like illness, as determined by the disease index, but have not yet developed proteinuria. Animals with early symptoms of disease are treated with various drugs, e. g., leflunomide, cyclosporin A, azathioprine, cyclophosphamide or prednisolone for 11 weeks and the survival rate and disease index of these animals are followed for 24 weeks. The disease index and urine protein level are determined once weekly.

Disease Index

The subsequent clinical parameters are taken into consideration:

1. Ears: reddening of the skin, deterioration of the pinna.
2. Nose: loss of hair, wasting of the skin.
3. Lymph nodes: detection of swollen lymph nodes on any part of the body, especially neck and extremities.
4. Fur: general condition of fur (e. g. shabby, mangy, etc.), loss of hair.
5. Skin: inflammation of the skin, scab and/ or granuloma formation.
6. Eyes: exophthalmos, deterioration due to inflammation, tumor formation around the eye, swelling of the eyelid with eventual closure of the eye.
7. Paws: reddening of the skin, swelling of the paw.

EVALUATION

A score for each of the above described parameters is given according to the severity of the symptoms as follows:

Points for clinical index

Involvement	Detectable	Moderate	Severe
Ears (each)	0.5	1.0	1.5
Nose	1.0	2.0	3.0
Lymph node (each)	1.0	2.0	3.0
Fur	1.0	2.0	3.0
Skin	1.0	2.0	3.0
Eyes (each)	1.0	2.0	3.0
Paws (each)	0.5	1.0	1.5

Body weight (one point for 5 g difference from week to week)

The determination of the disease index is performed, weekly, by the same individual, but without knowledge of the group being evaluated. The points, for each animal, are registered and the total score, of each group, summarized. The average score for the group is calculated, significance between the experimental group and the untreated diseased group is determined using the Student *t*-test.

Proteinuria

Pooled urine is collected from each experimental group and the amount of protein in the urine is calculated.

MODIFICATIONS OF THE METHOD

In addition to a lupus-like syndrome and massive T cell proliferation. MRL-1pr/1pr (MRL/1) mice develop an arthritic process very similar serologically and histologically to human rheumatoid arthritis. Boissier et al. (1989) found that in these animals mouse type II collagen is antigenic, but not arthritogenic.

Holmdahl et al. (1991) studied the involvement of macrophages and dendritic cells in synovial inflammation of collagen induced arthritis in DBA/1 mice and spontaneous arthritis in MRL/Lpr mice.

Rordorf-Adam et al. (1985) used serum amyloid P component and autoimmune parameters in the assessment of arthritis in MRL/lpr/lpr mice.

Furukawa et al. (1996) studied the autoimmune disease-prone genetic background in relation to Fas-defect in MRL/lpr mice.

Kanno et al. (1992) found spontaneous development of pancreatitis in the MRL/Mp strain of mice.

Kusakari et al. (1992) compared hearing acuity and inner ear disorders of MRL/lpr mice with those of BALB/c mice and found a significantly higher auditory brain stem response threshold. They recommended this as a model of sensorineuronal hearing loss.

Bundick and Eady (1992) investigated the effects of an immunosuppressive agent on the development of spontaneous lupus disease in female NZBW F_1 hybrid mice.

Walker et al. (1996) reported a powerful suppressive effect of testosterone on the autoimmune disease analogous to systemic lupus erythematodes spontaneously developed by F1-hybrids of New Zealand Black (NZB) × New Zealand White (NZW) mice. A model was developed in which NZB dams carrying NZB/NZW fetuses were treated with testosterone

in a dose adequate to masculinize the external genitalia in female fetuses.

Zoja et al. (1998) investigated bindarit, a compound devoid of immunosuppressive properties, in NZB/W F1 hybrid mice developing an immune complex glomerulonephritis with proteinuria and progression to renal insufficiency.

Kiberd and Stadnyk (1995) studied the role of endogenous interleukin-1 in established lupus nephritis in MRL lpr/lpr mice by administration of the IL-1 receptor antagonist IL-1ra.

Gleichmann et al. (1982), Schorlemmer et al. (1997) induced a systemic lupus erythematodes-like disease in mice by abnormal T- and B-cell cooperation. A chronic graft versus host reaction with the pathologic symptoms of severe glomerulonephritis is induced in B6D2 (C5Bl/6 × DBA/2) F1 hybrid mice receiving four i.v. injections (one per week) of 1×10^8 parental lymphoid spleen cells from DBA/2 donors. The inoculation of splenocytes into the BDF1 hybrid mice results in the development of a chronic GvH reaction with lymphoid hyperplasia, autoantibody production and immune-complex glomerulonephritis.

Chan et al. (1995) described ocular changes occurring in mice with experimental lupus erythematodes. The ocular disease is characterized by bilateral subacute and chronic inflammation of the eyelids (blepharitis) and hypertrophic Meibomian glands. The severity of the ocular changes is strain dependent. The authors recommend this experimental eye disease as an animal model for chronic blepharitis in humans.

The changes of lacrimal and salivary glands found in MRL/lpr mice and other mouse strains with autoimmune disorders were also regarded as model of Sjögren's syndrome in human (Sullivan and Edwards 1997; Toda et al. 1999).

REFERENCES AND FURTHER READING

Bartlett RR, Popovic S, Raiss RX (1988) Development of autoimmunity in MRL/lpr mice and the effect of drugs on this murine disease. Scand. J Rheumatol Suppl. 75:290–299

Bartlett RR, Mattar T, Weithmann U, Anagnostopulos H, Popovic S, Schleyerbach R (1989) Leflunomide (HWA 486): a novel immunorestoring drug. In: Lewis AJ, Doherty NS, Ackerman NR (eds) Therapeutic approaches to inflammatory diseases. New York, Elsevier Science Publishing Co., Inc., pp 215–228

Boissier MC, Texier B, Carlioz A, Fournier C (1989) Polyarthritis in MRL-1pr/1pr mice: Mouse type II collagen is antigenic, but not arthritogenic. Autoimmunity 4:31–41

Bundick RV, Eady RP (1992) The effects of CP 17193, an immunosuppressive pyrazoloquinoline, on the development of spontaneous lupus disease in NZBW F_1 hybrid mice. Clin Exp Immunol 89:179–184

Carlson RP, Baeder WL, Caccese RG, Warner LM, Sehgal SN (1992) Effects of orally administered rapamycin in animal models of arthritis and other autoimmune diseases. Ann NY Acad Sci 685:86–113

Chan CC, Gery I, Kohn LD, Nussenblatt RB, Mozes E, Singer SD (1995) Periocular inflammation in mice with experimental systemic lupus erythematodes. A new experimental blepharitis and its modulation. J Immunol 154:4830–4835

Furukawa F, Kanauchi H, Wakita H, Tokura Y, Tachibana T, Horiguchi Y, Imamura S, Ozaki S, Takigawa M (1996) Spontaneous autoimmune skin lesions of MRL/n mice: Autoimmune disease-prone genetic background in relation to Fas-defect MRL/lpr mice. J Invest Dermatol 107:95–100

Gleichmann E, van Elven EH, van der Veen JPW (1982) A systemic lupus erythematodes (SLE)-like disease in mice induced by abnormal T- and B-cell cooperation. Preferential formation of antibodies characteristic of SEL. Eur J Immunol 12:152

Gunn HC, Hiestand PC (1988) Cyclosporine A and cyclosporine G enhance IgG rheumatoid factor production in MRL/Ipr Mice. Transplant Proc 20, Suppl 4:238–242

Holmdahl R, Tarkowski A, Jonsson R (1991) Involvement of macrophages and dendritic cells in synovial inflammation of collagen induced arthritis in DBA/1 mice and spontaneous arthritis in MRL/Lpr mice. Autoimmunity 8:271–280

Kanno H, Nose M, Itoh J, Taniguchi Y, Kyogoku M (1992) Spontaneous development of pancreatitis in the MRL/Mp strain of mice in autoimmune mechanism. Clin Exp Immunol 89:68–73

Kiberd BA, Stadnyk AW (1995) Established murine lupus nephritis does not respond to exogenous interleukin-1 receptor antagonist: A role for the endogenous molecule? Immunopharmacology 30:131–137

Kusakari C, Hozawa K, Koike S, Kyogoku M, Takasaka T (1992) MRL/MP-lrp/Lrp mouse as a model of immune-induced sensorineuronal hearing loss. Ann Otol Rhinol Laryngol 101:82–86

Rordorf-Adam Ch, Serban D, Pataki A, Gruninger M (1985) Serum amyloid P component and autoimmune parameters in the assessment of arthritis in MRL/lpr/lpr mice. Clin Exp Immunol 61:509–516

Schorlemmer HU, Dickneite G (1992) Preclinical studies with 15-deoxyspergualin in various animal models for autoimmune diseases. Ann NY Acad Sci 685:155–174

Schorlemmer HU, Dickneite G, Enßle KH (1995) Immunoregulation of murine SLE-like diseases by interleukin-4-receptor. Lupus 4, Suppl 2:8

Schorlemmer HU, Kurrle R, Bartlett R (1997) The new immunosuppressants, the malononitrilamides MNA 279 and MNA 715, inhibit various graft-vs.-host diseases (GvHD) in rodents. Drugs Exp Clin Res 23:167–173

Sullivan DA, Edwards JA (1997) Androgen stimulation of lacrimal gland function in mouse models of Sjögren's syndrome. J Steroid Biochem Mol Biol 60:237–245

Theofilopoulos AN, Dixon FJ (1981) Etiopathogenesis of murine SLE. Immunological Rev 55:179–216

Toda I, Sullivan BD, Rocha EM, Da Silveira LA, Wickham LA, Sullivan DA (1999) Impact of gender on exocrine gland inflammation in mouse models of Sjögren's syndrome. Exp Eye Res 69:355–366

Walker SE, Keisler LW, Caldwell CW, Kier AB, Vom Saal FS (1996) Effects of altered prenatal hormonal environment on expression of autoimmune disease in NZB/NZW mice. Environ Health Perspect 104, Suppl 4:815–821

Zoja C, Corna D, Benedetti G, Morigi M, Donadelli R, Guglielmotti A, Pinza M, Bertani T, Remuzzi G (1998) Bindarit retards renal disease and prolongs survival in murine lupus autoimmune disease. Kidney Intern 53:726–734

I.2.2.18 Prevention of Experimentally Induced Myasthenia Gravis in Rats

PURPOSE AND RATIONALE

Myasthenia gravis is an organ specific autoimmune disease in man that results in skeletal muscles weakness. Typically, the sufferer has drooping eyelids, a blank facial expression, and weak, hesitant speech. This is due to the formation of autoantibodies against the nicotinic acetylcholine receptor (AChR). The formation of autoantibodies to acetylcholine's receptor leads to a gradual destruction of the receptors in skeletal muscles that receive nerve impulses and initiate muscle contractions. As a result, affected muscles fail to respond or react only weakly to nerve signals.

Experimental myasthenia gravis (EMG) can be induced in rats by injecting them with heterologous AChR, or with recombinant α subunits (two) of the AChR (portion of the AChR to which acetylcholine mainly binds) (Lennon et al. 1991). The animals display symptoms of myasthenia (electrophysiological evidence of altered neuromuscular function) and detectable antireceptor antibodies. The two α-subunits are plausible targets of pathogenic autoantibodies because they would allow mechanisms that depend on cross-linking, complement-mediated lysis, or hindrance of acetylcholine binding to the receptor (Schwartz 1993). The severity of the disease can vary, but most animals display, at the very least, a weakness and fatigability of foot grip. The disease gradually leads to abnormal gait and eventually the inability of the animals to walk or even right themselves.

PROCEDURE

Female rats of AO strain, 6–10 weeks old, are used. Three groups of rats are included in the experiment:

1. immunized with acetylcholine receptor (AChR)-protein and treated with test drug;
2. immunized with AChR-protein without drug, and
3. nonimmunized, nontreated control rats. The test drug is applied per os daily. First dose is administered on the day of immunization and the last on the day of sacrifice.

Immunization with AChR-Protein

AChR-protein isolated from Torpedo marmorata is emulsified with complete Freund's adjuvant and 100 µg/rat is injected intradermally in the hind foot pad. As additional adjuvant, 2.6×10^{10} *Bordetella pertussis* microorganisms is administered simultaneously by intramuscular injection in the hind leg.

Antibody Determination

Anti-AChR-protein antibodies are measured by enzyme linked immunosorbent assay (ELISA) as described by Norcross et al. (1980). AChR-protein is diluted to a final concentration of 2.5 µg/ml in 0.05 M carbonate buffer, pH 9.6. Two hundred ml of this solution is placed in each well of a microtitration plate (Flow Laboratories Inc.). After an over night incubation at 4°C, the plates are washed thoroughly with 0.01 M phosphate buffered saline (PBS) solution containing 0.05% Tween-20 (Sigma) subsequently referred to as PBS/T. Sera from all groups of rats are serially diluted in PBS/T and 200 µl is added to each micron well except in the background row (control row) and incubated at 4°C for 2 h. After washing, 200 µl of 1:1000 diluted peroxidase conjugated goat antirat immunoglobulin (Sera Lab. Sussex, England) in PBS/T are added to the micron wells and incubated for an additional 60 min at 4°C. After plates are washed, 200 µl of substrate-citrate buffer and 0.2 µl of 10% H_2O_2 are added and then incubated in the dark at room temperature for 30 min. The reaction is stopped by addition of 50 µl of 2M H_2SO_4 and the OD determined by using Titert Multiscan.

Two-color Flow Cytometry

Thymic cell suspensions are obtained by mincing tissue and passing it through 80 mm stainless mesh. After being washed three times in PBS, the cells are resuspended in PBS at a cell density of 10^7 viable cells/ml. The cell viability is determined by the trypan blue exclusion test. Erythrocytes are removed by addition of ammonium chloride. Cell staining and flow cytometric analyses are done as described by Itoyama et al. (1989). Thymocyte subsets expressing CD4 and/or CD8 molecules are defined by staining with monoclonal antibodies obtained from Serotec, Oxford, England: phycoerythrin (PE)-conjugated anti-W3/25 (CD4) and fluoresceinisothiocyanate (FITC)-conjugated anti-MRC OX8 (CD8). Two $\times 10^5$ to 1×10^6 cells suspended in 100 ml of PBS are exposed sequentially for 30 min to FITC-conjugated anti-CD8 and PE-conjugated anti-CD4 monoclonal antibodies. Isotype matched control monoclonal antibodies are used to prove the specificity of binding. Cell analysis is performed using FACScan flow cytometer from Becton Dickinson. One $\times 10^4$

events per sample are analyzed by Consort 30 and Lysis software. All data are collected and displayed on a log scale of increasing green and orange fluorescence intensity. This is presented as two-dimensional contour maps and as percentage of thymocytes by integrating counts in selected areas of the contour plots.

Stereologic Analysis of Thymuses

Thymuses of animals of all groups are prepared for light microscopic analysis. For this purpose thymus tissue is fixed in Carnoy's solution, embedded in paraffin and 3–5 µm thin sections are stained with hematoxylin and eosin. Cortex and medulla are analyzed stereologically using the point counting method described by Weible (1963). Volume density (*Vv*) of the examined structures is determined by the following equation: $Vv = Pi/Pt$, where *Pi* represents the number of points of the examined structure, and *Pt* the total number of points. *Vv* refers to the volume fraction i. e. volume of a feature per unit test volume (Williams 1981).

EVALUATION

EMG is evaluated clinically by daily examination of muscle weakness and scored as follows:

+ = weakness of grip with fatigability;
++ = abnormality of gait;
+++ = inability to walking and righting.

Immediately after appearance of clinical signs of EMG, rats are sacrificed, blood and thymuses are taken for determination of anti-AChR-protein antibodies, and histological analysis of thymuses and thymocyte subsets, respectively.

Statistical analysis of data is performed by Student's *t*-test (data of stereological analysis) and Mann-Whitney *U*-test (Results of flow cytometric analysis of thymocyte subsets).

MODIFICATIONS OF THE METHOD

McIntosh and Drachman (1987) described an *in vitro* suppressor assay using responder cells from the lymph nodes of Lewis rats immunized sc. with acetylcholine receptors emulsified in complete Freund's adjuvant and suppressor cells from spleens of rats immunized i.p. with acetylcholine receptors absorbed on bentonite. Antibodies were determined after stimulation with acetylcholine receptors from co-cultures of responder cells and putative suppressor cells treated previously with an immunosuppressant.

Araga and Blalock (1994) developed a method of altering B-cell-mediated autoimmune diseases by induction of anti-idiotypic antibodies by immunization with complementary peptides. A peptide encoded by RNA complementary to RNA for the Torpedo acetylcholine receptor main immunogenic region, AChR 67–16, was tested in the Lewis rat model of experimental autoimmune myasthenia gravis.

REFERENCES AND FURTHER READING

Arag S, Blalock JE (1994) Use of complementary peptides and their antibodies in B-cell-mediated autoimmune disease: prevention of autoimmune myasthenia gravis with a peptide vaccine. Immunomethods 5:130–135

Damjanovic M, Vidic-Dankovic B, Kosec D, Isakovic K (1993) Thymus changes in experimentally induced myasthenia gravis. Autoimmunity: 15:201–207

Drachman DB, Adams RN, McIntosh K, Pestronk A (1985) Treatment of experimental myasthenia gravis with cyclosporin A. Clin Immunol Immunopathol 34:174–188

Itoyama Y, Kira J, Fuji N, Goto I, Yamamoto N (1989) Increases in helper inducer T cells and activated T cells in HTLV-1 associated myelopathy. Ann Neurol:26:257–262

Lennon VA, Lambert EH, Leiby KR, Okarma TB, Talib S (1991) Recombinant human acetylcholine receptor α-subunit induces chronic experimental autoimmune myasthenia gravis. J Immunol, 146:2245–2248

McIntosh KR, Drachman DB (1986) Induction of suppressor cells specific for AChR in experimental autoimmune myasthenia gravis. Science 232:401–403

McIntosh KR, Drachman DB (1987) Properties of suppressor cells induced to acetylcholine receptor using cyclosporin A. Ann NY Acad Sci 505:628–638

Mrowka C, Thoenes GH, Langer KH, Bartlett RR (1994) Prevention of acute graft versus host disease (GVHD) in rats by the immunomodulating drug leflunomide. Ann Hematology 68:195–199

Norcross NL, Griffith IJ, Lettieri JA (1980) Measurement of acetylcholine receptors and anti-receptor antibodies by ELISA. Muscle Nerve 3:345–349

Oosterhuis H (1981) Observations of the natural history of myasthenia gravis and effect of thymectomy. Ann NY Acad Sci 377:678–682

Ulrichs K, Kaitschick J, Bartlett R, Müller-Ruchholtz W (1992) Suppression of natural xenophile antibodies with the novel immunosuppressive drug leflunomide. Transplant Proc 24:718–719

Williams JW, Xiao F, Foster P, Clardy C, McChesney L, Sankary H, Chong ASF (1994) Leflunomide in experimental transplantation. Control of rejection and alloantibody production, reversal of acute rejection, and interaction with cyclosporine. Transplantation 57:1223–1231

I.2.2.19 Glomerulonephritis Induced by Antibasement Membrane Antibody in Rats

PURPOSE AND RATIONALE

Masugi nephritis and other nephritis models of immunological origin in rats have been used for evaluation of immunosuppressive activity (Heymann et al. 1959; Shibata et al. 1966; Ito et al. 1983; Thoenes et al. 1989; Ogawa et al. 1990, 1991).

PROCEDURE

Preparation of Rabbit Antiserum against Rat Glomerular Basement Membrane

Glomeruli are separated from the homogenate of rat renal cortex by successive use of 3 metal sieves (150-, 180-, and 200-mesh). The basement membrane fraction is obtained by centrifugation and ultrasonic disruption. It is then digested with trypsin, dialyzed, and lyophilized. The resultant substance is employed as antigen. An emulsion of 1 mg of the antigen in 0.2 ml saline with 0.2 ml of complete Freund's adjuvant is injected intracutaneously into white rabbits once a week for 6 weeks. One week later, production of the antibasement membrane antibody is confirmed in guinea pigs by the passive cutaneous anaphylaxis test. Blood is collected from the carotid artery, incubated at 56°C for 30 min to inactivate components of the complement, and stored at –20°C until use.

Induction of Glomerulonephritis in Rats

Male Sprague-Dawley rats weighing about 300 g are injected with 0.5 ml of the rabbit antiserum via the tail vein. On the following day, they are further injected subcutaneously with an emulsion (0.25 ml) of physiological saline solution containing 5 mg of rabbit gamma-globulin in an identical volume of complete Freund's adjuvant.

Treatment

The rat antibasement antibody is injected 5 days before the start of administration of the test compound. Before the first dose, urinary total protein is determined and rats with nephritis are so assigned as to provide almost equal distribution of severity of the disease per group. The test compounds are administered orally for 14 days. The urine is collected at 7 and 14 days of treatment. After 14 days, the animals are sacrificed, blood is collected and thymus and kidneys are removed. Histopathological and immunohistochemical studies are performed in kidney tissue.

EVALUATION

Scores are given for **microscopic findings in the glomeruli:**

- cell proliferation in glomeruli
- PAS-positive granules in the epithelium of glomeruli
- fibrin deposits in Bowman's space
- adhesion to Bowman's capsule

and in **the tubuli:**

- hyaline cast
- dilation of tubuli

as well as for**immunofluorescence findings** for rat IgG, rat C3, and rabbit IgG.

Furthermore, total urinary protein, plasma total cholesterol, plasma fibrinogen, thymus/body weight ratio are compared between drug treated animals and controls by statistical means.

MODIFICATIONS OF THE METHOD

Lan et al. (1995) investigated the pathogenic role of interleukin-1 in the progression of established rat crescentic glomerulonephritis by administration of the interleukin-1 receptor antagonist IL-1ra.

Giménez et al. (1987), Thoenes et al. (1987) induced autoimmune tubulointerstitial nephritis in the brown Norway rat by injection of bovine tubular basement membrane.

Development of a systemic T-lymphocyte dependent autoimmune syndrome in brown Norway rats including glomerulonephritis with high proteinuria was induced with mercuric chloride by Baran et al. (1986), Aten et al. (1988), Lillevang et al. (1992).

Kokui et al. (1992) induced nephrosis with proteinuria in rats by intraperitoneal injection of puromycin aminonucleoside.

Lundstrom et al. (1993) studied the Heymann nephritis antigenic complex using a rat yolk sac carcinoma cell line that expresses glycoprotein 330, the main antigen in this autoimmune disease.

REFERENCES AND FURTHER READING

Aten J, Bosman CB, de Heer E, Hoedemaeker PJ, Weening JJ (1988) Cyclosporin A induces long-term unresponsiveness in mercuric chloride-induced autoimmune glomerulonephritis. Clin exp Immunol 73:307–311

Baran D, Vendeville B, Vial MC, Cosson C, Bascou C, Teychenne P, Druet P (1986) Effect of cyclosporin A on mercury-induced autoimmune glomerulonephritis in the Brown Norway rat. Clin Nephrol 25, Suppl 1:S175–S180

Cattran DC (1988) Effect of cyclosporin on active Heymann nephritis. Nephron 48:142–148

Fujita M, Ilida H, Asaka M, Izumino K, Takata M, Sasayama S (1991) Effect of the immunosuppressive agent, cyclosporin, on experimental immune complex glomerulonephritis in rats. Nephron 57:210–215

Giménez A, Leyva-Cobian F, Fiero C, Rio M, Bricio T, Mampaso F (1987) Effect of cyclosporin A on autoimmune tubulointerstitial nephritis in the brown Norway rat. Clin exp Immunol 69:550–556

Grönhagen-Riska C, von Willebrand E, Tikkanen T, Honkanen E, Miettinen A, Holthöfer H, Törnroth T (1990) The effect of cyclosporin A on the interstitial mononuclear cell

infiltration and the induction of Heymann's nephritis. Clin exp Immunol 79:266–272
Heymann W, Hackel DB, Harwood S, Wilson SGF, Hunter JLP (1959) Production of nephrotic syndrome in rats by Freund's adjuvants and rat kidney suspension. Proc Soc Exp Biol Med 100:660–664
Ito M, Yamada H, Okamoto K, Suzuki Y (1983) Crescentic type nephritis induced by anti-glomerular basement membrane (GMB) serum in rats. Jap J Pharmacol 33:1145–1154
Kokui K, Yoshikawa N, Nakamura H, Itoh H (1992) Cyclosporin reduces proteinuria in rats with aminonucleoside nephrosis. J Pathol 166:297–301
Lan HY, Nikolic-Paterson DJ, Mu W, Vannice JL, Atkins RC (1995) Interleukin-1 receptor antagonist halts the progression of established crescentic glomerulonephritis in the rat. Kidney Int 47:1303–1309
Lillevang ST, Rosenkvist J, Andersen CB, Larsen S, Kemp E, Kristensen T (1992) Single and combined effects of the vitamin D analogue KH1060 and cyclosporin A on mercuric-chloride-induced autoimmune disease in the BN rat. Clin exp Immunol 88:301–306
Lundstrom M, Orlando RA, Saedi MS, Woodward L, Kurihara H, Farquhar MG (1993) Immunocytochemical and biochemical characterization of the Heymann nephritis antigenic complex in rat L2 yolk sac cells. Am J Pathol 143:1423–1435
Ogawa T, Inazu M, Gotoh K, Hayashi S (1990) Effects of leflunomide on glomerulonephritis induced by antibasement membrane antibody in rats. Agents Actions 31:321–328
Ogawa T, Inazu M, Gotoh K, Inoue T, Hayashi S (1991) Therapeutic effects of leflunomide, a new antirheumatic drug, on glomerulonephritis induced by the antibasement antibody in rats. Clin Immunol Immunopathol 61:103–118
Reynolds J, Cashman SJ, Evans DJ, Pusey CD (1991) Cyclosporin A in the prevention and treatment of experimental autoimmune glomerulonephritis in the brown Norway rat. Clin Exp Immunol 85:28–32
Schorlemmer HU, Dickneite G (1992) Preclinical studies with 15-deoxyspergualin in various animal models for autoimmune diseases. Ann NY Acad Sci 685:155–174
Shibata S, Nagasawa T, Takuma T, Naruse T, Miyakawa Y, (1966) Isolation and properties of the soluble antigen specific for the production of nephrotoxic glomerulonephritis. I. Immunopathological demonstration of the complete antigenicity of the soluble antigen. Jpn J Exp Med 36:127–143
Shih W, Hines WH, Neilson EG (1988) Effects of cyclosporin A on the development of immune-mediated interstitial nephritis. Kidney Internat 33:1113–1118
Thoenes GH, Umscheid T, Sitter T, Langer KH (1987) Cyclosporin A inhibits autoimmune experimental tubulointerstitial nephritis. Immunol Lett 15:301–306
Thoenes GH, Sitter T, Langer KH, Bartlett RR, Schleyerbach R (1989) Leflunomide (HWA 486) inhibits experimental autoimmune tubulointerstitial nephritis in rats. Int J Immunopharmac 11:921–929
Tipping PG, Holdsworth SR (1985) Effect of cyclosporin A on antibody-induced experimental glomerulonephritis. Nephron 40:201–205
Tipping PG, Neale TJ, Holdsworth SR (1985) T lymphocyte participation in antibody-induced experimental glomerulonephritis. Kidney Internat 27:530–537
Wilson CB (1981) Nephritogenic antibody mechanisms involving antigens within the glomerulus. Immunol Rev 55:257–297
Wood A, Adu D, Birtwistle RJ, Brewer DB, Michael J (1988) Cyclosporin A and anti-glomerular basement membrane antibody glomerulonephritis in rats. Br J Path 69:189–193

I.2.2.20 Auto-Immune Uveitis in Rats

PURPOSE AND RATIONALE

The mechanisms of certain types of uveitis have been studied in animals implicating autoimmunity. Uveitis has been produced in guinea pigs following injections with homologous uveal tissue.

The method is described in detail in the Sect. O.7.3.

I.2.2.21 Inhibition of Allogenic Transplant Rejection

PURPOSE AND RATIONALE

Transplantation of allogenic organs to recipients results in rejection of the transplants. This effect can be suppressed or delayed by immunosuppressive agents. Various organs are used for allogenic transplantation in animal experiments, such as skin pieces (Schorlemmer et al. 1993), kidney (Lee 1967; Küchle et al. 1991), rat heart, rat small intestine (Xiao et al. 1944) and corneal buttons (Coupland et al. 1994). The immunosuppressive activity can be evaluated either by using a major histocompatibility complex variant strain combination or a strong allogenic system.

PROCEDURE

For **skin transplantation** male animals of inbred strains of Fischer (F334), Lewis (LEW), Brown Norway (BN), Dark Agouti (DA) rats are used. Rat tail skin (donor) is cut into square pieces of 0.5 to 1.0 cm and transplanted to the tails of recipient rats. Rejection is defined as the day when the skin graft is of red-brown color and hard consistency. As strain combination with a major histocompatibility variant, transplantation from LEW to F334 is performed. Using a strong allogenic system, the high responder DA to LEW donor recipient combination is used. The immunosuppressive agents, e. g., cyclosporine or leflunomide are given orally up to 20 days. Ten animals are used for each group.

EVALUATION

The mean values of rejection time of treated groups are compared statistically with vehicle treated controls using Student's *t*-test or the Mann Whitney U-test.

MODIFICATIONS OF THE METHOD

Schorlemmer and Kurrle (1997) used Lewis (LEW, Rtl*l) rats as receivers and Balb/c mice as donors

in a xenotransplantation model of mouse-to-rat skin grafts. Rejection was defined as the day when the skin graft turned red-brown and became hard. For quantification of xenospecific IgM and IgG antibody titers, the test sera (dilution 1:10) were incubated with 1×10^6 purified T-cells (by sheep anti-mouse dynabeads, Deutsche Dynal GmbH, Hamburg, Germany) from Balb/c donor spleens for 30 min at 4°C. The cells were washed 3 times with phosphate buffered saline (pH 7.2) and then stained for IgG or IgM xenoantibodies; 50 µl of either FITC-conjugated goat antibodies, specific for the Fc-portion of rat IgG or specific for the µ-chain of rat IgM were added. After 30 min at 4°C the cells were washed twice and analyzed by flow cytometry.

Techniques for transplantation of several organs have been elaborated.

For **kidney transplantation** male rats, 5–7 months of age, are used as donors and recipients for the orthotopic right kidney transplantation as described by Lee (1967) with a modification of ureter-ureter anastomosis (Thoenes et al. 1974). Because bilateral nephrectomy is performed at transplantation, animal survival is dependent upon the allograft's function. All rats that do not excrete urine on the first postoperative day are excluded from further studies. As a control concerning long survival, syngeneically transplanted rats are maintained up to 300 days.

Engelbrecht et al. (1992) described a new rapid technique for renal transplantation in the rat. The method combines a special sleeve anastomotic technique for the renal artery, convential end-to-end anastomosis of the renal vein, and implantation of the ureter into the bladder.

A porcine renal transplant model has been used by Almond et al. (1992).

Peters et al. (1993) reviewed the therapeutic potential of tacrolimus in renal and hepatic transplantation.

For studying **heart transplantation**, heterotopic implantation of hearts from BN to LEW rats is performed (Williams et al. 1993). The diagnosis of rejection is established once the palpable cardiac allograft impulse ceases. Further studies with rat cardiac allografts have been performed by Hancock et al. (1990). The Fischer 344 rat (donor)/Long Evans rat (recipient) combination was used by Kahn et al. (1991). Walpoth et al. (1993) used magnetic resonance spectroscopy for assessing myocardial rejection in the transplanted rat heart.

Shiraishi et al. (1995) evaluated the effectiveness of the interleukin-1 receptor antagonist IL-1ra in the immune and inflammatory responses to rat heart allografts.

Cardiac transplantation between inbred rat strains that differ for weak histocompatibility antigens is associated with the development of arteriosclerosis in arteries of the donor graft myocardium (Carmer et al. 1990; Adams et al. 1992).

A heterotopic rat **heart-transplant model** and the influence of infection was described by Kobayashi et al. (1993).

The **hamster to rat cardiac xenograft** model has been used by several authors (de Masi et al. 1990; Steinbrüchel et al. 1991; van den Bogaerde et al. 1991; Woo et al. 1993; Fujino et al. 1994; Schuurman et al. 1994). The hearts from Syrian hamsters were implanted heterotopically in male Lewis rats, with anastomoses between the infrarenal abdominal aorta and inferior vena cava of the recipient and the donor aorta and right pulmonary artery, respectively.

Primate cardiac xenografts were performed by McManus et al. (1993) using cynomolgus monkeys (*Macaca fascicularis*) as donors and baboons (*Papio anubis*) as recipients.

Chronic rejection of rat **aortic allograft** was studied by Mennander et al. (1991). Administration of cyclosporin induced accelerated allograft arteriosclerosis.

Heterotopic transplantation of small intestine has been performed from BN to LEW rats. The mesenteric venous drainage is reconstructed either via the vena cava or the portal vein (Xiao et al. 1994). An isolated Thiry–Vella-loop was prepared by Xia and Kirkman (1990). Kellnar et al. (1990) described allogenic transplantation of fetal rat intestine with anastomosis to the normal bowel of the host. Langrehr et al. (1991) investigated under which circumstances graft versus host disease occurs following fully allogenic small bowel transplantation in the rat. Kirsch et al. (1991) studied the extent to which intestinal transplants in rats undergo functional and morphologic compensation.

Liver transplantation procedure has been described by Svensson et al. (1995) allowing measurement of bile secretion.

Orthotopic left **lung transplantation** was performed in inbred rats by Katayama et al. (1991).

Tracheal allografts were implanted into the abdomen of recipient rats (Davreux et al. 1993).

In vivo electrophysiology of rat **peripheral nerve transplants** was studied by Yu et al. (1990). A sciatic-tibial nerve graft was harvested from the donor rat between the sciatic notch and the ankle. In the recipient, the tibial nerve and the sural nerve were resected. The

nerve graft was placed along the natural course of the native tibial nerve. Nerve repair was performed using standard end-to-end epineural microsuture technique.

A model of neurovascularized rectus femoris **muscle transplantation** in rats was established by Muramatsu et al. (1994).

The orthotopic **transplantation of vascularized skeletal allografts** (rat distal femur and surrounding muscular cuff) has been described by Lee et al. (1995).

Long-term surviving of **limb allografts** in rats was studied by Kuroki et al. (1991). The donor and recipient limbs were prepared simultaneously by amputation at midfemur. The donor limb was fixed orthotopically by Kirschner wire. The donor and recipient femoral arteries, veins and sciatic nerves were anastomosed using a microsurgical technique.

For **cornea transplantation** Brown Norway rats ($RT1^{1xn}$) serve as donors and Lewis rats ($RT1^{1}$) as recipients (Coupland et al. 1994). Both the donor and recipient rats are anesthetized with xylazine hydrochloride and ketamine hydrochloride. Twenty min prior to surgery the recipient rats also receive 0.5 mg/kg atropine sc. and phenylephrine hydrochloride 5% eyedrops. Under sterile conditions and using an operation microscope, two donor corneal buttons (3.5 mm) are harvested from the donor rat using a trephine and curved Castroviejo scissors. The donor animals are then sacrificed by ether inhalation. The left eyes of the recipient rats are prepared by removing a central 3.0-mm button using a trephine and curved Castroviejo scissors. A drop of sterile methylcellulose (1%) is placed over the 3.0-mm corneal opening before the donor cornea is fixed with 10 interrupted sutures. The anterior chamber is not re-established following surgery. Prior to closure of the eyelids with 3 or 4 interrupted sutures, Polyspectran eyelid gel is placed over the operated eye. Forty-eight hours following surgery, the eyelid sutures are removed, allowing for the first time assessment of the cornea on the slit-lamp microscope. Slit-lamp evaluations are performed every 2–3 days under i.m. anesthesia with ketamine, with assessment of the cornea by scoring graft opacity, edema and vascularization.

REFERENCES AND FURTHER READING

Adams DH, Tiney NL, Collins JJ, Karnovsky MJ (1992) Experimental graft arteriosclerosis. Transplantation 53:1115–1119

Almond PS, Moss A, Nakhleh R, Melin M, Chen S, Salazar A, Shirabe K, Matas A (1992) Rapamycin in a renal transplant model. Ann NY Acad Sci 685:121–122

Bartlett RR, Dimitrijevic M, Mattar T, Zielinski T, Germann T, Rüde E, Thoenes GH, Küchle CCA, Schorlemmer HU, Bremer E, Finnegan A, Schleyerbach R (1991) Leflunomide (HWA 486), a novel immunomodulating compound for the treatment of autoimmune disorders and reactions leading to transplantation rejection. Agents and Actions 32:11–21

Coupland SE, Klebe S, Karow AC, Krause L, Kruse H, Bartlett RR, Hoffmann F (1994) Leflunomide therapy following penetrating keratoplasty in the rat. Graefe's Arch Clin Exp Ophthalmol 232:622–627

Cramer DV, Chapman FA, Wu GD, Harnaha JB, Qian S, Makowka L (1990) Cardiac transplantation in the rat. Transplantation 50:554–558

Davreux CJ, Chu NH, Waddell TK, Mayer E, Patterson GA (1993) Improved tracheal allograft viability in immunosuppressed rats. Ann Thorac Surg 55:131–134

de Masi R, Alqaisi M, Araneda D, Nifong W, Thomas J, Gross U, Swanson M, Thomas F (1990) Reevaluation of total-lymphoid irradiation and cyclosporine therapy in the Syrian hamster-to-Lewis rat cardiac xenograft model. Transplantation 49:639–641

Engelbrecht G, Kahn D, Duminy F, Hickman R (1992) New rapid technique for renal transplantation in the rat. Microsurg 13:340–344

Fujino Y, Kawamura T, Hullett DA, Sollinger HW (1994) Evaluation of cyclosporine, mycophenolate mofetil, and brequinar sodium combination therapy on hamster-to-rat cardiac xenotransplantation. Transplantation 57:41–46

Hancock WW, diStefano R, Braun P, Schweizer RT, Tilney NL, Kupiec-Weglinski JW (1990) Cyclosporin and anti-interleukin 2 receptor monoclonal antibody therapy suppress accelerated rejection of rat cardiac allografts through different effector mechanisms. Transplantation 49:416–421

Kahn DR, Forrest DE, Otto DA (1991) Prolonged survival of rat cardiac allografts by donor pretreatment with methotrexate. Transplantation 51:697–700

Katayama Y, Yada I, Namikawa S, Kusagawa M (1991) Immunosuppressive effects of FK 506 in rat lung transplantation. Transplant Proc 23:3300–3301

Kellnar S, Herkomer C, Bae S, Schumacher U (1990) Allogenic transplantation of fetal rat intestine: anastomosis to the normal bowel of the host. J Pediatric Surg 25:415–417

Kirsch AJ, Kirsch SS, Kimura K, LaRosa CA, Jaffe BM (1991) The adaptive ability of transplanted rat small intestine. Surgery 109:779–787

Kobayashi J, Mavroudis C, Crawford SE, Zales VR, Backer CL (1993) A new rat infection-heart transplant model: effect of infection on graft survival studies. J Heart Lung Transplant 12:659–664

Küchle CCA, Thoenes GH, Langer KH, Schorlemmer HU, Bartlett RR, Schleyerbach R (1991) Prevention of kidney and skin graft rejection in rats by leflunomide, a new immunomodulating agent. Transplant Proc 23:1083–1086

Kuroki H, Ishida O, Daisaku H, Fukuhara K, Hatano E, Murakami T, Ikuta Y, Matsumoto AK, Akiyama M (1991) Morphological and immunological analysis of rats with long-term-surviving limb allografts induced by a short course of FK 506 or cyclosporine. Transplant Proc 23:516–520

Langrehr JM, Hoffman RA, Banner B, Stangl MJ, Monyhan H, Le KKW, Schraut WH (1991) Induction of graft-versus-host disease and rejection by sensitized small bowel allografts. Transplantation 52:399–405

Lee WP, Pan YC, Kesmarky S, Randolph MA, Fiala TS, Amarante MTJ, Weiland AJ, Yaremchuk MJ (1995) Experimental orthotopic transplantation of vascularized skeletal allografts: functional assessment and long-term survival. Plast Reconstr Surg 95:336–353

McManus RP, O'Hair DP, Komorowski R, Scott JP (1993) Immunosuppressant combinations in primate cardiac xenografts. Ann NY Acad Sci 969:281–284

Mennander A, Tiisala S, Paavonen T, Halttunen J, Häyry P (1991) Chronic rejection of rat aortic allograft. II. Administration of cyclosporin induces accelerated allograft arteriosclerosis. Transplant Int 4:173–179

Muramatsu K, Doi K, Kawai S (1994) The outcome of neurovascularized allogenic muscle transplantation under immunosuppression with cyclosporine. J Reconstr Microsurg 10:77–81

Murase N, Demetris AJ, Woo J, Tanabe M, Furuya T, Todo S, Strazl T E (1993) Graft-versus-host disease after Brown Norway-to-Lewis and Lewis-to-Brown Norway rat intestinal transplantation under FK 506. Transplantation 55:1–7

Nemoto K, Sugawara Y, Mae T, Hayashi M, Abe F, Fujii A, Takeuchi T (1992) Therapeutic activity of deoxyspergualin in comparison with cyclosporin A, and its combined use with cyclosporin A and prednisolone in highly allogeneic skin transplantation in the rat. Agents Actions 36:306–311

Peters DH, Fitton A, Plosker GL, Faulds D (1993) Tacrolimus. A review of its pharmacology, and therapeutic potential in hepatic and renal transplantation. Drug 46:746–794

Schorlemmer HU, Kurrle R (1997) Synergistic activity of malononitrilamides with cyclosporine to control and reverse xenograft rejection. Int J Tiss Reac 19:149–156

Schorlemmer HU, Seiler FR, Bartlett RR (1993) Prolongation of allogenetic transplanted skin grafts and induction of tolerance by leflunomide, a new immunosuppressive isoxazol derivative. Transplant Proc 25:763–767

Schuurman HJ, Joergensen J, Kuipers H, Meerloo T, Lardelli P, Hiestand P, White DH, Schreier MH (1994) Vascular transplantation of Syrian hamster heart into Lewis rat: effect of brequinar, cyclosporine, cobra venom factor, and splenectomy. Transplant Proc 26:1217–1219

Shaffer D, Muanza T, Blakely ML, Simpson MA, Monaco AP (1993) Prevention of graft-versus-host-disease by RS-61443 in two different rodent models. Transplantation 55:221–223

Shiraishi M, Csete M, Yasunaga C, McDiarmid SV, Vannice JL, Busuttil RW, Shaked A (1995) The inhibitor cytokine interleukin-1 receptor antagonist synergistically augments cyclosporine immunosuppression in a rat cardiac allograft model. J Surg Res 58:465–470

Steinbrüchel DA, Madsen HH, Nielsen B, Kemp E, Larsen S, Koch C (1991) The effect of combined treatment with total lymphoid irradiation, cyclosporin A, and anti-CD4 monoclonal antibodies in a hamster-to-rat heart transplantation model. Transplant Proc 23:579–580

Svensson G, Holmberg SB, Friman S (1995) Influence of liver transplantation and cyclosporin on bile secretion – an experimental study in the rat. Transpl Int 8:27–34

Ulrichs K, Kaitschick J, Bartlett R, Müller-Ruchholtz W (1992) Suppression of natural xenophile antibodies with the novel immunomodulating drug leflunomide. Transplant Proc 24:718–719

van den Bogaerde J, Aspinall R, Wang MW, Cary N, Lim S, Wright L, White D (1991) Induction of long-term survival of hamster heart xenografts in rats. Transplantation 52:15–20

Walpoth BH, Tschopp A, Lazeyras F, Galdikas J, Tschudi J, Altermatt H, Schaffner T, Aue WP, Althaus U (1993) Magnetic resonance spectroscopy for assessing myocardial rejection in the transplanted rat heart. J Heart Lung Transplant 12:271–282

Williams JW, Xiao F, Foster P, Chong A, Sharma S, Bartlett RR, Sankary HN (1993) Immunosuppressive effects of leflunomide in a cardiac allograft model. Transplant Proc 25:745–746

Williams JW, Xiao F, Foster P, Clardy C, McChesney L, Sankary H, Chong ASF (1994) Leflunomide in experimental transplantation. Control of rejection and alloantibody production, reversal of acute rejection, and interaction with cyclosporine. Transplantation 57:1223–1231

Woo J, Valdivia LA, Pan F, Celli S, Fung JJ, Thomson AW (1993) Cytidine potentiates the inhibitory effect of brequinar sodium on xeno-MLR, antibody production, and concordant hamster to rat cardiac xenograft survival. Ann NY Acad Sci 969:227–234

Xia W, Kirkman RL (1990) Immune function in transplanted small intestine. Transplantation 49:277–280

Xiao F, Chong ASF, Bartlett RR, Williams JW (1994) Leflunomide: a promising immunosuppressant in transplantation. In: Thomson AW, Starzl ThE (eds) Immunosuppressive Drugs. Edward Arnold, London, Boston, Melbourne, pp 203–212

Yu LT, England J, Sumner A, Larossa D, Hickey WF (1990) Electrophysiologic evaluation of peripheral nerve regeneration through allografts immunosuppressed with cyclosporin. J Reconstr Microsurg 6:317–323

Chapter J
Activity on the Gastrointestinal Tract[1]

[1] Reviewed by M. Bickel, contributions to former editions by A.W. Herling.

J.1 Salivary Glands

J.1.0.1 Measurement of Salivation

PURPOSE AND RATIONALE

Symptoms of several human diseases are manifested as increased salivation (e. g., Parkinson's disease) or decreased salivation (e. g., xerosis). Studies to find and to evaluate sialagogues, such as substance P and its synthetic derivatives, as well as to search for salivation inhibitors are necessary. Saliva excretion is greatly influenced by anesthetics. Wagner et al. (1991) proposed a simple method to study saliva secretion in conscious rats and to evaluate sialagogues and sialagogue antagonists.

PROCEDURE

Fed, male Sprague-Dawley rats (200–300 g) are weighed and distributed randomly into groups of 6 animals. Conscious rats are injected i.v., via the lateral tail vein, with either the vehicle or the sialagogue, e. g., substance P (0.3–3 µg/kg in 1 ml saline/kg). The rat's oral cavity is swabbed immediately after i.v. injection by placing and holding a pre-weighed, absorbent foam cube (e. g., 5/16", Texwipe Company, Upper Saddle River, NJ) sublingually for 10 s using a Triceps foam pencil (Texwipe Company, Upper Saddle River, NJ). Conscious rats are restrained during the 10 s collection period by gently holding the animal and opening the mouth using a plastic coated snare, which is looped around the maxillary incisors and drawn back over the animal's head and the hand holding the rat, drawn around in front of the rat and looped around the mandibular incisors. Gentle pressure on the snare opens the rat's mouth allowing the placement of the absorbent cube. Foam cubes are re-weighed immediately after use. The difference between the initial weight of the cube and the weight of the cube after use represents saliva secreted.

EVALUATION

Data are analyzed with Dunnett's *t*-test that compares several treated groups with a control group. Regression analysis is used to determine dose response and relative potency.

MODIFICATIONS OF THE METHOD

Martinez et al. (1978, 1981) inserted appropriate plastic cannulae into the main excretory ducts of the two submandibular glands in **rats**.

Giuliani et al. (1988) studied the relative contributions of various neurokinin receptors (NK-1, NK-2, NK-3) to the sialogogic response after i.v. application in urethane-anesthetized rats.

Direct cannulation of the glandular duct with polyethylene tubing was performed by Bodner et al. (1983) and Kohn et al. (1992).

Bianciotti et al. (1994, 1996) cannulated the ducts of both the submaxillary and parotid glands in male Wistar rats anesthetized with 10% ethyl urethane. No basal flow of saliva was observed from either gland, however dose-response curves could be established after intravenous injection of sialogogic agents, such as methacholine (0.3 to 10.0 µg/kg), norepinephrine (3 to 60 µg/kg), isoproterenol (1 to 30 µg/kg), methoxamine (30 to 300 µg/kg), substance P (0.3 to 10.0 µg/kg). Atrial natriuretic factor enhanced the salivary response to methacholine, methoxamine and substance P.

Lohinai et al. (1997) determined salivary amylase secretion in conscious rats. Under ether anesthesia a catheter was introduced into the esophagus for salivary juice collection and a cannula was inserted into the jugular vein for infusions. After post-anesthesia recovery, submaximal carbachol infusion was given as a background to obtain steady secretion because of the low basal secretory rate. After application of drugs, volume and amylase were determined in saliva samples collected for 30 min.

Iwabuchi et al. (1994) studied salivary secretion after administration of a muscarinic agonist in MRL/lpr **mice**. Saliva were collected from the floor of the mouth of anesthetized rats with a capillary micropipette every 5 min for 60 min.

A method for the quantitative comparison of atropine substitutes on the salivary secretion of the **cat** has been published by Bülbring and Dawes (1945). Cats anesthetized with pentobarbitone were used. A cannula is tied into Wharton's duct and attached to

a bottle containing tap-water. The tap-water, displaced by the saliva, passes out of the bottle through a tube which actuates a drop timer.

Ekström et al. (1994) used morphometric analyses to study the parotid acinar degranulation in cats after stimulation of the parasympathetic auriculo-temporal nerve.

Izumi and Karita (1994, 1995a, b) investigated the secretory and vasodilator effects of nerve stimulation in the submandibular gland of cats. Cats of either sex were anesthetized with ketamine and a mixture of chloralose and urethane, paralyzed by intravenous injection of pancuronium bromide and artificially ventilated. Blood flow changes in the submaxillary glands and lips of the cats were measured using a laser-Doppler flowmeter. The duct of the submandibular gland was cannulated with a polyethylene cannula inserted distal to the intersection between the chorda lingual nerve and the duct. The amount of saliva secreted in response to nerve stimulation was determined gravimetrically by collecting the saliva in pre-weighed tubes.

Boldyreff (1925) described the preparation of salivary fistulae in the **dog**.

For preparing a **parotid fistula**, a fine sound is introduced through the orifice of the parotid duct, which is found opposite to the largest upper molar tooth, to the depth of 6–8 cm. Around the orifice and at a distance of about 0.5 cm from it, four sutures are laid on the mucosa at equal distances one from the other. After this, a round piece of mucosae, about 1 cm in diameter around the orifice, with the sutures at the edge of this piece, is cut out with small sharp scissors. The duct is then separated from surrounding tissues about 2 cm from the orifice in the direction of its length. Then an opening is made through the cheek into the mouth (from the point half way on the vertical line from the front or the back corner of the eye to the mouth) to the base of the prepared duct. The orifice of the duct is now led outside by pulling out with the forceps. Four sutures on the piece of mucosa are made around it. The piece of mucosa is sutured carefully to the skin with knot sutures. The wound inside the mouth is closed with a continuous suture. The piece of mucosa must be covered daily with vaseline to prevent drying. Sutures must be taken out slowly, beginning 3 days after operation. For the first 10 days after operation it is necessary to produce on the dog an intensive salivary secretion, twice a day, by introducing into the mouth of the animal, dry bread or meat powder or 0.5% solution of hydrochloric acid. Saliva is collected into graduated test tubes.

In a similar way, one can produce a **fistula of the submaxillary or sublingual glands**, usually a common fistula for both glands, because their ducts have a common orifice.

Ogawa et al. (2003) developed a model of chronic parotitis in rats by a direct injection of complete Freund's adjuvant into the unilateral parotid gland via the parotid duct without skin incision.

Lambert et al. (1994) **cultured acinar cells** from lacrimal and submandibular glands as well as epithelial cells from rat small intestine in supplemented, serum-free media and measured the secretory components after treatment with various agents by radioimmunoassay.

REFERENCES AND FURTHER READING

Biancotti L, Elverdin JC, Vatta MS, Colatrella C, Fernández BE (1994) Atrial natriuretic factor enhances induced salivary secretion in the rat. Regul Pept 49:195–202

Biancotti L, Elverdin JC, Vatta MS, Fernández BE (1996) Atrial natriuretic factor modifies the composition of induced salivary secretion in the rat. Regul Pept 65:139–143

Bodner L, Qwarnstrom B, Omnell KA, Hand AR, Baum BJ (1983) Rat submandibular gland secretion: a bilateral and longitudinal comparative study. Comp Biochem Physiol 74A:829–831

Boldyreff WN (1925) Surgical method in the physiology of digestion. Description of the most important operations on digestive system. Ergebn Physiol 24:399–444

Bülbring E, Dawes GS (1945) A method for the assay of atropine substitutes on the salivary secretion. J Pharmacol Exp Ther 84:177–183

Ekström J, Asztély A, Helander AF, Tobin G (1994) Depletion of secretory granules from the feline parotid gland: action of NANC transmitters per se. Acta Physiol Scand 150:83–88

Guiliani S, Maggi CA, Regoli D, Drapeau G, Rovero P, Meli A (1988) NK-1 receptors mediate the tachykinin stimulation of salivary secretion: selective agonists provide further evidence. Eur J Pharmacol 150:377–379

Iwabuchi Y, Katagiri M, Masuhara T (1994) Salivary secretion and histopathological effects after single administration of the muscarinic agonist SNI-2011 in MRL/lpr mice. Arch Inter Pharmacodyn Ther 328:315–325

Izumi H, Karita K (1994) Parasympathetic-mediated reflex salivation and vasodilatation in the cat submandibular gland. Am J Physiol Regul Integr Comp Physiol 267:R747–R753

Izumi H, Karita K (1995a) Salivary secretion in cat submandibular gland mediated by chorda tympani afferents. Am J Physiol Regul Integr Comp Physiol 268:R438–R444

Izumi H, Karita K (1995b) Low-frequency subthreshold sympathetic stimulation augments maximal reflex parasympathetic salivary secretion in cats. Am J Physiol Regul Integr Comp Physiol 268:R1188–R1195

Johansson I, Linder J, Bratt P (1989) Comparison of saliva secretion rate and composition in the rat using a pentobarbital or a neuroleptanalgesic type of anesthesia. Caries Res 23:75–77

Kohn WG, Grossman E, Fox PC, Armando I, Goldstein DS, Baum BJ (1992) Effect of ionizing radiation on sympathetic nerve function in rat parotid glands. J Oral Pathol Med 21:134–137

Lambert RW, Kelleher RS, Wickham LA, Vaerman JP, Sullivan DA (1994) Neuroendocrine-immune modulation of secretory component production by rat lacrimal, salivary, and intestinal epithelial cells. Invest Ophthalmol Vis Sci 35:1192–1201

Lohnai Z, Burghardt B, Zelles T, Varga G (1997) The effect of L-arginine/nitric oxide pathway on salivary amylase secretion in conscious rats. J Physiol Paris 91:217–221

Martinez JR, Martinez AM (1981) Stimulatory and inhibitory effects of substance P on rat submandibular secretion. J Dent Res 60:1031–1038

Martinez JR, Quissell DO, Wood DL, Giles M (1978) Secretory response to parasympathomimetic and sympathomimetic stimulation from the submaxillary gland of rats treated with reserpine. J Pharmacol Exper Ther 194:384–395

Murray CW, Cowan A, Wright DL, Vaught JL, Jacoby HI (1987) Neurokinin-induced salivation in the anesthetized rat: A three receptor hypothesis. J Pharmacol Exp Ther 242:500–506

Ogawa A, Ren K, Tsuboi Y, Morimoto T, Sato T, Iwata K (2003) A new model of experimental parotitis in rats and its implication for trigeminal nociception. Exp Brain Res 152:307–316

Wagner LE, Tomczuk BE, Yanni JM (1991) Measurement of tachykinin-induced salivation in conscious rats. J Pharmacol Meth 26:67–72

J.2 Esophagus

J.2.0.1 Tunica Muscularis Mucosae of Esophagus In Vitro

PURPOSE AND RATIONALE

The tunica muscularis mucosae preparation of the rat esophagus (Bieger and Triggle 1985; Ohia et al. 1992) has been recommended for evaluation of 5-HT_4 receptor ligands since it possesses a homogeneous population of 5-HT_4 receptors which mediates a well defined relaxant response to 5-HT (Baxter et al. 1991, 1992; Reeves et al. 1991; Waikar et al. 1992; Eglen et al. 1993, 1995; Yang et al. 1993; Gale et al. 1994; Monge et al. 1994; Sagrada et al. 1994; Elz and Keller 1995; Hegde et al. 1995; Cohen et al. 1996, 1998; Wong and Eglen 1996; Nagakura et al. 1999; Takeda et al. 1999).

PROCEDURE

Male Sprague Dawley rats (200–300 g) are sacrificed by asphyxiation with CO_2, and 2 cm segments of intrathoracic esophagus, proximal to the diaphragm, are excised and placed in Tyrode solution of the following composition (mM): NaCl 136, KCl 2.7, $MgCl_2 \cdot 6H_2O$ 1.0, NaH_2PO_4 0.4, glucose 5.6, $NaHCO_3$ 11.9, $CaCl_2$ 1.8, pH 7.4. The external muscularis propria, containing the outer longitudinal and circular muscle layers of the esophagus, is carefully removed in order to isolate the inner smooth muscle tube of the tunica muscularis mucosae. The tunica muscularis mucosae is suspended in a 10 ml tissue bath containing Tyrode solution at 37°C and aerated continuously with 95% O_2/5% CO_2. Tissues are placed under 2.5 mN tension and are left to equilibrate with Tyrode solution for 60 min (washing every 15 min) prior to starting the experiment. Responses are recorded isometrically using a Hugo Sachs Electronic (Biegestab K30) transducer coupled to a Graphtec (Linearcorder WR3310) 4-channel chart recorder.

Preparation of tunica muscularis mucosae are contracted with carbachol (3 µM, approximate EC_{50}). Concentration-effect curves (relaxation) to 5-HT (or other agonists) are constructed in a cumulative fashion, followed by washout, with a 60-min interval between the first and second curve.

In antagonist studies, the antagonist is incubated with the tissue for 60 min following washout and the second concentration-effect curve is constructed in the presence of the antagonist. Responses are measured as decreases in isometric tension and are expressed as percentage relaxation of the carbachol-induced tone.

EVALUATION

Concentration-Effect Curves and Agonist Potencies

All agonist concentration-effect curves are fitted using an nonlinear, iterative curve fitting program according to the following relationship (Parker and Waud 1971):

$$E = E_{\max}[A]^n / \left([A]^n + EC_{50}^n\right) .$$

This relationship describes curves with a maximal response $E_{\max}$, half-maximal response EC_{50} (both in terms of molar concentration), and a slope factor determined by the power n. [A] represents agonist concentration and E is response.

Antagonist Potencies

pA_2 estimates of test compounds vs. 5-HT in the rat tunica muscularis mucosae are determined by the method of Arunlakshana and Schild (1959) and computed using Statview II (Brain Power Inc., Calabassas, CA). Concentration ratios are determined using the iterated EC_{50} values in the absence and the presence of the test compounds.

All remaining pA_2 estimates are determined by the method of Furchgott (1972) using a single concentration of agonist. The method assumes a competitive interaction and is calculated as follows:

$$pA_2 = -\log([\text{antagonist}]/[\text{concentration ratio} - 1])$$

Statistics

CL (95%) and statistical significance of the difference between samples (single comparisons; unpaired Student's *t*-test) are determined using Statview II.

MODIFICATIONS OF THE METHOD

De Boer et al. (1993) divided the **rat** esophagus into two parts, cervical and thoracic, each of a length of 10–15 mm. Both parts were cut longitudinally and pinned on a silicon mat with the outer, striated muscle coat up. After dissection of the striated muscle, the remaining muscularis mucosae was divided into 4 (5×2 mm, thoracic part) and 6 (5×1.5 mm, cervical part) strips. Strips from different parts showed no differences in pharmacological behavior.

Cohen et al. (1994) found 5-HT_4 receptors in rat but not guinea pig, rabbit or dog esophageal smooth muscle.

Several authors (de Boer et al. 1993, 1995; Kelly and Houston 1996; Lezama et al. 1996; Oriowo 1997, 1998) showed that β_3-adrenoceptors mediate the relaxation of the rat esophageal muscularis mucosae.

Eglen et al. (1996) studied the functional interactions between muscarinic M_2 receptors and 5-hydroxytryptamine 5-HT_4 receptors and β_3-adrenoceptors in the isolated esophageal muscularis mucosae of the rat.

Goldhill et al. (1997) investigated the 5-HT_4 receptor modulation of tachykinergic excitation of rat esophageal tunica muscularis mucosae.

The tunica muscularis mucosae of **guinea pigs** was used by various authors:

Yoshida et al. (1993) studied the effect of a gastroprokinetic agent on electrically-evoked contractions in tunica muscularis from isolated guinea pig esophagus.

Watson et al. (1995) investigated the interactions between muscarinic M_2-receptors and β-adrenoceptors in guinea-pig esophageal muscularis mucosae.

Uchida et al. (1998a, b) examined the effect of Ba^{2+} on acetylcholine- and KCl-induced contractions and characterized the endothelin-induced contraction of the guinea-pig esophageal muscularis mucosae.

Malmberg et al. (1991) studied muscle activity of isolated muscle strips from the middle pharyngeal constrictor, the inferior pharyngeal constrictor, the cricopharyngeal muscle, and the cervical esophagus from **rabbits** in organ baths in response to drugs and electrical field stimulation.

Kohjitani et al. (1993, 1996) divided the lower esophagus of rabbits into 3 regions (lower esophagus, transitional zone, lower esophageal sphincter) and studied the influence of anesthetics and peptides on contractions induced by acetylcholine or electrical field stimulation.

Percy et al. (1997) studied the pharmacological characteristics of rabbit esophageal muscularis mucosae *in vitro*.

Based on studies by Bitar and Mahklouf (1982), Biancani et al. (1987), isolated smooth muscle cells of the lower esophageal sphincter from **cats** were used by Hillemeier et al. (1996) to investigate the influence of protein kinase C on spontaneous muscle tone. Esophagus and stomach from sacrificed cats were removed and opened along the lesser curvature. The location of the squamocolumnar junction was identified, the mucosa was peeled and removed by sharp dissection under a microscope. The underlying circular muscle layer was cut into slices 0.5 mm thick with a tissue slicer. The last slices containing the myenteric plexus, longitudinal muscle and serosa were discarded. The slices of circular muscle were placed flat on a wax surface, and tissue squares were made by cutting twice with a 2-mm blade block, the second cut at right angle of the first. Isolated smooth muscle cells were obtained by enzymatic digestion with collagenase. Agonist-induced contraction of isolated muscle cells was achieved by exposing them to IP_3 and a protein kinase C agonist. The cells were fixed in acrolein at a final concentration of 1%. The length of 30 consecutive intact cells encountered at random was measured with a phase-contrast microscope and a closed-circuit video camera.

Muscle strips from *cat* lower esophageal sphincter were used by Dobreva et al. (1994), Kortezova et al. (1994), Preiksaitis and Laurier (1998).

Uy Dong Sohn et al. (1995) investigated muscle-type-specific signal transduction pathways in esophageal and lower esophageal sphincter circular smooth muscle of cats.

Tokuhara et al. (1993) studied the influence of adrenoceptor agonists on the striated muscle portion of the esophagus by use of isolated strips from **dogs**.

Saha et al. (1993) examined the effects of nitric oxide-containing compounds on **opossum** esophageal longitudinal smooth muscle *in vitro*.

La Rocca et al. (1992) examined the effects of metoclopramide in transverse muscular strips from **pigeon** esophagus.

REFERENCES AND FURTHER READING

Arunlakshana O, Schild HO (1959) Some quantitative uses of drug antagonism. Br J Pharmacol Chemother 14:48–58

Baxter GS, Clarke DE (1992) Benzimidazolone derivatives act as 5-HT4 receptor ligands in rat oesophagus. Eur J Pharmacol 212:225–229

Baxter GS, Craig DA, Clarke DE (1991) 5-Hydroxytryptamine$_4$ receptors mediate relaxation of the rat oesophageal tunica muscularis mucosae. Naunyn-Schmiedebergs Arch Pharmacol 343:439–446

Biancani P, Hillemeier C, Bitar KN, Mahklouf FM (1987) Contractions mediated by Ca^{2+} influx in esophageal muscle and by Ca^{2+} release in the LES. Am J Physiol 253:G760–G766

Bieger D, Triggle C (1985) Pharmacological properties of mechanical responses of the rat oesophageal muscularis mucosae to vagal and field stimulation. Br J Pharmacol 84:93–106

Bitar KN, Mahklouf GM (1982) Receptors on smooth muscle cells: Characterization by contraction and specific antagonists. Am J Physiol 242:G400–G407

Cohen ML, Susemichel AD, Bloomquist W, Robertson DW (1994) 5-HT$_4$ receptors in rat but not guinea pig, rabbit or dog esophageal smooth muscle. Gen Pharmacol 25:1143–1148

Cohen ML, Bloomquist W, Schaus JM, Thompson DC, Susemichel AD, Calligaro DO, Cohen I (1996) LY353433, a potent, orally effective, long-acting 5-HT$_4$ receptor antagonist: Comparison to cisapride and RS23597–190. J Pharmacol Exp Ther 277:97–104

Cohen ML, Bloomquist W, Calligaro D, Swanson S (1998) Comparative 5-HT$_4$ receptor antagonist activity of LY353433 and its active hydroxylated metabolites. Drug Dev Res 43:193–199

Da Rocca G, Fileccia R, Mule F, Abbadessa-Urso S (1992) Neurally mediated effects of metoclopramide on pigeon oesophageal muscle. Ital J Gastroenterol 24:198–202

De Boer REP, Brouwer F, Zaagsma J (1993) The β-adrenoceptors mediating relaxation of the rat oesophageal muscularis mucosae are predominantly of the β_3- but also of the β_2-subtype. Br J Pharmacol 110:442–446

De Boer REP, Brouwer F, Zaagsma J (1995) Noradrenaline-induced relaxation of rat oesophageal muscularis mucosae: Mediation solely by innervated β_3-adrenoceptors. Br J Pharmacol 116:1945–1947

Dobreva G, Mizhorkova Z, Kortezova N, Papasova M (1994) Some characteristics of the muscularis mucosae of the cat lower esophageal sphincter. Gen Pharmacol 25:639–643

Eglen RM, Bley K, Bonhaus DW, Clark RD, Hegde SS, Johnson LG, Leung E, Wong EHF (1993) RS 23597–190: A potent and selective 5-HT$_4$ receptor antagonist. Br J Pharmacol 110:119–126

Eglen RM, Bonhaus DW, Johnson LG, Leung E, Clark RD (1995) Pharmacological characterization of two novel and potent 5-HT$_4$ receptor agonists, RS 67333 and RS 67506, *in vitro* and *in vivo*. Br J Pharmacol 115:1387–1392

Eglen RM, Peele B, Pulido-Rios MT, Leung E (1996) Functional interactions between muscarinic M_2 receptors and 5-hydroxytryptamine 5-HT$_4$ receptors and β_3-adrenoceptors in isolated oesophageal muscularis mucosae of the rat. Br J Pharmacol 119:595–601

Elz S, Keller A (1995) Preparation and *in vitro* pharmacology of 5-HT$_4$ receptor ligands. Partial agonism and antagonism of metoclopramide analogous benzoic esters. Arch Pharm 328:585–594

Furchgott RF (1972) The classification of adrenoceptors (adrenergic receptors). An evaluation from the standpoint of receptor theory. In: Blaschko H, Muscholl E (eds) Handbook of Experimental Pharmacology Vol 33, pp 283–335, Springer-Verlag Berlin

Gale JD, Grossman CJ, Whitehead JWF, Oxford AW, Bunce KT, Humphrey PPA (1994) GR113808: A novel, selective antagonist with high affinity at the 5-HT$_4$ receptor. Br J Pharmacol 111:332–338

Goldhill J, Porquet MF, Angel I (1997) Post-synaptic 5-HT$_4$ receptor modulation of tachykinergic excitation of rat oesophageal tunica muscularis mucosae. Eur J Pharmacol 323:229–233

Hegde SS, Bonhaus DW, Johnson LG, Leung E, Clark RD, Eglen RM (1995) RS 39604, a potent, selective and orally active 5-HT$_4$ receptor antagonist. Br J Pharmacol 115:1087–1095

Hillemeier C, Bitar KN, Sohn U, Biancani P (1996) Protein kinase C mediates spontaneous sphincter tone in the cat lower esophageal sphincter. J Pharm Exp Ther 277:144–149

Kelly J, Houston G (1996) β_3-adrenoceptors mediating relaxation of the oesophageal tunica muscularis mucosae and distal colon of the rat: Comparative pharmacology and their desensitization by BRL 37344. J Auton Pharmacol 16:205–211

Kohjitani A, Shirakawa J, Obara H (1993) The effect of intravenous anesthetics on acetylcholine induced contraction of rabbit lower esophagus. J Jpn Dent Soc Anesthesiol 21:81–84

Kohjitani A, Shirakawa J, Okada S, Obara H (1996) Effects of various peptides on isolated rabbit lower esophageal sphincter. Peptides 17:927–931

Kortezova N, Velkova V, Mizhorkova Z, Bredy-Dobreva G, Vizi ES, Papasova M (1994) Participation of nitric oxide in the nicotine-induced relaxation of the cat lower esophageal sphincter. J Auton Nerv Syst 50:73–78

Lezama EJ, Konkar AA, Salazar-Bookaman MM, Miller DD, Feller DR (1996) Pharmacological study of atypical beta-adrenoceptors in rat esophageal smooth muscle. Eur J Pharmacol 308:69–80

Malmberg L, Ekberg O, Ekstrøm J (1991) Effect of drugs and electrical field stimulation on isolated muscle strips from the rabbit pharyngoesophageal segment. Dysphagia 6:203–208

Monge A, del Carmen-Pena M, Palop JA, Caldero JM, Roca J, Garcia E, Romero G, del Rio J, Lasheras B (1994) Synthesis of 2-piperazinylbenzothiazole and 2-piperazinylbenzoxazole derivatives with 5-HT$_3$ antagonist and 5-HT$_4$ agonist properties J Med Chem 37:1320–1325

Nagakura Y, Akuzawa S, Miyata K, Kamato T, Suzuki T, Ito H, Yamaguchi T (1999) Pharmacological properties of a novel gastrointestinal prokinetic benzamide selective for human 5-HT$_4$ receptor versus human 5-HT$_3$ receptor. Pharmacol Res 39:375–382

Ohia SE, Cheung YD, Bieger D, Triggle CR (1992) Pharmacological profile of the 5-hydroxytryptamine receptor that mediates relaxation of rat oesophageal smooth muscle. Gen Pharmacol 23:649–658

Oriowo MA (1997) β_3-adrenoceptors mediate smooth muscle relaxation in the rat lower oesophageal sphincter. J Auton Pharmacol 17:175–182

Oriowo MA (1998) Neural inhibition of the rat lower esophageal sphincter: Role of β_3-adrenoceptor activation. Gen Pharmacol 30:37–41

Parker RB, Waud DR (1971) Pharmacological evaluation of drug receptor dissociation constants. Statistical evaluation. I. Agonists. J Pharmacol Exp Ther 177:1–12

Percy WH, Miller AJ, Brunz JT (1997) Pharmacological characteristics of rabbit esophageal muscularis mucosae *in vitro*. Dig Dis Sci 42:2537–2546

Preiksaitis HG, Laurier G (1998) Pharmacological and molecular characterization of muscarinic receptors in cat esophageal smooth muscle. J Pharmacol Exp Ther 285:853–861

Reeves JJ, Bunce KT, Humphrey PPA (1991) Investigation into the 5-hydroxytryptamine receptor mediating smooth muscle relaxation in the rat oesophagus. Br J Pharmacol 103:1067–1072

Sagrada A, Schiavi GB, Cereda E, Ladinsky H (1994) Antagonistic properties of McNeil-A-343 at 5-HT_4 and 5-HT_3 receptors. Br J Pharmacol 113:711–716

Saha JK, Hirano I, Goyal RK (1993) Biphasic effect of sodium nitroprusside on esophageal longitudinal muscle: Involvement of cGMP and eicosanoids. Am J Physiol 265 (Gastrointest Liver Physiol 28):G403–G407

Takeda M, Tsukamoto K, Mizutani Y, Suzuki T, Taniyama K (1999) Identification of SK-951, a novel benzofuran derivative, as an agonist to 5-HT_4 receptors. Jpn J Pharmacol 79:203–212

Tokuhara T, Meulemans AL, de Ridder WJE, Higashino M, Kinoshita H, Schuurkes JAJ (1993) Effect of adrenoceptor agonists on striated muscle strips of the canine oesophagus. Br J Pharmacol 110:297–302

Uchida K, Yuzuki R, Kamikawa Y (1998a) Ba^{2+} selectively inhibits receptor mediated contraction of the esophageal muscularis mucosae. Eur J Pharmacol 362:83–86

Uchida K, Yuzuki R, Kamikawa Y (1998b) Pharmacological characterization of endothelin-induced contraction in the guinea-pig oesophageal muscularis mucosae. Br J Pharmacol 125:849–857

Uy Dong Sohn, Han B, Tashjian AH Jr, Behar J, Biancani P (1995) Agonist-independent, muscle-type-specific signal transduction pathways in cat esophageal and lower esophageal sphincter circular smooth muscle. J Pharmacol Exp Ther 273:482–491

Waikar MV, Hegde SS, Ford APDW, Clarke DE (1992) Pharmacological analyses of endo-6-methoxy-8-methyl-8-azabicyclo[3.2.1]oct-3-yl-2,3-dihydro-2-oxo-1H-benzimidazole-1-carboxylate hydrochloride (DAU 6285) at the 5-hydroxytryptamine$_4$ receptor in the tunica muscularis mucosae of rat esophagus and ileum of guinea pig: role of endogenous 5-hydroxytryptamine. J Pharmacol Exp Ther 264:654–661

Watson N, Reddy H, Eglen RM (1995) Characterization of muscarinic receptor and β-adrenoceptor interactions in guinea-pig oesophageal muscularis mucosae. Eur J Pharmacol 294:779–785

Wong EHF, Eglen RM (1996) Comparison of 5-HT_4 receptors in guinea-pig colon and rat oesophagus: Effects of novel agonists and antagonists. Naunyn-Schmiedebergs Arch Pharmacol 354:145–156

Yang DC, Goldstin B, Moormann AR, Flynn DL, Gullikson GW (1993) SC-53606, a potent and selective antagonist of 5-hydroxytryptamine$_4$ receptors in isolated rat esophageal tunica muscularis mucosae. J Pharmacol Exp Ther 266:1339–1347

Yoshida N, Omoya H, Seto Y, Kawashima K, Ito T (1993) Pharmacological studies on mosapride citrate (AS-4370), a gastro-prokinetic agent. II Effects on other gastrointestinal functions. Jpn Pharmacol Ther 21:265–275

J.2.0.2 Esophageal Sphincter In Vivo

PURPOSE AND RATIONALE

Salapatek et al. (1992), Xue et al. (1996) studied the control of esophageal peristalsis and function of the lower esophageal sphincter in anesthetized cats.

PROCEDURE

Adult cats of either sex are fasted overnight. Anesthesia is induced with 15 mg/kg ketamine i.m. and maintained with i.v. infusion of 15 mg/kg/h. The cats can tolerate intubation while continuing to swallow spontaneously or with pharyngeal stimulation. Esophageal motility is continuously monitored by a multi-lumen catheter passed orally. The catheter has a sleeve (Dent 1976) which is positioned within the lower esophageal sphincter, with recording ports 2, 4, 6, and 8 cm above the lower esophageal sphincter and one port just below the sleeve. The recording catheter channels are continuously perfused with distilled water at 0.3 ml/min by means of a pressurized infusion pump. At the recording ports within the esophageal body, the system is able to record a pressure rise of 300 mm Hg/s. Pressures are recorded using transducers. Respiration is continuously monitored with a belt pneumograph placed around the animal's chest. All pressures are recorded on a Beckman eight-channel direct writing chart recorder with input couplers, preamplifiers and amplifiers while simultaneously taped on an eight channel FM tape recorder. Drugs are administered intravenously.

For each esophageal contraction, amplitude is measured at each esophageal level, using mean intraesophageal pressure as baseline. Onset of contraction is determined as the point of rapid upstroke at each level, and progression of the wave along the esophagus is expressed as the lag of time or delay (in seconds) between two adjacent recording sites. Basal lower esophageal sphincter pressure is measured using intragastric pressure as reference. Maximum lower esophageal sphincter relaxation and lower esophageal sphincter after-contraction are also assessed.

EVALUATION

Statistical analysis is performed by using one-way analysis of variance and a Student's *t*-test where appropriate.

MODIFICATIONS OF THE METHOD

Greenwood et al. (1992) used a similar multi-lumen catheter assembly system in **cats** and registered additionally the electromyogram of the mylohyoid muscle.

Further studies in cats were performed by Preiksaitis et al. (1994) and Lichtenstein et al. (1994).

Using a miniature perfused sleeve/sidehole catheter, Kawahara et al. (1994) measured gastric, lower esophageal sphincter and esophageal pressure in urethane anesthetized **rats**.

Rouzade et al. (1996) monitored manometrically esophageal, lower esophageal sphincter and fundus pressure in conscious **dogs**.

Blackshaw et al. (1995), Blackshaw and Dent (1997) measured responses of the lower esophageal sphincter in urethane-anesthetized **ferrets**.

Smid et al. (1998) studied lower esophageal sphincter function in a model of oesophagitis in ferrets. Oesophagitis was induced by acid (0.15 M HCl) and 1% pepsin infusions in anesthetized ferrets. Lower esophageal sphincter strip responses were measured *in vitro* after various agents and after electrical field stimulation.

Knudsen et al. (1994) measured esophageal pressured with a four-channel, perfused catheter assembly in lightly anesthetized **opossums**.

Further studies in opossums were performed by Harrington et al. (1991), de Arruda-Henry and Uchida-Athanasio (1994).

REFERENCES AND FURTHER READING

Blackshaw LA, Dent J (1997) Lower oesophageal sphincter responses to noxious oesophageal chemical stimuli in the ferret: Involvement of tachykinin receptors. J Auton Nerv Syst 66:189–200

Blackshaw LA, Nisyrios V, Dent J (1995) Responses of ferret lower esophageal sphincter to 5-hydroxytryptamine pathways and receptor subtypes. Am J Physiol 268 (Gastrointest Liver Physiol 31):G1004–G1011

De Arruda-Henry MAC, Uchida-Athanasio EI (1994) Effect of metoclopramide, ranitidine and droperidol on lower esophageal sphincter. Experimental study in opossum (Didelphis albiventris). Arq Gastroenterol 31:103–107

Dent JA (1976) A new technique for continuous sphincter pressure measurement. Gastroenterology 71:263–267

Greenwood B, Blank E, Dodds WJ (1992) Nicotine stimulates esophageal peristaltic contractions in cats by a central mechanism. Am J Physiol 262 (Gastrointest Liver Physiol 25):G567–G571

Harrington SS, Dodds WJ, Mittal RK (1991) Identification of longitudinal muscle activity in opossum lower esophageal sphincter. Am J Physiol 261 (Gastrointest Liver Physiol 24):G974–G980

Kawahara H, Blackshaw LA, Nisyrios V, Dent J (1994) Transmitter mechanisms in vagal afferent-induced reduction of lower esophageal sphincter pressure in the rat. J Auton Nerv Syst 49:69–80

Knudsen MA, Frøbert O, Tøttrup A (1994) The role of the L-arginine-nitric oxide pathway for peristalsis in the opossum oesophageal body. Scand J Gastroenterol 29:1083–1087

Lichtenstein GR, Reynolds JC, Ogorek CP, Parkman HP (1994) Localization and inhibitory actions of galanin at the feline lower esophageal sphincter. Regul Pept 50:213–222

Preiksaitis HG, Tremblay L, Diamant NE (1994) Cholinergic responses in the cat lower esophageal sphincter show regional variation. Gastroenterol 196:381–388

Rouzade ML, Fioramonti J, Bueno L (1996) Role des recepteurs de 5-HT_3 dans le controle par la cystokinine des relaxantions transitoires du sphincter inferieur de l'oesophage chez le chien. Gastroenterol Clin Biol 20:575–580

Salapatek AMF, Hynna-Liepert T, Diamant NE (1992) Mechanism of action of cholecystokinin octapeptide on cat lower esophageal sphincter. Am J Physiol 263 (Gastrointest Liver Physiol 26):G419–G425

Smid SD, Page AJ, O'Donnell T, Langman J, Rowland R, Blackshaw LA (1998) Oesophagitis-induced changes in capsaicin-sensitive tachykinergic pathways in the ferret lower oesophageal sphincter. Neurogastroenterol Motil 10:405–411

Xue S, Valdez D, Collman PI, Diamant NE (1996) Effect of nitric oxide synthase blockade on esophageal peristalsis and the lower esophageal sphincter in the cat. Can J Physiol Pharmacol 74:1249–1257

J.2.0.3 Permanent Fistula of the Esophagus in the Dog

PURPOSE AND RATIONALE

Esophagostomy was made for the first time by Pavlov (1902) for the purpose of obtaining pure gastric juice from a dog. Pure gastric juice can obtained in great quantities only after shame feeding from a gastric fistula, so it is necessary that the dog shall have two fistulae: esophageal and gastric fistula. The technique to prepare a permanent gastric fistula in the dog was described by Boldyreff (1925).

PROCEDURE

It is necessary to obtain beforehand a well nourished dog with a gastric fistula. The operation must be done aseptically with the usual anesthesia. The incision on the neck is made on a median line 2–3 cm below the larynx and is 12–15 cm long. The esophagus is found under the trachea and a little to the left. It is separated as little as possible from the surrounding tissue with a knife handle and pulled outside. The esophagus is now divided, cross-section, and the ends of the dissected esophagus are carefully sutured into the respective corners of the wound. In suturing the mucosa of the esophagus with the skin of the wound it is necessary to take into the suture the muscle layer of the esophagus also. After the ends of the esophagus are sutured into the corners of the wound, the part of the wound between them is closed. The wound should be covered with thick antiseptic ointment. After the operation it is necessary to examine the wound daily. The sutures must be taken out gradually beginning five or six days after the operation.

Oesophagotomy can be performed more simply, if the esophagus is not divided but a longitudinal incision, 12–15 cm long is made through its wall. The edges of this incision are sutured together with the edges of the wound in the neck. When the wound is healed this fistula can be temporarily closed during feeding by means of a bandage or with a special de-

vice. The dog can then eat and drink normally and the saliva is not lost through the fistula.

MODIFICATIONS OF THE METHODS

Boldyreff (1925) described also the preparation of crop fistulas in the **rooster**. A longitudinal incision 2–3 cm long is made through the skin in the middle part of the crop. Then, with the aid of a pair of surgical forceps the front wall of the crop is lifted up and an opening about 2 cm long is made in it with scissors. After this a fistular tube is introduced into the crop with the aid of a large hook and, if necessary, the opening of the crop is sutured with one suture tightly around the tube.

REFERENCES AND FURTHER READING

Boldyreff WN (1925) Surgical method in the physiology of digestion. Description of the most important operations on digestive system. Ergebn Physiol 24:399–444

Pavlov IP (1902) Die physiologische Chirurgie des Verdauungskanals. Ergebn Physiol Abt. 1:246–286

J.3 Gastric Function

J.3.1 Acid Secretion

J.3.1.1 Acid Secretion in Perfused Rat Stomach (Gosh and Schild Rat)

PURPOSE AND RATIONALE

Gosh and Schild (1958) introduced a method for the continuous recording of acid gastric secretion in the rat. The acid secretion can be stimulated by histamine, acetylcholine and gastrin. Moreover, the stimulated secretion can be inhibited by anti-ulcer drugs.

PROCEDURE
(MODIFIED AFTER GOSH AND SCHILD 1958)

Male Sprague-Dawley or Wistar rats weighing about 250 g are used. They are withheld from food, but not from water 18 h prior to the experiment. Four animals are used per dose of test drug or standard. Anesthesia is induced by i.p. injection of 5 ml/kg of 25% urethane solution. Body temperature is artificially stabilized by means of a rectal thermometer and a heating pad. The trachea is exposed and cannulated for artificial respiration. The jugular veins are then exposed and cannulated with polyethylene tubes bevelled at the tip. The abdomen is opened through a midline incision, the pyloro-duodenal junction exposed and a double perfusion cannula (with two lumina) is introduced through a cut in the duodenum up to the cardiac part of the stomach and secured firmly by placing a ligature around the pylorus, care being taken not to include blood vessels within the ligature. Using a peristaltic pump, the stomach is perfused continuously with 0.9% NaCl solution at 37°C. In the effluent, pH is measured with a pH-meter and continuously recorded. Gastric secretion is stimulated by continuous intravenous infusion of 100 µg/kg/h of pentagastrin or 3 mg/kg/h histamine hydrochloride or 30 µg/kg/h carbachol. As soon as acid secretion has reached a plateau, test substances or standard are injected intravenously.

EVALUATION

The maximal inhibition of acid secretion (AI_{max}) and the inhibition of acid secretion during 1 h (AI_t) are calculated.

$\boldsymbol{AI_{max}} = (pH_i - pH_s) \times (pH_b - pH_s)^{-1} \times 100$

$\boldsymbol{AI_t} = 100 - F_i \times F_s^{-1} \times 100$ whereby,

$\mathbf{pH_b}$ = pH value at basal H^+ secretion

$\mathbf{pH_s}$ = pH value at stimulated H^+ secretion

$\mathbf{pH_i}$ = highest pH value after administration of test compound

$\boldsymbol{F_s}$ = integral of pH curve over 60 min before administration of test compound

$\boldsymbol{F_i}$ = integral of pH curve over 60 min after administration of test compound.

Moreover, using various doses of the test compound and of a standard, dose-response curves can be established and activity ratios with confidence limits can be calculated.

CRITICAL ASSESSMENT OF THE METHOD

The method of Gosh and Schild being modified by several authors can be used for standardization of secretagogues, like gastrin, and for evaluation of acid secretion inhibiting anti-ulcer drugs.

MODIFICATIONS OF THE METHOD

Burn et al. (1952) described the evaluation of substances which affect gastric secretion using perfusion of the stomach in anesthetized **cats**.

Lawrence and Smith (1974) described the measurement of gastric acid secretion in the **rat** by conductivity. The stomach of an anesthetized rat is continuously perfused with 2 ml/min of an isotonic (0.308 molar) glucose solution at 37°C. The conductance of a solution depends on the total ion concentration and is therefore not specific for hydrogen ions. Since hydrogen ions have an equivalent conductance nearly

5 times greater than any other ion found in gastric juice and since they are secreted in a far greater concentration than other ions, conductivity measurements can be regarded as a relatively specific measure of hydrogen ions. Using Mullard conductivity cells (type E 791/B) and a commercially available meter (Phillips PW 9501) simultaneous measurements in 6 rats were performed.

Gallo-Torres et al. (1979) described in detail a method for the bioassay of antisecretory activity in the conscious rat with acute gastric fistula with additional collection of the biliary and pancreatic secretion by means of a catheter in the common bile duct. The gastric secretions are collected by gravity via a cannula in the most gravity dependent site of the glandular stomach.

Larsson et al. (1983) described studies in the acutely vagotomized rat. Truncal vagotomy is performed under ether anesthesia by cutting the dorsal and ventral branches of nervus vagus just below the diaphragm. The pylorus is then ligated and a polyethylene catheter (PP 200) is inserted into the duodenum, close to the pylorus. Each animal is placed in a modified Bollman cage and is allowed to recover at least 1 h before the experiment. Gastric juice is collected by free drainage in 30 min samples.

Herling and Bickel (1986) showed that gastric acid secretion in stomach-lumen perfused rats can be stimulated *in vivo* on the subreceptor level by IBMX (phosphodiesterase inhibitor) and forskolin (non-receptor activation of the adenylate cyclase). H^+/K^+-ATPase inhibitors and H_2-antagonists show, according to their different modes of action, also a different inhibitory profile in this assay.

Hammer et al. (1992) used anesthetized female Sprague-Dawley rats weighing 200–320 g. After insertion of a tracheal cannula, a 3-mm silicon tubing is placed through the mouth and advanced to the stomach. The tubing is tied to the esophagus at the neck. A 4-mm drainage tube is inserted into the stomach through a laparotomy incision and an incision in the duodenum, and ligated in place at the pylorus. Gastric perfusate (0.9% saline at 37°C) is collected on ice every 5 min for titration to pH 7.0.

REFERENCES AND FURTHER READING

Barrett AM (1966) Specific stimulation of gastric acid secretion by a pentapeptide derivative of gastrin. J Pharm Pharmac 18:633–639

Burn JH, Finney DJ, Goodwin LG (eds) (1952) Biological standardization, Chapter XVII, Gastric secretion, Oxford University Press, London, pp 332–334

Gallo-Torres HE, Kuhn D, Witt C (1979) A method for the bio-assay of antisecretory activity in the conscious rat with acute gastric fistula: Studies with cimetidine, somatostatin, and the prostaglandin E_2-analog RO 21–6937. J Pharmacol Meth 2:339–355

Gosh MN, Schild HO (1958) Continuous recording of acid gastric secretion in the rat. Br J Pharmacol Chemother 13:54–61

Hammer RA, Ochoa A, Fernandez C, Ertan A, Arimura A (1992) Somatostatin as a mediator of the effect of neurotensin on pentagastrin-stimulated acid secretion in rats. Peptides 13:1175–1179

Herling AW, Bickel M (1986) The stimulatory effect of forskolin on gastric acid secretion in rats. Eur J Pharmacol 125:233–239

Herling AW, Bickel M, Lang HJ, Weidmann K, Rösner M, Metzger H, Rippel R, Nimmesgern H, Scheunemann KH (1988) A substituted thienol[3.4-d]imidazole versus substituted benzimidazoles as H^+,K^+-ATPase inhibitors. Pharmacology 36:289–297

Larsson H, Carlsson E, Junggren U, Olbe L, Sjöstrand SE, Skånberg I, Sundell G (1983) Inhibition of gastric acid secretion by omeprazole in the dog and rat. Gastroenterology 85:900–907

Lawrence AJ, Smith GM (1974) Measurement of gastric acid secretion by conductivity. Eur J Pharmacol 25:383–389

Smith GM, Lawrence AJ, Colin-Jones DG, Schild HO (1970) The assay of gastrin in the perfused rat stomach. Br J Pharmacol 38:206–213

Wissmann H, Schleyerbach R, Schölkens B, Geiger R (1973) Struktur-Wirkungsbeziehungen beim Gastrin. Der Beitrag von Carboxylgruppen von 9- und 10-Glutaminsäure zur biologischen Aktivität. Hoppe-Seyler's Z Physiol Chem 354:1591–1598

J.3.1.2 Isolated Rat Stomach

PURPOSE AND RATIONALE

The isolated whole stomach of the rat was recommended for evaluation of H_2-receptor antagonists (Bunce and Parsons 1976).

PROCEDURE

Fed immature rats of either sex weighing 38–42 g are anesthetized with sodium pentobarbitone i.p. The abdomen is opened and the esophagus ligated close to the stomach. An incision is made in the rumen of the stomach and the contents washed out with warm Krebs-Henseleit solution. A second incision is then made at the pyloric sphincter and polyethylene cannulae are inserted and tied into the stomach via these incisions. The stomach is rapidly dissected out and placed immediately into a 10 ml organ bath containing Krebs-Henseleit solution at 37°C. The lumen of the stomach is perfused at a rate of 1 ml/min with a modified Krebs-Henseleit solution (without Na_2CO_3 and KH_2PO_4) at 37°C. Both solutions are gassed with 95% O_2/5% CO_2. The effluent perfusate from the stomach is passed over a micro dual electrode. The changes in pH are converted to a function of hydrogen ion activity by an an-

tilog function generator and continuously recorded on a potentiometric pen recorder. The drugs are added, in a volume not exceeding 0.5 ml, to the complete Krebs-Henseleit solution bathing the serosal surface of the stomach. After setting up the stomach preparation the basal H^+ output is allowed to stabilize, both under control conditions and in presence of the H_2-antagonist, before the secretory responses to histamine are investigated. The response to a dose of histamine is assessed by measuring the amount of acid secreted at peak response above the preceding basal level.

EVALUATION

The rate of acid secretion is expressed as $[H^+]$ moles $\times$ 10^{-8} per min. The effect of the antagonist is assessed by measuring the potency of the agonist. An estimate of potency is firstly obtained using the agonist alone, and then a second estimate is obtained in the presence of the agonist-antagonist combination. The potency ratio is calculated according to Finney (1964).

MODIFICATIONS OF THE METHOD

A similar method was described by Szelenyi (1981) and Stanovnik et al. (1988) using the isolated stomach of the **mouse**.

Weigert et al. (1995) evaluated the effect of the opiate receptor antagonist naloxone on vagally stimulated secretion of bombesin-like immunoreactivity, somatostatin and gastrin from the isolated rat stomach which was perfused via the celiac artery with Krebs-Ringer buffer. Vagal stimulation was performed with 1 ms, 10 V and 2, 5, 0r 20 Hz, respectively.

REFERENCES AND FURTHER READING

Bunce KT, Parsons ME (1976) A quantitative study of metiamide, a histamine H_2-antagonist on the isolated whole rat stomach J Physiol 258:453–465

Finney DJ (1964) Statistical Method in Biological Assay. 2nd ed., pp 99–128, Charles Griffin, London

Shankley NP, Black JW, Ganellin CR, Mitchell RC (1988) Correlation between log $P_{oct/H2O}$ and pK_B estimates for a series of muscarinic and histamine H_2-receptor antagonists. Br J Pharmacol 94:264–274

Stanovnik L, Logonder-Mlinšek M, Erjavec F (1988) The effect of compound 48/80 and of electric field stimulation in mast cells in the isolated mouse stomach. Agents Actions 23:300–303

Szelenyi I (1981) An isolated mammalian stomach preparation for studying the effect of substances on gastric acid secretion. Arzneim Forsch/Drug Res 31:998–1000

Weigert N, Schäffler A, Reichenberger J, Madaus S, Classen M, Schusdziarra V (1995) Effect of endogenous opioids on vagally induced release of gastrin, somatostatin and bombesin-like immunoreactivity from the perfused rat stomach. Regul Peptides 55:207–215

J.3.1.3 Chronic Gastric Fistula in Rats

PURPOSE AND RATIONALE

A permanent gastric fistula using an especially designed Pavlov's type of cannula in the rat has been described by Lane et al. (1957) and Komarow et al. (1960, 1963). Moreover, the preparation of chronically denervated gastric pouches in the rat has been reported by Alphin and Lin (1959).

PROCEDURE

For a **permanent gastric fistula** in rats Komarow et al. (1960, 1963) developed a stainless steel cannula of the type extensively used in Pavlov's laboratories. The cannula is 10–12 mm in length with an inner bore of 3 mm diameter and a bevelled flange at each end. The inner bore at one flange is threaded to permit insertion of a removable screw which acts as a stopper between experiments. The lumen of the cannula permits a snug fit with a No. 8 French catheter.

Male Wistar rats weighing 280–300 g are used. Under ether anesthesia, the left upper quadrant of the abdomen is shaved and the animal placed on its right side. An incision of 5–10 mm in length is made about 5 mm below and parallel to the lower left costal margin between the parasternal and mammary lines and the deep abdominal muscles are divided. The area of the rumenal wall is then drawn up through the incision. This area should be close to the greater curvature but far enough away from the glandular portion of the stomach to avoid sacrificing secretory mucosa. A small incision is made in the exposed portion of the rumen and a purse string suture is loosely placed around the margin of the opening. The unthreaded flange of the cannula is inserted into the rumen and the suture is pulled tight around the shaft of the cannula and tied. The incision is then closed by two layers of interrupted sutures. The deep abdominal muscle is closed first by a suture at each side of the cannula, using a bit of rumen to ensure a tight fit. The incision is closed with skin sutures.

During the postoperative period of 2–3 weeks, the animals are conditioned to the experimental procedure by keeping them in a restraining cage for several hours each day. Food is withdrawn 18 h prior to the experiment. The animal is placed in a restraining cage, the stopper screw removed from the cannula and the stomach gently washed twice with 2–3 ml warm saline, and 6 cm length of rubber catheter is inserted through the lumen of the cannula. Hourly collections of gastric fluid in a graduated centrifuge tube are then started.

The animal model can be used for physiological studies as well as for standardization of secretagogues and for measuring the inhibition of gastric secretion by anti-secretory drugs.

For preparation of **chronic denervated gastric pouches** according to Alphin and Lin (1959) male Wistar or Sprague Dawley rats weighing 250–350 g are used. Under ether anesthesia, a mid-line incision is made along the abdominal wall and the stomach is gently pulled to the outside by means of a stainless steel hook. Two small clamps are then gently applied along the stomach between the smaller and greater curvature, care being taken not to injure the blood vessels supplying the glandular and the non-glandular portions of the stomach.

An incision is made between the clamps from one end to the other end of the greater curvature with as little involvement of the mesenteries as possible. The mucosa and the muscular wall are sewed up separately. A new opening is made midway along the greater curvature of the denervated pouch into which one end of a stainless steel cannula is secured by double purse-string sutures. The stainless steel cannula is 3 cm in length with an inside diameter of 3 mm. The other end of the cannula is led through a small puncture 1 cm on the left of the midline of the abdomen. The gastric end of the cannula is firmly anchored to the body wall by silk sutures. After closing the midline incision of the body wall by silk sutures, the animal receives 150 MU procaine penicillin. The animals receive a pasted diet for some days and are kept constantly in an air-conditioned room with constant temperature during the recovery period of 2–3 weeks.

For experiments, the animals are deprived of food, but not of water prior to the test, placed in restraining cages and the gastric juice is collected in graduated centrifugation tubes. The amount of secretion into the pouch and the acidity of the fluid are measured after secretagogues, e. g. 20 mg/kg histamine s.c., alone and then two hours later after administration of potential antisecretory drugs.

EVALUATION

The effect on volume and HCl secretion at 30 min intervals after administration of the test compound is compared with the control values. The decrease is expressed as percentage of control.

MODIFICATIONS OF THE METHOD

Larsson et al. (1983) described a modified technique for the chronic fistula rat. Under methohexital anesthesia a plastic cannula is implanted in the rumen of rats close to the glandular part of the stomach wall. At the same time, a polyethylene tube (PE 50) for compound administration is inserted into the upper part of duodenum and fixed to the cannula. The duodenal tube is subcutaneously guided to the neck, where the free end is guided through the skin. One week recovery is allowed before experiments. For the experiment, the rats are placed in modified Bollman cages and 6 consecutive 1-h samples of gastric juice are collected from the gastric cannulae. After the first two collection periods, the test compounds are given intraduodenally.

Altar (1980) described design and method of implantation of a chronic gastric cannula in adult rats.

Johnson et al. (1990) described a chronic gastric cannula for feeding ethanol liquid diet to rats.

Tsukamoto et al. (1984) reported an improved method for intragastric infusion in conscious rats with simultaneous implantation of a cannula into the jugular vein for blood sampling and drug administration.

Rossowski et al. (1997) measured the inhibition of gastric secretion by adrenomedullin, amylin, calcitonin-gene related peptide and their fragments in rats equipped with chronic gastric fistulas.

Bickel et al. (2004) measured sham-feeding in rats with chronically implanted gastric fistula after treatment with an anorectic compound.

REFERENCES AND FURTHER READING

Alphin RS, Lin TM (1959) Preparation of chronic denervated gastric pouches in the rat. Am J Physiol 197:257–262

Altar A (1980) A chronic subcutaneous gastric cannula in adult rats. Pharmacol Biochem Behav 12:629–621

Bickel M, Gossel M, Geisen K, Jaehne G, Lang HJ, Rosenburg R, Sandow J (2004) Analysis of the anorectic efficacy of HMR1426 in rodents and its effects on gastric emptying in rats. Int J Obes 28:211–221

Daly MJ, Humphray JM, Stables R (1980) Inhibition of gastric acid secretion in the dog by the H_2-receptor antagonists ranitidine, cimetidine and metiamide. Gut 21:408–412

Johnson DH, Kimura RE, Galinsky RE (1990) New chronic gastric cannula for feeding ethanol liquid diet to young and old rats. J Pharmacol Meth 24:37–42

Komarow SA, Brawlow SP (1960) Studies on basal gastric secretion in chronic fistula rats. Effect of urethane and chlorpromazine. Physiologist 3:96

Komarow SA, Brawlow SP, Boyd E (1963) A permanent gastric fistula. Proc Soc Exp Biol Med 112:451–453

Lane A, Ivy AC, Ivy EK (1957) Response of the chronic gastric fistula rat to histamine. Am J Physiol 190:221–228

Larsson H, Carlsson E, Junggren U, Olbe L, Sjöstrand SE, Skånberg I, Sundell G (1983) Inhibition of gastric acid secretion by omeprazole in the dog and rat. Gastroenterology 85:900–907

Lin TM, Alphin RS (1958) Cephalic phase of gastric secretion in the rat. Am J Physiol 192:23–26

Rossowski WJ, Jing N-Y, Coy DH (1997) Adrenomedullin, amylin, calcitonin-gene related peptide and their fragments

are potent inhibitors of gastric secretion in rats. Eur J Pharmacol 336:51–63
Tsukamoto H, Reidelberger RD, French SW, Largman C (1984) Long-term cannulation model for blood sampling and intragastric infusion in the rat. Am J Physiol 247 (Regulatory Integrative Comp Physiol 16):R595–R599

J.3.1.4 Chronic Gastric Fistula in Dogs

PURPOSE AND RATIONALE

A simple technique for preparing chronic gastric fistulas in dogs which does not require placement of cannulae or tubes has been described by Foschi et al. (1984).

PROCEDURE

Male mongrel or Beagle dogs weighing 12–18 kg are used. After thiopental and halothane anesthesia, a round incision (2 cm) is made on the left side of the abdomen below the costal arch. The muscular fascial layers are cut across to either the peritoneum or the abdominal cavity. The stomach is grasped on the greater curvature, as high as possible, and is gently pulled through the abdominal wall. A round excision of the serous-muscular layer (0.5 cm diameter) is made, and then the mucosa is cut and sutured to the serous layer with catgut. A purse string of 3–0 silk is placed 1.5 cm around the gastrostomy hole to invert the opening and to form an antireflux flap. The stomach is also sutured to the peritoneum, the fascial layer, and the skin with catgut. After 5 days, a silver cannula has to be inserted once a week to avoid closure of the gastrostomy.

After 10–14 days, the animals are trained to lie in a cage to their left sides, supported by a 30° angle with the caudal part of the body raised to avoid the passage of gastric juice into the duodenum. For secretion studies, a short plastic tube is inserted through the fistula and gastric juice is collected for periods of 15 min. After 30 min, secretagogues (e. g., pentagastrin 6 µg/kg/min) are given as continuous infusion and samples collected every 15 min.

EVALUATION

The samples are titrated with 0.1 N NaOH to pH 7.0 by a pH meter. The results are expressed as volume (ml), pH, acid concentration (µE/ml), and output (mE/h).

CRITICAL ASSESSMENT OF THE METHOD

The technique described by Foschi et al. (1984) has the advantage of simplicity.

MODIFICATIONS OF THE METHODS

Boldyreff (1925) reported improvements and details of the technique described by Pavlov (1902).

Thomas (1941) described an improved cannula for gastric and intestinal fistulas using a removable flange being inserted separately into the stomach or intestine.

Emås (1960) reported on gastric secretory responses to repeated intravenous infusions of histamine and gastrin in non-anaesthetized and anesthetized cats with gastric fistula. A gastric cannula as well as a duodenal cannula were inserted.

Daly et al. (1980) described an apparatus for intragastric titration in the conscious dog. A titration display unit provides a record of the secretory response both as a digital printout and a bar chart display.

REFERENCES AND FURTHER READING

Boldyreff WN (1925) Surgical method in the physiology of digestion. Description of the most important operations on digestive system. Ergebn Physiol 24:399–444
Brittain RT, Daly MJ (1981) A review of animal pharmacology of ranitidine – a new, selective histamine H_2-antagonist. Scand J Gastroenterol 16, Suppl 69:1–8
Daly MJ, Hartley RW, Stables R (1980) An improved apparatus for intragastric titration in the conscious dog. J Pharmacol Meth 3:63–69
Emås S (1960) Gastric secretory responses to repeated intravenous infusions of histamine and gastrin in non-anesthetized and anesthetized gastric fistula cats. Gastroenterology 39:771–782
Foschi D, Ferante F, Pagani F, Rovati V (1984) A new technique for preparing continent gastric fistulas in dogs. J Pharmacol Meth 12:167–170
Larsson H, Carlsson E, Junggren U, Olbe L, Sjöstrand SE, Skånberg I, Sundell G (1983) Inhibition of gastric acid secretion by omeprazole in the dog and rat. Gastroenterology 85:900–907
Pavlov IP (1902) Die physiologische Chirurgie des Verdauungskanals. Ergebn Physiol Abt. 1:246–286
Thomas JE (1941) An improved cannula for gastric and intestinal fistulas. Proc Soc exp Biol Med 46:260–261

J.3.1.5 Heidenhain Pouch in Dogs

PURPOSE AND RATIONALE

The preparation of a chronic gastric pouch, as described by Heidenhain in 1878, is one of the classic techniques in experimental surgery. This model has much contributed to the understanding of the physiology and pathology of the stomach and to modern techniques of abdominal surgery in man. The surgical technique has been described again in detail by deVito and Harkins (1957). A preparation of chronic denervated pouches in the rat has been described by Alphin and Lin (1959). Both preparations can be used as pharmacological models for testing antisecretory drugs.

PROCEDURE

Short-haired mongrel dogs or Harrier dogs weighing 15–20 kg are fasted 24 h preoperatively. Intravenous pentobarbital sodium, 30 mg/kg, provides satisfactory anesthesia. It can be supplemented, if necessary, during operation. The abdominal part is shaved with electric clippers, then with a razor. The skin is disinfected with Zephiran-70% alcohol. Sterile drapes are applied to cover the whole surgical field. A mid-line linea alba incision from xiphoid to umbilicus provides excellent exposure and ease for closure. As the posterior sheath is divided, the large ventral fat pad present in dogs should be excised completely. A self-retaining retractor is applied and the stomach is palpated for the absence of food. Then the spleen is displaced, wrapped in warm, moist pads and laid on the ventral wall below the incision.

The stomach is pulled into the operative field. The greater curvature is held at multiple points so that the stomach is stretched out and the line of incision for the pouch is selected. The pouch should be made from the corpus of the stomach so that true parietal cell juice can be obtained. A line projected from the incisura angularis perpendicular to the proximal lesser curvature will generally fall across the junction between corpus and antrum. Appropriate division of the gastric branches of the right gastroepiploic artery at the lower end of the proposed line of transsection clears the greater curvature for 1–2 cm. The gastroepiploic artery itself should be sectioned at this site and a long rent formed on the adjacent omentum, else the omentum vessels tend to tear during subsequent manipulations.

An index finger is then inserted through this defect dorsal to the stomach to emerge higher on the greater curvature through the gastrosplenic ligament at the upper end of the proposed line of transsection. This portion of the greater curve is cleared for 1–2 cm. Von Petz clamps with their staplings are used to control bleeding and to avoid leakage of gastric content. The stomach should be kept stretched and flattened while the clamps are applied. After division between the staples, any bleeding is controlled and the cut edges of the main stomach and pouch are then oversewn with continuous sutures of black silk. The suture should be of an inverting type. Surprisingly, leakage or excessive adhesions are not a problem when serosal apposition is neglected.

The pouch so formed is about 30% of the corpus volume and provides adequate secretory volume for further studies. A cannula, made of stainless steel, 3 cm long with a bevelled flange threaded at the other end is placed in the most ventral portion of the pouch through a small incision in the anterior wall. A single purse-string of silk holds it in place. A double sheet of omentum is then wrapped about the pouch and the cannula before being pulled through the abdominal wall, about 3 cm to the left of the mid-line subcostally. It is important that the cannula be held snugly by fascia, otherwise it will readily pull out of the pouch and abdominal wall. The linea alba is closed with a continuous suture of silk and the skin with subcuticular stitches of chromic catgut. On the outside of the cannula a stainless steel jacket is screwed. For further collections, a bag is connected to the cannula by a threaded adapter, facilitating removal for daily drainage of secretions.

At the end of surgery, 300 MU penicillin and 0.5 g of streptomycin are instilled intraperitoneally. Before recovery from anesthesia the dog receives 500 ml 5% glucose in saline intravenously. The same volume is given for 3 days postoperatively together with oral fluid ad libitum. From the 4th day onward, normal food is given. Twenty-four hours secretions are collected every morning and analyzed for free HCl. A period of 7–10 days is required for full recovery from the operation. Special care has to be taken for each animal being kept separately in a suitable cage with mesh bottom.

For pharmacological studies, food is withdrawn 18 h prior to the experiment with water ad libitum. The animals are placed in Pawlow stands and a continuous i.v. infusion of either pentagastrine at a dose of 8 µg/kg/h or histamine at a dose of 0.1 mg/kg/h is administered. Secreted fluid is collected at 15 or 30 min intervals and analyzed for free HCl. As soon as the secretion has reached a plateau, test compounds are given orally or intravenously.

EVALUATION

The effect on volume and HCl secretion at 15 or 30 min intervals after administration of the test compound is compared with the control values. Maximal inhibition is calculated as percentage change against the predrug value. Secretin inhibits gastric secretion volume in a dose-dependent manner. Activity ratios for unknown preparations of secretin can be calculated by 2+2 point assays in comparison with the international standard. Gastric secretion can be stimulated by slow continuous infusion of pentagastrin, e. g., (Gastrodiagnost) 8 µg/kg/h.

The Heidenhain pouch technique can also be used for evaluation and standardization of **gastrin analogues**. Two or more doses of the test compound and the standard are given intravenously. Dose-response

curves are established using gastric juice secretion, acid secretion, or pepsin secretion, within two 15-min collection periods as parameters. Activity ratios with confidence limits can be calculated.

For evaluation of **H_2-antagonists**, a continuous infusion of histamine is given over a period of 45 min, starting with 3×10^{-8} M/kg/h. Then, the dose of histamine is doubled and infused for the next 45 min. This procedure is repeated until secretion has reached a plateau. Secretory response curves are constructed in the presence or the absence of a H_2-antagonist at a concentration between 2×10^{-6} and 5×10^{-7} M/kg/h.

To evaluate the **type of gastric acid secretion inhibition**, e. g., cholinergic, histaminergic, or gastrinergic mechanisms, either carbachol (8 µg/kg/h), or histamine (80 µg/kg/h), or pentagastrin (8 µg/kg/h), are administered as continuous i.v. infusion until a plateau of acid secretion is reached. The experiments are performed at weekly intervals with and without the administration of various doses of test compounds. Regression lines of antisecretory effects of various doses of test drugs are constructed and used for calculation of ID_{50} values. Relative potencies versus a standard, e. g., cimetidine, can be calculated by four- or six-point assays.

MODIFICATIONS OF THE METHOD

Boldyreff (1925) described a simplified method for isolation of a portion of the stomach as compared to the original method of Heidenhain (1878).

Gastric motility can be measured by balloon manometry of the Heidenhain pouch in the conscious dog. The animals are deprived of food for 18 h before the experiment, but water is allowed ad libitum. A latex balloon, connected via a polyethylene catheter to a pressure transducer (Statham P 23 BB), is introduced through the fistula cannula into the accessory stomach. Changes in intragastric pressure are measured on a frequency measurement bridge and are recorded continuously. The number and height of the pressure waves are used as indices of gastric motor activity. Secretin inhibits gastric motility dose-dependent. After injection of gastrin or gastrin analogues, a dose-dependent increase of pressure is noted over a wide dose-range.

Jacobson et al. (1966, 1967) studied gastric secretion in relation to mucosal blood flow by an antipyrine clearance technique in conscious dogs with vagally denervated gastric fundic (Heidenhain) pouches. A vagally denervated fundic pouch was so constructed that the entire arterial blood supply was delivered by the splenic artery. A non-cannulating transducer (electromagnetic flowmeter) and a hydraulic occluder were implanted on the vessel.

The Heidenhain pouch preparation was used by Carter and Grossman (1978), Kauffman et al. (1980) to study the effect of luminal pH on acid secretion evoked by topical and parenteral stimulants and the effect of topical and intravenous 16,16-dimethyl prostaglandin E_2 on gastric bicarbonate secretion.

Baker (1979) and Roszkowski et al. (1986) developed a modified Heidenhain dog pouch preparation for collecting gastric juice exclusively from the pouch during experimental periods but allowed the pouch to be an integral part of the gastrointestinal tract during non-experimental periods. The pouch is prepared using conventional techniques but, instead of being fitted with a simple cannula through the abdominal wall, a three-way cannula is used which provides passage between the exterior orifice, the pouch and the main body of the stomach. By inserting an appropriate adapter, passage is available only to the pouch and not to the main stomach or vice versa.

The Heidenhain pouch technique in dogs has been used for preclinical evaluation of various drugs, such as:

- a histamine H_2 antagonist by Uchida et al. (1993),
- dual histamine H_2 and gastrin receptor antagonists by Kawanishi et al. (1997),
- a 5-HT_4 receptor antagonist by Bingham et al. (1995),
- an other 5-HT_4 receptor antagonist by Wardle et al. (1996),
- inhibition of motilin-induced phase III contractions by pentagastrin by Yamamoto et al. (1994),
- peptide YY by Zai et al. (1996),
- reversible K^+-competitive inhibitors of the gastric H^+/K^+-ATPase by Parsons et al. (1995),
- the antiulcer agent SWR-215 by Kataoka et al. (1997),
- a selective gastrin/CCK-B receptor antagonist by Yuki et al. (1997).

Descroix-Vagne et al. (1993) used Heidenhain pouch preparations in **cats** and **rabbits** to study the effect of perfusion at pH 5.5 on acid and pepsin secretion.

REFERENCES AND FURTHER READING

Alphin RS, Lin TM (1959) Preparation of chronic denervated gastric pouches in the rat. Am J Physiol 197:257–262

Baker SA (1979) A new dog fundic pouch preparation. Pharmacologist 21:176

Bickel M, Herling AW, Rising TJ, Wirth K (1986) Antisecretory effects of two new histamine H_2-receptor antagonists. Arzneim Forsch/Drug Res 36:1358–1363

Bingham S, King BF, Rushant B, Smith MI, Gaster L, Sanger GJ (1995) Antagonism by SE 204070 of 5-HT-evoked con-

tractions in the dog stomach: An *in vivo* model of 5-HT_4 receptor function. J Pharm Pharmacol 47:219–222
Boldyreff WN (1925) Surgical method in the physiology of digestion. Description of the most important operations on digestive system. Ergebn Physiol 24:399–444
Carter DC, Grossman MI (1978) Effect of luminal pH on acid secretion evoked by topical and parenteral stimulants. J Physiol (London) 281:227–237
Descroix-Vagne M, Perret JP, Daoud-El Baba M, Gros I, Rakotomalala H, Desvigne A, Jourdan G, Nicol P (1993) Interaction between pepsin and acid secretion during fundic perfusion in cat and rabbit. Comp Biochem Physiol A. Comp Physiol 104:283–286
deVito RV, Harkins HN (1959) Techniques in Heidenhain pouch experiments. J Appl Physiol 14:138–140
Gregory RA, Tracy HJ (1964) The constitution and properties of two gastrins extracted from hog antral mucosa. Gut 5:103–114
Heidenhain R (1878) Ueber die Pepsinbildung in den Pylorusdrüsen. Pflüger's Arch ges Physiol 18:169–171
Herling AW, Bickel M, Lang HJ, Weidmann K, Rösner M, Metzger H, Rippel R, Nimmesgern H, Scheunemann KH (1988) A substituted thienol[3.4-d]imidazole versus substituted benzimidazoles as H^+,K^+-ATPase inhibitors. Pharmacology 36:289–297
Jacobson ED, Linford RH, Grossman MI (1966) Gastric secretion in relation to mucosal blood flow studied by a clearance technique. J Clin Invest 45:1–13
Jacobson ED, Swan KG, Grossman MI (1967) Blood flow and secretion in the stomach. Gastroenterology 52:414–422
Kauffman Jr GL, Reeve JJ, Grossman MI (1980) Gastric bicarbonate secretion: Effect of topical and intravenous 16,16-dimethyl prostaglandin E_2. Am J Physiol 239:G44–G48
Kataoka H, Isoi T, Kiso T, Tanaka C, Shinkawa R, Kakita T, Shogaki T, Furukawa M, Ohtsubo Y (1997) Pharmacological profiles of a new antiulcer agent, SWR-215. Biol Pharm Bull 20:28–35
Kawanishi Y, Ishihara S, Kiyama R, Hagishita S, Tsushima T, Ishikawa M, Ishihara Y (1997) Synthesis and structure-activity relationships of dual histamine H_2 and gastrin receptor antagonists with noncyclic gastrin receptor antagonistic moieties. Bioorg Med Chem 5:1425–1431
Larsson H, Carlsson E, Junggren U, Olbe L, Sjöstrand SE, Skånberg I, Sundell G (1983) Inhibition of gastric acid secretion by omeprazole in the dog and rat. Gastroenterology 85:900–907
Parsons ME, Rushant B, Rasmussen TC, Leach C, Ife RJ, Postius S, Pope AJ (1995) Properties of the reversible K^+-competitive inhibitor of the gastric H^+/K^+-ATPase, SK and F 97574. II. Pharmacological properties. Biochem Pharmacol 50:1551–1556
Roszkowski AP, Garay GL, Baker S, Schuler M, Carter H (1986) Gastric antisecretory and antiulcer properties of enprostil, (±)-11α,15α,dihydroxy-16-phenoxy-17,18,19,20-tetranor-9-oxoprosta-4,5,13(*t*)-trienoic acid methyl ester. J Pharmacol Exper Ther 239:382–389
Rudick J, Szabo T (1976) The use of gastric pouches in gastric physiology: I. Techniques in the preparation of gastric pouches. Mt. Sinai J Med 43:423–439
Tracy HJ, Gregory RA (1964) Physiological properties of a series of synthetic peptides structurally related to gastrin I. Nature 204:935–938
Uchida M, Ohba S, Ikarashi Y, Misaki N, Kawano O (1993) Effect of the novel histamine H_2 antagonist: 5,6-dimethyl-2-[4-[3-(1-piperidinomethyl)phenoxy]-(z)-2-butenylamino]-4(1H)-pyrimidone dihydrochloride on histamine-induced gastric secretion in Heidenhain pouch dogs. Arzneim Forsch/Drug Res 43:873–876
Wardle KA, Bingham S, Ellis ES, Gaster LM, Rushant B, Smith MI, Sanger GJ (1996) Selective and functional 5-hydroxytryptamine$_4$ receptor antagonism by SB 207266. Br J Pharmacol 118:665–670
Yamamoto O, Matsunaga Y, Shiba Y, Haga N, Itoh Z (1994) Inhibition of motilin-induced phase III contractions by pentagastrin in Heidenhain pouch dogs. J Pharmacol Exp Ther 271:1471–1476
Yuki H, Nishida A, Miyake A, Ito H, Akuzawa S, Takinami Y, Takemoto Y, Miyata K (1997) YM022, a potent and selective gastrin/CCK-B receptor antagonist, inhibits peptone meal-induced gastric secretion in Heidenhain pouch dogs. Dig Dis Sci 42:707–714
Zai H, Haga N, Fujino MA, Itoh Z (1996) Effect of peptide YY on gastric motor and secretory activity in vagally innervated and denervated pouch dogs. Regul Pept 61:181–188

J.3.1.6 Gastrin Activity

PURPOSE AND RATIONALE

Biological activity of gastrin and its analogues can be determined with a bioassay using the acid secretion as determined by pH-metry (Gosh and Schild 1955, 1958; Barrett 1966; Smith et al. 1970) or by measurement of conductivity according to Lawrence and Smith (1974).

Radioimmunoassays for gastrin have been developed (Jaffe and Walsh 1979) and are available as commercial kits.

PROCEDURE

Male Sprague-Dawley or Wistar rats weighing about 250 g are used. They are withheld from food, but not from water, 18 h prior to the experiment. Four animals are used per dose of test drug or standard. Anesthesia is induced by i.p. injection of 5 ml/kg of 25% urethane solution. Body temperature is artificially stabilized by means of a rectal thermometer and a heated pad. The trachea is exposed and cannulated. The jugular veins are then exposed and cannulated with polyethylene tubes bevelled at the tip. The abdomen is opened through a midline incision, the pyloro-duodenal junction exposed and a catheter with two lumina is introduced through a cut in the duodenum up to the cardiac part of the stomach and secured firmly by tying a ligature around the pylorus. Care must be taken not to include blood vessels within the ligature.

Using a peristaltic pump, the stomach is perfused continuously with a phosphate-citrate buffer at 37°C. In the effluent pH is measured with a pH-meter and continuously recorded. At the beginning, gastric secretion is stimulated by an intravenous injection of 0.5 µg/kg pentagastrin. Then, the injections are repeated in 1 h intervals with alternating doses between

0.2, 0.4, 0.8, and 1.6 µg/kg of standard or test compound. Since in this dose range linearity of the response to gastrin can be assumed a 2+2 point parallel assay is allowed. After each injection, pH or conductivity is measured for 45 min. The area under the curve after each dosage is evaluated by planimetry.

EVALUATION

Each of 4 animals receives two doses of standard and test compound in the order of a Latin square. The dose differences have to follow a logarithmic scale. The evaluation is performed with the 4 × 4 assay according to Gosh and Schild (1958).

MODIFICATIONS OF THE METHOD

Wan (1977), Chang and Lotti (1986) used CF_1 female **mice**. The whole stomach was placed in tissue baths and perfused. The effluent of the perfused stomachs was collected at 15 min intervals, and the hydrogen ion concentration was determined by titration with 0.01 M NaOH to pH 7.0, or continuously recording with a pH-meter.

Lotti and Chang (1989) tested the inhibition of gastrin-induced acid secretion by a selective non-peptide gastrin antagonist in mice, rats and **guinea pigs**.

Black and Kalindjian (2002) reviewed gastrin agonists and antagonists.

REFERENCES AND FURTHER READING

Barrett AM (1966) Specific stimulation of gastric acid secretion by a pentapeptide derivative of gastrin. J Pharm Pharmacol 18:633–639

Black JW, Kalindjian SB (2002) Gastrin agonists and antagonists. Pharmacol Toxicol 91:275–281

Chang RS, Lotti VJ (1984) Biochemical and pharmacological characterization of an extremely potent and selective non-peptide cholecystokinin antagonist. Proc Natl Acad Sci, USA 83:4923–4926

Gosh MN, Schild HO (1955) A method for the continuous recording of gastric secretion in the rat. J Physiol, London, 128:97–109

Gosh MN, Schild HO (1958) Continuous recording of acid gastric secretion in the rat. Br J Pharmacol Chemother 13:54–61

Jaffe BM, Walsh JH (1979) Gastrin and related peptides. In: Jaffe BM, Behrman HR (eds) Methods of Hormone Radioimmunoassay. Academic Press, New York, pp 455–477

Lawrence AJ, Smith GM (1974) Measurement of gastric acid secretion by conductivity. Eur J Pharmacol 25:383–389

Lotti VJ, Chang RSL (1989) A new potent and selective non-peptide gastrin antagonist and brain cholecystokinin receptor (CCK_B) ligand: L-365260. Eur J Pharmacol 162:273–280

Smith GM, Lawrence AJ, Colin-Jones DG, Schild HO (1970) The assay of gastrin using the perfused rat stomach. Br J Pharmacol 38:206–213

Wan BYC (1977) Metiamide and stimulated acid secretion from the isolated non-distended and distended mouse stomach. J Physiol (London) 226:327–346

J.3.1.7 Receptor Binding for Gastrin

PURPOSE AND RATIONALE

The gastrin gene in all mammals consists of three exons and encodes a 101 (human, mouse) or 104 (rat) precursor peptide with an N-terminal signal peptide, which is removed at residues 21 or 25 to generate progastrin. The conversion of progastrin to smaller peptides is regulated by multiple mechanisms (Dockray et al. 2001).

Binding to gastrin receptors can be determined in isolated guinea pig gastric glands (Praissman et al. 1983; Gully et al. 1993).

PROCEDURE

The gastric glands of male guinea pigs weighing between 300 and 400 g are isolated according to Berglindh and Obrink (1976). The animals are anesthetized with 30 mg/kg Nembutal. The abdomen is opened and the aorta is cannulated in a retrograde direction. Heparin solution (250 IU/ml) is injected forcefully through the cannula. After one min, the animal is bled through the cannula and a ligature is placed around the mesenteric vessels. The chest is opened and the thoracic aorta clamped. A warm (37°C) phosphate buffered saline solution is pumped into the aorta, whereupon the portal vein is opened to allow a free outflow of the perfusate. By this procedure, most of the solution is forced through the gastric blood vessels. When the stomach appears totally exsanguinated, it is rapidly removed, opened along the lesser curvature and emptied. The cardial and antral regions are discarded. The corpus is rinsed several times with phosphate buffered saline solution and blotted with filter paper.

The thoroughly washed fundic mucosa from two guinea pigs is minced with fine scissors in a standard buffer consisting of 15 mM HEPES, 130 mM NaCl, 12 mM $NaHCO_3$, 3.0 mM NaH_2PO_4, 2.0 mM $MgSO_4$, 1.0 mM $CaCl_2$, 5.0 mM glucose, 4.0 mM L-glutamine, pH 7.4. The minced tissue is washed and then incubated with 0.1% collagenase in the above mentioned standard buffer containing 0.1% bovine serum albumin in a shaker bath at 37°C. After 40 min, the glands are liberated by a series of resuspensions through a 10 ml plastic pipette, filtered through 200 µ nylon mesh (Nytex), washed and collected by centrifugation. The glands are then resuspended in 40 ml of the standard binding buffer containing 0.1% bovine serum albumin at pH 7.4. Two ml aliquots are transferred into 15 ml plastic centrifuge tubes. The amount of protein

contained in fundic glands is determined according to Lowry et al. (1951).

[^{125}I]Gastrin binding is measured in the presence of 0.4 ml of gland suspension in triplicate tubes that contain 50 µl of either buffer, unlabeled gastrin (1 µM), or displacers at the desired concentration and 50 µl of [^{125}I] gastrin (70 pM final concentration). After 90 min of incubation at 37°C, the mixture is layered over 1 ml ice-cold incubation buffer in microcentrifuge tubes and is centrifuged at 10,000 *g* for 5 min. The supernatant is discarded and the radioactivity is measured in a γ-scintillation counter.

EVALUATION

IC_{50} values and K_i constants are calculated.

REFERENCES AND FURTHER READING

Berglindh T, öbrink KJ (1976) A method for preparing isolated glands from the rabbit gastric mucosa. Acta Physiol Scand 96:150–159

Brown J, Gallagher ND (1978) A specific gastrin receptor site in the rat stomach. Biochim Biophys Acta 538:42–49

Dockray GJ, Varro A, Dimaline R, Wang T (2001) The gastrins: their production and biological activities. Annu Rev Physiol 63:119–139

Gully D, Fréhel D, Marcy C, Spinazzé A, Lespy L, Neliat G, Maffrand JP, LeFur G (1993) Peripheral biological activity of SR 27897: a new potent non-peptide antagonist of CCK_A receptors. Eur J Pharmacol 232:13–19

Kopin AS, Lee YM, McBride EW, Miller LJ, Lu M, Lin HY, Kolakowski Jr LF, Beinborn M (1992) Expression cloning and characterization of the canine parietal cell gastrin receptor. Proc Natl Acad Sci, USA, 89:3605–3609

Leveland PM, Waldum HL (1991) The gastrin receptor assay. Scand J Gastroenterol 26:Suppl 180:62–69

Lowry OH, Rosebrough NJ, Farr AL, Randall RJ (1951) Protein measurement with the Folin phenol reagent. J Biol Chem 13:265–275

Praissman M, Walden ME, Pellecchia C (1983) Identification and characterization of a specific receptor for cholecystokinin on isolated fundic glands from guinea pig gastric mucosa using a biologically active ^{125}I-CCK-8 probe. J Receptor Res 3:647–665

J.3.1.8 Gastrin Releasing Peptide/Bombesin/Neuromedin

Bombesin is a tetradecapeptide originally isolated from frog skin by the group of Erspamer (Anastasi et al. 1971). Shortly before, Nakashima et al. (1970) isolated from the skin of *Rana pipiens* a peptide called ranatensin because of its contractile effects on smooth muscle. **Gastrin-releasing peptide**, which shares a C-terminus with amphibian bombesin, has been isolated from a variety of mammalian and non-mammalian species (Spindel et al. 1993). **Neuromedin B**, a decapeptide originally isolated from porcine spinal cord (Minamino et al. 1983), also shows sequence homology to bombesin and gastrin-releasing peptide. **Neuromedin N**, a six amino acid neurotensin-like peptide, shows a high affinity to brain neurotensin receptors and is rapidly inactivated by brain synaptic peptidases (Checler et al. 1990).

The peptides which belong to the bombesin family can be classified in three subgroups according to the sequence of their C-terminal tripeptide: bombesin (-His-Leu-MethNH_2), ranatensin and litorin (-His-Phe-MethNH_2), and phyllitorin (-Ser-Phe MethNH_2).

Bombesin and its homologues are known to affect a wide spectrum of biological processes (Tache et al. 1988; Parkman et al. 1994; Thomas et al. 1994; Konturek et al. 1995; Varga et al. 1994, 1995; Glad et al. 1996).

In the **gastrointestinal tract**, bombesin/gastrin-releasing peptide stimulates hormone and peptide release, stimulates gastric, pancreatic, bile and intestinal secretion, prevents gastric injury, causes smooth muscle contraction and induces epithelial growth (Dietrich et al. 1994; Kortezowa et al. 1994; Liu et al. 1995; Takehara et al. 1995; Wada et al. 1995; Weigert et al. 1995; Roberge et al. 1996; Yegen et al. 1996; Won Kyoo Cho 1997; Azay et al. 1998; Cox et al. 1998; Mercer et al. 1998; Milusheva et al. 1998; Nishino et al. 1998; Alvoro-Alonso et al. 1999; Bozkurt et al. 1999; Ladenheimer et al. 1999; Shahbazian et al. 1999).

Bombesin-related peptides inhibit **food intake** (Kirkham et al. 1994; Ladenheimer et al. 1996; Smith et al. 1997; Plamondon et al. 1998; Rushing and Gibbs 1998; Aalto et al. 1999; Edwards and Power 1999; Horstmann et al. 1999; Merali et al. 1999).

Several **central activities** of neuromedin B and gastrin-releasing peptide are reported, e. g. involvement in the hypothalamic-pituitary system (Pinski et al. 1992; Plamodon and Merali 1997; Garrido et al. 1998, 1999). Moody and Merali (2004) reviewed the behavioral implications of bombesin-like peptides and associated receptors within the brain. Roesler et al. (2004) discussed bombesin receptors as novel therapeutic targets in anxiety disorders. **Autocrine actions** of neuromedin B and gastrin-releasing peptide in small and non-small cell lung carcinomas are described (Gaudino et al. 1988; Siegfried et al. 1999).

REFERENCES AND FURTHER READING

Aalto Y, Forsgren S, Kjorell O, Funegard O, Franzen L, Henriksson P (1999) Does bombesin-like peptide mediate radiation-induced anorexia and satiety? Acta Oncol 38:1099–1102

Alvoro-Alonso I, Munoz-Acedo G, Rodriguez-Martin E, Schally AV, Arilla E (1999) Bombesin induces a reduction of somatostatin inhibition of adenyl cyclase activity, G_1 function, and somatostatin receptors in rat exocrine pancreas. Peptides 20:723–730

Anastasi A, Erspamer V, Bucci M (1971) Isolation and structure of bombesin and alytensin, two analogous peptides from the skin of European amphibians Bombina and Alytes. Experientia 27:166–167

Azay J, Nagain C, Llinares M, Devin C, Fehrentz JA, Bernad N, Roze C, Martinez J (1998) Comparative study of *in vivo* and *in vitro* activities of bombesin pseudopeptide analogs modified an the C-terminal dipeptide fragments. Peptides 19:57–63

Bozkurt A, Oktar BK, Kurtel H, Alican I, Coskun T, Yegen B (1999) Capsaicin-sensitive vagal fibres and 5-HT_3-, gastrin releasing peptide- and cholecystokinin A-receptors are involved in distension-induced inhibition of gastric emptying in the rat. Regul Pept 83:2–3

Checler F, Vincent JP, Kitabgi P (1986) Neuromedin N: High affinity interaction with brain neurotensin receptors and rapid inactivation by brain synaptic peptidases. Eur J Pharmacol 126:239–244

Cox MR, Padbury RTA, Snelling TL, Schloithe AC, Harvey JR, Toouli J, Saccone GTP (1998) Gastrin-releasing peptide stimulates gallbladder motility but not sphincter Oddi motility in Australian brush-tailed possum Dig Dis Sci 43:1275–1284

Dietrich JB, Hildebrand P, Baselgia-Jeker L, Pansky A, Eberle AN, Beglinger C (1994) Effect of BIM26226, a potent and specific bombesin receptor antagonist, on amylase release and binding of bombesin-like peptides to ARA-2J cells. Regul Pept 53:165–173

Edwards GL, Power JD (1999) The role of brain-gut peptides in the control of sodium appetite. Ann New York Acad Sci 897:192–197

Garrido MM, Martin S, Ambrosio E, Fuentes JA, Manzanares J (1998) Role of corticotropin-releasing hormone in gastrin-releasing peptide-mediated regulation of corticotropin and corticosterone secretion in male rats. Neuroendocrinology 68:116–122

Garrido MM, Manzanares J, Fuentes JA (1999) Hypothalamus, anterior pituitary and adrenal gland involvement in the activation of adrenocorticotropin and corticosterone secretion by gastrin-releasing peptide. Brain Res 828:20–26

Glad H, Svendsen P, Knuhtsen S, Olsen O, Schaffalitzki de Muckadell OB (1996) Importance of gastrin-releasing peptide on acid-induced secretin release and pancreatobiliary and duodenal bicarbonate secretion. Scand J Gastroenterol 31:993–1000

Gaudino G, Cirillo D, Naldini L, Rossino P, Comoglio PM (1988) Activation of the protein-tyrosin kinase associated with the bombesin receptor complex in small cell lung carcinomas. Proc Natl Acad Sci USA 85:2166–2170

Horstmann O, Nustede R, Schmidt W, Becker F, Stockmann H (1999) On the role of gastrin-releasing peptide in meal-stimulated exocrine pancreatic secretion. Pancreas 19:126–132

Kirkham TC, Walsh CA, Gibbs J, Smith GP, Leban J, McDermed J (1994) A novel bombesin receptor antagonist selectively blocks the satiety action of peripherally administered bombesin. Pharmacol Biochem Behav 48:808–811

Konturek SJ, Brzozowski T, Bielanski W, Schally AV (1995) Role of endogenous gastrin in gastroprotection. Eur J Pharmacol 278:203–212

Kortezova N, Mizhorkova Z, Milusheva E, Coy DH, Vizi ES, Varga G (1994) GRP-preferring bombesin receptor subtype mediates contractile activity in cat terminal ileum. Peptides 15:13331–1333

Ladenheimer E, Wirth KE, Moran TH (1996) Receptor mediation of feeding suppression by bombesin-like peptides. Pharmacol Biochem Behav 54:705–711

Ladenheimer EE, Wohn A, White WO, Schwartz GJ, Moran TH (1999) Inhibition of gastric emptying by bombesin-like peptides is depending on cholecystokinin-A receptor activation. Regul Pept 84:101–106

Liu F, Naruse S, Ozaki T, Sazi T, Kondo T, Toda Y (1995) Effect of gastrin-releasing peptide (GRP) on guinea pig gallbladder contraction *in vitro*. J Gastroenterol 30:764–767

Merali Z, McIntosh J, Anisman H (1999) Role of bombesin-related peptides in the control of food intake. Neuropeptides 33:376–386

Mercer DW, Cross JM, Chang L, Lichtenberger LM (1998) Bombesin prevents gastric injury in the rat: Role of gastrin. Dig Dis Sci 43:826–833

Milusheva EA, Kortezova NI, Mizhorkova ZN, Papasova M, Coy DH, Balint A, Vizi ES, Varga G (1998) Role of different bombesin receptor subtypes mediating contractile activity in cat upper intestinal tract. Peptides 19:549–556

Minamino N, Kangawa K, Matsuo H (1983) Neuromedin B: A novel bombesin-like peptide identified in porcine spinal cord. Biochem Biophys Res Commun 114:541–548

Moody TW, Merali Z (2004) Bombesin-like peptides and associated receptors within the brain: distribution and behavioral implications. Peptides 25:511–520

Nakajima T, Tanimura T, Pisano JJ (1970) Isolation and structure of a new vasoactive peptide Fed Proc 29:282

Nishino H, Tsunoda Y, Owyang C (1998) Mammalian bombesin receptors are coupled to multiple signal transduction pathways in pancreatic acini. Am J Physiol 274, Gastrointest Liver Physiol 37:G525–G534

Parkman HP, Vozzelli MA, Pagano AP, Cowan A (1994) Pharmacological analysis of receptors for bombesin–related peptides on guinea pig gall bladder smooth muscle. Regul Pept 52:173–180

Pinski J, Yano T, Schally AV (1992) Inhibitory effects of the new bombesin receptor antagonist RC-3095 on the luteinizing hormone release in rats. Neuroendocrinology 56:831–837

Plamondon H, Merali Z (1997) Anorectic action of bombesin requires receptor for corticotropin-releasing factor but not for oxytocin. Eur J Pharmacol 340:99–109

Plamondon H, Lambert C, Merali Z (1998) Sustained bombesin exposure results in receptor down-regulation and tolerance to the chronic but not acute effects of bombesin on ingestion. Brain Res 782:202–211

Roberge JN, Gronau KA, Brubaker PL (1996) Gastrin-releasing peptide is a novel mediator of proximal nutrient-induced proglucagon-derived peptide secretion from the distal gut. Endocrinology 137:2383–2388

Roesler R, Henriques JAP, Schwartsmann G (2004) Neuropeptides and anxiety disorders: bombesin receptors as novel therapeutic targets. Trends Pharmacol Sci 25:241–242

Rushing PA, Gibbs J (1998) Prolongation of intermeal interval by gastrin-releasing peptide depends on time of delivery. Peptides 19:1439–1442

Shahbazian A, Raichev P, Sandeva R, Kalfin R, Milenov K (1999) Effects of bombesin on the canine gallbladder motility: *In vivo* and *in vitro* experiments. Acta Physiol Pharmacol Bulg 23:39–45

Siegfried JM, Krishnamachary N, Gaither-Davis A, Gubish C, Hunt JD, Shriver SP (1999) Evidence for autocrine actions of neuromedin B and gastrin-releasing peptide in non-small lung cancer. Pulm Pharmacol Ther 12:291–302

Smith J, Perez S, Rushing PA, Smith GP, Gibbs J (1997) Gastrin releasing peptide-1–27 unlike bombesin, does not reduce sham feeding in rats. Peptides 18:1465–1467
Spindel AR, Giladi E, Segerson TP, Nagalla S (1993) Bombesin-like peptides: of ligands and receptors. Recent Progr Horm Res 48:365–391
Tache Y, Melchiorri P, Negri L (1988) Bombesin-like peptides in health and disease. Ann NY Acad Sci 547:217–267
Takehara Y, Sumii K, Sumii M, Kamiyasu T, Hamada M, Fukino Y, Yoshihara M, Tari A, Haruma K, Kajiyama G (1995) Effect of a bombesin antagonist on omeprazole-induced gastrin secretion in rats. Biomed Res Japan 16, Suppl 2:335–338
Varga G, Adrian TE, Coy DH, Reidelberger RD (1994) Bombesin receptor subtype mediation of gastroenteropancreatic hormone secretion in rats. Peptides 15:713–718
Varga G, Liehr RM, Scarpignato C, Coy DE (1995) Distinct receptors mediate gastrin-releasing peptide and neuromedin B-induced delay of gastric emptying of liquids in rats. Eur J Pharmacol 286:109–112
Wada M, Doi R, Hosotani R, Higashide S, Ibuka T, Habashita H, Nakai K, Fujii N, Imamura M (1995) Effect of a new bombesin receptor antagonist, (E)-alkene bombesin isostere, on amylase release from rat pancreatic acini. Pancreas 10:301–305
Weigert N, Schaffler A, Reichenberger J, Madaus S, Classen M, Schusdziarra V (1995) Effect of endogenous opioids on vagally induced release of gastrin, somatostatin and bombesin-like immunoreactivity from the perfused rat stomach. Regul Pept 55:207–215
Won Kyoo Cho (1997) Role of the neuropeptide, bombesin, in bile secretion. Yale J Biol Med 70:409–416
Yegen BÇ, Gürbüz V, Coúkun T, Bozkurt A, Kurtel H, Alican I, Dockray GJ (1996) Inhibitory effects of gastrin releasing peptide on gastric emptying in rats. Regul Peptides 61:175–180

J.3.1.9 Bombesin Receptor Binding

PURPOSE AND RATIONALE

Different types receptors have been described for bombesin-like peptides (von Schrenk et al. 1989; Battey et al. 1991; Rouissi et al. 1991; Severi et al. 1991; Fathi et al. 1993). The mammalian bombesin receptor subfamily of G protein coupled receptors consists of the gastrin-releasing peptide receptor (GRP-R), also called BB2, the neuromedin B receptor (NMB-R), also called BB1, and the bombesin receptor subtype 3 (BRS-3), also called bb3 (Fathi et al. 1993; Mantey et al. 1997; Donohue 1999; Jian 1999). A fourth subtype, bombesin receptor subtype 4, has been isolated from a cDNA library from the brain of the frog, *Bombina orientalis* (Katsuno et al. 1999). A ligand with high affinity to all four receptors has been identified (Pradhan et al. 1998).

Moody et al. (1978) studied the binding of the radiolabeled bombesin analogue [^{125}I]bombesin to rat brain membranes. Functional GRP-preferring bombesin receptors were identified in human melanoma cells by Pansky et al. (1997). Benya et al. (1995) expressed and characterized clones of human bombesin receptors.

PROCEDURE

BALB/3T3 fibroblasts devoid of gastrin-releasing peptide receptor (GRP-R) and neuromedin B receptor (NMB-R) are selected by clonal expansion after assaying for GRP-R or NMB-R by RNase protection and binding studies (Benya et al. 1992). These BALB/3T3 cells are stably transfected using a full length human GRP-R clone (huGRP-R transfected cells) or a full length human NMB-R clone (huNMB-R transfected cells) (Corgay et al. 1991). In both cases the receptor is subcloned into a modified version of the pCD2 plasmid and transfected using calcium phosphate precipitation. Stable transfectants are isolated in the presence of 800 µg/ml aminoglycoside G-418 (GIBCO, Waltham MA), identified by binding studies, and then maintained in DMEM containing 10% fetal bovine serum and 270 µg/ml G-418. Cells are passaged every 3–5 days at confluence by splitting 1:4.

[^{125}I-D-Tyr^{0}]NMB (2200 Ci/mmol), ^{125}I-GRP (2200 Ci/mmol), and [^{125}I-Tyr^{4}]Bn (2000 Ci/mmol) are prepared using Iodo-Gen and purified using high pressure liquid chromatography. Binding studies are performed by suspending disaggregated cells in binding buffer containing 75 pM levels of either [^{125}I-D-Tyr^{0}]NMB or [^{125}I-Tyr^{4}]Bn and 3×10^{6} cells/ml for 30 min at 22°C. Nonsaturable binding of either radiolabeled peptide is the amount of radioactivity associated with transfected cells when the incubation mixture contains either 1 µM NMB of 1 µM Bn.

The ability of various bombesin related agonists or antagonists to inhibit the binding of [^{125}I-Tyr^{4}]Bn to huGRP-R transfected cells and of [^{125}I-D-Tyr^{0}]NMB to huNMB-R transfected cells is compared.

EVALUATION

Data are expressed as the percentage of saturably bound reactivity in the absence of nonradioactive peptide. For each experiment each value is determined in duplicate, and the results are expressed as the means ± standard errors of at least 3 separate experiments.

MODIFICATIONS OF THE METHOD

Radulovic et al. (1991) studied biological effects and receptor binding affinities of pseudononapeptide bombesin/CRP receptor antagonists.

Fanger et al. (1993) identified a 63-kDa serum protein that binds somatostatin and gastrin-releasing peptide but not bombesin.

Wada et al. (1997), Ohki-Hamazaki et al. (1999), and Yamada et al. (2000a, 2000b) studied mice lacking the gastrin-releasing peptide receptor, the bombesin subtype-3 receptor or the neuromedin B receptor.

Mantey et al. (2004) and Boyle et al. (2005) described selective ligands for the bombesin receptor subtype 3.

Akeson et al. (1997) identified four amino acids in the gastrin-releasing peptide receptor that are required for high affinity agonist binding.

Ryan et al. (1998) studied the intracellular signaling of the human bombesin orphan receptor BRS-3 by various bombesin receptor agonists and antagonists.

Chave et al. (2000) analyzed the expression of bombesin-like peptides and their receptor subtypes in normal and neoplastic colorectal tissue.

Sun et al. (2000) investigated the presence and characteristics of the functional receptors for bombesin/GRP in human prostate adenocarcinoma specimens by radio-receptor assay and the mRNA expression of the three bombesin receptor subtypes by RT-PCR.

Weber et al. (2000) determined the structure of the mouse gastrin-releasing peptide receptor gene and investigated its basal promotor activity.

Radioligands for the **GRP receptor** are:

- [^{125}I][DTyr^{6}]bombesin-6–13-methylester, [^{125}I]GRP, [^{125}I][Tyr^{4}]bombesin,

for the **neuromedin B receptor:**

- [^{125}I]BH-NMB, [^{125}I][Tyr^{4}]bombesin,

for the **bombesin receptor subtype 3:**

- [^{125}I][Tyr^{6},βAla^{11},Phe^{13},Nle^{14}]bombesin-6–14 (Alexander et al. 2000).

REFERENCES AND FURTHER READING

Akeson M, Sainz E, Mantey SA, Jensen RT, Battey JF (1997) Identification of four amino acids in the gastrin-releasing peptide receptor that are required for high affinity agonist binding. J Biol Chem 272:17405–17409

Alexander S, Peters J, McKenzie G, Lewis S (2000) TiPS receptor and Ion Channel Supplement 2000, p 22

Battey JF, Way JM, Corjay HM (1991) Molecular cloning of the bombesin/gastrin-releasing peptide receptor from Swiss 3T3 cells. Proc Natl Acad Sci USA 88:395–399

Benya RV, Wada E, Battey JF, Fathi Z, Wang LH, Mantey SA, Coy DH, Jensen RT (1992) Neuromedin B receptors retain functional expression when transferred into BALB/3T3 fibroblasts: analysis of binding, kinetics, stoichiometry, modulation by guanine nucleotide binding proteins, signal transduction and comparison with natively expressed receptors. Mol Pharmacol 42:1058–1068

Benya RV, Kusui T, Pradhan TK, Battey JF, Jensen RT (1995) Expression and characterization of cloned human bombesin receptors. Mol Pharmacol 47:10–20

Boyle RG, Humphries J, Mitchell T, Showell GA, Apaya R, Iijima H, Shimada H, Arai T, Ueno H, Usui Y, Sakaki T, Wada E, Wada K (2005) The design of a new potent and selective ligand for the orphan bombesin receptor subtype 3 (BRS3) J Pept Sci 11:136–141

Chave HS, Gough AC, Palmer K, Preston SR, Primrose JN (2000) Bombesin family receptor and ligand gene expression in human colorectal cancer and normal mucosa. Br J Cancer 82:124–130

Corgay MH, Dobrzanski DJ, Way JM, Vialett J, Shapira H, Worland P, Sausville EA, Battey JF (1991) Two distinct bombesin receptor subtypes are expressed and functional in human lung carcinoma cells. J Biol Chem 266:18771–18779

Donohue PJ, Sainz E, Akeson M, Kroog GS, Mantey SA, Battey JF, Jensen RT, Northup JK (1999) An aspartate residue at the extracellular boundary of TMII and an arginine residue in TMVII of the gastrin-releasing peptide receptor interact to facilitate heterotrimeric G protein coupling. Biochemistry 38:9366–9372

Fanger BO, Wade AC, Cashman EA, Cardin AD (1993) Identification of a 63-kDa serum protein that binds somatostatin and gastrin-releasing peptide but not bombesin. Biochim Biophys Acta 1179:300–305

Fathi Z, Corjay MH, Shapira H, Wada E, Benya R, Jensen R, Viallet J, Sausville EA, Battey JF (1993) BRS-3: Novel bombesin receptor subtype selectively expressed in testis and lung carcinoma cells. J Biol Chem 268:5979–5984

Jian X, Sainz E, Clark WA, Jensen RT, Battey JF, Northup K (1999) The bombesin receptor subtypes have distinct G protein specificities. J Biol Chem 274:11573–11581

Katsuno T, Pradhan TK, Ryan RR, Mantey SA, Hou W, Donohue PJ, Akeson MA, Spindel ER, Battey JF, Coy DH, Jensen RT (1999) Pharmacology and cell biology of the bombesin receptor subtype 4 (BB-4-R). Biochemistry 38:7307–7320

Mantey SA, Weber HC, Sainz E, Akeson M, Ryan RR, Pradhan TK, Searles RP, Spindel ER, Battey JF, Coy DH, Jensen RT (1997) Discovery of a high affinity radioligand for the human orphan receptor, bombesin receptor subtype 3, which demonstrates that it has a unique pharmacology compared with other mammalian bombesin receptors. J Biol Chem 272:26062–26071

Mantey SA, Coy DH, Entsuah LK, Jensen RT (2004) Development of bombesin analogs with conformationally restricted amino acid substitutions with enhanced selectivity for the orphan receptor human bombesin receptor subtype 3. J Pharm Exp Ther 310:1161–1170

Moody TW, Pert CB, Rivier J, Brown MR (1978) Bombesin: Specific binding to rat brain membranes. Proc Natl Acad Sci USA 75:5372–5376

Ohki-Hamazaki H, Sakai Y, Kamata K, Ogura H, Okuyama S, Watase K, Yamada K, Wada K (1999) Functional properties of two bombesin-like receptors revealed by the analysis of mice lacking the neuromedin B receptor. J Neurosci 19:948–954

Pansky A, Pang F, Eberhard M, Baselgia L, Siegrist W, Baumann JB, Eberle AN, Beglinger C, Hildebrand B (1997) Identification of functional GRP-preferring bombesin receptors on human melanoma cells. Eur J Clin Invest 27:69–76

Pradhan TK, Katsuno T, Taylor JE, Kim SH, Ryan RR, Mantey SA, Donohue PJ, Weber HC, Sainz E, Battey JF, Coy DH, Jensen RT (1998) Identification of an unique ligand which has high affinity for all four bombesin receptor subtypes. Eur J Pharmacol 343:275–287

Radulovic S, Cai R-C, Serfozo P, Groot K, Redding TW, Pinski J, Schally AV (1991) Biological effects and receptor binding affinities of new pseudononapeptide bombesin/CRP receptor antagonists with N-terminal D-Trp or D-Tpi. Int J Peptide Protein Res 38:593–600

Rouissi N, Rhaleb NE, Nantel F, Dion S, Drapeau G, Regoli D (1991) Characterization of bombesin receptors in peripheral contractile organs. Br J Pharmacol 103:1141–1147

Ryan RR, Weber HC, Hou W, Sainz E, Mantey SA, Battey JF, Coy DH, Jensen RT (1998) Ability of various bombesin receptor agonists and antagonists to alter intracellular signalling of the human orphan receptor BRS-3. J Biol Chem 273:13613–13624

Severi C, Jensen RT, Erspamer V, D'Arpino L, Coy DH, Torsoli A, Delle Fabre G (1991) Different receptors mediate the action of bombesin-like peptides in gastric smooth muscle cells. Am J Physiol 260:G683–G690

Sun B, Halmos G, Schally AV, Wang X, Martinez M (2000) Presence of receptors for bombesin/gastrin-releasing peptide an mRNA for three receptor subtypes in human prostate cancers. Prostate 42:295–303

Von Schrenk T, Heinz-Erian P, Moran T, Mantey SA, Gardner JT, Jensen RT (1989) Neuromedin B receptor in esophagus: evidence for subtypes of bombesin receptors. Am J Physiol 256:G747–G758

Wada E, Watase K, Yamada K, Ogura H, Yamano M, Inomata Y, Eguchi J, Yamamoto K, Sunday ME, Maeno H, Mikoshiba K, Ohki-Kamazaki H, Wada K (1997) Generation and characterization of mice lacking gastrin-releasing peptide receptor. Biochem Biophys Res Commun 239:28–33

Weber HC, Jensen RTZ, Battey JF (2000) Molecular organization of the mouse gastrin-releasing peptide receptor and its promotor. Gene 244:137–149

Yamada K, Ohki-Hamazaki H, Wada K (2000a) Differential effects of social isolation upon body weight, food consumption, and responsiveness to novel and social environment in bombesin receptor subtye-3 (BRS-3) deficient mice. Physiol Behav 68:555–561

Yamada K, Wada E, Wada K (2000b) Bombesin-like peptides: studies on food intake and social behavior with receptor knock-out mice. Ann Med 32:519–529

J.3.1.10 Evaluation of Bombesin Receptor Antagonists as Anti-Cancer Drugs

PURPOSE AND RATIONALE

Bombesin and gastrin-releasing peptide affect the growth and differentiation of lung epithelium in the fetus and the adult. Gastrin-releasing peptide is an autocrine growth factor for various small cell carcinoma cell lines. Bombesin/gastrin-releasing peptide receptors were also identified in other human cancer tissue (Halmos et al. 1995). Therefore, bombesin- and gastrin-releasing peptide-antagonists were synthesized and tested as antitumor agents (Heimbrook et al. 1991; Qin et al. 1994a, 1995; Thomas et al. 1994; Azay et al. 1996; Casanueva et al. 1996; Halmos and Schally 1997; Moody and Jensen 1998).

The procedure of Qin et al. (1994a) on the inhibitory effect of an bombesin receptor antagonist on the growth of human pancreatic cells *in vivo* and *in vitro* is described as example of various similar studies.

PROCEDURE

Cancer Cell Line

Cancer cells of the CFPAC-1 human pancreatic cell line, originally established from a well differentiated ductal pancreatic adenocarcinoma of a 26-year-old white male with cystic fibrosis, are routinely maintained in a monolayer culture in Costar T75 culture flasks with IMDM medium containing 10% FCS, 0.5 g/liter L-glutamine, 25 mM HEPES, 3.7 g/liter $NaHCO_3$, 100 units/ml penicillin, 100 µg/ml streptomycin, and 0.25 µg/ml amphotericin B under humidified 5% CO_2 at 37°C. The cells growing exponentially are harvested by an incubation with 0.25% trypsin-EDTA in calcium- and magnesium-free Hank's balanced salt solution for 5 min at 37°C. For tumor cell implantation, a cell suspension is prepared in serum-free IMDM by repeatedly passing the cells through a G-22 needle; then the cells are diluted to a concentration of 5×10^6 cells/ml.

Implantation of Tumors in Nude Mice

Male athymic BALB/c (nu/nu) 6-week-old mice are housed in a laminar airflow cabinet under pathogen-free conditions throughout the experiments. Three nude mice receive s.c. injections in the flanks with 0.2 ml of cell suspension (1×10^6 cells) and serve as tumor donors. After 4 weeks, the implanted tumors grow to a size of about 5 mm in diameter and are removed from the mice. Tumor samples are dissected free of necrotic tissue and blood vessels and are cut into small fragments of about 8 mm^3. Under ether anesthesia, two pieces of tumor fragments are implanted s.c. by trocars on both sides of the flanks for each mouse. The mice bearing the implanted tumors are randomly divided into groups with 10 mice in each group.

The nude mice with implanted tumors start to receive injections of the bombesin antagonist or vehicle 7 days after the tumor cell injection. The treatment is continued for 25 days.

Evaluation of Tumor Growth

During the treatment, the size of the implanted tumors is measured by calipers in each mouse at 3–4 days intervals for 25 days to construct the tumor growth curve *in vivo*. Tumor volume is calculated by the formula: Tumor volume = length × width^2 × 0.5. Tumor volume

doubling time is defined as the time required for the tumors to grow from 50 mm^3 to 100 mm^3 for the control group and from 35 mm^3 to 70 mm^3 for the treatment group, respectively. The tumor growth delay time is estimated as the time difference for the treated tumors and the controls to reach a volume of 70 mm^3. At the end of the experiment, the animals are sacrificed by an overdose of ether. The tumors are removed from the animals, weighed, and immediately frozen in liquid nitrogen for measurement of DNA and protein content in tumor tissues.

Determination of DNA and Protein in Tumor Tissue

DNA in tumor tissue is determined by the method of Labara and Paigen (1979) which is based on the enhancement of fluorescence reaction upon binding bis-benzimidazole Hoechst 33528 to DNA in cell nuclei in a high ionic strength solution. Tumors collected in each group are pooled and homogenized in 10 times their volumes in a buffer consisting of 0.05 M NaH_2PO_4, 2.0 M NaCl, and 2 mM EDTA (pH 7.4). Hoechst 33528 is dissolved in the same buffer at a concentration of 1 µg/ml and filtered before use. An aliquot of tumor homogenate (0.4 ml) is suspended in 4 ml of Hoechst 33528 solution, followed by incubation in a dark room for 30 min. The reaction is measured by a fluorescence spectrophotometer at excitation and emission wavelengths of 356 and 492 nm, respectively. Calf thymus DNA type I is used as a standard.

Measurement of Cell Growth in Vitro

The effects of bombesin and the bombesin antagonist on the growth of CFPAC-1 human pancreatic cells *in vitro* is evaluated by direct cell counting and [^{3}H]thymidine incorporation assay.

Direct Cell Counting

CFPAC-1 cells collected from 60–70% confluent cultures are used for this study and seeded to 24-well culture plates (1×10^4 cells/well). After the cells are cultured in IMDM containing 10% FCS for 48 h, the medium is replaced by IMDM supplemented with 2.5% FCS and various concentrations of bombesin, bombesin antagonist, or a combination of both. The same volume of medium but without peptides is added to control wells. Following another 24 h of incubation, the culture is terminated by aspiration of the medium from the wells and washing with PBS (0.5 ml/well). The cells are trypsinized by a 10-min incubation with (0.5 ml/well) 0.25% Trypsin-EDTA. The detached cells are dispersed by repeated pipetting using a G-22 needle and syringe. The number of cells is counted by an automated electronic cell counter (Coulter Counter Model ZF).

[^{3}H]Thymidine Incorporation Assay

Single cell suspension is prepared in IMDM with 10% FCS and seeded to 24-well culture plates (1×10^4 cells/well). After 46 h of culture, the medium is changed to IMDM (0.5 ml/well) containing 2.5% FCS and various concentrations of bombesin, bombesin antagonist, or a combination of both. The same volume of medium but without peptides is added to control wells. After 24 h of culture [methyl-^{3}H]thymidine (radioactivity 25 Ci/mg) is added to each well (1µCi/well) to pulse the cells. After a 4-h incubation, the medium is removed from the wells, and the cells are fixed by Camoy's solution (1 ml/well; methanol:glacial acetic acid, 3:1, v/v) for 20 min. After washing 3 times with PBS, the cells in each well are dissolved with 0.5 ml of 0.3 N NaOH for 15 min at room temperature. The cell lysate is collected and mixed with 3 ml of Universal scintillation cocktail. The radioactivity is measured for 1 min by a liquid scintillation beta counter.

Receptor Binding Assay

Receptor binding assay is performed using intact CFPAC-1 cells in monolayer cultures. Tyr^4-bombesin is labeled with ^{125}I-Na using a Bio-Rad enzymobead iodination kit. Mono-^{125}I-Tyr^4-bombesin is purified by high performance liquid chromatography resulting in a specific activity of ^{125}I-Tyr^4-bombesin of about 2000 Ci/mmol. CFPAC-1 cells are seeded to 24-well culture plates (1×10^4 cells/well) and cultured with IMDM containing 10% FCS for 48 h. The cells in subconfluent culture are washed once with serum-free IMDM supplemented with 25 mM 4-(2-hydroxyethyl)-1-piperazineethanesulfonic acid, 10 mM $MgCl_2$, 1 mM EGTA, 10 mM monothioglycerol, 0.25 mM phenylmethylsulfonyl fluoride, aprotinin 10000 kallikrein inactivator units/liter, and 0.1% bovine serum albumin (pH 7.5), followed by an incubation for 2 h at 22°C with the same medium containing (0.5 nM) ^{125}I-Tyr^4-bombesin in the presence or absence of various concentrations of bombesin, bombesin antagonists or structurally unrelated peptides. The binding reaction is terminated by adding 0.5 ml of ice-cold medium to each well. After washing four times with ice-cold PBS (pH 7.4) the cells in each well are dissolved with 0.5 ml of 0.3 N NaOH. The resultant cellular lysate is collected from each well for measurement of radioactivity by a gamma counter.

EVALUATION

All data are expressed as the mean ± SEM of duplicate or triplicate observations from at least 2–3 repeated experiments. Mean values between the treatment and control group are analyzed by the Student *t*-test, Mann Whitney *U*-test, or one-way analysis of variance.

Data from receptor binding assays are analyzed by a ligand-PC computerized curve-fitting program created by Munson and Rodbard as modified by McPherson (1985) to determine the types of binding sites, the dissociation constants (K_d) and the maximal binding capacity of receptors (B_{max}).

MODIFICATIONS OF THE METHOD

Similar studies, mostly by Schally's group, as with tissue derived from human pancreatic cancer were performed with nitrosamine-induced pancreatic cancers in hamsters (Szepeshazi et al. 1993, 1994, 1999), with human prostate cancer (Pinski et al. 1993a, b), with rat prostate cancer (Pinski et al. 1994a), with human gastric cancer (Halmos et al. 1994; Qin et al. 1994b), with human small-cell and non-small-cell lung carcinoma (Pinski et al. 1994b; Moody et al. 1996; Koppan et al. 1998; Kiaris et al. 1999a), with human breast cancer (Yano et al. 1994; Miyazaki et al. 1998; Kahan et al. 2000), with mouse mammary cancer (Szepeshazi et al. 1992, 1997), with human colon cancer (Radulovic et al. 1994), with human glioblastoma (Kiaris et al. 1999b), and with human renal adenocarcinoma (Jungwirth et al. 1998).

REFERENCES AND FURTHER READING

Azay J, Gagne D, Devin C, Llinares M, Fehrentz JA, Martinez J (1996) JMV641: A potent bombesin receptor antagonist that inhibits Swiss 3T3 cell proliferation. Regul Pept 65:91–97

Casanueva FF, Perez FR, Casabiell X, Camiña JP, Cai RZ, Schally AV (1996) Correlation between the effects of bombesin antagonists on cell proliferation and intracellular calcium concentration in Swiss 3T3 and HT-29 cell lines. Proc Natl Acad Sci USA 93:1406–1411

Halmos G, Schally AV (1997) Reduction in receptors for bombesin and epidermal growth factor in xenografts of human small-cell lung cancer after treatment with bombesin antagonist RC-3095. Proc Natl Acad Sci USA 94:956–960

Halmos Pinski J, Szoke B, Schally AV (1994) Characterization of bombesin/gastrin-releasing peptide receptors in membranes of MKN45 human gastric cancer. Cancer Lett 85:111–118

Halmos G, Wittliff JL, Schally AV (1995) Characterization of bombesin/gastrin-releasing peptide receptors in human breast cancer and their relationship to steroid receptor expression. Cancer Res 55:280–287

Heimbrook DC, Saari WS, Balishin NL, Fisher TW, Friedman A, Kiefer DM, Rotberg S, Wallen JW, Oliff A (1991) Gastrin releasing peptide antagonists with improved potency and stability. J Med Chem 34:2102–2107

Jungwirth A, Schally AV, Halmos G, Groot K, Szepeshazi K, Pinski J, Armatis P (1998) Inhibition of the growth of Caki-I human renal adenocarcinoma *in vivo* by luteinizing hormone-releasing hormone antagonist cetrorelix, somatostatin analog RC-160, and bombesin antagonist RC-3940-II. Cancer 82:909–917

Kahan Z, Sun B, Schally AV, Arencibia JM, Cai C-R, Groot K, Halmos G (2000) Inhibition of growth of MDA-MB-468 estrogen-independent human breast cancer carcinoma by bombesin/gastrin-releasing peptide antagonists RC-3095 and RC3940-II. Cancer 88:1384–1392

Kiaris H, Schally AV, Nagy A, Sun B, Armatis P, Szepeshazi K (1999a) Targeted cytotoxic analog of bombesin/gastrin-releasing peptide inhibits the growth of H-69 human small-cell lung carcinoma in nude mice. Br J Cancer 81:966–971

Kiaris H, Schally AV, Sun B, Armatis P, Groot K (1999b) Inhibition of growth of human malignant glioblastoma in nude mice by antagonists of bombesin/gastrin-releasing peptide. Oncogene 18:7168–7173

Koppan M, Halmos G, Arencibia JM, Lamharzi N, Schally AV (1998) Bombesin/gastrin-releasing peptide antagonists RC-3095 and RC-3940-II inhibit tumor growth and decrease the levels and mRNA expression of epidermal growth factor receptors in H-69 small cell lung carcinoma. Cancer 83:1335–1343

Labara C, Paigen K (1979) A simple and sensitive DNA assay procedure. Anal Biochem 102:344–352

McPherson GA (1985) Analysis of radioligand binding experiments: a collection of computer programs for the IBM PC. J Pharmacol Meth 14:213–228

Miyazaki M, Lamharzi N, Schally AV, Halmos G, Szepeshazi K, Groot K, Cai R-Z (1998) Inhibition of growth of MDA-MB-231 human breast cancer xenografts in nude mice by bombesin/gastrin-releasing peptide (GRP) antagonists RC-3940-II and RC-3095. Eur J Cancer 34:710–717

Moody TW, Jensen RT (1998) Bombesin receptor antagonists. Drugs Future 23:1305–1315

Moody TW, Venugopal R, Hu V, Gozes Y, McDermed J, Leban JJ (1996) BW1023U90: A new GRP receptor antagonist for small-cell lung cancer cells. Peptides 17:1337–13343

Pinski J, Halmos G, Schally AV (1993a) Somatostatin analog RC-160 and bombesin/gastrin-releasing peptide antagonist RC-3095 inhibit the growth of androgen-independent DU-145 human prostate cancer line in nude mice. Cancer Lett 71:1–3

Pinski J, Schally AV, Halmos G, Szepeshazi K (1993b) Effect of somatostatin analog RC-160 and bombesin/gastrin-releasing peptide antagonist RC-3095 on growth of PC-3 human prostate cancer xenografts in nude mice. Int J Cancer 55:963–967

Pinski J, Reile H, Halmos G, Groot K, Schally AV (1994a) Inhibitory effects of somatostatin analog RC-160 and bombesin/gastrin-releasing peptide antagonist RC-3095 on growth of androgen-independent Dunning R-3327-AT-1 rat prostate cancer. Cancer Res 54:169–174

Pinski J, Schally AV, Halmos G, Szepeshazi K, Groot K, O'Byrne K, Cai R-Z (1994b) Effects of somatostatin analogue RC-160 and bombesin/gastrin-releasing peptide antagonists on the growth of human small-cell and non-small-cell lung carcinomas in mice. Br J Cancer 70:886–892

Qin Y, Ertl T, Cai R-Z, Halmos G, Schally AV (1994a) Inhibitory effect of bombesin receptor antagonist RC-3095 on the growth of human pancreatic cells *in vivo* and *in vitro*. Cancer Res 54:1035–1041

Qin Y, Halmos G, Cai R-Z, Szoke B, Ertl T, Schally AV (1994b) Bombesin antagonists inhibit *in vitro* and *in vivo* growth of

human gastric cancer and binding of bombesin to its receptors. J Cancer Res Clin Oncol 120:519–528
Qin Y, Ertl T, Cai R-Z, Horvath JE, Croot K, Schally AV (1995) Antagonists of bombesin/gastrin-releasing peptide inhibit growth of SW-1990 human pancreatic adenocarcinoma and production of cyclic AMP Int J Cancer 63:257–262
Radulovic S, Schally AV, Reile H, Halmos G, Szepeshazi K, Groot K, Milovanovic S, Miller G, Yang T (1994) Inhibitory effects of antagonists of bombesin/gastrin-releasing peptide (GRP) and somatostatin analog (RC-160) on growth of HT-29 human colon cancers in nude mice. Acta Oncol 33:693–701
Szepeshazi K, Schally AV, Halmos G, Groot K, Radulovic S (1992) Growth inhibition of estrogen-dependent and estrogen-independent MXT mammary cancers in mice by bombesin and gastrin-releasing peptide antagonist RC-3095. J Natl Cancer Inst 84:1915–1922
Szepeshazi K, Schally AV, Groot K, Halmos G (1993) Effect of bombesin gastrin-releasing peptide ($GRP^{14–27}$) and bombesin/GRP receptor antagonist RC-3095 on growth of nitrosamine-induced pancreatic cancers in hamsters. Int J Cancer 54:282–289
Szepeshazi K, Halmos G, Groot K, Schally AV (1994) Combination treatment of nitrosamine-induced pancreatic cancers in hamsters with analogues of LH-RH and a bombesin/GRP antagonist. Int J Pancreatology 16:141–149
Szepeshazi K, Schally AV, Halmos G, Lamharzi N, Groot K, Horvath JE (1997) A single *in vivo* administration of bombesin antagonist RC-3095 reduces the levels and mRNA expression of epidermal growth factor receptors in MXT mouse mammary cancers. Proc Natl Acad Sci USA 94:10913–10918
Szepeshazi K, Halmos G, Schally AV, Arencibia JM, Groot K, Vadillo-Buenfil M, Rodriguez-Martin E (1999) Growth inhibition of experimental pancreatic cancers and sustained reduction in epidermal growth factor receptors during therapy with hormonal peptide analogs. J Cancer Res Clin Oncol 125:444–452
Thomas F, Mormont C, Morgan B (1994) Gastrin-releasing peptide antagonists. Drugs Future 19:349–359
Yano T, Pinski J, Szepeshazi K, Halmos G, Radulovic S, Groot K, Schally AV (1994) Inhibitory effect of bombesin/gastrin-releasing peptide antagonist RC-3095 and luteinizing-releasing hormone antagonist SB-75 on the growth of MCF-7 MIII human breast cancer xenografts in athymic nude mice. Cancer 73:1229–1238

J.3.2 Mucus Secretion

J.3.2.1 Isolated Gastric Mucosal Preparation

PURPOSE AND RATIONALE

Main and Pearce (1978) described an isolated gastric mucosal preparation from rats for studying the pharmacology of gastric secretion and the synthesis or release of endogenous substances.

PROCEDURE

Rats of either sex weighing 100–120 g or guinea pigs weighing 400–600 g are anesthetized with 60 mg/kg pentobarbitone s.c. The abdomen is opened along the midline and the stomach exteriorized. The nonglandular portion is removed and the stomach rinsed with mucosal solution, containing 136 mM NaCl, 5 mM KCl, 3.6 mM $CaCl_2 \cdot 6H_2O$, 1.2 mM $MgCl_2 \cdot 6H_2O$, and 16.7 mM glucose. The muscular layer overlying the nonantral region is separated from the mucosa by blistering. The tip of a fine needle (27 gauge) is inserted just below the muscle and mucosal solution injected between the layers. The process is repeated as many times as is necessary to blister the whole area. Fine scissors are then used to cut the muscle along the greater curvature and then parallel to the cut edge. The muscle sheet is pulled back to expose the mucosa. The stomach is then removed, opened by cutting along the greater curvature, and rinsed with mucosal solution.

Two pieces are obtained from one stomach and each is placed, mucosal surface inwards, over a 1-cm^2-opening on a polyethylene vessel (titration cup). Both preparations, one each from the ventral and dorsal surfaces, are stretched lightly over the cup and tied in place. Each tissue is placed in an organ bath, at 37°C, containing 35 ml of serosal solution (110 mM NaCl, 5 mM KCl, 3.6 mM $CaCl_2 \cdot 6H_2O$, 1.2 mM $MgCl_2 \cdot 6H_2O$, 26 mM $NaHCO_3$, and 16.7 mM glucose) being gassed with a 95% O_2/5% CO_2 mixture. The mucosal surface is superfused by means of a peristaltic pump at a rate of 0.5 ml/min with an unbuffered solution of similar ionic composition and gassed with 100% O_2. The volume of solution on the mucosal side is kept constant by suction via the same pump using larger diameter tubing, varying between 1.6 and 2.0 ml. This small volume is used in order to follow changes in acid secretion more closely. Secretion is recorded continuously via a dual microelectrode in the mucosal solution connected with a potentiometric pen recorder. The H^+-ion concentration is noted every 15 min and expressed as apparent secretion rate. Drugs are added to the serosal solution in volumes not exceeding 1 ml. Contact times for drugs and hormones (e. g., gastrin or histamine) are between 30 and 60 min. Recovery periods before the next response are between 45 and 60 min. Responses are readily reversible on replacing the solution in the bath with fresh, warmed serosal solution.

EVALUATION

The secretory response is calculated as the increase in secretion rate at the peak of the response over the preceding basal value. Dose-response curves and time-response curves are established for histamine, gastrin,

and methacholine. The effects of drugs which inhibit acid secretion are evaluated by adding them either at the peak of a response, or 15 to 60 min prior to the secretagogue.

MODIFICATIONS OF THE METHOD

Wan et al. (1974) used the fundic glandular portion of the rat stomach mounted onto a glass tube without removing the muscular layer to study the inhibition of *in vitro* stimulated gastric acid secretion by a histamine H_2-receptor antagonist.

REFERENCES AND FURTHER READING

Main IHM, Pearce JB (1978) A rat isolated gastric mucosal preparation for studying the pharmacology of gastric secretion and the synthesis or release of endogenous substances. J Pharm Meth 1:27–38

Wan BYC, Assem KE, Schild HO (1974) Inhibition of *in vitro* stimulated gastric acid secretion by a histamine H_2-receptor antagonist, metiamide. Eur J Pharmacol 29:83–88

J.3.2.2 Primary Culture of Rat Gastric Epithelial Cells

PURPOSE AND RATIONALE

Zheng et al. (1994) described an *in vitro* model for evaluation of antisecretory agents using primary cultures of rat gastric epithelial cells.

PROCEDURE

Gastric mucosal cells from 1- to 2-week-old Sprague-Dawley rats are isolated according to Terano (1982). Gastric mucosal surface is washed thoroughly with sterile cotton and Hank's balanced salt solution (HBSS) and then rinsed with HBSS before being minced into approximately 1-mm^3 pieces. The minced tissues are incubated in HBSS containing 0.1% collagenase and 0.05% hyaluronidase at 37°C in a shaking water bath for 60 min, then pipetted several times and filtered through a sterile nylon mesh. The filtrate is washed twice with HBSS by centrifugation (200 *g* for 5 min) and resuspended in Coon's modified Ham's F-12 culture medium containing 100 µg/ml penicillin, 100 µg/ml streptomycin, 50 µg/ml gentamycine, 15 mM HEPES, 2 µg/ml fibronectin, and 10% fetal bovine serum. Cells are seeded at a density of $1.5–2 \times 10^5$ or $1–2 \times 10^4$ cells/cm^2 directly onto either 96-well plates or 6-well plates, and maintained in a Steri-Cult incubator at 37°C in a humidified atmosphere with 5% CO_2. The medium is changed daily. The confluent monolayers are formed after 4–5 days in 96-well plates.

Drug Treatment

To measure the effects of individual drugs on the viability of gastric mucosal cells, cells are incubated with 0.02–5 mg/ml drugs in culture medium for either 2 or 48 h for the uptake of MTT (3-[4,5-dimethyl-2-thiazolyl]-2,5-diphenyl-2*H*-tetrazolium bromide) or up to 8 days for the colony-forming efficiency assay. To measure the cytotoxicity of drugs, e. g., indomethacin, and acidified medium to gastric mucosal cells, cells are incubated in either serum-free medium containing 0.5–10 mM indomethacin for 1 h, or pH 3.5 at for 10–30 min.

To study the effect of various antacids, e. g., aluminium hydroxide or sucralfate preparations, cells are incubated for 1 h in culture medium containing these drugs. The drug suspensions are then aspirated away, followed by another hour of treatment with 3.5 mM indomethacin. Alternatively, cells are treated with drugs and 3.5 mM indomethacin concurrently for 1 h. The effects of antacids on acid-induced damage are investigated by incubating the cells with the agents for 2 h and then exposing them to pH 3.5 medium for 10 to 30 min.

MTT (3-[4,5-dimethyl-2-thiazolyl]-2,5-diphenyl-2H-Tetrazolium Bromide) Colorimetric Assay

Cells in 96-well plates are treated with the different drugs and then incubated in 100 µl of culture medium containing 10 µl of an MTT stock solution (5 mg/ml) for 4 h at 37°C according to Mosmann (1983). Following the incubation, 100 µl acid-isopropanol (0.04 N HCl in isopropanol) is added to the wells and incubated overnight at room temperature. The color changes are recorded at 540 nm on a microplate reader. To exclude the disturbance of precipitates in some samples, the samples are centrifuged and only the supernatants are read. For each experiment, a standard curve is generated by measuring the relationship of absorbance to a series of viable cell numbers.

Neutral Red Uptake Assay

Neutral red is prepared as a 1% stock solution in distilled water and diluted to 0.035% in HBSS immediately before each experiment. The cells are treated with the drugs and then stained with 0.1 ml of 0.035% neutral red for 30 min (Parish and Müllbacher 1983). The stain is discarded and the cells are washed twice in HBSS before the addition of 200 µl/well of acidified alcohol solution (50%, v/v, ethanol/water, containing 0.5% acetic acid). After a 2 h incubation period at room temperature, the color changes are measured in a microplate reader.

Colony-Forming Efficiency Assay

The cells are seeded into 6-well plates and incubated in culture medium containing 0.02 to 5 mg/ml of individual drugs for 8 days. Cells are then fixed in 10% formalin and stained with 1% aqueous crystal violet (Sundqvist et al. 1989). Colonies formed on each well are counted (crystal violet stains cell nuclei) and compared with those formed on drug-free wells.

EVALUATION

Data are expressed as mean ± standard error. A one-way analysis of variance followed by Scheffe's post hoc test is used to test the significance between control and drug-treated samples. Differences are considered significant at $P < 0.05$.

MODIFICATIONS OF THE METHOD

Buchan et al. (1993) used cultured human antral epithelial cells enriched for D cells to study the effect of cholecystokinin and secretin on somatostatin release.

REFERENCES AND FURTHER READING

Buchan AM, Meloche RM, Kwok YN, Kofod H (1993) Effect of cholecystokinin and secretin on somatostatin release from cultured antral cells. Gastroenterol 104:1414–1419

Mosmann T (1983) Rapid colorimetric assay for cellular growth and survival: Application to proliferation and cytotoxicity assays. J Immunol Methods 65:55–63

Parish CR, Müllbacher A (1983) Automated colorimetric assay for T cell cytotoxicity. J Immunol Methods 58:225–237

Sundqvist K, Liu Y, Nair J, Bartsch H, Arvidson K, Grafström C (1989) Cytotoxic and genotoxic effects of areca nut-related compounds in cultured human buccal epithelial cells. Cancer Res 49:5294–5298

Terano A, Ivey KJ, Stachura J, Sekhon S, Hosojima A, McKenzie WN, Krause WJ, Wyche JH (1982) Cell culture of rat gastric fundic mucosa. Gastroenterology 83:1280–1291

Zheng H, Shah PK, Audus KL (1994) Primary culture of rat gastric epithelial cells as an *in vitro* model to evaluate antiulcer agents. Pharmaceut Res 11:77–82

J.3.3
Gastric Motility

J.3.3.1
Measurement of Intragastric Pressure in Rats

PURPOSE AND RATIONALE

Gastric motor activity can be measured by recording intragastric pressure in anesthetized rats (Holzer 1992).

PROCEDURE

Sprague-Dawley rats of either sex weighing 220–240 g are deprived of food for 20 h prior experimentation but are allowed free access to tap water. After induction of anesthesia by i.p. injection of phenobarbital sodium (0.92 mmol/kg), the trachea is cannulated to facilitate spontaneous breathing. The left carotid artery is cannulated and connected to a pressure transducer to monitor mean arterial blood pressure. The left jugular vein is cannulated for i.v. injection of drugs and for continuous infusion of physiological saline at a rate of 0.6 ml/h to avoid dehydration of the animals. Intragastric pressure is measured by a catheter (outer diameter 1.9 mm) passed down to the stomach via the esophagus. The position of the catheter tip in the corpus region is verified at the end of each experiment. The catheter has two side holes in its tip segment and is continuously perfused with physiological saline at a rate of 0.6 ml/h. To record intragastric pressure, the catheter is connected to a pressure transducer.

EVALUATION

The gastric motor effect is quantitated by calculation of the area under the curve versus baseline intragastric pressure, measured immediately before injection of the stimulant (e. g., neurokinin A). To test inhibitors, the area under the curve after the stimulant is set as 100% and the effect of application of the inhibitor with the stimulant is calculated as percentage.

MODIFICATIONS OF THE METHOD

Lotti et al. (1986) described a simple mouse assay for the *in vivo* evaluation of cholecystokinin antagonists which is based on visual determination of the gastric emptying of a charcoal meal.

REFERENCES AND FURTHER READING

Holzer P (1992) Reflex gastric motor inhibition caused by intraperitoneal bradykinin: Antagonism by Hoe 140, a bradykinin antagonist. Peptides 13:1073–1077

Lotti VJ, Cerino DJ, Kling PJ, Chang RSL (1986) A new simple mouse model for the *in vivo* evaluation of cholecystokinin (CCK) antagonists: comparative potencies and durations of action of nonpeptide antagonists. Life Sci 39:1631–1638

J.3.3.2
Isolated Smooth Muscle Preparation of Guinea Pig Stomach

PURPOSE AND RATIONALE

Boyle et al. (1993) described a novel smooth muscle preparation from the guinea pig stomach for characterization of CCK receptors by use of selective antagonists.

PROCEDURE

Adult male guinea pigs weighing 330–400 g are sacrificed and the stomach rapidly removed. The fundus is discarded and the stomach is opened along the

greater curvature, pinned on a Petri-dish with the mucosa pointing up. The mucosal and submucosal layers are removed by dissection to reveal the underlying smooth muscle layer. Strips of circular muscle (2 × 25 mm) from the corpus region of the stomach are obtained by cutting inwards, following the striations of the lesser curvature. Muscle strips are mounted in siliconized 3 ml organ baths containing Krebs-Henseleit solution. The buffer is modified to include 5 µM indomethacin. The solution is maintained at 37°C and continuously gassed with a mixture of 95% O_2/5% CO_2. Isometric contractile responses are measured with force-displacement transducers (e. g., Grass FT.03) and recorded on a polygraph (e. g., Mark VII Graphtec Linearcorder).

Tissues are placed under 1 g tension and allowed to equilibrate for 30 min after which time they are contracted with a submaximal dose of carbamylcholine (10 nM). Using a 12 min dose cycle, concentration-response curves are established for agonists, e. g., gastrin, pentagastrin, CCK and CCK-analogues. For studies with antagonists, the tissues are exposed to antagonists for 15 min before re-exposure to agonists. The addition of 5 µM indomethacin removes the spontaneous activity due to the inherent myogenic tone existing in the tissue, but leaves the responses to the agonists unaffected.

EVALUATION

Contractile responses to exogenously applied agonists are expressed as absolute changes in tension and are transformed as a percentage of the maximal response achieved for that agonist in order to obtain potency values. EC_{50} values are obtained graphically for individual concentration-response curves. Responses to agonists in the presence of antagonists are expressed as a percentage of the control maximum response obtained in the same tissue preparation. Agonist concentration-response curves in the absence and presence of increasing concentrations of antagonists are obtained. The method of Arunlakshana and Schild (1959) is used to provide Schild plots of the data, and to obtain affinity constants for the antagonists.

MODIFICATIONS OF THE METHOD

Riazi-Farzad et al. (1996) described an improved preparation of the **isolated rat stomach fundus strip** based on the finding that the majority of the contractile response to 5-HT and carbachol was present in the left ventral longitudinal quartile of the tissue.

Van Nueten et al. (1978), Reyntjens et al. (1984), Schuurkes et al. (1985), Kishibayashi and Karasawa (1998) used an **isolated gastroduodenal preparation of the guinea pig**. After ligation of the esophagus, the stomach was filled with 20 ml saline and suspended in 200 ml of oxygenated Krebs-Henseleit solution, maintained at 37°C. The duodenum was cannulated and connected with an ultrasonic transit time transducer to record changes in intraluminal volume and with a bottle of saline to ensure constant hydrostatic pressure of 6 cm H_2O. Spontaneous phasic activity was always present on the stomach and recorded as rhythmic changes in gastric volume. Gastric peristaltic waves either stopped at the pylorus or were propagated to the duodenum. Antroduodenal coordination was quantified as the relative number of antral waves that were propagated to the duodenum. After 30 min stabilization, drugs were added in varying concentrations and the effects followed for 30 min. Three parameters were determined: (1) contractile amplitude, expressed as milliliters of expelled volume; (2) frequency, measured as number of contractions per minute; (3) percentage of antroduodenal coordination.

REFERENCES AND FURTHER READING

Arunlakshana O, Schild HO (1959) Some quantitative uses of drug antagonists. Br J Pharmacol Chemother 14:48–58

Boyle SJ, Tang KW, Woodruff GN, McKnight AT (1993) Characterization of CCK receptors in a novel smooth muscle preparation from the guinea pig stomach by use of the selective antagonists CI-988, L-365,260 and devazepide. Br J Pharmacol 109:913–917

Kishibayashi N, Karasawa A (1998) Effects of KW-5092, on antroduodenal coordination and gastric emptying in guinea-pigs. J Pharm Pharmacol 50:1045–1050

Reyntjens A, Verlinden M, Schuurkes J, van Nueten J, Janssen PAJ (1984) New approach to gastrointestinal motor dysfunction: non-antidopaminergic, non-cholinergic stimulation with cisapride. Curr Ther Res 36:1029–1037

Riazi-Farzad B, Nicholls PJ, Sewell RD (1996) Sensitivity differences to 5-HT and carbachol in subsections of the isolated rat stomach fundus strip: an improved preparation. J Pharmacol Toxicol Meth 35:217–221

Schuurkes JAJ, van Nueten JM, van Daele PGH, Reyntjens AJ, Janssen PAJ (1985) Motor-stimulating properties of cisapride on isolated gastrointestinal preparations of the guinea pig. J Pharmacol Exp Ther 234:775–783

Van Nueten JM, Ennis C, Helsen L, Laduron PM, Janssen PAJ (1978) Inhibition of dopamine receptors in the stomach: An explanation of the gastrokinetic properties of domperidone. Life Sci 23:453–458

J.3.4 Absorption

J.3.4.1 Measurement of Gastric Absorption of Drugs in Rats

PURPOSE AND RATIONALE

Although the stomach is not the prime absorptive site of drugs, the absorption of some drugs from the gas-

tric mucosa has been established (Doluisio et al. 1969; Welling 1977). Worland et al. (1983) described an *in situ* gastric pouch technique for direct measurement of the gastric absorption of drugs in the rat.

PROCEDURE

Male Wistar rats weighing 220–300 are anesthetized by i.p. injection of 50 mg/kg sodium pentobarbital. A cannula is placed in the jugular vein for administration of heparinized saline (3000 IU/kg) and whole blood replacement during the experiment. The replacement blood is collected from heparinized donor rats immediately prior to the experiment. Another cannula is placed into the carotid artery of the experimental animal for the collection of systemic blood samples. A midline incision is made in the abdominal wall. Double ligatures are placed on the superior epigastric vessels and transverse incisions are made between the ligatures. The branches of the right gastroepiploic veins and arteries are then ligated using surgical silk and the gastrohepatic ligament between the stomach and the posterior surface of the left hepatic lobe and the caudal hepatic lobe is separated. The gastrosplenic mesentery is also severed. A strip of gauze is employed to keep the liver lobes out of the surgical field. Using appropriately sized surgical silk, double ties are placed around the short gastric vessels and the esophagus, which are then severed between the ties. The pylorus and pyloric vessels are then ligated and an incision is made in the forestomach to allow the removal of gastric contents.

The pouch is then rinsed with warm saline until clear and the remaining fluid is removed using an adsorbent tissue. A Luer adapter modified from a three-way tap is tied into the incision to enable drug administration via a syringe. The gastric pouch is then transposed to the right of the animal exposing the left gastric vein. The vein is cannulated above the junction with the lienal (splenic) vein using a 21-gauge needle connected to a 15-cm length of polyethylene tubing (i.d. 0.75 mm, o.d. 1.45 mm). A small Oxford clamp with foam rubber insets is employed to prevent dislocation of the cannula during the changing of the sample vials. The drug is administered into the stomach and blood draining from the gastric pouch is collected over timed intervals. To determine the volume (ml) of blood collected, the venous effluent is weighed and hematocrit (HCT) readings are taken for each sample and converted to units using the formula:

$$\text{Volume (ml)} = \frac{\text{mass blood collected (g)}}{\text{HCT}\times\text{blood celldensity}+(1-\text{HCT})\times\text{plasma density}} .$$

Rat blood cell and plasma density measurements are obtained from five determinations from four rats, blood samples being separated at 3000 *g* for 10 min. Samples from the gastric pouch are kept on ice until the plasma can be separated by centrifugation at 3000 *g* for 10 min and the plasma frozen until assay.

Blood replacement is delivered at a rate of 0.7 ml/min from a gently oscillating reservoir using a peristaltic pump.

The compound to be tested is administered in a volume of 0.5 ml to the gastric pouch. Plasma levels are determined with a method specific for the compound under investigation. Plasma samples are collected at 4 min intervals over a period of 30–60 min. At the end of the experiment, the fluid in the gastric pouch is collected for determination of the dose remaining in the stomach.

EVALUATION

Mean values ± standard deviation of plasma concentration are calculated from 4–6 experiments and plotted versus time to demonstrate the absorption profile.

REFERENCES AND FURTHER READING

Doluisio JT, Billups NF, Dittert LW, Sugita ET, Swintowsky JV (1969) Drug absorption I: An *in situ* rat gut technique yielding realistic absorption rates. J Pharm Sci 58:1196–1200

Welling PG (1977) Influence of food and diet on gastrointestinal drug absorption: a review. J Pharmacokinet Biopharm 5:291–334

Worland PJ, Drummer OH, Jarrott B (1983) An *in situ* gastric pouch technique for direct measurement of the gastric absorption of drugs in the rat. J Pharmacol Meth 10:215–221

J.3.5 Antacid Activity

J.3.5.1 Evaluation of Antacids

PURPOSE AND RATIONALE

Antacids have been used for the treatment of gastroduodenal ulcerations since a long time (Konturek 1993). The main action of antacids is to reduce the acidity of the gastric content through neutralization and increasing intragastric pH. Since pepsin is not active at higher pH levels, antacids reduce peptic activity (Goldberg et al. 1968) and may also adsorb pepsin (Sepelyak et al. 1984). Binding of bile salts (Clain et al. 1977) by antacids may also have a beneficial influence on peptic ulcer disease. Most antacids contain magnesium and aluminum hydroxide, in some cases also calcium carbonate and sodium bicarbonate. The acid-neutralizing potency can be measured *in vitro*.

PROCEDURE

0.1 M HCl is added to the antacid to be tested. The acid neutralizing capacity is defined as the amount of 0.1 M HCl that can be added to a liquid antacid without reducing the pH of the mixture below pH 3.0. The determination of the acid neutralizing capacity of antacid tablets is performed *in vitro* by stirring a mixture of crushed tablets and water. The time at which all antacid is consumed is much longer for antacid in tablet as compared with the same amounts of antacid in liquid form. Magnesium hydroxide is very insoluble in water, but is readily soluble in hydrochloric acid. In combined preparations, the magnesium hydroxide reacts first to produce an almost immediate neutralizing effect and an increase of the pH within a few minutes. Aluminum oxide, on the other hand, has a weaker antacid activity, reacting more slow with acid (Fordtran et al. 1973; Richardson et al. 1988).

EVALUATION

In vitro titration curves of 0.1 M HCl with 5 ml liquid antacid or one tablet are measured over 3 h and compared with the standard.

CRITICAL ASSESSMENT OF THE METHOD

Acid neutralizing potency may be not the only factor which contributes to the therapeutic effect of antacids. Damage and protection in the stomach are essentially represented by acid secreted by the parietal cells and by bicarbonate released by the surface epithelial cells and mucous neck cells. Among various neurohumoral factors most important in the bicarbonate-secretion appear the prostaglandins, mainly of the E series. Mucosal bicarbonate secretion may be stimulated through the activation of prostaglandins by aluminum hydroxide containing antacids. Aluminum containing antacids were found to protect against mucosal damage due to topical irritants and against stress or aspirin induced lesions. Gastroprotection of aluminum-containing antacids has been attributed to the biological activity of nitric oxide interacting with mucosal prostanoids on the mucosal microcirculation. Therefore, these antacids were found to be active in various experimental ulcer models and to exert cytoprotective activity against ethanol induced gastric injury in rats (Szylenyi et al. 1983; Domschke et al. 1986; Hollander et al. 1986; Konturek et al. 1989, 1992; DiJoseph et al. 1989; Vergin and Kori-Lindner 1990). Konturek (1993) reported that aluminum hydroxide containing antacids protect growth factors, involved in the healing of ulcers, against acid degradation.

REFERENCES AND FURTHER READING

Clain JE, Malagelada JR, Chadwick VS, Hofmann AE (1977) Binding properties *in vitro* of antacids for conjugated bile salts. Gastroenterology 73:556–559

DiJoseph JF, Borella LE, Nabi Mir G (1989) Activated aluminium complex derived from solubilized antacids exhibits enhanced cytoprotective activity in the rat. Gastroenterology 96:730–735

Domschke W, Hagel J, Ruppin H, Kaduk B (1986) Antacids and gastric mucosal protection. Scand J Gastroenterol 21 (Suppl 125):144–149

Fordtran JS, Morawski SG, Richardson CT (1973) *In vivo* and *in vitro* evaluation of liquid antacids. N Engl J Med 288:923–928

Goldberg HI, Dodds WJ, Gee S, Montgomery C, Zboralske FF (1968) Role of acid and pepsin in acute experimental esophagitis. Gastroenterology 56:223–230

Hollander D, Tarnawski A, Gergely H (1986) Protection against alcohol-induced gastric mucosal injury by aluminium-containing compounds – Sucralfate, antacids and aluminium sulfate. Scand J Gastroenterol 21 (Suppl 125):151–153

Konturek SJ (1993) New aspects of clinical pharmacology of antacids. J Physiol Pharmacol 44, Suppl 1:5–21

Konturek SJ, Brzozowski T, Drozdowicz D, Nauert C (1989) Gastroprotection by an aluminium- and magnesium-hydroxide-containing antacid in rats. Role of endogenous prostanoids. Scand J Gastroenterol 24:1113–1120

Konturek SJ, Brzozowski T, Majka J, Szlachcic A, Nauert C, Slomiany B (1992) Nitric oxide in gastroprotection by aluminium-containing antacids. Eur J Pharmacol 229:155–162

Richardson CT, Peterson WL (1988) Clinical pharmacology of antacids In: Bianchi-Porro G, Richardson CT (eds) Antacids in Peptic Ulcer Disease. Raven Press, New York,pp 3–16

Sepelyak RJ, Feldkamp JR, Regnier FE, White JL, Hem SL (1984) Adsorption of pepsin by aluminium hydroxide. II. Pepsin inactivation. J Pharm Sci 73:1517–1522

Szelenyi I, Postius S, Engler H (1983) Evidence for a functional cytoprotective effect produced by antacids in the rat stomach. Eur J Pharmacol 88:403–410

Vergin H, Kori-Lindner C (1990) Putative mechanisms of cytoprotective effect of certain antacids and sucralfate. Digest Dis Sci 35:1320–1327

J.3.6 Inhibition of HCl Secretion

J.3.6.1 Anticholinergic Activity

J.3.6.1.1 General Considerations

Gastric motility and tonus, as well as gastric secretion are stimulated by cholinergic impulses. Anticholinergic compounds, such as the *Belladonna* alkaloid atropine, were the first drugs used in treatment of gastric ulcers. The doses that are necessary to reduce acid secretion also decrease mucus secretion and cause side effects, such as dry mouth, increase in heart rate and ocular disturbances. Inhibitors of specific muscarinic

receptors responsible for gastric acid secretion were found. Receptors for acetylcholine which play a major role in central and peripheral transmission have been studied extensively (Karlin et al. 1976; Hulme et al. 1990; Jones et al. 1992; Kebabian and Neumeyer 1994).

J.3.6.1.2 Acetylcholine Receptor Binding

PURPOSE AND RATIONALE

The search of specific muscarinic antagonists for inhibition of gastric acid secretion lead to the discovery of pirenzepine, a tricyclic compound, originally tested as psychotropic agent. This compound has a greater gastrointestinal selectivity than other muscarinic antagonists (Carmine and Brogden 1985; Longdong 1986). The activity of pirenzepine has been localized to M_1 receptors.

This, and the involvement of acetylcholine in many physiological processes, has stimulated the research on the various types of muscarinic receptors. At present, 5 types have been described but further subdivisions can be envisaged (Hulme et al. 1990; Jones et al. 1992; Kebabian and Neumeyer 1994; Caulfield and Birdsall 1998; Alexander et al. 2001; Eglen et al. 2001; Ma et al. 2004). The subtypes of muscarinic receptors have been characterized by the use of organs with a predominant subtype receptor population, e. g., rabbit vas deferens stimulated with electric impulses for M_1, electrically stimulated left atria from guinea pigs for M_2, and longitudinal smooth muscle preparations of guinea pig ileum or salivary gland of the rat for M_3 (Doods et al. 1987; Lambrecht et al. 1993), or by the use of selective antagonists (Pitschner et al. 1989; Richards 1990; Svensson et al. 1992,) or agonists (Lambrecht et al. 1993). Further characterization has been achieved by studies of the transduction mechanisms (Brown and Brown 1984; Brown et al. 1985; Parekh and Brading 1992) and by voltage clamp techniques (Bernheim et al. 1992). The five muscarinic receptor subtypes are referred to as M_1–M_5. The odd-numbered receptors (M_1, M_3, M_5) couple efficiently, through $G_{q/11}$, to activation of phospholipase C, which initiates the phosphatidyl-inositol turnover response. The even-numbered muscarinic receptors (M_2-M_4) inhibit adenylyl cyclase activity via activation of the G_i class of G proteins.

The genes for the muscarinic acetylcholine receptor subtypes have been cloned and expressed in Chinese ovary hamster cells (Buckley et al. 1989; Dörje et al. 1991) or in fibroblasts (Kashihara et al. 1992).

Many organs, e. g., rat brain (Luthin and Wolfe 1984; El-Fakahani et al. 1986) have been used for studies on acetylcholine receptor subtypes. Only the method using Chinese ovary hamster cells is presented here.

PROCEDURE

Preparation of Plasmid DNA

The coding sequences of the m1, m2, m3, m4, and m5 receptors are derived from a human genom library. The cDNAs are inserted into the Okayama/Berg pCD or pCD-PS expression vector (Bonner et al. 1987, 1988; Buckley et al. 1989). Plasmid DNA is isolated by two sequential density gradient centrifugations through CsCl (Maniatis et al. 1982).

Cell Culture

Chinese hamster ovary cells are incubated at 37°C in a humidified atmosphere (5% CO_2) as a monolayer culture in Dulbecco's modified Eagle's medium supplemented with 10% fetal calf serum, 100 units/ml each of penicillin G and streptomycin, and 4 mM glutamine.

Transfection Procedures

Cells are transfected using a modified calcium phosphate procedure (Chen and Okayama 1987) involving the use of cotransfected pcDneo as a selectable marker. Selection with the neomycin analog G 418 (600 µg/ml; Gibco NY) is started 72 h after transfection and continued for 2–3 weeks. Media are changed every 3 days. Clonal cell lines are obtained by single cell cloning and assayed for [^{3}H]NMS (N-methylscopolamine hydrochloride) binding capacity.

Membrane Preparation

Cells are grown to about 80% confluency, scraped into ice-cold binding buffer and homogenized for 30 s using a Brinkman homogenizer (setting 5). Membranes are pelleted at 16,000 *g* for 15 min and rehomogenized. Membrane protein is determined using a Bio-Rad protein assay dye reagent. Membranes are stored frozen at –80°C before use.

Radioligand Binding Studies

All membranes, drugs, and radioligands are made up in binding buffer consisting of 25 mM sodium phosphate (pH 7.4) containing 5 mM magnesium chloride. The assays are performed in 1 ml total volume. Final membrane concentrations are: m1 6 µg/ml; m2 10 µg/ml; m3 5 µg/ml; m4 3 µg/ml; and m5 4 µg/ml. In [^{3}H]NMS saturation experiments, 8–10 different concentrations

of the radioligand (2–1400 pM) are employed. For displacement experiments, [^{3}H]NMS in a concentration of 150 pM and 10 different concentrations of the displacer are used. Specific binding is defined as the difference in [^{3}H]NMS binding in the absence and presence of 1 μM atropine. Alternatively [^{3}H]pirenzepine is used. Incubations are carried out at 22°C for 3 h. Assays are terminated by filtration through a Brandell cell harvester onto Whatman GF/C filters. Membranes are washed three times with 5 ml of ice-cold binding buffer before being dried. They are transferred to 10 ml of scintillant (New England Nuclear Aquasol) and counted in a LKB β-counter.

EVALUATION

Data from direct binding experiments are fitted to the equation:

$$\alpha = (B_{\max} x^n/k)/(1 + x^n/k)$$

to derive the Hill coefficient n and to:

$$\alpha = (B_{\max} x/K_D)/(1 + x/K_D)$$

to obtain the dissociation constant K_D and the total number of binding sites $B_{\max}$ (α = [^{3}H]NMS specifically bound; x = [^{3}H]NMS concentration).

Data from displacement experiments are fitted to the equation:

$$\%[^3\text{H}]\text{NMS bound} = 100 - [100x^n/k/(1 + x^n/k)]$$

to obtain the Hill number n and to:

$$\%[^3\text{H}]\text{NMS bound} = 100 - [100 \times IC_{50}/(1 + x/IC_{50})]$$

to derive the IC_{50} value (x = concentration of the cold inhibitor).

K_i values are calculated by the method of Cheng and Prussoff (1973):

$$K_i = IC_{50}/(1 + L/K_D)$$

where L is the concentration of the radioligand, IC_{50} is the concentration causing 50% inhibition of the specific radioligand binding and K_D the dissociation constant of the radioligand receptor complex. Data are analyzed by a non-linear least-squares curve fitting procedure.

Results are expressed as mean values ± SEM of n experiments. Statistical significance is assessed using Student's t-test or Scheffé's method. $P < 0.05$ is accepted as being significant.

MODIFICATIONS OF THE METHOD

The selectivity towards muscarinic receptor subtypes can be tested by radioligand binding assays using either selective ligands or tissues possessing only one receptor subtype (Giachetti et al. 1986; Pitschner et al. 1989; Bickel et al. 1990). M_1-receptors from bovine cortex which has also M_2-and M_3-receptors are tested with the M_1-selective radioligand ^{3}H-pirenzepine. M_2-receptor from porcine heart possessing only this receptor type can be tested with the unselective ligand ^{3}H-N-methylscopolamine. M_3-receptors from rat submaxillary gland are likewise labelled with the unselective ligand ^{3}H-N-methylscopolamine, because this subtype is present predominantly in this tissue.

Measurement of the contractions of rabbit vas deferens after electrical stimulation was used to study the effects of prejunctional M_1 heteroreceptors and postjunctional M_2 receptors (Eltze et al. 1988; Dörje et al. 1991), of guinea pig atria for M_2-receptors and of guinea-pig ileum for M_3-receptors (Lambrecht et al. 1989, 1995). Cardiac muscarinic $M_{2\alpha}$ receptors have been discussed (Wess et al. 1988).

Coexistence of M_2 and M_3 subtypes of muscarinic receptors in canine colonic circular smooth muscle was reported by Zhang et al. (1991).

Investigations on the nature of muscarinic receptors present on parietal cell membranes using binding studies and polymerase chain reaction amplification or parietal cell messenger RNA revealed the existence of only a M_3 receptor responsible for acid secretion (Kajimura et al. 1992).

Spalding et al. (2002) described a novel muscarinic agonist, AC-42, and demonstrated its selectivity for the M_1 muscarinic subtype.

The phenotypes of knockout mice or the responses lost in these animals were used to characterize the properties of the subtypes of muscarinic receptors (Birdsall et al. 2001). Champtiaux et al. (2003) investigated the subunit composition of functional nicotinic receptors in dopaminergic neurons with knockout mice.

Owicki et al. (1990, 1992), McConnell et al. (1991, 1992) used a special apparatus, the 'cytosensor microphysiometer' which measures the rate of proton excretion from cultured cells. Chinese hamster ovary cells were transfected with the m_1 muscarinic acetylcholine receptor. Sequential addition of increasing doses of carbachol every 2.5 min induced an increasing acidification allowing the determination of an EC_{50} value. The effect was antagonized by atropine.

REFERENCES AND FURTHER READING

Alexander S, Peters J, Mathie A, MacKenzie G, Smith A (2001) TiPS Nomenclature Supplement 2001

Bernheim L, Matie A, Hille B (1992) Characterization of muscarinic receptor subtypes inhibiting Ca^{2+} current and M current in rat sympathetic neurons. Proc Natl Acad Sci USA 89:9544–9548

Bickel M, Bal-Tempe S, Blumbach J, Dohadwalla AN, Lal B, Palm D, Rajagopalan R, Rupp RH, Schmidt D, Volz-Zang C (1990) HL 752, a new enteral active muscarinic receptor antagonist. Med Sci Res 18:877–879

Birdsall NJM, Burgen ASV, Hulme EC (1978) The binding of agonists to brain muscarinic receptors. Mol Pharmacol 14:723–736

Birdsall NJM, Nathanson NM, Schwarz RD (2001) Muscarinic receptors: it's a knockout. Trends Pharmacol Sci 22:215–219

Bonner TI, Buckley NJ, Young AC, Brann MR (1987) Identification of a family of muscarinic receptor genes. Science 237:527–532

Bonner TI, Young AC, Brann MR, Buckley NJ (1988) Cloning and expression of the human and rat m5 muscarinic acetylcholine receptor genes. Neuron 1:403–410

Brown JH, Brown SL (1984) Agonists differentiate muscarinic receptors that inhibit cyclic AMP formation from those that stimulate phophoinositide metabolism. J Biol Chem 259:3777–3781

Brown JH, Goldstein D, Brown Masters S (1985) The putative M_1 muscarinic receptor does not regulate phophoinositide hydrolysis. Studies with pirenzepine and McN-A343 in chick heart and astrocytoma cells. Mol Pharmacol 27:525–531

Buckley NJ, Bonner TI, Buckley C, Brann MR (1989) Antagonist binding properties of five cloned muscarinic receptors expressed in CHO-K1 cells. Mol Pharmacol 35:469–476

Carmine AA, Brogden RN (1985) Pirenzepine: a review of its pharmacodynamic and pharmacokinetic properties and therapeutic efficacy in peptic ulcer disease and other allied diseases. Drugs 30:85–126

Caulfield MP, Birdsall NJM (1998) International Union of Pharmacology. XVII. Classification of muscarinic acetylcholine receptors. Pharmacol Rev 50:279–290

Champtiaux N, Gotti C, Cordero-Erausquin M, David DJ, Przybylski C, Lena C, Clementi F, Moretti M, Rossi FM, Le-Novere N, McIntosh JM, Gardier AM, Changeux JP (2003) Subunit composition of functional nicotinic receptors in dopaminergic neurons investigated with knock-out mice. J Neurosci 23:7820–7829

Chen C, Okayama H (1987) High efficiency transformation of mammalian cells by plasmid DNA. Mol Cell Biol 7:2745–2752

Cheng YC, Prussoff WH (1973) Relationship between the inhibition constant (K_I) and the concentration of inhibitor which causes 50 per cent inhibition (I_{50}) of an enzymatic reaction. Biochem Pharmacol 22:3099–3108

Doods HN, Mathy MJ, Davidesko D, van Charldorp KJ, de Jonge A, van Zwieten PA (1987) Selectivity of muscarinic antagonists in radioligand and *in vivo* experiments for the putative M_1, M_2 and M_3 receptors. J Pharm Exp Ther 242:257–262

Dörje F, Rettenmayr NM, Mutschler E, Lambrecht G (1991a) Effect of extracellular calcium concentration on potency of muscarinic agonists at M_1 and M2 receptors in rabbit vas deferens. Eur J Pharmacol 203:417–420

Dörje F, Wess J, Lambrecht G, Tacke R, Mutschler E, Brann MR (1991b) Antagonistic binding profiles of five cloned human muscarinic receptor subtypes. J Pharm Exp Ther 256:727–733

Eglen RM, Choppin A, Watson N (2001) Therapeutic opportunities from muscarinic receptor research. Trends Pharmacol Sci 22:409–414

El-Fakahani EE, Ramkumar V, Lai WS (1986) Multiple binding affinities of N-methylscopolamine to brain muscarinic acetylcholine receptors: Differentiation from M_1 and M_2 receptor subtypes. J Pharm Exp Ther 238:554–563

Eltze M, Gmelin G, Wess J, Strohmann C, Tacke R, Mutschler E, Lambrecht G (1988) Presynaptic muscarinic receptors mediating inhibition of neurogenic contractions in rabbit vas deferens are of the ganglionic M_1-type. Eur J Pharmacol 158:233–242

Ensinger HA, Doods HN, Immel-Sehr AR, Kuhn FJ, Lambrecht G, Mendla KD, Müller RE, Mutschler E, Sagrada A, Walther G, Hammer R (1993) WAL 2014 – a muscarinic agonist with preferential neuron-stimulating properties. Life Sci 52:473–480

Giachetti A, Giraldo E, Ladinski H, Montagna E (1986) Binding and functional profiles of the selective M_1 muscarinic receptor antagonists trihexylphenidyl and dicyclomine. Br J Pharmacol 89:83–90

Goyal RK (1989) Muscarinic receptor subtypes. Physiology and clinical implications. New Engl J Med 321:1022–1029

Hulme EC, Birdsall NJM, Buckley NJ (1990) Muscarinic receptor subtypes. Ann Rev Pharmacol Toxicol 30:633–673

Jones SVP, Levey AI, Weiner DM, Ellis J, Novotny E, Yu SH, Dorje F, Wess J, Brann MR (1992) Muscarinic acetylcholine receptors. In: Brann MR (ed) Molecular Biology of G-Protein-Coupled Receptors. Applications of Molecular Genetics to Pharmacology, Vol I, pp 170–197. Birkhäuser, Boston

Kajimura M, Reuben MA, Sachs G (1992) The muscarinic receptor gene expressed in rabbit parietal cells is the M_3 subtype. Gastroenterology 103:870–875

Karlin A, McNamee MG, Weill CL (1976) Methods of isolation and characterization of the acetylcholine receptor. In: Blecher M (ed) Methods in Receptor Research, Part I, Marcel Dekker, Inc., New York and Basel, pp 1–35

Kashihara K, Varga EV, Waite SL, Roeske WR, Yamamura HI (1992) Cloning of the rat M3, M4 and M5 muscarinic acetylcholine receptor genes by the polymerase chain reaction (PCR) and the pharmacological characterization of the expressed genes. Life Sci 51:955–971

Kebabian JW, Neumeyer JL (eds) (1994) The RBI Handbook of Receptor Classification. Research Biochemicals International, Natick, MA, pp 44–45

Lambrecht G, Feifel R, Wagner-Röder M, Strohmann C, Zilch H, Tacke R, Waelbroeck M, Christophe J, Boddeke H, Mutschler E (1989) Affinity profiles of hexohydrosiladifenidol analogues at muscarinic receptor subtypes. Eur J Pharmacol 168:71–80

Lambrecht G, Moser U, Grimm U, Pfaff O, Hermanni U, Hildebrandt C, Waelbroeck M, Christophe J, Mutschler E (1993) New functionally selective muscarinic antagonists. Life Sci 52:481–488

Lambrecht G, Gross J, Hacksell U, Hermanni U, Hildebrandt C, Hou X, Moser U, Nilsson BM, Pfaff O, Waelbroeck M, Werle J, Mutschler E (1995) The design and pharmacology of novel selective muscarinic agonists and antagonists. Life Sci 56:815–822

Lazareno S, Buckley NJ, Roberts FF (1990) Characterization of muscarinic M_4 binding sites in rabbit lung, chicken heart and NG108–15 cells. Mol Pharmacol 38:805–815

Longdong W (1986) Present status and future perspectives of muscarinic receptor antagonists. Scand J Gastroenterol 21:55–59
Luthin GR, Wolfe BB (1984) Comparison of [^{3}H]pirenzepine and [^{3}H]quinuclidinylbenzilate binding to muscarinic cholinergic receptors in rat brain. J Pharmacol Exp Ther 228:648–655
Ma W, Li BS, Zhang L, Pant HC (2004) Signaling cascades implicated in muscarinic regulation of peripheral neural stem and progenitor cells. Drug News Perspect 17:258–266
Maniatis T, Fritsch EF, Sambrook J (1982) Molecular Cloning. A Laboratory Manual. Cold Spring Harbor Laboratory, Cold Spring Harbor, NY
McConnell HM, Rice P, Wada GH, Owicki JC, Parce JW (1991) The microphysiometer biosensor. Curr Opin Struct Biol 1:647–652
McConnell HM, Owicki JC, Parce JW, Miller DL, Baxter GT, Wada HG, Pitchford S (1992) The Cytosensor Microphysiometer: biological applications of silicon technology. Science 257:1906–1912
McKinney M (1993) Muscarinic receptor subtype-specific coupling to second messengers in neuronal systems. In: Cuello AC (ed) Progress in Brain Research, Vol 98, Chapter 40, pp 333–340
Michel AD, Delmendo R, Stefanich E, Whiting RL (1989) Binding characteristics of the muscarinic receptor subtype of the NG108–15 cell line. Naunyn-Schmiedeberg's Arch Pharmacol 340:62–67
Norcoss NL, Griffith IJ, Lettieri JA (1980) Measurement of acetylcholine receptor and anti-receptor antibodies by ELISA. Muscle Nerve 3:345–349
Owicki JC, Parce JW, Kersco KM, Sigal GB, Muir VC, Venter JC, Fraser CM, McConnell HM (1990) Continuous monitoring of receptor-mediated changes in the metabolic rates of living cells. Proc Natl Acad Sci 87:4007–4011
Owicki JC, Parce JW (1992) Biosensors based on the energy metabolism of living cells: The physical chemistry and cell biology of extracellular acidification. Biosensors Bioelectronics 7:255–272
Parekh AB, Brading AF (1992) The M_3 muscarinic receptor links to three different transduction mechanisms with different efficacies in circular muscle of guinea pig stomach. Br J Pharmacol 106:639–643
Pitschner HF, Schlepper M, Schulte B, Volz C, Palm D, Wellstein A (1989) Selective antagonists reveal different functions of M cholinoceptor subtypes in humans. Trends Pharmacol Sci Suppl IV:92–96
Richards (1990) Rat hippocampal muscarinic autoreceptors are similar to the M_2 (cardiac) subtype: comparison with hippocampal M_1, atrial M_2 and ileal M_3 receptors. Br J Pharmacol 99:753–761
Spalding TA, Trotter C, Skjærbæk N, Messier TL, Currier EA, Burstein ES, Li D, Hacksell U, Brann MR (2002) Discovery of an ectopic activation site on the M_1 muscarinic receptor. Mol Pharmacol 61:1297–1302
Svensson AL, Alafuzoff I, Nordberg A (1992) Characterization of muscarinic receptor subtypes in Alzheimer and control brain cortices by selective muscarinic antagonists. Brain Res 596:142–148
Wamsley JK, Gehlert DR, Roeske WR, Yamamura HI (1984) Muscarinic antagonist binding site heterogeneity as evidenced by autoradiography after direct labeling with [^{3}H]QNB and [^{3}H]pirenzepine. Life Sci 34:1395–1402
Watson M, Yamamura HI, Roeske WR (1983) A unique regulatory profile and regional distribution of [^{3}H]pirenzepine binding in the rat provide evidence for distinct M_1 and M_2 muscarinic receptor subtypes. Life Sci 32:3001–3011
Wess J, Angeli P, Melchiorre C, Moser U, Mutschler E, Lambrecht G (1988) Methoctramine selectively blocks cardiac muscarinic M_2 receptors *in vivo*. Naunyn-Schmiedeberg's Arch Pharmacol 338:246–249
Zhang L, Horowitz B, Buxton ILO (1991) Muscarinic receptors in canine colonic circular smooth muscle. I. Coexistence of M_2 and M_3 subtypes. Mol Pharmacol 40:943–951

J.3.6.2 H_2-Antagonism

J.3.6.2.1 General Considerations

Three classes of histamine receptors with subtypes for the H_2 receptor have been identified by selective antagonists (Haaksma et al. 1990; Hill 1990; West et al. 1990; Clapham and Kilpatrick 1992). H_2-antagonists inhibit competitively the interaction of histamine with H_2-receptors responsible for acid secretion in the stomach. Although H_2-receptors are present in many tissues, including vascular and bronchial smooth muscle and the right atrium, H_2-antagonists interfere remarkably little with physiological functions other than gastric secretion.

The H_2 receptor was reported to be spontaneously active in transfected CHO cells (Smit et al. 1996). Based on this concept, the H_2 antagonists were reclassified; cimetidine, ranitidine and famotidine are in fact inverse agonists, whereas burimamide acts in this model system as a neutral agonist.

REFERENCES AND FURTHER READING

Black JW, Duncan WAM, Durant CJ, Ganellin CR, Parsons EM (1972) Definition and antagonism of histamine H_2-receptors. Nature 236:385–390
Clapham J, Kilpatrick GJ (1992) Histamine H_3 receptors modulate the release of [^{3}H]-acetylcholine from slices of rat entorhinal cortex: evidence for the possible existence of H_3 receptor subtypes. Br J Pharmacol 107:919–923
Haaksma EEJ, Leurs R, Timmerman H (1990) Histamine receptors: subclasses and specific ligands. Pharmac Ther 47:73–104
Hill SJ (1990) Distribution, properties and functional characteristics of three classes of histamine receptor. Pharmacol Rev 42:45–83
Leurs R, van der Goot H, Timmerman H (1991) Histaminergic agonists and antagonists. Recent Developments. Advanc Drug Res 20:217–304
Smit MJ, Leurs R, Alewijnse EA, Blauw J, van Nieuw-Amerongen GP, van der Vrede Y, Roovers E, Timmerman H (1996) Inverse agonism of histamine H_2 antagonists accounts for up-regulation of spontaneously active histamine H_2 receptors. Proc Natl Acad Sci USA 93:6802–6807
West RE Jr, Zweig A, Shih NY, Siegel MI, Egan RW, Clark MA (1990) Identification of two H_3-histamine receptor subtypes. Mol Pharmacol 38:610–613

J.3.6.2.2 Histamine H_2-Receptor Binding

PURPOSE AND RATIONALE

Histamine receptors have been classified on the basis of pharmacological analysis (Hill et al. 1997). Histamine exerts its action via at least four receptor subtypes. The H_1 receptor couples mainly to $G_{q/11}$, thereby stimulating phospholipase C, whereas the H_2 receptor interacts with G_s to activate adenylyl cyclase. The histamine H_3 and H_4 receptors couple to G_i proteins to inhibit adenylyl cyclase, and to stimulate MAPK.

Histamine H_2-receptor binding can be determined using homogenates from guinea pig cerebral cortex and ^{3}H-tiotidine as labeled ligand (Gajtkowski et al. 1983; Norris et al. 1984; Hill 1990). Using the polymerase chain reaction, the gene encoding the histamine H_2 receptor has been cloned (Gantz et al. 1991).

PROCEDURE

Preparation of Membranes

Guinea pigs of either sex weighing 400–600 g are sacrificed by exsanguination and the brains rapidly removed. The cerebral cortex is dissected away from the rest of the brain and homogenized in 50 mM sodium-potassium buffer, pH 7.4, using a Potter homogenizer. The homogenate is then centrifuged at 50,000 *g* for 10 min at 4°C. The resulting pellet is washed three times by being resuspended in phosphate buffer followed by recentrifugation. The pellet is finally resuspended in phosphate buffer, pH 7.4, at a protein concentration of 5 mg/ml.

Assay

An aliquot of 100 µl of the homogenate is incubated with 2 nM ^{3}H-tiotidine and varying concentrations of competing test substance, in triplicate, in a total volume of 250 µl, for 30 min at room temperature. The reaction is stopped by the addition of 2 ml of ice-cold phosphate buffer and immediately filtered under reduced pressure through Whatman GF/B glass-fiber filters, followed by 3 times 3 ml washes with room temperature buffer.

Radioactivity is determined by allowing the filters to remain for at least 18 h in NE 260 scintillator (Nuclear Enterprise), followed by liquid scintillation counting.

EVALUATION

K_i values (µM) are calculated for displacement of specific H_2-binding from the relationship

$$K_i = IC_{50}/(1 + [L]K_d^{-1})$$

where IC_{50} is the concentration of the drug required for 50% inhibition of specific binding, [L] is the concentration of ^{3}H-tiotidine in the assay and K_d is the dissociation constant for ^{3}H-tiotidine.

Data can be analyzed using a computer program as described by McPherson (1985).

MODIFICATIONS OF THE METHOD

Hirschfeld et al. (1992) performed photoaffinity labeling studies of the H_2 receptor using the radioactive probes [^{125}I]iodoaminopotentidine and its photolabile azido analogue [^{125}I]iodoazidopotentidine.

Martinez-Mir et al. (1990) studied the distribution of histamine H_1, H_2, and H_3 receptors in postmortem human and rhesus monkey brain by receptor autoradiography using [^{125}I]iodobolpyramine, [^{125}I]iodoaminopotentine, and [^{3}H](R)α-methylhistamine as ligands to label H_1, H_2, and H_3 receptors, respectively.

Traiffort et al. (1992) used [^{125}I]iodoaminopotentidine for pharmacological characterization and auto-radiographic localization of histamine H_2 receptors in human brain.

REFERENCES AND FURTHER READING

Bickel M, Herling AW, Rising TJ, Wirth K (1986) Antisecretory effects of two new histamine H_2-receptor antagonists. Arzneim Forsch/Drug Res 36:1358–1363

Eriks JC, van der Goot H, Sterk GJ, Timmerman H (1992) Histamine H_2-receptor agonists. Synthesis, *in vitro* pharmacology, and qualitative structure-activity relationships of substituted 4- and 5-(2-aminoethyl)-thiazoles. J Med Chem 35:3239–3246

Gajtkowski GA, Norris DB, Rising TJ, Wood TP (1983) Specific binding of [^{3}H]-tiotidine to histamine H_2 receptors in guinea pig cerebral cortex. Nature 304:65–67

Gantz I, Schäfer M, DelValle J, Logsdon C, Campell V, Uhler M, Yamada T (1991) Molecular cloning of a gene encoding the histamine H_2 receptor.

Hill SJ (1990) Distribution, properties and functional characteristics of three classes of histamine receptor. Pharmacol Rev 42:45–83

Hill SJ, Ganellin CR, Timmerman H, Schwartz JC, Shankley NP, Young JM, Schunack W, Levi R, Haas HL (1997) International Union of Pharmacology. XIII. Classification of histamine receptors. Pharmacol Rev 49:253–278

Hirschfeld J, Buschauer A, Elz S, Schunack W, Ruat M, Traiffort E, Schwartz J-Ch (1992) Iodoaminopotentidine and related compounds: A new class of ligands with high affinity and selectivity for the histamine H_2 receptor. J Med Chem 35:2231–2238

Martinez-Mir MI, Pollard H, Moreau J, Arrang JM, Ruat M, Traiffort E, Schwartz JC, Palacios JM (1990) Three histamine receptors (H_1, H_2, and H_3) visualized in the brain of human and non-human primates. Brain Res 526:322–327

McPherson GA (1985) Analysis of radioligand binding experiments. A collection of computer programs for the IBM PC. J Pharmacol Meth 14:213–228

Norris DB, Gajtkowski GA, Rising TJ (1984) Histamine H_2-binding studies in the guinea-pig brain. Agents Actions 14:543–545

Traiffort E, Pollard H, Moreau J, Ruat M, Schwartz JC, Martinez-Mir MI, Palacios JM (1992) Pharmacological characterization and autoradiographic localization of histamine H_2 receptors in human brain identified with [^{125}I]iodoaminopotentidine. J Neurochem 59:290–299

West RE Jr, Zweig A, Shih NY, Siegel MI, Egan RW, Clark MA (1990) Identification of two H_3-histamine receptor subtypes. Mol Pharmacol 38:610–613

J.3.6.2.3 H_2-Antagonism in Isolated Guinea Pig Right Atria

PURPOSE AND RATIONALE

H_2-antagonism can be determined in isolated guinea pig right atria which contain predominantly H_2-receptors. Compounds that inhibit the positive chronotropic effect mediated by histamine H_2-receptors in the isolated right guinea pig atrium (Reinhardt et al. 1974) can be classified as specific histamine H_2-antagonists. The test can be used as screening method for H_2-antagonists.

PROCEDURE

Male guinea pigs, e. g., Hartley strain, are sacrificed by exsanguination. The right atria are dissected and suspended at 0.7 g tension in a 25 ml organ bath with Tyrode's solution bubbled with carbogen (5% CO_2/95% O_2) at 38°C. After a stabilization period of 30 min, the contractions are recorded on a polygraph with a force-displacement transducer through a strain gauge. Cumulative concentration-response curves are obtained after sequential additions of histamine (10^{-7} to 10^{-4} M) in the absence of test drugs and the equilibration of test drugs or the standard (cimetidine).

EVALUATION

pA_2 values and relative potencies are calculated by a Schild plot (Arunlakshana and Schild 1959).

MODIFICATIONS OF THE METHOD

Hattori et al. (1990) studied the inotropic, electrophysiological and biochemical responses to histamine in rabbit papillary muscles and found evidence for coexistence of H_1- and H_2-receptors. Histamine increases force of contraction and decreases action potential duration in rabbit papillary muscles. H_2-antagonists antagonize the histamine-induced decrease in action potential duration, however, are less effective in antagonizing the increase in force of contraction produced by histamine. The positive inotropic response to histamine is abolished by sequential addition of a H_1-antagonist.

REFERENCES AND FURTHER READING

Arunlakshana O, Schild HO (1959) Some quantitative uses of drug antagonists. Br J Pharmacol Chemother 14:48–58

Daly MJ, Humphray JM, Stables R (1981) Some *in vitro* and *in vivo* actions of the new histamine H_2-receptor antagonist, ranitidine. Br J Pharmac 72:49–54

Hattori YS, Nakaya H, Endou M, Kanno M (1990) Inotropic, electrophysiological and biochemical responses to histamine in rabbit papillary muscles: evidence for coexistence of H_1- and H_2-receptors. J Pharm Exp Ther 253:250–256

Hirschfeld J, Buschauer A, Elz S, Schunack W, Ruat M, Traiffort E, Schwartz J-Ch (1992) Iodoaminopotentidine and related compounds: A new class of ligands with high affinity and selectivity for the histamine H_2 receptor. J Med Chem 35:2231–2238

Reinhardt D, Wagner J, Schümann HJ (1974) Differentiation of H_1- and H_2-receptors mediating positive chronotropic and inotropic responses to histamine on atrial preparations of the guinea-pig. Agents Actions 4:217–221

Tarutani M, Sakuma H, Shiratsuchi K, Mieda M (1985) Histamine H_2-receptor antagonistic action of N-3-[3-(1-piperidinyl)phenoxy]propyl acetoxyacetamide hydrochloride (TZU-0460). Arzneim Forsch/Drug Res 35:703–706

J.3.6.2.4 H_2-Antagonism in Isolated Rat Uterus

PURPOSE AND RATIONALE

Histamine inhibits spontaneous and electrically stimulated contractions of rat uterus horns. This effect can be antagonized by H_2-, but not by H_1-antagonists.

PROCEDURE

Adult, virgin Wistar rats weighing 180–200 g are used. By microscopic examination of vaginal smears, the stage of the estrus cycle is determined. Only animals in natural proestrus or metestrus are chosen. After sacrifice, the two uterus horns are removed and placed in modified de Jalon solution at room temperature and cleaned of mesenteric fat and connective tissue. Paired preparations from the same animal are used in parallel experiments. Two segments, about 2 cm in length, are taken from the ovarian end of the uterus horns and mounted separately on Perspex organ holders between two steel electrodes arranged at the end of the muscle. The organs are immediately superfused with modified de Jalon solution at 35°C at a rate of 2–3 ml/min being continuously gassed with air. Basal muscle tension is maintained at 0.5 g. The contractions of the preparations are recorded isometrically with a force-displacement transducer linked to a multipen recorder. The intrinsic rhythm of spontaneous and regular con-

tractions appears within 5–10 min after mounting the tissues in their holders.

Organs showing a frequency of only one contraction every two min or less are electrically stimulated with square wave impulses of 2 ms duration for 1 s every 1 min at 10 V and 80 Hz with a suitable stimulator. The organs are linked via a four-way stopcock to a set of reservoirs of modified de Jalon solution containing different concentrations of agonist and test substance. The preparations are superfused for 20–30 min with nutrient solution until mechanical activity of the uterus horns is stabilized in frequency and contraction height before addition of drugs.

The time interval between application of drugs is 15–20 min, the time of contact of the drugs with the uterus segments is about 4–5 min, being interrupted as soon as the contractions of the muscles reach a minimum. Logarithmic dose-response curves for histamine are constructed from mean effects of single doses, taking the average amplitude of 5 contractions immediately preceding the addition of histamine as 100% control activity. In experiments involving antagonists, a standard dose of histamine is used giving a response within the linear region of the log dose-response curve and is set as 100%. Reduction of histamine-induced inhibition is studied by superfusing increasing concentrations of antagonists in addition to the standard dose of histamine.

EVALUATION

Results are expressed in percentage of the reversal of initial depression of contraction height after histamine and plotted against –log mol/l concentration of the antagonist. pA_2 values are calculated according to Ariëns and van Rossum (1957).

REFERENCES AND FURTHER READING

Ariëns EJ, van Rossum JM (1957) $p\mathrm{D_x}$, $p\mathrm{A_x}$ and $p\mathrm{D'_x}$ values in the analysis of pharmacodynamics. Arch Int Pharmacodyn 110:275–299

Ash ASF, Schild HO (1966) Receptors mediating some actions of histamine. Br J Pharmacol Chemother 27:427–439

Eltze M (1979) Proestrus and metestrus rat uterus, a rapid and simple method for detecting histamine H_2-receptor antagonism. Arzneim Forsch/Drug Res 29:1107–1112

J.3.6.2.5 Activity at Histamine H_1- and H_2-Receptors In Vivo

PURPOSE AND RATIONALE

Owen and Pipkin (1985) described a technique that allows simultaneous and quantitative assay of the action of agonists and antagonists at histamine H_1- and H_2-receptors in anesthetized guinea pigs. The principle of the technique is based on H_1-receptor caused bronchoconstriction and H_2-receptor caused tachycardia.

PROCEDURE

Guinea pigs of either sex weighing about 500 g are anesthetized with 90 m/kg sodium pentobarbitone i.p. The trachea is cannulated to permit artificial respiration. Blood pressure is measured from a catheter tied into one carotid artery. Catheters are tied into one jugular and one femoral vein for the administration of drugs.

Airways resistance is measured using a modification of the Konzett–Rössler technique. By means of a small animal respiration pump, the lungs are inflated at a rate of 40 breaths/min. The inflow arm of the circuit includes a side-arm, the outlet of which is placed below 12 cm of H_2O. The volume of air used in the study has to be that which fills the lungs at a pressure of 12 cm H_2O, selected by adjusting the volume until no air escapes through the H_2O trap each time the lungs are filled. The side-arm is then clamped, and the animal is respired with the selected volume for the duration of the study. Airways resistance to inflow is measured using a pressure transducer connected to a second arm of the inflow circuit. Resistance is proportional to the maximum pressure required to inflate the lungs. Inflow pressure is registered on an electronic recorder.

Heart rate is measured from the blood pressure pulse using an instantaneous rate meter and is registered on an electronic recorder.

Intravenous injection of histamine causes simultaneously bronchoconstriction and tachycardia. The threshold dose needed to cause tachycardia may be less than that for bronchoconstriction, but both responses will be apparent over the dose range 1×10^{-8} to 5×10^{-7} mol/kg.

EVALUATION

Agonists

Dose-response curves for agonists compared to the dose-response curve for histamine for both parameters, bronchoconstriction and tachycardia, allow the calculation of potency ratios. Specific H_1-receptor agonists are more potent to cause bronchoconstriction than tachycardia, whereas H_2-agonists provoke tachycardia but are less active or inactive causing bronchoconstriction.

Antagonists

To evaluate antagonists, various doses of the test compound are injected i.v. and dose-response curves of

histamine are established for both parameters to be compared with the dose-response curve of histamine without pretreatment. From the ratios of shift to the right dose-response curves for both parameters can be established. These are similar for mixed antagonists, but a definitively higher potency is shown for H_1-antagonists in bronchoconstriction and a higher potency for H_2-antagonists in tachycardia.

REFERENCES AND FURTHER READING

Owen DAA, Pipkin MA (1985) A simple technique to simultaneously assess activity at histamine H_1- and H_2-receptors *in vivo*. J Pharmacol Meth 13:309–315

J.3.6.2.6 Inhibition of Histamine Stimulated Adenylate Cyclase from Gastric Mucosa

PURPOSE AND RATIONALE

The *in vitro* potencies of H_2-antagonists can be evaluated using determinations of adenylate cyclase activity in membrane preparations of guinea pig mucosa after stimulation with histamine.

PROCEDURE

Preparation of Membranes

Guinea pigs of either sex weighing 400–600 g are sacrificed. The fundic portion of the stomach is rapidly removed. Food particles are washed away with ice-cold 50 mM Tris buffer, pH 7.4, containing 4 mM EDTA and 0.25 M sucrose (homogenization buffer). The tissue is stretched, mucosal side up, on a glass Petri dish supported on ice and the mucosal layer is scraped off the muscle layer using a scalpel blade. The mucosal scrapings are transferred to 10 ml ice-cold homogenization buffer in a glass homogenization tube, and homogenized using an Ultra-Turrax homogenizer followed by four strokes using a Potter Teflon homogenizer. The resulting suspension is centrifuged at 700 *g* for 10 min at 4°C. The supernatant is discarded, and the pellet resuspended in 50 mM Tris buffer, pH 7.4, containing 4 mM EDTA followed by a further period of centrifugation. The resulting pellet is finally resuspended in Tris/EDTA buffer at a protein concentration of 2.4 mg/ml as determined by the method of Lowry et al. (1951) using bovine serum albumin as standard.

Stimulation of Adenylate Cyclase

Adenylate cyclase activity is measured according to Hegstrand et al. (1976). Aliquots (120 µg) of fundic mucosal homogenate are incubated in 100 mM Tris buffer, pH 7.8, containing 0.6 mM EGTA (ethylene-glycol-bis-(β-aminoethyl ether)-N,N′-tetra-acetic acid), 1 mM IBMX (isobutyl-methyl xanthine), 2 mM $MgCl_2$, 0.1 mM GPT (guanosine triphosphate), histamine at various concentrations between 0.1 µM and 100 µM and the compound under investigation at varying concentrations between 0.1 µM and 1 mM for 10 min at 0°C. The reaction is initiated by the addition of 1 mM ATP followed by a 10 min incubation at 30°C. The reaction is terminated by placing the assay tubes in a boiling water bath for 3 min. After cooling, 40 mg of Alumina 90 (E. Merck, 70–230 mesh) are added to each tube prior to mixing and centrifugation at 700 *g* for 15 min at 4°C.

Assay of Cyclic AMP

The cyclic AMP content of each sample is determined according to Brown et al. (1971) using ^{3}H-cyclic AMP in a competitive protein binding assay. Fifty µl aliquots from the adenylate cyclase assay are incubated with 50 µl of ^{3}H-cyclic AMP (14 nC at a specific activity of 62 Ci/mmol) and 100 µl of previously prepared cyclic AMP binding protein at 4°C. The bound and free ^{3}H-cyclic AMP are separated by the addition of 100 µl of charcoal reagent (2 g bovine serum albumin, 2.5 g Norit GSX charcoal in 100 ml of 50 mM Tris buffer, pH 7.4, containing 4 mM EDTA), followed by mixing and centrifugation at 1000 *g* for 15 min. Two hundred µl aliquots of the supernatant are decanted into scintillation vials containing 10 ml of NE 260 scintillator. Radioactivity is determined by liquid scintillation counting.

EVALUATION

Results are calculated from a standard curve using cyclic AMP as the standard. From these data IC_{50} values (µM) are derived.

REFERENCES AND FURTHER READING

Brown BL, Albano JDM, Ekins RP, Sgherzi AM (1971) A simple and sensitive assay method for the measurement of adenosine 3′,5′-cyclic monophosphate. Biochem J 121:561–562

Hegstrand LR, Kanof PhD, Greengard P (1976) Histamine-sensitive adenylate cyclase in mammalian brain. Nature 260:163–165

Lowry OH, Rosebrough NJ, Farr AL, Randall RJ (1951) Protein measurement with the Folin phenol reagent. J Biol Chem 13:265–275

Sewing KF, Beil W, Hannemann H, Hackbarth I (1985) The adenylate cyclase-cyclic AMP-protein kinase system in different cell populations of the guinea-pig gastric mucosa. Life Sci 12:1097–1106

Sewing KF, Beil W, Hannemann H (1988) Comparative pharmacology of histamine H_2-receptor antagonists. Drugs 33 (Suppl 3):25–29

J.3.6.3
H^+/K^+-ATPase (Proton Pump) Inhibition

J.3.6.3.1
General Considerations

The parietal cell of the stomach is activated by three major stimuli: histamine, acetylcholine, and gastrin. In addition to the direct action of gastrin and acetylcholine on the parietal cell, these two agents may release histamine from a histamine storage in the gastric mucosa. In this manner, histamine would act as the final mediator of acid secretion. One of the first events leading to acid secretion is a massive membrane transformation that occurs in the parietal cell. When the cell is stimulated, the tubulovesicles in the cytoplasma of the cell fuse and form an expanded secretory canaliculus in the apical membrane where the enzyme H^+/K^+-ATPase is located.

In this way, the ultimate mediator of acid secretion in the stomach is the proton pump H^+/K^+-ATPase which transports hydrogen in exchange for potassium. The rat stomach H^+/K^+-ATPase has been cloned by Shull and Lingrel (1986). Development of specific inhibitors of this enzyme is an approach to suppress acid secretion and ulcer formation since ulcers only exist in acidic medium.

Alderuccio et al. (1993) described an experimental autoimmune gastritis in BALB/c mice as a $CD4^+$ T cell-mediated organ-specific autoimmune disease induced by neonatal thymectomy. Transgenic expression of the gastric H^+/K^+-ATPase β subunit specifically prevented the onset of this form of autoimmune gastritis.

REFERENCES AND FURTHER READING

Alderuccio F, Toh BH, Tan SS, Gleeson PA, van Driel IR (1993) An autoimmune disease with multiple molecular targets abrogated by transgenic expression of a single autoantigen in the thymus. J Exp Med 178:419–426

Brändström PA, Wallmark B, Mattsson H, Rikner L, Hoffmann KJ (1990) Omeprazole: The first proton pump inhibitor. Medicin Res Rev 10:1–54

Herling AW, Weidmann K (1994) Gastric K^+/H^+-ATPase inhibitors. In: Ellis GP, Luscombe DK (eds) Progress in Medicinal Chemistry, Vol 31, Elsevier Science BV, pp 233–264

Sachs G, Shin JM, Besancon M, Pinz C (1993) The continuing development of gastric acid pump inhibitors. Aliment Pharmacol Ther 7 (Suppl 1):4–12

Sachs G, Shin JM, Briving C, Wallmark B, Hersey S (1995) The pharmacology of the gastric acid pump: the K^+/H^+-ATPase. Ann Rev Pharmacol Toxicol 35:277–305

Shull GE, Lingrel JB (1986) Molecular cloning of the rat stomach (H^+/K^+)-ATPase. J Biol Chem 261:16788–16791

J.3.6.3.2
H^+/K^+-ATPase Inhibition in Membrane Vesicles of Stomach Mucosa

PURPOSE AND RATIONALE

Several H^+/K^+-ATPase inhibitors contain a sulfhydryl group. At lower pH-values the compounds are protinated and rearrange to a sulphenic acid and a sulphenamide, that react with sulfhydryl groups in the enzyme. Therefore, the *in vitro* assays are performed both at neutral and at acidic pH levels.

PROCEDURE

Membrane vesicles containing H^+/K^+-ATPase are prepared from pig stomachs obtained from the local slaughter house (Ljungstrom et al. 1984). Pigs are fasted overnight before slaughter. The gastric mucosa of four stomachs is rinsed with cold saturated NaCl solution for 3–5 min. The superficial cells, cell debris plus the mucus are wiped off with the edge of a plastic ruler and with paper towels. The mucosa is scraped off. About 100 g scrapings are divided into portions of 10 g and homogenized in 0.25 M sucrose with seven strokes in a Potter-Elvehjem Teflon-glass homogenizer. The total volume is 600 ml which is centrifuged at 20,000 *g* for 40 min. The pellet is discarded. The supernatant is centrifuged at 75,000 *g* for 1 h. The resulting microsomal pellet is homogenized in 30 ml 0.25 M sucrose.

Aliquots of 15 ml are transferred to 100 ml centrifuge tubes and layered on top of step gradients, from the bottom comprising 25 ml 37% sucrose (w/v) and 45 ml 7.5% Ficoll (w/v) in 0.25 M sucrose. The tubes are centrifuged at 75,000 *g* for 1 h in a 6×100 ml ME angle rotor at 4°C. The gradient is then fractionated by pumping Fluoroinert 70 through a narrow tubing in a fractionating cap down to the bottom of the tube. Fractions are collected from top through a center hole in the fractionating cap. The yield of vesicles in a typical preparation is about 50–75 mg protein. In order to maintain a stable vesicular structure for a long period of time, the vesicles are frozen at –70°C under nitrogen. They can then be kept for several months without decrease of H^+/K^+-ATPase activity.

The ATPase activity is measured at 37°C as the release of inorganic phosphate (P_i) from ATP. The test drug and the standard (omeprazole) are pre-incubated in concentrations of 0.01 to 100.0 µM in enzyme containing buffers in parallel at pH 6.0 and 7.4 for 30 min at 37°C. Then, the medium of pH 6.0 is adjusted with

HEPES/Tris buffer to pH 7.4. The enzyme reaction is started by addition of nigericin and Tris/ATP. The total reaction volume is 1 ml, containing 20 µg vesicular protein, 4 mM $MgCl_2$, 10 mM KCl, 20 µM nigericin, 2 mM Tris-ATP, 10 mM HEPES and additionally 2 mM Pipes for the pre-incubation medium at pH 6.0.

After 4 min at 37°C, the reaction is stopped by the addition of 10 ml of 50% trichloroacetic acid. The denaturated protein is spun down and the P_i content is determined according to LeBel et al. (1978) based on the reduction of a phosphomolybdate complex by p-methylaminophenol sulfate in a copper acetate buffer or according to Carter and Karl (1982) based on the reaction of phosphomolybdate with the basic dye malachite green.

EVALUATION

IC_{50} values are calculated by probit analysis, whereby 0% corresponds to 4 mM Mg^{2+}-dependent and 100% to 4 mM Mg^{2+} plus 10 mM K^+-dependent ATP hydrolysis. IC_{50} values of the test compound at different pH values are compared with IC_{50} values of the standard. Statistical differences ($p < 0.05$) are calculated by Student's *t*-test.

MODIFICATIONS OF THE METHOD

Proton transport in gastric vesicles can be measured by acridine orange fluorescence quenching (Lee and Forte 1978; Beil et al. 1990). Membrane protein (0.12 mg) is incubated at 37°C in a volume of 2 ml containing: 10 mM Pipes/Tris buffer, pH 7.0 in the presence of 150 mM KCl, 2 mM $MgCl_2$, 2 mM ATP and 10 µM acridine orange. The pump reaction is started by the addition of valinomycine (ionophore for K^+). The decrease of fluorescence is studied at 530 mm as a measure for the intravesicular proton uptake.

CRITICAL ASSESSMENT OF THE METHOD

The pre-incubation period at the lowest possible pH of about 6 is used to initiate the acidic conversion of the test compound into its active principle. This reflects more the chemical instability of the test compound at neutral pH values than its effect during conditions of much higher acidity within the secretory cannaliculus of the parietal cell during acid secretion. Many chemically labile inhibitors are therefore very active in this test system. However, they do not cause an inhibition in more complex test systems and, therefore, are without any practical usefulness (Lindberg et al. 1990). Proton transport studies in gastric vesicles, using the acridine orange fluorescence quenching technique, where a pH gradient similar to *in vivo* conditions is formed (Lee and Forte 1978; Beil et al. 1990) are more suitable for studying the mechanism of action, acid-conversion, and structure-activity relationship of K^+/H^+-ATPase inhibitors (Herling and Weidmann 1994).

REFERENCES AND FURTHER READING

Beil W, Sewing KF (1984) Inhibition of partially purified K^+/H^+-ATPase from guinea-pig isolated and enriched parietal cells by substituted benzimidazoles. Br J Pharmacol 82:651–657

Beil W, Staar U, Sewing KF (1990) Substituted thieno[3,4-d]imidazoles, a novel group of K^+/H^+-ATPase inhibitors. Differentiation of their inhibition characteristics from those of omeprazole. Eur J Pharmacol 187:455–457

Carter SG, Karl DW (1982) Anorganic phosphate assay with malachite green: an improvement and evaluation. J Biochem Biophys Meth 7:7–13

Herling AW, Weidmann K (1994) Gastric K^+/H^+-ATPase inhibitors. In: Ellis GP, Luscombe DK (eds) Progress in Medicinal Chemistry, Vol 31, Elsevier Science BV, pp 233–264

LeBel D, Poirier GG, Beaudoin AR (1978) A convenient method for the ATPase assay. Anal Biochem 85:86–89

Lee HC, Forte JG (1978) A study of H^+ transport in gastric microsomal vesicles using fluorescent probes. Biochim Biophys Acta 508:339–356

Ljungström M, Norberg L, Olaisson H, Wernstedt C, Vega FV, Arvidson G, Mårdh S (1984) Characterization of proton-transporting membranes from resting pig gastric mucosa. Biochem Biophys Acta 769:209–219

Nagaya H, Satoh H, Maki Y (1987) Actions of antisecretory agents on proton transport in hog gastric mucosa. Biochem Pharmacol 36:513–519

Saccomani G, Stewart HB, Shaw D, Lewin M, Sachs G (1977) Characterization of gastric mucosal membranes. IX. Fractionation and purification of K^+-ATPase-containing vesicles by zonal centrifugation and free-flow electrophoresis technique. Biochim Biophys Acta 465:311–330

Sewing KF, Beil W, Hackbarth I, Hannemann H (1986) Effect of substituted benzimidazoles on H^+/K^+ATPase of isolated guinea-pig parietal cells. Scand J Gastroenterol 21, Suppl 118:52–53

Wallmark B, Jaresten BM, Larsson H, Ryberg B, Brandström A, Fellenius E (1973) Differentiation among inhibitory actions of omeprazole, cimetidine and SCN- on gastric secretion. Am J Physiol 245:G64–G71

J.3.6.3.3 Effect of H^+/K^+-ATPase Inhibitors on Serum Gastrin Levels

PURPOSE AND RATIONALE

It is known from the H^+/K^+-ATPase inhibitor omeprazole that the total acid blockade initiates a gastric antral feed back mechanism resulting in an excessive hypergastrinaemia (Arnold et al. 1986; Creutzfeldt et al. 1986; Larsson et al. 1986) which is believed to cause diffuse endocrine cell hyperplasia, characterized as carcinoids, in the gastric corpus after 2 years of treatment in the rat (Ekman et al. 1985).

PROCEDURE

Groups of 10–15 female Wistar rats weighing 90–110 g are treated daily for 10 weeks with omeprazole (10 or 30 mg/kg p.o.) or the test compound or serve as controls. The compounds are suspended in potato starch mucilage (20 mg/ml) and administered in a volume of 2 ml/kg. On days 1–3, the rats receive the H^+/K^+-ATPase inhibitors by intraperitoneal injection in order to cause gastric acid inhibition and therefore to reduce the gastric acid degradation of subsequent oral doses. After treatment for 2, 4, 7, and 10 weeks, blood samples are collected under ether anesthesia by retroorbital puncture. Gastrin is determined by radioimmunoassay using a commercially available kit, e. g. Gastrin RIAKit II; Dainabot Co., Ltd. At the end of the study of 10 weeks, the animals are studied for their gastric acid output using the pylorus ligation (Shay technique).

EVALUATION

Serum gastrin levels are determined as pg/ml. Statistical differences ($p < 0.05$) are calculated using Student's *t*-test.

MODIFICATIONS OF THE METHOD

Katz et al. (1987) described a five-day test to predict the long-term effects of gastric antisecretory agents on serum gastrin in rats.

REFERENCES AND FURTHER READING

Arnold R, Koop H, Schwarting H, Tuch K, Willemer B (1986) Effect of acid inhibition on gastric endocrine cells. Scand J Gastroenterol 21 (Suppl 125):14–19

Creutzfeldt W, Stöckmann F, Conlon JM, Fölsch UR, Bonatz G, Wülfrath M (1986) Effect of short- and long-term feeding of omeprazole on rat gastric endocrine cells. Digestion 35 (Suppl 1):84–97

Ekman L, Hansson E, Havu N, Carlsson E, Lundberg C (1985) Toxicological studies on omeprazole. Scand J Gastroenterol 20 (Suppl 108):53–69

Katz LB, Schoof RA, Shriver DA (1987) Use of a five-day test to predict the long-term effects of gastric antisecretory agents on serum gastrin in rats. J Pharmacol Meth 18:275–282

Larsson H, Carlsson E, Mattsson H, Lundell L, Sundler F, Sundell G, Wallmark B, Watanabe T, Håkanson R (1986) Plasma gastrin and gastric enterochromaffin-like cell activation and proliferation. Studies with omeprazole and ranitidine in intact and antrectomized rats. Gastroenterology 90:391–399

J.3.6.3.4 (^{14}C)-Aminopyrine Uptake and Oxygen Consumption in Isolated Rabbit Gastric Glands

PURPOSE AND RATIONALE

Isolated gastric glands from rabbits and other species can be used in studying the control of mechanism of gastric H^+ secretion (Berglindh and öbrink 1967; Berglindh et al. 1967; Sack and Spenny 1982; Sewing et al. 1983; Herling et al. 1987, 1988, 1990). In isolated gastric glands and parietal cells, H^+ secretion cannot be directly measured by titration; therefore, accumulation of weak bases such as aminopyrine is used as an indirect probe of H^+ secretion. Moreover, glandular oxygen consumption can be measured with the Warburg technique.

PROCEDURE

Preparation of Gastric Glands

Rabbits are anesthetized with 40 mg/kg pentobarbital i.v. The abdomen is opened and the aorta is cannulated in a retrograde direction. Five ml of a heparin solution (250 IU/ml) are injected with force through the cannula. After one min the rabbit is bled through the cannula and a ligature is placed around the mesenteric vessels. The chest is quickly opened and the thoracic aorta clamped. Phosphate buffered saline solution (containing 149.6 mM NaCl, 3 mM K_2HPO_4, 0.64 mM NaH_2PO_4, pH 7.3) at 37°C is pumped through the aorta, whereby the portal vein is opened to allow free outflow of the perfusate. By this procedure most of the solution is forced through the mesenteric vessels. The perfusion pressure, as measured proximal to the cannula, can be up to 600 mm Hg.

The stomach appears totally exsanguinated after perfusion with about 500 ml phosphate buffered saline solution and is then removed, cut open along the lesser curvature, and emptied. The cardial and antral regions are discarded. The corpus is rinsed several times with phosphate buffer solution and finally blotted with filter paper, whereby the remaining gastric content as well as some surface epithelial cells are removed. By blunt dissection the mucosa can easily be separated from the muscular and submuscular layers.

The mucosa is then minced into small pieces with a pair of scissors. The pieces are washed twice in warm oxygenated phosphate buffer solution and transferred to a 200 ml flask with 50 ml of a freshly prepared collagenase-enzyme solution containing 1 mg/ml collagenase (type I, Sigma), 1 mg/ml rabbit albumin (Sigma), 2 mg/ ml glucose in 130 mM NaCl, 10 mM $NaHCO_3$, 3 mM NaH_2PO_4, 3 mM Na_2HPO_4, 3 mM K_2HPO_4, 2 mM $MgSO_4$, 1 mM $CaCl_2$, and 10 mg/L phenol-red at pH 7.4. The flask is gassed with 100% oxygen, sealed, and kept in a 37°C water bath under gently stirring with a magnet for 90 min. The cloudy suspension containing the separated glands and some cells is filtered through a nylon mesh into 15 ml test tubes with conical bottoms. The glands rapidly sediment to the

bottom while the free cells remain in the solution. In this way centrifugation can be avoided and the glands can easily be washed free from isolated cells and collagenase by three washings with phosphate buffer at room temperature.

^{14}C-Aminopyrine Accumulation in Gastric Glands

The ability of gastric glands to form acid is measured based on aminopyrine accumulation. The glands are diluted to a final concentration of 2–4 mg dry weight/ml in a medium containing 100.0 mM NaCl, 5.0 mM KCl, 0.5 mM NaH_2PO_4, 1 mM Na_2HPO_4, 1.0 mM $CaCl_2$, 1.5 mM $MgCl_2$, 20.0 mM $NaHCO_3$, 20.0 mM HEPES, 2 g/ml glucose, 1 mg/ml rabbit albumin, adjusted with 1 M Tris to pH 7.4. Samples of 1 ml gland suspension are equilibrated in 1 ml medium containing 0.1 µCi/ml [^{14}C]aminopyrine at 37°C in a shaking water bath together with the agent to be tested. After 20 min either histamine or dibutyryl-cyclic-AMP is added, followed by a 30 min incubation period for histamine and a 45 min incubation period for dibutyryl-cyclo-AMP.

The glands are then separated from the medium by brief centrifugation. The supernatant is withdrawn, the pellets are dried at 80°C for 50 min, weighed and dissolved in 200 µl 1 M NaOH. Aliquots of the supernatant and the digested gland pellet are examined in a liquid scintillation counter. The ratio of intraglandular to extraglandular radioactivity is calculated. All determinations are made in triplicate.

Respiratory Studies

Glandular oxygen consumption is measured at 37°C using a Warburg respirometer and air as the gas phase. The 15 ml flasks with a central well 20% containing KOH solution on a filter paper as CO_2 adsorber are filled with 1 ml medium containing 100.0 mM NaCl, 5.0 mM KCl, 0.5 mM NaH_2PO_4, 1 mM Na_2HPO_4, 1.0 mM $CaCl_2$, 1.5 mM $MgCl_2$, 20.0 mM $NaHCO_3$, 20.0 mM HEPES, 2 g/ml glucose, 1 mg/ml rabbit albumin, adjusted with 1 M Tris to pH 7.4 and 1 ml gland suspension. After 20 min equilibration, the test compound and dbcAMP are added and the oxygen consumption is measured at 15 min intervals for the following 45 min. The recorded oxygen consumption is corrected according to the following formula:

$$O_2 \text{ consumption} = O_2 \text{ recorded} \times K$$

where

- $K = 273 \times (Pb/t{+}273) \times 760$
- t = ambient temperature in °C around the manometers
- Pb = Atmospheric pressure (mm Hg)

The respiratory activity is expressed in µl O_2 consumed per mg dry weight and time.

EVALUATION

IC_{50} values are calculated by probit analysis. Statistical differences ($P < 0.05$) are assessed by Student's t-test, n = the number of different gland preparations.

CRITICAL ASSESSMENT OF THE METHOD

Studies on (^{14}C)-aminopyrine uptake and oxygen consumption in isolated rabbit gastric glands have become a valuable approach for studying the effect of various H_2-receptor antagonists and proton pump inhibitors. When studying gastric acid production with the^{14}C-AP accumulation technique, the addition of basic drugs can be problematic (Fryklund and Wallmark 1986). The basic nature of a test compound can compete with accumulation of ^{14}C-AP. Nevertheless, it is generally accepted that oxygen consumption of gastric glands correlates well with acid formation (Berglindh et al. 1976).

MODIFICATIONS OF THE METHOD

Soll (1978) studied the actions of secretagogues on oxygen uptake by isolated mammalian parietal cells. Parietal cells were prepared from the stomach of dogs by collagenase digestion and counterflow centrifugation. Oxygen consumption was determined by polarography. Isobutyl methyl xanthine (IMX), carbamylcholine, histamine, and gastrin each independently stimulated oxygen uptake. The specificity of these responses was tested by use of an H_2-histamine receptor antagonist or atropine as anticholinergic agent.

Stoll (1980) investigated the [^{14}C]aminopyrine accumulation in isolated *canine* parietal cells when treated with histamine, gastrin and carbachol and the displacement by cimetidine or atropine.

Sewing et al. (1983, 1986) studied the effect of several benzimidazole derivatives on isolated and enriched guinea pig parietal cells using the ^{14}C-aminopyrine accumulation.

Schepp et al. (1994) determined the effects of exendin-4, a peptide from *Heloderma suspectum venom*, and exendin-(9–39)NH_2 on [^{14}C]aminopyrine accumulation in isolated rat parietal cells and compared these with those of glucagon-like peptide-1-(7–36)NH_2.

REFERENCES AND FURTHER READING

Beil W, Staar U, Sewing KF (1990) Substituted thieno[3.4-d]imidazoles, a novel group of H^+/K^+-ATPase inhibitors.

Differentiation of their inhibition characteristics from those of omeprazole. Eur J Pharmacol 187:455–467
Berglindh T, öbrink KJ (1976) A method for preparing isolated glands from the rabbit gastric mucosa. Acta Physiol Scand 96:150–159
Berglindh T, Helander HF, öbrink KJ (1976) Effects of secretagogues on oxygen consumption, aminopyrine accumulation and morphology in isolated gastric glands. Acta Physiol Scand 97:401–414
Fryklund J, Wallmark B (1986) Sulfide and sulfoxide derivatives of substituted benzimidazoles inhibit acid formation in isolated gastric glands by different mechanisms. J Pharm Exp Ther 236:248–253
Herling AW, Becht M, Kelker W, Ljungström M, Bickel M (1987) Inhibition of ^{14}C-aminopyrine accumulation in isolated rabbit gastric glands by the H_2-receptor antagonist Hoe 760 (TZU-0460) Agents Actions 20:35–39
Herling AW, Bickel M, Lang HJ, Weidmann K, Rösner M, Metzger H, Rippel R, Nimmesgern H, Scheunemann KH (1988) A substituted thieno[3.4-d]imidazole versus substituted benzimidazoles as H^+,K^+-ATPase inhibitors. Pharmacology 36:289–297
Herling AW, Becht M, Lang HJ, Scheunemann KH, Weidmann K, Scholl Th, Rippel R (1990) The inhibitory effect of Hoe 731 in isolated rabbit gastric glands. Biochem Pharmacol 40:1809–1814
Sack J, Spenney JG (1982) Aminopyrine accumulation by mammalian gastric glands: an analysis of the technique. Am J Physiol 243:G313–G319
Schepp W, Schmidtler J, Riedel T, Dehne K, Schusdziarra V, Holst JJ, Eng J, Raufman JP, Classen M (1994) Exendin-4 and exendin-(9–39)NH_2: Agonist and antagonist, respectively, at the rat parietal cell receptor for glucagon-like peptide-1-(7–36)NH_2. Eur J Pharmacol Mol Pharmacol Sect 269:183–191
Sewing KF, Harms P, Schulz G, Hannemann H (1983) Effect of substituted benzimidazoles on acid secretion in isolated and enriched guinea pig parietal cells. Gut 24:557–560
Sewing KF, Beil W, Hackbarth I, Hannemann H (1986) Effect of substituted benzimidazoles on H^+K^+ATPase of isolated guinea-pig parietal cells. Scand J Gastroenterol 21, Suppl 118:52–53
Soll AH (1978) The actions of secretagogues on oxygen uptake by isolated mammalian parietal cells. J Clin Invest 61:370–378
Stoll AH (1980) Secretagogue stimulation of [^{14}C]aminopyrine accumulation by isolated canine parietal cells. Am J Physiol 238 (Gastrointest Liver Physiol 1):G366–G375

J.3.6.3.5 Gastric Mucosal Blood Flow

PURPOSE AND RATIONALE

Hydrogen gas clearance has been used to measure blood flow in the basal portion of gastric mucosa in anesthetized rats (Leung et al. 1984, 1986; Pique et al. 1988).

PROCEDURE

Male Sprague Dawley rats are anesthetized with 1.5 g/kg of urethane subcutaneously. A tracheotomy is performed and a PE-250 tubing is inserted into the trachea to facilitate spontaneous breathing and for administration of 3% hydrogen in air. The right carotid artery is cannulated for blood pressure monitoring. A midline laparotomy is then performed and the stomach exteriorized. Through an incision in the forestomach the gastric contents are gently washed out with physiological saline. A double-lumen cannula (outer: Tygon with a diameter of 7 mm; inner: polyethylene with a diameter of 2 mm) are inserted into the stomach and secured by a ligature at the forestomach. The pylorus is ligated and a 0.9% sodium chloride solution is infused through the inner cannula at a rate of 0.8 ml/min and drained from the outer tubing. The gastric effluent is collected at 15-min intervals. Acid output (in micro-equivalents per min) is determined in the perfusate with 0.2 N NaOH with an automatic titrator.

An incision in the serosa and the muscularis externa is made in the gastric wall of the corpus, exposing 3–4 mm of the submucosa. Through this hole a platinum electrode is placed in contact with the exposed basal portion of the mucosa. The electrode is made with a ring of platinum wire, 125 µm in diameter, wound around a glass capillary tube and held in place inside a Teflon tube by epoxy. A Ag-AgCl reference electrode is placed inside the peritoneal cavity. The laparotomy incision is covered by Parafilm to minimize evaporation.

One femoral vein is cannulated for the infusion of saline or drugs. The rat is kept warm with a heat lamp to maintain rectal temperature at 37°C.

Hydrogen Gas Clearance Technique

Current is generated at the surface of a platinum electrode by oxidation of molecular hydrogen to hydrogen ions and electrons. This current, which is measured using a polarographic and amplifying unit, is proportional to the hydrogen tension gradient at the surface of the platinum electrode. When the experimental animal breathes 3% hydrogen in air, the current tracing, graphed on a recorder, gradually rises and reaches a plateau as the tissue adjacent to the electrode is saturated with hydrogen. After the external hydrogen source is removed, the current tracing gradually falls because of removal of tissue hydrogen by blood flow. The rate of dissipation of hydrogen estimates the tissue blood flow (Aukland et al. 1964).

The exponential decrease of the hydrogen gas clearing curves is evaluated by a computer program (Livingstone et al. 1986). Current from the platinum electrode is passed through an ADALAB analog-to-digital converter and discrete digitized values are sampled every 5 s. Blood flow is determined by an Newtonian-Gaussian nonlinear iterative regression program by

means of a biexponential formula:

$$f(x) = A + B\,e^{-k1t(t-T)} + B\,e^{-k2t(t-T)},$$

where *f(x)* is the electrode current, *A* is the baseline current, *B* is the initial current, e is the base of natural logarithms, k_1 is the rate constant for the fast component, k_2 is the rate constant for the slow component, *t* is the time at which the current is observed, and *T* is the time when hydrogen gas was removed.

Mucosal blood flow is expressed in milliliters per minute per 100 g of tissue.

Inhibition of Acid Secretion

Intravenous saline is infused during the first 45 min of the study. After this period, an infusion of 80 µg/kg· h of pentagastrin is administered for 135 min. During the last 75 min an intravenous infusion of the inhibitor or vehicle is administered simultaneously with pentagastrin. Corpus mucosal blood flow measurements are obtained during the resting period, 45 min after start for the pentagastrin infusion, and during the last 15 min of combined infusion of pentagastrin and inhibitor. Acid output is measured at 15 min intervals throughout the experiments.

EVALUATION

All data are expressed as mean ± standard error. The data are analyzed using a paired *t*-test for comparison of basal versus stimulated condition within the same animal, analysis of variance with contrasts, and linear and polynomial regression analysis for comparison between animals in different groups. A probability level of $P < 0.05$ is considered significant.

MODIFICATION OF THE METHOD

The hydrogen gas clearance technique has been used by many authors in experimental gastroenterology, e. g.: Hirose et al. (1991), Holzer and Guth (1991), Lippe and Holzer (1992), Pique et al. (1992), Tsukamoto et al. (1992), Lazaratos et al. (1993), Petho et al. (1994), Tanaka and Guth (1994), Goldin et al. (1996), Hisanaga et al. (1996), Doi et al. (1998), Heinemann et al. (1999).

REFERENCES AND FURTHER READING

Aukland K, Bower B, Berliner R (1964) Measurement of local blood flow with hydrogen gas. Circ Res 14:164–187

Doi K, Nagao T, Kawakubo K, Ibayashi S, Aoyagi K, Yano Y, Yamamoto C, Kanamoto K, Iida M, Sadoshima S, Fujishima M (1998) Calcitonin gene-related peptide affords gastric mucosal protection by activating potassium channel in Wistar rats. Gastroenterology 114:71–76

Goldin E, Casadevall M, Mourelle M, Cirera I, Elizalde JI, Panes J, Casamitjana R, Guth P, Pique JM, Teres J (1996) Role of prostaglandins and nitric oxide in gastrointestinal hyperemia of diabetic rats. Am J Physiol 270 (Gastrointest Liver Physiol 33):G684–G690

Heinemann A, Sattler V, Jocic M, Wienen W, Holzer P (1999) Effect of angiotensin II and telmisartan, an angiotensin-1 receptor antagonist, on rat gastric mucosa blood flow. Aliment Pharmacol Ther 13:347–355

Hirose H, Takeuchi K, Okabe S (1991) Effect of indomethacin on gastric mucosal blood flow around acetic acid-induced gastric ulcers in rats. Gastroenterology 100:1259–1265

Hisanaga Y, Goto H, Tachi K, Hayakawa T, Sugiyama A (1996) Implication of nitric oxide synthase activity in the genesis of water immersion stress-induced gastric lesions in rats: The protective effect of FK506. Aliment Pharmacol Ther 10:933–940

Holzer P, Guth PH (1991) Neuropeptide control of rats gastric mucosal blood flow. Increase by calcitonin gene-related peptide and vasoactive intestinal peptide, but not substance P and neurokinin A. Circ Res 68:100–105

Lazaratos S, Kashimura H, Nahakara A, Fukutomi H, Osuga T, Urushidani T, Miyauchi T, Goto K (1993) Gastric ulcer induced by submucosal injection of ET_1: Role of potent vasoconstriction and intraluminal acid. Am J Physiol 265 (Gastrointest Liver Physiol 28):G491–G498

Leung FW, Guth PH, Scremin OU, Golanska EM, Kauffman GL Jr (1984) Regional gastric mucosal blood flow measurements by hydrogen gas clearance in the anesthetized rat and rabbit. Gastroenterology 87:28–36

Leung FW, Kauffman GL Jr, Washington J, Scremin OU, Guth PH (1986) Blood flow limitation of stimulated gastric acid secretion in the rat. Am J Physiol 250:G794–799

Lippe IT, Holzer P (1992) Participation of endothelium-derived nitric oxide but not prostaglandin in the gastric mucosal hyperaemia due to acid back-diffusion. Br J Pharmacol 105:708–714

Livingston EH, Reedy T, Dao H, Leung FW, Guth PH (1986) Direct fitting of hydrogen gas clearance curves by computer. Gastroenterology 90:1523

Petho G, Jocic M, Holzer P (1994) Role of bradykinin in the hyperaemia following acid challenge of rat gastric mucosa. Br J Pharmacol 113:1036–1042

Pique JM, Leung FW, Tan HW, Livingston E, Scremin OU, Guth PH (1988) Gastric mucosal blood flow response to stimulation and inhibition of gastric acid secretion. Gastroenterology 95:642–650

Pique JM, Esplugues JV, Whittle BJR (1992) Endogenous nitric oxide as a mediator of gastric mucosal vasodilatation during acid secretion. Gastroenterology 102:168–174

Tanaka T, Guth PH (1994) Role of gastric mucosal blood flow in gastroprotective effects of novel xanthine derivative. Dig Dis Sci 39:587–592

Tsukamoto Y, Goto H, Hase S, Arisawa T, Ohara A, Suzuki T, Hoshino H, Endo H, Hamajima E, Omiya N (1992) Effect of duodenal mucosal blood flow on duodenal alkaline secretion in rats. Digestion 51:198–202

J.3.7
Anti-Ulcer Activity

J.3.7.1
Pylorus Ligation in Rats (SHAY Rat)

PURPOSE AND RATIONALE

A simple and reliable method for production of gastric ulceration in the rat based on ligature of the pylorus has

been published by Shay et al. (1945). The ulceration is caused by accumulation of acidic gastric juice in the stomach.

PROCEDURE

Female Wistar rats weighing 150–170 g are starved for 48 h having access to drinking water ad libitum. During this time they are housed single in cages with raised bottoms of wide wire mesh in order to avoid cannibalism and coprophagy. Ten animals are used per dose and as controls. Under ether anesthesia a midline abdominal incision is made. The pylorus is ligated, care being exercised that neither damage to the blood supply nor traction on the pylorus occurs. Grasping the stomach with instruments is to be meticulously avoided, else ulceration will invariably develop at such points. The abdominal wall is closed by sutures. The test compounds are given either orally by gavage or injected subcutaneously.

The animals are placed for 19 h in plastic cylinders with an inner diameter of 45 mm being closed on both ends by wire mesh. Afterwards, the animals are sacrificed in CO_2 anesthesia. The abdomen is opened and a ligature is placed around the esophagus close to the diaphragm. The stomach is removed, and the contents are drained in a centrifuge tube. Along the greater curvature the stomach is opened and pinned on a cork plate. The mucosa is examined with a stereomicroscope. In the rat, the upper two fifths of the stomach form the rumen with squamous epithelium and possess little protective mechanisms against the corrosive action of gastric juice. Below a limiting ridge, in the glandular portion of the stomach, the protective mechanisms are better in the mucosa of the medium two fifths of the stomach than in the lowest part, forming the antrum. Therefore, lesions occur mainly in the rumen and in the antrum. The number of ulcers is noted and the severity recorded with the following scores:

- 0 = no ulcer
- 1 = superficial ulcers
- 2 = deep ulcers
- 3 = perforation.

The volume of the gastric content is measured. After centrifugation, acidity is determined by titration with 0.1 n NaOH.

EVALUATION

An ulcer index U_I is calculated:

$$U_I = U_N + U_S + U_P \times 10^{-1}$$

- U_N = average of number of ulcers per animal
- U_S = average of severity score
- U_P = percentage of animals with ulcers

Ulcer index and acidity of the gastric content of treated animals are compared with controls. Using various doses, dose-response curves can be established for ulcer formation and gastric acid secretion. ID_{50} values can be calculated by probit analysis, whereby 0% corresponds to no and 100% to maximal stimulated gastric acid output.

CRITICAL ASSESSMENT OF THE METHOD

The "Shay-rat" has been proven to be a valuable tool to evaluate anti-ulcer drugs with various mechanisms of action.

REFERENCES AND FURTHER READING

Bickel M, Herling AW, Rising TJ, Wirth K (1986) Antisecretory effects of two new histamine H_2-receptor antagonists. Arzneim Forsch/Drug Res 36:1358–1363

Herling AW, Bickel M, Lang HJ, Weidmann K, Rösner M, Metzger H, Rippel R, Nimmesgern H, Bickel Scheunemann KH (1988) A substituted thienol[3.4-d]imidazole versus substituted benzimidazoles as H^+,K^+-ATPase inhibitors. Pharmacology 36:289–297

Selve N, Friderichs E, Graudums I (1992) EM 405: a new compound with analgesic and anti-inflammatory properties and no gastrointestinal side-effects. Agents Actions. Special Conference Issue, C84–C85

Shay H, Komarow SA, Fels SS, Meranze D, Gruenstein M, Siplet H (1945) A simple method for the uniform production of gastric ulceration in the rat. Gastroenterol 5:43–61

Shay H, Sun DCH, Gruenstein M (1954) A quantitative method for measuring spontaneous gastric secretion in the rat. Gastroenterology 26:906–913

J.3.7.2 Indomethacin Induced Ulcers in Rats

PURPOSE AND RATIONALE

Nonsteroidal anti-inflammatory agents, like indomethacin and acetyl-salicylic acid, induce gastric lesions in man and in experimental animals by inhibition of gastric cyclo-oxygenase resulting in less formation of prostacyclin, the predominant prostanoid produced in the gastric mucosa.

PROCEDURE

Groups of 8–10 Wistar rats weighing 150–200 g are used. The test drugs are administered orally in 0.1% Tween 80 solution 10 min prior to oral indomethacin in a dose of 20 mg/kg (4 mg/ml dissolved in 0.1% Tween 80 solution). Six hours later, the rats are sacrificed in CO_2 anesthesia and their stomachs removed. Formol-

saline (2% v/v) is then injected into the totally ligated stomachs for storage overnight. The next day, the stomachs are opened along the greater curvature, then washed in warm water, and examined under a 3-fold magnifier. The lengths of the longest diameters of the lesions are measured and summated to give a total lesion score (in mm) for each animal, the mean count for each group being calculated.

EVALUATION

The mean score in control rats is about 25 (range 20–28). Inhibition of the lesion production is expressed as percentage value.

MODIFICATION OF THE METHOD

Dose- and time dependency of the ulcerogenic action of indomethacin were studied by Djahanguiri (1969).

Instead of indomethacin, gastric lesions can be induced by intravenous or oral doses of aspirin which can be prevented by exogenous PGE_2 or PGI_2 (Konturek et al. 1981). Furthermore, reserpine at a dose of 8 mg/kg i.p., or cysteamine hydrochloride at a dose of 400 mg/kg s.c. was given in order to induce ulcers in rats (Tarutani et al. 1985).

Kitajima et al. (1993) studied the role of endothelin and platelet-activating factor in indomethacin-induced gastric mucosal injury in rats. Four hours after subcutaneous injection of 25 mg/kg indomethacin, the rats were sacrificed after ether anesthesia, and the stomach was removed. The stomach was filled with 1.5 ml of 2% buffered formalin for 10 min and then opened along the greater curvature. The total length of the lesions was measured.

Wallace et al. (1989) studied the ulcerogenic activity of endothelin in indomethacin pretreated rats using an *ex vivo* gastric chamber.

Scarpignato et al. (1995) evaluated NSAID-induced gastric mucosal damage by continuous measurement and recording gastric potential difference in the rat.

CRITICAL ASSESSMENT OF THE METHOD

According to West (1982) the cold stress induced ulcer formation, but not the indomethacin- or aspirin-induced ulcers are inhibited by H_2-receptor antagonists, whereas other authors reported protective effects of H_2-receptor antagonists under these conditions (Tarutani et al. 1985).

REFERENCES AND FURTHER READING

Djahanguiri B (1969) The production of acute gastric ulceration by indomethacin in the rat. Scand J Gastroenterol 4:265–267

Kitajima T, Yamaguchi T, Tani K, Kubota Y, Okuhira M, Inoue K, Yamda H (1993) Role of endothelin and platelet-activating factor in indomethacin-induced gastric mucosal injury in rats. Digestion 54:156–159

Konturek SJ, Piastucki I, Brzozowski T, Radecki T, Dembinska-Kiec A, Zmuda A, Gryglewski R (1981) Role of prostaglandins in the formation of aspirin-induced gastric ulcers. Gastroenterology 80:4–9

Scarpignato C, Corradi C, Gandolfi MA, Galmiche JP (1995) A new technique for continuous measurement and recording of gastric potential difference in the rat: evaluation of NSAID-induced gastric mucosal damage. J Pharmacol Toxicol Meth 34:63–72

Selve N, Friderichs E, Graudums I (1992) EM 405:a new compound with analgesic and anti-inflammatory properties and no gastrointestinal side-effects. Agents Actions. Special Conference Issue, C84–C85

Tarutani M, Sakuma H, Shiratsuchi K, Mieda M (1985) Histamine H_2-receptor antagonistic action of N-3-[3-(1-piperidinyl)phenoxy]propylacetoxyacetamide hydrochloride (TZU-0460). Arzneim Forsch/Drug Res 35:703–706

Wallace JL, Cirino G, de Nucci G, McKnight W, MacNaughton WK (1989) Endothelin has potent ulcerogenic and vasoconstrictor actions in the stomach. Am J Physiol (Gastrointest Liver Physiol 19):G661–G666

West GB (1982) Testing for drugs inhibiting the formation of gastric ulcers. J Pharmacol Meth 8:33–37

J.3.7.3 Ethanol Induced Mucosal Damage in Rats (Cytoprotective Activity)

PURPOSE AND RATIONALE

Intragastric application of absolute ethanol is a reproducible method to produce gastric lesions in experimental animals (Robert et al. 1979; Szabo et al. 1981). These lesions can be at least partially inhibited by various drugs, such as some prostaglandins. The protective effect against various irritants has been called cytoprotective activity (Robert 1979; Robert et al. 1979). The method has been modified by several authors. Witt et al. (1985) described a method to objectively quantify the extent of ethanol-induced gastric lesions utilizing a transmission densitometer to measure the optical density of the photographic negative of the stomach mucosa.

PROCEDURE

Male Wistar rats weighing 250–300 g are deprived of food 18 h prior to the experiment but are allowed free access to water. During this time they are kept in restraining cages to prevent coprophagy. The rats are administered either the appropriate vehicle or the cytoprotective drug, e. g. a prostanoid, intragastrally 30 min prior to administration of 1 ml absolute ethanol. Untreated animals are included as controls. One hour after administration of ethanol, the animals are euthanized with CO_2, the stomachs are excised, cut along

the greater curvature, and gently rinsed under tap water. The stomachs are stretched on a piece of foam core mat, mucosal site up.

The subjective scores of the treated tissues are recorded; the graded response is reflecting the least (0) to most (3) damage. A circular full thickness area, about 13 mm in diameter, is cut with a cork borer from each lobe of the fundus just below the ridge dividing the glandular from the non-glandular portion of the stomach. A Plexiglas template (19 × 14 × 0.3 cm), burnished on one side with emery cloth, and with four rows with six holes 13 mm in diameter is placed on a sheet of clear glass, burnished side up, and bound to the glass with photographic tape along the periphery. The excised pairs of tissue from each stomach are placed into the holes of the template.

Pairs of tissue from each stomach are examined to minimize sampling errors. The template is positioned on a rectangular central open area of an Aristo Model T-16 cold cathode transilluminator (38 × 38 cm) containing a W-45 blue-white lamp. A camera is mounted on a copy stand directly above the template. Photographs are taken, the film processed in a standard manner and a contact sheet is made from the negatives. A light transmission densitometer (e. g. MacBeth model TD-501) is used to evaluate the negatives. The optical density of the test tissues is determined by placing each area of the negative in sequence over the aperture through which the light is transmitted. The optical density is displayed on a digital read out and recorded. Hemorrhagic or damaged areas appear bright on the negative, whereas undamaged tissue appears dark. Hence, lower optical density values are indicative of damage while higher optical densities are associated with little, or, as in the case of control, no damage.

EVALUATION

The significance of differences in optical density between control and ethanol-treated tissue is evaluated by nonpaired single-tail Student's *t*-test.

MODIFICATIONS OF THE METHOD

Cytoprotection by prostaglandins was studied in rats by prevention of gastric necrosis produced by various agents such as alcohol, HCl, NaOH, hypertonic NaCl, and thermal injury (Robert et al. 1979) and against gastric injury produced by nonsteroidal anti-inflammatory compounds (Robert 1979; Franzone et al. 1988). The animals are fasted 48 h prior to the experiment and placed 18 h before the administration of drugs into plastic tubes to prevent coprophagy. Fifteen min after application of the test drug, the animals are given 1 ml of the irritant orally. After an additional hour, the animals are sacrificed, the stomachs removed and immediately opened along the greater curvature. Lesions are counted and scored (0 = no lesion; 1 = mild lesions; 2 = severe lesions; 4 = necrosis).

Starrett et al. (1989) employed 3.0 ml/kg ethyl alcohol (100%) or 3.0 ml/kg 0.75 N HCl as necrotizing agent.

Borella et al. (1989) studied the cytoprotective and anti-ulcer activities of the anorganic antacid Magaldrate in the rat using absolute ethanol as irritant.

Masuda et al. (1993) investigated the role of endogenous endothelin in the pathogenesis of ethanol-induced gastric mucosal injury in rats.

CRITICAL ASSESSMENT OF THE METHOD

Several prostaglandins provide cytoprotection, particularly in rats, in a dose-range which has no anti-secretory activity. However, clinical experience with prostaglandins showed that ulcer healing is only achieved at anti-secretory doses (Lindberg et al. 1990). Therefore, it seems very likely that the cytoprotective property of a compound in rats has very limited relevance to prediction of its ulcer healing potential in humans if cytoprotection is really separated from its antisecretory potential (Herling and Weidmann 1994).

REFERENCES AND FURTHER READING

Borella LE, DiJoseph JF, Nabi Mir G (1989) Cytoprotective and antiulcer activities of the antacid Magaldrate in the rat. Arzneim Forsch/Drug Res 39:786–789

Franzone JS, Cirillo R, Cravanzola C (1988) Cytoprotective activity of deboxamet: a possible interference with prostaglandin and prostacyclin metabolism in rat gastric mucosa. Int J Tiss Reac 10:149–158

Herling AW, Weidmann K (1994) Gastric K^+/H^+-ATPase inhibitors. In: Ellis GP, Luscombe DK (eds) Progress in Medicinal Chemistry, Vol 31, Elsevier Science BV, pp 233–264

Hollander D, Tarnawski A, Krause WJ, Gergely H (1985) Protective effect of sucralfate against alcohol-induced gastric mucosal injury in the rat. Gastroenterol 88:366–374

Lindberg P, Brändström A, Wallmark B, Mattson H, Rikner L, Hoffmann KJ (1990) Med Res Rev 10:1–54

Long JF, Chiu PJS, Derelanko MJ, Steinberg M (1983) Gastric antisecretory and cytoprotective activities of SCH 28080. J Pharmacol Exp Ther 226:114–120

Masuda E, Kawano S, Nagano K, Tsuji S, Takei Y, Hayashi N, Tsujii M, Oshita M, Michida T, Kobayashi I, Pen HB, Fusamoto H, Kamada T (1993) Role of endogenous endothelin in pathogenesis of ethanol-induced gastric mucosal injury in rats. Am J Physiol 265 (Gastrointest Liver Physiol 28):G474–G481

Robert A (1979) Cytoprotection by prostaglandins. Gastroenterology 77:761–767

Robert A, Nezamis JE, Lancaster C, Hanchar AJ (1979) Cytoprotection by prostaglandins in rats. Prevention of gas-

tric necrosis produced by alcohol, HCl, NaOH, hypertonic NaCl, and thermal injury. Gastroenterology 77:433–443
Starrett JE, Montzka TA, Crosswell AR, Cavanagh RL (1989) Synthesis and biological activity of 3-substituted imidazo[1,2-*a*]pyridines as antiulcer agents. J Med Chem 32:2204–2210
Szabo S, Trier JS, Frankel PW (1981) Sulfhydryl compounds may mediate gastric cytoprotection. Science 214:200–202
Witt CG, Will PC, Gaginella TS (1985) Quantification of ethanol-induced gastric mucosal injury by transmission densitometry. J Pharmacol Meth 13:109–116

J.3.7.4 Subacute Gastric Ulcer in Rats

PURPOSE AND RATIONALE

Ezer (1988) described a method for producing standard subacute gastric ulcers in rats and for the quantitative evaluation of the healing process.

PROCEDURE

Female Wistar rats weighing 120–150 g are fasted for 24 h having access to water at libitum in cages with wire sieves at the bottom. The rats are anesthetized with ether and a polyethylene catheter including a fine steel wire with a needle tip (1.2 mm diameter) at the lower end is orally inserted into the stomach. After the cannula reaches the gastric wall, the upper end of the steel wire is pressed in a definitive manner, so as to puncture the gastric wall. Each rat is kept in the same position during the intervention in order to localize the puncture at nearly the same region of the glandular part of the stomach. The test substances are administered orally, 30 min or 24 h after puncture. Free access to food and water is provided from 2 h up to the end of the experiment. Each group consists of 8–15 rats.

The animals are sacrificed by overdose of ether at definitive time intervals after puncture. The stomach is dissected and opened along the lesser curvature, extensively rinsed in tap water and fixed to the end of a polyethylene tube of 10 mm diameter (plastic tip of an automatic pipette) in a position with the punched ulcer in the center. The end of the tube with the gastric wall is suspended in a beaker containing physiological saline, and the pressure in the tube is gradually increased with a valved rubber ball connected to the other end of the tube. The third part of the system is a tonometer calibrated up to 1 bar. The value of tension at which bubbles appear at the ulcerous gastric wall is noted. This value is termed as tensile strength and can be expressed in mm Hg.

EVALUATION

The extent of the healing of gastric ulcers can be characterized by the healing rate (*HR*) according the following equation:

$$HR = (A - B)/C \quad \text{(mmHg/h)}$$

with

- A = tensile strength (mm Hg) at C time-point after puncture
- B = tensile strength 30 min after puncture (the average value is 143 mm Hg)
- C = time course (h) of the experiment.

Anti-ulcer drugs, such as H_2 antagonists, significantly increase the healing rate, which is decreased by nonsteroidal anti-inflammatory drugs.

CRITICAL ASSESSMENT OF THE METHOD

Similarly to the method of Takagi et al. (1969) who injected 50 µl of acetic acid into the stomach wall (Szelenyi et al. 1982), the method of Ezer (1988) allows to judge the time course of healing of the ulcers.

MODIFICATIONS OF THE METHOD

Okabe and Pfeiffer (1972) induced chronic gastric ulcer in rats by temporary instillation of acetic acid. In pentobarbital anesthesia, a cylindrical glass tube of 6 mm in diameter was tightly placed upon the anterior serosal surface of the glandular portion of the stomach one cm away from the pyloric end. A dose of 0.06 ml/animal of 50% acetic acid was instilled into the tube and allowed to remain one min on the gastric wall. After removal of the acid solution, the abdomen was closed in two layers and the animals brought back to their cages and fed normally. Test drugs were given orally on day 1 twice daily, 4 h after application of acetic acid and continued up to 10 days after induction of ulcer. The animals were sacrificed after 18 h of the last dose to assess ulcer size and healing. Ulcer index was calculated upon the product of length and width of ulcers.

Karmeli et al. (1996) induced gastric mucosal erosions in rats by addition of 0.1% iodoacetamide to the drinking water. The animals were sacrificed after various time intervals, the stomach was resected, washed, lesion area assessed, and mucosal inflammatory mediators determined. Myeloperoxidase was increased and nitric oxide synthase activity decreased. The damage induced by iodoacetamide was significantly ameliorated by treatment with a free radical scavenger, (4-hydroxy-2,2,6,6-tetramethyl-piperidine-1-oxyl, TEMPOL).

Piqueras et al. (2003) described gastric hypersecretion in **mice** due to mast cell activation associated with

mild gastritis induced by 0.1% iodoacetamide administered intragastrally and added to the drinking water for a 6-day period.

Marchetti et al. (1995) and Konturek et al. (1999) described a mouse model of *Helicobacter pylori* infection. Gastric function and healing of chronic acetic acid-induced ulcers in BALB/c mice were studied after inoculation with CagA and VacA positive (type I) or CagA and VacA negative (type II) *Helicobacter pylori* strains. This infection caused immediate suppression of gastric secretion and delayed the healing of ulcers.

Protell et al. (1976) described a reproducible model of acute bleeding ulcer in **dogs** – the "ulcer maker." An instrument has been developed for endoscopy or laparotomy, which creates gastric ulcers of reproducible diameter and depth.

REFERENCES AND FURTHER READING

Ezer E (1988) Novel method for producing standard subacute gastric ulcer in rats and for the quantitative evaluation of the healing process. J Pharmacol Meth 20:279–291

Karmeli F, Okon E, Rachmilewitz D (1996) Sulfhydryl blocker induced gastric damage is ameliorated by scavenging of free radicals. Gut 38:826–831

Konturek PCh, Brzozowski T, Konturek SJ, Stachura J, Karczewska E, Pajdo R, Ghiara P, Hahn EG (1999) Mouse model of Helicobacter infection: Studies of gastric function and ulcer healing. Aliment Pharmacol Ther 13:333–346

Marchetti M, Aricò B, Burroni D, Figura N, Rappouli R, Ghiara P (1995) Development of a mouse model of *Helicobacter pylori* infection that mimics human disease. Science 267:1655–1658

Okabe S, Pfeiffer CJ (1972) Chronicity of acetic acid ulcer in the rat stomach. Digest Dis 7:619–629

Piqueras L, Corpa JM, Martínez J, Martínez V (2003) Gastric hypersecretion associated to iodoacetamide-induced mild gastritis in mice. Naunyn-Schmiedebergs Arch Pharmacol 367:140–150

Protell RL, Silverstein FE, Piercey J, Dennis M, Sprake W, Rubin CE (1976) A reproducible animal model of acute bleeding ulcer – the "ulcer maker". Gastroenterology 71:961–964

Szelenyi I, Engler H, Herzog P, Postius S, Vergin H, Holtermüller KH (1982) Influence of nonsteroidal antiinflammatory compounds on healing of chronic gastric ulcers. Agents Actions 12:180–182

Takagi K, Okabe S, Saziki R (1969) A new method for production of chronic gastric ulcer in rats and the effect of several drugs on its healing. Jap J Pharmac 19:418–426

J.3.7.5 Gastric Ischemia-Reperfusion Injury in Rats

PURPOSE AND RATIONALE

Hassan et al. (1997) described the effect of an endothelin converting enzyme inhibitor on local gastric ischemia-reperfusion injury in rats. Endothelin-1 has potent ulcerogenic effects in the stomach (Wallace et al. 1988). Endogenous endothelin-1 has been implicated for ethanol-, indomethacin- and hemorrhagic shock-induced gastric ischemia-reperfusion injuries (Masuda et al. 1993; Kitajima et al. 1993; Michida et al. 1994; Kitajima et al. 1995).

PROCEDURE

Male Wistar rats weighing 200–250 g are fasted for 24 h with free access to water. The rats are anesthetized with 1.5 g/kg urethane i.p. The stomach is exposed by a medial laparotomy and instilled with 0.15 M HCl (1 ml/100 g) via the forestomach. The left gastric artery is clamped by a small vascular clamp for 5 min to induce ischemia and 30 min of reperfusion is done by releasing the clamp. Pretreatment with test drug or standard is given to groups of 5 rats immediately before the induction of ischemia. At the end of the experiment, the rats are sacrificed by cervical dislocation. The stomach is fixed with 10% buffered formalin and photographed for macroscopic evaluation of injuries. For the assessment of microscopic injuries, a sample of corpus 0.5 cm below the limiting ridge containing the entire width of the anterior wall is taken from each stomach and processed for subsequent histological evaluation.

A planimeter attached to a computer is used to trace the macroscopic mucosal injury from color photographs. The results are expressed as a percentage of the total glandular mucosal area.

Each histological section is stained with hematoxylin/eosin and examined under light microscope. An one cm length of each histological section is assessed for epithelial damage (score = 1), glandular disruption, vasocongestion or edema in the upper mucosa (score = 2), hemorrhagic damage in the mid to lower mucosa (score = 3) and deep necrosis and ulceration (score = 4). Each section is evaluated on a cumulative basis to give the histological index, the maximum score thus being 10.

EVALUATION

Data are expressed as mean ± SEM. Comparisons between different groups are made by one way analysis of variance followed by Fisher's least significant difference test. P-values of < 0.05 are considered as statistically significant.

REFERENCES AND FURTHER READING

Hassan M, Kashimura H, Matsumaru K, Nakahara A, Fukutomi H, Muto H, Goto K, Tanak M (1997) Phosphoramidon, an endothelin converting enzyme inhibitor, attenuates local gastric ischemia-reperfusion injury in rats. Life Sci 61:141–147

Kitajima T, Yamaguchi T, Tani K, Kubota Y, Okuhira M, Inoue K, Yamada H (1993) Digestion 54:156–159
Kitajima T, Tani K, Yamaguchi T, Kubota Y, Okuhira M, Mizuno T, Inoue K (1995) Digestion 56:111–116
Masuda E, Kawano S, Nagano K, Tsusi S, Takei Y, Hayashi N, Tsujii M, Oshita M, Michida T, Kobayashi I, Peng HB, Fusamoto H, Kamada T (1993) Am J Physiol G474–G481
Michida T, Kawano S, Masuda E, Kobayashi I, Nishimura Y, Tsujii M, Hayashi N, Takei Y, Tsuji S, Nagano K, Fusamoto H, Kamada T (1994) Gastroenterol 106:988–993
Wallace JL, Cirino G, de Nucci G, McKnight W, MacNaughton WK (1989) Am J Physiol 256:G661–G666

J.4 Intestinal Functions

J.4.1 Intestinal Secretion

J.4.1.1 Laxative Activity in Rats

PURPOSE AND RATIONALE

Laxatives of the sennoside type act mainly by acceleration of large intestine transit and inhibition of fluid absorption in the colon (Leng-Peschlow 1986).

PROCEDURE

For **measurement of large intestinal transit time**, female Wistar rats weighing approximately 200 g are anesthetized with ether. A PVC catheter is implanted into the caecum with the distal end fixed on the animal's neck. The animals are allowed to recover and are placed individually in a wire meshed cage to enable the feces to fall through onto blotting paper. Carmine red (10 mg in 0.4 ml distilled water per animal) is injected through the catheter immediately after administration of the test substance. The time until appearance of the first colored feces is registered.

For **measurement of fluid absorption in the colon**, female Wistar rats weighing approximately 200 g are anesthetized with 50 mg/kg pentobarbitone sodium. The colon is ligated and cannulated distal to the caecocolic junction (PE-tube, i.d. 1 mm) and, after a thorough rinse with 50 ml physiological saline to remove all contents, a second cannula (silicone, i.d. 3 mm) is inserted proximal to the rectum for fluid outflow. Four and 6 h after oral administration of the test compounds an open perfusion with an electrolyte solution (NaCl 6.72 g/l, KCl 0.37 g/l, $NaHCO_3$ 2.1 g/l, polyethylene glycol (PEG, mol wt 4000) 2.0 g/l, [^{14}C]PEG 5 µCi/l; pH 6.5, osmolality 275 milliosmol/kg) is started at a rate of 12 ml/h for two consecutive 2 h periods. [^{14}C]PEG activity is measured by liquid scintillation counting, Na^+ and K^+ by flame photometry, Cl^- by coulometric titration, osmolality by freezing point depression and mucus as protein-bound total hexoses by the orcinol-sulphuric acid method. Net H_2O, Na^+, K^+ and Cl^- transport are calculated and expressed as ml or µmol/h and per 10 cm colon length.

EVALUATION

All values are expressed as mean ± standard deviation. Statistical significance is assessed with Student's *t*-test.

MODIFICATIONS OF THE METHOD

Ogunti and Elujoba (1993) tested the laxative activity of *Cassia alata* in rats. Male Charles River rats were kept in individual cages during one week. Any rat producing wet feces was rejected. After administration of the test compounds to groups of 5 rats per dose, the feces were examined for wetness hourly for 12 h. The results were expressed as the mean percent of total feces that were wet per kg rat.

REFERENCES AND FURTHER READING

Leng-Peschlow E (1986a) Acceleration of large intestine transit time in rats by sennosides and related compounds. J Pharm Pharmacol 38:369–373
Leng-Peschlow E (1986b) Dual effect of orally administered sennosides on large intestine transit and fluid absorption in the rat. J Pharm Pharmacol 38:606–610
Ogunti EO, Elujoba AA (1993) Laxative activity of Cassia alata. Fitoterapia 64:437–439

J.4.1.2 Enteropooling Test

PURPOSE AND RATIONALE

The enteropooling assay in rats has been developed by Robert et al. (1976) to test the diarrheogenic property of prostaglandins for prediction of this clinically relevant side effect of several synthetic prostaglandins.

PROCEDURE

Female Sprague Dawley rats weighing 190–215 g are used. The animals are fasted overnight having free access to water. The test compounds are administered orally, and the animals, 12 per group, are sacrificed one hour later. The fluid accumulation occurs in the small intestine which is cut at the pylorus and the ileocecal junction, and its contents, consisting of a thick fluid (in controls) and a very watery fluid (in prostaglandin-treated animals) are collected into a graduated test tube by milking the whole length of the small intestine with the fingers. The volume of fluid is recorded.

EVALUATION

Using various doses, dose-response curves can be established and potency ratios calculated. 16,16-dimethyl PGE_2 was found to be the most active compound.

CRITICAL ASSESSMENT OF THE METHOD

Some other diarrheogenic agents, like $MgSO_4$, castor oil, bile, taurocholate and taurochenodesoxycholate cause enteropooling, whereas mineral oil and tragacanth are ineffective. The anticholinergic agent methylscopolamine partially counteracted the enteropooling. The assay, therefore, can be used to test the laxative or the antidiarrheal activity of compounds (Shook et al. 1989).

MODIFICATIONS OF THE METHOD

Beubler and Badhri (1990) used the PGE_2-induced net fluid secretion in the jejunum and colon in the rat to evaluate the antisecretory effects of antidiarrheal drugs. Polyethylene catheters were placed into the jejunum and colon and Tyrode solution was instilled into the loops. Net fluid transfer rates were determined gravimetrically 30 min after instillation of Tyrode solution.

REFERENCES AND FURTHER READING

Beubler E, Badhri P (1990) Comparison of the antisecretory effects of loperamide and loperamide oxide in the jejunum and the colon of rats *in vivo*. J Pharm Pharmacol 42:689–692

Pillai NR (1992) Anti-diarrhoeal activity of Punica granatum in experimental animals. Int J Pharmacognosy 30:201–204

Robert A, Nezamis JE, Lancaster C, Hanchar AJ, Klepper MS (1976) Enteropooling assay: a test for diarrhea produced by prostaglandins. Prostaglandins 11:809–828

Shook JE, Burks TF, Wasley JWF, Norman JA (1989) Novel calmodulin antagonist CGS 9343B inhibits secretory diarrhea. J Pharmacol Exp Ther 251:247–252

J.4.1.3 Inhibition of Chloride Secretion in Rabbit Colon[2]

PURPOSE AND RATIONALE

Epithelia have the ability to reabsorb or to secrete fluids and electrolytes. In 1958, Koefoed-Johnsen and Ussing first published a model of ion transport across frog skin epithelium. Ussing also introduced the measurement of the short-circuit current as a means of defining active ion transport (Koefoed-Johnsen and Ussing 1958). Mammalian colon is an example of epithelium which has the capacity to absorb and to secrete electrolytes.

[2]Contributed in the first edition by M. Hropot

Previous studies have shown that mammalian colon actively secretes chloride when exposed to prostaglandins and vasoactive intestinal peptides, which increase the cellular concentration of cAMP resulting in an electrogenic chloride secretion (Frizzell et al. 1976). The elevation of cAMP causes the opening of chloride channels, whereas the colonic epithelium absorbs sodium and chloride ions by an electroneutral mechanism under control conditions. In general it is assumed that absorption takes place mainly in the surface cells, whereas the crypts are the predominant site of secretion (Greger et al. 1985; Binder and Sandle 1987).

PROCEDURE

Rabbits of either sex (2.0 to 4.0 kg body weight) are killed by cervical dislocation. The distal colon is removed, immediately opened into a flat sheet and washed in the standard electrolyte solution. The epithelium with an area of 1.0 cm^2 is stripped from its underlying musculature and mounted in an Ussing chamber. The tissue is mounted vertically and bathed on both sides by electrolyte solutions, which are circulated and oxygenated by a water-jacketed bubble-lift apparatus maintained at 37°C. The carbogen gas used for bubbling contains O_2 and CO_2 in a mixture of 95% and 5%, respectively. The solutions used on the two sides have the following composition (in mmol/l): NaCl 120, $NaHCO_3$ 21, Na_2HPO_4 0.4, K_2HPO_4 1.6, $MgCl_2$ 1.2, glucose 5.

Tissues are continuously short-circuited by a four-electrode automatic voltage-clamp apparatus (AC-Microclamp, Aachen, Germany) which measures short-circuit current (I_{sc}) and automatically subtracts chamber fluid resistance. Transepithelial electrical potential difference is measured between Ag-AgCl electrodes, which make contact with the bathing solutions via agar bridges (5% agar in glucose-free standard electrolyte solution). I_{sc} is measured by passing sufficient current through Ag-AgCl electrodes to reduce the spontaneous transepithelial electrical potential difference to zero. Transepithelial conductance (G_t) is determined by passing 100-ms bipolar current pulses through the tissue.

The standard protocol consists of an initial equilibration period of 20 min. The I_{sc} measured in the presence of indomethacin (1 µmol/l, serosal and mucosal solution) corresponds mostly to the rheogenic reabsorption of sodium. In the next step, amiloride is added at 0.1 mmol/l to block sodium reabsorption. Then PGE_2 (1 µmol/l) is added to the serosal solution in the presence of amiloride in order to stimulate

chloride secretion. After a further equilibration period of 20 min putative blockers of chloride secretion are added to the mucosal or serosal solution.

EVALUATION

Each compound is examined at least 3 times and at three different concentrations (usually 1, 10 and 100 µmol/l). From the mean values a concentration-response curve is constructed, and from this curve the IC_{50} value is read as the concentration producing 50% inhibition of the stimulated I_{sc}.

Data are presented as means ± SEM. Paired *t*-test with a significance level of $p < 0.05$ may be used.

CRITICAL ASSESSMENT OF THE METHOD

The method can be used to study the antidiarrhoic activity of a test compound, but also generally its influence on active electrolyte transport across the cell membrane.

MODIFICATIONS OF THE METHOD

Warhurst et al. (1996) studied the effects of somatostatin analogues on electrogenic ion secretion in isolated rat colonic mucosa mounted in Ussing chambers.

REFERENCES AND FURTHER READING

Binder HJ, Sandle GI (1987) Electrolyte absorption and secretion in the mammalian colon. In: LR Johnson (ed) Physiology of the Gastrointestinal Tract, Raven Press New York, pp 1389–1418

Frizzell RA, Koch MJ, Schultz SG (1976) Ion transport by rabbit colon. I. Active and passive components. J Membr Biol 27:297–316

Greger R, Schlatter E, Gögelein H (1985) Cl^- channels in the apical cell membrane of the rectal gland "induced" by cAMP. Pflügers Arch 403:446–448

Koefoed-Johnsen V, Ussing HH (1958) The nature of the frog skin potential. Acta Physiol Scand 42 298–308

Warhurst G, Higgs NB, Fakhoury H, Warhurst AC, Garde J, Coy DH (1996) Somatostatin receptor subtype 2 mediates somatostatin inhibition of ion secretion in rat distal colon. Gastroenterology 111:325–333

J.4.2 Antidiarrhea Effect

J.4.2.1 Castor Oil Induced Diarrhea

PURPOSE AND RATIONALE

The induction of diarrhea with castor oil results from the action of ricinoleic acid formed by hydrolysis of the oil (Iwao and Terada 1962; Watson and Gordon 1962). Ricinoleic acid produces changes in the transport of water and electrolytes resulting in a hypersecretory response (Ammon et al. 1974). In addition to hypersecretion, ricinoleic acid sensitizes the intramural neurons of the gut.

PROCEDURE

Female Wistar rats weighing 210–230 g are used after overnight food deprivation. For the experiment, the rats are housed in individual cages with no access to drinking water. The potential antidiarrhoic agents are administered orally by gavage in various doses. Controls receive the solvent only. Each dose is given to 10 animals. One hour after dosage, 1 ml of castor oil is administered orally. Stools are collected on non-wetting paper sheets of uniform weight up to 24 h after administration of the castor oil. Every 15 min during the first 8 h, urine is drained off by gravity, and the net stool weight, termed early diarrheal excretion, is recorded. The diarrhea-free period is defined as the time in minutes between castor oil administration and the occurrence of the first diarrheal output. The acute diarrheal phase is the time between the first and the last diarrheal output of the 8-h observation period. Stools occurring between 8 and 24 h after castor oil administration are called late diarrheal excretion.

EVALUATION

With antidiarrheal agents dose-response curves are obtained for decrease of hypersecretion (stool weight) and for increase of the diarrhea-free period are obtained. Inhibitors of prostaglandin biosynthesis increase the diarrhea free period but do not affect early diarrheal secretion (Niemegeers et al. 1984).

MODIFICATIONS OF THE METHOD

Inhibition of castor oil-induced diarrhea in **mice** was tested by Bianchi and Goi (1977).

Dajani et al. (1977) tested antidiarrheal activity in castor-oil treated **monkeys**.

Mannitol-induced diarrhea was used as model in **calves** (Fioramonti and Buéno 1977) and in **pigs** (Théodorou et al. 1991).

REFERENCES AND FURTHER READING

Ammon HV, Thomas PJ, Phillips S (1974) Effects of oleic and ricinoleic acids on net jejunal water and electrolyte movement. J Clin Invest 53:374–379

Awouters F, Megens A, Verlinden M, Schuurkes J, Niemegeers C, Janssen PAJ (1993) Loperamide. Survey on mechanisms of its antidiarrheal activity. Dig Dis Sci 38:977–995

Bianchi C, Goi A (1977) On the antidiarrhoeal and analgesic properties of diphenoxylate, difenoxine and loperamide in mice and rats. Arzneim Forsch / Drug Res 27:1040–1043

Dajani EZ, Bianchi RG, East PF, Bloss JL, Adelstein GW, Yen CH (1977) The pharmacology of SC-27166: a novel anti-diarrheal agent. J Pharmacol Exp Ther 203:512–526

Fioramonti J, Buéno L (1977) Effects of loperamide hydrochloride in experimental diarrhea and gastrointestinal myoelectrical activity in calves. Am J Vet Res 48:415–419
Iwao I, Terada Y (1962) On the mechanism of diarrhea due to castor oil. Jpn J Pharmacol 12:137–145
Megens AAHP, Canters LLJ, Awouters FHL, Niemegeers CJE (1990) Normalization of small intestinal propulsion with loparamide-like antidiarrheals in rats. Eur J Pharmacol 17:357–364
Niemegeers CJE, Lenaerts FM, Janssen PAJ (1974) Loperamide (R 18 553), a novel type of antidiarrheal agent. Part 1: *In vivo* oral pharmacology and acute toxicity. Comparison with morphine, codeine, diphenoxylate and difenoxine. Arzneim Forsch/Drug Res 24:1633–1635
Niemegeers CJE, Colpaert FC, Awouters FHL (1981) Pharmacology and antidiarrheal effect of Loperamide. Drug Dev Res 1:1–20
Niemegeers CJE, Awouters F, Janssen PAJ (1984) The castor oil test in rats: An *in vivo* method to evaluate antipropulsive and antisecretory activity of antidiarrheals? Drug Dev Res 4:223–227
Pillai NR (1992) Anti-diarrhoeal activity of Punica granatum in experimental animals. Int J Pharmacognosy 30:201–204
Shook JE, Burks TF, Wasley JWF, Norman JA (1989a) Novel calmodulin antagonist CGS 9343B inhibits secretory diarrhea. J Pharmacol Exp Ther 251:247–252
Shook JE, Lemcke PK, Gehring CA, Hruby VJ, Burks TF (1989b) Antidiarrheal properties of supraspinal *mu, delta* and *kappa* opioid receptors: Inhibition of diarrhea without constipation. J Pharmacol Exp Ther 249:83–90
Théodorou V, Fioramonti J, Hachet T, Buéno L (1991) Absorptive and motor components of the antidiarrheal action of loperamide: an *in vivo* study in pigs. Gut 32:1335–1359
Van Nuetten JM, Schuurkes JAJ (1988) Pharmakologie der Motilitätstherapeutika. Z Gastroenterologie 26, Suppl 4:4–8
Watson WC, Gordon RS (1962) Studies on the digestion, absorption and metabolism of castor oil. Biochem Pharmacol 11:229–236

J.4.2.2 Antidiarrheal Effect in Cecectomized Rats

PURPOSE AND RATIONALE

Evaluation of antisecretory antidiarrheal agents in animal models is limited primarily to extrapolations of efficacy from enteropooling studies *in vivo* (DiJoseph et al. 1984), isolated intestinal loops (Nakaki et al. 1982), and Ussing flux chamber preparations *in vitro* (Dharmsathaphorn et al. 1984).These studies do not mimic secretory diarrhea. The method of Magnus (1915) using chronic diarrhea in cats induced by continuous milk diet and thereby proofing the antidiarrheal effect of morphine is of historical interest only.

Fondacaro et al. (1990) developed a model of secretory diarrhea utilizing conscious cecectomized rats by surgical resection of the cecum and by use of potent intestinal secretagogues. The rat has a pronounced cecum as part of its gastrointestinal tract. The rat cecum is not only a reservoir for intestinal contents where high concentrations of various microbial flora assist in the digestion of carbohydrates, cellulose and peptides through microbial fermentation processes (Ambuhl et al. 1979; Williams and Senior 1982) but also plays a role in handling of excess intestinal fluid.

PROCEDURE

Cecectomies are performed in unfasted rats weighing 200–250 g. Under anesthesia with methohexital (60 mg/kg i.p.) cecectomy is initiated with a 2-cm midventral incision. The cecum is lifted from the abdominal cavity and exteriorized onto a gauze drape. The cecal apex is freed by severing the avasclular area of the mesocecum. A ligature of no. 1 silk suture is positioned so as to occlude the cecum and its vasculature without compromising ileo-colonic patency. After the ligature is secured and ileo-colonic patency confirmed, the cecum is resected, and the remaining exposed cecal mucosa is washed with saline and cauterized. The intestinal segment is then returned to the abdominal cavity and the abdominal muscle fascia closed with sutures. The dermal incision is closed with wound clips that are removed about 1 week postsurgery. Immediately following the surgical procedure, the animals are returned to their cages and allowed free access to food and water. The animals are permitted at least a 48-h recovery period before being used in an experiment.

For the diarrhea assay, cecectomized rats are put into individual wire-bottomed cages placed over sheets of clean paper, and deprived of food and water for the duration of the assay. Rats are given a two hour's acclimatization period prior to the start of the assay in order to eliminate sporadic episodes of anxiety-induced defecation. During this period, they are observed also for consistent occurrences of pelleted feces; an animal producing other than pelleted stool is disqualified from the study. Diarrhea is induced with oral administration of secretagogues: either 16,16 dimethyl prostaglandin E_2 (0.3 mg/kg) in 3.5% ethanol, carbachol (15 mg/kg) in water, or cholera toxin (0.5 mg/kg) in an aqueous vehicle of 2% $NaHCO_3$ plus 2% casamino acids. Anti-diarrheal agents are administered by gavage after the onset of diarrheal episodes. The cage papers are removed and examined at 15 min intervals for carbachol-induced diarrhea, 30 min intervals for 16,16 dimethyl prostaglandin E_2 induced diarrhea, and hourly when cholera toxin is used as secretagogue. Fetal output is recorded at each interval and scored as follows:

- 1 = normal pelleted stool
- 2 = soft-formed stools
- 3 = water stool and/or diarrhea

Known antidiarrheal agents, such as chlorpromazine (10 mg/kg p.o.), or the alpha-2 receptor agonist clonidine (1.0 mg/kg p.o.), or morphine (10 mg/kg p.o.) reduce the fecal output and induce a cessation of diarrhea.

EVALUATION

The fecal output index is defined as the summation of the number of defecation periods and their ranked consistency score within an observation period and is expressed as mean ± SEM for each group. Student's *t*-test and analysis of variance are used for statistical comparisons of data points. Significance is accepted at $p < 0.05$ or less.

CRITICAL ASSESSMENT OF THE METHOD

The model of diarrhea induced by secretagogues in cecetomized rats has the advantage to mimic secretory diarrhea in man.

REFERENCES AND FURTHER READING

Ambuhl S, Williams VJ, Senior W (1979) Effects of cecectomy in the young adult female rat on digestibility of food offered ad libitum and in restricted amounts. Aust J Biol Sci 32:205–213

Dharmsathaphorn K, Yamshiro DJ, Lindeborg D, Mandel KG, McRoberts J, Ruffolo RR (1984) Effects of structure-activity relationships of a-adrenergic compounds on electrolyte transport in the rabbit ileum and rat colon. Gastroenterology 86:120–128

DiJoseph JF, Taylor JA, Nabi Mir G (1984) Alpha-2 receptors in the gastrointestinal system: A new therapeutic approach. Life Sci 35:1031–1042

Doherty NS, Hancock AA (1983) Role of alpha-2-adrenergic receptors in the control of diarrhea and intestinal motility. J Pharmacol Exp Ther 225:269–274

Fondacaro JD, McCafferty GP, Kolpak DC, Smith PhL (1989) Antidiarrheal activity of alpha-2 adrenoceptor agonist SK&F 35886. J Pharmacol Exp Ther 249:221–228

Fondacaro JD, Kolpak DC, Burnham DB, McCafferty GP (1990) Cecectomiced rat. A model of experimental secretory diarrhea in conscious animals. J Pharmacol Meth 24:59–71

Magnus R (1915) Die stopfende Wirkung des Morphins. Pflügers Arch ges Physiol 115:316–330

Nakaki T, Nakadate T, Yamamoto S, Kato R (1982) Alpha-2-adrenergic inhibition of intestinal secretion induced by prostaglandin E_1, vasoactive intestinal peptide, and dibutyryl cyclic AMP in rat jejunum. J Pharmacol Exp Ther 220:637–641

Williams VJ, Senior W (1982) Effects of caecetomy on the digestibility of food and rate of passage of digesta in the rat. Aust J Biol Sci 35:373–379

J.4.2.3 Evaluation of Antidiarrheal Effect in Cold-Restrained Rats

PURPOSE AND RATIONALE

Barone et al. (1990) tested the effect of various antidiarrheal and other drugs on increased fecal pellet output in cold-restrained rats resembling clinical observations that stressful situations can produce diarrhea in humans.

PROCEDURE

Male Sprague-Dawley rats weighing 260–310 g are maintained on Purina lab chow and water. Since gastric ulcers are reduced if cold-restrained rats are allowed free access to food and water, for studies on fecal output food was not withdrawn prior to the experiment. The rats are studied in normal living cages at room temperature (control, non-stressed animals) or in wire-mesh restraining cylinders placed in a cold (4°C) environment. Test drugs are administered by appropriate routes over optimal effective dose-ranges for their activities and at optimal pretreatment times to maximize their effects. The number of pellets expelled by each animal is measured at 1 and 3 h (fecal pellet output). Generally, the fecal pellets of stressed animals are less firm. Fecal pellet fluid content is determined by weighing fecal pellets, drying them in an oven at 37°C, and weighing them again.

EVALUATION

The dose in mg/kg that inhibits the cold restrained stress induced increase in fecal pellet output by 50% (ID_{50}) is determined using least-squares fit analysis directly from the regression line. If fecal pellet output is decreased by a drug but no clear dose-related effects occur, the maximum percent decrease is determined.

MODIFICATIONS OF THE METHOD

For colonic transit studies, rats are implanted with indwelling catheters in the proximal colon. Animals are anesthetized with 60 mg/kg pentobarbital i.p., and a chronic colonic catheter is positioned to enter the proximal colon 2 cm from the ileocecal junction. A catheter of about 20 cm of silicone tubing prepared with several drops of silicon rubber adhesive coating a 1-cm length along the catheter is positioned into the colon. The colon end of the tubing also is sealed with a 1-cm plug of petroleum jelly intraluminally. A small incision is made in the proximal colon, and the adhesive-coated portion of the Silastic tubing is tied in place with the use of a purse-string suture. The tubing is brought through the abdominal wall, led subcutaneously through the skin in the midscapular region and secured on the back of the neck with the use of a wound clip. The abdominal incision is closed with sutures and wound clips.

Experiments are performed in conscious animals 48–72 h after surgical preparation. At this time, the

radiolabeled marker (^{51}Cr as sodium chromate) is instilled into the proximal colon via the indwelling catheter. After 35, 60, or 120 min, cold-restrained rats and controls are sacrificed and their colons and large intestines are removed. The cecum and equal segments of the colon are dissected, placed into vials and subjected to gamma counting.

Ikeda et al. (1995) investigated the effect of a neurokinin$_1$ receptor antagonist on stress-induced defecation in rats placed in special restraint cages.

Kishibayashi et al. (1993) studied distal colonic function using wrap-restrained stress-induced defecation as described by Williams et al. (1988). The rats were lightly anesthetized with ether, and the foreshoulders, upper forelimbs and the thoracic trunk were wrapped in paper tape to restrict, but not prevent, movement. The animals recovered from anesthesia within 2–5 min and immediately moved around in cages and ate and drank, but had been restricted from mobility of forelimbs, which prevented them from grooming the face, upper head and the neck. Fecal pellet output induced by wrap-restraint stress was weighed during the 1st h after stress. The test drugs were given p.o. 1 h before stress. The ID_{50} values were calculated as the doses that reduced stress-induced defecation by 50%.

REFERENCES AND FURTHER READING

Barone FC, Deegan JF, Price WJ, Fowler PJ, Fondacaro JD, Ormsbee III HS (1990) Cold-restraint stress increases rat fecal output and colonic transit. Am J Physiol Gastrointest Liver Physiol 258:G329–G337

Ikeda K, MiYata K, Orita A, Kubota H, Yamata T, Tomioka K (1995) RP67580, a neurokinin$_1$ receptor antagonist, decreased restraint stress-induced defecation in rats. Neurosci Lett 198:103–106

Kishibayashi N, Ichikawa S, Yokoyama T, Ishii A, Karasawa A (1993) Pharmacological properties of KF18259, a novel 5-HT$_3$-receptor antagonist, in rats: inhibition of the distal colonic function. Japan J Pharmacol 63:495–502

Williams CL, Villar RG, Peterson JM, Burks TF (1988) Stress-induced changes in intestinal transit in the rat: A model for irritable bowel syndrome. Gastroenterology 94:611–621

J.4.3 Gut Motility

J.4.3.1 Isolated Ileum (MAGNUS Technique)

PURPOSE AND RATIONALE

The isolated ileum, as first described by Magnus (1904), is probably the most widely used model in experimental pharmacology. Magnus already studied simultaneously the spontaneous contractions of the longitudinal and circular musculature and the inhibiting effect of atropine. The method has been used for many purposes, such as the study on the effects of adrenaline on the lower segments causing contraction and on the segments of the upper end causing relaxation by Munro (1951) or the study on the origin of acetylcholine released from guinea-pig intestine and longitudinal muscle strips by Paton and Zar (1968) either retaining or being denervated from Auerbach's plexus. The model is used as a basic screening procedure for spasmolytic activity, whereby an anti-acetylcholine or anticarbachol effect indicates antimuscarinic activity and an anti-$BaCl_2$-effect indicates a musculotropic, papaverine-like effect. In addition to the isolated ileum, other parts of the gut such as the isolated duodenum and colon, have been used widely.

PROCEDURE

Guinea pigs of either sex weighing 300 to 500 g are used. They are sacrificed by stunning and exsanguination. The abdomen is opened with scissors. Just distal to the pylorus, a cord is tied around the intestine which is then severed above the cord. The intestine is gradually removed, with the mesentery being cut away as necessary. When the colon is reached, the intestine is cut. Below the cord, the intestine is cut halfway through, so that a glass tube can be inserted. Tyrode's solution is passed through the tube and the intestine until the effluent is clear. Mesentery is cut away from the intestine that was joined to the colon. Pieces of 2–3 cm length are cut. Preferable the most distal piece is used being the most sensitive one. This piece is fixed with a tissue clamp and brought into a 15 ml organ bath containing Tyrode's solution at 37°C being oxygenated with 95% O_2/5% CO_2. The other end is fixed to an isometric force transducer (UC 2 Gould-Statham, Oxnard USA). A preload of 1 g is chosen. Responses are recorded on a polygraph. After a pre-incubation time of 30 min, the experiment is started.

The following agonists and antagonists (standards) are used (concentrations in g/ml bath fluid):

Agonist	Antagonist
Acetylcholine 10^{-7} g/ml	Atropine 10^{-8}–19^{-9} g/ml
	Scopolamine 10^{-8}–10^{-9} g/ml
Carbachol 10^{-7} g/ml	Atropine 10^{-8}–10^{-9} g/ml
Histamine 10^{-6} g/ml	Histamine antagonists
$BaCl_2$ 10^{-4} g/ml	Papaverine 10^{-5}–10^{-6} g/ml
Serotonin 10^{-6} g/ml	Serotonin antagonists
PGE_2 2×10^{-7} g/ml	PG-antagonists

EVALUATION

Several methods for the quantitative evaluation of an antagonistic effect are available. One approach is the determination of pD'_2 values according to van Rossum and van den Brink (1963). Acetylcholine or histamine is added in $1/2 \log_{10}$ concentration increments until a maximum response is obtained. Control curves are recorded at 30 min intervals. After uniform control responses are obtained, the potential antagonist or the standard is added 5 min before the concentration-response curve is re-obtained. The potency of the antagonist is obtained by calculating the pD'_2 value which is defined as the negative logarithm of the molar concentration of an antagonist that causes a 50% reduction or the maximal response obtained with an agonist.

MODIFICATIONS OF THE METHOD

Many modifications of the Magnus technique have been described in the literature, mainly with the isolated ileum (e. g., Koelle et al. 1950).

Okwuasaba and Cook (1980) dissected the myenteric plexus and longitudinal muscle free of the underlying circular muscle according to the method of Paton (1957), Paton and Zar (1968) and stimulated the preparation with trains of supramaximal rectangular pulses of 1.0 ms duration at a frequency of 0.2 Hz.

Kilbinger et al. (1995) studied the influence of 5-HT_4 receptors on [^{3}H]-acetylcholine release from guinea pig myenteric plexus.

De Graaf et al. (1983) described a fully automated system for *in vitro* experiments with isolated tissues. The apparatus consists of an organ bath equipped with (a) a gradient pump supplying a logarithmic concentration/time gradient of agonist; (b) pumps and valves for dispensing bath fluid, antagonist solutions, and an oxygenation gas mixture; and (c) a transducer with automatic baseline adjustment. The information coming from the preparation is fed into a mini-computer. The data of various experiments can be accumulated and Schild-plots obtained.

Furukuwa et al. (1980) studied the effects of thyrotropin-releasing hormone on the isolated small intestine and taenia coli of the guinea pig.

Paiva et al. (1988) studied the role of sodium ions in angiotensin tachyphylaxis in the guinea-pig ileum and taenia coli.

Barnette et al. (1990) used electrically stimulated strips of circular smooth muscle from the lower esophageal sphincter of dogs to study the inhibition of neuronally induced relaxation by opioid peptides.

Bradykinin antagonism can be studied in the isolated guinea pig ileum bathed in a solution containing atropine (1.5 mM), diphenhydramine (3.4 mM), indomethacin (2.8 mM), and captopril (0.9 mM) (Rubin et al. 1978; Kachur et al. 1987).

Griesbacher and Lembeck (1992) used the isolated guinea-pig ileum for analysis of bradykinin antagonists.

Hew et al. (1990) used field stimulated (95% of maximum voltage, 0.1 Hz, 0.5 ms) guinea pig ileum, bathed in physiological salt solution at 37°C in the presence of 1 mM mepyramine for determination of histamine H_3 bioresponse. Reduction of contractile response by the test substance (>50% relative to control 0.3 mM R-α-methylhistamine) indicates possible H_3 agonism. At a test concentration where no significant activity is seen, ability to inhibit (>50%) R-α-methylhistamine-induced contractile reduction indicates antagonistic activity.

A similar technique was used by Conner et al. (1987) to study antagonist effects at functional 5-HT_{1A} receptors.

Feniuk et al. (1993) used the guinea-pig isolated ileum, vas deferens and right atrium to characterize somatostatin receptors. Transmural electrical stimulation was applied to guinea pig ileum (0.1 Hz, 0.1 ms continuously) and vas deferens (5 Hz, 0.5 ms for 1.5 s every 30 s) at supramaximal currents (approximately 800 mA) delivered from a Digitimer D330 multistimulator.

Radomirow et al. (1994) investigated opioid effects of short enkephalin fragments containing the Gly-Phe sequence on contractile responses of guinea pig ileum after addition of 10 nM acetylcholine or after electrical stimulation.

Coupar and Liu (1996) described a simple method for measuring the effects of drugs on intestinal longitudinal and circular muscle in **rats**. The preparation consists of a segment of rat ileum set up to measure the tension developed in the longitudinal muscle and intraluminal pressure developed in the circular muscle in response to transmural electrical stimulation.

Vassilev et al. (1993) exposed Wistar rats to subtoxic doses of Co^{2+} or Ni^{2+}, receiving $Co(NO_3)_2$ or $NiSO_4$ with drinking water for 30 days, and measured the changes in the contractile responses to carbachol and in the inhibitory effects of verapamil and nitrendipine on isolated smooth muscle preparations of the ileum and the trachea.

Pencheva and Radomirov (1993), Pencheva et al. (1999) studied the effects of GABA receptor agonists on the spontaneous activity of the circular layer in the terminal ileum of **cats**. Segments of the terminal ileum approximately 0.5 cm long were mounted in an organ

bath along the axis of the circular layer through a cotton thread with a large knot situated at the inner part of the gut wall.

Similar preparations of cat ileum were used by Kortezova et al. (1994) and Chernaeva and Mizhorkova (1995).

Vassilev and Radomirov (1992) used an isolated preparation of **rat rectum**. The rectal region, 1–6 cm proximal to the anal sphincter was removed and a 20 mm long segment suspended in an organ bath. The influence of prostaglandins and antagonists on spontaneous mechanical activity and electrically stimulated responses was investigated.

REFERENCES AND FURTHER READING

Barnette MS, Grous M, Manning CD, Callahan JF, Barone FC (1990) Inhibition of neuronally induced relaxation of canine lower esophageal sphincter by opioid peptides. Eur J Pharmacol 182:363–368

Bickel M, Bal-Tembe S, Blumbach J, Dohadwalla AN, Lal B, Palm D, Rajagopalan R, Rupp RH, Schmidt D, Volz-Zang C (1990) HL 752, a new enteral active muscarinic receptor antagonist. Med Sci Res 18:877–879

Chernaeva L, Mizhorkova Z (1995) Postnatal development of methionine-enkephalin modulation of cholinergic transmission in cat ileum. Mech Ageing Dev 83:117–124

Coupar I, Liu L (1996) A simple method for measuring the effects of drugs on intestinal longitudinal and circular muscle. J Pharmacol Toxicol Meth 36:147–154

De Graaf JS, de Vos CJ, Steenbergen HJ (1983) Fully automated experiments with isolated organs *in vitro*. J Pharmacol Meth 10:113–135

Feniuk W, Dimech J, Humphrey PPA (1993) Characterization of somatostatin receptors in guinea-pig isolated ileum, vas deferens and right atrium. Br J Pharmacol 110:1156–1164

Furukuwa K, Nomoto T, Tonoue T (1980) Effects of thyrotropin-releasing hormone (TRH) on the isolated small intestine and taenia coli of the guinea pig. Eur J Pharmacol 64:2179–287

Goldenberg MM, Burns RH (1973) Effectiveness of a unique antispasmodic 3,4-dihydro-5-phenoxy-benzo[*b*][1,7naphtyridin-1(2H)-one EU-1086, *in vivo* and *in vivo*. Arch Int Pharmacodyn 203:55–66

Griesbacher T, Lembeck F (1992) Analysis of the antagonistic actions of HOE 140 and other novel bradykinin analogues in the guinea-pig ileum. Eur J Pharmacol 211:393–398

Hew RW, et al (1990) Characterization of histamine H_3-receptor in guinea pig ileum with H_3-selective ligands. Br J Pharmacol 101:621–624

Kachur JF et al (1987) Bradykinin receptors: functional similarities in guinea pig muscle and mucosa. Regul Pept 17:63–70

Kilbinger H, Gebauer A, Hass J, Ladinsky H, Rizzi CA (1995) Benzimidazoles and renzapride facilitate acetylcholine release from guinea pig myenteric plexus via 5-HT_4 receptors. Naunyn-Schmiedeberg's Arch Pharmacol 351:229–236

Koelle GB, Koelle ES, Friedenwald JD (1950) The effect of inhibition of specific and non-specific cholinesterase on the motility of the isolated ileum. J Pharm Exp Ther 100:180–191

Kortezova N, Mizhorkova Z, Milusheva E, Coy DH, Vizi S, Varga G (1994) GRP-preferring bombesin receptor subtype mediates contractile activity in cat terminal ileum. Peptides 15:1331–1333

Magnus R (1904) Versuche am überlebenden Dünndarm von Säugethieren. Pflügers Arch 102:123–151

Moritoki H, Morita M, Kanbe T (1976) Effects of methylxanthines and imidazole on the contractions of guinea-pig ileum induced by transmural stimulation. Eur J Pharmacol 35:185–198

Munro AF (1951) The effect of adrenaline on the guinea-pig intestine. J Physiol 112:84–94

Okwuasaba FK, Cook MA (1980) The effect of theophylline and other methylxanthines on the presynaptic inhibition of the longitudinal smooth muscle of the guinea pig ileum induced by purine nucleotides. J Pharmacol Exp Ther 215:704–709

Paiva TB, Paiva ACM, Shimuta SI (1988) Role of sodium ions in angiotensin tachyphylaxis in the guinea-pig ileum and taenia coli. Naunyn-Schmiedeberg's Arch Pharmacol 337:656–660

Paton WDM (1957) The action of morphine and related substances on contraction and on acetylcholine output of coaxially stimulated guinea-pig ileum. Br J Pharmacol 12:119–127

Paton WDM, Zar MA (1968) The origin of acetylcholine released from guinea-pig intestine and longitudinal muscle strips. J Physiol 194:13–33

Pencheva N, Radomirov R (1993) Biphasic GABA-A receptor-mediated effect on the spontaneous activity of the circular layer in cat terminal ileum. Gen Pharmacol 24:955–960

Pencheva N, Itzev D, Milanov P (1999) Comparison of gamma-aminobutyric acid effects in different parts of the cat ileum. Eur J Pharmacol 368:49–56

Radimirow R, Pencheva N, Stoyneva I, Lazowa L (1994) Opioid effects of short enkephalin fragments containing the Gly-Phe sequence on contractile responses of guinea pig ileum. Gen Pharmacol 25:303–309

Rubin B, Laffan RJ, Kotler DG, O'Keefe EH, Demaio DA, Goldberg ME (1978) SQ 14,225 (D-3-mercapto-2-methylropanoyl-L-proline), a novel orally active inhibitor of angiotensin I-converting enzyme. J Pharmacol Exp Ther 204:71–280

Van Rossum JM, van den Brink (1963) Cumulative dose-response curves. Arch Int Pharmacodyn 143:240–246

Vassilev P, Radomirov R (1992) Contractile effects of prostaglandin E_2 in rat rectum: sensitivity to the prostaglandin antagonists diphloretin and SC 19220. Prostaglandins 44:471–484

Vassilev PP, Venkova K, Pencheva N, Staneva-Stoytcheva D (1993) Changes in the contractile responses to carbachol and in the inhibitory effects of verapamil and nitrendipine on isolated smooth muscle preparations from rats subchronically exposed to Co^{2+} and Ni^{2+}. Arch Toxicol 67:330–337

J.4.3.2 Cascade Superfusion Technique

PURPOSE AND RATIONALE

The technique of isolated organ superfusion was developed by Gaddum (1953) for the assay of biologically active substances. Extension of the technique for multiple tissue superfusion with particular reference to the identification and the assay of prostaglandin-like activity was used by various authors (Vane 1964;

Ferreira and Vane 1967; Ferreira et al. 1976; Gilmore et al. 1968; Hong 1974; Bult et al. 1977; Henman et al. 1978; Elliott and Adolfs 1984; Fournau et al. 1984).

PROCEDURE

The apparatus consists of a double-wall glass container (height 20–25 cm, inner diameter 7–8 cm) with an outlet at the bottom. A constant temperature of 38°C is maintained by circulation of warm water through the outer jacket. Inside the glass container can be suspended up to 5 pieces of tissue of various origins. The multiple preparation tissue holder consists of a vertical rectangular rod and plastic platforms for attachment of the tissues and for accurate deflection of the superfusate on to the lower tissue. The rod is grooved at 10 mm intervals with 1 mm deep slots set at an angle of 20° to the horizontal. To the upper surface of the nonwettable platform a small plastic hook is cemented at such a distance from the rod that when the tissue is in position its attachment thread passes between the V-shaped notch cut into the margin of the upper tissue platform. The individual platforms are inserted on to the vertical rod by slotting into the requisite grooves appropriate to the tissue length.

Thus, the superfusate passes at a uniform flow rate down the tissues of the cascade and the tension recording threads are separated from each other by about a 5-mm gap so that the responses can be conveniently recorded. The threads from the organs are connected over isotonic levers to isometric tension transducers. The lever is used for preloads according to the individual organ. Tension exerted by each tissue is recorded on a polygraph. Various media can be used for superfusion, e. g., Krebs-Henseleit solution gassed with 95% O_2 and 5% CO_2.

Many tissue preparations can be used for the cascade, such as rat fundic strip, rat duodenum, rat colon, rat bladder strip, guinea-pig ileum, guinea-pig proximal colon, rabbit stomach strip, rabbit coeliac/mesenteric artery, or rabbit aorta strip. Moreover, donor tissue can be superfused and its effluent be tested in the organs of the cascade.

EVALUATION

Many agonists and antagonists can be tested by appropriate selection of organs. Threshold doses and ED_{50} or ID_{50} values can be determined.

MODIFICATIONS OF THE METHOD

The superfusion technique has been used for several purposes, e. g., for the assay of catecholamines (Armitage and Vane 1964), for detecting active substances in the circulating blood (Vane 1964). A simple and inexpensive piece of apparatus for cascade superfusion procedures has been described by Naylor (1977).

Mombouli et al. (1996) described a bioassay of endothelium-derived hyperpolarizing factor (EDHF) using a perfusion-superfusion cascade where canine carotid arteries were used as donors of vasoactive substances and rings of coronary arteries without endothelium as detectors.

REFERENCES AND FURTHER READING

Armitage AK, Vane JR (1964) A sensitive method for the assay of catechol amines. Br J Pharmacol 22:204–210

Bult H, Parnham MJ, Bonta IL (1977) Bioassay by cascade superfusion using a highly sensitive laminar flow technique. J Pharm Pharmacol 29:369–370

Elliott GR, Adolfs MJP (1984) Continuous monitoring of prostacyclin production by the isolated, intact, rat aorta using a bioassay technique. J Pharmacol Meth 11:253–261

Ferreira SH, de Souza Costa F (1976) A laminar flow superfusion technique with much increased sensitivity for the detection of smooth muscle stimulating substances. Eur J Pharmacol 39:379–381

Ferreira SH, Vane JR (1967) Prostaglandins: Their disappearance from and release into the circulation. Nature (London) 216:868–876

Fournau P, Bonnet P, Bourgue MF, Paris J (1984) Prostacyclin bioassays using inhibition of platelet aggregation and relaxation of rabbit coeliac artery. J Pharmacol Meth 11:53–60

Gaddum JH (1953) The technique of superfusion. Br J Pharmacol 8:321–326

Gilmore N, Vane JR, Wyllie JH (1968) Prostaglandins released by the spleen. Nature (Lond) 218:1135–1140

Henman MC, Naylor IL, Leach GHD (1978) A critical evaluation of the use of a cascade superfusion technique for the detection and estimation of biological activity. J Pharmacol Meth 1:13–26

Henman MC, Naylor IL, Leach GHD (1983) Comparison of bioassay methods for the estimation of wound-released prostaglandin-like activity. J Pharmacol Meth 9:77–82

Hong E (1974) Differential pattern of activity of some prostaglandins in diverse superfused tissues. Prostaglandins 8:213–220

Mombouli JV, Bissiriou I, Agboton VT, Vanhoutte PM (1996) Bioassay of endothelium-derived hyperpolarizing factor. Biochem Biophys Res Commun 221:484–488

Naylor IL (1977) A simple and inexpensive piece of apparatus for cascade superfusion procedures. Br J Pharmacol 59:529P

Vane JR (1964) The use of isolated organs for detecting active substances in the circulating blood. Br J Pharmacol Chemother 23:360–373

J.4.3.3 In Vivo Evaluation of Spasmolytic Activity in Rats

PURPOSE AND RATIONALE

Maggi and Meli (1982) described an *in vivo* procedure for estimating spasmolytic activity in the rat by measuring smooth muscle contractions to topically applied acetylcholine.

PROCEDURE

Male albino rats weighing 350–400 g are anesthetized with subcutaneous urethane (1.2 g/kg). The left jugular vein is cannulated for administration of test compounds. After laparotomy occluding silk ligatures are applied at a distance of 2 cm from each other in the gut (colon or rectum). Through a small incision the flanged tip of a polyethylene tubing (1 mm i.d., 1.5 mm o.d.) is inserted into the lumen of this pocket-like space and secured in place by a purse string ligature. The free end of the tubing is connected to a pressure transducer and the whole system filled with saline. The same procedure is performed with the urinary bladder. The organs are filled with warm saline (37°C) to obtain a resting pressure of 4–12 mm Hg. Warm saline soaked cotton wool swabs are laid around the exteriorized organs which are maintained warm and moist with warm (37°C) saline dropping from a reservoir at a rate of 10–15 drops/min.

After 15 min stabilization period, saline flow is stopped and a dose-response curve to acetylcholine determined. A volume of 0.5 ml (an amount sufficient to put the whole outer surface of the organ into contact with the bathing solution) of acetylcholine at the desired concentration is applied within 2–3 s from a syringe to the outer surface of the target organ. To construct a dose-response curve of acetylcholine, increasing concentrations are applied to the target organ until maximal contraction is obtained. After at least 3 or more control curves have been obtained at 10 min intervals, the antagonist is administered.

EVALUATION

The quantitative analysis of the data is carried out by plotting the results of each experiment as log (acetylcholine dose ratio-1) against log dose antagonist (Arunlakshana and Schild 1959). The regression line is calculated according to the method of least squares and ED_{50} values and 95% confidence limits according to Litchfield and Wilcoxon (1949). From ED_{50} values, the dose of the antagonist (mg/kg i.v.) to produce an acetylcholine dose ratio of 10 is calculated according to Daly et al. (1975). Parallel displacement to the right of the agonist dose response curve and a slope of unity for the regression line indicate competitive antagonism. The DR_{10} values from different organs are compared by means of Student's *t*-test for unpaired data.

MODIFICATIONS OF THE METHOD

In vivo registration of gut motility in guinea pigs was already described by Straub and Viaud (1933). A four cm long part of the gut was ligated and filled with Tyrode solution. Gut motility was measured at variable intraluminal pressure.

REFERENCES AND FURTHER READING

Arunlakshana O, Schild HO (1959) Some quantitative use of drug antagonists. Br J Pharmacol 14:48–58

Daly MJ, Flook JJ, Levy GP (1975) The selectivity of β-adrenoceptor antagonists on cardiovascular and bronchodilator responses to iso-prenaline in the anaesthetized dog. Br J Pharmacol 53:173–181

Khairallah PA, Page LH (1961) Mechanism of action of angiotensin and bradykinin on smooth muscle *in situ*. Am J Physiol 200:51–54

Litchfield JT, Wilcoxon F (1949) A simplified method of evaluating dose-effect experiments. J Pharm Exp Ther 96:99–113

Maggi CA, Meli A (1982) An *in vivo* procedure for estimating spasmolytic activity in the rat by measuring smooth muscle contractions to topically applied acetylcholine. J Pharmacol Meth 8:39–46

Straub W, Viaud P (1933) Studien über Darmmotilität. I. Methodik. Arch Exper Path Pharmakol 169:1–8

J.4.3.4 Colon Motility in Anesthetized Rats

PURPOSE AND RATIONALE

The influence of spasmolytic drugs on carbachol induced increase of colonic motility can be measured in anesthetized rats. The method has also be used to study the stimulation of colonic motility by an enkephalin analogue pentapeptide (Bickel 1983).

PROCEDURE

Male Sprague-Dawley rats weighing 350–500 g are anesthetized with pentobarbital i.v. A pressure sensitive tip catheter is inserted into the colon ascendens and the signals of the intraluminal pressure changes are recorded. The colonic contractions are stimulated by i.v. injection of 3 mg/kg carbachol. The height and the duration of the contractions are recorded. Then, the test compound is injected intravenously. The decrease of contractions is measured and the duration of the spasmolytic activity determined by repeated administration of carbachol at 15 min intervals, until the contractions are not significantly different from the response obtained with carbachol alone.

EVALUATION

Significant differences are calculated using Student's unpaired *t*-test.

MODIFICATIONS OF THE METHOD

Maggi and Meli (1984) used eserine-induced hypertonus of **guinea pig** distal colon *in vivo* as a phar-

macological procedure for testing smooth muscle relaxants. Male albino guinea pigs weighing 240–300 g are anesthetized with 1.5 g/kg urethane s.c. Through a midline abdominal incision, the proximal part of the hypogastric loop of the distal colon is exposed and occluding silk ligatures are applied at a distance of 2 cm from each other, taking great care to avoid any lesion to the vascular and nervous supply. Through a small incision, the flanged tip of a polyethylene tube (1 mm i.d., 1.5 mm o.d.) is inserted into the lumen and secured by means of a purse-string ligature. The free end of the tube is connected to a pressure transducer and the whole system is filled with saline. Intraluminal pressure and its variations are recorded on a polygraph. The effect of drugs is assessed as inhibition of eserine induced hypertonus.

Théodorou et al. (1991) studied the absorptive and motor components of the antidiarrheal action of loperamide in **pigs**. Motility was recorded by implantation of intraparietal electrodes into various parts of the gut.

Raffa et al. (1987) used a method utilizing the insertion of a 3 mm glass bead into the distal colon in **mice** to evaluate the activity of intracerebroventricularly administered μ- and δ-opioid agonists on colonic bead expulsion time.

REFERENCES AND FURTHER READING

Bickel M (1983) Stimulation of colonic motility in dogs and rats by an enkephalin analogue pentapeptide. Life Sci 33, Suppl 1:469–472

Bickel M, Bal-Tempe S, Blumbach J, Dohadwalla AN, Lal B, Palm D, Rajagopalan R, Rupp RH, Schmidt D, Volz-Zang C (1990) HL 752, a new enteral active muscarinic receptor antagonist. Med Sci Res 18:877–879

Maggi CA, Meli A (1984) Eserine-induced hypertone of guinea pig distal colon *in vivo*: a new pharmacological procedure for testing smooth muscle relaxants. J Pharmacol Meth 12:91–96

Raffa RB, Mathiasen JR, Jacoby HI (1987) Colonic bead expulsion time in normal and μ-opioid receptor deficient (CXBK) mice following central (icv) administration of μ- and δ-opioid agonists. Life Sci 41:2229–2234

Théodorou V, Fioramonti J, Hachet T, Buéno L (1991) Absorptive and motor components of the antidiarrhoeal action of loperamide: an *in vivo* study in pigs. Gut 32:1355–1359

J.4.3.5 Continuous Recording of Electrical and Mechanical Activity in the Gut of the Conscious Rat

PURPOSE AND RATIONALE

Bueno et al. (1981) described a method for continuous electrical and mechanical activity recording in the gut of the conscious rat. In this study two methods for the continuous recording of motor events – microtransducers and the electromyogram – are compared for the rat stomach and intestine.

PROCEDURE

Male Wistar rats weighing 200–300 g are housed singly in wire-bottomed cages and allowed lab chow and water ad libitum during the training period of 30 days. Under halothane anesthesia pairs of electrodes are implanted along the greater curvature of the pyloric antrum 5 and 2 cm from the pylorus, on the antimesenteric border of the duodenum 2 and 5 cm beyond the pylorus, and along the jejunum, 4 cm from the pylorus using a procedure described by Ruckebusch and Fioramonti (1975).

The contractions of the circular muscle layer are recorded with strain gauge microtransducers sutured onto the serosa at less than 1 cm from each set of electrodes (Pascaud et al. 1978). The free ends of the electrodes and strain gauge wires are carried subcutaneously and exteriorized on the back of the neck. The wires are inserted into a glass tube (15 cm and 0.5 cm external diameter) to prevent twisting and any contact with the metallic lids of the cage.

EVALUATION

Both electrical and mechanical activities are continuously recorded starting 5–7 days after surgery on a multichannel recorder (e. g., 8-channel Dynograph, Beckman, USA) using lead selector couplers (type 9856, Beckman) at a constant time of 0.1 s for the electrical spiking activity and strain gauge couplers (type 9863, Beckman) for the contractile force minitransducers. Simultaneously low frequency signals (frequency < 3 Hz) of the electromyogram are eliminated through filters and the spiking activity, integrated for each 20 s, is recorded on a potentiometric recorder. The electrical and mechanical activities are also recorded simultaneously on a magnetic tape recorder.

The index of motility, expressed as mcoul/min is calculated from the integrated records of electrical activity. The index of mechanical motility is calculated as the area under all contraction waves occurring during 1 min, and is expressed as gs/min. Mechanical and electrical activities during a test period of 30 min after administration of stimulant drugs, e. g., the gastrointestinal hormones gastrin and cholecystokinin, or relaxing drugs, like anticholinergic agents, are compared with the values of a 30 min pretest period.

MODIFICATIONS OF THE METHOD

Wright et al. (1981) described a similar method for long-term recording of intestinal mechanical and elec-

trical activity in the unrestrained rat. Mechanical activity is detected using miniaturized half-bridge metal foil strain-gauge force transducers. The electrical activity is monitored by silver/silver chloride bipolar electrodes. The lead wires from the recording units are encased in a metal compression spring and are permanently joint to a ball connector positioned on the top of the cage, such allowing the animal free access to all parts of the cage.

Stam et al. (1995) described computer analysis of the migrating motility complex of the small intestine recorded in freely moving rats. Myoelectric activity of the small intestine was recorded digitally in fasted, freely moving rats with multiple pairs of electrodes in the antimesenterial smooth muscle. A computer program was developed to distinguish the three characteristic phases of the migrating motility complex.

Fändriks (1993) measured duodenal wall motility, mucosal fluid transport and alkaline secretion in anesthetized **cats**. A triple-lumen tube supplied with two small balloons was positioned via the esophagus in the duodenal lumen and its distal end was led through a small incision in the antimesenteric border of the distal duodenum at the level of the ligament of Treitz. The most oral of the balloons was positioned immediately to the pylorus. After filling with air, the balloons occluded the lumen and isolated a 2 cm segment of the proximal duodenum. A double-lumen tube was inserted into the stomach for luminal perfusion.

Martinez et al. (1993), Jimenez et al. (1994) studied gastrointestinal motility and coordination in **chickens**. Animals were chronically implanted with electrodes in stomach, duodenum, ileum, caeca and rectum.

Nakajima et al. (1996) used a telemetric device (supplied by Data Sciences International, Inc., St Paul, MN) which can be implanted in the abdominal cavity of small animals. Gastric motility of freely moving rats could be continuously recorded for up to 60 days.

REFERENCES AND FURTHER READING

Bueno L, Ferre JP, Ruckebusch M, Genton M, Pascaud X (1981) Continuous electrical and mechanical activity recording in the gut of the conscious rat. J Pharmacol Meth 6:129–136

Fändriks L (1993) Measurements of duodenal wall motility, mucosal fluid transport and alkaline secretion. Description and evaluation of a methodological approach in the anesthetized cat. Acta Physiol Scand 149:59–66

Jimenez M, Martinez V, Rodriguez-Membrilla A, Rodriguez-Sinovas A, Gonalons E, Vergara P (1994) Rhythmic oscillating complex: Characterization, induction, and relationship to MMC in chickens. AM J Physiol 266 (Gastrointest Liver Physiol 29):G585–G595

Martinez V, Jimenez M, Gonalons E, Vergara P (1993) Effects of cholecystokinin and gastrin on gastroduodenal motility and coordination in chickens. Life Sci 52:191–198

Nakajima M, Sakai T, Mizumoto A, Itoh Z (1996) Development of a new telemetric system for measuring gastrointestinal contractile activity in unrestrained and conscious small animals. J Smooth Musc Res 32:1–7

Pascaud XB, Genton MJH, Bass P (1978) A miniature transducer for recording intestinal motility in unrestrained chronic rats. Am J Physiol 235:E523–E 538

Ruckebusch M, Fioramonti J (1975) Electrical spiking activity and propulsion in small intestine in fed and fasted rats. Gastroenterology 68:1500–1508

Stam R, Kroese ABA, Croiset G, Wiegant VM, Akkermans LM (1995) Computer analysis of the migrating motility complex of the small intestine recorded in freely moving rats. J Pharmacol Toxicol Meth 33:129–136

Wright JW, Healy TEJ, Balfour TW, Hardcastle JD (1981) A method for long-term recording of intestinal mechanical and electrical activity in the unrestrained rat. J Pharmacol Meth 6:233–242

J.4.3.6 Propulsive Gut Motility in Mice

PURPOSE AND RATIONALE

The passage of a charcoal meal through the gastrointestinal tract in mice is used as parameter for intestinal motility and to study the effect of laxatives.

PROCEDURE

Groups of 10 female mice (e. g., NMRI strain) weighing 15 g are fed an oat diet for 3 days. Eighteen hours prior to the experiment food, but not water, is withdrawn. The animals are treated either subcutaneously 15 min or orally 60 min before administration of the charcoal meal (0.2 ml of a 4% suspension of charcoal in 2% carboxymethylcellulose solution). The mice are sacrificed after various time intervals, 20 min, 40 min, 60 min and 120 min. Ten animals serve as controls for each time interval. The entire intestine is immediately removed and immersed in 5% formalin to halt peristalsis; then washed in running water. The distance the meal has traveled through the intestine as indicated by the charcoal is measured and expressed as percent of the total distance from the pylorus to the caecum.

EVALUATION

Student's *t*-test is used to compare the control and the drug-treated group.

CRITICAL ASSESSMENT OF THE METHOD

The charcoal passage test can be used for evaluation of laxative activity as well as for inhibition of intestinal motility.

MODIFICATIONS OF THE METHOD

Instead of charcoal, unsubstituted Hostapermblau (CuPcB) suspended in gummi arabicum mucilage can be used.

Carmine red (15) suspended in a 1% tragacanth solution was used for measurement of small intestine transit in **rats** (Leng-Peschlow 1986).

Miller et al. (1981) measured the intestinal transit in the rat by the use of radiochromium (^{51}Cr). Female Sprague Dawley rats weighing approximately 200 g were implanted with indwelling silastic cannulae in the proximal duodenum. Following a 3 day recovery period, the animals were fasted for 18 h and then treated with the test compounds. Thirty min later, 0.2 ml of radiochromium (0.5 mCi $Na^{51}CrO_4$) was instilled into the small intestine via the indwelling silastic cannula. Twenty-five min after chromium instillation, the animals were sacrificed. The small intestine was carefully removed and divided into 10 equal segments. The radioactivity was determined with an automatic gamma counting system. The effect of drugs could be quantified by determining the geometric center of the distribution of chromium through the small intestine.

Shook et al. (1989) used radiolabeled chromium to measure gastrointestinal transit in mice.

Megens et al. (1989) used the charcoal test to study the *in vivo* dissociation between the antipropulsive and antidiarrheal properties of opioids in rats.

Lish and Peters (1957) recommended an intestinal antipropulsive test in intact insulin-treated rats providing certain advantages over the commonly used charcoal meal test for screening of synthetic antispasmodic and antipropulsive agents.

REFERENCES AND FURTHER READING

Goldenberg MM, Burns RH (1973) Effectiveness of an unique antispasmotic 3,4-dihydro-5-phenoxy-benzol[*b*][1,7naphthyridin-1(2H)-one EU-1086, *in vivo* and *in vitro.* Arch Int Pharmacodyn 203:55–66

Leng-Peschlow E (1986) Acceleration of large intestine transit time in rats by sennosides and related compounds. J Pharm Pharmacol 38:369–373

Lish PM, Peters EL (1957) Antagonism of insulin-induced gastrointestinal hypermotility in the rat. Proc Soc Exp Biol Med 94:664–668

Macht DI, Barba-Gose J (1931) Two new methods for the pharmacological comparison of insoluble purgatives. J Am Pharm Ass 20:558–564

Megens AAHP, Canters LLJ, Awouters FHL, Niemegeers CJE (1989) Is *in vivo* dissociation between the antipropulsive and antidiarrheal properties of opioids in rats related to gut selectivity? Arch Int Pharmacodyn 298:220–229

Miller MS, Galligan JJ, Burks TF (1981) Accurate measurement of intestinal transit in the rat. J Pharmacol Meth 6:211–217

Niemegeers CJE, Lenaerts FM, Janssen PAJ (1974) Loperamide (R18 553), a novel type of antidiarrheal agent. Part 2: *In vivo* parenteral pharmacology and acute toxicity in mice. Comparison with morphine, codeine and diphenoxylate. Arzneim Forsch/Drug Res 24:1636–1638

Shook JE, Lemcke PK, Gehring CA, Hruby VJ, Burks TF (1989) Antidiarrheal properties of supraspinal *mu, delta* and *kappa* opioid receptors: Inhibition of diarrhea without constipation. J Pharmacol Exp Ther 249:83–90

J.4.3.7 Nerve-Jejunum Preparation of the Rabbit

PURPOSE AND RATIONALE

Perivascular nerve stimulation induces cessation of peristalsis of rabbit jejunum (Finkelman 1930). Effects of test compounds on this phenomenon can be tested.

PROCEDURE

Albino rabbits are sacrificed and the jejunal part of the gut prepared. The nerve lies in the mesentery along with the arterial blood supply. Nerve-jejunum preparations are suspended in an organ bath. The preparation is stimulated with pulses at a frequency of 20 Hz with 0.5 ms and about 5 volt for 10 s at 3 min intervals. Test compounds are applied to the organ bath in a cumulative manner at 6 min intervals. Peristalsis movements for each period of 3 min between drug application or of the period of cessation of peristalsis induced by nerve stimulation of the rabbit jejunum preparation are recorded. The effect of drugs on spontaneous peristalsis movement and on the cessation of peristalsis movement exerted by perivascular nerve stimulation is tested.

EVALUATION

The areas of peristalsis movement for each period of 3 min are measured using a planimeter. The effects are expressed as percentage of change between controls and test compound treated preparations.

REFERENCES AND FURTHER READING

Finkelman B (1930) On the nature of inhibition in the intestine. J Physiol 70:145–157

J.4.3.8 Motility of Gastrointestinal Tract in Dogs

PURPOSE AND RATIONALE

Intraluminal pressure and motility of the small intestine can be measured in unanesthetized dogs with balloon catheter systems via a duodenal Mann-Bollman (1931) fistula according to Tasaka and Farrar (1976) or in the loop of a Thiry–Vella fistula (see below).

PROCEDURE

Fistulas of the small intestine are created in male Beagle dogs weighing 15–20 kg. The animals are anesthetized with 40 mg/kg pentobarbital i.v. and fixed on an operation table. After shaving and careful disinfection of the skin a midline incision is made. A 10–15 cm length of ileum, approximately 15 cm proximal to the caecum, is excised. The remaining ileum is anastomosed end-to-end. The excised ileum is anastomosed, end to side, to the proximal or middle jejunum. Radiopaque tantalum markers are sutured to the serosa distal to this anastomosis in order to guide the direction for subsequent intubation. The other end is sutured to the skin. To create a skin ileostomy which does not shrink rapidly, a small amount of muscle, fascia and subcutaneous tissue are excised from the abdominal wall.

For the measurement of the pressure inside the intestine, an air-filled system is employed. Air-filled latex balloons (Cementex), 5 mm in diameter, are attached to air-filled PE 190 polyethylene catheters (ID 1.19 mm) with a length of 120 cm. Three balloon-catheter pressure assemblies are tied together with the balloons 5 cm apart. The catheters are connected to Statham p23 db pressure transducers and to a polygraph. The transducers are rendered airtight by repeated applications of latex to all the connections.

The dogs are withheld from food, but not from water 18 h prior to the experiment. The balloon-catheter assemblies are introduced through the fistula and secured in an appropriate position. The system is filled with air to a pressure of 10 mm Hg. Similarly, balloon-catheter assemblies can be introduced into a Thiry–Vella fistula.

Intraluminal pressure is measured continuously; frequency and amplitude of pressure waves are recorded. After a period of 1 h, the test drug is administered orally or subcutaneously and the above mentioned parameters recorded for 10 min intervals.

EVALUATION

For 10 min intervals amplitude frequency (f_A), average degree and duration of amplitudes (A) and average pressure performance (PL_i) are calculated. Post-drug values are compared with pre-drug readings.

MODIFICATIONS OF THE METHOD

Goldenberg and Burns (1973) reported on a technique using rubber balloon catheters inserted in the duodenum, ileum, or colon of dogs, secured by purse-string sutures and filled with water to record intraluminal pressure monitored by Statham pressure transducers connected to a polygraph. Furthermore, an antispasmodic agent can be tested for relaxation of morphine sulfate (0.3 mg/kg i.v.) induced spasms of the intestinal tract.

Fox et al. (1985) implanted chronically extraluminal strain gage force transducers on the serosal surface of the gastrointestinal tract of dogs.

REFERENCES AND FURTHER READING

Fox DA, Bauer R, Bass P (1985) Use of gut cyclic motor activity to evaluate a stimulant (narcotic) and inhibitor (anticholinergic) of gastrointestinal-tract activity in the unanesthetized dog. J Pharmacol Meth 13:147–155

Goldenberg MM, Burns RH (1973) Effectiveness of an unique antispasmotic 3,4-dihydro-5-phenoxy-benzol[*b*][1,7naphthyridin-1(2H)-one EU-1086, *in vivo* and *in vitro.* Arch Int Pharmacodyn 203:55–66

Mann FC, Bollman JL (1931) A method for making a satisfactory fistula at any level of the gastrointestinal tract. Ann Surg 93:794–797

Tasaka K, Farrar JT (1976) Intraluminal pressure of the small intestine of the unanesthetized dog. Pflüger's Arch 364:35–44

J.4.3.9 Thiry–Vella Fistula

PURPOSE AND RATIONALE

As described first by Thiry (1864) and improved by Vella (1892), a part of the jejunum is isolated and the ends are exteriorized through the abdominal wall allowing to measure *in vivo* motility and function of the intestines in dogs and other species (Boldyreff 1925).

PROCEDURE

Male Beagle dogs weighing 15–20 kg are used. They are fasted 24 h preoperatively. Intravenous pentobarbital sodium, 30 mg/kg, provides satisfactory anesthesia. It can be supplemented, if necessary, during operation. The abdominal part is shaved with electric clippers, then with a razor. The skin is disinfected with Zephiran –70% alcohol. Sterile drapes are applied to cover the whole operative field. A mid-line linea alba incision is made. A loop of the jejunum, about 70 cm in length, is separated leaving the blood supply through the mesenterium intact. Both distal and proximal ends are exteriorized through the abdominal wall and provided with stomata. An end-to-end jejuno-jejunal anastomosis is performed.

EVALUATION

The preparation can be used to evaluate intestinal motility. A latex balloon connected via a polyethylene catheter to a pressure transducer (Statham P 23 BB) is introduced through the proximal ostium. Changes in

intragastric pressure are measured on a frequency measurement bridge and are recorded continuously. The number and height of the pressure waves are used as indices of intestinal motor activity. Secretin inhibits motility of the small intestine dose-dependent.

MODIFICATIONS OF THE METHOD

Sarr et al. (1981) and Bastidas et al. (1990) used **dogs** with Thiry–Vella loops to study jejunal absorption.

Bilchik et al. (1993) examined the effects of physiological doses of peptide YY in dogs with jejunal and ileal exteriorized, neurovascularly intact Thiry–Vella fistulas.

Ashton et al. (1996) created Thiry–Vella fistulas using a 20 cm segment of distal colon under general anesthesia in dogs. Colonic absorption of water and electrolytes was evaluated in awake, conscious animals.

Liu et al. (1996a) studied the effects of intravenous peptide YY on colonic water and electrolyte transport in awake dogs which had 20 cm neurovascularly intact colon Thiry–Vella fistulas.

In an other study, Liu et al. (1996b) evaluated the effects of cholecystokinin and peptide YY on intestinal absorption of water and electrolytes using colonic, ileal, or jejunal fistulas in dogs.

These authors (Liu et al. 1995) also examined the effects of intraluminal administration of a new substituted peptide YY analog on intestinal absorption of water and electrolytes in dog with jejunal, ileal and colonic Thiry–Vella fistulas.

Barry et al. (1995) investigated the effect of luminally administered dopamine, the D_1-receptor agonist SKF 38393, the α_1-receptor antagonist terazosin, and the α_2-receptor antagonist yohimbine on ileal water and electrolyte transport in dogs with Thiry–Vella fistulas.

Walters et al. (1994) described the effect of a model of canine jejuno-ileal orthotopic autotransplantation on jejunal and ileal transport of water and electrolytes. For neurally intact jejunal loops, myoneural continuity between the loop and the proximal duodenum and jejunum was maintained by preserving a bridge of tunica muscularis devoid of mucosa between the proximal jejunum and the loop. All intrinsic neural and lymphatic continuity to the loop was carefully maintained by not transecting any of the mesentery to the loop.

For the autotransplanted jejunal loop the dogs underwent construction of an identical loop with the muscular bridge after preparation of an jejuno-ileal autotransplantation. For this purpose, all neural, lymphatic, myogenous, and connective tissue connections with the jejuno-ileum were transected except for the fully isolated and stripped superior mesentery artery and vein at the base of the small bowel mesentery. The perivascular and adventitial tissue of these two vessels were carefully dissected away and transected under optical magnification. From here, the mesenteries to the distal duodenum and to the distal ileum were transected in radial fashion and the distal duodenum and distal ileum 5 cm from the ileo-colonic junction were also transected. At this point, the jejuno-ileum was completely isolated from any neural/lymphatic continuity with the dog except for any neural/lymphatic elements travelling within the media of the mesenteric artery and vein.

Neurally intact and autotransplanted ileal loops were prepared in a similar way.

Remie et al. (1990) described in detail the preparation of a Thiry–Vella loop in the **rat**. After laparotomy the segment to be isolated has to be located carefully. The segment should be vascularized by two or more tributary arteries. For ligation of the arcade, two ligatures are placed around the blood vessels 2–3 mm from each other. The two ligatures are tightened, the gut wall is disinfected with iodine solution, and both the vessels of the arcade and the gut wall are cut. The same procedure is performed at the other end of the segment to be isolated. This segment is laid on gauze moistened with warm saline avoiding torsion of the vessels. For end-to-end anastomosis the remaining parts of the gut are approximated and two corner sutures are placed. A continuous suture with transfixing stitches is placed on the anterior and posterior wall. Using a pair of sharp scissors two holes are made in the abdominal wall and the skin. Subsequently, standard end-to-side anastomosis technique is used to sew the gut to the internal abdominal muscle. The two stay sutures are at 180° and the posterior wall is sutured first. Following this, the skin is sutured to the abdominal muscle, using a running suture.

Chu et al. (1995) used Thiry–Vella fistulas of either the jejunum or ileum in rats in order to determine whether the trophic effects of bombesin on the small bowel mucosa are mediated by nonluminal factors or endogenous luminal secretion.

Bárdos and Nagy (1995) prepared double Thiry–Vella fistulas in rats. The first Thiry–Vella loop was created from the lower duodenum. After 1 month or more, a similar fistula was prepared from the upper part of the colon. The two loops were positioned along the midline and formed a line of 4 openings of the abdominal wall providing an easy access for inserting stimulatory devices to either of the loops in the same animal. A rubber balloon made of latex rubber was tied

to a silicon rubber tube, inserted into the isolated loop via one of its orifices and then fixed to the body by a tape. Stimulation was performed by injection of various volumes of water into the balloon from an attached syringe. Behavioral reactions of the animals were recorded as scores during 10 s stimulation periods.

In order to purify the putative luminal cholecystokinin-releasing factor, Spannagel et al. (1996) collected intestinal secretions by perfusing a modified Thiry–Vella fistula of jejunum in conscious rats.

Snoj et al. (1992) found that phosphatidylcholine inhibited postoperative adhesions after small bowel anastomosis in the rat.

Gianotti and Tchervenkov (1992) used a Thiry–Vella loop in **guinea pigs** to study the stimulatory effect of intraluminal nutriment on burned guinea pig intestinal mucosa.

Philpott et (1993) created Thiry–Vella loops in 21 week old **rabbits** in order to study the influence of luminal factors on intestinal repair during refeeding of malnourished infant rabbits.

Silbart et al. (1996) examined the ability of several bacterial endotoxins and their subunits to act as adjuvants or carrier proteins in stimulating an intestinal secretory Ig4 response to 2-acetylaminoflourene using Thiry–Vella loops in rabbits.

REFERENCES AND FURTHER READING

Anthone GJ, Zinner MJ, Yeo CJ (1993) Small bowel origin and caloric dependence of a signal for meal-induced jejunal absorption. Ann Surg 217:57–63

Ashton KA, Chang LK, Anthone GJ, Ortega AE, Simons AJ, Beart RW Jr (1996) Basal and meal-stimulated colonic absorption. Dis Colon Rectum 39:865–870

Bárdos G, Nagy K (1995) A new method: double Thiry-Vella fistulas in rats to compare the effects of small and large intestinal stimulation on behaviour. Physiol Behav 57:591–593

Barry MK, Maher MM, Gontarek JD, Jimenez RE, Yeo CJ (1995) Luminal dopamine modulates canine water and electrolyte transport. Dig Dis Sci 40:1738–1743

Bastidas JA, Orandle MS, Zinner MJ, Yeo CJ (1990) Small-bowel origin of the signal for meal-induced jejunal absorption. Surgery 108:376–383

Bastidas JA, Zinner MJ, Bastidas JA, Orandle MS, Yeo CJ (1992) Influence of meal composition on canine jejunal water and electrolyte absorption. Gastroenterology 102:486–492

Bilchik AJ, Hines OJ, Adrian TE, McFadden DW, Berger JJ, Zinner MJ, Ashley SW (1993) Peptide YY is a physiological regulator of water and electrolyte absorption in the canine small bowel *in vivo*. Gastroenterology 105:1441–1448

Boldyreff WN (1925) Surgical method in the physiology of digestion. Description of the most important operations on digestive system. Ergebn Physiol 24:399–444

Chu KU, Higashide S-I, Evers BM, Ishikuza J, Townsend CM Jr, Thompson CJ, Jones RS, Souba WW Jr, Hanks JB, Fischer JE, Gadacz TR, Chu KU (1995) Bombesin stimulates mucosal growth in jejunal and ileal Thiry–Vella fistulas. Ann Surg 221:602–611

Gianotti L, Tchervenkov JI (1992) Stimulatory effect of intraluminal nutriment on burned guinea pig intestinal mucosa. Rivista Italiana Nutrizione Parent Enter 10:112–118

Konturek SJ, Radecki T, Thor P (1974) Comparison of endogenous release of secretin and cholecystokinin in proximal and distal duodenum in the dog. Scand J Gastroenterol 9:153–157

Liu CD, Hines OJ, Whang EE, Balasubramaniam A, Newton TR, Zinner MJ, Ashley SW, McFadden DW (1995) A novel synthetic analog of peptide YY, BIM-43004, given intraluminally, is proabsorptive. J Surg Res 59:80–84

Liu CD, Adrian TE, Newton TR, Bilchik AJ, Zinner MJ, Ashley SW, McFadden DW (1996a) Peptide YY: A potential proabsorptive hormone for the treatment of malabsorptive disorders. Am Surg 62:232–236

Liu CD, Hines OJ, Newton TR, Adrian TE, Zinner MJ, Ashley SW, McFadden DW (1996b) Cholecystokinin mediation of colonic absorption via peptide YY: Foregut-hindgut axis. World J Surg 20:221–227

McFadden DW, Jaffe BM, Ferrara A, Zinner MJ (1984) Jejunal absorptive response to a test meal and its modification by cholinergic and calcium channel blockade in the awake dog. Surg Forum 35:174–176

Philpott DJ, Kirk DR, Butzner JD (1993) Luminal factors stimulate intestinal repair during refeeding of malnourished infant rabbits. Can J Physiol Pharmacol 71:650–656

Remie R, Rensema JW, Van Dongen JJ (1990) Perfusion of the isolated gut *in vivo*. In: Van Dongen JJ, Rensema JW, Van Wunnik (eds) Manual of microsurgery in the rat. Part I. Elsevier Science Publ., pp 255–274

Sarr MG, Kelly KA, Phillips SF (1981) Feeding augments canine jejunal absorption via a hormonal mechanism. Dig Dis Sci 26:961–965

Silbart LK, McAleer F, Rasmussen MV, Goslinoski L, Keren DF, Finley A, Kruningen HJV, Winchell MJ (1996) Selective induction of mucosal immune response to 2-acetylaminofluorene. Anticancer Res 16:651–660

Snoj M, Ar'Rajab A, Ahrén B, Bengmark S (1992) Effect of phosphatidylcholine on postoperative adhesions after small bowel anastomosis in the rat. Br J Surg 79:427–429

Spannagel AW, Green GM, Guan D, Liddle RA, Faull K, Reeve JR Jr (1996) Purification and characterization of a luminal cholecystokinin-releasing factor from rat intestinal secretion. Proc Natl Acad Sci USA 93:4415–4420

Thiry L (1864) über eine neue Methode, den Dünndarm zu isolieren. Natur Kl 50:77–79

Tracy HJ, Gregory RA (1964) Physiological properties of a series of synthetic peptides structurally related to gastrin I. Nature 204:935–938

Walters AM, Zinsmeister AR, Sarr MG (1994) Effect of a model of canine jejunoileal orthotopic autotransplantation on jejunal and ileal transport of water and electrolytes. Digest Dis Sci 39:843–850

Yeo CJ, Bastidas JA, Schmieg RE, Zinner MJ (1990) Meal-stimulated absorption of water and electrolytes in canine jejunum. Am J Physiol 259:G402–G409

J.4.3.10 Continuous Recording of Mechanical and Electrical Activity in the Intestine of Conscious Dogs

PURPOSE AND RATIONALE

Cyclic motor activity occurring in almost all parts of the gastrointestinal tract is due to a migrating electric complex (Szurszewski 1969; Fioramonti et al. 1980;

Sarna and Condon 1984; Sarna et al. 1984; Sarna 1985). Smooth muscle cells of the gut show periodic oscillations of membrane potentials called electrically controlled activity; they are also named slow waves, basic electrical rhythm, or pacesetter potentials. If the membrane potential depolarizes beyond a certain threshold during such an oscillation, the smooth muscle contracts. This is usually associated with a rapid burst of electrical oscillations, called electrical response activities or spikes. Electrical response activity is, therefore, associated with contractions on a 1:1 basis.

Implantation of extraluminal force transducers allows the monitoring of contractile activity in conscious animals (Bass and Wiley 1972; Ormsbee and Bass 1976; Ormsbee et al. 1981). The data can be analyzed by computer (Ehrlein and Hiesinger 1982; Schemann et al. 1985). The effects of opiate agonists, morphine, natural enkephalins, endorphins, and synthetic enkephalins and opiate antagonists, like nalorphine, as well as other gastrointestinal hormones, such as motilin, can be studied (Bickel and Belz 1985, 1988; Bickel et al. 1985).

PROCEDURE

Male Beagle dogs weighing 15–20 kg are anesthetized with thiobarbital and anesthesia is then maintained with halothane and a mixture of N_2O and O_2 (3:1). Under aseptic conditions several miniaturized strain gauge force transducers are sutured onto the muscular layers of the gastrointestinal tract. Before implantation, the transducers are externally calibrated giving linear signals over a range from 10 to 300 mN. Each transducer has its recording axis perpendicular to the longitudinal axis of the intestine to record contractions of the circular smooth muscles. The proximal ends of the strain gauge transducers are fitted to a plug embedded in a stainless-steel cannula implanted into the abdominal wall. The signals are continuously recorded and stored in a HP 9835A Hewlett Packard computer, allowing later analysis of the data.

For measuring electrical activity, bipolar electrodes are implanted at several parts of the intestinal tract. The lead wires from the electrodes are externalized via a stainless-steel cannula. Electromyogram is recorded on an electroencephalograph.

The animals are kept in a standardized environment with one daily feeding at 9:00 A.M. The dogs are trained to stand in a Pawlov stand. Eighteen hours prior to the beginning of the experiment, the animals are fasted with access to water. Motility data and electrical activity are first recorded for fasting dogs without drug treatment. Then the drug is injected intravenously during the period of quiescence of the migrating motor complex.

EVALUATION

Recordings are analyzed for duration of cycles (min) and motor complexes (min), mean height (mN) and frequency (*n*/min). The length of the cycles is measured from the beginning of one complex to the beginning of the next complex. Electromyogram is analyzed for slow waves (cycles/min), maximum amplitude of the spike bursts (mV), duration of the spike bursts (ms) and duration of the effect (min). The data before and after administration of various doses of the test compound are compared by statistical means (Student's *t*-test).

MODIFICATIONS OF THE METHOD

Itoh et al. (1977) and Nagakura et al. (1996) used extraluminal force transducers for recording contractile motility of the gastrointestinal smooth muscle in conscious dogs.

Nakada (1995) recorded gastrointestinal and gallbladder contractions in conscious dogs by chronically implanted strain gauge transducers and gallbladder volume changes by a chronically indwelling gallbladder catheter.

Orihata and Sarna (1994) investigated contractile mechanism of gastroprokinetic agents in conscious dogs. The spatial and temporal parameters of gastric, pyloric and duodenal contractions during the entire period of gastroduodenal emptying, during a 60-min period of drug infusion and during the post-drug-infusion period were analyzed by a computer method.

REFERENCES AND FURTHER READING

Bass P, Wiley JN (1972) Contractile force transducer for recording muscle activity in unanesthetized animals. J Appl Physiol 32:567–570

Bickel M, Belz U (1985) Initiation of the interdigestive migrating motor complex by a synthetic enkephalin analogue in the dog. IRCS Med Sci 13:525–526

Bickel M, Belz U (1988) Motilin and a synthetic enkephalin induce colonic motor complexes (CMC) in the conscious dog. Peptides 9:501–507

Bickel M, Alpermann HG, Roche M, Schemann M, Ehrlein HJ (1985) Pharmacology of a gut motility stimulating enkephalin analogue: Arzneim Forsch/Drug Res 35:1417–1426

Ehrlein HJ, Hiesinger E (1982) Computer analysis of mechanical activity of gastroduodenal junction in unanesthetized dogs. Quart J Exp Physiol 67:17–29

Fioramonti J, Garcia-Villar R, Bueno L, Ruckebusch Y (1980) Colonic myoelectrical activity and propulsion in the dog. Digest Dis Sci 25:641–646

Itoh Z, Honda R, Takeuchi S, Aizawa I, Takayanagi R (1977) An extraluminal force transducer for recording contractile motility of the gastrointestinal smooth muscle in conscious dogs: Its construction and implantation. Gastroenterol Jpn 12:275–283

Nagakura Y, Kamato T, Nishida A, Ito H, Yamano M, Miyata K (1996) Characterization of 5-hydroxytryptamine (5-HT) receptor subtypes influencing colonic motility in conscious dogs. Naunyn-Schmiedeberg's Arch Pharmacol 353:489–498

Nakada K (1995) Effect of gastrectomy on gallbladder motility: An experimental study. J Smooth Muscle Res 31:23–32

Orihata M, Sarna SK (1994) Contractile mechanisms of action of gastroprokinetic agents: Cisapride, metoclopramide, and domperidone. Am J Physiol 266 (Gastrointest Liver Physiol 29):G665–G676

Ormsbee III HS, Bass P (1976) Gastroduodenal motor gradients in the dog after pyloroplasty. Am J Physiol 230:389–397

Ormsbee III HS, Telford GL, Suter CM, Wilson PD, Mason GR (1981) Mechanism of canine migrating motor complex – a reappraisal. Am J Physiol 240:G141–G146

Sarna SK (1985) Cyclic motor activity migrating complex. Gastroenterology 89:894–913

Sarna SK, Condon RE (1984) Morphine-initiated migrating myoelectric complexes in the fed state in dogs. Gastroenterology 86:662–669

Sarna SK, Condon R, Cowles V (1984) Colonic migrating and nonmigrating motor complexes in dogs. Am J Physiol 246:G355–G360

Schemann M, Ehrlein HJ, Sahyoun H (1985) Computerised method for pattern recognition of intestinal motility: functional significance of the spread of contractions. Med Biol Eng Comput 23:143–149

Szurszewski JH (1969) A migrating electric complex of the canine small intestine. Am J Physiol 217:1757–1763

J.4.4 Absorption

J.4.4.1 Everted Sac Technique

PURPOSE AND RATIONALE

The everted sac technique is used to study the transport of substances from the mucosal to the serosal surface (Wilson and Wiseman 1954).

PROCEDURE

Male Wistar rats weighing 150–220 g are anesthetized with 30 mg/kg pentobarbitone s.c. A midline abdominal incision is made. The rats are sacrificed by cardiac puncture. The small intestine from the ligament of Treitz to the ileocaecal junction with a length of 6–7 cm is rapidly removed and everted with a glass rod. The sac is securely ligated at both ends and filled with Krebs-Henseleit bicarbonate buffer solution (pH 7.4) containing 0.4% glucose and pre-gassed with 95% O_2/5% CO_2. The sac is incubated at 37°C in a glass vessel containing the same buffer solution and gassed with 95% O_2/5% CO_2.

After 5 min, the drug solution is added to the glass vessel and the preparation is further incubated. After given time intervals, the fluid from the everted sac is removed and the volume determined. The concentration of the drug transported from the mucosal to the serosal side is determined by appropriate analytical methods.

EVALUATION

Determinations of the drug in the everted sac at different time intervals allow evaluation of pharmacokinetic parameters.

MODIFICATIONS OF THE METHOD

Madar (1983) used the small intestine everted sac of **chicken** for demonstration of amino acid and glucose transport.

Harnett et al. (1989) used everted segments of distal ileum of **rats** to study taurocholate absorption.

Turner et al. (1990) used everted sacs of ileum in **sheep** to study selenate and selenite absorption.

Goerg et al. (1992) used the stripped descending colon of the **rat** as everted sac to study the inhibition of neuronally mediated secretion in rat colonic mucosa by prostaglandin D_2.

Under ether anesthesia, the descending colon is removed and transferred into ice-cold bathing solution. The colon is placed on a plastic rod. After a circular incision with a blunt scalpel, the serosa and muscularis propria are stripped away, leaving the mucosal-submucosal preparation consisting of the mucosa, the muscularis mucosae, and a part of the submucosa with the completely preserved submucosal plexus. The tube-like mucosal-submucosal preparation is mounted as an everted sac in a holding apparatus (volume of the outer compartment 25 ml). The potential difference between the outer mucosal side and inner serosal side is measured by two agar bridges. The tissue is short-circuited by a voltage clamp after correcting for the offset potential and compensating for the solution resistance.

Moreover, transmural ion fluxes can be determined with the everted sac technique. Net fluxes of sodium, chloride, and potassium are studied by direct measurements of volume changes and changes of electrolyte concentrations in the inner volume of the everted sacs. Unidirectional fluxes can be determined simultaneously with the direct measurement of net fluxes by adding the isotopes $^{22}Na^+$ and $^{36}Cl^-$ to one side of the everted sac.

Schilling and Mitra (1990) used the everted gut technique in rats to study enteral insulin absorption.

Mizuma et al. (1993) studied the active absorption in the intestine and metabolism of the β- and α-anomers of the glucoside and galactoside of p-nitrophenol to find a more suitable prodrug for poorly absorbed drugs. The everted sac technique was used to investigate the intestinal absorption of these glycosides from the mucosal to the serosal side of the rat jejunum.

Kitagawa et al. (1996) investigated the influence of various factors, such as temperature, on the absorption of methochlorpromazine in the small intestinal everted sac of rats.

Tanaka et al. (1996) estimated the transport characteristics of thyrotropin-releasing hormone (TRH) and its chemically modified derivative with lauric acid (Lau-TRH) across the rat small or large intestine by means of an *in vitro* everted sac experiment.

Sasaki et al. (1995) studied the absorption characteristics of azetirelin, a new thyrotropin-releasing hormone analogue in rats by means of *in situ* closed loop and *in vitro* everted sac experiments.

Toskulkao et al. (1995) examined the effects of stevioside (a natural non-nutritive sweetening agent) and of steviol (a product of enzymatic hydrolysis of stevioside) on intestinal glucose absorption in hamster jejunum using the everted sac technique.

Motozono et al. (1994) determined the effect of age on gastrointestinal absorption of tobramycin in suckling, weanling and adult rats by an everted sac method.

REFERENCES AND FURTHER READING

Fujioka Y, Mizuno N, Morita E, Motozono H, Takahashi K, Yamanaka Y, Shinkuma D (1991) Effect of age on the gastrointestinal absorption of acyclovir in rats. J Pharm Pharmacol 43:465–469

Goerg KJ, Wanitschke R, Diener M, Rummel W (1992) Inhibition of neuronally mediated secretion in rat colonic mucosa by prostaglandin D_2. Gastroenterology 103:781–788

Harnett KM, Walsh CT, Zhang L (1989) Effects of Bay o 2752, a hypocholesterolemic agent, on intestinal taurocholate absorption and cholesterol esterification. J Pharm Exp Ther 251:502–509

Kitagawa S, Sato K, Sasaki M (1996)Absorption of methochlorpromazine in rat small intestinal everted sac. Biol Pharm Bull 19:998–1000

Madar Z (1983) Demonstration of amino acid and glucose transport in chick small intestine everted sac as a student laboratory exercise. Biochem Educ 11 9–11

Mizuma T, Ohta K, Hayashi M, Awazu S (1993) Comparative study of active absorption by the intestine and disposition of anomers of sugar-conjugated compounds. Biochem Phamacol 45:1520–1523

Motozono H, Mizuno N, Morita E, Fujioka Y, Takahashi K (1994) Effect of age on gastrointestinal absorption of tobramycin in rats. Int J Pharm 108:39–48

Sasaki I, Tanaka K, Fujita T, Murakami M, Yamamoto A, Muranishi S (1995) Intestinal absorption of azetirelin, a new thyrotropin-releasing hormone analogue. II. *In situ* and *in vitro* absorption characteristics of azetirelin from the rat intestine. Biol Pharm Bull 18:976–979

Schilling RJ, Mitra AK (1990) Intestinal mucosal transport of insulin. Int J Pharm 62:53–64

Tanaka K, Fuijita T, Yamamoto Y, Murakami M, Yamamoto A, Muranishi S (1996) Enhancement of intestinal transport of thyrotropin-releasing hormone via a carrier-mediated transport system by chemical modification with lauric acid. Biochim Biophys Acta – Biomembr 1283:119–126

Turner JC, Osborn PJ, McVeagh (1990) Studies on selenate and selenite absorption by sheep ileum using an everted sac method and an isolated, vascular perfused system. Comp Biochem Physiol 95A:297–301

Tuskulkao C, Sutheerawattananon M, Piyachaturawat P (1995) Inhibitory effect of steviol, a metabolite of stevioside, on glucose absorption in everted hamster intestine *in vitro*. Toxicol Lett 80:153–159

Wilson TH, Wiseman G (1954) The use of sacs of everted small intestine for the study of transfer of substances from the mucosal to the serosal surface. J Physiol 123:116–125

Witkowska D, Sendrowicz L, Oledzka R, Szablicka E, Garszel J (1992) The study of leucine and methionine transport in the gut of rats intoxicated with Thiram. Arch Toxicol 66:267–271

J.4.4.2 Stomach Emptying and Intestinal Absorption in Rats

PURPOSE AND RATIONALE

Reynell and Spray (1956) described a method for the simultaneous measurements of gastric emptying, intestinal transit and absorption of test substances in the rat using phenol red as marker.

PROCEDURE

Adult male Wistar rats weighing 200–300 g are allowed water but are deprived of food 24 h before the experiment. They are treated orally or subcutaneously with the test compound 15 min prior to oral administration by gavage of 1.5 ml 0.07% phenol red in 2% carboymethylcellulose solution. Fifteen min later the animal is sacrificed and the stomach is immediately removed. The whole stomach including the stomach content is alkalized with 1 N NaOH and homogenized. The homogenate is filtered, and after precipitation of the protein with 10% trichloroacetic acid, centrifuged for 15 min at 3000 rpm. The concentration of phenol red in the supernatant is measured colorimetrically in a photometer at 546 nm.

EVALUATION

Percentage of stomach emptying (S_e) is calculated according to the following formula:

$$S_e = 100 - P_s \times P_a^{-1} \times 100$$

- P_s = Concentration of phenol red in the stomach (µg/ml)

- P_a = Concentration of phenol red in the initial solution after addition of equal volumes of 1 N NaOH and trichloroacetic acid (μg/ml)

MODIFICATIONS OF THE METHOD

By selective ligations of the different parts of the gastrointestinal tract and analysis for phenol red contents and for drug substance, as well as by sacrificing the animals after various time intervals, the degree and time course of absorption can be studied.

Droppleman et al. (1980) described a simplified method for assessing drug effects on gastric emptying in **rats**. Three ml of a semi-solid test meal, based on methylcellulose, are given to rats fasted 24 h prior to the experiment. At a specified time following the test meal, the rats are sacrificed, laparatomized, and the stomachs removed. The full stomachs are weighed on an analytical balance; they are opened and rinsed. Excess moisture is removed and the empty stomach weighed again. The difference is subtracted from the weight of 3 ml of the test meal, indicating the quantity emptied from the stomach during the test period. Gastric motor stimulants, e. g., metoclopramide increase, and anticholinergic compounds decrease gastric emptying.

Megens et al. (1990) used phenol red as marker to measure gastrointestinal propulsion after castor oil or paraffin oil challenge in **rats**.

Hedge et al. (1995) studied 5-HT_4 receptor mediated stimulation of gastric emptying in rats using a specially prepared semi-solid test meal containing charcoal.

Bonnafous et al. (1995) investigated benzodiazepine-withdrawal-induced gastric emptying disturbances in rats. Male Wistar rats, weighing 200–250 g, fasted for 16 h, received by gavage 2 ml of a test meal containing 1 μCi/ml of ^{51}Cr sodium chromate, 15 min after drug administration. Thirty min later, the animals were sacrificed by cervical dislocation. The stomach, small intestine (10 segments) and the colon were excised and placed into tubes. Radioactivity was determined by placing the tubes in a gamma counter. Gastric emptying was calculated as the percentage of total counts found in the small intestine and the colon.

Varga et al. (1995) determined gastric emptying in rats 5 min after a 3-ml intragastric load of 0.9% NaCl using phenol red as marker in order to define which bombesin receptors are involved in the delay of gastric emptying by bombesin-like peptides.

Lasheras et al. (1996) studied gastric emptying in rats. Sixty min after oral administration of vehicle or test compounds, the rats received by gavage 40 steel spheroids (1 mm diameter) in 2 ml 3% carboxymethylcellulose. Sixty min later, the animals were sacrificed and the spheroids remaining inside the stomach counted.

Yegen et al. (1996) studied the inhibitory effects of gastrin releasing peptide on gastric emptying in rats using methyl cellulose and phenol red as non-absorbable marker.

Haga et al. (1994) studied gastric emptying in **mice**. Male mice, weighing 18–22 g, had free access to food and water before the experiment. The test compounds were administered orally in 10 ml/kg 0.5% methylcellulose solution. The mice were deprived of food an water and sacrificed 4 h later by cervical dislocation. The stomachs were removed and opened. The contents of the stomach were mixed with 10% trichloroacetic acid, and centrifuged at 3000 rpm for 30 min. The weight of the sediment was taken as the food remaining in the stomach.

Ding and Håkanson (1996) examined the effect of drugs on a cholecystokinin-A receptor-mediated response by gastric emptying of a charcoal meal in mice.

Costall et al. (1987) used the **guinea pig** to study the influence of a 5-HT_3 antagonist on gastric emptying.

Brighton et al. (1987) used scintigraphy following indium-111-labeled meals in Beagle **dogs** and **baboons**. Indium-111-labeled polystyrene beads (500 mCi per dog) were mixed into a meal consisting of 50 g of finely crushed commercial dog food and 50 ml of milk. Images of 1 min duration were taken every 5 min for a period of 1 h using a large field of view gamma camera (ON Sigma 410).

Gullikson et al. (1991, 1993) studied gastric emptying of a solid meal in dogs.

REFERENCES AND FURTHER READING

Bonnafous C, Lefevre P, Bueno L (1995) Benzodiazepine-withdrawal-induced gastric emptying disturbances in rats: Evidence for serotonin receptor involvement. J Pharm Exp Ther 273:995–1000

Briejer MR, Akkermans LMA, Schuurkes JAJ (1995) Gastrointestinal prokinetic benzamides: the pharmacology underlying stimulation of motility. Pharmacol Rev 47:631–651

Brighton SW, Dormehl IC, du Pleussis M, Maree M (1987) The effect of an oral gold preparation on the gastrointestinal tract motility in two species of experimental animals. J Pharmacol Meth 17:185–188

Costall B, Gunning SJ, Naylor RJ, Tyers MB (1987) The effect of GR 38032F, a novel 5-HT_3 antagonist on gastric emptying in the guinea pig. Br J Pharmacol 91:263–264

Ding X-Q, Håkanson R (1996) Evaluation of the specificity and potency of a series of cholecystokinin-B/gastrin receptor antagonists *in vivo*. Pharmacol Toxicol 79:124–130

Droppleman DA, Gregory RL, Alphin RS (1980) A simplified method for assessing drug effects on gastric emptying in rats. J Pharmacol Meth 4:227–230

Gullikson GW, Löffler RF, Virña MA (1991) Relationship of serotonin-3 receptor antagonist activity on gastric emptying and motor-stimulating actions of prokinetic drugs in dogs. J Pharmacol Exp Ther 258:103–110

Gullikson GW, Virña MA, Löffler RF, Yang DC, Goldstin B, Wang SX, Moummi C, Flynn DL, Zabrowski DL (1993) SC-49518 enhances gastric emptying of solid and liquid meals and stimulates gastric motility in dogs by a 5-hydroxytryptamine$_4$ receptor mechanism. J Pharmacol Exp Ther 264:240–248

Haga K, Asano K, Inaba K, Morimoto Y, Setoguchi M (1994) Effect of Y-25130, a selective 5-hydroxytryptamine$_3$ receptor antagonist, on gastric emptying in mice. Arch Int Pharmacodyn 328:344–355

Hegde SS, Wong AG, Perry MR, Ku P, Moy TM, Loeb M, Eglen RM (1995) 5-HT$_4$ receptor mediated stimulation of gastric emptying in rats. Naunyn-Schmiedeberg's Arch Pharmacol 351:589–595

Lasheras B, Berjón A, Montañes R, Roca J, Romero G, Ramírez MJ, Del Rio J (1996) Pharmacological properties of quinoxaline derivatives as a new class of 5-HT$_3$ receptor antagonists. Arzneim Forsch/Drug Res 46:401–406

Megens AAHP, Canters LLJ, Awouters FHL, Niemegeers CJE (1990) Normalization of small intestinal propulsion with loperamide-like antidiarrheal agents. Eur J Pharmacol 17:357–364

Reynell PC, Spray GH (1956) The simultaneous measurement of absorption and transit in the gastrointestinal tract of the rat. J Physiol 131:452–462

Varga G, Liehr RM, Scarpignato C, Coy DE (1995) Distinct receptors mediate gastrin-releasing peptide and neuromedin B-induced delay of gastric emptying of liquids in rats. Eur J Pharmacol 286:109–112

Yegen BÇ, Gürbüz V, Coúkun T, Bozkurt A, Kurtel H, Alican I, Dockray GJ (1996) Inhibitory effects of gastrin releasing peptide on gastric emptying in rats. Regul Peptides 61:175–180

J.4.4.3 Intestinal Drug Absorption

PURPOSE AND RATIONALE

Doluisio et al. (1969) described an *in situ* rat gut technique to determine absorption rates of drugs.

PROCEDURE

Male Sprague-Dawley albino rats weighing 220–260 g are fasted 16–24 h prior to surgery allowing, however, drinking water ad libitum. They are kept in cages having wide mesh floors to prevent coprophagia. One hour prior to surgery, the animals are anesthetized with 1 g/kg ethylurethane i.p. The small intestine is exposed by a midline abdominal incision, and two L-shaped glass cannulae are inserted through small slits at the duodenal and ileal ends. Care has to be taken to handle the small intestine gently in order to maintain an intact blood flow. The cannulae are secured by ligation with silk suture, and the intestine is returned to the abdominal cavity. Four cm long segments of tubings are attached to the exposed ends of both cannulae, and a 30-ml hypodermic syringe fitted with a three-way stopcock and containing perfusion fluid warmed to 37°C is attached to the duodenal cannula. As a means of clearing the gut, perfusion fluid is passed slowly through it and out the ileal cannula to be discarded until the effluent is clear. The remaining perfusion solution is carefully expelled from the intestine by means of air pumped through from the syringe.

Immediately afterwards, 10 ml of drug solution are introduced into the intestine by means of a syringe. The stopwatch is started, and the ileal cannula is connected to another 30 ml syringe fitted with a three-way stopcock. This arrangement enables the operator to pump the lumen solution into either the ileal or the duodenal syringe, remove 0.1-ml aliquots, and return the remaining solution to the intestine within 10–15 s. To assure uniform drug solution concentrations throughout the gut segment, aliquots are removed from the syringes alternatively. Samples are collected every 5 min. Depending on the drug to be studied, the concentration is determined by chemical methods.

EVALUATION

The concentrations of the drug are plotted on a logarithmic scale on the ordinate versus time on the abscissa on a linear scale. Half-life values can be calculated.

MODIFICATIONS OF THE METHOD

Ochsenfahrt (1979) described a more sophisticated method to measure the absorption of drugs in the vascularly perfused, isolated intestine of the rat. Male rats weighing about 350 g are anesthetized with urethane. The abdomen is opened by a midline incision. The mesentery of the ascending and transverse colon is gently pulled away from the mesentery of the small intestine. The vessels to the colon are ligated and cut. The superior mesenteric artery is freed from the surrounding mesentery. The duodenal vessels are ligated and cut. A suitable segment of the jejunum of about 7 cm length is selected. The proximal cannula is tied into the lumen of this segment, and the duodenum is cut. The lumen of the segment is washed with 3–4 ml warm Krebs-Henseleit solution. Then, the distal cannula is tied. After the mesenteric vessels distal to the experimental segment are ligated, the rest of the small intestine, ileum, and colon is excised. Temporarily, the intestine is covered with gauze soaked with saline solution.

The preparation of the rat is interrupted for 8–10 min, while a second rat (donor rat), which has been anesthetized with urethane, is prepared. The donor rat supplies the arterial blood; the sponta-

neous respiration is supported with a respiration pump through a tracheal cannula. The right jugular vein of the donor rat is cannulated for the blood infusion and 2 mg heparin dissolved in 0.1 saline solution is administered. A cannula is placed into the left carotid artery of the donor rat; this tube is later connected to the superior mesenteric artery of the test segment. Blood lost by the donor rat is replaced with heparinized blood taken from other rats immediately before the beginning of the experiment.

In the test animal, a thin silicon tube is inserted in the left carotid artery. Two mg heparin, dissolved in 0.1 ml saline, are injected. The superior mesenteric vein is ligated distal to the splenic vein and a plastic cannula is inserted for venous outflow. The cannula is then connected to a drop counter. The luminal cannulae of the segment are connected to a recirculation unit which is filled with Krebs-Henseleit solution at 37°C, and the luminal perfusion of the segment (mucosal solution) is started. The mucosal solution is oxygenated and recirculated. The superior mesenteric artery is ligated with a thread at its origin at the aorta and then cannulated. This cannula is first connected to the carotid artery of the test animal and later to the carotid artery of the donor animal. The isolated vascularly perfused segment is suspended in a serosal bath containing Krebs-Henseleit solution at 37°C. Venous blood outflow is collected in plastic vials at 15 min intervals. Samples are taken from the mucosal and serosal solutions at the beginning and the end of each period. By this way, the mucosal disappearance rate, the venous appearance rate, and the serosal appearance rate can be measured.

Schilling and Mitra (1992) measured insulin absorption from the distal duodenum/proximal jejunum and from the distal jejunum/proximal ileum in anesthetized rats by the closed-loop technique.

Schümann and Hunder (1996) described a modified device for the differentiated study of intestinal transfer in isolated intestinal segments from mice and suckling rats *in vitro*. A luminal perfusion system for small intestinal segments was adapted for the use in mice and rat pups to investigate longitudinal differences in drug and toxin transfer.

REFERENCES AND FURTHER READING

Doluisio JT, Billups NF, Dittert LW, Sugita ET, Swintowsky JV (1969) Drug absorption I: An *in situ* rat gut technique yielding realistic absorption rates. J Pharm Sci 58:1196–1200

Ochsenfahrt H (1979) The relevance of blood flow for the absorption of drugs in the vascularly perfused, isolated intestine of the rat. Naunyn-Schmiedeberg's Arch Pharmacol 306:105–112

Schilling RJ, Mitra AK (1992) Pharmacodynamics of insulin following intravenous and enteral administrations of porcine-zinc insulin to rats. Pharmaceut Res 9:1003–1009

Schümann K, Hunder G (1996) A modified device for the differentiated study of intestinal transfer in isolated intestinal segments from mice and suckling rats *in vitro*. J Pharmacol Toxicol Meth 36:211–217

J.4.5 Duodenal Ulcer Formation

J.4.5.1 Cysteamine-Induced Duodenal Ulcers in Rats

PURPOSE AND RATIONALE

Duodenal ulcers can be induced in rats by repeated administration of cysteamine or propionitrile in rats (Dzan et al. 1975; Szabo 1978; Szabo et al. 1979).

PROCEDURE

Male Sprague-Dawley rats with an initial weight of 200 g are used. Cysteamine-HCl is administered three times on day 1 in a dose of 280 mg/kg orally. Protective drugs, such as H_2-antagonists, are given 30 min prior cysteamine treatment. The rats are sacrificed on the third day. For histological evaluation, the stomach and duodenum are fixed in 10% aqueous buffered formaldehyde and paraffin-embedded sections are stained with hematoxylin and eosin. Duodenal ulcers develop in the anterior (antimesenteric) and posterior wall of the proximal duodenum, about 2–4 mm from the pylorus. The more severe ulcers, located on the anterior wall, frequently perforate, resulting in focal or generalized peritonitis, or penetrate into the liver. The opposite ulcer invariably penetrates into the pancreas.

EVALUATION

The intensity of the duodenal ulcer is evaluated using scores from 0 to 3.

- 0 = no ulcer
- 1 = superficial mucosal erosion
- 2 = deep ulcer usually with transmural necrosis
- 3 = perforated or penetrated ulcer

CRITICAL ASSESSMENT OF THE METHOD

In view of the development of modern gastric K^+/H^+-ATPase inhibitors the predictive value of methods using experimental ulcers in the rat for clinical healing rates in man has been challenged (Herling and Weidmann 1994).

MODIFICATIONS OF THE METHOD

The cysteamine-induced duodenal ulcer has been used for pharmacological studies by many authors, e. g.:

Evangelista et al. (1992), Krantis et al. (1993), Pascaud et al. (1993), Tanaka et al. (1993), Morimoto et al. (1994), Pendley et al. (1995), Sikiric et al. (1997), Drago et al. (1999).

Okabe et al. (1971), Sato et al. (1989) described a method for experimental, penetrating gastric and duodenal ulcers in rats. Rats were anesthetized with ether and an incision was made in the abdomen. A round metal mold, 6 mm in diameter, was placed in close contact with the serosal surface of the duodenal wall, about 7 mm distal to the pylorus. **Glacial acetic acid** (60 ml) war poured into the mold and was left in place for 20 s. After the acetic acid was removed, the treated surface was rinsed with 50 ml of 0.02 N NaOH and the abdomen was closed. A drug or the vehicle was given p.o. once a day for 14 consecutive days beginning 2 days after the operation. The animals were sacrificed on the 16th day after the operation and the ulcerated area (mm^2) was measured.

Mepirizole-induced duodenal ulcers were described by Okabe et al. (1982), Sato et al. (1989), Tanaka et al. (1989). A drug or the vehicle was given p.o. 30 min before mepirizole (200 mg/kg) was administered s.c. Twenty-four hours later, 1 ml of 0.5% Evan's blue solution was injected via the tail vein of each rat and the rats were sacrificed by CO_2 asphyxiation. The gastroduodenal region was removed and examined for lesions.

REFERENCES AND FURTHER READING

Drago F, Montoneri C, Varga C, Laszlo F (1999) Dual effect of female sex steroids on drug-induced gastroduodenal ulcers in the rat. Life Sci 64:2341–2350

Dzan VJ, Haith LR Jr, Szabo S, Reynolds ES (1975) Effect of metiamide on the development of duodenal ulcers produced by cysteamine or propionitrile in rats. Clin Res 23:576A

Evangelista S, Renzi D, Tramontana M, Surrenti C, Theodorsson E, Maggi CA (1992) Cysteamine induced-duodenal ulcers are associated with a selective depletion in gastric and duodenal calcitonin gene-related peptide-like immunoreactivity in rats. Regul Pept 39:19–28

Herling AW, Weidmann K (1994) Gastric K^+/H^+-ATPase inhibitors. In: Ellis GP, Luscombe DK (eds) Progress in Medicinal Chemistry, Vol 31, Elsevier Science BV, pp 233–264

Krantis A, Harding RK, McKay AE, Morris GP (1993) Effects of compound U74500A in animal models of gastric and duodenal ulceration. Dig Dis Sci 38:722–729

Morimoto Y, Shimohara K, Tanaka K, Hara H, Sukamoto T (1994) 4-Methoxyphenyl-4-(3,4,5-trimethoxybenzyl)-1-piperazine-acetate monofumarate monohydrate (KB 5492), a new anti-ulcer agent with selective affinity for the sigma receptor, prevents cysteamine-induced duodenal ulcers in rats by a mechanism different from that of cimetidine. Jpn J Pharmacol 64:221–224

Okabe S, Roth JL, Pfeiffer CJ (1971) A method for experimental, penetrating gastric and duodenal ulcers in rats. Am J Dig Dis 16:277–284

Okabe S, Ishihara Y, Inoo H, Tanaka H (1982) Mepirizole-induced duodenal ulcers in rats and their pathogenesis. Dig Dis Sci 27:242–249

Pascaud XB, Chovet M, Soulard P, Chevalier E, Roze C, Junien JL (1993) Effects of a new sigma ligand, JO 1784, on cyste-amine ulcers and duodenal alkaline secretion in rats. Gastroenterology 104:427–434

Pendley CE, Fitzpatrick LR, Capolino AJ, Davis MA, Esterline NJ, Jakubowska A, Bertrand P, Guyon C, Dubroeucq MC, Martin GE (1995) RP 73780, a gastrin/cholecystokinin$_B$ receptor antagonist with potent anti-ulcer activity in the rat. J Pharmacol Exp Ther 273:1015–1022

Robert A, Nezamis JE, Lancaster C, Badalamenti JM (1974) Cysteamine-induced duodenal ulcers: A new model to test anti-ulcer drugs. Digestion 11:199–214

Roszkowski AP, Garay GL, Baker S, Schuler M, Carter H (1986) Gastric antisecretory and antiulcer properties of enprostil, (±)-11α ,15α ,dihydroxy-16-phenoxy-17,18,19,20-tetranor-9-oxoprosta-4,5,13(*t*)-trienoic acid methyl ester. J Pharmacol Exper Ther 239:382–389

Satoh H, Inatomi M, Nagaya H, Inada I, Nohara A, Nakamura N, Maki Y (1989) Antisecretory and antiulcer activities of a novel proton pump inhibitor AG-1749 in dogs and rats. J Pharm Exp Ther 248:806–815

Selye H, Szabo S (1973) Experimental model for production of perforating duodenal ulcer by cysteamine in the rat. Nature 244:458–459

Sikiric P, Mikus D, Seiwerth S, Grabarevic Z, Rucman R, Petec M, Jagic V, Turkuvic B, Rotkvic I, Mise S, Zorocic I, Peric J, Konjevoda P, Perovic D, Jurina L, Hanzevacki M, Separovic J, Gjurasin M, Jadrijevic S, Jelovac N, Miklic P, Buljat G, Marovic A (1997) Pentadecapeptide BCP 157, cimetidine, ranitidine, bromocryptine, and atropine effect in cysteamine lesions in totally gastrectomized rats: A model for cytoprotection studies. Dig Dis Sci 42:1029–1037

Szabo S (1978) Animal model: Cysteamine-induced acute and chronic duodenal ulcer in the rat. Am J Pathol 93:273–276

Szabo S, Haith LR Jr, Reynolds ES (1979) Pathogenesis of duodenal ulceration produced by cysteamine or propionitrile. Influence of vagotomy, sympathectomy, histamine depletion, H-2 receptor antagonists and hormones. Dig Dis Sci 24:471–477

Tanaka H, Takeuchi K, Okabe S (1989) The relation of intraduodenal pH and delayed gastric emptying in duodenal ulceration induced by mepirizole or cysteamine in rats. Jpn J Pharmacol 51:483–492

Tanaka T, Morioka Y, Gebert U (1993) Effect of a novel xanthine derivative on experimental ulcers in rats. Arzneim Forsch/Drug Res 43:558–562

J.4.6 Models of Inflammatory Gut Disease

J.4.6.1 Experimental Ileitis

PURPOSE AND RATIONALE

An experimental model of inflammatory bowel disease produced by the intraluminal administration of the cytotoxic plant lectin ricin into the rabbit ileum was developed by Sjogren et al. (1994), Goldhill et al. (1995, 1997). *In vitro*, electric field stimulation results

in larger non-cholinergic excitatory junction potentials in ricin-treated circular muscles than in controls.

PROCEDURE

Inflammation

Acute ileitis is induced with ricin in male New Zealand white rabbits. The animals are anesthetized with intramuscular xylazine (9 mg/kg) and ketamine (50 mg/kg) and maintained with intravenous pentobarbital (15 mg/kg). A midline incision is made, a ligated terminal ileal loop (~10 cm in length) is constructed in each animal and 1 ml of ricin (1 mg/ml) or vehicle is injected into the lumen. The loop is removed after 5 h, a time period that allows development of ileitis, abnormal myoelectric activity and increased response to electric field stimulation. Animals are sacrificed with an overdose of pentobarbital. The loop is opened along its length, gently flushed of luminal contents with cold oxygenated Krebs-bicarbonate-saline and prepared for contractility studies.

Contractility Studies

Muscle strips (~1 × 0.4 cm) with mucosa removed are cut in the axis of the circular muscle and attached to isometric tension transducers in 10-ml organ baths with modified oxygenated Krebs-bicarbonate-saline at 37.5 ± 0.5°C. Tissues are allowed to equilibrate at L_i (the length at which no tension can be measured) for 20 min. The strips are then stretched to L_0, which is determined as the length at which maximum force is generated in response to acetylcholine (0.5–1 mM). Strips are then allowed to equilibrate for an additional 20 min.

Effect of Inflammation on Response to Tachykinins

Concentration-response curves are constructed to substance P and neurokinin agonists (or analogues) on separate muscle strips in vehicle- and ricin-treated tissues. Studies are performed in the presence or absence of tetrodotoxin to distinguish between neural and non-neural effects of ricin treatment.

Effects of Ricin Treatment to Responses to Electrical Field Stimulation

Muscle strips are passed through a pair of ring electrodes (2-mm diameter) and stimulated for 10 s by square-wave pulses (0.5 ms duration, supramaximal voltage) at 1–10 Hz. Stimulation is performed in the presence of atropine (1 mM) and N^G-nitro-L-arginine methyl ester) (L-NAME) (0.1 mM).

EVALUATION

Maximum increases in muscle tone in response to tachykinin addition of electrical field stimulation are obtained through visual analysis of chart recorder outputs. Responses to tachykinins are expressed as absolute tension development. Electrical field stimulation data are expressed as a percentage of the response to 1 μM acetylcholine added at L_0 to reduce the variation of the data. Values are given as mean ± SEM Tachykinin concentration responses are fitted to sigmoid curves and EC_{50} values (with 95% confidence intervals) are determined from these curves. Differences between frequency or concentration-response curves are assessed statistically by multivariate analysis of variance, with adjustments made for multiple comparisons. In cases in which curves are significantly different to one another, maximal responses were compared statistically using Student's *t*-test.

MODIFICATIONS OF THE METHOD

Miller et al. (1991) induced ileitis in **rabbits** by luminal perfusion with histamine monochloramine or with acetic acid.

Rachmilewitz et al. (1997) induced inflammation in the small intestine in **rats** by intrajejunal administration of 0.1 ml 2% iodoacetamide.

Sukumar et al. (1997) induced ileitis in rats by two doses of indomethacin (7.5 mg/kg) administered subcutaneously 24 h apart.

Ileitis in **guinea pigs** was induced by intraluminal trinitrobenzene sulfonic acid (Miller et al. 1993; Izzo et al. 1998; Mazelin et al. 1998).

Likewise, ileitis in **hamsters** was induced by intraluminal injection of trinitrobenzene sulfonic acid (Boyd et al. 1995).

Shibata et al. (1993) induced ileitis in **dogs** by administration of 10 ml 100% ethanol and 1 g trinitrobenzene sulfonic acid dissolved in 10 ml water through a tube inserted into the ileum.

Interleukin-10 (IL-10) is produced by T cells, B cells, and macrophages. It down-regulates the function of T helper (Th) -1 cells, natural killer (NK) cells, and macrophages. In 1993, Kuhn et al. reported that, in IL-$10^{-/-}$ mice, inflammation occurred in the whole intestine. The lesions were observed mainly in the duodenum, proximal jejunum, and ascending colon. Pathological thickening of the intestinal wall, due to hyperplastic changes, was observed in the duodenum and jejunum. In the colon, goblet cell depletion, degeneration of the epithelium, infiltration of IgA-producing plasma cells, and an increase in major histocompatibility complex (MHC) class II expression were detected. As in the IL-$2^{-/-}$ mice, the activation of $CD4^+$ cells and the depletion of their inhibitor, the regulatory T cells, are presumed to be the cause of the inflam-

mation. In 2000, Jijon et al. assessed the mechanism behind a poly (ADP-ribose) polymerase (PARP) induced increase in epithelial permeability that is associated with chronic, non-resolving colitis, which develops spontaneously in the IL-10-gene-deficient mouse. They demonstrated that treatment of IL-10-deficient mice with the PARP inhibitor 3-aminobenzamide reversed the typical signs of Crohn's disease in these mice, namely increased permeability, high levels of mucosal interferon-α (IFN-α) and tumor necrosis factor α (TNF-α), and increased nitric oxide (NO) production. In the same year, Cantorna et al. (2000) used the IL-10-deficient mouse model to investigate the role of vitamin D on the course of inflammatory bowel disease (IBD). The animals were divided into three groups: vitamin D deficient, vitamin D sufficient, and active vitamin D supplemented. In contrast with vitamin D-deficient IL-10 knockout (KO) mice, vitamin-D-sufficient mice did not develop diarrhea, waste, or die prematurely. To the authors' surprise, supplementation with active vitamin D for only 2 weeks blocked the progression and significantly ameliorated the symptoms in the mice that had established spontaneously developed IBD. The importance of animal models for the evaluation of pharmacological strategies was further emphasized in a straightforward mini-study conducted by Gratz et al. (2002), who administered murine monoclonal anti-TNF-α antibodies intraperitoneally into IL-10 KO mice that had established IBD. Demonstration of significant histological improvement of inflammation that correlated well with a resolution of diarrhea and rectal bleeding accentuated the pivotal role that TNF-α appears to play in the pathogenesis of IBD and emphasized the importance of this model. Recently, a pioneer therapeutic approach to IBD was tested in the IL-10 KO model by Watanabe et al. (2003a, 2003b). The group developed poly-DL-lactic acid microspheres containing dichloromethylene diphosphonate that, once administered rectally, were specifically taken up by macrophages, subsequently depleting them. The authors showed reduced numbers of resident macrophages in the intestinal lymphoid follicles in this model, associated with suppression of development of chronic colitis.

REFERENCES AND FURTHER READING

Boyd AJ, Sherman IA, Saibil FG (1995) Effects of plain and controlled-ileal-release budesonide formulations in experimental ileitis. Scand J Gastroenterol 30:974–981

Cantorna MT, Munsick C, Bemiss C, Mahon BD (2000) 1, 25-Dihydroxycholecalciferol prevents and ameliorated symptoms of experimental murine inflammatory bowel disease. J Nutr 130:2648–2652

Goldhill JM, Sanders K, Shea-Donohue T, Sjogren R (1995) *In vitro* changes in neural control of muscle function in experimental ileitis. Am J Physiol 268:G823–G830

Goldhill SM, Shea-Donohue T, Ali N, Piñeiro-Carrero VM (1997) Tachykinergic neurotransmission is enhanced in small intestinal circular muscle in a rabbit model of inflammation. J Pharmacol Exp Ther 282:1373–1378

Gratz R, Becker S, Sokolowski N, Schumann M, Bass D, Malnick SD (2002) Murine monoclonal anti-TNF antibody administration has a beneficial effect on inflammatory bowel disease that develops in IL-10 knockout mice. Dig Dis Sci 47:1723–1727

Izzo AA, Mascolo N, Capasso F (1998) Nitric oxide as a modulator of intestinal water and electrolyte transport. Dig Dis Sci 43:1605–1620

Jijon HB, Churchill T, Malfair D, Wessler A, Jewell LD, Parsons HG, Madsen KL (2000) Inhibition of poly (ADP-ribose) polymerase attenuates inflammation in a model of chronic colitis. Am J Physiol 279:G641–G651

Kuhn R, Lohler J, Rennick D, Rajewsky K, Muller W (1993) Interleukin-10-deficient mice develop chronic enterocolitis. Cell 75:263–274

Mazelin L, Theodorou V, More J, Edmonds-Alt X, Fioramonti J, Bueno L (1998) Comparative effects of nonpeptide tachykinin receptor antagonists on experimental gut inflammation in rats and guinea pigs. Life Sci m63:293–304

Miller MJS, Zhang XJ, Barkemeyer B, Sadowska-Krowicka H, Eloby-Childress S, Gu X, Clark DA (1991) Potential role of monochloramine in a rabbit model of ileitis. Scand J Gastroenterol 26:852–858

Miller MJS, Chotinaruemol S, Sadowska-Krowicka H, Zhang XJ, McIntyre JA, Clark DA (1993) Guinea pig ileitis is attenuated by the leumedin N-(fluorenyl-9-methoxycarbonyl)-leucine (NPC 15199). J Pharmacol Exp Ther 266:468–472

Rachmilewitz D, Okon E, Karmell F (1997) Sulfhydryl blocker induced small intestinal inflammation in rats: A new model mimicking Crohn's disease. Gut 41:358–365

Shibata Y, Taruishi M, Ashida T (1993) Experimental ileitis in dogs and colitis in rats with trinitrobenzene sulfonic acid – Colonoscopic and histopathologic studies. Gastroenterol Jpn 28:518–527

Sjogren RW, Colleton C, Shea-Donohue T (1994) Intestinal myoelectric response in two different models of acute enteric inflammation. Am J Physiol 30:G329–G337

Sukumar P, Loo A, Magur E, Nandi J, Oler A, Levine RA (1997) Dietary supplementation of nucleotides and arginine promotes healing of small bowel ulcers in experimental ulcerative colitis. Dig Dis Sci 42:1530–1536

Watanabe M, Yamazaki M, Kanai T (2003) Mucosal T cells as a target for treatment of IBD. J Gastroenterol 38 [Suppl. 15]:48–50

Watanabe N, Ikuta K, Okazaki K, Nakase H, Tabata Y, Matsuura M, Tamaki H, Kawanami C, Honjo T, Chiba T (2003) Elimination of local macrophages in intestine prevents chronic colitis in interleukin-10-deficient mice. Dig Dis Sci 48:408–414

J.4.6.2 Experimental Colitis

PURPOSE AND RATIONALE

Inflammatory bowel diseases, ulcerative colitis and Crohn's disease, represent chronic alteration of the

gastrointestinal tract of unknown etiology perhaps involving immunological events. The immunological parameters have been described as secondary but may possibly be attributed to the chronicity of the disease. Several compounds have been described to elicit cell-mediated immune responses in the gut, such as dinitrochlorobenzene (DNCB) (Rosenberg and Fischer 1964; Norris et al. 1982; Norris 1989) or 2,4,6,-trinitrobenzene sulfonic acid (TNBS) (Morris et al. 1989; Selve and Wöhrmann 1992).

PROCEDURE

A three-step concept is realized to mimic the human disease, using 2,4,6-trinitrobenzene sulfonic acid (TNBS) as a defined hapten:

1. specific hypersensitivity by active immunization,
2. local inflammation by local challenge,
3. chronicity by chronic application of the immunogen.

Female Sprague Dawley rats weighing 150–200 g are sensitized by intradermal injection of 0.8% TNBS (Fluka, Neu-Ulm, Germany) solution into a shaved area on the back once daily for three consecutive days. TNBS is dissolved in 0.05 ml Freund's incomplete adjuvant together with 1 mg/ml ovalbumin. After 18 days, the animals receive a further intradermal booster injection. Intradermal challenge of 0.08% TNBS in 0.05 ml 0.9% NaCl solution with or without ovalbumin, or ovalbumin solution without TNBS, is given 14 days later in order to determine the type and specificity of the immunological reaction.

Ten days after the intradermal challenge, a flexible polyethylene tube of 0.5 mm diameter is implanted under ketamine (100 mg/kg i.p.) anesthesia 15 cm proximal to the cecum and emerging at the neck for TNBS or drug administration. After a 10-day recovery phase, the animals are treated daily for 3 weeks with 0.08% TNBS in saline (0.2 mg/rat) given through the catheter. Control groups receive only saline. Drugs are applied either by gavage twice a day. suspended in carboxymethyl cellulose, or intraluminally once a day, suspended in saline. The animals are sacrificed by CO_2 inhalation 24 h after the last intraluminal application of TNBS. The distal 10 cm of small intestine anterior to the ileo-caeco-colic junction (5 cm distance to the open end of the catheter) including Peyer's patches are dissected, cut open longitudinally and rinsed with saline.

Immediately after dissection, the distal small intestine is visually assessed for inflammation according to the following scores:

Enteritis score	*Gross morphology*
0	No visible damage of the whole 10 cm the small intestine
1	Slight inflammation, slight redness (hyperemia), villi visible under 15 fold magnification
2	Intermediate inflammation, discontinuous hyperemia, intermediate redness of villi
3	Intensive inflammation, intensive hyperemia, intensive redness of villi

The dissected gut segments, precisely 10 cm long, are weighed for measurement of edema formation. They are then incubated in Tris buffer for 30 min at 37°C in a shaking water bath (1 ml/100 mg tissue, Tris 50 mM, pH 7.4, 100 mM NaCl, 1 mM $CaCl_2$, 1 mg/ml glucose). Following incubation, aliquots of the solutions are centrifuged (13,000 *g*, 2 min, 20°C) for determination of leucotriene B_4 (TB_4) by a commercial radioimmuno-assay (e. g., Amersham Buchler, Brunswick).

EVALUATION

Results are expressed as means ± SEM of (n) experiments. Differences between control and inflamed tissue, and influence of drug treatment are compared. Statistical significance is calculated by Wilcoxon-Mann-Whitney U-test for unpaired data. The level of significance is taken as $p < 0.05$.

MODIFICATIONS OF THE METHOD

Several authors used the trinitrobenzene sulfonic acid model in *rats* with slight modifications (Hogaboam et al. 1996; Kitano et al. 1996; Yue et al. 1996; Lora et al. 1997; Taniguchi et al. 1997; Cruz et al. 1998; Fries et al. 1998; Goldhill et al. 1998).

Zea-Ariate et al. (1994) studied chronic colitis in Wistar rats after intracolonic instillation of 20 or 42 mg of trinitrobenzene sulfonic acid in 30% and 40% ethanol and compared the effect with the administration of ethanol alone.

Alternatives to the 2,4,6-trinitrobenzene sulfonic acid model in **rats** were proposed:

Wallace et al. (1995), Hawkins et al. (1997) recommended dinitrobenzene sulfonic acid to produce experimental colitis in the rat.

Patterson and Colony (1983) tested sulphasalazine and 5-aminosalicylic acid in experimental colitis induced in **guinea pigs** by topical dinitrochlorobenzene.

Neurath et al. (1996) studied chronic intestinal inflammation induced by 2,4,6-trinitrobenzene sulfonic acid (TNBS) in **mice**.

These authors (Neurath et al. 1997) investigated the role of tumor necrosis factor in this mouse model and showed that no significant TNBS-induced colitis could be induced in mice in which the TNF-alpha gene had been inactivated by homologous recombination.

Cuzzocrea et al. (2004) found that 5-amino-isoquinolinone reduces colon injury in experimental colitis induced by dinitrobenzene sulfonic acid in mice.

Antony et al. (1997), Oyen et al. (1997) used trinitrobenzene sulfonic acid to induce experimental colitis in **rabbits**.

Dams et al. (1998) compared gamma-camera imaging in rabbits with colitis after retrograde instillation of trinitrobenzene sulfonic acid with technetium-99m-labeled liposomes after various time intervals with macroscopically scored severity of inflammation.

A model of diffuse colitis in **rats** induced by intraluminal colonic instillation or serosal application of dilute **acetic acid** was described by MacPharson and Pfeiffer (1976, 1978). Ritzpatrick et al. (1990) tested the anti-inflammatory effects of various drugs on acetic acid induced colitis in the rat.

For instillation into the colon of rats, a 2 cm length of soft polyethylene tubing is fitted to a Luer stub adapter. The open end of the tubing is sealed with glue. The whole length of the tubing is perforated with a needle at 0.5 mm length by four holes, 90° apart. A 1 ml syringe containing 10% acetic acid in saline is fitted to the adapter. The tubing is inserted intrarectally into the colon of rats and 0.2 ml is injected into the lumen. After 10 s contact *in situ*, the remaining acid is withdrawn and the lumen washed with three successive 0.5 ml volumes of isotonic saline. Test drugs are administered daily during the following days. Diffuse colonic lesions appear after 3 days in control animals and the animals experience a bloody diarrhea. An initial mucosal inflammation develops into submucosal edema; petechial hemorrhages become enlarged with subsequent neutrophil invasion, and pseudopolyps become evident.

Terzioglu et al. (1997) studied the effect of prostaglandin E_1 on the experimental colitis induced by rectal instillation of 10% acetic acid in rats.

Fabia et al. (1994) induced colitis in rats in an exteriorized colonic segment by administration of 4% acetic acid for 15 s. Four days later, this colonic segment was examined using a morphological scoring system, and measurements of myeloperoxidase activity and plasma exudation into the colonic segment.

Eliakim et al. (1995) demonstrated that ketotifen ameliorated capsaicin-augmented acetic acid-induced colitis. Rats were pretreated with subcutaneous injections of 20, 30, and 50 mg/kg capsaicin. Colitis was induced 2 weeks later by flushing 2 ml 5% acetic acid into the proximal colon.

Higa et al. (1997) studied the role of neutrophils in the pathogenesis of acetic acid-induced colitis in mice.

Millar et al. (1996) evaluated the antioxidant potential of new treatments for inflammatory bowel disease using acetic acid-induced colitis in rats.

Myers et al. (1997) determined colonic transit in rats by calculating the geometric center of distribution of a radiolabeled marker (^{51}Cr) instilled into the proximal colon after induction of distal colitis by intracolonic administration of 4% acetic acid.

Palmen et al. (1998) studied the effects of local butesonide treatment on cell-mediated immune response in acute and relapsing colitis in rats.

Several **other agents** can induce experimental colitis in animals (Kim and Berstadt 1992), such as

- **phorbol esters** (Fretland et al. 1990),
- **carrageenan** (Marcus and Watt 1969; Benitz et al. 1973; Watt and Marcus 1973; Abraham et al. 1974; Jensen et al. 1984. Kitano et al. 1994; Pricolo et al. 1996),
- **amylopectin-sulfate** (Watt and Marcus 1972),
- **dextran sulfate** (Ohkusa 1985; Okayasu et al. 1990; Axelsson et al. 1966; Shintani et al. 1997; Kanauchi et al. 1998),
- the **chemotactic peptide FMLP** (Magnusson et al. 1985; *von Ritter et al. 1988;* LeDuc and Nast 1990).

Ekstrom (1998) described **oxazolone**-induced colitis in rats. Dark Agouti rats were skin-sensitized with oxazolone and further challenged intra-rectally with oxazolone dissolved in carmellose sodium/peanut oil.

Suzuki et al. (1997) developed a rat model for human ulcerative colitis by using **1-hydroxy-anthraquinone** to cause severe inflammation of colonic mucosa.

Aiko et al. (1997), Satdnicki et al. (1998) induced chronic granulomatous colitis in female Lewis rats via intramural (subserosal) injections of **peptidoglycan-polysaccharide** into the distal colon.

Surfactants being used to enhance drug absorption may cause intestinal damage. Oberle et al. (1995) evaluated mucosal damage by surfactants in a single-pass *in situ* perfusion model in the rat. The release of LDH and mucus into the lumen of jejunum and colon following perfusion of the nonionic surfactants Tween 80 and Triton X-100 was determined.

Axelsson and Ahlstedt (1993) reviewed the actions of sulfasalazine and analogues in various animal models of experimental colitis, in particular in the hapten-, immune complex- and dextran models.

Bach et al. (1985) studied the inhibition of LTC synthetase and of rat liver glutathione *S*-transferases by sulfasalazine.

Stein et al. (1993) determined arachidonic acid oxidation and damage in the colon in rats stressed by the **cold-restraint** method.

Kirsner et al. (1959), Kraft et al. (1963) induced severe colitis in **rabbits** which had previously been sensitized to egg albumin and had mild colonic inflammation induced by intrarectal instillation of a small amount of diluted **formalin**.

Meenan et al. (1996) induced immune-complex colitis in rabbits by using various formalin concentrations (2%, 0.75%, and 0.5%).

Hodgson et al. (1978) induced colitis in rabbits by a modified technique. Preformed immune complex of human serum albumin and anti-HSA with antigen excess was injected to non-sensitized rabbits after provocation of mild inflammation in the colon with diluted formalin.

Kuroe et al. (1996a, b) induced granulomatous enterocolitis in rabbits by repeated submucosal injection of **muramyl dipeptide** emulsion into the rectum and colon with a flexible endoscope. Extraintestinal manifestations, such as pericholangitis, were observed.

Walsh and Zeitlin (1987) studied the effects of salazopyrin, 5-aminosalicylic acid and prednisolone on immune complex-mediated colitis in **mice**.

A survey on various genetic and immune manipulations which lead to inflammatory bowel disease in mice was given by Powrie and Leach (1995).

$CD4^+$ T lymphocytes injected into severe immunodeficient (SCID) mice lead to an inflammatory and lethal bowel disease (Claesson et al. 1996; Leach et al. 1996; Rudolphi et al. 1996; Bregenholt et al. 1998).

Hermiston and Gordon (1995) described an inflammatory bowel disease in mice expressing a dominant negative N-cadherin resembling Crohn's disease.

Watanabe et al. (1998) reported that interleukin7 transgenic mice develop chronic colitis with decreased interleucin7 protein accumulation in the colonic mucosa.

Mitchell and Turk (1990) described a model of **granulomatous bowel disease in guinea pigs**. Epithelioid cell granulomas and primary macrophage granulomas were induced by the inoculation of BCG (Pasteur) and irradiated Mycobacterium leprae, respectively, into the terminal ileum.

Wallace et al. (1998) induced colitis in guinea pigs and in rats by intracolonic administration of trinitrobenzene sulfonic acid.

Some **monkeys**, such as the cotton-top tamarin, *Saguinus oedipus* (Chalifoux and Bronson 1981; Madara et al. 1985; Lushbach et al. 1985; Podolsky et al. 1988; Hesterberg et al. 1996; Warren 1996), and juvenile rhesus monkeys (Adler et al. 1990), develop **spontaneous colitis**.

CRITICAL ASSESSMENT OF THE METHODS

The relevance of animal models for the pathogenesis and treatment of human inflammatory bowel disease was reviewed by Dieleman et al. (1997) and by Sartor (1997).

A critical review of *in vitro* models in inflammatory bowel disease was given by McKay et al. (1997).

REFERENCES AND FURTHER READING

Abraham R, Fabian RJ, Goldberg L, Coulston F, (1974) Role of lysosomes in carrageenan-induced cecal ulceration. Gastroenterology 67:1169–1181

Adler R, Hendrickx A, Rush J, Fondacaro JD (1990) Chronic colitis of juvenile rhesus macaques: mucosal tissue levels of interleukin-1 (IL-1) and leucotriene B4 (LTB-4). Gastroenterol 98:A436

Aiko S, Conner EM, Fuseler JA, Grisham MB (1997) Effects of cyclosporine and FK506 in chronic colitis. J Pharmacol Exp Ther 280:1075–1084

Antony D, Savage F, Boulos P, Hembry R, Sams V, Trevethick M (1997) Effect of methylprednisolone on the ulceration, matrix metalloproteinase distribution and eicosanoid production in a model of colitis in the rabbit. Int J Exp Pathol 78:411–419

Aparigio-Pages MN, Verspaget HW, Pena AS, Weterman IT, de Bruin PA, Mierement-Ooms MA, van der Zon JM, van Tol EA, Lamers CB (1989) *In vitro* cellular cytotoxicity in Crohn's disease and ulcerative colitis: Relation with disease activity and treatment, and the effect of recombinant gamma interferon. J Clin Lab Immunol 29:119–124

Axelsson LG, Ahlstedt S (1993) Actions of sulfosalazine and analogues in animal models of experimental colitis. Immunopharmacology 2:219–232

Axelsson L-G, Landstrom E, Goldschmidt TJ, Gronberg A, Bylund-Fellenius AC (1996) Dextran sulfate sodium induced experimental colitis in immunodeficient mice. Inflamm Res 45:181–191

Bach MK, Brashler JR, Jahnson MA (1985) Inhibition by sulfasalazine of LTC synthetase and of rat liver glutathione *S*-transferases. Biochem Pharmacol 34:2695–2704

Benitz KF, Goldberg L, Coulston F (1973) Intestinal effects of carrageenan in the rhesus monkeys. Food Cosmet Toxicol 11:565–575

Bregenholt S, Claesson MH (1998) Splenic T helper cell type 1 cytokine profile and extramedullary haematopoesis in severe combined immunodeficient (scid) mice with inflammatory bowel disease (IBD). Clin Exp Immunol 111:166–172

Brogden RN, Sorkin EM (1989) Mesalazine. A review of its pharmacodynamic and pharmacokinetic properties, and

therapeutic potential in chronic inflammatory bowel disease. Drugs 38:500–523
Chalifoux LV, Bronson RT (1981) Colonic adenocarcinoma associated with chronic colitis in cotton-top marmosets, Saguinus oedipus. Gastroenterol 80:942–946
Claesson MH, Rudolphi A, Kofoed S, Pulsen SS, Reimann J (1996) $CD4^+$ T lymphocytes injected into severe combined immunodeficient (SCID) mice lead to an inflammatory and lethal bowel disease. Clin Exp Immunol 104:491–500
Cruz T, Galvez J, Ocete MA, Crespo ME, Sanchez de Medina LH, Zarzuelo A (1998) Oral administration of rutoside can ameliorate inflammatory bowel disease in rats. Life Sci 62:687–695
Cuzzocrea S, Mazzon E, Di Paola R, Genovese T, Patel NSA, Muià C, Threadgill MD, de Sarro A, Thiemermann C (2004) 5-Aminoisoquinolinone reduces colon injury by experimental colitis. Naunyn-Schmiedebergs Arch Pharmacol 370:464–473
Damms ETM, Oyen WJG, Boerman OC, Storm G, Laverman P, Koenders EB, Van der Meer JWM, Corstens FHM (1998) Technetium-99m-labeled liposomes to image experimental colitis in rabbits. J Nucl Med 39:2172–2178
Dieleman LA, Peña AS, Meuwissen SGM, van Rees EP (1997) Role of animal models for the pathogenesis and treatment of inflammatory bowel disease. Scand J Gastroenterol 32, Suppl 223:99–104
Ekstrom GM (1998) Oxazolone-induced colitis in rats: Effects of butesonide, cyclosporine A, and 5-aminosalicylic acid. Scand J Gastroenterol 22:174–179
Eliakim R, Karmeli F, Okon E, Rachmilewitz D (1995) Ketotifen ameliorates capsaicin-augmented acetic acid-induced colitis. Dig Dis Sci 40:503–509
Fabia R, Ar'Rajab A, Willén R, Brattsand R, Erlansson M, Svensjö E (1994) Topical anticolitic efficacy and selectivity of the glucocorticoid budesonide in a new model of acetic acid-induced acute colitis in the rat. Aliment Pharmacol Ther 8:433–446
Fiocchi C (1990) Immune events associated with inflammatory bowel disease. Gastroenterol 25, Suppl 172:4–12
Fretland DJ, Widomski DL, Levin S, Gaginella TS (1990) Colonic inflammation in the rabbit induced by phorbol-12-myristate-13-acetate. Inflammation 14:143–150
Fries W, Pagiaro E, Canova E, Carrato P, Gasprini G, Pomerri F, Martin A, Carlotto C, Mazzon E, Sturniolo GC, Longo G (1998) The effect of heparin on trinitrobenzene sulphonic acid-induced colitis in the rat. Aliment Pharmacol Ther 12:229–236
Goldhill J, Pichat P, Roome N, Angel I, Arbilla S (1998) Effect of mizolastine on visceral sensory afferent sensitivity and inflammation during experimental colitis. Arzneim Forsch/Drug Res 48:179–184
Hawkins JV, Emmel EL, Feuer JJ, Nedelman MA, Harvey CJ, Klein HJ, Rozmiarek H, Kennedy AR, Lichtenstein GR, Billings PC (1997) Protease activity in a hapten-induced model of ulcerative colitis in rats. Dig Dis Sci 42:1969–1980
Hermiston ML, Gordon JI (1995) Inflammatory bowel disease and adenomas in mice expressing a dominant negative N-cadherin. Science 270:1203–1207
Hesterberg PE, Wisnor-Hines D, Briskin MJ, Soler-Feran D, Merrill C, Mackay CR, Newman W (1996) Rapid solution of chronic colitis in the cotton-top tamarin with an antibody to a gut-homing integrin $\alpha_4\beta_7$. Gastroenterol 111:1373–1380
Higa A, Eto T, Nawa Y (1997) Evaluation of the role of neutrophils in the pathogenesis of acetic acid-induced colitis in mice. Scand J Gastroenterol 32:564–568
Hogaboam CM, Muller MJ, Collins SM, Hunt RH (1996) An orally active non-selective endothelin receptor antagonist, bosentan, markedly reduces injury in a rat model of colitis. Eur J Pharmacol 309:261–269
Jensen BH, Andersen JO, Poulsen SS, Olsen PS, Rasmussen SN (1984) The prophylactic effect of 5-aminosalicylic acid and salazosulphapyridine on degraded-carrageenan-induced colitis in guinea pigs. Scand J Gastroenterol 19:299–303
Kanauchi O, Nakamura T, Agata K, Mitsuyama K, Iwanaga T (1998) Effects of germinated barley foodstuff on dextran sulfate sodium-induced colitis in rats. J Gastroenterol 801:179–188
Kim HS, Berstadt A (1992) Experimental colitis in animal models. Scand J Gastroenterol 27:529–537
Kirsner JB, Elchlepp JG, Goldgraber ME, Ablaza J, Ford H (1959) Production of an experimental 'colitis' in rabbits. Arch Pathol 68:392–408
Kitano A, Matsumoto T, Tabata A, Obayashi M, Nakagawa M, Yasuda K, Watanabe Y, Okabe H, Kashima K, Fukushima R, Nakamura S, Oshitani N, Obata A, Okawa K, Kobayashi K (1994) Anti-inflammatory effect of bucillamine on carrageenan-induced colitis in the rabbit. Int J Immunotherapy 10:135–143
Kitano A, Oshitani N, Okabe H, Hara J, Suzuki N, Aoki T, Adachi K, Watanabe Y, Yasuda K, Tabata A, Obayashi M, Nakamura S, Obata A, Matsumoto T, Okawa K, Kobayashi K (1996) Effect of bucillamine in the rat trinitrobenzene sulfonic acid induced model of colitis. Inflamm Res 45:491–493
Kraft SC, Fitch FW, Kirsner JB (1963) Histologic and immunochemical features of 'Auer' colitis in rabbits. Am J Pathol 43:913–927
Kuroe K, Haga Y, Funakoshi O, Mizuki I, Kanazawa K, Yoshida Y (1996a) Extraintestinal manifestations of granulomatous enterocolitis induced in rabbits by long-term submucosal administration of muramyl dipeptide emulsified with Freund's complete adjuvant. J Gastroenterol 31:199–206
Kuroe K, Haga Y, Funakoshi O, Kanazawa K, Mizuki I, Yoshida Y (1996b) Pericholangitis in a rabbit colitis model induced by injection of muramyl dipeptide emulsified with a long-chain fatty acid. J Gastroenterol 31:347–352
Leach MW, Bean AGD, Mauze S, Coffman RL, Powrie F (1996) Inflammatory bowel disease in C.B-17 scid mice reconstituted with the $CD45RB^{high}$ subset of CD^+ T cells. Am J Pathol 148:1503–1515
LeDuc LE, Nast CC (1990) Chemotactic peptide-induced colitis in rabbits. Gastroenterol 98:929–935
Lora L, Mazzon E, Martines D, Fries W, Muraca M, Martin A, D'Odorico A, Naccarato R, Citi S (1997) Hepatocyte tight-junctional permeability is increased in rat experimental colitis. Gastroenterol 113:1347–1354
Lushbach C, Humason G, Clapp N (1985) Histology of colitis: Sanguinus oedipus and other marmosets. Dig Dis Sci 30, Suppl:45–51
MacPherson B, Pfeiffer CJ (1976) Experimental colitis. Digestion 14:42–452
MacPherson BR, Pfeiffer CJ (1978) Experimental production of diffuse colitis in rats. Digestion 17:136–150
Madara JL, Podolsky DK, King NW, Sehgal PK, Moore R, Winter HS (1985) Characterization of spontaneous colitis in cotton-top tamarin (Sanguinis oedipus) and its response to sulfasalazine. Gastroenterology 88:13–19
Magnusson KE, Dahlgren C, Sjolander A (1985) Effect of N-formylated-methionyl-leucyl-phenylalanine on gut permeability. Inflammation 9:365–373

Marcus R, Watt J (1969) Seaweeds and ulcerative colitis in laboratory animals. Lancet 2:489–490

McKay DM, Philpott DJ, Perdue MH (1997) Review Article: *In vitro* models in inflammatory bowel disease research – a critical review. Aliment Pharmacol Ther 11, Suppl 3:70–80

Meenan J, Hommes DW, Mevissen M, Dijkhuizen S, Soule H, Moyle M, Buller HR, Ten Kate FW, Tytgat GNJ, Van Deventer SJH (1996) Attenuation of the inflammatory response in an animal colitis model by neutrophil inhibitory factor, a novel β_2-integrin antagonist. Scand J Gastroenterol 31:786–791

Millar AD, Rampton DS, Chander CL, Claxson AWD, Blades S, Coumbe A, Panetta J, Morris CJ, Blake DR (1996) Evaluating the antioxidant potential of new treatments for inflammatory bowel disease using a rat model of colitis. Gut 39:407–415

Mitchell IC, Turk JL (1990) Effect of the immune modulating agents cyclophosphamide, methotrexate, hydrocortisone, and cyclosporin A on an animal model of granulomatous bowel disease. Gut 31:674–678

Morris CP, Beck PL, Herridge MS, Depew WT, Szewczuk MR, Wallace HJ (1989) Hapten-induced model of chronic inflammation and ulceration in the rat colon. Gastroenterology 96:795–803

Myers BS, Dempsey DT, Ysar S, Martin JS, Parkman HP, Ryan JP (1997) Acute experimental distal colitis alters colonic transit in rats

Neurath MF, Pettersson S, Meyer zum Büschenfelde K-H (1996) Local administration of antisense phosphorothionate oligonucleotides to the p65 subunit of NF-kappaB abrogates established experimental colitis in mice. Nat Med 2:998–1004

Neurath MF, Fuss I, Pasparakis M, Alexopoulou L, Haralambous S, Meyer zum Büschenfelde KH, Strober W, Kollias G (1997) Predominant pathogenic role of tumor necrosis factor in experimental colitis in mice. Eur J Immunol 27:1743–1750

Norris AA (1989) Animal models of inflammatory bowel disease. In: Pharmacological Methods in the Control of Inflammation. Alan R. Liss, Inc. pp 321–342

Norris AA, Lewis AJ, Zeitlein IJ (1982) Changes in colonic tissue levels of inflammatory mediators in a guinea-pig model of immune colitis. Agents Actions 12:239–242

Oberle RL, Moore TJ, Krummel DAP (1995) Evaluation of mucosal damage of surfactants in rat jejunum and colon. J Pharmacol Toxicol Meth 33:75–81

Ohkusa T (1985) Production of experimental ulcerative colitis in hamsters by dextran sulfate sodium and change in intestinal microflora. Jpn J Gastroenterol 82:1327–1336

Okayasu I, Hatekeyama S, Yamada M, Ohkusa T, Inagaki Y, Nakaya R (1990) A novel method in the induction of reliable experimental acute and chronic ulcerative colitis in mice. Gastroenterol 98:694–702

Oyen WJG, Boerman OC, Dams ETM, Storm G, Van Bloois L, Koenders EB, Van Haelst UJGM, Van der Meer JWM, Cortens FHM (1997) Scintigraphic evaluation of experimental colitis in rabbits. J Nucl Med 38:1596–1600

Palmen MJHJ, Dieleman LA, Soesatyo M, Peña AS, Meuwissen SGM, van Rees EP (1998) Effects of local butesonide treatment on cell-mediated immune response in acute and relapsing colitis in rats. Dig Dis Sci 43:2516–2525

Patterson DJ, Colony PC (1983) Anti-secretory effect of sulphasalazine and 5-aminosalicylic acid in experimental colitis. Gastroenterology 84:1271

Podolsky DK, Madara JL, King NW, Sehgal PK, Moore R, Winter HS (1988) Colonic mucin composition in primates: selective alterations associated with spontaneous colitis in the cotton-top tamarin. Gastroenterology 88:20–25

Powrie F, Leach MW (1995) Genetic and spontaneous models of inflammatory bowel disease in rodents: evidence for abnormalities in mucosal immune regulation. Ther Immunol 2:115–123

Pricolo VE, Madhere SM, Finkelstein SD, Reichner JS (1996) Effects of lambda-carrageenan induced experimental enterocolitis on splenocyte function and nitric oxide production. J Surg Res 66:6–11

Ritzpatrick R, Bostwick JSD, Renzetti M, Pendleton RG, Decktor DL (1990) Antiinflammatory effects of various drugs on acetic acid induced colitis in the rat. Agents Actions 30:393–402

Rosenberg EW, Fischer RW (1964) DNCB allergy in the guinea-pig colon. Arch Dermatol 89:99–112

Rudolphi A, Bonhagen K, Reimann J (1996) Polyclonal expansion of adoptively transferred $CD4^+$ α β T cells in the colonic lamina propria of scid mice with colitis. Eur J Immunol 26:1156–1163

Sartor RB (1997) Review article: How relevant to human inflammatory bowel disease are current animal models of intestinal inflammation? Aliment Pharmacol Ther 11, Suppl 3:70–89–97

Selve N, Wöhrmann T (1992) Intestinal inflammation in TNBS sensitized rats as a model of chronic inflammatory bowel disease. Mediat Inflamm 1:121–126

Shintani N, Nakajima T, Nakaburo H, Nagai H, Kagitani Y, Takizawa H, Asakura H (1997) Intravenous immunoglobulin (IVIG) treatment of experimental colitis induced by dextran sulfate in rats. Clin Exp Immunol 108:340–345

Stadnicki A, Sartor RB, Janardham R, Majluf-Cruz A, Kettner CA, Adam AA, Colman RW (1998) Specific inhibition of plasma kallikrein modulates chronic granulomatous intestinal and systemic inflammation in genetically susceptible rats. FASEB J 12:325–333

Stein TA, Keegan L, Auguste LJ, Bailey B, Wise L (1993) Stress induced experimental colitis. Mediat Inflamm 2:253–256

Suzui M, Ushijama T, Yoshimi N, Nakagama H, Hara A, Sugimura T, Nagao M, Mori H (1997) No involvement of APC gene mutations in ulcerative colitis-associated rat colon carcinogenesis induced by 1-hydroxyanthraquinone and methylazoxymethanol acetate. Mol Carcinog 20:389–393

Taniguchi T, Tsukada H, Nakamura H, Kodama M, Fukuda K, Tominaga M, Seino Y (1997) Effects of a thromboxane A_2 receptor antagonist in an animal model of inflammatory bowel disease. Digestion 58:476–478

Terzioglu T, Yalti T, Tezelman S (1997) The effect of prostaglandin E_1 on experimental colitis in the rat. Int J Colorectal Dis 12:63–66

von Herbay A, Gebbers JO, Otto HF (1990) Immunopatholgy of ulcerative colitis: A review. Hepato-Gastroenterol 37:99–107

von Ritter, Sekizuka E, Grisham MB, Granger DN (1988) The chemotactic peptide N-formyl-methionyl-leucyl-phenylalanin increases mucosal permeability in the distal ileum of the rat. Gastroenterology 95:778–780

Wallace JL, Le T, Carter L, Appleyard CB, Beck PL (1995) Hapten-induced chronic colitis in the rat: alternatives to trinitrobenzene sulfonic acid. J Pharmacol Toxicol Meth 33:237–239

Wallace JL, McCafferty DM, Sharkey KA (1998) Lack of beneficial effect of a tachykinin receptor antagonist in experimental colitis. Regul Peptides 73:95–101

Walsh LP, Zeitlin IJ (1987) Effect of salazopyrin, 5-aminosalicylic acid and prednisolone on an immune complex-mediated colitis in mice. Br J Pharmacol 92/Suppl:741P

Warren BF (1996) Cytokines in the cotton top tamarin model of human ulcerative colitis. Aliment Pharmacol Ther Suppl 10:45–47

Watanabe M, Ueno Y, Yajima T, Okamoto S, Hayashi T, Yamazaki M, Iwao Y, Ishii H, Habu S, Uehira M, Nishimoto H, Ishikawa H, Hata JI, Hibi T (1998) Interleukin7 transgenic mice develop chronic colitis with decreased interleucin7 protein accumulation in the colonic mucosa. J Exp Med 187:389–402

Watt J, Marcus R (1972) Ulceration of the colon in rabbits fed sulfated amylopectin. J Pharm Pharmacol 24:68–69

Watt J, Marcus R (1973) Progress report. Experimental ulcerative disease of the colon in animals. Gut 14:506–510

Yue G, Sun FF, Dunn C, Yin K, Wong PYK (1996) The 21-aminosteroid tirilazad mesylate can ameliorate inflammatory bowel disease in rats. J Pharmacol Exp Ther 276:265–270

Zea-Ariarte W, Makiyama K, Itsuno M, Umene Y, Hara K (1994) Experimental induced colitis in rats by ethanolic solution of trinitrobenzene sulfonic acid and ethanol alone: A comparative study. Acta med Nagasaki 39:1–10

J.5 Emetic and Anti-Emetic Activity

J.5.0.1 Assessment of Emetic and Anti-Emetic Activity in Dogs

PURPOSE AND RATIONALE

Emesis comparable to man occurs only in a few animal species. Among laboratory animals, the dog is a suitable species to test anti-emetic drugs. Apomorphine-induced emesis is also used to evaluate neuroleptic drugs (see E.5.3.8). Burkman (1982) described a technique relying upon the use of apomorphine either as a reference standard against which other emetics can be compared, or as a challenging agent against which anti-emetic compounds can be evaluated.

PROCEDURE

Beagle dogs weighing between 15 and 20 kg are used. Each dog is given 200 g food 30 min prior to an assay session. The threshold emetic dose of apomorphine hydrochloride is established for each dog by administering single doses at 5 day intervals in gradually increasing amounts. The starting dose is 0.07 mM/kg (22 mg/kg) body weight, i.m., and is subsequently increased (or decreased) as required. Injection sites alternate between contralateral gluteus muscles. After every third or fourth dose of the emetic, the animals receive an equivalent volume of vehicle under similar conditions in order to detect the presence of a conditioned emetic response.

The threshold dose is defined as the concentration provoking an emetic episode and determined for each individual animal. The threshold emetic dose is relatively stable for a given group of dogs over a period of 2 months. Continued administration to the same dogs for longer periods of time is inadvisable as Pavlovian emetic conditioning becomes evident after 8–10 doses of apomorphine. Establishment of an emetic threshold for a test compound using a similar dosing schedule allows to quantitatively express the test compound's emetic potency as a ratio compared with the reference standard. Usually, 4–6 animals are sufficient to provide a reliable estimate of the test compound's emetic efficacy and potency.

In the anti-emetic assay, dogs whose apomorphine threshold emetic dose has been determined receive various concentrations of the potential anti-emetic drug at a given time interval prior to apomorphine. The dose initially selected for the anti-emetic is a fraction of the acute LD_{50} of this drug in mice. A new threshold dose is estimated in the presence of the test anti-emetic and compared to the threshold dose in the presence of the reference standard chlorpromazine.

EVALUATION

Using the threshold doses, the relative potency of an emetic compared to apomorphine, or the relative potency of an anti-emetic compared to chlorpromazine, is calculated.

MODIFICATIONS OF THE METHOD

Cisplatin-induced emesis in the **dog**, as described by Gylys et al. (1979), was used by Turconi et al. (1991) to test the anti-emetic properties of 5-HT_3 receptor antagonists.

Heaslip and Evans (1995) studied the emetic, central nervous system, and pulmonary activities of rolipram in the dog after i.v. and intragastral application.

Gupta and Sharma (1996) tested the activity of antioxidants against emesis induced by an intravenous dose of 3 mg/kg cisplatin in healthy mongrel dogs.

Szelenyi et al. (1994) described emesis in **domestic pigs** as a new experimental tool for detection of anti-emetic drugs and for evaluation of the emetogenic potential of new anticancer agents. Healthy young, 12–15-week-old domestic pigs of either sex were lightly anesthetized with ketamine (10 mg/kg, i.v.) and xylazine (2 mg/kg, i.v.) and a cannula inserted into a superficial vein of one of the extremities. The challenging agents, e. g., cisplatin, carboplatin, cyclophosphamide, or ifosfamide were infused intravenously at different doses during a total administration time of 15 min. After removing of the cannula the animals

were placed in their boxes for observation of emesis over 24 h. Drugs with anti-emetic potential were given intravenously 15 min prior cisplatin infusion.

Göthert et al. (1995) found a dose-dependent inhibition of cisplatin-induced emesis in pigs by anpirtoline, a mixed 5-HT_1 receptor agonist/5-HT_3 receptor antagonist.

Gardner et al. (1995, 1998) used the **house musk shrew** (*Suncus murinus*) to test antagonism against cisplatin-induced emesis.

Kwiatkowska et al. (2004) performed a comparative analysis of the potential of cannabinoids and ondansetron to suppress cisplatin-induced emesis in *Suncus murinus* (house musk shrew).

REFERENCES AND FURTHER READING

Bigaud M, Elands J, Kastner PR, Bohnke RA, Emmert LW, Galvan M (1995) Pharmacology of the human metabolites of Dolasetron, an antiemetic 5-HT_3 receptor antagonist. Drug Dev Res 34:289–296

Burkman AM (1982) Assessment of emetic and antiemetic activity. J Pharmacol Meth 8:165–171

Gardner C, Perren M (1998) Inhibition of anesthetic-induced emesis by a NK_1 or 5-HT_3 receptor antagonist in the house musk shrew, Suncus murinus. Neuropharmacology 37:1643–1644

Gardner CJ, Twissell DJ, Dale TJ, Gale DJ, Jordan CC, Kilpatrick GJ, Bountra C, Ward P (1995) The broad-spectrum anti-emetic activity of the novel non-peptide tachykinin NK_1 receptor antagonist GR203040. Br J Pharmacol 116:3158–3163

Göthert M, Hamon M, Barann M, Bönisch H, Gozlan H, Laguzzi R, Metzenauer P, Nickel B, Szelenyi I (1995) 5-HT_3 receptor antagonism by anpirtoline, a mixed 5-HT_1 receptor agonist/5-HT_3 receptor antagonist. Br J Pharmacol 114:269–274

Gupta YK, Sharma SS (1996) Antiemetic activity of antioxidants against cisplatin-induced emesis in dogs. Environ Toxicol Pharmacol 1:179–184

Gylys JA, Doran KM, Buyinski JP (1979) Antagonism of cisplatin-induced emesis in the dog. Commun Chem Pathol Pharmacol 23:61–68

Gylys JA, Wright RN, Nicolosi WD, Buyniski JP, Crenshaw RR (1988) BMY 25801, an anti-emetic agent free of D_2 dopamine antagonist properties. J Pharmacol Exp Ther 244:830–837

Heaslip RJ, Evans DY (1995) Emetic, central nervous system, and pulmonary activities of rolipram in the dog. Eur J Pharmacol 286:281–290

Kwiatkowska M, Parker LA, Burton P, Mechoulam R (2004) A comparative analysis of the potential of cannabinoids and ondansetron to suppress cisplatin-induced emesis in *Suncus murinus* (house musk shrew). Psychopharmacology 174:254–259

Szelenyi I, Herold H, Göthert M (1994) Emesis induced in domestic pigs: a new experimental tool for detection of antiemetic drugs and for evaluation of the emetogenic potential of new anticancer agents. J Pharmacol Toxicol Meth 32:109–116

Turconi M, Donetti A, Schiavone A, Sagrada A, Montagna E, Nicola M, Cesana R, Rizzi C, Micheletti R (1991) Pharmacological properties of a novel class of 5-HT_3 receptor antagonists. Eur J Pharmacol 203:203–211

J.5.0.2 Anti-Emetic Activity in Ferrets

PURPOSE AND RATIONALE

The ferret is a well established animal model of emesis which responds to cancer chemotherapeutic agents in a manner similar to that observed in man (Florczyk et al. 1982). The animals react with vomiting and retching after challenge with central (loperamide and apomorphine), peripheral ($CuSO_4$), or mixed central and peripheral (ipecacuanha, cisplatin) emetic stimuli. The model has been used to test the anti-emetic properties of 5-HT_3 receptor antagonists and tachykinin NK_1 receptor antagonists.

PROCEDURE

Adult male ferrets weighing 1 to 1.5 kg are randomly assigned to the different treatment groups. Each animal is anesthetized by inhalation with methoxyflurane. A jugular vein is cannulated and exteriorized from the outside of the neck. Following recovery from the anesthesia, the animals are dosed with the test drug or the standard or the vehicle 30 min prior i.v. administration of 10 mg/kg cisplatin. The numbers of retches and vomits occurring following the administration of the emetogen are recorded in each animal for 5 h. Retching is defined as rhythmic inspiratory movements against a closed glottis, and vomiting as forced expulsion of upper gastrointestinal contents.

EVALUATION

Duration of action of the compounds is assessed by determining the period of time for which the inhibitory effects remain significantly different from vehicle controls.

Statistical analysis of the data is performed by a repeated measure analysis of variance (ANOVA) followed by pairwise comparisons against control at each time period using Fisher's LSD multiple comparison test.

MODIFICATIONS OF THE METHOD

Fink-Jensen et al. (1992) reported that the excitatory amino acid receptor antagonists, 2,3-dihydroxy-6-nitro-7-sulphamoylbenzo(f)quinoxaline (NBQX) and 6-cyano-7-nitroqinoxaline-2,3-dione (CNQX), which preferentially block non-NMDA subtypes of excitatory amino acid receptors, effectively inhibit cisplatin-induced emesis in ferrets.

Emesis in ferrets was induced by X-irradiation or oral doses of copper sulfate (Andrews and Bhandari 1993).

Watson et al. (1995) studied the anti-emetic effects of a selective NK_1 receptor antagonist using the gag reflex in ferrets. The gag reflex is mediated by mechanoreceptors in the superior laryngeal nerve, which projects to the nucleus tractus solitarius. (Mifflin 1993). The gag reflex was evoked in conscious ferrets by gentle tactile stimulation of the pharynx and larynx and was recorded as an all or none response before and after drug administration.

Furthermore, the authors induced retching in the ferret by electrical stimulation of the vagal afferents under urethane anesthesia (Andrews et al. 1990). The dorsal or ventral abdominal vagus was isolated and ligated and the central cut-end stimulated before and after drug administration.

Duplantier et al. (1996) studied the emetic behavior in the ferret induced by inhibitors of phosphodiesterase type IV (PDE IV) and by rolipram comparing with the [^{3}H]rolipram binding activity. Robichaud et al. (1999, 2001) compared several PDE IV inhibitors and studied the mode of action inducing emesis in ferrets.

REFERENCES AND FURTHER READING

Andrews PLR, Bhandari P (1993) Resinferatoxin, an ultrapotent capsaicin analogue, has anti-emetic properties in the ferret. Neuropharmacology 32:799–806

Andrews PLR, Davis CJ, Bingham S, Davidson HIM, Hawthorn J, Maskell L (1990) The abdominal visceral innervation and the emetic reflex: pathways, pharmacology and plasticity. Can J Physiol Pharmacol 68:325–345

Beattie DT, Beresford IJ, Connor HE, Marshall FM, Hawcock AB, Hagan R, Bowers J, Birch PJ, Ward P (1995) The pharmacology of GR203040, a novel, potent and selective non-peptide tachykinin NK_1 receptor antagonist. Br J Pharmacol 116:3149–3157

Bingham S, Blower PR, Davey PT, King PD, Sanger GJ, Wardle KA, Nishioka Y (1994) Differences in the anti-emetic efficacies of the 5-HT_3 receptor antagonists granisetron and azasetron in the conscious ferret. Pharmacometrics 47:21–28

Bountra C, Bunce K, Dale T, Gardner C, Jordan C, Twissell D, Ward P (1993) Anti-emetic profile of an non-peptide neurokinin NK_1 receptor antagonist, CP 99,994, in ferrets. Eur J Pharmacol 249:R3–R4

Cohen ML, Bloomquist W, Gidda JS, Lacefield W (1989) Comparison of the 5-HT_3 receptor antagonist properties of ICS 205–930, GR38032 and zacopride. J Pharmacol Exp Ther 248:197–201

Duplantier AJ, Biggers MS, Chambers RJ, Cheng JB, Cooper K, Damon DB, Eggler JF, Kraus KG, Marfat A, Masamune H, Pillar JS, Shirley JT, Umland JP, Watson JW (1996) Biarylcarboxylic acids and -amides: inhibition of phosphodiesterase type IV versus [^{3}H]rolipram binding activity and their relationship to emetic behavior in the ferret. J Med Chem 39:120–125

Eglen RM, Lee CH, Smith WL, Johnson LG, Clark R, Whiting RL, Hedge SS (1995) Pharmacological characterization of RS 25259–197, a novel and selective 5-HT_3 receptor antagonist, *in vivo*. Br J Pharmacol 114:860–866

Fink-Jensen A, Judge ME, Hansen JB, Jacobsen B, Turski L, Olney J, Honoré T (1992) Inhibition of cisplatin-induced emesis in ferrets by non-NMDA receptor antagonists NBQX and CNQX. Neurosci Lett 137:173–177

Fitzpatrick LR, Lambert RM, Pendley CE, Martin GE, Bostwick JS, Gessner GW, Aitey JE, Youssefyeh RD, Pendeton RG, Decktor DL (1990) RG 12915, a potent hydroxytryptamine$_3$ antagonist that is an orally effective inhibitor of cytotoxic drug-induced emesis in the ferret and dog. J Pharmacol Exp Ther 254:450–455

Florczyk AP, Schurig JE, Bradner WT (1982) Cisplatin-induced emesis in the ferret: a new animal model. Cancer Treat Rep 66:187–189

Gardner CJ, Twissell DJ, Dale TJ, Gale DJ, Jordan CC, Kilpatrick GJ, Bountra C, Ward P (1995) The broad-spectrum anti-emetic activity of the novel non-peptide tachykinin NK_1 receptor antagonist GR203040. Br J Pharmacol 116:3158–3163

Gonsalves S, Watson J, Ashton C (1996) Broad spectrum anti-emetic effects of CP-122,721, a tachykinin NK_1 receptor antagonist, in ferrets. Eur J Pharmacol 305:181–185

Gylys JA, Wright RN, Nicolosi WD, Buyniski JP, Crenshaw RR (1988) BMY 25801, an anti-emetic agent free of D_2 dopamine antagonist properties. J Pharmacol Exp Ther 244:830–837

Mifflin SW (1993) Laryngeal afferent inputs to the nucleus of the solitary tract. Am J Physiol 265:R269–R276

Miller RC, Galvan M, Gittos MW, van Giersbergen PLM, Moser PC, Fozard JR (1993) Pharmacological properties of dolasetron, a potent and selective antagonist at 5-HT_3 receptors. Drug Dev Res 28:87–93

Robichaud A, Tattersall FD, Choudhury I, Rodger IW (1999) Emesis induced by inhibitors of type IV cyclic nucleotide phosphodiesterase (PDE IV) in the ferret. Neuropharmacology 38:289–297

Robichaud A, Savoie C, Stamatiou PB, Tattersall FD, Chan CC (2001) PDE4 inhibitors induce emesis in ferrets via a noradrenergic pathway. Neuropharmacology 40:262–269

Rudd JA, Jordan CC, Naylor RJ (1996) The action of the NK_1 tachykinin receptor antagonist, CP 99,994 in antagonizing the acute and delayed emesis induced by cisplatin in the ferret. Br J Pharmacol 119:931–936

Rupniak NMJ, Tattersall FD, Williams AR, Rycroft W, Carlson EJ, Cascieri MA, Sadowski S, Ber E, Hale JJ, Mills SG, McCoss M, Seward E, Huscroft I, Owen S, Swain CJ, Hill RG, Hargreaves RJ (1997) *In vitro* and *in vivo* predictors of the anti-emetic activity of tachykinin NK_1 receptor antagonists. Eur J Pharmacol 326:201–209

Watson JW, Gonsalves SF, Fossa AA, McLean S, Seeger T, Obach S, Andrews PLR (1995) The anti-emetic effects of CP-99,994 in the ferret and the dog: Role of the NK_1 receptor. Br J Pharmacol 115:84–94

J.5.0.3 Assessment of Emetic and Anti-Emetic Activity in Pigeons

PURPOSE AND RATIONALE

Emesis in pigeons can be induced by various agents. Formerly, the phenomenon has been used for standardization of cardiac glycosides (Hanzlik 1929). More re-

cently, dose response curves of emesis have been determined for various agents and anti-emetic effects were evaluated (Wolff and Leander 1994, 1995).

PROCEDURE

Male White Carneaux pigeons are kept in individual stainless steel cages at constant temperature and humidity. They are maintained at 90% of their free-feeding body weights by once-daily feeding of approximately 20 g Purina Pigeon Checkers.

All testing is conducted during the illuminates phase of the light-dark cycle. On test days, the birds are fed 5 min before the start of an emetic trial. If vomiting occurs, the pigeons are given an additional 20 g of feed before being returned to their home cages at the conclusion of the observation period. Individual subjects are allowed a recovery period of at least 3 days between each drug test.

For the following compounds emetic doses are reported:

- Cisplatin 10 mg/kg, injected into a wing vein.,
- Ipecac syrup, 1 to 3 ml/kg, administered via a feeding needle passed through the crop to the opening of the proventriculus,
- emetine, 1 to 20 mg/kg, injected into the pectoralis muscle,
- m-(chlorphenyl)-biguanide (mCBG), 0.32 to 5 mg/kg, injected intramuscularly,
- ditolyganidine (DTG), 5.6 mg/kg, injected intramuscularly.

Test substances with potential anti-emetic activity are injected at various doses 15 min before the emetic challenge. The animals are observed for vomiting during 2 h.

EVALUATION

ED_{50} values for with 95% confidence limits are calculated for the activity of emetic substances, as well as for the inhibition of emesis by anti-emetic drugs after a high dose of the emetic compound.

REFERENCES AND FURTHER READING

Chaney SG, Kare MR, (1966) Emesis in birds. J Am Vet Med Assoc 149:938–943

Hanzlik JP (1929) New method of estimating the potency of digitalis in pigeons: Pigeon emesis. J Pharmacol Exp Ther 35:363–391

Hudzik TJ (1991) Sigma ligand-induced emesis in the pigeon. Pharmacol Biochem Behav 41:215–217

Hudzik TJ, De Costa BR, McMillan DA (1993) Sigma receptor-mediated emetic response in pigeons. Agonists, antagonists, and modifiers. Eur J Pharmacol 236:279–287

Koster R (1957) Comparative studies of emesis in pigeons and dogs. J Pharmacol Exp Ther 119:406–417

Preziosi P, D'Amato M, Del Carmine R, Martire M, Pozzoli G, Navarra P (1992) The effects of 5-HT_3 receptor antagonists on cisplatin-induced emesis in the pigeon. Eur J Pharmacol 221:343–350

Wolff MC, Leander JD (1994) Antiemetic effects of 5-HT_{1A} agonists in the pigeon. Pharmacol Biochem Behav 49:385–391

Wolff MC, Leander JD (1995) Comparison of the antiemetic effects of a 5-HT_{1A} agonist, LY228729, and 5-HT_3 antagonists in the pigeon. Pharmacol Biochem Behav 52:571–575

J.5.0.4 Activity Against Motion-Induced Emesis

PURPOSE AND RATIONALE

The house musk shrew (*Suncus murinus*) is a small insectivore that has been shown to exhibits emesis when exposed to linear reciprocation motion (Ueno et al. 1988; Okada et al. 1994).

PROCEDURE

Adult male (body weight range 55–90 g) and female (body weight range 35–50 g) are used. The animals receive a dose of the test drug or vehicle in a volume of 4 ml/kg 15 min before motion testing. The animals are placed in a Perspex chamber (11 cm wide × 22 cm long × 11 cm high) that is attached to the platform of a shaker set to execute a linear horizontal movement of 4 cm at a frequency of 1 Hz along the long axis of the chamber. The animals are allowed approximately 3 min to become accustomed to the chamber before exposure to motion for a period of 5 min, during which the number and timing of emetic episodes are recorded. An emetic episode usually consists of a short period of rapid retching followed by a vomit. A cross-over design is used for the experiment, with animals exposed to motion testing following treatment with vehicle control on one occasion, and following treatment with test drug on another. An interval of 12 days is allowed between treatments.

EVALUATION

Group results are expressed as mean ± SEM. Either Student's *t*-test or the Wilcoxon signed rank test is used as a measure of significance.

MODIFICATIONS OF THE METHOD

Gardner and Perren (1998) described a model of post-anesthesia-induced emesis in Suncus murinus.

Parker et al. (2004) tested the effect of cannabinoids on lithium-induced vomiting in the *Suncus murinus* (house musk shrew).

Lucot (1989) used cats to test the activity of HT_3 antagonists against motion-induced sickness.

REFERENCES AND FURTHER READING

Gardner C, Perren M (1998) Inhibition of anaesthetic-induced emesis by a NK_1 or 5-HT_3 receptor antagonist in the house musk shrew, Suncus murinus. Neuropharmacology 37:1643–1644

Gardner CJ, Twissell DJ, Dale TJ, Gale DJ, Jordan CC, Kilpatrick GJ, Bountra C, Ward P (1995) The broad-spectrum anti-emetic activity of the novel non-peptide tachykinin NK_1 receptor antagonist GR203040. Br J Pharmacol 116:3158–3163

Lucot JB (1989) Blockade of 5-hydroxytryptamine$_3$ receptors prevents cisplatin-induced but not motion- or xylazine-induced emesis in the cat. Pharmacol Biochem Behav 32:207–210

Okada F, Torii Y, Saito H, Matsuki N (1994) Antiemetic effects of serotonergic 5-HT_{1A}-receptor agonists in Suncus murinus. Jpn J Pharmacol 64:109–114

Parker LA, Kwiatkowska M, Burton P, Mechoulam R (2004) Effect of cannabinoids on lithium-induced vomiting in the *Suncus murinus* (house musk shrew). Psychopharmacology 171:156–161

Torii Y, Saito H, Matsuki N (1991) Selective blockade of cytotoxic drug-induced emesis by 5-HT_3 receptor antagonists in Suncus murinus. Jpn J Pharmacol 55:107–113

Ueno S, Matsuki N, Saito H (1988) Suncus murinus as a new experimental model for motion sickness. Life Sci 43:413–420

J.5.0.5 Foot Tapping in Gerbils

PURPOSE AND RATIONALE

Foot tapping in gerbils, a centrally mediated behavior (Graham et al. 1993; Bristow and Young 1994; Rupniak and Williams 1994; Vassout et al. (1994), has been claimed to be highly predictive for NK_1 antagonists to prevent cisplatin-induced retching in ferrets and to be a simple *in vivo* assay for CNS penetration (Rupniak et al. 1997).

PROCEDURE

Mongolian gerbils of either sex weighing 35–70 g are anesthetized by inhalation of an isoflurane/oxygen mixture to permit exposure of the jugular vein through a skin incision in the neck, using blunt dissection to clear surrounding salivary gland and connective tissues. Test compounds or vehicle are administered using an injection volume of 5 ml/kg i.v. The wound is closed and a second incision is made in the midline of the scalp to expose the skull. The highly selective, peptidase-resistant NK_1 receptor agonist GR73632 (D-Ala-[D-Pro^9,Me-Leu^8]substance P-(1–17) (Hagan et al. 1991) is infused directly into the cerebral ventricles (3 pmol in 5 µl i.c.v.) by vertical insertion of a cuffed 27-gauge needle to a depth of 4.5 mm below bregma. The scalp incision is closed and the animal allowed to recover from anesthesia in a clear Perspex observation box (25 × 20 × 20 cm). The duration of hind foot stepping is then recorded continuously for 5 min using a stopclock. The time relapse from induction to recovery from anesthesia, with intervening i.v. and i.c.v. injections is about 3–4 min.

EVALUATION

Data are subjected to one-way analysis of variance (ANOVA), followed by Dunnett's or Newman-Keuls multiple comparison *t*-tests.

CRITICAL ASSESSMENT OF THE METHOD

The specificity of the method to predict anti-emetic activity has to be proven.

REFERENCES AND FURTHER READING

Bristow LJ, Young L (1994) Chromodacryorrhea and repetitive hind paw tapping: models of peripheral and central tachykinin NK_1 receptor activation in gerbils. Eur J Pharmacol 254:245–249

Graham EA, Turpin MP, Stubbs CM (1993) Characterization of the tachykinin-induced thumping response in gerbils. Neuropeptides 4:228

Rupniak NMJ, Williams AR (1994) Differential inhibition of foot tapping and chromodacyorrhea in gerbils by CNS penetrant and non-penetrant tachykinin NK_1 receptor antagonists. Eur J Pharmacol 265:179–183

Rupniak NMJ, Tattersall FD, Williams AR, Rycroft W, Carlson EJ, Cascieri MA, Sadowski S, Ber E, Hale JJ, Mills SG, McCoss M, Seward E, Huscroft I, Owen S, Swain CJ, Hill RG, Hargreaves RJ (1997) *In vitro* and *in vivo* predictors of the anti-emetic activity of tachykinin NK_1 receptor antagonists. Eur J Pharmacol 326:201–209

Vassout A, Schaub M, Gentsch C, Ofner S, Schilling W, Veenstra S (1994) CGP 49823, a novel NK1 receptor antagonist: behavioural effects. Neuropeptides 26 (Suppl 1):38

J.6 Gall Bladder Functions

J.6.1 Bile Secretion

J.6.1.1 Cholagogic Activity in Mice

PURPOSE AND RATIONALE

A rapid method for standardization of cholagogues in mice by simple weighing the gall bladder filled with bile was published by Litvinchuk (1976).

PROCEDURE

Groups of 10 female mice (e. g., NMRI strain) weighing 15–20 g are used. Food, but not water, is withdrawn 24 h prior to the experiment. The test compound or the control solution is administered subcutaneously or

orally. After 1 h, the animals are sacrificed and bled from the carotid artery. Laparotomy is performed, the liver exposed, and a No. 75 silk ligature is tied around the cystic duct, which is detached from the bile ducts and removed from the peritoneal cavity. If a large volume of bile has been accumulated, the full gall bladder is removed together with the bile ducts. The isolated gall bladder is weighed on a suitable balance, after which the contents are removed, the gall bladder walls are washed with distilled water, dried on filter paper, and the organ is weighed again. The difference in weight of the full and the empty gall bladder indicates the quantity of bile secreted during a measured time. The concentration of cholates, bilirubin, and cholesterol in the bile can be determined.

EVALUATION

The average of secreted bile in groups of 10 treated mice is compared with the average value of the control group using Student's *t*-test.

CRITICAL ASSESSMENT OF THE METHOD

The method has the clear advantage of simplicity but does not measure the true bile excretion since the outflow from the bile bladder during the test period is neglected.

MODIFICATIONS OF THE METHOD

Sterczer et al. (1996) studied the effect of cholagogues on the volume of the gallbladder in healthy dogs fasted for 24 h by two-dimensional ultrasonography. The volume was measured immediately before the administration of each test substance and at 10-min intervals for 120 min thereafter.

REFERENCES AND FURTHER READING

Gully D, Fréhel D, Marcy C, Spinazzé A, Lespy L, Neliat G, Maffrand JP, LeFur G (1993) Peripheral biological activity of SR 27897: a new potent non-peptide antagonist of CCK_A receptors. Eur J Pharmacol 232:13–19

Litvinchuk MD (1976) Rapid method for standardization cholagogues in mice. Byul Eksp Biol Med 82:889–890

Makovec FL, Revel L, Rovati L, Setnikar I (1986) *In vivo* spasmodic activity on the gall bladder of the mouse of new glutamic acid derivatives with CCK antagonistic activity. Gastroenterol 90:1531–1535

Sterczer A, Voros K, Karsal F (1996) Effect of cholagogues on the volume of the gallbladder of dogs. Res Vet Sci 60:44–47

J.6.1.2 Choleretic Activity in Rats

PURPOSE AND RATIONALE

In contrast to other animals, rats do not possess a bile bladder. Therefore, cannulation of the bile duct in rats can be used as a suitable model to measure choleresis, i. e. bile production.

PROCEDURE

Male rats (e. g. Sprague-Dawley strain) weighing 300–500 g are used. Food, but not water, is withdrawn 18 h prior to the experiment. The animals are anesthetized with 5 ml/kg 25% urethane solution. The trachea is cannulated and the abdomen opened by a midline incision. The pylorus is ligated and the bile duct cannulated from the duodenum with a thin (0.05 mm diameter) polyethylene catheter which is pushed up to the liver. The secreted bile volume is measured for 30 min intervals and then the bile is returned to the duodenum. After a preperiod of 60 min, the test substances are administered subcutaneously or intraduodenally. The bile volume is registered in 30 min intervals for 2 h.

EVALUATION

The average values of the post-drug periods are compared with the pre-drug readings.

MODIFICATIONS OF THE METHOD

Several authors tested the choleretic activity of plant extracts and essential oils (De la Puerta et al. 1993; Peana et al. 1994; Trabace et al. 1994) and of synthetic compounds (Grella et al. 1992; Paglietti et al. 1994) in rats.

Tripodi et al. (1993) investigated the anticholelithogenic and choleretic activities of taurohyodeoxycholic acid by measurement of biliary flow and biliary solids content in rats.

Bouchard et al. (1993) induced cholestasis in rats by treatment with 17-α-ethinyl estradiol and studied the influence of oral treatment with ursodeoxycholic and tauroursodeoxycholic acids.

Vahlensieck et al. (1995) studied the effect of *Chelidonium majus* herb extract on choleresis in the isolated perfused rat liver.

Miki et al. (1993) investigated the metabolism and the choleretic activity of homochenodeoxycholic acid in **hamsters** with bile fistula.

Pesson et al. (1959) recommended the**guinea pig** as the best choice among the common laboratory animals to study choleretic agents.

Cohen et al. (1992) reported a study in male **black-tailed prairie dogs** (*Cynomys ludovicianus*) weighing 1.0 ± 0.2 kg anesthetized with 20 mg/kg xylazine i.m. and 20 min later with 100 mg/kg ketamine i.m. Through an abdominal incision, the cystic duct is ligated, and gallbladder bile is aspirated. A PE-

50 polyethylene cannula is inserted into the common bile duct and secured with silk sutures, thereby completely diverting bile flow for collection. The bile duct cannula is externalized, the abdominal incision closed, and the prairie dog placed in a restraining cage with access to food and water.

Matsumura et al. (1996) analyzed hypercholeresis in **dogs** with pigment gallstones after cholate infusion.

REFERENCES AND FURTHER READING

Bouchard G, Yousef IM, Tuchweber B (1993) Influence of oral treatment with ursodeoxycholic and tauroursodeoxycholic acids on estrogen induced cholestasis in rats: Effects on bile formation and liver plasma membranes. Liver 13:193–202

Cohen DE, Leighton LS, Carey MC (1992) Bile salt hydrophobicity controls vesicle secretion rates and transformation in native bile. Am J Physiol Gastrointest Liver 263:G386–G395

De la Puerta R, Saenz MT, Garcia MD (1993) Choleretic effect of the essential oil from Helichrysum picardi Boiss. and Reuter in rats. Phytother Res 7:376–377

Grella G, Paglietti G, Sparatore F, Satta M, Manca P, Peana A (1992) Synthesis and choleretic activity of 3-[2-(3-R', 4-R", 5-R"'-benzyl)-5-R-benzimidazol-1-yl]butanoic acids. Farmaco 47:21–35

Matsumura JS, Neri K, Rege RV (1996) Hypercholeresis with cholate infusion in dogs with pigment gallstones. Dig Dis Sci 41:272–281

Miki S, Cohen BI, Mikami T, Mosbach EH (1993) Metabolism and choleretic activity of homochenodeoxycholic acid in the hamster. J Lipid Res 34:915–921

Pesson M, Salle J, Auffret C (1959) Activités cholérétique et cholagogue des dérivés del l'acide cinnamique et de l'acide a-phénylcinnamique. Arch Int Pharmacodyn 119:443–482

Roda A, Aldini R, Grigolo B, Simoni P, Roda E, Pellicciari R, Lenzi PL, Natalini B (1988) 23-Methyl-3a,7b-dihydroxy-5b-cholan-24-oic acid: Dose-response study of biliary secretion in rat. Hepatol 8:1571–1576

Paglietti G, Sanna P, Carta A, Sparatore F, Vazzana I, Peana A, Satta M (1994) Choleretic activity of 3-[ring substituted benzotriazol-1(2)yl]alkanoic and alkenoic acids. Farmaco 49:693–702

Peana A, Satta M, Luigi-Moretti MD, Orecchioni M (1994) A study on choleretic activity of Salvia desoleana essential oil. Planta Med 60:478–479

Trabace L, Avato P, Mazzoccoli M, Siro-Brigiani G (1994) Choleretic activity of Thapsia chem I, II and III in rats: Comparison with terpenoid constituents and peppermint oil. Phytother Res 8:305–307

Tripodi AS, Contos S, Germogli R (1993) Pharmacological studies on taurohyodeoxycholic acid. Arzneim Forsch/Drug Res 43:877–887

Vahlensieck U, Hahn R, Winterhoff H, Gumbinger GH, Nahrstedt A, Kemper FH (1995) The effect of Chelidonium majus herb extract on choleresis in the isolated perfused rat liver. Planta Med 61:267–271

J.6.1.3 Chronic Bile Fistula in Rats

PURPOSE AND RATIONALE

Most of the techniques for collection of bile in rats use restrained or anesthetized animals. Such factors as well as the surgical intervention itself may profoundly influence the results. Therefore, Remie et al. (1990, 1991) developed a technique for a permanent double bile fistula in rats. The procedure is described in detail.

PROCEDURE

Preparation of Cannulae

Cannulae are made of silicon rubber. The proximal bile cannula, which will be inserted into the common bile duct in the direction to the liver, is 18 cm long (Silastic tubing, Dow Corning, no. 605–135; 0.51 i.d. and 0.94 o.d.) and has one square cut and one bevelled end. Two silicon rings are wrapped around the cannula at 7 mm and 50 mm, respectively, from the bevelled end.

The distal bile cannula, which will be inserted into the common bile duct in the direction of the gut, is made of the same material, is also 18 cm long and has one square cut and one bevelled end. This cannula, however must have a smaller tip-diameter (Silastic tubing, Dow Corning, no. 605–105: 0.31 i.d. and 0.64 o.d.). To serve this purpose, the square cut end of the cannula is immersed in ether, causing the tubing to dilate. When the tubing is wide enough, a 13 mm piece of small diameter Silastic tubing is inserted. Subsequently, two silicon rings are wrapped around the cannula, one at the joint of the two tubes and the other 5 cm from the tip. The tip in then cut at a 45° angle, 7 mm from the first silicon ring.

The duodenal cannula (Silastic tubing, Dow Corning, no. 605–135) is also 18 cm long, and has one square and one bevelled end. An additional ring is placed 30 mm from the tip. Before the cannulae are fixed to the skull, they must be connected to a stainless steel needle bent in a 90° angle.

Anesthesia

The animal is anesthetized with halothane/N_2O/O_2.

Preparation of the Crown of the Head

The head of the animal is shaved and disinfected. An incision of about 1 cm is made and the bregma exposed. Three stainless steel screws (1.0 × 4.2 mm) are mounted in the crown, two in the left and one on the right side of the bregma. The screws are tightened that approximately 2 mm is left between the skull and the head of the screws.

Double Cannulation of the Bile Duct

The abdominal wall is shaved and disinfected and the animal secured on the operation board with adhesive tape. A midline incision is made from the level of the

pubic bones to the xyphoid cartilage. The abdomen is then opened by making an incision over the linea alba towards the sternum up to the distal part of the fourth sternebra, thus exposing the xiphoid cartilage.

Then, the intestines are lifted out and are laid next to the animal on moistened gauze. Using jewelers forceps, the bile duct is stripped off its surrounding tissue and ligated with a 7–0 suture. The duct is placed under tension with an artery forceps for cannulation. With the aid of a microscope, a V-shaped hole is made just cranial of the first ligature with iridectomy scissors. The sterile proximal cannula is inserted into the duct. The second ligature is tied and pulled tight ensuring that the cannula is not obstructed. The bile is now flowing into the cannula. The first ligature is released and the threads are tied behind the silicon ring. The rat is then turned and the ligature reclamped, thereby putting the distal part of the duct under tension. A third ligature is loosely introduced around the duct, distal to the first ligature. Another V-shaped aperture is made between the first and third ligature for insertion of the distal bile cannula. The third ligature is tied and pulled tight. The first ligature is released from the artery forceps and tied around the second cannula behind the silicon ring. All the loose threats are cut close to the knots. The sections of the cannulae which lie between the silicon rings are placed kink-free in the abdominal cavity. The cannulae are fixed using 7–0 silk suture to the abdominal muscle near the xiphoid cartilage.

Cannulation of the Duodenum

After location of the place where the bile duct enters the duodenum (sphincter of Oddi), a four fine-stitch purse-string suture (7–0) is made in the wall of the duodenum at the outer border at about 1 cm proximal to the sphincter. Using a 20G needle, an incision is made inside the purse string. The cannula is inserted into the duodenum until the first, smaller silicon ring has entered the lumen, and the purse string is tightened between the first and the second ring. This cannula together with the bile cannula is placed kink-free in the abdominal cavity and anchored to the internal muscle.

The abdomen is closed of resorbable sutures leaving 1 cm of the skin unclosed.

Subcutaneous Tunneling and Anchoring of the Cannulae

>From the back of the neck, a slender needle holder is pushed subcutaneously through the connective tissue in caudal direction as near as possible to the skin down to the xiphoid cartilage. The cannulae are then grasped and pulled through to emerge at the crown of the head. The abdominal wall is closed completely.

With a 5 cm piece of polyethylene tubing (0.75 × 1.45 mm), the two long ends of the L-shaped stainless steel adapters are connected and the short ends inserted into the respective cannulae. The cannulae together with the tubing are fixed to the skull with acrylic glue flowing under the heads of the screws.

Postoperative Care

The animals are allowed to recover in a warm and quiet place. They reach usually preoperative weight within 2–3 days, and display normal feeding and drinking behavior. Supplementation with saline besides the normal tap water may be necessary.

Collection of Bile

The animals are housed in individual metabolic cages. For bile collection, they are attached to long swiveled PE-cannulae (0.75 × 1.45 mm). A stainless steel coil is used to protect the rats from gnawing on the tubing. For continuous collection of bile, the cannula can be connected to a fraction collector.

CRITICAL ASSESSMENT OF THE METHOD

Among other applications, the method is suited to study the enterohepatic circulation of compounds.

MODIFICATIONS OF THE METHOD

Castilho et al. (1990) studied the intestinal mucosal cholesterol synthesis in rats using a chronic bile duct-ureter fistula model. Male Wistar rats weighing 300–350 g were anesthetized with 50 mg/kg pentobarbital i.p. and submitted to a bile duct-right ureter fistula utilizing a PE-50 catheter after a right-kidney nephrectomy.

REFERENCES AND FURTHER READING

Castilho LN, Sipahi AM, Bettarello A, Quintão ECR (1990) Bile acids do not regulate the intestinal mucosal cholesterol synthesis: Studies in the chronic bile duct-ureter fistula rat model. Digestion 45:147–152

Duane WC, Gilberstadt ML, Wiegand DM (1979) Diurnal rhythms of bile acid production in the rat. Am J Physiol 236:R175–R179

Gebhard RL, Prigge WF (1992) Thyroid hormone differentially augments biliary sterol secretion in the rat. II. The chronic bile fistula model. J Lipid Res 33:1467–1473

Pandak WM, Vlahcevic ZR, Heuman DM, Hylemon PB (1990) Regulation of bile acid synthesis. V. Inhibition of conversion of 7-dehydrocholesterol to cholesterol is associated with down-regulation of cholesterol 7a-hydoxylase activity and inhibition of bile acid synthesis. J Lipid Res 31:2149–2158

Remie R, Rensema JW, van Wunnik GHJ, van Dongen JJ (1990) Permanent double bile fistula (with intact enterohepatic circulation). In: van Dongen JJ, Remie R, Rensema JW, van

Wunnik GHJ (eds) Manual of microsurgery on the laboratory rat. Vol I, Elsevier, Amsterdam, pp 201–212
Remie R, Rensema JW, Havinga R, Kuipers F (1991) The permanent bile fistula rat model. Progr Pharmacol Clin Pharmacol 8:127–145

J.6.1.4 Chronic Bile Fistula in Dogs

PURPOSE AND RATIONALE

Herrera et al. (1968) described a special cannula which can be used to obtain bile or pancreatic juice from a duodenal pouch after appropriate surgical procedures.

PROCEDURE

Male Beagle dogs weighing 15–20 kg are used. The abdomen is opened through a midline epigastric incision under barbiturate anesthesia. The duodenum is mobilized at the pyloric and jejunal ends, and a 5-cm duodenal segment containing the common bile duct is isolated. The distal stoma of the duodenum is closed and continuity restored by end-to-side duodenojejunostomy. The duodenal pouch is closed at both ends.

The cannula to be inserted is made of stainless steel and consists of 3 parts. The main casement measures 10.5 cm in length, with an external diameter of 1.0 cm. The internal end is flanged, and 1.5 cm from this point there is a short lateral limb, also 1.5 cm in length. The lateral limb is also flanged but, in addition, possesses a small V-shaped defect to facilitate insertion into the pouch. When not in use, the cannula is sealed from the exterior by inserting a threaded plug which allows bile to enter the duodenum in the normal manner. For collection of bile this plug is removed and a long obturator is inserted. The latter effectively isolates the bile secretion from duodenal contents. A similar hollow obturator is reserved for use when duodenal perfusion is studied, the obturator being connected via a plastic tube to the irrigating fluid.

Through a small antimesenteric incision in the duodenal pouch, the lateral limb of the cannula is inserted; the V-shaped defect in the flange facilitates entry into the pouch. A purse string secures the cannula in position. The defunctioned loop of duodenum is then brought anterior to the pancreas, and the remaining limb of the cannula inserted through a small duodenotomy and secured by a further purse-string suture. The whole system is then generously wrapped in omentum and the cannula exteriorized through a stab incision toward the flank. An external collar stabilizes the cannula. The cannula is left open to drain blood and secretions for 24 h postoperatively, after which time the plug is inserted. Physiologic saline is administered subcutaneously for a period of 3 days, after which the animals are permitted to drink water. Daily checks of the cannula are advisable to ensure that the plug remains tight. The animals receive normal kennel food and water ad libitum.

The dogs are allowed at least 4 weeks to recover. Eighteen hours prior to the experiment food is withdrawn but water allowed ad libitum. The long hollow obturator is inserted and bile collected for 15 min periods. After 1 h pretest time, the test compound is given either orally or intravenously.

EVALUATION

Secretion of bile is measured at 15 min intervals and volume and bile contents are determined from 1 ml samples. The values are compared with pretest data. The remaining bile is re-infused into the duodenum via the hollow obturator.

MODIFICATIONS OF THE METHOD

Boldyreff (1925) described several techniques for fistulae of the gall bladder and also for the fistula of the ductus choledochus in dogs.

An abdominal incision about 10 cm is made on the median line. The duodenum is pulled out and the orifice of the large (first) pancreatic duct is found. The orifice of the ductus choledochus with the orifice of the small (second) pancreatic duct is situated on the other side of the intestine some 2 or 3 cm nearer the stomach. The ductus choledochus goes straight from the gallbladder to the duodenum; further it lies parallel to is and at its end it is attached to the wall of the duodenum. The small pancreatic duct goes from the gland straight to the duodenum.

At the very beginning of the operation it is useful to cut the ligamentum that goes from the liver to the duodenum, because this facilitates orientation and operating. It is necessary to cut out a piece of the intestinal wall with the orifice of the ductus choledochus. But before this one must prepare off a little bit the intestine from the pancreas so as to be able to close conveniently and securely the hole in the intestine and divide between double ligatures the second pancreatic duct.

On the duodenum around the orifice of the ductus choledochus an incomplete oval figure is now marked with a knife, so that the duct enters this figure through the incomplete part of the oval and has its orifice in the middle of this figure. The length of the oval is about 1.5 cm and its width 1 cm. A suture is then made on the edge of this oval, which is cut out not completely but

leaving a small bridge about 0.5 cm wide between the intestine and the oval; through the bridge the duct enters the oval. The mucosa of this bridge must be completely destroyed with a knife.

The oval piece of the intestine is now turned with the mucosa up and its serosa is sutured to the serosa of the intestine The hole in the intestine is very carefully closed with two layers of sutures. Two heavy threads are then passed underneath the intestine on either side of the place of operation; they are laid through the abdominal wall and tied after the operation is over. They serve as temporary supporting sutures. The oval piece of the intestine is now sutured with the skin of the abdominal wound and the wound is closed in the usual manner. The supporting sutures must be taken out one day or two days after the operation.

REFERENCES AND FURTHER READING

Boldyreff WN (1925) Surgical method in the physiology of digestion. Description of the most important operations on digestive system. Ergebn Physiol 24:399–444

Herrera F, Kemp DR, Tsukamoto M, Woodward ER, Dragstedt LR (1968) A new cannula for the study of pancreatic function. J Appl Physiol 25:207–209

J.6.1.5 Prevention of Experimental Cholelithiasis

PURPOSE AND RATIONALE

Several animal species develop gallstones, either spontaneously or induced by diet, such as **tupaias** (Schwaier 1979; Schwaier et al. 1979), **ground squirrels** (Fridhandler et al. 1983; MacPherson et al. 1987; MacPherson and Pemsingh 1997), **hamsters** (Holzbach 1984; Cohen et al. 1995) and **owl monkeys** (Pekow et al. 1995).

The **prairie dog** (*Cynomys ludovicianus*) is the animal model that has been used most extensively to study diet-induced cholesterol gallstone formation and the inhibition thereof (Holzbach 1984; Conter et al. 1986; Matoba et al. 1989; Cohen et al. 1990; Broughton et al. 1991; Afdhal et al. 1993; Kam et al. 1996).

Davis et al. (2003) and Saunders et al. (1991) studied the use of statins for the prevention of gallstones in cholesterol-fed prairie dogs.

PROCEDURE

Wild-caught male prairie dogs weighing about 1 kg were kept in quarantine for 3 weeks and fed normal rodent chow. Then the diet was changed to a lithogenic diet consisting of a 1.2% cholesterol formulation for the study period of 28 days. Medication (drug or placebo) was applied through a gastric tube under slight sedation twice a day. Blood chemistry analysis for total cholesterol and triglycerides was performed on study days 0, 14, and 28.

At the completion of the study period, all animals were placed under general anesthesia and underwent an open cholecystectomy. A subcostal incision was made in the right upper quadrant, and the gallbladder removed using clips on the cystic duct. The gallbladder was then opened and visually inspected for gallstones. Bile from the gall bladder was the aspirated for microscopic analysis.

A sample of bile of each animal was examined using light microscopy to determine the presence of cholesterol crystals.

EVALUATION

Statistical analysis was performed using Student's *t*-test for cholesterol and triglyceride data. The Fisher exact test was utilized for analysis of gallstone and cholesterol crystal formation data.

MODIFICATIONS OF THE METHOD

Chapman et al. (1998) established and characterized primary gallbladder epithelial cell cultures in the prairie dog.

Chen et al. (1999) studied biliary sludge and pigmented stone formation in bile duct-ligated guinea pigs.

Stone et al. (1987) developed a rat model to explain the ciclosporin-induced cholestasis observed in transplantation patients.

REFERENCES AND FURTHER READING

Afdhal NH, Gong D, Niu N, Turner B, LaMont JT, Offner GT (1993) Cholesterol cholelithiais in the prairie dog. Role of mucin and nonmucin glycoproteins. Hepatology 17:693–700

Broughton G, Tseng A, Fitzgibbons R, Tyndall S, Stanislav G, Rongone EL (1991) The prevention of cholelithiasis with infused sodium chenodeoxycholate in the prairie dog (*Cynomys ludovicianus*). Comp Biochem Physiol A 99:609–613

Chapman WC, Fisk J, Schot D, Debelak JP, Washington MK, Bluth RF, Pierce D, Williams RF (1998) Establishment and characterization of primary gallbladder epithelial cell cultures in the prairie dog. J Surg Res 80:35–43

Chen CY, Shiesh SC, Lin XZ (1999) Biliary sludge and pigmented stone formation in bile duct-ligated guinea pigs. Dig Dis Sci 44:203–209

Cohen BI, Mosbach EH, Matoba N, Suh SO, McSherry CK (1990) The effect of alfalfa-corn diets on cholesterol metabolism and gallstones in prairie dogs. Lipids 25:143–148

Cohen BI, Mikami T, Ayyad N, Ohshima A, Infante R, Mosbach EH (1995) Hydrophilic bile acids: prevention and dissolution experiments in two animal models of cholesterol cholelithiasis. Lipids 30:855–861

Conter RL, Roslyn J, Pitt HA, DenBesten L (1986) Carbohydrate diet-induced calcium bilirubinate sludge and pigment gall stones in the prairie dog. J Surg Res 40:580–587
Davis KG, Wertin TM, Schriver JP (2003) The use of simvastatin for the prevention of gallstones in the lithogenic prairie dog model. Obes Surg 13:865–868
Fridhandler TM, Davison JS, Shaffer EA (1983) Defective gallbladder contractility in the ground squirrel and prairie dog during early stages of cholesterol gallstone formation. Gastroenterology 85:830–836
Holzbach RT (1984) Animal models of cholesterol gallstone disease. Hepatology 4 [Suppl 5]:191S–198S
Kam DM, Webb PA, Sandman G, Chugh A, Vertz Ma, Scheeres DE (1996) A novel 5-lipoxygenase inhibitor prevents gallstone formation in a lithogenic prairie dog model. Am Surg 62:551–556
MacPherson BR, Pemsingh RS, Scott GW (1987) Experimental cholelithiasis in the ground squirrel. Lab Invest 56:138–145
MacPherson BR, Pemsingh RS (1997) Ground squirrel model for cholelithiasis: role of epithelial glycoproteins. Microsc Res Tech 3:39–55
Matoba N, Cohen BI, Mosbach EH, Stenger RJ, Kuroki S, Une M, McSherry CK (1989) 7-Methyl bile acids: effects of chenodeoxycholic acid, cholic acid, and their 7-α-methyl analogues on the formation of cholesterol gallstones in the prairie dog. Gastroenterology 96:178–185
Pekow CA, Weller RE, Schulte SJ, Lee SP (1995) Dietary induction of cholesterol gallstones in the owl monkey: preliminary findings in a new animal model. Lab Anim Sci 45:657–662
Saunders KD, Cates JA, Abedin MZ, Rege S, Festekdjian SF, Howard W, Roslyn JJ (1991) Lovostatin inhibits gallstone formation in the cholesterol-fed prairie dog. Ann Surg 214:149–154
Schwaier A (1979) Tupaias (tree shrews) – a new animal model for gallstone research. I. First observation of gallstones. Res Exp Med (Berl) 176:15–24
Schwaier A, Weis HJ, van der Linden J (1979) Tupaias (tree shrews) – a new animal model for gallstone research. II. Influence of fat, sugar, and cholesterol on bile composition. Exp Med (Berl) 176:157–172
Stone BG, Udani M, Sanghvi A, Warty V, Plocki K, Bedetti CD, Van Thiel DH (1987) Cyclosporin-A-induced cholestasis. The mechanism in a rat model. Gastroenterology 93:344–351

J.6.2 Gall Bladder Motility

J.6.2.1 Activity on Isolated Gall-Bladder Strips from Guinea Pigs

PURPOSE AND RATIONALE

Effects on the smooth musculature of the gall bladder can be studied in isolated strips of gall bladder from guinea pigs or cats (Chowdhury et al. 1975; Fara and Erde 1978; Cabrini et al. 1995).

PROCEDURE

Guinea pigs of either sex weighing approximately 400 g are anesthetized with 3 g/kg urethane i.p. The gall bladder is removed and cut into longitudinal strips 10×3 mm. The strips are suspended in a Krebs solution bath between a stationary hook and an isometric strain gauge. Tension is recorded on a polygraph. The bath is maintained at 37°C and aerated with a gas mixture of 95% O_2 and 5% CO_2. After a half-hour stabilization period, test doses of acetylcholine (1 mg/ml) are added to determine viability of the preparation. Dose-response curves for the muscle strips are obtained by introducing one dose of the stimulating agent and waiting until the maximal response to that dose is reached (usually 5–15 min). The bath is then rinsed three times and 15 min allowed before a new dose is tested.

EVALUATION

Concentrations for the maximal response and ED_{50} values are calculated.

MODIFICATIONS OF THE METHOD

Eltze et al. (1997) found that contractions of the isolated guinea-pig gallbladder elicited by muscarinic stimuli are mediated by functional muscarinic M_3 receptors.

REFERENCES AND FURTHER READING

Cabrini DA, Silva AM, Calixto JB (1995) Mechanisms of bradykinin-induced contraction of the guinea-pig gall bladder *in vitro*. Br J Pharmacol 114:1549–1556
Chowdhury JR, Berkowitz JM, Praissman M, Fara JW (1975) Interaction between octapeptide-cholecystokinin, gastrin, and secretin on cat gall bladder *in vitro*. Am J Physiol 229:1311–1315
Eltze M, König H, Ullrich B, Grebe T (1997) Contraction of guinea-pig gallbladder: Muscarinic M_3 or M_4 receptors? Eur J Pharmacol 332:77–87
Fara JW, Erde SM (1978) Comparison of *in vivo* and *in vitro* responses to sulfated and non-sulfated ceruletide. Eur J Pharmacol 47:359–363

J.6.2.2 Gallbladder Motility in Dogs

PURPOSE AND RATIONALE

Gall bladder motility can be measured in anesthetized dogs with intraluminal manometry.

PROCEDURE

Beagle dogs weighing 15–18 kg are fasted for 16 h prior to the experiment. Median laparotomy is performed under pentobarbital anesthesia (25 mg/kg i.v.). An incision is made in the bile bladder and a 2 mm diameter polyethylene catheter introduced. The catheter is advanced as far as possible to the neck of the gall bladder and tied. The pressure in the interior of the gall

bladder is recorded on a pen recorder via a Statham pressure transducer (P 23 BB) and a frequency measuring bridge.

EVALUATION

Cholecystokinin increases dose-dependent the intraluminal pressure. The preparation can be used for evaluation of cholecystokinin or cholecystokinin-like activity.

MODIFICATIONS OF THE METHOD

Ryan and Cohen (1976) used adult opossums (*Didelphis viginiana*) of either sex, weighing 2.5–3.0 kg.

REFERENCES AND FURTHER READING

Ryan J, Cohen S (1976) Gallbladder pressure-volume response to gastrointestinal hormones. Am J Physiol 230:1461–1465

J.6.2.3 Cholecystokinin Activity (Isolated Gallbladder or Intestine)

PURPOSE AND RATIONALE

A sensitive bioassay for cholecystokinin utilizing strips of rabbit gall bladder has been described by Amer and Becvar (1969). Segments of ileum and colon have been used by Paton and Zar (1968) and by Zetler (1984).

PROCEDURE

Male albino rabbits weighing 1.5–2.5 kg are fasted 18 h prior to the experiment. The animals are sacrificed by cervical dislocation and the liver is quickly dissected out. The gallbladder is teased away from the liver and immediately placed in Locke-Ringer solution. The biliary contents are emptied and the gall bladder is cut spirally (right-handed spiral starting from the bile duct) into a strip of muscle tissue 30–40 mm in length and about 5 mm wide. The muscle strip is placed in an organ bath containing Locke-Ringer solution at 37°C continuously bubbled with carbogen. The initial tension of the muscle is adjusted to 0.5 g. The bath fluid is changed every 30 min. The test compound and the standard (range 5–20 mIDU (Ivy dog units) are added alternatively. The maximum of contractions is usually reached after 5 min. Then, the bath fluid is changed. The next dose is applied when the tension has achieved again the starting value.

EVALUATION

The maximum of contraction is taken as endpoint. Using at least two doses of test compound and standard, parallel line assays can be carried out and potencies ratios can be calculated.

CRITICAL ASSESSMENT OF THE METHOD

This bioassay has the advantage to be sensitive and less time consuming than *in vivo* assays, such as measuring gall bladder motility in the anesthetized dog (see J.6.2.2). However, the assay is not specific for cholecystokinin, since also gastrin and gastrin analogues cause contractions of the isolated bile bladder. This assay allows also to calculate potency ratios of different gastrin analogues.

MODIFICATIONS OF THE METHOD

The whole gallbladder of the mouse or a strip of guinea pig gallbladder is used for evaluation of cholecystokinin-like peptides, ceruletide, ceruletide analogues, and cholecystokinin octapeptide by Zetler (1979, 1984)

Paton and Zar (1968), Zetler (1984), Chang and Lotti (1986), Barthol and Holzer (1987) used isolated segments of ileum and colon from guinea pigs for determination of CCK-like activity.

Makovec et al. (1986), Tachibana et al. (1996) studied the *in vivo* activity of derivatives of CCK in emptying the gallbladder in mice.

Henke et al. (1997) tested CCK-A agonists in the isolated guinea pig gall bladder.

Singh et al. (1995) used gall bladder strips from guinea pigs to evaluate CCK receptor antagonists.

Fukamizu et al. (1998) tested the effect of a cholecystokinin-A receptor antagonist against CCK-8 induced contractions in isolated smooth muscle fibers of gall bladders and longitudinal fibers of ileum from guinea pigs.

REFERENCES AND FURTHER READING

Amer MS, Becvar WE (1969) A sensitive*in vitro* method for the assay of cholecystokinin. J Endocrin 43:637–642

Barthol L, Holzer P (1987) Evaluation of a new and potent cholecystokinin antagonist on motor response of the guinea pig intestine. Br J Pharmacol 90:753–761

Chang RS, Lotti VJ (1984) Biochemical and pharmacological characterization of an extremely potent and selective nonpeptide cholecystokinin antagonist. Proc Natl Acad Sci, USA, 83:4923–4926

Fara JW, Erde SM (1978) Comparison of *in vivo* and *in vitro* responses to sulfated and non-sulfated ceruletide. Eur J Pharmacol 47:359–363

Fukamizu Y, Nakajima T, Kimura K, Kanda H, Fujii M, Saito T, Kasai H (1998) Biochemical and pharmacological profile of Loxiglumide, a novel cholecystokinin-A antagonist. Arzneim Forsch/Drug Res 48:58–64

Henke BR, Aquino CJ, Birkemo LS, Croom DK, Dougherty RW Jr, Ervin GN, Grizzle MK, Hirst GC, James MK, Johnson MF, Queen KL, Sherill RG, Sugg EE, Suh EM,

Szewczyk JW, Unwalla RJ, Yingling J, Wilson TM (1997) Optimization of 3-(1H-indazol-3-ylmethyl)-1,5-benzodiazepines as potent, orally active CCK-A agonists. J Med Chem 40:2706–2725

Makovec F, Revel L, Rovati L, Setnikar I (1986) *In vivo* antispasmotic activity on the gall bladder of the mouse of new glutamic acid derivatives with CCK-antagonistic activity. Gastroenterology 90:1531

Paton WDM, Zar MA (1968) The origin of acetylcholine released from guinea-pig intestine and longitudinal muscle strips. J Physiol (London) 194:13–33

Singh L, Field MJ, Hill DR, Horwell DC, McKnight AT, Roberts E, Tang KW, Woodruff GN (1995) Peptoid CCK receptor antagonists: pharmacological evaluation of CCK_A, CCK_B and mixed $CCK_{A/B}$ receptor antagonists. Eur J Pharmacol 286:185–191

Tachibana I, Kanagawa K, Yamamoto Y, Otsuki M (1996) Pharmacological profile of a new serine derivative cholecystokinin receptor antagonist TP-680 on pancreatic, biliary and gastric function. J Pharmacol Exp Ther 279:1404–1412

Zetler G (1984) Ceruletide, ceruletide analogues and cholecystokinin octapeptide (CCK-8): Effects on isolated intestinal preparations and gallbladders of guinea pigs and mice. Peptides 5:729–736

Zetler G, Cannon D, Powell D, Skrabanek P, Vanderhaeghen JJ (1979) A cholecystokinin-like peptide in crude substance P from human and bovine brain. Arch intern Pharmacodyn 238:128–141

J.6.3 Sphincter Oddi Function

J.6.3.1 Relaxation of Sphincter of Oddi In Vitro

PURPOSE AND RATIONALE

The integrity of the relaxation function the sphincter of Oddi is a prerequisite for normal delivery of bile into the duodenum. Sphincter of Oddi relaxation is mainly executed by non-adrenergic, non-cholinergic (NANC) nerves that are essentially nitrergic in several species including guinea pigs (Pauletzki et al. 1993) and rabbits (Lonovics et al. 1994).

PROCEDURE

Biliary sphincter of Oddi muscle rings of approximately 6 mm length from adult male New Zealand white rabbits weighing form 3500–4000 g pretreated with various drugs or diet are prepared. The papilla Vater is eliminated and the ampullary part of the muscle rings of approximately 3 mm length are mounted horizontally on two small L-shaped glass hooks one of which is connected to a force transducer attached to a polygraph for measurement and recording of isometric tension. The experiments are carried out in an organ bath (5 ml) containing Krebs bicarbonate buffer which is maintained at 37°C and aerated continuously with carbogen. The initial tension is set at 10 mN and the rings are allowed to equilibrate over 1 h during which period the sphincters develop characteristic 14–19 per min rhythmic contractions. Atropine (1 μM) and guanethidine (4 μM) are continuously present (NANC solution). Changes in isometric tension in response to two consecutive trains of impulses of electrical field stimulation (40 stimuli, 50 V, 0.1 ms and 20 Hz) are then studied.

EVALUATION

The data representing changes in isometric tension expressed as means ± standard deviation are evaluated by means of analysis of variance (ANOVA) followed by a modified Student's *t*-test for multiple comparisons according to Bonferroni's method. Changes are considered statistically significant at P-values smaller than 0.05.

MODIFICATIONS OF THE METHOD

In addition to studies with the isolated sphincter of Oddi of rabbits (Slivka et al. 1994; Sari et al. 1998; Jia and Stamler 1999) and guinea pigs (Harrington et al. 1992; Gocer et al. 1995; Lu et al. 1997), several pharmacological studies were reported with the isolated sphincter of Oddi of **opossum** (Perodi et al. 1990; Allescher et al. 1993), and of the **Australian brush-tailed possum** (*Trichosurus vulpecula*) (Baker et al. 1992, 1996).

REFERENCES AND FURTHER READING

Allescher HD, Daniel EE, Classen M (1993) Nitric oxide as putative nonadrenergic noncholinergic inhibitory transmitter in the opossum sphincter of Oddi. Can J Physiol Pharmacol 71:525–530

Baker RA, Saccone GTP, Costi D, Thune A, Toouli J (1992) Motilin and erythromycin enhance the *in vitro* contractile activity of the sphincter of Oddi of the Australian brush-tailed possum. Naunyn-Schmiedeberg's Arch Pharmacol 345:71–77

Baker RA, Wilson TC, Padbury RTA, Toouli J, Saccone GTP (1996) Galanin modulates sphincter of Oddi function in the Australian brush-tailed possum. Peptides 17:933–941

Gocer F, Yaris E, Tuncer M, Kayaalp SO (1995) Effect of vasodilators on the rhythmic contractions of guinea-pig isolated sphincter of Oddi. Arzneim Forsch/Drug Res 45:809–812

Harringtom K, Bomzon A, Sharkey KA, Davison JS, Shaffer EA (1992) Differential sensitivities of the sphincter Oddi and gallbladder to cholecystokinin in the guinea pig: Their role in transsphincteric bile flow. Can J Physiol Pharmacol 70:1336–1341

Jia L, Stamler JS (1999) Dual actions of S-nitrosylated derivative of vasoactive intestinal peptide as a vasoactive intestinal peptide-like mediator and a nitric oxide carrier. Eur J Pharmacol 366:79–86

Lonovics J, Jacab I, Szilvássy J, Szilvássy Z (1994) Regional differences in nitric oxide-mediated relaxation in the rabbit sphincter of Oddi. Eur J Pharmacol 255:117–122

Lu XQ, Zhang F, Huang M (1997) Effects of dihydroetorphine hydrochloride on contraction and electric discharge of Oddi' sphincter. Chin J Pharmacol Toxicol 11:275–277
Pauletzki JG, Sharkey KA, Davison JS, Bomzon A, Shaffer EA (1993) Involvement of L-arginine-nitric oxide pathways in the neural relaxation of the sphincter of Oddi. Eur J Pharmacol 232:263–270
Perodi JR, Cho N, Zenilman ME, Barteau JA, Soper NJ, Becker JM (1990) Substance P stimulates the opossum sphincter of Oddi *in vitro*. J Surg Res 49:197–204
Sari R, Szilvássy Z, Jacab I, Nagy I, Lonovics J (1998) Cross tolerance between nitroglycerine and neural relaxation of the rabbit sphincter of Oddi. Pharmacol Res 37:505–512
Slivka A, Chuttani R, Carr-Locke DL, Kobzik L, Bredt DS, Loscalzo J, Stamler JS (1994) Inhibition of sphincter Oddi function by the nitric oxide carrier S-nitroso-N-acetylcystein in rabbits and humans. J Clin Invest 94:1792–1798
Szilvássy Z, Sari R, Nemeth J, Nagy I, Csati S, Lonovics J (1998) Improvement of nitrergic relaxation by farnesol of the sphincter of Oddi from hypercholesterolaemic rabbits. Eur J Pharmacol 353:75–78

J.6.3.2 Function of Sphincter of Oddi In Vivo

PURPOSE AND RATIONALE

Dogs were used for *in vivo* studies of the function of the sphincter of Oddi (Sarles 1986; Pozo et al. 1990; Matsumara et al. 1991; Kobayashi et al. 1994; Wang et al. 1998). Shima et al. (1998) recorded the spontaneous motility and the response to cerulein on the canine sphincter of Oddi using a constant-perfusion technique.

PROCEDURE

Mongrel dogs weighing 7–9 kg fasted overnight are anesthetized with 25 mg/kg intravenous pentobarbital sodium and are maintained under adequate anesthesia with 12.5 mg/kg intravenous pentobarbital sodium as required. Systemic blood pressure is monitored through a catheter placed into the femoral artery. A femoral vein is cannulated and used for systemic administration of Ringer's solution and drugs.

After an upper median laparotomy, a small longitudinal incision is made in the common bile duct. Two catheters (outer diameter 2.0 mm) are cannulated and tied in the bile duct to avoid any leaks and the occlusion of the orifice of the catheters. One is distally placed at 5 mm proximal to the choledochoduodenal junction and is used to perfuse the sphincter of Oddi with saline at a rate of 0.12 ml/min using an infusion pump. The other is proximally placed and used to siphon off the hepatic bile. Pressure changes are recorded on a polygraph through a pressure transducer which is placed between the infusion pump and the catheter.

EVALUATION

To evaluate the effects of intravenously administered drugs on the sphincter of Oddi, a motility index is calculated by measuring the square between the zero line and the trace of the sphincter of Oddi pressure changes per minute.

Results are expressed as means ± SEM; n is the number of independent observations of different animals. The paired and unpaired t-tests are used for statistical analysis. $P < 0.05$ is considered significant.

MODIFICATIONS OF THE METHOD

Thune et al. (1992, 1995) studied simultaneously the flow resistances in the common bile duct and main pancreatic duct sphincters in anesthetized **cats** using a perfusion technique.

Elbrønd et al. (1994) prepared the sphincter of Oddi and duodenum in anesthetized **rabbits** with perfused catheters and bipolar electrodes. Increasing, successive doses of cholecystokinin were administered intravenously every 15th min. The digitized recordings were scored on a computer in control and stimulatory cholecystokinin sequences.

Further studies in **rabbits** were performed by Nakamura (1996), Chiu et al. (1998).

Opossums were used by Calabuig et al. (1990), Hanyu et al. (1990),Cullen et al. (1996), Herrmann et al. (1999) to study the function of the sphincter of Oddi.

Several authors used the **Australian brush-tailed possum** (*Trichosurus vulpecula*) for studies of the function of the sphincter of Oddi *in vivo* (Baker et al. 1990; Saccone et al. 1992; Cox et al. 1998a, b; Huang et al. 1998).

The **prairie dog** was used by several authors to study the function of the sphincter of Oddi (Ahrend et al. 1992; Kaufman et al. 1993; Thierney et al. 1994).

Pasricha et al. (1995) reported a model in **pigs** for endoscopic biliary manometry, similar in technique to the procedure in humans.

REFERENCES AND FURTHER READING

Ahrendt SA, Ahrendt GM, Lillemoe KD, Pitt HA (1992) Effect of octreotide on sphincter of Oddi and gallbladder motility in prairie dogs. Am J Physiol 262 (Gastrointest Liver Physiol 25):G909–G914
Baker RA, Saccone GTP, Toouli J (1990) Cisapride inhibits motility of the sphincter of Oddi in the Australian possum. Dig Dis Sci 35:711–715
Calabuig R, Weems WA, Moody FG (1990) Choledochoduodenal flow: effect of the sphincter of Oddi in opossums and cats. Gastroenterology 99:1641–1646
Chiu JH, Lui WY, Chen YL, Hong CY (1998) Local somatothermal stimulation inhibits the motility of sphincter of Oddi in

cats, rabbits and humans through nitrergic neural release of nitric oxide. Life Sci 63:413–428
Cox MR, Padbury RT, Snellin TL, Schloithe AC, Harvey JR, Toouli J, Saccone GTP (1998a) Gastrin-releasing peptide stimulates gall bladder motility bot not sphincter of Oddi motility in Australian brush-tailed possum. Dig Dis Sci 43:1275–1284
Cox MR, Padbury RT, Harvey JR, Baker RA, Toouli J, Saccone GTP (1998b) Substance P stimulates sphincter of Oddi motility and inhibits trans-sphincteric flow in the Australian brush-tailed possum. Neurogastroenterol Motil 10:165–173
Cullen JJ, Conklin JL, Murray J, Ledlow A, Rosenthal G (1996) Effect of recombinant human hemoglobin on opossum sphincter of Oddi motor function *in vivo* and *in vitro*. Dig Dis Sci 41:289–294
Elbrønd H, østergaard L, Huniche B, Skovgaard Larsen L, Andersen MB (1994) Rabbit sphincter Oddi and duodenal pressure and slow-wave activity. Scand J Gastroenterol 29:537–544
Hanyu N, Dodds WJ, Layman RD, Hogan WJ (1990) Cholecystokinin-induced contraction of opossum sphincter of Oddi. Mechanism of action. Dig Dis Sci 35:567–576
Herrmann BW, Cullen JJ, Ledlow A, Murray JA, Conklin JL (1999) The effect of peroxynitrite on sphincter of Oddi. J Surg Res 81:55–58
Huang J, Padbury RTA, Schloithe AC, Cox MR, Simula ME, Harvey JR, Baker RA, Toouli J, Saccone GTP (1998) Somatostatin stimulates the brush-tailed possum sphincter of Oddi *in vitro* and *in vivo*. Gastroenterology 115:672–679
Kaufman HS, Ahrendt SA, Pitt HA, Lillemoe KD (1993) The effect of erythromycin on motility of the duodenum, sphincter of Oddi, and gallbladder in the prairie dog. Surgery 114:543–548
Kobayashi T, Hosoba T, Mori M, Mimura H, Miyake J, Hamazaki K, Tsuge H, Orita K, Yamasato T, Neya T, Mizutani M, Nakayama S (1994) Effects of gastrectomy on motility, perfusion pressure, and caerulein-induced relaxation of sphincter of Oddi in dogs. Jpn J Smooth Muscle Res 30:85–96
Matsumara T, Yada S, Miyoshi Y, Komi N (1991) Effect of synthetic protease inhibitor on the sphincter of Oddi function in dogs. Jpn J Gastroenterol 88:2663–2670
Nakamura M (1996) Effects of prostaglandins on motility of rabbit sphincters of Oddi *in vivo*. J Osaka City Med Cent 45:29–41
Pasricha PJ, Tietjen TG, Kalloo AN (1995) Biliary manometry in swine: An unique endoscopic model for teaching and research. Endoscopy 27:70–72
Pozo MJ, Salido GM, Madrid JA (1990) Action of cholecystokinin on the dog sphincter of Oddi: Influence of anticholinergic agents. Arch Int Physiol Biochim 98:353–360
Saccone GTP, Liu YF, Thune A, Harvey JR, Baker RA, Toouli J (1992) Erythromycin and motilin stimulate sphincter of Oddi motility and inhibit trans-sphincteric flow in the Australian possum. Naunyn-Schmiedeberg's Arch Pharmacol 346:701–706
Sarles JC (1986) Hormonal control of sphincter of Oddi. Dig Dis Sci 31:208–212
Shima Y, Mori M, Harano M, Tsuge H, Tanak N, Yamazato T (1998) Nitric oxide mediates cerulein-induced relaxation of canine sphincter of Oddi. Dig Dis Sci 43:547–553
Thierney S, Qian Z, Burrow C, Lipsett PA, Pitt HA, Lillemoe KD (1994) Estrogen inhibits sphincter of Oddi motility. J Surg Res 57:69–73
Thune A, Jivegård L, Pollard H, Moreau J, Schwartz JC, Svanvik J (1992) Location of enkephalinase and functional effects of [Leu^5]enkephalin and inhibition of enkephalinase in the feline main pancreatic and bile duct sphincters. Clin Sci 82:169–173
Thune A, Delbro DS, Nilsson B, Friman S, Svanvik J (1995) Role of nitric oxide in motility and secretion of the feline hepatobiliary tract. Scand J Gastroenterol 30:715–720
Wang HJ, Tanaka M, Konomi H, Toma H, Yokohata K, Pasricha PJ, Kalloo AN (1998) Effect of local injection of botulinum toxin on sphincter of Oddi cyclic motility in dogs. Dig Dis Sci 43:694–701

J.7 Pancreatic Function

J.7.0.1 Acute Pancreatic Fistula in Rats

PURPOSE AND RATIONALE

The effect of exogenous hormones, e. g. secretin, or other drugs on pancreas secretion can be measured in rats with acute pancreas fistula.

PROCEDURE

Male Sprague Dawley rats weighing 150–200 g are used. Eighteen hours prior to the experiment food is withdrawn with free access to water. Groups of 4–5 rats are used for each dose of drug evaluation, the control group consists of at least 7 rats. The animals are anesthetized with 5 ml 25% urethane solution i.m. and the is trachea cannulated. The abdomen is opened by a mid-line incision and the pylorus ligated. The proximal part of the bile duct is ligated near the hepatic porta. The bile is drained via a thin polyethylene tube into the duodenum. The distal part of the bile duct with the orifices of pancreatic ducts is cannulated with another thin polyethylene tube. The pancreatic juice is collected in graduated microvessels. After a pre-test period of 60 min, the test compounds are applied intravenously or intraduodenally.

EVALUATION

The secretion after injection of the test compound is compared with the pre-test values. Secretin increases pancreatic secretion volume in a dose-dependent manner. Activity ratios for unknown preparations can be calculated by 2+2 assays in comparison with the international standard.

MODIFICATIONS OF THE METHOD

Guan et al. (1990) inserted two separate cannulae for bile and pancreatic juice to Wistar **rats** under methoxyfluorane anesthesia. Both fluids were returned to the intestine. Placing the rats in modified Bollman-

type restraint cages, experiments could be performed after a few days in conscious animals.

Ito et al. (1994) studied the inhibition of CCK-8-induced pancreatic amylase secretion by a cholecystokinin type-A receptor antagonist in rats.

Niederau et al. (1989) compared the effects of CCK receptor antagonists on rat pancreatic secretion *in vivo*. Output of amylase in pancreatico-biliary secretion was measured after various doses of caerulein. The effects of high caerulein doses were dose-dependent inhibited by CCK-antagonists.

Alvarez and Lopez (1989) studied the effect of alloxan diabetes on exocrine pancreatic secretion in the anesthetized **rabbit**. After a 14–15 h fasting period, but with free access to water, rabbits weighing about 2.0 kg are anesthetized by intravenous injection of 1.0 g/kg urethane. After tracheotomy, a median laparotomy is performed, the main pancreatic duct is exposed and cannulated near its entrance to the duodenum following ligation of the pylorus and cannulation of the bile duct for deviation of bile to the exterior.

Kim et al. (1993) studied the effect of [(CH_2NH) 4,5]secretin on pancreatic exocrine secretion in **guinea pigs** and rats using an acute pancreatic fistula preparation.

Niederau et al. (1990), Tachibana et al. (1996) determined pancreatic exocrine secretion in **mice**. Because the cannulation of mouse pancreatic duct is not possible for technical reasons, the amount of amylase was determined *in vivo*. Five min after i.v. administration of test drugs, mice were sacrificed and a 5 cm-duodenal loop was removed. The duodenal contents were washed out with 1.0 ml ice-cold saline and collected for amylase activity.

REFERENCES AND FURTHER READING

Alphin RS, Lin TM (1959) Effect of feeding and sham feeding on pancreatic secretion of the rat. Am J Physiol 197:260–262

Alvarez C, Lopez MA (1989) The effect of alloxan diabetes on exocrine pancreatic secretion in the anesthetized rabbit. Intern J Pancreatol 5:229–238

Colwell AR (1950) The relation of bile loss to water balance in the rat. Am J Digest Dis 17:270–276

Guan D, Maouyo D, Sarfati P, Morisset J (1990) Effects of SMS 201–995 on basal and stimulated pancreatic secretion in rats. Endocrinology 127:298–304

Ito H, Sogabe H, Nakari T, Sato Y, Tomoi M, Kadowaki M, Matsuo M, Tokoro K, Yoshida K (1994) Pharmacological profile of FK480, a novel cholecystokinin type-A receptor antagonist: comparison with loxiglumide. J Pharmacol Exp Ther 268:571–575

Kim CD, Li P, Lee KY, Coy DH, Chey WY (1993) Effect of [(CH_2NH)4,5]secretin on pancreatic exocrine secretion in guinea pigs and rats. Am J Physiol, Gastrointest Liver Physiol 265:G805–G810

Lin TM, Ivy AC (1957) Relation of secretin to the parasympathetic mechanism for pancreatic secretion. Am J Physiol 187:361–368

Lin TM, Karvinen E, Ivy AC (1957) Role of pancreatic digestion in cholesterol absorption. Am J Physiol 190:214–220

Niederau M, Niederau G, Strohmeyer G, Grendell JH (1989) Comparative effects of CCK receptor antagonists on rat pancreatic secretion *in vivo*. Am J Physiol (Gastrointest Liver Physiol) 19:G150

Niederau C, Niederau M, Luthen R, Strohmeyer G, Ferrell LD, Grendell JH (1990) Pancreatic exocrine secretion in acute experimental pancreatitis. Gastroenterology 99:1120–1127

Tachibana I, Kanagawa K, Yamamoto Y, Otsuki M (1996) Pharmacological profile of a new serine derivative cholecystokinin receptor antagonist TP-680 on pancreatic, biliary and gastric function. J Pharmacol Exp Ther 279:1404–1412

J.7.0.2 Exocrine Secretion of Isolated Pancreas

PURPOSE AND RATIONALE

Procedures for isolation and perfusion of rat pancreas in order to record membrane potential and effective membrane resistance during the collection of perfusates and for simultaneous measuring of flow of pancreatic juice were described by Kanno (1972), Kanno and Saito (1976), Kanno et al. (1976), Saito et al. (1980). Similar techniques to measure exocrine secretion of the isolated pancreas have been used by other groups (Penhos et al. 1969; Mann and Norman 1984; Trimble et al. 1985; Norman and Mann 1986, 1987; Norman et al. 1989; Park et al. 1993).

PROCEDURE

Male Sprague Dawley rats weighing about 250 g are fasted for 24 h before the experiments but are allowed to drink water. Under ether anesthesia and after cannulation, the vascular system and the common duct are separately perfused. The rectum and the transverse colon are separated from the pancreas following ligation and sectioning of their vascular supply. Perfusion is performed through the hepatic end of the common duct with the outlet at the duodenal end. The **flushing preparation** is used when continuously recording the transmembrane potential and, in this preparation, the common duct is flushed at a constant pressure of 5 cm H_2O following cannulation of both ends with stainless steel tubes. The **draining preparation** is used during the electrical measurements are made from as many acinar cells as possible in every 10 min. In the draining preparation, the hepatic end of the duct is ligated and the pancreatic juice collected from the duodenal end following cannulation with a stainless steel tube. In both preparations, the inlets of the vascular perfusion are the superior mesenteric artery and the coeliac artery, and the outlet is the portal vein. The rate of vas-

cular flow is kept constant at 1 ml/min with the aid of a roller pump. The animal is then killed by cutting the carotid arteries and the perfusion begins. The spleen is removed after section of its vascular supply close to the hilum, care being taken to avoid interference with the supply from the splenic artery. The blood supplying stomach and liver is stopped by tying the hepatic artery and gastric arteries. The superior mesenteric vein and the descending branch of the superior mesenteric artery are then ligated. The mesentery with its embedded whole pancreas and the attached duodenum is then removed and mounted on a paraffin block in a lucite chamber containing 20 ml of standard Krebs-Henseleit solution. The contents of the duodenum is then drained with a polyethylene tube. The level of the standard Krebs-Henseleit solution in the bath is kept constant with a siphon. The temperature of the preparation and perfusing Krebs-Henseleit solution containing 8 vol% erythrocytes is maintained at 37°C. The perfusion solution in the reservoir is continuously bubbled with 5% CO_2 in O_2.

The rate of flow of pancreatic juice is measured by attaching a calibrated tube made of silicone-rubber to the free end of the pancreatic duct cannula. Every 10th min the tube is replaced and the rate of flow of pancreatic juice is noted. The sample is diluted with Krebs-Henseleit solution up to 100 ml and the amount of amylase assessed.

Intracellular recordings are made from the pancreatic acinar cells by manually advancing KCl-filled microelectrodes under direct visual control. The microelectrode is connected to the probe of a solid state pre-amplifier. Resting potentials are observed at the screen of a cathode ray oscilloscope and simultaneously recorded on a direct visual oscillograph.

Measurements are made every 10 min for half an hour as base level, followed by measurements every 10 min during infusion of drug for one hour.

EVALUATION

All results are expressed as mean ± SEM. Statistical analysis is performed using Student's *t*-test.

REFERENCES AND FURTHER READING

Kanno T (1972) Calcium-dependent amylase release and electrophysiological measurements in cells of the pancreas. J Physiol (London) 226:353–371

Kanno T, Saito A (1976) The potentiating influences of insulin on pancreozymin-induced hyperpolarization and amylase release in the pancreatic acinar cell. J Physiol 261:505–521

Kanno T, Suga T, Yamamoto M (1976) Effects of oxygen supply on electrical and secretory responses of humorally stimulated acinar cells in isolated rat pancreas. Jap J Physiol 26:101–115

Mann GE, Norman PSR (1984) Regulatory effects of insulin and experimental diabetes on neutral amino acid transport in the perfused rat exocrine pancreas. Kinetics of unidirectional L-serine influx and efflux at the basolateral plasma membrane. Biochim Biophys Acta 778:618–622

Norman PSR, Mann GE (1986) Transport characteristics of system A in the rat exocrine pancreatic epithelium analyzed using the specific non-metabolized amino acid analogue α-methylaminobutyric acid. Biochim Biophys Acta 861:389–394

Norman PSR, Mann GE (1987) Ionic dependence of amino-acid transport in the exocrine pancreatic epithelium: calcium dependence of insulin action. J Membr Biol 96:153–163

Norman PSR, Habara Y, Mann GE (1989) Paradoxical effects of endogenous and exogenous insulin on amino acid transport activity in the isolated rat pancreas: somatostatin-14 inhibits insulin action. Diabetologia 32:177–184

Park HJ, Lee YL, Kwon HY (1993) Effects of pancreatic polypeptide on insulin action in exocrine secretion of isolated rat pancreas. J Physiol 463:421–429

Penhos JC, Wu C-H, Basabe JC, Lopez N, Wolff FW (1969) A rat pancreas-small gut preparation for the study of intestinal factor(s) and insulin release. Diabetes 18:733–738

Saito A, Williams JA, Kanno T (1980) Potentiation of cholecystokinin-induced exocrine secretion by both endogenous and exogenous insulin in isolated and perfused rat pancreata. J Clin Invest 65:777–782

Trimble ER, Bruzzone R, Gjinovci A, Renold AE (1985) Activity of insulin-acinar axis in the isolated perfused rat pancreas. Endocrinology 117:1246–1252

J.7.0.3 Chronic Pancreatic Fistula in Rats

PURPOSE AND RATIONALE

Suguiyama et al. (1996) described the preparation of a chronic pancreatic fistula in the WBN/Kob rat, a strain which develops spontaneously chronic pancreatitis (Ohashi et al. 1990; see also J.7.0.14).

PROCEDURE

Male WBN/Kob rats at an age of 2 months are used. Before surgery, the rats have free access to chow and water. After an 18-h fast, laparotomy is performed through a midline incision under general anesthesia with ether. A polyethylene catheter (inside diameter 0.28 mm; outside diameter 0.61 mm, length 30 cm), as an external pancreatic fistula, is inserted into the common biliary pancreatic duct immediately proximal to the ampulla of Vater. The bile duct is ligated proximally to the pancreas. Another catheter is introduced into the bile duct distal to the confluence of the hepatic ducts, and the opposite end of the catheter is inserted into the duodenum near the ampulla through the stomach to drain the bile into the intestine. A third catheter is inserted in the duodenum through the stomach to return pancreatic juice. A fourth catheter is placed in the femoral vein, and 0.15 M sodium chloride is continuously administered at a flow rate of 1 ml/h with a sy-

ringe pump. All catheters are brought into the abdominal cavity or the femoral region through a subcutaneous tunnel starting in the middle portion of the tail. The rat is then placed prone in a cage with the proximal portion of the tail fixed to a side wall of the cage. When awakened, the rat is allowed access to food and water ad libitum. Pancreatic juice is collected and continually re-circulated with a syringe pump every 6 h until the secretion test.

The secretion test is started 3 days after surgery. After a 12-h fast, pancreatic juice is collected every 30 min in a plastic syringe. The juice volume is determined by weighing. A 50-µl sample is taken for the analysis of juice composition, and the remaining juice is returned to the duodenum for the next 30-min collection period.

After a 30-min basal period, the test compound is administered in graded doses, each dose for 30 min.

The bicarbonate concentration of pancreatic juice is measured with a microgasometer (Natelson 1958) in a sample size of 10 µl. Protein concentration is determined by measuring optical density at 280 nm with purified bovine trypsinogen as standard.

EVALUATION

All values are presented as mean ± SEM. Results are analyzed by means of the Wilcoxon test. Differences are considered significant at $p < 0.05$.

REFERENCES AND FURTHER READING

Arai T, Komatsu Y, Sasaki K, Taguchi S (1998) Reduced reactivity of pancreatic exocrine secretion in response to gastrointestinal hormone in WBN/Kob rats. J Gastroenterol 33:247–253

Natelson S (1958) Routine use of ultra-micro-methods in the clinical laboratory. Am J Clin Pathol 21:1153–1170

Ohashi K, Kim JH, Hara H, Aso R, Akimoto T, Nakama K (1990) A new spontaneously occurring model of chronic pancreatitis. Int J Pancreatol 6:231–247

Sugiyama M, Kobory O, Atomi Y, Wada N, Kuroda A, Muto T (1996) Effect of oral administration of protease inhibitor on pancreatic exocrine function in WBN/Kob rats with chronic pancreatitis. Pancreas 13:71–79

J.7.0.4 Acute Pancreatic Fistula in Dogs

PURPOSE AND RATIONALE

The effect of exogenous hormones, e. g. secretin or gastrin, or of vagal stimulation, on pancreatic secretion can be measured in dogs with acute pancreas fistulas.

PROCEDURE

Beagle dogs of either sex weighing 12–20 kg are used. The animals are fasted for a 24-h period and then anesthetized with 25 mg/kg sodium pentobarbital i.v. After opening the abdomen along the mid-line, the pyloric sphincter is ligated and the common bile duct cannulated to prevent the entry of acid chyme and bile into the duodenum. The bile is allowed to drain. The pancreas is gently exposed and the major pancreatic duct ligated. A polyethylene tube of 2 mm diameter is inserted into the minor pancreatic duct for collection of the secretion. The left femoral vein is cannulated for continuous infusion or i.v. injection. The pancreatic juice is collected in an ice-bath in a special tapered tube with fine calibrations for measuring volumes of less than 1 ml.

At the end of each collection period, the volume is recorded, and the bicarbonate content determined titrimetrically. Furthermore, pancreatic enzymes, such as amylase, are determined in the samples. Determination of protein concentrations in the pancreatic juice can be used as end-point since the total protein concentration is proportional to the individual enzymes (Keller et al. 1958). In a pretest period of 10 min, samples are collected every 2 min. Then, the test compound is injected intravenously and the pancreatic juice is collected every 2 min.

EVALUATION

The secretion after injection of the test compound is compared with the pre-test values. Secretin increases pancreatic volume and bicarbonate secretion in a dose-dependent manner. Activity ratios for unknown preparations can be calculated by 2+2 points assays in comparison with the international standard.

Moreover, the model can be used for standardization of gastrin analogues.

MODIFICATIONS OF THE METHOD

Glad et al. (1996) tested the influence of gastrin-releasing peptide on acid-induced secretin release and pancreatobiliary and duodenal bicarbonate secretion in Danish country strain **pigs** weighing between 22 and 30 kg. The animals, starved overnight with free access to water, were premedicated with 4 mg/kg i.m azaperone, and with 5 mg/kg i.p. metomidate. After 20 min a cannula was placed in an ear vein, and 5–10 mg/kg metomidate was given i.v. followed by intubation and artificial respiration with 50% O_2 and 50% N_2O. Anesthesia was maintained with an intravenous bolus infusion of 0.53% α-chloralose.

Both external jugular veins were cannulated for infusion of saline or drugs. A femoral artery was cannulated for withdrawal of blood samples and recording of blood pressure. After laparotomy the cystic duct

was ligated, and the common hepatic duct and the pancreatic duct were catheterized. The duodenal segment was defined as extending from the pylorus to the ligament of Treitz. A Foley catheter was passed through the pylorus into the proximal part of the duodenum and inflated. Distal to the pylorus the pancreaticoduodenal arteries, veins and nerves were dissected, and a double ligature was passed under these structures and tied around the duodenum. At the ligament of Treitz an inflated Foley catheter was placed in the distal part of the duodenum and tied with a suture around the duodenum. A catheter was placed through a splenic branch of the left gastroepiploic vein and advanced through the lienal vein to the portal vein.

The flow of pancreatic juice and bile was tested before and after the experiment by means of an intravenous bolus of 5 pmol/kg secretin. Before the experiment the duodenum was continuously perfused at a rate of 2 ml/min for 435 min with isotonic saline containing phenol red (10 mg/l) as a marker. After drug treatment (intravenous infusion of gastrin-releasing peptide or duodenal HCl perfusion) pancreatic and hepatic secretions were collected in 15-min periods and the volumes determined by weighing. Duodenal effluents were collected in 15-min periods and phenol red concentrations determined spectrophotometrically. Blood sampled were withdrawn for determination of secretin by radioimmunoassay.

REFERENCES AND FURTHER READING

Glad H, Svendsen P, Knuhtsen S, Olsen O, Schaffalitzki de Muckadell OB (1996) Importance of gastrin-releasing peptide on acid-induced secretin release and pacreatobiliary and duodenal bicarbonate secretion. Scand J Gastroenterol 31:993–1000

Ivy AC, Janecek HM (1959) Assay of Jorpes-Mutt secretin and cholecystokinin. Acta Physiol Scand 45:220–230

Keller PJ, Cohen E, Neurath H (1958) The proteins of bovine pancreatic juice. J Biol Chem 233:344–349

Lehnert P, Stahlheber H, Forell MM, Dost FH, Fritz H, Hutzel M, Werle E (1969) Bestimmung der Halbwertszeit von Secretin. Klin Wschr 47:1200–1204

Lin TM, Ivy AC (1957) Relation of secretin to the parasympathetic mechanism for pancreatic secretion. Am J Physiol 187:361–368

J.7.0.5 Chronic Pancreatic Fistula in Dogs

PURPOSE AND RATIONALE

Herrera et al. (1968) described a special cannula which can be used to obtain pancreatic juice or bile from a duodenal pouch after appropriate surgical procedures (Preshaw and Grossman 1965).

PROCEDURE

Male Beagle dogs weighing 15–20 kg are used. The abdomen is opened through a midline epigastric incision under barbiturate anesthesia. The duodenum is mobilized at the pyloric and jejunal ends, and a 5-cm duodenal segment containing the main pancreatic duct is isolated. The proximal level of the duodenal section lies immediately distal to the opening of the common bile duct and the distal level of section lies 2.5 cm distal to the main pancreatic duct. The distal stoma of the duodenum is closed and continuity restored by end-to-side duodeno-jejunostomy. The duodenal pouch is closed at both ends.

The cannula to be inserted is made of stainless steel and consists of 3 parts. The main casement measures 10.5 cm in length, with an external diameter of 1.0 cm. The internal end is flanged, and 1.5 cm from this point there is a short lateral limb, also 1.5 cm in length. The lateral limb is also flanged but, in addition, possesses a small V-shaped defect to facilitate insertion into the pouch.

When not in use, the cannula is sealed from the exterior by inserting a threaded plug which allows pancreatic juice to enter the duodenum in the normal manner. For collection of juice this plug is removed and a long obturator is inserted. The latter effectively isolates the pancreatic secretion from other duodenal contents. A similar hollow obturator is reserved for use when duodenal perfusion is studied, the obturator being connected via a plastic tube to the irrigating fluid.

Through a small antimesenteric incision in the duodenal pouch, the lateral limb of the cannula is inserted; the V-shaped defect in the flange facilitates entry into the pouch. A purse string secures the cannula in position. The defunctioned loop of duodenum is then brought anterior to the pancreas, and the remaining limb of the cannula inserted through a small duodenotomy and secured further by a purse-string suture. The whole system is then generously wrapped in omentum and the cannula exteriorized through a stab incision toward the flank. An external collar stabilizes the cannula.

The cannula is left open to drain blood and secretions for 24 h postoperatively, after which time the plug is inserted. Physiologic saline is administered subcutaneously for a period of 3 days, after which the animals are permitted to drink water. Checking the cannula daily is advisable to ensure that the plug remains tight. The animals receive normal kennel food and water ad libitum.

The dogs are allowed at least 2 weeks to recover. Eighteen hours prior to the experiment food is with-

drawn but water allowed ad libitum. The long obturator is inserted and pancreatic juice collected for 15 min periods. After 1 h pretest time, the test compound is given either orally or intravenously.

EVALUATION

Secretion of pancreas juice is measured at 15 min intervals and volume and enzyme content determined. The values are compared with pretest data.

MODIFICATIONS OF THE METHOD

Boldyreff (1925) described details of the technique as recommended by Pavlov (1902) as well as his own modification.

Konturek et al. (1976, 1984) performed experiments with chronic gastric fistulas in **cats** as well as in **dogs** to compare the species-specific activities of vasoactive intestinal peptide and secretin in stimulation of pancreatic secretion.

Ninomiya et al. (1998) studied the effects of a cholecystokinin A receptor antagonist on pancreatic exocrine secretion stimulated by exogenously administered CCK-8 in conscious dogs with chronic pancreatic fistula.

Garvin et al. (1993) described distal pancreatectomy with autotransplantation and pancreaticocystostomy in dogs.

Kuruda et al. (1995) developed a new technique in dogs for pancreatico-gastrointestinal anastomosis that consists of pancreatectomy using the ultrasonic dissector and implantation of the pancreatic duct into the gastrointestinal tract without suturing the pancreatic parenchyma.

REFERENCES AND FURTHER READING

Boldyreff WN (1925) Surgical method in the physiology of digestion. Description of the most important operations on digestive system. Ergebn Physiol 24:399–444

Garvin PJ, Niehoff M, Burton FR (1993) A laboratory model for evaluation of posttransplant pancreatic exocrine secretion. J Invest Surg 6:53–63

Herrera F, Kemp DR, Tsukamoto M, Woodward ER, Dragstedt LR (1968) A new cannula for the study of pancreatic function. J Appl Physiol 25:207–209

Hosotani R, Chowdhury P, Rayford PhL (1989) L-364,718, a new CCK antagonist, inhibits postprandial pancreatic secretion and PP release in dogs. Dig Dis Sci 34:462–467

Konturek SJ, Radecki T, Thor P (1974) Comparison of endogenous release of secretin and cholecystokinin in proximal and distal duodenum in the dog. Scand J Gastroenterol 9:153–157

Konturek SJ, Pucher A, Radecki T (1976) Comparison of vasoactive intestinal peptide and secretin in stimulation of pancreatic secretion. J Physiol 255:497–509

Konturek SJ, Cieszkowski M, Kwiecien N, Konturek J, Tasler J, Bilski J (1984) Effects of omeprazole, a substituted benzimidazole, on gastrointestinal secretions, serum gastrin, and gastric mucosal blood flow in dogs. Gastroenterol 86:71–77

Kuroda Y, Tanioka Y, Matsumoto SI, Kim Y, Fujita H, Ajiki T, Suzuki Y, Ku Y, Saitoh Y (1995) A new technique for pancreaticogastrointestinal anastomosis without suturing the pancreatic parenchyma. J Am Coll Surg 181:311–314

Ninomiya K, Saito T, Wakatsuki K, Saeki M, Kato T, Kasai H, Kimura F, Fujii M (1998) Effects of loxiglumide on pancreatic exocrine secretion stimulated by cholecystokinin-8 in conscious dogs. Arzneim Forsch/Drug Res 48:52–54

Pavlov IP (1902) Die physiologische Chirurgie des Verdauungskanals. Ergebn Physiol Abt. 1:246–286

Preshaw RM, Grossman MI (1965) Stimulation of pancreatic secretion by extracts of the pyloric gland area of the stomach. Gastroenterology 48:36–44

J.7.0.6 Somatostatin Activity

PURPOSE AND RATIONALE

Somatostatin is a neuropeptide, also called somatotrophin release inhibiting factor (SRIF or SRIF-14), which occurs not only in the brain, but also in a variety of peripheral tissues. Two other related peptides somatostatin-28 (SRIF-28) and cortistatin (Vasilaki et al. 1999), also occur naturally (Humphrey 1998). Somatostatin acts via G-protein coupled receptors of which five subtypes are cloned (Hoyer 1998).

Somatostatin analogues and antagonists have been tried for a variety of indications (Bass et al. 1996; Coy and Taylor 1996; Papageorgiou and Borer 1996; Rohrer et al. 1998; Yang et al. 1998; Hocart et al. 1999). The long-acting octapeptide somatostatin analog, octreotide, has been studied thoroughly (Ambler et al. 1996; Danesi and Del Tacca 1996; Hoffmann et al. 1996; Paran et al. 1996) and gained clinical use as gastric antisecretory agent.

Somatostatin inhibits basal pancreatic secretion as well as secretion stimulated by food, cholecystokinin, and secretin. Inhibition of pancreatic secretion can be used as bioassay to compare synthetic analogues with the original somatostatin.

PROCEDURE

Male Wistar rats weighing 300–400 g are anesthetized with methoxyfluorane and prepared with silastic cannulae. Two cannulae drain pancreatic juice and bile separately, one cannula is inserted into the duodenum for return of bile and pancreatic juice to the intestine and for intestinal infusion. Another cannula is located in the abdominal cavity and a fifth cannula into the right jugular vein for drug infusion. After surgery, the rats are placed into modified Bollman-type restrain cages. The rats have free access to food and water. Dur-

ing recovery and between the experiments, pancreatic juice and bile are collected and continuously returned to the intestine by a servo-system consisting of a collection tube in a liquid-level photodetector coupled to a peristaltic pump.

Experiments are performed on the third to eighth days postoperatively. The rats are assigned to treatment groups on a random basis and, treatment days are equally divided among the third to eighth postoperative days. The rats are fasted overnight before each experiment. Bile and pancreatic juice are collected separately every 30 min; the volume of pancreatic juice is measured, and 10 ml is taken for protein assay. Different doses of the test drug and the standard are given as continuous i.v. infusion over a period of 2 h.

EVALUATION

Inhibition of pancreatic fluid and protein output is calculated compared to control infusion and expressed as percentage. From dose-response curves activity ratios can be calculated.

MODIFICATIONS OF THE METHOD

Konturek et al. (1985) and Susini et al. (1980) studied the effect of somatostatin analogues on pancreas secretion in dogs.

Cai et al. (1986) reported on the biological activity of octapeptide analogs of somatostatin assaying GH concentrations in blood samples of anesthetized rats by RIA and studying the inhibition of gastric secretion on dogs.

Biological actions of prosomatostatin have been described by Meyers et al. (1980) using *in vitro* and *in vivo* GH bioassays.

Taylor et al. (1996) employed the technique of cytosensor microphysiometry for real-time evaluation of somatostatin subtype receptor activity in CHO-K_1 cells stably expressing the human sst_2 receptors.

Cytotoxic analogs of somatostatin have been synthesized and evaluated (Nagy et al. 1998).

Gilon et al. (1998) studied a synthetic receptor 5-selective somatostatin analogue *in vivo* in rats. The compound inhibited bombesin- and caerulein-induced amylase and lipase release from the pancreas without inhibiting growth hormone or glucagon release.

Jeandel et al. (1998) described the effects of two somatostatin variants on receptor binding, adenyl cyclase activity and growth hormone release from the frog pituitary.

Hofland et al. (1994) determined relative potencies of somatostatin analogs on the inhibition of growth hormone release by cultured human endocrine tumor cells and normal rat anterior pituitary cells.

Rohrer et al. (1998) and Rohrer and Schaeffer (2000) described rapid identification of subtype-selective agonists of the somatostatin receptor through combinatorial chemistry.

Hoyer et al. (2004) characterized *in vitro* a non-peptide somatostatin sst_1 receptor antagonist.

Reubi et al. (2000) described SST_3-selective potent peptidic somatostatin receptor antagonists.

Nunn et al. (2003a, 2003b) reported properties of putative small-molecule somatostatin sst_2 receptor-selective antagonists.

Using high-throughput parallel synthesis, Moinet (2001) prepared non-peptide ligands for the somatostatin sst_3 receptor.

Gademann et al. (2001) reported that peptide folding induces high and selective affinity of a linear and small β-peptide to the human somatostatin receptor 4.

Nunn (2003c) described β^2/β^3-di- and α/β^3-tetrapeptide derivatives as potent agonists at somatostatin sst_4 receptors.

Somatostatin analogs labeled with ^{99m}technetium, ^{111}indium, and ^{90}yttrium were developed for tumor diagnosis and therapy (O'Byrne and Carney 1996; Pearson et al. 1996; Stolz et al. 1996, 1998; Thakur et al. 1996).

Radioimmunoassays for somatostatin have been developed (Arimura et al. 1975; Gerich et al. 1979; Patel and Reichlin 1979; Patel 1984) and are available as commercial kits.

Siehler et al. (1998) reported that [^{125}I]Tyr^{10}-cortistatin$_{14}$ labels all five somatostatin receptors.

REFERENCES AND FURTHER READING

Ambler GL, Butler AA, Padmanabhan I, Breier BH, Gluckman PD (1996) The effects of octreotide on GH receptor and IGF-I expression in the GH-deficient rat. J Endocrinol 149:223–231

Arimura A, Sato H, Coy DH, Schally AV (1975) Radioimmunoassay for GH-release inhibiting hormone. Proc Soc Exp Biol Med 148:784–789

Bass RT, Buckwalter BL, Patel BP, Pausch HM, Price LA, Strnad J, Hadcock JR (1996) Identification and characterization of novel somatostatin antagonists. Mol Pharmacol 50:709–715

Cai RZ, Szoke B, Lu R, Fu D, Redding TW, Schally AV (1986) Synthesis and biological activity of highly potent octapeptide analogs of somatostatin. Proc Natl Acad Sci, USA, 83:1896–1900

Chariot J, Roze C, Vaille C, Debray C (1978) Effects of somatostatin on the external secretion of the pancreas in the rat. Gastroenterology 75:832–837

Coy DH, Taylor JE (1996) Receptor-specific somatostatin analogs: Correlation with biological activity. Metab Clin Exp 45, Suppl:21–23

Danesi R, Del Tacca M (1996) The effects of the somatostatin analog octreotide on angiogenesis *in vitro*. Metab Clin Exp 45, Suppl:49–50

Fölsch UR, Lankisch PG, Creutzfeldt W (1978) Effect of somatostatin on basal and stimulated pancreatic secretion in the rat. Digestion 17:194–203

Gademann K, Kimmerlin T, Hoyer D, Seebach D (2001) Peptide folding induces high and selective affinity of a linear and small β-peptide to the human somatostatin receptor 4. J Med Chem 44:2460–2468

Gerich J, Greene K, Hara M, Rizza R, Patton G (1979) Radioimmunoassay of somatostatin and its application in the study of pancreatic somatostatin secretion *in vitro*. J Lab Clin Med 93:1009–1017

Green GM, Nasset ES (1980) Importance of bile in regulation of intraluminal proteolytic enzyme activities in the rat. Gastroenterology 79:695–702

Guan D, Maouyo D, Sarfati P, Morisset J (1990) Effects of SMS 201–995 on basal and stimulated pancreatic secretion in rats. Endocrinology 127:298–304

Gilon C, Huenges M, Matha B, Gellerman G, Hornik V, Afargan M, Amitay O, Ziv O, Feller E, Gamliel A, Shohat D, Wanger M, Arad O, Kessler H (1998) A backbone-cyclic, receptor 5-selective somatostatin analogue: Synthesis, bioactivity, and nuclear resonance conformational analysis. J Med Chem 41:919–929

Hocart SJ, Jain R, Murphy WA, Taylor JE, Coy DH (1999) Highly potent cyclic disulfide antagonists of somatostatin. J Med Chem 42:1863–1871

Hoffmann TF, Uhl E, Messmer K (1996) Protective effect of the somatostatin analogue octreotide in ischemia/reperfusion induced acute pancreatitis in rats. Pancreas 12:286–293

Hofland LJ, van Koetsfeld PM, Waaijers M, Zuyderwijk J, Lamberts SWJ (1994) Relative potencies of the somatostatin analogs octreotide, BIM-23014, and RC-160 on the inhibition of growth hormone release by cultured human endocrine tumor cells and normal rat anterior pituitary cells. Endocrinology 134:301–306

Hoyer D (1998) Distribution and localization of somatostatin (SRIF) receptor transcripts and proteins. Naunyn Schmiedeberg's Arch Pharmacol 358, Suppl 2:R381

Hoyer D, Nunn C, Hannon J, Schoeffter P, Feuerbach D, Schuepbach E, Langeneeger D, Bouhelal R, Hurth K, Neumann P, Troxler T, Pfaeffli P (2004) SRA880, in vitro characterization of the first non-peptide somatostatin sst_1 receptor antagonist. Neurosci Lett 361:132–135

Humphrey PPA (1998) The pharmacology of somatostatin receptors. Naunyn Schmiedeberg's Arch Pharmacol 358, Suppl 2:R381

Jeandel L, Okuno A, Kobayashi T, Kikuyama S, Tostivint H, Lihrmann I, Chartrel N, Conlon JM, Fournier A, Tonon MC, Vaudry H (1998) Effects of the two somatostatin variants somatostatin-14 and Pro^2,Met^{13}somatostatin-14 on receptor binding, adenyl cyclase activity and growth hormone release from the frog pituitary. J Neuroendocrinol 10:187–192

Konturek SJ, Cieskowski M, Bilski J, Konturek j, Bielansky W, Schally AV (1985) Effects of cyclic hexapeptide analog of somatostatin on pancreatic secretion in dogs. Proc Soc Exp Biol Med 178:68–72

Meyers CA, Murphy WA, Redding TW, Coy DH, Schally AV (1980) Synthesis and biological actions of prosomatostatin. Proc Natl Acad Sci USA, 77:6171–6174

Moinet C, Contour-Galcéra MO, Poitout L, Morgan B, Gordon T, Roubert P, Thurieau C (2001) Novel nonpeptide ligands for the somatostatin sst_3 receptor. Bioorg Med Chem Lett 11:991–995

Nagy A, Schally AV, Halmos G, Armatis P, Cai RZ, Csernus V, Kovacs M, Koppa M, Szepeshazi K, Kahan Z (1998) Synthesis and biological evaluation of cytotoxic analogs of somatostatin containing doxorubicin or its intensely potent derivative, 2-pyrrolinodoxorubicin. Proc Natl Acad Sci, USA, 402:1794–1799

Nunn C, Langenegger D, Hurth K, Schmidt K, Fehlmann D, Hoyer D (2003a) Agonist properties of putative small-molecule somatostatin sst_2 receptor selective antagonists. Eur J Pharmacol 465:211–218

Nunn C, Schoeffter P, Langenegger D, Hoyer D (2003b) Functional characterization of the putative somatostatin sst_2 receptor antagonist CYN 154806. Naunyn-Schmiedebergs Arch Pharmacol 367:1–9

Nunn C, Rueping M, Langenegger D, Schuepbach E, Kimmerlin T, Micuch P, Seebach D, Hoyer D (2003c) β^2/β^3-di- and α/β^3-tetrapeptide derivatives as potent agonists at somatostatin sst_4 receptors. Naunyn-Schmiedebergs Arch Pharmacol 367:95–103

O'Byrne KJ, Carney DN (1996) Radiolabeled somatostatin analogue scintigraphy in oncology. Anti-Cancer Drugs 7, Suppl 1:33–44

Papageorgiou C, Borer X (1996) A non-peptide ligand for the somatostatin receptor having a benzodiazepinone structure. Bioorg Med Chem Lett 6:267–272

Paran H, Klausner J, Siegal A, Graff E, Freund U, Kaplan O (1996) Effect of the somatostatin analogue octreotide on experimental pancreatitis in rats. J Surg Res 62:201–206

Patel YC (1984) Radioimmunoassay of somatostatin-related peptides. In: Larner J, Pohl SL (eds) Methods in Diabetes Research, Vol I: Laboratory Methods, Part B, John Wiley & Sons, New York, pp 307–327

Patel YC, Reichlin S (1979) Somatostatin. In: Jaffe BM, Behrman HR (eds) Methods of Hormone Radioimmunoassay. 2nd edn, Academic Press, New York, pp 77–99

Pearson DA, Lister-James J, McBride JW, Wilson DM, Martel LJ, Civitello ER, Taylor JE, Moyer BR, Dean RT (1996) Somatostatin receptor-binding peptides labeled with technetium^{99m}: Chemistry and initial biological studies. J Med Chem 39:1361–1371

Reubi JC, Schaer JC, Wenger S, Hoeger C, Erchegyi J, Waser B, Rivier J (2000) SST3-selective potent peptidic somatostatin receptor antagonists. Proc Natl Acad Sci USA 97:13973–13978

Rohrer SP, Birzin ET, Mosley ET, Berk SC, Hutchins SM, Shen DM, Xiong Y, Hayes EC, Parmar RM, Foor F, Mitra SW, Degrado SJ, Shu M, Klopp JM, Cai SJ, Blake A, Chan WWS, Pasternak A, Yang L, Patchett AA, Smith RG, Chapman KT, Schaeffer JM (1998) Rapid identification of subtype-selective agonists of the somatostatin receptor through combinatorial chemistry. Science 282:737–740

Rohrer SP, Schaeffer JM (2000) Identification and characterization of subtype selective somatostatin receptor agonists. J Physiol (Paris) 94:211–215

Siehler S, Seuwen K, Hoyer DF (1998) [^{125}I]Tyr^{10}-cortistatin$_{14}$ labels all five somatostatin receptors. Naunyn-Schmiedebergs Arch Pharmacol 357:483–489

Srikant CB, Heisler S (1985) Relationship between receptor binding and biopotency of somatostatin-14 and somatostatin-28 in mouse pituitary tumor cells. Endocrinology 117:271–278

Stolz B, Smith-Jones P, Albert R, Tolcsvai L, Briner U, Ruser G, Macke H (1996) Somatostatin analogues for somatostatin-receptor-mediated radiotherapy of cancer. Digestion 57, Suppl 1:17–21

Stolz B, Weckbecker G, Smith-Jones PM, Albert R, Raulf F, Bruns C (1998) The somatostatin receptor-targeted ra-

diotherapeutic ^{90}Y-DOTA-DPhe^{1}-Tyr^{3}-octreotide (^{90}Y-SMT487) eradicates experimental rat pancreatic Ca 20948 tumors. Eur J Nucl Med 25:668–674
Susini C, Esteve JP, Vaysse N, Pradayrol L, Ribet A (1980) Somatostatin 28: effect on exocrine pancreatic secretion in conscious dogs. Gastroenterology 79:720–724
Taylor JE, Nelson R, Woon CW (1996) Real-time evaluation of somatostatin subtype receptor activity employing the technique of cytosensor microphysiometry. Peptides 17:1257–1259
Thakur ML, Kolan HR, Rifat S, Li J, Rux A, John E, Halmos G, Schally AV (1996) Vapreotide labeled with Tc^{99m} for imaging tumors: Preparation and preliminary evaluation. Int J Oncol 9:445–451
Vale W, Brazeau P, Rivier C, Brown M, Boss M, Rivier J, Burgus R, Ling N, Guillemin R (1974) Somatostatin. Rec Progr Horm Res 31:365–397
Vasilaki A, Lanneau C, Dournaud P, De Lecca L, Gardette R, Epelbaum J (1999) Cortistatin affects glutamate sensitivity in mouse hypothalamic neurones through activation of sst_2 somatostatin receptor subtypes. Neuroscience 88:359–364
Yang L, Berk SC, Rohrer SP, Mosley RT, Guo L, Underwood DJ, Arison BH, Birzin ET, Hayes EC, Mitra SW, Parmar RM, Cheng K, Wu TJ, Butler BS, Foor F, Pasternak A, Pan Y, Silva M, Freidinger RM, Smith RG, Chapman K, Schaeffer JM, Patchett AA (1998) Synthesis and biological activities of potent peptidomimetics selective for somatostatin receptor subtype 2. Proc Natl Acad Sci USA 95:10836–10941

J.7.0.7 Receptor Binding for Somatostatin

GENERAL CONSIDERATIONS

A family of five somatostatin receptor subtypes from various species including man has been described (Yamada et al. 1992; Reisine and Bell 1995; Hoyer et al. 1995; Bruns et al. 1996; Liapakis et al. 1996; Patel and Srikant 1994; Hoyer et al. 1995; Patel et al. 1996; Nilsson and Folkesson 1997; Patel 1997; Pscherer et al. 1996; Shimon et al. 1997; Humphrey et al. 1998; Moller et al. 2003; Olias et al. 2004). There are several endogenous ligands, such as somatostatin-14, somatostatin-28 and the corticostatins (Meyerhoff et al. 1992; De Lecea 1996; Fukusumo 1997). A number of synthetic peptide analogues have been developed and their relative affinities at human recombinant receptors in radioligand receptor studies have been established (Raynor et al. 1992; Bass et al. 1996; Coy and Taylor 1996; Pearson et al. 1996; Piwko et al. 1996, 1997a, b).

Greenmman and Melmed (1994) evaluated the expression of three somatostatin receptor subtypes (SSTR3, SSTR4, and SSTR5) in pituitary tumor specimens. SSTR3 expression was studied by reverse transcription coupled to polymerase chain reaction, whereas SSTR4 and SSTR5 expression was determined by ribonuclease protection assay.

Somatostatin occurs not only in the hypothalamus and in the gut, but also in several other organs. Somatostatin$_1$ receptors in the nucleus accumbens have been found to mediate the stimulatory effect of somatostatin on locomotor activity in rats (Raynor et al. 1993a). Molecular cloning and expression of a pituitary somatostatin receptor with preferential affinity for somatostatin-28 has been described by O'Carroll et al. (1992).

Cloning and expression of a mouse somatostatin receptor (SSTR 2B) has been reported by Vanetti et al. (1992). Pharmacological properties of two cloned somatostatin receptors have been described by Rens-Domiano et al. (1992).

Subtype-selective peptides have been identified by Raynor et al. (1993b). The somatostatin receptor, SSTR3, coupled to adenyl cyclase, has been cloned by Yasuda et al. (1992). Somatostatin receptors SSTR4 and SSTR5 have been cloned and characterized by Raynor et al. (1993c).

The somatostatin receptor SST_1 mediates inhibition of central neurons (Viollet et al. 1997).

The somatostatin receptor SST_2 inhibits growth hormone release (Raynor et al. 1993b), inhibits parietal cell function and ion secretion in rat distal colon (McKeen et al. 1996; Warhurst et al. 1996; Wyatt et al. 1996), and inhibits neurons in the rat locus coeruleus (Chessell et al. 1996). High basal gastric acid secretion has been found in somatostatin receptor subtype 2 knockout mice (Martinez et al. 1998). The cytoplasmatic tail of the somatostatin receptor SST_2 undergoes alternative splicing giving rise to two isoforms, SST_{2A} and SST_{2B} (Schulz et al. 1998).

The somatostatin receptor sst_3 mediates relaxation of isolated gastric smooth muscle cells (Gu et al. 1995).

The fourth human somatostatin receptor has been cloned and characterized by Rohrer et al. (1993).

The somatostatin receptor sst_5 may have a role in inhibition of hormone release from the pituitary (Tallent et al. 1996) and pancreas (Rossowski and Coy (1994) and mediates the antiproliferative effect of somatostatin in vascular smooth muscle (Lauder et al. 1997).

PROCEDURE

Crude membrane preparations are obtained by homogenizing (Polytron, setting 6, 15 s) tumor cell cultures (e. g. human SCLC line NCI-H69, rat pancreatic tumor AR42J) or rat tissues (lung, pancreas, cerebral cortex) in ice-cold 50 mM Tris-HCl and centrifuging twice at 39,000 *g* (10 min), with an intermediate resuspen-

sion in fresh buffer. The final pellets are resuspended in 10 mM Tris-HCl for assay. Aliquots of the membrane preparation are incubated for 25 min at 30°C with [^{125}I-Tyr^{11}]SRIF (2000 Ci/mmol, Amersham) in 50 mM HEPES (pH 7.4) containing bovine serum albumin (10 mg/ml; fraction V, Sigma), $MgCl_2$ (5 mM), Trasylol (200 KIU/ml), bacitracin (0.02 mg/ml), and phenyl-methyl-sulfonyl fluoride (0.02 mg/ml). The final assay volume is 0.3 ml. The incubations are terminated by rapid filtration through Whatman GF/C filters (pre-soaked in 0.3% polyethylenimine) under reduced pressure. Each tube and filter is then washed three times with 5 ml aliquots of ice-cold buffer. Specific binding is defined as the total [^{125}I-Tyr^{11}]SRIF bound minus that bound in the presence of 200 nM unlabeled SRIF.

EVALUATION

The binding parameters are calculated from the experimental data by non-linear least-squares regression analysis using an appropriate computer program.

CRITICAL ASSESSMENT OF THE METHOD

Somatostatin occurs in many organs and has more activities than anticipated at its discovery. Therefore, the occurrence of a family of receptors rather than a single receptor is not surprising.

MODIFICATIONS OF THE METHOD

Receptor scintigraphy with a radioiodinated somatostatin analogue has been described by Bakker et al. (1990).

The tissue-selective binding of somatostatin-14 and somatostatin-28 in rat brain was studied by Srikant et al. (1990).

Feniuk et al. (1993) characterized somatostatin receptors in guinea-pig isolated ileum, vas deferens and right atrium.

Yang et al. (1998) reported synthesis and biological activities of potent peptidomimetics selective for somatostatin receptor subtype 2 by testing inhibition of forskolin-stimulated cAMP accumulation in a mouse cell line that contains a cAMP response element fused to the *E. coli* β-galactosidase gene and by measuring growth hormone release from primary cultures of rat anterior pituitary cells.

REFERENCES AND FURTHER READING

Bakker WH, Krenning EP, Breeman WA, Koper JW, Kooij PP, Reubi JC, Klijn JG, Visser ThJ, Docter R, Lamberts SW (1990) Receptor scintigraphy with a radioiodinated somatostatin analogue: Radiolabeling, biologic activity, and *in vivo* application in animals. J Nucl Med 31:1501–1509

Bass RT, Buchwalter BL, Patel BP, Pausch MH, Price LA, Stemad J, Hadcock JR (1996) Identification and characterization of novel somatostatin antagonists. Mol Pharmacol 50:709–715

Bruno JF, Xu Y, Song J, Berelowitz M (1992) Molecular cloning and functional expression of a brain-specific somatostatin receptor. Proc Natl Acad Sci, USA 89:1151–1155

Bruns C, Raulf F, Hoyer D, Schloos J, Lubbert H, Weckbecker G (1996) Binding properties of somatostatin receptor subtypes. Metab Clin Exp 45, Suppl:17–20

Chessell IP, Black M, Feniuk W, Humphrey PPA (1996) Operational characteristics of somatostatin receptors mediating inhibitory actions on rat locus coeruleus neurons. Br J Pharmacol 117:1673–1678

Coy DH, Taylor JE (1996) Receptor-specific somatostatin analogs: Correlations with biological activity. Metab Clin Exp 45, Suppl:21–23

De Lecea L, Criado JR, Prospero-Garcia O, Gautvick KM, Schweitzer P, Danielson PE, Dunlop CL, Siggins GR, Henriksen SJ, Sutcliffe GJ (1996) A cortical neuropeptide with neuronal depressant and sleep-modulating properties. Nature 381:242–245

Feniuk W, Dimech J, Humphrey PPA (1993) Characterization of somatostatin receptors in guinea-pig isolated ileum, vas deferens and right atrium. Br J Pharmacol 110:1156–1164

Fukusumi S, Kitada C, Takekawa S, Kizawa H, Sakamoto J, Miyamoto M, Hinuma S, Kitano K, Fujino M (1997) Identification and characterization of o novel human corticostatin-like peptide. Biochem Biophys Res Commun 232:157–163

Greenman Y, Melmed S (1994) Expression of three somatostatin receptor subtypes in pituitary adenomas: Evidence for preferential SSTR5 expression in the mammosomatotroph lineage. J Clin Endocrin Metab 79:724–729

Gu ZF, Corleto VD, Mantey SA, Coy DH, Maton PN, Jensen RT (1995) Somatostatin receptor subtype 3 mediates the inhibitory action of somatostatin on gastric smooth muscle cells. Am J Physiol 268:G739–G748

Hoyer D, Bell GI, Berelowitz M, Epelbaum J, Feniuk W, Humphrey PPA, O'Carroll AM, Patel YC, Schonbrunn A, Taylor JE, Reisine T (1995) Classification and nomenclature of somatostatin receptors. Trends Pharmacol Sci 16:86–88

Humphrey PPA, Epelbaum J, Feniuk W, Hoyer D, Taylor JE, Reisine TR (1998) Somatostatin receptors. In: Girdlestone D (ed) The IUPHAR Compendium of Receptor Characterization and Classification, IUPHAR Media, London, pp 246–255

Liapakis G, Tallent M, Reisine T (1996) Molecular and functional properties of somatostatin receptor subtypes. Metab Clin Exp 45, Suppl:12–13

Lauder H, Sellers LA, Fan TP, Fenluk W, Humphrey PPA (1997) Somatostatin sst_5 inhibition of receptor mediated regeneration of rat aortic vascular smooth muscle cells. Br J Pharmacol 122:663–670

Martinez V, Curi AP, Torkian B, Schaeffer JM, Wilkinson HA, Walsh JH, Tache Y (1998) High basal gastric acid secretion in somatostatin receptor subtype 2 knockout mice. Gastroenterology 114:1125–1132

McKeen ES, Feniuk W, Michel AD, Kidd EJ, Humphrey PPA (1996) Identification and characterization of heterogeneous somatostatin binding sites in rat distal colon mucosa. Naunyn Schmiedeberg's Arch Pharmacol 354:543–549

Meyerhof W, Wulfsen I, Schönrock Ch, Fehr S, Richter D (1992) Molecular cloning of a somatostatin-28 receptor

and comparison of its expression pattern with that of a somatostatin-14 receptor in rat brain. Proc Natl Acad Sci 89:10267–10271

Moller LN, Stidsen CE, Hartmann B, Holst JJ (2003) Somatostatin receptors. Biochim Biophys Acta 1616:1–84

Murphy WA, Taylor JE, Moreau JP, Coy DH (1989) Novel heptapeptide somatostatin analog displays anti-tumor activity independent of effects on growth hormone secretion. Peptide Res 2:128–132

Nilsson L, Folkesson R (1997) Coexistence of somatostatin receptor subtypes in the human neuroblastoma cell line LA-N_2. FEBS Lett 401:83–88

O'Carroll AM, Lolait StJ, König M, Mahan LC (1992) Molecular cloning and expression of a pituitary somatostatin receptor with preferential affinity for somatostatin-28. Molecul Pharmacol 42:936–946

Olias G, Viollet C, Kusserow H, Epelbaum J, Meyerhof W (2004) Regulation and function of somatostatin receptors. J Neurochem 89:1057–1091

Patel YC (1997) Molecular pharmacology of somatostatin receptor subtypes. J Clin Invest 20:348–367

Patel YC, Greenwood M, Panetta R, Hukovic N, Grigorakis S, Robertson LA, Srikant CB (1996) Molecular biology of somatostatin receptor subtypes. Metab Clin Exp 45, Suppl:31–38

Patel YC, Srikant CB (1994) Subtype selectivity of peptide analogs for all five cloned somatostatin receptors (hsstr 1–5). Endocrinology 135:2814–2817

Pearson DA, Lister-James J, McBride WJ, Wilson DM, Martel LJ, Civitello ER, Taylor JE, Moyer BR, Dean RT (1996) Somatostatin receptor-binding peptides labeled with technetium-99m: Chemistry and initial biological studies. J Med Chem 39:1361–1371

Pinski J, Milanovic S, Yano T, Hamaoui A, Radulovic S, Cai RZ, Schally AV (1992) Biological activity and receptor binding characteristics to various human tumors of acetylated somatostatin analogs. Proc Soc Exp Biol Med 200:49–56

Piwko C, Thoss VS, Probst A, Hoyer D (1996) Localization and pharmacological characterization of somatostatin recognition sites in the human cerebellum. Neuropharmacol 35:713–723

Piwko C, Thoss VS, Probst A, Hoyer D (1997a) The elusive nature of cerebellar somatostatin receptors: Studies in rat, monkey and human cerebellum. J Recept Signal Transduction Res 17:385–405

Piwko C, Thoss VS, Schupbacvh E, Kummer J, Langenecker D, Probst A, Hoyer D (1997b) Pharmacological characterization of human cerebral cortex somatostatin SRIF-1 and SRIF-2 receptors. Naunyn Schmiedeberg's Arch Pharmacol 355:161–167

Pscherer A, Dörflinger U, Kirfel J, Gawlas K, Rüschoff J, Buettner R, Schüle R (1996) The helix-loop-helix transcription factor SEF-2 regulates the activity of a novel initiator element in the promoter of the somatostatin receptor II gene. EMBO J 15:6680–6690

Raynor K, Coy DC, Reisine T (1992) Analogues of somatostatin bind selectively to brain somatostatin receptor subtypes. J Neurochem 59:1241–1250

Raynor K, Lucke I, Reisine T (1993a) Somatostatin$_1$ receptors in the nucleus accumbens selectively mediate the stimulatory effect of somatostatin on locomotor activity in rats. J Pharmacol Exp Ther 265:67–73

Raynor K, Murphy WA, Coy DH, Taylor JE, Moreau JP, Yasuda K, Bell GI, Reisine T (1993b) Cloned somatostatin receptors: Identification of subtype-selective peptides and demonstration of high affinity binding of linear peptides. Molecul Pharmacol 43:838–844

Raynor K, O'Carroll AM, Kong H, Yasuda K, Mahan LC, Bell GI, Reisine T (1993c) Characterization of cloned somatostatin receptors SSTR4 and SSTR5. Mol Pharmacol 44:385–392

Rens-Domiano S, Law SF, Yamada Y, Seino S, Bell GI, Reisine T (1992) Pharmacological properties of two cloned somatostatin receptors. Mol Pharmacol 42:28–34

Reisine T, Bell GI (1995) Molecular properties of somatostatin receptors. Neurosci 67:777–790

Rohrer L, Raulf F, Bruns Ch, Buettner R, Hofstaedter F, Schüle R (1993) Cloning and characterization of a fourth human somatostatin receptor. Proc Natl Acad Sci, USA, 90:4196–4200

Rossowski WJ, Coy DH (1994) Specific inhibition of rat pancreatic insulin or glucagon release by receptor-selective somatostatin analogs. Biochem Biophys Res Commun 205:341–346

Schonbrunn A, Lee AB, Brown PJ (1993) Characterization of a biotinylated somatostatin analog as a receptor probe. Endocrinology 132:146–154

Schulz S, Schmidt H, Handel M, Schreff M, Hollt V (1998) Differential distribution of alternatively spliced somatostatin receptor 2 isoforms SST_{2A} and SST_{2B} in rat spinal cord. Neurosci Lett 257:37–40

Shimon I, Taylor JE, Dong JZ, Bitonte RA, Kim S, Morgan B, Coy DH, Culler MD, Melmed S (1997) Somatostatin receptor subtype specificity in human fetal pituitary cultures. Differential role of SSTR2 and SSTR5 for growth hormone, thyroid-stimulating hormone, and prolactin regulation. J Clin Invest 99:789–798

Simon MA, Romero B, Calle C (1988) Characterization of somatostatin binding sites in isolated rat adipocytes. Regul Pept 23:261–270

Srikant CB, Dahan A, Craig C (1990) Receptor binding of somatostatin-14 and somatostatin-28 in rat brain: differential modulation by nucleotides and ions. Regul Pept 27:181–194

Tallent M, Liapakis G, O'Carroll AM, Lolait SJ, Dichter M, Reisine T (1996) Somatostatin receptor subtypes SSTR2 and SSTR5 couple negatively to an L-type Ca^{2+} current in the pituitary cell line AtT20. Neurosci 71:1073–1081

Thermos K, Reisine T (1988) Somatostatin receptor subtypes in the clonal anterior pituitary cell lines AtT-20 and GH3. Mol Pharmacol 33:370–377

Vanetti M, Kouba M, Wang X, Vogt G, Höllt V (1992) Cloning and expression of a novel mouse somatostatin receptor (SSTR 2B). FEBS Lett 311:290–294

Viollet C, Lanneau C, Faivre-Bauman A, Zhang J, Djordjijevic D, Loudes C, Gardette R, Kordon C, Epelbaum J (1997) Distinct patterns of expression and physiological effects of sst_1 and sst_2 receptor subtypes in mouse hypothalamic neurons and astrocytes in culture. J Neurochem 68:2273–2280

Warhurst G, Higgs NB, Fakhoury H, Warhurst AC, Garde J, Coy DH (1996) Somatostatin receptor subtype 2 mediates somatostatin inhibition of ion secretion in rat distal colon. Gastroenterology 111:325–333

Wyatt MA, Jarvie E, Humphrey PPA (1996) Somatostatin sst_2 receptor-mediated inhibition of parietal cell function in rat isolated gastric mucosa. Br J Pharmacol 119:905–910

Yamada Y, Post SR, Wang K, Tager HS, Bell GI, Seino S (1992) Cloning and functional characterization of a family of human and mouse somatostatin receptors expressed in brain, gastrointestinal tract, and kidney. Proc Natl Acad Sci, USA, 89:251–255

Yang L, Berk SC, Rohrer SP, Mosley RT, Guo L, Underwood DJ, Arison BH, Birzin ET, Hayes EC, Mitra SW, Parmar RM, Cheng K, Wu T-J, Butler BS, Foor F, Pasternak A,

Pan Y, Silva M, Freidinger RM, Smith RG, Chapman K, Schaeffer JM, Patchett AA (1998) Synthesis and biological activities of potent peptidomimetics selective for somatostatin receptor subtype 2. Proc Natl Acad Sci USA 95:10836–10841

Yasuda R, Rens-Damiano S, Breder ChD, Law SR, Saper CB, Reisine T, Bell GI (1992) Cloning of a novel somatostatin receptor, SSTR3, coupled to adenyl cyclase. J Biol Chem 267:20422–20428

J.7.0.8 Secretin Activity

PURPOSE AND RATIONALE

Synthetic derivatives of secretin can be tested for activity against the standard using the bioassay of a chronic pancreatic fistula in dogs. Moreover, stability of secretin preparations has to be checked when using this bioassay.

PROCEDURE

Dogs with a chronic pancreatic fistula prepared according to Preshaw and Grossman (1965), Herrera et al. (1968) (see J.6.1.4) are used. Eighteen hours prior to the experiment food is withdrawn but water allowed ad libitum. Pancreatic juice is collected for 15 min periods. After 1 h pretest time, a test dose of 0.2 KE/kg Karolinska-secretin is given intravenously. In one hour intervals the test preparation or the standard is given alternatively in logarithmic doses between 0.1 and 1.6 KE/kg intravenously. The volume of pancreas juice secreted during 30 min after injection is used as parameter.

EVALUATION

Using at least two doses of test compound and standard, parallel line assays can be carried out and potencies can be calculated. Each of 4 animals receives two doses test compound and two doses standard, the application scheduled according to a Latin square. Potency ratios with confidence limits are calculated.

CRITICAL ASSESSMENT OF THE METHOD

The method is time consuming and needs dogs with chronic fistula. Nevertheless, for final evaluation of a test compound this bioassay can not be avoided.

MODIFICATIONS OF THE METHOD

The standardization of secretin has been described as early as 1952 by Burn et al. using anesthetized **cats**. After laparotomy the pylorus and first duodenal loop are brought outside and turned to the animal's left side. The bile duct is identified by gently squeezing the bile-bladder. The pancreatic duct usually enters the duodenum about 2 mm below the entry of the bile-duct. Starting about 2 cm below the bile duct, the pancreas is separated from the duodenum by blunt dissection, the blood vessels being tied and divided where necessary. When the pancreatic duct is reached, two silk ligatures are placed around and a length of 5 mm is dissected. A dose of secretin is injected intravenously and one of the ligatures is then tied as near the duodenum as possible. The duct is then cut and a flow of juice is usually visible. A small cannula is tied into the duct and attached to a rubber tube and L-piece whose position is adjusted so that the flow of juice continues. The cannula and the L-piece are clamped in position and the abdomen is closed.

The relation between the dose injected and the number of drops of pancreatic juice secreted is almost linear, but the slope differs in different cats. In making a comparison between two preparations, the dose-response relation is first determined for the standard preparation by administration of three or more different doses. A dose of the test preparation is then injected and the effect compared with the curve of the standard. Further doses of the test preparation and comparison of the dose-response curves allow the calculation of the relative potency.

Izzo et al. (1989) studied the internalization of labelled secretin into isolated pancreatic acinar cells of **rats**.

REFERENCES AND FURTHER READING

Burn JH, Finney DJ, Goodwin LG (1952) Biological Standardization, Oxford University Press, London, New York, Toronto, Chapter XVIII, Secretin and Pancreozymin, pp 335–339

Herrera F, Kemp DR, Tsukamoto M, Woodward ER, Dragstedt LR (1968) A new cannula for the study of pancreatic function. J Appl Physiol 25:207–209

Izzo RS, Chen AI, Pellecchia C, Praisman M (1989) Secretin internalization and adenosine 3′,5′-monophosphate levels in pancreatic acinar cells. Endocrinology 124:2252–2260

Preshaw RM, Grossman MI (1965) Stimulation of pancreatic secretion by extracts of the pyloric gland area of the stomach. Gastroenterology 48:36–44

J.7.0.9 Receptor Binding for Secretin

PURPOSE AND RATIONALE

Secretin receptor antagonists, such as reduced peptide bond pseudopeptide analogues of secretin, inhibit the binding of ^{125}I-secretin to secretin receptors in pancreatic acini (Haffar et al. 1991).

Radioimmunoassays for secretin have been developed (Boden and Wilson 1979; Chang and Chey 1980) and are available as commercial kits.

PROCEDURE

Dispersed acini from guinea pig pancreas are prepared according to Peikin et al. (1978) and Jensen et al. (1982). After sacrifice, the pancreas of a guinea pig is immediately removed and trimmed of fat and mesentery. A suspension of dispersed acini is prepared by injecting the pancreas 5 times with 5 ml of digestion solution composed of standard incubation solution plus purified collagenase (0.12 mg/ml). The pancreas is incubated for 4 sequential 10-min periods at 37°C in a Dubnoff incubator at 160 oscillations per min. The gas phase is 100% O_2. The digestion solution is discarded, and the tissue is washed 3 times with 5 ml of standard incubation solution. The tissue is dispersed by passing it 5 times through each of a series of siliconized glass pipettes of decreasing bore (3, 1, and 0.5 mm). Large fragments and the duct system are discarded. The suspension of dispersed acini is layered over standard incubation solution containing 4% albumin and centrifuged at 800 *g*. The supernatant is discarded, and the acini are washed twice with standard incubation solution containing 4% albumin.

^{125}I-Secretin and ^{125}I-labeled analogues are prepared using chloramine T and a method described by Chang and Chey (1980), Jensen et al. (1983), Zhou et al. (1989). They are separated from ^{125}I using a disposable C_{18} cartridge (Sep-Pak) and then separated from unlabeled peptide with reverse phase HPLC using a 4.6-mm × 25-cm column of mBondapak C_{18}. The column is eluated with a linear gradient of acetonitrile in 0.1% trifluoroacetic acid (v/v) from 0 to 54% acetonitrile in 60 min using a flow rate of 1.0 ml/min.

For binding of ^{125}I-secretin incubations are performed containing 0.25 ml of cell suspension of pancreatic acini (one pancreas in 10 ml of standard incubation buffer) and 50 pM ^{125}I-secretin with or without 1 mM secretin. Nonsaturable binding of ^{125}I-secretin is measured as the amount of radioactivity associated with acini when the incubation contains 50 pM ^{125}I-secretin plus 1 mM secretin. Secretin antagonists are added in various concentrations. Saturable binding of ^{125}I-secretin is expressed as percentage of radioactivity bound in the absence of the antagonists.

EVALUATION

K_i values are calculated from percent of controls of bound ^{125}I-secretin using the equation:

$$K_i = [R/(R-1)][S\,B/(S+A)]$$

where R = the observed saturable binding of ^{125}I-secretin in the presence of the antagonist (B) expressed as a fraction of that obtained when B is not present. A is the concentration of ^{125}I-secretin (0.05 nM), S is the k_d determined by Scatchard analysis.

MODIFICATIONS OF THE METHOD

Bawab et al. (1991) characterized the down regulation of the ^{125}I-secretin binding sites and the associated desensitization of the secretion receptor-cAMP system in rat gastric glands.

Molecular cloning and expression of a cDNA encoding the secretin receptor in COS cells was reported by Ishihara et al. (1991).

Steiner et al. (1993) localized secretin receptors mediating rat stomach relaxation by autoradiography of frozen sections of the rat stomach with ^{125}I-labeled porcine secretin.

Ulrich et al. (1993) studied the intrinsic photoaffinity labeling of native and recombinant rat pancreatic secretin receptors.

Vilardaga et al. (1994) investigated the properties and regulation of the coupling to adenylate cyclase of secretin receptors stabile transfected in Chinese hamster ovary cells.

Molecular cloning, expression and functional characterization of a human secretin receptor was reported by Chow (1995), Patel et al. (1995), of the rabbit secretin receptor by Svoboda et al. (1996). The full-length human secretin receptor cDNA was subcloned into the mammalian expression vector pRc/CMV and expressed in cultured CHO cells (Ng et al. 1999). Intracellular cAMP accumulation of the stably transfected cells was measured by a radioimmunoassay, while the extracellular acidification rate was measured by the Cytosensor microphysiometer.

REFERENCES AND FURTHER READING

Bawab W, Chastre E, Gespach C (1991) Functional and structural characterization of the secretin receptors in rat gastric glands: desensitization and glycoprotein nature. Biosci Rep 11:33–42

Boden G, Wilson RM (1979) Secretin. In: Jaffe BM, Behrman HR (eds) Methods of Hormone Radioimmunoassay. Academic Press, New York, pp 479–494

Chang TM, Chey WY (1980) Radioimmunoassay of secretin. A critical review and current status. Dig Dis Sci 25:529–552

Chow BKC (1995) Molecular cloning and functional characterization of a human secretin receptor. Biochem Biophys Res Commun 212:204–211

Haffar BM, Hocart SJ, Coy DH, Mantey S, Chiang HCV, Jensen RT (1991) Reduced peptide bond pseudopeptide analogues of secretin. A new class of secretin receptor antagonists. J Biol Chem 266:316–322

Ishihara T, Nakamura AS, Kaziro Y, Takahashi T, Takahashi K, Nagata S (1991) Molecular cloning and expres-

sion of a cDNA encoding the secretin receptor. EMBO J 10:1635–1641
Jensen RT, Lemp GF, Gardner JD (1982) Interactions of COOH-terminal fragments of cholecystokinin with receptors on dispersed acini from guinea pig pancreas. J Biol Chem 257:5554–5559
Jensen RT, Charlton CG, Adachi H, Jones SW, O'Donohue TL, Gardner JD (1983) Use of ^{125}I-secretin to identify and characterize high-affinity secretin receptors on pancreatic acini. Am J Physiol 245:G186–G195
Ng SSM, Pang RTK, Chow BKC, Cheng CHK (1999) Real-time evaluation of human secretin receptor activity using cytosensor microphysiometry. J Cell Biochem 72:517–527
Patel DR, Kong Y, Sreedharan SP (1995) Molecular cloning and expression of a human secretin receptor. Mol Pharmacol 47:467–473
Peikin SR, Rottman AJ, Batzri S, Gardner JD (1978) Kinetics of amylase release by dispersed acini prepared from guinea pig pancreas. Am J Physiol 235:E743–E749
Steiner TS, Mangel AW, McVey DC, Vigna SR (1993) Secretin receptors mediating rat stomach relaxation. Am J Physiol, Gastrointest Liver Physiol 264:G863–G867
Svoboda M, Tastenoy M, De Neef P, Delporte C, Waelbroeck M, Robberecht P (1998) Molecular cloning and *in vitro* properties of the recombinant rabbit secretin receptor. Peptides 19:1055–1062
Ulrich II CD, Pinon DI, Hadac EM, Holicki EL, Chang-Miller A, Gates LK, Miller LJ, (1993) Intrinsic photoaffinity labeling of native and recombinant rat pancreatic secretin receptors. Gastroenterology 105:1534–1543
Vilardaga JP, Ciccarelli E, Dubeaux C, de Neff P, Bollen A, Robberecht P (1994) Properties and regulation of the coupling to adenylate cyclase of secretin receptors stably transfected in Chinese hamster ovary cells. Mol Pharmacol 45:1022–1028
Zhou Z-C, Gardner JD, Jensen RT (1989) Interaction of peptides related to VIP and secretin with guinea pig pancreatic acini. Am J Physiol 256:G283–G290

J.7.0.10 Cholecystokinin Activity (Isolated Rat Pancreatic Acini)

PURPOSE AND RATIONALE

Cholecystokinin (CCK) is one of the first discovered gastrointestinal hormones and one of the most abundant neuropeptides in the brain (Crawley and Corwin (1994). CCK is found in high concentrations in the mammalian brain and may be implicated in the neurobiology of anxiety and panic disorder (Bourin et al. 1996). Two types of CCK receptors have been identified (Wank 1995; Noble et al. 1999; Miyasaka and Funakoshi 2003): CCK-A receptors are mainly located in the periphery, but are also found in some areas of the CNS. CCK-B receptors (Noble and Roques 1999) are widely distributed in the brain. Major biological actions of CCK are the reduction of food intake (Moran and Kinzig 2004) and the induction of anxiety-related behavior. Inhibition of feeding is mainly mediated by the A-type receptors, whereas anxiety-like behavior is induced by stimulating B-type receptors (Fink et al. 1998).

Isolated pancreatic acini of rats can be used for evaluation of cholecystokinin activity of synthetic derivatives and for plasma CCK-like activity (Liddle et al. 1984; Höcker et al. 1990; Schmidt et al. 1991).

PROCEDURE

For plasma determinations, CCK or inhibitors are extracted from a plasma sample using PR-18 cartridges (Merck, Darmstadt, Germany). One ml plasma is diluted with 4 ml 0.1% trifluoroacetic acid and applied to a cartridge. After a wash (15 ml), CCK and inhibitor are eluted with acetonitrile/water (80:20, v/v) and lyophilized. Pancreatic acini are prepared from female Sprague-Dawley rats weighing 180–200 g, 1 to 2 weeks post ovarectomy, by enzymatic digestion of pancreas with collagenase (Jensen et al. 1982). Test compounds, or extracted material reconstituted with Krebs-Ringer HEPES buffer, or CCK standard is incubated with acini (final volume 0.25 ml). Lipase is measured with an autoanalyser (e. g., Hitachi type 705 or 805). Release is calculated as percent of the initial content determined in each incubation vial.

EVALUATION

CCK bioactivity is determined by comparison with a CCK-8 standard curve. Results are expressed as CCK-like bioactivity.

MODIFICATIONS OF THE METHOD

Amblard et al. (1998) evaluated cyclic cholecystokinin analogues for their ability to stimulate amylase secretion from isolated pancreatic acini.

Inhibition of CCK-8 induced release of amylase from pancreatic cells was used for measurement of CCK_A antagonism (Yamazaki et al. 1995; Akiyama et al. 1996; Patel et al. 1996; Taniguchi et al. 1996; Ballaz et al. 1997; Martin-Martinez et al. 1997).

Deyer et al. (1993) reported on acetylcholine and cholecystokinin induced acid extrusion in mouse isolated pancreatic acinar cells as measured by the microphysiometer. The microphysiometer continually measures the pH of the medium bathing a cell sample. EC_{50} values for the acidification rate were determined for CCK and CCK analogues. Dunlop et al. (1997) used the Cytosensor microphysiometer to analyze the activity of cholecystokinin antagonists against the CCK-4-mediated response in hCCK-B CHO cells.

REFERENCES AND FURTHER READING

Akiyama T, Tachibana I, Hirohata Y, Shirohara H, Yamamoto M, Otsuki M (1996) Pharmacological profile of TP-680,

a new cholecystokinin$_A$ receptor antagonist. Br J Pharmacol 117:1588–1564
Amblard M, Rodriguez M, Lignon MF, Galas MC, Bernad N, Aumelas A, Martinez J (1998) Modification of receptor selectivity and functional activity of cyclic cholecystokinin analogues. Eur J Med Chem 33:171–180
Amsterdam A, Jamieson JD (1972) Structural and functional characterization of isolated pancreatic exocrine cells. Proc Natl Acad Sci, USA 69:3028–3032
Ballaz S, Barber A, Fortuño A, Del Río J, Martín-Martínez M, Gómez-Monterrey I, Herranz R, Gonzáles-Muñiz R, García-López MT (1997) Pharmacological evaluation of IQM-95,333, a highly selective CCK_A receptor antagonist with anxiolytic-like activity in animal models. Br J Pharmacol 121:759–767
Bourin M, Malinge M, Vasar E, Bradwejn J (1996) Two faces of cholecystokinin: Anxiety and schizophrenia. Fundam Clin Pharmacol 10:116–126
Crawley JN, Corwin RL (1994) Biological actions of cholecystokinin. Peptides 15:731–755
Deyer JC, Thorn P, Bountra C, Jordan CC (1993) Acetylcholine and cholecystokinin induced acid extrusion in mouse isolated pancreatic acinar cells as measured by the microphysiometer. J Physiol 459:390P
Dunlop J, Brammer N, Evans N, Ennis C (1997) YM022 [(R)-1-[2,3-dihydro-1-(2′-methylphenacyl)-2-oxo-5-phenyl-1H-1,4-benzodiazepin-3yl]-3-(3-methylphenyl)urea]: an irreversible cholecystokinin type-B receptor antagonist. Biochem Pharmacol 54:81–85
Fink H, Rex A, Voits M, Voigt JP (1998) Major biological actions of CCK. A critical evaluation of research findings. Exp Brain Res 123:77–83
Höcker M, Schmidt WE, Wilms HM, Lehnhoff F, Nustede R, Schafmayer A, Fölsch UR (1990) Measurement of tissue cholecystokinin (CCK) concentrations by bioassay and specific radioimmunoassay. Characterization of the bioactivity of CCK-58 before and after tryptic cleavage. Eur J Clin Invest 20 (Suppl 1):S45–S50
Jensen RT, Lemp GF, Gardner JD (1982) Interactions of COOH-terminal fragments of cholecystokinin with receptors on dispersed acini from guinea pig pancreas. J Biol Chem 257:5554–5559
Lewis LD, Williams JA (1990) Regulation of cholecystokinin secretion by food, hormones, and neural pathways in the rat. Am J Physiol 258 (Gastrointest Liver Physiol 21):G512–G518
Liddle RA, Goldfine ID, Williams JA (1984) Bioassay of plasma cholecystokinin in rats: effects of food, trypsin inhibitor, and alcohol. Gastroenterology 87:542–549
Martin-Martinez M, Bartolome-Nebreda JM, Gomez-Monterrey I, Gozalez-Muniz R, Garcia-Lopez MT, Ballaz S, Barber A, Fortuno A, Del Rio J, Herranz R (1997) Synthesis and stereochemical structure activity relationships of 1,3-dioxyperhydropyrido[1,2c]pyrimidine derivatives: Potent and selective cholecystokinin A receptor antagonists. J Med Chem 40:3402–3407
Miyasaka K, Funakoshi A (2003) Cholecystokinin and cholecystokinin receptors. J Gastroenterol 38:1–13
Moran TH, Kinzig KP (2004) Gastrointestinal satiety signals. II. Cholecystokinin. Am J Physiol 286:G183–G188
Noble F, Wank SA, Crawley JN, Bradwejn J, Seroogy KB, Hamon M, Roques BP (1999) International Union of Pharmacology. XXI. Structure, distribution, and functions of cholecystokinin receptors. Pharmacol Rev 51:745–781
Noble F, Roques BP (1999) CCK-B receptor: chemistry. Molecular biology, biochemistry and pharmacology. Progr Neurobiol 58:349–379
Patel S, Chapman KL, Smith AJ, Bailey I, Freedman SB (1996) Are radioligand antagonist / agonist binding ratios in rat pancreas predictive of functional efficacy of cholecystokinin receptor agonists and antagonists? Regul Pept 65:29–35
Taniguchi H, Yazaki N, Endo T, Nagasaki M (1996) Pharmacological profile of T-0632, a novel potent and selective CCK_A receptor antagonist, *in vitro*. Eur J Pharmacol 304:147–154
Schmidt WE, Creutzfeldt C, Höcker M, Nustede R, Choudhury AR, Schleser A, Rovati LC, Fölsch UR (1991) Cholecystokinin receptor antagonist loxiglumide modulates plasma levels of gastro-entero-pancreatic hormones in man. Eur J Clin Invest 21:501–511
Wank SA (1995) Cholecystokinin receptors. Am J Physiol 269:G628–G646
Yamazaki Y, Shinagawa K, Takeda H, Kobayashi M, Akahane M, Ajisawa Y (1995) Cholecystokinin-A specific antagonism of KSG-504 to cholecystokinin receptor binding and pancreatic secretion in mammals. Jpn J Pharmacol 69:367–373

J.7.0.11 Receptor Binding of Cholecystokinin

PURPOSE AND RATIONALE

Receptor binding assays for CCK have been described by several authors, such as Innis and Snyder (1980) for rat pancreas; Gaisano et al. (1989), Doi et al. (1990), Blevis et al. (1990), Maletínská et al. (1992) for isolated pancreatic acini; Saito et al. (1981), Chang et al. (1983) for guinea pig cerebral cortex, Praissman et al. (1983) for guinea pig mucosa, Van Dijk et al. (1984) for rat brain and pancreas; Steigerwalt et al. (1984), Chang and Lotti (1986) for gallbladder membranes; Kaufmann et al. (1993) for guinea-pig cerebral cortex and rat pancreas.

Using transfected COS cells, Talkad et al. (1994) identified three different states of the pancreatic CCK receptor, with the very-low-affinity state being the most abundant.

DeTullio et al. (1999) and Herranz (2003) reviewed advances in the chemistry of cholecystokinin receptor agonists and antagonists.

Radioimmunoassays for cholecystokinin have been developed (Harvey 1979) and are available as commercial kits.

PROCEDURE

Membranes of rat (Sprague Dawley) pancreas, guinea pig (Hartley) cerebral cortex, and bovine gallbladder are prepared by homogenization in 50–100 vol of 50 mM Tris-HCl (pH 7.4 at 37°C) using a Polytron (Brinkman, PT 10, setting 4 for 10 s for pancreas or brain and maximal speed for bovine gallbladder). Homogenates are centrifuged at 50,000 *g* for 10 min, and

the pellets are resuspended in the same buffer and centrifuged as described above. The resulting pellets are resuspended in 4000, 80, and 25 ml of binding assay buffer for each g of original tissue wet weight of pancreas, brain, and gallbladder, respectively. ^{125}I-CCK-8 binding assay buffer contains 5 mM dithiothreitol, 50 mM Tris-HCl (pH 7.4 at 37°C), 5 mM $MgCl_2$, 2 mg of bovine serum albumin, and bacitracin at 0.14 mg/ml for pancreas; 10 mM HEPES, 5 mM $MgCl_2$, 1 mM EGTA, bacitracin at 0.25 mg/ml, and 130 mM NaCl (pH adjusted to 6.5 with NaOH) for brain; and 10 mM HEPES, 5 mM $MgCl_2$, 1 mM EGTA, bacitracin at 0.25 mg/ml, soybean trypsin inhibitors at 0.2 mg/ml, and 130 mM NaCl (pH 6.5) for bovine gallbladder.

^{125}I Bolton-Hunter labeled CCK-8 (New England Nuclear) is used. Free and bound ^{125}I-CCK-8 are separated by filtration using Whatman G/F B glass fiber filters that are presoaked with 50 mM Tris-HCl (pH 7.4) containing bovine serum albumin (1 mg/ml). Immediately after the filtration, the filters are washed rapidly three times with 4 ml of Tris-HCl containing bovine serum albumin (0.1 mg/ml). Radioactivity is counted with a gamma counter, e. g. Beckman Instruments. Specific ^{125}I-CCK-8 binding is defined as the difference between total binding and nonspecific binding in the presence of 1 mM CCK.

EVALUATION

IC_{50} values are determined by regression analysis of displacement curves. Inhibitor constants (K_i) are calculated from the formula

$$K_i = I/(K_{d'}/K_{d-1})$$

where I is the concentration of the inhibitor, and K_d and $K_{d'}$ are the dissociation constants of ^{125}I-CCK-8 in the absence and presence of the inhibitor, respectively.

MODIFICATIONS OF THE METHOD

Subtypes of the cholecystokinin receptor, forming a cholecystokinin receptor family, have been described, such as CCK_A from pancreas and other parts of the gastrointestinal tract and in a few discrete brain regions (Kachur et al. 1991; Poirot et al. 1992; Wank et al. 1992a).

According to the IUPHAR Compendium of Receptor Characterization and Classification 1998; CCK_A and CCK_B receptors are designated as CCK_1 and CCK_2, respectively.

A survey on ligands for cholecystokinin receptors was given by Trivedi (1994).

Van der Bent et al. (1994) described molecular modeling of **CCK-A receptors**.

For CCK_A receptor binding assays (Fossa et al. 1997), the pancreas from a male Hartley guinea pig is dissected and placed in saline. Fatty tissue and blood vessels are dissected away and the tissue placed in 20 vol of buffer (50 mM Tris HCl, pH 7.4, 0.35 mg/ml bacitracin and 0.5 mg/ml soybean trypsin inhibitor) at 4°C and minced using scissors. The tissue is homogenized (Polytron, setting no. 9 for two 15-s bursts), strained through gauze and centrifuged at 100,000 *g* for 15 min at 4°C. The supernatant is discarded and the pellet resuspended in 20 vol of buffer and recentrifuged. The final pellet is diluted to a concentration of 1.25 mg/ml (original wet weight) in buffer and kept on ice until used. The incubation reaction is initiated by the addition of 100 µl of tissue to 96-well plates containing 150 µl of incubation buffer (50 mM Tris HCl, pH 7.4, and a final concentration of 5 mM $MgCl_2$, 5 mM dithiothreitol and 1% DMSO) with 60 pM final concentration of ^{125}I-BH-CCK_{8S}, and drug or vehicle. After a 30-min incubation the reaction is terminated by rapid filtration using a Skatron cell harvester (Skatron Instruments, Inc. VA) onto GF/B filters that were soaked for 2 h in 50 mM Tris HCl, 0.1 mg/ml bovine serum albumin. The filters are dried and counted on a Betaplate counter (Wallac Inc. Gaithersburg, MD) for 45 s per sample.

Povoski et al. (1994) reported cholecystokinin receptor characterization and cholecystokinin A receptor messenger RNA expression in transgenic mouse pancreatic carcinomas and dysplastic pancreas.

Yule et al. (1993), Blevins et al. (1994) recorded intracellular Ca^{2+} concentration signaling stimulated by cholecystokinin or by a partial CCK agonist in Chinese hamster ovary-CCK-A cells or in isolated pancreatic acini.

Ghanekar et al. (1997) established a Chinese hamster ovary cell line bearing the mouse type A cholecystokinin receptor.

CCK-A agonists were evaluated as anorectic agents (Pierson et al. 1997; Simmons et al. 1998).

CCK_B receptors occur predominantly in the central nervous system indicating involvement in behavioral functions (Moran et al. 1986; Wank et al. 1992b; Derrien et al. 1994; Schäfer et al. 1994) but also in pancreatic cancer cells (Smith et al. 1993; Zhou et al. 1992) and small lung cell cancer lines (Sethi et al. 1993).

For CCK_B receptor binding assays (Fossa et al. 1997), guinea pig cortex is homogenized with a Teflon homogenizer in 20 vol of 50 mM Tris HCl (pH 7.4) containing 5 mM $MgCl_2$ at 4°C and centrifuged at

100,000 *g* for 30 min. The supernatant is discarded and the pellet resuspended and spun again. The pellet is diluted to a concentration of 10 mg/ml (original wet weight) with assay buffer (10 mM HEPES, 5 mM $MgCl_2$, 1 mM EGTA, 130 mM NaCl, and 0.2 mg/ml bacitracin, pH 6.5) before use. The incubation reaction is initiated by the addition of 50 µl of tissue to 96-well plates containing 150 µl of assay buffer with 1% DMSO final concentration, 50 pM final concentration of ^{125}I-BH-CCK_{8S} and the appropriate concentration of drug or vehicle. Non-specific binding is estimated using 1 µM CCK_{8S}. The reaction is terminated by spinning the plates using a H1000B rotor at 3000 rpm for 5 min at 4°C. The pellet is washed with 200 µl of 50 mM Tris HCl and respun. The supernatant is again discarded, the pellet resuspended and the tissues harvested onto Betaplate filters soaked in 0.2% polyethylenimine for 2 h using a Skatron cell harvester (Skatron Instruments, Inc., VA). The filtermats are dried and counted on a Betaplate counter (Wallac Inc. Gaithersburg, MD) for 45 s per sample.

Lee et al. (1993) described cloning and characterization of the human brain cholecystokinin-B/gastrin receptor.

Kaufmann et al. (1993) studied the binding of a series of succinylated cholecystokinin tetrapeptide derivatives to different tissues and their effects on intracellular calcium mobilization ($[Ca^{2+}]_i$) in the human T-cell line Jurkat and rat pituitary (GH3) cells.

Durieux et al. (1989) described [^{3}H]pBC 264 as the first highly potent and very selective radioligand for CCK_B receptors.

Slaninova et al. (1995) recommended the radioiodinated CCK_8 analogue, SNF 8702, as a selective radioligand for CCK_B receptors.

Knapp et al. (1990) found CCK-B receptor heterogeneity in various brain areas of the guinea pig using a highly selective CCK-B receptor radioligand.

Dunlop et al. (1996) described the functional characterization of a Chinese hamster ovary cell line transfected with the human CCK-B receptor gene. Functional coupling in these cells was demonstrated using agonist stimulated mobilization of intracellular Ca^{2+}, measured with the FURA-2 technique.

Kaufmann et al. (1995) described the effects of guanyl nucleotides on CCK_B receptor binding in brain tissue and continuous cell lines, such as Jurkat T-cells, rat pituitary GH3 cells, rat glioma C6 cells, and small cell lung cancer NCI-H69 cells.

Cuq et al. (1997) reported that mRNAs encoding CCK_B but not CCK_A receptors are expressed in human T lymphocytes and Jurkat lymphoblastoid cells.

CCK_A receptor antagonists have been described (Chang and Lotti 1986; Makovec et al. 1986; Evans 1993; Gully et al. 1993) as well as **CCK_B receptor antagonists** (Hill and Woodruff 1990; Ohtsuka et al. 1993; Pendley et al. 1993).

Selective non-peptide **CCK_B/gastrin receptor antagonists** have been described by Bertrand et al. (1994, Makovec et al. 1999; Takeuchi et al. 1999). Harper et al. (1999) analyzed some of them in radioligand binding assays in mouse and rat cerebral cortex.

Cholecystokinin dipeptoid antagonists with anxiolytic properties which bind preferably to CCK_B receptors have been reported by Boden et al. (1993).

CCK_A receptor antagonists (Ballaz et al. 1997) and **CCK_B receptor antagonists** (Revel et al. 1998) with anxiolytic-like activity in animal models were described.

REFERENCES AND FURTHER READING

Ballaz S, Barber A, Fortuno A, del Rio J, Martin-Martinez M, Gomez-Monterrey I, Herranz R (1997) Pharmacological evaluation of IQM-95,333, a highly selective CCK_A receptor antagonist with anxiolytic-like activity in animal models. Br J Pharmacol 121:759–767

Bertrand P, Böhme GA, Durieux C, Guyon C, Capet M, Jeantaud B, Boudeau P, Ducos B, Pendley CE, Martin GE, Floch A, Doble A (1994) Pharmacological properties of ureido-acetamides, new potent and selective non-peptide CCK_B/gastrin receptor antagonists. Eur J Pharm 262:233–245

Blevins GT Jr, Doi R, Tangoku A, Chowdhury P, McKay D, Rayford PL (1992) Simultaneous measurement of cholecystokinin-stimulated amylase release and cholecystokinin receptor binding in rat pancreatic acini. J Lab Clin Med 119:566–573

Blevins GT Jr, van de Westerloo EMA, Yule DI, Williams JA (1994) Characterization of cholecystokinin$_A$ receptor agonist activity by a family of cholecystokinin$_B$ receptor antagonists. J Pharmacol Exp Ther 269:911–916

Boden PR, Higginbottom M, Hill DR, Horwell DC, Hughes J, Rees DC, Roberts E, Singh L, Suman-Chauhan N, Wooruff GN (1993) Cholecystokinin dipeptoid antagonists: Design, synthesis, and anxiolytic profile of some novel CCK-A and CCK-B selective and "mixed" CCK-A/CCK-B antagonists. J Med Chem 36:552–565

Chang RS, Lotti VJ (1986) Biochemical and pharmacological characterization of an extremely potent and selective non-peptide cholecystokinin antagonist. Proc Natl Acad Sci, USA, 83:4923–4926

Chang RS, Lotti VJ, Chen TB, Kunkel KA (1986) Characterization of the binding of [^{3}H]-(±)-L-364,718: a new potent, non-peptide cholecystokinin antagonist radioligand selective for peripheral receptors. Mol Pharmacol 30:212–217

Chang RSL, Lotti VJ, Martin GE, Chen TB (1983) Increase in brain ^{125}I-cholecystokinin (CCK) receptor binding following chronic haloperidol treatment, intracisternal 6- hydroxydopamine or ventral tegmental lesions. Life Sci 32:871–878

Cuq P, Gross A, Terraza A, Fourmy D, Clerc P, Dornand J, Magous R (1997) mRNAs encoding CCK_B but not CCK_A

receptors are expressed in human T lymphocytes and Jurkat lymphoblastoid cells. Life Sci 61:543–555

Derrien M, McCort-Tranchepain I, Ducos B, Roques BP, Durieux C (1994) Heterogeneity of CCK_B receptors involved in animal models of anxiety. Pharmacol Biochem Behav 49:133–141

DeTullio P, Delarge J, Pirotte B (1999) Recent advances in the chemistry of cholecystokinin receptor ligands (agonists and antagonists). Curr Med Chem 6:433–455

Doi R, Hosotani R, Inoue K, Fujii N, Najima H, Rayford PhL, Tobe T (1990) Receptor binding of cholecystokinin analogues in isolated rat pancreatic acini. Biochem Biophys Res Commun 166:286–292

Dunlop J, Brammer N, Ennis C (1996) Pharmacological characterization of a Chinese hamster ovary cell line transfected with the human CCK-B receptor gene. Neuropeptides 30:359–363

Durieux C, Corringer JP, Bergeron F, Roques BP (1989) [^{3}H]pBC 264, first highly potent and very selective radioligand for CCK-B receptors. Eur J Pharmacol 168:269–270

Evans BE (1993) MK-329: A non-peptide cholecystokinin A antagonist. Drug Dev Res 29:255–261

Fossa AA, DePasquale J, Morrone J, Zorn SH, Bryce D, Lowe JA, McLean S (1997) Cardiovascular effects of cholecystokinin-4 are mediated by the cholecystokinin-B receptor subtype in the conscious guinea pig and dog. J Pharmacol Exp Ther 281:180–187

Gaisano HY, Klueppelberg UG, Pinon DI, Pfenning MA, Powers StP, Miller LJ (1989) Novel tool for the study of cholecystokinin-stimulated pancreatic enzyme secretion. J Clin Invest 83:321–325

Ghanekar D, Hadac EM, Holicky EL, Miller LJ (1997) Differences in partial agonistic action at cholecystokinin receptors of mouse and rat are dependent on parameters extrinsic to receptor structure: Molecular cloning, expression and functional characterization of the mouse type A cholecystokinin receptor. J Pharm Exp Ther 282:1206–1212

Gully D, Fréhel D, Marcy C, Spinazzé A, Lespy L, Neliat G, Maffrand JP, LeFur G (1993) Peripheral biological activity of SR 27897: a new potent non-peptide antagonist of CCK_A receptors. Eur J Pharmacol 232:13–19

Harper EA, Griffin EP, Shankley NP, Black JW (1999) Analysis of the behavior of selected CCK_B/gastrin receptor antagonists in radioligand binding assays in rat and mouse cerebral cortex. Br J Pharmacol 126:1496–1503

Harvey RF (1979) Cholecystokinin – Pancreozymin. In: Jaffe BM, Behrman HR (eds) Methods of Hormone Radioimmunoassay. Academic Press, New York, pp 495–526

Herranz R (2003) Cholecystokinin antagonists: pharmacological and therapeutic potential. Med Res Rev 23:559–605

Hill DR, Woodruff GN (1990) Differentiation of central cholecystokinin receptor binding sites using the non-peptide antagonists MK-329 and L-365,260. Brain Res 526:276–283

Innis RB, Snyder SH (1980) Distinct cholecystokinin receptors in brain and pancreas. Proc Natl Acad Sci, USA, 77:6917–6921

Kachur JF, Wang SX, Gullikson GW, Gaginella TS (1991) Cholecystokinin-mediated ileal electrolyte transport in the guinea pig. Gastroenterology 101:1428–1431

Kaufmann R, Lindschau C, Henklein P, Boomgaarden M, Haller H, Schöneberg T, Arnswald A, Kölske C, Ott T (1993) Studies with succinylated CCK-4 derivatives: characterization of CCK_B receptor binding and measurement of $[Ca^{2+}]_i$ mobilization. Mol Neuropharmacol 3:147–151

Kaufmann R, Schöneberg T, Henklein P, Meyer R, Martin H, Ott T (1995) Effects of guanyl nucleotides on CCK_B receptor binding in brain tissue and continous cell lines: a comparative study. Neuropeptides 29:63–68

Knapp RJ, Vaughn LK, Fang S-N, Bogert CL, Yamamura MS, Hruby VJ, Yamamura HI (1990) A new, highly selective CCK-B receptor radioligand ([^{3}H][N-methyl-Nle^{28,31}] $CCK_{26–33}$): evidence for CCK-B receptor heterogeneity. J Pharmacol Exp Ther 255:1278–1286

Lee Y-M, Beinborn M, McBride EW, Lu M, Kolakowski LF Jr, Kopin AS (1993) The human brain cholecystokinin-B/gastrin receptor. Cloning and characterization. J Biol Chem 268:8164–8169

Lin CW, Miller T (1985) Characterization of cholecystokinin receptor sites in guinea-pig cortical membranes using [^{125}I]Bolton-Hunter cholecystokinin octapeptide. J Pharmacol Exp Ther 232:755–780

Makovec F, Revel L, Rovati L, Setnikar I (1986) *In vivo* antispasmodic activity on the gall bladder of the mouse of new glutamic acid derivatives with CCK antagonistic activity. Gastroenterol 90:1531

Makovec F, Revel L, Letari O, Mennuni L, Impicciatore M (1999) Characterization of antisecretory and antiulcer activity of CR 2945, a new potent and selective gastrin/CCK_B receptor antagonist. Eur J Pharmacol 369:81–90

Maletínská L, Lignon MF, Galas MCh, Bernad N, Pírková J, Hlavácek J, Slaninová J, Martinez J (1992) Pharmacological characterization of new cholecystokinin analogues. Eur J Pharmacol 222:233–240

Moran TH, Robinson PH, Goldrich MS, McHugh PR (1986) Two brain cholecystokinin receptors: implications for behavioral actions. Brain Res 362:175–179

Ohtsuka T, Kotaki H, Nakayama N, Itezono Y, Shimma N, Kudoh T, Kuwahara T, Arisawa M, Yokose K (1993) Tetronothiodin, a novel cholecystokinin type-B receptor antagonist produced by Streptomyces sp. NR0489. II. Isolation, characterization and biological activities. J Antibiotics 46:11–17

Pendley ChE, Fitzpatrick LR, Ewing RW, Molino BF, Martin GE (1993) The gastrin/cholecystokinin-B receptor antagonist L-365,260 reduces basal acid secretion and prevents gastrointestinal damage induced by aspirin, ethanol and cysteamine in the rat. J Pharmacol Exp Ther 265:1348–1354

Pierson ME, Comstock JM, Simmons RD, Kaiser F, Julien R, Zongrone J, Rosamond JD (1997) Synthesis and biological evaluation of potent, selective, hexapeptide CCK-A agonist anorectic agents. J Med Chem 40:4302–4207

Poirot SS, Dufresne M, Jiménez J, Vaysse N, Fourmy D (1992) Biochemical characterization of a subtype pancreatic cholecystokinin receptor and its agonistic binding domain. J Receptor Res 12:233–253

Povoski SP, Zhou W, Longnecker DS, Bell RH Jr (1994) Cholecystokinin receptor characterization and cholecystokinin A receptor messenger RNA expression in transgenic mouse pancreatic carcinomas and dysplastic pancreas. Oncol Res 6:411–417

Praissman M, Martinez PA, Saladino CF, Berkowitz JM, Steggles AW, Finkelstein JA (1983a) Characterization of cholecystokinin binding sites in rat cerebral cortex using a ^{125}I-CCK-8 probe resistant to degradation. J Neurochem 40:1406–1413

Praissman M, Walden ME, Pellecchia C (1983b) Identification and characterization of a specific receptor for cholecystokinin on isolated fundic glands from guinea pig gastric mucosa using a biologically active ^{125}I-CCK-8 probe. J Receptor Res 3:647–665

Revel L, Mennuni L, Garofalo P, Makovec F (1998) CR 2945: a novel CCK_B receptor antagonist with anxiolytic-like activity. Behav Pharmacol 9:183–194
Saito A, Goldfine ID, Williams JA (1981) Characterization of receptors for cholecystokinin and related peptides in mouse cerebral cortex. J Neurochem 37:483–490
Schäfer U, Harhammer R, Boomgaarden M, Sohr R, Ott T, Henklein P, Repke H (1994) Binding of cholecystokinin-8 (CCK-8) peptide derivates to CCK_A and CCK_B receptors. J Neurochem 62:1426–1431
Sethi T, Herget T, Wu SV, Walsh JH, Rozengurt E (1993) CCK_A and CCK_B receptors are expressed in small cell lung cancer lines and mediate Ca^{2+} mobilization and clonal growth. Cancer Res 53:5208–5213
Simmons RD, Kaiser FC, Pierson ME, Rosamond JR (1998) ARL 15849: A selective CCK-A agonist with anorectic activity in the rat and dog. Pharmacol Biochem Behav 59:439–444
Slaninova J, Knapp RJ, Weber SJ, Davis TP, Fang SN, Hruby VJ, Yamamura HI (1995) [^{125}I]SNF 8702: A selective radioligand for CCK_B receptors. Peptides 16:221–224
Smith JP, Rickabaugh CA, Mc Laughlin PJ, Zagon IS (1993) Cholecystokinin receptors and PANC-1 human pancreatic cancer cells. Am J Physiol, Gastrointest Liver Physiol 265:G149–G155
Steigerwalt RW, Goldfine ID, Williams JA (1984) Characterization of cholecystokinin receptors on bovine gallbladder membranes. Am J Physiol 247:G709–G714
Takeuchi K, Hirata T, Yamamoto H, Kunikata T, Ishikawa M, Ishihara Y (1999) Effects of S-0509, a novel CCK_B/gastrin receptor antagonist, on acid secretion and experimental duodenal ulcers in rats. Aliment Pharmacol Ther 13:87–96
Talkad VD, Forune KP, Pollo DA, Shah GN, Wank SA, Gardner JD (1994) Direct demonstration of three different states of the pancreatic cholecystokinin receptor. Proc Natl Acad Sci USA 91:1868–1872
Tilley JW, Danho W, Shiuey SJ, Kulesha I, Sarabu R, Swistok J, Makofske R, Olson GL, Chiang E, Rusiecki VK, Wagner R, Michalewsky J, Triscari J, Nelson D, Chiruzzo FY, Weatherford S (1992) Structure activity of *C*-terminal modified analogs of Ac-CCK-7. Int J Peptide Protein Res 39:322–336
Trivedi BK (1994) Ligands for cholecystokinin receptors: Recent developments. Curr Opin Ther Pat 4:31–44
Van der Bent A, Ijzerman AP, Soudijn W (1994) Molecular modelling of CCK-A receptors. Drug Design Disc 12:129–148
Van Dijk A, Richard JG, Trzeciak A, Gillessen D, Möhler H (1984) Cholecystokinin receptors: biochemical demonstration and autoradiographical localization in rat brain and pancreas using [^{3}H]cholecystokinin$_8$ as radioligand. J Neurosci 4:1021–1033
Wank SA, Harkins R, Jensen JT, Shapira H, deWeerth A, Slattery T (1992a) Purification, molecular cloning, and functional expression of the cholecystokinin receptor from rat pancreas. Proc Natl Acad Sci, USA, 89:3125–3129
Wank SA, Pisegna JR, deWeerth A (1992b) Brain and gastrointestinal cholecystokinin receptor family: structure and functional expression. Proc Natl Acad Sci, USA, 89:8691–8695
Yule DI, Tseng M-J, Williams JA, Logsdon CD (1993) A cloned CCK-A receptor transduces multiple signals in response to full and partial agonists. Am J Physiol 265 (Gastrointest Liver Physiol 28):G999–G1004
Zhou W, Povovski SP, Longnecker DS, Bell RH Jr (1992) Novel expression of gastrin (cholestystokinin B) receptors in azaserine-induced rat pancreatic carcinoma: Receptor determination and characterization. Cancer Res 52:6905–6911

J.7.0.12 Acute Experimental Pancreatitis

PURPOSE AND RATIONALE

Acute interstitial pancreatitis can be induced in the rat by excessive doses of a pancreatic secretagogue (Lampel and Kern 1987) such as caerulein (Renner et al. 1986; Ito et al. 1991; Yazu et al. 1991).

PROCEDURE

Induction of Pancreatitis

Male Wistar rats weighing 200 g are used. Pancreatitis is induced by caerulein given as 5 intraperitoneal injections of 40 µg/kg each at hourly intervals on day 1. Controls receive saline injections only. Treatment with potential drugs is started at day 1 and continued for 7 or 14 days. The rats are sacrificed after 1 or 2 weeks following caerulein injection.

Preparation of Pancreatic Acini

The rats are decapitated after overnight fasting and the pancreata are quickly removed. The pancreata are injected with digestion medium containing 170 U/ml collagenase and incubated for 15 min at 37°C. The medium is changed for the second incubation for 60 min with 15 ml digestion medium containing 200 U/ml collagenase. Acini are dissociated by sequential passage through 4 pipettes of different diameters in a standard medium containing 0,1% soybean inhibitor. The suspension is filtered through a single layer of gauze and layered over 15 ml of 4% bovine albumin. After centrifugation for 2 min at 400 rpm, the pellet is washed 3 times with 20 ml of incubation medium containing 0.5 mM $CaCl_2$. Finally, the acini are resuspended in 10–20 ml of the incubation medium containing 10 mM HEPES, 145 mM NaCl, 4.7 mM KH_2PO_4, 1.0 mM $CaCl_2$, 1.2 mM $MgCl_2$, 16.5 mM glucose, 0.1% bovine serum albumin, 0.01% soybean trypsin inhibitor, Eagles minimal essential amino acids and vitamins, adjusted to pH 7.4 and bubbled with 100% oxygen.

Measurement of [^{3}H]-Thymidine Uptake Into Pancreatic Acini

Aliquots (5 ml) of the acini suspension are incubated at 37°C for 30 min, and 6-[^{3}H]-thymidine (5 mCi/mmol) is added as a final concentration of 0.8 mCi/mol. After incubation for 60 min, 200 ml aliquots are filtered by vacuum through Whatman GF/B glass fiber filters. Filters which trapped the acini are washed with 15 ml ice-cold buffer. After adding 5 ml of Aquazol II to

each vial, the radioactivity of the filters is counted with a scintillation spectrometer.

Measurement of Amylase Secretion from Pancreatic Acini

Acini are resuspended in 5 ml of the incubation medium and pre-incubated at 37°C for 30 min. Carbachol at concentrations between 10^{-7} and 10^{-4} M or CCK-8 at concentrations between 10^{-11} and 10^{-8} M is added and the acini suspension is incubated at 37°C for an additional 30 min. Triplicate 300 ml aliquots are centrifuged for 5 s at 3000 rpm. The amylase activity in the supernatant is measured by a commercial amylase test. Triplicate 500 ml aliquots are sampled before adding the secretagogue and the amylase contents (total amylase) are measured after sonification.

EVALUATION

Thymidine uptake is compared between control, caerulein treated animals and animals treated with drugs. Dose-response curves of amylase secretion after carbachol and CCK-8 are established for each group. Moreover, amylase concentrations in the acini are compared.

MODIFICATIONS OF THE METHOD

Griesbacher and Lembeck (1992), Griesbacher et al. (1993) studied the prevention of **caerulein-induced** experimental acute pancreatitis in the rat by the bradykinin antagonist HOE 140.

Several authors (Ito et al. 1994; Ogden et al. 1994; Liu et al. 1995; Sledzinski et al. 1995; Weidenbach et al. 1995; Chen et al. 1996; Lembeck and Griesbacher 1996; Asano et al. 1997; Ito et al. 1997) used different dose regimens of caerulein administration to induce acute pancreatitis in rats.

Niederau et al. (1995) used caerulein to induce acute necrotizing pancreatitis in mice and evaluated the protective effects of secretin and of the cholecystokinin-receptor antagonists proglumide and benzotript.

Huch et al. (1995) induced necrotizing pancreatitis by intraductal infusion of low-dose glycodeoxycholic acid (10 mmol/l) followed by intravenous cerulein (6 µg/kg/h) for 6 h.

Several other chemicals and drugs may induced acute pancreatitis (Vogel 1994).

Merkord et al. (1997) studied the pathogenesis and the time course of lesions of acute interstitial pancreatitis in rats induced by intravenous injection of 6 mg/kg **dibutyltin dichloride** (DBTC), an organotin compound used in chemical industry and in veterinary medicine. First, the cytotoxic effects on the biliopancreatic duct epithelium lead to epithelial necrosis with obstruction of the duct, subsequent cholestasis, and interstitial pancreatitis; and second, the hematogenic effects of DBTC cause direct injury of pancreatic cells followed by interstitial edema and inflammation. A chronic course is found when the obstruction of the duct and cholestasis persist.

Destruction of acinar cells has been found after the administration of **ethionine** in rats (Herman and Fitzgerald 1962).

Niederau et al. (1985), Neuschwander-Tetri et al. (1994), Norman et al. (1995), Van Laethem et al. (1995), Taniguchi et al. (1996) described acute necrotizing pancreatitis induced by caerulein in **mice**.

Pancreatitis can be induced in mice by a **choline-deficient diet** (Lombardi et al. 1975; Niederau et al. 1990). Mice weighing 10–14 g are fed regular laboratory chow ad libitum before the experiment. A choline-deficient diet supplemented with 0.5% ethionine is given for a period of 66 h, after which it is replaced by regular chow.

Lake-Bakaar and Lyubsky (1995), Hirano (1997), Niederau et al. (1995) induced acute pancreatitis in female Swiss-Webster mice by feeding a choline- and methionine-deficient diet supplemented with 1% ethionine.

Emanuelli et al. (1994) demonstrated that a single injection of endotoxin (lipopolysaccharides, *E. coli* 0111-B4) into the superior pancreaticoduodenal artery of **rabbits** induced a dose-dependent acute necrotizing pancreatitis.

Watanabe et al. (1993) induced acute hemorrhagic pancreatitis in rats by surgically **closing a 1 cm length of duodenal loop** at points proximal and distal to the orifice of the pancreatic duct for 6 h with bypassing the bile from the liver hilus distal to the closed loop. The effects of Hoe 140, a bradykinin antagonist, were studied.

Ha et al. (1994, 1996) used the closed duodenal loop technique to study the role of endogenous and exogenous cholecystokinin in experimental pancreatitis and the effect of a cholecystokinin receptor antagonist on the early stage of the healing process in acute pancreatitis.

Kimura et al. (1988) found beneficial effects of a cholecystokinin A receptor antagonist in three methods of acute experimental pancreatitis: pancreatitis in mice induced by 6 intraperitoneal injections of 50 µg/kg caerulein, necrotizing pancreatitis in rats induced by injection of sodium taurocholate into the common

bile duct followed by 4 subcutaneous injections of 50 µg/kg caerulein, and in closed duodenal loop induced pancreatitis in rats.

Obermaier et al. (2001, 2004a, 2004b) described **ischemia/reperfusion-induced pancreatitis** in rats. Male Wister rats weighing 290–330 g were anesthetized by intraperitoneal injection of 60 mg/kg pentobarbital. The were placed on a heating pad and ventilated after tracheotomy with normal air (TSE, Bad Homburg, Germany). Polyethylene catheters were placed in the right carotid artery and the left jugular vein. The upper abdomen was opened by transverse laparotomy. The intestine was exteriorized to the right. The stomach was turned up cranially, and fixed on the skin by sutures. All exteriorized segments were moistened and covered with transparent foil to prevent drying. The pancreas was separated from the stomach and the short gastric vessels were ligated. The border to the caudal apart of the pancreas tail segment was the constant branch of the pancreaticoduodenal artery running to the caudal part of the spleen. Pancreatic and connective tissue in the area of the celiac axis were dissected. Thus the complete vascular isolation of the pancreatic tail pedunculated on the splenic vessels was accomplished.

The common hepatic artery was identified in order to allow PO_2 measurements, the pancreas was fixed on an oval plastic pad with sutures to the connective tissue and splenectomy was performed. A PO_2-sensitive Clark-type probe was inserted into the pancreatic tissue. The probe was fixed to connective tissue on its distal end with a suture. For local intra-arterial access, a small polyethylene catheter was inserted in the retrograde direction into the left gastric artery and fixed. The pancreatic tail-segment was covered with foil to prevent access of ambient air and drying. After a stabilization period of 10 min, the pancreatic tail segment was flushed with 1 ml of heparinized saline via the catheter in the left gastric artery, after clamping the celiac axis and the common hepatic artery. Paleness of the pancreatic tail segment indicated successful flushing.

For the induction of isolated pancreatic tail ischemia two clamps were put on the splenic vessels and then the clamps of the celiac axis and the common hepatic artery were removed. Continuously decreasing tissue PO_2 indicated successful ischemia. The clamps on the splenic vessels were removed after an ischemic period of 120 min, and disappearing paleness always indicated successful reperfusion. The animals were observed for a further 2 h. At the end of the experiment, the pancreas was excised for histological examination. Biopsy samples from the non-ischemic head served as control tissue to exclude experimental side-effects on the non-ischemic pancreatic head.

Microcirculatory measurements were done by intravital fluorescence microscopy. Histological examinations of the perfused pancreas tail were performed after staining with hematoxylin and eosin.

REFERENCES AND FURTHER READING

Adler G, Hupp T, Kern HF (1979) Course and spontaneous regression of acute pancreatitis in the rat. Virchow's Arch 382:31–37

Amsterdam A, Jamieson JD (1972) Structural and functional characterization of isolated pancreatic exocrine cells. Proc Natl Acad Sci, USA 69:3028–3032

Asano M, Hatori C, Inamura N, Sawai H, Hirosumi J, Fujiwara T, Nakahara K (1997) Effects of a nonpeptide bradykinin B_2 receptor antagonist, FR167344, on different *in vivo* animal models of inflammation. Br J Pharmacol 122:1436–1440

Chen YZ, Ikei S, Yamaguchi Y, Sameshima H, Sugita H, Moriyasu M, Ogawa M (1996) The protective effect of long-acting recombinant human pancreatic secretory inhibitor (R44S-PSTI) in a rat model of cerulein-induced pancreatitis. J Int Med Res 24:59–68

Emanuelli G, Montrucchio G, Dughera A, Gaia E, Lupia E, Battaglia E, De Martino A, De Giuli P, Gubetta L, Camussi G (1994) Role of platelet activating factor in acute pancreatitis induced by lipopolysaccharides in rabbits. Eur J Pharmacol 26:265–272

Griesbacher T, Lembeck F (1992) Effects of the bradykinin antagonist, HOE 140, in experimental acute pancreatitis. Br J Pharmacol 107:356–360

Griesbacher T, Tiran B, Lembeck F (1993) Pathological events in experimental acute pancreatitis prevented by the bradykinin antagonist, Hoe 140. Br J Pharmacol 108:405–411

Ha S-S, Satake K, Hiura A, Sowa M, Nishiwaki H (1994) Effect of a new cholecystokinin receptor antagonist (KSG 504) on the early stage of the healing process in acute pancreatitis induced by the closed duodenal loop technique. Pancreas 9:501–507

Ha S-S, Satake K, Hiura A (1996) Role of endogenous and exogenous cholecystokinin in experimental acute pancreatitis induced in rats by the closed duodenal loop technique. J Gastroenterol 31:404–413

Herman L, Fitzgerald PJ (1962) Restitution of pancreatic acinar cells following ethionine. J Cell Biol 12:279–312

Hirano T (1997) Somatostatin analogue improves survival rate in mice with CDF-diet-induced acute pancreatitis. Med Sci Res 25:279–281

Huch K, Schmidt J, Schratt W, Sinn HP, Buhr H, Herfarth C, Klar E (1995) Hyperoncotic dextran and systemic aprotinin in necrotizing rodent pancreatitis. Scand J Gastroenterol 30:812–816

Ito T, Kimura T, Furukawa M, Yamaguchi H, Nakano I, Nawata H (1991) Effects of cyclosporin A on caerulein-induced pancreatitis in rats. Med Sci Res 19:585–586

Ito T, Kimura T, Furukawa M, Yamaguchi H, Goto M, Nakano I, Nawata H (1994) Protective effects of gabexate mesilate on acute pancreatitis induced by tacrolimus (FK-506) in rats in which the pancreas was stimulated by caerulein. J Gastroenterol 29:305–313

Ito T, Ogoshi K, Nakano I, Ueda F, Sakai H, Kinjo M, Nawata H (1997) Effect of irsogladine on gap junctions in cerulein-induced acute pancreatitis in rats. Pancreas 15:297–303

Kimura K, Tominaga K, Fujii M, Saito T, Kasai H (1998) Effects of loxiglumide on experimental acute pancreatitis in comparison with gabexate mesilate. Arzneim Forsch/Drug Res 48:65–69

Lampel M, Kern HF (1987) Acute interstitial pancreatitis in the rat induced by excessive doses of a pancreatic secretagogue. Virchow's Arch A Path Anat Histol 373:97–117

Lake-Bakaar G, Lyubsky S (1995) Dose-dependent effect of continuous subcutaneous verapamil infusion on experimental acute pancreatitis in mice. Dig Dis Sci 40:2349–2355

Lembeck F, Griesbacher T (1996) Pathophysiological and possible physiological roles of kinins in the pancreas. Immunopharmacol 33:336–338

Liu XH, Kimura T, Ishikawa H, Yamaguchi H, Furukawa M, Nakano I, Kinjoh M, Nawata H (1995) Effect of endothelin$_1$ on the development of hemorrhagic pancreatitis in rats. Scand J Gastroenterol 30:276–282

Lombardi B, Estes LW, Longnecker DS (1975) Acute hemorrhagic pancreatitis (massive necrosis) with fat necrosis induced in mice by DL-ethionine fed with a choline-deficient diet. Am J Pathol 79:464–480

Merkord J, Jonas L, Weber H, Kröning G, Nizze H, Henninghausen G (1997) Acute interstitial pancreatitis in rats induced by dibutyltin dichloride (DBTC): Pathogenesis and natural course of lesions. Pancreas 15:392–401

Neuschwander-Tetri BA, Barnidge M, Janney CG (1994) Cerulein-induced pancreatic cysteine depletion: Prevention does not diminish acute pancreatitis in the mouse. Gastroenterology 107:824–830

Niederau C, Ferrell LD, Grendell JH (1985) Caerulein-induced acute necrotizing pancreatitis in mice: Protective effects of proglumide, benzotript, and secretin. Gastroenterology 88:1192–1204

Niederau C, Niederau M, Lüthen R, Strohmeyer G, Ferrell LD (1990) Pancreatic exocrine secretion in acute experimental pancreatitis. Gastroenterology 99:1120–1127

Niederau C, Brinsa R, Niederau M, Luthen R, Strohmeyer G, Ferrell LD (1995) Effects of C_1-esterase inhibitor in three models of acute pancreatitis. Int J Pancreatol 17:189–196

Norman J, Franz M, Messina J, Riker A, Fabri PJ, Rosemurgy AS, Gower WR Jr (1995) Interleukin-1 receptor antagonist decreases severity of experimental acute pancreatitis. Surgery 117:648–655

Obermaier R, Benz S, Kortmann B, Benthues A, Ansorge N, Hopf UT (2001) Ischemia/reperfusion-induced pancreatitis in rats: a new model of complete normothermic in situ ischemia of a pancreatic tail-segment. Clin Exp Med 1:51–59

Obermaier R, von Dobschuetz E, Benthues A, Ansorge N, Schareck W, Hopt UT, Benz S (2004a) Exogenous and endogenous nitric oxide donors improve post-ischemic tissue oxygenation in early pancreatic ischemia/reperfusion injury in the rat. Eur Surg Res 36:219–225

Obermanier R, von Dobschuetz E, Muhs O, Keck T, Drognitz O, Jonas L, Schareck W, Hopt UT, Benz S (2004b) Influence of nitric oxide on microcirculation in pancreatic/reperfusion injury: an intravital microscopic study. Transpl Int 17:208–214

Ogden JM, Modlin IM, Gorelick GS, Marks IN (1994) Effect of buprenorphine on pancreatic enzyme synthesis and secretion in normal rats and rats with acute edematous pancreatitis. Dig Dis Sci 39:2407–2415

Renner IG, Wisner JR, Lavingne BC (1986) Partial restoration of pancreatic function by exogenous secretin in rats with caeruletide-induced acute pancreatitis. Dig Dis Sci 31:305–313

Sledzinski Z, Wozniak M, Antosiewicz J, Lezoche E, Familiari M, Bertoli E, Greci L, Brunelli A, Mazera N, Wajda Z (1995) Protective effect of 4-hydroxy-TEMPO, a low molecular weight superoxide dismutase mimic, on free radical toxicity in experimental pancreatitis. Int J Pancreatol 18:153–160

Taniguchi H, Yakazi N, Yomota M, Shikano T, Endo T, Nagasaki M (1996) Pharmacological profile of T-0632, a novel potent and selective CCK_A receptor antagonist, *in vivo*. Eur J Pharmacol 312:227–233

Van Laethem JL, Marchant A, Delvaux A, Goldman M, Robberecht P, Velu T, Deviere J (1995) Interleukin 10 prevents necrosis in murine experimental pancreatitis. Gastroenterol 108:1017–1922

Vogel S (1994) Pankreatitis durch Arzneimittel. Arzneimitteltherapie 3:90–92

Watanabe S, Nishino T, Chang JH, Shiratori K, Moriyoshi Y, Takeuchi T (1993) Effect of Hoe 140, a new potent bradykinin antagonist, on experimental acute pancreatitis in rats. Gastroenterol 104, Suppl:A342

Weidenbach H, Lerch MM, Gress TM, Pfaff D, Turi S, Adler G (1995) Vasoactive mediators and the progression from oedematous to necrotising experimental acute pancreatitis. Gut 37:434–440

Yazu T, Kimura T, Sumii T, Nawata H (1991) Alteration of cholecystokinin receptor binding after caerulein-induced pancreatitis in rats. Digestion 50:142–148

J.7.0.13
Taurocholate-Induced Pancreatitis in the Rat

PURPOSE AND RATIONALE

Retrograde infusion of bile salts into the pancreatic duct induces severe necrotizing pancreatitis indicated by reduced amylase output and histological changes.

PROCEDURE

Male Sprague-Dawley or Wistar rats weighing 200–300 g are anesthetized by i.m injection of a mixture of 87 mg/kg ketamine and 13 mg/kg xylazine. After laparotomy, the pancreaticobiliary duct is cannulated through the duodenal papilla with a polyethylene catheter (P10, Clay Adams) which is introduced by means of a puncture in the duodenum. A precision pump is used to infuse 0.6 ml 5% sodium taurocholate into the pancreaticobiliary duct during a 10-min period at an infusion rate of 6 ml/h. The catheter is then withdrawn and the abdominal cavity surgically closed.

After various time intervals (several hours up to 2 weeks), the animals are anesthetized and the pancreaticobiliary duct is cannulated again. The response to various doses of caerulein is measured.

EVALUATION

The degree of amylase output (mg/h) is taken as parameter. Dose response curves after various doses of caerulein are established.

MODIFICATIONS OF THE METHOD

The effects of various agents on experimental pancreatitis induced by retrograde intraductal injection of **taurocholate** solution or bile acid in rats have been studied by various authors (Bielecki et al. (1994), Hietaranta et al. 1995; Nakae et al. 1995; Niederau et al. 1995; Kimura et al. 1996; Mithofer et al. 1996; Paran et al. 1996; Tachibana et al. 1996; Norman et al. 1997; Plusczyk et al. 1997; Manso et al. 1998).

Tanaka et al. (1995), Sakai (1996) induced necrotizing pancreatitis by retrograde injection of **deoxycholate** solution into the biliopancreatic duct of rats.

REFERENCES AND FURTHER READING

Bielecki K, Wiedmann M, Meyer F, Kimura W, Mossner J (1994) Effect of 5-fluorourazil on secretion and synthesis of pancreatic digestive enzymes: Studies in isolated pancreatic acini and perfused pancreas derived from normal rats and rats with acute necrotizing pancreatitis. Pancreas 9:518–525

Hietaranta AJ, Peurovuori HJ, Nevalainen TJ (1995) Phospholipase A_2 in sodium taurocholate-induced experimental hemorrhagic pancreatitis in the rat. J Surg Res 59:271–278

Kimura W, Okubo K, Han I, Kanai S, Matsushita A, Muto T, Miyasaka K (1996) Effects of pancreatic duct ligation and aging on acute taurocholate-induced pancreatitis: Experiments in the perfused pancreas in rats. Int J Pancreatol 19:117–127

Lankisch PG, Winckler K, Bokermann M, Schmidt H, Creutzfeldt W (1974) The influence of glucagon on acute experimental pancreatitis in the rat. Scand J Gastroenterol 9:725–729

Mithofer K, Fernandez-Del Castillo C, Ferraro MJ, Lewandrowski K, Rattner DW, Warshaw AL (1996) Antibiotic treatment improves survival in acute necrotizing pancreatitis. Gastroenterol 110:232–240

Nakae Y, Naruse S, Kitagawa M, Hirao S, Yamamoto R, Hayakawa T (1995) Activation of trypsinogen in experimental models of acute pancreatitis in rats. Pancreas 10:306–313

Niederau C, Niederau M, Lüthen R, Strohmeyer G, Ferrell LD (1990) Pancreatic exocrine secretion in acute experimental pancreatitis. Gastroenterology 99:1120–1127

Niederau C, Brinsa R, Niederau M, Luthen R, Strohmeyer G, Ferrell LD (1995) Effects of C_1-esterase inhibitor in three models of acute pancreatitis. Int J Pancreatol 17:189–196

Norman J, Yang J, Fink G, Carter G, Ku G, Denham W, Livingston D (1997) Severity and mortality of experimental pancreatitis are dependent on interleukin$_1$ converting enzyme. J Interferone Cytokine Res 17:113–118

Manso MA, Orfao A, Tabernero MD, Vicente S, De Dios I (1998) Changes in both the membrane and the enzyme content of individual zymogen granules are associated with sodium taurocholate-induced pancreatitis in rats. Clin Sci 94:293–301

Paran H, Klausner J, Siegal A, Graff E, Freund U, Kaplan O (1996) Effect of the somatostatin analogue octreotide on experimental pancreatitis in rats. J Surg Res 62:201–206

Plusczyk T, Westermann S, Rathgeb D, Feifel G (1997) Acute pancreatitis in rats: Effects of sodium taurocholate, CCK-8, and Sec on pancreatic microcirculation. Am J Physiol, Gastrointest Liver Physiol 272:G310–320

Sakai Y (1996) Experimental study on roles of endotoxin and PAF (platelet activating factor) in the development of severe acute pancreatitis. J Saitama Med Sch 23:145–157

Tanaka N, Murata A, Uda KI, Toda H, Kato T, Hayashida H, Matsuura N, Mori T (1995) Interleukin-1 receptor antagonist modifies the changes in vital organs induced by acute necrotizing pancreatitis in a rat experimental model. Crit Care Med 23:901–908

Tachibana I, Watanabe N, Shirohara H, Akiyama T, Nakano S, Otsuki M (1996) Effects of MCI-727 on pancreatic exocrine secretion and acute pancreatitis in two experimental rat models. Pancreas 12:165–172

J.7.0.14 Chronic Pancreatitis

PURPOSE AND RATIONALE

Chronic pancreatitis was induced by various means in rats (Zhou 1990, 1994; Goto et al. 1995; Puig-Diví et al. 1996), golden hamsters (Rutishauser et al. 1991, 1995), cats (Reber et al. 1992, 1999; Zhao et al. 1996), dogs (Hayakawa et al. 1993; Tanaka et al. 1994, 1998), and pigs (Vinter-Jensen et al. 1997).

Puig-Diví et al. (1996) induced chronic pancreatitis in rats by trinitrobenzene sulfonic acid infusion into the pancreatic ducts.

PROCEDURE

Male Sprague Dawley rats weighing 300–350 g are anesthetized with ketamine (100 mg/kg i.p.) after an overnight fast. Access to the pancreas is gained through a ventral midline incision. The duodenum is opened and the biliopancreatic duct cannulated through the papilla using polyethylene tubing (PE 10). The biliopancreatic secretion is allowed to drain freely for 15 min. To prevent liver damage, the duct is tied close to the liver. Retrograde infusion is initiated by means of a controlled pressure device that uses the height of a liquid column (trinitrobenzene sulfonic acid or vehicle) in a vertical pipette connected to the infusion cannula to control the intraductal pressure and infusion volume. Ductal pressure is never allowed to exceed 20 cm H_2O. In the treated group 0.4 ml of 2% trinitrobenzene sulfonic acid in phosphate buffered saline + 10% ethanol (pH 8) is infused. Ethanol is employed as an epithelial "barrier breaker" to facilitate trinitrobenzene sulfonic acid penetration into the tissue. Rats in the control group undergo the same procedure, except that trinitrobenzene sulfonic acid in absent from the infusion medium.

The total exposure time of the gland to the instillate is 60 min, followed by a washout period of 30 min. Ligatures are then released, the duodenum and the abdominal wall are sutured, and the animals are kept under observation for 2 h after surgery. Rats are then

transferred to individual cages, where they are fasted for 24 h. Thereafter they receive standard chow and their weight gain is recorded weekly.

Blood is withdrawn after various time intervals by cardiac puncture under light ether anesthesia for determination of glucose and serum α-amylase (EPS test, Boehringer Mannheim GmbH).

Groups of treated rats and controls are sacrificed at 3, 4, and 6 weeks after the surgical procedure. Pancreata are fixed in 10% neutral buffered formaldehyde and embedded in paraffin. Several sections are cut and stained with haematoxylin-eosin for light microscopy evaluation. The degree of periductal and intralobular fibrosis, patchy acute and chronic inflammatory cell infiltrates, common duct stenosis, and segmentary gland atrophy is evaluated.

EVALUATION

Data are expressed as means ± SEM. A two-tailed Student's *t*-test for unpaired values is used for statistical comparison of mean values of serum amylase, glucose and rat weight.

MODIFICATIONS OF THE METHOD

Chung and Richter (1971), Zhou et al. (1990, 1994) induced chronic pancreatitis in rats by **ligation of the pancreatic duct**.

Injection of oleic acid (Goke et al. 1989; Goldstein et al. 1989; Andersen et al. 1994; Kakugawa 1996; Seymour et al. 1995, 1998) or of a viscous solution of zein – oleic acid – linoleic acid (Kataoka et al. 1998) into the pancreatic duct was used to induce chronic pancreatitis in rats.

Goto et al. (1995) described a chronic pancreatitis model with diabetes induced by intraperitoneal **cerulein** injection plus water immersion stress in rats.

Pancreatic blood flow was measured in **cats** with chronic pancreatitis induced by partial ligation of the pancreatic duct by Austin et al. (1980), Reber et al. (1992, 1999), Widdison et al. (1992).

Zhao et al. (1996, 1998) induced progressing lesions of chronic pancreatitis in cats by intraductal injection of alcohol or by a combination of intraductal and intraparenchymal injection of ethanol together with partial obstruction of the main pancreatic duct to 70% of its original lumen by fixation of a small catheter in the papilla.

Hayakawa et al. (1993) induced pancreatolithiasis in **dogs** by partial obstruction of the major pancreatic duct.

Rats of the diabetic strain WBN/Kob (Tsuchitani et al. 1985; Nakama et al. 1985) develop **spontaneously chronic pancreatitis** (Ohashi et al. 1990; Sato et al. 1993; Sugiyama et al. 1996a, b; Arai et al. 1998; Ito et al. 1998) with pancreatic fibrosis and parenchymal destruction and both endocrine and exocrine pancreatic dysfunction (see also K.2.0.2).

Transgenic mice overexpressing $TGF_{\beta 1}$ (Sanvito et al. 1995) develop tissue changes in the pancreas resembling changes found in chronic pancreatitis.

Shetzline et al. (1998) identified target tissues of pancreatic polypeptide using an *in vivo* radioreceptor assay in order to further elucidate the function of this hormone.

REFERENCES AND FURTHER READING

Andersen DK, Ruiz CL, Burant CF, Nealon WH, Thompson JC, Hanks JB (1994) Insulin regulation of hepatic glucose transporter protein is impaired in chronic pancreatitis. Ann Surg 219:679–687

Arai T, Komatsu Y, Sasaki K, Taguchi S (1998) Reduced reactivity of pancreatic exocrine secretion in response to gastrointestinal hormone in WBN/Kob rats. J Gastroenterol 33:247–253

Austin JL, Roberts C, Rosenholtz MJ, Reber HA (1980) Effect of partial duct obstruction and drainage on pancreatic function. J Surg Res 28:426–433

Chung A, Richter WR (1971) Early changes in the exocrine pancreas of the dog and rat after ligation of the pancreatic duct: A light and electron microscopy study. Am J Patol 63:521–546

Goke B, Glock J, Richter G, Adler G (1989) CAMOSTAT in chronic pancreatitis: effects on oleic acid-induced pancreatic insufficiency in rats. Biomed Res 10, Suppl 1:83–86

Goldstein JA, Kirwin JD, Seymour NE, Trachtenberg JE, Rademaker EA, Anderson DK (1989) Reversal of *in vitro* hepatic insulin resistance in chronic pancreatitis by pancreatic polypeptide in the rat. Surgery 106:1128–1133

Goto M, Nakano I, Kimura T, Miyahara T, Kinjo M, Nawata H (1995) New chronic pancreatitis model with diabetes induced by cerulein plus stress in rats. Digest Dis Sci 40:2356–2363

Hayakawa T, Kondo T, Shibata T, Kitagawa M, Sobajima H, Sakai Y, Ishiguro H, Nakae Y, Tanikawa M, Naruse S (1993) Longitudinal changes of plasma pancreatic enzymes and hormones in experimental pancreatolithiasis in dogs. Digest Dis Sci 38:2098–2103

Ito H, Sogabe H, Kuno M, Satoh Y, Ogawa T, Konishi K, Yoshida K (1998) Effect of FK480, a CCK-A receptor antagonist, on spontaneously developed chronic pancreatitis in WBN/Kob rats. Pancreas 17:295–300

Kakugawa Y, Paraskevas S, Metrakos P, Giaid A, Qi SJ, Duguid WP, Rosenberg L (1996) Alterations in pancreatic microcirculation and expression of endeothelin-1 in a model of chronic pancreatitis. Pancreas 13:89–95

Kataoka K, Sasaki T, Yorizumi H, Sakagami J, Kashima K (1998) Pathophysiologic studies of experimental chronic pancreatitis in rats induced by injection of zein – oleic acid – linoleic acid into the pancreatic duct. Pancreas 16:289–299

Nakama K, Schichinohe K, Kobayashi K (1998) Spontaneous diabetes-like syndrome in WBN/Kob rats. Acta Diabetol Lat 22:335–342

Ohashi K, Kim JH, Hara H, Aso R, Akimoto T, Nakama K (1990) A new spontaneously occurring model of chronic pancreatitis. Int J Pancreatol 6:231–247
Puig-Diví V, Molero X, Salas A, Guarner F, Guarner L, Malagelada JR (1996) Induction of chronic pancreatic disease by trinitrobenzene sulfonic acid infusion into rat pancreatic ducts. Pancreas 13:417–424
Reber HA, Karanjia ND, Alvarez C, Widdison AL, Leung FW, Ashley SW, Lutrin FJ (1992) Pancreatic blood flow in cats with chronic pancreatitis. Gastroenterol 103:652–659
Reber PU, Patel AG, Toyama MT, Ashley SW, Reber HA (1999) Feline model of chronic obstructive pancreatitis: effects of acute pancreatic duct decompression on blood flow and interstitial pH. Scand J Gastroenterol 34:439–444
Rutishauser SCB, Ali AE, Yates N, Jeffrey IJM, Brannigan S, Guyan PM, Hunt LP, Braganza JM (1991) Comparison of pancreatic and hepatic secretory function in hamsters fed low and high fat diets. Eur J Gastroenterol Hepatol 3:613–621
Rutishauser SCB, Ali AE, Jeffrey IJM, Hunt LP, Braganza JM (1995) Towards an animal model of chronic pancreatitis: Pancreatobiliary secretion in hamsters with long-term treatment with chemical inducers of cytochromes P450. Int J Pancreatology 18:117–126
Sanvito F, Nichols A, Herrere PL, Huarte J, Wohlwend A, Vassalli JD, Orci L (1995) $TGF_{\beta 1}$ overexpression in murine pancreas induces chronic pancreatitis and, together with TNF_{α}, triggers insulin-dependent diabetes. Biochem Biophys Res Commun 217:1279–1286
Sato M, Furukawa F, Nishikawa A, Imazawa T, Yoshimura H, Suzuki J, Nakamura K, Takahshi M (1993) Effect of cyclohexamide on spontaneous testicular and pancreatic lesions in WBN/Kob rats. Bull Nat Inst Hyg Sci 111:34–38
Seymour NE, Volpert AR, Lee EL, Andersen DK, Hernandez C, Nealon WH, Brunicardi CF, Gadacz TR (1995) Alterations in hepatocyte insulin binding in chronic pancreatitis: effects of pancreatic polypeptide. Am J Surg 169:105–110
Seymour NE, Spector S, Andersen DK, Elm MS, Whitcomb DC (1998) Overexpression of hepatic pancreatic polypeptide receptors in chronic pancreatitis. J Surg Res 76:47–52
Shetzline MA, Zipf WB, Nishikawara MT (1998) Pancreatic polypeptide: Identification of target tissues using an *in vivo* radioreceptor assay. Peptides 19:279–289
Sugiyama M, Kobori O, Atomi Y, Wada N, Kuroda A, Muto T (1996a) Effect of oral administration of protease inhibitor on pancreatic exocrine function in WBN/Kob rats with chronic pancreatitis. Pancreas 13:71–79
Sugiyama M, Kobori O, Atomi Y, Wada N, Kuroda A, Muto T (1996b) Pancreatic exocrine function during acute exacerbation in WBN/Kob rats with spontaneous chronic pancreatitis. Int J Pancreatology 20:191–196
Tanaka T, Ichiba Y, Miura Y, Ito H, Dohi K (1994) Canine model of chronic pancreatitis due to chronic ischemia. Digestion 55:86–89
Tanaka T, Miura Y, Matsugu Y, Ichiba Y, Ito H, Dohi K (1998) Pancreatic duct obstruction is an aggravating factor in the canine model of chronic alcoholic pancreatitis. Gastroenterol 115:1248–1253
Tsuchitani M, Saeguisa T, Namara I, Nishikawa T, Gonda T (1985) A new diabetic strain of rat (WBN/Kob). Lab Anim 19:200–207
Vinter-Jensen L, Juhl CO, Teglbjaerg PS, Poulsen SS, Dajani EZ, Nexo E (1997) Systemic treatment with epidermal growth factor in pigs induces ductal proliferations in the pancreas. Gastroenterology 113:1367–1374
Widdison AL, Alvarez C, Schwarz M, Reber HA (1992) The influence of ethanol on pancreatic blood flow in cats with chronic pancreatitis. Surgery 112:202–210
Zhao P, Tu J, van den Oord JJ, Fevery J (1996a) Damage to duct epithelium is necessary to develop progressing lesions of chronic pancreatitis in the cat. Hepato-Gastroenterol 43:1620–1626
Zhao P, Tu J, Martens A, Ponette E, van Steenbergen W, van den Oord J, Fevery J (1996b) Radiologic investigations and pathologic results of experimental chronic pancreatitis in cats. Acad Radiol 5:850–856
Zhou W, Chao W, Levine BA, Olson MS (1990) Evidence of platelet-activating factor as a late-phase mediator of chronic pancreatitis in the rat. Am J Pathol 137:1501–1508
Zhou W, Levine BA, Olson MS (1996) Lipid mediator production in acute and chronic pancreatitis in the rat. J Surg Res 56:37–44

J.8 Liver Function

J.8.1 Hepatocellular Function

J.8.1.1 Hepatitis in Long Evans Cinnamon Rats

PURPOSE AND RATIONALE

The Long Evans Cinnamon strain of rats has been recommended as a useful model to study genetically transmitted fulminant hepatitis and chronic liver disease (Yoshida et al. 1987; Hawkins et al. 1995). The underlying cause is thought to be due to excessive copper accumulation in the liver of Long Evans Cinnamon rats, thus making this animal a model for Wilson's disease in humans (Okayasu et al. 1992). Chelation therapy or feeding a copper-deficient diet can ameliorate the symptoms in Long Evans Cinnamon rats and Wilson's disease (Togashi et al. 1992).

PROCEDURE

Male Long Evans Cinnamon rats obtained from a commercial breeder at an age of 5 weeks are housed in temperature- und humidity-controlled rooms at a 12:12 light/dark cycle. Groups of 6–10 rats are given different diets based on a 15% purified egg protein diet and supplemented with vitamins or drugs. Drugs are applied via minipumps intraperitoneally implanted under ether anesthesia.

The occurrence of jaundice is easily observable as the time when the ears and tail turn yellow and the urine becomes bright orange, staining the fur in the lower abdominal region. Usually, the jaundice progressively worsens, ending in death of the animal within about a week. Incidence of jaundice and mortality vs. time are used as parameters.

EVALUATION

Statistics are performed using StatView II software package for Student's *t*-test, ANOVA, and the Scheffé F-test for comparison between means. All data are expressed as means. A p-value < 0.05 is used as the threshold of significance.

MODIFICATIONS OF THE METHOD

Several drugs which are known to be effective or which are potentially effective in treatment of Wilson's disease were studied in this animal model, such as D-penicillamine (Togashi et al. 1992; Yokoi et al. 1994; Shimizu et al. 1997), trientine (= triethylenetetramine) (Iseki et al. 1992; Sone et al. 1996; Yamamoto et al. 1997), tetrathiomolybdate (Ogra et al. 1995; Suzuki 1997; Sugawara et al. 1999), or the investigative drug TJN-101 (Yokoi et al. 1995).

The interferon-γ transgenic mouse which carries the mouse INF-γ gene develops chronic hepatitis from the age of 6–10 weeks and was recommended by Okamoto et al. (1999) as a model for **chronic hepatitis**.

REFERENCES AND FURTHER READING

Hawkins RL, Mori M, Inoue M, Torii K (1995) Proline, ascorbic acid, or thioredoxin affect jaundice and mortality in Long Evans Cinnamon rats. Pharmacol Biochem Behav 52:509–515

Iseki K, Kobayashi M, Ohba A, Miyazaki K, Li Y, Togashi Y, Takeichi N (1992) Comparison of disposition behavior and decoppering effect of triethylenetramine in animal model of Wilson's disease (Long-Evans Cinnamon rat) with normal Wistar rat. Biopharm Drug Dispos 13:273–283

Ogra Y, Ohmichi M, Suzuki KT (1995) Systemic dispositions of molybdenum and copper after tetrathiomolybdate injection on LEC rats. J Trace Elem Med Biol 9:165–169

Okamoto T, Yamamura K, Hino O (1999) The mouse interferon-γ transgene chronic hepatitis model. Int J Mol Med 3:517–520

Okayasu T, Tochimaru H, Hyuga T, Takahashi T, Takekoshi Y, Li Y, Togashi Y, Takeichi N, Kasai N, Arashima S (1992) Inherited copper toxicity in Long-Evans Cinnamon rats exhibiting spontaneous hepatitis: A model of Wilson's disease. Pediatric Res 31:253–257

Shimizu N, Fujii Y, Saito Y, Yamaguchi Y, Aoki T (1997) Age-related copper, zinc, and iron metabolism in Long-Evans cinnamon rats and copper eliminating effects of D-penicillamine and trienthine 2 HCl. J Trace Elem Exp Med 10:49–59

Sone H, Maeda M, Wakabayashi K, Takeichi N, Mori M, Sigimura T, Nagao M (1996) Inhibition of hereditary hepatitis and liver tumor development in Long-Evans cinnamon rats by the copper chelating agent trientine dihydrochloride. Hepatology 23:764–770

Sugawara N, Ikeda T, Lai YR, Sugawara C (1999) The effect of subcutaneous tetrathiomolybdate administration on copper and iron metabolism, including their regional distribution in the brain, in the Long-Evans Cinnamon rat, a bona fide animal model for Wilson's disease. Pharmacol Toxicol 84:211–217

Suzuki KT (1997) Selective removal of copper accumulating in a form bound to metallothionein in the liver of LEC rats by tetrathiomolybdate. J Trace Elem Exp Med 10:101–109

Togashi Y, Li Y, Kang KJ, Takeichi N, Fujioka Y, Nagashima K, Kobayashi H (1992) D-Penicillamine prevents the development of hepatitis in Long-Evans Cinnamon rats with abnormal copper metabolism. Hepatology 15:82–87

Yamamoto Y, Sone H, Yamashita S, Nagata Y, Niikawa H, Hara K, Nagao M (1997) Oxidative stress in LEC rats evaluated by plasma antioxidants and free fatty acids. J Trace Elem Exp Med 10:129–134

Yokoi T, Nagayama S, Kajiwara R, Kawaguchi Y, Kamataki T (1994) Effects of cyclosporin A and D-penicillamine on the development of hepatitis an the production of antibody to protein disulfide isomerase in LEC rats. Res Commun Mol Pathol Pharmacol 85:73–81

Yokoi T, Nagayama S, Kajiwara R, Kawaguchi Y, Aizawa T, Otaki Y, Aburada M, Kamataki T (1995) Occurrence of autoimmune antibodies to liver microsomal proteins associated with lethal hepatitis in LEC rats: Effects of TJN-101 ((+)-(6S,7S,R-biar)-5,6,7,8-tetrahydro-1,2,3,12-tetramethoxy-6,7-dimethyl-10,11-methylenedioxy-6-dibenzo[a,c]cyclooctenol) in the development of hepatitis and the antibodies. Toxicol Lett 76:33–38

Yoshida MC, Masuda C, Sasaki M, Takeichi N, Kobayashi H, Dempo K, Mori M (1987) New mutation causing hereditary hepatitis in the laboratory rat. J Hered 78:361–365

J.8.1.2 Temporary Hepatic Ischemia

PURPOSE AND RATIONALE

Hepatocellular function is altered by temporary hepatic ischemia as occurring during surgical management of acute hepatic trauma and being essential during hepatic transplantation. To study this, total hepatic ischemia in rats is produced by placing a ligature around the hepatic artery, portal vein, and the common bile duct.

PROCEDURE

Hepatic Ischemia Procedure

Male albino Holtzman rats, weighing 300–350 g are fasted for 16 h prior to the experiment but are allowed water ad libitum. The rats are anesthetized lightly with ether and the abdominal cavity is opened through a midline incision. Splenectomy is performed following which a temporary extracorporal splenofemoral shunt is established between the splenic vein and the right femoral vein using a PE-190 tubing. To insure total hepatic ischemia, the portal vein as the hepatic artery and the bile duct are occluded by placing a tourniquet around the vessels. Blood pressure is measured via a catheter inserted into the right femoral artery. After heparinization (10 mg/kg), hepatic ischemia is produced for 60 min. During the ischemic period, 0.7 ml of saline is given i.v. at 20-min intervals for volume replacement. At the end of the 60-min is-

chemic period, the tourniquet around the portal vein, hepatic artery and the bile duct is removed in order to re-establish blood flow to the liver. The abdominal incision is then closed and the animals receive either saline (nontreated) or the drug. Following administration of saline or the drug the catheters are removed and the animals are returned to their home cages.

Sham-operated animals are prepared exactly in the same manner except that the tourniquet around the portal vein, hepatic artery, and the bile duct are not placed.

Measurement of Indocyanine Green Clearance

Three hours following the end of ischemia, the experimental as well as the sham-operated rats are lightly anesthetized with ether and a femoral artery and vein of each animal cannulated. Sodium heparin (400 units) is given i.v. and the animals are allowed to awake. Indocyananine green is given i.v. at 5 mg/kg (low) or 25 mg/kg (high) to the animals via the femoral vein and 0.2 ml arterial blood samples are taken at 5, 6, 8, 10, 12, 15, 18, and 20 min later. The blood samples are diluted with 0.8 ml of 1% bovine serum albumin in normal saline and centrifuged at 6000 rpm for 20 min at 4°C. The spectrophotometric absorbance of the supernatant is read at 800 nm and the indocyanine green concentration determined from a standard curve.

EVALUATION

The $t_{1/2}$ of indocyanine green clearance is computed for each animal using a computer program which calculates the least square line of log indocyanine green vs. time. Mean and standard errors for each group are compared using the Student *t*-test.

MODIFICATIONS OF THE METHOD

Daemen et al. (1989) compared the electromagnetic versus the microsphere and the clearance method for liver blood flow measurement in the rat.

Kawaguchi et al. (2004) described the protective effect of a Rho kinase inhibitor against hepatic ischemia-reperfusion injury in rats.

REFERENCES AND FURTHER READING

Chaudry IH, Clemens MG, Ohkawa M, Schleck S, Baue AE (1982) Restoration of hepatocellular function and blood flow following hepatic ischemia with ATP-$MgCl_2$. Adv Shock Res 8:177–186

Daemen MJAP, Thijssen HHW, van Essen, Veroort-Peters HTM, Prinzen FW, Struyker Boudier HAJ, Smits JFM (1989) Liver blood flow measurement in the rat. The electromagnetic versus the microsphere and the clearance methods. J Pharmacol Meth 21:287–297

Hirisawa H, Chaudry IH, Baue AE (1978) Improved hepatic function and survival with adenosine triphosphate magnesium chloride after hepatic ischemia. Surgery 83:655–662

Kawaguchi A, Ohmori M, Fujimura A (2004) Partial protective effect of Y-27632, a Rho kinase inhibitor, against hepatic ischemia-reperfusion injury in rats. Eur J Pharmacol 493:167–171

Koo A, Liang IYS (1977) Blood flow in hepatic sinusoids in experimental hemorrhagic shock in the rat. Microvasc Res 13:315–325

Levy CM, Smith F, Longueville J, Paumgartener G, Howart M (1967) Indocyanine green as a test for hepatic function. JAMA 200:236–237

Nuxmalo JL, Teranaka M, Schenk WG (1978) Hepatic blood flow measurement. Total hepatic blood flow measured by ICG clearance and electromagnetic flow meters in a canine septic shock model. Ann Surg 183:299–302

Paumgartener G, Probst P, Kraines R, Levy CM (1970) Kinetics of indocyanine green removal from the blood. Ann NY Acad Sci 170:134–147

Ritz R, Cavanilles J, Michaels SBA, Shubin H, Weil MH (1973) Disappearance of indocyanine green during circulatory shock. Surg Gynecol Obstet 136:57–62

J.8.1.3 Model for Direct Transhepatic Studies in Dogs

PURPOSE AND RATIONALE

A chronic conscious dog model for repeated transhepatic studies over a period of 6–8 weeks was developed by O'Brien et al. (1991). This model can be applied to the study of the hepatic effects of pancreatic hormone secretion and glucose metabolism, to studies of the hepatic mechanisms associated with high first-pass metabolism and food interactions of drugs (Semple et al. 1990), and to studies of insulin balance in dogs that have undergone previous pancreatectomy and islet cell auto-transplantation.

PROCEDURE

Four silastic catheters, 0.062 in. ID × 0.125 in. OD (lengths: carotid 70 cm; jugular 70 cm; hepatic 80 cm; and portal 70 cm) and two ultrasonic transit time flow probes suitable for long-term implants (Burton and Gorewit 1984), 4 mm for the hepatic artery and 6 mm for the portal vein, are cleaned with chlorhexidine scrub and rinsed with distilled water. Double velour dacron cuffs are placed 15 cm from the external ends of all the devices.

Male dogs weighing 20–25 kg are sedated and anesthetized with a 2% halothane/L O_2 mixture. Skin interface sites and subcutaneous pockets for placement of catheters are prepared. After skin closure the external ends of the catheters are sealed. Then the catheters and flow probes are placed into the abdomen by retrieving them from the subcutaneous pockets. First, the hepatic artery flow probe is placed, then, the portal venous

flow probe inserted. To eliminate extrahepatic blood flow, the gastroduodenal artery is ligated. Then, the portal vein and the hepatic vein catheters are placed. After ensuring catheter patency, the abdomen is closed. Finally, a carotid artery catheter and a jugular venous catheter are placed.

EVALUATION

Blood samples can be withdrawn from the catheters placed into the carotid artery, the right external jugular vein, the portal vein, and the hepatic vein. Blood flow is measured by flow probes in the hepatic artery and the hepatic portal vein.

The following values are measured:

- Plasma flow in the portal vein and plasma flow in the hepatic artery,
- drug concentration in the portal vein, in the hepatic artery, in the hepatic vein, and in the right external jugular vein.

From these data plasma flux in the portal vein, in the hepatic artery, and in the hepatic vein and the interval areas under the curve for these vessels are calculated.

REFERENCES AND FURTHER READING

Burton RG, Gorewit RC (1984) Ultrasonic flowmeter uses wide beam transit time technique. Medical Electronics 15:68–73

Semple HA, Tam YK, O'Brien DW (1990) Physiological modelling of the hepatic interaction between food and hydralazine in the conscious dog. Pharmaceut Res 7:S223

O'Brien DW, Semple HA, Molnar GD, Tam Y, Coutts RT, Rajotte RV, Bayens-Simmonds J (1991) A chronic conscious dog model for direct transhepatic studies in normal and pancreatic islet cell transplanted dogs. J Pharmacol Meth 25:157–170

J.8.2 Liver Cirrhosis and Necrosis

J.8.2.1 General Considerations

Various factors induce liver cirrhosis in man, such as alcoholism, viral hepatitis, intoxications, bile duct disorders, inborn diseases, and others. In the process leading to cirrhosis, accumulation of connective tissue and parenchymal regeneration are competing events. Excessive formation of connective tissue with collagen overproduction in the liver reduces hepatic blood flow, impairs the metabolic functions of the liver, and increases portal vein pressure. These mechanisms result in hepatic failure, esophageal bleeding, portal hypertension and ascites. Therefore, the search for agents to prevent liver cirrhosis is focused on inhibitors of excessive connective tissue formation in the liver (Kervar et al. 1976; Nolan et al. 1978). The main component of connective tissue formed as a response to chronic injury is collagen. The collagenous fibers consist of triple helical molecules. Their formation depends on the presence of hydrogen bonds involving the post-translationally hydroxylated amino acid hydroxyproline. If the number of hydrogen bonds is reduced due to a decrease of hydroxylated amino acids, the resulting collagen can not form the triple helix and is degraded instead of being deposited in the extracellular matrix.

Insoluble collagen is responsible for most of the mechanical functions of connective tissue, e. g., bone, tendon and skin, being influenced by hormones, desmotropic drugs, such as D-penicillamine, and by maturation and age (Vogel 1969, 1972, 1974a, b, 1976, 1978, 1980, 1989; Bickel et al. 1990, 1991). The aim of fibrosuppressive compounds is to reduce only the excessive formation of insoluble collagen in the liver leaving collagen synthesis and turnover in other tissues intact. Fibrosuppressive effects by inhibition of proline hydroxylation can be screened with *in vitro* methods, however, the desired organ specificity has to be tested in models of liver cirrhosis and fibrosis *in vivo* together with functional studies of the connective and supporting tissue. Detailed description of methods for studying collagen metabolism and mechanical function of connective tissue is given in the Sect. M.2.1.3 (hormones).

REFERENCES AND FURTHER READING

Baader E, Bickel M, Brocks D, Engelbart K, Günzler V, Schmidts HL, Vogel G (1990) Liver selective fibrosuppression in the rat by HOE 077, an inhibitor of prolyl-4-hydroxylase. Hepatology 12:947

Bickel M, Baader E, Brocks D, Burghard H, Günzler V, Engelbart K, Hanauske-Abel M, Vogel HG (1990) Liver selective fibrosuppression in the rat by a derivative of pyridine-2,4-dicarboxylate. Gastroenterology 98:A 570

Bickel M, Baader E, Brocks DG, Engelbart K, Günzler V, Schmidts HL, Vogel HG (1991) Beneficial effects of inhibitors of prolyl-4-hydroxylase in CCl_4-induced fibrosis of the liver in rats. J Hepatol 13, Suppl 3:S26–S34

Kervar SS, Felix AM (1976) Effect of L-3,4-dehydroproline on collagen synthesis and prolyl hydroxylase activity in mammalian cell cultures. J Biol Chem 251:503–509

Kervar SS, Oronsky AL, Choe D, Alvarez B (1976) Studies on the effect of 3,4-dehydroproline on collagen metabolism in carbon tetrachloride-induced hepatic fibrosis. Arch Biochem Biophys 182:118–123

Nolan JC, Ridge S, Oronsky AL, Kervar SS (1978) Studies on the mechanism of reduction of prolyl hydroxylase activity by D,L-3,4 dehydroproline. Arch Biochem Biophys 189:448–453

Prockop DJ, Berg RA, Kivirikko KI, Uitto J (1976) Intracellular steps in the biosynthesis of collagen. In: Ramachandran GN, Reddi AH (eds) Biochemistry of Collagen. Plenum Press, New York and London, pp 163–273

Vogel HG (1969) Zur Wirkung von Hormonen auf physikalische und chemische Eigenschaften des Binde- und Stützgewebes. Arzneim Forsch/Drug Res 19:1495, 1732, 1790, 1981
Vogel HG (1972) Effects of D-penicillamine and prednisolone on connective tissue in rats. Conn Tiss Res 1:283–289
Vogel HG (1974a) Organ specificity of the effects of D-Penicillamine and of lathyrogen (aminoacetonitrile) on mechanical properties of connective and supporting tissue. Arzneim Forsch/Drug Res 24:157–163
Vogel HG (1974b) Correlation between tensile strength and collagen content in rat skin. Effect of age and cortisol treatment. Conn Tiss Res 2:177–182
Vogel HG (1976) Tensile strength, relaxation and mechanical recovery in rat skin as influenced by maturation and age. J Med 7:177–188
Vogel HG (1978) Influence of maturation and age on mechanical and biochemical parameters of connective tissue of various organs in the rat. Conn Tiss Res 6:161–166
Vogel HG (1980) Influence of maturation and aging on mechanical and biochemical properties of connective tissue in rats. Mechanism Aging Develop 14:283–292
Vogel HG (1989) Mechanical properties of rat skin with aging. In: Balin AK, Kligman AM (eds) Aging and the Skin. Raven Press, New York, pp 227–275

J.8.2.2 Inhibition of Proline Hydroxylation

PURPOSE AND RATIONALE

The thermal stability of the triple helix of collagenous proteins is crucially dependent upon the intramolecular hydrogen bonds involving the 4-hydroxyproline residues synthesized by the enzyme prolyl 4-hydroxylase. This makes the enzyme a possible target for therapeutic antifibrotic agents.

PROCEDURE

Enzyme activity is assayed in sealed test tubes. The reaction volume of 1 ml contains 50 mM Tris buffer, pH 7.5, 10–100 mM (60000 d.p.m.) 2-oxo[1-^{14}C]glutarate, 1–50 mM $FeSO_4$, 0.1–1 mM ascorbate, 10–100 mg (Pro-Pro-Gly)$_{10}$, 0.1 mg catalase, 2 mg bovine serum albumin, 100 mM dithiotreitol, 0.05–0.2 mg enzyme, and inhibitors in various concentrations. After incubation at 37°C for 30 min, the generated $^{14}CO_2$ is trapped and determined.

EVALUATION

Inhibition modes are determined by plotting 1/v versus 1/concentration of the variable substrate (Lineweaver-Burk plot). The K_i values are derived from a secondary transformation (slopes or intercepts vs. inhibitor concentrations). The lines of best fit for primary plots and secondary transformations are calculated by using the method of least squares. The mean K_i value of 4–6 experiments is calculated.

MODIFICATIONS OF THE METHOD

The collagen hydroxylases lysyl hydroxylase and prolyl 3-hydroxylase have similar reaction mechanisms as prolyl 4-hydroxylase, differing only in the specificity for the amino acid sequence of the substrate (Kivirikko and Myllylä 1982). Instead of (Pro-Pro-Gly)$_{10}$, 50–500 mg Arg-Ala-Gly-Ile-Lys-Gly-Ile-Arg-Gly-Phe-Ser-Gly are used.

The activity of prolyl 3-hydroxylase is assayed in a reaction volume of 1.5 ml containing 50 mM Tris buffer, pH 7.5, 1,000,000 d.p.m. of biologically obtained [2,3-^{3}H]proline-labeled protocollagen substrate in which all proline residues recognized by proline 4-hydroxylase are converted to hydroxyproline, 2 mM ascorbate, 0.2 mg/ml catalase, 2 mg/ml bovine serum albumin, 15 mM 2-oxoglutarate, 50 mM Fe^{2+}, 100 mM dithiothreitol, 0.2–2 mg enzyme, and inhibitors at various concentrations. After incubation at 37°C for 30 min, the reaction is stopped by addition of 0.5 ml 10% trichloroacetic acid (w/v). The reaction mixture is then distilled, and 1.6 ml of ^3H_2O is counted for radioactivity.

REFERENCES AND FURTHER READING

Hanauske-Abel HM, Günzler V (1982) A stereochemical concept for the catalytic mechanism of prolylhydroxylase. Applicability to classification and design of inhibitors. J Theor Biol 94:421–455
Kivirikko KI, Myllylä R (1982) The hydroxylation of prolyl and lysyl residues. In: Freedman RB, Hawkins HC (eds) The enzymology of post-translational modification of proteins. Academic Press, London, pp 53–104
Majamaa K, Hanauske-Abel HM, Günzler V, Kivirikko KI (1984) The 2-oxoglutarate binding site of prolyl 4-hydroxylase. Identification of distinct subsites and evidence for 2-oxoglutarate decarboxylation in a ligand reaction at the enzyme-bound ferrous ion. Eur J Biochem 138:239–245
Majamaa K, Turpeenniemi-Hujanen TM, Latipää P, Günzler V, Hanauske-Abel HM, Hassinen IE, Kivirikko KI (1985) Differences between collagen hydroxylases and 2-oxoglutarate dehydrogenase in their inhibition by structural analogues of 2-oxoglutarate. Biochem J 229:127–133
Majamaa K, Günzler V, Hanauske-Abel HM, Myllylä R, Kivirikko KI (1986) Partial identity of 2-oxoglutarate and ascorbate binding sites of prolyl 4-hydroxylase. J Biol Chem 261:7819–7823
Peterkofsky B, DiBlasio R (1975) Modification of the tritium-release assays for prolyl and lysyl hydroxylases using Dowex-50 columns. Anal Biochem 66:279–286

J.8.2.3 Influence on Collagen Synthesis in Human Skin Fibroblasts

PURPOSE AND RATIONALE

Secretion of collagen by fibroblasts and other cells capable of synthesizing extracellular matrix is dependent on the hydroxylation of proline residues by prolyl 4-

hydroxylase. This enzyme is located in the cisternae of the endoplasmic reticulum. An agent aimed at inhibition of this enzyme must therefore pass both the external cell membrane and the endoplasmic reticular membrane. Organ specificity of a prolyl 4-hydroxylase inhibitor can be achieved by applying a prodrug which can be converted to the active agent only in cells of specialized tissues, e. g., in the liver, but not generally in fibroblasts.

PROCEDURE

Confluent cultures of human skin fibroblasts are preincubated for 24 h at 37°C without serum in glutamine-free Dulbecco's minimal essential medium supplemented with 50 mg/ml sodium ascorbate, 60 mg/ml 3-aminopropionitrile, and 100 U/ml penicillin G. The cells are then exposed to the potential inhibitor at various concentrations for 20 min, followed by the addition of 2 mCi [U-^{14}C]proline/ml. The incubation is continued for 5 h at 37°C. Then, the cells are separated from the medium. After removal of non-incorporated [^{14}C]proline, the proteins from medium and cells are hydrolyzed, and the hydroxyproline content is determined by amino acid analysis. The total incorporation of radioactivity serves as marker for protein synthesis.

EVALUATION

Two individual samples are taken for each concentration of the inhibitor and 6 samples for the controls. Proline incorporation is expressed as % of control radioactivity. Hydroxyproline synthesis is expressed as relative Hyp/Pro ratio according to the formula:

$$(\mathrm{Hyp/Pro_{sample}}/\mathrm{Hyp/Pro_{control}}) \times 100\,.$$

REFERENCES AND FURTHER READING

Negro A, Garbisa S, Gotte L, Spina M (1987) The use of reverse-phase high-performance liquid chromatography and pre-column derivatization with dansyl chloride for quantitation of specific amino acids in collagen and elastin. Anal Biochem 160:39–46

Tschank G, Raghunath M, Günzler V, Hanauske-Abel HM (1987) Pyridinedicarboxylates, the first mechanism-derived inhibitors for prolyl 4-hydroxylase, selectively suppress cellular hydroxyprolyl biosynthesis. Biochem J 248:625–633

Tschank G, Hanauske-Abel HM, Peterkofsky B (1988) The effectiveness of inhibitors of soluble prolyl hydroxylase against the enzyme in the cisternae of isolated bone microsomes. Arch Biochem Biophys 261:312–323

J.8.2.4 Influence on Collagen Synthesis in Chicken Calvaria

PURPOSE AND RATIONALE

To find fibrosuppressive agents for therapeutic use, it is necessary to have prodrugs which cross cell membranes readily and are converted intracellularly to the active agent. Proinhibitors which are cleaved hydrolytically can suppress collagen synthesis in chicken calvaria.

PROCEDURE

Calvaria are removed from chicken embryos, age 15 days, and washed for 3 min with DMEM at 37°C. They are then transferred into Pyrex tubes (8–10 calvaria/tube) containing 3 ml medium supplemented with 2 mM glutamine, 6 mCi [U-^{14}C-]proline, and various concentrations of the inhibitor. The samples are incubated for 1.5 to 6 h at 37°C. The experiment is terminated by placing the tubes in ice and separation of calvaria from the culture medium. The calvaria are washed once with 3 ml of fresh medium, which is then pooled with the incubation medium. Bovine serum albumin and phenyl methyl sulfonyl fluoride are added (final concentration 1 mg/ml and 6 mg/ml, respectively). The calvaria are extracted for 16 h with 25 ml of 0.5 M acetic acid.

The following procedure is identical for the medium and the calvaria extracts. The samples are extensively dialyzed against 0.5 M acetic acid at 4°C. Aliquots are withdrawn for SDS-PAGE1 and the triple-helix stability assay is performed. The remaining material is lyophilized, resuspended in 2 ml 6 N HCl and hydrolyzed at 105°C for 24 h. After evaporation of the acid, the samples are dissolved in 2 ml H_2O, and the hydroxyproline content is determined according to Juva and Prockop (1967).

In order to study the degree of collagen hydroxylation and proportion of collagen biosynthesis, calvaria are incubated in the presence of 10 mCi [3,4-^{3}H]-proline/ml and 2 mCi [U-^{14}C]-proline/ml for 3 h under the conditions described above. After lyophilization, aliquots of media and calvaria samples are digested with collagenase according to Peterkofsky et al. (1982). The degree of hydroxylation is calculated from the ^{3}H/^{14}C ratio in the digested material; the amount of collagen as a proportion of total protein synthesis is determined by the relation of collagenase degradable vs. collagenase resistant radioactivity. The stability of the extracted collagenous material against digestion by a trypsin/chymotrypsin mixture is tested according to the procedure proposed by Bruckner and Prockop (1981): An aliquot of either culture medium or calvaria extract is incubated for 15 min at a temperature between 25°C and 45°C in a total volume of 800 µl of 0.04 M NaCl/0.1 Tris, pH 7.4. After quenching to 0°C the sample is digested with 200 µl of a mixture of each 1 mg trypsin and chymotrypsin/ml buffer

for 15 min at room temperature. One hundred µl of 1 mg BSA/ml buffer is added, and the protease-resistant radioactivity, consisting of triple-helical collagen, is precipitated with 100 µl 100% trichloroacetic acid (w/v). The sample is transferred in total to a Schleicher and Schüll OE 67 filter paper of 2.5 cm diameter. The digested material is removed by repeated washing with cold 5% trichloroacetic acid and methanol. The filters are then dried and the radioactivity is determined. Unhydrolyzed samples are studied by SDS-polyacrylamide gel electrophoresis, and autofluorography. The morphologic appearance of the control and treated cultures is studied by electron microscopy.

EVALUATION

IC_{50}-values of hydroxyproline synthesis are read graphically from concentration response curves. Total protein synthesis is estimated as the incorporation of proline; the mean ± standard deviation is calculated from four samples.

MODIFICATIONS OF THE METHOD

Canalis et al. (1977) used cultured calvaria from 21 day fetal rats to study the effects of insulin and glucagon on bone collagen synthesis.

REFERENCES AND FURTHER READING

Bruckner P, Prockop DJ (1981) Proteolytic enzymes as probes for the triple-helical conformation of procollagen. Anal Biochem 110:360–368

Canalis EM, Dietrich JW, Maina DA, Raisz LG (1977) Hormonal control of bone collagen synthesis *in vitro*. Effects of insulin and glucagon. Endocrinology 100:668–674

Juva K, Prockop DJ (1966) Modified procedure for the assay of H^3- or C^{14}-labeled hydroxyproline. Anal Biochem 15:77–83

Peterkofsky B, Assad R (1976) Submicrosomal localization of prolyl hydroxylase from chick embryo limb bone. J Biol Chem 251:4770–4777

Peterkofsky B, Chojkier M, Bateman J (1982) Determination of collagen synthesis in tissue and cell culture systems. In: Furthmayr H (ed) Immunochemistry of the extracellular matrix. Vol II: Applications. CRC Press, Boca Raton, pp 19–47

J.8.2.5 Allyl Alcohol Induced Liver Necrosis in Rats

PURPOSE AND RATIONALE

Administration of allyl alcohol induces focal liver necrosis in rats which can be partially prevented by treatment with several drugs such as antibiotics.

PROCEDURE

Female Wistar rats weighing 120–150 g are used. At 8:00 A.M. of the first day food but not water is withdrawn. At 3:00 P.M. the compounds to be tested for protective activity are administered i.p. or orally. One hour later, the animals are dosed orally with 0.4 ml/kg of a 1.25% solution of allyl alcohol in water. At 8:00 A.M. of the second day the treatment with the potentially protective drugs is repeated. Food but not water is withheld until the third day. At 8:00 A.M. of the third day the animals are sacrificed and the liver removed. The parietal sides of the liver (left, medium and right lobe and lobus caudatus) are checked using a stereomicroscope with 25 times magnification. Focal necrosis is observed as white-green or yellowish hemorrhagic areas clearly separated from unaffected tissue. The diameter of the necrotic areas is determined using a ocular-micrometer. These values are added for each animal to obtain an index for necrosis.

EVALUATION

Using 10 animals for controls and for each treatment group, the mean of necrosis index is calculated and compared with Student's *t*-test. The protective effect is expressed as percentage decrease of the necrosis index versus controls.

REFERENCES AND FURTHER READING

Eger W (1954) Das Verhalten der Phosphoamidase in der Leber bei Tetrachlorkohlenstoff- und Allylalkoholvergiftung. Virchows Arch 325:648–656

Eger W (1955) Der Einfluß von Antibiotika und Sulfonamiden auf Lebernekrosen im Allylalkoholtest. Med Mschr 9:294–295

J.8.2.6 Carbontetrachloride Induced Liver Fibrosis in Rats

PURPOSE AND RATIONALE

Chronic administration of tetrachloride to rats induces severe disturbances of hepatic function together with histologically observable liver fibrosis.

PROCEDURE

Groups of 20 female Wistar rats with a starting body weight of 100–150 g are used. The animals are treated orally twice a week with 1 mg/kg carbontetrachloride, dissolved in olive oil 1:1, over a period of 8 weeks. The animals are kept under standard conditions (day/night rhythm 8:00 A.M. to 8:00 P.M., 22°C room temperature, standard diet, e. g. Altromin 1321 pellets, and water ad libitum). Twenty animals serve as controls receiving olive oil only, 40–60 animals receive the carbontetrachloride only, and groups of 20 rats receive in addition the compound under investigation in various doses by gavage twice daily (with the exception of the weekends, when only one dose is given) on the basis

of the actual body weight. The animals are weighed weekly.

At the end of the experiment (8 weeks), the animals are anesthetized and exsanguinated through the caval vein.

In the *serum*, the following parameters are determined:

- Total bilirubin,
- total bile acids,
- 7S fragment of type IV collagen,
- procollagen III N-peptide.

The following organs are prepared for determination of hydroxyproline:

- Liver,
- kidney,
- aortic wall, and
- tail tendons.

The specimens of the organs are weighed and completely hydrolyzed in 6 N HCl. Hydroxyproline is measured by HPLC and expressed as mg/mg wet weight of the organs.

To measure **mechanical properties of connective tissue**, the following organs are prepared: Femur and tibia of both sides, tail tendons, and strips from dorsal skin (Bickel et al. 1990, 1991; detailed description of the methods see N.2.1.3). Furthermore, the influence on the healing process of skin wounds is studied (Method see N.2.1.3.5).

For **histological analysis**, 3–5 pieces of the liver weighing about 1 g are fixed in formalin and Carnoy solution. Three – 5 sections of each liver are embedded, cut and stained with azocarmine aniline blue (AZAN) and evaluated for the development of fibrosis using a score of 0–IV.

Grade 0:	Normal liver histology.
Grade I:	Tiny and short septa of connective tissue without influence on the structure of the hepatic lobules.
Grade II:	Large septa of connective tissue, flowing together and penetrating into the parenchyma. Tendency to develop nodules.
Grade III:	Nodular transformation of the liver architecture with loss of the structure of the hepatic lobules.
Grade IV:	Excessive formation and deposition of connective tissue with subdivision of the regenerating lobules and with development of scars.

EVALUATION

For detection of significant differences ($p < 0.05$), the unpaired *t*-test is used. For comparison of the scores in the histological evaluation, the χ^2-test is used.

MODIFICATIONS OF THE TEST

Instead of chronic intoxication with carbontetrachloride resulting in liver fibrosis, acute hepatocellular damage can be achieved by short term application of carbontetrachloride.

Wistar rats with a starting body weight of 120–150 g are treated daily for 5 days with various oral doses of the compound under investigation. From day 2 to day 5 (4 applications) the rats receive by gavage a dose of 1 mg/kg carbontetrachloride dissolved in olive oil (1:1). Blood is withdrawn every day and the aminotransferases ALAT and ASAT, as well as total bilirubin are determined in the serum.

Niederberger et al. (1995, 1998) induced liver cirrhosis and ascites in rats by treatment with carbon tetrachloride.

Sakamoto et al. (2005) induced liver cirrhosis in rats by intraperitoneal injection of 10 mg/kg dimethylnitrosamine three times a week for 3 weeks.

Kawaura et al. (1993) produced liver cirrhosis with ascites in **dogs** by administration of 2 ml carbontetrachloride per kg body weight once a week for 4 weeks. Eight weeks afterwards, the supradiaphragmatic inferior vena cava was constricted to 50% resulting in ascites formation of 500 to 1000 ml. The dogs could be treated by ligation of the common hepatic artery and hepatocyte inoculation into the spleen.

Wirth et al. (1997) studied the effects of a bradykinin B_1 receptor antagonist in rats with CCl_4-induced liver cirrhosis.

In the model of CCl_4-induced liver fibrosis, the antifibrotic agents HOE077 and safironil decreased collagen accumulation in the liver by inhibition of stellate cell activation, which was more pronounced in female than it was in male rats (Wang et al. 1998). In the same model (Bickel et al. 1998) demonstrated powerful antifibrotic effects of a new prolyl 4-hydroxylase (P4-H) inhibitor, S4682, having a K_i of 155 nM at the purified enzyme P4-H. Inhibition of prolyl hydroxylation in stellate cells was inhibited with an IC_{50} of 39 μM by S4682. In drug-treated rats, ascites was significantly lower compared with controls. Histological examination proved a significantly lesser score of liver fibrosis after drug treatment.

REFERENCES AND FURTHER READING

Abe H, Sakaguchi M, Odashima S, Arichi S (1982) Protective effect of saikosaponin-d isolated from Bupleurum falcatum L. on CCl_4-induced liver injury in the rat. Naunyn Schmiedeberg's Arch Pharmacol 320:266–271

Ala-Kokko L, Stenbäck F, Ryhänen L (1987) Preventive effect of malotilate on carbon tetrachloride-induced liver damage and collagen accumulation in the rat. Biochem J 246:503–509

Bickel M, Baader E, Brocks D, Burghard H, Günzler V, Engelbart K, Hanauske-Abel HM, Vogel HG (1990) Liver selective fibrosuppression in the rat by a derivative of pyridine-2,4-dicarboxylate, S 0885. Gastroenterology 98:A 570

Bickel M, Baader E, Brocks D, Günzler V, Schmidts HL (1991a) Effects of a prolyl-4-hydroxylase inhibitor on collagen synthesis in different rat organs. Eur J Gastroenterol Hepatol 3, Suppl 1:S65, Abstr. 260

Bickel M, Baader E, Brocks DG, Engelbart K, Günzler V, Schmidts HL, Vogel HG (1991b) Beneficial effects of inhibitors of prolyl 4-hydroxylase in CCl_4-induced fibrosis of the liver in rats. J Hepatol 13, Suppl 3:S26–S34

Bickel M, Baringhaus KH, Gerl M, Guenzler V, Kanta J, Schmidts HL, Stapf M, Tschank G, Weidmann K, Werner U (1998) Selective inhibition of hepatic collagen accumulation in experimental liver fibrosis in rats, by a new prolyl 4-hydroxylase inhibitor. Hepatology 28:404–411

Brocks D, Bickel M, Engelbarth K (1986) Type IV collagen antigens in serum of rats with experimental fibrosis of the liver. Alcohol Alcoholism Suppl 1:497–500

Hirayama C, Morotomi I, Hiroshige K (1979) Quantitative and metabolic changes of hepatic collagens in rats after tetrachloride poisoning. Biochem J 118:229–232

Kawaura Y, Dohden K, Ogawa S, Koichi K (1993) A new surgical procedure consisting of ligation of common hepatic artery and auto-transplantation of hepatocytes into the spleen for end stage liver cirrhosis accompanied by ascites. Gastroenterol Jpn 28:259–267

Niederberger M, Martin PY, Gines P, Morris K, Tsai P, Xu DL, McMurtry I, Schrier RW (1995) Normalization of nitric oxide production corrects arterial vasodilation and hyperdynamic circulation in cirrhotic rats. Gastroenterology 109:1624–1630

Niederberger M, Gines P, Martin PY, St. John J, Woytaszek P, Xu L, Tsai P, Nemenoff RA, Schrier RW (1998) Increased renal and vascular cytosolic phospholipase A_2 activity in rats with cirrhosis and ascites. Hepatology 27:42–47

Sakamoto M, Ueno T, Nakamura T, Sakata R, Hasimoto O, Torimura R, Sata M (2005) Improvement of portal hypertension and hepatic blood flow in cirrhotic rats by oestrogen. Eur J Clin Invest 35:220–225

Wang YJ, Wang SS, Bickel M, Guenzler V, Gerl M, Bissell DM (1998) Two novel antifibrotics, HOE 077 and Safironil, modulate stellate cell activation in rat liver injury. Differential effects in males and females. Am J Pathol 152:279–287

Wirth KJ, Bickel M, Hropot M, Günzler V, Heitsch H, Ruppert D, Schölkens BA (1997) The bradykinin B_1 receptor antagonist icatibant (HOE 140) corrects avid Na^+ retention in rats with CCl_4-induced liver cirrhosis: Possible role of enhanced microvascular leakage. Eur J Pharmacol 337:45–53

J.8.2.7 Bile Duct Ligation Induced Liver Fibrosis in Rats

PURPOSE AND RATIONALE

Bile duct ligation in rats induces liver fibrosis which can be evaluated by histological means and by determination of serum collagen parameters.

PROCEDURE

Male Sprague Dawley rats weighing approximately 250 g are anesthetized with ketanest (Rompun). Laparotomy is performed under antiseptic conditions. A mid-line incision in the abdomen is made from the xiphosternum to the pubis, exposing the muscle layers and the linea alba, which is then incised over a length corresponding to the skin incision. The edge of the liver is then raised and the duodenum pulled down to expose the common bile duct, which pursues an almost straight course of about 3 cm from the hilum of the liver to its opening into the duodenum. There is no gallbladder, and the duct is embedded for the greater part of its length in the pancreas, which opens into it by numerous small ducts. A blunt aneurysm needle is passed under the part of the duct selected, stripping the pancreas away with care, and the duct is divided between double ligatures of cotton thread. The peritoneum and the muscle layers as well as the skin wound are closed with cotton stitches.

The animals receive normal diet and water ad libitum throughout the experiment. Groups of 5–10 animals receive the test compound in various doses or the vehicle twice daily for 6 weeks. Then, they are sacrificed and blood is harvested for determination of bile acids, 7S fragment of type IV collagen, and procollagen III N-peptide. The liver is used for histological studies and for hydroxyproline determinations. Control animals show excessive bile duct proliferation as well as formation of fibrous septa. The picture is consistent with complete biliary cirrhosis.

EVALUATION

For detection of significant differences ($p < 0.05$), the unpaired *t*-test is used.

MODIFICATIONS OF THE METHOD

Alpini et al. (1994) found an upregulation of secretin receptor gene expression in rat cholangiocytes after bile duct ligation.

Fiorucci et al. (2003) used 4-week bile-duct-ligated cirrhotic rats to study the effects of a nitric oxide-releasing derivative of ursodeoxycholic acid.

REFERENCES AND FURTHER READING

Alpini G, Ulrich II CD, Phillips JO, Pham LD, Miller LJ, LaRusso NF (1994) Upregulation of secretin receptor gene expression in rat cholangiocytes after bile duct ligation. Am J Physiol, Gastrointest Liver Physiol 266:G922–G928

Cameron GR, Oakley CL (1932) Ligation of the common bile duct. J Path 35:769–798

Fiorucci S, Antonelli E, Brancaleone V, Sanpaolo L, Orlandi S, Distrutt E, Acuto G, Clerici C, Baldoni M, Del Soldato P, Morelli A (2003) NCX-1000, a nitric oxide-releasing derivative of ursodeoxycholic acid, ameliorates portal hypertension and lowers norepinephrine-induced intrahepatic resistance in the isolated and perfused rat liver. J Hepatol 39:932–939

Kountouras J, Billing BH, Scheuer PJ (1984) Prolonged bile duct obstruction: a new experimental model for cirrhosis in the rat. Br J Exp Path 65:305–311

J.8.2.8 Galactosamine Induced Liver Necrosis

PURPOSE AND RATIONALE

Single dose or a few repeated doses of D-galactosamine cause acute hepatic necrosis in rats (Decker and Keppler 1972). Prolonged administration leads to cirrhosis (Lesch et al. 1970).

PROCEDURE

For induction of acute experimental hepatotoxicity, divided doses of 100 to 400 mg/kg D-galactosamine are injected to rats i.p. or i.v. during one day.

For induction of liver cirrhosis, male Wistar rats weighing 110–180 g are injected intraperitoneally three times weekly with 500 mg/kg D-galactosamine over a period of one to 3 months. Potential protective substances are administered orally with the food or by gavage every day. The rats are sacrificed at various time intervals and the livers obtained by autopsy.

EVALUATION

The livers are evaluated by light microscopy and immunohistology using antibodies against macrophages, lymphocytes and the extracellular matrix components, e. g., laminin, fibronectin, desmin, collagen type I, III, and IV. The extent of liver cell necrosis and immunoreactivity for macrophages, lymphocytes and the extracellular matrix components is graded semiquantitatively on a 0 to 4+ scale (0 = absent, 1+ = trace, 2+ = weak, 3+ = moderate, and 4+ = strong). Furthermore, serum enzyme activities, such as GOT and GPT, are determined.

MODIFICATIONS OF THE METHOD

Other agents used to induce experimental cirrhosis are ethionine, thioacetamide (Dashti et al. 1996), dialkylnitrosamines, tannic acid, aflatoxins, pyrrolidizine alkaloids, and hepatotoxic components from mushrooms, such as amatoxins and phallotoxins (Zimmerman 1976).

Bruck et al. (1996) found an inhibition of thioacetamide-induced liver cirrhosis in rats by a nonpeptidic mimetic of the extracellular matrix-associated Arg-Gly-Asp epitope.

Intrahepatic cholestasis can be induced by alpha-naphthylisothiocyanate in rats (Krell et al. 1982).

Fulminant liver destruction can be induced with anti-Fas antibody.

Rodriguez et al. (1996) injected inbred female C57BL mice with anti-Fas antibody. The animals died within a few hours due to massive apoptosis of hepatocytes. This was accompanied by the sequential activation of cysteine proteases of the interleukin$_{1\beta}$-converting enzyme (ICE) and CPP32 (caspase-3) types in the cytosol of the hepatocytes. Systemic injection of the tripeptide *N*-benzyloxycarbonyl-Val-Ala-Asp-fluoromethylketone inhibited the intracellular activation of CPP32-like proteases *in vivo* and fully protected mice against Fas-mediated fulminant liver destruction and death.

Suzuki (1998) showed that the CPP32 subfamily, rather than the ICE subfamily, plays the dominant role in Fas antibody-induced hepatitis.

REFERENCES AND FURTHER READING

Bruck R, Hershkowviz R, Lider O, Aed H, Zaidel L, Matas Z, Barg J, Halpern Z (1996) Inhibition of experimentally-induced liver cirrhosis in rats by a nonpeptidic mimetic of the extracellular matrix-associated Arg-Gly-Asp epitope. J Hepatol 24:731–738

Dashti HM, Abul H, Behbehani A, Hussain T, Madda JP (1996) Interleukin-8 and trace element alterations in experimentally induced liver cirrhosis: The influence of zinc, selenium, and allopurinol treatment. J Trace Elem Exp Med 9:27–40

Decker K, Keppler D (1972) Galactosamine induced liver injury. In: Popper H, Schaffner F (eds) Progress in Liver Disease, Vol IV, Grune and Stratton Inc, New York, pp 183–199

Eggstein S, Kreisel W, Gerok W, Eggstein M (1989) Dipeptidylaminopeptidase IV in einem klinischen Krankengut und bei Galaktosaminhepatitis der Ratte: Aktivität und Lektinaffinitätschromatographie in Serum und Leberplasmamembran. J Clin Chem Clin Biochem 27:547–554

Galanos C, Freudenberg MA, Reutter W (1979) Galactosamine-induced sensitization to the lethal effects of endotoxin. Proc Natl Acad Sci USA 76:5939–5943

Jonker AM, Dijkhuis FWJ, Hardonk MJ, Moerkerk P, Kate JT, Grond J (1994) Immunohistochemical study of hepatic fibrosis induced in rats by multiple galactosamine injections. Hepatology 19:775–781

Keppler D, Lesch R, Reutter W, Decker K (1968) Experimental hepatitis induced by D-galactosamine. Exp Mol Pathol 9:279–290

Krell H, Höke H, Pfaff E (1982) Development of intrahepatic cholestasis by a-naphthylisothiocyanate in rats. Gastroenterology 82:507–514

Leighton JA, Bay MK, Maldonato AL, Johnson RF, Schenker St, Speeg KV (1990) The effect of liver dysfunction on colchicine pharmacokinetics in the rat. Hepatology 11:210–215

Lesch R, Keppler D, Reutter W, Rudigier J, Oehlert W, Decker K (1970) Entwicklung einer experimentellen Leberzirrhose durch D-Galaktosamin. Histologische, biochemische und autoradiographische Untersuchungen an Ratten. Virchows Arch, Abt B Zellpath 6:57–71

Rodriguez I, Matsuura K, Ody C, Nagata S, Vassalli P (1996) Systemic injection of a tripeptide inhibits the intracellular activation of CPP32-like proteases in vivo and fully protects mice against Fas-mediated fulminant liver destruction and death. J Exp Med 184:2067–2072

Suzuki A (1998) The dominant role of CPP32 subfamily in fas-mediated hepatitis. Proc Soc Exp Biol Med 217:450–454
Zieve L, Anderson WR, Dozeman R (1988) Hepatic regenerative enzyme activity after diffuse injury with galactosamine: relationship to histologic alterations. J Lab Clin Med 112:575–582
Zimmerman HJ (1976) Experimental hepatotoxicity. In: Born GVR, Eichler O, Farah A, Herken H, Welch AD (eds) Handbook of Experimental Pharmacology, Vol XVI: Experimental production of diseases. Part 5: Liver. Springer-Verlag Berlin, Heidelberg, New York, pp 1–120

J.8.2.9
Liver Fibrosis Induced by Schistosome Cercariae

CCl_4-induced liver fibrosis is the most commonly used model in liver fibrosis. The major shortcoming of this method is the high relative variability of the amount of collagen produced in the liver by treatment with the toxin. Determination of hydroxyproline, as a parameter of collagen deposition in the liver, showed a large relative variability of 75% after 8 weeks of treatment with twice-weekly administration of CCl_4. To ensure adequate statistical interpretation, 50 rats/group are needed (Bickel et al. 1996).

Exposure of mice tails to *Schistosome cercariae* causes infiltration of the cercariae into the circulation and subsequent deposition of the schistosome eggs in the liver. Thereafter liver fibrosis is produced in the liver in a time-dependent fashion. Hydroxyproline of the liver increases by threefold and sevenfold, 10 and 18 weeks after infection. The relative variabilities of the hydroxyproline content of the liver were 10% to 20%, 10 and 18 weeks after infection, respectively (Phillips et al. 1977, 1987). The advantages of this model are the simplicity of fibrosis induction, the uniform generation of liver fibrosis with a very low variability with regard to the collagen produced in the liver, and, most of all, that it represents a disease model which accurately corresponds to the human disease. One should not forget that at least 200 million people suffer from schistosomiasis, most of them living in developing countries.

In this model the antifibrotic active compound Safironil caused a significant reduction of collagen type I and fibronectin in the liver. The beneficial effects of Safironil were at least in part due to a decrease in stellate cell activation by a mechanism sensitive to tumour growth factor $(TGF)_{\beta 1}$ (Phillips et al. 1997).

REFERENCES AND FURTHER READING

Bickel M, Gerl M, Günzler V (1996) Die CCl_4 induzierte Leberfibrose der Ratte. Validierung eines experimentellen Modells. Z Gastroenterol Suppl 34: Abstr. 49
Phillips SM, Diconza JJ, Gold JA, Reid WA (1977) Schistosomiasis in the congenitally athymic (nude) mouse. Thymic dependency of eosinophilia granuloma formation and host morbidity. J Immunol 118:594–599
Phillips SM, Linette GP, Doughty BL, Byram JE, von Lichtenberg F (1987) In vivo T cell depletion regulates resistance and morbidity in murine schistosomiasis. J Immunol 139:919–924
Phillips M, Ramadan M, Hilliard B, Sugaya H, Zekavat A, Günzler V, Bickel M (1997) The regulation of schistosome granuloma formation and fibrosis by anti-fibrogenic treatment: Safironil (HOE 277) and $TGF_{\beta 1}$ Mab. Gastroenterology Suppl 122: Abstr. 1358

J.9
Eviscerated Animals

J.9.1
Evisceration in Rats

PURPOSE AND RATIONALE

Eviscerated animals have been used to study the influence of hormones and other drugs on carbohydrate disposal (Russell 1942; Creutzfeldt et al. 1961; Wick and Drury 1963; Willms et al. 1969; Tanira and Furman 1999).

"Functional" evisceration has been performed by most authors (Russell 1942; Creutzfeldt et al. 1961; Creutzfeldt and Deuticke 1962; Willms et al. 1969; Penhos et al. 1970; Smith 1986; Smith et al. 1990; Tanira and Furman 1999). The abdominal viscera, with the exception of the liver, are removed, and the blood vessels supplying the liver – the coeliac axis and the portal vein – are tied and cut.

PROCEDURE

Male Wistar rats weighing 180 to 280 g are allowed free access to food and water until the experiment. They are anesthetized with 55 mg/kg pentobarbitone sodium i.p. Cannulae are placed in the left femoral vein and in the abdominal aorta via the left femoral artery.

The abdominal cavity is opened and the anterior mesenteric artery, posterior mesenteric artery and the coeliac axis are cut between double ligatures close to the abdominal aorta. The hepatic portal vein is ligated and cut in the same manner. After ligating and cutting the esophagus and the rectum, the abdominal portion of the gastrointestinal tract is removed, together with the pancreas and the spleen. The muscle and the skin incisions are sutured. After completion of the operation the rats are left for 15 min to equilibrate.

Drugs are injected intravenously through the venous cannula. Blood samples are withdrawn from the aortic cannula before and at various intervals after drug ad-

ministration to be assayed for insulin, blood glucose and non-esterified fatty acids.

EVALUATION

All results are expressed as mean ± SEM. Statistical analysis is performed using ANOVA.

CRITICAL ASSESSMENT OF THE METHOD

The described "functional" evisceration can be performed within 2–3 min without any hemorrhage or any signs of shock, even in hypophysectomized or adrenalectomized animals. That the liver remaining *in situ* is effectively cut off from the blood stream is proven by the fact that rats eviscerated in this way will die within 1–2 h without infusion of glucose.

MODIFICATIONS OF THE METHOD

Some authors removed also the kidneys and the adrenals in rats (Creutzfeldt and Deuticke 1962).

Dogs were eviscerated and nephrectomized under sodium pentobarbital anesthesia by Levine et al. (1950).

REFERENCES AND FURTHER READING

Creutzfeldt W, Deuticke U (1962) Beeinflussung der Insulinempfindlichkeit der eviscerierten Ratte durch Nebennieren-Exstirpation, Nebennierenhormone und Glukagon. Acta endocrin 39:262–284

Creutzfeldt W, Deuticke U, Söling HD (1961) Potenzierung der Wirkung von exogenem Insulin durch N-(4-Methylbenzolsulfonyl)-N′-butylcarbamid und N_1,-n-Butylbiguanid beim eviscerierten Tier. Klin Wschr 39:790–795

Levine R, Goldstein MS, Huddlestun B, Klein SP (1950) Action of insulin on the 'permeability' of cells to free hexoses, a studied by its effect on the distribution of galactose. Am J Physiol 163:70–76

Penhos JC, Voyles N, Lazaraus N, Tanese T, Gutman R, Recant L (1970) Hypoglycemic action of porcine proinsulin in eviscerated, functionally hepatectomized rats. Horm Metab Res 2:43–44

Russell JA (1942) The anterior pituitary in the carbohydrate metabolism of the eviscerated rat. Am J Physiol 136:95–104

Smith OLK (1986) Protein degradation in skeletal muscles after evisceration of fed or fasted rats. Am J Physiol 251:E379–E384

Smith OLK, Wong CY, Gelfand RA (1990) Influence of glucocorticoids on skeletal muscle proteolysis in normal and diabetic-adrenalectomized eviscerated rats. Metabolism 39:641–646

Tanira MOM, Furman BL (1999) The *in vivo* interaction between gliclazide and glibenclamide and insulin on glucose disposal in the rat. Pharmacol Res 39:349–356

Wick AN, Drury DR (1963) Influence of glucose concentration on the action of insulin. Am J Physiol 174:445–447

Willms B, Appels A, Söling HD, Creutzfeldt W (1969) Lack of hypoglycemic effect of bovine proinsulin in eviscerated, hepatectomized rats. Horm Metab Res 1:199–200

J.9.2 Evisceration in Rabbits

PURPOSE AND RATIONALE

Evisceration in rabbits was performed by Drury (1935), Wick and Drury (1963), Lippmann and Hommel (1968, 1969), Menzel and Haupt (1972). A detailed description of the technique was given by Lippmann and Hommel (1968).

PROCEDURE

Rabbits of both sexes weighing 2.6–3.2 kg kept on standard diet and tap water ad libitum are used. Food is withdrawn 12 h before surgery and the abdominal skin is shaved. The animals are anesthetized with 50 mg/kg hexobarbital sodium intravenously. After fixation of the animal, the abdominal cavity is opened by electrocautery from the xyphoid process until 3 cm cranial of the symphysis. The rectum is cut between double ligatures as far caudally as possible. Bleeding from the arteria rectalis has to be avoided. The arteria mesenterica inferior, which is a tiny vessel in the rabbit, is ligated close to the aorta. The root of the mesentery is cut up to the superior mesenteric artery which is tightly ligated. Then the arteria coeliaca is ligated in the same manner allowing complete removal of the root of the mesentery. The esophagus is ligated close to the cardia. After double ligature of the portal vein the whole gastrointestinal tract including the pancreas and the spleen is isolated and the liver is functionally cut off. To eliminate the function of the kidneys, the renal arteries are ligated close to the aorta and the ureters close to the hilus. Cannulae are introduced into the caval vein via the renal veins. The right renal vein is ligated close to the hilus and the tip of a polyethylene catheter placed 4–6 cm caudal from the inferior caval vein for blood withdrawal; the left renal vein is also ligated close to the hilus and the tip of a polyethylene catheter placed 6 cm cranial from the inferior caval vein for infusion.

The animal receives via the catheter 750 IU heparin, 0.3 mg/kg lobeline hydrochloride, 3 mg/kg pentylenetetrazole, 0.01 mg/kg ouabain, and 1.3 mg/kg synephrine to stabilize the cardiovascular function.

Drugs are injected intravenously through the infusion cannula. Blood samples are withdrawn from the other cannula before and at various intervals after drug administration to be assayed for insulin and blood glucose.

EVALUATION

All results are expressed as mean ± SEM. Statistical analysis is performed using ANOVA.

MODIFICATIONS OF THE METHOD

Schäfer (1990) measured glucose disappearance rates into peripheral tissues *in vivo* in adult eviscerated, nephrectomized and adrenalectomiced rabbits, Wistar rats and non-diabetic sand rats with physiological insulin concentrations in the blood.

REFERENCES AND FURTHER READING

Drury DR (1935) Sugar utilization in eviscerated rabbits. Am J Physiol 111:289–292

Lippmann GH, Hommel H (1968) Bestimmung der biologischen Aktivität des Insulin am eviszerierten Kaninchen. I. Versuchsanordung und Methodenkritik. Acta biol med germ 21:723–732

Lippmann GH, Hommel H (1969) Bestimmung der biologischen Aktivität des Insulin. II Wirkung auf den Glukoseabstrom. Acta biol med germ 22:23–33

Menzel R, Haupt I (1972) Untersuchungen zur *in vitro* und *in vivo*-Insulinbindung mit Anti-Rinderinsulinserum vom Kaninchen. Acta biol med germ 28:3249–356

Schäfer H (1990) Glucose disappearance rates into peripheral tissues of adult rabbits (*Sivilagus floridans*), Wistar rats (*Rattus rattus*) and sand rats (*Psammomys obesus*) in relation to body weight and blood glucose concentration. Com Biochem Physiol Comp Physiol 95:209–213

Wick AN, Drury DR (1963) Influence of glucose concentration on the action of insulin. Am J Physiol 174:445–447

J.10
Safety Pharmacology of Gastrointestinal Drugs

See Hering (2006).

REFERENCES AND FURTHER READING

Herling AW (2006) Metabolism pharmacology. In: Vogel HG, Hock FJ, Maas J, Mayer D (eds) Drug Discovery and Evaluation Safety and Pharmacokinetic Assays, Chap. I.M. Springer-Verlag, Berlin Heidelberg New York, pp 255–318

Chapter K
Antidiabetic Activity[1]

[1] Completely rewritten by G. Müller, with reviews and contributions for this and the former edition by A.W. Herling, and by J. Sandow.

K.1 Methods to Induce Experimental Diabetes Mellitus

K.1.1 Pancreatectomy in Dogs

GENERAL CONSIDERATIONS

Dysfunction of the visceral tract has been considered for a long time to be the cause of diabetes mellitus. Bomskov in 1910 reported severe diabetic symptoms in dogs after cannulation of the ductus lymphaticus. This observation, however, could not be confirmed in later experiments (Vogel 1963). The technique was similar to that described by Gryaznova (1962, 1963) for ligation of the thoracic duct in dogs.

Von Mehring and Minkowski in 1890 noted polyuria, polydipsia, polyphagia, and severe glucosuria following removal of the pancreas in dogs. The final proof for the existence of a hormone in the pancreas was furnished by Banting and Best (1922) who could reduce the elevated blood sugar levels in pancreatectomized dogs by injection of extracts of the pancreatic glands. The role of the pituitary gland in development of diabetes has first been elucidated by Houssay (1930, 1931) in pancreatectomized dogs (Survey by Beyer and Schöffling 1986).

PURPOSE AND RATIONALE

The technique of complete pancreatectomy in the dog as described in detail by Foà (1971) and by Sirek (1986) has been used by many scientists as a relevant animal model for insulin-deficient diabetes mellitus in man. Some remarks of our own experiences are added to an abbreviated version of Sirek's description.

PROCEDURE

Male Beagle dogs weighing 12–16 kg are used. After appropriate premedication the animal is placed on its back intubated with a tracheal tubus and anaesthesia is achived and maintained by an inhalation anaesthetics (e. g. fluroane). After removal of the fur and disinfection of the skin a midline incision is made from the xyphoid process reaching well below the umbilicus. Bleeding vessels are ligated and the abdomen is entered through the linea alba. The falciform ligament is carefully removed and the vessels ligated. A self-retaining retractor is applied. By passing the right hand along the stomach to the pylorus, the duodenum with the head of the pancreas is brought into the operating field. First, the mesentery at the unicate process is cut and the process itself is dissected free. The glandu-

lar tissue is peeled off from the inferior pancreaticoduodenal artery and vein. The vessels themselves are carefully preserved. Along a line of cleavage which exists between the pancreas, the pancreaticoduodenal vessels and the duodenal wall, the pancreas is separated from the duodenum and from the carefully preserved pancreatico-duodenal vessels. The small vessels to the pancreas are ligated. The dissection is carried out from both sides of the duodenum. In the area of the accessory pancreatic duct the glandular tissue being attached very firmly has to be carefully removed in order to leave no residual pancreatic tissue behind.

The pancreatic duct is cleaned, doubly ligated and cut between the ligatures. The dissection proceeds until one encounters a small lobe containing the main pancreatic duct. The glandular tissue adheres here firmly to the duodenum. Blunt dissection and ligation of the vessels is followed by ligation of the pancreatic duct. By pulling on the pylorus and the stomach, the pyloric and the splenic parts of the pancreas are delivered into the wound. The duodenal part is placed back into the abdominal cavity. The mesentery of the body and tail of the pancreas is cut with scissors. The small vessels are doubly ligated and cut. The pancreatic tissue is bluntly dissected from the splenic vessels. The pancreatic branches of the splenic vessels are doubly ligated and cut. Working in direction from the spleen to the pylorus, the pyloric part of the pancreas is the last one to be dissected. Finally, all pancreatic tissue is removed.

The surgical field is checked once more for pancreatic remnants. The concavity of the duodenum and its mesentery is approximated by a few silk stitches and the omentum is wrapped around the duodenum. Retroperitoneal injection of 5 ml 1% procaine solution is given to prevent intussusception of the gut. 250,000 IU penicillin G in saline solution are instilled into the peritoneal cavity. The abdominal wall and the subcutaneous layer are closed by sutures and finally the skin is sutured with continuous everting mattress stitches.

After the operation, the animal receives via a jugular vein catheter for 3–4 days the following treatment: 1000 ml 10% glucose solution with 10 IU human insulin Regular, 3 ml 24% Borgal (sulfadioxin/trimethoprim) solution, 2 ml 50% metamizol and 400 IU secretin. On the third day, the animal is offered milk. After the animal has passed the first milk feces, commercially available dry food together with a preparation of pancreatic enzymes for substitution. Insulin is substituted with a single daily subcutaneous dose of a long-acting insulin (e. g. Lantus) and the insulin dose is individually adjusted according to the blood glucose levels achieved. Vitamin D_3 is given every three months as a intramuscular injection of 1 ml Vigantol forte.

MODIFICATIONS OF THE METHOD

Experiments performed by Houssay (1930, 1931) performing hypophysectomy in pancreatectomized dogs revealed amelioration of the diabetic state. These experiments contributed to the understanding of hormonal control in diabetes mellitus.

Rappaport and coworkers (1966) and Lau and coworkers (1976) used a pedunculated subcutaneous autotransplant of an isolated pancreas remnant for the temporary deprivation of internal secretion in the dog.

Subtotal pancreatectomy in **rats** was described by Scow (1957), Scow and coworkers (1957), Wagner and Cardeza (1957), Bonner-Weir and coworkers (1983), Noguchi and coworkers (1994), Tanigawa and coworkers (1997). The pancreatic tissue between the common bile duct, duodenal loop, and portal vein in the duodenal segment, along the greater curvature in the gastric segment, and along the splenic vein in the splenic segment, was surgically excised in 3- to 4-weeks old rats weighing 80–100 g.

Greeley (1937) proposed a 3-stage procedure with 3–4 weeks intervening between operations for pancreatectomy in **rabbits**.

Itoh and Maki (1996) reported surgical removal of 90% of pancreatic tissue in 7 or 13 weeks old **mice**. Under sodium pentobarbital anesthesia (65 mg/kg i.p.), the pancreas and the spleen were surgically removed with careful conservation of the common bile duct and major vessels surrounding the duodenum. Approximately 10% (by weight and by insulin content) of the pancreas tissue was left intact adjacent to the lower duodenal loop.

REFERENCES AND FURTHER READING

Banting FG, Best CH (1922) The internal secretion of the pancreas. J Lab Clin Med 7:251–266

Beyer J, Schöffling K (1968) Die Houssay-Präparation (Methodisches Vorgehen und Auswirkungen der Versuchsanordnung auf Stoffwechsel und endokrines System). In: Pfeiffer EF (ed) Handbook of Diabetes mellitus, Pathophysiology and Clinical Considerations. Vol. I, Lehmanns Verlag, München, pp 745–761

Bonner-Weir S, Trent DF, Weir GC (1983) Partial pancreatectomy in the rat and subsequent defect in glucose-induced insulin release. J Clin Invest 71:1544–1553

Foà PP (1971) Pankreatektomie. In: Dörzbach E (ed) Handbook of Experimental Pharmacology Vol 32/1, Insulin, Springer-Verlag, Berlin Heidelberg New York, pp 146–158

Geisen K (1988) Special pharmacology of the new sulfonylurea glimepiride. Arzneim Forsch/Drug Res 38:1120–1130

Greeley PO (1937) Pancreatic diabetes in the rabbit. Proc Soc Exp Biol 37:390
Gryaznova AV (1962) Ligation of the thoracic duct in dogs. Arkhiv Anatomii, Gistologii i Embriologii 42:90–95
Gryaznova AV (1963) Ligation of the thoracic duct in dogs. Fed Proc 22/II,T886
Houssay BA (1930) Le diabète pancréatique des chiens hypophysectomisés. Les troubles diabétiques chez les chiens privés d'hypophyse et de pancréas. Compt rend Soc Biol, Paris 105:121–126
Houssay BA, Biasotti A (1931) Pankreasdiabetes und Hypophyse am Hund. Pflüger's Arch ges Physiol 227:664–685
Itoh A, Maki T (1996) Protection of nonobese diabetic mice from autoimmune diabetes by reduction of islet mass before insulitis. Proc Natl Acad Sci 93:11053–11056
Lau TS, McMillan N, Cherrington A, Lo S, Drucker WR, Koven IH (1976) Insulin metabolism in depancreatized dogs during hemorrhagic shock. J Surg Oncol 8:49–52
von Mehring J, Minkowski O (1890) Diabetes mellitus nach Pankreasexstirpation. Arch exper Path Pharmakol 26:371–387
Noguchi Y, Younes RN, Konlon KC, Vydelingum NA, Matsumoto A, Brennan MF (1994) The effect of prolonged hyperglycemia on metabolic alterations in the subtotally pancreatectomized rat. Surg Today, Jpn J Surg 24:987–994
Rappaport AM, Vranic M, Wrenshall GA (1966) A pedunculated subcutaneous autotransplant of an isolated pancreas remnant for the temporary deprivation of internal secretion in the dog. Surgery 59:792–798
Scow RO (1957) "Total" pancreatectomy in the rat: operation, effects and post-operative care. Endocrinology 60:359–367
Scow RO, Wagner EM, Cardeza A (1957) Effect of hypophysectomy on the insulin requirement and response to fasting of "totally" pancreatectomized rats. Endocrinology 61:380–391
Sirek A (1968) Pancreatectomy and diabetes. In: Pfeiffer EF(ed) Handbook of Diabetes mellitus, Pathophysiology and Clinical Considerations. Vol. I, Lehmanns Verlag, München, pp 727–743
Tanigawa K, Nakamura S, Kawaguchi M, Xu G, Kin S, Tamura K (1997) Effect of aging on B-cell function and replication in rat pancreas after 90% pancreatectomy. Pancreas 15:53–59
Vogel HG (1963) Unpublished data
Wagner EM, Cardeza A (1957) Effect of hypophysectomy on the insulin requirement and response to fasting of totally pancreatectomized rats. Endocrinology 61:380–388

K.1.2 Alloxan-Induced Diabetes

PURPOSE AND RATIONALE

Surveys on chemically induced diabetes in animals were given by Frerichs and Creutzfeldt (1968, 1971). This kind of diabetes predominantly based on insulin-deficiency due to chemically (beta cell toxicity) destroyed pancreatic beta-cells.

Hyperglycemia and glucosuria after administration of alloxan has been described in several species, such as in dogs (Brunschwig et al. 1943, Tasaka et al. 1988), in rabbits (Baily and Baily 1943), in rats (Dunn and McLetchie 1943, Goldner and Gomori 1944) and in other species (Frerichs and Creutzfeldt 1968, 1971). Guinea pigs have been found to be resistant (Maske and Weinges 1957). Dosage and treatment regimen have been elaborated for the most frequently used species. In most species a triphasic time course is observed: an initial rise of glucose is followed by a decrease, probably due to depletion of islets from insulin, again followed by a sustained increase of blood glucose.

PROCEDURE

Rabbits weighing 2.0 to 3.5 kg are infused via the ear vein with 150 mg/kg alloxan monohydrate (5.0 g/100 ml, pH 4.5) for 10 min resulting in 70% of the animals to become hyperglycemic and uricosuric. The rest of the animals either die or are only temporarily hyperglycemic (Baily and Baily 1943, Pincus et al. 1954, Bänder et al. 1969).

Rats of Wistar or Sprague-Dawley strain weighing 150–200 g are injected subcutaneously with 100–175 mg/kg alloxan (Blum and Schmid 1954, Katsumata and Katsumata 1990, Katsumata et al. 1993).

Male **Beagle dogs** weighing 15–20 kg are injected intravenously with 60 mg/kg alloxan. Subsequently, the animals receive daily 1000 ml 5% glucose solution with 10 IU Regular insulin for one week and canned food ad libitum. Thereafter, a single daily dose of a long-acting insulin (e. g. Lantus) is administered subcutaneously and the insulin dose is individually adjusted according to the blood glucose levels achieved. (Brunschwig at al 1943, Geisen 1988).

MODIFICATIONS OF THE METHOD

Kodoma and coworkers (1993) described a new diabetes model induced by neonatal alloxan treatment in rats. Male Sprague Dawley rats 2, 4, or 6 days of age were injected intraperitoneally with 200 mg/kg of alloxan monohydrate after a 16 h fast. The most severe diabetic symptoms occurred in rats injected on day 6.

Keikkila and coworkers (1974) reported the prevention of alloxan-induced diabetes by ethanol administration in mice.

REFERENCES AND FURTHER READING

Baily CC, Baily OT (1943) Production of diabetes mellitus in rabbits with alloxan. A preliminary report. J Am Med Ass 122:1165–1166
Bänder A, Pfaff W, Schmidt FH, Stork H, Schröder HG (1969) Zur Pharmakologie von HB 419, einem neuen, stark wirksamen oralen Antidiabeticum. Arzneim Forsch/Drug Res 19:1363–1372
Blum F, Schmid R (1954) Über den Einfluss der Konzentration auf den Ablauf des experimentellen Alloxandiabetes. Helv Physiol Acta 12:181–183

Brunschwig A, Allen JG, Goldner MG, Gomori G (1943) Alloxan. J Am Med Ass 122:966
Dunn JS, McLetchie NGB (1943) Experimental alloxan diabetes in the rat. Lancet II:384–387
Frerichs H, Creutzfeldt W (1968) Diabetes durch Beta-Zytotoxine. In: Pfeiffer EF (ed) Handbook of Diabetes mellitus, Pathophysiology and Clinical Considerations. Vol. I, Lehmanns Verlag, München, pp 811–840
Frerichs H, Creutzfeldt W (1971) Der experimentelle chemische Diabetes. In: Dörzbach E (ed) Handbook of Experimental Pharmacology Vol 32/1, Insulin, Springer-Verlag, Berlin Heidelberg New York, pp 159–202
Geisen K (1988) Special pharmacology of the new sulfonylurea glimepiride. Arzneim Forsch/Drug Res 38:1120–1130
Goldner MG, Gomori G (1944) Studies on the mechanism of alloxan diabetes. Endocrinology 35:241–248
Heikkila RE, Barden H, Cohen G (1974) Prevention of alloxan-induced diabetes by ethanol administration. J Pharm Exp Ther 190:501–506
Katsumata K, Katsumata Y (1990) Effect of single administration of tolbutamide on the occurrence of alloxan diabetes in rats. Horm Metabol Res 22:192–193
Katsumata K, Katsumata Y, Ozawa T, Katsumata Jr (1993) Potentiating effect of combined usage of three sulfonylurea drugs on the occurrence of alloxan diabetes in rats. Horm Metab Res 25:125–126
Kodoma T, Iwase M, Nunoi K, Maki Y, Yoshinari M, Fujishima M (1993) A new diabetes model induced by neonatal alloxan treatment in rats. Diab Res Clin Pract 20:183–189
Pincus IJ, Hurwitz JJ, Scott ME (1954) Effect of rate of injection of alloxan on development of diabetes in rabbits. Proc Soc Exp Biol Med 86:553–558
Tasaka Y, Inoue Y, Matsumoto H, Hirata Y (1988) Changes in plasma glucagon, pancreatic polypeptide and insulin during development of alloxan diabetes mellitus in dog. Endocrinol Japon 35:399–404

K.1.3 Streptozotocin-Induced Diabetes

PURPOSE AND RATIONALE

Rakieten and coworkers (1963) reported the diabetogenic activity of the antibiotic streptozotocin. The compound turned out to be specifically cytotoxic to beta-cells of the pancreas.

PROCEDURE

Male Wistar rats weighing 150–220 g fed with a standard diet are injected with 60 mg/kg streptozotocin (Calbiochem) intravenously. As with alloxan, three phases of blood glucose changes are observed. Initially, blood glucose is increased, reaching values of 150–200 mg% after 3 h. Six–eight h after streptozotocin, the serum insulin values are increased up to 4 times, resulting in a hypoglycemic phase which is followed by persistent hyperglycemia. Severity and onset of diabetic symptoms depend on the dose of streptozotocin. After the dose of 60 mg/kg i.v., symptoms occur already after 24–48 h with hyperglycemia up to 800 mg%, glucosuria and ketonemia. Histologically, the beta-cells are degranulated or even necrotic. A steady state is reached after 10–14 days allowing to use the animals for pharmacological tests.

CRITICAL ASSESSMENT OF THE METHOD

Streptozotocin induced diabetes in laboratory animals, mostly in rats, has become a valuable tool in diabetes research being used by many investigators.

MODIFICATIONS OF THE METHOD

A survey on susceptibility of various species to streptozotocin was given by Frerichs and Creutzfeldt (1971). Multiple low doses of streptozotocin induce immune pancreatic insulitis in rats thereby mimicking immune type 1 diabetes in humans (Like and Rossini 1976, Rossini et al. 1977). Miller (1990) described the effect of streptozotocin on the golden Syrian hamster using a single i.p injection of 50 mg/kg streptozotocin. Enhancement of streptozotocin induced diabetes in CD-1 mice by cyclosporin A was reported by Iwakiri and coworkers (1987). Grussner and coworkers (1993) induced long-lasting diabetes mellitus in Yorkshire Landrace pigs with a dosage of 150 mg/kg streptozotocin.

Stosic-Grujicic and coworkers (1999) described protection of mice from multiple low dose streptozotocin-induced insulitis and diabetes by the immunosuppressive drug leflunomide. Bleich and coworkers (1999) found that elimination of leukocyte 12-lipoxygenase in mice ameliorates low dose streptozotocin-induced diabetes by increasing islet resistance to cytokines and decreasing macrophage production of nitric oxide. Masutani and coworkers (1998) studied the role of poly(ADP-ribose)-polymerase (Parp) in streptozotocin-induced diabetes. Parp-deficient ($Parp^{-/-}$) mice were established by disrupting *Parp* exon 1 using the homologous recombination technique. These mice were almost resistant to streptozotocin-induced diabetes.

REFERENCES AND FURTHER READING

Bleich D, Chen S, Zipser B, Sun D, Funk CD, Nadler JL (1999) Resistance to tpye1 diabetes induction in 12-lipoxygenase knockout mice. J Clin Invest 103:1431–1436
Frerichs H, Creutzfeldt W (1971) Der experimentelle chemische Diabetes. In: Dörzbach E (ed) Handbook of Experimental Pharmacology Vol 32/1, Insulin, Springer-Verlag, Berlin Heidelberg New York, pp 159–202
Geisen K (1988) Special pharmacology of the new sulfonylurea glimepiride. Arzneim Forsch/Drug Res 38:1120–1130
Grussner R, Nakleh R, Grussner A, Tomadze G, Diem P, Sutherland D (1993) Streptozotocin-induced diabetes mellitus in pigs. Horm Metab Res 25:199–203
Iwakiri R, Nagafuchi S, Kounoue E, Nakano S, Koga T, Nakayama M, Nakamura M. Niho Y (1987) Cyclosporin A

enhances streptozotocin induced diabetes in CD-1 mice. Experientia 43:324–327
Katsumata K, Katsumata K Jr, Katsumata Y (1992) Protective effect of diltiazem hydrochloride on the occurrence of alloxan- or streptozotocin-induced diabetes in rats. Horm Met Res 24:508–510
Like AA, Rossini AA (1976) Streptozotocin-induced pancreatic insulitis: A new model of diabetes mellitus. Science 193:415–417
Masutani M, Suzuki H, Kamada N, Watanabe M, Ueda O, Nozaki T, Jishage K-I, Watanabe T, Sugimoto T, Nakagama H, Ochiya T, Sugimura T (1998) Poly(ADP-ribose)polymerase gene disruption conferred mice resistant to streptozotocin-induced diabetes. Proc Natl Acad Sci USA 96:2301–2304
Miller DL (1990) Experimental diabetes: Effect of streptozotocin on the golden Syrian hamster. Lab Anim Sci 40:539–540
Rakieten N, Rakieten ML, Nadkarni MV (1963) Studies on the diabetogenic action of streptozotocin (NSC-37917). Cancer Chemother Rep 29:91–102
Rossini AA, Like AA, Chick A, Appel MC, Cahill GF (1977) Studies of streptozotocin-induced insulitis and diabetes. Proc Natl Acad Sci, 74:2485–2489
Stisic-Grujicic S, Dimitrijevic M, Bartlett R (1999) Leflunomide protects mice from multiple low dose streptozotocin (MLD-SZ)-induced insulitis and diabetes. Clin Exp Immunol 117:44–50
Tancrède G, Rousseau-Migneron S, Nadeau A (1983) Long-term changes in the diabetic state induced by different doses of streptozotocin in rats. Br J Exp Path 64:117–123

K.1.4 Other Diabetogenic Compounds

PURPOSE AND RATIONALE

Several other compounds have been found to induce symptoms of diabetes and/or obesity, such as dithizone (Maske and Weinges 1957, Frerichs and Creutzfeldt 1971, Hansen et al. 1989, Goldberg et al. 1991) or gold-thioglucose (Stauffacher et al. 1967, Caterson et al. 1988, Silva and Hernandez 1989, Heydrick et al. 1995) or monosodium glutamate (Sartin et al. 1985).

PROCEDURE

Goldberg and coworkers (1991) injected various chelators, such as dithizone, 8-(p-toluene-sulfonylamino)-quinoline (8-TSQ), and 8-(benzenesulfanylamino)-quinoline (8-BSQ) in a single i.v. dose of 40–100 mg/kg to cats, rabbits, golden hamsters and mice. Dithizone injection causes a triphasic glycemic reaction in rabbits. A phase of initial hyperglycemia is detected after 2 h, followed by a normoglycemic phase after 8 h and a secondary permanent hyperglycemic phase after 24–72 h. Histologically, complete and partial degranulation of beta cells is observed.

REFERENCES AND FURTHER READING

Bavelsky ZE, Zavyazkina TV, Moisev YS, Medvedev VI (1992) Zinc content in pancreatic islets in experimental diabetes induced by chelating agents. Patol Fiziol Eksp Ter 36:29–32
Caterson ID, Cooney GJ, Vanner MA, Nicks JL, Williams PF (1988) The activities of the pyruvate dehydrogenase complex and of acetyl-CoA carboxylase in various tissues in experimental obesity: tissue differences and insulin resistance. Diab Nutr Metab 1:65–70
Frerichs H, Creutzfeldt W (1971) Der experimentelle chemische Diabetes. In: Dörzbach E (ed) Handbook of Experimental Pharmacology Vol 32/1, Insulin, Springer-Verlag, Berlin Heidelberg New York, pp 159–202
Goldberg ED, Eshchenko VA, Bovt VD (1991) The diabetogenic and acidotropic effects of chelators. Exp Pathol 42:59–64
Hansen WA, Christie MR, Kahn R, Norgard A, Abel I, Petersen AM, Jorgensen DW, Baekkeskov S, Nielsen JH, Lernmark A, Egeberg J, Richter-Olesen H, Grainger T, Kristensen JK, Brynitz S, Bilde T (1989) Supravital dithizone staining in the isolation of human and rat pancreatic islets. Diabetes Res 10:53–57
Heydrick SJ, Gautier N, Olichon-Berte C, Van Obberghen E, Le Marchand Brustel Y (1995) Early alteration of insulin stimulation of PI 3-kinase in muscle and adipocyte from gold thioglucose obese mice. Am J Physiol Endocrinol Metab 268:E604–E612
Maske H, Weinges K (1957) Untersuchungen über das Verhalten der Meerschweinchen gegenüber verschiedenen diabetogenen Noxen. Alloxan und Dithizon. Naunyn-Schmiedeberg's Arch exper Path Pharmakol 230:406–420
Sartin JL, Lamperti AA, Kemppainen RJ (1985) Alterations in insulin and glucagon secretion by monosodium glutamate lesions of the hypothalamic arcuate nucleus. Endocr Res 11:145–155
Silva E, Hernandez L (1989) Goldthioglucose causes brain and serotonin depletion correlated with increased body weight. Brain Res 490:192–195
Stauffacher W, Lambert AE, Vecchio D, Renold AE (1967) Measurement of insulin activities in pancreas and serum of mice with spontaneous ("obese" and "New Zealand obese") and induced (goldthioglucose) obesity and hyperglycemia, with considerations on the pathogenesis of the spontaneous syndrome. Diabetologia 3:230–237

K.1.5 Growth Hormone-Induced Diabetes

Cotes and coworkers (1949) described the diabetogenic action of pure anterior pituitary growth hormone in cats. In intact adult dogs and cats the repeated administration of growth hormone induces an intensively diabetic condition with all symptoms of diabetes including severe ketonuria and ketonemia. Rats of any age subjected to a similar treatment do not become diabetic but grow faster (Young 1945) and show striking hypertrophy of the pancreatic islets.

REFERENCES AND FURTHER READING

Cotes PM, Reid E, Young FG (1949) Diabetogenic action of pure anterior pituitary growth hormone. Nature 164:209–211
Martin TE, Young FG (1968) Experimental diabetes following growth hormone. In: Pfeiffer EF (ed) Handbook of Diabetes mellitus, Pathophysiology and Clinical Considerations. Vol. I, Lehmanns Verlag, München, pp 763–770

Young FG (1945) Growth and diabetes in normal animals treated with pituitary (anterior lobe) diabetogenic extract. Biochem J 39:515–536

K.1.6 Corticosteroid-Induced Diabetes

Ingle (1941) described hyperglycemia and glucosuria in forced fed rats treated with cortisone. In the guinea pig and in the rabbit, experimental corticoid diabetes could be obtained without forced feeding (Hausberger and Ramsay 1953, Abelove and Paschkis 1954). In the rat, the adrenal cortex, stimulated by corticotrophin, has the capacity to secrete amounts of steroids which induce steroid diabetes (Ingle et al. 1946).

REFERENCES AND FURTHER READING

Abelove WA, Paschkis KE (1954) Comparison of the diabetogenic action of cortisone and growth hormone in different species. Endocrinology 55:637–654

Bellens R, Bastenie PA (1968) Experimental steroid diabetes. In: Pfeiffer EF (ed) Handbook of Diabetes mellitus, Pathophysiology and Clinical Considerations. Vol. I, Lehmanns Verlag, München, pp 797–810

Hausberger FX, Ramsay AJ (1953) Steroid diabetes in guinea pigs. Effect of cortisone administration on blood- and urinary glucose, nitrogen excretion, fat deposition, and the islets of Langerhans. Endocrinology 53:423–435

Ingle DJ (1941) The production of glycosuria in the normal rat by means of 17-hydroxy-11-dehydrocorticosterone. Endocrinology 29:649–652

Ingle DJ, Li CH, Evans HM (1946) The effect of adrenocorticotropic hormone on the urinary excretion of sodium, chloride, potassium, nitrogen and glucose in normal rats. Endocrinology 39:32–39

K.1.7 Insulin Deficiency Due to Insulin Antibodies

PURPOSE AND RATIONALE

A transient diabetic syndrome can be induced by injection of guinea pig anti-insulin serum in various species (Moloney and Coval 1955, Wright 1968).

PROCEDURE

Bovine insulin, dissolved in acidified water (pH 3.0), is incorporated in a water-oil emulsion based on complete Freund's adjuvant or a mixture of paraffin oil and lanolin. A dose of 1 mg insulin is injected in divided doses subcutaneously to male guinea pigs weighing 300–400 g. Injections are given at monthly intervals and the guinea pigs are bled by cardiac puncture two weeks after the second and subsequent doses of antigen. It is possible to get 10 ml blood from every animal once a month.

Intravenous injection of 0.25–1.0 ml guinea pig anti-insulin serum to rats induces a dose-dependent increase of blood glucose reaching values up to 300 mg%. This effect is unique to guinea pig anti-insulin serum and is due to neutralization by insulin antibodies of endogenous insulin secreted by the injected animal. In this way a state of insulin deficiency is induced. It persists as long as antibodies capable of reacting with insulin remain in the circulation. Slow rate intravenous infusion or intraperitoneal injection prolongs the effect for more than a few hours. However, large doses and prolonged administration accompanied by ketonemia, ketonuria, glucosuria, and acidosis are fatal to the animals. After lower doses, the diabetic syndrome is reversible after a few hours.

REFERENCES AND FURTHER READING

Arnim J, Grant RT, Wright PH (1960) Acute insulin deficiency provoked by single injections of anti-insulin serum. J Physiol (London) 153:131–145

Moloney PJ, Coval M (1955) Antigenicity of insulin: diabetes induced by specific antibodies. Biochem J 59:179–185

Wright PH (1968) Experimental insulin-deficiency due to insulin antibodies. In: 841–865. Pfeiffer EF (ed) Handbook of Diabetes mellitus, Pathophysiology and Clinical Considerations. Vol. I, Lehmanns Verlag, München, pp 841–865

K.1.8 Virus-Induced Diabetes

Juvenile-onset (type I) diabetes mellitus may be due to virus infections and β-cell specific autoimmunity (Craighead 1978). The D-variant of encephalomyocarditis virus (EMC-D) selectively infects and destroys pancreatic β-cells in susceptible mouse strains similar to human insulin-dependent diabetes (Yoon et al. 1980, Giron and Patterson 1982, Giron et al. 1983, Vialettes et al. 1983). Adult, male ICR Swiss mice are susceptible to the diabetogenic effect of the D-variant of encephalomyocarditis virus in contrast to adult C3H/HeJ male mice which are relatively resistant. Pretreatment with cyclosporin A, a potent immunosuppressive drug, results in increased severity and incidence of diabetes in susceptible ICR Swiss mice and induction of diabetes in resistant C3H/HeJ mice (Gould et al. 1985).

MODIFICATIONS OF THE METHOD

Hirasawa and coworkers (1997) studied the possible role of macrophage-derived soluble mediators in the pathogenesis of encephalomyelitis virus-induced diabetes in mice. The inactivation of macrophages prior to viral infection resulted in the prevention of diabetes. Utsugi and coworkers (1992) demonstrated that intraperitoneal inoculation with NDK25, a variant of encephalomyocarditis virus which has been cloned from

the M variant of encephalomyocarditis virus, caused DBA/2 mice to develop non-insulin-dependent diabetes mellitus. See and Tilles (1995) challenged CD-1 mice with a diabetogenic strain (E2) of coxsackievirus B4. Islet cell destruction was associated with chronic islet cell inflammation, elevation of islet cell antibody, and prolonged presence of viral RNA in the pancreas. Stubbs and coworkers (1994) investigated the effect of Kilham rat virus (KRV) infection on GLUT2 expression in diabetes-resistant BB/Wor rats. Viral antibody-free diabetes resistant rats did not develop spontaneous diabetes, but inoculation with Kilham rat virus induced autoimmune beta cell-destruction and hyperglycemia. Hayashi and coworkers (1995) investigated the role of adhesion molecules in the reovirus type2-induced diabetes-like syndrome in mice. Ellerman and coworkers (1996) studied Kilham rat virus induced autoimmune diabetes in multiple strains of rat.

REFERENCES AND FURTHER READING

Craighead J (1978) Current views on the etiology of insulin-dependent diabetes mellitus. New Engl J Med 299:1439–1445

Ellerman KE, Richards CA, Guberski DL, Shek WR, Like AA (1996) Kilham rat virus triggers T-cell-dependent autoimmune diabetes in multiple strains of rat. Diabetes 45:557–562

Giron DJ, Patterson RR (1982) Effect of steroid hormones on virus-induced diabetes mellitus. Infect Immun 37:820–822

Giron DJ, Cohen SJ, Lyons SP, Trombley ML, Gould CL (1983) Virus-induced diabetes mellitus in ICR Swiss mice is age dependent. Infect Immun 41:834–836

Gould CL, McMannama KG, Bigley NJ, Giron DJ (1985) Virus-induced murine diabetes. Enhancement by immunosuppression. Diabetes 34:1217–1221

Hayashi T, Yamamoto S, Onodera T (1995) Prevention of reovirus type2-induced diabetes-like syndrome in DBA/1 suckling mice by treatment with antibodies against intracellular adhesion molecule – 1 and lymphocyte function-associated antigen – 1. Int J Exp Path 76:403–409

Hirasawa K, Jun HS, Maeda K, Kawaguchi Y, Itagaki S, Mikami T, Baek HS, Doi K, Yoon JW (1997) Possible role of macrophage-derived soluble mediators in the pathogenesis of encephalomyelitis virus-induced diabetes in mice. J Virol 71:4024–4031

See DM, Tilles JG (1995) Pathogenesis of virus-induced diabetes in mice. J Infect Dis 171:1131–1138

Stubbs M, Guberski DL, Like AA (1994) Preservation of GLUT2 expression in islet beta cells of Kilham rat virus (KRV)-infected diabetes-resistant BB/Wor rats. Diabetologia 37:1186–1194

Utsugi T, Kanda T, Tajima Y, Tomono S, Suzuki T, Murata K, Dan K, Seto Y, Kawazu S (1992) A new animal model of non-insulin-dependent diabetes mellitus induced by the NDK25 variant of encephalomyocarditis virus. Diab Res 20:109–119

Vialettes B, Baume D, Charpin C, De Maeyer-Guignard J, Vague P (1983) Assessment of viral and immune factors in EMC virus-induced diabetes: effects of cyclosporin A and interferon. J Lab Clin Immunol 10:35–40

Yoon JW, McClintock PR, Onodera T, Notkins AL (1980) Virus-induced diabetes mellitus. XVII. Inhibition by a nondiabetogenic variant of encephalomyocarditis virus. J Exp Med 152:878–892

K.2
Genetically Diabetic Animals

GENERAL CONSIDERATIONS

Several animal species, mostly rodents, were described to exhibit spontaneously diabetes mellitus on a hereditary basis. These findings were highly appreciated with the expectation to get more insight into the pathogenesis of diabetes in humans. During the last few years since the discovery of leptin (Zhang et al. 1994) and its downstream signal transduction cascade (Friedman and Halaas 1998) tremendous new insight of the genetics of diabetic and obese animal disease models derived. Up to now at least 6 genetically diabetic animal models exhibit defects in the leptin pathway: The*ob* mutation in the mouse resulted in leptin deficiency. The*db* mutation in the mouse and the *cp* and*fa* mutations in the rat are different mutations of the leptin receptor gene. The *fat* mutation in the mouse results in a biologically inactive carboxipeptidase E, which processes the prohormone conversion of POMC into α-MSH, which activates the hypothalamic MC4 receptor. Finally the Agouti yellow (*y*) mouse exhibit an ubiquitous expression of the Agouti protein which represents an antagonist of the hypothalamic MC4 receptor.

Symptoms of diabetes and obesity are overlapping in many animal models (see also L.2. Genetically obese animals).

CRITICAL ASSESSMENT

The pathophysiological mechanisms which finally lead to the diabetes phenotype (hyperglycemia, hyperinsulinemia and insulin resistance) exhibited of the various animal disease models for non-insulin dependent diabetes do not necessarily be identical to those in human disease. Therefore, detailed knowledge about the (patho-)physiology of these animal disease models is a prerequisite for interpretation of experimental results and their value for the human disease.

REFERENCES AND FURTHER READING

Brunk R (1971) Spontandiabetes bei Tieren. In: Dörzbach E (ed) Handbook of Experimental Pharmacology Vol 32/1, Insulin, Springer-Verlag, Berlin Heidelberg New York, pp 203–272

Friedman JF, Halaas JL (1998) Leptin and the regulation of body weight in mammals. Nature 395:763–770

Herberg L, Coleman DL (1977) Laboratory animals exhibiting obesity and diabetes syndromes. Metabolism 26:59–99

Herberg L, Berger M, Buchanan KD, Gries FA, Kern H (1976) Tiermodelle in der Diabetesforschung: metabolische und hormonelle Besonderheiten. Z Versuchstierk 18:91–105
Shafrir E (1992) Animal models of non-insulin-dependent diabetes. Diabetes/Metab Rev 8:179–208
Velasquez MT, Kimmel PL, Michaelis OE,IV (1990) Animal models of spontaneous diabetic kidney disease. FASEB J 4:2850–2859
Zhang Y, Proenca R, Maffei M, Barone M, Leopold L, Friedman JF (1994) Positional cloning of the mouse obese gene and its human homologue. Nature 372:425–432

K.2.1 Spontaneously Diabetic Rats

The occurrence of spontaneous diabetes has been reported in several strains of rats.

BB Rat

The BB rat (Bio Breeding (BB) rat) is a model of spontaneous diabetes associated with insulin deficiency and insulitis due to autoimmune destruction of pancreatic beta cells. (Nakhooda et al. 1977 and 1978, Like et al. 1982, Oschilewski et al. 1985, Lee et al. 1988, Solomon et al. 1989, Papaccio and Mezzogiorno 1989, Kolb et al. 1990, Velasquez et al. 1990, Lefkowith et al. 1990, Gottlieb et al. 1990, Ellerman et al. 1993). Diabetes is inherited as an autosomal recessive trait and develops with equal frequency and severity among males and females. The onset of clinical diabetes is sudden, and occurs at about 60–120 days of age. Within several days, diabetic animals are severely hyperglycemic,hypoinsulinemic, and ketotic unless insulin treatment is instituted. Pipeleers and coworkers (1991) described the transplantation of purified islet cells in diabetic BB rats. Hao and coworkers (1993) reported that the immunosuppressive agent mycophenolate mofetil can prevent the development of diabetes in BB rats. Klöting and Vogt (1991) characterized the features of a subline of diabetes-prone BB rats (BB/OK rats). The circadian variations in blood pressure and heart rate of this strain were compared with spontaneously hypertensive rats (Berg et al. 1997).

REFERENCES AND FURTHER READING

Berg S, Dunger A, Vogt L, Schmidt S (1997) Circadian variations in blood pressure and heart rate in diabetes prone and resistant rat strains compared with spontaneously hypertensive rats. Exp Clin Endocrinol Diabetes 105, Suppl 2:7–9
Ellerman K, Wroblewski M, Rabinovitch A, Like A (1993) Natural killer cell depletion and diabetes mellitus in the BB/Wor rat. Diabetologia 36:596–601
Gottlieb PA, Berrios JP, Mariani G, Handler ES, Greiner D, Mordes JP, Rossini AA (1990) Autoimmune destruction of islets transplanted into RT6-depleted diabetes-resistant BB/Wor rats. Diabetes 39:643–645
Hao L, Chan SM, Lafferty KJ (1993) Mycophenolate mofetil can prevent the development of diabetes in BB rats. Ann NY Acad Sci 969:328–332
Klöting I, Vogt L (1991) BB/O(TTAWA)K(ARLSBURG) rats: features of a subline of diabetes prone BB rats. Diabetes Res 18:79–87
Kolb H, Burkart V, Appels B, Hanenberg H, Kantwerk-Funke G, Kiesel U, Funda J, Schraermeyer U, Kolb-Bachofen V (1990) Essential contribution of macrophages to islet cell destruction *in vivo* and *in vitro*. J Autoimmun 3 Suppl):117–120
Lee KU, Pak CY, Amano K, Yoon JW (1988) Prevention of lymphocytic thyroiditis and insulitis in diabetes-prone BB rats by the depletion of macrophages. Diabetologia 31:400–402
Lefkowith J, Schreiner G, Cormier J, Handler ES, Driscoll HK, Greiner D, Mordes JP, Rossini AA (1990) Prevention of diabetes in the BB rat by essential fatty acid deficiency. J Exp Med 171:729–743
Like AA, Butler L, Williams RM, Appel MC, Weringer EJ, Rossini AA (1982) Spontaneous autoimmune diabetes mellitus in the BB rat. Diabetes 31 (Suppl 1):7–11
Nakhooda AF, Like AA, Chappel CI, Murray FT, Marliss EB (1977) The spontaneously diabetic Wistar rat; metabolic and morphologic studies. Diabetes 26:100–112
Nakhooda AF, Like AA, Chappel CI, Wei CN, Marliss EB (1978) The spontaneously diabetic Wistar rat (the "BB" rat). Studies prior to and during development of the overt syndrome. Diabetologia 14:199–207
Papaccio G, Mezzogiorno V (1989) Morphological aspects of glucagon and somatostatin islet cells in diabetic Bio Breeding and low-dose streptozotocin-treated Wistar rats. Pancreas 4:289–294
Pipeleers D, Pipeleers-Marichal M, Markholst H, Hoorens A, Klöppel G (1991) Transplantation of purified islet cells in diabetic BB rats. Diabetologia 34:390–396
Sima AAF (1984) Neuropathic and ocular complications in the BB-Wistar rat. In: Shafrir R, Reynold A (eds) Lesson from Diabetes, London, pp 447–453
Solomon SS, Deaton J, Harris G, Smoake JA (1989) Studies of insulin resistance in the streptozotocin diabetic and BB rat: Activation of low Km cAMP phosphodiesterase by insulin. Am J Med Sci 297:372–376
Velasquez MT, Kimmel PL, Michaelis OE (1990) Animal models of spontaneous diabetic kidney disease. FASEB J 4:2850–2859

WBN/Kob RAT

Spontaneous hyperglycemia, glucosuria and glucose intolerance have been observed in aged males of an inbred Wistar strain, named the WBN/Kob rat (Nakama et al. 1985, Tsuchitani et al. 1985, Koizumi 1989, Shimoda et al. 1993).These animals exhibit impaired glucose tolerance and glucosuria at 21 weeks of age. Obvious decreases in the number and size of islets are found already after 12 weeks of age. Fibrinous exudation and degeneration of pancreatic tissue are observed in the exocrine part, mainly around degenerated islets and pancreatic ducts in 16 weeks old males. These rats develop demyelinating, predominantly motor neuropathy, later accompanied by axonal changes (Yagihashi et al. 1993).

REFERENCES AND FURTHER READING

Koizumi M, Shimoda I, Sato K, Shishido T, Ono T, Ishizuka J, Toyota T, Goto Y (1989) Effects of CAMOSTAT on development of spontaneous diabetes in the WBN/Kob rats. Biomed Res 10, Suppl 1:45–50

Nakama K, Shichinohe K, Kobayashi K, Naito K, Ushida O, Yasuhara K, Zobe M (1985) Spontaneous diabetes-like syndrome in WBN/Kob rats. Acta Diabetol Lat. 122:335–342

Shimoda I, Koizumi M, Shimosegawa T, Shishido T, Ono T, Sato K, Ishizuka J, Toyota T (1993) Physiological characterization of spontaneously developed diabetes in male WBN/Kob rat and prevention of development of diabetes by chronic oral administration of synthetic trypsin inhibitor (FOY-305). Pancreas 8:196–203

Tsichitani M, Saegusa T, Narama I, Nishikawa T, Gonda T (1985) A new diabetic strain of rat (WBN/Kob) Laboratory Animals 19:200–207

Yagihashi S, Wada RI, Kamijo M, Nagai K (1993) Peripheral neuropathy in the WBN/Kob rat with chronic pancreatitis and spontaneous diabetes. Lab Invest 68:296–307

Cohen Diabetic Rat

Diabetes in Cohen rats is characterized by hyperglycemia, glucosuria, and hyperinsulinemia, with late development of hypoinsulinemia, insulin resistance, and a decrease in the number and sensitivity of insulin receptors. The rats develop overt diabetes and diabetes related complications when fed a diet rich in sucrose or other refined sugars and poor in copper content, but not when fed a starch or stock diet (Cohen 1972, Velasquez et al. 1990).

REFERENCES AND FURTHER READING

Cohen AM, Teitelbaum A, Saliternik R (1972) Genetics and diet as factors in the development of diabetes mellitus. Metabolism 21:235–240

Velasquez MT, Kimmel PL, Michaelis OE (1990) Animal models of spontaneous diabetic kidney disease. FASEB J 4:2850–2859

Goto–Kakizaki Rat

Non-obese, insulin-resistant Goto–Kakizaki (GK) rats are a highly inbred strain of Wistar rats that spontaneously developed type II diabetes. Defects in glucose-stimulated insulin secretion, peripheral insulin resistance, and hyperinsulinemia are seen as early as 2 to 4 weeks after birth. Impaired skeletal muscle glycogen synthase activation by insulin was observed, accompanied by chronic activation of diacylglycerol-sensitive protein kinase C.

REFERENCES AND FURTHER READING

Avignon A, Yamada K, Zhou X (1996) Chronic activation of protein kinase C in soleus muscles and other tissues of insulin-resistant type II diabetic Goto–Kakizaki (GK), obese/aged and obese/Zucker rats. A mechanism for inhibiting glycogen synthesis. Diabetes 45:1396–1404

Begum N, Ragiola L (1998) Altered regulation of insulin signaling components in adipocytes of insulin-resistant type II diabetic Goto–Kakizaki rats. Metabolisms 47:54–62

Goto Y, Kakizaki M, Masaki N (1975) Spontaneous diabetes produced by selective breeding of normal Wistar rats. Proc Jpn Acad 51:80–85

Portha B, Serradas P, Bailbe D (1991) β Cell insensivity in the GK rat, a spontaneous non-obese model for type II diabetes. Diabetes 40:486–491

Villar-Palsi C, Farese RV (1994) Impaired skeletal muscle glycogen synthase activation by insulin in the Goto–Kakizaki (G/K) rat. Diabetologia 37:885–888

Zucker-Fatty Rat

The Zucker-fatty rat is a classic model of hyperinsulinemic obesity. (Zucker 1965). Obesity is due to a simple autosomal recessive (*fa*) gene and develops at an early age. Obese Zucker rats manifest mild glucose intolerance, hyperinsulinemia, and peripheral insulin resistance similar to human type 2 diabetes. However, their blood sugar level is usually normal throughout life (Bray 1977, Clark et al. 1983, McCaleb and Sredy 1992, Abadie et al. 1993, Alamzadeh et al. 1993, Kasim et al. 1993, Galante et al. 1994).

REFERENCES AND FURTHER READING

Abadie JM, Wright B, Correa G, Browne ES, Porter JR, Svec F (1993) Effect of dihydro-epiandrosterone on neurotransmitter levels and appetite regulation of the obese Zucker rat. Diabetes 42:662–669

Alamzadeh R, Slonim AE, Zdanowicz MM (1993) Modification of insulin resistance by diazoxide in obese Zucker rats. Endocrinology 133:705–712

Bray GA (1977) The Zucker-fatty rat: A review. Fed Proc 36:148–153

Clark JB, Palmer CJ, Shaw WN (1983) The diabetic Zucker fatty rat. Proc Soc Exp Biol Med 173:68–75

Fujiwara T, Yoshioka S, Yoshioka T, Ushiyama I, Horikoshi H (1988) Characterization of new oral antidiabetic agent CS-045. Studies in KK and *ob/ob* mice and Zucker fatty rats. Diabetes 37:1549–1558

Galante P, Maerker E, Scholz R, Rett K, Herberg L, Mosthaf L, Häring HU (1994) Insulin-induced translocation of GLUT 4 in skeletal muscle of insulin-resistant Zucker rats. Diabetologia 37:3–9

Kasim SE, Elovson J, Khilnani S, Almario RU, Jen KLC (1993) Effect of lovostatin on the secretion of very low density lipoproteins and apolipoprotein B in the hypertriglyceridemic Zucker obese rat. Atherosclerosis 104:147–152

Kava R, Greenwoof MRC, Johnson PR (1990) Zucker (*fa/fa*) rat. Ilar News 32:4–8

McCaleb ML, Sredy J (1992) Metabolic abnormalities of the hyperglycemic obese Zucker rat. Metabolism 41:522–525

Shafrir E (1992) Animal models of non-insulin-dependent diabetes. Diabetes/Metab Rev 8:179–208

Stern J, Johnson PR, Greenwood RC, Zucker LM, Hirsch J (1972) Insulin resistance and pancreatic insulin release in the genetically obese Zucker rat. Proc Soc Exp Biol Med 139:66–69

Stern JS, Johnson PR, Batchelor BR, Zucker LM, Hirsch J (1975) Pancreatic insulin release and peripheral tissue resistance in Zucker obese rats fed high- and low-carbohydrate diets. Am J Physiol 228:543–548

Vasselli JR, Flory T, Fried KS (1987) Insulin binding and glucose transport in adipocytes of acarbose-treated Zucker lean and obese rats. Int J Obesity 11:71–75
Yoshioka S, Nishino H, Shiraki T, Ikeda K, Koike H, Okuno A, Wada M, Fujiwara T, Horikoshi H (1993) Antihypertensive effects of CS-045 treatment in obese Zucker rats. Metabolism 42:75–80
Zucker LM (1965) Hereditary obesity in the rat associated with hyperlipidemia. Ann NY Acad Sci 131:447–458
Zucker LM, Antoniades HN (1972) Insulin and obesity in the Zucker genetically obese rat "Fatty". Endocrinology 90:1320–1330

Zucker Diabetic Fatty Rat (Zdf/Drt-Fa)

The obese Zucker Diabetic Fatty rat originally derived from the Zucker fatty rat (Peterson et al. 1990). and has the identical mutation (fa) in th leptin receptor. In addition a defect in the insulin promoter has been described (Griffen et al. 2001). Insulin promoter activity is reduced 30–50% in homozygous ZDF fetal islets, and insulin mRNA levels are similarly reduced by 45%. Only the males become diabetic at the age of around 10 weeks spontaneously with hyperglycemia of about 20 mmol/l; the females develop diabetes only when feeding a high-fat diet.. Diabetes phenotype develops due to lipotoxicity to the β-cell (Lee et al. 1994). These rats are characterized besides hyperglycemia by insulin resistance, moderate hyperinsulinemia, extreme hyperphagia due to the loss of calories by glucosuria and obesity.

REFERENCES AND FURTHER READING

Peterson RG, Shaw WN, Neel M-AN, Little LA, Eicheberg J (1990) Zucker Diabetic Fatty rat as a model for non-insulin-dependent diabetes mellitus. ILAR News 32:16–19
Lee Y, Hirose H, Ohneda M, Johnson JH, McGarry JD, Unger RH (1994) β-cell lipotoxicity in the pathogenesis of non-insulin-dependent diabetes mellitus of obese rats: impairment in adipocytes-β-cell relationships. Proc Natl Acad Sci 91:10878–10882

Wdf/Ta-Fa Rat

The WDF/Ta-fa rat, commonly referred to as the Wistar fatty rat, is a genetically obese, hyperglycemic rat established by the transfer of the fatty *(fa)* gene from the Zucker rat to the Wistar Kyoto rat. (Ikeda et al. 1981, Kava et al. 1989, Velasquez et al. 1990). The Wistar fatty rat exhibits obesity, hyperinsulinemia, glucose intolerance, hyperlipidemia, and hyperphagia similar to Zucker rats being, however, more glucose intolerant and insulin resistant than Zucker rats. Hyperglycemia is usually not observed in females but can be induced by addition of sucrose to the diet. Kobayashi and coworkers (1992) found an increase of insulin sensitivity by activation of insulin receptor kinase by Pioglitazone in Wistar fatty rats (*fa/fa*). Sugiyma and coworkers (1992) found a reduction of glucose intolerance and hypersecretion of insulin in Wistar fatty rats after treatment with pioglitazone for 10 days.

REFERENCES AND FURTHER READING

Griffen SC, Wang J, German MS (2001) A genetic defect in beta-cell gene expression segregates independently from the fa locus in the ZDF rat. Diabetes. 50:63–68
Ikeda H, Shino A, Matsuo T, Iwatsuka H, Suzuoki Z (1981) A new genetically obese-hyperglycemic rat (Wistar fatty). Diabetes 30:1045–1050
Kava RA, West DB, Lukasik VA, Greenwood MRC (1989) Sexual dimorphism of hyperglycemia and glucose tolerance in Wistar fatty rats. Diabetes 38:159–163
Kava RA, Peterson RG, West DB, Greenwood MRC (1990) Ilar News 32:9–13
Kobayashi M, Iwanshi M, Egawa K, Shigeta Y (1992) Pioglitazone increases insulin sensitivity by activating insulin receptor kinase. Diabetes 41:476–483
Madar Z, Omusky Z (1991) Inhibition of intestinal α-glucosidase activity and postprandial hyperglycemia by α-glucosidase inhibitors in *fa/fa* rats. Nutr Res 11:1035–1046
Peterson RG, Little LA, Neel MA (1990) WKY fatty rat as a model of obesity and non-insulin dependent diabetes mellitus. Ilar News 32:13–15
Sugiyama Y, Taketomi S, Shimura Y, Ikeda H, Fujita T (1990) Effects of pioglitazone on glucose and lipid metabolism in Wistar fatty rats. Arzneim Forsch/Drug Res 40:263–267
Velasquez MT, Kimmel PL, Michaelis OE,IV (1990) Animal models of spontaneous diabetic kidney disease. FASEB J 4:2850–2859

OLETF Rat

A spontaneously diabetic rat with polyuria, polydipsia, and mild obesity was discovered in 1984 in an outbred colony of Long-Evans rats. A strain of rats developed from this rat by selective breeding has since been maintained at the Tokushima Research Institute (Otsuka Pharmaceutical, Tokushima, Japan) and named OLETF. The characteristic features of OLETF rats are: (1) late onset of hyperglycemia (after 18 weeks of age), (2) a chronic course of disease, (3) mild obesity, (4) inheritance by males, (5) hyperplastic foci of pancreatic islets, and (6) renal complications (nodular lesions). The clinical and pathological features of disease in OLETF rats resemble those of human NIDDM. Administration of diazoxide (0.2% in diet), an inhibitor of insulin secretion, to OLETF rats from the age of 4 to 12 weeks completely prevented the development of obesity and insulin resistance (Aizawa et al. 1995). Ishida and coworkers (1995) found that insulin resistance preceded impaired insulin secretion in OLETF rats.

REFERENCES AND FURTHER READING

Aizawa T, Taguchi N, Sato Y, Nakabayashi T, Kobuchi H, Hidaka H, Nagasawa T, Ishihara F, Itoh N, Hashizume K (1995) Prophylaxis of genetically determined diabetes by

diazoxide: a study in a rat model of naturally occurring obese diabetes. J Pharmacol Exp Ther 275:194–199
Ishida K, Mizuno A, Sano T, Shima K (1995) Which is the primary etiologic event in Otsuka Long-Evans Tokushima fatty rats, a model of spontaneous non-insulin-dependent diabetes mellitus, insulin resistance, or impaired insulin secretion? Metabolism 44:940–945
Kawano K, Hirashima T, Mori S, Kurosumi M, Saitoh Y (1991) A new rat strain with non-insulin dependent diabetes mellitus, "OLETF". Rat News Lett 25:24–26
Kawano K, Hirashima T, Mori S, Saitoh YA, Kurosumi M, Natori T (1992) Spontaneous long-term hyperglycemic rat with diabetic complications. Otsuka Long-Evans Tokushima fatty (OLETF) strain. Diabetes 41:1422–1428

ESS-Rat

The occurrence of spontaneous diabetes in a colony of rats (Stilman Saldago), called eSS-rat was reported by Tarrés and coworkers (1981). The animals show abnormal glucose tolerance tests from the age of 2 months onwards. The syndrome consists of a mild type of diabetes that does not diminish the longevity of the animals. Six-months old rats show disruption of the islet architecture and fibrosis of the stroma (Dumm et al. 1990).

REFERENCES AND FURTHER READING

Dumm CLAG, Semino MC, Gagliardino JJ (1990) Sequential changes in pancreatic islets of spontaneously diabetic rats. Pancreas 5:533–539
Herberg L, Coleman DL (1977) Laboratory animals exhibiting obesity and diabetes syndromes. Metabolism 26:59–99
Tarrés MC, Martínez SM, Liborio MM, Rabasa SL (1981) Diabetes mellitus en una línea endocrinada de rata. Mendeliana 5:39–48

Obese SHR Rat

The strain of obese SHR rats was developed by Koletsky (1973, 1975) by mating a spontaneous hypertensive female rat of the Kyoto-Wistar strain with a normotensive Sprague Dawley male. After several generations of selective inbreeding, these obese SHR exhibited obesity, hypertension, and hyperlipidemia. In addition, some rats developed hyperglycemia and glucosuria associated with giant hyperplasia of pancreatic islets. From these rats, several substrains were developed, such as the JCR:LA-corpulent rat which exhibits a syndrome characterized by obesity, hypertriglyceridemia and hyperinsulinemia with impaired glucose tolerance (Russell et al. 1994). Reduced insulin receptor signaling was found in the obese spontaneously hypertensive Koletsky rat (Friedman et al. 1997).

REFERENCES AND FURTHER READING

Friedman JE, Ishizuka T, Liu S, Farrell CJ, Bedol D, Koletsky RJ, Kaung HL, Ernsberger P (1997) Reduced insulin receptor signaling in the obese spontaneously hypertensive Koletsky rat. Am J Physiol Endocrinol Metab 273:E1014–1023
Koletsky S (1973) Obese spontaneous hypertensive rats – a model for study of arteriosclerosis. Exp Mol Pathol 19:53–60
Koletsky S (1975) Pathologic findings and laboratory data in a new strain of obese hypertensive rats. Am J Pathol 80:129–142
Russell JC, Graham S, Hameed M (1994) Abnormal insulin and glucose metabolism in the JCR:LA-corpulent rat. Metabolism 43:538–543
Velasquez MT, Kimmel PL, Michaelis OE (1990) Animal models of spontaneous diabetic kidney disease. FASEB J 4:2850–2859

SHR/N-cp Rat

The congenic SHR/N-cp rat strain, developed at the National Institutes of Health, USA, (Hansen 1983, Michaelis et al. 1986, Hansen 1988, Adamo et al. 1989) was derived by mating a male Koletsky rat heterozygous for the corpulent gene (cp/+) to a female rat of the Okamoto strain. After a minimum of 12 backcrosses, homozygous (cp/cp) SHR/N-cp rats exhibit obesity, mild hypertension, hyperinsulinemia, and glucose intolerance.

REFERENCES AND FURTHER READING

Adamo M, Shemer J, Aridor M, Dixon J, Carswell N, Bhathena SJ, Michaelis OE,IV, LeRoith D (1989) Liver insulin receptor tyrosine kinase activity in a model of type II diabetes mellitus and obesity. J Nutr 119:484–489
Hansen CT (1983) Two new congenic rat strains for nutrition and obesity research. Fed Proc 42:573
Hansen CT (1988) The development of the SRH/N- and LA/N-cp (corpulent) congenic rat strains. In: Hansen CT, Michaelis OE,IV (eds) New models of genetically obese rats for studies in diabetes, heart disease, and complications of obesity. Summaries of Workshop Papers and Current Bibliography. National Institutes of Health, Bethesda, MD, pp 7–10
McCune SA, Baker PB, Stills HF (1990) SHHF/Mcc-cp rat: a model of obesity, non-insulin-dependent diabetes, and congestive heart failure. Ilar News 32:23–27
Michaelis OE, Hansen CT (1990) The spontaneous hypertensive/NIH corpulent rat: a new rodent model for the study of non-insulin dependent diabetes mellitus and its complications. Ilar News 32:19–22
Michaelis OE, Patrick DH, Hansen A, Canry JJ, Werner RM, Carswell N (1986) Spontaneous hypertensive/NIH- corpulent rat. An animal model for insulin-independent diabetes mellitus (type II). Am J Pathol 123:398–400
Velasquez MT, Kimmel PL, Michaelis OE (1990) Animal models of spontaneous diabetic kidney disease. FASEB J 4:2850–2859

BHE Rat

The BHE rat colony was originally developed by breeding black and white hooded rats of the Pennsylvania State College strain and albino rats of the Yale (Osborne Mendell) strain. The BHE rat is a model in

which the diabetic state is manifested only at maturity. BHE rats have hyperinsulinemia at 50 days of age associated with glucose intolerance and tissue resistance to insulin. Later on, BHE rats have less hyperinsulinemia with reduced pancreatic insulin stores, and show mild hyperglycemia and hyperlipidemia.

REFERENCES AND FURTHER READING

Berdanier CD (1974) Metabolic abnormalities in BHE rats. Diabetologia 10:691–695

Durand AMA, Fisher M, Adams M (1964) Histology in rats as influenced by age and diet. Arch Pathol 77:268–277

Velasquez MT, Kimmel PL, Michaelis OE (1990) Animal models of spontaneous diabetic kidney disease. FASEB J 4:2850–2859

LEW.1AR1/Ztm-iddm RAT

Lenzen et al. (2001), Jörns et al. (2004) described a Type I (insulin-dependent) diabetes mellitus rat model (LEW.1AR1/Ztm-*iddm*), which arose through a spontaneous mutation in a congenic Lewis rat strain with a defined MHC haplotype (RT1.Aa B/Du Cu). Diabetes appeared in the rats with an incidence of 20% without major sex preference at 58+/-2 days. The disease was characterised by hyperglycaemia, glycosuria, ketonuria and polyuria. In peripheral blood, the proportion of T lymphocytes was in the normal range expressing the RT6.1 differentiation antigen. Islets were heavily infiltrated with B and T lymphocytes, macrophages and NK cells with beta cells rapidly destroyed through apoptosis in areas of insulitis.

REFERENCES AND FURTHER READING

Jörns A, Kubat B, Tiedge M, Wedekind D, Hedrich HJ, Klöppel G, Lenzen S (2004) Pathology of the pancreas and other organs in the diabetic LEW.1AR1/Ztm- *iddm* rat, a new model of spontaneous insulin-dependent diabetes mellitus. Virchows Arch 444:183–189

Lenzen S, Tiedge M, Elsner M, Lortz S, Weiss H, Jörns A, Koppel G, Wedekínd D, Prokop Sm, Hedrich HJ (2001) The LEW.1AR1/Ztm-*iddm* rat: a new model of spontaneous insulin-dependent diabetes mellitus.

K.2.2 Spontaneously Diabetic Mice

KK Mouse

Nakamura (1962, 1967) reported on a diabetic strain of the KK-mouse. The animals were moderately obese and showed polyphagia and polyuria. Mice at the age of seven months or older showed glucosuria and blood sugar levels up to 320 mg%. The pancreatic insulin content was increased, but histologically degranulation of the β-cells and hypertrophy of the islets were found. Sections of the liver showed a reduction of glycogen and an increase in lipid content.

REFERENCES AND FURTHER READING

Fujiwara T, Yoshioka S, Yoshioka T, Ushiyama I, Horikoshi H (1988) Characterization of new oral antidiabetic agent CS-045. Studies in KK and *ob/ob* mice and Zucker fatty rats. Diabetes 37:1549–1558

Herberg L, Coleman DL (1977) Laboratory animals exhibiting obesity and diabetes syndromes. Metabolism 26:59–99

Kondo K, Nozawa K, Tomida T, Ezaki K (1957) Inbred strains resulting from Japanese mice. Bull Exp Animals 6:107–112

Nakamura M (1962) A diabetic strain of the mouse. Proc Jap Acad 38:348–352

Nakamura M, Yamada K (1967) Studies on a diabetic (KK) strain of the mouse. Diabetologia 3:212–221

KK-A^y Mouse

Iwatsuka and coworkers (1970) reported on yellow KK mice (also named KK-A^y mice), carrying the yellow obese gene (A^y). These mice develop marked adiposity and diabetic symptoms in comparison with their littermates, black KK mice. Blood glucose and circulating insulin levels as well as HbA_{1c} levels were increased progressively from 5 weeks of age. Degranulation and glycogen infiltration of B cells were followed by hypertrophy and central cavitation of islets. Lipogenesis by liver and adipose tissue were increased. Insulin sensitivity of adipose tissue was more remarkably reduced than in black KK mice to its complete loss at 16 weeks of age. Renal involvement is uniquely marked by early onset and rapid development of glomerular basement membrane thickening (Diani et al. 1987).

KK-A^y mice can be used to demonstrate the extrapancreatic action of antidiabetic drugs, such as glimepiride, a novel sulfonylurea (Satoh et al. 1994). Sohda and coworkers (1990) evaluated ciglitazone and a series of 5-[4-(pyridylalkoxy)benzyl]-2,4-thiazolidinediones for hypoglycemic and hypolipemic activities in yellow KK mice. Hofmann and coworkers (1992) evaluated the expression of the liver glucose transporter GLUT2 and the activity and the expression of phosphoenolpyruvate carboxykinase in the liver of obese KKA^Y mice after treatment with the oral antidiabetic agent pioglitazone.

REFERENCES AND FURTHER READING

Diani AR, Sawada GA, Zhang NY, Wyse BM, Connell CL, Vidmar TJ, Connell MA (1987) The KKA^y mouse: a model for the rapid development of glomerular capillary basement membrane thickening. Blood Vessels 24:297–303

Hofmann CA, Edwards CW, Hillman RM, Colca JR (1992) Treatment of insulin-resistant mice with the oral antidiabetic agent pioglitazone: evaluation of liver GLUT2 and

phosphoenolpyruvate carboxykinase expression. Endocrinol 130:735–740
Iwatsuka H, Shino A, Suzouki Z (1970) General survey of diabetic features of yellow KK mice. Endocrinol Japon 17:23–35
Shafrir E (1992) Animal models of non-insulin-dependent diabetes. Diabetes/Metab Rev 8:179–208
Sohda T, Momose Y, Meguro K, Kawamatsu Y, Sugiyama Y, Ikeda H (1990) Studies on antidiabetic agents. Synthesis and hypoglycemic activity of 5-[4-(pyridylalkoxy)benzyl]-2,4-thiazolidinediones. Arzneim Forsch/Drug Res 40: 37–42

NOD Mouse

The NOD mouse strain was established by inbreeding diabetic CTS mice derived originally from the JCL-ICR strain. Like the BB rat, the NOD mouse is a model of insulin dependent diabetes mellitus and develops hypoinsulinemia secondary to autoimmune destruction of pancreatic β cells in association with insulitis and auto antibody production. Following insulitis, destruction of the insulin-producing pancreatic β cells ensues in many (but not all) mice, with physiologic manifestations of insulin depletion appearing between 3 and 7 months of age. The onset of diabetes can be prevented by an immunmodulating drug (Baeder et al. 1992) or by a soluble interleukin-1 receptor (Nicoletti et al. 1994). Hutchings and Cooke (1995) compared the protective effects afforded by intravenous administration of bovine or ovine insulin to young NOD mice. Bergerot and coworkers (1997) reported that feeding small amounts (2–20 µg) of human insulin conjugated to cholera toxin B subunit can effectively suppress β-cell destruction and clinical diabetes in adult NOD mice. Insulin-dependent diabetes mellitus in NOD Mice is the result of a $CD4^+$ and $CD8^+$ T cell-dependent auto-immune process directed against the pancreatic β-cells (Serreze and Leiter 1994, Verdaguer et al. 1997).

Elias et al. (1990) described induction and therapy of autoimmune diabetes in the non-obese diabetic (NOD/Lt) mouse by a 65-kDa heat shock protein.

REFERENCES AND FURTHER READING

Baeder WL, Sredy J, Sehgal SN, Chang JY, Adams LM (1992) Rapamycin prevents the onset of insulin dependent diabetes mellitus (IDDM) in NOD mice. Clin Exp Immunol 89:174–178
Bergerot I, Ploix C, Petersen J, Moulin V, Rask C, Fabien N, Lindblad M, Mayer A, Czerkinsky C, Holmgren J, Thivolet C (1997) A cholera toxoid-insulin conjugate as an oral vaccine against spontaneous autoimmune diabetes. Proc Natl Acad Sci, USA, 94:4610–4614
Charlton B, Bacelj A, Mandel TE (1988) Administration of silica particles or anti-Lyt2 antibody prevents β-cell destruction in NOD mice given cyclophosphamide. Diabetes 37:930–935
Elias D, Markovits D, Reshef T, van der Zee R, Cohen IR (1990) Induction and therapy of autoimmune diabetes in the non-obese diabetic (NOD/Lt) mouse by a 65-kDa heat shock protein. Proc Natl Acad Sci USA 87:1576–1580
Geisen K, Deutschländer H, Gorbach S, Klenke C, Zimmermann U (1990) Function of barium alginate-microencapsulated xenogenic islets in different diabetic mouse models. In: Shafrir E (ed) Frontiers in Diabetes Research. Lessons from Animal Diabetes III. Smith-Gordon, pp 142–148
Hutchings PR, Cooke A (1995) Comparative study of the protective affect afforded by intravenous administration of bovine or ovine insulin to young NOD mice. Diabetes 44:906–910
Lee KU, Amano K, Yoon JW (1988) Evidence for initial involvement of macrophage in development of insulitis in NOD mice. Diabetes 37:989–991
Matsuba H, Jitsukawa T, Yamagata N, Uchida S, Watanabe H (1994) Establishment of rat glutamic acid decarboxylase (GAD)-reactive T-cell clones from NOD mice. Immunol Lett 42:101–103
Nicoletti F, Di Marco R, Barcellini W, Magro G, Schorlemmer HU, Kurrle R, Lunetta M, Grasso S, Zaccone P, Meroni PL (1994) Protection from experimental autoimmune diabetes in the non-obese diabetic mouse with soluble interleukin-1 receptor. Eur J Immunol 24:1843–1847
Serreze DV, Leiter EH (1994) Genetic and pathogenetic basis of autoimmune diabetes in NOD mice. Curr Opin Immunol 6:900–906
Tochino Y (1984) Breeding and characteristics of a spontaneously diabetic non obese strain (NOD mouse) of mice. In: Shafrir E, Renold AE (eds) Lessons from Animal Diabetes. John Libbey, London, pp 93–98
Velasquez MT, Kimmel PL, Michaelis OE (1990) Animal models of spontaneous diabetic kidney disease. FASEB J 4:2850–2859
Verdaguer J, Schmidt D, Amrani A, Anderson B, Averill N, Santamaria P (1997) Spontaneous autoimmune diabetes in monoclonal T cell nonobese diabetic mice. J Exp Med 186:1663–1676

Obese Hyperglycemic Mice

Ingalls and coworkers (1950), Mayer and coworkers (1951), Bleisch and coworkers (1952) observed hereditary diabetes in genetically obese mice. The obese hyperglycemic mice were glycosuric, the non-fasting blood sugar levels were about 300 mg%, but neither ketonuria nor coma were observed. One of the most interesting features was insulin-resistance; doses as high as 400 IU/kg had little effect on blood sugar. The serum insulin-like activity was high, the islands of Langerhans were hypertrophic, their insulin content was increased and the liver glycogen stores were decreased. Kidneys and other organs did not show pathological changes. Obviously, the diabetic condition of this and other strains of obese hyperglycemic mice is different from that of the human diabetic patient. The*ob* mutation was identified as a mutation in the leptin gene in adipose tissue (Zhang et al. 1994) and the substitution of leptin reverses the obese and diabetic phenotype completely (Halaas et al. 1995). Other strains or substrains of mice with obesity and hyper-

glycemia have been described by Dickie (1962), Westman (1968), Stein and coworkers (1970), Coleman and Hummel (1973), and Herberg and Coleman (1977). Gill and Yen (1991) studied the effect of ciglitazone on endogenous plasma islet amyloid polypeptide (amylin) and insulin sensitivity in obese-diabetic viable yellow mice (VY/Wfl-A^{vy}/a).

REFERENCES AND FURTHER READING

Bleisch VR, Mayer J, Dickie MM (1952) Familial diabetes mellitus in mice associated with insulin resistance, obesity and hyperplasia of the islands of Langerhans. Am J Pathol 28:369–385

Coleman DL, Hummel KP (1973) The influence of genetic background on the expression of obese (ob) gene in the mouse. Diabetologia 9:287–293

Dickie MM (1962) New mutations. Mouse News Letter 27:37

Gill AM, Yen TT (1991) Effects of ciglitazone on endogenous plasma islet amyloid polypeptide and insulin sensitivity in obese-diabetic viable yellow mice. Life Sci 48:703–710

Halaas JL, Gajiwala KS, Maffei M, Cohen SL, Chait BT, Rabinowitz D, Lallone RL, Burley SK, Friedman JM (1995) Weight-reducing effects of the plasma protein encoded by the obese gene. Science 269:543–546

Hellman B (1967) Some metabolic aspects of the obese-hyperglycemic syndrome in mice. Diabetologia 3:222–229

Herberg L, Coleman DL (1977) Laboratory animals exhibiting obesity and diabetes syndromes. Metabolism 26:59–99

Ingalls AM, Dickie MM, Snell GT (1950) Obese, a new mutation in the house mouse. J Hered 14:317–318

Mayer J, Bates MW, Dickie MM (1951) Hereditary diabetes in genetically obese mice. Science 113:746–747

Sirek A (1968) Spontaneous hereditary diabetes in laboratory animals. in: Pfeiffer EF (ed) Handbook of Diabetes mellitus, Pathophysiology and Clinical Considerations. Vol. I, Lehmanns Verlag, München, pp 715–726

Stauffacher W, Lambert AE, Vecchio D, Renold AE (1967) Measurement of insulin activities in pancreas and serum of mice with spontaneous ("obese" and "New Zealand obese") and induced (goldthioglucose) obesity and hyperglycemia, with considerations on the pathogenesis of the spontaneous syndrome. Diabetologia 3:230–237

Stein JM, Bewsher PD, Stowers JN (1970) The metabolism of ketones, triglyceride and monoglyceride in livers of obese hyperglycaemic mice. Diabetologia 6:570–574

Westman S (1968) Development of the obese-hyperglycaemic syndrome in mice. Diabetologia 4:141–149

Zhang Y, Proenca R, Maffei M, Barone M, Leopold L, Friedman JF (1994) Positional cloning of the mouse obese gene and its human homologue. Nature 372:425–432

Diabetic db/db Mice

The diabetes *db/db* mouse strain is derived from an autosomal recessive mutation having occurred spontaneously in mice of the C57BL/KsJ strain which was identified as a mutation in the leptin receptor gene (Tartaglia et al. 1995). On this basis, the diabetes mouse (C57BL/6J *db/db*) consistently develops a severe diabetic syndrome similar to that found in the C57BL/KsJ *ob/ob* mouse, characterized by early onset of hyperinsulinemia, and hyperglycemia up to 20 to 25 mmol/l. (Hummel et al. 1966, Coleman and Hummel 1967, Like et al. 1972). The *db/db* mouse, in contrast to the *ob/ob* mouse, develops significant nephropathy (Gardner 1978). Mutations on the leptin receptor result in an obese phenotype identical to that of *ob* mice (Li et al. 1998). C57BL/KsJ *ob/ob* mice are phenotypically the same as other strains of *db* mice. The leptin receptor (Ob-R) gene encodes 5 alternatively spliced forms, Ob-Ra, Ob-Rb, Ob-Rc, Ob-Rd (Lee et al. 1996). In the *db/db* mouse strain, the Ob-Rb transcript contains an insert with a premature stop codon as a result if abnormal splicing (Chen et al. 1996, Friedman and Halaas 1998).

Coleman and Hummel (1969) joined adult diabetic mice (*db/db*) of the C57BL/Ks strain in parabiosis with normal mice of the same sex. Little, if any, amelioration of the disease was observed in parabiont diabetics and no symptoms of diabetes were observed in the normal parabiont. Instead, the normal partners lost weight, became hypoglycemic, and died of apparent starvation 50 days after surgery. In contrast, the diabetic partners gained weight rapidly and remained diabetic. Raizada and coworkers (1980) demonstrated a decrease of insulin receptors and impaired responses to insulin in fibroblastic cultures from the diabetic *db/db* mouse.

REFERENCES AND FURTHER READING

Berglund O, Frankel BJ, Hellman B (1980) Development of the insulin secretory defect in genetically diabetic (*db/db*) mouse. Acta Endocrinol 87:543–551

Chen H, Charlat O, Tartaglia LA, Woolf EA, Weng X, Ellis SJ, Lakey ND, Culpepper J, Moore KJ, Breitbart RE, Duyk GM, Tepper RI, Morgenstern JP (1996) Evidence that the diabetes gene encodes the leptin receptor. Identification of a mutation in the leptin receptor gene in *db/db* mice. Cell 84:491–495

Coleman DL, Hummel KP (1967) Studies with the mutation diabetes in the mouse. Diabetologia 3:238–248

Coleman DL, Hummel KP (1969) Effects of parabiosis of normal with genetically diabetic mice. Am J Physiol 217:1298–1304

Friedman JF, Halaas JL (1998) Leptin and the regulation of body weight in mammals. Nature 395:763–770

Gardner K (1978) Glomerular hyperfiltration during the onset of diabetes mellitus in two strains of diabetic mice (C57BL/6J *db/db* and C57BL/KsJ *db/db*) Diabetologia 15:59–63

Herberg L, Coleman DL (1977) Laboratory animals exhibiting obesity and diabetes syndromes. Metabolism 26:59–99

Hummel KP, Dickie MM, Colemann DL (1966) Diabetes, a new mutation in the mouse. Science 153:1127–1128

Lee SM (1982) The effect of chronic α-glycosidase inhibition on diabetic nephropathy in the *db/db* mouse. Diabetes 13:249–254

Lee GH, Proenca R, Montez JM, Carroll KM, Darvishzadeh JG, Li JI, Friedman JM (1996) Abnormal splicing in the leptin receptor in diabetic mice. Nature 379:632–635

Leiter EH, Coleman DL, Ingram DK, Reynold MA (1983) Influence of dietary carbohydrate on the induction of diabetes in C5BL/KsJ-*db/db* diabetes mice. J Nutr 113:184–195

Li C, Ioffe E, Fidahusein N, Connolly E, Friedman JM (1998) Absence of soluble leptin receptor in plasma from db^{Pas}/db^{Pas} and other *db/db* mice. J Biol Chem 10078–10082
Like AA, Lavine RL, Poffenbarger PL, Chick WI (1972) Studies on the diabetic mutant mouse. VI Evolution of glomerular lesions and associated proteinuria. Am J Pathol 66:193–224
Raizada MK, Tan G, Fellows RE (1980) Fibroblastic cultures from the diabetic*db/db* mouse. Demonstration of decreased insulin receptors and impaired responses to insulin. J Biol Chem 255:9149–9155
Stearns SB, Benz CA (1978) Glucagon and insulin relationships in genetically diabetic (*db/db*) and streptozotocin-induced diabetic mice. Horm Metab Res 10:20–33
Tartaglia LA, Dembski M, Wenig X, Deng N, Culpepper J, Devos R, Richards GJ, Campfield LA, Clark FT, Deeds J (1995) Identification and expression cloning of a leptin receptor, OB-R. Cell 83:1263–1271

Diabetes Obesity Syndrome in CBA/Ca mice

A spontaneous maturity onset diabetes obesity syndrome occurs in a small proportion (10–20%) of male CBA/Ca mice. Inbreeding can increase the incidence to 80%. It occurs at 12–16 weeks of age, and is characterized by hyperphagia, obesity, hyperglycemia, hypertriglyceridemia, hyperinsulinemia, and an impaired glucose tolerance. The mice are also resistant to exogenous insulin. Female mice remain normal except for a slight increase in serum insulin. The male obese diabetic mice have a normal life expectancy.

REFERENCES AND FURTHER READING

Campbell IL, Das AK (1982) A spontaneous diabetic syndrome in the CBA/Ca laboratory mouse. Biochem Soc Trans 10:392
Connelly DM, Taberner PV (1985) Insulin independent diabetes in male mice from an inbred CBA strain. Endocrinol 104 (Suppl):139
Connelly DM, Taberner PV (1989) Characterization of spontaneous diabetes obesity syndrome in mature CBA/Ca mice. Pharmacol Biochem Behav 34:255–259
Sclafani A (1984) Animal models in obesity: classification and characterization. Int J Obes 8:491–508

Wellesley Mouse

The Wellesley mouse, described first by Jones (1964), is a hybrid with predisposition to diabetes mellitus. The diabetic animals have elevated levels of immunoreactive insulin in serum, enlarged pancreatic islets and reduced insulin responsiveness in peripheral tissues (Cahill et al. 1967, Gleason et al. 1967, Like and Jones 1967).

REFERENCES AND FURTHER READING

Cahill GF, Jones EE, Lauris V, Steinke J, Soeldner JS (1967) Studies on experimental diabetes in the Wellesley hybrid mouse. II. Serum insulin levels and response of peripheral tissues. Diabetologia 3:171–174
Gleason RE, Lauris V, Soeldner JS (1967) Studies on experimental diabetes in the Wellesley hybrid mouse. III. Dietary effects and similar changes in a commercial Swiss-Hauschke strain. Diabetologia 3:175–178
Jones E (1964) Spontaneous hyperplasia of the pancreatic islets associated with glycosuria in hybrid mice. In: Brolin SE, Hellman B, Knutson H (eds) The structure and metabolism of pancreatic islets. Pergamon Press, Oxford, pp 189–191
Like AA, Jones EE (1967) Studies on experimental diabetes in the Wellesley hybrid mouse. IV. Morphologic changes in islet tissue. Diabetologia 3:179–187

K.2.3 Chinese Hamster

Meier and Yerganian (1959, 1961) described the occurrence of hereditary diabetes mellitus in the Chinese hamster (*Cricetulus griseus*). Blood sugar levels of diabetic hamsters were elevated from a normal of 110 mg% up to 600 mg%. Severe polyuria, glucosuria, ketonuria, and proteinuria were observed. The diabetic condition could be improved by administration of insulin, and oral antidiabetic drugs were effective in mildly diabetic hamsters. Pathological changes were seen in histological sections of pancreas, liver and kidney. The number of pancreatic islets was decreased, and the cells of the remaining islets were abnormal. This animal model has been studied by several authors.

REFERENCES AND FURTHER READING

Butler L (1967) The inheritance of diabetes in the Chinese hamster. Diabetologia 3:124–129
Frenkel BJ, Gerich JE, Hagura R, Fanska RE, Gerritsen GC, Grodsky GM (1974) Abnormal secretion of insulin and glucagon by the *in vitro* perfused pancreas of the genetically diabetic Chinese hamster. J Clin Invest 53:1637–1646
Gerritsen GC (1982) The Chinese hamster as a model for the study of diabetes mellitus. Diabetes 31 (Suppl 1):14–23
Gerritsen GC, Dulin WE (1967) Characterization of diabetes in the Chinese hamster. Diabetologia 3:74–78
Gundersen K, Yerganian G, Lin BJ, Gagnon H, Bell F, McRae W, Onsberg T (1967) Diabetes in the Chinese hamster. Some clinical and metabolic aspects. Diabetologia 3:85–91
Luse SA, Caramia F, Gerritsen G, Dulin WE (1967) Spontaneous diabetes mellitus in the Chinese hamster: An electron microscopic study of the islets of Langerhans. Diabetologia 3:97–108
Malaisse W, Malaisse-Lagae F, Gerritsen GC, Dulin WE, Wright PH (1967) Insulin secretion *in vitro* by the pancreas of the Chinese hamster. Diabetologia 3:109–114
Meier H, Yerganian GA (1959) Spontaneous hereditary diabetes mellitus in Chinese hamster (*Cricetulus griseus*). I. Pathological findings. Proc Soc Exper Biol Med 100:810–815
Meier H, Yerganian G (1961a) Spontaneous diabetes mellitus in the Chinese hamster (*Cricetulus griseus*). II. Findings in the offspring of diabetic parents. Diabetes 10:12–18
Meier H, Yerganian G (1961b) Spontaneous hereditary diabetes mellitus in the Chinese hamster (*Cricetulus griseus*).

III. Maintenance of a diabetic hamster colony with the aid of hypoglycemic therapy. Diabetes 10:19–21
Shirai T, Welsh GW, Sims EAH (1967) Diabetes mellitus in the Chinese hamster. II. The evolution of renal glomerulopathy. Diabetologia 3:266–286
Sims EAH, Landau BR (1967) Diabetes mellitus in the Chinese hamster. I. Metabolic and morphologic studies. Diabetologia 3:115–123
Sirek A (1968) Spontaneous hereditary diabetes in laboratory animals. in: Pfeiffer EF (ed) Handbook of Diabetes mellitus, Pathophysiology and Clinical Considerations. Vol. I, Lehmanns Verlag, München, pp 715–726
Sirek OV, Sirek A (1967) The colony of Chinese hamsters of the C.H. Best institute. A review of experimental work. Diabetologia 3:65–73
Soret MG, Dulin WE, Matthew's J, Gerritsen GC (1974) Morphologic abnormalities observed in retina, pancreas and kidney of diabetic Chinese hamsters. Diabetologia 10:567–579

K.2.4 Other Species with Inherited Diabetic Symptoms

SAND Rat

The sand rat (*Psammomys obesus*) lives in the desert regions of North Africa and the Near East. In the laboratory the animals develop diabetic symptoms when fed Purina laboratory chow instead of an all vegetable diet (Hackel et al. 1965 and 1967, Miki et al. 1967, deFronzo et al. 1967, Brodoff et al. 1967, Strasser 1968). The diabetic syndrome in the sand rat usually develops within 2–3 months with variations in severity between the animals. Severely hyperglycemic animals die prematurely from ketosis. Initially, the pancreatic islets appear normal. In the intermediate stage of the disease, degranulation of pancreatic β cells is observed. This is followed by β cell degeneration and necrosis with resultant insulinopenia and ketonuria. Histological studies by Dubault and coworkers (1995) showed insulitis in animals who became insulin-dependent in later stages and recommended *Psammomys obesus* as a model of latent progression to insulin-deficiency in type 2 diabetes patients.

REFERENCES AND FURTHER READING

Brodoff BN, Penhos JC, Levine R, White R (1967) The effect of feeding and various hormones on the glucose tolerance of the sand rat (*Psammomys obesus*) Diabetologia 3:167–170
DeFronzo R, Miki E, Steinke J (1967) Diabetic syndrome in sand rats. Diabetologia 3:140–142
Dubault J, Boulanger M, Espinal J, Marquie G, Petkov P, du Boistesselin R (1995) Latent autoimmune diabetes mellitus in adult humans with non-insulin-dependent diabetes: Is *Psammomys obesus* a suitable animal model? Acta Diabetol 32:92–94
Hackel BB, Frohman LA, Mikat E, Lebovitz HE, Schmidt-Nielsen K (1965a) Review of current studies on the effect of diet on the glucose tolerance of the sand rat (*Psammomys obesus*). Ann N Y Acad Sci 131:459–463
Hackel DB, Schmidt-Nielson K, Haines HB, Miai E (1965b) Diabetes mellitus in the sand rat (*Psammomys obesus*) – pathologic studies. Lab Invest 14:200–207
Hackel DB, Mikat E, Lebovitz HE, Schmidt-Nielsen K, Horton ES, Kinney TD (1967) The sand rat (*Psammomys obesus*) as an experimental animal in studies of diabetes mellitus. Diabetologia 3:130–134
Haines H, Hackel DB, Schmidt-Nielsen K (1965) Experimental diabetes mellitus induced by diet in the sand rat. Am J Physiol 208:297–300
Kalderon B, Gutman A, Levy E, Shafrir E, Adler JH (1986) Characterization of stages in the development of obesity-diabetes syndrome in the sand rat (*Psammomys obesus*). Diabetes 35:717–724
Marquie G, Duhault J, Jacotot B (1984) Diabetes mellitus in sand rats (*Psammomys obesus*). Metabolic pattern during development of the diabetic syndrome. Diabetes 33:438–443
Miki E, Like AA, Steinke J, Soeldner JS (1967) Diabetic syndrome in sand rats. Diabetologia 3:135–139
Schmidt-Nielsen K, Haines HB, Hackel DB (1964) Diabetes mellitus in the sand rat induced by standard laboratory diets. Science 143:689–690
Shafrir E (1992) Animal models of non-insulin-dependent diabetes. Diabetes/Metab Rev 8:179–208
Strasser H (1968) A breeding program for spontaneously diabetic experimental animals.: *Psammomys obesus* (sand rat) and *Acomys cahirinus* (spiny mouse). Lab Anim Care 18:328–338

Spiny Mouse

The spiny mouse (*Acomys cahirinus*) is a small rodent living in the semi-desert areas of the Eastern Mediterranean (Pictet et al. 1967). Diabetes occurs in about 15% of the animals under laboratory conditions accompanied by hyperplasia of the endocrine pancreas. Great variations in the appearance and severity of diabetes and obesity occur in this species. Some animals show obesity, mild hyperglycemia, and hyperinsulinemia. Others have frank hyperglycemia with glucosuria that leads to fatal ketosis. Regardless of the stage of the disease, all spiny mice characteristically have massive hyperplasia of pancreatic islets and increased pancreatic insulin content. Despite the large insulin stores, plasma insulin response to glucose is delayed or impaired suggesting an impairment of the insulin release mechanism.

REFERENCES AND FURTHER READING

Brunk R (1971) Spontandiabetes bei einer weiteren Stachelmausform (*Acomys c. cahirinus* Desmarest, 1819) Z Versuchstierk 13:81–86
Gonet AE, Stauffacher W, Pictet R, Renold AE (1965) Obesity and diabetes mellitus with striking congenital hyperplasia of the islets of Langerhans in spiny mice (*Acomys cahirinus*). I. Histological findings and preliminary metabolic observations. Diabetologia 1:162–171
Junod A, Letarte J, Lambert AE, Stauffacher W (1969) Studies in spiny mice (*Acomys cahirinus*): Metabolic state and pancreatic insulin release *in vitro*. Horm Metab Res 1:45–52

Pictet R, Orci L, Gonet AE, Rouiller Ch, Renold AE (1967) Ultrastructural studies of the hyperplastic islets of Langerhans of spiny mice (*Acomys cahirinus*) before and during the development of hyperglycemia. Diabetologia 3:188–211
Renold AE, Dulin WE (1967) Spontaneous diabetes in laboratory animals. Diabetologia 3:63–64
Shafrir E, Teitelbaum A, Cohen AM (1972) Hyperlipidemia and impaired glucose tolerance in *Acomys cahirinus* maintained on synthetic carbohydrate diets. Isr J Med Sci 8:990–992

African Hamster (Mystromys albicaudatus)

Spontaneous diabetes mellitus was described in South African hamsters (*Mystromys albicaudatus*) by Packer and coworkers (1970), Stuhlman and coworkers (1972, 1974, 1975), Schmidt and coworkers (1974). Characteristics established as part of the diabetic syndrome in this species include hyperglycemia, glucosuria, ketonuria, polyuria, polyphagia and polydipsia. Pancreatic lesions include β-cell vacuolization, glycogen infiltration, nuclear pycnosis, margination of organelles, and β-cell death.

REFERENCES AND FURTHER READING

Packer JT, Kraner KL, Rose SD, Stuhlman A, Nelson RL (1970) Diabetes mellitus in *Mystromys albicaudatus*. Arch Pathol 89:410–415
Schmidt G, Martin AP, Stuhlman RA, Townsend JF, Lucas FV, Vorbeck ML (1974) Evaluation of hepatic mitochondrial function in the spontaneously diabetic *Mystromys albicaudatus*. Lab Invest 30:451–457
Stuhlman RA, Packer JT, Doyle RE (1972) Spontaneous diabetes mellitus in *Mystromys albicaudatus*. Repeated glucose values from 620 animals. Diabetes 21:715–721
Stuhlman RA, Srivastava PK, Schmidt G, Vorbeck ML, Townsend JF (1974) Characterization of diabetes mellitus in South African Hamsters (*Mystromys albicaudatus*). Diabetologia 10:685–690
Stuhlman RA, Packer JT, Doyle RE, Brown RV, Townsend JF (1975) Relationship between pancreatic lesions and serum glucose values in *Mystromys albicaudatus*. Lab Anim Sci 25:168–174

Tuco-Tuco

The diabetic syndrome in Tuco-tucos (*Ctenomis talarum*) is similar to that in sand rats and spiny mice (Wise et al. 1972). However, Tuco-tucos tend to have less hyperglycemia and are less prone to ketosis. Many animals, mainly males, become hyperphagic and quite obese. Degranulation of β cell is the usual lesion in the pancreas, but amyloid hyalinization of islets has been observed in a few animals.

REFERENCES AND FURTHER READING

Velasquez MT, Kimmel PL, Michaelis OE (1990) Animal models of spontaneous diabetic kidney disease. FASEB J 4:2850–2859
Wise PH, Weir BJ, Hime JM, Forrest E (1972) The diabetic syndrome in the Tuco-Tuco (*Ctenomis talarum*). Diabetologia 8:165–172

Macaca Nigra

A high incidence of spontaneous diabetes mellitus was found in *Macaca nigra* (Celebes black apes) with analogies to human diabetes (Howard 1972, 1974a, b, 1975). Abnormal signs include hyperglycemia, decreased clearance of glucose, in intravenous tolerance tests, reduced insulin secretion and increased serum lipids. Insulin secretory capacity is lost concomitant with amyloid infiltration into the islets of Langerhans. Secondary manifestations are atherosclerosis, thickened basement membranes of muscle capillaries, and cataracts. The genetic predisposition in these monkeys is exacerbated by changes in diet and environment.

REFERENCES AND FURTHER READING

Howard CF Jr (1972) Spontaneous diabetes in *Macaca nigra*. Diabetes 21:1977–1090
Howard CF Jr (1974a) Diabetes in *Macaca nigra*: metabolic and histologic changes. Diabetologia 10:671–677
Howard CF Jr (1974b) Correlations of serum triglyceride and prebetalipoprotein levels to the severity of spontaneous diabetes in *Macaca nigra*. J Clin Endocr Metab 38:856–860
Howard CF Jr (1975) Basement membrane thickness in muscle capillaries of normal and spontaneously diabetic *Macaca nigra*. Diabetes 24:201–206

K.2.5 Transgenic Animals and Knockout Mice

GENERAL CONSIDERATIONS

Insulin exerts its diverse biological effects by binding to and activating the membrane-bound insulin receptor (IR), thereby initiating the insulin signal transduction cascade (see K.6.3 and K.6.3.2). IRs are not only present in the classical insulin target tissues, i. e., adipose tissue, skeletal muscle, and liver, but are also widely expressed throughout the organism in tissues such as pancreas, the central nervous system (CNS), lymphatic cells, and kidney. Signals initiated by the activated IR result in the diverse biological effects of insulin, such as the stimulation of glucose transport, the inhibition of gluconeogenesis, the stimulation of protein and lipid synthesis, and the regulation of gene transcription. Because the roles of many components of the signaling pathway were initially characterized *in vitro*, more recent research has focused on the analysis of insulin action *in vivo* by generating mice with targeted disruption of genes for these components. Since the pattern of inheritance of type II diabetes points to a disease of polygenic nature, not only single gene-deficient mice but also models with combined genetic

disruptions have been created in an attempt to represent the polygenic nature of the disease.

Realization that metabolic diseases do not only involve many genes but also many organs necessitated engineering the mouse genome with spatial and temporal controls. This requires the generation of premutant mice whereby the alleles of interest is flanked by recognition sites for DNA recombinases such as Cre (loxP sites) or Flp (Frt sites; Branda and Dymecki 2004). When such premutant mice are bred with transgenic mice that express the corresponding DNA recombinase in a tissue-specific fashion, the gene of interest is inactivated only in that particular tissue. An added sophistication of spatially controlled mutagenesis is the inclusion of temporal control, which is achieved by using ligand-activated chimeric recombinases composed of fusion of the recombinase with the ligand binding domain of a nuclear receptor (Metzger and Chambon 2001). Employing spatially and temporally controlled mutagenesis revealed that metabolic perturbation in one tissue encroaches on the metabolism of another. This tissue communication and crosstalk allows for metabolic flexibility, with respect to the use or production of metabolic fuel. Understanding this may ultimately reveal the genetic determinants that limit the degree of metabolic flexibility, thus promoting metabolic diseases in humans (Bickel 2004).

The first knockout models of insulin resistance aimed at the disruption of major molecules in IR signaling in each tissue. The successful generation of viable, heterozygous IR knockout mice showed that 50% of IR expression is sufficient for the maintenance of physiological blood glucose concentrations. In contrast, homozygous IR-deficient mice rapidly develop diabetic ketoacidosis and die within 3–7 days after birth (Accili et al. 1996, Joshi et al. 1996), showing the indispensability of IR for the control of glucose metabolism. The new techniques for conditional gene inactivation in mice are particularly helpful if conventional knockout of a gene results in embryonic lethality, preventing the analysis of gene function in the adult. Conditional mutagenesis enables the inactivation of a gene of interest in a specific tissue or in a temporally controlled manner, thereby providing new insights into the contribution of a gene to a complex physiological phenotype such as insulin resistance.

Skeletal Muscle and Insulin Resistance

Because insulin resistance in skeletal muscle is one of the earliest detectable defects in type II diabetic patients, muscle-specific insulin receptor knockout (MIRKO) mice have been generated as a model for muscle-specific insulin resistance. MIRKO mice displayed elevated fat mass, serum triglycerides, and free fatty acids, indicating that insulin resistance in muscle contributes to the altered fat metabolism associated with type II diabetes (Brüning et al. 1998). Additionally, Kim and coworkers (2001) demonstrated that IR deficiency in muscle promotes redistribution of substrates to adipose tissue, thereby contributing to increased adiposity in MIRKO mice. Surprisingly, blood glucose, serum insulin, and glucose tolerance were normal in these mice, initially leading to the interpretation that tissues other than muscle are more essential for insulin-regulated glucose disposal than previously assumed. However, Zisman and coworkers (2000) disrupted the gene for the glucose transporter 4 (GLUT4), which mediates glucose transport in response to insulin, selectively in mouse muscle tissue. They found that Glut4-mediated glucose uptake in muscle was indeed essential for the maintenance of normal glucose homeostasis. Consistently, mice with a combined muscle-specific functional inactivation of IR and the closely related insulin-like growth factor receptor (IGF-1R) also display a complete type II diabetic phenotype, implicating a compensatory role of IGF-1R for mediating insulin's stimulation of glucose transport *via* Glut4 in muscle (Fernandez et al. 2001).

Adipose Tissue and Insulin Resistance

The strong association between the world-wide epidemic of obesity and dramatically increasing prevalence of insulin resistance and type II diabetes has prompted recent research to focus on the mechanisms linking adipose tissue to whole body insulin sensitivity, β-cell function, and overall glucose metabolism. Newborn mice with IR deficiency show a marked reduction in white adipose tissue mass, pointing to a role for IR in the regulation of adipocyte growth and differentiation (Accili et al. 1996). Mice with an adipose tissue-specific knockout of the IR (FIRKO) also display a reduced fat mass, loss of the normal correlation of plasma leptin and body weight, and protection against both obesity and obesity-related glucose intolerance. Interestingly, they also exhibit an 18% extended lifespan (Bluher et al. 2003). Strikingly, whereas adipocytes of control mice exhibit a bell-shaped size distribution, adipocytes of FIRKO mice demerge into groups of small and large cells. Interestingly, these differently sized cells also show different expression of fatty acid synthase and the transcription factors CCAAT enhancer binding protein (C/EBP)-α as well as sterol regulatory element-binding protein 1 (SREBP1). Thus inactivation of the IR revealed a pre-

viously unrecognized heterogeneity of adipose tissue. Consistent with the phenotype of GLUT4-null mice, which display a depletion of fat stores (Katz et al. 1995), the selective disruption of GLUT4 in adipose tissue caused an impaired glucose transport, followed by development of insulin resistance. The role of adipose tissue in muscle-specific IR deficiency was addressed in mice with a targeted inactivation of IR-mediated signaling in both muscle and adipose tissue (Lauro et al. 1998). These mice did not become diabetic despite peripheral insulin resistance and a mild impairment of β-cell function. Together, these data suggest that there may be a critical threshold in whole body insulin resistance that finally leads to a diabetic phenotype. Moreover, this insulin resistance might result in excessive demands on the pancreatic β-cells to secrete insulin, leading to consecutive decompensation of these cells. These data clearly assign adipocytes an important role in lipid storage, development of obesity, and regulation of glucose homeostasis.

Role of the β-Cell in Impaired Glucose Tolerance

Mice with a specific disruption of the IR gene in β-cells show a selective loss of insulin secretion in response to glucose and a progressive impairment of glucose tolerance (Kulkarni et al. 1999), indicating that insulin stimulates its own secretion via IRs on β-cells, thus playing an important functional role in glucose sensing by the pancreatic β-cell. Therefore, defects in insulin signaling at the level of the β-cell may contribute to the observed alterations in insulin secretion in type 2 diabetes. Interestingly, a β-cell-specific IGF-1R knockout model also underscored a role for this receptor in the control of glucose-stimulated insulin secretion and glucose tolerance (Kulkarni et al. 2002). The interplay between insulin resistance and insulin secretory defects has also been addressed by the generation of mice deficient for insulin receptor substrate 1 (IRS-1) and β-cell glucokinase (GK). The heterozygous β-cell GK knockout is characterized by decreased insulin secretion in response to glucose, whereas IRS-1-deficient mice are insulin resistant but do not develop overt diabetes (Abe et al. 1998). In contrast to either individual mutation, the double-knockout mice developed a diabetic phenotype (Terauchi et al. 1997), demonstrating that the combination of individual minor defects in insulin action or insulin secretion can cause overt diabetes.

Insulin Resistance in the Brain

The liver-specific insulin receptor knockout (LIRKO) mouse, as expected, exhibits a dramatic phenotype with severe insulin resistance and progressive liver failure (Michael et al. 2000), mirroring the critical role of insulin signaling in liver for regulating glucose homeostasis and maintaining normal hepatic function. However, IRs and insulin-signaling proteins are not exclusively expressed in classic insulin target tissues; they are also widely distributed throughout the CNS. CNS-specific disruption of the IR gene (NIRKO) revealed an important role of IRs in the regulation of energy disposal, fuel metabolism, and reproduction (Brüning et al. 2000). It has very recently been shown in conventional IR-deficient mice that combined restoration of IR function selectively in brain, liver, and pancreatic β-cells rescues these mice from neonatal death, prevents diabetes in a majority of animals, and restores adipose tissue content, lifespan, and reproductive function. Interestingly, IR substitution either limited to brain or liver and pancreatic β-cells was sufficient to prevent neonatal death but not lipatrophic diabetes, leading to the surprising finding that IR signaling in nontypical insulin target tissues like the brain seems to be crucial to maintain fuel homeostasis and prevent diabetes.

Inactivation of IRS Proteins

Aside from IR knockouts, various molecules of the signal transduction pathway initiated by IR have been disrupted, such as IRS-1, which was believed to be the principal substrate for the IR and IGF-1R. Mice deficient for IRS-1 exhibit impaired glucose tolerance and a decrease in insulin/IGF-1-stimulated glucose uptake *in vivo* and *in vitro*, thereby providing a mouse model of genetically determined insulin resistance (Abe et al. 1998, Jenkins and Storlien 1997). Additionally, elevated blood pressure and plasma triglyceride levels were observed, as well as impaired endothelium-dependent vascular relaxation, indicating that insulin resistance plays an important role in the clustering of coronary risk factors leading to accelerated atherosclerosis. The residual insulin/IGF-1 action in IRS-1-deficient mice correlated with the existence of an alternative tyrosine-phosphorylated protein (IRS-2) (Araki et al. 1994), which is also capable of activating the signaling cascade. Surprisingly, disruption of IRS-2 impaired peripheral insulin signaling and pancreatic β-cell function, resulting in progressive deterioration of glucose homeostasis (Withers et al. 1998). This phenotype results from insulin resistance in liver and skeletal muscle and β-cell dysfunction. Succeeding studies indicated tissue-specific functions for IRS-1 and IRS-2 in mediating the metabolic effects of insulin *in vivo*, IRS-1 having a major role in skeletal

muscle and IRS-2 in liver, muscle, adipose tissue, pancreatic β-cells, and reproductive tissue. Interestingly, mice with a double knockout of IRS-1 and the subsequently identified IRS-3 (Lavan et al. 1997) displayed a phenotype of early-onset severe lipatrophy associated with hyperglycemia, hyperinsulinemia, and decreased plasma levels of the anorexigenic hormone leptin. The IRS-1/IRS-3 double-knockout phenotype in mice (Lausten et al. 2002) might mimic the situation in humans better than the single IRS-1 knockout.

The concept that several subclinical genetic alterations in insulin action can synergize to result in overt diabetes was tested in mice double heterozygous for IR and IRS-1 alleles with a ~50% reduction in expression of either protein (Brüning et al. 1997). In these mice, the combined genetic defects led to aggravation of insulin resistance with 5- to 50-fold elevated plasma insulin levels and respective β-cell hyperplasia, and ~ 40% of the animals developed overt diabetes at the age of 4–6 mo. This mouse model of type II diabetes, in which diabetes arises in an age-dependent manner from the interaction between two genetically determined, subclinical defects in the insulin-signaling cascade, demonstrates the important role of epistatic interactions in the pathogenesis of common diseases with non-Mendelian genetics. Moreover, this model has been used successfully to identify further modifying C57BL/6 loci regulating insulin sensitivity (Almind et al. 2003).

Inactivation of PPARs

It has been shown that the abnormal accumulation of lipids in tissues other than adipose adversely affects insulin sensitivity, indicating a complex system for the comprehensive control of lipid and glucose homeostasis. The key coordinators in this metabolic axis are members of the nuclear hormone receptor superfamily. Among those, PPARs (see K.6.4.4) respond to small lipid agents, e. g., dietary fatty acids, and contribute a key mechanism in the regulation of lipid and glucose metabolism (reviewed by Rangwala and Lazar 2004). The important physiological role of the PPARs, i. e., PPAR-α,-β/δ and -γ, was deduced from findings identifying the PPARs as primary targets of two key classes of synthetic compounds that have been used in the successful treatment of diabetes and dyslipidemia. In particular, thiazolidinedione (TZD) insulin sensitizers are potent and specific PPAR-γ ligands and activators. Fibrates have predominant activity as PPAR-α agonists, favorably affecting serum lipid levels. Diverse knockout models have been created to study the function of the single PPAR isoforms *in vivo*.

Consistent with the concept that PPAR-α is the member of the PPAR family that mediates cellular lipid utilization, pharmacological inhibition of cellular fatty acid flux in mice lacking PPAR-α caused massive hepatic and cardiac lipid accumulation, hypoglycemia, and death in 100% of male and 25% of female animals, demonstrating a pivotal role for PPAR-α in lipid and glucose homeostasis *in vivo*. Nevertheless, there was no major phenotypic defect detectable in PPAR-α knockouts without pharmacological challenge (Djouadi et al. 1998). Muoio and coworkers (2002) showed that skeletal muscle of PPAR-α-deficient mice exhibited only minor changes in fatty acid homeostasis, and even mRNA expression of known PPAR-α target genes in muscle tissue was not significantly affected. They proposed that this finding might be explained by high levels of PPAR-β/δ compensating for the lack of PPAR-α, suggesting redundancy in the functions of PPARs as transcriptional regulators of fatty acid homeostasis.

In contrast to the embryonic lethality of homozygous PPAR-γ knockouts (Barak et al. 1999), mice deficient only for the PPAR-γ2 isoform survived, exhibiting an overall reduction in white adipose tissue, less lipid accumulation, and decreased expression of adipogenic genes in adipose tissue (Zhang et al. 2004). Consistently, embryonic fibroblasts of PPAR-γ2 knockouts showed a dramatically reduced capacity for adipogenesis *in vitro*. In addition, insulin sensitivity was impaired in these mice, with decreased expression of IRS-1 and Glut4 in skeletal muscle, but TZDs were able to normalize this insulin resistance (Zhang et al. 2004). In contrast, heterozygous PPAR-γ knockouts show reduced disposition to insulin resistance. Strikingly, this phenotype is blunted by treatment with a synthetic PPAR-γ ligand of the TSD class, indicating that optimal levels of PPAR-γ activity are crucial for its beneficial effects. To address these obvious incongruities, PPAR-γ has been selectively disrupted in liver, adipose tissue, and muscle. Briefly, although adipose tissue appears to be the main site of TZD action, the conditional knockouts highlight important functions for muscle and liver PPAR-γ in the control of body composition and insulin sensitivity. PPAR-γ deficiency in adipose tissue leads to progressive loss of fat, hyperlipidemia, fatty liver, and accompanying hepatic insulin resistance (He et al. 2003). The mice can maintain normal whole body glucose homeostasis and normal insulin sensitivity only as long as some adipose tissue is present. These studies identify a molecular link between blood glucose homeostasis and lipid metabolism, providing a genetic basis for the observed

phenotypic correlation between obesity and type II diabetes mellitus.

Transgenic Animal Model for Type I Diabetes

Aichele and coworkers (1994) used a synthetic peptide corresponding to an immunodominant epitope of lymphocytic choriomeningitis virus glycoprotein (LCMV GP) to prime or to tolerize $CD8^+$ T cells *in vivo*. Peptide-specific tolerance was then examined in transgenic mice expressing LCMV GP in the β islet cells of the pancreas. These mice developed $CD8^+$ T cell-mediated diabetes within 8–14 days after LCMV infection. Specific peptide-induced tolerance prevented autoimmune destruction of β islet cells and diabetes in this transgenic mouse model.Oldstone and coworkers (1991) showed that virus infection triggers insulin-dependent diabetes mellitus in a transgenic mouse model. Ablation of tolerance and induction of diabetes by virus infection in viral antigen transgenic mice was reported by Ohashi and coworkers (1991). Von Herrath and coworkers (1994) investigated how virus induces a rapid or slow onset insulin-dependent diabetes mellitus in two distinct transgenic mouse models. Von Herrath and coworkers (1995) evaluated the role of the costimulatory molecule B7-1 in overcoming peripheral ignorance in transgenic mice which expressed the glycoprotein or nucleoprotein of lymphocytic choriomeningitis virus as the self-antigen in pancreatic β-cells. Von Herrath and Holz (1997) reported that pathological changes in the islet milieu precede infiltration of islets and destruction in β-cells by autoreactive lymphocytes in a transgenic model of virus-induced IDDM. RIP-LCMV transgenic mice that express the viral glycoprotein or nucleoprotein from lymphocytic choriomeningitis virus (LCMV) under control of the rat insulin promoter (RIP) in pancreatic β-cells develop autoimmune diabetes after infection with LCMV. Upregulation of MHC class II molecules associated with the attraction/activation of antigen presenting cells to the islets occurs as soon as 2 days after LCMV inoculation of transgenic mice, clearly before $CD4^+$ and $CD8^+$ lymphocytes are found entering the cells. Possibilities of treatment of virus-induced autoimmune diabetes were discussed (von Herrath et al. 1997). Moritani and coworkers (1996) reported the prevention of adoptively transferred diabetes in nonobese diabetic mice with IL-10-transduced islet-specific Th1 lymphocytes as a gene therapy model for autoimmune diabetes. Birk and coworkers (1996) generated transgenic NOD mice carrying a murine Hsp60 transgene driven by the $H°2E_\alpha$ class II promoter in order to examine the hypothesis of a pathogenic role for self-reactive cells against the stress protein Hsp60 in autoimmune destruction of pancreatic cells in the diabetes of NOD mice.

Future Developments

The employment of even more sophisticated strategies in conditional gene targeting may overcome these limitations in the future. Conditional inactivation of genes is mainly achieved by the Cre-loxP system (Lewandoski 2001). Moller (1994) and Plum and coworkers (2005) recently summarized our current knowledge about the use of knockout and transgenic animal models in diabetes research. Animal models of insulin resistance has recently been reviewed by Nandi and coworkers (2004).

K.2.6 Metabolic Systems Biology

With the completion of the many genomes, genetics is positioned to meet physiology. Argmann and coworkers (2005) predicted the coming of "systems metabolism" in mammals through the use of the mouse, as a model system to study metabolism. Building on mouse genetics with increasingly sophisticated clinical and molecular phenotyping strategies has enabled scientists to now tackle complex biomedical questions, such as those related to the pathogenesis of the common metabolic disorders. The ultimate goal of such strategies will be to mimic human metabolism with the click of a mouse.

Techniques in mouse genetics and phenomics have rapidly evolved over the past decade, which with the renaissance of integrative physiology positioned scientists well for the emergence of the discipline, systems biology. Such systems biology approaches hold great promise in the area of metabolism. The efficient conversion of metabolic parts to metabolic systems will depend on the integration of discovery-based and hypothesis-driven phenogenomic approaches, which rely on the study of mouse models derived from both reverse- and forward genetic strategies. A stable marriage of *in silico* with wet biology that allows for reiterative testing of the computationally identified networks will be crucial for the success of systems biology approaches. Such integrated approaches will become indispensable future resources for drug target identification as well as drug discovery and evaluation. It is expected that such insight into complex metabolic networks will ultimately translate into better therapeutic strategies for metabolic diseases.

REFERENCES AND FURTHER READING

Abe H, Yamada N, Kamata K, Kuwaki T, Shimada M, Osuga J, Shionoiri F, Yahagi N, Kadowaki T, Tamemoto H, Ishibashi S, Yazaki Y, Makuuchi M (1998) Hypertension, hypertriglyceridemia, and impaired endothelium-dependent vascular relaxation in mice lacking insulin receptor substrate-1. J Clin Invest 101:1784–1788

Accili D, Drago J, Lee EJ, Johnson MD, Cool MH, Salvatore P, Asico LD, Jose PA, Taylor SI, Westphal H (1996) Early neonatal death in mice homozygous for a null allele of the insulin receptor gene. Nat Genet 12:106–109

Aichele P, Hyburtz D, Ohashi POS, Odermatt B, Zinkernagel, Hengartner H, Pircher H (1994) Peptide-induced T-cell tolerance to prevent autoimmune diabetes in a transgenic mouse model. Proc Natl Acad Sci USA 91:444–448

Aizawa T, Asanuma N, Terauchi Y, Suzuki N, Komatsu M, Itoh N, Nakabayashi T, Hidaka H, Ohnota H, Yamauchi K, Yasuda K, Yazaki Y, Kodawaki T, Hashizume K (1996) Analysis of the pancreatic β-cell in the mouse with targeted disruption of the pancreatic β-cell-specific glucokinase gene. Biochem Biophys Res Commun 229:460–465

Almind K, Kulkarni RN, Lannon SM, Kahn CR (2003) Identification of interactive loci linked to insulin and leptin in mice with genetic insulin resistance. Diabetes 52:1535–1543

Araki E, Lipes MA, Patti ME, Brüning JC, Haag B, Johnson RS, Kahn CR (1994) Alternative pathway of insulin signalling in mice with targeted disruption of the IRS-1 gene. Nature 372:128–129

Argmann CA, Chambon P, Auwerx J (2005) Mouse phenogenomics: The fast track to "systems metabolism". Cell Metabolism 2:349–360

Barak Y, Nelson MC, Ong ES, Jones YZ, Ruiz-Lozano P, Chien KR, Koder A, Evans RM (1999) PPARγ is required for placental, cardia and adipose tissue development. Mol Cell 4:585–595

Bickel PE (2004) Metabolic fuel selection: the importance of being flexible. J Clin Invest 114:1547–1549

Birk OS, Douek DC, Elias D, Takacs K, Dewchand H, Gur SL, Walker MD, Van der Zee R, Cohen IR, Altman DM (1996) A role Hsp60 in autoimmune diabetes: Analysis of a transgenic model. Proc Natl Acad Sci USA 93:1032–1037

Bluher M, Kahn BB, Kahn CR (2003) Extended longevity in mice lacking the insulin receptor in adipose tissue. Science 299:572–574

Branda C, Dymecki S (2004) Talking about a revolution: The impact of site-specific recombinases on genetic analyses in mice. Dev Cell 6:7–28

Brünning JC, Gautam D, Burks DJ, Gillette J, Schubert M, Orban PC, Klein R, Krone W, Müller-Wieland D, Kahn CR (2000) Role of brain insulin receptor incontrol of body weight and reproduction. Science 289:2122–2125

Brüning JC, Michael MD, Winnay JN, Hayashi T, Horsch D, Accili D, Goodyear LJ, Kahn CR (1998) A muscle-specific insulin receptorknockout exhibits features of the metabolic syndrome of NIDDMwithout altering glucose tolerance. Mol Cell 2:559–569

Brüning JC, Winnay J, Bonner-Weir S, Taylor SI, Accili D, Kahm CR (1997) Development of a novel polygenic model of NIDDM in mice heterozygous for IR and IRS-1 null alleles. Cell 88:561–572

Djoudi F, Weinheimer CJ, Saffitz JE, Pitchford C, Bastin J, Gonzalez FJ, Kelly DP (1998) A gender-related defect in lipid metabolism and glucose transport and glucose homeostasis in peroxisome proliferator-activated receptor α-deficient mice. J Clin Invest 102:1083–1091

Fernandez AM, Kim JK, Yakar S, Dupont J, Hernandez-Sanchez C, Castle AL, Filmore J, Shulman GI, Le Roith D (2001) Functional inactivation of the IGF-1 and insulin receptors in skeletal muscle causes type 2 diabetes. Genes Dev 15:1926–1934

He W, Barak Y, Hevener A, Olson P, Liao D, Le J, Nelson M, Ong E, Olefsky JM, Evans RM (2003) Adipose-specific peroxisome-activated receptor γ knockout causes insulin resistance in fat and liver but not in muscle. Proc Natl Acad Sci USA 100:15712–15717

Jenkins AB, Storlien LH (1997) Insulin resistance and hyperinsulinaemia in insulin receptor substrate-1 knockout mice. Diabetologia 40:1113–1114

Joshi RL, Lamothe B, Cordonnier N, Mesbah K, Monthioux E, Jami J, Bucchini D. (12996) Targeted disruption of the insulin receptor gene in the mouse results in neonatal lethality. EMBO J 15:1542–1547

Katz EB, Stenbit AE, hatton K, DePinho R, Charron MJ (1995) Cardiac and adipose tissue abnormalities but not diabetes in mice deficient in GLUT4. Nature 377:151–155

Kim JK, Zisman A, Fillmore JJ, Peroni OD, Kotani K, Perret P, Zong H, Dong J, Kahn CR, Kahn BB, Shulamn GI (2001) J Clin Invest 108:153–160

Kulkarni RN, Brüning JC, Winnay JN, Postic C, Magnuson MA, Kahn RC (1999) Tissue specific knockout of the insulin receptor in pancreatic β cells creates an insulin secretory defect similar to that in type 2 diabetes. Cell 96:329–339

Kulkarni RN, Holzenberger M, Shih DQ, Ozcan U, Stoffel M, Magnuson MA, Kahn CR (2002) β-cell-specific deletion of the Igf1 receptor leads to hyperinsulinemia and glucose intolerance but does not alter β-cell mass. Nat Genet 31:111–115

Lauro D, Kido Y, Castle AL, Zarnowski MJ, Hayashi H, Ebina Y, Accili D (1998) Impaired glucose tolerance in mice with a targeted impairment of insulin action in muscle and adipose tissue. Nat Genet 20:294–298

Laustsen PG, Michael MD, Crute BE, Cohen SE, Ueki K, Kulkarni RN, Keller SR, Lienhard GE, Kahn CR (1998) Lipoatrophic diabetes in Irs(-/-)Irs(-/-) double knockout mice. Genes Dev 16:3213–3222

Lavan BE, Lane WS, Lienhard GE (1997) The 60-kDa phosphotyrosine protein in insulin-treated adipocytes ia a new member of the insulin receptor substrate family. J Biol Chem 272:11439–11443

Metzger D, Chambon P (2001) Site- and time-specific gene targeting in the mouse. Methods 24:71–80

Michael MD, Kulkarni RN, Postic C, Previs SF, Shulman GI, Magnuson MA, Kahn CR (2000) Loss of insulin signaling in hepatocytes leads to severe insulin resistance and progressive hepatic dysfunction. Mol Cell 6:87–97

Moller DE (1994) Transgenic approaches to the pathogenesis of NIDDM. Diabetes 43:1394–1401

Moritani M, Yoshimoto K, Ii S, Kondo M, Iwahana H, Yamaoka T, Sano T, Nakano N, Kikutani H, Itakura M (1996) Prevention of adoptively transferred diabetes in nonobese diabetic mice with IL-10-transduced islet-specific Th1 lymphocytes: A gene therapy model of autoimmune diabetes. J Clin Invest 98:1851–1859

Muoio DM, MacLean PS, Lang DB, Li S, Houmard JA, Way JM, Winegar DA, Corton JC, Dohm GL, Kraus WE (2002) Fatty acid homeostasis and induction of lipid regulatory genes in skeletal muscles of peroxisome proliferator-activated receptor (PPAR) α knock-out mice. Evidence for compensatory regulation by PPARδ. J Biol Chem 277:26089–26097

Nandi A, Kitamura Y, Kahn CR, Accilli D (2004) Mouse models of insulin resistance. Physiol Rev 84:623–647

Ohashi PS, Oehen S, Buerki K, Pircher H, Ohashi CT, Odermatt B, Malissen B, Zinkernagel RM, Hengartner H (1991) Ablation of "tolerance" and induction of diabetes by virus infection in viral antigen transgenic mice. Cell 65:305–317

Oldstone MBA, Nerenberg M, Southern P, Price J, Lewicki H (1991) Virus infection triggers insulin-dependent diabetes mellitus in a transgenic model: role of anti-self (virus) immune response. Cell 65:319–331

Palmiter RD, Behringer RR, Quaife CJ, Maxwell F, Maxwell IH, Brinster RL (1987) Cell lineage ablation in transgenic mice by cell-specific expression of a toxin gene. Cell 50:435–443

Plum L, Wunderlich FT, Baudler S, Krone W, Brüning C (2005) Transgenic and knockout mice in diabetes research: Novel insights into pathophysiology, limitations, and perspectives. J Physiol 20:152–161

Rangwala SM, Lazar MA (2004) Peroxisome proliferator-activated receptor γ in diabetes and metabolism. Trends Pharmacol Sci 25:331–336

Terauchi Y, Iwamoto K, Tamemoto H, Komeda K, Ishii C, Kanazawa Y, Asanuma N, Aizawa T, Akanuma Y, Yasuda K, Kodama T, Tobe K, Yazaki Y, Kadowaki T (1997) Development of non-insulin-dependent diabetes mellitus in the double knockout mice with disruption of insulin receptor substrate-1 and β-cell glucokinase genes. Genetic reconstruction of diabetes as a polygenic disease. J Clin Invest 99:861–866

Von Herrath MG, Holz A (1997) Pathological changes in the islet milieu precede infiltration of islets and destruction in β-cells by autoreactive lymphocytes in a transgenic model of virus-induced IDDM. J Autoimmun 10:231–238

Von Herrath MG, Dockter J, Oldstone MBA (1994) How virus induces a rapid or slow onset insulin-dependent diabetes mellitus in a transgenic mouse model. Immunity 1:231–242

Von Herrath MG, Guerder S, Lewicki H, Flavell RA, Oldstone MBA (1995) Coexpression of B7–1 and viral ("self") transgenes in pancreatic β-cells can break peripheral ignorance and lead to spontaneous autoimmune diabetes. Immunity 3:727–738

Von Herrath MG, Hormann D, Gairin JE, Oldstone MBA (1997) Pathogenesis and treatment of virus-induced autoimmune diabetes: novel insights gained from the RIP-LCVM transgenic mouse model. Biochem Soc Transact 25:630–635

Withers DJ, Gutierrez JS, Towery H, Burks DJ, Ren J-M, Previs S, Zhang Y, Bernal D, Pons S, Shulman GI, Bonner-Weir S, White MF (1998) Disruption of IRS-2 caused type 2 diabetes. Nature 391:900–907

Zhang J, Fu M, Cui T, Xiong C, Xu K, Zhong W, Xiao Y, Floyd D, Liang J, Li E, Song Q, Chen YE (2004) Selective disruption of PPARγ2 impairs the development of adipose tissue and insulin sensitivity. Proc Natl Acad Sci USA 101:10703–10708

Zisman A, Peroni OD, Abel ED, Michael MD, Mauvais-Jarvis F, Lowell BB, Wojtaszewski JF, Hirshman MF, Virkamaki A, Goodyear LJ, Kahn CR, Kahn BB (2000) Targeted disruption of the glucose transporter 4 selectivity in muscle causes insulin resistance and glucose intolerance. Nat Med 6:924–928

K.3
Measurement of Blood Glucose-Lowering and Antidiabetic Activity

K.3.1
Hypoglycemic Effects

K.3.1.1
Blood Glucose-Lowering Effect in Rabbits

PURPOSE AND RATIONALE

The rabbit has been used since many years for standardization of insulin (see K.4.1). Therefore, it has been chosen as primary screening model for screening of blood glucose lowering compounds as well as for establishing time-response curves and relative activities (Bänder et al. 1969, Geisen 1988).

PROCEDURE

Groups of 4–5 mixed breed rabbits (e. g. Hoe:BASK, SPFWiga) of either sex weighing 3.0–4.5 kg are used. For insulin evaluation, food is withheld overnight. For evaluation of sulfonylureas and other blood glucose lowering agents the animals are on a normal diet (e. g. Era mixed feed 8300) prior to the experiment. The animals are gently placed into special restraining boxes allowing free access to the rabbit's ears.

Oral blood glucose lowering substances are applied by gavage in 1 ml/kg of 0.4% starch suspension or intravenously in solution. Several doses are given to different groups. One control group receives the vehicle only. By puncture of the ear veins, blood is withdrawn immediately before and 1, 2, 3, 4, 5, 24, 48, and 72 h after treatment. For time-response curves values are also measured after 8, 12, 16, and 20 h. Blood glucose is determined in 10 µl blood samples with the hexokinase enzyme method (Glucoquant test kit).

Evaluation

Average blood sugar values are plotted versus time for each dosage. Besides the original values, percentage data related to the value before the experiment are calculated. Mean effects at a time interval are calculated using the trapezoidal rule. The values of the experimental group are compared statistically with the *t*-test or the WILCOXON test for each time interval with those of the control group. Differences between several treated groups and the control group are tested using a simultaneous comparison according to Dunnett or Nemenyi/Dunnett. Dose dependencies and relative activities are determined by means of linear regression analysis after Fieller (1944) and Sidak (1967). All data

for statistical comparisons have to be tested for homogeneity of variances according to Levene (1960) and for normal distribution according to Shapiro and Wilk (1965). In the case of regression analyses, the lines are additionally tested for parallelism according to Tuckey (1966) and for linearity according to Scheffé (1959). The level of significance for all procedures is chosen as 5%.

MODIFICATIONS OF THE METHOD

For special purposes the effect of blood sugar lowering agents is studied in glucose loaded animals. Rabbits of either sex weighing 3.0–4.5 kg are treated either once (0.5 h after test compound) or twice (0.5 and 2.5 h after test compound) orally with 2 g glucose/kg body weight in 50% solution.

A biological assay of insulin preparations in comparison with a stable standard using the blood sugar lowering effect in rabbits has been proposed by Harrison and coworkers (1925).

The biological assay of insulin using the blood sugar lowering effect in rabbits has been until recently the official assay in several pharmacopoeias, such as European Pharmacopoeia, 2nd edn 1980; Deutsches Arzneibuch 1986; British Pharmacopoeia 1988; United States Pharmacopoeia 23 and The National Formulary 18, 1995.

The rabbit blood glucose bioassay as well as the mouse convulsion assay and the mouse glucose assay were used for establishing international standards for highly purified human, porcine and bovine insulins (Bristow et al. 1988).

In several pharmacopoeias, the biological assays have been replaced by chemical methods (British Pharmacopoeia 1999; European Pharmacopoeia, 3rd edn 1997; but the rabbit blood sugar method is still valid in the United States Pharmacopeia USP 24, 2000.

PROCEDURE

Four groups of at least 6 randomly distributed rabbits weighing at least 1.8 kg are kept in the laboratory and maintained on a uniform diet for not less than one week before use in the assay. About 24 h before the test each rabbit is provided with an amount of food that will be consumed within 6 h. The same feeding schedule is followed before each test day. During the test all food and water is withheld until the final blood sample has been taken. The rabbits are placed into comfortable restraining cages to avoid undue excitement.

Immediately before use two solutions of the standard preparation are made, containing 1 unit and 2 units of insulin per ml, respectively, and two dilutions of the preparation being examined which, if the assumption of potency is correct, contain amounts of insulin equivalent to those in the dilutions of the standard preparation. As diluent, a solution is used of 0.1–0.25% w/v of either m-cresol or phenol and 1.4 to 1.8 w/v of glycerol being acidified with hydrochloric acid to a pH between 2.5 and 3.5.

Each of the prepared solutions is injected subcutaneously to one group of rabbits, using the same volume, which should usually be between 0.3 and 0.5 ml for each rabbit, the injections being carried out according to a randomized block design. Preferably on the following day, but in any case not more than 1 week later, each solution is administered to a second group of rabbits following a twin crossover design. One hour and 2.5 h after each injection a suitable blood sample is taken from the ear vein of each rabbit. Blood sugar is determined by a suitable method, preferably using glucose oxidase.

EVALUATION

The results of the assay are calculated by standard analytical methods (e. g., USP 23, 1995).

CRITICAL ASSESSMENT OF THE METHOD

The classical bioassay based on blood-sugar lowering activity in rabbits has been replaced by chemical methods in some pharmacopoeias (Underhill et al. 1994), but is still included in USP 24 (2000) and will be still necessary for evaluation of synthetic insulin derivatives.

MODIFICATIONS OF THE METHOD II

An assay of insulin activity after intraperitoneal injection in rats has been described by Rafaelsen and coworkers (1965) and Young (1967). Shults and coworkers (1994) reported as one of the first on an implantable potentiostat-radiotelemetry system for *in vivo* sensing of glucose, implanted into the paravertebral thoracic subcutaneous tissue of a dog. An enzyme electrode sensor measures the oxidation current of hydrogen peroxide formed by the stoichiometric conversion of the substrate glucose and oxygen as a cofactor in an immobilized glucose oxidase layer. Salehi and coworkers (1996) described the development of a compact, low power, implantable system for *in vivo* monitoring of oxygen and glucose concentrations.

REFERENCES AND FURTHER READING

Bänder A, Pfaff W, Schmidt FH, Stork H, Schröder HG (1969) Zur Pharmakologie von HB 419, einem neuen, stark wirk-

samen oralen Antidiabeticum. Arzneim Forsch/Drug Res 19:1363–1372
Biological Assay of Insulin. British Pharmacopoeia (1988) Vol. II, London, Her Majesty's Stationary Office, pp A168–A170
Bristow AF, Gaines Das RE, Bangham DR (1988) World Health Organization. International standards for highly purified human, porcine and bovine insulins. J Biol Standard 16:165–178
British Pharmacopoeia (1999) Vol I, London: The Stationery Office, pp 789–794
European Pharmacopoeia (1980) 2nd edn, V.2.2.3. Assay of Insulin
European Pharmacopoeia (1997) 3rd edn, Insulin, pp 1020–1022
Fieller EC (1944) A fundamental formula in the statistics of biological assay, and some applications. Quart J Pharm Pharmacol 17:117–123
Geisen K (1988) Special pharmacology of the new sulfonylurea glimepiride. Arzneim Forsch/Drug Res 38:1120–1130
Harrison GA, Lawrence RD, Marks HP, Dale HH (1925) The strength of insulin preparations: a comparison between laboratory and clinical measurements. Br Med J 2:1102–1105
Insulin assay (1990) Rabbit blood-sugar method. United States Pharmacopoeia XXII. The National Formulary XVII. United States Pharmacopoeial Convention, Inc., Rockville, MD, pp 1513–1514
Levene H (1960) Robust tests for equality of variances. In Olkin I, Ghury SG, Hoeffding W, Madow WG, Mann HB (eds) Contributions to probability and statistics. Essays in honor of Harold Hotteling. Stanford University Press, Stanford, CA., pp 278–292
Miller RG (1966) Simultaneous statistical inference. McGraw-Hill Book Company, New York
Rafaelsen OJ, Lauris V, Renold AE (1965) Localized intraperitoneal action of insulin on rat diaphragm and epididymal adipose tissue *in vivo*. Diabetes 14:19–26
Salehi C, Atanasov P, Yang SP, Wilkins E (1996) A telemetry-instrumentation system for long-term implantable glucose and oxygen sensors. Anal Lett 29:2289–2308
Scheffé H (1959) The analysis of variance. Wiley, New York
Shapiro SS, Wilk MB (1965) An analysis of variance test for normality (Complete samples) Biometrika 52:591–611
Shults MC, Rhodes RK, Updike ST, Gilligan BJ, Reining WN (1994) A telemetry-instrumentation system for monitoring multiple subcutaneously implanted glucose sensors. IEEE Trans Biomed Eng 41:937–942
Sidak Z (1967) Rectangular confidence regions for the means of multivariate normal distributions. J Am Statist Assoc 62:626–631
Tuckey (1966)
Underhill LA, Dabbah R, Grady LT, Rhodes CT (1994) Alternatives to animal testing in the USP-NF: Present and future. Drug Devel Industr Pharmacy 20:165–216
USP 23 (1995) Design and analysis of biological assays. The United States Pharmacopeia. pp 1705–1715
USP 23 (1995) Insulin assay. The United States Pharmacopeia. pp 1716–1717
USP 24 (2000) Insulin assays. The United States Pharmacopeia. pp 1848–1849
Young DAB (1967) A serum inhibitor of insulin action on muscle. I. Its detection and properties. Diabetologia 3:287–298

K.3.1.2 Blood Glucose-Lowering Effect in Rats

PURPOSE AND RATIONALE

Rats are used for screening as well as for quantitative evaluation of blood glucose lowering agents.

PROCEDURE

Male Wistar rats (e. g. Hoe:WISKf, SPF 71) weighing 180–240 g are kept on standard diet (e. g. Altromin 1324). Groups of 4–7 non-fasted animals are treated orally or intraperitoneally with various doses of the test compounds suspended in 0.4% starch suspension. One control group receives the vehicle only. Blood is withdrawn from the tip of the tail immediately before, and 1, 2, 3, 5, and 24 h after administration of the test compound. Blood glucose is determined in 10 µl blood samples with the hexokinase enzyme method (Glucoquant test kit).

EVALUATION

Average blood sugar values are plotted versus time for each dosage. Besides the original values, percentage data related to the value before the experiment are calculated. Mean effects over a time period are calculated using the trapezoidal rule. Statistical evaluation is performed as described for tests in rabbits.

MODIFICATIONS OF THE METHOD

Studies in Glucose-Loaded Rats

For special purposes the effect of blood sugar lowering agents is studied in glucose loaded animals. One g glucose/kg body weight is given in a 50% solution either orally 5 min after oral administration or subcutaneously 5 min after intraperitoneal administration of the test compound.

Studies in Streptozotocin-Diabetic Rats

Male Wistar rats (e. g. Hoe:WISKf, SPF 71 strain) weighing 170–220 g are kept on standard diet (e. g. Altromin 1324). Ten–fourteen days prior to the study they are injected with 60 mg/kg streptozotocin (Calbiochem) intravenously. Blood sugar levels rise from 5.5–6.0 mmol/l up to 25.0–28.0 mmol/l and glucosuria occurs. Plasma insulin levels fall below 4 µU/ml. Compounds which release insulin from pancreatic islets as sole hypoglycemic activity are not effective in rats with severe streptozotocin induced diabetes.

K.3.1.3 Blood Glucose-Lowering Effect in Mice

PURPOSE AND RATIONALE

Eneroth and Ahlund (1968, 1970a and b) recommended a twin crossover method for bioassay of insulin using blood glucose levels in mice instead of hypoglycemic seizures giving more precise results. This test was induced into the British Pharmacopoeia 1980 and continued up to 1988. Moreover, the test is included as alternative in the European Pharmacopoeia, 2nd edn 1980; and in Deutsches Arzneibuch, 9. Ausgabe, 1986.

PROCEDURE

Non-fasting mice of the same strain and sex are used having body masses such that the difference between the heaviest and lightest mouse is not more than 2 g. The mice are assigned at random to four equal groups of not less than 10 animals. Two dilutions of a solution of the substance or of the preparation to be examined and 2 dilutions of the reference solution are prepared using as diluent 0.9% NaCl solution adjusted to pH 2.5 with 0.1 N hydrochloric acid and containing a suitable protein carrier. In a preliminary experiment, concentrations of 0.02 IU and 0.10 IU are tested. Each of the prepared solutions (0.1 ml/10 g body weight) is injected subcutaneously to one group of mice according to a randomized block design. Not less than 2.5 h later, each solution is administered to a second group of mice following a twin crossover design. Exactly 30 min after each injection, a sample of 50 µl of blood is taken from the orbital venous sinus of each mouse. Blood glucose concentration is determined by a suitable method, such as described by Hoffman (1937).

EVALUATION

The potency is calculated by the usual statistical methods for the twin-cross-over assay.

REFERENCES AND FURTHER READING

Biological Assay of Insulin (1988) British Pharmacopoeia, Vol. II, London, Her Majesty's Stationary Office, pp A168–A170

Eneroth G, Åhlund K (1968) Biological assay of insulin by blood sugar determination in mice. Acta Pharm Suecica 5:691–594

Eneroth G, Åhlund K (1970a) A twin crossover method for bioassay of insulin using blood glucose levels in mice – a comparison with the rabbit method. Acta Pharm Suecica 7:457–462

Eneroth G, Åhlund K (1970b) Exogenous insulin and blood glucose levels in mice. Factors affecting the dose-response relationship. Acta Pharm Suecica 7:491–500

European Pharmacopeia (1980) 2nd edn, V.2.2.3. Assay of Insulin

Hoffman WS (1937) A rapid photoelectric method for the determination of glucose in blood and urine. J Biol Chem 120:51–55

Wertbestimmung von Insulin (1986) Deutsches Arzneibuch, 9. Ausgabe, Deutscher Apotheker Verlag Stuttgart, pp 50–52

K.3.1.4 Blood Glucose-Lowering Effect in Dogs

PURPOSE AND RATIONALE

Besides experiments in rats and rabbits studies in dogs are necessary to predict the effect of a new compound in man due to differences in species related metabolism.

PROCEDURE

Male Beagle dogs weighing 15–20 kg are kept on standard diet (e. g. Erka mixed feed 8500). Food is withdrawn 18 h prior to the administration of the test compound which is given either orally or intravenously in various doses. Control animals receive the vehicle only. Blood is collected at different time intervals up to 48 h. Blood glucose is determined with the hexokinase enzyme method (Glucoquant test kit) and plasma insulin with an immunological method (Riagnost-kit).

EVALUATION

Average blood sugar values are plotted versus time for each dosage. Besides the original values, percentage data related to the value before the experiment are calculated. Mean effects over a time period are calculated using the trapezoidal rule. Similarly, plasma insulin levels are plotted versus time and compared with control values. Statistical evaluation is performed as described for tests in rabbits.

MODIFICATIONS OF THE METHOD

Studies in Pancreatectomized Dogs

The surgical technique of pancreatectomy in dogs is described in Sect. K.1.0.1. The animals are pancreatectomized up to 2–3 years prior to the study. They are kept on dry feed (Vipromix) together with 2–3 g pancreatic enzymes (Viveral). Insulin is substituted with a single daily subcutaneous dose of 32 IU Insulin Ultratard HM. For substitution of vitamin D an intramuscular dose of 1 ml Vigantol is given every 3 months.

On the day before the study, the animals receive 32 IU of the shorter acting Basal-H insulin. This insulin is administered at the same time when food and test compound are given in the morning. The test drug

is applied as oral suspension in tap water. Blood glucose is determined before and up to 6 h after treatment in hourly intervals. Control animals receive tap water only.

Studies in Alloxan-Diabetic Dogs

Chemical diabetes can be induced by a single intravenous dose of 60 mg/kg alloxan. Afterwards, the animals receive infusions of 1000 ml 5% glucose together with 10 IU Regular Insulin via a jugular vein catheter daily during one week and canned food ad libitum. Thereafter, a single dose of 28 IU Insulin Ultratard HM is given daily and the animals are fed commercial diet (Altromin pellets). On the day before the study, the dogs receive 28 IU of the shorter acting Basal-H insulin. This insulin is given at the same time as food and test compound in the morning. The test drug is applied as oral suspension in tap water. Blood glucose is determined before and up to 6 h after treatment in hourly intervals. Control animals receive tap water only.

Continuous Blood Glucose Monitoring

A device for continuous blood glucose monitoring and infusion in freely mobile dogs was described by Geisen and coworkers (1981, 1988) and Bänder and coworkers (1969).

REFERENCES AND FURTHER READING

Bänder A, Pfaff W, Schmidt FH, Stork H, Schröder HG (1969) Zur Pharmakologie von HB 419, einem neuen, stark wirksamen oralen Antidiabeticum. Arzneim Forsch/Drug Res 19:1363–1372

Geisen K (1988) Special pharmacology of the new sulfonylurea glimepiride. Arzneim Forsch/Drug Res 38:1120–1130

Geisen K, Reisig E, Härtel D (1981) Kontinuierliche Blutglucosemessung und Infusion bei wachen, frei beweglichen Hunden. Continuous blood glucose monitoring and infusion in freely mobile dogs. Res Exp Med (Berl) 179:103–111

K.3.1.5 Blood Glucose-Lowering Effect in Other Species

Instead of rats male guinea pigs (e. g., Pirbright white, Hoe:DHPK, SPF Lac) weighing 250–380 g can be used. Blood is withdrawn by puncture of ear veins before, and 1, 3, and 5 h after administration of the test compound or the vehicle. Blood sugar determinations and statistical evaluations are performed as described for rabbits and rats.

Genetically obese and diabetic yellow KK mice have been used by Sohda and coworkers (1990) for evaluation of hypoglycemic activity of potential antidiabetic drugs. Gill and Yen (1991) studied the effect of ciglitazone in obese-diabetic viable yellow mice (VY/Wfl-A^{vy}/a).

REFERENCES AND FURTHER READING

Gill AM, Yen TT (1991) Effects of ciglitazone on endogenous plasma islet amyloid polypeptide and insulin sensitivity in obese-diabetic viable yellow mice. Life Sci 48:703–710

Sohda T, Momose Y, Meguro K, Kawamatsu Y, Sugiyama Y, Ikeda H (1990) Studies on antidiabetic agents. Synthesis and hypoglycemic activity of 5-[4-(pyridylalkoxy)benzyl]-2,4-thiazolidinediones. Arzneim Forsch/Drug Res 40:37–42

K.3.2 Euglycemic Clamp Technique

PURPOSE AND RATIONALE

The euglycemic glucose clamp technique has provided a useful method of quantifying *in vivo* insulin sensitivity in humans (DeFronzo et al. 1979). In this technique a variable glucose infusion is delivered to maintain euglycemia during insulin infusion. Whole-body tissue sensitivity to insulin, as determined by net glucose uptake, can be quantitated under conditions of near steady state glucose and insulin levels. Kraegen and coworkers (1983, 1985) developed the euglycemic glucose clamp technique for use in the intact conscious rat.

PROCEDURE

Male Wistar rats weighing 150–200 g are fasted overnight and anesthetized with pentobarbital (40 mg/kg, i.p.). Catheters are inserted into a jugular vein and a femoral vein for blood collections and insulin and glucose infusion, respectively. To evaluate the insulin action under physiological hyperinsulinemia (steady state plasma insulin concentration during the clamp test around 100 µU/dl), and maximal hyperinsulinemia (under which maximal insulin action may appear) two insulin infusion rates, 6 and 30 mU/kg/min, are used. The blood glucose concentrations are determined from samples collected at 5-min intervals during the 90-min clamp test. The glucose infusion rate is adjusted so as to maintain the blood glucose at its basal level during the clamp test. The final glucose infusion rate is calculated from the amount of glucose infused for the last 30 min (from 60 to 90 min after start of the clamp) in which the blood glucose levels are in a steady state. The glucose metabolic clearance rate is obtained by dividing the glucose infusion rate by the steady state blood glucose concentration. The steady state plasma insulin concentration is calculated from the insulin concentrations at 60 and 90 min after the start of the

clamp. At the start and end of the euglycemic clamp test, free fatty acid concentration is also determined and the free fatty acid suppression rate is calculated.

EVALUATION

All values are analyzed by one-way ANOVA. When the steady state plasma insulin is maintained at submaximal concentration by the euglycemic clamp technique, the glucose infusion rate and glucose metabolic clearance rate value are considered to reflect the state of receptor binding levels in the peripheral tissue as an index for insulin sensitivity. Under maximal hyperinsulinemia these values are thought to reflect the state of the enzymes and glucose transport system activated after the binding to receptors, indicating mainly insulin responsiveness.

MODIFICATIONS OF THE METHOD

Burnol and coworkers (1983) used the euglycemic insulin clamp technique coupled with isotopic measurement of glucose turnover to quantify insulin sensitivity in the anesthetized rat.

Bryer-Ash and coworkers (1995) used this technique to demonstrate reduction of insulin sensitivity by amylin corresponding to reduced insulin receptor kinase activity.

The effects of counterregulatory hormones on insulin-induced glucose utilization by individual tissues in rats, using the euglycemic hyperinsulinemic clamp technique combined with an injection of 2-[1-^{3}H]-deoxyglucose, were studied by Marfaing and coworkers (1991).

Lang (1992) determined the insulin-mediated glucose uptake in normal and streptozotocin-diabetic rats using the euglycemic-hyperinsulinemic clamp technique.

Hirshman and Horton (1990) reported increased insulin sensitivity and responsiveness in peripheral tissues of the rat after glyburide as determined by the glucose clamp technique.

Lee and coworkers (1994) studied the metabolic effects of troglitazone on fructose-induced insulin resistance with the euglycemic hyperinsulinemic clamp technique in rats.

Tominaga and coworkers (1992, 1993) studied the influence of insulin antibodies in anesthetized rats and of thiazolidinediones on hepatic insulin resistance in streptozotocin-induced diabetic rats by the glucose clamp technique.

Gelardi and coworkers (1991) used the hyperinsulinemic-euglycemic clamp technique to evaluate the insulin sensitivity in the obese offspring of streptozotocin-induced mildly hyperglycemic rats.

Hulman and coworkers (1993) studied insulin resistance in the conscious spontaneously hypertensive rat with the euglycemic hyperinsulinemic clamp technique.

Cheung and Bryer-Ash (1994) described a modified method for the performance of glucose insulin clamp studies in conscious rats under local anesthesia.

Burvin and coworkers (1994) developed a modification of the euglycemic insulin clamp technique and used it to repeatedly assess *in vivo* insulin effects in awake streptozotocin-induced diabetic rats.

Xie and coworkers (1996) described a modified euglycemic clamp technique in cats.

Finegood and coworkers (1987) estimated endogenous glucose production during hyperinsulinemic-euglycemic glucose clamps using unlabeled and labeled glucose infusates in dogs.

Xie and coworkers (1996) described an insulin sensitivity test using a modified euglycemic clamp in **cats** and rats. This test uses the amount of glucose required to be infused to maintain euglycemia over a 30-min period in rats and 60 min in cats following a bolus administration of insulin as the index of insulin sensitivity. Glucose levels are determined a short intervals and variable glucose infusion is used to hold glucose levels with-in a few percentage points of the basal pre-test glucose level. A new blood sampling technique is described that allows each insulin sensitivity test to be carried out using a total of only 0.5 ml of blood.

REFERENCES AND FURTHER READING

Bryer-Ash M, Follett L, Hodges N, Wimalawansa S (1995) Amylin-mediated reduction in insulin sensitivity corresponds to reduced insulin receptor kinase activity in the rat *in vivo*. Metabolism 44:705–711

Burnol A, Leturque A, Ferre P (1983) A method for quantifying insulin sensitivity in the anesthetized rat: The euglycemic insulin clamp technique coupled with isotopic measurement of glucose turnover. Reprod Nutr Dev 23:429–435

Burvin R, Armoni M, Karnieli E (1994) *In vivo* insulin action in normal and streptozotocin-induced diabetic rats. Physiol Behav 56:1–6

DeFronzo RA, Tobin JD, Andres R (1979) Glucose clamp technique: a method for quantifying insulin secretion and resistance. Am J Physiol 237:E214–223

Cheung A, Bryer-Ash M (1994) Modified method for the performance of glucose insulin clamp studies in conscious rats. J Pharmacol Toxicol Meth 31:215–220

Finegood DT, Bergman RN, Vranic A (1987) Estimation of endogenous glucose production during hyperinsulinemic-euglycemic glucose clamps. Comparison of unlabeled and labeled glucose infusates. Diabetes 36:914–924

Gelardi NL, Cha CM, Oh W (1991) Evaluation of insulin sensitivity in obese offspring of diabetic rats by hyperinsulinemic-euglycemic clamp technique. Pediatric Res 30:40–44

Hirshman MF, Horton ES (1990) Glyburide increases insulin sensitivity and responsiveness in peripheral tissues of the rat as determined by the glucose clamp technique. Endocrinol 126:2407–2412
Hulman S, Falkner B, Freyvogel N (1993) Insulin resistance in the conscious spontaneously hypertensive rat: euglycemic hyperinsulinemic clamp study. Metabolism 42:14–18
Kraegen EW, James DE, Bennett SP, Chishol DJ (1983) *In vivo* insulin sensitivity in the rat determined by euglycemic clamp. Am J Physiol 245 (Endocrinol Metab 8):E1–E7
Kraegen EW, James DE, Jenkins AB, Chisholm DJ (1985) Dose-response curves for *in vivo* sensitivity in individual tissues in rats. Am J Physiol; Endocrin Metab 11:E353–E362
Lang CH (1992) Rates and tissue sites of noninsulin- and insulin-mediated glucose uptake in diabetic rats. Proc Soc Exp Biol Med 199:81–87
Lee MK, Miles PDG, Khoursheed M, Gao KM, Moossa AR, Olefsky JM (1994) Metabolic effects of troglitazone on fructose-induced insulin resistance in rats. Diabetes 43:1435–1439
Marfaing P, Ktorza A, Berthault MF, Predine J, Picon L, Penicaud L (1991) Effects of counterregulatory hormones on insulin-induced glucose utilization by individual tissues in rats. Diabete and Metabolisme (Paris) 17:55–60
Ohsawa I, Sato J, Oshida Y, Sato Y, Sakamoto N (1991) Effect of glimepiride on insulin action in peripheral tissues of the rat determined by the euglycemic clamp technique. J Japan Diab Soc 34:873–874
Tominaga M, Matsumoto M, Igarashi M, Eguchi H, Sekikawa A, Sasaki H (1992) Insulin antibody does not cause insulin resistance during glucose clamping in rats. Diabet Res Clin Pract 18:143–151
Tominaga M, Igarashi M, Daimon M, Eguchi H, Matsumoto M, Sekikawa A, Yamatani K, Sasaki H (1993) Thiazolidinediones (AD-4833 and CS-045) improve hepatic insulin resistance in streptozotocin-induced diabetic rats. Endocr J 40:343–349
Xie H, Zhu L, Zhang YL, Legare DJ, Lautt WW (1996) Insulin sensitivity test with a modified euglycemic technique in cats and rats. J Pharmacol Toxicol Meth 35:77–82

K.3.3 Hypoglycemic Seizures in Mice

PURPOSE AND RATIONALE

The biological assay of insulin using hypoglycemic seizures in mice has been suggested already in 1923 by Fraser. The biological standardization of insulin using the mouse convulsion method has been published in detail by the Health Organisation of the League of Nations in 1926 (Trevan and Boock, Hemmingsen and Krogh) and has been until recently the official assay in several pharmacopoeias, such as European Pharmacopeia, 2nd edn 1980; Deutsches Arzneibuch 1986; British Pharmacopoeia 1988. In most pharmacopoeias, the biological assays have been replaced by chemical methods (British Pharmacopoeia 1999; European Pharmacopoeia, 3rd edn 1997).

PROCEDURE

Ninety-six mice of either sex (but not of mixed sexes) weighing 20 ± 5 g are randomly distributed into 4 groups. The mice are deprived of food 2–20 h immediately preceding the test. Solutions of the insulin standard and of the test preparation containing 30 and 60 milliUnits/ml are prepared by diluting the original solution with 0.9% NaCl solution, pH 2.5. 0.5 ml/20 g mouse of these solutions are injected subcutaneously. The mice are kept at a uniform temperature, between 29 and 35°C, in transparent containers within an air incubator with a transparent front. The mice are observed for 1.5 h and the number of mice is recorded that are dead, convulse or lie still for more than 2 or 3 s when placed on their backs.

EVALUATION

The percentage of mice of each group showing the afore mentioned symptoms is calculated and the relative potency of the test solution calculated using a $2 + 2$ point assay.

CRITICAL ASSESSMENT OF THE METHOD

Attempts to replace the tests in mice and rabbits by *in vitro* tests, such as the rat diaphragm test, the rat epididymal fat pad test, or even the radioimmunoassay failed due to several reasons (Trethewey 1989). Nevertheless, for industrial production and for stability studies, the classical bioassays based on hypoglycemic seizures in mice or hypoglycemia in rabbits have been replaced by chemical methods (Stewart 1974, Underhill et al. 1994).

MODIFICATIONS OF THE METHOD

A modification of the mice seizure method using rotating hollow cylinders has been proposed by Young and Lewis (1947). A similar technique which increases the sensitivity of the mice seizure method has been used by Vogel (1964). The equipment consisted of seven perforated metal drums with a diameter of 15 cm. The drums were rotated in oblique position at 10 rotations per minute. Female mice weighing 16 to 20 g were deprived of feed at the afternoon before the test. On the test day, groups of 6 mice received doses of 0.5; 1.0 or 1.5 IU/kg of test preparation or standard subcutaneously and were placed after 20 min into the rotating drums. Controls received saline only. Mice with insulin-induced seizures dropped out from the rotating drum. The number of animals dropping out was counted after 15; 30; 45 and 60 min. Mice dropping out due to hypoglycemic seizures received 0.5 ml of 10% glucose solution intraperitoneally. ED_{50} values and activity ratios were calculated according to Litchfield and Wilcoxon (1949).

REFERENCES AND FURTHER READING

Biological Assay of Insulin (1988) British Pharmacopoeia, Vol. II, London, Her Majesty's Stationary Office, pp A168–A170

British Pharmacopoeia (1999) Vol I, London: The Stationery Office, pp 789–794

European Pharmacopeia (1980) 2nd edn, V.2.2.3. Assay of Insulin

European Pharmacopoeia (1997) 3rd edn, Insulin, pp 1020–1022

Fraser DT (1923) White mice and the assay of insulin. J Lab Clin Med 8:425–428

Hemmingsen AM, Krogh A (1926) The assay of insulin by the convulsive-dose method on white mice. In: League of Nations; Health Organisation; The Biological Standardisation of Insulin. Publications of The League of Nations. III. Health, 1926, III. 7. pp 40–46

Litchfield JT, Wilcoxon F (1949) A simplified method for evaluating dose-effect experiments. J Pharmacol Exp Ther 96:99

Stewart GA (1974) Historical review of the analytical control of insulin. Analyst 99:913–928

Trethewey J (1989) Bioassays for the analysis of insulin. J Pharm Biomed Anal 7:189–197

Trevan JW, Boock E (1926) The standardisation of insulin by the determination of the convulsive dose for mice. In: League of Nations; Health Organisation; The Biological Standardisation of Insulin. Publications of The League of Nations. III. Health, 1926, III. 7. pp 47–56

Vogel HG (1964) Unpublished data

Wertbestimmung von Insulin. Deutsches Arzneibuch, 9. Ausgabe 1986, Deutscher Apotheker Verlag Stuttgart, pp 50–52

Young DM, Lewis AH (1947) Detection of hypoglycemic reactions in the mouse assay for insulin. Science 105:368–369

K.3.4 Effects of Insulin Sensitizer Drugs

PURPOSE AND RATIONALE

Insulin sensitizer drugs are reported to improve symptoms in patients with established type 2 diabetes (NIDDM = non-insulin dependent diabetes mellitus) (Colca 1995; Kuehnle 1996). In contrast to sulfonylureas, these compounds do not lower blood glucose in normal animals. Various animal models resembling type 2 diabetes are used for evaluation. Details of these models are described in the respective chapters. *In vitro* techniques showed an increased glucose uptake into muscle tissue and into adipocytes.

PROCEDURE

In Vivo Studies

Chang et al. (1983) studied ciglitazone in *ob/ob* and *db/db* mice, diabetic Chinese hamsters, and normal and streptozotocin-diabetic rats.

Fujita et al. (1983) investigated the effects of ciglitazone in obese-diabetic yellow *KK* (*KK-A*^{y}) mice and obese Zucker-fatty rats.

Diani et al. (1984) treated C5BL/6J-*ob/ob* and C57BL/KsJ-*db/db* mice for several weeks with ciglitazone and studied the morphological effects on pancreatic islets.

Fujiwara et al. (1988) performed studies in *KK* and *ob/ob* mice and Zucker fatty rats.

Moreover, Fujiwara et al. (1991) studied the effects of CS-045 on glycemic control and pancreatic islet structure at a late stage of the diabetes syndrome in C57BL/KsJ-*db/db* mice.

Ikeda et al. (1990), Sohda et al. (1990) used insulin resistant animals (yellow *KK* mice, Zucker fatty rats, and obese Beagle dogs with moderate insulin resistance).

Gill and Yen (1991) studied the effects on endogenous plasma islet amyloid polypeptide and insulin sensitivity in obese-diabetic viable yellow mice.

Hofmann et al. (1991, 1992) treated insulin resistant KKA^y mice.

Stevenson et al. (1991) studied the effects of englitazone in nondiabetic rats and found no overt hypoglycemia but an enhancement of insulin action.

Kobayashi et al. (1992) found an increase of insulin sensitivity by activating insulin receptor kinase in genetically obese Wistar fatty rats treated with various doses of pioglitazone.

Sugiyma et al. (1992) found a reduction of glucose intolerance and hypersecretion of insulin in Wistar fatty rats after treatment with pioglitazone for 10 days.

Tominaga et al. (1993) used the glucose clamp-technique in streptozotocin-induced diabetic rats.

Yoshioka et al. (1993) found antihypertensive effects in obese Zucker rats.

Lee et al. (1994) studied the metabolic effects on fructose-induced insulin resistance in rats.

Apweiler et al. (1995) administered BM 13.09143 to lean and obese Zucker rats and performed hyperinsulinemic-euglycemic clamp studies in these animals.

Fujiwara et al. (1995) found a suppression of hepatic gluconeogenesis in long-term troglitazone treated diabetic KK and C57BL/ksJ-*db/db* mice.

Lee and Olefsky (1995) studied the effects of troglitazone in normal rats with the euglycemic glucose clamp technique.

In Vitro Studies

Kirsch et al. (1984) found a reversal of cAMP-induced post-insulin receptor resistance in rat adipocytes *in vitro*.

Ciaraldi et al. (1990) performed *in vitro* studies using cultured hepatoma cells (Hep G2) and muscle cells (BC3H-1) and found an increased glycogen synthase I activity in both cell types.

Murano et al. (1994) found a stimulation of fructose-2,6-bisphosphate production in rat hepatocytes.

Kellerer et al. (1994) reported the prevention of glucose-induced insulin resistance of insulin receptor in rat-1 fibroblasts.

Bader et al. (1993) found an increased [^{32}P]incorporation in the 95 kD β-subunit of the insulin receptor and an increased phosphorylation of the synthetic substrate Poly[GluNa4:1Tyr] in receptors isolated from skeletal muscle of obese Zucker rats treated with CS 045.

Teboul et al. (1995) found that thiazolidinediones convert myogenic cells (C_2C_{12}N myoblasts, a subclone of the C_2C_{12} cell line) into adipose-like cells. Thiazolidinediones or fatty acids prevented the expression of myogenin, α-actin, and creatine kinase and abolished the formation of multinucleated myotubes. In parallel, these treatments induced the expression of a typical adipose differentiation program including acquisition of adipocyte morphology and activation of adipose-related genes.

Tafuri (1996) reported that troglitazone enhanced the rate and percent differentiation of fibroblasts to adipocytes. Basal glucose transport and synthesis of GLUT1 transporter messenger RNA were increased.

Stevenson et al. (1990) examined the effects of racemic englitazone (CP 68722) in adipocytes and soleus muscles from *ob/ob* mice and in 3T3-L1 adipocytes. Administration of the drug in various doses lowered plasma glucose and insulin dose-dependently without producing frank hypoglycemia in either diabetic or nondiabetic animals. Basal and insulin-stimulated lipogenesis were enhanced in adipocytes from *ob/ob* mice. Glycogenesis and basal glucose oxidation in isolated soleus muscles were stimulated.

Kreutter et al. (1990) used 3T3-L1 adipocytes and found a stimulation of 2-deoxyglucose uptake.

Masuda et al. (1995) found an insulinotropic mechanism distinct from glibenclamide in isolated rat pancreatic islets and HIT cells.

REFERENCES AND FURTHER READING

Apweiler R, Kühnle HF, Ritter G, Schell R, Freund P (1995) Effect of the nee antidiabetic agent (–)-BM 13.0913.Na on insulin resistance in lean and obese Zucker rats. Metabolism 44:577–583

Bader S, Kiehn R, Häring HU (1993) Effekt von CS 045 auf die Kinaseaktivität des Insulinrezeptors im Skelettmuskel insulin-resistenter Zucker-Ratten. Diab Stoffw 2:56–61

ChangAY, Wyse BM, Gilchrist BJ, Peterson T, Diani AR (1983) Ciglitazone, a new hypoglycemic agent. I: Studies in *ob/ob* and *db/db* mice, diabetic Chinese hamsters, and normal and streptozotocin-diabetic rats. Diabetes 32:830–838

Ciaraldi TP, Gilmore A, Olefsky JM, Goldberg M, Heidenreich KA (1990) *In vitro* studies on the action of CS-045, a new antidiabetic agent. Metabolism 39:1056–1062

Colca JR (1995) Insulin sensitiser drugs in development for the treatment in diabetes. Expert Opin Invest Drugs 4:27–29

Diani AR, Peterson T, Samada GA, Wyse BM, Gilchrist BJ, Chang AY (1984) Ciglitazone, a new hypoglycemic agent. 4. Effects on pancreatic islets of C5BL/6J-*ob/ob* and C57BL/KsJ-*db/db* mice. Diabetologia 27:225–234

Fujita T, Sugiyama Y, Taketomi S, Sohda T, Kawamatsu Y, Iwatsuka H, Suzuki Z (1983) Reduction of insulin resistance in obese and/or diabetic animals by 5-[4-(1-methylcyclohexylmethoxy)benzyl]-thizolidine-2,4-dione (ADD-3878, U-63,287, ciglitazone), a new antidiabetic agent. Diabetes 32:804–810

Fujiwara T, Yoshioka S, Yoshioka T, Ushiyama I, Horikoshi H (1988) Characterization of new oral antidiabetic agent CS-045. Studies in KK and *ob/ob* mice and Zucker fatty rats. Diabetes 37:1549–1558

Fujiwara T, Wada M, Fukuda K, Fukami M, Yoshioka S, Yoshioka T, Horikoshi H (1991) Characterization of CS-045, a new oral antidiabetic agent, II. Effects on glycemic control and pancreatic islet structure at a late stage of the diabetes syndrome in C57BL/KsJ-*db/db* mice. Metabolism 40:1213–1218

Fujiwara T, Akuno A, Yoshioka S, Horikoshi H (1995) Suppression of hepatic gluconeogenesis in long-term troglitazone treated diabetic KK and C57BL/ksJ-*db/db* mice. Metabolism 44:486–490

Gill AM, Yen TT (1991) Effects of ciglitazone on endogenous plasma islet amyloid polypeptide and insulin sensitivity in obese-diabetic viable yellow mice. Life Sci 48:703–710

Hofmann C, Lorenz K, Colca JR (1991) Glucose transport deficiency in diabetic animals is corrected by treatment with the oral antihyperglycemic agent pioglitazone. Endocrinol 129:1915–1925

Hofmann CA, Edwards CW, Hillman RM, Colca JR (1992) Treatment of insulin-resistant mice with the oral antidiabetic agent pioglitazone: evaluation of liver GLUT2 and phosphoenolpyruvate carboxykinase expression. Endocrinol 130:735–740

Ikeda H, Taketomi S, Sugiyama Y, Shimura Y, Sohda T Meguro K, Fujita T (1990) Effects of pioglitazone on glucose and lipid metabolism in normal and insulin resistant animals. Arzneim Forsch/Drug Res 40:156–162

Kellerer M, Kroder G, Tippmer S, Berti L, Kiehn R, Mosthaf L, Häring H (1994) Troglitazone prevents glucose-induced insulin resistance of insulin receptor in rat-1 fibroblasts. Diabetes 43:447–453

Kirsch DM, Bachmann W, Häring HU (1984) Ciglitazone reverses cAMP-induced post-insulin receptor resistance in rat adipocytes *in vitro*. FEBS Lett 176:49–54

Kobayashi M, Iwanshi M, Egawa K, Shigeta Y (1992) Pioglitazone increases insulin sensitivity by activating insulin receptor kinase. Diabetes 41:476–483

Kreutter DK, Andrews KM, Gibbs EM, Hutson NJ, Stevenson RW (1990) Insulinlike activity of new antidiabetic agent CP 68722 in 3T3-L1 adipocytes. Diabetes 39:1414–1419

Kuehnle HF (1996) New therapeutic agents for the treatment of NIDDM. Exp Clin Endocrinol Diabetes 104:93–101

Lee MK, Olefsky JM (1995) Acute effects of troglitazone on *in vivo* insulin action in normal rats. Metabolism 44:1166–1169

Lee MK, Miles PDG, Khoursheed M, Gao KM, Moossa AR, Olefsky JM (1994) Metabolic effects of troglitazone on fructose-induced insulin resistance in rats. Diabetes 43:1435–1439

Masuda K, Okamoto Y, Tuura Y, Kato S, Miura T, Tsuda K, Horikoshi H, Ishida H, Seino Y (1995) Effects of troglitazone (CS-045) on insulin secretion in isolated rat pancreatic islets and HIT cells: an insulinotropic mechanism distinct from glibenclamide. Diabetologia 38:24–30

Murano K, Inoue Y, Emoto M, Kaku K, Kaneko T (1994) CS-045, a new oral antidiabetic agent, stimulates fructose-2,6-bisphosphate production in rat hepatocytes. Eur J Pharmacol 254:257–262

Sohda T, Momose Y, Meguro K, Kawamatsu Y, Sugiyama Y, Ikeda H (1990) Studies on antidiabetic agents. Synthesis and hypoglycemic activity of 5-[4-(pyridylalkoxy)benzyl]-2,4-thiazolidinediones. Arzneim Forsch/Drug Res 40:37–42

Stevenson RW, Hutson NJ, Krupp MN, Volkmann RA, Holland GF, Eggler JF, Clark DA, McPherson RK, Hall KL, Danbury BH, Gibbs EM, Kreutter DK (1990) Actions of novel antidiabetic agent englitazone in hyperglycemic hyperinsulinemic *ob/ob* mice. Diabetes 39:1218–1227

Stevenson RW, McPherson RK, Genereux PE, Danbury BH, Kreutter DK (1991) Antidiabetic agent englitazone enhances insulin action in nondiabetic rats without producing hypoglycemia. Metabolism 40:1268–1274

Sugiyama Y, Taketomi S, Shimura Y, Ikeda H, Fujita T (1990) Effects of pioglitazone on glucose and lipid metabolism in Wistar fatty rats. Arzneim Forsch/Drug Res 40:263–267

Tafuri SR (1996) Troglitazone enhances differentiation, glucose uptake, and Glut1 protein levels in 3T3-L1 adipocytes. Endocrinology 137:4706–4712

Teboul L, Gaillard D, Staccini L, Inadera H, Amri EZ, Grimaldi PA (1995) Thiazolidinediones and fatty acids convert myogenic cells into adipose-like cells. J Biol Chem 270:28183–28187

Tominaga M, Igarashi M, Daimon M, Eguchi H, Matsumoto M, Sekikawa A, Yamatani K, Sasaki H (1993) Thiazolidinediones (AD-4833 and CS-045) improve hepatic insulin resistance in streptozotocin-induced diabetic rats. Endocr J 40:343–349

Yoshioka S, Nishino H, Shiraki T, Ikeda K, Koike H, Okuno A, Wada M, Fujiwara T, Horikoshi H (1993) Antihypertensive effects of CS-045 treatment in obese Zucker rats. Metabolism 42:75–80

K.3.5 Effects of Thiazolidinediones on Peroxisome Proliferator-Activated Receptor-γ

PURPOSE AND RATIONALE

Peroxisome proliferator-activated receptors (PPARs) compose a subfamily of the nuclear hormone receptors. Three distinct PPARs, termed α, δ, and γ, each encoded by a separate gene and showing a distinct tissue distribution pattern, have been described (Keller and Wahli 1993; Green 1995; Devchand et al. 1996; Lemberger et al. 1996; Schoonjans et al. 1996a, b, 1997, Willson et al. 2000), Walczak and Tontomoz 2002). Ligands that induce the transcriptional activity of PPARα and γ have been identified (Forman et al. 1995; Devchand et al. 1996; Lehmann 1995). Fatty acids and eicosanoids regulate gene expression through direct interactions with peroxisome proliferator-activated receptors α and γ (Kliewer et al. 1997). PPARγ is a central regulator of adipocyte gene expression and differentiation (Tortonoz et al. 1995; Brun et al. 1996; Wu 1998, Lowell 1999). Thiazolidinedione derivatives which are antidiabetic agents are potent and selective activators of PPARγ (Young et al. 1997; Henke et al. 1998, Murakami et al. 1998; Reginato et al. 1998; Ribon et al. 1998, Vázquez et al. 2002).. Berger et al. (1996) found a correlation of antidiabetic actions of thiazolidinediones in *db/db* mice with the conformational change in peroxisomal proliferator-activated receptor-γ: Murphy and Holder (2000) suggested a therapeutic potential of PPARγ agonists in the treatment of inflammatory diseases and certain cancers.

Steppan et al. (2001), Berger (2001) showed that adipocytes secrete a signaling molecule which they called resistin (for resistance to insulin). Circulating resistin levels in mice are decreased by thiazolidindiones and are increased in diet-induced and genetic forms of obesity. On the other hand adipocytes secrete another adipocytokine called adiponectin. Serum levels of adiponectin correlate with insulin sensitivity and are increased by the treatment with thiazolidindiones (Choi et al. 2005, Do et al. 2006).

PROCEDURE

Plasmids

The pSG5-haPPARγ1 expression construct is generated by inserting the hamster PPARγ complementary DNA into the EcoRI site of the pSG5 expression vector (Strategene, La Jolla, CA). As reporter construct, pPPRE-chloramphenicol acetyltransferase (CAT) is used containing two copies of the peroxisomal proliferator response element from the enhancer region of the murine acyl coenzyme A-oxidase gene adjacent to the glutathione-S-transferase minimal promotor and the CAT gene.

Cell Culture and Transfections

COS-1 cells are seeded at 2.1×10^5 cells per dish in 35-mm dishes (for transactivation assays) and 3×10^6 cells/dish in 150-mm dishes (for binding assays) in DMEM (high glucose) containing 10% charcoal-stripped fetal calf serum, nonessential amino acids, 100 U/ml penicillin G, and 100 µg/ml streptomycin sulfate at 37°C in a humidified atmosphere of 10% CO_2. After 24 h, transfections are performed with Lipofectamine (Life Technologies, Gaithersburg, MD). For transactivation experiments, transfection mixes are used containing 1 µg receptor expression vector, and 1 µg pCH110 (Pharmacia, Piscataway, NJ)

as an internal control and, for binding studies 20 µg receptor expression vector.

Binding Assay

Transfected cells are grown for 48 h after transfection with the receptor expression vector. Receptor preparation is performed according to Tilley et al. (1989). Cell lysates containing receptor are prepared in TEGM (10 mM Tris-HCl, pH 7.2; 1 mM EDTA; 10% glycerol; 7 µl/100 ml β-mercaptoethanol; 10 mM Na molybdate; 1 mM dithiothreitol; 5 µg/ml aprotinin; 2 µg/ml leupeptin; 2 mg/ml benzamide; and 0.5 mM phenylmethylsulfonylfluoride). Plates are placed on ice, rinsed with TEG (10 mM Tris-HCl, pH 7.2; 50 mM EDTA; and 10% glycerol), and scraped into 0.5 ml TEGM. The material is pooled, frozen in liquid nitrogen to lyse the cells, and thawed on ice. The lysate is centrifuged at 22,000 *g* for 20 min at 4°C to remove the debris and stored frozen (–80°C) until use. For each assay, an aliquot of receptor-containing lysate (0.1–0.25 mg protein) is incubated with 10 nM ditritiated AD-5075 (21 Ci/mmol) with or without test compound for ~16 h at 4°C in TEGM (300 µl final volume). Unbound ligand is removed by incubation on ice for ~10 min after the addition of 200 µl dextran/gelatin-coated charcoal. After centrifugation at 3000 rpm for 10 min at 4°C, 200-µl aliquots of supernate are counted in an liquid scintillation counter.

PPAR binding assays using gel filtration to separate the bound radioactivity ligand from the free ligand (Kliewer et al. 1997) have been replaced by the scintillation proximity assay (SPA) which increases the throughput of PPAR competition assays (Nichols et al. 1998, Elbrecht et al. 1999). In this technique the ligand binding domain is labeled with biotin and immobilized on streptavidin-modified scintillation proximity beads. When a potential radioligand of PPARγ, binds to the PPARγ ligand binding domain, light, which leads to a detectable signal, is emitted. Competition with a nonlabeled ligand avoids the binding of the radioligand to the PPARγ ligand binding domain and no signal is emitted. With this binding assay, there is no need to separate free radioligands from bound ligands, thus simplifying the process.

Su et al. (1999) described the use of a PPARγ-specific monoclonal antibody to demonstrate thiazolidinediones induced PPARγ receptor expression *in vitro.*

Transactivation Assay

After transfection, cells are incubated for 48 h in culture medium with or without increasing concentrations of test compounds. Cell lysates are produced using reporter lysis buffer (Promega Corp., Madison, WI). CAT activity is determined using radiolabeled butyryl CoA as substrate in a diffusion based assay. β-Galactosidase activity is determined according to Hollons and Yoshimura (1989).

Lipogenesis Assay

PPARγ plays an important role in the regulation of cell differentiation (Lowell 1999). Adipogenesis requires combined high levels of PPARγ and other transcription factors such as CAAT/enhancer binding protein (C/EBP) and adipocyte determination and differentiation-dependent factor 1/sterol regulatory binding protein (ADD-1/SREBP-1). PPARγ plays an essential role in the molecular control of adipogenesis. Ectopic expression of PPARγ induces adipocyte differentiation (Tontonoz et al. 1994), whereas in the absence of PPARγ adipocytes fail to develop (Lowell 1999). Adipocyte differentiation leads to expression of adipocyte-specific genes, such as aP2 (Tontonoz et al. 1994) or lipoproteinlipase (Schoonjans et al. 1996c) which are under the control of PPARγ. The lipogenesis assay, based on preadipocytes differentiation to adipocytes, where PPARγ plays an important role, has been used to select PPARγ agonists for *in vivo* studies. Henke et al. (1998) tested compounds for their ability to promote differentiation of C3H10T1/2 stem cells via measurement of glucose incorporation into total lipid of the cells.

Protease Digestion Assay

The protease digestion assay is performed according to the method of Allan at al (1992) with minor modifications. The plasmid pSG5-haPPARγ1 is used to synthesize ^{35}S-radiolabeled PPARγ1 in a coupled transcription/translation system. The transcription/translation reactions are subsequently aliquoted into 22.5-µl volumes, and 2.5 µl PBS with or without a thiazolidinethione are added. The mixtures are incubated for 20 min at 25°C, separated into 4.5-µl aliquots, and 0.5 µl distilled water or distilled water-solubilized trypsin are added. The protein digestions are allowed to proceed for 10 min at 25°C, then terminated by the addition of 20 µl denaturing gel loading buffer and boiling for 5 min. The products of the digestion are separated by electrophoresis through a 1.5-mm 12% polyacrylamide-SDS gel. After electrophoresis, the gels are fixed in 10% acetic acid-40% methanol for 30 min, treated in EN^{3}HANCE for an additional 30 min. and dried under vacuum for 2 h at 80°C. Autoradiography is then performed to visualize the radiolabeled digestion products.

EVALUATION

Binding Assays

For binding assays, competition curves are generated by incubation of 10 nM [^{3}H]AD-5075 with hamster PPARg1 produced by transient transfection of COS-1. The percentage of ligand bound after incubation in the presence of the indicated concentration of each unlabeled compound for 16 h is plotted.

Activation Assays

For activation assays of PPARg in COS-1 cells transiently cotransfected with pSG5-haPPARg1 and pPPRE-CAT, normalized CAT activity is plotted after incubation in the presence of the indicated concentration of each compound for 48 h.

Lipogenesis Assays

The lipogenic activity of PPAR agonists can be assessed by determining radioactive glucose uptake into the total lipids of cells. The amount of glucose incorporation into lipids in these cells provides a measure of cell differentiation. Moreover, the expression of adipocyte marker genes (aP2, lipoprotein lipase, leptin) and the accumulation of triglycerides in the cytoplasm confirmed by oil red O staining are other methods to evaluate the lipogenic activity of PPARγ agonists.

Protease Digestion Assay

For evaluation of the protease digestion assay, the partially protease-resistant conformation product of PPARγ is visualized by autoradiography on SDS-PAGE after incubation with the thiazolidinedione and increasing concentrations of trypsin.

MODIFICATIONS OF THE METHOD

Berger et al. (1999) reported distinct biological effects of PPARγ and PPARδ ligands.

Desvergne and Wahli (1999) reviewed nuclear control of metabolism by peroxisome proliferator-activated receptors.

Lin et al. (1999) reported a fluorescence-based method for investigating the interactions of PPAR with ligands.

Brown et al. (2001) described identification of a subtype selective human PPARα agonist through parallel-array synthesis.

Xu et al. (2001) investigated the structural determinants of ligand binding selectivity between the peroxisome proliferator-activated receptors.

Lee et al. (2003) reviewed metabolic disorders and peroxisome proliferator-activated receptors.

Ram (2003) underlined the therapeutic significance of peroxisome proliferator-activated receptor modulators in diabetes.

Norris et al. (2003) found that muscle-specific PPARγ-deficient mice develop increased adiposity and insulin resistance but respond to thiazolidines.

Vikramadithyan et al. (2003) studied a peroxixome proliferators-activated receptor alpha (PPARα) and PPARγ agonist as body weight lowering, hypolipidemic and euglycemic agent. HEK 293 cells were used to conduct the reporter-based transactivation of PPARα and PPARγ.

Matsusue et al. (2003) found that liver-specific disruption of PPARγ in leptin-deficient mice improves fatty liver but aggravates diabetic phenotypes.

Stanley et al. (2003) studied subtype-specific effects of peroxisome proliferator-activated receptor ligands on co-repressor activity.

Wurch et al. (2002) described pharmacological analysis of wild-type α, γ and δ subtypes of the human peroxisome proliferator-activated receptor.

REFERENCES AND FURTHER READING

Allan GF, Xiaohua L, Tsai SY, Weigel NL, Edwards DP, Tsai MJ, O'Malley BW (1992) Hormone and antihormone induce distinct conformational changes which are central to steroid receptor activation. J Biol Chem 267:19513–19520

Berger A (2001) Resistin, a new hormone that links obesity with type 2 diabetes. Br Med J 322:193

Berger J, Bailey P, Biswas C, Cullinan CA, Dobber TW, Hayes NS, Saperstein R, Smith RG, Leibowitz MD (1996) Thiazolidinediones produce a conformational change in peroxisomal proliferator-activated receptor-γ: Binding and activation correlate with antidiabetic actions in *db/db* mice. Endocrinology 137:4189–4195

Berger J, Leibowitz MD, Doebber TW, Elbrecht A, Zhang B, Zhou G, Biswas C, Cullinan CA, Hayes NS, Li Y, Tanen M, Ventre J, Wu MS, Berger DG, Mosley R, Maequis R, Santini C, Sahoo SP, Tolman RL, Smith RG, Moller DE (1999) Novel peroxisome proliferator-activated receptor (PPAR)γ and PPARδ ligands produce distinct biological effects. J Biol Chem 274:6718–6726

Brown PJ, Stuart WL, Hurley KP, Lewis MC, Winegar DA, Wilson JG, Wilkison WO, Ittoop OR, Willson TM (2001) Identification of a subtype selective human PPARα agonist through parallel-array synthesis. Bioorgan Med Chem Lett 11:1225–1227

Brun RP, Kim JB, Hu E, Altiok S, Spiegelman BM (1996) Adipocyte differentiation: a transcriptional regulatory cascade. Curr Opin Cell Biol 8:826–832

Choi KC, Ryu OH, Lee KW, Kim HY, Seo JA, Kim SG, Kim NH, Choi DS, Baik SH, Choi KM (2005) Effect of PPAR-alpha and -gamma agonist on the expression of visfatin, adiponectin, and TNF-alpha in visceral fat of OLETF rats. Biochem Biophys Res Commun. 336:747–53

De Vos P, Lefebre AM, Miller SG, Guerre-Millo M, Wong K, Saladin R, Hamann LG, Briggs MR, Auwerx J (1996) Thiazolidinediones repress ob gene expression in rodents via activation of peroxisome proliferator-activated receptor-γ J Clin Invest 98:49

Desvergne B, Wahli W (1999) Peroxisome proliferator-activated receptors: nuclear control of metabolism. Endocr Rev 20:649–688

Devchand PR, Keller H, Peters JM, Vazquez M, Gonzalez FJ, Wahli E (1996) The PPARα-leucotriene B4 pathway to inflammation control. Nature 384:39–43

Do D, Alvarez J, Chiquette E, Chilton R (2006) The good fat hormone: adiponectin and cardiovascular disease. Curr Atheroscler Rep. 8:94–99

Elbrecht A, Chen Y, Adams A, Berger J, Griffin P, Klatt T, Zhang B, Menke J, Zhou G, Smith RG, Moller DE (1999) L-764406 is a partial agonist of human peroxisome proliferator-activated receptor γ. J Biol Chem 274:7913–7922

Forman BM, Totonoz P, Chen J, Brun RP, Spiegelman PE, Evans RM (1995) 15-Deoxy-$\Delta^{12,14}$-prostagandin J_2 is a ligand for the adipocyte determination factor PPARγ. Cell 83:803–812

Green S (1995) PPAR: A mediator of peroxisome proliferator action. Mutation Res 333:101–109

Henke BR, Blanchard SG, Brackeen MF, Brown KK, Cobb JE, Collins JL, Harrington WW, Hashim MA, Hull-Ryde EA, Kaldor I, Kliewer SA, Lake DSH, Leesnitzer LM, Lehmann JM, Lenhard JM, Orband-Miller LA, Miller JF, Mook RA, Noble SA, Oliver W, Parks DJ, Plunket KD, Szewczyk JR, Willson TM (1998) N-(2-Benzoylphenyl)-L-tyrosine PPARγ agonists. 1. Discovery of a novel series of potent antihyperglcemic and antihyperlipemic agents. J Med Chem 41:5020–5036

Hollons T, Yoshimura FK (1989) Variation in enzymatic transient gene expression assays. Anal Biochem 182:411–418

Keller H, Wahli W (1993) Peroxisome proliferator-activated receptors. A link between endocrinology and nutrition? Trends Endocrinol Metab 4:291–296

Kliewer SA, Sundseth SS, Jones SA, Brown PJ, Wisely GP, Knoble SS, Devchand P, Wahli W, Willson TM, Lenhard JM, Lehmann JM (1997) Fatty acids and eicosanoids regulate gene expression through direct interactions with peroxisome proliferator-activated receptors α and γ. Proc Natl Acad Sci USA 94:4318–4323

Lee CH, Olson P, Evans RM (2003) Minireview: Lipid metabolism, metabolic disorders and peroxisome proliferator-activated receptors. Endocrinology 144:2201–2207

Lehmann JM, Moore LB, Smith-Oliver TA, Wilkison WO, Willson TM, Kliewer SA (1995) An antidiabetic thiazolidinedione is a high affinity ligand for peroxisome proliferator-activated receptor-γ (PPAR-γ). J Biol Chem 270:121953–12956

Lemberger T, Desvergne B, Wahli W (1996) Peroxisome proliferator–activated receptors: A nuclear receptor signaling pathway in lipid physiology. Annu Rev Cell Dev Biol 12:335–363

Lin Q, Ruuska SE, Shaw NS, Dong D, Noy N (1999) Ligand selectivity of the peroxisome proliferator-activated receptor α. Biochemistry 38:185–190

Lowell BB (1999) Minireview. An essential regulator of adipogenesis and modulator of fat cell function: PPARγ. Cell 99:239–242

Matsusue K, Haluzik M, Lambert G, Yim SH, Gavrilova O, Ward JM, Brewer B, Reitman ML, Gonzalez FJ (2003) Liver-specific disruption of PPARγ in leptin-deficient mice improves fatty liver but aggravates diabetic phenotypes. J Clin Invest 111:737–747

Murakami K, Tobe K, Die T, Mochizuki T, Ohashi M, Akanuma Y, Yazaki Y, Kadowaki T (1998) A novel insulin sensitizer acts a coligand for peroxisome proliferator-activated receptor-α (PPAR-α) and PPAR-γ. Effect of PPAR-α activation on abnormal lipid metabolisms in liver of Zucker fatty rats. Diabetes 47:1841–1847

Murphy GJ, Holder JC (2000) PPAR-γ agonists: therapeutic role in diabetes, inflammation and cancer. Trends Pharmacol Sci 21:469–474

Nichols JS, Parks DJ, Consler TG, Blanchard SG (1998) Development of a scintillation proximity assay for peroxisome proliferators-activated γ ligand binding domain. Anal Biochem 257:112–119

Norris AW, Chen L, Fisher SJ, Szanto I, Ristow M, Jozsi AC, Hirshman MF, Rosen ED, Goodyear LJ, Gonzalez FJ, Spiegelman BM, Kahn RC (2003) Muscle-specific PPARγ-deficient mice develop increased adiposity and insulin resistance but respond to thiazolidines. J Clin Invest 112:608–618

Ram VJ (2003) Therapeutic significance of peroxisome proliferator-activated receptor modulators in diabetes. Drugs Today (Barc) 39:609–632

Reginato MJ, Bailey ST, Krakow SL, Minami C, Ishii S, Tanaka H, Lazar MA (1998) A potent antidiabetic thiazolidinedione with unique peroxisome proliferator-activated receptor γ-activating properties. J Biol Chem 273:32679–32684

Ribon V, Johnson JH, Camp HS, Saltiel AR (1998) Thiazolidinediones and insulin resistance: Peroxisome proliferator-activated receptor γ activation stimulates expression of the CAP gene. Proc Natl Acad Sci USA 95:14751–14756

Schoonjans K, Staels B, Auwerx J (1996a) The peroxisome proliferator activated receptors (PPARs) and their effects on lipid metabolism and adipocyte differentiation. Biochem Biophys Acta 1302:93–109

Schoonjans K, Staels B, Auwerx J (1996b) Role of the peroxisome proliferator activated receptor (PPAR) in mediating effects of fibrates and fatty acids on gene expression. J Lipid Res 37:907–925

Schoonjans K, Peinado-Onsurbe J, Lefebvre AM, Heyman RA, Briggs M, Deeb S, Staels B, Auwerx J (1996c) PPARα and PPARγ activators direct a distinct tissue-specific transcriptional response via the PPRE in the lipoprotein lipase gene. EMBO J 15:5336–5348

Schoonjans K, Martin G, Staels B, Auwerx J (1997) Peroxisome proliferator-activated receptors, orphans with ligands and functions. Curr Opin Lipidol 8:159–166

Stanley TB, Leesnitzer LM, Montana VG, Galardi CM, Lambert MH, Holt JA, Xu HE, Moore LB, Blanchard SG, Stimmel JB (2003) Subtype specific effects of peroxisome proliferator-activated receptor ligands on corepressor activity. Biochemistry 42:9278–9287

Steppan CM, Bailey ST, Bhat S, Brown EJ, Banerjee RR, Wright CM, Patel HR, Ahima RS, Lazar MA (2001) The hormone resistin links obesity to diabetes. Nature 409:307–312

Stumvoll M (1998) Troglitazone. Diab Stoffw 7:136–143

Su JL, Winegar DA, Wisely GB, Sigel CS, Hull-Ryde EA (1999) Use of PPAR gamma-specific monoclonal antibody to demonstrate thiazolidinediones induce PPAR gamma receptor expression *in vitro*. Hybridoma 18:273–280

Tilley WD, Marcelli M, Wilson JD, McPhaul MJ (1989) Characterization and expression of a cDNA encoding the human androgen receptor. Proc Natl Acad Sci USA 86:327–331

Tortonoz P, Hu E, Spiegelman BM (1994) Stimulation of adiposogenesis in fibroblasts by PPARγ2, a lipid-activated transcription factor. Cell 30:1147–1156

Tortonoz P, Hu E, Spiegelman BM (1995) Regulation of adipocyte gene expression and differentiation by peroxisome proliferator activated receptor γ. Curr Opin Genet

Devel 5:571–576Vázquez M, Silvesatre JS, Prous JR (2002) Experimental approaches to study PPARγ agonists as antidiabetic drugs. Methods Find Exp Clin Pharmacol 24:515–523
Vikramadithyan RK, Hiriyan J, Suresh J, Gershome C, Babu RK, Misra P, Rajagopalan, Chakrabarti R (2003) DRF 2655: a unique molecule tha reduced body weight and ameliorates abnormalities. Obesity Res 11:292–303
Walczak R, Tontonoz P (2002) PPARadigms and PPARadoxes: expanding roles for PPARγ in the control of lipid metabolism. J Lipid Res 43:177–186
Willson TM, Brown PJ, Sternbach DD, Henke BR (2000) The PPARs: From orphan receptors to drug discovery. J Med Chem 43:527–550
Wu Z, Xie Y, Morrison RF, Bucher NLR, Farmer SR (1998) PPAR-γ induces the insulin-dependent glucose transporter GLUT4 in the absence of C/EBP$_\alpha$ during the conversion of 3T3 fibroblasts into adipocytes. J Clin Invest 101:22–32
Wurch T, Junquero D, Delhon A, Pauwels PJ (2002) Pharmacological analysis of wild-type α, γ and δ subtypes of the human peroxisome proliferator-activated receptor. Naunyn-Schmiedebergs Arch Pharmacol 365:133–140
Xu HE, Lambert MH, Montana VG, Plunket KD, Moore LB, Collins JL, Oplinger JA, Kliewer SA, Gampe RT, McKee DD, Moore JT, Willson TM (2001) Structural determinants of ligand binding selectivity between the peroxisome proliferator-activated receptors. Proc Natl Acad Sci USA 98:13919–13924
Young PW, Buckle DR, Cantello BCC, Chapman H, Clapham JC, Coyle PJ, Haigh D, Hindley RM, Holder JC, Kallender H, Latter AJ, Lawrie KWM, Mossakowska D, Murphy GJ, Cox LR, Smith SA (1998) Identification of high-affinity binding sites for the insulin sensitizer Rosiglitazone (BRL-49653) in rodent and human adipocytes using a radioiodinated ligand for peroxisomal proliferator-activated receptor γ. J Pharmacol Exp Ther 284:751–759

K.3.6 Antidiabetic Effects of Liver X Receptor Agonists

PURPOSE AND RATIONALE

The nuclear receptors liver X receptor (LXR)α and LXRβ which are sensors of cholesterol metabolism and lipid biosynthesis are also regulators of inflammatory cytokines, suppressors of hepatic glucose production, and involved in different cell-signaling pathways. LXRα is a target gene of the peroxisome proliferators-activated receptor-γ, a target of drugs used in treating elevated levels of glucose seen in diabetes (Steffensen and Gustafsson 2004). Furthermore, insulin induces LXRα in hepatocytes, resulting in increased expression of lipogenic enzymes and suppression of key enzymes in gluconeogenesis, including phosphoenolpyruvate carboxykinase (PEPCK). Mukherjee et al. (1997) observed sensitization of diabetic and obese mice to insulin by retinoid X receptor agonists. Treatment of diabetic rodents with a LXRα agonist resulted in dramatic reduction of plasma glucose (Cao et al. 2003).

PROCEDURE

Oral Glucose Tolerance Study in fa/fa Rats

Obese insulin-resistant female Zucker (*fa/fa*) rats, 10 weeks of age, are orally gavaged for 9 days with either vehicle of the LXRα agonist. Eight h after the last dose, animals are fasted overnight and on the following morning subjected to an oral glucose tolerance test. Blood was obtained from the animals via the tail vein at time 0 and times 15, 30, 60, and 120 min after an oral glucose challenge (2.5 g of glucose/kg body weight). Plasma glucose and insulin levels are analyzed on all samples, and the results are expressed as the product of glucose AUC and insulin AUC.

Glucose Output with ZDF Rat Liver Slices

Precision-cut liver slices are generated from control, treated for 7 days with the LXRα agonist after an overnight fast. After preincubation and wash phases, the slices are incubated for 2 h at 29° C in Krebs-Henseleit bicarbonate buffer containing 40 mM mannitol in either the presence or absence of 10 mM lactate. Incubation media glucose levels are assessed at the 2-h time by subtracting the basal rate of glucose output per gram liver tissue from the substrate-stimulated rate of glucose output per gram of liver tissue.

Nuclear Run-On Experiment

A nuclear run-on experiment (Cao et al. 2002) is performed in the livers of diabetic *db/db* mice treated for 7 days with the LXRα agonist. Mouse liver nuclei are isolated (Schibler et al. 1983) and *in vivo* elongation reaction is performed (Goldman et al. 1985). The radiolabeled RNA is then subjected to slot blot (Mauvieux et al. 1998) in probes.

mRNA Measurement

Total RNAs are prepared from frozen tissue samples or cells with TRIzol reagent (Invitrogen) or Qiagen RNA prep kit. Mouse phosphoenolpyruvate carboxykinase and G6P mRNA are measured by RNase protection assay and quantified with a Molecular Dynamics Phaosphorimager Model 51. Rat mRNA is subjected to reverse transcription reactions using the Omniscript reverse transcriptase kit (Qiagen). The resulting cDNA is amplified using TaqMan 2 × PCR master mix (Applied Biosystems). The PCR products are detected in real time using an ABI-7900HT sequence detection system (Applied Biosystems). The rat PEPCK branched cDNA is analyzed according to Burris et al. (1999).

CRITICAL ASSESSMENT OF THE METHOD

Chisholm et al. (2003) reported that a LXR ligand induces severe lipogenesis in db/db diabetic mice.

MODIFICATIONS OF THE METHOD

Stulnig et al. (2002a, 2002b) concluded that LXR ligands mediate beneficial metabolic effects in insulin resistance syndromes including type 2 diabetes by interfering with peripheral glucocorticoid activation.

REFERENCES AND FURTHER READING

Burris TP, Pelton PD, Zhou L, Osborne MC, Cryan E, Demarest KT (1999) A novel method for analysis of nuclear receptor function at natural promoters: Peroxisome proliferators-activated receptor γ agonist actions on aP2 gene expression detected using branch DNA messenger RNA quantification. Mol Endocrinology 13:410–417

Cao G, Beyer TP, Yang XP, Schmidt RJ, Zhang Y, Bensch WR, Kauffman RF, Gao H, Ryan TP, Liang Y, Eacho PI, Jiang XC (2002) Phospholipid transfer protein is regulated by liver X receptors *in vivo*. J Biol Chem 277:39561–39565

Cao G, Yu L, Broderick CL, Oldham BA, Beyer TP, Schmidt RJ, Zhang Y, Stayrook KR, Suen C, Otto KA, Miller AR, Dai J, Foxworthy P, Gao H, Ryan TP, Jiang XC, Burris TP, Eacho PI, Etgen GJ (2003) Antidiabetic action of a liver X receptor agonist mediated by inhibition of hepatic gluconeogenesis. J Biol Chem 278:1131–1136

Chisholm JW, Hong J, Mills SA, Lawn RM (2003) The LXR ligand T0901317 induces severe lipogenesis in db/db diabetic mouse. J Lipid Res 44.2039–2048

Goldman MJ, Back DW, Goodridge AG (1985) Nutritional regulation of the synthesis and degradation of malic enzyme messenger RNA in duck liver. J Biol Chem 260:4404–4408

Mauvieux L, Canioni D, Hermine O, Valensi F, Radford-Weiss I, Azagury M, Magen M, Flandrin G, Brousse N, Varet B, Macintyre EA (1998) Quantitative RNA slot-blot analysis of CCND1/cyclin D1 expression in suspected mantle cell lymphomas. Leukemia 12:78–85

Mukherjee R, Davies PJ, Crombie DL, Bischoff ED, Cesaario RM, Jow L, Hamann LG, Boem MF, Mondon CE, Nadzan AM, Paterniti JR, Heyman RA (1997) Sensitization of diabetic and obese mice to insulin by retinoid X receptor agonists. Nature 386:407–410

Schibler U, Hagenbuchle O, Wellauer PK, Pittet AC (1983) Two promoters of different strength control the transcription of the mouse α-amylase gene Amy-1a in the parotid gland and the liver. Cell 32:501–508

Steffensen KR, Gustafsson JÅ (2004) Putative metabolic effects of the liver X receptor (LXR) Diabetes 53 (Suppl.1):S36-S42

Stulnig TM, Oppermann U, Steffensen KR, Schuster GU, Gustafsson JÅ (2002a) Liver X receptors downregulate 11β-hydroxysteroid dehydrogenase type 1 expression and activity Diabetes 51:2426–2433

Stulnig TM, Steffensen KR, Gao H, Reimers M, Dahlman-Wright K, Schuster GU, Gustafsson JÅ (2002b) Novel roles of liver X receptors exposed by gene expression profiling in liver and adipose tissue. Mol Pharmacol 62:1299–1305

K.4
Measurement of Insulin and Other Glucose-Regulating Peptide Hormones

K.4.1
Radioimmunoassays for Insulin, Glucagon and Somatostatin

PURPOSE AND RATIONALE

Insulin activity is an important laboratory parameter in the clinical evaluation of several diseases such as diabetes mellitus types I and II, states of impaired glucose tolerance, and insulin-producing tumors (insulinomas), where the insulin secretion released from pancreas β-cells is altered.

The first description of an immunoassay of endogenous plasma insulin in man has been given by Yalow and Berson (1959, 1960). Yalow and coworkers (1960) provided evidence that the bioassays hitherto being used (isolated rat diaphragm, epididymal fat pad tissue) measure insulin-like activity but not true insulin levels in blood. Since that time, the method has been used and modified by many investigators, e. g., Grodsky and Forsham (1960), Morgan and Lazarow (1963), Hales and Randle (1963), Melani and coworkers (1965, 1967), Wright and coworkers 1968. Survey on the radioimmunoassay of insulin have been given by Ditschuneit and Faulhaber (1975), Freedlender and coworkers (1984).The introduction of radioimmunoassay (RIA) by Berson and Yalow (1959) provided a novel method for measuring insulin in plasma and serum. In order to improve reliability and practicability, various technologies have appeared in the field of immunoassays. Variety is seen in the choice of labels (radioactive, enzymatic, fluorescent, etc.), separation methods (precipitation of antigen-antibody complexes, coated solid-phase antibody technology, etc.), detection methods (spectrophotometry, fluorimetry, amperometry, potentiometry, and calorimetry), and principles such as the competitive or noncompetitive immunoassay. These immunoassay techniques have become important analytical methods in clinical chemistry laboratories for the selective detection of drugs or proteins as well as hormones such as insulin at trace levels.

PROCEDURES

Immunization

Semisynthetic or biosynthetic human insulin is used as immunogen and as standard. Formerly, porcine insulin has been used since Yalow and Berson (1960) and subsequently many other authors have shown that

antisera raised against porcine insulin react identically with human and porcine insulin. Guinea pigs weighing 350–450 g are injected subcutaneously with 0.4 ml of an emulsion of 5 mg human insulin dissolved in 1.0 ml 0.01 N HCl and 3.0 ml complete Freund's adjuvant (Difco Laboratories). For boostering, 0.2 ml of an identically prepared emulsion is injected in monthly intervals. Fourteen days after the third booster injection, the animals are slightly anesthetized and 8–10 ml blood are withdrawn by cardiac puncture. Boosting is continued at monthly intervals and the animals are bled 2 weeks following each booster injection.

The optimal antiserum titer for use in the radioimmunoassay is determined using conditions identical to those employed in routine immunoassays. The percentage binding of 1 µU ^{125}I insulin is determined for dilutions of antisera ranging from 10^3 to 10^6 fold. The steepness of the antisera dilution curve is a measure of the affinity of the antiserum and therefore the potential sensitivity of the radioimmunoassay. Antisera with the steepest slopes, but not necessarily the highest titer, are selected for further study. The selected antisera dilutions are then run in an immunoassay using a full range of standards. A reduction in the percent ^{125}I-insulin bound to antibody from 50% (in the absence of unlabeled insulin) to 45% (in the presence of unlabeled insulin) (B/Bo = 0.9) is a reasonable measure of assay sensitivity.

Assay

The antibody-bound ^{125}I-insulin prepared as described above can be separated from free ^{125}I-insulin in various ways, such as by paper electrophoresis, as originally described by Yalow and Berson (1960), or by a two-antibody system, as described by Morgan and Lazarow (1963), Starr and coworkers (1979). In this method, the soluble insulin-anti-insulin complex is precipitated by an anti-guinea pig serum antibody. The following procedure is recommended (Freedlender et al. 1984):

- A buffer is prepared from a solution of 8.25 g boric acid and 2.70 g NaOH dissolved in 1 l water. After dissolving 5.0 g of purified bovine serum albumin (BSA), pH is adjusted with concentrated HCl to 8.0.
- In disposable plastic tubes, 10 × 75 mm, the following volumes are added:
  - 100 µl serum or standard
  - 900 µl buffer
  - 100 µl 1 mU ^{125}I-insulin in assay buffer
  - 100 µl guinea pig anti-insulin antiserum diluted in assay buffer (at a concentration to bind 50% of the ^{125}I-insulin in the absence of unlabeled hormone)
- The mixture is incubated at 4°C for 72 h. Then, the following solutions are added:
  - 100 µl normal guinea pig serum diluted 1:400 in the assay buffer
  - 100 µl rabbit anti-guinea pig globulin serum diluted in assay buffer
- The mixture is again incubated at 4°C for 72 h and then centrifuged (2,000 × *g*, 20 min, 4°C). The supernatant is decanted and radioactivity counted in the precipitate for 5 min.

EVALUATION

Counts in the nonspecific binding tubes are subtracted from counts in all other tubes. Data are linearized using an unweighted logit-log transformation (Rodbard and Frazier 1975). Micro-units insulin in a logarithmic scale are plotted against the ratio B/Bo ^{125}I-insulin on a logit scale. The range of B/Bo between 0.4 and 0.9 is the most suitable for determination of insulin concentration in plasma.

CRITICAL ASSESSMENT OF THE METHOD

The immunoassay of insulin as described by Yalow and Berson (1960) has been a break-through for many immunological assays of peptide hormones and other drugs. At present, not only guinea pig anti-insulin antisera, but also complete RIA kits are available from a number of commercial firms.

MODIFICATIONS OF THE METHOD

Cam and McNeill (1996) published a sensitive radioimmunoassay optimized for reproducible measurement of rat plasma insulin. Relatively small volumes (25 µl) of plasma from control, diabetic, and fasted rats can be assayed reproducibly with charcoal in the final separation step.

The hormones, insulin, glucagon and somatostatin are determined radioimmunologically: insulin with the RIAgnost-kit and rat insulin as standard; glucagon with a rabbit antibody, ^{125}I-glucagon as tracer, and polyethylene glycol as precipitant; somatostatin with a rabbit antibody, ^{125}I-tyrosyl-somatostatin as tracer and charcoal dextran for separation of free and bound hormone. At least 3 experiments per concentration are performed. The values of each collection period of 1 min are averaged and plotted *vs* time. The effects of the test compound (increase or decrease of the secreted hormones) are compared with the control periods and the effect of elevated glucose.

K.4.2 Bioassay for Glucagon

PURPOSE AND RATIONALE

Glucagon is a 29-amino-acid, single-chain polypeptide which is secreted by the α-cells in the islets of Langerhans. It is synthesized from preproglucagon, a 180-amino-acid precursor (Bell et al. 1983). Proglucagon is processed in islet and intestinal cell lines (Tucker et al. 1996). Glucagon interacts with a 60-kDa glycoprotein receptor on the plasma membrane of target cells (Sheetz and Tager 1988).

A biological assay of glucagon is described in the British Pharmacopoeia 1988. The potency of glucagon is estimated by comparing its hyperglycemic activity with that of the standard preparation of glucagon using the rabbit blood sugar assay as performed for insulin determinations.

PROCEDURE

Rabbits of either sex, weighing 1.8 to 2.8 kg are maintained under uniform conditions and an adequate uniform diet for at least one week. Forty-eight hours before the beginning of the test, each rabbit is injected with 1 ml of cortisone acetate injection. The animals are deprived of food, but not water, from 16 h before each test day until the withdrawal of the last blood sample on that day. The rabbits are randomly distributed into 4 groups of at least 6 animals.

The standard preparation to be used is the 1st International Standard for Glucagon, porcine, established in 1973, consisting of freeze-dried porcine glucagon with lactose and sodium chloride (supplied in ampoules containing 1.49 Units), or another suitable preparation the potency of which has been determined in relation to the International Standard.

The entire contents of one ampoule of the standard preparation are reconstituted with 2 ml of saline solution, acidified to pH 3.0 with hydrochloric acid and diluted with the same solvent to a convenient concentration, for example 100 milliUnits per ml. Two dilutions are made containing 24 and 6 milliUnits per ml, respectively, and at the same time two dilutions are made of the preparation being examined. The rabbits are injected subcutaneously with doses of 1 ml of each of the four solutions, giving the doses in random order following a twin cross-over design on two consecutive days at the same time each day. At 20 and 60 min after injection, a blood sample is taken from a marginal ear vein of each rabbit. Blood glucose concentrations are determined using a suitable method, such as the glucose-oxidase procedure.

EVALUATION

The result of the assay is calculated by standard statistical methods using the means of the two blood glucose levels found for each rabbit.

MODIFICATIONS OF THE METHOD

Glucagon can be determined by radioimmunoassay (Unger 1959, Harris et al. 1978, von Schenk 1984). Commercial kits are available.

REFERENCES AND FURTHER READING

Bell GI, Sanchez-Pescador R, Laybourn PJ, Najarian RC (1983) Exon duplication and divergence in the human preproglucagon gene. Nature 304:368–371

Biological assay of glucagon. British Pharmacopoeia 1988, Vol II, London, Her Majesty's Stationary Office, pp A70–A171

Cam MC, McNeill JH (1996) A sensitive radioimmunoassay optimized for reproducible measurement of rat plasma insulin. J Pharmacol Toxicol Meth 35:111–119

Ditschuneit H, Faulhaber JD (1975) Radioimmunoassay of insulin. In: Hasselblatt A, v. Bruchhausen F (eds) Insulin, Part 2, Handbook of Experimental Pharmacology, Vol 32/2, Springer-Verlag, Berlin Heidelberg New York, pp 655–670

Freedlender AE, Vandenhoff GE, Macleod MS, Malcolm RR (1984) Radioimmunoassay of insulin. In: Larner J, Pohl SL (eds) Methods in Diabetes Research, Vol I: Laboratory Methods, Part B. Wiley, New York, pp 295–305

Grodsky GM, Forsham PH (1960) An immunochemical assay of total extractable insulin in man. J Clin Invest 39:1070–1079

Hales CN, Randle PJ (1963) Immunoassay of insulin with insulin-antibody precipitate. Biochem J 88:137–146

Harris V, Faloona GR, Unger RH (1978) Glucagon. In: Jaffe BM, Behrman HR (eds) Methods of Hormone Radioimmunoassay. Second edition, Academic Press New York, San Francisco, London, pp 643–656

Melani F, Ditschuneit H, Bartelt KM, Friedrich H, Pfeiffer EF (1965) Über die radioimmunologische Bestimmung von Insulin im Blut. Klin Wschr 43:1000–1007

Melani F, Lawecki J, Bartelt KM, Pfeiffer EF (1967) Immunologisch nachweisbares Insulin (IMI) bei Stoffwechselgesunden, Fettsüchtigen und adipösen Diabetikern nach intravenöser Gabe von Glukose, Tolbutamid und Glucagon. Diabetologia 3:422–426

Morgan CR, Lazarow A (1963) Immunoassay of insulin: Two antibody system. Plasma insulin levels of normal, subdiabetic and diabetic rats. Diabetes 12:115–126

Rodbard D, Frazier GR (1975) Statistical analysis of radioligand assay data. Methods Enzymol 37B:3–22

Sheetz MJ, Tager HS (1988) Receptor-linked proteolysis of membrane-bound glucagon yields a membrane associated hormone fragment. J Biol Chem 263:8509–8514

Starr JI, Horwitz DL, Rubenstein AH, Mako ME (1979) Insulin, proinsulin and C-peptide. In: Jaffe BM, Behrman HR (eds) Methods of Hormone Radioimmunoassay, 2nd ed., Academic Press, New York, pp 613–642

Tucker JD, Dhanvantari S, Brubaker PL (1996) Proglucagon processing in islet and intestinal cell lines. Regul Pept 62:29–35

Unger RH, Eisentraut AM, McCall MS, Keller S, Lanz HC, Madison LL (1959) Glucagon antibodies and their use for immunoassay for glucagon. Proc Soc Exp Biol Med 102:621–623

von Schenk H (1984) Radioimmunoassay of glucagon. In: Larner J, Pohl SL (eds) Methods in Diabetes Research,

Vol I: Laboratory Methods, Part A. Wiley, New York, pp 327–345
Wright PH, Makulu DR, Malaisse WJ, Roberts NM, Yu PL (1968) A method for the immunoassay of insulin. Diabetes 17:537–546
Yalow R, Black H, Villazon M, Berson SA (1960) Comparison of plasma insulin levels following administration of tolbutamide and glucose. Diabetes 9:356–362
Yalow RS, Berson SA (1959) Assay of plasma insulin in human subjects by immunological methods. Nature (London) 21:1648–1649
Yalow RS, Berson SA (1960) Immunoassay of endogenous plasma insulin in man. J Clin Invest 39:1157–1175

K.4.3 Receptor Binding and In Vitro Activity of Glucagon

PURPOSE AND RATIONALE

The binding of glucagon to its receptor is assayed with rat liver plasma membranes (Neville 1968, Pohl et al. 1971, Goldstein and Blecher 1976). Displacement of ^{125}I-labeled glucagon is measured for synthetic glucagon analogs in comparison to natural glucagon. Cyclic AMP formation as the first step in glucagon action on liver is measured as a bioassay in liver plasma membranes.

PROCEDURE

Preparation of Membranes

Male Sprague-Dawley rats weighing 160–200 g are decapitated and the livers rapidly removed and trimmed of fat and connective tissue. The pooled livers are placed on a pre-chilled glass plate and chopped finely with a stainless steel blade. Ten-gram portions of the mincate are suspended in 35 ml of ice-cold 1 mM $NaHCO_3$ and homogenized in a loose fitting Dounce homogenizer. Two homogenates are combined, brought to 500 ml with ice-cold medium, stirred magnetically for 5 min, and finally filtered once through two layers of cheesecloth. The filtrate is centrifuged ($1{,}500 \times g$, 10 min). Supernatant fluid is aspirated to waste using a serum pipette attached to a water pump. Homogenizations and centrifugations are continued until all of the tissue has been processed. The pooled pellets are again homogenized. The suspension is adjusted to $44 \pm 0.1\%$ (wt/wt) sucrose solution by the addition of 70% sucrose solution. Sucrose gradients are prepared in 1×3.5-in. tubes by pipetting 26 ml of the tissue suspension followed by an overlay of 13 ml of $42.3 \pm 0.1\%$ sucrose. Centrifugation is carried out ($95{,}100 \times g$, 2 h). The float containing the plasma membranes can be removed by pinching the tube slightly above the float, then lifting off the float with a spoon-shaped Teflon-coated spatula. These floats are transferred to a pre-weighed plastic centrifuge tube (50 ml), and the well-mixed suspension centrifuged at ($40{,}000 \times g$, 30 min). Following aspiration of the supernatant to waste, the tubes are reweighed in order to estimate the yield of plasma membranes. After addition of an equal volume of medium, the pellet is aspirated repeatedly through a 20-gauge needle fitted to a syringe. The plasma membrane suspension is distributed in 0.2 or 1.0 ml aliquots to screwcap plastic vessels for storage in liquid nitrogen.

Radioiodination of Glucagon

Three nmol glucagon are allowed to react with a 1.0 nmol sample of carrier-free $Na^{125}I$ (2.0 mC) in the presence of 1.5 nmol chloramine-T, added at a regular interval of 30 s (0.5 nmol each time). Reaction is terminated by addition of 0.5% sodium metabisulfite solution (Hagopian and Tager 1983). By chromatographic purification (Jørgensen and Larsen 1972), fractions of 2 ml are collected, and the monoiodinated glucagon as determined by reverse phase HPLC is stored at –20°C for receptor binding assays.

Receptor Binding

Membrane suspensions adjusted to 50 µg protein in 400 µl of Tris-HCl buffer (25 mM, pH 7.5, with 1% BSA) are incubated for 10 min with 50 µl peptide solution (Tris-HCl buffer) and 50 µl of [^{125}I]glucagon (10^6 cpm, 25 fmol). The samples are then filtered through Oxoid filters and washed three times with 1 ml of Tris-HCl buffer. The radioactivity retained in the filters is counted by a γ-counter.

Adenylate Cyclase Assay

The assay is carried out with a membrane suspension containing 25–30 µg protein in a volume of 0.1 ml of 25 mM Tris/HCl (pH 7.5) containing 1% BSA, 1 mM ATP with 4×10^6 cpm [α^{32}P]ATP, 5 mM $MgCl_2$, 1 nM cAMP containing 10,000 cpm of [^{3}H]cAMP, 10 mM GTP, 20 mM phosphocreatine and 0.72 mg/ml creatinine phosphokinase (100 U/ml). Assays are run in triplicate.

EVALUATION

Results are expressed as the percentage inhibition of [^{125}I]glucagon specific binding for receptor binding assays. For adenylate cyclase assays the results are expressed as percent potency relative to the maximal stimulation by glucagon which is defined as 100%.

MODIFICATIONS OF THE METHOD

Azizeh and coworkers (1995, 1997) synthesized and tested a glucagon antagonist and multiple replacement

analogs of glucagon by adenylate cyclase assay according to Lin and coworkers (1975) and receptor binding assay according to Wright and Rodbell (1979).

REFERENCES AND FURTHER READING

Azizeh BY, Van Tine BA, Sturm NS, Hutzler AM, David C, Trivedi D, Hruby VJ (1995) [des His^1, des Phe^6, Glu^9]-glucagon amide: a newly designed "pure" glucagon antagonist. Bioorg Med Chem Lett 5:1849–1852

Azizeh BY, Ahn J-M, Caspari R, Shenderovich MD, Trivedi D, Hruby VJ (1997) The role of phenylalanine in position 6 in glucagon's mechanism of action: multiple replacement analogs of glucagon. J Med Chem 40:2555–2562

Goldstein St, Blecher M (1976) Isolation of glucagon receptor proteins from rat liver plasma membranes. In: Blecher M (ed) Methods in Receptor Research, Part I, Marcel Decker, Inc., New York and Basel, pp 119–142

Hagopian WA, Tager HS (1983) Receptor binding and cell-mediated metabolism of [^{125}I]monoiodoglucagon by isolated hepatocytes. J Biol Chem 259:8986–8993

Jørgensen KH, Larsen UD (1972) Purification of ^{125}I-glucagon by ion exchange chromatography. Horm Metab Res 4:223–224

Lin MC, Wright DE, Hruby VJ, Rodbell M (1975) Structure-function relationships in glucagon: Properties of highly purified des-His^1-, monoiodo-, and [des-Asn^{28}, Thr^{29}](homoserine lactone^{27})-glucagon. Biochemistry 14:1559–1563

Neville DM (1968) Isolation of an organ specific protein antigen from cell-surface membrane of rat liver. Biochim Biophys Acta 154:540–552

Pohl SL, Birnbaumer L, Rodbell M (1971) The glucagon-sensitive adenyl cyclase system in plasma membranes of rat liver. J Biol Chem 246:1849–1856

Wright DE, Rodbell M (1979) $Glucagon_{1-6}$ binds to the glucagon receptor and activates hepatic adenylate cyclase. J Biol Chem 254:268–269

K.4.4 Glucagon-Like Peptide I

PURPOSE AND RATIONALE

Several intestinal peptides have been described to have insulinotropic or incretin activity, e. g. GIP (gastric inhibitory peptide, glucose-dependent insulin releasing peptide) (Creutzfeldt 1985, Baer and Dupré 1989, Volz et al. 1995). More recently, glucagon-like peptide-1 (7–37) or the (7–36)amide is described as a new incretin (Kreymann et al. 1987, Fehmann et al. 1989, 1990, 1991a, 1992, 1995, Holz et al. 1993). The insulinotropic activity has been confirmed in diabetic and non diabetic subjects (Gutniak 1992, Nathan et al. 1992, Nauck et al. 1993, Ørskov 1993). The insulin stimulatory effect of glucagon-like peptide-1(7–36)amide is glucose-dependent (Göke et al. 1993a). The peptide does not only stimulate insulin release but also inhibits glucagon secretion (Komatsu et al. 1989). Cloning and functional expression of the rat (Thorens 1992) and human (Dillon et al. 1993) glucagon-like peptide1 (GLP-1) receptor has been achieved. The sequence of glucagon-like peptide-1 (7–36)amide is completely conserved in all mammalian species studied, implying that it plays a critical physiological role. Intracerebroventricular administration of GLP-1 powerfully inhibits feeding in fasted rats, which is blocked by the GLP-1-receptor antagonist exendin(9–39) (Turton et al. 1996; Meurer et al. 1999).

Peptides isolated from reptile venoms, such as exendin-4, were found to have similar activity as glucagon-like peptide-1(7–36)amide (Göke et al. 1993b; Adelhorst et al. 1994; Schepp et al. 1994). Gedulin et al. (2005) found that exendin-4 improves insulin sensitivity and β-cell mass in insulin-resistant obese *fa/fa* Zucker rats independent of glycemia and body weight. Shechter et al. (2003) described [2-sulfo-9-fluorenylmethoxycarbony]$_3$-exendin-4 as a long-acting glucose-lowering prodrug. Analogs and antagonists of glucagon-like peptide-1(7–36)-amide have been synthesized and evaluated in pharmacological experiments (Watanabe et al. 1994, Hjorth and Schwartz 1996, Montrose-Rafizadeh et al. 1997).

Besides insulin release from perfused pancreas (see K.6.6), the receptor binding according to Göke and Conlon (1988) on rat insulinoma-derived cells (RINm5F cells), the cAMP formation and the insulin release were studied (Göke et al. 1989a, b).

PROCEDURE

Binding Studies with RINm5F Cells

The RINm5F cell line is derived from a radiation-induced insulin-producing rat tumor (Gazdar et al. 1980). The RINm5F cells are grown in plastic culture bottles (Praz et al. 1983). They are detached from the surface of the bottles before the experiment using phosphate-buffered saline (PBS, 136 mM NaCl, 2.7 mM KCl, 8.1 mM Na_2HPO_4, 1.5 mM KH_2PO_4, pH 7.3) containing 0.7 mM EDTA, and centrifuged ($100 \times g$, 5 min). The pelleted cells are resuspended in an incubation buffer (2.5 mM Tris-HCl, 120 mM NaCl, 1.2 mM $MgSO_4$, 1.5 mM KCl, and 15 mM CH_3COONa, pH 7.4) containing 1% human serum albumin, 0.1% bacitracin and 1 mM EDTA. Approximately 3×10^6 cells/tube are incubated for 5 min at 37°C, followed by the addition of unlabeled peptide (final concentration range from 10 pmol to 1 mmol) and radiolabeled tracer (approximately 40,000 c.p.m.). Iodination of the glucagon-like peptide-1(7–36)amide is carried out using the lactoperoxidase method. The total volume of incubation is 0.3 ml. After incubation for 60 min, aliquots (200 µl) of the cell sus-

pensions are centrifuged (11,500 × *g*, 2 min) through an oil layer (dibutylphthalate/dinonylphthalate, 10/4, v/v). Cell-surface associated radioactivity in the pellet is counted using a γ-counter (e. g. Gamma 5500, Beckman).

Determination of cAMP Production in RINm5F Cells

Approximately 1×10^6 cells in 0.45 ml buffer (113 mM NaCl, 4.7 mM KCl, 1.2 mM KH_2PO_4, 10 mM HEPES, 2.5 mM $CaCl_2$ and 1.2 mM $MgSO_4$, pH 7.4) containing 1% human serum albumin are pre-incubated for 10 min at 37°C, and then incubated for 10 min after the addition of 2 µl 3-isobutyl-1-methylxanthine (IBMX, 50 mM) in order to prevent the breakdown of cAMP. The reaction is then started by the addition of 50 µl of a peptide solution dissolved in the above buffer (final concentration range from 10 pM to 1 µM). After incubation for 10 min at 37°C, the reaction is stopped by the addition of 200 µl 12% trichloroacetic acid (TCA). The reaction mixture is sonicated for 30 s at 25 W (e. g., Heat system, Ultrasonics) and centrifuged (11,500 × *g*, 2 min). 25 µl of 1 M HCl is added to 0.5 ml supernatant. TCA dissolved in the supernatant is removed by diethyl ether (3 × 1 ml) and the resulting supernatant is stored at –40°C until cAMP assays being performed by use of a RIA kit.

REFERENCES AND FURTHER READING

Adelhorst K, Hedegaard BB, Knudsen LB, Kirk O (1994) Structure-activity studies of glucagon-like peptide-1. J Biol Chem 289:6275–6278

Baer AR, Dupré J (1989) Suppression of insulin binding by prolonged enteral or parenteral nutrient infusion in the rat: role of gastric inhibitory polypeptide. Can J Physiol Pharmacol 67:1105–1109

Creutzfeldt W, Ebert R (1985) New developments in the incretin concept. Diabetologia 28:565–573 Dillon JS, Tanizawa Y, Wheeler MB, Leng XH, Ligon BB, Rabin DU, Yoo-Warren H, Permutt MA, Boyd III AE (1993) Cloning and functional expression of the human glucagon-like peptide 1 (GLP-1) receptor. Endocrinology 133:1907–1910

Dillon JS, Tanizawa Y, Wheeler MB, Leng XH, Ligon BB, Rabin DU, Yoo-Warren H, Permutt MA, Boyd III AE (1993) Cloning and functional expression of the human glucagon-like peptide 1 (GLP-1) receptor. Endocrinology 133:1907–1910

Fehmann HC, Habener JF (1991a) Homologous desensitization of the insulinotropic glucagon-like peptide-1(7–37) receptor in insulinoma (HIT-T15) cells. Endocrinology 128:2880–2888

Fehmann HC, Habener JF (1991b) Functional receptors for the insulinotropic hormone glucagon-like peptide-1(7–37) on a somatostatin secreting cell line. FEBS Lett 279:335–340

Fehmann HC, Habener JF (1992) Insulinotropic hormone glucagon-like peptide-1(7–37) stimulation of proinsulin gene expression and proinsulin biosynthesis in insulinoma βTC-1 cells. Endocrinology 130:159–166

Fehmann HC, Göke B, Göke R,Trautmann ME, Arnold R (1989) Synergistic effect of glucagon-like peptide-1 (7–36) amide and glucose-dependent insulin-releasing polypeptide on the endocrine rat pancreas. FEBS Lett 252:109–112

Fehmann HC, Göke B, Weber V, Göke R, Trautmann ME, Richter G, Arnold R (1990) Interaction of glucagon-like peptide-1 (7–36)amide and cholecystokinin-8 in the endocrine and exocrine rat pancreas. Pancreas 5:361–365

Fehmann HC, Göke R, Göke B, Bächle R, Wagner B, Arnold R (1991a) Priming effect of glucagon-like peptide-1 (7–36) amide, glucose-dependent insulinotropic polypeptide and cholecystokinin-8 at the isolated perfused rat pancreas. Biochem Biophys Acta 1091:356–363

Fehmann HC, Göke R, Eissele R, Arnold R (1991b) Helodermin and islet hormone release in isolated rat pancreas. Int J Pancreatol 8:289–303

Fehmann HC, Göke R, Göke B (1992) Glucagon-like peptide-1(7–37)/(7–36)amide is a new incretin. Mol Cell Endocrin 85:C39–C44

Fehmann HC, Göke R, Göke B (1995) Cell and molecular biology of the incretin hormones glucagon-like peptide-I and glucose-dependent insulin releasing polypeptide. Endocr Rev 16:390–410

Gazdar AF, Chick WL, Oie HK, Sims HL, King DL, Weir GC, Lauris V (1980) Continuous, clonal insulin- and somatostatin-secreting cell line established from a transplantable rat islet cell tumor. Proc Natl Acad Sci, USA 77:3519–3523

Gedulin BR. Nikoulina SE, Smith PA, Gedulin G, Nielsenn LL, Baron AD, Parkes DG, Young AA (2005) Exenatide (exendin-4) improves insulin sensitivity and β-cell mass in insulin-resistant obese *fa/fa* Zucker rats independent of glycemia and body weight. Endocrinology 146:2069–2076

Göke R, Conlon JM (1988) Receptors for glucagon-like peptide-1(7–36)amide on rat insulinoma-derived cells. J Endocrinol 116:357–362

Göke R, Fehmann HC, Richter G, Trautmann M, Göke B (1989a) Interaction of glucagon-like peptide-1(7–36)amide and somatostatin-14 in RINm5F cells and in the perfused rat pancreas. Pancreas 4:668–673

Göke R, Trautmann ME, Haus E, Richter G, Fehmann HC, Arnold R, Göke B (1989b) Signal transmission after GLP-1(7–36)amide binding in RINm5F cells. Am J Physiol 257 (Gastrointest Liver Physiol 20):G397–G401

Göke R, Oltmer B, Sheikh SP, Göke B (1992) Solubilization of active GLP-1(7–36)amide receptors from RINm5F plasma membranes. FEBS Lett 300:232–236

Göke R, Wagner B, Fehmann HC, Göke B (1993a) Glucose-dependency of the insulin stimulatory effect of glucagon-like peptide-1(7–36)amide on the rat pancreas. Res Exp Med 193:97–103

Göke R, Fehmann HC, Linn Th, Schmidt H, Krause M, Eng J, Göke B (1993b) Exendin-4 is a high potency agonist and truncated exendin-(9–39)-amide an antagonist at the glucagon-like peptide-1(7–36)amide receptor of insulin-secreting β-cells. J Biol Chem 268:19650–19655

Gutniak M, Ørskov C, Holst JJ, Ahrén B, Efendic S (1992) Antidiabetogenic effect of glucagon-like peptide-1(7–36)amide in normal subjects and patients with diabetes mellitus. New Engl J; ed 326:1316–1322

Hjorth SA, Schwartz TW (1996) Glucagon and GLP-1 receptors: lessons from chimeric ligands and receptors. Acta Physiol Scand 157:343–345

Holz GG, Kühtreiber WM, Habener JF (1993) Pancreatic beta-cells are rendered glucose-competent by the insulinotropic hormone glucagon-like peptide-1(7–37). Nature 361:362–365

Jehle PM, Jehle D, Fußgänger RD, Adler G (1995) Effects of glucagon-like peptide-1 (GLP-1) in RINm5F insulinoma cells. Exp Clin Endocrinol 103:31–36
Komatsu R, Matsuyama T, Namba M, Watanabe N, Itoh H, Kono N, Tarui S (1989) Glucagonostatic and insulinotropic action of glucagon-like peptide 1(7–36)-amide. Diabetes 38:902–905
Kreymann B, Williams G, Ghatei MA, Bloom SR (1987) Glucagon-like peptide-1 7–37: a physiological incretin in man. Lancet, Dec 1987:1300–1303
Lankat-Buttgereit B, Göke R, Fehmann HC, Richter G, Göke B (1994) Molecular cloning of a cDNA encoding for the GLP-1 receptor expressed in rat lung. Exp Clin Endocrinol 102:341–347
Meurer JA, Colca JR, Burton PS, Elhammer AP (1999) Properties of native and in vitro glycosylated forms of the glucagon-like peptide-1 receptor antagonist exendin(9–39). Metabolism 48:716–724
Montrose-Rafizadeh C, Yang H, Rodgers BD, Beday A, Pritchette LA, Eng J (1997) High potency antagonists of the pancreatic glucagon-like peptide-1 receptor. J Biol Chem 272:21201–21206
Nathan DM, Schreiber E, Fogel H, Mojsov S, Habener JF (1992) Insulinotropic action of glucagon-like peptide-1-(7–37) in diabetic and nondiabetic subjects. Diabetes Care 15:270–276
Nauck MA, Heimesaat MM, Ørskov C, Holst JJ, Ebert R, Creutzfeldt W (1993) Preserved incretin activity of glucagon-like peptide 1 [7–36 amide] but not of synthetic human gastric inhibitory peptide in patients with type-2 diabetes mellitus. J Clin Invest 91:301–307
Ørskov C, Wettergren A, Holst JJ (1993) Biological effects and metabolic rates of glucagonlike peptide-1 7–36 amide and glucagonlike peptide-1 7–37 in healthy subjects are indistinguishable. Diabetes 42:658–661
Praz GA, Halban PA, Wollheim CB, Blondel B, Strauss JA, Reynold AE (1983) Regulation of immunoreactive insulin release from a rat cell line (RINm5F) Biochem J 210:345–352
Schepp W, Schmidtler J, Riedel T, Dehne K, Schusdziarra V, Holst JJ, Eng J, Raufman JP, Classen M (1994) Exendin-4 and exendin-(9–39)NH_2: Agonist and antagonist, respectively, at the rat parietal cell receptor for glucagon-like peptide-1-(7–36)NH_2. Eur J Pharmacol Mol Pharmacol Sect 269:183–191
Schepp W, Dehne K, Riedel T, Schmidtler J, Schaffer K, Classen M (1996) Oxyntomodulin: A cAMP-dependent stimulus of rat parietal cell function via the receptor for glucagon-like peptide-1 (7–36)NH_2. Digestion 57:398–405
Shechter Y, Tsubery H, Fridkin M (2003) [2-Sulfo-9-fluorenylmethoxycarbony]$_3$-exendin-4 – a long-acting glucose-lowering prodrug. Biochem Biophys Res Commun 305:386–391
Thorens B (1992) Expression cloning of the pancreatic β cell receptor for the gluco-incretin hormone glucagon-like peptide 1. Proc Natl Acad Sci, USA 89:8641–8645
Turton MD, O'Shea D, Gunn I, Beak SA, Edwards CMB, Meeran K, Chol SJ, Taylor GM, Heath MM, Lambert PD, Wilding JPH, Smith DM, Ghatei MA, Herbert J, Bloom SR (1996) A role for glucagon-like peptide-1 in the central regulation of feeding. Nature 379:69–72
Valverde I, Merida E, Delgado E, Trapote MA, Villanueva-Penacarillo ML (1993) Presence and characterization of glucagon-like peptide-1(7–36)amide receptors in solubilized membranes of rat adipose tissue. Endocrinol 132:75–79
Van Delft J, Uttenthal LO, Hermida OG, Fontela T, Ghiglione M (1997) Identification of amidated forms of GLP-1 in rat tissues using a highly sensitive radioimmunoassay. Regul Pept 70:191–198
Volz A, Göke R, Lankat-Buttgereit B, Fehmann HC, Bode HP, Göke B (1995) Molecular cloning, functional expression, and signal transduction of the GIP-receptor cloned from a human insulinoma. FEBS Lett 373:23–29
Watanabe Y, Kawai K, Ohashi S, Yokota C, Suzuki S, Yamashita K (1994) Structure-activity of glucagon-like peptide-1(7–36)amide: insulinotropic activities in perfused rat pancreas, and receptor binding and cyclic AMP production in RINm5F cells. J Endocrinol 140:45–52

K.4.5 Insulin-Like Growth Factors

PURPOSE AND RATIONALE

Three different lines of research have led to the discovery of insulin-like growth factors (Froesch et al. 1985): Growth hormone does not stimulate growth processes by itself but induces factors, named sulfation factors or somatomedins, that mediate the message of growth hormone (Salmon and Daughaday 1957, Nevo 1982, Laron 1999). Pierson and Temin (1972) extracted factors from serum with multiplication-stimulating activity (MSA) for chicken fibroblasts in the cell culture and with non-suppressible insulin-like activity. Serum exerts insulin-like effects on insulin target tissues such as muscle and adipose tissues to a much greater extent than it can be expected on the basis of the insulin content in serum. The activity of factors other than insulin in the epididymal fat pad assay was proven by the persistence of serum insulin-like activity after pancreatectomy (Steinke et al. 1962). Since this activity could not be suppressed by insulin antibodies, the factors were called 'non-suppressible insulin-like activity' or NSILA.

They were finally identified as insulin-like growth factors I and II (Rinderknecht and Humbel 1978a, b) structurally related to insulin. These polypeptide hormones are present in serum in high concentrations but are bound to specific carrier proteins (Zapf et al. 1975). Most of IGF and also the IGF-binding protein are synthesized and secreted, but apparently not stored by the liver (Schwander et al. 1983, Sara and Hall 1990).

Insulin-like growth factor 1 (IGF-1) is a polypeptide of 70 amino acids, whose function of is more or less clarified (Cascieri et al. 1988, Moxley et al. 1990, Salamon et al. 1991, Schmitz et al. 1991, Vikman et al. 1989, Laron 1999). The metabolic activity of IGF-1 is regulated by at least 6 IGF-binding proteins, the most important being IGFBP-3. The effects of growth hormone on protein metabolism are mediated by IGF-1,

whereas these 2 hormones are antagonistic in their effects on insulin and some aspects of lipid metabolism. IGF-1 has been shown to improve glycemic control and to reduce insulin requirements in both IDDM and NIDDM (Simpson et al. 1998). One important clinical use is replacement therapy in primary IGF-1 deficiency, such as Laron syndrome, which is characterized by dwarfism due to primary GH resistance or insensitivity (Laron 1999). IGF-1 improves bone healing *in vivo* (Kobayashi et al. 1996). A truncated variant of human IGF-1 with the tripeptide Gly-Pro-Glu absent from the N-terminus, has been isolated from bovine colostrum, human brain and porcine uterus which is about 10-fold more potent than IGF-1 at stimulating hypertrophy and proliferation of cultured cells (Ballard et al. 1999).

The function of insulin-like growth factor II is less defined (Roth 1988). IGF-II has an insulin-like effect *in vitro* and *in vivo* (Shizume et al. 1996, Burvin et al. 1998). IGF-II, administered acutely, affects glucose homeostasis in a manner very similar to insulin, probably via the insulin receptors, although with significantly lower potency.

Two subtypes of IGF receptors exist which are different from the insulin receptor and different in their affinity for IGF I and IGF II (Rechler 1985; Verspohl et al. 1988). They belong to the insulin receptor family of receptor tyrosine kinases (Ullrich and Schlessinger 1990, Schlessinger and Ullrich 1992, Fantl et al. 1993). Although insulin and IGF bind with high affinity to their own specific receptors, each can also bind to the heterologous receptor with reduced binding affinity (DeMeyts 1994).

With recombinant DNA technology insulin analogs with modified amino acid sequence can be produced which may bind differently to the insulin and IGF receptor resulting in different biological activities (Drejer 1992, Schäffer 1993). It has been speculated whether the unexpected carcinogenic effect of an insulin analog (Dideriksen et al. 1992) is related to the mitogenic effect in mouse NIH 3T3 fibroblasts which express IGF receptors but not insulin receptors (Gammeltoft and Drejer 1991). Biosynthesis of 10 kDa and 7.5 kDa insulin-like growth factor II in a human rhabdomyosarcoma cell line has been described by Nielsen et al. (1993).

For new insulin analogs the kinetics of association and dissociation to the receptors should be studied and *in vivo* metabolic activity should be compared with insulin and IGF I.

The *in vivo* metabolic action of insulin-like growth factor I can be compared with insulin in adult rats using the following methods (Schmitz et al. 1991): Dose-dependence and time-dependence of blood sugar decrease after intravenous injection, antilipolytic effect (decrease of non-esterified fatty acids) after i.v. injection, stimulation of glucose disposal during euglycemic clamping after intravenous infusion. Furthermore, all other assays described for insulin can be applied. Gazzano-Santoro and coworkers (1998) described a cell-based potency assay for insulin-like growth factor-1.

PROCEDURE

Cells from the human cell line HU-3, established from the bone marrow of a patient with acute megakaryoblastic leukemia, are adapted to grow in the presence of human thrombopoietin. Removal of thrombopoietin results in decreased proliferation and rapid loss of viability. Cells are cultured in RPMI-1640 medium with 2% heat-inactivated human serum, 2 mM glutamine, 10 mM HEPES (pH 7.2) and 5 ng/ml thrombopoietin in culture flasks. They are grown in suspension at 37°C in a humidified 5% CO_2 incubator and are routinely subcultured every two or three days when densities reach $0.8–1.5 \times 10^6$ cells/ml.

The cell growth assay is performed under serum-free conditions in assay medium consisting of RPMI-1640 supplemented with 0.1% BSA, 10 mM HEPES (pH 7.2) and 50 µg/ml gentamycin. Cells are washed twice in the assay medium and resuspended at a density of 0.25×10^6 cells/ml. In a typical assay, 100 µl of a cell suspension (25,000 cells/well) and 100 µl of IGF-1 at varying concentrations are added to flat bottomed 96-well tissue culture plates at 37°C and 5% CO_2 and cultured for 2 days. 40 µl of Alamar Blue™ (undiluted) are then added and the incubation continued for 7–24 h. The plates are allowed to cool to room temperature for 10 min on a shaker and the fluorescence is read using a 96-well fluorometer with excitation at 530 nm and emission at 590 nm.

EVALUATION

Results, expressed as relative fluorescence units, are plotted against IGF-1 concentrations using a 4-parameter curve-fitting program. Test compounds are compared with the standard.

MODIFICATIONS OF THE METHOD

Boge and coworkers (1994) described an enzyme immunoreceptor assay for the quantitation of insulin-like growth factor-1 and insulin receptors in bovine muscle tissue.

Hodgson and coworkers (1995) tested mutations at positions 11 and 60 of insulin-like growth factor-1 using (a) quantification of affinities for the human insulin receptor overexpressed on NIH 3T3 cells, (b) quantification of affinities for the type 1 IGF receptor via competition for binding to a monolayer of MDA-MB-231 cells, (c) promotion of the *in vitro* mitogenesis of growth-arrested MCF-7 cells in the presence of 17-β-oestradiol, and (d) a competition assay for binding to IGF-binding proteins secreted by MCF-7 cells.

In order to investigate the influence of insulin-like growth factor-1 and IGF-binding protein-1 on wound healing, Lee and coworkers (1996) measured the contraction of collagen gels with embedded fibroblasts.

Ernst and White (1996) studied the hormonal regulation of IGF-binding protein-2 expression in C_2C_{12} myoblasts.

Frystyk and Baxter (1998) described a competitive assay for rat insulin-like growth factor (IGF)-binding protein-3 (rIGFBP-3) based on the ability of IGFBP-3 to form a ternary complex with the acid labile subunit (ALS) in the presence of IGF. Human ALS was bound to test tubes pre-coated with anti-human ALS antibody. The assay depends on a competition between a covalent complex of ^{125}I-hIGF-I and hIGFBP-3, added as tracer, and hIGFBP-3 or rIGFBP-3 in standards or test samples, for binding to the immobilized hALS. Purified natural hIGFBP-3 served as standard.

Damon and coworkers (1997) used the C_2 skeletal myogenic cell line to characterize an insulin-like growth factor-binding protein, named Mac25/IGFBP-7.

To explore the possible relationship between insulin-like growth factor I and diabetic retinopathy, Naruse and coworkers (1996) examined the effects of glucose on IGF-I stimulated thymidine incorporation into DNA and IGF-I binding in cultured bovine retinal pericytes.

Jonsson and coworkers (1997) used a fluorometric proliferation assay with AlamarBlue to study the proliferative capacity of isolated human osteoblasts which were dose-dependently stimulated by IGF-I.

REFERENCES AND FURTHER READING

Ballard FJ, Wallace JC, Francis GL, Read LC, Tomas FM (1996) Des(1–3)IGF-I: A truncated form of insulin-like growth factor-I. Int J Biochem Cell Biol 28:1085–1087

Boge A, Sauerwein H, Meyer HHD (1994) An enzyme immunoreceptor assay for the quantitation of insulin-like growth factor-1 and insulin receptors in bovine muscle tissue. Anal Biochem 216:406–412

Burvin R, LeRoith D, Harel H, Zloczower M, Marbach M, Karnieli E (1998) The effect of acute insulin-like growth factor-II administration on glucose metabolism in the rat. Growth Horm IGF Res 8:205–210

Cascieri MA, Saperstein R, Hayes NS, Green BG, Chicchi GG, Applebaum J, Bayne ML (1988) Serum half-live and biological activity of mutants of human insulin-like growth factor I which do not bind to serum binding proteins. Endocrinol 123:373–381

Damon SE, Haugk KL, Swisshelm K, Quinn LS (1997) Developmental regulation of mac25/insulin-like growth factor-binding protein-7 expression in skeletal myogenesis. Exp Cell Res 237:192–195

DeMeyts P (1994) The structural basis of insulin and insulin-like growth factor-I receptor binding and negative cooperativity, and its relevance to mitogenic versus metabolic signalling. Diabetologia 37[Suppl 2]:S135–S148

Dideriksen LH, Jørgensen LN, Drejer K (1992) Carcinogenic effect on female rats after 12 months administration of the insulin analog B10 Asp. Diabetes 41 (Suppl I):143A

Drejer K (1992) The bioactivity of insulin analogs from *in vitro* receptor binding to *in vivo* glucose uptake. Diabetes/Metab Rev 8:259–286

Ernst CW, White ME (1996) Hormonal regulation of IGF-binding protein-2 expression in C_2C_{12} myoblasts. J Endocrinol 149:417–429

Fantl WJ, Johnson DE, Williams LT (1993) Signalling by receptor tyrosine kinases. Annu Rev Biochem 62:453–481

Froesch ER, Schmid C, Schwander J, Zapf J (1985) Actions of insulin-like growth factors. Ann Rev Physiol 47:443–467

Frystyk J, Baxter RC (1998) Competitive assay for determination of rat insulin-like growth factor binding protein-3. Endocrinology 139:1454–1457

Gammeltoft S, Drejer K (1991) Increased mitogenic potency of high affinity insulin analogs in mouse NIH 3T3 fibroblasts. J Cell Biol (Suppl 15B):54

Gazzano-Santoro H, Chen A, Mukku V (1998) A cell-based potency assay for insulin-like growth factor-1. Biologicals 26:61–68

Hodgson D, May FEB, Westley BR (1995) Mutations at positions 11 and 60 of insulin-like growth factor 1 reveal differences between its interaction with the type I insulin-like-growth-factor receptor and the insulin receptor. Eur J Biochem 233:299–309

Jonsson KB, Frost A, Larrson R, Ljunghall S, Ljunggren O (1997) A new fluorometric assay for the determination of osteoblastic proliferation: Effects of glucocorticoids and insulin-like growth factor-1. Calcif Tissue Int 60:30–36

Kobayashi K, Agrawal K, Jackson IT, Vega JB (1996) The effect of insulin-like growth factor 1 on cranofacial bone healing. Plast Reconstr Surg 97:1129–1135

Laron Z (1999) Somatomedin-1 (recombinant insulin-like growth factor-1): Clinical pharmacology and potential treatment of endocrine and metabolic disorders. Biodrugs 11:55–70

Lee Y-R, Oshita Y, Tsuboi R, Ogawa H (1996) Combination of insulin-like growth factor (IGF)-I and IGF-binding protein-1 promotes fibroblast-embedded collagen gel contraction. Endocrinology 137:5278–5283

Moxley RT, Arner P, Moss A, Skottner A, Fox M, James D, Livingston JN (1990) Acute effects of insulin-like growth factor I and insulin on glucose metabolism *in vivo*. Am J Physiol; Endocrinol Metab 259:E561–E567

Naruse K, Sakakibara F, Nakamura J, Koh N, Hotta N (1996) Enhancement and inhibition of mitogenic action of insulin-like growth factor I by high glucose in cultured bovine retinal pericytes. Life Sci 58:267–276

Nevo Z (1982) Somatomedins as regulators of proteoglycan synthesis. Conn Tiss Res 10:109–113

Nielsen FC, Haselbacher G, Christiansen J, Lake M, Grønborg M, Gammeltoft S (1993) Biosynthesis of 10 kDa and 7.5 kDa insulin-like growth factor II in a human rhabdomyosarcoma cell line. Mol Cell Endocrinol 93:87–95

Pierson RW, Temin HM (1972) The partial purification from calf serum of a fraction with multiplication-stimulating activity for chicken fibroblasts in the cell culture and with non-suppressible insulin-like activity. J Cell Physiol 79:319–330

Rechler MM (1985) The nature and regulation of the receptors for insulin-like growth factors. Ann Rev Physiol 47:425–442

Rinderknecht E, Humbel RE (1978a) The amino acid sequence of human insulin-like growth factor I and its structural homology with proinsulin. J Biol Chem 253:2769–2776

Rinderknecht E, Humbel RE (1978b) Primary structure of human insulin-like growth factor II. FEBS Lett 89:283–286

Roth RA (1988) Structure of the receptor for insulin-like growth factor II: the puzzle amplified. Science 239:1269–1271

Salamon EA, Luo J, Murphy LJ (1989) The effect of acute and chronic insulin administration on insulin-like growth factor expression in the pituitary-intact and hypophysectomized rat. Diabetologia 32:348–353

Salmon WD, Daughaday WH (1957) A hormonally controlled serum factor which stimulates sulfate incorporation by cartilage *in vivo*. J Lab Clin Med 49:825–836

Sara VR, Hall K (1990) Insulin-like growth factors and their binding proteins. Physiol Rev 70:591–614

Schäffer L, Kjeldsen T, Andersen AS, Wiberg FC, Larsen UD, Cara JF, Mirmira RG, Nakagawa SH, Tager HS (1993) Interaction of a hybrid insulin/insulin-like growth factor-I analog with chimeric insulin/type I insulin-like growth factor receptors. J Biol Chem 268:3044–3047

Shizume K, Marumoto Y, Sakano KI (1996) Hypoglycemic effect of insulin-like growth factor II (IGF-II) is mediated mainly through insulin and/or IGF-I receptor bot not IGF-II receptor. Clin Pediatric Endocrinol 5, Suppl 8:77–83

Schlessinger J, Ullrich A (1992) Growth factor signaling by receptor tyrosine kinases. Neuron 9:383–391

Schmitz F, Hartmann H, Stümpel F, Creutzfeldt W (1991) *In vivo* metabolic action of insulin-like growth factor I in adult rats. Diabetologie 34:144–149

Schwander J, Hauri C, Zapf J, Froesch ER (1983) Synthesis and secretion of insulin-like growth factor and its binding protein by the perfused rat liver: Dependence on growth hormone status. Endocrinol 113:297–305

Simpson HL, Umpleby AM, Russell-Jones DL (1998) Insulin-like growth factor-1 and diabetes. A review. Growth Horm IGF Res 8:83–95

Steinke J, Sirek A, Lauris V, Lukens FDW, Renold AE (1962) Measurement of small quantities of insulin-like activity with rat adipose tissue. III. Persistence of serum insulin-like activity after pancreatectomy. J Clin Invest 41:1699–1707

Ullrich A, Schlessinger J (1990) Signal transduction by receptors with tyrosine kinase activity. Cell 61:203–212

Verspohl EJ, Maddux BA, Goldfine ID (1988) Insulin and insulin-like growth factor I regulate the same biological functions in HEP-G2 cells via their own specific receptors. J Clin Endocr Metab 67:169–174

Vikman K, Isgaard J, Edén S (1991) Growth hormone regulation of insulin-like growth factor-I mRNA in rat adipose tissue and isolated rat adipocytes. J Endocrinol 131:139–145

Zapf J, Waldvogel M, Froesch ER (1975) Binding of nonsuppressible insulin-like activity to human serum: Evidence for a carrier protein. Arch Biochem Biophys 168:638–645

K.4.6 Amylin

GENERAL CONSIDERATIONS

Amylin, also named islet amyloid polypeptide, is a pancreatic islet peptide consisting of 37 amino acids with a role in the maintenance of glucose homeostasis. The peptide is predominantly present in the β-cells of the pancreas and to a lesser extent in the gastrointestinal tract and in the nervous system, where amylin mRNA is also present along with specific binding sites.

Amylin has structural and functional relationships to two other messenger proteins, calcitonin and calcitonin gene-related peptide (Rink et al. 1993, Pittner et al. 1994, van Rossum et al. 1997, Wimalawansa 1996).

Amylin inhibits food intake in rodents when given centrally as well as peripherally (Morley et al. 1997, Lutz et al. 1998). Bhavsar and coworkers (1998) found a synergy between amylin and cholecystokinin for inhibition of food intake in mice.

Amylin reduces insulin-stimulated incorporation of glucose into glycogen in skeletal muscle. Young and coworkers (1992) found that increasing concentrations of amylin progressively depressed the maximal insulin-stimulated radioglucose incorporation into soleus muscle glycogen.

Castle and coworkers (1998) reported an inhibition of 3-O-methyl-D-glucose transport in perfused rat hindlimb muscle under hyperinsulinemic conditions.

Bryer-Ash and coworkers (1995) found that amylin-mediated reduction in insulin sensitivity corresponds to reduced insulin receptor kinase activity in the rat *in vivo*.

Transgenic mice expressing human islet amyloid polypeptide develop diabetes mellitus by 8 weeks of age, which is associated with selective β-cell death and impaired insulin secretion (Janson et al. 1996).

Mulder and coworkers (2000) showed that amylin-deficient mice develop a more severe form of alloxan-induced diabetes.

In single β-cells exhibiting normal glucose sensing, amylin causes membrane hyperpolarization, increases net outward current and reductions in insulin secretion. In contrast, in cells with abnormal glucose sensing (e. g., from *db/db* diabetic mice) amylin has no effect on electrical activity or secretion (Wagoner et al. 1993).

Amylin suppressed the cAMP generation induced by glucagon-like peptide 1 (GLP-1) in RINm5F cells dose-dependently (Göke et al. 1993).

Amylin, also named human islet amyloid polypeptide (hIAPP) according to van Hulst and coworkers (1997), may be implicated in the pathogenesis of pancreatic islet amyloid formation and type 2 diabetes mellitus (Wimalawansa 1997). Van Hulst and coworkers (1997) used transgenic mice for the study of (patho)physiological roles of hIAPP *in vivo*. Leckstrom and coworkers (1997) studied plasma levels and immunoreactivity of insulin and islet amyloid polypeptide in *Psammomys obesus* (sand rat) under low-energy and high-energy diet.

Amylin given peripherally or centrally inhibits acid gastric secretion in a dose dependent manner and has a protective effect against indomethacin- or ethanol-induced ulcers only when injected centrally. Subcutaneous or central injection of amylin produces a dose-dependent inhibition of gastric emptying, which may contribute to the activity of amylin in the regulation of carbohydrate absorption. In addition, amylin inhibits food intake both when injected peripherally or centrally. Amylin is considered to take part in the rapid endocrine response during digestion to maintain euglycemia (Guidobono 1998).

Amylin slows the rate of gastric emptying in spontaneously diabetic BB/Wistar rats (Macdonald 1997) and inhibits gastric acid secretion in rats (Rossowski et al. 1997).

Guidobono and coworkers (1997) reported a cytoprotective effect of amylin against indomethacin- and ethanol-induced ulcers when given intracerebroventricularly, but not when given subcutaneously.

Clementi and coworkers (1997) found a protective, dose-dependent effect of amylin against reserpine- and serotonin-induced gastric damage in rats, however, no anti-ulcer effect after pylorus ligation.

The search for a superior compound with the biological actions of human amylin resulted in the identification of [$Pro^{25,28,29}$]human amylin, assigned the USAN name pramlintide. Young and coworkers (1996) compared this compound with human and rat amylin in various pharmacological tests, such as receptor assays (binding to rat nucleus membranes, amylin receptors; binding to membranes from SK-N-MC cells, CGRP receptors; binding to membranes from T46D cells, calcitonin receptors), gastric emptying in rats, plasma glucose after oral glucose gavage. When studying glycogen metabolism in the isolated soleus muscle of rats, pramlintide was slightly more potent than human amylin, but not different from rat amylin in inhibiting insulin-stimulated incorporation of [U-^{14}C]glucose into muscle glycogen. After intravenous infusion of amylin or pramlintide, a dose-dependent increase of plasma glucose, plasma lactate and ionized calcium was found. Mean arterial blood pressure decreased with higher doses.

Clementi and coworkers (1995) found an anti-inflammatory activity of amylin in mouse ear edema induced by Croton oil and acetic acid-induced peritonitis in the rat, but not in serotonin-induced rat paw edema and plasma protein extravasation induced by dextran in rat skin.

Bell and coworkers (1995), Bell and McDermont (1995) reported that amylin has an hypertrophic effect in rat ventricular cardiomyocytes and exerts the contractile response via $CGRP_1$-preferring receptors.

In anesthetized rats, amylin increased after intravenous infusion urine flow, sodium excretion, glomerular filtration rate and renal plasma flow (Vine et al. 1998).

Clementi and coworkers (1996) reported that intracerebroventricularly injected amylin induced in rats a dose-dependent decrease of locomotor activity without affecting grooming and sniffing.

Amylin dose-dependently stimulated cell proliferation of human osteoblast like (hOB) cells and increased osteocalcin production (Villa et al. 1997). Cornish and coworkers (1998) found in adult male mice after daily subcutaneous injection of amylin for 4 weeks an increase of histomorphometric indices of bone formation and a reduction of bone resorption. Muff and coworkers (1995) and Poyner (1997) identified, characterized and cloned the receptors for calcitonin, calcitonin-gene-related peptide and amylin.

PURPOSE AND RATIONALE

Binding sites with high affinity for amylin are present in several brain regions, with the nucleus accumbens and surrounding tissue containing more than twice as many banding sites as any other regions (Beaumont et al. 1993).

PROCEDURE

Membrane Preparation

Membranes are prepared from male Sprague-Dawley rats (150–200 g). Following decapitation, the basal forebrain regions (nucleus accumbens) are removed to PBS (pH 7.4) at 4°C. The tissues are weighted, then placed in 10 ml/g tissue of ice-cold 20 mM HEPES/KOH (pH 7.4) and homogenized with a Polytron (10 s at setting 4). An additional 30 ml of cold HEPES/KOH is added, and the homogenate centrifuged (48,000 × *g*, 15 min). After discarding the supernatant fluid, membrane pellets are resuspended by homogenization in 40 ml of fresh HEPES/KOH and

centrifuged as before. Membranes are washed again by homogenization in buffer and centrifugation. The final membrane pellet is resuspended in a volume of 20 mM HEPES/KOH containing 0.2 mM PMSF added immediately before use from a stock 0.2 M solution in ethanol. A volume of buffer is used to yield a concentration of about 80 mg original tissue/ml. Membranes are kept frozen at –80°C until use.

Binding Assay

Membranes from 4 mg of original wet weight of tissue are incubated with ^{125}I-BH-amylin (rat amylin, BH-labeled at the amino-terminal lysine, (Amersham Corp.) in 20 mM HEPES/KOH (pH 7.4), containing 0.5 mg/ml bacitracin, 0.5 mg/ml BSA and 0.2 mM phenylmethylsulfonyl fluoride (PMSF), for 60 min at 23°C. Incubations are carried out in duplicate tubes and are started by addition of membranes. Incubations are terminated by filtration through glass fiber filters that have been presoaked in 0.3% polyethylene-imine, followed by washing with 15 ml of cold PBS.

EVALUATION

Competition curves are generated by measuring binding of 13 pM ^{125}I-BH-amylin in the presence of 10^{-11} to 10^{-6} unlabeled peptide. Data are fitted to a four-parameter logistic equation to derive half-maximal inhibitory concentrations (IC_{50} values) and slope factors (Hill coefficients).

MODIFICATIONS OF THE METHOD

Sheriff and coworkers (1992) characterized amylin binding sites in the human hepatoblastoma cell line, HepG2. Perry and coworkers (1997) studied amylin and calcitonin receptor binding in the mouse α-thyroid-stimulating hormone thyrotroph cell line.

REFERENCES AND FURTHER READING

Beaumont K, Kenney MA, Young AA, Rink TJ (1993) High affinity amylin binding sites in rat brain. Mol Pharmacol 44:493–497

Bell D, McDermont BJ (1995) Activity of amylin at $CGRP_1$-preferring receptors coupled to positive contractile response in rat ventricular cardiomyocytes. Regul Pept 60:125–133

Bell D, Schluter KD, Zhou X-J, McDermont BJ, Piper HM (1995) Hypertrophic effect of calcitonin gene-related peptide (CGRP) and amylin on adult mammalian ventricular cardiomyocytes. J Mol Cell Cardiol 27:2433–2443

Bhasvar S, Watkins J, Young A (1998) Synergy between amylin and cholecystokinin for inhibition of food intake in mice. Physiol Behav 64:557–561

Bryer-Ash M, Follett L, Hodges N, Wimalawansa SJ (1995) Amylin-mediated reduction in insulin sensitivity corresponds to reduced insulin receptor kinase activity in the rat *in vivo*. Metab Clin Exp 44:705–711

Castle AL, Kou CH, Han DH, Ivy JL (1998) Amylin-mediated inhibition of insulin-stimulated glucose transport in skeletal muscle. Am J Physiol 275; Endocrinol Metab 38:E531–536

Clementi G, Caruso A, Cutulli VCM, Prato A, de Bernardis E, Fiore CE, Amico-Roxas M (1995) Anti-inflammatory activity of amylin and CGRP in different experimental models of inflammation. Life Sci 57: PL193–PL197

Clementi G, Valerio C, Emmi I, Prato A, Drago F (1996) Behavioral effects of amylin injected intracerebroventricularly in the rat. Peptides 17:589–591

Clementi G, Caruso A, Cutuli VMC, Prato A, de Bernardis A, Amico-Roxas M (1997) Effect of amylin in various experimental models of gastric ulcer. Eur J Pharmacol 332:209–213

Cornish J, Callon KE, King AR, Cooper GJS, Reid IR (1998) Systemic administration of amylin increases bone mass, linear growth, and adiposity in male mice. Am J Physiol 275; Endocrinol Metab 38:E694–E699

Göke R, McGregor GP, Göke B (1993) Amylin alters biological effects of GLP-1 in the beta-cell. Digestion 54:355–356

Guidobono F, Pagani F, Ticozzi C, Sibilia V, Pecile A, Netti C (1997) Protection by amylin of gastric erosions induced by indomethacin or ethanol in rats. Br J Pharmacol 120:581–596

Guidobono F (1998) Amylin and gastrointestinal activity. Gen Pharmacol 31:173–177

Janson J, Soeller WC, Roche PC, Nelson RT, Torchia AJ, Kreutter DK, Butler PC (1996) Spontaneous diabetes mellitus in transgenic mice expressing human islet amyloid polypeptide. Proc Natl Acad Sci USA 93:7283–7288

Leckstrom A, Ziv E, Shafrir E, Westermark P (1997) Islet amyloid polypeptide in *Psammomys obesus* (sand rat): Effects of nutritionally induced diabetes and recovery on low-energy diet or vanadyl sulfate treatment. Pancreas 15:358–366

Lutz TA, Rossi R, Althaus J, Del Prete E, Scharrer E (1998) Amylin reduces food intake more potently than calcitonin gene-related peptide (CGRP) when injected into the lateral brain ventricle in rats. Peptides 19:1533–1540

Macdonald IA (1997) Amylin and the gastrointestinal tract. Diabetes Med 14/Suppl 2:S24–S28

Morley JE, Suarez MD, Mattamal M, Flood JF (1997) Amylin and food intake in mice: Effect on motivation to eat and mechanism of action. Pharmacol Biochem Behav 56:123–129

Muff R, Born W, Fischer JA (1995) Receptors for calcitonin, calcitonin gene related peptide, amylin, and adrenomedullin. Can J Physiol Pharmacol 73:963–967

Mulder H, Gebre-Medhin S, Betsholtz C, Sundler F, Ahrén B (2000) Islet amyloid polypeptide (amylin)-deficient mice develop a more severe form of alloxan-induced diabetes. Am J Physiol Endocrinol Metab 278:E684–E691

Perry KJ, Quiza M, Myers DE, Morfis M, Christopoulos G, Sexton PM (1997) Characterization of amylin and calcitonin receptor binding in the mouse α-thyroid-stimulating hormone thyrotroph cell line. Endocrinol 138:3486–4396

Pittner RA, Albrandt K, Beaumont K, Gaeta LSL, Koda JE, Moore CX, Ritterhouse J, Rink TJ (1994) Molecular physiology of amylin. J Cell Biochem 555:19–28

Poyner DR (1997) Molecular pharmacology of receptors for calcitonin-gene-related peptide, amylin and adrenomedullin. Biochem Soc Transact 25:1032–1036

Rossowski WJ, Jiang NY, Coy DH (1997) Adrenomedullin, amylin, calcitonin gene-related peptide and their fragments

are potent inhibitors of gastric acid secretion in rats. Eur J Pharmacol 336:51–63
Rink TJ, Beaumont K, Koda J, Young A (1993) Structure and biology of amylin. Trends Pharmacol Sci 14:113–118
Sheriff S, Fischer JE, Balasubramaniam A (1992) Characterization of amylin binding sites in a human hepatoblastoma cell line. Peptides 13:1193–1199
Van Hulst KL, Born W, Muff R, Oosterwijk C, Blankenstein MA, Lips CJM, Fischer JA, Höppener JWM (1997) Biologically active human islet amyloid polypeptide/Amylin in transgenic mice. Eur J Endocrinol 136:107–113
Van Rossum D, Hanisch UK, Quirion R (1997) Neuroanatomical localization, pharmacological characterization and functions of CGRP, related peptides and their receptors. Neurosci Biobehav Rev 21:649–678
Villa I, Rubanacci A, Ravasi F, Ferrara AF, Guidobono F (1997) Effects of amylin on human osteoblast-like cells. Peptides 18:537–540
Vine W, Smith P, LaChappell R, Blase E, Young A (1998) Effects of amylin on renal function in the rat. Horm Metab Res 30:518–522
Wagoner PK, Chen C, Worley JF, Dukes ID, Oxford GS (1993) Amylin modulates β-cell glucose sensing via effects on stimulus-secretion coupling. Proc Natl Acad Sci, USA 90:9145–9149
Wimalawansa SJ (1996) Calcitonin gene-related peptide and its receptors: molecular genetics, physiology, pathophysiology, and therapeutic potentials. Endocrine Rev 17:533–585
Wimalawansa SJ (1997) Amylin, calcitonin gene-related peptide, calcitonin, and adrenomedullin: a peptide superfamily. Crit Rev Neurobiol 11:167–239
Young AA, Gedulin B, Wolfe-Lopez D, Greene HE, Rink TJ, Cooper GJS (1992) Amylin and insulin in rat soleus muscle: dose response for cosecreted noncompetitive antagonists. Am J Physiol 263, Endocrinol Metab 26:E274–E281
Young AA, Vine W, Gedulin BR, Pittner R, Janes S, Gaeta LSL, Percy A, Moore CX, Koda JE, Rink TJ, Beaumont K (1996) Preclinical pharmacology of pramlintide in the rat: comparison with human and rat amylin. Drug Dev Res 37:231–248

K.5 Insulin Target Tissues and Cells

K.5.1 Adipose Tissue and Adipocytes

GENERAL CONSIDERATIONS

Rodent adipose tissue and cells represent the targets exhibiting the most prominent insulin sensitivity (i. e. lowest EC/IC_{50}) and responsiveness (i. e. highest fold stimulation/inhibition above basal) of the relevant insulin signaling cascades (e. g. insulin receptor activation) and metabolic end effector systems (e. g. lipolysis) in comparison to liver (e. g. gluconeogenesis) and muscle cells (e. g. glucose transport). This might be based in part on technical advantages of the adipose tissue/adipocyte preparation in comparison to that of muscle/myocytes. But more likely it reflects the exquisite physiological role of the adipose tissue in the regulation and coordination of glucose and lipid metabolism, i. e. insulin stimulation of lipid synthesis (lipogenesis) and insulin inhibition of lipolysis. On basis of their relatively easy technical preparation, functional adipose tissue fragments (epididymal fat pads) and primary adipocytes (isolated epididymal adipocytes) from rats as well as adipocyte cell lines derived from mice (3T3-L1, F442A) are the first choice for the development of robust and reliable cell/tissue-based assay systems for insulin-like activity.

K.5.1.1 Epididymal Fat Pads of Rats

GENERAL CONSIDERATIONS

Insulin-like activity can be measured by the uptake of glucose into fat cells, which at low extracellular glucose concentrations (see K.6.1.6) represents the rate-limiting step for the conversion of glucose in and its storage as lipids, or for the oxidative (glycolysis plus citric acid cycle) and non-oxidative (glycogen synthesis) metabolism of glucose. Adipose tissue from the epididymal fat pads from rodents has been found to be very suitable for the analysis of non-oxidative and oxidative glucose metabolism. Early studies (Beigelman 1959, Steelman et al. 1961) determined the difference of glucose concentration in the medium after incubation of pieces of epididymal rat adipose tissue for the direct determination of glucose uptake (encompassing non-oxidative and oxidative glucose metabolism) or measured oxygen consumption in Warburg vessels (Ball and Merill 1961, Froesch et al. 1963) or the release of radiolabeled $^{14}CO_2$ from [^{14}C]glucose after its trapping and counting (Martin et al. 1958, Slater et al. 1961, Gliemann 1965a and 1967b, 1972) monitoring glucose oxidation, exclusively. The latter principle was used by Martin and coworkers (1958) using epididymal fat pads from the rat. This method has been used by various authors (Humbel 1959, Ditschuneit et al. 1959) and described in detail by Renold and coworkers (1960) and Siess and coworkers (1965). Sönksen and coworkers (1965) found a close correlation between "suppressible" insulin-like activity measured by the fad pad method and insulin concentration determined by immunoassay. Ball and Merrill (1961) used the manometric measurement of the net gas exchange of rat adipose tissue to quantitate small amounts of insulin. A survey of the biological assays of insulin-like serum activity was given by Faulhaber and Ditschuneit (1975).

The use of serum from pancreatectomized animals revealed the presence of factors apparently exerting insulin-like activity other than insulin (Steinke et al. 1962, 1965). Subsequently, the nature of these insulin-

like activities has been characterized (see K.6.3.6.4), but so far they escaped their unequivocal characterization and molecular identification, presumably due to their structural heterogeneity and low abundance.

PURPOSE AND RATIONALE

The epididymal fat pad assay, originally developed as bioassay of insulin-like activity in serum samples, can also be used for measuring activity of synthetic insulin derivatives and analogs as well as for the evaluation of peripheral insulin-like effects of antidiabetic compounds, such as sulfonylureas and biguanides, which have long been assumed to exert their blood glucose decreasing activity exclusively *via* stimulation of insulin release and improvement of peripheral insulin sensitivity, respectively. However, in the subsequent decades this tissue-based system has been replaced by cell-based assays (see below) which for most applications offer the advantages of higher sensitivity, accuracy, reproducibility and test capacity (throughput) despite lower expenditure in the number of animals (*per* data point) required.

K.5.1.2 Primary Rat Adipocytes

PURPOSE AND RATIONALE

The worldwide dramatic increase in obesity with its associated health problems and the identification of adipocyte-secreted proteins that apparently have major impact on the regulation of whole-body glucose, lipid and energy metabolism have generated major interest in adipocyte biology. Adipocytes are the primary storage site for energy in vertebrate animals. During fasting, adipocytes release energy-rich molecules that provide metabolic fuels to other tissues. Adipocytes also secrete hormones that orchestrate the storage, release, and oxidation of energy-rich molecules throughout the body and that control behavior, including feeding and appetite. Primary adipocytes maintain a large dynamic pool of triacylglycerol (TAG) and express a specific set of proteins to maintain circulating metabolic fuel levels. Primary adipocytes and adipose tissue have been used to study basic adipocyte biology.

Rodbell (1964) and Gliemann (1965, 1967a and b) used primary adipocytes isolated by digestion of epididymal fat pads from rats with collagenase. The conversion of (3- ^{3}H) glucose into total adipocyte TAG has been used as a very sensitive parameter in an improved assay for insulin-like activity by Moody and coworkers (1974) which during the subsequent decades turned out to represent the golden standard for assays for insulin-like activity. Alternatively to primary rat adipocytes, Etherton and Chung (1981) and Etherton and Walker (1982) characterized the insulin sensitivity of isolated swine adipocytes.

Preparation of Rat Adipocytes

Male Wistar or Sprague-Dawley rats weighing 140–200 g are sacrificed and both epididymal fat pads are removed under sterile conditions. The fat pads are cut into pieces and incubated for 20 min at 37°C with 1 mg/ml collagenase (e. g. type CLS II, Worthington, NJ) in Krebs-Ringer HEPES bicarbonate buffer, KRHB, (25 mM HEPES/KOH, pH 7.4, 0.1 mM glucose, 1% wt/vol BSA). The cell suspension is filtered through a 100-µm nylon screen and washed 3 times by flotation (accumulation of a thin cell layer on top of the medium after centrifugation ($1{,}000 \times g$, 1 min, swing-out rotor) with KRHB lacking glucose and finally suspended in the same solution. The suspension is adjusted to a final titer of 3.5×10^5 cells/ml.

Stimulation of Rat Adipocytes with Insulin

Adipocytes are suspended in buffer S (Dulbecco's minimal essential medium ([DMEM] for primary culture to induce insulin resistance, see K.6.3.5) or KRHB (for short-term measurement of insulin-like activity) both containing 5 mM glucose, 0.5 M mM sodium pyruvate, 4 mM L-glutamine, 200 nM 1-methyl-2-phenylethyl)adenosine, 100 µg/ml gentamycine, 1% BSA and 25 mM HEPES/KOH, pH 7.4) at 5% cytocrit (corresponding to about 7×10^5cells/ml). For determination of the packed cell volume, small aliquots of the cell suspension are aspirated into capillary hematocrit tubes and centrifuged for 90 s in a micro-hematocrit centrifuge in order to measure the fractional occupation of the suspension by the adipocytes (= cytocrit). A 20-ml portion of the adipocyte suspension (5% cytocrit) is added to 20 ml of buffer S containing human insulin as indicated. Incubations (20 min, 37°C) are performed under 5% CO_2 in 200-ml polyethylene vials during shaking at 110 cycles/min with a stroke length of 3.5 cm.

Permeabilization of Rat Adipocytes

Studies of intermediary metabolism and its regulation by insulin often require the use of agents that do not readily penetrate the plasma membrane of intact cells due to the size and charge of substrates (e. g. sugar phosphates, nucleotides, hydrophilic inhibitors, antibodies). Such studies would greatly benefit if the permeability of the plasma membrane to these compounds or the release of freely diffusible cytoplas-

mic molecules (e. g. metabolites, proteins) across the plasma membrane could be increased. Thus, permeabilized cells can be useful for the analysis of complicated metabolic processes as well as for the study of the insulin-like activity of agents which do not readily pass the plasma membrane of adipocytes including the elucidation of the molecular mechanism(s) of the insulin(-like) action induced or inhibited by a certain compound/drug. For this, it may be useful to block known signal transduction or metabolic pathways in adipocytes by introducing specific inhibitory antibodies (against key signaling proteins/metabolic enzymes) or peptide substrates (competing for the endogenous protein substrate; e. g. synthetic peptide as kinase substrate) prior to stimulation of the adipocytes with the compound/drug. In conclusion, permeabilized cells should be looked upon as a method that rapidly makes the interior of the cells accessible (for a review see Declercq and Baes 2000).

In general, the widely used methods of short incubation under hypoxic conditions (Gordon et al. 1985) and electroporation (i. e. subjecting cells to a short series of high-voltage electrical discharges permeabilize cells transiently. These cells are characterized by the formation of small protuberances (blebs) indicative of localized cell surface damage. It is conceivable that the stretched plasma membrane of such blebs act as a high-permeability region. Disappearance of blebs and restoration of normal plasma membrane impermeability is achieved again by short (15-min) incubation at 37°C. During the period of enhanced permeability small compounds can be introduced. Upon alternative physical treatment, such as osmotic shock and brief freezing/thawing, the cells are also temporarily permeabilized. Such cells reseal under appropriate conditions (Lepers et al. 1990). These physical methods are probably not selective for the plasma membrane necessitating other permeabilization techniques if intact intracellular membranes are required.

In addition, intactness of intracellular organelles will also benefit from the use of permeabilizing media that are isotonic with the cell content (Bijleveld and Geelen 1987). The cholesterol-sequestering approach produces very fast holes of about 8 nm (Schulz 1990) and is most suited to rapidly measuring cellular enzyme activities as the lesions are sufficiently large to allow entry of large molecular substrates or proteins and to allow cytosolic proteins of at least 285 kDa to leave the cell (Bijleveld and Geelen 1987). Apart from transient permeabilization, all the other techniques for permeabilizing cells have severe limitations due to the fact that cellular integrity is destroyed. The degree of loss of integrity determines the application of a particular permeabilizing procedure. The use of digitonin-permeabilized mammalian cells for measuring enzyme activities in the course of studies on lipid metabolism has been reviewed by Geelen (2005).

Electroporation of Rat Adipocytes

For the introduction of antibodies and peptides as well as compounds/drugs into isolated rat adipocytes without significant loss of cell viability and insulin sensitivity, the method of electroporation has been used successfully. For this, 0.4 ml of buffer E (4.74 mM NaCl, 118 mM KCl, 0.38 mM $CaCl_2$, 1 mM EGTA, 1.19 mM $MgS0_4$, 1.19 mM KH_2PO_4, 25 mg/ml BSA, 3 mM sodium pyruvate and 25 mM HEPES/KOH, pH 7.4) is placed in a 0.4-cm gap-width electroporation cuvette (Bio-Rad, Munich, Germany) together with the antibodies or peptides or compounds/drugs. 0.4 ml of adipocyte suspension (50% cytocrit in buffer E) is added to each cuvette and gently mixed. Electroporation is performed using a Gene Pulser Transfection Apparatus (Bio-Rad, Munich, Germany) which is set at a capacitance of 25 µF and voltage of 800 V (2 kV/cm), at 25°C for six shocks (Shibata et al. 1991, Quon et al. 1993). After the third treatment, the adipocyte suspension is gently stirred with a plastic stick and the electric polarity is reversed. The time constant of electroporation is typically 0.6 ms during the final shock. Routinely, 4 ml of adipocyte suspension (25% cytocrit) is electroporated in five cuvettes. The time required for treatment of the five cuvettes is about 3 min. After electroporation, the cells from five electroporations are pooled and transferred to 50-ml polystyrene tubes. After incubation (30 min, 37°C) in 5% CO_2/95% O_2, the cells are centrifuged ($200 \times g$, 1 min, swing-out-rotor) and the infranatant is aspirated. Thereafter the cells are washed once with 40 ml of buffer E containing 5 mM glucose and 4% BSA, suspended in 20 ml of the same buffer and then incubated (1 h, 37°C) under 5% CO_2 prior to challenge with the appropriate stimulus. Using this electroporation technology Müller and coworkers (2000) introduced into rat adipocytes inhibitory antibodies against tyrosine kinases mediating insulin-like signaling in response to stimuli different from insulin (see K.6.3.6.4).

REFERENCES AND FURTHER READING

Ball EG, Merrill MA (1961) A manometric assay of insulin and some results of the application of the method to sera and islet-containing tissue. Endocrinology 69:596–607

Beigelman PM (1959) Insulin-like activity of normal and diabetic human serum. Diabetes 8:29–35

Bijleveld C, Geelen MJH (1987) Mesurement of acetyl-CoA carboxylase activity in isolated hepatocytes. Biochim Biophys Acta 918:274–283
Ditschuneit H, Chang SA, Pfeiffer M, Pfeiffer EF (1959) Über die Bestimmung von Insulin im Blute am epididymalen Fettanhang der Ratte mit Hilfe markierter Glukose. Klin Wschr 37:1234–1239
Etherton TD, Chung CS (1981) Preparation, characterization, and insulin sensitivity of isolates swine adipocytes: comparison with adipose tissue slices. J Lipid Res 22:1053–1059
Etherton TD, Walker OA (1982) Characterization of insulin binding to isolated swine adipocytes. Endocrinol 110:1720–1724
Faulhaber JD, Ditschuneit H (1975) The biological assay of insulin-like serum activity (ILA) in: Hasselblatt A, v. Bruchhausen F (eds) Insulin, Part 2, Handbook of Experimental Pharmacology, Vol 32/2, Springer-Verlag, Berlin Heidelberg New York, pp 671–691
Froesch ER, Bürgi H, Ramseier EB, Bally P, Labhart A (1963) Antibody-suppressible and nonsuppressible insulin-like activities in human serum and their physiologic significance. An insulin assay with adipose tissue of increased precision and specificity. J Clin Invest 42:1816–1834
Geelen MJH (2005) The use of digitonin-permeabilized mammalin cells for measuring enzyme activities in the course of studies on lipid metabolism. Anal Biochem 347:1–9
Gliemann J (1965) Insulin-like activity of dilute human serum assayed by an isolated adipose cell method. Diabetes 14:643–649
Gliemann J (1967a) Assay of insulin-like activity by the isolated fat cell method. II. The suppressible and non-suppressible insulin-like activity of serum. Diabetologia 3:389–394
Gliemann J (1967b) Insulin assay by the isolated fat cell method. I. Factors influencing the response to crystalline insulin. Diabetologia 3:382–388
Gliemann J, Sørensen HH (1970) Assay of insulin-like activity by the isolated fat cell method. IV. The biological activity of proinsulin. Diabetologia 6:499–504
Gliemann J, Østerlind K, Vinten J, Gammeltoft S (1972) A procedure for measurement of distribution spaces in isolated fat cells. Biochim Biophys Acta 286:1–9
Gordon PB, Tolleshaug H, Seglen PO (1985) Autophagic sequestration of [14C]sucrose introduced into isolated rat hepatocytes by electrical and non-electrical methods. Exp Cell Res 160:449–458
Humbel RE (1959) Messung der Serum–Insulin-Aktivität mit epididymalem Fettgewebe *in vitro*. Experientia (Basel) 15:256–258
Lepers A, Cacan R, Verbert A (1990) Permeabilized cells as a way of gaining access to intracellular organelles: an approach to glycosylation reactions. Biochemistry 72:1–5
Martin DB, Renold AE, Dagenais YM (1958) An assay for insulin-like activity using rat adipose tissue. Lancet II/76–77
Moody AJ, Stan MA, Stan M (1974) A simple free fat cell bioassay for insulin. Horm Metab Res 6:12–16
Müller G, Wied S, Frick W (2000) Cross talk of $pp125^{FAK}$ and $pp59^{LYN}$ non-receptor tyrosine kinases to insulin-mimetic signaling in adipocytes. Mol Cell Biol 20:4708–4723
Quon MJ, Zarnowski MJ, Guerre-Millo M, de la Luz Sierra M, Taylor SI, Cushman SW (1993) Transfection of DNA into isolated rat adipose cells by electroporation. Biochem Biophys Res Commun 194:338–346
Renold AE, Martin DB, Dagenais YM, Steinke J, Nickerson RJ, Lauris V (1960) Measurement of small quantities of insulin-like activity using rat adipose tissue. I. A proposed procedure. J Clin Invest 39:1487–1498
Rodbell M (1964) Metabolism of isolated fat cells. I. Effect of hormones on glucose metabolism and lipolysis. J Biol Chem 239:375–380
Shibata H, Robinson FW, Benzing CF, Kono T (1991) Evidence that protein kinase C may not be involved in the insulin action on cAMP phosphodiesterase: Studies with electroporated rat adipocytes that were highly responsive to insulin. Arch Biochem Biophys 285:97–104
Siess E, Teinzer A, Wieland O (1965) Eine vereinfachte Methode zur Insulinbestimmung im Serum. Diabetologia 1:201–207
Slater JDH, Samaan N, Fraser R, Stillman D (1961) Immunological studies with circulating insulin. Br Med J I:1712–1715
Sönksen PH, Ellis JP, Lowy C, Rutherford A, Nabarro JDN (1965) Plasma insulin: a correlation between bioassay and immunoassay. Br Med J (1965 II):209–210
Steelman SL, Oslapas R, Busch RD (1961) An improved *in vitro* method for determination of "insulin-like" activity. Proc Soc Exp Biol Med 105:595–598
Steinke J, Miki E, Cahill GF (1965) Assay of crystalline insulin and of serum insulin-like activity of different species on adipose tissue of the rat, mouse and guinea pig. New Engl J Med 273:1464–1467
Steinke J, Sirek A, Lauris V, Lukens FDW, Renold AE (1962) Measurement of small quantities of insulin-like activity with rat adipose tissue. III. Persistence of serum insulin-like activity after pancreatectomy. J Clin Invest 41:1699–1707

K.5.1.3 Insulin-Resistant Primary Rat Adipocytes

PURPOSE AND RATIONALE

Primary rat adipocytes can be maintained in culture for long-term treatment with compounds/drug candidates to study their insulin-like activity upon chronic challenge or for the induction of insulin resistance to study the insulin-sensitizing activity of compounds/drugs for up to 24 h without significant loss of viability by incubation in buffer S (see K.6.3.5) containing 5 mM glucose and 0.5 mM sodium pyruvate under 95% O_2/5% CO_2 and continuous gentle shaking with moderate loss of insulin sensitivity and responsiveness, only (Müller and Wied, 1993). The conditions can be modified for the (subsequent) induction of insulin resistance *in vitro*, which might reflect the hyperglycemic and hyperinsulinemic state promoting insulin resistance *in vivo*.

PROCEDURE

For induction of insulin resistance, primary rat adipocytes are incubated in buffer S in the presence of 25 mM glucose, 0.5 mM sodium pyruvate and 10 nM insulin for 4 to 20 h at 37°C under slow shaking. When assayed for insulin-stimulated glucose transport following a 15- to 30-min incubation period in buffer S

containing 0.5 mM glucose and sodium pyruvate but lacking insulin (which enables downregulation of the glucose transport system from the chronically insulin-stimulated to basal levels).

EVALUATION

The adipocytes made insulin-resistant *in vitro* show a right-ward shift of the concentration-response curve (decreased insulin sensitivity) and a reduced maximal glucose transport velocity at constant or only slightly elevated basal glucose transport (decreased insulin responsiveness) (see Müller and Wied 1993). During prolonged incubation in suspension culture, the adipocytes tend to increase their basal glucose uptake which might reflect elevated energy demands due to stress conditions or loss of plasma membrane integrity. It is therefore most critical to choose culture conditions which preserve the energy status of the rat adipocytes and are compatible with 5- to 6-fold stimulations of glucose transport, at least, at low glucose concentrations corresponding to the normal insulin-sensitive state. This allows monitoring of the induction of insulin resistance by culturing of the adipocytes at high glucose and insulin and its blockade by the concomitant presence of compounds/drugs which may act as insulin senitizers. The use of 25 mM glucosamine instead of high glucose/insulin as initially proposed by Marshall and coworkers (1984; see K.6.3.5) on basis of the apparent activation of the hexosamine pathway during glucose/insulin-induced desensitization of rat adipocytes in culture is not recommended. It has meanwhile been demonstrated that intracellular accumulation of glucosamine results in depletion of cytosolic ATP and accompanying induction of the stress response (Hresko et al. 1998) causing apparent loss of insulin responsiveness which is based on massive increment of the basal glucose transport rate rather than on impairment of insulin signaling to the glucose transport system.

K.5.1.4 Cultured Mouse Adipocytes

GENERAL CONSIDERATIONS

Primary adipocytes have several limitations. They do not propagate in culture, they are difficult to transfect with DNA, they usually have a single huge TAG lipid droplet (LD) that interferes with biochemistry and microscopy, their properties vary as a result of the genetics and conditions of the animals from which they have been isolated, and the isolation procedure is tedious and introduces variation. In addition, harvesting primary adipocytes or adipose tissue from animals generally requires the euthanasia of a vertebrate animal and the expense of specialized facilities and protocols. For these reasons and likely others, cell lines have been developed that can be induced to store TAG, to express proteins that are hallmarks of primary adipocytes, exert many of the functional and physiological features of primary adipocytes and presumably to recapitulate key events in adipocyte ontogeny.

K.5.1.4.1 3T3-L1 Adipocytes

PURPOSE AND RATIONALE

Three decades ago, Kehinde and Green (1974) reported that a clonal subline of mouse 3T3 cells had a propensity to differentiate into adipocytes when in a "resting state". This 3T3-L1 cell culture model of adipogenesis has been exploited extensively to investigate the molecular mechanisms of adipocyte differentiation, lipid metabolism, insulin signaling, and glucose transport as well as to identify physiologically important adipocyte-secreted proteins (adipokines or adipocytokines), such as adiponectin, visfatin and resistin (for reviews see Banerjee and Lazar 2003, Stefan and Stumvoll 2002, McGillis 2005).

Green and Kehinde (1974) isolated from the established mouse fibroblast line 3T3 two subclonal lines that accumulate large amounts of TAG after they had undergone stimulus-induced differentiation from confluent fibroblasts *via* the state of preadipocytes to mature adipocytes. The cell line 3T3-L1 has been used extensively by many authors (Spooner et al. 1979, Frost and Lane 1985, Zuber et al. 1985, Chan et al. 1988, Clancy and Czech 1990, Wieland et al. 1990, Müller et al. 1993). For some purposes (e. g. analysis of the endogenous leptin production), the F442A mouse fibroblastic cell line has been used successfully (Zhang et al. 2002, Teta et al. 2005). Kletzien and coworkers (1992) studied the effect of pioglitazone, an insulin-sensitizing agent, on the expression of the adipocyte fatty acid-binding protein in *ob/ob* mice and 3T3 L1 cells.

PROCEDURES

Culture and Differentiation

3T3-L1 fibroblasts (American Type Culture Collection, Rockville, MD) are seeded in 12-well (60,000 cells/well) or 96-well (15,000 cells/well) plates and maintained in DMEM (high glucose), 10% fetal bovine serum (FBS), 5 mM L-glutamine and 2% BSA. Following three days at 90–100% conflu-

ence, differentiation is initiated by the addition of DMEM containing 10% FBS, 400 nM human insulin, 1 µM dexamethasone and 1 mM IBMX. Three days later, the medium is replaced with DMEM, 10% FBS and 100 nM insulin. After additional two days, the medium is changed to DMEM (low glucose) and 10% FBS. The presence of putative insulin-sensitizing compounds, such as glitazones (e. g. 1–10 µM pioglitazone) in the various differentiation media considerably may improve the degree of differentiation as has been shown in numerous studies since the introduction of these drugs into the anti-diabetic therapy. The differentiated adipocytes are used 5 to 12 d after completion of the differentiation protocol, when more than 85% of the cells expressed the adipocyte phenotype (LD accumulation as observed with "Oil Red" staining). Prior to experimentation, the cells are rinsed two times with low serum medium (DMEM containing 5 mM glucose, 0.5% BSA, 0.1% FBS, 25 mM HEPES/KOH, pH 7.4, 10 mM glutamine, 100 units/ml streptomycin/penicillin), then incubated (12 to 14 h) in this medium lacking FBS (for down-regulation of the insulin signal transduction cascade) and finally washed twice with PBS containing 2 mM sodium pyruvate prior to incubation (30 min, 37°C) with insulin or compounds/drug candidates.

K.5.1.4.2 OP9 Adipocytes

PURPOSE AND RATIONALE

The 3T3-L1 adipocyte model has significant limitations. First, from the time of initial plating, the generation of 3T3-L1 adipocytes from preadipocytes requires at least two weeks (Student et al. 1980). Second, if 3T3-L1 cells become confluent and are further propagated or if they are passaged extensively, they no longer differentiate robustly into adipocytes. These issues make culturing of 3T3-L1 cells demanding and limit their utility in the generation of stable cell lines. Third, it is difficult to efficiently detect RNAs and proteins encoded by transiently transfected DNA in 3T3-L1 adipocytes. This limitation derives from the facts that most plasmid transfection protocols require subconfluent cells and that levels of RNAs and proteins expressed from such transfections dramatically decline before 3T3-L1 cells become adipocytes. Finally, because the 3T3-L1 cell line originated from a single clone and thus has clone-specific traits, it fails to recapitulate the primary cells it models. Thus, an alternative, tractable adipocyte model system would be desirable. A new adipocyte cell culture model, OP9 mouse stromal cells, has been characterized recently that provides a tractable alternative system for studies of adipocyte biology (Wolins et al. 2006). The OP9 cell line was established from the calvaria of newborn mice genetically deficient in functional macrophage colony-stimulating factor (M-CSF) (Nakano et al. 1994).

PROCEDURE

Propagation and Differentiation

OP9 cells are available from the American Type Culture Collection (ATCC, catalog no. CRL-2749), however, have to be tested and selected for those capable of consistent differentiation into adipocytes. OP9 cells are grown in OP9 propagation medium (α-MEM, 20% FBS, 2 mM L-glutamine, 100 U/ml penicillin, and 100 µg/ml streptomycin). The optimal differentiation potential of OP9 cells is achieved when cells are replated every three days at a density of at least 7,000 cells/cm^2. OP9 cells grown in this manner are flat with broad cell processes. In contrast, OP9 cells maintained at low cell density adopt a spindly morphology and differentiate into adipocytes poorly. Three methods can be used to differentiate OP9 preadipocytes into adipocytes.

Serum Replacement Method (SR)

OP9 cells are grown to confluence and then cultured for two additional days in either OP9 or 3T3-L1 propagation medium as described above. The cells are then cultured up to 4 more days in serum replacement medium (α-MEM, 15% KnockOut™ SR [Invitrogen], 100 U/ml penicillin, and 100 µg/ml streptomycin). For the purpose of studying effects of insulin/compounds/drugs, it is important to change the SR medium to OP9 propagation medium after day 2 of differentiation, because KnockOut™ SR contains very high concentrations of insulin (final concentration of 1.7 µM) and 5 ng/ml bone morphogenic protein 4 (BMP-4; R&D Systems). However, BMP-4 makes no significant difference in adipocyte differentiation, so all experiments can be performed without BMP-4 with the exception of the assay for insulin-stimulated glucose uptake.

Insulin/Oleate Method (IO)

OP9 cells are plated at 5,000 cells/cm^2. When cells adhered to the plate, the OP9 propagation medium is replaced with insulin/oleate medium (α-MEM, 0.2% FBS, 175 nM insulin, 900 µM oleate bound to BSA [5.5/1 molar ratio] prepared according to Wolins and coworkers (2005); 100 U/ml penicillin, and 100 µg/ml streptomycin).

Adipogenic Cocktail Method (AC)

This method is very similar to that used for 3T3-L1 cells (see K.5.1.4.1 and Student et al. 1980). Cells are grown to confluence and then cultured for two additional days in 3T3-L1 adipocyte medium (DMEM, 10% FBS, 2 mM L-glutamine, 100 U/ml penicillin, and 100 µg/ml streptomycin). Cells are then cultured for two days in DM1 (DMEM, 10% FBS, 175 nM insulin, 0.25 µM dexamethasone, 0.5 mM IBMX, 2 mM L-glutamine, 100 U/ml penicillin, and 100 µg/ml streptomycin). The cells are cultured for two additional days in DM2 (DMEM, 10% FBS, 175 nM insulin, 2 mM L-glutamine, 100 U/ml penicillin, and 100 µg/ml streptomycin). Differentiated OP9 cells are maintained in OP9 propagation medium.

EVALUATION

OP9 mouse stromal cells represent a new model of rodent adipocytes that will be useful for further studies of the mechanisms of adipocyte differentiation and of mature adipocyte function (Wolins et al. 2006). When OP9 cells are given any one of three adipogenic stimuli, they rapidly accumulate TAG to form numerous, large LD, exert adipocyte morphology, express adipocyte late marker proteins, including glucose transporter 4 (GLUT4), adiponectin, perilipin, and S3–12 and exhibit robust insulin-stimulated glucose transport. OP9 cells can differentiate into adipocytes within two days. This rapid rate of differentiation allows for the detection of transiently expressed proteins in mature OP9 adipocytes. Adipogenesis in OP9 cells involves the master transcriptional regulator of adipocyte differentiation, peroxisome proliferator-activated receptor (PPAR-γ). OP9 cells are late preadipocytes in that, before the addition of adipogenic stimuli, they express the adipocyte proteins CCAAT/enhancer binding proteins α and β, PPAR-γ, sterol-regulatory element binding protein-1, S3–12, and perilipin. OP9 differentiation is not diminished by maintenance in culture at high cell density or by long periods in continuous culture, thereby facilitating the generation of stable cell lines that retain adipogenic potential.

Several practical features of OP9 cells make this cell line a particularly convenient model for adipocyte studies. First, OP9 adipocytes can be rapidly produced from either preconfluent cells (IO method) or confluent cells (SR and AC methods). Second, in contrast to 3T3-L1 cells, OP9 cells can be maintained at high density without loss of potential to differentiate into adipocytes. Third, OP9 cells continue to differentiate well even at high passage number. These features permit large numbers of OP9 cells to be conveniently maintained in culture and OP9 adipocytes to be produced for experiments within a few days.

K.5.1.5 Cultured Human Adipocytes

Murine cell models, most notably the 3T3-L1 cell line, have been the basis for the majority of studies of lipogenesis and lipolysis including their regulation as well as of adipogenesis at the transcriptional and post-transcriptional levels. However, there is a growing concern that the regulation of lipid metabolism may differ between human and murine adipocytes. For example, the resistin gene and its secreted protein product as well as its putative role in the regulation of lipid synthesis and degradation were first identified in the 3T3-L1 cells. Subsequent *in vivo* analysis in mice demonstrated an association between resistin levels, obesity, and type II diabetes. In contrast, clinical studies do not demonstrate a comparable association between serum resistin levels, obesity, and insulin resistance in non-obese and obese human subjects. Likewise the expression of the agouti gene in adipose tissue and its involvement in lipolysis regulation differs between man and mouse. These discrepancies argue for the increased use of human preadipocyte cell models in exploratory research and drug discovery relating to obesity and type II diabetes. Recently, the culturing of human adipocytes has been introduced successfully. The dramatically increasing incidence of diabetes and obesity in the industrialized countries immediately argues for the need of *in vitro* studies with human adipocytes, which justifies a more detailed evaluation of their generation and characterization. Two different sources for differentiated human adipocytes are available so far which differ in their accessibility for daily use and reflection of the primary adipocyte phenotype.

K.5.1.5.1 Adipocytes Derived from Human Adipose-Derived Adult Stem (ADAS) Cells

PURPOSE AND RATIONALE

ADAS cells can be reproducibly isolated from liposuction aspirates through a procedure involving collagenase digestion, differential centrifugation, and expansion in culture. A single milliliter of tissue yields over 400,000 cells (Aust et al. 2004). The undifferentiated human ADAS cells express a distinct immunophenotype based on flow cytometric analyses and, following

induction, produce additional adipocyte-specific proteins (Aust et al. 2004, Gronthos et al. 2001, Halvorsen et al. 2001, Sen et al. 2001, Zuk et al. 2002). The human ADAS cells display multipotentiality with the capability of differentiating along the adipocyte, chondrocyte, myogenic, neuronal, and osteoblast lineages (Aust et al. 2004, Zuk et al. 2002). In the presence of dexamethasone, insulin, IBMX, and a thiazolidinedione, the undifferentiated human ADAS cells undergo adipogenesis. Between 30 and 80% of the cells, based on flow cytometric methods, accumulate LD, which can be stained for neutral lipids with the "Oil Red" dye.

PROCEDURE

LD proteomicsProteomic procedures for the analysis of human (ADAS) and rodent fat cells have been used by DeLany and coworkers (2005), Lee and coworkers (2006), Chen and coworkers (2005) and Brasaemle and coworkers (2004). For the evaluation of ADAS cells (DeLany et al. 2005), liposuction aspirates from subcutaneous adipose tissue sites can be obtained from male and female subjects (30–40 years, 25–30 BMI) undergoing elective procedures in local plastic surgical offices. Tissues are washed three to four times with PBS and suspended in an equal volume of PBS supplemented with 1% bovine serum and 0.1% collagenase type I prewarmed to 37°C. The tissue is placed in a shaking water bath at 37°C with continuous agitation for 60 min and centrifuged ($300 \times g$, 5 min, room temperature). The supernatant is removed, and the pelleted stromal vascular fraction (SVF) is resuspended in Stromal Medium (DMEM/F-12 Ham's, 10% FBS, antibiotics/antimycotics) and plated at a density of 0.156 ml of tissue digest/cm^2 of surface area in T225 flasks using Stromal Medium for expansion and culture according to the procedure of Hauner and coworkers (1989). This initial passage of the primary cell culture is referred to as "Passage 0." Following the first 48 h of incubation at 37°C at 5% CO_2, the cultures are washed with PBS and maintained in Stromal Medium until they achieve 100% confluence (mean cell density of ~30,000 cells/cm^2 after 4 d in culture). The cells are passaged by trypsin/EDTA digestion and seeded at a density of 30,000 cells/cm^2 ("Passage 1") on 10-cm plates.

One day after seeding, plates are either harvested for protein (day 0), or the medium is replaced with an adipogenic differentiation (AD) medium composed of DMEM/F-12 with 3% FBS, 33 µM biotin, 17 µM pantothenate, 1 µM bovine insulin, 1 µM dexamethasone, 0.25 mM IBMX, 5 µM rosiglitazone, and 100 units of penicillin, 100 µg of streptomycin, 0.25 µg of Fungizone. After three days, AD medium is changed to adipocyte maintenance medium, which is identical to the AD medium except for the removal of both IBMX and rosiglitazone. Cells are fed every 3rd day and usually maintained in culture for 9 d prior to harvest.

EVALUATION

The studies published so far provide a composite profile of the proteome of undifferentiated human ADAS cells obtained from multiple donors. Overall, the results confirm the adipocyte-specific protein expression. However, not all of the proteins identified derive from ADAS cells and may be qualified as contaminants. The most striking examples are hemoglobins A and B, reported in the undifferentiated cell lysates. The presence of hemoglobin apparently reflects the cell isolation procedure. The SVF population prepared by collagenase digestion of the adipose tissue and subsequent centrifugation routinely contains erythrocytes that are washed away after a 48-h period during which the ADAS cells adhere to the plastic surface. Typically, nucleated hematopoietic cells, expressing the marker CD45, account for less than 1% of the ADAS cell population by Passage 1 according to previous flow cytometric studies (Aust et al. 2004, Gronthos et al. 2001). Nevertheless it is feasible that some hemoglobin remains bound to the adherent ADAS cell population either as intact erythrocytes or as membrane-bound protein.

Proteomic analyses of total cell lysates from murine 3T3-L1 adipocytes have identified between eight and 100 protein features by one- and two-dimensional gel electrophoresis/mass spectroscopy (Welsh et al. 2004, Wilson et al. 2003, Brasaemle et al. 2004, Choi et al. 2004). The ADAS cell proteome includes a high percentage of identical or similar proteins (DeLany et al. 2005).

K.5.1.5.2 Adipocytes Derived from Commercially Available Human Preadipocytes

PROCEDURE

Frozen human preadipocytes (PromoCell) are thawed and cultured in preadipocyte expansion medium (DMEM/F12 supplemented with 10% FBS, human epidermal growth factor (2.5 ng/ml), hTGF-β (0.25 ng/ml), bovine fibroblast growth factor (bFGF, 0.5 ng/ml), and antibiotics until the cells are confluent. For adipocyte terminal differentiation, preadipocytes are induced with differentiation medium contain-

ing DMEM/F12, 3% rabbit serum, biotin (33 µM), pantothenate (17 µM), human recombinant insulin (0.1 µM), dexamethasone (1 µM), IBMX (0.5 mM), and a peroxisome proliferator-activated receptor (PPAR) γ-ligand, such as troglitazone (3 µM) or F-moc-L-leucine (30 µM). After a 6-d induction period, with fresh medium added every 3rd day, the cells are fed with the same medium without IBMX or a PPAR γ-ligand (adipocyte medium) every 3–4 d for 6 additional days. Cells at passages 3–4 are routinely used for adipocyte differentiation. TAG accumulation is confirmed by staining formaldehyde-fixed cells with the neutral lipid-specific dye, Bodipy, at 1 µg/ml. Microscopic images are obtained using an inverted microscope with iluminator and image acquisition system (Carl Zeiss, Inc., Germany).

EVALUATION

Differentiated adipocytes are fixed in formaldehyde (5%), and TAG is stained with Bodipy. After the fluorescence of each well has been read at 530 nm, the Bodipy-stained lipid is removed, and cells are permeabilized using isopropanol. Isopropanol is subsequently removed, and cellular DNA is stained with EthD-1 (2 µM) for 30 min before measuring EthD-1 fluorescence at 620 nm. The EthD-1 readout is directly correlated with cell density between 2,000 and 40,000 cells/cm^2. Fluorescence units of Bodipy and EthD-1 per well are used to determine the lipid/DNA ratio.

K.5.1.6 Adipocyte–Myocyte Co-Culture

PURPOSE AND RATIONALE

There is growing evidence that paracrine/endocrine communication between adipose and muscle cells may be involved in the induction of insulin resistance during the pathogenesis of type II diabetes. This negative cross-talk, which may be mediated by soluble factors secreted by the adipocytes (e. g. adipokines) can be mimicked *in vitro* by using a co-culture based on human primary skeletal muscle and human primary adipose cells as has been recently introduced by Eckel and coworkers (Dietze et al. 2002).

PROCEDURE

Culture of Human Skeletal Muscle Cells

Satellite cells are isolated from M. rectus abdominis by enzymatic digestion with trypsin followed by a purification step with fibroblast-specific magnetic beads to prevent contamination with fibroblasts. After two passages, the myoblasts are characterized by the manufacturer (PromoCell) using immunohistochemical detection of sarcomeric myosin in differentiated cultures at 100% confluence (8 d). Primary human skeletal muscle cells of four healthy donors are usually supplied as proliferating myoblasts (5×10^5 cells). These cells are grown up to confluence in 25 cm^2 flasks, trypsinized, and subsequently seeded in 175 cm^2 flasks at a density of 1×10^6 cells. After two passages 5–7.5 $\times 10^7$ cells are harvested and stored until further use as frozen aliquots containing 2×10^6 myoblasts. For an individual experiment, myoblasts are seeded in 6-well culture dishes (9.6 cm^2/well) at a density of 10^5 cells per well and are cultured in α-MEM/Hams F-12 medium containing "Skeletal Muscle Cell Growth Medium Supplement Pack" to up to near confluence. The cells are then differentiated and fused by culture in α-MEM for 4 days.

Isolation and Culture of Human Adipocytes

Adipose tissue samples are obtained from the mammary fat of normal or moderate overweight women (BMI 20–30 kg/m^2, 20 and 50 years) undergoing surgical mammary reduction. All subjects should be healthy and have no evidence of diabetes according to routine laboratory tests. Adipose tissue samples are dissected from other tissues and minced into pieces of about 10 mg in weight. Preadipocytes are isolated by collagenase digestion as described (K.5.1.2). Isolated cell pellets are resuspended in DMEM/Hams F12 medium supplemented with 10% FCS, seeded on membrane inserts (3.5×10^5/4.3 cm^2) or in a 6-well culture dish, and kept in culture for 16 h. After washing, culture is continued in an adipocyte differentiation medium. After a period of 15 days, 60–80% of seeded preadipocytes develop into differentiated adipose cells as defined by cytoplasm completely filled with small or large LD.

Co-Culture

Co-culture of human fat and muscle cells is conducted according to a recently published protocol (Dietze et al. 2002, Dietze-Schroeder et al. 2005). Briefly, after *in vitro* differentiation of preadipocytes on membrane inserts, the adipocytes are washed once with PBS and then incubated for 24 h in skeletal muscle cell differentiation medium containing 1 pM insulin. Thereafter, adipocytes are washed twice with PBS and individual membrane inserts are subsequently transferred to the culture plates containing differentiated (4 d) myocytes in α-MEM containing 1 pM insulin. This results in

an assembly of the two cell types sharing the culture medium but being separated by the membrane of the insert. The typical distance from the bottom of the culture dish to the membrane is 0.9 mm. Co-culture is conducted for 48 h.

EVALUATION

Integrity of both cell types is routinely checked by light microscopy at the end of the co-culture period. Following co-culture, the effect of insulin or compounds/drugs are studied as described below for normal myocytes and adipocytes.

K.5.1.7 Adipocytes Derived from Mouse Embryonic Fibroblasts (MEF)

It is often useful to study the effects of insulin/compounds/drugs in adipocytes derived from knockout (KO) mice deficient for one (or several) gene(s) relevant for adipocyte differentiation or function. This may lead to the confirmation/exclusion of the affected gene (product) in the molecular mechanism of insulin/compound/drug action on the regulation of lipid metabolism or differentiation in adipocytes. For this, MEF from the KO mice are isolated and differentiated to adipocytes *in vitro*. Stable lines of MEF adipocytes are generated from 12.5–14.5 d embryos of wildtype or homozygous KO mice as described. Selected MEF cells are cultured in DMEM with 10% FBS. At confluence cells are exposed to a pro-differentiation regimen 1 µM dexamethasone, 5 µg/ml insulin, 0.5 mM IBMX and 5 µM rosiglitazone. After two days cells are maintained in medium containing insulin for 4 d, then in medium without insulin for an additional 3–4 d before use.

K.5.1.8 Brown Adipocytes

Brown fat precursor cells are isolated from the interscapular brown adipose tissue of 5–6 week old C57BL/6 wildtype, KO or transgenic mice. Cells are cultured in maintenance medium (DMEM, 10% FBS, 10 mM HEPES, 100 nM sodium selenite, 3 nM insulin, 15 mM ascorbic acid, 50 µg/ml tetracycline, 50 µg/ml streptomycin, 50 µg/ml ampicillin 1 µg/ml Fungizone [Invitrogen]). Precursors are seeded at 15–20,000 cells/cm^2 in 12-well plates or in 35-mm coverslip-bottom dishes for biochemical and cell biological assays. After they attained confluence (d 0), cells are cultured for two days in differentiation medium (DMEM, 0.5 mM IBMX, 0.5 mM dexamethasone, 125 µM indomethacin after which they are maintained in maintenance medium for an additional three days before use.

K.5.1.9 Conditionally Immortalized Cell Strains

PURPOSE AND RATIONALE

Cell lines provide the cell count and homogenous populations for throughput applications, but do not behave as a primary cell can. It is well accepted that primary cells behave more normally than cell lines. Yet, key limitations exist that preclude one from using primary cells during initial phases of drug discovery. The limitations include cost, homogeneity of cell population and total cell count achievable, donor-to-donor variability, and loss of key cellular behaviours when the cell is outside its home organ.

Conditionally immortalized cell strains are primary cells that behave normally in cell culture, can be expanded beyond 40 population doublings, yet maintain normal behaviours throughout the culture time. This is achieved by combining the telomerase rejuvenating effect of telomerase with a specifically modified temperature-sensitive large-T (ts LT) antigen in the same cell. The ts LT mutant codes for a gene product that is functional at 33°C but non-functional at 37°C. Though the construct overcomes the cells' natural senescence behaviour at low passage and provides a strong proliferative signal, the cells are not able to exhibit a full range of differentiated functions. By switching the culture conditions to 37°C one stops cell proliferation and the cells are responsive to media growth factors that drive differentiation. If the line is carried at 37°C for sufficient time, the strain permanently looses its ability to proliferate. A second mutation in the construct controls SV40's ability to auto-excise. Consequently, this mutant conveys a higher level of karyotype stability to the host genomic background over multiple population doublings. Telomerase, also called telomere terminal transferase, elongates chromosomes by adding TTAGGG sequences to the end of existing chromosomes thereby preventing chromosomes from losing base pair sequences at their ends and from fusing to each other. However, each time a cell divides, some of the telomere is lost (25–200 bp per division). When the telomere becomes too short, the chromosome reaches a critical length and can no longer replicate. At this point cells senescence and may be removed by apoptosis. In somatic and aging cells telomerase activity is usually very low. If telomerase is activated in cell, the cell will continue to grow and divide. Consequently,

the conditionally immortalized cell strain with active telomerase acts like a primary cell but provides homogenous cell populations at the high cell counts of cell lines.

EXPERIMENTAL PROCEDURES

Sequential retroviral (MMLV-based vector possessing the Neomycin selection marker) transfection at low passage using ts LT (u197sA58), followed by the telomerase construct hTERT, leads to highly proliferative strains which are highly responsive to differentiation. The conditional immortalization allows at a permissive temperature production of large uniform cell populations while active telomerase is reversing telomere shortening. Concurrently, at the permissive temperature ts LT is actively driving cell proliferation while maintaining karyotype stability over >40 population doublings. By increasing the culture temperature the cells stop dividing. One then converts to a differentiation medium so that the cells can express normal differentiated function and phenotype once again.

Conditionally Immortalized Human Skeletal Muscle Cells

The XM13A1 cell line introduced from Cambrex, Clonetics Bio Science Walkersville Inc. contains a mixed cell population derived from human skeletal muscle of normal 30–40 year old female subjects. These cells can finally be differentiated from myoblasts into well-developed myotubes (e. g. in 96-well plates) that have morphological and phenotypic characteristics of differentiated muscle. These include creatine kinase activity and stimulation (2- to 2.5-fold above basal) of glycogen synthesis by 0.1–1 μM insulin up to passage 21. Other markers of differentiation found include myogenin, GLUT4, uncoupling protein-3 and GS. Functional activities include stimulation of glycogen synthesis by LiCl and IGF-1, stimulation of glucose transport by AICAR and induction of insulin resistance by glucosamine (see K.5.1.3) or fatty acids.

Conditionally Immortalized Human Preadipocytes

The XA15A1 and XM18B1 cell lines introduced from Cambrex, Clonetics Bio Science Walkersville Inc. represent mixed cell populations derived from subcutaneous adipose tissue of normal 31–40/60 year old male subjects. Both strains are highly responsive, given the correct media conditions (even in the absence of PPARγ ligands glitazones), to differentiate from the primary normal human preadipocytes into functional mature adipocytes after more than 40 population doublings in culture. Markers of differentiation found include glycerol-3-phosphate dehydrogenase and aP2. The differentiated cells secrete leptin and adiponectin into the culture medium and exhibit insulin stimulation of glycogen synthesis (up to 2-fold with EC_{50} of 10–50 nM) and of glucose transport (up to 2.5-fold at 1 μM).

REFERENCES AND FURTHER READING

Aust L, Devlin BH, Foster SJ, Halvorsen Y-DC, Hicok K, Kloster AL, du Laney TV, Sen A, Willlingmyre D, Gimble JM (2004) Recovery of human adipose derived adult stem cells from liposuction aspirates. Cytotherapy 6:1–8

Banerjee RR, Lazar MA (2003) Resistin: molecular history and prognosis. J Mol Med 81:218–226

Brasaemle DL, Dolios G, Shapiro L, Wang R (2004) Proteomic analysis of proteins associated with lipid droplets of basal and lipolytically stimulated 3T3-L1 adipocytes. J Biol Chem 279:46835–46842

Chen X, Cushman SW, Pannell LK, Hess S (2005) Quantitative proteomic analysis of the secretory proteins from rat adipose cells using a 2D liquid chromatography – MS/MS approach. J Prot Res 4:570–577

Choi KL, Wang Y, Tse CA, Lam KS, Cooper GJ, Xu A (2004) Proteomic analysis of adipocyte differentiation: evidence that α2 macroglobulin is involved in the adipose conversion of 3T3L1 preadipocytes. Proteomics 4:1840–1848

Clancy BM, Czech MP (1990) Hexose transport stimulation and membrane redistribution of glucose transporter isoforms in response to cholera toxin, dibutyryl cyclic AMP, and insulin in 3T3-L1 adipocytes. J Biol Chem 265:12434–12443

Dietze D, Koenen M, Röhrig K, Horikoshi H, Hauner H, Eckel J (2002) Impairment of insulin signaling in human skeletal muscle cells by co-culture with human adipocytes. Diabetes 51:2369–2376

Dietze-Schroeder D, Sell H, Uhlig M, Koenen M, Eckel J (2005) Autocrine action of adiponectin on human fat cells prevents the release of insulin resistance-inducing factors. Diabetes 54:2003–2011

DeLany JP, Floyd ZE, Zvonic S, Smith A, Gravois A, Reiners E, Wu X, Kilroy G, Lefevre M, Gimble JM (2005) Proteomic analysis of primary cultures of human adipose-derived stem cells. Mol Cell Proteomics 4:731–740

Fauth C, O'Hare MJ, Lederer G, Jat PS, Speicher MR (2004) Order of genetic events is critical determinant of aberrations in chromosome count and structure. Chron Cancer 40:298–306

Frost SC, Lane MD (1985) Evidence for the involvement of vicinal sulfhydryl groups in insulin-activated hexose transport by 3T3-L1 adipocytes. J Biol Chem 260:2646–2652

Green H, Kehinde O (1974) Sublines of mouse 3T3 cells that accumulate lipid. Cell 1:113–116

Gronthos S, Franklin DM, Leddy HA, Storms R, Gimble JM (2001) Characterization of surface protein expression on human adipose tissue-derived stromal cells. J Cell Physiol 189:54–63

Halvorsen Y-DC, Bond A, Sen A, Franklin DM, Lea-Currie YR, Ellis PN, Wilkison WO, Gimble JM (2001) Thiazolidinediones and glucocorticoids synergistically induce differentiation of human adipose tissue stromal cells: biochemical, cellular and molecular analysis. Metabolism 50:407–413

Hauner H, Entenmann G, Wabitsch M, Gaillard D, Ailhaud G, Negrel R, Pfeiffer EF (1989) Promoting effect of glucocorticoids on the differentiation of human adipocyte precursor cells cultured in a chemically defined medium. J Clin Investig 84:1663–1670

Kletzien RF, Foellmi LA, Harris PKW, Wyse BM, Clarke SD (1992) Adipocyte fatty acid-binding protein: Regulation of gene expression *in vivo* and *in vitro* by an insulin-sensitizing agent. Mol Pharmacol 42:558–562
Lee H-K, Lee B-H, Park S-A, Kim C-W (2006) The proteomic analysis of an adipocyte differentiated from human mesenchymal stem cells using two-dimensional gel electrophoresis. Proteomics 6:1223–1229
Marshall S, Garvey WT, Geller M (1984) Primary culture of adipocytes. J Biol Chem 259:6376–6384
McGillis JP (2005) White adipose tissue, inert no more. Endocrinology 146:2154–2156
Müller G, Wied S (1993) The sulfonylurea drug, glimepiride, stimulates glucose transport, glucose transporter translocation, and dephosphorylation in insulin-resistant rat adipocytes *in vitro*. Diabetes 42:1852–1867
Nakano T, Kodama H, Honjo T (1994) Generation of lymphohematopoietic cells from embryonic stem cells in culture. Science 265:1098–1101
O'Hare MJ, Bond J, Clarke C, Takeuchi Y, Atherton AJ, Berry C (2001) Conditional immortalization of freshly isolated mammary fibroblasts and endothelial cells. Proc Natl Acad Sci USA 98:646–651
Sen A, Lea-Currie YR, Sujkowska D, franklin DM, Wilkison WO, Halvorsen Y-DC, Gimble JM (2001) The adipogenic potential of human adipose derived stromal cells from multiple donors is heterogenous. J Cell biochem 81:312–319
Spooner PM, Chernick SS, Garrison MM, Scow RO (1979) Insulin regulation of lipoprotein lipase activity and release in 3T3-L1 adipocytes. J Biol Chem 254:10021–10029
Student AK, Hsu RY, Lane MD (1980) Induction of fatty acid synthase synthesis in differentiating 3T3-L1 preadipocytes. J Biol Chem 255:4745–4750
Teta D, Tedjani A, Burnier M, Bevington A, Brown J, Harris K (2005) Glucose-containing peritoneal dialysis fluids regulate leptin secretion from 3T3-L1 adipocytes. Nephrol Dial Transplant 20:1329–1335
Welsh GI, Griffiths MR, Webster KJ, Page MJ, Tavare JM (2004) Proteome analysis of adipogenesis. Proteomics 4:1042–1051
Wieland M, Brandenburg C, Brandenburg D, Joost HG (1990) Antagonistic effect of a covalently dimerized insulin derivative on insulin receptors in 3T3-L1 adipocytes. Proc Natl Acad Sci USA 87:1154–1158
Wilson-Fritch L, Burkart A, Bell G, Mendelson K, Leszyk J, Nicoloro S, Czech M, Corvera S (2003) Mitochondrial biogenesis and remodelling during adipogenesis and in response to the insulin sensitizer rosiglitazone. Mol Cell Biol 23:1085–1094
Wolins NE, Quaynor BK, Skinner JR, Schoenfish MJ, Tzekov A, Bickel PE (2005) S3–12, adipophilin, and TIP47 package lipid in adipocytes. J Biol Chem 280:19146–19155
Wolins NE, Quaynor BK, Skinner JR, Tzekov A, Park C, Choi K, Bickel PE (2006) OP9 mouse stromal cells rapidly differentiate into adipocytes: characterization of a useful new model of adipogenesis. J Lipid Res 47:450–46
Zhang P, Klenk ES, Lazzaro MA, Williams LB, Considine RV (2002) Hexosamines regulate leptin production in 3T3-L1 adipocytes through transcriptional mechanisms. Endocrinol 143:99–106
Zuber MX, Wang S-M, Thammavaram KV, Reed DK, Reed BC (1985) Elevation of the number of cell-surface insulin receptors and the rate of 2-deoxyglucose uptake by exposure of 3T3-L1 adipocytes to tolbutamide. J Biol Chem 260:14045–14052
Zuk PA, Zhu M, Ashjian P, De Ugarte DA, Huang JI, Mizuno H, Alfonso ZC, Fraser JK, Benhaim P, Hedrick MH (2002) Human adipose tissue is a source of multipotent stem cells. Mol Biol Cell 13:4279–4295

K.5.2 Liver and Hepatocytes

GENERAL CONSIDERATIONS

In type II diabetic patients with moderate fasting hyperglycemia, the liver production of glucose is increased by about 50 g/d above normal (DeFronzo et al. 1992). This modest increase is the consequence of reduced suppression of hepatic glucose production by insulin (Firth et al. 1987) and could be nullified by reducing dietary carbohydrate by 50 g/d. The increased hepatic glucose production in type II diabetes is probably caused by a combination of lack of an insulin-mediated reduction in glucagon secretion (Müller et al. 1970) and hepatic resistance to insulin action at the level of both the insulin signaling transduction cascade and its coupling to the metabolic end effector enzymes of gluconeogenesis. The importance of increased hepatic glucose production is underlined by the fact that when phosphoenolpyruvate carboxykinase (PEPCK), the key rate-limiting regulatory enzyme of gluconeogenesis, is overexpressed in mice carrying a transgene expressing the protein hyperglycemia results (Valera et al. 1994). Independent of whether increased hepatic glucose production plays a primary or only secondary role in the pathogenesis of human type II diabetes, analysis of insulin signaling and metabolic action in liver is important for gaining a complete picture of the pathophysiology of type II diabetes. The model of the isolated perfused rat liver offers advantages in determining insulin action, which, compared to primary and cultured liver cells, are the intact tissue, the near physiological function of the liver, and, compared to the *in vivo* situation, the separation from other effects which may also affect hepatic metabolism, like basal glucagon secretion from α-cells, increased sympathetic activity and/or hypothalamic effects (Nonogaki 2000). Taken together, liver cells harbor a number of important targets for compounds/drugs with insulin-like and anti-diabetic activity, which can be assayed using the intact liver and primary or cultured hepatocytes of human and rodent origin.

K.5.2.1 Perfused Rat Liver

Male Wistar rats weighing 200–250 g are anesthetized with 150 mg/kg hexobarbital intraperitoneally. After opening the abdomen, two ligatures are tied around

the stomach, one around the esophageal end to include the adjacent blood vessels and the other around the pylorus. The stomach is removed between these ligatures, a procedure that facilitates the remaining dissection and the subsequent removal of the liver from the animal. A ligature is placed around the bile duct. The portal vein is tied and cannulated with PP10 tubing. The thorax is opened and the vena cava is cannulated via the right atrium. The lower vena inferior cava is tied and the liver is removed from the animal. From the portal vein the liver is washed with 100 ml heparinized (5 IU/ml) physiological saline solution at 37°C for 3 min whilst the outflow occurs via the vena cava. The preparation is then transferred to a perfusion apparatus, where the portal vein cannula is attached to tubing containing the oxygenated medium.

KRBH with 25% bovine erythrocytes, 1.6% BSA, and 22.5 mM Na-L-lactate is used as perfusion medium. The perfusion rate is 30 ml/min. 70 ml of this solution are used for recirculation over 2 h. The test compounds/drug candidates are added in a concentration of 40–100 µM to the perfusate medium. The central element of the perfusion apparatus is a gas-tight, thermostatized, double-walled suction filter with an insertable sieve base as support of the organ. The discharge tube is elongated with a Plexiglas tube of 18 cm length and 10 mm inside diameter. The lower end of this tube is connected to a peristaltic pump by means of a Luer safety joint. The suction filter for perfusion of the liver has an internal diameter of 95 mm. On the return of the perfusate to the organ, it passes through a heat exchanger (glass spiral) and a filter holder with a sieve membrane of stainless steel (diameter 25 mm, mesh size 50 µm). A variable carbogen/oxygen mixture, the ratio of which is depending on the pH value of the perfusate, is used for gassing. The perfusate in the Plexiglas tube is bubbled with 70 ml gas mixture/min. To avoid foam formation, a detergent (14 µl/ml 0.1% Genapol PF-10) has to be added to the perfusate. Samples for analyses are withdrawn by catheter immediately in front of the Luer joint in the Plexiglas tube.

K.5.2.2 Primary Rat Hepatocytes

Sprague-Dawley rats (100–200 g) are fed *ad libitum* prior to the hepatocyte isolation. Hepatocytes are isolated from rat livers thoroughly perfused with buffer containing collagenase, hyaluronidase and trypsin inhibitor as described by Van den Berghe and coworkers (1980). The rat livers are perfused for 4 min at 25 ml/min flow rate with perfusion buffer and then with collagenase buffer until the digestion is complete (~6 min). At the end of the perfusion, connective tissue and large blood vessels are removed. The hepatocytes are then passed through a 100-µm nylon mesh sieve. The cells are washed twice with 125 ml of wash buffer and collected by centrifugation ($50 \times g$, 2 min). The hepatocytes are suspended in plating medium (DMEM, 10% FBS, 100 nM insulin, 25 nM dexamethasone, 6.3 µg/ml transferrin, 22 µg/l gentamycin) and passed through a 100-µm nylon mesh sieve. Cells (1.6×10^5) are plated in 48-well cell culture plates for the various metabolic assays.

K.5.2.3 Cultured Human Hepatocytes

HepG2/C3A (ATCC) human hepatoma cells are cultured in minimal essential medium (α-MEM, GIBCO) supplemented with 10% FBS), 100 µM non-essential amino acid mix, 1 mM sodium pyruvate, and 1 mM L-glutamine and are seeded in 48-well plates at 1.4×10^5 cells per well three days prior to the experiment.

REFERENCES AND FURTHER READING

DeFronzo RA, Bonadonna RC, Ferrannini E (1992) Pathogenesis of NIDDM: a balanced overview, Diabetologia 35:389–394

Firth R, Bell P, Rizza R (1987) Insulin action in non-insulin-dependent diabetes mellitus: the relationship between hepatic and extrahepatic insulin resistance and obesity, Metabolism 36:1091–1095

Müller WA, Faloona GR, Aguilar-Parada E (1970) Abnormal alpha-cell function in diabetes: response to carbohydrate and protein ingestion, N Engl J Med 283:109–115

Nonogaki K (2000) New sights into sympathetic regulation of glucose and fat metabolism, Diabetologia 43:533–549

Valera A, Pujol A, Pelegin M (1994) Transgenic mice overexpressing phosphoenolpyruvate carboxykinase develop non-insulin-dependent diabetes mellitus, Proc Natl Acad Sci USA 91:9151–9154

Van den Berghe G, Bontemps F, Hers H-G (1980) Purine catabolism in isolated rat hepatocytes. Biochem J 188:913–920

K.5.3 Muscle Tissue and Myocytes

GENERAL CONSIDERATIONS

Muscle cell lines have been used to study skeletal muscle glucose metabolism in response to acute insulin stimulation. Subcellular fractionation followed by immunoblotting as well as photoaffinity labeling followed by immunoprecipitation has demonstrated that in cultured muscle cells insulin causes rapid translocation of the glucose transporter isoform, GLUT4, to the plasma membrane as has been well established for primary and cultured adipocytes. Over decades,

numerous studies have demonstrated that insulin affects many signalling events (e. g. IR and insulin receptor substrate tyrosine phosphorylation) as well as metabolic end effector systems (e. g. glucose transport and glycogen synthesis) in similar fashion. Despite the considerably higher complexity in gaining access to insulin-responsive cells/tissues from muscle compared to adipose tissue, the eminent physiological role of the human skeletal muscle as the predominant acute and short-term storage site for the daily carbohydrate intake necessitates the use of adequate cell- and tissue-based muscle model systems for assaying the insulin-like activity of compounds/candidate drugs. Moreover, these systems may be helpful for analysis of the molecular mechanisms of muscle insulin resistance and of its abrogation by putative insulin-sensitizing compounds/drugs. According to recent findings culminating in the "lipotoxicity hypothesis" (see K.6.3.4), peripheral insulin resistance seems to be correlated to the deposition or loss, respectively, of TAG or its precursors/degradation products in the cytoplasm of skeletal muscle cells, the so-called intramyocellular lipids. Thus, cell- and tissue-based muscle assay systems are also prerequisite for the analysis of myocellular lipid metabolism.

K.5.3.1 Perfused Rat Hindlimb

Female Wistar rats weighing 170–230 g are starved 48 h before the experiment. They are anesthetized by i.p. injection of 50 mg/kg pentobarbital. After an midline incision, the skin is reflected and the superficial epigastric vessels are ligated. The abdominal wall is then incised from the pubic symphysis to the xyphoid process using electrocautery. After ligation of the uterine, ovarian and inferior mesenteric arteries, the upper half of the uterus, the ovaries and part of the descending colon are excised, together with adhering adipose tissue. Next, branches of the hypogastric and pudoepigastric trunks supplying pelvic viscera are ligated. Ligatures are also placed around the neck of the bladder and the residual portions of the uterus and descending colon. Adipose tissue in the perineal and retroperitoneal regions is removed.

Two pairs of ligatures are placed around the aorta and the vena cava, one just above the origin of the iliolumbar vessels and the other above the origin of the renal vessels. The inferior epigastric, iliolumbar and renal vessels are then ligated as are the coeliac axis and the portal vein. A ligature is also placed around the tail. The ligatures previously placed around the vena cava and aorta above the origin of the renal vessels are then tied. The aorta is incised between the left renal and iliolumbar vessels and a no. 18 polyethylene catheter filled with 0.85% NaCl containing 200 units of heparin/ml is introduced, passed to a point midway between the iliolumbar vessels and the aortic bifurcation, and after flushing with heparin-NaCl solution finally tied in place. The vena cava is cannulated with a no. 16 needle which is secured in a position so that its tip is at the same level as the aortic catheter. The needle is connected with a transparent vinyl tubing. The preparation is then transferred to a perfusion apparatus, where the aorta cannula is attached to tubing containing the oxygenated medium.

KRBH with 25% bovine erythrocytes, 4% BSA, and 10 mM D-glucose is used as perfusion medium. The perfusion rate is 8 ml/min. 70 ml are used for recirculation over 2 h. The test compounds/drug candidate are added in a concentration of 40–100 µM to the perfusate medium. The central element of the perfusion apparatus is a gas-tight, thermostatized, double-walled suction filter with an insertable sieve base as support of the organ. The discharge tube is elongated with a Plexiglas tube of 18 cm length and 10 mm inside diameter. The lower end of this tube is connected to a peristaltic pump by means of a Luer safety joint. The suction filter for perfusion of the hind limb has an internal diameter of 145 mm. On the return of the perfusate to the organ, it passes through a heat exchanger (glass spiral) and a filter holder with a sieve membrane of stainless steel (diameter 25 mm, mesh size 50 µm). A variable carbogen/oxygen mixture, the ratio of which is depending on the pH value of the perfusate, is used for gassing. The perfusate in the Plexiglas tube is bubbled with 70 ml gas mixture/min. To avoid foam formation, a detergent (14 µl/ml 0.1% Genapol PF-10) has to be added to the perfusate. Samples for analyses are withdrawn by catheter immediately in front of the Luer joint in the Plexiglas tube.

K.5.3.2 Rat Diaphragms

Sprague Dawley rats weighing 70–100 g are used. The animals are sacrificed during anesthesia and the diaphragms still attached to the rib cages are carefully removed, released from the rib cages and adhering connective and fat tissues, washed in PBS, spread out and divided into two equal pieces as described by Müller and coworkers (1994). For assaying the effects of insulin/compounds/drugs, the hemidiaphragms are incubated in KRH buffer gassed with

carbogen (95% O_2/5% CO_2) in the presence of 5 mM glucose or other ingredients as indicated for the specific assays. In some cases, diaphragms attached to the rib cage instead of hemidiaphragms are used to prevent spontaneous contraction to less than physiological length.

K.5.3.3 Rat Soleus and Extensor Digitorum Longus

In studies of soleus muscle and extensor digitorum longus (EDL), the hindquarters are perfused for 3 min (25 ml/min) to wash out the blood. The two soleus or EDL muscles from each rat are removed with tendons intact, placed in perforated baskets and incubated in separate test tubes. Muscles from three rats are incubated together with insulin/compounds/drug candidates. The perfusing and incubation medium is KRB (pH 7.4) containing 8 mM glucose, 1 mM pyruvate and 0.2% (w/v) BSA. The incubation medium was gassed continuously with 95% O_2/5% CO_2. At the end of the incubation, muscles are freeze-clamped with aluminium tongs cooled in liquid nitrogen, and then trimmed of connective tissue and visible fat while kept in liquid nitrogen. In order to further ensure that findings reflected the biology of muscle cells, these are before analysis in most experiments isolated from other tissue components by microdissection using a stereomicroscope after freeze-drying.

K.5.3.4 Human Muscle Strips

A human muscle preparation has been introduced successfully by Dohm and coworkers (1988). For this, immediately after the surgical incision, muscle strips (abdominal rectus muscle) are mounted at *in vivo* length by using one set of clamps, which is 2.5-cm wide and constructed from two pairs of hemostats. The clamp is placed by the surgeon on the muscle, and a 0.5–1 g muscle piece is clamped, excised, and immediately transferred to oxygenated (KRBH) for immediate transfer to the laboratory. Muscle fiber strips, weighing between 20 and 50 mg, are dissected free from the mounted specimen, secured with a small Plexiglas support, and cut free. Particular care has to be taken to remove all visible fat. From one muscle piece, it is possible to obtain 5–10 muscle strips. After preparation, the muscle strips are washed for 30 min in KRBH supplemented with 38 mM mannitol, 2 mM pyruvate, and 10 mg/l BSA. The viability of muscle is usually investigated by analysis of 3–0-methylglucose transport (see below). Typically, insulin-stimulated glucose transport follows concentration-dependent fashion with the maximum effect of about 2-fold above the basal glucose transport rate ($\sim$1 µmol/ml · h).

K.5.3.5 Cultured Human Skeletal Muscle Cells

Human skeletal muscle cell cultures are handled as described by Aas and coworkers (2004). A cell bank of satellite cells is established from muscle biopsy samples of the vastus lateralis muscle from four healthy volunteers (age 25–30 years, BMI 22–25, fasting glucose and insulin within the normal range and no family history of diabetes). The biopsies have to obtained with informed consent and approval by the National Committee for Research Ethics. Muscle cell cultures free of fibroblasts were established as previously described (Henry et al. 1995) with minor modifications. Briefly, muscle tissue is dissected in Ham's F-10 media at 4°C, dissociated by three successive treatments with 0.05% trypsin/EDTA, and then satellite cells were resuspended in skeletal cell growth medium with 2% FCS and no added insulin. The cells are grown on culture wells coated with extracellular matrix gel (Gaster et al. 2001). After 2 to 3 weeks at about 80% confluence, fusion of myoblasts into multinucleated myotubes is achieved by growth for 8 d in α-MEM with 2% FCS. Hyperglycaemic medium can be made by the addition of glucose (to a concentration of 10 or 20 mM) to α-MEM with 2% FCS. All cells used in the experiments should be at passage 3 to 6.

K.5.3.6 L6 Myotubes

Stock cultures of L6 rat skeletal muscle cells from the ATCC are grown in α-MEM containing 10% (v/v) FBS, 100 U/ml penicillin, 100 µg/ml streptomycin, and antimycotics (growth medium) in a humidified atmosphere of 95% air and 5% CO_2 at 37°C. For the experiments, stocks are trypsinized and the myocytes reseeded on 6-well cell culture plates or 60 × 15 mm Petri dishes at a density of 4,000 cells/cm^2. After 24 h ($\sim$80% confluence), the medium is changed to α-MEM containing 2% (v/v) FBS and antibiotics/antimycotics as described above (differentiation medium) that is replaced after 2, 4, and 6 d of culture. After 7 d, myotube differentiation is complete, and experimental procedures are initiated. In all experiments, L6 myotubes are serum-starved for 4 h before expo-

sure to insulin/compounds/drugs. All controls are incubated with equal concentrations of the vehicle (e. g. DMSO) and the respective concentrations of fat-free albumin (e. g. BSA) as present in the treated cells.

K.5.3.7 L6 Myotubes Transfected with GLUT4

L6 myotubes express a detectable but rather moderate amount of the insulin-regulated GLUT4 which may account, in part, for the limited insulin stimulation of their glucose transport system. To increase the insulin responsiveness of glucose transport, L6 myocytes are transfected with myc-tagged GLUT4 (L6 GLUT4-myc cells) (Dr. Amira Klip, Davison of Cell Biology, The Hospital for Sick Children, Toronto, Canada). After growth in 96-well tissue culture plates using 200 µl of α-MEM containing 2% FBS, 100 units/ml penicillin G, and 100 mg/ml streptomycin sulfate at 37°C in a humidified atmosphere of 8.5% CO_2, myoblasts are seeded in medium containing 2% (v/v) FBS at a density of $\sim 2 \times 10^4$ cells/ml and used 6–8 d postseeding. Cells are fed fresh medium every 48 h and used at the stage of myocytes or after the differentiation to myotubes.

K.5.3.8 BC_3H_1 Myocytes

GENERAL CONSIDERATIONS

The BC_3H_1 cell line is a non-fusing spontaneously and reversibly differentiating mouse muscle cell line derived from a mouse neoplasm (Schubert et al. 1974). As for other cultured cell lines, the BC_3H^1 myocytes demonstrate intermediate characteristics, possessing electron-microscopic features of both smooth and skeletal muscle but with a nicotinic acetylcholine receptor and an action potential more characteristic of skeletal muscle (Standaert et al. 1984). Unfortunately, BC_3H_1 myocytes do not express GLUT4 and therefore the limited insulin stimulation of glucose transport relies on the glucose transporter isoform 1, GLUT1, exclusively.

PROCEDURE

BC_3H_1 myocytes are cultured to confluence in 100-mm dishes over 10–14 d in DMEM supplemented with 15% "Process Serum Replacement-I" (Sigma) and 25 mM glucose are added 18 h before the experiment. Cells are rinsed and pre-incubated at 37°C for 20 min in Dulbecco's PBS with 0.1 mM $CaCl_2$ and 1 mg/ml BSA, then treated with vehicle or compounds/drug candidates in vehicle for 30 min or overnight.

K.5.3.9 C_2C_{12} Myotubes

PURPOSE AND RATIONALE

C_2C_{12} cells, a mouse skeletal muscle cell line, has been isolated from dystrophic mouse muscle by Yaffe and Saxel (1977), McMahon and coworkers (1994), Ernst and White (1996). Subsequently, the myocytes have been shown to express a limited amount of GLUT4 and to be suitable for stable transfection experiments of exogenous cDNA, making this cell line a candidate for stable transfections of cDNAs that encode mutant skeletal muscle and cardiac protein isoforms.

PROCEDURE

Monolayers of mouse C_2C1_2 myoblasts (ATCC CRL-1772) are grown in Dulbecco's modified high-glucose Eagle's medium (DMEMH; 90%/10% (v/v) FBS/4.0 mM glutamine/50 µg/ml gentamycin, in a humidified incubator at 37°C, 5% CO_2 as has been described by Muoio and coworkers (1999) Cells are grown in 100-mm dishes, sub-cultured at 60–80% confluence, and split at a ratio of 1:10 using trypsin (0.25% (w/v) in MEM with 1.0 mM EDTA). Cells grown to 60% confluence are sub-cultured at a ratio of 1:15 into 6-well dishes that had been coated with 0.01% (w/v) collagen. When cells are 80% confluent, myoblasts are induced to differentiate into myotubes by changing to low-serum differentiation medium (98% DMEMH/2% (v/v) horse serum/4.0 mM glutamine/25 mM HEPES/50 µg/ml gentamycin). Differentiation medium is changed daily. By day 5, cells are typically fully confluent and had differentiated into multinucleated, contracting myotubes.

K.5.3.10 Cardiomyocytes

Cardiomyocytes are isolated by perfusion of hearts from adult rats with collagenase according to established protocols (Eckel et al. 1983 and 1991, Bähr et al. 1995).

REFERENCES AND FURTHER READING

Aas V, Kase ET, Solberg R, Jensen J, Rustan AC (2004) Chronic hyperglycaemia promotes lipogenesis and triacylglycerol accumulation in human skeletal muscle cells. Diabetologia 47:1452–1461

Dohm GL, Tapscott EB, Pories WJ, Dabbs DJ, Flickinger EG, Meelheim D, Fushiki T, Atkinson SM, Elton WE, Caro JF

(1988) An in vitro human muscle preparation suitable for metabolic studies. J Clin Invest 82:486–494
Bähr M, von Holtey M, Müller G, Eckel J (1995) Direct stimulation of myocardial glucose transport and glucose transporter-1 (GLU1) and GLUT4 protein expression by the sulfonylurea glimepiride. Endocrinology 136:2547–2553
Eckel J, Pandalis G, Reinauer H (1983) Insulin action on the glucose transport system in isolated cardiocytes from adult rat. Biochem J 212:385–392
Eckel J, Asskamp B, Reinauer H (1991) Induction of insulin resistance in primary cultured adult cardiac myocytes. Endocrinology 129:345–352
Ernst CW, White ME (1996) Hormonal regulation of IGF-binding protein-2 expression in C_2C_{12} myoblasts. J Endocrinol 149:417–429
Gaster M, Beck-Nielsen H, Schroder HD (2001) Proliferation conditions for human satellite cells. The fractional content of satellite cells. APMIS 109:726–734
Henry RR, Abrams L, Nikoulina S, Ciaraldi TP (1995) Insulin action and glucose metabolism in nondiabetic control and NIDDM subjects-comparison using human skeletal muscle cell-cultures. Diabetes 44:936–946
McMahon DK, Anderson PAW, Nassar R, Bunting JB, Saba Z, Oakeley AE, Malouf NN (1994) C_2C_{12} cells: biophysical, biochemical, and immunocytochemical properties. Am J Physiol Cell Physiol 266:C1795–C1802
Müller G, Wied S, Wetekam EM, Crecelius A, Pünter J (1994) Stimulation of glucose utilization in 3T3 adipocytes and rat diaphragm *in vitro* by the sulfonylureas glimiperide and glibenclamide, is correlated with modulations of the cAMP regulatory cycle. Biochem Pharmacol 48:985–996
Muoio DM, Seefeld K, Witters LA, Coleman RA (1999) AMP-activated kinase reciprocally regulates triacylglycerol synthesis and fatty acid oxidation in liver and muscle: evidence that sn-glycerol-3-phosphate acyltransferase is a novel target. Biochem J 338:783–791
Schubert D, Harris AJ, Devine CE, Heinemann S (1974) Characterization of a unique muscle cell line. J Cell Biol 61:398–413
Standaert ML, Shimmel SD, Pollet RJ (1984) The development of insulin receptors and responses in the differentiating non-fusing muscle cell line BC_3H_1. J Biol Chem 259:2337–2345
Yaffe D, Saxel O (1977) Serial passaging and differentiation of myogenic cells isolated from dystrophic mouse muscle. Nature, Lond. 270:725–727

K.5.4
Pancreas and Pancreatic β-Cells

GENERAL CONSIDERATIONS

Concurrent with the obesity epidemic, the incidence of type II diabetes is increasing at an alarming rate. Type II diabetes arises when the endocrine pancreas fails to secrete sufficient insulin to cope with the metabolic demand, because of aquired β-cell secretory dysfunction and/or decreased β-cell mass. Insulin secretory dysfunction is well documented. Whether insulin secretory dysfunction is a cause or consequence of the disease (in response to chronic challenge for compensation of the peripheral insulin resistance) is still debated, but there is mounting evidence that it may be symptomatic of changes in β-cell mass. Although proposed 50 years ago, the hypothesis that β-cell loss plays an important role in the pathogenesis of type II diabetes has only recently come to the fore. β-cell mass in the adult is plastic, and adjustments in β-cell growth and survival maintain a balance between insulin supply and metabolic demand. For example, obese individuals who do not develop diabetes exhibit an increase in β-cell mass that appears to compensate for the increased metabolic load and obesity-associated insulin resistance. However, this β-cell adaptation eventually fails in the subset of obese individuals who develop type II diabetes. Indeed, most individuals with type II diabetes whether obese or lean, show a net decrease in β-cell mass. Thus, type II diabetes is a disease of relative insulin deficiency. Given the pivotal role of β-cell mass in determining whether an individual will progress to type II diabetes, there is growing interest in understanding the mechanism that controls the life and death of β-cells. The molecular mechanisms involved in the decision between β-cell life and death have been reviewed by Rhodes (2005). Furthermore, assay systems based on the isolated perfused pancreas, perifused islets, insulinoma cells and cultured β-cells are required to study the effects of compounds/drugs on insulin secretion, β-cell growth and β-cell survival.

K.5.4.1
Perfused Rat Pancreas

PROCEDURE

Male Wistar rats (e. g. Hoe:WISKf, SPF 71-strain) weighing 200–250 g serve as donors. Prior to the experiment, the animals have free access to food and water. The pancreas is removed under pentobarbital (50 mg/kg i.p.) anesthesia. The mesenteric artery is doubly ligated and cut, and the entire intestine below the duodenum is separated and removed from the rat to simplify the exposure. The esophagus is ligated as high as possible and cut above the ligature. A loose ligature is placed, but not tied, around the entire gastrohepatic ligament. The aorta is cautiously exposed through the crura of the diaphragm well above the point of origin of the celiac axis. The ligature around the gastrohepatic ligament is then tied as tightly as possible, and the ligament cut above the ligature. The aorta is cut between the double clamps and below the lower clamp, and the preparation is lifted out from the abdomen. The clamps are removed from the aorta which is slit open on the side opposite to the origin of the celiac axis, revealing the opening of the latter. The arterial cannula

is inserted and tied in place. An opening is made close to the ligature, as near as the end of the portal vein as possible.

EVALUATION

Circulation through the preparation is initiated and fluid is observed to flow from the slit in the portal vein. After a minute or two, the flow is stopped and a cannula is inserted into the portal vein and tied in place. Flow is then resumed at a perfusion pressure of about 100 mm Hg. Carbogenated Krebs-Ringer bicarbonate buffer with 2% BSA and 5.5 mM glucose is used as perfusion medium at a temperature of 37.5°C with a perfusion rate of 1.75 ml/min. The perfusate is collected every minute for 30 min. After 5 min perfusion with 5.5 mM glucose, the test compound is added until the 15th min (concentrations between 0.05 and 0.5 mM for highly active substances), followed by perfusion with 5.5 mM glucose and finally with 16.6 mM glucose. The perfusate medium samples are stored at –20°C until further processing.

K.5.4.2 Perifused Islets

Male Wistar rats weighing 200–250 g serve as donors. Before the study, the animals have free access to food and water. Two donor rats are used for each test. The pancreas is removed under pentobarbital anesthesia. The islets are obtained by the collagenase (e. g. collagenase type IV, Worthington) method and collected under a stereomicroscope. In each test, up to 10 chambers each with 15 islets are perifused. Cut-off Microfuge tubes, sealed with Tuohy-Borst adapters, serve as perfusion chambers. Two thick-walled, small-diameter Teflon catheters are passed through the adapter into the chamber. One of the catheters extends to the bottom of the chamber and acts as the perifusate inlet, the other extends to the lower edge of the adapter cone and acts as outlet. The latter is connected to a multi-channel peristaltic pump which delivers the perifusate to a fraction collector. The chamber volume is 0.15 ml. The perifusate flow rate is 0.1 ml/min. The perifusate consists of a carbogenated Krebs-Ringer bicarbonate buffer with 1.0 mM glucose, 0.25% BSA, and 5 mM theophylline. The storage vessels for the perifusate, the chambers, and the inlet catheters are immersed in a water bath of 37°C.

EVALUATION

After a pre-perifusion phase of one hour, the perifusate is collected every min for 46 min. From the 2nd until the 18th min, the test compound is added at concentrations between 0.1 and 2.5 μM, and from the 34th to the 46th min, the glucose concentration is raised to 20.0 mM. The hormones: insulin, glucagon and somatostatin are determined by using a commercially available RIA-kit or ELISA-kit.

K.5.4.3 Insulinoma Cells

PURPOSE AND RATIONALE

Chick and coworkers (1977) described a transplantable insulinoma in the rat which was originally observed as primary tumor in the pancreas of an old male NEDH albino rat being previously irradiated during a parabiosis experiment. Fragments of this tumor were transplanted to young NEDH rats in many passages inducing severe hypoglycemia in host rats. Gazdar and coworkers (1980) reported the establishment of a continuous cell line of a rat islet cell tumor which secretes primarily insulin and some somatostatin. Bhatena and coworkers (1982) studied insulin, glucagon, and somatostatin receptors on cultured cells and clones from rat islet cell tumor.

PROCEDURE

The insulinoma is transplanted when the tumor has reached a diameter of about 2 cm and the carrier animal exhibits distinct manifestations of insulin excess. The tumor is removed, cut open, mixed briefly in a mortar and one tenth to one twentieth is injected between the shoulder blades of another animal. No metastases are observed. The histological examination also shows a nonmalignant adenoma. The tumors grow only in rats of the strain NEDH (New England Deaconess Hospital).

K.5.4.4 Cultured β-Cells

GENERAL CONSIDERATIONS

Reliable β-cell models are of paramount importance for diabetes research (see above). It is generally accepted that the use of primary cells is preferable. However, this requires large quantities of isolated pancreatic islets, which is work-intensive and has the inherent inconvenience of representing a mixed population of β-, α-, δ-, and F cells. Consequently, rodent β-cell lines have proven their usefulness, and their continuous development is still essential until clonal human β-cells become available. The intrinsic challenge when establishing a β-cell line is the maintenance of

tissue-specific differentiation combined with adequate cell proliferation. As a result, only a limited number of β-cell lines are available to date, all of rodent origin. Several insulin-secreting cell lines are reported in the literature (review by Poitout et al. 1996). The most widely used are RINm5F, βHC9, βTC6-F7 and, more recently, MIN6. Among the mouse-derived β-cell lines (Miyazaki et al. 1990, Knaack et al. 1994), MIN6 cells (Miyazaki et al. 1990, Ishihara et al. 1993) represent a valuable model, which was further improved by isolation of the clonal subline MIN6m9 (Minami et al. 2000). However, MIN6 cells exhibit secretory responses to pyruvate, which is not a secretagogue for normal islets (Skelly et al. 1998). Mouse βHC9 grow very slowly and are thus difficult to study. Of rat origin, RINm5F cells are poorly differentiated, have low insulin content and do not respond to glucose in the physiological concentration range (Halban et al. 1983, Praz et al. 1983, McClenaghan et al. 1998), and BRIN-BD11 cells are poorly differentiated, exhibiting low insulin content and weak secretory responses to glucose (McClenaghan and Flatt, 1999). Finally, loss of differentiated features as a function of time in tissue culture has been reported for several rodent cell lines, including RIN1046–38 and βTC6 (Clark et al. 1990, Ferber et al. 1994). Genetic engineering of RIN1046–38 cells results in clones with stable glucose responsiveness but with maximal insulin secretion occurring at subphysiological glucose concentrations because of a high level of low K_m hexokinase activity in these cells (Ferber et al. 1994, Hohmeier et al. 1997). Stable glucose responsiveness has also been reported for βTC cells after clonal selection in soft agar (Knaack et al. 1994), but even these cloned cell lines (e. g. βTC6-F7) appear to lose glucose responsiveness after prolonged tissue culture (Zhou et al. 1998). Currently, clonal INS-1 cells (e. g. INS1–832/13 or 1E; Hohmeier et al. 2000) appear to represent the most attractive vehicles for studying β-cell function.

PROCEDURE

RINm5F

Insulin-producing cells from the RINm5F cell line are grown in RPMI medium containing 10% (v/v) heat inactivated FCS, 50 IU/ml penicillin, 0.25 µg/ml amphotericin B, and 50 µg/ml streptomycin at 37°C in an atmosphere of humidified air/CO_2 (19:1) (Praz et al. 1983). The cells are seeded at a density of 3.5×10^4 cells/ml in 20 ml of medium (75 cm^2 culture flasks). The medium is replaced 4 times a week (one passage). Thereafter, the cells are treated with trypsin (0.02% trypsin in 0.9% NaCl/0.2 mM EDTA) for 2–5 min at 37°C. The trypsin-treated cells are diluted, re-seeded at a density of 2×10^6 cells per 75 cm^2 culture flask and grown to 70% confluency.

For single-cell patch clamp studies, RINm5F cells are maintained in RPMI 1640 tissue culture media, containing 11 mM glucose, supplemented with 10% FCS, 2 mM glutamine and 50 µg/ml gentamycine. Cells are seeded out every 2–3 d onto Petri dishes and kept in a humidified atmosphere of 95% O_2 and 5% CO_2 at a temperature of 37°C. The cells are isolated by incubation in a Ca^{2+}-free medium containing 0.25% trypsin for about 3 min. Single cells and clusters of 2–3 cells are obtained after centrifugation with 800 rpm and are stored on ice until use. The tight-seal whole-cell patch-clamp technique can be applied to single cells.

MIN6

The MIN6 cell has been derived from transgenic mice expressing a comparable transgene (Miyazaki et al. 1990). MIN6 cells cultured on a gelatine layer have been shown to form spherical cell clusters (pseudo-islets) similar to those in islets. (Hauge-Evans et al. 1999). Two rodent insulin genes have been identified in MIN6 cell pseudo-islets (Roderigo-Milne et al. 2002). The glucose-induced biphasic insulin secretion pattern observed in isolated mouse islets was also demonstrated in MIN6 pseudo-islets. Differences between pancreatic islets representing a complete endocrine organ and the artificial MIN6-pseudo-islets containing only β-cells were observed cautioning the use of the pseudo-islets for evaluation of compounds/drugs (Brenner and Mest 2003).

For culture, MIN6 cells (starting passage 40) are maintained in DMEM containing 25 mM glucose and supplemented with 15% heat-inactivated FBS in humidified 5% CO_2/95% air at 37°C. Cells are exposed to glucose-free extracellular solution for 30 min prior to measurement of insulin secretion or intracellular calcium.

Palmitate-Treated MIN6

Busch and coworkers (2005) studied the effect of fatty acids on the viability and functionality of pancreatic β-cells. For this, palmitate-treated MIN6 cell pools are selected and routinely passaged in 75-cm^2 flasks with 20 ml DMEM containing 25 mM glucose, 24 mM $NaHO_3$, 10 mM HEPES, 10% (by vol.) FCS, 50 IU/ml penicillin, 50 mg/ml streptomycin, and 1 mM palmitate coupled to 2.3% BSA (wt/vol). This selection procedure is carried out twice, giving rise to two independent pools of palmitate-treated cells. Both pools

are used for transcript profiling experiments and functional studies. Control MIN6 cells are taken through the same selection process but using BSA-medium without palmitate. Cells are seeded in DMEM as follows. For [^{14}C]palmitate-labeling and protein measurement, 2×10^5 cells per well in 24-well dishes (0.5 ml) are used, for microarray experiments, 5×10^6 cells per 25-cm^2 flask (5 ml) are used, for analysis of lipid composition, 6×10^6 cell per 10-cm dish (15 ml) are used. At 48 h before the experiments (24 h after seeding), the medium is replaced with DMEM (as above but with 5 mM glucose) supplemented with either BSA alone or BSA coupled to palmitate. Couplings are prepared in DMEM (25 or 5 mM glucose) as desribed by Busch and coworkers (2002). The couplings are diluted 1:8 (for culture and for experiments), giving a final concentration of 1 mM palmitate to 2.3% BSA (wt/vol), corresponding to a molar ratio of 3:1.

HIT-T15

The insulin secreting HIT cell line has been developed by Santerre and coworkers (1981) by isolating pancreatic islets from the hamster, dispersing the islets into single cells, transforming the cell isolates with the simian virus 40 (SV40), and cloning out the insulin-secreting cell lines. These clonal cells retain a differentiated function and respond to secretagogues and inhibitors of insulin secretion (Boyd et al. 1991).

INS-1/2

Asfari and coworkers (1992) derived INS-1 cells and INS-2 cells from parental radiation-induced RINm5F cells. In the course of a co-culture of lymphocytes and RINm5F cells in the presence of 2-mercaptoethanol, the authors observed the formation of free-floating cell aggregates which appeared to be morphologically different from the parental cells. These clusters were isolated and gave rise to the INS-cell lines, whose viability is dependent on the presence of 2-mercaptoethanol in the media and whose secretory characteristics are similar to those of native islets with its modulation by free radicals upon challenge of the cells by alloxan has been reported by Janjic and coworkers (1995). Due to the nonclonal nature of these cells, limited stability over passages probably explains some of the discrepancies observed among the numerous laboratories using parental INS-1 cells worldwide. To circumvent this problem, Hohmeier and coworkers (2000) stably transfected INS-1 cells with the human proinsulin gene, followed by selection of clones based on robust glucose-stimulated insulin secretion. The resulting INS-1–832/13 cells are highly glucose responsive. However, these cells overexpress human insulin driven by the ubiquitous cytomegalovirus promoter in addition to the endogenous rat insulin, rendering it impossible to judge the differentiated state based on insulin content. An alternative approach would be the cloning of well differentiated INS-1 cells without genetic manipulation. Hence, the clonal INS-1E cells has been isolated from the parental cells based on both their insulin content and their secretory response to glucose as well as adequate proliferation (Hohmeier et al. 2002).

INS-1E

Clonal INS-1E cells, derived from parental INS-1 cells (Asfari et al. 1992) on basis of selection for insulin content and adequate proliferation (Janjic et al. 1999), are cultured in a humidified atmosphere containing 5% CO_2 in complete medium composed of RPMI 1640 supplemented with 5% heat-inactivated FCS, 1 mM sodium pyruvate, 50 µM 2-mercaptoethanol, 2 mM glutamine, 10 mM HEPES, 100 U/ml penicillin, and 100 µg/ml streptomycin. The maintenance culture is passaged once a week by gentle trypsinization, and cells are seeded at a density of 4×10^4 cells/cm^2, i. e. 3×10^6 cells, in 75-cm^2 Falcon bottles with 20 ml complete medium. The potential presence of mycoplasma is regularly checked using a photometric enzyme immunoassay for the detection of PCR-amplified mycoplasma DNA (Roche, Diagnostics). INS-1E are seeded at 2×10^5 cells/ml in Falcon 24-well plates and used 4–5 days thereafter, with one medium change on d 3 or 4. For generation of INS-1E cell clusters, cells are seeded in nonadherent bacterial 10-cm petri dishes and cultured in complete medium for 5–6 d before use. The stable differentiated INS-1E β-cell phenotype was reported for over more than 100 passages corresponding to a 2-year continuous follow-up. INS-1E cells can be safely cultured and used within passages 40–100 with high insulin contents. Glucose-induced insulin secretion is concentration-dependent and similar to rat islet responses as are the secretion responses to amino acids and sulfonylureas. Moreover, INS-1E cells retained the amplifying pathway, as judged by glucose-induced augmentation of insulin release in a depolarized state. Finally, spheroid clusters, sometimes referred to as pseudoislets (Hauge-Evans et al. 1999), composed of reaggregated INS-1E cells, can be prepared and tested for their ability to respond to secretagogues. Thus, INS-1E cells represent a stable and valuable β-cell model for the analysis of insulin secretion induced by compounds/drug/candidates.

β-TC

Hanahan (1985) applied gene transfer technology to the establishment of β-cell lines. In order to target the expression of viral DNA to the β-cell, recombinant oncogenes have been designed by fusion of the 5′-regulatory region of the rat insulin II gene with the early coding region of SV40. The transgenes have been microinjected into fertilized mice embryos, which were then implanted in the oviduct of pseudopregnant females. The offspring specifically expressed SV40 in their β-cells and spontaneously developed β-cell tumors at 10–20 weeks of age. Tumors were subsequently excised, isolated and propagated in culture, giving rise to β-tumor cell (***β*-TC**) lines (Erfrat et al. 1988). Because these cells do not grow in culture at low density, the have not been cloned, and several subpopulations have been derived. Hamaguchi and coworkers (1991) applied this technique to the development of the NIT1 cell line from transgenic NOD mice in order to establish an immortalized source of NOD β-cells.

Betacyt

The betacyte, also called the HepG2Ins/β-cell, is a genetically engineered insulin-secreting human liver cell line that is glucose responsive (Simpson et al. 1995 and 1996, Tuch et al. 1997). The clone was constructed by doubly transfecting the HepG2 cell line with insulin cDNA under the control of the constitutive CMV promoter and the cDNA for the glucose transporter isoform 2 (GLUT2), which is specific to β-cells and hepatocytes. Interestingly, this cell is capable not only of synthesizing, storing and secreting insulin in a regulated fashion when challenged with physiological concentrations of glucose, but also of acting as a liver cell and secreting albumin.

REFERENCES AND FURTHER READING

Asfari M, Janjic D, Meda P, Li G, Halban PA, Wollheim CB (1992) Establishment of 2-mercaptoethanol-dependent differentiated insulin-secreting cell lines. Endocrinology 130:167–178

Bhatena SJ, Oie HK, Gazdar AF, Voyles NR, Wilkins SD, Recant L (1982) Insulin, glucagon, and somatostatin receptors on cultured cells and clones from rat islet cell tumor. Diabetes 31:521–531

Boyd III AE, Aguilar-Bryan L, Bryan J, Kunze DL, Moss L, Nelson DA, Rajan AS, Raef H, Xiang H, Yaney GC (1991) Sulfonylurea signal transduction. In: Bardin CW (ed) Proceedings of the 1990 Laurentian Hormone Conference. Rec Progr Horm Res 47:299–317

Brenner M, Mest HJ (2003) Comparison of the insulin secretory kinetics from MIN6 pseudoislets and mouse islets. Naunyn Schmiedeberg's Arch Pharmacol 367, Suppl 1, R73, A279

Busch AK, Cordery D, Denyer GS, Biden TJ (2002) Expression profiling of pamitate- and oleate-regulated genes provides novel insights into the effects of chronic lipid exposure on pancreatic β-cell function. Diabetes 51:977–987

Busch AK, Gurisik E, Cordery DV, Sudlow M, Denyer GS, Laybutt DR, Hughes WE, Biden TJ (2005) Increased fatty acid desaturation and enhanced expression of stearoyl coenzyme A desaturase protects pancreatic β-cells from lipoapoptosis. Diabetes 54:2917–2924

Chick WL, Warren S, Chute RN, Like AA, Lauris V, Kitchen KC (1977) A transplantable insulinoma in the rat. Proc Natl Acad Sci, USA 74:628–632

Clark SA, Burnham BL, Chick WL (1990) Modulation of glucose-induced insulin secretion from a rat clonal β-cell line. Endocrinology 127:2779–2788

Erfrat S, Linde S, Kofod H, Spector D, Delannoy M, Grant S, Hanahan D, Baekkekov S (1988) Beta-cell lines derived from transgenic mice expressing a hybrid insulin gene-oncogene. Proc Natl Acad Sci USA 85:9037–9041

Ferber S, BeltrandelRio H, Johnson JH, Noel R, Becker T, Cassidy LE, Clark S, Hughes SD, Newgard CB (1994) Transfection of rat insulinoma cells with GLUT-2 confers both low and high affinity glucose-stimulated insulin release: relationship to glucokinase activity. J Biol Chem 269:11523–11529

Gazdar AF, Chick WL, Oie HK, Sims HL, King DL, Weir GC, Lauris V (1980) Continuous, clonal, insulin-, and somatostatin-secreting cell lines established from a transplantable rat islet cell tumor. Proc. Natl Acad Sci, USA 77:3519–3523

Halban PA, Praz GA, Wollheim CB (1983) Abnormal glucose metabolism accompanies failure of glucose to stimulate insulin release from a pancreatic cell line (RINm5F). Biochem J 212:439–443

Hamaguchi K, Gaskins HR, Leiter EH (1991) NIT-1, a pancreatic β-cell line established from a transgenic NOD/Lt mouse. Diabetes 40:842–849

Hanahan D (1985) Heritable formation of pancreatic β-cell tumors in transgenic mice expressing recombinant insulin/SV40 oncogenes. Nature 315:115–122

Hauge-Evans AC, Squires PE, Persaud SJ, Jones PM (1999) Pancreatic beta-cell-to-beta-cell interactions are required for integrated responses to nutrient stimuli: enhanced Ca^{2+} and insulin secretory responses of MIN6 pseudoislets. Diabetes 48:1402–1408

Hohmeier HE, BeltrandelRio H, Clark S, Henkel-Rieger R, Normington K, Newgard CB (1997) Regulation of insulin secretion from novel engineered insulinoma cell lines. Diabetes 46:958–967

Hohmeier HE, Mulder H, Chen G, Henkel-Rieger R, Prentki M, Newgard CB (2000) Isolation of INS-1-derived cell lines with robust ATP-sensitive K^+ channel-dependent and independent glucose-stimulated insulin secretion. Diabetes 49:424–430

Ishihara H, Asano T, Tsukuda K, Katagiri H, Inukai K, Anai M, Kikuchi M, Yazaki Y, Miyazaki JI, Oka Y (1993) Pancreatic β cell line MIN6 exhibits characteristics of glucose metabolism and glucose-stimulated insulin secretion similar to those of normal islets. Diabetologia 36:1139–1145

Janjic D, Maechler P, Sekine N, Bartley C, Annen AS, Wollheim CB (1999) Free radical modulation of insulin release in INS-1 cells exposed to alloxan. Biochem Pharmacol 57:639–648

Knaack D, Fiore DM, Surana M, Leiser M, Laurance M, Fusco-DeMane D, Hegre OD, Fleischer N, Efrat S (1994) Clonal insulinoma cell line that stably maintains correct glucose responsiveness. Diabetes 43:1413–1417

McClenaghan NH, Elsner M, Tiedge M, Lenzen S (1998) Molecular characterization of the glucose-sensing mechanism in the clonal insulin-secreting BRIN-BD11 cell line. Biochem Biophys Res Commun 242:262–266
McClenaghan NH, Flatt PR (1999) Engineering cultured insulin-secreting pancreatic B-cell lines. J Mol Med 77:235–243
Minami K, Yano H, Miki T, Nagashima K, Wang CZ, Tanaka H, Miyazaki JI, Seino S (2000) Insulin secretion and differential gene expression in glucose-responsive and –unresponsive MIN6 sublines. Am J Physiol 279:E773-E781
Miyazaki J, Araki K, Yamato E, Ikegami H, Asano T, Shibasaki Y, Oka Y, Yamamura K (1990) Establishment of a pancreatic β cell line that retains glucose-inducible insulin secretion: special reference to expression of glucose transporter isoforms. Endocrinology 127:126–132
Poitout V, Olson LK, Robertson RP (1996) Insulin-secreting cell lines: Classification, characteristics and potential applications. Diabet Metabol (Paris) 22:7–14
Praz GA, Halban PA, Wollheim CB, Blondel B, Strauss AJ, Renold AE (1983) Regulation of immunoreactive-insulin release from a rat cell line (RINm5F). Biochem J 210:345–352
Rhodes CJ (2005) Type 2 diabetes – a matter of beta-cell life and death. Science 21:380–384
Roderigo-Milne H, Hauge-Evans AC, Persaud SJ, Jones PM (2002) Differential expression of insulin genes 1 and 2 in MIN6 cells and pseudoislets. Biochem Biophys Res Commun 296:589–595
Santerre RF, Cook RA, Crisek RMD, Sharp JD, Schmidt RJ, William DC, Wilson CP (1981) Insulin synthesis in a clonal cell line of simian virus 40-transformed hamster pancreatic beta cells. Proc Natl Acad Sci USA 78:4339–4343
Skelly RH, Bollheimer LC, Wicksteed BL, Corkey BE, Rhodes CJ (1998) A distinct difference in the metabolic stimulus-response coupling pathways for regulating proinsulin biosynthesis and insulin secretion that lies at the level of a requirement of fatty acyl moieties. Biochem J 331:553–561
Simpson AM, Tuch BE, Swan MA, Tu J, Marshall GM (1995) Functional expression of the human insulin gene in a human hepatoma cell line (HEP G2). Gene Therapy 2:223–231
Simpson AM, Beynon S, Maxwell L, Tuch BE, Marshall GM (1996) Dynamic insulin secretion and storage in a human hepatoma cell line – HEP G2ins/g. Diabetes 45, Suppl 2:27A
Tuch BE, Beynon S, Tabiin MT, Sassoon R, Goodman RJ, Simpson AM (1997) Effect of β-cell toxins on genetically engineered insulin-secreting cells. J Autoimmun 10:239–244
Zhou D, Sun AM, Li X, Mamujee SN, Vacek I, Gerogiou J, Wheeler MB (1998) In vitro and *in vivo* evaluation of insulin-producing βTC6-F7 cells in microcapsules. Am J Physiol 43:C1356–1362

K.6
Assays for Insulin and Insulin-Like Metabolic Activity

EVALUATION

Data from the metabolic assays (and signaling assays, see below) are calculated as stimulation factor above basal activity (absence of insulin/compound/drug candidate) for processes stimulated (e. g. lipogenesis, glucose transport and GLUT4 translocation) or as difference between the basal and insulin/compound/drug candidate-induced values for processes down-regulated (e. g. lipolysis). In each case, these data, which reflect the responsiveness of the metabolic effector system studied toward the respective stimulus (insulin/compound/drug candidate), are normalized to the basal (set at 0%) and maximal insulin action (set at 100%; elicited by maximally effective concentration of insulin). For characterization of the sensitivity of the metabolic effector system toward the respective stimulus, effective concentrations for the induction of 150% (or higher) of the basal activity (set at 100%) can be given. These so-called EC_{150}-values facilitate the insulin-independent comparison of the relative potency of the insulin-like activity between compounds/drug candidates, in general, and in particular for those frequently observed stimuli, which do not elicit the same maximal response in % stimulation or inhibition and/or fail to approach the maximal insulin response.

Typically, at least three different cell/tissue preparations with two to four independent incubations with insulin/compound/drug candidate and two to four independent activity measurements (i. e. assays) should be performed. Concentration/response curves can be fitted to the equation

$$y = a + b[x/(x + k)]$$

using a Marquardt-Levenberg non-linear least squares algorithm. When plotted on linear-log axes, this equation gives a sigmoidal curve where the parameters are associated with the following properties:

$$\begin{aligned} a &= \text{basal response;} \\ a + b &= \text{maximal response;} \\ k &= \text{half-maximal concentration}(EC_{50}); \\ x &= \text{concentration of insulin.} \end{aligned}$$

The term “insulin-like activity” is used in a wide range of definitions varying in the type and number of parameters evaluated by the respective assays which

have to be fullfilled by a given compound/drug candidate. An appropriate criterium for a compound/drug candidate with insulin-like activity may represent that it exerts at least 20% of the maximal insulin response in at least three major metabolic insulin actions (e. g. glucose transport, lipogenesis, anti-lipolysis) in at least one insulin target cell/tissue. However, the final judgement of a compound/drug candidate as being appropriate for further evaluation and development has to rely on the complete data set of its profiling in many metabolic and signaling assays rather than to stick to the fullfillment of fixed criteria for one or a few parameters.

K.6.1 Assays for Insulin and Insulin-Like Activity Based on Adipocytes

K.6.1.1 Differentiation

PURPOSE AND RATIONALE

The increase in obesity and the identification of adipocyte-secreted proteins that regulate energy metabolism (Drevon 2005) have generated huge interest in adipocyte biology. Adipocytes are the primary storage site for energy in vertebrate animals. During fasting, adipocytes release energy-rich molecules that provide metabolic fuels to other tissues. Adipocytes also secrete hormones that orchestrate the storage, release, and oxidation of energy-rich molecules throughout the body and that control behavior, including feeding (Rajala and Scherer 2003). Insulin as anabolic hormone is of critical importance for the differentiation of adipocytes in humans. Consequently, assays that monitor the quantitative analysis of adipocyte differentiation may be helpful for studying the effects of insulin/compounds/drugs on pathways which are engaged both directly in the regulation of the differentiation and in the molecular mechanisms of metabolic insulin action.

PROCEDURE

Understanding the molecular mechanism underlying adipocyte differentiation has been one of the major focuses of many researchers in the field of metabolic disorders. Methods in use for the assessment of fat cell development and maturation after initiation of adipogenesis in cell culture include microscopic examination of cellular LD formation and cellular lipid staining by Oil Red O (von Goor et al. 1986). These methods, although excellent in detecting the presence of intracellular lipid, are ineffective in objectively quantifying the degree of fat accumulation if not used in conjunction with other extraction and analytic systems. Particularly, during the process of adipogenesis of preadipocytes, it is observable that cells are heterogeneous in their response to adipogenic agents in terms of speed of adipogenic conversion and degree of fat accumulation (Shigematsu et al. 2001). This heterogeneity of response may cause difficulties when evaluating and comparing the effects of several treatments that target only fat cells of certain status due to the masking influence of those non-targeted cells. Thus, an effective method to detect and classify cells with similar fat content will certainly increase analytical precision in monitoring fat cell development and the ability to quantify the effects of therapeutic agents. Currently, flow cytometry and fluorescence-activated cell sorters (FACSs) are extensively used in the analysis of adipocyte differentiation and lipid accumulation as well as their modulation by compounds/drugs as is exemplified best by the study from Lee and coworkers (2004).

EVALUATION

A simple and sensitive method to detect and quantify lipid accumulation inside cells by flow cytometry has been introduced (Lee et al. 2004). Using this method, elevated levels of cytoplasmic granularity can be detected that correlate well with an increased level of lipid accumulated inside cells after adipogenic conversion. Furthermore, this method is appropriate to monitor and quantify adipose cell maturation within a complex population of cells and to identify and collect the adipose cells with similar lipid storage for further analysis. Flow cytometry offers distinct advantages over existing detection systems for cytoplasmic lipid staining and lipid extraction and can represent a powerful analytical tool to monitor the effect of chemicals and biological molecules, including compounds and putative anti-obesity drugs on adipose cell conversion and maturation. Moreover, in combination with a cell sorting facility, this method offers a simple and efficient means of collecting adipose cells of specific status for further analysis. In conclusion, flow cytometry enables the direct measurement of the lipid content of specific cells in a complex population of adipose cells. Not only is the system simple, sensitive, and quantitative, but it also offers an advantage over the existing methodology, with its capability of monitoring the degree of intracellular lipid accumulation in a precise, fast, and selective manner. These results provide a basis for developing a variety of applications in com-

pound and drug screening procedures to monitor adipose cell development.

K.6.1.2 Lipogenesis

GENERAL CONSIDERATIONS

Lipogenesis encompasses the complete biosynthetic pathways for TAG stored in cytoplasmic LD and phospholipids building up the internal and plasma membranes (including their lipidic intermediary and degradation products). The type as well as the concentration of the labeled precursor (e. g. glucose, fatty acids) whose conversion or incorporation into TAG and phospholipids is followed determines which step(s) of the lipogenic pathway is monitored by the lipogenesis assay (e. g. glucose transport, acylation). Thus, simple variations of the assay conditions allow the selective analysis of individual rate-limiting steps of lipogenesis and their modulation by compounds/drug candidates.

K.6.1.2.1 Method Based on the Incorporation of Radiolabeled Glucose

PURPOSE AND RATIONALE

This assay measures the complete pathway of lipid synthesis (lipogenesis) encompassing the transport of the radiolabelelled glucose across the plasma membrane of the adipocytes, its conversion into glycerol and/or fatty acids and their subsequent esterification into predominantly neutral TAG and phospholipids and finally the deposition of TAG in LD in the cytoplasm of the adipocytes. Since in adipocytes each of these steps is stimulated by insulin, albeit to varying degrees, the lipogenesis assay is perfectly suited for the analysis of effects of compounds/drugs on the complex insulin signaling cascade regulating lipogenesis. Dependent on the experimental conditions chosen (i. e. low or high glucose), the assay monitors predominantly the effect of insulin/compound/drug on glucose transport or on the subsequent esterification. At low glucose concentrations (up to 0.1 mM glucose), when according to TLC-analysis of the total TAG after enzymatic digestion the majority of the radiolabel is incorporated into the glycerol backbone, the glucose transport step is rate-limiting and monitored. In contrast, at higher glucose concentrations (above 2 mM), when two thirds of the radiolabel are recovered with the fatty acid moieties of TAG, the rate-limiting and monitored step is the esterification rather than glucose transport, which is driven by mass action. Since in adipocytes the insulin stimulation of glucose transport is significantly more pronounced than that of esterification, the lipogenesis assay performed at low glucose concentration (< 0.1 mM glucose) exhibits the highest insulin responsiveness whereas at intermediary glucose concentrations (0.1–2 mM), it represents a compromise for the measurement of both transport and esterification with intermediary insulin responsiveness and at high glucose concentrations (> 2 mM glucose) it predominantly monitores the esterification with lowest insulin responsiveness.

PROCEDURE

For measurement of lipogenesis monitoring effects on both glucose transport and esterification, isolated rat adipocytes are incubated with D-[^{3}H]glucose (0.55 mM final concentration, 0.1–1 μCi). The cells are lysed and the total lipids separated from water-soluble products and the incubation medium including the unincorporated [^{3}H]glucose by addition of toluene-based scintillation cocktail. After phase separation, radioactivity incorporated into total lipids/phospholipids is determined by liquid scintillation counting directly without removal of the lipid phase based on determination of the radiolabel of the lipidic products partitioned into the toluene phase containing the scintillator rather than of the [^{3}H]glucose left in the aqueous phase lacking scintillator (Moody et al. 1974).

The reaction is started by the transfer of 0.2 ml of adipocyte suspension (3.5×10^5 cells/ml) in KRHB to scintillation vials containing 0.1 ml of [3-^{3}H]glucose (2 μCi/ml, 4.4 mM), 0.4 ml of 2-fold KRHB and 0.3 ml of insulin or compound/drug with insulin-mimetic activity dissolved in vehicle (e. g. DMSO) and diluted with KRHB to the appropriate concentration of compound and vehicle (e. g. 3% DMSO). The scintillation vials are placed under a stream of carbogen for 10 s, then closed and placed in a very slowly shaking water bath (37°C). After incubation for 90 min, the reaction is terminated by the addition of 10 ml of toluene-based scintillation cocktail. The vials are mixed rigorously using a vortexer and subsequently left standing for 2–4 h to allow phase separation. The ^{3}H-radioactivity is determined with a liquid scintillation counter.

EVALUATION

Blank values obtained from a typical reaction mixture containing buffer and [3-^{3}H]glucose but lacking either adipocytes or compound/drug/insulin have to be included in each experiment. Since the quality of the cells decreases with time (resulting in increased lipogenesis in the basal state), it is recommended to

set up 2 basal incubations for every 20–25 test mixtures. In addition, for direct comparisons (e. g. of insulin analogs) incubations with identical (insulin) concentrations should be performed immediately for one agent (insulin) after the other rather than with the complete concentration series for one agent (insulin) after the other. This procedure allows the resolution of potency differences of less than 10% between two insulin analogs as reflected in corresponding shifts of the apparent EC_{50}-values with identical maximal responses. The blank values lacking adipocytes (usually 500–600 dpm) are subtracted from the values measured for the corresponding set of test mixtures containing adipocytes to correct for ^{3}H-radiation originating from the aqueous phase (i. e. [^{3}H]glucose left in the incubation medium). Fold stimulations reflecting the responsiveness of the glucose transport and/or esterification systems of the adipocytes toward insulin/compound/drug are calculated as ratio between the corrected test values (presence of insulin/compound/drug) and basal values (absence of insulin/compound/drug). Typically, insulin induces 15- to 20-fold, 8- to 12-fold and 2.5- to 4-fold stimulations in lipogenesis at 50 µM, 0.55 mM and 2 mM glucose, respectively. Due to the very limited number of pipetting steps (with the most critical one being the transfer of an equal number of cells to each assay mixture), the standard deviations are rather low. Usually, 2–4 measurements per data point are sufficient.

An insulin-concentration/response curve should be performed for each experiment to test the insulin sensitivity and responsiveness (and thus the quality) of the adipocytes prepared. Appropriate insulin concentrations are 0.01, 0.02, 0.04, 0.06, 0.08, 0.1, 0,12, 0.15, 0.2, 0.5, 1, 5 nM (final concentration in the assay). Typically, the EC_{50} for human insulin is 0.06–0.10 nM. The insulin-like activity of compounds/drugs can be expressed as % of the maximal insulin stimulation (that is as the ratio between the fold stimulation provoked by the compounds/drugs with insulin-like activity at the maximally effective concentration and that induced by 5 nM insulin) to correct for the varying quality (i. e. insulin responsiveness) of the cells from different preparations.

K.6.1.2.2 Method Based on the Incorporation of a Fluorescent Fatty Acid Analog

PURPOSE AND RATIONALE

Usually lipogenesis is studied by the incorporation of radiolabeled glucose into toluene-extractable acylglycerols in the presence of glucose at concentrations below 2 mM (see above). Under these conditions glucose transport and, in consequence, supply of glycerol-3-phosphate is rate-limiting. For uncoupling of glucose transport/glycerol-3-phosphate synthesis from (re)esterification, lipogenesis has to be performed in the presence of high glucose. To circumvent analysis of lipogenesis at high glucose (> 2 mM) by (radio)labeling the glycerol moiety of TAG, which necessitates the application of glucose of high specific radioactivity, a fluorescent fatty acid analog can be used for its insulin-sensitive incorporation into TAG in isolated rat adipocytes.

Several recent reports suggest that the fluorescent fatty acid derivative, NBD-stearate, behaves like naturally occurring fatty acids, since it has been shown to enter rat hepatocytes by the same uptake mechanism as that described for unmodified fatty acids (Elsing et al. 1995, Storch et al. 1995). Furthermore, measurement of the uptake of a fluorescent long-chain fatty acid derivative into COS7 cells transfected with a 3T3-L1 adipocyte cDNA library led to the identification of fatty acyl-CoA synthetase and a putative fatty acid transport protein (Schaffer and Lodish 1994). Recently the efficient incorporation of NBD-FA, 12-((7-nitrobenz-2-oxa-1,3-diazol-4-yl)amino)dodecanoic acid, into mono- and diacylglycerol(-3-phosphate) in isolated rat adipocytes and its significant stimulation by insulin has been reported by Müller and coworkers (1997).

PROCEDURE

Incubation of the Adipocytes

200 µl of adipocyte suspension is supplemented with 190 µl of KRHB containing 0.1/2 mM glucose (= KRHBlow/KRHBhigh) and 10 µl of an insulin solution (routinely 200 nM) or compound/drug candidate (routinely 200 µM in 20% DMSO) and incubated for 15 min at 37°C in a slowly shaking water bath. The assay is started by the addition of 50 µl of 0.9 mM NBD-FA (prepared daily from a 100 mM stock solution in ethanol by dilution with KRHBlow/KRHBhigh under mild heating). After incubation at 37°C under mild shaking (stage 11, thermomixer, Eppendorff) for 90 min, lipogenesis is terminated by filtration of the total mixtures over GF/C-filters under vacuum. The filters are rapidly washed three times with 1 ml of KRHBlow/KRHBhigh each, placed in 20-ml plastic scintillation vials and extracted with 400 µl THF for 15 min under rigorous shaking. 300 µl of the extract is transferred into new tubes and centrifuged (15,000 × *g*, 5 min). The supernatant is dried (SpeedVac) and sus-

pended in 50 µl THF. 5-µl samples are analysed by TLC on silica gel Si-60 plates using 78 ml diethyl ether, 22 ml petrol ether, 1 ml acetic acid as solvent system. Fluorescent lipid products on the dried plates are visualized under UV (312 nM) and photographed (Polaroid CU5). The amount of acylglycerols (AG) is determined by fluorescence scanning with excitation at 342 nm and emission at 505 nm or fluorescence imaging with excitation at 460 nm and emission at 540–560 nm. The relative peak area of each lipid product minus a background value (derived from an equal-sized region of the TLC plate which does not contain any lipid product) is calculated as arb. units.

Characterization of the Fluorescent Lipids

For elucidation of the type of lipid(s), the synthesis of which is stimulated by insulin/compound/drug, the fluorescently labeled lipids are analyzed. This enables the characterization of the signaling and enzymatic steps preferentially activated during stimulus-induced lipogenesis. For this, adipocytes are labeled with 0.5 mM NBD-FA for 4 h at 37°C. Total lipids are extracted from the washed cells with chloroform/methanol (3/1 by vol.), dried and suspended in THF. NBD-fatty acylglycerol-3-phosphate, NBD-fatty acyl-palmitoylglycerol-3-phosphate and NBD-fatty acyl-palmitoylglycerol and NBD-fatty acyl-dipalmitoylglycerol are separated by TLC (Silica Gel Si-60 F_{254}) using toluene/ethylacetate (9/1 by vol.) as solvent system and subsequently eluted from the plate using the line elution method with ethylacetate as eluent. Larger amounts are separated by flash column chromatography (Still et al. 1978) on YMC-spherical silica (60 A, 40 µM, YMC Europe GmbH, Schermbeck).

EVALUATION

The nitrobenzyldiazolyl (NBD) moiety of NBD-FA is a strong fluorophore and is located far away from the carboxyl terminus. Furthermore, the apparent overall length of NBD-FA (carbon backbone including NBD moiety) is comparable to palmitic acid. It has been shown that insulin stimulation of the synthesis of the three lipid species harboring one NBD-fatty acyl residue each, in isolated rat adipocytes, closely resembles that of radioactive labeling of total lipids by [3-^{3}H]glucose with regard to both insulin responsiveness and sensitivity. The data available suggest that incorporation of one residue of NBD-FA into glycerol-3-phosphate blocks further acylation, resulting in the accumulation of mono-NBD-fatty-acylglycerol-3-phosphate, NBD-fatty-acylpalmitoylglycerol-3-phosphate and NBD-fatty-acylpalmitoylglycerol rather than of NBD-fatty acyl-dipalmitoylglycerol. One possibility is a stringent substrate specificity of diacylglycerol transferase (DGAT), for both the acceptor, diacylglycerol, and the donor acyl-CoA.

Stimulation of the rate-limiting enzyme of the esterification steps, GPAT, by insulin has been well established (Sooranna and Saggerson 1976, Vila and Farese 1991, Farese et al. 1994). It is generally accepted that in rat adipocytes the glucose transport step is rate-limiting for insulin-stimulated lipogenesis in the presence of 0.1 mM glucose in the incubation medium (see above). Thus under these conditions, the stimulation of synthesis of these AG by insulin may mainly reflect the effect of insulin on glucose transport. At 2 mM glucose, however, processes subsequent to glucose transport and glycerol-3-phosphate production will become rate-limiting. Both transport and esterification may be studied more conveniently using incorporation of NBD-FA rather than of [3-^{3}H]glucose into lipids (see K.6.1.2.1), in particular under conditions of screening for compounds/drug candidates. Thus, assaying lipogenesis with NBD-FA can be used as a sensitive and reliable (non-radioactive) method for analyzing insulin signaling and lipid synthesis in rat adipocytes, in particular, if there is interest on the impact of high glucose concentrations in the incubation medium (and thus of conditions of insulin resistance; see K.6.3.5) on these processes.

K.6.1.3 Glucose Transport

GENERAL CONSIDERATIONS

Glucose transport is generally assumed to represent the rate-limiting step for lipogenesis in adipose tissue *in vivo* and in adipocytes *in vitro*, at least under conditions of low to moderate concentrations of glucose in the plasma and incubation medium, respectively (see above). Its stimulation by insulin is of exquisite sensitivity and responsiveness. Insulin resistance is defined as the reduced ability of cells or tissues to respond to physiological levels of insulin and is characteristic of non-insulin-dependent diabetes mellitus (type II diabetes). Skeletal muscle is the primary tissue responsible for the postprandial uptake of glucose from the blood in humans. The two major transporters expressed in adipose tissue/skeletal muscle are the muscle/fat-specific glucose transporter GLUT4 and the ubiquitous transporter GLUT1. The insulin-stimulated acute activation of glucose transport mainly occurs by one of two mechanisms: translocation of GLUT4 and GLUT1 from intracellular vesicles to the

plasma membrane and augmentation of the intrinsic catalytic activities of the transporters. The molecular mechanisms underlying the glucose transport and its regulation are similar for adipose and muscle cells. Consequently, adipocytes are more widely used for transport studies than myocytes due to their more convenient accessibility and more pronounced insulin responsiveness. However, studies for clarification of the mechanism by which compounds/drugs with insulin-ike and/or insulin-sensitizing activity stimulate glucose uptake in skeletal muscle for the treatment of type II diabetes have to be performed with assay systems based on muscle cells or tissues. When differentiated into myotubes, cultured L6 muscle cells possess many of the properties of mature skeletal muscle tissue. They express both GLUT4 and GLUT1 and are capable of increasing glucose transport *via* insulin stimulation.

PURPOSE AND RATIONALE

Uptake of glucose in cultured cells is commonly determined by using non-metabolizable radioactive hexoses, such as 3-*O*-methylglucose (3MG) or 2-deoxyglucose (2DG), labeled with a high specific activity of tritium. [^{3}H]3MG necessitates a very short incubation time due to fast equilibration of the analog across plasma membranes and requires either rapid separation of the cells from the aqueous incubation medium of the reaction mixture, usually by centrifugation through a suitable oil cushion with a buoyant density of less than 1, or the prevention of 3MG efflux by washing with a mercuric chloride solution. Uptake assays based on [^{3}H]2DG are more convenient because 2DG is phosphorylated to a stable and membrane-impermeable derivative, 2-deoxyglucose-6-phosphate (2DG6P), by hexokinase or glucokinase, which may accumulate at a specific intracellular compartment, ensuring less rapid equilibration, slower kinetics and more convenient measurement of 2DG transport compared to 3MG (Frost and Lane 1985). However, routine use of these radiolabeled analogs is costly and requires a specialized institution where isotopes can be handled. Consequently, considerable efforts have been spent during the last decade in the development of assays using non-radioactive tracers, which are compatible with the analysis of glucose transport with sufficient insulin responsiveness.

K.6.1.3.1 Method Based on Radiolabeled 2-Deoxyglucose

Isolated Tissues

[2-^{3}H]2DG (12 mCi/mouse) is injected i.p. into mice fasted for 6 h. After 40 min, mice are sacrificed and tissues are excised and rinsed in ice-cold PBS, 1 mM EDTA. Tissue samples are homogenized in 0.5% perchloric acid and centrifuged. The protein pellet is solubilized in 0.3 N NaOH, 0.1% SDS for protein determination. The supernatant is neutralized with KOH and an aliquot is counted to yield total tissue counts (2DG and 2DGP). A second aliquot is treated with $Ba(OH)_2$ and $ZnSO_4$ to remove 2DGP and counted to yield [2-^{3}H]2DG. Specific [2-^{3}H]2DGP accumulation in itssues is calculated as difference between total tissue counts and [2-^{3}H]2DG counts.

Primary and Cultured Adipocytes

50-µl portions of adipocyte cell suspension (1×10^6 cells/ml) are pipetted into minisorp tubes (Nunc, Denmark) and equilibrated at 25°C for 30 min. Insulin (80 nM stock in KRH/5% BSA) and compounds/drugs (lyophilized, 2 mg/ml or 2% DMSO, 30 µM) are added in 50 µl KRHB and incubated for 30 min at 25°C. Thereafter, 50 µl of 2-deoxy-D-[1-^{3}H]glucose (2 µCi per ml of KRHB containing 10 µl/ml of ^{3}H-stock, 0.2 mCi/ml specific activity 20–30 Ci/mmol, 0.3 mM) are added (total volume of the final incubation mixture = 150 µl). After further incubation for 20 min at 25°C in a shaking water bath, the assay is terminated by transfer of 100 µl samples on top of 250 µl dinonylphthalate (density < 0.93–0.96 g/ml, Merck, Darmstadt, FRG) in 500-µl plastic tubes (Beckman) and centrifugation in a microfuge (10,000 × *g*, 1 min, room temperature). The adipocytes remain on top of the oil layer, while the buffer is below the oil layer. The tube is cut with a special knife at the position of the oil layer below the adipocyte layer, then transferred into scintillation vials containing 5 ml aqueous scintillation cocktail (Zinsser Nr. 312 or Beckman Ready Safe) and counted for radioactivity. To correct for 2DG unspecifically associated with the adipocyte plasma membrane or entrapped in extracellular spaces or penetrated into the adipocytes by diffusion, 2 µl of cytochalasin B (20 µM final conc.) from a 1 mM stock solution (in 10% ethanol, diluted with H_2O from a 10 mM stock in ethanol at the day of use) and, as a control, 2 µl of 10% ethanol are added prior to addition of radiolabeled 2DG and incubated under identical conditions (Gliemann et al. 1972, Foley and Gliemann 1981, Müller and Wied 1993).

EVALUATION

Specific transport is calculated as the difference between total cell-associated radioactivity (absence of cytochalasin B) and unspecifically associated/

entrapped radioactivity (presence of cytochalasin B). Under the conditions used, 2DG transport is linear with time up to 20 min. The fold stimulation for glucose transport is calculated as ratio between stimulated specific transport (presence of insulin/compound/drug) and basal specific transport (absence of insulin/compound/drug). For insulin (2 nM), this stimulation factor usually lies in the range between 15 and 25. To compensate for the varying insulin responsiveness of different adipocyte preparations, the insulin-like activity of compounds/drugs can be calculated as percentage of the maximal effect as described above for lipogenesis.

This assay measures the total glucose uptake encompassing the transport of the non-metabolizable glucose analog, 2DG, *via* the specific glucose transporters, GLUT1 and GLUT4, and the molecular mechanism of their movement from intracellular vesicles to the plasma membrane (GLUT translocation) including the underlying signaling cascade through which insulin stimulates glucose transport in adipocytes. Since 2DG taken up the cell is immediately phosphorylated by hexokinase, the assay actually monitors the accumulation of 2DG6P (presumably in specialized intracellular compartments). However, the rate-limiting step of glucose uptake at low glucose concentrations is the transport *via* GLUT1/4 rather than the phosphorylation. This results in apparently longer linear periods of glucose uptake in comparison to the use of non-phosphorylatable glucose analogs, such as 3MG (see K.6.1.3.3) and thereby considerably facilitates the experimental procedure and kinetic analysis. Subsequent conversion of the 2DG6P into lipids and glycogen or its oxidation does not occur. Thus, the use of 2DG is a reliable measure for glucose transport into adipocytes.

K.6.1.3.2 Method Based on Unlabeled 2-Deoxyglucose

PURPOSE AND RATIONALE

A non-radioisotope, enzymatic assay based on the methods of Manchester and coworkers (1990) and Sasson and coworkers (1993) for measuring of 2-deoxyglucose-6-phosphate (2DG6P) in tissues and cultured cells has been developed by Yamamoto and coworkers (2006). These methods enable the detection of 2DG6P accumulating in cells by measurement of the fluorescence of NADPH produced from $NADP^+$, which is coupled to the oxidation of 2DG to 2DG6P by glucose-6-phosphate dehydrogenase (G6PDH). This approach, however, requires the cultivation of many cells on large plates and the preparation of cell extracts because the fluorescence of NADPH is rather weak. Consequently and more recently, a diaphorase–resazurin system that produces a potent fluorescent substance in the presence of NADPH has been linked. Uptake of 2DG into the cells can be measured by the addition of a single assay solution to the cell culture, followed by a simple incubation.

PROCEDURE

The differentiated 3T3-L1 adipocytes or L6 myotubes are incubated with 170 µl/well of α-MEM with 2% FBS in the presence of compounds/drugs/insulin for 10–30 min. After incubation, the cells are washed twice with Krebs–Ringer–phosphate–Hepes (KRPH) buffer (pH 7.4, 20 mM HEPES, 5 mM KH_2PO_4, 1 mM $MgSO_4$, 1 mM $CaCl_2$, 136 mM NaCl, 4.7 mM KCl) containing 0.1% BSA. The washed cells are then incubated with KRPH buffer containing 1 mM 2DG and 0.1% BSA for 1–2 h (termed the 2DG-uptake period) at 37°C in 95% O_2/5% CO_2. After incubation, the cells are washed twice with KRPH buffer containing 0.1% BSA and then 25 µl of 0.1 N NaOH was added. To degrade NAD(P)H, $NAD(P)^+$ and any enzymes in the cells, the culture plate is subjected to one freeze–thaw cycle and incubated at 85°C for 40 min on a temperature-controlled bath. The components in the wells are then neutralized by the addition of 25 µl of 0.1 N HCl and then 25 µl of 150 mM triethanolamine (pH 8.1) is added.

To determine the low concentrations of 2DG and/or 2DG6P present in a 96-well microplate, a diaphorase–NADPH amplifying system is combined with previous methods (Sasson et al. 1993, Manchester et al. 1990) for measuring 2DG6P in tissues and cultured cells. 50 µl of 2DG solution at various concentrations is dispensed into each well of a 96-well plate and incubated for 90 min at 37°C after the addition of 150 µl of an assay cocktail of 50 mM triethanolamine (pH 8.1), 50 mM KCl, 0.5 mM $MgCl_2$, 0.02% BSA, 670 µM ATP, 0.12 µM $NADP^+$, 25 µM resazurin sodium salt, 5.5 units/ml hexokinase, 16 units/ml G6PDH, and 1 unit/ml diaphorase. The assay cocktail is prepared before each assay from stock solutions of enzyme, coenzyme, and substrate that are maintained in the freezer or refrigerator. At the end of the incubation, fluorescence at 590 nm with excitation at 530 nm is measured by a microplate reader to detect the resorufin derived from reduced resazurin. A standard curve is generated by placing 2DG standard solutions in wells of the culture plate that had been prepared without cells.

EVALUATION

Glucose uptake in cultured cells is routinely determined by using non-metabolizable radioactive hexoses, such as 3MG or 2DG, labeled with a high specific activity of tritium. Assaying the uptake of [^{3}H]2DG is more convenient than assaying the uptake of [^{3}H]3MG because 2DG is converted to a stable and impermeable derivative 2DG6P through phosphorylation by hexokinase or glucokinase (see above). Because both methods rely on the use of substantial amounts of radioactive material, the concentration of the unlabeled analog is usually kept low (50–500 µM) in the uptake mixture to maintain a high specific activity. Measuring the uptake of these analogs at concentrations comparable to normal or pathological blood glucose levels (5–10 mM) is not practical because of the excessive amount of radioactive analog that would be required to maintain a specific activity high enough to obtain reliable data. Furthermore, the high concentration of analog needed is very expensive and a specialized institution registered for using radioactive isotopes is required. Although new fluorescently labeled glucose analogs for use as tracers of glucose uptake have been synthesized, none of these molecules has been found to show the same biological behavior as 2DG (Perret et al. 2004). Therefore, 2DG is often considered to be the gold standard in reference tracers of glucose transport and phosphorylation.

The resazurin–diaphorase-amplifying system facilitates the measurement of NADPH in the 2DG uptake assay, because the resorufin fluorophore produced is water-soluble and has high fluorescence intensity. In addition, there will be little background interference from other biochemical entities in the cell or from chemical compounds/drugs added during the assay because the emission wavelength of resorufin is longer and its fluorescence wavelength is much longer than those of NADPH. Furthermore, analysis of resorufin can be measured on standard, clear tissue-culture plates because the material comprising the culture plate, such as polystyrene, does not interfere with the fluorescence signal of resorufin.

K.6.1.3.3 Method Based on 3-*O*-Methylglucose

The rate of 3MG transport is determined according to Whitesell and Gliemann (1979), Karnieli and coworkers (1981), Basi and coworkers (1992) by a modification of the L-arabinose uptake method described by Foley and coworkers (1978).

PROCEDURE

5-ml polyethylene miniscintillation vials are prepared with 50 µl of incubation medium containing L-[1-^{3}H]glucose and 3-*O*-[methyl-^{14}C]glucose such that their concentration is 0.5 mM (58.2 and 11.6 µCi/µmol, respectively). L-Glucose is included as a marker for the extracellular space. Sugar uptake is initiated by the rapid addition of 200 µl of adipose cell suspension (2×10^8 cell/ml) and then rapidly stopped by the addition of 10 µl of a 10 mM solution of cytochalasin B in 25% ethyl alcohol. The duration of this 'pulse' incubation is adjusted from 3 to 25 s so that the uptake achieved will be approximately one third of the equilibrium level. The equilibrium level of uptake is determined by incubating cells for 5 to 6 min in the presence of 3MG only and then for one additional min following the addition of L-glucose. Experimental blanks are obtained by adding cytochalasin B to the labeled sugar solution prior to the addition of cells. Following incubation, two 100-µl portions of each incubation mixture are separated from the incubation medium by centrifugation through dinonylphthalate, and the separated cells are counted for radioactivity (see above for 2DG transport). The net uptake of 3MG is then counted, and the initial uptake velocity or rate of transport is determined.

EVALUATION

3MG is a non-phosphorylatable glucose analog which can be used for the accurate measurement of the true initial glucose transport rate without interference with the subsequent glucose-metabolizing steps (e. g. phosphorylation to glucose-6-phosphate). Since the volume of the adipocyte cytosol is rather small, the time period required for equilibration of the extracellular and intracellular glucose concentration is rather short. This necessitates sophisticated experimental procedures enabling start and termination of the transport reaction within a few seconds. Therefore, for routine purposes 2DG rather than 3MG is commonly preferred.

K.6.1.3.4 Method Based on a Fluorescent Glucose Analog

Zou and coworkers (2005) described a sensitive and non-radioactive assay for direct and rapid measuring glucose transport in single living cells. The assay is based on direct incubation of mammalian cells with a fluorescent D-glucose analog, 2-[*N*-(7-nitrobenz-2-oxa-1,3-diazol-4-yl)amino]-2-deoxy-D-glucose (2-NBDG) followed by flow cytometric detection of total fluorescence produced by the cells due to accumu-

lation of 2-NBDG-6-phosphate with time. However, despite a series of experiments has been conducted to define the optimal conditions for this assay, Zou and coworkers (2005) failed to demonstrate a clear-cut stimulation of 2-NBDG transport into these cells by insulin.

REFERENCES AND FURTHER READING

Basi NS, Thomaskutti KG, Pointer RH (1992) Regulation of glucose transport in isolated adipocytes by levamisole. Can J Physiol Pharmacol 70:1190–1194

Drevon CA (2005) Fatty acids and expression of adipokines. Biochim Biophys Acta 1740:287–292

Elsing C, Winn Borner U, Stremmel W (1995) Confocal analysis of hepatocellular long-chain fatty acid uptake. Am J Physiol 269:G842-G851

Farese RV, Standaert ML, Yamada K, Huang LC, Zhang C, Cooper DR, Wang Z, Yang Y, Suzuki S, Toyota T, Larner J (1994) Insulin-induced activation of glycerol-3-phosphate acyltransferase by chiro-inositol-containing insulin mediator is defective in adipocytes of insulin-resistant, type II diabetic, Goto–Kakizaki rats. Proc Natl Acad Sci USA 91:11040–11044

Foley JE, Gliemann J (1981) Accumulation of 2-deoxyglucose against its concentration gradient in rat adipocytes. Biochim Biophys Acta 648:100–106

Foley JE, Cushman SW, Salans LB (1978) Glucose transport in isolated rat adipocytes with measurement of L-arabinose uptake. Am J Physiol 234:E112–E119

Frost SC, Lane MD (1985) Evidence for the involvement of vicinal sulfhydryl groups in insulin-activated hexose transport by 3T3-L1 adipocytes. J Biol Chem 260:2646–2652

Gliemann J, Østerlind K, Vinten J, Gammeltoft S (1972) A procedure for measurement of distribution spaces in isolated fat cells. Biochim Biophys Acta 286:1–9

Humbel RE (1959) Messung der Serum–Insulin-Aktivität mit epididymalem Fettgewebe *in vitro*. Experientia (Basel) 15:256–258

Karnieli E, Zarnowski MJ, Hissin PJ, Simpson IA, Salans LB, Cushman SW (1981) Insulin-stimulated translocation of glucose transport systems in the isolated rat adipose cell. J Biol Chem 256:4772–3777

Lee Y-H, Chen S-Y, Wiesner RJ, Huang Y-F (2004) Simple flow cytometric method used to assess lipid accumulation in fat cells. J Lipid Res 45:1162–1167

Lingsøe J (1961) Determination of the insulin-like activity in serum using rat epididymal adipose tissue. Scand J Clin Lab Invest 13:628–636

Manchester JK, Chi MM, Carter JG, Pusateri ME, McDougal DB, Lowry OH (1990) Measurement of 2-deoxyglucose and 2-deoxyglucose 6-phosphate in tissues. Anal Biochem 185:118–124

Moody AJ, Stan MA, Stan M (1974) A simple free fat cell bioassay for insulin. Horm Metab Res 6:12–16

Müller G, Jordan H, Petry S, Wetekam E-M, Schindler P (1997) Analysis of lipid metabolism in adipocytes using fluorescent fatty acids I. Insulin stimulation of lipogenesis. Biochim Biophys Acta 1347:23–39

Perret P, Ghezzi C, Ogier L, Abbadi M, Morin C, Mathieu JP, Fagret D (2004) Biological studies of radiolabeled glucose analogs iodinated in positions 3, 4 or 6. Nucl Med Biol 31:241–250

Rajala MW, Scherer PE (2003) Minireview. The adipocyte-at the crossroads of energy homeostasis, inflammation, and atherosclerosis. Endocrinology 144:3765–3773

Sasson S, Oron R, Cerasi E (1993) Enzymatic assay for 2-deoxyglucose 6-phosphate for assessing hexose uptake rates in cultured cells. Anal Biochem 215:309–311

Schaffer JE, Lodish HF (1994) Expression cloning and characterization of a novel adipocyte long chain fatty acid transport protein. Cell 97:427–436

Sooranna SR, Saggerson ED (1976) Interactions of insulin and adrenaline with glycerol phosphate acylation processes in fat-cells from rat. FEBS Lett 64:36–39

Shigematsu S, Miller SL, Pessin JE (2001) Differentiated 3T3L1 adipocytes are composed of heterogenous cell population with distinct receptor tyrosine kinase signaling properties. J Biol Chem 276:15292–15297

Still MC, Khan M, Mitra A (1978) J Org Chem 43:2923–2925

Storch J, Lechene C, Kleinfeld AM (1995) Direct determination of free fatty acid transport across the adipocyte plasma membrane using quantitative fluorescence microscopy. J Biol Chem 266:13473–13476

Vila M, Farese RV (1991) Insulin rapidly increases glycerol-3-phosphate-acyltransferase activity in rat adipocytes. Arch Biochem Biophys 284:366–368

Von Goor H, Gerrits PO, Groud J (1986) The application of lipid-soluble stains in plastic-embedded sections. Histochemistry 85:251–253

Whitesell RR, Gliemann J (1979) Kinetic parameters of 3-*O*-methylglucose and glucose in adipocytes. J Biol Chem 254:5276–5283

Yamamoto N, Sato T, Kawasaki K, Murosaki S, Yamamoto Y (2006) A nonradioisotope, enzymatic assay for 2-deoxyglucose uptake in L6 skeletal muscle cells cultured in a 96-well microplate. Anal Biochem 351:139–145

Zou C, Wang Y, Shen Z (2005) "-NBDG as a fluorescent indicator for direct glucose uptake measurement. J Biochem Biophys Methods 64:207–215

K.6.1.4 Glucose Transporter Translocation

PURPOSE AND RATIONALE

The transport of glucose across the plasma membrane of mammalian cells represents one of the most important nutrient transport events, since glucose plays a central role in cellular energy homeostasis and intermediary metabolism. Apparently, rather than mediated by a single transporter molecule, glucose transport is mediated by a family of highly related transporters characterized by 12 transmembrane regions and amino-/carboxy-termini facing the cytoplasm (Assimacopoulos-Jeannet et al. 1991, Gould and Holman 1993, Mueckler 1994), the most important ones with regard to carbohydrate metabolism and regulation by insulin are:

GLUT1: the erythrocyte-type glucose transporter,

GLUT2: the liver-type glucose transporter,

GLUT3: the brain-type glucose transporter,

GLUT4: the insulin-responsive glucose transporter

GLUT5: the small intestine sugar/fructose transporter

GLUT8: a small intestine/hypothalamic glucose sensor and ion channel lacking a transport function

Among these isoforms, the insulin-responsive GLUT4 is the only one, which is expressed in mammalian muscle and adipose tissue, exclusively, and localized in cytoplasmic vesicles (GLUT4 vesicles) derived from the tubulo-vesicular structures of the trans-Golgi network in the unstimulated state. In animal and human adipose and muscle tissues insulin induces several-fold increases in glucose transport by causing the movement and fusion of GLUT4 vesicles to and with the plasma membrane, respectively. This so-called GLUT4 translocation leads to increase in the number of GLUT4 molecules exposed at the plasma membrane which results in elevated glucose transport velocity (i. e. increase in v_{max}). Numerous cellular, animal and human studies have revealed significant impairment of GLUT4 translocation in the insulin-resistant and diabetic state. The molecular basis remains unclear so far but may include alterations in the complex machinery regulating the targeting, docking and fusion of the GLUT4 vesicles as well as in the phosphorylation of protein (SNARE) components involved (see below). This is suggested by the findings that GLUT4 is inactivated by phosphorylation in the insulin-resistant state and activated by dephosphorylation (Reusch et al. 1993) and that the phosphorylation state of GLUT4 is increased in primary rat adipocytes made insulin-resistant *in vitro* by incubation with high glucose and insulin (Müller and Wied 1993, see K.5.1.3).

K.6.1.4.1 Methods Based on the Determination of GLUT Molecules in Isolated Plasma Membranes

GENERAL CONSIDERATIONS

The insulin-stimulated GLUT4 translocation in adipocytes can be assayed by a number of different procedures either dependent on or independent of subcellular fractionation, i. e. the preparation of plasma membranes of high purity. This admittedly tedious and time-consuming procedure is prerequisite for the majority of techniques appropriate for the analysis of cell surface expression of GLUT4 (and thus reflecting GLUT4 translocation) in primary rat adipocytes, which had been challenged with insulin/compounds/drugs. These techniques rely on the determination of the amount of immunoreactive GLUT4 by immunoblotting with the recently introduced specific anti-GLUT4 antibodies in isolated and sufficiently pure plasma membrane vesicles. Alternatively, radioactively or fluorescently labeled glucose analogs which are recognized but not transported by GLUT4 can be used for determination of the number of GLUT4 at the plasma membrane of intact rat adipocytes upon covalent crosslinking (see K.6.1.4.2.3). In contrast, in cultured murine or human adipocytes GLUT4 translocation can be followed upon transfection with a recombinant GLUT4 which is tagged with an extracellular epitope recognized by a specific antibody thereby circumventing the necessity for subcellular fractionation or covalent crosslinking (see K.6.1.4.1.2 and K.6.1.4.2).

Preparation of Rat Adipocyte Plasma Membrane Vesicles

Adipocytes are isolated from epididymal fat pads of 160–180 g male Wistar rats by collagenase digestion under sterile conditions and incubated with insulin or compounds/drugs as described (see K.5.1.2). The subcellular fractionation is performed according to McKeel and Jarett (1970) and Simpson and coworkers (1983) with the following modifications: The postnuclear supernatant is centrifuged (12,000 × *g*, 15 min). The washed pellet is suspended in 35 ml of buffer and recentrifuged (1000 × *g*, 10 min). The washed pellet (12,000 × *g*, 20 min) is suspended in 5 ml of buffer, layered onto a 20 ml cushion of 38% (w/v) sucrose, 20 mM Tris/HCl (pH 7.4), 1 mM EDTA and centrifuged (110,000 × *g*, 60 min, 4°C). The membranes at the interface between the two layers (1 ml) are removed by suction, diluted with three volumes of buffer and layered on top of a 8 ml cushion of 24% Percoll, 250 mM sucrose, 20 mM Tris/HCl (pH 7.4), 1 mM EDTA. After centrifugation (45,000 × *g*, 30 min) the plasma membranes are withdrawn with a Pasteur pipette from the lower fourth of the gradient (1 ml), diluted with 10 volumes of buffer and recentrifuged (150,000 × *g*, 90 min, 4°C). The pellet is suspended, recentrifuged, finally dissolved in buffer at 2–5 mg protein/ml and stored at –80°C. The majority of plasma membranes are recovered as outside-out vesicles as revealed by the low cryptic activity of exofacial 5′-nucleotidase which is detected after detergent solubilization of the vesicles.

K.6.1.4.1.1 Determination by Immunoblotting

The methods described above lost their importance with the introduction of antibodies specific for GLUT4 representing the major (insulin-)regulated GLUT isoform which accounts for more than 90% of the max-

imal insulin-stimulated glucose transport activity in primary rat adipocytes and is localized in the basal state almost exclusively (95%) at intracellular vesicles and in the maximally stimulated state with 50% at the plasma membrane. Consequently, the amount of GLUT4 in plasma membrane vesicles derived from basal and stimulated (by insulin/compound/drug) rat adipocytes is now usually determined by immunoblotting for GLUT4. In case of weak expression of GLUT4 (e. g. cultured human adipocytes) or limited availability of starting materials (e. g. human adipose tissue), the sensitivity of the immunological detection can be considerably improved by immunoprecipitation of GLUT4 from the solubilized plasma membrane vesicles prior to immunoblotting.

Polyclonal affinity-purified rabbit antibodies have bee successfully raised against a synthetic peptide corresponding to the COOH-terminal domain of rat GLUT4 (residues 495–509) (James et al. 1989). The plasma membrane vesicles are subjected to SDS-PAGE (25 µg protein/lane) and electrophoretically transferred onto nitrocellulose filters (Towbin et al. 1979). Incubations of the filters with primary and secondary antibodies (^{125}I-labeled or peroxidase-labeled anti-rabbit IgG from goat) and quantitative evaluation of the immunoreactive material by autoradiography and densitometry or enhanced chemiluminescence and luminescence imaging, respectively, are carried out as described previously (Müller and Wied 1993) for the demonstration of the sulfonylurea-induced GLUT4 translocation in isolated rat adipocytes, which may be based on phosphorylation of GLUT4. Evidence has been presented suggested that insulin promotes serine phosphorylation of GLUT4 at the carboxyl terminus (Lawrence et al. 1990a, b) arguing for a causal relationship between GLUT4 translocation and phosphorylation in response to insulin and insulin-like acting sulfonylureas, such as glimepiride.

K.6.1.4.1.2 Determination of GLUT Molecules in Plasma Membrane "Sheets"

PURPOSE AND RATIONALE

In non-recombinant adherent murine and human adipocytes as well as non-adherent primary adipocytes which express endogenous GLUT4, only, its translocation can be monitored by the plasma membrane "sheet" assay. This is based on placing glass coverslips onto the adherent cells (6- or 12-well culture plates) following incubation with insulin/compounds/drugs. Upon removal of the coverslips the adherent cells are sheared and their plasma membranes attached to the coverslip become disrupted, leaving the cytosolic components and the intracellular particulate materials (including the intracellular GLUT4 vesicles) with the medium of the plate. Subsequent immunofluorescent detection of GLUT4 remaining attached to the coverslips enables the semi-quantitative determination of GLUT4 located at the plasma membrane and apparently deprived from intracellular GLUT4.

PROCEDURE

The protocol for the preparation of plasma membrane sheets is derived from that of Moore and coworkers (1987) with modifications adapted from Robinson and coworkers (1992) and Fingar and coworkers (1993). 3T3-L1 adipocytes or human cultured adipocytes are plated on poly-D-lysine-coated coverslips the day before an experiment. Adipocytes are incubated for 1.5 h at 37°C in Leibovitz's L-15 medium containing 0.2% BSA and treated in the absence or presence of insulin/compounds/drug candidatess. The cells are washed twice in ice-cold buffer A (100 mM NaCl, 50 mM HEPES/KOH, pH 7.3) and once in buffer B (100 mM KCl, 2 mM $CaCl_2$, 1 mM $MgCl_2$, 10 µM leupeptin, 2 µg/ml trypsin inhibitor, 0.5 mM benzamidine, 20 mM HEPES/KOH, pH 7.2) and then sonified in buffer B for 3 sec using a Branson 250 sonifier with a microtip placed 1 cm above the coverslip (output control = 4, duty cycle = 30). Adherent plasma membrane sheets are washed twice in ice-cold buffer B, fixed in 3% paraformaldehyde for 10 min, and processed for indirect immunofluorescence using affinity-purified anti-GLUT4 antisera and rhodamine-conjugated secondary antibodies as described (Garcia de Herreros and Birnbaum 1989).

K.6.1.4.2 Methods Based on the Determination of GLUT Molecules at the Plasma Membranes of Intact Cells

GENERAL CONSIDERATIONS

For recombinant cultured murine and human adipocytes, the need for subcellular fractionation (i. e. preparation of plasma membrane vesicles of sufficient purity) can be circumvented by heterologous expression of GLUT4 tagged at the extracellular loop with an epitope for which specific antibodies are available (e. g. c-myc) and subsequent immunological detection of GLUT4 in the intact and appropriately fixed cells. Alternatively, GLUT exposed at the plasma membrane of intact adipocytes can be photoaffinity-labeled with membrane-impermeable specific and radioactive probes which enable the subsequent

detection upon immunoprecipitation of GLUT4/1 from total membranes. Moreover, the methods of "in-cell" immunoblotting or colorimetry enable accurate and straightforward detection of plasma membrane GLUT4 of cultured and subsequent to the treatment fixed adipocytes without the need for cell fractionation or plasma membrane sheet generation.

K.6.1.4.2.1 In-cell Immunoblotting

PURPOSE AND RATIONALE

The "in-cell immunoblot" is an immunocytochemical assay performed in microtiter plate formate. Target-specific primary antibodies and infrared-labeled secondary antibodies are used to detect target proteins in fixed cells, and fluorescent signal from each well is quantified. Two targets at 700 and 800 nm using two spectrally distinct dyes are monitored. Separate lasers and fluorescence detectors are used for each dye and offer a wide linear detection range. With two detection channels two separate targets can be probed or the quantification accuracy is increased by using the second channel for normalization against a second target or DNA stain. Quantification accuracy is maximized by normalization because adjustments can be made for differences in cell number from well to well. Two-color normalization also helps to prevent false negatives and provides more accurate evaluation of the treatment of cells with compounds/drug candidates. The use of near-infrared probes yields high sensitivity for measuring small changes in the protein amount. The direct detection of proteins (e. g. GLUT4) in their cellular context eliminates variabilities and artifacts caused by cell lysis, gel loading, electrophoresis, and membrane transfer.

This method enables the analysis of cell surface expression of proteins (e. g. GLUT4) in adherent cells without the need for cumbersome and labor-intensive cell fractionation procedures. Upon incubation of the adherent adipocytes with insulin/compounds/drug candidates, GLUT4 expression at the plasma membrane is detected by "in-cell" immunoblotting using conditions for fixation and permeabilization of the adipocytes, which enable access of the anti-epitope antibodies to plasma membrane GLUT4, only, rather than to intracellular GLUT4 vesicles.

PROCEDURE

3T3-L1 fibroblasts or human adipocytes are seeded in 96-well clear round bottom plates (BD Bioscience cat# 353077) at 200,000 cells/well, grown to confluency and then differentiated into mature adipocytes as described above. After serum deprivement overnight by replacement of the differentiation medium with serum-free DMEM, the adipocytes are incubated with insulin/compound/drug in 200 µl of the same medium for 15 min at 37°C. For fixation, 25 µl of 36% formaldehyde is added gently to each well using side of the wells (to avoid detaching of the cells from the well bottom). After incubation for 20 min at room temperature with very gentle rotation, the fixation solution is removed. For permeabilization, the cells are washed three times with 100 µl of PBS containing 0.1% TX-100 for 5 min each by carefully pipetting the permeabilization solution down the sides of the wells to avoid detaching the cells from the well bottom. Thereafter, the permeabilization solution is removed and the washing step is repeated two more times. After addition of 100 µl of blocking buffer (Odyssey, LICOR Biosciences) to each well and incubation for 1 h at room temperature with very gentle shaking on a rotator, 50 µl of anti-GLUT4 antibody (1:200–1:500, Calbiochem) is added and the incubation continued overnight at 4°C. Thereafter, the primary antibody solution is removed and the plates are washed five times with 200 µl of PBS containing 0.1% Tween-20 for 5 min each. 50 µl of fluorescently labeled secondary antibody solution (goat anti-rabbit IRDye 800CW, Rockland Immunochemicals, 1:800 diluted in Odyssey blocking buffer with 0.2% Tween-20) is added to each well. After incubation for 1 h at room temperature on a rotator under protection from light, the secondary antibody solution is removed and the plates are washed five times with 200 µl of PBS containing 0.1% Tween-20 at room temperature for 5 min each. After the final wash, the washing solution is completely removed from the wells. The plates are immediately scanned by placing on the Odyssey scan surface with detection in the 800 nm channel and at 169 µm resolution at 3.0 to 3.5 mm focus offset and an intensity setting of 5 or less.

K.6.1.4.2.2 In-cell Colorimetry

PURPOSE AND RATIONALE

Understanding the molecular mechanisms of insulin action has been of major interest since the discovery, several decades ago, that insulin stimulates glucose transport *in vivo*. Subcellular fractionation (see K.6.1.4.1 and K.6.3.6.1), cell photolabeling coupled to immunoprecipitation and immunofluorescence (see below) or immunoelectron microscopy have been used to detect translocation of GLUT4 to the cell surface (Wilson and Cushman 1994, Kozka et al. 1991, Smith

et al. 1991). All of these methods are laborious and suffer from methodological inaccuracies. Subcellular fractionation is cumbersome and produces membranes that are rarely pure. Moreover, quantitative recovery of all membrane compartments is difficult or impossible. Affinity labeling of surface glucose transporters followed by immunoprecipitation depends on the ability to obtain quantitative immunoprecipitation and recovery upon SDS-PAGE. This technique results in the incorporation of about 1/10.000 of the label added, thus the signal to noise ratio is low. Moreover, the reactivity of the photolabel can depend on the level of activity of the transporter (Vannucci et al. 1992) in addition to the amount of transporter exposed at the cell surface. Immunofluorescence detection does not distinguish the native GLUT4 molecules incorporated into the cell membrane from molecules in subplasmalemmal vesicles, and is not a quantitative technique. Immunogold electron microscopy detects antigens at the plasma membrane accurately, but has not been successfully used in a quantitative fashion. None of the above techniques is suitable for large numbers of experiments, as would be required for screening of antidiabetic drugs stimulating insulin signaling or GLUT4 translocation. Therefore, Wang and coworkers (1998) intended to develop a fast and quantitative approach to measure GLUT4 translocation in intact cells. The method described uses cells in culture and does not require subsequent immunoprecipitation, SDS-PAGE or use of radioactivity, as required by the photolabeling technique. It does not require large amounts of cells nor laborious subcellular fractionation and is rapid, sensitive and quantitative.

PROCEDURE

Construction of L6 Cells Expressing c-myc Epitope-Tagged GLUT4 (GLUT4myc)

GLUT4myc cDNA is constructed by inserting the human c-myc epitope (14 amino acids) into the first ectodomain of GLUT4 as described by Kanai and coworkers (1993). The epitope does not affect GLUT4 activity. GLUT4myc cDNA is subcloned into the mammalian expression vector pCXN (pCXN-GLUT4myc) as described by Niwa and coworkers (1991). L6 myoblasts are transfected with pCXN-GLUT4myc and pSV2-bsr, a blasticidin S deaminase expression plasmid, and selected with blasticidin S hydrochloride.

Cell Culture

L6-GLUT4myc myoblasts in cell monolayers are maintained in α-MEM supplemented with 10% FBS in a humidified atmosphere containing 10% CO_2 and 90% air at 37°C. Cells are grown in 12- or 24-well plates and, prior to experiments, incubated with serum-free α-MEM supplemented with 25 mM glucose for 5 h.

Colorimetric Assay of Surface GLUT4myc

Quiescent L6-GLUT4myc cells are incubated with compounds/drug candidates, then washed once with PBS, fixed in 3% paraformaldehyde in PBS for 3 min at room temperature. The fixative is immediately neutralized by incubation with 1% glycine in PBS at 4°C for 10 min. The cells are blocked with 10% goat serum and 3% BSA in PBS at 4°C for at least 30 min. Primary monoclonal antibody (anti-c-myc, 9E10) is then added into the cultures at a dilution of 1:100 and maintained for 30 min at 4°C. The cells are extensively washed with PBS before introducing peroxidase-conjugated rabbit anti-mouse IgG (1:1,000). After 30 min at 4°C, the cells are extensively washed and 1 ml *o*-phenylenediamine dihydrochloride reagent is added to each well. The colorimetric reaction is stopped by addition of 0.25 ml of 3 N HCl for 10 min at room temperature. The supernatant is collected and the optical absorbance is measured at 492 nm.

EVALUATION

Standard curves can be generated using either peroxidase conjugated anti-mouse IgG alone or myc-tag peptide. For this, myc-tag peptide at various concentrations is coated onto 24-well plates by incubation at 4°C for 24 h and then allowed to dry. The plates are rinsed with PBS to move excess salt and the uncoated spaces are blocked with 10% goat serum and 3% BSA.

K.6.1.4.2.3 Exofacial Labeling

PURPOSE AND RATIONALE

Alternatively, in non-recombinant primary and cultured adipocytes GLUT translocation can be analyzed by exofacial labeling of the GLUT molecules. For this, the membrane-impermeable photoreactive substrate analogs, radiolabeled bismannose propylamine (ATB-BMPA; Ryder et al. 2000) and biotinylated and spacer-equipped glucose compound (GP15; Hashimoto et al. 2001), which are all recognized but not transported by GLUT1 and GLUT4. In addition, a series of photoaffinity probes based on a dihexose structure, in which the hexose moieties (d-mannose or d-glucose) are linked through their 4-OH positions to a 2-aminopropyl spacer, to probe the cell-surface exposure of GLUT4 has been generated. Comparisons

of aryl azide, benzophenone and aryl diazirinetrifluoroethane photoaffinity labelling derivatives of hexoses (Holman et al. 1986, 1988, 1990) have suggested that the latter are most suitable as they are highly efficient cross-linkers with good specificity. A (diazirinetrifluoroethyl)benzoyl moiety has been attached through an amide link to the central amine group. More recently a biotinylated version of this compound has been developed in which a linker to biotin is attached through the hydroxy group of the 2-hydroxy-4-(1-diazirine-2,2,2-trifluoroethyl)benzoyl moiety (Koumanov et al. 1998). This compound has been used to assess the cell-surface exposure of GLUT4 in the human muscle of control and type II diabetic patients and marked impairments in the insulin-stimulated translocation of GLUT4 have been identified using this technique (Ryder et al. 2000). All these substrate analogs can be covalently crosslinked to the GLUT isoforms by photoaffinity-labeling *via* the attached diazirinetrifluorobenzoyl moiety upon UV-irradiation following incubation of the cells with insulin/compounds/drugs. After removal of free substrate analog by washing of the adipocytes, total membranes are prepared from the lysed cells and counted for radioactivity (ATB-BMPA) or detected by immunoblotting for interaction with streptavidin (GP15). Both measures reflect the amount of total GLUT1/4 located at the plasma membranes at the time point of cell lysis, exclusively. For specific analysis of GLUT4 or GLUT1 translocation, the isoforms have to be immunoprecipitated with specific antibodies since the substrate analogs do not discriminate between GLUT4 and 1 (Holman et al. 1990).

PROCEDURE

For the use of photoaffinity labeling with GP15, (Hashimoto et al. 2001), primary rat adipocytes, which have been incubated with insulin/compounds/drugs are maintained at 18 C in the presence of 300–500 µM photoreactive probe for 1 min either in the presence or absence of 0.5 M glucose. The samples are then irradiated for 1 min in a Rayonet photochemical reactor using 300 nm bulbs. Excess reagent is removed by extensive washing in physiological buffers and then 0.3 µM avidin is added to block the cell-surface tagged transporters. Excess avidin is then removed by washing the cells. For detection of biotinylated GLUT4 by blotting, adipocyte samples are homogenised in HEPES/EDTA/sucrose (HES) buffer (255 mm sucrose, 1 mM EDTA, 20 mM HEPES (pH 7.2), 1 µg/ml antipain, aprotinin, pepstatin and leupeptin, each, and 100 µM 4-(2-aminoethyl)benzenesulfonyl fluoride hydrochloride (AEBSF). Homogenates are washed once with HES buffer and subjected to centrifugation (554,000 × *g*, 30 min, 4 C) to obtain a total membrane fraction. This pellet is solubilized in PBS, pH 7.2, with 2% of Thesit ($C_{12}E_9$) and 1 µg/ml each of antipain, aprotinin, pepstatin and leupeptin, and 100 µM AEBSF. The samples are solubilized for 50 min at 4 C with rotation and then subjected to centrifugation (20,000 × *g*, 20 min, 4 C). Biotinylated proteins in the supernatants are either immunoprecipitated using a GLUT4 antiserum as described above or precipitated with streptavidin beads (Pierce, Rockford). Following GLUT4 immunoprecipitation, complexes are released into electophoresis-sample buffer (62.5 mM Tris/HCl, pH 6.8, 2% SDS, 10% glycerol) at room temperature. The steptavidin precipitates are washed four times with PBS buffer containing 1% Thesit with protease inhibitors, four times with PBS containing 0.1% Thesit *plus* protease inhibitors and once in PBS. Electrophoresis-sample buffer is added to each pellet. The sample is then heated to 95 C for 30 min and subjected to centrifugation (2,300 × *g*, 1 min). After removal of the supernatants, the pellets are washed with additional electrophoresis-sample buffer, heated to 95 C for 30 min and resubjected to centrifugation. Mercaptoethanol is added (10% final concentration) to the above samples in electrophoresis-sample buffer and these samples are then subjected to SDS-PAGE (10% gel). Proteins are transferred to nitrocellulose membranes. Membranes are blocked with 5% non-fat milk in Tris-buffered saline containing 0.1% Tween (TBS-T) and washed six times with TBS-T. Membranes are either incubated with streptavidin-HRP (Amersham) or with affinity-purified anti-GLUT4 C-terminal antibody in TBS-T containing 1% BSA (2 h, room temperature), followed by washing (six times in TBS-T) and detection using secondary antibody linked to horseradish peroxidase. GLUT4 protein is visualized with enhanced chemiluminescence (ECL).

K.6.1.4.3 Method Based on the Reconstitution of GLUT4 Translocation

PURPOSE AND RATIONALE

Insulin action on peripheral tissues including fat, heart, and skeletal muscle leads to increased glucose transport. The basis for this action lies in the increased translocation of GLUT4-containing vesicles from an intracellular reservoir compartment and ultimately exposure of the GLUT4 at the cell surface where it facilitates transport (see K.6.1.3 and K.6.1.4). Kinetic

studies have identified that GLUT4 traffics through multiple intracellular compartments involving endosomes, the trans-Golgi network (TGN), and a specialized compartment in which GLUT4 is enriched and it is the exocytosis process that is stimulated by insulin (Satoh et al. 1993, Yang and Holman 1993). However, the site of insulin action along the exocytic pathway is unknown and potentially could involve increased release or budding of GLUT4 vesicles from tubular-vesicular structures, increased movements of vesicles along microtubules, increased transit through cortical actin near the cell surface, increased docking and then fusion of GLUT4 vesicles at the plasma membrane, and then possibly stimulation of catalytic activity of plasma-membrane-inserted GLUT transporters. For further resolution of the key-regulated step, an *in vitro* fusion reaction has been developed in which GLUT4 vesicles are immunoisolated and fused with reconstituted plasma membrane in the presence of cell cytoplasm. The separate analysis of this partial reaction in the exocytic limb of the translocation sequence allows direct analysis of the extent to which fusion is stimulated by insulin or insulin-like compounds/drug candidates. Remarkably, the magnitude and time course for insulin's action on glucose transport is fully recapitulated in the vesicle fusion reaction.

Cell-free reconstitution of vesicle fusion reactions have many advantages for studying cell biology processes, as the separate components of the fusion reaction can be separately manipulated and combined. The cell-free approach is particularly powerful in studying insulin-regulated fusion as separate mixing of vesicles containing insulin-activated and non-activated components is feasible. With this approach, it can be studied whether the action of insulin/compounds/drugs leads to activation of GLUT4 vesicles, activation of components of the cytoplasm fraction, or activation of components of the plasma-membrane fraction. For insulin, recent data reveal that it is the activation of that plasma-membrane fraction that is the key-regulated step in the stimulation of fusion (Koumanov et al. 2005).

However, the exact nature of insulin signals that regulate GLUT4 translocation and how they affect the donor membrane, plasma membranes, or some other components in the translocation machinery remain unclear. In attempts to further characterize the translocation machinery and to study its modulation by insulin/compounds/drugs, two distinct *in vitro* reconstitution assays for GLUT4 translocation have been developed (Inoue et al. 1999, Koumanov et al. 2005).

K.6.1.4.3.1 Analysis by Immunoblotting

Preparation of Plasma Membranes and Donor Membranes

In an attempt to define the mechanism of insulin-regulated GLUT4 translocation, Inoue and coworkers (1999) developed an *in vitro* reconstitution assay based on immunoblotting detection of the membrane fusion reaction. For this, differentiated 3T3-L1 adipocytes (stably transfected with mycGLUT4 cDNA by using a retroviral expression plasmid for the preparation of donor membranes) in 10-cm dishes are serum-starved for 18 h and then incubated in the presence or absence of insulin/compounds/drugs. After washing twice with ice-cold PBS, the cells are homogenized immediately by using 20 strokes of a 1-ml Teflon-in-glass homogenizer in a buffer containing 10 mM HEPES/KOH (pH 7.4), 1 mM EDTA, 250 mM sucrose, 1 mM DTT, 1 mM Na_3VO_4, 50 nM okadaic acid, 1 mM PMSF, and 0.1 mg/ml aprotinin. For preparing the donor membranes containing mycGLUT4, the homogenization buffer is supplemented with 0.5 mM $ZnCl_2$. The homogenate is centrifuged ($500 \times g$, 1 min). For collection of plasma membranes, the supernatant is centrifuged ($1{,}500 \times g$, 5 min). The supernatant is centrifuged ($12{,}000 \times g$, 15 min). For collection of donor membranes (consisting of both low- and high-density microsomes), the supernatant is centrifuged ($100{,}000 \times g$, 1 h). The resulting pellets of plasma membranes and donor membranes are suspended in the homogenization buffer without $ZnCl_2$, adjusted to a protein concentration of 2–4 mg/ml using the Bradford method and immediately used for the *in vitro* association assay.

In Vitro Association Assay

Donor membranes and plasma membranes (15–30 µg each) are mixed at 4°C in 75 µl of assay buffer (20 mM HEPES/KOH, pH 7.0, 250 mM sucrose, 0.5 mM EDTA, 1.5 mM $MgCl_2$, 0.5 mM $CaCl_2$, 1 mM DTT, 50 µg/ml BSA, 50 mM KCl), supplemented with an ATP-regenerating system (1 mM ATP, 8 mM creatine phosphate, 25 units/ml creatine phosphokinase). The amount of protein for plasma membranes and donor membranes in the assay is equal. The reactions are initiated by incubation at 37°C. After 2–10 min, the reactions are returned to 4°C and subjected to one of two procedures to separate the plasma membranes or plasma membrane-associated donor membrane vesicle structures from the donor membranes. Two different methods for the demonstration of the fusion of donor membranes and plasma membranes have been used successfully by Inoue and coworkers (1999).

Method I

The mixture is applied to the top of a discontinuous 28–44% sucrose gradient with 2% steps and subjected to centrifugation (100,000 × *g*, 18 h). Each 4-ml step layer is diluted with ice-cold water and centrifuged (200,000 × *g*, 1 h). The final pellets are dissolved in SDS-sample buffer.

Method II

The mixture is centrifuged (15,000 × *g*, 15 min) after dilution with 1 ml of the ice-cold homogenization buffer supplemented with 0.5 M KCl. The final pellet is dissolved in SDS-sample buffer. For detection of mycGLUT4 translocated from the donor membranes into the re-isolated plasma membranes during the *in vitro* association reaction, plasma membrane proteins are tested for the myc epitope by immunoblotting with appropriate primary antibodies and secondary anti-IgG antibodies coupled to peroxidase. The chemiluminescent signals for mycGLUT4 on the blot, which are quantitated by densitometric scanning have to be proportional to the load over the range used.

K.6.1.4.3.2 Analysis by Fluorescent Resonance Energy Transfer (FRET)

Isolation of Tagged GLUT4 Vesicles

For demonstration of GLUT4 translocation in the reconstitution system introduced by Koumanov and coworkers (2005), rat adipocytes at 40% cytocrit are stimulated with 5 nM insulin for 20 min at 37°C. In a typical experiment 10 ml of cells are used. After cooling the cells to 18°C, the surface GLUT4 is labeled with 500 µM biotinylated photolabel GP15 (see K.6.1.4.2.3) and incubated with 10 µg/ml of cells DyLight647 streptavidin for a further 15 min. Insulin/compound/drug is removed and GLUT4 is internalized. The cells are then homogenized and processed as described by Simpson and coworkers (Simpson et al. 1983) to obtain a post-high-density-microsome supernatant, containing the fluorescently tagged GLUT4 vesicles. The GLUT4 vesicles are purified by immunoisolation using an anti-GLUT4 antibody (Satoh et al. 1993) prebound to the MBP-pa construct attached to a 0.7 ml amylose resin column. After 2 h incubation, the column is washed with intracellular buffer (IC buffer, 20 mM HEPES/KOH, pH 7.4, 140 mM potassium glutamate, 5 mM NaCl, 1 mM EGTA) and the GLUT4 vesicles are eluted in 500 µl fractions with 20 mM maltose in IC buffer. The presence of GLUT4 in each fraction is monitored by measuring the DyLight 647 fluorescence. Usually, fractions 1–3 are pooled together and used as a source of purified GLUT4 vesicles. GLUT4 in the fractions is analyzed using a sheep anti-GLUT4 antibody.

Preparation of Cytosol and Plasma Membrane-Liposomes

Concentrated cytosol is prepared from rat adipocytes in the basal state or following treatment with insulin/compounds/drugs for 20 min. Cells are washed once with buffer without BSA and once with IC buffer. As much buffer as possible is removed and the cells are vortexed and then spun (265,000 × *g*, 70 min). The cytosol is recovered between the pellet of crude membranes at the bottom and the fat layer at the top and kept frozen at −70°C until further use. Basal and insulin/compound/drug-treated plasma membranes are prepared (Simpson et al. 1983) and reconstituted in phospholipid-liposomes using an adaptation of previously described methods (Kono 1983, Schurmann et al. 1989). Purified plasma membrane is solubilized in 1.25% octyl glucoside and applied to Sephadex G50 column. 200-µl aliquots of solubilized eluted protein (300 µg/ml) are gently vortex mixed with 40 µl of 150 mg/ml Soya bean phosphatidylcholine (Type IV-S, Sigma) in 20 mM HEPES (pH 7.4). A biotin-Europium (TMT) ligand is added at 55 nM final concentration and the mixture is sonicated for 15 s and frozen to −70°C for at least 2 h. The samples are then thawed, resonicated and purified on flotation Histodenz gradients. The liposomes are mixed 1:1 with 80% Histodenz in reconstitution buffer (25 mM HEPES, pH 7.4, 100 mM KCl, 1 mM DTT) containing 10% glycerol. This is overlayed with 30% Histodenz in reconstitution buffer containing glycerol, and then with buffer only. After centrifugation (35,000 rpm, 12 h, SW41Ti rotor), liposomes are collected at the 0/30% Histodenz interface. The amount of encapsulated biotin-Eu(TMT) is monitored by measuring the fluorescence against a standard curve. Typically 1–2 nM of Biotin-Eu(TMT) is encapsulated in 1 ml of isolated liposomes.

Fusion Assays

Fusion assays are performed in duplicate. 50 µl of GLUT4 vesicles, liposomes and cytosol are mixed with 25 µl of IC buffer containing 1 µM biocytin on ice. Fusion is initiated by adding 50 µl of ATP regenerating system (final concentrations: 1 mM ATP, 5 mM $MgCl_2$, 8 mM phosphocreatine, and 31 U/ml creatine phosphokinase Type 1) at 37°C. In some cases GLUT4 vesicles and plasma membrane liposomes are mixed with the ATP regenerating system on ice and the reac-

tion is initiated by adding cytosol. Fusion is stopped by returning the samples on ice and addition of 1% TX-100 containing excess biocytin.

EVALUATION

The extent to which fusion had occurred prior to this endpoint is detected by TR-FRET between Europium (TMT) and DyLight 647 in a FARCyte microplate reader. The TR-FRET signal is calculated from the ratio of the emission at 670 nm/612 nm with excitation at 340 nm. The zero time point is used as a measure of the background and is subtracted from each value. Generally the extent of fusion at 5 min is compared with the maximal fusion obtained by incubation at 37°C for 30 min.

The*in vitro* reconstitution approach for GLUT4 translocation provides an unequivocal evaluation of the role of compounds/drug candidates in the fusion step as it represents a partial reaction in the GLUT4 vesicle translocation process. Although several recent microscopy studies on GLUT4 movement in cells have suggested that a regulated fusion step is likely (van Dam et al. 2005, Kanda et al. 2005, Lizunov et al. 2005), it is difficult to interpret such studies as many factors before and after the fusion step can influence the appearance of tagged-GLUT4 at the cell surface. Although the use of TIRF microscopy (Lizunov et al. 2005) has narrowed down the number of partial reactions involved in the insulin stimulation of exocytosis, the interpretation of these microscopy images is equivocal because the net incorporation of GLUT4 into the plasma membrane can be interpreted as indicating an involvement of the cytoskeleton, docking and fusion and endocytosis. In addition, fusion and endocytosis may be tightly coupled and the location of the membrane site at which these partial reactions occur may not be distinct. The *in vitro* analysis of the fusion reaction allows the fusion step to be studied in isolation from any involvement of the cytoskeleton or the endocytosis steps.

Applications

Li and McNeill (1997) reviewed various quantitation methods for the insulin-regulatable glucose transporter GLUT4 including reconstituted glucose transport, cytochalasin B binding assays, immunocytochemistry, immunoblots, ELISA, and exofacial labels. The effect of streptozotocin-induced diabetes on GLUT4 phosphorylation in rat adipocytes has been studied by Begum and Draznin (1992). The effect on glucose transporters by sulfonylureas was studied by Jacobs and Jung (1985), Jacobs and coworkers (1989), that of metformin by Matthei and coworkers (1991). Cusin and coworkers (1990) found that hyperinsulinemia increases the amount of GLUT4 mRNA in white adipose tissue and decreases that of muscles. Hofmann and coworkers (1991) determined GLUT4 content by Western immunoblot protein analysis and by Northern blot analysis of GLUT4 mRNA in epididymal fat or soleus muscle tissue of streptozotocin-treated rats and of obese male KKA^Y mice after treatment with pioglitazone. The effect of *in vivo* thyroid hormone status on insulin signaling and GLUT1 and GLUT4 glucose transport systems in rat adipocytes was studied by Matthei and coworkers (1995). Galante and coworkers (1994) studied insulin-induced translocation of GLUT4 in skeletal muscle of insulin-resistant Zucker rats. Recycling of GLUT4 was studied by Laurie and coworkers (1993), Rampal and coworkers (1995). Bähr and coworkers (1995) studied the stimulation of myocardial glucose transport and glucose transporter-1 (GLUT1) and GLUT4 protein expression in cultured cardiomyocytes from rats. Teresaki and coworkers (1998) studied the influence of an insulin sensitizer on GLUT4 translocation in adipocytes of rats fed a high fat diet. Ren and coworkers (1995) evaluated the effect of increased GLUT4 protein expression in muscle and fat on the whole body glucose metabolism by the euglycemic hyperinsulinemic clamp technique in conscious mice. Uphues and coworkers (1995) used cardiac ventricular tissue of lean and genetically obese (fa/fa) Zucker rats to study the expression, subcellular distribution and insulin-induced recruitment of the glucose transporter GLUT4. Zeller and coworkers (1995) studied the GLUT1 distribution in adult rat brains using a newly developed immuno-autoradiographic method. Abe and coworkers (1997) reported molecular cloning of bovine GLUT4. Dalen and coworkers (2003) reported that the expression of the insulin-responsive glucose transporter GLUT4 in adipocytes is dependent in liver X receptor α.

REFERENCES AND FURTHER READING

Abe H, Morimatsu M, Nikami H, Miyashige T, Saito M (1997) Molecular cloning and mRNA expression of the bovine insulin-responsive glucose transporter GLUT4. J Anim Sci 75:182–188

Assimacopoulos-Jeannet F, Cusin I, Greco-Perotto RM, Terrettaz J, Rohner-Jeanrenaud F, Zarjevski N, Jeanrenaud B (1991) Glucose transporters: structure, function, and regulation. Biochemie 73:76–70

Begum N, Draznin B (1992) The effect of streptozotocin-induced diabetes on GLUT-4 phosphorylation in rat adipocytes. J Clin Invest 90:1254–1262

Cusin I, Terrettaz J, Rohner-Jeanrenaud F, Zarjevski N, Assimacopoulos-Jeannet F, Jeanrenaud B (1990) Hyperinsulinemia increases the amount of GLUT4 mRNA in white adipose tissue and decreases that of muscles: a clue for

increased fat depot and insulin resistance. Endocrinology 127:3246–3248

Dalen KT, Ulven SM, Bamberg K, Gustafsson JÅ (2003) Expression of the insulin-responsive glucose transporter GLUT4 in adipocytes is dependent in liver X receptor α. J Biol Chem 278:48283–48291

Fingar DC, Hausdorff SF, Blenis J, Birnbaum MJ (1993) Dissociation of pp70 ribosomal protein S6 kinase from insulin-stimulated glucose transport in 3T3-L1 adipocytes. J Biol Chem 268:3005–3008

Galante P, Maerker E, Scholz R, Rett K, Herberg L, Mosthaf L, Häring HU (1994) Insulin-induced translocation of GLUT4 in skeletal muscle of insulin-resistant Zucker rats. Diabetologia 37:3–9

Garcia de Herreros A, Birnbaum MJ (1989) The acquisition of increased insulin-responsive hexose transport in 3T3-L1 adipocytes correlates with expression of a novel transporter proteins. J Biol Chem 264:19994–19999

Gould GW, Holman GD (1993) The glucose transporter family: structure, function and tissue-specific expression. Biochem J 295:329–341

Hashimoto M, Yang J, Holman GD (2001) Cell-surface recognition of biotinylated membrane proteins requires very long spacer arms: An example from glucose-transporter arms. Chembiochem 2:52–59

Hofmann C, Lorenz K, Colca JR (1991) Glucose transport deficiency in diabetic animals is corrected by treatment with the oral antihyperglycemic agent pioglitazone. Endocrinol 129:1915–1925

Holman GD, Karim AR, Karim B (1988) Photolabeling of erythrocyte and adipocyte hexose transporters using a benzophone derivative of bis(D-mannose). Biochim Biophys Acta 946:75–84

Holman GD, Kozka IJ, Clark AE, Flower CJ, Saltis J, Habberfield AD, Simpson IA, Cushman SW (1990) Cell surface labeling of glucose transporter isoform GLUT4 by bismannose photolabel. Correlation with stimulation of glucose transport in rat adipose cells by insulin and phorbol ester. J Biol Chem 265:18172–18179

Holman GD, Parkar BA, Midgley PJW (1986) Exofacial photoaffinity labelling of the human erythrocyte sugar transporter. Biochim Biophys Acta 855:115–126

Inoue G, Cheatham B, Kahn CR (1999) Development of an *in vitro* reconstitution assay for glucose transporter 4 translocation. Proc Natl Acad Sci USA 96:14919–14924

Jacobs DB, Jung CY (1985) Sulfonylurea potentiates insulin-induced recruitment of glucose transport carrier in rat adipocytes. J Biol Chem 260:2593–2596

Jacobs DB, Hayes GR, Lockwood DHl (1989) *In vitro* effect of sulfonylurea on glucose transport and translocation of glucose transporters in adipocytes from streptozotocin-induced diabetic rats. Diabetes 38:205–211

James DE, Strube M, Mueckler M (1989) Molecular cloning and characterization of an insulin-regulatable glucose transporter. Nature 338:83–87

Kanai F, Nishioka Y, Hayashi H, Kamohara S, Todaka M, Ebina Y (1993) Direct demonstration of insulin-induced GLUT4 translocation to the surface of intact cells by insertion of a c-myc epitope into an exofacial GLUT4 domain. J Biol Chem 268:14523–14526

Kanda H, Tamori Y, Shinoda H, Yoshikawa M, Sakaue M, Udagawa J, Otani H, Tashiro F, Miyazaki JI, Kasuga M (2005) Adipocytes from Munc18c-null mice show increased sensitivity to insulin-stimulated GLUT4 externalization. J Clin Invest 115:291–301

Kono T (1983) Recycling of insulin-sensitive glucose transporter in rat adipocytes. Methods Enzymol 98:431–444

Koumanov F, Jin B, Yang J, Holman GD (2005) Insulin signaling meets vesicle traffic of GLUT4 at a plasma-membrane-activated fusion step. Cell Metab 3:179–189

Koumanov F, Yang, Jones AE, Hatanaka Y, Holman GD (1998) Cell-surface biotinylation of GLUT4 using bis-mannose photolabels. Biochem J 330:1209–1215

Kozka IJ, Clark AE, Holman GD (1991) Chronic treatment with insulin selectively down-regulates cell-surface GLUT4 glucose transporters in 3T3-L1 adipocytes. J Biol Chem 266:11726–11731

Laurie SM, Cain CC, Lienhard GE, Castle JD (1993) The glucose transporter GLUT4 and secretory membrane proteins (SCAMPs) colocalize in rat adipocytes and partially segregate during insulin stimulation. J Biol Chem 268:19110–19117

Lawrence JC, Hiken JF, James DE (1990) Stimulation of glucose transport and glucose transporter phosphorylation by okadiac acid in rat adipocytes. J Biol Chem 265:19768–19776

Lawrence JC, Hiken JF, James DE (1990) Phosphorylation of the glucose transporter in rat adipocytes. Identification of the intracellular domain at the carboxyl terminus as a target for phosphorylation in intact cells and in vitro. J Biol Chem 265:2324–2332

Li W-M, McNeill JH (1997) Quantitative methods for measuring the insulin-regulatable glucose transporter (Glut4). J Pharmacol Toxicol Meth 38:1–10

Lizunov VA, Matsumoto H, Zimmerberg J, Cushman SW, Frolov VA (2005) Insulin stimulates the halting, tethering, and fusion of mobile GLUT4 vesicles in rat adipose cells. J Cell Biol 169:481–489

Matthei S, Hamann A, Klein HH, Benecke H, Kreymann G, Flier JS, Greten H (1991) Association of metformin's effect to increase insulin-stimulated glucose transport with potentiation of insulin-induced translocation of glucose transporters from intracellular pool to plasma membrane in rat adipocytes. Diabetes 40:850–857

Matthei S, Trost B, Hammann A, Kausch C, Benecke H, Greten H, Höppner W, Klein HH (1995) The effect of *in vivo* thyroid hormone status on insulin signalling and GLUT1 and GLUT4 glucose transport systems in rat adipocytes. J Endocrinol 144:347–357

McKeel DW, Jarett L (1970) Preparation and characterization of a plasma membrane fraction from isolated fat cells. J Cell Biol 44:417–432

Moore MS, Mahafferey DT, Brodsky FM, Anderson RGW (1987) Assembly of clathrin-coated pits onto purified plasma membranes. Science 236:558–563

Mueckler M (1994) Facilitative glucose transporters. Eur J Biochem 219:713–725

Müller G, Wied S (1993) The sulfonylurea drug, glimepiride, stimulates glucose transport, glucose transporter translocation, and dephosphorylation in insulin-resistant rat adipocytes *in vitro*. Diabetes 42:1852–1867

Niwa H, Yamamura K, Miyazaki J (1991) Efficient selection for high-expression transfectants with a novel eukaryotic vector. Gene 108:193–199

Rampal AL, Jhun BH, Kim S, Liu H, Manka M, Lachaal M, Spangler RA, Jung CY (1995) Okadaic acid stimulates glucose transport in rat adipocytes by increasing the externalization rate constant of GLUT4 recycling. J Biol Chem 270:3938–3943

Ren JM, Marshall BA, Mueckler MM, McCaleb M, Amatruda JM, Shulman GI (1995) Overexpression of Glut4 protein in muscle increases basal and insulin-stimulated whole body glucose disposal in conscious mice. J Clin Invest 95:429–432

Reusch JEB, Sussman KE, Draznin B (1993) Inverse relationship between GLUT-4 phosphorylation and its intrinsic activity. J Biol Chem 268:3348–3351

Robinson LJ, Pang S, Harris DS, Heuser J, James DE (1992) Translocation of the glucose transporter (GLUT4) to the cell surface in permeabilized 3T3-L1 adipocytes: effects of ATP, insulin, and GTP gamma S and localization of GLUT4 to clathrin lattices. J Cell Biol 117:1181–1196

Ryder JW, Yang J, Galuska D, Rincon J, Björnholm M, Krook A, Lund S, Pedersen O, Wallberg-Henriksson H, Zierath JR, Holman GD (2000) Diabetes 49:647–654

Satoh S, Nishimura H, Clark AE, Kozka IJ, Vannucci SJ, Simpson IA, Quon MJ, Cushman SW, Holman GD (1993) Use of bis-Mannose photolabel to elucidate insulin-regulated GLUT4 subcellular trafficking kinetics in rat adipose cells: Evidence that exocytosis is a critical site of hormone action. J Biol Chem 268:17820–17829

Schürmann A, Rosenthal W, Hinsch KD, Joost HG (1989) Differential sensitivity to guanine nucleotides of basal and insulin-stimulated glucose transporter activity reconstituted from adipocyte membrane fractions. FEBS Lett 255:259–264

Simpson IA, Yver DR, Hissin PJ, Wardzala LJ, Karnieli E, Salans LB, Cushman SW (1983) Insulin-stimulated translocation of glucose transporters in the isolated rat adipose tissue cells: characterization of subcellular fractions. Biochim Biophys Acta 763:393–407

Smith RM, Charron MJ, Shah N, Lodish HF, Jarett L (1991) Immunoelectron microscopic demonstration of insulin-stimulated translocation of glucose transporters to the plasma membrane of isolated rat adipocytes and masking of the carboxyl-terminal epitope of intracellular GLUT4. Proc Natl Acad Sci USA 88:6893–6897

Terasaki J, Anai M, Funaki M, Shibata T, Inukai K, Ogihara T, Ishihara H, Katagiri H, Onishi Y, Sadoka H, Fukushima Y, Yataki Y, Kikuchi M, Oka Y, Asana T (1998) Role of JTT-501, a new insulin sensitizer, in restoring impaired GLUT4 translocation in adipocytes of rats fed a high fat diet. Diabetologia 41:400–409

Towbin H, Staehelin T, Gordon J (1979) Electrophoretic transfer from polyacrylamide gels to nitrocellulose sheets: procedure and some applications. Proc Natl Acad Sci USA 76:4350–4354

Uphues I, Kolter T, Eckel J (1995) Failure of insulin-regulated recruitment of the glucose transporter GLUT4 in cardiac muscle of obese Zucker rats is associated with alterations of small-molecular-mass GTP-binding proteins. Biochem J 311:161–166

van Dam EM, Govers R, James DE (2005) Akt activation is requieed at a late stage of insulin-induced GLUT4 translocation to the plasma membrane. Mol Endocrinol 19:1067–1077

Vannucci SJ, Nishimura H, Satoh S, Cushman SW, Holman GD, Simpson IA (1992) Cell surface accessibility of GLUT4 glucose transporters in insulin-stimulated rat adipose cells. Modulation by isoprenaline and adenosine. Biochem J 288:325–330

Wang Q, Khayat Z, Kishi K, Ebina Y, Klip A (1998) GLUT4 translocation by insulin in intact muscle cells: detection by a fast and quantitative assay. FEBS Lett 427:193–197

Wilson CM, Cushman SW (1994) Insulin stimulation of glucose transport activity in rat skeletal muscle: increase in cell surface GLUT4 as assessed by photolabeling. Biochem J 299:755–759

Yang J, Holman GD (1993) Comparison of GLUT4 and GLUT1 subcellular trafficking in basal and insulin-stimulated 3T3-L1 cells. J Biol Chem 268:4600–4603

Zeller K, Vogel J, Rahner-Welsch S, Kuschinsky W (1995) GLUT1 distribution in adult rat brains. Pflügers Arch Eur J Physiol 429:R63/201

K.6.1.5 Fatty Acid Transport

PURPOSE AND RATIONALE

To gain knowledge of the biochemical pathways of fat metabolism in human physiology is central to understanding the derangements and pathology in the adipocyte handling of fatty acids associated with obesity and type II diabetes. The adipocyte stores large amounts of TAG, which continually turn over during lipolytic hydrolysis and reacylation of exogenous fatty acids. Human adipocytes do not have the capacity to synthesize significant amounts of fatty acids *de novo*. The large part of TAG synthesis comes from fatty acids provided by lipoprotein lipase hydrolysis of chylomicron or very low density lipoprotein TAG in the capillary blood vessels provided by the intestinum and the liver, respectively. Fatty acids act as detergents that rapidly dissolve the plasma membrane, causing cell lysis if allowed to accumulate. More conflicting, the abnormal storage of TAG in the LD of cells from non-adipose tissues (muscle, liver, pancreatic β-cells) may interfere with the insulin regulation of lipid and carbohydrate metabolism as well as with glucose-induced insulin secretion *via* ill-defined molecular mechanisms which are collectively termed the lipotoxicity hypothesis for the pathogenesis of type II diabetes. The flow of fatty acids into the adipocyte can be high and these fatty acids have to be efficiently and rapidly converted to TAG and stored away in the cytoplasmic LD. The synthesis of lipids, in particular of TAG, including the biogenesis of LD by adipocytes depends on the uptake of free fatty acids (FFA) from the blood stream. FFA transport across the adipocyte plasma membrane involves both passive diffusion (at high FFA concentrations) and facilitated diffusion *via* specific transport proteins (at low concentrations). Current evidence indicates that several classes of fatty acid transport proteins, long-chain fatty acyl-CoA synthetases (ACS) and cytosolic fatty binding-proteins participate in fatty acid transport and activation. In eukaryotic systems, both fatty acid transport proteins (FATPs), fatty acid-binding proteins (FABPs), ACS and fatty acyl-CoA binding proteins are suggested to function in concert to facilitate long chain fatty acid uptake. There is considerable evidence that insulin stimulates fatty acid transport up to 3-fold in adipocytes by inducing the translocation of specific FATPs (CD36) from intra-

cellular vesicles to the plasma membranes, a molecular mechanism resembling GLUT4 translocation (see above). Potential drugs targeting these proteinaceous components of the transport pathway are promising. They may specifically block fatty acid uptake, cytoplasmic trafficking and/or activation in adipocytes for the pharmacotherapy of obesity, diabetes and the metabolic syndrome in humans. Conversely, stimulation of fatty acid uptake into adipocytes by potential drugs with insulin-like activity may be beneficial for the anti-diabetic therapy on basis of storage of excess of FFA in adipose tissue, the site specifically designed for the deposition of carbons taken in by daily food. The removal of FFA from the circulation would thereby circumvent the putative lipotoxic effects of FFA in other non-adipose tissues. It is hypothesized that high circulating levels of FFA occur when uptake and activation of fatty acids exceed the adipocyte's capacity for storage or β-oxidation. This leads to excess fatty acid internalization and resultant lipotoxicity of non-adipose cells and tissues (muscle, liver, pancreas). However, so far no drugs are available, which either increase or decrease the storage of TAG (by stimulation/inhibition of fatty acid transport and esterification or inhibition/stimulation of lipolysis in adipose tissue or non-adipose tissues, respectively. Their identification requires the development of assay systems for monitoring fatty acid transport, esterification and lipolysis appropriate for throughput screening.

K.6.1.5.1 Method Based on Radiolabeled Fatty Acids

Adipocytes

The [^{3}H]oleic acid uptake assays are performed with confluent 3T3-L1 adipocyte cell monolayers according to the procedure developed by Stremmel and coworkers (1986) and Pohl and coworkers (2005). [^{3}H]Oleic acid (173 µM, 0.05–0.20 µCi) is dissolved in a defatted BSA solution (173 µM) at a ratio of 1:1.2 ml of the oleate/BSA solution is incubated with the cell monolayer of each well of a 6-well culture dish at 37°C. The uptake is terminated after 5 min by removal of the solution followed by addition of 5 ml of an ice-cold stop solution (PBS containing 0.5% BSA and 200 µM phloretin). The stop solution is discharged after 2 min, and the culture dishes are washed by dipping them six times in ice-cold oleate/BSA solution (173 µM). NaOH (2 M) is added to lyse the cells. After neutralization, aliquots of the lysates are used for protein and radioactivity determination (in a liquid scintillation counter after addition of 10 ml of scintillation cocktail Ultima-Gold).

Hepatocytes

For measurement of fatty acid uptake into hepatocytes according to the procedure described by Chang and coworkers (2006), 200 µl of a suspension of freshly isolated hepatocytes (5×10^5 cells in PBS with > 95% viability according to trypan blue exclusion) are added to 200 µl of oleate-BSA buffer solution containing 40 µM of oleic acid, 10 µM BSA and 5 µCi/ml [^{3}H]oleate in PBS. At increasing periods of time (0–120 s) afterwards, 5 ml of buffer containing 0.1% BSA and 500 µM phloretin in BSA are added to the mixture to stop the uptake. The entire mixture is immediately run through a glass fiber filter under low vacuum (< 10 mm Hg) to collect the cells. The glass fiber is placed in a vial with scintillation fluid to count radioactivity. A blank vial and a vial with an aliquot of oleate-BSA buffer solution is used as negative and positive controls, respectively. The assays done at the time point zero are used as the background uptake activity and subtracted from the activity measured at each time point. The final values are corrected for cell viability, determined after isolation of the hepatocytes by trypan blue exclusion or MTT.

Viability of Cultured Cells – MTT Assay

To evaluate the cytotoxic effect of the drugs, an MTT [3-(4,5-dimethylthiazol-2-yl)-2,5-diphenyltetrazolium bromide] assay is performed. Cells are seeded in 12-well plates and incubated with compounds/drug candidates. Subsequently, 200 µl of 0.25% (w/v) MTT is added to each well, and cells are further incubated for 2 h. The resulting formazan crystals are then solubilized by adding 1 ml of MTT lysis solution (10% SDS and 1 mM acetic acid in DMSO). Absorbance at 570 nm is measured. The results are expressed as the percentage of absorbance related to control cells.

Viability of Cultured Cells – Trypan Blue Assay

After incubation of the cells in the absence (control group) or presence of compound/drug candidate, the cells are exposed to the membrane-impermeant dye, trypan blue (0.1%, w/v) for 15 min at 37°C. The presence of dye is determined by light microscopy and the numbers of unstained and stained cells in the field are counted to obtain an estimate of the percentage of the cells taking up the dye.

Viability of Cultured Cells – Lactate Dehydrogenase (LDH) Release

After incubation of the cells with compound/drug candidate, LDH release into the medium is measured by

determining LDH activity (cytotoxicity detection kit-LDH, Roche Applied Science). The amount of color formed in the assay is proportional to the number of lysed cells. The LDH activity in the total of dead islet cells (high control) is measured after solubilization of the cells with 5% (by vol.) Triton X-100.

EVALUATION

To determine the percentage cytotoxicity, the absorbance at 490 nm is measured in multiple samples with subtraction of values obtained in control incubation (low control with cells but without compound) using the following equation:

$$Cytotoxicity(\%) = \frac{\text{compound value} - \text{low control}}{\text{high control} - \text{low control}} \times 100$$

K.6.1.5.2 Method Based on Fluorescent Fatty Acids

GENERAL CONSIDERATIONS

Fatty acid transport can be more easily studied in yeast compared to mammalian cells, which makes a yeast-based assay system attractive for throughput screening in drug discovery. Fatty acid uptake has been demonstrated to be essential for growth of yeast under conditions of blocked *de novo* synthesis. This occurs in the natural state when cells are grown under hypoxic conditions due to the requirement of the acyl-CoA desaturase for oxygen. During hypoxia, cells specifically require an exogenous source of long-chain unsaturated fatty acids. Fatty acid uptake is dependent upon two proteins, Fat1p, the orthologue of the mammalian FATPs and an ASCL, either Faa1p or Faa4p. Yeast with deletions in the structural gene encoding Fat1p (FAT1) or Faa1p and Faa4p (FAA1 and FAA4) cannot grow anaerobically whether or not unsaturated fatty acids are added to the growth media due to a defect in fatty acid activation (Faergeman et al. 1997 and 2001 , Dirusso et al. 2000). These deficiencies in transport and growth can be alleviated by expression of a selected group of FATPs (mmFATP1, mmFATP2 and mmFATP4 ; Johnson et al. 2000). The yeast system was recently successfully exploited as a method for screening fatty acid uptake inhibitors, which function by specific interaction with a mammalian FATP conditionally expressed in yeast (Li et al. 2005).

PURPOSE AND RATIONALE

This method (Li et al. 2005) is based on the use of the fluorescent fatty acid analog, 4,4-difluoro-5-methyl-4-bora-3*a*,4a-diaza-*s*-indacene-3-dodecanoic acid (C_1-Bodipy-C_{12}). The length of C_1-Bodipy-C_{12} is approximately equivalent to that of an 18-carbon fatty acid. The Bodipy fluorophore is 11 carbons away from the carboxylate group. Both a non-homogenous and homogenous assay designs have been developed. Cellular uptake of C_1-Bodipy-C_{12} can be monitored using fluorescence microscopy. For this, cells are first incubated with C_1-Bodipy-C_{12} to allow uptake and then unincorporated ligand is removed using repeated washes with the fatty acid-binding protein BSA. For detection of fatty acid uptake, the cells are attached to microscope slides by coating with polylysine and then visualized using confocal microscopy. For high-throughput screening, this is not practical, however, due to the requirement of several washing cycles and centrifugations or of microscopy as detection method. The homogenous assay avoids multiple washing steps and relies on a standard microtiter plate fluorescence reader. In this method, extracellular fluorescence is quenched by the addition of trypan blue which does not penetrate into intact 3T3-L1 adipocytes. The assay has been validated with the non-fluorescent natural fatty acid, oleic acid, in addition to sodium azide and Triacsin C, compounds that interfere with fatty acid uptake by blockade of the fatty acid activation step.

PROCEDURE

Yeast cells with the genes for Fat1p and Faa1p deleted and transformed with the expression vector encoding murine FATP2 (mmFATP2) under the control of the GAL10 promoter are grown to 0.1 A_{600} (mid-log phase) in yeast-supplemented minimal media containing 2% galactose and 2% raffinose (without leucine and histidine) at 30°C to induce expression of the mmFATP2. Cells are harvested by centrifugation (5,000 × *g*, 5 min) and then resuspended in PBS at a cell density of 6×10^7/ml prior to use. In a standard uptake assay, 50 µl of yeast cells (3×10^6) is dispensed into each well and incubated with 5 µM C_1-Bodipy-C_{12} in the dark for 3 min in 100 µl total volume. C_1-Bodipy-C_{12} is prepared in PBS containing BSA (7.5 µM final concentration in the assay). Then, 50 µl of trypan blue (0.33 mM final concentration) is added to the reaction to quench the extracellular fluorescence of C_1-Bodipy-C_{12}. Fluorescence intensity is measured on a fluorescence microtiter plate reader (e. g. Molecular Devices) with filter set at 485 nm excitation and 528 nm emission. Fluorescence intensity is recorded after adding trypan blue at room temperature for various times (0, 30, 60 min). The ratio of measured fluorescence intensity of yeast cells expressing

and lacking mmFATP2 is calculated and used to assess the C_1-Bodipy-C_{12} uptake activity of the corresponding mammalian FATP. Cells are incubated with compounds/drugs on an orbital shaker (250 rpm, 30°C) for 2 h prior to assaying C_1-Bodipy-C_{12} uptake.

EVALUATION

This yeast-based assay system introduced by Li and coworkers (2005) for the identification of compounds/drug candidates that target the mammalian FATPs is critically dependent on the bypass of the time-consuming repeated washing steps with BSA required to limit the fluorescent signal from unincorporated ligand. For this, a quenching reagent was chosen, that decreases the signal of non-cell-associated C_1-Bodipy-C_{12}, which obscures the cell-associated fluorescence. Consequently, the quenching dye must have an absorbance spectrum that significantly overlaps the fluorescence emission of the Bodipy fluorophor, such as Trypan blue, with a peak absorbance at 607 nm. This dye has been shown to quench the extracellular fluorescent probes used in phagocytosis assays but does not quench internal fluorescence since it is effectively excluded from living cells due to impermeability of the cell membrane to this compound. BSA is added to the assay mixture to solubilize the hydrophobic fatty acid analog. It has been found that the apparent fluorescence measured in the presence of BSA is much more consistent compared to that measured in the absence of BSA. The signal difference between the positive and the negative controls (ratio of cells expressing and lacking the mammalian FATP) is usually in the range of 4- to 5-fold. Therefore, utilizing trypan blue to quench the non-cell associated C_1-Bodipy-C_{12} it is possible to omit the washing cycles for monitoring fatty acid uptake.

One advantage of the yeast cell-based assay to target the mammalian FATPs is that it relies on a phenotype (i. e. fluorescence signal) specific to the target protein. Thus, it mimics the biological context of the protein more closely than the cell-free system (Fernandes 1998). A draw-back of the cell-based assay, however, is the lack of knowledge about the mechanism of interaction with and specificity toward the target protein. Therefore, secondary screens must be performed, which are required to eliminate toxic compounds. Compounds which kill the cells allow the nonspecific entry of trypan blue leading to quench of the internalized ligand. Additionally, some selected compounds might work by non-FATP-mediated mechanisms, including those that increase the permeability of the cell membrane and facilitate trypan blue entry into the cells. In conclusion, the data presented so far demonstrate that the yeast cell-based fatty acid uptake assay employing a *S. cerevisiae* strain deficient in fatty acid uptake, that expresses mmFATP2 and tests the mmFATP2-dependent C_1-Bodipy-C_{12} transport activity can be used for high-throughput screening of inhibitors or activators of the fatty acid transport and may be successfully applied to other members of the FATP and ACS families.

REFERENCES AND FURTHER READING

Chang BH-J, Li L, Paul A, Taniguchi S, Nannegari V, Heird WC, Chan L (2006) Protection against fatty liver but normal adipogenesis in mice lacking adipose differentiation-related protein. Mol Cell Biol 26:1063–1076

DiRusso CC, Connell EJ, Faergeman NJ, Knudsen J, Hansen JK, Black PN (2000) Murine FATP alleviates growth and biochemical deficiences of yeast *fat1*Delta strains. Eur J Biochem 267:4422–4433

Faergeman NJ, Black PN, Zhao XD, Knudsen J, DiRusso CC (2001) The Acyl-CoA synthetases encoded within *FAA1* and *FAA4* in *Saccharomyces cerevisiae* function as components of the fatty acid transport system linking import, activation, and intracellular utilization. J Biol Chem 276:37051–37059

Faergeman NJ, DiRusso CC, Elberger A, Knudsen J, Black PN (1997) Disruption of the *Saccharomyces cerevisiae* homologue to the murine fatty acid transport protein impairs uptake and growth on long-chain fatty acids. J Biol Chem 272:8531–8538

Fernandes PB (1998) Technological advances in high-throughput screening. Curr Opin Chem Biol 2:597–603

Johnson DR, Knoll LJ, Levin DE, Gordon JI (1994) *Saccharomyces cerevisiae* contains four fatty acid activation (*FAA*) genes: an assessment of their role in regulating protein N-myristoylation and cellualr lipid metabolism. J Cell Biol 127:751–762

Li H, Black PN, DiRusso CC (2005) A live-cell high-throughput screening assay for identification of fatty acid uptake inhibitors. Anal Biochem 336:11–19

Pohl J, Ring A, Korkmaz Ü, Ehehalt R, Stremmel W (2005) FAT/CD36-mediated long-chain fatty acid uptake in adipocytes requires plasma membrane rafts. Mol Biol Cell 16:24–31

Stremmel W, Strohmeyer G, Berk PD (1986) Hepatocellular uptake of oleate is energy dependent, sodium linked, and inhibited by an antibody to a hepatocyte plasma membrane fatty acid binding protein. Proc Natl Acad Sci USA 83:3584–3588

K.6.1.6 Cellular Esterification

PURPOSE AND RATIONALE

The following assay monitors the complete pathway of esterification of glycerol-3-phosphate synthesized *via* glycolysis from glucose, which is transported into the adipocytes upon insulin-dependent GLUT4 translocation with fatty acids taken up by the adipocytes *via* the fatty acid transport proteins (in insulin-dependent fashion) (see K.6.1.2 and K.6.1.5).

PROCEDURE

For this assay described by Sooranna and Saggerson (1976), adipocytes are treated with low concentrations of saponin to permeabilize the plasma membrane (without disrupting internal membranes) and subsequently incubated with L-[U-^{14}C]glycerol-3-phosphate for 10 min at 25°C. Toluene-based scintillation cocktail is added and the lipid and aqueous phases are separated by centrifugation. The lipid phase is removed and counted for radioactivity.

EVALUATION

This assay measures the complete esterification pathway of glycerol-3-phosphate into lipid-soluble products (TAG, phospholipids, lipidic intermediates such as [lyso]phosphatidic acid) including the regulatory cascade which is stimulated by insulin. One or the other of the activation or acylation steps may be affected by compounds/drug candidates. Glucose transport does not interfere due to the use of the permeabilized adipocytes as is revealed by lack of inhibition of basal esterification by cytochalasin B.

K.6.1.7 Lipid-Synthesizing Enzymes

PURPOSE AND RATIONALE

The effects of insulin/compounds/drugs on the three acylating enzymes involved in the esterification pathway, glycerol-3-phosphate-acyltransferase (GPAT), monoacylglycerol-3-phosphate-acyltrans-ferase (AGPAT) and 1,2-diacylglycerol-acyltrans-ferase (DGAT) (for a review see Coleman and Lee 2004) can be assayed individually using microsomes (GPAT, AGPAT, DGAT) and mitochondria (GPAT, AGPAT) prepared from adipocytes which have been pretreated correspondingly. Care must be taken to preserve the activation state of the acylating enzymes during preparation of the microsomes after challenge of the adipocytes with insulin/compounds/drugs by the inclusion of mixtures of phosphatase and protease inhibitors. For the analysis of putative direct effects of compounds/drugs on the acylation enzymes, they are added to the cell-free incubation mixtures containing microsomes/mitochondria from untreated adipocytes.

Preparation of Microsomes/Mitochondria

Isolated rat adipocytes, which have been incubated with insulin/compounds/drugs, are homogenized by 10 strokes in a motor-driven Teflon-in-glass homogenizer in TES buffer (20 mM Tris/HCl, pH 7.4, 250 mM sucrose, 1 mM EDTA) supplemented with 10 µM okadaic acid, 10 mM sodium pyrophosphate, 100 mM NaF, 10 mM glycerol-3-phosphate, 1 mM sodium orthovanadate, 0.1 mM PMSF, 10 µg/ml each of antipain, leupeptin, pepstatin and E-64. After differential centrifugation steps for the removal of cell debris (500 × *g*, 5 min), plasma membranes (2,000 × *g*, 15 min) and mitochondria (10,000 × *g*, 20 min), the supernatant is centrifuged (100,000 × *g*, 60 min, 4°C). The pellet is resuspended in TES buffer and centrifuged (16,000 × *g*, 10 min). The microsomes are recovered from the supernatant by centrifugation (100,000 × *g*, 60 min, 4°C). Microsomes and mitochondria are resuspended in TES buffer (at 4 mg protein/ml) and finally stored at −80°C and used only once after thawing. According to the distribution of the marker enzymes (NADPH-cytochrome-c reductase, GRP-78 and BiP for microsomes, succinate dehydrogenase and porin for mitochondria, adenylate cyclase and Na^+/K^+-ATPase for plasma membranes), the microsomes are contaminated to varying degree with mitochondria and are significantly deprived of plasma membranes.

K.6.1.7.1 Glycerol-3-Phosphate Acyltransferase (GPAT)

PROCEDURE

Radioactive Assay

The incubation mixture contains 50 mM Tris/HCl (pH 7.4), 200 mM KCl, 1 mM DTT, 150 µM palmitoyl-CoA, 4 mM $MgCl_2$, 10 mM NaF, 2 mg/ml BSA, 0.2 mM [^{3}H]glycerol-3-phosphate (2 µCi) and microsomes from primary rat adipocytes (25–100 µg) in a final volume of 0.5 ml. The reaction is started by addition of the microsomes in the absence or presence of 2 mM *N*-ethylmaleimide (NEM). After incubation (3 min, 37°C), the reaction is stopped with 2 ml of water-saturated butanol, followed by 1.5 ml of butanol-saturated water. The butanol phase is separated and washed twice. An aliquot is counted for radioactivity. Under these conditions the rate of product formation is linear for up to 15 min.

Fluorescent Assay

Up to 100 µl of microsomes/mitochondria are incubated with 100 µl of reaction mixture containing 40 mM Tris/HCl (pH 7.4), 8 mM $MgCl_2$, 4 mg/ml BSA, 10 mM NaF, 1 mM NDC, 0.3 mM glycerol-3-phosphate in a total volume of 200 µl. After incubation (60–180 min, 25–30°C) in the absence or presence of 2 mM NEM, the reaction is terminated by the addition of 300 µl of chloroform/methanol (2/1, by vol.) containing 0.1 M HCl and thoroughly mix-

ing. After phase separation (5000 × *g*, 10 min), 180 µl of the lower organic phase are removed and dried. The resin is solubilized in 50 µl of dichloromethane by thorough mixing. Portions (5 µl) are analyzed by thin layer chromatography (Merck, silicagel Si-60) using acetic acid methylester/toluol (2/1 or 1/1, by vol.) with synthetic NBD-labeled mono-, di- and tridodecanoylglycerol run in parallel as markers.

EVALUATION

In case of using of microsomes which are equipped with the complete lipid-synthesizing machinery, the predominant radiolabeled/fluorescent product formed is TAG with accumulation of only minor amounts of its precursors, phosphatidic acid (3–8%) and lysophosphatidic acid (1–4%) as determined by thin layer chromatography and fluorography. However, under the conditions used GPAT activity is rate-limiting for the formation of radiolabeled or fluorescent TAG and consequently, the rate of TAG formation is a direct reflection of the activity of GPAT. In case of using mitochondria, which are typically contaminated by microsomes, their total GPAT activity is determined in the absence of NEM. mtGPAT1 activity, which is resistant to inhibition of NEM (Bell and Coleman 1980), is determined in the presence of 2 mM NEM and subtracted from the total activity to yield the NEM-sensitive GPAT activity, representing the activity from the microsomal GPAT and mtGPAT2 (Bell and Coleman 1980, Lewin et al. 2004). Typically, 2 mM NEM is sufficient to inhibit all of the microsomal GPAT and mtGPAT2 activity.

Time- and concentration dependence of sulfonylurea-stimulated GPAT was tested by Müller and coworkers (1994). Insulin has been reported to stimulate microsomal GPAT by 2- to 3-fold in primary rat adipocytes. The molecular mechanism of this regulation remains to be elucidated. Phosphorylation (by casein kinase II and allosteric activators (polar head groups derived from glycosyl-phosphatidylinositol lipids) have been discussed (Vila et al. 1990; see K.6.3.6.4).

K.6.1.7.2 Acylglycerol-3-Phosphate Acyltransferase (AGPAT)

PROCEDURE

Radioactive Assay

1-ml incubation mixtures are prepared by sonication of monoacyl-glycerol-3-phosphate (MAGP) (up to 100 µM), TX-100 (0.5%), phosphatidylcholine (0.2 mg/ml), [^{14}C]palmitoyl-CoA (40 µM), NaF (50 mM), $MgCl_2$ (1.5 mM) in 150 mM Tris/HCl (pH 8.0). The reaction is started by addition of up to 20 µg of microsomes. After incubation (10 min, 37°C, constant shaking), the reaction is terminated by the addition of 4.5 ml of chloroform/methanol (1/2, by vol.), then of 1.5 ml of chloroform and 1.5 ml of 2 M KCl/0.2 M H_3PO_4. Diacylglycerol-3-phosphate contained in the chloroform layer is dried, redissolved in chloroform/methanol (2/1, by vol.) and then analyzed by TLC using chloroform/methanol/acetic acid/water (25/10/3/1, by vol.). Dried TLC plates are subjected to fluorography (ENHANCE spray, NEN/DuPont; Kodak X-Omat AR films).

Spectrophotometric Assay

AGPAT can be assayed by measuring the reaction of released CoA-SH with 5,5′-dithiobis(2-nitrobenzoic acid) (DTNB = Ellman's reagent) spectrophotometrically. The reaction mixture consists of 100 mM Tris/HCl (pH 7.4), 20 µM oleoyl-CoA, 50 µM 1-acylglycerol-3-phosphate, 1 mM DTNB (10 mM stock in 1 M Tris/HCl, pH 8.0) and up to 50 µl of sample (~200 µg microsomal protein) in the presence of compounds/drug candidates in the wells of a 96-well microtiter plate (200 µl total vol.). The reaction is initiated by the addition of oleoyl-CoA after preincubation of the microsomes with all other components for 2–4 min. The increase in absorbance at 405 nm is followed at 37°C with a microtiterplate spectrophotometer. Control incubations are performed in the absence of 1-acylglycerol-3-phosphate, and the observed rates are subtracted from the rates measured in the presence of acyl acceptor.

K.6.1.7.3 Diacylglycerol Acyltransferase (DGAT)

PROCEDURE

The incubation mixture (250 µl) contains 150 mM Tris/HCl (pH 8.0), 10 mM $MgCl_2$, 1 mg/ml BSA, 50 µM [^{14}C]palmitoyl-CoA (3 µCi, 25,000 cpm/nmol). The reaction is started by the addition of up to 50 µl of a mixture containing 1.5 mM 1,2-diacylglycerol and phosphatidylcholine (0.2 mg/ml) in absolute ethanol and up to 100 µg of microsomal protein. After incubation (15 min, 37°C), the reaction is terminated by the addition of 1 ml of 2-propanol/heptane/water (80/20/2, by vol.). TAG contained in the heptane layer is further purified. The dried samples are redissolved in chloroform/methanol (2/1, by vol.) and analyzed by TLC using petroleum ether/diethyl ether/acetic acid (80/20/1,

by vol.) or hexan/diethylether/acetic acid (70/291/1, by vol.) and fluorography or radioactivity scanning.

K.6.1.8 Formation of Lipid Droplets (LD)

GENERAL CONSIDERATIONS

In vertebrate animals the most abundant energy reserve is stored as TAG in the LD of adipocytes. These LD can be as large as 100 µm and are composed of a core of TAG surrounded by a phospholipid and cholesterol monolayer into which numerous proteins are embedded (DeLany et al. 2005, Brasaemle et al. 2004, Wolins et al. 2005, Robenek et al. 2004, 2005a, 2005b). Most other types of cells contain tiny LD that store primarily cholesterol esters and serve as a reservoir of cholesterol for the synthesis and maintenance of membranes. Steroidogenic cells of the adrenal cortex, testes, and ovaries use stored cholesterol additionally as a source of substrate for steroid hormone synthesis. Little is known about the mechanisms that control the flux of neutral lipids into and out of LD in any type of cell, but it is clear that the processes that control lipid traffic in adipocytes are central to the regulation of whole body energy metabolism. Moreover, the biogenesis of these structures, in general, and in adipocytes, in particular, remains to be elucidated. Several proteins have been identified on their surface, including adipocyte differentiation-related protein (ADRP or adipophilin), perilipins, and caveolin, but their roles in LD assembly are unknown.

ADRP and perilipins are abundant on LD. ADRP is found mostly on smaller LD. Caveolin is a 21-kDa membrane protein with a hairpin structure whose N and C termini face the cytosol. This is in agreement with the model proposed for the assembly of LD. According to this model the TAG will during the biosynthesis "oil-out" between the leaflets of the bilayers, forming lens-shaped structures in the membrane. The LD, covered by a monolayer, will be formed by the budding of such a lens from the membrane. The structure will be stabilized by proteins bound to both the luminal and cytosolic surface of the membrane.

PURPOSE AND RATIONALE

Cell-free systems are extremely useful for studies of sorting processes, such as the budding of transport vesicles and are the only method for determining the mechanism by which such complex structures are formed. A microsome-based, cell-free system has been developed by Marchesan and coworkers (2003) to study the transport of TAG from microsomes to the cytosol. This system assembles TAG-containing LD similar to the small LD isolated from 3T3-L1 cells. Caveolin, ADRP, vimentin, and the GRP-78 are present on these LD and the release of the LD from microsomes is dependent on PLD and the formation of PA. This cell-free system may be helpful for the screening and characterization of compounds/drug candidates activating or inhibiting LD biogenesis by interference downstream of TAG synthesis (e. g. DGAT activity, assembly of LD-associated proteins at the ER, LD release from the ER) as well as for the elucidation of the mode of action of compounds/drug candidates identified in cell-based assays for lipogenesis (see K.6.1.2).

K.6.1.8.1 Preparation of Microsomes

3T3-L1 cells are cultured and differentiated for 2 days (unless stated otherwise) as described above. The cells (2×10^6 cells/incubation) are homogenized (30 strokes in a Dounce glass homogenizer in 10 mM Tris/HCl (pH 7.5) containing 250 mM sucrose, 1 mM EDTA, 100 KIU/ml Trasylol, 0.1 mM leupeptin, 0.1 µM pepstatin, and 1 mM PMSF, and the microsomes are isolated by two distinct gradient ultracentrifugation methods as described (see K.6.1.8.2). To remove loosely bound (non-integral) proteins from the microsomes, the pellet is resuspended in 500 mM Tris/HCl (pH 7.5) containing 1.2 M KCl (high salt wash) and incubated (30 min, 4°C) with head-over-tail mixing. The microsomes are then recovered by ultracentrifugation (160,000 × *g*, 70 min, 12°C). The washed microsomes are resuspended in 10 mM Tris/HCl (pH 7.5) containing 250 mM sucrose.

K.6.1.8.2 Cell-Free System

Incubation

The *in vitro* system used to investigate the formation of LD and introduced by Marchesan and coworkers (2003) is based on microsomes that had been subjected to a high salt wash, an activator from the 160,000 × *g*-supernatant from homogenized rat adipocytes, and a substrate for DGAT. To prepare the DGAT substrate, 0.25 mg of 1,2-diacylglycerol is dissolved in 40 µl of 10 mM Tris/HCl (pH 7.5) with 1.0 mM palmitoyl-CoA by gentle vortexing: 1.25 µl of [^{14}C]palmitoyl-CoA (55 mCi/mmol; total 0.06 µCi) and 360 µl of 10 mM Tris/HCl (pH 7.5) are added, and the mixture is vortexed again. To start the reaction, 600 µl of the partially purified cytosolic activator in 10 mM Tris/HCl

(pH 7.5) containing 250 mM sucrose, 150 µl of 1.4 M $MgCl_2$ (in the same buffer), and 50 µl of the microsome solution (0.5–1 mg of microsomes) are added to the DGAT substrate. Incubation is carried out (37°C, 60 min) (the production of LD plateaued between 30 and 60 min). After the incubation, the total production of radioactive TAG is measured, and the incubation mixture is subjected to gradient ultracentrifugation as described below. Before centrifugation, the mixture is supplemented with (final concentrations) Trasylol (100 KIU/ml), leupeptin (0.1 mM), PMSF (1 mM), pepstatin A (1 µM), N-acetyl-Leu-Leu-norleucinal (5 µM), and EDTA (0.5 mM).

Gradient Ultracentrifugation

For gradient I, the samples are adjusted to 25% sucrose, and 1 ml is layered under 2 ml of 50 mM Tris/HCl (pH 7.5) with 10% sucrose and 10 mM EDTA, which in turn is overlaid with 2 ml of 50 mM Tris/HCl (pH 7.5), 10 mM EDTA, and centrifuged (160,000 × *g*, 17 h, 4°C, Beckman SW55 Ti rotor). Homogenates of 3T3-L1 cells (differentiated for 10 days) are used to establish the gradient. The gradient is divided into four fractions with mean densities of < 1.018 (2 ml), 1.034 (1 ml), 1.055 (1 ml), and 1.098 (1 ml) g/ml, respectively. The major amount of TAG (∼60%) is recovered in the d < 1.018 g/ml fraction. The pellet (microsomes and cell debris) contains only ∼3% of the total amount of TAG recovered from the gradient. Caveolin is present in all fractions and in the pellet.

For gradient II, the samples are adjusted to 40% sucrose, and 1.2 ml is layered under 3 ml of 50 mM Tris/HCl (pH 7.5) with 25% sucrose and 10 mM EDTA, which is in turn overlaid with 1 ml of 50 mM Tris/HCl (pH 7.5) and 10 mM EDTA. After centrifugation (160,000 × *g*, 17 h, 4°C Beckman SW55 Ti rotor) the gradient is arbitrarily divided into 5 fractions with mean densities of 1.055 (1.2 ml), 1.099 (1 ml), 1.112 (1 ml), 1.141 (1 ml), and 1.161 (1 ml) g/ml, respectively. Most (75%) of the TAG is present in the top fraction (d < 1.055 g/ml). Caveolin is present in the top fraction and in the two bottom fractions.

K.6.1.8.3 Characterization of Lipid Droplets

SDS-PAGE

LD fractions in microcentrifuge tubes are delipidated with 1.5 ml of cold acetone overnight at –20°C followed by centrifugation (14,000 × *g*, 30 min, 4°C) and removal of solvent from the protein pellet. The pellet is further extracted with acetone (20°C) followed by acetone/ether (1/1, by vol.) and ether. Residual solvents are evaporated under nitrogen, and proteins are solubilized in 2 × Laemmli sample buffer by incubation in a bath sonicator at 65°C for 4–5 h with frequent mixing using a vortex mixer. Additional 2-mercaptoethanol is added to samples before loading onto SDS-PAGE gels. Typically, LD proteins from 28 dishes of adipocytes are loaded onto 30-cm-long SDS-PAGE gels for staining and further identification. Typically, proteins from two dishes of cells are loaded onto gels for transfer to nitrocellulose membranes and immunoblotting. Gels containing greater protein loads are stained for 2 h in 0.25% Coomassie Blue G250 in 10% acetic acid, 50% methanol and then destained in 7% acetic acid, 5% methanol for 4–6 h. To confirm the identification of known LD-associated proteins, nitrocellulose membranes containing LD proteins are probed with antisera raised against the amino terminus of rat perilipin A, mouse adipophilin (Research Diagnostics Inc., NJ), mouse TIP47 (Research Diagnostics), mouse S3–12), and caveolin-1 (Signal Transduction Inc.).

In-Gel Tryptic Digestion of LD-Associated Proteins

Coomassie-stained protein bands are excised from the gels and destained with 45% acetonitrile in 100 mM ammonium bicarbonate. The resulting gel slices are incubated with 10 mM Tris(2-carboxyethyl)phosphine hydrochloride, alkylated by the addition of 50 mM iodoacetamide, and then digested in situ with trypsin (100 ng per band in 50 mM ammonium bicarbonate). The tryptic peptides are extracted using POROS 20 R2 beads (Applied Biosystems) in 0.2% trifluoroacetic acid in 5% formic acid. The extracted peptides are concentrated using C_{18} zip-tips and eluted with 0.1% trifluoroacetic acid in 30% acetonitrile followed by 0.1% trifluoroacetic acid in 75% acetonitrile. The eluates are dried under vacuum using a SpeedVac concentrator.

Mass Spectrometry

The resulting peptides are dissolved in 2–25 µl of HPLC sample solvents containing water/methanol/acetic acid/trifluoroacetic acid (70/30/0.5/0.01, by vol.). The volume used is proportional to the staining intensity of the given band. Micro-HPLC-MS/MS analysis is conducted on an LCQ electrospray ionization ion trap mass spectrometer coupled with an online MicroPro-HPLC system. Two microliters of tryptic peptide solution is injected into a Magic C18 column (0.2 × 50 mm, 5 µm, 200 Å, Michrom BioResources) which had been equilibrated with 70% solvent A (0.5% acetic acid and 0.01% trifluoroacetic

acid in water/methanol (95/5, by vol.) and 30% solvent B (0.5% acetic acid and 0.01% trifluoroacetic acid in methanol:water (95/5, by vol.). Peptides are separated and eluted from the HPLC column with a linear gradient from 30 to 95% solvent B in 15 min at a flow rate of 2.0 µl/min. The eluted peptides are sprayed directly into the LCQ mass spectrometer (2.8 kV). The LCQ mass spectrometer is operated in a data-dependent mode for measuring the molecular masses of peptides (parent peptides) and collecting MS/MS peptide fragmentation spectra.

Database Search and Protein Identification

The measured molecular masses of parent peptides and their MS/MS data are used to search for information of non-redundant DNA/protein sequence database using the program KNEXUS (Genomic Solutions). The mass error tolerance used in the database search is usually ± 3 Da for the parent ions and ± 0.5 Da for the fragment ions, respectively. Protein identifications are made based on expectation values $< 1 \times 10^{-2}$ or the quality of MS/MS spectra of peptides identified. BLAST searches are performed for hypothetical and unknown proteins.

K.6.1.9 Re-Esterification

PURPOSE AND RATIONALE

In adipose tissue under conditions of enhanced lipolysis, i. e. during fasting or β-adrenergic stimulation, synthesis of TAG from endogenous fatty acids released from the LD during lipolysis is usually not completely repressed. This apparently vicious cycle of the so-called re-esterification is regulated in complex fashion and critically depends on the concentration of the exogenous fatty acids, which in combination with the lipolytically released fatty acids form a common pool for re-esterification. Thus, the supply from/removal by the circulation of fatty acids ultimately determines the rate of re-esterification which thereby ensures rapid and hormone-independent delivery of fatty acids into the circulation in case of immediate demand for nutrients. Previous studies of the regulation of FFA re-esterification *in vitro* have used the balance technique (Vaughan 1962), in which re-esterification is calculated from the difference between glycerol and FFA release (Gilbert et al. 1974, Hammond and Johnston 1987). This method does not distinguish between FFA re-esterification and TAG synthesis. Other studies that measured both processes simultaneously did not provide exogenous FFA in the incubation medium (Brooks 1982), and so do not accurately mimic the situation *in vivo*, in which FFA substrate may be derived from the plasma, either from hydrolysis of circulating lipoproteins or from albumin-bound FFA.

Whether FFA re-esterification may be regulated independently from TAG synthesis can be addressed by the recently developed dual-isotopic technique for measuring FFA re-esterification in adipose tissue Leibel and Hirsch 1985). This method allows TAG synthesis and re-esterification to be measured independently and simultaneously. Studies using this technique hace suggested that the rate of FFA re-esterification is not regulated at the cellular level, but rather by changes in the extracellular environment (Leibel et al. 1989, Edens et al. 1990).

PROCEDURE

Pre-incubation medium consistes of Krebs-Henseleit bicarbonate buffer containing 5 g/100 ml BSA and 4.17 mM glucose. Dual isotope incubation medium is a composition identical to pre-incubation medium, except that it also contains 0.5 mM palmitic acid and both [U-^{14}C]glucose and [9,10-^{3}H]palmitic acid. Palmitic acid is complexed to BSA as described by Leibel and coworkers (1984) with minor modifications. Briefly, a film of mixed unlabeled and [^{3}H]palmitic acid is dissolved with ethanol and a small (12%) molar excess of NaOH. This solution is heated at 60°C for 30 min with gentle shaking. It is then dried under a stream of N_2. Pre-warmed (60°C) 10% BSA in distilled, deionized water is added. The 10% BSA is heated and gently shaken until clear. The 10% BSA (now containing 1 mM palmitic acid) is combined with an equal volume of double-strength KHB bicarbonate buffer with glucose to make the incubation medium. The final medium specific activity of [^{14}C]glucose ranges from 0.4 µCi/ µmol to 0.9 µCi/ µmol, that of [^{3}H]palmitate is 2.0 µCi/µmol. The final concentration of glucose in the incubation medium is 5 mM. The gas phase above both pre-incubation and incubation media is 5% CO_2/95% O_2. All incubations are carried out 2 h at a shaking speed of 80 cycles/min and temperature of 37°C. Zero time samples are run and all other values are corrected accordingly. The isolated rat adipocytes are suspended at a 50% concentration and aliquoted (200 µl) into 2 ml of incubation medium. Incubations are done in 20-ml polypropylene, screw-top vials at 37°C, with shaking at 80 cycles/min. Incubations in medium containing either no added FFA or 0.5 mM palmitic acid are done in the basal state (no additions) and either with adenosine deaminase to prevent inhibition of lipoly-

sis or with isoproterenol (1 µM) to stimulate lipolysis. At the end of the incubations (2 h), the adipocytes and medium are poured into iced Falcon tubes containing PE90 catheters. The tubes are spun gently for 1–2 min at 0°C to float the adipocytes. Incubation medium is withdrawn from beneath the adipocytes through the catheter and frozen for subsequent glycerol assay by the method of Laurell and Tibbling (1966). The cells remaining in the tube are extracted by the method of Dole and Meinertz (1960). The extracted lipids are subjected to TLC to isolate TAG. The TAG is recovered and counted simultaneously for both ^{3}H and ^{14}C. The incorporation of [^{14}C]glucose into TAG calculate the rate of re-esterification as described (Leibel and Hirsch, 1985).

EVALUATION

Under these experimental conditions, ^{14}C is not incorporated into the fatty acid moiety of AG and ^{3}H is not incorporated into the glycerol moiety. FFA re-esterifcation can be measured because both unlabeled FFA arising from lipolysis and medium-derived [^{3}H]palmitate are esterified in newly synthesized [^{14}C]AG. The degree of dilution of [^{3}H]palmitate by unlabeled, endogenous FFA in [^{14}C]TAG is an index of the rate of re-esterification. Re-esterification is calculated as the difference between the total theoretical moles of FFA in TAG (µmol[^{14}C]TAG × 3) minus the actual total µmoles of [^{3}H]palmitate esterified into TAG. Therefore, FA re-esterification, or the esterification of unlabeled FFA in TAG equals [(3 × µmol[^{14}C]TAG)-µmol[^{3}H]TAG], where µmoles of [^{3}H]TAG represents the amount of [^{3}H]palmitate esterified into [^{14}C]TAG. The data are expressed as µmol FFA re-esterified per µmol newly synthesized TAG (3 × µmol[^{14}C]TAG - µmol[^{3}H]TAG/µmol[^{14}C]TAG), a value that theoretically can vary between zero (no re-esterification) and three (all newly esterified fatty acids derived from lipolysis). Adipocyte size is measured in aliquots of isolated adipocytes by microscopy. The lipid content of aliquots of isolated adipocytes is determined gravimetrically in Dole extracts. Adipocyte concentration in the incubation mixture is calculated by dividing lipid content by cell size (assumed to be 100% lipid).

K.6.1.10 Cellular Lipolysis

GENERAL CONSIDERATIONS

Deregulation of lipid metabolism has long been recognized as essential in the development of obesity and the metabolic syndrome. White adipose tissue (WAT) lipolysis plays a pivotal role in controlling the quantity of TAG stored in fat depots and in determining plasma free fatty acid levels (Frayn 2002). Hence, targeting critical steps of this catabolic process constitutes one of the strategies to combat obesity and the metabolic syndrome (Nisoli and Carruba 2004).

Activators of lipolysis represent a pharmacological interest only if the same molecule or another compound stimulates oxidation of fatty acid and energy expenditure. The lipolytic and thermogenic β3-adrenergic agonists highly efficient in rodents to decrease fat mass and insulin resistance have so far not been effective in humans. There are several potential explanations. Unlike rodents, adult humans have very little brown adipose tissue, the tissue specialized in thermogenesis in rodents, which possesses a lot of β3-adrenoceptors. The receptors are expressed at low levels in human white adipocytes, again a major difference with rodents. Finally, the first generation of β3-adrenergic agonists may have low efficacies and potencies for the human β3-adrenergic receptor. Nevertheless, the approach is interesting conceptually. Ideally, a strategy could be to stimulate lipolysis and use of the fatty acids by newly formed brown fat cells (Tiraby and Langin 2003, Langin 2006). Concomitant stimulation of fat oxidation in skeletal muscle is an alternative strategy. The recently characterized lipolytic receptors (e. g., natriuretic peptide and pituitary adenylate cyclase-activating polypeptide receptors) and pathways (e. g., residual lipolytic effect of catecholamines in mice with no β-adrenoceptors) may constitute novel drug targets.

Since the launching of nicotinic acid (niacin) as a lipid-lowering drug a long time ago, suppression of lipolysis to decrease free fatty acid level has attracted much interest (Karpe and Frayn 2004). However, most known antilipolytic receptors are expressed in several organs raising the risk for side-effects. The recent cloning of the receptor for nicotinic acid which is mainly expressed in WAT has undoubtedly led to important screening efforts for the identification of agonists with less side-effects than niacin and its long-lasting form, acipimox (Tunaru et al. 2003, Wise et al. 2003). Inhibition of HSL is also attractive as the enzyme has little homology with other mammalian lipases and show a rather limited tissue distribution. Indeed, several series of agonists have been synthesized (Slee et al. 2003, Ebdrup et al. 2004) with an apparent high specificity for some of them (Langin et al. 2005). The effect of chronic treatment in rodent models of obesity and dyslipidaemia is now awaited.

PURPOSE AND RATIONALE

The inhibition of lipolysis induced by starvation or β-adrenergic stimulation in response to insulin is of exquisite sensitivity ($IC_{50} < 0.1$ nM) and responsiveness (lipolysis rate less than 5% of that in the basal state) toward the hormone. This reflects the enormous physiological importance of a tight regulation of fatty acid release from adipose tissue to ensure both adequate nutrient supply and prevention from the detrimental so-called lipotoxic effects of FFA in the circulation. The complex molecular mechanism of the signal transduction in the adipocytes from the insulin receptor downstream to the lipolytic end effector systems, i. e. the TAG-degrading lipases (see K.6.1.13) has been characterized in detail (for a review see Müller and Petry 2005). It encompasses the translocation of lipases (HSL) and LD surface proteins (perilipins) from the cytosol to the LD and *vice versa*, respectively, which is stimulated in the fastened/β-adrenergic state and blocked in response to insulin. These translocation processes are regulated by (PKA-dependent) phosphorylation of both the lipases and LD surface proteins and presumably additional regulatory proteins. These phosphorylations are down-regulated by insulin through stimulation of cAMP degradation by phosphodiesterase 3B which is linked directly to distal elements of the insulin signaling cascade in adipocytes. Basal and stimulated lipolysis as well as its inhibition is monitored *in vitro* with cultured and primary rodent and human adipocytes and can be used to study insulin-like effects on the negative regulation (i. e. activation of the insulin signaling) or direct inhibition of lipolysis (i. e. of the lipases involved) by compounds/drug candidates. Several procedures are available based on the determination of glycerol and fatty acids released from unlabeled, fluorescently labeled or radiolabeled TAG.

K.6.1.10.1 Method Based on Isolated Fat Pads

Gonadal fat pads are removed from male rats and washed several times with PBS. Tissue pieces (~20 mg) are incubated in DMEM containing 2% fatty acid-free BSA with or without 10 µM isoproterenol at 37°C. Portions are collected after 30, 60, 120, 180 and 240 min and analyzed for the FFA and glycerol content by using commercial kits (Wako Chemicals).

K.6.1.10.2 Method Based on the Release of Fluorescent Fatty Acids from Isolated Adipocytes

PROCEDURE

This method which avoids the use of radioactivity but nevertheless enables the visualization and quantitative evaluation of the released fatty acids has been introduced by Müller and coworkers (2003). For fluorescent labeling of adipocyte TAG, 250-µl portions of adipocyte suspension in 1.5-ml plastic cups are incubated (15 min, 37°C) with 200 µl of KRH containing 1% BSA in the presence of 0.55 nM insulin prior to addition of 50 µl of NBD-FA (500 µM, prepared daily by dissolving 39.8 mg NBD-FA in 1 ml ethanol under moderate heating and subsequent 1:200 dilution with KRH containing 1% BSA) and further incubation (1 h, 37°C) under mild shaking (thermomixer 5436, setting 10, Eppendorf, Hamburg, Germany). For removal of free NBD-FA left in the incubation medium, the adipocyte suspensions are combined in 50-ml plastic vials and centrifuged ($500 \times g$, 1 min, swing-out rotor). The infranatant below the cell surface layer is aspirated. The adipocytes are suspended in 30 ml of medium L (Medium 199 containing 25 mM HEPES, 4 mM L-glutamine, 5.5 mM glucose, 3% BSA). After two further cycles of centrifugation and resuspension, the washed adipocytes are finally adjusted to 2.5×10^6 cells/ml in medium L. For treatment with compounds/drug candidates directly inhibiting relevant lipases which may bind to proteins, the adipocytes are washed with medium L lacking BSA and then incubated (15 min, 37°C) with the inhibitors in the same medium. For initiation of lipolysis, 400-µl portions of adipocyte suspension are supplemented with 500 µl of medium L containing 2 or 4% BSA (in case of preincubation with inhibitors) and 5.5 mM glucose and incubated (37°C) for 30–180 min in the presence or absence of combinations of isoproterenol and ADA in plastic scintillation vials (total vol. 1 ml) under mild shaking in a water bath. 150-µl Portions of the suspension are transferred into pre-cooled Eppendorf cups containing 750 µl chloroform/heptane/methanol (3/3/2 by vol.), mixed vigorously and centrifuged ($12{,}000 \times g$, 1 min). The lower organic phase is removed, dried (SpeedVac) and then suspended in 20 µl of THF. 5- to 10-µl portions are analyzed by TLC using Si-60 F_{254} plates (Merck, Darmstadt, Germany) and diethylether/petrolether/acetic acid (78/22/1, by vol.) as solvent system.

EVALUATION

Quantitative evaluation of the amount of NBD-FA is performed by fluorescence imaging (Storm 860, Molecular Dynamics, Germany) using imaging software (Molecular Dynamics, ImageQuant). Alternatively, 20-µl aliquots of the lower phase are supplemented with 325 µl of methanol/chloroform/ heptane (10/9/7, by vol.) and 1.05 ml of 0.1 M potassium carbonate, 0.1 M boric acid (pH 10.5), vortexed and then centrifuged (12,000 × *g*, 1 min). 150-µl Portions of the upper phase are removed and measured for fluorescence (automatic fluorometric analyzer, Cobas Bio, Roche Diagnostics, Germany).

K.6.1.10.3 Method Based on the Release of Glycerol from Isolated Adipocytes

PROCEDURE

The determination of glycerol released from unlabeled adipocytes is the most common and convenient method and can be performed according to published procedures (Petry et al. 2005) with the following modifications. 300-µl aliquots of the incubation mixtures are rapidly transferred into 1.5-ml Eppendorf cups precooled to 4°C and containing 300 µl of 10% (w/v) $HClO_4$. After incubation (1 h, 4°C), the precipitates are removed by centrifugation (12,000 × *g*, 2 min). The infranatants recovered are neutralized with 20% KOH, followed by addition of 60 µl of 1 M Tris/HCl (pH 7.4). 150-µl samples are removed for glycerol determination, frozen in liquid N_2 and stored at –20°C. Glycerol is measured fluorometrically by a modified version of the enzymatic method (Wieland 1974). The reaction mixture contains 0.1 M Tris/HCl (pH 9.3), 0.9 mM ATP, 1.25 mM NAD, 0.1 M $MgCl_2$, 0.25% (v/v) hydrazine hydrate, 5–50 µl sample or glycerol standard, and a mixture of glycerol kinase (0.2 U/ml final conc.) and glycerol 3-phosphate dehydrogenase (0.7 U/ml final conc.) in a total volume of 240 µl. Fluorescence is determined using an automatic fluorometric analyzer.

K.6.1.10.4 Method Based on the Release of [^{3}H]Oleic Acid from Isolated Adipocytes

PROCEDURE

Adipocytes are washed with KRPH buffer (128 mM NaCl, 4.7 mM KCl, 1 mM $MgCl_2$, 1.25 mM $CaCl_2$, 25 mM sodium phosphate, 1 mM sodium pyruvate, 5.5 mM glucose, 50 mM HEPES/KOH, pH 7.4) and then incubated (2 h, 37°C) in fresh KRPH containing [^{3}H]oleic acid (50 µCi *per* 2×10^6 cells and ml) and 1% BSA in the presence of 0.55 nM human insulin. The adipocytes are washed with KRPH (10°C) containing 5.5 mM glucose and 2% BSA or lacking BSA (for subsequent treatment with direct lipase inhibitors for 15 min at 37°C) three times by centrifugation and then incubated (2 h, 37°C) under mild shaking in KRPH containing 5.5 mM glucose, 2% BSA and 400 µM phloretin (for reduction of fatty acid uptake by 85%) at 1×10^6 cells/ml in the presence of lipolytic stimuli. Thereafter, 150-µl portions of the adipocyte suspension are transferred into narrow centrifugation tubes (Beckman) and then overlayed with 100 µl of dinonylphtalate (Merck, Darmstadt, Germany). After centrifugation (2,000 × *g*, 30 sec, 25°C), the tubes are cut through the oil layer and the lower parts of the tubes containing the incubation medium transferred into 5-ml scintillation vials and mixed with 3 ml of chloroform/heptane (1/1, by vol.) containing 2% methanol. After centrifugation (2,000 × *g*, 5 min), the upper aqueous phase is removed by suction. Following addition of 5 ml of liquid scintillation cocktail to the lower organic phase, radioactivity is measured.

EVALUATION

Control values of the 0-min incubation with the corresponding lipolytic stimulus are subtracted in each case to correct for [^{3}H]oleic acid left from the labeling period and accounting for 2–7% of the total radioactivity recovered with the medium. TLC and phosphorimaging analysis revealed that both under basal and lipolytic conditions, [^{3}H]oleic acid accounts for more than 70% of the total radioactivity measured, radiolabeled degradation products (recovered mainly with the aqueous phase) for 15–20% and TAG for up to 6%.

K.6.1.10.5 Method Based on the Release of Unlabeled Fatty Acids from Isolated Adipocytes

PURPOSE AND RATIONALE

Studying lipolysis with human adipocytes and adipose tissues is hampered by methodological problems. The amount of human adipose tissue that is available is usually limited and the rate of lipid mobilization from human adipocytes is low compared to that of rat adipocytes. Both chemical and enzymatic methods for determination of FFA in human blood and serum have been developed (e. g. Matsubara et al. 1983, Shimizu et al. 1980, Duncombe and Rising 1973, Miles et al. 1983, Okabe et al. 1980). However, incomplete recovery of FFA from plasma (Duncombe and Rising 1973)

and interference of BSA with the FFA assays (Matsubara et al. 1983, Shimizu et al. 1980, Okabe et al. 1980) have been reported, which results in an underestimation of FFA values in serum and plasma samples. To overcome this, the extraction method has been modified (Duncombe and Rising 1973), BSA has been included in the standard curve (Miles et al. 1983) or p-toluenesulfonic acid has been used (Matsubara et al. 1983).

These methods are unsuited for FFA determination for human *in vitro* studies since the detection limit is too high using small amounts of human adipose cells with usually low lipolytic activity. Näslund and coworkers (1989) have established a chemiluminometric method for the determination of low levels of FFA based on H_2O_2 determination in a peroxidase luminescence reaction. Since albumin (which must be added to the incubation medium as FFA carrier) inferes with this assay resulting in non-linear FFA standard curves, Näslund and coworkers (1993) modified the chemiluminometric assay for compatibility with biological samples containing albumin.

PROCEDURE

A semiautomatic luminometric method for determination of small amounts of FFA released from human adipocytes *in vitro* has been introduced by Näslund and coworkers (1993). BSA is used as acceptor of FFA in the incubation medium of isolated fat cells. The assay involves pretreatment with the detergent SDS to liberate the FFA from the BSA before activation by acyl-CoA synthetase (ACS). This is followed by oxidation of the resulting thioesters by acyl-CoA oxidase (ACO). The H_2O_2 formed is subsequently measured in a horseradish peroxidase (HRP)-catalyzed luminol reaction. The assay is linear in the interval of 0.01–1 nmol in the cuvette corresponding to 2–200 µmoles in the sample, and 25 samples can be automatically assayed in the luminometer within 75 min. FFA release can easily be studied in a small incubation volume (200 µl) of very diluted (10^4 cells/ml) human adipocyte suspensions. Samples (25 µl) containing 0.25% BSA from incubates of adipose tissue cells do not interfere with the standard curve. This method (Näslund et al. 1993) is sensitive, simple and inexpensive luminometric assay for FFA release. It is many 100-fold more sensitive than standard spectrophotometric methods and can be used for serial studies of lipid metabolism (lipolysis, FFA re-esterification) in small amounts of human adipose tissue or for investigations of FFA release from very diluted human adipose cell samples.

K.6.1.11 Cell-Free Lipolysis

PURPOSE AND RATIONALE

For analysis of effects of compounds/drug candidates on the translocation to the LD and direct activation of HSL including the increase in accessibility of the TAG of LD for degradation by HSL (or other/additional lipases), these individual steps of lipolysis can be reconstituted in a cell-free system consisting of purified LD and crude HSL (and other lipases) prepared from primary rat adipocytes.

PROCEDURE

Preparation of LD from Adipocytes

LD are prepared according to Egan and coworkers (1992) and adaptions from Wolins and coworkers (2005) with the following modifications: After the incubation, the adipocytes are washed two times with KHH by flotation and removal of the infranatant by suction and then homogenized in 25 mM Tris/HCl (pH 7.4), 250 mM sucrose, 5 mM NaF, 10 mM $NaPP_i$, 1 mM Na_3VO_4, 1 mM EDTA, 20 µg/ml leupeptin, 1 mM benzamidine, 0.5 mM PMSF at 15°C. After centrifugation (1,000 × *g*, 5 min, 15°C), 1 ml of the supernatant is combined with 1.5 ml of 65% sucrose (w/v) and poured into a 5-ml centrifuge tube. 1.5 ml of 10% sucrose (w/v) is then layered on top of the sucrose cushion. The tube is filled to capacity with buffer A. The gradient is centrifuged (172,000 × *g*, 60 min, 15°C) and then allowed to coast to rest. The floating fraction of LD is visualized as the upper white layer of the gradient, and is isolated by suction with a syringe (0.8 ml). After one washing cycle with buffer A, the LD are suspended in an equal volume of 4-fold sample buffer containing 10% SDS by incubation (10 min, 65°C) and treatment in a bath sonicator (10 min, 25°C, max. power) for extraction of proteins. After centrifugation (10,000 × *g*, 5 min, 25°C), proteins contained in the infranatant are separated by SDS-PAGE. Alternatively, the gradient is fractionated from bottom to top by suction with a syringe (0.8 ml each). Proteins of fractions 1–5 are precipitated with 5% TCA (15 min, 2°C, 15,000 × *g*, 10 min), washed three times with ice-cold acetone, dried and finally suspended in sample buffer. Fraction 6 is extracted for protein (see above). All samples are analysed by SDS-PAGE and immunoblotting.

Cell-Free System

Adipocytes labeled with NBD-FA (see K.6.1.2.2) are washed with KRH containing 0.5% BSA, suspended

in the same medium at 3.5×10^5 cells/ml and incubated (5 min, 37°C) in plastic scintillation vials under mild shaking in a water bath in the presence or absence of isoproterenol, insulin or compound/drug candidate. Adipocytes (3.5×10^6 cells) are washed twice with BSA-free KRH by flotation ($500 \times g$, 1 min) and then suspended in 2.5 ml of homogenization medium (50 mM Tris/HCl, pH 7.4, 1 mM EDTA, 0.25 M sucrose, 2 mM DTT, 50 mM glycerol-3-phosphate, 10 mM sodium pyrophosphate, 25 mM NaF, 1 µM microcystin, 2 µM cantharidin, 1 mM benzamidine, 5 µg/ml leupeptin, 10 µg/ml pepstatin, 2 µg/ml antipain, 25 µg/ml soy bean trypsin inhibitor, 5 µg/ml PKA inhibitor). The mixture is vortexed, homogenized in a teflon-in-glass homogenizer (10 strokes using a rotating teflon pestle) at 15°C, transferred into plastic vials (under rinsing of the homogenization vessel with homogenization medium) and then centrifuged ($12{,}000 \times g$, 30 min, 4°C, swing-out rotor). The infranatant (cytosol) is separated from the (fluorescent) TAG-containing LD by aspiration with a syringe. To eliminate entrapped unbroken cells, the LD are resuspended in 8 ml of homogenization medium (15°C) containing 120 mM sucrose and 140 mM KCl, vortexed vigorously, and subsequently subjected to centrifugation ($200{,}000 \times g$, 1 h). The infranatant (washing medium) is removed by suction. For initiation of NBD-FA release, 1 ml of ice-cold homogenization medium containing 2% BSA is added to the plastic vial while the LD adhering to the vessel wall are removed by repeated pipetting. A teflon-coated magnetic stirring disc is placed into the vial. The mixture is warmed up to 30°C and incubated under stirring (250 rpm) for 1 to 4 h. The digestion is terminated by addition of 2 ml of chloroform/methanol (3/1; by vol.). The extracts are dried (SpeedVac), suspended in 50 µl of THF and then analyzed by TLC as described below.

Cell-free lipolysis is performed in glass tubes as described by Okuda and coworkers (1994) and Morimoto and coworkers (2000, 2001) with the following modifications: 40 µl of packed NBD-FA-labeled LD are incubated (90 min, 30°C, constant shaking) with 80 µl of a solution enriched for HSL (100–200 µg protein) and 120 µl of buffer C containing 2% BSA, 2 mM DTT with or without 4.2 mg gum arabic. For incubation of the cell-free lipolysis system, compounds are added directly from the 10-mM stock solutions in DMSO to the reaction mixture containing the LD without prior dilution. The final DMSO concentration during all incubations is kept constant at 0.1%. Portions of the lipolysis reaction are terminated by extraction of the total incubation mixture with 720 µl of chloroform/methanol/0.1 N HCl (3/1/1, by vol.). After vortexing and centrifugation ($2{,}000 \times g$, 2 min) of the mixture, the organic phase is collected, dried under a stream of N_2 and resuspended in 40 µl of tetrahydrofurane. 10-µl portions are analyzed by TLC (Silica Gel G plates, Merck Darmstadt, Germany; diethylether/petrolether/acetic acid, 78/22/1 by vol.). NBD-FA released from the total NBD-FA-labeled AG is quantitatively evaluated by phosphorimaging (e. g. Storm 860, Molecular Dynamics, Germany) using imaging software (ImageQuant, Molecular Dynamics), as described previously (Müller et al. 2003).

EVALUATION

A blank value of a control reaction terminated immediately after addition of HSL-solution to the LD is subtracted in each case. Other portions of the lipolysis reaction are supplemented with 760 µl of buffer C containing protease inhibitors and centrifuged through sucrose cushions for the recovery of LD which are then analyzed for protein composition, in particular for the amount of HSL (HSL translocation, see K.6.1.12).

K.6.1.12 Translocation of Hormone-Sensitive Lipase (HSL)

PURPOSE AND RATIONALE

The molecular mechanism of the regulation of lipolysis in adipocytes by starvation, β-adrenergic stimuli and insulin as well as compounds/drugs (e. g. nicotinic acid relies on the movement of HSL from the cytosol, its predominant location in the basal state, to the LD (Egan et al. 1992, Brasaemle et al. 2000, Clifford 2000, for reviews see Holm 1999 and 2003, Londos 2005, Müller et al. 2005). Candidate components involved in this HSL translocation initiated by β-adrenergic stimuli and inhibited by insulin and lipid-lowering durgs are elements of the cytoskeleton and LD-associated proteins, such as perilipin. Interestingly, perilipin has been observed to undergo reverse translocation from the LD to the cytosol upon challenge of adipocytes with insulin. The relative contribution of HSL and perilipin translocation to lipolysis stimulation seems, however, to depend on size, age and origin of the adipocytes. HSL translocation blocked by insulin or compounds can be easily monitored by immunoblotting of isolated LD for HSL

PROCEDURE

For the identification of HSL associated with LD in the induced compared to the basal state of the adipocytes, LD are prepared, purified, suspended in 20% SDS,

vortexed vigorously, then incubated (10 min, 95°C) and finally centrifuged (12,000 × *g*, 5 min). Solubilized LD-associated proteins recovered from the infranatant by suction are analyzed by SDS-PAGE (7.5% separating gel). The proteins are then transferred onto polyvinylidine difluoride (PVDF) membranes for 4 h at 200 mA using 20 mM 3-(cyclohexylamino)-1-propanesulphonic acid (pH 11.0) in 10% methanol. Transfer efficiency is evaluated by Amido black staining in control lanes. The membrane is washed with PBS containing 0.1% Tween-20, then incubated (1 h, 25°C) with PBS containing 0.5 M NaCl and 0.75% BSA and subsequently incubated (18 h, 4°C) in the same buffer with anti-HSL antibody (1:1,000 dilution, 0.5–2 µg/ml). This antibody was raised in white New Zealand rabbits against recombinant full-length His-tagged human HSL. This 84-kD polypeptide was encoded by a pET-derived expression vector under the control of the T7 promoter, expressed in *E.coli*, then partially purified from inclusion bodies by SDS-PAGE and subsequent elution from the gel band and finally homogenized in PBS prior to emulsification in Ribi Adjuvant System (RIBI Immunochem Research Inc., USA) and subsequent intraperitoneal injection into rabbits. The antibody was purified by chromatography on protein A-Sepharose. Subsequently, the blotting membrane is washed two times with PBS containing 0.1% SDS, 0.2% Nonidet P-40, and 0.25% sodium deoxycholate and then once with PBS. Thereafter the filters are incubated (2 h, 25°C) with horseradish peroxidase conjugated anti-rabbit-IgG (1:5,000 dilution) in PBS containing 0.75% BSA.

EVALUATION

Following three washing cycles (see K.6.1.4.3.1, K.6.3.1.3.2.1 and K.6.3.4.3), the amount of HSL is determined by ECL Western blotting detection reagents (Amersham-Pharmacia, Germany) according to the manufacturer's instructions. Quantitative evaluation is performed by luminometric scanning (Roche Diagnostics, Germany) using ImageQuant software.

K.6.1.12.1 Protein Composition of LD

PURPOSE AND RATIONALE

Stimulation as well as inhibition of lipolysis in adipocytes by hormones, nutritional signals or compounds/drug candidates exerts marked effects on the protein composition of LD favoring TAG/LD degradation or TAG/LD synthesis, respectively. These alterations can be monitored by modern proteomic analysis as has already been performed by Brasaemle and coworkers (2004) for 3T3-L1 adipocytes, Liu and coworkers (2004) for CHO fibroblasts, Fujimoto and coworkers (2004) for cultured human HuH7 hepatoma cells, Umlauf and coworkers (2004) for cultured human A431 epithelial cells and Wu and coworkers (2000) for mouse mammary glands. The unexpected identification of caveolin as LD-associated protein in adipocytes (for a review see Liu et al. 2002) demonstrates the power of modern proteomic analysis. These data may be useful to characterize and differentiate the molecular mechanisms of compounds which interfere with the lipid metabolism of physiologically relevant cells, such as adipocytes, at unknown site(s).

PROCEDURE

For proteomic analysis of adipocyte LD, six days after the initiation of differentiation, 40 dishes of 3T3-L1 adipocytes are incubated either under lipolytically stimulated conditions (e. g. 10 µM isoproterenol and 0.5 mM IBMX for 15 min at 37°C) or without the additions for basal conditions and subsequently in the absence or presence of anti-lipolytic stimuli (e. g. insulin or compounds/drug candidates for 2 h) before harvest. Culture medium is removed, and cells are rinsed twice with ice-cold PBS before scraping of the cells into PBS using typical cell scrapers. Cells from sets of 10 dishes of cells are pooled into 15-ml conical screw-capped tubes (Falcon) and centrifuged (500 × *g*, 5 min). Cell pellets are resuspended in a hypotonic medium containing 10 mM Tris (pH 7.4), 1 mM EDTA, 10 mM sodium fluoride, 20 µg/ml leupeptin, 1 mM benzamidine, and 100 µM 4-(2-aminoethyl)benzenesulfonylfluoride hydrochloride by pipetting and incubated on ice for 10 min before homogenization by 10 strokes in a Teflon-glass homogenizer. Cell lysates are centrifuged (26,000 × *g*, 30 min, 4°C, SW41 Ti-rotor Beckman), and the rotor is allowed to coast to a stop. The floating LD layers are harvested using a tube slicer, and the harvested fractions are adjusted to 25% sucrose and 100 mM sodium carbonate (pH 11.5) using a 60% sucrose stock solution and a 1 M sodium carbonate stock solution with protease inhibitors followed by gentle mixing by pipetting. The density-adjusted fractions (~4 ml) are layered into centrifuge tubes containing 1-ml cushions of 60% sucrose and then overlaid with ~5 ml of 100 mM sodium carbonate (pH 11.5) with protease inhibitors followed by ~3.5 ml of the hypotonic lysis medium with protease inhibitors. Tubes are centrifuged (26,000 × *g*, 30 min, 4°C, SW41 Ti-rotor Beckman) and the rotor is allowed to coast to a stop.

Floating LD are harvested using a tube slicer into 1.5-ml microcentrifuge tubes. Residual carbonate solution is removed by centrifuging tubes (14,000 × *g*, 20 min, 4°C, Eppendorf microcentrifuge). The infranatant is removed with an 18-gauge needle from below the floating LD fraction, and the LD fraction is rinsed once with hypotonic lysis solution containing protease inhibitors.

EVALUATION

Typically, LD are isolated from 8 separate sets of 40 dishes of adipocytes grown and differentiated at different times. 4 sets of dishes are used for basal conditions, and 4 sets of dishes are used for lipolytically stimulated conditions. Proteins from LD preparations from 3 sets of 28 dishes of basal adipocytes are separated in 3 lanes of a single SDS-PAGE gel. Coomassie-stained bands are compared and found to be equivalent for all lanes. Bands from one lane are excised for analysis by mass spectrometry. Proteins from LD preparations from 3 sets of 28 dishes of lipolytically stimulated adipocytes are separated in 3 lanes of a single SDS-PAGE gel and compared with a single lane containing proteins from 28 dishes of basal adipocytes on the same gel. Coomassie-stained bands are compared and found to vary slightly between the three preparations from the lipolytically stimulated adipocytes and significantly between basal and stimulated preparations. Bands are excised for all stained proteins from two lanes of stimulated preparations and analyzed by mass spectrometry.

The LD of adipocytes are unique among LD of many types of cells with respect to size, the perilipin-enriched protein composition, and the dynamic rearrangements in structure that occur in response to stimulation of the β-adrenergic signaling pathway. Although perilipin A is the most abundant protein associated with the large LD of basal adipocytes, when lipolysis is stimulated, these LD fragment into myriad micro-LD. Interestingly, the total mass of perilipin does not increase in proportion to the greatly increased surface area of the micro-LD. Some of the excess surface becomes coated with other PAT family members, adipophilin, TIP47, and S3–12 (Wolins et al. 2005). Additionally, the association of numerous unrelated proteins with the LD increases.

Adipophilin was found by proteomic analysis of proteins on LD isolated from lipolytically stimulated 3T3-L1 adipocytes but not basal adipocytes. This finding was confirmed by immunofluorescence microscopy experiments. The appearance of adipophilin on the LD of lipolytically stimulated adipocytes may be a consequence of increased availability of binding sites on micro-LD to stabilize nascent adipophilin. The results strongly suggest that adipophilin plays a role in lipolysis. The identification of caveolin-1 on LD isolated from lipolytically stimulated but not basal adipocytes is consistent with previous observations (Cohen et al. 2004). Caveolin-1, perilipin, and the catalytic subunit of PKA can be co-immunoprecipitated from lysates of adipocytes preincubated with β-adrenergic receptor agonists but not from basal adipocytes (Cohen et al. 2004). Thus, the three proteins form a complex in stimulated cells with caveolin-1 thereby bridging between perilipin and the catalytic subunit of PKA to facilitate the phosphorylation of perilipin. The identifications of lipid metabolic enzymes on the LD of adipocytes and several other types of cells shows that these structures are not passive repositories for neutral TAG but, instead, comprise a dynamic pool of lipids.

The identifications of several proteins in the adipocyte LD preparations carry implications regarding the immediate subcellular neighborhood of LD. The intermediate filament protein, vimentin, is identified in the basal and stimulated state. Previous studies show that fibrous vimentin intermediate filaments collapse into a cage structure around developing LD in differentiating adipocytes (Franke et al. 1987). The disruption of vimentin cage formation halts LD formation (Lieber et al. 1996). Identification of the Eps-15 homology domain protein EHD2, a protein that binds to actin filaments in differentiated 3T3-L1 adipocytes (Guilherme et al. 2004), provides additional evidence of a close link between LD and the cytoskeleton. The identification of calnexin in basal and lipolytically stimulated LD preparations, as confirmed by immunofluorescence microscopy, suggests that segments of endoplasmic reticulum come into close contact with LD. Finally, several mitochondrial proteins can be identified in both preparations, including a subunit of ATP synthase, prohibitin, and pyruvate carboxylase, indicating that mitochondria are closely associated with and difficult to separate from LD. Several studies have illustrated the tight packing of mitochondria around LD in adipocytes (Cohen et al. 2004, Blanchette-Mackie et al. 1995).

In conclusion, surface proteins on adipocyte LD include enzymes involved in many aspects of lipid metabolism, as found on LD in other types of cells. However, unlike other types of LD, perilipins are a major protein component that controls lipid traffic and the association of adipophilin (Brasaemle et al. 1997, Tansey et al. 2001, 2003), HSL (Sztalryd et al. 2003),

CGI-58 (Yamaguchi et al. 2004, Subramanian et al. 2004), and likely of other proteins with the LD. The stimulation of lipolysis is accompanied by the fragmentation of large LD into numerous dispersed micro-LD accompanied by major changes in the overall protein composition. Although most of the changes appear to affect the relative mass of various proteins that also associate with basal LD, adipophilin and caveolin-1 selectively associate with LD in stimulated cells. It is expected that this type of analysis will be useful for the future characterization including elucidation of the mode of action of compounds/candidate drugs which affect lipid metabolism by either stimulating or inhibiting TAG synthesis or degradation and in consequence LD biogenesis in adipose as well as in non-adipose tissues.

K.6.1.12.2 Interaction of HSL and Perilipin

PURPOSE AND RATIONALE

Recently, the differential effects of blocking perilipin phosphorylation on HSL translocation and lipolysis have been dissected (Miyoshi et al. 2006). Employing adenoviral and transgenic expression of a perilipin construct deficient in all 6 PKA sites (Peri A Δ1–6), PKA-dependent phosphorylation of perilipin has been demonstrated not to be required for HSL translocation to the LD, but is essential for the lipolytic actions of LD-associated HSL in adipocytes. Crosslinking and immunoprecipitation studies suggest that PKA-dependent phosphorylation of perilipin promotes close-range interaction with LD-associated HSL. It is conceivable that compounds/drug candidates promoting or abrogating TAG synthesis/LD biogenesis or their degradation modify the HSL-perilipin in negative or positive fashion, which can be monitored with the following assay systems.

PROCEDURE

Construction of Perilipin KO Mice Expressing the Perilipin Mutant Transgene Lacking the 6 PKA Consensus Phosphorylation Sites in BAT

A targeted disruption of the perilipin gene is performed by replacing exon 3 with a neomycin cassette, thereby disrupting coding of all known perilipin mRNAs. The perilipin KO mice are viable and exhibit predicted reductions in adipocyte size and adipose mass (Martinez-Botas et al. 2000). Perilipin KO mice are backcrossed for 10 generations to C57BL/6 mice. For generation of mice expressing a peri Δ1–6 transgene in adipose tissue, a mouse peri Δ1–6 cDNA, FLAG-tagged at the carboxy-terminal using PCR is generated and then ligated into a SmaI site of pBluescript SK vector containing the aP2 enhancer/promoter region, the SV40 small tumor antigen splice site and polyadenylation signal sequence. A fragment containing the entire aP2-perilipin A-FLAG transgene is microinjected into fertilized eggs of C57BL/6 mice using well-described procedures (Brinster et al. 1981). Transgenic mice expressing the peri Δ1–6 transgene almost exclusively in BAT are obtained. These mice are fully viable, exhibit no apparent adipose phenotype and are mated with backcrossed perilipin KO mice to generate perilipin A Δ1–6 mice (Miyoshi et al. 2006).

HSL-Perilipin Crosslinking and Coimmunoprecipitation

Differentiated adipocytes expressing GFP and wild-type or mutant (e. g. deletion of the 6 PKA consensus phosphorylation sites) FLAG-tagged perilipin A are incubated in differentiation medium containing palmitic and oleic acid (240 µM each) for 48 h. After overnight serum depletion, adipocytes are treated for 15 min with 200 nM phenylisopropyl adenosine (PIA, basal state) or 20 µM forskolin *plus* 0.5 mM IBMX (stimulated state), washed with PBS and then maintained for 10 min in hypotonic lysis buffer (20 mM HEPES/KOH, pH 7.5, 2 mM EDTA, 50 mM sodium fluoride, 100 µM sodium orthovanadate, protease inhibitor cocktail) and either PIA or forskolin *plus* IBMX. Cells are then harvested and homogenized (10 strokes with a teflon-in-glass homogenizer on ice). 3,3′-Dithiobis sulfosuccinimidylpropionate (DTSSP), a cross-linker with 12A spacer arm length (Pierce, Rockford) is added to the homogenates and incubated with rotation at 22°C for 30 min. The crosslinking reaction is terminated by addition of Tris/HCl (50 mM final). After addition of Triton X-100 (2% final) and NaCl (75 mM final), samples are drawn through a 23-gauge needle and then centrifuged (10,000 × *g*, 20 min, 4°C) to separate the LD (upper layer), infranatant (lower layer) and a membrane pellet. The LD are isolated with a tube cutter and placed in a fresh tube. The infranatant is subjected to multiple rounds of centrifugation and removal of the residual LD, until almost no LD are visible. The pooled LD fractions are washed with 1 ml of fresh lysis buffer, collected after centrifugation and resuspended in fresh lysis buffer. Half of this LD suspension is used for TAG measurement. The other half is incubated with SDS lysis buffer (10% final) at 37°C for 30 min with vortexing and then centrifuged for 10 min, after which the final LD fraction is harvested. Portions of each fraction are loaded on SDS-PAGE gels and

then immunoblotted for perilipin and HSL. This confirmed that more than 95% of perilipin is removed from the LD and present in the infranatant fraction. The infranatant fraction is immunoprecipitated using the FLAG-Tagged protein immunoprecipitation kit (Sigma) at 4°C for 24 h with rotation. Immunoprecipitates are eluted from the pelleted anti-FLAG agarose beads by boiling in SDS-PAGE sample buffer containing 2-mercaptoethanol. The reducing conditions are sufficient to break the DTSSP-induced protein crosslinks. Eluted samples are electrophoresed and immunoblotted for the LD-associated proteins, perilipin and HSL. To assess potential non-specific crosslinking of perilipin with membrane or cytosolic proteins, immunoblots are also probed with corresponding antibodies (e. g. toward clathrin, adiponectin).

EVALUATION

With respect to the phosphorylation-dependent mechanism by which perilipin promotes lipolysis, the assay monitoring the interaction of HSL and perilipin reveals that the lipolytic action(s) of LD-associated HSL require a novel event(s) mediated by PKA-dependent perilipin phosphorylation. The prpecise nature of this event(s) remains to be elucidated. However, it is likely to involve conformational changes in perilipin that bring LD-associated HSL into proximity with stored neutral TAG. The effected LD-associated HSL presumably includes the pool of HSL that is prepositioned at the LD in the basal state (Moore et al. 2005, Morimoto el al. 2001, Brasaemle et al. 2004). The crosslinking studies suggest that PKA-dependent phosphorylation of perilipin alters the spatial relationship between perilipin and LD-associated HSL in such a way as to facilitate close-range interaction between the two (or between HSL and a perilipin-associated moiety). This interaction may facilitate access of LD-associated HSL to stored neutral TAG, thereby initiating lipolysis. Recently, chronic PKA-dependent phosphorylation of perilipin A has been shown to induce LD remodeling (i. e. fragmentation and dispersion) independently of lipase action (Marcinkiewicz et al. 2006). This suggests that this remodeling promotes lipolysis and supports the concept that PKA-dependent phosphorylation induces dramatic conformational changes in perilipin.

Thus, perilipin seems to act as the critical component of a scaffold that stabilizes LD structure and composition for optimal TAG storage and regulated lipolysis (Moore et al. 2005, Brasaemle et al. 2004). Compounds/drug candidates interfering with lipolysis may directly modify the perilipin-HSL interaction without affecting perilipin phosphorylation. Those compounds could be identified using the crosslinking assay.

K.6.1.13 Triacylglycerol (TAG) Lipases (HSL, ATGL) Activity

GENERAL CONSIDERATIONS

A direct effect of a compound on the activity of HSL rather than its translocation can be assayed in a cell-free system consisting of emulsified TAG rather than intact LD (see K.6.1.12.1). Lipases play a key role in human lipid metabolism as they degrade dietary nutritional as well as intracellular stored lipids and thereby initiate and regulate the release of FFA into the serum. Therefore, they represent potential targets for the development of drugs aimed at obesity, diabetes and atherosclerosis (for a review see Petry et al. 2004). Pancreatic lipase (PL), gastric lipase (GL) and HSL are responsible for the cleavage of dietary and stored lipids, respectively, to fatty acids and glycerol (and MAG) in the stomach and duodenum (GP; for a review see Lengsfeld et al. 2004), enterocytes (PL; for a review see Tiss et al. 2004) and adipocytes (HSL), which finally will appear in the blood stream directly or as lipoproteins after passage across and esterification/assembly into lipoproteins (chylomicrons) in enterocytes. In addition, lipases are responsible for the degradation of lipoproteins (TAG in chylomicrons) in the liver by hepatic lipase or of lipoproteins (VLDL, LDL from the liver, chylomicrons from enterocytes) in muscle and adipose tissue endothelium by lipoprotein lipase (LPL) and endothelial lipase (EL; for a review see Badellino et al. 2004). The activities of LPL and HSL are under tight hormonal control by a complex interplay of transcriptional and post-transcriptional mechanisms.

The rate-limiting role of HSL in the breakdown of adipose tissue TAG, postulated for decades (Fredrikson et al. 1981, Holm 2003, Kraemer and Shen 2002, Yeaman 2004, Osterlund 2001) has been challenged by the data from HSL knockout mice (Hämmerle et al. 2002, Osuga et al. 2000, Wang et al. 2001, for a review see Raben and Baldassare 2005). Catecholamine-induced lipolysis is abrogated, but residual basal lipolysis is observed in adipocytes from HSL-null mice, which surprisingly display a non-obese phenotype and the accumulation of DAG in their adipose tissues. These data suggest the existence of non-HSL lipases in adipose tissue (of rodents, at least), that preferentially hydrolyze the first ester bond of the TAG molecules. To search for such TAG lipases, gene and protein databases for murine and human pro-

teins with structural homologies to known lipases, i. e. the GXSXG motif for serine esterases and the α/β-hydrolase folds, have been screened. Candidates have been analyzed for TAG-hydrolase activity and expression in mouse adipose tissues and during differentiation of 3T3-L1 adipocytes. Only one previously undescribed enzyme fulfilled these requirements and has been named adipocyte TAG lipase (ATGL), desnutrin, or iPLA2ζ (Zimmermann et al. 2004, Jenkins et al. 2004, Villena et al. 2004). The 260 amino-terminal amino acids of this 54-kD protein contains a predicted esterase domain in the α/β-hydrolase fold as well as a GXSXG site with a putative active serine (amino acid 47). Moreover, a "patatin" domain is present in the same domain. Patatin domain-containing proteins have been shown to exert acyl-hydrolase activity on phospholipid, MAG and DAG substrates and is thought to be involved in the ATP and acyl-CoA-independent transacylation reaction. Consistent with this, ATGL catalyze the CoA-independent transfer of oleate from a mono-olein donor to a mono- or diolein acceptor, which generates DAG and TAG, respectively. Using antibodies directed against ATGL, it has been suggested that ATGL is responsible for 75% of the cytosolic acylhydrolase activity in white adipose tissue of HSL-deficient mice. ATGL could therefore participate together with HSL in adipose tissue lipolysis. Although HSL catalyzes the rate-limiting step in TAG hydrolysis, the major physiological substrate for this enzyme is DAG, not TAG. Hämmerle and coworkers generated ATGL-deficient mice (Haemmerle et al. 2006) and thereby confirmed that ATGL is the rate-limiting lipase for the initiation of TAG catabolism in adipose and many non-adipose tissues. The association of ATGL deficiency with increased glucose tolerance, increased insulin sensitivity, and increased respiratory quotient during fasting provides compelling evidence that the decreased availability of FFAs promotes the use of glucose as metabolic fuel despite the presence of massive amounts of fat in adipose tissue and muscle. The inability to mobilize these fat stores leads to energy starvation, resulting in reduced energy expenditure, a decline in body temperature and premature death when ATGL knockout mice are stressed by cold temperature or food deprivation. Thus, ATGL plays a crucial role in energy homeostasis in mice. The observations that ATGL contributes to adipocyte lipolysis in human adipose tissue (Kershaw et al. 2006) and that genetic variation in the human ATGL gene is associated with plasma FFA, TAG and type II diabetes suggest that ATGL may be of similar relevance in humans. However, by comparing human adipose tissue gene expression of HSL and ATGL as well as total triolein lipase activity and lipolytic capacity in adipocytes from lean *vs.* obese human subjects and in addition the tri- and diglyceride hydrolase activities of Cos-7 cell transfected with HSL and ATGL cDNAs, Mairal and coworkers (2006) found evidence for a down-regulation by body fat and for association with *in vitro* hydrolysis of triolein by HSL rather than ATGL. Moreover, their data argue for a predominant role of HSL as both tri- and diglyceride-hydrolysing lipase in human adipocytes. The findings reinforce the necessity for the use of appropriate human cellular assay systems for the identification and characterization of compounds/drug candidates interfering with lipid metabolism, in general, and lipolysis, in particular.

PURPOSE AND RATIONALE

Since neutral lipases are water-soluble enzymes hydrolysing insoluble long-chain TAG substrates and sometimes, in addition, phospholipids to a varying degree (LPL, EL), the cleavage reaction has to occur at the lipid-water interface (Petry et al. 2005, Hide et al. 1992, Verger 1997, Schmid and Verger 1998). This distinguishes lipases from other hydrolytic enzymes and makes them unique target proteins with regard to selectivity and mode of inhibition. The insolubility of neutral TAG has several striking consequences. Both in the serum compartment and in the cytoplasm of cells neutral lipids are never in direct contact with the aqueous milieu. They are organized as high-molecular-mass aggregates in emulsified droplets consisting of an interior TAG core and surrounded by a monolayer shell of phospholipids and embedded proteins (cytoplasmic LD and serum lipoproteins). Alternatively, lipids are organized in smaller complexes bound to serum or intracellular fatty acid/lipid-binding proteins, such as albumin and caveolin. Lipases interact with these special substrate complexes or "super-substrates" using hydrophobic domains which are exposed/unmasked upon contact as a consequence of substrate-induced conformational change, which sometimes has been called "interfacial activation" (Petry et al. 2005, Hide et al. 1992, Verger 1997, Schmid and Verger 1998). The apparently "two-dimensional" reaction of lipases does not simply follow Michaelis-Menten kinetics of enzyme reactions in aqueous milieu and critically depends on the quality of the interface. In PL the free access of lipidic substrates to the catalytic site is hampered by a so-called lid domain. This blockade is released upon interaction of lipase with the water-lipid interface inducing a conformational change. However, there is considerable evidence that HSL lacks a sim-

ilar lid domain (Ben Ali et al. 2004). The authentic, i. e. substrate-specific, measurement of lipase activity as well as the development of reliable lipase assay systems has to take these unique features into account.

Beisson and co-workers (2000) critically reviewed the lipase assay systems used most widely so far. The most sensitive and reliable assays are discontinuous "time-stop" assays using radiolabeled emulsified TAG or phosphoglycerides as substrates. The substrate has to be separated from the product by chromatographic methods or partitioning. Enzymatic fluorescence- or bioluminescence-based or chromatographic methods for determination of the unlabeled products of lipolysis are highly sensitive but are discontinuous, which is also true for even more sensitive radioactive methods. Titrimetric and potentiometric assays are continuous, but are relative insensitive and may interact with acidic or basic assay constituents, such as test compounds. To overcome these handicaps, Beisson and coworkers (1999) have developed an elegant continuous lipase assay using naturally occurring fluorescent TAG isolated from *parinari glaberrimum.* Synthetic octadeca-9,11,13,15-tetronic-3hydroxy-octadecyloxypropylester, a 1 acyl-2 alky glyceride from *parinaric acid*, represents as DAG analog an efficient substrate for HSL, but it is too sensitive toward oxidation to be used under routine conditions. An alternative ultraviolet spectrophotometric assay has been introduced by the same group which is less sensitive to oxidation using TAG from *aleutris fordii* seeds (Pencreac'h et al. 2002).

Whereas continuous assays based on soluble fluorescent substrates are frequently and successfully being used for esterases, they have rarely been described for lipases. Some of these soluble substrates have been proposed for the measurement of lipolytic activity (Hendrickson 1994, Meshulam et al. 1992). These assay systems turned out to be simple, easy-to-handle and of sufficient sensitivity. But one has to keep in mind, that they do not account for the special features of the lipase-substrate interaction and therefore do not discriminate lipases from esterases. In consequence, lipase activity may be underestimated or even remain undetected, in particular in case of assays being performed with crude enzyme sources, such as body fluids or tissue samples. Moreover, the use of water-soluble substrates may lead to gross misinterpretations of the inhibitory profiles of compounds. Consequently, lipidic substrates resembling the native substrate with regard to chain length and amphiphilic nature, equipped with appropriate fluorophores, should be applied whenever feasible.

Importantly, even huge fluorophores, such as BODIPY (Meshulam et al. 1992), rhodamine (Agmon et al. 1993) or pyrene (Scholze et al. 1999) coupled to lipase substrates apparently do not interfere with their cleavage by lipolytic enzymes. Thus, the nature of the fluorescence label does not seem to be very critical. In general, it should be as small and of hydrophobic character as possible to guarantee optimal interaction with the lipase, should not interact with coloured compounds and should be insensitive toward oxidation. For these reasons, the *p*-nitrobenzodifurazan (NBD) moiety has often been chosen as fluorescence label. NBD is a relative small fluorophore and is well accepted by various lipid-handling enzymes/proteins without grossly influencing their recognition and catalytic mechanisms. For instance, NBD-labelling has been used previously for determination of phospholipase A_2 activity in a time-stop assay design (Dagan and Yedgar 1987, Wittenauer et al. 1984). Müller and coworkers (1997) have shown, that 12-(7-nitrobenzo[1,2,3]oxadiazol-4-ylamino)dodecanoic acid (NBD-FA) is taken up by adipocytes and incorporated into TAG in insulin-sensitive fashion. This demonstrates acceptance of NBD-modified fatty acid and lipid precursors as substrates by lipid-handling enzymes, in general.

Starting from NBD-FA a non-soluble lipase substrate, NBD-MAG, has been introduced which upon presentation in mixed phospholipid-NBD-MAG micelles represents a "super-substrate" and is well accepted by a number of neutral lipases. Incorporation of NBD-MAG into mixed micelles and subsequent release of NBD-FA from the micelles in course of lipase action can easily be followed by a change in extinction thereby enabling the design of an assay system for a variety of neutral lipases in crude tissue samples on a routine basis.

PROCEDURE

Preparation of Rat Adipocyte Extract

Adipocytes are isolated from epididymal fat pads of Wistar rats by digestion with collagenase and subsequent separation from undigested tissue using a nylon web as described (see K.5.1.2). Cells obtained from 10 rats are washed three times with 50 ml each of homogenization buffer (25 mM Tris/HCl (pH 7.4), 0.25 M sucrose, 1 mM EDTA, 1 mM DTT, 10 µg/ml each of leupeptin, antipain and pepstatin) by flotation ($500 \times g$, 2 min, 25°C, swing-out rotor), suspended in 10 ml of homogenization buffer and then homogenized by 10 strokes at 1500 rpm in a loosely fitting Teflon-in-glass homogenizer (15°C). The homogenate is centrifuged ($3{,}000 \times g$, 10 min, 4°C). The infranatant be-

low the fat layer is aspirated and recentrifuged. This procedure is repeated three times for complete removal of residual lipid left at the top after the centrifugations. The final infranatant is centrifuged (48,000 × *g*, 45 min, 4°C). The resulting fat-free supernatant is mixed with 1 g of heparin-Sepharose (washed five times with 25 mM Tris/HCl (pH 7.4), 150 mM NaCl), incubated at 4°C for 1 h (under head-to-end rotation of the vial) and then centrifuged (1,000 × *g*, 10 min, 4°C). The supernatant is adjusted to pH 5.2 and incubated (30 min, 4°C). The precipitates are collected by centrifugation (25,000 × *g*, 10 min, 4°C), suspended in 2.5 ml of 20 mM Tris/HCl (pH 7.0), 1 mM EDTA, 1 mM DTT, 70 mM NaCl, 13% sucrose, 10 µg/ml each of leupeptin, antipain and pepstatin and finaly dialyzed (20 h, 4°C) against 3 × 500 ml of 25 mM Tris/HCl (pH 7.4), 50% glycerol, 1 mM EDTA, 1 mM DTT and 10 µg/ml each of leupeptin, antipain and pepstatin. Adipocyte extract is frozen in liquid N_2 and stored at –70°C for up to four weeks.

Preparation of Tissue Extracts

The tissues are surgically removed and washed in PBS containing 1 mM EDTA. Homogenization is performed on ice in lysis buffer A (0.25 M sucrose, 1 mM EDTA, 1 mM dithiothreitol, 20 µg/ml leupeptin, 2 µg/ml antipain, 1 µg/ml pepstatin) using a ultraturax. The infranatants are obtained after centrifugation (20,000 × *g*, 90 min, 4°C). The reaction is performed in a water bath at 37°C for 60 min with 0.1 ml of substrate and 0.1 ml of infranatant.

K.6.1.13.1 Method Based on Fluorescently Labeled Monoacylglycerol (NBD-MAG)

PROCEDURE

Preparation and Immunoprecipitation of HEK293 Cell Lysates Ectopically Expressing Lipases

Expression constructs encoding only the open reading frame of the relevant lipase with or without epitope tags are constructed by subcloning PCR amplification products into a mammalian expression with CMV promoter or into the Gateway entry vector followed by recombination into the Gateway destination vector. Each expression vector is used to transiently transfect HEK293 cells. HEK293 cells are grown in DMEM supplemented with 10% FCS at 37°C in an atmosphere of 5% CO_2. 10-cm tissue culture dishes with 90% confluent HEK293 cells are transfected using Lipofectamine2000 (Invitrogen). 72 h after transfection, cells are washed with ice-cold TBS and harvested. Cells are pelleted by centrifugation (1,000 × *g*, 5 min) and stored at –80°C until lysate preparation. For this, frozen cells are suspended in 1 ml of lipase reaction buffer (20 mM Tris/HCl, pH 8.0, 150 mM NaCl, 0.53% sodium taurodeoxycholate, 1.33 mM $CaCl_2$) containing the complete proteinase inhibitor mix. The resulting suspensions are then sonicated on ice with 4 bursts of 10 s from a probe sonicator. Homogenized lysate is centrifuged (1,000 × *g*, 10 min) for removal of cell debris. 50-µl portions of the resulting cleared lysates are used for direct activity measurements. For immunoprecipitation, portions are supplemented with anti-V5 mouse monoclonal antibody (7.2 µg) and incubated at 4°C overnight with tumbling. Next, 20 µl of protein A-bead suspension is added and tumbled at 4°C for 2 h. Beads are then pelleted with gentle centrifugation, washed four times with 900 µl of lipase reaction buffer followed by resuspension in 100 µl of lipase reaction buffer.

Activity Measurement

Since HSL cleaves MAG in addition to DAG and TAG albeit a rather low rate, Petry and coworkers (2005) introduced the use of NBD-MAG as substrate for a convenient, non-radioactive and homogeneous activity assay for HSL. For preparation of the NBD-MAG substrate, 41.5 µl of a PC solution (6 mg/ml in chloroform), 83.5 µl of a PI solution (6 mg/ml in chloroform) and 100 µl of a NBD-MAG solution (10 mg/ml in chloroform) are added to plastic scintillation vials are dried over a stream of N_2 and stored until use at 4°C for up to three days. The dried lipids are then re-suspended in 20 ml of 25 mM Tris/HCl buffer (pH 7.4), 150 mM NaCl and then subjected to an ultrasonic treatment in a ice bath using a Branson Sonifier (type II, standard microtip; 2 × 1 min at a setting 2 followed by 2 × 1 min at a setting 4 with 1-min intervals). During the ultrasonic treatment, the color of the substrate suspension shifts from yellow (maximum absorbance at 481 nm) to pink (maximum absorbance at 550 nm). It is used after a period of 15 min (minimum) to up to 2 h (maximum). To start the assay procedure, 180 µl of NBD-MAG substrate solution are warmed up to 30°C, supplemented with either 30 µl of an adipocyte extract (appropriately diluted with, 25 mM Tris/HCl buffer, pH 7.4, 150 mM NaCl, 0.2 mM EDTA, 0.5 mM DTT containing 0.1% BSA) or 20 µl of recombinant human HSL in the wells of 96-well microtiter plates.

EVALUATION

The optical density (OD) at 481 nm is recorded continuously at regular time intervals (from 1 to 30

min) using a microplate scanning spectrophotometer. Buffer alone is used as a control experiment. Alternatively, the products generated in the reaction mixture are analyzed by TLC. For this purpose 200 µl of the reaction mixture are transferred into 2-ml reaction vials and supplemented with 1.3 ml of a methanol/chloroform/heptane (10/9/7, by vol.) and then with 0.4 ml of 0.1 M HCl. After intense vortexing, phase separation is initiated by centrifugation (800 × *g*, 20 min, 25°C), 200-µl aliquots of the lower organic phase are removed, then dried under vacuum (SpeedVac evaporator) and finally suspended in 50 µl of tetrahydrofuran (THF). Samples of 5- to 10-µl are separated by TLC on silica gel Si-60 plates using diethylether/petrol ether/acetic acid (78/22/1, by vol.) as elution solvent system. The amount of NBD-FA acid released is evaluated by fluorescence imaging using a phosphorimager (Molecular Dynamics, storm 860 and ImageQuant software) with an excitation wavelength of at 460 nm and emission wavelength of at 540–550 nm.

K.6.1.13.2 Method Based on Fluorescently Labeled TAG

For substrate preparation, NBD-TAG (total mixture of NBD-MAG/DAG/TAG) are extracted with chloroform/heptane from adipocytes, which had been incubated with NBD-FA in the presence of insulin, and purified as described (Müller et al. 1997). For 4 ml of substrate emulsion, 2 mg of dried NBD-TAG is emulsified with 0.2 mg of phosphatidylcholine/phosphatidylinositol, 3/1, w/w) in chloroform. After evaporation of the solvent (SpeedVac), 2 ml of 0.1 M potassium phosphate (pH 7.0) is added and the substrate is sonicated (4 × 1 min, Branson Sonifier 250, setting 2–3, 22°C). Subsequently, 1.6 ml of potassium phosphate is added and the sonication is repeated on ice. After the second sonication, 0.4 ml of potassium phosphate containing 10% BSA is added. 100 µl of substrate emulsion is mixed with 100 µl of rat adipocyte extract as a source for crude HSL (prepared as above) in homogenization medium and incubated (1 h, 30°C). The digestion is terminated by addition of 400 µl of chloroform/methanol (3/1; by vol.) and analyzed as described above for cell-free lipolysis (see K.6.1.11).

K.6.1.13.3 Method Based on Radiolabeled Trioleoylglycerol (TOG)

For assaying trioleoylglycerol (TOG = triolein) cleavage, the TOG droplet emulsion (final conc. 1.7 mM) is prepared by mixing 25–50 µCi glycerol-tri[^{3}H]oleate (in toluene/ethanol, 1/1), 6.8 µmol TOG (in chloroform), 0.6 mg PC and 0.2 mg PI, subsequent drying over a stream of N_2 and final suspending in 2 ml of 0.1 M KP_i (pH 7.0) under ultrasonic treatment (Branson sonifier B-12, standard microtip, setting 2, 2 × 1 min with 1-min intervalls on ice). After addition of 1 ml of 0.1 M KP_i (pH 7.0) and ultrasonic treatment (see above, 4 × 30 sec with 1-min intervalls on ice), the TOG substrate suspension is supplemented with 1 ml of 20% BSA (in 0.1 M KP_i) and stored until use at 4°C (for up to two weeks). The reaction is started by addition of 10 µl of rat adipocyte extract (appropriately diluted with 20 mM M KP_i, pH 7.0, 1 mM EDTA, 1 mM DTT, 0.02% BSA, 10 µg/ml of each leupeptin, pepstatin and antipain) to 10 µl of TOG suspension. After incubation (30 min, 37°C), the reaction is terminated by addition of 325 µl of methanol/chloroform/heptane (10/9/7, by vol.). Phase separation is initiated by addition of 105 µl of 0.1 M K_2CO_3, 0.1 M boric acid (pH 10.5), intense vortexing and centrifugation (8,000 × *g*, 15 min). 150 µl of the upper aqueous phase is transferred into scintillation vials and supplemented with 5 ml of scintillation cocktail (Beckman Ready Safe) for measurement of radioactivity by liquid scintillation counting. This method has been used by Vertesy and coworkers (2002) for the identification of novel inhibitors of HSL with putative anti-diabetic activity from natural sources, such as funghi.

K.6.1.13.4 Method Based on Radiolabeled Tributyrin

For assaying tributyrin cleavage, 10 µl of [^{14}C]tributyrin (20 mM, 0.1 µCi, in ethanol) are dried, then suspended in 25 µl of 0.1 M KP_i (pH 7.25), 140 mM NaCl, 1 mM DTT, 0.2 mM EDTA and finally incubated (30 min, 37°C) with 25 µl of rat adipocyte extract (appropriately diluted with the same buffer). The reaction is terminated by the addition of 325 µl of methanol/chloroform/heptane (10/9/7, by vol.) and 125 µl of 0.1 M NaOH and subsequently processed and described as above (see K.6.1.13.3).

K.6.1.13.5 Method Based on Resorufin Ester

The assay uses 1,2-dilauryl-rac-glycero-3-glutaric acid (6′-methylresorufin) ester (DGGR) as a substrate (Lehner and Verger 1997). DGGR is cleaved by lipase, resulting in an unstable dicarbonic acid ester that is spontaneously hydrolyzed to yield glutaric acid and

methylresorufin, a bluish-purple chromophore with peak absorption at 581 nm. The rate of methylresorufin formation is directly proportional to the lipase activity in the sample. Hydrolysis of DGGR (final conc. 100 µM) is determined at 37°C in a final volume of 1 ml. For this, substrate solution is prepared by mixing 40 µl of the ester (2 mg/ml dioxane) with 160 µl of 20 mM Tris/HCl (pH 8.0), 150 mM NaCl, and 0.05% TX-100. 790 µl of 20 mM Tris/HCl (pH 8.0), 150 mM NaCl, 0.53% sodium taurocholate and 1.33 mM $CaCl_2$ is added, and the reaction is started by addition of 10 µl of rat adipocyte extract. The release of resorufin is monitored at 572 nm. For high-throughput screening of compounds/drug candidates activating or inhibiting lipases, 10 µl of whole-cell lysate or immunoprecipitation beads is added to the wells of a 96-well plate. After adjustment of the samples to 125 µl in lipase reaction buffer, 125 µl of reaction buffer containing DGGR is added (final conc. of 36 µg/ml in a final assay volume of 250 µl per volume). After mixing, OD 581 is monitored at 5 min-intervals for 2 h to assess lipase activity. This procedure has been used by Lake and coworkers (2005) for the analysis of the expression, regulation, and triglyceride hydrolase activity of the adiponutrin family members.

K.6.1.13.6 Method Based on p-Nitrophenylbutyrate

For assaying *p*-nitrophenylbutyrate (PNPB) cleavage according to the procedure described by Holm and Osterlund (1999) with modifications from Soni and coworkers (2004), 10 µl of 2 mM PNPB (in acetonitrile) are added to 890 µl of 0.1 M KP_i (pH 7.25), 140 mM NaCl, 1 mM DTT, 0.2 mM EDTA and then incubated (10 min, 37°C) in the presence of 100 µl of rat adipocyte extract (appropriately diluted with the same buffer) in the absence or presence of 0.01% TX-100. The reaction is terminated by adding 3.25 ml of methanol/chloroform/heptane (10/9/7), vigorously vortexed for 10 s, and then centrifuged ($800 \times g$, 20 min, 21°C). The upper phase is collected and thereafter subjected to incubation at 42°C for 2 min. The absorbance of the released *p*-nitrophenol (extinction coefficient of 12,000) is measured at 405 nm.

K.6.1.13.7 Method Based on Potentiometry

For a potentiometric assay, the hydrolysis of short- and medium-chain TAG is determined at pH 8.0 and 37°C with a pH-stat (TTT 80 Radiometer) by titrating liberated fatty acids with 0.1 N NaOH. The standard mixture using tributyrin contains 14.9 ml of 150 mM NaCl and 100 µl of tributyrin (final vol. 15 ml). With TOG, the assay mix is composed of 14.5 ml of 150 ml NaCl, 2 mM sodium taurodeoxycholate, 0.1 mg/ml BSA and 0.5 ml of TOG.

K.6.1.14 Neutral Cholesterylester Hydrolase Activity

HSL possesses pronounced neutral cholesterylester hydrolase activity in addition to its neutral TAG hydrolase activity in contrast to ATGL, which exhibits the latter, exclusively (Zimmermann et al. 2004, Jenkins et al. 2004). Consequently, assaying cholesterylester hydrolase activity can be used to discriminate between HSL and ATGL activity in crude cell lysates. Cholesterylester hydrolase is measured according to the procedure described by Holm and Osterlund (1999) with modifications from Soni and coworkers (2004) and Ben Ali and coworkers (2005). 1.17 mg of cholesteryl oleate, including 2×10^7 dpm of [^{14}C]cholesteryl oleate, plus a phospholipid mixture (71.4 µl, including phosphatidylcholine [15 mg/ml] and phosphatidylinositol [5 mg/ml], dissolved in chloroform) are placed in a 4-ml glass vial. Solvents are evaporated under a gentle stream of N_2. 2 ml of 0.1 M potassium phosphate (pH 7.5) is added. After incubation (10 min, 37°C), the mixtures are sonicated (twice for 1 min each, separated by a 1-min interval). An additional 1 ml of 0.1 M potassium phosphate (pH 7.5) is added and incubated (10 min, 37°C). The mixtures are sonicated again (four times for 30 s each on ice, separated by 30-s intervals). After sonication, 1 ml of 20% fatty acid-free BSA prepared in 0.1 M potassium phosphate (pH 7.5) is added. For each assay, 100 µl of substrate is mixed with 100 µl of sample and incubated (30 min, 37°C). The reactions are terminated, extracted and counted for radioactivity as described above for the method based on radiolabeled TOG.

K.6.1.15 Lipoprotein Lipase (LPL) Activity

For assaying LPLaccording to Dichek and coworkers (1993) and Iverius and coworkers (1985) with modifications, substrate is prepared by evaporation of 5 mg of unlabeled TOG together with 50 µCi glycerol-tri[^{3}H]oleate and 0.24 mg PC from the solvent, toluene, under a stream of N_2. The dried lipids are emulsified in 1 ml of 1 M Tris/HCl (pH 8.5), 0.1 M NaCl and 2.5% BSA in the absence or presence of 1 M

NaCl and in the presence of 8% heated rat serum under sonication (Branson Sonifier B-12, standard microtip, setting 2, 10 s on, 10 s off, for 10 cycles on ice). Affinity-purified LPL from bovine milk in 15 µl of 10 mM Tris/HCl (pH 7.4), 0.5 mM DTT are incubated (60 min, 37°C) with 5 µl of substrate emulsion. Reactions are terminated by addition of 325 µl of methanol/chloroform/heptane (10/9/7, by vol.) and subsequently of 105 µl of 0.1 M K_2CO_3, 0.1 M boric acid (pH 10.5). After vortexing, the phases are separated and 100-µl portions of the upper aqueous phase are mixed with 5 ml of scintillation cocktail (Beckman, Ready Safe) and counted for radioactivity. LPL activity is determined by subtracting the non-LPL-dependent lipolytic activity (presence of 1 M NaCl) from the total activity (absence of 1 M NaCl).

K.6.1.16 Analysis of Lipolysis Products

TAG Hydrolysis Rate

For the quantitation of DAG and MAG formed by the TAG lipase actions, the reaction is terminated by adding 1 ml of chloroform/methanol (2/1, by vol.) containing 1% acetic acid, oleic acid (10 µg/ml) and standards for monooleoylglycerol (MOG) and dioleoylglycerol DOG (10 µg/ml, sn-1,2 and sn-1,3). The mixture is vortexed vigorously three times over 15 min. After centrifugation (4,000 × *g*, 10 min), 0.5 ml of the lower phase is collected and evaporated under nitrogen. The lipid pellet is dissolved in chloroform and applied onto TLC (Merck, silica gel 60) with chloroform/acetone/acetic acid (96/4/1, by vol.) as solvent. Lipids are visualized with iodine vapor and the bands corresponding to MOG, DOG and TOG and oleic acid are cut out. The comigrating radioactivity is determined by liquid scintillation counting.

Alternatively, for determination of the rate of DAG formation, the lipolysis reaction is terminated by adding 25 µl of 1 M HCl and 1 ml of hexane/isopropyl alcohol (3/2, by vol.) containing oleic acid (10 µg/ml) and standards for MOG, DOG (*sn*-1.2 and *sn*-1.3, Sigma) and TOG (10 µg/ml each). The mixture is vortexed vigorously three times over a period of 15 min. After centrifugation (4,000 × *g*, 10 min), 0.4 ml of the upper phase is collected and evaporated under nitrogen. The lipid pellet is dissolved in chloroform and loaded onto a TLC plate (Merck, silica gel 60). The TLC is developed with chloroform/acetone/acetic acid (96/4/1) as solvent. The lipids and FFA are visualized with iodine vapor, and the bands corresponding to MOG, DOG and TOG and oleic acid are cut out. The comigrating radioactivity is determined by liquid scintillation counting, and the molar concentrations of the products are calculated.

EVALUATION

The specific TAG hydrolase activity (TAG to DAG conversion) is calculated from the total AG lipolytic activity and the DAG formed during the reaction (considering that MAG does not accumulate) by the equation given by Hämmerle and coworkers (2002).

REFERENCES AND FURTHER READING

Agmon V, Cherbu S, Dagan A, Grace M, Grabowski GA, Gatt S (1993) Synthesis and use of novel fluorescent glycosphingolipids for estimating beta-glucosidase activity in vitro in the absence of detergents and subtyping Gaucher disease variants following administration into intact cells. Biochim Biophys Acta 1170:72–79

Badellino K, Jin W, Rader DJ (2004) Endothelial lipase: a novel drug target for HDL and atherosclerosis ? in "Lipases and phospholipases in drug development" (Müller G, Petry S Eds.) pp 139–154, Wiley-VCH, Weinheim, Germany

Beisson F, Ferte N, Nari J, Noat G, Arondel V, Verger R (1999) use of naturally fluorescent triacylglycerols from *Parinari glaberrimum* to detect low lipase activities from *Arabidopsis thaliana* seedlings. J Lipid Res 40:2313–2321

Beisson F, Tiss A, Riviere C, Verger R (2000) Methods for lipase detection and assay: a critical review. Eur j Lipid Sci Technol 1.133–153

Bell RM, Coleman RA (1980) Enzymes of glycerolipid synthesis in eukaryotes. Annu Rev Biochem 49:459–487

Ben Ali Y, Carriere F, Verger R, Petry S, Müller G, Abousalham A (2005) Continuous monitoring of cholesterol oleate hydrolysis by hormone-sensitive lipase and other cholesterol esterases. J Lipid Res 46:994–1000

Ben Ali Y, Chahinian H, Petry S, Müller G, Carriere F, Verger R, Abousalham A (2004) Might the kinetic behavior of hormone-sensitive lipase reflect the absence of the lid domain ? Biochemistry 43:9298–9306

Blanchette-Mackie EJ, Dwyer NK, Barber T, Coxey RA, Takeda T, Rondinone CM, Theodorakis JL, Greenberg AS, Londos C (1995) Perilipin is located on the surface layer of intracellular lipid droplets in adipocytes. J Lipid Res 36:1211–1226

Brasaemle DL, Barber T, Wolins NE, Serrero G, Blanchette-Mackie EJ, Londos C (1997) Adipose differentiation-related protein is an ubiquitously expressed lipid storage droplet-associated protein. J Lipid Res 38:2249–2263

Brasaemle DL, Dolios G, Shapiro L, Wang R (2004) Proteomic analysis of proteins associated with lipid droplets of basal and lipolytically stimulated 3T3-L1 adipocytes. J Biol Chem 279:46835–46842

Brasaemle DL, Levin D, Adler-Wailes D, Londos C (2000) The lipolytic stimulation of 3T3-L1 adipocytes promotes the translocation of hormone-sensitive lipase to the surfaces of lipid storage droplets. Biochim Biophys Acta 1483:251–262

Brinster RL, Chen HY, Trumbauer M, Senear AW, Warren R, Palmiter RD (1981) Somatic expression of herpes thymidine kinase in mice following injection of a fusion gene into eggs. Cell 27:223–231

Brooks B, Arch JRS, Newsholme EA (1982) Effects of hormones on the rate of the triacylglycerol/fatty acid substrate

cycle in adipocytes and epididymal fat pads. FEBS Lett 146:327–330
Clifford G, Londos C, Kraemer F, Vernon R, Yeaman S (2000) Translocation of hormone-sensitive lipase and perilipin upon lipolytic stimulation of rat adipocytes. J Biol Chem 275:5011–5015
Cohen AW, Razani B, Schubert W, Williams TM, Wang XB, Iyengar P, Brasaemle DL, Scherer PE, Lisanti MP Role of caveolin-1 in the modulation of lipolysis and lipid droplet formation. (2004) Diabetes 53:1261–1270
Coleman RA, Lee DP (2004) Enzymes of triacylglycerol synthesis and their regulation. Progress Lipid Res 43:134–176
Dagan A, Yedgar S (1987) A facile method for direct determination of phospholipase A_2 activity in intact cells. Biochem Int 15:801–808
DeLany JP, Floyd ZE, Zvonic S, Smith A, Gravois A, Reiners E, Wu X, Kilroy G, Lefevre M, Gimble JM (2005) Proteomic analysis of primary cultures of human adipose-derived stem cells: modulation by adipogenesis. Mol Cell Proteomics 4:731–740
Dichek HL, Parrott C, Ronan R, Brunzell JD, Brewer HB, Sanamarina-Fojo S (1993) Functional characterization of a chimeric lipase genetically engineered from human lipoprotein lipase and human hepatic lipase. J Lipid Res 34:1393–1401
Dole VP, Meinertz H (1960) Microdetermination of long chain fatty acids in plasma and tissue. J Biol Chem 235:2595–2599
Duncombe WG, Rising TJ (1973) Quantitative extraction and determination of nonesterified fatty acids in plasma. J Lipid Res 14:258–261
Ebdrup S, Sorensen LG, Olsen OH, Jacobsen P (2004) Synthesis and structure-activity relationship for a novel class of potent and selective carbamoyl-triazole based inhibitors for hormone sensitive lipase. J Med Chem 47:400–410
Edens NK, Leibel RL, Hirsch J (1990) Mechanism of free fatty acid re-esterification in human adipocytes in vitr. J Lipid Res 31:1423–1431
Egan J, Greenberg A, Chang M-K, Wek S, Moos J, Londos C (1992) Mechanism of hormone-stimulated lipolysis in adipocytes: translocation of hormone-sensitive lipase to the lipid storage droplet. Proc Natl Acad Sci USA 89:8537–8541
Folch J, Lees M, Sloane Stanley GH (1957) A simple method for the isolation and purification of total lipids from animal tissues. J Biol Chem 226:497–509
Franke WW, Hergt M, Grund C (1987) Rearrangement of the vimentin cytoskeleton during adipose conversion: formation of an intermediate filament cage around lipid globules. Cell 49:131–141
Frayn KN (2002) Adipose tissue as a buffer for daily lipid flux. Diabetologia 45:1201–1210
Fredrikson G et al (1981) Hormone-sensitive lipase of rat adipose tissue. Purification and some properties. J Biol Chem 256:6311–6320
Fujimoto Y, Iabe H, Sakai J, Makita M, Noda J, Mori M, Higashi Y, Kojima S, Takano T (2004) Identification of major proteins in the lipid droplet-enriched fraction isolated from the human hepatocyte cell line HuH7. Biochim Biophys Acta 1644:47–59
Gilbert CH, Kaye J, Galton DJ (1974) The effect of a glucose load on plasma fatty acids and lipolysis in adipose tissue of obese diabetic and non-diabetic patients. Diabetologia 10:135–138
Guilherme A, Soriano NA, Bose S, Holik J, Bose A, Pomerleau DP, Furcinitti P, Leszyk J, Corvera S, Czech MP (2004) CGI-58 interacts with perilipin and is localized to lipid droplets: Possible involvement of GCI-58 misloacalization in Chanarin-Dorfman syndrome. J Biol Chem 279:30490–30497
Hämmerle G, Zimmermann R, Hayn M, Theussi C, Waeg G, Wagner E, Sattler W, Magin TM, Wagner EF, Zechner R (2002) Hormone-sensitive lipase deficiency in mice causes diglyceride accumulation in adipose tissue, muscle and testis. J Biol Chem 277:4806–4815
Hammond VA, Johnston DG (1987) Substrate cycling between triglyceride and fatty acid in human adipocytes. Metabolism 36:308–313
Hendrickson HS (1994) Fluorescence-based assays of lipases, phospholipases, and other lipolytic enzymes. Anal Biochem 219:1–8
Hide WA, Chan L, Li WH (1992) Structure and evolution of the lipase superfamily. J Lipid Res 33:315–336
Holm C (2003) Molecular mechanisms regulating hormone-sensitive lipase and lipolysis. Biochem Soc Trans 31:1120–1124
Holm C, Osterlund T (1999) Methods Mol Biol 109:109–121
Iverius P-H, Brunzell JD (1985) Human adipose tissue lipoprotein lipase: changes with feeding and relation to postheparin plasma enzyme. Am J Physiol 249:E107-E114
Jenkins CM, Mancuso DJ, Yan W, Sims HF, Gibson B, Gross RW (2004) Identification, cloning, expression, and purification of three novel human calcium-independent phospholipase A2 family members possessing triacylglycerol lipase and acylglycerol transacylase activities. J Biol Chem 279:48968–48975
Karpe F, Frayn KN (2004) The nicotinic acid receptor-a new mechanism for an old drug. Lancet 363:1892–1984
Kershaw EE, Hamm JK, Verhagen LAW, Peroni O, Katic M, Flier JS (2006) Adipose triglyceride lipase, function, regulation by insulin, and comparison with adiponutrin. Diabetes 55:148–157
Kraemer FB, Shen WJ (2002) Hormone-sensitive lipase: control of intracellular tri-(di-)acylglycerol and cholesterylester hydrolysis. J Lipid Res 43:1585–1594
Lake AC, Sun Y, Li J-L, Kim JE, Johnson JW, Li D, Revett T, Shih HH, Liu W, Paulsen JE, Gimeno RE (2005) Expression, regulation, and triglyceride hydrolase activity of adiponutrin family members. J Lipid Res 46:2477–2487
Langin D (2006) Adipose tissue lipolysis as a metabolic pathway to define pharmacological strategies against obesity and the metablic syndrome
Langin D, Dicker A, Tavernier G, Hoffstedt J, Mairal A, Ryden M (2005) Adipocyte lipases and defect of lipolysis in human obesity. Diabetes 54:3190–3197
Laurell S, Tibbling G (1966) An enzymatic fluorometric micromethod for the determination of glycerol. Clin Chim Acta 13:317–322
Lehner R, Verger R (1997) Purification and characterization of a porcine liver microsomal triacylglycerol hydrolase. Biochemistry 36:1861–1868
Leibel RL, Forse RA, Hirsch J (1989) Effects of rapid glucose infusion on *in vivo* and in vitro free fatty acid re-esterification by adipose tissue of fasted obese subjects. Int J Obes 13:661–671
Leibel RL, Hirsch J (1985) A radioisotopic technique for analysis of free fatty acid re-esterification in human adipose tissue. Am J Physiol 248:E140-E147
Leibel RL, Hirsch J, Berry EM, Gruen RK (1984) Radioisotopic method for the measurement of lipolysis in small samples of human adipose tissue. J Lipid Res 25:49–57
Lengsfeld H, Beaumier-Gallon G, Chahinian H, De Caro A, Verger R, Laugier R, Carriere F (2004) Physiology of gastrointestinal lipolysis and therapeutical use of lipases and

digestive lipase inhibitors. in "Lipases and phospholipases in drug development" (Müller G, Petry S Eds.) pp 195–229, Wiley-VCH, Weinheim, Germany

Lewin TM, Schwerbrock NM, Lee DP, Coleman RA (2004) Identification of a new glycerol-3-phosphate acyltransferase isoenzyme, mtGPAT2, in mitochondria. J Biol Chem 279:13488–13495

Lieber JG, Evans RM (1996) Disruption of the vimentin intermediate filament system durign adipose conversion of 3T3-L1 cells inhibits lipid droplet accumulation. J Cell Sci 109:3047–3058

Liu P, Rudick M, Anderson RG (2002) Multiple functions of caveolin-1. J Biol Chem 277:41295–41298

Liu P, Ying Y, Zhao Y, Mundy DI, Zhu M, Anderson RG (2004) Chinese hamster ovary K2 cell lipid droplets appear to be metabolic organelles involved in membrane traffic. J Biol Chem 279:3787–3792

Londos C, Sztalryd C, Tansey JT, Kimmel AR (2005) Role of PAT proteins in lipid metabolism. Biochimie 87:45–49

Marchesan D, Rutberg M, Andersson L, Asp L, Larsson T, Boren J, Johansson BR, Olofsson S-O (2003) A phospholipase D-dependent process forms lipid droplets containing caveolin, adipocyte differentiation-related protein, and vimentin in a cell-free system. J Biol Chem 278:27293–27300

Marcinkiewicz A, Gauthier D, Garcia A, Brasaemle DL (2006) The phosphorylation of serine 492 of perilipin a directs lipid droplet fragmentation and dispersion. J Biol Chem 281:11901–11909

Marial A, langin D, Arner P, Hoffstedt J (2006) Human adipose triglyceride lipase (*PNPLA2*) is not regulated by obesity and exhibits low in vitro trigyceride hydrolase activity. Diabetologia 49:1629–1636

Martinez-Botas J, Andreson J, Tessler D, Lapillojnne A, Hung-Junn Chang B, Quast M, Gorenstein D, Chen K-H, Chan L (2000) Absence of perilipin results in leanness and reverses obesity in Lepr(db/db) mice. Nature Genetics 26:474–479

Matsubara C, Nishikawa Y, Yoshida Y, Takamura K (1983) A spectrophotometric method for the determination of free fatty acid in serum using acyl-coenzyme A synthase and acyl-coenzyme A oxidase. Anal Biochem 130:128–133

Meshulam T, Herscovitz H, Casavant D, Bernardo J, Roman R, Haugland RP, Strohmeier GS, Diamond RD, Simons ER (1992) Flow cytometric kinetic measurements of neutrophil phospholipase A activation. J Biol Chem 267:21465–21470

Miles J, Glasscock R, Aikens J, Gerich J, Haymond M (1983) A microfluorometric method for the determination of free fatty acids in plasma. J Lipid Res 24:96–100

Miyoshi H, Souza SC, Zhang H-H, Strissel KJ, Christoffolete A, Kovsan J, Rudich A, Kraemer FB, Bianco AC, Obin MS, Greenberg AS (2006) Perilipin promotes HSL-mediated adipocyte lipolysis via phosphorylation-dependent and independent mechanisms. J Biol Chem

Morimoto C, Kameda K, Tsujita T, Okuda H (2001) Relationships between lipolysis induced by various lipolytic agents and hormone-sensitive lipase in rat fat cells. J Lipid Res 42:120–127

Morimoto C, Tsujita T, Sumida M, Okuda H (2000) Substrate-dependent lipolysis induced by isoproterenol. Biochem Biophys Res Commun 274:631–634

Moore HP, Silver RB, Mottillo EP, Bernlohr DA, Granneman JG (2005) Perilipin targets a novel pool of lipid droplets for lipolytic attack by hormone-sensitive lipase. J Biol Chem 280:43109–43120

Müller G, Jordan H, Jung C, Kleine H, Petry S (2003) Analysis of lipolysis in adipocytes using a fluorescent fatty acid derivative. Biochimie 85:1245–1256

Müller G, Jordan H, Petry S, Wetekam E-M, Schindler P (1997) Analysis of lipid metabolism in adipocytes using fluorescent fatty acids I. Insulin stimulation of lipogenesis. Biochim Biophys Acta 1347:23–39

Müller G, Petry S (2005) Triacylglycerol storage and mobilization, regulation of in "Encyclopedia of molecular cell biology and molecular medicine" (Meyers RA, Ed.) vol 14, pp 621–704, Wiley-VCH, Weinheim, Germany

Müller G, Wied S, Wetekam E-M, Crecelius A, Unkelbach A, Pünter J (1994) Stimulation of glucose utilization in 3T3 adipocytes and rat diaphragm *in vitro* by the sulfonylureas, glimepiride and glibenclamide, is correlated with modulations of the cAMP regulatory cascade. Biochem Pharmacol 48:985–996

Näslund B, Bernström K, Lundin A, Arner P (1989) Free fatty acid determination by peroxidase-catalysed luminol chemiluminescence. J Biolumin Chemilumin 3:115–124

Näslund B, Bernström K, Lundin A, Arner P (1993) Release of small amounts of free fatty acids from human adipocytes as determined by chemiluminescence. J Lipid Res 34.633–641

Nisoli E, Carruba MO (2004) Emerging aspects of pharmacotherapy for obesity and metabolic syndrome. Pharmacol Res 50:453–469

Okabe H, Uji Y, Nagashima K, Noma A (1980) Enzymic determination of free fatty acids in serum. Clin Chem 26:1540–1543

Okuda H, Morimoto C, Tsujita T (1994) Effect of substrates on the cyclic AMP-dependent lipolytic reaction of hormone-sensitive lipase. J Lipid Res 35:1267–1273

Osterlund T (2001) Structure-function relationships of hormone-sensitive lipase. Eur J Biochem 268:1899–1907

Osuga J, Ishibashi S, Oka T, Yagyu H, Tozawa R, Fujimoto A, Shionoiri F, Yahagi N, Kraemer FB, Tsutsumi O, Yamada N (2000) Targeted disruption of hormone-sensitive lipase results in male sterility and adipocyte hypertrophy, but not in obesity. Proc Natl Acad Sci USA 97:787–792

Pencreac'h G, Graille J, Pina M, Verger R (2002) An ultraviolet spectrophotometric assay for measuring lipase activity using long-chain triacylglycerols from *Aleurites fordii* seeds. Anal Biochem 303:17–24

Petry S, Ben Ali Y, Chahinian H, Jordan H, Kleine H, Müller G, Carriere F, Abousalham A (2005) Sensitive assay for hormone-sensitive lipase using NBD-labeled monoacylglycerol to detect low activities in rat adipocytes. J Lipid Res 46:603–614

Petry S, Baringhaus K-H, Schönafinger K, Jung C, Kleine H, Müller G (2004) in "Lipases and phospholipases in drug development" (Müller G, Petry S Eds.) pp 121–138, Wiley-VCH Weinheim Germany

Raben DM, Baldassare JJ (2005) A new lipase in regulating lipid mobilization: hormone-sensitive lipase is not alone. Trends Endocrinol Metab 16:35–36

Robenek H, Robenek MJ, Buers I, Lorkowski S, Hofnagel O, Troyer D, Severs NJ (2005a) Lipid droplets gain PAT family proteins by interaction with specialized plasma membrane proteins. J Biol Chem 280:26330–26338

Robenek H, Robenek MJ, Troyer D (2005b) PAT family proteins pervade lipid droplet cores. J Lipid Res 46:1331–1338

Robenek MJ, Severs NJ, Schlattmann K, Plenz G, Zimmer KP, Troyer D, Robenek H (2004) Lipids partition caveoln-1 from ER membranes into lipid droplets: updating the model of lipid droplet biogenesis. FASEB J 18:866–868

Schmid RD, Verger R (1998) Lipases: interfacial enzymes with attractive applications. Angew. Chem Int Ed Engl 37:1608–1633

Scholze H, Stutz H, Paltauf F, Hermetter A (1999) Fluorescent inhibitors for the qualitative and quantitative analysis of lipolytic enzymes. Anal Biochem 276:72–80
Shimizu S, Tani Y, Yamada M, Tabata M, Murachi T (1980) Enzymatic determination of serum-free fatty acids: a colorimetric method. Anal Biochem 107:193–198
Slee DH, Bhat AS, Nguyen TN, Kish M, Lundeen K, Newman MJ (2003) Pyrrolopyrazinedione-based inhibitors of human hormone-sensitive lipase. J Med Chem 46:1120–1122
Sooranna SR, Saggerson ED (1976) Interactions of insulin and adrenaline with glycerol phosphate acylation processes in fat cells from rat. FEBS Lett 64:36–39
Subramanian V, Rothenberg A, Gomez C, Cohen AW, Garcia A, Bhattacharyya S, Shapiro L, Dolios G, Wang R, Lisanti M, Brasaemle DL (2004) Hydrophobic sequences target and anchor perilipin A to lipid droplets. J Biol Chem 279:42062–42071
Sztalryd C, Xu G, Dorward H, Tansey J, Contreras J, Kimmel A, Londos C (2003) Perilipin A is essential for the translocation of hormone-sensitive lipase during lipolytic activation. J Cell Biol 161:1093–1103
Tansey JT, Huml AM, Vogt R, Davis KE, Jones JM, Fraser KA, Brasaemle DL, Kimmel AR, Londos C (2003) J Biol Chem 278:8401–8406
Tansey JT, Sztalryd C, Gruia-Gray J, Roush DL, Zee JV, Gavrilova O, Reitman ML, Deng CX, Li C, Kimmel AR, Londos C (2001) Proc Natl Acad Sci USA 98:6494–6499
Tiraby C, Langin D (2003) Conversion of white into brown adipocytes: a strategy for the control of fat mass ? Trends Endocrinol Metab 14:439–441
Tiss A, Miled N, Verger R, Gargouri Y, Abousalham A (2004) Digestive lipases inhibition: an in vitro study. in "Lipases and phospholipases in drug development" (Müller G, Petry S Eds.) pp 155–193, Wiley-VCH, Weinheim, Germany
Tunaru S, Kero J, Schaub A, Wufka C, Blaukat A, Pfeffer K (2003) PUMA-G and HM74 are receptors for nicotininc acid and mediate its anti-lipolytic effect. Nat Med 9:352–355
Umlauf E, Csaszar E, Moertelmaier M, Schuetz GJ, Parton RG, Prohaska R (2004) Association of stomatin with lipid bodies. J Biol Chem 279:23699–23709
Vaughan M (1962) The production and release of glycerol by adipose tissue incubated in vitro. J Biol Chem 237:3354–3358
Verger R (1997) 'Interfacial activation' of lipases: facts and artefacts. Trends Biotechnol 15:32–38
Vertesy L, Beck B, Brönstrup M, Ehrlich K, Kurz M, Müller G, Schummer D, Seibert G (2002) Cyclipostins, novel hormone-sensitive lipase inhibitors from *Streptomyces* sp. DSM 13381. II. Isolation, structure elucidation and biological properties. J Antibiotics 55:480–494
Vila MDC, Milligan G, Standaert ML, Farese RV (1990) Insulin activates glycerol-3-phosphate-acyltransferase (de novo phosphatidic acid synthesis) through a phospholipid-derived mediator. Apparent involvement of Gi? and activation of a phospholipase C. Biochem 29:8735–8740
Villena JA, Roy S, Sarkadi-Nagy E, Kim KH, Sul HS (2004) Desnutrin, an adipocyte gene encoding a novel patatin domain-containing protein, is induced by fasting and glucocorticoids: ectopic expression of desnutrin increases triglyceride hydrolysis. J Biol Chem 279:47066–47075
Wang SP, Laurin N, Himms-Hagen J, Rudnicki MA, Levy E, Robert MF, Pan I, Oligny L, Mitchell GA (2001) The adipose tissue phenotype of hormone-sensitive lipase deficiency in mice. Obes Res 9:119–128
Wieland O (1974) Glycerin UV-Methode. In: Bergmeyer HU (ed) Methoden der enzymatischen Analyse. Verlag Chemie Weinheim, pp 1448–1453
Wise A, Foord SM, Fraser NJ, Barnes AA, Elshourbagy N, Eilert M (2003) Molecular identification of high and low affinity receptors for nicotinic acid. J Biol Chem 278:9869–9874
Wittenauer LA, Shirai K, Jackson RL, Johnson JD (1984) Hydrolysis of a fluorescent phospholipid substrate by phospholipase A2 and lipoprotein lipase. Biochem Biophys. Res Commun 118:894–901
Wolins NE, Quaynor BK, Skinner JR, Schoenfish MJ, Tzekov A, Bickel PE (2005) S3–12, adipophilin, and TIP47 package lipid in adipocytes. J Biol Chem 280:19146–19155
Wu CC, Howell KE, Neville MC, Yates JR, McManaman JL (2000) Proteomics reveal a link between the endoplasmic reticulum and lipid secretory mechanisms in mammary epithelial cells. Electrophoresis 21:3470–3482
Yamaguchi T, Omatsu N, Matsushita S, Osumi T (2004) CGI-58 interacts with perilipin and is localized to lipid droplets. Possible involvement of CGI-58 mislocalization in Chanarin-Dorfman syndrome. J Biol Chem 279:30490–30497
Yeaman SJ (2004) Hormone-sensitive lipase: new roles for an old enzyme. Biochem J 379:11–22
Zimmermann R, Strauss JG, Hämmerle G, Schoiswohl G, Birner-Grünberger R, Riederer M, Lass A, Neuberger G, Eisenhaber F, Hermetter A, Zechner R (2004) Fat mobilization in adipose tissue is promoted by adipose triglyceride lipase. Science 306:1383–1386

K.6.1.17 Affinity Labeling of TAG Lipases

PURPOSE AND RATIONALE

Compounds which interfere with lipolysis by direct blockade of TAG cleavage can be directed to various lipases in differential fashion. So far, in addition to HSL, ATGL, GS-2 and adiponutrin have been identified as putative TAG degrading lipases in rodent adipocytes. Their differential targeting by compounds/drug candidates can be analyzed by activity tagging (for a review see Petry et al. 2004).A fluorescence technology for selectively screening for lipolytic enzymes developed by Schmidinger and coworkers (2005) is based on the so-called click chemistry utilizing the copper(I)-catalyzed azide-alkyne [3+2] cycloaddition reaction (Speers and Cravatt 2004a and b, Wang et al. 2003). Lipase- and esterase-mediated hydrolysis of acyl esters is based on a mechanism involving a nucleophilic serine, which in most cases is part of a catalytic triad with histidine and asparate. In the first reaction step, the active serine attacks the carbonyl group of the scissile fatty acid to give a tetrahedral transition state. This intermediate state is cleaved to yield the free fatty acid, the alcohol component and the nucleophilic serine. Although many lipases show strong structural and sequential similarities (Pleiss et al. 1998, Arpigny and Jaeger 1999), their substrate and stereospecificities can

vary significantly (Martinelle et al. 1995). It is known that *p*-nitrophenylesters of alkylphosphonic acids irreversible and stoichiometrically react with the nucleophilic serine of lipases and esterases, freezing the reaction at the point of the tetrahedral transition state. In the past, they have been applied to the determination of serine hydrolase activity by using different approaches (Oskolkova et al. 2003, Rotticci et al. 2000). If fluorescent inhibitors are used, the tagged enzyme becomes visible (Mannesse et al. 1995). Thus, it can be detected and quantified on the basis of its fluorescent signal (Scholze et al. 1999). Fluorescently labeled alkyl phosphonates detect active enzymes in electrophoretically pure proteins and in complex proteosome samples (Speers and Cravatt 2004a, Adam et al. 2002, Greenbaum et al. 2002).

PROCEDURE

Activity tagging of lipases contained in adipocyte tissue can be performed according to the protocol of Birner-Grünberger and coworkers (2005). For this, gonadal fat pads (white adipose tissue) of fed and fasted mice are surgically removed and washed in PBS. Homogenization is performed on ice in lysis buffer (0.25 M sucrose, 1 mM EDTA, 1 mM DTT, 20 µg/ml leupeptin, 2 µg/ml antipain, 1 µg/ml pepstatin) using a motor-driven Teflon-in-glass homogenizer (8 strokes, 1,500 rpm). Cell debris is removed by centrifugation (1,000 × *g*, 15 min) to obtain cytoplasmic extracts. Protein concentrations is determined using the BIORAD protein assay based on the method of Bradford. 50 µg of protein sample dissolved in lysis buffer, 10 µl of 10 mM Triton X-100 in methanol (final conc. 1 mM) and 20 µl of activity tag (NBD-labeled single-chain phosphonic acid ester, TAG phosphonates and cholesteryl phosphonates which react with the nucleophilic serine in the active site of lipolytic enzymes due to the active phosphonate moiety with the good leaving PNPB group and then remain covalently attached leading to irreversible inactivation of the lipases) dissolved in methanol (1 nmol/10 µl, final conc. 20 µM) are mixed and the organic solvent is evaporated under a stream of argon. 100 µl of protein sample (0.5 mg protein/ml) is added and the resultant mixture is incubated (2 h, 37°C) under light protection. Proteins are precipitated in 10% ice-cold TCA (1 h, on ice) and collected by centrifugation (10,000 × *g*, 15 min, 4°C). The pellet is washed once with ice-cold acetone and resuspended in 1D sample buffer (20 mM KH_2PO_4, 6 mM EDTA, 60 mg/ml SDS, 100 mg/ml glycerol, 0.5 mg/ml bromophenol blue, 20 µl/ml mercaptoethanol, pH 6.8) or 2D sample buffer (7 M urea, 2 M thiourea, 4% CHAPS, 60 mM DTT, 2% Pharmalyte pH 3–10, 0.002% bromophenol blue). SDS-PAGE is performed in a Tris/glycine buffer system by aligning proteins (50 or 100 µg protein/lane) in a 5% stacking gel and separating them in a 10% resolving gel at 20–50 mA constant current. 2D-gel electrophoresis is performed in the first dimension by isoelectric focusing of 50–500 µg protein in 7 or 18 cm immobilized non-linear pH 3–10 gradients at 6.5/12 kVh and in the second dimension by SDS-PAGE on 7 or 20 cm gels as described by Gorg and coworkers (1985, 1988). Gels are fixed in 7.5% acetic acid and 10% ethanol and scanned at a resolution of 100 µm. NBD fluorescence is detected at 530 nm and an excitation wavelength of 488 nm. For visualization of the whole protein pattern, gels are stained with SYPRO Ruby following the manufacturer's instructions (Molecular Probes) and scanned at 605 nm and an excitation wavelength of 488 nm. For LC-MS/MS-analysis, the fluorescent protein spots are excised and tryptically digested according to the method by Shevchenko and coworkers (1996). Peptide extracts are dissolved in 0.1% formic acid and separated on a nano-HPLC-system. 20-µl samples are injected and concentrated on the loading column (LC packings PepMap™ C-18, 5 µm, 100 A, 300 µm ID × 1 mm) for 5 min using 0.1% formic acid as isocratic solvent at a flow rate of 20 µ l/min. The column is then switched into the nano-flow-circuit and the sample is loaded on the nano-column at a flow rate of 300 nl/min and separated using a gradient from 0.3% formic acid and 5% acetonitrile to 0.3% formic acid and 50% acetonitrile over 60 min. The sample is ionized in a Finnigan nano-ESI source equipped with NanoSpray tips and analyzed in a Thermo-Finnigan LCQ Deca XPplus iontrap mass-spectrometer. Acceptance parameters are two or more identified distinct peptides (Carr et al. 2004). Identified protein sequences are subjected to BLAST and motif search for identification of potential serine hydrolases.

EVALUATION

In pilot experiments, 50 µg of cleared cell lysate (see above) is incubated with 1 nmol of fluorescently labeled lipase inhibitor O-((6-(7-nitrobenz-2-oxa-1,3-dia-zol-4-yl)amino)hexanoyl)-aminoethyl-O-(n-hexyl)phosphonic acid *p*-nitrophenyl ester () and 1 mM TX-100 at 37°C for 2 h under shaking. Total protein is then precipitated with 10% TCA for 1 h on ice, washed once with acetone and subjected to 10% SDS-PAGE. After treatment of the gels with 10% ethanol and 7% acetic acid, the fluorescent signals are detected with laser scanner (excitation 488 nm, emission 530 nm).

K.6.1.18 Interaction of ATGL and CGI-58

PURPOSE AND RATIONALE

In contrast to HSL, which undergoes PKA-dependent phosphorylation and translocation from the cytoplasm to LD upon β-adrenergic stimulation of adipocytes, the regulation of ATGL may rely on protein-protein interaction. It has been demonstrated by Lass and coworkers (2006) that efficient enzymic activity of ATGL depends on interaction with and activation by CGI-58. Mutations in the human *CGI-58* gene are associated with Chanarin-Dorfman Syndrome (CDS), a rare genetic disease where TG accumulates excessively in multiple tissues (Chanarin et al. 1975, Dorfman et al. 1974, Lefevre et al. 2001). CGI-58 interacts with ATGL, stimulating its TAG hydrolase activity up to 20-fold. Alleles of *CGI-58* carrying point mutations associated with CDS fail to activate ATGL. Moreover, CGI-58/ATGL coexpression attenuates lipid accumulation in COS-7 cells. Antisense RNA-mediated reduction of CGI-58 expression in 3T3-L1 adipocytes inhibits TAG mobilization. These data establish an important biochemical function for CGI-58 in the lipolytic degradation of TAG and raise the question whether defects in CGI-58 may contribute to the pathogenesis of type II diabetes and obesity. The following assays allow the analysis of the functional interaction of ATGL with CGI-58 and its modulation by compounds/drug candidates.

PROCEDURE

Preparation of ATGL

Monkey embryonic kidney cells (COS-7, ATCC CRL-1651) are transfected using Metafectene (Biontex, Germany) as described (Zimmermann et al. 2004). For the preparation of cell extracts, cells are collected by trypsin treatment, washed three times with PBS and disrupted in buffer A (0.25 M sucrose, 1 mM EDTA, 1 mM dithiothreitol, 20 µg/ml leupetine, 2 µg/ml antipain, 1 µg/ml pepstatin, 20 mM Tris/HCl, pH 7.0) by sonication. Nuclei and unbroken cells are removed by centrifugation (1,000 × *g*, 4°C, 5 min). The expression of the His-tagged proteins is detected using immunoblotting as described (Zimmermann et al. 2004). COS-7 cells expressing His-tagged mouse ATGL are lysed in buffer C (25 mM NaPO4, pH 7.0, 20% glycerol, 2 mM β-mercaptoethanol, 0,01% NP-40) and incubated with TALON Co^{2+} resin (BD Biosciences). The resin-cell extract suspension is then poured into a micro bio-spin column (Bio-Rad) and washed with 10 column volumes of buffer C containing 500 mM NaCl. Recombinant His-tagged ATGL is eluted by a step-gradient of imidazole (200 mM final concentration) in buffer C. For determination of the purity of the protein, fractions are subjected to SDS-PAGE gel electrophoresis and immunoblotting.

Preparation of GST-Tagged CGI-58

The coding sequence of mouse CGI-58 is cloned into pYex4T-1 vector and transformed into the *S. cerevisiae* BY4742 (Matα; his3; leu2; lys2; ura3) strain. Large-scale overexpression of GST-CGI is achieved by maintaining transformed *S. cerevisiae* carrying in YNB-urea containing 0.5 mM $CuSO_4$ to induce copper promoter-driven expression of the fusion cassette. After induction, cells are harvested and protoplasts are generated with zymolyase and disrupted by sonication in the presence of 0.2% NP-40. The supernatant containing the GST-fusion protein is purified using glutathione-Sepharose beads. Purified GST-CGI is dialyzed overnight with 150 mM KCl, 10 mM potassium phosphate buffer (pH 7.4), and 0.01% NP-40.

Interaction Assay

For the detection of interacting proteins, ELISA plates are coated with 3 µg GST-CGI or GST in buffer D (50 mM Tris, pH 8.0, 150 mM NaCl, 5 mM $CaCl_2$). The wells are blocked with 5% BSA in buffer D and incubated with 50 µg protein/well of COS-7 cell extracts containing His-tagged ATGL in 50 mM potassium phosphate buffer (pH 7.0) in the absence or presence of compounds/drug candidates. After washing with buffer D containing 0.05% Tween 20, the mouse anti-His antibody is added in the same buffer containing 0.5% BSA. Subsequent to three further washes, horseradish peroxidase-conjugated anti-mouse antibody is added. After washing three times with buffer D containing 0.05% Tween 20, the absorbance of tetramethyl-benzidine is determined at 450 nm using 620 nm as reference wavelength. The absorbance of GST coated wells is subtracted from that coated with GST-CGI.

REFERENCES AND FURTHER READING

Adam GC, Sorensen EJ, Cravatt BF (2002) Trifunctional chemical probes for the consolidated detection and identification of enzyme activities from complex proteomes. Mol Cell Proteomics 1:781–790

Arpigny JL, Jaeger KE (1999) Bacterial lipolytic enzymes: classification and properties. Biochem J 343:177–183

Birner-Grünberger R, Susani-Etzerodt H, Waldhuber M, Riesenhuber G, Schmidinger H, Rechberger G, Kollroser M, Strauss JG, Lass A, Zimmermann R, Hämmerle G, Zechner R, Hermetter A (2005) The lipolytic proteome of mouse adipose tissue. Mol Cell Biol

Carr S, Aebersold R, Baldwin M, Burlingame A, Clauser K, Nesvizhskii A (2004) The need for guidelines in publicaiton of peptide and protein identification data: Working group on publication guidelines for peptide and protein identification data. Mol Cell Prot 3:531–533

Chanarin I, Patel A, Slavin G, Wills EJ, Andrews TM, Stewart G (1975) Neutral-lipid storage disease: a new disorder of lipid metabolism. BMJ 1:553–555

Dorfman ML, Hershko C, Eisenberg S, Sagher F (1974) Ichthyosiform dermatosis with systemic lipidosis. Arch Dermatol 110:261–266

Gorg A, Postel W, Gunther S, Weser J (1985) Improved horizontal two-dimensional electrophoresis with hybrid isoelectric-focusing in immobilized ph gradients in the 1st-dimension and laying-on transfer in the 2nd-dimension. Electrophoresis 6:599–604

Gorg A, Postel W, Gunther S (1988) The current state of two-dimensional electrophoresis with immobilized ph gradients. Electrophoresis 9:531–54

Greenbaum DC, Arnold WD, Lu F, Hayrapetian L, Baruch A, Krumrine J, Toba S, Chehade K, Bromee D, Kuntz ID, Bogyo M (2002) Small molecule affinity fingerprinting, a tool for enzyme family subclassification, target identification, and inhibitor design. Chem Biol 9:1085–1094

Lass A, Zimmermann R, Hämmerle G, Riederer M, Schoiswohl G, Schweiger M, Kienesberger P, Strauss JG, Gorkiewicz G, Zechner R (2006) Adipose triglyceride lipase-mediated lipolysis of cellular fat stores is activated by CGI-58 and defective in Chanarin-Dorfman syndrome. Cell Metabol 3:309–319

Lefevre C, Jobard F, Caux F, Bouadjar B, Karaduman A, Heilig R, Lakhdar H, Wollenberg A, Verret A, Weissenbach J (2001) Mutations in CGI-58, the gene encoding a new protein of the esterase/lipase/thioesterase subfamily, in Chanarin-Dorfman syndrome. Am J Hum Genet 69:1002–1012

Manesse MLM, Boots J-WP, Dijkman R, Slotboom AT, van der Hjiden HTWM, Egmond MR, Verhij HM, de Haas GH. Biochim Biophys Acta 1259:56–64

Martinelle M, Holmquist M, Hult K (1995) On the interfacial activation of Candida antarctica lipase A and B as compared with Humicola lanuginosa lipase. Biochim Biophys Acta 1258:272–276

Oskolkova OV, Saf R, Zenzmaier E, Hermetter A (2003) Fluorescent organophosphonates as inhibitors of microbial lipases. Chem Phys Lipids 125:103–114

Petry S, Baringhaus K-H, Schönafinger K, Jung C, Kleine H, Müller G (2004) High-throughput screening of hormone-sensitive lipase and subsequent computer-assisted compound optimization in "Lipases and phospholipases in drug development" (Müller G, Petry S Eds.) pp 121–136, Wiley-VCH, Weinheim, Germany

Pleiss J, Fischer M, Schmid RD (1998) Anatomy of lipase binding sites: the scissile fatty acid binding site. Chem Phys Lipids 93:67–80

Rotticci D, Norin T, Hult K, Martinelle M (2000) An active-site titration method for lipases. Biochim Biophys Acta 1483:132–140

Schmidinger H, Birner-Grünberger R, Riesenhuber G, Saf R, Susani-Etzerodt H, Hermetter A (2005) Novel fluorescent phosphonic acid esters for discrimination of lipases and esterases. ChemBioChem 6:1–6

Scholze H, Stutz H, Paltauf F, Hermetter A (1999) Fluorescent inhibitors for the qualitative and quantitative analysis of lipolytic enzymes. Anal Biochem 276:72–80

Shevchenko A, Wilm M, Vorm O, Mann M (1996) Mass spectrometric sequencing of proteins from silver stained polyacrylamide gels. Anal Chem 68:850–858

Speers AE, Cravatt BF (2004a) Chemical strategies for activity-based proteomics. ChemBioChem 5:41–47

Speers AE, Cravatt BF (2004b) Profiling enzyme activities *in vivo* using click chemistry methods. Chem Biol 11:535–546

Wang Q, Chan TR, Hilgraf R, Fokin VV, Sharpless KB, Finn MG (2003) Bioconjugation by copper(I)-catalyzed azide-alkyne [3+2] cycloaddition. J Am Chem Soc 125:3192–3193

Zimmermann R, Strauss JG, Hämmerle G, Schoiswohl G, Birner-Grünberger R, Riederer M, Lass A, Neuberger G, Eisenhaber F, Hermetter A, Zechner R (2004) Fat mobilization in adipose tissue is promoted by adipose triglyceride lipase. Science 306:1383–1386

K.6.1.19 Measurement of cAMP Levels

PURPOSE AND RATIONALE

Activation of lipolysis in adipocytes by β-adrenergic stimuli and its inhibition by insulin critically depends on the generation by adenylate cyclase and degradation by phosphodiesterase 3B (PDE3B), respectively (for a review see Müller and Petry 2004). The intracellular cAMP levels can be determined in adipocytes which have been exposed to isoproterenol prior to incubation with insulin/compounds/drug candidates.

PROCEDURE

400 µl of adipocyte suspension (lipocrit 10%) are suspended in 600 µl KRH containing 0.75% BSA, 1.5 mM glucose, and incubated in the absence or presence of lipolytic stimuli (isoproterenol, adenosine deaminase) in combination with insulin or compounds/drug candidates at 37°C in a mildly shaking water bath. 200-µl aliquots are transferred into Eppendorf cups containing 20 µl $HClO_4$ (70%), vortexed vigorously and centrifuged (12,000 × *g*, 15 min, room temperature). 110 µl of the infranatant is removed, taking care not to aspirate any of the precipitate, supplemented with 60 µl of 1 M Tris/HCl (pH 7.5), incubated for 15 min on ice and then centrifuged (13,000 × *g*, 15 min, 4°C). 150 µl of the infranatant is removed for glycerol determination, frozen in liquid N_2 and stored at –20°C prior to determination of glycerol and cAMP levels. cAMP is determined by a modification of the protein kinase binding procedure. Samples and standards are incubated with 8 µg of R-subunit of PKA and 175 nCi [8-^{3}H]cAMP in a buffer composed of 50 mM Tris/HCl (pH 7.4), 4 mM EDTA in a final volume of 200 µl for 4 h at 4°C to reach equilibrium. Charcoal suspension (30 g/l) is added and after vortexing, the mixture is centrifuged at 16,000 × *g*, 2 min, 4°C). The supernatant is transferred into scintillation vials, supplemented with 5 ml water-compatible scintillation fluid

and counted for radioactivity using a liquid scintillation counter.

EVALUATION

The concentration of endogenous unlabeled cAMP in the samples is determined from a linear standard curve.

K.6.1.20 cAMP-Specific Phosphodiesterase (PDE) Activity

PURPOSE AND RATIONALE

Membrane-bound phosphodiesterase of rat epididymal adipose cells is stimulated when intact cells are exposed to insulin. The localization at the endoplasmic reticulum (corresponding to the low density microsomal fraction) and properties of the insulin-sensitive particulate cGMP-inhibitable cAMP phosphodiesterase have been described by Kono and coworkers (1975), Osegawa and coworkers (1982), Saltiel and Steigerwalt (1985), Solomon and coworkers (1986). Recently, the phosphodiesterase isoform, PDE3B, has been identified as target for phosphorylation and activation by protein kinase PKB/Akt, which is a key element of the downstream insulin signaling cascade.

PROCEDURE

The low density microsomal fraction (LDM) of primary or cultured adipocytes (pellet of a 100,000 × *g*/60 min-centrifugation of the post-mitochondrial supernatant prepared from the homogenate of adipocytes exposed to lipolytic stimuli in the absence or presence of compounds; see above) is incubated in the absence or presence of compounds at various concentrations for 20 min. For the assay of cAMP-specific PDE up to 50 µg of LDM protein are incubated (5 min, 30°C) with 500 nM [2,8-^{3}H]cAMP (100 nCi) in 50 mM Tris/HCl (pH 7.4), 0.5 mM DTT, 5 mM $MgCl_2$, 50 µM PMSF in a total volume of 0.25 ml. The incubation is terminated by the sequential addition of 30 µl of 10 mM IBMX and 120 µl of 0.1 N HCl and heating (5 min, 95°C). After neutralization (120 µl of 0.1 N KOH, 80 ml of 250 mM Tris/HCl (pH 7.4), 10 µl of crude 5′-nucleotidase (5 mg/ml) (*Crotalus atrox*) is added to the mixture. The reaction (30 min, 37°C) is terminated by the addition of 60 µl of 200 mM EDTA, 5 mM adenosine. Unreacted cAMP is removed by the addition of 1 ml of a 1:3 slurry of Dowex AG-1X8 (Bio-rad). Solutions are shaken (5 min, 4°C) and centrifuged (1,000 × *g*, 5 min).

EVALUATION

Radiolabeled adenosine left in the supernatant after enzymic degradation of 5′-AMP and chromatographic removal of cAMP is determined by liquid scintillation counting. The assay is proportional to up to 100 µg of protein and linear throughout 20 min. It monitores the putative insulin-like effects of compounds on the regulation of cAMP degradation *via* the insulin signaling cascade (or alternative pathways) as well as directly on the activity state of PDE3B depending on whether or not the compound is present during the incubation of the adipocytes or LDM.

K.6.1.21 Activity State of Protein Kinase A (PKA)

PURPOSE AND RATIONALE

The cAMP levels generated in response to β-adrenergic stimulation in the absence or presence of insulin or compounds in adipocytes determine the activity of PKA phosphorylating both HSL and perilipin which which play key roles in the regulation of lipolysis in adipocytes (see K.6.1.10 and K.6.1.12.2). Thus, the PKA activity ultimately determines the lipolytic state of the adipocytes in response to insulin/compounds/drug candidates. The assay monitors the activity state of PKA in adipocytes in response to β-adrenergic stimuli in the absence or presence of insulin/compounds/drug candidates at the time point of homogenization. This activity ratio is a parameter for the portion of PKA active *in vivo* toward total cellular PKA at the time point of homogenization.

K.6.1.21.1 Radioactive Method

For determination of the activity state of PKA, 500-µl adipocyte suspension (5×10^6 cells/ml) are transferred to 2-ml microfuge tubes, pre-cooled to 4°C, containing at final concentrations: 20 mM Tris/HCl (pH 7.4), 10 mM EDTA and the cAMP PDE inhibitor, Ro 20–1724 (100 µM). The mixture is vortexed briefly, decanted into a 5-ml Teflon-in-glass homogenizer and homogenized with 10 strokes of the rotating (1,500 rpm) Teflon pestle. The homogenate is transferred to pre-cooled microfuge tubes and centrifuged (16,000 × *g*, 10 min, 4°C). The infranatant is removed and immediately assayed for PKA activity. 25 µl of assay medium (20 mM MOPS/KOH, pH 7.0, 10 mM $MgCl_2$, 0.1 mM ATP, 0.5 mg/ml histone H1, 5 mM DTT, 50 µCi/ml [γ-^{32}P]ATP) is added to 25 µl infranatant. After vortexing and incubation for 20 min

at 30°C, the reaction is terminated by addition of 1 ml of ice-cold 20% TCA containing 5 mM sodium pyrophosphate and incubation (1 h, 4°C). The precipitates are sedimented by centrifugation (16,000 × *g*, 5 min, 4°C) and, after removal of the supernatant, dissolved in 100 µl of cold 1 N NaOH and re-precipitated with 20% TCA and 5 mM sodium pyrophosphate. The precipitate is then filtered under vacuum over GF/C-glass microfiber filter that had been pre-wetted with 5% TCA, 5 mM sodium pyrophosphate. The filters are washed with 4 ml of the same medium, dried and counted for radioactivity.

EVALUATION

Each adipocyte infranatant is assayed in quadruplicate under four separate conditions: (I) with no further additions; (II) in the presence of 15 µM cAMP; (III) in the presence of 2 µM PKA inhibitor synthetic peptide and (IV) in the presence of 15 µM cAMP and 2 µM PKA inhibitor synthetic peptide. The results are expressed as corrected PKA activity ratios (I)–(III)/(II)–(IV) according to Honnor and coworkers (1985a and b) and Londos and coworkers (1985).

K.6.1.21.2 Fluorescent Method

PROCEDURE

The method based on fluorescently labeled kemptide has been introduced by Müller and coworkers (2000) and Schölch and coworkers (2004) and can be used for determination of the activity ratio in cells or tissues from rats treated with compounds/drug candidates. For the *ex vivo* experimental design, frozen tissue samples are minced under liquid N_2 in 2 ml of 25 mM MES (pH 6.0), 140 mM NaCl, 2 mmol/l EDTA, 0.5 mM EGTA, 0.25 M sucrose, 50 mM NaF, 10 mM sodium pyrophosphate, 20 mM glycerol-3-phosphate, 1 mM sodium orthovanadate, 2 µM microcystin, 1 µM okadaic acid, and protease inhibitors per gram of wet weight and then homogenized by sequential use of an Ultraturrax homogenizer (30 s, maximum speed) and a Teflon-in-glass homogenizer (tightly fitting, five strokes, 3,000 rpm, on ice). After centrifugation (500 × *g*, 5 min, 4°C), the infranatant below the fat layer is carefully removed, adjusted to 0.5% Triton X-100, and after incubation (30 min, 4°C) and homogenization (Teflon-in-glass, 10 strokes, 500 rpm, 4°C) centrifuged (10,000 × *g*, 15 min, 4°C). The supernatant is re-centrifuged (100,000 × *g*, 1 h, 4°C). Twenty-five microliters of the supernatant (cytosol) are incubated (30 min, 30°C) with 12.5 µl of assay buffer (200 mM Tris/HCl, pH 7.5, 40 mM $MgCl_2$, 4 mM ATP, 400 µM rhodamine-labeled kemptide [PepTag A1 peptide obtained from Serva/Promega Heidelberg, Germany]) in the absence or presence of 10 µM mono-butyryl-cAMP and 50 µM heat-stable PKA inhibitor peptide (Sigma, Germany) in a total volume of 50 µl. The reaction is terminated by placing the tube into a boiling water bath for 2 min, and the mixture is stored at –20°C for further analysis. Portions of this mixture (10 µl) supplemented with 1 µl of 80% glycerol are separated by agarose gel electrophoresis (0.8% in 50 mM Tris/HCl, pH 8.0, 15 min at 100 V). Phosphorylated kemptide (net charge –1) migrating toward the anode and separated from the nonphosphorylated species (net charge +1) moving toward the cathode is visualized under UV light. For quantitative evaluation, the gel material that contained the phosphorylated band is excised (125 µl), heated (95°C), and supplemented with 75 µl of gel solubilization solution and 50 µl of glacial acetic acid, and finally its absorbance is determined at 570 nm using a 96-well plate reader (normalized for liquefied agarose containing no kemptide).

EVALUATION

The PKA activity ratio is calculated as the ratio between the absorbance in the absence and presence of cAMP corrected in each case for unspecific phosphorylation in the presence of the PKA inhibitor (which typically is < 15% of total) and reflects the portion of PKA activity (i. e., cAMP concentration) present at the time point of removal of the tissue or cell samples. Control experiments demonstrated that the activity ratio is independent of dilution of the tissue or cell homogenates (and protein concentration) from 2 g wet wt/ml to 0.03 g/ml (limit of detection) corresponding to 20–0.02 mg protein/ml and of incubation period (up to 2 h), thereby excluding formation of inactive PKA dephosphorylated holoenzyme during homogenization and subsequent assay.

K.6.1.22 PKA Catalytic Activity

PURPOSE AND RATIONALE

In addition to the regulation of the PKA activity by modulation of the cytosolic cAMP levels, insulin and insulin-like compounds/drug candidates may affect PKA by modulating its regulation *via* signaling mechanisms as provoked by insulin or by its direct allosteric activation or blockade by small molecule inhibitors.

PROCEDURE

PKA activity is assayed according to Roskoski and coworkers (1983) and Honnor and coworkers (1985a). The reaction mixture contains 25 µl of rat adipocyte cytosol, 0.4 µM kemptide (consensus substrate peptide), 40 mM Tris/HCl (pH 7.2), 2 mM DTT, 12.5 mM $MgCl_2$, 0.1 mM PMSF, 1 mM IBMX, 100 µM [γ-^{32}P]ATP (1 µCi) with or without 1 µM cAMP in a total volume of 100 µl. After incubation (10 min, 30°C), the reaction mixture is chilled on ice, then supplemented with 3 ml of 75 mM phosphoric acid, 100 mM NaF, 10 mM ATP and immediately spotted on phosphocellulose filters (Whatman P18). After extensive washing with 75 mM phosphoric acid, the filters are dried and counted for radioactivity.

MODIFICATIONS OF THE METHOD

The inhibition of isoproterenol-stimulated PKA by sulfonylureas in rat adipocytes was tested by Müller and coworkers (1994). The direct effect of tolbutamide and glyburide on the activity of PKA in rat liver cytosol was investigated by Okuno and coworkers (1988).

K.6.1.23 Protein Phosphatase (PP) Activity

PURPOSE AND RATIONALE

Insulin inhibits lipolysis by decreasing the phosphorylation and thus the activation state of HSL in adipose tissue *via* both the inhibition of PKA and the stimulation of protein phosphatase 2A (PP2A) *via* ill-defined mechanisms. They may involve the phosphoinositol-3′-kinase (PI3K) signaling pathway, the mitogen-activated protein kinase (MAPK) signaling pathway or soluble mediators of the phosphoinositolglycan (PIG) class (Vila et al. 1990; see K.6.3.6.4).

PROCEDURE

For measurement of PP2A activity, the adipocytes (3×10^7 cells) are washed once with 25 ml of ice-cold 100 mM Tris/HCl (pH 8.5), 10 mM EDTA, 25 mM DTT and immediately resuspended in 0.5 ml of 100 mM Tris/HCl (pH 7.0), 2 mM EDTA, 10 mM DTT, 0.5 mM benzamidine, 0.2 mM PMSF, 2 µg/ml leupeptin, 5 µg/ml pepstatin. After addition of the same volume of ice-cold glass beads, cell extracts are prepared by vigorous vortexing (5 times 5 s each with cooling intervals on ice) and centrifuged (13,000 × *g*, 5 min, 4°C). The supernatant (S13) is diluted with 3 volumes of the same buffer containing 1% BSA. Protein phosphatase activity is assayed as the ability to dephosphorylate ^{32}P-labeled myelin basic protein (MBP). 10 µl of S13 is added to an assay mixture (total volume 50 µl) containing 50 mM Tris/HCl (pH 7.5), 1 mM EDTA, 0.5 mM EGTA, and 0.2 nmol ^{32}P-labeled myelin basic protein (900 dpm/pmol) for 20 min at 30°C in the absence or presence of 2 nM okadaic acid. The reaction is terminated by the addition of 50 µl of ice-cold 10% TCA. After incubation for 15 min on ice and centrifugation (12,000 × *g*, 5 min, 4°C), the supernatant is neutralized with NaOH and measured for radioactivity by liquid scintillation counting (10 ml Aquasol).

EVALUATION

PP2A activity is determined as the difference between ^{32}P-radiolabeled MBP measured in the presence of okadaic acid (10 nM) corresponding to the PP2A independent phosphatase portion and radiolabeled MBP determined after uninhibited incubation corresponding to the total phosphatase activity. Under these conditions, release of $^{32}P_i$ is linear for up to 10 min. One unit of activity is defined as the amount of enzyme that catalyzes the release of 1 µmol of $^{32}P_i$-radiolabel from labeled myelin basic protein in one min under conditions of the standard assay (Müller et al. 2000).

REFERENCES AND FURTHER READING

Honnor RC, Dhillon GS, Londos C (1985a) cAMP-dependent protein kinase and lipolysis in rat adipocytes I. Cell preparation, manipulation, and predictability in behavior. J Biol Chem 260:15122–15129

Honnor RC, Dhillon GS, Londos C (1985b) cAMP-dependent protein kinase and lipolysis in rat adipocytes II. Definition of steady-state relationship with lipolytic and antilipolytic modulators. J Biol Chem 260:15130–15138

Kono T, Robinson FW, Sarver JA (1975) Insulin-sensitive phosphodiesterase. Its localization, hormonal stimulation, and oxidative stabilization. J Biol Chem 250:7826–7835

Londos C, Honnor RC, Dhillon GS (1985) cAMP-dependent protein kinase and lipolysis in rat adipocytes III. Multiple modes of insulin regulation of lipolysis and regulation of insulin responses by adenylate cyclase regulators. J Biol Chem 260:15139–15145

Müller G, Petry S (2004) Physiological and pharmacological regulation of triacylglycerol storage and mobilization in "Lipases and phospholipases in drug development" (Müller G, Petry S Eds.) pp 231–332, Wiley-VCH, Weinheim, Germany

Müller G, Wied S, Wetekam EM, Crecelius A, Pünter J (1994) Stimulation of glucose utilization in 3T3 adipocytes and rat diaphragm *in vitro* by the sulfonylureas glimiperide and glibenclamide, is correlated with modulations of the cAMP regulatory cycle. Biochem Pharmacol 48:985–996

Müller G, Grey S, Jung C, Bandlow W (2000) Insulin-like signaling in yeast: Modulation of protein phosphatase 2A, protein kinase A, cAMP-specific phosphodiesterase, and glycosyl-phosphatidylinositol-specific phospholipase C activities. Biochemistry 39:1475–1488

Okuno S, Inaba M, Nishizawa Y, Inoue A, Morii H (1988) Effect of tolbutamide and glyburide on cAMP-dependent protein kinase activity in rat liver cytosol. Diabetes 37:857–861

Osegawa M, Makino H, Kanatsuka A, Kumagai A (1982) Effects of sulfonylureas on membrane-bound low K_m cyclic AMP phosphodiesterase in rat fat cells. Biochim Biophys Acta 721:289–296

Roskoski R (1983) Assays of protein kinase. Meth Enzymol 99:3–6

Saltiel AR, Steigerwalt RW (1985) Purification of putative insulin-sensitive cAMP phosphodiesterase or its catalytic domain from adipose tissue. Diabetes 35:698–704

Schölch C, Kuhlmann J, Gossel M, Müller G, Neumann-Häfelin C, Belz U, Kalisch J, Biemer-Daub G, Kramer W, Juretschke H-P, Herling A (2004) Characterization of adenosine-A1-receptor-mediated antilipolysis in rats by tissue-microdialysis, ^{1}H-spectroscopy and glucose clamp studies. Diabetes 53:1920–1926

Solomon SS, Deaton J, Shankar TP, Palazzolo M (1986) Cyclic AMP phosphodiesterase in diabetes. Effect of glyburide. Diabetes 35:1233–1236

Vila MDC, Milligan G, Standaert ML, Farese RV (1990) Insulin activates glycerol-3-phosphate-acyltransferase (de novo phosphatidic acid synthesis) through a phospholipid-derived mediator. Apparent involvement of Giα and activation of a phospholipase C. Biochem 29:8735–8740

K.6.2 Assays for Insulin and Insulin-Like Metabolic Activity Based on Hepatocytes, Myocytes and Diaphragms

GENERAL CONSIDERATIONS

Despite the eminent importance of studies with primary and cultures adipocytes or adipose tissues on basis of their physiological role in the regulation of lipid and carbohydrate metabolism in humans in combination with the relative low expenditure in preparing adipocytes of high quality and number, compounds and drug candidates for future anti-diabetic and anti-obesity therapy have to be analyzed for their effects in primary and cultured hepatocytes and myocytes or liver and muscle tissues, too. In principle, the majority of the assays described above for adipocytes can be adapted for the use with hepatocytes and myocytes. However, the following selection takes into account the relative contribution of each process monitored to its role in the whole-body regulation of intermediary metabolism in the normal and disease state. Moreover, technical aspects, such as requirement for a special equipment and applicability in throughput screening assays for drug discovery were additional criteria.

K.6.2.1 Glucose Oxidation

PROCEDURE

Cultured Myocytes and Hepatocytes

For the measurement of glucose oxidation on basis of $^{14}CO_2$ release, varying amounts of [^{14}C]glucose (0.1 mCi/ml) are used. Alternatively, glucose oxidation is determined as the formation of [^{3}H]water from [5-^{3}H]glucose. After culture in DMEM medium in 24-well culture dishes, cells are incubated at 37°C for 2 h in 10 µl of KRB solution containing [5-^{3}H]glucose at various concentrations of glucose as described by Wang and coworkers (2004). Control wells containing no cells are included to allow for correction of the conversion of [^{3}H]water into [^{3}H]glucose.

Diaphragm

Glucose utilization by isolated diaphragms can be monitored according to the procedure described by Jeoung and coworkers (2006). For this, diaphragms are removed from 48-h starved mice, rinsed in KHB buffer, blotted, weighed, and placed in 10-ml Erlenmeyer flasks containing 1.5 ml of KHB buffer (pH 7.4), 5 mM glucose, and 0.2% BSA. The flasks are flushed with 95% O_2/5% CO_2 sealed with rubber stoppers, placed in a shaking (60 cycles/min) water bath at 37°C, and pre-incubated for 30 min. Diaphragms are removed from the flasks, blotted, and transferred to new flasks containing 1.5 ml of KHB buffer supplemented with 5 mM glucose containing 20–500 µCi/mmol [U-^{14}C]glucose and 80 µCi/mmol [5-^{3}H]glucose and 1 mU/ml insulin as described by Clark and coworkers (1987). Flasks are flushed with 95% O_2/5% CO_2, sealed with rubber serum caps fitted with hanging center wells and incubated for 1 h with shaking at 37°C. Reactions are terminated by the injection of 0.25 ml of phenethylamine/methanol (1/1, by vol.) into the center wells and 0.1 ml of 60% (w/v) perchloric acid into the incubation medium.

EVALUATION

The rate of glucose oxidation is determined from the production of $^{14}CO_2$, the rate of glycolysis from the difference between the rate of ^3H_2O formed (Ashcroft et al. 1975) and the rate of substrate cycling, and the rate of substrate cycling from the difference between the rates of glycogen synthesis from [U-^{14}C]glucose and [5-^{3}H]glucose. Glucose utilization rates are calculated as pmol of glucose utilized/hour/cell or mg tissue as: Glucose utilized (pmol) = [^{3}H]water formed (cpm)/specific radioactivity of [5-^{3}H]glucose (cpm/pmol).

K.6.2.2 Pyruvate Oxidation

PURPOSE AND RATIONALE

Pyruvate oxidation can be monitored in isolated rat adipocytes as the incorporation of the acetyl-CoA generated into lipophilic products along the fatty acid syn-

thesis and esterification (into TAG) pathways. Under conditions of glucose deprivation pruvate dehydrogenase (PDH) is rate-limiting for the overall conversion of 3-[^{14}C]pyruvate into radiolabeled products (e. g. fatty acids, TAG) which are separated from the unincorporated ^{14}C-labeled pyruvate, acetyl-CoA and hydrophilic intermediates by partitioning into the toluene phase.

PROCEDURE

Isolated rat adipocytes are prepared by collagenase digestion as described above (K.5.1.2), however, in KRHB lacking glucose. 3.5×10^4 cells are incubated (2 h, 37°C) with 0.1 mM [3-^{14}C]sodium pyruvate (0.5 µCi) in 1 ml of KRHB lacking glucose. After addition of 5 ml toluene, the samples are vortexed and incubated overnight at 4°C. 1 ml of the upper toluene phase is removed, supplemented with 10 ml toluene-based scintillation cocktail (e. g. Beckman Quickszint 501) and counted for radioactivity.

EVALUATION

Dichloroacetate (DCA), which acts as unspecific inhibitor of PDH kinase leading to activation of PDH and thereby stimulation of pyruvate oxidation, should be used as control (0.2–5 mM final conc.). Data each corrected for a blank value lacking cells are calculated as fold-stimulation of ^{14}C-incorporation into toluene-soluble products in response to DCA *vs.* basal. In isolated rat adipocytes 5 mM DCA stimulates pyruvate oxidation by 3- to 4-fold. The assay may be useful for the identification of compounds/drug candidates which stimulate pyruvate oxidation by inhibition of PDK (PDK2 in adipocytes) or different modes of action.

K.6.2.3 Pyruvate Dehydrogenase Complex (PDC) Activity

PDC activity is determined according to the method of Jeoung and coworkers (2006). For this, deep-frozen and pulverized diaphragms are homogenized in 5 volumes of extraction buffer containing 30 mM HEPES/KOH (pH 7.5), 0.5 mM thiamine pyrophosphate, 3% Triton X-100, 5 mM EDTA, 2% BSA, 5 mM DTT, 10 µM tosyl-phenylalanyl-chloromethyl ketone, 10 µg/ml trypsin inhibitor, 1 µM leupeptin, 2 mM dichloroacetate (DCA), and 50 mM KF. The supernatant obtained by centrifugation (10,000 × *g*, 10 min, 4°C) is made 9% (w/v) in PEG6000 to precipitate PDC. Pellet produced by centrifugation (12,000 × *g*, 10 min) is suspended in a suspension buffer containing 30 mM HEPES/KOH (pH 7.5), 1% Triton X-100, 0.2 mM EDTA, 2% BSA, 1 µM leupeptin, 5 mM DTT. For determination of total PDC activity, diaphragms are homogenized in 5 volumes of the extraction buffer lacking DCA and KF. The supernatant (200 µl) obtained by centrifugation of the homogenate (10,000 × *g*, 10 min, 4°C) is added to 100 µl of an activation buffer (suspension buffer containing 25 mM $MgCl_2$, 1.5 mM $CaCl_2$, and 1 µg of recombinant pyruvate dehydrogenase phosphatase 1 protein. After incubation (20 min, 30°C) to dephosphorylate and activate PDC, samples are treated with PEG6000 (final 9%, w/v) to precipitate PDC. An aliquot of an extract of the pellet is used to assay of total PDC activity. PDC activity is measured spectrophotometrically in a 96-well plate reader with a coupled assay based on the reaction catalyzed by arylamine acetyltransferase (Nakai et al. 1999, Coore et al. 1971). One unit of PDC activity corresponds to the acetylation of 1 µmol of *p*-(*p*-aminophenylazo)-benzenesulphonate per min at 30°C.

K.6.2.4 Pyruvate Dehydrogenase Kinase (PDK) Activity

GENERAL CONSIDERATIONS

The PDC multienzyme complex (5–10 million Da) catalyzes a key regulatory step in oxidative glycolysis, the irreversible decarboxylation of pyruvate. Its activity is reduced under conditions of increased fatty acid oxidation, i. e. when tissue [acetyl-CoA]/[CoA] and [NADH]/[NAD^+] ratios are elevated. Thus, PDC activity is down-regulated during fasting and in pathological conditions associated with insulin resistance, such as diabetes and obesity (Fuller and Randle 1984, Orfali et al. 1993, Kelley et al. 1992).

The mammalian PDC is composed of multiple copies of three enzymes: pyruvate decarboxylase (E1 subunit), dihydrolipoyl acetyltransferase (E2 subunit, a modular protein which contains a transacetylase and so-called outer and inner lipoyl domains, $E2_c$, $E2_{L1}$ and $E2_{L2}$, respectively), and dihydrolipoyl dehydrogenase (E3 subunit). It is regulated by reversible phosphorylation (Linn et al. 1969, Yeaman 1978). Four pyruvate dehydrogenase kinase (PDK) and two pyruvate dehydrogenase phosphatase (PDP) isozymes have been identified to date (Gudi et al. 1995). PDKs inactivate PDC by catalyzing the ATP-dependent phosphorylation of three serine residues on the PDC E1 subunits.

PURPOSE AND RATIONALE

The blood glucose lowering effect of dichloroacetate (DCA) in diabetic rodents (Lorini and Ciman 1962) and type II diabetic patients (Stacpoole et al. 1978)

has been ascribed to its ability to inhibit PDKs and thereby activate PDC *in vivo*. The primary structures of PDK isozymes 1–4 share little sequence homology with other eukaryotic protein kinases and are more homologous to prokaryotic histidine kinases (Popov et al. 1993). These findings increased the attractiveness for drug discovery projects to identify novel inhibitors of PDK activity as possible therapeutic agents for diabetes and other pathological conditions in which PDC activity is reduced (e. g. lactic acidosis, ischemia) (Bersin and Stacpoole 1997). Until recently, the only known small molecule inhibitors of PDK activity were pyruvate, DCA, halogenated acetophenones and analogs of ATP (e. g. adenosine 5′-[β,γ-imido]triphosphate (p[NH]ppA). The following assays may be useful for the identification of structurally novel PDK inhibitors.

PROCEDURE

Functional PDK Assay

Compounds are assessed for their ability to inhibit the ATP-dependent inactivation of porcine heart PDC. The assay essentially consisted of three steps. First, a BSA-stabilized PDC preparation is acetylated to enhance its intrinsic PDK activity. Second, the PDK reaction is initiated by the addition of ATP. Third, after 7 min the PDK reaction is terminated and the residual PDC activity is assessed by monitoring the formation of NADH at 340 nm. In some experiments, the PDC is either supplemented with rPDK and/or ATP is omitted during the second step.

E1 Subunit Phosphorylation Assay

For phosphorylation of the PDC E1 subunit by endogenous PDK (Jackson et al. 1998), the reaction is initiated by the addition of [γ-^{33}P]ATP (80 mCi/mmol) to intact porcine PDC. The reaction is terminated after 45 s by the addition of TCA. Precipitated protein is recovered by centrifugation, dissolved in 1 M NaOH and the radioactivity of the entire sample is determined by liquid scintillation counting.

PDK Peptide Phosphorylation Assay

PDK activity is determined by measuring the PDK-catalyzed phosphorylation of an acetylated tetradecapeptide substrate, Ac-YHGHSMSDPGVSYR, as previously described (Jackson et al. 1998), except that the reaction volume is 25 µl. Effects of compounds/drug candidates on PDK activity are usually determined in the presence of 0.2 mM [γ-^{33}P]ATP (0.05 µCi/nmol ATP) and 0.5 mM peptide substrate. In experiments where the [γ-^{33}P]ATP (0.05–0.85 µCi/nmol ATP) concentration is varied, the final peptide concentration is 0.5 mM. When the peptide concentration is varied, the final [γ-^{33}P]ATP concentration is adjusted to 0.2 mM. Results are expressed as specific activity (nmol of phosphate transferred per mg of PDK protein per 30 min).

Kinase Autophosphorylation Assay

PDK1 or PDK2 (50 µg/ml) is incubated in a 25-µl reaction mixture containing MOPS (40 mM, pH 7.2), KH_2PO_4 (20 mM), EDTA (0.5 mM), $MgCl_2$ (1.8 mM), KCl (30 mM), DTT (2 mM), NaF (10 mM), [γ-^{32}P]ATP (0.2 mM, 0.01 mCi/mmol) and compounds/drug candidates at 37°C for up to 5 min. The reaction is terminated by the addition of 0.1 volume of a mixture of 425 mM H_3PO_4 and 5 mM p[NH]ppA. The sample is then adjusted to pH 7.4 by the addition of 125 µl of a mixture of 60 mM Tris (pH 8.7) and NaCl (500 mM). The entire sample is then applied to a nitrocellulose membrane and rinsed with TBS (20 mM Tris, 500 mM NaCl, pH 7.5) using a Dot-slot blotting apparatus. Phosphorylated proteins are visualized using a phosphor screen and a phosphorimager (e. g. Storm 840).

Phosphorylation of E1 Protein by PDKs

PDK1 or PDK2 (7.5 µg) is incubated in the presence or absence of 95 µg of acetylated PDC without BSA (Jackson et al. 1998) in a 75-µl reaction mixture containing MOPS (40 mM, pH 7.2), KH_2PO_4 (20 mM), EDTA (0.5 mM), $MgCl_2$ (1.8 mM), KCl (30 mM), DTT (2 mM), NaF (10 mM) and [γ-^{32}P]ATP (0.2 mM, 0.01 mCi/mmol). Following a 45-min incubation at 37°C, the reaction is terminated by the addition of an equal amount of Laemmli sample buffer. 40-µl portions are subjected to SDS/PAGE.

Assay for Direct Inhibition by Supplemental PDKs

PDK2 is added to the functional PDK assay described above, which is performed in the absence and presence of ATP. Alternatively, a PDC preparation which is neither stabilized with BSA nor pre-acetylated is incubated (14 µg/ml) in 180 µl of 40 mM MOPS (pH 7.4), 0.36 mM EDTA, 30 mM KCl, 1.5 mM $MgCl_2$, 120 mM ADP, 2 mM DTT, 10 mM NaF and the additions indicated, at 37°C for up to 10 min. During this step, ADP is omitted in some experiments. The PDC reaction is initiated by the addition of 20 µl of 40 mM MOPS (pH 7.4), 0.36 mM EDTA, 1.5 mM $MgCl_2$, 1 mM DTT, 1.1 mM CoASH, 2.2 mM NAD^+, 2.2 mM pyruvate and 2.2 mM thiamine pyrophosphate. NADH formation over 5 min is monitored at 340 nm.

EVALUATION

The functional PDK assay has a spectrophotometric read-out and measures the effect of PDK activity on PDC function. However the PDK isozyme composition and the stoichiometry of PDK relative to PDC are unknown. Obviously this assay is more difficult to optimize and validate than a traditional kinase assay based upon a model fluorescent peptide substrate. However, the functional PDK assay should identify not only compounds acting at known or presumed sites on the kinase (ATP, lipoamide, or pyruvate binding sites) but also those interfering with interactions between PDK and other PDC protein components (e. g. E1 subunit or the inner lipoyl domain (E2L2) of the E2 subunit of PDC). Although inhibitors of protein–protein interactions are rare, it is desirable that an initial screening assay allows for this possibility.

In contrast to the functional PDK assay, the E1 phosphorylation assay enables PDK activity to be measured directly by testing the compounds/drug candidates for a more specific effect. The ability to inhibit phosphorylation of the E1 subunit by PDK activity intrinsic to the PDC preparation. This assay was used to confirm PDK inhibition in the functional assay. At least one of the concentrations selected for each compound approximated its IC_{50} value determined in the functional assay. The recombinant inner lipoyl domain of the PDC dihydrolipoyl acetyltransferase ($rE2_{L2}$) is a known inhibitor of PDK activity in this assay and is included as a control (Jackson et al. 1998).

The E1 phosphorylation assay is able confirm that apparent PDK inhibition in the functional assay is due to inhibition of E1 phosphorylation. However, this assay suffers from the drawback that the PDK isozyme composition and stoichiometry are undefined. Therefore, a much simpler assay with defined stoichiometry of a synthesized tetradecapeptide (a fragment of the E1 subunit which contains all three of the serines which are phosphorylated by PDK [Yeaman et al. 1978]) can be used. This assay has been modified by Mullinax and coworkers (1985) who demonstrated that this tetradecapeptide is a specific substrate for PDK and the PDH phosphatase. Therefore, this assay is in principle the most amenable to kinetic characterization of inhibitors acting at the active site of PDKs.

REFERENCES AND FURTHER READING

Ashcroft SJH, Weerasinghe LCCC, Bassett JM, Randle PJ (1975) The pentose cycle and insulin release in mouse pancreatic islets. Biochem J 126:525–532

Bersin RM, Stacpoole PW (1997) Dichloroacetae as metabolic therapy for myocardial ischemia and failure. Am Heart J 134:841–855

Clark AS, Mitch WE, Goodman MN, Fagan JM, Goheer MA, Curnow RT (1987) Dichloroacetate inhibits glycolysis and augments insulin-stimulated glycogen synthesis in rat muscle. J Clin Invest 79:588–594

Coore HG, Denton RM, Martin BR, Randle PJ (1971) Regulation of adipose tissue pyruvate dehydrogenase by insulin and other hormones. Biochem J 125:115–127

Fuller SJ, Randle PJ (1984) Reversible phosphorylation of pyruvate dehydrogenase in rat skeletal-muscle mitochondria. Effects of starvation and diabetes. Biochemistry 219:635–646

Gudi R, Bowker-Kinley MM, Kedishvili NY, Zhao Y, Popov KM (1995) Diversity of the pyruvate dehydrogenase kinase gene family in humans. J Biol Chem 270:28989–28994

Jackson JC et al. (1998) Heterologously expressed inner lipoyl domain of dihydrolipoyl acetyltransferase inhibits ATP-dependent inactivation of pyruvate dehydrogenase complex. Identification of important amino acid residues. Biochem J 334:703–711

Jeoung NH, Wu P, Joshi MA, Jaskiewicz J, Bock CB, DePaoli-Roach AA, Harris RA (2006) Role of pyruvate dehydrogenase kinase 4 (PDK4) in glucose homeostasis during starvation. Biochem J

Kelley DE, Mokan M, Mandarino LJ (1992) Intracellular defects in glucose metabolism in obese patients with NIDDM. Diabetes 41:698–706

Linn TC, Pettit FH, Reed LJ (1969) Alpha-keto acid dehydrogenase complexes. X. Regulation of the activity of the pyruvate dehydrogenase complex from beef kidney mitochondria by phosphorylation and dephosphorylation. Proc Natl Acad Sci USA 62:234–241

Lorini M, Ciman M (1962) Hypoglycaemic action of diisopropyl-ammonium salts in experimental diabetes. Biochem Pharmacol 11:823–827

Mullinax TR, Stepp LR, Brown JR, Reed LJ (1985) Synthetic peptide substrates for mammalian pyruvate dehydrogenase kinase and pyruvate dehydrogenase phosphatase. Arch Biochem Biophys 243:655–659

Nakai N, Sato Y, Oshida Y, Fujitsuka N, Yoshimura A, Shimomura Y (1999) Insulin activation of pyruvate dehydrogenase complex is enhanced by exercise training. Metabolism 48:865–869

Orfali KA, Fryer LG, Holness MJ, Sugden MC (1993) Long-term regulation of pyruvate dehydrogenase kinase by high-fat feeding. Experiments *in vivo* and in cultured cardiomyocytes.FEBS Lett 336:501–505

Popov KM, Kedishvili NY, Zhao Y, Shimomura Y, Crabb DW, Harris RA (1993) Primary structure of pyruvate dehydrogenase kinase establishes a new family of eukaryotic protein kinases. J Biol Chem 268:26602–26606

Stacpoole PW, Moore GW, Kornhauser DM (1978) Metabolic-effects of dichloroaceate in patients with diabetes mellitus and hyperlipoproteinemia. New Engl J Med 298:526–530

Wang X, Wang R, Nemcek TA, Cao N, Pan JY, Frevert EU (2004) A self-contained 48-well fatty acid oxidation assay. Assay Drug Develop Technol 2:63–69

Yeaman SJ, Hutcheson ET, Roche TE, Pettit FH, Brown JR, Reed LJ, Watson DC, Dixon GH (1978) Sites of phosphorylation on pyruvate dehydrogenase from bovine kidney and heart. Biochemistry 17:2364–2370

K.6.2.5 Fatty Acid Oxidation

GENERAL CONSIDERATIONS

The development of obesity and the associated insulin resistance results from increases in the ratio of food in-

take to energy expenditure. Loss of body weight can be achieved through a reduction in food intake, a stimulation of energy expenditure, or a combination of both. At the same time, a reduction of fatty acid oxidation has been described in obese and diabetic patients, and the resulting accumulation of fatty acid oxidation has been described in obese and diabetic patients and the resulting accumulation of fatty acids or metabolites of fatty acids in tissues such as skeletal muscle and liver seems to play a direct role in the development of insulin resistance. Recent observations in animal models suggest that a stimulation of fatty acid oxidation reduces the accumulation of fatty acids in tissues and increases overall energy expenditure, leading to lean, insulin-sensitive phenotypes. The modulation of fatty acid oxidation is therefore an attractive new therapeutic strategy for the treatment of obesity and insulin resistance.

Fatty acid oxidation modulated by compounds/drug candidates can be measured with myocytes and hepatocytes by indirect (generation of $^3H_20$) or direct (generation of $^{14}CO_2$) procedures with the advantages of lower expenditure in equipment and handling inherent to the former and higher accuracy and physiological relevance associated with the latter. In any case current assays using cultured cells are cumbersome and of low-throughput. Most published procedures utilizing ^{14}C-labeled lon-chain fatty acid substrates (e. g. palmitate or oleate) are performed in tissue culture flasks, in which a center well captures the radioactive CO_2 product (Angelini et al. 1980, Alam and Saggerson 1998, Kaushik et al. 2001). Alternatively, ^{3}H-labeled fatty acids can be used, but a labor-intensive extraction of ^3H_2O is needed (Ibrahimi et al. 1999). These low-throughput assay methods are not suitable for rapid screening of potential drug candidates. More recently, a variant of the $^{14}CO_2$-capturing method has been introduced by Collins and coworkers (1998) which facilitates the accurate, reproducible and safe throughput measurement of the released of $^{14}CO_2$.

K.6.2.5.1 CO_2 Release

PURPOSE AND RATIONALE

The measurement of fatty acid oxidation using a self-contained 48-well assay has been described by Wang and coworkers (2004). Palmitate is conjugated with essentially fatty acid-free BSA to generate a stock solution of 25% (w/v) BSA and 6 mM fatty acid in serum-free medium. After conjugation with albumin, the concentration of fatty acids in the solution is measured using a NEFA kit (Wako Chemicals, Inc.). The stock solution is diluted into the final culture medium to obtain concentrations of 1 to 1000 µM fatty acid. Palmitate oxidation is measured by the production of $^{14}CO_2$ from [1-^{14}C]palmitic acid.

PROCEDURE

For throughput analysis, the cells are incubated for 1 to 3 h at 37°C in 6- to 24-well culture dishes with medium containing 0.2–1 µCi/ml [1-^{14}C]palmitic acid and nonlabeled palmitate (1–1000 µM), 2.5 mM glucose and 0.8 mM carnitine in the presence or absence of compounds/drug candidates. Each culture dish is sealed using a special technique, for instance by covering with Parafilm, which had a piece of Whatman paper taped facing the inside of the Petri dish. Alternatively and for low-throughput application, the cells can be handled according to the protocol published by Fediuc and coworkers (2006). For this, the L6 myotubes are serum-starved for 4 h before exposure to fatty acids [i]and then incubated for 1 h in 60 × 15 mm culture dishes with medium containing 0.2 µCi/ml [1-^{14}C]palmitic acid (1–10 mM) in the absence or presence of compounds/drug candidates. Each culture dish is sealed with Parafilm, which has a piece of Whatman paper taped facing the inside of the Petri dish. After the incubation, CO_2 generated during this period has to be trapped using a special technique, for instance by wetting the Whatman paper with 100 µl of phenylethylamine/methanol (1/1) and subsequent addition of 200 µl of H_2SO_4 (4 M) to the cells. After additional incubation (1 h, 37°C), the amount of $^{14}CO_2$ is determined by careful removal of the Whatman paper and transfer to scintillation vials for radioactivity counting as described by Ceddia and coworkers (2000, 2004).

Alternatively, cultured hepatocytes or myocytes are grown to confluence in the odd-numbered rows of 48-well plates. For standard assays, the cells are washed with PBS twice and then incubated with 125 µl of KRB buffer supplemented with 5 mM glucose at 37°C for 1 h. After removal of this buffer, 125 µl of reaction mixture in KRB buffer containing 0.2 µCi [1-^{14}C]palmitate (~500,000 cpm) and 0.5% BSA is added to the wells. Palmitate is conjugated with essentially fatty acid-free BSA to generate a stock solution of 25% (w/v) BSA and 6 mM fatty acid in serum-free medium. After conjugation with BSA, the concentration of fatty acids in the solution is measured using a NEFA kit (Wako Chemicals). The reactions are performed in the sealed environment of the device at room temperature for 3 h. The reactions are termi-

nated by injection of 250 µl of 1 M HCl into the cell-containing wells to release CO_2. This injection is performed through the pierceable septum using a syringe. The CO_2 is captured in 250 µl of 1 M NaOH in the adjacent connected well as room temperature overnight. The NaOH solution is removed into a scintillation vial and mixed with 4 ml of OptiPhase (HiSafe 3) scintillation cocktail and counted.

For measurement of fatty acid in isolated hepatocytes in suspension according to the procedure of Chang and coworkers (2006), cells (5×10^5) are incubated for 1 h in buffer containing carnitine, NAD, ATP, cytochrome c, $MgCl_2$, coenzyme A, and [^{14}C]palmitic acid complexed with fatty acid-free BSA. The reaction is stopped with 60% perchloric acid. The released CO_2 is trapped by hyamine hydroxide at the top of a hanging center well and counted for radioactivity in a β-scintillation counter. Fatty acid oxidation is calculated as percentage of the maximal value obtained by stimulation of the cells with epinephrine (1 µg/ml).

For measurement of fatty oxidation in native liver tissues according to the procedure introduced by Wu and coworkers (2006), liver slices (0.5 mm thick) are prepared using a tissue slicer and placed in 25-ml Erlenmeyer center-well flasks with 2 ml KRP buffer. [^{14}C]oleic acid bound to fatty acid-free BSA in KRP buffer is added to a final concentration of 0.5 mM and equilibrated for 30 s with a humidified 95% O_2/5% CO_2 gas mix. Flasks are then capped with a rubber stopper containing a centered well enclosing a loosely folded filter paper moistened with 0.2 ml of 1 N NaOH solution. After incubation for 4 h at 37°C, the reaction is stopped by injecting 0.2 ml of H_2SO_4 (1 M). The radioactivity trapped in the filter paper is determined by scintillation counting.

To improve the throughput, a device that accommodates four 48-well culture dishes in a single unit has been designed (Collins et al. 1998). Two adjacent wells form a single experimental unit by means of a coneting chamber, which is sealed from other experimental units and from the outside environment to prevent the release of radioactive material. In this design, obne well of the experimental unit contains the cells and ^{14}C-labeled fatt acid. The [^{14}C]CO_2 produced by β-oxidation of the fatty acids is then released from the culture medium upon addition of HCl and is subsequently captured in the adjacent NaOH-containing well. The data published demonstrate that the use of this device, which has a simple desing and is easy to use, allows highly reproducible evaluation of long-chain fatty acid oxidation in cultured cells with low variability, can be used with a variety of substrates, such as long- and medium-chain fatty acids, and cell lines, such as HepG2, primary rat hepatocytes and HEK293, and unlike previously reported center-well capture methods for β-oxidation assays, can be run in medium-throughput making it suitable for compound characterization and drug discovery. The ability to use primary hepatocytes opens the possibility to evaluate cells after exposure to drugs *in vivo*.

K.6.2.5.2 Release of Acid-Soluble Metabolites (ASM)

PROCEDURE

Determination of fatty acid oxidation as the release of ASM, which predominantly consist of tritiated water and ketone bodies, follows the proccdure described by Moon and Rhead (1987) with modifications introduced by Minnich and coworkers (2001). The reaction mixture is prepared by complete evaporation of the solvent from [9,10-^{3}H]palmitic acid with a 5% CO_2/95% air stream. The [^{3}H]palmitate is resuspended in Hanks' basic salt solution (HBSS) containing 10 mg/ml BSA and brought to a final concentration of 22 µM [^{3}H]palmitate and 0.5 mg/ml BSA with HBSS. 0.2 ml of this mixture is applied to the wells of 24-well culture dishes containing HepG2 cells or L6 myotubes rinsed twice with 1.5 ml of Dulbecco's PBS. Blanks are prepared by applying 0.1 ml methanol for 30 s. After incubation (2 h, 37°C) in humidified 5% CO_2/95% air, the reaction mixture is removed and added to a centrifuge tube containing 0.2 ml of 10% TCA. Each well is rinsed with 0.1 ml of Dulbecco's PBS, which is added to the tube. After 2 min at room temperature, the reaction mixture is centrifuged ($8{,}500 \times g$, 5 min). The supernatants are immediately removed, then supplemented with 70 µl of 6 N NaOH and loaded onto a 1-ml Dowex-1 column in a pasteur pipette. Columns are rinsed with 1 ml of distilled water. The eluate is collected in a scintillation vial containing 10 ml of scintillation cocktail and then counted for radioactivity.

Alternatively, for bypassing the removal of non-oxidized fatty acids by column adsorption, the ASM can be measured directly by transfer of the cells to plastic tubes according to the protocol introduced by Aas and coworkers (2004). The flasks are rinsed with 1.5 ml of perchloric acid (1 M) that is subsequently added to the same plastic tube. The tubes are then centrifuged ($1{,}800 \times g$, 10 min) and 1.0 ml of the supernatant is counted by liquid scintillation. ASM are also measured in the growth media of cells grown on 6-well plates that had been incubated with [1-^{14}C]oleic

acid and [1-^{14}C]palmitic acid. A 250-µl aliquot of the cell medium is precipitated with 100 µl of 6% BSA and 1.0 ml of 1 M perchloric acid. After centrifugation (1,800 × *g*, 2 min), 500 µl of the supernatant is counted by liquid scintillation. No-cell controls have to be included.

EVALUATION

The sensitivity of this assay critically depends on the substrate concentration, cell density, BSA concentration and incubation time. Though the concentration of [^{3}H]palmitate employed routinely (22 µM) is not fully saturating, less than 2% of the substrate is converted to ^3H_2O by L6 myotubes. The [^{3}H]palmitate concentration is thus virtually constant throughout the incubation period. ^3H_2O formation is linear to up to ~60 µg of cell protein per well, at which point the response levels off, and to up to 4 h of incubation. Optimal activity is typically observed in HBSS containing 0.5 mg/ml fatty acid-free BSA in comparison to other media (e. g. MEM). In conclusion, the ^3H_2O release assay combines the advantages of relatively low requirements of cells, radiolabeled substrate and assay time.

ASM, a measure of ketone bodies in the liver and of tricarboxylic-acid-cycle intermediates and acetyl esters in muscle, are assayed in supernatants of the acid precipitate. In myocytes, ASM routinely accounts for over 90% of total oxidation products. Minimal increases in ^{14}C-radioactivity over background levels occur in media in which myocytes have been incubated, indicating that insignificant amounts (< 15% of the counts recovered as CO_2) of ASM are released into the medium.

REFERENCES AND FURTHER READING

Alam N, Saggerson ED (1998) Malonyl-CoA and the regulation of fatty acid oxidation in soleus muscle. Biochem J 334:233–241

Angelini C, Philippart M, Borrone C, Bresolin N, Cantini M, Lucke S (1980) Multisystem triglyceride storage disorder with impaired long-chain fatty acid oxidation. Ann Neurol 7:5–10

Aas V, Kase ET, Solberg R, Jensen J, Rustan AC (2004) Chronic hyperglycaemia promotes lipogenesis and triacylglycerol accumulation in human skeletal muscle cells. Diabetologia 47:1452–1461

Ceddia RB, Sweeney G (2004) Creatine supplementation increases glucose oxidation and AMPK phosphorylation and reduces lactate production in L6 rat skeletal muscle cells. J Physiol 555:409–421

Ceddia RB, William WN, Lima FB, Flandin P, Curi R, Giacobino JP (2000) Leptin stimulates uncoupling protein-2 mRNA expression and Krebs cycle activity and inhibits lipid synthesis in isolated rat white adipocytes. Eur J Biochem 267:5952–5958

Chang BH-J, Li L, Paul A, Taniguchi S, Nannegari V, Heird WC, Chan L (2006) Protection against fatty liver but normal adipogenesis in mice lacking adipose differentiation-related protein. Mol Cell Biol 26:1063–1076

Collins CL, Bode BP, Souba WW, Abcouwer SF (1998) Multiwell $^{14}CO_2$-capture assay for evaluation of substrate oxidation rates of cells in culture. BioTechniques 24:803–808

Fediuc S, Gaidhu MP, Ceddia RB (2006) Regulation of AMP-activated protein kinase and acetyl-CoA carboxylase phosphorylation by palmitate in skeletal muscle cells. J Lipid Res 47:412–420

Ibrahimi A, Bonen A, Blinn WD, Hajri T, Li X, Zhong K, Cameron R, Abumrad NA (1999) Muscle-specific overexpression of FAT/CD36 enhances fatty acid oxidation by contracting muscle, reduces plasma triglycerides and fatty acids, and increases plasma glucose and insulin. J Biol Chem 274:26761–26766

Kaushik VK, Young ME, Dean DJ, Kurowski TG, Saha AK, Ruderman NB (2001) Regulation of fatty acid oxidation and glucose metabolism in rat soleus muscle: effects of AICAR. Am J Physiol Endocrinol Metab 281:E335-E340

Minnich A, Tian N, Byan L, Bilder G (2001) A potent PPARα agonist stimulates mitochondrial fatty acid β-oxidation in liver and skeletal muscle. Am J Physiol Endocrinol Metab 280:E270-E279

Moon A, Rhead WJ (1987) Complementation analysis of fatty acid oxidation disorders. J Clin Invest 79:59–64

Wang X, Wang R, Nemcek TA, Cao N, Pan JY, Frevert EU (2004) A self-contained 48-well fatty acid oxidation assay. Assay Drug Develop Technol 2:63–69

Wu Q, Ortegon AM, Tsang B, Doege H, Feingold KR, Stahl A (2006) FATP1 is an insulin-sensitive fatty acid transporter involved in diet-induced obesity. Mol Cell Biol 26:3455–3467

K.6.2.6 Carnitine Palmitoyltransferase I (CPTI) Activity

PURPOSE AND RATIONALE

Carnitine palmitoyltransferase I (CPT I) which mediates the uptake of long-chain fatty acids into mitochondria, is the rate-limiting enzyme for mitochondrial fatty acid oxidation in mammalian cells. Pharmacological inhibition of CPT I in course of an increase in its physiological negative regulator, malonyl-CoA, as consequence of the inhibition of fatty acid synthase by a natural small molecule (C75) has been demonstrated to lead to appetite suppression. This apparent anti-obesity therapeutic action is presumably based on an alteration in the metabolism of neurons in the hypothalamus, where an increase in malonyl-CoA serves as a secondary messenger of the nutrient status, thereby mediating satiety (Loftus et al. 2000, Hu et al. 2003). In addition, in peripheral tissues (Thupari et al. 2002), C75 has been postulated not only to increase the level of malonyl-CoA but also to act as a malonyl-CoA analog that antagonizes the inhibitory effect on CPT I (McGarry and Brown 1997). Both its central and the peripheral actions could reduce weight in lean and fat mice. Furthermore, both direct activation and direct inhibition of CPT I and the resulting increased

and decreased fatty acid oxidation, respectively, have been implicated as putative target for the improvement of impaired insulin signaling and glucose metabolism in muscle and liver cells in course of reduced lipid accumulation (i. e. reduced lipotoxicity, see K.6.3.2) and of enhanced glucose oxidation according to the inverse relationship between glucose and fatty acid oxidation (i. e. Randle cycle), respectively.

Mammalian tissues express three isoforms of CPT I, liver (L-CPT I), muscle (M-CPT I) (McGarry and Brown, 1997), and brain (CPT I-C) (Price et al. 2002). The liver and muscle isoforms are tightly regulated by their physiological inhibitor malonyl-CoA, which allows CPT I to signal the availability of lipid and carbohydrate fuels to the cell. The malonyl-CoA sensitivity of L-CPT I in the adult rat depends on the physiological state. It is increased by renewed feeding of carbohydrates to fasted rats, by obesity, or following administration of insulin to diabetic rats, whereas it is decreased by starvation and diabetes (Grantham and Zammit 1986, 1988). CPT I activity can be measured with mitochondria from cultured cells and tissues.

PROCEDURE

Preparation of Mitochondrial Fractions

Mitochondria-enriched cell fractions from various cell types (INS, L6 myotubes, HEK293 cells) cultured in 15-cm dishes are obtained with a glass homogenizer as described by Rubi and coworkers (2002). The pellet, in which the mitochondria remain largely intact, is used directly for CPT I activity assays. Mitochondria-enriched fractions are obtained from rat and mouse muscle according to published procedures (Saggerson and Carpenter 1981) with minor modifications. Two soleus muscle samples of each animal are homogenized separately in 250 mM sucrose buffer using an omni-mixer and then centrifuged (1,000 × *g*, 15 min). The pellet is homogenized and centrifuged (600 × *g*, 10 min). The resulting supernatant is centrifuged (15,000 × *g*, 15 min) and the pellet is resuspended in 100 µl of a buffer containing 250 mM sucrose and 150 mM KCl. Mitochondria-enriched fractions from rat and mouse liver are obtained by homogenization in a buffer containing 250 mM sucrose, 1 mM EDTA, and 10 mM Tris-HCl (pH 7.4). The liver suspension is centrifuged (560 × *g*, 15 min), and the supernatant is further centrifuged (12,000 × *g*, 20 min). The pellet is resuspended in 2 mL of homogenization buffer, centrifuged (7,000 × *g*, 10 min), washed and resuspended in 1 ml of the homogenization buffer. To obtain mitochondria-enriched fractions from mice pancreas, tissue is homogenized in a buffer containing 250 mM sucrose, 20 mM Tris-HCl (pH 7.4), 0.5 mM EDTA, 0.5 mM EGTA, 1 mM DTT, 10 µg/ml leupeptin, 4 µg/ml aprotinin, 2 µg/ml pepstatin, and 100 µM PMSF. The homogenate is subjected to differential centrifugation (900 × *g*, 10 min and 5,500 × *g*, 10 min). The pellet is resuspended with a Dounce homogenizer and centrifuged (2,000 × *g*, 2 min and 4,000 × *g*, 8 min). Finally, the pellet is resuspended in 250 µl of 250 mM sucrose (Li et al. 1996). All the processes are performed at 4°C, and fractions are assayed immediately for CPT I activity.

Determination of CPT I Activity

CPT I activity is measured in mitochondria-enriched fractions obtained from cultured cells or tissues. CPT I activity in 10–15 µg of mitochondria-enriched cell fractions, or 20 µg of mitochondrial fractions from tissues is determined by the radiometric method as described by Morillas and coworkers (2001). Extracts are pre-incubated at 30°C for different times in the presence or absence of compounds/drug candidates. Enzyme activity is assayed for 4 min at 30°C in a total volume of 200 µl. The substrates are 50 µM palmitoyl-CoA and 400 or 1000 µM L-[*methyl*-^{3}H]carnitine for L- and M-CPT I isoforms, respectively. In tissues and cell culture extracts, both CPT I (malonyl-CoA-sensitive) and CPT II (insensitive to malonyl-CoA) are present. Thus, in these fractions, CPT I activity is determined as the malonyl-CoA/etomoxiryl-CoA-sensitive CPT activity. CPT II activity, which is also present in mammalian mitochondrial extracts, is always subtracted from the total activity to calculate specific CPT I activity. The presence of CPT activity insensitive to malonyl-CoA (CPT II activity) in mitochondria obtained from cell cultures is typically less than 5% and thus is not taken into consideration. Compounds/drug candidates are pre-incubated with the enzyme for 1–5 min depending on the assay. Compound/drug candidate concentrations ranging from 0.01 to 50 µM are used to estimate the IC_{50} value. Malonyl-CoA (50 µM) is used for malonyl-CoA inhibition assays. In all cases, the molar ratio of palmitoyl-CoA to BSA is kept at 5:1 to avoid the presence of free acyl-CoA and its deleterious detergent effects and to prevent the formation of micelles. Kinetic constants (K_m and V_{max}) are determined by Lineweaver-Burk analysis. Inhibition constants (K_I and k_{inact}) are determined at 20 µM palmitoyl-CoA by nonlinear parameter estimation (Maurer and Fung 2000) using SigmaPlot version 8.0. All protein concentrations are determined using the Bio-Rad protein assay with BSA as a standard.

Binding of Compounds/Drugs to CPT I

The binding of compounds/drugs to CPT I is assessed as described by Tutwiler and Ryzlak (1980) with some modifications. Mitochondria-enriched fractions are pre-incubated for 5 min at 30°C with compounds/drugs at 50 µM. One aliquot is used directly for the CPT I activity assay (unwashed), and the other aliquot is centrifuged (13,000 × *g*, 5 min, 4°C) and resuspended (washed) in 5 mM Tris-HCl (pH 7.2), 150 mM KCl, 2 µg/ml leupeptine, 0.5 µM benzamidine, 1 µg/ml pepstatin, and 1 mM PMSF before the activity assay.

To verify the reversibility of the interaction of compounds/drug candidates with CPT I, dialysis assays are performed. Mitochondria-enriched fractions (160 µg) are pre-incubated at 30°C for 5 min (without the compound/drug) or with a final concentration of 50 µM compound and then dialyzed in buffer containing 10 mM HEPES (pH 7.4), 1 mM EDTA, and 10% glycerol at 4°C. Aliquots are taken before dialysis (0 h), and 24 and 36 h thereafter, and assayed for CPT I activity. This method has been used by Bentebibel and coworkers (2006) to demonstrate novel effects of C75 on CPI I activity and palmitate oxidation.

K.6.2.7 Respiratory Quotient (RQ)

Respiratory quotient changes during variable periods of fasting of rodents are monitored at 24°C ambient temperature in an open respirometric system. Individual O_2-consumption and CO_2-production are recorded every 5 min at a flow rate of ~40 l/h. RQ equals volumes of CO_2 released/volumes of O_2 consumed. During the 18-h measurement period mice are maintained in metabolic cuvettes (5 l9, which contained bedding material (~50 g) and provided access to water *ad libitum*. In each trial, typically 4 mice are investigated. Before and after the experiment, mice are weighed and body temperature are recorded by inserting a rectal probe.

K.6.2.8 Phosphoryation of Acetyl-CoA Carboxylase (ACC) and AMP-Dependent Protein Kinase (AMPK)

PURPOSE AND RATIONALE

In recent years, a large body of evidence has been published showing that in mammals AMP-activated protein kinase (AMPK) responds to hormonal and nutrient signals in the central nervous system and peripheral tissues, modulating food intake and whole-body energy homeostasis (for a review see Carling 2005). AMPK is a heterotrimeric enzyme that has been proposed to function as a "fuel gauge" that monitors changes in the energy status of cells. When activated, AMPK shuts down anabolic pathways and promotes catabolism in response to an increase in the AMP/ATP ratio by downregulating the activity of key enzymes of intermediary metabolism. In its activated state, AMPK phosphorylates serine residues 79, 1,200, and 1,215 of acetyl-coenzyme A carboxylase (ACC), producing an 80–90% decrease in the V_{max} of the enzyme, suggesting that AMPK is the physiological ACC kinase. There is also evidence that long-chain fatty acids (LCFAs) act as potent feedback suppressors of lipogenesis by inhibiting ACC activity. ACC is a multifunctional enzyme that, when active (dephosphorylated form), catalyzes the conversion of acetyl-CoA to malonyl-CoA in the *de novo* lipid synthesis pathway. Malonyl-CoA is a potent inhibitor of CPT I) a rate-limiting step for the entry of LCFAs into mitochondria for oxidation (see above). When ACC is inactive (phosphorylated form), a decrease in malonyl-CoA occurs and disinhibits CPT I, thereby increasing the mitochondrial import and oxidation of LCFAs (for reviews see McGarry and Brown 1997, Carling 2005). Therefore, the AMPK/ACC system is thought to play a central role in the regulation of cellular lipid homeostasis (Spiegelman and Flier 2001). In certain metabolic disorders, such as obesity and type II diabetes, lipid metabolism is dysfunctional, causing fatty acids to increase in the circulation and also in intracellular compartments. High levels of fatty acids are toxic to the cells and may cause deleterious metabolic abnormalities (lipotoxicity). By increasing fatty acid oxidation in peripheral tissues, the AMPK/ACC system may play an important role by protecting the cells from these metabolic abnormalities. Of special interest are the mechanisms that regulate the AMPK/ACC system in skeletal muscle, because this tissue plays a major role in determining whole-body energy expenditure, accounts for 70% of total-body glucose disposal, and may modify substrate utilization toward substantially increasing fatty acid oxidation.

The classical view is that AMPK is activated allosterically by an increase in the intracellular AMP/ATP ratio, by phosphorylation of threonine 172 (Thr-172) within the α-subunit, catalyzed by the upstream kinase LKB1 (the upstream kinase of AMPK), and by inhibition of the dephosphorylation of Thr-172 by protein phosphatases. To date, a wide range of physiological stressors, pharmacological agents, and hormones associated with increases in the intracellular

AMP/ATP ratio have been demonstrated to activate AMPK (Corton et al. 1994, for a review see Carling 2005). Fatty acids, another major cellular energy source, may also regulate AMPK activity in skeletal muscle. It has been reported that in perfused rat cardiac muscle, palmitate and oleate significantly increases AMPK activity without causing any significant alteration in AMP/ATP ratio. Another study has reported that exposure to acetate, octanoate, or palmitate causes a significant reduction in AMP/ATP ratio followed by a significant increase in AMPK activity in primary rat hepatocytes (for reviews see Kemp et al. 1999, Ruderman et al. 1999). In contrast to these observations are reports that the AMPK activity of rat liver purified LKB1/STRAD/MOM25 (the upstream kinase complex of AMPK) was inhibited by long-chain acyl-CoA esters *in vitro* (Lizano et al. 2004, Hawley et al. 2003, Boudeau et al. 2003). Consequently, AMPK and ACC represent important targets for future anti-diabetic and anti-obesity therapy *via* activation of fatty acid oxidation in course of activation of the former and inhibition of the latter. The identification of activators of AMPK or inhibitors of ACC, which act directly at the enzyme level or affect the regulation of the enzymes (i. e. induce their phosphorylation) requires reliable cell-based assay systems for measurement of the activity and phosphorylation state of AMPK and ACC in cultured muscle and liver cells and tissues.

Procedure

Cells are grown on six-well plates and incubated for 60 min in the presence or absence of palmitic acid (1–10 µM). AICAR, a synthetic nucleotide precursor taken up by the cells and phosphorylated to the monophosphate form ZMP, which can accumulate in the cell, mimicks the effect of AMP on AMPK phosphorylation and activation. Therefore, incubation with AICAR (2 mM, 60 min) is used as a positive control for AMPK and ACC phosphorylation in L6 myotubes. Because ACC is a substrate for AMPK, the determination of ACC phosphorylation also serves as an indicator of AMPK activity. Immediately after all treatments, cells are lysed in buffer containing 135 mM NaCl, 1 mM $MgCl_2$, 2.7 mM KCl, 20 mM Tris/HCl (pH 8.0), 1% Triton X-100, 10% glycerol, and protease and phosphatase inhibitors (0.5 mM Na_3VO_4, 10 mM NaF, 1 µM leupeptin, 1 µM pepstatin, 1 µM okadaic acid, and 0.2 mM PMSF), heated (65°C, 5 min), and passed five times through a 25 gauge syringe. An aliquot of the cell lysates is used to determine the protein concentration in each sample by the Bradford method. Before loading onto SDS-PAGE gels, the samples are diluted 1:1 with 2 × Laemmli sample buffer (62.5 mM Tris/HCl, pH 6.8, 2% SDS, 50 mM DTT, and 0.01% bromophenol blue). Aliquots of cell lysates containing 30 µg of protein are subjected to SDS-PAGE (12% and 7.5% resolving gels for P-AMPK and P-ACC, respectively) and then transferred to polyvinylidene difluoride membranes (Bio-Rad Laboratories). The phosphorylation of AMPK is determined using phospho-AMPK(Thr172) antibody (1:1,000 dilution), which detects AMPK-α only when activated by phosphorylation at Thr-172 (Cell Signaling Technology). ACC phosphorylation is detected using phospho-ACC-specific antibody (1:500 dilution; Upstate Biotechnology), which recognizes ACC when phosphorylated at serine 79 (Ser-79). Equal loading of samples is also confirmed by Coomassie blue staining of all gels.

K.6.2.9 AMPK Activity

Regulating energy levels is a fundamental process in every living organism. At a cellular level ATP must be maintained at relatively high levels (normally about 10-fold above the concentration of ADP) in order to drive essential metabolic processes. At a whole body level, maintaining a balance between energy supply and energy demand is also crucial. Within the Western world the consequences of failing to regulate energy metabolism is ever more obvious as demonstrated by the huge increase in the prevalence of metabolic disorders, such as obesity and type II diabetes (Jonsson 2002). One system that is emerging as a key player in the overall regulation of energy balance is the AMP-activated protein kinase (AMPK) cascade. AMPK is activated in response to ATP depletion (Hardie et al. 1998, Hardie et al. 2003, Carling 2004 and 2005), which causes a concomitant increase in the AMP:ATP ratio (Corton et al. 1994). Once activated AMPK phosphorylates a number of downstream substrates, the overall effect of which is to switch-off ATP utilising pathways, e. g. fatty acid synthesis, and switch-on ATP-generating pathways e. g. fatty acid oxidation (Hardie et al. 1998, Kemp et al. 1999). In addition to the acute effects of AMPK, activation of AMPK has longer-term effects, altering both gene expression (Foretz et al. 1998) and protein expression (Winder et al. 2000). Although the physiological consequence of these longer-term effects of AMPK are not fully understood, it seems likely that they are involved in the overall regulation of energy metabolism.

AMPK is activated allosterically by AMP and by phosphorylation. AMPK is phosphorylated on T172 which lies within the activation loop of the kinase catalytic domain, a region where many protein kinases require phosphorylation for their activation (Johnson et al. 1996). Phosphorylation of T172 is catalysed by an upstream kinase, the molecular identity of which remained elusive until very recently. Through advances made in the investigation of the regulation by upstream kinases of SNF1, the yeast counterpart of AMPK, the identity of the upstream kinase appears finally to have been revealed. Three closely related yeast kinases, Elm1, Pak1 and Tos3 have been identified that phosphorylate and activate SNF1 *in vitro* (Hong et al. 2003, Sutherland et al. 2003). The amino acid sequences of the catalytic domains of Elm1, Pak1 and Tos3 are most closely related to members of the mammalian Ca^{2+}/calmodulin dependent protein kinase kinase (CAMKK) subgroup. Another kinase sharing significant amino acid sequence identity with the three yeast kinases was LKB1 (also known as STK11). Recent studies have shown that LKB1 phosphorylates and activates a number of AMPK-related kinases (Lizcano et al. 2004), and although the physiological role of these kinases is largely unknown, it is possible that some of the tumor suppressor functions of LKB1 are mediated via these kinases rather than AMPK itself. The finding that LKB1 lies upstream of AMPK, however, does provides the intriguing possibility that there may be a link between metabolic regulation and cell proliferation, mediated by AMPK (Carling 2005). The following assays enable the measurement of AMPK activity as a consequence of appropriate phosphorylation/dephosphorylation by upstream kinases or by direct activation/inhibition by compounds/drug candidates which may be helpful for future anti-diabetic and anti-obesity therapy, respectively.

K.6.2.9.1 Measurement with Recombinant AMPK

PURPOSE AND RATIONALE

For analysis of direct effects of compounds/drug candidates on the activity of AMPK, the enzyme has to be purified (e. g. from rat liver, isoform mixture) or heterogeneously expressed (e. g. in E. coli or insect cells, specific isoforms) and subjected to kinase assay in the presence of the agents. These test systems may be used for the identification and characterization of activators or inhibitors for AMPK, which both might helpful for future therapy of diabetes and obesity, respectively.

PROCEDURE

Expression of Recombinant AMPK

A new polycistronic bacterial expression system has been introduced by Neumann and coworkers (2003), which yields milligram amounts of heterotrimeric and functional AMPK. For this, the cDNA sequences encoding the subunits of AMPK (GenBank Accession Nos. X95578, X95577, and U40819) are subcloned by PCR and inserted into individual pET-plasmids (*Nde*I/*Spe*I sites of pET3-ax, γ1-subunit, resulting in pγ1; *Nco*I/*Spe*I sites of pET-3dx, β1-subunit, resulting in pβ1; *Nco*I/*Spe*I sites of pET14dx, α1-subunit, resulting in pHis-α1r), harboring an ampicillin resistance gene (ampR). Successive restriction and ligation of individual cistrons to the acceptor vector pγ1 lead to a polycistronic gene consisting of a promoter, ribosome-binding sites (RBS), the sequences of γ-, β-, and His-tagged α-subunits of AMPK, as well as a transcriptional terminator.

Purification of Recombinant AMPK

The tricistronic plasmid pγ1β1His-α1 is transformed into competent host cells (*E. coli* BL21-CodonPlus (DE3)-RIL) and incubated overnight at 37°C on LB agar containing 150 µg/ml ampicillin and 25 µg/ml chloramphenicol. Resuspended cells are used to inoculate LB medium containing appropriate antibiotics. Cultures are grown in a shaker incubator at 37°C. Protein expression is induced with 0.4 mM isopropyl β-D-thiogalactopyranoside final concentration at an O.D. (600 nm) of 0.6 and cultures were grown for additional 4 h. Cells are harvested, washed twice with 0.9% NaCl, resuspended in lysis buffer (15% sucrose, 50 mM sodium phosphate, pH 8.0, 50 mM NaCl, 10 mM imidazole and 1 mM β-mercaptoethanol), and sonicated on ice in a Branson 250 sonifier (50% duty, output 5, 2 min, three times). Insoluble material is removed by centrifugation and the supernatant is loaded onto Ni–NTA agarose (Qiagen). After washing (three column volumes with lysis buffer, 20 mM imidazole) and elution (lysis buffer, containing 250 mM imidazole), the protein is stored at −20°C until use.

Gel filtration Chromatography

For confirmation of complex formation of AMPK holoenzyme, the size of purified AMPK in solution is determined by gel filtration chromatography with a Superose 12 HR 10/30 column (Amersham-Pharmacia) connected to HPLC. Minor non-protein contaminants in Ni^{2+}-purified AMPK are removed by batch affinity purification with Blue Sepharose (Amersham-Pharmacia), using elution with 50 mM sodium phos-

phate (pH 8.5), 1 M NaCl, 50 mM AMP, and 1 mM β-mercaptoethanol. One hundred micrograms of protein is then separated in 25 mM sodium phosphate (pH 7.0), 200 mM NaCl, and 1 mM β-mercaptoethanol at a flow rate of 0.75 ml/min and a temperature of 22°C. The column is calibrated for Stokes radii with the following marker proteins: carbonic anhydrase (24.0 Å, 29 kDa), albumin (35.5 Å, 67 kDa), aldolase (48.1 Å, 158 kDa), catalase (52.2 Å, 232 kDa), ferritin (61 Å, 440 kDa), and thyroglobulin (70.0 Å, 669 kDa).

Alternatively, partially purified AMPK holoenzyme from rat liver (up to the blue-Sepharose step according to the protocol of Carling and coworkers [1989] can be used instead of the recombinant version. It is usually obtained in a partially phosphorylated state and therefore does not require the activation step by exogenous upstream kinases, such as LKB1.

Phosphorylation/Activation In Vitro

Ni^{2+}-purified recombinant AMPK is activated with a partially purified preparation of AMPKK (purified up to the Q-Sepharose step (Hawley et al. 1996), with the exception that NaF and sodium pyrophosphate are omitted from the buffers) in the presence of 100 µM ATP, 5 mM $MgCl_2$, and 1 mM DTT in 50 mM HEPES (pH 7.4), for 30 min at 37°C in a thermostated shaker. Samples are then diluted in HEPES assay buffer (50 mM HEPES, pH 7.4, 1 mM EDTA, 10% glycerol, 50 mM NaF, 5 mM sodium pyrophosphate, and 1 mM DTT) and assayed for AMPK activity. For labelling of AMPK with [^{32}P]ATP, Ni^{2+}-purified recombinant AMPK is incubated in the presence or absence of AMPKK (Q-Sepharose pure) in the presence of 100 µM [γ-^{32}P]ATP (approx. 400 cpm/pmol), 100 µM AMP, 5 mM $MgCl_2$, and 1 mM DTT for 30 min at 37°C in a thermostated shaker. After dilution, AMPK is repurified on NTA–Nickel magnetic agarose beads (Qiagen, Basel) before adding SDS sample buffer and running on 12% acrylamide SDS gels. Radiolabeled AMPK is visualized by autoradiography or phosphorimaging.

Alternatively, for phospho-AMPK (Thr172) detection, the 35%-ammonium sulfate precipitate from treated myotubes or hepatocytes can be used for immunoblotting with polyclonal antibodies to AMPK phosphorylated at Thr172 (Cell Signaling Technology, USA) according to the protocoll of Zhou and coworkers (2001).

Radioactive Assay Method

The radioactive AMPK filter assay with [γ-^{33}P]ATP and a consensus substrate, the so-called SAMS peptide (HMRSAMSGLHLVKRR) (Dale et al. 1995) is conducted as described by Zhou and coworkers (2001) and Davies and coworkers (1989). The 100-µl reaction mixture contained 100 µM AMP, 100 µM ATP (0.5 µCi ^{33}P-ATP per reaction), and 50 µM SAMS in a buffer (40 mM HEPES, pH 7.0, 80 mM NaCl, 0.8 mM EDTA, 5 mM $MgCl_2$, 0.025% BSA, and 0.8 mM DTT). The reaction is initiated with addition of the enzyme. After 30-minute incubation at 30°C, the reaction is stopped by addition of 80 µl 1% H_3PO_4. Aliquots (100 µl) are transferred to 96-well MultiScreen plates (MAPHNOB50; Millipore Corp., USA). The plate is washed three times with 1% H_3PO_4 followed by radioactivity detection in a microtiter plate TopCount apparatus.

AlphaScreenAssay Method

The enzymatic reactions for the Alphascreen are carried out according to Li and coworkers (2003) in white round-bottomed 96-well plates (Packard). Each reaction mixture contained (in a total volume of 0.015 ml) ACC-CREBp (100 nM), ATP (200 µM), buffer A (50 mM HEPES, pH 7.0, 100 mM NaCl, 0.01% BSA (w/v), 5 mM $MgCl_2$, 0.8 mM DTTl), and AMPK (0.74 mU, 1 mU = 1 pmol phosphate incorporated into 200 µM SAMS per min at 30°C in the radioactive filter assay). The reaction is initiated by the addition of the enzyme. Incubation is at 30°C for 30 min. The reaction is terminated by the addition of the detection mixture which contained donor and acceptor beads (40 µg/ml each), Anti-pS^{133}-CREB antibody (4 nM), and EDTA (16 mM) in buffer A (0.015 ml) without $MgCl_2$. The plate is read on an ALPHAQuest instrument (Packard Biosignal) after incubation at room temperature in the dark for 2–24 h.

HTRF Assay Method

The enzymatic reactions for HTRF are identical to those for the Alphascreen but are carried out in black round-bottomed 96-well Optiplates (Packard) as described by Li and coworkers (2003). The reaction is terminated by the addition of detection mixture (0.035 ml) which contained SA-XL665 (14 nM), LANCE Eu-W1024-labeled Anti-pS^{133}-CREB antibody (140 pM), and EDTA (3 mM) in buffer A without $MgCl_2$. The plate is incubated for 1 h at room temperature followed by determination of fluorescence with a Discovery instrument (Packard). The 620- and 665-nm fluorescence signals are counted simultaneously and the ratio (665 nm/620 nm × 10,000) is recorded for each well.

EVALUATION

Inhibition

The *in vitro* AMPK inhibition data are fit to the following equation for competitive inhibition by non-linear regression using a least-squares Marquardt algorithm in a computer program: $V_i/V_o = (K_m + S)/[S + K_m \times (1 + I/K_i)]$, where V_i is the inhibited velocity, V_o is the initial velocity, S is the substrate (ATP) concentration, K_m is the Michaelis constant for ATP, I is the inhibitor concentration, and K_i is the dissociation constant for the inhibitor. For determination of K_m, AMPK is assayed at varying concentrations of SAMS peptide in the presence of 200 µM AMP. Kinetic analysis is performed using Graphpad Prism software as has been introduced for AMPK analysis by Stein and coworkers (2000).

Activation

The availability of ultrafast, ultrasensitive, and robust assays suited to high-throughput screening is key to obtaining small-molecule AMPK activators. In the absence of high-affinity and selective anti-phospho Ser/Thr antibodies for AMPK substrates, two homogeneous AMPK assays have been developed with the commercially available antibody Anti-pS^{133}-CREB and an engineered peptide ACC-CREBp. Anti-pS^{133}-CREB antibody was raised against the phospho-CREB peptide derived from cAMP response element binding protein (CREB). ACC-CREBp is a variant (Arg to Pro) of ACC-CREB, a hybrid peptide consisting of a 9-amino-acid peptide from rat ACC, CREB peptide, and the addition of two hydrophobic Leu residues. ACC-CREBp shows increased suitability as a substrate for AMPK, eliminates phosphorylation by PKA, and preserves antibody binding. The homogeneous time-resolved fluorescence and AlphaScreen AMPK assays are developed using both Anti-pS^{133}-CREB antibody and ACC-CREBp that are either labeled with a fluorescent probe or linked to a photoactivated bead, respectively. Very similar biphasic ATP titration curves are generated by both the filter assay and the AlphaScreen. The inhibitory effect observed at higher ATP concentrations most likely results from ATP competing with AMP binding at the allosteric site. Consistent with this hypothesis, an increase in the AMP concentration (from 30 to 200 µM) shifted the curves to the right, suggesting that more ATP is required to compete with AMP. Nearly identical AMP titration curves are generated by the filter assay and the AlphaScreen.

A small molecule AMPK activator of the thienopyridone class has been identified in a high-throughput screening effort (Anderson et al. 2004, Cool et al. 2006), which directly stimulates partially purified rat liver and recombinant human AMPK ($EC_{50} \sim 1$ µM) and inhibits fatty acid synthesis in primary rat hepatocytes ($IC_{50} \sim 3$ µM) and is lower plasma glucose in ob/ob mice. These results demonstrate that small molecule-mediated activation of AMPK *in vivo* is feasible and represents a promising approach for the treatment of type II diabetes.

K.6.2.9.2 Immunecomplex Kinase Assay

PURPOSE AND RATIONALE

For analysis of the AMPK activity and its regulation *ex vivo* in (muscle and liver) tissues or cells upon treatment of rodents or cultured cells with putative AMPK modulators, AMPK is immunoprecipitated from total cell or tissue homogenates and then subjected to immunecomplex kinase assay using a consensus substrate peptide.

PROCEDURE

Cultured myotubes or hepatocytes, incubated with AICAR or compounds/drug candidates in KRH containing 20 mM glucose for 15 min at 37°C, or alternatively, muscle and liver tissues from rodents, treated with compounds/drug candidates, are homogenized by direct addition of an equivalent volume of ice-cold homogenization buffer (50 mM Tris/HCl, pH 7.4, 250 mM mannitol, 1 mM EDTA, 1 mM EGTA, 50 mM NaF, 5 mM $Na_4P_2O_7$, 1 mM PMSF, 1 DTT and 10% glycerol, 0.1% Triton X-100, 1 µl/ml protease inhibitor cocktail [Sigma]) before snap-freezing in liquid nitrogen. The crude homogenate is sonicated with 4 pulses of 3 s each before centrifugation (18,000 × *g*, 3 min). Alternatively, Witters and Kemp (1992) lysed treated hepatocytes directly in digitonin-containing and phosphatase-containing buffer, followed by precipitation with ammonium sulfate at 35% saturation.

To 200 µl of the sample, 2 µl of α-AMPK antibody (Cell Signaling Technologies) are added, and the immunoprecipitation is incubated overnight at 4°C with gentle mixing. After 12 h immunoprecipitation, 30 µl of protein-A beads (50% slurry) is added to each sample and incubated for 2 h at 4°C with gentle mixing. The assay is started by the addition of the immunecomplexes to assay buffer (80 mM HEPES, pH 7.4, 160 mM NaCl, 1.6 mM EDTA, 200 µM SAMS peptide, 200 µM AMP, 200 µM ATP, 16% glycerol, 0.1% Triton X-100) containing [γ-^{32}P]ATP (0.5 µCi per sample). After the addition of enzyme to the reaction tube, samples are vortex-mixed for 5 s and in-

cubated for 10 min at 30°C. Following the incubation, the reaction mixture is vortex-mixed and spotted on P81 Whatman filter paper, briefly allowed to dry, and washed three times in 1% $HClO_4$ before a single wash in acetone. After sufficient time to allow the filter papers to air dry, they are immersed in a scintillant-fluor cocktail and the activity of each sample is measured in a scintillation counter.

K.6.2.9.3 Selectivity vs. Glycogen Phosphorylase (GP) and Fructose 1,6-bis-Phosphatase (FBP)

RATIONALE AND PURPOSE

The enzymes, glycogen phosphorylase (GP) and fructose 1,6-bis-phosphatase (FBP) are allosterically modulated by AMP and ZMP (Longus et al. 2003, Vincent et al. 1991). AMP activates GP, whereas it inhibits FBP. To assess the specificity of small molecules directly activating AMPK, it may be useful to study the effects of the compounds on the activity of GP and FBP. Lack of increase or decrease, respectively, in their activity indicates that unlike AICAR/ZMP these compounds do not act as general AMP mimetics, but selectively activates AMPK. The possibilities of direct interaction with the AMP-binding site of AMPK (but apparently not with those of GP and FBP) or with a distinct allosteric site of AMPK can then be tackled by investigating the putative additive, subadditive or potentiating effects on AMPK activity of combinations of maximally efficacious concentrations of compounds and increasing concentrations of AMP (and *vice versa*). On basis of additive effects obtained by following this strategy between AMP and a newly identified small molecule AMPK activator, which inhibited fatty acid synthesis in primary rat hepatocytes and increases whole-body fatty acid oxidation in normal rats, Cool and coworkers (2006) suggested its binding to a unique site that differs from that of AMP binding.

GP Activity Assay

To assay GP activity according to Kaiser and coworkers (2001), 1.5 µg/ml of rabbit muscle GPb (Sigma) is added to a reaction mix containing 20 mM Na_2HPO_4 (pH 7.2), 2 mM $MgSO_4$, 1 mM β-NADP (β-nicotinamide adenine dinucleotide phosphate), 1.4 U/ml G-6-PDH (glucose-6-phosphate-dehydrogenase) and 3 U/ml PGM (phosphoglucomutase). AMP or compounds/drug candidates are added to the assay medium followed by the addition of glycogen (final concentration 1 mg/ml) to initiate the reaction. After incubating 10 min at 25°C, GPb activity is assessed by measuring absorbance at 340 nm.

FBPase Activity Assay

FBPase (0.01 U/ml final concentration) in 2 × assay buffer (100 mM Tris/HCl, pH 7, 4 mM $MgCl_2$, 300 mM NaCl, 0.2 mg/ml BSA and 6 mM DTT) is added to the compounds/drug candidates to result in the final desired concentrations. Substrate, D-fructose-1,6-diphosphate, at a final concentration of 0.1 mM is added to the reaction. The reaction mix is incubated at 30°C for 20 min. Following the incubation, 2 volumes of Malachite Green solution (Upstate, USA) containing 0.001% Tween 20 is added and absorbance at 640 nm read immediately.

K.6.2.9.4 AMP:ATP Levels

PURPOSE AND RATIONALE

To confirm that effects elicited by small molecule AMPK activators (e. g. inhibition of fatty acid synthesis, stimulation of fatty acid oxidation) are mediated by direct upregulation of AMPK activity rather than by cytotoxic effects (e. g. uncoupling of mitochondria, blockade of mitochondrial respiration) ultimately leading to decreased levels of ATP and increased levels of AMP, the AMP:ATP ratio of cells can be measured upon challenge with the putative AMPK activator. Lack of effect on AMP:ATP is compatible with the compound exerting its cellular effects by direct activation of AMPK and not as a consequence of cellular stress, toxicity or other means of increasing the AMP:ATP.

PROCEDURE

Primary rat hepatocytes are plated and treated as described above. Following the 4-h incubation with compounds/drug candidates, cells are washed with ice-cold PBS and the adenine nucleotides are extracted by Corton and coworkers (1994) with 500 µl/well $HClO_3$. The acid is extracted with three treatments of 1.1 volumes of 1/1 tri-n-octylamine:1,1,2-trichlorotriflouroethane. 50–100 µl of the aqueous sample is injected in a Whatman Partisil 10 SAX column preequilibrated in buffer A (10 mM K_2PO_4, pH 6.75) according to the procedure of Cool and coworkers (2006). For elution, sample columns are run for 5 min in buffer A, then for 15 min in a linear gradient to buffer B (500 mM K_2HPO_4, pH 5) and finally for 35 min in buffer B at a flow rate of 2 ml/min. To measure nucleotide concentration absorbance is read at 254 nm.

K.6.2.9.5 Malonyl-CoA Levels

PURPOSE AND RATIONALE

Since AMPK activation inhibits ACC activity, one expected *in vivo* consequence is a decrease in cellular malonyl CoA levels, leading to reduced lipid synthesis and elevated fatty acid oxidation (see K.6.2.5). Thus, in conjunction with increased ACC phosphorylation in primary rat hepatocytes, a reduction in malonyl CoA levels may be anticipated in the liver of rats following treatment with compounds/drug candidates.

PROCEDURE

Malonyl CoA levels in rat tissues from animals treated with the appropriate feeding paradigm and sacrificed 1.5 h after treatment with compounds/drug candidates are measured according to the procedure of Cool and coworkers (2006). Tissues are harvested, immediately frozen in liquid nitrogen and then homogenized in a 1:10 volume (w/v) of ice-cold 5% sulfosalicylic acid containing 50 µM dithioerythritol. Homogenates are centrifuged (15,000 × *g*, 60 min, 2°C) and the supernatants filtered through a 0.22-µm filter (Ultrafree-MC, Millipore USA). Samples are stored at −80°C prior to liquid chromatography mass spectrometry analysis. HPLC is run at binary mode (A: 5 mM dimethylbutylamine and 6 mM HOAc; B: 0.1% formic acid in CH_3CN) at 200 µl/min with the third pump to deliver post column mixing solvent CH_3CN. The data are acquired on a TOF mass spectrometer using positive ion TOF-MS mode.

REFERENCES AND FURTHER READING

Anderson SN, Cool BL, Kifle L, Chiou W, Egan DA, Barrett LW, Richardson PL, Frevert EU, Warrior U, Kofron JL, Burns DJ (2004) Microarrayed compound screening (microARCS) to identify activators and inhibitors of AMP-activated protein kinase. J Biomol Screen 9:112–121

Bentebibel A, Sebastian D, Herrero L, Lopez-Vinas E, Serra D, Asins G, Gomez-Puertas P, Hegardt FG (2006) Novel effect of C75 on carnitine palmitoyltransferase I activity and palmitate oxidation. Biochemistry 45:4339–4350

Boudeau J, Baas AF, Deak M, Morrice NA, Kieloch A, Schutkowski M (2003) MO25α/β interact with STRAD α/β enhancing their ability to bind, activate and localize LKB1 in the cytoplasm. EMBO J 22:5102–5114

Carling D (2005) AMP-activated protein kinase: balancing the scales. Biochimie 87:87–91

Carling D (2004) The AMP-activated protein kinase cascade-a unifying system for energy control. Trends Biochem Sci 29:18–24

Carling D, Clarke PR, Zammit VA, Hardie DG (1989) Purification and characterization of the AMP-activated protei kinase. Copurification of acetyl-CoA carboxylase kinase and 3-hydroxy-3-methylglutaryl-CoA reductase kinase activities. Eur J Biochem 186:129–136

Corton JM, Gillespie JG, Hardie DG (1994) Role of the AMP-activated protein kinase in the cellular stress response. Curr Biol 4:315–324

Cool B, Zinker B, Chiou W, Kifle L, Cao N, Perham M, Dickinson R, Adler A, Gagne G, Iyengar R, Zhao G, Marsh K, Kym P, Jung P, Camp HS, Frevert E (2006) Identification and characterization of a small molecule AMPK activator that treats key components of type 2 diabetes. Cell Metabolism 3:403–416

Corton JM, Gillespie JG, Hardie (1994) Role of the AMP-activated protein kinase in the cellular stress response. Curr Biol 4:315–324

Dale S, Wilson WA, Edelman AM, Hardie DG (1995) Similar substrate recognition motifs for mammalian AMP-activated protein kinase, higher plant HMG-CoA reductase kinase-A, yeast SNF1, and mammalian calmodulin-dependent protein kinase I. FEBS Lett 361:191–195

Davies SP, Carling D, Hardie DG (1989) Tissue distribution of the AMP-activated protein kinase, and lack of activation by cyclic-AMP-dependent protein kinase, studied using a specific and sensitive peptide assay. Eur J Biochem 186:123–128

Foretz M, Carlind D, Guichard C, Ferre P, Foufelle F (1998) AMP-activated protein kinase inhibits the glucose-activated expression of fatty acid synthase gene in rat hepatocytes. J Biol Chem 272:14767–14771

Grantham BD, Zammit VA (1986) Restoration of the properties of carnitine palmitoyltransferase I in liver mitochondria during re-feeding of starved rats. Biochem J 239:485–488

Grantham BD, Zammit VA (1988) Role of carnitine palmitoyltransferase I in the regulation of hepatic ketogenesis during the onset and reversal of chronic diabetes. Biochem J 249:409–414

Hardie DG, Carling D, Carlson M (1998) The AMP-activated/SNF1 protein kinase subfamily: metabolic sensors of the eukaryotic cell Annu Rev Biochem 67:821–855

Hardie DG, Scott JW, Pan DA, Hudson ER (2003) Management of cellular energy by the AMP-activated protein kinase system. FEBS Lett 546:113–120

Hawley SA, Boudeau J, Reid JL, Mustard KJ, Udd L, Makela TP (2003) Complexes between LKB1 tumor suppressor, STRADα/β and MO25α/β are upstream kinases in the AMP-activated protein kinase cascade. J Biol 2:

Hawley SA, Davison M, Woods A, Davies SP, Beri RK, Carling D, Hardie DG (1996) Characterization of the AMP-activated protein kinase kinase from rat liver and identification of threonine 172 as the major site at which it phosphorylates AMP-activated protein kinase. J Biol Chem 217:27879–27887

Hong SP, Leiper FC, Woods A, Carling D, Carlson M (2003) Activation of yeast Snf1 and mammalian AMP-activated protein kinase by upstream kinases. Proc Natl Acad Sci USA 100:8839–8843

Hu Z, Cha SH, Chohnan S, Lane MD (2003) Hypothalamic malonyl-CoA as a mediator of feeding behaviour. Proc Natl Acad Sci USA 100:12624–12629

Johnson LN, Noble MEM, Owen DJ (1996) Active and inactive protein kinases: structural basis for regulation. Cell 85:149–158

Jonsson B (2002) Revealing the cost of Type II diabetes in Europe. Diabetologia 45:S5-S12

Kaiser A, Nishi K, Gorin D, Walsh DA, Bradbury EM, Schnier JB (2001) The cyclin-dependent kinase (CDK) inhibitor flavopiridol inhibits glycogen phosphorylase. Arch Biochem Biophys 386:179–187

Kemp BE, Mitchelhill KI, Stapleton D, Michell BJ, Chen Z-P, Witters LA (1999) Dealing with energy demand:

the AMP-activated protein kinase. Trend Biochem Sci 24:22–25
Li G, Kowluru A, Metz SA (1996) Characterization of prenylcysteine methyltransferase in insulin-secreting cells. Biochem J 316:345–351
Li Y, Cummings RT, Cunningham BR, Chen Y, Zhou G (2003) Homogeneous assays for adenosine 5′-monophosphate-activated protein kinase. Anal Biochem 321:151–156
Lizcano JM, Goransson O, Toth R, Deak M, Morrice NA, Boudeau J, Hawley SA, Udd L, Makeka TP, Hardie DR (2004) LKB1 is a master kinase that activates 13 kinases of the AMPK subfamily, including MARK/PAR-1. EMBO J 23:833–843
Loftus TM, Jaworsky DE, Frehywot GL, Townsend CA, Ronnett GV, Lane MD, Kuhajda FP (2000) Reduced food intake and body weight in mice treated with fatty acid synthase inhibitors. Science 288:2379–2381
Longus SL, Wambolt RB, Parsons HL, Brownsey RW, Allard MF (2003) 5-Aminoimidazole-4-carboxamide 1-beta-D-ribofuranoside (AICAR) stimulates myocardial glycogenolysis by allosteric mechanisms. Am J Physiol Regul Integr. Comp Physiol 284:R936-R944
Maurer T, Fung HL (2000) Comparison of methods for analyzing kinetic data from mechanism-based enzyme inactivation: Application to nitric oxide synthase. AAPS Pharm Sci 2:E8
McGarry JD, Brown NF (1997) The mitochondrial carnitine palmitoyltransferase system. From concept to molecular analysis. Eur J Biochem 244:1–14
Morillas M, Gomez-Puertas P, Roca R, Serra D, Asins G, Valencia A, Hegardt FG (2001) Structural model of the catalytic core of carnitine palmitoyltransferase I and carnitine octanoyltransferase (COT). J Biol Chem 276:45001–45008
Neumann D, Woods A, Carling D, Wallimann T, Schlattner U (2003) Mammalain AMP-activated protein kinase: functional, heterotrimeric complexes by co-expression of subunits in *Escherichia coli*. Protein Express Purif 30:230–237
Price N, van der Leij F, Jackson V, Corstorphine C, Thomson R, Sorensen A, Zammit VA (2002) A novel brain-expressed protein related to carnitine palmitoyltransferase I. Genomics 80:433–442
Rubi B, Antinozzi PA, Herrero I, Ishihara H, Asins G, Serra D, Wollheim CB, Maechler P, Hegardt FG (2002) Adenovirus-mediated overexpression of liver carnitine palmitoyltransferase I in INS1E cells: Effects on cell metabolism and insulin secretion. Biochem J 364:219–226
Ruderman NB, Saha AK, Vavvas D, Witters LA (1999) Malonyl-CoA, fuel sensing, and insulin resistance. Am J Physiol 276:E1-E18
Saggerson ED, Carpenter CA (1981) Carnitine palmitoyltransferase and carnitine octanoyltransferase activities in liver, kidney cortex, adipocyte, lactating mammary gland, skeletal muscle and heart. FEBS Lett 129:229–232
Spiegelman BM, Flier JS (2001) Obesity and the regulation of energy balance. Cell 104:531–543
Stein SC, Woods A, Jones NA, Davison MD, Carling D (2000) The regulation of AMP-activated protein kinase by phosphorylation. Biochem J 345:437–443
Sutherland CM, Hawley SA, McCartney RR, Leech A, Stark MJR, Schmidt MC (2003) Elm1p is one of three upstream kinases for the *Saccharomcyes cerevisiae* SNF1 complex. Curr Biol 13:1299–1305
Thupari JN, Landree LE, Ronnett GV, Kuhajda FP (2002) C75 increases peripheral energy utilization and fatty acid oxidation in diet-induced obesity. Proc Natl Acad Sci USA 99:9428–9502
Tutwiler GF, Ryzlak MT (1980) Inhibition of mitochondrial carnitine palmitoyltransferase by 2-tetradecylglycidic acid. Life Sci 26:393–397
Vincent MF, Marangos PJ, Gruber HE, Van den Berghe G (1991) Inhibition by AICA riboside of gluconeogenesis in isolated rat hepatocytes. Diabetes 40:1259–1266
Winder W, Holmes B, Rubink D, Jensen E, Chen M, Holloszy J (2000) Activation of AMP-activated protein kinase increases mitochondrial enzymes in skeletal muscle. J Appl Physiol 88:2219–2226
Witters LA, Kemp BE (1992) Insulin activation of acteyl-CoA carboxylase accompanied by inhibition of the 5′-AMP-activated protein kinase. J Biol Chem 267:2864–2867
Zhou G, Myers R, Li Y, Chen Y, Shen X, Fenyk-Melody J, Wu M, Ventre J, Doebber T, Fujii N, Musi N, Hirshman MF, Goodyear LJ, Moller DE (2001) Role of AMP-activated protein kinase in mechanism of metformin action. J Clin Invest 108:1167–1174

K.6.2.10 Acetyl-CoA Carboxylase (ACC) Activity

GENERAL CONSIDERATIONS

Activation of AMPK increases phosphorylation of various downstream target proteins including ACC, a key component in the regulation and coordination of fatty acid metabolism and catabolism (Carling 2004). ACC, the rate-limiting enzyme for fatty acid biosynthesis, produces malonyl-CoA *via* the catalysis of the carboxylation of acetyl-CoA which acts as inhibitor of CPT1 (Ruderman et al. 2003). Thereby, ACC controls mitochondrial β-oxidation in negative fashion coordinating fatty acid synthesis and degradation in reciprocal fashion. Inhibition of ACC may lead to stimulation of fatty acid oxidation in both muscle and liver with beneficial effects for the therapy of type II diabetes and obesity.

In theory, any component of ACC could be a potential target for drug discovery. In fact, a high-throughput screening assay that screens for inhibitors of the holoenzyme has been described by Soriano and coworkers(2006). However, a more robust assay could increase the potential for finding inhibitors. One assay commonly used to measure CT activity is an enzyme-coupled assay that relies on the absorbance of NADH (Guchhait et al. 1974). High-throughput assay formats based on the UV detection of NADH are problematic because the screening libraries often contain many compounds that absorb strongly at 340 nm, thereby generating false negatives.

K.6.2.10.1 DTNB Method

PURPOSE AND RATIONALE

A modification of the coupled enzyme assay for carboxyltransferase, that avoids the use of NADH de-

tection and therefore offers a potential advantage in a typical HTS environment, has been introduced by Santoro and coworkers (2006). The CT reaction is assayed in the reverse direction in which malonyl-CoA reacts with biocytin (an analog of the biotin carboxyl carrier protein) to form acetyl-CoA and carboxybiotin. The production of acetyl-CoA is coupled to citrate synthase, which produced citrate and coenzyme A. The amount of coenzyme A formed is detected using 5,5′-dithiobis-2-nitrobenzoic acid (DTNB = Ellman's reagent). The assay has been developed for use in both 96- and 384-well microplate formats and validated using a known bisubstrate analog inhibitor of CT. The spectrophotometric readout in the visible absorbance range used in this assay does not generate the number of false negatives associated with frequently used NAD/NADH assay systems that rely on detection of NADH using UV absorbance.

PROCEDURE

The assay buffer consists of 100 mM potassium phosphate (pH 7.6) with 0.1% Tween 20. In preparing the reagent stock solutions, 10 mM malonyl-CoA is dissolved in water, 100 mM OAA is dissolved in assay buffer, 1.2 mM DTNB is dissolved in assay buffer, 100 mM biocytin is sonicated in assay buffer, and ACC is dissolved in assay buffer. Commercially obtained citrate synthase solution is diluted 1:10 in assay buffer. Using the above stock solutions, assay solutions are prepared. "CT solution" contains 30 ml of OAA stock, 3 ml of ACC, and 67 ml of assay buffer, and "CS solution" contains 6 ml of malonyl-CoA stock solution, 36 ml of biocytin stock solution, 6 ml of citrate synthase solution, and 52 ml of assay buffer. Final concentrations of reagents in the assay are as follows: 200 µM malonyl-CoA, 12 mM biocytin, 10 mM OAA, 200 µM DTNB, 21.9 nM ACC, and 104 nM citrate synthase.

Automated screening is performed on an integrated core system (e. g. Beckman SAGIAN). The assay plates used are prespotted with 1 µl of each test compound/drug candidate per well. Using an automated liquid dispenser, 30 µl of CT solution is added to each assay well. The plates are incubated at room temperature for 5 min 40 s to allow for association of potential slow-binding inhibitors with ACC. An automated liquid handler with 384-tip pod (e. g. Beckman Biomek FX) is used to add 9 µl of DTNB to each well. The reaction is then initiated by the addition of 20 µl of CS solution using the liquid handler (with gentle aspiration mixing). The plate is promptly transferred (40 s after the beginning of the CS addition step) to an automated 384-detector (e. g. Molecular Devices SPECTRAmax Plus), and the absorbance at 412 nm is recorded. A second reading is taken 5 min 40 s later. The HTS assay is carried out at room temperature.

EVALUATION

The quality of this assay for throughput assay for inhibitors to the CT subunit of ACC is demonstrated by a large assay signal window, low data variation among controls, and strong Z' factors. The assay is reliable for many hours and reproducible from day to day. The screening assay described here will be a useful tool in the discovery of potential anti-diabetic and anti-obesity drugs targeting human ACC.

K.6.2.10.2 Phosphate Measurement

Colorimetric Method

All assays are performed using clear 96-well plates (e. g. Costar). The order of addition of assay components depended on the type of experiment performed. For initial velocity measurements, all assay components except the substrate with variable concentration are premixed in 200 mM HEPES/KOH (pH 8). The reaction is initiated by adding an equal volume of the missing substrate. Solutions of varying ATP and acetyl-CoA concentrations are prepared in doubly distilled/deionized water; holo biotin carboxyl carrier protein solutions are prepared in 50 mM HEPES (pH 7.3) and 10% glycerol. Aliquots (50 µl) are removed from the reaction mix at fixed time points and placed in a 96-well plate preloaded with 100 µl BioMol Green reagent (BIOMOL) to quench the reaction. Incubation time for color development, typically 30 min, is the same for all mixtures. Absorbance is read at 620 nm using a microplate spectrophotometer. Initial rates are measured within a 10% turnover range of the limiting substrate. Phosphate concentration is determined using a standard curve.

Charcoal Adsorption-Scintillation Counting Method

Alternatively, phosphate can be measured using the charcoal adsorption–scintillation counting method adapted from Stitt and Xu (1988). All assay solutions included a trace of [γ-^{33}P]-labeled ATP. Initial velocity measurements are as described for the colorimetric method. At various time points, a 30-µl aliquot is transferred to an Eppendorf tube, fitted with a 0.45-µm filter, containing 120 µl of 5% TCA and 50 µl of 80 mg/ml activated charcoal. After vigorous mixing, the tube is spun in a microcentrifuge (11,000 × g, 30 s) to filter out the charcoal. A 50-µl aliquot of the fil-

trate is added to 7 ml of aqueous scintillation fluid and counted for 1 min in a scintillation counter. To obtain the 100% turnover count (*plus* background), a 30-µl reaction mix is placed in 170 µl of 5% TCA without charcoal and a 50-µl aliquot is counted as above. Background counts, measured by repeating the assay adding water instead of enzyme, are subtracted from all measurements to determine percentage turnover.

Scintillation Proximity Assay (SPA) Method

Assay solutions (33 µl) containing 5 (or 10) µM ATP, 1 (or 2) nCi/µl [γ-^{33}P]-labeled ATP, 20 µM acetyl-CoA, 40 nM AccC, 40 nM AccA/D, and 80 nM BCCP in buffer A (100 mM HEPES/KOH, pH 8, 150 mM NaCl, 10% glycerol, and 1 mM DTT) are incubated for 1 h. The reaction is quenched by the addition of 10 µl of freshly made solution A (two volumes of solution B [30 mg/ml wheat germ agglutinin-coated polystyrene imaging beads or 30 mg/ml streptavidin-coated SPA scintillation beads, Amersham-Pharmacia Biosciences, in 50 mM HEPES/KOH, pH 7.3] mixed with one volume of 16 mM ammonium heptamolybdate in 2.4 N HCl solution). Shortly thereafter (but no longer than 40 min after), 10 µl of 256 mM citrate solution is added. The beads are spun down (2,000–3,000 rpm, 5 min). For experiments using SPA imaging beads, the plate is kept in the dark for at least 2 h before reading the signal using the Leadseeker instrument (Amersham-Pharmacia Biosciences). For experiments using SPA scintillation beads, radioactivity is determined in a TopCount instrument (e. g. Packard) after the plate has been centrifuged.

EVALUATION

Initial velocity measurements as a function of substrate concentration are carried out using either the charcoal adsorption–scintillation counting method, the colorimetric method, or the SPA method. Data are fitted to the Michaelis–Menten equation (using e. g. the GraphPad Prism software).

In general, phosphate determination is a simple and robust method for the measurement of the overall activity of ACC. The monitoring of phosphate production, at low (nanomolar) protein concentrations, is demonstrated to represent the overall activity of ACC due to the coupled activities of biotin carboxylase and CT and the cycling of biotin cofactor attached to BCCP between the two half-reactions. The method has been adapted for a 384-well screening assay format and validated to monitor competitive inhibitors of either biotin carboxylase or CT. The use of holo-BCCP instead of free biotin, as well as the use of physiologically relevant concentrations of the protein components, makes this assay a good model for the *in vivo* ACC system and will facilitate the identification of physiologically relevant inhibitors.

REFERENCES AND FURTHER READING

Carling D (2004) The AMP-activated protein kinase cascade-a unifying system for energy control. Trends Biochem Sci 29:18–24

Guchhait RB, Polakis SE, Dimroth P, Stoll E, Moss J, Lane MD (1974) Acetyl coenzyme A carboxylase system of *Escherichia coli*. J Biol Chem 249:6633–6645

Ruderman N, Saha AK, Kraegen EW (2003) Minireview: malonyl CoA, AMP-activated protein kinase, and adiposity. Endocrinology 144:5166–5171

Santoro N, Brtva T, Roest SV, Siegel K, Waldrop GL (2006) A high-throughput screening assay for the carboxyltransferase subunit of acetyl-CoA carboxylase. Anal Biochem

Soriano A, Radice AD, Herbitter AH, Langsdorf EF, Stafford JM, Chan S, Wang S, Liu Y-H, Black TA (2006) *Escherichia coli* acetyl-coenzyme A carboxylase: characterization and development of a high-throughput assay. Anal Biochem 349:268–276

Stitt BL, Xu Y (1988) Sequential hydrolysis of ATP molecules bound in interacting catalytic sites of *Escherichia coli* transcription termination protein Rho. J Biol Chem 273:26477–26486

K.6.2.11 Gluconeogenesis, Ketone Body Formation and TCA Cycle

PURPOSE AND RATIONALE

De novo synthesis of glucose in the liver from precursors such as fructose, pyruvate, lactate, gluconeogenic amino acids, and glycerol is a central mechanism to provide the organism with glucose in times of starvation (Cherrington 1997, Nordlie et al. 1999). On the other hand, when glucose is directly available from external resources, gluconeogenesis is dispensable and consequently needs to be shut off. Integration of these events is complex and occurs through various hormonal and nutritional factors (Barthel et al. 2005). The principal parameters affecting hepatic glucose output are the concentrations of the available glucogenic substrates and the activity of a few regulatory enzymes. The activity of the key gluconeogenic enzymes phosphoenolpyruvate carboxykinase (PEPCK) and glucose-6-phosphatase (G-6-Pase) is regulated by transcriptional and non-transcriptional mechanisms, whereas the third key enzyme, fructose-1,6-bisphosphatase (FBPase), is also regulated through competitive inhibition by fructose 2,6-bisphosphate. Insulin is the most important hormone that inhibits gluconeogenesis. It acts predominantly by suppressing the expression of the genes for the key gluconeogenic enzymes, PEPCK and G-6-Pase (Barthel and Schmoll 2003).

Over the recent years, considerable progress has been made in understanding the mechanisms and molecular details involved in the regulation of hepatic glucose production and its impairment in diabetes. A spectrum of different experimental approaches, ranging from genetic manipulations like knockout models and use of gain or loss of function-mutated constructs in cellular models to the development and application of selective pharmacological compounds, has provided evidence for the convergence of multiple signaling pathways in particular on the level of the transcriptional regulation of PEPCK and G-6-Pase gene expression, the key gluconeogenic genes in liver cells. Analogous to multiple braking systems in cars or motorbikes, the redundancy in the regulation of hepatic glucose production emphasizes the critical importance of this process in the glucose homeostasis of the organism. On the other hand, our increasing knowledge in this field has made it possible to identify a group of promising pharmacological targets, therefore providing a solid basis for the development of new and more potent anti-diabetic drugs.

K.6.2.11.1 Hepatocytes

PURPOSE AND RATIONALE

Isolated hepatocytes can be used to study the effect of drugs on hepatic gluconeogenesis and other hepatic metabolic reactions such as ketone body formation and the tricarboxylic acid cycle.

PROCEDURE

Male Wistar rats weighing 200–300 g are used. The hepatocytes are isolated by perfusion of the liver with collagenase (Berry and Friend 1969, Seglen 1976,Alvarez et al. 1987). The viability of the isolated hepatocytes can be evaluated by the Trypan blue test. Usually 90–95% of the cells exclude the stain and can therefore be regarded as intact. The isolated hepatocytes (20×10^6 cells/vial) are suspended in 3.0 ml of KRB containing 4% BSA. The cell suspension is pre-incubated for 15 min at 37°C in a Dubnoff metabolic shaking incubator gassed with carbogen. The following substrates are added in various combinations, and each sample is incubated for 60 min with 1 mM each of alanine, fructose, glycerol and lactate, and 10 mM pyruvate, or 2 mM sodium palmitate bound to albumin. Compounds/drug candidates are added in concentrations between 0.05 and 5.0 mM. At the end of the 60-min incubation period, 0.2 ml of 70% $HClO_4$ is added into the medium to stop the reaction. The reaction mixture is then centrifuged, and the supernatant obtained is used to determine the intermediate metabolites. Glucose is assayed by the glucose-oxidase method, lactate (Gutmann and Wahlefeld 1974), pyruvate (Czok and Lamprecht 1974), acetoacetate (Mellanby and Williamson 1974), and β-hydroxybutyrate (Williamson and Melanby 1974) by appropriate enzymatic methods.

In order to measure the influence on the tricarboxylic acid cycle, (U-^{14}C) alanine, (1-^{14}C) glutamate, (1-^{14}C) pyruvate, (1-^{14}C) palmitate, or (1-^{14}C) glucose is added after pre-incubation together with various combinations of compounds and substrates, and incubated for 60 min. The radioactivity is measured by the $^{14}CO_2$-capturing method (Gliemann 1965).

K.6.2.11.2 Perfused Isolated Rat Liver

PURPOSE AND RATIONALE

The technique of liver perfusion has been described extensively by Ross (1972), mentioning in his introductory remarks that the isolated liver was first used by Claude Bernard in 1885. Derived from several modifications, the perfusion of rat liver from the portal vein is the most widely used technique.

EVALUATION

Several parameters can be determined in the effluate, such as net glucose production from lactate and net lactate utilization. The values are plotted against time before and after addition of the compounds and drug candidates, such as insulin or sulfonylureas.

MODIFICATIONS OF THE METHOD

This method has been widely used for studying carbohydrate and lipid intermediary metabolism (Herling et al. 1998) as well as drug metabolism (Milne et al. 1997; 2000; Vuppugalla, 2004). Many variations have been reported predominantly with respect to the animal species used. Chaib et al. (2004) compared isolated perfused livers of rats with those of guinea pigs. Den Butter (1994) used livers from rabbits. Further modifications are related to the direction of perfusion via hepatic artery or portal vein or both simultaneously or in connection with the isolated jointly perfused small intestine (Stumpel et al. (1997 and 2000) as well as the continuous perfusion in a recirculated (see above) or open (non-recirculated) manner (Lopez et al. 1998).

Alexander and coworkers (1992) studied hepatic blood flow regulation in an isolated dual-perfused

rabbit liver preparation. Alexander and coworkers (1995) described a miniaturized perfusion circuit using a novel design of organ bath, to maintain a buoyant preparation, and a high-efficiency miniaturized membrane tubing oxygenator for testing hepatic function during prolonged isolated rat liver perfusion. Kobayashi and coworkers (1991) found inhibition of gluconeogenesis in isolated hepatocytes from normal, fasted rats by the sulfonylurea, glimepiride.

REFERENCES AND FURTHER READING

Alexander B, Mathie RT, Ralevic V, Burnstock G (1992) An isolated dual-perfused rabbit liver preparation for the study of hepatic blood flow regulation. J Pharm Meth 27:17–22

Alexander B, Aslam M, Benjamin IS (1995) Hepatic function during prolonged isolated rat liver perfusion using a new miniaturized perfusion circuit. J Pharmacol Toxicol Meth 34:203–210

Alvarez JF, Cabello MA, Felíu JE, Mato JM (1987) A phosphooligosaccharide mimics insulin action on glycogen phosphorylase and pyruvate kinase activities in isolated rat hepatocytes. Biochem Biophys Res Commun 147:765–771

Barthel A, Schmoll D (2003) Novel concepts in insulin regulation of hepatic gluconeogenesis. Am J Physiol Endocrinol Metab 285:E685-E692

Barthel A, Schmoll D, Unterman TG (2005) FoxO proteins in insulin action and metabolism. Trends Endocrinol Metab 16:183–189

Berry MN, Friend DS (1969) High-yield preparation of isolated rat liver parenchymal cells. A biochemical and fine structural study. J Cell Biol 43:506–520

Cherrington AD (1999) Banting lecture 1997. Control of glucose uptake and release by the liver *in vivo*. Diabetes 48:1198–1214

Chaib S, Charrueau C, Neveux N, Coudray-Lucas C, Cynober L, De Bandt JP (2004) Isolated perfused liver model: the rat and guinea pig compared. Nutrition. 20:458–64

Chowdhury MH, Agius L (1987) Epidermal growth factor counteracts the glycogenic effect of insulin in parenchymal hepatocyte cultures. Biochem J 247:307–314

Czok R, Lamprecht W (1974) Pyruvate, phosphoenol-pyruvate and D-glycerate-2-phosphate. In: Bergmeyer HJ (ed) Methods of Enzymatic Analysis, Vol 3, Verlag Chemie Weinheim, Academic Press New York, London. pp 1446–1451

den Butter G, Marsh DC, Lindell SL, Belzer FO, Southard JH (1994) Effect of glycine on isolated, perfused rabbit livers following 48-hour preservation in University of Wisconsin solution without glutathione. Transpl Int.7:195–200

Forsayeth JR, Maddux BA, Goldfine IA (1986) Biosynthesis and processing of the human insulin receptor. Diabetes 35:837–846

Forsayeth JR, Montemurro A, Maddux BA, DePirro R, Goldfine ID (1988) Effect of monoclonal antibodies on human insulin receptor autophosphorylation, negative cooperativity, and down-regulation. J Biol Chem 262:4134–4140

Gliemann J (1965) Insulin-like activity of dilute human serum assayed by an isolated adipose cell method. Diabetes 14:643–649

Gutmann I, Wahlefeld AM (1974) L-(+)-lactate determination with lactate dehydrogenase and NAD. In: Bergmeyer HJ (ed) Methods of Enzymatic Analysis, Vol 3, Verlag Chemie Weinheim, Academic Press New York, London. pp 1464–1468

Herling AW, Burger HJ, Schwab D, Hemmerle H, Below P, Schubert G (1998) Pharmacodynamic profile of a novel inhibitor of the hepatic glucose-6-phosphatase system. Am J Physiol 274:G1087–93

Kobayashi M, Hotta N, Komori T, Haga T, Koh N, Sakakibara F, Sakamoto N (1991) Antigluconeogenetic effect of a new potent sulfonylurea drug, Hoe 490, in isolated hepatocytes from normal, fasted rats. J Japan Diab Soc 34:767–774

Lopez CH, Bracht A, Yamamoto NS, dos Santos MD (1998) Metabolic effects and distribution space of flufenamic acid in the isolated perfused rat liver. Chem Biol Interact. 116:105–22

Mellanby J, Williamson DH (1974) Acetoactetate. In: Bergmeyer HJ (ed) Methods of Enzymatic Analysis, Vol 4, Verlag Chemie Weinheim, Academic Press New York, London. pp 1840–1843

Milne RW, Jensen RH, Larsen C, Evans AM, Nation RL (1997) Comparison of the disposition of hepatically-generated morphine-3-glucuronide and morphine-6-glucuronide in isolated perfused liver from the guinea pig. Pharm Res 14:1014–8

Milne RW, Larsen LA, Jorgensen KL, Bastlund J, Stretch GR, Evans AM (2000) Hepatic disposition of fexofenadine: influence of the transport inhibitors erythromycin and dibromosulphothalein. Pharm Res17:1511–5

Nordlie RC, Foster JD, Lange AJ (1999) Regulation of glucose production by the liver. Annu Rev Nutr 19:379–406

Ross BD (1972) Endocrine organs: Pancreas. In Ross BD: Perfusion Techniques in Biochemistry. A Laboratory Manual in the Use of Isolated Perfused Organs in Biochemical Experimentation. Clarendon Press, Oxford, pp 321–355

Seglen PO (1976) Preparation of isolated rat liver cells. In: Prescott DM (ed) Methods in Cell Biology, Vol XIII, Academic Press, New York, pp 29–83

Stumpel F, Scholtka B, Jungermann K (2000) Stimulation by portal insulin of intestinal glucose absorption via hepatoenteral nerves and prostaglandin E2 in the isolated, jointly perfused small intestine and liver of the rat. Ann N Y Acad Sci. 915:111–6

Stumpel F, Jungermann K (1997) Sensing by intrahepatic muscarinic nerves of a portal-arterial glucose concentration gradient as a signal for insulin-dependent glucose uptake in the perfused rat liver. FEBS Lett. 406:119–22

Williamson DH, Mellanby J (1974) D-(–)-3-hydroxybutyrate. In: Bergmeyer HJ (ed) Methods of Enzymatic Analysis, Vol 4, Verlag Chemie Weinheim, Academic Press New York, London. pp 1836–1839

K.6.2.11.3 Phosphoenolpyruvate Carboxykinase (PEPCK) Activity

PEPCK is measured using the $NaH^{14}CO_3$ fixation assay as described by Noce and Utter (1975) and Burcelin and coworkers (1995) with some modifications. 490 µl of rat liver cytosol is added to 500 µl of reaction buffer containing 150 µmol Tris/acetate (pH 7.2), 5 µmol sodium IDP, 10 µmol $MnCl_2$, 250 µmol KCl, 10 mM DTT, 2 mM GSH, 400/150 µmol $KHCO_3$ and 15 µCi $NaH[^{14}C]O_3^-$ (10 µmol, Amersham-Pharmacia). The reaction is started by the addition of 10 µl of 0.4 M phosphoenolpyruvate and terminated after 10 min incubation at 25°C by addition of 1 ml of 6 N HCl and placing the

tube on ice. After dilution with 1 ml of deionized water, unreacted CO_2 ($H[^{14}C]O_3^-$) is removed by bubbling with N_2 and CO_2 for 30 min each. The reaction mixture is supplemented with 10 ml of aqueous scintillation cocktail (Beckman ReadySafe) and measured for radioactivity by liquid scintillation counting. From each value appropriate blanks are subtracted containing the same ingredients but lacking either cytosol or IDP. Under these conditions and up to the maximal amount of cytosol used, the incorporation rates are linear with both cytosol concentration and time during the first 15 min at least.

K.6.2.12 Glucose Transport

GENERAL CONSIDERATIONS

Skeletal muscle contains several glucose transporters. Evidence indicates that GLUT4 translocation to the cell surface is the major mechanism responsible for regulated glucose uptake in this tissue. Insulin and muscle contractions are the most important stimuli for GLUT4 mobilization from the intracellular storage compartment to the plasma membrane. Nevertheless, other factors like hypoxia, catecholamines and glucocorticoids can alter this mobilization. Contraction and insulin cause increases in the maximal velocity of glucose transport (Nesher et al. 1985) through three mechanisms: (1) a conformational alteration in cell surface glucose transporter leading to increased transport activity, (2) increase in the number of GLUT4 in the plasma membrane, and (3) rapid synthesis of new transporters (Hayashi et al. 1997, Rea and James 1997). The current knowledge on the differential effects of insulin and contraction on glucose transport in skeletal muscle has recently been reviewed by Pereira and Lancha (2004).

PURPOSE AND RATIONALE

Some studies have been developed with the purpose of explaining the two different mechanisms that stimulate glucose transport due to the action of insulin and muscle contraction. One hypothesis is that there are two separate pools of GLUT4 in the skeletal muscle. GLUT4 from one pool is thus translocated by the action of insulin but not of contraction, whereas GLUT4 from another pool is translocated by contraction stimulation, but not by insulin. In any case, on basis of the major contribution of the skeletal muscle in the insulin-stimulated whole-body glucose disposal in humans, compounds/drug candidates which activate the muscle glucose transport by engagement of either the insulin- or contraction-induced signaling pathway may be helpful for the future anti-diabetic therapy. The following tissue- and cell-based assays can be used for their identification and characterization.

K.6.2.12.1 Method Based on Diaphragms

PROCEDURE

Intact washed rat diaphragms are incubated (30 min, 37°C) in HEPES-buffered saline (25 mM HEPES, 120 mM NaCl, 5 mM KCl, 1.5 mM $CaCl_2$, 1 mM $MgCl_2$, 5 mM glucose, 0.5 mM sodium pyruvate, 1.5 mM KH_2PO_4, pH 7.4) under constant bubbling with 95% O_2/5% CO_2. The diaphragms are then washed two times with the same buffer lacking glucose and further incubated (30 min) in 5 ml of glucose-free buffer in the presence of insulin/compounds/drug candidates. Glucose transport is initiated by addition of 50 µl of 10 µM 2-[1-^{3}H]deoxyglucose (10 µCi/ml) in the absence or presence of 25 µM cytochalasin B (control). After 15 min, the diaphragms are rinsed four times with ice-cold buffer containing 10 mM glucose, 25 µM cytochalasin B, blotted with filter paper and homogenized. Portions of the homogenate are used for protein determination (BCA method).

EVALUATION

1-ml portions of the supernatant of a centrifugation ($10{,}000 \times g$, 15 min) are mixed with 10 ml scintillation cocktail and counted for radioactivity.

K.6.2.12.2 Method Based on Myocytes

PROCEDURE

Transport studies are carried out using six-well Falcon plates. Cells are routinely plated at a density of 1.5×10^5 cells/well. Medium is aspirated and each well is washed with 10 ml of PBS. Nine hundred microlitres of uptake buffer (PBS containing 1 mg/ml BSA) are added to each well. Transport studies are carried out at 23°C and are initiated by adding 100 µl of 2-[1-^{3}H]deoxyglucose (10 µCi/ml) to the desired final concentration (up to 500 µM). At appropriate times, uptake is terminated by rapidly washing the cells twice (less than 15 s) with 10 ml of ice-cold PBS. In the case of 3MG uptake, cells are washed with cold PBS containing 1 mM mercuric chloride. Samples are taken at 15, 30, 45 and 60 s after the addition of radioactive substrate. Cells are solubilized with 1 ml of 0.1% Triton X-100, and 0.8 ml aliquots are counted in 10 ml of

scintillation fluid. Under these conditions, the uptake of 3MG and 2DG is linear with time, and over 95% of the internalized 2DG are phosphorylated. Cells in two wells from each plate are detached with 0.1% trypsin, and counted using a Coulter counter. Studies are carried out in duplicate and each experiment is repeated at least twice. Results are consistent in all cases. Data are analysed by a linear least squares regression fit program (e. g. SlideWrite Plus, version 4.0, Advanced Graphics Software, CA), and by a non-linear regression data analysis program (e. g. Enzfitter program, Biosoft, UK).

EVALUATION

Specific glucose transport (dpm/mg of protein) is calculated as the difference between diaphragm-associated radioactivity measured in the absence (total uptake) and presence of cytochalasin B (non-specific uptake). Under these experimental conditions, transport of 2DG is linear for up to 30 min.

K.6.2.12.3 GLUT4 Translocation in Myocytes

GENERAL CONSIDERATIONS

Understanding the molecular mechanisms of insulin action has been of major interest since the discovery, several decades ago, that insulin stimulates glucose transport *in vivo* by inducing GLUT4 translocation (see aove). GLUT4 translocation is a complex vesicular traffic process which includes fusion and docking steps. Herbst and coworkers (1995) showed previously that introduction of a peptide corresponding to tyrosine-phosphorylated IRS-1 motifs into 3T3-L1 adipocytes resulted in a significant increase in the translocation of GLUT4 to the plasma membrane by immunofluorescence staining which mimicked the response to insulin. However, no relative increase in the rate of glucose uptake was observed in those cells. This led to the speculation that some stimulus may bring GLUT4 vesicles to the plasma membrane (docking) but is not sufficient to trigger fusion with the membrane. A converse phenomenon was observed by others upon introducing isoproterenol to rat adipocytes whereby the insulin-dependent gain in glucose transporter detected in isolated plasma membrane was not changed while glucose transport was decreased. It is therefore conceivable that immunostaining of isolated membranes or of permeabilized cells cannot distinguish GLUT4 proteins docked on the plasma membrane from those which are fully fused with it. It is well conceivable that compounds/drug candidates provoke GLUT4 translocation without concomitant glucose transport activation and, *vice versa*, transport activation in the absence of translocation.

PURPOSE AND RATIONALE

Subcellular fractionation, cell photolabeling coupled to immunoprecipitation and immunofluorescence or immunoelectron microscopy have been used to detect translocation of GLUT4 to the cell surface. All of these methods are laborious and suffer from methodological inaccuracies. Subcellular fractionation is cumbersome and produces membranes that are rarely pure. Moreover, quantitative recovery of all membrane compartments is difficult or impossible. Affinity labeling of surface GLUT4/1 followed by immunoprecipitation depends on the ability to obtain quantitative immunoprecipitation and recovery upon SDS-PAGE. This technique results in the incorporation of about 1/10 000 of the label added, thus the signal to noise ratio is low. Moreover, the reactivity of the photolabel can depend on the level of activity of the GLUT in addition to the amount of GLUT exposed at the cell surface. Immunofluorescence detection does not distinguish the native GLUT4 molecules incorporated into the cell membrane from molecules in subplasmalemmal vesicles, and is not a quantitative technique. Immunogold electron microscopy detects antigens at the plasma membrane accurately, but has not been successfully used in a quantitative fashion. None of the above techniques is suitable for large numbers of experiments, as would be required for throughput screening and even characterization of anti-diabetic drugs or of agents interfering with insulin signaling or intracellular trafficking. Therefore, a fast, sensitive and quantitative technique is needed to measure GLUT4 translocation in intact cultured myocytes, which does not rely on immunoprecipitation, SDS-PAGE or use of radioactivity, as required by the photolabeling technique and does not require large amounts of cells or laborious subcellular fractionation.

Previous studies have shown that in CHO cells or other fibroblasts stably expressing heterologous GLUT4, insulin-stimulated translocation of the transfected GLUT4 is not detectable by immunoblot analysis of subcellular fractions, nor by immunofluorescence microscopy (Kanai et al. 1993). However, transfection of GLUT4myc allowed for detection of the exofacial epitope by ^{125}I-labeled secondary antibody. By this approach, insulin-induced GLUT4myc translocation was observed in CHO cells (Wang et al. 2000). For study of GLUT4 translocation in L6 myocytes, GLUT4myc has to be introduced into L6 in-

sulin-sensitive muscle cells which express endogenous GLUT4 as well as GLUT1 and GLUT3. The amount of GLUT4myc expressed at the surface of basal cells (5 fmol/mg protein) is usually in the range of that of native GLUT4 (about 12 fmol/mg). This discrete level of expression of GLUT4myc likely allows for its correct localization without saturation of the proteins determining its intracellular sorting.

PROCEDURE

Construction and Culture of GLUT4 Ectopically Expressing L6 Myocytes

For the construction of GLUT4myc-expressing L6 myocytes, the human c-myc epitope (14 amino acids) is inserted into the first ectodomain of GLUT4 as described by Kanai and coworkers (1993). The epitope does not affect GLUT4 activity. GLUT4myc cDNA is subcloned into the mammalian expression vector pCXN (pCXN-GLUT4myc). L6 myocytes are transfected with pCXN-GLUT4myc and pSV2-bsr, a blasticidin S deaminase expression plasmid, and selected with blasticidin S hydrochloride. L6-GLUT4myc myocytes in cell monolayers are maintained in α-MEM supplemented with 10% FBS in a humidified atmosphere containing 10% CO_2/90% air at 37°C. Cells are grown in 12- or 24-well plates for immunofluorescence and on glass coverslips for fixation. Prior to experiments, cells are incubated with serum-free α-MEM supplemented with 25 mM glucose for 5 h.

K.6.2.12.3.1
Method Based on Indirect Immunofluorescence

Quiescent L6-GLUT4myc cells grown on glass coverslips are treated with insulin/compounds/drugs, then rinsed once with PBS, fixed with 3% paraformaldehyde in PBS for 3 min at room temperature, and neutralized with 1% glycine in PBS at 4°C for 10 min. The cells are incubated with PBS containing 10% goat serum and 3% BSA at 4°C for at least 30 min. Primary antibody (anti-c-myc 9E10) is added at a dilution of 1:100 and maintained at 4°C for 30 min. The cells are extensively washed with cold PBS before introducing the secondary antibody (Cy3-IgG, 1:1,000) for 30 min at 4°C. The cells are washed, then mounted and immediately examined by immunofluorescence microscopy.

K.6.2.12.3.2
Method Based on Cell Fixation

PROCEDURE

Quiescent L6-GLUT4myc cells treated with insulin/compounds/drugs are washed once with PBS, fixed in 3% paraformaldehyde in PBS for 3 min at room temperature. Thereafter, the fixative is immediately neutralized by incubation with 1% glycine in PBS at 4°C for 10 min. The cells are blocked with 10% goat serum and 3% BSA in PBS at 4°C for at least 30 min. Primary antibody (anti-c-myc, 9E10) is then added into the cultures at a dilution of 1:100 and maintained for 30 min at 4°C. The cells are extensively washed with PBS before introducing peroxidase-conjugated rabbit anti-mouse IgG (1:1,000). After 30 min at 4°C, the cells are extensively washed and 1 ml OPD reagent is added to each well. The colorimetric reaction is stopped by addition of 0.25 ml of 3 N HCl for 10 min at room temperature. The supernatant is collected and the optical absorbance is measured at 492 nm. Standard curves are generated using either peroxidase conjugated anti-mouse IgG alone or myc-tag peptide. Myc-tag peptide at various concentrations is coated onto 24-well plates by incubation at 4°C for 24 h then allowed to dry. The plates are rinsed with PBS to remove excess salt and the uncoated spaces are blocked with 10% goat serum and 3% BSA.

EVALUATION

Introduction of a tag c-myc epitope (14 amino acids) into the first exofacial loop of GLUT4 cDNA allows for the direct detection of GLUT4myc molecules translocated to the plasma membrane upon fixation of the intact myocytes under conditions which do not allow access of the anti-myc antibodies to intracellular structures, such as the GLUT4 vesicles. The efficacy of this method has been compared with that of the conventionally used subcellular fractionation and immunofluorescence approaches. Virtually similar effects of insulin on GLUT4 translocation are detected by all three approaches.

REFERENCES AND FURTHER READING

Burcelin R, Eddouks M, Maury J, Kande J, Assan R, Girard J (1995) Excessive glucose production, rather than insulin resistance, accounts for hyperglycemia in recent-onset streptocotozin-diabetic rats. Diabetologia 38:283–290

Hayashi T, Wojtaszewski JFP, Goodyear LJ (1997) Exercise regulation of glucose transport in skeletal muscle. Am J Physiol 273:E1039-E1051

Herbst JJ, Andrews GC, Contillo LC, Singleton DH, Genereux PE, Gibbs EM, Lienhard GE (1995) Effect of the activation of phosphatidylinositol3-kinase by a thiophosphotyrosine peptide on glucose transport in 3T3-L1 adipocytes. J Biol Chem 270:26000–26005

Kanai F, Nishioka Y, Hayashi H, Kamohara S, Todaka M, Ebina Y (1993) Direct demonstration of insulin-induced GLUT4 translocation to the surface of intact cells by insertion of a c-myc epitope into an exofacial GLUT4 domain. J Biol Chem 268:14523–14526

Noce PS, Utter MF (1975) Decarboxylation of oxalacetate to pyruvate by purified avian liver phosphoenolpyruvate carboxykinase. J Biol Chem 250:9099–9105
Pereira LO, Lancha AH (2004) Effect of insulin and contraction up on glucose transport in skeletal muscle. Prog Biophys Mol Biol 84:1–27
Rea S, James DE (1997) Moving GLUT4, the Kristiansen biogenesis and trafficking of GLUT4 storage vesicle. Diabetes 46:1667–1677
Wang L, Hayashi H, Kishi K, Huang L, Hagi A, Tamaoka K, Hawkins PT (2000) Gi-mediated translocation of GLUT4 is independent of p85/p110α and p110γ phosphoinositide 3-kinases but might involve the activation of Akt kinase. Biochem J 345:543–555

K.6.2.13 Glycogen Synthesis

GENERAL CONSIDERATIONS

Insulin and contractile activity are major regulators of glycogen metabolism in skeletal muscle (Pederson et al. 2005). Insulin stimulates glycogen synthesis, and postprandially, ~80% of ingested glucose is taken up by skeletal muscle and converted to glycogen (Jue et al. 1989a and b, Shulman et al. 1990). Under these conditions, insulin activates glycogen synthase (GS), as well as glucose transport, *via* translocation of the GLUT4 transporter. Glycogen is a major fuel for the contractile activity of skeletal muscle. During contraction, glycogen is utilized as a source of energy, and it has been demonstrated that, perhaps paradoxically, glycogen resynthesis occurs while glycogen is being broken down (Price et al. 1991, 1994). Presumably, this represents a mechanism for the rapid replenishment of glycogen stores when exercise ceases (Bloch et al. 1994, Ivy and Kuo 1998). The period following exercise is characterized by increased glucose uptake and net glycogen synthesis in skeletal muscle, a scenario similar to insulin stimulation of muscle. Despite the fact that the mechanism of GS activation in response to insulin has been extensively studied, the molecular details of both insulin and contraction-induced activation remain mostly unknown. The following assays enable the demonstration of stimulatory effects on glycogen synthesis in muscle cells of compounds with insulin-like activity which may contribute significantly to their blood glucose-decreasing potency.

K.6.2.13.1 Method Based on Diaphragms

PROCEDURE

Male Sprague Dawley rats weighing 70–100 g are used. The animals are sacrificed during anesthesia and the diaphragms are carefully removed, spread out and divided into two equal pieces. The hemidiaphragms are incubated in Krebs-Henseleit buffer gassed with carbogen (95% O_2/5% CO_2) with 5 mM [U-^{14}C]glucose (0.5 µCi/ml) in the presence of insulin/compounds/drugs. After 30 min incubation at 37°C, the hemidiaphragms are blotted on tissue, frozen in liquid nitrogen, and ground in a porcelain mortar and pestle chilled with liquid nitrogen. Samples of the powdered tissue are weighed and dissolved by heating for 45 min at 100°C in 30% KOH (1 ml/100 mg tissue) before ethanol is added to a final concentration of 70%. After 4 h at –20°C, the samples are centrifuged (2,000 × *g*, 10 min). The glycogen pellets are washed 3 times with 70% ethanol before the amount of ^{14}C-labeled glycogen is determined by liquid scintillation counting. Total glycogen is determined according to Lowry and Passoneau (1972) after hydrolysis to glucose (1 N HCl at 100°C for 3 h). The incorporation of [^{14}C]glucose into radiolabeled glycogen is normalized for the total amount of glycogen.

EVALUATION

The concentration dependence of [U-^{14}C]glucose uptake and conversion into glycogen by insulin/compounds/drug candidates is determined. The isolated diaphragm of rats or mice is the preferable organ to study the effect of insulin and substances with insulin-like effects, such as sulfonylureas, on muscle tissue or the influence of denervation (Standing and Foy 1970, Smith and Lawrence 1984, Ishizuka et al. 1990, Hothersall et al. 1990).

K.6.2.13.2 Method Based on Myotubes

L6 myotubes are washed three times with Krebs-Ringer phosphate HEPES (KRPH) buffer (150 mM NaCl, 5 mM KCl, 2.9 mM Na_2HPO_4, 1.25 mM $MgSO_4$, 1.2 mM $CaCl_2$, 10 mM HEPES, pH 7.4) supplemented with 0.1% BSA. The cells are then incubated for 30 min to up to 2 h with 25 µl of reaction medium (glucose-free α-MEM containing 20 mM HEPES, pH 7.4, 0.1% BSA, 100–500 µM [^{14}C]glucose [0.1–0.5 µCi]) in the presence of increasing concentrations of insulin/compounds/drug candidates at 37°C in a humified atmosphere of 8.5% CO_2. Subsequently, the reaction medium is removed by aspiration and the cells are washed with 100 µl of ice-cold PBS. The cells are then disrupted by incubation in 50 µl of 1 N NaOH for 10 min at 60°C. The cell homogenates are cooled to room temperature and trans-

ferred to 96-well FC/DV filter plates (Millipore) containing 100 µl of ice-cold ethanol. The plates are then incubated for 2–3 h at 4°C. The precipitate is filtered under vacuum and washed three times with 250 ml of ice-cold 66% ethanol. The filters are dried under a 100-W incandescent lamp. 50 µl of scintillation cocktail (e. g. Microscint 20, Packard) are added and the wells are sealed. The [^{14}C]glucose incorporated into cellular glycogen is quantified in a TopCount 96-well liquid scintillation counter.

EVALUATION

In order to identify hypoglycemic drugs with insulin-like or insulin-sensitizing activity, Berger and Hayes (1998) developed an assay for activators of glucose incorporation into glycogen utilizing differentiating L6 muscle cells in 96-well plates. In general, *in vitro* assays of glucose incorporation into glycogen in insulin-sensitive tissue have been used culture media containing the normal physiological concentration, ~5.5 mM, of unlabeled glucose and tracer levels of radiolabeled glucose (e. g. Chou et al. 1987, Robinson et al. 1993). Similarily, using this assay design and L6 myotubes, Berger and Hayes (1998) observed that such conditions do not produce glycogen of a high enough specific activity to be accurately quantified in single-well extracts from a 96-well plate. In contrast, use of glucose-free α-MEM as the reaction media increases the signal by more than one order of magitude, thereby allowing quantification of single wells in the 96-well format. Consequently, addition of exogenous (non-radioactive) glucose is omitted, which apparently does not lead to physiological alterations in course of the brief incubation with compounds/drug candidates and the subsequent assay period. Glucose incorporation follows in a time and concentration-dependent fashion and is blocked by typical inhibitors of glucose transport. Both insulin and pervanadate exerting insulin-like activity increase glycogen synthesis in concentration-dependent manner. This assay may serve as a high-capacity screen to identify novel compounds that upregulate glucose anabolic metabolism in skeletal muscle.

K.6.2.14 Glycogen Synthase (GS) Activity

GENERAL CONSIDERATIONS

Glycogen metabolism is controlled largely by the coordinated action of the two enzymes glycogen synthase (GS) and glycogen phosphorylase (GP). Both enzymes are controlled by covalent phosphorylation and by allosteric effectors (Cohen 1986, Roach 1991, Roach et al. 2001). GS undergoes a complex multisite phosphorylation at nine sites by several protein kinases (Roach et al. 2001), most notably PKA, casein kinase I, casein kinase II, GSK-3, and AMPK (Carling and Hardie 1989) which generally lead to inactivation.Important regulatory phosphorylation sites are distributed between the amino- (sites 2 and 2a) and the carboxyl-termini (sites 3a and 3b) of the GS molecule (Lawrence et al. 1983, Skurat et al. 1994, 2000). Full activity can be restored to phosphorylated enzyme by the presence of the allosteric activator glucose-6-phosphate (G-6P). GP is activated by phosphorylation of a single site (GP *a*) by phosphorylase kinase (Cohen 1987). The less active, dephosphorylated form (GP *b*) acquires full activity in the presence of the allosteric effector AMP. Dephosphorylation of all three of these key regulatory proteins, GS, GP, and phosphorylase kinase, is believed to be catalyzed primarily by glycogen-associated phosphatases (PP1G) (Hubbard and Cohen 1989a, b).

K.6.2.14.1 Method Based on Diaphragms

PROCEDURE

GS is assayed according to Oron and Larner (1979), Guinovart and coworkers (1979), Altan and coworkers (1985) with the following modifications: Intact hemidiaphragms are dissected from male Wistar rats and incubated in DMEM (10 ml/hemidiaphragm) with constant bubbling of 95% O_2/5% CO_2. For treatment with insulin/compounds/drug candidates, the hemidiaphragms are incubated (37°C) in the same medium containing 5 mM glucose. For preparation of homogenates, the diaphragms are blotted and frozen in liquid nitrogen. The frozen diaphragms (pool of four) are manually ground in a porcelain mortar and then homogenized at 0°C in 10 vol. of 25 mM Tris/HCl (pH 7.4), 100 mM NaF, 5 mM EDTA, 0.1 mM PMSF. The homogenate is centrifuged (10,000 × *g*, 20 min). The supernatant is used for the GS assay. After addition of 10 µl of diaphragm homogenate to 200 µl of 25 mM Tris/HCl (pH 7.4), 50 mM NaF, 10 mM EDTA (pre-incubated at 30°C) containing either 0.1 or 10 mM G6P, the reaction is initiated by supplementing 0.2 mM [U-^{14}C]UDP-glucose (10 µCi) and terminated after 15 min by the addition of 2.5 ml of ice-cold 66% ethanol and filtration over pre-wetted Whatman GF/C glass fiber disks. The filters are washed, dried and counted for radioactivity. Blanks are assayed by

adding the homogenate to tubes containing the complete reaction mixture plus ice-cold ethanol.

EVALUATION

The fractional velocity as parameter for the portion of GS active *in vivo* (l-form) toward the total enzyme contents (l-+d-forms) at the time point of homogenization is calculated as ratio between the activities measured at 0.1 (l-form) and 10 mM G-6P (l-+d-forms).

The concentration-dependence of sulfonylurea stimulated GS and its potentiation by insulin in the isolated rat diaphragm were studied by Müller and coworkers (1994).

K.6.2.14.2 Method Based on Myotubes/Hepatocytes

PROCEDURE

GS activity is assayed by measuring the incorporation of D-[^{14}C]glucose from UDP-[^{14}C]glucose into glycogen. L6 myotubes or HepG2 cells cultured in 6- or 12-well plates and serum-deprived overnight are incubated with insulin/compounds/drugs in serum-free α-MEM under an atmosphere of 5% CO_2 for 30 min at 37°C. After removal of the incubation medium and washing, the cells are scraped into 0.2–0.5 ml of 10 mM Tris/HCl (pH 7.5) containing 10 mM EDTA, 150 mM KF, 5 mM DTT. The cell lysates are centrifuged (5,500 × *g*, 2 min, 10°C). The infranatant below the lipid layer is cleared from residual lipids by two additional centrifugations (defatted homogenate) and served as source for GS. The reaction is started by adding 30 µl of the homogenate to 60 µl of a reaction mixture (prewarmed at 30°C) containing 33 mM Tris/HCl (pH 7.8), 0.2 mM UDP-[U-^{14}C]glucose (4 µCi), 6.7 mg glycogen, 150 mM KF and 0.1 mM/10 mM G-6P. After incubation for 20 min at 30°C, the reaction is terminated by addition of 2 ml of 66% ethanol, 10 mM LiBr (–20°C), rapid mixing and filtration over pre-wetted Whatman GF/C glass-fiber discs. The filters are washed 5 times with 5 ml of 66% ethanol each at 25°C, dried and measured for radioactivity. Blank values determined by adding the homogenate to tubes containing the complete reaction mixture plus ice-cold ethanol are subtracted from the total values each.

EVALUATION

The fractional velocity is calculated as the ratio of GS activity in the presence of 0.1 mM and 10 mM G6P. Measurements of GS activity in defatted homogenates from myotubes/hepatocytes which had been incubated in the presence of 0.1 mM glucose instead of 5 mM glucose (the concentration routinely used) did not reveal significant differences with respect to both the activity ratio and the effect of insulin. Presumably, the dilution of the limited amount of G6P, which accumulates during incubation with 5 mM extracellular glucose, during the subsequent preparation of the homogenate and the GS assay is high enough to prevent allosteric activation of GS. According to our experience incubation of the isolated rat adipocytes in the presence of 5 mM glucose has a positive impact on their viability, in general, and insulin sensitivity (glucose transport, glycogen synthesis), in particular.

K.6.2.15 Phosphorylation State of GS

PURPOSE AND RATIONALE

A large body of evidence suggests that insulin activation of GS proceeds via the PI-3K/Akt pathway that leads to phosphorylation and inhibition of GSK-3 (Shepherd et al. 1995, Cross et al. 1995). However, GSK-3 alone is not sufficient to account for GS dephosphorylation and activation by insulin (Lawrence and Roach 1997, Skurat et al. 2000). The mTOR, mammalian target for the immunosuppressant drug rapamycin, pathway is also activated by insulin. Rapamycin has been shown to block insulin-mediated activation of GS in muscle and 3T3-L1 adipocytes (Azpiazu et al. 1996, Shepherd et al. 1995) without affecting insulin-induced inactivation of GSK-3 (Cross et al. 1997), opening the possibility that mTOR could control GS phosphorylation *via* a phosphatase. Therefore, insulin may promote glycogen synthesis both *via* inhibition of GSK-3 *and* stimulation of a glycogen-associated type 1 serine/threonine protein phosphatase, PP1G. Studies with mice deficient in the regulatory subunit of PP1G indicate that although PP1G is not necessary for activation of GS by insulin, it is essential for regulation of glycogen metabolism under basal conditions and in response to contractile activity, and may explain the reduced muscle glycogen content in the KO mice, despite the normal activation of GS (Aschenbach et al. 2001). Contractions may utilize a separate signaling pathway from insulin to activate GS in response to contractions. Changes in GS activity in human muscle biopsy samples obtained during isometric contractions are associated with changes in protein phosphatase activity (Katz and Raz 1995), but the identity of this enzyme has not been determined. The phosphorylation state of GS in muscle and liver cells and the impact of compounds/drug candidates can be

monitored by ^{32}P- labeling and subsequent immunoprecipitation of GS.

PROCEDURE

Myotubes/hepatocytes are washed twice by flotation in low phosphate medium composed of KRP-HEPES modified to contain 50 µM KH_2PO_4, 2 mM glucose, 2% BSA and then suspended in the same medium (7.5×10^5 cells/ml). 5-ml portions are incubated with [^{32}P]phosphate (0.2 mCi/ml) for 2 h prior to addition of insulin/compounds/drug candidates and of 0.5 ml of 50 mM glucose. After incubation (20 min, 37°C), the cells are floated by centrifugation (1,000 × *g*, 1 min) and the infranatant is aspirated. The cells are suspended in 1.5 ml of cold 50 mM Tris/HCl (pH 7.6), 100 mM KF, 20 mM glycerol-3-phosphate, 10 mM $K_4P_2O_7$, 10 mM EDTA, 1 mM benzamidine, 0.2 mM PMSF and homogenized by 10 strokes using a tight-fitting Teflon-in-glass homogenizer in the same Eppendorf cup. The homogenate is centrifuged (18,000 × *g*, 30 min, 4°C). 1 ml of the post-mitochondrial supernatant is incubated with 10 µl of GS antiserum raised in guinea pigs by immunization with purified GS from rabbit skeletal muscle. After incubation for 2 h at 4°C, 50 µl of protein A-Sepharose (10% w/v in TES, see below) is added and the incubation continued overnight. The immunoprecipitates are collected by centrifugation (12,000 × *g*, 2 min, 4°C) and washed twice with 1 ml each of TES (50 mM Tris/HCl, pH 7.4, 1 mM EDTA, 150 mM NaCl) containing 1% TX-100, twice with TES and finally once with 50 mM Tris/HCl (pH 7.4). The beads are suspended in 25 µl of 2xLaemmli sample buffer, heated (95°C, 5 min) and centrifuged. The supernatant is subjected to SDS-PAGE (8% resolving gel). The amount of [^{32}P] contained in GS is determined by excising the corresponding gel pieces and measuring their radioactivity by liquid scintillation counting.

K.6.2.16 Protein Phosphatase 1G (PP1G) Activity and Phosphorylation

PP-1 Activity

Muscle PP1 activity is measured according to a protocol from Begum and Ragolia (1996). L6 myotubes treated with insulin/compounds/drug candidates are scraped off the 24-well dishes with 0.3 ml of phosphatase extraction buffer containing 20 mM Tris/HCl (pH 7.2), 2 mM EDTA, 2 mM EGTA with 10 µg/ml each of aprotinin, leupeptin, antipain, soy bean trypsin inhibitor, 1 mM benzamidine, 1 mM PMSF. The cells are sonicated for 10 sec, centrifuged (2,000 × *g*, 5 min) and the supernatants are used for the assay of PP1G activity in the presence and absence of 2 nM okadaic acid to inhibit PP2A activity. The conditions of the assay allow measurement of PP1 and PP2A activities and not PP2B and PP2C enzymes, which require divalent ions. Okadaic acid at 2 nM inhibits PP2A, only, and the PP-1 activity remaining in the assay is comparable with the activity inhibited by inhibitor 2 (Srinivasan an Begum 1994). Purified [^{32}P]-labeled GP *b* is used as a substrate. [^{32}P]-labeled GP *b* is prepared by reacting γ[^{32}P]ATP with purified phosphorylase kinase and GP *a* (Cohen 1983).

In Vivo Phosphorylation and Immunoprecipitation of PP1

Differentiated L6 myotubes are serum-starved overnight. The next day, the medium is removed and replaced by 1 ml of phosphate-free DMEM and incubation is continued for 1 h. [^{32}P]-orthophosphate is added (0.5 mCi/ml), and the cells are incubated for 4 h followed by incubation with compound/drug candidate for up to 1 h. Subsequently, the cells were rinsed four times with 1 ml of ice-cold PBS containing phosphatase and protease inhibitors and harvested in 0.5 ml of lysis buffer (20 mM triethanolamine, pH 7.2, 0.5 mM EGTA, 1 mM EDTA, 2 mM sodium vanadate, 100 mM sodium pyrophosphate, 100 mM sodium fluoride, 40 mM glycerol-3-phosphate, 1 mM benzamidine, 0.1 mM PMSF, 10 µg/ml each of leupeptin, aprotinin, antipain, trypsin inhibitor, and pepstatin A, 140 mM NaCl, and 1% Triton X-100. The cell lysates are centrifuged (16,000 rpm, 10 min) to remove cell debris. 100 µg of cell lysate protein are diluted to 1 ml with lysis buffer and precleared by incubation with rat IgG (5 µg/ml, coupled to protein A sepharose) at 4°C for 1 h. The supernatants are immunoprecipitated with PP1G subunit antibody (10 µg/ml) for 1 h at 4°C followed by treatment with 50 µl protein A sepharose CL6B (50%, by vol.). The pellets are washed four times with 1 ml of lysis buffer and resuspended in 40 ml of 2-fold SDS-sample buffer. The samples are incubated (37°C, 10 min) followed by centrifugation (10,000 × *g*, 1 min) to pellet the sepharose beads. Electrophoresis of the immunoprecipitates is performed in 7.5% SDS-polyacrylamide gels followed by autoradiography. The protein contents of PP1G regulatory subunit are determined by immunoprecipitating unlabeled cell lysates with anti-G subunit antibody, followed by separation of immunoprecipitated proteins on SDS-PAGE. The proteins are transferred to polyvinylidene difluoride membrane and probed with PP1G subunit antibody. The regulatory subunit

of PP1 is identified by incubating with [^{125}I]protein A (0.2 µCi/ml) followed by autoradiography. The intensity of the signal is evaluated by densitometric analysis of the autoradiograms as well as by radioactivity scanning.

REFERENCES AND FURTHER READING

Altan N, Altan VM, Mikolay L, Larner J, Schwartz CFW (1985) Insulin-like and insulin-enhancing effects of the sulfonylurea glyburide on rat adipose tissue glycogen synthase. Diabetes 34:281–286

Aschenbach WG, Suzuki Y, Breedeb K, Prats C, Hirshman MF (2001) The muscle-specific protein phosphatase PP1G/R_{GL} (G_M) is essential for activation of glycogen synthase by exercise. J Biol Chem 276:39959–39967

Azpiazu I, Saltiel AR, DePaoli-Roach AA, Lawrence JC (1996) Regulation of both glycogen synthase and PHAS-1 by insulin in rat skeletal muscle involves mitogen-activated protein kinase-independent and rapamycin-sensitive pathways. J Biol Chem 271:5033–5039

Begum N, Ragolia L (1996) Effect of tumor necrosis factor-α on insulin action in cultured rat skeletal muscle cells. Endocrinology 137:2441–2446

Berger J, Hayes NS (1998) A high-capacity assay for activators of glucose incorporation into glycogen in L6 muscle cells. Anal Biochem 261:159–163

Bloch G, Chase JR, Meyer DB, Avison MJ, Shulman GI, Shulman RG (1994) *In vivo* regulation of rat muscle glycogen resynthesis after intense exercise. Am J Physiol 266:E85-E91

Carling D, Hardie DG (1989) The substrate and sequence specificity of the AMP-activated protein kinase. Phosphorylation of glycogen synthase and phosphorylase kinase. Biochim Biophys Acta 1012:81–86

Chou CK, Dull T, Russell DS, Gherzi R, Lebowl D, Ulrich A, Rosen OM (1987) Human insulin receptors mutated at the ATP-binding site lack protein tyrosine kinase activity and fail to mediate postreceptor effects of insulin. J Biol Chem 262:1842–1847

Cohen P (1983) Protein phosphatases and their regulation. Methods Enzymol 99:243–250

Cohen P (1987) Molecular mechanisms involved in the control of glycogenolyis in skeletal muscle by calcium ions and cyclic AMP. Biochem Soc Trans 15:999–1001

Cohen P (1986) in The Enzymes (Boyer P, Krebs EG, eds) pp 461–497, 3rd Ed, Academic Press, Orlando, USA

Cross DA, Watt PW, Shaw M, van der Kaay J, Downes CP, Holder JC, Cohen P (1997) Insulin activates protein kinase B, inhibits glycogen synthase kinase-3 and activates glycogen synthese by rapamycin-insensitive pathways in skeletal muscle and adipose tissue. FEBS Lett 406:211–215

Guinovart JJ, Salavert A, Massagué J, Ciudad CJ, Salsas E, Itarte E (1979) Glycogen synthase: A new activity ratio assay expressing a high sensitivity to the phosphorylation state. FEBS Lett 106:284–288

Hothersall JS, Muirhead RP, Wimalawansa S (1990) The effect of amylin and calcitonin gene-related peptide on insulin-stimulated glucose transport in the diaphragm. Biochem Biophys Res Commun 169:451–454

Hubbard MJ, Cohen P (1989a) Regulation of protein phosphatase-1G from rabbit skeletal muscle. 2. Catalytic subunit translocation is a mechanism for reversible inhibition of activity toward glycogen-bound substrates. Eur J Biochem 180:457–465

Hubbard MJ, Cohen P (1989b) Regulation of protein phosphatase-1G from rabbit skeletal muscle. 1. Phosphorylation by cAMP-dependent protein kinase at a site 2 releases catalytic subunit from the glycogen-bound holoenzyme. Eur J Biochem 186:701–709

Ishizuka T, Cooper DR, Hernandez H, Buckley D, Standaert M, Farese RV (1990) Effects of insulin on diacylglycerol-protein kinase C signaling in rat diaphragm and soleus muscle and relationship to glucose transport. Diabetes 39:181–190

Ivy JL, Kuo CH (1998) Regulation of GLUT4 protein and glycogen synthase during muscle glycogen synthesis after exercise. Acta Physiol Scand 162:295–304

Jue T, Rothman DL, Tavitian BA, Shulman RG (1989a) Natural-abundance 13C NMR study of glycogen repletion in human liver and muscle. Proc Natl Acad Sci USA 86:1439–1442

Jue T, Rothman DL, Shulman GI, Tavitian BA, DeFronzo RA, Shulman RG (1989b) Direct observation of glycogen synthesis in human muscle with 13C NMR. Proc Natl Acad Sci USA 86:4489–4491

Katz A, Raz I (1995) Rapid activation of glycogen synthase and protein phosphatase in human skeletal muscle after isometric contraction requires an intact circulation. Pflügers Arch Eur J Physiol 431:259–265

Lawrence JC, Hiken JF, DePaoli-Roach AA, Roach PJ (1983) Hormonal control of glycogen synthase in rat hemidiaphragms. Effects of insulin and epinephrine on the distribution of phosphate between two cyanogen bromide fragments. J Biol Chem 258:10710–10719

Lawrence JC, Roach PJ (1997) New insights into the role and mechanism of glycogen synthase activation by insulin. Diabetes 46:541–547

Lowry OH, Passonneau JV (1972) A flexible system of enzymatic analysis. Chapter 9: A collection of metabolite assays. Academic Press, New York, pp 174–177

Müller G, Wied S, Wetekam EM, Crecelius A, Pünter J (1994) Stimulation of glucose utilization in 3T3 adipocytes and rat diaphragm *in vitro* by the sulfonylureas glimiperide and glibenclamide, is correlated with modulations of the cAMP regulatory cycle. Biochem Pharmacol 48:985–996

Murano K, Inoue Y, Emoto M, Kaku K, Kaneko T (1994) CS-045, a new oral antidiabetic agent, stimulates fructose-2,6-bisphosphate production in rat hepatocytes. Eur J Pharmacol 254:257–262

Oron Y, Larner J (1979) A modified rapid filtration assay of glycogen synthase. Anal Biochem 94:409–410

Pederson BA, Schroeder JM, Parker GE, Smith MW, DePaoli-Roach AA, Roach PJ (2005) Glucose metabolism in mice lacking muscle glycogen synthase. Diabetes 54:3466–3473

Price TB, Rothman DL, Avison MJ, Buonamico P, Shulman RG (1991) 13C-NMR measurements of muscle glycogen during low-intensity exercise. J Appl Physiol 70:1836–1844

Price TB, Taylor R, Mason GF, Rothman DL, Shulman GI, Shulman RG (1994) Turnover of human muscle glycogen with low-intensity exercise. Med Sci Sports Exercise 26:983–991

Roach PJ (1991) Multisite and hierarchal protein phosphorylation. J Biol Chem 266:14139–14142

Roach PJ, Skurat AV, Harris RA (2001) in Handbook of Physiology: The Endocrine Pancreas and Regulation of Metabolism (Jefferson LS, Cherrington AD, Eds) pp 609–647, Oxford University Press, New York, USA

Robinson KA, Boggs KP, Buse MG (1993) Okadaic acid, insulin, and denervation effects on glucose and amino acid transport and glycogen synthesis in muscle. Am J Physiol; Endocrinol Metab 265:E36–E43

Robinson KA, Sens DA, Buse MG (1993) Pre-exposure to glucosamine induces insulin resistance of glucose trans-

port and glycogen synthesis in isolated rat skeletal muscles. Study of mechanisms in muscle and in rat-1 fibroblasts overexpressing the human insulin receptor. Diabetes 42:1333–1346
Shepherd PR, Nave BT, Siddle K (1995) Insulin stimulation of glycogen synthesis and glycogen synthase activity is blocked by wortmannin and rapamycin in 3T3-L1 adipocytes: evidence for the involvement of phosphoinositide 3-kinase and p70 ribosomal protein S6 kinase. Biochem J 305:25–28
Shulman GI, Rothman DL, Jue T, Stein P, DeFronzo RA, Shulman RG (1990) Quantitation of muscle glycogen synthesis in normal subjects and subjects with non-insulin-dependent diabetes by 13C nuclear magnetic resonance spectroscopy. N Engl J Med 322:223–228
Skurat AV, Dietrich AD, Roach PJ (2000) Glycogen synthase sensitivity to insulin and glucose-6-phosphate is mediated by both NH2- and COOH-terminal phosphorylation sites. Diabetes 49:1096–1100
Skurat AV, Wang Y, Roach PJ (1994) Rabbit skeletal muscle glycogen synthase expressed in COS cells. Identification of regulatory phosphorylation sites. J Biol Chem 269:25534–25542
Smith RL, Lawrence JC (1984) Insulin action in denervated rat hemidiaphragm. J Biol Chem 259:2201–2207
Srinivasan M, Begum N (1994) Regulation of protein phosphatase 1 and 2A activities by insulin during myogenesis in rat skeletal muscle in culture. J Biol Chem 269:12514–12520
Standing VF, Foy JM (1970) The effect of glibenclamide on glucose uptake in the isolated rat diaphragm. Postgrad Med J, Dec Suppl 16–20

K.6.2.17 Lipid Metabolism in Muscle and Liver Cells

GENERAL CONSIDERATIONS

Type II diabetes is characterized by hyperglycemia, hyperinsulinemia, reduced ability to oxidize fat, and TAG accumulation in skeletal muscle fibers. Impaired glucose transport and glycogen synthesis are well documented in insulin-resistant subjects (Richter et al. 1988, Hansen et al. 1992, Boden et al. 1996, Kawanaka et al. 2001), but lipid metabolism is less clearly understood (Goodpaster and Kelley 1998). Especially, focus has been put on the increased intramyocellular TAG content, since an inverse correlation between insulin resistance and intramyocellular TAG has been demonstrated (Pan et al. 1997, Koyama et al. 1997, Simoneau et al. 1995, Phillips et al. 1996, Boesch et al. 1997, Szczepaniak et al. 1999). The mechanism responsible for TAG accumulation remains unclear, but it may depend on either an increased lipid uptake or a decreased lipid oxidation as *de novo* lipogenesis within skeletal muscle is low. Increased plasma-free fatty acid (FFA) availability induces insulin resistance within hours by lipid infusion or within weeks by feeding rats a high-fat diet or in massively obese humans accompanied with intramyocellular TAG accumulation (Storlien et al. 1991, Oakes et al. 1997, Griffin et al. 1999, Boden et al. 2001, Perseghin et al. 1999, Chalkley et al. 1998). Weight loss and lowering of plasma free fatty acids reduced insulin resistance and the TAG content (Roden et al. 1996, Boden et al. 2001). Several studies have shown an association between obesity, insulin resistance, and reduced oxidative capacity in skeletal muscle (Bachmann et al. 2001, for reviews see Guo 2001, Saloranta and Groop 1996, Boden 1997), as demonstrated by the finding of decreased mitochondrial number, altered mitochondrial morphology and decreased expression of mitochondrial genes of the oxidative metabolism (Morino et al. 2005, Petersen et al. 2004, Mootha et al. 2003, Pati et al. 2003). Deficiency of CPT leads to pathological TAG accumulation in muscle tissue further emphasizing the role of mitochondria for lipid homeostasis. Our current knowledge on TAG accumulation in relation to insulin resistance and type II diabetes originates mainly from *in vivo* studies rendering it difficult to determine the contribution of genetic and environmental factors to TAG accumulation in type II diabetes and obesity. Cultured myotubes offer a unique model for separating the genetic influence on insulin resistance and type II diabetes from environmental factors. The following assays can be used for the analysis of lipid metabolism in cultured muscle cells and its modulation by compounds and drug candidates.

K.6.2.17.1 Incubation with Fatty Acids

Solutions containing fatty acids are prepared according to the procedure described by Montell and coworkers (2002). Sodium salt of oleic acid is prepared immediately prior to utilization by dissolving the fatty acid in deionized water containing 1.2 eq of NaOH at 70°C with stirring until an optically clear dispersion is obtained. The fatty acid-salt solution is immediately added to DMEM containing fatty acid-free BSA with continuous agitation to avoid precipitation. Typically, the fatty acid:BSA molar ratio is 5:1. Myocyte cultures are grown in a DMEM/M199 medium (3/1) supplemented with 10% fetal bovine serum, 10 µg/ml insulin, 2 mM glutamine, 25 ng/ml fibroblast growth factor, 10 ng/ml epidermal growth factor. Immediately after myotube differentiation, cells are rinsed in Hanks' balanced salt solution, and a medium devoid of fibroblast growth factor, epidermal growth factor, and glutamine is added. Myotube cultures are maintained in this medium for up to 2 weeks.

K.6.2.17.2 Lipid Synthesis

Incorporation of [^{14}C]Glycerol into Lipids

For qualitative analysis of esterification of glycerol into AG, cells are incubated with 5 mM [U-^{14}C]glycerol (100 µCi/mmol), 5 mM glucose, and 1 mM sodium oleate (BSA:oleate molar ratio of 1:5) for 15 h (Montell et al. 2002). The cell monolayers are then washed three times in Hanks' balanced salt solution, and the lipids are extracted twice with hexane/isopropanol (3/2). After drying under nitrogen, the residual lipid extract is redissolved in chloroform/methanol (2/1) as described (Folch et al. 1957) and separated by TLC by use of hexane/diethyl ether/acetic acid (70/30/1). The lipid spots are identified by iodine vapor and counted in a phosphorimager.

Incorporation of [^{14}C]Glucose into Lipids

The synthesis of neutral lipids starting from glucose can be followed according to the protocol of Aas and coworkers (2004). Myotubes are incubated with either [1-^{14}C]oleic acid (18.5 kBq/ml, 0.6 mM) or [1-^{14}C]palmitic acid (18.5 kBq/ml, 0.6 mM) in the absence or presence of insulin/compound/drug candidate for 4 h before they are harvested into ice-cold PBS, centrifuged (1,000 × *g*, 5 min), resuspended in distilled water and sonicated. Cell-associated lipids are extracted with chloroform/methanol as described (Folch et al. 1957). Briefly, 400 µl of cell homogenate is mixed with 8 ml of chloroform/methanol (2/1, by vol.), and FCS (30 µl) was added as a carrier. After 30 min, 1.6 ml of 0.9% NaCl (pH 2) is added and the mixture is centrifuged (1,000*xg*, 5 min). The organic phase is evaporated under a steam of nitrogen at 40°C. The residual lipid extract is re-dissolved in 200 µl of n-hexane and separated by TLC using hexane/diethylether/acetic acid (65/35/1) as the mobile phase. The bands are visualised with iodine, excised and counted by liquid scintillation. Lipids are also extracted after incubation of myotubes with D-[^{14}C(U)]glucose (74 and 111 kBq/ml, 5.5 mM or 20 mM) for 24 h.

EVALUATION

Extraction of lipids is carried out after incubation of myotubes with D-[^{14}C(U)]glucose for 4 h. Myotubes are exposed to DMEM supplemented with 0.24 mM fatty acid-free BSA, 0.5 mM L-carnitine, 20 mM HEPES, 5.5 or 20 mM [D-^{14}C(U)]glucose [(2.0 µCi/ml), and insulin/compound/drug candidate. On the basis of the typically very low incorporation, the overall glucose incorporation into lipids is determined by counting the total lipid extract washed with a water phase that contained 0.5 M glucose to displace all glucose labeled.

Incorporation of [^{14}C]Palmitate into Lipids

For analysis of lipid synthesis starting with fatty acids accrding to the protocol of Busch and coworkers (2005), cells are treated for 48 h with insulin/compounds/drug candidates. Two hours before the end of the treatment 2.5 µCi [^{14}C]palmitate in ethanol is added to each well (24-well dish, 0.5 ml culture medium). The labeled cells are put on ice, washed in 3 × 0.5 ml ice-cold PBS, scraped off the dish in 1 ml cold PBS, and spun (3,000 × *g*, 10 min). The supernatant is discarded, and lipids in the cell pellet are extracted overnight in 1 ml chloroform/methanol (2/1, by vol.). The extractions are washed in 250 µl H_2O, followed by an additional wash in 125 µl H_2O, and the resulting lipid-containing, organic phase is dried under a stream of nitrogen. The lipids are redissolved in 50 µl chloroform/methanol (2/1, by vol.), and a small fraction is used to determine the total amount of counts in the extracted lipids. The rest of the sample is spotted onto silica plates. The lipids are separated by TLCD-^{14}C(U) in petroleum ether/diethyl ether/methanol/acetic acid (180/14/4/1, by vol.). Spots comigrating with TAG and cholesterol ester standards are individually scraped and counted by liquid scintillation spectrometry. Protein is measured in parallel using a bicinchoninic acid protein assay.

Incorporation of [^{14}C]Acetate into Lipids

This protocol has been adapted from methods previously described (Foretz et al. 1998, Garcia-Villafranca et al. 2003, Cool et al. 2006). Primary rat hepatocytes are isolated as described (see K.5.2.2) and plated at 5×10^4 cells per well on collagen-coated, black-walled 96-well plates in DMEM supplemented with 10% FBS, 5 mM glucose, 1 mM sodium pyruvate, 2 mM L-glutamine, 25 mM HEPES/KOH (pH 7.4), 0.1 mM non-essential amino acids, 5 µg/ml transferrin, 100 nM dexamethasone, 100 nM insulin and 25 µg/ml gentamycin. After 4 h incubation, medium is replaced with medium as described above but lacking FBS and containing 100 nM triiodothyronine. Following a 16 h incubation at 37°C, the medium is removed and replaced with medium containing [^{14}C]acetate (2 µCi/ml) and as a control, AICAR or compounds/drug candidates. Cells are incubated (4 h, 37°C). Subsequently, the plates are rinsed with PBS three times. The final wash is replaced with scintillation cocktail (e. g. Mi-

croscint20, Perkin Elmer) and radioactivity incorporated into fatty acid monitored on a microplate β-reader.

REFERENCES AND FURTHER READING

Aas V, Kase ET, Solberg R, Jensen J, Rustan AC (2004) Chronic hyperglycaemia promotes lipogenesis and triacylglycerol accumulation in human skeletal muscle cells. Diabetologia 47:1452–1461

Bachmann OP, Dahl DB, Brechtel K, Machann J, Haap M, Maier T, Loviscach M, Stumvoll M, Claussen CD, Schick F, Häring HU, Jacob S (2001) Effects of intravenous and dietary lipid challenge on intramyocellular lipid content and the relation with insulin sensitivity in humans. Diabetes 50:2579–2584

Boden G (1997) Role of fatty acids in the pathogenesis of insulin resistance and NIDDM. Diabetes 46:3–10

Boden G, Lebed B, Schatz M, Homko C, Lemieux S (2001) Effects of acute changes of plasma free fatty acids on intramyocellular fat content and insulin resistance in healthy subjects. Diabetes 50:1612–1617

Boesch C, Slotboom J, Hoppeler H, Kreis R (1997) *In vivo* determination of intra-myocellular lipids in human muscle by means of localized ^{1}H-NMR spectroscopy. Magn Reson Med 37:484–493

Busch AK, Gurisik E, Cordery DV, Sudlow M, Denyer GS, Laybutt DR, Hughes WE, Biden TJ (2005) Increased fatty acid desaturation and enhanced expression of stearoyl coenzyme A desaturase protects pancreatic β-cells from lipoapoptosis. Diabetes 54:2917–2924

Chalkley SM, Hettiarachchi M, Chisholm DJ, Kraegen EW (1998) Five-hour fatty acid elevation increases muscle lipids and impairs glycogen synthesis in the rat. Metabolism 47:1121–1126

Cool B, Zinker B, Chiou W, Kifle L, Cao N, Perham M, Dickinson R, Adler A (2006) Identification and characterization of a small molecule AMPK activator that treats key components of type 2 diabetes and the metabolic syndrome. Cell Metabolism 3:403–416

Folch J, Lees M, Sloane Stanley GH (1957) A simple method for the isolation and purification of total lipids from animal tissues. J Biol Chem 226:497–509

Foretz M, Carling D, Guichard C, Ferre P, Foufelle F (1998) AMP-activated protein kinase inhibits the glucose-activated expression of fatty acid synthase gene in rat hepatocytes. J Biol Chem 273:14767–14771

Garcia-Villafranca J, Guillen A, Castro J (2003) Involvement of nitric oxide/cyclic GMP signaling pathway in the regulation of fatty acid metabolism in rat hepatocytes. Biochem Pharmacol 65:807–812

Goodpaster BH, Kelley DE (1998) Role of muscle in triglyceride metabolism. Curr Opin Lipidol 9:231–236

Griffin ME, Marcucci MJ, Cline GW, Bell K, Barucci N, Lee D, Goodyear LJ, Kraegen EW, White MF, Shulman GI (1999) Free fatty acid-induced insulin resistance is associated with activation of protein kinase C-τ and alterations in the insulin signaling cascade. Diabetes 48:1270–1274

Guo ZK (2001) Triglyceride content in skeletal muscle: variability and the source. Anal Biochem 296:1–8

Itani SI, Ruderman NB, Schmieder F, Boden G (2002) Lipid-induced insulin resistance in human muscle is associated with changes in diacylglycerol, protein kinase C and IκB-α. Diabetes 51:2005–2011

Koyama K, Chen G, Lee Y, Unger RH (1997) Tissue triglycerides, insulin resistance, and insulin production: implications for hyperinsulinemia of obesity. Am J Physiol 273:E708–713

Mootha VK et al (2003) PGC-1alpha-responsive genes involved in oxidative phosphorylation are coordinately downregulated in human diabetes. Nat Genet 34:267–273

Morino K, Petersen KF, Dufour S, Befroy D, Frattini J, Shatzkes N, Neschen S, White MF, Bilz S, Sono S, Pypaert M, Shulman GI (2005) Reduced mitochondrial density and increased IRS-1 serine phosphorylation in muscle of insulin-resistant offspring of type 2 diabetic parents. J Clin Invest 115:3587–3593

Oakes ND, Cooney GJ, Camilleri S, Chisholm DJ, Kraegen EW (1997) Mechanisms of liver and muscle insulin resistance induced by chronic high-fat feeding. Diabetes 46:1768–1774

Pan DA, Lillioja S, Kriketos AD, Milner MR, Baur LA, Bogardus C, Jenkins AB, Storlien LH (1997) Skeletal muscle triglyceride levels are inversely related to insulin action. Diabetes 46:983–988

Patti ME et al (2003) Coordinated reduction of genes of oxidative metabolism in humans with insulin resistance and diabetes: potential role of PGC1 and NRF1. Proc Natl Acad Sci USA 100:8466–8471

Perseghin G, Scifo P, De Cobelli F, Pagliato E, Battezzati A, Arcelloni C, Vanzulli A, Testolin G, Pozza G, Del Maschio A, Luzi L (1999) Intramyocellular triglyceride content is a determinant of *in vivo* insulin resistance in humans. Diabetes 48:1600–1606

Petersen KF, Dufour S, Befroy D, Garcia R, Shulman GI (2004) Impaired mitochondrial activity in the insulin-resistant offspring of patients with type 2 diabetes. N Engl J Med 350:664–671

Phillips DIW, Caddy S, Ilic V, Fielding BA, Frayn KN, Borthwick AC, Taylor R (1996) Intra-muscular triglyceride and muscle insulin sensitivity: evidence for a relationship in nondiabetic subjects. Metabolism 45:947–950

Roden M, Price TB, Perseghin KF, Petersen KF, Rothman DL, Cline GW, Shulman GI (1996) mechanisms of free fatty acid induced insulin resistance in humans. J Clin Invest 17:2859–2865

Saloranta C, Groop L (1996) Interactions between glucose and FFA metabolism in man. Diabetes Metab Rev 12:15–36

Simoneau JA, Colberg SR, Theate FL, Kelley DE (1997) Skeletal muscle glycolytic and oxidative enzyme capacities are determinants of insulin sensitivity and muscle composition in obese women. FASEB J 9:273–278

Storlien LH, Jenks AB, Chisholm DJ, Pascoe WS, Khouri S, Kraegen EW (1991) Influence of dietary fat composition on development of insulin resistance in rats: relationship to muscle triglyceride and ω-3 fatty acids in muscle phospholipids. Diabetes 40:280–289

Szczepaniak LS, Babcock EE, Schick F, Dobbins RL, Garg A, Burns DK, McGarry JD, Stein DT (1999) Measurement of intracellular triglyceride stores by ^{1}H spectroscopy: validation *in vivo*. Am J Physiol 276:E977-E989

K.6.2.17.3 Lipolysis

GENERAL CONSIDERATIONS

TAG is accumulated in LD in the cytoplasm of skeletal muscle cells (Schick et al. 1993, Oscai et al. 1990). The energy content of this TAG store is higher than the energy content of the muscle glycogen pool. The

muscle TAG concentration is increased by a high-fat diet (Van der Vusse et al. 1996) and in poorly controlled diabetes (Standl et al. 1980, Stearns et al. 1979), and is inversely related to whole-body insulin action (Pan et al. 1997). On the other hand, although existing studies are not unambiguous, the general view is that the intramuscular TAG stores can be mobilized by catecholamines (Froberg et al. 1975, Abumrad et al. 1980) and by exercise (Oscai et al. 1990, Van der Vusse et al. 1996). The exercise-induced decrease in muscle TAG concentration can be reduced by β-adrenergic blockade, and must accordingly be due to some extent to sympathetic stimulation (Stankiewicz-Choroszucha and Gorski 1978). While it seems that the intramuscular TAG constitute a dynamic energy store, the enzymic regulation of TAG breakdown in muscle is poorly understood (Van der Vusse et al. 1996, Martin 1996, Hagstrom-Toft et al. 1997, Kerckhoffs et al. 1998). The expression of HSL and its regulation by adrenaline has been investigated by Langfort and coworkers (1999).

It is thought that HSL is the major enzyme responsible for the hydrolysis of stored TAG in skeletal muscle similar to in adipose tissue. HSL protein or mRNA has been detected in rodent (Holm et al. 1987, Langfort et al. 1999) and in human (Roepstorff et al. 2004) skeletal muscle but with a considerable lower expression than in adipose tissue. The HSL protein expression also varies between fiber types, being higher in oxidative than glycolytic fibers (Langfort et al. 1999). Furthermore, it was recently shown (Hämmerle et al. 2002) that HSL-deficient mice accumulated DAG in adipose tissue and skeletal muscle, indicating that when HSL is missing this leads to an incomplete hydrolysis of TAG with an interruption of the lipolytic cascade at the stage of diacylglycerol hydrolysis. This observation was supported by the findings of a marked reduction in the formation of fatty acids in skeletal muscle as in several other tissues (Hämmerle et al. 2002). Interestingly, when the specific TAG hydrolase activity (the enzymatic conversion of TAG to DAG) was calculated, the specific TAG hydrolase activity was reduced 50% in adipose tissue, whereas no reduction was found in skeletal muscle when comparing HSL-deficient mice with wild type (Hämmerle et al. 2002). These data suggest that HSL is rate-limiting in the catabolism of DAG but not of TAG hydrolysis in skeletal muscle and furthermore points to the existence of one or more lipases with considerable activity, specifically to TAG hydrolysis in skeletal muscle. Further support for the existence of lipases other than HSL involved in basal TAG hydrolysis in skeletal muscle appears from recent studies, where neutral lipase activity in human skeletal muscle only decreased by ~25% when antiserum against HSL was added to the assay medium (Roepstorff et al. 2004, Watt et al. 2004). When a similar approach was taken in basal, resting rat soleus muscle (Langfort et al. 2000, Langfort et al. 1999), HSL activity was decreased by ~60%, indicating that HSL may be less dominating in human skeletal muscle than in rat skeletal muscle and that more lipases than HSL are involved in TAG hydrolysis in the resting state. It has been shown that electrically induced muscle contractions increase the neutral lipase activity of soleus muscle of rats (Langfort et al. 2000). It is surprising from the point of view that exercise is accompanied by increases in circulating catecholamine concentrations, and there is evidence for activation of HSL by epinephrine. Thus, in incubated rat soleus muscle, HSL was activated by epinephrine (Langfort et al. 1999). The impact of skeletal muscle lipid metabolism on exercise and insulin resistance has been reviewed by Kiens (2006). The following assays can be used for investigation of the effects of compounds/drug candidates on the regulation and activity of muscle lipases.

K.6.2.17.3.1 Lipolysis in Isolated Muscle Strips

PROCEDURE

In studies of glycerol release, muscle strips are incubated for indicated periods of time (usually 90 min) in 2 ml of KRB buffer supplemented with 20 mg/ml BSA (pH 7.4), 1 mg/ml glucose, and 0.1 mg/ml ascorbic acid in a shaking water bath (37°C), with air as gas phase according to the protocol of Enoksson and coworkers (2005). After incubation, an aliquot of the medium is removed for analysis of glycerol using an ultrasensitive bioluminescent method (Hellmer et al. 1989). Strips are incubated in duplicate or triplicate in the absence (basal) or presence of various concentrations of isoproterenol, which is a non-selective β-adrenoceptor agonist. The muscle strip is removed from the medium and frozen in liquid nitrogen. It is then removed from the clamps and weighed. Lipolysis is expressed as millimole of glycerol per total incubation medium per time unit per milligram of muscle strip. In studies of FFA release, muscle strips are incubated and analyzed as described for glycerol release, except that 20 mg/ml of fatty acid-free BSA is used as the protein component in the incubation buffer, the number of strips in each type of incubation should range between five and ten, and FFA is analyzed by an ultrasensitive chemiluminescence method as described for adipocytes (Näslund et al. 1993; see K.6.1.10.5).

K.6.2.17.3.2 TAG Lipase Activity in Soleus Muscle

Incubation and Electrical Stimulation

For electrical stimulation of the isolated soleus muscle after 1 h pre-incubation with compound/drug, the isolated soleus muscle with is transferred to fresh incubation medium and fixed in the vertical position and at resting length by small clips attached to the tendons according to the procedure introduced by Langfort and coworkers (2000). The upper tendon is connected to a force transducer. If subsequent electrical stimulation required, the muscles either remain resting or are stimulated electrically through electrodes in both ends to perform repeated ($1 \cdot s^{-1}$) maximal tetanic contractions (200-ms trains of 100 Hz, impulse duration 0.2 ms, 25 V) for 1, 5, 10 or 60 min while tension is recorded.

At the end of the incubation, muscles are freeze-clamped with aluminium tongs cooled in liquid nitrogen, and then trimmed of connective tissue and visible fat while kept in liquid nitrogen. In order to further ensure that findings reflected the biology of muscle cells, these are isolated before analysis from other tissue components by microdissection using a stereomicroscope after freeze-drying. Sometimes single fibres are isolated from fresh, non-frozen muscle by microdissection after collagenase digestion (one muscle being incubated for 3 h at 37°C in 5 ml of DMEM containing 2% (w/v) collagenase).

Preparation of Homogenates

Generally, muscles are homogenized (e. g. Polytron PT 3100, maximum speed) on ice in 10 vol. of 0.25 M sucrose, 1 mM DTT, 40 mM β-glycerophosphate, 10 mM sodium pyrophosphate, 20 mM HEPES/KOH (pH 7.0), 0.31 µM okadaic acid, 20 µg/ml leupeptin, 10 µg/ml antipain and 1 µ/ml pepstatin. The crude homogenate is centrifuged (15,800 × g, 1 min, 4°C). The supernatant is recovered and stored at −80°C until analysis within 1 week. In experiments evaluating the effect of phosphatase treatment on muscle homogenate, the homogenization buffer contained 20 mM Pipes (pH 7.0) instead of sodium pyrophosphate and glycerophosphate.

HSL Assay

HSL assays are based on measurement of release of [^{3}H]oleic acid from 1(3)-mono[^{3}H]oleoyl-2-oleylglycerol, a DAG analog not hydrolysable at position 2 (referred to as MOME activity), and from tri[^{3}H]olein (referred to as TOG activity). Upon phosphorylation by PKA, the TOG activity of adipose tissue HSL increases markedly (Fredrikson et al. 1981, Cook et al. 1982), whereas the MOME activity does not change significantly (Cook et al. 1982, Cook et al. 1983, Greenberg et al. 2001, for a review see Yeaman 2004). Accordingly, MOME activity is a measure of the total enzyme concentration, whereas TOG activity is a measure of the activated form of HSL, and represents the assay of choice for monitoring changes in the activation state of HSL. The TOG and MOME substrates are emulsified with phospholipids by sonication, and BSA is used as fatty acid acceptor. Samples of 14 µl (for TOG activity measurements) or 7 µl (for MOME activity measurement) of muscle supernatant (protein concentration ∼3 mg/ml) or pellet (resuspended to initial volume in homogenization buffer; protein concentration ∼4.4 mg/ml) are incubated for 30 min at 37°C with 100 µl of 5 mM TOG (1.25×10^6 cpm) or MOME (0.4×10^6 cpm) substrate and enzyme dilution buffer (to a total volume of 200 µl). Hydrolysis is stopped by the addition of 3.25 ml of methanol/chloroform/heptane (10/9/7, by vol.), followed by 1.1 ml of 0.1 M potassium carbonate/0.1 M boric acid (pH 10.5). The mixture is vortexed vigorously for 10 s and centrifuged (1,100 × g, 20 min). A 1-ml portion of the upper phase containing the released fatty acids is mixed with 10 ml of scintillation liquid. Radioactivity is determined in a scintillation counter.

K.6.2.17.3.3 Magnetic Resonance Spectroscopy Study of Intramyocellular Lipid Content

Kuhlmann et al. (2003) performed a longitudinal *in vivo* ^{1}H-spectroscopic study of intramyocellular lipid content in Zucker diabetic fatty (ZDF) rats. Magnetic resonance spectroscopy (MRS) has been established as a dependable method for selective detection and quantification of intramyocellular lipid (IMCL) in humans. To validate the interrelation between insulin sensitivity and IMCL in an animal model of type 2 diabetes, volume-selective ^{1}H-MRS at 7 Tesla to non-invasively assess IMCL in the rat was established. In male obese ZDF rats and their lean littermates, IMCL levels were determined repeatedly over 4 months, and insulin sensitivity was measured by the euglycemic-hyperinsulinemic clamp method at 6–7 and at 22–24 weeks of age.

In vivo MRS studies were performed using a 7-T Biospec system (Bruker BioSpin, Ettlingen, Germany), a resonator for excitation and an actively decoupled surface coil for signal detection. Rats were anesthetized with 2–3 vol% isoflurane and 1:2

O_2:N_2O, and their temperature was kept at 37.5°C. The animals were fixed in a non-magnetic device allowing for accurate alignment of their hindleg on top of the surface coil. Voxels of ≈8 mm^3 size were located in M. soleus and in M. tibialis anterior, avoiding vascular structures and gross adipose tissue deposits. Volume-localized ^{1}H-MR spectra [PRESS sequence, echo time (TE) = 17 ms, repetition time (TR) = 1 s, CHESS water suppression, 1024 averages] were obtained with Bruker's ParaVision acquisition software. The integral of the IMCL signal (1.3 ppm) was related to that of total creatine (tCr; 3.05 ppm; program MRUI 97.2, cf. http://www.mrui.uab.es). The IMCL/tCr ratio corresponded to the total muscle IMCL value. In all cases, a clear distinction between EMCL and IMCL was possible. As the IMCL/tCr ratio did not change on using a relaxation delay TR of 2 s instead of 1 s ($n = 4$), the influence of relaxation time changes on observed IMCL values could be excluded. The tCr values for the M. soleus and M. tibialis anterior were determined in obese ZDF rats at 8 weeks and 15 months of age ($n = 8$ each). In both muscles, tCr concentrations proved to be constant (soleus 89 ± 1.1 and 81 ± 1.7 µmol/g dry wt.; tibialis 136 ± 2.2 and 132 ± 1.0 µmol/g dry wt., respectively) and therefore to be a good reference for quantification of IMCL.

For assessing hepatic fat content, the rats were placed prone with their upper abdomen on top of the detecting surface coil. Volume-localized, respiration-triggered ^{1}H-MR spectra were obtained without water suppression (TE = 28 ms, TR = 1 s, 8 mm^3). Fat content was expressed as the ratio of the fat-to-water signal (in percentage).

K.6.2.18 Determination of Other Metabolites in Muscle

Muscle non-lipidic metabolites are determined according to the procedure of Watt and coworkers (2004). For this, muscle samples are divided into aliquots under liquid nitrogen. One piece of muscle (~80 mg wet muscle) is freeze-dried, dissected free of non-muscle contaminants under magnification, and divided into four aliquots. Muscle for glycogen analysis (3 mg) is extracted in 2 M HCl and neutralized with 0.67 M NaOH, and glycogen content is determined as described above and adapted from Passoneau and Lauderdale (1974). A second aliquot of muscle (2 mg) is extracted according to Harris and coworkers (1974), and ATP, phosphocreatine, creatine, and lactate are determined by enzymatic fluorometric techniques according to well-established procedures (Passoneau and Lowry 1993). Intramyocellular TAG content is determined by extraction of the TAG from ~6 mg of tissue in chloroform/methanol (2/1), saponification of the TAG in an ethanol-KOH solution at 60°C, and fluorometric determination of glycerol (Froberg and Mossfeldt 1971, 1975).

REFERENCES AND FURTHER READING

Abumrad NA, Tepperman HM, Tepperman J (1980) J Lipid Res 21:149–155

Cook KG, Colbran RJ, Snee J, Yeaman SJ (1983)Cytosolic cholesterol ester hydrolase from bovine corpus luteum. Its purification, identification and relationship to hormone-sensitive lipase. Biochim Biophys Acta 752:46–53

Cook KG, Yeaman SJ, Stralfors P, Fredrikson G, Belfrage P (1982) Direct evidence that cholesterol ester hydrolase from adrenal cortex is the same enzyme as hormone-sensitive lipase from adipose tissue. Eur J Biochem 125:245–249

Enoksson S, Hagström-Toft E, Nordahl J, Hultenby K, Pettersson N, Isaksson B, Permert J, Wibom R, Holm C, Bolinder J, Arner P (2005) Marked reutilization of free fatty acids during activated lipolysis in human skeletal muscle. J Clin Endocrinol Metab 90:1189–1195

Folch J, Lees M, Stanley GHS (1957) A simple method for the isolation and purification of total lipids from animal tissues. J Biol Chem 226:497–509

Fredrikson G, Stralfors P, Nilsson NO, Belfrage P (1981) Hormone-sensitive lipase from rat adipose tissue. Purification and some properties. J Biol Chem 256:6311–6320

Froberg SO, Hultman E, Nilsson LH (1975) Effect of noradrenaline on triglyceride and glycogen concentrations in liver and muscle from man. Metab Clin Exp 24:119–126

Froberg SO, Mossfeldt PF (1971) Effect of prolonged strenous exercise on the concentration of triglycerides, phospholipids and glycogen in muscle of man. Acta Physiol Scand 82:167–171

Greenberg AS, Shen W-J, Muliro K, Patel S, Souza SC, Roth RA, Kraemer FB (2001) Stimulation of lipolysis and hormone-sensitive lipase via the extracellular signal-regulated kinase pathway. J Biol Chem 276:45456–45461

Hämmerle G, Zimmermann R, Hayn M, Theusl C, Waeg G, Wagner E, Sattler W, Magin TM, Wagner EF, Zechner R (2002) Hormone-sensitive lipase deficiency in mice causes diglyceride accumulation in adipose tissue, muscle, and testis. J Biol Chem 277:4806–4815

Hagstrom-Toft E, Enoksson S, Moberg E, Bolinder J, Arner P (1997) Absolute concentrations of glycerol and lactate in human skeletal muscle, adipose tissue, and blood. Am J Physiol 273:E584-E592

Harris RC, Hultman E, Nordesjo L-O (1974) Glycogen, glycolytic intermediates and high-energy phosphates determined in biopsy samples of musculus quadriceps femoris of man at rest. Methods and variance of values. Scan J Clin Lab Invest 33:109–120

Hellmer J, Arner P, Lundin A (1989) Automatic luminometric kinetic assay of glycerol for lipolysis studies. Anal biochem 15:132–137

Holm C, Belfrage P, Fredrikson G (1987) Immunological evidence for the presence of hormone-sensitive lipase in rat tissues other than adipose tissue. Biochim Biophys Res Commun 148:99–105

Kerckhoffs DAJM, Arner P, Bolinder J (1998) Lipolysis and lactate production in human skeletal muscle and adipose tissue following glucose ingestion. Clin Sci 94:71–77

Kiens B (2006) Skeletal muscle lipid metabolism in exercise and insulin resistance. Physiol Rev 86:205–243
Kuhlmann J, Neumann-Haefeli C, Belz U, Kalisch J, Juretschke HP, Stein M, Kleinschmidt E, Kramer W, Herling AW (2003) Intracellular lipid and insulin resistance. A longitudinal *in vivo* ^{1}H-spectroscopic study in Zucker diabetic fatty rats. Diabetes 52:136–144
Langfort J, Ploug T, Ihlemann J, Holm C, Galbo H (2000) Stimulation of hormone-sensitive lipase activity by contractions in rat skeletal muscle. Biochem J 351:207–214
Langfort J, Ploug T, Ihleman J, Saldo M, Holm C, Galbo H (1999) Expression of hormone-sensitive lipase and its regulation by adrenaline in skeletal muscle. Biochem J 340:459–465
Martin III WH (1996) Effects of acute and chronic exercise on fat metabolism. Exercise Sport Sci Rev 24:203–231
Näslund B, Bernström K, Lundin A, Arner P (1993) Release of small amounts of free fatty acids from human adipocytes as determined by chemiluminescence. J Lipid Res 34:633–641
Oscai LB, Essing DA, Palmer WK (1990) Lipase regulation of muscle triglyceride hydrolysis. J Appl Physiol 69:1571–1577
Pan DA, Lillioja S, Kriketos AD, Milner MR, Baur LA, Bogardus C, Jenkins AB, Storlien LH (1997) Skeletal muscle triglyceride levels are inversely related to insulin action. Diabetes 46:983–988
Passoneau JA, Lowry OH (1993) Enzymatic analysis: A practical guide. Totowa, NJ: Humana
Passoneau JV, Lauderdale VR (1974) A comparison of three methods of glycogen measurement in tissues. Anal Biochem 60:405–412
Roepstorff C, Vistisen B, Donsmark M, Nielsen JN, Galbo H, Green KA, Hardie DG, Wojtaszewski JF, Richter EA, Kiens B (2004) Regulation of hormone-sensitive lipase activity and Ser563 and Ser565 phosphorylation in human skeletal muscle during exercise. J Physiol 560:551–562
Schick F, Eismann B, Jung W-F, Bongers H, Bunse M, Lutz O (1993) Comparison of localized proton NMR signals of skeletal muscle and fat tissue *in vivo*: two lipid compartments in muscle tissue. Magn Reson Med 29:158–167
Standl E, Lotz N, Dexel T, Janka H-U, Kolb HJ (1980) Muscle triglycerides in diabetic subjects. Effect of insulin deficiency and exercise. Diabetologia 18:463–469
Stankiewicz-Choroszucha J, Gorski J (1978) Effect of decreased availability of substrates on intramuscular triglyceride utilization during exercise. Eur J Appl Physiol Occup Physiol 15:27–35
Stearns SB, Tepperman HM, Tepperman J (1979) Studies on the utilization and mobilization of lipid in skeletal muscles from streptozotocin-diabetic and control rats. J Lipid Res 20:654–662
Van de Vusse GJ, Reneman RS (1996) Handb. Physiol Sect 12: Exercise Regul Integr Mult Syst pp 952–994
Watt MJ, Holmes AG, Steinberg GR, Meas JL, Kemp BE, Febbraio MA (2004) Reduced plasma FFA availability increases net triacylglycerol degradation, but not GPAT or HSL activity, in human skeletal muscle. Am J Physiol Endocrinol Metab 287:E120-E127
Watt MJ, Steinberg GR, Chan S, Garnham A, Kemp BE, Febbraio MA (2004) Beta-adrenergic stimulation of skeletal muscle HSL can be overridden by AMPK signaling. FASEB J 18:1445–1446
Yeaman SJ (2004) Hormone-sensitive lipase: new roles for an old enzyme. Biochem J 379:11–22

K.6.3 Assays for Insulin and Insulin-Like Signal Transduction Based on Adipocytes, Hepatocytes and Myocytes

GENERAL CONSIDERATION

After having established insulin-like activity of compounds/drug candidates in primary or cultured adipose, muscle, and liver cells or tissues with one or several of the metabolic assays described above (see K.6.1 and K.6.2), it is often useful to elucidate the molecular mode of action of these compounds/drug candidates for further characterization and optimization, in particular regarding selectivity and potency. For this, detailed knowledge in the molecular mechanisms of the insulin signal transduction cascade as well as of cross-talking insulin-like signaling pathways as well as the availability of appropriate reliable and robust cell-free and cell-based assays reflecting these events are required. The following view results from the current experimental findings but due to limitations in space and rapid progress still made in this area has to be considered as simplified and temporary, only.

Upon binding of insulin to the IR (insulin receptor) in the major insulin-responsive target cells (adipocytes, myocytes, hepatocytes), the insulin signal transduction machinery, a complex network of protein-protein interactions and protein (serine/threonine/tyrosine) phosphorylation and dephosphorylation cascades between a multitude of cellular signaling components (e. g. enzymes, adaptor proteins, structural proteins), is activated and transmits the insulin signal to a variety of metabolic (predominantly) and mitogenic (to a minor degree) effector systems (e. g. glucose transport, GLUT4 translocation, glycogen synthesis, gene expression, cell differentiation, DNA synthesis) (Biddinger and Kahn 2006, Myers and White 1995, Saltiel 1996, Yenush and White 1997, White 1998, Watson and Pessin 2006). For compounds/drug candidates with insulin-like/sensitizing activity, it is important to differentiate between metabolic and mitogenic signaling in cells of both high (e. g. adipocytes) and low insulin responsiveness (e. g. fibroblasts).

Two major pathways within the insulin signaling cascade have been dissected and are thought to mediate the different biological functions of the hormone: (I) Activation of phosphatidylinositol-3′-kinase (PI3-K) plays a pivotal role for regulation of glucose transport and cellular trafficking as well as glycogen synthesis and lipolysis by insulin. (II) Formation of

the Shc-Grb2 complex leads to activation of the Ras-pathway which has been linked to insulin regulation of both cell growth and gene expression, although this has been questioned recently. Many of the proteins involved in these two cascades have been identified at the molecular level (White 1997, Holman and Kasuga 1997, White 2002). The most upstream located one, the insulin receptor (IR) is a transmembrane tyrosine kinase which when activated by insulin binding, undergoes rapid autophosphorylation and phosphorylates a number of intracellular substrates, among them one or more 50- to 60-kDa proteins, including Shc, a 15-kDa fatty acid binding protein and several so-called insulin receptor substrate proteins, IRS-1/2/3/4, and Gab, which act as adaptor proteins lacking any enzymatic activity. Following tyrosine phosphorylation, the phosphotyrosine residues of the IRS polypeptides act as docking sites for several Src homology 2 (SH2) domain-containing adaptor molecules and enzymes, including PI3-K, Grb2, SHP2, Nck, and Fyn. The interaction between the IRS proteins and PI3-K occurs through the p85 regulatory subunit of the enzyme and results in an increase in catalytic activity of the p110 subunit.

PI3-K is essential and may even be sufficient for many of the insulin-regulated metabolic processes, including stimulation of glucose transport and glycogen synthesis and inhibition of lipolysis (Yeh el al 1997, Alessi and Downes 1998, Shepherd et al. 1998, Shepherd 2005, Cheatham et al. 1994, Herbst et al. 1995, Yeh et al. 1997). PI3-K activation results in the production of phosphatidylinositol (3,4,5)-trisphosphate and phosphatidylinositol (3,4)-bisphosphate which leads to binding and concomitant activation of the membrane-associated serine/threonine protein kinases, PDK1/2 (the nature of PDK2 remaining unclear so far). The binding of the pleckstrin-homology domain of PKB to the PI3-K-generated phosphoinositides both recruits PKB to the plasma membrane and *via* phosphorylation by PDK1/2 stimulates its kinase activity. Activation of Akt requires that it undergoes phosphorylation at two sites (Welsh et al. 2005). PDK1 phosphorylates Akt at Thr308, a residue located in its kinase-domain activation loop. In addition, Ser473 in the C-terminal hydrophobic motif of Akt has long been known to undergo phosphorylation but the identity of the kinase responsible has been controversial. Recently, however, an enzyme complex consisting of mTOR (mammalian target of rapamycin) and RICTOR (rapamycin insensitive companion of mTOR) has been shown to phosphorylate Akt at Ser473 in response to insulin (Hresko and Mueckler 2006, Sarabassov et al. 2005).

Thus the current knowledge favors the view that most metabolic insulin signals emerge from insulin-dependent tyrosine phosphorylation of the IRS proteins (and additional adaptor proteins located in lipid rafts, see K.6.3.6), whereas the mitogenic insulin action is apparently coupled to tyrosine phosphorylation of the Shc proteins. The latter serve as docking sites for the Grb-SOS complex which possesses GDP-GTP exchange activity for the small G-protein Ras and is activated by binding to Shc. In turn GTP-loaded Ras interacts with and activates the Raf serine kinase which phosphorylates the dual specificity kinase, mitogen/extracellular signal-activated kinase MEK (= MAPKK). Activated MEK phosphorylates the mitogen-activated protein kinases MAPK, ERK1 (p44) and ERK2 (p42), which in turn phosphorylate and activate a number of transcription factors (e. g. c-jun, c-fos) and structural proteins ultimately leading to increased gene and protein expression as well as DNA synthesis in insulin-like fashion (Gustafson et al. 1998).

In addition to the identification of the signal transduction pathways directly leading from the IR to downstream targets, several cross talks have been delineated between signal transmission by insulin and other hormones/growth factors (e. g. EGF, angiotensin) or diverse exogenous stimuli (e. g. H_2O_2, phosphoinositolglycans, see K.6.3.6.4) which either mimic to a certain degree (insulin-like activity) or modulate in a positive or negative fashion (insulin-sensitizing or desensitizing activity) metabolic and/or mitogenic insulin action in various cellular systems. Since none of these ligands activates the IR kinase directly, their signalling pathways may converge with that of insulin at a more distal signalling step (Argetsinger et al. 1995, Huppertz et al. 1996, Kowalski-Chauvel et al. 1996, Velloso et al. 1996, Verdier et al. 1997, Baron et al. 1998). Soluble phosphoinositolglycan molecules (PIG) which have been shown to exert partial insulin-like effects in diverse cellular and subcellular systems (Müller et al. 1997, Kessler et al. 1998, Frick et al. 1998, Leon and Varela-Nieto 2004, Müller et al. 2005) can also be classified into the latter category. Interestingly, the second-generation sulfonylureas, glibenclamide and, in particular, glimepiride have been demonstrated to stimulate glucose transport and non-oxidative metabolism in adipose and muscle cells *in vitro* by causing IR-independent tyrosine phosphorylation of IRS-1/2 and stimulating the downstream located insulin signaling events (Müller et al. 1994, Müller and Geisen 1996, Müller 2005). This insulin-like signaling in cells of peripheral tissues

may explain the insulin-independent blood glucose-lowering activity of glimepiride/glibenclamide as has been reported in a number of animal studies (Geisen 1988, Müller et al. 1995, Müller 2000, 2005), which supplements the potent blood glucose decrease *via* insulin release provoked by these widely used antidiabetics.

K.6.3.1 Insulin Receptor (IR) Activation

GENERAL CONSIDERATIONS

Insulin exerts its biological effects through a plasma membrane receptor that possesses a tyrosine kinase activity. Binding of insulin to the α-subunits of the IR induces autophosphorylation *in trans* on tyrosine residues of its β-subunits and thereby stimulates the intrinsic tyrosine kinase activity toward intracellular substrates (such as IRS proteins and Shc) that play crucial roles in the transmission of the signal (see K.6.3). Alterations in tyrosine phosphorylation of the IR have been described in insulin resistant states, such as diabetes and obesity (Combettes-Souverain and Issad 1998). The discovery of pharmacological agents that specifically activate the tyrosine kinase activity of the IR in cell-free and cell-based assay systems has recently been reported (Zhang et al. 1999) and apparently formed the starting point for a number of drug discovery efforts for future insulin-like or sensitizing drugs for the treatment of insulin-resistant patients.

The first critical node in the insulin-signaling network is, by definition, IR and the associated IRS. The IR is a tetrameric protein that consists of two extracellular α-subunits and two intracellular β-subunits. It belongs to a subfamily of receptor tyrosine kinases (RTKs) which also includes the insulin-like growth factor-1 receptor (IGF1R) and an orphan receptor, known as the IR-related receptor (IRR). Each of these receptors is the product of a separate gene, in which the two subunits are derived from a single-chain precursor or proreceptor that is processed by a furin-like enzyme to give a single α-β dimers linked with disulfide bonds to form the tetrameric $\alpha 2 \beta 2$ holoreceptor. This configuration allows for the creation of a hybrid IR-IGF1R complex, which serves as an additional receptor isoform modulated by insulin-like/sensitizing stimuli in differential fashion. The activity of the IR is tightly regulated, as unchecked activation or inactivity would lead to profound metabolic (and presumably proliferative) consequences. There are two splice isoforms of the IR, and each has a different affinity for insulin and IGF-1 (DeMeyts 1976).

Functionally, the IR behaves like a classical allosteric enzyme in which the α-subunit inhibits the tyrosine-kinase activity that is intrinsic to the β-subunit. Insulin binding to the α-subunit, or removal of the α-subunit by proteolysis or genetic deletion, leads to partial derepression, i. e. activation of the kinase activity in the β-subunit by stabilizing the open/relaxed rather than the closed/tense conformation of the activation loops of the two receptor halves. Following this initial activation, transphosphorylation of the β-subunits at tyrosines 1158, 1162, and 1163, leads to an additional stabilization of this conformational change even in the absence of ongoing insulin binding (Ellis et al. 1986,). The determination of the crystal structure of the tyrosine kinase domain of the human IR has provided a better understanding of the molecular mechanism involved in the stimulation of its kinase activity. In the unphosphorylated state, Tyr-1162 is located in the active site of the enzyme and plays an autoinhibitory role by competing with the binding of protein substrates. This tyrosine remains in the unphosphorylated form in the basal state, because other residues in the activation loop also impair ATP binding. The crystallization of the tris-phosphorylated form of the kinase domain has shown that autophosphorylation of these three tyrosines results in a dramatic change in the conformation of the activation loop (Hubbard 1997). This conformation change permits unrestricted access to the binding sites for ATP and protein substrates. It has been postulated that conformational changes induced by ligand binding move the kinase domain of the two β-subunits of the IR nearer to each other, thereby allowing *trans*-phosphorylation of tyrosine 1162 and adjacent tyrosines in the activation loop.

It is important to note that unlike other RTK that bind directly to the cytoplasmic tails of downstream effectors, the IR and IGF-1R engage specific proteins that are known as the IRS proteins and mediate the binding of intracellular effectors (see above). In addition, the IR and the IRS proteins share common mechanisms of regulation: They are negatively regulated by dephosphorylation by protein tyrosine phosphatases (PTPs), phosphorylation by serine/threonine kinases which interfere with IR/IRS function by sterically blocking interaction of IR and IRS or modifying IR kinase activity or downstream signaling of IRS, binding of inhibitory adaptor and signaling proteins (e. g. suppressor of cytokine signalling SOCS1/3, plasma membrane glycoprotein PC-1) and ligand-induced down-regulation of IRS at the translational and transcriptional level. Furthermore, the IR is also down-regulated at the protein level by ligand-induced inter-

nalization and degradation. Some of these regulatory processes may be dysregulated during the pathogenesis of insulin-resistant, hyperinsulinemic states, including obesity, type II diabetes and metabolic syndrome. The following methods may be helpful for the identification and characterization of insulin-like and sensitizing compounds/drug candidates as well as of insulin analogs with favorable kinetic (short- or long-lasting) action profiles using cell-free and cell-based assay systems.

K.6.3.1.1 Insulin Binding

PURPOSE AND RATIONALE

IR binding studies have been performed with various animal tissues and primary and cultured cells of rodent and human origin. Human adipocytes can be used to study simultaneously IR binding and metabolic effects of insulin (Hjøllund 1991). The binding tests are of value to characterize newly synthesized insulin analogs (Schwartz et al. 1987, Ribel et al. 1990, Vølund et al. 1991, Robertson et al. 1992).

K.6.3.1.1.1 Preparation of ^{125}I-Insulin

Most investigators use the "chloramine-T procedure" to iodinate insulin. The reaction is carried out in a 20 ml glass vial in an ice-bath with continuous magnetic stirring. To 2.5 ml 0.05 M phosphate buffer (pH 7.5), 2.0 mCi $Na^{125}I$, and 15 µl of a 1 mg/ml insulin solution are added. Then, 0.5 ml of a chloramine T (50 mg/ml) solution is added dropwise over the course of 1 min. After 10 min, 0.7 ml of a freshly prepared sodium metabisulfite solution (50 mg/ml in 0.05 M phosphate buffer, pH 7.5) is added. One ml of this reaction mixture is transferred to 10 ml 2% BSA for determination of specific activity. In order to absorb unreacted ^{125}I and damaged products, 2.0 g 20–50 mesh AG 1X-8 resin (BioRad) are added (equilibrated in 1 ml 0.05 M phosphate buffer, pH 7.5, containing 0.1 mg/ml thiomerosal and 20 mg/ml crystalline BSA). The reaction mixture is stirred for 10 min, decanted from the resin and diluted to a concentration of less than 25 µC/ml in a solution of 0.8 M glycine, 0.2 M NaCl, 0.05 M phosphate (pH 7.5), and 2.5 mg/ml crystalline BSA. The final solution is stored in multiple aliquots at –70°C.

K.6.3.1.1.2 Binding to Purified Insulin Receptor

IR are partially purified by affinity chromatography on WGA-Sepharose according to the procedure introduced by Ellis and coworkers (1986). Confluent flasks of cells are solubilized with 50 mM HEPES/KOH (pH 7.6), 1 mM PMSF, 1 mg/ml bacitracin. The lysate is then centrifuged (100,000 × *g*, 1 h, 4°C) and loaded on a 2-ml WGA-Sepharose column for 2 h at 4°C. After washing of the column with buffer C (50 mM HEPES/KOH, pH 7.6, 150 mM NaCl, 0.1% TX-100), bound proteins are eluted with 0.3 M N-acetyl-D-glucosamine in buffer C. The IR is further affinity-purified batch-wise by adsorption to monoclonal anti-hIR antibodies which are subsequently bound to anti-mouse IgG coupled to Sepharose beads. After several washing cycles with buffer C (10,000 × *g*, 2 min, 4°C), portions of the hIR-mAb-anti-IgG-beads are suspended in 50 µl of 20 mM HEPES/KOH (pH 7.4), 150 mM NaCl, 20 mg/ml BSA, 0.05% TX-100 and then incubated with ^{125}I-labeled insulin (300 mCi/mg, 0.2 µCi, 5 pM) in the presence of increasing concentrations of unlabeled insulin for 1 h at 4°C. Subsequently, the hIR-mAb-anti-IgG-beads are collected by centrifugation (10,000 × *g*, 2 min, 4°C), rapidly washed with 500 µl of buffer C containing 20 mg/ml BSA and finally counted in a gamma-counter.

K.6.3.1.1.3 Binding to Cultured Cells

Chinese hamster ovary (CHO) cells expressing the wild-type human IR (CHO-hIR) are maintained in Ham's F12 medium supplemented with 10% FCS, penicillin (100 U/ml) and streptomycin (100 µg/ml) (F12 medium). Cells (~ 10^6 cells/100-mm plate) are cotransfected with plasmid DNA (10 µg of expression plasmid *plus* 2 µg of pSV2NEO) in the form of a calcium phosphate precipitate with the addition of a glycerol shock (20% glycerol in F12 medium) after 4 h. After 36 h, the cells are split 1:20 and allowed to grow for 24 h prior to addition of G418 (400 µg/ml). 10–14 d later, colonies from 5 plates (~250–500 colonies) are harvested with trypsin/EDTA (0.05% trypsin, 0.02% EDTA in Ca^{2+}-free and Mg^{2+}-free Hank's basic salt solution and are replated in 24-well culture plates in F12 medium. 2 d later, semi-confluent cells (~4×10^4 cells/well) are washed twice with buffer B (100 mM HEPES/KOH, pH 7.8, 120 mM NaCl, 1.2 mM $MgSO_4$, 1 mM EDTA, 15 mM sodium acetate, 10 mM glucose, 1% BSA) and are then incubated with 16 h at 4°C with 0.5 ml of buffer B containing ^{125}I-labeled insulin (30,000 cpm, 120 Ci/g) *plus* increasing concentrations of unlabeled insulin. Cells are washed twice, solubilized with 0.5 ml of 0.03% SDS and counted in a γ-counter.

K.6.3.1.1.4 Binding to Human Primary Adipocytes

PROCEDURE

Subcutaneous adipose tissue (~4–5 g) is obtained from the abdomen of patients undergoing gastroenterological surgery. Patients suffering from any endocrine or metabolic disorder or taking drugs known to affect metabolism should be excluded. Other exclusion criteria are impaired glucose tolerance measured by determination of fasting blood glucose and the 2 h value after a 75-g oral glucose load. The adipose tissue is finely chopped and incubated for 90 min at 37°C in 25 mM HEPES/KOH (pH 7.4), containing HSA (25 g/l) and collagenase (0.5 g/l). The isolated adipocytes are subsequently washed five times in HEPES/KOH (see above) containing 50 g/l HSA.

IR binding studies with isolated human adipocytes are performed in a 300 µl cell suspension containing about 1×10^5 cells/ml in 10 mM HEPES (pH 7.4), 50 g/l HSA at 37°C. The iodine labeled ligand ([^{125}I]Tyr^{A14}-monoiodinated insulin, specific activity about 350 mCi/mg) in a final concentration of 20 pM is incubated with increasing amounts of unlabeled human insulin and the insulin analog/compound/drug candidate to be tested. The reaction is stopped by adding 10 ml of chilled 0.150 M NaCl and subsequent centrifugation through silicone oil (Pedersen et al. 1981 and 1982, Zeuzem et al. 1984). Non-specific binding is measured by incubating tracer in the presence of a large excess of unlabeled insulin.

For kinetic analysis of binding, the association is studied by incubation of the ([^{125}I]Tyr^{A14}-monoiodinated insulin for various times (1 to 240 min) and the reaction is terminated as described above. At each time point, the non-specific binding is measured and subsequently subtracted from the corresponding data for total binding. Dissociation rates are determined by first incubating isolated human adipocytes at 37°C with either [^{125}I]Tyr^{A14}-insulin or the test compound labeled in the same position for 90 min to achieve steady-state binding conditions. Each incubation mixture is then centrifuged for 60 s The adipocytes are rapidly washed twice by diluting with buffer to the original volume at 4°C and the centrifugations and aspirations are repeated. After the third aspiration, the cells are diluted to the original volume with buffer alone or native insulin or the insulin analog or compound to be tested at a final concentration of 0.2 µM at 22°C. At this hormone concentration a maximal effect of ^{125}I-insulin dissociation is reported (Podlecki et al. 1984, DeMeyts et al. 1976). The reaction is stopped at various times between 10 and 180 min and cell-associated radioactivity is determined.

K.6.3.1.2 IR Conformational Change Using BRET and FRET

PURPOSE AND RATIONALE

BRET is a natural phenomenon in which resonance energy transfer occurs between luminescent donor and fluorescent acceptor proteins (Xu et al. 1999, Angers et al. 2000). Resonance energy transfer occurs when part of the energy of an excited donor is transferred to an acceptor fluorophore, which re-emits light at another wavelength. Resonance energy transfer only takes place if the emission spectrum of the donor molecule and the absorption spectrum of the acceptor molecule overlap sufficiently and if the donor and the acceptor are in proper distance (10–100 Å) and relative orientation (Tsien et al. 1993, Wu and Brand 1994). In the BRET methodology, the first protein partner is fused to *Renilla* luciferase (Rluc), whereas the second protein partner is fused to a fluorescent protein (e. g. yellow fluorescent protein YFP). If the two partners do not interact, only one signal, emitted by the luciferase, can be detected after addition of its substrate cœlenterazine. If the two partners interact, resonance energy transfer occurs between Rluc and the YFP, and an additional signal, emitted by the YFP, can be detected. The strict dependence of BRET on the molecular proximity between energy donors and acceptors makes it a system of choice to study changes in the interaction between two proteins, which usually (in the unstimulated state of the target cell) exist as separate entities or are already assemblied in a preformed complex susceptible to changes in their relative neighborhood or orientation in response to appropriate stimuli.

Binding of insulin to the IR induces a conformational change that brings the two β-subunits of the IR into close proximity, allowing trans-phosphorylation of one IR β-subunit by the other subunit (Hubbard 1997, Combettes-Souverain and Isaad 1998). This autophosphorylation stimulates the tyrosine kinase activity of the IR towards intracellular substrates, such as IRS-1 and initiated downstream signaling to the terminal metabolic insulin effector systems, such as GLUT4 translocation, which are impaired in insulin-resistant and diabetic states. Therefore, methods that allow monitoring of the activity of the IR constitute important tools for the search for insulin-like compounds and putative anti-diabetic drugs.

Biazzo-Ashnault and coworkers (2001) developed a FRET-based assay for monitoring IR kinase activ-

ity. In this assay, the IR has to be immobilized on a microtiter plate with anti-IR antibody. A kinase reaction is then performed using a phosphorylation cocktail containing a biotinylated substrate. After incubation with a fluorescent donor, a strpetavidin-labeled fluorescent acceptor that to the biotinylated substrate is added. Energy transfer only occurs if the fluorescent donor coupled to anti-phosphotyrosine antibody is in close proximity to the streptavidin-labeled fluorescnet acceptor, i. e. if the peptide substrate is phosphorylated on tyrosine residues. Obviously, this is still a heterogeneous assay involving time-consuming incubations and washing steps.

By contrast, Boute and coworkers (2001) developed a completely homogeneous test, based on the BRET methodology, to follow IR kinase activity. A chimeric human IR, in which one IR β-subunit is fused to *Renilla* luciferase (Rluc) and the other IR β-subunit is fused to yellow fluorescent protein (YFP) is produced in HEK cells and partially purified by wheat germ lectin chromatography. Insulin-induced conformational change could be detected as an increase in energy transfer (BRET signal) between Rluc and YFP. This BRET signal corresponds to the ligand-induced conformational changes of the IR before any phosphorylation event, and faithfully reflects the activation state of the IR (Boute et al. 2001).

PROCEDURE

Cell-Based Assay

HEK-293 cells maintained in DMEM supplemented with 4.5 g/l glucose and 10% FBS (Invitrogen) are seeded at a density of 1.2×10^6 cells per 100-mm dish. Transient transfection is performed 1 day later using FuGene 6 (Roche Diagnostics) with either 0.3 µg of IR-Rluc cDNA and 0.3 µg of empty vector or with 0.3 µg of IR-Rluc and 0.3 µg of IR-YFP cDNAs per 100-mm dish. BRET measurements on intact cells are performed essentially as described by Angers and coworkers (2000). 2 days after transfection, HEK-293 cells are detached with Trypsin-EDTA and resuspended in PBS. Approximately 60,000 cells per well are distributed in a 96-well microplate. Cells are incubated for 2 to 10 min in absence or presence of 100 nM insulin. Coelenterazine is added at a final concentration of 5 µM, and light-emission acquisition is started immediately. For use of adherent cells, cells are transfected exactly as described above, but 1 day after transfection, cells are transferred into 96-well microplates (white CulturPlate-96, Packard) at a density of 30,000 cells per well.

In Vitro Assay on Partially Purified Fusion IR

BRET measurements are performed using partially purified fusion IR. Two days after transfection, cells are extracted in buffer containing 1% Triton X-100, 20 mM MOPS, 2.5 mM-benzamidine, 1 mM-EDTA, 1 mM-4-(2aminoethyl) benzenesulfonyl fluoride hydrochloride, and 1 µg/ml each of aprotinin, pepstatin, antipain, and leupeptin. Fusion receptors are partially purified by chromatography on wheat-germ lectin Sepharose by Tavare and Denton (1988). Partially purified fusion IR are aliquoted and stored at −80°C for subsequent use. *In vitro* measurement of BRET signal is performed using 4.5 µl of wheat-germ lectin (WGL) eluate (approximately 2 µg of proteins) preincubated in 96-well microplates for 45 min at 20°C in a total volume of 60 µl containing 30 mM MOPS, 1 mM Na_3VO_4, and different concentrations of ligands. Coelenterazine (7 µl, 2.6 µM final concentration, Molecular Probes, USA) is added to the preparation and light emission acquisition at 485 nm (filter window 20 nm) and 530 nm (filter window 25 nm) is started immediately using a microplate analyser (e. g. Fusion, Packard).

EVALUATION

The BRET ratio has been defined previously (Angers et al. 2000) as [(emission at 530 nm) – (emission at 485 nm) × Cf]/(emission at 485 nm), where Cf corresponds to (emission at 530 nm)/(emission at 485 nm) for the Rluc fusion protein expressed alone in the same experimental conditions (i. e., IR-Rluc transfected alone).

The BRET signal detected in this assay closely reflects the activation state of the IR independently of any phosphorylation reaction. It is a completely homogeneous procedure, requiring no washing step.Thus, the procedure allows for very rapid determination of the activation state of the IR and can be easily used in throughput screening tests for the search of novel compounds/drug candidates with insulin-like activity. Indeed, partially purified fusion IR can be prepared on a large scale by WGL-chromatography and stored at −80°C for subsequent use. This preparation can be distributed in an automated way in 96-well microplates and the effect of molecules on IR activity can be measured within a few minutes using the BRET method. Therefore, the same preparation can be used for multiple screening rounds. Similar procedures should be applicable to any receptor in which lignad binding induces dimerization or conformational changes de-

tectable by BRET. Thus, this assay could be a valuable tool for the search of compounds/drug candidates with anti-diabetic properties.

For screening purposes it turned out that the *in vitro* rather than the cell-based assay has to be used (Boute et al. 2001). The chimeric IR are correctly expressed and functional in HEK293 cells, but an unexpected high basal BRET signal was observed. Obviously, the choice between an *in vivo* and *in vitro* assay has to be done on a case-by-case basis. However, it must be kept in mind that in an intact cell assay, cells have to be distributed and cultured in microtiter plates for each screening round, which is highly time-consuming.

Comparison with FRET Technology

Before the development of BRET in 1999, fluorescence resonance energy transfer (FRET) has been used widely to study protein-protein interactions or to monitor conformational changes within a given protein. In the FRET methodology, luciferase is replaced by a fluorophore that is excited using monochromatic light at the appropriate wavelength (Cubitt et al. 1995, Hovius et al. 2000, Zacharias et al. 2000). A major advantage of FRET is to permit, under microscopic observation, visualization in a single living cell of protein-protein interactions at the subcellular level (Wouters et al. 2001). This is difficult to perform with the present version of the BRET methodology because of the low intensity of light emission by luciferase.

However, FRET presents several disadvantages that make BRET a technology of choice in many cases. In FRET, the donor fluorophore must be excited using monochromatic light. Because of the overlapping absorption and emission spectra of the existing mutants of GFP, direct excitation of the acceptor fluorophore by the light used to excite the donor often complicates the interpretation of the results. This obviously does not occur in BRET because excitation of the donor partner does not require exogenous illumination. Therefore, the quantification of resonance energy transfer is much easier in BRET than in FRET (Tsien 1998). Another related advantage of BRET is that the relative levels of expression of donor and acceptor partners can be quantified independently by measuring the luminescence of the donor and the fluorescence of the acceptor (Xu et al. 2002). Moreover, in FRET, excitation of the donor by illumination of the sample can induce photobleaching of the donor fluorophore, which results in loss of signal with time (Tsien et al. 1993, Cubitt et al. 1995). In addition, in FRET, illumination of the sample often induces autofluorescence that is emitted by endogenous cell components. The resulting background can easily be dealt with when FRET is assessed in a single cell with imaging techniques, by using an unlabeled region of the cell as an internal reference for the autofluorescence background (Tsien 1998). However, this background might become a serious problem when interactions are measured on populations of cells or molecules using non-imaging methods, such as fluorometry in microtiter plates (as would be desirable for throughput screening assays). Recent studies indicate that a tenfold improvement in sensitivity could be attained by using BRET rather than FRET, in an otherwise identical assay (Arai et al. 2000, 2001). Finally, it must be taken into account that the instrumentation requirements for BRET are simpler than those for FRET, which needs an excitation light source. A comparative evaluation of BRET *vs.* FRET technologies with emphasis in their putative application in high-throughput screening has been provided by Boute and coworkers (2002). A chimeric human insulin receptor, in which one-receptor β-subunit was fused to *Renilla* luciferase and the other receptor β-subunit was fused to yellow fluorescent protein, was produced in HEK cells and partially purified by wheat germ lectin chromatography. Insulin-induced conformation change could be detected as an increase in energy transfer (BRET signal) between *Renilla* luciferase and the yellow fluorescent protein.

K.6.3.1.3
IR Tyrosine Phosphorylation

K.6.3.1.3.1
Phosphorylation with Purified IR

PROCEDURE

Preparation of Purified IR

IR is extracted and purified from human placenta as described by Yamaguchi and coworkers (1983) with modifications from Ozawa and coworkers (1998). After preparation of placental membranes from one piece of fresh normal human placenta by differential centrifugation, a suspension containing the membrane proteins is mixed with the same volume of a 50 mM Tris/HCl buffer (pH 7.4) containing 2% Triton X-100 and protein inhibitors (2 mM BAEE, 1 mg/ml pepstatin, 1 mg/ml aprotinin, 1 mg/ml leupeptin and 0.1 mM PMSF) for 45 min at 4°C with stirring. A clear supernatant is obtained by centrifugation (100,000 × *g*, 90 min, 4°C) and is transferred to 40 ml of a WGA-Sepharose affinity column. The fractions including the protein are pooled and applied to 6.3 ml of an insulin-Sepharose column. After thorough washing of the column with 50 mM Tris-HCl (pH 7.4) containing 1.0 M

NaCl, 0.1% Triton X-100 and 0.1 mM PMSF, the IR is eluted with 50 mM acetate buffer (pH 5.0) containing 1.0 M NaCl and 0.1% Triton X-100. The active fractions assessed by ^{125}I-insulin binding activity are collected and concentrated by pressured dialysis using a Diaflo ultrafiltration membrane PM-30 (Amicon Inc.). The purified IR is stored at −80°C. The purity of the IR is assessed by SDS-PAGE and silver staining. The purified IR results in two bands of 135 and 90 kDa, which correspond to α- and β-subunits of the IR, respectively. The stability of the purified IR is determined by the kinase activity of IR at various time intervals after elution of the insulin-Sepharose column. There is no apparent change for the kinase activity up to 1 month, which is evaluated from the magnitude of phosphorylated artificial substrate, poly(Glu^{80}Tyr^{20}), incubated with insulin and its receptor. The IR prepared by the present method is thus of sufficient stability. Kinase activities of purified IR are typically found to change from one extraction to another. In order to control this kinase activity so that it would to be the same throughout the experiment, the concentration of the purified IR has to be adjusted by dilution before the IR is applied for measurements in the present method.

Radioactive Assay

The direct effect of insulin/compounds/drug candidates on the purified IR is assessed by using random copolymers of (Glu^{80}Tyr^{20})$_n$ serving as a substrate for the IR kinase according to Braun and coworkers (1984). The purified IR is pre-incubated with 0.48 µM insulin at 22°C for 1 h in 630 µl of a solution (solution A) containing 25 µM ATP and 5.0 mM $MnCl_2$. The random copolymer of (Glu^{80}Tyr^{20})$_n$ is dissolved in a buffer solution (solution B) containing 0.1% Triton X-100, 5.0 mM $MnCl_2$, 10 mM $MgCl_2$, 50 µCi [γ-^{32}P]ATP, and 50 mM HEPES/KOH (pH 7.4) to its final concentration of 0.5 mg/ml. A 30-µl portion of solution B is taken into a microtube. Phosphorylation of (Glu^{80}Tyr^{20})$_n$ is initiated by adding 15 µl of the pre-incubated IR solution into the microtube, and the solution is incubated for 2 to 120 min. After each incubation time, the sample is applied to filter paper (Whatman 3MM). The filter paper is washed 6 times with 10% TCA and then with acetone and finally air-dried. Radioactivity is counted with a liquid scintillation counter. The magnitude of phosphorylated random copolymers incubated with maximally effective concentrations of insulin is about 4- to 6- times higher than that without insulin at each time, demonstrating the activity of the IR preparation by the present purification method. The insulin-like activity of compounds/drug candidates is calculated as percentage of the maximal insulin effect.

K.6.3.1.3.2 Phosphorylation with Intact Cells

K.6.3.1.3.2.1 Detection by Immunoblotting

IR is immunoprecipitated from cell lysates (9×10^6 cells) by incubating with rabbit anti-IR antibody (3 µg) in buffer A (10 mM sodium phosphate, pH 7.4, 150 mM NaCl, 1% Nonidet-P40, 1% sodium deoxycholate, 0.1% SDS, 1 mM sodium pyrophosphate, 100 µM pervanadate, complete protease inhibitor mix tablets) overnight at 4°C with rotating. Prewashed protein G-sepharose beads (50 µl of packed beads) are added and the solution is mixed in a rotator for 2 h at 4°C. The beads are washed three times in buffer A and protein is eluted using SDS sample buffer (65 mM Tris/HCl, pH 6.8, 1.3% SDS, 13% glycerol, and bromophenol blue) with heating at 95°C for 5 min. SDS-PAGE is carried out by the method of Laemmli on 10% polyacrylamide gels using a mini-apparatus (e. g. Novex) in 25 mM Tris base, pH 8.3, 192 mM glycine, 0.1% SDS at 140 V constant voltage. Electrophoretic transfer from SDS-polyacrylamide gels to polyvinylidene fluoride (PVDF) (antiphosphotyrosine probing) or nitrocellulose (anti-IR probing) is carried out in a mini-blot apparatus (e. g. Novex). The blotting conditions are 40 V for 2 h in 12 mM Tris base, pH 8.3, 96 mM glycine, 20% methanol. Membranes are blocked in 1% polyvinylpyrrolidone (PVP-40, PVDF membranes) or 5% non-fat milk (nitrocellulose) and washed in 25 mM Tris (pH 7.2), 150 mM NaCl, 0.1% Tween 20. Phosphotyrosine-containing proteins are detected using antiphosphotyrosine (4G10) antibody-HRP-conjugated diluted 1:2,000 in 1% PVP-40. The β-subunit of the IR is detected using rabbit anti-IR diluted 1:1,000 in 5% milk followed by 1:2,000 dilution of anti-rabbit-HRP. Reactive proteins are visualized using chemiluminescent detection and a LumiImager.

K.6.3.1.3.2.2 Detection by ELISA

PURPOSE AND RATIONALE

A new assay method has been introduced by Ozawa and coworkers (1998) for the identification and evaluation of compounds/drug candidates with insulin-like activity and interfering with the insulin signaling pathway. It is based on the on/off switching mechanism of the IR-mediated insulin signaling. The Y939 sub-

strate peptide, a synthetic peptide of 12 amino acid residues, consists of a tyrosine-phosphorylated domain of IRS-1 and of a binding domain of IRS-1 to PI-3K. The Y939 peptide is immobilized on an avidin-coated 96-well microtiter plate. Upon binding of insulin to the IR prepared in total or immunoprecipitated from lysates of treated cells, insulin stimulates its receptor kinase activity in a sample solution and phosphorylates the tyrosine residue of the Y939 peptide immobilized on the well surface. The sample solution is washed out, and a selective binding protein for the phosphorylated tyrosine, monoclonal anti-phosphotyrosine antibody labeled with horseradish peroxidase, is added and forms a phosphorylated peptide-antibody complex. The amount of complex thus formed is detected by enzymatic amplification with horseradish peroxidase that can produce a green-color product with an absorbance at 727 nm capable of being detected by colorimetry. The amount of phosphorylated Y939 peptide thus measured is expected to be a selective and sensitive measure of the extent of the insulin signaling induced by compounds/drug candidates.

PROCEDURE

Preparation of Biotin-Y939 Substrate Peptide

The Y939 substrate peptide is biotinylated by reaction of a maleimide group of biotin-$PEAC_5$-maleimide with a thiol group of cysteine introduced at the carboxy-terminal end of the Y939 peptide. 1.0 mg of Y939 peptide (7.2×10^{-7} mol) is dissolved in 160 µl of PBS buffer (150 mM NaCl, 3.0 mM KCl, 10 mM phosphate buffer, pH 7.2), and 2.5 mg of biotin-$PEAC_5$-maleimide (3.6×10^{-6} mol) dissolved in 40 µl of DMSO is added dropwise to the Y939 peptide solution with gentle stirring. The reaction mixture is left for 12 h at 25°C. The reactants are purified by reverse phase HPLC performed on a 801-SC system (Japan Spectroscopic Co., Japan), equipped with a Kaseisorb LC ODS-300–5 column and a UV detector, using a linear gradient of 0–80% acetonitrile in 0.05% trifluoroacetic acid at a constant flow rate of 1.0 ml/min over 60 min. The eluents are monitored by UV absorbance at 220 nm. 10 ml of an eluent containing biotinylated peptide are collected and lyophilized. To evaluate the ratio of covalently immobilized biotin molecules to the Y939 peptide, the amounts of the Y939-immobilized biotin and the Y939 peptide in the eluent are determined as follows. After lyophilization, the biotin-Y939 conjugate is dissolved in 1.0 ml of a PBS buffer and its absorbance at 280 nm is measured. Assuming that the observed absorbance is due to a tyrosine residue in a Y939 peptide, total amount of Y939 peptide is obtained from the absorbance and molar absorptivity for tyrosine of 1.34×10^3 M^{-1} cm^{-1}. The amount of Y939-conjugated D-biotin is evaluated by a spectrophotometric assay method.

Immobilization of the Y939 Peptide on a 96-Well Microtiter Plate

All 96 wells of a microtiter plate are incubated with 150 µl each of avidin solution (0.1 mg/ml avidin in PBS buffer) over 18 h at 4°C. After the immobilization of avidin on the well, each well of the plate is washed with a PBS-T buffer solution (0.05% Tween 20 in PBS buffer). To fill up space between the immobilized avidin molecules with BSA molecules, a 200-µl portion of a BSA solution (1.0% BSA in PBS buffer) is added to each well and the plate is left for 4 h at 4°C. The BSA solution is discarded, and each well is washed four times with the PBS-T solution. After washing with the PBS-T solution, 150 µl of biotin-Y939 conjugates (1.0 µg/ml in the PBS-T solution) is added to each well and biotin-avidin complexation is carried out for 1 h at 4°C. An excess of the conjugates is discarded, and the well is washed four times with the PBS-T solution.

Kinase Reaction

A sample solution is prepared in a microtube, consisting of 0.05% Triton X-100, 50 µM ATP, 1.7 mM $MnCl_2$, a given concentration of IR, 50 mM HEPES/NaOH (pH 7.4), and each concentration of insulin. The sample solution is incubated in a microtube at 25°C for 10 min, and 150-µl portion of the sample solution thus prepared is introduced in a given well. For obtaining a background absorbance, the sample solution without insulin is also introduced in one of the wells. The plate is shaken on a mixer for 1 h at 37°C to react the IR immunecomplex with the Y939 peptide immobilized on the well surface. The plate is washed three times with the PBS-T solution and then two times with a TBS solution (20 mM NaCl, 3.0 mM KCl, and 20 mM Tris/HCl, pH 7.4).

Enzymatic Reaction and Absorptiometric Assay

After dilution of monoclonal anti-phosphotyrosine antibody labeled with horseradish peroxidase in the TBS solution to its final concentration of 0.5 µg/ml, 150-µl of the solution is added into each well. After standing for 2 h at room temperature without shaking, the plate is washed six times with a TBS-T (0.05% Tween 20 in the TBS buffer) solution. To evaluate the amount of the antibody specifically bound to the phosphorylated Y939 peptide, 175 µl of a DA-64 solution

(0.4 mg/mL of DA-64 in 2.0% H_2O_2, 50 mM citric acid, and 100 mM Na_2HPO_4) is added to each well and is incubated with shaking for 1 h at 37°C in the dark. After the enzymatic reaction, the DA-64 solution is subjected to absorbance measurement. A 150-µl portion of the DA-64 solution is diluted with 1.0 ml of Milli-Q water, and the absorbance of the solution in a 1.0-ml cuvette is measured at 727 nm against water with a spectrophotometer.

EVALUATION

For obtaining net insulin-dependent signals (absorbance), a background absorbance obtained by introducing a buffer solution without insulin is subtracted from the observed absorbance in the presence of a given concentration of insulin. Changes in absolute value of this net absorbance are not negligible from one microtiter plate to another, seemingly because of unexpected alteration in the experimental conditions such as concentration of antibody and/or a decrease in activities for IR kinase. In order for the net absorbances obtained from one microtiter plate to be comparable to those obtained from another, the measured net absorbance for a given concentration of insulin is normalized against absorbance for 1.0 µM insulin in terms of $B/B_{max} \times 100$, where B is the absorbance for each concentration of insulin and B_{max} that for 1.0 µM insulin.

K.6.3.1.3.2.3 Detection by TRF

PURPOSE AND RATIONALE

A time-resolved fluorescent assay using Wallac's DELFIA system (DELFIA assay) has been developed to monitor changes in IR tyrosine phosphorylation. Usually phosphorylation levels are analyzed by measuring the incorporation of radioactive phosphate (Tornqvist and Avruch 1988), by immunoblotting, or by ELISA (Krutzfeldt et al. 1999) using phosphotyrosine antibodies (see K.6.3.1.3). These methods suffer from various drawbacks including the use of radioisotopes, tedious and limited sample analysis with respect to immunoblotting, and low dynamic range, in particular in colorimetric assays using ELISA. In contrast, the DELFIA assay using time-resolved fluorometry is a highly sensitive, non-radioactive assay performed in microtiter plates amenable to automation. A formate similar to that of the DELFIA assay has been used by Okada and coworkers (1998) to measure the effect of sodium orthovanadate on IR autophosphorylation of erythrocytes from normal and diabetic patients.

PROCEDURE

Cell Culture

Chinese hamster ovary (CHO) cells overexpressing the hIR (CHO-hIR) are maintained in DMEM, 10% (by vol.) FBS and 1% (by vol.) penicillin-streptomycin at 37°C under 5% CO_2. Before treatment with insulin/compounds/drug candidates, cells are serum-starved for at least 14 h by incubation in DMEM, 0.5% (w/v) BSA, 1% penicillin–streptomycin.

In Vitro Phosphorylation of the IR

Wheat germ agglutinin-purified hIR is prepared from total membranes of CHO-hIR as described (K.6.3.1.1.2 and K.6.3.1.3.1) and then phosphorylated by incubating 700 µg of hIR with 50 mM HEPES (pH 7.4), 10 mM $MnCl_2$, 0.1% (by vol.) Triton X-100, 1 µM insulin, 0.5 mM ATP, and 100 µM sodium orthovanadate for 1 h at room temperature. The phosphorylated hIR is purified by passing the solution over a PD-10 column (Pharmacia) in 50 mM HEPES (pH 7.4), 0.1% Triton X-100, 100 µM sodium orthovanadate and concentrated by centrifugation in a 2-ml Amicon concentrator (30MWCO).

Biotinylation of Anti-IR Antibody

Anti-IR antibody Ab-3 (800 µl of 1.3 mg/ml, Upstate Biotechnology) is biotinylated by incubating overnight at 4°C with 60 µM of freshly prepared Sulf-NHS-LC-biotin (Pierce) dissolved in 4 mM bicarbonate (pH 7.8), 35 mM NaCl, 1% (by vol.) glycerol (final vol. 1 ml). Buffer exchange (PBS) and excess biotin removal are facilitated by diluting and concentrating in centricon units (30MWCO). The level of biotin incorporation is quantitated by comparing to a standard curve constructed using the biotin-induced displacement of avidin from the dye 2-(4-hydroxybenzene azo benzoic acid (HABA; Pierce; absorption of HABA–avidin 500 nm) according to the manufacturer's instructions. The typical yield is between 4 and 10 moles of biotin per mole of protein.

Preparation of Phosphorylated IR from Cells

Cells are grown in 6-well plates until ~60% confluency and serum-starved overnight. The cells are washed with DMEM, incubated in 2 ml of the same medium, and treated with various concentrations of insulin/compounds/drug candidates for 5–10 min. Following the treatments the medium is removed and the cells are immediately frozen in liquid nitrogen and then stored at −80°C until cell lysis. Cells are lysed in 200 µl of lysis buffer (50 mM Tris, pH 7.4,

150 mM NaCl, 1% Triton X-100, 1 mM pyrophosphate, 100 µM pervanadate, "Complete" protease inhibitor tablet). The cells are gently scraped from the dishes and centrifuged (14,000 rpm, 15 min, 4°C, Eppendorf centrifuge). The supernatants are used in the DELFIA assay.

Quantitation of Receptor Phosphorylation

All incubations of the DELFIA assay are carried out at room temperature with agitation in a final volume of 200 µl of DELFIA assay buffer unless otherwise stated. Streptavidin-coated plates are washed with DELFIA wash buffer for 15 min. After removal of wash buffer, anti-IR–biotin or anti-EGFR–biotin (100 ng/well) is added for 30 min. The plate is washed three times with wash buffer and cell lysates are added and the plate is incubated for 1 h. The plate is again washed three times with wash buffer, europium-labeled anti-phosphotyrosine antibody (100 ng/well) is added, and the plate is incubated for 1 h. Following extensive washing (at least five times), 180 µl of enhancement solution is added. The plate is shaken vigorously for 30 min and read in a microtiter plate reader using an europium protocol (excitation at 340 nm, emission at 615 nm, delay 400 µs, 1000 µs/cycle).

Optimization of Conditions

This time-resolved fluorescent (TRF) assay for measuring tyrosine-phosphorylated proteins in cells has been optimized by Waddleton and coworkers (2002). For this, biotinylated anti-IR antibody is used to capture both phosphorylated and non-phosphorylated IR from cells and for immobilization to the streptavidin-coated plate. Europium-labeled anti-phosphotyrosine antibody is used to bind only the phosphorylated IR. Time-resolved fluorometry of europium is then used to measure the level of phosphorylated IR. To establish conditions for the DELFIA assay, *in vitro* phosphorylated IR partially purified from CHO hIR cells is used. The optimum concentrations of both the capture antibody (anti-IR antibody) and the anti-phosphotyrosine antibody is typically ~100 ng. Using *in vitro* phosphorylated partially purified CHO hIR (0.13–0.52 µg/ml) the Eu signal typically reaches three orders of magnitude and remains linear to up to ~ 800,000 Eu counts. The minimal amount of phosphorylated IR necessary for a reliable signal is ~ 0.1 pmole (in 200 µl). The signal is specific for the phosphorylated form of IR since non-phosphorylated IR tested at similar concentrations does not produce a significant increase in background signal. Establishing the optimal conditions for the DELFIA assay it has been demonstrated that the phosphorylation status of the IR does not affect the ability of the capture antibody to immunoprecipitate IR from cell lysates.

EVALUATION

Stimulation of the cells with insulin followed by measurement of IR phosphorylation by DELFIA resulted in an EC_{50} of ~25 nM. This is similar to that reported by Biazzo-Ashnault and coworkers (2001) who used a FRET assay to measure IR tyrosine kinase activity by following phosphorylation of a synthetic peptide. Using the non-specific, protein tyrosine phosphatase (PTP) inhibitor, pervanadate, a 10-fold increase in basal IR phosphorylation is typically detected by the DELFIA assay, whereas analysis of the same samples by immunoblotting reveals a 3-fold increase, only. This difference is likely due to enhanced sensitivity of the DELFIA assay, particularly in the lower range where quantitation of scanned immunoblots is less accurate. Pervanadate results in a 50% increase in insulin-induced IR phosphorylation compared to treatment with ligand alone (10 nM), as measured by both DELFIA and immunoblotting. Comparing the well-established technique of immunoblotting with anti-phosphotyrosine antibodies to the DELFIA assay, similar results are usually obtained. In addition, Waddleton and coworkers (2002) demonstrated that this assay can be used to monitor IR phosphorylation in a normal (i. e. IR non-overexpressing) cell line and in response to phosphatase inhibitors. They also show the rapid and easy adaptation of the Delphia format assay to monitor changes in the phosphorylation status of other cellular proteins. These findings provide strong evidence that changes in the phosphorylation status of the IR in response to PTP inhibitors and most likely insulin-like compounds/drug candidates can be monitored using the DELFIA assay.

K.6.3.1.3.2.4 Yeast-Based Method

GENERAL CONSIDERATIONS

A number of mammalian cell-based assays have been developed in order to analyze IR kinase activity in response to compounds/candidate drugs in a cellular environment that most closely resembles the natural physiological conditions (see K.6.3.1.3.2 and K.6.3.1.2; Sims and Allbritton 2003, Sato et al. 2002). However, mammalian cell-based assays are expensive and time-consuming. Moreover, the effects of redundant processes on the measured output can be difficult to control and to distinguish from the effects that are specific for the IR. The yeast *Saccharomyces cere-*

visiae represents an inexpensive and rapid alternative for measuring the activity of the IR in a heterologous, yet eukaryotic environment. The fact that yeast does not have any endogenous RTKs and no *bona fide* non-receptor tyrosine kinases offers the advantage of a null background for the expression of the mammalian IR and for the measurement of the effects of compounds/drug candidates on the specific target (Barberis 2002, Gunde 2004, Hughes 2002). A yeast growth selection system for monitoring mammalian RTK activities and for detecting inhibition by specific inhibitors, which is based on the Ras-recruitment system (RRS) developed by Aronheim and collaborators has been introduced recently (Broder et al. 1998, Aronheim et al. 1994, 1998) and further modified and improved by Gunde and Barberis (2005). In particular, it may be useful for the throughput-screening for insulin-like compounds/drug candidates acting directly at the IR.

PURPOSE AND RATIONALE

Cdc25p, the yeast homolog of mammalian son of sevenless (Sos), is a Ras guanyl nucleotide exchange factor (Ras-GEF) functioning upstream of the Ras proteins in *S. cerevisiae*. The yeast temperature sensitive *cdc25–2* strain cannot grow at 37°C, because the mutant Cdc25 protein carried by this strain is unable to activate the endogenous Ras protein at this non-permissive temperature. Aronheim and coworkers (1994, 1998) have shown that membrane targeting of the mammalian Sos is sufficient to activate Ras leading to complementation of the *cdc25–2* temperature sensitive allele. The yeast growth selection system for monitoring human IR is based on the RRS.

PROCEDURE

Yeast Strains and Yeast Spotting Assay

Cells from the yeast strain cdc25–2 (Matα, ade5, cdc25–2, his7, lys2, met10, trp1, ura3–52, leu2) transformed with the hIR are plated on 2% glucose agar plates. Four different colonies of each transformation are picked and spotted onto two sets of galactose plates (3% galactose, 2% raffinose, and 2% glycerol) that are incubated at 25°C or 37°C. For this spotting assay, the yeast suspensions are not adjusted to the same concentration prior to spotting, whereas for the serial dilutions, the yeast cultures are adjusted to the same concentration. Plates incubated at 25°C are scanned after 4 days, whereas plates incubated at 37°C are scanned after 7 days. For serial dilutions, exponentially growing cultures are serially diluted in sterile water starting with a concentration of 4×10^7 cells/ml. 5 µl of each dilution are spotted onto two sets of galactose plates, corresponding to about 100,000, 20,000, 4000, 800, 160, and 32 cells *per* spot. Plates are incubated at 25°C and 37°C and scanned after 4 and 11 days, respectively.

Preparation of Yeast Extracts and Immunoblot Analysis

Exponentially growing *S. cerevisiae* cultures expressing the hIR are diluted to a final absorbance at 600 nm (A_{600}) of 0.5 in 4 ml of Ura/-Leu/-Trp dropout medium containing 2% glucose and are grown for 4 h. Cells are harvested by centrifugation, and whole cell extracts are prepared as described (Kaiser et al. 1994). Samples of whole cell extracts subjected to SDS-PAGE and blotted on nitrocellulose membranes following standard protocols.

Growth

Exponentially growing cultures expressing hIR are washed once with water and diluted to a final A_{600} of 0.1 ml of Ura/-Leu/-Trp dropout medium containing 3% galactose, 2% raffinose, and 2% glycerol. As a control, cells expressing M-Grb2-Ras(Q61L)ÄF are similarly grown, washed, and diluted to a final A_{600} of 0.03. 150 µl of the diluted cells are added to 96-well plates containing 1.5 µl of the compounds/drug candidates at the desired concentrations (1% final DMSO concentration). The plates are incubated at 37°C, and growth at the indicated time points is quantified by measuring A_{595} with a microtiter plate reader.

EVALUATION

As alternatives to this yeast Sos-recruitment system (RRS) to monitor protein-protein interactions at the plasma membrane, the reverse RRS for the identification of protein-protein interactions with integral membrane proteins (Köhler and Muller 2003), the split-ubiquitin system (Hubsman et al. 2001), and the SCINEX-P system (Stagljar et al. 2001) have been developed during the last decade. The split-ubiquitin system has been used to detect novel proteins that are associated with the mammalian ErbB3 RTK (Thaminy et al. 2003). Ehrhard and coworkers (2000) developed a method that uses the yeast G-protein signaling pathway as readout to select for protein-protein interactions. This assay has been validated with known binding partners, such as the RTK fibroblast growth factor receptor 3 (FGFR3) and SNT-1, that constitutively binds to the FGFR3 intracellular domain. The latter two methods are feasible for detection of interactions between an integral membrane protein and a soluble cytoplasmic protein, but, in contrast to the direct RTK assays, the binding of cytoplasmic proteins to the RTKs is independent of receptor activity.

Furthermore, Köhler and Muller (2003) recently applied an adaptation of the RRS to the analysis of interactions between two membrane-associated proteins, namely the myristylated and phosphorylated EGFR intracellular domain and a myristylated Grb2-Ras fusion protein. Due to the fact that yeast cells do not have endogenous mammalian-type tyrosine kinases, the yeast-based growth selection system offers the advantage of a null background eukaryotic organism for expression of these mammalian membrane-bound kinases, such as the IR. This assay may be of value in throughput screenings for the identification of cell-active activators (and inhibitors) of RTKs.

K.6.3.2 Phosphorylation of Signaling Components by Insulin and Insulin-Like Stimuli

GENERAL CONSIDERATIONS

Protein kinases (PK) and phosphatases (PP) have been implicated in a variety of cellular processes such as proliferation, differentiation, metabolism and apoptosis. Over one-third of the proteins in the human proteome are phosphoproteins and the family of PK and PP represents up to 5% of the human genome. These enzymes may cause an increase in or suppression of the activity of other enzymes, receptors, regulatory proteins or transcription factors, mark proteins for destruction, allow proteins to move from one subcellular compartment to another, or enhance or impede protein–protein interactions. In many cases these components and processes are embedded in various signaling pathways, such as the insulin signal transduction cascades. Thus, any change in the level, activity, or localization of PK and PP has a major impact on the regulation of these processes. Not surprisingly, the dysregulation of protein phosphorylation has been associated with diabetes.

There are estimated to be over 500 different PK in the human proteome that catalyze the transfer of phosphate from ATP to serine, threonine, and tyrosine. PK can be divided into two broad classes, serine/threonine and tyrosine kinases, although a few PK are able to phosphorylate both types of amino acid residues (dual-specificity kinases). Because of the key role that PK play in cellular functions, they have become one of the most important drug targets. As such, protein phosphorylation is in the focus of much interest for the development of compounds to selectively regulate the activity of diabetes-related PK. Thus, there is a need for assay systems that monitor the activity of these enzymes under a variety of experimental conditions and for the development of selective inhibitors or activators of these enzymes for a variety of therapeutic applications, among them metabolic diseases, such as diabetes.

PURPOSE AND RATIONALE

One strategy is based on the identification of selective novel inhibitors of PK, which have been implicated with interference of insulin signal transduction *via* serine phosphorylation of key signaling components, such as IRS-1 (see K.6.3 and K.6.3.4), thereby blocking activation of downstream components, such as PI3-K. These compounds/drug candidates should act as insulin-sensitizers bypassing the insulin resistance in muscle and liver tissues of type II diabetic patients. The other strategy relies on the identification of activators of PK, which function as positive elements in the insulin signal transduction cascade, such as the IR. These compounds/drug candiates may induce insulin-like signals in muscle and liver tissues of type II diabetic patients. In any case, the effect of large libraries of compounds on the phosphorylation of specific insulin signaling components has to be analyzed in a rapid, reliable and sensitive fashion.

PROCEDURE

Numerous methods have been designed to measure PK activity. Early methods require physical separation of substrate protein or peptide from its phosphorylated product. One method is to use radiolabeled ATP that allows the incorporated phosphate to be detected after the capture of the protein/peptide substrate by binding to phosphocellulose membranes (Witt and Roskoski 1975). This type of PK assay requires multiple steps and the use of radioactivity with its accompanying hazards and costs. Previously, a very selective and highly sensitive assay for various protein kinases was developed that is based on the use of biotinylated peptide substrates and [γ-^{32}P]ATP. This assay is fast, quantitative, and does not require any alteration of the peptide consensus sequence of the optimal PK substrate, which is routinely done with phosphocellulose membrane-based kinase assays. Although this assay system offers many advantages such as specificity, sensitivity, and convenience, it suffers from the fact that it is not homogeneous, i. e., it requires transfer of reaction products to a filter plate, and it is radioactive. Others have developed assays for measuring the enzyme activity of PK that are homogeneous and increase throughput for measuring the PK activity of many samples. Some of these are radioactivity-based assays, such as the scintillation proximity assays (SPA) or fluorescence-based

assays, such as time-resolved fluorescence resonance energy transfer (FRET) and fluorescence polarization (FP). The SPA and flashplate assay have been used as a high-throughput homogeneous assay of PK activity that does not require an antibody (Braunwalder et al. 1996, Antonsson et al. 1999), but still has some disadvantages. Although the signal-to-noise ratio (S/N) is high for the SPA, it uses radioactivity ([γ-^{33}P]ATP), and its efficiency is dependent on the energy of the isotope used ([γ-^{33}P]ATP is preferred over ([α-^{32}P]ATP). It also requires centrifugation or washing steps. Homogeneous non-radioactive assay formats measuring PK activity, that include FP and FRET, have been developed to eliminate the disadvantages of radioactivity and washing steps (Seethala and Menzel 1997, Park et al. 1999). FP is a ratiometric technique that reflects the rotational motion of a fluorescent molecule in solution with the rotational velocity dependent on the apparent molecular size (Pope et al. 1999). Although FRET and FP are non-radioactive, their signal-to-noise ratios are low and they rely on the availability of very high affinity and selective antibodies. This represents a major drawback of FRET, its reliability on the dual-label format in which an anti-phosphopeptide antibody is labeled with a fluorescence donor and is brought into close proximity to the peptide conjugated to a fluorescence acceptor, and only when these two molecules are within close proximity does transfer occur. FP on the other hand, uses only one labeled fluorescent molecule and it is ratiometric and thus minimizes interference by sample quenching. The disadvantages, however, are the very low S/N ratio that in some cases is less than 1.5, depending on the assay. The optimization of the assay may be difficult to attain because one cannot easily predict the appropriate location and spatial configuration for the fluorescent label. A major disadvantage of both FP and FRET assays is that they are dependent on the availability of a phospho-specific antibody. Another drawback to the use of antibodies is that their high specificity for a given phosphopeptide often prevents the same antibody from being used with different substrates. Anti-phosphotyrosine-specific antibodies are broadly reactive since they are relatively insensitive to the surrounding amino acid context. In contrast, anti-phosphoserine-/phosphothreonine-specific antibodies are highly dependent on the amino acid sequence surrounding the phosphorylated residue and thus tend to only bind a limited diversity of phosphorylated sites (Wu et al. 2000). In general, a new antibody must be generated for each different substrate, which can be both time consuming and expensive. There are also ELISA-based assays for PK activity, but these also require multiple steps in addition to being dependent on availability of a phospho-specific antibody to capture product (Angeles et al. 1996).

Several antibody-free non-radioactive assays for PK activity have been reported. One of these is based on the differential electrophoretic mobility of the fluorescent peptide substrate and its phosphorylated product using capillary electrophoresis and is compatible with throughput formats. This type of assay requires specialized high-throughput capillary electrophoresis setup and equipment. Another assay method replaces ATP in the reaction with ATPγS leading to the formation of a thiophosphorylated peptide product (Jeong and Nikiforov 1999). This product is then chemically biotinylated by a sulfur-specific biotinylation reagent. Streptavidin is then added to the fluorescently tagged peptide and an FP measurement is taken to measure the amount of product formed. The potential disadvantages of this assay include long incubation times and altered kinetics for some PK due to the ATPγS. Another antibody-free FP assay of PK activity that has been reported uses polyarginine to discriminate fluorescently labeled phosphorylated and non-phosphorylated peptides based on charge interaction of the phosphate group and the positively charged high molecular weight polyarginine (see K.6.3.2.3; Coffin et al. 2000, Simeonov et al. 2002). Another potential antibody-free assay of PK activity is the so-called IMAP assay that employs trivalent metal ions immobilized on nanoparticles to bind phosphate groups on molecules and thus increase their FP values (Huang et al. 2002). This approach is similar in concept to immobilized metal affinity chromatography (IMAC) used to specifically isolate phosphopeptides from mixtures containing both phosphorylated and non-phosphorylated peptides (Anderson and Porath 1986). Finally, the development of microchip instruments has led to an additional approach for measuring the PK activity (Cohen et al. 1999). In the microfluidic assay of PK activity, fluorophore-labeled peptide substrate and product are separated based on a difference in their charge-to-mass ratio. Separation of product and substrate is achieved by electrophoresis through an electric field, followed by quantitation of the individual fluorescent peaks. The currently most important and widely used PK assay technologies as well as novel ones with interesting future applications are described briefly.

K.6.3.2.1 Scintillation Proximity Assay (SPA)

For the scintillation proximity assay (SPA), the final assay conditions are 50 mM Tris (pH 8.0), 10 mM $MgCl_2$, 0.01% Triton X-100, 1 mM DTT, 1 or 3.75 µM ATP, 0.375 µM biotinylated peptide substrate, 160 ng/reaction kinase, 10 µM compound (in 10 mM DMSO, diluted 1:100 at least) and 0.125 µCi/reaction of [^{33}P]ATP. The 40-µl reactions are incubated at room temperature for 4 h. A stop reagent (40 µl per well) containing 0.2 mg streptavidin-coated SPA beads (Amersham), 40 mM EDTA, and 74% CsCl is added to the reaction. After sealing the plates and incubating for 2 h at room temperature, the plates are read on a microtiter plate TopCount scintillation counter.

K.6.3.2.2 Fluorescence Polarization (FP) Assay

PURPOSE AND RATIONALE

FP is a solution-based non-radioactive homogeneous assay that requires no separation of components for the analysis and in many but not all cases (see below) depends on the availability of appropriate phosphosite-specific antibodies. FP, first described in 1926, depends on the differing rotational properties of small (<10,000 Da) *vs.* large (> 100,000 Da) molecules. Fluorescent molecules excited by a plane of polarized light emit light in that same plane if the molecules do not move or rotate during the course of the excited state (1–5 ns). If the fluorescent molecules change position during their existence in the excited state, the polarized light will be emitted in a plane different with respect to the excitation plane. Large molecules such as proteins (or small molecules bound to proteins) do not rotate or move significantly during the lifetime of the excited state. Therefore, they do not become depolarized during the course of an FP experiment. Small molecules, such as peptides, tumble more rapidly and thus become depolarized during the course of the FP experiment. This change in polarization can be detected by monitoring the amount of fluorescence in the vertical *vs.* the horizontal plane following excitation in the vertical plane. Mathematically this can be expressed as polarization value $(P) = (I_V\text{-}I_H)/(I_V+I_H)$, where I_V and I_H are the intensities of the vertical and horizontal components of the emission light, respectively. FP is a dimensionless entity and is not dependent on the intensity of the emitted light or on the concentration of the fluorophore. This is a fundamental advantage of FP, in that each sample has an internal calibration that thus limits variations in intensity due to source fluctuation, fluorescence quenching by contaminants or inhibitors, or scattering caused by turbidity. The major limitation of FP lies in the limited sensitivity and signal-to-noise ratio, requiring specialized fluorimeters.

PROCEDURE

Most commercially available FP-based assays of PK activity require a anti-phospho-specific antibody. There are several disadvantages to the use of antibodies in FP assays. Although anti-phosphotyrosine-specific antibodies are common and relatively amino acid context independent, they are expensive. Anti-phosphoserine- or phosphothreonine-specific antibodies can be difficult and costly to produce and are sensitive to amino acid sequence surrounding the phosphorylation site and hence cannot be used for all serine/threonine peptide substrates (see K.6.3.2 and K.6.3.3.4). Unlike most other homogeneous fluorescent assays of PK activity, reagents required for the zinc FP assay are simply a fluorescein-labeled peptide and commonly used, inexpensive laboratory reagents, with no antibody required.

Modifications of the method have been established which are based on the use of Zinc (Scott and Carpenter 2003, polyarginine (Coffin et al. 2000) and competitive mode of assaying (Seethala and Menzel 1998, Turek et al. 2001, Kristjansdottir and Rudolph 2003).

K.6.3.2.3 Fluorescence-Based Assay

PURPOSE AND RATIONALE

To address the various drawbacks of existing assays, a novel, robust system to measure the activity of several PK has been developed. This assay is rapid, can be completed in less than 2 h, and can be carried out in multiwell plate formats such as 96- or 384-well plates. The signal-to-noise ratio is very high, and unlike FRET or FP, it uses a simple measure of fluorescence intensity. The assay also does not rely on the availability of high-affinity and selective antibodies, as is the case with other existing technologies. Finally, the assay is easily adapted to robotic systems for drug discovery programs.

PROCEDURE

It has been reported that phosphorylation of peptides on serine (Murray et al. 1996) or tyrosine (Dass and Mahalakshmi 1996) decreases the proteolytic activity of proteases. Thus, phosphorylation of peptides by PK

can be monitored by the increase in resistance to protease cleavage of the phosphorylated product. The difference in cleavage rate of the peptide in the absence and presence of phosphorylation can be used as a measure of the PK activity. It is noteworthy that the activity of PP can also be determined using a similar approach. The cleavage rate can be monitored by HPLC separation of the peptides before and after phosphorylation. However, this approach is tedious, time-consuming, requires large amounts of substrates and PK/PP, and is not practical for a large number of samples. To develop a PK assay based on this principle that is sensitive, simple, and scalable to high-throughput formats, Kupcho and coworkers (2003) introduced a fluorescence technology based on the use of Rhodamine 110 (R110)-modified peptide substrates.

Free R110 is a fluorescent molecule but when it is covalently linked *via* both its amino groups in a bisamide form both its visible absorption nd its fluorescence are suppressed. Upon enzymatic cleavage, the non-fluorescent bisamide substrate is converted in a two-step process, first to the fluorescent monoamide and then to the fluorescent monoamide and then to the even more fluorescent free R110. Both of these hydrolysis products exhibit spectral properties similar to those of fluorescein, with peak excitation and emission wavelengths of 496 and 520 nm, respectively. When the peptide substrate is not phosphorylated, it can be digested by aminopeptidase, which releases free R110 and thus enhances fluorescence at 520 nm. Phosphorylation of the peptide slows down the proteolytic cleavage of the peptide and thus minimal change is observed in the fluorescence. Using the appropriate consensus sequence for the peptide substrates, which have to be coupled to R110 in a bisamide form according to the protocol from Kupcho and coworkers (2003), the activity of a multitude of different PK can be monitored.

K.6.3.2.4 Capillary Electrophoresis-Based Assay

PURPOSE AND RATIONALE

Separation of non-phosphorylated substrate from the phosphorylated product can be accomplished by capillary zone electrophoresis. Dawson and coworkers (1994). Although the separations are very efficient, each separation run takes about 10–15 min, making this apporach too slow for the screening of large chemical libraries. The microchip is uniquely suited for the development of PK assays based on separation of substrate and product. Using computer control, it is possible to dispense nanoliter volumes of reagent solutions into the channel network. Enzymatic phosphorylation of the substrate takes place while the mixture is flowing through a reaction channel. An aliquot of the mixture is then injected into a separation channel where substrates and product are electrophoretically separated. The separation requires only a fraction of the time needed in traditional capillary electrophoresis. Cohen and coworkers (1999) presented the successful development of a microchip-based assay for a model PK, PKA, activity. This assay format may be applied to a wide range of different PK, for which fluorogenic substrates do not exist but where the outcome of the enzymatic reaction can be assessed by the separation of substrate from product.

PROCEDURE

The assay buffer for on-chip experiments using PKA is 100 mM HEPES/KOH (pH 7.5), 5 mM MgCl2, 100 μM ATP, 50 μM cAMP, and 1 M NDSB-195 (dimethylethylammonium propane sulfate) and is filtered through a 0.22-μm disposable Millipore syringe filter. The design and fabrication of the chips is given in the published report (Cohen et al. 1999). Prior to use, the chips are thoroughly cleaned with deionized water, 2-propanol, a filtered solution of 1 N NaOH for 15–30 min, rinsed with water and finally filled with assay buffer. To run experiments, the microchips are filled with the required reagents and placed in a specially constructed holder on the stage of an epifluorescent inverted microscope (480/40-nm excitation filter; 535/40-nm emission filter). A lid containing Pt electrodes is placed over the chip. Upon lid closure, the electrodes are inserted into the wells of the chip. These electrodes are connected to the high-voltage controller. Currents and voltages are applied to platinum wire electrodes immersed in reagent wells on the microchip.

EVALUATION

The capillary electrophoresis-based assay format may replace other methods of analysis of PK, namely radiolabel assays and other more cumbersome heterogeneous formats, the true appeal of the microchip is its potential for application to high-throughput screening. Significant reductions in assay time and reagent consumption will offset the expense by the need for instrumentation and software development. Optimization of channel dimension for the direct introduction of compounds/drug candidates from a microtiter plate into the on-chip reagent stream of substrate and enzyme as well as of reagent concentrations as methods to manipulate on-chip incubation times for enzymes of varying turnover rates have meanwhile been achieved.

K.6.3.3 Dephosphorylation of Insulin and Insulin-Like Signaling Components

GENERAL CONSIDERATIONS

The PTP (protein tyrosine phosphatases) are a structurally diverse family of both receptor-like and non-transmembrane hydrolases that have been implicated in the control of numerous physiological processes, including growth, differentiation and metabolism (Johnson et al. 2002). Approximately 75 PTPs have been identified to date. These enzymes are characterized by the presence of a conserved catalytic domain of 240 residues which contains the unique signature motif, $C(X_5)R$, that defines this enzyme superfamily (Andersen et al. 2001, Alonso et al. 2004). The structural diversity is manifested by the variability in non-catalytic sequences fused to the amino- or carboxy-terminus of the catalytic domain. These non-catalytic segments frequently serve a regulatory function, including ligand binding for receptor PTPs and targeting of cytoplasmic PTPs to defined subcellular locations. Despite variations in primary structure and differences in substrate specificity, key structural features in the catalytic site and mechanism are conserved among all members of the PTP superfamily (Barford et al. 1994 and 1998, Zhang 2003). Although great progress has been made in illustrating the, somewhat unexpected, structural diversity within this large enzyme family, relatively little is known of the physiological function of individual PTP. Presumably this structural diversity reflects a broad range of functions for the PTP family *in vivo*. However, it is clear on the basis of the role of protein tyrosine phosporylation in insulin signal transduction that PTP play important roles in the down-regulation of the insulin signal either for the physiological termination of insulin action after removal of insulin from the circulation or during the pathogenesis of type II diabetes in course of the development of insulin resistance in peripheral tissues. In particular, the potential role of PTP1B as a negative regulator of insulin action, causally related to the pathogenesis of insulin resistance and type II diabetes has been suggested by a number of studies using knock-out animals and cultured cells with ectopic overexpression and inhibition by small molecules or antisence oligonucleotides (Johnson et al. 2002, Elchebly et al. 1999). Consequently, PTP, in general, and PTP1B, in particular, have been recognized as attractive targets for the identification of insulin-like/sensitizing drugs for future anti-diabetic therapy.

PURPOSE AND RATIONALE

Considerable work has been directed at identifying PTP that dephosphorylate IR as possible targets for insulin-like compounds/drug candidates. Several receptor PTP (e. g. PTP-α, LAR) and non-receptor PTP (PTEN, PTP1B) have been considered candidates based on studies of their overexpression, substrate-trapping mutants, mouse knockout models, and other approaches (Cheng et al. 2002, Tonks 2003, Bourdeau et al. 2005). Since the inhibition of PTP1B causes prolonged and increased IR phosphorylation, it is a potential therapeutic target in the treatment of type II diabetes and insulin resistance.

As interest in understanding PTP1B and its role in the regulation of insulin signal transduction and pathogenesis of type II diabetes grows, the accurate measurement of tyrosine phosphorylation on proteins becomes increasingly important. Therefore to aid in the identification of selective, potent PTP1B inhibitors novel assays have recently been designed to follow changes in tyrosine phosphorylation of the IR and of additional so far unknown substrate proteins as well as for the identification of novel PTP1B substrate proteins in normal and insulin-resistant muscle, adipose and hepatoma cell lines which all express functional PTP1B and IR.

In addition to PP, lipid phosphatases have also been implicated as negative regulators of insulin signaling and ac tion, in general, and insulin-stimulated GLUT4 translocation, in particular. In addition to positive regulators of GLUT4 translocation, negative regulators have also been studied intensely because they might provide opportunities for pharmacological interventions. For example, the endogenous attenuation of PI3-K signaling occurs through the dephosphorylation of phosphatidylinositol-3,4,5-trisphosphate [PtdIns(3,4,5)P_3,]. Two phosphoinositide phosphateses, SHIP2 (type-II SH2-domain-containing inositol 5′-phosphatase) and PTEN (phosphatase and tensin homolog deleted on chromosome ten), have been implicated in negatively regulating insulin signaling (Jiang and Zhang, 2002). SHIP2 removes the 5′ phosphate from PtdIns(3,4,5)P_3 to generate phosphatidylinositol-3,4-bisphosphate [PtdIns(3,4)P_2]. Although the *Ship2* KO mice die shortly after birth and are severely hypoglycemic, heterozygous animals show improved glucose tolerance and enhanced insulin sensitivity (Clement et al. 2001).

In contrast to SHIP2, PTEN is a 3′-specific PtdIns(3,4,5)P_3 phosphatase that generates PtdIns(4,5)P_2). Overexpression of PTEN prevents the accumulation of PtdIns(3,4,5)P_3 and also inhibits

insulin-stimulated GLUT4 translocation in 3T3L1 adipocytes (Nakashima et al. 2000). Moreover, the genetic ablation of PTEN in adipose tissue of mice has recently been shown to enhance insulin sensitivity and resistance to pharmacologically induced diabetes (Kurlawalla-Martinez et al. 2005).

K.6.3.3.1 Protein Tyrosine Phosphatase (PTP) Activity Measurement Using DIFMUP

PURPOSE AND RATIONALE

A variety of substrates have been developed for measurement of the hydrolytic activity of PTP with the rather unspecific *para*-nitrophenylphosphate (PNPP) and specific phosphotyrosine-containing peptides being most widely used. These assays have significantly improved our understanding of substrate specificity and catalytic mechanism of PTP. However, their use for routine inhibitor screening is rather limited due to a variety of reasons, in particular, the requirement for synthesis of a phosphopeptide, low sensitivity in detection, susceptibility to color interference, and discontinuous nature (i. e. termination of the reaction by addition of acidic malachite green reagent or alkaline solution; Zhang and Dixon 1994, Zhang et al. 1993). A number of fluorogenic compounds used for the analysis and characterization of PTP have been described. Recently, Huang and coworkers (1999) and Wang and coworkers (1999) described the development of fluorescein monosulfate monophosphate as a dual fluorogenic substrate for both phosphoserine/threonine phosphatases and PTP. The similarity in their reaction mechanisms seems to be the reason that phosphatases from the different families can use these small non-peptidic substrates, albeit with pronounced differences in their catalytic efficiencies. Wang and coworkers (1999) described the development of fluorescein monosulfate monophosphate and their use as sensitive fluorogenic substrates for several PTP. The demonstrated catalytic efficiencies which are comparable to those of phosphopeptide substrates favor their use in alternative more sensitive assay designs. Recently, another fluorogenic substrate, 6,8-difluoro-4-methylumbiliferyl phosphate (DIFMUP) was found to be appropriate for measurement of PTP activity (Welte et al. 2003). This substrate has initially been developed for phosphoserine/threonine phosphatases (Gee et al. 1999) and subsequently optimized for use in the high-throughput assay format (Welte et al. 2005). The DIFMUP-based assay may be helpful for the kinetic analysis and characterization of small-molecule inhibitors for PTP, which have been implicated as negative regulators in insulin signalling (e. g. PTPα, LAR, CD45, TC-PTP, YOP, SHP2), in general, and PTP1B, in particular.

PROCEDURE

All reactions are carried out at 37°C in black polystyrol 96-well plates with flat bottoms. For measurement of PTP1B, PTPα, LAR, CD45, TC-PTP, YOP, and SHP2, the reaction buffer contains 50 mM HEPES (pH 6.9), 150 mM NaCl, 1 mM EDTA, 2 mM DTT, and for VHR, the reaction buffer contains 50 mM sodium acetate (pH 5.6), 100 mM NaCl, 1 mM EDTA, 2 mM DTT. The substrate stock solution is prepared in DMSO at a final concentration of 10 mM and stored at −20°C. For measurement, DIFMUP is diluted 10-fold in the desired reaction buffer, yielding a final concentration of 1 mM. Fluorescence excitation of hydrolyzed DIFMUP (Molecular Probes) and the fluorescent standard DIFMU is measured at 358 nm and emission is detected at 455 nm in a fluorescence plate reader (e. g. Spectramax, Molecular Devices).

For kinetic analysis, the DIFMUP stock solution is pre-diluted in reaction buffer and added to the reaction mixture to yield final concentrations of 0–300 µM. The assay is initiated by adding 10 µl of substrate to 90 µl of reaction buffer containing the prediluted PTP (final concentrations: PTP1B, 100 ng/ml; PTPα, 500 ng/ml; LAR, 125 ng/ml; CD45, 100 ng/ml; TC-PTP, 100 ng/ml; SHP2, 2 µg/ml, YOP, 50 ng/ml).

Compounds/drug candidates are pre-diluted in reaction buffer containing 100 ng PTP1B to the indicated final concentrations ranging from 0.8 to 80 µM in a final volume of 90 µl. The reaction is started by adding 10 µl of substrate buffer containing 1 mM DIFMUP and the intensity of released DIFMU is monitored continuously for 5 min. Malachite green and PNPP assays are performed as described (Zhang and Dixon 1994, Zhang et al. 1993). Initial velocities of the reactions are used to calculate kinetic constants using Sigma Plot software. The initial velocities are plotted against the inhibitor concentrations and the IC_{50} is calculated.

Detailed analysis of the binding mode of compounds/candidate drugs is performed as follows. For analysis of the time dependence of inhibition, different inhibitors are incubated at their IC_{50} concentrations with PTP1B for 0, 10, and 15 min. The reaction is started by adding 10 µl of substrate buffer containing 1 mM DIFMUP and the reaction is followed for 10 min. For analysis of the reversibility of inhibition, compounds/drug candidates are incubated for 10 min

with PTP1B. After addition of DIFMUP to a final concentration of 10 µM, the reactions are followed continuously until the fluorescence emission do not increase further. The reactions are restarted by adding DIFMUP to a final concentration of 100 µM and the release of DIFMU is monitored for an additional 10 min.

EVALUATION

The fluorogenic substrate, DIFMUP, was developed as a substrate for phosphoserine/threonine phosphatases to enable continuous measurement of activity (Gee et al. 1999). Its hydrolysis by a phosphatase results in the release of fluorescent DIFMU, which can be easily followed in continuous mode by a fluorescence reader. A great advantage of this substrate is its low pK_a value of 4.7 compatible with pH 7.0 during the reaction without prior alkalization (Sun et al. 1998). Furthermore, the substrate yields a higher fluorescence quantum than other frequently used fluorogenic substrates, such as 4-methylumbelliferyl phosphate. This substrate is accepted a recombinant fragment of human PTP1B (Welte et al. 2003). This finding has meanwhile been extended by a detailed kinetic and comparative analysis of PTP reactions using DIFMUP and other substrates (Welte et al. 2005). Compared to PNPP, DIFMUP is a better substrate for PTP1B as reflected in both its lower K_m and higher turnover number. However, dephosphorylation of a phosphotyrosine-containing peptide derived from the IR is even more efficient, indicating the requirement of amino acids adjacent to the phosphoamino acids.

DIFMUP is accepted by other PTP from different families. These include CD45, PTPα, SHP2, YOP, LAR, and TC-PTP. For these PTP a clear relationship between the relative fluorescence signal and the enzyme concentration is detected, which, however, with regard to the protein amount required differed by two orders of magnitude between LAR, TC-PTP, CD45, YOP (50–500 µg) and PTPα, SHP2 (0.5–2 µg) with PTP1B and the closely related TC-PTP showing the highest affinity for DIFMUP (Welte et al. 2005). These findings hint at subtle differences in the catalytic sites between these PTP for hydrolysis of optimally bound DIFMUP. Taken together, differences in the substrate recognition and catalytic sites of the various PTP are presumably monitored in the course of DIFMUP binding and cleavage. In contrast, no major kinetic differences between a number of phosphatases were reported for the hydrolysis of 3,6-fluorescein diphosphate and other fluorogenic substrates (Huang et al. 1999, Wang et al. 1999), arguing for similar and more flexible binding modes to the substrate recognition and catalytic sites of these apparently more unspecific substrates.

The search for inhibitors of PTPs requires a robust test system to assay a large number of compounds for a multitude of different enzymes. A novel non-peptidic inhibitor, a benzooxathiazoldioxide derivative (Petry et al. 2002, Liu et al. 2002) exhibits in different PTP1B assays using either DIFMUP, PNPP, or the IR phosphopeptide as substrate an IC_{50} of 3.8, 5.1 and 3.9 µM, respectively. DMSO used as solvent for the inhibitors did not affect cleavage of DIFMUP to up to 4% final concentration during the assay, reflecting the robustness of the assay.

PTP all share a nucleophilic cysteine residue located in the catalytic cleft, which is sensitive to oxidation or covalent modification (Zhang 2003, Johnson et al. 2002). Therefore, characterization of the nature of their inhibition by small-molecule inhibitors is important, which requires detailed kinetic studies. The possibility of continuous measurement of DIFMUP hydrolysis allows rapid characterization of the reversible nature of inhibition. For this, the enzyme is incubated in the absence or presence of inhibitor in the presence of 10 µM DIFMUP. After incubation for 10 min, when hydrolysis of DIFMUP stops due to substrate depletion (as revealed by approaching a plateau level of fluorescent DIFMU generated), a 10-fold excess of fresh DIFMUP is added to the reaction. This leads to complete reversion of inhibition of DIFMUP hydrolysis as reflected in the almost identical initial velocities of the reactions containing or lacking (control) the inhibitor after fresh DIFMUP has been added. The degree of inhibition is often found to depend strictly on the incubation time of the inhibitor with PTP1B prior to DIFMUP addition.

In summary, the high sensitivity and compatibility with a broad pH range of the fluorogenic DIFMUP assay provide advantages with regard to saving enzyme and miniaturization. Consequently, the DIFMUP assay will be useful for the development of throughput screening assays for a variety of physiologically important PTP as has been already been demonstrated for the receptor PTP, LAR (Pastula et al. 2003). In addition to its technical advantages, DIFMUP seems to reflect the binding mode of phosphotyrosine-containing peptide substrates more closely than the widely used non-peptidic substrates, PNPP and 3,6-fluorescein diphosphate. These characteristics may facilitate the future search for competitive and reversible PTP inhibitors as.

K.6.3.3.2 PTP Identification Using Substrate Trapping

PURPOSE AND RATIONALE

To understand fully the role of PTP in cellular function, in general, and in insulin signal transduction, in particular, it will be necessary to identify multitude of the physiological substrates of the individual members of the PTP family. It has shown in numerous studies that alteration of the nucleophilic Cys to Ser or Ala allows some PTPs to be isolated in a complex with their target substrates. Thus it appears that the Cys ⟶ Ser/Ala mutants may be utilized to isolate all combinations of PTP1B and its substrates. Additional alternative "substrate-trapping" PTP mutants have been identified by systematic mutational analysis of the invariant residues that were predicted from the crystal structure to be important in catalysis. In one such mutant form of PTP1B Asp-181, the residue that functions as a general acid to facilitate cleavage of the scissile P–O bond in the substrate, has been altered to Ala. Clearly, a definition of the spectrum of phosphotyrosyl proteins dephosphorylated by PTP1B *in vivo* will be a prerequisite for the elucidation of the physiological function of that enzyme. Such substrate identification or trapping may be achieved by the following method.

PROCEDURE

Immunoprecipitation, Immunofluorescence and Activity Assay

Cells transformed or transfected with vectors coding for PP are lysed 44–48 h after transfection in 50 mM Tris/HCl (pH 7.5), 5 mM EDTA, 150 mM NaCl, 1% Triton X-100, 5 mM iodoacetic acid, 10 mM sodium pyrophosphate, 10 mM NaF, 5 µg/ml leupeptin, 5 µg/ml aprotinin, 1 mM benzamidine (1 ml per 10-cm dish, 0.5 ml per 6-cm dish). PTP1B is immunoprecipitated from lysates with a monoclonal antibody (mAb). GST-PTP1B fusion proteins are precipitated with glutathione-Sepharose. Precipitates are collected by centrifugation (5,000 × *g*, 15 s, 4°C), washed four times with 0.7 ml of ice-cold lysis buffer, and finally heated at 95°C for 5 min in 60 µl of 2 × Laemmli sample buffer. mAb to phosphotyrosine are typically used for immunoblotting at the following concentrations: 4G10 (Upstate Biotechnology) 2 µg/ml, RC20b (Transduction Laboratories) 0.5 µ g/ml. The levels of expression of wild-type, C215A, and mutant PTP1B should always be equivalent. For immunofluorescence experiments, cells are seeded onto glass coverslips at $2.5–3 \times 10^5$ per 6-cm dish, transfected with 10 µg of PTP1B cDNA, wild-type or mutant, and processed for immunofluorescence staining at 36 h after transfection as described by Lorenzen and coworkers (1995).

EVALUATION

Considering that the substrate-trapping mutant, PTP have the ability, through interaction with phosphotyrosine residues, to increase the basal phosphorylation of their target substrates, one might expect them to promote ligand-independent signaling. However because these mutants form stable complexes with target substrates, they may also interfere with signaling *in vivo* in a manner analogous to the wild-type phosphatase. Thus, if the site of tyrosine phosphorylation on the substrate is critical for a protein-protein interaction required for signaling or if the substrate is an enzyme and the phosphorylation site is located close to the active site, steric hindrance resulting from binding of the mutant PTP may exert an effect that is functionally equivalent to dephosphorylation.

The successful application of this technique to identify additional substrates of PTP1B, and substrates of other PTP, will require expression of the Asp ⟶ Ala mutant PTP in cells and selection of an appropriate stimulus to trigger tyrosine phosphorylation of the substrate and accumulation of a complex with the mutant PTP. For PTP1B, IR is naturally abundant in myocytes, hepatocytes and adipocytes, and its basal rate of autophosphorylation generates enough tyrosine-phosphorylated protein to be trapped by PTP1B-D181A and to be detected by anti-phosphotyrosine immunoblotting. Its high molecular weight, characteristic of growth factor receptors, facilitates identification. Of the less-phosphorylated substrates of PTP1B, the finding that phosphorylation of p70 is enhanced upon cotransfection with v-src and D181A may enable enough of this substrate to be isolated to allow its identification by peptide sequencing. In addition to the use of trapping mutants to identify novel PTP substrates, it also may be possible to identify the site within the cell at which a PTP acts on a particular target, through colocalization of the substrate and the Asp ⟶ Ala mutant PTP.

These findings indicate that PTP1B can display substrate specificity *in vivo* and bolster the hypothesis that the subcellular targeting is an important mechanism by which such specificity is achieved. The substrate-trapping mutant introduced by Flint and coworkers (1997) is altered in a residue that is an invariant catalytic acid in all members of the PTP family. Therefore, the use of this mutation should be generally applicable to any PTP and may represent a powerful tool with which

to delineate the physiological substrate specificity of other members of the family, thereby revealing important insights into their function *in vivo* and their potential as drug targets.

K.6.3.3.3 Lipid Phosphatase Activity Measurement

PURPOSE AND RATIONALE

The methods currently available for the assay of lipid-metabolizing enzymes, in general, and lipid phosphatases, in particular, rely on the release of radioactive isotopes with some form of substrate/product separation step before quantitation. Estimation of cellular mass of phosphoinositides usually requires labeling of cells with [^{3}H]inositol or [^{32}P]orthophosphate followed by deacylation and HPLC analysis. Estimation of phosphoinositide mass in tissues is at present restricted to PtdIns(3,4,5)P_3 and requires extraction of the lipids and removal of the phosphoinositol head groups followed by a radiometric displacement assay which also requires synthesis of radiolabeled inositol(1,3,4,5)tetrakisphosphate. These assays also suffer from the drawback that the labeled substrates or precursors required are expensive and samples require extensive processing before analysis.

A novel assay for quantification of phosphoinositides based on their ability to bind specifically to certain pleckstrin homology (PH) domains (Gray et al. 2003). PH domains are the major intracellular targets of PtdIns(3,4,5)P_3, PtdIns(3,4)P_2, and several other phosphoinositides. Recently the number of characterized PH domains binding inositol lipids with a broad range of affinity and specificity has increased (Lemmon and Fergusson, 2001). Other recently discovered phosphoinositide binding domains, like the phox homology domain (Xu et al. 2001, Bravo et al. 2001) and FYVE domains (Gillooly et al. 2001), could potentially also be used in the assay formats described herein. Other critical components of the assay concept are biologically active short acyl chain phosphoinositides that recently have become commercially available. Important structural features of these include short acyl side chains (diC4 to diC8), rendering them water soluble, and the addition of biotin to the terminus of the *sn*-1 acyl chain while still allowing selective recognition of the inositol head group. Finally, sensitive non-radioactive detection of lipid/PH domain complexes relies on either TR-FRET using Lance reagents (e. g. Perkin–Elmer Wallac) or the recently introduced AlphaScreen technology (BioSignal Packard). In both cases, PtdIns(3,4)P_2 or PtdIns(3,4,5)P_3 present in samples is detected in competition assays by its ability to dissociate signal-generating complexes between PH domain, biotinylated lipid, and detection reagents. The assay systems presented here allow the assay of lipid phosphatases in a homogeneous format compatible with throughput screening and, in the case of the TR-FRET format, capable of real-time kinetic measurements.

PROCEDURE

Detection of Biotinylated Phosphoinositide/PH Domain Complexes

The GRP1 PH domain (amino acids 263 to 380) is PCR cloned from a mouse brain cDNA library as described by Gray and coworkers (1999). The protein is expressed from the pGEX 4T1 vector (Amersham Pharmacia) in *Escherichia coli* and affinity purified on glutathione–agarose using the manufacturer's standard protocols. The purified PH domains are labeled with Lance chelate according to the manufacturer's protocols.

AlphaScreen detection is performed in 384-well microtiterplates in 50 mM HEPES/KOH (pH 7.4), 50 mM NaCl, and 0.1% BSA. Biotinylated, short-chain (diC6) phosphoinositides and GRP1 PH–GST are added at 15 and 3.75 nM, respectively. Donor and acceptor AlphaScreen beads (Perkin–Elmer) are added at 5 µg/ml to a final volume of 50 µl. Plates are incubated in the dark for 5 h to ensure binding is complete and then read in an AlphaQuest AD instrument (Perkin–Elmer) using standard settings. The TR-FRET sensor complex consists of 50 mM HEPES (pH 7.4), 150 mM NaCl, 5 mM DTT, and 0.05% CHAPS with APC–streptavidin) 32 nM and 120 nM biotinylated, short-chain (diC6) phosphoinositides, and 35 nM Lance chelate labeled GST-PH domain. Alternatively the TR-FRET sensor complex contains 21 nM Lance chelate labeled anti-GST antibody and unlabeled PH domain in a final volume of 50 µl. All assays contain CHAPS at low concentration to prevent loss of lipids by adsorption onto plastic surfaces.

For all assays plates are read with the following settings: excitation 360–35 nm filter, emission 665 nm filter, dichroic filter 505 nm, PMT 1000 V set to digital sensitivity 2, 100 flashes per well, 10-ms interval between flashes, read 50 ms after flash, and integration 1000 ms.

The TR-FRET assays are conducted in 50 mM HEPES/KOH (pH 7.4), 150 mM NaCl, 5 mM $MgCl_2$, 5 mM DTT, 0.05% CHAPS (assay buffer) using a two-component reaction. The first component is a twofold-concentrated sensor complex consisting

of 32 nM APC–Streptavidin, 120 nM biotinylated diC6PtdIns(3,4,5)P_3, and 35 nM Lance chelate labeled GST–PH domain. Alternatively the sensor complex contains 21 nM Lance chelate labeled anti-GST antibody and unlabeled PH domain. The first component also contains 100 ng recombinant PI3-kinase γ in a final volume of 25 µl assay buffer. The second component contains the diC8PtdIns(4,5)P_2 at two times the required final concentrations and ATP at 100 µM again in 25 µl assay buffer. The assays are started by mixing the two components in a 96-well plate and reading at the required time intervals to obtain rates of reaction.

EVALUATION

A novel approach to quantitation of phosphoinositides in cell extracts and *in vitro* enzyme-catalyzed reactions using suitably tagged and/or labeled PH domains as probes (Gray et al. 2003). Stable complexes are formed between the biotinylated target lipid and an appropriate PH domain, and phosphoinositides present in samples are detected by their ability to compete for binding to the PH domain. Complexes are detected using AlphaScreen technology or time-resolved FRET. The assay procedure has been validated using recombinant PI3-K γ with diC8PtdIns(4,5)P_2 as substrate and general receptor for phosphoinositides-1 (GRP1) PH domain as a PtdIns(3,4,5)P_3-specific probe. This PI3-K assay is robust and suitable for throughput screening,. The approach is adaptable to lipid phosphatases as demonstrated by assays for PTEN, a phosphoinositide 3-phosphatase, which is measured using the same reagents but with diC8PtdIns(3,4,5)P_3 as substrate. PtdIns(3,4,5)P_3 present in lipid extracts of growth factor-stimulated Swiss 3T3 and HL60 cells is also detectable at picomole sensitivity. Gray and coworkers (2003) therefore proposed that similar procedures should be capable of measuring any known phosphoinositide present in cell and tissue extracts or produced in PK and PP assays by using one of several well-characterized protein domains with appropriate phosphoinositide-binding specificity

PtdIns(3,4,5)P_3 Measurements

Alternatively to the above method of quantification of phosphoinositides by using phosphoinositide-binding proteins, PtdIns(3,4,5)P_3 can be measured directly by prior radiolabeling as described by Blero and coworkers (2005). For this, cells (1.5×10^6), which have been pretreated with compounds/drug candidates, are cultured in 10% serum overnight. Cells are washed twice in medium without serum and twice in medium without either phosphate or serum. They are labeled for at least 4 h in medium with [^{32}P]orthophosphate (250 µCi/ml) but without serum. Cells may be stimulated with compounds/drug candidates during the labeling period, in addition or alternatively. The reaction is terminated by 5 ml cold PBS. Cells are lysed in 3.75 ml of 2.4 N HCl. Lipids are extracted in 3 ml methanol and 4.5 ml $CHCl_3$. After TLC and deacylation of the phosphoinositides, separation is performed by HPLC on Whatman SAX columns (Pesesse et al. 2001). Radioactivity is estimated with an online detector (e. g. Raytest, Germany). PtdIns(4,5)P_2 is also determined by labelling the cells with [^{3}H]inositol as reported by Serunian and coworkers (1991). The various 3-phosphorylated phosphoinositides standards have to be prepared in insulin-stimulated CHO-IR cells or in platelets as reported (Blero et al. 2001, Giuriato et al. 2003).

Measurement of Recombinant SHIP2 Activity

For the identification and characterization of compounds/drug candidates which directly interfere with the activity of SHIP2 and may represent future antidiabetic drugs the activity of SHIP2 can be assayed with cells transfected with recombinant SHIP2 by HPLC analysis of their phosphoinositides after radiolabeling *in vivo* according to the procedure of Wada and coworkers (2001).

In Vivo Generation of ^{32}P-Labeled Phosphoinositides and HPLC Analysis

The same numbers of 3T3-L1 adipocytes transfected with LacZ, wildtype WT-SHIP2, or phosphatase-defective ΔIP-SHIP2 are phosphate-starved overnight in phosphate-free DMEM, followed by serum starvation for 3 h. [^{32}P]orthophosphate (0.1 mCi/ml) is then added, and the cells are cultured for an additional 2 h. Following the labeling period, the cells are incubated without or with compounds/drug candidates for 15 min. The reaction is terminated by washing once with ice-cold PBS, followed by the addition of methanol/1 N HCI (1/1). The labeling of the cells with [^{32}P]orthophosphate is conducted at the same time in all three sets of transfected cells. Phospholipids are then extracted with chloroform. The extracted lipid is deacylated and subjected to amino-exchange HPLC using a Partisphere strong anion-exchange column as described previously (Serunian et al. 1991, Funaki et al. 1999). The PI(3,4)P2 and PI(3,4,5)P3 levels in the same sample for each cell line are measured within a single HPLC run. The radioactivity is detected with an on-line radiochemical detector.

MODIFICATION OF THE METHOD

Lin and coworkers (2003) reported about the separation of phospholipids, such as phosphoinositides, in microfluidic chip devices and its application to homogeneous high-throughput screening assays for lipid-modifying enzymes. The method takes advantage of the high-separation power of the microchips that separate lipids based on micellar electrokinetic capillary chromatography (MEKC) and the high sensitivity of fluorescence detection. The assay format consists of two steps: an on-plate enzymatic reaction using fluorescently labeled substrates followed by an on-chip MEKC separation of the reaction products from the substrates. The utility of the assay format for screening is demonstrated using phospholipase A_2 but may be extended to other phospholipases and lipid phosphatases with the advantages of avoidance of the use of radioactive substrates and tedious separation/washing steps and the detection of both substrate and product simultaneously.

K.6.3.3.4 Generic Assay for Protein Kinases (PK) and Phosphatases (PP) Based on Phosphate Release

PURPOSE AND RATIONALE

PK and PP produce or consume inorganic phosphate (P_i). Detection of an increase or decrease of the P_i concentration in the environment of these enzymes is a common way to monitor the enzymatic activity. Assays capable of measuring a change in the inorganic phosphate concentration serve as uniform readout for the activity of these enzymes (Ellen Chan and Swaminathan 1986, Brune et al. 1994). A number of colorimetric and fluorometric assays have been reported for the determination of inorganic phosphate (Itaya and Ui 1966, Kirkbright et al. 1972, Sebbon and Fynn 1973). Most of these assays are based on complexation reactions with the free phosphate. In addition, some methods for phosphate measurements have been developed based on the enzymatic conversion of phosphate and a substrate to a UV-absorbing product (Webb 1992, Ungerer et al. 1993). The disadvantages of all these methods are that they are slow, lack sensitivity or are sensitive to interfering compounds (Ellen Chang and Swaminathan, 1986, Tashima 1975, Hwang 1976).

To circumvent these problems, Brune and coworkers (1994, 1998) developed a continuous-flow phosphate assay. As an improvement Schenk and coworkers (2003) introduced a probe for the rapid measurement of P_i, in particular to follow its release in real time from enzymes such as phosphatases. The probe consists of phosphate-binding protein (PBP) labeled with a fluorophore, *N*-(2-(1-maleimidyl)ethyl]-7-(diethylamino)coumarin-3-carboxamide (MDCC). Upon binding of P_i under physiological conditions a ~13-fold increase in fluorescence is observed. The binding of Pi to MDCC-PBP is very fast, has a high affinity, and is very sensitive. These characteristics make the reaction between P_i and MDCC-PBP very suitable for dynamic P_i detection assays and thus for application in a continuous-flow phosphate assay. A further increase in sensitivity of a continuous-flow generic fluorescent assay for PK and PP was achieved by Schenk and coworkers (2003) by coupling to liquid chromatography (LC).

K.6.3.3.5 Cellular PTP Assays

The development of cell-based assays for the identification as well as evaluation of the biological activity of PTP inhibitors which positively affect insulin signaling and reduce insulin resistance (e. g. PTP1B, see above) is hampered by a number of issues. The typical functional readout for PTP1B inhibition has been to measure IR phosphorylation (see K.6.3.1.3). Yet, the increase in IR phosphorylation due to PTP1B inhibition is usually variable, dependent on cell type and at most two- to three-fold over controls, thus, making it unsuitable for screening. Furthermore, because many of the current potent PTP1B inhibitors contain a phosphonate or a phosphate mimetic they are highly charged and therefore cell permeability becomes an issue. Without a robust cellular functional readout and questionable cell permeability of PP inhibitors, it becomes difficult to reconcile the reason for the lack of activity of PTP inhibitors in cell-based assays. In order to circumvent some of these issues, yeast- and insect cell-based PTP1B assays have been developed.

K.6.3.3.5.1 Yeast-Based Assay

PURPOSE AND RATIONALE

Yeast has been used as a model system for the screening of various compounds/drug candidates. It provides a cellular environment to prevent PP oxidation and measuring yeast growth is both an easy and sensitive screening assay (Melese and Hieter 2002). In addition, yeast cell permeability has been shown not to be an issue in concentrating compounds internally, but like mammalian cells, the rate-limiting factor in internalization of compounds has been due to the function of

efflux pumps. v-Src, a tyrosine kinase from the Rous Sarcoma virus, is lethal when overexpressed in the yeast Saccharomyces cerevisiae (Brugge et al. 1987). the lethality of v-Src has been attributed to the hypertyrosine phosphorylation of multiple yeast proteins leading to mitotic dysfunction but the exact target responsible for the toxicity remains to be identified (Kornbluth et al. 1987, Florio et al. 1994, Trager et al. 1997). Yeast can be rescued from the v-Src lethality by co-expressing the catalytic domain of PTP1B (Florio et al. 1994). This rescue is presumably due to the activity of PTP1B in dephosphorylating the various yeast proteins phosphorylated by v-Src. Based on these observations Montalibet and Kennedy (2004) developed and optimized a yeast-based assay to screen for PTP1B inhibitors.

PROCEDURE

Yeast with leucine and uracil deficiency markers are transformed with the plasmids coding for v-Src and the appropriate PTP (here PTP1B) and the colonies formed three days after are transferred to leucine and uracil dropout media containing raffinose as the sole carbon source and grown overnight. Serial dilutions of the inhibitors are arrayed in 96-well plates containing leucine and uracil dropout media with 4% galactose. The plates are inoculated with the overnight yeast cultures at a final concentration of 10^6 per ml in the absence or presence of increasing concentrations of compounds/drug candidates (Hammonds et al. 1998). The wells are overlaid with mineral oil, incubated at 30°C and read periodically at 600 nm for 4 days. The growth curves generated are used to obtain EC_{50}-values for the putative PTP1B inhibitors.

EVALUATION

Based on the previous observation that co-expression of PTP1B can rescue yeast from v-Src lethality, Montalibet and Kennedy (2004) optimized the expression levels of PTP1B and v-Src such that inhibition of PTP1B activity results in growth interference. PTP1B catalytic activity was shown to be absolutely required for yeast growth since the catalytically inactive PTP1B mutants C215S and D181A failed to overcome the lethality of v-Src. A certain stoichiometry between PTP1B and v-Src expression is required to obtain a robust growth phenotype and at the same time to ensure sensitivity toward inhibitors. Screening can be carried out in 96-well plates and growth of th eliquid culture measured by absorbance at 600 nm. The PTP inhibitor, vanadate, specifically inhibited PTP1B-dependent growth in a concentration-dependent manner with an EC_{50} of 0.92 mM. This simple yeast growth interference assay may be useful for throughput screening for inhibitors of PTP1B, in particular, and PTP, in general.

K.6.3.3.5.2 Insect Cell-Based Assay

PURPOSE AND RATIONALE

Cromlish and coworkers (1999) described an intact cell-based assay for the discovery of cell-permeable, selective PTP inhibitors utilizing the baculovirus expression system, where a PTP of interest is expressed in Sf9 insect cells and a direct readout of the PP activity within these cells is obtained from the amount of hydrolysis of the cell-permeable substrate, *para*-nitrophenylpyrophosphate (pNPP).

PROCEDURE

Baculoviruses recombinant for the cDNA coding for the desired PTP (e. g. PTP1B) is prepared using the Bac-to-Bac Baculovirus Expression System and recovered from the supernatant medium from transfected Sf9 insect cells after three rounds of amplification to up to a total viral stock volume of 500 ml. Sf9 cells are infected with the recombinant or control baculovirus (Cromlish and Kennedy 1996), collected 29 hpi by centrifugation ($48 \times g$, 5 min), washed once in assay buffer (Hanks' solution buffered with 15 mM HEPES/KOH, pH 7.4) and re-centrifuged ($21 \times g$, 10 min). The cells are resuspended gently in assay buffer and examined using a hemocytometer and microscope for cell density as well as trypan blue exclusion. Assays are performed using a pipetting robot, programmed to mix gently after each addition. 200-µl Hanks' solution containing the cells. Following a 15-min incubation with compounds/drug candidates at 37°C, the cells are challenged with 1–50 mM of tissue culture-grade pNPP for 15 min. The cells are centrifuged ($410 \times g$, 3 min, 4°C). 100-µl samples of the supernatants are transferred to fresh clear polystyrene 96-well plates, and the amount of hydrolysis of pNPP is determined spectrophotometrically at OD of 405 nm. The pNPP hydrolysis window obtained between PTP-expressing cells and control-infected cells represents the amount of phosphatase activity due to the PTP of interest.

EVALUATION

Inhibitions are calculated by comparing pNPP hydrolysis of the inhibitor-treated PTP-expressing cells with that of DMSO-treated PTP-expressing cells. For the PTP Sf9 cell-based assay to be useful in screening for

PTP inhibitors, it is necessary to harvest the cells at a time point when sufficient amounts of the protein of interest are produced, yet the cells are healthy and viable prior to the deleterious effects associated with the later stages of the viral infection.

K.6.3.3.5.3 Bacterial Cell-Based Assay

PURPOSE AND RATIONALE

Senn and Wolosiuk (2005) developed a high-throughput screening assay for the detection of phosphatase activity in bacterial colonies overexpressing mammalian phosphatases. Unlike the insect cell-based method, this procedure is compatible with the use of physiological substrates but nevertheless is versatile, since it is based on the detection of the common product of all phosphatase reactions, P_i. In this method, substrates diffuse from a filter paper across a nitrocellulose membrane to bacterial colonies located on the opposite face, and then the reaction products flow back to the paper. Finally, a colorimetric reagent discloses the presence of orthophosphate in the filter paper.

PROCEDURE

Escherichia coli cells are transformed with vectors coding for the corresponding PP under a strong inducible promoter and after appropriate dilution grown directly over a nitrocellullose membrane that lay on Luria-Bertani (LB) agar supplemented with 100 µg/ml ampicillin. When the diameter of colonies is 1 mm (~24 h), the expression of the PP is induced by spreading 0.2 ml of inducer (e. g. 40 mM IPTG, 10% agarose) onto the agar surface. After 3 h, the nitrocellulose membrane (pore size 0.2 µm; Bio-Rad, USA) is withdrawn from the Petri dish and placed with bacteria facing up for 10 min on a Whatman filter paper soaked in water. After this washing step has been repeated twice, the nitrocellulose membrane is similarly placed for 5–10 min on another Whatman filter paper previously soaked in the corresponding solution for catalysis. The catalytic solution employed to detect the PP activity is 50 mM Tris/HCl (pH 7.8), 10 mM $MgCl_2$, and 0.1–1 mM phosphopeptide designed according to the consensus sequence for the relevant PP. The nitrocellulose membrane is withdrawn and can be stored for additional PP assays. The filter paper is first dipped gently for 2 s into the reagent (1.2 N sulfuric acid, 0.5% ammonium molybdate, 2% ascorbic acid) of Chen and coworkers (1956) for the assay of P_i and subsequently placed onto an absorbent paper to remove the excess of liquid until blue spots appeared.

EVALUATION

The bacterial cell-based procedure is sensitive enough to detect endogenous phosphate activity of bacteria under some experimental conditions. Although this feature appears to be useful for searching bacterial phosphatases, it can be a drawback when studying cloned mammalian PP. In those cases, *E. coli* strains with diminished phosphatase activity at the pH of interest should be used. In addition, plasmids of a high number of copies could be employed to reduce the time of catalysis and the background signal generated by chromosomal phosphatases. In most cases, the differentiation between the cloned PP activity and background phosphatase activity should be feasible.

Many currently used high-throughput procedures for the detection of compounds modulating PP activity are based on non-physiological substrates holding a colored or fluorescent moiety that facilitates the analysis of the reaction (Wahler and Reymond 2001) but generally impairs the intrinsic activity (Goddard and Reymond 2004). The bacterial cell-based assay for phosphatase activity offers the advantages of the use of specific protein or peptide substrates and the possibility of testing different experimental conditions using the same bacterial lawn. This feature may be helpful for the evaluation of the selectivity of PP.

REFERENCES AND FURTHER READING

Alessi DR, Downes CP (1998) The role of PI 3-kinase in insulin action. Biochim Biophys Acta 1436:151–164

Alonso A, Sasin J, Bottini N, Osterman A, Godzik A, Hunter T, Dixon J, Mustelin T (2004) Protein tyrosine phosphatases in the humane genome. Cell 117:699–711

Andersen JN, Mortensen OH, Peters GH, Drake PG, Iversen LF, Olsen OH, Jansen PG, Andersen HS, Tonks NK, Moller NP (2001) Structural and evolutionary relationships among protein tyrosine phosphatase domains. Mol Cell Biol 21:7117–7136

Andersson L, Porath J (1986) Isolation of phosphoproteins by immobilized metal (Fe^{2+}) affinity chromatography. Anal Biochem 155:250–254

Angeles TS, Steffler C, Bartlett BA, Hudkins RL, Stephens RM, Kaplan DR, Dionne CA (1996) Enzyme-linked immunosorbent assay for trkA tyrosine kinase activity. Anal Biochem 236:49–55

Angers S, Salahpour A, Joly E, Hilairet S, Chelsky D, Dennis M, Bouvier M (2000) Detection of beta 2-adrenergic receptor dimerization in living cells using bioluminescence resonance energy transfer (BRET). Proc Natl Acad Sci USA 97:3684–3689

Antonsson B, Marshall CJ, Montessuit S, Arkinstall S (1999) An in vitro 96-well plate assay of the mitogen-activated protein kinase cascade. Anal Biochem 267:294–299

Arai R (2000) Fluorolabeling of antibody variable domains with green fluorescent protein variants: application to an energy transfer-based homogeneous immunoassay. Protein Eng 13:369–376

Arai R (2001) Demonstration of a homogeneous noncompetitive immunoassay based on bioluminescence resonance energy transfer. Anal Biochem 289:77–81

Aronheim A, Broder YC, Cohen A, Fritsch A, Belisle B, Abo A (1998) Chp, a homologue of the GTPase Cdc42Hs, activates the JNK pathway and is implicated in reorganizing the actin cytoskeleton. Curr Biol 8:1125–1128

Aronheim A, Engelberg D, Li N, al-Alawi N, Schlessinger J, Karin M (1994) Membrane targeting of the nucleotide exchange factor Sos is sufficient for activating the Ras signaling pathway. Cell 78:949–961

Barberis A (2002) cell-based high-throughput screens for drug discovery. Eur Biopharm Rev Winter:93–96

Barford D, Das AK, Egloff MP (1998) The structure and mechanism of protein phosphatases: insights into catalysis and regulation. Annu Rev Biophys Biomol Struct 27:133–164

Barford D, Keller JC, Flint AJ, Tonks NK (1994) Purification and crystallization of the catalytic domain of human protein tyrosine phosphatase 1B expressed in Escherichia coli. J Mol Biol 239:726–730

Baron V, Calleja V, Ferrari P, Alengrin F, Van Obberghen E (1998) $pp125^{FAK}$ focal adhesion kinase is a substrate for the insulin and insulin-like growth factor-I tyrosine kinase receptors. J Biol Chem 273:7162–7166

Biazzo-Ashnault DE, Park Y-W, Cummings RT, Ding V, Moller DE, Ahang BB, Quershi SA (2001) Detection of insulin receptor tyrosine kinase activity using time-resolved fluorescence energy transfer technology. Anal biochem 291:155–158

Biddinger SB, Kahn CR (2006) From mice to men: insights into the insulin resistance syndromes. Annu Rev Physiol 68:123–158

Blero D, De Smedt F, Pesesse X, Paternotte N, Moreau C, Payrastre B, Erneux C (2001) The SH2 domain containing inositol 5-phosphatase SHIP2 controls phosphatidylinositol 3,4,5-trisphosphate levels in CHO-IR cells stimulated by insulin. Biochem Biophys Res Commun 282:839–843

Blero D, Zhang J, Pesesse X, Payrastre B, Dumont JE, Schurmans S, Erneux C (2005) Phosphatidyl 3,4,5-trisphosphate modulation in SHIP2-deficient mouse embryonic fibroblasts. FEBS J 272:2512–2522

Bourdeau A, Dube N, Tremblay ML (2005) Cytoplasmic protein tyrosine phosphatases, regulation and function: the roles of PTP1B and TC-PTP. Curr Opin Cell Biol 17:203–209

Boute N, Pernet K, Isaad T (2001) Monitoring the activation state of the insulin receptor using bioluminescence resonance energy transfer. Mol Pharmacol 60:640–645

Boute N, Jockers R, Issad T (2002) The use of resonance energy transfer in high-throughput screening: BRET versus FRET. Trends Pharmacol Sci 23:351–354

Braun S, Raymond WE, Racker E (1984) Synthetic tyrosine polymers as substrates and inhibitors of tyrosine-specific protein kinases. J Biol Chem 259:2051–2054

Braunwalder AF, Yarwood DR, Hall T, Missbach M, Lipson KE, Sills MA (1996) A solid phase assay for the determination of protein tyrosine kinase activity of c-src using scintillation microtitration plates. Anal Biochem 234:23–26

Bravo J, Karathanassis D, Pacold CM, Pacold ME, Ellson CD, Anderson KE, Butler PJ, Lavenir I, Perisic PT, Hawkins L, Stephens L, Williams RL (2001) The crystal structure of the PX domain from p40(phox) bound to phosphatidylinositol 3-phosphate. Mol Cell 8:829–839

Broder YC, Katz S, Aronheim A (1998) The ras recruitment system, a novel approach to the study of protein-protein interactions. Curr Biol 8:1121–1124

Brugge JS, Jarosik G, Andersen J, Queral-Lustig A, Fedor-Chaiken M, Broach JR (1987) Expression of Rous sarcoma virus transforming protein pp60v-src in Saccharomyces cerevisiae cells. Mol Cell Biol 7:2180–2187

Brune M, Hunter JL, Corrie JET, Webb MR (1994) Direct, real-time measurement of rapid inorganic phosphate release using a novel fluorescent probe and its application to actomyosin subfragment 1 ATPase. Biochemistry 33:8262–8271

Brune M, Hunter JL, Howell SA, Martin SR, Hazlett ThL, Corrie JET, Webb MR (1998) Mechanism of inorganic phosphate interaction with phosphate binding protein from *Escherichia coli*. Biochemistry 37:10370–10380

Cheatham RB, Vlahos CJ, Cheatham L, Wang L, Blenis J, Kahn CR (1994) Phosphatidylinositol 3-kinase activation is required for insulin stimulation of pp70S6 kinase, DNA synthesis, and glucose transporter translocation. Mol Cell Biol 14:4902–4911

Chen PS, Toribara TY, Warner H (1956) Microdetermination of phosphorus. Anal Chem 28:1756–1758

Cheng A, Dube N, Gu F, Tremblay ML (2002) Coordinated action of protein tyrosine phosphatases in insulin signal transduction. Eur J Biochem 269:1050–1059

Clement S et al (2001) The lipid phosphatase SHIP2 controls insulin sensitivity. Nature 409:92–97

Coffin J, Latev M, Bi X, Nikiforov TT (2000) Detection of phosphopeptides by fluorescence polarization in the presence of cationic polyamino acids: application to kinase assays. Anal Biochem 278:206–212

Cohen CB, Chin-Dixon E, Jeong S, Nikiforov TT (1999) A microchip-based enzyme assay for protein kinase A. Anal Biochem 273:89–97

Combettes-Souverain M, Isaad T (1998) Molecular basis of insulin action. Diabetes Metab 24:477–489

Cromlish WA, Kennedy B (1996) Selective inhibition of cyclooxygenase-1 and –2 using intact insect cells assays. Biochem Pharmacol 52:1777–1785

Cromlish WA, Payette P, Kennedy BP (1999) Development and validation of an intact cell assay for protein tyrosine phosphatases using recombinant baculoviruses. Biochem Pharmacol 58:1539–1546

Cubitt AB (1995) Understanding, improving and using green fluorescent protein. Trends Biochem Sci 20:448–455

Dass C, Mahalakshmi P (1996) Phosphorylation of enkephalins enhances their proteolytic stability. Life Sci 58:1039–1045

Dawson JF, Boland MP, Holmes CFB (1994) A capillary electrophoresis-based assay protein kinases and protein phosphatases using peptide substrates. Anal Biochem 220:340–345

DeMeyts P, Bianco AR, Roth J (1976) Site-site interactions among insulin receptors. Characterization of the negative cooperativity. J Biol Chem 251:1877–1888

Ehrhard KN, Jacoby JJ, Fu XY, Jahn R, Dohlman HG (2000) Use of G-protein fusions to monitor integral membrane protein-protein interactions in yeast. Nat Biotechnol 18:1075–1079

Elchebly M, Payette P, Michaliszyn E, Cromlish W, Collins S, Loy AL, Normandin D, Cheng A, Himms-Hagen J, Chan CC, Ramachandran C, Gresser MJ, Tremblay ML, Kennedy BP (1999) Science 283:1544–1548

Ellen Chan LP, Swaminathan R (1986) Adenosine triphosphate interferes with phosphate determination. Clin Chem 32:1981–1982

Ellis L, Clauser E, Morgan DO, Edery M, Roth RA, Rutter WJ (1986) Replacement of insulin receptor tyrosine residues 1162 and 1163 compromises insulin-stimulated kinase activity and uptake of 2-deoxyglucose. Cell 45:721–732

Flint AJ, Gebbink MFBG, Franza BR, Hill DE, Tonks NK (1993) Multi-site phosphorylation of the protein tyrosine

phosphatase, PTP1B: identification of cell cycle regulated and phorbol ester stimulated sites of phosphorylation. EMBO J 12:1937–1946

Flint AJ, Tiganis T, Barford D, Tonks NK (1997) Development of "substrate-trapping" mutants to identify physiological substrates of protein tyrosine phosphatases. Proc Natl Acad Sci USA 94:1680–1685Florio M, Wilson LK, Trager JB, Thorner J, Martin GS (1994) Aberrant protein phosphorylation at tyrosine is responsible for the growth-inhibitory action of pp60v-src expressed in the yeast Saccharomyces cerevisiae. Mol Biol cell 5:282–296

Florio M, Wilson LK, Trager JB, Thorner J, Martin GS (1994) Aberrant protein phosphorylation at tyrosine is responsible for the growth-inhibitory action of $pp60^{v\text{-}src}$ expressed in the yeast *Saccharomyces cerevisiae*. Mol Cell Biol 5:283–296

Frick W, Bauer A, Bauer J, Wied S, Müller G (1998) Insulin-mimetic signalling of synthetic phosphoinositolglycans in isolated rat adipocytes. Biochem J 336:163–181

Funaki M, Katagiri H, Kanda A, Anai M, Nawano M, Ogihara K, Inukai Y, Fukushima H, Ono H (1999) p85/p110-type phosphatidylinositol kinase phosphorylates not only the D-3, but also the D-4 position of the inositol ring. J Biol Chem 274:22019–22024

Gee KR, Sun WC, Bhalgat MK, Upson RH, Klaubert DH, Lataham KA, Haugland RP (1999) Fluorogenic substrates based on fluorinated umbelliferones for continuous assays of phosphatases and beta-galactosidases. Anal Biochem 273:41–48

Geisen K (1988) Special pharmacology of the new sulfonylurea glimepiride. Drug Res 38:1120–1130

Gillooly DJ, Simonsen A, Stenmark H (2001) Cellular functions of phosphatidylinositol 3-phosphate and FYVE domain proteins. Biochem J 355:249–258

Giuriato S, Pesesse X, Bodin S, Sasaki T, Viala C, Marion E, Penninger J, Schurmans S, Erneux C, Payrastre B (2003) SH2-containing inositol 5-phosphatases 1 and 2 in blood platelets. Their interactions and roles in the control of phosphatidylinositol 3,4,5-trisphosphate levels. Biochem J 376:199–207

Goddard J-P, Reymond J-L (2004) Enzyme assays for high-throughput screening. Curr Opin Biotechnol 15:314–322

Gray A, Olsson H, Batty IH, Priganica L, Downes CP (2003) Nonradioactive methods for the assay of phosphoinositide 3-kinases and phosphoinositide phosphatases and selective detection of signaling lipids in cell and tissue extracts. Anal Biochem 313:234–245

Gray A, Van Der Kaay J, Downes CP (1999) The plackstrin homology domains of protein kinase b- and GRP1 (general receptor for phosphoinositides-1) are sensitive and selective probes for the cellular detection of phosphatidylinositol 3,4-bisphosphate and/or phosphatidylinositol 3,4,5-trisphosphate *in vivo*. Biochem J 344:929–936

Gunde T (2004) *In vivo veritas ?* Cell-based assays for identifying RTK inhibitors. Eur Biopharm Rev Spring:56–60

Gunde T, Barberis A (2005) Yeast growth selection system for detecting activity and inhibition of dimerization-dependent receptor tyrosine kinase. Biotechniques 39:541–549

Gustafson TA, Moodie SA, Lavan BE (1998) The insulin receptor and metabolic signaling. In: Reviews Physiology, Biochemistry and Pharmacology, vol. 137, pp 71–192, Springer-Verlag, Berlin, Heidelberg, New York. The insulin receptor and metabolic signaling

Hammonds TR, Maxwell A, Jenkins JR (1998) Use of a rapid throughput *in vivo* screen to investigate inhibitors of eukaryotic topoisomerase II enzymes. Antimicrob Agents Chemother 42:889–894

Herbst JJ, Andrews GC, Contillo LG, Singleton PH, Genereux PE, Gibbs EM, Lienhard GE (1995) Effect of the activation of phosphatidylinositol 3-kinase by a thiophosphotyrosine peptide on glucose transport in 3T3-L1 adipocytes. J Biol Chem 270:26000–26005

Hjøllund E (1991) Insulin receptor binding and action in human adipocytes. Dan Med Bull 38:252–270

Holman GD, Kasuga M (1997) From receptor to transporter: insulin signalling to glucose transport. Diabetologia 40:991–1003

Hovius R (2000) Fluorescence techniques: shedding light on ligand-receptor interactions. Trends Pharmacol Sci 21:266–273

Hresko RC, Mueckler M (2006) mTOR/RICTOR is the Ser473 kinase for Akt/PKB in 3T3-L1 adipocytes. J Biol Chem, in press

Huang W, Zhang Y, Sportsman JR (2002) A fluorescence polarization assay for cyclic nucleotide phosphodiesterases. J Biolmol Screen 7:215–222

Huang Z, Wang Q, Ly HD, Govindarajan A, Scheigetz J, Zamboni R, Desmarais S, Ramachandran C (1999) 3,6-Fluorescein diphosphate: a sensitive fluorogenic and chromogenic substrate for protein tyrosine phosphatases. J Biomol Screen 4:327–334

Hubbard SR (1997) Crystal structure of the activated tyrosine kinase in complex with peptide substrate and ATP analog. EMBO J 16:5572–5581

Hubsman M, Yudkovsky G, Aronheim A (2001) A novel approach for the identification of protein-protein interaction with integral membrane proteins. Nucelic Acids Res 29:E18

Hughes TR (2002) Yeast and drug discovery. Funct Integr Genomics 2:199–211

Huppertz C, Schwartz C, Becker W, Horn F, Heinrich PC, Joost H-G (1996) Comparison of the effects of insulin, PDGF, interleukin-6, and interferon-γ on glucose transport in 3T3-L1 cells: lack of cross-talk between tyrosine kinase receptors and JAK/STAT pathways. Diabetologia 39:1432–1439

Hwang KJ (1976) Interference of ATP and acidity in the determination of inorganic phosphate by the Fiske and Subbarow method. Anal Biochem 75:40–44

Itaya K, Ui M (1966) A new micromethod for the colorimetric determination of inorganic phosphate. Clin Chim Acta 14:361–366

Jeong S, Nikiforov TT (1999) A kinase assay based on thiophosphorylation and biotinylation. BioTechniques 27:1232–1238

Jiang G, Zhang BB (2002) PI 3-kinase and its up- and downstream modulators as potential targets for the treatment of type II diabetes. Front Biosci 7:d902-d907

Johnson TO, Ermolieff J, Jirousek MR (2002) Protein tyrosine phosphatase 1B inhibitors for diabetes. Nat Rev Drug Dis 1:696–709

Kaiser C, Michaelis S, Mitchell A (1994) Methods in Yeast genetics. CSH Laboratory press, Cvold Spring Harbor, NY

Kessler A, Müller G, Wied S, Crecelius A, Eckel J (1998) Signalling pathways of an insulin-mimetic phosphoinositolglycanpeptide in muscle and adipose tissues. Biochem J 330:277–286

Kirkbright GF, Narayanaswamy R, West TS (1972) The spectrofluorimetric determination of orthophosphate as quinine molybdophosphate. Analyst 97:174–181

Kohler F, Muller KM (2003) Adaptation of the Ras-recruitment system to the analysis of interactions between membrane-associated proteins. Nucleic Acids Res 31:e28

Kornbluth S, Jove R, Hanafusa H (1987) Characterization of avian and viral p60src proteins expressed in yeast. Proc Natl Acad Sci USA 84:4455–4459

Kowalski-Chauvel A, Pradayrol L, Vaysse N, Seva C (1996) Gastrin stimulates tyrosine phosphorylation of insulin receptor substrate 1 and its association with Grb2 and the phosphatidylinositol 3-kinase. J Biol Chem 271:26356–26361

Kristjansdottir K, Rudolph J (2003) A fluorescence polarization assay for native protein substrates of kinases. Anal Biochem 316:41–49

Krutzfeldt J, Grunweller A, Raasch W, Drenckhan M, Klein HH (1999) Microtiter well assays for protein tyrosine phosphatase activities directed against phosphorylated insulin receptor or insulin receptor substrate-1. Anal Biochem 271:97–99

Kupcho K, Somberg R, Bulleit B, Goueli SA (2003) A homogeneous, nonradioactive high-throughput fluorogenic protein kinase assay. Anal Biochem 317:210–217

Kurlawalla-Martinez C (2005) Insulin hypersensitivity and resistance to streptozotocin-induced diabetes in mice lacking PTEN in adipose tissue. Mol Cell Biol 25:2498–2510

Lemmon MA, Ferguson KM (2001) Molecular determinants in pleckstrin homology domains that allow specific recognition of phosphoinositides. Biochem Soc Trans 29:377–384

Leon Y, Varela-Nieto I (2004) Glycosyl-phosphatidylinositol cleavage products in signal transduction in "Lipases and Phospholipases in Drug Development" (Müller G, Petry S Eds.) pp 101–119, Wiley-VCH Weinheim Germany

Lin S, Fischl AS, Bi X, Parce W (2003) Separation of phospholipids in microfluidic chip device: application to high-throughput screening assays for lipid-modifying enzymes. Anal Biochem 314:97–107

Liu G, Trevillyan JM (2002) Protein tyrosine phosphatase 1B as a target for the treatment of impaired glucose tolerance and type II diabetes. Curr Opin Invest Drugs 11:1608–1616

Lorenzen JA, Dadabay CY, Fischer EH (1995) COOH-terminal sequence motifs target the T cell protein tyrosine phosphatase to the ER and nucleus. J Cell Biol 131:631–643

Melese T, Hieter P (2002) From genetics and genomics to drug discovery: yeast rises to the challenge. Trends Pharmacol Sci 23:544–547

Montalibet J, Kennedy BP (2004) Using yeast to screen for inhibitors of protein tyrosine phosphatase 1B. Biochem Pharmacol 68:1807–1814

Müller G (2000) The molecular mechanism of the insulin-mimetic/sensitizing activity of the anti-diabetic sulfonylurea drug amaryl. Mol Med 6:907–933

Müller G, Geisen K (1996) Characterization of the molecular mode of action of the sulfonylurea, glimepiride, at adipocytes. Horm Metab Res 28:469–487

Müller G, Schulz A, Wied S, Frick W (2005) Regulation of lipid raft proteins by glimepiride- and insulin-induced glycosylphosphatidylinositol-specific phospholipase C in rat adipocytes. Biochem Pharmacol 69:761–780

Müller G, Wied S, Wetekam E-M, Crecelius A, Unkelbach A, Pünter J (1994) Stimulation of glucose utilization in 3T3 adipocytes and rat diaphragm *in vitro* by the sulfonylureas, glimepiride and glibenclamide, is correlated with modulations of the cAMP regulatory cascade. Biochem Pharmacol 48:985–996

Müller G, Satoh Y, Geisen K (1995) Extrapancreatic effects of sulfonylureas – a comparison between glimepiride and conventional sulfonylureas. Diabetes Res Clin Pract 28 (Suppl.):S115–S137

Müller G, Wied S, Crecelius A, Kessler A, Eckel J (1997) Phosphoinositolglycan-peptides from yeast potently induce metabolic insulin actions in isolated rat adipocytes, cardiomyocytes, and diaphragms. Endocrinology 138:3459–3475

Murray PF, Hammerschmidt P, Samela A, Passeron S (1996) Peptide degradation: effect of substrate phosphorylation on aminopeptidasic hydrolysis. Int J Biochem Cell Biol 28:451–456

Myers MG, White MF (1995) New frontiers in insulin receptor substrate signaling. Trends Endocrinol Metab 6:209–215

Nakashima N et al (2000) The tumor suppressor PTEN negatively regulates insulin signaling in 3T3-L1 adipocytes. J Biol Chem 275:12889–12895

Okada Y, Yoshida M, Baba S, Shii K (1998) Development of vanadate sensitive human erythrocyte insulin receptor tyrosine phosphatase assay. Diabetes Res Clin Practice 41:157–163

Ozawa T, Sato M, Sugawara M, Umezawa Y (1998) An assay method for evaluating chemical selectivity of agonists for insulin signaling pathways based on agonist-induced phosphorylation of a target peptide. Anal Chem 70:2345–2352

Park Y-W, Cummings RT, Wu L, Zheng S, Cameron PM, Woods A, Zaller DM, Marcy AI, Hermes JD (1999) Homogeneous proximity tyrosine kinase assays: scintillation proximity assay versus homogeneous time-resolved fluorescence. Anal Biochem 289:94–104

Pastula C, Johnson I, Beechem JM, Patton WF (2003) Development of fluorescence-based assays for serine/threonine and tyrosine phosphatases. Comb Chem High Throughput Screen 6:341–346

Pedersen O, Hjøllund E, Beck-Nielsen H, Lindskov HO, Sonne O, Gliemann J (1981) Insulin receptor binding and receptor-mediated insulin degradation in human adipocytes. Diabetologia 20:636–641

Pedersen O, Hjøllund E, Linkskov HO (1982) Insulin binding and action on fat cells from young healthy females and males. Am J Physiol 243:E158–E167

Podlecki DA, Frank BH, Olefsky JM (1984) *In vitro* characterization of human proinsulin. Diabetes 33:111–118

Pesesse X, Dewaste V, De Smedt F, Laffargue M, Giuriato S, Moreau C, Payrastre B, Erneux C (2001) The Src homology 2 domain containing inositol 5-phosphatase SHIP2 is recruited to the epidermal growth factor (EGF) receptor and dephosphorylates phosphatidylinositol 3,4,5-trisphosphate in EGF-stimulated COS-7 cells. J Biol Chem 276:28348–28355

Petry S, Baringhaus KH, Hoelder S, Müller G (2002) Substituted and non-substituted benzooxathiazoles and compounds derived there from. Eur patent appl WO 2004/11722A1

Pope AJ, Haupts UM, Moore KJ (1999) Homogenous fluorescence readouts for miniaturized high-throughput screening: theory and practice. Drug Discovery Today 4:350–362Ricort JM, Tanti JF, Obberghen E, Le Marchand-Brustel Y (1997) Cross-talk between the platelet-derived growth factor and the insulin signaling pathways in 3T3-L1 adipocytes. J Biol Chem 272:19814–19818

Ribel U, Hougaard P, Drejer K, Sørensen AR (1990) Equivalent *in vivo* biological activity of insulin analogs and human insulin despite different *in vitro* potencies. Diabetes 39:1033–1039

Robertson DA, Singh BM, Hale PJ, Jensen I, Nattrass M (1992) Metabolic effects of monomeric insulin analogs of different receptor affinity. Diabetes Med 9:240–246

Saltiel AR (1996) Diverse signaling pathways in the cellular actions of insulin. Am J Physiol 270:375–385

Sarbassov DD, et al (2005) Phosphorylation and regulation of Akt/PKB by the rictor-mTOR complex. Science 307:1098–1101

Sato M, Ozawa T, Inukai K, Asano T, Umezawa Y (2002) Fluorescent indicators for imaging protein phosphorylation in single living cells. Nat Biotechnol 20:287–294

Schenk T, Appels NMGM, van Elswijk DA, Irth H, Tjaden UR, van der Greef J (2003) A generic assay for phosphate-consuming or –releasing enzymes coupled on-line to liquid chromatography for lead finding in natural products. Anal Biochem 316:118–126

Schwartz GP, Burke GT, Katsoyannis PG (1987) A superactive insulin: [B10-aspartic acid]insulin(human). Proc Natl Acad Sci USA 84:6408–6411

Scott JE, Carpenter JW (2003) A homogeneous assay of kinase activity that detects phosphopeptide using fluorescence polarization and zinc. Anal Biochem 316:82–91

Sebbon B, Fynn GH (1973) Orthophosphate analysis by the Fiske-Subbarow method and interference by adenosine phosphates and pyrophosphate at variable acid pH. Anal Biochem 56:566–570

Seethala R, Menzel R (1997) A homogeneous, fluorescence polarization assay for src-family tyrosine kinases. Anal Biochem 253:210–218

Seethala R, Menzel R (1998) A fluorescence polarization competition immunoassay for tyrosine kinases. Anal Biochem 255:257–262

Senn AM, Wolosiuk RA (2005) A high-throughput screening for phosphatases using specific substrates. Anal Biochem 339:150–156

Serunian LA, Auger K, Cantley LC (1991) Identification and quantification of polyphosphoinositides produced in response to platelet-derived growth-factor stimulation. Methods Enzymol 198:78–87

Simeonov A, Bi X, Nikiforov TT (2002) Enzyme assays by fluorescence polarization in the presence of polyarginine: study for kinase, phosphatase, and protease reactions. Anal Biochem 304:193–199

Sims CE, Allbritton NL (2003) Single-cell kinase assays: opening a window onto cell behavior. Curr Opin Biotechnol 14:23–28

Shepherd PR (2005) Mechanisms regulating phosphoinositide 3-kinase signaling in insulin-sensitive tissues. Acta Physiol Scand 183:3–12

Shepherd PR, Withers DJ, Siddle K (1998) Phosphoinositide 3-kinase: the key switch mechanism in insulin signalling. Biochem J 333:471–490

Stagljar I, Korostensky C, Johnsson N, te Heesen S (1998) A genetic system based on split-ubiquitin for the analysis of interactins between membrane proteins *in vivo*. Proc Natl Acad Sci USA 95:5187–5192

Sun WC, Gee KR, Haughland RP (1998) Synthesis of novel fluorinated coumarins: excellent UV-light excitable fluorescent dyes. Bioorg Med Chem Lett 8:3107–3110

Tashima Y (1975) Removal of protein interference in the Fiske-Subbarow method by sodium dodecyl sulfate. Anal Biochem 69:410–414

Tavare JM, Denton RM (1988) Studies on the autophosphorylation of the insulin receptor from human placenta. Biochem J 252:607–615

Thaminy S, Auerbach D, Arnoldo A, Stagljar I (2003) Identification of novel ErbB3-interacting factors using the split-ubiquitin membrane yeast two-hybrid system. Genome Res 13:1744–1753

Tonks NK (2003) Minireview: PTP1B: from the sidelines to the front lines! FEBS lett 546:140148

Tornqvist HE, Avruch J (1988) Relationship of site-specific β subunit tyrosine autophosphorylation to insulin activation of the insulin receptor protein kinase activity. J Biol Chem 263:4593–4601

Trager JB, Martin GS (1997) The role of the Src homology-2 domain in the lethal effect of Src expression in the yeast Saccharomyces cerevisiae. Int J Biochem Cell Biol 29:635–648

Tsien RY (1993) FRET for studying intracellular signalling. Trends Cell Biol 3:243–245

Tsien RY (1998) The green fluorescent protein. Annu Rev Biochem 67:509–544

Turek TC, Small EC, Bryant RW, Hill WAG (2001) Development and validation of a competitive AKT serine/threonine kinase fluorescence polarization assay using a product-specific anti-phospho-serine antibody. Anal Biochem 299:45–53

Ungerer JP, Oosthuizen MH, Bissbort SH (1993) An enzymatic assay of inorganic phosphate in serum using nucleoside phosphorylase and xanthine oxidase. Clin Chim Acta 223:149–157

Velloso lA, Folli F, Sun X-U, White MF, Saad MJA, Kahn CR (1996) Cross-talk between the insulin and angiotensin signaling systems. Proc Natl Acad Sci USA 93:12490–12495

Verdier F, Chretien S, Billat C, Gisselbrecht S, Lacombe C, Mayeux P (1997) Erythropoietin induces the tyrosine phosphorylation of insulin receptor substrate-2. J Biol Chem 272:26173–26178

Vølund A, Brange J, Drejer K, Jensen I, Markussen J, Ribel U, Sørensen AR (1991) *In vitro* and *in vivo* potency of insulin analogs designed for clinical use. Diabetes Med 8:839–847

Wada T, Sasaoka T, Funaki M, Hori H, Murakami M, Ishiki M, Haruta T, Asano T, Ogawa W, Ishihara H, Kobayashi M (2001) Overexpression of SH2-containing inositol phosphatase 2 rsults in negative regulation of insulin-induced metabolic actions in 3T3-L1 adipocytes via its 5′-phosphatase catalytic activity. Mol Cell Biol 21:1633–1646

Waddleton D, Ramachandran C, Wang Q (2002) Development of a time-resolved fluorescent assay for measuring tyrosine-phosphorylated proteins in cells. Anal Biochem 309:150–157

Wahler D, Reymond J-L (2001) High-throughput screening for biocatalysts. Curr Opin Biotechnol 12:535–544

Wang Q, Scheigetz J, Gilbert M, Snider JS, Ramachandran C (1999) Fluorescein monophosphates as fluorogenic substrates for protein tyrosine phosphatases. Biochim Biophys Acta 1431:14–23

Watson RT, Pessin JE (2006) Bridging the GAP between insulin signaling and GLUT4 translocation. Trends Biochem Sci 31:215–222

Webb MR (1992) A continuous spectrophotometric assay for inorganic phosphate and for measuring phosphate release kinetics in biological systems. Proc Natl Acad Sci USA 89:4884–4887

Welsh GI et al (2005) Role of protein kinase B in insulin-regulated glucose uptake. Biochem Soc Trans 33:350–353

Welte S, Baringhaus K-H, Schmider W, Müller G, Petry S, Tennagels N (2005) 6,8–4-methylumbiliferyl phosphate: a fluorogenic substrate for protein tyrosine phosphatases. Anal Biochem 338:32–38

Welte S, Tennagels N, Petry S (2003) Highly sensitive and continuous protein tyrosine phosphatase (PTPase) test using 6,8 difluoro-4-methyl-umbelliferylphosphate. Int patent no WO03/056029 A2

White MF (1997) The insulin signalling system and the IRS proteins. Diabetologia 40:S2–S17

White MF (1998) The IRS-signalling system: a network of docking proteins that mediate insulin action. Mol Cell Biochem 182:3–11

White MF (2002) IRS proteins and the common path to diabetes. Am J Physiol Endocrinol Metab 283: E413-E422

Witt JJ, Roskoski R (1975) Rapid protein kinase assay using phosphocellulose-paper absorption. Anal Biochem 66:253–258
Wouters FS (2001) Imaging biochemistry inside cells. Trends Cell Biol 11:203–211
Wu JJ, Yarwood DR, Pham Q, Sills MA, Identification of a high-affinity anti-phosphoserine antibody for development of a homogeneous fluorescence polarization assay for protein kinase C. J Biolmol Screen 5:23–30
Wu P, Brand L (1994) Resonance energy transfer: methods and applications. Anal Biochem 218:1–13
Xu J, Seet LF, Hanson B, Hong W (2001) The Phox homology (PX) domain, a new player in phosphoinositide signalling. Biochem J 360:513–530
Xu Y (2002) Resonance energy transfer as an emerging technique for monitoring protein-protein interactions *in vivo*: BRET *vs* FRET. Luminscence Biotechnology: Instruments and Applications, (Van Dyke K, eds.) CRC Press, pp 529–538
Xu Y, Piston DW, Johnson CH (1999) A bioluminescence resonance energy transfer (BRET) system: application to interacting circadian clock proteins. Proc Natl Acad Sci USA 96:151–156
Yamaguchi Y, Choi S, Sakamoto Y, Itakura K (1983) Purification of insulin receptor with full binding activity. J Biol Chem 258:5045–5049
Yeh JI, Gulve EA, Rameh L, Birmbaum MJ (1997) The effects of wortmannin on rat skeletal muscle. Dissociation of signalling pathways for insulin- and contraction-activated hexose transport. J Biol Chem 270:2107–2111
Yenush L, White MF (1997) The IRS-signalling system during insulin and cytokine action. Bioassays 19:491–500
Zacharias DA (2000) Recent advancesin technology for measuring and manipulating cell signals. Curr Opin Nueorbiol 10:416–421
Zeuzem S, Taylor R, Agius L, Albisser AM, Alberti KGMM (1984) Differential binding of sulphated insulin to adipocytes and hepatocytes. Diabetologia 27:184–188
Zhang B, Salituro G, Szalkowski D, Zhibua L, Zhang Y, Royo I, Vilella D, Diez MT, Pelaez F, Ruby C, Kendall RL, Mao X, Griffin P, Calaycay J, Zierath JR, Heck JV, Smith RG, Moller DE (1999) Discovery of a small molecuale insulin mimetic with antidiabetic activity in mice. Science 284:974–977
Zhang ZY (2003) Mechanistic studies on protein tyrosine phosphatases. Prog Nucleic Acid Res Mol Biol 73:171–220
Zhang ZY, Dixon JE (1994) Protein tyrosine phosphatases: emchanisms of catalysis and substrate specificity. Adv Enzymol 68:1–36
Zhang ZY, Maclean D, Thieme-Sefler AM, Roeske RW, Dixon JE (1993) A continuous spectrophotometric and fluorimetric assay for protein tyrosine phosphatase using phosphotyrosine-containing peptides. Anal Biochem 211:7–15

K.6.3.4 Expression, Phosphorylation, Activity and Interaction of Insulin Signaling Components

PURPOSE AND RATIONALE

Signal transduction from the cell surface to the nucleus was found to occur predominantly by serine/threonine- and tyrosine-specific PK participating in cascades involving phosphorylation of multiple substrates. The role of protein phosphorylation in signal transduction is well characterized in the case of the insulin signaling cascade in insulin-responsive target cells, such as liver, muscle and adipose cells (for reviews see Chen 2006, White et al. 1994, 1998, 2003).

In the past decade, it has been increasingly recognized that insulin resistance is associated with chronic, low-grade systemic inflammation. These celllar inflammatory responses are thought to be mediated by serine/threonine phosphorylation by PK, such as IKKβ (Yuan et al. 2001, Gao et al. 2002), JNK1 (Hirosumi et al. 2002), PKCθ (Yu et al. 2002), or direct interaction with inhibitory proteins, such as SOCS (Mooney et al. 2001, Steppan et al. 2005, Ueki et al. 2004), of key components of insulin signaling, such as the IRS proteins, which thereby undergo inactivation or downregulation. The molecular mechanism of insulin-like compounds/drug candidates can be studied in appropriate assay systems monitoring the phosphorylation state or protein-protein interaction of the individual insulin signaling components.

K.6.3.4.1 Preparation of Cytosolic Extracts

PROCEDURE

Cultured Adipocytes

Cultured mouse or human adipocytes are incubated with insulin/compounds/drugs in 12- or 24-well plates for 10–20 min, then washed twice with 50 mM HEPES/KOH (pH 7.5), 150 mM NaCl, 1 mM $CaCl_2$, 1 mM $MgCl_2$, 10 mM EDTA, 10 mM glycerol-3-phosphate, 10 mM $Na_4P_2O_7$, 2 mM Na_3VO_4, 100 mM NaF. Cells are solubilized in the above buffer containing 1% (by vol.) Triton X-100, 0.1% sodium deoxycholate, 10% glycerol and protease inhibitors (20 µg/ml leupeptin, 10 µg/ml pepstatin A, 50 µg/ml aprotinin, 10 µM E-64, 0.5 mM PMSF = lysis buffer) by scraping with a Teflon policeman (adherent cells). Total lysates are centrifuged (25,000 × *g*, 20 min, 18°C). The infranatant is aspirated taking care to avoid contamination by the upper fat layer and recentrifuged to obtain the defatted cell lysate (cytosolic extract).

Primary Rat Adipocytes

Adipocytes ($1–3 \times 10^6$ cells/ml) are incubated with insulin/compounds/drug candidates and then separated from the medium by flotation and lysed in 1 ml of chilled buffer containing 20 mM Tris/HCl (pH 7.4), 150 mM NaCl, 10% glycerol, 2 mM EDTA, 1 mM Na_3VO_4, 50 mM $Na_4P_2O_7$, 10 mM NaF, 10 mM glycerol-3-phosphate, 0.2 mM PMSF, 20 µg/ml leupeptin, 10 µg/ml pepstatin, 25 µg/ml aprotinin by

10 strokes in a loose-fitting Teflon-in-glass homogenizer at 15°C. The fat-free homogenate, prepared by centrifugation (500 × *g*, 3 min, 15°C), is supplemented with Triton X-100 (1% final conc.) and sodium deoxycholate (0.5% final conc.), incubated for 30 min at 4°C and finally centrifuged (13,000 × *g*, 10 min).

Liver

Portions of frozen liver (0.2–1 g wet weight), which has been perfused as described (see K.5.2.1) are homogenized in a buffer containing 50 mM HEPES/KOH (pH 7.4), 140 mM NaCl, 250 mM sucrose, 1 mM $MgCl_2$, 1 mM $CaCl_2$, 2 mM EDTA, 2.5 mM Na_3VO_4, 10 mM glycerol-3-phosphate, 20 mM $NaPP_i$, 20 mM NaF, 1 mM phenylphosphate, 5 µM okadaic acid (sodium salt), 1% Nonidet P-40, 10% glycerol and protease inhibitors (10 µg/ml leupeptin, 5 µg/ml pepstatin A, 75 µg/ml aprotinin, 100 µM benzamidine, 2 µg/ml antipain, 10 µg/ml soybean trypsin inhibitor, 5 µM microcystin, 5 µM E-64, 0.2 mM PMSF) using an Ultraturrax T25 basic (three 10-s cycles at 2,000 rpm on ice) and then a tight-fitting Teflon-in-glass homogenizer (5 strokes at 500 rpm on ice). The total homogenate is centrifuged (48,000 × *g*, 30 min, 4°C). The supernatant is carefully removed to avoid contamination with the upper fat layer and re-centrifuged. The fat-free supernatant obtained is stored in liquid N_2 and used as cytosolic extract (3–5 mg protein per ml).

Diaphragm

After incubation with insulin/compounds/drug candidates, the hemidiaphragms (80–100 mg wet weight) are rapidly liberated from the rib cage, rinsed once with homogenization buffer (25 mM Hepes/KOH, pH 7.4, 140 mM NaCl, 10% glycerol, 1 mM EDTA, 1 mM sodium vanadate, 50 mM sodium pyrophosphate, 100 mM NaF, 10 mM glycerol-3-phosphate, 0.2 mM PMSF, 10 µg/ml leupeptin, 10 µg/ml pepstatin, 5 µg/ml antipain, 25 µg/ml aprotinin), frozen in liquid N_2 and then homogenized in 2 ml of ice-cold homogenization buffer in a porcelain mortar on ice. After centrifugation (1,500 × *g*, 10 min, 4°C), the fat-free supernatant is supplemented with Triton X-100 (0.5% final conc.), incubated (30 min, 4°C) and centrifuged (18,000 × *g*, 20 min, 4°C) to yield the cytosolic extract.

Skeletal Muscle

Rats at week 10 of age and housed in a temperature-controlled room (22°C) with a 12:12-h light-dark cycle with free access to chow and water are deeply anesthetized with an i.p. injection of pentobarbital sodium (50 mg/kg). Intact epitrochlearis muscles (type II muscle consisting primarily of both type IIa and IIb fibers) and strips of soleus muscles (consisting primarily of type I fibers) are prepared (~30 mg). Soleus strips and epitrochlearis muscles are incubated for 60 min at 37°C in 3 ml of oxygenated (95% O_2/5% CO_2) KHB containing 14 mM $NaHCO_3$ and then for 10 min with KHB supplemented with 8 mM glucose, 32 mM mannitol, 0.1% BSA in the presence of insulin/compounds/drugs. Thereafter, the muscles are rinsed for 10 min at 37°C in 3 ml of oxygenated KHB containing 40 mM mannitol, 0.1% BSA, then trimmed of fat and connective tissue, quickly frozen between aluminium blocks cooled with liquid N_2 and weighed. Frozen muscles are homogenized in 8 vol. of ice-cold lysis buffer (50 mM HEPES/KOH, pH 7.5, 150 mM NaCl, 20 mM sodium pyrophosphate, 20 mM glycerolphosphate, 10 mM NaF, 2 mM Na_3VO_4, 2 mM EDTA, 1% TX-100, 10% glycerol, 1 mM $MgCl_2$, 1 mM $CaCl_2$, 10 µg/ml aprotinin, 10 µg/ml leupeptin, 0.5 µg/ml pepstatin, 2 mM PMSF). Lysates are incubated on ice for 20 min and then centrifuged (13,000 × *g*, 20 min, 4°C) to yield the cytosolic extract.

K.6.3.4.2 Immunoprecipitation

Up to 1 -ml portions of cytosol (equal amounts of protein) are precleared (30 -min incubation at 4°C, 2-min centrifugation at 10,000 × *g*) with protein A/G-Sepharose (50 mg, Pharmacia) and then supplemented with typically 2–10 µg/ml appropriate antibodies: anti-IRS-1 (rabbit, polyclonal, protein A-purified, raised against a peptide corresponding to amino acids 1220–1235 of rat IRS-1, Upstate Biotechnology), anti-IRS-2 (raised against peptide mixture corresponding to amino acids 618–747 and 976–1094 of mouse IRS-2), anti-IRβ (raised against a peptide corresponding to the 100 carboxy-terminal amino acids of human IR, Upstate Biotechnology), anti-GSK-3β (mouse monoclonal, protein G-purified, raised against a peptide corresponding to amino acids 203–219 of Drosophila GSK-3β, Upstate Biotechnology, preadsorbed on protein A-Sepharose). After incubation (4 -20 h, 4°C, end-over-end rotation) and centrifugation (10,000 × *g*, 2 min, 4°C), the collected immune complexes are washed twice with 1 ml each of immunoprecipitation buffer (50 mM HEPES/KOH, pH 7.4, 500 mM NaCl, 100 mM NaF, 10 mM EDTA, 20 mM glycerol-3-phosphate, 10 mM NaP_i, 2.5 mM Na_3VO_4) containing 1% Nonidet P-40 (omitted for sequential immunoprecipitation), then twice with 1 ml each of im-

munoprecipitation buffer containing 150 mM NaCl and 0.1% NP-40 and once with 1 ml of immunoprecipitation buffer containing 150 mM NaCl and twice with immunoprecipitation buffer lacking detergent and salt. The washed immune complexes are finally suspended in 50 µl of Laemmli buffer (2% SDS, 5% 2-mercaptoethanol), heated (95°C, 2 min) and centrifuged. The supernatant samples are analyzed by SDS-PAGE. 4–12% Bis-Tris precast gel, pH 6.4, morpholinoethanesulfonic acid (MES)/SDS running buffer, e. g. Novex) under reducing conditions. For sequential immunoprecipitation, the supernatant samples (50 µl) are supplemented with 1 ml of immunoprecipitation buffer containing 1% NP-40 and 1–10 µl of the relevant antiserum. After incubation (12 h, 4°C), 50 µl of protein A-Sepharose (100 mg/ml in immunoprecipitation buffer) is added and the incubation continued (4 h, end-over-end rotation). The immunecomplexes are collected, washed and processed for SDS-PAGE.

K.6.3.4.3 Immunoblotting

Immunoblotting is performed as described previously by Towbin (1979), Frick and coworkers (1998) and Müller and coworkers (2000) with minor modifications. Briefly, after SDS-PAGE and electrophoretic transfer of the proteins (2 h, 400 mA in 20% methanol, 192 mM glycine, 25 mM Tris, 0.005% SDS) to PVDF membranes (Immobilon, Millipore, Germany), the blocked membrane (1 h in blotting buffer containing 20 mM Tris/HCl, pH 7.6, 150 mM NaCl, 0.05% Tween 20, 0.1% Brij, 0.01% NP-40 and supplemented with either 1% ovalbumin or 1% BSA or 5% nonfat dried milk according to manufacturer's instructions and the unspecific background signal obtained) is incubated (2 h, 25°C) with the appropriate antibodies (often 1:200–1:5,000). The membranes are washed (four times with Tris-buffered saline (TBS) containing 1% (by vol.) Nonidet-P40 and 0.5% Tween 20, twice with TBS containing 0.5% Tween 20, three times with TBS containing 0.05% Tween 20, twice with TBS). After incubation (1 h, 25°C) of the membranes with either [^{125}I]protein A (5 µCi/ml, Amersham-Pharmacia) or secondary goat anti-mouse or anti-rabbit antibody conjugated with horse-radish peroxidase (HRP, Santa Cruz Biotechnology) in the same blocking medium, the membranes are washed five times and then subjected in case of the radioactive method to autoradiography (Kodak X-Omat AR) or phosphorimaging (Molecular Dynamics, Storm 860) or in case of the non-radioactive method to an enhanced chemiluminescence (ECL, Amersham-Pharmacia or Renaissance Chemiluminescence Detection System, NEN/DuPont) detection system.

EVALUATION

The band intensities on the autoradiographs are quantified on a scanning densitometer. The ECL-blots are visualized by a LumiImager (Roche) and quantified using IMAGEQUANT software (Roche). The recovery in the amounts of immunoprecipitated protein is corrected (data on fold- or % stimulation) for the amount of protein actually applied onto the gel as revealed by homologous immunoblotting. Each experiment should be performed with samples from at least four different cell incubations or tissue preparations with antibody incubations/blots performed in triplicate, each.

K.6.3.4.4 Immunecomplex Kinase Assay

PURPOSE AND RATIONALE

In case of high expression and/or high specific activity, the relevant PK can be assayed directly using total cytosolic extracts from cells/tissues which have been incubated with compounds/drug candidates, provided the assay used displays sufficient specificity (e. g. due to specific substrate peptide). However, in most cases the relevant kinase has to be enriched by specific immunoprecipitation (see K.6.3.4.2) using antibodies which do not interfere with the subsequent measurement of the PK activity within the immunecomplex. This immunecomplex kinase assay also eliminates the need for specific peptide or protein substrates not accepted by PK which may be contained in the total cytosolic extracts used and lead to unspecific activity measurements.

The immunecomplexes prepared as described (see K.6.2.9.2) are washed in kinase buffer (50 mM HEPES/KOH, pH 7.4, 100 mM NaCl, 5 mM $MnCl_2$, 1 mM $MgCl_2$, 0.5 mM DTT, 20 mM NaF, 1 mM Na_3VO_4) and then suspended in 25 µl of kinase buffer. The PK reactions are started by addition of ATP (unlabeled or ^{32}P- or ^{33}P-labeled, final conc. 5 µM, 0.2 mCi/ml to up to 100 µM, 0.5 mCi/ml) and incubated (often 3–15 min, 22°C) in the absence (autophosphorylation) or presence of recombinant substrate protein (often 0.1–1 µg) or peptide (5–25 µg) in a final volume of 50 µl. Autophosphorylation reactions are terminated by addition of 50 µl of ice-cold 2-fold stop buffer (100 mM HEPES/KOH, pH 7.4, 300 mM NaCl, 200 mM ATP, 0.1% Triton X-100) and wash-

ing of the beads (10,000 × *g*, 2 min, 4°C) twice with 1 ml of stop buffer and once with 1 ml of stop buffer lacking detergent and salt prior to addition of 20 µl of Laemmli sample buffer and boiling (95°C, 5 min). Substrate phosphorylation reactions are terminated by addition of 20 µl of 4-fold concentrated Laemmli sample buffer and boiling. The phosphoproteins contained in the supernatant of a spin (10,000 × *g*, 5 min) are separated on SDS-PAGE (10% Bis-Tris resolving gel, morpholinopropanesulfonic acid/SDS running buffer) and analyzed by phosphorimaging directly (use of [$^{32/33}$P]ATP) or after immunoblotting with anti-phosphotyrosine or anti-pan-phosphoserine/ threonine antibodies (use of unlabeled ATP). Under these conditions the PK reactions are linear with time for the assay period. Protein concentration is determined by the BCA protein assay with crystalline BSA as standard. Phosphorimaging is performed with a phosphorimager Storm 860 and quantitatively evaluated using ImageQuant software (Molecular Dynamics).

EVALUATION

Differences in recovery in the amounts of immunoprecipitated protein during a specific experiment are corrected in each case (data on fold- or % stimulation) for the amount of protein actually applied onto the gel by homologous immunoblotting. The data should be confirmed by running independent experiments with different batches of cytosolic fractions prepared from independent cell/tissue incubations, each, with two to five parallel independent immunoprecipitation/kinase assay analyses.

K.6.3.4.4.1 Phosphatidylinositol-3′-Kinase (PI3-K)

Portions of the anti-IRS-1/2 immunecomplexes (see K.6.3.4.4) are assayed for PI3-K activity by incubating in 100 µl of 20 mM Tris/HCl (pH 7.0), 50 µM [γ-^{32}P]ATP (5 µCi), 10 mM $MgCl_2$, 2 mM $MnCl_2$, 100 mM NaCl, 2 mM EDTA, 0.5 µM wortmannin (for control incubations, only) containing 10 µg of phosphatidylinositol and 1 µg of phosphatidylserine (Avanti Polar Lipids) for 15 min at 22°C. After addition of 20 µl of 8 M HCl and 160 µl of a 1/1 mixture of methanol/chloroform, the extracted phospholipids are resolved by TLC on plates (Silica Gel 60, Merck, Darmstadt) coated with 1% oxalate and developed in chloroform/methanol/water/ammonia (60/47/11.3/3.2, by vol.). Radiolabeled phosphatidylinositol-3-phosphate (PI3-P, average R_f value of 0.41 under these conditions) is visualized by autoradiography and quantitated by phosphorimage analysis. For calculation of wortmannin-sensitive PI3-K, all values are corrected for PI3-P radiolabeled in the presence of wortmannin.

K.6.3.4.4.2 Phosphoinositide-Dependent Kinase-1/2 (PDK-1/2)

Akt-1/2 represents the major substrate of PDK-1/2 within the insulin signaling cascade (see K.6.3). Its phosphorylation can therefore be used as measure for specific increases in PDK-1/2 activity in response to insulin/compounds/drug candidates. For this, cytosolic extracts are prepared (see K.6.3.4.1) from cells/tissues which have been incubated with insulin/compounds/drug candidates. After centrifugation (150,000 × *g*, 60 min, 4°C), 1-ml portions of the supernatant are immunoprecipitated with 10 µg anti-Akt-1/2 antibodies coupled to protein G-Sepharose beads. The immunoprecipitates are washed and finally suspended in 50 µl of Laemmli sample buffer (2% SDS), heated (95°C, 2 min) and centrifuged (12,000 × *g*, 2 min). After dilution with 1 ml of immunoprecipitation buffer containing 10 µg/ml aprotinin, 20 µg/ml pepstatin, 10 µg/ml leupeptin, 1 mM PMSF and subsequent centrifugation again (12,000 × *g*, 2 min), the supernatant is supplemented with 20 µg of a kit containing four different monoclonal anti-phosphoserine antibodies (Biomol, Hamburg, Germany; clones 1C8, 4A3, 4A9, 4H4) and the monoclonal anti-phosphothreonine antibodies (clone 1E11). After incubation (4 h, 4°C), the antibodies complexes are precipitates during a 2-h incubation with 50 µl of 50 mg protein A-Sepharose per ml of 50 mM HEPES/KOH (pH 7.4), 0.1% Triton X-100. The collected immunoprecipitates (12,000 × *g*, 2 min) are washed three times with 1 ml each of 50 mM HEPES/KOH (pH 7.4), 150 mM NaCl, 100 mM NaF, 0.2 mM Na_3VO_4, 0.1% SDS, 1% Triton X-100 and finally twice with buffer lacking Triton X-100. Phosphoproteins are eluted from the washed precipitates by incubation with 500 µl of 50 mM HEPES/KOH (pH 7.4) containing 50 mM *p*-nitrophenylphosphate for 30 min at 4°C. The supernatants obtained by centrifugation are precipitated with TCA. The acetone-washed pellets are suspended in 50 µl of Laemmli sample buffer and analyzed by SDS-PAGE. Phosphorylated Akt-1/2 is detected by immunoblotting with anti-Akt-1/2 antibodies as described above. In case of high expression/phosphorylation of Akt, immunoblotting with the anti-AktpS473 (PDK-1) or pT307 (PDK-2) antibody (1:400) may be sufficient for the direct detection of Akt phosphorylation and consequently for evaluation of PDK-1/2 activity.

K.6.3.4.4.3 Protein Kinase B (Akt-1/2)

Cytosolic fractions prepared from cells/tissues which have been incubated with insulin/compounds/drug candidates. 900 µl of cytosolic extract are incubated with 100 µl of anti-Akt-1/2 antibody (raised in rabbits by immunization with a synthetic peptide corresponding to residues 465–480 of the human PKB sequence, 10 µg pre-coupled to 10 mg of protein A-Sepharose in 100 µl of lysis buffer for 2 h at 4°C). The immunoprecipitates are collected by centrifugation (12,000 × *g*, 2 min, 4°C), washed twice with 1 ml each of Akt assay buffer (20 mM Mops, pH 7.0, 1 mM EDTA, 1 mM EGTA, 10 mM $Na_4P_2O_7$, 50 mM NaF, 1 mM Na_3VO_4, 1 µM microcystin, 1 µM okadaic acid, 10 µg/ml pepstatin, 25 µg/ml leupeptin, 1 µg/ml antipain, 10 µg/ml aprotinin, 0.1 mM PMSF, 0.01% Brij35, 5% glycerol) containing 1% Nonidet P-40, 0.5 M NaCl and three times with 1 ml each of assay buffer lacking salt and detergent. The immunoprecipitates are finally resuspended in 45 µl of PKB assay buffer containing 10 mM $MgCl_2$, 1 mM DTT, 2.5 µM PKA inhibitor peptide (IP_{20}) and either the synthetic substrate peptide, Crosstide (100 µM final conc.), which is based on the sequence surrounding the serine phosphorylation site of GSK-3 (Ser21 of GSK-3α and Ser9 of GSK-3β) or alternatively, histone 2B (150 µg/ml). The assay is initiated by the addition of 5 µl of [γ-^{32}P]ATP (50 µM, 4 µCi) and terminated after incubation for 15 min at 30°C by placing the test tubes on ice. For determination of Crosstide phosphorylation, the 10-µl portions of the samples are adsorbed on p81 phosphocellulose paper and extensively washed as described for the MAPK assay (see K.6.3.4.4.6). The radioactivity associated with the paper is counted by liquid scintillation counting. For determination of histone 2B phosphorylation, the samples are separated on a 12% SDS-PAGE. The autoradiogram is quantitated by densitometry. Exposure times are chosen which guarantee that the intensity of the bands is linearly related to the quantity of protein contained in the bands.

K.6.3.4.4.4 Glycogen Synthase-3β (GSK-3β)

GSK-3β activity is determined using immunecomplexes from cytosolic extracts of treated cells/tissues (see K.6.3.4.1 and K.6.3.4.2) with phospho-glycogen synthase peptide 2 (P-GS 2) as a substrate (Eldar-Finkelman et al. 1996, Wang et al. 1994). The GSK-3β immunecomplexes (with antibodies raised in sheep by immunization with a synthetic peptide corresponding to amino acids 471–483 of rat GSK-3β and coupled to BSA) are precipitated with 2 mg of anti-sheep IgG coupled to agarose in 50 µl of lysis buffer (under rotation for 2 h at 4°C). The beads are collected by centrifugation (12,000 × *g*, 2 min), washed once with 1 ml of 100 mM Tris/HCl (pH 7.4) containing 0.2% Nonidet P-40, 0.5 M NaCl, 0.5 M LiCl, once with 10 mM Tris/HCl and twice with GSK-3 assay buffer (20 mM HEPES/KOH, pH 7.4, 10 mM $MgCl_2$, 1 mM DTT, 10 mM NaF, 10 mM $Na_4P_2O_7$) and then suspended in 20 µl of assay buffer containing 0.4 mg/ml BSA, 30 µM [γ-^{32}P]ATP (3,000 Ci/mmol, 1 mCi/ml) and 20 µM P-GS2. After incubation (15 min, 30°C), the reactions are terminated by addition of 20 µl of 20% TCA and centrifugation (10,000 × *g*, 5 min). Then, 15-µl portions of the supernatant are spotted on 1 × 1-cm pieces of Whatman P81 phosphocellulose paper. 20 s later, the filters are washed five times with 0.75% phosphoric acid (for at least 5 min each time) and once with acetone. The dried filters are counted for radioactivity in the presence of 5 ml of scintillation fluid (e. g. ACS, Amersham-Pharmacia). $^{32}P_i$ incorporation into the negative control peptide (glycogen synthase peptide 2 [Ala21]) is subtracted from values obtained using P-GS 2. No activity is typically measured with immunoprecipitates using non-immune IgG. In some experiments recombinant PP2A inhibitor (PP2AI, 1 µg, Calbiochem) is used as substrate instead of P-GS1. In this case the PK reaction (conditions as above) is terminated by rapid centrifugation (12,000 × *g*, 1 min, 4°C) and separation of the supernatant from the immunecomplex pellet. The supernatant of a precipitation (10% TCA for 1 h on ice, 15,000 × *g*, 15 min, 4°C) containing the phosphorylated PP2AI is suspended in 50 µl of 2-fold Laemmli sample buffer, heated (95°C, 5 min) and centrifuged (12,000 × *g*, 2 min). The supernatants are run on SDS-PAGE and phosphorylated PP2AI and GSK-3 are visualized by autoradiography and quantitated by phosphorimaging.

K.6.3.4.4.5 MAPK/ERK Kinase (MEK)

MEK activity is determined using immunecomplexes from cytosolic extracts of treated cells/tissues (see K.6.3.4.1 and K.6.3.4.2) with recombinant MAPK/ERK2 (Upstate Biotechnology) as substrate. The assay mix contains 4 mM MOPS buffer (pH 7.5), 5 mM glycerol-3-phosphate, 1.25 mM EGTA, 0.2 mM sodium orthovanadate, 0.2 mM DTT, 10 mM $MgCl_2$, 0.15 mM ATP, and 0.04 µCi/µl [γ-^{32}P]ATP. The concentration of MAPK/ERK2 (0.5 ng/µl) is chosen to

approximate the concentration of MAPK/ERK2 that would be assayed in rat adipocyte cell lysates.

K.6.3.4.4.6 Mitogen-Activated Protein Kinase (MAPK)

MAPK activity is determined using immunecomplexes from cytosolic extracts of cells/tissues treated with compounds/drug candidates (see K.6.3.4.1 and K.6.3.4.2) with myelin basic protein (MBP) as substrate. Adipocytes incubated with insulin/compounds/drugs are washed with KRP-HEPES by flotation and then lysed in 1 ml of 50 mM HEPES/KOH (pH 7.2), 100 mM NaCl, 2 mM EDTA, 1% Nonidet P-40, 0.5 mM Na_3VO_4, 40 mM *p*-nitrophenylphosphate, 10 mM glycerol-3-phosphate, 10 mM NaF, 0.2 mM PMSF, 25 µg/ml leupeptin, 25 µg/ml aprotinin by incubation for 30 min on ice and vigorous vortexing three times for 10 s at 10-min intervals. Lysates are cleared by centrifugation (12,000 × *g*, 10 min, 4°C). The infranatant below the fat cake is removed using a syringe, re-centrifuged and used for measurement of MAPK by addition of 250-µl portions to 250 µl of protein A-Sepharose (50 mg/ml of 50 mM HEPES/KOH, pH 7.2, 100 mM NaCl), which had been precoupled with 10 µl of rabbit anti-p42MAPK antiserum (raised against rat p42MAPK, Upstate Biotechnology) and 5 µl of rabbit anti-p44MAPK antiserum (raised against the carboxyl-terminal 14 amino acids of rat p44MAPK), and incubation for 2 h at 4°C. The beads are collected by centrifugation (12,000 × *g*, 2 min, 4°C), washed three times with 1 ml each of lysis buffer and three times with 1 ml each of 10 mM HEPES/KOH (pH 7.4), 10 mM $MgCl_2$ and then resuspended in 45 µl of kinase buffer (50 mM glycerol-3-phosphate, pH 7.3, 5 mM $Na_4P_2O_7$, 10 mM NaF, 0.5 mM EDTA, 15 mM $MgCl_2$, 2 mM DTT, 4.4 mM PK inhibitor peptide) containing 0.5 mg/ml MBP. The kinase reaction is initiated by the addition of 5 µl of 0.5 mM [γ-^{32}P]ATP (700 mCi/mmol). Following a 10-min incubation at 30°C, reactions are terminated by spotting 10 µl of the reaction mixture onto p81 phosphocellulose papers (Whatman), which are immediately immersed in 0.85% orthophosphoric acid under stirring and washed once in 95% ethanol for 5 min. Papers are dried and ^{32}P is quantitated by liquid scintillation counting.

K.6.3.4.5 Phosphoproteomics

GENERAL CONSIDERATIONS

The above methods for the detection of the phosphorylation state of insulin signalling components encompassing the IR and its downstream elements enable their individual analysis, only. Taking into account the expenditure in time and costs, their simultaneous analysis in a phosphoproteomic approach may be of great advantage. Innovations in the area of 2-D gel electrophoresis, protein analysis and computer databases are moving proteomics from futuristic possibilities into common laboratory procedures. The main aim of classic proteome studies is the separation of complex protein mixtures in order to visualize the relative levels of as many proteins as possible. Improvements of analytical techniques for protein identification, such as peptide mass fingerprinting, have enabled analysis of changes in proteomes on a large scale. However, obtaining information on co- and post-translational modifications within the analyzed proteome remains a major challenge. A wide variety of post-translational modifications, such as phosphorylation, glycosylation, acylation, methylation and acetylation, are known to play key roles in regulating the function, localization, binding specificity and stability of target proteins. To analyze this additional layer of protein diversity and to reveal its complexity, the traditional protein-by-protein approach clearly will not suffice to meet the huge magnitude of variation created by post-translational modifications. Therefore, development of proteome-based technology is required to analyze post-translational modifications of proteins, in general and phosphorylation, in particular.

PURPOSE AND RATIONALE

Since protein phosphorylation is an essential post-translational process in a variety of cellular processes, it is not surprising that perturbations in the equilibrium of PK and PP activities are fundamentally involved in metabolic diseases, such as type II diabetes and obesity. These pathogenetic changes in protein phosphorylation are preferably analyzed in parallel ("phosphoproteomics") rather than sequential fashion (e. g. immunoblotting, immunoprecipitation).

PROCEDURE

Various techniques can be used to detect phosphorylated proteins. In many approaches detection of phosphorylated proteins separated on 2-D gels is activated by incubating cells with [^{32}P] or [^{33}P]orthophosphate. However, when radiolabeling is used to detect phosphoproteins it has to be considered that constitutively phosphorylated proteins with slow phosphate turnover rates, which hence only incorporate small amounts of radioactive phosphate, may be poorly detected. Furthermore, care is necessary when comparing ra-

tios of phosphorylated threonine, serine and tyrosine residues. Similarly, different metabolic phosphorylation/dephosphorylation rates cause unequal incorporation of [^{32}P] into different types of amino acids. The use of poly- and monoclonal antibodies directed against phosphoamino acids represents an alternative procedure to detect phosphorylated proteins blotted onto a membrane. This method is very sensitive since antibodies can detect as little as a few fmol of epitope. Among other strategies, antibodies recognizing phosphotyrosine (pY), phosphothreonine (pT) and phosphoserine (pS) have been generated by cross-linking of a phosphoamino acid-containing hapten to keyhole limpet hemocyanin or BSA. Anti-pT, pY and pS antibodies are commercially available and particularly pY antibodies are now widely used. It was found that different anti-pY antibodies bind to essentially the same proteins in immunoblotting analysis, independent of the exact nature of the immunogen against which the antibodies were raised. Little to no cross-reactivity to non-phosphorylated tyrosine, pT, pS, AMP or ATP has been observed. The sensitivity of the anti-pY antibody is very high, since tyrosine phosphorylation in normal and unstimulated cells and tissues is 100- to 1,000-fold less abundant than pS, accounting for only 0.02% of phosphoamino acids. However, phosphorylation-specific antibodies may not detect certain phosphorylated proteins due to steric hindrance of the recognition site, which is especially true for anti-pT and pS antibodies. In addition, lack of antigenicity conferred by pT and pS (in contrast to pY) has precluded rigorous and unquestionable detection of threonine and serine phosphorylation in proteins. More often pT and pS can be identified specially in the context of a larger epitope, only, thus precluding whole proteome analysis. However, many groups of substrates have overlapping epitopes, for example those with a proline in the +1 position of a phosphorylated Ser or Thr (the archetypal MAPK or CIK sites) forwhich monoclonal antibodies have recently been introduced. Once more common phosphorylation motifs have been determined, more antibodies will become available, thus facilitating phosphorylation analysis of the whole proteome (= phosphoproteomics; for a review see Kaufmann et al. 2001).

Extensive reviews cover the most critical tasks of lysis of mammalian cells, sequential extraction (Mollow et al. 1999), pre-fractionation (Cordwell et al. 2000), sample preparation (Herbert 1999, O'Farrell 1975), sample solubilization for isoelectric focusing (Rabilloud et al. 1997) and two-dimensional gel electrophoresis (Görg et al. 2000) and finally detection of phosphoproteins by immunoblotting (see K.6.3.1.3.2.1 and K.6.3.4.3) and ot total proteins by chemical staining (Dunn 1999, Birkelund et al. 1997)

EVALUATION

Detection of phosphorylated proteins within complex protein mixtures separated by 2-D gel electrophoresis followed by immunoblotting represents a relatively simple and sensitive method. Antibodies directed against pT, pS and pY have been successfully used in proteome studies to identify and characterize phosphoproteins. A strategy is recommended that allows high-throughput identification of phosphorylated proteins. The protein-by-protein approach for elucidating complex biological regulatory processes mediated by protein phosphorylation can now be replaced by analysis of the phospho-proteome under varying conditions.

However, the described methodology has its limits. Especially specific anti-pS and anti-pT antibodies are not able to recognize all proteins harboring phosphates on these residues. Therefore, immunoblotting analysis should be combined with radiolabelling techniques to obtain highly accurate and complete pictures of the phospho-proteome. A major challenge in creating phospho-proteome maps remains the low abundance of many phosphorylated key regulatory proteins, such as signal transduction molecules. Improvement of the sensitivity of protein identification techniques, such as peptide-mass fingerprinting by matrix-assisted laser-desorption-ionization-time-of-flight (MALDI-TOF) mass spectrometry will be the key to overcome this obstacle.

K.6.3.4.6 Multiplex Bead Immunoassay

PURPOSE AND RATIONALE

The introduction of methodologies that allow the simultaneous measurement of interrelated markers, e. g. phosphoproteins within a common signal transduction pathway, has revoltionized the drug discorvery and evaluation process. Monitoring multiple proteins in a single sample and experiment saves time, labor costs and sample volume. The multiplex bead immunoassay developed by BioSource Inc. (CA, USA) in conjunction with the Luminex xMAP™ detection system and fluorescently encoded microspheres enables the simultaneous measurement of up to 100 different biological markers depending on the availability of appropriate (phosphosite-specific) antibodies. Each microsphere is labeled with a distinguishable fluorophore that allows

it to be assigned or gated to a particular region by the scanner. Antibodies specific for the (phospho-)protein of interest, are covalently linked to beads of a unique fluorescent region. The combination of different beads allows the user to simultaneously measure various protein markers of interest. The reagent and antibody bead kits offered by BioSource are intended for the quantitative determination of the (phospho-)protein in total cellular lysates and tissue homogenates.

The multiplex bead immunoassay is a solid phase sandwich immunoassay, which is designed to be analyzed with a Luminex 100™ instrument. The spectral properties of 100 distinct bead regions can be monitored with this instrument, a capability that affords this assay system the potential for measuring up to 100 different marker (phospho-)proteins ina single sample. Beads of defined spectral properties conjugated to marker-specific capture antibodies and samples (including standards of known marker concentration, blank controls etc.) are pipetted into wells of a filter bottom microplate and incubated for 2 h. During this first incubation, the marker (phospho-) proteins bind to the capture antibodies on the beads. After washing the beads, marker (phosphosite-) specific detector antibodies are added and incubated with the beads for 1 h. During this second incubation, the marker specific detector antibodies recognize their (phosphorylated) epitopes and bind to the appropriate immobilized marker (phospho-)proteins. After removal of excess detector antibodies, an anti-rabbit R-phycoerythrin (RPE) conjugated secondary antibody is added for 30 min. During this final incubation, the anti-rabbit RPE binds to the detector antibodies associated with the immunecomplexes on the beads, forming four-membered solid phase sandwiches. After washing to remove unbound anti-rabbit RPE, the beads are analyzed with the Luminex 100™ instrument. By monitoring the spectral properties of the beads and the amount of associated RPE fluorescence, the concentration of one or more analytes can be determined.

The multiple bead immunoassay has been initially introduced for the determination of the concentration of a panel of cytokines circulating in human serum (e. g. of patients suffering from primary Sjorens syndrome or bacterial infection; Szodoray et al. 2004, Pickering et al. 2004), but can meanwhile be applied successfully for the analysis of phosphorylation state of a number (currently seven) of key components of the insulin signal transduction cascade undergoing either tyrosine phosphorylation (IR, IGF-1 receptor, IRS-1) or serine/threonine phosphorylation (GSK-3, Akt, p70S6 kinase, p42/44 MAPK). Using this method the quantitative evaluation of changes in their phosphorylation state in response to treatment of insulin target cells requires one single-well reaction, only, rather than seven separate immunoprecipitation reactions followed by seven immunoblotting and fluorescent/luminescent imaging procedures. Thus, this method will significantly facilitate the throughput characterization of compounds/drug candidates with insulin-like and/or insulin-sensitzing activity and concomitantly increase its accuracy and resolution.

K.6.3.4.7 Protein Interaction Analysis

PURPOSE AND RATIONALE

In addition to protein phosphorylation, protein-protein interaction represents the major molecular mechanism for insulin signal transduction in insulin target cells (see K.6.3 and K.6.3.4), as exemplified by binding to and activation by IRS of PI3-K. Protein-protein interaction can be measured by (i) coimmunoprecipitation of one partner and subsequent immunoblotting of the coimmunoprecipitate for presence of the binding partner, (ii) pull-down of one partner *via* its tag (e. g. GST, His) and subsequent immunoblotting of the recovered material for presence of the (tagged) binding partner and (iii) the optical phenomenon called surface plasmon resonance (SPR). More than one decade after its introduction (Jönsson et al. 1991), latter method (iii) combined with a miniaturized flow system and a sophisticated surface designhas gained a lot of attractiveness since it enables many biomolecular interactions to be investigated conveniently in real time and does depend neither on the availability of a pair of compatible antibodies as is the case for coimmunoprecipitation (i) nor on the generation of recombinant tagged or labeled binding partners as is required for pull-down (ii) and furthermore allows kinetic and real-time rather than sole steady-state analysis of the interaction.

SPR defines the characteristics of proteins interms of their specificity of interaction with other molecules, the rates at which they interact (association and dissociation) and their affinity, which can be determined from the level of binding at equilibrium (seen as a constant signal) as a function of sample concentration as well as from kinetic measurements. Even the formation of multimolecular complexes can be monitored.

The natural phenomenon of SPR is utilized by the Biacore protein interaction analysis system (Biacore

AB, Sweden) to deliver high-quality data in real time, without the use of labels. The SPR phenomenon occurs when polarised light, under conditions of total internal reflection, strikes an electrically conducting gold layer at the interface between media of different refractive index, the glass of a sensor surface (high refractive index) and a buffer (low refractive index). In Biacore systems, a sensor chip and microfluidics system form flow cells through which samples flow over the sensor surface. As molecules from the injected sample bind to the immobilised molecules, an alteration in refractive index occurs that is proportional to the change in mass concentration at the surface. Using the SPR phenomenon, these changes are detected in real time and data is presented as a sensorgram (SPR response plotted against real time).

PROCEDURE

In a typical experiment one of the components (binding partner, ligand) in a biospecific pair is immobilized on the sensor chip surface (Löfas et al. 1995), and the counterpart (the analyte) which interacts with the ligand is in solution and passed over the gold film in a continuous flow. In the flow system (Sjölander and Urbaniczky 1991), samples and reagents can be introduced over the sensor surface. Automation of flow properties and sample injection gives the experiment control over temperature, flow and concentration properties as well as permitting reaction conditions on the surface to be changed easily.

The surface properties of the sensor chips are central to BiaCore technology. The surface of the gold film that is needed for SPR detection is modified to avoid protein adsorption to the detector surface itself. This is achieved by a self-assembled monolayer of alkanethiols to which dextran is coupled by epoxy chemistry (Johnsson et al. 1991, Löfas 1995). the surface properties are of great importance for the evaluation of results from real-time biomolecular interaction analysis. Unwanted interactions can be identified and to some extent compensated for by proper control surfaces in multidetection approaches (Karlsson and Stählberg 1995). Nordin and coworkers (2005) analyzed small molecule interactions with PK using SPR biosensors

EVALUATION

A range of methods based on BiaCore technology have been developed for different purposes over the past years which have been reviewed by Malmqvist and Karlsson (1997). Biacore's system facilitates the elucidation of disease mechanisms and the discovery of drug candidates by characterising native and recombinant protein interactions. The system enables the definition of potential drug targets, and the development of assays to characterize the interaction of target proteins with low-molecular-weight compounds. Other applications may include the selection of protein therapeutic candidates (e. g. recombinant insulin analogs) according to their on-/off-rates of binding to the target (e. g. IR) as well as the detection and characterization of immune responses during preclinical and clinical development.

Regarding application of BiaCore technology to PK-inhibitor interaction, Nordlin and coworkers (2005) found the immobilization conditions to be critical and they developed several strategies for preserving the binding capacity for inhibitors and ATP. The composition of the assay buffer is developed for optimized kinase assay performance. The assays include kinetic characterization of inhibitor binding to PK and analysis of binding characteristics in the presence of ATP for identification of ATP-competitive binders. The effect of PK phosphorylation on the binding of ATP and inhibitors can also be investigated, as is the PK isotype specificity. Furthermore, a complementary activity assay revealed the correlation between binding to the PK and inhibition of the PK. Thus, the biosensor technology offers a useful tool in PK-targeted compound identification and drug evaluation.

K.6.3.5 *O*-Linked Glycosylation (*O*-GlcNAc) of Insulin Signaling Components

GENERAL CONSIDERATIONS

Hyperglycemia is a consequence of type II diabetes and constitutes a self-perpetuating condition that contributes to poor metabolic control by impairing both insulin action and insulin secretion (Kruszynska and Olefsky 1996, Karam 1996, Yki-Järvinen 1992). The deleterious effects of hyperglycemia have been collectively referred to as "glucose toxicity" (Rossetti et al. 1990 and 1995, Rossetti 1996), the most prominent one of which is insulin resistance. Studies of humans and animals with spontaneous or experimentally induced insulin resistance have revealed much about the multiple pathways that can lead to insulin resistance. However, the primary events that trigger insulin resistance remain incompletely understood. Experimental induction of insulin resistance in isolated cells or tissues can be a useful approach for the identification of early events because it provides considerable experimental control.

Marshall and coworkers provided ample evidence that excessive flux of glucose through the hexosamine biosynthesis pathway (HBP) triggers various adaptive responses that restore intracellular glucose homeostasis. One such response is reduction of glucose uptake through desensitization of the insulin-responsive glucose transport system (GTS). Since the glucose-sensing/signal transductional capability of the HBP constitutes only one function of this ubiquitous pathway, this regulatory arm of the HBP has been named the hexosamine signaling pathway (HSP) (Marshall and Rumberger 2000, Marshall 2002).

In exploring the functional role of the HSP and the underlying mechanisms, glucosamine (GlcN) is often used as a pharmacological tool since it can readily undergo internalization through the GLUT1/4 and directly enter the HBP at the level of GlcN-6-P (Marshall et al. 1991a, 2004). Thus, GlcN was found to mimic glucose-induced desensitization in adipocytes and was shown to be > 40 times more potent than glucose. Although it was originally thought of that glucose and GlcN were causing desensitization through a common mechanism, this premise was later questioned when actinomycin-D was found to completely block glucose-induced desensitization but not GlcN-induced desensitization (Marshall et al. 1991b, Han et al. 2003). Thus, glucose-induced desensitization is mediated through a mechanism involving changes in gene expression, whereas GlcN-induced desensitization occurs through an alternate and unidentified mechanism. In conclusion, Marshall and colleagues hypothesized that flux through the HBP serves as a glucose sensor in adipocytes, and potentially other insulin target cells, and by some unknown negative feedback loop, regulates glucose transport provoking glucose-induced insulin resistance.

PURPOSE AND RATIONALE

The studies of Hebert and coworkers (1996), Cooksey and McClain (2002) and Gazdag and coworkers (2000) demonstrated an inverse relationship between cellular UDP-GlcNAc levels and insulin action, but did not reveal a specific mechanism for the association. UDP-GlcNAc is a substrate for O-GlcNAc transferase (uridine diphospho-*N*-acetyl-glucosamine/polypeptide-*N*-acetylglucosaminyltrans-ferase) that transfers single *N*-acetylglucosamine moieties to the hydroxyl group of serine and threonine residues on cellular target proteins in a dynamic and reversible process known as O-GlcNAcylation (Wells et al. 2001). The extent of cellular O-GlcNAcylation appears to be regulated, at least in part, by the cellular concentration of the UDP-GlcNAc substrate (Kreppel and Hart 1999). McClain and coworkers (2002) recently found direct evidence that O-GlcNAc transferase plays an important role in insulin action by overexpressing O-GlcNAc transferase in skeletal muscle and fat in transgenic mice and inducing insulin resistance.

O-GlcNAcase (β-*N*-acetylglucosaminidase) is responsible for specific removal of single O-GlcNAc modifications from cellular proteins. Both O-GlcNAc transferase and O-GlcNAcase exhibit nuclear and cytoplasmic localization and are highly conserved (Dong and Hart 1994). Wells and coworkers (2001) have hypothesized that O-GlcNAcylation of proteins is a type of post-translational modification that may be analogous to PK and PP regulation of phosphorylation and thus compete for similar or adjacent phosphorylation sites in a reciprocal manner. It seems possible that, in addition to flux through the HBP, regulation of either O-GlcNAc transferase (McClain et al. 2002) or O-GlcNAcase (Vosseller et al. 2001, 2002) may influence insulin action. O-(2-acetamido-2-deoxy-D-glucopyranosylidene) amino-*N*-phenylcarbamate (PUGNAc) is a potent and nontoxic inhibitor of O-GlcNAcase in various cell lines (Haltiwanger et al. 1998). Arias and coworkers (2004) found that prolonged incubation in PUGNAc results in increased protein-O-linked glycosylation and insulin resistance in rat skeletal muscle. The following assays represent model systems for the induction and analysis of glucose-induced insulin resistance which is mediated by O-GlcNAcylation and can be modified by compounds/drug candidates.

K.6.3.5.1 Induction of *O*-Glc-NAc Modification in Adipocytes, Myocytes and Muscles

Primary Adipocytes

Isolated adipocytes are obtained from the epididymal fat pads of male Sprague–Dawley rats (180–225 g) by collagenase digestion as described above with modifications introduced by Marshall and coworkers (2005). After digestion, cells are washed three times in HEPES-buffered balanced saline solution (HBSS) consisting of 25 mM HEPES (pH 7.6), 120 mM NaCl, 0.8 mM $MgSO_4$, 2 mM $CaCl_2$, 5.4 mM KCl, 1 mM NaH_2PO_4, 1 mM sodium pyruvate, 100 U/ml penicillin, 100 µg/ml streptomycin, and 1% BSA. Cells are then diluted to a final concentration of 5×10^5 cells/ml (12 ml HBSS per 1 g initial fat weight). From a common pool of cells, 200-µl portions of the adipocyte suspension in 12 × 75-mm sterile polystyrene tubes are in-

cubated at 37°C in the absence or presence of insulin (10 nM final conc.) to stimulate the glucose transport system and to facilitate the subsequent uptake of GlcN. After 20–30 min, GlcN is added and adipocytes are further incubated at 37°C.

3T3-L1 Adipocytes

3T3-L1 adipocytes are cultured for 16 h in DMEM containing 4 mM glucose in the absence of serum and containing PUGNAc (100 µM). After 16 h, cells are refed with identical media for 3 h. For GlcN and/or chronic insulin/glucose treatment of cells, 3T3-L1 adipocytes are cultured for 16 h in DMEM containing 4 mM glucose in the absence of serum with 0.2% BSA and containing 5 mM GlcN/5 mM HEPES (pH 7.6) and/or insulin (1 nM). After 16 h, cells are washed twice and refed with identical media used during 16-h treatment, but lacking insulin. Cells are then washed twice with Krebs-Ringer's phosphate buffer (KRP) and stimulated in KRP with various concentrations of insulin for the indicated time at 37°C.

Myocytes

C2C12 cells are cultured to confluence in growing conditions in DMEM containing 25 mM glucose and 10% fetal bovine serum (FBS) in collagen type I-coated culture plate according to the procedure described by Fujita and coworkers (2005). When cell confluence is attained, cells are cultured for 4 days with DMEM containing 25 mM glucose, 2% horse serum, and with or without 10 mM GlcN. After 4 d, the change in cell morphology induced by GlcN is observed by an optical microscope.

Muscles

Epitrochlearis muscles are quickly excised from rats (140–160 g) anesthetized with an intraperitoneal injection of sodium pentobarbital (5 mg/100 g body weight) upon loss of pedal reflexes and then transferred into the tissue incubation medium. Muscles are incubated (18 h) in flasks containing 1.5 ml of low glucose (5.5 mM) DMEM supplemented with $CaCl_2$ (final conc. 2.5 mM), $NaHCO_3$ (final conc. 25 mM), insulin (final conc. 0.6 nM) and BSA (0.1%). Insulin is included for the initial 18 h of incubation because this prevents the increase in basal glucose transport observed with prolonged incubation of isolated skeletal muscle. Flasks are placed in a shaking water bath at 35°C and continuously gassed with 95% O_2/5% CO_2. The media are replaced with fresh DMEM every 6 h during the initial 18-h incubation. To minimize bacterial contamination during prolonged incubation, 100 µU/ml penicillin and 100 µg/ml streptomycin are added to the DMEM and Teflon air filters are used to minimize aerosol contaminants.

Following the 18-h incubation in supplemented DMEM, muscles are rinsed in KHB supplemented with 0.1% BSA, 100 µU/ml penicillin, 100 µg/ml streptomycin, 2 mM sodium pyruvate and 5 mM mannitol for two 30-min periods at 30°C for removal of glucose and DMEM. During the rinse steps, the KHB buffer is supplemented with 0, 0.6 or 12 nM insulin. Muscles treated with inhibitors of GFAT in the initial incubation steps continued to be exposed to up to 100 µM inhibitor during the subsequent rinse steps. Muscles are then rapidly blotted, trimmed, clamp frozen with aluminium tongs cooled to the temperature of liquid N_2 and stored at −80°C until further processing. Total frozen muscles are weighed, transferred to pre-chilled glass tissue grinding tubes and homogenized in ice-cold lysis buffer (1 ml/muscle) containing 20 mM Tris/HCl (pH 7.4), 150 mM NaCl, 1% NP-40, 2 mM EDTA, 2 mM EGTA, 1 mM DTT, 2.5 mM sodium pyrophosphate, 10 mM NaF, 2 mM Na_3VO_4, 20 mM glycerol-3-phosphate, 1 µg/ml leupeptin, 1 µg/ml pepstatin, 1 µg/ml aprotinin, 1 mM PMSF in the absence or presence of up to 100 µM of PUGNAc. Homogenates are transferred to microfuge tubes, rotated for 1–2 h at 4°C, and then centrifuged (12,000 × *g*, 15 min, room temperature) to remove insoluble material. Following homogenization, processed muscle samples are used for determination of the levels of GlcNAc-6-phosphate and UDP-GlcNAc as well as the amount of *O*-GlcNAc-modified proteins.

K.6.3.5.2 Assay for Glutamine/Fructose-6-Phosphate Amidotransferase (GFAT)

Fluorometric Method

GFA activity is assayed according to previously described methods (Yki-Järvinen et al. 1997) with modifications. Cells corresponding to 5–15 mg protein is homogenized for 10 s on ice and sonicated for 10 bursts in a Branson 250 sonifier in 10 ml of homogenization buffer (50 mM sodium phosphate, pH 7.5, 100 mM KCl, 1 mM EDTA). The sample is then centrifuged (60,000 × *g*, 15 min, 4°C) and the supernatant is used for assay of GFA activity. All samples are assayed immediately after homogenization. 50 µl of homogenate is incubated (45 min, 37°C) in a reaction mix (final volume 100 µl) containing 12 mM fructose-6-phosphate, 12 mM glutamine, 40 mM sodium phosphate (pH 7.4), 1 mM EDTA, 1 mM DTT in the ab-

sence or presence of 0.5 mM of UDP-GlcNAc. The reaction is terminated with 50 µl of 1 M perchloric acid, vortexed, and centrifuged (15,000 × *g*, 15 min, 4°C). The deproteinized supernatant (145 µl) is then treated with 258 µl of a 1/4 mixture of tri-N-ocytlamine/1,1,2-trifluoroethane, vortexed and centrifuged (15,000 × *g*, 1 min). The aqueous phase is then filtered through a 0.2-µm filter and 50 µl is derivatized with an equal volume of O-phtaldialdehyde (OPA) solution (4 mg OPA dissolved in 50 µl of ethanol and added to 5 ml of 0.1 M sodium borate and 10 µl mercaptoethanol). Immediately thereafter samples are separated over a reverse-phase C18 column (25 cm × 4.6 mm) equilibrated with 15 mM sodium phosphate (pH 7.2), 5% acetonitril, and 5% isopropanol. Absorbance of the sample eluent is analyzed using a fluorescent detector and the peak area is integrated. OPA-derivatized GlcN6P standards are run separately to determine the retention time and to generate a standard curve for correlation of area to activity. The correlation coefficient between the concentration of GlcN6P standards and the area under the GlcN6Ppeak is typically 0.999 or higher. The recovery of samples spiked with GlcN6P prior to derivatization is usually more than 95%.

Radiometric Method

A highly sensitive and rapid method for the separation of radiolabeled fructose-6-phosphate from glucosamine-6-phosphate has been developed by Broschat and coworkers (2002), which can be used in a disposable column or a 96-well formate and is > 10-fold more sensitive than the HPLC method. The column assay has a broad range of linearity with low variation between samples. When performed in the 96-well formate, the assay is linear with time and enzyme concentration and greatly improves the rapidity and accuracy with which GFAT activity can be measured.

Research Formate

Cells are homogenized as described for the fluorometric assay using the cytosolic fraction obtained by 100,000 × *g* spin for 1 h. The final assay conditions contain 20 µM fructose-6-phosphate (300,000 cpm), 400 µM glutamine, 20 mM imidazole buffer (pH 6.8), 1 mM EDTA, 10 mM KCl, 1 mg/ml BSA and 1 mM DTT in a total volume of 50 µl. All assays are conducted at room temperature. Just prior to the assay, the samples prepared in stabilizing buffer containing glucose-6-phosphate (Zhou et al. 1995) are buffer-exchanged on PD-10 columns equilibrated in the GFAT assay buffer. The reaction is stopped by dilution of the enzyme reaction with 1 ml of 10 mM $NaHCO_3$ (pH 3.0). Separation of GlcN-6-phosphate from substrate is performed immediately at room temperature. Unbound [^{14}C]GlcN-6-phosphate is collected in scintillation vials and quantified by scintillation counting.

Screening Formate

Strong anion exchange resin (AG1X8, 400 mesh, formate form) is prepared prior to the assay and stored for 2 weeks at room temperature or at 4°C for longer periods. The resin is suspended in batch in a 5-volume excess of 10 mM $NaHCO_3$ (pH 3.0) and allowed to settle for 20 min. The fines and excess buffer are decanted, and the procedure is repeated until no fine material remained, usually three to four times. The pH of the formate buffer above the resin should be unchanged by the resin after the equilibration is complete. GFAT activity is measured in a total volume of 50 µl in U-bottomed deep-well 96-well plates. The substrates, 20 µM [^{14}C]fructose-6-phosphate (75,000 cpm per well) and 400 µM glutamine are mixed and the reaction is terminated by the addition of a 150-µl suspension of Dowex AG1X8 (400 mesh) in 10 mM $NaHCO_3$, containing 50 µl resin and 100 µl buffer by volume. Suspension of the resin is maintained using a stir plate prior to transfer. The resin is allowed to settle for 5 min, after which a 50-µl aliquot of the supernatant is removed using a programmable liquid transfer device and transferred to a 96-well topcount plate. After addition of 150 µl of scintillation cocktail, the plates are sealed, shaken for 5 min and counted for radioactivity in a topcount reader.

K.6.3.5.3 Assay for *O*-GlcNAc Transferase

Cells corresponding to 2–5 mg protein (bicinchoninic acid method using BSA as standard) are homogenized in 6 × volume (µl/mg) of homogenizing buffer containing 20 mM HEPES/KOH (pH 7.0), 10 mM $MgCl_2$, 0.4 mM Na_3VO_4, 1 mM EDTA, 4 µM benzamidine, 0.5 mM PMSF, 1 µg/ml pepstatin, 1 ng/ml leupeptin, 0.5 µg/ml antipain and 250 mM sucrose (HBS) in a glass homogenizer for 30 sec on ice. The homogenate is centrifuged (100,000 × *g*, 25 min, 4°C). The supernatant (cytosol) is mixed with an equal volume of 30% PEG8000 and incubated on ice for 30 min to precipitate proteins. The precipitated material is pelleted by brief centrifugation (10,000 × *g*, 2 min). The supernatant is discarded and the pellet is washed once with HBS and resuspended in half the original volume of HBS. *O*-GlcNAc transferase is measured as described by Haltiwanger and cowork-

ers (1992) with slight modifications. Both methods derive their specificity by utilizing peptide substrates that are modelled after *O*-glucosaminylation motifs of known *O*-GlcNAcylated proteins. The method recommended utilizes an Arg-tagged peptide which binds firmly to phosphocellulose paper. Reactions are conducted in 45-µl mixtures containing 1–5 µg of cytosolic protein in 20 mM HEPES/KOH (pH 8.0), 250 mM sucrose, 0.5 mM EDTA, 5 mM peptide substrate (TITSETPSSTTTQITKR) and 0.2 µCi UDP-[6-^{3}H]-N-acetylglucosamine (25 Ci/mmol). The reactions are incubated (60 min, 25°C). At the end of the incubations, 40-µl portions are spotted onto 1-cm^2 Whatman P81 ion exchange papers. The paper squares are immediately immersed in 50 mM formic acid, washed extensively with 4 × 4 ml of 50 mM formic acid per square and then counted for radioactivity in 5 ml scintillation cocktail per square. All assays should be conducted in the linear range for time, peptide concentration and homogenate protein.

K.6.3.5.4 Measurement of GlcN-6-P Levels

For determination of the GlcN-6-P levels according to the procedure of Marshall and coworkers (2005b), adipocytes or myocytes after treatment with compounds/drug candidates are transferred to 1.5-ml microfuge tubes and washed 3 times with ice-cold, BSA-free HBSS. During the final wash, the cell volume is reduced to 150 µl and 0.4 ml of cold perchloric acid (0.3 M) is added to the cells for 10 min. The mixture is then centrifuged (20,800 × *g*, 10 min, 4°C) and the deproteinated metabolite extract (420 µl) is transferred to a new microfuge tube. After the extract is neutralized by adding a small amount of K_2CO_3 (5 M), extracts are frozen and stored at −20°C. The concentration GlcN-6-P is measured in the extracts by HPLC as previously described (Marshall et al. 2004, 2005a) by a method that entailed derivatization of GlcN-6-P with O-pthaldialdehyde (OPA) so that it can be detected fluorometrically (following separation by reverse phase HPLC).

K.6.3.5.5 Measurement of UDP-GlcNAc Levels

This assay is performed essentially as described previously by Robinson and coworkers (1995). To avoid degradation of UDP-GlcNAc, isolated tissue samples are frozen immediately in liquid nitrogen, and then the procedure for the extraction of UDP-GlcNAc is carried out as quickly as possible. Frozen muscle or liver tissue (~150 mg) is homogenized at 4°C in 5 volumes of PBS. A small aliquot of tissue homogenate is used for protein assay. 100% (w/v) TCA is added to tissue homogenate (10% final conc.). Samples are mixed well and the precipitates are pelleted by centrifugation (10,000 × *g*, 15 min, 4°C). To eliminate TCA from the supernatant, two volumes of diethylether are added and mixed well. After centrifugation (1,000 × *g*, 3 min, room temperature), the diethylether phase is discarded. This TCA elimination step is repeated 10 times. The aqueous samples are dried up and dissolved in 30 µl distilled water. The extracts are centrifuged (20,000 × *g*, 10 min, room temperature), and high pressure liquid chromatography (HPLC) is performed on a SAX anion-exchange column (4.6 × 250 mm, e. g. Whatman Partisil) eluted with 40 mM ammonium phosphate at a flow rate of 1 ml/min. The amount of UDP-GlcNAc in the samples is quantified by ultraviolet absorption (A_{254}), and calculated from the height of peak against standard series of UDP-GlcNAc. The retention-time of the peak of UDP-GlcNAc is 12.0 min.

K.6.3.5.6 Detection of *O*-GlcNAc-Modified Proteins

Immunological Detection

For immunological detection of O-GlcNAc-modified proteins according to the procedure introduced by Vosseller and coworkers (2002), whole-cell lysates for immunoblotting are prepared by scraping 3T3-L1 cells from 6-cm culture dishes in 400 µl of 1% SDS, transferring to Eppendorf tubes, and boiling for 10 min. Laemmli sample buffer is added directly to lysates for SDS-PAGE. Lysates for immunoprecipitations are obtained by scraping cells in 1% Nonidet P-40 buffer containing 15 mM Tris/HCl (pH 7.5), 150 mM NaCl, 1 mM EDTA, protease inhibitors, and 1 µM PUGNAc to inhibit deglycosylation during lysis. Protein concentrations in lysates are determined by using the Bio-Rad protein reagent. The anti-O-GlcNAc antibody used is a mouse monoclonal IgM from ascites designated 110.6 (Comer et al. 2001). For these immunoprecipitations, antibody is bound and covalently coupled by using dimethyl pimelimidate (Pierce) to agarose-conjugated anti-IgM. For immunoblotting, secondary antibody is horseradish peroxidase-conjugated goat anti-mouse IgM (µ chain-specific). In all cases, immunoblots are developed with ECL reagent and imaged on hyperfilm (Amersham Pharmacia). Immunoprecipitations with indicated antibodies are performed

overnight at 4°C and captured with protein A/G-Sepharose (Santa Cruz Biotechnology) unless otherwise indicated, washed in RIPA buffer (1% Nonidet P-40 buffer described above, but including 0.1% SDS, 0.25% sodium deoxycholate, and not containing protease inhibitors or PUGNAc), followed by washing in TBS. Proteins are boiled off Sepharose beads in Laemmli sample buffer for SDS-PAGE with precast minigels (Bio-Rad). The separated proteins are transferred to polyvinylidene difluoride (Immobilon-P, Millipore), blocked at least 1 h in TBS containing 4% BSA and 0.1% Tween20, and probed with indicated antibodies overnight at 4°C. After binding of appropriate horseradish peroxidase-coupled secondary antibodies, ECL detection is used. In cases where densitometry is used to quantitate Western blot signals, the Flourchem imaging system and software (Alpha Innotech, CA) are used.

Enzymatic Detection

Terminally *O*-GlcNAc-modified membrane proteins are identified by the galactosyltransferase probe method using purified UDP-Gal-GlcNAc-Galβ-(1–4) galactosyltransferase (Gal-transferase) and UDP-[^{3}H]galactose as described by Roquemore and coworkers (1994) with modifications introduced by Buse and coworkers (2002). Briefly, 0.5 or 1 mg of total crude membrane proteins in 50 mM HEPES (pH 7.4), 150 mM NaCl, and 0.5% CHAPS is incubated for 1 h at 37°C with the addition of 10 mM HEPES (pH 7.3), 10 mM galactose, 5 mM $MnCl_2$, 1 mM DTT, 25 mM 5′-AMP, 20 µCi/ml UDP-[6-^{3}H]galactose (40 Ci/mmol), and 1 U/ml galactosyltransferase (previously autogalactosylated for 30 min at 37°C in 50 mM Tris/HCl, pH 7.3, 5 mM $MgCl_2$, 1 mM mercaptoethanol, 0.4 mM UDP-galactose, and 0.1 mg/ml aprotinin). Enzyme reactions are terminated by the addition of 10 mM EDTA. Immunoprecipitation of galactosylated membranes is described below.

REFERENCES AND FURTHER READING

Arias EB, Kim J, Cartee GD (2004) Prolonged incubation in PUGNAc results in increased protein O-linked glycosylation and insulin resistance in rat skeletal muscle. Diabetes 53:921–930

Birkelund S, Bini L, Pallini V, Sanchez-Campillo, Liberatori S, Clausen JD, Ostergaard S, Holm A, Christiansen G (1997) Characterization of Chlamydia trachomatis 12-induced tyrosine-phosphorylated HeLa cell proteins by two-dimensional gel electrophoresis. Electrophoresis 18:563–567

Broschat KO, Gorka C, Kasten TP, Gulve EA, Kilpatrick B (2002) A radiometric assay for glutamine:fructose-6-phosphate amidotransferase. Anal Biochem 305:10–15

Buse MG, Robinson KA, Marshall BA, Hresko RC, Mueckler MM (2002) Enhanced *O*-GlcNAc protein modification is associated with insulin resistance in GLUT1-overexpressing muscles. Am J Physiol Endocrinol Metab 283:E241-E250

Chen H (2006) Cellular inflammatory responses: Novel insights for obesity and insulin resistance. Pharmacol Res 53:469–477

Comer FI, Vosseller K, Wells L, Accavitti MA, Hart GW (2001) Characterization of a mouse monoclonal antibody specific for O-linked N-acetylglucosamine. Anal Biochem 293:169–177

Cooksey RC, McClain DA (2002) Transgenic mice overexpressing the rate-limiting enzyme for heosamine synthesis in skeletal muscle or adipose tissue exhibit total body insulin resistance. Ann N Y Acad Sci 967:102–111

Cordwell SJ, Nouwens AS, Verrills NM, Basseal DJ, Walsh BJ (2000) Subproteomics based upon protein cellular location and relative solubilities in conjunction with composite two-dimensional electrophoresis gels. Electrophoresis 21:1094–1103

Dong DL, Hart GW (1994) Purification and characterization of an O-GlcNAc selective N-acetyl-beta-D-glucosaminidase from rat spleen cytosol. J Biol Chem 269:19321–19330

Dunn MJ (1999) Methods Mol Biol 112:319–329

Eldar-Finkelman H, Argast GM, Foord O, Fischer EH, Krebs EG (1996) Expression and characterization of glycogen synthase kinase-3 mutants and their effect on glycogen synthase activity in intact cells. Proc Natl Acad Sci USA 93:10228–10233

Frick W, Bauer A, Bauer J, Wied S, Müller G (1998) Insulin-mimetic signalling of synthetic phosphoinositolglycans in isolated rat adipocytes. Biochem J 336:163–181

Fujita T, Furukawa S, Morita K, Ishihara T, Shiotani M, Matsushita Y, Matsuda M, Shimomura I (2005) Glucosamine induces lipid accumulation and adipogenic change in C2C12 myoblasts. Biochem Biophys Res Commun 328:369–374

Gazdag AC, Wetter TJ, Davidson RT, Robinson KA, Buse MG, Yee AJ, Turcotte LP, Cartee GD (2000) Lower calorie intake enhances muscle insulin action and reduces hexosamine levels. Am J Physiol Regul Integr Comp Physiol 278:R504-R512

Görg A, Obermaier C, Boguth G, Harder A, Scheibe B, Wildgruber R, Weiss W (2000) The current state of two-dimensional electrophoresis with immobilized pH gradients. Electrophoresis 21:1037–1053

Gao Z, Hwang D, Bataille F, Lefebre M, York D, Quon MJ (2002) Serine phosphorylation of insulin receptor substrate 1 by inhibitor kappa B kinase complex. J Biol Chem 277

Haltiwanger RS, Blomber MA, Hart GW (1992) Glycosylation of nuclear and cytoplasmic proteins. Purification and characterization of a uridine diphospho-N-acetyl-glucosamine:polypeptide N-acetyltransferase. J Biol Chem 267:9005–9013

Haltiwanger RS, Grove K, Philipsberg GA (1998) Modulation of O-linked N-acetylglucosamine levels on nuclear and cytoplasmic proteins *in vivo* using the peptide O-GlcNAc-beta-N-acetylglucosaminidase inhibitior O-(2-acet-amido-2-deoxy-D-glucopyranosylidene)amino-N-phenylcarbamate. J Biol Chem 273:3611–3617

Han D-H, Chen MM, Holloszy JO (2003) Glucosamine and glucose induce insulin resistance by different mechanisms in rta skeletal muscle. Am J Physiol Endocrinol Metab 285:E1267-E1272

Hebert LF, Daniels MC, Zhou JX, Crook ED, Turner RL, Simmons ST, Neidigh JL, Zhu JS, Baron AD, McClain DA

(1996) Overexpression of glutamine:fructose-6-phosphate amidotransferase in transgenic mice leads to insulin resistance. J Clin Invest 98:930–936

Herbert B (1999) Advances in protein solubilisation for two-dimensional electrophoresis. Electrophoresis 20:660–663

Hirosumi J, Tuncman G, Chang L, Gorgun CZ, Usyal KT, Maeda K (2002) A central role for JNK in obesity and insulin resistance. Nature 420:333–336

Johnsson B, Löfas S, Lindqvist G (1991) Immobilization of proteins to a carboxymethyldextran modified gold surface for biospecific interaction analysis in surface plasmon resonance. Anal Biochem 198:268–277

Jönsson U, Fägerstam L, Johnsson B, Karlsson R, Lundh K, Löfas S, Persson B, Roos H, Rönnberg I (1991) Real-time biospecific interaction analysis using surface plasmon resonance and a sensor chip technology. BioTechniques 11:620–627

Karam JH (1996) Reversible insulin resistance in non-insulin-dependent diabetes mellitus. Horm Metab Res 28:440–444

Karlsson R, Stählberg R (1995) Surface plasmon resonance detection and multi-spot sensing for direct monitoring of interactions involving low molecular weight analytes and for determination of low affinities. Anal Biochem 228:274–280

Kaufmann H, Bailey JE, Fussenegger M (2001) Use of antibodies for detection of phosphorylated proteins separated by two-dimensional gel electrophoresis. Proteomics 1:194–199

Kreppel LK, Hart GW (1999) Regulation of a cytosolic and nuclear O-GlcNAc transferase: role of the tetratricopeptide repeats. J Biol Chem 274:32015–32022

Kruszynska YT, Olefsky JM (1996) Cellular and molecular mechanisms of non-insulin dependent diabetes mellitus. J Invest Med 44:413–428

Löfas S (1995) Dextran modified self-assembled monolayer surfaces for use in biointeraction analysis with surface plasmon resonance. Pure Appl Chem 67:829–834

Löfas S, Johnsson B, Edström A, Hansson A, Lindquist G, Müller Hillgren R-M, Stigh L (1995) Methods for site controlled coupling to carbosymethyldextran surfaces in surface plasmon resonance sensors. Biosens Bioelectron 10:9–10

Malmqvist M, Karlsson R (1997) Biomolecular interaction analysis: affinity biosensor technologies for functional analysis of proteins. Curr Opin Chem Biol 1:378–383

Marshall S (2002) The hexosamine signaling pathway: a new road to drug discovery. Curr Opin Endocrinol Diab 9:160–167

Marshall S, Bacote V, Traxinger RR (1991a) Discovery of a metabolic pathway mediating glucose-induced desensitization of the glucose transport system: role of hexosamine biosynthesis in the induction of insulin resistance. J Biol Chem 266:4706–4712

Marshall S, Garvey WT, Traxinger RR (1991b) New insights into the metabolic regulation of insulin action and insulin resistance: role of glucose and amino acids. FASEB J 5:3031–3036

Marshall S, Nadeau O, Yamasaki K (2004) Dynamic actions of glucose and glucosamine on hexosmaine biosynthesis in isolated adipocytes: differential effects on glucosamine 6-phosphate, UDP-*N*-acetylglucosamine, and ATP levels. J Biol Chem 279:35313–35319

Marshall S, Nadeau O, Yamasaki K (2005a) Glucosamine-induced activation of glycogen biosynthesis in isolated adipocytes: evidence for a rapid allosteric control mechanism with the hexosamine biosynthesis pathway. J Biol Chem, in press

Marshall S, Rumberger I (2000) in: Walker M, Butler P, Rizza RA (Eds) The Diabetes Annual/13, Elsevier, New York, pp 97–112

Marshall S, Yamasaki K, Okuyama R (2005) Glucosamine induces rapid desensitization of glucose transport in isolated adipocytes by increasing GlcN-6-P levels. Biochem Biophys Res Commun 329:1155–1161

McClain DA, Lubas WA, Cooksey RC, Hazel M, Parker GJ, Love DC, Hanover JA (2002) Altered glycan-dependent signaling induces insulin resistance and hyperleptinemia. Proc Natl Acad Sci USA 99:10695–10699

Molloy MP, Herbert BR, Williams KL, Gooley AA (1999) Extraction of Escherichia coli proteins with organic solvents prior to two-dimensional electrophoresis. Electrophoresis 20:701–704

Mooney RA, Senn J, Cameron S, Inamdar N, Boivin LM, Shang Y (2001) Suppressors of cytokine signaling-1 and –6 associate with and inhibit the insulin receptor. A potential mechanism for cytokine-mediated insulin resistance. J Biol Chem 276:25889–258993

Müller G, Wied S, Frick W (2000) Cross talk of $pp125^{FAK}$ and $pp59^{Lyn}$ non-receptor tyrosine kinases to insulin-mimetic signaling in adipocytes. Mol Cell Biol 20:4708–4723

Myers MG, Sun X-J, White MF (1994) The IRS-1 signaling system. Trends Biochem Sci 19:289–293

Nordin H, Jungnelius M, Karlsson R, Karlsson OP (2005) Kinetic studies of small molecule interactions with protein kinases using biosensor technology. Anal Biochem 340:359–368

O'Farrell PH (1975) High resolution two-dimensional electrophoresis of proteins. J Biol Chem 250:4007–4021

Pickering AK (2004) Cytokine response to infection with *Bacillus anthacis* spores. Infect Immun 72:6382–6389

Rabilloud T, Adessi C, Giraudel A, Lunardi J (1997) Improvement of the solubilization of proteins in two-dimensional electrophoresis with immobilized pH gradients. Electrophoresis 21:1094–1103

Robinson KA, Weinstein ML, Lindenmayer GE, Buse MG (1995) Effects of diabetes and hyperglycemia on the hexosamine synthesis pathway in rat muscle and liver. Diabetes 44:1438–1446

Roquemore EP, Chou T, Hart GW (1994) Detection of *O*-linked n-acetylglucosamine (*O*-GlcNAc) on cytoplasmic and nuclear proteins. Methods Enzymol 230:443–460

Rossetti L (1996) in: LeRoith D, Taylor SI, Olefsky JM (Eds) Diabetes mellitus, Lippincott-Raven, Philadelphia, pp 544–553

Rossetti L, Giaccari A, DeFronzo RA (1990) Glucose toxicity. Diabetes Care 13:610–630

Rossetti L, Hawkins M, Chen W, Gindi J, Barzilai N (1995) *In vivo* glucoamine infusion induces insulin resistance in normoglycemic but not in hyperglycemic conscious rats. J Clin Invest 96:132–140

Sjölander S, Urbaniczky C (1991) Integrated fluid handling system for biomolecular interaction analysis. Anal Chem 63:2338–2345

Steppan CM, Wang J, Whiteman EL, Birnbaum MJ, Lazar MA (2005) Activation of SOCS-3 by resistin. Mol Cell Biol 25:1569–1575

Szodoray P (2004) Circulating cytokines in primary Sjorens syndrome determined by a multiplex cytokine system. Scan J Pharmacol 59:592–599

Towbin H, Staehelin T, Gordon J (1979) Electrophoretic transfer from polyacrylamide gels to nitrocellulose sheets: procedure and some applications. Proc Natl Acad Sci USA 76:4350–4354

Ueki K, Kondo T, Kahn CR (2004) Suppressor of cytokine signaling 1 tyrosine phosphorylation of insulin receptor substrate proteins by discrete mechanisms. Mol Cell Biol 24:5434–5446
Vosseller K, Wells L, Lane MD, Hart GW (2002) Elevated nucleocytoplasmic glycosylation by O-GlcNAc results in insulin resistance associated with defects in Akt activation in 3T3-L1 adipocytes. Proc Natl Acad Sci USA 99:5313–5318
Vosseller K, Wells L, Hart GW (2001) Nucleocytoplasmic O-glycosylation: O-GlcNAc and functional proteomics. Biochimie 83:575–581
Wang QM, Fiol CJ, DePaoli-Roach AA, Roach PJ (1994) Glycogen synthase kinase-3β is a dual specificity kinase differentially regulated by tyrosine and serine/threonine phosphorylation. J Biol Chem 269:14566–14574
Wells L, Vosseller K, Hart GW (2001) Glycosylation of nucleocytoplasmic proteins: signal transduction and O-GlcNAc. Science 291:2376–2378
White MF (1998) The IRS-signalling system: A network of docking proteins that mediate insulin action. Mol Cell Biochem 182:3–11
White MF (2003) Insulin signaling in health and disease. Science 302:1710–1711
Yki-Järvinen H (1992) Glucose toxicity. Endocr Rev 13:415–431
Yki-Järvinen, Vogt C, Iozzo P, Pipek R, Daniels MC, Virkamäki A, Mäkimattila S, Mandarino L, DeFronzo RA, McClain D, Gottschalk WK (1997) UDP-N-acetylglucosamine transferase and glutamine:fructose 6-phosphate amidotransferase activities in insulin-sensitive tissues. Diabetologia 40:76–81
Yu C, Chen Y, Cline GW, Zhang D, Zong H, Wang Y (2002) Mechanism by which fatty acids inhibit insulin activation of insulin receptor substrate (IRS-1)-associated phosphatidylinositol 3-kinase activity in muscle. J Biol Chem 277:50230–50236
Yuan M, Konstantopoulos N, Lee J, Hansen L, Li ZW, Karin M (2001) reversal of obesity- and diet-induced insulin resistance with salicylates or targeted disruption of Ikkbeta. Science 293:1673–1677
Zhou J, Neidigh JL, Espinosa R, LeBeau MM, McClain DA (1995) Human glutamine:fructose-6-phosphate amidotransferase: Characterization of mRNA and chromosomal assignment to 2p13. Hum Genet 96:99–101

K.6.3.6 Insulin-Like Signal Transduction via Plasma Membrane Microdomains (Caveolae and Lipid Rafts)

GENERAL CONSIDERATIONS

Caveolae

Caveolae were discovered as non-coated small flask-shaped invaginations (25–100 nm) of the plasma membrane by electron microscopy of endothelial cells (Fan et al. 1983, for a review see Anderson 1993a, 1993b, 1998, 1999, 2002, Shaul and Anderson 1998). It is possible that caveolae are formed from non-invaginated lipid rafts in the presence of the principal structural caveolae protein, caveolin (Kurzchalia et al. 1994, Lisanti et al. 1994, Parton 1996, Schlegel et al. 1998, Müller 1999 and 2000, Müller and Welte 2002e). Caveolae and the so called lipid rafts are believed to be enriched in the bulk membrane lipids, such as phosphatidylinositol, cholesterol, sphingomyelin and glycolipids, such as glycosylphosphatidylinositol and the ganglioside GM1 (for reviews see Rietveld and Simons 1998, Bickel 2002). Due to the high concentration of cholesterol and sphingomyelin, caveolae and lipid rafts are much more resistant to solubilization by detergents than are other parts of the plasma membrane and intracellular membranes (Brown and Rose 1992, Brown and London 1997 and 1998, Harder et al. 1998, Müller 2002d, Edidin 2003). The concentrations of various lipids in caveolae and rafts suggest great variations between different cell types, but also reflect the different experimental approaches used. Moreover, caveolae constitute between cell types a very variable, and usually unknown, fraction of the plasma membrane. Figures for enrichment of various components in caveolae compared to the total plasma membrane therefore reflect, to a large extent, this property of the particular cell type under investigation. In addition to the high content of cholesterol and sphingolipids, caveolae are stabilized by one or more caveolin isoforms. The caveolins are a family of 21–25-kDa integral membrane proteins that from the coat structure of caveolae (Glenney 1992, Okamoto et al. 1998, Smart et al. 1999). An unsual hairpin membrane domain results in both the amino- and carboxy-termini facing the cytoplasm. Caveolins avidly bind cholesterol, which may be the basis for their association with the liquid-ordered phase of the plasma membrane. In adipocytes caveolin-1 is the most prominent isoform (Rothberg et al. 1992) and its ablation leads to a total loss of caveolae.

Caveolae are believed to be involved in a number of cellular processes, such as receptor mediated uptake and organization of transmembrane signaling (Shaul and Anderson 1998). Caveolae and lipid rafts harbor a number of components of various intracellular signal transduction pathways including G-protein-coupled receptors, heterotrimeric G-proteins, RTK (Src family tyrosine kinases), components of the Ras-mitogen-activated protein kinase (MAPK) pathway, protein kinase C isoforms, and endothelial nitric oxide synthase (eNOS) (Schlegel et al. 1999, Shaul and Anderson 1998, Smart et al. 1999). As a consequence, they may function as locations for the direct physical interaction of signaling elements where the cross-talk between the corresponding signaling pathways takes place (Okamoto et al. 1998). Lisanti and coworkers demonstrated direct binding of a common domain within caveolin, the caveolin-scaffolding do-

main (CSD) to the corresponding caveolin-binding domain (CBD) of a variety of signaling proteins which are thereby kept in a basal inactive state, however competent for future activation (Couet et al. 1997a, Ju et al. 1997, Mineo et al. 1998, Müller 2001b, Moffett et al. 2000). The inhibitory interaction between caveolin and signaling molecules should be accessible for modulation in response to extracellular/intracellular signals. Activation of signaling pathways engaging CBD-harboring signaling molecules requires their relief from binding to/inhibition by caveolin both in short and long term (Couet et al. 1997a and b, Kobzik et al. 1996).

Lipid Rafts

Discovery of the intracellular molecules and pathways that mediate insulin action has preoccupied many investigators for many years, but controversy and confusion remain. An emerging concept to explain such signaling specificity in the face of molecular promiscuity is that specialized scaffold, anchor, and adapter proteins segregate signaling molecules into specific cellular compartments *via* protein-protein interactions (Mastick et al. 1998). One level of spatial organization proposed for the plasma membrane is that of the liquid-ordered phase. According to a model proposed by Simons and Ikonen (1997) and Simons and Toomre (2000), lipids in the liquid-ordered phase pack together to form dynamic "rafts" in the plasma membrane, and these lipid rafts either recruit or exclude specific molecules, including signaling proteins. The biophysical and biochemical microenvironment of the rafts (e. g., membrane fluidity) may influence the function of the raft proteins. Also, the physical segregation of proteins into such "microdomains" may regulate the accessibility of those proteins to regulatory or effector molecules. The structural bases suggested for protein association with rafts include glycophosphatidylinositol (GPI) anchors (e. g., folate receptor), dual fatty acylation by myristylation and palmitoylation (e. g., Src family tyrosine kinases), transmembrane domain structure (e. g., influenza hemagglutinin polypeptide), cholesterol binding (e. g., caveolins), and protein-protein interactions (e. g., caveolin-interacting proteins). On the basis of their ability to sort proteins, rafts have been implicated in a number of cell functions, including signal transduction.

Signaling Function of Lipid Rafts and Caveolae

A pathway for insulin activation of glucose transport has been identified in insulin-sensitive cells which involves rafts/caveolae and the in- and out-movement of signaling proteins (Baumann et al. 2000, Ribon et al. 1998). Thus, rafts/caveolae seem to harbor signaling components for insulin-stimulated glucose transport and regulate their activity by interaction with caveolin and additional caveolar structural proteins that may serve as scaffolding proteins for concentrating and activating/inhibiting specific insulin signaling components. In addition, Baumann (2001) and coworkers presented a large body of evidence that a signal generated at the lipid rafts of adipocytes in response to insulin is required for insulin-stimulated glucose transport, in addition to that elicited by the PI3-K pathway (see K.6.3.6.3).

Interestingly, compounds which manage to modulate the interaction of caveolin/caveolae with CBD-containing signaling proteins and, in consequence, the activation state of the corresponding downstream signaling cascades have been described. A study by Müller and coworkers (2001a, b) demonstrated that in isolated rat adipocytes, the non-RTK, $pp59^{Lyn}$ and $pp125^{Fak}$, are down-regulated by localization in caveolae/binding to caveolin and up-regulated by release from caveolae/dissociation from caveolin in response to phosphoinositolglycans (PIG), degradation products of GPI membrane protein anchors (Jones and Varela-Nieto 1999, Müller and Frick 1999), and the sulfonylurea drug, glimepiride (Langtry and Balfour 1998). The short term redistribution of these kinases from caveolae/rafts induces insulin-independent activation of the metabolic insulin signaling cascade. These findings suggest that the concentration of signaling proteins at caveolae/caveolin may be regulated by diverse physiological and pharmacological stimuli thereby integrating cross-talk to various signal transduction pathways.

PURPOSE AND RATIONALE

In rat adipocytes and in 3T3-L1 adipocytes the IR is localized to caveolae (Müller et al. 2002c, Gustavsson et al. 1999). The immediate downstream signaling molecule, IRS1, on the other hand, has been reported not to be associated with the plasma membrane in rat adipocytes. In rat adipocytes the disruption of caveolar integrity by cholesterol depletion using β-cyclodextrin, reversibly makes the cells insulin resistant by inhibiting the IR from phosphorylating IRS1. On the other hand, insulin signalling for mitogenic control *via* MAPK, ERK1 and 2, is not impaired in the rat cells (Gustavsson et al. 1996). The importance of caveolae for insulin action is reinforced by the finding that, in response to insulin stimulation, the insulin-regulated glucose transporter, GLUT4, is translocated

to caveolae for glucose uptake (Gustavsson et al. 1996, Kandror et al. 1995), and that some of the downstream signalling for enhanced glucose uptake may take place in caveolae.

In addition, destruction of caveolae causes a reduced uptake of long-chain fatty acids in 3T3-L1 cells and HepG2 cells (Pohl et al. 2002, Meshulam et al. 2006), and the major structural protein of caveolae, caveolin, and the caveolae-localized protein, CD36, both bind fatty acids. Caveolin has been implicated in TAG metabolism through its association with lipid bodies and LD in 3T3-L1 adipocytes and other cell lines (Fujimoto et al. 2001, Ostermeyer et al. 2001, Pol et al. 2001) and its mediation of the interaction between perilipin and the catalytic subunit of PKA which is required for β-adrenergic-dependent phosphorylation of perilipin and activation of lipolysis in adipocytes (Cohen et al. 2004). Caveolin-$1^{-/-}$ mice that are deficient in caveolin and caveolae have, moreover, been found to have deranged lipid metabolism and atrophied adipose tissue (Drab et al. 2001, Razani et al. 2001, 2002a, for a review see Razani et al. 2002b). Furthermore, caveolin-$1^{-/-}$ mice show a 90% decrease in IR expression selectively in adipose tissue, greatly reduced insulin-induced phosphorylation of PKB, and insulin resistance (Capozza et al. 2005, Oshikawa et al. 2004, for a review see Ishikawa et al. 2005). These findings indicate that intact caveolae are important for normal insulin signalling and (insulin) regulation of metabolism of carbohydrates and lipids in adipocytes. The following methods enable the analysis of the role of rafts/caveolae in insulin and insulin-like signal transduction in adipocytes as well as of their participation in the insulin-like activity of compounds/drug candidates.

K.6.3.6.1 Preparation of Plasma Membranes

Lipid rafts are routinely prepared from the plasma membranes of differentiated mammalian cells, preferably primary and cultured adipocytes or lung endothelial cells, due to their relative abundance.

K.6.3.6.1.1 Sucrose Gradient-Based Method

Basal and insulin/compound-stimulated adipocytes are homogenized in 10 mM Tris/HCl (pH 7.4), 1 mM EDTA, 0.5 mM EGTA, 0.25 M sucrose, 25 mM NaF, 1 mM pyrophosphate with protease inhibitors (10 µM leupeptin, 1 µM pepstatin, 1 µM aprotinin, 4 mM iodoacetate and 50 mM PMSF) using a motor-driven Teflon-in-glass homogenizer at room temperature. Subsequent procedures are carried out at 4°C. Cell debris and nuclei are removed by centrifugation at (1,000 × *g*, 10 min). A plasma membrane-containing pellet, obtained by centrifugation (16,000 × *g*, 20 min) is resuspended in 10 mM Tris/HCl (pH 7.4), 1 mM EDTA and protease inhibitors. The plasma membranes are purified by sucrose density gradient centrifugation (Avruch and Wallach 1971).

K.6.3.6.1.2 OptiPrep-Step Gradient-Based Method

Purification of plasma membranes from total membranes is performed by fractionation using the OptiPrep gradient (AXIS-Shield) according to the procedure of Pohl and coworkers (2005). Monolayers of confluent 3T3-L1 adipocytes are washed once in PBS to remove the culture medium and then once in the homogenization buffer (10 mM Tris/HCl, pH 7.4, 25 mM sucrose, 0.5 mM EDTA). Thereafter, cells are scraped in 3 ml of homogenization buffer and centrifuged (1,000 × *g*, 5 min). The pellet is resuspended in 2 ml of homogenization buffer. Cells are lysed by 10 passages through a fine syringe needle followed by treatment with a tight-fitting Dounce homogenisator. The homogenate is centrifuged (1,000 × *g*, 10 min). The resulting post-nuclear supernatant is centrifuged (100,000 × *g*, 40 min). The resulting total membrane pellet is resuspended in 1 ml of homogenization buffer containing 25% (w/v) iodixnol and loaded onto a nine-step OptiPrep gradient, which consisted of 25, 22, 19, 16, 13, 10, 7, 4, and 1% (w/v) iodixnol. After centrifugation (200,000 × *g*, 3 h, 4°C, Beckman SW41Ti), 18 fractions are collected from the bottom of each centrifuge tube. A portion of each fraction can be analyzed by SDS-PAGE and immunoblotting for markers of the plasma membranes. Fractions 5, 6 and 7 are used as purified plasma membranes according to their enrichment of Na^+/K^+-ATPase, CD36 and caveolin-1.

K.6.3.6.1.3 Affinity Partitioning-Based Method

All work including the two-phase systems is done at 4°C in a well-tempered cold room as two-phase partitioning is critically dependent on temperature. Male Sprague–Dawley rats, weighing 200–300 g, are starved overnight and killed by decapitation. Lungs are excised and thoroughly perfused with ice-cold homogenization medium (0.25 M sucrose, 5 mM Tris/HCl, pH 8.0). They are cut into pieces and squashed in a garlic press. Four grams of lungs are transferred to a Potter–Elvehjem homogenizer containing a 30-g

two-phase system including the lung tissue. The two-phase system consisted of 5.7% (w/w) dextran T500 (bottom phase) and 5.7% (w/w) PEG 3350 (top phase) in 15 mM Tris/H_2SO_4 (pH 7.8) (final concentrations in the system). Homogenization is done by 5 up and down strokes by a motor-driven homogenizer with a Teflon pestle at 1,000 rpm. The homogenate is transferred to a Dounce homogenizer and further homogenized by 10 strokes with a loose-fitting pestle followed by 10 strokes with a tight-fitting one. After homogenization, the phases are separated by gentle centrifugation (270 × *g*, 5 min, Sorvall SS-34 rotor). The PEG-rich top phase is collected and the dextran-rich bottom phase re-extracted with fresh top phase by mixing and phase separation as above. The two top phases collected are combined and further subjected to affinity partitioning. The fresh top phase for re-extraction is obtained from a similar 30-g two-phase system as above, replacing the lung tissue with 4 g of 15 mM Tris/H_2SO_4 (pH 7.8). After weighing in the components, the system is thoroughly mixed and allowed to settle overnight before collecting the top phase to be used for re-extraction. The phases for affinity partitioning are obtained as follows: a 20-g system containing 6.0% (w/w) PEG 3350 and 6.0% (w/w) dextran T500, including 1.3 mg WGA coupled to dextran T500, in 15 mM borate/Tris (pH 7.8) (final concentrations), is weighed in. After thoroughly mixing the system and letting settle overnight, the phases are collected individually, the WGA–dextran-containing bottom phase to be used for the initial affinity partitioning step and the PEG-enriched top phase for re-extraction (Persson et al. 2001). The combined top phases from the partitioning step above are mixed thoroughly with the WGA-containing bottom phase by 20 inversions, vortexing, and another 20 inversions. After phase separation through gentle centrifugation as above, the top phase is removed and the bottom phase re-extracted in the same manner with the fresh top phase obtained from the pre-equilibrated 20-g system. The final bottom phase is collected, diluted 10-times with 0.1 M *N*-acetylglucosamine in 5 mM Tris/HCl (pH 8.0) to dissociate membranes from WGA-dextran, and centrifuged (100,000 × *g*, 90 min). The plasma membrane pellet is resuspended in homogenization medium.

K.6.3.6.2 Preparation of Lipid Rafts and Caveolae

PURPOSE AND RATIONALE

Typical preparations of lipid rafts use 1% Triton X-100 to extract whole cells and the low-density, detergent-resistant material is separated from other solubilized membrane fractions by centrifugation on a 5% to 30% sucrose gradient (Brown and Rose 1992). Subsequently, lipid rafts have been prepared using a variety of other detergents, including Lubrol WX, Lubrol PX, Brij58, Brij96, Brji98, Nonidet P40, CHAPS, and octylglucoside (for a review see Macdonald and Pike 2005). Although preparations of detergent-resistant membranes are readily isolated, several observations have raised concerns that extraction of cells with detergent may be generating clusters of raft lipids and proteins that did not exist in the intact cell. For example, examination of cells grown on coverslips and then extracted with Triton X-100 reveals a continuous membrane sheet pock-marked by large holes (Major and Maxfield 1995). Because rafts are thought to be < 50 nm in diameter (Anderson and Jacobson 2002, Edidin 2003), the residual "detergent-resistant" membranes probably form from individual rafts that coalesced as a result of the detergent treatment.

To avoid the complications associated with preparing rafts using detergent extraction procedures, several methods have been established for isolating rafts from cells fractionated in the absence of detergent. Song and coworkers (1996) sonicated cells in a pH 11 sodium carbonate buffer and isolated caveolae by centrifugation of the lysate in a discontinuous 5%/35%/45% sucrose gradient. Although this procedure is relatively easy, the spin time of 16–20 h is long and the resulting raft fraction is significantly contaminated with other membranes. A more carful fractionation of lipid rafts (Smart et al. 1995), which is based on lysis of the cells in an isotonic buffer containing EDTA and purified plasma membranes on a Percoll gradient. The plasma membranes are then sonicated and the lipid rafts isolated by flotation through a 10–20% gradient OptiPrep. This method results in the production of a relatively clean raft preparation. However, it is time-consuming and yields are poor. Furthermore, there is significant variability from preparation to preparation and from cell type to cell type. Because of the drawbacks associated with those procedures for isolating detergent-free lipid rafts, Macdonald and Pike (2005) developed an improved method that allows the rapid isolation of purified rafts in good yield. It is based on lysis of cells by shearing in an isotonic buffer containing calcium and magnesium and apparently allows isolation of a highly purified raft fraction in a single step by flotation in a 0–20% OptiPrep gradient.

Studies on caveolae structure and function would be facilitated by a convenient high-yield isolation procedure. Most isolation protocols developed involve the

detachment of caveolae from crude membranes either by Triton X-100 treatment (Sargiocomo et al. 1993, Chang et al. 1994) or by sonication (Smart et al. 1995) followed by density gradient centrifugation in either sucrose (Sargiocomo et al. 1993, Chang et al. 1994) or OptiPrep gradients (Smart et al. 1995). To obtain highly purified caveolae, however, extensive purification of a suitable plasma membrane fraction is required prior to detachment and centrifugation as was demonstrated using lung endothelial cells (Schnitzer et al. 1995a, b). Alternatively, immunoisolation protocols may be used (Oh and Schnitzer 1999, Abedinpour and Jergil 2003), although these also require prepurification steps.

PROCEDURE

Conventional plasma membrane purification protocols based on centrifugation techniques usually result in low yields. In an alternative approach rat liver plasma membranes are purified by affinity partitioning in a PEG–dextran aqueous two-phase system (see above). Partitioning conditions are chosen to direct the bulk of unfractionated membranes to the PEG-rich top phase and then selectively to attract plasma membranes to the dextran-rich bottom phase by including WGA conjugated to dextran as an affinity ligand. This lectin specifically binds to *N*-acetylglucosamine and sialic acid residues on the plasma membrane surface. The affinity purification method is rapid and resulted in plasma membranes of high purity and yield (Persson et al. 1991, Persson and Jergil 1992). The possibility of combining two-phase affinity purification of plasma membranes with density gradient centrifugation to isolate caveolae has been explored (Abedinpour and Jergil 2003). Such a method should be generally applicable for the preparation of caveolae from various tissues and cells. The isolation of a vesicular fraction from rat lung highly purified in caveolin, a caveolar marker protein, by this approach is reported.

K.6.3.6.2.1 Carbonate-Based Method

Purified plasma membranes are pelleted and resuspended in 0.5 M Na_2CO_3 (pH 11), and sonicated with a probe-type sonifier 3 × 20 s. The homogenate is then adjusted to 45% (w/v) sucrose in 12 mM MES (pH 6.5), 75 mM NaCl, 0.25 M Na_2CO_3, with protease inhibitors, and loaded under a 5–35% (w/v) discontinuous sucrose gradient in the same solution and centrifuged (39,000 rpm, 16–20 h, 4°C, Beckman SW41 rotor). The light-scattering band at the 5–35% sucrose interface is collected and referred to as standard caveolae fraction. The recovery of caveolin in the caveolae fraction is typically 25 ± 5%as determined by immunoblotting. Alternatively, for preparation from intact adipocytes, washed cells (0.5×10^7 cells) are suspended in 2 ml of sodium carbonate buffer (0.5 M Na_2CO_3, pH 11) containing protease inhibitors and homogenized sequentially using a loosely fitting Dounce homogenizer (10 strokes) and a sonicator (3x20 s bursts). The homogenate (2 ml) is then adjusted to 45% sucrose by addition of 2 ml of 90% sucrose, 50 mM MES/KOH (pH 6.5), 150 mM NaCl (final pH of the mixture 10.2). A discontinuous sucrose gradient is formed by overlaying this solution with 4 ml of 35% sucrose and 4 ml of 5% sucrose, both in the same buffer containing 0.25 M Na_2CO_3. After centrifugation (see above), 0.85-ml gradient fractions are collected to yield a total of 14 fractions. The individual gradient fractions are pooled into rafts (Fr. 4–7) and non-raft areas (Fr. 10–14). The membranes from each pooled gradient fractions obtained by either method are diluted 2- to 3-fold with 25 mM MES (pH 6.5), 150 mM NaCl, 1% TX-100, collected by centrifugation (50,000 × *g*, 30 min, 4°C) and resuspended in non-dissociating buffer (10 mM Tris/HCl, pH 7.4, 150 mM NaCl, 1% Nonidet P-40, 5 mM EDTA, 0.5 mM EGTA, 1 mM sodium orthovanadate, 50 mM NaF and protease inhibitors) or dissociating buffer (= non-dissociating buffer supplemented with 60 mM octylthioglucoside, 0.3% deoxycholate) as indicated, incubated (1 h, on ice) and used for (co)immunoprecipitation, immunoblotting or photoaffinity labeling.

K.6.3.6.2.2 Detergent-Based Method

For preparation from intact adipocytes, washed adipocytes (3.5×10^7) are suspended in 1.5 ml of lysis buffer (25 mM MES, pH 6.0, 150 mM NaCl, 5 mM EDTA, 1% TX-100, 0.2 mM sodium orthovanadate, and protease inhibitors) and incubated for 20 min on ice. The cells are lysed with 10 strokes in a manual Teflon-in-glass homogenizer over the course of 1 h at 4°C. The lysate is centrifuged (1,300 × *g*, 5 min) to pellet unbroken cells, cellular debris, nuclei and large unsoluble material. One ml of the postnuclear supernatant is subjected to sucrose gradient centrifugation by mixing with an equal volume of 85% sucrose, 25 mM MES (pH 6.0), 150 mM NaCl, 5 mM EDTA at the bottom of a 12-ml centrifuge tube which is overlayed with 5.5 ml of 35% sucrose, and then 3.5 ml of 5% sucrose in the same medium. After centrifugation (230,000 × *g*, 18 h, 4°C, Beckman SW41 rotor), 0.9-ml

fractions are collected from top to bottom, and termed fraction Fr. 1, 2, 3, etc. The bottom fraction is Fr. 12. Fr. 5 appears as a white, light-scattering band under illumination located at 5–7% sucrose at the 35-% sucrose interface. The rafts contained in Fr. 5 are pelleted by dilution of the sucrose with 5 volumes of 50 mM HEPES/KOH containing protease inhibitors and centrifugation (200,000 × *g*, 2 h).

Alternatively, for preparation from plasma membrane fractions, Triton X-100 is added to the purified plasma membrane fraction to a final concentration of 1% (w/v) (approximately a 100-fold excess of detergent to membrane protein). The sample is incubated for 30 min at 4°C and centrifuged (100,000 × *g*, 90 min). The pellet is resuspended in homogenization medium by 10 strokes in a tight-fitting Dounce homogenizer. The resulting sample is transferred to a Beckman SW40 ultracentrifuge tube. The sample is adjusted to 40% (w/v) sucrose by addition of 80% (w/v) sucrose, before layering 5.5 ml each of 24 and 5% (w/v) sucrose on top of the sample. All sucrose solutions are made in 5 mM Tris/HCl (pH 8.0). After centrifugation (100,000 × *g*, 21 h, 4°C, Beckman SW41 rotor), 12 1-ml fractions are collected by upward displacement. The light-scattering band at the 5–35% (w/v) sucrose interface is collected as lipid rafts. The recovery of caveolin is typically 15 % as determined by immunoblotting.

K.6.3.6.2.3 Immunopurification

Lipid rafts prepared from rat adipocytes (originating from 500 µl of packed cell volume) are resuspended in 0.5 ml of homogenisation buffer (buffer H). 1% Triton X-100, 2% CHAPS, 60 mM D-octyl glycoside (final concentrations) are added to 50 µl of resuspended rafts to a final volume of 100 µl. After 1 h on ice, the fractions are centrifuged (104,000 × *g*, 1 h). The pellets containing detergent resistant rafts are resuspended in 100 µl buffer H and analyzed. For immunoprecipitations the rafts (corresponding to 750 µl of packed cell volume) and resistant to 1% Triton X-100 treatment are suspended in 300 µl buffer H and incubated for 4 h with 6 µl caveolin-1 antibody supplemented with 10 µl of packed Protein A-Sepharose during the last hour. Non-bound material is removed and the Sepharose gel is washed five times in 600 µl buffer H. The bound proteins are eluted by boiling for 15 min in buffer H supplemented with 0.6% $C_{13}E_{12}$, 48 mM NaF, 48 mM NaCl, 5% SDS, 2% β-mercaptoethanol and 5% glycerol. For GLUT-4 analysis, rafts (corresponding to 500 µl packed cell volume) are treated with 1% $C_{13}E_{12}$ and centrifuged (7000 × *g*, 10 min). The supernatant is incubated for 4 h with 4 µl caveolin-1 antibody supplemented with 7 µl packed protein A-Sepharose during the last hour. The gel is washed and eluted as described above. Each step in the immunoprecipitation procedures is performed at 4°C. The recovery of immunopurified lipid rafts is normalized by homologous immunoblotting with anti-caveolin antibodies of the same blot following stripping of the membrane.

EVALUATION

A generally applicable method for the preparation of highly purified caveolae and/or lipid rafts based on a combination of affinity preparation of plasma membranes and density gradient centrifugation has been developed. To test this approach lung tissue have been chosen as endothelial cells lining vascular ducts are rich in caveolae. In earlier studies caveolae were prepared from plasma membranes of these cells isolated by an in situ silica-coating procedure (Schnitzer et al. 1995b). Alternatively, a crude lung homogenate can be used as starting material, preparing a plasma membrane-enriched fraction by affinity partitioning (Abedinpour and Jergil 2003). To improve purity the affinity step is preceded by homogenization of the tissue directly in a conventional aqueous two-phase system followed by phase separation to remove material disturbing the affinity step. A similar approach was elaborated successfully for the purification of plasma membranes from liver (Persson and Jergil 1992, Ekblad and Jergil 2001), suggesting that the method might be applicable also to other tissues. Lung membranes have been shown similarly to liver membranes both in the conventional and in the affinity two-phase step. The overall yield of the plasma membrane marker enzyme, 5′-nucleotidase, is somewhat lower from lung (30–35%) than from liver (50–70%), however. This is primarily due to a low recovery of 5′-nucleotidase in the affinity step rather than an unfavorable distribution of the enzyme in this step or the preceding conventional two-phase step. The enrichment of 5′-nucleotidase (8-fold) compares favorably with the 5- to 10-fold enrichment of various plasma membrane markers in the earlier isolation procedure involving silica coating of lung endothelial plasma membranes. The silica coating procedure isolates the luminal part of the plasma membrane (Schnitzer et al. 1995b), while all regions of the plasma membrane are isolated by the affinity partitioning procedure (Persson et al. 1991, Persson and Jergil 1992, Ekblad and Jergil 2001).

The plasma membrane fraction obtained by the affinity procedure is suitable for the isolation of a frac-

tion highly enriched in the caveolar marker, caveolin, after dispersion of the membranes in Triton X-100 and floatation in a sucrose density gradient. The enrichment of caveolin is approximately 20-fold in this density gradient step, slightly higher than the 13-fold enrichment observed when caveolae-rich vesicles are isolated from silica-coated endothelial plasma membranes (Schnitzer et al. 1995b). However, both the affinity partitioning method presented here and the silica coating procedure result in plasma membrane material suitable for obtaining highly purified caveolae by sucrose gradient centrifugation regardless of the enrichment of caveolin attained.

Caveolae may be isolated also by a detergent-free method, gradient centrifugation by sonication of affinity purified plasma membranes. Although the yield is much lower, this nevertheless shows that the separation also works for the detergent-free preparation of caveolae-enriched material. It may be possible to optimize shearing of the plasma membrane preparation and the gradient separation to increase the yield, particularly since much vesicular material containing caveolin remained in the high-density part of the gradient. The caveolin-enriched fraction isolated after Triton X-100 treatment consists of morphologically similar closed vesicles of the same size (50–100 nm) as that of caveolae previously isolated from lung endothelial cells (Schnitzer et al. 1995a and 1995b, Stan et al. 1997). Notably no vesicles in the size range 200–700 nm are observed. Such vesicles are common in Triton-insoluble membranes prepared from crude lung homogenates, being either non-caveolar membranes or membranes occasionally having attached caveolae (Schnitzer et al. 1995d). They are not present, however, in caveolar preparations obtained by Triton X-100 treatment of endothelial plasma membranes isolated by the silica coating procedure followed by sucrose gradient centrifugation. The thin-section micrographs indicated that many of the isolated vesicles are not smoothly rounded but had an irregular shape.

K.6.3.6.3 Lipid Raft- and Caveolae-Based Assays in Insulin and Insulin-Like Signal Transduction

PURPOSE AND RATIONALE

For studying signal transduction processes which involve caveolae, these structures are isolated as rafts by biochemical methods (carbonate or detergent extraction) from primary or cultured differentiated cells, such as muscle and fat cells, after incubation with external stimuli. Rafts can be prepared either directly from total cells, or total cell lysates or (preferably) isolated (purified) plasma membranes. The use of rafts from total cells or lysates may obscure subtle changes in signaling since the (considerable) fraction of rafts present in membranes of the Golgi apparatus (where their biogenesis takes place) may respond differently (or not at all) toward external stimuli compared to the plasma membrane rafts. Subsequent analysis for the presence in/cofractionation with caveolae, direct interaction with caveolin and changes in activity of signaling proteins in response to the external stimuli requires the methods of enrichment/purification of rafts, photoaffinity labeling (of GPI proteins), coimmunoprecipitation with caveolin (of signaling proteins), immunoblotting (of signaling proteins) and immune complex kinase assays (in case of kinase activity of signaling proteins).

K.6.3.6.3.1 Co-Immunoprecipitation of Lipid Raft Proteins

Total cell lysates (25–50 µg protein) or rafts in non-dissociating buffer (10–15 µg protein) are pre-cleared (1 h, 4°C) with protein G/A-Sepharose (50 mg/ml) in a total volume of 100 µl and then supplemented with appropriate antibodies (e. g. $pp125^{Fak}$, 2 µg/sample; IRS-1, 1:50 dilution; IRS-2, 10 µg/sample; $pp59^{Lyn}$, 5 µg/sample; caveolin, 0.7 µg/sample; IRβ, 1:175 dilution) pre-adsorbed on protein G-Sepharose (monoclonal antibodies) or protein A-Sepharose (rabbit antibodies) in a total volume of 100 µl. After incubation (4 h, 4°C, end-over-end rotation) and centrifugation (3,000 × g, 2 min, 4°C), the collected immune complexes are washed twice with 1 ml each of immunoprecipitation buffer (50 mM HEPES/KOH, pH 7.4, 500 mM NaCl, 100 mM NaF, 10 mM EDTA, 10 mM sodium pyrophosphate, 1 mM sodium orthovanadate) containing 0.2% Nonidet P-40 and 0.3% deoxycholate, then twice with 1 ml each of immunoprecipitation buffer containing 150 mM NaCl and 0.2% Nonidet P-40 and once with 1 ml of immunoprecipitation buffer lacking salt and detergent and finally suspended in 50 µl of Laemmli sample buffer (4% SDS, 115 mM Tris/HCl, pH 6.8, 1 mM EDTA, 10% glycerol, 4 mg/ml bromophenol blue) supplemented with 1.2% β-mercaptoethanol (except for anti-caveolin immunoprecipitates), heated (95°C, 2 min) and centrifuged. The supernatant samples are analyzed by SDS-PAGE (4–12% Bis-Tris precast gel, pH 6.4, MES/SDS running buffer under reducing conditions) and subsequent immunoblotting (see K.6.3.4.3 and K.6.3.6.3.2). The centrifugation conditions for collection of the protein A/G-Sepharose-bound immune

complexes, do not lead to sedimentation of (non-dissociated rafts) to any significant degree according to immunoblotting with anti-caveolin antibody. The coimmunoprecipitation of proteins with caveolin from non-dissociated rafts is specific for raft-associated components, such as the GPI protein, Gce1, and the dual-acylated non-RTK, pp59^{Lyn}, since the use of non-immune IgG instead of anti-caveolin antibody or of dissociated DIGs and anti-caveolin antibody do not result in immunoprecipation of Gce1 and pp59^{Lyn}.

K.6.3.6.3.2 Immunoblotting of Lipid Raft Proteins

Immunoblotting is performed as described (see K.6.3.1.3.2.1 and K.6.3.4.3) with minor modifications. After SDS-PAGE and transfer of the proteins to PVDF membranes (2 h, 400 mA in 20% methanol, 192 mM glycine, 25 mM Tris, 0.005% SDS), the blocked membrane (1 h in 20 mM Tris/HCl, pH 7.6, 150 mM NaCl, 0.05% Tween 20, 0.1% Brij, 0.01% NP-40 and with 1% ovalbumin and 1% BSA (anti-phosphotyrosine, anti-pp59^{Lyn}, anti-IRβ) or with 5% non-fat dried milk (anti-caveolin, anti-IRS-1/2) is incubated (2 h, 25°C) with antibodies against IRS-1 (1:500), IRS-2 (1:750), caveolin (1:2,000), pp59^{Lyn} (1 µg/ml) or IRβ (2 µg/ml) diluted in the same medium, and then washed five times with the same medium. After incubation of the membranes (1 h, 25°C) with horseradish peroxidase-coupled goat anti-mouse IgG antibody or goat anti-rabbit IgG antibody diluted in the appropriate blocking buffer (1:5,000 or 1:2,500) and subsequent washing with detergent-containing (two times) and detergent-free (two times) buffer (20 mM Tris/HCl, pH 7.6, 150 mM NaCl), the labeled proteins are visualized by the enhanced chemiluminescence method.

K.6.3.6.3.3 Immunecomplex Assay for Lipid Raft PK

Immunecomplex kinase assays are performed as described (see K.6.2.9.2 and K.6.3.4.4) with minor modifications. Immune complexes are suspended 30 µl of kinase buffer (50 mM HEPES/KOH, pH 7.4, 100 mM NaCl, 1.25 mM $MnCl_2$, 12.5 mM $MgCl_2$, 1.25 mM EGTA, 0.5 mM DTT, 1 mM Na_3VO_4) containing [γ-^{32}P]ATP (final conc. 40 µM, 0.2 mCi/ml) or 1 mM ATP and incubated (e. g. for pp59^{Lyn}: 15 min, 22°C) in the presence of 1 µg heat-denatured enolase. Phosphorylation is terminated by addition of 10 µl of four-fold concentrated Laemmli buffer and boiling. The phosphoproteins are separated on SDS-PAGE (10% Bis-Tris resolving gel, MOPS/SDS running buffer) and analyzed for phosphotyrosine by phosphorimaging ([γ-^{32}P]ATP) or immunoblotting (ATP). Under these conditions the kinase reactions are linear with time for the assay period. IRS-1 immune complexes are assayed for PI3-K by incubating (10 min, 22°C) in 50 µl of 20 mM Tris/HCl (pH 7.0), 50 µM [γ-^{33}P]ATP (5 µCi), 10 mM $MgCl_2$, 2 mM $MnCl_2$, 100 mM NaCl, 2 mM EDTA, 0.5 µM wortmannin (for control incubations, only) containing 10 µg of phosphatidylinositol (PI) and 1 µg of phosphatidylserine. After addition of 10 µl of 8 M HCl and 160 µl of a 1/1 mixture of methanol/chloroform, the extracted phospholipids are resolved by TLC on plates coated with 1% oxalate and developed in chloroform/methanol/water/ammonia (60/47/11.3/3.2, by vol.). Radiolabeled PI3-P is quantitated by phosphorimage analysis. For calculation of wortmannin-sensitive PI3-K, all values are corrected for PI3-P radiolabeled in the presence of wortmannin. SDS-PAGE and subsequent immunoblotting for caveolin and the PK assumed to localize permanently or transiently at lipid rafts (e. g. protein kinase C) is performed as described (K.6.3.6.3.2).

K.6.3.6.3.4 Electron Microscopic Analysis of Caveolae

PURPOSE AND RATIONALE

Several laboratories have localized important elements of the insulin signal transduction machinery to caveolae or rafts, including the IR itself. Baumann and coworkers (2000) and Chiang and coworkers (2001) have reported the discovery of a novel insulin-signaling pathway in adipocytes that relies on proper localization of signaling molecules to lipid rafts and that is required for insulin-stimulated glucose uptake. Using a detergent-based method of lipid raft preparation, Mastick and coworkers (1995) found only trace levels of insulin receptor in the rafts of 3T3-L1 adipocytes. Müller and coworkers (2001a, b) characterized the composition of rafts from isolated rat adipocytes. The rafts and non-rafts were prepared by both detergent and detergent-free methods from total cell lysates and from plasma membranes, respectively. Representative fractions were analyzed by immunoblotting for known raft and nonraft proteins. Despite the methodological differences, there was good agreement between the proteins enriched in rafts and non-rafts by the two procedures. By both methods, the β-subunit of the IR was relatively depleted from the rats and relatively enriched in the non-rafts. However, Gustavsson and coworkers (1999) reached the opposite result by double immunogold transmission EM and detergent-free isolation of rafts. In these experiments, caveolin and

both subunits of the IR colocalized in ~50-nm-round structures that corresponded to individual caveolae and in clusters of these structures. This colocalization was confirmed by immunofluorescence microscopy in paraformaldehyde-fixed 3T3-L1 adipocyte plasma membrane sheets. The immunofluorescence labeling pattern appeared as doughnut-like spots of 0.3–0.5 μm diameter, a size that was noted to be similar to that of the caveolae clusters visualized by EM. Biochemically, the IR cofractionated with caveolin in detergent-free isolation of rafts from rat adipocyte plasma membranes. The addition of insulin was not associated with a significant change in localization of the IR, as assessed biochemically or by immunofluorescence. Even low concentrations of Triton X-100 (0.1%) completely solubilized the β-subunit of the IR from the caveolin-enriched fractions. This observation may explain why Mastick and coworkers (1998) found only trace amounts of the IR in rafts prepared on the basis of detergent insolubility. The molecular basis for the (partial or transient) localization of IR at lipid rafts may rely on the interaction of IR with caveolin-1, which is assumed to differentially modulate insulin signaling, as has been demonstrated by Nystrom and coworkers (1999).

PROCEDURE

Samples of appropriate fractions from the sucrose gradient are mixed with 10 volumes of 3% paraformaldehyde and 1.5% glutaraldehyde in 0.1 M sodium cacodylate, pH 7.4 (final conc.). The sample is incubated (40 min, 4°C) followed by centrifugation (100,000 × *g*, 90 min). The pellet is washed twice with 0.1 M sodium cacodylate (pH 7.4), treated with 1% OsO_4 for 1 h, and washed twice with 0.1 M sodium cacodylate. Samples were stepwise dehydrated in ethanol, treated with 1% uranyl acetate in ethanol, and embedded in Epon. Thin sections (50 nm) were stained with uranyl acetate and lead by standard procedures and examined and micrographed in an electron microscope.

Samples of the caveolae-enriched fractions are also examined following negative staining after fixation with 2% paraformaldehyde. The material is attached to carbon and pioloform-coated nickel grids for 20 min. The grids are washed three times for 5 min with phosphate-buffered saline before staining with 1% uranyl acetate for 2 min and micrographing in an electron microscope.

EVALUATION

An insulin-independent pathway has been described that mimics the metabolic actions of insulin in adipocytes (Müller et al. 2001a, b). This pathway can be stimulated in adipocytes by exogenous phosphoinositolglycans (PIG), cleavage products of the glycosyl-phophatidylinositol (GPI) anchor of GPI-linked proteins, which have initially been proposed to act as soluble mediators of insulin action, but do not share structural and functional similarity with the typical second messengers regulating glycogen metabolism in response to adrenergic hormones (Wasner et al. 2003). PIG treatment of isolated rat adipocytes leads to concentration-dependent increases in tyrosine phosphorylation of IRS-1, IRS-1-associated PI3-K activity, and glucose uptake in an insulin-independent fashion. A critical mechanism in this pathway may involve the dissociation of the non-RTK, Lyn and Fak, from caveolin-1 (Müller et al. 2000), their activation by tyrosine phosphorylation, and their redistribution from rafts to non-raft membranes (Müller et al. 2001b, Müller et al. 2005). Incubation of adipocytes with PIG, as with insulin, is followed by tyrosine phosphorylation of caveolin-1. The same research group succeeded in the characterization and identification of a specific binding protein for synthetic PIG in the lipid rafts of the adipocyte plasma membrane (Müller et al. 2002a, b). The involvement of lipid rafts in insulin-mimetic signaling by PIG was demonstrated by complete abrogation of redistribution of signaling proteins and IRS-1 tyrosine phosphorylation in response to PIG challenge of rat adipocytes, which have been depleted of lipid rafts by prior cholesterol removal from the plasma membrane (Müller et al. 2002e). The physiological role of this pathway and its potential cross talk with the insulin-signaling pathway in caveolae remain to be determined (Müller 2002d). These questions will be facilitated by molecular cloning and inactivation or overexpression of the gene coding for this PIG receptor in 3T3-L1 adipocytes.

Several laboratories have investigated whether there is overlap between membrane compartments that contain caveolin and GLUT4. Using biochemical isolation techniques, Scherer and coworkers (1994) detected a transient increase in GLUT4 immunoreactivity in rafts after insulin stimulation of 3T3-L1 adipocytes. Also, insulin stimulation led to an increase in plasma membrane caveolin and a corresponding decrease in caveolin detected in low-density microsomes. These investigators detected caveolin in GLUT4 vesicles immunoisolated from rat adipocytes. Kandror and coworkers (1995) conducted similar studies but arrived at a different conclusion. They found that intracellular caveolin and GLUT4 were detectable on vesicles of similar size and buoyant density and

that these vesicles translocated to the plasma membrane in response to insulin. However, in contrast to the findings of Scherer and coworkers (1994), only limited amounts of caveolin protein were present in immunoabsorbed GLUT4 vesicles, which suggested that the intracellular pools of these proteins, although biophysically similar, were distinct. Gustavsson and coworkers (1996) isolated subcellular membrane fractions from rat adipocytes and performed glucose uptake assays on intact adipocytes at various times during an insulin pulse. On basis of the results obtained, the authors propose a model such that, upon insulin stimulation, GLUT4 moves first to the PM and then to detergent-resistant plasma membrane microdomains (caveolae?), where GLUT4-mediated glucose transport occurs. Taken together, at this point the weight of the published data supports localization of a significant subset of plasma membrane IR and GLUT4 to caveolae in adipocytes, nut the issue is not settled (for a review see Bickel 2002).

REFERENCES AND FURTHER READING

Abedinpour P, Jergil B (2003) Isolation of a caveolae-enriched fraction from rat lung by affinity partitioning and sucrose gradient centrifugation. Anal Biochem 313:1–8

Anderson RGW (1993a) Caveolae: where incoming and outgoing messengers meet. Proc Natl Acad Sci USA 90:10909–10913

Anderson RGW (1993b) Plasmalemmal caveolae and GPI-anchored membrane proteins. Curr Opin Cell Biol 5:647–652

Anderson RGW (1998) The caveolae membrane system. Annu Rev Biochem 67:199–225

Anderson RGW, Jacobson K (2002) A role for lipid shells in targeting proteins to caveolae, rafts, and other lipid domains. Science 296:1821–1825

Avruch J, Wallach DFH (1971) Preparation and properties of plasma membrane and endoplasmatic reticulum fragments from isolated fat cells. Biochim Biophys Acta 233:334–347

Baumann CA, Brady MJ, Saltiel AR (2001) Activation of glycogen synthase by insulin in 3T3-L1 adipocytes involves c-Cbl-associating protein (CAP)-dependent and CAP-independent signaling pathways. J Biol Chem 276:6065–6068

Bauman CA, Ribon V, Kanzaki M, Thurmond DC, Mora S, Shigematsu S, Bickel PE, Pessin JE, Saltiel AR (2000) CAP defines a second signalling pathway required for insulin-stimulated glucose transport. Nature 407:202–207

Bickel PE (2002) Lipid rafts and insulin signaling Am J Physiol Endocrinol Metab 282:E1-E10

Brown DA, Rose JK (1992) Sorting of GPI-anchored proteins to glycolipid-enriched membrane subdomains during transport to the apical cell surface. Cell 68:533–544

Brown DA, London E (1997) Breakthroughs and Views. Structure of detergent-resistant membrane domains: Does phase separation occur in biological membranes ? Biochem Biophys Res Commun 240:1–7

Brown DA, London E (1998) Structure and origin of ordered lipid domains in biological membranes. J Membr Biol 164:103–114

Capozza F, Combs TP, Cohen AW, Cho Y-R, Park S-Y, Scherer PE, Kim JK, Lisanti MP (2005) Caveolin-3 knockout mice show increased adiposity and whole body insulin resistance, with ligand-induced insulin receptor instability in skeletal muscle. Am J Physiol Cell Physiol 288:C1317-C1331

Chang W-J, Ying Y, Rothberg KG, Hooper NM, Turner AJ, Gambliel HA, Gunzberg JD, Munmby SM, Gilamn AG, Anderson RGW (1994) Purification and characterization of smooth muscle cell caveolae. J Cell Biol 126:127–138

Chiang SH, Baumann CA, Kanzaki M, Thurmond DC, Watson RT, Neudauer CL, Macara IG, Pessin JE, Saltiel AR (2001) Insulin-stimulated GLUT4 translocation requires the CAP-dependent activation of TC10. Nature 410:944–948

Cohen AW, Razani B, Schubert W, Williams TM, Wang XB, Iyengar P, Brasaemle DL, Scherer PE, Lisanti MP (2004) Role of caveolin-1 in the modulation of lipolysis and lipid droplet formation. Diabetes 53:1261–1270

Couet J, Li S, Okamoto T, Ikezu T, Lisanti MP (1997a) Identification of peptide and protein ligands for the caveolin-scaffolding domain. J Biol Chem 272:6525–6533

Couet J, Sargiacomo M, Lisanti MP (1997b) Interaction of a receptor tyrosine kinase, EGF-R, with caveolins. Caveolin binding negatively regulates tyrosine and serine/threonine kinase activities. J Biol Chem 272:30429–30438

Drab M, Verkade P, Elger M, Kasper M, Lohn M, Lauterbach B, Menne J, Lindschau C, Mende F, Luft FC (2001) Loss of caveolae, vascular dysfunction and pulmonary defects in caveolin-1 gene-disrupted mice. Science 293:2449–2452Edidin M (2003) The state of lipid rafts: from model membranes to cells. Annu Rev Biophys Biomol Struct 32:257–283

Ekblad L, Jergil B (2001) Localization of phosphatidylinositol 4-kinase isoenzymes in rat liver plasma membrane domains. Biochim Biophys Acta 1531:209–221

Fan JY, Carpentier JL, van Obberghen E, Grunfeld C, Gordon P, Orci L (1983) Morphological changes of the 3T3-L1 fibroblast plasma membrane upon differentiation to the adipocyte form. J Cell Sci 61:219–230

Glenney JR (1992) The sequence of human caveolin reveals identity with VIP 21, a component of transport vesicles. FEBS Lett 314:45–48

Gustavsson J, Parpal S, Karsson M, Ramsing C, Thorn H, Borg M, Lindroth M, Peterson KH, Magnusson KE, Stralfors P (1999) Localization of the insulin receptor in caveolae of adipocyte plasma membrane. FASEB J 13:1961–1971

Gustavsson J, Parpal S, Stralfors P (1996) Insulin-stimulated glucose uptake involves the transition of glucose transporters to a caveolae-rich fraction within the plasma membrane. Implications for Type II diabetes. Mol Med 2:367–372

Harder TP, Scheiffele P, Verkade P, Simons K (1998) Lipid domain structure of the plasma membrane revealed by patching of membrane components. J Cell Biol 141:929–942

Ishikawa Y, Otsu K, Oshikawa J (2005) Caveolin, different roles for insulin signal. Cell Signal 17:1175–1182

Jones DR, Varela-Nieto I (1999) Diabetes and the role of inositol-containing lipids in insulin signaling. Mol Med 5:505–514

Ju H, Zou R, Venema VJ, Venema RC (1997) Direct interaction of endothelial nitric-oxide synthase and caveolin-1 inhibits synthase activity. J Biol Chem 272:18522–18525

Kandror KV, Stephens JM, Pilch PF (1995) Expression and compartimentalization of caveolin in adipose cells: co-

ordinate regulation with and structural segregation from GLUT4. J Cell Biol 129:999–1006
Kobzik T, Smith W, Kelly RA, Michel T (1996) Endothelial nitric oxide synthase targeting to caveolae. J Biol Chem 271:22810–22814
Kurzchalia TV, Dupree P, Monier S (1994) VIP-21 Caveolin, a protein of the trans-Golgi network and caveolae. FEBS Lett 346:88–91
Langtry HD, Balfour JA (1998) Glimepiride – A review of its pharmacological and clinical efficacy in the management of type 2 diabetes mellitus. Drugs 55:563–584
Lisanti MP, Scherer PE, Tang ZL, Sargiacomo M (1994) Caveolae, caveolin and caveolin-rich membrane domains: A signaling hypothesis. Trends Cell Biol 4:231–235
Macdonald JL, Pike LJ (2005) A simplified method for the preparation of detergent-free lipid rafts. J Lipid Res 46:1061–1067
Mastick CC, Brady MJ, Printen JA, Ribbon V, Saltiel AR (1998) Spatial determinants of specificity of insulin action. Mol Cell Biochem 182:65–71
Mastick CC, Brady MJ, Saltiel AR (1995) Insulin stimulates the tyrosine phosphorylation of caveolin. J Cell Biol 129:1523–1531
Mayor S, Maxfield FR (1995) Insolubility and redistribution of GPI-anchored proteins at the cell surface after detergent treatment. Mol Biol Cell 6:929–944
Meshulam T, Simard JR, Wharton J, Hamilton JA, Pilch PF (2006) Role of caveolin-1 and cholesterol in transmembrane fatty acid movement. Biochemistry 45:2882–2893
Mineo C, Ying Y-S, Chapline C, Jaken S, Anderson RGW (1998) Targeting of protein kinase C alpha to caveolae. J Cell Biol 141:601–610
Moffett S, Brown DA, Linder ME (2000) Lipid-dependent targeting of G proteins into rafts. J Biol Chem 275:2191–2198
Müller G (2000) The molecular mechanism of the insulin-mimetic/sensitizing activity of the antidiabetic sulfonylurea drug Amaryl. Mol Med 6:907–933
Müller G (2002d) Dynamics of plasma membrane microdomains and Cross-Talk to the Insulin Signalling Cascade (Invited Review) FEBS Lett 531:81–87
Müller G, Frick W (1999) Signalling via caveolin: involvement in the cross-talk between phosphoinositolglycans and insulin. CMLS, Cell Mol Life Sci 56:945–970
Müller G, Hanekop N, Kramer W, Bandlow W, Frick W (2002a) Interaction of phosphoinositolglycan(-peptides) with plasma membrane lipid rafts of rat adipocytes. Arch Biochem Biophys 408:17–32
Müller G, Hanekop N, Wied S, Frick W (2002c) Cholesterol depletion blocks redistribution of lipid raft components and insulin-mimetic signaling by glimepiride and phosphoinositolglycans in rat adipocytes. Mol Med 8:120–136
Müller G, Jung C, Frick W, Bandlow W, Kramer W (2002b) Interaction of phosphoinositolglycan(-peptides) with plasma membrane lipid rafts triggers insulin-mimetic signaling in rat adipocytes. Arch Biochem Biophys 408:7–16
Müller G, Jung C, Wied S, Welte S, Frick W (2001a) Insulin-mimetic signaling by the sulfonylurea glimepiride and phosphoinositolglycans involves distinct mechanisms for redistribution of lipid raft components. Biochemistry 40:14603–14620
Müller G, Jung C, Wied S, Welte S, Jordan H, Frick W (2001b) Redistribution of glycolipid raft domain components induces insulin-mimetic signaling in rat adipocytes. Mol Cell Biol 21:4553–4567
Müller G, Schulz A, Wied S, Frick W (2005) Regulation of lipid raft proteins by glimepiride- and insulin-induced glycosylphosphatidylinositol-specific phospholipase C in rat adipocytes. Biochem Pharmacol 69:761–780
Müller G, Welte S (2002e) Lipid raft domains are the targets for the insulin-independent blood glucose-decreasing activity of the sulfonylurea glimepiride. Recent Res Develop Endocrinol 3:401–423
Müller G, Wied S, Frick W (2000) Cross talk of $pp125^{FAK}$ and $pp59^{Lyn}$ non-receptor tyrosine kinases to insulin-mimetic signaling in adipocytes. Mol Cell Biol 20:4708–4723
Nystrom FH, Chen H, Cong LN, Li Y, Quon MJ (1999) Caveolin-1 interacts with the insulin receptor and can differentially modulate insulin signaling in transfected Cos-7 cells and rat adipose cells. Mol Endocrinol 13:2013–2024
Oh P, Schnitzer JE (1999) Immunoisolation of caveolae with high affinity antibody binding to the oligomeric caveolin cage. Toward understanding the basis of purification. J Biol Chem 274:23144–23154
Okamoto T, Schlegel A, Scherer PE, Lisanti MP (1998) Caveolins, a family of scaffolding proteins for organizing "preassembled signaling complexes" at the plasma membrane. J Biol Chem 273:5419–5422
Oshikawa J, Otsu K, Toya Y, Tsunematsu T, Hankins R, Kawabe J-I, Minamisawa S, Umemura S, Hagiwara Y, Ishikawa Y (2004) Insulin resistance in skeletal muscles of caveolin-3 null mice. Proc Natl Acad Sci USA 101:12670–12675
Parton RG (1996) Caveolae and caveolins. Curr Opin Cell Biol 8:542–548
Persson A, Johansson B, Olsson H, Jergil B (1991) Purification of rat liver plasma membranes by wheat-germ-agglutinin partitioning. Biochem J 237:173–177
Persson A, Jergil B (1992) Purification of plasma membranes by aqueous two-phase affinity partitioning. Anal Biochem 204:131–136
Pohl J, Ring A, Korkmaz Ü, Ehehalt R, Stremmel W (2005) FAT/CD36-mediated long-chain fatty acid uptake in adipocytes requires plasma membrane rafts. Mol Biol Cell 16:24–31
Pohl J, Ring A, Stremmel W (2002) Uptake of long-chain fatty acids in HepG2 cells involves caveolae: analysis of a novel pathway. J Lipid Res 43:1390–1399
Razani B, Combs TP, Wang XB, Frank PG, Park DS, Russel RG, Li M, Tang B, Jelicks LA, Scherer PE, Lisanti MP (2002) Caveolin-1 deficient mice are lean, resistant to diet-induced obesity and show hypertriglyceridemia with adipocyte abnormalities. J Biol Chem 277:8635–8647
Razani B, Engelman JA, Wang XB, Schubert W, Zhang XL, marks CB, Macaluso F, Russell RG, Li M, Pestell RG (2001) Caveolin-1 null mice are viabele, but show evidence for hyper-proliferative and vascular abnormalities. J Biol Chem 276:38121–38138
Razani B, Woodman SE, Lisanti MP (2002) Caveolae: From cell biology to animal physiology. Pharmacol Rev 54:431–467
Ribon V, Printen JA, Hoffman NG, Kay BK, Saltiel RA (1998) A novel, multifunctional c-Cbl binding protein in insulin receptor signaling in 3T3-L1 adipocytes. Mol Cell Biol 18:872–879
Rietveld A, Simons K (1998) The differential miscibility of lipids as the basis for the formation of functional membrane rafts. Biochim Biophys Acta 1376:467–479
Rothberg KG, Henser JE, Donzell WC, Ying Y-S, Glenney JR, Anderson RGW (1992) Caveolin, a protein component of caveolae membrane coats. Cell 68:673–682
Sargiacomo M, Sudol M, Tang Z, Lisanti MP (1993) Signal transducing molecules and glycosyl-phosphatidylinositol-linked proteins from a caveolin-rich insoluble complex in MDCK cells. J Cell Biol 122:789–807

Scherer PE, Lisanti MP, Baldini G, Sargiocomo M, Mastick CC, Lodish HF (1994) Induction of caveolin during adipogenesis and association of GLUT4 with caveolin-rich vesicles. J Cell Biol 127:1233–1243

Schlegel A, Volonte D, Engelman JA, Galbiati F, Mehta P, Zhang X-L (1998) Crowded little caves: structure and function of caveolae. Cell Signal 10:457–463

Schnitzer JE, McIntosh DP, Dvorak AM, Liu J, Oh P (1995a) Separation of caveolae from associated microdomains of GPI-anchored proteins. Science 269:1435–1439

Schnitzer JE, Oh P, Jaconson BS, Dvorak AM (1995b) Caveolae from luminal plasmalemma of rat lung endothelium: Microdomains enriched in caveolin, Ca2+-ATPase, and inositol trisphosphate receptor. Proc Natl Acad Sci USA 92:1759–1763

Shaul PW, Anderson RG (1998) Role of plasmalemmal caveolae in signal transduction. Am J Physiol Lung Cell Mol Physiol 275:L843-L851

Simons K, Ikonen E (1997) Functional rafts in cell membranes. Nature 387:569–572

Simons K, Toomre D (2000) Lipid rafts and signal transduction. Nat Rev Mol Cell Biol 1:31–39

Smart EJ, Graf GA, McNiven MA, Sessa WC, Engelman JA, Scherer PE, Okamoto T, Lisanti MP (1999) Caveolins, liquid-ordered somains, and signal transduction. Mol Cell Biol 19:7289–7304

Smart EJ, Ying Y, Mineo C, Anderson RGW (1995) A detergent-free method for purifying caveolae membrane from tissue culture cells. Proc Natl Acad Sci USA 92:10104–10108

Song KS, Li S, Okamoto T, Quilliam LA, Sargiacomo M, Lisanti MP (1996) Co-purification and direct interaction of Ras with caveolin, an integral membrane protein of caveolae microdomains. J Biol Chem 271:9690–9697

Stan R-V, Roberts WG, Predescu K, Ihida L, Saucan L, Ghitescu L, Palade GE (1997) Immunoisolation and partial characterization of endothelial plasmalemmal vesicles (caveolae). Mol Biol Cell 8:595–605

Wasner HK, Müller G, Eckel J (2003) Direct comparison of inositol phosphoglycan with prostaglandylinositol cyclic phosphate, two potential mediators of insulin action. Exp Clin Endocrinol. Diabetes 111, 358–363

K.6.3.6.4 Glycosyl-Phosphatidylinositol-Specific Phospholipase (GPI-PL) and Insulin-Like Signaling

GENERAL CONSIDERATIONS

Insulin-responsive mammalian cells and tissues express a number of GPI-proteins, the majority of them with their GPI anchor embedded in the outer leaflet of the plasma membranes as well as some lipases, the (G)PI-PLC/D, which may control down-regulation of GPI-protein cell surface expression and simultaneously up-regulation of the soluble protein moiety released into circulation (Romero et al. 1988, Low 1989 and 1990, Thomas 1990, Romero and Larner 1993, Saltiel 1990, Saltiel et al. 1986, Müller and Bandlow 1991, Varela-Nieto et al. 1996, Nosjean et al. 1997, Jones and Varela-Nieto 1999, Müller et al. 2005). In fact, soluble forms of GPI-proteins have been detected in human plasma, such as 5′-nucleotidase, Thy-1, alkaline phosphatase and CD16 receptors, and GPI-PLC have been found in human neutrophils, bovine brain, rat intestine and a human carcinoma cell line. The GPI anchor consisting of three mannose residues and a non-acetylated glucosamine, one end of which amide-linked to the protein moiety *via* a phosphoethanolamine bridge and the other end glycosidically linked to the 6-hydroxyl group of PI, is cleaved by (G)PI-PLC/D releasing diacylglycerol or phosphatidic acid, respectively, and leaving a terminal inositolglycan structure at the protein moiety harbouring (PIG) or lacking a (cyclic) phosphate residue (for reviews see Chan et al. 1988, Cross 1990, Ferguson 1991, Müller 2000).

In eukaryotes, some GPI-PLC/D are up-regulated by glucose as well as certain hormones, growth factors and drugs (e. g. insulin, glimepiride) in rodent adipocytes, myocytes and human endothelial cells (Müller et al. 1993, 1994a, 1994c, Mohavedi and Hooper 1997). In particular, the antidiabetic drug, glimepiride, which lowers blood glucose predominantly by stimulation of insulin release from pancreatic β-cells and, in addition, to a minor degree by mimicking metabolic insulin action in peripheral tissues, such as activation of glucose transport in muscle cells and inhibition of lipolysis in adipocytes (Müller et al. 1994d, Bähr et al. 1995), has been demonstrated to activate a GPI-PLC. Upon treatment of primary or cultured rodent adipocytes with pharmacological concentrations of this sulfonylurea, a potent amphiphilic-to-hydrophilic conversion of a subset of GPI-proteins by activation of a GPI-PLC has been observed (Müller et al. 1993, 1994b). The functional and physiological significance of the insulin- and glimepiride-regulated lipolytic cleavage of GPI-proteins in mammalian cells is not well understood at present, albeit initially a role as soluble mediators for metabolic insulin action has been proposed (Farese 1990, Fonteles et al. 1996, Gaulton 1994, Larner 1987, Lazar et al. 1994, Lisanti et al. 1989, Mato 1989, Low and Saltiel 1988, Lawrence et al. 1986, Müller 2002a, Romero 1990, Shaskin et al. 1997, Saltiel et al. 1988).

PURPOSE AND RATIONALE

Recently, a synthetic inositol derivative, GPI-2350, has been described which inhibits the well-characterized bacterial, trypanosomal and serum (G)PI-PLC/D with high potency and selectivity (Müller et al. 2005). Using GPI-2350, which almost completely down-regulates the insulin- and glimepiride-inducible GPI-PLC in intact rat adipocytes, a major role for this enzyme in metabolic insulin signalling and action in

these cells could be excluded. In contrast, activation of the GPI-PLC turned out to be indispensable for the insulin-mimetic effects of glimepiride *via* the recently described IR-independent cross-talk from lipid rafts to the IRS-1 protein (see above). Based on the criteria for lipid rafts, certain GPI-anchored, acylated and transmembrane signalling proteins have been found to be enriched in rafts *vs* non-raft areas of the plasma membranes. Furthermore, rafts are not homogenous in composition and structure since subspecies of higher (hcRafts) and lower cholesterol (lcRafts) content can be distinguished from one another on the basis of their lower and higher buoyant density, respectively (Müller 2005, Müller et al. 2005). Strikingly, the stimulus-induced redistribution of certain GPI-anchored as well as acylated signalling proteins from hcRafts to lcRafts (Müller et al. 2001a, b) is blocked by GPI-2350. This finding hints to a role of the mammalian GPI-PLC in the control of the localization and activation of signalling proteins within rafts during signal transduction across the plasma membrane of adipocytes. The following assays enable the analysis of the role of the GPI-PL for insulin-like signaling and metabolic action in insulin target cells as well as of the effects of compounds/drug candidates on the activity of the GPI-PL. The GPI-PL may turn out as promising target for future anti-diabetic drugs (Müller and Frick 1999, Müller 2002b, Müller and Welte 2002).

K.6.3.6.4.1 Activity Assay for GPI-PL

PROCEDURE

Adipocyte GPI-PLC

Adipocyte GPI-PLC (5–25 µg PM or hc/lcRafts) is assayed as the conversion of GPI-protein, acetylcholinesterase (AchE) from its amphiphilic version (containing the intact GPI anchor) into its hydrophilic version (containing the lipolytically cleaved GPI anchor) are assayed according to a protocol adapted from Müller and coworkers (1994b) by incubation with 10 µl of bovine erythrocyte AChE solution (12 U/ml in 10 mM Tris/HCl, pH 7.4, 144 mM NaCl, 0.1% TX-100) in 100 µl of 20 mM HEPES/KOH (pH 7.8), 144 mM NaCl, 0.1% TX-100, 0.2 mM $MgCl_2$ for 1 h at 25°C and subsequent termination by adding 5 µl of glacial acetic acid and then 0.4 ml of 10 mM Tris/HCl (pH 7.4), 144 mM NaCl. Each reaction mixture is subjected to TX-114 partitioning (see below). The GPI-PLC activity is calculated as the amphiphilic-to-hydrophilic conversion of the GPI-protein substrates from the ratio of the activities of hydrophilic 5′-Nuc or AChE measured in the TX-114-depleted phase and the total activity measured before partitioning and corrected for the non-enzymatic background in the TX-114-depleted phase (accounting for 10–20% of the total activity) as revealed by blank incubations lacking (G)PI-PLC.

TX-114 partitioning

Pelleted hc/lcRafts (10–50 µg protein) or GPI-PL reaction mixtures (0.5 ml) are separated into amphiphilic and hydrophilic proteins using partitioning between TX-114-enriched and depleted phases according to Bordier (1981) and Pryde and Phillips (1986) by suspending in 1 ml or mixing with 0.5 ml, respectively, of ice-cold 25 mM Tris/HCl (pH 7.4), 144 mM NaCl containing 1 or 2% TX-114. After incubation for 1 h on ice, the mixture is layered onto a cushion of 0.4 ml of 0.25 M sucrose and 25 mM Tris/HCl (pH 7.4) on ice. Phase separation is induced by warming up to 37°C and subsequent centrifugation (10,000 × *g*, 1 min). After re-extraction of the lower TX-114-enriched phase, aliquots of the pooled upper TX-114-depleted phase are measured for AChE activity or precipitated (15% polyethylene glycol 4000) for SDS-PAGE analysis.

EVALUATION

Concentration-response curves are established using various concentrations of standard (human insulin) and the test compounds, e. g. sulfonylureas, allowing calculation of EC_{50} values and potency ratios.

K.6.3.6.4.2 GPI-PL-Dependent Translocation of GPI Proteins Within Lipid Rafts

PROCEDURE

Photoaffinity Labeling of the GPI Protein, Gce1

Solubilized plasma membranes and rafts (5–10 µg protein) are incubated (30 min, 4°C) with 50 µCi 8-N_3-[^{32}P]cAMP (0.5 nmol) in 50 µl of 10 mM Tris/HCl (pH 7.4), 1 mM EDTA, 0.5 mM EGTA, 140 mM NaCl, 10 mM $MgCl_2$, 2 mM $MnCl_2$, 1 mM isobutylmethylxanthine, 1 mM DTT, 1 mM AMP, and protease inhibitors in the wells of microtiter plates (96-formate) and then irradiated with UV light (254 nm, 8000 µW/cm^2) at a distance of 0.5 cm for 1 min (Müller et al. 1993, 1994a, b). Subsequently, the photoaffinity labeling reaction is quenched by addition of 100 µl of the same buffer containing 10 mM cAMP. Gce1 is precipitated (5% trichloroacetic acid, 1 h on ice, 10,000 × *g*, 15 min) and solubilized in sample buffer for SDS-PAGE. Protein concentration is determined using the BCA protein determination kit from Pierce. Autoradiographs and direct photoimages

are processed and quantified by computer-assisted video densitometry (e. g. Storm 860 PhosphorImager system, Molecular Dynamics). The recovery in the amounts of immunoprecipitated protein has to be corrected (data on fold- or % stimulation) for the amount of protein actually applied onto the gel as revealed by homologous immunoblotting.

Preparation of lc/hcRafts

Pre-treated and subsequently washed adipocytes are homogenized in lysis buffer (25 mM MES, pH 6.0, 140 mM NaCl, 2 mM EDTA, 0.5 mM EGTA, 0.25 M sucrose, 50 mM NaF, 5 mM sodium pyrophosphate, 10 mM glycerol-3-phosphate, 1 mM sodium orthovanadate and protease inhibitors) using a motor-driven Teflon-in-glass homogenizer (10 strokes). Plasma mmebranes are obtained by differential centrifugation of the defatted postnuclear infranatant (= cytosolic fraction) and then purified by two sequential centrifugation steps through sucrose and Percoll cushions as described above and finally suspended in 25 mM Tris/HCl (pH 7.4), 0.25 M sucrose, 1 mM EDTA at 2 mg protein/ml. hc/lcRafts are obtained by the detergent method and discontinuous sucrose gradient centrifugation as reported above. The light-scattering opalescent bands at the 0.5–0.65 M (fractions 3 + 4) and 0.8–0.9 M (fractions 5 + 6) sucrose interfaces are collected as hcRafts and lcRafts, respectively, with density measurement using the refractive index. hc/lcRafts are collected by centrifugation (50,000 × *g*, 30 min, 4°C) after three-fold dilution of the pooled gradient fractions with 25 mM MES (pH 6.5), 1% TX-100, 150 mM NaCl, and then characterized (immunoblotting, enzyme assays) by enrichment/deprivation of relevant marker proteins as described above or subjected to TX-114 partitioning (see K.6.3.6.4.1). For immunoprecipitation of caveolin, rafts are solubilized (1 h, 4°C) in 10 mM Tris/HCl (pH 7.4), 150 mM NaCl, 1% TX-100, 60 mM β-octylglucoside, 0.3% deoxycholate, 5 mM EDTA, 0.5 mM EGTA, 1 mM sodium orthovanadate, 50 mM NaF, 1 µM microcystin and protease inhibitors and centrifuged (50,000 × *g*, 30 min). For direct immunoblotting, rafts are solubilized in two-fold Laemmli sample buffer and centrifuged (10,000 × *g*, 5 min). The supernatants are used.

EVALUATION

The following working hypothesis for signal generation in and transduction across the PM of rat adipocytes on the basis of the redistribution of lipid-modified signalling proteins, such as GPI-proteins and acylated tyrosine kinases, within rafts has been deduced from the present experimental findings (Müller 2005). (1) Amphiphilic GPI-proteins with intact GPI anchor as well as hydrophilic GPI-proteins with lipolytically cleaved GPI anchor preferentially accumulate at hcRafts versus lcRafts. (2) Only uncleaved GPI-proteins redistribute from hcRafts to lcRafts in response to glimepiride and insulin. Apparently, the GPI anchor functions as a signal for the recruitment to rafts *versus* non-raft areas, but does not determine the targeting to lcRafts or hcRafts. The current working model implicates that the PIG core structure of the GPI anchor functions as the only hcRafts-targeting signal (*via* recognition through the receptor protein, p115) for a subset of GPI-proteins which are amenable to stimulus-induced redistribution to lcRafts. The present findings strongly suggest the expression of three distinct subspecies of rafts in the plasma membranes of rat adipocytes: (i) TX-100- and Lubrol-WX-insoluble hcRafts, (ii) TX-100-soluble and Lubrol-WX-insoluble lcRafts in the basal state and (iii) TX-100- and Lubrol-WX-insoluble lcRafts upon glimepiride challenge. This is more compatible with the model of heterogenous rafts rather than that of layered rafts or homogenous rafts with selective lipid extraction as has been recently proposed for their heterogenous structure as well as their biogenesis and maintenance (Macdonald and Pike 2005). Accordingly, layered rafts are constituted of rings ranging from a liquid-ordered cholesterol- and glycosphingolipid-enriched core through less ordered regions into the liquid-disordered non-raft areas of the residual PM, the core of which is left as hcRafts after TX-100 solubilization, whereas core and immediately surrounding areas are left unsolubilized by Lubrol-WX. Homogenous rafts are liquid-ordered domains of a uniform mixture of the protein and lipid constituents are surrounded by the liquid-disordered phase of the plasma membranes which are selectively solubilized by TX-100 and Lubrol-WX (Macdonald and Pike 2005). Both models can hardly explain the existence of TX-100-insoluble lcrafts or their generation from hcrafts in response to glimepiride. In contrast, heterogenous rafts of different lipid and protein composition could coexist as separate structural entities in the membrane and be differentially solubilized by TX-100 and Lubrol-WX. It is conceivable that the glimepiride-induced translocation of certain GPI-anchored and acylated signalling proteins from distinct hcRafts accompanied by the limited loss of cholesterol results in the *de novo* generation of lcRafts of increased buoyant density retaining TX-100 insol-

ubility to a partial degree. Alternatively, the translocated raft protein components may be recruited directly from discrete hcRafts into pre-existing Lubrol-WX-insoluble (TX-100-soluble) lcRafts thereby rendering them partially insoluble in TX-100.

In conclusion, the adipocyte GPI-PL has now been recognized as a critical component specifically operating in the insulin-like signalling cascade triggered by glimepiride rather than in insulin signalling. Furthermore, insulin-like signalling by glimepiride is not significantly impaired in the insulin-resistant state as reported previously for rat adipocytes *in vitro* (Müller and Wied 1993). Therefore, the adipocyte GPI-PLC might represent a useful target for the therapy of type II diabetes mellitus.

REFERENCES AND FURTHER READING

Bordier C (1981) Phase separation of integral membrane proteins in Triton X-114 solution. J Biol Chem 256:1604–1607

Chan BL, Lisanti MP, Rodriguez-Boulan E, Saltiel AR (1988) Insulin-stimulated release of lipoprotein lipase by metabolism of its phosphatidinylinositol anchor. Science 241:1670–1672

Cross GAM (1990) Glycolipid anchoring of plasma membrane proteins. Ann Rev Cell Biol 6:1–39

Farese RV (1990) Lipid-derived mediators in insulin action. Proc Soc Exp Biol Med 195:312–324

Ferguson MAJ (1991) Lipid anchors on membrane proteins. Curr Opin Struct Biol 1:522–529

Fonteles MC, Huang LC, Larner J (1996) Infusion of pH 2.0 D-chiro-inositol glycan insulin putative mediator normalizes plasma glucose in streptozotocin diabetic rats at a dose equivalent to insulin without inducing hypoglycemia. Diabetologia 39:731–734

Gaulton GN, Pratt JC (1994) Glycosylated phosphatidylinositol molecules as second messengers. Semin Immunol 6:97–104

Jones DR, Varela-Nieto I (1998) The role of glycosyl-phosphatidylinositol in signal transduction. Int J Biochem Cell Biol 30:313–326

Larner J (1987) Banting lecture: Insulin signaling mechanisms. Lessons from the old testament of glycogen metabolism and the new testament of molecular biology. Diabetes 37:262–275

Lawrence JC, Hiken JF, Inkster M, Scott CW, Mumby MC (1986) Insulin stimulates the generation of an adipocyte phosphoprotein that is isolated with a monoclonal antibody against the regulatory subunit of bovine heart cAMP-dependent protein kinase. Proc Natl Acad Sci USA 83:3649–3653

Lazar DF, Knez JJ, Medof ME, Cuatrecasas P, Saltiel AR (1994) Stimulation of glycogen synthesis by insulin in human erythroleukemia cells requires the synthesis of glycosyl-phosphatidylinositol. Proc Natl Acad Sci USA 91:9665–9669

Lewis KA, Garigapati VR, Zhou C, Roberts MF (1993) Substrate requirements of bacterial phosphatidinylinositol-specific phospholipase C. Biochem 32:8836–8841

Lisanti MP, Darnell JC, Chan BL, Rodriguez-Boulan E, Saltiel AR (1989) The distribution of glycosyl-phosphatidylinositol anchored proteins is differentially regulated by serum and insulin. Biochem Biophys Res Comm 164:824–832

Low MG (1989) The glycosyl-phosphatidylinositol anchor of membrane proteins. Biochim Biophys Acta 988:427–454

Low MG (1990) Degradation of glycosyl-phosphatidylinositol anchors by specific phospholipases. In: Turner AJ (ed) Molecular and Cell Biology of Membrane Proteins. Glycolipid Anchors of Cell-surface Proteins. Ellis Horwood, New York, pp 35–63

Low MG, Saltiel AR (1988) Structural and functional roles of glycosyl-phosphatidylinositol in membranes. Science 239:268–275

Low MG, Stiernberg J, Waneck GL, Flavell RA, Kincade PW (1988) Cell-specific heterogeneity in sensitivity of phosphatidinylinositol-anchored membrane antigens to release by phospholipase C. J Immunol Meth 113:101–111

Macdonald JL, Pike LJ (2005) A simplified method for the preparation of detergent-free lipid rafts. J Lipid Res 46:1061–1067

Mato JM (1989) Insulin mediators revisited. Cell Signal 1:143–146

Movahedi S, Hooper NM (1997) Insulin stimulates the release of the glycosyl phosphatidylinositol-anchored membrane dipeptidase from 3T3-L1 adipocytes through the action of a phospholipase C. Biochem J 326:531–537

Müller G (2000) The molecular mechanism of the insulin-mimetic/sensitizing activity of the antidiabetic sulfonylurea drug Amaryl. Mol Med 6:907–933

Müller G (2002a) Dynamics of plasma membrane microdomains and Cross-Talk to the Insulin Signalling Cascade (Invited Review) FEBS Lett 531:81–87

Müller G (2002b) Concepts and options for current insulin research and future anti-diabetic therapy. Recent Res Develop Endocrinol 3:199–218

Müller G (2005) The mode of action of the antidiabetic drug glimepiride-beyond insulin secretion. Curr Med Chem – Immune Metab Agents 5:499–518

Müller G, Bandlow W (1991) A cAMP binding ectoprotein in the yeast*Saccharomyces cerevisiae*. Biochemistry 30:10181–10190

Müller G, Dearey E-A, Korndörfer A, Bandlow W (1994a) Stimulation of a glycosyl phosphatidylinositol-specific phospholipase by insulin and the sulfonylurea, glimepiride, in rat adipocytes depends on increased glucose transport. J Cell Biol 126:1267–1276

Müller G, Dearey EA, Pünter J (1993) The sulfonylurea drug, glimepiride, stimulates release of glycosylphosphatidylinositol-anchored plasma membrane proteins from 3T3 adipocytes. Biochem J 289:509–521

Müller G, Frick W (1999) Signalling via caveolin: involvement in the cross-talk between phosphoinositolglycans and insulin. CMLS, Cell Mol Life Sci 56:945–970

Müller G, Hanekop N, Wied S, Frick W (2002) Cholesterol depletion blocks redistribution of lipid raft components and insulin-mimetic signaling by glimepiride and phosphoinositolglycans in rat adipocytes. Mol Med 8:120–136

Müller G, Jung C, Wied S, Welte S, Frick W (2001a) Insulin-mimetic signaling by the sulfonylurea glimepiride and phosphoinositolglycans involves distinct mechanisms for redistribution of lipid raft components. Biochemistry 40:14603–14620

Müller G, Jung C, Wied S, Welte S, Jordan H, Frick W (2001b) Redistribution of glycolipid raft domain components induces insulin-mimetic signaling in rat adipocytes. Mol Cell Biol 21:4553–4567

Müller G, Korndörfer A, Saar K, Karbe-Thönges B, Fasold H, Müllner S (1994b) 4′-amino-benzamido-taurocholic acid selectively solubilizes glycosyl-phosphatidylinositol-anchored membrane proteins and improves lipolytic cleav-

age of their membrane anchors by specific phospholipases. Arch Biochem Biophys 309:329–340
Müller G, Schulz A, Wied S, Frick W (2005) Regulation of lipid raft proteins by glimepiride- and insulin-induced glycosylphosphatidylinositol-specific phospholipase C in rat adipocytes. Biochem Pharmacol 69:761–780
Müller G, Welte S (2002) Lipid raft domains are the targets for the insulin-independent blood glucose-decreasing activity of the sulfonylurea glimepiride. Recent Res Develop Endocrinol 3:401–423
Müller G, Wetekam E-A, Jung C, Bandlow W (1994c) Membrane association of lipoprotein lipase and a cAMP-binding ectoprotein in rat adipocytes. Biochemistry 33:12149–12159
Müller G, Wied S (1993) The sulfonylurea drug, glimepiride, stimulates glucose transport, glucose transporter translocation, and dephosphorylation in insulin-resistant rat adipocytes *in vitro*. Diabetes 42:1852–1867
Müller G, Wied S, Wetekam EM, Crecelius A, Pünter J (1994d) Stimulation of glucose utilization in 3T3 adipocytes and rat diaphragm *in vitro* by the sulfonylureas glimiperide and glibenclamide, is correlated with modulations of the cAMP regulatory cycle. Biochem Pharmacol 48:985–996
Nosjean O, Briolay A, Roux B (1997) Mammalian GPI proteins: sorting, membrane residence and functions. Biochim Biophys Acta 1331:153–186
Pryde JG, Phillips JH (1986) Fractionation of membrane proteins by temperature-induced phase separation in Triton X-114. Biochem J (1986) 233.525–533
Romero G, Larner J (1993) Insulin mediators and the mechanism of insulin action. Adv Pharm 24:21–50
Romero G, Luttrell L, Rogol A, Zeller K, Hewlett E, Larner J (1988) Phosphatidylinositol-glycan anchors of membrane proteins: Potential precursors of insulin mediators. Science 240:509–512
Romero GL, Gamez G, Huang LC, Lilley K, Luttrell L (1990) Antiinositolglycan antibodies selectively block some of the actions of insulin in intact BC_3H_1 cells. Proc Natl Acad Sci USA 87:1476–1480
Satiel AR (1990) Second messengers of insulin action. Trends Endocrinol Metab 1:158–163
Saltiel AR, Fox JA, Sherline P, Cuatrecasas P (1986) Insulin stimulates the generation from hepatic plasma membranes of modulators derived from an inositol glycolipid. Science 233:967–972
Saltiel AR, Osterman DG, Darnell JC, Sorbara-Cazan LR, Chan BL, Low MG, Cuatrecasas P (1988) The function of glycosyl phosphoinositides in hormone action. Phil Trans R Soc Lond B320:345–358
Shashkin PN, Shashkina EF, Fernqvist-Forbes E, Zhou Y-P, Grill V, Katz A (1997) Insulin mediators in man: Effects of glucose and insulin resistance. Diabetologia 40:557–563
Thomas JR, Dwek RA, Rademacher TW (1990) Structure, biosynthesis and function of gylcosylphosphatidinylinositols. Biochem 29:5413–5422
Varela-Nieto I, Leon Y, Caro HN (1996) Cell signalling by inositol phosphoglycans from different species. Comp Biochem Physiol 115B:223–241

K.6.4 Assays for Insulin and Insulin-Like Regulation of Gene and Protein Expression

Part of the blood glucose-lowering activity of insulin is based on massive and specific up- or downregulation of the gene expression for proteins/enzymes which directly regulate carbohydrate and lipid metabolism (e. g. GLUT4, PEPCK). Furthermore, changes in the intermediary metabolism provoked by insulin may secondarily lead to alterations in the gene/protein expression of other signalling/metabolic pathways. Consequently, it is important for the identification as well as characterization of compounds/drug candidates with insulin-like activity to analyze their effect on the expression of gene and proteins. For practical reasons, this analysis can be restricted to those genes/proteins which according to the present knowledge are relevant for mode of action of the compound/drug candidate. However, undoubtedly whole-genome or proteome searches for changes in the expression levels have important advantages, in particular due to its unbiased nature. However, they require considerable experimental expenditure and time on basis of conventional technology. This may change completely with the successful introduction of protein chips and DNA microarrays for the study of protein and gene expression and further increase its attractiveness for routine application in characterization of novel compounds/drug candidates.

K.6.4.1 Protein Chips

GENERAL CONSIDERATIONS

Currently, mapping the proteome and understanding the roles of these proteins are still in the very early stages, but scientists are hopeful that individual proteins, as well as constellations or "fingerprints" made up of multiple proteins (even if those proteins' functions are unknown), will soon be used regularly for the characterization of compounds/drug candidates in drug discovery programmes, in addition to application in the characterization of the probands for clinical trials regarding both desired and undesired effects of drug candidate envisioned. Indeed, the promise of these tests is so significant that many companies are already using such markers to select the most appropriate patients for clinical trials and to choose better drug candidates. Meanwhile, pharmaceutical and biotechnology companies have become acutely aware of the value of biomarkers for identifying those patients who may disproportionately benefit from a drug and those at highest risk of experiencing serious adverse effects. Biomarkers are regarded as a vital tool in streamlining drug discovery and development and accelerating approvals.

Proteins are the workhorses of the cell. Although genes represent the blueprint of life, proteins are the molecules that actually carry out the gene's instructions. In addition, because proteins are not confined to the cell that created them (as is mRNA) but float throughout the bloodstream, they are easier to find and measure. During the pre- and post-genome-sequencing euphoria of the late 1990s and early 2000, many researchers declared that the proteosome was the next frontier.

K.6.4.1.1 Challenges for Development

A major obstacle in protein chip development is the fact that proteins greatly outnumber genes. A single gene can code for multiple proteins, and each protein can undergo modifications that substantially change its activity. As a result, potentially several hundred thousand proteins can be required for the estimated 30,000 genes to do their work in the human body. This scenario helps explain the complexity of the human body despite the fact that it has relatively few genes compared with lower organisms. It also makes it much harder for scienists to completely map the proteosome. In addition, in contrast to the strandlike construction of mRNA and DNA, proteins have extremely complex structures. Within each protein's convoluted architecture there are certain "active" sites that make the most difference in terms of the protein's activity (It is in these sites that other molecules, including drugs, exert their activity). When they are placed on a substrate, such as a chip, proteins may unfold, becoming inactive and useless for study.

In terms of the technology, the traditional method of using 2-D gels for measuring the protein expression in a clinical or experimental sample is tedious and cumbersome. Initially, there was great interest in finding ways to industrialize this approach by using mass spectrometry and automated systems. With the arrival of DNA microarrays and their success in the RNA measurement field, the dawn of "proteome-wide chips" seemed imminent. But the technological hurdles facing the field have not diminished substantially and throughput in proteomics is still far behind what is achievable in areas such as gene sequencing and gene expression analysis.

As a result of the aforementioned challenges, many groups have taken a tip from the surging interest in gene-expression-profiling patterns. To develop such "signatures" of disease, researchers realized that they need only capture several proteins accurately and reproducibly. The protein marker signature does not need to be understandable. It just needs to be robust. Thus, interest in proteomics has now switched from being able to accurately quantify and identify all of the proteins in a particular sample to being able to distinguish "fingerprints" that are sufficient to separate one sample (e. g. progressive disease) from another (e. g. mild disease).

K.6.4.1.2 Technologies

Protein chips are mainly used to either identify protein-protein interactions or to find proteins in a sample. The former type of chip is primarily a drug discrovery and development tool, while the latter type can be used either in drug discovery and development or in diagnostic development. The type of molecule used to capture the proteins is the fundamental difference between chips for research purposes, which can be used to find biomarkers, and those chips that will be used to diagnose disease or predict outcomes. When searching for protein biomarker signatures, one must be sure they are examining a wide range of proteins and accurately measuring the relative levels of all of these proteins. Once the markers have been identified, one can then concentrate on a particular subset of proteins and find the ideal binding-molecules for use in a diagnostic system. Therefore, the key intermediate step is to locate the important marker proteins among the several hundred thousand proteins present in the body. A variety of molecules can be used to bind proteins, but antibodies are most often used. Primary antibodies are used to capture the protein (antigen) which is recognized by secondary antibodies (not sharing the antigenic determinant with the primary antibody but often labeled with biotin), and some type of read-out (e. g. Cy5-labeled streptavidin) signals presence of the protein (antigen). To build such arrays, each antibody placed on the chip (often in the wells of a microtiter plate) must be generated and then thoroughly tested for its cross-reactivity and binding affinity. Because proteins can share domains, or certain common structures, cross-reactivity can cause serious problems. Determining that a protein is cross-reactive requires extensive screening against other proteins. In addition, it is very difficult to get antibodies that bind tightly to a particular protein. Haab and coworkers (2001) showed that as few as 20% of antibodies out of hundreds could provide specific and accurate measurements of matching proteins on a chip. Antibodies can be exquisitely specific, however, and researchers are only now begin-

ning to learn some general rules on how to design good antibodies for proteins microarrays. A certain number of antibodies are already very well characterized. The pharmaceutical industry has been heavily reliant on these identified antibodies. The technology for making protein chips has also advanced, largely through the development of new methods to capture the proteins without degrading them.

New approaches to protein microarrays are also emerging. For example, mass spectrometry has recently been demonstrated to be useful for selection of certain proteins from a mixture and then to "soft land" these proteins onto a microarray while retaining their shape and activity to a very high degree. Meanwhile, a bench-top system of arrays of silicon-nitride microcantilevers with customizable surfaces has been introduced to detect interactions between proteins, antigens and DNA. This system does not require labelling because the microcantilevers bend due to the interaction between two molecules. Furthermore, a digital proteome chip has been developed for a comprehensive protein expression analysis. The technology is predicted of being unusually rapid (a single sample can be processed in one hour or less) and has unprecedented sensitivity, reproducibility, and accuracy. Very recently, isothermal rolling-circle amplification technology (RCAT) has been linked to antibodies as a means of signal amplification on traditional sandwich immunoassay-based protein chips. This detection method may be particularly useful because it remains localized and can detect protein analytes with zeptomole sensitivity and across a very broad dynamic range. Protein microarrays for interaction studies and other functional genomics studies will be most useful for drug discovery and development. By using a parallel procedure for protein production and purification technology it is assumed to generate and purify thousands of different proteins for the generation of the most diverse "portfolio of functional protein content". A comparative evaluation of selected suppliers of protein chip technology including their applications reported so far has been provided by Branca (2004).

K.6.4.2 DNA-Microarrays

PURPOSE AND RATIONALE

Changes and improvement in microarray technology have enhanced the ability to analyze transcription-factor-binding events genome-wide. Early versions of microarrays used for location analysis were manufactured by amplifying the promoter regions of genes from genomic DNA using PCR, and spotting the amplicons on glass slides. In addition to being reasonable accessible and affordable, PCR-generated probes could cover the entire proximal promoter region of a gene with a single probe. But these arrays had limitations. Double-stranded PCR products are less effective hybridization probes than single-stranded oligomers. PCR-generated probes are more susceptible to variations in quality due to the processing required to generate them and with only one probe reporting for each promoter, there is a relatively high rate of error associated with bad probes. Finally, the binding may occur anywhere within the probe sequence, which may be as long as 1 or 2 kB.

PROCEDURE

Emerging microarray applications such as aCGH (array-based comparative genomic hybridization), SNP (single nucleotide polymorphism) analysis, location analysis (ChIP, on-chip-chromatin immunoprecipitation on a microarray), methylation analysis, splice variant analysis and microRNA studies are all growing faster even than the already popular microarray application of gene expression. Inkjet-based array manufacturing processes provide the flexibility, long probe lengths and density required by these applications. The use of ChIP and microarray technology has proved a powerful combination for analyzing transcriptional regulation (for a review see Lee and Volkert 2006). One of the primary advantages of ChIP is that protein-DNA interactions are first fixed by the addition of a cross-linking agent to living cells, thus allowing for the identification of dynamic *in vivo* interactions between transcriptions factors and the genome. However, this approach has been relatively limited for exploring protein-DNA interactions across the genome as detection of the enrichment on this scale can be difficult. Enrichment is often detected by use of PCR-based assays, which are easy to perform and highly informative, but detection is limited because it is difficult to perform these assays in a sufficiently high-throughput format for genome analysis. Alternative approaches, such as cloning and sequencing of enriched DNA or direct sequencing of enriched DNA, have also been used, but are relatively labour-intensive and depend on sequencing large numbers of fragments to approach complete genome coverage. Using microarrays for the identification of enriched DNA regions has circumvented some of the difficulties in detecting enrichment genome-wide. Immuno-enriched DNA can be labeled, hybridized to arrays and compared to control DNA that has been hybridized at the same time. As arrays can be

designed to probe all known promoter regions (Boyer et al. 2005) or even the entire genome (Kim et al. 2005), this ensures complete coverage of the genome in a rapid and highly parallel fashion.

The current versions of arrays used for location analysis take advantage of newer printing technology. Features are now commonly composed of 60-mer oligonucleotides rather than long PCR amplicons. Several studies have shown that oligonucleotide probes are more sensitive than PCR probes in microarray analysis (Carter et al. 2003, Hughes et al. 2001, Li et al. 2002). Furthermore, it has been shown that results using longer oligonucleotides are more sensitive and reproducible than shorter ones. The 5070-base range seems to represent the "sweetspot" where hybridization efficiency, specificity and sensitivity are co-optimized. These oligonucleotide arrays are manufactured by commercial vendors, which translates to an increase in both the quality and consistency of the arrays. For instance, there are currently three array designs for the study of transcription factor binding in the human genome available (for a review see Lee and Volkert 2006).

EVALUATION

Future studies will focus on expanding the transcriptional regulatory network for metabolic genes. It will be interesting to identify the targets of transcription factors that are themselves targets of metabolic transcriptions factors, thus expanding the transcriptional regulatory network responsible for the genetic programme underlying the coordination of glucose and lipid metabolism. Transcription factors are responsible for recruiting additional components of the transcription apparatus, most notably chromatin-remodelling and –modifying complexes that affect transcription by regulating higher-order DNA structure. Consequently, one area of interest is identifying the targets of these various remodelling and modifying complexes and linking the network of transcriptions factors with the network of chromatin modifiers in liver, muscle, adipose and pancreatic β-cells.

K.6.4.3 siRNA

During the past decade a panel of methods has been developed for the validation of drug targets at the cellular level encompassing constitutive or regulated overexpression of the gene envisioned or its downregulation (antisense RNA, mouse embryonic fibroblasts from knockout mice and RNAi). RNAi displays a number of advantages regarding the expenditure in equipment, costs and time required. Moreover, the incomplete efficacy of RNAi in downregulating gene expression (usually by up to 80%) more closely reflects the pharmacological inhibition of transcription by small molecule compounds. In addition, there are considerable efforts to use RNAi as future therapeutics albeit many challenges have to be overcome.

RNA interference (RNAi) is an ancient mechanism of gene regulation, found in eukaryotes as diverse as yeast and mammals, and probably plays a central role in controlling gene expression in all eukaryotes (Tijsterman et al. 2002). Using small interfering RNA (siRNA) molecules, RNAi can selectively silence essentially any gene in the genome. Once in a cell, a short double-stranded RNA (dsRNA) molecule is cleaved by an RNase III, called "Dicer", into 21- to 23-nucleotide guide RNA duplexes with two-nucleotide 3′-overhangs, called siRNAs that become bound to the RNA-induced silencing complex (RISC). Within the RISC, one of the two strands of the siRNA is chosen as the antisense strand *via* cleavage of the passenger strand (Gregory et al. 2005, Rand et al. 2005), so that they can target complementary sequences in messenger RNAs involved in a disease. An RISC-associated "slicer" RNase belonging to the Argonaute2 (Ago2) family then cleaves the target in the middle of the homology, which is followed by further degradation mediated by an exosome complex (Liu et al. 2004, Rand et al. 2004) thereby interrupting the synthesis of the disease-causing protein. The RISC complex is naturally stable within the cell, enabling siRNA to cut multiple mRNA molecules consecutively and, therefore, suppressing protein synthesis in a potent and targeted way.

K.6.4.3.1 Design

The bulk of pharmaceutical applications of RNAi uses siRNA or its precursor. A completely foolproof algorithm of siRNA design for every target may remain an unattainable dream due to the inherent difficulty of predicting the various parameters that affect siRNA function (Heale et al. 2005, Amarzguioui et al. 2004, Gong and Ferrell 2004). However, some significant factors have been recognized. First, a successful application of RNAi demands that it be as specific to the target RNA as possible. Kim and coworkers (2004) demonstrated that 27-bp siRNAs are 10- to 100-times more potent and specific *in vivo* than their 21-bp counterparts. Second, Schwarz and coworkers (2003) found

that the formation of RISC is an asymmetric process in that only one strand of the siRNA is incorporated, not both. Third, it is now clear that the local secondary structure of the target RNA has dramatic influence on the accessibility for the siRNA (Vickers et al. 2003, Kretschmer-Kazemi and Sczakiel 2003, Luo and Chang 2004). Although siRNA designs have been proposed to incorporate this parameter (Heale et al. 2005, Amarzguioui and Prydz 2004, Gong and Ferrel 2004), the empirical nature of RNA structure prediction has left room for uncertainty. Fourth, a number of studies havc reported various degrees of positive and negative regulation of genes besides the intended target leading to "off-target" effects that are not easily explained by a fortuitous sequence homology of the siRNA to the off-target mRNAs (Sledz et al. 2003, Jackson et al. 2003, Bridgeet al. 2003). In conclusion, one should follow all the guidelines suggested above but remember that the ultimate test is experimental.

K.6.4.3.2 Source

It is to be realized that RNAi-based target validation or therapy exploits the physiological machinery constitutively present in the normal cell and that dsRNA is the only entity needed to activate it. In other words, therapeutic RNAi is triggered by the simple introduction of target-specific siRNA. This is commonly achieved by one of the following methods. The 21-mer siRNA with the 3′-dinucleotide overhangs can be chemically synthesized and introduced into the cell. Alternately, relatively long sense and antisense strands are transcribed *in vitro* from recombinant DNA templates, annealed to produce the dsRNA, which is digested with Dicer to generate siRNA that is then transfected into the cells. Lastly, the dsRNA can be generated *in vivo* by transfection of the corresponding DNA clone, which is then processed by the intracellular Dicer to generate the siRNA.

Synthetic siRNA

The chemistry of RNA synthesis has significantly improved over the years with an additional boost from the recent demands of the RNAi market. Short RNAs containing a variety of modifications are now commercially available (Dorsett and Tuschl 2004, Manoharan 2004). Modifications are explored for a variety of goals, such as improved RNAi activity and lower IC_{50}, enhanced stability, particularly against nucleases, and better pharmacokinetics and organ targeting. Effect of terminal and internal modifications of the siRNA on the silencing activity has been tested, and the consensus is summarized here. Additions at the 5′-end of the sense strand had little or no effect (Chiu and Rana 2003). A 5′-phosphate group on the antisense strand is essential for the incorporation into RISC. However, additions to the phosphate group are generally tolerated (Nykanen et al. 2001, Martinez et al. 2002). Tolerance at the 3′- end of the antisense depends on the derivative. While biotin, ddC, aminopropyl group and puromycin do not inhibit siRNA activity, 2-hydroxyethylphosphate, ethylene thymidine, and some fluorescent derivatives do (Schwarz et al. 2002). Of all the internal modifications, substitutions of the 2′-OH of ribose are the best studied and include -H, -OMe, -F and -NH_2. In general, all 2′-substitutions in the 3′- overhangs are tolerated (Elbashir et al. 2001, Amarzguioui et al. 2003). siRNAs with internal 2′-F are RNase-resistant and may perform better than unmodified siRNA in cell culture (Capodici et al. 2002), but not necessarily so in animals (Layzer et al. 2004). Internally, 2′-*O*-methylated siRNAs also exhibit significantly greater stability in serum with sustained silencing activity, and siRNAs with alternate 2′-OMe and 2′-F substitutions have similar advantages as well. For reasons that are unclear, 2′-NH_2 substitutions in either sense or antisense strand cause significant loss of silencing activity (Parrish et al. 2000). Replacement of the phosphodiester (P = O) backbone with phosphorothioates (P = S) or boranophosphonates (P = B) also offers nuclease resistance, but excessive substitution leads to loss of activity and/or increased toxicity (Manharan et al. 2004, Amarzguioui et al. 2003). Lastly, siRNA containing synthetic RNA-like nucleotide analog, known as "locked nucleic acid" (LNA), exhibits greatly improved biostability and enhanced inhibition of certain RNA targets (Braasch et al. 2003).

siRNA Transcribed In Vitro

Exogenous siRNA is also produced by the transcription of both strands of recombinant DNA templates, usually from a bacteriophage promoter, such as T7 or SP6 (Dudek and Picard 2004). As the resultant transcripts have 5′-triphosphates that may activate the undesirable IFN pathway, as mentioned before (Kim et al. 2005), the dsRNA product is either treated with phosphatase or trimmed with Dicer (Myers et al. 2003) *in vitro* before transfection.

Recombinant siRNA

The other common technique is to transfect target cells with DNA clones expressing shRNA, also known as DNA-directed RNAi or ddRNAi (Smith et al. 2000).

The corresponding complementary DNA (cDNA) is cloned between two converging promoters, generating dsRNA in the recipient cells that is cleaved by cellular Dicer into siRNA. In an alternate strategy, a DNA segment containing a hyphenated inverted repeat produces an shRNA of 19 bp or longer upon transcription. The shRNA is processed essentially by the miRNA pathway using Drosha and Dicer as described previously to eventually generate the siRNA. Both strategies employ RNA polymerase III promoters, such as human and mouse U6, human H1, and human 7SK promoters. The commonly used vectors are of adenoviral, lentiviral, or retroviral origin. Recombinant expression opens the avenue for inducible and/or tissue-specific expression of the siRNA (Wiznerowicz et al. 2003, Matsukura et al. 2003), which is not possible with synthetic siRNA. It also allows more sustained siRNA production over longer periods, critical in therapy for chronic diseases (see below). The potential hazards include viral infection, adverse immune reactions, and disruption or dysregulation of important genes via chromosomal integration of the viral genome (Bartosch and Cosset 2004). Furthermore, the parameters of shRNA design (such as the optimal length of the stem and the loop regions) are still ill defined and need further experimentation.

K.6.4.3.3 Delivery

There are two strategies for delivering siRNAs*in vivo*. One is to stably express siRNA precursors, such as short hairpin RNAs (shRNAs) from viral vector using gene therapy. The other is to deliver synthetic siRNAs by complexing or covalently linking the duplex RNA with lipids and/or delivery proteins. To solve the problem of cell penetration, most researchers have either complexed the RNA with a lipid or modified the RNA's phosphate backbone to minimize its charge. Despite the questions and unresolved problems, several companies are moving ahead to develop RNAi therapy for many diseases, including diabetes. The standard lipid reagents that were originally developed for DNA transfection, such as Oligofectamine (Invitrogen), continue to be the reagents of choice for cell culture studies (Spagnou et al. 2004). Recent formulations claim to be specifically improved for RNA delivery and can be used in the presence of serum in cell culture and in live animals. Current options for the synthesis and design has been reviewed by Baric (2005).

K.6.4.3.4 Use for Metabolic Diseases

Numerous studies using highly sensitive microarray analyses have demonstrated that siRNAs can have off-target effects by silencing genes relevant for the regulation of carbohydrate and lpid metabolism in adipose, liver, muscle and pancreatic β-cells. This makes siRNA to an ideal tool for the cellular validation of molecular targets (e. g. enzymes, transcription factors) for the terapy of metabolic disorders, such as diabetes and obesity, as has been demonstrated elegantly by Zhou and coworkers (2004). In addition, RNAi-based therapeutics have potentially significant advantages over traditional approaches of treating diseases, including broad apllicability, therapeuice precision, and selectivity avoiding side effects. This widespread applicability, coupled to relative ease of synthesis and low cost of production make siRNAs an attractive new class of small-molecule drugs. RNAi-based drugs are designed to destroy the target RNA and therefore stop the associated undesirable protein production required for disease progression. The putative therapeutic potential for the use of siRNA, in general, and the cure of metabolic diseases, particular, has been reviewed by Dallas and Vlassov (2006) and Rondinone (2006).

REFERENCES AND FURTHER READING

Amarzguiou M, Holen T, Babaie E, Prydz H (2003) Toleracne for mutations and chemical modifications in a siRNA. Nucleic Acids Res 31:589–595

Amarzguiou M, Prydz H (2004) An algorithm for selection of functional siRNA sequences. Biochem Biophys Res Commun 316:1050–1058

Baric S (2005) Silence of the transcripts: RNA interference in medicine. J Mol Med 83:764–773

Bartosch B, Cosset FL (2004) Strategies for retargeted gene delivery using vectors derived from lentiviruses. Curr Gene Ther 4:427–443

Boyer LA, Lee TI, Cole MF, Johnstone SE, Levine SS, Zucker JP, Guenther MG, Kumar RM, Murray HL, Jenner RG, Gifford DK, Melton DA, Jaenisch R, Young RA (2005) Core transcriptional regulatory circuitry in human embryonic stem cells. Cell 122:947–956

Branca MA (2004) Protein chips: Advancing toward clinical diagnostic applications. Spectrum Diagnostic Rel Technol 1:1–13

Braasch DA, Jensen S, Liu Y, Kaur K, Arar K, White MA, Corey DR (2003) RNA interference in mammalian cells by chemically-modified RNA. Biochemistry 42:7967–7975

Bridge AJ, Pebernard S, Ducraux A, Nicoulaz AL, Iggo R (2003) Induction of an interferon response by RNAi vectors in mammalian cells. Nat Genet 34:263–264

Capodici J, Kariko K, Weissman D (2002) Inhibition of HIV-1 infection by small interfering RNA-mediated RNA interference. J Immunol 169:5196–5201

Carter MG, Hamatani T, Sharov AA (2003) In situ-synthesized novel microarray optimized for mouse stem cell and

early developmental expression profiling. Genome Res 13:1011–1021
Chiu YL, Rana TM (2003) siRNA function in RNAi: a chemical modification analysis. RNA 9:1034–1048
Dallas A, Vlassov AV (2006) RNAi: A novel antisense technology and its therapeutic potential. Med Sci Monit 12:RA67–74
Dorsett Y, Tuschl T (2004) siRNAs: applications in functional genomics and potential as therapeutics. Nat Rev Drug Discov 3:318–329
Dudek P, Picard D (2004) TROD: T7 RNAi oligo designer. Nucleic Acids Res 32:W121–123
Elbashir SM, Harborth J, Lendeckel W, Yalcin A, Weber K, Tuschl T (2001) Duplexes of 21-nucleotide RNAs mediate RNA interference in cultured mammalian cells. Nature 411:494–498
Gong D, Ferrell JE (2004) Picking a winner: new mechanistic insights into the design of effective siRNAs. Trends Biotechnol 22:451–454
Gregory RI, Chendrimada TP, Cooch N, Shiekhattar R (2005) Human RISC couples microRNA biogenesis and posttranciptional gene silencing. Cell 123:631–640
Haab BB (2001) Protein microarrays for highly parallel detection and quantitation of specific proteins and antibodies in complex solutions. Genome Biology 2:2–25
Heale BS, Soifer HS, Bowers C, Rossi JJ (2005) siRNA target site secondary structure predictions using local stable substructures. Nucleic Acid Res 33:e30
Hughes TR, Mao M, Jones AR, Burchard J, Marton MJ, Shannon KW, Lefkowitz SM, Ziman M, Schelter JM, Meyer MR, Kobayashi S, Davis C, Dai H, He YD, Stephaniants SB, Cavet G, Walker WL, West A, Coffey E, Shoemaker DD, Stoughton R, Blanchard AP, Friend SH, Linsley PS (2001) Expression profiling using microarrays fabricated by an ink-jet oligonucleotide synthsizer. Nat Biotechnol 19:342–347
Jackson AL, Bartz SR, Schelter J, Kobayashi SV, Burchard J, Mao M, Li B, Cavet G, Linsley PS (2003) Expression profiling reveals off-target gene regulation by RNAi. Nat Biotechnol 21:635–637
Kim TH, Barrera LO, Zheng M, Qu C, Singer MA, Richmond TA, Wu Y, Green RD, Ren B (2005) A high-resolution map of active promoters in the human genome. Nature 436:876–880
Kim DH, Behlke MA, Rose SD, Chang MS, Choi S, Rossi JJ (2004) Interferon induction by siRNAs and ssRNAs synthesized by phage polymerase. Nat Biotechnol 22:321–325
Kretschmer-Kazemi FR, Sczakiel G (2003) The activity of siRNA in mammalian cells is related to structural target accessibility: a comparison with antisense oligonucleotides. Nucleic Acids Res 31:4417–4424
Layzer JM, McCaffrey AP, Tanner AK, Huang Z, Lay MA, Sullenger BA (2004) *In vivo* activity of nuclease-resistant siRNAs. RNA 10:766–771
Lee T, Volkert T (2006) Transcription factors – Analysing regulation in stem cells. The Biochemist February 2006: 29–31
Li J, Pankratz M, Johnson JA (2002) Toxicol Sci 69:383–390
Liu J, Carnell MA, Rivas FV, Marsden CG, Thompson JM, Song JJ, Hammond SM, Joshua-Tor L, Hannon GJ (2004) Argonaute2 is the catalytic engine of mammalian RNAi. Science 305:1437–1441
Luo KO, Chang DC (2004) The gene-silencing efficiency of siRNA is strongly dependent on the local structure of mRNA at the targeted region. Biochem Biophys Res Commun 318:303–310
Manoharan M (2004) RNA interference and chemically modified small interfering RNAs. Curr Opin Chem Biol 8:570–579
Martinez J, Patkaniowska A, Urlaub H, Luhrmann R, Tuschl T (2002) Single-stranded siRNAs guide target RNA cleavage in RNAi. Cell 110:563–574
Matsukura S, Jones PA, Takai D (2003) Establishment of conditional vectors for hairpin siRNA knockdowns. Nucleic Acids Res 31:e77
Myers JW, Jones JT, Meyer T, Ferrell JE (2003) Recombinant Dicer efficiently converts large dsRNAs into siRNAs suitable for gene silencing. Nat Biotechnol 21:324–328
Nykanen A, Haley B, Zamore PD (2001) ATP requirements and small interfering RNA structure in the RNA interference pathway. Cell 107:309–321
Parrish S, Fleenor J, Xu S, Mello C, Fire A (2000) Functional anatomy of a dsRNA trigger: differential requirement for the two trigger strands in RNA interference. Mol Cell 6:1077–1087
Rand TA, Ginalski K, Grishin NV, Wang X (2004) Biochemical identification of Argonaute 2 as the sole protein required for RNA-induced silencing complex activity. Proc Natl Acad Sci USA 101:14385–14389
Rand TA, Petersen FD, Wang X (2005) Argonaute2 cleaves the anti-guide strand of siRNA during RISC activation. Cell 123:621–629
Rondinone CM (2006) The therapeutic potential of RNAi in metabolic diseases. BioTechniques 40:S31-S36
Schwarz DS, Hutvagner G, Du T, Xu Z, Aronin N, Zamore PD (2003) Assymmetry in the assembly of the RNAi enzyme complex. Cell 115:199–208
Schwarz DS, Hutvagner G, Haley B, Zamore PD (2002) Evidence that siRNAs function as guides, not primers, in the *Drosophila* and human RNAi. Cell 110:563–574
Sledz CA, Holko M, de Veer MJ, Silverman RH, Williams BR (2003) Activation of the interferon system by short-interfering RNAs. Nat Cell Biol 5:834–839
Smith NA, Singh SP, Wang MB, Stoutjesdijk (PA) Green AG, Waterhouse PM (2000) Total silencing by intron-spliced hairpin RNAs. Nature 407:319–320
Spagnou S, Miller AD, Keller M (2004) Lipidic carriers of siRNA: differences in the formulation, cellular uptake, and delivery with plasmid DNA. Biochemistry 43:13348–13356
Tijsterman M, Ketting RF, Plasterk RH (2002) The genetics of RNA silencing. Annu Rev Genet 36:489–519
Vickers TA, Koo S, Bennett CF, Crooke ST, Dean NM, Baker BF (2003) Efficient reduction of target RNAs by small interfering RNA and RNAase H-dependent antisense agents. A comparative analysis. J Biol Chem 278:7108–7118
Wiznerowicz M, Trono D (2003) Conditional suppression of cellular genes. Lentivirus vector-mediated drug-inducible RNA interference. J Virol 77:8957–8961
Zhou QL, Park JG, Jiang ZY, Holik JJ, Mitra P, Semiz S, Guilherme A, Powelka AM, Tang X, Virbasius J, Czech MP (2004) Analysis of insulin signalling by RNAi-based gene silencing. Biochem Soc Trans 32:817–821

K.6.4.4 Effect on Peroxisome Proliferator-Activated Receptor

GENERAL CONSIDERATIONS

The peroxisome proliferator-activated receptors (PPARs) are ligand-activated transcription factors of

the nuclear receptor superfamily (Issemann and Green 1990, Dreyer et al. 1992). They regulate glucose, lipid, and cholesterol metabolism in response to fatty acids and their derivatives, eicosanoids, and drugs used in the treatment of hyperlipidemia and diabetes. The PPAR subfamily contains three members known as PPARα, PPARβ/δ, and PPARγ. Each PPAR subtype shows a distinct tissue distribution (Keller and Wahli 1993, Green 1995, Devchand et al. 1996, Lemberger et al. 1996, Schoonjans et al. 1996a, b, c, 1997, Willson et al. 2000, Walczak and Tontomoz 2002) and ligand preference.

PPARα is expressed predominantly in metabolically active tissues, including liver, kidney, skeletal muscle, and brown fat (Sher et al. 1993, Mukherjee et al. 1994), and its ligands include fatty acids, hypolipidemic drugs, eicosanoids and xenobiotics (Forman et al. 1997, Kliewer et al. 1997, Forman et al. 1995, Devchand et al. 1996, Lehmann 1995).

PPARγ is highly expressed in adipocytes (Elbrecht et al. 1996, Mukherjee et al. 1997), is involved in control of lipid storage, and plays a critical role in the regulation of adipocyte gene expression and the induction of adipogenesis and adipocyte differentiation (Tortonoz et al. 1994 and 1995, Brun et al. 1996, Wu 1998, Lowell 1999). Thiazolidinedione derivatives which are antidiabetic agents are potent and selective activators of PPARγ (Young et al. 1997, Henke et al. 1998, Murakami et al. 1998, Reginato et al. 1998, Ribon et al. 1998, Vázquez et al. 2002). The meanwhile widely used anti-diabetic drugs, pioglitazone and rosiglitazone, preferentially bind to the γ-isoform and modulate the expression of a number of genes in predominantly adipose tissue, but presumably also in muscle and liver tissues, ultimately leading to substantial increase in insulin sensitivity (Lehmann et al. 1995). Berger and coworkers (1996) found a correlation of antidiabetic actions of thiazolidinediones in *db/db* mice with the conformational change in PPARγ. Su and coworkers (1999) described the use of a PPARγ-specific monoclonal antibody to demonstrate thiazolidinediones induced PPARγ receptor expression *in vitro.*

Murphy and Holder (2000) suggested a therapeutic potential of PPARγ agonists in the treatment of inflammatory diseases and certain cancers. Steppan and coworkers (2001) and Berger (2001) showed that adipocytes secrete a signaling molecule which they called resistin (for resistance to insulin). Circulating resistin levels in mice are decreased by thiazolidindiones and are increased in diet-induced and genetic forms of obesity.

Although the function of PPARδ, which is expressed ubiquitously, is less well known, this nuclear receptor may be involved in the regulation of cholesterol and lipid metabolism (Oliver et al. 2001, Shi et al. 2001). Fatty acids and cyclooxygenase 2-derived prostacyclin (PGI_2) are natural ligands for PPARδ (Gupta et al. 2000). Several highly selective and potent synthetic ligands (e. g., L-165041, GW501516) activate PPARδ at nanomolar concentrations (Oliver et al. 2001, Glinghammar et al. 2003).

All subtypes share a common structural organization with a highly conserved N-terminal DNA binding domain (DBD) and a moderately conserved C-terminal ligand-binding domain (LBD) that contains a carboxy-terminal activation function motif (AF2). All of the PPAR subfamily members heterodimerize with the receptor for 9-*cis* retinoic acid (RXR) and bind to target gene peroxisome proliferator elements (PPREs), a direct repeat of the sequence AGGTCA separated by one nucleotide (DR-1) (Dreyer et al. 1992, Kliewer et al. 1992).

Unliganded nuclear receptors, such as retinoic acid receptors (RARα) and T3Rα, are able to repress basal transcription through recruitment of corepressors (Chen and Evans 1995). Among the three PPARs, PPARδ distinguishes itself by displaying remarkably potent transcriptional repression activity. In contrast, unliganded PPARα and PPARγ do not repress PPRE-mediated transcription, presumably due to their inability to bind nuclear receptor corepressors SMRT and NCoR on the PPRE DNA element (Shi et al. 2001). Agonist binding to nuclear receptor LBD provokes a conformational change of the AF-2 motif that produces a suitable binding surface for recruitment of coactivators (Xu et al. 1999).

K.6.4.4.1 Recombinant Cell Lines

PURPOSE AND RATIONALE

Because of involvement of PPARs in many critical physiological and pathological functions, in particular with regard to metabolic diseases, the identification of high-affinity ligands would create useful tools for studying the PPAR role in the normal physiological and disease states as well as for drug discovery, in particular for the therapy of metabolic diseases, such as type II diabetes. To characterize PPAR specificity of synthetic ligands, stable HeLa-derived reporter cell lines in which PPARα, PPARβ, and PPARγ agonists induce luciferase activity have been constructed. These cell lines stably express a chimeric protein con-

taining the yeast transactivator GAL4 DBD fused to LBD regions of PPARs (GAL4-PPARs) and contain a luciferase reporter gene driven by a pentamer of the GAL4 recognition sequence in front of the β-globin promoter. The GAL4-PPAR chimeric receptors has been chosen because this assay format eliminates background activity from endogenous receptors and allowed quantitation of relative activity across the three PPAR subtypes with the same reporter gene. Additional assays for the characterization of PPAR-modulating compounds and drug candidates are given in K.3.5.

K.6.4.4.2 Lipogenesis Assay

The lipogenic activity of PPARγ agonists can be assessed by determining the uptake of radioactive glucose uptake and its incorporation into the total lipids of cells (see K.6.1.2.1). The amount of glucose incorporation into lipids in these cells provides a measure of cell differentiation, since preadipocytes are less efficient in *de novo* lipogenesis compared to mature adipocytes on basis of their different expression levels of lipogenic genes, such as GLUT4 and GPAT. Moreover, the analysis of the expression of adipocyte marker genes (aP2, LPL, leptin) and of the accumulation of TAG in the cytoplasm confirmed by oil red O staining are other methods to evaluate the lipogenic activity of PPARγ agonists and thereby indirectly their binding affinity to PPARγ.

K.6.4.4.3 Protease Digestion Assay

PROCEDURE

The protease digestion assay can be performed according to the method of Allan and coworkers (1992) with minor modifications. The plasmid pSG5-hPPARγ1 is used to synthesize ^{35}S-radiolabeled PPARγ1 in a coupled transcription/translation system. The transcription/translation reactions are subsequently divided into portions of 22.5-µl volume. 2.5 µl PBS with or without a thiazolidinethione are added. The mixtures are incubated for 20 min at 25°C, separated into 4.5-µl aliquots, and 0.5 µl distilled water or distilled water-solubilized trypsin are added. The protein digestions are allowed to proceed for 10 min at 25°C, then terminated by the addition of 20 µl denaturing gel loading buffer and boiling for 5 min. The products of the digestion are separated by electrophoresis through a 1.5-mm 12%-polyacrylamide-SDS gel. After electrophoresis, the gels are fixed in 10% acetic acid/40% methanol for 30 min, treated in EN^{3}HANCE for an additional 30 min. and dried under vacuum for 2 h at 80°C. Autoradiography is then performed to visualize the radiolabeled digestion products.

EVALUATION

For evaluation of the protease digestion assay, the partially protease-resistant conformation product of PPARγ is visualized by autoradiography on SDS-PAGE after incubation with the thiazolidinedione and increasing concentrations of trypsin.

K.6.4.4.4 Living Cell Luciferase Assay

The luciferase assays were used by Seimandi and coworkers (2005) to investigate the differential responses of PPARα, PPARδ and PPARγ reporter cell lines to selective PPAR synthetic ligands. For this, cells are seeded at a density of 40,000 cells per well in 96-well white opaque tissue culture plates. Tested compounds are added 8 h later, and cells are incubated for 16 h. Experiments are performed in quadruplicate. At the end of incubation, culture medium is replaced by medium containing 3×10^{-4} M luciferin. Luciferase activity is measured for 2 s in intact living cells using a MicroBeta Wallac luminometer (Perkin-Elmer).

K.6.4.4.5 Lysed Cell Luciferase Assay

PROCEDURE

Cells are seeded at a density of 200,000 cells per well in 24-well test plates. Test compounds/drug candidates are added 8 h later, and cells are then incubated for 16 h. Cell extract preparation is done essentially as recommended by Promega. Compound-containing medium is removed, and cells are washed with PBS. Cells are lysed in 25 mM Tris/phosphate (pH 7.8), 2 mM EDTA, 1% Triton X-100, 2 mM DTT, 10% glycerol. Protein concentration is estimated with the Bradford assay kit and BSA as standard.

Cell protein extracts (100 µl) are loaded onto 96-well white opaque tissue plates, and luciferase activity is measured after injection of luciferase detection buffer (20 mM Tricine, pH 7.8, 1.1 mM ($MgCO_3$) 4.0 mM $Mg(OH)_2{\cdot}5H_2O$, 2.7 mM $MgSO_4$, 0.1 mM EDTA, 33 mM DDT) and luciferase assay substrate (0.5 mM luciferin, 0.5 mM ATP, 0.3 mM coenzyme A)

using a luminometer (e. g. Berthold Technologies). Luminescence is measured for 2 s.

EVALUATION

In the transactivation assay, each compound is tested at various concentrations in at least two independent experiments. For each experiment, tests are performed in duplicate or triplicate for each concentration, and data are analysed as means and standard deviations. Individual agonist concentration-response curves, in the absence and presence of antagonist, are fitted using the sigmoidal dose-response function of a graphics and statistics software program (e. g. GraphPad Prism, version 4.0). EC_{50} (effective concentration for half-maximal luciferase activity) and IC_{50} (half-maximal inhibitory concentration) values are calculated from equations used to fit the data in this graphic software. Transactivation data are presented as EC_{50} and IC_{50} values for each compound tested. To analyze significance of PPAR isotype activation, PPAR agonist treatment is compared with controls using one-way analysis of variance (ANOVA) with the help of GraphPad Prism software.

In this assay system, the expression of PPAR isotypes differentially modulates the reporter gene basal activity and thus provides interesting information on the recruitment of cell type-specific coregulators by PPARs. Using specific PPAR agonists and antagonists, these cell lines permit an easy, rapid, and specific identification of subtype-selective PPAR ligands in a standardized microtiter plate assay. Furthermore, since HG5LN cells are putative host cells for other GAL4 nuclear receptor chimeras, RAR, thyroid hormone receptors, and steroid receptors, the assay system may be helpful to characterize the nuclear receptor selectivity of their nuclear receptor ligands which could also play important roles in the pathogenesis and therapy of metabolic diseases.

REFERENCES AND FURTHER READING

Allan GF, Xiaohua L, Tsai SY, Weigel NL, Edwards DP, Tsai MJ, O'Malley BW (1992) Hormone and antihormone induce distinct conformational changes which are central to steroid receptor activation. J Biol Chem 267:19513–19520

Berger A (2001) Resistin, a new hormone that links obesity with type 2 diabetes. Br Med J 322:193

Berger J, Bailey P, Biswas C, Cullinan CA, Dobber TW, Hayes NS, Saperstein R, Smith RG, Leibowitz MD (1996) Thiazolidinediones produce a conformational change in peroxisomal proliferator-activated receptor-γ: Binding and activation correlate with antidiabetic actions in *db/db* mice. Endocrinology 137:4189–4195

Brun RP, Kim JB, Hu E, Altiok S, Spiegelman BM (1996) Adipocyte differentiation: a transcriptional regulatory cascade. Curr Opin Cell Biol 8:826–832

Chen JD, Evans RM (1995) A transcriptional co-repressor that interacts with nuclear hormone receptors. Nature 377:454–457

Devchand PR, Keller H, Peters JM, Vazquez M, Gonzalez FJ, Wahli E (1996) The PPARα-leucotriene B4 pathway to inflammation control. Nature 384:39–43

Dreyer C, Krey G, Keller H, Givel F, Helftenberg G, Wahli W (1992) Control of the peroxisomal beta-oxidation pathway by a novel family of nuclear hormone receptors. Cell 68:879–887

Elbrecht A, Chen Y, Cullinan CA, Hayes N, Leibowitz M, Moller DE, Berger J (1996) Molecular cloning, expression, and characterization of human peroxisome proliferator activated receptor γ1 and γ2. Biochem Biophys Res Commun 224:431–437

Forman BM, Chen J, Evans RM (1997) Hypolipidemic drugs, polyunsaturated fatty acids, and eicosanoids are ligands for peroxisome proliferator-activator receptors alpha and delta. Proc Natl Acad Sci USA 94:4312–4317

Forman BM, Totonoz P, Chen J, Brun RP, Spiegelman PE, Evans RM (1995) 15-Deoxy-$\Delta^{12,14}$-prostagandin J_2 is a ligand for the adipocyte determination factor PPARγ. Cell 83:803–812

Glinghammar B, Skogsberg J, Hamsten A, Ehrenborg E (2003) PPARδ activation induces COX-2 gene expression and cell proliferation in human hepatocellular carcinoma cells. Biochem Biophys Res Commun 308:361–368

Green S (1995) PPAR: A mediator of peroxisome proliferator action. Mutation Res 333:101–109

Gupta RA, Tan J, Krause WF, Geraci MW, EWillson TM, dey SK, DuBois RN (2000) Prostacyclin-mediated activation of peroxisome proliferator-activated receptor delta in colorectal cancer. Proc Natl Acad Sci USA 97:13275–13280

Henke BR, Blanchard SG, Brackeen MF, Brown KK, Cobb JE, Collins JL, Harrington WW, Hashim MA, Hull-Ryde EA, Kaldor I, Kliewer SA, Lake DSH, Leesnitzer LM, Lehmann JM, Lenhard JM, Orband-Miller LA, Miller JF, Mook RA, Noble SA, Oliver W, Parks DJ, Plunket KD, Szewczyk JR, Willson TM (1998) N-(2-Benzoylphenyl)-L-tyrosine PPARγ agonists. 1. Discovery of a novel series of potent antihyperglcemic and antihyperlipemic agents. J Med Chem 41:5020–5036

Issemann I, Green S (1990) Activation of a member of the steroid hormone receptor superfamily by peroxisome proliferators. Nature 347:645–650

Keller H, Wahli W (1993) Peroxisome proliferator-activated receptors. A link between endocrinology and nutrition? Trends Endocrinol Metab 4:291–296

Kliewer SA, Sundseth SS, Jones SA, Brown PJ, Wisely GP, Knoble SS, Devchand P, Wahli W, Willson TM, Lenhard JM, Lehmann JM (1997) Fatty acids and eicosanoids regulate gene expression through direct interactions with peroxisome proliferator-activated receptors α and γ. Proc Natl Acad Sci USA 94:4318–4323

Kliewer Sa, Umesono K, Mangelsdorf DJ, Evans RM (1992) Retinoid X receptor interacts with nuclear receptors in retinoic acid, thyroid hormone, and vitamin D3 signalling. Nature 355:446–449

Lehmann JM, Moore LB, Smith-Oliver TA, Wilkison WO, Willson TM, Kliewer SA (1995) An antidiabetic thiazolidinedione is a high affinity ligand for peroxisome proliferator-activated receptor-γ (PPAR-γ). J Biol Chem 270:121953–12956

Lemberger T, Desvergne B, Wahli W (1996) Peroxisome proliferator–activated receptors: A nuclear receptor signaling pathway in lipid physiology. Annu Rev Cell Dev Biol 12:335–363

Lowell BB (1999) Minireview. An essential regulator of adipogenesis and modulator of fat cell function: PPARγ. Cell 99:239–242

Mukherjee R, Jow L, Croston GE, Paterniti JR (1997) Identification, characterization, and tissue distribution of human peroxisome proliferator-activated receptor (PPAR) isoforms PPARγ2 versus PPARγ1 and activation with retinoid X receptor agonists and antagonists. J Biol Chem 272:8071–8076

Mukherjee R, Jow L, Noonan D, McDonnell DP (1994) Human and rat peroxisome proliferator activated receptors (PPARs) demonstrate similar tissue distribution but different responsiveness to PPAR activators. J Steroid Biochem Mol Biol 51:157–166

Murakami K, Tobe K, Die T, Mochizuki T, Ohashi M, Akanuma Y, Yazaki Y, Kadowaki T (1998) A novel insulin sensitizer acts a coligand for peroxisome proliferator-activated receptor-α (PPAR-α) and PPAR-γ. Effect of PPAR-α activation on abnormal lipid metabolisms in liver of Zucker fatty rats. Diabetes 47:1841–1847

Murphy GJ, Holder JC (2000) PPAR-γ agonists: therapeutic role in diabetes, inflammation and cancer. Trends Pharmacol Sci 21:469–474

Oliver WR, Shenk JL, Snaith MR, Russell CS, Plunket KD, Bodkin NL, Lewis MC, Winegar DA, Sznaidman ML, Lambert MH, Xu HE, Sternbach DD, Kliewer SA, Hansen BC, Willson TM (2001) A selective peroxisome proliferator-activated receptor delta agonist promotes reverse cholesterol transport. Proc Natl Acad Sci USA 98:5306–5311

Reginato MJ, Bailey ST, Krakow SL, Minami C, Ishii S, Tanaka H, Lazar MA (1998) A potent antidiabetic thiazolidinedione with unique peroxisome proliferator-activated receptor γ-activating properties. J Biol Chem 273:32679–32684

Ribon V, Johnson JH, Camp HS, Saltiel AR (1998) Thiazolidinediones and insulin resistance: Peroxisome proliferator-activated receptor γ activation stimulates expression of the CAP gene. Proc Natl Acad Sci USA 95:14751–14756

Schoonjans K, Staels B, Auwerx J (1996a) The peroxisome proliferator activated receptors (PPARs) and their effects on lipid metabolism and adipocyte differentiation. Biochem Biophys Acta 1302:93–109

Schoonjans K, Staels B, Auwerx J (1996b) Role of the peroxisome proliferator activated receptor (PPAR) in mediating effects of fibrates and fatty acids on gene expression. J Lipid Res 37:907–925

Schoonjans K, Peinado-Onsurbe J, Lefebvre AM, Heyman RA, Briggs M, Deeb S, Staels B, Auwerx J (1996c) PPARα and PPARγ activators direct a distinct tissue-specific transcriptional response via the PPRE in the lipoprotein lipase gene. EMBO J 15:5336–5348

Schoonjans K, Martin G, Staels B, Auwerx J (1997) Peroxisome proliferator-activated receptors, orphans with ligands and functions. Curr Opin Lipidol 8:159–166

Seimandi M, Lemaire G, Pillon A, Perrin A, Carlavan I, Voegel JJ, Vignon F, Nicolas J-C, Balaguer P (2005) Differential responses of PPARα, PPARδ, and PPARγ reporter cell lines to selective PPAR synthetic ligands. Anal Biochem 344:8–15

Sher T, Yi HF, McBride OW, Gonzalez FJ (1993) cDNA cloning, chromosomal mapping, and functional characterization of the human peroxisome proliferator activated receptor. Biochemistry 32:5598–5604

Shi Y, Hon M, Evans RM (2001) The peroxisome proliferator-activated receptor delta, an integrator of transcriptional repression and nuclear receptor signaling. Proc Natl Acad Sci USA 99:2613–2618

Steppan CM, Bailey ST, Bhat S, Brown EJ, Banerjee RR, Wright CM, Patel HR, Ahima RS, Lazar MA (2001) The hormone resistin links obesity to diabetes. Nature 409:307–312

Su JL, Winegar DA, Wisely GB, Sigel CS, Hull-Ryde EA (1999) Use of PPAR gamma-specific monoclonal antibody to demonstrate thiazolidinediones induce PPAR gamma receptor expression *in vitro*. Hybridoma 18:273–280

Tortonoz P, Hu E, Spiegelman BM (1994) Stimulation of adiposogenesis in fibroblasts by PPARγ2, a lipid-activated transcription factor. Cell 30:1147–1156

Tortonoz P, Hu E, Spiegelman BM (1995) Regulation of adipocyte gene expression and differentiation by peroxisome proliferator activated receptor γ. Curr Opin Genet Devel 5:571–576

Vázquez M, Silvesatre JS, Prous JR (2002) Experimental approaches to study PPARγ agonists as antidiabetic drugs. Methods Find Exp Clin Pharmacol 24:515–523

Walczak R, Tontonoz P (2002) PPARadigms and PPARadoxes: expanding roles for PPARγ in the control of lipid metabolism. J Lipid Res 43:177–186

Willson TM, Brown PJ, Sternbach DD, Henke BR (2000) The PPARs: From orphan receptors to drug discovery. J Med Chem 43:527–550

Wu Z, Xie Y, Morrison RF, Bucher NLR, Farmer SR (1998) PPAR-γ induces the insulin-dependent glucose transporter GLUT4 in the absence of C/EBP$_\alpha$ during the conversion of 3T3 fibroblasts into adipocytes. J Clin Invest 101:22–32

Xu HE, Lambert MH, Montana VG, Parks DJ, Blanchard SG, Brown PJ, Sternbach DD, Lehmann JM, Wisely GB, Willson TM, Kliewer SA, Milburn MV (1999) Molecular recognition of fatty acids by peroxisome proliferator-activated receptors. Mol Cell 3:397–403

Young PW, Buckle DR, Cantello BCC, Chapman H, Clapham JC, Coyle PJ, Haigh D, Hindley RM, Holder JC, Kallender H, Latter AJ, Lawrie KWM, Mossakowska D, Murphy GJ, Cox LR, Smith SA (1998) Identification of high-affinity binding sites for the insulin sensitizer Rosiglitazone (BRL-49653) in rodent and human adipocytes using a radioiodinated ligand for peroxisomal proliferator-activated receptor γ. J Pharmacol Exp Ther 284:751–759

K.6.4.5 Effect on Proliferation

PURPOSE AND RATIONALE

Both, insulin and IGF-1 stimulate growth and proliferation of cells which express the corresponding receptors at adequate number. However, they differ considerably in their relative potency with IGF-1 exerting at least 100-fold higher/lower mitogenic/metabolic activities compared to those of insulin. The *in vivo* metabolic action of IGF-1 can be compared with insulin in adult rats using the following methods (DeMeyts 1994, Ulrich and Schlessinger 1990, Schlessinger and Ulrich 1992, Simpson et al. 1998), (i) dose-dependence and time-dependence of blood sugar decrease after intravenous injection, (ii) the antilipolytic effect (decrease of non-esterified fatty acids) after i.v. injection, (iii) stimulation of glucose disposal dur-

ing euglycemic clamping after intravenous infusion. Furthermore, all other assays described for insulin can be applied. Gazzano-Santoro and coworkers (1998) described a cell-based potency assay for IGF-1.

PROCEDURE

Cell Culture

Cells from the human cell line HU-3, established from the bone marrow of a patient with acute megakaryoblastic leukemia, are adapted to grow in the presence of human thrombopoietin. Removal of thrombopoietin results in decreased proliferation and rapid loss of viability. Cells are cultured in RPMI-1640 medium with 2% heat-inactivated human serum, 2 mM glutamine, 10 mM HEPES (pH 7.2) and 5 ng/ml thrombopoietin in culture flasks. They are grown in suspension at 37°C in a humidified 5% CO_2 incubator and are routinely subcultured every two or three days when densities reach $0.8–1.5 \times 10^6$ cells/ml.

Alternatively, the proliferative potency of insulin analogs can be determined by measuring the proliferation of human mammary epithelial cells (HMEC, Clonetics USA) in culture. HMEC obtained at passage 7 and expanded and frozen at passage 8 are used at passage 10 for all experiments. Cells are cultured in growth medium (fuly supplemented MEGM, Bio Whittaker, 10 ng/ml hEGF, 5 µg/ml insulin, 0.5 µg/ml hydrocortisone, 50 µg/ml gentamycin, 50 ng/ml amphotericin-B, 13 mg/ml bovine pituitary extract) which is changed every day. For a growth experiment, the medium is changed to assay medium lacking insulin but containing 0.1% BSA.

Assay

The HU-3 cell growth assay is performed under serum-free conditions in assay medium consisting of RPMI-1640 supplemented with 0.1% BSA, 10 mM HEPES (pH 7.2) and 50 µg/ml gentamycin. HU-3 cells are washed twice in the assay medium and resuspended at a density of 0.25×10^6 cells/ml. In a typical assay, 100 µl of a cell suspension (25,000 cells/well) and 100 µl of IGF-1 at varying concentrations are added to flat bottomed 96-well tissue culture plates at 37°C and 5% CO_2 and cultured for 2 d. 40 µl of Alamar Blue™ (undiluted) are then added and the incubation continued for 7–24 h. The plates are allowed to cool to room temperature for 10 min on a shaker and the fluorescence is read using a 96-well plate fluorometer with excitation at 530 nm and emission at 590 nm.

The HMEC cell growth assay is performed in 96-well Cytostart scintillation microplates (Amerham Pharmacia). One day one, HMEC cells are seeded at a density of 4,000 cells/well in 100 µl of assay medium. Insulin in the growth medium is replaced with graded doses of recombinant human insulin or insulin analog/compounds from 0–1 µM final concentration. After 4-h incubation, 0.1 µCi of ^{14}C-thymidine in 10 µl of assay medium is added to each well and plates are read at 48 h and/or 72 h in a microtiter plate scintillation counter.

EVALUATION

Recombinant human insulin and IGF-1 are controls used in each assay run, and recombinant human insulin is on each assay plate. Results, expressed as relative fluorescence units, are plotted against IGF-1/compound concentrations using a 4-parameter curve-fitting program. Test compounds are compared with the standard. Typically, the maximal growth response is between 3- to 4-fold stimulation over basal. Response data are normalized to between 0 and 100% response equal to 100 X (response at concentration X – response at concentration zero) divided by (response at maximal concentration – response at zero concentration). Concentration-response data are fit by non-linear regression employing appropriate software. Analysis of the proliferative capacity of novel recombinant insulin analogs with improved kinetic profile in comparison to IGF-1 and insulin is of tremendous importance.

REFERENCES AND FURTHER READING

DeMeyts P (1994) The structural basis of insulin and insulin-like growth factor-I receptor binding and negative co-operativity, and its relevance to mitogenic versus metabolic signalling. Diabetologia 37[Suppl 2]:S135–S148

Gazzano-Santoro H, Chen A, Mukku V (1998) A cell-based potency assay for insulin-like growth factor-1. Biologicals 26:61–68

Schlessinger J, Ullrich A (1992) Growth factor signaling by receptor tyrosine kinases. Neuron 9:383–391

Simpson HL, Umpleby AM, Russell-Jones DL (1998) Insulin-like growth factor-1 and diabetes. A review. Growth Horm IGF Res 8:83–95

Ullrich A, Schlessinger J (1990) Signal transduction by receptors with tyrosine kinase activity. Cell 61:203–212

K.6.5
Assays for Insulin and Insulin-Like Regulation of Energy Metabolism

K.6.5.1
Determination of Oxygen Consumption and Extracellular Acidification Rates

PURPOSE AND RATIONALE

Accumulating experimental evidence indicates that dysregulation of energy metabolism is a fundamen-

tal process that is associated with the phenotype of metabolic disorders, in particular type II diabetes and obesity. Many current anti-diabetic drugs (metformin, glitazones) target the pathways that control glucose metabolism. Very recently, a technologies (Bionas Inc. Germany, Seahorse Bioscience Inc. USA) have been developed that manages to rapidly profile the bioenergetic pathways in a variety of cell types. These include alterations caused by drugs that target the specific metabolic pathways the cell uses to ensure its energy demands, normal metabolic functions and survival. These technologies allow a more detailed analysis of the link between glucose/lipid metabolism and energy metabolism, including interference of one or the other by compounds/drug candidates, as well as the screening for or characterization of drug candidates affecting or leaving unaffected those pathways. For this, both the oxygen consumption rate (OCR), which primarily reflects mitochondrial respiration, and the extracellular acidification rate (ECAR), which primarily reflects lactic acid production (glycolysis), are measured using the Bionas or Seahorse technology. Furthermore, the OCR and ECAR readings allow to profile the metabolic sensitivities and degree of inhibition/stimulation of a number of cell lines relevant for the study of glucose and lipid metabolism and its regulation toward modulators of anaerobic and aerobic energy metabolism (e. g. phloretin, 2-deoxyglucose, dinitrophenol). Analysis of the sensitivities of the cell lines to these modulators provides insights into their bioenergetic preferences/dependencies and their global physiological responses to the modulation. This characterization may be useful for the selection of cell lines appropriate for use in screening for compounds with anti-proliferative activity (ECAR for anaerobic energy metabolism; Boros et al. 2002) as well as insulin-like metabolic activity (OCR for aerobic energy metabolism; Wolf et al. 1997), with regard to sensitivity and responsiveness of their energy metabolism and the relevant bioenergetic pathways (Ehret et al. 2001). During the last decade multiparametric cellular microelectronic interdigitated biosensor chips for microphysiological and screening applications with living cells have been developed (Ehret et al. 2001, Lehmann et al. 2000).

PROCEDURE

Bionas 2500 Analyzing System

The Bionas 2500 analyzing system is an automated system suitable for online cell-based compound/drug candidate identification and profiling. The innovative aspect of this bioanalytical device is the adaptation of electronic chip design for a completely non-invasive and multiparametric sampling of metabolically relevant readouts in long-term tissue and cell culture. The system uses a silicon-based technology to continuously monitor minute changes in (i) solution pH resulting from the output of acid metabolites excreted by living cells into their immediate microenvironment (Lehmann et al. 2001), (ii) oxygen content resulting from oxygen consumed by living cells from their immediate microenvironment and (iii) electrical impedance resulting from the electrical isolation of intact cell membranes close to the sensor surface (adhesion/confluence) (Ehret et al. 1998). The Bionas 2500 analyzing system works in real-time, allowing the rapid and continuous monitoring of cellular activity and the measurement of recovery from a particular challenge and the process of desensitization.

Cells are seeded onto Bionas metabolic chips the day prior to the experiment and left to attach to the sensor surface overnight. The sensor chips are then transferred into the Bionas 2500 analyzing system. The system has the capacity to measure the acidification, respiration and adhesion/confluence rate from six separate sensor chips. Modified, low-buffered medium is pumped across the cells at a rate of 56 µl/min during which time the pH and the oxygen content of the microenvironment surrounding the sensor is maintained constant. To measure the rates for acidification and respiration from cells the fluid flow is periodically halted, allowed a build-up of acid metabolites and a depletion of oxygen in the chamber and, therefore, an alteration in the fluid pH and oxygen content. Flow is resumed and the acid and oxygen-depleted fluid flushed out of the chamber. This flow-on, flow-off cycle is repeated throughout the experiment. To measure the adhesion/confluence, no fluid perfusion is necessary. After collecting baseline acidification, respiration and adhesion rates, the compound/drug candidate is introduced and the effect on acidification, respiration and adhesion rates are monitored.

Seahorse XF Instrument

Adherent 3T3-L1 adipocytes, L6-myoblasts/myotubes or HepG2 cells are seeded in 24-well Seahorse cell culture microplates at various cell densities per chamber per well. Approximately 45 min prior to the assay, the culture medium is exchanged with a low-buffered RPMI assay medium to ensure accurate ECAR readings. For detection of acute drug responses, OCR and ECAR are measured for 5 min in each well to establish a baseline. Compound/drug solution is then added and followed by measurement of OCR and ECAR.

For time resolved measurements, test measurements are made at a series of time points. Non-adherent cells (primary hepatocytes and adipocytes) are seeded onto Cell-Tak-coated Seahorse cell culture microplates either before or after the compound/drug treatment. Cell-Tak treatment of plates is performed according to manufacturers instruction. Cells remain attached to the surface of the well after the measurement as determined by light microscopy. Cells are lifted from the culture surface by simple pipetting without trypsin treatment.

A unique feature of the Seahorse instrument is its ability to make accurate and repeatable measurements in as little as 5 minutes. This is accomplished by isolating an extremely small volume (less than 10 µl) of medium above the cell monolayer. Cellular metabolism causes rapid, easily measurable changes to the "microenvironment" in this small volume. Typically, a measurement cycle is performed for 2–10 min. During the time, analyte levels are measured every 8 sec until oxygen concentration drops approximately 10% and medium pH declines approximately 0.1 unit. The measurement is performed using fluorescent biosensors embedded in a sterile disposable cartridge that is placed above a 24-well tissue culture microtiterplate.

EVALUATION

Baseline metabolic rates are typically measured twice and are reported in nmol/min for OCR and mpH/min for ECAR. Compound/drug is then added to the medium and mixed for 5 min, and then the post-treatment OCR and ECAR measurements are made and repeated. As cells shift metabolic pathways, the relationship between OCR and ECAR changes. Because these measurements are non-destructive, cells can be profiled over a period of minutes, hours or days.

K.6.5.2 Metabolomics

GENERAL CONSIDERATIONS

The flow of information from DNA to cellular building blocks is the central dogma of biology. DNA is transcribed into RNA, then translated to proteins, which then make small molecules. While there may be over 25,000 genes, 100,000 to 200,000 transcripts and up to 1,000,000 proteins, it is estimated that there may be as few as 2,500 small molecule species in the human metabolome. Metabolomics is the study of the metabolome, i. e. of the repertoire of these non-proteinaceous, endogenously-synthesized small molecules present in an organism. Representative small molecules include well-known compounds such as glucose, cholesterol, ATP and soluble signaling molecules, such as cAMP, AMP, diacylglycerol. These molecules are the ultimate product of cellular metabolism. The metabolome refers to the catalogue of those roughly 2,400 known endogenous metabolites in a specific organism. Most important, the normal physiological and disease states are ultimately manifest at the level of biochemistry and more precisely, at the level of the metabolome. It is more clear-cut and more quantitative because it is known where metabolites fit in biochemical pathways and the metabolites' relative concentrations are measurable. This makes a clear difference to many of the other "omics" sciences. It seems very likely that intelligent application of this methodology in appropriate animal disease models will considerably facilitate the identification and characterization of compounds/drugs for most indications and for metabolic diseases, in particular, with regard to potency, safety, accuracy, predictability and the time required. The putative "systems" contribution of metabolomics to pharmaceutical drug discovery and development has been reviewed by Harrigan (2006).

PURPOSE AND RATIONALE

Metabolomics technology determines the small molecule repertoire of a cell or a biological sample typically using a proprietary approach of simultaneous, multidimensional molecular analysis, followed by sophisticated data analysis and visualization. Biological samples are extracted using special protocols and the resulting extracts are separated and analyzed using a variety of detection techniques. Chromatographic outputs are analyzed using multiple mass spectrometers, which accurately identify the mass for a particular molecular species. Electrochemical detectors monitor additional broad classes of compounds. By choosing appropriate types of separation and detection technologies and mass spectrometers, the cellular metabolites are analyzed according to their various properties. Modified mass spectrometers produce data streams that are automatically processed and stored in proprietary information management systems. The data are quality-checked, reduced, refined and abstracted using custom algorithms and software. Data visualization is then used to compare experimental data to a large data base of control information. Hundreds of compounds of known identity are measured in a sample and contrasted to controls. Unique unknowns are brought to light for structure elucidation.

PROCEDURE

Metabolomics research is characterized, at least I part, by two different (but not necessarily mutually exclusive) conceptual approaches broadly defined as "targeted" and "non-targeted" (Harrigan and Goodacre 2003, Goodacre et al. 2003, Vaidyanathan et al. 2005). Non-targeted approaches provide a hypothesis-free global overview of high abundance metabolites most affected by experimental perturbation or disease. Targeted approaches which highlight identified and preselected metabolic pathways may prove more relevant in evaluating the impact of a compound/drug candidate on metabolic regulation. Technology platforms for targeted approaches are based on discrete optimized analytical strategies for different classes of metabolites or pathways. This approach represents both an accommodation with the wide differences in physicochemical structure, stability and differential abundance of metabolome components. It clearly facilitates greater evaluation of low-abundance, biologically important metabolites, such as eicosanoids, other signalling lipids and hormones. A key challenge for vendors providing instrumentation to support metabolomics is in establishing an optimal balance between the accuracy and range of metabolite measurements. Targeted metabolomics approaches additionally allow adoption of flux-based methodology where specifically designed tracer-labeled substrates can be incorporated into test biological systems and their distribution and metabolic fate recorded. Metabolic flux analyses provide an operational "moving picture" rather than a compositional "snapshot" of a biological system. At present, this approach is somewhat underpresented in metabolomics but it may be pointed out that the data acquisition technologies used here are essentially that used in compositional studies. The data acquisition technologies utilised in metabolomics, primarily nuclear magnetic resonance spectroscopy and mass spectrometry have been extensively reviewed (Weljie et al. 2006).

Applications in Early Drug Discovery

There is considerably emphasis on metabolomic applications in later stages of drug discovery, including clinical trials. However, strategies to reduce attrition may be most cost-effectively implemented at the earliest stages of drug discovery, which encompasses disciplines such as target validation and high-throughput screening. In current drug discovery projects substrate/product ratios are used as mechanistic markers of enzyme function in increasing number. It is critical that a drug candidate be shown to act on its target throughout all stages of the value chain and that modulation of that target does indeed impact disease progression.

Applications in the Analysis of Animal Models

The development of drugs for the regulation of metabolic diseases, such as cardiovascular diseases, obesity and type II diabetes, clearly requires considerable efficacy and toxicological testing in animal models. Efficacy assessments also require that regulation of metabolism in animal models is reasonably well understood. A metabolomics study utilising an analytical platform developed by Lipidomics Technologies Inc. that allows quantitative measurement of more than 500 lipid metabolites in blood and tissue samples has recently been employed to probe metabolic regulation in the low density lipoprotein receptor null (LDLrKO) mouse, a model for atherosclerotic progression (Krul et al. 2006).

Correlation of Metabolome, Proteome and Transcriptome Data Sets

An increasing area of interest is correlation of metabolomic data sets with proteomic and transcriptomic data sets (Davidov et al. 2004). While the goal of such studies is presumably to provide a deeper understanding of biological systems it may be worth pointing out that if the metabolome were truly closer to phenotype, then the use of complementary data from genomics, transcriptomics and proteomics could be perceived as merely ancillary or even potentially confounding. In an integrated transcriptomic and NMR-based metabolomic study of fatty liver in the rat, an inverse correlation between stearoyl CoA desaturase mRNA levels and levels of unsaturated fatty acids described as "surprising" by the authors was revealed (Griffin et al. 2004). This observation is somewhat less surprising when placed in the context of a metabolomic demonstration that gene expression patterns in the adipose tissue of obese mice resulted in assessments of rates of fatty acid synthesis and lipogenesis that are inconsistent with direct measurements of the metabolic fluxes (Hellerstein 2003).

Future Metabolomics Technologies

The development of a new methodology for determining the concentration of protein-unbound FFA in intracellular and extracellular milieu entitled "Fluorescent Probes for Hydrophobic Metabolites" represents a particularly intriguing programme. Although FFA levels are clearly critical in many diseases, monitoring of

unbound FFA profiles remains technically challenging and improved detection methodologies can only help facilitate drug candidate progression in a range of therapeutic areas. The use of fluorescently labeled metabolite probes is also a theme in a proposal "Glycolipid Metabolism in Single Cells" to dissect glycolipid metabolism in single neurons. This proposal will focus on the development of different fluorescently labeled substrates within two different glycolipid metabolite pathways and offers particular promise in pharmacological evaluations of neuroactive agents. Another cellular neuro-metabolomic proposal "Technologies for Cellular Neurometabolomics" addresses the use of a suite of technology developments including unique sampling protocols, microfluidically-based sample conditioning unit with integrated electrophoretic separations, followed by native fluorescence and mass spectrometric detection and capture of appropriate metabolites into nl-volume capillaries for nl-volume NMR spectroscopic characterization.

EVALUATION

Companies (e. g. Metabolon Inc.) have developed proprietary software to link the resulting profile directly to metabolic pathway maps. This linkage greatly facilitates the identification of particular pathways that are affected in the biological sample relative to controls. In this way, the genes, RNAs, and proteins involved in a disease can be quickly and efficiently elucidated. By analyzing a sample using multiple mass spectrometry-based technologies, integrating the data, and analyzing through proprietary software and algorithms, the characterization of compounds/drugs in animal disease models, in general, for metabolic diseases such as type II diabetes, in particular, can be achieved much faster and more accurately than previously possible. Moreover, academic efforts have recently been initiated supporting well-conceived and technically feasible innovations that have the potential to drive metabolomics as a biologically informed science and provide metabolomic data that can be integrated into early drug candidate evaluation and also guide subsequent biomarker-enabled *in vivo* studies.

REFERENCES AND FURTHER READING

Boros LG, Cascante M, Lee WN (2002) Metabolic profiling of cell growth and death in cancer: applications in drug discovery. Drug Discovery Today 7:364–372

Davidov E, Clish CB, Oresic M, Meys M, Stochaj W, Snell P, Lavine G, Londo TR, Adourian A, Zhang X, Johnston M (2004) Methods for the differential intergrative omic analysis of plasma from a transgenic disease animal model. Omics 8:267–288

Ehret R, Baumann W, Brischwein M, Lehmann M, Henning T, Freund I (2001) Multiparametric cellular biosensor chips for screening applications. Fresenius J Anal Chem 369:30–35

Ehret R, Baumann W, Brischwein M, Schwinde A, Wolf B (1998) On-line control of cellular adhesion with impedance measurements using interdigitate electrode structures. Med Biol Engineer Comput 36:365–370

Goodacre R, Vaidyanathan S, Dunn WB, Harrigan GG, Kell DB (2004) Metabolomics by numbers-aquiring and understanding global metabolite data. Trends Biotechnol 22:245–252

Griffin JL, BonneySA, Mann C, Hebbachi AM, Gibbons GF, Nicholson JK, Shoulders CC, Scott J (2004) An integrative reverse functional genomic and metabolic approach to understanding orotic acid induced fatty liver. Physiol Genomics 17:140–149

Harrigan GG (2006) Metabolomics, a "systems" contribution to pharmaceutical discovery and drug development. Drug Discovery World Spring 2006:39–46

Harrigan GG, Goodacre R (Eds) (2003) Metabolic profiling: its roloe in biomarker discovery and gene function analysis. Kluwer Academic Publishers, MA, USA

Hellerstein MK (2003) *In vivo* measurement of fluxes through metabolic pathways; the missing link in functional genomics and pharmaceutical research. Annu Rev Nutr 23:379–402

Krul E, Butteiger D, Flickinger A, Harrigan GG, Wiest MM, German BG, Watkins SM (2006) Lipid metabolome analysis of the LDL receptor null mouse. In preparation

Lehmann M, Baumann W, Brischwein M, Ehret R, Kraus M, Schwinde A, Bitzenhofer M, Freund I, Wolf B (2000) Noninvasive measurement of cell membrane associated proton gradients by ionsensitive field effect transistor arrays for microphysiological and bioelectronical applications. Biosensors&Bioelectronics 15:117–124

Lehmann M, Baumann W, Brischwein M, Gahle HJ, Freund I, Ehret R, Drechsler S, Palzer H, Kleintges M, Sieben U, Wolf B (2001) Simultaneous measurement of cellular respiration and acidification with a single CMOS ISFET. Biosensors&Bioelectronics 16:195–203

Vaidyanathan S, Harrigan GG, Goodacre R (Eds) (2005) Metabolome analyses: strategies for systems biology. Springer Science+Business Media, MA, USA

Weljie AM, Newton J, Mercier P, Carlson E, Slupsky CM (2006) Targeted profiling: quantitative anaylsis of ^{1}H NMR metabolomics data. Anal Chem 78:4430–4442

Wolf B, Brischwein M, Baumann W, Ehret R, Kraus M (1997) Monitoring of cellular signalling and metabolism with modular sensor-technique. The PhysioControl-Microsystem (PCM). Biosensors&Bioelectronics 13:501–509

K.6.6
Assays for the Expression and Release of Insulin and Glucose-Regulating Peptide Hormones from Pancreatic β-Cells

K.6.6.1
Insulin Release from the Isolated Perfused Rat Pancreas

PURPOSE AND RATIONALE

The *in vitro* perfusion of the isolated rat pancreas as described by Anderson and Long (1947), Ross (1972), Grodsky and coworkers (1983, 1984) and Muñoz and

coworkers (1995) offers the advantage to study the influence of carbohydrates, hormones and drugs such as sulfonylureas not only on insulin but also on glucagon and somatostatin secretion without interference of secondary effects resulting from changes in hepatic, pituitary or adrenal functions.

PROCEDURE

The insulin concentration of the perfusate of the rat pancreas prepared as described (see K.5.4.1) is determined with the RIAgnost kit using rat insulin as standard in every second sample. The determination is done immediately after the end of an experiment.

K.6.6.2 Insulin Release from the Isolated Perifused Rat Pancreatic Islets

PURPOSE AND RATIONALE

An assay with isolated pancreatic islets to study the dynamic response and transitions between various metabolic states has been recommended by Idahl (1972). A further description and discussion of the method were given by Malaisse-Lagae and Malaisse (1984).

PROCEDURE

The insulin concentration of the perifusate of the rat islets prepared as described (K.5.4.2) is determined with the RIAgnost kit using rat insulin as standard in every second sample. The determination is done immediately after the end of an experiment.

EVALUATION

The raw data are expressed in µU insulin per islet/min. Mean and standard error of the mean of each time interval are calculated for graphical representation. The values under exposure to drug are compared with the values under perifusion with glucose only, and with the effect of elevated glucose.

REFERENCES AND FURTHER READING

Anderson E, Long JA (1947) The effect of hyperglycemia on insulin secretion as determined with the isolated rat pancreas in a perfusion apparatus. Endocrinology 40:92–97

Fletcher DJ, Weir G (1984) Tissue culture of dispersed islet cells. In: Larner J, Pohl StL (eds) Methods in Diabetes Research. Vol I: Laboratory Methods. Part A. Wiley, New York, pp 167–173

Geisen K (1988) Special pharmacology of the new sulfonylurea glimepiride. Arzneim Forsch/Drug Res 38:1120–1130

Grodsky GM, Batts AA, Bennett LL, Vicella C, McWilliams NB, Smith DF (1983) Effects of carbohydrates on secretion of insulin from isolated rat pancreas. Am J Physiol 205:638–644

Grodsky GM, Heldt A (1984) Method for the *in vitro* perfusion of the pancreas. In: Larner J, Pohl SL (eds) Methods in Diabetes Research. Vol. I.: Laboratory Methods, Part B. Wiley, New York, pp 137–146

Horaguchi A, Merrell RC (1981) Preparation of viable islet cells from dogs by a new method. Diabetes 30:455–458

Idahl LÅ (1972) A microperifusion device for pancreatic islets allowing concomitant recordings of intermediate metabolites and insulin release. Analyt Biochem 50:386–398

Kaiser N, Cerasi E (1991) Long term monolayer culture of adult rat islet of Langerhans. An experimental model for studying chronic modulation of β-cell function. In: Greenstein B (ed) Neuroendocrine Research Methods. Vol 1, Chapter 6, Harwood Academic Publ, pp 131–147

Lernmark Å (1974) The preparation of, and studies on, free cell suspensions from mouse pancreatic islets. Diabetologia 10:431–438

Malaisse-Lagae F, Malaisse WJ (1984) Insulin release by pancreatic islets. In: Larner J, Pohl StL (eds) Methods in Diabetes Research. Vol. I.: Laboratory Methods, Part B. Wiley, New York, pp 147–152

Marchetti P, Giannarelli R, di Carlo A, Zappella A, Masoni A, Masiello P, Marchetti A, Picaro L, Navalesi R (1989) *In vitro* function of porcine islets of Langerhans. Diabetes Nutr Metab Clin Exper 2:105–109

McDaniel ML, Colca JR, Kotagal N (1984) Islet cell membrane isolation and characterization. In: Larner J, Pohl StL (eds) Methods in Diabetes Research. Vol I: Laboratory Methods. Part A. Wiley, New York, pp 153–166

Muñoz M, Sweiry JH, Mann GE (1995) Insulin stimulates cationic amino acid transport in the isolated perfused rat pancreas. Exper Physiol 80:745–753

Panten U, Ishida H, Schauder P, Frerichs H, Hasselblatt A (1977) A versatile microperifusion system. Anal Biochem 82:317–326

Pipeleers DG (1984) Islet cell purification. In: Larner J, Pohl StL (eds) Methods in Diabetes Research. Vol. I.: Laboratory Methods, Part B. Wiley, New York, pp 185–211

Ross BD (1972) Endocrine organs: Pancreas. In Ross BD: Perfusion Techniques in Biochemistry. A Laboratory Manual in the Use of Isolated Perfused Organs in Biochemical Experimentation. Clarendon Press, Oxford, pp 321–355

Schatz H, Maier V, Hinz M, Nierle C, Pfeiffer EF (1972) The effect of tolbutamide and glibenclamide on the incorporation of [^{3}H] leucine and on the conversion of proinsulin to insulin in isolated pancreatic islets. FEBS Lett 26:237–240

K.6.6.3 Insulin Release from Cultured β-Cells

PURPOSE AND RATIONALE

Insulin released into the supernatant of monolayers of cultured β-cells grown in 96-well culture dishes as described above is determined radioimmunochemically (see above) using a guinea pig anti-rat insulin antibody, ^{125}I-labeled human insulin as tracer and rat insulin as standard. Free and bound radioactivity is separated using an anti-IgG (goat anti-guinea pig) antibody. Typically, the sensitivity of this assay is 17 pM, and the coefficient of variation is less than 3% at both low and high levels.

PROCEDURE

Insulin Secretion from MIN6 Cells

Cultured MIN6 cells (1×10^5) are replated and cultured (see K.5.4.4) for 24 h before being used in secretion assays. Insulin secretion is measured during 1 h static incubations in KRBH(118.5 mM NaCl, 2.54 mM $CaCl_2$, 1.19 mM KH_2PO_4, 4.74 mM KCl, 25 mM $NaHCO_3$, 1.19 mM $MgSO_4$, 10 mM HEPES, pH 7.4) containing 0–20 mM glucose (basal or glucose-induced secretion) and/or compounds/drugs. Samples of the supernatant are assayed for insulin. To determine total insulin content, insulin is extracted using 95/5 ethanol/acetic acid. Insulin is measured using a mouse insulin ELISA kit.

Insulin Secretion from RINm5F Cells

One day prior to the experiment, approximately 1×10^6 RINm5F cells, grown as described above, are seeded into 24-well test plates. At the time of the experiment, the culture medium is aspirated, and the cells are washed with 1 ml of a modified KRBH containing 10 mM HEPES/KOH (pH 7.4), 5 mM $NaHCO_3$, 0.5% BSA and 0–20 mM glucose. After pre-incubation for 30 min at 37°C with the above buffer, compounds/drug candidates dissolved in DMSO at 10 mM are added (final concentration range from 10 nM to 100 µM) and incubated for 30 min at 37°C. The incubation is stopped by aspiration of the buffer which is stored at −80°C until measurement of insulin by ELISA or RIA. After the aspiration, the cells are washed with PBS and dissolved in 0.5 ml NaOH (0.1 M). After overnight incubation, the resulting solution is collected for assay of cellular protein content.

Insulin Secretion from INS1 Cells

INS1 cells (5×10^4 per well in 12-well plates) are treated with RPMI 1640 medium containing 3–20 mM glucose and 0.5 mM FFA or a mixture of oleic and palmitic acids in equal ratio, with a total concentration of 0.5 mM. Control wells contained 0.5% fatty acid-free BSA in medium. After 24 h, the cells are washed in PBS and pre-incubated for 2 h in KRBH containing 0–20 mM glucose (119 mM NaCl, 4.75 mM KCl, 5 mM $NaHCO_3$, 1.2 mM $MgSO_4$, 1.18 mM KH_2PO_4, 20 mM HEPES, pH 7.4, 2.54 mM $CaCl_2$). Glucose responsiveness is evaluated by an initial 30-min incubation in KRH containing 3 mM glucose followed by incubation for 30 min in KRH containing 20 mM glucose. Samples are collected for insulin measurement using RIA or ELISA with CV 4.5% and minimal detection 0.15 µg/l.

Insulin Secretion from Attached INS-1E Cells

The secretory responses to glucose and other secretagogues are tested in INS-1E cells between passages 54–95 according to the procedure of Merglen and coworkers (2004). Before the experiments, cells are maintained for 2 h in glucose-free culture medium. The cells are then washed twice and preincubated for 30 min at 37 C in glucose-free KRBH (135 mM NaCl, 3.6 mM KCl, 5 mM $NaHCO_3$, 0.5 mM NaH_2PO_4, 0.5 mM $MgCl_2$, 1.5 mM $CaCl_2$, and 10 mM HEPES, pH 7.4) BSA (0.1%) is added as an insulin carrier. Next, cells are washed once with glucose-free KRBH and then incubated for 30 min in KRBH and compounds/drug candidates. Incubation is stopped by putting the plates on ice. The supernatants are collected for insulin secretion, and cellular insulin contents are determined from acid-ethanol extracts. Insulin secretion is measured by RIA or ELISA using rat insulin as standard (see K.4.1).

Perifusion of INS-1E Cell Clusters

Spheroid clusters composed of INS-1E cells are preincubated for 2 h in glucose-free culture medium. After low speed centrifugation (500 rpm), cell clusters are resuspended in glucose-free KRBH and counted, and about 500 spheroids are distributed per chamber in a 250-µl volume thermostated at 37°C. The flow rate is set at 0.5 ml/min, and fractions are collected every minute after a 20-min washing period at basal 2.5 mM glucose. At the end of the perifusion, cell clusters are collected, and insulin contents are determined from acid-ethanol extracts.

Total Insulin Content

Cells from 4 wells of 24-well culture dishes are scraped into ice-cold PBS containing 5.5 mM glucose and 0.1% fatty acid-free BSA and immediately frozen in liquid N_2. Frozen cells are sonicated in acidic ethanol (0.2 M HCl in 87.5% ethanol). The samples are then centrifuged. The supernatant is used for measurement of total insulin content. Insulin in the perifusion fractions and cell extracts is determined by RIA or ELISA (see K.4.1).

K.6.6.4 Lipolysis in β-Cells

PURPOSE AND RATIONALE

Besides the *de novo* synthesis of LC-CoA starting with the ACC reaction and malonyl-CoA formation, leading to inhibition of the translocation of LC-CoA into mitochondria, lipid-derived signaling molecules involved

in insulin secretion may also originate from the breakdown of TAG stores in β-cells. This may occur through activation of HSL, the enzyme that exerts a major control in TAG hydrolysis in adipose tissue (for a review see Yeaman 2004).

It was first demonstrated in 1999 that HSL is expressed and active in the β-cells of the pancreatic islet (Mulder et al. 1999). Two isoforms are expressed in the β-cell, the 84-kDa protein seen in adipocytes and other tissues and an 89-kDa protein (Mulder et al. 1999) encoded by exons 1–9 *plus* exon A, which is spliced to exon 1, introducing an additional 43 amino acids into the polypeptide (Lindvall et al. 2004).

The role of HSL in the β-cell has yet to be fully established. Two studies have independently looked at insulin secretion in HSL-knockout mice (Roduit et al. 2001, Fex et al. 2004). Both demonstrate features of insulin resistance in peripheral tissues, but differ in the effect of the knockout on insulin secretion from the pancreas. In one study, the glucose-responsiveness of insulin secretion was impaired (Roduit et al. 2001), both *in vivo* and in pancreatic islets isolated from the mice. The islets from the HSL knockout mice were totally unresponsive to glucose, but showed a normal response to depolarizing concentrations of KCl. This work is consistent with a key role for HSL in coupling of glucose metabolism to increased insulin secretion, perhaps by generating a lipid messenger such as DAG or fatty acyl-CoA from intracellular stores of TAG (Mulder et al. 1999, Roduit et al. 2001, Yaney et al. 2000). Also consistent with this role is the increased expression of HSL in response to high concentrations of glucose, with the elevated glucose ensuring an appropriate supply of the lipid mediators (Sorhede-Winzell 2001). The second study in HSL null mice demonstrated that insulin secretion was essentially unimpaired, with an increase in islet mass being found, presumably as a result of the insulin resistance in peripheral tissues (Fex et al. 2004). Possible reasons for the apparent discrepancies between the two studies may rely on the genetic background of the mice.

However, recent studies on transgenic mice that overexpress HSL specifically in the β-cell have provided evidence for a role for HSL in mediating the lipotoxicity associated with type II diabetes. These mice showed impaired glucose tolerance and had defective GSIS when fed a high-fat diet, accompanied by lower levels of β-cell TAG than found in control mice fed the same diet (Sorhede-Winzell 2003a). One proposed mechanism for this is that HSL provides endogenous ligands for lipid-activated transcription factors, including the PPAR-activated receptors. In this regard, it would appear that, in control animals, the accumulation of intracellular TAG is actually a protective mechanism (Listenberger et al. 2003), with the lipotoxicity being manifested when the storage capacity is exceeded or when the lipid stores are mobilized by HSL. Consistent with this is the observation that long-term feeding with a high-fat diet leads to down-regulation of pancreatic HSL levels by as much as 75%, presumably as a protective mechanism against the generation of these lipid metabolites (Sorhede-Winzell 2003b).

PROCEDURE

Lipolysis in cultured β-cells is determined as the release of glycerol into the incubation medium. Since FFA and glycerol are the end-products of lipolysis and glycerol is not metabolized by the β-cell due to low expression of glycerol kinase, glycerol release actually reflects the degree of lipolysis in cultured β-cells. Cells grown in 24-well culture dishes are incubated in 500 µl of RPMI 1640 medium containing 10% (by vol.) heat-inactivated fetal calf serum, 50 IU/ml penicillin, 0.25 µg/ml amphotericin B and 50 µg/ml streptomycin in the presence of increasing concentrations of glucose (2.8–16.7 mM) at 37°C for up to 4 h in an atmosphere of humidified air/CO_2 (19/1). After certain periods of time, 20-µl portions are transferred to a 96-well culture plate and incubated with glycerol kinase (50 U/ml) and luciferin/luciferase reagent. After addition of 10 µl of 1 mM ATP, the luminescence is measured in a luminometer after 4, 8 and 12 min. The glycerol concentration is calculated from the standard curve.

REFERENCES AND FURTHER READING

Lindvall H, Nevsten P, Strom K, Wallenberg R, Sundler F, Langin D, Sorhede-Winzell M, Holm C (2004) A novel hormone-sensitive lipase isoform expressed in pancreatic β-cells. J Biol Chem 279.3828–3836

Listenberger LL, Han X, Lewis SE, Cases S, Farese RV, Ory DS, Schaffer JE (2003) Triglyceride accumulation protects against fatty acid-induced lipotoxicity. Proc Natl Acad Sci USA 100:3077–3082

Merglen A, Theander S, Rubi B, Chaffard G, Wollheim CB, Maechler P (2004) Glucose sensitivity and metabolism-secretion coupling studied during two-year continuous culture in INS-1E insulinoma cells. Endocrinology 145:667–678

Mulder H, Holst LS, Svensson H, Degerman E, Sundler F, Ahren B, Rorsman P, Holm C (1999) Hormone-sensitive lipase, the rate-lmiting enzyme in triglyceride hydrolysis is expressed and active in β-cells. Diabetes 48:228–232

Mulder H, Sorhede-Winzell M, Contreras JA, Fex M, Strom K, Ploug T, Galbo H, Arner P, Lundberg C, Sundler F (2003) Hormone-sensitive lipase null mice exhibits signs of im-

paired insulin sensitivity whereas insulin secretion is intact. J Biol Chem 278:36380–36388
Roduit R, Masiello P, Wang SP, Li H, Mitchell GA, Prentki M (2001) A role for hormone-sensitive lipase in glucose-stimulated insulin secretion. A study in hormone-sensitive lipase-deficient mice. Diabetes 50:1970–1975
Sorhede-Winzell M, Holm C, Ahren B (2003a) Downregulation of islet hormone-sensitive lipase during long-term high-fat feeding. Biochim Biophys Res Commun 304:273–278
Sorhede-Winzell M, Svensson H, Arner P, Ahren B, Holm C (2001) The expression of hormone-sensitive lipase in clonal β-cells and rat islets is induced by long-term exposure to high glucose. Diabetes 50:2225–2230
Sorhede-Winzell M, Svensson H, Enerback S, Ravnskjaer K, Mandrup S, Esser V, Arner P, Alves-Guerra M-C, Miroux B, Sandler F (2003b) Pancreatic β-cell lipotxicity induced by overexpression of hormone-sensitive lipase. Diabetes 52:2057–2065
Yaney GC, Korchak HM, Corkey BE (2000) Long-chain acyl-CoA regulation of protein kinase C and fatty acid potentiation of glucose-stimulated insulin secretion in clonal beta-cells. Endocrinology 141:1989–1998
Yeaman SJ (2004) Hormone-sensitive lipase-new roles for an old enzyme. Biochem J 379:11–22

K.6.6.5 Measurement of Ca^{2+} Levels

Imaging

For imaging of cultured β-cells according to the protocol of Toye and coworkers (2005) with the modifiactions adapted from Freeman and coworkers (2006), MIN6 cells are cultured on 35-mm Fluorodishes (World Precision Instruments) and incubated with DMEM *plus* 3 µM Fura-2-AM (Molecular Probes) for 40 min at 37°C. They are imaged at room temperature (20–24°C) using an IonOptix fluorescence system with 340 nm and 380 nm dual excitation. The 510 nm emission ratio is collected at 1 Hz. Background subtraction is performed by measuring fluorescence from a cell-free region in the field of view. Cells are perfused continuously with extracellular solution containing 137 mM NaCl, 5.6 mM KCl, 2.6 mM $CaCl_2$, 1.2 mM $MgCl_2$, 10 mM HEPES/NaOH (pH 7.4) *plus* glucose or compounds/drug candidates.

Fluorometry

Calcium levels are monitored in cells transduced the day before the experiment with the calcium-sensitive photoprotein aequorin. Measurements of mitochondrial and cytosolic calcium are performed using the corresponding adenovirus constructs, AdCA-mtAeq and AdCA-cyAeq, respectively. The 2-h preincubation period also serves to load cells with the aequorin prosthetic group, i. e. 5 µM coelenterazine [2-(*p*-hydroxybenzyl)-6-(*p*-hydroxyphenyl)-8-benzyl-imidazo[1,2-]pyrazin-3-(7H)-one; Calbiochem]. Calibration is calculated based on the total counts obtained at the end of the trace following permeabilization of the cells with 50 µM digitonin and 10 mM $CaCl_2$ exposure.

K.6.6.6 Measurement of $^{86}Rb^+$ Efflux

PURPOSE AND RATIONALE

The binding of a sulfonylurea to its receptor SUR1, a subunit of the ATP-sensitive K^+ channel of β-cells, leads to blockade of the channel activity and concomitant decrease in the K^+ efflux (Boyd III et al. 1991). The resulting depolarization of the β-cell plasma membrane causes opening of the voltage-gated Ca^{2+} channel (Nelson et al. 1987, Niki et al. 1989, Rorsman and Trube 1986, Nichols et al. 1996). The rise in the intracellular [Ca^{2+}] triggers the exocytosis of insulin. $^{86}Rb^+$ efflux can be used as marker for K^+ efflux and analyzed in response to treatment of cultured β-cells with compounds/drug candidates.

PROCEDURE

RINm5F cells are grown and plated at a density of 200,000 cells/well (24-well tissue culture plates). $^{86}Rb^+$ efflux experiments are performed at 37°C and overnight equilibration of cells in RPMI 1640 medium supplemented with 10% FCS, 0.1 µCi/ml $^{86}RbCl$ and 0.2 µCi/ml L-[^{3}H]leucine (internal marker of cell recovery). After removing the medium, cells are preincubated in a medium containing 120 mM NaCl, 1.8 mM $CaCl_2$, 0.8 mM $MgCl_2$, 10 mM KCl, 20 mM HEPES/NaOH (pH 7.5) supplemented with 0.1 µCi $^{86}RbCl$, 0.24 mg/ml oligomycin, 1 mM 2-deoxy-D-glucose and several concentrations of compounds/drug candidates as well as sulfonylureas (as positive controls). $^{86}Rb^+$ efflux studies are initiated by removing the pre-incubation medium and incubating the cells with 200 µl of the same medium/well without $^{86}Rb^+$, oligomycin, and 2-deoxy-D-glucose. Efflux is stopped by removing this medium and washing the cells three times with 1 ml of 0.1 M $MgCl_2$ at 37°C. Cells are extracted with 2 × 1 ml of 0.1 N NaOH and counted. Total intracellular concentrations of ATP are measured after extracting the cells with 1% Triton X-100 by using the luciferase-luciferin technique.

EVALUATION

Inhibition is measured as percent of maximum $^{86}Rb^+$ efflux. Half maximum inhibition constants can be calculated.

MODIFICATIONS OF THE METHOD

Daniel and coworkers (1991) recommended a high through-put ^{86}Rb efflux assay in human medulloblastoma cells TE671 for screening of potassium channel modulators. Hu and coworkers (1995) cloned a voltage-regulated K channel from human hippocampus for transfection into CHO cells. The authors recommended this method as a high through-put assay to identify isotype-specific K-channel modulators.

REFERENCES AND FURTHER READING

Boyd III AE, Aguilar-Bryan L, Bryan J, Kunze DL, Moss L, Nelson DA, Rajan AS, Raef H, Xiang H, Yaney GC (1991) Sulfonylurea signal transduction. Rec Progr Horm Res 47:299–317

Daniel S, Malkowitz L, Wang HC, Beer B, Blume AJ, Ziai MR (1991) Screening for potassium channel modulators by a high through-put 86-Rubidium efflux assay in a 96-well microtiter plate. J Pharmacol Meth 25:185–193

Freeman H, Shimomura K, Horner E, Cox RD, Ashcroft FM (2006) Nicotinamide nucleotide transhydrogenase: A key role in insulin secretion. Cell Metabol 3:35–45

Hu W, Toral J, Cernovi P, Ziai R, Sokol PT (1995) Depolarization-induced $^{86}Rb^+$ efflux in CHO cells expressing a recombinant potassium channel. J Pharmacol Toxicol Meth 34:1–7

Nelson TY, Gaines KL, Rajan AS, Berg M, Boyd III AE (1987) Increased cytosolic calcium. A signal for sulfonylurea-stimulated insulin release from beta cells. J Biol Chem 262:2606–2612

Nichols CG, et al (1996) Adenosine diphosphate as an intracellular regulator of insulin secretion. Science 272:1785–1887

Niki I, Kelly RP, Ashcroft SJH, Ashcroft FM (1989) ATP-sensitive K-channels in HIT T15 β-cells studied by patch-clamp methods, ^{86}Rb efflux and glibenclamide binding. Pflügers Arch 415:47–55

Rorsman P, Trube G (1986) Calcium and delayed potassium currents in mouse pancreatic β-cells under voltage-clamp conditions. J Physiol 374:531–550

Toye AA, Lippiat JD, Proks P, Shimomura K, Bentley L, Hugill A, Mijat V, Goldsworthy M, Moir L, Haynes A, Quarterman J, Freeman HC, Ashcroft FM, Cox RD (2005) A genetic and physiological study of impaired glucose homeostasis control in C57BL/6J mice. Diabetologia 48:675–686

K.6.6.7 Measurement of Cell Membrane Potential

PURPOSE AND RATIONALE

ATP-sensitive potassium (K_{ATP}) channels couple cell metabolism to electrical activity of the plasma membrane by regulating membrane K^+ fluxes (for a review see Ashcroft 2005). A reduction in metabolism opens K_{ATP} channels, producing K^+ efflux, membrane hyperpolarization, and suppression of electrical activity. Conversely, increased metabolism closes K_{ATP} channels. The consequent membrane depolarization stimulates electrical activity and may thereby trigger cellular responses such as the release of hormones and neurotransmitters, or muscle contraction.

Studies on isolated cells and tissues, and more recently on genetically modified mice and patients with mutations in K_{ATP} channel genes, have demonstrated that K_{ATP} channels play a multitude of physiological roles (Seino and Miki 2004). They contribute to glucose homeostasis by regulating insulin secretion from pancreatic β-cells (Ashcroft and Rorsman 1989, Henquin 2000, Gribble and Reimann 2003, Rorsman et al. 1994, Koster et al. 2000, Seghers et al. 2000, Dunne et al. 2004), glucagon secretion from pancreatic α-cells (Gopel et al. 2000a), somatostatin secretion from D cells (Gopel et al. 2000b), and GLP-1 secretion from L cells (Gribble et al. 2003). In ventromedial hypothalamic neurons they mediate the counter-regulatory response to glucose (Miki et al. 2001), and in arcuate nucleus neurons they may be involved in appetite regulation. In these glucose-sensing cells, K_{ATP} channels respond to fluctuating changes in blood glucose concentration. In many other tissues, however, they are largely closed under resting conditions and open only in response to ischemia, hormones, or neurotransmitters. In cardiac muscle and central neurons the resulting reduction in electrical activity helps protect against cardiac stress and brain seizures (Zingman et al. 2002, Yamada et al. 2001). K_{ATP} channels are involved in ischemic preconditioning in heart (Gumina et al. 2003) and the regulation of vascular smooth muscle tone (opening of K_{ATP} channels leads to relaxation) (Daut et al. 1994, Chutkow et al. 2002). Given their critical role in regulating electrical excitability in many cells, it is perhaps not surprising that disruption of K_{ATP} channel function can lead to disease. To date, mutations in K_{ATP} channel genes have been shown to cause neonatal diabetes (Gloyn et al. 2004, Magge et al. 2004), hyperinsulinemia (Dunne et al. 2004, Glaser et al. 2000, Thomas and Lightner 1996, Huopio et al. 2000). The effect of compounds/drug candidates on the open/closed state of K_{ATP} channel and the electrical activity of β-cell plasma membranes can be assayed with the following assays, which may be helpful for the identification of insulin secretagogues and sensitizers for GSIS as potential drug in the anti-diabetic therapy.

PROCEDURE

Rat insulinoma cells RINm5F (Gögelein et al. 1998) or cultured pancreatic β-cells from NMRI mice (Rorsman and Trube 1985, Zünkler et al. 1985) or HIT T15 β-cells (Niki et al. 1989) are used. Whole cell patch-clamp experiments are performed according to Hamill and coworkers (1981), Rajan and coworkers

(1993), Lindau and Neher (1988) at room temperature with cells bathed in an external solution of 140 mM NaCl, 4 mM KCl, 10 mM HEPES (pH 7.4). The patch pipettes are mounted on a suction pipette holder. The outlet is connected to silicon rubber tubing through which the suction is applied. The pipette solution contains 135 mM KCl, 1 mM $MgCl_2$, 1 mM EGTA, 10 mM HEPES (pH 7.5), 0.3 mM NaATP. Pipettes are prepared by pulling from borosilicate glass, coated with silicon rubber, and heat polished at the tip. Pipette resistances are ranging between 4 and 7 MΩ. A patch-clamp amplifier (e. g. EPC 7, List Electronic, Darmstadt, FRG) is used which allows capacitance and series resistance compensation. The series resistance after achieving the whole cell recording configuration is 5–20 MΩ and 50% series resistance compensation is used to keep the voltage error during current flow below 2 mV. The cell membrane potential is held at –70 to –80 mV and hyper- and depolarizing voltage pulses of 10 mV amplitude are applied alternatively every 2 s. Voltage-dependent currents, i. e., the Ca^{2+} inward current and the delayed K^+ outward current are not activated by these low pulse amplitudes and, therefore, most of the current is flowing through ATP-dependent K^+ channels. Inside-out patches are prepared according to Hamill and coworkers (1981) by disrupting the outer vesicle membrane.

EVALUATION

The current and voltage signals are stored on magnetic tape or filtered by a 4-pole Bessel filter and displayed on a digital oscilloscope. Outward currents flowing from the cell to the bath are indicated by upward deflections and inward currents by downward deflections. Half maximal effective concentrations are calculated as EC_{50} values.

MODIFICATIONS OF THE METHOD

Henquin and Meissner (1984), Henquin and coworkers (1984, 1985), Meissner (1990) measured membrane potential of mouse pancreatic β-cells. Hu and coworkers (2000) compared the effects of netaglinide, a non-sulfonylurea hypoglycemic agent, with sulfonylureas on pancreatic β-cell K_{ATP} channel activity with the whole-cell configuration of the patch-clamp technique in primary cultures of rat pancreatic β-cells. Wang and Giebisch (1991) reported a dual modulation of the renal ATP-sensitive K^+ channel by PKA and PKC in cells of the cortical collecting duct of rabbit kidneys using the cell-attached and inside-out modification. Shieh and coworkers (2000) characterized K_{ATP} channel opener-activated currents in pig and guinea pig bladder smooth muscle cells using the whole-cell patch-clamp technique. Shindo and coworkers (2000) examined with the whole-cell configuration of the patch-clamp technique the effects of a vascular relaxing agent on the heterologously expressed pancreatic-type ATP-sensitive K^+ channels SUR1/Ki6.2, SUR2A/Ki6.2, and SUR2B/Ki6.2 in human embryonic kidney 293T cells. Using whole-cell and single-channel patch-clamp recording, Gomora and Enyeart (1999) studied pharmacological properties of a cyclic AMP-sensitive potassium channel, I_{AC}, which is distinctive among K^+ channels both in its activation by ATP and inhibition by cyclic AMP. Alternatively, Maechler and coworkers (2004) monitored the cell membrane potential using 100 nM of the fluorescent probe bis-oxonol [bis-(1,3-diethylthiobarbituric acid) trimethine oxonol; Molecular Probes]. Filters used for excitation and emission had wavelength optima at 544 and 590 nm, respectively.

K.6.6.8 Measurement of Mitochondrial Membrane Potential

PROCEDURE

Mitochondrial membrane potential ($\Delta\psi_m$) is measured using the fluorescent probe, rhodamine 123. Cells cultured in 24-well plates are maintained for 2 h in 2.5 mM glucose medium at 37°C before loading with 10 µg/ml rhodamine 123 (Molecular Probes) for 20 min at 37 C in KRBH. The $\Delta\psi_m$ is monitored with excitation and emission filters set at 485 and 520 nm, respectively. Glucose (additions on top of the basal concentration of 2.5 mM) and then the protonophore carbonyl cyanide *p*-trifluoromethoxyphenylhydrazone (FCCP) is added to each well.

K.6.6.9 Measurement of cAMP Production

Approximately 1×10^6 cultured β-cells (grown as described above) in 0.45 ml buffer (113 mM NaCl, 4.7 mM KCl, 1.2 mM KH_2PO_4, 10 mM HEPES, pH 7.4, 2.5 mM $CaCl_2$ and 1.2 mM $MgSO_4$) containing 1% human serum albumin are pre-incubated for 10 min at 37°C, and then incubated for 10 min after the addition of 2 µl of IBMX (50 mM) in order to prevent the breakdown of cAMP. The reaction is then started by the addition of 50 µl of a peptide solution dissolved in the above buffer (final concentration range from 10 pM to 1 µM). After incubation for 10 min at 37°C, the reaction is stopped by the addition of 200 µl of 12% TCA. The reaction mixture is sonicated for 30 s at

25 W (e. g., Heat system, Ultrasonics) and centrifuged (11,500 × *g*, 2 min). HCl (25 µl, 1 M) is added to 0.5 ml supernatant. TCA dissolved in the supernatant is removed by diethyl ether (3 × 1 ml) and the resulting supernatant is stored at −80°C until cAMP assays being performed by use of a RIA kit.

K.6.6.10 Measurement of Cytosolic ATP Levels

Cytosolic ATP levels are monitored in cells expressing the ATP-sensitive bioluminescent probe luciferase 1 d after transduction with the specific AdRIP-Luc viral construct according to Maechler and coworkers (1998) and Rubi and coworkers (2001). After the preincubation steps described above, the 24-well plates are transferred to the plate reader in the luminometer mode. The luciferase substrate, 100 µM beetle luciferin (Promega), is added to the KRBH. After a 10-min period in basal 2.5 mM glucose, cells are stimulated with the indicated glucose concentrations, and 20 min later the mitochondrial poison NaN_3 (2 mM) is added (as a control).

K.6.6.11 Analysis of Lipotoxicity

GENERAL CONSIDERATIONS

There is increasing experimental evidence that sustained elevated plasma and intracellular lipid concentrations result in impaired insulin action and secretion *in vivo* and *in vitro*. This has implications for the causal relationship between the pathogenesis of obesity and type II diabetes (Carpentier et al. 2001, Dobbins et al. 2002). It is known that increased plasma FFA concentrations reduce insulin-mediated glucose uptake and metabolism in muscle tissue presumably *via* the glucose-fatty acid (Randle) cycle (Randle et al. 1963), but the exact mechanism of action of FFA on the β-cell to modulate glucose-stimulated insulin secretion (GSIS) (Zhou and Grill 1994, Roche et al. 1998, Unger and Orci 2002) remains to be elucidated. A complex interrelationship between the metabolism of glucose and lipids in β-cells has been described (Prentki and Corkey 1996), and this critically depends on the duration of exposure (acute or chronic) to the lipid metabolites (Zhou et al. 1994, Roche et al. 1998). In conclusion, it is now generally accepted that in rodent β-cells and islets lipids and/or lipid precursors/metabolites interfere with GSIS and β-cell functionality (Maedler et 2001, El Assaad et al. 2003, Cnop et al. 2001), but their nature (e. g. TAG, FFA, acyl-CoA, DAG) and molecular mode of action still remains a matter of intense research and debate.

However, serious doubts have been raised against the hypothesis of FFA-induced impairment of GSIS and β-cell death as playing a major role in the pathophysiology of human type II diabetes. Although increased plasma FFA and lipid (as lipoprotein TAG) concentrations and alterations in their composition occur in obesity in humans (Wang et al. 2003), this condition is not invariably linked to the onset of type II diabetes. Fewer than 12% of obese subjects with elevated lipid profiles suffer from diabetes (Ford et al. 2002). Furthermore, the concept of glucolipotoxity (Poitout and Robertson 2002) proposes that, in type II diabetes, the elevation of both glucose and FFA could contribute to the decrease in pancreatic islet function as a result of both β-cell apoptotic death and decreased insulin secretion.

PURPOSE AND RATIONALE

The following assay systems enable the determination of effects of compounds/drug candidates on the fatty acid-induced (and glucose-induced) modulation of GSIS, cell death and TAG concentration, composition and localisation in cultured β-cells. They may be helpful for the identification and characterization of compounds/drugs with the potential of abrogating the lipo(gluco)toxic effects of lipid (metabolites) in β-cells in response to certain (patho)physiological stimuli (e. g. stress, reactive oxygen species, see K.8.8).

PROCEDURE

Viability Assay

INS1 cells are plated into 8-well Permanox slides (Gibco) and treated for 24 h with 0.1, 0.25, 0.5 and 1 mM of FFA in 3 or 20 mM glucose. Adjustments to the stock solution are made to ensure a constant BSA concentration. Following incubation, cells are rinsed in PBS, incubated for a further 30 min in PBS containing 10 µM calcein-AM (Sigma) at 37°C and fixed in 2.5% paraformaldehyde for 30 min. Slides are rinsed twice more in PBS and the slides mounted in Vectorshield containing propidium iodide (Vector Laboratories). Viability is quantified by counting the propidium-iodide-positive nuclei and calcein-AM-positive cells (average cell count = 60 cells per field) and determining the percentage of propidium-iodide-positive nuclei in at least three fields of view per condition.

TAG and Phospholipid Content and Composition

INS1 or COS7 cells are seeded into 6-well plates at 2×10^5 cells per well and treated for 24 h with 0.5 mM

specific fatty acids. Total lipids are extracted from cells in chloroform/methanol (2/1) and lipid fractions are separated using solid-phase extraction (Burdge et al. 2000). The TAG and phospholipid fractions are collected and fatty acid methyl esters prepared using methanolic sulphuric acid. The fatty acid methyl esters are separated by gas chromatography (e. g. Agilent 6890 GC equipped with a DB-Wax 30 m capillary column coated with a polyethylene glycol stationary phase, internal diameter 0.25 mm, film thickness 0.25 µm; Agilent Technologies). Fatty acids are separated according to fatty acyl carbon chain length and degree of saturation. Intact TAG analyses are performed by high-temperature gas chromatography (HTGC; e. g. Hewlett Packard 5890 series II GC with a DB1-HT 15 m fused silica capillary column, internal diameter 0.32 mm, film thickness 0.1 mm). Hydrogen is the carrier gas and a flame ionisation detector is employed to monitor column eluent. HTGC analyses separates the TAG according to their carbon number. The absolute concentrations of individual fatty acids and TAG are determined typically by reference to internal standards (heptadecanoic acid [17:0] for NEFA; tripentadecanoin [15:0] for TAG; phosphatidylcholine, diheptadecanoyl [17:0] for phospholipid).

Light Microscopy

INS1 and cells are incubated in 8-well Permanox or glass slides (Gibco) with compounds/drug candidates for 24 h in the absence or presence of 3 or 20 mM glucose and 1 mM FFA. Cells are washed in PBS and fixed in 2.5% PFA and then stained for lipids. A stock solution of 0.5% (saturated) oil red O in propan-2-ol is freshly diluted (three parts stock solution in two parts distilled water) and filtered immediately before use. Cells are stained for 30 min at 37°C, then briefly destained in 60% isopropanol and washed in water before mounting in PBS/glycerol. A freshly prepared 1% Nile blue-solution in distilled water is filtered and an aliquot is further diluted in water to 0.02%. Fixed cells are washed twice in PBS. Nile blue solution (1%) is added to the cells for 10 min at 65°C or 70°C, after which the cells are washed in water and destained in 1% acetic acid (65°C) for 30 s. Cells are restained for 15 min in 0.02% Nile blue at 65°C or 70°C before being washed in water and mounted in PBS/glycerol.

Electron Microscopy

INS1 cells for morphological analysis are incubated with compounds/drug candidates in 25-cm^2 flasks for 24 h as described above. Cells are removed and gently prepared as a pellet, fixed in 2.5% glutaraldehyde (minimum 1 h) at room temperature (or for a 10-min period at 70°C), post-fixed in 2% osmium, dehydrated and embedded in Spurr resin. Cells for immunoelectron microscopy are fixed in ice-cold 4% paraformaldehyde (10 min) followed by 8% paraformaldehyde at room temperature (50 min), washed in PBS, dehydrated in methanol and embedded in LR Gold resin. Ultrathin sections are cut onto nickel grids and contrast-enhanced with uranyl acetate and lead citrate. Sections are examined in an electron microscope with an accelerating voltage of 80 kV.

REFERENCES AND FURTHER READING

Ashcroft FM (2005) ATP-sensitive potassium channelopathies: focus on insulin secretion. J Clin Invest 115:2047–2058

Ashcroft FM, Rorsman P (1989) Electrophysiology of the pancreatic β-cell. Prog Biophys Mol Biol 54:87–143

Bryan J, Aguilar-Bryan (1997) The ABCs of ATP-sensitive potassium channels. Curr Opin Cell Biol 9:553–559

Burdge GC, Wright P, Jones AE, Wooton SA (2000) A method for separation of phosphatidylcholine, triacylglycerol, non-esterified fatty acids and cholesterol esters from plasma by solid-phase extraction. Br J Nutr 84:781–787

Carpentier A, Giacca A, Lewis GF (2001) Effect of increased plasma non-esterified fatty acids (NEFA) on arginine-stimulated insulin secretion in obese humans. Diabetologia 44:1989–1997

Chutkow WA, Simon MC, Beau MML, Burant CF (1996) Cloning, tissue expression, and chromosomal localization of SUR2, the putative drug-binding subunit of cardiac, skeletal muscle and vascular K_{ATP} channels. Diabetes 45:1439–1445

Cnop M, Hannaert JC, Hoorens A, Eizirik DL, Pipeleers DG (2001) Inverse relationship between cytotoxicity of free fatty acids in pancreatic islet cells and cellular triglyceride accumulation. Diabetes 50:1771–1777

Daut J, Klieber HG, Cyrys S, Noak T (1994) K_{ATP} channels and basal coronary vascular tone. Cardiovasc Res 28:811–817

Dobbins RL, Szczepaniak LS, Myhill J (2002) The composition of dietary fat directly influences glucose-stimulated insulin secretion in rats. Diabetes 51:1825–1833

Dunne MJ, Cosgrove KE, Shepherd RM, Aynsley-Green A, Lindley KJ (2004) Hyperinsulinemia in infancy: from basic science to clinical disease. Physiol Rev 84:239–275

El-Assaad W, Buteau J, Peyot ML (2003) Saturated fatty acids synergize with elevated glucose to cause pancreatic beta-cell death. Endocrinology 144:4154–4163

Fex M, Olofsson CS, Fransson U, Bacos K, Lindvall H, Sörhede-Winzell M, Rorsman P, Holm C, Mulder H (2004) Hormone-sensitive lipase deficiency in mouse islets abolishes neutral cholesterol ester hydrolase activity but leaves lipolysis, acylglycerides, fat oxidation, and insulin secretion intact. Endocrinology 145:3746–3753

Gloyn AL et al (2004) Activating mutations in the ATP-sensitive potassium channel subunit Kir6.2 gene are associated with permanent neonatal diabetes. N Engl J Med 350:1838–1849

Gögelein H, Hartung J, Englert HC, Schölkens BA (1998) HMR 1883, a novel cardioselective inhibitor of the ATP-sensitive potassium channel. Part I. Effects on cardiomyocytes, coronary flow and pancreatic β-cells. J Pharmacol Exp Ther 286:1453–1464

Gomora JC, Enyeart JJ (1999) Dual pharmacological properties of a cyclic AMP-sensitive potassium channel. J Pharmacol Exp Ther 290:266–275

Gopel SO et al (2000a) Regulation of glucagon release in mouse alpha-cells by K_{ATP} channels and inactivation of TTX-sensitive Na^+ channels. J Physiol 528:509–520

Gopel SO, Kanno T, Barg S, Rorsman P (2000b) Patch-clamp characterization of somatostatin-secreting δ-cells in intact mouse pancreatic islets. J Physiol 528:497–507

Gribble FM, Reimann F (2003) Sulphonylurea action revisited: the post-cloning era. Diabetologia 46:875–891

Gribble FM, Williams L, Simpson AK, Reimann F (2003) A novel glucose-sensing mechanism contributing to glucagon-like peptide-1 secretion from the GLUTag cell line. Diabetes 52:1147–1154

Gumina RJ et al (2003) Knockout of Kir6.2 negates ischemic preconditioning-induced protection of myocardial energetics. Am J Physiol Heart Circ Physiol 284:H2106–H2113

Hamill OP, Marty A, Neher E, Sakmann B, Sigworth FJ (1981) Improved patch-clamp techniques for high-resolution current recordings from cells and cell-free membrane patches. Pflüger's Arch 391:85–100

Henquin JC (2000) Triggering and amplifying pathways of regulation of insulin secretion by glucose. Diabetes 49:1751–1760

Henquin JC, Meissner HP (1984) Effects of theophylline and dibutyryl cyclic adenosine monophosphate on the membrane potential of mouse pancreatic β-cells. J Physiol 351:595–612

Henquin JC, Schmeer W, Henquin M, Meissner HP (1984) Forskolin suppresses the slow cyclic variations of glucose-induced electrical activity in pancreatic β cells. Biochem Biophys Res Commun 120:797–803

Henquin JC, Schmeer W, Henquin M, Meissner HP (1985) Effects of a calcium channel agonist on the electrical, ionic and secretory events in mouse pancreatic β-cells. Biochem Biophys Res Commun 131:980–986

Hu S, Wang S, Fanelli B, Bell PA, Dunning BE, Geisse S, Schmitz R, Boettcher BR (2000) Pancreatic β-cell K_{ATP} channel activity and membrane binding studies with nateglinide: a comparison with sulfonylureas and repaglinide. J Pharmacol Exp Ther 293:444–452

Huopio H, et al (2000) Dominantly inherited hyperinsulinism caused by a mutation in the sulfonylurea receptor type I. J Clin Invest 106:897–906

Koster JC, Marshall BA, Ensor N, Corbett JA, Nichols CG (2000) Targeted overactivity of beta cell K(ATP) channels induces profound neonatal diabetes. Cell 100:645–654

Lindau M, Neher E (1988) Patch-clamp techniques for time-resolved capacitance measurements in single cells. Pflüger's Arch 411:137–146

Maechler P, Wang H, Wollheim CB (1998) Continuous monitoring of ATP levels in living insulin secreting cells expressing cytosolic firefly luciferase. FEBS Lett 422:328–332

Maedler K, Spinas GA, Dyntar D (2001) Distinct effects of saturated and monounsaturated fatty acids on beta-cell turnover and function. Diabetes 50:69–76

Magge SN et al (2004) Familial leucine-sensitive hypoglycemia of infancy due to a dominant mutation of the beta-cell sulfonylurea receptor. J Clin Endocrinol Metab 89:4450–4456

Meissner HP (1990) Membrane potential measurements in pancreatic β cells with intracellular microelectrodes. Meth Enzymol 192:235–246

Miki T et al (2001) ATP-sensitive K^+ channels in the hypothalamus are essential for the maintenance of glucose homeostasis. Nat Neurosci 4:507–512

Mulder H, Holst LS, Svensson H (1999) Hormone-sensitive lipase deficiency in mouse islets abolishes neutral cholesterol ester hydrolase activity but leaves lipolysis, acylglycerides, fat oxidation, and insulin secretion intact. Endocrinology 145:3746–3753

Niki I, Kelly RP, Ashcroft SJH, Ashroft FM (1989) ATP-sensitive K-channels in HIT T15 β-cells studied by patch-clamp methods, ^{86}Rb efflux and glibenclamide binding. Pflügers Arch 415:47–55

Poitout V, Robertson RP (2002) Minireview: secondary beta-cell failure in type 2 diabetes-a convergence of glucotoxicity and lipotoxicity. Endocrinology 143:339–342

Prentki M, Corkey BE (1996) Are the beta-cell signalling molecules malonyl-CoA and cytosolic long-chain acyl-CoA implicated in multiple tissue defects of obesity and NIDDM ? Diabetes 45:1086–1094

Rajan AS, Aguilar-Bryan L, Nelson DA, Nichols CG, Wechsler SW, Lechago J, Bryan J (1993) Sulfonylurea receptors and ATP-sensitive K^+ channels in clonal pancreatic β cells. Evidence for two high affinity sulfonylurea receptors. J Biol Chem 268:15221–15228

Randle PJ, Garland PB, Hales CN, Newsholme EA (1963) The glucose fatty acid cycle. Its role in insulin sensitivity and the metabolic disturbances of diabetes mellitus. Lancet 1:785–789

Roche E, Farfari S, Witters LA (1998) Long-term exposure of beta-INS cells to high glucose concentrations increases anaplerosis, lipogenesis, and lipogenic gene expression. Diabetes 47:1086–1094

Roduit R, Masiello P, Wang SP, Li H, Mitchell GA, Prentki M (2001) A role for hormone-sensitive lipase in glucose-stimulated insulin secretion. A study in hormone-sensitive lipase-deficient mice. Diabetes 50:1970–1975

Rorsman P, Trube G (1985) Glucose dependent K^+ channels in pancreatic B-cells are regulated by intracellular ATP. Pflüger's Arch 405:305–309

Rorsman P, Bokvist K, Ämmälä C, Eliasson L, Renström E, Gäbel J (1994) Ion channels, electrical activity and insulin secretion. Diabete and Metabolisme (Paris) 20:138–145

Rubi B, Ishihara H, Hegardt FG, Wollheim CB, Maechler P (2001) GAD65-mediated glutamate decarboxylation reduces glucose-stimulated insulin secretion in pancreatic β cells. J Biol Chem 276:36391–36396

Seino S, Miki T (2004) Gene targeting approach to clarification of ion channel function: studies of Kir6.x null mice. J Physiol 554:295–300

Shieh C-C, Feng J, Buckner SA, Brioni JD, Coghlan MJ, Sullivan JP, Gopalakrishnan M (2000) Functional implication of spare ATP-sensitive K^+ channels in bladder smooth muscle cells. J Pharmacol Exp Ther 296:669–675

Shindo T, Katayama Y, Horio Y, Kurachi Y (2000) MCC-134, a novel vascular relaxing agent, is an inverse agonist for the pancreatic-type ATP-sensitive K^+ channel. J Pharmacol Exp Ther 292:131–135

Thomas P, Ye Y, Lightner E (1996) Mutation of the pancreatic islet inward rectifier Kir6.2 also leads to familial persistent hyperinsulinemia hypoglycemia of infancy. Hum Mol Genet 5:1809–1812

Unger RH, Orci L (2002) Lipoapoptosis: its mechanism and its diseases. Biochim Biophys Acta 1585:202–212

Wang L, Folsom AR, Zheng ZJ, Pankow JS, Eckfeldt JH (2003) Plasma fatty acid composition and incidence of diabetes in middle-aged adults: the Atherosclerosis Risk in Communities (ARIC) Study. Am J Clin Nutr 78:91–98

Wang W, Giebisch G (1991) Dual modulation of renal ATP-sensitive K^+ channel by protein kinases A and C. Proc Natl Acad Sci USA 88:9722–9725

Yamada K et al (2001) Protective role of ATP-sensitive potassium channels in hypoxia-induced generalized seizure. Science 292:1543–1546
Zhou YP, Grill VE (1994) Long-term exposure of rat pancreatic islets to fatty acids inhibits glucose-induced insulin secretion and biosynthesis through a glucose fatty acid cycle. J Clin Invest 93:870–876
Zingman LV et al (2002) Kir6.2 is required for adaptation to stress. Proc Natl Acad Sci USA 99:13278–13283
Zünkler BJ, Lenzen S, Männer K, Panten U, Trube G (1988) Concentration-dependent effects of tolbutamide, meglitinide, glipizide, glibenclamide and diazoxide on ATP-regulated K^+ currents in pancreatic B-cells. Naunyn-Schmiedeberg's Arch Pharmacol 337:225–230

K.6.6.12 Interaction with β-Cell Plasma Membranes and K_{ATP} Channels

It is now established that increasing the closed probability of the β-cell ATP-dependent potassium channel (K_{ATP}) is the major mechanism through which sulfonylureas as well as glucose (*via* transport, phosphorylation and metabolism for generation of ATP) stimulate insulin release from pancreatic β-cells (for reviews see Ashcroft and Ashcroft 1992, Ashcroft 2005, Bryan and Aguilar-Bryan 1997, Gribble and Reimann 2003, Henquin 2000, Inagaki et al. 1996). The resulting reduction in potassium ion efflux causes depolarization of the β-cell plasma membrane which in turn leads to opening of voltage-sensitive Ca^{2+} channels of the L-type. The increased influx of Ca^{2+} and thus the elevated cytosolic Ca^{2+} levels trigger the fusion of insulin-containing secretory granules with the plasma membrane, presumably mediated by Ca^{2+}/calmodulin-dependent protein kinase and additional unknown mechanisms (Philipson 1995, Aguilar-Bryan and Bryan 1999). The β-cell K_{ATP} consists of the regulatory sulfonylurea receptor subunits (SUR), such as SUR1, and the physically associated pore-forming potassium ion inwardly rectifying subunit, KIR6.2, in a multimeric assembly with the SUR and KIR6.2 subunits in 1:1-stoichiometry and four identical SUR/KIR6.2 complexes per functional channel unit (size of the channel holocomplex $[SUR/KIR6.2]_4$ about 1000 kDa; Skeer et al. 1994, Clement et al. 1997a and b, Bryan and Aquilar-Bryan 1999, Shyng and Nichols 1997). SUR1, which is predominantly expressed in neuronal/pancreatic β-cells, is an ATP-binding cassette (ABC) protein or transport ATPase, which closely resembles members of the multidrug resistance associated protein family with 17 predicted transmembrane domains (TMD) and two nucleotide-binding folds (NBF), which bind specifically (Mg^{2+})ATP/ADP (Bryan et al. 1995, Inagaki et al. 1995 and 1996, Ueda et al. 1999, Gribble et al. 1997). The KIR6.2 subunits have two TMDs which somehow contribute to the K^+ conductivity and selectivity (Babenko et al. 1998). The glibenclamide-binding site of SUR1 is proposed to consist of a benzamido (meglitinide)-binding site on TMDs 1–5 and the sulfonylurea (tolbutamide)-binding site on TMDs 12–17 based on photolabeling with [^{125}I]iodoglibenclamide and chimeric receptors (Ashfield et al. 1999, Babenko et al. 1999, Chutkow et al. 1996, Isomoto et al. 1996, Tanabe et al. 1999, Aguilar-Bryan et al. 1995). Interaction with both the benzamido- and sulfonylurea-binding sites could account for the several thousand-fold increase in affinity of glibenclamide vs. tolbutamide. SUR2A/B are splice variants of a single SUR2 gene differing in 42 amino acids at the carboxy-terminus, exclusively, with SUR2A expressed mainly in cardiac/skeletal muscle cells (Chutkow et al. 1996, Inagaki et al. 1996) and SUR2B in vascular/non-vascular smooth muscle cells and brain (Isomoto et al. 1996, Aguilar-Bryan et al. 1998). K^+-channel openers (KCOs) bind to SURs at the tolbutamide-binding site encompassing those (flanking) TMDs 12–17 which surround the central core region of the tolbutamide-binding site (Uhde et al. 1999). SURs define the sensitivity of the K_{ATP} channel holocomplex for its sensitivity toward both sulfonylureas and KCOs with SUR1 mediating high sensitivity for sulfonylureas/low sensitivity toward KCOs and *vice versa* SUR2A/2B mediating low sensitivity for sulfonylureas/high sensitivity for KCOs (for a review see Ashcroft 2005).

The following assays enable the investigation of the direct binding of compounds/drug candidates to the K_{ATP} channels and their SUR subunits, which may be helpful for the identification of insulin releasers acting like sulfonylureas or glinides, which have been used successfully in the anti-diabetic therapy since decades.

K.6.6.12.1 Isolation of Membranes

PROCEDURE

For receptor binding studies, membranes are isolated from adenoma tissue suspension, cerebral cortex of Wistar rats (Kaubisch et al. 1982, Geisen et al. 1985) or from RINm5F cells (Müller et al. 1994a).

Cerebral Cortex Homogenates

The homogenates are prepared from decapitated Wistar rats. The cortices are immersed in ice-cold buffer, pH 7.5, and are homogenized under cooling in an Ultraturrax tissue homogenizer. The cell membranes are

centrifuged (50,000 × *g*, 1 h, 4°C) resuspended in fresh phosphate buffer and recentrifuged at thea same speed. The resulting pellet is suspended in phosphate buffer, the final dilution being 1:50, based on wet weight of the cerebral cortex. One ml aliquot of this cell suspension is used for the incubations.

β-Cell Adenoma Tissue

The tissue is dissected from rats of the strain NEDH, is homogenized in 25 mM HEPES/KOH (pH 7.4), 0.25 M sucrose, 0.5 mM EDTA, 100 µM PMSF (50 ml/g tissue) under cooling with ice (3 × 5 s) with an Ultraturrax homogenizer. After centrifugation (3,000 × *g*, 5 min) the supernatant is transferred into new tubes and centrifuged (200,000 × *g*, 1 h, 4°C). The pellet is washed with 2 × 5 ml of the same buffer, resuspended in 2 volumes of the same buffer and centrifuged again (75,000 × *g*, 30 min). The pellet is resuspended again in the membrane buffer.

Membranes from Cultured β-Cells

Insulin producing cells from RINm5F cell culture (one culture flask) are washed twice with 25 mM HEPES/KOH (pH 7.4), 0.25 M sucrose, 0.5 mM EDTA, scraped with 20 ml of the same buffer and homogenized with 10 strokes of a tight fitting Potter-Elvehjem homogenizer followed by sonication (bath sonicator, 4°C, 10 s, maximal power). After centrifugation (200,000 × *g*, 45 min, 4°C) the pellet is suspended in 10 ml of 25 mM HEPES/KOH (pH 7.4), 0.25 M sucrose, 100 mM NaCl, 0.5 mM EDTA, 200 µM PMSF and recentrifuged (1,000 × *g*, 10 min). The supernatant is transferred to a new tube and centrifuged (50,000 × *g*, 30 min, 4°C). The pellet is washed once with 25 mM HEPES/KOH (pH 7.4) and finally suspended in membrane buffer (25 mM HEPES/KOH, pH 7.4, 150 mM NaCl, 1 mM EDTA, 100 µM PMSF, 10 µg/ml soybean/trypsin inhibitor, 10 µM leupeptin, 1 mM iodoacetamide at 5 mg protein/ml). Aliquots are stored at –80°C.

K.6.6.12.2 Binding to Membranes

PURPOSE AND RATIONALE

Sulfonylureas block K_{ATP} channel in the β-cell plasma membrane (Schmid-Antomarchi et al. 1987a, b). Binding to the receptor and depolarization of the membrane initiates a chain of events leading to the release of insulin (Boyd 1992). The high affinity sulfonylurea receptor is considered to be an integral part of the K_{ATP} channel (Aguilar-Bryan et al. 1992). Binding studies of sulfonylureas and other drugs can be performed with isolated pancreatic islets, isolated insulinoma cells, isolated intact membranes or solubilized membranes from primary or cultured cells or intact cells (Geisen et al. 1985, Gaines et al. 1988, Panten et al. 1989, 1992, 1993, Müller et al. 1994a).

PROCEDURE

Filter binding assays are performed in a total volume of 1 ml containing 5 mg membrane protein, 25 mM MOPS/KOH (pH 7.4), 0.1 mM $CaCl_2$ and labeled sulfonylurea, e. g. [^{3}H]glibenclamide or [^{3}H]glimepiride at concentrations between 0.1 and 20 nM. After incubation for 45 min at 25°C, the binding reaction is terminated by rapid filtration through Whatman GF/F filters soaked with the same buffer. The filters are washed three times with 5 ml of ice-cold 25 mM HEPES/KOH (pH 7.4), 100 mM NaCl, 1 mM EDTA, 200 µM PMSF, 0.5 µg/ml leupeptin, 0.75 µg/ml pepstatin and two times with 5 ml of ice-cold HEPES/KOH (pH 7.4), placed in 10 ml of ACSII scintillation cocktail and after incubation overnight counted for radioactivity in a liquid scintillation counter. Non-specific binding is determined in parallel samples in the presence of 1 µM unlabeled ligand.

K.6.6.12.3 Binding to Cells

Culture

Cultured cells producing the β-cell sulfonylurea receptor, SUR1, include the hamster insulin secreting tumor cell line, HIT-T15 (passage 65–75; CRL1777 ATCC). Cells are maintained in T-175 culture flasks as monolayers in DMEM containing high glucose supplemented with 10% fetal bovine serum, 100 U, 7 ml penicillin and 0.1 mg/ml streptomycin. Cells are grown in 5% CO_2 at 37°C, maintained in subconfluent cultures, fed three times a week, and subcultured as needed. To subculture, confluent cells are detached with 0.05% trypsin/EDTA, resuspended in supplemented DMEM/high glucose and replated at 1/10 of the original density.

Steady-State Analysis

After growth to 70% confluency, cells are treated with trypsin (0.02% trypsin in 0.9% NaCl/0.2 mM EDTA), washed with 3 × 10 ml KRBH containing 20 mM HEPES/KOH (pH 7.4), 125 mM NaCl, 5 mM KCl, 7.5 mM $NaHCIO_3$, 2 mM $CaCl_2$, 0.8 mM $MgSO_4$, suspended at a density of 2×10^7cells/ml in the same buffer and then incubated for 45 min at 4°C at

a density of 4×10^6 cells per 0.5 ml assay volume with labeled sulfonylurea, e. g., [^{3}H]glibenclamide or [^{3}H]glimepiride at concentrations between 0.1 and 20 nM. For determination of non-specific binding, 1 µM unlabeled ligand is included. The incubation mixture is rapidly filtered on Whatman GF/C filters soaked with ice-cold buffer under reduced pressure. Filtration and washing has to take less than 30 s. The filters are washed three times with 6 ml ice-cold buffer containing 100 µM PMSF, 0.5 µg/ml leupeptin, 0.75 mg/ml pepstatin, 1 µg/ml aprotinin, 50 mg/ml antipapain dihydrochloride, placed in 10 ml of ACSII scintillation cocktail and after incubation overnight counted for radioactivity in a liquid scintillation counter.

Kinetic Analysis

For studying the association kinetics, the binding reaction is started by addition of radiolabeled ligand and terminated after predetermined periods of time by rapid filtration. For studying the dissociation kinetics, displacement of radiolabeled ligand at equilibrium (60 min incubation) is initiated by addition of unlabeled drug (final concentration 1 µM) and terminated after given periods of time. For termination, the incubation mixtures are rapidly chilled to 2–4°C by placing the assay tube in a dry ice/methanol bath for 1 s immediately prior to filtration in a filtration apparatus located in a cool bench. Further processing is performed as described above.

EVALUATION

K_d as well as B_{max}-values are calculated from Scatchard plot analyses and K_{on} and K_{off} values from kinetic studies. Curvilinear Scatchard plots allow the assumption of more than one binding site. IC_{50} values for half maximal inhibition of [^{3}H]sulfonylurea binding can be calculated from competition-inhibition plots.

MODIFICATIONS OF THE METHOD

Masuda and coworkers (1995) tested the effect of troglitazone on sulfonylurea receptor binding in rat pancreatic islet cells and in HIT cells. They concluded that troglitazone has a non-competitive binding site at, or in the vicinity of, the sulfonylurea receptor.

K.6.6.12.4 Photoaffinity Labeling of Membranes

PURPOSE AND RATIONALE

Binding sites of sulfonylureas have been identified in pancreatic β-cell membranes and in other tissues such as brain. The technique of photoaffinity labeling allows the identification and purification of membrane receptors (Bernardi et al. 1988, Yip 1984, Kramer et al. 1994, Aguilar-Bryan et al. 1990, Boyd III 1991, Müller et al. 1994a, Geisen et al. 1985, Gaines et al. 1988, Kaubisch et al. 1982, Rajan et al. 1993, Sakura et al. 1995, Tanabe et al. 1998).

PROCEDURE

Photoaffinity Labeling with Glibenclamide

Samples of membrane suspension are prepared as described above. 600 µg of β-cell membranes, suspended in 100 mM sodium phosphate buffer (pH 7.4), are incubated in a total volume of 200 µl with 40–60 nM (0.3–0.4 µCi) [^{3}H]glibenclamide at 20°C in the dark for 60 min. Irradiation is performed in a Rayonet RPR 100 photochemical reactor (Southern Ultraviolet Co., CT), equipped with RPR 2530 Å lamps at a distance of 10 cm from the lamps. After irradiation at 254 nm for 2 min the membranes are diluted with 1 ml of 10 mM Tris/HEPES buffer (pH 7.4) containing 4 mM EDTA, 4 mM iodoacetamide, 4 mM PMSF and centrifuged (48,000 × g, 30 min). The resulting pellet is resuspended in 200 µl water and protein precipitated according to Wessel and Flügge (1984).

Differential Photoaffinity Labeling

600 µg of β-cell membranes are incubated with various concentrations (10^{-9} to 10^{-4} M) of glibenclamide or the test compounds. After incubation with 60 nM (0.37 µCi) [^{3}H]glibenclamide in the dark, the membranes are photolabeled at 254 nm for 2 min. After washing of the membranes, the proteins are separated by SDS gel electrophoresis.

SDS-PAGE Analysis

The protein precipitates are dissolved in 70 µl of 62.5 mM Tris/HCl buffer (pH 6.8) containing 2% SDS, 5% mercaptoethanol, 0.005% bromophenol blue by shaking on a mixer for 60 min. After centrifugation (15,000 × g, 10 min), the clear supernatants are subjected to SDS gel electrophoresis on 150 × 180 × 1.5 mm slab gels (Kramer et al. 1988). After fixing and staining, the gels are scanned with a densitometer (e. g. CD50, Desaga, Heidelberg). The radioactivity is determined by liquid scintillation counting after slicing the gels into 2 mm pieces and after digestion of proteins with Biolute.

EVALUATION

The radioactive peak of [^{3}H]glibenclamide bound to the receptor protein is decreased depending on the

concentration of unlabeled glibenclamide or test compounds. IC_{50} values can be calculated.

K.6.6.12.5 Binding to Recombinant SUR1

PROCEDURE

Heterologous Expression of SUR1

Chinese hamster ovary and COS (1, m6, 7) cell lines do not produce SUR1 and are used for heterologous SUR1 expression. For transient transfection, COS cells are plated at 50–60% confluence. Cells are transfected using either a DEAE-dextran or a lipofectamine protocol. 3-day-old cultures of COS cells are trypsinized and replated at a density of 3.5×10^5 cells per 35-mm well (six-well dish) and allowed to attach overnight. Typically, 5 µg of a SUR1 plasmid is mixed with 5 µg of a KIR6.2 plasmid and brought up to 7.5 µl final volume in TBS (8 g/l NaCl, 0.4 g/l KCl, 0.2 g/l Na_2HPO_4, 3 g/l Tris base, 0.2 g/l $CaCl_2$, 0.1 g/l $MgCl_2$, pH 7.5) before addition of DEAE-dextran (30 µl of a 5 mg/ml solution in TBS). The samples are vortexed, collected by spinning in a microfuge, then incubated (15 min, 22°C) prior to addition of 0.5 ml of 10% FBS in TBS. Cells are washed twice with Hanks' balanced salt solution (HBSS), the DNA mix is added, and the cells are maintained in a CO_2 incubator at 37°C. After 4 h incubation, the DNA mix is decanted and the cells shocked for 5 min in 1 ml HBS and 10% dimethyl sulfoxide, then placed in 2 ml of DMEM/high glucose containing 2% FBS and 10 µM chloroquine and kept in the incubator for 4 h. Thereafter the cells are washed three times with HBSS and incubated in normal growth media until assayed.

Alternatively, lipofectamine is used for transfection instead of DEAE-dextran. COS cells are plated in six-well dishes and are used at 70–80% confluency. Typically 1 µg of a SUR1 plasmid and 1 µg of a KIR6.2 plasmid are mixed with 375 µl of Opti-Mem reduced serum medium (Life Technologies, Inc.), then added to 375 µl of Opti-Mem containing 9 µl of lipofectamine. After 1 h incubation, the mixture is supplemented with Opti-Mem to 1 ml final volume and added to the cells, which had been washed twice with 3 ml of Opti-Mem each. After 5 h incubation, the Opti-Mem is replaced with DMEM/high glucose containing 10% FBS. Transfections are scaled up based on the area of the plates used. For instance, 150-mm plates used for membrane isolations are transfected with 100 µg of each plasmid using the DEAE-dextran protocol. Transfected cells are used for determination of sulfonylurea binding and photolabeling or $^{86}Rb^+$ efflux 36–72 h post-transfection.

Membrane Preparation

Membranes are prepared from 15–25 150-mm dishes. Cells are washed three times in PBS (pH 7.4), then scraped in PBS and collected in 10-ml plastic tubes. The cells are pelleted, resuspended in 10 ml of hypotonic buffer (10 mM Tris/HCl, pH 7.4, 1 mM EDTA), and allowed to swell for 1 h on ice. Cells are then homogenized, transferred to a 15-ml glass tube, and spun ($2{,}000 \times g$, 20 min, 4°C) to remove nuclei and unbroken cells. The supernatant is then transferred to a polycarbonate centrifuge tube and membranes are collected by centrifugation (50,000 rpm, 90 min, Ti80 fixed-angle rotor). The pelleted membranes are resuspended in 5–200 µl of membrane buffer (25 mM Tris/HCl, pH 7.4, 2 mM EDTA, 250 mM sucrose, 0.2 mM PMSF, 10 µg/ml leupeptin) and stored frozen in aliquots in liquid N_2.

Membrane Solubilization

Membranes are rapidly thawed, resuspended using a Teflon-in-glass homogenizer, and mixed with ice-cold digitonin (25% w/v, in deionized water, prepared daily) to a final protein concentration of 3 mg/ml and 1% digitonin. Subsequent steps are performed at 25°C in the presence of 0.2 mM PMSF, 10 µg/ml leupeptin, 20 µg/ml pepstatin, 0.2 mM phenanthroline). After 30 min of incubation, solubilized membrane proteins are separated from insoluble material by centrifugation ($100{,}000 \times g$, 1 h, 4°C). Alternatively, the thawed and re-homogenized membranes are mixed with the same volume (resulting in 3 mg/ml protein) of ice-cold 0.2% (w/v) phosphatidylcholine, 20% (w/v) glycerol, 280 mM KCl, 4 mM EDTA, 0.4 mM PMSF, 20 µg/ml leupeptin, 50 mM HEPES/KOH (pH 7.4), 2.5% (w/v) Triton X-100 or CHAPS, incubated on ice for 1 h (under gentle stirring) and then centrifuged ($150{,}000 \times g$, 1 h, 4°C). The supernatants are collected and stored frozen in liquid N_2.

Partial Purification of SUR1

For purification of the 140-kDa core glycosylated species of SUR1, 4-ml aliquots of digitonin-solubilized membranes are cycled for times over a 1-ml concanavalin A-Sepharose column equilibrated with 40 mM Tris/HCl (pH 7.5), 0.2 M NaCl, 1 mM EDTA, 1% digitonin. The column is washed with 8 ml of the equilibrating buffer and eluted with 4 ml of the equilibrating buffer containing 0.5 M methyl α-methylmannopyranoside. The eluted protein is stored

in liquid nitrogen. For purification of the 150-kDa complex glycosylated SUR1, wheat germ agglutinin-Sepharose is used instead of concanavalin A-Sepharose. The procedure is the same as described with the exception of elution of the receptor using 0.3 M N-acetylgluosamine.

The eluate for the lectin columns is cycled twice over a 1-ml column of Reactive Green 19-agarose equilibrated with 40 mM HEPES/KOH (pH 8.5), 1 mM EDTA, 0.5% (w/v) digitonin. After washing with 10 ml of equilibrating buffer, and 10 ml of the same buffer supplemented with 0.5 M NaCl, the protein is eluted with 4 ml of equilibrating buffer containing 1.5 M NaCl. The eluate from the Reactive Green-19 purification step is diluted 1:2 with 40 mM HEPES/KOH (pH 8.5), 1 mM EDTA, 0.2% digitonin, then cycled twice over a 1-ml phenylboronate-10 Sepharose column. The phenylboronate column is washed with 10 ml of the HEPES buffer, followed by 2 ml of 0.1 M Tris/HCl (pH 7.5), 1 mM EDTA, and 0.2% digitonin. The protein is eluted with 4 ml of 0.1 M Tris/HCl (pH 7.5), 1 mM EDTA, 0.15% (w/v) sodium dodecyl sulfate. Prior to binding measurements, pooled samples from the various column steps are concentrated by centrifugation ($3{,}000 \times g$, 30 min, 4°C) through 100,000 molecular weight cut-off filters (Amicon), which have been pretreated with 5% (v/v) Tween 20 for 14 h at 4°C.

K.6.6.12.6 Interaction with Extrapancreatic Tissues

In addition to β-cells and hypothalamic neurons (Angel and Bidet 1991), SUR1 is also expressed in human adipocytes (Shi et al. 1999). Closure of the K_{ATP} by sulfonylurea binding to the adipocyte SUR1 leads to depolarization of the plasma membrane, opening of voltage-dependent Ca^{2+} channels and concomitant increase of the cytosolic Ca^{2+} concentration. Thus, adipocytes and determination of intracellular Ca^{2+} may be used for assaying the potency of sulfonylureas with regard to binding to SUR1.

Prior to fluorometric Ca^{2+} measurement, the adipocytes are washed three times (by flotation) with HBSS (140 mM NaCl, 0.8 mM $MgSO_4$, 1.8 mM $CaCl_2$, 0.9 mM NaH_2PO_4, 4 mM $NaHCO_3$, 5 mM glucose, 2 mM sodium pyruvate, 2 mM glutamine, 20 mM HEPES, 1% BSA). The cells are then loaded with Fura-2-acetoxymethyl ester (10 µM) in the same buffer for 45 min at 37°C in the dark with continuous shaking. For removal of extracellular dye, the cells are washed three times with HBSS and resuspended in HBSS at 3.5×10^5 cells/ml. Cytosolic Ca^{2+} is determined using dual excitation (340 and 380 nm) and single emission (510 nm) fluorometry. After establishment of a stable baseline in the absence or presence of the K_{ATP} channel openers, diazoxide and nitrendipine, the response to sulfonylureas is determined. Digitonin (25 µM) and Tris/EGTA (100 mM) are used to measure maximal and minimal fluorescence to calibrate the signals. Cytosolic Ca^{2+} is calculated by the equation of Grynkiewicz and coworkers (1985).

Direct effects of sulfonylurea agents on glucose transport (Cooper et al. 1990, Rogers et al. 1987, Müller 2000), insulin-induced decrease in 5′-nucleotidase activity in skeletal muscle membranes (Klip et al. 1987), diacylglycerol-like activation of protein kinase C (Cooper et al. 1990) were studied in BC_3H_1 myocytes, rat cardiomyocytes (Bähr et al. 1995) and rat diaphragms (Müller et al. 1994b). Augmentation of the effects of insulin and insulin-like growth factors I and II on glucose uptake by sulfonylureas (Wang et al. 1987), coordinate regulation of glucose transporter function, and gene expression by insulin and sulfonylureas (Wang et al. 1989), glyburide-stimulated glucose transport *via* PKC-mediated pathway (Davidson et al. 1991) were studied in the same cell line. For glimepiride, a sulfonylurea of the 3rd generation, but not for sulfonylureas of the 2nd or 1st generation (glibenclamide or tolbutamide, respectively), its direct interaction with lipid rafts at the plasma membranes of rat adipocytes, presumably *via* spontaneous intercalation between raft glyco(sphingo)lipids has been reported (Müller and Geisen 1996, Müller and Welte 2002). This is associated with activation of the GPI-PL (see K.6.3.6.4) and the translocation of certain GPI-proteins and non-RTK from high cholesterol-containing rafts to low cholesterol-containing rafts accompanied by their activation. This redistribution of signaling components which ultimately leads to the IR-independent tyrosine phosphorylation of IRS-1 and downstream signaling to the glucose transport system in rat adipocytes (Müller et al. 2001, for reviews see Müller 2002, 2005) may represent the molecular basis for the so-called extrapancreatic activity of certain sulfonylurea drugs, i. e. the blood glucose lowering in the absence of additional insulin release. The effects of compounds/drug candidates on the redistribution and activation of lipid raft proteins in rat adipocytes can be assayed as described (see K.6.3.6.4.2).

REFERENCES AND FURTHER READING

Aguilar-Bryan L, et al (1995) Cloning of the β-cell high-affinity sulfonylurea receptor: a regulator of insulin secretion. Science 268:423–426

Aguilar-Bryan L, Bryan J (1999) Molecular biology of adenosine triphosphate-sensitive potassium channels. Endocr Rev 20:101–135

Aguilar-Bryan L, Clement JP, Gonzalez G, Kunjilwar K, Babenko A, Bryan J (1998) Toward understanding the assembly and structure of K_{ATP} channels. Physiol Rev 78:227–245

Aguilar-Bryan L, Nelson DA, Vu QA, Humphrey MB (1990) Photoaffinity labeling and partial purification of the b cell sulfonylurea receptor using a novel, biologically active glyburide analog. J Biol Chem 265:8218–8224

Angel I, Bidet S (1991) The binding site for [^{3}H]glibenclamide in the rat cerebral cortex does not recognize K-channel agonists or antagonists other than sulfonylureas. Fundam Clin Pharmacol 5:107–115

Ashcroft FM (2005) ATP-sensitive potassium channelopathies: focus on insulin secretion. J Clin Invest 115:2047–2058

Ashcroft SJH, Ashcroft FM (1992) The sulfonylurea receptor. Biochem Biophys Acta 1175:45–59

Ashfield R, Gribble FM, Ashcroft SJ, Ashcroft FM (1999) Identification of the high-affinity tolbutamide site on the SUR1 subunit of the K(ATP) channel. Diabetes 48:1341–1347

Babenko AP, Aguilar-Bryan L, Bryan J (1998) A view of SUR/KIR6.X, K_{ATP} channels. Annu Rev Physiol 60:667–687

Babenko AP, Gonzalez G, Bryan J (1999) The tolbutamide site of SUR1 and a mechanism for its functional coupling to K_{ATP} channel closure. FEBS Lett 459:367–376

Bähr M, von Holtey M, Müller G, Eckel J (1995) Direct stimulation of myocardial glucose transport and glucose transporter-1 (GLUT1) and GLUT4 protein expression by the sulfonylurea glimepiride. Endocrinology 136:2547–2553

Bernardi H, Fosset M, Lazdunski M (1988) Characterization, purification, and affinity labeling of the brain [^{3}H]glibenclamide-binding protein, a putative neuronal ATP-regulated K^+ channel. Proc Natl Acad Sci USA 85:9816–9820

Boyd III AE, Aguilar-Bryan L, Bryan J, Kunze DL, Moss L, Nelson DA, Rajan AS, Raef H, Xiang H, Yaney GC (1991) Sulfonylurea signal transduction. Rec Progr Horm Res 47:299–317

Bryan J, Aguilar-Bryan L (1997) The ABCs of ATP-sensitive potassium channels. Curr Opin Cell Biol 9:553–559

Bryan J, Aguilar-Bryan L (1999) Sulfonylurea receptors: ABC transporters that regulate ATP-sensitive K^+ channels. Biochim Biophys Acta 1461:285–303

Bryan LA, Nichols CG, Wechsler SW, Clement JP, Boyd AE, Gonzales G, Sosa HH, Nguy K, Bryan J, Nelson DA (1995) Cloning of the β cell high-affinity sulfonylurea receptor: a regulator of insulin secretion. Science 268:423–426

Chutkow WA, Simon MC, Beau MML, Burant CF (1996) Cloning, tissue expression, and chromosomal localization of SUR2, the putative drug-binding subunit of cardiac, skeletal muscle and vascular K_{ATP} channels. Diabetes 45:1439–1445

Clement JP et al (1997a) Association and stoichiometry of K_{ATP} channel subunits. Neuron 18:827–838

Clement IV JP, Kunjilwar K, Gonzalez G, Schwanstecher M, Panten U, Aguilar-Bryan L, Bryan J (1997b) Association and stoichiometry of K_{ATP} channel subunits. Neuron 18:827–838

Cooper DR, Vila MC, Watson JE, Nair G, Pollet RJ, Standaert M, Farese RV (1990) Sulfonylurea-stimulated glucose transport association with diacylglycerol-like activation of protein kinase C in BC_3H_1 myocytes. Diabetes 39:1399–1407

Davidson MB, Molnar IG, Furman A, Yamaguchi D (1991) Glyburide-stimulated glucose transport in cultured muscle cells via protein kinase C-mediated pathway requiring new protein synthesis. Diabetes 40:1531–1538

Gaines KL, Hamilton S, Boyd III AE (1988) Characterization of the sulfonylurea receptor on beta cell membranes. J Biol Chem 263:2589–2592

Geisen K, Hitzel V, Ökonomopoulos R, Pünter J, Weyer R, Summ HD (1985) Inhibition of ^{3}H-glibenclamide binding to sulfonylurea receptors by oral antidiabetics. Arzneim Forsch/Drug Res 35:707–712

Glaser B, Thornton P, Otonkoski T, Junien C (2000) Genetics of neonatal hyperinsulinism. Arch Dis Child Fetal Neonatal ed 82:F79-F86

Gribble FM, Reimann F (2003) Sulphonylurea action revisited: the post-cloning era. Diabetologia 46:875–891

Gribble FM, Tucker SJ, Ashcroft FM (1997) The essential role of the Walker A motifs of SUR1 in K_{ATP} channel activation by MgADP and diazoxide. EMBO J 16:1145–1152

Grynkiewicz G, Pocnic M, Tsien RY (1985) A new generation of Ca^{2+} indicators with greatly improved fluorescent properties. J Biol Chem 260:3440–3450

Henquin JC (2000) Triggering and amplifying pathways of regulation of insulin secretion by glucose. Diabetes 49:1751–1760

Inagaki N, et al (1995) Cloning and functional characterisation of a novel ATP-sensitive potassium channel ubiquitously expressed in rat tissues, including pancreatic islets, pituitary, skeletal muscle, and heart. J Biol Chem 270:5691–5694

Inagaki N, et al (1996) A family of sulfonylurea receptors determines the pharmacological properties of ATP-sensitive K^+ channels. Neuron 16:1011–1017

Isomoto S, et al (1996) A novel sulfonylurea receptor forms with BIR (Kir6.2) a smooth muscle type ATP-sensitive K^+ channel. J Biol Chem 271:24321–24324

Kaubisch N, Hammer R, Wollheim C, Renold AE, Offord R (1982) Specific receptors for sulfonylureas in brain and in a β-cell tumor of the rat. Biochem Pharmacol 31:1171–1174

Klip A, Ramlal RJ, Douen AG, Burdett E, Young D, Cartee GD, Holloszy JO (1987) Insulin-induced decrease in 5′-nucleotidase activity in skeletal muscle membranes. FEBS Lett 238:419–423

Koster JC, Marshall BA, Ensor N, Corbett JA, Nichols CG (2000) Targeted overactivity of beta cell K(ATP) channels induces profound neonatal diabetes. Cell 100:645–654

Kramer W, Müller G, Girbig F, Gutjahr U, Kowalewski S, Hertz D, Summ HD (1994) Differential interaction of glimepiride and glibenclamide with the β-cell sulfonylurea receptor. II. Photoaffinity labeling. Biochem Biophys Acta 119:278–290

Kramer W, Oekonomopulos R, Pünter J, Summ HD (1988) Direct photolabeling of the putative sulfonylurea receptor in rat b-cell tumor membranes by [^{3}H]glibenclamide. FEBS Lett 229:355–359

Müller G (2002) Dynamics of plasma membrane microdomains and cross-talk to the insulin signaling cascade. FEBS Lett 531:81–87

Müller G (2000) The molecular mechanism of the insulin-mimetic/sensitizing activity of the antidiabetic sulfonylurea drug amaryl. Mol Med 6:907–933

Müller G (2005) The mode of action of the antidiabetic drug glimepiride-beyond insulin secretion. Curr Med Chem Immun Endoc Metab Agents 5:499–518

Müller G, Jung C, Wied S, Welte S, Jordan H, Frick W (2001) Redistribution of glycolipid raft domain components induces insulin-mimetic signaling in rat adipocytes. Mol Cell Biol 21:4553–4567

Müller G, Geisen K (1996) Characterization of the molecular mode of action of the sulfonylurea, glimepiride, at adipocytes. Horm Metab Res 28:469–487
Müller G, Hartz D, Pünter J, Ökonomopoulos R, Kramer W (1994a) Differential interaction of glimepiride and glibenclamide with the β-cell sulfonylurea receptor. I. Binding characteristics. Biochim Biophys Acta 1191:267–277
Müller G, Welte S (2002) Lipid raft domains are the targets for the insulin-independent blood glucose-decreasing activity of the sulfonylurea glimepiride. Recent Res Develop Endocrinol 3:401–423
Müller G, Wied S, Wetekam EM, Crecelius A, Pünter J (1994) Stimulation of glucose utilization in 3T3 adipocytes and rat diaphragm *in vitro* by the sulfonylureas glimiperide and glibenclamide, is correlated with modulations of the cAMP regulatory cycle. Biochem Pharmacol 48:985–996
Philipson LH (1995) ATP-sensitive K^+ channels: paradigm lost, paradigm regained. Science 270:1159
Rajan AS, Aguilar-Bryan L, Nelson DA, Nichols CG, Wechsler SW, Lechago J, Bryan J (1993) Sulfonylurea receptors and ATP-sensitive K^+ channels in clonal pancreatic β cells. Evidence for two high affinity sulfonylurea receptors. J Biol Chem 268:15221–15228
Rogers BJ, Standaert ML, Pollet (1987) Direct effects of sulfonylurea agents on glucose transport in the BC_3H_1 myocyte. Diabetes 39:1292–1296
Sakura H, Ammala C, Smith PA, Gribble FM, Ashcroft FM (1995) Cloning and functional expression of the cDNA encoding a novel ATP-sensitive potassium channel subunit expressed in pancreatic β-cells, brain, heart and skeletal muscle. FEBS Lett 377:338–344
Schmid-Antomarchi H, DeWeille J, Fosset M, Lazdunski M (1987a) The receptor for the antidiabetic sulfonylureas controls the activity of the ATP-modulated K^+-channels in insulin-secreting cells. J Biol Chem 262:15840–15844
Schmid-Antomarchi H, DeWeille J, Fosset M, Lazdunski M (1987b) The antidiabetic sulfonylurea glibenclamide is a potent blocker of the ATP-modulated K^+-channel in insulin-secreting cells. Biochem Biophys Res Commun 146:21–25
Shi H, Moustaid-Moussa N, Wilkison WO, Zemel MB (1999) Role of the sulfonylurea receptor in regulating human adipocyte metabolism. FASEB J 13:1833–1838
Shyng SL, Nichols GG (1997) Octameric stoichiometry of the K_{ATP} channel complex. J Gen Physiol 110:655–664
Skeer JM, Degano P, Coles B, Potier M, Ashcroft FM, Ashcroft SJH (1994) Determination of the molecular mass of the native beta-cell sulfonylurea receptor. FEBS Lett 338:98–102
Tanabe K et al (1999) Direct photoaffinity labeling of the Kir6.2 subunit of the ATP-sensitive K^+ channel by 8-azido-ATP. J Biol Chem 274:3931–3933
Ueda K, Komine J, Matsuo M, Seino S, Amachi T (1999) Cooperative binding of ATP and MgADP in the sulfonylurea receptor is modulated by glibenclamide. Proc Natl Acad Sci USA 96:1268–1272
Uhde I, Toman A, Gross I, Schwanstecher C, Schwanstecher M (1999) Identification of the potassium channel opener site on sulfonylurea receptors. J Biol Chem 274:28079–28082
Wang PH, Beguinot F, Smith RJ (1987) Augmentation of the effects of insulin and insulin-like growth factors I and II on glucose uptake in cultured rat skeletal muscle cells by sulfonylureas. Diabetologia 30:797–803
Wang PH, Moller D, Flier JS, Nayak RC, Smith RJ (1989) Coordinate regulation of glucose transporter function, number, and gene expression by insulin and sulfonylureas in L6 skeletal muscle cells. J Clin Invest 84:62–67
Wessel D, Flügge UI (1984) A method for the quantitative recovery of protein in dilute solution in the presence of detergents and lipids. Anal Biochem 138:141–143
Yip CC (1984) Photoaffinity probes for hormone receptor characterization. In: Larner J, Pohl SL (eds) Methods in Diabetes Research Vol I: Laboratory Methods, Part A. Wiley, New York, pp 3–14

K.7 Measurement of Glucose Absorption

K.7.1 Inhibition of Polysaccharide-Degrading Enzymes

GENERAL CONSIDERATIONS

Starch as the predominant ingredient of human food is rapidly degraded in the gastrointestinal tract by salivary and pancreatic α-amylase to maltose which is further hydrolyzed by maltase localized in the brush border of the small intestine to glucose. Glucose is immediately absorbed leading to hyperglycemia and consequently to hyperinsulinemia. Both phenomena are undesirable in diabetics and in obese patients. Inhibition of the digestion of starch leads to a decrease and a retardation of glucose absorption. In nature, α-amylase inhibitors are found in wheat and other grains (Shainkin and Birk, 1970). Several inhibitors of amylase and α-glucosidase have been developed (Bischoff 1991). Animal experiments with high doses of absorbable α-glucosidase inhibitors indicate that lysosomal storage of glycogen may occur (Lembcke et al. 1991).

REFERENCES AND FURTHER READING

Bischoff H (1991) Wirkung von Acarbose auf diabetische Spätkomplikationen und Risikofaktoren – Neue tierexperimentelle Ergebnisse. Akt Endokrin Stoffw 12:25–32
Bischoff H (1994) Pharmacology of α-glucosidase inhibition Eur J Clin Invest 24, Suppl 3:3–10
Bischoff H, Puls W, Krause HP, Schutt H, Thomas G (1985) Pharmacological properties of the novel glucosidase inhibitors BAY M1099 (Miglitol) and BAY O 1248. Diab Res Clin Pract Suppl 1:S53
Lembcke B, Lamberts R, Creutzfeldt W (1991) Lysosomal storage of glycogen as a sequel of α-glucosidase inhibition by the absorbed deoxynojirimycin derivative emiglitate (BAYo1248). A drug-induced pattern of hepatic glycogen storage mimicking Pompe's disease (glycogenosis type II). Res Exp Med 191:389–404
Shainkin R, Birk Y (1970) α-Amylase inhibitors from wheat. Isolation and characterization. Biochim Biophys Acta 221:502–513

K.7.1.1 Assay for α-Amylase

PURPOSE AND RATIONALE

α-Amylase activity can be measured by determination of the reducing groups arising from hydrolysis of soluble starch by isolated pancreatic α-amylase according to the protocol of Rick and Stegbauer (1970). The reduction of 3,5-dinitrosalicylic acid to nitroaminosalicylic acid produces a color shift which is followed photometrically by changes in the absorbance at 546 nm. Inhibition of starch hydrolysis by an α-amylase inhibitor results in a diminished absorbance at 546 nm in comparison with the controls.

PROCEDURE

Commercially available pancreatic α-amylase (Merck, Germany) is used. Various concentrations of the α-amylase inhibitor are dissolved in 1 ml 20 mM Sörensen buffer, pH 6.9 and 10 mM NaCl. 0.1 ml pancreatic α-amylase solution in 0.4% BSA is added. After prior incubation at 25°C, the enzymatic reaction is started by addition of 1.0 ml soluble starch solution. The reaction is stopped after 10 min with 1.0 ml of dinitrosalicylic acid reagent. The mixture is heated in a boiling water bath for 10 min, and after cooling measured at 546 nm against the reagent blank.

REFERENCES AND FURTHER READING

Rick W, Stegbauer HP (1970) α-Amylase. Messung der reduzierenden Gruppen. In: Bergmeyer H (ed) Methoden der enzymatischen Analyse, Vol II, 2nd ed., pp 848–853

K.7.1.2 Assay for α-Glucosidase

PURPOSE AND RATIONALE

Inhibition of glucosidase can be measured *in vitro* using glucosidase from porcine small intestinal mucosa.

PROCEDURE

Glucosidase is prepared from rat or porcine small intestinal mucosa or porcine pancreas. The enzyme activity is assayed according to Dahlqvist (1964). The inhibitory activity is determined by incubating a solution (20 µl) of an enzyme preparation with 80 mM sodium phosphate buffer, pH 7.0 (500 µl) containing 37 mM sucrose or maltose, or 3.7 mM isomaltose and a solution (20 ml) containing various concentrations of the inhibitor at 37°C for 20 min. The reaction mixture is heated for 2 min in a boiling water bath to stop the reaction. The amount of liberated glucose is measured by the glucose oxidase method. Matsuo and coworkers (1992), Ikeda and coworkers (1991) and Glick and Bray (1983) studied the effect of intestinal disaccharidase inhibitors on obesity and diabetes.

REFERENCES AND FURTHER READING

Dahlqvist A (1964) Method for assay of intestinal disaccharidases. Anal Biochem 7:18–25

Glick Z, Bray GA (1983) Effects of acarbose on food intake, body weight and fat depots in lean and obese rats. Pharmacol Biochem Behav 19:71–78

Ikeda H, Odaka H, Matsuo T (1991) Effect of a disaccharidase inhibitor, AO-128, on a high sucrose-diet-induced hyperglycemia in female Wistar fatty rats. Jpn Pharmacol Ther 19:155–150

Matsuo T, Odaka H, Ikeda H (1992) Effect of an intestinal disaccharidase inhibitor (AO-128) on obesity and diabetes. Am J Clin Nutr 55, Suppl 1:314S–317S

K.7.1.3 Everted Sac Technique for Assaying α-Glucosidase

PURPOSE AND RATIONALE

The everted sac technique allows to study the effects of intestinal enzymes on substrates in an incubation vial.

PROCEDURE

Male rats weighing 120–140 g are sacrificed and the small intestines removed by cutting across the upper end of the duodenal junction. The intestine is stripped of the mesentery and the entire intestinal content is rinsed with cold saline solution. The intestine is divided into 7 to 8 cm-segments and turned inside out using a Pasteur pipette. The everted intestine is ligated at one end with a cotton thread and a second ligature is placed loosely around the opposite end ready for tying. A 1 ml syringe with Krebs-Henseleit-buffer is introduced into the lumen sac. The end of the sac is ligated and placed in a 25 ml Erlenmeyer flask containing 6 ml of 1% starch, dissolved in Krebs-Henseleit-buffer, with or without various concentrations of the α-amylase inhibitor. Pork α-amylase (4000 U/g starch) is also included in the 6 ml starch solution. Following gassing with 95% O_2/5% CO_2, the flask is tightly capped and incubated in a shaking bath at 37°C for 120 min. The reaction is terminated by the addition of 10 µl 1 N HCl. At the end of the incubation period, the sac is removed from the flask and the inner fluid is collected by cutting one end of the sac. The final volumes of the solute in the serosal and the mucosal side and the level of glucose liberation are measured.

EVALUATION

Glucose liberated in the presence of various concentrations of the α-amylase inhibitor is expressed as percentage of glucose found without the inhibitor. Dose-

response curves can be drawn plotting percent inhibition versus concentration of the inhibitor

REFERENCES AND FURTHER READING

Madar Z (1983) Demonstration of amino acid and glucose transport in chicken small intestine everted sac as a student laboratory exercise. Biochem Educ 11:9–11

Madar Z, Omusky Z (1991) Inhibition of intestinal α-glucosidase activity and postprandial hyperglycemia by α-glucosidase inhibitors in *fa/fa* rats. Nutr Res 11:1035–1046

Lembcke B, Fölsch UR, Creutzfeldt W (1985) Effect of 1-desoxynojirimycin derivatives on small intestinal disaccharidase activities and on active transport *in vitro*. Digestion 31:120–127

K.7.2 Assays for GLUT2 Transport Activity

GENERAL CONSIDERATIONS

Diabetes management is directed toward control of postprandial fluctuations or excursions in blood glucose, which reflect the relative rates of delivery from the intestine and disposal to the tissues. While much is known about the impact of disposal mechanisms on blood glucose, rather less is known about delivery mechanisms, including gastric emptying, membrane hydrolysis, and sugar absorption itself.

Intestinal sugar absorption is increased in experimental diabetes (Csaky and Fischer 1981, Debnam et al. 1990, Thomson et al. 1981). Knowledge of sugar absorption has been based primarily on the mechanism of Na^+/glucose cotransport by Na^+/glucose cotransporter (SGLT1) and its long-term regulation by diet (Ferraris 2001). Recently, however, we have discovered a new pathway of sugar absorption, the apical GLUT2 pathway, which operates within minutes when high concentrations of primary digestion products, i. e., sugars, disaccharides, and α-dextrins, are presented to or generated at the apical membrane of the small intestine. This process is reversed when these sugars are absent from the lumen *in vivo*. The first indication of the existence of this mechanism was obtained in a study of the increase in fructose absorption in experimental diabetes (Corpe et al. 1996).

Dietary glucose crosses the apical membrane of the enterocyte by SGLT1 and exits across the basolateral membrane through the facilitative transporter GLUT2 (Thorens et al. 1990). Plasma glucose is maintained at ~5 mM. When the glucose concentration in the lumen is lower than in plasma, SGLT1 transports glucose uphill against its concentration gradient. This transcellular pathway is powered by a downhill gradient of Na^+ across the apical membrane, maintained by the basolateral Na^+/K^+-ATPase. The cloning of SGLT1 by Wright′s laboratory (Hediger et al. 1987) and GLUT2 by Thorens' laboratory (Thorens et al. 1990) began the molecular biological era of intestinal nutrient transport

PURPOSE AND RATIONALE

Recent experimental evidence hints to a refined model for intestinal glucose absorption (for a review see Kellett and Brot-Laroche 2005, Kellett and Helliwell 2000) whereby a long-term diet containing high–glycemic index sugars is priming the rapid induction of the translocation to and insertion into the apical plasma membrane of GLUT2 by simple dietary sugars. Most importantly, the apical GLUT2 component of absorption seems to be several times greater than the active component at high glucose concentrations. According to this hypothesis, apical GLUT2 and SGLT1 act in tandem to cover the entire concentration range with SGLT1 playing an important regulatory role in the control of apical GLUT2. Apical GLUT2 is not only tightly regulated by long- and short-term supply of dietary sugars, but also by local and endocrine hormones, cellular energy status, stress, and diabetes; regulation occurs through a network of intracellular signaling pathways. Accordingly, apical GLUT2 can provide a major route of sugar absorption by which absorptive capacity is rapidly and precisely upregulated to match the dietary intake of sugars during assimilation of a meal (for a review see Kellett and Brot-Laroche 2005). Apical GLUT2 provides a safety factor by preventing high sugar loads from reaching the colon (Cheeseman 2002). Moreover, the consequent rapid delivery of sugar into the blood might increase the postprandial excursions, especially when glycemic control is poor. Apical GLUT2 is therefore a potential therapeutic target for novel dietary or pharmacological approaches to control intestinal sugar delivery and thereby improve glycemic control. The following assays enable the analysis of effects of compounds/drug candidates on the regulation (*via* insertion into the apical memebrane) and transport activity of GLUT2 and may be helpful for the identification and characterization of a new class of glucose absorption inhibitors as putative future anti-diabetic drugs.

K.7.2.1 Perfusion of Jejunal Loops

PROCEDURE

Helliwell and coworkers (2000) described the perfusion of jejunal loops. Male Wistar rats (240–260 g) fed *ad libitum* on standard diet with free access to water are anaesthetized with an intraperitoneal injec-

tion of a mixture of 1.0 ml of Hypnorm (Janssen U.K.) and 0.4 ml of Hypnovel (Roche Diagnostics) per kg of body weight. The intestine is exposed by a laparotomy. A 30-cm segment just below the ligament of Trietz is cannulated, flushed free of nutrients and perfused with a single-pass system at a flow rate of 0.5ml/min with a modified Krebs bicarbonate saline (118 mM NaCl, 4.74 mM KCl, 1.2 mM KH_2PO_4, 1.25 mM $CaCl_2$ and 24.8 mM $NaHCO_3$) segmented with 95% O_2/5% CO_2. The effluent is collected every 5-min using a fraction collector. The jugular vein is cannulated with a silastic tube and infused with saline at a flow rate of 3 ml/h. Radiolabeled substrate is added to the perfusate and radiolabeled PEG4000 is included as a non-absorbable marker to allow for the correction of fluid movements. At the end of the perfusion period the intestine is removed, weighed wet and then dried overnight before reweighing. For the addition of phloretin the luminal solution required the use of modified Krebs bicarbonate saline (see above) to keep the inhibitor in solution. Phloretin is initially made up as a stock solution in DMSO and 200 µl of stock, then added to 150 ml of perfusate to give a final concentration of 1 mM. Final DMSO concentration is therefore 0.13% (v/v), which has been demonstrated previously to have no effect on tissue permeability. Phloretin can be used in solution for the length of the experiment.

Compound Application

Because compounds take some time to become effective in whole tissue and because there is a limit to the time of viability for isolated loops *in vitro*, the following procedure for the treatment of jejunum with drugs has been adopted. Jejunum is first perfused luminally *in vivo* with 5 mM D-fructose (plus 1 mM β-hydroxybutyrate as an energy source) in the presence or absence of compound. The perfusion system is a gas-segmented, single-pass system with perfusate and gas flow rates of 0.75 and 0.38 ml/min respectively. Jejunum is perfused with compound for 30 min. At the end of the *in vivo* treatment period, the cannulated loop is then excised and perfused *in vitro* using the gas-segmented, recirculated flow system: 5 mM D-glucose or fructose in combination with the compound at the end of the *in vivo* treatment period are perfused luminally through the jejunum for 60 min; the flow rates of perfusate and gas were 7.0 and 3.4 ml/min respectively. Control perfusions are performed in which no compounds are present. These show that there is no falling off in the glucose/fructose uptake rate after the initial approach to the steady state, confirming that this approach to compound treatment and perfusion ensured that the jejunum is viable for the whole experimental period from the start of the *in vivo* to the finish of the *in vitro* perfusion. Samples (0.05 ml) are taken from the perfusate at 5-min intervals throughout the *in vitro* perfusion. After measurement of glucose/fructose concentration with a COBAS automatic analyser (Roche Diagnostics) using a test kit from the same supplier, the amount of glucose/fructose remaining in the perfusate is calculated, with correction for losses in perfusate volume caused by water transport. Because the perfusate is recirculated, the concentration of fructose decreases with time; it is therefore necessary to limit the period over which the rate of transport is measured to one in which the concentration decreased by no more than 20%. Over such periods, plots of luminal perfusate content versus time are effectively linear. The rate of glucose/fructose transport, expressed as µmol/min· (g of dry weight)$^{-1}$, is therefore determined by linear regression analysis as the average rate of disappearance over this period from the luminal perfusate *in vitro*.

Dually Perfused in Situ Jejunum

Dual perfusion of the jejunum is typically performed as described by Hirsh and Cheeseman (1998). Male Sprague-Dawley rats (200–350 g) are fed a standard chow diet and water *ad libitum*. Before the start of the experiment, food is withdrawn for approximately 24 h to minimize intestinal lumenal contents during surgery. All rats are anesthetized prior to surgery using sodium pentobarbital given by intraperitoneal injection (60 mg/kg body weight) and placed on a heated (37°C) surgical table. After performing a laparotomy, the blood supply to the spleen, rectum, colon, cecum, stomach, and ileum are tied off and the tissues removed. The vasculature to the pancreas and duodenum are also ligated. A 35-cm segment of jejunum, starting 5 cm distal from the ligament of Trietz, is isolated and the lumenal contents removed by gently flushing with 20 ml of warm saline (0.9%), and the jejunum is cannulated at both ends. The lumen is perfused with a Krebs-bicarbonate saline solution (120 mM NaCl, 4 mM KCl, 2.5 mM $MgSO_4$, 1.2 mM KH_2PO_4, 25 mM $NaHCO_3$, 1 mM $CaCl_2$) using a pump. The solution containing 5 mM 3-*O*-MG or 5 mM 3-*O*-MG and 5 mM D-fructose, is maintained at 37°C and gassed with 95% O_2, 5% CO_2. Isotopically labeled hexoses, 10 µCi of either 3-*O*-methyl-D-[1-^{3}H]glucose, or both 3-*O*-methyl-D-[1-^{3}H]glucose and D-[U-^{14}C]fructose, are added to the lumenal circuit immediately after portal vein cannulation. The single-pass lumenal circuit is perfused at a flow rate of 1.6 ml/min, and the so-

lution is segmented by 95% O_2/5% CO_2 gas bubbles. The gas bubbles are introduced into the lumenal perfusate through a Y piece at a flow rate which ensured that bubbles occupied the diameter of the perfusion tube. This not only exposes the tissue to a saturating gas partial pressure, but also helps to mix the solution in the tissue lumen. After a single-pass through the segment of jejunum the lumenal perfusate is discarded. The aorta, proximal to the superior mesenteric artery, is ligated just prior to insertion of a cannula into the superior mesenteric artery. The single-pass vascular circuit is perfused at a rate of 1.6 ml/min with fresh Krebs-bicarbonate saline solution, containing 5 mM D-glucose, 0.034 mM streptomycin sulfate, 5 mM L-glutamine, 1120 USP units heparin, and 10% w/v Ficoll 70 as a plasma expander, which is maintained at 37°C and gassed with 95% O_2/5% CO_2 maintaining the pH at 7.4. Once the vascular circuit is established, the rat is euthanized and the vascular perfusate is collected *via* cannula placed in the hepatic portal vein. The effluent is collected continuously for up to 80 min using a fraction collector.

Washout Studies in the Dually Perfused Jejunum

This procedure is similar to the one used by Boyd and Parsons (1979). This washout model is useful for indirectly indicating the locus of compound/drug action. When the labeled 3-*O*-MG is washed out in the presence of an equimolar concentration of unlabeled mannitol in the lumen, the rate of washout into the vascular bed can be described by the sum of two exponential terms (assuming a two-compartmental model applies). The contributing compartments are a fast releasing (vascular flow rate dependent) and a slow releasing one (vascular flow rate independent), which represent: 1) Q_{01} mucosal epithelium layer and 2) Q_{02} deeper submucosal (muscle) layer. Assuming that each pool unloads independently, then each pool will have its own rate constant: the fast, K_1 and the slow, K_2.

EVALUATION

Tissue ion conductance (G) is calculated from PD and I_{sc} according to Ohm's law. For the measurement of basal glucose fluxes, the tissue is clamped at zero voltage by continuously introducing an appropriate I_{sc} with an automatic voltage clamp every 5 min, except for 5–10 s when PD is measured by removing the voltage clamp. Tissue pairs are matched for conductance and discarded if conductance varied by >20%. The non-metabolizable glucose analog 3-*O*-methyl-D-[1-^{3}H]glucose (5 μCi) is added either to the serosal or mucosal side after mounting and the tissue is allowed to equilibrate for 20 min. Net directional flux from mucosal-to-serosal surface is determined for conductance-matched tissues by measuring four consecutive 5-min fluxes before the addition of compound/drug candidate and four 5-min fluxes following the addition of the agent.

MODIFICATION OF THE METHOD

Epithelial glucose uptake can be measured according to the method described by Walker and coworkers (2005).

K.7.2.2 Transport Activity of Brush Border Membrane Vesicles

Preparation of Intestinal Brush Border Membrane Vesicles

Brush-border membrane vesicles (BBMV) are prepared from mucosal scrapings as described by Corpe and coworkers (1996) on basis of a standard procedure introduced by Maenz and Cheeseman (1986). Every stage of the preparation is performed at 0–4°C to prevent changes in trafficking after the intestine had been excised. Briefly, the jejuna of two rats are perfused with compounds/drugs as described above. The timing of the final *in vitro* perfusion is such as to get as direct a correspondence as possible between rates of transport and extent of trafficking. Perfusions for vesicle preparations are therefore terminated at a point corresponding to half the time period over which the average rate of transport is determined, as described above. Immediately after perfusion, each jejunum is rinsed with ice-cold buffered mannitol (20 mM imidazole buffer, pH 7.5, containing 250 mM mannitol and 0.1 mM PMSF), placed on an ice-cold glass plate and slit longitudinally so that the muscle of the jejunum flattened out on to the cold plate. The mucosa is scraped off with a microscope slide and placed in 65 ml of ice-cold mannitol/Tris buffer (300 mM mannitol, 5 mM EGTA, 12 mM Tris/HCl, pH 7.4, and 0.1 mM PMSF). The tissue is homogenized in a Polytron homogenizer (four 30 s bursts using the large probe at setting 7) before addition of $MgCl_2$ to a final concentration of 12 mM. After stirring the solution on ice for 15 min the solution is centrifuged (1,600 × *g*, 15min) to remove debris. The supernatant is further centrifuged (20,000 × *g*, 30 min) and the pellet homogenized in half-strength mannitol/Tris buffer (150 mM mannitol, 2.5 mM EGTA, 6 mM Tris/HCl, pH 7.4, and 0.05 mM PMSF) with a glass homogenizer before further addition of $MgCl_2$. After stirring on ice the centrifugation is repeated as before, and the pellet is then washed

(300 mM mannitol/5mM Tris/HCl, pH7.4) before repelleting (20,000 × *g*). This BBMV preparation is diluted to a protein concentration of 8 mg/ml. Enrichment of sucrase activity in these highly purified preparations typically range from 16- to 20-fold. There is no significant enrichment of Na^+/K^+-ATPase activity.

Preparation of Renal Brush Border Membrane Vesicles

Both kidneys are removed from anaesthetized animals and placed in ice-cold 154 mM NaCl. After removal of the renal capsule, the kidneys are weighed and then sliced into 2-mm thick sections and the cortex dissected away. Cortical fragments from six kidneys are pooled, weighed and suspended in 30 ml of 300 mM mannitol, 12 mM Tris/HCl (pH 7.4), 5 mM EGTA. The resulting suspension was homogenized for 2 min (Ultra Turrax homogenizer) at half speed, followed by the addition of 42 ml of cold distilled water and $MgCl_2$ to a concentration of 12 mM, and then stirred on ice for 15 min. The solution is then centrifuged (2,000 × *g*, 15 min) and the supernatant then re-centrifuged (21,000 × *g*, 30 min). The pellet is suspended in 20 ml of 150 mM mannitol, 6 mM Tris/HCl (pH 7.4), 2.5 mM EGTA using 10 cycles of a hand-operated glass-Teflon homogenizer. $MgCl_2$ is added to a concentration of 12 mM and, after stirring on ice for 15 min, low and high-speed centrifugations described above are repeated. The pellet is then re-suspended in 20 ml of 300 mM mannitol, 12 mM Tris/HCl (pH 7.4), 2.5 mM EGTA and centrifuged (21,000 × *g*, 30 min). The purified BBMV pellet is finally resuspended in the same buffer to a protein concentration of 3–6 mg/ml using 5–6 passes through a syringe fitted with a 21-gauge needle. All steps are carried out at 4°C. The concentration of protein (Bradford 1976) and activity of alkaline phosphatase and Na^+/K^+-ATPase in the initial homogenate and BBMV preparation are determined in order to derive values for enrichment of these marker enzymes (see Corpe et al. 1996).

Glucose Transport

Transport studies are carried out at 20°C on freshly prepared BBMV as described (Sharp and Debnam, 1994). The transport process is initiated by mixing equal volumes of BBMV suspension and uptake buffer consisting of 200 mM NaSCN, 20 mM HEPES, 0.1 mM $MgSO_4$ containing D-[^{3}H]glucose (9 Ci/mmol) and such that the final concentration of glucose is 5–500 µM. Due to the wide glucose concentration range used, the osmotic balance is maintained by adding mannitol to give a final glucose *plus* mannitol concentration of 100 mM. Uptake is terminated after 4 s by the addition of 3 ml of ice-cold 154 mM NaCl containing 0.5 mM phlorizin, followed by vacuum filtration through 0.45-µm nitrocellulose filters (Sartorius, Germany). Three further washes with stop solution are carried out.

EVALUATION

Scintillation counting of the filters is used to calculate glucose accumulation and this is expressed as nmol (mg protein)$^{-1}$ (4 s)$^{-1}$. The kinetic parameters of V_{max} (maximum transport capacity) and K_t (glucose concentration at half V_{max}) for phlorizin-sensitive uptake were derived using a non-linear least squares curve-fitting program.

Parallel uptakes using buffer containing 1 mM phlorizin to block SGLT-mediated transport indicated that uptake is > 90% phlorizin-sensitive. In order to assess GLUT-mediated transport, a higher glucose concentration (20 mM) is used in the presence of 1 mM phlorizin. This value is consistent with the low affinity of GLUT transporters for glucose binding. In addition, uptake of L-glucose at both 100 µM and 20 mM should be performed to establish the contribution of passive glucose transport.

K.7.2.3 Apical Expression of GLUT2

Biotinylation of Surface Proteins

The method of surface protein biotinylation for analysis of GLUT2 expression at apical membranes has been introduced by Au and coworkers (2002). For the detection of GLUT2 in the apical membrane of enterocytes, i. e. of the translocation of GLUT2 from intracellular vesicles to the apical cell surface, proteins expressed on the apical surface of jejunal enterocytes are labeled with *N*-hydroxysuccinimido (NHS)-SS-biotin introduced into the intestinal lumen. At the end of the *in vivo* perfusion the intestine is maintained *in situ*, but cooled on ice. The luminal solution containing NHS-SS-biotin, 1.5 mg/ml in 10 mM triethanolamine/2.5 mM $CaCl_2$/250 mM sucrose buffer (pH 9.0), is introduced into the lumen and left for 30 min. The lumen is then flushed with a PBS/100 mM glycine buffer to quench the free biotin before two final washings with PBS. Mucosal scrapings are then used to make protein extracts as described below.

Isolation of Biotinylated Proteins

Proteins are extracted from the homogenate for 1h at 4°C using the following buffer: 1% Triton X-100, 150 mM NaCl, 5 mM EDTA and 50 mM Tris (pH7.5).

After centrifugation (14,000 × *g*, 10 min) the supernatant is collected and incubated overnight with streptavidin beads. After washing twice with the Triton X-100 buffer to remove non-linked protein, the beads are washed with a high-salt buffer (500 mM NaCl) and finally with a no-salt buffer (10 mM Tris, pH 7.5). The isolated biotinylated proteins are then solubilized in Laemmli sample buffer to be run on SDS-PAGE for immunoblotting. Comparisons of total cell GLUT2 with apical GLUT2 are made by running samples of the supernatant after spinning down the streptavidin-coated beads on the same immunoblots as samples of recovered biotinylated protein.

Detection of Apical GLUT2 by Immunoblotting

Membranes (15 µg of protein) are solubilized in Laemmli sample buffer and separated by SDS-PAGE (10% gel). The proteins are blotted on to nitrocellulose membrane by electrotransfer for 75 min at 4°C. The membranes are stained for total protein with Ponceau S to ascertain that equivalent amounts of protein are loaded and transferred from each lane. Blocking of the membrane is carried out in 3% non-fat milk in PBST (0.05% Tween 20/PBS, pH 7.4) for 1 h and then incubated with 1:1,000 rabbit polyclonal antibody to rat GLUT2 in 3% non-fat dry milk in PBST overnight at 4°C. The membrane is washed three times in 3% non-fat dry milk/PBST for 15 min, 1 h and 15 min respectively. The nitrocellulose membrane was then incubated with a secondary antibody, anti-rabbit IgG coupled to horseradish peroxidase diluted 1:2,000 in 3% non-fat dry milk/PBST for 1 h. Three subsequent washes followed as described above. Finally, the membrane is treated with the ECL detection solution (Amersham-Pharmacia) before autoradiography for 30 s using Kodak XAR-5 film with an intensifying screen. The specificity of the antibody was determined by running parallel lanes of isolated biotinylated proteins and probing them with the native antibody or with antiserum which had been pre-incubated at room temperature for 1 h with the peptide used to raise the antibody. Two antibodies are employed, one that recognizes an epitope in the large extracellular loop between transmembrane segments 1 and 2, amino acids 40–55 (SHYRHVLGVPLDDRRA; Biogenesis, UK) and a second which recognized a portion of the C-terminal sequence of rat GLUT2 (CVQMEFLGSSETV; Research Diagnostics, USA).

K.7.3 Evaluation of Glucose Absorption In Vivo

PURPOSE AND RATIONALE

The inhibition of glucose absorption can be determined by measuring blood glucose after administration of starch or disaccharides with and without the inhibitor. In addition, non-absorbed starch or disaccharides can be determined in the intestine.

PROCEDURE

Male Wistar rats are kept on a standard diet with free access to tap water at constant temperature (24 ± 1°C). Sixteen hours prior to the experiment food but not water is withheld. Groups of rats receive by stomach tube 2.5 g/kg raw starch in a water suspension without or with various doses of the α-amylase inhibitor. After 10, 20, 30, 60, 120 and 240 min, blood is withdrawn for determination of blood glucose and non-esterified fatty acids. The animals are sacrificed after these intervals and the residual starch in the stomach and the intestine determined. Definitely more starch is found in the intestine after simultaneous application of the α-amylase inhibitor. Similar experiments are performed in dogs for determination of serum insulin. The increase of blood glucose and serum insulin as well as the decrease of NEFA are inhibited.

EVALUATION

The values of starch content in stomach and intestine, as well as the blood glucose-, serum insulin- and NEFA-values are compared between control and treated animals.

MODIFICATIONS OF THE METHOD

In order to test the inhibition of glucosidase in addition, loading tests with sucrose or other disaccharides are performed (Puls and Keup 1973, Puls et al. 1977, Matsuo et al. 1992). Matsuo and coworkers (1992) performed experiments with genetically or experimentally obese rats (female Zucker fatty rats or female ventromedial hypothalamic nuclei-lesioned rats) and male yellow *KK*-mice. LeMarchand-Brustel and coworkers (1990) studied the effect of an α-glycosidase inhibitor on experimentally induced obesity in mice. Male Swiss albino mice were rendered obese by injection of goldthioglucose at the age of 3 weeks. Since goldthioglucose treatment does not produce obesity in all injected mice, pro-obese mice were selected at 8 weeks of age on the basis of their body weight gain. They were divided in a control group receiving chow without drug and a treated group receiv-

ing chow containing the glycosidase inhibitor. Weight gain, glycemia and insulinemia were followed over 120 days. Madar and Omusky (1991) studied the inhibition of intestinal α-glucosidase activity and postprandial hyperglycemia by α-glucosidase inhibitors in *fa/fa* rats. Various starch sources were used. Blood samples were taken at various intervals after starch load. Takami and coworkers (1991) studied the antidiabetic actions of a disaccharidase inhibitor in spontaneously diabetic (GK) rats. Okada and coworkers (1992) reported anti-obesity and antidiabetic actions of a new potent disaccharidase inhibitor in genetically obese-diabetic mice.

REFERENCES AND FURTHER READING

Au A, Gupta A, Schembri P, Cheeseman CI (2002) Rapid insertion of GLUT2 into the rat jejunal brush-border membrane promoted by glucagon-like peptide 2. Biochem J 367:247–254

Boyd CA, Parsons DS (1979) Movements of monosaccharides between blood and tissues of vascularly perfused small intestine. J Physiol 287:371–391

Bradford MM (1976) A rapid and sensitive method for the quantification of microgram quantities of protein utilising the principle of pprotein-dye binding. Anal Biochem 72:248–254

Cheeseman CI (2002) Intestinal hexose absorption: transcellular or paracellular fluxes. J Physiol 544:336

Corpe CP, Basaleh MM, Affleck J, Gould GW, Jess TJ, Kellett GL (1996) The regulation of GLUT5 and GLUT2 activity in the adaptation of intestinal brush-border fructose transport in diabetes. Pflüglers Archiv Eur J Physiol 432:192–201

Czaky TZ, Fischer E (1981) Intestinal sugar transport in experimental diabetes. Diabetes 30:568–574

Debnam ES, Ebrahim HY, Swaine DJ (1990) Diabetes mellitus and sugar transport across the brush border and basolateral membranes of rat jejunal enterocytes. J Physiol 424:13–25

Ferraris RP (2001) Dietary and developmental regulation of intestinal sugar transport. Biochem J 360:265–276

Hediger MA, Coady MJ, Ikeda TS, Wright EM (1987) Expression cloning and sequencing of the Na+/glucose cotransporter. Nature 330:379–381

Helliwell PA, Richardson M, Affleck J, Kellett GL (2000) Stimulation of fructose transport across the intestinal brush-border membrane by PMA is mediated by GLUT2 and dynamically regulated by protein kinase C. Biochem J 350:149–154

Hirsh AJ, Cheeseman CI (1998) Cholecystokinin decreases intestinal hexose absorption by a parallel reduction in SGLT1 abundance in the brush-border membrane. J Biol Chem 273:14545–14549

Kellett GL, Brot-Laroche E (2005) Apical GLUT2, A major pathway of intestinal sugar absorption. Diabetes 54:3056–3062

Kellett GL, Helliwell PA (2000) The diffusive component of intestinal glucose absorption is mediated by the glucose-induced recruitment of GLUT2 to the brush border membrane. Biochem J 350:155–162

Le Marchand-Brustel Y, Rochet N, Grémeaux T, Marot I, Van Obberghen E (1990) Effect of an a-glycosidase inhibitor on experimentally induced obesity in mice. Diabetologia 33:24–30

Madar Z, Omusky Z (1991) Inhibition of intestinal α-glucosidase activity and postprandial hyperglycemia by α-glucosidase inhibitors in *fa/fa* rats. Nutr Res 11:1035–1046

Maenz DD, Cheeseman CI (1986) Effect of hyperglycemia on D-glucose transport across the brush-border and basolateral membrane of rat small intestine. Biochim Biophys Acta 860:277–285

Matsuo T, Odaka H, Ikeda H (1992) Effect of an intestinal disaccharidase inhibitor (AO-128) on obesity and diabetes. Am J Clin Nutr 55, Suppl 1:314S–317S

Okada H, Shino A, Ikeda H, Matsuo T (1992) Anti-obesity and antidiabetic actions of a new potent disaccharidase inhibitor in genetically obese-diabetic mice, KKA^y. J Nut Sci Vitaminol 38:27–37

Puls W, Keup U (1973) Influence of an α-amylase inhibitor (BAY d 7791) on blood glucose, serum insulin and NEFA in starch loading tests in rats, dogs and man. Diabetologia 9:97–101

Puls W, Keup U, Krause HP, Thomas G, Hoffmeister F (1977) Glucosidase inhibition. A new approach to the treatment of diabetes, obesity, and hyperlipoproteinaemia. Naturwiss 64:536–537

Sharp PA, Debnam ES (1994) The role of cyclic AMP in the control of sugar transport across the brush-border and basolateral membranes of rat jejunal enterocytes. Exp Physiol 70:203–214

Takami K, Okada H, Tsukuda R, Matsuo T (1991) Antidiabetic actions of a disaccharidase inhibitor, AO-128, in spontaneously diabetic (GK) rats. Jpn J Pharmacol Ther 19:161–171

Thomson AB (1981) Uptake of glucose into the intestine of diabetic rats: effects of variations in the effective resistance of the unstirred water layer. Diabetes 30:247–255

Thorens B, Cheng ZQ, Brown D, Lodish HF (1990) Liver glucose transporter: a basolateral protein in hepatocytes and intestine and kidney cells.Am J Physiol 259:C279-C285

Walker J, Jijon HB, Diaz H, Salehi P, Churchill T, Madsen KL (2005) 5-Aminoimidazole-4-carboxamide riboside (AICAR) enhances GLUT2-dependent jejunal glucose transport: a possible role for AMPK. Biochem J 385:485–491

K.8 Monitoring of Diabetic Late Complications

K.8.1 Aldose Reductase Activity

GENERAL CONSIDERATIONS

Secondary symptoms of long lasting diabetes mellitus are diabetic neuropathy with sensory symptoms, motoric disturbances due to reduced nerve conduction velocity and diabetic cataracts. Both are related to enhanced conversion of glucose to polyols, such as sorbitol, by the enzyme aldose reductase (van Heyningen 1959, Clements 1979). Sorbitol is converted to fructose by sorbitol-dehydrogenase. A low activity of this enzyme enhances the accumulation of sorbitol, thus contributing to cellular damage. Inhibitors of aldose reductase have been developed with positive results in diabetic patients (Kador et al. 1985).

There are even some experimental hints for the benefit of aldose reductase inhibitors in diabetic cardiomyopathy (Cameron et al. 1989). Experimental data provide also evidence for possible beneficial effects in diabetic neuropathy, retinopathy, measured by nerve conduction velocity or electroretinography, lens cataract formation, vascular permeability and filtration (Williamson et al. 1987, Tilton et al. 1988 and 1989, Pugliese et al. 1990) and nephropathy (Sarges and Oates 1993).

Geisen and coworkers (1994) reported on sorbitol-accumulating pyrimidine derivatives which inhibited sorbitol dehydrogenase, induced a dose-dependent increase of tissue sorbitol and accelerated cataract development. Surprisingly, an acceleration of motor nerve conduction velocity in normal and diabetic rats and a normalization of glomerular filtration rates in diabetic rats were found.

REFERENCES AND FURTHER READING

Cameron NE, Cotter MA, Robertson S (1989) Contractile properties of cardiac papillary muscle in streptozotocin-diabetic rats and the effects of aldose reductase inhibition. Diabetologia 32:365–370

Clements RS (1979) Diabetic neuropathy – new concepts in its etiology. Diabetes 28:604–611

Geisen K, Utz R, Grötsch H, Lang HJ, Nimmesgern H (1994) Sorbitol-accumulating pyrimidine derivatives. Arzneim Forsch/Drug Res 44:1032–1043

Kador PF, Robison WG, Kinoshita JH (1985) The pharmacology of aldose reductase inhibitors. Ann Rev Pharmacol Toxicol 25:691–714

Pugliese G, Tilton RG, Speedy A, Chang K, Province MA, Kilo C, Williamson JR (1990) Vascular filtration function in galactose-fed versus diabetic rats: the role of polyol pathway activity. Metabolism 39:690–697

Sarges R, Oates PJ (1993) Aldose reductase inhibitors: Recent developments. Progr Drug Res 40:99–161

Tilton RG, Chang K, Weigel C, Eades D, Sherman WR, Kilo C, Williamson JR (1988) Increased ocular blood flow and ^{125}I-albumin permeation in galactose-fed rats: Inhibition by sorbinil. Invest Ophthalm Vis Sci 29:861–868

Tilton RG, Chang K, Pugliese G, Eades DM, Province MA, Sherman WR, Kilo C, Williamson JR (1989) Prevention of hemodynamic and vascular filtration changes in diabetic rats by aldose reductase inhibitors. Diabetes 38:1258–1270

van Heyningen R (1959) Formation of polyols by the lens of the rat with "sugar" cataract. Nature 184:194–195

Williamson JR, Chang K, Tilton RG, Prater C, Jeffrey JR, Weigel C, Sherman WR, Eades DM, Kilo C (1987) Increased vascular permeability in spontaneously diabetic BB/W rats and rats with mild versus severe streptozotocin-induced diabetes. Diabetes 36:813–821

K.8.1.1 Measurement with Normal Lenses

PURPOSE AND RATIONALE

The enzyme aldose reductase from bovine lens has been characterized by Hayman and Kinoshita (1965). Using this preparation, the *in vitro* effectiveness of various aldose reductase inhibitors can be determined (Varma and Kinoshita 1976, Billon et al. 1990).

PROCEDURE

Aldose reductase from lenses of calf eyes is isolated from the homogenates by ammonium sulfate precipitation of the concomitant proteins and by column chromatography on DEAE-cellulose. DL-Glyceraldehyde is used as substrate. The activity is expressed as the rate of OD_{340} [nm] due to the utilization of NADPH in the reaction. The reaction mixture contains 0.1 M phosphate buffer (pH 6.2), NADPH 2.5×10^{-4} M, DL-glyceraldehyde 1.5×10^{-3} M and the enzyme. The total volume of the reaction mixture is 1 ml. The reference blank consists of all the above compounds except the substrate. The effects of inhibitors on the enzyme activity are determined by including the compound being tested at the desired concentration in the reaction mixture. Appropriate blanks are used to correct for nonspecific reduction of NADPH and absorption by the compounds being tested. The test compounds are added first in 10^{-3} M solution and diluted as desired.

EVALUATION

Percentage of inhibition is tested at various concentrations and IC_{50}-values are calculated.

REFERENCES AND FURTHER READING

Billon F, Delchambre Ch, Cloarec A, Sartori E, Teulon JM (1990) Aldose reductase inhibition by 2,4-oxo and thioxo derivates of 1,2,3,4-tetrahydroquinazoline. Eur J Med Chem 25:121–126

Hayman S, Kinoshita JH (1965) Isolation and properties of lens aldose reductase. J Biol Chem 240:877–882

Varma S, Kinoshita JH (1976) Inhibition of lens aldose reductase by flavonoids – their possible role in the prevention of diabetic cataracts. Biochem Pharmacol 25:2505–2513

K.8.1.2 Measurement with Cataract Lenses

PURPOSE AND RATIONALE

The effect of aldose reductase inhibitors can be tested by determining the level of aldose reductase, NADPH and $NADP^+$ in the lenses of galactose treated or streptozotocin diabetic rats after treatment with the inhibitor compared to controls.

PROCEDURE

Galactose Treatment

Cataract formation can be induced by galactose feeding to young rats. Male Sprague-Dawley rats weighing 40–50 g are randomly divided into 2 groups. One

group is fed a laboratory chow, the other group is fed a galactose diet containing 50% galactose, 20% cornstarch, 15% casein, 9% hydrogenated oil, 4% salt mixture, and 2% cod liver oil. Diabetes is induced in male Sprague-Dawley rats weighing 80–90 g by a single intravenous dose of 100 mg/kg streptozotocin.

Streptozotocin Treatment

Diabetes is induced in 230–260 g male Sprague-Dawley rats by administration of a single tail vein injection of streptozotocin (55 mg kg^{-1}) 2–4 weeks prior to study. Streptozotocin is dissolved in freshly prepared 0.05 M citrate buffer (pH 4.5) and administered under light isoflurane anaesthesia. Animals are glycosuric 24 h after streptozotocin treatment. The weight of the control animals is matched to that of the 2–4 week diabetics. Animals were allowed *ad libitum* access to a standard rat chow (Diet RM1, SDS Ltd, UK) and water until the time of experimentation, with the exception of those subjected to an overnight fast. For all experimental procedures animals are terminally anaesthetized with intraperitoneal pentobarbitone sodium (90 mg kg^{-1}) before removal of eyes. The progression of cataracts is observed in controls and in rats treated with the aldose reductase inhibitor.

Assay

At appropriate times, the rats are sacrificed and the lenses are dissected. They are frozen on solid CO_2 and stored at –70°C until analysis. Single rat lenses are homogenized in 200 µl of 10 mM sodium phosphate buffer containing 5 mM 2-mercaptoethanol (pH 7.0) for 0.5 min at 0°C. A cell-free extract is obtained by centrifuging (17,300 × *g*, 10 min) the total lens homogenate. The enzyme reaction mixture (final volume 1 ml) contains 0.4 M $(NH_4)_2SO_4$, 0.1 M HEPES/NaOH buffer (pH 7.0), 10 mM DL-glyceraldehyde and 0.12 mM NADPH. A 20-ml aliquot of supernatant is added to initiate the reaction. Decrease in absorbance at 340 nm is followed spectrophotometrically. Enzymatic activity is expressed as nM of NADPH oxidized per min.

EVALUATION

Results are expressed as aldose reductase units/mg lens (wet weight). Means ± SE are calculated and compared using Student's non-paired *t*-test.

MODIFICATIONS OF THE METHOD

Naeser and coworkers (1988) studied sorbitol metabolism in the retina, optic nerve, and sural nerve of diabetic rats treated with an aldose reductase inhibitor. Activities of aldose reductase, sorbitol-dehydrogenase, and content of sorbitol were assayed in these tissues.

Freeze-dried tissue samples are sonicated for 5–10 s in 215 µl of 0.04 M Tris (pH 6.8). For determination of aldose reductase, the homogenate is centrifuged for 45 min at 37,000 rpm and 100 µl is taken from the supernatant for analysis. The remaining sample is centrifuged further (96,000 rpm, 2 h) and the supernatant used for sorbitol determination. For determination of aldose reductase, 10 µl of the sample are mixed with 15 µl buffer solution containing 0.14 mM Tris, 151 µM NADH, and 0.6 M glucose. After incubation in a water bath for 20 min at 38°C, the incubation is stopped by transfer to ice. Samples mixed with buffer solution without glucose serve as blanks. Twenty µl of the incubated material are then mixed with 1.25 ml of 0.04 M NaOH solution containing 1.7 mM NaCl. Fluorescence is measured in a Farrand Ratio Fluorometer with primary filters 5860 and 5970 (Corning Glass Works) and secondary filters 2A (Turner Optical Co), 4308 and 3387 (Corning Glass Works). The amount of NADPH consumed serves as measure for aldose reductase activity.

Sorbitol-dehydrogenase is measured by adding 5 µl of fresh homogenate to 20 µl of a buffer composed of 0.1 mM Tris (pH 6.8), 1.25 mM NAD and 50 mM sorbitol. After incubation for 30 min at 38°C, the reaction is stopped by the addition of 5 µl 0.1 N NaOH and transfer to ice. The amount of NAD^+ converted to NADH is determined luminometrically in 10 µl samples with 100 µl of NAD(P)H reagent (Roche Diagnostics) containing 5 mg/L luciferase, 25 mM potassium phosphate, 100 mM dithiothreitol, 38 U/L Triton-X 100, and 20 mM myristic aldehyde. The flux of light is instantly registered, using a photomultiplier.

Sorbitol is determined in the centrifugation supernatant. After immersion in boiling water for 5 min, aliquots of 15 µl are added to 10 µl buffer containing 0.1 M Tris (pH 8.6), 3.5 mM NAD, and 2.7 U/ml sorbitol-dehydrogenase. Tissue blanks are run without sorbitol-dehydrogenase. The incubation is terminated and the amount of NADH formed is determined as for the sorbitol-dehydrogenase assay.

Gonzales and coworkers (1986) studied the effect of an aldose reductase inhibitor on integration of polyol pathway, pentose phosphate pathway and glycolytic route in diabetic rat lens. Diabetes was induced in male Wistar rats weighing about 230 g by subcutaneous injection of 200 mg/kg alloxan monohydrate. After one week, in the diabetic rat lens was an ap-

parent increase in the flux of glucose through the pentose phosphate pathway, as measured by the difference in the yields of $^{14}CO_2$ from [1-^{14}C]glucose and [6-^{14}C]glucose [C1–C6]. Treatment with the aldose reductase inhibitor reduced the values toward normal. With glucose tritiated on carbons 2 or 3, it has been shown that the flux of glucose through the polyol route is increased, whereas the flux through the glycolytic pathway is decreased in the diabetic rat lens. Both parameters were restored to normal in diabetic rats treated with the aldose reductase inhibitor.

Meydani and coworkers (1994) investigated the onset and progression of cataract in weanling Sprague Dawley rats fed 10, 15, 20 and 30% dietary galactose for 45–226 days.

Ohta and coworkers (1999) studied cataract development in 12-months-old rats fed a 25% galactose diet and its relation to osmotic stress and oxidative damage.

Using phosphorus-31 nuclear magnetic resonance spectroscopy, Sakagami and coworkers (1999) investigated the metabolic kinetics of organophosphate compounds in the rat lens during cataract development induced by different doses of galactose added to rat chow.

Mackic and coworkers (1994) developed a model of galactose-induced cataract formation in guinea pigs and studied the morphologic changes and accumulation of galactitol.

Sato and coworkers (1998) demonstrated that the formation and progression sugar cataracts in galactose-fed dogs can be dose-dependently inhibited by the aldose reductase inhibitors.

REFERENCES AND FURTHER READING

Gonzales AM, Sochor M, Hothersall JS, McLean P (1986) Effect of aldose reductase inhibitor (sorbinil) on integration of polyol pathway, pentose phosphate pathway and glycolytic route in diabetic rat lens. Diabetes 35:1200–1205

Mackic JB, Ross-Cisneros FN, McComb JG, Bekhor I, Weiss MH, Kannan R, Zlokovic BV (1994) Galactose-induced cataract formation in guinea pigs: Morphologic changes and accumulation of galactitol. Invest Ophthalm Vis Sci 35:804–810

Meydani M, Martin A, Sastre J, Smith D, Dallal G, Taylor A, Blumberg J (1994) Dose-response characteristics of galactose-induced cataract in the rat. Ophthalm Res 26:368–374

Naeser et al (1988) Sorbitol metabolism in the retina, optic nerve, and sural nerve of diabetic rats treated with an aldose reductase inhibitor

Ohta Y, Yamasaki T, Niwa T, Goto H, Majima Y, Ishiguro I (1999) Cataract development in 12-months-old rats fed a 25% galactose diet and its relation to osmotic stress and oxidative damage. Ophthalm Res 31:321–331

Sakagami K, Igarashi H, Tanaka K, Yoshida A (1999) Organophosphate metabolic changes in the rat lens during the development of galactose-induced cataract. Hokkaido J Med Sci 74:457–466

Sato S, Mori K, Wyman M, Kador FP (1998) Dose-dependent prevention of sugar cataracts in galactose-fed dogs by the aldose reductase inhibitor M79175. Exp Eye Res 66:217–222

K.8.2 Nerve Conduction Velocity

PURPOSE AND RATIONALE

Aldose reductase inhibitors can be tested in rats with diabetes induced with streptozotocin by measuring nerve conduction velocity (Miyoshi and Goto 1973, Mayer and Tomlinson 1983, Tomlinson et al. 1882, 1984, Yue et al. 1982) and resistance to ischemic conduction block (Price et al. 1988).

PROCEDURE

Male Wistar rats weighing 100–150 g are rendered diabetic with an i.v. injection of 60 mg/kg streptozotocin. Diabetes is confirmed by the presence of glucosuria and elevated blood glucose levels 24 h after injection. The rats are kept on standard diet and water ad libitum for 28 days after streptozotocin treatment. Groups of rats are treated with the test compound (aldose reductase inhibitor) or the vehicle once daily by gavage starting 24 h after streptozotocin injection. One group of age-matched rats serves as control.

For measurement of sciatic nerve conduction velocity, rats are anesthetized with 2% halothane in oxygen and placed in a Perspex chamber that is maintained at a constant temperature by a copper coil in the base through which warm water is circulated. A fine needle thermocouple is inserted in the lateral aspect of the left hind limb, and the subcutaneous temperature is measured with an electronic thermometer. The conduction velocity of the left sciatic-tibial nerve is measured by a modification of the method of Sharma and Thomas (1974). Two fine platinum stimulating electrodes are inserted in the sciatic notch, and two more are inserted through the skin of the ankle to lie adjacently to the tibial nerve. The electrodes are 5 mm apart, the distal end being the cathode. A recording electrode is inserted under the skin of the lateral side of the foot and another between the third and fourth toes. A ground electrode is inserted under the skin on the dorsum of the foot. Both stimulation and recording are carried out with a neurophysiological unit (e. g., model MS92a, Medelec, Old Woking, UK). The nerve is stimulated supramaximally with square-wave pulses of 0.1 ms duration. The conduction velocity is calculated as the distance between the distal electrodes divided by the difference between the latencies at the two stimulation points. The mean of three recordings

is taken. The coefficient of variation of nerve conduction velocity is calculated by measuring nerve conduction velocity six times in one rat from each treatment group, withdrawing and reinserting the electrodes each time.

To measure resistance to ischemic conduction block, two fine platinum stimulating electrodes (1 cm apart) are inserted in the lateral aspect of the tail 3 cm from the base. Two recording electrodes are inserted near the tip, and a ground electrode is inserted midway between these and the stimulating electrodes. A thermocouple is attached to the middle of the tail. Both stimulation and recording are carried out as described above. To render the tail ischemic, a small sphygmomanometer cuff is inflated to 240 mm Hg around the base of the tail. The nerve is stimulated at 2.5 min intervals until the action potential disappears. The tail temperature is maintained at 32°C. At the end of the experiment, 5 ml blood is taken by cardiac puncture. The animal is then sacrificed, the sciatic nerves are removed, cleaned, weighed, snap-frozen in liquid nitrogen and stored at –20°C for subsequent estimation of polyol level.

Nerve polyol estimation is performed by the method of Stribling and coworkers (1985). Frozen nerves are thawed, placed in 1 ml water containing 60 µg of α-methylmannoside as an internal standard, and boiled for 20 min. Zinc sulfate (200 µl of a 5% solution) is added, samples are homogenized with a Polytron homogenizer, 200 µl 0.3 N barium hydroxide solution is added, and the samples rehomogenized. After centrifugation, the supernatant is freeze-dried overnight. The residue is silylated with 250 ml of a mixture of pyridine/hexamethyldisilazane/ trimethylchlorosilane (10/2/1, Pierce) at room temperature for 24 h. The reaction is stopped by adding 2 ml water, and 200 µl cyclohexane is added. Samples are shaken and 2 µl of the organic phase is injected into a gas chromatograph. Plasma glucose levels are measured with the use of a glucose analyzer. Plasma fructosamine, which reflects plasma protein glycosylation, is measured with the use of a commercial kit. Plasma glucose, plasma fructosamine and nerve sorbitol are increased and nerve conduction velocity decreased in streptozotocin treated rats.

EVALUATION

Data from diabetic rats treated with the aldose-reductase inhibitor are compared with the values of untreated diabetic rats and normal controls. Statistical comparisons are made by use of the Mann-Whitney *U* test.

MODIFICATIONS OF THE METHOD

Sima and coworkers (1990) studied motor nerve conduction velocity and neuroanatomical abnormalities in insulin-deficient diabetic Bio-Breeding rats (BB-rat) with and without long-term administration of an aldose reductase inhibitor. Their findings of a significant, but incomplete prevention of neuropathy in these animals by aldose reductase inhibition suggest that additional mechanisms besides polyol-pathway activation may be of importance in the pathogenesis of diabetic neuropathy. Carrington and coworkers (1991) studied effects on impulse conduction after aldose reductase inhibition with imirestat in sciatic nerves of streptozotocin-diabetic rats both *in vivo* and *in vitro*. Cameron and coworkers (1991) studied nerve blood flow monitored by microelectrode polarography and hydrogen clearance in experimental diabetes in rats in relation to conduction deficits. Using these methods, Cameron and Cotter (2003) studied the effects of 5-hydroxytryptamine 5-HT_2 receptor antagonists on nerve conduction velocity and endoneurial perfusion in diabetic rats.

Schmidt and coworkers (1991) performed ultrastructural studies in mesenteric nerves of streptozotocin-induced diabetic rats.

REFERENCES AND FURTHER READING

Cameron NE, Cotter MA, Low AP (1991) Nerve blood flow in early experimental diabetes in rats: relation to conduction deficits. Am J Physiol 261 E1–E8

Cameron NE, Cotter MA (2003) The effects of 5-hydroxytryptamine 5-HT_2 receptor antagonists on nerve conduction velocity and endoneurial perfusion in diabetic rats. Naunyn-Schmiedbergs Arch Pharmacol 367:607–614

Carrington AL, Ettlinger CB, Calcutt NA, Tomlinson DR (1991) Aldose reductase inhibition with imirestat-effects on impulse conduction and insulin-stimulation of Na^+/K^+-adenosine triphosphatase activity in sciatic nerves of streptozotocin-diabetic rats. Diabetologia 34:397–401

Mayer JH, Tomlinson DR (1983) Prevention of defects of axonal transport and nerve conduction velocity by oral administration of myo-inositol or an aldose reductase inhibitor in streptozotocin-diabetic rats. Diabetologia 25:433–438

Miyoshi T, Goto I (1973) Serial *in vivo* determinations of nerve conduction velocity in rat tails. Physiological and pathological changes. Electroencephalogr Clin Neurophysiol 35:125–131

Schmidt RE, Plurad SB, Coleman BD, Williamson JR, Tilton RG (1991) Effects of sorbinil, dietary *myo*-inositol supplementation, and insulin on resolution of neuroaxonal dystrophy in mesenteric nerves of streptozotocin-induced diabetic rats. Diabetes 40:573–582

Sharma AK, Thomas PK (1974) Peripheral nerve structure and function in experimental diabetes. J Neurol Sci 23:1–15

Sima AAF, Prashar A, Zhang WX, Chakrabarti S, Greene DA (1990) Preventive effect of long-term aldose reductase inhibition (Ponalrestat) on nerve conduction and sural nerve structure in the spontaneously diabetic Bio-Breeding rat. J Clin Invest 85:1410–1420

Stribling D, Mirrlees DJ, Harrison HE, Earl DCN, (1985) Properties of ICI 128,436, a novel aldose reductase inhibitor and its effects on diabetic complications in the rat. Metabolism 34:336–344

Tomlinson DR, Holmes PR, Mayer JH (1982) Reversal, by treatment with an aldose reductase inhibitor, of impaired axonal transport and motor nerve conduction velocity in experimental diabetes mellitus. Neurosci Lett 31:189–193

Yue DK, Hanwell MA, Satchell PM, Turtle JR (1982) The effect of aldose inhibition on motor nerve conduction velocity in diabetic rats. Diabetes 31:789–794

K.8.3 Nerve Blood Flow (Doppler Flux)

PURPOSE AND RATIONALE

In addition to nerve conduction studies, Calcutt and coworkers (1994) described a method to measure nerve blood flow by laser Doppler flowmetry in rats with streptozotocin induced diabetes treated with aldose reductase inhibitors.

PROCEDURE

Diabetes is induced in female Sprague-Dawley rats weighing 200–280 g by a single i.p. injection of 50 mg/kg streptozotocin after an overnight fast and is confirmed 2 days later by blood glucose determinations. Aldose-reductase inhibitor treated rats receive the test compound orally by gavage once a day for 2 months. For the experiment, the animals are anesthetized with an intraperitoneal injection (2 ml/kg) consisting of pentobarbital (12.5 mg/ml) and diazepam (1.25 mg/ml) in 0.9% NaCl. For estimation of nerve blood flow, a laser Doppler flowmeter (TSI model BPM 403A, MN) with a wavelength of 780 nm is used. Flow determinations are made with a filter frequency of 30 Hz to 18 kHz and, depending on the magnitude of the reflected signal, one of four band widths (30 Hz to 1.3 kHz, 30 Hz to 3 kHz, 30 Hz to 7.5 kHz, or 30 Hz to 18 kHz). The flow meter continuously displays a moving average for the preceding 5 s in units of $\text{Hz} \times 10^2$. For flow measurements, the sciatic nerve is exposed and the probe tip of the flow-meter placed 1 mm above the mid-thigh region of the nerve using a micromanipulator. After a 10 s stabilization period, the first measurement is recorded. The probe is then advanced 1 mm distally for a second measurement and this process repeated until 10 readings are recorded over 1 cm of nerve. The mean of 10 values is taken as average nerve laser Doppler flow. Blood flow velocity, expressed in m/s, is reduced in diabetic rats.

EVALUATION

The effects of streptozotocin diabetes and of aldose reductase treatment are assessed by one factor analysis of variance (ANOVA). Individual post-hoc comparisons are made with the Newman-Keuls method when the F ratio is $P < 0.05$.

K.8.4 Electroretinogram

PURPOSE AND RATIONALE

Diabetic neuropathy is one of the important symptoms of long-lasting diabetes (Engerman 1989). Several animal studies with aldose reductase inhibitors have been performed (Lightman et al. 1987, Hotta et al. 1988, Nagata and Robison 1988). Segawa and coworkers (1988) measured the development of electroretinogram abnormalities and the possible role of polyol pathway activity in diabetic hyperglycemia and galactosemia in the rat.

PROCEDURE

Male Sprague-Dawley rats weighing 310–400 g are dark-adapted for 20 min and anesthetized with i.p injections of ketamine, 50–80 mg/kg and atropine sulfate, 2 mg/kg. Electroretinography is performed monocularly with the pupil maximally dilated. Photic stimulation is delivered with an intensity of one J in 20 s interstimulus intervals. Using a contact lens-type electrode, electroretinograms (ERG) evoked by strong flushes are amplified by a preamplifier, displayed on an oscilloscope and summed using a signal averager which also provides a copy of the averaged ERG. The amplitudes of the a- and b-waves are measured from the base line to the trough of the a-wave and from the trough of the a-wave to the crest of the b-wave, respectively. The amplitudes of the oscillatory potentials are measured. The peak latencies are measured as the intervals between the stimulus onset and the peak of the corresponding a- and b-waves and oscillatory potentials. The oscillatory potentials (designated O_1, O_2, and O_3 in order of appearance on the ascending limb of the b-wave) are added together. The sum of these amplitudes is expressed as the wavelet index.

For inducing galactosemia, male Sprague-Dawley rats weighing 140–185 g at the beginning of the study, receive a diet of 30% galactose. Test compounds are given as 0.1% to the diet.

EVALUATION

Data are calculated as mean ± SEM and significance levels are estimated using the Wilcoxon rank sum test for unpaired data (two-sided). Linear regression is calculated by the least square method. A p-value of < 0.05 is regarded as statistically significant.

MODIFICATIONS OF THE METHOD

De la Cruz et al. (2003) studied the effects of clopidogrel and ticlopidine on experimental ischemic retinopathy in streptozotocin-diabetic rats. The percentage of the retinal surface occupied by horseradish peroxidase-permeable vessels was recorded.

REFERENCES AND FURTHER READING

Calcutt NA, Mizisin AP, Kalichman MW (1994) Aldose reductase inhibition, Doppler flux and conduction in diabetic rat nerve. Eur J Pharmacol 251:27–33

De la Cruz J, Arrebola M, González-Correa J, Martinez-Cerdán E, Moreno A, de la Cuesta SF (2003) Effects of clopidogrel and ticlopidine on experimental ischemic retinopathy in rats. Naunyn-Schmiedebergs Arch Pharmacol 367:204–210

Engerman RL (1989) Pathogenesis of diabetic retinopathy. Diabetes 38:1203–1206

Hotta N, Kakuta H, Fukasawa H, Koh N, Matsumae H, Kimura M, Sakamoto N (1988) Prevention of diabetic neuropathy by an aldose reductase inhibitor in fructose-fed streptomycin-diabetic rats. In: Sakamoto N, Kinoshita JH, Kador PF, Hotta N (eds) Polyol pathway and its role in diabetic complications. Excerpta Medica, Amsterdam, pp 311–318

Lightman S, Rechthand E, Terubayashi H, Palestine A, Rapoport A, Kador P (1987) Permeability changes in blood-retinal barrier of galactosemic rats are prevented by aldose reductase inhibitors. Diabetes 36:1271–1275

Nagata M, Robison WG (1988) Basement membrane thickening in retina and muscle of animal models of diabetes. In: Sakamoto N, Kinoshita JH, Kador PF, Hotta N (eds) Polyol pathway and its role in diabetic complications. Excerpta Medica, Amsterdam, pp 276–285

Segawa M, Hirata Y, Fujimori S, Okada K (1988a) The development of electroretinogram abnormalities and the possible role of polyol pathway activity in diabetic hyperglycemia and galactosemia. Metabolism 37:454–460

Segawa M, Takahashi N, Namiki H, Masuzawa K (1988b) Electrophysiological abnormalities and polyol accumulation in retinas of diabetic and galactosemic rats. In: Sakamoto N, Kinoshita JH, Kador PF, Hotta N (eds) Polyol pathway and its role in diabetic complications. Excerpta Medica, Amsterdam, pp 306–310

K.8.5 Streptozotocin-Induced Cataract

PURPOSE AND RATIONALE

The increased incidence of cataracts, i. e. changes in the transparency or of the refractory index of the lens, in diabetic patients is well known. Evidence has accumulated for the involvement of polyol metabolism and the enzyme aldose reductase in diabetic cataractogenesis (van Heyningen 1959, Pirie and van Heyningen 1964). The enzyme aldose reductase catalyzes the reduction of aldoses such as glucose and galactose to the corresponding polyols, i. e., sorbitol and dulcitol. Sugar-induced cataractogenesis has been shown to parallel lenticular polyol accumulation (Kinoshita 1965). Since polyols do not readily diffuse through intact cellular membranes, they create a severe osmotic stress within the lenticular cells which leads to cellular swelling and loss of integrity of the cellular membrane (Kinoshita 1974). Aldose reductase inhibitors have been shown to prevent sugar induced cataracts (Dvornik et al. 1973, Varma and Kinoshita 1976, Kinoshita et al. 1979, Muller et al. 1985).

PROCEDURE

Experimental diabetes is induced in Wistar rats weighing 150–180 g by intravenous injection of 50 mg/kg streptozotocin (Griffin et al. 1984).

EVALUATION

The values of animals treated with the aldose reductase inhibitor are compared with the values of rats treated with streptozotocin only.

MODIFICATION OF THE METHOD

Instead of systemic application, the aldose reductase inhibitor is applied twice daily for 6 weeks in solution as eye drops to female Sprague-Dawley rats with a starting weight of 120–140 g after diabetes induction with 70 m/kg streptozotocin i.v. Body weight and blood sugar are registered twice a week. The progression of cataractous changes is followed by slit-lamp and Scheimpflug photography analysis every second week. At the end of the experiment, the animals are sacrificed and the lenses analyzed for their content of ATP, ADP, AMP, glucose, sorbitol, fructose, glucose-6-phosphate, and fructose-6-phosphate.

REFERENCES AND FURTHER READING

Dvornik D, Simard-Duquesne, Krami M, Sestanj K, Gabbay KH, Kinoshita JH, Varma SD, Merola LO (1973) Polyol accumulation in galactosemic and diabetic rats: Control by an aldose reductase inhibitor. Science 182:1146–1148

Griffin BW, Chandler ML, DeSantis L (1984) Prevention of diabetic cataract and neuropathy in rats by two new aldose reductase inhibitors. Invest Ophthalm Vis Sci 25:136

Kinoshita JH (1965) Cataracts in galactosemia. Invest Ophthalm 4:786–799

Kinoshita JH (1974) Mechanisms initiating cataract formation. Invest Ophthalm 13:713–724

Kinoshita JH, Fukushi S, Kador P, Merola LO (1979) Aldose reductase in diabetic complications of the eye. Metabolism 28 (Suppl 1):462–469

Müller P, Hockwin O, Ohrloff C (1985) Comparison of aldose reductase inhibitors by determination of IC_{50} with bovine and rat lens extracts. Ophthalm Res 17:115–119

Pirie A, van Heyningen R (1964) Effect of diabetes on the content of sorbitol, glucose, fructose and inositol in the human lens. Exp Eye Res 3:124–131

van Heyningen R (1959) Formation of polyols by the lens of the rat with "sugar" cataract. Nature 184:194–195

Varma SD, Kinoshita JH (1976) Inhibition of lens aldose reductase by flavonoids – their possible role in the prevention of diabetic cataracts. Biochem Pharmacol 25:2505–2513
Wegener A, Hockwin O (1991) Benefit/risk assessment of ophthalmic anti-infectives. Chibret Intern J Ophthalmol 8:43–45

K.8.6 Naphthalene-Induced Cataract

PURPOSE AND RATIONALE

Systemic application of naphthalene induces cataract in Brown-Norway rats. Aldose reductase inhibitors are tested for prevention of the cataract changes by parallel systemic or topical application (as eye drops).

PROCEDURE

Female Brown-Norway rats at an age of 6–7 weeks with a starting weight of 70–100 g are used. They are fed standard lab chow and receive water ad libitum. Naphthalene is dissolved in warm paraffin oil (10 g/100 ml) and is administered orally by gavage every second day in a dose of 1 g/kg. The test compound is administered orally every day or applied topically as suspension every day once, twice or four times to the right eye. The duration of the treatment is 6 weeks. Slit lamp microscopy (Zeiss photo slit lamp) during mydriasis with 1% atropine eye drops is performed in weekly intervals, including a baseline examination before the start of the treatment and a final examination prior to sacrifice. Scheimpflug photography of the anterior eye segment (Topcon SL-45 Scheimpflug camera) is carried out at the baseline examination, after 3 weeks of treatment and at the end of the experiment. Prior to sacrifice blood samples are taken by cardiac puncture under ether anesthesia. After sacrifice, lens fresh weight, concentration of oxidized and reduced glutathione, and the concentration of the aldose reductase inhibitor in the lenses and in blood samples are determined.

EVALUATION

The values of animals treated with the aldose reductase inhibitor are compared with the values of rats treated with naphthalene only.

MODIFICATIONS OF THE METHOD

Rathbun and coworkers (1996a) induced rapid-onset cataracts in SPF C57 bl/6 mice by i.p. administration of naphthalene following cytochrome P-450 induction with phenobarbital. Rathbun and coworkers (1996b) assessed the activity of a L-cysteine prodrug suitable for glutathione biosynthesis rat lenses *in vitro* and as an agent for the prevention of acetaminophen- and naphthalene-induced murine cataract in genetically susceptible mice. Holmen and coworkers (1999) compared different methods of photographic evaluation of cataract formation in rats in response to different regimes of naphthalene treatment.

REFERENCES AND FURTHER READING

Hockwin O (1989) Die Scheimpflug-Photographie der Linse. Fortschr Ophthalmol 86:304–311
Hockwin O, Wegener A, Sisk DR, Dohrmann B, Kruse M (1985) Efficacy of AL-1576 in preventing naphthalene cataract in three rat strains. Slit lamp and Scheimpflug photographic study. Lens Res 2:321–335
Holmen JB, Ekesten B, Lundgren B (1999) Naphthalen-induced cataract model in rats: A comparative study between slit and retroillumination images, biochemical changes and naphthalene dose and duration. Curr Eye Res 19:418–425
Rathbun WB, Nagasawa HT, Killen CE (1996a) Prevention of naphthalene-induced cataract and hepatic glutathione loss by the L-cysteine prodrugs, MTCA and PTCA. Exp Eye Res 62:433–441
Rathbun WB, Holleschau AM, Cohen JF, Nagasawa HT (1996b) Prevention of acetaminophen- and naphthalene-induced cataract and glutathione loss by CySSME. Invest Ophthalmol Vis Sci 37:923–929
Wegener A, Hockwin O (1991) Benefit/risk assessment of ophthalmic anti-infectives. Chibret Intern J Ophthalmol 8:43–45

K.8.7 Determination of Advanced Glycation End Products (AGE)

GENERAL CONSIDERATIONS

Common to both type I and type II diabetes is the development of inflammatory and vascular complications that, over time, might portend significant morbidity and early mortality in affected subjects. Although multiple studies have suggested a direct role for adverse effects of glucose itself in modulating cellular properties, both in the extra- and intracellular milieu (Greene et al. 1987, Inoguchi et al. 1994, Xia et al. 1994, Nishikawa et al. 2000), recent observations suggest an emerging role for the products of non-enzymatic glycoxidation of proteins and/or lipids, the advanced glycation endproducts (AGE), in the pathogenesis of diabetic complications.

Formation of AGE

The non-enzymatic glycation and oxidation of proteins and/or lipids is a well-recognized phenomenon that occurs naturally, albeit at a very slow rate, during the course of aging. However, certain conditions within the cellular environment might enhance the formation of these modified structures. Specifically in the context of diabetes, hyperglycemia is a major trigger for the accelerated formation and deposition of

AGEs (Brownlee 1995, Ruderman et al. 1992). Multiple specific AGE, formed by glycation and/or oxidation, such as carboxy(methyl)lysine (CML), pentosidine and pyralline, have been identified in diabetic tissues (Ikeda et al. 1996, Reddy et al. 1995). It is speculated that, in diabetes, hyperglycemia alone might not be the sole perturbant driving formation of these modified structures, as AGE formation is enhanced in pro-oxidant states, such as that observed in diabetes itself (Baynes 1991). The observation that products of glycoxidation have been noted in hyperlipidemic atherosclerotic lesions, even in euglycemia, supports this concept. A recent suggestion is that *in vitro* AGE formation might be driven by the myeloperoxidase–hydrogen peroxide–chloride system, thereby providing a mechanism for conversion of hydroxy-amino-acids into glycolaldehyde, a precursor in the steps leading to formation of CML. Thus, these findings could have implications for AGEs in inflammatory settings, once confirmation *in vivo* has been established. It is important to note that, in diverse conditions, such as renal failure and Alzheimer's disease, AGE epitopes have also been identified within affected structures (Miyata et al. 1996), thereby providing a contributory mechanism for the cellular stress observed in these settings.

AGE and Mechanisms of Cellular Perturbation

It is likely that AGEs exert their effects *via* a number of mechanisms. Accumulation of cross-linking AGEs that tend to become insoluble, such as pentosidine, are thought to contribute to the tissue perturbation and rigidity that typify advanced diabetes, especially in the skin and basement membranes (Sell et al. 1992, Beiswenger et al. 1993). These factors are potentially linked to vascular leakiness and hyperpermeability. Vlassara and coworkers (1995) identified galectin-2 as a high-affinity binding protein for AGE. In addition, work from M. Brownlee's laboratory suggests that intracellular formation of AGE might modify the activity of growth factors, such as basic fibroblast growth factor.

Beyond the direct effects of AGEs on modulating cellular structure and function are those effects postulated to occur during ligation of specific cell surface receptors. In this context, the best-characterized receptor for AGEs (RAGE) is a multi-ligand member of the immunoglobulin (Ig) superfamily of cell surface molecules (Schmidt et al. 1992, Neeper et al. 1992). RAGE is composed of an extracellular region containing one 'V'-type Ig domain, followed by two 'C'-type Ig domains. This portion of the molecule confers the ligand-binding properties, which are probably specific to the 'V'-domain. This portion of the molecule is followed by a hydrophobic transmembrane-spanning domain and, lastly, by a highly charged, short cytosolic domain that is essential for RAGE-mediated cellular effects upon engagement of ligand (Kislinger et al. 1999a, b; Yamamoto et al. 2001; Arancio et al. 2004; Hadding et al. 2004).

PURPOSE AND RATIONALE

Interactions between AGE and their binding proteins lead to the activation of a range of secondary messenger systems and increases the production of cytokines, including TGF-β, PDGF, and IL-1 (Ikeda et al. 1996). Recently, compounds that can cleave established AGE cross-links (Reddy et al. 1995), such as ALT711, a stable 4,5-dimethylthiazolium derivative of the prototype compound *N*-phenyl-thiazolium bromide, have been investigated. *In vivo* efficacy has been demonstrated in animal models, showing that these compounds can result in reduced AGE accumulation and can reverse age- and diabetes-dependent increases in arterial stiffness (Baynes 1991). RAGE as target for the prevention and treatment of the vascular and inflammatory complications of diabetes has been critically reviewed by Schmidt and Stern (2000a, b). The following assays enable the study of the AGE-RAGE interaction including its cellular effects as well as the modulation of both processes by compounds/drug candidates, which may be helpful for future therapy of diabetic late complications.

PROCEDURE

Cell Culture

The well-characterized normal rat kidney epithelial cell line (NRK-52E) can be obtained from the American Tissue Culture Collection. NRK-52E cells are believed to be of a proximal tubular origin on the basis of patterns of collagen secretion, C-type natriuretic peptide secretion, and the presence of EGF receptors. Cells are maintained in DMEM containing 4.5 g/l glucose with 10% FCS at 37°C in a 5% CO_2 atmosphere and passaged twice a week.

In Vitro Preparation of AGE Ligands

Procedures for the preparation of AGE ligands have been given by Oldfield and coworkers (2001) and Kislinger and coworkers (1999a and b). For preparation of AGE-BSA and AGE-RNase, BSA (10 mg/ml) or RNase (10 mg/ml) is incubated at 37°C for 6 weeks with D-glucose (90 g/l) in a 0.4-M phosphate buffer

containing azide (Vlassara et al. 1985). Control preparations are treated identically except that glucose is omitted. Preparations are extensively dialyzed against phosphate buffer to remove free glucose. The extent of advanced glycation is assessed by characteristic fluorescence (excitation 370, emission 440 nm). Advanced glycation is associated with an approximately 10-fold increase in fluorescence compared with controls.

For preparation of human AGE-IgG, human IgG (5 mg/ml in PBS) is subjected to non-enzymatic glycation by incubation in PBS containing 25 mM D-ribose. The solution is sterile-filtered (0.2 µm) and then incubated at 37°C for 6 weeks under aerobic conditions. At the end of that time, the mixture is extensively dialyzed *versus* PBS at 4°C to remove unreacted ribose. This material is then chromatographed onto resin containing Affi-Gel 10 (Bio-Rad) to which had previously been adsorbed to recombinant human soluble RAGE. After incubation, the resin is washed extensively with 10-column volumes of TBS (20 mM Tris, pH 7.4, 100 mM NaCl). Bound components are eluted by 20 mM glycine (pH 2.5). The absorbance at 280 nm of each fraction is determined. Positive fractions are immediately neutralized and dialyzed *versus* TBS.

For preparation of carboxymethyl lysine–modified BSA (CML-BSA) (Kislinger et al. 1999a, b), 50 mg/ml aliquots of BSA are incubated with increasing concentrations of glyoxylic acid (5–90 mM) in the presence of approximately 5-fold molar excess of sodium cyanoborohydride. Control proteins are prepared under the same conditions, except that glyoxylic acid was omitted. The extent of chemical modification of lysine residues is determined as described previously using 2,4,6-trinitrobenzenesulfonic acid (Cayot and Tainturier 1997). The extent of lysine modification was up to 34% for CML-BSA preparations.

Iodination of AGE-BSA

AGE-BSA was iodinated by incubating AGE-BSA with chloramine-T (Greenwood et al. 1963). Bound ^{125}I was separated from free ^{125}I using a Biogel P6DG desalting gel (Bio-Rad Laboratories Inc.). Specific activity of the tracer is typically 400 Ci/mM.

Membrane Preparation

Membranes are prepared based on the method of Skolnik and coworkers (1991). NRK-52E cells are grown to confluence in 150-cm^2 tissue-culture flasks. Cells are washed twice with PBS, then detached from plates using a HEPES (100 mM) solution containing BSA (0.1%) and Triton X-100 (0.1%) with EDTA (5 mM), leupeptin (1 µM), and PMSF (2 mM). Cells are centrifuged (2,000 × *g*, 5 min) and resuspended in the above buffer before disruption by ultrasound. Cell debris is removed by further centrifugation (2,000 × *g*, 10 min) and the supernatant centrifuged (100,000 × *g*, 1 h, 4°C). The supernatant is discarded, and the cell membranes in the precipitate are resolubilized in the above buffer. Protein concentrations are determined by the method of Bradford. The membrane preparation is used in binding studies and for ligand and Western blot analysis.

Binding Assay with Radiolabeled AGE

For binding studies according to the procedure of Oldfield and coworkers (2001), cell membrane extracts are incubated with ^{125}I-AGE-BSA (0.5 nM) and increasing concentrations of unlabeled AGE-BSA (0.015–7.46 µmol) in the absence or presence of compounds/drug candidates for 3 h at 4°C in HEPES (100 mM) binding buffer with BSA (0.1%), Triton X-100 (0.1%), leupeptin (1 µM), and PMSF (2 mM). A Brandel cell filter (Biomedical Research and Development Laboratories) is used to separate bound and free radioligand. A Tris-HCl (10 mM) polyethylene glycol (6.6%) buffer is used to wash components through the apparatus onto glass filter papers, which are counted in a γ-counter for 1 min. Binding experiments are performed in duplicate in five separate experiments, and the specificity of binding is assessed in further experiments using unlabeled, unmodified BSA (1 µmol) as the competitor. Binding data were analyzed using a specific binding program (LIGAND).

Binding Assay with Radiolabeled RAGE

Human soluble recombinant RAGE (sRAGE) prepared as described above is radiolabeled with ^{125}I by incubation with IODO-BEADS (Pierce) to a specific activity of ~4,000–5,000 cpm/ng protein. In all cases, after radioiodination, precipitation of the radiolabeled material in TCA exceeded 90%. CML modifications of proteins or native, unmodified proteins are loaded onto the wells of plastic dishes (5 ng/well) in bicarbonate/carbonate buffer (pH 9.6) and incubated for 16 h at 4°C. Material in the wells is aspirated, and unoccupied sites are blocked by incubation with PBS containing 1% BSA for 2 h at 37°C. Wells are washed twice with PBS containing 0.005% octyl β-glucoside. Radioligand binding assay is performed in PBS containing 0.2% BSA with increasing concentrations of ^{125}I-human sRAGE alone or in the presence of a 50-fold molar excess of unlabeled human sRAGE or compounds/drug candidates for 2 h at 37°C. At the end of that time, wells are washed rapidly five times with

washing buffer. Elution of bound material is performed in a solution containing 1 mg/ml heparin. Solution is aspirated from the wells and counted in a γ-counter.

EVALUATION

Equilibrium binding data are analyzed according to the equation of Klotz and Hunston (1984): $B = nKA/1 + KA$, where B indicates specifically bound ligand (total binding, wells incubated with tracer alone, minus nonspecific binding, wells incubated with tracer in the presence of excess unlabeled material), n indicates sites/cell, K indicates the dissociation constant, and A indicates free ligand concentration) using non-linear least squares analysis. Specific binding of CML-BSA to radiolabeled RAGE is further determined by subtraction of nonspecific binding (counts obtained upon binding of radiolabeled sRAGE to immobilized BSA) from that obtained upon binding of radiolabeled sRAGE to immobilized CML-BSA. In case of binding to immobilized BSA, counts are negligible and less than 10% that observed in the presence of CML-BSA. Pretreatment with either antibodies, soluble RAGE, or the potential competitors and competitors/drug candidates is performed for 2 h prior to binding assay. Sometimes, it may be helpful to use materials eluted from the RAGE-Affi-Gel 10 columns (after passage of AGE-IgG) isolated RAGE domains for testing as unlabeled competitor in the binding assay. For this, human RAGE cDNA encoding the V, C1, or C2 domain is inserted into the *Eco*RI site of pGEX4T vector containing GST. Fusion proteins, V-GST, C1-GST, and C2-GST, are expressed in *E. coli*, purified on a glutathione-Sepharose column, and cleaved with thrombin (Amersham Pharmacia). RAGE domains are then purified to homogeneity using glutathione-Sepharose and characterized by SDS-PAGE and amino-terminal sequencing prior to testing in the radioligand binding assay.

Ligand and Immunoblotting Analysis

Cell membrane extracts (20 µg of membrane protein per lane) are subjected to non-reducing SDS (12–15%) PAGE and electroblotted onto nitrocellulose membranes (Hybond, Amersham Pharmacia). For ligand blotting the membranes are blocked overnight at 4°C in 10 mM Tris (pH 7.4), 150 mM NaCl, 0.1% Tween buffer containing 2.5% BSA, before incubation with ^{125}I-AGE-BSA (110 ng/ml) for 2 h at room temperature. After washing with 10 mM Tris (pH 7.4), 150 mM NaCl, and 0.1% Tween, the membrane is exposed to Kodak Biomax MS film for 1–4 h. Receptor-ligand binding specificity is studied in competitive experiments where unlabeled AGE-BSA, AGE-RNase, BSA, and RNase (all 100 µg/ml) are added as competing ligands.

In immunoblotting experiments, the nitrocellulose membrane is incubated at room temperature for 1 h with a polyclonal goat Ab against human RAGE 1:2,000 (Soulis et al. 1997, Brett et al. 1993). Membranes are washed before a 15-min incubation with a biotinylated secondary antibody and a streptavidin-horseradish peroxidase conjugate. Immunoreactivity is detected using an enhanced chemiluminescence kit (Amersham Pharmacia Biotech). Primary antibodies are omitted in experiments as negative controls and RAGE antibody specificity is confirmed by preincubation of the membrane with recombinant RAGE before the addition of RAGE antibody.

Isolation of Human Serum Albumin and Immunoblotting for AGE

Plasma samples are obtained from human donors with diabetes, renal failure, or age-matched healthy controls in accordance with the laws of the respective national ethics committees. Samples (2 ml) are dialyzed for 16 h at 4°C in 20 mM phosphate buffer (pH 7.1) in a total volume of 4 ml. After dialysis, samples are subjected to filtration (0.8 µm), and then chromatographed onto columns containing Affi-Gel blue resin (Bio-Rad) previously equilibrated in 20 mM phosphate buffer (pH 7.1). 5 ml of resin are employed per ml of plasma. The resin is washed in 2.5 column volumes of phosphate buffer as above, and human serum albumin is eluted by application of phosphate buffer containing 1.4 M NaCl. The absorbance at 280 nm for each fraction is determined, and positive fractions are determined by SDS-PAGE followed by staining with silver. For immunoblotting, the materials (30 µg of protein, each) are employed to SDS-PAGE gels (8%). Simultaneously, marker proteins are added. After electrophoretic separation and transfer of the proteins to nitrocellulose membranes, the unoccupied sites on the membranes are blocked in the presence of non-fat dry milk (13.5%) in TBS for 4 h at room temperature. Immunoblotting is performed using affinity-purified anti-CML IgG as above (10–20 µg/ml) in milk buffer (5%) for 1.5 h at 37°C. Membranes are washed extensively in TBS containing 0.1% Tween 20 . The membranes are incubated with goat anti-rabbit IgG labeled with horseradish peroxidase for 1 h at 37°C, washed extensively in the above buffer. Visualization of antibody binding was performed employing the ECL detection system (Amersham Pharmacia). Quantitative evalua-

tion of band intensity is performed using Molecular Dynamics/ImageQuant.

K.8.8 Measurement of Reactive Oxygen Species (ROS) Production

GENERAL CONSIDERATIONS

All forms of diabetes, both inherited and aquired, are typified by hyperglycemia, a relative or absolute lack of insulin, and the development of diabetes-specific microvascular pathology in the retina (retinopathy), renal glomerulus (nephropathy) and peripheral nerve (neuropathy). At the molecular cell biology level, three major hypotheses regarding the mechanisms by which hyperglycemia causes diabetic complications, i. e. the aldose reductase pathway (see above), formation of AGE (see above) and activation of PKC, have each generated a great deal of supporting data (Brownlee 1995, Koya and King 1998, Schmidt and Stern 2000b). Seminal work from Michael Brownlee's laboratory has shed new light on the mechanisms by which elevated concentrations of glucose perturb cellular properties in a fundamental way, thereby joining these three pathways into a unifying hypothesis for hyperglycemia-induced late complications (Nishikawa et al. 2000). In endothelial cells subjected to physiologically relevant glucose concentrations as a model system, the non-insulin-dependent uptake of glucose *via* GLUT1 leads to oxidative stress (OS) with concomitant generation of reactive oxygen species (ROS), the increase of both is positively correlated to the glucose concentration. Several pathways are considered as likely candidates for the emergence of OS and the formation of oxygen free radicals in cells, including the accelerated flux of glucose through glycolysis and feeding of pyruvate, thus formed, to the tricarboxylic acid cycle, which overloads mitochondria and thereby causes excessive generation of ROS. In turn, OS and ROS has recently been shown to cause upregulation of the mitochondrial uncoupling protein 2 (UCP-2), leading to a vicious cycle of increased electron flux *via* the respiratory chain and concomitant elevated production of ROS. Most importantly, it has been demonstrated recently, that suppression of intracellular ROS, using low molecular weight inhibitors or by expression of the anti-oxidant enzyme, manganese-dependent superoxide dismutase (MnSOD), prevents each of the three molecular mechanisms mentioned above (Nishikawa et al. 2000). Consequently, glucose-induced formation of oxidants is a proximal step in cellular perturbation prelevant during diabetes. Thus, assays which monitor the generation of OS and ROS in response to compounds/drug candidates may be helpful for the finding and characterization of future anti-diabetic drugs, which may reduce the risk for the development of diabetic late complications.

PURPOSE AND RATIONALE

Although there are various methods to assess oxidative damage of cells, such as measuring lipid peroxidation products and DNA adducts (Holley and Cheeseman 1993), none of them evaluate the OS directly. With the first description of using 2′,7′-dichlorofluorescin diacetate (DCFH-DA) as a fluorometric assay for hydrogen peroxide (Keston and Brandt 1965), it became popular to use dichlorofluorescin (DCFH) as a probe to evaluate intracellular hydrogen peroxide formation by flow cytometry. The theory behind using DCFH-DA is that nonfluorescent fluorescin derivatives will emit fluorescence after being oxidized by hydrogen peroxide (LeBel et al. 1992). The emitted fluorescence is directly proportional to the concentration of hydrogen peroxide. When applied to intact cells, the nonionic, nonpolar DCFH-DA crosses cell membranes and is hydrolyzed enzymatically by intracellular esterases to nonfluorescent DCFH (LeBel et al. 1992, Bass et al. 1982). In the presence of reactive oxygen species (ROS), DCFH is oxidized to highly fluorescent dichlorofluorescein (DCF) (LeBel et al. 1992). Therefore, the intracellular DCF fluorescence can be used as an index to quantify the overall OS in cells.

Many studies have used fluorescent microscopy to quantify OS in cells using DCFH-DA. This method has the problem of inducing photooxidation of DCFH to DCF intracellularly and emitting fluorescence, because it is difficult to control the time of light exposure when trying to locate and focus cells under the microscope. In addition to the problem of photooxidation, there is no standard way to quantify the OS using a microscope. In order to prevent the overestimation of the OS due to photooxidation, an instrument equipped with fast light excitation and fast fluorescence capturing, which will not induce excessive photooxidation, is needed. Wang and Joseph (1999) have introduced a fluorescent microplate reader-based method to evaluate OS in cultured cells, induced by applying various free radical generators extracellularly, using DCFH as the probe.

PROCEDURE

Measurement of OS

Cells (e. g. PC12) are grown in growth medium containing 85% RPMI-1640 with *l*-glutamine, 10% heat-

inactivated horse serum, 5% FBS, 100 U/ml penicillin G sodium, and 100 µg/ml streptomycin sulfate. The cells are maintained in collagen-coated plates in 5% CO_2/95% air at 37°C. The culture medium is changed twice every week and the cells are split 1:4 or 1:8 every week. Cells were split and counted by trypan blue exclusion. Viable cells (10^4/well) are plated into 96-well collagen-coated plates one day before the experiments. On the day of the experiments, after removing the medium, the cells in the plates are washed with KRH buffer and then incubated with 100 µM 6-carboxy-2′,7′-dichlorofluorescin diacetate (DCFH-DA; Molecular Probes Inc. USA) in the loading medium in 5% CO_2/95% air at 37°C for 30 min. For loading the cells with DCFH, DCFH-DA from a 10-mM stock solution in DMSO is mixed with loading medium (99% RPMI-1640 and 1% FBS) to a final concentration of 100 µM. After DCFH-DA is removed, the cells are washed and incubated with KRH buffer (with different concentrations of one of the free radical generators, e. g. H_2O_2, dopamine) in the absence of presence of high glucose concentration. The fluorescence of the cells from each well is measured and recorded.

For OS measurement, DCFH-DA-loaded cells are placed in a CytoFluor Series 4000 multiwell fluorescence plate reader with temperature maintained at 37°C. The excitation filter is set at 485 nm and the emission filter is set at 530 nm. The fluorescence from each well is captured, digitized, and stored on a computer using Cytofluor (Version 4.0) (PerSeptive Biosystems Inc. USA). Data points are taken every 5 min for 30 min and the data are exported to Excel (Microsoft, USA) spreadsheet software for analysis.

Measurement of ROS

For measurement of ROS production according to the procedure of Freeman and coworkers (2006), a 10-mM stock solution of H_2DCFDA-SE (2′,7′-dichlorofluorescein diacetate with a succinimidyl ester group, DCF, Molecular Probes) is prepared in DMSO, stored at −70°C, and diluted with KRB (pH 7.0) just before use to a final concentration of 10 µM. The cells are plated in 24-well cell culture plates overnight. They are then washed twice with PBS, incubated in PBS *plus* DCF for 30 min at 37°C, washed with PBS, and incubated in KRB containing 5.5 or 20 mM glucose for a further 30 min. They are imaged at room temperature using an IonOptix fluorescence system, with 495 nm excitation and 520 nm emission. The background fluorescence is subtracted. 0.5 mM menadione is used as a generator of ROS as a control. The Ros concentrations are determined from a standard curve of H_2O_2 (5–50 µM). To confrom that glucose generates ROS, dihydroethidium (DHE) conversion to ethidium by oxidation can be measured according the procedure of Russell and coworkers (2002). The ratio of DHE:ethidium is determined using a fluorimeter and standarized against cellular protein. DHE is measured using 355 nm excitation and 430 nm emission, and ethidium is measured using 518 nm excitation and 605 nm emission.

Measurement of Mitochondrial ROS Production

To evaluate the direct production of mitochondrial ROS in cells, the DCFDA measurements have to be combined with ROS-specific staining by using the reduced Mito Tracker Red probe (CM-H_2Xros; Molecular Probes Inc. USA) according to the procedure described by Degli Esposti and coworkers (1999). For this, the cells suspended in growth medium at 1×10^6/ml are incubated for 15 min at room temperature with freshly prepared CM-H_2XRos (0.5 µM), then washed twice with PBS, and collected on a slide using a Cytospin apparatus (Wolvetang et al. 1994). The cells are fixed with 3.7% formaldehyde in PBS, followed by washing first with PBS containing 30 mM NH_4Cl and then with distilled water. In some experiments, the fixed cells are counterstained with Hoechst 33342 before mounting with anti-fade medium, and the slides are stored at 4°C in the dark. In parallel experiments, mitochondrial staining to analyze membrane potential can be performed using 100 nM oxidized Mito Tracker Red (CM-XRos) following the same protocol as outlined above for CM-H_2XRos. Confocal microscopy is undertaken with a Krypton/Argon instrument, usually with a 40 × oil objective and intermediate laser and photomultiplier voltage. The 590-nm bandpass filter is used to detect the red fluorescence of CM-XRos staining (Wolter et al. 1997). Epifluorescence is evaluated with a microscope using a Texas Red filter and a CCD camera attached to a microcomputer image analyzer.

EVALUATION

The percentage increase in fluorescence per well is calculated by the formula $[(Ft_{30}\text{-}Ft_0)/Ft_0 * 100]$, where Ft_{30} = fluorescence at time 30 min and Ft_0 = fluorescence at time 0 min. This method of analysis has advantages over analyzing just the net change in fluorescence in that, not only did the calculated data directly reflect the percentage changes of fluorescence over time from the cells in the same well, they also effectively control for variability among wells. This method also cancels out the background

fluorescence in each well, and therefore, a "no cell" control is not needed.

Various free radical generators produce concentration-dependent changes in DCF fluorescence, indicating the indiscriminate nature of DCF. Due to the indiscriminate nature of DCFH, which can be oxidized by various ROS and not just H_2O_2, the increase of intracellular DCF fluorescence does not necessarily reflect the levels of ROS directly, but rather an overall OS index in cells. Quantifying cellular OS by the DCF assay using a fluorescent microplate reader is an easy and efficient method with low variability which can be used to quantify the potency of pro-oxidants or can be adapted to evaluate the efficacy of antioxidants against ROS in various cell lines. The use of a 96-well microplate reader enables the generation of a large amount of data with low variability.

Measurement of Mitochondrial Size

Since glucose-induced ROS production and swelling of mitochondria seem to be correlated (Russell et al. 2002), determination of alterations in the size of mitochondria exposed to OS may be indicative for the generation of mitochondrial ROS. For measurement of the mitochondrial size, cells are loaded with Mitotracker orange (CMTMRos; Molecular Probes Inc. USA) using confocal microscopy with 540 nm excitation. Each mitochondrion is a complex fractal-like network, making accurate analysis of volume difficult. Therefore, the maximum cross-sectional area is determined from identification of each individual mitochondrion throughout the z-series. All distinguishable mitochondria at each step level in the z-series are measured at the largest cross-sectional area of the mitochondrion. The size of the mitochondria is determined using the perimeter of visible CMTMRos and reflects the mitochondrial area at the measured level. Identical methods of identification and measurement are applied to each mitochondrion in each cell and in each condition, thus reducing the effect of technical artifact. The mitochondrial areas are then averaged for each neuron and, where necessary, results are first converted to a log normal distribution before obtaining descriptive statistics or performing tests of inference about the data set. Results are obtained for > 100 mitochondria in at least 10 randomly measured neurons per condition.

REFERENCES AND FURTHER READING

Arancio O, Zhang HP, Chen X, Lin C, Trinchese F, Puzzo D, Liu S, Hedge A, Yan SF, Stern A, Luddy JS, Lue LF, Walker DG, Roher A, Buttini M, Mucke L, Li W, Schmidt AM, Kindy M, Hyslop PA, Stern DM, Du-Yan SS (2004) RAGE potentiates Abeta-induced perturbation of neuronal function on transgenic mice. EMBO J 23:4096–4105

Bass DA, Parce JW, Dechatelet LR, Szejda P, Seeds MC, Thomas M (1982) Flow cytometry studies of oxidative product formation by neutrophils: a graded response to membrane stimulation. J Immunol 130:1910–1917

Baynes J (1991) Role of oxidative stress in development of complications in diabetes

Brett J et al (1993) Survey of the distribution of a newly characterized receptor for advanced glycation end products in tissues. Am J Pathol 143:1699–1712

Brownlee M (1995) Advanced glycosylation in diabetes and aging. Annu Rev Med 46:223–234

Cayot P, Tainturier G (1997) The quantification of protein amino groups by the trinitrobenzenesulfonic acid method: a reexamination. Anal Biochem 249:184–200

Degli Esposti M, Hatzinisiriou I, McLennan H, Ralph S (1999) Bcl-2 and mitochondrial oxygen radicals. J Biol Chem 274:29831–29837

Freeman H, Shimomura K, Horner E, Cox RD, Ashcroft FM (2006) Nicotinamide nucleotide transhydrogenase: A key role in insulin secretion. Cell Metabol 3:35–45

Greene D et al (1987) Sorbitol, phosphoinositides, and sodium-potassium-ATPase in the pathogenesis of diabetic complications. New Engl J Med 316:599–606

Greenwood PC, Hunter WM, Glover JS (1963) The preparation of 131I-labeled human growth hormone of high specific radioactivity. Biochem J 89:114–123

Hadding A, Kaltschmidt B, Kaltschmidt C (2004) Overexpression of receptor of advanced glycation end products hypersensitizes cells for amyloid beta peptide-induced cell death. Biochim Biophys Acta 1691:67–72

Holley AE, Cheeseman KH (1993) Measuring free radical reactions *in vivo*. Br Med Bull 49:494–505

Ikeda K, Higashi T, Sano H, Jinnouchi Y, Yoshida M, Araki T, Ueda S, Horiuchi S (1996) Carboxymethyllysine protein adduct is a major immunological epitope in proteins modified with AGEs of the Maillard reaction. Biochemistry 35:8075–8083

Inoguchi et al (1994) Insulin's effect on protein kinase C and diacylglycerol induced by diabetes and glucose in vascular tissues. Am J Physiol 267:E369-E379

Keston AS, Brandt R (1965) The fluorometric analysis of ultramicro quantities of hydrogen peroxide. Anal Biochem 11:1–5

Kislinger T, Fu C, Huber B, Qu W, Taguchi A, Yan SD, Hofmann M, Yan SF, Pischetsrieder M, Stern D, Schmidt AM (1999a) N-(Carboxymethyl)lysine adducts of proteins are ligands for receptor for advanced glycation products that activate cell signaling pathways and modulate gene expression. J Biol Chem 274:31740–31749

Kislinger T et al (1999b) N-(carboxy-methyl)lysine modifications of proteins are ligands for RAGE that activate cell signaling pathways and modulate gene expression. J Biol Chem 274:31740–31749

Klotz I, Hunston D (1984) Mathematical models for ligand-receptor binding. Real sites, ghost sites. J Biol Chem 259:10060–10062

Koya D, King G (1998) PKC activation and the development of diabetic complications. Diabetes 47:859–866

LeBel CP, Ishiropoulos H, Bondy SC (1992) Evaluation of the probe 2′,7′-dichlorofluorescein as an indicator of reactive oxygen species formation and oxidative stress. Chem Res Toxicol 5:227–231

Miyata T et al (1996) RAGE mediates the interaction of AGE-beta-2-microglobulin with human mononuclear phagocytes

via an oxidant-sensitive pathway: implications for the pathogenesis of dialysis-related amyloidosis. J Clin Invest 98:1088–1094
Neeper M et al (1992) Cloning and expression of RAGE: a cell surface receptor for advanced glycosylation end products of proteins. J Biol Chem 267:14998–15004
Nishikawa et al (2000) Normalizing mitochondrial superoxide production blocks three pathways of hyperglycemic damage. Nature 404:787–790
Oldfield MD, Bach LA, Forbes JM, Nikolic-Paterson D, McRoberts A, Thallas V, Atkins RC, Osicka T, Jerums G, Cooper ME (2001) Advanced glycation end products cause epithelial-myofibroblast transdifferentiation via the receptor for advanced glycation end products (RAGE). J Clin Invest 108:1853–1863
Reddy et al (1995) Carboxymethyllysine is a dominant AGE antigen in tissue proteins. Biochemistry 34:10872–10878
Ruderman N et al (1992) Glucose and diabetic vascular disease. FASEB J 6:2905–2914
Russell JW, Golovoy D, Vincent AM, Mahendru P, Olzmann JA, Mentzer A, Feldman EL (2002) High glucose-induced oxidative stress and mitochondrial dysfunction in neurons. FASEB J 16:1738–1748
Schmidt AM et al (1992) Isolation and characterization of binding proteins for advacned glycosylation end products from lung tissue which are present on the endothelial cell surface. J Biol Chem 267:14987–14997
Schmidt AM, Stern D (2000a) A radical approach to the pathogenesis of diabetic complications. Trends Pharmacol Sci 21:367–369
Schmidt AM, Stern DM (2000b) RAGE: A new target for the prevention and treatment of the vascular and inflammatory complications of diabetes. Trends Endocrinol Metab 11:368–375
Sell D et al (1992) Pentosidine formation in skin correlates with severity of complications in individuals with longstanding IDDM. Diabetes 41:1286–1292
Skolnik EY et al (1991) Human and rat mesangial cell receptors for glucose-modified proteins: potential role in kidney tissue remodelling and diabetic nephropathy. J Exp Med 174:931–939
Soulis T et al (1997) Advanced glycation end products and their receptors co-localise in rat organs susceptible to diabetic microvascular injury. Diabetologia 40:619–628
Vlassara H, Brownlee M, Cerami A (1985) High-affinity-receptor-mediated uptake and degradation of glucose-modified proteins: a potential mechanism for the removal of senescent macromolecules. Proc Natl Acad Sci USA 82:5588–5592
Vlassara H et al (1995) Galectin-2 as a high affinity binding protein for AGE: a new member of the AGE-receptor complex. Mol Med 1:634–646
Wang H, Joseph JA (1999) Quantifying cellular oxidative stress by dichlorofluorescein assay using microplate reader. Free Radical Biol Med 27:612–616
Wolter KG, Hsu YT, Smith CL, Nechushtan A, Xi XG, Youle RJ (1997) Movement of Bax from the cytosol to mitochondria during apoptosis. J Cell Biol 139:1281–1292
Wolvetang EJ, Johnson KL, Krauer K, Ralph SJ, Linnane AW (1994) Mitochondrial respiratory chain inhibitors induce apoptosis. FEBS Lett 339:40–44
Xia et al (1994) Characterization of the mechanism for the chronic activation of diacylglycerol-protein kinase C pathway in diabetes and hypergalactosemia. Diabetes 43:1122–1129
Yamamoto Y, Kato I, Doi T, Yonekura H, Ohashi S, Takeuchi M, Watanabe T, Yamagishi SI, Sakurai S, Takasawa S, Okamoto H, Yamamoto H (2001) Development and prevention of advanced diabetic nephropathy in RAGE-overexpressing mice. J Clin Invest 108:261–268

K.9 Insulin Analogs: Assessment of Insulin Mitogenicity and IGF-I Activity[2]

K.9.1 Introduction and Application to Insulin Analogs

The metabolic activity of insulin has been studied extensively in-vitro and in-vivo, based on the initial assessment of insulin receptor affinity, followed by methods to estimate the metabolic activity in vitro. These estimates provides some guidance about the biological activity which will be found in-vivo, they need to be confirmed and supplemented by testing the glucose lowering activity in animals (mice, rats, dogs, pigs). The biological effects (hypoglycemic activity) are related to the direct activation of the insulin receptor and subsequent signaling through intracellular mechanisms. The second group of biological effects is related to cell proliferation (mitogenic activity), which may be mediated by the insulin receptor, by the IGF-I receptor and by hybrids of the two receptors. The evaluation of the relevance of mitogenicity estimates may be performed in in vitro and in-vivo. One approach is cell proliferation in benign and malignant cell lines, for example on mammary epithelial cell lines MCF-10 and MCF-7 (Milazzo et al. 1997).

In the in-vivo evaluation, the metabolic activity is determined in animals (see chapter K.3) using the rat or rabbit bioassay (Lin et al. 1999) by intravenous injection, to confirm the blood glucose lowering activity after direct receptor activation. This initial test confirms intrinsic activity at the receptor level, However, it does not indicate depot activity and is applicable in the same manner to fast acting insulin analogs (lispro, aspart, glulisine), and to long-acting analogs (glargine, detemir). The rat bioassay by intravenous injection is preferred is the initial test for in-vivo biological activity. In order to evaluate depot activity, the time action profile after subcutaneous injection may be determined subsequently, in order to distinguish between the rapid acting insulin analogs and long acting insulin analogs. This has been done in clinical studies by measuring the glucose lowering, and the residence of 125-I-labeled insulin analogs at the subcutaneous injection site (Kang et al. 1991a).

[2] Amendment by J. Sandow

In a practical approach, testing for depot activity may be performed by the pharmacodynamics of glucose lowering, preferably in intact dogs. Such studies may be later be followed up by euglycemic clamp studies. The pharmacokinetics can be based on nonspecific measuring of immunoreactive insulin, and concentration changes of C-peptides. More specific determination of the insulin analog concentrations require advanced methods, for example there is the specific radioimmunoassay for lispro insulin (Bowsher et al. 1999, von Mach et al. 2002).

GENERAL CONSIDERATIONS

A general approach may be suggested for the in vitro evaluation of new insulins. This approach is based on the consideration that insulin has metabolic as well as mitogenic activity which is mediated predominantly by signaling via the insulin receptor, and at high concentrations - as used in vitro - may also be mediated by signaling via the IGF-I receptor. The primary step is determination of insulin receptor affinity, followed by IGF-I receptor affinity (Baehr et al. 1997). There is one important reference compounds, [B10-Asp] insulin which should be used in these evaluations as comparator (Berti et al. 1998), because of the toxicological findings with [B10-Asp] insulin which have raised concern about enhanced mitogenic activity of insulins with prolonged residence time at the insulin receptor (Jorgensen et al. 1992). [B10-Asp] insulin was evaluated as fast acting insulin analog in early clinical trials (Kang et al. 1991b, Nielsen etal. 1995), and was subsequently found to induce benign and malignant mammary gland tumours in rats, during twelve-month toxicology studies. This has been attributed to enhanced mitogenic signaling via the insulin receptor, and alternatively to increased affinity for the IGF-I receptor with subsequent growth promoting effects on mammary gland tissue. A guideline regarding the evaluation of new insulin analogs for carcinogenicity was issued by the European Agency for the Evaluation of Medicinal Products (EMEA 2001), with specific guidance about the in vitro and in-vivo evaluation to be performed. In this guideline, the specific reference compounds mentioned a human insulin, [B10-Asp] insulin and IGF-I (somatomedin C).

PURPOSE AND RATIONALE

The structure and approach to the evaluation of new insulins is directed towards efficacy in terms of glucose lowering, in the predictive manner to differentiate between monomeric insulins with fast absorption kinetics, and long acting insulins with delayed absorption from the subcutaneous injection site.

PROCEDURE

The initial steps are performed in vitro, focused on receptor interaction. Subsequent steps in vitro to explore the receptor-mediated signaling, which is however at the present time difficult to attribute precisely to biological and clinical effects. This is due to the wide concentration range permissible during in vitro studies, whereas the narrowly limited clinical concentration range needs to be kept in mind during any interpretation of clinical relevance (Zib and Raskin 2006).

The main aim of the in vitro evaluation is to establish the relation of metabolic activity to mitogenic activity, as previously done for structure activity studies on insulin analogs, and subsequently directed to predicting clinical relevance of these observations, when comparing new compounds with the established biochemical and toxicological profile of [B10-Asp] insulin, and the clinically used fast acting and long-acting insulin analogs.

MODIFICATIONS OF THE METHOD

The primary step of measuring insulin receptor affinity may be performed in several modifications, depending on the receptor preparation, and on the source of insulin receptors e. g. from fibroblasts, placental membranes, skeletal muscle cells and other sources. The second step of measuring IGF-I receptor affinity also has several options, for research on the IGF-I receptor a human osteosarcoma cell line (SAOS B10) was in several instances applied due to the high number of IGF receptors and lower number of insulin receptors on the cells (Kurtzhals et al. 2000).

The biological profile in animals is directed at predicting clinical utility either as a fast acting (mealtime) insulin, or at establishing depot activity in a suitable animal species. Blood glucose lowering (hypoglycemic) activity is also important for the design of safety studies depending on the preclinical metabolic to mitogenic ratio. In the chronic toxicity studies, and where applicable in carcinogenicity studies, the dose range from biologically effective dose to maximum tolerated dose may be 50–100fold, the results than need to be interpreted carefully for their relevance in relation to the therapeutic concentrations found in clinical therapy.

CRITICAL ASSESSMENT OF THE METHOD

When considering the extensive knowledge on three fast acting insulins and two long acting insulins cur-

rently in clinical use, the predictive relevance of the methods described here can be assessed in each case, and selection of the appropriate study design is based on existing clinical experience.

REFERENCES AND FURTHER READING

Baehr M, Kolter T, Seipke G, Eckel J (1997) Growth promoting and metabolic activity of the human insulin analog [GlyA21, ArgB31, ArgB32] insulin (HOE 901) in muscle cells. Eur J Pharmacol 320:259–265

Berti L, Kellerer M, Bossenmaier B, Seffer E, Seipke G, Haring H (1998) The long-acting human insulin analog HOE901: Characteristics of insulin signalling in comparison to Asp(B10) and regular insulin. Horm Metab Res 30:123–129

Bowsher RR, Lynch RA, Brown-Augsburger P, Santa PF, Legan WE, Woodworth JR, Chance RE (1999) Sensitive RIA for the specific determination of insulin lispro. Clin Chem. 45(1):104–10. EMEA (European Agency for the Evaluation of Medical Products). 2001. Points to consider document on the non-clinical assessment of the carcinogenic potential of insulin analogs. European Agency for the Evaluation of Medicinal Products. 2001

Hamel FG, Siford GL, Fawcett J, Chance RE, Frank BH, Duckworth WC (1999) Metabolism 48(5):611–7. Differences in the cellular processing of AspB10 human insulin compared with human insulin and LysB28ProB29 human insulin

Hennige AM, Strack V, Metzinger E, Seipke G, Haring HU, Kellerer M (2005) Effects of new insulin analogs HMR1964 (insulin glulisine) and HMR1423 on insulin receptors. Diabetologia. 48(9):1891–7. Epub 2005 Jul 29

Jorgensen L, Dideriksen L, Drejer K (1992) Carcinogenic effect of the human insulin analog B10Asp in female rats. Diabetologia 35(Suppl 1):A3

Kang S, Brange J, Burch A, Volund A, Owens DR (1991a) Diabetes Care 14(11):942–8. Subcutaneous insulin absorption explained by insulin's physicochemical properties. Evidence from absorption studies of soluble human insulin and insulin analogs in humans

Kang S, Brange J, Burch A, Volund A, Owens DR (1991b) Diabetes Care 14(11):1057–65. Absorption kinetics and action profiles of subcutaneously administered insulin analogs (AspB9GluB27, AspB10, AspB28) in healthy subjects

Kellerer M, Haering HU (2001) Insulin analogs: impact of cell model characteristics on results and conclusions regarding mitogenic properties. Exp Clin Endocrinol Diabetes 109 63–64

Kurtzhals P, Schaffer L, Sorenson A, Kristensen C, Jonassen I, Schmid C, Trub T (2000) Correlations of recepwtor binding and metabolic and mitogenic potencies of insulin analogs designed for clinical use. Diabetes 49:999–1005

Lin S, Wang SY, Chen EC, Chien YW (1999) Insulin lispro: in-vivo potency determination by intravenous administration in conscious rabbits. J Pharm Pharmacol 51(3):301–6

Milazzo G, Sciacca L, Papa V, Goldfine ID, Vigneri R (1997) ASPB10 insulin induction of increased mitogenic responses and phenotypic changes in human breast epithelial cells: evidence for enhanced interactions with the insulin-like growth factor-I receptor. Mol Carcinog 18(1):19–25

Nielsen FS, Jorgensen LN, Ipsen M, Voldsgaard AI, Parving HH (1995) Long-term comparison of human insulin analog B10Asp and soluble human insulin in IDDM patients on a basal/bolus insulin regimen. Diabetologia 38:592–598

Rakatzi I, Stosik M, Gromke T, Siddle K, Eckel J (2006) Arch Physiol Biochem 112(1):37–47. Differential phosphorylation of IRS-1 and IRS-2 by insulin and IGF-I receptors

Slieker LJ, Brooke GS, DiMarchi RD, Flora DB, Green LK, Hoffmann JA, Long HB, Fan L, Shields JE, Sundell KL, Surface PL, Chance RE (1997) Diabetologia. 40 Suppl 2:S54–61. Modifications in the B10 and B26–30 regions of the B chain of human insulin alter affinity for the human IGF-I receptor more than for the insulin receptor

von Mach MA, Brinkmann C, Hansen T, Weilemann LS, Beyer J (2002) Differences in pharmacokinetics and pharmacodynamics of insulin lispro and aspart in healthy volunteers. Exp Clin Endocrinol Diabetes. 110(8):416–9

Zib I, Raskin P (2006) Novel insulin analogs and its mitogenic potential. Diabetes Obes Metab 8(6):611–20

K.9.2 Insulin Receptor Affinity

GENERAL CONSIDERATIONS

An initial step in the evaluation of insulin analogs is determination of their affinity for the insulin receptor (Lee and Pilch 1994). The studies may include receptor association and dissociation as well as the signalling via the insulin receptor (insulin receptor tyrosine kinase activity and tyrosine phosphorylation of substrates). These methods provide some guidance about the biological potency to be expected, although they provide only limited information about the time action profile.

Receptor affinity data to be extended by evaluation of post-receptor events (signaling), The time action profile in animals and humans, which may differ considerably from the predictions derived from the receptor affinity alone.

PURPOSE AND RATIONALE

These methods described the initial binding of insulin analogs to the receptor preparation obtained from different sources. Tissues differ in their receptor content, the early methods used membrane receptors isolated from different organs, and more recent methods use solubilised human insulin receptor protein.

PROCEDURE

There are several important modifications of the assay principle. This depends on selection of the initial source of receptor (tissue), the preparation of the receptor protein, and the procedure to determine receptor affinity using a radioactive labeled insulin preparation. Some details of the methods are described in section K.6.3.2.1.1of this chapter.

Slieker et al. 1997 described the method using placental membranes and mammary epithelial cells as the receptor preparations for [125I]-Insulin and [125I]-IGF-I binding assays. The placental assay employed incubating 30–40 mg of membrane protein with approximately 10 fmol of iodinated ligand in a final volume of 500 ml of 100 mmol/l HEPES, pH 7.8, 120 mmol/l NaCl, 5 mmol/l KCl, 1.2 mmol/l MgSO4, 8 mmol/l glucose and 0.25% BSA for 16–18 h at 4°C. Membranes were collected on glass fiber filters pre-treated with 0.1% polyethyleneimine by using a cell harvester (Skatron, Lier, Norway). Binding assays with mammary epithelial cells were performed under similar conditions using confluent cells on either P12 (IGF-I receptor) or P6 (insulin receptor) plates (Costar, Cambridge, Mass., USA). Monolayers were incubated in insulin-free medium for 24 h prior to initiating the binding assay. Cells were incubated in the above buffer containing iodinated IGF-I and cold competing ligands for 16–18 h at 4°C. After washing the monolayers with cold assay buffer, cells were solubilized in 0.1 N NaOH and counted for 125I. EC50 values were determined by fitting displacement data to a four-parameter model by nonlinear regression. Dissociation constants for TyrA14-[125I]-Insulin, – LysB28ProB29 HI, and -AspB10 HI were obtained according to the method of Drejer et al. (1991).

For the quantification of receptor numbers of insulin and IGF-I on Chinese hamster ovary cells (CHO) using the [125-I] labeled ligands, Hansen et al. (1996) are applied the method which was also modified for time course studies of binding to these receptors.

CHO-hIR and CHO-K1 cells were seeded on 24-well Nunclon plates at a density of 5x10% cells/well in DMEM containing 20 mM Hepes, 1ug/l human albumin, 10% fetal calf serum, 1% non-essential amino acids and 0.1% bacitracin (pH 7.4); cells were used at confluence. The numbers of insulin and IGF-1 receptors present at the surface of the CHO-K1 and CHO-hIR cells were determined by saturation of the respective receptors with unlabeled ligand. Cells were incubated overnight at 4°C with 50 pM 125I-labeled insulin or [125I]IGF-1 in the presence of increasing amounts of unlabeled insulin or IGF-1 respectively. The number of receptors was estimated with the aid of the LIGAND program fitting a two-site model [Munson and Rodbard 1980]. The native CHO-K1 cells were estimated to express approx. 3.000 high-affinity binding sites for insulin and 50.000 IGF-1 receptors, whereas CHO-hIR cells were found to express 60.000 IRs and 50.000 IGF-1 receptors.

For the time course of receptor association, the procedure was as follows (Hansen et al. 1996). CHO-hIR cells were cultivated in DMEM containing 2 mM glutamine, 50 units/ml penicillin, 50ug/ml streptomycin, 10% fetal calf serum, 1% non-essential amino acids and 1 lM methotrexate. Cells were grown to 80% confluence in 60 mm dishes, 6-well plates (IRTK activity assay) or 12-well plates before the experiments were carried out. Before stimulation with insulin or analog, the cells were starved for 18 h in serum-free medium supplemented with 0.5% insulin-free BSA. The cells were stimulated with 1 ml of 0.1 lM insulin or analog for 30 min, then washed thoroughly 3–5 times (2–5 ml each wash) and subsequently incubated in serum- and insulin-free medium. Because of the large variations in receptor kinetics and potencies of the analogs, the high concentration of 0.1 μM and the 30 min stimulation time were used to ensure maximal stimulation. At various times post-stimulation (0–180 min) the medium was removed and the cells processed further (insulin receptor tyrosine kinase activity IRTK and tyrosine phosphorylation of IR, IRS-1 and Shc).

Kurtzhals et al. (2000) used a preparation of human solubilised insulin receptor protein. Human insulin receptor (hIR) (isoform without exon 11) was isolated from transfected baby hamster kidney (BHK) cells by solubilization and partial purification on a wheat germ agglutinin column. For binding experiments, human insulin receptor (hIR) was incubated with 3 pmol/l TyrA14[125I] human insulin and various concentrations of unlabeled human insulin or insulin analog in a binding buffer containing 0.1 mol/l HEPES, 0.1 mol/l NaCl, 0.01 mol/l MgSO4, 0.5% HSA, 0.2% g-globulin, and 0.025% Triton X-100, pH 7.8, for 42 h at 4°C. Bound tracer was isolated by precipitation with 400 μl 25% PEG 8000 and washing with 1 ml 15% PEG 8000. The data were fitted to a 4-parameter logistic function where *B*max and *B*min were fixed and slope and concentration required for half-maximal effect (EC50) varied. The relative affinity of an insulin analog was calculated as the ratio between the EC50 value for human insulin and that of the insulin analog.

Dissociation from the insulin receptor was determined by Kurtzhals et al. (2000) using CHO cells. Dissociation constants for A14Tyr[125I]-insulins were determined as previously described using Chinese hamster ovary (CHO) cells overexpressing the human insulin receptor (CHOhIR cells) (9). The cells were cultured at 37°C in a 5% CO2 humidified atmosphere in Dulbecco's modified Eagle's

medium (DMEM) supplemented with 10% (vol/vol) fetal calf serum (FCS), 1% nonessential amino acids, 50 µg/ml streptomycin, 50 U/ml penicillin, and 1 µmol/l methotrexate. Cells were subcultured at a 1:5 split ratio every 3–4 days for maintenance. For dissociation studies, cells were seeded on 24-well plates at a density of 5 3 104 cells/well in DMEM containing 10% FCS, 1% nonessential amino acids, 20 mmol/l HEPES, 0.1% HSA, and 0.1% bacitracin (pH 7.4). Cells were used at confluence and were incubated with 50 pmol/l A14Tyr[125I]-insulin or analog for 3 h at 4°C. Cells were washed quickly twice with ice-cold HEPES-buffered DMEM (pH 7.4), and the dissociation of radioactivity was measured after the addition of HEPES-buffered DMEM containing 0.1 µmol/l unlabeled human insulin to measure the maximal accelerated dissociation rate. Cell-associated radioactivity was measured as a function of time, and the dissociation rate constant (*k*d) was calculated from the fitted monoexponential dissociation profiles using the following equation: $B = B_{min} + (B_{max} - B_{min})$ 3 exp(–*k*d 3*t*), where *B* represents cell-associated radioactivity.

MODIFICATIONS OF THE METHOD

The main modifications are related to the selection of receptor protein (membranes or solubilised receptor protein, cells transfected with the human insulin receptor – CHOhIR cells)

CRITICAL ASSESSMENT OF THE METHOD

It is important to use the same system when comparing the insulin receptor affinity of several insulins. To some extent, this can be used as the selection tool in structure activity studies. There are however considerable limitations when comparing affinities with in vitro potency, and ultimately with in-vivo hypoglycemic activity. Therefore, results of the insulin receptor affinity need to be supplemented by data on receptor association and dissociation, as well as post-receptor signaling mechanisms.

REFERENCES AND FURTHER READING

De Meyts P, Christoffersen CT, Ursø B et al (1993) Insulin potency as a mitogen is determined by the half-life of the insulin-receptor complex. Exp Clin Endocrinol Leipzig 101:22–23

Drejer K, Kruse V, Larsen UD, Hougaard P, Bjørn S, Gammeltoft S (1991) Receptor binding and tyrosine kinase activation by insulin analogs with extreme affinities studied in human hepatoma HepG2 cells. Diabetes 40:1488–1495

Gammeltoft S (1984) Insulin receptors: binding kinetics and structure-function relationship of insulin. Physiol Rev: 1321–1378

Hansen BF, Danielsen GM, Drejer K et al (1996) Sustained signalling from the insulin receptor after stimulation with insulin analogs exhibiting increased mitogenic potency. Biochem J 315:271–279

Kohanski RA, Lane MD (1983) Binding of insulin to solubilized insulin receptor from human placenta. Evidence for a single class of noninteracting binding sites. J Biol Chem 258:7460–8

Kohanski RA, Lane MD (1985) Homogeneous functional insulin receptor from 3T3-L1 adipocytes. Purification using N alpha B1-(biotinyl-epsilon-aminocaproyl)insulin and avidin-sepharose. J Biol Chem 260:5014–25

Kurtzhals P, Schaffer L, Sorenson A, Kristensen C, Jonassen I, Schmid C, Trub T (2000) Correlations of recepwtor binding and metabolic and mitogenic potencies of insulin analogs designed for clinical use. Diabetes 49:999– 1005

Lee J, Pilch PF (1994) The insulin receptor: structure, function, and signaling. Am J Physiol 266:C319–34

Munson PJ, Rodbard D (1980) LIGAND: a versatile computerized approach for characterization of ligand-binding systems. Anal Biochem 107:220–239

Slieker LJ, Brooke GS, DiMarchi RD, Flora DB, Green LK, Hoffman JA, Long HB, Fan L, Shields JE, Sundell KL, Surface PL, Chance RE (1997) Modifications in the B10 and B26–30 regions of the B chain of human insulin alter affinity for the human IGF-I receptor more than for the insulin receptor. Diabetologia 40(Suppl 2):S54–S61

Woldin CN, Hing FS, Lee J, Pilch PF, Shipley GG (1999) Structural studies of the detergent-solubilized and vesicle- reconstituted insulin receptor. J Biol Chem 274:34981–92

K.9.3 Signaling Via Insulin Receptor

GENERAL CONSIDERATIONS

The postreceptor events after stimulation of the insulin receptor are of considerable interest for understanding the effects on different tissues, changes associated with insulin resistance and mitogenic activation of normal tissue and tumor tissues. This is a very complex area of research, because the mitogenic signalling is concentration dependent and many effects may be obtained in vitro which have no equivalent within the therapeutic range of insulin application in patients. Due to the complexities of the signaling mechanisms, and their redundancy with regard to cell proliferation, apoptosis and tissue growth, these investigations are necessary for better understanding, but not sufficient at the present time to fully explained the antiapoptotic and mitogenic activities *in vivo* and the clinical relevance.

PURPOSE AND RATIONALE

Studies on signaling of insulin analogs via the insulin receptor over a wide range of concentrations in vitro are performed to elucidate the intracellular mechanisms, and the components of the signaling chain.

PROCEDURE

Among the many procedures and protocols used for investigation of signaling in cells stimulated with insulin analogs, Hennige et al. (2005) provide an example for the assessment of the fast acting insulin glulisine. Their tests were performed in 10-week-old male C57BL/6 mice from Charles River acclimatized for 2 weeks before entering the study. The mice were maintained on a normal light/dark cycle and kept on a regular diet. Glucose levels were sampled from mouse tail bleeds using a Glucometer Elite (Bayer, Elkhart, IN).

The procedures for in -vivo insulin stimulation and Western blot analysis were described for a short term experiment, by single dose stimulation with regular human insulin or insulin glulisine (1 IU/kg body wt) injected intraperitoneally. For short-term stimulation, 2 IU of insulin were injected into the inferior vena cava. Control animals received a comparable amount of diluent. Tissues (liver, muscle, and hypothalamus) were removed at the indicated time points and homogenized at 4°C, as previously described (8). Homogenates were allowed to solubilize for 30 min on ice and were clarified by centrifugation at 12,000 *g* for 20 min. To detect insulin-stimulated tyrosine phosphorylation, supernatants containing 0.5 mg of total protein were immunoprecipitated with antibodies directed against the COOH-terminal sequences of the insulin receptor, and of the insulin receptor substrates IRS-1 and IRS-2 . Visualization of immunocomplexes after gel electrophoresis and Western blotting with the antiphosphotyrosine antibody 4G10 was performed with the nonradioactive enhanced chemiluminescence system. Blots were subsequently stripped and reprobed to reveal expression of total protein. To assess activation of downstream signaling elements, tissue lysates were separated by SDS-PAGE and transferred to nitrocellulose. Membranes were probed with anti–phospho-AKT and anti–phosphomitogen-activated protein (MAP) kinase antibodies (Cell Signaling, Beverly, MA), respectively.

Assay of PI 3-kinase activity: Tissue lysates were immunopurified with anti-PY20 (Santa Cruz Biotechnology, Santa Cruz, CA) antibodies and immunocomplexes were absorbed to protein a-sepharose for 12 h. Immunoprecipitates were washed three times and pellets were directly incubated with 0.1 mg/ml L-PI (Sigma) and 50 mol/l [32P]-ATP (Perkin Elmer) at room temperature for 10 min. After 1501 of 1 mol/l HCl was added, lipids were extracted twice with 4501 chloroform/methanol (1:1 by vol). Products were separated by thin-layer chromatography, as previously described (9). ^{32}P-labeled phospholipids were detected by autoradiography.

[3H]thymidine incorporation into C2C12 myoblasts: To measure [3H]thymidine incorporation, C2C12 cells were grown in Dulbecco's modified Eagle's medium (4.5 g/l glucose and 10% FCS) in six-well culture plates, and subsequently starved for 24 h in serum-free medium. After cells were stimulated with insulin for 16 h, [3H]thymidine (0.5 Ci/ml) was added for 4 h. The dishes were then rinsed twice with ice-cold PBS and once with 10% trichloroacetic acid. After 20 min, dishes were washed once with ice-cold 10% trichloroacetic acid. Cells were then lysed with 5001 of 0.2 N NaOH/1% SDS and neutralized with 0.5 ml of 0.2 N HCl. Radioactivity was determined by liquid scintillation counting.

MODIFICATIONS OF THE METHOD

There are many options to analyze the postreceptor events to characterise signaling in insulin stimulated cells (Gronborg et al. 1993, Chang et al. 2004), with considerable overlap towards the IGF-I stimulated signaling (Valentinis and Baserga 2001). For the practical approach of risk assessment for insulin analogs, these methods are not suitable, due to the complexity and the as yet only partially defined relation to proliferative activity in normal tissues, and in pre-existing tumors. The research potential of these methods in defined cell lines in culture is very important, the application to insulin stimulated animals and their tissues is also of considerable heuristic relevance.

CRITICAL ASSESSMENT OF THE METHOD

Exploration of the insulin receptor related signaling mechanisms is at present an active research area with many a well-defined methods (see Sect. K.6 in this chapter).

REFERENCES AND FURTHER READING

De Meyts P, Ursø B, Christoffersen CT, Shymko RM (1995) Mechanism of insulin and IGF-I receptor activation and signal transduction specificity. Receptor dimer crosslinking, bell-shaped curves, and sustained versus transient signalling. Ann New York Acad Sci 766:388–401

Hennige AM, Lehmann R, Weigert C, Moeschel K, Schauble M, Metzinger E, Lammers R, Haring HU (2005a) Insulin glulisine: Insulin receptor signaling characteristics *in vivo*. Diabetes 54:361–366

Ish-Shalom D, Tzivion G, Christoffersen CT, Ursø B, De Meyts P Naor D (1995) Mitogenic potential of insulin on lymphoma cells lacking IGF-I receptors. Ann N Y Acad Sci 766:409–415

Lamphere L, Lienhard GE (1992) Components of signaling pathways for insulin and insulin-like growth factor-I in muscle myoblasts and myotubes. Endocrinology. 131(5):2196–202

Shymko RM, De Meyts P, Thomas R (1997) Logical analysis of timing-dependent receptor signalling specificity: Application to the insulin receptor metabolic and mitogenic signalling pathways. Biochem J 326(Pt 2):463– 469
Gronborg M, Wulff BS, Rasmussen JS, Kjeldsen T, Gammeltoft S (1993) Structure-function relationship of the insulin-like growth factor-I receptor tyrosine kinase. J Biol Chem 268(31):23435–40
Chang L, Chiang SH, Saltiel AR (2004) Insulin signaling and the regulation of glucose transport. Mol Med 10(7–12):65–71
Valentinis B, Baserga R (2001) IGF-I receptor signalling in transformation and differentiation. Mol Pathol 54(3):133–137

K.9.4 IGF-I Receptor Affinity

GENERAL CONSIDERATIONS

IGF-I receptor affinity is characterised by binding of IGF-I to receptors on cell membranes, or to the IGF-I receptor protein. The cell lines which have been selected for their high density of IGF-I receptors provide estimates of affinity which may vary considerably, and need to be supplemented by methods for interaction of insulin analogs with the receptor (dissociation, residence time), and receptor-mediated effects on proliferation in normal tissues, and in tumor cell lines.

For the IGF-1 receptor affinity of insulin analogs, cell lines have been used with a favorable relation of IGF-I receptors to insulin receptors. Clearly, results differ with the test system used, therefore the determination of IGF-I receptor affinity is considered a preselection step for the further investigation of signalling via the IGF-I receptor and the insulin receptor. Placental membranes or mammary epithelial cell lines (Slieker et al. 1997), and human skeletal muscle cells (Ciaraldi et al. 2001) have been used for structure activity studies, and full investigations on signaling (Ciaraldi et al. 2005),

PURPOSE AND RATIONALE

Studies are performed to obtain an estimate of the proliferative and antiapoptotic activity to be expected raised on the affinity for the IGF-I receptor (DeMeyts et al. 1994, Rubin and Baserga 1995), and to explore the mitogenic/metabolic ratio in preparation of detailed investigation of the effects on cells (e. g. thymidine incorporation), and on postreceptor signaling (Leroith et al. 994).

PROCEDURE

Human skeletal muscle cells (Ciaraldi et al. 2001) are used for the assessment of insulin analog interaction with insulin receptors and IGF-I receptors.

Cell Culture

Biopsy of the vastus lateralis muscle was performed according to published procedures (19). Human skeletal muscle cells were isolated and grown in culture as described in detail previously (Henry et al. 1995). When myoblasts attained 80–90% confluence, the growth medium was changed to MEM supplemented with 2% FBS and antibiotics to induce fusion to multinucleated myotubes. The medium was changed every other day during cell fusion. All studies were performed on cells after one passage.

Insulin and IGF-I Binding Assays

Hormone binding assays were performed by the modification of a method described previously (Henry et al. 1995). Fully differentiated human skeletal muscle cells from nondiabetic subjects and patients with type 2 diabetes were washed four times with reaction buffer, then incubated with reaction buffer and [125I-Tyr A14]insulin (final concentration, 67 pm) or [125I-Tyr A14]IGF-I (final concentration, 39 pm) for 4 h at 12 C in the absence or presence of varying concentrations of unlabeled hormone. Results were calculated based on the displacement of specific insulin/ IGF-I binding normalized to protein concentrations in cells from both nondiabetic subjects and patients with type 2 diabetes.

MODIFICATIONS OF THE METHOD

One particular assay based on IGF receptor affinity in an osteosarcoma cell line SAOS B10 was used extensively in the preclinical evaluation of mitogenic activity (Kurtzhals et al. 2000). This cell line was initially selected for research on IGF-I, and subsequently adapted to structure activity studies. The finding of slightly increased IGF-1 receptor affinity in the presence of a rate of receptor dissociation similar to human insulin is not associated with any biological consequences, as shown by the subsequent extensive studies on absence of toxicity and carcinogenicity mice and rats (Stammberger et al. 2002).

CRITICAL ASSESSMENT OF THE METHOD

It remains the highly active and controversial area of research to define which mechanisms are involved and contribute to a significant extent to cell proliferation and apoptosis via the insulin receptor and/or the IGF-I receptor (Blakesley et al. 1996, DeMeyts 1994, DeMeyts et al. 1995a, DeMeyts et al. 1995b). Evidence for these mechanisms relies to significant extent on the time factor of interaction with the insulin receptor, prolonged residence time as conclude from the incidence

of [B10-Asp] insulin would be dissociated with stimulation of tissue proliferation, and could have an effect on tumor progression (Prager and Melmed 1993, LeRoith 1994, DeMeyts 1995b, Strobl et al. 1995).

The assessment of IGF-I receptor affinity and its that the physiological role becomes even more complicated with the unresolved role of insulin/IGF-I hybrid receptors (Soos et al. 1993, Takata and Kobayashi 1994), which may also have a role in the microvascular and macrovascular complications of diabetes (Li et al. 2005). At present time, there is no evidence for a pathophysiological role of slightly increased IGF-I receptor affinity in the presence of physiological residence time at the receptor, with dissociation rates similar to human insulin. Investigation of insulin glargine has shown that there is no effect on proliferation of benign and malignant mammary cell lines (Staiger etal 20059, and no effect on tumor formation in rodent carcinogenicity studies (Stammberger et al. 2002). There is also no evidence for any proliferative effect of the clinically used fast acting insulin analogs in animal toxicology studies (EPARs for insulin lispro, insulin aspart, and insulin glulisine). Investigation of mammary gland tissue for proliferation markers after a six-month and twelve-months treatment in rats has shown no proliferative effect (Stammberger etal 2006).

REFERENCES AND FURTHER READING

Blakesley VA, Scrimgeour A, Esposito D, Le Roith D (1996) Signaling via the insulin-like growth factor-I receptor: does it differ from insulin receptor signaling? Cytokine Growth Factor Rev 7(2):153–9

Ciaraldi TP, Phillips SA, Carter L, Aroda V, Mudaliar S, Henry RR (2005) Effects of the rapid-acting insulin analog glulisine on cultured human skeletal muscle cells: comparisons with insulin and insulin-like growth factor I. J Clin Endocrinol Metab 90(10):5551–8

Ciaraldi TP, Carter L, Seipke G, Mudaliar S, Henry RR (2001) Effects of the Long-Acting Insulin Analog Insulin Glargine on Cultured Human Skeletal Muscle Cells: Comparisons to Insulin and IGF-I J Clin Endocrinol Metab/86 (5838–5847)

De Meyts P, Christoffersen CT, Urso B, Wallach B, Gronskov K, Yakushiji F, Shymko RM (1995a) Role of the time factor in signaling specificity: application to mitogenic and metabolic signaling by the insulin and insulin-like growth factor-I receptor tyrosine kinases. Metabolism 44(10 Suppl 4):2–11

De Meyts P, Urso B, Christoffersen CT, Shymko RM (1995b) Mechanism of insulin and IGF-I receptor activation and signal transduction specificity. Receptor dimer cross-linking, bell-shaped curves, and sustained versus transient signaling. Ann N Y Acad Sci 766:388–401

De Meyts P,Wallach B, Christoffersen CT et al (1994) The insulin-like growth factor-I receptor. Structure, ligand binding mechanism and signal transduction. Horm Res 42:152–169

De Meyts P (1994) The structural basis of insulin and insulin-like growth factor-I receptor binding and negative cooperativity, and its relevance to mitogenic versus metabolic signalling. Diabetologia 37 Suppl 2:S135–48

Henry RR, Abrams L, Nikoulina S, Ciaraldi TP (1995) Insulin action and glucose metabolism in non-diabetic control and NIDDM subjects: comparison using human skeletal muscle cell cultures. Diabetes 44:935–945

LeRoith D, Sampson PC, Roberts CT Jr (1994) How does the mitogenic insulin-like growth factor I receptor differ from the metabolic insulin receptor? Horm Res 41 Suppl 2:74–8; discussion 79

Li G, Barrett EJ, Hong Wang H, Weidong C, Zhenqi L (2005) Insulin at Physiological Concentrations Selectively Activates Insulin But Not Insulin-Like Growth Factor I (IGF-I) or Insulin/IGF-I Hybrid Receptors in Endothelial Cells. Endocrinology 146:4690–4696

Prager D, Melmed S (1993) Insulin and insulin-like growth factor I receptors: are there functional distinctions? Endocrinology 132(4):1419–20

Rosenzweig SA, Oemar BS, Law NM, Shankavaram UT, Miller BS (1993) Insulin like growth factor 1 receptor signal transduction to the nucleus. Adv Exp Med Biol 343:159–68

Rubin R, Baserga R (1995) Insulin-like growth factor-I receptor. Its role in cell proliferation, apoptosis, and tumorigenicity. Lab Invest 73(3):311–31

Sepp-Lorenzino L (1998) Structure and function of the insulin-like growth factor I receptor. Breast Cancer Res Treat 47(3):235–53

Soos MA, Nave BT, Siddle K (1993) Immunological studies of type I IGF receptors and insulin receptors: characterisation of hybrid and atypical receptor subtypes. Adv Exp Med Biol 343:145–57

Staiger K, Hennige AM, Schweitzer MA, Staiger H, Haering HU, Monika Kellerer M (2005) Effect of Insulin Glargine Versus Regular Human Insulin on Proliferation of Human Breast Epithelial Cells. ADA Annual Symposium San Diego Abstract 451-P

Stammberger I, Bube A, Durchfeld-Meyer B, Donaubauer H, Troschau G (2002) Evaluation of the Carcinogenic Potential of Insulin glargine in Rats and Mice. Int J Toxicol 21(3):171–179

Stammberger I, Seipke G, Bartels T (2006) Insulin glulisine—a comprehensive preclinical evaluation. Int J Toxicol. Jan-Feb;25(1):25–33

Strobl JS, Wonderlin WF, Flynn DC (1995) Mitogenic signal transduction in human breast cancer cells. Gen Pharmacol 26(8):1643–9

Takata Y, Kobayashi M (1994) Insulin-like growth factor I signalling through heterodimers of insulin and insulin-like growth factor I receptors. Diabete Metab 20(1):31–6

K.9.5 Signaling via IGF-1 Receptor

The insulin receptor (IR) and the insulin-like growth factor I receptor (IGF-IR) belong to the same subfamily of receptor tyrosine kinases with two extracellular ·-subunits and two transmembrane β-subunits. They share a high similarity of structure and intracellular signalling events (Dupont and Leroith 2002). However, the IR and the IGF-IR mediate different effects on metabolism, cell proliferation, apoptosis and differentiation. Although some of the variation can be attributed to a different tissue distribution or subcellu-

lar localization, it can also be explained by structural differences in the β-subunit, which may result in activation of specific substrates and signal pathways.

The presence and formation of hybrid receptors, heterodimers composed of the subunits of the insulin receptor and IGF-I receptor has been documented both in normal tissue and in tumor tissue samples (Salzman et al. 1984, Schumacher etal 1991, Soos et al. 1993, Siddle et al. 1994). It has been proposed that signaling in tumor tissue may proceed via such hybrid receptors.

In cells expressing the insulin receptor isoform A (IRA) and the insulin like growth factor-1 receptor (IGF1R), the presence of hybrid receptors, constituted of an alphabeta-IRA chain associated with an alphabeta-IGF1R chain, has been demonstrated. These heterodimers are found in normal cells, and also appear to play crucial roles in a number of cancers (Belfiore etal 1999, Frasca et al. 2003, Pandini et al. 1999). However, they remain difficult to study, due to the concomitant presence of IRA and IGF1R homodimers. Using bioluminescence resonance energy transfer (BRET), Siddle and Blanquart et al. (2005) have developed assays to specifically monitor the activation state of IRA/IGF1R hybrids, both in vitro and in living cells. In the first assay, only hybrid receptors were BRET competent. In the second assay, the activation state of IRA/IGF1R hybrids was monitored in real time, in living cells. In hybrid receptors, trans-phosphorylation of the kinase-dead alpha/beta-Rluc moiety by the wild-type alpha/beta moiety induced the recruitment of YFP-PTP1B-D181A-Cter, resulting in a hybrid-specific ligand-induced BRET signal. Both methods allow monitoring of the activity of IRA/IGF1R hybrid receptor and could be used to detect molecules of therapeutic interest for the treatment of cancer (Blanquart et al. 2005).

CRITICAL ASSESSMENT OF THE METHOD

There are presently a number of methods applicable for the detection of insulin/IGF-I hybrid receptors, and their state of activation. It will be important to investigate insulin analogs with reference to their effects on hybrid receptors, and signaling in normal tissue (Lamphere and Lienhard 1992) as well as in tumor tissue. There are observations of adaptive changes in the formation of insulin/IGF-I hybrid receptors in type 2 diabetic patients, attributed to chronic hyperinsulinaemia (Mosthaf et al. 1991, Federici et al. 1998a, 1998b), as well as alterations of the hybrid receptor ratio in tumor as such as thyroid cancer (Belfiore et al. 1999), and breast cancer (Pandini et al. 1999, Frasca et al. 2003).

REFERENCES AND FURTHER READING

Belfiore A, Pandini G, Vella V, Squatrito S, Vigneri R (1999) Insulin/IGF-I hybrid receptors play a major role in IGF-I signaling in thyroid cancer. Biochimie 81(4):403–7

Blanquart C, Gonzalez-Yanes C, Issad T (2006) Monitoring the activation state of insulin/IGF-1 hybrid receptors using Bioluminescence Resonance Energy Transfer. Mol Pharmacol [Epub ahead of print]

Dupont J, LeRoith D (2001) Insulin and insulin-like growth factor I receptors: similarities and differences in signal transduction. Horm Res 55:22–6

Entingh-Pearsall A, Kahn CR (2004) Differential roles of the insulin and insulin-like growth factor-I (IGF-I) receptors in response to insulin and IGF-I. J Biol Chem 279(36):38016–24. Epub 2004 Jul 7

Federici M, Lauro D, D'Adamo M, Giovannone B, Porzio O, Mellozzi M, Tamburrano G, Sbraccia P, Sesti G (1998a) Expression of insulin/IGF-I hybrid receptors is increased in skeletal muscle of patients with chronic primary hyperinsulinemia. Diabetes 47(1):87–92

Federici M, Porzio O, Lauro D, Borboni P, Giovannone B, Zucaro L, Hribal ML, Sesti G (1998b) Increased abundance of insulin/insulin-like growth factor-I hybrid receptors in skeletal muscle of obese subjects is correlated with *in vivo* insulin sensitivity. J Clin Endocrinol Metab 83(8):2911–2915

Frasca F, Pandini G, Vigneri R, Goldfine ID (2003) Insulin and hybrid insulin/IGF receptors are major regulators of breast cancer cells. Breast Dis 17:73–89

Kim J, Accili D (2002) Signalling through IGF-I and insulin receptors: where is the specificity? Growth Horm IGF Res 12:84

Lamphere L, Lienhard GE (1992) Components of signaling pathways for insulin and insulin-like growth factor-I in muscle myoblasts and myotubes. Endocrinology 131(5):2196–202

Li G, Barrett EJ, Wang H, Chai W, Liu Z (2005) Insulin at physiological concentrations selectively activates insulin but not insulin-like growth factor I (IGF-I) or insulin/IGF-I hybrid receptors in endothelial cells. Endocrinology 146(11):4690–6. Epub 2005 Aug 11

Mosthaf L, Vogt B, Haring HU, Ullrich A (1991) Altered expression of insulin receptor types A and B in the skeletal muscle of non-insulin-dependent diabetes mellitus patients. Proc Natl Acad Sci U S A 88:4728–30

Nitert MD, Chisalita SI, Olsson K, Bornfeldt KE, Arnqvist HJ (2005) IGF-I/insulin hybrid receptors in human endothelial cells. Mol Cell Endocrinol 229(1–2):31–7

Pandini G, Frasca F, Mineo R, Sciacca L, Vigneri R, Belfiore A. Insulin/insulin-like growth factor I hybrid receptors have different biological characteristics depending on the insulin receptor isoform. Biochem J 290(Pt 2):419–26

Pandini G, Vigneri R, Costantino A, Frasca F, Ippolito A, Fujita-Yamaguchi Y, Siddle K, Goldfine ID, Belfiore A (1999) Insulin and insulin-like growth factor-I (IGF-I) receptor overexpression in breast cancers leads to insulin/IGF-I hybrid receptor overexpression: evidence for a second mechanism of IGF-I signaling. Clin Cancer Res 5(7):1935–44

Sakai K, Lowman HB, Clemmons DR (2002) Increases in free, unbound insulin-like growth factor I enhance insulin responsiveness in human hepatoma G2 cells in culture. J Biol Chem 277(16):13620–7. Epub 2002 Feb 7

Salzman A, Wan CF, Rubin CS (1984) Biogenesis, transit, and functional properties of the insulin proreceptor and modified insulin receptors in 3T3-L1 adipocytes. Use of monensin to probe proreceptor cleavage and generate altered receptor subunits. Biochemistry 23:6555–65

Schumacher R, Mosthaf L, Schlessinger J, Brandenburg D, Ullrich A (1991) Insulin and insulin-like growth factor-1 binding specificity is determined by distinct regions of their cognate receptors. J Biol Chem. 266(29):19288–95
Siddle K, Soos MA, Field CE, Nave BT (1994) Hybrid and atypical insulin/insulin-like growth factor I receptors. Horm Res 41 Suppl 2:56–64
Soos MA, Field CE, Siddle K (1993) Purified hybrid insulin/insulin-like growth factor-I receptors bind insulin-like growth factor-I, but not insulin, with high affinity
Whitehead JP, Clark SF, Urso B, James DE (2000) Signalling through the insulin receptor. Curr Opin Cell Biol 12:222–8

K.9.6 Mitogenic Activity

GENERAL CONSIDERATIONS

The determination of mitogenic activity on benign and malignant cell lines is a preliminary approach which has been proposed in the points-to-consider.document of the EMEA safety working party. Enhanced cell proliferation may be the result of signaling via the insulin receptor at near physiological concentrations, via the IGF-I receptor at supraphysiological concentrations, and presumably also related to the presence of hybrid receptors which are preferentially stimulated by IGF-I (Li et al. 2005, Slaaby et al. 2006)

PURPOSE AND RATIONALE

The tests for mitogenic activity are considered to be in early toxicology procedure which provides guidance about the subsequent toxicological evaluation to be performed. In case of enhanced mitogenicity found with the particular cell line, the six-month of 12 month toxicology studies may include histological investigation of specific organ tissues, together with proliferation markers in these tissues (as an example, referred to Stammberger et al. 2006 for investigation of mammary gland tissue in rats).

PROCEDURE

The procedure by Slieker et al. (1996) is based on stimulation of human mammary epithelial cells (HMEC)**.** Mitogenicity was assessed by measuring insulin analog- stimulated growth of human mammary epithelial cells (HMEC) in culture. HMECwere obtained from Clonetics Corporation (San Diego, Calif., USA) at passage 7 and were expanded and frozen at passage 8. A fresh ampule was used for each experiment so that cells were not grown beyond passage 9. Cells were maintained inMCDB 170 medium containing bovine insulin (5 mg/ml), recombinant human epidermal growth factor (10 ng/ml), hydrocortisone (0.5 mg/ml), bovine pituitary extract (50 mg/ml) and gentamycin/amphotericin B. For a growth experiment, cells were plated in 96-well trays at adensity of 12500 cells/cm2 in the above-medium modified as follows: 0.1%BSAwas added and 5 mg/ml bovine insulin was substituted by a graded dose of human insulin or analog from 0 to 1000 nmol/l final concentration. Trays were incubated for 72 h and the cells were counted by Coulter counter (Coulter Electronics, Hialeah, Fla., USA) after trypsinization. Typically, the maximal growth response was between 3- and 4-fold stimulation over basal and did not differ between analogs. Response data were normalized to between 0 and 100% response equal to 100 ' (response at dose X – response at zero dose) divided by (response at maximal dose – response at zero dose). Dose-response data were fit by non-linear regression employing JMP (SAS Institute, Inc., Cary, N.C., USA).

The method by Trueb and Froesch in human osteosarcoma cells (SAOS-B10) for determination of the binding of insulin analogs to the IGF receptor, and proliferative activity was developed in 1995 and subsequently applied by Kurtzhals et al. (2000). Human osteosarcoma cells (B10, a subline of Saos-2, supplied by S.B. and G.A.Rodan, West Point, Pennsylvania) are used because they exhibit a high rate of proliferation and high number of IGF-1 receptors on the cell surface. From competition of 125-I-insulin by unlabeled human insulin, a number of only 740 insulin binding sites per cell has been calculated whereas 21,000 or 39,000 IGF-1 binding sites per cell were determined in two separate experiments. IGF-1 receptor binding is measured (Competition with 125-I IGF-I). The dilution of the stock solutions of the various analogs and natural insulins are performed with HBB/1% HSA (HBB: 118 mM NaCI, 5 mM KCI, 1.2 mM MgSO4, 8.8 mM D-Glucose, 100 mM Hepes, pH 8.0). In the studies by Froesch, possible concentration of the stock dilution was 5.5–10" M for insulin glargine and the related Arg(B31)Arg(B32) insulin due to a lower solubility of both substances at neutral pH.

Therefore, the maximum final concentration in the competition experiment was limited to 5.10∼M for these analogs (10- M for human insulin and the animal insulins). The limitations of preparing stock solutions for insulin analogs with a marked change in isoelectric point should be considered in the experimental design. In another series, initial stock solutions with a standard concentration of 5.5 + 10" M were used, again limiting the final maximum concentration to 5.1 0" M for the insulin analogs in the competition experiment.

Osteosarcoma cells (BlO, passage 27, 125,000 or 150,000 per well) were seeded in 24-well tissue cul-

ture plates and kept overnight at 37°C in DMEM/F12 (1:1) with the addition of 10% fetal calf serum. For deinduction the medium was changed to 500 µl serum-free medium for 4 hours, then the cells were incubated with 200 µl HBB/1% HSA-[125-I] -IGF-1 tracer (0.03 pick/well = 52,000 cam, 8.1×10^{-13} M final concentration) + 20 µl insulin analog or reference in the respective dilution overnight at 4°C. Plates are washed three times with cold PBS and dried at room temperature. Then 200 µl 2 N NaOH are added to each well for 1 hour at room temperature. The lysed cells are transferred to scintillation vials (each well washed with additional 200 µl NaOH) counted for bound radioactivity with a gamma-counter (triplicate measurements).

Mitogenic activity was tested by thymidine incorporation. The dilution of the stock solutions of the various analogs and natural insulins was performed with the basic medium (F12/1 g BSA). The concentration range used was between 10(-11) and 10(-6) M. Cells (50,000) were seeded in 24-well tissue culture plates and kept overnight in DMEM/F12 (1:l) with the addition of 10% fetal calf serum at 37°C. The medium was changed to DMEM/F12 1:l with 5% fetal calf serum for a second overnight incubation period, followed by F12/1 g BSA/L for 30 minutes. The medium was then changed to 400 µl (200 µl in another study) F12/1 BSA + 40 µl (20 µl in another study) insulin analog or reference compound in the respective dilution. Cells were kept at 37°C for 17 hours, then 30 µl (20 µl in another study) 3H-methylthymidine was added (0.3 pCi/well). After 3 to 4 hours at 37°C the medium was aspirated, plates were washed three times in cold PBS, and 500 µl 10% TCA added to each well for 30 minutes at 4°C. After aspiration, wells are washed twice with 10% TCA and dried at room temperature (30 minutes). Then 500 µl 1 N KOH is added to each well for 1 hour at room temperature. 250 µl are removed from each well for liquid scintillation counting (gamma-counter, triplicate counting) after mixing the sample first with 250 µl 1N-HCI and second with 5 ml scintillation fluid.

The method for mitogenic potency described by Kurtzhals etal (2000) is based on thymidine incorporation of the SAOS-B10 line with predominant IGF-I receptors and very few insulin receptors, previously used as SAOS cells extensively for research on chondrocytes and bone formation. The human osteosarcoma cell line Saos/B10 (20), a subclone of Saos-2 (ATCC HTB-85), was used by Kurtzhals. B10 cells express ~30,000 IGF-I receptors and < 1,000 insulin receptors per cell. Cells were cultured in DMEM/F12 supplemented with 10% FCS, L-glutamine, and penicillin/streptomycin. During the entire experiment, cells were grown and kept at 37°C in a humidified atmosphere with 5% CO2. For experiments, cells were trypsinized, plated in 24-well dishes at ~75–100 3 103 cells per well, and cultured for 16 h. Growth medium was then removed and replaced with test buffer (DMEM/F12 without FCS but with 0.5% BSA), and the cells were starved for 4 h. Then, the medium was withdrawn, and cells were incubated with test buffer containing 0.8 pmol/l to 0.8 mmol/l insulin analog for 16 h at 37°C before addition of [3H]methyl-thymidine. [3H]thymidine incorporation was allowed to take place for 4 h at 37°C. The cells were then washed 3 times with ice-cold phosphate-buffered saline and lysed in 10% trichloroacetic acid for 15 min under constant gentle rocking at 4°C. The soluble free [3H]thymidine was removed by 3 consecutive washes in ice-cold 10% trichloroacetic acid. The high molecular weight part of the cell lysates was resolubilized in 1 mol/l KOH and neutralized with an equal volume of 1 mol/l HCl, and DNA-incorporated [^{3}H]thymidine was measured in a b-counter. Each concentration was assayed in triplicate for each experiment. The experiments were repeated 3 times. To compare the mitogenic potential of the insulin analogs with that of human insulin, log-dose response profiles were generated, and EC50 values were estimated using a 4-parameter logistic function (19). Relative mitogenic potency was calculated as the ratio between the estimated EC_{50} values (EC50,HI/EC50,analog), assuming parallelism of the log-dose response profiles.

The relevance of these mitogenicity estimates in a special cell line with predominant IGF-I receptors has been challenged, in a particular because insulin glargine, which showed slightly enhanced mitogenic activity in this test dissociate is rapidly from the insulin receptor (similar to human insulin), and does not stimulate the IGF-I receptor at therapeutic concentrations in humans, because it's affinity for the IGF receptor over the therapeutic dose range is much lower than that of endogenous IGF-I at physiological concentrations.

MODIFICATIONS OF THE METHOD

These tests may be performed on cell lines in vitro, or on tissue specimens ex-vivo.

CRITICAL ASSESSMENT OF THE METHOD

Mitogenicity estimates our guidance for subsequent evaluation of tissues in animal toxicology studies.

REFERENCES AND FURTHER READING

Dalle S, Ricketts W, Imamura T, Vollenweider P, Olefsky JM (2001) Insulin and insulin-like growth factor I receptors uti-

lize different G protein signaling components, J Biol Chem 276:15688–15695
De Meyts P, Christoffersen CT, Ursø B et al (1995) Role of the time factor in signalling specificity. Application to mitogenic and metabolic signalling by the insulin and insulin-like growth factor-I receptor tyrosine kinases. Metabolism 44[Suppl 4]:1–11
De Meyts P, Ursø B, Christoffersen CT, Shymko RM (1995) Mechanism of insulin and IGF-I receptor activation and signal transduction specificity. Receptor dimer crosslinking, bell-shaped curves, and sustained versus transient signalling. Ann New York Acad Sci 766:388–401
DeMeyts P, Whittaker J (2002) Structural biology of insulin and IGF1 receptors: implications for drug design, Nat Rev Drug Discov 1:769–783
DeMeyts P, Whittaker J (2002) Structural biology of insulin and IGF-I receptors: Implications for drug design. Nature Rev 1:769. Baserga R, Peruzzi F, Reiss K (2002) The IGF-1 receptor in cancer biology. Int J Cancer 107:873
Hankinson SE, Willett WC, Colditz GA, et al (1998) Circulating concentrations of insulin-like growth factor-I and risk of breast cancer, Lancet 351 1393–1396
Ish-Shalom D, Tzivion G, Christoffersen CT, Ursø B, De Meyts P, Naor D (1995) Mitogenic potential of insulin on lymphoma cells lacking IGF-I receptors. Ann N Y Acad Sci 766:409–415
Jones JI, Clemmons DR (1995) Insulin-like growth factors and their binding proteins: biological actions. Endocr Rev 16:3–34
Kellerer M, Haering HU (2001) Insulin analogs: impact of cell model characteristics on results and conclusions regarding mitogenic properties. Exp Clin Endocrinol Diabetes 109:63–64
Koontz JW, Iwahashi M (1981) Insulin as a potent, specific growth factor in a rat hepatoma cell line. Science 211:947–949
Kurtzhals P, Schaffer L, Sorenson A, Kristensen C, Jonassen I, Schmid C, Trub T (2000) Correlations of recepwtor binding and metabolic and mitogenic potencies of insulin analogs designed for clinical use. Diabetes 49:999–1005
Mamounas M, Gervin D, Englesberg E (1989) The insulin receptor as a transmitter of a mitogenic signal in Chinese-hamster ovary CHO-K1 cells. Proc Natl Acad Sci U.S.A. 86:9294–9298
Pandini G, Frasca F, Mineo R, Sciacca L, Vigneri R, Belfiore A (2002) Insulin/insulin-like growth factor I hybrid receptors have different biological characteristics depending on the insulin receptor isoform involved. J Biol Chem 277:39684–39695
Prisco M, Romano G, Peruzzi F, Valentinis B, Baserga R (1999) Insulin and IGF-I receptors signaling in protection from apoptosis. Horm Metab Res 31:80–89
Renehan AG, Zwahlen M, Minder C, O'Dwyer ST, Shalet SM, Egger M (2004) Insulin-like growth factor (IGF)-I, IGF binding protein-3, and cancer risk: systematic review and meta-regression analysis. Lancet 363:1346–53. Ullrich A, Schlessinger J (1990) Signal transduction by receptors with tyrosine kinase activity. Cell 61:203–212
Slaaby R, Schaffer L, Lautrup-Larsen I, Andersen AS, Shaw AC, Mathiasen IS, Brandt J (2006) Hybrid receptors formed by insulin receptor (IR) and insulin-like growth factor I receptor (IGF-IR) have low insulin and high IGF-1 affinity irrespective of the IR splice variant. J Biol Chem 281(36):25869–74
Schmid C, Keller C, Gosteli-Peter M, Zapf J (1999) Mitogenic and antiapoptotic effects of insulin-like growth factor binding protein-6 in the human osteoblastic osteosarcoma cell line Saos-2/B-10. Biochem Biophys Res Commun 263(3):786–9

K.9.7 Insulin and IGF-1 Assays

GENERAL CONSIDERATIONS

Methods for the quantitation the determination of plasma concentrations of insulin, IGF-I and the IGF binding proteins (not considered here in detail) have been developed based on diverse analytical principles such as radioimmunoassay, enzyme-linked assays, chemiluminescence assays and other principles. Their particular application is to the measurement of concentration changes of insulin, IGF-I and binding proteins during repeated dose treatment of animals, and of course the main application in clinical chemistry is to the evaluation of type 2 diabetes, and growth disorders in children.

PURPOSE AND RATIONALE

The main purpose is to establish a relation of pharmacokinetics and pharmacodynamics, namely in states of insulin resistance (increased insulin concentrations) and during the treatment of diabetes (from decompensation before treatment to established glycemic control).

MODIFICATIONS OF THE METHOD

Specific methods for determination have been established for insulin analogs, for example aspart insulin (Andresen et al. 2000), lispro insulin (Bowsher et al. 1999; Cao et al. 2001), and some of these assays are available commercially (e. g., Linco assay for lispro insulin). For other insulin analogs, methods have been adapted for pharmacokinetic determination (e. g., Mudaliar et al. 2000;Kuerzel et al. 2003 for insulin glargine). There are many sensitive assays for animal insulins and for human insulin, which can be adapted for animal experimentation (Temple et al. 1992; Clark and Hales 1994), the insulin assays have been particularly useful in establishing physiological and pathological secretory patterns (Polonsky et al. 1988a, 1988b). Many of the studies have been extended and supplemented by the measurement of human or animal C-peptide in order to assess endogenous insulin production, and suppression of endogenous insulin during treatment (Ashby and Frier 1981; Bonser and Garcia-Webb 1981; Tillil et al. 1988). Measurement of excretion of C-peptide in the urine is also a helpful method of evaluating secretion rates.

Concerning the methods for determination of IGF-1, many methods were developed for pediatric applications and subsequently their use has been extended to other questions (Teale and Marks 1986; Quarmby et al. 1988; Tchao et al. 1995; Moses et al. 1996; Frystyk et al. 1999; Juul 2003; Elmlinger et al. 2004, 2005; Khosravi et al. 2005; Yakar et al. 2005). Methods for the determination of IGF binding proteins have been reviewed (Rutanen and Pekonen 1991), and several options are now available. In this context, the classical assays for IGF-I activity also need to be mentioned but no longer have practical relevance for the evaluation of the effects of insulin analogs (Zapf 1998).

In the context of measuring circulating concentrations, it may also be helpful to measure of the adaptation of receptor concentrations in tissues by using the appropriate insulin and IGF receptor assays *ex vivo* (Pedersen 1983; Taylor 1984; Johansson and Arnquist 2006).

CRITICAL ASSESSMENT OF THE METHOD

Selection of the appropriate methods for the measurement of insulin, C-peptide, IGF-I and IGF binding proteins is facilitated by a number of options, based on laboratory developed methods and an increasing number of commercially available assays which have been extensively validated.

REFERENCES AND FURTHER READING

Andersen L, Jorgensen PN, Jensen LB, Walsh D (2000) A new insulin immunoassay specific for the rapid-acting insulin analog, insulin aspart, suitable for bioavailability, bioequivalence, and pharmacokinetic studies. Clin Biochem 33(8):627–633

Ashby JP, Frier BM (1981) Circulating C peptide: measurement and clinical application. Ann Clin Biochem 18(Pt 3):125–130

Blum WF, Breier BH (1994) Radioimmunoassays for IGFs and IGFBPs. Growth Regul 4 [Suppl 1]:11–19

Bonser AM, Garcia-Webb P (1981) C-peptide measurement and its clinical usefulness: a review. Ann Clin Biochem 18(Pt 4):200–206

Bowsher RR, Lynch RA, Brown-Augsburger P, Santa PF, Legan WE, Woodworth JR, Chance RE (1999) Sensitive RIA for the specific determination of insulin lispro. Clin Chem 45(1):104–110

Cao Y, Smith WC, Bowsher RR (2001) A sensitive chemiluminescent enzyme immunoassay for the bioanalysis of carboxyl-terminal B-chain analogs of human insulin. J Pharm Biomed Anal 26(1):53–61

Clark PM, Hales CN (1994) How to measure plasma insulin. Diabetes Metab Rev 10(2):79–90

Elmlinger MW, Kuhnel W, Weber MM, Ranke MB (2004) Reference ranges for two automated chemiluminescent assays for serum insulin-like growth factor I (IGF-I) and IGF-binding protein 3 (IGFBP-3). Clin Chem Lab Med42(6):654–664

Elmlinger MW, Zwirner M, Kuhnel W (2005) Stability of insulin-like growth factor (IGF)-I and IGF binding protein (IGFBP)-3 measured by the IMMULITE automated chemiluminescence assay system in different blood specimens. Clin Lab 51(3–4):145–152

Froesch ER, Hussain MA, Schmid C, Zapf J (1996) Insulin-like growth factor I: physiology, metabolic effects and clinical uses. Diabetes Metab Rev 12(3):195–215

Frystyk J, Skjaerbaek C, Vestbo E, Fisker S, Orskov H (1999) Circulating levels of free insulin-like growth factors in obese subjects: the impact of type 2 diabetes. Diabetes Metab Res Rev 15(5):314–322

Hill DJ, Milner RD.(1985) Insulin as a growth factor. Pediatr Res 19(9):879–886

Khosravi J, Anastasia D, Umesh B, Najmuddin K, Radha GK (2005) Pitfalls of immunoassay and sample for IGF-I: comparison of different assay methodologies using various fresh and stored serum samples. Clin Biochem 38/7:659–666

Johansson GS, Arnqvist HJ (2006) Insulin and IGF-I action on insulin receptors, IGF-I receptors, and hybrid insulin/IGF-I receptors in vascular smooth muscle cells. Am J Physiol 291(5):E1124–1130 [Epub 2006 Jun 27]

Juul A (2003) Serum levels of insulin-like growth factor I and its binding proteins in health and disease. Growth Horm IGF Res 13:113

Kuerzel GU, Shukla U, Scholtz HE, Pretorius SG, Wessels DH, Venter C, Potgieter MA, Lang AM, Koose T, Bernhardt E (2003) Biotransformation of insulin glargine after subcutaneous injection in healthy subjects. Curr Med Res Opin 19(1):34–40

Lassarre C, Duron F, Binoux M (2001) Use of the ligand immunofunctional assay for human insulin-like growth factor (IGF) binding protein-3 (IGFBP-3) to analyze IGFBP-3 proteolysis and IGF-I bioavailability in healthy adults, GH-deficient and acromegalic patients, and diabetics. J Clin Endocrinol Metab 86(5):1942–1952

Moses AC, Young SC, Morrow LA et al (1996) Recombinant human insulin-like growth factor I increases insulin sensitivity and improves glycemic control in type II diabetes. Diabetes 45:91

Mudaliar S, Mohideen P, Deutsch R, Ciaraldi TP, Armstrong D, Kim B, Sha X, Henry RR (2002) Intravenous glargine and regular insulin have similar effects on endogenous glucose output and peripheral activation/deactivation kinetic profiles. Diabetes Care 25(9):1597–1602

Pedersen O (1983) Insulin receptor assays used in human studies: merits and limitations. Diabetes Care 6(3):301–319

Polonsky KS, Given BD, Hirsch LJ, Tillil H, Shapiro ET, Beebe C, Frank BH, Galloway JA, Van Cauter E (1988a) Abnormal patterns of insulin secretion in non-insulin-dependent diabetes mellitus. N Engl J Med 318(19):1231–1239

Polonsky KS, Given BD, Van Cauter E (1988b) Twenty-four-hour profiles and pulsatile patterns of insulin secretion in normal and obese subjects. J Clin Invest 81(2):442–448

Quarmby V, Quan C, Ling V, Compton P, Canova-Davis E (1998) How much insulin-like growth factor I (IGF-I) circulates? Impact of standardization on IGF-I assay accuracy. J Clin Endocrinol Metab 83:1211–1216

Rutanen EM, Pekonen F (1991) Assays for IGF binding proteins. Acta Endocrinol (Copenh) 124 [Suppl 2]:70–73

Taylor R (1984) Insulin receptor assays – clinical application and limitations (2). Diabet Med 1(3):181–188

Tchao A, Wong A, Bondy G (1995) Technical and clinical validation of a serum IGF-1 assay. Clin Biochem 28:331–331

Teale JD, Marks V (1986) The measurement of insulin-like growth factor I: clinical applications and significance. Ann Clin Biochem 23 (Pt 4):413–424
Temple R, Clark PM, Hales CN (1992) Measurement of insulin secretion in type 2 diabetes: problems and pitfalls. Diabet Med 9(6):503–512
Tillil H, Shapiro ET, Given BD, Rue P, Rubenstein AH, Galloway JA, Polonsky KS (1988) Reevaluation of urine C-peptide as measure of insulin secretion. Diabetes 37(9):1195–1201
Yakar S, LeRoith D, Brodt P (2005) The role of the growth hormone/insulin-like growth factor axis in tumor growth and progression: lessons from animal models. Cytokine Growth Factor Rev 16:407–420
Zapf-J (1998) Growth promotion by insulin-like growth factor I in hypophysectomized and diabetic rats. Mol Cell Endocrinol 140(1–2):143–149

K.9.8 Assessment of Metabolic-Mitogenic Ratio In Vitro

GENERAL CONSIDERATIONS

When structure activity studies are performed with insulin analogs, it is useful to determine the relative contributions of the hypoglycemic activity (metabolic), and the proliferative activity (mitogenic). Both activities are intrinsic to the insulin molecule, it is important to realise that they are activated at vastly different concentrations in vitro, and that the wide concentration range for testing is permissible in such studies. The metabolic-mitogenic ratio needs to be supplemented by data on the receptor association/dissociation, because experimental evidence for the [B10-Asp] insulin with enhanced mitogenic activity and causing tumor stimulation in rodent toxicology studies indicates that prolonged residence time and decreased rate of dissociation from the insulin receptor may be the critical factor. As a consequence, this information is critical a required for a new insulin analogs. When additional information about enhanced affinity for the IGF-I receptor is obtained, mitogenicity may be tested by methods described here in K9.6 and needs to be followed up by studies on mammary epithelial cells, when available also on other benign and malignant tissue derived cell lines, and ultimately by assessment of carcinogenic potential in animals.

REFERENCES AND FURTHER READING

EMEA (European Agency for the Evaluation of Medical Products) (2001) Points to consider document on the nonclinical assessment of the carcinogenic potential of insulin analogs. European Agency for the Evaluation of Medicinal Products

K.9.9 Assessment of Hypoglycemic Activity In Vivo

GENERAL CONSIDERATIONS

Methods for the assay of hypoglycemic activity in animals are reviewed in section K.3 and will be discussed here only with reference to the application and structure activity studies with insulin analogs. For the two classes of insulin analogs of clinical interest, a different experimental design is needed.

Tests by intravenous injection indicate the intrinsic activity, human insulin may be used as the comparator (Lin et al. 1999).

The time-action profiles of fast acting insulins are tested by subcutaneous injection in rats, rabbits or dogs, with regular human insulin as the reference preparation. The drug concentration of test insulin and reference human insulin needs to be identical, for meaningful comparisons. When dilution is a compared, they should have the same insulin concentration. The preferred test is by using the under eluted insulin analog at the concentration equivalent to U-100. The test interval depends on the insulin dose selected, for fast acting insulins test periods of four to six hours are considered sufficient.

The time-action profiles of long acting insulin analogs are tested by subcutaneous injection preferably in dogs or pigs, as a preliminary procedure they may also be tested in rabbits. Human NPH insulin is used as the comparator. The preferred test concentrations are those equivalent to U-100 insulin. The zinc content of formulations is often of interest and will be tested at increasing zinc content, keeping the insulin drug concentration constant.

PURPOSE AND RATIONALE

The biological activity predicted by in vitro studies needs to be confirmed in animals, there may be considerable differences between the in vitro result and the *in vivo* activity due to the pharmacokinetics of the selected drug candidate. The first stage is always testing by intravenous injection to enable immediate contact with the insulin receptor.

K.9.9.1 Depot Activity of Insulin Analogs in Rabbits

PROCEDURE

This test by subcutaneous injection is suitable for the evaluation of depot activity of long acting insulins and insulin depot preparations. Adult male rabbits body weight 2,5–3,5 kg are suitable for the test, the animals

may be used repeatedly when treatment free intervals of at least two weeks (recovery periods) are inserted after each treatment day. In each group, eight to 10 Rabbits are treated on the test day. Insulin analogs and insulin depot preparations are compared for reference. The insulin analogs (long acting) or depot preparations of human insulin as reference compounds (NPH insulin) are injected subcutaneously for example at a dose 0.3 IU/kg by microliter syringes, using the undiluted original concentration (straight concentrations) equivalent to U-100 insulin.

Blood samples for glucose determination are obtained from an ear vein immediately before treatment, and then hourly up to 8 hours after subcutaneous injection. The blood glucose may be determined by enzymatic assay, for example in 10 µl of native blood using a commercial test kit.

Evaluation of blood glucose data is was performed descriptively and by explorative statistics.For descriptive evaluation of time-action blood glucose profiles (time point and extent of maximum decrease, centroid time, duration/maximal decrease ratio and total area of blood glucose decrease are used.

In this experimental design, the concentration of the insulins and the composition may be varied, for example by changing the zinc content. To test statistically for dependency on insulin concentration or zinc content of the formulation, the drug concentration-dependency and/or the zinc concentration-dependency of two or more groups is compared using exact one-sided Wilcoxon tests (Hollander and Wolfe 1973, Streitberg and Röhmel 1987).

The test parameters are total peak area and ratio of duration to maximal decrease, accepting an increase within each of these parameters as the relevant test direction for increasing concentrations of drug (insulin) or zinc content (formulation). Each test is performed separately at a significance level of 5 %.

REFERENCES AND FURTHER READING

Hollander M, Wolfe DA (1973) Nonparametric statistical methods; Wiley Series in Probability and Mathematical Statistics; John Wiley & Sons, Inc., New York

Streitberg B, Röhmel J (1987) Exakte Verteilung für Rang- und Randomisierungstests im allgemeinen Stichprobenproblem; EDV in Medizin und Biologie 18; pp 12–19: Verlag Eugen Ulmer GmbH & Co., Stuttgart; Gustav Fisher Verlag KG, Stuttgart

MODIFICATIONS OF THE METHOD

The principal modifications of this method are the selection of insulin concentrations to be tested. It is established that depot activity depends on local concentration at the injection site, therefore it is advisable to inject smaller volumes by microsyringe, rather than use dilution is of the original concentration to be evaluated.

CRITICAL ASSESSMENT OF THE METHOD

Testing of depot activity in rabbits is an earlier option, but not as trustworthy as extended testing for depot activity in dogs or pigs.

K.9.9.2 Depot Activity of Insulin Analogs in Fasted Dogs

GENERAL CONSIDERATIONS

The time action profile of long acting insulin analogs after subcutaneous injection varies considerably depending on the species used for testing. In general, proof of depot activity cannot be obtained in mice and rats, is difficult to obtain in rabbits unless high dose is a tested, and is readily obtained by testing in in dogs or pigs.

PURPOSE AND RATIONALE

The test procedure in dogs is based on experience with human NPH insulin and with insulin zinc suspensions (intermediate acting insulins). It has shown to be very reliable in the preclinical evaluation of insulin glargine (Seipke et al. 2000),

PROCEDURE

Adult male beagle dogs are used for this study, feed is withheld for 17 hours. Groups of dogs (six to 10 animals) are treated with the insulin to be tested for depot activity. Human regular insulin (soluble) and/or human NPH insulin are used as the reference compounds. Tests may be performed sequentially, in parallel or by cross over. Insulin preparations are injected subcutaneously at the flank of the animal, alternating between the right and left flank. Blood samples for glucose determination are obtained by leg vein puncture, immediately before treatemnt and hourly up to 10 hours after treatment, additional samples may be obtained 12, 14 and 16 hours after administration,. Blood glucose iss determined enzymatically, for example in 10 µl native blood using the Glucoquant test kit (Boehringer Mannheim) with the EPOS Analyzer 5060 (Eppendorf). For evaluation of the glucose data, means and standard error of the mean at each measuring point of the raw data [or using data converted to percent of the initial values] were used for tabular and/ or graphical representation of the time response curves.

For statistical evaluation of the depot activity, centroid times are calculated and, for evaluation of the blood glucose decreasing activity, the area of blood glucose decrease for each group is calculated. In both cases, a two-way ANOVA is performed at a significance level of 5%.

The mean blood glucose decrease was calculated by the trapezoidal rule and the centroid time (C_t) by

$$C_t = \frac{\sum_{i=1}^{n}(T_i * F_i)}{\sum_{i=1}^{n} F_i} \quad \text{where} \quad T_i = \frac{t_{i+1} + t_i}{2} \quad \text{and}$$

$$F_i = \frac{(t_{i+1} - t_i)(c_{i+1} - c_i)}{2}$$

t_i = times of measurement (i = 1,...,n),
c_0 = base line glucose concentration and
c_i = glucose concentration at measurement time t_i.

Calculation of the centroid time and of the areas of blood glucose decrease is performed with the raw data. The point of onset and endpoint of the blood glucose decrease are defined by intersection of the blood glucose curve with the baseline in the descending or ascending phase, respectively.

REFERENCES AND FURTHER READING

Holm S (1979) A simple sequentially rejective multiple test procedure. Scandinavian J Stat 6:65–70

Lin FO, Hasemann JK (1975) A modified Jonckeere test against ordered alternatives when ties are present at a single extreme value. National Institute of Environmental Health Sciences, North Carolina Environmental Biometric Branch

Lin S, Wang SY, Chen EC, Chien YW (1999) Insulin lispro: invivo potency determination by intravenous administration in conscious rabbits. J Pharm Pharmacol 51(3):301–6

Seipke G, Sandow J, Geisen K, Stammberger I (2000) Preclinical Profile of the New Long-Acting Insulin Glargine (HOE 901). Endocrine Society Annual Meeting 2000, Toronto, Canada, Poster #83

K.9.10 Mitogenic Risk and Safety Evaluation In Vivo

GENERAL CONSIDERATIONS

An intense discussion was raised by the findings that one fast acting insulin analog [B10-Asp] insulin showed unexpected toxicity on proliferation and tumor development of rat mammary glands. This finding was attributed tentatively to mitogenic signaling via the insulin receptor, and/or mitogenic signaling via the IGF-I receptor, based on the finding that on the insulin receptor residence time was prolonged and the rate of dissociation was much lower than found with human insulin, and that affinity for the IGF-I receptor was enhanced. This compound has therefore become the reference standard for the assessment of enhanced mitogenicity and its effect in toxicology. The preclinical evaluation of insulin analogs for the risk of enhanced mitogenicity therefore includes determination of the metabolic and mitogenic in vitro characteristics, by affinity for the insulin receptor and rate of association/dissociation, affinity for the IGF-I receptor, evaluation of enhanced mitogenic signaling e. g. by thymidine incorporation into proliferating cells, and details of signaling via the insulin receptor and IGF-I receptor (e. g. tyrosin phosphorylation, phosphorylation of receptor substrates).

REFERENCES AND FURTHER READING

Stammberger I, Bube A, Durchfeld-Meyer B, Donaubauer H, Troschau G (2002) Evaluation of the Carcinogenic Potential of Insulin Glargine in Rats and Mice. Int J Toxicol 21(3):171–179

Stammberger I, Seipke G, Bartels T (2006) Insulin glulisine—a comprehensive preclinical evaluation. Int J Toxicol 25(1):25–33

Staiger K, Hennige AM, Schweitzer MA, Staiger H, Haering HU, Monika Kellerer M (2005) Effect of Insulin Glargine Versus Regular Human Insulin on Proliferation of Human Breast Epithelial Cells. ADA Annual Symposium San Diego Abstract 451-P

Zib I, Raskin P (2006) Novel insulin analogs and its mitogenic potential. Diabetes Obes Metab 8(6):611–20

Milazzo G, Sciacca L, Papa V, Goldfine ID, Vigneri R (1997) ASPB10 insulin induction of increased mitogenic responses and phenotypic changes in human breast epithelial cells: evidence for enhanced interactions with the insulin-like growth factor-I receptor. Mol Carcinog 18(1):19–25

Leroith D, Baserga R, Helman L, Roberts CT (1995) Insulin-like growth-factors and cancer. Ann Intern Med 122:54–59

Kellerer M, Haering HU (2001) Insulin analogs: impact of cell model characteristics on results and conclusions regarding mitogenic properties. Exp Clin Endocrinol Diabetes 109:63–64

Hennige AM, Kellerer M, Strack V, Metzinger E, Seipke G, Haring HU (1999) New human insulin analogs: Characteristics of insulin signalling in comparison to ASP (B10) and regular insulin. Diabetologia 42:A178 (Abstract 665)

EPAR EMEA Novorapid (2004) Document 272799en6 aspart, scientific discussion in the public assessment report for Novorapid (insulin aspart NN) http://www.emea.europa.eu/humandocs/Humans/EPAR/novorapid

EPAR EMEA Lantus (2006) Document 061500en6 glargine, scientific discussion in the public assessment report for Lantus (insulin glargine INN) http://www.emea.europa.eu/humandocs/Humans/EPAR/lantus

EPAR EMEA Humalog (2006) Document 060195en6 lispro, scientific discussion in the public assessment report for Humalog (insulin lispro INN) http://www.emea.europa.eu/humandocs/Humans/EPAR/humalog

EPAR EMEA Levemir (2006) Document 093604en6 detemir, scientific discussion in the public assessment report for Levemir (insulin detemir INN) http://www.emea.europa.eu/humandocs/Humans/EPAR/levemir

Chapter L
Anti-obesity Activity[1]

[1] Reviewed by M. Bickel, contributions by A.W. Herling

L.1 Methods to Induce Experimental Obesity

L.1.0.1 General Considerations

Influence of the central nervous system, in particular of the hypothalamus, on development of obesity has been suspected since the early clinical observations of Babinski (1900) and Fröhlich (1901), Biedl 1916). Experiments reported by Smith (1927, 1930) showed that injections of chromic acid into the suprasellular region of rats with lesion of the hypothalamus induced obesity in rats (Bomskov 1939). Hetherington and Ranson (1939) found that electrolytic lesions, restricted to the ventromedial region of the hypothalamus, could be associated with the development of obesity.

A virally induced obesity syndrome in mice was described by Lyons et al. (1982).

Chan (1995) gave a review on β-cell stimulus-secretion coupling defects in rodent models of obesity.

Leiter and Herberg (1997) reviewed the advances in understanding the molecular bases for monogenic obe-

sity mutations capable of producing obesity-induced diabetes, or diabesity in mice.

Astrup and Lundsgaard (1998) discussed pharmacological mechanisms of anti-obesity drugs.

REFERENCES AND FURTHER READING

Astrup A, Lundsgaard C (1998) What do pharmacological approaches to obesity management offer? Linking pharmacological mechanisms of obesity management agents to clinic practice. Exp Clin Endocrinol Diabetes 106, Suppl 2:29–34

Babinski MJ (1900) Tumeur de corps pituitaire sans acromegalie et avec manquer de developpement des organes genitaux. Rev Neurol 8:531–533

Biedl A (1916) Innere Sekretion. Ihre physiologischen Grundlagen und ihre Bedeutung für die Pathologie. Zweiter Teil. Urban und Schwarzenberg, Berlin/Wien, pp 173–179

Bomskov C (1939) Methodik der Hormonforschung, Zweiter Band, Georg Thieme Verlag Leipzig, pp 614–615

Bray G, York DA (1979) Hypothalamic and genetic obesity in experimental animals: an autonomic and endocrine hypothesis. Physiol Rev 59:719–809

Chan CB (1995) β-Cell stimulus-secretion coupling defects in rodent models of obesity. Can J Physiol Pharmacol 73:1414–1424

Fröhlich A (1901) Ein Fall von Tumor der Hypophysis cerebri ohne Akromegalie. Wien Klin Rundsch 15:883–886

Hetherington AW, Ranson SW (1939) Experimental hypothalamico-hypophyseal obesity in the rat. Proc Soc Exp Biol Med 41:465–466

Leiter EH, Herberg (1997) The polygenetics of diabesity in mice. Diabetes Rev 5:131–148

Lyons MJ, Faust IM, Hemmes RB, Buskirk DR, Hirsch J, Zabriskie JB (1982) A virally induced obesity syndrome in mice. Science 216:82–85

Scalfani A (1984) Animal models of obesity: classification and characterization. Int J Obesity 8:491–508

Smith PE (1927) The disabilities caused by hypophysectomy and their repair. The tuberal (hypothalamic) syndrome in the rat. J Amer Med Assoc 88:158–161

Smith (1930) Amer J Anat 45:265

L.1.0.2 Food-Induced Obesity

PURPOSE AND RATIONALE

Obesity can be induced in rats by offering a diet containing corn oil and condensed milk.

PROCEDURE

Male Sprague Dawley rats are housed in individual wire-bottom suspended cages in rooms maintained at 22–23°C with 12 h light-dark cycles. At the age of 6 months (body weight about 450 g) the animals are divided in 2 groups: group I is fed ordinary Purina Rodent Chow, group II a special diet containing Purina Rodent Chow, corn oil and condensed milk, resulting in a composition of 14.7% protein, 44.2% carbohydrate, 15.8% lipid, 2.5% fiber, 1.2% vitamin mixture, and 19% water. Body weight and food intakes are measured, and diet replaced, every 3 to 4 days.

Three months from the start of the experiment, the rats are sacrificed by decapitation for determination of adipose tissue cell size and number, carcass composition and plasma lipids, and hormone and glucose levels.

The dorsal subcutaneous (inguinal) pad, the retroperitoneal pad, and one epididymal fat pad are sampled for determination of lipid content by the method of Folch et al. (1957). The method consists of homogenizing the tissue with a 2:1 chloroform-methanol mixture and washing the extract by addition to it of 0.2 its volume of water. The resulting mixture separates into two phases. The lower phase is the total pure lipid extract. Cell number in each pad is determined by the osmium fixation method of Hirsch and Gallian (1968) using a Coulter counter. Total epididymal pad weights are based on doubling the weight of the individual pads sampled.

EVALUATION

Intergroup comparisons are made with the use of a two-tailed Student's *t*-test.

MODIFICATIONS OF THE METHOD

Scalfani and Springer (1976) induced obesity in adult female rats by adding a variety of supermarket foods to lab chow (**"cafeteria diet"**). In behavioral tests, the authors found similarities to hypothalamic and human obesity syndromes.

Rothwell et al. (1982) compared the effects of feeding a cafeteria diet on energy balance and diet-induced thermogenesis in four strains of rats.

Stock and Rothwell (1979) discussed the influence of various forms of feeding, high-fat diets, insulin injections, tube-feeding, and cafeteria feeding on energy balance in laboratory animals.

Rolls et al. (1980) found persistent obesity in rats following a period of consumption of a mixed, high energy diet. When the high energy foods were withdrawn after 90 days and just chow was available, the obese rats maintained their elevated body weights.

Hill et al. (1992) studied the influence of amount and composition of dietary fat on development of obesity in rats. Adult male Wistar rats were fed high fat (HF; 60% of calories) or low fat (LF; 20% of calories) diets for 28 weeks. Half of the rats in each condition received diets with saturated fat (lard) or with polyunsaturated fat (corn oil). There was some indication that unsaturated fat diets were associated with greater ac-

cumulation of fat in subcutaneous tissue depots than saturated fat diets. The effects of the type of fat were less than those of the amount of dietary fat.

Wade and Gray (1979) reviewed the gonadal effects on food intake and adiposity in rats. Estradiol and testosterone decrease adiposity, while progesterone increases carcass fat content.

Thermogenesis induced by various diets has been discussed by Rothwell and Stock (1986).

Harris (1993) studied the impact of high- or low-fat cafeteria foods on nutrient intake and growth of rats consuming a diet containing 30% energy as fat.

Segues et al. (1994) studied long-term effects of cafeteria diet feeding on young female Wistar rats by comparing the circulating levels of glucose, lactate, glycerol, 3-hydroxybutyrate and urea, and liver glycogen.

Llado et al. (1997) studied fatty acid composition of brown adipose tissue in dietary obese rats. Long time exposure to a hypercaloric high-fat diet such as the cafeteria diet induced an important fatty acid accumulation in brown adipose tissue, mainly for the major saturated and monounsaturated fatty acids.

LeBlanc and Labrie (1997) investigated the role of palatability of the food in diet-induced thermogenesis.

Selective breeding for diet-induced obesity and resistance in Sprague-Dawley rats was reported by Levin et al. (1997).

Herberg et al. (1974) reported the effects of either a high-carbohydrate diet or a high-fat diet over prolonged periods in metabolically intact and in obese NZO **mice**.

West et al. (1992) evaluated the effects of a 7 week consumption of a diet containing 32.6% of kilocalories as fat (condensed milk) on body composition and energy intake in nine strains of inbred mice. Relative to Chow diet controls, the condensed milk diet significantly increased carcass lipid content in six strains (AKR/J, C57L/J, A/J, C3H/HeJ, DBA/2J, and C57BL/6J), but had no or a marginal effect on adiposity in 3 strains of mice (SJL/J, I/STN, and SWR/J).

West et al. (1994) studied the genetics of dietary obesity in AKR/J x RWR/J mice. Pups were weaned between the ages of 29 and 34 days onto Purina Chow ad libitum until they were switched to a high fat, condensed milk diet containing 32.6%, 15.0%, and 52.4% of kilocalories as fat, protein, and carbohydrate, respectively.

Strain-specific response to β_3-adrenergic receptor agonist treatment of diet-induced obesity in mice was reported by Collins et al. (1997).

REFERENCES AND FURTHER READING

Collins S, Daniel KW, Petro AE, Surwit RS (1997) Strain-specific response to β_3-adrenergic receptor agonist treatment of diet-induced obesity in mice. Endocrinology 138:405–413

Folch J, Lees M, Sloane-Stanley GH (1957) A simple method for the isolation and purification of total lipids from animal tissue. J Biol Chem 226:497–509

Foster DO, Ma SWY (1989) The effector of diet-induced thermogenesis: brown adipose tissue or liver? In: Lardy H, Stratman F (eds) Hormones, Thermogenesis and Obesity. Elsevier, New York, pp 165–171

Harris RB (1993) The impact of high- or low-fat cafeteria foods on nutrient intake and growth of rats consuming a diet containing 30% energy as fat. Int J Obes 17:307–315

Herberg L, Döppen W, Major E, Gries FA (1974) Dietary-induced hypertrophic-hyperplastic obesity in mice. J Lipid Res 15:580–585

Hill JO, Lin D, Yakubu F, Peters JC (1992) Development of dietary obesity in rats: influence of amount and composition of dietary fat. Int J Obes 16:321–333

Hirsch J, Gallian E (1968) Methods for determination of adipose cell size in man and animals. J Lipid Res 9:110–119

LeBlanc J, Labrie A (1997) A possible role for palatability of the food in diet-induced thermogenesis. Int J Obes 21:1100–1103

Llado I, Pons A, Palou A (1997) Fatty acid composition of brown adipose tissue in dietary obese rats. Biochem Mol Biol Int 43:1129–1136

Levin BE, Dunn-Meynell AA, Balkan B, Keesey R (1997) Selective breeding for diet-induced obesity and resistance in Sprague-Dawley rats. Am J Physiol (Regul Integr Comp Physiol) 273:R725–R730

Mayer J (1953) Genetic, traumatic and environmental factors in the etiology of obesity. Physiol Rev 33:472–508

Rolls BJ, Rowe RA, Turner RC (1980) Persistent obesity in rats following a period of consumption of a mixed, high energy diet. J Physiol 298:415–427

Rothwell NJ, Stock MJ (1986) Brown adipose tissue and diet-induced thermogenesis. In: Trayhurn P, Nicholls DG (eds) Brown Adipose Tissue. Edward Arnold, Ltd., London, pp 269–298

Rothwell NJ, Saville ME, Stock MJ (1982) Effects of feeding a "cafeteria" diet on energy balance and diet-induced thermogenesis in four strains of rats. J Nutr 112:1515–1524

Salmon DMV, Flatt JP (1985) Effect of dietary fat content on the incidence of obesity among ad libitum fed mice. Int J Obes 9:443–449

Scalfani A, Springer D (1976) Dietary obesity in adult rats: similarities to hypothalamic and human obesity syndromes. Physiol Behav 17:461–471

Segues T, Salvado J, Arola L, Alemany M (1994) Long-term effects of cafeteria diet feeding on young Wistar rats. Biochem Mol Biol Int 33:321–328

Stock MJ, Rothwell NJ (1979) Energy balance in reversible obesity. In: Festing MFW (ed) Animal Model of Obesity. MacMillan Press Ltd., pp 141–151

Tiscari J, Nauss-Karol C, Levin BE, Sullivan AC (1985) Changes in lipid metabolism in diet-induced obesity. Metabolism 34:580–587

Wade GN, Gray JM (1979) Gonadal effects on food intake and adiposity: a metabolic hypothesis. Physiol Behav 22:583–593

West DB, Boozer CN, Moody DL, Atkinson RL (1992) Dietary obesity in nine inbred mouse strains. Am J Physiol 262:R1025–R1032

West DB, Waguespack J, York B, Goudey-Lefevre J, Price RA (1994) Genetics of dietary obesity in AKR/J x RWR/J mice: segregation of the trait and identification of a linked locus on chromosome 4. Mammalian Genome 5:546–552

L.1.0.3 Hypothalamic Obesity

PURPOSE AND RATIONALE

Hyperphagia in rats has been reported after hypothalamic lesions (Liu and Yin 1974). Surgical techniques were described by Leibowitz et al. (1981), Vander Tuig et al. (1985).

PROCEDURE

Female Sprague Dawley rats, weighing about 190 g body weight, receive during a 5–9 days initial period of adjustment a high-fat diet. They are then fasted overnight, anesthetized with 35 mg/kg pentobarbital sodium and additionally 1 mg atropine methyl nitrate intraperitoneally. Bilateral wire knife cuts or electrolytic lesions are sterotaxically positioned in the hypothalamus (David Kopf Instruments, CA). With the incision bar positioned at –3.0 mm, parasagittal wire knife cuts are placed between the medial and lateral hypothalamus using a retractable wire knife according to Gold et al. (1973). The cuts are made 1.0 mm lateral to the midline and extended from 8.5 to 5.5 mm anterior to the ear bars and from the base of the brain dorsally 3.0 mm.

To produce electrolytic lesions in the ventromedial hypothalamus, the incision bar is positioned at +5.0 mm and a stainless steel electrode, insulated except for 0.5 mm at the tip, is lowered 0.6 mm lateral to the midline and 5.8 mm anterior to the ear bars. With the tip of the electrode 0.7 mm above the base of the brain, lesions are made by passing 2.0 mA of anodal current for 20 s to a rectal electrode.

Sham-operated rats serve as controls. Separate rats that are fasted overnight are killed at the time of surgery to provide data on initial body composition.

Histological verification of placement of knife cuts and lesions is made in brains fixed in 10% buffered formaldehyde solution and embedded in paraffin. Serial sections through the hypothalamic area of the brain are examined histologically.

EVALUATION

Not only food consumption and increase of body weight can be determined after hypothalamic lesions, but also brown adipose tissue enzymes and guanosine diphosphate binding to brown adipose tissue mitochondria and noradrenaline turnover in various organs.

MODIFICATIONS OF THE METHOD

A survey on hypothalamic and genetic obesity in experimental animals was given by Bray and York (1979).

Caloric compensation to gastric loads in rats with hypothalamic hyperphagia was reported by Liu and Yin (1974).

Sclafani and Aravich (1983) adapted adult female Sprague Dawley rats to a macronutrient self-selection regimen which allowed them ad libitum access to separate sources of protein, carbohydrate, and fat. The rats were then given either ventromedial hypothalamic lesions, paraventricular hypothalamic lesions, parasagittal knife cuts through medial hypothalamus or sham lesions. Following surgery, all lesioned rats overate and became obese as compared to sham operated controls. The group with parasagittal knife cuts through medial hypothalamus gained more weight than the groups with ventromedial hypothalamic lesions and paraventricular hypothalamic lesions.

Enhanced expression of rat obese (ob) gene in adipose tissue of ventromedial hypothalamus (VMH)-lesioned rats was described by Funahashi et al. (1995).

Elmquist et al. (1999) discussed the role of leptin and other peptide hormones in different areas of the hypothalamus in controlling food intake and body weight.

REFERENCES AND FURTHER READING

Bray GA, York DA (1979) Hypothalamic and genetic obesity in experimental animals: An autonomic and endocrine hypothesis. Physiol Rev 59:719–809

Elmquist JK, Elias CF, Saper CB (1999) From lesions to leptin: Hypothalamic control of food intake and body weight. Neuron 22:221–232

Funahashi T, Shimomura I, Hiraoka H, Arai T, Takahashi M, Nakamura T, Nokazi S, Yamashita S, Takemura K, Tokonuga K, Matsusawa Y (1995) Enhanced expression of rat obese (ob) gene in adipose tissue of ventromedial hypothalamus (VMH)-lesioned rats. Biochem Biophys Res Commun 211:469–475

Gold RM, Kapatos G, Carey RJ (1973) A retracting wire knife for stereotaxic brain surgery made from a microliter syringe. Physiol Behav 10:813–815

Himms-Hagen J, Tokuyama K, Eley J, Park IRA, Cui J, Zaror-Behrens G, Coscina DV (1989) Hypothalamic regulation of brown adipose tissue in lean and obese rodents. In: Lardy H, Stratman F (eds) Hormones, Thermogenesis and Obesity. Elsevier, New York, pp 173–184

Leibowitz SF, Hammer NJ, Chang K (1981) Hypothalamic paraventricular nucleus lesions produce overeating and obesity in the rat. Physiol Behav 27:1031–1040

Liu CM, Yin TH (1974) Caloric compensation to gastric loads in rats with hypothalamic hyperphagia. Physiol Behav 13:231–238

Sclafani A, Aravich PF (1983) Macronutrient self-selection in three forms of hypothalamic obesity. Am J Physiol (Regul Integr Comp Physiol 13):R686–694

Vander Tuig, Kerner J, Romsos DR (1985) Hypothalamic obesity, brown adipose tissue, and sympathoadrenal activity in rats. Am J Physiol 248 (Endocrinol Metab 11):E607–E617

L.1.0.4 Goldthioglucose-Induced Obesity

PURPOSE AND RATIONALE

Intraperitoneal or intramuscular injection of goldthioglucose induces obesity in mice. The effect is related to destruction of hypothalamic and extrahypothalamic areas of the brain (Perry and Liebelt 1961).

PROCEDURE

Swiss albino mice of either sex are fed with commercial mouse chow (Altromin R) ad libitum. At the age of 6 weeks, the animals receive a single intraperitoneal injection of 30–40 mg/kg goldthioglucose.

EVALUATION

Food intake is registered for 2 weeks and body weight for a period of 3 months and compared with untreated controls.

MODIFICATIONS OF THE METHOD

Debons et al. (1962, 1968, 1977) administered 800 mg/kg goldthioglucose by a single intraperitoneal injection to female CBA mice.

Obesity was induced in rats by implants of goldthioglucose in the hypothalamus (Smith and Britt 1971; Smith 1972).

Several other compounds produce obesity concomitantly with brain lesions.

Single intraperitoneal injection of bipiperidyl mustard (N,N′-bis-[β-chloroethyl]-4,4′-bipiperidine) in doses between 5 to 50 mg/kg induced obesity in mice (Rutman et al. 1966). Brain lesions and obesity by bipiperidyl mustard could also produced in rats (Laughton and Powley 1981).

Massive and persistent obesity was induced in mice by a single intracerebral injection with 4-nitroquinoline 1-oxide (Mizutani 1977).

REFERENCES AND FURTHER READING

Brecher G, Waxler SH (1949) Obesity in albino mice due to single injections of goldthioglucose. Proc Soc Exp Biol Med 70:498–501

Debons AF, Silver L, Cronkite EP, Johnson A, Brecher G, Tenzer D, Schwartz IL (1962) Localization of gold in mouse brain in relation to gold thioglucose obesity. Am J Physiol 202:743–750

Debons AF, Krimsky I, Likuski HJ, From A, Cloutier RJ (1968) Goldthioglucose damage to the satiety center: inhibition in diabetes. Am J Physiol 214:562–658

Debons AF, Krimsky I, Maayan ML, Fani K, Jimenez FA (1977) Goldthioglucose obesity syndrome. Fed Proc 36:143–137

Deter RL, Liebelt RA (1964) Goldthioglucose as an experimental tool. Texas Rep Biol Med 22:229–243

Laughton W, Powley TL (1981) Bipiperidyl mustard produces brain lesions and obesity in the rat. Brain Res 221:415–420

Marshall NB, Barrnett RJ, Mayer J (1955) Hypothalamic lesions in goldthioglucose injected mice. Proc Soc Exp Biol Med 90:240–244

Mizutani T (1977) Characterization of obesity in mice induced with 4-nitroquinoline 1-oxide. Jap J Vet Sci 39:141–147

Perry JH, Liebelt RA (1961) Extra-hypothalamic lesions associated with gold-thioglucose induced obesity. Proc Soc Exp Biol Med 106:55–57

Rutman RJ, Lewis FS, Bloomer WD (1966) Bipiperidyl mustard, a new obesifying agent in the mouse. Science 153:1000–1002

Smith CJV (1972) Hypothalamic glucoreceptors – the influence of gold thioglucose implants in the ventromedial and lateral hypothalamic areas of normal and diabetic rats. Physiol Behav 9:391–396

Smith CJV, Britt DL (1971) Obesity in the rat induced by hypothalamic implants of gold thioglucose. Physiol Behav 7:7–10

Stauffacher W, Lambert AE, Vecchio D, Renold AE (1967) Measurement of insulin activities in pancreas and serum of mice with spontaneous ("obese" and "New Zealand obese") and induced (goldthioglucose) obesity and hyperglycemia, with considerations on the pathogenesis of the spontaneous syndrome. Diabetologia 3:230–237

L.1.0.5 Monosodium Glutamate-Induced Obesity

PURPOSE AND RATIONALE

Adiposity can be induced in mice by repeated subcutaneous injections of monosodium-L-glutamate at an early stage of life (Olney 1969).

PROCEDURE

Male Charles River mice are treated immediately after birth with daily subcutaneous injections of 2 g/kg monosodium-L-glutamate for 5 consecutive days. Control mice are treated with physiological saline. The animals are weaned at 3 weeks of age, housed under controlled temperature and artificial light/dark cycle and provided with commercial powdered chow and tap water at libitum.

EVALUATION

Food consumption and weight gain is measured at weekly intervals.

MODIFICATIONS OF THE METHOD

Tokuyama and Himms-Hagen (1986) studied brown adipose tissue thermogenesis, torpor, and obesity in glutamate-treated C57B1/6J mice offered either normal chow or a cafeteria diet and found that the high metabolic efficiency and obesity of the glutamate-obese animals are principally a consequence of their

maintenance of a hypothermic torpid state for more than 50% of the time.

Seress (1982) injected young albino **rats** with either single or repeated doses of 0.1–6.0 mg/g body weight of monosodium L-glutamate between the ages of 2 and 40 days. The smallest, single effective dose was 0.25 mg/g body weight administered during the first week of life. The sensitivity to monosodium L-glutamate decreased with age. In adult rats an 80–90% loss of neurons in the anterior part of the arcuate nucleus was found.

Remke et al. (1988) reported on development of hypothalamic obesity after subcutaneous administration of monosodium glutamate to neonate rats.

REFERENCES AND FURTHER READING

Bunyan D, Merrell EA, Shah PD (1976) The induction of obesity in rodents by means of monosodium glutamate. Br J Nutr 35:25–39

Olney JW (1969) Brain lesions, obesity, and other disturbances in mice treated with monosodium glutamate. Science 164:719–721

Pizzi WJ, Barnhart JE (1976) Effects of monosodium glutamate on somatic development, obesity and activity in the mouse. Pharmacol Biochem Behav 5:551–557

Poon TKY, Cameron DP (1978) Measurement of oxygen consumption and locomotor activity in monosodium glutamate-induced obesity. Am J Physiol 234:E532–E534

Redding TW, Schally AV, Arimura A, Wakabayashi I (1971) Effect of monosodium glutamate on some endocrine functions. Neuroendocrinology 8:245–255

Remke H, Wilsdorf A, Müller F (1988) Development of hypothalamic obesity in rats. Exp Pathol 33:223–232

Seress L (1982) Divergent effects of acute and chronic monosodium L-glutamate treatment on the anterior and posterior parts of the arcuate nucleus. Neuroscience 7:2207–2216

Tokuyama K, Himms-Hagen J (1986) Brown adipose tissue thermogenesis, torpor, and obesity in glutamate-treated mice. Am J Physiol 251 (Endocrin Metab 14):E407–E415

Yoshida T, Nishioka H, Nakamura Y, Kondo M (1984) Reduced norepinephrine turnover in mice with monosodium glutamate-induced obesity. Metabolism 33:1060–1063

Yoshida T, Nishioka H, Nakamura Y, Kanatsuna T, Kondo M (1985) Reduced norepinephrine turnover in brown adipose tissue of pre-obese mice treated with monosodium-L-glutamate. Life Sci 36:931–938

Yoshida T, Sakane N, Wakabayashi Y, Umekawa T, Kondo M (1994) Anti-obesity effect of CL 316,243, a highly specific β_3-adrenoceptor agonist, in mice with monosodium-L-glutamate-induced obesity. Eur J Endocrinol 131:97–102

L.2 Genetically Obese Animals

L.2.0.1 General Considerations

Obesity and diabetes are syndromes quite often linked in patients (maturity onset diabetes) and hereditary animal models. Hunt et al. (1976) described animal models of diabetes and obesity including the PBB-Ld mouse. A survey on hypothalamic and genetic obesity in experimental animals was given by Bray and York (1979). The inheritance of obesity in animal models of obesity was discussed by Festing (1979). Cawthorne (1979) discussed the use of animal models in the detection and evaluation of compounds for the treatment of obesity. The regulation of body weight in animals by leptin was reviewed by Friedman and Halaas (1998).

Symptoms of diabetes and obesity are overlapping in many animal models (see also K.2: Genetically diabetic animals).

REFERENCES AND FURTHER READING

Bray GA, York DA (1979) Hypothalamic and genetic obesity in experimental animals: An autonomic and endocrine hypothesis. Physiol Rev 59:719–809

Cawthorne (1979) The use of animal models in the detection and evaluation of compounds for the treatment of obesity. In: Festing MFW (ed) Animal Model of Obesity. MacMillan Press Ltd., pp 79–90

Coleman DL (1978) Obese and diabetes: two mutant genes causing diabetes-obesity syndromes in mice

Festing MFW (1979) The inheritance of obesity in animal models of obesity. In Festing MFW (ed) Animal Model of Obesity. MacMillan Press Ltd., pp 15–37

Friedman JM, Halaas JL (1998) Leptin and the regulation of body weight in mammals. Nature 395:763–770

Hunt CE, Lindsey JR, Walkley SU (1976) Animal models of diabetes and obesity including PBB-Ld mouse. Fed Proc 35:1206–1217

Westman S (1968) Development of the obese-hyperglycaemic syndrome in mice. Diabetologia 4:141–149

L.2.0.2 Spontaneously Obese Rats

The occurrence of spontaneous obesity has been reported in several strains of rats:

WBN/KOB RAT

Spontaneous hyperglycemia, glucosuria and glucose intolerance have been observed in aged males of an inbred Wistar strain, named the WBN/Kob rat (Nakama et al. 1985; Tsuchitani et al. 1985; Koizumi 1989). These animals exhibit impaired glucose tolerance and glucosuria at 21 weeks of age. Obvious decreases in the number and size of islets are found already after 12 weeks of age. Fibrinous exudation and degeneration of pancreatic tissue are observed in the exocrine part, mainly around degenerated islets and pancreatic ducts in 16 weeks old males.

REFERENCES AND FURTHER READING

Koizumi M, Shimoda I, Sato K, Shishido T, Ono T, Ishizuka J, Toyota T, Goto Y (1989) Effects of CAMOSTAT on development of spontaneous diabetes in the WBN/Kob rats. Biomed Res 10, Suppl 1:45–50

Nakama K, Shichinohe K, Kobayashi K, Naito K, Ushida O, Yasuhara K, Zobe M (1985) Spontaneous diabetes-like syndrome in WBN/Kob rats. Acta Diabetol Lat. 122:335–342
Tsichitani M, Saegusa T, Narama I, Nishikawa T, Gonda T (1985) A new diabetic strain of rat (WBN/Kob) Laboratory Animals 19:200–207

Zucker-Fatty Rat

The Zucker-fatty rat is a classic model of hyperinsulinemic obesity. (Zucker 1965). Obesity is due to a simple autosomal recessive (*fa*) gene and develops at an early age. Obese Zucker rats manifest mild glucose intolerance, hyperinsulinemia, and peripheral insulin resistance similar to human NIDDM. However, their blood sugar level is usually normal throughout life (Bray 1977; Clark et al. 1983; McCaleb and Sredy 1992; Abadie et al. 1993; Alamzadeh et al. 1993; Kasim et al. 1993; Galante et al. 1994).

Truett et al. (1991) found evidence that the rat obesity gene fatty (*fa*) has homology with the mouse gene diabetes (*db*).

Triscari and Sullivan (1987) reported a normalizing effect of an inhibitor of thromboxane synthase on the hyperinsulinemic state of obese Zucker rats and diet-induced obese rats.

Rouru et al. (1993) described the effect of chronic treatment with a 5-HT_1 receptor agonist on food intake, weight gain, plasma insulin and neuropeptide Y mRNA expression in obese Zucker rats.

Santti et al. (1994) studied the potentiation of the anti-obesity effect of a β_3-adrenoceptor agonist in obese Zucker rats by exercise.

Savontaus et al. (1997) investigated the anti-obesity effect of a imidazoline derivative in genetically obese (*fa*/*fa*) Zucker rats.

Zhang et al. (1996) reported downregulation of the expression of the *obese* gene by an antidiabetic thiazolidinedione in Zucker diabetic fatty rats and *db/db* mice.

Lynch et al. (1992) identified several adipocyte proteins, among them pyruvate decarboxylase contributing to the increased lipogenic capacity of young obese Zucker adipocytes.

REFERENCES AND FURTHER READING

Abadie JM, Wright B, Correa G, Browne ES, Porter JR, Svec F (1993) Effect of dihydro-epiandrosterone on neurotransmitter levels and appetite regulation of the obese Zucker rat. Diabetes 42:662–669
Alamzadeh R, Slonim AE, Zdanowicz MM (1993) Modification of insulin resistance by diazoxide in obese Zucker rats. Endocrinology 133:705–712
Bray GA (1977) The Zucker-fatty rat: A review. Fed Proc 36:148–153
Cleary MP (1989) Antiobesity effect of dehydroepiandrosterone in the Zucker rat. In: Lardy H, Stratman F (eds) Hormones, Thermogenesis and Obesity. Elsevier, New York, pp 365–376
Clark JB, Palmer CJ, Shaw WN (1983) The diabetic Zucker fatty rat. Proc Soc Exp Biol Med 173:68–75
Fujiwara T, Yoshioka S, Yoshioka T, Ushiyama I, Horikoshi H (1988) Characterization of new oral antidiabetic agent CS-045. Studies in KK and *ob/ob* mice and Zucker fatty rats. Diabetes 37:1549–1558
Galante P, Maerker E, Scholz R, Rett K, Herberg L, Mosthaf L, Häring HU (1994) Insulin-induced translocation of GLUT 4 in skeletal muscle of insulin-resistant Zucker rats. Diabetologia 37:3–9
Kasim SE, Elovson J, Khilnani S, Almario RU, Jen KLC (1993) Effect of lovostatin on the secretion of very low density lipoproteins and apolipoprotein B in the hypertriglyceridemic Zucker obese rat. Atherosclerosis 104:147–152
Kava R, Greenwoof MRC, Johnson PR (1990) Zucker (*fa/fa*) rat. Ilar News 32:4–8
Lynch CJ, McCall KM, Billingsley ML, Bohlen LM, Hreniuk SP, Martin LF, Witters LA, Vannucci SJ (1992) Pyruvate carboxylase in genetic obesity. Am J Physiol 262 (Endocrinol Metab 25):E608–618
McCaleb ML, Sredy J (1992) Metabolic abnormalities of the hyperglycemic obese Zucker rat. Metabolism 41:522–525
Rouru J, Pesonen U, Isaksson K, Huupponen R, Koulu M (1993) Effect of chronic treatment with TFMPP, a 5-HT_1 receptor agonist, on food intake, weight gain, plasma insulin and neuropeptide Y mRNA expression in obese Zucker rats. Eur J Pharmacol 234:191–198
Santti E, Huupponen R, Rouro J, Hänninen V, Pesonen U, Jhanwar-Uniyal M, Koulu M (1994) Potentiation of the anti-obesity effect of the β_3-adrenoceptor agonist BRL 35135 in obese Zucker rats by exercise. Br J Pharmacol 113:1231–1236
Savontaus E, Raasmaja A, Rouru J, Koulu M, Pesonen U, Virtanen R, Savola JM, Huupponen R (1997) Anti-obesity effect of MPV-1743 A III, a novel imidazoline derivative, in genetic obesity. Eur J Pharmacol 328:207–215
Shafrir E (1992) Animal models of non-insulin-dependent diabetes. Diabetes/Metab Rev 8:179–208
Triscari J, Sullivan AC (1987) A pharmacotherapeutic approach to the regulation of hyperinsulinemia and obesity. Int J Obesity 11, Suppl 3:43–51
Truett GE, Bahary N, Friedman JM, Leibel RL (1991) Rat obesity gene fatty *(fa)* maps to chromosome 5: Evidence for homology with the mouse gene diabetes (*db*). Proc Natl Acad Sci USA 88:7806–7809
Vasselli JR, Flory T, Fried KS (1987) Insulin binding and glucose transport in adipocytes of acarbose-treated Zucker lean and obese rats. Int J Obesity 11:71–75
Yoshioka S, Nishino H, Shiraki T, Ikeda K, Koike H, Okuno A, Wada M, Fujiwara T, Horikoshi H (1993) Antihypertensive effects of CS-045 treatment in obese Zucker rats. Metabolism 42:75–80
Zhang B, Graziano MP, Doebber TW, Leibowitz MD, White-Carrington S, Szalkowski DM,. Hey PJ, Wu M, Cullinan CA, Bailey P, Lollmann B, Frederich R, Flier JS, Strader CD, Smith RG (1996) Down-regulation of the expression of the *obese* gene by an antidiabetic thiazolidinedione in Zucker diabetic fatty rats and *db/db* mice. J Biol Chem 271:9455–9459
Zucker LM (1965) Hereditary obesity in the rat associated with hyperlipidemia. Ann NY Acad Sci 131:447–458

WDF/TA-FA RAT

The WDF/Ta-fa rat, commonly referred to as the Wistar fatty rat, is a genetically obese, hyperglycemic rat established by the transfer of the fatty (*fa*) gene from the Zucker rat to the Wistar Kyoto rat. (Ikeda et al. 1981; Kava et al. 1989; Velasquez et al. 1990). The Wistar fatty rat exhibits obesity, hyperinsulinemia, glucose intolerance, hyperlipidemia, and hyperphagia similar to Zucker rats being, however, more glucose intolerant and insulin resistant than Zucker rats. Hyperglycemia is usually not observed in females but can be induced by addition of sucrose to the diet.

Kobayashi et al. (1992) found an increase of insulin sensitivity by activation of insulin receptor kinase by Pioglitazone in Wistar fatty rats (*fa/fa*).

Mazusaki et al. (1996) found an augmented expression of the *obese* (*ob*) gene during the process of obesity in genetically obese-hyperglycemic Wistar fatty (*fa/fa*) rats.

REFERENCES AND FURTHER READING

Ikeda H, Shino A, Matsuo T, Iwatsuka H, Suzuoki Z (1981) A new genetically obese-hyperglycemic rat (Wistar fatty). Diabetes 30:1045–1050

Kava R, Peterson RG, West DB, Greenwood MRC (1990) Ilar News 32:9–13

Kava RA, West DB, Lukasik VA, Greenwood MRC (1989) Sexual dimorphism of hyperglycemia and glucose tolerance in Wistar fatty rats. Diabetes 38:159–163

Kobayashi M, Iwanshi M, Egawa K, Shigeta Y (1992) Pioglitazone increases insulin sensitivity by activating insulin receptor kinase. Diabetes 41:476–483

Madar Z, Omusky Z (1991) Inhibition of intestinal α-glucosidase activity and postprandial hyperglycemia by α-glucosidase inhibitors in *fa/fa* rats. Nutrit Res 11:1035–1046

Mazusaki H, Hosoda K, Ogawa Y, Shigemoto M, Satoh N, Mori K, Tamura N, Nishi S, Yoshimasa Y, Yamori Y, Nakao K (1996) Augmented expression of *obese (ob)* gene during the process of obesity in genetically obese-hyperglycemic Wistar fatty *(fa/fa)* rats. FEBS Lett 378:267–271

Peterson RG, Little LA, Neel MA (1990) WKY fatty rat as a model of obesity and non-insulin dependent diabetes mellitus. Ilar News 32:13–15

Velasquez MT, Kimmel PL, Michaelis OE,IV (1990) Animal models of spontaneous diabetic kidney disease. FASEB J 4:2850–2859

OLETF Rat

A spontaneously diabetic rat with polyuria, polydipsia, and mild obesity was discovered in 1984 in an outbred colony of Long-Evans rats. A strain of rats developed from this rat by selective breeding has since been maintained at the Tokushima Research Institute (Otsuka Pharmaceutical, Tokushima, Japan) and named OLETF. The characteristic features of OLETF rats are: (1) late onset of hyperglycemia (after 18 weeks of age), (2) a chronic course of disease, (3) mild obesity, (4) inheritance by males, (5) hyperplastic foci of pancreatic islets, and (6) renal complications (nodular lesions). The clinical and pathological features of disease in OLETF rats resemble those of human NIDDM.

Administration of diazoxide (0.2% in diet), an inhibitor of insulin secretion, to OLETF rats from the age of 4 to 12 weeks completely prevented the development of obesity and insulin resistance (Aizawa et al. 1995).

Ishida et al. (1995) found that insulin resistance preceded impaired insulin secretion in OLETF rats.

Umekawa et al. (1997) determined induction of uncoupling protein and activation of GLUT4 in OLETF rats after administration of a specific β_3-adrenoceptor agonist.

REFERENCES AND FURTHER READING

Aizawa T, Taguchi N, Sato Y, Nakabayashi T, Kobuchi H, Hidaka H, Nagasawa T, Ishihara F, Itoh N, Hashizume K (1995) Prophylaxis of genetically determined diabetes by diazoxide: a study in a rat model of naturally occurring obese diabetes. J Pharmacol Exp Ther 275:194–199

Ishida K, Mizuno A, Sano T, Shima K (1995) Which is the primary etiologic event in Otsuka Long-Evans Tokushima fatty rats, a model of spontaneous non-insulin-dependent diabetes mellitus, insulin resistance, or impaired insulin secretion? Metabolism 44:940–945

Kawano K, Hirashima T, Mori S, Kurosumi M, Saitoh Y (1991) A new rat strain with non-insulin dependent diabetes mellitus, "OLETF". Rat News Lett 25:24–26

Kawano K, Hirashima T, Mori S, Saitoh YA, Kurosumi M, Natori T (1992) Spontaneous long-term hyperglycemic rat with diabetic complications. Otsuka Long-Evans Tokushima fatty (OLETF) strain. Diabetes 41:1422–1428

Umekawa T, Yoshida T, Sakane N, Saito M, Kumamoto K (1997) Anti-obesity and anti-diabetic effects of CL316,243, a highly specific β_3-adrenoceptor agonist, in Otsuka Long Evans Tokushima Fatty rats: induction of uncoupling protein and activation of glucose transporter 4 in white fat. Eur J Endocrinol 136:429–437

Yamamoto M, Dong MJ, Fukumitsu KI, Imoto I, Kihara Y, Hirohata Y, Otsuki M (1999) Metabolic abnormalities in the genetically obese and diabetic Otsuka Long Evans Tukushima fatty rat can be prevented by α-glucosidase inhibitor. Metab Clin Exp 48:347–354

Obese SHR Rat

The strain of obese SHR rats was developed by Koletsky (1973, 1975) by mating a spontaneous hypertensive female rat of the Kyoto-Wistar strain with a normotensive Sprague Dawley male. After several generations of selective inbreeding, these obese SHR exhibited obesity, hypertension, and hyperlipidemia. In addition, some rats developed hyperglycemia and glucosuria associated with giant hyperplasia of pancreatic islets.

REFERENCES AND FURTHER READING

Ernsberger P, Koletsky RJ, Friedman JE (1999) Molecular pathology in the obese spontaneous hypertensive Koletsky rat: A model of syndrome X. Ann New York Acad Sci 892:272–288

Koletsky S (1973) Obese spontaneous hypertensive rats – a model for study of arteriosclerosis. Exp Mol Pathol 19:53–60

Koletsky S (1975) Pathologic findings and laboratory data in a new strain of obese hypertensive rats. Am J Pathol 80:129–142

Russell JC, Graham S, Hameed M (1994) Abnormal insulin and glucose metabolism in the JCR:LA-corpulent rat. Metabolism 43:538–543

Velasquez MT, Kimmel PL, Michaelis OE,IV (1990) Animal models of spontaneous diabetic kidney disease. FASEB J 4:2850–2859

Yen T, Shaw WN, Yu PL (1977) Genetics of obesity in Zucker rats and Koletsky rats. Heredity 38:373–377

JCR:LA-Corpulent Rat

Several substrains were developed from obese SHR rats, such as the JCR:LA-corpulent rat which exhibits a syndrome characterized by obesity, hypertriglyceridemia and hyperinsulinemia with impaired glucose tolerance and is susceptible to vascular arteriosclerotic lesions (Russell et al. 1986a, b, 1994).

Compared to fatty Zucker rats, the JCR:LA-corpulent rats have higher levels of the insulin releasing hormone gastric inhibitory polypeptide and higher insulin levels (Pederson et al. 1991).

Vydelingum et al. (1995) found an overexpression of the obese gene in the JCR:LA-corpulent rat.

REFERENCES AND FURTHER READING

Dophin PJ, Stewart B, Amy RM, Russell JC (1987) Serum lipids and lipoproteins in the atherosclerotic-prone LA/N-corpulent rat. Biochem Biophys Acta 919:140–148

Pederson RA, Campos RV, Buchan AMJ, Chisholm CB, Russell JC, Brown JC (1991) Comparison of the enteroinsular axis in two strains of obese rat, the fatty Zucker and the JCR:LA-corpulent. Int J Obesity 15:461–470

Russell JC, Amy RM (1986a) Early arteriosclerotic lesions in a susceptible rat model: the LA/N-corpulent rat. Arteriosclerosis 60:119–129

Russell JC, Amy RM (1986b) Myocardial and vascular lesions in the LA/N-corpulent rat. Can J Physiol Pharmacol 64:1272–1280

Russell JC, Graham S, Hameed M (1994) Abnormal insulin and glucose metabolism in the JCR:LA-corpulent rat. Metabolism 43:538–543

Vydelingum S, Shillabeer G, Hatch G, Russell JC, Lau DCW (1995) Overexpression of the obese gene in the genetically obese JCR:LA-corpulent rat. Biochem Biophys Res Commun 216:148–153

Growth Hormone-Deficient Dwarf Rat

Clark et al. (1996) described the obese growth hormone-deficient dwarf rat as a new model of obesity.

REFERENCES AND FURTHER READING

Clark RG, Mortensen DL, Carlsson LMS, Carlsson B, Carmignac D, Robinson ICAF (1996) The obese growth hormone (GH)-deficient dwarf rat: Body fat responses to patterned delivery of GH and insulin-like growth factor-I. Endocrinology 137:1904–1912

L.2.0.3 Spontaneously Obese Mice

Yellow Obese (A^YA) Mouse

The yellow obese mouse in the only example of obesity inherited through a dominant gene and was described as early as 1883 by Lataste and in 1905 by Cuenot. It is located on chromosome 2 at linkage group 5, the agouti locus (Bateson 1903). Since the genes controlling obesity and the agouti coat colors are so closely linked, the obesity is associated with a change of pigmentation from black to yellow. Such an association allows the early identification of pre-obese mice as soon as the coat hair begins to grow.

Since the original description of the yellow (A^ya) mouse, a number of additional alleles have appeared at the agouti locus. The homozygous dominant yellow mutation (A^y/A^y) is lethal in utero (Robertson 1942; Eaton and Green 1962) with approximately 25% of any litter from A^ya matings dying from an abnormal development after the trophoblast stage (Pedersen 1974).

Yellow (A^ya) mice develop a moderate form of obesity and diabetes. Increased body weight first appears at the time of puberty (8–12 wk) (Dickie and Wooley 1946; Carpenter and Mayer 1958), after which body weight increases slowly to reach values of approximately 40 g. In contrast to other forms of obesity, yellow mice are characterized by increased linear growth. Plasma insulin concentrations are increased and food is stored more efficiently than in lean mice (Dickerson and Gowan 1967). Food intake returns to normal in older A^ya mice and the animals lose body weight (Hollifield and Parson 1957). The obesity may be exaggerated by being fed high-fat diets (Fenton and Chase 1951; Silberberg and Silberberg 1957; Carpenter and Mayer 1958). Food restriction may normalize body weight but the animals still remain obese (Fenton and Chase 1951; Hollifield and Parson 1957). Metabolic rate of A^ya mice is depressed when related to body surface, although oxygen consumption per animal is identical to the homozygous recessive agouti (a/a) mouse (Bartke and Gorecki 1968).

Gill and Yen (1991) studied the effect of ciglitazone on endogenous plasma islet amyloid polypeptide

(amylin) and insulin sensitivity in obese-diabetic viable yellow mice (VY/Wfl-A^{vy}/a).

REFERENCES AND FURTHER READING

Bartke A, Gorecki A (1968) Oxygen consumption by obese yellow mice and their normal littermates. Am J Physiol 214:1250–1252

Bateson W (1903) The present state of knowledge of colors heredity in mice and rats. Proc Zool Soc London 2:71–99

Carpenter KJ, Mayer J (1958) Physiological observations on yellow obesity in the mouse. Am J Physiol 193:499–504

Cuenot L (1905) Les races pures et leur combinaisons chez les souris. Arch Zool Exp Gen 122:123–132

Dickerson GE, Gowan JW (1967) Hereditary obesity and efficient food utilization in mice. Science 105:496–498

Dickie MM, Wooley GW (1946) The age factor in weight of yellow and "thin-yellows" revealed in litter-mate comparisons. J Hered 37:365–358

Eaton GJ, Green MM (1962) Implantation and lethality of the yellow mouse. Genetica 33:106–112

Fenton PF, Chase HB (1951) Effect of diet on obesity of yellow mice in inbred lines. Proc Soc Exp Biol Med 77:420–422

Gill AM, Yen TT (1991) Effects of ciglitazone on endogenous plasma islet amyloid polypeptide and insulin sensitivity in obese-diabetic viable yellow mice. Life Sci 48:703–710

Hollifield G, Parson W (1957) Food drive and satiety in yellow mice. Am J Physiol 189:36–38

Lataste F (1883) Trois questions: naturaliste. Bull Sci du Dep du Nord 8:364

Pedersen RA (1974) Development of lethal yellow (A^y/A^y) mouse embryos *in vitro*. J Exp Zool 188:307–320

Robertson GG (1942) An analysis of the development of homozygous yellow mouse embryos. J Exp Zool 89:197–230

Silberberg R, Silberberg M (1957) Lesions in "yellow" mice fed stock, high-fat or high-carbohydrate diets. Yale J Biol Med 29:525–539

KK-A^Y Mouse

Iwatsuka et al. (1970) reported on yellow KK mice (also named KK-A^y mice), carrying the yellow obese gene (A^y). These mice develop marked adiposity and diabetic symptoms in comparison with their littermates, black KK mice. Blood glucose and circulating insulin levels as well as HbA_{1c} levels were increased progressively from 5 weeks of age. Degranulation and glycogen infiltration of B cells were followed by hypertrophy and central cavitation of islets. Lipogenesis by liver and adipose tissue were increased. Insulin sensitivity of adipose tissue was more remarkably reduced than in black KK mice to its complete loss at 16 weeks of age. Renal involvement is uniquely marked by early onset and rapid development of glomerular basement membrane thickening (Diani et al. 1987).

KK-A^y mice can be used to demonstrate the extra-pancreatic action of antidiabetic drugs, such as glimepiride, a novel sulfonylurea (Satoh et al. 1994).

Sohda et al. (1990) evaluated ciglitazone and a series of 5-[4-(pyridylalkoxy)benzyl]-2,4-thiazolidinediones for hypoglycemic and hypolipemic activities in yellow KK mice.

Hofmann et al. (1992) evaluated the expression of the liver glucose transporter GLUT2 and the activity and the expression of phosphoenolpyruvate carboxykinase in the liver of obese KKA^Y mice after treatment with the oral antidiabetic agent pioglitazone.

Yoshida et al. (1991) compared brown adipose tissue thermogenesis, resting metabolic rate, insulin receptors in adipocytes, and blood glucose and serum insulin levels during a glucose overloading test in yellow KK mice with C57B1 control mice after a β_3-adrenoceptor agonist.

Yoshida et al. (1996) determined body weight, food intake, white adipose tissue weight, brown adipose tissue weight and its thermogenesis, noradrenaline turnover, blood glucose and serum insulin levels and GLUT4 in diabetic yellow KK mice compared with C57B1 mice after mazindol.

REFERENCES AND FURTHER READING

Diani AR, Sawada GA, Zhang NY, Wyse BM, Connell CL, Vidmar TJ, Connell MA (1987) The KKA^y mouse: a model for the rapid development of glomerular capillary basement membrane thickening. Blood Vessels 24:297–303

Hofmann CA, Edwards CW, Hillman RM, Colca JR (1992) Treatment of insulin-resistant mice with the oral antidiabetic agent pioglitazone: evaluation of liver GLUT2 and phosphoenol-pyruvate carboxykinase expression. Endocrinol 130:735–740

Iwatsuka H, Shino A, Suzouki Z (1970) General survey of diabetic features of yellow KK mice. Endocrinol Japon 17:23–35

Shafrir E (1992) Animal models of non-insulin-dependent diabetes. Diabetes/Metab Rev 8:179–208

Sohda T, Momose Y, Meguro K, Kawamatsu Y, Sugiyama Y, Ikeda H (1990) Studies on antidiabetic agents. Synthesis and hypoglycemic activity of 5-[4-(pyridylalkoxy)benzyl]-2,4-thiazolidinediones. Arzneim Forsch/Drug Res 40:37–42

Yoshida T, Hiraoka N, Yoshioka K, Hasegawa G, Kondo M (1991) Anti-obesity and anti-diabetic actions of a, BRL 28630A, in yellow kk mice. Endocrinol Japon 38:397–403

Yoshida T, Umekawa T, Wakabayashi Y, Yoshimoto K, Sakane N, Kondo M (1996) Anti-obesity and anti-diabetic effects of mazindol in yellow kk mice: its activating effect on brown adipose tissue thermogenesis. Clin Exp Pharmacol Physiol 23:476–482

OBESE HYPERGLYCEMIC (OB/OB) MICE

Ingalls et al. (1950), Mayer et al. (1951), Bleisch et al. (1952) observed hereditary diabetes in genetically obese mice. The obese hyperglycemic mice were glycosuric, the non-fasting blood sugar levels were about 300 mg%, but neither ketonuria nor coma were observed. One of the most interesting features was insulin-resistance; doses as high as 400 IU/kg had little effect on blood sugar. The

serum insulin-like activity was high, the islands of Langerhans were hypertrophic, their insulin content was increased and the liver glycogen stores were decreased. Kidneys and other organs did not show pathological changes. Obviously, the diabetic condition of this and other strains of obese hyperglycemic mice is different from that of the human diabetic patient.

Reduced oxygen consumption has been noted as early as 10–18 days of age in *ob/ob* mice (Boissenault et al. 1976; Trayhurn 1977).

Other strains or substrains of mice with obesity and hyperglycemia have been described by Dickie (1962), Westman (1968), Stein et al. (1970), Coleman and Hummel (1973), Herberg and Coleman (1977).

Strautz (1970) implanted *ob/ob* mice with Millipore diffusion chambers containing islets isolated from pancreas of normal littermates.

Trayhurn et al. (1977) found a thermogenic defect in pre-obese *ob/ob* mice. Rectal temperature of 17 days old pre-obese mice in response to an environmental temperature of 4°C fell much more than in lean controls.

Chlouverakis (1972) performed parabiotic experiments of obese-hyperglycemic mice (*ob/ob*) with lean littermates and determined body weight, glucose, serum insulin and triglycerides as well as insulin-sensitivity of diaphragm muscle and epididymal fat pad.

Parabiosis of obese (*ob/ob*) with diabetes (*db/db*) mice caused the obese partner to become hypoglycemic, to lose weight and to die of starvation, while no abnormal changes were observed in the diabetic partner (Coleman 1973).

Cresto et al. (1977) compared the rate of insulin degradation in normal and in*ob/ob* mice.

Zhang et al. (1994) succeeded in positional cloning of the mouse *obese* gene and its human homologue.

Pelleymounter et al. (1995) investigated the effects of the *obese* gene product on body weight regulation in *ob/ob* mice. The OB protein was expressed in *E. coli* and purified to homogeneity as a 16-kilodalton monomer. Daily intraperitoneal injections of the recombinant OB protein to *ob/ob* mice lowered their body weight, percent body fat, food intake, and serum concentrations of glucose and insulin.

Halaas et al. (1995) reported that daily intraperitoneal injections of either mouse or human recombinant OB protein reduced the body weight of *ob/ob* mice but had no effect on *db/db* mice.

Campfield et al. (1995) found that peripheral and central administration of microgram doses of recombinant mouse OB protein reduced food intake and body weight of *ob/ob* and diet-induced obese mice but not in *db/db* obese mice.

Trayhurn et al. (1996) studied the effects of fasting and refeeding on *ob* gene expression in white adipose tissue of lean and obese *(ob/ob)* mice using a 33-mer antisense oligonucleotide as a probe for the rapid chemiluminescence-based detection of *ob* mRNA.

Sterility defect in homozygous obese female mice could be corrected by treatment with the human recombinant OB protein leptin (Chehab et al. 1996).

Roupas et al. (1990) used isolated adipocytes from *ob/ob* mice to study the diabetogenic action of growth hormone.

REFERENCES AND FURTHER READING

Bleisch VR, Mayer J, Dickie MM (1952) Familial diabetes mellitus in mice associated with insulin resistance, obesity and hyperplasia of the islands of Langerhans. Am J Pathol 28:369–385

Boissenault GA, Hornshuh MJ, Simons JW, Romsos DR, Leveille GA (1976) Oxygen consumption of lean and obese (*ob/ob*) mice from birth to 16 weeks of age. Fed Proc 36:1150

Campfield LA, Smith FJ, Guisez Y, Devos R, Burn P (1995) Recombinant mouse OB protein: evidence for a peripheral signal linking adiposity and central neural networks. Science 269:546–549

Chehab FF, Lim ME, Lu R (1996) Correction of the sterility defect in homozygous obese female mice by treatment with the human recombinant leptin. Nature Genet 12:318–322

Chlouverakis C (1972) Insulin resistance of parabiotic obese-hyperglycemic mice (obob). Horm Metab Res 4:143–148

Chlouverakis C, White PA (1969) Obesity and insulin resistance in the obese-hyperglycemic mouse (obob). Metabolism 18:998–1006

Coleman DL (1973) Effects of parabiosis of obese with diabetes and normal mice. Diabetologia 9:294–298

Coleman DL (1989) Therapeutic effects of dehydroepiandrosterone and its metabolites in diabetes-obesity mutants. In: Lardy H, Stratman F (eds) Hormones, Thermogenesis and Obesity. Elsevier, New York, pp 377–383

Coleman DL, Hummel KP (1973) The influence of genetic background on the expression of obese (ob) gene in the mouse. Diabetologia 9:287–293

Cresto JC, Lavine RL, Buchly ML, Penhos JC, Bhathena SJ, Recant L (1977) Half life of injected ^{125}I-insulin in control and *ob/ob* mice. Acta Physiol Lat Am 27:7–15

Dickie MM (1962) New mutations. Mouse News Letter 27:37

Halaas JL, Gajiwala KS, Maffei M, Cohen SL, Chait BT, Rabinowitz D, Lallone RL, Burley SK, Friedman JM (1955) Weight-reducing effects of the plasma protein encoded by the *obese* gene. Science 269:543–546

Hellman B (1967) Some metabolic aspects of the obese-hyperglycemic syndrome in mice. Diabetologia 3:222–229

Herberg L, Coleman DL (1977) Laboratory animals exhibiting obesity and diabetes syndromes. Metabolism 26:59–99

Ingalls AM, Dickie MM, Snell GT (1950) Obese, a new mutation in the house mouse. J Hered 14:317–318

Mayer J, Bates MW, Dickie MM (1951) Hereditary diabetes in genetically obese mice. Science 113:746–747

Pelleymounter MA, Cullen MJ, Baker MB, Hecht R, Winters D, Boone T, Collins F (1995) Effects of the *obese* gene

product on body weight regulation in *ob/ob* mice. Science 269:540–543
Roupas P, Towns RJ, Kostyo JL (1990) Isolated adipocytes from growth hormone-treated obese*(ob/ob)* mice exhibit insulin resistance. Biochim Biophys Acta 1052:341–344
Sirek A (1968) Spontaneous hereditary diabetes in laboratory animals. in: Pfeiffer EF (ed) Handbook of Diabetes mellitus, Pathophysiology and Clinical Considerations. Vol. I, Lehmanns Verlag, München. pp 715–726
Stauffacher W, Lambert AE, Vecchio D, Renold AE (1967) Measurement of insulin activities in pancreas and serum of mice with spontaneous ("obese" and "New Zealand obese") and induced (goldthioglucose) obesity and hyperglycemia, with considerations on the pathogenesis of the spontaneous syndrome. Diabetologia 3:230–237
Stein JM, Bewsher PD, Stowers JN (1970) The metabolism of ketones, triglyceride and monoglyceride in livers of obese hyperglycaemic mice. Diabetologia 6:570–574
Strautz RL (1970) Studies of hereditary-obese mice (obob) after implantation of pancreatic islets in Millipore filter capsules. Diabetologia 6:306–312
Trayhurn P, Thurlby PL, James WPT (1977) Thermogenic defect in pre-obese *ob/ob* mice. Nature 266:60–62
Trayhurn P, Thomas MEA, Duncan JS, Rayner DV (1996) Effects of fasting and refeeding on *ob* gene expression in white adipose tissue of lean and obese *(ob/ob)* mice. FEBS Lett 368:488–490
Westman S (1968) Development of the obese-hyperglycaemic syndrome in mice. Diabetologia 4:141–149
Zhang Y, Proenca R, Maffei M, Barone M, Leopold L, Friedman JM (1994) Positional cloning of the mouse *obese* gene and its human homologue. Nature 372:425–432

BL/6 Obese Mice

An obese mutation occurred in a noninbred stock (Ingalls et al. 1950) but was established later, and has been maintained, in the C5BL/6J (BL/6) strain. BL/6 obese mice are characterized by marked obesity, hyperphagia, transient hyperglycemia and markedly elevated plasma insulin concentrations associated with an increase in number and size of beta cells in the islets of Langerhans (Coleman and Hummel 1973; Genuth et al. 1971). The mutation is autosomal recessive and homozygous mutants of both sexes are infertile. Obese mutants are obtained by mating known heterozygotes. A primary metabolic disturbance in the adipocyte has been postulated since increased adipocyte size has been observed as early as 14 days of age well before any obesity or hyperinsulinemia are observed (Joosten and van der Kroon 1974).

REFERENCES AND FURTHER READING

Coleman DL, Hummel KP (1973) The influence of genetic background on the expression of the obese (*ob*) gene in the mouse. Diabetologia 9:287–293
Genuth SM, Przybyslski RS, Rosenberg DM (1971) Insulin resistance in genetically obese hyperglycemic mice. Endocrinology 88:1230–1238
Ingalls AM, Dickie MM, Snell GD (1950) Obese, a new mutation in the mouse. J Hered 41:317–318
Joosten HFP, van der Kroon PHW (1974) Enlargement of epididymal adipocytes in relation to hyperinsulinemia in obese mice (obob). Metabolism 23:59–66

NZO Mouse

The New Zealand obese (NZO) mouse was first described in 1953 by Bielschowsky and Bielschowsky. The strain was developed by selective inbreeding of obese mice from a mixed colony, beginning from a pair of agouti mice, which also gave rise to the NZB black strain (Melez et al. 1980). NZO mice develop obesity, mild hyperglycemia, glucose intolerance, hyperinsulinemia, and insulin resistance. The adult NZO mouse normally attains a body weight of 50–70 g by 6–8 months, although weight gain continues slowly after this age (Crofford and Davis 1965; Herberg et al. 1970). Hyperglycemia and glucose intolerance increase continuously with advancing age of the animals.

Renal disease in NZO mice is seen by 6 months of age. NZO mice have a high prevalence of autoimmune disorders.

REFERENCES AND FURTHER READING

Bielschowsky M, Bielschowsky F (1953) A new strain of mice with hereditary obesity. Proc Univ Otago Med School 31:29–31
Cofford OB, Davis CK (1965) Growth characteristics, glucose tolerance and insulin sensitivity of New Zealand obese mice. Metabolism 14:271–280
Herberg L, Major E, Hennings U, Grüneklee G, Freytag G, Gries FA (1970) Differences in the development of the obese-hyperglycemic syndrome in obob and NZO mice. Diabetologia 6:292–299
Melez KA, Harrison LC, Gilliam JN, Steinberg AD (1980) Diabetes is associated with autoimmunity in the New Zealand obese (NZO) mouse. Diabetes 29:835–840
Seemayer TA, Colle E (1980) Pancreatic cellular infiltrates in autoimmune-prone New Zealand black mice. Diabetologia 19:216–221
Shafrir E (1992) Animal models of non-insulin-dependent diabetes. Diabetes/Metab Rev 8:179–208
Velasquez MT, Kimmel PL, Michaelis OE (1990) Animal models of spontaneous diabetic kidney disease. FASEB J 4:2850–2859
Veroni MC, Proietto J, Larkins RG (1991) Insulin resistance in New Zealand obese mice. Diabetes 40:1480

Diabetes Obesity Syndrome in CBA/CA Mice

A spontaneous maturity onset diabetes obesity syndrome occurs in a small proportion (10–20%) of male CBA/Ca mice. Inbreeding can increase the incidence to 80%. It occurs at 12–16 weeks of age, and is characterized by hyperphagia, obesity, hyperglycemia, hypertriglyceridemia, hyperinsulinemia, and an impaired glucose tolerance. The mice are also resistant to exogenous insulin. Female mice remain normal except

for a slight increase in serum insulin. The male obese diabetic mice have a normal life expectancy.

REFERENCES AND FURTHER READING

Campbell IL, Das AK (1982) A spontaneous diabetic syndrome in the CBA/Ca laboratory mouse. Biochem Soc Trans 10:392

Connelly DM, Taberner PV (1985) Insulin independent diabetes in male mice from an inbred CBA strain. Endocrinol 104 (Suppl):139

Connelly DM, Taberner PV (1989) Characterization of spontaneous diabetes obesity syndrome in mature CBA/Ca mice. Pharmacol Biochem Behav 34:255–259

Sclafani A (1984) Animal models in obesity: classification and characterization. Int J Obes 8:491–508

FAT/FAT Mice

Fat mice carry an autosomal recessive mutation and display a rang of abnormalities, including progressive adult onset obesity, hyperinsulinemia and infertility (Coleman and Eicher 1990). The mutant allele of *fat* was identified and shown to be a missense (serin ⟶ proline) mutation in carboxypeptidase E which abolishes enzyme activity in a variety of neuroendocrine tissues (Naggert et al. 1995). Carboxypeptidase E is required for both sorting and proteolytic processing of a variety of prohormones including proinsulin and POMC (Cool et al. 1997). As carboxypeptidase E is expressed in the CNS, defective processing of a variety of hypothalamic neuropeptides – such as POMC and MCH – may trigger obesity in these animals (Rovere et al. 1996).

REFERENCES AND FURTHER READING

Coleman DL, Eicher EM (1990) Fat *(fat)* and*tubby (tub)*: two autosomal recessive mutations causing obesity syndromes in the mouse. J Hered 88:424–427

Cool DR, Normant E, Shen F, Chen H, Pannell L, Zhang Y, Loh YP (1997) Carboxypeptidase E is a regulated secretory pathway sorting receptor: genetic obliteration leads to endocrine disorders in Cpe/fat mice. Cell 88:73–83

Naggert JK, Fricker DL, Varlamov O, Nishina PM, Rouille Y, Steiner DF, Carroll RJ, Paigen BJ, Leiter EH (1995) Hyperproinsulinaemia in obese *fat/fat* mice associated with a carboxypeptidase E mutation which reduces enzyme activity. Nat Genet 10:135–142

Naggert J, Harris T, North M (1997) The genetics of obesity. Curr Opin Genet Devel 7:398–404

Rovere C, Viale A, Nahon J, Kitabgi P (1996) Impaired processing of brain proneurotensin and promelanin-concentrating hormone in obese *fat/fat* mice. Endocrinology 137:2954–2958

Tubby Mice

Tubby is an autosomal recessive mutation in mice (Coleman and Eicher 1990) which display a tripartite phenotype of blindness, deafness and maturity onset obesity. In response to weight gain, these mice gradually increase their food intake in proportion to body weight and increase plasma insulin levels thereby maintaining normoglycemia. The progressive retinal degeneration in *tubby* mice results from apoptotic loss of photoreceptor cells, with abnormal electroretinograms detected as early as 3 weeks of age (Heckenlively et al. 1955). The mouse obesity gene *tubby* has been identified and characterized (Noben-Trauth et al. 1996; Kleyn et al. 1996).

REFERENCES AND FURTHER READING

Coleman DL, Eicher EM (1990) Fat *(fat)* and*tubby (tub)*: two autosomal recessive mutations causing obesity syndromes in the mouse. J Hered 88:424–427

Heckenlively JR, Chang B, Erway LC, Peng C, Hawes NL, Hageman GS, Roderick TH (1995) Mouse model for Usher syndrome: linkage mapping suggests homology to Usher type I reported at human chromosome 11p15. Proc Natl Acad Sci USA 92:11100–11104

Kleyn PW, Fan W, Kovats SG, Lee JJ, Pulido JC, Wu Y, Berkemeier LR, Misumi DJ, Holmgren L, Charlat O (1996) Identification and characterization of the mouse gene *tubby*: a member of a novel gene family. Cell 85:281–290

Noben-Trauth K, Naggert JK, North MA, Nishina PM (1996) A candidate gene for the mouse mutation *tubby*. Nature 380:534–538

L.2.0.4 Transgenic ANIMALS

PURPOSE AND RATIONALE

Transgenic animals will offer a new approach to study development of obesity and therapeutic possibilities. Lowell et al. (1993) used a transgenic toxigene approach to create transgenic mice with primary deficiency of brown adipose tissue.

The potential for inserting new genetic material into mammals has produced numerous transgenic mice with increased or decreased quantities of body fat (Bray and Bouchard 1997).

Jensen et al. (1997) reported prevention of diet-induced obesity in transgenic mice overexpressing skeletal muscle lipoprotein lipase. The authors hypothesized that the potential to increase lipoprotein lipase activity in muscle by gene or drug delivery may prove an effective tool in preventing and/or treating obesity in humans.

REFERENCES AND FURTHER READING

Bray G, Bouchard C (1997) Genetics and human obesity: research directions. FASEB J 11:937–945

Jensen DR, Schlaepfer IR, Morin CL, Pennington DS, Marcell T, Ammon SM, Gutierrez-Hartmann A, Eckel RH (1997) Prevention of diet-induced obesity in transgenic mice overexpressing skeletal muscle lipoprotein lipase. Am J Physiol (Regul Integr Comp Physiol) 273:R683–R689

Lowell BB, Susulic VS, Haman A, Lawitts JA, Himms-Hagen J, Boyer BB, Kozak LP, Flier JS (1993) Development of obesity in transgenic mice after genetic ablation of brown adipose tissue. Nature 366:740–742

L.3 Assays of Anti-obesity Activity

L.3.1 Anorectic Activity

L.3.1.1 Food Consumption in Rats

PURPOSE AND RATIONALE

Food intake is measured in acute experiments in normal or obese rats. Additionally, in semichronic experiments body weight gain is recorded.

PROCEDURE

Female Zucker rats weighing 250–350 g are maintained under standard conditions (temperature, light-dark cycle, ground rodent pellet chow, tap water). Measurements of food intake begin on day –2. The food is offered in special dishes to reduce spillage. Food intake and body weight are measured daily between 8:00 and 9:00 A.M. At this time any spilled food from the collecting paper under the cage is gathered, air-dried if necessary, and weighed. Individual food intakes in grams are recorded. The tests compounds are either administered with the food or injected intraperitoneally. Groups of 5–10 animals are used for control or treatment with various doses of the test compound or the standard. Mazindol, 3 m/kg i.p. or 10 mg/kg p.o. can serve as standard. Treatment is continued for 7 days.

EVALUATION

Average food intake and body weight is recorded for each day. Average values of test drugs are compared statistically for each day with the control group. Results after oral administration have to be confirmed by parenteral route in order to exclude errors due to palatability.

MODIFICATIONS OF THE METHOD

Hull and Maher, Maher and Hull (1990) used male Sprague-Dawley rats placed on a mush diet composed of equal parts of ground rodent chow and of 4% nutrient agar solution. The agar-based chow allows a more accurate measurement of food intake and has been shown to be sufficient for maintaining normal growth in rats. The rats were made hyperphagic by food deprivation for 4 h at the beginning of the dark cycle.

Mennini et al. (1991) and Anelli et al. (1992) studied the anorectic activity of various compounds in different species, such as mice, rats, and guinea pigs.

Bowden et al. (1988) used metabolism cages equipped with automated feeding monitors. Food was provided as 45 mg pellets which were singly delivered to a feeding trough. A photodetector sensed the removal of the pellet, and the number of pellets delivered over a specified time interval was recorded.

Samanin et al. (1979) described anorexia in rats induced by the central serotonin agonist m-chlorophenylpiperazine.

Blavet et al. (1982) studied food intake in fasted rats after treatment with several typical anorexigenic agents.

Dourish et al. (1985) investigated the effects of the serotonin agonist 8-OH-DPAT on food intake in non-deprived male rats. This effect was prevented by p-chlorophenylalanine (Dourish et al. 1986).

The anxiolytics gespirone, buspirone and ipsapirone increased free feeding in rats and did not inhibit feeding induced by 8-OH-DPAT (Gilbert and Dourish 1987).

Jackson et al. (1997) investigated the mechanisms underlying the hypophagic effects of the 5-HT and noradrenaline reuptake inhibitor, sibutramine, in the rat.

Simansky and Vaidya (1990) tested the anorectic action of a serotonin uptake inhibitor by measuring the volume of milk consumed by food-deprived rats.

Stevens and Edwards (1996) induced anorexia by subcutaneous injection of 5 mg/kg 5-hydroxytryptamine in Wistar rats habituated to a restricted feeding regime and tested the effects of a 5-HT_3 antagonist.

Rouru et al. (1992) investigated in genetically obese male Zucker rats the effect of subchronic metformin treatment on food intake, weight gain and plasma insulin and corticosterone levels and somatostatin concentrations in the pancreas.

Robert et al. (1989) found an enhanced food intake after intracerebroventricular administration of the tetrapeptide FMRF-amide (Phe-Met-Arg-Phe-NH_2) in obese "cafeteria" rats.

Cooper et al. (1990a, b) used non-deprived rats to study anorectic effects in a test of palatable food consumption and in nocturnal free-feeding.

Cooper et al. (1990c) tested not only food consumption but also the frequency of feeding bouts and duration of individual feeding episodes.

Eberle-Wang and Simansky (1992) studied the influence on the anorectic action of CCK and serotonin by measuring the uptake of sweetened mash mixture in rats.

Voigt et al. (1995) studied the involvement of the 5-HT_{1A} receptor in CCK induced satiety by recording food intake during a 2 h test meal in food deprived and in freely feeding rats.

Influence on postprandial satiety in rats was tested by Rosofsky and Geary (1989). Rats were given pelleted chow and water ad libitum. Near the middle of the bright phase of the light-dark cycle, pellets were removed, the animals treated and condensed milk presented 30 min later. Milk consumption was measured at 4-min intervals for 40 min.

Rats show a dramatic and reliable reduction of food intake if they are prefed a low-protein basal diet and then offered a diet that is imbalanced in any of the essential amino acids (Leung and Rogers 1969). This anorectic response has been used by Hammer et al. (1990) to test $serotonin_3$ receptor antagonists.

Tail pinch is an effective stimulant of eating in rats (Antelman and Szechtman 1975; Fray et al. 1982). Clark et al. (1992) reported that N-methyl-D-aspartate lesions of the lateral hypothalamus do not reduce amphetamine or fenfluramine anorexia but enhance the acquisition of eating in response to tail pinch in the rat.

Thurlby and Samanin (1981) studied the effect of anorectic drugs on food-rewarded runway behavior.

Ferrari et al. (1992) studied the effects on anorexia induced by ACTH and immobilization in rats in an X-maze with alternate open and covered arms, each baited with laboratory chow.

Cooper et al. (1993) studied dopamine D-1 receptor antagonists in rats with chronic gastric fistula which were trained to sham-feed a 10% sucrose solution in a 60 min test.

Bickel et al. (2004) analyzed anorectic effects in rodents by measurement of food consumption. Mice or rats were individually placed in Macrolon cages equipped with a device for continuous monitoring of food consumption consisting of a container filled with feed, hanging on an electronic balance. The balance transmits the weight changes of the feed container continuously to a central unit. Data were stored and processed at the end of the experiment. This system, obtained from TSE, Bad Homburg, Germany, can measure food consumption for up to 3 weeks from more than 199 feeding sensors simultaneously. Similar equipment was used by Bauhofer et al. (2002) and Gaetani et al. (2003).

In wild rodents, **hoarding of food** covers the long term alimentary need. In the laboratory, hoarding behavior does not occur in ad libitum fed rats. On the contrary, rats whose energy balance is threatened by previous food restriction hoard as soon as experimental conditions allow to do so. When such a rat gets free access to a food stock (placed outside its usual territory), it carries food into its shelter and accumulates an amount proportionate to its body weight. Fantino et al. (1980, 1986, 1988), Nishida et al. (1990) used the reduction of the amount of food hoarded during a period of 3 h as parameter for anorectic activity of drugs.

Caccia et al. (1993) studied the anorectic effect of D-fenfluramine in the **marmoset** (*Callithrix jacchus*).

Knoll (1979, 1984) described satietin, a anorectic substance which has been isolated from serum of humans and several animal species. Satietin has been reported to be a 50000–70000 dalton MW glycoprotein, containing 14–15% amino acids and 70–75% carbohydrates, surviving digestion with proteases and boiling. Purification of bovine serum satietin was reported by Nagy (1994). These factors suppressed feeding in rats after peripheral and after intracerebroventricular administration.

REFERENCES AND FURTHER READING

Abadie JM, Wright B, Correa G, Browne ES, Porter JR, Svec F (1993) Effect of dihydro-epiandrosterone on neurotransmitter levels and appetite regulation of the obese Zucker rat. Diabetes 42:662–669

Anelli M, Bizzi A, Caccia S, Codegoni AM, Fracasso C, Garattini S (1992) Anorectic activity of fluoxetine and norfluoxetine in mice, rats, and guinea pigs. J Pharm Pharmacol 44:696–698

Antelman SM, Szechtman H (1975) Tail pinch induces eating in sated rats which appears to depend on nigrostriatal dopamine. Science 189:731–733

Bauhofer A, Witte K, Lemmer B, Middeke M, Lorenz W, Celik I (2002) Quality of life in animals as a new outcome for surgical research: G-CSF as a quality of life improving factor. Eur Surg Res 34:22–29

Bickel M, Gossel M, Geisen K, Jaehne G, Lang HJ, Rosenburg R, Sandow J (2004) Analysis of the anorectic efficacy of HMR1426 in rodents and its effects on gastric emptying in rats. Int J Obes 28:211–221

Blavet N, DeFeudis FV, Clostre F (1982) Studies on food intake in the fasted rat. Gen Pharmacol 13:293–297

Bowden CR, Karkanias CD, Bean AJ (1988) Re-evaluation of histidyl-proline diketopiperazine [cyclo(his-pro)] effects on food intake in the rat. Pharmacol Biochem Behav 29:357–363

Caccia S, Anelli M, Fracasso C, Frittoli E, Giorcelli P, Gobbi M, Taddei C, Garattini S, Mennini T (1993) Anorectic effect and brain concentrations of D-fenfluramine in the marmoset: relationship to the *in vivo* and *in vitro* effects on serotonergic mechanisms. Naunyn Schmiedeberg's Arch Pharmacol 347:306–312

Clark JM, Clark AJM, Winn P (1992) *N*-methyl-D-aspartate lesions of the lateral hypothalamus do not reduce amphetamine or fenfluramine anorexia but enhance the acquisition of eating in response to tail pinch in the rat. Psychopharmacology 109:331–337

Cooper SJ, Dourish CT, Barber DJ (1990a) Fluoxetine reduces food intake by a cholecystokinin-independent mechanism. Pharmacol Biochem Behav 35:51–54

Cooper SJ, Dourish CT, Barber DJ (1990b) Reversal of the anorectic effect of (+)-fenfluramine in the rat by the selective cholecystokinin receptor antagonist MK-329. Br J Pharmacol 99:65–70

Cooper SJ, Francis J, Rusk IN (1990c) The anorectic effect of SK&F 38393, a selective dopamine D_1 agonist: a microstructural analysis of feeding and related behavior. Psychopharmacology 100:182–187

Cooper SJ, Francis J, Barber DJ (1993) Selective dopamine D-1 receptor antagonists, SK&F 38393 and CY 208–243 reduce sucrose sham-feeding in the rat. Neuropharmacol 32:101–102

Dourish CT, Hutson PH, Curzon G (1985) Low doses of the putative serotonin agonist 8-hydroxy-2-(di-n-propylamino)tetralin (8-OH-DPAT) elicit feeding in the rat. Psychopharmacology 86:197–204

Dourish CT, Hutson PH, Curzon G (1986) Para-chlorophenylalanine prevents feeding induced by the serotonin agonist 8-hydroxy-2-(di-n-propylamino)tetralin (8-OH-DPAT). Psychopharmacology 89:467–471

Eberle-Wang K, Simansky KJ (1992) The CCK-A receptor antagonist, devazipide, blocks the anorectic action of CCK but not peripheral serotonin in rats. Pharmacol Biochem Behav 43:943–947

Fantino M, Cabanac M (1980) Body weight regulation with a proportional hoarding response. Physiol Behav 24:939–942

Fantino M, Faïon F, Roland Y (1986) Effect of dexfenfluramine on body weight set-point: Study in the rat with hoarding behavior. Appetite 7 (Suppl):115–126

Fantino M, Boucher H, Faïon F, Mathiot P (1988) Dexfenfluramine and body weight regulation: experimental study with hoarding behavior. Clin Neuropharmacol 11 (Suppl 1):S97–S104

Ferrari F, Pelloni F, Giuliani D (1992) B-HT 920 stimulates feeding and antagonizes anorexia induced by ACTH and immobilisation. Eur J Pharmacol 210:17–22

Fray PJ, Koob GF, Iversen SD (1982) Tail-pinch-elicited behavior in rats: preference, plasticity and learning. Behav Neural Biol 36:108–136

Gaetani S, Oveisi F, Piomelli D (2003) Modulation of meal pattern in the rat by the anorectic lipid mediator oleoylethanolamide. Neuropsychopharmacology 28:1311–1316

Garattini S (1992) An update on the pharmacology of serotoninergic appetite-suppressive drugs. Int J Obesity 16/ Suppl l4:S41–S48

Garattini S, Bizzi A, Codegoni AM, Caccia S, Mennini T (1992a) Progress report on the anorexia induced by drugs believed to mimic some of the effects of serotonin on the central nervous system. Am J Clin Nutr 55:160S–166S

Garattini S, Bizzi A, Caccia S, Mennini T (1992b) Progress report on the anorectic effects of dexfenfluramine, fluoxetine and sertaline. Intern J Obesity 16/Suppl 3:S43–S50

Gilbert F, Dourish CT (1987) Effects of the novel anxiolytics gespirone, buspirone and ipsapirone on free feeding and on feeding induced by 8-OH-DPAT. Psychopharmacology 93:349–352

Hammer VA, Gietzen DW, Beverly JL, Rogers QR (1990) Serotonin$_3$ receptor antagonists block anorectic responses to amino acid imbalance. Am J Physiol, Regul Integr Comp Physiol 259:R627–R636

Hull KM, Maher TJ (1990) L-Tyrosine potentiates the anorexia induced by mixed-acting sympathomimetic drugs in hyperphagic rats. J Pharm Exp Ther 255:403–409

Jackson HC, Bearham MC, Hutchins LJ, Mazurkiewicz SE, Needham AM, Heal DJ (1997) Investigation of the mechanisms underlying the hypophagic effects of the 5-HT and noradrenaline reuptake inhibitor, sibutramine, in the rat. Br J Pharmacol 121:1613–1618

Knoll J (1979) Satietin: A highly potent anorexogenic substance in human serum. Physiol Behav 23:497–502

Knoll J (1984) Satietin: A 50000 dalton glycoprotein in human serum with potent, long-lasting and selective anorectic activity. J Neural Transmiss 59:163–194

Leung PMB, Rogers QR (1969) Food intake: regulation by plasma amino acid pattern. Life Sci 8:1–9

Maher TJ, Hull KM (1990) Effects of L-tyrosine on the anorectic activity of mixed-acting sympathomimetics in hyperphagic rats. Eur J Pharmacol 183:429–430

Mennini T, Bizzi A, Caccia S, Codegoni A, Fracasso C, Frittoli E, Guiso G, Padura IM, Taddei C, Uslenghi A, Garattini S (1991) Comparative studies on the anorectic activity of *d*-fenfluramine in mice, rats and guinea pigs. Naunyn Schmiedeberg's Arch Pharmacol 343:483–490

Nagy J (1994) Purification of the anorectic agents satietin from bovine serum. Pharmacol Biochem Behav 48:17–22

Nishida KJ, Dougherty GG, Ellinwood EH, Rockwell WJK (1990) Effects of chronic chlorimipramine and imipramine administration on food hoarding behavior in male rats. Res Commun Psychol Psychiatry Behav 15:115–128

Robert JJ, Orosco M, Rouch C, Jacquot C, Cohen Y (1989) Unexpected responses of the obese "cafeteria" rat to the peptide FMRF-amide. Pharmacol Biochem Behav 34:341–344

Rosofsky M, Geary N (1989) Phenylpropanolamine and amphetamine disrupt postprandial satiety in rats. Pharmacol Biochem Behav 34:797–803

Rouru J, Huuponen R, Pesonen U, Koulu M (1992) Subchronic treatment with metformin produces anorectic effect and reduces hyperinsulinemia in genetically obese Zucker rats. Life Sci 50:1813–1820

Samanin R, Mennini T, Ferraris A, Bendotti C, Borsini F, Garattini S (1979) m-Chlorophenylpiperazine: A central serotonin agonist causing powerful anorexia in rats. Naunyn-Schmiedeberg's Arch Pharmacol 308:159–163

Simansky KJ, Vaidya AH (1990) Behavioral mechanisms for the anorectic action of the serotonin (5-HT) uptake inhibitor sertaline in rats: comparison with directly acting 5-HT agonists. Brain Res Bull 25:953–960

Simmons RD, Blosser JC, Rosamond JR (1994) FPL 14294: A novel CCK-8 agonist with potent intranasal anorectic activity in the rat. Pharmacol Biochem Behav 47:701–708

Stevens R, Edwards S (1996) Effect of a 5-HT$_3$ antagonist on peripheral 5-hydroxytryptamine-induced anorexia. Psychobiology 24:67–70

Thurlby PL, Samanin R (1981) Effects of anorectic drugs and prior feeding on food-rewarded runway behavior. Pharmacol Biochem Behav 14:799–804

Vergoni AV, Poggioli R, Marrama D, Bertolini A (1990) Inhibition of feeding by ACTH-(1–24): behavioral and pharmacological aspects. Eur J Pharmacol 179:347–355

Voigt JP, Fink H, Marsden CA (1995) Evidence for the involvement of the 5-HT$_{1A}$ receptor in CCK induced satiety in rats. Naunyn-Schmiedeberg's Arch Pharmacol 351:217–220

L.3.1.2 Computer-Assisted Measurement of Food Consumption in Rats

PURPOSE AND RATIONALE

Techniques have been developed for continuous measurement of food consumption in rats.

PROCEDURE

Animals are placed individually in cages (Macrolon cage Type 4, size: 44 × 26 × 15 cm) equipped with a device for continuous monitoring of feed consumption. This device is a container filled with feed and hanging on an electronic balance in the cage. The balance transmits the weight changes of the feed container continuously to a central unit. The data are stored and processed at the end of the experiment. This system can measure feed consumption continuously for up to 2 weeks from up to 64 feeding sensors (animals) simultaneously. The feeding monitoring system and data processing hardware and software (Release V3.07) can be obtained from TSE-Systems, Bad Homburg, Germany. Software options: the data are presented in the form of a matrix. The matrix delivers cumulatively or sequentially feed consumption in grams (g) for given time intervals for each individual animal. The advantages of this system are that the animals are kept in their home cages, that the feed monitoring period is long and, most of all, the animals are left undisturbed during the experimental session. An additional program for microstructural analysis calculates the parameters for feed consumption over a given time (24 h). Parameters delivered are: number of meals (Nm/time), inter-meal breaks (IMB) (min), average meal size (g) and average meal duration (min). In the present study, a meal was defined to be $\geq$0.5 g and the IMB $\geq$15 min. Using this system we have determined the anorectic activity of the central acting anorectic agents amphetamine, sibutramine, and dexfenfluramine (Bickel et al. 2000), as well as the peripheral acting anorectic SR146131, a CCK_A-receptor antagonist (Bickel et al. 2002), and HMR1426, an anorectic drug that powerfully inhibits gastric emptying rate (Bickel et al. 2004).

A 2-week treatment with HMR1426 in Zucker fatty rats fed a normal standard rat diet (1 g feed = 12.1 kJ) reduced the body weight increase significantly by 5% (Gossel et al. 2001). In Zucker fatty rats fed a fat-rich diet (1 g feed = 20.2 kJ), 3 weeks of treatment with HMR1426 caused a significant loss of body weight of 33% (Bickel et al. 2003).

REFERENCES AND FURTHER READING

Bickel M, Jaehne G, Stapf M, Wandschneider J, Gossel M (2000) Microstructural analysis of feeding behavior after amphetamine, sibutramine and dexfenfluramine in rats. Int J Obes 24 [Suppl 1]: Abstract 413

Bickel M, Gossel M, Jaehne G (2002) Acute and chronic effects of the CCK_A-receptor agonist (SR146131) on body weight development, feed consumption and the pancreas in rodents. In: Benedetti E, Pedone C (eds) Peptides 2002. Proceedings of the 27th European Peptide Symposium, 31 August to 6 September 2002, Sorrento, Italy. Edizioni Zino, Naples, pp 436–437

Bickel M, Gossel M, Jaehne G, Lang HJ, Sandow J (2003) Antiobesic effect of HMR1426 and obesity and diabetes related serum parameters in female Zucker fatty rats. Int J Obes 27 [Suppl 1]: Abstract T4:P4–012

Bickel M, Gossel M, Geisen K, Jaehne J, Lang HJ, Rosenburg R, Sandow J (2004) Analysis of the anorectic efficacy of HMR1426 in rodents and its effects on gastric emptying in rats. Int J Obes 28:211–221

Gossel M, Bickel M, Jaehne G, Stapf M, Wandschneider J, Sandow J (2001) Effect of 14 days treatment with HMR1426, a new anorectically acting drug, on body weight development and obesity related serum parameters in Zucker fatty rats. Obes Res Suppl 9: Abstract PG72

L.3.1.3 The Endocannabinoid System

PURPOSE AND RATIONALE

Recent discovery of cannabinoid receptors and their natural ligands, the endocannabinoids, has initiated the development of synthetic antagonists and agonist of these receptors to better understand the physiological role of the endocannabinoid system. Two types of receptors have been so far identified: the CB_1-receptor present in brain and periphery and the CB_2-receptor found in the periphery only. Both types of receptors are negatively coupled to Ca^{2+} channels through G-proteins (Pertwee 1997; Howlett et al. 2002). Kogan and Mechoulam (2006) gave an overview on the chemistry of endocannabinoids as well as of some synthetic molecules that affect the endocannabinoid system. Matias and Di Marzo (2006) described the enzymes involved in endocannabinoid synthesis and degradation. The endocannabinoid system has emerged as an important neuromodulatory system in the brain (Marsicano and Lutz 2006). Endocannabinoids play important roles in the gastrointestinal tract (Massa and Monory 2006) and in energy metabolism (Pagotto and Pasquali 2006).

For further studies on the pharmacological effects of cannabinoids and cannabinoid antagonists and on cannabinoid receptor binding see Sects. H.1.1.8, H.1.1.8.1, and H.1.1.8.2.

The appetite-stimulating effect of marijuana with its main active ingredient Δ^9-tetrahydrocannabinoid (Δ^9-

THC) has been known for a long time. The demonstration that the endogenous endocannabinoid anandamide induces overeating in rats suggests a physiological role for endocannabinoids (Williams and Kirkham 1999). Further support for this hypothesis came from CB1 receptor knockout mice ($CB1^{-/-}$) which were hypophagic and lean compared to wild-type mice (Cota et al. 2003).

The search for CB_1-receptor antagonists with anorectic properties led to the discovery of SR141716 (rimonabant). The compound inhibited CB_1-receptors in rat brain synaptosomes with an $IC_{50} = 2.35 \pm 0.47$ nM (Rinaldi-Carmona et al. 1996). A large number of different investigators have confirmed the powerful anorectic and antiobesic effect of this drug in various models. Simiand et al. (1998) investigated the anorectic effect in marmosets. Colombo et al. (1998) tested the anorectic effect and body weight reduction in non-obese Wistar rats. Ravinet-Trillou et al. (2003) showed anorectic properties of SR141716 in diet-induced obese mice.

PROCEDURE

Mice were housed on a reverse light-dark cycle (lights off 0900–2100 hours) in a room with temperature (22±2°C) and humidity control. They were fed either a high-fat diet (HFD) of 4.7 cal/g energy density (TD 97366, Harlan; 49% fat, 18% protein, 33% carbohydrate) or a standard mouse diet (STD) containing 2.9 kcal/g (A04C, UAR; 8% fat, 19% protein, 73% carbohydrate). SR141716 [*N*-piperidino-5-(4-chlorophenyl)-1-(2,4-dichlorophenyl)-4-methylpyrazole-3-carboxamide] was administered orally in distilled water with 0.1% Tween 80 just before the onset of the dark phase. A habituation to treatment with the vehicle was performed during the week before the start of treatment.

SR141716 Treatment in DIO Mice

Six-week-old C57BL/6J male mice were given HFD or STD diets for 12–17 weeks before drug treatment started. The mice were weight matched and assigned to one of the following three groups: high-fat diet fed/vehicle-treated (HFD-Veh), high-fat diet fed/SR141716-treated (10 mg/kg) (HFD-SR 10 mg), and standard-diet fed/vehicle-treated (STD-Veh). Body weight and individual food intake were recorded daily. The energy intake was determined taking into account the caloric density of each diet and the average daily energy intake was calculated weekly for each of the 5 weeks of treatment. To balance the wide difference in body weight between the groups, the relative energy intake was calculated by correcting for body weight and was expressed as kilocalories per gram mouse per day × 100. After a 30-day treatment, body fat and lean masses of anesthetized mice were estimated using a small research animal body composition analyzer (model SA-3000, EM-SCAN). The measurement principle is based on the high electrical conductivity in all lean tissues relative to lipids when exposed to an oscillating radio frequency. We previously calibrated the device by using carcass analysis of mice fed a standard or a high-fat diet. Regression models integrating total body electrical conductivity (TOBEC) values and body weights were fitted to chemically analyzed whole-body protein and fat contents (adjusted $r^2 = 0.96$, $P < 0.0001$ for protein, adjusted $r^2 = 0.93$, $P < 0.0001$ for fat). Food deprivation was shown to produce a reduction of metabolic rate in rodents and body weight loss during fasting was reported to be an indicator of this metabolic rate. Thus body weight change during a 24-h fast was measured after 5 weeks of treatment. Finally, additional 18-h-fasted mice were injected intraperitoneally with human recombinant insulin (Sigma) at the dose of 0.6 U/kg. Glycemia was measured before and 30, 60, 90, 120, and 180 min after insulin injection using a glucose analyzer (Bayer Diagnostics) to assess insulin sensitivity.

Another experiment compared a 3-day SR141716 treatment with a caloric restriction. Obese mice were randomized into one of the three treatment groups: a group treated with vehicle, a group treated with SR141716 at the dose of 10 mg/kg per day for 3 days, and a vehicle-treated pair-fed group (HFD-PFVeh) that was fed the same quantity of diet as that consumed by the animals receiving SR141716. Food intake and body weight were monitored daily; lumbar white adipose pads were weighed after death.

SR141716 Treatment in CB1 Receptor Knockout Mice

CB1 receptor knockout ($CB1^{-/-}$) mice were generated. For constructing the targeting vector, a 9-kb *Kpn*I-*Kpn*I fragment including the entire coding region of the CB1-receptor gene was cloned from a 129SvJ6 mouse genomic library. An *Apa*I-*Apa*I fragment containing part of the coding region was inactivated by substitution with a neomycin resistance cassette. The targeting vector was transfected into embryonic stem cells from the 129/Ola line. Then, mutated ES cells were injected into C57BL/6 blastocytes to generate chimeric founder mice. Germline transmission of the targeted allele was determined by PCR analysis of mouse tail genomic DNA. The homozygous $CB1^{-/-}$ mice used in this work were on a C57BL/6X129/Ola

F2 genetic background. The lack of binding of the synthetic CB1 receptor agonist [^{3}H]CP55,940 in these mice was checked by autoradiography in various brain sections. After 6 weeks of a high-fat diet, 15-week-old male CB1$^{-/-}$ mice were either given SR141716 orally at the dose of 10 mg/kg per day or treated with vehicle alone. Body weight and food intake were monitored daily throughout the 3-week treatment period as previously described.

EVALUATION

ANOVA and post hoc analyses were performed using SAS version 8.2. A repeated two-way ANOVA for treatment and time (repeated measures on food intake and body weight) or one-way ANOVA for treatment (all other variables) was used to determine statistical significance. When a single dose of SR141716 was included in the experiment, post hoc comparisons between the SR141716-treated group, obese, and lean control groups were performed after Holm's adjustment. When two doses of SR141716 were studied, comparisons among dietary obese mice receiving each of SR141716 doses versus vehicle were performed by Dunnett's test. When the hypotheses necessary for the application of parametric tests were not achieved, appropriate transformations were applied. The results are presented as means ± SEM.

MODIFICATIONS OF THE METHOD

SR147778, a CB_1-receptor antagonist, was shown to cause a long-lasting anorectic effect in fasted and non-deprived rats and to reduce ethanol drinking in mice. In CHO-cells expressing the *h*CB1-receptor the K_i was 3.5 ± 0.29 nM, whereas the K_i for *h*CB2-receptors was 442 ± 30 nM (Rinaldi-Carmona et al. 2004).

Animals

Male Sprague-Dawley rats (180–250 g) were used for *in vitro* and food intake studies. Male Wistar rats (300 g) obtained from Charles River were used for schedule-induced polydipsia (SIP) studies.

Drug Preparation and Administration

For *in vivo* experiments, drugs were suspended with 0.01% Tween 80 plus DMSO in saline (NaCl 0.9%) for i.v. administration or distilled water for other routes. SR147778 was administered by i.p., p.o., or s.c. routes in a volume of 20 ml/kg body weight.

Voluntary Ethanol Consumption

The test was performed as described by Arnone et al. (1997). One week before testing, mice were singly housed in cages equipped with two bottles of plain water. Mice were then subjected to five daily 6-h test sessions during which they had a free choice between one bottle of water or one filled with a 10% (v/v) non-sweetened ethanol solution. The quantities of the different liquids consumed were measured by weighing the bottle before and after each session. The bottles were regularly checked for possible leakage. SR147778 was administered 30 min before each experiment session.

Spontaneous Sucrose Drinking

Two weeks prior to testing, rats caged individually were given access to a sucrose solution (5%) in their home cage during daily 4-h sessions (without food and water). At the end of the training periods, rats displaying a poor sucrose drinking response were discarded from the study. On the day of the test, rats were administered orally with SR147778 or vehicle in a volume of 2 ml/kg 1 h before the presentation of the sucrose solution. The amount of the sucrose solution drunk by each rat (n = 6–8 per group) was measured by weighing each bottle before and at the end of the 4-h drinking period.

Food Intake in 18-h Fasted Rats

Over a period of 10 days before the experiment, rats were fasted for 18 h and allowed access to food for only 6 h between 10:00 a.m. and 4:00 p.m. each day. Water was available ad libitum. At the end of this adaptation phase, SR147778 or vehicle was administered orally, in a volume of 5 ml/kg, at 9:00 a.m., 1 h after a preweighed amount of food (A04 standard rat laboratory diet) was introduced into the cage, and then food intake was measured (taking into account spillage) at different times.

Spontaneous Feeding in Non-deprived Rats

Rats were maintained in a reversed light/dark cycle (lights off 9:00 a.m. to 9:00 p.m.) with food and water ad libitum. On the day of the experiment, food was removed from the cage at 8:00 a.m., and animals were administered orally with SR147778 or vehicle in a volume of 5 ml/kg at 9:00 a.m. (at the beginning of the dark phase). One hour after, a preweighed amount of food (A04 standard rat laboratory diet) was introduced into the cage, and then food intake was measured (taking into account spillage) at different times.

Schedule-Induced Ethanol Polydipsia

Rats were randomly allocated to drinking either water or ethanol in a protocol of SIP (Falk et al. 1972). They were food deprived (food available for 1 h per

day) but not water deprived. They were trained in operant chambers (40.5 × 31 × 31 cm; Imetronic, Pessac, France) fitted with a food tray where food pellets (45 mg; Bioserv, Phymep, Paris) were delivered every 60 s (FT-60s). Visits to the food tray were automatically recorded. A metal drinking tube protruded into the chamber near the food magazine and was connected to a drinking bottle. Licks of the drinking tube were numbered by the closure of an electric circuit. Bottles were weighed to the nearest 0.1 g at the end of each SIP session. Both groups were trained for 2 weeks, 5 days per week, under the SIP procedure until they drank about 10 ml of plain water, which was then substituted for slightly sweetened solutions (0.05% weight/volume saccharose) of either water or ethanol. Over the next 2 weeks of training, the concentration of ethanol was progressively increased by steps of 2% to reach the final 10% concentration. Fluid consumption was allowed to stabilize over five daily training sessions. Then, each group (ethanol or water) was divided into two subgroups: one treated with one dose of SR147778 administered i.p. 1 h before testing and the other subgroup administered with the corresponding vehicle. As a control, SR141716 was tested at 10 mg/kg in the same conditions. The four subgroups of rats were tested once a week (1-h test session) with a different dose of SR147778 and trained daily (1-h training session) on the 4 remaining days. In the same rats and in the same experimental conditions, the activity of the reference CB1 antagonist, SR141716, had previously been investigated at 10 mg/kg i.p. Data are presented as the mean quantities of water or ethanol consumed during each test session; they were analyzed with Student's *t*-test to compare the quantities of water or ethanol rats drank after administration of SR147778 or vehicle during a given test session.

Data Analysis

Data from competition experiments (IC_{50}, EC_{50}, and DE_{50}) were analyzed using a non-linear least-squares method. K_d values of 0.09± 0.01 nM (brain), 0.309± 0.031 nM (hCB1), 0.17± 0.03 nM (spleen), and 0.49± 0.11 nM (hCB2) were used to determine K_i values. A Schild plot was constructed to estimate the pA_2 value in mouse vas deferens and adenylyl cyclase studies. Statistical significance was determined by Student's *t*-test, and $p < 0.05$ was considered significant. For *in vivo* pharmacological tests, statistical analysis was performed using ANOVA followed by Dunnett's *t*-test. ID_{50} values were calculated using the Pharmacofit method.

Matias et al. (2006a) described regulation of the levels of endogenous cannabinoids in the brain and peripheral tissues and the control of food intake.

Mechoulam et al. (2006) reviewed the effects of endocannabinoids on feeding and suckling.

Regulation, function and dysregulation of endocannabinoids in models of adipose and β-pancreatic cells and in obesity and hyperglycemia are described by Matias et al. (2006b).

REFERENCES AND FURTHER READING

Arnone M, Maruani J, Chaperon F, Thiébot MH, Poncelet M, Soubrié P, LeFur G (1997) Selective inhibition of sucrose and ethanol intake by SR141716, an antagonist of the central (CB1) receptors. Psychopharmacology 132:104–106

Colombo G, Agabio R, Diaz G, Lobina C, Reali R, Gessa GL (1998) Appetite suppression and weight loss after the Cannabinoid antagonist SR 141716. Life Sci 8:113–117

Cota D, Marsicano G, Tschöp M, Grübler Y, Flachskamm C, Schubert M, Auer D, Yassouridis A, Thöne-Reineke C, Ortmann S, Thomassoni F, Cervino C, Nisoli E, Linthorst ACE, Pasquali R, Lutz B, Stalla K, Pagotto U (2003) The endogenous cannabinoid system affects energy balance via central orexigenic drive and peripheral lipogenesis. J Clin Invest 112:423–431

Falk JL, Samson HH, Winger G (1972) Behavioral maintenance of high concentrations of blood ethanol and physical dependence in the rat. Science 177:811–813

Howlett AC, Barth F, Bonner TI, Cabral G, Casellas P, Devane WA, Felder CC, Herkenham M, Mackie K, Martin BR, Mechoulam R, Pertwee RG (2002) International Union of Pharmacology XXVII. Classification of cannabinoid receptors. Pharmacol Rev 54:161–202

Kogan NM, Mechoulam R (2006) The chemistry of endocannabinoids. J Endocrinol Invest 29 [Suppl 3]:3–14

Marsicano G, Lutz B (2006) Neuromodulatory functions of the endocannabinoid system. J Endocinol Invest 29 [Suppl 3]: 27–46

Massa F, Monory K (2006) Endocannabinoids and the gastrointestinal tract. J Endocrinol Invest 29 [Suppl 3]:47–57

Matias I, Di Marzo V (2006) Endocannabinoid synthesis and degradation, and their regulation in the framework of energy balance. J Endocrin Invest 29 [Suppl 3]:15–26

Matias I, Bisogno T, Di Marzo V (2006a) Endogenous cannabinoids in the brain and peripheral tissues: regulation of their levels and control of food intake. Int J Obes 30:S7–S12

Matias I, Gonthier MP, Orlando P, Martiadis V, De Petrocellis L, Cervino C, Petrosino S, Hoareau L, Festy F, Pasquali R, Roche R, Maj M, Pagotto U, Monteleone P, Di Marzo V (2006b) Regulation, function and dysregulation of endocannabinoids in models pf adipose and β-pancreatic cells and in obesity and hyperglycemia. Clin Endocrin Metab 91:3171–3180

Mechoulam R, Berry EM, Avraham Y, Di Marzo V, Fride E (2006) Endocannabinoids, feeding and suckling – from our perspective. Int J Obes 30 [Suppl 1]:S24–S28

Pagotto U, Pasquali R (2006) Endocannabinoids and energy metabolism. J Endocrinol Invest 29 [Suppl3]:58–68

Pertwee RG (1997) Pharmacology of cannabinoid CB1 and CB2 receptors. Pharmacol Ther 74:129–180

Ravinet-Trillou C, Arnone M, Delgorge C, Gonalons N, Keane P, Maffrand JP, Soubrié P (2003) Anti-obesity effects of SR141716, a CB1 receptor antagonist, in diet-induced obese mice. Am J Physiol 284:R345–R353

Rinaldi-Carmona M, Pialot F, Congy C, Redon E, Barth F, Bachy A, Brelière J-C, Soubrié P, Le Fur G (1996) Characterization and distribution of binding sites for [^{3}H]-SR 141716A, a selective brain (CB1) cannabinoid receptor antagonist, in rodent brain. Life Sci 58:1239–1247

Rinaldi-Carmona M, Barth F, Congy C, Martinez S, Oustric D, Pério A, Poncelet M, Maruani J, Arnone M, Finance O, Soubrié P, Le Fur G (2004) SR147778 [5-(4-bromophenyl)-1-(2,4-dichlorophenyl)-4-ethyl-N-(1-piperidinyl)-1*H*-pyrazole-3-carboxamide], a new potent and selective antagonist of the CB1 cannabinoid receptor: biochemical and pharmacological characterization. J Pharmacol Exp Ther 310:905–914

Simiand S, Keane M, Keane PE, Soubrié P (1998) SR 141716, a CB1 cannabinoid receptor antagonist, selectively reduces sweet food intake in marmoset. Behav Pharmacol 9:179–181

Williams CM, Kirkham TC (1999) Anandamide induces overeating: mediation by central cannabinoid (CB1) receptors. Psychopharmacology 143:315–317

L.3.2 Metabolic Activity

L.3.2.1 GDP-Binding in Brown Adipose Tissue

PURPOSE AND RATIONALE

Brown adipose tissue is the major site for non-shivering thermogenesis in rodents (Ricquier and Mory 1984; Foster 1986). Drugs activating brown adipose tissue thermogenesis via β-adrenoceptors cause uncoupling of oxidative phosphorylation from electron transport (Arch et al. 1984; Nicholls et al. 1986). The binding of the nucleotide guanosine diphosphate (GDP) to brown adipose tissue membrane protein, the uncoupling protein or thermogenin (Ricquier and Bouillaud 1986), is an established indicator of the thermogenetic activity of brown adipose tissue (Milner et al. 1988).

PROCEDURE

Obese male fatty Zucker rats at the age of 13 weeks weighing about 450 g receive various doses of the test compound in the drinking water or tap water as control for 21 days. Food intake is measured every day and body weight every other day. At the end of the treatment, the rats are sacrificed by decapitation and interscapular brown adipose tissue is quickly dissected from surrounding tissue.

According to the method published by Nicholls (1976) brown adipose tissue is minced, diluted with 250 mM sucrose and homogenized with a Potter S homogenizer (B. Braun Melsungen, Germany). The homogenate is centrifuged for 10 min at 8500 *g*. The pellet is diluted with 250 mM sucrose and centrifuged at 700 *g* for 10 min. The supernatant is collected and centrifuged at 8500 *g* for 10 min. Bovine serum albumin at 0.2% is added to wash the suspension of the pellet, which now consists of mitochondria. After centrifugation (8500 *g*) the resulting pellet is suspended in albumin-free sucrose buffer. The binding of [3H]-GDP (DuPont NEN, Boston MA) to mitochondria of single rats is determined by incubating mitochondria in a basic medium containing 100 mM sucrose, 20 mM TES (*N*-tris-[hydroxymethyl]-methyl-2-aminoethanesulphonic acid), 1 mM EDTA, 10 mM choline chloride, 2 µM rotenone, [^{14}C]sucrose (0.125 µCi ml^{-1}) and 10 µM [^{3}H]-GDP (0.53 Ci mmol^{-1}) at room temperature. Non-specific binding is assessed in the presence of unlabelled GDP (1 mM). After 10 min of incubation, the reaction is terminated by filtration the mixture through Thomas A/E glass fibre filters by using a Brandel cell harvester. The radioactivity is measured with the Opti Phase 'High Safe' II scintillation cocktail and a scintillation counter enabling the samples to be counted for both ^{3}H and ^{14}C. The protein content of the mitochondrial suspensions is assayed according to the method of Peterson (1977).

EVALUATION

GDP binding is assessed from ^{3}H radioactivity with a correction for trapped medium using [^{14}C]-sucrose. Two way analysis of variance (ANOVA) is performed.

MODIFICATIONS OF THE METHOD

Glucose is a minor substrate for isolated brown adipocytes, fuelling thermogenesis by a maximum of 16% (Isler et al. 1987).

The mechanism of anti-obesity action of a dihydropyridine calcium antagonist was studied by Yoshida et al. (1994b). Obesity was induced by subcutaneous injection of 2 g/kg monosodium-L-glutamate immediately after birth for 5 consecutive days in ICR female mice. Binding of GDP and cytochrome c oxidase activity in brown adipose tissue mitochondria were significantly increased after 4 weeks drug treatment incorporated in the diet.

Yoshida et al. (1984, 1985) found a reduced norepinephrine turnover in brown adipose tissue of mice with monosodium glutamate-induced obesity.

Kajita et al. (1994), Takahashi et al. (1994) determined regional blood flow in brown adipose tissue by the microsphere method in anesthetized rats.

Yoshida et al. (1996) determined the effect of mazindol on noradrenaline turnover in brown adipose tissue of yellow KK mice and C57B1 control mice.

REFERENCES AND FURTHER READING

Arch JRS, Ainsworth AT, Cawthorne MA, Piercy V, Sennitt MV, Thody VE, Wilson C, Wilson S (1984) Atypical β-adrenoceptor on brown adipocytes as target for anti-obesity drugs. Nature 309:163–165

Foster DO (1986) Quantitative role of brown adipose tissue in thermogenesis. In: Trayhurn P, Nicholls DG (eds) Brown Adipose Tissue. Edward Arnold, Ltd., London, pp 31–51

Halloway BR (1989) Selective β-agonists of brown fat and thermogenesis. In: Lardy H, Stratman F (eds) Hormones, Thermogenesis and Obesity. Elsevier, New York, pp 477–484

Himms-Hagen J (1989) Brown adipose tissue thermogenesis and obesity. Progr Lipid Res 28:67–115

Isler D, Hill HP, Meier MK (1987) Glucose metabolism in isolated brown adipocytes under β-adrenergic stimulation. Quantitative contribution of glucose to total thermogenesis. Biochem J 245:789–793

Kajita J, Kobayashi S, Yoshida T (1994) Effect of benidipine hydrochloride on regional blood flow of the adipose tissue in anesthetized rats. Arzneim Forsch/Drug Res 44:297–300

Milner RE, Wilson S, Arch JRS, Trayhurn A (1988) Acute effects of a β-adrenoceptor agonist (BRL 26830A) on rat brown adipose tissue mitochondria. Biochem J 249:759–763

Nedergaaard J, Jacobsson A, Cannon B (1989) Adrenergic regulation of thermogenin activity and amount in brown adipose tissue. In: Lardy H, Stratman F (eds) Hormones, Thermogenesis and Obesity. Elsevier, New York, pp 105–116

Nicholls DG (1976) Hamster-brown-adipose tissue mitochondria: purine nucleotide control of the ionic conductance of the inner membrane, the nature of the nucleotide binding site. Eur J Biochem 62:223–228

Nicholls DG, Cunningham SA, Rial E (1986) The bioenergetic mechanisms of brown adipose tissue thermogenesis. In: Trayhurn P, Nicholls DG (eds) Brown Adipose Tissue. Edward Arnold, Ltd., London, pp 52–85

Peterson GL (1977) A simplification of the protein assay method of Lowry et al. which is generally more applicable. Anal Biochem 83:346–356

Ricquier D, Mory G (1984) Factors affecting brown adipose tissue in animals and man. Clinics Endocrinol Metab 13:501–521

Ricquier D, Bouillaud F (1986) The brown adipose tissue mitochondrial uncoupling protein. In: Trayhurn P, Nicholls DG (eds) Brown Adipose Tissue. Edward Arnold, Ltd., London, pp 86–104

Santti E, Huupponen R, Rouro J, Hänninen V, Pesonen U, Jhanwar-Uniyal M, Koulu M (1994) Potentiation of the anti-obesity effect of the β_3-adrenoceptor agonist BRL 35135 in obese Zucker rats by exercise. Br J Pharmacol 113:1231–1236

Savontaus E, Raasmaja A, Rouru J, Koulu M, Pesonen U, Virtanen R, Savola JM, Huupponen R (1997) Anti-obesity effect of MPV-1743 A III, a novel imidazoline derivative, in genetic obesity. Eur J Pharmacol 328:207–215

Swick RW, Henningfield MF (1989) Changes in the number of GDP binding sites on brown adipose tissue (BAT) mitochondria and its uncoupling protein. In: Lardy H, Stratman F (eds) Hormones, Thermogenesis and Obesity. Elsevier, New York, pp 117–127

Takahashi H, Nakano K, Yasuda TT, Komiyma Y, Muakami T, Nishimura M, Nakanishi T, Sakamoto SH, Nanbu A, Yoshimura M (1994) Anti-obesity and anti-diabetic effects of carterenol in non-insulin dependent diabetic mice. Clin Exp Pharmacol Physiol 21:477–483

Yoshida T, Nishioka H, Nakamura Y, Kondo M (1984) Reduced norepinephrine turnover in mice with monosodium glutamate-induced obesity. Metabolism 33:1060–1063

Yoshida T, Nishioka H, Nakamura Y, Kanatsuna T, Kondo M (1985) Reduced norepinephrine turnover in brown adipose tissue of pre-obese mice treated with monosodium-L-glutamate. Life Sci 36:931–938

Yoshida T, Hiraoka N, Yoshioka K, Hasegawa G, Kondo M (1991) Anti-obesity and anti-diabetic actions of a β_3-adrenoceptor agonist, BRL 28630A, in yellow kk mice. Endocrinol Japon 38:397–403

Yoshida T, Sakane N, Wakabayashi Y, Umekawa T, Kondo M (1994a) Anti-obesity and anti-diabetic effects of CL 316,243, a highly specific β_3-adrenoceptor agonist, in yellow KK mice. Life Sci 54:491–498

Yoshida T, Umekawa T, Wakabayashi Y, Sakane N, Kondo M (1994b) Mechanism of anti-obesity action of bendipine hydrochloride in mice. Int J Obesity 18:776–779

Yoshida T, Umekawa T, Wakabayashi Y, Yoshimoto K, Sakane N, Kondo M (1996) Anti-obesity and anti-diabetic effects of mazindol in yellow kk mice: its activating effect on brown adipose tissue thermogenesis. Clin Exp Pharmacol Physiol 23:476–482

Umekawa T, Yoshida T, Sakane N, Saito M, Kumamoto K (1997) Anti-obesity and anti-diabetic effects of CL316,243, a highly specific β_3-adrenoceptor agonist, in Otsuka Long Evans Tokushima Fatty rats: induction of uncoupling protein and activation of glucose transporter 4 in white fat. Eur J Endocrinol 136:429–437

L.3.2.2 Uncoupling Protein and GLUT4 in Brown Adipose Tissue

PURPOSE AND RATIONALE

Uncoupling proteins (UCPs) are a family of inner mitochondrial membrane transporters which dissipate the proton gradient, releasing stored energy as heat. UCP1 is expressed exclusively in brown adipocytes, UCP2 is expressed widely, while UCP3 is found in skeletal muscle and brown adipose tissue (Vidal-Puig et al. 1997; Fleury et al. 1997; Masaki et al. 1997; Matsuda et al. 1997; Boss et al. 1997; Gong et al. 1997; Larkin et al. 1997). They are upregulated by thyroid hormones (Larkin 1997; Masaki 1997; Branco et al. 1999; Lanni et al. 1999). Mao et al. (1999) identified and characterized a novel member of the human uncoupling protein family, termed uncoupling protein-4 (UCP4).

In addition to the binding of the nucleotide guanosine diphosphate (GDP) to brown adipose tissue membrane protein, the uncoupling protein itself, and the glucose transporter 4 (GLUT4) were determined by RNA (Northern blot) analysis and by protein (Western blot) analysis as indicators of the thermogenetic activity of brown adipose tissue.

PROCEDURE

Male fatty (OLETF fatty) rats at the age of 10 weeks are given subcutaneous injection of test compound or

solvent once daily. After 14 weeks treatment, the rats are sacrificed and brown and white adipose tissue samples rapidly removed.

Northern Blot Analysis

Total RNA is extracted from 0.1–1 g of tissue using TRIzol (Gibco) and the concentration determined from the absorbance at 260 nm. Total RNA (20 mg) is separated on a 1.5% agarose/formaldehyde gel, and transferred to and fixed on a nylon membrane. A 488 bp uncoupling protein cDNA probe corresponding to the coding region of rat uncoupling protein is prepared by digesting the whole uncoupling protein cDNA with BamHI. The uncoupling protein probe and GLUT4 cDNA are labeled with α-[^{32}P]dCTP (deoxy-cytidine-triphosphate). The blots are hybridized to the labeled probes at 42°C for 20 h in the presence of 500 µg/ml salmon sperm DNA, and exposed to an X-ray film for autoradiography and an imaging plate of BAS1000 (Fuji Film) for quantitative analysis.

Western Blot Analysis

Each tissue is homogenized in 5–10 volumes of a solution containing 10 mmol/l Tris-HCl and 1 mmol/l EDTA (pH 7.4) for 30 s with a Polytron. After centrifugation at 1500 *g* for 5 min, the fat cake is discarded, and the infranatant (fat-free extract) is used for protein determination according to Lowry et al. (1951) and cytochrome C oxidase activity (Yonetani and Ray 1965). Uncoupling protein and GLUT4 protein in the fat-free extract is measured by Western blot analysis. The fat-free extracts (10 µg protein of brown adipose tissue, 20 µg of white adipose tissue) are solubilized, subjected to sodium dodecyl sulfate-polyacrylamide gel electrophoresis, and transferred to a nitrocellulose filter. After blocking with 5% non-fat dry milk, the filter is incubated with rabbit antiserum against rat uncoupling protein or GLUT4. The rabbit antisera against rat uncoupling protein and GLUT4 are prepared by immunizing purified rat uncoupling protein (Lin and Klingenberg 1980) and a 12-amino acid peptide corresponding to GLUT4 (residues 498–509, TELEYLGPDEND) (Shimizu et al. 1993) respectively, coupled with keyhole limpet hemocyanin. Then the filter is incubated with [^{125}I]protein A (ICN). The dry blot is exposed to an X-ray film for autoradiography and an imaging plate of BAS1000 (Fuji Film) for quantitative analysis.

EVALUATION

Data are expressed as means ± SEM and are analyzed by two-way ANOVA followed by Bonferroni *t*-test.

MODIFICATIONS OF THE METHOD

A radioimmunoassay to measure uncoupling protein was used by Milner et al. (1988).

Scarpace et al. (2000) performed unilateral surgical denervation of the interscapular BAT in rats under pentobarbital anesthesia according to Bartness et al. (1986). A transverse incision was made just anterior to the BAT, separating the BAT from the muscles of the scapulae. The BAT was raised to expose the five intercostal nerve bundles entering each pad. On one side, a section of each nerve bundle was removed with scissors. Denervation can be verified by assessing norepinephrine levels in the innervated compared with the denervated BAT pads (Scarpace and Matheny 1996).

Puigserver et al. (1996) studied the effects of retinoic acid isomers on the appearance of uncoupling protein in primary cultures of brown adipocytes, in the brown adipocyte cell line HIB 1B and directly in intact mice.

Shimabukuro et al. (1997) reported the induction of uncoupling protein-2 mRNA in the pancreatic islets of Zucker diabetic fatty rats by troglitazone.

Foellmi-Adams et al. (1996) found a synergy between norepinephrine and pioglitazone in induction of uncoupling protein in mice.

Kotz et al. (2000) determined uncoupling protein 1 (UCP1) in brown adipose tissue, UCP2 in white adipose tissue and UCP3 in muscle of male Sprague Dawley rats after injection of neuropeptide Y into the hypothalamic paraventricular nucleus.

Great efforts have been devoted to study the influence of **β_3-adrenergic agonists** on formation of uncoupling protein.

Umekawa et al. (1997) found an induction of uncoupling protein and activation of GLUT4 in white fat of Otsuka Long-Evans Tokushima fatty rats after treatment with a specific β_3-adrenoceptor agonist.

Ghorbani and Himms-Hagen (1997) found appearance of abundant densely-stained brown adipocytes expressing uncoupling protein in white adipose tissue during reversal of obesity and diabetes in Zucker fa/fa rats induced by the β_3-adrenoceptor agonist CL316,243.

Nagase et al. (1996) found in yellow obese KK mice after treatment with a β_3-adrenergic agonist a significant reduction of body weight, associated with a marked decrease of white fat pad weight and hypertrophy of the interscapular brown adipose tissue with a sixfold increase in mitochondrial uncoupling protein content.

Liu et al. (1995, 1996), Stock (1997) reported an increase of glucose utilization in rat brown adipose tis-

sue after treatment with a β_3-adrenoreceptor agonist or with sibutramine, a serotonin and noradrenaline reuptake inhibitor.

Savontaus et al. (1998) reported an increase of UCP3 and UCP1 in brown adipose tissue of obese fa/fa Zucker rats after chronic administration of a β_3-adrenoreceptor agonist.

The effects of β_3-adrenoceptor agonists on uncoupling protein-1 and leptin in culture-differentiated rat brown fat cells are antagonized by a β_3-adrenoreceptor antagonist (Tonello et al. 1998).

Berraondo et al. (2000) found an up-regulation of muscle UCP2 gene expression by a β_3-adrenoreceptor agonist in obese rodents, but down-regulation in lean animals.

Paulik and Lennard (1997) found an increased expression of uncoupling protein in C3H10T1/2 cells, a pluripotent stem-cell line, after addition of **thiazolidinediones**.

REFERENCES AND FURTHER READING

Bartness TJ, Billington CJ, Levine AS, Morley JE, Brown DM, Rowland ME (1986) Insulin and metabolic efficacy in rats. I. Effects of sucrose feeding and BAT axotomy. Am J Physiol 251:R1108–R1117

Berraondo B, Matrti A, Duncan JS, Trayhurn P, Martinez JA (2000) Up-regulation of muscle UPC2 gene expression by a new β_3-adrenoceptor agonist, trecadrine, in obese (cafeteria) rodents, but down-regulation in lean animals. Int J Obes 24:156–163

Boss O, Samec S, Paolini-Giacobino A, Rossier C, Dulloo A, Seydoux J, Muzzin P, Giacobino JP (1997) Uncoupling protein-3: A new member of the mitochondrial carrier family with tissue-specific expression. FEBS Lett 408:39–42

Branco M, Ribeiro M, Negrao N, Bianco C (1999) 3,5,3′-Triiodothyronine actively stimulates UCP in brown fat under minimal sympathetic activity. Am J Physiol 276; Endocrinol Metab 39:E179–E187

Fleury C, Neverova M, Collins S, Raimbault S, Champigny O, Levi-Meyrueis C, Bouillaud F, Seldin MF, Surwit RS, Ricquier D, Warden CH (1997) Uncoupling protein-2: A novel gene linked to obesity and hyperinsulinemia. Nat Genet 15:269–272

Foellmi-Adams LA, Wyss BM, Herron D, Nedergaard J, Kletzien RF (1996) Induction of uncoupling protein in brown adipose tissue. Synergy between norepinephrine and pioglitazone, an insulin-sensitizing agent. Biochem Pharmacol 52:693–701

Ghorbani M, Himms-Hagen J (1997) Appearance of brown adipocytes in white adipose tissue during CL316,243-induced reversal of obesity and diabetes in Zucker fa/fa rats. Int J Obes 21:465–475

Gong DW, He Y, Karas M, Reitman M (1997) Uncoupling protein-3 is a mediator of thermogenesis regulated by thyroid hormone, β_3-adrenergic agonists, and leptin. J Biol Chem 272:24129–24132

Kotz CM, Wang CF, Briggs JE, Levine AS, Billington CJ (2000) Effect of NPY in the hypothalamic paraventricular nucleus on uncoupling protein 1, 2, and 3 in the rat. Am J Physiol 278, Regul Integr Comp Physiol 47:R494–R498

Lanni A, Beneduce L, Lombardi A, Moreno M, Boss O, Muzzin P, Giacobino JP, Goglia F (1999) Expression of uncoupling protein-3 and mitochondrial activity in the transition from hypothyroid to hyperthyroid state in rat skeletal muscle. FEBS Lett 444:250–254

Larkin S, Mull E, Miao W, Pittner R, Albrandt K, Moore C, Young A, Denaro M, Beaumont K (1997) Regulation of the third member of the uncoupling protein family, UCP3, by cold and thyroid hormone. Biochem Biophys Res Commun 240:222–227

Lin CS, Klingenberg M (1980) Isolation of the uncoupling protein from brown adipose tissue mitochondria. FEBS Lett 133:299–303

Liu YL, Stock MJ, (1995) Acute effects of the β_3-adrenocptor agonist, BRL 35135, on tissue glucose utilization. Br J Pharmacol 114:888–894

Liu YL, Kashani SMZ, Heal DJ, Stock MJ, (1996) Effect of sibutramine on tissue glucose utilization in the rat. Br J Pharmacol 117:324P

Lowry OH, Rosebrough NJ, Farr AL, Randall RJ (1951) Protein measurement with the Folin phenol reagent. J Biol Chem 193:265–275

Mao W, Yu XX, Zhong A, Li W, Brush J, Sherwood SW, Adams SA, Pan G (1999) UCP, a novel, brain-specific mitochondrial protein that reduces membrane potential in mammalian cells. FEBS Lett 443:326–330

Masaki T, Yoshimatsu H, Kakuma T, Hidaka S, Kurakawa M, Sataka T (1997) Enhanced expression of uncoupling protein 2 gene in rat white adipose tissue and skeletal muscle following chronic treatment with thyroid hormone. FEBS Lett 418:323–326

Matsuda J, Hosada K, Itoh H, Son C, Doi K, Tanaka T, Fukunaga Y, Inoue G, Nishimura H, Yoshimasa Y, Yamori Y, Nakao K (1997) Cloning of rat uncoupling protein-3 and uncoupling protein-2 cDNAs: Their gene expression in rats fed a high fat diet. FEBS Lett 418:200–204

Milner RE, Wilson S, Arch JRS, Trayhurn P (1988) Acute effects of a β-adrenoceptor agonist (BRL 26830A) on rat brown-adipose-tissue mitochondria. Biochem J 249:759–763

Nagase I, Yoshida T, Kumamoto K, Umekawa T, Sakane N, Nikami H, Kawada T, Saito M (1996) Expression of uncoupling protein in skeletal muscle and white fat of obese mice treated with thermogenic β_3-adrenergic agonist. J Clin Invest 97:2898–2094

Paulik MA, Lenhard M (1997) Thiazolidinediones inhibit alkaline phosphatase activity while increasing expression off uncoupling protein, deiodinase, and increasing mitochondrial mass in C3H10T1/2 cells. Cell Tiss Res 290:79–87

Puigserver P, Vazquez F, Bonet ML, Pico C, Palou A (1996) *In vitro* and *in vivo* induction of brown adipocyte uncoupling protein (thermogenin) by retinoic acid. Biochem J 317:827–833

Ricquier D, Raimbault S, Champigny O, Miroux B, Bouillaud F (1992) The uncoupling protein is not expressed in rat liver. FEBS Lett 303:103–106

Savontaus E, Rouro J, Boss O, Huupponen R, Koulu M (1998) Differential regulation of uncoupling proteins by chronic treatments with β_3-adrenergic agonist BRL 35135 and metformin in obese fa/fa Zucker rats. Biochem Biophys Res Commun 246:899–904

Scarpace PJ, Matheney M (1996) Thermogenesis in brown adipose tissue with age: post-receptor activation by forskolin. Eur J Physiol 431:388–394

Scarpace PJ, Matheny M, Moore RL, Kumar MV (2000) Modulation of uncoupling protein 2 and uncoupling protein 3:

regulation by denervation, leptin and retinoic acid treatment. J Endocrinol 164:331–337
Shimabukuro M, Zhou YT, Unger RH (1997) Induction of uncoupling protein-2 mRNA by troglitazone in the pancreatic islets of Zucker diabetic fatty rats. Biochem Biophys Res Commun 237:359–361
Shimizu Y, Nikami H, Tsukazaki K, Machado UF, Yano H, Seino Y, Saito M (1993) Increased expression of glucose transporter GLUT-4 in brown adipose tissue of fasted rats after cold exposure. Am J Physiol 264:E890–E895
Shrago E, McTigue J, Katiyar S, Woldegiorgis C (1989) Preparation of highly purified reconstituted uncoupling protein to study biochemical mechanism(s) of proton conductance. In: Lardy H, Stratman F (eds) Hormones, Thermogenesis and Obesity. Elsevier, New York, pp 129–136
Stock MJ (1997) Sibutramine: a review of the pharmacology of a novel anti-obesity agent. Int J Obesity 21 (Suppl 1): S25–S29
Tonello C, Dioni L, Briscini L, Nisoli E, Carruba MO (1998) SR59230A blocks β_3-adrenoreceptor-linked modulation of uncoupling protein-1 and leptin in rat brown adipocytes. Eur J Pharmacol 352:125–129
Umekawa T, Yoshida T, Sakane N, Saito M, Kumamoto K, Kondo M (1997) Anti-obesity and anti-diabetic effects of CL316,243, a highly specific β_3-adrenoceptor agonist, in Otsuka Long-Evans Tokushima fatty rats: induction of uncoupling protein and activation of GLUT4 in white fat. Eur J Endocrinol 136:429–437
Viadal-Puig A, Solanes G, Grujic D, Flier JS, Lowell BB (1997) UCP3: An uncoupling protein homologue expressed preferentially and abundantly in skeletal muscle and brown adipose tissue. Biochem Biophys Res Commun 235:79–82
Yonetani T, Ray GS (1965)A study on cytochrome oxidase: kinetics of the aerobic oxidation of ferrocytochrome c by cytochrome oxidase. J Biol Chem 240:3392–3398

L.3.2.3 Resting Metabolic Rate

PURPOSE AND RATIONALE

Resting metabolic rate can be influenced by various drugs both in normal and obese animals.

PROCEDURE

Female yellow KK mice and female C57B1 mice at the age of 12 weeks are housed under controlled temperature and artificial light/dark conditions and are fed with commercial powdered chow and tap water ad libitum. Groups of each strain are treated with doses of test drug or solvent by daily intramuscular injections for 2 weeks. Daily food intake and body weight is measured.

Resting metabolic rate is estimated by means of a closed-circuit metabolic system (Molnar et al. 1986). The system consists of a chamber, circulating pump, desiccant and CO_2-absorbent canisters, solenoid valve, regulated gas source, and modified liquid crystal display calculator. The internal volume of a chamber for a single rat should be 4.5 liters. Food cups are placed on the door for convenient access when refilling. Water is supplied in a tray filled intermittently by means of a stopcock in the chamber wall. A shallow stainless steel funnel-shaped tray for urine collection is located in the bottom of the chamber.

Animals are placed in the chamber and the door is sealed airtight. Chamber air circulates by means of a peristaltic pump at a rate of 2.3 l/min through an external loop containing canisters of desiccant and CO_2-absorbent. In this manner, water vapor pressure remains constant and the respiration by-product, CO_2, is removed. Consumption of O_2 produces a pressure drop in the sealed system which actuates the pressure sensor for O_2 replacement.

The pressure sensor has two input ports, low and high, producing a simple contact closure whenever the high pressure exceeds the low by ~1 Torr. The low port is connected to the interior of the metabolic chamber by a length of tubing attached to a threaded connector, whereas the high port is open to the atmosphere. Thus the contact closes whenever the pressure within the chamber falls to more than 1 Torr below atmospheric pressure.

The contact closure is routed to the control unit where a precise pulse of fixed duration is triggered. This pulse activates a solid-state relay through an emitter-follower transistor circuit. The relay output is in series with a solenoid valve and line voltage, so that contact closure results in opening of the valve for a fixed duration. Since the input port of the valve is at a constant pressure, a predictable, highly repeatable volume of gas flows into the chamber. This raises the chamber pressure and opens the pressure sensor contacts. The entire cycle repeats after sufficient metabolism to again decrease the chamber pressure and close the sensor contacts.

After a stable baseline has been achieved after 30 min, drugs are administered and resting metabolic rate is measured for one hour at an ambient temperature of 22°C.

EVALUATION

Data are presented as means ± SEM. Statistical analysis is performed by Student's *t*-test.

MODIFICATIONS OF THE METHOD

Poon and Cameron (1978) measured oxygen consumption utilizing a standard Machlett manometer connected to a desiccator that accommodated a single mouse. The desiccator was placed in a 20°C water bath to ensure constant temperature throughout and CO_2 was absorbed by means of soda lime UPS. After a 5-min equilibration period, measurements of oxy-

gen consumption were obtained over a 5-min period. The procedure was repeated twice within 1 h for each mouse.

In order to study differential antagonism to amphetamine-induced oxygen consumption and agitation by psychoactive drugs Niemegeers and Janssen (1979) placed groups of 3 rats with a total weight of 235 ± 5 g consisting of 2 parts, a bottom and a cover, both made up from clear glass. The cover, containing a thermometer, was used to seal the chamber airtight. Inside the chamber a perforate plate was placed as animal platform. Containers filled with calcium oxide were placed below and above the animal holder. The chamber was flushed with oxygen for 3 min at an overpressure of 50 units as measured by a manometer connected to one outlet of the chamber. Test drugs were administered subcutaneously 60 min before the animals were placed in the test chambers and 45 min before 2.5 mg/kg amphetamine were injected. Oxygen consumption was measured as decrease of manometer pressure over one hour.

Rothwell (1989) measured central activation of thermogesesis by prostaglandins by resting oxygen consumption in individual closed-circuit calorimeters (Stock 1975) and by registration of colonic temperature in conscious rats.

Jensen et al. (2001) described a self-correcting indirect calorimeter system for the measurement of energy balance in small animals.

Himms-Hagen et al. (1994) tested the effect of a thermogenic β_3-agonist on energy balance in rats. Twenty-four hours energy expenditure, resting metabolic rate, and thermic effect of food were measured using open-circuit indirect calorimetry. The rat was placed in a respiration chamber (44 × 22 × 18 cm), airflow was measured with a Brooks thermal mass flowmeter (Brooks Instrument Division, Emerson Electric, Hatfield, PA), and the flow of outside air through the chamber was controlled at a variable rate by two adjustable peristaltic pumps that maintained CO_2 concentration at <1%. Temperature was maintained at 23 ± 1.0°C. Humidity was measured by an electronic psychrometer, barometric pressure was recorded, and feeding activity was monitored by an infrared detector. The rat was placed into the chamber at 09:30 and removed at 08:30 at the following morning. Food was available to the rat only between 16:30 and 07:30. Total energy expenditure was measured for 23. Resting metabolic rate was determined from the lowest energy expenditure at rest between 11:00 and 16:00. Thermic effect of food was determined from the difference between resting metabolic rate and the lowest energy expenditure at rest between 24:00 and 07:00. For the measurement of minimum metabolic rate, the rat was anesthetized (pentobarbital sodium, 60 mg/kg) and then placed in a small chamber filled with warm circulating water in which it was submerged except for the head. Core temperature was measured with a digital thermometer immediately after induction of anesthesia, and this temperature was maintained (± 0.1°C) by adjusting the temperature of the circulating water bath. The chamber was sealed and minimum metabolic rate determined with the same equipment as was used for the 24-h energy expenditure. Measurements of minimum metabolic rate were made for 5–15 min between 08:30 and 09:30 after a stabilization period of 5–10 min.

Ghorbani et al. (1997) tested the effect of a β_3-adrenoreceptor agonist on resting metabolic rate in rats by placing the animal in a water-jacketed chamber at 28°C, volume 1 liter, through which air, also at 28°C, was drawn at a rate of 1 l/min. Oxygen entering and leaving the chamber was measured with an oxygen analyzer (Beckman Industrial Oxygen Analyzer, model 755).

Paulik et al. (1998) described a robust technique to measure thermogenesis of **yeast cells** cultured in microtiter plates using infrared thermography. Thermogenesis increased after exposing yeast to uncoupling protein-2, or troglitazone or β_3-adrenoreceptor agonists.

REFERENCES AND FURTHER READING

Ghorbani M, Claus TH, Himms-Hagen J (1997) Hypertrophy of brown adipocytes in brown and white adipose tissue and reversal of diet-induced obesity in rats treated with a β_3-adrenoceptor agonist. Biochem Pharmacol 54:121–131

Himms-Hagen J, Cui J, Danforth E Jr, Taatjes DJ, Lang SS, Waters BL, Claus TH (1994) Effect of CL-316,243, a thermogenic β_3-agonist, on energy balance and brown and white adipose tissue in rats. Am J Physiol 266 (Regul Integr Comp Physiol 35):R1371–1382

Jensen DR, Gayles EC, Ammon S, Phillips R, Eckel RH (2001) A self-correcting indirect calorimeter system for the measurement of energy balance in small animals. J Appl Physiol 90:912–918

Molnar JA, Cunningham JJ, Miyatani S, Vizulis A, Write JD, Burke JF (1986) Closed-circuit metabolic system with multiple applications. J Appl Physiol 61:1582–1585

Niemegeers CJE, Janssen PAJ (1979) Differential antagonism to amphetamine-induced oxygen consumption and agitation by psychoactive drugs. In: Fielding S, Lal H (eds) Industrial Pharmacology, Vol II, Antidepressants., pp 125–141

Paulik MA, Buckholz RG, Lancaster ME, Dallas WS, Hull-Ryde EA, Weiel JE, Lenhard JM (1998) Thermogenic effects of uncoupling protein-2, troglitazone, and β-adrenoceptor agonists. Pharm Res 15:944–949

Poon TKY, Cameron DP (1978) Measurement of oxygen consumption and locomotor activity in monosodium glutamate-induced obesity. Am J Physiol 234:E532–E534

Rothwell NJ (1989) Central activation of thermogesesis by prostaglandins: dependence on CRF. Horm Metab Res 22:616–618
Stock MJ (1975) An automatic close-circuit oxygen consumption apparatus for small animals. J Appl Physiol 253:1271–1276
Yoshida T, Yoshioka K, Kamanaru K, Hiraoka N, Kondo M (1990) Mitigation of obesity by BRL 26830A, a new β-adrenoceptor agonist, in MSG obese mice. J Nutr Sci Vitaminol 36:75–80
Yoshida T, Hiraoka N, Yoshioka K, Hasegawa G, Kondo M (1991) Anti-obesity and anti-diabetic actions of a β_3-adrenoceptor agonist, BRL 28630A, in yellow kk mice. Endocrinol Japon 38:397–403

L.3.2.4 β_3-Adrenoceptor

PURPOSE AND RATIONALE

β_3-adrenoreceptor agonists produce weight loss in obese rodents (Yoshida et al. 1994; Weyer et al. 1999) which is almost entirely accounted for a reduction in body fat. As this effect is observed without a decrease in food intake, it is thought to be due to increased thermogenesis in brown adipose tissue, increased lipolysis in white adipose tissue, and suppression of leptin gene expression and serum leptin levels (Arch and Wilson 1996; Kumar et al. 1999).

The β_3-adrenoreceptor has been cloned and characterized in animals (Granneman et al. 1991; Nahmias et al. 1991; Evans et al. 1996) as well as from man (Emorine et al. 1989; Strosberg 1997). However, the physiological function of the human β_3-adrenoreceptor, the significance of animal data with β_3-adrenoreceptor agonists, and even the presence of a putative fourth β-adrenoreceptor in human adipose tissue are still a matter of debate (Emorine et al. 1994; Galitzky et al. 1998; Kaumann et al. 1998; Sarsero et al. 1998; Strosberg et al. 1998; Weyer et al. 1999).

The development of a Chinese hamster ovary cell transfection system, using the human β_3-adrenoreceptor gene resulted in potential new selective β_3-agonists being identified (Carruba et al. 1998). Human β_1-, β_2- and β_3-adrenoreceptors expressed in Chinese hamster ovary (CHO) cells were used to evaluate potential β_3-adrenoreceptor agonists by He et al. (2000).

PROCEDURE

cAMP Response Element-Luciferase Receptor Gene Assay

CHO cells stably expressing human β_1-, β_2- or β_3-adrenoreceptor populations are transfected with cAMP response element-luciferase plasmids using electroporation with a single 70-ms, 150-V pulse (Vansal and Fellner 1999). The transfected cells are seeded at a density of 40000/well in 96-well microtiter plates and allowed to grow for 20 h. After 20 h, the cells are treated with varying drug concentrations (10^{-11} to 10^{-4} M) for 4 h. Following drug exposure, the cells are lysed and luciferase activity is measured using the LucLite assay kit (Packard). Changes in light production are measured by a Topcount luminometer (Packard).

EVALUATION

Data are analyzed in duplicate at each concentration and expressed as percent luciferase response relative to the maximum response to (–)-isoproterenol (10^{-6} M). Results are expressed as the mean ± SEM.

MODIFICATIONS OF THE METHOD

Gettys et al. (1996) reported that the β_3-adrenergic receptor inhibits insulin-stimulated leptin secretion from isolated rat white adipocytes.

Using reverse transcription-polymerase chain reaction, Evans et al. (1998) compared levels of β_3-adrenoreceptor mRNA in white adipose tissue, brown adipose tissue, ileum and colon from genetically obese (*ob/ob*) and lean (+/+) C57BL/6J mice.

Bioassays

Tomiyama et al. (1998) studied β-adrenoreceptor subtypes mediating ureteral relaxation in rats, rabbits and dogs. β_3-adrenoreceptor agonists were more effective in relaxing canine ureter than β_1- and β_2-adrenoreceptor agonists.

Koike et al. (1997) reported that the relaxant responses in the guinea pig taenia caecum are mediated by both the β_2- and β_3-adrenoreceptors.

REFERENCES AND FURTHER READING

Arch JRS, Wilson S (1996) Prospects for β_3-adrenoceptor agonists in the treatment of obesity and diabetes. Int J Obes 20:191–199
Carruba M, Tomello C, Briscini L, Nisoli E, Astrup A (1998) Advances in pharmacotherapy for obesity. Int J Obes 22; Suppl 1:S13–S17
Emorine L, Blin N, Strosberg AD (1994) The human β_3-adrenoceptor: the search for a physiological function. Trends Pharmacol Sci 15:3–7
Emorine LJ, Marullo S, Briend-Sutren MM, Patey G, Tate K, Delavier-Klutchko C, Strosberg AD (1989) Molecular characterization of the human β_3-adrenergic receptor. Science 245:1118–1121
Evans BA, Papaioannou M, Bonazzi VR, Summers RJ (1996) Expression of β_3-adrenoreceptor mRNA in tissues. Br J Pharmacol 117:210–216
Evans BA, Papaioannou M, Anastasopoulos F, Summers RJ (1998) Differential regulation of β_3-adrenoceptors in gut and adipose tissue of genetically obese (*ob/ob*) C57BL/6J mice. Br J Pharmacol 124:763–771

Galitzky J, Langin D, Montastruc JL, Lafontan M, Berlan M (1998) On the presence of a fourth β-adrenoceptor in human adipose tissue. Trends Pharmacol Sci 19:164–165
Gettys TW, Harkness PJ, Watson PM (1996) The β_3-adrenergic receptor inhibits insulin-stimulated leptin secretion from isolated rat adipocytes. Endocrinology 137:4054–4057
Granneman JG, Lahners KN, Chaudry A (1991) Molecular cloning and expression of the rat β_3-adrenergic receptor. Mol Pharmacol 40:895–899
He Y, Nikulin VI, Vansal SS, Feller DR, Miller DD (2000) Synthesis and human β_3-adrenoceptor activity of 1-(3,5-diiodo-4-methoxybenzyl)-1,2,3,4-tetrahydroisoquinolin-6-ol derivatives *in vitro*. J Med Chem 43:591–598
Kaumann AJ, Preitner F, Sarsero D, Molenaar P, Revelli JP, Giacobino JP (1998) (–)-CGP 12177 causes cardiostimulation and binds to cardiac putative β_4-adrenoceptors in both wild-type and β_3-adrenoceptor knockout mice. Mol Pharmacol 53:670–675
Koike K, Ichino T, Horinouchi T, Takayanagi I (1997) The β_2- and β_3-adrenoceptor-mediated relaxation induced by isoprenaline and salbutamol in guinea pig taenia caecum. J Smooth Muscle Res 33:99–106
Kumar MV, Moore RL, Scarpace PJ (1999) β_3-adrenergic regulation of leptin, food intake, and adiposity is impaired with age. Pflügers Arch Eur J Physiol 438:681–688
Nahmias C, Blin N, Elalouf JM, Mattei MG, Stroberg AD, Emorine LJ (1991) Molecular characterization of the mouse β_3-adrenergic receptor: relationship with the atypical receptor of adipocytes. EMBO J 10:3721–3727
Sarsero D, Molenaar P, Kaumann AJ (1998) Validity of (–)-[^{3}H]-CGP 12177A as a radioligand for the 'putative β_4-adrenoceptor' in rat atrium. Br J Pharmacol 123:371–380
Strosberg AD (1997) Structure and function of the β_3-adrenergic receptor. Annu Rev Pharmacol Toxicol 37:421–450
Strosberg AD, Gerhardt CC, Gros J, Jockers R, Rouxel FP (1998) On the putative existence of a fourth β-adrenoceptor: proof is still missing. Trends Pharmacol Sci 19:165–166
Tomiyama Y, Hayakawa K, Shinagawa K, Akahane M, Ajisawa Y, Park YC, Kurita T (1998) β_3-adrenoceptor subtypes in the ureteral smooth muscle of rats, rabbits and dogs. Eur J Pharmacol 352:269–278
Vansal SS, Fellner DR (1999) An efficient cyclic AMP assay for the functional elevation of β-adrenergic receptor ligands. J Receptor Signal Transduct Res 19:853–863
Weyer C, Gautier JF, Danforth E Jr (1999) Development of β_3-adrenoceptor agonists for the treatment of obesity and diabetes – An update. Diabetes Metab 25:11–21
Yoshida T, Sakane N, Wakabajashi Y, Umekawa T, Kondo M (1994) Anti-obesity and anti-diabetic effects of CL 316,243, a highly specific beta$_3$-adrenoceptor agonist, in yellow KK mice. Life Sci 54:491–498

L.4 Assays of Obesity-Regulating Peptide Hormones

L.4.0.1 Hormonal Regulation of Food Intake

Food intake and fat deposition are regulated by neurotransmitters peptides, most of the located in the brain, particularly in the hypothalamus (Elmquist et al. 1999; Kalra et al. 1999) and in the gut. This includes peptides that are **orexigenic** (appetite-stimulating) signals and **anorectic** peptides. A review was given on investigational antiobesity agents and obesity therapeutic treatment targets by Bays (2004).

Neuropeptide Y (NPY), orexins A and B, galanin, melanin concentrating hormone (MCH), and **agouti-related peptide (AgRP)** all act to stimulate feeding, while **alpha-melanocyte stimulating hormone (αMSH)**, (see N.10.1), **corticotropin releasing hormone (CRH)**, (see N.9.4), **cholecystokinin (CCK)**, (see J.7.0.10), **cocaine and amphetamine regulated transcript (CART), neurotensin, glucagon-like peptide 1 (GLP_1)**, (see K.4.0.3), **calcitonin gene related peptide (CGRP)**, (see N.10.3), **bombesin** (see J.3.1.8) and **ciliary neurotropic factor** (Xu et al. 1998) have anorectic actions (Tritos et al. 1999).

Mutations reducing the functional activity of leptin, the leptin receptor, α-MSH, and the melanocortin-4 receptors lead to obesity in animals. *Mc4r*-deficient ($Mc4r^{-/-}$) mice do not respond to the anorectic actions of MTII, an MSH-like antagonist, suggesting that α-MSH inhibits feeding primarily by activating Mc4r (Marsh et al. 1999).

Leptin (see L.4.1) is a 167 amino acid protein that is synthesized and secreted primarily by white adipose tissue, circulates in the blood and acts on receptors in the hypothalamus to decrease food intake and increase energy expenditure (Friedman and Halaas 1998; Trayhurn et al. 1999). Leptin and its derivatives are candidates for treatment of obesity, however, clinical studies (Considine et al. (1996) showed that most of obese humans have higher plasma levels of leptin than non-obese individuals, suggesting that obesity is associated with leptin resistance rather than leptin deficiency.

Neuropeptide Y (NPY) (see L.4.2) is a 36 amino acid peptide that is widely distributed throughout both the central and peripheral nervous systems and which plays a key role in the control of body weight. Central administration of NPY increases food intake (Stanley et al. 1992), while a reduction in endogenous neuropeptide Y leads to a decrease of food intake (Lambert et al. 1993). NPY antagonists are candidates for anti-obesity drugs.

Orexin-A and orexin-B (see L.4.3) are 33- and 28-residue peptides, also called hypocrites, which were originally isolated from rat hypothalamus (Sakurai et al. 1998). These peptides are located predominantly in the hypothalamus and locus coeruleus but are also found elsewhere in the brain. The orexins have a broad range of physiological functions, including the con-

trol of feeding and energy metabolism. Food consumption is dose-dependently increased after intracerebroventricular infusion of orexin A and orexin B to rats (Jain et al. 2000). Orexin antagonists are potential anti-obesity drugs (Parker 1999).

Galanin (see L.4.4) is 29 amino acid C-terminally amidated peptide (30 amino acids in humans) which is localized mainly in the mammalian CNS, but also in other organs. Central administration of galanin increases and administration of galanin receptor antagonists (Crawley et al. 1990; Leibowitz and Kim 1992) decreases food intake. These data suggest the use of galanin receptor antagonists as anti-obesity agents.

Agouti-related protein affects pigmentation when its expression is limited to the skin, but ubiquitous expression causes obesity (Ollmann et al. 1997). The hypothalamic expression of agouti related protein is regulated by leptin, and overexpression of agouti related protein results in obesity and diabetes (Rosenfeld et al. 1998). Recombinant Agouti-related protein is a potent, selective antagonist at MC3R and MC4R, melanocortin receptor subtypes implicated in weight regulation (Fong et al. 1997; Shutter et al. 1997; Tota et al. 1999). Ubiquitous expression of human Agouti-related protein complementary DNA in transgenic mice caused obesity without altering pigmentation. Agouti-related protein is a neuropeptide implicated in the normal control of body weigh downstream of leptin signaling. Ollmann et al. (1998) used a sensitive bioassay based on *Xenopus* melanophores to characterize pharmacological properties of recombinant Agouti protein.

Melanin concentrating hormone (MCH) is a cyclic 19 amino acid neuropeptide that was originally found to regulate pigmentation in fish. It plays a role in the central feeding behavior increasing food consumption (Qu et al. 1996; Rossi et al. 1999). Mice carrying a targeted deletion of the MCH gene are hypophagic and lean (Shimada et al. 1998). Among other factors, MCH may be a target of leptin signaling in the hypothalamus (Sahu 1998; Huang et al. 1999). Melanin-concentrating hormone is a functional melanocortin antagonist in the hypothalamus (Ludwig et al. 1998). MCH has been identified as the natural ligand for the orphan somatostatin-like receptor 1 (SLC-1) (Bacher et al. 1999; Chambers et al. 1999; Shimomura et al. 1999) which has been characterized by Saito et al. (1999). High binding capacity for MCH was found in human keratinocytes (Burgaud et al. (1997). Radioligands for the mammalian MCH receptor were described by Hintermann et al. (1999).

Cocaine- and amphetamine-regulated transcript (CART), a brain located peptide, has potent appetite suppressing activity and is closely associated with the actions of leptin and neuropeptide Y (Lambert et al. 1998; Kuhar and Dall-Vechia 1999). When injected intracerebroventricularly into rats, recombinant CART peptide inhibits both normal and starvation-induced feeding, and completely blocks the feeding response induced by neuropeptide Y (Kristensen et al. 1998). In the rat the CART gene encodes a peptide of either 129 or 116 amino acids whereas only the short form exists in humans (Thim et al. 1998a, b). A role of CART peptides in substance abuse and addiction is suggested by psychomotor-stimulant regulation of CART transcription in the striatum, as well as its localization within neural circuits that mediate reward and reinforcing behaviors (Couceyro and Lambert 1999). CART has been found not only in the hypothalamus and other brain areas (Broberger 1999; Koylu et al. 1998, 1999) but also in other organs, such as the pancreas (Jensen et al. 1999), in the rat sympatho-adrenal axis (Dun et al. 2000), or in the vagal afferent neurons sensitive to cholecystokinin (Broberger et al. 1999). CART can cross the blood-brain barrier (Kastin and Akerström 1999). CART receptor agonists are potential anti-obesity drugs (Couceyro and Lambert 1999).

Resistin

Steppan et al. (2001a), Berger (2001), Steppan and Lazar (2002, 2004), and Banerjee and Lazar (2004) showed that adipocytes secrete a signaling molecule with 114 amino acids in length which is called **resistin** (for resistance to insulin) and which links obesity to diabetes (Haluzik and Haluzikova (2006). Circulating resistin levels in mice are increased in diet-induced and genetic forms of obesity and are decreased by thiazolidindiones (see K.5.0.6). Central administration of resistin promotes short-term satiety in rats (Tovar et al. 2005). Administration of anti-resistin antibody improves blood sugar and insulin action in mice with diet-induced obesity. Treatment of normal mice with recombinant resistin impairs glucose tolerance and insulin action. Insulin-stimulated glucose uptake by adipocytes ins enhanced by neutralization of resistin and is reduced by resistin treatment. Resistin with slightly modified amino acid sequence has also been found in humans.

Steppan et al. (2001b) described a family of tissue-specific **resistin-like-molecules (RELMs).** RELMα is a secreted protein that has a restricted tissue distribution with highest levels in adipose tissue. Another family member, RELMβ, is a secreted protein expressed

only in the gastrointestinal tract, particularly in the colon, in both mouse and human. RELMβ gene expression is highest in proliferative epithelial cells and is markedly increased in tumors, suggesting a role in intestinal proliferation.

Banerjee et al. (2004) generated mice deficient in resistin by replacing the coding exons of the resistin gene(*rstn*) with the reporter gene *lacZ*. The mice exhibited low blood glucose levels after fasting due to reduced hepatic glucose production indicating a physiological function of resistin in maintenance of blood glucose during fasting. The lack of resistin diminished the increase in post-fast glucose associated with increased weight, suggesting a role for resistin in mediating hyperglycemia associated with obesity.

REFERENCES AND FURTHER READING

Ahima RS, Flier JS (2000) Adipose tissue as an endocrine organ. Trends Endocrin Metab 11:327–332

Bacher D, Kreienkamp HJ, Weise C, Buck F, Richter D (1999) Identification of melanin concentrating hormone (MHC) as the natural ligand for the orphan somatostatin-like receptor 1 (SLC-1) FEBS Lett 467:522–524

Banerjee RR, Lazar MA (2004) Resistin: molecular history and prognosis. J Mol Med 81:218–226

Banerjee RR, Rangwala SM, Shapiro JS, Rich AS, Rhoades B, Qi Y, Wang J, Rajala MW, Pocai A, Scherer PE, Steppan CM, Ahima RS, Obici S, Rosetti L, Lazar MA (2004) Regulation of fasted blood glucose by resistin. Science 303:1195–1198

Bays HE (2004) Current and investigational antiobesity agents and obesity therapeutic treatment targets. Obes Res 12:1197–1211

Berger A (2001) Resistin, a new hormone that links obesity with type 2 diabetes. Br Med J 322:193

Broberger C (1999) Hypothalamic cocaine- and amphetamine-regulated transcript (CART) neurons. Histochemical relationship to thyrotropin-releasing hormone, melatonin-concentrating hormone, orexin/hypocretin and neuropeptide Y. Brain Res 848:101–113

Broberger C, Holmberg K, Kuhar MJ, Hökfelt T (1999) Cocaine- and amphetamine-regulated transcript in the rat vagus nerve: A putative mediator of cholecystokinin-induced satiety. Proc Natl Acad Sci USA 96:13506–13511

Burgaud JL, Poosti R, Fehrentz JA, Martinez J, Nahon JL (1997) Melanin-concentrating hormone binding sites in human SVK14 keratinocytes. Biochem Biophys Res Commun 241:622–629

Chambers J, Ames RS, Bergsma D, Muir A, Fitzgerald LR, Hervieu G, Dytko GM, Foley JJ, Martin S, Liu WS, Park J, Ellis C, Ganguly S, Konchar S, Cluderay J, Leslie R, Wilson S, Sarau HM (1999) Melanin-concentrating hormone is the cognate ligand for the orphan G-protein-coupled receptor SLC-1. Nature 400:261–265

Considine RV, Sinha MK, Heiman ML, Kriauciunas A, Stephens TW, Nyce MR, Ohannesian JP, Marco CC, McKee JL, Bauer TL, Caro JF (1996) Serum immunoreactive leptin concentrations in normal-weight and obese humans. N Engl J Med 334:292–295

Couceyro PR, Lambert PD (1999) CART peptides: Therapeutic potential in obesity and feeding disorders. Drug News Perspect 12:133–136

Crawley JN, Austin MC, Fiske SM, Martin B, Consolo S, Berthold M, Langel U, Fisone G, Bartfai T (1990) Activity of centrally administered galanin fragments on stimulation of feeding behavior and on galanin receptor binding in the rat hypothalamus. J Neurosci 10:3695–3700

Dun NJ, Dun SL, Kwok EH, Yang J, Chang J-K (2000) Cocaine- and amphetamine-regulated transcript-immunoreactivity in the rat sympatho-adrenal axis. Neurosci Lett 283:97–100

Elmquist JK, Elias CF, Saper CB (1999) From lesions to leptin: hypothalamic control of food intake and body weight. Neuron 22:221–232

Fong TM, Mao C, MacNeil T, Kalyani R, Smith T, Weinberg T, Tota MR, Van der Ploeg LH (1997) ART (protein product of agouti-related transcript) as an antagonist of MC-3 and MC-4 receptors. Biochem Biophys Res Commun 237:629–631

Friedman JM, Halaas JL (1998) Leptin and the regulation of body weight in mammals. Nature 395:763–770

Haluzik M, Haluzikova D (2006) The role of resistin in obesity-induced insulin resistance. Curr Opin Invest Drugs 7:306–311

Hintermann E, Drozdz R, Tanner H, Eberle AN (1999) Synthesis and characterization of new radioligands for the mammalian melanin-concentrating hormone (MCH) receptor. J Recept Signal Transduction Res 19:411–422

Huang Q, Viale A, Picard F, Nahon JL, Richard D (1999) Effect of leptin on melanin-concentrating hormone expression in the brain of lean and obese Lep(ob)/Lep(ob) mice. Neuroendocrinology 69:145–153

Jain MR, Horvath TL, Kalra PS, Kalra SP (2000) Evidence that NPY Y1 receptors are involved in stimulation of feeding by orexins (hypocretins) in sated rats. Regul Pept 87:19–24

Jensen PB, Kristensen P, Clausen JT, Judge ME, Hastrup S, Thim L, Wulff BS, Foged C, Jensen J, Holst JJ, Madsen OD (1999) The hypothalamic satiety peptide CART is expressed in anorectic and non-anorectic pancreatic islets tumors and in the normal islet of Langerhans. FEBS Lett 447:139–143

Kalra SP, Dube MG, Pu S, Xu B, Horvath TL, Kalra PS (1999) Interacting appetite-regulating pathways in the hypothalamic regulation of body weight. Endocr Rev 20:68–100

Kastin AJ, Akerström V (1999) Entry of CART into brain is rapid but not inhibited by excess CART or leptin. Am J Physiol 277; Endocrinol Metab 40:E901–E904

Koylu EO, Couceyro PR, Lambert PD, Kuhar MJ (1998) Cocaine- and amphetamine-regulated transcript peptide immunohistochemical localization in the rat brain. J Comp Neurol 391:115–132

Koylu EO, Smith Y, Couceyro PR, Kuhar MJ (1999) CART peptides colocalize with tyrosine hydroxylase neurones in rat locus coeruleus, Synapse 31:309–311

Kristensen P, Judge ME, Thim L, Ribel U, Christjansen KN, Wulff BS, Clausen JT, Jensen PB, Madsen OD, Vrang N, Larsen PJ, Hastrup S (1998) Hypothalamic CART is a new anorectic peptide regulated by leptin. Nature 393:72–76

Kuhar MJ, Dall-Vechia SE (1999) CART peptides: Novel addiction- and feeding-related peptides. Trends Neurosci 22:316–320

Lambert PD, Wilding JPH, al Dokhayel AAM, Bohuon C, Comoy E, Gilbey SG, Bloom SR (1993) A role for neuropeptide Y, dynorphin, and noradrenaline in the central control of food intake after food deprivation. Endocrinology 133:29–33

Lambert PD, Couceyro PR, McGirr KM, Vechia SED, Smith Y, Kuhar MJ (1998) CART peptides in the central control of feeding and interaction with neuropeptide Y. Synapse 29:293–298

Leibowitz SF, Kim T (1992) Impact of a galanin antagonist on exogenous galanin and natural patterns of fat ingestion. Brain Res 599:148–152
Ludwig DS, Mountjoy KG, Tatro JB, Gillette JA, Frederich RC, Flier JS, Marato-Flier E (1998) Melanin-concentrating hormone: A functional melanocortin antagonist in the hypothalamus. Am J Physiol 274; Endocrinol Metab 37:E627–E633
Marsh DJ, Hollopeter G, Huszar D, Laufer R, Yagaloff KA, Fisher SL, Burn P, Palmiter RD (1999) Response of melanocortin-4 receptor-deficient mice to anorectic and orexigenic peptides. Nature Genetics 21:119–122
Ollmann MM, Wilson BD, Yang Y-K, Kerns JA, Chen Y, Gantz I, Barsh GS (1997) Antagonism of central melanocortin receptors *in vitro* and *in vivo* by agouti-related protein. Science 278:135–138
Ollmann MM, Lamoreux ML, Wilson BD, Barsh GS (1998) Interaction of Agouti protein with the melanocortin-1 receptor *in vitro* and *in vivo*. Genes Dev 12:316–3330
Parker EM (1999) The role of central neuropeptide, neurotransmitter and hormonal systems in the regulation of body weight. Neurotransmiss 15:3–11
Qu D, Ludwig DS, Gammeltoft S, Piper M, Pellemounter A, Cullen MJ. Foulds-Mathes W, Przypek J, Kanarek R, Maratos-Flier E (1996) A role for melatonin-concentrating hormone in the control of feeding behavior. Nature 380:243–237
Rosenfeld RD, Zeni L, Welcher AA, Narhi LO, Hale C, Marasco J, Delaney J, Gleason T, Philo JS, Katta V, Hui J, Baumgartner J, Graham M, Stark KL, Karbon W (1998) Biochemical and biophysical characterization of bacterially expressed human agouti-related protein. Biochemistry 37:16041–16052
Rossi M, Beak SA, Choi SJ, Small CJ, Morgan DGA, Ghatei MA, Smith DM, Bloom SR (1999) Investigation of the feeding effects of melanin concentrating hormone on food intake. Action independent of galanin and the melanocortin receptors. Brain Res 846:164–170
Sahu A (1998) Evidence that galanin (GAL), melanin-concentrating hormone (MHC), neurotensin (NT) proopiomelanocortin (POMC) and neuropeptide Y (NPY) are targets of leptin signaling in the hypothalamus. Endocrinology 139:795–798
Shutter JR, Graham M, Kinsey AC, Scully S, Lüthy R, Stark KL (1997) Hypothalamic expression of ART, a novel gene related to agouti, is up-regulated in obese and diabetic mice. Genes Dev 11:593–602
Saito Y, Nothacker HP, Wang Z, Lin SHS, Leslie F, Civelli O (1999) Molecular characterization of the melanin-concentrating hormone receptor. Nature 400:265–269
Sakurai T, Amemiya A, Ishii M, Matsuzaki I, Chemelli RM, Tanaka H, Williams SC, Richardson JA, Kozlowski GP, Wilson S, Arch JRS, Buckingham RB, Haynes AC, Carr SA, Annan RS, McNulty DE, Liu W-S, Terrett JA, Elshourbagy NA, Bergsma DJ, Yanagisawa M (1998) Orexins and orexin receptors: A family of hypothalamic neuropeptides an G protein-coupled receptors that regulate feeding behavior. Cell 92:573–585
Shimada M, Tritos NA, Lowell BB, Flier JS, Maratos-Flier E (1998) Mice lacking melanin-concentrating hormone are hypophagic and lean. Nature 396:670–674
Shimomura Y, Mori M, Sugo T, Ishibashi Y, Abe M, Kurokawa T, Onda H, Nishimura O, Sumino Y, Fujino M (1999) Isolation and identification of melanin-concentrating hormone as the endogenous ligand for the SLC-1 receptor. Biochem Biophys Res Commun 261:622–626
Stanley BG, Magdalin W, Seirafi A, Nguyen MM, Leibowitz SF (1992) Evidence for neuropeptide Y mediation of eating produced by food deprivation and for a variant of the Y-1 receptor mediating this peptide's effect. Peptides 13:581–587
Steppan CM, Lazar MA (2002) Resistin and obesity-associated insulin resistance. Trends Endocrinol Metab 13:18–23
Steppan CM, Lazar MA (2004) The current biology of resistin. J Intern Med 255:439–447
Steppan CM, Bailey ST, Bhat S, Brown EJ, Banerjee RR, Wright CM, Patel HR, Ahima RS, Lazar MA (2001a) The hormone resistin links obesity to diabetes. Nature 409:307–312
Steppan CM, Brown EJ, Wright CM, Bhat S, Banerjee RR, Dai CY, Enders GH, Silberg DG, Wen X, Wu GD, Lazar MA (2001b) A family of tissue-specific resistin-like molecules. Proc Natl Acad Sci USA 98:502–506
Thim L, Nielsen PF, Judge ME, Andersen AS, Diers I, Egel-Mitani M, Hastrup S (1998a) Purification and characterization of e new hypothalamic satiety peptide, cocaine and amphetamine regulated transcript (CART), produced in yeast. FEBS Lett 428:263–268
Thim L, Kristene P, Larsen PJ, Wulff BS (1998b) CART, a new anorectic peptide. Int J Biochem Cell Biol 30:1281–1284
Tota MR, Smith TS, Mao C, McNeil T, Mosley RT, Van der Ploeg LTH, Fong TM (1999) Molecular interaction of Agouti protein and Agouti-related protein with human melanocortin receptors. Biochemistry 38:897–904
Tovar S, Nogueiras R, Tung LYC, Castañeda TR, Vásquez MJ, Morris A, Williams LM, Dickson SL, Diéguez C (2005) Central administration of resistin promotes short-term satiety in rats. Eur J Endocrinol 153:R1–R5
Trayhurn P, Hoggard N, Mercer JG, Rayner DV (1999) Leptin: Fundamental aspects. Int J Obes 23, Suppl 1:22–28
Tritos NA, Maratos-Flier E (1999) Two important systems in energy homeostasis: Melanocortins and melanin-concentrating hormone. Neuropeptides 33:339–349
Xu B, Dube MG, Kalra PS, Farmeie WG, Kaibara A, Moldawer LL, Martin D, Kalra SP (1998) Anorectic effects of the cytokine, ciliary neurotropic factor, are mediated by hypothalamic neuropeptide Y: Comparison with leptin. Endocrinology 139:466–473

L.4.1
Leptin

L.4.1.1
General Considerations on the Obese Gene Product Leptin

The obese gene product leptin is a cytokine-like nonglycosylated peptide of 146 amino acids that is secreted from adipose tissue. It is an important circulating hormone for the regulation of body weight (Arch and Beeley 1996; Hamann and Matthaei 1996; Friedman and Halaas 1998; Trayhurn 1999). MacDougald et al. (1995) described the expression of the obese gene product (leptin) in white adipose tissue and 3T3-L1 adipocytes.

The mouse obese gene and its human homologue which show approximately 85% amino acid homology have been cloned by Zhang et al. (1994). Leptin binding was first reported in rat hypothalamic membranes (Stephens et al. (1995).

A **leptin receptor** was subsequently identified by expression cloning from a mouse chorioid plexus cDNA library (Tartaglia et al. 1995). Several transcripts of the leptin receptor as a result of alternative splicing which have different length of cytoplasmatic region have been identified in mice and rats (Guan et al. 1997; Igel et al. 1997; Murakami et al. 1997) as well as leptin receptors in man (Maffei et al. 1995, 1996; Liu et al. 1997; Strosberg and Issad 1999). There are at least five different isoforms of the leptin receptor in mice. Mutations in the leptin receptor lead to massive obesity in *db* mice and *fa* rats (Friedman and Halaas 1998).

Administration of recombinant human leptin to mice increases thermogenesis and lipid oxidation in brown fat coupled with increased lipolysis and decreased fat synthesis in white and brown fat, which lead to a rapid reduction in the body weight (Sarmiento et al. 1997).

Leptin increases uncoupling protein expression in brown adipose tissue and oxygen consumption in mice (Scarpace et al. 1997).

Intracerebroventricular injection of recombinant murine leptin produces a dose-dependent reduction of laboratory diet in normal rats. This effect is attenuated in rats with diet-induced obesity (Widdowson et al. 1997).

The role of leptin in human obesity is controversial. Rare forms of human obesity have been identified where mutations in leptin or its receptor play a major role in the development of the disease. Leptin may be a signal for the onset of puberty in humans (Strosberg and Issad 1999). Leptin activates leptin-receptor expressing neurons in the arcuate region of the hypothalamus. Projections from these neurones stimulate melanocortin MC_4 receptors and neuropeptide Y-containing neurones to activate the sympathetic nervous system which controls lipolysis in white adipose tissue. The firing of gonadotrophin-releasing hormone-containing neurons and secretion of gonadotrophin-releasing hormone to the pituitary is elicited by leptin-mediated activation of leptin-receptor-expressing neurons and by other factors that control the reproductive axis (Chebab 2000).

Grasso et al. (1997, 1999) found inhibitory effects of leptin-related synthetic peptides on food intake and body weight gain after intraperitoneal administration in female C57BL/6J*ob/ob* mice which may have potential application to the treatment of human obesity.

Ducy et al. (2000) and Takeda et al. (2002) suggest that leptin inhibits bone formation, probably via the sympathetic nervous system.

Dumond et al. (2003) showed in rats that leptin strongly stimulated anabolic functions of chondrocytes and induced the synthesis of IGF-1 and TGFβ 1 in cartilage at both the messenger RNA and protein levels. A key role of leptin in osteoarthritis was assumed.

REFERENCES AND FURTHER READING

Arch JRS, Beeley LJ (1996) Leptin: The hormone that directs the regulation of energy balance. Pharmacol Commun 7:317–322

Ahima RS, Flier JS (2000) Leptin. Annu Rev Physiol 62:413–437

Barinaga M (1995) "Obese" protein that slims mice. Science 269:475–476

Chebab FF (2000) Leptin as a regulator of adipose mass and reproduction. Trends Pharmacol Sci 21:309–314

Ducy P, Amling M, Takeda S, Priemel M, Schilling AF, Beil FT, Shen J, Vinson C, Rueger JM, Karsenty G (2000) Leptin inhibits bone formation through a hypothalamic relay: a central control of bone mass. Cell 100:197–207

Dumond H, Presle N, Terlain B, Mainard D, Loeuille D, Netter P, Pottie P (2003) Evidence for a key role of leptin of osteoarthritis. Arthritis Rheum 48:3118–3129

Friedman JM, Halaas JL (1998) Leptin and the regulation of body weight in mammals. Nature 395:763–770

Grasso P, Leinung MC, Ingher SP, Lee DW (1997) *In vivo* effects of leptin-related synthetic peptides on body weight and food intake in female *ob/ob* mice. Endocrinology 138:1413–1418

Grasso P, White DW, Tartaglia LA, Leinung MC, Lee DW (1999) Inhibitory effects of leptin-related synthetic peptide 116–130 on food intake and body weight gain in female C57BL/6J *ob/ob* mice may not be mediated by peptide activation of the long form of the leptin receptor. Diabetes 48:2204–2209

Guan XM, Hess JF, Yu H, Hey PJ, Van der Ploeg LHT (1997) Differential expression of mRNA for leptin receptor isoforms in the rat brain. Mol Cell Endocrinol 133:1–7

Hamann A, Matthaei S (1996) Regulation of energy balance by leptin. Exp Clin Endocrinol Diabetes 104:293–300

Igel M, Becker W, Herberg L, Joost HG (1997) Hyperleptinemia, leptin resistance, and polymorphic leptin receptor in the New Zealand obese mouse. Endocrinology 138:4234–4239

Liu C, Liu XJ, Barry G, Ling N, Maki RA, De Souza EB (1997) Expression and characterization of a putative high affinity human soluble leptin receptor. Endocrinology 138:3548–3554

MacDougald OA, Hwang CS, Fan H, Lane MD (1995) Regulated expression of the obese gene product (leptin) in white adipose tissue and 3T3-L1 adipocytes. Proc Natl Acad Sci USA 92:9034–9037

Maffei M, Halaas J, Ravussin E, Pratley RE, Lee GH, Zhang Y, Fei H, Kim S, Lallone R, Ranganathan S, Kern PA, Friedman JM (1995) Leptin levels in human and rodent: measurement of plasma leptin and ob RNA in obese and weight-reduced subjects. Nature Med 1:1155–1161

Maffei M, Stoffel M, Berone M, Moon B, Dammerman M, Ravussin E, Bogardus C, Ludwig DS, Flier JS, Talley M, Auerbach S, Friedman JM (1996) Absence of mutations in the human OB gene in obese/diabetic subjects. Diabetes 45:679–682

Murakami T, Yamashita T, Iida M, Kuwajima M, Shima K (1997) A short form of leptin receptor performs signal transduction. Biochem Biophys Res Commun 231:26–29

Sarmiento U, Benson B, Kaufman S, Ross L, Qi M, Scully S, DiPalma C (1997) Morphologic and molecular changes induced by recombinant human leptin in the white and brown adipose tissues of C57BL/6 mice. Lab Invest 77:243–256

Scarpace PJ, Matheny M, Pollock BH, Tumer N (1997) Leptin increases uncoupling protein expression and energy expenditure. Am J Physiol (Endocrin Metab) 273:E226–E230

Stephens TW, Caro JF (1998) To be lean or not to be lean. Is leptin the answer? Exp Clin Endocrin Diab 106:1–15

Stephens TW, Basinski M, Birstow PK, Bue-Valleskey JM, Burgett SG, Craft L, Hale J, Hoffmann J, Hsuing HM, Kriauciuneas A, Mackelar W, Rosteck PR Jr Schoner B, Smith D, Tinsley FC, Zhang X, Heiman M (1995) The role of neuropeptide Y in the antiobesity action of the obese gene product. Nature 377:530–532

Strosberg D, Issad T (1999) The involvement of leptin in humans revealed by mutations in the leptin and leptin receptor genes. Trends Pharmacol Sci 20:227–230

Takeda S, Elefteriou F, Levasseur R, Liu X, Zhao L, Parker KL, Armstrong D, Ducy P, Karsenty G (2002) Leptin regulates bone formation via the sympathetic nervous system. Cell 111:305–317

Tartaglia LA, Dembski M, Weng X, Deng N, Culpepper J, Devos R, Richards GJ, Campfield LA, Clark FT, Deeds J, Muir C, Sanker S, Moriarty A, Moore KJ, Smutko JS, Mays GG, Woolf EA, Monroe CA, Tepper RI (1995) Identification and expression cloning of a leptin receptor, OB-R. Cell 83:1263–1271

Trayhurn P, Hoggard N, Mercer JG, Rayner DV (1999) Leptin: Fundamental aspects. Int J Obes 23, Suppl 1:22–28

Widdowson PS, Upton R, Buckingham R, Arch J, Williams G (1997) Inhibition of food response to intracerebroventricular injection of leptin is attenuated in rats with diet-induced obesity. Diabetes 46:1782–178

Zhang Y, Proenca R, Maffei M, Barone M, Leopold L, Friedman JM (1994) Positional cloning of the mouse obese gene and its human homologue. Nature 372:425–432

L.4.1.2 Determination of Leptin mRNA Level in Adipose Tissue

PURPOSE AND RATIONALE

Leptin mRNA levels in adipose tissue can be determined by Northern blot analysis (Friedrich et al. 1995; Harris et al. 1996; Zachwieja et al. 1997; Kochan et al. 1999).

PROCEDURE

Male Wistar rats weighing approximately 230 g treated for 14 days with test drug are sacrificed by decapitation. Liver, epididymal white adipose tissue and intracapsular brown adipose tissue are rapidly removed and frozen in liquid nitrogen. Total RNA is extracted from frozen tissues by a guanidinium thiocyanate-phenol/chloroform method (Chomczynski and Sacchi 1987). The RNA (10 µg per lane) is fractionated by horizontal gel electrophoresis. The RNA is transferred to a positively charged nylon membrane and fixed with UV-light. Pre-hybridization is performed at 42°C for 45 min in pre-hybridization solution containing 7% sodium dodecyl sulfate, 50% formamide, 5× saline-sodium citrate buffer, 2% blocking reagent (Boehringer Mannheim, Mannheim, Germany), 50 mM sodium phosphate (pH 7.0) and 0.1% N-laurylsarcosine. Hybridization is performed at 42°C overnight in pre-hybridization solution containing oligonucleotide probe (25 ng/ml) specific to leptin, malic enzyme or 185 RNA. The following post-hybridization washes are performed: twice for 5 min in 2× saline-sodium citrate buffer/0.1% sodium dodecyl sulfate (at room temperature): twice for 15 min in 0.1× saline-sodium citrate buffer/0.1% sodium dodecyl sulfate (at 48°C). The membranes are then rinsed briefly with washing buffer containing 0.1 M maleic acid (pH 7.5), 0.15 M NaCl and 0.3% Tween 20. They are blocked by incubation for 30 min at room temperature with blocking buffer (1% blocking agent, 0.1 M maleic acid (pH 7.5), 0.15 M NaCl) and incubated (at the same conditions as described above) with blocking buffer containing a polyclonal antibody against digoxigenin conjugated to alkaline phosphatase. After washing twice for 15 min with washing buffer, the membranes are rinsed for 5 min with detection buffer (0.1 M Tris-Cl, pH 9.5, 0.1 M NaCl) and immersed for 5 min in CDP-Star solution (Boehringer Mannheim, Mannheim, Germany). Membranes are exposed to Kodak XAR film for 15 min to 1 h (Karbowska et al. 1999).

EVALUATION

Signals are scanned and quantified using the NIH-Image software. The level of mRNA for leptin and malic enzyme as well as for 185 RNA is estimated using PeakFit software (Jandel Scientific). The values for leptin and malic enzyme mRNA are normalized to the corresponding amount of 185 RNA. Results expressed in arbitrary units are presented as means ± SEM of samples of 10 rats. The statistical difference between groups is assessed by one-way analysis of variance (ANOVA) followed by Student's *t*-test or by Mann-Whitney test.

MODIFICATIONS OF THE METHOD

Richards et al. (2000) described quantitative analysis of leptin mRNA using competitive reverse transcription polymerase chain reaction and capillary electrophoresis with laser-induced fluorescence detection.

Shintani et al. (2000) determined leptin mRNA levels in primary cultured rat adipocytes.

Li et al. (1999) used an anti-leptin polyclonal antiserum to detect leptin-immunoreactivity in the central nervous system in rats.

REFERENCES AND FURTHER READING

Chomczynski P, Sacchi N (1987) Single-step method of RNA isolation by acid guanidinium thiocyanate-phenol-chloroform extraction. Anal Biochem 162:156–159

Frederich RC et al (1995) Expression of ob mRNA and its encoded protein in rodents: Impact of nutrition and obesity. J Clin Invest 96:1658–1663

Frederich RC, Hamann A, Anderson S, Löllmann B, Lowell BB, Flier JS (1995) Leptin levels reflect body lipid content in mice: evidence for diet-induced resistance to leptin action. Nature Med 1:1311–1314

Harris RBS, Ramsay TG, Smith SR, Bruch RC (1996) Early and late stimulation of ob mRNA expression in meal-fed and over-fed rats. J Clin Invest 97:2020–2026

Karbowska J, Kochan Z, Zelewski L, Swierczynski J (1999) Tissue-specific effect of clofibrate on rat lipogenic enzyme gene expression. Eur J Pharmacol 370:329–336

Kochan Z, Karbowska J, Swierczynski J (1999) Effect of clofibrate on malic enzyme and leptin mRNA level in rat brown and white adipose tissue. Horm Metab Res 31:536–542

Li HY, Wang LL, Yeh RS (1999) Leptin-immunoreactivity in the central nervous system in normal and diabetic rats. NeuroReport 10:437–442

Richards MP, Ashwell CM, McMurtry JP (2000) Quantitative analysis of leptin mRNA using competitive reverse transcription polymerase chain reaction and capillary electrophoresis with laser-induced fluorescence detection. Electrophoresis 21:792–798

Shintani M, Nishimura H, Yonemitsu S, Masuzaki H, Ogawa Y, Hosoda K, Inuoe G, Yoshimasa Y, Nakao K (2000) Down-regulation of leptin by free fatty acids in rat adipocytes: Effects of triacsin C, palmitate, and 2-bromopalmitate. Metab Clin Exp 49:326–330

Zachwieja JJ, Hendry SL, Smith SR, Harris RBS (1997) Voluntary wheel running decreases adipose tissue mass and expression of leptin mRNA in Osborne-Mendel rats. Diabetes 46:1159–1166

L.4.1.3 Determination of Plasma Leptin

PURPOSE AND RATIONALE

Plasma leptin levels are determined by radioimmunoassay using a rat-specific antibody (Ciba-Geigy, Basel, Switzerland) (Zachwieja et al. 1997) or with a double-antibody radioimmunoassay kit based on a mouse standard (Linco Research, St. Louis, MO) (Surwit et al. 1997; Van Heek et al. 1997). A radioimmunoassay for leptin in human plasma was described McGregor et al. (1996).

PROCEDURE

The peptide VPIQKVQDDTKTLIKTIVT representing the first twenty amino acids of the predicted sequence of mature leptin protein (leptin 1–20) was synthesized with 9-fluorenyl methyl oxycarbonyl-(Fmoc)-protected L-amino acids on a applied Biosystems peptide synthesizer and purified by HPLC on a Dynamax column developed with a 0.1% trifluoroacetic acid (TFA)/H_2O/acetonitrile (8% to 40%) gradient. The peptide is conjugated to thyroglobulin using carbodiimide as coupling reagent. Rabbits are immunized by intradermal injections and boosted at 4 weeks intervals.

A peptide identical to the one used for antibody generation except for a tyrosine residue added to the C-terminal end is labelled with ^{125}I using the oxidizing agent Iodogen (Pierce, USA) and purified on HPLC. For radioimmunoassay, the buffer consists of Tris-HCl 1 M, pH 7.4; 0.1% gelatin; 0.1% Triton X-100, and 0.01% NaN_3. Unlabelled ob peptide is used for standards. 100 µl of standard or unknown, 200 µ l buffer, 100 µl antibody at a final concentration of 1:80000 and 100 µl ^{125}I-leptin peptide (approximately 5000 cpm) are added to polystyrene tubes and incubated for 48 h at 4°C. Antibody-bound and unbound peptide are separated by addition of goat anti-rabbit immunoglobulin antibody followed by centrifugation. The precipitates are counted on a computer-linked gamma-counter and the leptin concentrations of the samples are obtained using the "RIA-Calc" program.

EVALUATION

Results are expressed as means ± SD, and statistical comparisons are made with the use of Student's *t*-test. Linear regression analysis is performed with the method of least squares.

MODIFICATIONS OF THE METHOD

Maffei et al. (1995) used an immunoprecipitation assay to measure plasma leptin levels. A quantitative increase of the signal intensity was seen on Western blots when increasing amounts of recombinant protein were added to *ob* mouse serum, which does not have leptin. Densitometry was used to compare the signal intensity of the native protein in mouse plasma to the standard. The level of leptin-like immunoreactivity was quantified as nanograms per ml.

REFERENCES AND FURTHER READING

Maffei M, Halaas J, Ravussin E, Pratley RE, Lee GH, Zhang Y, Fei H, Kim S, Lallone R, Ranganathan S, Kern PA, Friedman JM (1995) Leptin levels in human and rodent: measurement of plasma leptin and ob RNA in obese and weight-reduced subjects. Nature Med 1:1155–1161

McGregor GP, Desaga JF, Ehlenz K, Fischer A, Heese F, Hegele A, Lämmer C, Peiser C, Lang RE (1996) Radioimmunological measurement of leptin in plasma of obese and diabetic human subjects. Endocrinology 137:1501–1504

Surwit RS, Petro AE, Parekh P, Collins S (1997) Low plasma leptin in response to dietary fat in diabetes- and obesity-prone mice. Diabetes 46:1516–1520

Van Heek M, Compton DS, France CF, Tedesco RP, Fawzi AB, Graziano MP, Sybertz EJ, Strader CD, Davis HR Jr (1997)

Diet-induced obese mice develop peripheral, but not central, resistance to leptin. J Clin Invest 99:385–390
Zachwieja JJ, Hendry SL, Smith SR, Harris RBS (1997) Voluntary wheel running decreases adipose tissue mass and expression of leptin mRNA in Osborne-Mendel rats. Diabetes 46:1159–1166

L.4.2 Neuropeptide Y

L.4.2.1 General Considerations on Neuropeptide Y and Related Peptides

Neuropeptide Y (NPY), peptide YY (PYY) and pancreatic polypeptide (PP) are endogenous 36-amino acid peptides belonging to the same family, which is characterized by a tertiary structure termed 'PP-fold' (Larhammar 1996; Berglund et al. 2003). They have different tissue distributions (Sundler et al. 1993) and act in different physiological systems, mostly neuronal for NPY and endocrine for PYY and PP (Wettstein et al. 1995; Playford and Cox 1996; Goumain et al. 1998).

Neuropeptide Y plays a key role in the control of body weight (Leibowitz 1994; Kalra and Kalra 2004). Central administration of neuropeptide Y increases food intake and decreases thermogenesis in satiated animals (Billington et al. (1991, Stanley et al. 1992), while a reduction in endogenous neuropeptide Y leads to a decrease of food intake (Lambert et al. 1993). Hypothalamic neuropeptide Y and mRNA levels are increased after fasting and in genetically obese mice (Stephens et al. 1995). Neuropeptide Y is required for the maintenance of the obese phenotype of the leptin-deficient *ob/ob* mice (Erickson et al. 1996). Conversely, leptin appears to decrease food intake and body weight in part by decreasing neuropeptide Y synthesis and release (Stephens et al. 1995). These data suggest that neuropeptide Y is a key modulator of body weight and that neuropeptide Y receptor antagonists may be useful anti-obesity agents.

Neuropeptide Y mediates its physiological effects via interaction with at least six distinct G protein-coupled receptors, designated Y_1, Y_2, Y_3, Y_4, Y_5 and Y_6.(Marsh et al. 1998; Michel et al. 1998; Wyss et al. 1998; Iyengar et al. 1999; Larhammer and Salaneck 2004; Lin et al. 2004).

Central administration of peptide analogues of neuropeptide Y has been used to study the physiological roles of neuropeptide Y, especially the role of the peptide in feeding behavior. Kanatani et al. (1999) demonstrated an anorexogenic effect against NPY induced feeding in rats by an Y_1 antagonist with high selectivity and potency for the Y_1 receptor. Central administration of peptides that activate the Y_5 receptor, peptide YY (PYY), PYY(3–36), [Leu^{31},Pro^{34}]NPY, and human pancreatic polypeptide elicit feeding, whereas central administration of central administration of peptides that are inactive at the Y_5 receptor do not elicit feeding (Gerald et al. 1996). Fuhlendorff et al. (1990) described [Leu^{31}, Pro^{34}]neuropeptide Y as a specific Y_1 receptor agonist. While other neuropeptide Y analogues or fragments interacts with several neuropeptide Y receptors, [D-Trp^{32}]NPY is a completely selective Y_5 agonist that elicits feeding at relatively high doses (Gerald et al. 1996). Peptides with activity on the Y_1 receptor produce conflicting effects on feeding. $DesAA^{10–17}$[$Cys^{7–21}$,Pro^{34}]NPY is a Y_1 receptor agonist with a potency equivalent to neuropeptide Y, but does not elicit feeding after central administration (Kirby et al. 1995).

Schaffhauser et al. (1997) described inhibition of food intake after intracerebroventricular injection of neuropeptide Y Y_5 receptor antisense oligodeoxynucleotides in rats.

Dumont et al. (2004) recommended receptor autoradiography as means to explore the possible functional relevance of neuropeptides such as neuropeptide Y.

Criscione et al. (1998) reported inhibition of food intake in rats by an Y_5 receptor antagonist under various conditions. Several neuropeptide Y antagonists were synthesized which inhibit food intake in rodents and may be used as anorectic agents (Matthews et al. 1997; Kask et al. 1998; Parker et al. 1998; Shigeri et al. 1998; Wieland et al. 1998; Zarrinmayeh et al. 1998).

Besides the stimulation of feeding, NPY and PYY show several other activities: influence on gastric motility (Chen et al. 1997), antisecretory effects in the gastrointestinal tract (Souli et al. 1997), anti-stress activity (Heilig 2004), anti-epileptic activity (Baraban 2004; Vezzani and Sperk 2004), central and peripheral control of the cardiovascular system (Lew et al. 1996; Tadepalli et al. 1996; Hudspith and Muglani 1997; McCloskey et al. 1997), effects on renal function (Blaze et al. 1997; Bischoff et al. 1997), antinociceptive effects (Broqua et al. 1996), or release of ACTH (Small et al. 1997). Kask et al. (2001) described the effects of a neuropeptide Y Y_5 receptor antagonist on food intake and anxiety-related behavior in the rat.

Sajdyk et al. (1999) found that amygdalar neuropeptide Y Y_1 receptors mediate the anxiolytic-like actions of neuropeptide Y in the social interaction test, whereas neuropeptide Y-Y_2 receptors mediate anxiety in the amygdala (Sajdyk et al. 2002).

Neuropeptide Y plays a role in neurobiological responses to ethanol and drugs of abuse (Thiele et al. 2004).

NPY receptor agonists show anxiolytic effects in rat conflict tests (Britton et al. 1997; Kask et al. 2002); neuropeptide Y_1 antagonists have anxiogenic-like effects (Kask et al. 1996).

Goumain et al. (1998) generated a rat Y_5 clone by reverse transcription from rat brain, polymerase chain reaction and transfection to COS-7 cells. Isolated jejunal crypt and villus cells and colon epithelial cells were analyzed for the Y_5 receptor by reverse transcription and polymerase chain reaction. Inhibition of binding of [^{125}I]peptide YY in these cells by various peptides was studied.

Mullins et al. (2000) characterized the cloned neuropeptide Y y_6 receptor in mice.

REFERENCES AND FURTHER READING

Baraban SC (2004) Neuropeptide Y and epilepsy: recent progress, prospects and controversies. Neuropeptides 38:261–266

Berglund MM, Hipskind PA, Gehlert DR (2003) Recent developments in our understanding of the physiological role of PP-fold peptide receptor subtypes. Exp Biol Med 228:217–244

Billington CJ, Briggs JE, Grace M, Levine AS (1991) Effect of intracerebroventricular injection of neuropeptide Y on energy metabolism. Am J Physiol 260, Regul Integr Comp Physiol 29:R321–R327

Bischoff A, Avramidis P, Erdbrugger W, Munter K, Michel MC (1997) Receptor subtypes Y_1 and Y_5 are involved in the renal effects of neuropeptide Y. Br J Pharmacol 120:1335–1343

Blaze CA, Mannon PJ, Vigna SR, Kherani AR, Benjamin BA (1997) Peptide YY receptor distribution and subtype in the kidney: Effect on renal hemodynamics and function in rats. Am J Physiol 273: Renal Physiol 42:F545–F553

Britton KT, Southerland S, Van Uden E, Kirby D, Rivier J, Koob G (1997) Anxiolytic activity of NPY receptor agonists in the conflict test. Psychopharmacology 132:6–13

Broqua P, Wettstein JG, Rocher MN, Gauthier-Martin B, Riviere PJM, Junien JL, Dahl SG (1996) Antinociceptive effects of neuropeptide Y and related peptides in mice. Brain Res 724:25–32

Chen CH, Stephens RL Jr, Rogers RC (1997) PYY and NPY: Control of gastric motility via action on Y_1 and Y_2 receptors in the dorsal vagal complex. Neurogastroenterol Motil 9:109–116

Criscione L, Rigollier P, Batzl-Hartmann C, Rueger H, Stricker-Krangrad A, Wyss P, Brunner L, Whitebread S, Yamaguchi Y, Gerald C, Heurich RO, Walker MW, Chiesi M, Schilling W, Hofbauer KG, Levens N (1998) Food intake in free-feeding and energy-deprived lean rats is mediated by the neuropeptide Y_5 receptor. J Clin Invest 102:2136–2145

Dumont Y, Chabot JG, Quirion R (2004) Receptor autoradiography as means to explore the possible functional relvance of neuropeptides: focus on new agonists and antagonists to study natriuretic peptides, neuropeptide Y and calcitonin gene-related peptides. Peptides 25:365–391

Erickson JC, Hollopeter G, Palmiter RD (1996) Attenuation of the obesity syndrome of *ob/ob* mice by the loss of neuropeptide Y. Science 274:1704–1707

Fuhlendorff J, Gether U, Aakerlund L, Langeland-Johansen N, Thøgersen H, Melberg SG, Olsen UB, Thastrup O, Schwartz TW (1990) [Leu^{31}, Pro^{34}]neuropeptide Y: a specific Y_1 receptor agonist. Proc Natl Acad Sci USA 87:182–186

Gerald C, Walker MW, Criscione L, Gustafson EL, Batzl-Hartmann C, Smith KE, Vaysse P, Durkin MM, Laz TM, Linemeyer DL, Schaffhauser AO, Whitebread S, Hofbauer KG, Taber RI, Branchek TA, Weinshank RL (1996) A receptor subtype involved in neuropeptide Y-induced food intake. Nature 382:168–171

Goumain M, Voisin T, Lorinet AM, Balsubramaniam A, Laburthe M (1998) Pharmacological profile of the rat intestinal crypt peptide YY receptor vs. the recombinant Y5 receptor. Eur J Pharmacol 362:245–249

Heilig M (2004) The NPY system in stress, anxiety and depression. Neuropeptides 38:213–224

Hudspith MJ, Munglani R (1997) The therapeutic potential of neuropeptide Y in cardiovascular disease. Exper Opin Invest Drugs 6:437–445

Iyengar S, Li DL, Simmons RMA (1999) Characterization of neuropeptide Y-induced feeding in mice: Do Y1-Y6 receptor subtypes mediate feeding? J Pharmacol Exp Ther 289:1031–1040

Kalra SP, Kalra PS (2004) NPY and cohorts in regulating appetite, obesity and metabolic syndrome: beneficial effects of gene therapy. Neuropeptides 38:201–211

Kanatani A, Kanno T, Ishihara A, Hata M, Sakuraba A, Tanaka T, Tsuchiya Y, Mase T, Fukuroda T, Fukami T, Ihara M (1999) The novel neuropeptide Y Y_1 receptor antagonist J-104870: A potent feeding suppressant with oral bioavailability. Biochem Biophys Res Commun 266:88–91

Kask A, Rago L, Harro J (1996) Anxiogenic-like effect of the neuropeptide Y Y_1 receptor antagonist BIBP3226. Eur J Pharmacol 317:R3–R4

Kask A, Rago L, Harro J (1998) Evidence for involvement of neuropeptide Y receptors in the regulation of food intake: Studies with Y-1-selective antagonist BIBP3226. Br J Pharmacol 124:1507–1515

Kask A, Vasar E, Heidmets LT, Allikmets L, Wikberg JES (2001) Neuropeptide Y Y_5 receptor antagonist CGP71683A: the effects on food intake and anxiety-related behavior in the rat. Eur J Pharmacol 414:215–224

Kask A, Harro J, von Hörsten S, Redrobe JP, van Dumont Y, Quirion R (2002) The neurocircuitry and receptor subtypes mediating anxiolytic-like effects od neuropeptide Y. Neurosci Biobehav Rev 26:259–283

Kirby DA, Koerber SC, May JM, Hagaman C, Cullen MJ, Pelleymounter MA, Rivier JE (1995) Y_1 and Y_2 receptor selective neuropeptide Y analogues: Evidence for a Y_1 receptor subclass. J Med Chem 38:4579–4586

Lambert PD, Wilding JPH, al Dokhayel AAM, Bohuon C, Comoy E, Gilbey SG, Bloom SR (1993) A role for neuropeptide Y, dynorphin, and noradrenaline in the central control of food intake after food deprivation. Endocrinology 133:29–33

Larhammar D (1996) Structural diversities for neuropeptide Y, peptide YY and pancreatic polypeptide. Regul Pept 65:165–174

Larhammar D, Salaneck E (2004) Molecular evolution of NPY receptor subtypes. Neuropeptides 38:141–151

Leibowitz SF (1994) Hypothalamic neuropeptide Y in regulation to energy balance. Ann NY Acad Sci 739:12–35

Lew MJ, Murphy R, Angus JA (1996) Synthesis and characterization of a selective peptide antagonist of neuropeptide Y vascular postsynaptic receptors. Br J Pharmacol 117:1768–1772

Lin S, Boey D, Herzog H (2004) NPY and Y receptors: lessons from transgenic and knockout models. Neuropeptides 38:189–200

Marsh DJ, Hollopeter G, Kafer KE, Palmiter RD (1998) Role of Y5 neuropeptide Y receptor in feeding and obesity. Nat Med 4:718–721

Matthews JE, Jansen M, Lyerly D, Cox R, Chen WJ, Koller KJ, Daniels AJ (1997) Pharmacological characterization and selectivity of the NPY antagonist GR231118 (1229U91) for different NPY receptors. Regul Pept 72:113–119

McCloskey MJD, Moriarty MJ, Tseng A, Shine J, Potter EK (1997) Activities of centrally truncated analogues of neuropeptide Y at Y_1 and Y_2 receptor subtypes *in vivo*. Neuropeptides 31:193–197

Michel MC, Beck-Sickinger A, Cox H, Doods HN, Herzog H, Larhammar D, Quirion R, Schwartz T, Westfall T (1998) XVI. International Union of Pharmacology recommendations for the nomenclature of neuropeptide Y, peptide YY, and pancreatic polypeptide receptors. Pharmacol Rev 50:143–150

Mullins DE, Guzzi M, Xia L, Parker EM (2000) Pharmacological characterization of the cloned neuropeptide Y y_6 receptor. Eur J Pharmacol 395:87–93

Parker EM (1999) The role of central neuropeptide, neurotransmitter and hormonal systems in the regulation of body weight. Neurotransmiss 15:3–11

Parker EM, Babij CK, Balasubramaniam A, Burrier RE, Guzzi M, Hamud F, Mukhopadhyay G, Rudinski MS, Tao Z, Tice M, Xia L, Mullins DE, Salisbury BG (1998) GR231118 (1229U91) and other analogues of the C-terminus of neuropeptide Y are potent neuropeptide Y Y_1 receptor antagonists and neuropeptide Y Y_4 receptor agonists. Eur J Pharmacol 349:97–105

Playford RJ, Cox HM (1996) Peptide YY and neuropeptide Y: two peptides intimately involved in electrolyte homeostasis. Trends Pharmacol Sci 17:436–438

Sajdyk TJ, Vandergriff MG, Gehlert DR (1999) Amygdalar neuropeptide Y Y_1 receptors mediated the anxiolytic-like actions of neuropeptide Y in the social interaction test. Eur J Pharmacol 368:143–147

Sajdyk TJ, Schober DA, Smiley DL, Gehlert DR (2002) Neuropeptide Y-Y_2 receptors mediate anxiety in the amygdale. Pharmacol Biochem Behav 71:419–423

Schaffhauser AO, Stricker-Krongrad A, Brunner L, Cumin F, Gerald C, Whitebread S, Criscione L, Hofbauer KG (1997) Inhibition of food intake by neuropeptide Y Y5 receptor antisense oligodeoxynucleotides. Diabetes 46:1792–1798

Shigeri Y, Ishikawa M, Ishihara Y, Fujimoto M (1998) A potent nonpeptide neuropeptide Y Y1 receptor antagonist, a benzodiazepine derivative. Life Sci 63:151–160

Small CJ, Morgan DGA, Meeran K, Heath MM, Gunn I, Edwards CMB, Gardiner J, Taylor GM, Hurley JD, Rossi M, Goldstone AP, O'Shea D, Smith DM, Ghatei MA, Bloom SR (1997) Peptide analogue studies of the hypothalamic neuropeptide Y receptor mediating pituitary adrenocorticotropic hormone release. Proc Natl Acad Sci USA 94:11686–11691

Souli A, Chariot J, Voisin T, Presset O, Tsocas A, Balasubramaniam A, Laburthe M, Roze C (1997) Several receptors mediate the antisecretory effects of peptide YY, neuropeptide Y and pancreatic polypeptide on VIP-induced fluid secretion in the rat jejunum *in vivo*. Peptides 18:551–557

Stanley BG, Magdalin W, Seirafi A, Nguyen MM, Leibowitz SF (1992) Evidence for neuropeptide Y mediation of eating produced by food deprivation and for a variant of the Y-1 receptor mediating this peptide's effect. Peptides 13:581–587

Stephens TW, Basinski M, Bristow PK, Bue-Valleskey JM, Rosteck PR, Schoner B, Smith D, Tinsley FC, Zhang X-Y, Heiman M (1995) The role of neuropeptide Y in the antiobesity action of the obese gene product. Nature 377:530–532

Sundler P, Boettcher G, Ekblad E, Hakanson R (1993)PP, PYY and NPY: occurrence and distribution in the periphery. In: Colmers WF, Walestedt C (eds) The Biology of Neuropeptide Y and Related Peptides. Humana Press, Inc., pp 157–196

Tadepalli AS, Harrington WW, Hashim MA, Matthews J, Leban JJ, Spaltenstein A, Daniels AJ (1996) Hemodynamic characterization of a novel neuropeptide Y receptor antagonist. J Cardiovasc Pharmacol 27:712–718

Thiele TE, Sparta DR, Hayes DM, Fee JR (2004) The role of neuropeptide Y in neurobiological responses to ethanol and drugs of abuse. Neuropeptides 38:235–243

Vezzani A, Sperk G (2004) Overexpression of NPY and Y2 receptors in epileptic brain tissue: an endogenous neuroprotective mechanism in temporal lobe epilepsy? Neuropeptides 38:245–252

Wettstein JG, Early B, Junien JL, (1995) Central nervous system pharmacology of neuropeptide Y. Pharmacol Ther 65:397–414

Wieland HA, Engel W, Eberlein W, Rudolf K, Doods HN (1998) Subtype selectivity of the novel nonpeptide neuropeptide Y Y1 receptor antagonist BIBO 3304 and its effect on feeding in rodents. Br J Pharmacol 125:549–555

Wyss P, Stricker-Krongard A, Brunner L, Miller J, Crossthwaite A, Whitebread S, Criscione L (1998) The pharmacology of neuropeptide Y (NPY) receptor-mediated feeding in rats characterizes better Y5 than Y1, but not Y2 or Y4 subtypes. Regul Pept 75–76:363–371

Zarrinmayeh H, Nunes AM, Ornstein PL, Zimmermann DM, Arnold MB, Schober DA, Gackenheimer SL, Bruns RF, Hipskind BA, Britton TC, Cantrell BE, Gehlert DL (1998) Synthesis and evaluation of a series of novel 2-[(4-chlorophenoxy)methyl]benzimidazoles as selective neuropeptide Y Y_1 receptor antagonists. J Med Chem 41:2709–2719

L.4.2.2 Receptor Assay of Neuropeptide Y

PURPOSE AND RATIONALE

At least six distinct G protein-coupled receptors of neuropeptide Y have been identified, designated Y_1, Y_2, Y_3, Y_4, Y_5 and Y_6 (Doods and Krause 1991; Marsh et al. 1998; Michel et al. 1998; Bischoff and Michel 1999).

Sheikh et al. (1989) described a receptor binding assay for neuropeptide Y.

PROCEDURE

^{125}*I-Labeling*

^{125}I-labeled NPY is prepared using carrier-free Na^{125}I and 1,3,4,6-tetrachloro-3α,α6-diphenylglycouril (Ser-

va Heidelberg, Germany) as oxidizing agent. Synthetic porcine NPY (7 nmol) in 40 µl of sodium phosphate buffer (pH 7.4, 0.1 M) and 1 mCi of $Na^{125}I$ in 10 µl of dilute NaOH is added to a reaction vial which has been coated with 20 µg of chlorglycouril by evaporation of 20 µ l of a solution of glycouril in methylene chloride. Following incubation in ice for 5 min, 50 µl of 35% acetonitrile is added prior to HPLC.

Purification by Reverse Phase-High Performance Liquid Chromatography

A prepacked Nucleosil 300–5 C_{18} cartridge is used. The chromatography is performed at 50°C with a flow rate of 1 ml 35% acetonitrile/min. Fractions of 0.5 ml are collected into tubes containing 0.1 ml of acetic acid (0.5 M) containing 10 mg/liter bovine serum albumin. Aliquots of 10 µl are counted in a γ-counter, and fractions containing the radiolabeled peptide are pooled and stored at –20°C.

Preparation of Synaptosomal Membranes

Synaptosomal membranes are prepared from the hippocampus of Danish LYY-strain landrace/Yorkshire pigs. The tissue is homogenized in 0.32 M sucrose in a Sorval Omni-Mixer at 0°C for 5 min, followed by centrifugation (1000 *g*, 10 min). The supernatant is removed and centrifuged (20,000 *g*, 30 min) to form the crude mitochondrial fraction. After resuspension in 3 ml of sucrose, this fraction is subfractionated on a discontinuous density gradient consisting of 0.8 M and 1.2 M sucrose (3 ml of each) in a SW 27 rotor and a Beckman ultracentrifuge (100,000 *g*, 90 min). The synaptosomes which concentrate at the interface between the two sucrose concentrations are collected and recentrifuged (50,000 *g*, 10 min). The resulting pellet is washed with HEPES buffer (pH 7.4, 25 mM) containing $CaCl_2$ (2.5 mM) and $MgCl_2$ (1 mM), centrifuged (50,000 *g*, 10 min), and resuspended in HEPES buffer. The protein concentration is determined using the Bio-Rad protein assay with bovine serum albumin as standard. The membrane preparation is diluted in binding buffer to a protein concentration of 2 g/liter and stored at –80°C.

Receptor Binding Assay

The binding buffer is a HEPES buffer (pH 7.4, 25 mM) containing $CaCl_2$ (2.5 mM) and $MgCl_2$ (1 mM), bovine serum albumin (10 g/liter), and bacitracin (0.5 g/liter). The incubation mixture consists of 0.5 ml of membrane suspension, diluted with binding buffer to a protein concentration of 200 mg/liter, 0.05 ml of unlabeled peptide, and 0.5 ml of ^{125}I-labeled peptide (40,000 cpm). After 1 h of incubation, triplicate aliquots of the incubation medium are transferred to polypropylene tubes (0.4 × 4.5 cm), containing 200 µl of ice-cold buffer. Membrane-bound, radiolabeled peptide is separated from the free peptide by centrifugation (7500 *g*, 2 min) in a Beckman Microfuge B. The supernatant is aspirated, and the tube and pellet are gently washed with buffer (0.5 ml). The tip of the tube is the cut off and counted in the γ-counter.

EVALUATION

The specific binding is calculated as the difference between the amount of ^{125}I-labeled peptide bound in the absence (total binding) and presence (nonspecific binding) if 10 µM unlabeled peptide.

The concentration dependence of the receptor binding is determined by incubating the membranes with increasing concentrations of radiolabeled peptide in the absence or presence of unlabeled peptide.

MODIFICATIONS OF THE METHOD

Rose et al. (1995) reported cloning and functional expression of a cDNA encoding a human type 2 neuropeptide Y receptor.

Gehlert et al. (1996) recommended [^{125}I][Leu^{31}, Pro^{34}]peptide YY as selective radioligand for the neuropeptide Y Y_1 receptor and for human pancreatic polypeptide 1 receptors.

Robin-Jagerschmidt et al. (1998) investigated the ligand binding site of neuropeptide Y at the rat Y_1 receptor by construction of mutant receptors and [^3H]NPY binding studies.

Dumont et al. (1998) investigated the respective distribution of neuropeptide Y Y_1, Y_2, Y_4, and Y_5 receptor subtypes in rodents (rat and mouse), guinea pig, and primates (marmoset and vervet monkey and human) brains, representing three orders of mammals.

Primus et al. (1998) measured guanyl 5′(γ[^{35}S]-thio)-triphosphate binding to NPY receptor-activated G-proteins in adult rat brain sections in order to determine the neuroanatomical distribution of NPY receptor subtypes.

Wyss et al. (1998) administered various doses of synthetic neuropeptide Y agonists intracerebroventricularly to rats in order to establish dose-response curves and to estimate ED_{50} values of feeding. These values were compared with binding affinities (IC_{50}) for rat NPY receptor subtypes Y_1, Y_2, Y_4, and Y_5 *in vitro*. Mouse fibroblast cell lines (LMTK–) were stably transfected with the rat Y_1, Y_2 and the Y_4 recep-

tor, whereas human embryonic kidney HEK-293 cells were used for transfection with the rat Y_5 receptor.

Parker et al. (1998) determined the agonist and antagonist potency of neuropeptide Y and various analogues for cloned human and rat neuropeptide Y receptors expressed in CHO or 293 cells.

Wieland et al. (1998) studied the subtype selectivity of a nonpeptide Y_1 receptor antagonist using membranes from rat hypothalamus, from SK-N-MC (neuroblastoma) cells and from SMS-KAN (neuroblastoma) cells; human Y_1 receptor stably expressed in baby hamster kidney (BHK) cells, rat Y_1 receptor expressing human embryonic kidney (HEK) 293 cells, human Y_2 receptor stably expressed in BHK cells, rat Y_4 stably transfected in BHK cells, and human Y_5 receptor stably transfected in HEK 293 cells.

Several groups reported screening results of neuropeptide Y antagonists mostly using receptor binding experiments (Murakami et al. 1999; Fotsch et al. 2001; Islam et al. 2002; Poindexter et al. 2002; Andres et al. 2003; Hammond et al. 2003; Blum et al. 2004; Gillman et al. 2006; Kakui et al. 2006).

Dautzenberg et al. (2005) established robust functional assays for the characterization of neuropeptide Y receptors. The human neuropeptide Y (NPY) receptors 1 (hY_1), 2 (hY_2), 4 (hY_4), and the mouse type 5 (mY_5) receptor were expressed in human embryonic kidney 293 (HEK293) cells. The receptors bound a radioiodinated NPY ligand with high affinity and various NPY analogs competed for binding in a receptor-selective manner. Similarly, cAMP inhibition and GTPγ S binding assays were established. The four NPY receptors were further tested in the fluorimetric imaging plate reader (FLIPR) format, a cellular high-throughput assay, in the absence and presence of chimeric G proteins, Gq_{o5}, Gq_{i5} and Gq_{i9}.

PROCEDURE

Cell Transfections

cDNAs of the four NPY receptors inserted into pcDNA3 (5 µg each) or Gq_{i5}, Gq_{o5} and Gq_{i9} (10 µg each) inserted into pcDNA5 (Invitrogen) were transiently transfected into HEK293 cells with the FUGENE reagent (Roche Molecular Biochemicals, Mannheim, Germany) according to the manufacturer's protocol. Cell lines stably expressing the various NPY receptors together with Gq_{i9} were generated by transfecting receptor cDNA (0.5 µg each), the Gq_{i9} cDNA (1 µg) and the pOG44 vector (10 µg) encoding the cDNA for the DNA recombinase used in the Flip-in system (Invitrogen) with the FUGENE reagent. Two days after transfection, Geneticin (500 µg/ml) and hygromycin (50 µg/ml) selection was initiated and stable cell clones robustly responding in the FLIPR assay were selected.

Radioreceptor Binding Assays

Membranes from NPY-receptor-expressing HEK cells were prepared according to Dautzenberg et al. 2005. Competition binding assays were performed with 5 (hY_2 or hY_4), 25 (mY_5) and 40 µg (hY_1) of membrane proteins prepared from the four NPY receptors under assay conditions according to Rist et al. (1996), using 96-well plates (Beckmann Instruments, Fullertown, Calif., USA) and a scintillation proximity assay (SPA; Dautzenberg et al. 2000}). The membranes, 1 mg wheat germ agglutinin SPA beads (Amersham Pharmacia Biotech), 100 pM [^{125}I]PYY and unlabeled peptides (10^{-5} M to 10^{-11} M) were added. The reaction mixture was incubated on a shaker for 120 min at 22°C and then read in a TopCount (Packard). Nonspecific binding was determined as residual binding in the presence of 10 µM PYY. The dissociation constant K_d, the inhibition constant K_i, and the maximum receptor concentration, B_{max}, were calculated using the interactive curve fitting program Xlfit (Hoffmann-La Roche). Under these conditions less than 10% of the total radioactivity was specifically bound by the various receptor constructs.

cAMP Inhibition Assay

The inhibition of forskolin-mediated cAMP accumulation by NPY analogs in 96-well plates was determined as previously described (Dautzenberg et al. 2001). Briefly 20,000 cells were incubated in Krebs-Ringer-HEPES-buffered solution (KHR; 124 mM NaCl, 5 mM KCl, 1.25 mM $MgSO_4$, 1.5 mM $CaCl_2$, 1.25 mM KH_2PO_4, 25 mM HEPES, pH 7.4) in the presence of 1 µM forskolin (Sigma, Munich, Germany) with increasing concentrations of agonists (10 pM to 10 µM) for 60 min at 37°C. Reactions were stopped by the addition of 0.12 ml ice-cold ethanol and stored at –80°C for at least 4 h. The cAMP content was determined from the supernatant using the Biotrak non-radioactive cAMP kit (Amersham Pharmacia Biotech) according to the manufacturer's instructions.

GTPγ S Binding Assay

Agonist-mediated binding of GTPγ^{35}S was investigated in the SPA format using 96-well plates (Rover et al. 2000}) and membranes prepared from cells transfected with the hY_1, hY_2, hY_4 and mY_5 receptors. Binding was performed in 200 µ l of 20 mM HEPES-buffer (pH 7.4, plus 6 mM $MgCl_2$ and 100 mM NaCl),

supplemented with 20 µM GDP, 10 µM cold GTPγ S and 0.3 nM GTPγ^{35}S. Then, 20 µg (hY_2, hY_4, mY_5) to 40 µg (hY_1) membranes, 1 mg wheatgerm agglutinin SPA beads, NPY analogs or synthetic compounds (10^{-4} M to 10^{-11} M) were added. For antagonist assays, a submaximal (EC_{80}) concentration of PYY was added together with increasing antagonist concentrations (10^{-4} to 10^{-11} M). The reaction mixture was incubated on a shaker for 60 min at 22°C and then centrifuged for 5 min at 1500 rpm in an Eppendorf 5403 centrifuge. Finally the plates were read in a TopCount reader (Packard).

Calcium Mobilization Assays

HEK293 transiently stably expressing the four NPY receptors with or without chimeric G-proteins were seeded at a density of 100,000 cells into poly-D-lysine-coated 96-well blackwall, clear-bottom microtiter plates (Corning, NY) (Dautzenberg et al. 2004). One day later, the medium was removed and 100 µl loading medium [DMEM high glucose, without serum, supplemented with 10 mM HEPES acid, 0.1% BSA, 5 mM probenecid and 2 µM Fluo-3AM (Molecular Probes, Leiden, The Netherlands)] was added. Cells were loaded for 1 h at 37°C, washed twice with 100 µl assay buffer (5 mM HEPES acid, 140 mM NaCl, 1 mM $MgCl_2$, 5 mM KCl, 10 mM glucose) and then 150 µl assay buffer was added. Cells were further preincubated at room temperature before adding agonists or agonists plus antagonists in 50 µl assay buffer and then measured on a T-channel fluorimetric imaging plate reader (FLIPR, Molecular Devices, Sunnyvale, Calif., USA). Maximum change in fluorescence over baseline was used to determine agonist response.

EVALUATION

Statistical analyses of the binding, cAMP, GTPγ S and calcium mobilization data were performed on a Macintosh PC using StatView software (SAS, Cary, N.C., USA) by one-way analyses of variance (ANOVAs) across experimental groups followed by the Dunnett's test with the alpha set at 0.05.

Beauverger et al. (2005) characterized antagonists specific to human neuropeptide Y receptor subtype 5 using a **luciferase reporter gene assay**.

PROCEDURE

CRE-Luciferase Reporter Assay

Standardization of this assay consisted of testing various cell densities and incubation times to optimize the signal-to-background ratio. Briefly, HEK293-hMT1 cells grown to ≈ 80% confluence were transfected in batches with lipofectAMINE Plus (Life Technologies) using 20 ng of pcDOR8, 500 ng of pΔ MC16-Luc and 1 µg of either pcDNA3.1 or pcDNA3.1-Y5 per million of cells. Then, 24 h after transfection, cells were detached by agitation, centrifuged and recovered at 10^6 cells/ml in phenol-red-free DMEM medium supplemented with 2% fetal calf serum. They were then seeded as 50-µl aliquots into white 96-well tissue culture plates containing the drugs previously diluted in the same medium and distributed as 50-µ l aliquots. After a 20-h incubation period, the luciferase activity was measured by adding 100 µl per well of Luclite buffer (Packard) followed by a 30-min incubation in the dark at room temperature and a use of a Topcount (Packard).

Savontaus et al. (1998) measured expression of preproneuropeptide Y mRNA in the arcuate nucleus and preprocorticotropin-releasing factor mRNA in the paraventricular nucleus by *in situ* hybridization technique after short and long-term treatment with a β_3-adrenoreceptor agonist.

Bioassays have been used for characterization and classification of neuropeptide Y receptors (Hedge et al. 1995; Pheng and Regoli 1998; Dumont et al. 2000a, b). Some isolated organs appear to be "monoreceptor" systems, e. g., the rat tail artery (Gicquiaux et al. 1996), the rabbit saphenous vein (Pheng and Regoli 1998; Feletou et al. 1999) or the isolated perfused kidney of the rat (Hedge et al. 1995) for the Y_1 receptor. The dog saphenous vein, the rat vas deferens and the rat colon can be used for the Y_2 receptor, the rat colon for the Y_4 receptor, and the rabbit ileum for the Y_5 receptor (Pheng et al. 1997).

REFERENCES AND FURTHER READING

Andres CJ, Antal Zimanyi I, Deshpande MS, Iben LG, Grant-Young K, Mattson GK, Zhai W (2003) Differentially functionalized diamines as novel ligands for the NPY_2 receptor. Bioorg Med Chem Lett 13:2883–2885

Beauverger P, Rodriguez M, Nicolas JP, Audinot V, Lamamy V, Dromaint S, Nagel N, Macia C, Léopold O, Galizzi JP, Caignard DH, Aldana I, Monge A, Chomarat P, Boutin JA (2005) Functional characterization of human neuropeptide Y receptor subtype five specific antagonists using an luciferase reporter gene assay. Cell Signalling 17:489–496

Bischoff A, Michel MC (1999) Emerging functions for neuropeptide Y5 receptors. Trends Pharmacol Sci 20:104–106

Blum CA, Zheng X, de Lombaert S (2004) Design, synthesis and biologic evaluation of substituted 2-cyclhexyl-4-phenyl-1*H*-imidazoles. Potent and selective neuropeptide Y Y5-receptor antagonists. J Med Chem 47:2318–2325

Dautzenberg FM, Huber G, Higelin J, Py-Lang G, Kilpatrick G (2000) Evidence for the abundant expression of arginine 185 containing human $CRF_{2\alpha}$ receptors and the role of position 185 for receptor-ligand selectivity. Neuropharmacology 39:1368–1376

Dautzenberg FM, Wichmann J, Higelin J, Py-Lang G, Kratzeisen C, Malherbe P, Kilpatrick GJ, Jenck F (2001) Pharmacological characterization of the novel nonpeptide orphanin FQ/nociceptin receptor agonist Ro 64–6198: rapid and reversible desensitization of the ORL1 receptor in vitro and lack of tolerance in vivo. J Pharmacol Exp Ther 298:812–819

Dautzenberg FM, Gutknecht E, Van der Linden I, Olivares-Reyes JA, Dürrenberger F, Hauger RL (2004) Cell type specific calcium signaling by corticotropin-releasing factor type 1 (CRF_1) and 2a ($CRF_{2\alpha}$) receptors: phospholipase C-mediated responses in human embryonic kidney 293 but not SK-N-MC neuroblastoma cells. Biochem Pharmacol 68:1833–1844

Dautzenberg FM, Higelin J, Pflieger P, Neidhart W, Guba W (2005) Establishment of robust functional assays for the characterization of neuropeptide Y (NPY) receptors: identification of 3-(5-benzoyl-thiazol-2-ylamino)-benzonitrile as selective NPY type 5 receptor antagonist. Neuropharmacology 48:1043–1055

Doods HN, Krause J (1991) Different neuropeptide Y receptor subtypes in rat and rabbit vas deferens. Eur J Pharmacol 204:101–103

Dumont Y, Jacques D, Bouchard P, Quirion R (1998) Species differences in the expression and distribution of the neuropeptide Y Y_1, Y_2, Y_4, and Y_5 receptors in rodents, guinea pig, and primate brains. J Comp Neurol 402:372–384

Dumont Y, Cadieux A, Doods H, Pheng LH, Abounader R, Hamel E, Jacques D, Regoli D, Quirion J (2000a) BIIE0246, a potent and highly selective non-peptide neuropeptide Y Y_2 receptor antagonist. Br J Pharmacol 129:1075–1088

Dumont Y, Cadieux A, Doods H, Fournier A, Quirion R (2000b) Potent and selective tools to investigate neuropeptide Y receptors in the central and peripheral nervous system: BIBO3304 (Y_{-1}) and CGP71683A (Y_5). Can J Physiol Pharmacol 78:116–125

Feletou M, Nicolas JP, Rodriguez M, Beauverger P, Galizzi JP, Boutin JA, Dehault J (1999) NPY receptor subtype in the rabbit isolated ileum. Br J Pharmacol 127:795–801

Fotsch C, Sonnenberg JD, Chen N, Hale C, Karbon W, Norman MH (2001) Synthesis and structure-activity relationships of trisubstituted phenyl urea derivatives as neuropeptide Y5 antagonists. J Med Chem 44:2344–2356

Gehlert DR, Gackenheimer SL, Schober DA, Beavers L, Gadski R, Burnett JP, Mayne N, Lundell I, Larhammer D (1996) The neuropeptide Y Y_1 receptor selective radioligand, [^{125}I][Leu^{31},Pro^{34}]peptide YY, is also a high affinity radioligand for human pancreatic polypeptide 1 receptors. Eur J Pharmacol 318:485–490

Gicquiaux H, Tschopl M, Doods HN, Bucher B (1996) Discrimination between neuropeptide Y and peptide YY in the rat tail artery by the neuropeptide Y_1-selective antagonist BIBP 3226. Br J Pharmacol 119:1313–1318

Gillman KW, Higgins MA, Poindexter GS, Browning M, Clarke WJ, Flowers S, Grace JE, Hogan JB, McGovern RT, Iben LG, Mattson GK, Ortiz A, Rassnick S, Russell JW, Antal-Zimanyi I (2006) Synthesis and evaluation of 5.5-diphenylimidazolones as potent human neuropeptide Y5 receptor antagonists. Bioorg Med Chem 14:5517–5526

Hammond M, Elliott RL, Gillapsy ML, Hager DC, Hank RF, LaFlamme JA, Oliver RM, DaSilva-Jardine PA, Stevenson RW, Mack CM, Cassella JV (2003) Structure-activity relationships in a series of NPY Y5 antagonists: 3-amido-9-ethylcarbazoles, core-modified analogues and amide isosteres. Bioorg Med Chem Lett 13:1989–1992

Hedge SS, Bonhaus DW, Stanley W, Eglen RM, Moy TM, Loeb M, Shetty SG, Desouza A, Krstenansky J (1995) Pharmacological evaluation of 1229U91, a novel high-affinity and selective neuropeptide Y Y_1 receptor. J Pharmacol Exp Ther 275:1261–1266

Islam I, Dhanoa D, Finn J, Du P, Walker MW, Salon JA, Zhang J, Gluchowski C (2002) Discovery of potent and selective small molecule NPY Y5 receptor antagonists. Bioorg Med Chem Lett 12:1767–1769

Kakui N, Tanaka J, Tabata Y, Asai K, Masuda N, Miyara T, Nakatani Y, Ohsawa F, Nishikawa N, Sugai M, Suzuki M, Aoki K, Kitaguchi H (2006) Pharmacological characterization and feeding-suppressive property of FMS586 [3-(5,6,7,8-tetrahydro-9-isopropyl-carbazol-3yl)-1-methyl-1-(2-pyridin-4-yl-ethyl) urea hydrochloride], a novel, selective, and orally active antagonist for neuropeptide Y Y5 receptor. J Pharmacol Exp Ther 317:562–570

Marsh DJ, Hollopeter G, Kafer KE, Palmiter RD (1998) Role of Y5 neuropeptide Y receptor in feeding and obesity. Nat Med 4:718–721

Michel MC, Beck-Sickinger A, Cox H, Doods HN, Herzog H, Larhammar D, Quirion R, Schwartz T, Westfall T (1998) XVI. International Union of Pharmacology recommendations for the nomenclature of neuropeptide Y, peptide YY, and pancreatic polypeptide receptors. Pharmacol Rev 50:143–150

Murakami Y, Hagishita S, Okada T, Kii M, Hashizume H, Yagami T, Fujimoto M (1999) 1,3-Disubstituted benzazepines as neuropeptide Y Y1 receptor antagonists. Bioorg Med Chem 7:1703–1714

Parker EM, Babij CK, Balasubramaniam A, Burrier RE, Guzzi M, Hamud F, Mukhopadhyay G, Rudinski MS, Tao Z, Tice M, Xia L, Mullins DE, Salisbury BG (1998) GR231118 (1229U91) and other analogues of the C-terminus of neuropeptide Y are potent neuropeptide Y Y_1 receptor antagonists and neuropeptide Y Y_4 receptor agonists. Eur J Pharmacol 349:97–105

Pheng LH, Regoli D (1998) Bioassays for NPY receptors: Old and new. Regul Pept 75–76:79–87

Pheng LH, Quirion R, Iyengar S, Fournier A, Regoli D (1997) The rabbit ileum; a sensitive and selective preparation for the neuropeptide Y Y_5 receptor. Eur J Pharmacol 333:R3–R5

Poindexter GS, Bruce MA, LeBoulluec KL, Monkovic I, Martin SW, Parker EM, Iben LG, McGovern RT, Ortiz AA, Stanley JA, Mattson GK, Kozlowski M, Arcuri M, Antal-Zimanyi I (2002) Dihydropyridine neuropeptide Y Y1 receptor antagonists. Bioorg Med Chem Lett 12 :379–382

Primus RJ, Yevich E, Gallagher DW (1998) *In vitro* autoradiography of GTP γ [^{35}S] binding at activated NPY receptor subtypes in adult rat brain. Mol Brain Res 58:74–82

Rist B, Zerbe O, Ingenhoven N, Scapozza L, Peers C, Vaughan PF, McDonald RL, Wieland HA, Beck-Sickinger AG (1996) Modified, cyclic dodecapeptide analog of neuropeptide Y is the smallest full agonist at the human Y2 receptor, FEBS Lett 394:169–173

Robin-Jagerschmidt C, Sylte I, Bihoreau C, Hendricksen L, Calvet A, Dahl SG, Bénicourt C (1998) The ligand binding site of NPY at the rat Y_1 receptor investigated by site-directed mutagenesis and molecular modeling. Mol Cell Endocrinol 139:187–198

Rose PM, Fernandes P, Lynch JS, Frazier ST, Fisher SM, Kodokula K, Kienzle B, Seethala R (1995) Cloning and functional expression of a cDNA encoding a human type 2 neuropeptide Y receptor. J Biol Chem 270:22661–22664

Rover S, Adam G, Cesura AM, Galley G, Jenck F, Monsma FJ Jr, Wichmann J, Dautzenberg FM (2000) High-affinity, non-peptide agonists for the ORL1 (orphanin FQ/nociceptin) receptor. J Med Chem 43:1329–1338

Savontaus E, Pesonen U, Rouru J, Huupponen R, Koulu M (1998) Effects of ZD7114, a selective β_3-adrenoceptor agonist, on neuroendocrine mechanisms controlling energy balance. Eur J Pharmacol 374:265–274

Wieland HA, Engel W, Eberlein W, Rudolf K, Doods HN (1998) Subtype selectivity of the novel nonpeptide neuropeptide Y Y_1 receptor antagonist BIBO 3304 and its effect on feeding in rodents. Br J Pharmacol 125:549–555

Wyss P, Stricker-Krongard A, Brunner L, Miller J, Crossthwaite A, Whitebread S, Criscione L (1998) The pharmacology of neuropeptide Y (NPY) receptor-mediated feeding in rats characterizes better Y5 than Y1, but not Y2 or Y4 subtypes. Regul Pept 75–76:363–371

L.4.3 Orexin

L.4.3.1 General Considerations on Orexin

Orexin-A and orexin-B are 33- and 28-residue peptides, also called hypocretins, which were originally isolated from rat hypothalamus (De Lecea et al. 1998; Sakurai et al. 1998). Both peptides are derived from a 130 amino acid precursor, preproorexin, which is encoded by a gene localized to chromosome 17q21 in humans. These peptides are located predominantly in the hypothalamus and locus coeruleus (Evans et al. 1999), but are also found elsewhere in the brain, and in the spinal cord (Smart 1999; Van den Pol 1999). The orexins have a broad range of physiological functions, including the control of feeding and energy metabolism (Dube et al. 1999; Mondal et al. 1999; Sakurai 1999, 2006), stimulation of insulin secretion (Nowak et al. 2000, 2005), modulation of neuro-endocrine function (Date et al. 1999), regulation of the sleep-wake cycle (Piper et al. 2000), narcolepsy (Taheri et al. 2002; Wille et al. 2003; Mieda et al. 2004), stress and anxiety, behavioral activities (Ida et al. 1999; Siegel 2003), cardiovascular (Shirasaka et al. 1999; Chen et al. 2000), adrenal function (Jöhren et al. 2004), and sexual and reproductive functions (Pu et al. 1998; deLecea and Sutcliffe 1999; Tamura et al. 1999). Food consumption is dose-dependently increased after intracerebroventricular infusion of orexin A and orexin B to rats which can be suppressed by a NPY Y_1 antagonist (Jain et al. 2000). Food intake could inhibited by central injection of an anti-orexin antibody in fasted rats (Yamada et al. 2000). Novak et al. (2000) found an increase of insulin secretion after subcutaneous injection of orexins to rats.

Orexin antagonists are potential anti-obesity drugs (Parker 1999).

REFERENCES AND FURTHER READING

Cai XJ, Widdowson PJ, Harrold J, Wilson S, Buckingham RE, Arch JRS, Tadayyon M, Clapham JC, Wilding J, Williams G (1999) Hypothalamic orexin expression. Modulation by blood glucose and feeding. Diabetes 48:2132–2137

Chen C-T, Hwang L-L, Chang J-K, Dun NJ (2000) Pressor effects of orexins injected intracisternally and to the rostral ventrolateral medulla of anesthetized rats. Am J Physiol 278; Regul Integr Comp Physiol 47:R692–R897

Date Y, Ueta Y, Yamashita H, Yamaguchi H, Matsukura S, Kangawa K, Sakurai T, Yanagisawa M, Nakazato M (1999) Orexins, orexigenic hypothalamic peptides, interact with autonomic, neuroendocrine and neuroregulatory systems. Proc Natl Acad Sci USA 96:748–753

De Lecea L, Sutcliffe JG (1999) The hypocretins/orexins: Novel hypothalamic neuropeptides involved in different physiological systems. Cell Mol Life Sci 56:473–480

De Lecea L, Kilduff TS, Peyron C, Gao XB, Foye PE, Danielson PE, Fukuhara C, Battenberg ELF, Gautvik VT, Bartlett II FS, Frankel WN. Van der Pol AN, Bloom FE, Gautvik KM, Sutcliffe JG (1998) The hypocretins: hypothalamus-specific peptides with neuroexcitatory activity. Proc Natl Acad Sci USA 95:322–327

Dube MG, Kalra SP, Kalra PS (1999) Food intake elicited by central administration of orexins/hypocretins: Identification of hypothalamic sites of action. Brain Res 842:473–477

Evans ME, Harries M, Patel S, Benham CD (1999) Orexin-A depolarizes neurons in the rat locus coeruleus brain slice *in vitro*. J Physiol 515:121P

Ida T, Nakahara K, Katayama T, Murakami M, Nakazato M (1999) Effect of lateral cerebroventricular injection of the appetite-stimulating neuropeptide, orexin and neuropeptide Y, on the various behavioral activities of rats. Brain Res 821:526–529

Jain MR, Horvath TL, Kalra PS, Kalra SP (2000) Evidence that NPY Y1 receptors are involved in stimulation of feeding by orexins (hypocretins) in sated rats. Regul Pept 87:19–24

Jöhren O, Brüggemann N, Dominiak P (2004) Orexins (hypocretins) and adrenal function. Hormon Metab Res 36:370–375

Mieda M, Willie JT, Hara J, Sinton CM, Sakurai T, Yanagisawa M (2004) Orexin peptides prevent catalepsy and improve wakefulness in an orexin neuron-ablated model of narcolepsy in mice. Proc Natl Acad Sci USA 101:4649–4654

Mondal MS, Nakazato M, Date Y, Murakami N, Yanagisawa M, Matsukura S (1999) Widespread distribution of orexin in the rat brain and its regulation upon fasting. Biochem Biophys Res Commun 256:495–499

Nowak KW, Mackowiak P, Switonska MM, Fabis M, Malendowicz LK (2000) Acute orexin effects on insulin secretion in the rat: *In vivo* and *in vitro* studies. Life Sci 66:449–454

Nowak KW, Strowski MZ, Switonska M, Kaczmarek P, Singh V, Fabis M, Mackowiak P, Nowak M, Malendowicz LK (2005) Evidence that orexins A and B stimulate insulin secretion from rat pancreas via both receptor subtypes. Int Mol Med 15:969–972

Parker EM (1999) The role of central neuropeptide, neurotransmitter and hormonal systems in the regulation of body weight. Neurotransmiss 15:3–11

Piper DC, Upton N, Smith MI, Hunter AJ (2000) The novel neuropeptide, orexin A, modulates the sleep-wake cycle of rats. Eur J Neurosci 12:726–730

Pu S, Jain MR, Kalra PS, Kalra SP (1998) Orexins, a novel family of hypothalamic neuropeptides, modulate pituitary

luteinizing hormone secretion in an ovarian steroid-dependent manner. Regul Pept 78:133–136
Sakurai T (1999) Orexin and orexin receptors: implication of feeding behavior. Regul Pept 85:25–30
Sakurai T (2006) Roles of orexins and orexin receptors in central regulation of feeding behavior and energy homeostasis. CNS Neurol Disord Drug Targets 5:313–325
Sakurai T, Amemiya A, Ishii M, Matsuzaki I, Chemelli RM, Tanaka H, Williams SC, Richardson JA, Kozlowski GP, Wilson S, Arch JRS, Buckingham RB, Haynes AC, Carr SA, Annan RS, McNulty DE, Liu W-S, Terrett JA, Elshourbagy NA, Bergsma DJ, Yanagisawa M (1998) Orexins and orexin receptors: A family of hypothalamic neuropeptides an G protein-coupled receptors that regulate feeding behavior. Cell 92:573–585
Shirasaka T, Nakazato M, Matsukura S, Takasaki M, Kannan H (1999) Sympathetic and cardiovascular actions of orexins in conscious rats. Am J Physiol 277; Regul Integr Comp Physiol 46:R1780–R1785
Siegel JM (2003) Hypocretin (Orexin): role in normal behavior and neuropathology. Annu Rev Psychol 55:125–148
Smart D (1999) Orexins: A new family of neuropeptides. Br J Anaesth 83:695–697
Smart D, Jerman JC, Brough SJ, Rushton SL, Murdock PR, Jewitt F, Elshourbagy NA, Ellis JC, Middlemiss DN, Brown F (1999) Characterization of recombinant orexin receptor pharmacology in a Chinese hamster ovary cell-line using FLIPR. Br J Pharmacol 128:1–3
Taheri S, Zeitzer JM, Mignot E (2002) The role of hypocretins (orexins) in sleep regulation and narcolepsy. Annu Rev Neurosci 25:283–313
Tamura T, Irahara M, Tezuka M, Kiyokawa M, Aono T (1999) Orexins, orexigenic hypothalamic neuropeptides, suppress the pulsatile secretion of luteinizing hormone in ovarectomized female rats. Biochem Biophys Res Commun 264:759–762
Van den Pol AN, Gao XB, Obrietan K, Kilduff TS, Belousov AB (1999) Presynaptic and postsynaptic actions and modulation of neuroendocrine neurons by a new hypothalamic peptide, hypocretin/orexin. J Neurosci 18:7962–7971
Willie JT, Chemelli RM, Sinton CM, Tokita S, Williams SC, Kisanuki YY, Marcus JN, Lee C, Elmquist JK, Kohlmeier KA, Leonard CS, Richardson JA, Hammer RE, Yanagisawa M (2003) Distinct narcolepsy syndromes in orexin receptor-2 and orexin null mice: molecular genetic dissection of non-REM and REM sleep regulatory processes. Neuron 38:715–730
Yamada H, Okumura T, Motomura W, Kobayashi Y, Kohgo Y (2000) Inhibition of food intake by central injection of anti-orexin antibody in fasted rats. Biochem Biophys Res Commun 267:527–531

L.4.3.2 Receptor Assay of Orexin

PURPOSE AND RATIONALE

The peptides orexin A and orexin B bind both to two receptors, orexin-1 (OX_1) and orexin-2 (OX_2), although orexin B has a low affinity for OX_1 (Sakurai et al. 1998). Differential expression of orexin receptor 1 and 2 in rat brain was reported by Marcus et al. (2001) and distinct recognition of OX_1 and OX_2 receptors by orexin peptides by Ammoun et al. (2005).

PROCEDURE

Orexin OX_1 and OX_2 receptors are produced by polymerase chain reaction from foetal and adult brain cDNA libraries, using primers located across the start and stop codons. The receptors are subcloned into the pCDN vector (with neomycin resistance) and transfected into CHO cells using lipofectamine (Life Technologies). Clones are selected using 400 µg/ml G418 (Life Technologies) and single clones are produced by limiting dilution cloning.

CHO-OX_1 and CHO-OX_2 cells are routinely grown as monolayers in MEM-Alpha medium supplemented with 10% fetal calf serum and 400 µ g/ml G418 and maintained under 95% O_2/5% CO_2 at 37°C. Cells are passaged every 3–4 days.

Synthetic human orexin A is ^{125}I-labeled at Tyr17 by chloramine-T oxidation in the presence of $Na^{125}I$ (2000 Ci/mmol). Monoiodinated peptide is purified by C^{18} reverse-phase HPLC (Takigawa et al. 1995). Stable transfectant CHO cell lines expressing human OX_1R or OX_2R are each seeded onto 12-well plates at a density of 3×10^3 cells per well. After an overnight culture, medium is discarded and cells are incubated at 20°C for 90 min with binding buffer (HEPES-buffered saline/5% bovine serum albumin) containing 10^{-10} M [^{125}I]orexin A plus designated concentrations of unlabeled competitors. Cells are then washed three times with ice-cold phosphate-buffered saline and lysed in 0.1 N NaOH. Cell-bound radioactivity is determined by a γ-counter.

EVALUATION

Data are expressed as the percentage of saturably bound reactivity in the absence of nonradioactive peptide. For each experiment each value is determined in duplicate, and the results are expressed as the means ± standard errors of at least 3 separate experiments.

MODIFICATIONS OF THE METHOD

Smart et al. (1999) studied the pharmacology of recombinant orexin receptors using the fluorescence imaging plate recorder (FLIPR). CHO-OX_1 or CHO-OX_2 cells were seeded into black walled clear base 96 well plates at a density of 20000 cells per well in MEM-Alpha medium supplemented with 10% fetal calf serum and 400 µg/ml G418 and cultured overnight. The cells were then incubated with MEM-Alpha medium containing the cytoplasmatic calcium indicator, Fluo-3AM (4 µM) and 2.5 mM probenecid at 37°C for 60 min. The cells were washed four times with, and finally resuspended in, Tyrode's medium containing 2.5 mM probenecid and 1% gelatin, be-

fore being incubated for 30 min at 37°C with either buffer alone (control) or buffer containing various signal transduction modifying agents. The plates were then placed into an FLIPR (Molecular Devices, U.K.) to monitor cell fluorescence ($\lambda = 488$ nM, $\lambda = 540$ nM) (Sullivan et al. 1999) before and after the addition of orexin A or orexin B.

REFERENCES AND FURTHER READING

Ammoun S, Holmquist T, Shariatmadari R, Oonk HB, Detheux M, Parmentier M, Åkerman KEO, Kukkonen JP (2005) Distinct recognition of OX_1 and OX_2 receptors by orexin peptides. J Pharmacol Exp Ther 305:507–514

Marcus JN, Aschkenasi CJ, Chemelli RM, Saper CB, Yanagisawa M, Elmquist JK (2001) Differential expression of orexin receptor 1 and 2 in rat brain. J Comp Neurol 435:6–25

Sakurai T, Amemiya A, Ishii M, Matsuzaki I, Chemelli RM, Tanaka H, Williams SC, Richardson JA, Kozlowski GP, Wilson S, Arch JRS, Buckingham RB, Haynes AC, Carr SA, Annan RS, McNulty DE, Liu W-S, Terrett JA, Elshourbagy NA, Bergsma DJ, Yanagisawa M (1998) Orexins and orexin receptors: A family of hypothalamic neuropeptides an G protein-coupled receptors that regulate feeding behavior. Cell 92:573–585

Smart D, Jerman JC, Brough SJ, Rushton SL, Murdock PR, Jewitt F, Elshourbagy NA, Ellis JC, Middlemiss DN, Brown F (1999) Characterization of recombinant orexin receptor pharmacology in a Chinese hamster ovary cell-line using FLIPR. Br J Pharmacol 128:1–3

Sullivan E, Tucker EM, Dale IL (1999) Measurement of [Ca^{2+}] using the fluorometric imaging plate reader (FLIRP). In: Lambert DG (ed) Calcium Signaling Protocols. Humana Press, NJ, pp 125–136

Takigawa M, Sakurai T, Kasuya Y, Abe Y, Masaski T, Goto K (1995) Molecular identification of guanine-nucleotide-binding regulatory proteins which couple to endothelin receptors. Eur J Biochem 228:102–108

L.4.3.3 Radioimmunoassay for Orexin

PURPOSE AND RATIONALE

A radioimmunoassay for orexin A has been developed by Mitsuma et al. (2000).

PROCEDURE

Synthetic orexin A is conjugated on an equal weight basis to BSA using glutaraldehyde. New Zealand white rabbits are immunized with an emulsion of this conjugate in one ml of water and complete Freund's adjuvant (1:2, v/v) which is injected into the foot pad at intervals of 3 weeks. Blood is withdrawn one week after each injection, and the presence of anti-orexin is checked by radioimmunoassay.

Radioiodination of orexin A is performed with the chloramine T method. The radioiodinated materials are chromatographed on Sephadex G-25, eluted with 0.01 M phosphate buffer (pH 7.4), and collected in 1.0 ml fractions. The first peak is orexin A-I^{125}.

For determination of tissue concentrations, brain tissues of rats are dissected into the hypothalamus, cerebral cortex, thalamus, striatum, hippocampal formation, brain stem and cerebellum.

For the extraction of orexin A, the freshly obtained tissues are weighed and placed in 5.0 ml acid-acetone, homogenized and centrifuged.

For the double antibody radioimmunoassay, 0.1 ml of standard or samples, 0.1 ml of antibody (1:1000), 0.1 ml orexin A I^{125}, and 0,5 ml buffer are incubated for 24 h at 4°C. Then 0.1 ml of the second antibody solution is added and incubated again for 24 h at 4°C. The samples are centrifuged, the supernatants decanted and radioactivity counted in the precipitates.

EVALUATION

Bound/total count is calculated and standard curves versus synthetic orexin A are established.

MODIFICATIONS OF THE METHOD

Using separate radioimmunoassays for orexin A and orexin B, Mondal et al. (1999) determined their distribution in microdissected nuclei of the diencephalon and brainstem of rats.

REFERENCES AND FURTHER READING

Mondal MS, Nakazato M, Date Y, Murakami N, Handa R, Sakata T, Matsukura S (1999) Characterization of orexin A and orexin B in the microdissected brain nuclei and their contents in two obese rat models. Neurosci Lett 273:45–48

Mitsuma T, Hirooka Y, Kayama M, Mori Y, Yokoi Y, Rhue N, Ping J, Izumi M, Ikai R, Adachi K, Nogimori T (2000) Radioimmunoassay for orexin A. Life Sci 66:897–904

Sakurai T, Amemiya A, Ishii M, Matsuzaki I, Chemelli RM, Tanaka H, Williams SC, Richardson JA, Kozlowski GP, Wilson S, Arch JRS, Buckingham RB, Haynes AC, Carr SA, Annan RS, McNulty DE, Liu W-S, Terrett JA, Elshourbagy NA, Bergsma DJ, Yanagisawa M (1998) Orexins and orexin receptors: A family of hypothalamic neuropeptides an G protein-coupled receptors that regulate feeding behavior. Cell 92:573–585

L.4.4 Galanin

L.4.4.1 General Considerations on Galanin

Galanin is a neuropeptide of 29 amino acids in length (30 amino acids in humans) which was first isolated from porcine intestine (Tatemoto et al. 1983) and is localized mainly in the mammalian CNS (Skofitsch and

Jacobowitz 1985; Melander et al. 1986), but also in other organs (Baltazar et al. 2000). Central administration of galanin increases food intake in satiated rats (Crawley et al. 1990). Conversely, reduction of central galanin levels by antisense oligonucleotide techniques (Akabayashi et al. 1994) or central administration of galanin receptor antagonists (Leibowitz and Kim 1992) decreases food intake. The activity of galanin in the hypothalamus is modulated by metabolic hormones and by the ingestion of nutrients (Wang et al. 1998).

These data suggest the use of galanin receptor antagonists as anti-obesity agents. More recent studies concentrate on pain and CNS effects (Kask et al. 1997; Holmes et al. 2000; O'Meara et al. 2000; Xu et al. 2000; Counts et al. 2003; Elliott-Hunt et al. 2004; Krasnow et al. 2004; Badie-Mahdavi et al. 2005a; Lundström et al. 2005).

Physiological actions of peripherally administered galanin include contraction of smooth muscle (Ekblad et al. 1989; Ahtaridis et al. 1998; Korolkiewicz et al. 1998; Niiro et al. 1998), inhibition of glucose-stimulated insulin release (McDonald et al. 1985; Leonhardt et al. 1989), influence on learning and memory behavior (McDonald and Crawley 1997; McDonald et al. 1998a, b; Gleason et al. 1999; ögren et al. 1999; Zachariou et al. 1999), antinociceptive activity in rats with experimentally induced neuropathy (Burazin and Gundlach 1998; Ma and Bisby 1999; Yu et al. 1999; Kerr et al. 2000; Wang et al. 2000). Based on pharmacological and molecular biological evidence, Mazarati et al. (2001) discussed the hypothesis that galanin works as an endogenous anticonvulsant. A nonpeptide galanin receptor agonist showed anticonvulsant activity (Shi et al. 2002).

Galanin-overexpressing transgenic mice showed no anxiety-related behaviors in three different tests (Holmes et al. 2002), whereas galanin GAL-R1 receptor null mutant mice displayed increased anxiety-like behavior (Holmes et al. 2003).

Galanin has been found to influence secretion of growth hormone (Ottlecz et al. 1988; Murakami et al. 1987), LH (Todd et al. 1998), luteinizing hormone (Finn et al. 1998), and prolactin (Koshiyama et al. 1987; Cai et al. 1998; Wynick et al. 1998), to inhibit dopamine release from the median eminence (Nordström et al. 1987), to influence ACh release from rat brain (Fisone et al. 1987; Kasa et al. 1998), to inhibit norepinephrine release from the hypothalamus (Tsuda et al. (1989) and to modulate 5-HT_{1A} receptors in the ventral limbic cortex of the rat (Diaz-Cabiale et al. 2000).

A fragment of the galanin precursor protein, galanin message-associated peptide (GMAP), is present in dorsal root ganglion cells and influences the spinal nociceptor flexor reflex in rats (Xu et al. 1996).

A galanin-like peptide, named GALP, was isolated by Ohtaki et al. (1999) from porcine hypothalamus.

Some synthetic **galanin receptor agonists** were described, such as galnon (Saar et al. 2002; Bahdie-Mahdavi et al. 2005b) or galmic (Ceide et al. 2004; Bartfai et al. 2004).

Various **galanin receptor antagonists**, such as galantide (Lindskog et al. 1992; Sahu et al. 1994; Arletti et al. 1997; Ceresini et al. 1998), and other compounds (Bartfai et al. 1991; Pramanik and ögren 1992; Kask et al. 1995; Xu et al. 1995; Kakuyama et al. 1997; Pooga et al. 1998; Koegler et al. 1999; Park and Baum 1999; Katoh and Ohmori 2000; Kisfalvi et al. 2000; Swanson et al. 2005; ögren et al. 2005) were synthesized and tested.

REFERENCES AND FURTHER READING

Akabayashi A, Koenig JI, Watanabe Y, Alexander JT, Leibowitz SF (1994) Galanin-containing neurons in the paraventricular nucleus: A neurochemical marker for fat ingestion and body weight gain. Proc Natl Acad Sci 91:10375–10379

Ahtaridis SA, Katoch SS, Moreland RS (1998) Mechanism of galanin-induced contraction of longitudinal smooth muscle of the rat jejunum. Am J Physiol 274; Gastrointest Liver Physiol 37:G306–G313

Arletti R, Benelli A, Cavazzuti E, Bertolini A (1997) Galantide improves social memory in rats. Pharmacol Res 35:317–319

Bahdie-Mahdavi H, Lu X, Behrens MM, Bartfai T (2005a) Role of galanin receptor 1 and galanin receptor 2 activation on synaptic plasticity associated with 3′,5′-cyclic AMP response element-binding protein phosphorylation in the dentate gyrus. Studies with a galanin receptor agonist and galanin receptor knockout mice. Neuroscience 132:591–604

Bahdie-Mahdavi H, Behrens MM, Rebek J, Bartfai T (2005b) Effect of galnon on induction of long-term potentiation in dentate gyrus of C57BL/6 mice. Neuropeptides 39:249–251

Baltazar ET, Kitamura N, Hondo E, Narreto EC, Yamada J (2000) Galanin-like immunoreactive endocrine cells in bovine pancreas. J Anat 196:285–291

Bartfai T, Bedecs K, Land T, Langel ü, Bertorelli R, Girotti P, Consolo S, Xu X (1991) M-15: High-affinity chimeric peptide that blocks the neuronal actions of galanin in the hippocampus, locus coeruleus, and spinal cord. Proc Natl Acad Sci USA 88:10961–10965

Bartfai T, Lu X, Badie Mahdavi H, Barrr AM, Mazarati A, Hua XY, Yaksh T, Haberhauer G, Ceide SC, Trembleau L, Somogyi L, Kröck L, Rebek J (2004) Galmic, a nonpeptide galanin recptor agonist, affects behaviors in seizure, pain, and forced-swim tests. Proc Natl Acad Sci USA 101:10470–10475

Burazin TCD, Gundlach AL (1998) Inducible galanin and GalR2 receptor system in motor neuron injury and regeneration. J Neurochem 71:879–882

Cai A, Bowers RC, Moore JP Jr, Hyde JF (1998) Function of galanin in the anterior pituitary of estrogen-treated Fischer 344 rats: Autocrine and paracrine regulation of prolactin secretion. Endocrinology 139:2452–2458

Ceide SC, Trembleau L, Haberhauser G, Somogyi L, Lu X, Bartfai T, Rebek J (2004) Synthesis of galmic: a nonpeptide galanin receptor agonist. Proc Natl Acad Sci USA 101:16727–16732

Ceresini G, Sgoifo A, Freddi M, Musso E, Parmigiani S, Del-Rio G, Valenti G (1998) Effects of galanin and the galanin receptor antagonist galantide on plasma catecholamine levels during a psychosocial stress in rats. Neuroendocrinology 67:67–72

Counts SE, Perez SE, Ginsberg SD, de Lacalle S, Mufson EJ (2003) Galanin in Alzheimer disease. Mol Interventions 3:137–156

Crawley JN, Austin MC, Fiske SM, Martin B, Consolo S, Berthold M, Langel U, Fisone G, Bartfai T (1990) Activity of centrally administered galanin fragments on stimulation of feeding behavior and on galanin receptor binding in the rat hypothalamus. J Neurosci 10:3695–3700

Diaz-Cabiale Z, Narvaez JA, Finnman UB, Bellido I, ögren SO, Fuxe K (2000) Galanin-(1–16) modulates 5-HT_{1A} receptors in the ventral limbic cortex of the rat. NeuroReport 11:515–519

Ekblad E, Håkanson R, Sundler F, Wahlestedt C (1989) Galanin: neuromodulatory and direct contractile effects in smooth muscle preparations. Br J Pharmacol 86:241–246

Elliott-Hunt CR, Marsh B, Bacon A, Pope R, Vanderplank P, Wynick D (2004) Galanin acts as a neuroprotective factor to the hippocampus. Proc Natl Acad Sci USA 101:5105–5110

Holmes A, Yang RJ, Crawley JN (2002) Evaluation of an anxiety-related phenotype in galanin overexpressing transgenic mice. J Mol Neurosci 18:151–165

Holmes A, Kinney JW, Wrenn CC, Li Q, Yang RJ, Ma L, Vishwanath J, Saavedra MC, Innerfield S, Jacoby AS, Shine J, Iismaa TP, Crawley JN (2003) Galanin GAL-R1 receptor null mutant mice display increased anxiety-like behavior specific to the elevated plus-maze. Neuropsychopharmacology 28:1031–1044

Holmes FE, Mahoney S, King VR, Bacon A, Kerr NCH, Pachnis V, Curtis R, Priestley JV, Wynick D (2000) Targeted disruption of the galanin gene reduces the number of sensory neurons and their regenerative capacity. Proc Natl Acad Sci USA 97:11563–11568

Kask K, Berthold M, Bartfai T (1997) Galanin receptors: involvement in feeding, pain, depression and Alzheimer's disease. Life Sci 60:1523–1533

Koshiyama H, Hato Y, Inoue T, Muarkami Y, Yanaihara N, Imura H (1987) Central galanin stimulates pituitary prolactin secretion in rats: possible involvement of hypothalamic vasoactive intestinal polypeptide. Neurosci Lett 7:49–54

Krasnow SM, Hohmann JG, Gragerov A, Clifton DK, Steiner RA (2004) Analysis of the contribution of galanin receptors 1 and 2 to the central actions of galanin-like peptide. Neuroendocrinology 79:268–277

Finn PD, Clifton DK, Steiner RA (1998) The regulation of galanin gene expression in gonadotropin-releasing hormone neurons. Mol Cell Endocrinol 140:137–142

Fisone G, Langel U, Carlquist M, Bergman T, Consolo S, Höckfelt T (1989) Galanin receptor and its ligands in the rat hippocampus. Eur J Biochem 181:269–276

Gleason TC, Dreiling JL, Crawley JN (1999) Rat strain differences in response to galanin in the Morris water test. Neuropeptides 33:265–270

Kakuyama H, Mochizuki T, Iguchi K, Yamabe K, Hosoe H, Hoshino M, Yanaihara M (1997) [Ala^6,D-$Tryp^8$]-galanin(1–5)ol is a potent galanin antagonist on insulin release. Biomed Res Japan 18:49–56

Kasa P, Farkas Z, Forgon M, Papp H, Balaspiri L (1998) Effects of different galanins on the release of acetylcholine in the various areas of rat brain. Ann New York Acad Sci 863:435–437

Kask K, Berthold M, Bourne J, Andell S, 'Langel ü, Bartfai T (1995) Binding and agonist/antagonist actions of M35, galanin(1–13)-bradykinin(2–9)amide chimeric peptide, in Rin m5F insulinoma cells. Regul Pept 59:341–348

Katoh T, Ohmori O (2000) Studies on the total synthesis of Sch 202596, an antagonist of the galanin subtype GalR1: Synthesis of geodin, the spirocoumarone subunit of Sch 202596. Tetrahedron Lett 41:465–469

Kerr BJ, Cafferty WBJ, Gupta YK, Bacon A, Wynick D, McMahon SB, Thompson SWN (2000) Galanin knockout mice reveal nociceptive deficits following peripheral nerve injury. Eur J Neurosci 12:793–802

Kisfalvi I Jr, Burghardt B, Balint A, Zelles T, Vizi ES, Varga G (2000) Antisecretory effects of galanin and its putative antagonists M15, M35, and C7 in the rat stomach. J Physiol Paris 94:37–42

Koegler FH, York DA, Bray GA (1999) The effects on feeding of galanin and M40 when injected into the nucleus of the solitary tract, the lateral parabrachial nucleus, and the third ventricle. Physiol Behav 67:259–267

Korolkiewicz R, Rekowski P, Szyk A, Kato S, Yasuhiro T, Kubomi M, Tashima K, Takeuchi K (1998) Effect of diabetes mellitus on the contractile activity of carbachol and galanin in isolated gastric fundus strips of rats. Pharmacology 57:65–78

Leibowitz SF, Kim T (1992) Impact of a galanin antagonist on exogenous galanin and natural patterns of fat ingestion. Brain Res 599:148–152

Leonharst U, Siegel EG, Köhler H, Barthel M, Tytko A, Nebendahl K, Creutzfeldt W (1989) Galanin inhibits glucose-induced insulin release *in vitro*. Horm Metab Res 21:100–101

Lindskog S, Ahren B, Land T, Langel ü, Bartfai T (1992) The novel high-affinity antagonist, galantide, blocks the galanin-mediated inhibition of glucose-induced insulin secretion. Eur J Pharmacol 210:183–188

Lu X, Mazarati A, Sanna P, Shinmei S, Bartfai T (2005) Distribution and differential regulation of galanin receptor subtypes in rat brain: effects of seizure activity. Neuropeptides 39:147–152

Lundström L, Elmquist A, Bartfai T, Langel U (2005) Galanin and its receptors in neurological disorders. Neuromol Med 7:157–180

Ma W, Bisby MA (1999) Increase of galanin mRNA in lumbar dorsal root ganglion neurones of adult rats after partial sciatic nerve ligation. Neurosci Lett 262:195–198

Mazarati A, Langel U, Bartfai T (2001) Galanin: an endogenous anticonvulsant? Neuroscience 7:506–517

McDonald TJ, Dupre J, Tatemoto K, Greenberg GR, Rasziuk J, Mutt V (1985) Galanin inhibits insulin secretion and induces hyperglycemia in dogs. Diabetes 34:192–196

McDonald MP, Crawley JN (1997) Galanin-acetylcholine interactions in rodent memory tasks and Alzheimer's disease. J Psychiatry Neurosci 22:303–317

McDonald MP, Williard LB, Wenk GL, Crawley JN (1998a) Coadministration of galanin antagonist M40 with a muscarinic M_1 agonist improves delayed nonmatching to position choice accuracy in rats with cholinergic lesions. J Neurosci 18:5078–5085

McDonald MP, Gleason TC, Robinson JK, Crawley JN (1998b) Galanin inhibits performance on rodent memory tasks. Ann New Acad Sci 863:305–322
Melander T, Hökfelt T, Rökaeus Å (1986) Distribution of galaninlike immunoreactivity in the rat central nervous system. J Comp Neurol 248:475–517
Murakami Y, Kato Y, Koshiyama H, Inoue T, Yanaihara N, Imura H (1987) Galanin stimulates growth hormone (GH) secretion via GH-releasing factor (GRF) in conscious rats. Eur J Pharmacol 136:415–418
Niiro M, Nishimura J, Hirano K, Nakano H, Kanaide H (1998) Mechanism of galanin-induced contraction in the rat myometrium. Br J Pharmacol 124:1623–1632
Nordström ö, Melander T, Höckfelt T, Bartfai T, Goldstein M (1987) Evidence for an inhibitory effect of the peptide galanin on dopamine release from the rat medial eminence. Neurosci Lett 73:21–26
ögren SO, Schott PA, Kehr J, Misane T, Razani H (1999) Galanin and learning. Brain Res 848:174–182
ögren SO, Kuteeva E, Hökfelt T, Kehr J (2005) Galanin receptor antagonists: a potential novel pharmacological treatment for mood disorders. CNS Drugs 20:633–654
Ohtaki T, Kumano S, Ishibashi Y, Ogi K, Matsui H, Harada M, Kitada C, Kurokawa T, Onda H, Fujino M (1999) Isolation and cDNA of a novel galanin-like peptide (GALP) from porcine hypothalamus. J Biol Chem 274:37041–37045
O'Meara G, Coumis U, Ma SY, Kehr J, Mahoney S, Bacon A, Allen SH, Holmes F, Kahl U, Wang FH, Kearns JR, Ove-Ogren S, Dawbarn D, Mufson EJ, Davis C, Dawson G, Wynick D (2000) Galanin regulates the postnatal survival of a subset of basal forebrain cholinergic neurons. Proc Natl Acad Sci USA 97:11569–11574
Ottlecz A, Snyder GD, McCann SM (1988) Regulatory role of galanin in control of hypothalamic-anterior pituitary function. Proc Natl Acad Sci USA 85:9861–9865
Park JJ, Baum MJ (1999) Intracerebroventricular infusion of the galanin antagonist M40 attenuates heterosexual partner preference in ferrets. Behav Neurosci 113:391–400
Parker EM (1999) The role of central neuropeptide, neurotransmitter and hormonal systems in the regulation of body weight. Neurotransmiss 15:3–11
Pooga M, Jureus A, Rezaei K, Hasanvan H, Saar K, Kask K, Kjellen P, Land T, Halonen J, Maeorg U, Uri A, Solyom S, Bartfai T, Langel ü (1998) Novel galanin receptor ligands. J Pept Res 51:65–74
Pramanik A, ögren SO (1992) Galanin-evoked acetylcholine release in the rat striatum is blocked by the putative galanin antagonist M15. Brain Res 574:317–319
Saar K, Mazarati AM, Mahlapuu R, Hallnemo G, Soomets U, Kilk K, Hellberg S, Pooga M, Tolf BR, Shi TS, Hökfelt T, Wasterlain C, Bartfai T (2002) Anticonvulsant activity of a nonpeptide galanin receptor agonist. Proc Natl Acad Sci USA 99:7136–7141
Sahu A, Xu B, Kalra SP (1994) Role of galanin in stimulation of pituitary luteinizing hormone secretion as revealed by a specific receptor antagonist, galantide. Endocrinology 134:529–536
Shi TS, Hökfelt T, Wasterlain C, Bartfai T, Langel U (2002) Anticonvulsant activity a nonpeptide galanin receptor antagonist. Proc Natl Acad Sci USA 99:7136–7141
Skofitsch G, Jacobowitz DM (1985) Immunohistochemical mapping of galanin-like neurons in the rat central nervous system. Peptides 6:509–546
Swanson CJ, Blackburn TP, Zhang X, Zheng K, Xu ZQD, Hökfelt T, Wolisky TD, Konkel MJ, Chen H, Zhong H, Walker MW, Craig DA, Gerald CPG, Branchek TA (2005) Anxiolytic- and antidepressant-like profiles of the galanin-3 receptor (Gal_3) antagonists SNAP 37889 and SNAP 398299- Proc Natl Acad Sci USA 102:17489–17494
Tatemoto K, Rökaeus Å, Jörnvall H, McDonald TJ, Mutt V (1983) Galanin, a novel biologically active peptide from porcine intestine. FEBS Lett 164:124–128
Todd JF, Small CJ, Akinsanya KO, Stanley SA, Smith DM, Bloom SR (1998) Galanin is a paracrine inhibitor of gonadotroph function in the female rat. Endocrinology 139:4222–4229
Tsuda K, Yokoo H, Goldstein M (1989) Neuropeptide Y and galanin in norepinephrine release in hypothalamic slices. Hypertension 14:81–86
Wang J, Akabayashi A, Hi J-Y, Dourmashkin J, Alexander JT, Silva I, Lighter J, Leibowitz SF (1998) Hypothalamic galanin: Control by signals from fat metabolism Brain Res 804:7–20
Wang D, Lundeberg T, Yu L-C (2000) Antinociceptive role of galanin in periaqueductal grey of rats with experimentally induced mononeuropathy. Neuroscience 96:767–771
Wynick D, Small CJ, Bacon A, Holmes FE, Norman M, Ormandy CJ, Kilic E, Kerr NCH, Ghatei M, Talamantes F, Bloom SR, Pachnis V (1998) Galanin regulates prolactin release and lactotroph proliferation. Proc Natl Acad Sci USA 95:12671–12676
Xu X-J, Wiesenfeld-Hallin Z, Langel ü, Bedecs K, Bartfai T (1995) New high affinity peptide antagonists to the spinal galanin receptor. Br J Pharmacol 116:2076–2080
Xu X-J, Andell S, Bartfai T, Wiesenfeld-Hallin Z (1996) Fragments of the galanin message-associated peptide (GMAP) modulate the spinal reflex in rat. Eur J Pharmacol 318:301–306
Xu X-J, Hökfelt R, Bartfai T, Wiesenfeld-Hallin Z (2000) Galanin and spinal nociceptive mechanisms: recent advances and therapeutic implications. Neuropeptides 34:137–147
Yu L-C, Lundeberg S, An H, Wang F-X, Lundeberg T (1999) Effects of intrathecal galanin on nociceptive response in rats with mononeuropathy. Life Sci 64:1145–1153
Zachariou V, Parikh K, Picciotto MR (1999) Centrally administered galanin blocks morphine place preference in the mouse. Brain Res 831:33–42

L.4.4.2 Receptor Assay of Galanin

PURPOSE AND RATIONALE

Galanin mediates its physiological effects via interaction with at least three G protein-coupled receptors, designated GAL1, GAL2, and GAL3 receptor (Wang and Parker 1998; Iismaa and Shine 1999; Branchek et al. 2000; Waters and Krause 2000).

The first known galanin receptor GAL1 has been isolated from the human Bowes melanoma cell line (Habert-Ortoli 1994). Human GAL1 contains 349 amino acids with the structure of a G protein-coupled receptor. A rat GAL1 homologue, cloned from Rin14B cells, contains 346 amino acids (Parker et al. 1995). Human GAL1 mRNA has been detected by northern blot analysis in fetal brain and small intestinal tissue, and also by reverse transcriptase-polymerase chain reaction in the human gastrointestinal tract from

the esophagus to the rectum. Rat GAL1 mRNA has been detected by northern blot analysis in the brain, spinal cord and Rin14B cells. Human and rat GAL1 share similar binding profiles in [^{125}I]galanin binding assays (Sullivan et al. 1997).

Heuillet et al. (1994) described ligand binding and functional characteristics of the human galanin receptor in the Bowes melanoma cell line.

Jungnickel and Gundlach (2005) studied [^{125}I]-galanin binding in brain of wild-type, and galanin- and GALR1-knockout mice.

The rat GAL2 receptor has been cloned and characterized by Wang et al. (1997), Ahmad et al. (1998), the mouse GAL2 receptor by Pang et al. (1998) and the human GAL2 receptor by Bloomquist et al. (1998) and Fathi et al. (1998). Unlike GAL1, mRNA encoding rat GAL2 is widely distributed in all tissues examined including the brain and peripheral tissues. Likewise, the human GAL2 receptor is detectable by RT-PCR in several central and peripheral tissues. GalR2 plays a key role in neurite outgrowth from adult sensory neurons (Mahoney et al. 2003). Rat GAL1 and GAL2 share similar pharmacological profiles in that they possess high affinity for full-length and N-terminal fragments of galanin.

Rat and human GAL3 receptors were described by Kolakowski et al. (1998), Smith et al. (1998). Human and rat GAL3 share similar profiles in [^{125}I]galanin receptor binding assays.

Lee et al. (1999) reported the isolation of a cDNA clone named GPR54 which encodes a G-protein coupled receptor related to the galanin receptors.

PROCEDURE

Preparation of the radioligand ^{125}I-galanin is performed by iodination of galanin at room temperature by the chlor-amine-T method. Galanin, 10 µg, in 20 µl 0.05 M sodium phosphate buffer (pH 7.5) and 20 µl chloramine-T (5 mg/ml) are added in a batch containing 2 mCi Na^{125}I (245 mCi/ml). The reaction is terminated by adding 100 µl of a solution of sodium metabisulfite (1.2 mg/ml). The reaction mixture is transferred onto a column packed with SP-Sephadex C25, equilibrated with a solution of 100 µg/ml BSA, then washed and equilibrated with 0.05 M sodium phosphate buffer (pH 5.0). The excess of Na^{125}I is first eluted with 0.05 M sodium phosphate buffer (pH 5.0), while the iodinated galanin is eluted as a single peak with 0.05 M sodium phosphate buffer (pH 8.1). Fractions corresponding to a peak of ^{125}I-galanin are pooled, the pH adjusted to 6.0 with acetic acid, and the aliquots stored at –18°C until use.

Male Sprague-Dawley rats are sacrificed and their brains quickly removed. The hypothalamus is dissected for **preparation of membranes**. The tissue is homogenized (10% mass/vol) in 0.32 M sucrose buffered with 5 mM HEPES (pH 7.4). The homogenate is diluted 10-fold and centrifuged at 1000 *g* for 10 min. The supernatant is centrifuged at 10,000 *g* for 45 min, and the pellet is resuspended in 5 mM HEPES-buffered Krebs-Ringer solution (pH 7.4).

Displacement experiments are carried out with various test compounds in a final volume of 400 µl HEPES/Krebs-Ringer solution, 0.05% BSA (pH 7.4), containing 1 mM ^{125}I-galanin and 70–100 µg membrane preparation. Samples are incubated for 30 min at 37°C. Incubation is terminated by the addition of 10 ml ice-cold HEPES/Krebs-Ringer solution, followed by rapid filtration over Whatman GF/B filters, precoated for 5–6 h in 0.3% polyethyleneimine solution. Specific binding is defined as that displaceable by 1 mM rat galanin1–29.

EVALUATION

Bound/total count is calculated and displacement curves versus the standard are established.

REFERENCES AND FURTHER READING

Ahmad S, O'Donnell D, Payza K, Ducharma J, Menard D, Brown W, Schmidt R, Wahlestedt C, Shen SH, Walker P (1998) Cloning and evaluation of the role of rat GALR-2, a novel subtype of galanin receptor, on the control of pain reception. Ann New York Acad Sci 863:108–119

Bloomquist BT, Beauchamp MR, Zhelnin L, Brown SE, Gore-Willse AR, Gregor P, Cornfield LJ (1998) Cloning and expression of the human galanin receptor GalR2. Biochem Biophys Res Commun 243:474–479

Branchek TA, Smith KE, Gerald C, Walker MW (2000) Galanin receptor subtypes. Trends Pharmacol Sci 21:109–116

Fathi Z, Battaglino PM, Iben LG, Li H, Baker E, Zhang D, McGovern R, Lahle CD, Sutherland GR, Iismaa TP, Dickinson KEJ, Antal-Zimanyi I (1998) Molecular characterization, pharmacological properties and chromosomal localization of the human GALR2 receptor. Mol Brain Res 58:156–169

Habert-Ortoli E, Aminranoff B, Loquet I, Laburthe M, Mayaux JF (1994) Molecular cloning of a functional human galanin receptor. Proc Natl Acad Sci USA 91:9780–9783

Heuillet E, Bouaiche Z, Ménager J, Dugay P, Munoz N, Dubois H, Amiranoff B, Crespo A, Lavavre J, Blanchard JV (1994) The human galanin receptor: ligand binding and functional characteristics in the Bowes melanoma cell line. Eur J Pharmacol 269:139–147

Iismaa TP, Shine J (1999) Galanin and galanin receptors. Results Probl Cell Differ 26:257–291

Jungnickel SRF, Gundlach AL (2005) [^{125}I]-Galanin binding in brain of wildtype, and galanin- and GALR1-knockout mice: strain and species differences in GALR1 density and distribution. Neuroscience 131:407–421

Kolakowski LF Jr, O'Neill GP, Howard AD, Broussard SR, Sullivan KA, Feighner SD, Sawzdargo M, Nguyen T,

Kargman S, Shiao L-L, Hreniuk DL, Tan CP, Evans J, Abramovitz M, Chateauneuf A, Coulombe N, Ng G, Johnson MP, Tharian A, Khoshbouei H, George SR, Smith RG, O'Dowd BF (1998) Molecular characterization and expression of cloned human galanin receptors GALR2 and GALR3. J Neurochem 71:2239–2251

Lee DK, Nguyen T, O'Neill GP, Cheng R, Liu Y, Howard AD, Coulombe N, Tan CP, Tang-Nguyen AT, George SR, O'Dowd BF (1999) Discovery of a receptor related to the galanin receptors. FEBS Lett 446:103–107

Mahoney SA, Hosking R, Farrant S, Holmes FE, Jacoby AS, Shine J, Iismaa TP, Scott MK, Schmidt R, Wynick D (2003) The second galanin receptor GalR2 plays a key role in neurite outgrowth from adult sensory neurons. J Neurosci 23:416–421

Pang L, Hashemi T, Lee-H JJ, Maguire M, Graziano MP, Bayne M, Hawes B, Wong G, Wang S (1998) The mouse GalR2 receptor: Genomic organization, cDNA cloning, and functional characterization. J Neurochem 71:2252–2259

Parker EM, Izzarelli DG, Nowak HP, Mahle CD, Iben LG, Wang J, Goldstein ME (1995) Cloning and characterization of the rat GALR1 galanin receptor from Rin14B insulinoma cells. Mol Brain Res 34:179–189

Saar K, Valkna A, Soomets U, Rezaei K, Zorko M, Zilmer M, Langel ü (1997) Role of the third cytoplasmatic loop in signal transduction by galanin receptors. Biochem Soc Transact 25:1036–1040

Smith KE, Walker MW, Artymyshyn R, Bard J, Borowsky B, Tamm JA, Yoa W-J, Vaysse PJ-J, Brancheck TA, Walker MW, Jones KA (1998) Cloned human and rat GAL3 receptors: Pharmacology and activation of G-protein inwardly rectifying K^+ channels. J Biol Chem 273:23321–23326

Sullivan KA, Shiao L-L, Cascieri MA (1997) Pharmacological characterization and tissue distribution of the human and rat GALR1 receptors. Biochem Biophys Res Commun 233:823–828Wang S, Parker EM (1998) Galanin receptor subtypes as potential therapeutic targets. Expert Opin Ther Pat 8:1225–1235

Wang S, Hashemi T, He C, Strader C, Bayne M (1997) Molecular cloning and pharmacological characterization of a new galanin receptor subtype. Mol Pharmacol 52:337–343

Waters SM, Krause JE (2000) Distribution of galanin-1, -2 and -3 receptor messenger RNAs in central and peripheral rat tissues. Neuroscience 95:265–171

L.4.5 Adipsin

L.4.5.1 General Considerations on Adipsin

Proteins of the alternative complement pathway are secreted by adipose tissue (Choy et al. 1992; Peake et al. 1997). **Adipsin (complement D)** was the first to be cloned from an adipose tissue cell line and shown to be synthesized and secreted by adipose tissue (Cook et al. 1987; Flier et al. 1987; Johnson et al. 1991; White et al. 1992). Adipsin is markedly suppressed in *ob/ob, db/db*, monosodium glutamate-induced obese mice, in obese JCR:LA-cp rats and in cafeteria-fed rats (Rosen et al. 1989; Dugail et al. 1990; Shillabeer et al. 1992; Spurlock et al. 1996), and is regulated by glucocorticoids, retinoic acid, sympathomimetic drugs and insulin (Kitagawa et al. 1989; Spiegelman et al. 1989; Lowell and Flier 1990; Lowell et al. 1990; Moustaid et al. 1990; Antras et al. 1991; Miner et al. 1993). In contrast to rodents, adipsin increases with adiposity in humans and in response to feeding and is decreased during fasting, cachexia and lipatrophy (Napolitano et al. 1994).

Adipsin is required for the synthesis of **acylation stimulating protein (ASP)**, a protein implicated in fat metabolism (Sniderman and Cianflone 1994; Cianflone et al. 1999; van Harmelen et al. 1999). ASP is produced by the cleavage of C3a by carboxypeptidase and is highly expressed by mature adipocytes. The synthesis of C3a from C3 requires complement factor B and adipsin. Plasma ASP increases with meals and facilitates the synthesis and storage of triglycerides. Consistent with its role as a mediator of lipogenesis, ASP deficiency increases postprandial fatty acid levels and decreases weight gain and trigylceride synthesis in mice (Murray et al. 1999, 2000).

Several other factors, such as adiponectin (Takahashi et al. 2000) are involved in the function of adipose tissue acting as target as well as an endocrine organ (Ahima and Flier 2000).

REFERENCES AND FURTHER READING

Ahima RS, Flier JS (2000) Adipose tissue as an endocrine organ. Trends Endocrin Metab 11:327–332

Antras J, Lasnier F, Pairault J (1991) Adipsin gene expression in 3T3-F442A adipocytes is posttranscriptionally downregulated by retinoic acid. J Biol Chem 266:1157–1161

Choy LN, Rosen BS, Spiegelman BM (1992) Adipsin and an endogenous pathway of complement from adipose cells. J Biol Chem 267:12736–12741

Cianflone K, Maslowska M, Sniderman AD (1999) Acylation stimulating protein (ASP) an adipocyte autocrine: new directions. Sem Cell Dev Biol 10:31–34

Cook KS, Min HY, Johnson D, Chaplinsky RJ, Flier JS, Hunt CR, Spiegelman BM (1987) Adipsin: a circulating serine protease homologue secreted by adipose tissue and sciatic nerve. Science 237:402–405

Dugail I, Quignard-Boulange A, le Liepvre X, Lavau M (1990) Impairment of adipsin expression is secondary to the onset of obesity in *db/db* mice. J Biol Chem 265:1831–1833

Flier JS, Cook KS, Usher P, Spiegelman BM (1987) Severely impaired adipsin expression in genetic and acquired obesity. Science 237:405–408

Johnson PA, Greenwood MRC, Horwitz BA, Stern JS (1991) Animal models of obesity: Genetic aspects. Annu Rev Nutr 11:325–352

Kitagawa K, Rosen SB, Spiegelman BM, Lienhard GE, Tanner LI (1998) Insulin stimulates acute release of adipsin from 3T3-L1 adipocytes. Biochem Biophys Acta 1014:83–89

Lowell BB, Flier JS (1990) Differentiation dependent biphasic regulation of adipsin gene expression by insulin and insulin-like growth factor-1 in 3T3-F442A adipocytes. Endocrinology 127:2898–2906

Lowell BB, Napolitano A, Usher P, Dulloo AG, Rosen BS, Spiegelman BM, Flier JS (1990) Reduced adipsin expression in murine obesity: effect of age and treatment with

the sympathomimetic-thermogenic drug mixture ephedrine and caffeine. Endocrinology 126:1514–1520
Miner JL, Byatt CA, Baile CA, Krivi GG (1993) Adipsin expression and growth rate in rats as influenced by insulin and somatotropin. Physiol Behav 54:207–212
Murray I, Sniderman AD, Cianflone K (1999) Enhanced triglyceride clearance with intraperitoneal human acylation stimulating protein in C5BL/6 mice. Am J Physiol 277:E474–E480
Murray I, Havel PJ, Sniderman AD, Cianflone K (2000) Reduced body weight, adipose tissue, and leptin levels despite increased energy intake in female mice lacking acylation-stimulating protein. Endocrinology 141:1041–1049
Moustaid N, Lasnier F, Hainque B, Quignard-Boulange A, Pairault J (1990) Analysis of gene expression during adipogenesis in 3T3-F442A preadipocytes: insulin and dexamethasone control. J Cell Biochem 42:243–254
Napolitano A, Lowell BB, Damm D, Leibel RL, Ravussin E, Jimerson DC, Lesem MD, Van Dyke DC, Daly PA, Chatis P (1994) Concentrations of adipsin in blood and rates of adipsin secretion by adipose tissue in humans with normal, elevated and diminished adipose tissue mass. Int J Obes Relat Metab Disord 18:213–218
Peake PW, O'Grady S, Pussell BA, Charlesworth JA (1997) Detection and quantification of the control proteins of the alternative pathway of complement in 3T3-L1 adipocytes. Eur J Clin Invest 27:922–927
Rosen BS, Cook KS, Yaglom J, Groves DL, Volanikis JE, Damm D, White T, Spiegelman BM (1989) Adipsin and complement factor D activity: an immune-related defect in obesity. Science 23:1483–1487
Shillabeer G, Hornford J, Forden JM, Wong NC, Russell JC, Lau DC (1992) Fatty acid synthase and adipsin mRNA levels in obese and lean JCR:LAS-cp rats: effect of diet. J Lipid Res 33:31–39
Sniderman AD, Cianflone K (1994) The adipsin-ASP pathway and regulation of adipocyte function. Ann Med 26:388–393
Spiegelman BM, Lowell B, Napolitano A, Dubuc P, Barton D, Francke U, Groves DL, Cook KS, Flier JS (1989) Adrenal glucocorticoids regulate adipisin gene expression in genetically obese mice. J Biol Chem 264:1811–1815
Spurlock ME, Hahn KJ, Miner JL (1996) Regulation of adipsin and body composition in the monosodium glutamate (MSG)-treated mouse. Physiol Behav 60:1217–1221
Takahashi M, Arita Y, Yamagata K, Matsukawa Y, Okutomi K, Horie M, Shimomura I, Hotta K, Kuriyama H, Kihara S, Nakamura T, Yamashita S, Funahashi T, Matsuzawa Y (2000) Genomic structure and mutations in adipose-specific gene, adiponectin. Int J Obese Relat Metab Disord 24:861–868
Van Harmelen V, Reynisdottir S, Cianflone K, Degerman E, Hoffstedt J, Nisell K, Sniderman A, Arner P (1999) Mechanisms involved in the regulation of free fatty acid release from isolated human fat cells by acylation-stimulating protein and insulin. J Biol Chem 274:18243–18251
White RT, Damm D, Hancock N, Rosen BS, Lowell BE, Usher P, Flier S, Spiegelman BM (1992) Human adipsin is identical to complement factor D and is expressed at high levels in adipose tissue. J Biol Chem 267:9210–9213

L.4.5.2 Adipsin Expression in Mice

PURPOSE AND RATIONALE

Adipsin expression at the protein and mRNA levels was studied in mice (Flier et al. 1987; Spiegelman et al. 1989; Lowell et al. 1990; Dugail et al. 1990) and rats (Miner et al. 1993).

PROCEDURE

Various strains of mice (CD-1 mice, C57BL6 *ob/ob* mice, C57BL/Ks misty diabetes (m db/m db) mice, and mice with monosodium glutamate induced obesity are treated with drugs, e. g., ephedrine (1 g/kg chow) and caffeine (1.4 g/kg chow) mixed in the diet. The effects of these regimens on fat pad weight, specific mRNAs in white epididymal and brown adipose tissue and serum adipsin concentrations are assessed.

RNA is extracted from epididymal adipose tissue, brown intercapsular adipose tissue, 3T3-F422A adipocytes and isolated rat adipocytes by the guanidium-cesium chloride technique. Total RNA is denaturated, electrophoresed in 1.5% agarose, transferred to nylon filters, and hybridized to random primed adipsin, uncoupling protein (UCP), or actin cDNAs (Flier et al. 1987).

Serum adipsin and adipsin released by 3T3-F442A cultured adipocytes are assessed by RIA. Mouse adipsin purified from Chinese hamster ovary cells stably transfected with an adipsin expression vector is iodinated using the Bolton-Hunter reagent. The labeled protein is separated from unincorporated ^{125}I using G-50 Sephadex chromatography. The first rabbit polyclonal antibody is raised to purified mouse adipsin overexpressed using a baculovirus expression system. The assay is carried out in PBS, pH 7.4, supplemented with $CaCl_2$ (0.1 g/liter), $MgCl_2$ (0.1 g/liter), and BSA (0.1%). Serum adipsin is assessed in a dilution of 1:1000–1:5000 and in culture media at a dilution of 1:100. After adding tracer, standards, and serum, the tubes are mixed and the first antibody is added at a dilution of 1:800. After an overnight incubation, the bound and unbound tracer are separated using goat anti-rabbit immunoglobulin C fixed to heat killed staphylococcus at a ratio 1:1.2.

EVALUATION

Standard curves are generated using mouse adipsin purified from stably transfected CHO cells. Serial dilutions of standards, serum, and culture media are compared.

MODIFICATIONS OF THE METHOD

Dugail et al. (1989) showed that, in sharp contrast with genetically obese mice, adipsin mRNA is not suppressed in genetically obese Zucker rats.

Platt et al. (1994) found that a tissue-specific transcription factor that regulates adipsin expression is less active in the adipose tissue of obese animals.

Napolitano et al. (1994) determined concentrations in blood and rates of adipsin secretion by adipose tissue in humans using a two-monoclonal 'sandwich' ELISA assay.

REFERENCES AND FURTHER READING

Dugail I, Le Liepvre X, Quignard-Boulangé A, Pairault J, Lavau M (1989) Adipsin mRNA amounts are not decreased in the genetically obese Zucker rat. Biochem J 257:917–919

Dugail I, Quignard-Boulangé A, Le Liepvre X, Lavau M (1990) Impairment of adipsin gene expression is secondary to the onset of obesity in *db/db* mice. J Biol Chem 265:1831–1833

Flier JS, Cook KS, Usher P, Spiegelman BM (1987) Severely impaired adipsin expression in genetic and acquired obesity. Science 237:405–408

Lowell BB, Napolitano A, Usher P, Dulloo AG, Rosen BS, Spiegelman BM, Flier JS (1990) Reduced adipsin expression in murine obesity: Effect of age and treatment with the sympathomimetic-thermogenic drug mixture ephedrine and caffeine. Endocrinology 126:1514–1520

Miner JL, Byatt JC, Baile CA, Krivi GG (1993) Adipsin gene expression and growth in rats as influenced by insulin and somatotropin. Physiol Behav 54:207–212

Napolitano A, Lowell BB, Damm D, Leibel RL, Ravussin E, Jimerson DC, Lesem MD, Van Dyke DC, Daly PA, Chatis P, White RL, Spiegelman BM, Flier JS (1994) Concentrations of adipsin in blood and rates of adipsin secretion by adipose tissue in humans with normal, elevated and diminished adipose tissue mass. Intern J Obesity 18:213–218

Platt KA, Claffey KP, Wilkison WO, Spiegelman BM, Ross SR (1994) Independent regulation of adipose tissue specificity and obese response of the adipsin promoter in transgenic mice. J Biol Chem 269:28558–28562

Spiegelman BM, Lowell B, Napolitano A, Dubuc P, Barton D, Francke U, Groves DL, Cook KS, Flier JS (1989) Adrenal glucocorticoids regulate adipsin gene expression in obese mice. J Biol Chem 264:1811–1815

L.4.6 Ghrelin

Small synthetic molecules called growth hormone secretagogues (GHSs) (Bowers et al. 1980, 1984) stimulate the release of growth hormone (GH) from the pituitary. They act through the GHS-R, a G-protein-coupled receptor (Howard et al. 1996). The natural ligand of this receptor was discovered as a 28-amino-acid-containing peptide, called ghrelin (Kojima et al. 1999, 2000, 2001; Davenport et al. 2005), produced in the XA-like cells of the stomach (Kojima et al. 1999; Date et al. 2000); however, smaller amounts of ghrelin are also found in the small and large intestine (Hosada et al. 2000). Ghrelin and the growth hormone secretagogue receptor are expressed in the rat adrenal cortex (Andreis et al. 2003). GH, GH receptor, GH secretagogue receptor, and ghrelin are also expressed in human T cells, B cells, and neutrophils (Hattori et al. 2001).

Ghrelin is the first peptide hormone in which the third amino acid serine is modified by a fatty acid; this modification is essential for the peptide's biological activity. Beside ghrelin's GH-releasing effect, it is a powerful appetite-simulating peptide. Plasma ghrelin concentration is increased in fasting conditions and reduced after habitual feeding (Kojima and Kangawa 2005), suggesting that ghrelin may act as an initiation signal for food intake. Chronic systemic or intracerebroventricular application to rats produced hyperphagia and obesity in rats (Wren et al. 2001). The appetite-stimulatory signal of ghrelin is mediated through action on the hypothalamic neuropeptide Y (NPY) and the Y1 receptor (Asakawa et al. 2001).

[^{125}I-His^{9}]-ghrelin was recommended as a radioligand for localizing GHS and GH receptors in human and rat tissue (Katugampola et al. 2001).

Various heterocyclic compounds acting as ghrelin receptor agonists have been developed, which might be useful for the treatment of anorexia nervosa (Palucki et al. 2001). Multiple ghrelin-derived molecules produced by post-translational processing were identified indicating structural divergence of human ghrelin (Hosoda et al. 2003). Until now, however, no specific ghrelin receptor antagonist has been described, although such a compound might be an attractive approach to reduce feed intake and to decrease obesity.

REFERENCES AND FURTHER READING

Andreis PG, Malendowicz LK, Trejter M, Neri G, Spinazzi R, Rossi GP, Nussdorfer GG (2003) Ghrelin and growth hormone secretagogue receptor are expressed in the rat adrenal cortex. Evidence that ghrelin stimulates the growth, but not the secretory activity of adrenal cells. FEBS Lett 536:173–179

Asakawa A, Inui A, Kaga T, Yuzriha H, Nagata T, Ueno N, Makino S, Fujimiya M, Niijima A (2001) Ghrelin is an appetite-stimulating signal from the stomach with structural resemblance to Motilin. Gastroenterology 120:337–345

Bowers CY, Momany F, Reynolds GA, Chang D, Hong A, Chang K (1980) Structure–activity relationships of a synthetic pentapeptide that specifically releases growth hormone in vitro. Endocrinology 106:663–667

Bowers CY, Momany FA, Reynolds GA, Hong A (1994) On the in vitro and in vivo activity of a new synthetic hexapeptide that acts on the pituitary to specifically release growth hormone. Endocrinology 114:1537–1545

Date Y, Kojima M, Hosoda H, Sawaguchi A, Mondal MS, Suganuma T, Matsukura S, Kangawa K, Nakazato M (2000) Ghrelin, a novel growth hormone-releasing acetylated peptide, is synthesized in a distinct endocrine cell type in the gastrointestinal tract of rats and humans. Endocrinology 141:4255–4261

Davenport AP, Bonner TI, Foord SM, Harmar AJ, Neubig RR, Pin JP, Spedding M, Kojima M, Kangawa K (2005) International Union of Pharmacology. LVI. Ghrelin receptor nomenclature, distribution, and function. Pharmacol Rev 57:541–546

Hattori N, Saito T, Yagyu T, Jiang BH, Kitagawa K, Inagaki C (2001) GH, GH receptor, GH secretagogue receptor, and ghrelin expressed in human T cells, B cells, and neutrophils. J Clin Endocrinol Metab 86:4284–4291

Hosada A, Kojima M, Matsuo H, Kanmgawa K (2000) Ghrelin and des-acyl ghrelin: two major forms of rat ghrelin in gastrointestinal tissue. Biochem Biophys Res Commun 279:909–913

Hosoda H, Kojima M, Mizushima T, Shimizu S, Kangawa K (2003) Structural divergence of human ghrelin. Identification of multiple ghrelin-derived molecules produced by post-translational processing. J Biol Chem 278:64–70

Howard AD, Feighner SD, Cully DF, Arena JP, Liberator PA, Rosenblum CI, Hamelin M, Hreniuk DL, Palyha OC, Anderson J, Paress PS, Diaz C, Chou M, Liu KK, McKee KK, Pong SS, Chaung LY, Elbrecht A, Dashkevicz M, Heavens R, Rigby M, Sirinathsinghji DJ, Dean DC, Melillo DG, Patchett AA, Nargund R, Patrick RG, DeMartino JA, Gupta SK, Schaeffer JM, Smith RG, Van der Ploeg LHY (1996) A receptor in pituitary and hypothalamus that functions in growth hormone release. Science 273:974–977

Katugampola SD, Pallikaros Z, Davenport AP (2001) [^{125}I-His^{9}]-ghrelin, a novel radioligand for localizing GHS and GH receptors in human and rat tissue: upregulation of receptors with atherosclerosis. Br J Pharmacol 134:143–149

Kojima M, Kangawa K (2005) Ghrelin: structure and function. Physiol Rev 85:495–522

Kojima M, Hosoda H, Date Y, Nakazato M, Matsuo H, Kangawa K (1999) Ghrelin is a growth-hormone-releasing acylated peptide from stomach. Nature 402:656–660

Kojima M, Hosoda H, Kangawa K (2000) Purification and distribution of ghrelin: the natural endogenous ligand for the growth hormone secretagogue receptor. Horm Res 56 [Suppl 1]:93–97

Kojima M, Hosoda H, Matsuo H, Kangawa K (2001) Ghrelin: discovery of the natural endogenous ligand for the growth hormone secretagogue receptor. Trends Endocrinol Metab 12:118–126

Palucki B, Feighner SD, Pong SS, McKee KK, Hreniuk DL, Tan C, Howard AD, Van der Ploeg LHY, Patchett AA, Nardund (2001) Spiro(indole-3,4-piperdine) growth hormone secretagogues as ghrelin mimetics. Bioorg Med Chem Lett 11:1955–1957

Wren AM, Small CJ, Abbott CR, Dhillo WS, Seal LJ, Cohen MA, Batterham RL, Taheri ST, Stanley SA, Ghatei A, Bloom SR (2001) Ghrelin causes hyperphagia and obesity in rats. Diabetes 50:2540–2547

L.5 Safety Pharmacology of Drugs with Anti-obesity Activity

See Herling (2006).

REFERENCES AND FURTHER READING

Herling AW (2006) Metabolism pharmacology. In: Vogel HG (ed), Hock FJ, Maas J, Mayer D (co-eds) Drug discovery and evaluation safety and pharmacokinetic assays. Springer, Berlin Heidelberg New York, Chap. I.G., pp 151–193

Chapter M
Anti-Atherosclerotic Activity[1]

[1] Reviewed and amended by H.-L. Schäfer

M.1 Induction of Experimental Atherosclerosis

M.1.0.1 General Considerations

Experimental atherosclerosis was first successfully induced in rabbits by Saltykow (1908) and Ignatowski (1909). During the following years, various scientists found that dietary cholesterol was the responsible stimulus for development of atherosclerosis. Other species are also susceptible to diet-induced atherosclerosis (Reviews by Kritchevsky 1964; Hadjiinky et al. 1991). Mouse models of atherosclerosis were reviewed by Reardon and Getz (2001) and by Daugherty (2002). Tailleux et al. (2003) underlined the importance of nuclear receptors, e. g., peroxisome proliferators-activated receptors (PPARs), liver X receptors (LXR) (Joseph and Totonoz 2003; Terasaka et al. 2003) and retinoid receptors (RXR) (Staels 2001; Li et al. 2005), which are implicated in lipid metabolism and inflammation.

REFERENCES AND FURTHER READING

Daugherty A (2002) Mouse models of atherosclerosis. Am J Med Sci 323:3–10
Hadjiinky P, Bourdillon MC, Grosgogeat Y (1991) Modèles expérimentaux d'athérosclérose. Apports, limites et perspectives. Arch Mal Ceut Vaiss 84:1593–1603
Ignatowski A (1909) Über die Wirkung des tierischen Eiweißes auf die Aorta und die parenchymatösen Organe der Kaninchen. Virchow's Arch pathol Anat Physiol 198:248–270
Joseph SB, Totonoz P (2003) LXRs: new therapeutic targets in atherosclerosis? Curr Opin Pharmacol 3:192–197
Kritchevsky D (1964) Experimental Atherosclerosis. In Paoletti R (ed) Lipid Pharmacology, Academic Press, New York, London, Chapter 2, pp 63–130
Li AC, Binder CJ, Guttierrez A, Brown KK, Plotkin CR, Pattiso JW, Vallendor AF, Davis RA, Willson TM, Witztum JL, Palinski W, Glass CK (2005) Different inhibition of macrophage foam-cell formation and atherosclerosis in mice by PPARα, β/δ and γ. J Clin Invest 114:1564–1576
Reardon CA, Getz GS (2001) Mouse models of atherosclerosis. Cur Opin Lipidol 12:167–173
Saltykow S (1908) Die experimentell erzeugten Arterienveränderungen in ihrer Beziehung zu Atherosklerose und verwandten Krankheiten des Menschen. Zentralbl Allgem Pathol Pathol Anat 19:321–368
Staels B (2001) Regulation of lipid and lipoprotein metabolism by retinoids. J Am Acad Dermatol 45:S158–S167
Tailleux A, Torpier G, Mezdour H, Fruchart JC, Staels B, Fiévet C (2003) Murine models to investigate pharmacological compounds acting as ligands of PPARs in dyslipemia and atherosclerosis. Trend Pharmacol Sci 24:530–534
Terasake N, Hiroshima A, Koieyama T, Ubukata N, Morikawa Y, Nakai D, Inaba T (2003) T-0901317, a synthetic liver X receptor ligand, inhibits development of atherosclerosis in LDL-deficient mice. FEBS Lett 536:6–11

M.1.0.2 Cholesterol-Diet-Induced Atherosclerosis in Rabbits and Other Species

PURPOSE AND RATIONALE

Rabbits are known to be susceptible to hypercholesterolemia and arteriosclerosis after excessive cholesterol feeding. Therefore, this approach has been chosen by many authors to study the effect of potential anti-arteriosclerotic drugs.

PROCEDURE

Several modifications of the protocol have been described. Usually, male rabbits from an inbred strain, e. g., white New Zealand, at an age of 8–10 weeks are used. Body weight variation should be as low as possible. At the beginning of the experiment, blood is withdrawn from the marginal ear vein for determination of total cholesterol, total glycerides, and blood sugar. Groups of 10 animals are used for treatment with drugs or as controls. The rabbits are switched from commercial food to a diet supplemented with 0.3–2% cholesterol and kept on this regimen for a period of 10–12 weeks. One group is kept on normal diet. During and at the end of the experiment blood is taken for analysis. Usually, cholesterol and triglyceride levels increase several-fold over the original values.

The animals are sacrificed and the thoracic aorta is removed, cleaned of surrounding tissues, and longitudinally cut and opened for fixation with formaldehyde. The tissue is stained with oil red. The percentage of

the intimal surface covered by the oil red positive lesions is calculated with a computerized planimeter. In animals fed a normal diet, the aorta does not show any staining, whereas in cholesterol-fed rabbits the aorta shows severe atherogenic lesions.

EVALUATION

Data are expressed as means ± standard deviation. Statistical evaluation is performed by Dunnett's or Scheffé's test. A p-value of < 0.05 is regarded as statistically significant.

MODIFICATIONS OF THE METHOD

Shore and Shore (1976) studied two **different strains of rabbits** (New Zealand White and Dutch Belt) as models of hyperlipoproteinemia and atherosclerosis.

Tao et al. (2003) studied antioxidative, antinitrative, and vasculoprotective effects of a PPAR-γ agonist in New Zealand White rabbits with hypercholesterolemia induced by a high-cholesterol diet.

Studies of Kritchevsky et al. (1989) on experimental atherosclerosis in **rabbits** fed **cholesterol-free diets** revealed a greater influence of animal protein and of partially hydrogenated soybean oil on development of atherosclerosis than plant protein and unsaturated soybean oil.

Cockerels (Tennent et al. 1960) and **turkeys** (Simpson and Harms 1969) are very susceptible to cholesterol feeding and develop marked hypercholesterolemia in rather short periods. Atherosclerosis could also be induced in cockerels by high doses of estrogen without atherogenic diet (Caldwell and Suydam 1959).

Spontaneous arteriosclerosis in **pigeons** has been described by Clarkson and Lofland (1961).

The **Japanese sea quail** (*Coturnix coturnix japonica*) is highly susceptible to the rapid development of severe experimental atherosclerosis (Day et al. 1975, 1977, 1979, 1990; Chapman et al. 1976).

Out of 13 strains of **mice**, Roberts and Thompson (1976) selected the C57BR/cdJ and the CBA/J strain und used these strains and their hybrids as models for atherosclerosis research.

Paigen et al. (1987) described quantitative assessment of atherosclerotic lesions in mice. After 14 weeks on an atherogenetic diet C57BL/6J female mice had aortic lesions at each of the coronary arteries, at the junction of the aorta to the heart and in scattered areas of the aortic surface. The lesions increased after 9 months of atherogenic diet. Methods of evaluating the number and size of lesions were compared including sizing with a microscope eyepiece grid and computer-assisted planimetry.

Atherosclerosis susceptibility differences among progenitors of recombinant inbred strains of mice were described by Paigen et al. (1990).

Yamaguchi et al. (1993) found that addition of 10% linoleic acid to a high-cholesterol diet enhanced cholesterol deposition in the aorta of male ICR strain mice.

In **rats** hypercholesterolemia can be induced by daily administration by gavage of 1 ml/100 g body weight of a cocktail containing in 1 l peanut oil: 100 g cholesterol, 30 g propylthio-uracil, and 100 g cholic acid over a period of 7 days. The test compounds are administered simultaneously with the cocktail (Fillios et al. 1956; Lustalot et al. 1961).

Inoue et al. (1990) induced experimental atherosclerosis in the rat carotid artery by balloon de-endothelialization and atherogenic diet. A balloon catheter was introduced into the rat's carotid arteries from the iliac arteries and the endothelium was denuded.

The **hamster** is susceptible to atherosclerosis. Nistor et al. (1987) fed male hamsters a hyperlipidemic diet consisting of standard chow supplemented with 3% cholesterol and 15% commercial butter for 12 months. Serum total cholesterol doubled after 3 weeks and attained a 17-fold value after 10 months. Up to 6 months, smooth muscle cells in the intima and media of the aorta as well as endothelial cells began to load with lipids. After 10 months the affected zones looked like human atherosclerotic plaque with huge cholesterol crystal deposits, calcium deposits and necrosis.

Especially the hybrid hamster strain Bioä F_1B (Bio Breeders Fitchburg, MA, USA) is more susceptible to dietary induced atherosclerosis than other strains (Kowala et al. 1991). Early atherosclerotic lesions can be induced within a 3-months-feeding of a cholesterol/butter enriched diet. In these animals simvastin dose-dependently inhibited the development of hyperlipidemia and the plaque formation by cholesterol synthesis inhibition The histopathological examination of the aortas showed that the cholesterol/butter fed F_1B hamster developed atherosclerotic lesions and functional changes in the aorta which are closely related to man (Schäfer et al. 1999).

Soret et al. (1976) studied the diet-induced hypercholesterinemia in the diabetic and non-diabetic Chinese hamster.

Beitz and Mest (1991) used cholesterol-fed **guinea pigs** to study the antihyperlipemic effects of a potentially anti-atherosclerotic drug. Fernandez (2001) reviewed the advantages of the guinea pig as an animal model to study hepatic cholesterol, lipoprotein metabolism, and early atherosclerosis. Guinea pigs de-

velop fatty streaks after 12 weeks on a cholesterol diet; the response to cholesterol is highly individualized, and animals can be a hyper-responder or a hyporesponder to dietary cholesterol.

During the last 30 years **minpigs** have become a popular animal model for testing lipid-lowering drugs and their anti-atherosclerotic properties (Jacobsson 1987; Huff et al. 2002; Telford et al. 2003). Jacobsson and Lundholm investigated the lipid-lowering and anti-atherosclerotic effects of clofibrate, nicotinic acid, and other drugs (Lundholm 1978; Jacobsson and Lundholm 1982; Jacobsson 1987). Huff and Telford investigated the effect of atorvastatin and a bile acid absorption inhibitor on lipid metabolism and serum LDL kinetics (Huff et al. 2002; Telford et al. 2003). The benefits of the minipig are the absence of rodent-specific peroxisomal proliferation by PPAR α-agonists and closer homology to humans in absolute and relative organ sizes. The effective doses of the tested drugs in the minpig were close to clinically effective doses in humans.

Malinow et al. (1976) recommended the **cynomolgus monkey** as a model for therapeutic intervention on established coronary atherosclerosis.

This species was used by Hollander et al. (1978) to study the development atherosclerosis after a cholesterol and fat enriched diet.

Beere et al. (1992) described experimental atherosclerosis at the carotid bifurcation of the cynomolgus monkey by a cholesterol-enriched diet.

Eggen et al. (1991) studied the progression and the regression of diet-induced atherosclerotic lesions in aorta and coronary arteries on **rhesus monkeys**.

Howard (1976) recommended the **baboon** as model in atherosclerosis research because of the similarity of cholesterol metabolism and composition of the lipoproteins to man.

Kushwaha et al. (1991) determined the effect of estrogen and progesterone on plasma cholesterol concentrations and on arterial lesions in ovarectomized and hysterectomized baboons fed a high-cholesterol/high-saturated-fat diet.

Blaton an Peeters (1976) reported studies on the **chimpanzee**, the **baboon** and the **rhesus macacus** as models for atherosclerosis.

The use of normal adult **marmosets**, a species with a lipoprotein profile similar to that of humans, may be an alternative (Crook et al. 1990; Baxter et al. 1992).

Ming-Peng et al. (1990) studied high density lipoproteins and prevention of experimental atherosclerosis in **tree shrews** (*Tupaia belangera yunalis*). In contrast to rabbits, no increased lipid deposition in aortic intima after cholesterol feeding was found in tree shrews.

CRITICAL ASSESSMENT OF THE METHOD

Diet-induced hypercholesterolemia is useful for the detection of agents that interfere with the adsorption, degradation, serum clearance, and excretion of cholesterol to receive a broader effect range. It must be considered whether the effects of agents that interfere with cholesterol absorption will be enforced and therefore whether the efficacy is overestimated in those models.

REFERENCES AND FURTHER READING

Baxter A, Fitzgerald BJ, Hutson JL, McCarthy AD, Motteram JM, Ross BC, Sapra M, Snowden MA, Watson NS, Williams RJ, Wright C (1992) Squalestatin 1, a potent inhibitor of squalene synthase, which lowers cholesterol *in vivo*. J Biol Chem 267:11705–11708

Beere PA, Glagov S, Zarins ChK (1992) Experimental atherosclerosis at the carotid bifurcation of the cynomolgus monkey. Arterioscl Thrombos 12:1245–1253

Beitz J, Mest HJ (1991) A new derivative of tradipil (AR 12456) as a potentially new antiatherosclerotic drug. Cardiovasc Drug Rev 9:385–397

Blaton V, Peeters H (1976) The nonhuman primates as models for studying atherosclerosis: Studies on the chimpanzee, the baboon and the rhesus macacus. In: Day CE (ed) Atherosclerosis Drug Discovery, Plenum Press, New York and London, pp 33–64

Bretherton KN, Day AJ, Skinner SL (1977) Hypertension-accelerated atherogenesis in cholesterol-fed rabbits. Atherosclerosis 27:79–87

Caldwell CT, Suydam DE (1959) Quantitative study of estrogen-induced atherosclerosis in cockerels. Proc Soc Exp Biol Med 101:299–302

Chapman KP, Stafford WW, Day CE (1976) Produced by selective breeding of Japanese quail animal model for experimental atherosclerosis. In: Day CE (ed) Atherosclerosis Drug Discovery, Plenum Press, New York and London, pp 347–356

Clarkson TB, Lofland HB (1961) Therapeutic studies on spontaneous arteriosclerosis in pigeons. In: Garattini S, Paoletti R (eds) Drugs affecting lipid metabolism. Elsevier Publ Comp., Amsterdam, pp 314–317

Crook D, Weisgraber KH, Rall SC Jr, Mahley RW (1990) Isolation and characterization of several plasma apolipoproteins of common marmoset monkey. Arteriosclerosis 10:625–632

Day CE (1990) Comparison of hypocholesterolemic activities of the bile acid sequestrants cholestyramine and cholestipol hydrochloride in cholesterol fed sea quail. Artery 17:281–288

Day CE, Stafford WW (1975) New animal model for atherosclerosis research. In: Kritchevsky D, Paoletti R, Holmes WL (eds) Lipids, Lipoproteins, and Drugs. Plenum Press, New York, pp 339–347

Day CE, Stafford WW, Schurr PE (1977) Utility of a selected line (SEA) of the Japanese quail (*Coturnix coturnix japonica*) for the discovery of new anti-atherosclerosis drugs. Anim Sci 27:817–821

Day CE, Phillips WA, Schurr PE (1979) Animal models for an integrated approach to the pharmacologic control of atherosclerosis. Artery 5:90–109

Eggen DA, Bhattacharyya AK, Strong JP, Newman III WP, Guzman MA, Restrepo C (1991) Use of serum lipid and apolipoprotein concentrations to predict extent of diet-induced atherosclerotic lesions in aortas and coronary arteries and to demonstrate regression of lesions in individual Rhesus monkeys. Arterioscl Thrombos 11:467–475

Fernandez ML (2001) Guinea pigs as model for cholesterol and lipoprotein metabolism. J Nutr 131:10–20

Fillios LC, Andrus StB, Mann GV, Stare FJ (1956) Experimental production of gross atherosclerosis in the rat. J Exper Med 104:539–552

Fukushima H, Nakatani H (1969) Cholesterol-lowering effects of DL-*N*-(α-methylbenzyl)-linoleamide and its optically active isomers in cholesterol-fed animals. J Atheroscler Res 9:65–71

Henry PD, Bentley KI (1981) Suppression of atherogenesis in cholesterol-fed rabbit treated with nifedipine. J Clin Invest 68:1366–1369

Hollander W, Prusty S, Nagraj S, Kirkpatrick B, Paddock J, Colombo M (1978) Comparative effects of cetaben (PHB) and dichlormethylene diphosphonate (Cl_2MDP) on the development of atherosclerosis in the cynomolgus monkey. Atherosclerosis 31:307–325

Howard AN (1976) The baboon in atherosclerosis research: Comyparison with other species and use in testing drugs affecting lipid metabolism. In: Day CE (ed) Atherosclerosis Drug Discovery, Plenum Press, New York and London, pp 77–87

Huff MW, Telford DE, Edwards JY, Burnett JR, Barrett HP, Rapp SR, Napawan N, Keller BT (2002) Inhibition of the apical sodium-dependent bile acid transporter reduced LDL cholesterol and apoB by enhanced plasma clearance of LDL apoB. Arterioscler Thromb Vasc Biol 22:1884–1891

Inoue Y, Goto H, Horinuki R, Kimura Y, Toda T (1990) Experimental atherosclerosis in the rat carotid artery induced by balloon de-endothelialization and hyperlipemia. A histological and biochemical study. J Jpn Atheroscler Soc 18:1147–1154

Jacobsson L (1987) Influence of clofibrate on the plasma lipoprotein pattern and on lipid content and protein and collagen synthesis in atherosclerotic coronary arteries and abdominal aorta from hypercholesterolemic mini-pigs. Atherosclerosis 63:173–180

Jacobsson L, Lundholm L (1982) Experimental atherosclerosis in hypercholesterolemic mini-pigs. Atherosclerosis 45:129–148

Kowala MC, Nunnari JJ, Durham SK, Nicolosi RJ (1991) Doxazin and cholestyramine similarly decrease fatty streak formation in the aortic arch of hyperlipidemic hamsters. Atherosclerosis 91:35–49

Kritchevsky D (1964) Animal techniques for evaluating hypocholesteremic drugs. In: Nodine JH, Siegler PE (eds) Animal and Clinical Pharmacologic Techniques in Drug Evaluation. Year Book Medical Publishers, Inc., Chicago, pp 193–198

Kritchevsky D, Tepper SA, Davidson LM, Fisher EA, Klurfeld DM (1989) Experimental atherosclerosis in rabbits fed cholesterol-free diets. 13. Interactions of protein and fat. Atherosclerosis 75:123–127

Kushwaha RS, Lewis DS, Dee Carey K, McGill Jr HC (1991) Effects of estrogen and progesterone on plasma lipoproteins and experimental atherosclerosis in the baboon (*Papio* sp.) Arterioscl Thrombos 11:23–31

Lundholm L (1978) Influence of nicotinic acid, nicitrol and ß-pyridicarbinol on experimental hyperlipidemia and atherosclerosis in mini-pigs. Atherosclerosis 29:217–239

Lustalot P, Schuler W, Albrecht W (1961) Comparison of drug actions in a spectrum of experimental anti-atherosclerotic test systems. In: Garattini S, Paoletti R (eds) Drugs affecting lipid metabolism. Elsevier Publ Comp., Amsterdam, pp 271–276

Malinow MR, McLaughlin P, Papworth L, Naito HK, Lewis L, McNulty WP (1976) A model for therapeutic intervention on established coronary atherosclerosis in a nonhuman primate. In: Day CE (ed) Atherosclerosis Drug Discovery, Plenum Press, New York and London, pp 3–31

Ming-Peng S, Ren-Yi X, Bi-Fang R, Zong-Li W (1990) High density lipoproteins and prevention of experimental atherosclerosis with special reference to tree shrews. Ann New Acad Sci 598:339–351

Moss JN, Dajani EZ (1971) Antihyperlipidemic agents. In: Turner RA, Hebborn P (eds) Screening Methods in Pharmacology. Vol. II, Academic Press, New York and London, pp 121–143

Nistor A, Bulla A, Filip DA, Radu A (1987) The hyperlipidemic hamster as a model of experimental atherosclerosis. Atherosclerosis 68:159–173

O'Meara NMG, Devery RAM, Owens D, Collins PB, Johnson AH, Tomkin GH (1991) Serum lipoproteins and cholesterol metabolism in two hypercholesterolaemic rabbit models. Diabetologia 34:139–143

Paigen B, Morrow A, Holmes PA, Mitchell D, Williams RA (1987) Quantitative assessment of atherosclerotic lesions in mice. Atherosclerosis 68:231–240

Paigen B, Ishida BY, Verstuyft J, Winters RB, Albee D (1990) Atherosclerosis susceptibility differences among progenitors of recombinant inbred strains of mice. Atherosclerosis 10:316–323

Riezebos J, Vleeming W, Beems RB, van Amsterdam JGC, Meijer GW, de Wildt DJ, Porsius AJ, Wemer J (1994) Comparison of Israpidine and Ramipril in cholesterol-fed rabbits: effect on progression of atherosclerosis and endothelial dysfunction. J Cardiovasc Pharmacol 23:415–423

Roberts A, Thompson JS (1976) Inbred mice and their hybrids as an animal model for atherosclerosis research. In: Day CE (ed) Atherosclerosis Drug Discovery, Plenum Press, New York and London, pp 313–327

Schäfer H-L, Linz W, Bube A, Falk E, Hennig A, Hoffmann A, Leineweber M, Matthäi U, Schmalz M, Sendlbeck E, Kramer W, Schölkens BA (1999) The Syrian hamster as animal model for atherosclerosis. Naunyn-Schmiedeberg's Arch Pharmacol 359S: R111

Scholz W, Albus U, Hropot M, KLaus E, Linz W, Schölkens BA (1990) Zunahme des Na^+/H^+-Austausches an Kaninchenerythrozyzen unter atherogener Diät. In: Assmann G, Betz E, Heinle H, Schulte H (eds) Arteriosklerose. Neue Aspekte aus Zellbiologie und Molekulargenetik, Epidemiologie und Klinik. Tagung der Deutschen Gesellschaft für Arteriosklerose-Forschung. pp 296–302

Shore B, Shore V (1976) Rabbits as a model for the study of hyperlipoproteinemia and atherosclerosis. In: Day CE (ed) Atherosclerosis Drug Discovery, Plenum Press, New York and London, pp 123–141

Simpson CF, Harms RH (1969) Aortic atherosclerosis of turkeys induced by feeding of cholesterol. J Atheroscler Res 10:63–75

Soret MG, Blanks MC, Gerritsen GC, Day CE, Block EM (1976) Diet-induced hypercholesterinemia in the diabetic and non-diabetic Chinese hamster. In: Day CE (ed) Atherosclerosis Drug Discovery, Plenum Press, New York and London, pp 329–343

Tao L, Liu HR, Gao E, Teng ZP, Lopez BL, Christopher TA, Ma XL, Batinic-Haberle I, Willette RN, Ohlstein EH, Yue TL (2003) Antioxidative, antinitrative, and vasculoprotective effects of a peroxisome proliferator-activated receptor-γ agonist in hypercholesterolemia. Circulation 108:2805–2811

Telford DE, Edwards JY, Lipson SM, Hugh P, Barrett HP, Burnett JR, Krul ES, Keller BT, Huff MW (2003) Inhibition of both the apical sodium-dependent bile acid transporter and HMG-CoA reductase markedly enhances the clearance of LDL apoB. J Lipid Res 44:943–952

Tennent DM, Siegel H, Zanetti ME, Kuron GW, Ott WH, Wolf FJ (1960) Plasma cholesterol lowering action of bile acid binding polymers in experimental animals. J Lipid Res 1:469–473

Yamaguchi Y, Kitagawa S, Imaizumi N, Kunitomo M, Fujiwara M (1993) Enhancement of cholesterol deposition by dietary linoleic acid in cholesterol-fed mice: an animal model for primary screening of antiatherosclerotic agents. J Pharm Toxicol Meth 30:169–175

M.1.0.3
Hereditary Hypercholesterolemia in Rats

A strain of genetically hypercholesterolemic rats (RICO) was described by Müller et al. (1979). In contrast to Zucker-rats, these animals are normo-triglyceridemic and non-obese. The hypercholesterolemia of the RICO rat is related to a decreased rate of catabolism of chylomicrons and LDL, but more specifically to an excessive production of these two types of lipoproteins. This strain has been proposed to study hypolipidemic drugs, particularly those designed to decrease the plasma concentrations of chylomicrons and LDL. Hypolipidemic effects of β-cyclodextrin were found in this model (Riottot et al. 1993).

REFERENCES AND FURTHER READING

Lutton C, Ouguerram K, Sauvage M, Magot T (1990) Turnover of [^{14}C]sucrose HDL and uptake by organs in the normal or genetically hypercholesterolemic (RICO) rat using a constant infusion method. Reprod Nutr Dev 30:97–101

Müller KR, Li JR, Dinh DM, Subbiah MTR (1979) The characteristics and metabolism of a genetically hypercholesterolemic strain of rats (RICO). Biochim Biophys Acta 574:334–343

Ougueram K, Magot T, Lutton C (1991) Alterations in cholesterol metabolism in the genetically hypercholesterolemic RICO rat: an overview. In: Malmedier CL, Alaupovic P, Brewer Jr HB (eds) Hypercholesterolemia, hypocholesterolemia, hypertriglyceridemia, *in vivo* kinetics. Adv Exp Med Biol 285:257–274. Plenum Press, New York and London

Ougueram K, Magot T, Lutton C (1992) Metabolism of intestinal triglyceride-rich lipoproteins in the genetically hypercholesterolemic rat (RICO). Atherosclerosis 93:210–208

Riottot M, Olivier Ph, Huet A, Caboche JJ, Parquet M, Khallou J, Lutton C (1993) Hypolipidemic effects of β-cyclodextrin in the hamster and in the genetically hypercholesterolemic RICO rat. Lipids 28:181–188

M.1.0.4
Hereditary Hyperlipemia in Rabbits

Watanabe et al. (1977, 1980) described a strain of rabbits with hereditary hyperlipemia (WHHL rabbit) which has been used by several scientists to study development of atherosclerosis, as well as for histological and functional changes of the aorta. At the age of 10–14 months homozygous animals exhibit an atheromatous plaque, distributed heterogeneously over the luminal surface of the aorta. Serum cholesterol is increased up to 400–600 mg/dl. The increased levels of LDL have been studied in detail (Kita et al. 1981, 1982).

REFERENCES AND FURTHER READING

Bilheimer DW, Watanabe Y, Kita T (1982) Impaired receptor-mediated catabolism of low density lipoprotein in the WHHL rabbit, an animal model of familial hypercholesterolemia. Proc Natl Acad Sci, USA, 79:3305–3309

Gallagher PJ, Nanjee MN, Richards T, Roche WR, Miller NE (1988) Biochemical and pathological features of a modified strain of Watanabe heritable hyperlipidemic rabbits. Atherosclerosis 71:173–183

Kita T, Brown MS, Watanabe Y, Goldstein JL (1981) Deficiency of low density lipoprotein receptors in liver and adrenal gland of the WHHL rabbit, an animal model of familial hypercholesterolemia. Proc Natl Acad Sci, USA, 78:2268–2272

Kita T, Brown MS, Bilheimer DW, Goldstein JL (1982) Delayed clearance of very low density and intermediate density lipoproteins with enhanced conversion to low density lipoprotein in WHHL rabbits. Proc Natl Acad Sci, USA, 79:5693–5697

Makheja AN, Bloom S, Muesing R, Simon T, Bailey JM (1989) Anti-inflammatory drugs in experimental atherosclerosis. 7. Spontaneous atherosclerosis in WHHL rabbits and inhibition by cortisone acetate. Atherosclerosis 76:155–161

Rosenfeld ME, Tsukada T, Gown AM, Ross R (1987) Fatty streak initiation in Watanabe heritable hyperlipemic and comparably hypercholesterolemic fat-fed rabbits. Arteriosclerosis 7:9–23

Schneider WJ, Brown MS, Goldstein JL (1983) Kinetic defects in the processing of the low density lipoprotein receptor in fibroblasts from WHHL rabbits and a family with familial hypercholesterolemia. Mol Biol Med 1:353–367

Tagawa H, Tomoike H, Nakamura M (1991) Putative mechanisms of the impairment of endothelium-dependent relaxation of the aorta with atheromatous plaque in heritable hyperlipidemic rabbits. Circ Res 68:330–337

Watanabe Y (1980) Serial inbreeding of rabbits with hereditary hyperlipidemia (WHHL)-rabbit). Incidence and development of atherosclerosis and xanthoma. Atherosclerosis 36:261–268

Watanabe Y, Ito T, Kondo T (1977) Breeding of a rabbit strain of hyperlipidemia and characteristic of these strain. Exp Anim 26:35–42

Watanabe Y, Ito T, Shiomi M (1985) The effect of selective breeding on the development of coronary atherosclerosis in WHHL rabbits. An animal model for familial hypercholesterolemia. Atherosclerosis 56:71–79

M.1.0.5 Studies in Transgenic Mice

Mice do not develop atherosclerotic lesions spontaneously. Paigen et al. (1985) fed ten inbred strains of mice an atherogenic diet containing 1.25% cholesterol, 0.5% cholic acid and 15% fat in order to study the variation in susceptibility to atherosclerosis among these strains. The strains were examined for plasma cholesterol and triglyceride levels and for formation of lipid-containing lesions in the aortic wall. The most susceptible strain was C57BL/6J mice.

Several transgenic animals as disease model were created during the last decade, mostly mice (Stoltzfus and Rubin 1993), but also rats and rabbits.

The widely used model is the Apo E knockout mouse originally created by Nubuyo Maeda, University of North Carolina, Chapell Hill, NC. These Apo E knockout mice have spontaneously elevated plasma cholesterol levels, and develop atherosclerosis even on regular chow within 3–4 months. The time dependent progression of atherosclerosis leads to lesions similar in histopathology to those observed in humans. This animal model is used as background for atherosclerosis research and target validation. Duez et al. (2002) used apolipoprotein E-deficient mice and human apoA-I transgenic apoE-deficient mice fed a Western diet to investigate the reduction of atherosclerosis by the PPARα agonist fenofibrate.

Walsh et al. (1989) and Rubin et al. (1991) integrated human apolipoprotein A-I gene in transgenic mice resulting in an increase of HDL levels.

Linton et al. (1993) described the development of transgenic mice expressing high levels of human apolipoprotein B48 and human apolipoprotein B100 which are considered to be atherogenic.

Transgenic mice expressing high levels of human apoliprotein B develop severe atherosclerotic lesions in response to a high-fat diet (Purcell-Huynh et al. 1995).

Ishibashi et al. (1994) found massive xanthomatosis of the skin and subcutaneous tissue and atherosclerosis in cholesterol-fed low density lipoprotein receptor-negative mice.

Sasan et al. (1998) reported that low density lipoprotein receptor-negative mice expressing human apolipoprotein B-100 develop complex atherosclerotic lesions on a chow diet.

Li et al. (2000) used LDL receptor-deficient mice to study the inhibition of development of atherosclerosis by PPARγ-specific agonists.

Joseph et al. (2002) investigated the inhibition of development of atherosclerosis in *LDL receptor* knockout mice and *ApoE* knockout mice by a synthetic LXR ligand.

Terasaka et al. (2003) reported inhibition of development of atherosclerosis in LDL-receptor-deficient mice by a synthetic liver X receptor ligand.

Transgenic mice lacking apolipoprotein E showed severe hypercholesterolemia and atherosclerosis (Plump et al. 1992; Zhang et al. 1992). ApoE-deficient mice develop lesions of all phases of atherosclerosis throughout the arterial tree (Nakashima et al. 1994).

Fu et al. (2003) reported that the PPARα agonist ciprofibrate severely aggravates hypercholesterolemia and accelerates the development of atherosclerosis in mice lacking apolipoprotein E.

Wang (2005) described the cardiovascular functional phenotype of ApoE knockout mice and reported that simvastatin paradoxically increased serum lipids and atherosclerosis, but decreased serum lipids and atherosclerosis in LDL receptor knockout mice.

Meier and Leitersdorf (2004) reviewed nutritional, pharmacologic, and genetic atherosclerosis intervention studies in ApoE knockout mice. Several known beneficial nutritional interventions are effective, as well as ACE inhibitors, Ang II receptor blockers, the cholesterol absorption inhibitor ezetimibe and PPARγ agonists. Meier pointed out that the model helps the understanding that atherosclerosis is a form of chronic inflammation and that, despite being imperfect, the ApoE knockout mouse is currently the most popular mouse model used by researchers around the globe.

Overexpression of apolipoprotein E in transgenic mice reduced plasma cholesterol and triglyceride levels, prevented hypercholesterolemia and inhibited the formation of fatty streak lesions (Harada et al. 1996).

Transgenic mice overexpressing the human dysfunctional apolipoprotein E variant APOE*3 Leiden develop hyperlipidemia and are highly susceptible to diet-induced atherosclerosis (Groot et al. 1996).

Sullivan et al. (1998) reported type III hyperlipoproteinemia and spontaneous atherosclerosis in mice resulting from gene replacement of mouse ApoE with human ApoE*2.

Severe hypercholesterolemia, hypertriglyceridemia, and atherosclerosis were observed in ob/ob mice lacking both leptin and the LDL receptor (Hasty et al. 2001).

Based on animal knockout, transgenic, and gene therapy studies, Bursill et al. (2004) highlighted the importance of chemokines, particularly the CC-chemokines and fractalkine, in atherosclerosis.

REFERENCES AND FURTHER READING

Bursill CA, Channon KM, Greaves DC (2004) The role of chemokines in atherosclerosis: recent evidence from experimental models and population genetics. Curr Opin Lipidol 15:145–149

Duez H, Chao YS, Hernandez M, Torpier G, Poulain P, Mundt S, Mallat Z, Teissier E, Burton CA, Tedgui A, Fruchart JC, Fiévet C, Wright SD, Staels B (2002) Reduction of atherosclerosis by the peroxisome proliferators-activated receptor α agonist fenofibrate in mice. J Biol Chem 277:48051–48057

Fu T, Kashireddy P, Borensztajn J (2003) The peroxisome-proliferator-activated receptor α agonist ciprofibrate severely aggravates hypercholesterolaemia and accelerates the development of atherosclerosis in mice lacking apolipoprotein E. Biochem J 373:941–947

Groot PH, van Vlijmen BJ, Benson GM, Hofker MH, Schiffelers R, Vidgeon-Hart M, Haveskes LM (1996) Quantitative assessment of aortic atherosclerosis in APOE*3 Leiden transgenic mice and its relationship to serum cholesterol exposure. Arterioscler Thromb Vasc Biol 16:926–933

Harada K, Shimano H, Ishibashi S, Yamada N (1996) Transgenic mouse and gene therapy. Diabetes 45 (Suppl 3): S129–S132

Hasty AH, Shimano H, Osuga J, Namatama I, Takahashi A, Yahagi N, Perrey S, Iizuka Y, Tamura Y, Amemiya-Kudo M, Yoshikawa T, Okazaki H, Harada K, Matsuzaka T, Sone H, Gotoda T, Nagai R, Ishibashi S, Yamda N (2001) Severe hypercholesterolemia, hypertriglyceridemia and atherosclerosis in mice lacking both leptin and the low density lipoprotein receptor. J Biol Chem 276:37402–37408

Ishibashi S, Goldstein JL, Brown MS, Herz J, Burns DK (1994) Massive xanthomatosis and atherosclerosis in cholesterol-fed low density lipoprotein receptor-negative mice. J Clin Invest 93:1885–1893

Joseph SB, McKilligin E, Pei L, Watson MA, Collins AR, Laffitte BA, Chen M, Noh G, Goodman J, Hagger GH, Tran J, Tippin TK, Wang X, Lusis AJ, Hsueh WA, Law RE, Collins JL, Willson TM, Tontonoz P (2002) Synthetic LXR ligand inhibits the development of atherosclerosis in mice. Proc Natl Acad Sci USA 99:7604–7609

Li AC, Brown KK, Silvestre MJ, Willson TM, Paliski W, Glass CK (2000) Peroxisome proliferator-activated receptor γ ligands inhibit development of atherosclerosis in LDL receptor-deficient mice. J Clin Invest 106:523–531

Linton MF, Farese RV, Chiesa G, Grass DS, Chin P, Hammer RE, Hobbs HH, Young SG (1993) Transgenic mice expressing high plasma concentrations of human apolipoprotein B100 and apolipoprotein (a). J Clin Invest 92:3029–3037

Meier KS, Leitersdorf E (2004) Atherosclerosis in the apolipoprotein E-deficient mouse; a decade of progress. Arterioscler Thromb Vasc Biol 24:1006–1014

Nakashima Y, Plump AS, Raines EW, Breslow JL, Ross R (1994) ApoE-deficient mice develop lesions of all phases of atherosclerosis throughout the arterial tree. Arterioscler Thromb 14:133–140

Paigen B, Morrow A, Brandon C, Mitchell D, Holmes P (1985) Variation in susceptibility to atherosclerosis among inbred strains of mice. Atherosclerosis 57:65–73

Plump AS, Smith JD, Hayek T, Aalto-Setälä K, Walsh A, Verstuyft JG, Rubin EM, Breslow JL (1992) Severe hypercholesterolemia and atherosclerosis in apolipoprotein E-deficient mice created by homologous recombination in ES cells. Cell 71:343–353

Purcell-Huynh DA, Farese RV, Johnson DF, Flynn LM, Pierotti V, Newland DE, Linton MF, Young SG (1995) Transgenic mice expressing high levels of human apoliprotein B develop severe atherosclerotic lesions in response to a high-fat diet. J Clin Invest 95:2246–2257

Rubin EM, Ishida BY, Clift SM, Kraus RM (1991) Expression of human apolipoprotein A-I in transgenic mice results in reduced plasma levels of murine apolipoprotein A-I and the appearance of two new high density lipoprotein subclasses. Proc Natl Acad Sci USA 88:434–438

Sasan DA, Newland DE, Tao R, Marcovina S, Wang J, Mooser V, Hammer RE, Hobbs HH (1998) Low density lipoprotein receptor-negative mice expressing human apolipoprotein B-100 develop complex atherosclerotic lesions on a chow diet: no accentuation by apolipoprotein(s). Proc Natl Acad Sci USA 95:4544–4549

Stoltzfus L, Rubin EM (1993) Atherogenesis. Insights from the study of transgenic and gene-targeted mice. Trends Cardiovasc Med 3:130–134

Sullivan PM, Mazdour H, Quarfordt SH, Maeda N (1998) Type III hyperlipoproteinemia and spontaneous atherosclerosis in mice resulting from gene replacement of mouse ApoE with human ApoE*2. J Clin Invest 102:130–135

Terasaka N, Hiroshima A, Koieyama T, Ubukata N, Morikawa Y, Nakai D, Inaba T (2003) T-0901317, a synthetic liver X receptor ligand, inhibits development of atherosclerosis in LDL receptor-deficient mice. FEBS Lett 536:6–11

Walsh A, Ito Y, Breslow JL (1989) High levels of human apolipoprotein A-I in transgenic mice result in increased plasma levels of small high density lipoprotein (HDL) particles comparable to human HDL_3. J Biol Chem 264: 6488–6494

Wang YX (2005) Cardiovascular functional phenotypes and pharmacological responses in apolipoprotein E deficient mice. Neurobiol Aging 26:309–316

Zhang SH, Reddick RL, Piedrahita JA, Maeda N (1992) Spontaneous hypercholesterolemia and arterial lesions in mice lacking apolipoprotein E. Science 258:468–471

M.1.0.6 Evaluation of Endothelial Function in Rabbits with Atherosclerosis

PURPOSE AND RATIONALE

Cholesterol feeding of rabbits impairs the endothelium-dependent relaxation evoked by acetylcholine in the aorta. This phenomenon can be used to study the influence of vasodilators as well as the prevention by ACE-inhibitors (Becker et al. 1991).

PROCEDURE

Male white New Zealand rabbits weighing 3–4 kg receive a hypercholesterolemic diet containing 0.25 to 1% cholesterol and 3% coconut oil. Rabbits of the same weight receiving standard diet serve as controls. After several weeks, the serum cholesterol levels are increased from 30–40 mg/dl in the control group up to 900–1000 mg/dl in the cholesterol-fed group. At the end of the treatment period, the animals are sacrificed by intravenous injection of sodium pentobarbital and a complete autopsy is performed.

Intact proximal parts of the thoracic aorta are sectioned into 2 mm wide rings, cut off to strips,

and suspended at 2 g gauge in 25 ml organ chambers filled with a buffer solution of 37°C comprising 113.8 mM NaCl, 20 mM $NaHCO_3$, 4.7 mM KCl, 1.2 mM KH_2PO_4, 1.1 mM $MgSO_4$, 2.5 mM $CaCl_2$, and 5.5 mM glucose being gassed with a 95% O_2/5% CO_2 mixture to achieve a pH of 7.4. After 2 h, when a stable contractile tone is established, norepinephrine is added at a final concentration of 1×10^{-8} M, which produces a stable submaximum isotonic contraction. Then, acetylcholine is added in 10 fold incremental doses from 1×10^{-8} M up to final concentrations of 10^{-5} M. Relaxation of aortic strips is assessed as percentage decrease in contraction. Acetylcholine induced concentration-dependent relaxation is greatly impaired in aorta rings from cholesterol-fed rabbits whereas contractions to norepinephrine are only slightly diminished.

EVALUATION

The data are expressed as mean ± SEM and compared by Student's *t*-test for unpaired data.

MODIFICATIONS OF THE METHOD

Verbeuren et al. (1986, 1990) and Tagawa et al. (1991) used a bioassay for the determination of EDRF (Rubanyi et al. 1985). The donor thoracic aorta segments (3 cm long) are mounted horizontally in perfusion chambers filled with physiological salt solution which contains indomethacin (3×10^{-6} M) at 37°C; the solution is gassed with a mixture of 20% O_2, 5% CO_2, and 75% N_2. The aortas (control and atherosclerotic tissue) and a piece of glass tubing are perfused continuously with the same solution at 3 ml/min. The perfusate is dripping directly onto a segment (5 mm long) of either a control or an atherosclerotic abdominal aorta from which the endothelium was mechanically removed. The detector abdominal aortas are mounted vertically over two hooks and the development of isometric tension is monitored continuously. The initial tension of the detector aortas is set at 8 g. The perfusate of each donor aorta is analyzed both on a control and on an atherosclerotic detector preparation: the order of this double analysis is selected at random. A control and an atherosclerotic donor aorta are always analyzed in parallel and thus on the same detector tissue. Drugs are added to the perfusion medium. Before the start of the experiments, the tissues are allowed to equilibrate for 45 min in the perfusion chambers. By means of a three-way system, placed at the outlet of the donor aortas, atropine (10^{-6} M) is added to the perfusate to block any muscarinic contractile effect of acetylcholine on the detector tissue. Noradrenaline (2×10^{-6} M) is infused into the perfusate via this 3-way system causing a sustained contraction in the detector tissue.

After the stabilization of the contraction to noradrenaline, the highest dose of acetylcholine (1.6×10^{-8} mol) is added to the solution for perfusion of the tubing in order to confirm no change in the contractile response to noradrenaline in the detector tissues. Moreover, the perfusate from the control and atherosclerotic donor aortas under basal conditions does not significantly affect the contraction of the detector tissues. The tissues are allowed to equilibrate and then increasing doses of acetylcholine (0.01 to 160×10^{-10} mol) are injected into the perfusion medium close to the donor aortas. Relaxation is less pronounced in the detector tissues when atherosclerotic aortas are stimulated with acetylcholine indicating that the cholinergic agent causes a smaller release of EDRF from atherosclerotic donor aortas than from control donor aortas. The degree of the arteriosclerotic lesion can be assessed by this functional assay.

REFERENCES AND FURTHER READING

Becker RHA, Wiemer G, Linz W (1991) Preservation of endothelial function by ramipril in rabbits on a long-term atherogenic diet. J Cardiovasc Pharmacol 18 (Suppl 2):S110–S115

Bossaller C, Habib GB, Yamamoto H, Williams C, Wells S, Henry PD (1987) Impaired muscarinic endothelium-dependent relaxation and cyclic guanosine 5′-monophosphate formation in atherosclerotic human coronary artery and rabbit aorta. J Clin Invest 79:170–174

Finta KM, Fischer MJ, Lee L, Gordon D, Pitt B, Webb RC (1993) Ramipril prevents impaired endothelium-dependent relaxation in arteries from rabbits fed an atherogenic diet. Atherosclerosis 100:149–156

Jayakody L, Kappagoda T, Senaratne MPJ, Thomson ABR (1988) Impairment of endothelium-dependent relaxation: an early marker for atherosclerosis in the rabbit. Br J Pharmacol 94:335–346

Rubanyi GM, Lorenz RR, Vanhoutte PM (1985) Bioassay of endothelium-derived relaxing factor(s): inactivation by catecholamines. Am J Physiol 249:H95–H110

Tagawa H, Tomoike H, Nakamura M (1991) Putative mechanisms of the impairment of endothelium-dependent relaxation of the aorta with atheromatous plaque in heritable hyperlipidemic rabbits. Circ Res 68:330–337

Verbeuren TJ, Jordaens FH, Zonnekeyn LL, Van Hove CE, Coene MC, Herman AG (1986) Effect of hypercholesterolemia on vascular reactivity in the rabbit. I. Endothelium-dependent and endothelium-independent contractions and relaxations in isolated arteries of control and hypercholesterolemic rabbits. Circ Res 58:552–564

Verbeuren TJ, Jordaens FH, Van Hove CE, Van Hoydonk AE, Herman AG (1990) Release and vascular activity of endothelium-derived relaxing factor in atherosclerotic rabbit aorta. Eur J Pharmacol 191:173–184

M.1.0.7 Intimal Reactions After Endothelial Injury

PURPOSE AND RATIONALE

Several attempts have been made to induce intimal injury in animals which is followed by proliferation and formation of fatty streaks similar to the alterations found in human atherosclerosis. One approach is the "balloon catheterization".

PROCEDURE

Male New Zealand White rabbits weighing 2.0–3.5 kg or male Sprague-Dawley rats weighing 350–400 g are used. An embolectomy catheter (Edwards Laboratories, size 4 French for rabbits, size 2 French for rats) is introduced into the right femoral artery under surgical anesthesia and passed to the aortic arch. After inflation with room air, the catheter is withdrawn to the iliac bifurcation, deflated and removed.

The incorporation of [^{3}H]thymidine into DNA of rabbit or rat aorta is measured 48 h after balloon catheterization. Animals are sacrificed 45 min after intravenous injection of [^{3}H]thymidine. Intima-media is prepared from whole aorta by scraping with blunt forceps. The specific activity of ^{3}H in DNA is determined after extraction of the DNA in the washed tissue homogenate using hot dilute perchloric acid. DNA is assayed by the diphenylamine method. ^{3}H Incorporation is measured in a liquid scintillation counter.

For histological examination, rabbits are injected 2 weeks after balloon catheterization intravenously with heparin (500 U/kg) and then sacrificed. Fixative (2% glutaraldehyde in 0.15 M phosphate buffer, pH 7.4) is infused at a constant pressure of 100 mm Hg via a carotid cannula and the aorta is pressure fixed *in situ* for 60 min. Intimal proliferation is quantified in the upper abdominal aorta, in the lower abdominal aorta and half-way between these points.

EVALUATION

[^{3}H]Thymidine incorporation and intimal proliferation is compared between drug treated animals and controls.

MODIFICATIONS OF THE METHOD

DeCampli et al. (1988) studied the effects of various drugs on accelerated myointimal proliferation in canine veno-arterial allografts by histological methods. An 8-cm length of femoral vein was removed, reversed, divided, and sewn end-to-end into carotid or femoral arteries of a recipient dog.

Berkenboom et al. (1989) induced experimental atherosclerosis in **canine** and **porcine** coronary arteries by endothelial denudation followed by a high-cholesterol diet.

Kawata et al. (1990) described the detection of regenerating cells in the aorta after ballooning by immunocytochemical demonstration of the thymidine analogue 5-bromo-2′-deoxyuridine.

Manderson et al. (1990) described changes in vascular reactivity of carotid arteries in rabbits following endothelial denudation.

Bocan et al. (1991) tested an ACAT inhibitor and selected lipid-lowering agents for anti-atherosclerotic activity in iliac-femoral and thoracic aortic lesions. Atherosclerotic lesion comparable in composition to human fatty streaks were induced by chronic endothelial denudation in the iliac-femoral artery inserting a sterile, indwelling, 18-cm nylon filament with a diameter of 200 µm into the lumen of the right femoral artery in hypercholesterolemic New Zealand White rabbits. Naturally occurring fatty streaks developed in the thoracic aorta following cholesterol feeding. The effect of treatment on lesion regression was evaluated in the iliac-femoral artery, while changes in the lesion progression were evaluated in the thoracic artery.

Davies et al. (1993) performed right common carotid artery bypass grafting using the ipsilateral external jugal vein in New Zealand White rabbits and studied the response to endothelin-1 in normolipidemic and hyperlipidemic animals.

Groves et al. (1993) studied platelet adhesion and thrombus formation in a **porcine** model of balloon angioplasty.

ACE inhibitor treatment reduced the neointima formation after endothelial denudation in the carotid artery of **rats** using a balloon catheter (Farhy et al. 1992; Linz and Schölkens 1992; Linz et al. 1993, 1994).

Lyle et al. (1995) tested the effect of inhibitors of factor X_a or platelet adhesion, heparin, and aspirin on platelet deposition in an atherosclerotic rabbit model of angioplastic injury. Acute ^{111}indium-labelled platelet deposition and thrombosis were assessed 4 h after balloon-injury in femoral arteries subjected to prior endothelial damage (air desiccation) and cholesterol supplementation (1 month).

REFERENCES AND FURTHER READING

Berkenboom G, Unger P, Fontaine J (1989) Atherosclerosis and responses of human isolated coronary arteries to endothelium-dependent and -independent vasodilators. J Cardiovasc Pharmacol 14, Suppl 11:S35–S39

Bocan TMA, Mueller SB, Uhlendorf PD, Newton RS, Krause BR (1991) Comparison of CI-976, an ACAT inhibitor, and

selected lipid-lowering agents for antiatherosclerotic activity in iliac-femoral and thoracic aortic lesions. Arterioscler Thrombosis 11:1830–1843
Davies MG, Klyachkin ML, Kim JH, Hagen PO (1993) Endothelin and vein bypass grafts in experimental atherosclerosis. J Cardiovasc Pharmacol 22, Suppl 8:S348–S351
DeCampli WM, Kosek JC, Mitchell RS, Handen CE, Miller DC (1988) Effects of aspirin, dipyridamole, and cod liver oil on accelerated myointimal proliferation in canine venoarterial allografts. Ann Surg 208:746–754
Farhy RD, Ho KL, Carretero OA, Scicli AG (1992) Kinins mediate the antiproliferative effect of ramipril in rat carotid artery. Biochem Biophys Res Commun 182:283–288
Groves PH, Levis MJ, Cheadle HA, Penny WJ (1993) SIN-1 reduces platelet adhesion and thrombus formation in a porcine model of balloon angioplasty. Circulation 87:590–597
Jackson CL, Bush RC, Bowyer DE (1988) Inhibitory effects of calcium antagonists on balloon catheter-induced arterial smooth muscle cell proliferation and lesion size. Atherosclerosis 69:115–122
Kawata M, Lee KT, Makiat T (1990) Detection of regenerating cells in the aorta after ballooning by immunocytochemical demonstration of the thymidine analogue 5-bromo-2′-deoxyuridine (BrUdR). In: Lee KT, Onodera K, Tanaka K (eds) Atherosclerosis II: Recent Progress in Atherosclerosis Research. Ann NY Acad Sci 598:514–516
Linz W, Schölkens BA (1992) Role of bradykinin in the cardiac effects of angiotensin-converting enzyme inhibitors. J Cardiovasc Pharmacol 20(Suppl 9):S83–S90
Linz W, Wiemer G, Schölkens BA (1993) Contribution of bradykinin to the cardiovascular effects of ramipril. J Cardiovasc Pharmacol 22(Suppl 9):S1–S8
Linz W, Wiemer G, Gohlke P, Unger T, Schölkens BA (1994) The contribution of bradykinin to the cardiovascular actions of ACE inhibitors. In Lindpaintner K, Ganten D (eds) The Cardiac Renin Angiotensin System. Futura Publ Co., Inc., Armonk, NY, pp 253–287
Lyle EM, Fujita T, Conner MW, Connolly TM, Vlasuk GP, Lynch JL (1995) Effect of inhibitors of factor X_a or platelet adhesion, heparin, and aspirin on platelet deposition in an atherosclerotic rabbit model of angioplastic injury. J Pharmacol Toxicol Meth 33:53–61
Manderson JA, Cocks TM, Campbell GR (1990) Changes in vascular reactivity following endothelial denudation. In: Lee KT, Onodera K, Tanaka K (eds) Atherosclerosis II: Recent Progress in Atherosclerosis Research. Ann NY Acad Sci 598:564–566

M.2 Influence on Lipid Metabolism

M.2.0.1 General Considerations

Elevated lipid levels, especially hypercholesterolemia, result from increased absorption from the gut, enhanced endogenous synthesis, or inadequate clearance from serum. Therefore, there are three feasible ways to reduce hyperlipidemia: to block endogenous synthesis, decrease absorption or enhance clearance from serum. These three factors can be evaluated in normal animals without artificial diets. Clinically used lipid-lowering compounds such as PPARα agonists (fibrates), cholesterol absorption inhibitors (ezetimibe), bile acid sequestrants, and HMG-CoA reductase inhibitors (statins) can be tested in this way, and their pharmacological activity further investigated with additional tests. For the investigation of the effects on plasma lipids, the right animal model has to be chosen. For fibrates, rats and mice are appropriate models; for LDL-lowering compounds, hamster, guinea and rabbits. Earlier attempts to interfere with endogenous cholesterol synthesis resulted in the accumulation of sterols other than cholesterol (Holmes 1964). To date only the inhibition of cholesterol biosynthesis with HMG-CoA reductase inhibitors has been a clinically effective approach for LDL cholesterol lowering. Inhibition of other enzymes of the cholesterol biosynthesis pathway upstream from HMG-CoA reductase, such as squalene synthetase, were investigated by several pharmaceutical companies until the 1990s, but this development was discontinued for safety reasons. Inhibition of cholesterol biosynthesis upstream from HMG-CoA reductase leads to nonphysiological accumulation of metabolic intermediates. In the past the inhibition of cholesterol absorption by ACAT-inhibitors was a widely followed approach. ACAT-inhibitors inhibit cholesterol absorption in rodents effectively, but so far all ACAT-inhibitors have been ineffective in humans. The only compound that is effective in humans is ezetimibe, an azetidinone. The compound was discovered fortuitously in an ACAT-inhibitor program. During the development of that compound, it was found that ezetimibe inhibits cholesterol absorption independently from ACAT (Van Heek et al. 2000, 2001, 2003; Harris et al. 2003; Clader 2004). Ezetimibe inhibits cholesterol absorption in several animal models and is effective against plasma LDL-cholesterol in humans. Another approach to enhance hepatic LDL clearance is to interrupt bile acid recirculation. Compounds that inhibit bile acid absorption increase the conversion of cholesterol into bile acids, enhance hepatic clearance, and lower LDL cholesterol by LDL receptor upregulation in the liver.

Protective effects of calcium antagonists against experimental arteriosclerosis acting mainly on other mechanisms than lipid metabolism have been claimed by various authors but the clinical relevance is still questionable (Kjeldsen and Stender 1989; Fronek 1990; Knorr and Kazda 1990; Fleckenstein-Grün et al. 1992).

REFERENCES AND FURTHER READING

Clader JW (2004) The discovery of ezetimibe: a view from outside the receptor. J Med Chem 47:1–9

Fleckenstein-Grün, Frey M, Thimm F, Fleckenstein A (1992) Protective effects of various calcium antagonists against experimental arteriosclerosis. J Human Hypertens 6, Suppl 1:S13–S18

Fronek K (1990) Calcium antagonists and experimental atherosclerosis. Cardiovasc Drug Rev 8:229–237

Harris M, Davis W, Brown WV (2003) Ezetimibe. Drugs Today (Barc) 39:229–247

Holmes WL (1964) Drugs affecting lipid synthesis. In: Paoletti R (ed) Lipid Pharmacology, Academic Press, New York, London, chapter 3, pp 131–184

Illingworth DR (1987) Lipid-lowering drugs. An overview of indications and optimum therapeutic use. Drugs 33:259–279

Kjeldsen K, Stender S (1989) Calcium antagonists and experimental atherosclerosis. Proc Soc Exp Biol Med 190:219–228

Knorr AM, Kazda S (1990) Influence of nifedipine on experimental arteriosclerosis. Cardiovasc Drugs Ther 4:1027–1032

McCarthy PA (1993) New approaches to atherosclerosis: An overview. Med Res Rev 13:139–159

Van Heek M, Farley C, Compton DS, Hoos L, Alton KB, Sybertz EJ, Davis HR (2000) Comparison of the activity and disposition of the novel cholesterol absorption inhibitor, SCH5835, and its glucuronide, SCH60663. Br J Pharmacol 129:1748–1754

Van Heek M, Compton DS, Davis HR (2001) The cholesterol adsorption inhibitor, ezetimibe, decreases diet-induced hypercholesterolemia in monkeys. Eur J Pharmacol 415:79–84

Van Heek M, Farley C, Copton DS, Hoos LM, Smith-Torhan A, Davois HR (2003) Ezetimibe potently inhibits cholesterol absorption but does not affect acute hepatic or intestinal cholesterol synthesis in rats. Br J Pharmacol 138:1459–1464

M.2.0.2 Hypolipidemic Activity in Rats

PURPOSE AND RATIONALE

Hyperlipoproteinemia with increased concentrations of cholesterol- and triglyceride-carrying lipoproteins is considered to be the cause of arteriosclerosis with its dual sequelae of thrombosis and infarction. Lipoproteins are divided into 6 major classes: chylomicrons, chylomicron remnants, VLDL (very low density lipoproteins), IDL (intermediate density lipoproteins), LDL (low density lipoproteins), and HDL (high density lipoproteins). HDL promotes the removal of cholesterol from peripheral cells and facilitates its delivery back to the liver. Therefore, increased levels of HDL are desirable. On the contrary, high levels of VLDL and LDL promote arteriosclerosis. LDL, especially in its oxidized form, is taken up by macrophages via a scavenger mechanism. Therefore, anti-arteriosclerotic drugs should reduce VLDL and LDL and/or elevate HDL.

PROCEDURE

Groups of ten male Wistar or Sprague Dawley rats weighing 180–200 g are used. They are given once daily in the morning over a period of 5–8 days the test compounds or the standard in various doses ranging from 1 to 100 mg/kg via a stomach tube in a volume of 5 ml/kg. The control group is given the solvent (e. g., 0.5% HEC with 0.4% Tween 80) only. The body weight of each animal is recorded at the beginning and at the end of the experiment. If the effect on VLDL and triglycerides is the focus of the experiment, animals should be non-fasted or postprandial, and food should be withdrawn for no longer than 4 h before blood sampling. On the morning of the first day, blood samples are taken under light isoflurane or CO_2 anesthesia by retro-orbital puncture. Then, the first dose is applied. During the whole period, the animals have free access to food and water. At the end of the experiment, blood samples are taken by retro-orbital puncture. Immediately thereafter, the animals are sacrificed and the liver removed, blotted free from blood and weighed. Samples of liver are frozen in liquid nitrogen and stored at –25°C for lipid analysis. The blood samples are centrifuged for 2 min at 16,000 *g*. Total cholesterol and triglycerides in each blood sample are determined.

To estimate the serum lipoproteins two methods are available: ultracentrifugation and liquid chromatography. For ultracentrifugation more than 1 ml serum is needed, so the serum has to be group-vice pooled. The serum lipoproteins are separated by means of a preparative ultracentrifuge.

The separation of fractions VLDL, LDL, HDL, and of the subnatant of HDL is carried out as follows:

VLDL	native density of the serum (1.006), 16 h at 40,000 rpm,
LDL	density range from 1.006 to 1.04, 18 h at 40,000 rpm,
HDL	density range from 1.04 to 1.21, 18 h at 40,000 rpm,
Subnatant of HDL	density > 1.21

The density is adjusted by addition of a calculated amount of NaBr solution.

Another faster approach is the separation of lipoprotein by fast protein liquid chromatography (FPLC).

Distribution of cholesterol to lipoprotein fractions is performed after separation of fractions by gel permeation chromatography, using a published method (März et al. 1993). The cholesterol and triglyceride content in the isolated lipoprotein fractions after ultracentrifugation or FPLC separation is determined using standard enzymatic assays for clinical diagnostics

(e. g., Roche-Diagnostics, CHOD-PAP method, Siedel et al. 1983). Triglycerides are also determined with standard enzymatic assays for clinical diagnostic (e. g., Roche Diagnostics, GPO-PAP method; Eggstein and Kreutz 1966a, 1966b; Wahlefeld 1974). The method of Lowry et al. (1951) is applied to determine protein content.

Frozen samples of liver are thawed, homogenized and aliquots are extracted with chloroform/methanol or dichloromethane/methanol 2:1 (v/v). The extracts are purified according to Folch et al. (1957). Solvents of aliquots of the extracts are evaporated and dissolved in isopropanol for determinations of cholesterol and triglycerides, using enzymatic assays for serum diagnostics (Herling et al. 1999).

EVALUATION

Average values of body weight, cholesterol and triglycerides are expressed as percentage of initial values for each group at the end of the experiment. Statistical differences between the controls and the treatment groups are evaluated by covariance analysis.

CRITICAL ASSESSMENT OF THE METHOD

Studies with normocholesterinemic animals are faced with the difficulty that starting cholesterol levels are relatively low, and to achieve significance for lowering of cholesterol levels requires large groups of animals. LDL cholesterol lowering can be investigated in normocholesterolemic hamster, guinea pigs or minpigs, not in mice or rats. Triglyceride-lowering drugs such as fibrates are very effective against serum triglycerides and cholesterol in normolipemic male Sprague Dawley rats.

MODIFICATIONS OF THE METHOD

Similar tests can be performed in various species, e. g.:

- male NMRI mice, weighing 25–30 g, male or female C57/bl6 mice weighing 18–24 g,
- male New Zealand obese (NZO) mice, weighing 35–40 g,
- male Syrian golden hamsters, weighing 80–120 g,
- male Pirbright guinea pigs, weighing 200–250 g,
- male miniature pigs, weighing 14–22 kg.

To study long term effects, the experiments are extended for 4 weeks or 3 months.

Schurr et al. (1976) proposed high volume screening procedures for hypobetalipoproteinemic activity in rats.

März et al. (1993) described fast lipoprotein chromatography as a new method of analysis for plasma lipoproteins.

Adipokinetic actions of several hormones in slices of perirenal adipose tissue of various species were determined by Rudman et al. (1963).

REFERENCES AND FURTHER READING

Allain CC, Poon LS, Chan CSG, Richmond W, Fu PC (1974) Enzymatic determination of total serum cholesterol. Clin Chem 20:470–475

Balasubramaniam S, Simons LA, Chang S, Roach PD, Nestel PJ (1990) On the mechanism by which an ACAT inhibitor (CL 277,082) influences plasma lipoproteins in the rat. Atherosclerosis 82:1–5

Cardin AD, Holdsworth G, Jackson RL (1984) Isolation and characterization of plasma lipoproteins and apolipoproteins. In: Schwartz A (ed) Methods in Pharmacology, Vol 5, Plenum Oress, New York and London, pp 141–166

Dole VP, Meinertz H (1960) Microdetermination of long-chain fatty acids in plasma and tissues. J Biol Chem 235:2595–2599

Eggstein M, Kreutz FH (1966a) Eine neue Bestimmung der Neutralfette im Blutserum und Gewebe. I. Mitteilung. Prinzip, Durchführung und Besprechung der Methode. Klin Wschr 44:262–267

Eggstein M, Kreutz FH (1966b) Eine neue Bestimmung der Neutralfette im Blutserum und Gewebe. II. Mitteilung. Zuverlässigkeit der Methode, andere Neutralfettbestimmungen, Normalwerte für Triglyceride und Gycerin im menschlichen Blut. Klin Wschr 44:267–273

Folch J, Lees M, Sloane Stanley GH (1957) A simple method for the isolation and purification of total lipids from animal tissues. J Biol Chem 226:497–509

Friedewald WT, Levy RI, Fredrickson DS (1972) Estimation of low-density lipoprotein cholesterol in plasma, without use of the preparative centrifuge. Clin Chem 18:499–502

Getz GS (1990) The involvement of lipoproteins in atherogenesis: evolving concepts. In: Lee KT, Onodera K, Tanaka K (eds) Atherosclerosis II: Recent Progress in Atherosclerosis Research. Ann NY Acad Sci 598:17–28

Hatch FT, Lees RS (1968) Practical methods for plasma lipoprotein analysis. In: Paoletti R, Kritchevsky D (eds) Advances in Lipid Research, Vol 6, pp 1–68, Academic Press, New York

Havel RJ, Eder HA, Bragdon JH (1955) The distribution and chemical composition of ultracentrifugally separated lipoproteins in human serum. J Clin Invest 34:1345–1353

Herling AW, Burger HJ, Schubert G, Hemmerle H, Schäfer HL, Kramer W (1999) Alteration of carbohydrate and lipid intermediary metabolism during inhibition of glucose-6-phosphatase in rats. Eur J Pharmacol 386:75–82

Holub WR, Galli FA (1972) Automated direct method for measurement of serum cholesterol, with use of primary standards and a stable reagent. Clin Chem 18:239–243

Keul J, Linnet N, Eschenbruch E (1968) The photometric autotitration of free fatty acids. Z Klin Chem Klin Biochem 6:394–398

Kita T, Yokode M, Ishii K, Arai H, Nagano Y (1990) The role of atherogenic low density lipoproteins (LDL) in the pathogenesis of atherosclerosis. In: Lee KT, Onodera K, Tanaka K (eds) Atherosclerosis II: Recent Progress in Atherosclerosis Research. Ann NY Acad Sci 598:188–193

Koga S, Horwitz DL, Scanu AM (1969) Isolation and properties of lipoproteins from normal rat serum. J Lipid Res 10:577–588

Lopez A, Vial R, Gremillion L, Bell L (1971) Automated simultaneous turbidimetric determination of cholesterol in β- and pre-β-lipoproteins. Clin Chem 17:994–997

Lowry OH, Rosebrough NJ, Farr AL, Randall RJ (1951) Protein measurement with the Folin phenol reagent. J Biol Chem 193:265–275

März W, Siekmeier R, Scharnagl H, Seiffert UB, Gross W (1993) Fast lipoprotein chromatography: a new method of analysis for plasma lipoproteins. Clin Chem 39:2276–2281

Moss JN, Dajani EZ (1971) Antihyperlipidemic agents. In: Turner RA, Hebborn P (eds) Screening Methods in Pharmacology. Vol. II, Academic Press, New York and London, pp 121–143

Rudman D, Brown SJ, Malkin MF (1963) Adipokinetic actions of adrenocorticotropin, thyroid-stimulating hormone, vasopressin, α- and β-melanocyte-stimulating hormones, fraction H, epinephrine and norepinephrine in the rabbit, guinea pig, hamster, rat and dog. Endocrinology 72:527–543

Schurr PE, Schultz JR, Day CE (1976) High volume screening procedures for hypobetalipoproteinemic activity in rats. In: Day CE (ed) Atherosclerosis Drug Discovery, Plenum Press, New York and London, pp 215–229

Siedel J, Hägele EO, Ziegenhorn J, Wahlefeld AW (1983) Reagent for the enzymatic determination of serum total cholesterol with improved lipolytic efficiency. Clin Chem 29:1075–1080

Sperry WM (1956) Lipid analysis. In: Glick D (ed) Methods in biochemical analysis, Vol. II, pp 83–111

Wahlefeld AW (1974) Triglyceride. Bestimmung nach enzymatischer Verseifung. In: Bergmeier HU (ed) Methoden der enzymatischen Analyse, 3. Auflage, Band II, Verlag Chemie, pp 1878–1882

M.2.0.3 Hypolipidemic Activity in Syrian Hamsters

PURPOSE AND RATIONALE

The Syrian hamster (*Mesocricetus auratus*) is a widely used animal to study the effects of drugs and diet on lipoprotein metabolism. Several in human approved lipid lowering drug like HMG-Co A reductase inhibitors, cholestyramine or ezetimibe lower plasma cholesterol in hamster. The lipoprotein and bile acid metabolism of the hamster is closer to human than the lipoprotein and bile acid metabolism of rats and mice (Bravo et al. 1994; Suckling et al. 1991; Kris-Etheron and Dietschy 1997). The hamster has in contrast to pig, rat and mouse CETP (Cholesteryl Ester Transfer Protein) activity, similarly as seen in humans (Ha and Barter 1982, 1986; Ahn et al. 1994).

Increase in plasma cholesterol can be easily induced by adding small, physiological amounts of cholesterol to the diet (0.05–0.01 weight%). Additional saturated fat like coconut oil (5–10 weight%) has synergistic effects for induction of hyperlipidemia. (Kowala et al. 1991) A stable hyperlipidemia with a human like lipoprotein pattern can be induced in hamster within 2–3 weeks by adding 10 weight% coconut butter and 0.2% cholesterol into the diet. Hamster HDL cholesterol can be easily measured after precipitation of VLDL+LDL cholesterol with phoshotungstic acid/$MgCl_2$ (Weingand and Daggy 1990, 1991). LDL and HDL cholesterol can also be measured directly with Kits from Roche Diagnostics. A complete separation of all lipoprotein fractions can be done by FPLC on Superose 6 columns (Pharmacia) with a modified method of März et al. (1993).

PROCEDURE

Male Syrian hamsters weighing 95–125 g at the start of the experiment are randomly assigned to form groups of 6–15 animals each. Test compounds can be administrated by oral gavage, once or twice daily or mixed into the diet. If compounds are administered with diet, a different diet has to be prepared for each group. One control receives powdered or pellet standard hamster chow only; a second control and the treated groups, a cholesterol-enriched diet. If compounds are administered with diet a daily food consumption of 8 g should be taken in account for dose calculation. Cholestyramine, for example, is active when mixed into the diet in a concentration range between 0.3% to 2%. After 1–3 weeks on these diets, the animals are anesthetized with isoflurane, a blood sample is taken from the retroorbital vene plexus, the superior vena cava or the abdominal aorta, and the liver is removed and weighed. Microsomes are prepared by ultracentrifugation from the livers.

Preparation of Plasma Lipoprotein Profiles

The blood is centrifuged at 6000 *g* for 5 min and the plasma removed. The plasma is analyzed for total cholesterol and triglycerides using colorimetric enzymatic assays for clinical diagnostics, as described in the previous chapter for rats (e. g., Roche Diagnostics). The cholesterol content of HDL and LDL was determined using enzymatic assays for clinical diagnostics (Roche Diagnostics, HDL-C plus and LDL-C plus).

Quantification of High-Density-Lipoprotein Cholesterol by Differential Precipitation

Weingand and Daggy (1990) compared the validity of differential precipitation with Mg^{2+}-phosphotungstate for quantification of plasma high-density-lipoprotein cholesterol with ultracentrifugal flotation.

As precipitating agent, 0.55 mmol/l phoshotungstic acid and 25 mmol/l magnesium chloride is added. Cholesterol is determined spectrophotometrically with an

enzymatic cholesterol reagent containing microbial cholesterol esterase, in a Hitachi 705 clinical chemistry analyzer.

Fast Lipoprotein Chromatography

März et al. (1989, 1993) developed fast lipoprotein chromatography for rapid and quantitative analysis of lipoprotein fractions.

Fast lipoprotein chromatography is carried out with a chromatography system from Kontron consisting of two Model 420 pumps, a Model 432 variable-wavelength detector, and a Model 450 data system. Without using a pretreatment, 20 µl of plasma are applied to a 300-mm Superose column 6 equilibrated with 100 mmol/l Na_2HPO_4, pH 7.4, and 200 mmol/l NaCl. Lipoproteins are detected on-line at 500 nm after post-column derivatization with CHOD-PAP cholesterol reagent (Roche Diagnostics, Mannheim, Germany). The column eluate and the cholesterol reagent are mixed in a motor-driven microchamber attached to the column outlet, and the mixture is then passed through a "knitted" capillary (20–22). The flow rate of the reagent is 70 µl/min; the run time is 80 min. Under these conditions, it takes the column eluate 2 min to pass the derivatization capillary. VLDL-C, LDL-C and HDL-C are calculated on the basis of relative peak areas and total cholesterol, previously measured with an enzymatic assay in serum as described above.

Tissue Preparation

The liver is homogenized in a KCl (0.104 M) solution containing NaF (50 mM) using a glass Teflon homogenizer. The homogenate is centrifuged at 30,000 *g*, 5°C for 25 min. The supernatant is then centrifuged at 100,000 *g*, 5°C for 60 min to pellet the microsomes, which are resuspended in potassium phosphate buffer (50 mM) containing NaF (50 mM) adjusted to pH 7.4.

Determination of Enzyme Activities in Microsomal Fractions

Protein for all the following assays is determined using the method described by Bradford (1976).

HMG-CoA reductase activity is determined by quantifying the conversion of [^{14}C]HMG-CoA to [^{14}C]mevalonic acid lactone, based on the method described by Ingebritsen and Gibson (1981). ACAT activity in liver microsomes and intestinal cell homogenates is determined by the method described by Suckling et al. (1982), measuring the incorporation of [^{14}C]oleoyl-CoA into cholesteryl oleate. The cholesterol 7α-hydroxylase activity in the microsomes is quantified by determination of the percentage conversion of [^{14}C]cholesterol to 7α-hydroxy[^{14}C]cholesterol. 3 mg of microsomal protein is diluted to a volume of 5.3 ml with a potassium phosphate buffer (50 mM, pH 7.4) containing NaF (50 mM), cysteamine (31.4 mM), glucose-6-phosphate (12.7 mM) NADP (1.4 mM) and [^{14}C]cholesterol (0.22 µCi, 55 Ci/mol). After a short pre-incubation (5 min at 37°C), the reaction is started by the addition of glucose-6-phosphate dehydrogenase suspension (7 µg). The reaction is stopped 1 h later by adding methanol (5 ml). The cholesterol and 7α-hydroxy-cholesterol are extracted into a mixture of chloroform and methanol (2:1, v/v, 2 × 5 ml). The product and substrate are separated by thin-layer chromatography on silica gel eluting with toluene/ethyl acetate (3:7, v/v). The radioactive regions corresponding to cholesterol and 7α-hydroxy-cholesterol are scraped off the plates and quantified by liquid scintillation counting. An alternative non-radioactive method to determine 7α-hydroxylase activity is described in detail in Sect. M.2.0.8.

EVALUATION

Dose–response curves for standard and test drug are established using the serum LDL cholesterol value of the standard chow fed as the maximal effect and the cholesterol control data as zero.

CRITICAL ASSESSMENT OF THE METHOD

Potent drugs acting on cholesterol or bile acid absorption lower serum LDL cholesterol below the level measured in animals on standard chow. PPARα agonists (fibrates) increase liver triglycerides in hamsters on a normal or high-fat diet (Planke et al. 1988). HMG-CoA reductase inhibitors (statins) are not well tolerated, the therapeutic range of statins which is effective against LDL cholesterol is very narrow, and the animals have to been treated for longer than 3 weeks to see the maximal effects of statins on serum LDL cholesterol.

REFERENCES AND FURTHER READING

Ahn YS, Smith D, Osada J, Li Z, Schaefer EJ, Ordovas M (1994) Dietary fat saturation affects apolipoprotein gene expression and high density lipoprotein size distribution in golden Syrian hamsters. J Nutr 124:2147–2155

Bradford MM (1976) A rapid and sensitive method for the quantitation of microgram quantities of protein utilizing the principle of protein-dye binding. Anal Biochem 72:248

Bravo E, Cantafora A, Calcobrini A, Ortu G (1994) Why prefer the golden Syrian hamster (Mesocricetus auratus) to

the Wistar rats in experimental studies on plasma lipoprotein metabolism. Comp Biochim Physiol Vol. 107B: pp 347–355
Ingebritson GS, Gibson MD (1981) Assay of enzymes that modulate *S*-3-hydroxy-3-methylglutaryl coenzyme A reductase by reversible phosphorylation. Meth Enzymol 71:486
März W, Scharnagel H, Siekmeier R, Träger L, Gross W (1989) Fast lipoprotein chromatography (FPLC) of plasma lipoproteins. J Clin Chem Clin Biochem 27:719
März W, Siekmeier R, Scharnagel H, Seiffert UB, Gross W (1993) Fast lipoprotein chromatography: new method of analysis for plasma lipoproteins. Clin Chem 39:2276–2281
Ha Y-C, Barter PJ (1982) Differences in plasma cholesteryl ester transfer activity in sixteen vertebrate species. Comp Biochem Physiol Vol 71B:265–269
Ha Y-C, Barter PJ (1986) Effects of sucrose feeding and injection of lipid transfer protein on rat plasma lipoproteins. Comp Biochem Physiol B 83:463–466
Kowala MC, Nunnari JJ, Durham SK, Nicolosi RJ (1991) Doxazin and cholestyramine similarly decrease fatty streak formation in the aortic arch of hyperlipidemic hamsters. Atherosclerosis 91:35–49
Kris-Etheron PM, Dietschy J (1997) Design criteria for studies examining individual fatty acid effects on cardiovascular diseases risk factors: human and animal studies. Am J Clin Nutr 65 Suppl:1590S–1596S
Planke MO, Olivier P, Clavey V, Marzin D, Fruchart JC (1988) Aspects of cholesterol metabolism in normal and hypercholesterolemic Syrian hamster. Methods Find Exp Clin Pharmacol 10:575–579
Suckling KE, Boyd GS, Smellie CG (1982) Properties of a solubilised and reconstituted preparation of acyl-CoA:cholesterol acyltransferase from rat liver. Biochem Biophys Acta 710:154
Suckling KE, Benson GM, Bond B, Gee A, Glen A, Haynes C, Jackson B (1991) Cholesterol lowering and bile acid excretion in the hamster with cholestyramine treatment. Atherosclerosis 89:183–190
Weingand KW, Daggy BP (1990) Quantification of high-density-lipoprotein cholesterol in plasma from hamsters by differential precipitation. Clin Chem 36:575–576
Weingand KW, Daggy BP (1991) Effects of dietary cholesterol and fasting on hamster lipoprotein lipids. Eur J Clin Chem Clin Biochem 29:425–428

M.2.0.4 Triton-Induced Hyperlipidemia

PURPOSE AND RATIONALE

The systemic administration of the surfactant Triton to mice or rats results in a biphasic elevation of plasma cholesterol and triglycerides. Triton inhibits lipoprotein lipase (LPL) activity and so VLDL particle clearance (Frantz and Hinkelman 1955; Garattini et al. 1958, 1961; Holmes 1964; Tamasi et al. 1968; Millar et al. 2005).

PROCEDURE

Male Sprague Dawley or Wistar rats weighing 200–350 g were starved for 18 h and then injected intravenously with 200 mg/kg Triton WR 1339 (isooctyl-polyoxy-ethylene phenol). Serum triglycerides increased 20-fold in a nearly linear fashion within 1 and 8 h and serum cholesterol levels increased sharply 2–3 times within 24 h (phase I). The hypercholesterolemia decreased nearly to control levels within the next 24 h (phase II). The test drugs employed or the vehicle for the controls were administered simultaneously with the Triton injection if only the acute effect of a drug was investigated or ad 1–3 days before. Serum triglyceride cholesterol analyses were carried out 0, 2, 4, 6, and 8 h after Triton injection in order to investigate drugs that interfere with triglyceride synthesis; and 0, 6, 24, and 48 h after Triton injection for investigation of drugs that are effective against cholesterol synthesis. In 1951 it was described by Kellner et al. that intravenous injection of nonionic detergents increased serum lipids up to 48 h. Later it was shown by Schotz et al. (1957) that the hyperlipidemia is induced by inhibition of triglyceride hydrolysis by lipoprotein lipase. Since then, lipolysis inhibition has been used to determine hepatic VLDL secretion rates. The VLDL secretion rate can be calculated from the increase in triglyceride and cholesterol over time after the Triton injection. Drugs interfering with hepatic triglyceride and cholesterol biosynthesis were shown to be active in phase I, while drugs interfering with cholesterol clearance, excretion and metabolism were active in phase II.

EVALUATION

Mean values ± standard deviation are calculated for each group and time interval and compared statistically with the controls.

CRITICAL ASSESSMENT OF THE METHOD

The method employing Triton hypercholesterolemia is rather simple and rapid for detection of compounds interfering with the synthesis of triglycerides or synthesis and excretion of cholesterol. Since the test is rather artificial, the results have to be validated by other methods, e. g., *ex vivo* measurement of liver cholesterol synthesis.

REFERENCES AND FURTHER READING

Frantz ID, Hinkelman BT (1955) Acceleration of hepatic cholesterol synthesis by Triton WR-1339. J Exper Med 101:225–232
Garattini S, Paoletti P, Paoletti R (1958) The effect of diphenylethylacetic acid on cholesterol and fatty acid biosynthesis. Arch Int Pharmacodyn 117:114–122
Garattini S, Paoletti R, Bizzi L, Grossi E, Vertua R (1961) A comparative evaluation of hypocholesteremizing drugs on several tests. In: Garattini S, Paoletti R (eds) Drugs

affecting lipid metabolism. Elsevier Publ Comp., Amsterdam, pp 144–157
Holmes WL (1964) Drugs affecting lipid synthesis. In: Paoletti R (ed) Lipid Pharmacology, Academic Press, New York, London, chapter 3, pp 131–184
Keller AJ, Correll JW, Ladd AT (1951) Sustained hyperlipemia induced in rabbits by means of intravenous injected surface-active agents. J Exp Med 93:373–384
Millar JS, Cromley DA, McCoy MG, Rader DJ, Billheimer JT (2005) Determining hepatic triglyceride production in mice: comparison of poloxamer 407 with Triton WR-1339. J Lipid Res 46:2032–2028
Moss JN, Dajani EZ (1971) Antihyperlipidemic agents. In: Turner RA, Hebborn P (eds) Screening Methods in Pharmacology. Vol. II, Academic Press, New York and London, pp 121–143
Schotz MC, Scanu A, Page IH (1957) Effect of Triton on lipoprotein lipase of rat plasma. Am J Physiol 188:399–402
Tamasi G, Borsy J, Patthy A (1968) Comparison of the antilipemic effect of nicotinic acid (NA) and 4-methylpyrazole-5-carboxylic acid (MPC) in rats. Biochem Pharmacol 17:1789–1794
Tubbs PK, Garland PB (1969) Assay of coenzyme A and some acyl derivatives. Meth Enzymol 13:535–551

M.2.0.5 Fructose-Induced Hypertriglyceridemia in Rats

PURPOSE AND RATIONALE

Rats switched from a diet low in carbohydrates and high in protein to a high intake of fructose, develop an acute hypertriglyceridemia. Compounds are tested for inhibition of this phenomenon.

PROCEDURE

Male Sprague Dawley rats weighing 200–250 g were fed over a period of 1 week a diet enriched in protein with reduced carbohydrate content, e. g., Altromin C1080 or C1009. Groups of ten animals were treated for 3 days daily with the test compound or the standard (fenofibrate 30–100 mg/kg) or the vehicle (0–5% hydroxyl-ethyl-cellulose) by oral gavage. From the second to the third day water was withheld for a period of 24 h. Immediately afterwards, the animals were offered 20% fructose solution ad libitum for a period of 20 h. After this time, which was also 20 h after the last application of the test compound, the animals were anesthetized with isoflurane or CO_2/O_2 (70/30 v/v) and 1.2 ml blood was withdrawn by retro-orbital puncture. The blood was centrifuged at 6000 *g* for 5 min and the serum removed. The serum was analyzed for total cholesterol and triglycerides and glycerol using a colorimetric enzymatic assay for clinical diagnostics, as described in the previous chapter for rats (e. g. Roche Diagnostics).

EVALUATION

The average values of total glycerol for the treated groups are compared with those for the control group using ANOVA.

REFERENCES AND FURTHER READING

Eggstein M, Kreutz FH (1966a) Eine neue Bestimmung der Neutralfette im Blutserum und Gewebe. I. Mitteilung. Prinzip, Durchführung und Besprechung der Methode. Klin Wschr. 44:262–267
Eggstein M, Kreutz FH (1966b) Eine neue Bestimmung der Neutralfette im Blutserum und Gewebe. II. Mitteilung. Zuverlässigkeit der Methode, andere Neutralfettbestimmungen, Normalwerte für Triglyceride und Glycerin im menschlichen Blut. Klin Wschr 44:267–273
Moss JN, Dajani EZ (1971) Antihyperlipidemic agents. In: Turner RA, Hebborn P (eds) Screening Methods in Pharmacology. Vol. II, Academic Press, New York and London, pp 121–143
Richterich R, Lauber K (1962) Bestimmung des Gesamt-Cholesterins im Serum. VIII. Mitteilung über Ultramikromethoden im klinischen Laboratorium. Klin Wschr 40:1252–1256

M.2.0.6 Intravenous Lipid Tolerance Test in Rats

PURPOSE AND RATIONALE

Intravenous injection of a lipid emulsion results in an increase of triglycerides in serum. The lipolytic activity can be determined by measuring lipid elimination.

PROCEDURE

Male Wistar rats weighing 200–240 g are treated daily with various doses of the test compound or the vehicle over a period of 5 days. On the fifth day, two hours after the last administration of the test compound, the animals are anesthetized with isoflurane or 40–60 mg/kg sodium pentobarbital i.p. Then they are injected intravenously with 2 ml/kg of a 10% lipid emulsion (Intralipid Vitrum, Hausmann AG, St. Gallen, Switzerland). Prior to the injection and 10, 20, 30, and 40 min thereafter blood is withdrawn by retro-orbital puncture for determination of triglycerides.

EVALUATION

Peak levels as well as elimination constant and half life are determined.

REFERENCES AND FURTHER READING

Carlson LA, Rössner S (1972) A methodological study of an intravenous fat tolerance test with Intralipid emulsion. Scand J Clin Lab Invest 29:271–280
D'Costa MA, Smigura FC, Kulhay K, Angel A (1977) Effects of clofibrate on lipid synthesis, storage, and plasma intralipid clearance. J Lab Clin Med 90:823–836

M.2.0.7 Influence on Lipoprotein-Lipase Activity

PURPOSE AND RATIONALE

Post-heparin plasma lipolytic activity is measured by at least two lipase activities: hepatic lipase (HL) and lipoprotein lipase (LPL). Hypothyroid rats show a selective decline of post-heparin plasma hepatic lipase (Murase and Uchimura 1980).

For patients with familial lipoprotein lipase deficiency a rapid diagnostic test was developed (Gotoda et al. 1991). The method was used to study the influence of drugs on lipoprotein lipase activity (Tsusumi et al. 1993).

PROCEDURE

Male Wistar rats weighing 180–200 g receive either various single doses or one daily dose of test compounds over a period of several days. Blood samples are drawn from the tail vein into tubes containing 1 mg EDTA/ml. The animals are then injected with 100 U/kg heparin via the tail vein and blood samples are collected 5 min later. Plasma samples are used to determine lipoprotein lipase and hepatic lipase activity.

Lipoprotein lipase activity in postheparin plasma is measured using glycerol tri[1-^{14}C]oleate as substrate and selective blocking of hepatic lipase activity with antiserum to rat hepatic lipase. Hepatic triglyceride lipase activity in postheparin plasma is obtained by subtracting lipoprotein lipase activity from total plasma lipase activity.

EVALUATION

The dose-related increase of plasma lipoprotein lipase activity and the time course after drug administration are evaluated.

REFERENCES AND FURTHER READING

Gotoda T, Yamada N, Kawamura M, Kozaki K, Mori N, Ishibashi S, Shimano H, Takaku F, Yazaki Y, Furuichi Y, Murase T (1991) Heterogeneous mutations in the human lipoprotein lipase gene in patients with familial lipoprotein lipase deficiency. J Clin Invest 88:1856–1864

Murase T, Uchimura H (1980) A selective decline of postheparin plasma hepatic triglyceride lipase in hypothyroid rats. Metabolism 29:797–801

Nilsson-Ehle P, Schotz MC (1976) A stable, radioactive substrate emulsion for assay of lipoprotein lipase. J Lipid Res 17:536–541

Tsusumi K, Inoue Y, Shima A, Iwasaki K, Kawamura M, Murase T (1993) The novel compound NO-1886 increases lipoprotein lipase activity with resulting elevation of high density lipoprotein cholesterol, and long term administration inhibits atherogenesis in the coronary arteries of rats with experimental atherosclerosis. J Clin Invest 92:411–417

M.2.0.8 Influence on Several Steps of Cholesterol Absorption and Formation

PURPOSE AND RATIONALE

Cholesterol levels in the body result from two sources: absorption from the gut and endogenous *de novo* synthesis. Certain natural products and the azetidinone drug ezetimibe inhibit cholesterol absorption and reduce plasma cholesterol levels in experimental animals and are therefore of potential pharmacologic interest in the treatment of hypercholesterolemia. In rodents cholesterol absorption can be decreased by inhibition of acyl coenzyme A:cholesterol acyltransferase (ACAT). In humans ACAT-inhibitors are not effective. Inhibition of cholesterol resorption results in a compensatory increase of hepatic 3-hydroxy-3-methylglutaryl-coenzyme A (HMG-CoA) reductase activity, which can be decreased by (HMG-CoA) reductase inhibitors (statins). The hepatic cholesterol biosynthesis can be measured with several radioactive tracers as described later in Sect. M.3, by conversion of radioactive precursors into cholesterol. In addition to serum LDL cholesterol, hepatic cholesterol biosynthesis is a biomarker for the *in vivo* efficacy of cholesterol absorption inhibitors. Harwood et al. (1993) and van Hek and Davis (2002) studied the pharmacologic consequences of cholesterol absorption inhibition: alteration in cholesterol metabolism and reduction in plasma cholesterol concentration induced by a synthetic saponin β-tigogenin cellobioside or ezetimibe.

PROCEDURE

Male golden Syrian hamsters, weighing 100–120 g, are housed in a reversed light-dark cycle room (light between 3:00 P.M. and 3:00 A.M.) and receive a cholesterol-poor or cholesterol-enriched diet and water ad libitum 1 week prior to use. The animals are assigned to groups of 6 animals each and are given free access to water and chow that contains the compounds to be tested in appropriate concentrations for 4 days. At 9:00 A.M. of the fourth day of the study, the animals receive a 1.0-ml oral bolus of liquid formulation of cholesterol and radiolabeled cholesterol dissolved in Intralipidcontaining 15 mg of [^{3}H]cholesterol (2.25 μCi) and 7.5 mg cholic acid for determining cholesterol absorption. At 9:00 A.M. of the fifth day (peak of the diurnal cycles of HMG-CoA reductase and cholesterol 7α-hydroxylase activities) animals are anesthetized with pentobarbital and blood samples are obtained by cardiac puncture for deter-

mining plasma cholesterol and triglyceride levels, and cholesterol absorption.

Livers are removed, weighed, rinsed in 4°C saline, and apportioned for determining hepatic cholesterol levels, hepatic HMG-CoA reductase, cholesterol 7α-hydroxylase activities, hepatic LDL receptor concentration, and cholesterol absorption.

For determination of total hepatic cholesterol, one aliquot of the liver tissue (0.5 g) is saponified in 5 ml ethanolic KOH, 3.3% (v/v) at 65°C for 1 h. After addition of 5 ml water and 2 mg 5-cholestene (internal standard), lipids are extracted with 15 ml petroleum ether. Samples are shaken several times to extract the sterols into the petroleum ether phase. Then 100 µl of the petroleum ether phase (upper phase) is transferred into an HPLC autosampler vial and the solvent is removed by air-stream. For final HPLC analysis, the samples are mixed with an equal volume of HPLC eluent. The total cholesterol content is detected at 210 nm after isocratic HPLC separation on an RP C18 column (Merck Lichrospher 100, 250 × 4 mm, 5 µm) with 2-propanol-acetonitrile (55:45 v/v) as eluent solution (0.8 ml/min) using 5-cholestene as an internal standard.

Alternatively, hepatic cholesterol concentration can also be measured with a colorimetric enzymatic assay. Frozen samples of liver are thawed, homogenized and aliquots are extracted with chloroform/methanol and analyzed as described earlier in Sect. M.2.0.2 (Herling et al. 1999).

Hepatic microsomes for measurement of hepatic HMG-CoA reductase activity and cholesterol 7α-hydroxylase activity are prepared according to Harwood et al. (1984) and Junker and Story (1985). For measurement of HMG-CoA reductase activity, 0.5 g liver are immediately homogenized at 4°C in 1 ml TEDK buffer (containing 50 mM Tris (pH 7.5), 1 mM EDTA, 5.0 mM dithiothreitol, and 70 mM KCl) using 15 strikes in a Dounce homogenizer. For measurement of cholesterol 7α-hydroxylase activity, 0.5 g liver pieces are immediately homogenized at 4°C in 1 ml PEDSKF buffer (containing 40 mM phosphate (pH 7.4), 5 mM EDTA, 5 mM DTT, 250 mM sucrose, 50 mM KCl, and 50 mM KF) using 20 strokes of a Dounce homogenizer. Homogenates are first centrifuged at 4°C for 20 min at 10,000 *g* and the resultant supernatant is then centrifuged at 4°C for 90 min at 178,000 *g*. The resulting microsomal pellets are resuspended in either 1.0 ml TEDK per g liver (HMG-CoA reductase determination) or 1 ml PEDSKF per g liver (cholesterol 7α-hydroxylase determination) by 5 strokes of a Potter-Elvehjem pestle and are stored frozen in liquid nitrogen.

For measurement of hepaticHMG-CoA reductase activity, 50 µg of microsomal protein is incubated for 30 min at 37°C in a final volume of 75 µl of TEDK buffer containing 3.4 mM $NADP^+$, 30 mM glucose-6-phosphate, 66.7 µM [^{14}C]HMG-CoA (10 cpm/pmol), 15000–20,000 cpm [^{3}H]mevalonate (0.6–1.2 Ci/mmol) as an internal standard, and 68 mM EDTA to prevent conversion of mevalonate to phosphomevalonate during incubation. After incubation, 10 µl of 6 M HCl are added to terminate the enzyme reaction and to convert the newly formed mevalonate to mevalonolactone. The mevalonolactone is then separated from unreacted substrate by silica gel thin-layer chromatography. After development in toluene-acetone 1:1, the region of the chromatogram corresponding to $R_f = 0.4–1.0$ is removed, immersed in liquid scintillation fluid, and counted using a dual channel $^3H/^{14}C$ program. HMG-CoA reductase activity is expressed as pmoles of mevalonate formed from HMG-CoA per min of incubation at 37°C per mg of microsomal protein.

Cholesterol 7 α-hydroxylase activity was determined with a modified method according to the procedure of Hylemon (1989) with the following modifications. To measure 7α-hydroxylase activity, 2 mg microsomal protein (1 ml in assay buffer) is pre-incubated for 10 min at 37°C with 20 µl cholesterol solution (1 mg/ml) in 45% hydroxypropyl-ß-cyclodextrin (ICN) in order to saturate the enzyme with cholesterol substrate. 7α-Hydroxycholesterol is measured with isocratic HPLC analysis on a C-18 reversed-phase column (Merck 250 × 4 mm, 5 µm), at 240 nm with acetonitrile:methanol (70:30 v/v) as eluent (0.7 ml/min) using 7ß-hydroxycholesterol as internal standard. The protein content of the microsomes is measured by the BCA method (Pierce).

Cholesterol 7α-hydroxylase activity is expressed as pmoles of 7α-hydroxycholesterol formed from cholesterol per minute of incubation per milligram of microsomal protein.

Hepatic *in vivo* cholesterol biosynthesis is determined with a method according to Dietschy and Spady (1984). [^{14}C]Octanoic acid sodium salt (NEC 092H, concentration 0.1 mCi/ml in ethanol, NEN, Cologne, Germany) is used as tracer. The metabolism of the tracer into liver cholesterol is investigated using the following procedure. The solution is concentrated about 20-fold under a nitrogen stream and dissolved in 0.9% NaCl to a final concentration of 50 µCi/ml. This

solution is injected into the femoral vein at a dose of 10 µCi/100 g body weight under ether anesthesia.

The animals are killed 1 h after administration and the liver removed and washed in isotonic NaCl solution. Three aliquots (0.5 g) are extracted in 30 ml of 6.6% ethanolic KOH at 65°C for 2 h. After cooling down to room temperature, 5 ml aqua is added and the cholesterol is extracted twice with 15 ml petroleum ether into a volumetric flask. The petroleum ether is removed under an air stream. The lipid phase is resolved and transferred three times with 2 ml ethanol acetone 1:1 (v/v) into a 15-ml glass vial after heating the glass container used. The cholesterol is precipitated with digitonin after adding one drop of 1M HCl, 2 ml 10% aqueous aluminum chloride, 3 ml 0.5% digitonin in ethanol water 1:1 (v/v), and incubated for 1 h at 45°C in a water bath. The liquid phase is discarded after centrifugation. The pellet is washed with 5 ml acetone three times and once with ether. Each pellet is rolled out by hand on a table until completely dry.

To cleave the digitonin–cholesterol complex, the vials are heated to 80°C and the cholesterol resolved with 0.6 ml pyridine. When the samples are cooled to room temperature, 5 ml ether is added twice, the samples are centrifuged, and the liquid phase is transferred into scintillation vials. The ether is removed under air stream, and the residual cholesterol resolved with 1 ml methanol and 10 ml scintillation cocktail (Ecolite ICN, Eschwege, Germany).

The radioactivity is counted in a ß-scintillation counter. The disintegrations per minute (DPM) are calculated per gram of liver tissue after background correction and correlated with the liver cholesterol concentration in a graph plotting liver cholesterol on the *x*-axis and radioactivity (dpm/g liver tissue) on the *y*-axis. Orientation of treated groups relative to cholesterol-fed and non-cholesterol-fed control animals gives information about sterol turnover.

Hepatic LDL receptor levels are measured by enzyme immune blotting (Cosgrove et al. 1992). One hundred –150 µl of the soluble extracts containing 100–600 µg protein are adjusted to 2% SDS and 0.2 M sucrose by addition of 0.33 volumes of electrophoresis sample buffer (containing 320 mM Tris (pH 6.8), 8% SDS, and 0.8 M sucrose). Mixtures are applied without heating and without addition of β-mercaptoethanol to 6-mm wells of a 7.5% (w/w) 0.1% SDS-containing polyacrylamide slab gel of 1.5 mm thickness. Electrophoresis is conducted at room temperature with a constant current of 15 mA/gel. Prestained molecular weight markers are included in a separate lane to monitor separation. After electrophoresis, proteins migrating into the gel are electrophoretically transferred to S&S BA85 nitrocellulose membranes at 18°C with a constant voltage of 120 V for 6–8 h in 25 mM Tris, 192 mM glycine buffer (pH 8.3), containing 20% methanol.

After transfer, the nitrocellulose paper is incubated with 100 ml of Tris buffered saline containing 3% gelatin for 30 min at room temperature with gentle shaking. After incubation, the nitrocellulose sheet is removed from the blocking solutions, immersed without rinsing into 50 ml Tris buffer solution (TBS) containing 1% gelatin and 250 µl of anti-LDL receptor peptide antiserum (final dilution 1:200) and incubated for 2 h at room temperature with gentle shaking. The nitrocellulose sheet is washed twice for 10 min each with TBS containing 0.05% Tween-20 and once for 10 min with TBS. The washed nitrocellulose sheet is incubated with 50 ml TBS containing 1% gelatin and 100 µl of goat anti-rabbit IgG-horseradish conjugate (final dilution 1:500) at room temperature for 1 h with gentle shaking. After incubation, the nitrocellulose is washed again as described above. During this final wash, 40 mg of 4-chloro-1-naphthol is dissolved in 10 ml methanol, and 50 µl cold 30% hydrogen peroxide is added to 50 ml TBS containing 1% gelatin. After draining the final TBS wash from the nitrocellulose, the two solutions are mixed and immediately added to the nitrocellulose. The mixture is incubated at room temperature with gentle shaking until the desired color development is observed. The nitrocellulose sheet is washed with running tap water for 15 min. The nitrocellulose is dried between pieces of filter paper and the intensity of color formation is quantitated by reflectance densitometry using a suitable instrument (e. g., Hoefer Scientific Instruments GS300 Transmittance/Reflectance Scanning Densitometer). Color intensity, which is a linear function of the number of LDL receptors in the analyzed fraction, is expressed in terms of mm peak height (arbitrary reflectance units).

Intestinal cholesterol absorption is estimated with the dual isotope feces ratio method using [^{3}H]sitostanol and [^{14}C]cholesterol. Each hamster received an intragastric dose of a mixture of [^{3}H]sitostanol and [^{14}C]cholesterol dissolved in Intralipid or plant oil, or in detergent mix (Tricaprin/Tricapril). The feces is collected for 48 h after dosing and homogenized with water; aliquots are oxidized in a sample oxidizer, which traps CO_2 and H_2O in separate vials mixed with liquid scintillation fluid, and counted using a background correction program. The absorption ratio can be calculated by changes of the $^{14}C/^3H$ ratio in application solution and feces with

the following formula ($^{14}C/^{3}H$ application solution – $^{14}C/^{3}H$ feces)/ $^{14}C/^{3}H$ application solution.

If a sample oxidizer is not available an alternative method is the recovery of radioactivity present in the liver and plasma 24 h after an oral bolus of [^{3}H]cholesterol. For assessment of hepatic radioactivity, 1.0-g liver pieces are placed in 50-ml polypropylene tubes and incubated with 2.5 ml of 2.5 M KOH for 2 h at 75°C. After allowing the saponification mixture to cool to room temperature, 5.0 ml of 80% ethanol, 0.1 ml [^{14}C]cholesterol (40,000 dpm, 15 dpm/nmol) as carrier and extraction standard and 10 ml of hexane are added. Tubes are capped and shaken vigorously for 1 min. Mixtures are permitted to stand to allow phase separation, and are shaken vigorously for an additional minute. Mixtures are the centrifuged at 1000 *g* for 5 min. Duplicate 3.0-ml aliquots of each hexane layer are removed, transferred to 20-ml liquid scintillation vials, mixed with 10 ml liquid scintillation fluid, and counted using a dual channel $^{3}H/^{14}C$ program.

After correction for recovery losses, hepatic radioactivity is calculated based on total liver weights. For assessment of total plasma radioactivity, 200-µl aliquots of plasma are added to 20-ml liquid scintillation vials and decolorized by addition of 25 µl of hydrogen peroxide. Then 10 ml aqueous scintillation fluid is added and the mixture assessed for radioactivity. Total radioactivity in the plasma is calculated based on the assumption that hamsters possess approximately 4.0 ml plasma per 100 g body weight. The degree of cholesterol absorption is expressed as a percentage of the total radioactivity administered that is present in the liver plus plasma 24 h after bolus administration.

For **determination of bile acids in feces**, pooled feces from each group of animals is collected over a period of 48 h (about 20 g). After addition of 9 ml ethanol, 1 ml water and hyodeoxycholate (internal standard) the mixture is continuously shaken at 90°C overnight. Samples are centrifuged and an aliquot of the liquid phase is diluted 1:5 with methanol for quantification of bile acids. Individual bile acids (deoxycholate; lithocholate; 12-oxo lithocholate) are separated and quantified by HPLC-MS (HPLC: RP C18 column Merck Purospher™, end-capped, 5 µm, 125 × 3 mm; gradient elution (20%–60% eluent B, 15 min, 0.6 ml/min; eluent A: 90% H_2O, 10% acetonitrile; eluent B: 10% H_2O, 90% acetonitrile, buffered at pH 8 with 20 mM ammonium acetate; MS detection: electrospray negative mode Hewlett Packard, 1100 MSD).

For **lipid and lipoprotein determinations**, serum or plasma can be used. Blood samples are treated either with EDTA or heparin to prevent clotting or without an anticoagulant and are then centrifuged, as described earlier in Sects. M.2.0.2 and M.2.0.3.

EVALUATION

Inhibition of cholesterol resorption results in a decrease of hepatic cholesterol and a compensatory increase of hepatic HMG-CoA reductase activity resulting from de novo cholesterol synthesis and an increase of hepatic LDL receptor levels.

MODIFICATIONS OF THE METHOD

Ogishima and Okuda (1986) described an improved method for assay of cholesterol 7α-hydroylase activity. Cholesterol 7α-hydroxylation is performed in liver microsomes utilizing cholesterol as substrate. 7α-Hydroycholesterol is converted by the action of cholesterol oxidase into 7α-hydro-4-cholesten-3-one having an intense absorption at 240 nm.

Hylemon et al. (1989) reported a modified HPLC-spectrophotometric method for measuring cholesterol 7α-hydroxylase activity by using a C-18 reverse-phase column to separate 7α-hydroxy-4-cholesten-3-one and 4-cholestene-3-one and by adding 7β-hydroxycholesterol to each reaction mixture as an internal recovery standard. This method measures simultaneously cholesterol 7α-hydroxylase activity using endogenous cholesterol and exogenous [4-^{14}C]cholesterol as substrate.

Princen and Meijer (1990) measured cholesterol 7α-hydroxylase activity in cultured rat hepatocytes.

REFERENCES AND FURTHER READING

Assmann G, Shriewer H, Schmitz G, Hägele EO (1983) Quantification of high-density-lipoprotein cholesterol by precipitation with phosphotungstic acid/$MgCl_2$. Clin Chem 29:2026–2030

Bernini F, Corsini A, Fumagalli R, Paoletti R (1994) Pharmacology of lipoprotein receptors. J Lipid Mediat Cell Signal 9:9–17

Cosgrove PG, Gaynor BJ, Harwood HJ (1992) Quantitation of hepatic low density lipoprotein receptor levels in the hamster. FASEB J 4:A533

Dietschy JM, Spady DK (1984) Measurement of rates of cholesterol synthesis using tritiated water. J Lipid Res; 25:1469–1476

Harwood HJ, Schneider M, Stacpoole PW (1984) Measurement of human leukocyte microsomal HMG-CoA reductase activity. J Lipid Res 25:967–978

Harwood HJ, Chandler CE, Pellarin LD, Bangerter FW, Wilkins RW, Long CA, Cosgrove PG, Malinow MR, Marzetta CA, Pettini JK, Savoy YE, Mayne JT (1993) Pharmacologic consequences of cholesterol absorption inhibition: alteration in cholesterol metabolism and reduction in

plasma cholesterol concentration induced by the synthetic saponin β-tigogenin cellobioside (CP-88818; tiqueside). J Lipid Res 34:377–395
Herling AW, Burger HJ, Schubert G, Hemmerle H, Schäfer HL, Kramer W (1999) Alteration of carbohydrate and lipid intermediary metabolism during inhibition of glucose-6-phosphatase in rats. Eur J Pharmacol 386:75–82
Hylemon PB, Stude EJ, Pandak WM, Heuman DM, Vlahcevic ZR, Chinag JYL (1989) Simultaneous measurement of cholesterol 7α-hydroxylase activity by reverse-phase high-performance liquid chromatography using both endogenous cholesterol and exogenous [4-^{14}C]cholesterol as substrate. Anal Biochem 182:212–216
Junker LH, Story JA (1985) An improved assay for cholesterol 7α-hydroxylase activity using phospholipid liposome-solubilized substrate. Lipids 20:712–718
Ogishima T, Okuda K (1986) An improved method for assay of cholesterol 7α-hydroylase activity. Analyt Biochem 158:228–232
Princen HMG, Meijer P (1990) Maintenance of bile acid synthesis and cholesterol 7α-hydroxylase activity in cultured rat hepatocytes. Biochem J 272:273–275

M.3 Inhibition of Cholesterol Biosynthesis

M.3.1 General Considerations on Cholesterol Biosynthesis

The following steps are involved in cholesterol biosynthesis:

- HMG-CoA synthase (hydroxymethylglutaryl-coenzyme A synthase)
- forming **hydroxymethylglutaryl-CoA** from acetyl-CoA and acetoacetyl-CoA
- HMG-CoA reductase (hydroxymethylglutaryl-coenzyme A reductase)
- forming **mevalonic acid** from hydroxymethylglutaryl-CoA.

Inhibition of cholesterol synthesis on this step is used at present successfully for therapy (see below)

- Mevalonate kinaseforming **5-phospho-mevalonic acid** from mevalonic acid,
- Phospho-mevalonate kinase forming **5-pyrophospho-mevalonic acid** from 5-phospho-mevalonic acid,
- Pyrophospho-mevalonate decarboxylase forming **3-isopentyl-pyrophosphate** from 5-pyrophospho-mevalonic acid,
- Isopentyl-pyrophosphate isomerase forming **3,3-dimethyl-pyrophosphate** from 3-isopentyl-pyrophosphate,
- Dimethylallyl-transferase forming in a two step process **geranyl pyrophosphate** from 3,3-dimethyl-pyrophosphate, and
- **Farnesyl pyrophosphate** from geranyl pyrophosphate,
- Squalene synthetaseforming **squalene** from farnesyl pyrophosphate,
- Squalene epoxidaseforming **2,3-oxidosqualene** from squalene,
- 2,3-Oxidosqualene cyclase forming **lanosterol** from 2,3-oxidosqualene.

Following the formation of lanosterol (4,4,14α-trimethylcholesta-8(9),24-dien-3β-ol), a series of enzyme reactions is required to produce cholesterol (Bae et al. 1999):

- to 4,4,14α-trimethylcholesta-8(9)-en-3β-ol,
- to 4,4-dimethylcholesta-8(9),14-dien-3β-ol,
- to 4,4-dimethylcholesta-8(9)-en-3β-ol,
- to cholesta-8(9)-en-3β-ol,
- to cholesta-7-en-3β-ol,
- to cholesta-5,7-dien-3β-ol (7-dehydrocholesterol), and finally
- to cholesta-5-en-3β-ol (cholesterol) by 7-dehydrocholesterol reductase.

Besides **inhibition of HMG-CoA reductase** (detailed description below) other approaches to inhibit biosynthesis of cholesterol are reported:

- **inhibition of HMG-CoA synthase** (Goldstein and Brown 1990; Miller et al. 1980; Greenspan et al. 1987; Grayson and Westkaemper 1988);
- **inhibition of squalene synthase** (Ness et al. 1994; Sliskovic and Picard 1997; Rosenberg 1998; Hiyoshi et al. 2000; Squalene synthase plays an important role in sterol biosynthesis by catalyzing the head-to-head condensation of two molecules of farnesylpyrophosphate. The enzyme is a single 47,000 Da polypeptide that is bound to the subcellular membranes of the endoplasmatic reticulum in yeast and mammalian liver (see below);
- **inhibition of squalene epoxidase** (Ryder 1992); Squalene epoxidase catalyzes the conversion of squalene to (3S)-2,3-oxidosqualene, an essential step in the biosynthesis of sterols in mammals, plants, and microorganisms (see below)
- **inhibition of 2,3-oxidosqualene cyclase** (Gerst et al. 1986; Cattel et al. 1989; Sen and Prestwich 1989; Dollis and Schuber 1994; Mark et al. 1996; Eisele et al. 1997; Morand et al. 1997; Abe et al.

1998a); The enzyme 2,3-oxidosqualene cyclase is of special interest due to its dual function: cyclization of 2,3-monoepoxysqualene to lanosterol and 2,3:22,23-diepoxysqualene to oxylanosterol. An orally active oxidosqualene:lanosterol cyclase inhibitor (Ro48–8071) showed potent noncompetitive inhibition of bacterial squalene:hopene cyclase from *Alicyclobacillus acidocaldarius*. A tritium-labeled isotopomer of this nonterpenoid inhibitor, which possesses a benzophenone photophore, was chemically synthesized as a photoaffinity label (Abe et al. 1998b);

- **inhibition of 7-dehydrocholesterol reductase** (Amin et al. 1996); Deficiency of this enzyme causes a severe developmental disorder with multiple congenital and morphogenic abnormalities, the Smith-Lemli-Opitz syndrome (Waterham and Wanders 2000).

Search and development of new cholesterol-lowering drugs is continued (Abe and Prestwich 1998). Whether the efficacy and safety of these agents in man will be on the long run superior to currently available therapies remains to be determined.

REFERENCES AND FURTHER READING

Abe I, Prestwich GD (1998) Development of new cholesterol-lowering drugs. Drug Dev Today 3:389–390

Abe I, Zheng YF, Prestwich GD (1998a) Mechanism based inhibitors and other active-site targeted inhibitors of oxidosqualene cyclase and squalene cyclase. J Enzyme Inhib 13:385–398

Abe I, Zheng YF, Prestwich GD (1998b) Photoaffinity labeling of oxidosqualene cyclase and squalene cyclase by a benzophenone-containing inhibitor. Biochemistry 37:5779–5784

Amin D, Rutledge RZ, Needle SN, Galczenski HF, Neuenschwander K, Scotese AC, Maguire MP, Bush RC, Hele DJ, Bilder GE, Perrone MH (1997) RPR 107393, a potent squalene synthase inhibitor and orally effective cholesterol-lowering agent: comparison with inhibitors of HMG-CoA reductase. J Pharmacol Exp Ther 281:746–752

Bae S-H, Lee JN, Fitzky BU, Seong J, Paik Y-K (1999) Cholesterol biosynthesis from lanosterol. Molecular cloning, tissue distribution, expression, chromosomal location and regulation of rat 7-dehydrocholesterol reductase, a Smith-Lemli-Opitz syndrome-related protein. J Biol Chem 274:14624–14631

Cattel L, Ceruti M, Balliano G, Viola F, Grosa G, Schuber F (1989) Drug design based on biosynthetic studies: synthesis, biological activity, and kinetics of new inhibitors of 2,3-oxidosqualene cyclase and squalene epoxidase. Steroids 53:363–391

Dollis D, Schuber F (1994) Effects of a 2,3-oxidosqualene-lanosterol cyclase inhibitor 2,3:22,23-dioxidosqualene and 24,25-epoxycholesterol on the regulation of cholesterol biosynthesis in human hepatoma cell line HepG2. Biochem Pharmacol 48:49–57

Eisele B, Budzinski R, Müller P, Maier R, Mark M (1997) Effects of a novel 2,3-oxidosqualene cyclase inhibitor on cholesterol biosynthesis and lipid metabolism *in vivo*. J Lipid Res 38:564–575

Gerst N, Schuber F, Viola F, Cattel L (1986) Inhibition of cholesterol biosynthesis in 3T3 fibroblasts by 2-aza-2,3-dihydrosqualene, a rationally designed 2,3-oxidosqualene cyclase inhibitor. Biochem Pharmacol 35:4243–4250

Goldstein JL, Brown MS (1990) Regulation of mevalonate pathway. Nature 343:425–430

Grayson NA, Westkaemper RB (1988) Stable analogs of acyl adenylates. Inhibition of acetyl- and acyl-CoA synthetase by adenosine 5′-alkylphosphates. Life Sci 43:437–444

Greenspan MD, Yudkowitz JB, Lo CYL, Chen JS, Alberts AW, Hunt VM, Chang MN, Yang SS, Thompson KL, Chiang YCP, Chabala JC, Monaghan RL, Schwartz RL (1987) Inhibition of hydroxymethylglutaryl-coenzyme A synthase by L-659,699. Proc Natl Acad Sci USA 84:7488–7492

Mark M, Müller P, Maier R, Eisele B (1996) Effects of a novel 2,3-oxidosqualene cyclase inhibitor on the regulation of cholesterol biosynthesis in HepG2 cells. J Lipid Res 37:148–158

Miller LR, Pinkerton FT, Schroepfer GJ (1980) 5α-Cholest-8(14)-en-3β-ol-15-one, a potent inhibitor or sterol synthesis, reduces the levels of activity of enzymes involved in the synthesis and reduction of 3-hydroxy-3-methylglutaryl coenzyme A in CHO-K1 cells. Biochem Intern 1:223–228

Morand OH, Aebi JD, Dehmlow H, Ji Y-H, Gains N, Lengsfeld H, Himber J (1997) Ro 48–8071, a new 2,3-oxidosqualene:lanosterol cyclase inhibitor lowering plasma cholesterol in hamsters, squirrel monkeys, and minipigs: comparison to simvastin. J Lipid Res 38:373–390

Ness GC, Zhao Z, Keller RK (1994) Effect of squalene synthase inhibition on the expression of hepatic cholesterol biosynthesis enzymes, LDL receptor, and cholesterol 7-alpha-hydroxylase. Arch Biochem Biophys 311:277–285

Rosenberg SH (1998) Squalene synthase inhibitors. Exp Opin Ther Patents 8:521–530

Ryder NS (1992) Terbenafine: mode of action and properties of the squalene epoxidase inhibition. Br J Dermatol 126: Suppl 39:2–7

Sen SE, Prestwich GD (1989) Squalene analogs containing isopropylidene mimics as potential inhibitors of pig liver squalene epoxidase and oxidosqualene cyclase. J Med Chem 32:2152–2158

Sliskovic DR, Picard JA (1997) Squalene synthase inhibitors. Emerg Drugs 2:93–107

Waterham HR, Wanders RJA (2000) Biochemical and genetic aspects of 7-dehydrocholesterol reductase and Smith-Lemli-Opitz syndrome. Biochem Biophys Acta 1529:340–356

M.3.2 Determination of HMG-CoA-Reductase Inhibitory Activity

M.3.2.1 General Considerations on HMG-CoA-Reductase

More than 70% of the total production of body cholesterol in humans is derived from de novo synthesis. 3-Hydroxy-3-methylglutaryl-coenzyme A (HMG-CoA) reductase is the rate limiting enzyme governing cholesterol biosynthesis and the synthesis of other isoprenoids in mammalian cells (Rodwell et al. 1976).

The development of HMG-CoA reductase inhibitors (called statins) offers an advance in the treatment of hypercholesterolemia by interfering with the crucial step of cholesterol biosynthesis. When inhibiting hepatic HMG-CoA reductase, the inhibitors trigger an increased production of LDL receptors in the liver. As LDL receptor activity increases, more LDL is extracted from the blood and thus the level of circulating LDL-cholesterol is reduced. Pharmacological evaluation of HMG-CoA reductase inhibitors is based on studies on the inhibition of the isolated enzyme HMG-CoA -reductase *in vitro*, on the inhibition of the incorporation of ^{14}C sodium acetate into cholesterol in isolated liver cells, and on the effect of HMG-CoA -reductase inhibitors *in vivo*. HMG-CoA reductase activity has a diurnal rhythm in liver and intestine which has to be considered for *in vivo* studies (Shapiro and Rodwell 1969; Shefer et al. 1972).

HMG-CoA reductase inhibitors have been associated with skeletal myopathy (rhabdomyolysis) in humans and experimental animals (Flint et al. 1997; Klotz 2003). The rhabdomyolysis is probably mechanism based, from the cerivastatin cases it could be concluded that the risk of rhabdomyolysis is related to active drug levels in the systemic circulation and peripheral tissues (Graham et al. 2004).

REFERENCES AND FURTHER READING

Clinkenbeard KD, Sugiyama T, Reed WD, Lane MD (1975) Cytoplasmatic 3-hydroxy-3-methylglutaryl coenzyme A synthase from liver. Purification, properties, and role in cholesterol synthesis. J Biol Chem 250:3124–3135

Flint OP, Masters BA, Gregg RE, Durham SK (1997) Inhibition of cholesterol synthesis by squalene synthase inhibitors does not induce myotoxicity *in vitro*. Toxicol Appl Pharmacol 145:91–98

Gotto AM (1990) Pravastatin: A hydrophilic inhibitor of cholesterol synthesis. J Drug Dev 3:155–161

Graham DJ, Staffa JA, Shatin D, Andrade SE, Schech SD, Grenade LL, Gurwitz JH, Chan KA, Goodman MJ, Platt R (2004) Incidence of hospitalized rhabdomyolysis in patients treated with lipid-lowering drugs. J Am Med Assoc 2992:2585–2590

Jendralla H, Baader E, Bartmann W, Beck G, Bergmann A, Granzer E, v. Kerekjarto B, Kesseler K, Krause R, Schubert W, Wess G (1990) Synthesis and biological activity of new HMG-CoA reductase inhibitors. 2. Derivatives of 7-(1*H*-pyrrol-3-yl)-substituted-3,5-dihydroxyhept-6(E)-enoic(-heptanoic) acids. J Med Chem 33:61–70

Jungnickel PW, Cantral KA, Maloley PA (1992) Pravastin: A new drug for the treatment of hypercholesterinemia. Clin Pharm 11:677–689

Klotz U (2003) Pharmacological comparison of the statins. Arzn Forsch/Drug Res 53:605–611

Krause R, Neubauer H, Leven M, Kesseler K (1990) Inhibition of cholesterol synthesis in target tissues and extrahepatic organs after administration of HMG-CoA reductase inhibitors in normolipidaemic rats: organ selectivity and time course of the inhibition. J Drug Dev 3 (Suppl 1):255–257

Mauro VF, MacDonald JL (1991) Simvastatin: A review of its pharmacology and clinical use. DICP, Annal Pharmacother 25:257–264

Parish EJ, Nanduri VBB, Kohl HH, Taylor FR (1986) Oxysterols: Chemical synthesis, biosynthesis and biological activities. Lipids 21:27–30

Rodwell VW, Nordstrom JL, Mitschelen JJ (1976) Regulation of HMG-CoA reductase. In: Paoletti R, Kritchevsky D (eds) Advances in Lipid Research Vol 14:1–74, Academic Press, New York

Saito Y, Kitahara MKS, Sakashita MSK, Toyoda KSK, Shibazaki TSK (1993) Novel inhibitors of atherosclerotic intimal thickening. Curr Opin Therap Patents 3:1241–1242

Scott WA (1990) Hydrophilicity and the differential pharmacology of pravastin. In: Wood C (ed) Lipid management: Pravastin and the differential pharmacology of HMG-CoA reductase inhibitors. Royal Soc Medi Serv, Round Table Series, No 16:17–25

Shapiro DJ, Rodwell VW (1969) Diurnal variation and cholesterol regulation of hepatic HMG-CoA reductase activity. Biochem Biophys Res Commun 37:687–872

Shefer S, Hauser S, Lapar V, Mosbach EH (1972) Diurnal variation of HMG CoA reductase activity in rat intestine. J Lipid Res 13:571–573

Sirtori CR (1990) Pharmacology and mechanism of action of the new HMG-CoA reductase inhibitors. Pharmacol Res 22:555–563

Soma MR, Corsini A, Paoletti R (1992) Cholesterol and mevalonic acid modulation in cell metabolism and multiplication. Toxicology Letters 64/65:1–15

Trzaskos JM, Magolda RL, Favata MF, Fischer RT, Johnson PR, Chen HW, Ko SS, Leonard DA, Gaylor JL (1993) Modulation of 3-hydroxy-3-methylglutaryl-CoA reductase by 15α-fluorolanost-7-en-3β-ol. A mechanism-based inhibitor of cholesterol biosynthesis. J Biol Chem 268:22591–22599

Tsujita Y (1990a) A potent HMG-CoA reductase inhibitor, pravastatin sodium. Tissue selective inhibition of cholesterogenesis and preventive effect on atherosclerosis in WHHL rabbits. J Drug Dev 3 (Suppl 1):155–159

Tsujita Y (1990b) HMG-CoA reductase inhibitors. J Jpn Atheroscler Soc 18:165–171

M.3.2.2 Inhibition of the Isolated Enzyme HMG-CoA-Reductase in Vitro

PURPOSE AND RATIONALE

For screening purposes, studies on the inhibition of HMG-CoA reductase obtained from rat liver microsomal fraction can be used (Avigan et al. 1975; Philipp and Shapiro 1979).

PROCEDURE

The inhibitory activity of the test compound on HMG-CoA reductase is estimated with soluble enzyme preparations obtained from the microsomal fraction of rat liver (Philipp and Shapiro 1979). The enzyme reaction is carried out with 50 µl partially

purified HMG-CoA reductase in buffer containing 25 mM Tris, 10 mM EDTA, and 10 mM dithiothreitol at pH 7.5, 20 µl of 910 µM HMG-CoA solution containing 100 nCi (3.7 KBq) of ^{14}C-HMG-CoA and 20 µl of NADPH regenerating system (5.2×10^{-2} M glucose-6-phosphate, 1 unit glucose-6-phosphate dehydrogenase, 5.3×10^{-3} M NADP), with the actual concentration of 50 mM NADPH. The final incubation volume is 200 µl. The main reaction is preceded by 20 min preincubation with the NADPH regenerating system at 37°C, followed by 20 min incubation at 37°C of the completed samples with the test compound or the standard and stopped by addition of 75 µl 2 N $HClO_4$. After 60 min at room temperature, the samples are cooled in an ice-bath and neutralized by addition of 75 µl 3 N potassium acetate. Supplementing the volume with water to 500 µl, the precipitate is centrifuged and 250 µl of the clear supernatant are applied to a column (0.6 × 8.0 cm) of BIORAD AG 1-X8 (100–200 mesh). Mevalonolactone is eluted with water discarding the first 750 µl and collecting the next 3500 µl. Five hundred µl of the eluate are used for measurement in duplicate, mixed in vials with 10 ml Quickscint (Zinsser) and measured in a liquid scintillation counter (Beckman). The assay is generally performed in triplicate. Lovastatin sodium is used as standard.

EVALUATION

The mean values with and without inhibitors are compared for the calculation of inhibition. IC_{50} values are calculated.

REFERENCES AND FURTHER READING

Avigan J, Bhathena SJ, Schreiner ME (1975) Control of sterol synthesis and of hydroxymethylglutaryl CoA reductase in skin fibroblasts grown from patients with homozygous type II hyperlipoproteinemia. J Lipid Res 16:151–154

Baker FC, Schooley DA (1979) Analysis and purification of acyl coenzyme A thioesters by reversed-phase ion-pair liquid chromatography. Analyt Biochem 94:417–424

Heller RA, Gould RG (1973) Solubilization and partial purification of hepatic 3-hydroxy-3-methylglutaryl coenzyme A reductase. Biochem Biophys Res Comm 50:859–865

Kramer W, Wess G, Enhsen A, Bock K, Falk E, Hoffmann A, Neckermann G, Gantz D, Schulz S, Nickau B, Petzinger E, Turley S, Dietschy JM (1994) Bile acid derived HMG-CoA reductase inhibitors. Biochim Biophys Acta 1227:137–154

Kubo M, Strott CA (1987) Differential activity of 3-hydroxy-3-methylglutaryl coenzyme A reductase in zones of the adrenal cortex. Endocrinol 120:214–221

Philipp BW, Shapiro DJ (1979) Improved methods for the assay and activation of 3-hydroxy-3-methylglutaryl coenzyme A reductase. J Lipid Res 20:588–593

Wess G, Kramer W, Han XB, Bock K, Enhsen A, Glombik H, Baringhaus KH, Böger G, Urmann M, Hoffmann A, Falk E (1994) Synthesis and biological activity of bile acid-derived HMG-CoA reductase inhibitors. The role of the 21-methyl in recognition of HMG-CoA reductase and the ileal bile acid transport system. J Med Chem 37:3240–3246

M.3.2.3 Inhibition of the Incorporation of ^{14}C-Sodium Acetate into Cholesterol in Isolated Liver Cells

PURPOSE AND RATIONALE

De novo synthesis of cholesterol from labelled acetate can be measured in isolated liver cells. This synthesis can be inhibited by incubation with HMG-CoA reductase inhibitors.

PROCEDURE

Monolayers of primary cell cultures from hepatocytes of female rats or of cultures of HEP-G2 cells (human hepatoma cells) are incubated in a lipoprotein deficient medium for 1 h with various concentrations of the potential HMG-CoA reductase inhibitor or the standard (Lovastatin). Thereafter, the labelled precursor ^{14}C sodium acetate is added to the medium and the incubation continued for further 3 or 24 h. To one part of the cells an internal standard of ^{3}H-cholesterol is added and the cells are saponified by alkaline. The lipids of these saponified cells are extracted with chloroform/methanol. The lipid mixture is separated by preparative thin layer chromatography. The localization of cholesterol is identified by exposure to iodine vapor and the amount of newly synthesized ^{14}C-cholesterol is determined in a scintillation counter.

Cell protein is determined in another part of the cells. A third part of the cell culture is used to control the integrity of the cells by light microscopy and tested biologically by determination of the release of lactate dehydrogenase into the incubation medium.

EVALUATION

The amount of newly synthesized cholesterol per mg cell protein is calculated. The inhibitory capacity of the test drug is estimated against a solvent control. IC_{50} values are calculated from the results of various concentrations.

MODIFICATIONS OF THE METHOD

Chen and Kandutsch (1976) studied the effects of cholesterol derivatives on sterol biosynthesis in cultures of various cell types.

Liver specificity of inhibition of sterol synthesis is studied by *in vitro* uptake into hepatocytes and human

skin fibroblasts (Scott 1990) or in slices of various tissues after oral treatment with HMG-CoA reductase inhibitors (Tsujita 1990).

Shaw et al. (1990), however, caution against the use of HEP-G2 cells which may not be the cell system of choice to demonstrate liver selectivity of inhibitors of HMG-CoA reductase.

Cultures of HEP-G2 cells have also be used to test inhibition of cytoplasmic acetoacetyl-CoA thiolase (Greenspan et al. 1989) or inhibition of squalene epoxidase (Hidaka et al. 1991).

Pearce et al. (1992) used HEP G2 cells to study the hypocholesterolemic activity of synthetic and natural tocotrienols *in vitro*.

Raiteri et al. (1997) investigated drugs acting at different steps of the mevalonate pathway on arterial smooth muscle cell proliferation. Competitive HMG-CoA reductase inhibitors dose-dependently decreased smooth muscle cell proliferation.

REFERENCES AND FURTHER READING

Beck G, Kesseler K, Baader E, Bartmann W, Bergmann A, Granzer E, Jendralla H, von Kerekjarto B, Krause R, Paulus E, Schubert W, Wess G (1990) Synthesis and biological activity of new HMG-CoA reductase inhibitors. 1. Lactones of pyridine- and pyrimidine-substituted 3,5-dihydroxy-6-heptenoic (heptanoic) acids. J Med Chem 33:52–60

Chen HW, Kandutsch AA (1976) Effects of cholesterol derivatives on sterol biosynthesis. In: Day CE (ed) Atherosclerosis Drug Discovery, Plenum Press, New York and London, pp 405–417

Gebhardt R (1993) Multiple inhibitory effects of garlic extracts on cholesterol biosynthesis in hepatocytes. Lipids 28:613–619

Gotto AM (1990) Pravastatin: A hydrophilic inhibitor of cholesterol synthesis. J Drug Dev 3:155–161

Greenspan MD, Yudkovitz JB, Chen JS, Hanf DP, Chang MN, Chiang PYC, Chabala JC, Alberts AW (1989) The inhibition of cytoplasmatic acetoacetyl-CoA thiolase by a triyne carbonate (L-660,631) Biochem Biophys Res Commun 163:548–553

Hidaka Y, Hotta H, Nagata Y, Iwasawa Y, Horie M, Kamei T (1991) Effect of a novel squalene epoxidase inhibitor, NB-598, on the regulation of cholesterol metabolism in HEP G2 cells. J Biol Chem 266:13171–13177

Parker RA, Clark RW, Sit SY, Lanier TL, Grosso RA, Kim Wright JJ (1990) Selective inhibition of cholesterol synthesis in liver versus extrahepatic tissues by HMG-CoA reductase inhibitors. J Lipid Res 31:1271–1282

Pearce BC, Parker RA, Deason ME, Qureshi AA, Kim Wright JJ (1992) Hypocholesterolemic activity of synthetic and natural tocotrienols. J Med Chem 35:3595–3606

Raiteri M, Amaboldi L, McGeady P, Gelb MH, Veri D, Tagliabue C, Quarato P, Ferraboschi P, Santaniello E, Paoletti R, Fumagalli R, Corsini A (1997) Pharmacological control of mevalonate pathway: Effect on arterial smooth muscle cell proliferation. J Pharmacol Exp Ther 281:1144–1153

Scott WA (1990) Hydrophilicity and the differential pharmacology of pravastin. In: Wood C (ed) Lipid management: Pravastin and the differential pharmacology of HMG-CoA reductase inhibitors. Royal Society of Medicine Services, London, pp 17–25

Shaw MK, Newton RS, Sliskovic DR, Roth BD, Ferguson E, Krause BR (1990) HEP-G2 cells and primary rat hepatocytes differ in their response to inhibitors of HMG-CoA reductase. Biochem Biophys Res Commun 170:726–734

Tsujita Y (1990) A potent HMG-CoA reductase inhibitor, pravastatin sodium. Tissue selective inhibition of cholesterogenesis and preventive effect on atherosclerosis in WHHL rabbits. J Drug Dev 3 (Suppl 1):155–159

M.3.2.4 Ex Vivo Inhibition of Cholesterol Biosynthesis in Isolated Rat Liver Slices

PURPOSE AND RATIONALE

Inhibition of cholesterol biosynthesis in rat livers can be measured in an *ex vivo* assay after oral treatment with HMG-CoA reductase inhibitors by cholesterol synthesis from labelled sodium octanoate.

PROCEDURE

Male Sprague Dawley rats weighing 110–130 g are kept on a reverse light cycle (lights 3:00 P.M. to 3:00 A.M.) for 14 days prior to use. Throughout the period of adaptation, the rats have free access to a low cholesterol diet and tap water. On the day of the experiment, the test compounds are given orally between 9:00 and 11:00 A.M. as suspensions in 0.5% methylcellulose. After one hour, the rats are sacrificed, the livers removed and transferred to chilled oxygenated Krebs-Ringer-bicarbonate buffer (pH 7.4). The livers are then chopped into 0.8-mm^2 pieces using a McIlwain tissue chopper (e. g., Brinkmann Instr., Westbury, USA) and are suspended in the same buffer. Aliquots of the suspension are pipetted, in triplicate, into culture tubes which contain [^{14}C]sodium octanoate (300 µM/l, 6.67 Ci/M). The assay volume is 1 ml. The tubes are gassed with 95% O_2/5% CO_2 for 10 s, stoppered with a serum cap, and incubated at 37°C in a metabolic shaker at 150 oscillations/min for 90 min.

The reaction is stopped by addition of 1 ml 15% KOH in ethanol. An aliquot of the mixture is assayed for protein concentration. An internal standard [^{3}H]cholesterol (30,000 dpm) is added to determine recovery, which ranges from 70–80%. The tubes are saponified at 75°C for 2 h and then extracted with 10 ml of petroleum ether for 30 min. The lower aqueous phase is frozen in a dry ice/alcohol mixture, and the ether phase is removed, washed with 2 ml glass-distilled water and then evaporated to dryness. The [^{14}C]cholesterol synthesized is separated by thin layer chromatography on plastic silica gel plates using chloroform as eluent. After visualization with iodine, the

cholesterol spots are cut out, and radioactivity quantitated by liquid scintillation counting.

EVALUATION

Results are expressed as percentage inhibition compared to vehicle-treated control values. Using various doses, ED_{50} values of inhibition can be calculated from dose-response curves.

MODIFICATIONS OF THE METHOD

Koga et al. (1990) tested the tissue-selective inhibition of cholesterol synthesis *in vivo* by pravastin sodium in mice. Drugs were orally administered to mice 2 h prior to an intraperitoneal injection of [^{14}C]acetate. The animals were sacrificed 1 h afterwards and the cholesterol synthesis determined in various organs.

REFERENCES AND FURTHER READING

Amin D, Gustafson SK, Weinacht JM, Cornell SA, Neuenschwander K, Kosmider B, Scotese AC, Regan JR, Perrone MH (1993) RG 12561 (Dalvastatin): A novel synthetic inhibitor of HMG-CoA reductase and cholesterol-lowering agent. Pharmacology 46:13–22

Beck G, Kesseler K, Baader E, Bartmann W, Bergmann A, Granzer E, Jendralla H, von Kerekjarto B, Krause R, Paulus E, Schubert W, Wess G (1990) Synthesis and biological activity of new HMG-CoA reductase inhibitors. 1. Lactones of pyridine- and pyrimidine-substituted 3,5-dihydroxy-6-heptenoic (heptanoic) acids. J Med Chem 33:52–60

Bocan TMA, Ferguson E, McNally W, Uhlendorf PD, Mueller SB, Dehart P, Sliskovic DR, Roth BD, Krause BR, Newton RS (1992) Hepatic and non hepatic sterol synthesis and tissue distribution of a liver selective HMG-CoA reductase inhibitor, CI-981: comparison with selected HMG-CoA reductase inhibitors. Biochim Biophys Acta 1123:133–144

Brown MS, Goldstein JL, Dietschy JM (1979) Active and inactive forms of 3-hydroxyx-3-methylglutaryl coenzyme A reductase in the liver of the rat. J Biol Chem 254:5144–5149

Koga T, Shimada Y, Kuroda M, Tsujita Y, Hasegawa K, Yamazaki M (1990) Tissue-selective inhibition of cholesterol synthesis *in vivo* by pravastin sodium, a 3-hydroxy-3-methylglutaryl-coenzym A reductase inhibitor. Biochim Biophys Acta 1045:115–120

M.3.2.5 Effect of HMG-CoA-Reductase Inhibitors in Vivo

PURPOSE AND RATIONALE

A strain of rabbits with heritable hyperlipidemia, the WHHL strain, has been described by Watanabe et al. (1980, 1985, 1988). These animals develop digital xanthoma and aortic and coronary atherosclerosis already at an early age. This animal is considered to be a suitable model for the evaluation of preventive or even regressive effects of drugs on hyperlipidemia and atherosclerosis.

PROCEDURE

Male heterozygous WHHL rabbits weighing 1.8 to 2.5 kg at an age between 8 and 20 weeks are used. The animals are housed individually under standard conditions (standard rabbit diet and water ad libitum) and are allowed to accommodate 2 weeks prior to treatment. The test compounds are suspended in 0.5% methylcellulose and are administered each day orally by gavage in the afternoon to insure an increased plasma level at night, since in man HMG-CoA reductase activity has been found to be higher at night than during daytime (Shapiro and Rodwell 1969; Shefer et al. 1972) similar to the enzyme in rodents. The treatment is continued for 14 days.

Blood samples are taken in the morning without previous feeding. Two ml of blood are drawn from the outer ear vein 5 days prior to the beginning of treatment, on days 3 and 8 of treatment and 30 days after the end of treatment for the determination of biochemical parameters. In addition, 6 ml blood are drawn at the first and the last day of treatment and 10 days after the end of treatment for determination of biochemical parameters and lipoprotein profile. In order to obtain serum, blood is allowed to clot at room temperature and then centrifuged twice at 10,000 rpm.

The following biochemical parameters are determined in non-frozen samples (kept at 4°C): total cholesterol, HDL-cholesterol, triacylglycerol, as well as creatinine, total bilirubin, alkaline phosphatase, alanine amino transferase (ALAT), aspartate amino transferase (ASAT), and γ-glutamyl transferase (γ-GT) using commercially available kits.

The separation of serum lipoproteins by gel permeation chromatography is performed according to Ha and Barter (1985). This method is particularly well suited for the metabolic studies of lipoproteins, because the elution profile can be obtained from the same sample under more gentle conditions than by sequential ultracentrifugation. According to their descending particle size, the elution profile of lipoproteins in the same fraction of density (< 1.21 g/ml) shows, as the elution progresses, three major peaks which correspond to very low density lipoproteins (VLDL), low density lipoproteins (LDL) and high density lipoproteins (HDL), respectively.

Since the amount of serum collected from one rabbit is too low to determine the lipoprotein profile from each sample, the total lipoproteins are isolated by ultracentrifugation at a density < 1.21 g/ml and the lipoproteins thus obtained in each group are pooled two by two prior to injection onto the cross-linked agarose HR 50 column (Superose 6B). As a result,

each lipoprotein profile represents the lipoprotein size distribution of an equal volume of lipoproteins obtained from two rabbits. Cholesterol and triacylglycerol concentrations are determined in each 1 ml elution fraction.

EVALUATION

The data at 5 days before beginning of treatment and of day 0 of each animal are pooled and the mean is taken as reference value. Student's paired *t*-test is used to calculate for each group the significance of difference between mean values.

MODIFICATIONS OF THE METHOD

Extension of the treatment period up to 24 weeks allows to evaluate the meanwhile apparent atherosclerotic lesions in the aorta and the coronaries by gross observation and light microscopy (Tsujita 1990).

Kasim et al. (1993) studied the effect of lovastatin on the secretion of very low density lipoprotein lipids and apolipoprotein B in the Zucker obese rat which is basically a model for genetic hypertriglyceridemia.

Soma et al. (1993) studied the effects of HMG-CoA reductase inhibitors on carotid intimal thickening induced by placing a nonocclusive, biologically inert, soft, hollow Silastic collar around both carotid arteries in normocholesterolemic rabbits (Booth et al. 1989).

Bocan et al. (1994) assessed atherosclerotic lesion development in the thoracic artery and chronically denuded iliac-femoral artery of hypercholesterolemic New Zealand White rabbits using inhibitors of HMG-CoA reductase.

Krause and Newton (1995) tested the lipid-lowering activity of atorvastatin and lovostatin in several rodent species (rat models, guinea pigs, rabbits). They concluded that normal rats can be used as a preclinical tool to assess the efficacy of HMG-CoA reductase inhibitors since triglyceride lowering correlates with cholesterol lowering in LDL animal models.

Johnston et al. (2001) induced atheroma formation in the aortas of C57BL/6 mice by long-term administration of Poloxamer-407, a nonionic surfactant, and tested the potency of selected statin drugs in this model of hyperlipidemia and atherosclerosis.

Delsing et al. (2003) studied differential effects of a calcium antagonist and a statin and their combination on atherosclerosis in ApoE*3-Leiden transgenic mice.

Aoki et al. (2002) induced postprandial lipemia in rats by administration of a lipid emulsion and measured the triglyceride-lowering effect of a statin.

Ugawa et al. (2002) established an experimental model of the escape phenomenon in hamsters in which plasma cholesterol, initially reduced by statins, increases again on long-term administration, and tested the effectiveness of a squalene synthase inhibitor in this model.

Yokota et al. (2003) tested the protective effect of a HMG-CoA reductase inhibitor on experimental renal ischemia-reperfusion injury in mice.

Abletshauser et al. (2002) reported a new method for biosensing of arteriosclerotic nanoplaque formation and interaction with an HMG-CoA reductase inhibitor and recommended this method for experimental and clinical studies.

REFERENCES AND FURTHER READING

Abletshauser C, Klüßendorf D, Schmidt A, Winkler K, März W, Buddecke E, Malmstan M, Siegel G (2002) Biosensing of arteriosclerotic nanoplaque formation and interaction with an HMG CoA reductase inhibitor. Acta Physiol Scand 176:131–145

Aoki T, Yoshinaka Y, Yamazaki H, Suzuki H, Tamaki T, Sato F, Kitahara M, Saito Y (2002) Triglyceride-lowering effect of pivastatin in a rat model of postprandial lipemia. Eur J Pharmacol 444:107–113

Bocan TMA, Mazur MJ, Mueller SB, Brown EQ, Sliskovic DR, O'Brien PM, Creswell MW, Lee H, Uhlendorf PD, Roth BD, Newton RS (1994) Antiatherosclerotic activity of inhibitors of 3-hydroxy-3-methylglutaryl coenzyme A reductase in cholesterol-fed rabbits: a biochemical and morphological evaluation. Atherosclerosis 111:127–142

Booth RGF, Martin JF, Honey AC, Hassall DG, Beesley JE, Moncada S (1989) Rapid development of atherosclerotic lesions in the rabbit carotid artery induced by perivascular manipulation. Atherosclerosis 76:257–268

Delsing DJ, Jukema JW, van de Wiel MA, Emeis JJ, van der Laarse A, Havekes LM, Princen HM (2003) Differential effects of amlodipin and atorvastin treatment and their combination on atherosclerosis in ApoE*3-Leiden transgenic mice. J Cardiovasc Pharmacol 42:63–70

Ha YC, Barter PJ (1985) Rapid separation of plasma lipoproteins by gel permeation chromatography on agarose gel Superose 6B. J Chromatogr 341:154–159

Johnston TP, Nguyen LB, Chu WA, Shefer S (2001) Potency of selected statin drugs in a new mouse model of hyperlipidemia and atherosclerosis. Int J Pharm 229:75–86

Kasim SE, Elovson J, Khilnani S, Almario RU, Jen KLC (1993) The effect of lovastatin on the secretion of very low density lipoprotein lipids and apolipoprotein B in the hypertriglyceridemic Zucker obese rat. Atherosclerosis 104:147–152

Krause BR, Newton SB (1995) Lipid-lowering activity of atorvastatin and lovostatin in rodent species: triglyceride-lowering in rats correlates with efficacy in LDL animals. Atherosclerosis 117:237–244

Soma MR, Donetti E, Paroline C, Mazzini G, Ferrari C, Fumagalli R, Paoletti R (1993) HMG-CoA reductase inhibitors. *In vivo* effects on carotid intimal thickening in normocholesterolemic rabbits. Arterioscler Thrombos 13:571–578

Tsujita Y (1990) A potent HMG-CoA reductase inhibitor, pravastatin sodium. Tissue selective inhibition of choles-

terogenesis and preventive effect on atherosclerosis in WHHL rabbits. J Drug Dev 3 (Suppl 1):155–159
Tsujita Y, Kuroda M, Shimada Y, Tanzawa K, Arai M, Kaneko I, Tanaka M, Masuda H, Tarumi Ch, Watanabe Y, Fujii S (1986) CS-514, a competitive inhibitor of 3-hydroxy-3-methylglutaryl coenzyme A reductase: tissue-selective inhibition of sterol synthesis and hypolipidemic effect on various animal species. Biochim Biophys Acta 877:50–60
Ugawa T, Kakuta H, Moritani H, Shikama H (2002) Experimental model of escape phenomenon in hamsters and the effectiveness of YM-53601 in the model. Br J Pharmacol 135:1572–1578
Watanabe Y (1980) Serial inbreeding of rabbits with hereditary hyperlipidemia (WHHL)-rabbit). Incidence and development of atherosclerosis and xanthoma. Atherosclerosis 36:261–268
Watanabe Y, Ito T, Shiomi M (1985) The effect of selective breeding on the development of coronary atherosclerosis in WHHL rabbits. An animal model for familial hypercholesterolemia. Atherosclerosis 56:71–79
Watanabe Y, Ito T, Shiomi M, Tsujita Y, Kuroda M, Arai M, Fukami M, Tamura A (1988) Preventive effect of pravastatin sodium, a potent inhibitor of 3-hydroxy-3-methylglutaryl coenzyme A reductase, on coronary atherosclerosis and xanthoma in WHHL rabbits. Biochim Biophys Acta 960:294–302
Yokota N, O'Donnell M, Daniels F, Burne-Taney M, Keane W, Kasiske B, Rabb H (2003) Protective effect of HMG CoA reductase inhibitor on experimental renal ischemia-reperfusion injury. Am J Nephrol 23:13–17

M.3.2.6 Influence of Statins on Endothelial Nitric Oxide Synthase

PURPOSE AND RATIONALE

Several studies indicate that the beneficial effects of 3-hydroxy-3-methylglutaryl coenzyme A reductase inhibitors (statins) on endothelial function and cardiovascular ischemic events may be attributed not only to their lipid-lowering effect but also to direct effects on the atherosclerotic vessel wall. One such effect is the upregulation of nitric oxide synthase, which generally leads to vasorelaxation (Kano et al. 1999; Amin-Hanjani et al. 2001; Rikitake et al. 2001; Sata et al. 2001; Sumi et al. 2001; Jones et al. 2002; Laufs et al. 2002; Mitani et al. 2003a, 2003b; Parker et al. 2003; Wassmann and Nickenig 2003; Yamamoto et al. 2003; Kumai et al. 2004).

Parker et al. (2003) compared different statins for e-NOS subcellular localization, formation of prooxidants, and endothelial-dependent vascular function.

PROCEDURE

Endothelium-Dependent Vascular Relaxation Ex Vivo in Statin-Treated Rats

Sprague Dawley rats (~160 g) on standard chow are treated with HMG-CoA reductase inhibitors for 8 days at doses that do not result in plasma cholesterol reductions as determined in previous experiments. To assay vascular relaxation, aortas are dissected out and perivascular tissue removed. Aortic rings (~5 mm) are incubated at 37°C in pH 7.4 Krebs-bicarbonate buffer with 5.mM glucose and 95% O_2/5% CO_2, and suspended on a strain gauge transducer to measure isometric circumferential tension. After adjustment basal tension to 2.0 g over 90 min, aortic rings are contracted submaximally with a thromboxane receptor agonist (U-46619) and exposed to increasing concentrations of acetylcholine (or nitroprusside as control), which is known to induce endothelium-dependent relaxation by activating e-NOS.

Data are expressed as mean (±SEM) percentage decrease in tension from the level of induced tone. Significance is determined with Student's *t*-test/two-way ANOVA.

Vascular Endothelial Cell Culture

Human arterial endothelial cells (HAECs) and human umbilical vein endothelial cells (HUVECs) are used at passages 3–8. Culture and statin incubations are conducted in Clonetics complete EGM medium (M-188-derived) with 2% serum. For experiments using redox probes, cells are grown in 24-well plates or collagen-coated glass chamber-slides to near confluency. For cell-based assays using oxyhemoglobin and cytochrome c, endothelial cell cultures are pretreated with statins in flasks, then harvested by brief trypsinization, centrifuged and suspended in KREBS-Ringer buffer with 5.5 mM glucose and 95% O_2/5% CO_2 for assay in cuvettes.

Fluorescence Assays for Intracellular Reactive Nitrogen and Oxygen Species

As peroxynitrite indicator DHR-123 is used, which is non-fluorescent and enters cells readily where it is oxidized (with limited selectivity by $^{=}$ONOO and $^{=}$OH) to the cationic, fluorescent rhodamine-123 (RH-123), which is entrapped in mitochondria (Kelm et al. 1997). Statins are added to endothelial cell cultures for 4–16 h followed by addition of DHR-123 (5 μM), bradykinin (1 μM) and A23187 (1 μM) to activate e-NOS. At the indicated times, cells are washed with PBS, and intracellular fluorescence is assayed using a fluorescent plate reader (Cytofluor-4000, $\lambda ex = 485 \pm 20$, $\lambda em = 530 \pm 25$ nm).

DHR oxidation is also assayed *ex vivo* in aortic specimens isolated from statin-treated rats. Aortic rings are incubated in 300 μl of EGM medium containing DHR-123 (5 μM), bradykinin (1 μM) and A23187 (1 μM) at 37°C for 90 min. Samples are washed twice in PBS, the homogenized in PBS + 0.1% Tween-20 +

0.1% SDS, and duplicate aliquots are taken for fluorescence readings. Protein is determined by the Bradford method. A fluorescence standard curve for DHR-123 oxidation product (HR-123) is generated and results are calculated as pmol product per mg protein.

Spectrophotometric Assay for Superoxide Anion

The assay of superoxide anion in the presence of NO in intact cells is accomplished by an adaptation of the spectrophotometric method described by Kelm et al. (1977). Endothelial cells are treated with statins in monolayer culture, then detached and resuspended in Krebs-Ringer buffer. Cells are added to cuvettes (7.5×10^5 to 1.25×10^6 cells/ml) with oxyhemoglobin (3 µM), ferricytochrome c (10 µM) and $CaCl_2$ (0.1 mM) and assayed at 37°C with continuous stirring and 95% O_2/5% CO_2 flow. Agonists are added at 5-min intervals. Absorbance spectra from 400 to 600 nm are collected at 1-min intervals using a Beckman DU-7500 diode array spectrophotometer with data capture software. The superoxide anion-specific reduction of cytochrome c is measured as the change over time in absorbance difference between 465 nm and the isosbestic wavelength 525 nm.

Fluorescence Microscopy with DHR-123 and e-NOS Immunofluorescence

Human arterial endothelial cells are grown on glass chamber slides and incubated for several hours with the statins and 10 µM DHR-123. Localization of the DHR-123 oxidized product is analyzed by epifluorescence using Nikon Microphot-FXA with Chroma High-Q resorufin filter and interference contrast optics. Images are captured using a Photometric Image Point CCD video camera. For e-NOS localization, human arterial endothelial cells are fixed and processed for immunofluorescence using rabbit polyclonal anti-eNOS antibody at 2 µg/ml and LRSC-conjugated donkey anti-rabbit IgG second antibody (Jackson Immunoresearch). Images comparing control and treated cells are obtained using the same CCD exposure times and video amplifier gain.

Subcellular Fractionation and Immunoblotting of Endothelial Cells

Human umbilical vein endothelial cells are incubated with statins followed by harvesting by scraping into 50 mM HEPES, 150 mM NaCl, 5 mM EDTA, pH 7.4, with protease inhibitors (Sigma, P-8340), and lysed by brief sonification in a glass homogenizer. Cell lysates are cleared at 500 *g* and fractionated by centrifugation at 16,000 *g*. The 16,000 *g* pellet is resuspended and ultracentrifuged in a discontinuous sucrose gradient (20 mM Tris-HCl, 1 mM EDTA, pH 7.4, with steps of 0.50 and 1.12 M sucrose) to isolate plasma membranes and Golgi/mitochondria-rich intracellular membranes. Microsomes and cytosol are isolated from the 16,000 *g* supernatant. Samples are assayed for e-NOS protein level by SDS-PAGE (4%–20% gradient gels) and western transfer to PVDF membranes (Novex LC-2002), and probed using rabbit polyclonal anti-eNOS antibody with peroxidase-linked anti-rabbit IgG for chemoluminescence and densitometry. Data are given as percentage of control absorbance units from densitometry.

Sterol Synthesis in Endothelial CELLS

Cholesterol synthesis is assayed in human arterial endothelial cells (Parker et al. 1990) grown to confluence and incubated for 16 h in serum-free standard medium + 1.0% serum albumin. Statins are added in various concentrations in DMSO vehicle and 0.5 h sterol synthesis is assayed by addition of Na-[1-^{14}C] acetate (4.0 µCi/well, 2.0 mCi/ml, 58 mCi/mmol) and incubation for 4 h at 37°C. Radiolipids in washed and lysed cells are extracted into chloroform–methanol and cell cholesterol is resolved by silica gel thin-layer chromatography. Radioactivity is determined by phosphoimager, and the 50% inhibitory concentration (IC_{50}) calculated and compared to that in vehicle controls.

EVALUATION

Data obtained by these methods suggest that the action of lipophilic statins in endothelium can shift e-NOS localization towards intracellular domains, thereby increasing the encounter with metabolically generated superoxide anion to produce peroxynitrite and related oxidants. Under some conditions, the direct action of lipophilic HMG-CoA reductase inhibitors may unbalance NO and superoxide anion fluxes and promote oxidant stress, compromising the beneficial vascular effects of e-NOS.

MODIFICATIONS OF THE METHOD

Kano et al. (1999) measured upregulation of eNOS mRNA in the rabbit aorta by a HMG-CoA reductase inhibitor using competitive reverse-transcriptase polymerase chain reaction methods.

Laufs et al. (2002) determined the expression and activity of eNOS by reverse-transcriptase polymerase chain reaction, Western blotting and arginine-citrulline assays.

Yamamoto et al. (2003) investigated the effect of a HMG-CoA reductase inhibitor on inducible nitric

oxide synthase expression in rat vascular smooth muscle cells using a modification of the semi-quantitative reverse transcription-polymerase chain reaction.

Ikeda et al. (2003) reported the protection of ischemic-reperfused myocardium in normocholesterolemic rats by a HMG-CoA reductase inhibitor.

Baetta et al. (2002) found that in the absence of lipid lowering, tissue factor expression in infiltrated inflammatory cells and macrophage accumulation in carotid lesions of cholesterol-fed rabbits are reduced by statin treatment.

Shimizu et al. (2003) performed heterotopic murine cardiac transplants in total allogenic or histocompatibility class II-mismatched combinations. Direct anti-inflammatory mechanisms of statins may contribute to the attenuation of experimental allograft arteriosclerosis.

REFERENCES AND FURTHER READING

Amin-Hanjani S, Stagliano NE, Yamada M, Huang PL, Liao JK, Moskowitz MA (2001) Mevastin, an HMG-CoA reductase inhibitor, reduces stroke damage and upregulates endothelial nitric oxide synthase in mice. Stroke 32:980–986

Baetta R, Camera M, Comparato C, Altana C, Ezekowitz MD, Tremoli E (2002) Fluvastatin reduces tissue factor expression and macrophage accumulation in carotid lesions of cholesterol-fed rabbits in the absence of lipid lowering. Arterioscler Thromb Vasc Biol 22:692–698

Ikeda Y, Young LH, Lefer AM (2003) Rosuvastin, a new HMG-CoA reductase inhibitor, protects ischemic reperfused myocardium in normocholesterolemic rats. J Cardiovasc Pharmacol 41:649–656

Jones SP, Gibson MF, Rimmer DM, Gibson TM, Sharp BR, Lefer DJ (2002) Direct vascular and cardioprotective effects of rosuvastatin, a new HMG-CoA reductase inhibitor. J Am Coll Cardiol 40:1172–1178

Kano H, Hayashi T, Sumi D, Esaki T, Asai Y, Thakur NK, Jayachandran M, Iguchi A (1999) A HMG-CoA reductase inhibitor improved regression of atherosclerosis in the rabbit aorta without affecting serum lipid levels: possible relevance of up-regulation of endothelial NO synthase mRNA. Biochem Biophys Res Commun 259:414–419

Kelm M, Dahmann R, Wink D, Feelisch M (1997) The nitric oxide/superoxide assay. J Biol Chem 272:9922–9932

Kumai T, Oonuma S, Matsumoto N, Takeba Y, Taniguchi R, Kamio K, Miyazu O, Koitabashi Y, Sekine S, Tadokoro M, Kobayashi S (2004) Anti-lipid deposition effect of HMG-CoA reductase inhibitor, pitavastin, in a rat model of hypertension and hypercholesterolemia. Life Sci 74:2129–2142

Laufs U, Gertz K, Dirnagl U, Böhm M, Nickenig G, Endres M (2002) Rosuvastatin, a new HMG-CoA reductase inhibitor, upregulates endothelial nitric oxide synthase and protects from ischemic stroke in mice. Brain Res 942:23–30

Mitani H, Egashira K, Ohashi N, Yoshikawa M, Niwa S, Nonomura K, Nakashima A, Kimura M (2003a) Preservation of endothelial function by the HMG-CoA reductase inhibitor fluvastatin through its lipid-lowering independent antioxidant properties in atherosclerotic rabbits. Pharmacology 68:121–130

Mitani H, Egashira K, Kimura M (2003b) HMG-Ca reductase inhibitor, fluvastatin, has cholesterol-lowering independent "direct" effects on atherosclerotic vessels in high cholesterol diet-fed rabbits. Pharmacol Res 48:417–427

Parker RA, Clark RW, Sit SY, Lanier TL, Grosso RA, Wright JJ (1990) Selective inhibition of cholesterol synthesis in liver vs. extrahepatic tissues by HMG CoA reductase inhibitors. J Lipid Res 31:1271–1282

Parker RA, Huang Q, Tesfamariam B (2003) Influence of 3-hydroxy-3-methylglutaryl-CoA (HMG-CoA) reductase inhibitors on endothelial nitric oxide synthase and the formation of oxidants in the vasculature. Atherosclerosis 169:19–29

Rikitake Y, Kawashima S, Takeshita S, Yamashita T, Azumi H, Yasuhara M, Nishi H, Inoue N, Yokoyama M (2001) Antioxidative properties of fluvastatin, an HMG-CoA reductase inhibitor, contribute to prevention of atherosclerosis in cholesterol-fed-rabbits. Atherosclerosis 154:87–96

Sata M, Nishimatsu H, Suzuki E, Sugiura S, Yoshizumi M, Ouchi Y, Hirata Y, Ngai R (2001) Endothelial nitric oxide synthase is essential for the HMG-CoA reductase inhibitor cerivastin to promote collateral growth ion response to ischemia. FASEB J 15:2530–2532

Shimizu K, Aikawa M, Takayama K, Libby P, Mitchell RN (2003) Direct anti-inflammatory mechanisms contribute to attenuation of experimental allograft arteriosclerosis by statins. Circulation 108:2113–2120

Sumi D, Hayashi T, Thakur NK, Jayachandran M, Asai Y, Kano H, Matsui H, Iguchi A (2001) A HMG-CoA reductase inhibitor possesses a potent anti-atherosclerotic effect other than lipid lowering effects – the relevance of endothelial nitric oxide reductase and superoxide anion scavenging action. Atherosclerosis 155:347–357

Wassmann S, Nickenig G (2003) Interrelationship of free oxygen radicals and endothelial dysfunction – modulation by statins. Endothelium 10:23–33

Yamamoto T, Takeda K, Harada S, Nakata T, Azuma A, Sasaki S, Nakagawa M (2003) HMG-CoA reductase inhibitor enhances inducible nitric oxide synthase expression in rat vascular smooth muscle cell; involvement of the Rho/Rho kinase pathway. Atherosclerosis 166:213–222

M.3.3 Inhibition of Squalene Synthase

PURPOSE AND RATIONALE

Squalene synthase (farnesyl-diphosphate:farnesyl diphosphate farnesyl-transferase) is an enzyme vital for cholesterol biosynthesis. It catalyzes the dimerization of two farnesyl pyrophosphate molecules to form squalene, a key cholesterol precursor. Unlike HMG-CoA reductase inhibitors, squalene synthase inhibitors do not lower the levels of ubiquinone and dolicol *in vivo*, both essential for cell growth and viability. Several natural and synthetic squalene synthase inhibitors have been described (Biller et al. 1991a, 1991b; Oehlschlager et al. 1991; Baxter et al. 1992; Ciosek et al. 1993; Harris et al. 1995; Lindsey and Harwood 1995; Chan et al. 1996; Dufresne et al. 1996; McTaggart et al. 1996; Amin et al. 1996, 1997; Sliskovic and Picard 1997; Rosenberg 1998; Vaidya et al. 1998; Hiyoshi et al. 2000, 2003; Ugawa et al. 2000, 2002, 2003; Amano et al. 2003; Ishihara

et al. 2003; Nishimoto et al. 2003). Ugawa et al. (2000) determined squalene synthase activities in microsomes.

PROCEDURE

Microsomes are prepared from the livers of rats, hamsters, guinea pigs, beagle dogs and rhesus monkeys as well as from HepG2 cells. The tissues or harvested cells are homogenized in 50 mM HEPES buffer using a glass homogenizer. Homogenates are centrifuged at 500 *g* for 15 min at 4°C and the resulting supernatants are further centrifuged at 8000 *g* for 15 min at 4°C. Microsomes are then isolated from this second supernatant by ultra-centrifugation at 100,000 *g* for 60 min at 4°C. The microsome precipitates are suspended in HEPES buffer (1–5 mg/ml) and stored in aliquots at –80°C.

Squalene synthase activities of these microsomes are assayed using a modification of the technique of Amin et al. (1992). The test compounds are dissolved in DMSO and the assays carried out in 50 mM HEPES buffer, pH 7.5, containing (in mM): NaF 11, $MgCl_2$ 5.5, DTT 3, NADPH 1, farnesyl pyrophosphate (FPP) 5 µM, [^{3}H]-FPP (0.017 µM, 15 Ci/mmol), NB-598, a squalene oxidase inhibitor, 10 µM and sodium pyrophosphate decahydrate 1 mM. After preincubation of these components at 30°C for 5 min, the reaction is started by the addition of microsomes (10 µg protein). The reaction is carried out at 30°C for 20 min, then terminated by addition of 100 µl of 1:1 solution of 40% (w/v) KOH:ethanol. Synthesized [^{3}H]squalene is extracted in petroleum ether and counted in Aquasol-2 using a Beckman liquid scintillation counter.

EVALUATION

Results are expressed as mean ±SEM and compared using two-way repeated analysis of variance (ANOVA).

REFERENCES AND FURTHER READING

Amano Y, Nishimoto T, Tozawa R, Ishikawa E, Imura Y, Sugiyama Y (2003) Lipid-lowering effects of TAK-475, a squalene synthase inhibitor: animal models of familial hypercholesterolemia. Eur J Pharmacol 466:155–161

Amin D, Cornell SA, Gustafson DK, Needle SJ, Ullrich JW, Bilder GE, Perrone MH (1992) Biphosphonates used for the treatment of bone disorders inhibit squalene synthase and cholesterol biosynthesis. J Lipid Res 33:1657–1663

Amin D, Rutledge RZ, Needle SN, Hele DJ, Neuenschwander K, Bush RC, Bilder GE, Perrone MH (1996) RPR 101821, a new potent cholesterol-lowering agent: inhibition of squalene synthase and 7-dehydrocholesterol reductase. Naunyn-Schmiedebergs Arch Pharmacol 353:233–240

Amin D, Rutledge RZ, Needle SN, Hele DJ, Galczenski HF, Neuenschwander K, Scotese AC, Maguire MP, Bush RC, Hele DJ, Bilder GE, Perrone MH (1997) RPR 101821, a potent squalene synthase inhibitor and orally effective cholesterol-lowering agent: comparison with inhibitors of HMG-CoA reductase. J Pharmacol Exp Ther 281:746–752

Baxter A, Fitzgerald BJ, Hutson JL, McCarthy AD, Motteram JM, Ross BC, Sapra M, Snowden MA, Watson NS, Williams RJ, Wright C (1992) Squalestatin 1, a potent inhibitor of squalene synthase, which lowers cholesterol *in vivo*. J Biol Chem 267:11705–11708

Biller SA, Forster C, Gordon EM, Harrity T, Rich LC, Marretta J, Ciosek CP (1991a) Isoprenyl phosphinylformates: new inhibitors of squalene synthetase. J Med Chem 34:1912–1914

Biller SA, Sofia MJ, DeLange B, Forster C, Gordon EM, Harrity T, Rich LC, Ciosek CP (1991b) The first potent inhibitor of squalene synthase: a profound contribution of an ether oxygen to inhibitor-enzyme interaction. J Am Chem Soc 113:8522–8524

Chan C, Andreotti D, Cox B, Dymock BW, Hutson JL, Keeling SE, McCarthy AD, Procopiou PA, Ross BC, Sareen M, Scicinski JJ, Sharatt PJ, Snowden MA, Watson MS (1996) The squalestatins: decarboxy and 4-deoxy analogues as potent squalene synthase inhibitors. J Med Chem 39:207–215

Ciosek CP Jr, Magnin DR, Harrity DW, Logan JV, Dickson JK Jr, Gordon EM, Hamilton KA, Jolibois KG, Kunselman LK, Lawrence RM (1993) Lipophilic 1,1-bisphosphonates are potent squalene synthase inhibitors and orally active cholesterol lowering agents *in vivo*. J Biol Chem 268:24832–24837

Dufresne C, Jones ETT, Omstead MN, Bergstrom JD, Wilsin KE (1996) Novel zaragozic acids from *Leptodontidium elatius*. J Nat Prod 59:52–54

Harris GH, Dufresne C, Joshua H, Koch LA, Zink DL, Salmon PM, Goklen KE, Kurtz MM, Rew DJ, Bergstrom JD, Wilson KE (1995) Isolation, structure determination and squalene synthase activity of L-731,120 and L-731,128, alkyl citrate analogs of zaragozic acids A and B. Bioorg Med Chem Lett 5:2403–2408

Hiyoshi H, Yanagimachi M, Ito M, Ohtsuka I, Yoshida I, Saeki T, Tanaka H (2000) Effect of ER-27856, a novel squalene synthase inhibitor, on plasma cholesterol in monkeys: comparison with 3-hydroxy-3-methylglutaryl-CoA reductase inhibitors. J Lipid Res 41:1136–1144

Hiyoshi H, Yanagimachi M, Ito M, Yasuda N, Okada T, Ikuda H, Shinmyo D, Tanaka K, Kuruso Y, Yoshida I, Saeki T, Tanaka H (2003) Squalene synthase inhibitors suppress triglyceride biosynthesis through the farnesol pathway in hepatocytes. J Lipid Res 44:128–135

Ishihara T, Kakuta H, Moritani H, Ugawa T, Sakamoto S, Tsukamoto S, Yanagishawa I (2003) Syntheses and biological evaluation of novel quinuclidine derivatives as squalene synthase inhibitors. Bioorg Med Chem 11:2403–2414

Lindsey S, Harwood HJ (1995) Inhibition of mammalian squalene synthase activity by zaragozig acid A is a result of competitive inhibition followed by mechanism-based irreversible inactivation. J Biol Chem 270:9083–9096

McTaggart F, Brown GR, Davidson RG, Freeman S, Holdgate GA, Mallion KB, Mirrlees DJ, Smith GJ, Ward WH (1996) Inhibition of squalene synthase of rat liver by novel 3′substituted quinuclidines. Biochem Pharmacol 51:1477–1487

Nishimoto T, Amano Y, Tozawa R, Ishikawa E, Imura Y, Yukimasa H, Sugiyama Y (2003) Lipid-lowering properties of TAK-475, a squalene synthase inhibitor in vivo and in vitro. Br J Pharmacol 139:911–918

Oehlschlager AC, Singh SM, Sharma S (1991) Squalene synthetase inhibitors: synthesis of sulfonium ion mimics of the carbocationic intermediates. J Org Chem 56:3856–3861
Rosenberg SH (1998) Squalene synthase inhibitors. Exp Opin Ther Pat 8:521–530
Sliskovic DR, Picard JA (1997) Squalene synthase inhibitors. Emerg Drugs 2:93–107
Ugawa T, Kakuta H, Moritani H, Matsuda K, Ishihara T, Yamaguchi M, Naganuma S, Iizumi Y, Shikama H (2000) YM-53601, a novel squalene synthase inhibitor, reduces plasma cholesterol and triglyceride levels in several animal species. Br J Pharmacol 131:63–70
Ugawa T, Kakuta H, Inagaki O (2002) Effect of YM-53691, a novel squalene synthase inhibitor, on the clearance rate ofplasma LDL and VLDL in hamsters. Br J Pharmacol 137:561–569
Ugawa T, Kakuta H, Moritani H, Inagaki O, Shikama H (2003) YM-53601. a novel squalene synthase inhibitor, suppresses lipogenic biosynthesis and lipid secretion in rodents. Br J Pharmacol 139:140–146
Vaidya S, Bostedor R, Kurtz MM, Bergstrom JD, Bansal VS (1998) Massive production of farnesol-derived dicarboxylic acids in mice treated with the squalene synthase inhibitor zaragozic acid A. Arch Biochem Biophys 355:84–92

M.3.4 Inhibition of Squalene Epoxidase

PURPOSE AND RATIONALE

Squalene epoxidase is a microsomal enzyme that catalyses the oxidation of squalene to 2,3-oxidosqalene, the last reaction of non-sterol metabolites in the cholesterol biosynthesis pathway (Hidaka et al. 1990). Inhibitors of this enzyme are unlikely to block the production of biologically important non-sterol products, such as isoprenyl adenine, dolichol, coenzyme Q, or heme A, in contrast with HMG-CoA reductase inhibitors, which inhibit their production (Ghirlanda et al. 1993; Chugh et al. 2003). Several squalene epoxidase inhibitors have been described (Horie et al. 1990, 1991; Hikada et al. 1991; Moore et al. 1992; Gotteland et al. 1998; Sawada et al. 2001, 2004).

Sawada et al. (2001) described a modified squalene epoxidase assay.

PROCEDURE

HepG2 cells are cultured routinely in medium A (Eagle's modified minimum essential medium supplemented with 1 mM pyruvate and non-essential amino acids with 10% heat-inactivated fetal calf serum) at 37°C in a humidified 95% O_2/5% CO_2 air atmosphere.

For the assay, the cells are grown in 225-cm^2 culture flasks, and incubated for 18 h in medium A containing 10% human lipoprotein-deficient serum and 1 μM of the squalene synthase inhibitor L-654,949, to increase the squalene epoxidase activity. The HepG2 cells are washed and harvested by trypsin treatment. After centrifugation (100 *g*, 5 min at 4°C), the supernatant fraction is removed by aspiration. The cell pellet is frozen and kept at –80°C until use. On the day of the experiment, the cell pellet is thawed, ruptured by sonication (5 s at 4°C) in 0.1 M Tris-HCl, pH 7.5 containing 1 mM EDTA, mixed4$:1 with 2% Triton X-100, allowed to stand at 4°C for 30 min, and assayed for squalene epoxidase activity (Tai and Bloch 1972). Aliquots of the mixture are incubated for 90 min at 37°C with or without test compound dissolved in 1% DMSO in a final volume of 0.3 ml containing 0.1 M Tris-HCl, pH 7.5, 1 mM EDTA, 1 mM NADPH, 1 mM FAD, 0.3 mM AMO1618 (an inhibitor of 2,3-oxidosqualene cyclase), 0.17% Triton X-100, and 8 μM [^{3}H]-squalene (3.7 kBq) dispersed in 0.075% Tween 80. The reaction is stopped by the addition of 0.3 ml of 10% ethanolic KOH. After incubation for 90 min at 75°C, non-saponifiable materials are extracted with 2 ml of petroleum ether. The extracts are evaporated under a nitrogen stream. The residue is taken up in a small volume of diethyl ether, spotted on a silica gel thin layer chromatography plate and developed in benzene/ethyl acetate (99.5:0.5, v/v). The radioactivity corresponding to 2,3-oxidosqualene is counted by autoradiography.

EVALUATION

The results are expressed as means ±SD and evaluated by repeated-measures analysis of variance, followed by Dunnett's multiple comparisons.

MODIFICATIONS OF THE METHOD

A simplified squalene epoxidase assay based on HPCL separation and time-dependent UV/visible determination of squalene is published by Grieveson et al. (1997).

REFERENCES AND FURTHER READING

Chugh A, Ray A, Gupta JB (2003) Squalene epoxidase as hypocholesterolemic drug revisited. Prog Lipid Res 42:37–50
Ghirlanda G, Oradei A, Manto A, Lippa S, Uccioli L, Caputo S, Greco AV, Littarru GP (1993) Evidence of plasma CoQ10-lowering effect by HMG-CoA reductase inhibitors. A double-blind, placebo-controlled study. J Clin Pharmacol 33:226–229
Gotteland JP, Loubat C, Planty B, Junquero D, Delhon A, Halazy S (1998) Sulfonamide derivatives of benzylamine block cholesterol biosynthesis in HepG-2 cells: a new type of squalene epoxidase inhibitors. Bioorg Med Chem Lett 8:1337–1342
Grieveson LA, Ono T, Sakakibara J, Derrick JP, Dickinson JM, McMahon A, Higson SPJ (1997) A simplified squalene epoxidase assay based on an HPCL separation and time-

dependent UV/visible determination of squalene. Anal Biochem 252:19–23
Hidaka Y, Sato T, Kamei T (1990) Regulation of squalene epoxidase in HepG2 cells. J Lipid Res 31:2087–2094
Hikada Y, Hotta H, Nagata Y, Iwasawa Y, Horie M, Kamei T (1991) Effect of a novel squalene epoxidase inhibitor, NB-598, on the regulation of cholesterol metabolism in HepG2 cells. J Biol Chem 266:13171–13177
Horie M, Tsuchiya Y, Hayashi M, Iida Y, Iwasawa Y, Nagata Y, Sawasaki Y, Fukuzumi H, Kitani K, Kamei T (1990) NB-598: a potent competitive inhibitor of squalene epoxidase. J Biol Chem 265:18075–18078
Horie M, Sawasaki Y, Fukuzumi H, Watanabe K, Iuzuka Y, Tsuchiya Y, Kamei T (1991) Hypolipidemic effects of NB-598 in dogs. Atherosclerosis 88:183–192
Moore WR, Schatzman GL, Jarvi ET, Gross RS, McCarthy JR (1992) Terminal difluoro olefin analogues of squalene are time-dependent inhibitors of squalene epoxidase. J Am Chem Soc 114:360–361
Sawada M, Matsuo M, Hagihara H, Tenda N, Nagayoshi A, Okumura H, Washizuka KI, Seki J, Goto T (2001) Effect of FR194738, a potent inhibitor of squalene epoxidase, on cholesterol metabolism in HepG2 cells. Eur J Pharmacol 431:11–16
Sawada M, Washizuka K, Okumura H (2004) Synthesis and biological activity of a novel squalene epoxidase inhibitor, FR194738. Bioorg Med Chem Lett 14:633–637
Tai HH, Bloch K (1972) Squalene epoxidase of rat liver. J Biol Chem 247:3767–3773

M.4 Inhibition of Cholesterol Absorption

M.4.1 Inhibition of ACAT (Acyl Coenzyme A: Cholesterol Acyltransferase)

M.4.1.1 General Considerations

Acyl coenzyme A:cholesterol acyltransferase (ACAT), which catalyses the intracellular formation of cholesteryl esters, plays an important role in the intestinal absorption of cholesterol, foam cell formation within the arterial wall and VLDL production in the liver. Two isoforms of the enzyme exist, ACAT1 expressed in macrophages and ACAT2 expressed in intestine and liver. Cholesterol is absorbed from the gut exclusively in the unesterified form, but appears in the lymph esterified with various long-chain unsaturated fatty acids. The enzyme responsible is ACAT, a microsomal enzyme, that utilizes long-chain fatty acyl coenzyme A and cholesterol as substrates. ACAT inhibitors also have potential actions beyond inhibition of cholesterol absorption. Inhibition of hepatic ACAT could reduce the production of cholesteryl esters for packaging into lipoproteins, while inhibition of ACAT1 in macrophages could reduce the deposition of cholesteryl esters and prevent the formation of foam cells and atherosclerotic lesions. Nevertheless, from investigations in ACAT2 knockout mice it is known that ACAT2 is not the only rate-limiting pathway for cholesterol absorption. On normal chow these mice absorp cholesterol as efficiently as wild-type mice, only if mice were fed a cholesterol-enriched diet. ACAT2 is important for cholesterol absorption (Lee et al. 2004; Repa et al. 2004). Under physiological conditions alternative pathways compensate for the ACAT2 deficiency in mice (Hussain et al. 2005).

Human ACAT cDNA was cloned from a human macrophage cDNA library and expressed in an ACAT deficient line of Chinese hamster ovary cells. The cDNA, labelled K1, encoded an integral membrane protein of 550 amino acids (Chang et al. 1993). The inhibition of ACAT as treatment for hypercholesterolemia and atherosclerosis is an attractive target.

REFERENCES AND FURTHER READING

Chang CCY, Huh HY, Cadigan KM, Chang TY (1993) Molecular cloning and functional expression of human acyl-coenzyme A:cholesterol acyltransferase cDNA in mutant Chinese hamster ovary cells. J Biol Chem 268:20747–20755
Clark SB, Tercyak AM (1984) Reduced cholesterol transmucosal transport in rats with inhibited mucosal acyl CoA:cholesterol acyltransferase and normal pancreatic function. J Lipid Res 25:148–159
Field FJ, Albright E, Mathur S (1991) Inhibition of acyl-coenzyme A:cholesterol acyltransferase activity by PD 128042: effect on cholesterol metabolism and secretion in CaCo-2 cells. Lipids 26:1–8
Fukushima H, Aono S, Nakamura Y, Endo M, Imai T (1969) The effect of *N*-(α-methylbenzyl)linoleamide on cholesterol metabolism in rats. J Atheroscler Res 10:403–414
Harnett KM, Walsh CT, Zhang L (1989) Effects of Bay o 2752, a hypocholesterolemic agent, on intestinal taurocholate absorption and cholesterol esterification. J Pharm Exp Ther 251:502–509
Heider JG, Pickens CE, Kelly LA (1983) Role of acyl CoA:cholesterol acyltransferase in cholesterol absorption and its inhibition by 57–118 in the rabbit. J Lipid Res 24:1127–1134
Hussain MM, Fatma S, Pan X, Iqbal J (2005) Intestinal lipoprotein assembly. Curr Opin Lipidol 16:281–285
Krause BR, Anderson M, Bisgaier CL, Bocan T, Bousley R, DeHart P, Essenburg A, Hamelehle K, Homan R, Kieft K, McNally W, Stanfield R, Newton RS (1993) *In vivo* evidence that the lipid-regulating activity of the ACAT inhibitor CI-976 in rats is due to inhibition of both intestinal and liver ACAT. J Lipid Res 34:279–294
Largis EE, Wang CW, DeVries VG, Schaffer SA (1989) CL 277,082, a novel inhibitor of ACAT-catalyzed cholesterol esterification and cholesterol absorption. J Lipid Res 30:681–690
Lee RG, Kelly KL, Sawyer JK et al (2004) Plasma cholestery ester provided by lecithin: cholesterol acyltransferase and acyl-coenzyme a: cholesterol acyltransferase 2 have opposite atherosclerotic potential. Circ Res 95:998–1004

Matsuda K (1994) ACAT inhibitors as antiatherosclerotic agents: Compounds and mechanisms. Med Res Rev 14:271–305
Nervi F, Brinfman M, Allalón W, Depiereux E, Del Pozo R (1984) Regulation of biliary cholesterol secretion in the rat. Role of hepatic esterification. J Clin Invest 74:2226–2237
O'Brien PM, Sliskovic DR (1992) ACAT inhibitors: A potential new approach to the treatment of hypercholesterolaemia and atherosclerosis. Curr Opin Ther Pat 2:507–526
Picard JA (1993) ACAT inhibitors. Curr Opin Ther Pat 3:151–160
Repa JJ, Buhmann KK, Farese RV Jr et al (2004) ACAT2 deficiency limits cholesterol absorption in the cholesterol-fed mouse: impact on hepatic cholesterol homeostasis. Hepatology 40:1088–1097
Roark WH, Roth BC (1994) ACAT inhibitors: preclinical profiles of clinical candidates. Expert Opin Invest Drugs 3:1143–1152
Rodgers JB (1969) Assay of acyl-CoA:monoglyceride acyltransferase from rat small intestine using continuous recording spectroscopy. J Lipid Res 10:427–432
Sliskovic DR, White AD (1991) Therapeutic potential of ACAT inhibitors as lipid lowering and anti-atherosclerotic agents. Trends Pharmacol Sci 12:194–199
Tanaka H, Kimura T (1994) ACAT inhibitors in development. Expert Opin Invest Drugs 3:427–436
Tso P, Morshed KM, Nutting DF (1991) Importance of acyl CoA:cholesterol acyltransferase (ACAT) on the esterification of cholesterol by enterocytes. FASEB J 5:A709
Windler E, Rücker W, Greeve J, Reimitz H, Greten H (1990) Influence of the acyl-coenzyme A:cholesterol-acyltransferase inhibitor octimibate on cholesterol transport in rat mesenteric lymph. Arzneim Forsch/Drug Res 40:1108–1111

M.4.1.2 In Vitro ACAT Inhibitory Activity

PURPOSE AND RATIONALE

In vitro ACAT inhibitory activity can be determined in microsomal preparations from liver or intestine of rabbits.

PROCEDURE

Hepatic or intestinal microsomes are prepared from rabbits. Prior to sacrifice, the animals receive chow supplemented with 2% cholesterol and 10% safflower oil for 6 weeks. Each assay contains 0.2 mg of microsomal protein and fatty acid-poor bovine serum albumin (3 mg/ml) in 0.04 M KH_2PO_4 buffer, pH 7.4, containing 0.05 M KCl, 0.03 M EDTA, and 0.3 M sucrose. Drug dilutions are made in DMSO (5 µl DMSO/200 µl total incubation volume). The reaction is started by the addition of [^{14}C]oleyl CoA (50 µM, 7 dpm/pmol). After 3 min the reaction is stopped by the addition of chloroform-methanol 2:1. [^{3}H]Cholesteryl oleate is used as an internal standard. Lipid extracts are dissolved in chloroform, spotted on TLC plates (silica gel G) and developed in hexane-petroleum ether-acetic acid 80:20:1. Unlabeled, carrier cholesterol oleate is added to the internal standard to aid band visualization with iodine vapor. The band corresponding to cholesteryl esters is then scraped into scintillation vials and radioactivity is determined by liquid scintillation spectroscopy.

EVALUATION

For each compound four concentrations are evaluated in duplicate. IC_{50} values are determined by performing a nonlinear least-squares fit of the data to a log dose-response curve.

MODIFICATIONS OF THE METHOD

Rothblatt et al. (1977) studied ACAT activity in Fu5 rat hepatoma cells under the influence of hyperlipemic serum lipoproteins.

Mathur et al. (1981) studied ACAT activity in hepatic microsomes of cynomolgus monkeys during diet-induced hypercholesterolemia.

Einarsson et al. (1989) studied acyl-CoA: cholesterol acyltransferase activity in human liver microsomes.

Largis et al. (1989) found CL 277,082 to be a potent inhibitor of ACAT in microsomes from a variety of tissues and smooth muscle cells in culture.

Heffron et al. (1990) studied ACAT inhibition in microsomal fractions of the transformed mouse macrophage J774.

Bell et al. (1992) measured ACAT inhibition in cultured Fu5AH cells.

Field et al. (1991), Krause et al. (1993) tested the inhibition of ACAT in CaCo-2 cells.

REFERENCES AND FURTHER READING

Bell FP, Gammil RB, John LCS (1992) U-73482: A novel ACAT inhibitor that elevates HDL-cholesterol, lowers plasma triglyceride and facilitates hepatic cholesterol mobilization in the rat. Atherosclerosis 92:115–122
Einarsson K, Benthin L, Ewerth S, Hellers G, Stwåhlberg D, Angelin B (1989) Studies on acyl-CoA:cholesterol acyltransferase activity in human liver microsomes. J Lipid Res 30:739–746
Field FJ, Salome RG (1982) Effect of dietary fat saturation, cholesterol and cholestyramine on acyl CoA:cholesterol acyltransferase activity in rabbit intestinal microsomes. Biochim Biophys Acta 712:557–570
Field FJ, Albright E, Mathur S (1991) Inhibition of acylcoenzyme A:cholesterol acyltransferase by PD 128042: effect on cholesterol metabolism and secretion in CaCo-2 cells. Lipids 26:1–8
Heffron F, Middleton B, White DA (1990) Inhibition of acyl coenzyme A:cholesterol acyl transferase by trimethylcyclohexanylmandelate (Cyclandelate). Biochem Pharmacol 39:575–580
Helgerud P, Saarem K, Norum KR (1981) Acyl-CoA:cholesterol acyltransferase in human small intestine: its activity and

some properties of the enzymic reaction. J Lipid Res 22:271–277
Krause BR, Anderson M, Bisgaier CL, Bocan T, Bousley R, DeHart P, Essenburg A, Hamelehle K, Homan R, Kieft K, McNally W, Stanfield R, Newton RS (1993) *In vivo* evidence that the lipid-regulating activity of the ACAT inhibitor CI-976 in rats is due to inhibition of both intestinal and liver ACAT: J Lipid Res 34:279–294
Largis EE, Wang CH, DeVries VG, Schaffer SA (1989) CL 277,082: a novel inhibitor of ACAT-catalyzed cholesterol esterification and cholesterol absorption. J Lipid Res 30:681–690
Mathur SN, Armstrong ML, Alber CA, Spector AA (1981) Hepatic acyl-CoA:cholesterol acyltransferase activity during diet-induced hypercholesterolemia in cynomolgus monkeys. J Lipid Res 22:659–667
Roth BD, Blankley CJ, Hoefle ML, Holmes A, Roark WH, Trivedi BK, Essenburg AD, Kieft A, Krause BR, Stanfield RL (1992) Inhibitors of acyl CoA:cholesterol acyltransferase. 1. Identification and structure-activity relationships of a novel series of fatty acid anilide hypocholesterolemic agents. J Med Chem 35:1609–1617
Rothblatt GH, Naftulin M, Arbogast LY (1977) Stimulation of acyl-CoA:cholesterol acyltransferase activity by hyperlipemic serum lipoproteins. Proc Soc Exp Biol Med 155:501–506
Schmitz G, Niemann R, Brennhausen B, Krause R, Assmann G (1985) Regulation of high density lipoprotein receptors in cultured macrophages: role of acyl-CoA:cholesterol acyltransferase. EMBO J 4:2773–2779

M.4.1.3 In Vivo Tests for ACAT Inhibitory Activity

PURPOSE AND RATIONALE

Most authors test the *in vivo* anti-atherosclerotic and antihyperlipemic effect of ACAT inhibitors in cholesterol-fed hypercholesterolemic animals (Balasubramaniam et al. 1990; Harris et al. 1992; Tanaka et al. 1944). Krause et al. (1993a) used the Zilversmit dual isotope technique (Zilversmit 1972; Cayen and Dvornik 1979) for determining cholesterol absorption in rats.

PROCEDURE

Male Sprague-Dawley rats weighing 200–225 g are fed with a diet containing 5.5% peanut oil, 0.5% cholic acid and 1.5% cholesterol with or without (controls) drugs for 1 week. On the last day, food is removed at 8:00 A.M. and the isotopes are administered beginning at 2:00 P.M. [^{3}H]cholesterol (13 µCi/rat) is given by oral gavage and [^{14}C]cholesterol (1.5 µCi/rat) is given is given by tail vein injection. The [^{3}H]cholesterol is prepared as an emulsion by dissolving 125 mg cholesterol in 1625 mg olive oil. The oil phase is suspended by sonication in 25 ml of water containing 156 mg taurocholate (sodium salt). Each animal receives 1 ml. The intravenous dose is prepared by drying the labeled cholesterol (50 µCi), and then adding 300 µl warm ethanol followed by 12.5 ml of saline. Each animal receives 0.5 ml of this colloidal suspension. The rats are allowed to consume their respective diets at 3:00 P.M., and are sacrificed 48 h after the isotope administration.

EVALUATION

The percentage of an oral dose of cholesterol absorbed is calculated from the plasma isotope ratio (% of the oral dose in 2 ml plasma/of the intravenous dose in 2 ml plasma × 100).

FURTHER IN VIVO METHODS

Heider et al. (1983) measured cholesterol absorption via the Zilversmit dual isotope method in rabbits.

Gillies et al. (1990) studied the regulation of ACAT activity by a cholesterol substrate pool during the progression and regression phases of atherosclerosis in rabbits with dietary induced atherosclerosis.

Krause et al. (1993b) compared the activities of two ACAT-inhibitors in normocholesterolemic and hypercholesterolemic rats, rabbits, guinea pigs and dogs.

Nagata et al. (1995) tested a new ACAT inhibitor in diet-induced atherosclerosis formation in female C57BL/6J mice.

Bocan et al. (1993) described a reduction of VLDL and vessel wall cholesteryl ester content in Yucatan micropigs after treatment with an ACAT inhibitor.

REFERENCES AND FURTHER READING

Balasubramaniam S, Simons LA, Chang S, Roach PD, Nestel PJ (1990) On the mechanisms by which an ACAT inhibitor (CL 277,082) influences plasma lipoproteins in the rat. Atherosclerosis 82:1–5
Bocan TMA, Muellers BAK, Uhlendorf PD, Quenby-Brown E, Mazur MJ, Black AE (1993) Inhibition of acyl-CoA:cholesterol *O*-acyl transferase reduces the cholesterol enrichment of atherosclerotic lesions in the Yucatan micropig. Atherosclerosis 99:175–186
Cayen MN, Dvornik D (1979) Effect of diosgenin on lipid metabolism in rats. J Lipid Res 20:162–174
Gillies PJ, Robinson CS, Rathgeb KA (1990) Regulation of ACAT activity by a cholesterol substrate pool during the progression and regression phases of atherosclerosis: implications for drug discovery. Atherosclerosis 83:177–185
Harris NV, Smith C, Ashton MJ, Bridge AW, Bush RC, Coffee ECJ, Dron DI, Harper MF, Lythgoe DJ, Newton CG, Riddell D (1992) Acyl-CoA:cholesterol *O*-acyl transferase (ACAT) inhibitors. 1. 2-(Alkylthio)-4,5-diphenyl-1*H*-imidazoles as potent inhibitors of ACAT. J Med Chem 35:4384–4392
Heider JG, Pickes CE, Kelly LA (1983) Role of acyl-CoA:cholesterol acyltransferase in cholesterol absorption and its inhibition by 57–118 in the rabbit. J Lipid Res 24:1127–1134
Krause BR, Anderson M, Bisgaier CL, Bocan T, Bousley R, DeHart P, Essenburg A, Hamelehle K, Homan R, Kieft K, McNally W, Stanfield R, Newton RS (1993a) *In vivo* evidence

that the lipid-regulating activity of the ACAT inhibitor CI-976 in rats is due to inhibition of both intestinal and liver ACAT: J Lipid Res 34:279–294

Krause BR, Black A, Bousley R, Essenburg A, Cornicelli J, Holmes A, Homan R, Kieft K, Sekere C, Shaw-Hes MK, Stanfield R. Trivedi B, Woolf T (1993b) Divergent pharmacological activities of PD 132301–2 and CL 277,082, urea inhibitors of acyl-CoA:cholesterol acyltransferase. J Pharm Exp Ther 267:734–743

Nagata Y, Yonemoto M, Iwasawa Y, Shimuzi-Nagumo A, Hattori H, Sawazaki Y, Kamei T (1995) *N*-[2-[*N*'-Pentyl-(6,6-dimethyl-2,4-heptadinyl)amino]ethyl]-(2-methyl-1-naphthylthio)acetamide (FY-087). A new acyl coenzyme A:cholesterol acyltransferase (ACAT) inhibitor of diet-induced atherosclerosis formation in mice. Biochem Pharmacol 49:643–651

Tanaka H, Ohtsuka I, Kogushi M, Kimura T, Fujimori T, Saeki T, Hayashi K, Kobayashi H, Yamada T, Hiyoshi H, Saito I (1994) Effect of the acyl-CoA:cholesterol acyltransferase inhibitor, E5324, on experimental atherosclerosis in rabbits. Atherosclerosis 107:187–210

Zilversmit DB (1972) A single blood sample dual isotope method for the measurement of cholesterol absorption in rats. Proc Soc Exp Biol Med 140:862–865

M.4.1.4 Lymph Fistula Model for Cholesterol Absorption

PURPOSE AND RATIONALE

Direct evidence for an inhibitory effect on cholesterol absorption can be obtained by the lymph-fistula model in rats. This model also provides an indication as to the duration of inhibition and the relative selectivity of the compound on the absorption of cholesterol versus triglyceride and phospholipid.

PROCEDURE

Rats are anesthetized by an intramuscular injection of tiletamine/zolazepam (Telazol, 40 mg/kg). Silicon rubber cannulae are placed into the main mesenteric lymph duct and into the duodenum and secured with sutures. Animals are allowed to recover from surgery overnight in restraining cages while infused intraduodenally with 2% dextrose in saline containing 0.03% KCl (2.5 ml/h). Drinking water is allowed at libitum during this recovery period.

At 6:00 A.M. the following day, the drinking water is removed and a 2-h basal lymph sample is collected. Then, the animals are given the ACAT inhibitor at a specified dose as a single bolus into the duodenal cannula using a aqueous CMC/Tween suspension vehicle. Controls receive a bolus injection of the vehicle alone. Immediately after the drug dose, a lipid emulsion containing 0.1% cholesterol, 0.11% sodium taurocholate, 15% Intralipid (20%, Kabivitrium Inc.), 2.4% safflower oil, and 82.6% saline is infused into the duodenal cannula (3 ml/h). Then, four 2-h lymph collections are obtained. The lymph samples are extracted into hexane in the presence of a stigmasterol internal standard. Total and free cholesterol are quantitated by liquid gas chromatography.

EVALUATION

Esterified cholesterol of lymph is determined from difference between total and free cholesterol.

MODIFICATIONS OF THE METHOD

The lymph fistula model can also be used to examine the effect of ACAT inhibitors on the absorption of endogenous (i. e. biliary) cholesterol. Cannulated rats are infused intraduodenally with the saline/dextrose solution to which 2% whole rat bile is added containing [^{14}C]cholesterol. No nonradiolabeled lipid other than that in bile is infused into the animals, and hence, lymph cholesterol is exclusively of biliary origin. Hourly collections of lymph are obtained with the use of fraction collectors. Lymph is extracted with 3 volumes of ethylacetate-acetone 2:1 (Slayback et al. 1977). The total ^{14}C label of an aliquot of lymph extract is determined by liquid scintillation spectroscopy. The lymph extracts are resuspended in 100 µl chloroform-methanol 2:1 and spotted on Whatman LK6D TCL plates. The plates are developed in hexane-diethylether-acetic acid 85:15:1. The distribution of ^{14}C label between the cholesteryl ester and cholesterol bands are visualized and quantified by exposing the plates to phosphor imaging plates for 16 h and then scanning the imaging screens on a Molecular Dynamics Phosphorimager.

Clark and Tercyak (1984) studied the absorption of cholesterol during inhibition of mucosal acyl-CoA: cholesterol acyltransferase in mesenteric lymph fistula rats with normal pancreatic function.

Åkerlund and Björkhem (1990), Björkhem et al. (1993) used the lymph-fistula model in rats for studies on the link between HMG-CoA reductase and cholesterol 7α-hydroxylase. The thoracic lymph duct was cannulated just proximal to the cisterna magna through an abdominal approach. The proximal part of the lymph duct was ligated. The cannula exited at the back of the animal. The lymph was allowed to flow freely from the animal to the bottom of the metabolic cages. Under these conditions, the rats could move freely in the cages during the lymphatic drainage.

CRITICAL ASSESSMENT OF THE METHOD

Gallo et al. (1987) found normal cholesterol absorption in rats in which intestinal acyl coenzyme A:cholesterol acyltransferase activity was significantly reduced by

ACAT-inhibitors. This challenges the value of ACAT-inhibition at least in normal individuals.

REFERENCES AND FURTHER READING

Åkerlund JE, Björkhem I (1990) Studies on the regulation of cholesterol 7α-hydroxylase and HMG-CoA reductase in rat liver: effects of lymphatic drainage and ligation of the lymph duct. J Lipid Res 31:2159–2166

Björkhem I, Andersson U, Sudjama-Sugiaman E, Eggertsen G, Hylemon Ph (1993) Studies on the link between HMG-CoA reductase and cholesterol 7α-hydroxylase in lymph-fistula rats: evidence for both transcriptional and post-transcriptional mechanisms for down-regulation of the two enzymes by bile acids. J Lipid Res 34:1497–1503

Clark SB, Tercyak AM (1984) Reduced cholesterol transmucosal transport in rats with inhibited mucosal acyl-CoA:cholesterol acyltransferase and normal pancreatic function. J Lipid Res 25:148–159

Gallo LL, Wadsworth JA, Vahouny GV (1987) Normal cholesterol absorption in rats deficient in intestinal acyl coenzyme A:cholesterol acyltransferase activity. J Lipid Res 28:381–387

Krause BR, Sloop CH, Castle CK, Roheim PS (1981) Mesenteric lymph apolipoproteins in control and ethinyl estradiol-treated rats: a model for studying apolipoproteins from intestinal origin. J Lipid Res 22:610–619

Krause BR, Anderson M, Bisgaier CL, Bocan T, Bousley R, DeHart P, Essenburg A, Hamelehle K, Homan R, Kieft K, McNally W, Stanfield R, Newton RS (1993) *In vivo* evidence that the lipid-regulating activity of the ACAT inhibitor CI-976 in rats is due to inhibition of both intestinal and liver ACAT. J Lipid Res 34:279–294

Krause BR, Anderson M, Bisgaier CL, Bocan T, Bousley R, DeHart P, Essenbug A, Hamelehle K, Homan R, Kieft K, McNally W, Stanfield R, Newton RS (1993b) *In vivo* evidence that the lipid-regulating activity of the ACAT inhibitor CI-976 in rats is due to inhibition of both intestinal and liver ACAT: J Lipid Res 34:279–294

Slayback JRB, Cheung LWY, Geyer RP (1977) Quantitative extraction of microgram amounts of lipid from cultured human cells. Anal Biochem 83:372–384

Sugiyama Y, Ishikawa E, Odaka H, Miki N, Tawada H, Ikeda H (1995) TMP-153, a novel ACAT inhibitor, inhibits cholesterol absorption and lowers cholesterol in rats and hamsters. Atherosclerosis 113:71–78

M.5 Interruption of Bile Acid Recirculation

M.5.0.1 Cholestyramine Binding

PURPOSE AND RATIONALE

Cholesterol is metabolized in the liver by oxidation to bile acids which undergo enterohepatic circulation. In the untreated state, approximately 95% of the bile acids that are secreted are reabsorbed and returned to the liver, while the small loss is replaced by de novo biosynthesis from cholesterol. Increased excretion of bile acids with the feces increases the rate of oxidation of cholesterol in the liver leading to a partial depletion of the hepatic cholesterol pool. A compensatory increase in uptake via the LDL receptors results in lower serum LDL levels. This can be achieved by addition of a bile acid binding resin, e. g., cholestyramine, to the food. The binding of unconjugated and conjugated bile-salt anions can be tested *in vitro* (Johns and Bates 1969).

PROCEDURE

Rabbits weighing 2.5–3 kg are switched from standard food to a diet containing 10–20% polymeric basic-anion exchanging resin, e. g. cholestyramine. Cholesterol levels in serum are measured at the beginning and at the end of a 4 weeks feeding period.

EVALUATION

Cholesterol levels as means ±SD are calculated for controls and treated animals and compared by statistical analysis.

MODIFICATION OF THE METHOD

Tennent et al. (1960) tested polymeric organic bases for action on blood cholesterol in 4-day experiments and in experiments of 7–8 weeks duration in cholesterol-fed White Leghorn cockerels. The birds were given a diet containing 2% cholesterol and 5% cotton-seed oil with or without addition of polymeric bases. The increase of cholesterol and the incidence of aortic atheromatosis was decreased by polymeric organic bases.

Day (1990) compared the hypocholesterolemic activities of the bile acid sequestrants cholestyramine and cholestipol hydrochloride in cholesterol fed sea quail.

Quaternary ammonium conjugates of bile acid inhibited cholic acid binding and transport in everted ileal sacs of guinea pigs *in vitro* (Fears et al. 1990).

REFERENCES AND FURTHER READING

Ast M, Frishman WH (1990) Bile acid sequestrants. J Clin Pharmacol 30:99–106

Curtius HCh, Bürgi W (1966) Gaschromatographische Bestimmung des Serumcholesterins. Z klin Chem klin Biochem 4:38–42

Day ChE (1990) Comparison of hypocholesterolemic activities of the bile acid sequestrants cholestyramine and cholestipol hydrochloride in cholesterol fed sea quail. Artery 17:281–288

Fears R, Brown R, Ferres H, Grenier F, Tyrell AWR (1990) Effects of novel bile salts on cholesterol metabolism in rats and guinea-pigs. Biochem Pharmacol 40:2029–2037

Johns W, Bates T (1969) Quantification of the binding tendencies of cholestyramine I: Effect of structure and added electrolytes on the binding of unconjugated and conjugated bile salt anions. J Pharmac Sci 58:179–183

Kihara K, Toda H, Mori M, Hashimoto M, Mizogami S (1988) The bile acid binding and hypocholesterolemic activity of anion-exchange resins bearing the imidazolium salt group. Eur J Med Chem 23:411–415

Tennent DM, Siegel H, Zanetti ME, Kuron GW, Ott WH, Wolf FJ (1960) Plasma cholesterol lowering action of bile acid binding polymers in experimental animals. J Lipid Res 1:469–473

Toda H, Kihara K, Hashimoto M, Mizogami S (1988) Bile acid binding and hypocholesterolemic activity of a new anion exchange resin from 2-methylimidazol and epichlorhydrin. J Pharm Sci 77:531–533

M.6
Inhibition of Lipid Oxidation

M.6.0.1
General Considerations

Oxidative modification of the low density lipoproteins (LDL) has been shown to cause accelerated degradation of LDL via the scavenger receptor pathway. Under conditions of high serum LDL levels, LDL particles can migrate into the subendothelial space where oxidation of LDL can occur. The actual oxidation process is believed to begin with lipid peroxidation, followed by fragmentation to result in short-chain aldehydes. These aldehydes can form adducts with the lysine residues of apo B, creating a new epitope which is recognized by the scavenger receptor of macrophages.

During the same process, lecithin is converted to lysolecithin, which is a selective chemotactic agent for monocytes. The monocytes adhere to the arterial wall and penetrate through to the subendothelium. Once there, the monocyte changes to a tissue macrophage which takes up the oxidized LDL via the scavenger receptor. The uptake of oxidized LDL continues until the macrophage is engorged with cholesteryl esters ultimately forming a foam cell. Groups of these foam cells constitute a fatty streak. By inhibiting the oxidation of LDL, it is hoped that the modification of apo B and the production of chemotactic lysolecithin can be prevented.

The family of receptors for mammalian low-density proteins has been reviewed by Hussain et al. (1999).

REFERENCES AND FURTHER READING

Bruckdorfer KR (1990) Free radicals, lipid peroxidation and atherosclerosis. Curr Opin Lipidol 1:529–535

Esterbauer H, Rotheneder M, Striegl G, Waeg G, Ashy A, Sattler W, Jürgens G (1989) Vitamin E and other lipophilic anti-oxidants protect LDL against oxidation. Fat Sci Technol 91:316–324

Hussain MM, Strickland DK, Bakillah A (1999) The mammalian low-density lipoprotein receptor family. Annu Rev Nutr 19:141–172

Jürgens G (1989) Modified serum lipoproteins and atherosclerosis. Ann Rep Med Chem 25:169–176

McCarthy PA (1993) New approaches to atherosclerosis: An overview. Med Res Rev 13:139–159

Parthasarathy S, Wieland E, Steinberg D (1989) A role for endothelial cell lipoxygenase in the oxidative modification of low density lipoprotein. Proc Natl Acad Sci USA 86:1046–1050

Rankin SM, Parthasarathy S, Steinberg D (1991) Evidence for a dominant role of lipoxygenase(s) in the oxidation of LDL by mouse peritoneal macrophages. J Lipid Res 32:449–456

Steinberg D (1990) Arterial metabolism of lipoproteins in relation to atherogenesis. In: Lee KT, Onodera K, Tanaka K (eds) Atherosclerosis II: Recent Progress in Atherosclerosis Research. Ann NY Acad Sci 598:188–193

Steinbrecher UP (1987) Oxidation of human low density lipoprotein results in derivatization of lysine residues of apolipoprotein B by lipid peroxide decomposition products. J Biol Chem 262:3603–3608

Steinbrecher UP (1990) Oxidatively modified lipoproteins. Curr Opin Lipidol 1:411–415

Steinbrecher UP, Witztum JL, Parthasarathy S, Steinberg D (1987) Decrease in reactive amino groups during oxidation or endothelial cell modification of LDL. Arteriosclerosis 7:135–143

Steinbrecher UP, Zhang H, Lougheed M (1990) Role of oxidatively modified LDL in atherosclerosis. Free Rad Biol Med 9:155–158

Witztum JL, Steinberg D (1991) Role of oxidized low density lipoprotein in atherogenesis. J Clin Invest 88:1785–1792

M.6.0.2
Inhibition of Lipid Peroxidation of Isolated Plasma Low-Density Lipoproteins

PURPOSE AND RATIONALE

Hypercholesterolemic Watanabe rabbits are considered to be a suitable model to study the effect of antioxidants as anti-atherosclerotic agents (Carew et al. 1987; Kita et al. 1987; Steinberg et al. 1988; Dresel et al. 1990). Plasma of Watanabe heritable hyperlipidemic (WHHL) rabbits is used to test the inhibition of Cu^{2+}-induced lipid peroxidation of isolated low density lipoproteins (LDL).

PROCEDURE

Animals of a modified Watanabe heritable hyperlipidemic rabbit strain (Gallagher et al. 1988) are used. The animals are fed over a period of 12 weeks with Purina rabbit chow diet with or without 1% of test compound or standard (probucol). Plasma samples are collected in Na_2EDTA (0.1% final concentration). LDL are isolated from each rabbit plasma using a sequential ultracentrifugation technique at $d = 1.019–1.063$ g/ml (Mao et al. 1983). LDL are then dialyzed against phosphate buffered saline (PBS, 0.01 M sodium phosphate, 0.12 M NaCl, pH 7.4) at 4°C for 24 h.

For determination of LDL lipid peroxidation induced by Cu^{2+}, 100 µg of each LDL sample is adjusted

to a volume of 1.5 ml with distilled water. Lipid peroxidation is initiated by addition of $CuSO_4$ to a final concentration of 5 µM followed by an incubation at 37°C for 3 h. The reaction is stopped by adding 100 µl of 50 mM Na_2EDTA. Fifty micrograms of LDL from the reaction mixture are added to 1.5 ml of 20% trichloroacetic acid and vortexed. Finally, 1.5 ml of 0.67% thiobarbituric acid (TBA) in 0.05 N NaOH is added and the mixture is incubated at 90°C for 30 min. Samples are centrifuged at 1500 rpm for 10 min. The absorbance of the supernatant fractions is determined at 532 nm to estimate the content of lipid peroxides (thiobarbituric acid-reactive substances). A standard curve (0–5 nmol) of malondialdehyde is generated using malondialdehyde bis(dimethyl acetal) as reference to determine the lipid peroxidation content in Cu^{2+}-treated LDL.

EVALUATION

The content of lipid peroxide in LDL is plotted against the drug concentration in LDL fractions. The extent of Cu^{2+}-induced peroxidation decreases with increasing drug concentrations. The effects of test compounds are compared to the standard.

MODIFICATIONS OF THE METHOD

Inhibition of iron-dependent lipid peroxidation by test compounds was measured by Braughler et al. (1987), Yoshioka et al. 1989).

Yamamoto et al. (1986) studied the effects of probucol on lipid storage in macrophages *in vitro* in the presence of acetylated low density lipoprotein using macrophage-like cells (UE-12) established from a human histiocytic lymphoma cell line.

Barnhart et al. (1989) used LDL from human plasma to study the concentration-dependent antioxidant activity of probucol.

Parthasarathy et al. (1986) incubated LDL from human plasma samples with rabbit aortic endothelial cells and measured the increase in electrophoretic mobility, the increase in peroxides, and the increase in subsequent susceptibility to macrophage degradation.

Mansuy et al. (1986) studied the inhibition of lipid peroxidation induced in liver microsomes either chemically by $FeSO_4$ and reducing agents (cysteine or ascorbate) or enzymatically by NADPH and CCl_4.

REFERENCES AND FURTHER READING

Asakawa T, Matsushita S, (1980) Coloring conditions of thiobarbituric acid test for detecting lipid hydroperoxides. Lipids 15:137–140

Barnhart RL, Busch SJ, Jackson RL (1989) Concentration-dependent antioxidant activity of probucol in low density lipoproteins *in vitro*: probucol degradation precedes lipoprotein oxidation. J Lipid Res 30:1703–1710

Bernheim F, Bernheim MLC, Wilbur KM (1948) The reaction between thiobarbituric acid and the oxidation products of certain lipids. J Biol Chem 174:257–264

Braughler JM, Pregenzer JF, Chase RL, Duncan LA, Jacobsen EJ, McCall JM (1987) Novel 21-amino steroids as potent inhibitors of iron-dependent lipid peroxidation. J Biol Chem 262:10438–10440

Carew TE, Schwenke DC, Steinberg D (1987) Antiatherogenic effect of probucol unrelated to its hypocholesterolemic effect: Evidence that antioxidants *in vivo* can selectively inhibit low density lipoprotein degradation in macrophage-rich fatty streaks and slow the progression of atherosclerosis in the Watanabe heritable hyperlipidemic rabbit. Proc Natl Acad Sci USA 84:7725–7729

Dresel HA, Deigner HP, Frübis J, Strein K, Schettler G (1990) LDL-metabolism of the arterial wall – new implications for atherogenesis. Z Kardiol 79: Suppl. 3:9–16

Gallagher PJ, Nanjee MN, Richards T, Roche WR, Miller NE (1988) Biochemical and pathological features of a modified strain of Watanabe heritable hyperlipidemic rabbits. Atherosclerosis 71:173–183

Kita T (1991) Oxidized lipoproteins and probucol. Curr Opin Lipidol 2:35–38

Kita T, Nagano Y, Yokode M, Ishii K, Kume N, Ooshima A, Yoshida H, Kawai Ch (1987) Probucol prevents the progression of atherosclerosis in Watanabe heritable hyperlipidemic rabbit, an animal model for familial hypercholesterolemia. Proc Natl Acad Sci USA 84:5928–5931

Mansuy D, Sassi A, Dansette PM, Plat M (1986) A new potent inhibitor of lipid peroxidation *in vitro* and *in vivo*, the hepatoprotective drug anisyldithiolthione. Biochem Biophys Res Commun 135:1015–1021

Mao SJT, Patton JG, Badimon JJ, Kottke BA, Alley MC, Cardin AD (1983) Monoclonal antibodies to human plasma low-density lipoproteins. I. Enhanced binding of ^{125}I-labeled low-density lipoproteins by combined use of two monoclonal antibodies. Clin Chem 29:1890–1897

Mao SJT, Yates MT, Rechtin AN, Jackson RL, Van Sickle WA (1991) Antioxidant activity of probucol and its analogues in hypercholesterolemic Watanabe rabbits. J Med Chem 34:298–302

McLean LR, Hagaman KA (1989) Effect of probucol on the physical properties of low-density lipoproteins oxidized by copper. Biochemistry 28:321–327

Parthasarathy S, Young SG, Witztum JL, Pittman RC, Steinberg D (1986) Probucol inhibits oxidative modification of low density lipoprotein. J Clin Invest 77:641–644

Steinberg D, Parthasaraty S, Carew TE (1988) *In vivo* inhibition of foam cell development by probucol in Watanabe rabbits. Am J Cardiol 62:6B–12B

Yamamoto A, Takaishi S, Hara H, Nishikawa O, Yokoyama S, Yamamura T, Yamaguchi T (1986) Probucol prevents lipid storage in macrophages. Atherosclerosis 62:209–217

Yoshioka T, Fujita T, Kanai T, Aizawa Y, Kurumada T, Hasegawa K, Horikoshi H (1989) Studies with hindered phenols and analogues. 1. Hypolipidemic and hypoglycemic agents with ability to inhibit lipid peroxidation. J Med Chem 32:421–428

Zhang H, Basra HJK, Steinbrecher UP (1990) Effects of oxidatively modified LDL on cholesterol esterification in cultured macrophages. J Lipid Res 31:1361–1369

M.7 Internalization of Labeled LDL into HepG2 Cells

PURPOSE AND RATIONALE

Enhanced uptake of low density lipoproteins (LDL) via the LDL receptor into liver cells results in reduced plasma cholesterol levels. This can be tested in the cultured hepatoma cell line HepG2.

PROCEDURE

Heterozygous WHHL rabbits are treated with the test compound over a period of 4 weeks. Blood is withdrawn twice weekly before, during, and after treatment for determination of total plasma cholesterol, low density lipoprotein cholesterol, total triglycerides, and high density lipoprotein cholesterol. Lipoprotein-deficient serum is prepared by ultracentrifugation (Goldstein et al. 1983). Serum of treated and untreated animals is used for the uptake assay being prepared by centrifugation to remove the clots, followed by heat inactivation of the complement system and sterilization through a 0.45-µm filter. In each preparation, 2 mg LDL (*d*, 1.019 to 1.050 g/ml) at 10 mg/ml are iodinated by the monochloride method to a specific activity of 300 cpm/ng (Huettinger et al. 1984).

HepG2 cells are grown in 5 cm dishes in Eagle's minimum essential medium to 60% confluence. Serum prepared from treated animals and from the same animals in the pretreatment period is added from 1% to 50% to the medium used to grow HepG2 cells. After incubation of 18 h, cells are washed and incubated in Eagle's minimum essential medium plus 2% bovine serum albumin and 8 µg labeled LDL for 3 h. The cells are then washed and solubilized in sodium hydroxide, and the content of each dish is counted for radioactivity. An aliquot is used to determine protein content.

EVALUATION

Values are given for specific uptake, which is calculated from the difference of total uptake minus uptake measured when a 40-fold excess of unlabeled LDL is present in the incubation medium of duplicate or triplicate incubations. The effect of the test drug is demonstrated by an increase of uptake with increasing percentage of serum of treated animals containing the active drug.

MODIFICATIONS OF THE METHOD

Sprague et al. (1993) measured the inhibition of scavenger receptor-mediated modified low-density lipoprotein endocytosis in cultured bovine aortic endothelial cells.

Takano and Mowri (1990) produced a monoclonal antibody which recognizes peroxidized lipoproteins.

REFERENCES AND FURTHER READING

Cosgrove PG, Gaynor BJ, Harwood HJ Jr (1992) Quantitation of hepatic LDL receptor levels in the hamster. FASEB J 4:A533

Goldstein JL, Basu SK, Brown MS (1983) Receptor mediated endocytosis of LDL in cultured cells. Meth Enzymol 98:241–260

Huettinger M, Schneider WJ, Ho YK, Goldstein JL, Brown M (1984) Use of monoclonal anti-receptor antibodies to probe the expression of the low density lipoprotein receptor in tissues of normal and Watanabe heritable hyperlipidemic rabbits. J Clin Invest 74:1017–1026

Huettinger M, Herrmann M, Goldenberg H, Granzer E, Leineweber M (1993) Hypolipidemic activity of HOE-402 is mediated by stimulation of the LDL receptor pathway. Atheroscl Thromb 13:1005–1012

Sprague EA, Kothapalli R, Kerbacher JJ, Edwards EH, Schwartz CJ, Elbein AD (1993) Inhibition of scavenger receptor-mediated modified low-density lipoprotein endocytosis in cultured bovine aortic endothelial cells by the glycoprotein processing inhibitor castanospermine. Biochemistry 32:8888–8895

Takano T, Mowri HO (1990) Peroxidized lipoproteins recognized by a new monoclonal antibody (DLR1a/104G) in atherosclerotic lesions. In: Lee KT, Onodera K, Tanaka K (eds) Atherosclerosis II: Recent Progress in Atherosclerosis Research. Ann NY Acad Sci 598:136–142

M.8 Influence of Peroxisome Proliferator-Activated Receptors (PPARs) and Liver X Receptors (LXRs) on Development of Atherosclerosis

M.8.1 General Considerations

Peroxisome proliferator-activated receptors (PPARs) and liver X receptors (LXRs) are nuclear receptors that regulate systemic glucose and lipid metabolism. They are expressed by macrophages in which they modulate cholesterol homeostasis and inflammation. These receptors heterodimerize with retinoid X receptors (RXRs) to modulate transcription at the promoters of target genes. They act as lipid sensors and bind with micromolar affinities to ligands derived from either intracellular metabolism or dietary lipids. Endogenous ligands of PPARs include fatty acids and eicosanoids, whereas metabolites of oxidized cholesterol activate the LXRs.

REFERENCES AND FURTHER READING

Barish GD, Evans RM (2004) PPARs and LXRs: atherosclerosis goes nuclear. Trends Endocrinol Metab 15:158–165

Desvergne B, Wahli W (1999) Peroxisome proliferator-activated receptors: nuclear control of metabolism. Endocrinol Rev 20:649–688
Kersten S, Desvergne B, Wahli W (2000) Roles of PPARs in health and disease. Nature 405:421–424
Kersten S (2002) Peroxisome proliferator activated receptors and obesity. Eur J Pharmacol 440:223–234
Leo C, Chen JD (2000) The SRC family of nuclear receptor coactivators. Gene 245:1–11
Li AC, Glass CK (2004) PPAR- and LXR-dependent pathways controlling lipid metabolism and the development of atherosclerosis. J Lipid Res 45:2161–2173
Marx N, Duez H, Fruchart JC, Staels B (2004) Peroxisome proliferator-activated receptors and atherogenesis. Regulators of gene expression in vascular cells. Circ Res 94:1168–1178
Nuclear Receptors Nomenclature Committee (1999) A unified nomenclature system for the nuclear receptor superfamily. Cell 97:161–163
Savkur RS, Bramlett KS, Clawson D, Burris TP (2004) Pharmacology of nuclear receptor-coregulator recognition. Vitam Horm 68:145–183

M.8.2 Influence of PPAR Activation

PURPOSE AND RATIONALE

Peroxisome proliferator-activated receptors (PPARs) play a major role in atherosclerosis (Brun et al. 1996; Pineda Torra et al. 1999; Duval et al. 2002; Tailleux et al. 2003). The PPAR family consists of three proteins: α, β/δ and γ. Experimental data suggest that PPAR-α and PPAR-γ activation decreases atherosclerosis progression not only by correcting metabolic disorders, but also through direct effects on the vascular wall. PPARs modulate the recruitment of leukocytes to endothelial cells, control the inflammatory response and lipid homeostasis of monocytes/macrophages and regulate inflammatory cytokine production by smooth muscle cells. PPAR agonists, such as fibrates and thiazolidinediones, are recommended for the treatment of atherosclerosis, diabetes and obesity (Willson et al. 2000; Etgen and Mantio 2003; Francis et al. 2003; Wang and Tafuri 2003; Ferré 2004; Kota et al. 2005). Scavenger receptors are expressed in atherosclerotic lesion macrophages and regulated by activators of peroxisome proliferator-activated receptors (Chinetti et al. 2000). PPARγ is a regulator of monocyte/macrophage function (Ricote et al. 1999).

REFERENCES AND FURTHER READING

Brun RP, Tontonoz P, Forman B, Ellis R, Chen J, Evans RM, Spiegelman BM (1996) Differential activation of adipogenesis by multiple PPAR isoforms. Genes Dev 15:974–984
Chinetti G, Gbaguidi FG, Griglio S, Mallat Z, Antonucci M, Poulain P, Chapman J, Fruchart JC, Tedgui A, Najib-Fruchart J, Staels B (2000) CLA-1/SR-BI is expressed in atherosclerotic lesion macrophages and regulated by activators of peroxisome proliferator-activated receptors. Circulation 101:2411–2417
Duval C, Chinetti G, Trottein F, Fruchart JC, Staels B (2002) The role of PPARs in atherosclerosis. Trends Mol Med 8:422–430
Etgen GJ, Mantio N (2003) PPAR ligands for metabolic disorders. Curr Top Med Chem 3:1649–1661
Ferré P (2004) The biology of peroxisome proliferator-activated receptors. Relationship with lipid metabolism and insulin sensitivity. Diabetes 53 [Suppl 1]:S43–S50
Francis GA, Annicotte JS, Auwerx J (2003) PPAR agonists in the treatment of atherosclerosis. Curr Opin Pharmacol 3:186–191
Kota BP, Huang THW, Roufogalis BD (2005) An overwiew on biological mechanisms of PPARs. Pharmacol Res 51:85–94
Pineda Torra I, Gervois P, Stels B (1999) Peroxisome proliferator-activated receptor alpha in metabolic disease, inflammation, atherosclerosis and aging. Curr Opin Lipidol 10:151–159
Ricote M, Huang JT, Welch JS, Glass CK (1999) The peroxisome proliferator-activated receptor (PPARγ) as a regulator of monocyte/macrophage function. J Leukoc Biol 66:733–739
Tailleux A, Torpier G, Mezdour H, Fruchart JC, Staels B, Fièvet C (2003) Murine models to investigate pharmacological compounds acting as ligands of PPARs in dyslipidemia and atherosclerosis. Trends Pharmacol Sci 24:530–534
Wang M, Tafuri S (2003) Modulation of PPARγ activity with pharmaceutical agents: treatment of insulin resistance and atherosclerosis. J Cell Biochem 89:38–47
Willson TM, Brown PJ, Sternbach DD, Henke BR (2000) The PPARs: From orphan receptors to drug discovery. J Med Chem 43:527–550

M.8.2.1 PPARα

PURPOSE AND RATIONALE

Several studies indicate the lipid-lowering role of PPARα in rodents (Chinetti et al. 2001; Vosper et al. 2002). PPARα is highly expressed in the rodent liver where activation of these receptors with fibrates induces a massive increase in peroxisomal fatty acid oxidation in hepatocytes. This provides a powerful action for the clearance of fat from the serum. Fibrates also increase the expression of the liver fatty-acid-binding protein (Lawrence et al. 2000) and the hepatocyte-secreted apolipoproteins apoAI and apoAII (Vu-Dac et al. 1995). Lee et al. (1995) demonstrated that PPARα is responsible for clofibrate-induced fatty acid oxidation by disrupting the PPARα gene in mice. Mice lacking apolipoprotein E are characterized by severe hypercholesterolemia. Tordjman et al. (2001) reported that PPARα deficiency reduces insulin resistance and atherosclerosis in apoE-null mice. Fu et al. (2003) found that the PPARα agonist ciprofibrate severely aggravates hypercholesterolemia and accelerates the development of atherosclerosis in mice lack-

ing apolipoprotein E. Species differences have to be taken in account. Lawrence et al. (2001) reported that PPARα fails to induce peroxisome proliferation-associated genes in human cells independent of the level of receptor expression.

REFERENCES AND FURTHER READING

Chinetti G, Lestavel S, Bocher V, Remaley AT, Neve B, Pineda Torra I, Teissier E, Minnich A, Jaye M, Duverger N, Brewer HB, Fruchart JC, Clavey V, Staels B (2001) PPAR-α and PPAR-γ activators induce cholesterol removal from human macrophage foam cells through stimulation of the ABCA1 pathway. Nature Med 7:53–38

Fu T, Kashireddy P, Borensztajn J (2003) The peroxisome-proliferator-activated receptor α agonist ciprofibrate severely aggravates hypercholesterolaemia and accelerates the development of atherosclerosis in mice lacking apolipoprotein E. Biochem J 373:941–947

Lawrence JW, Kroll DJ, Eacho PI (2000) Ligand-dependent interaction of hepatic acid-binding protein with the nucleus. J Lipid Res 41:1390–1401

Lawrence JW, Li Y, Chen S, DeLuca JG, Berger JP, Umbenhauer DR, Moller DE, Zhou G (2001) Differential gene regulation in human versus rodent hepatocytes by peroxisome proliferator-activated receptor (PPAR)α. J Biol Chem 276:31521–31527

Lee SST, Pineau T, Drago J, Lee EJ, Owens JW, Kroetz DL, Fernadez-Salguero PM, Westphal H, Gonzalez FJ (1995) Targeted disruption of the α isoform of the peroxisome proliferator-activated receptor gene in mice results in abolishment of the pleiotropic effects of peroxisome proliferators. Mol Cell Biol 15:3012–3022

Tordjman K, Bernal-Mizrachi C, Zermany L, Weng S, Feng C, Zhang F, Leone TC, Coleman T, Kelly DP, Semenkovich CF (2001) PPARα deficiency reduces insulin resistance and atherosclerosis in apoE-null mice. J Clin Invest 107:1025–1034

Vosper H, Khoudoli GA, Graham TL, Palmer CNA (2002) Peroxisome proliferator-activated agonists, hyperlipidaemia, and atherosclerosis. Pharmacol Ther 95:47–62

Vu-Dac N, Schoonjans K, Kosykh, Dallongeville J, Fruchart JC, Staels B, Auwerx J (1995) Fibrates increase human apolipoprotein A-II through activation of the peroxisome proliferators-activated receptor. J Clin Invest 96:741–750

M.8.2.1.1 Effect of PPARα Agonists in Mice

PURPOSE AND RATIONALE

Duez et al. (2002) described reduction of atherosclerosis by the peroxisome proliferator-activated receptor α agonist fenofibrate in mice.

PROCEDURE

Animals

Homozygous human apoA-I transgenic (Rubin et al. 1991) and apoE-deficient C57Bl/6 mouse strains were used. Human apoA-I transgenic mice were crossed with apoE-deficient mice to generate heterozygous human apoA-I transgenic mice in a heterozygous apoE-deficient background. These mice were further mated with homozygous apoE-deficient mice to generate human apoA-I transgenic mice in a homozygous apoE-deficient background (hapoA-I Tg × apoE-deficient mice). Human apoA-I expression was analyzed in plasma by enzyme-linked immunosorbent assay using specific antibodies (Berthou et al. 1996). Homozygous apoE-deficient mice were identified after determination of total cholesterol levels. After weaning, apoE-deficient and hapoA-I Tg × apoE-deficient male mice were maintained on a standard pellet rodent chow.

Ten-week-old apoE-deficient male mice were given a Western diet containing 20% fat and 0.2% cholesterol before the treatment period. Then one group was treated for 8 weeks with fenofibrate (0.05% added to the diet, corresponding to 100 mg/kg per day), the other group served as control. At the end of the study, blood was collected under anesthesia by retro-orbital puncture and tissues collected for further analysis.

ApoE-deficient male mice on a C57Bl/6 background were treated at an age of 20 weeks with 100 mg/kg per day fenofibrate by gavage. Another group served as control. After 6 weeks, the animal were sacrificed and their aortic cholesterol and cholesteryl ester content were determined.

Ten-week-old hapoA-I Tg × apoE-deficient male mice were given a Western diet for 2 weeks before treatment with either control or fenofibrate (0.05% added to the diet, corresponding to 100 mg/kg per day) for another 8 weeks. At the end of the study, blood and tissue samples were collected for further analysis.

Lipids, Apolipoprotein, and Lipoprotein Measurements

Plasma cholesterol and triglyceride concentrations were determined by an enzymatic assay adapted to microtiter plates using commercially available reagents. Plasma human apoA-I levels were measured by an immunoelectrophoretic assay using species-specific polyclonal antibodies (Berthou et al. 1996). Lipoprotein cholesterol profiles were obtained by fast-protein liquid chromatography. This system allows the separation of three major lipoprotein classes, very low density lipoprotein (VLDL), intermediate density lipoprotein (IDL) + LDL and HDL according to their size.

Cholesterol Measurement in the Descending Aorta

After collection of the blood, the vasculature was gently perfused through the left ventricle with cold PBS and 5 mM EDTA. For collection of aorta for biochemical analysis, all branches and adipose tissue connected to the aorta were removed, and each aorta was carefully excised from the aortic root to the right renal

artery. The aortas were kept briefly on ice in PBS, and then blotted dry, weighed, minced, and extracted with chloroform/methanol (2:1) according to Folch et al. (1957). The lipid extracts were dried down, resuspended quantitatively in chloroform/ methanol (2:1) and stored at –20°C until the time of assay. Total and free cholesterol levels in the aortic extracts were determined with an enzymatic fluorometric assay (Sparrow et al. 2001). The solvent was evaporated and the lipid residue was re-dissolved in 100 µl of reagent-grade ethanol. Aliquots of cholesterol and cholesteryl oleate standard solutions in chloroform/ ethanol (1:1) were treated similarly. To determine free cholesterol, samples and standard were incubated for 1 h at 39°C in a total volume of 1.01 ml of 0.1 M potassium phosphate buffer, pH 7.4, containing 0.03% Triton X-100 and 0.9 mM sodium cholate. Cholesterol oxidase (Roche Molecular Biochemicals), peroxidase (Roche Molecular Biochemicals) and *p*-hydroxyphenylacetic acid (Aldrich) were added for an additional 1-h incubation at 37°C. The fluorescent product was measured (excitation 325 nm, emission 425 nm). For total cholesterol determinations, cholesterol esterase (Calbiochem) was included in the first incubation step, and cholesteryl oleate was used as standard. The esterified cholesterol content in each sample was calculated by subtracting the value of free cholesterol from that of total cholesterol. All values were expressed as nmol/aorta.

Analysis of Atherosclerotic Lesions in the Aorta

Hearts and ascending aortas were fixed in formaldehyde, and serial 10-mm-thick cryosections were cut from the aortic arch to the ventricles for quantitative analysis of atherosclerosis. The distance between each section was 50 mM, and the final magnification 2.5-fold. Sections were stained with Oil Red O and counterstained with hematoxylin. The atherosclerotic lesion and the Oil Red O-stained areas of each section were quantified using a computer-assisted video imaging system. To avoid morphological heterogeneity between mice, the expression of average atherosclerotic lesion areas in the region of the aortic sinus, from the appearance to the disappearance of the aortic valves, was normalized at ten equal sections.

EVALUATION

A non-parametric Mann-Whitney test was used to analyze for significant differences between the experimental groups. Analysis of variance (ANOVA) and Tukey post-hoc tests were used for analysis of the lesion area data.

REFERENCES AND FURTHER READING

Berthou L, Duverger N, Emmanuel F, Langouët S, Auwerx J, Guillouzo A, Fruchart JC, Rubin E, Denèfle P, Staels B, Branellec D (1996) Opposite regulation of human versus mouse apolipoprotein A-I by fibrates in human apolipoprotein A-I transgenic mice. J Clin Invest 97:2408–2416

Duez H, Chao YS, Hernandez M, Torpier G, Poulain P, Mundt S, Mallat Z, Teissier E, Burton CA, Tedgui A, Fruchart JC, Fiévet C, Wright SD, Staels B (2002) Reduction of atherosclerosis by the peroxisome proliferators-activated receptor α agonist fenofibrate in mice. J Biol Chem 277:48051–48057

Folch J, Lees M, Sloane Stanley GH (1957) A simple method for the isolation and purification of total lipids from animal tissues. J Biol Chem 226:497–509

Rubin EM, Ishida BY, Clift SM, Krauss RM (1991) Expression of human apolipoprotein A-I in transgenic mice results in reduced plasma levels of murine apolipoprotein A-I and the appearance of two new high density lipoprotein size subclasses. Proc Natl Acad Sci USA 88:434–438

Sparrow CP, Burton CA, Hernandez M, Mundt S, Hassing H, Patel S, Rosa R, Hermanowski-Vosatka A, Wang PR, Zhang D, Peterson L, Detmers PA, Chao YS, Wright SD (2001) Simvastin has anti-inflammatory and antiatherosclerotic activities independent of plasma cholesterol lowering. Arterioscler Thromb Vasc Biol 21:115–121

M.8.2.1.2 Effect of PPARα and PPARγ Agonists in Human Macrophages

PURPOSE AND RATIONALE

Lee and Evans (2002) reviewed the role of the peroxisome proliferator-activated receptor-γ in macrophage lipid homeostasis.

Chinetti et al. (1998) reported that PPARα and PPARγ activators induce cholesterol removal from human macrophage foam cells through stimulation of the ABCA1 pathway.

PROCEDURE

Transactivation Assays of the RPR-5 Compound

Transactivation assays are performed with the RPR-5 compound in A10 cells (a rat smooth muscle cell line) using full-length human PPARα and PPARγ and the PGL3-J_3-TK vector (Vu-Dac et al. 1995). After 24 h, luciferase activity is measured with LucLite (Packard, Meridian, Conn., USA) according to the manufacturer's instructions.

Cell Culture

Mononuclear cells are isolated from the blood of healthy normolipidic donors by Ficoll gradient centrifugation and cultured (Chinetti et al. 1998). Mature monocytes are used for experiments after 10 days of culture. For treatment with the different activators, medium is changed to medium without human serum but supplemented with 1% Nitridoma

HU (Boehringer). Efflux studies are performed in the absence of any serum. Human monocytic THP-1 cells (ATCC, Rockville, Md., USA) are maintained in RPMI 1640 medium containing 10% of FCS and differentiated for 48 h with 100 nM PMA.

RNA Extraction and Analysis

After incubation with the PPAR activators, cells are washed with PBS and used for RNA extraction. Total RNA is extracted after 10 days from differentiated macrophages and THP-1 cells treated for 24 h with the compounds using Trizol (Life Technologies, France). For Northern blot analysis, membranes are hydrolyzed containing 10 µg of total RNA with radiolabeled ABCA1 or 36B4 control cDNA probes. An *Eco*RI LXR-β and a *Hin*dIII-*Hin*cII LXR-α cDNA fragment are used as probes. For the human ABCA1 probe, a 1.1-kb cDNA fragment is cloned into a pCR4–4-TOPO vector (Invitrogen).

Transient Transfection Assay

At 24 h before transduction, COS1 cells are plated in 24-well plates at a density of 5×10^4 cells/well and cultured in Dulbecco's modified Eagle's medium supplemented with 10% fetal calf serum. Cells are transfected by lipofection using ExGen 500 (Euromedex) in OPITMEM 1 medium, with 50 ng of reporter plasmid and increasing quantities of LXR-α and RXR expression plasmids (10, 25, and 50 ng) in the presence of 50 ng of the internal control β-gal expression vector, for 3 h in serum-free medium. Fresh medium containing 0.2% fetal calf serum and 10 µM 22(R)-hydroxycholesterol (Sigma) or its solvents are subsequently added and cells are further incubated for 48 h.

Cholesterol Loading and Efflux

Ten day-old human macrophages were pretreated for 24 h and thereafter every 24 h with PPAR activators (e. g., rosiglitazone 100 nM, Wy14643 50 µM) and cholesterol loaded by incubation with AcLDL (50 µg/ml, with or without [^{3}H]cholesterol) in RPMI 1640 medium supplemented with 1% Nutridoma (Boehringer) for 48 h. After this incubation period, cells are washed twice in PBS and apoAI-mediated cholesterol efflux studies are immediately performed by adding fresh RMPI medium without Nutridoma with or without 100 µg/ml of apoAI for 24 h. Because, in macrophages, the equilibrium between esterified and free cholesterol is not obtained even after a 24-h additional incubation period, the experiments are performed in the absence of equilibrium.

EVALUATION

For transactivation assays

ED_{50} values are calculated after curve fitting with XLFit (human PPARα $EC_{50} = 0.13$ µM, PPARγ $EC_{50} = 5$ µM).

For transient transfection assay

Cell extracts are prepared and assayed for luciferase activity (Delerive et al. 2000). Results are normalized to internal control β-gal activity.

For cholesterol binding and efflux

At the end of the incubation, intracellular lipids are extracted in hexane/isopropanol, dried under nitrogen, and free cholesterol, total cholesterol and phospholipids are measured by enzymatic assays (Boehringer). Esterified cholesterol is measured as the difference between total and free cholesterol. Cellular proteins are collected by digestion in NaOH and measured by Bradford assay (BioRad). The percent change of intracellular cholesterol amounts in the presence of apoAI relative to apoAI-free medium is expressed according to the following equation:

$$\begin{aligned}&\text{Percent decrease in cellular cholesterol}\\&= \{[(\text{cellular cholesterol})_{\text{RPMI}}\\&\quad - (\text{cellular cholesterol})_{\text{apoAI}}]\\&\quad + (\text{cellular cholesterol})_{\text{RPMI}}\} \times 100\,.\end{aligned}$$

In the experiments with [^{3}H]cholesterol, radioactivity is measured, by scintillation counting, in centrifuged medium and in cellular lipids extracted with hexane/isopropanol. ApoAI-induced [^{3}H]cholesterol is measured as the fraction of total labeled cholesterol appearing in the medium in the presence of apoAI after subtraction of values for apoAI-free medium. For the phospholipid efflux study, lipids are isolated from culture medium by chloroform/methanol extraction. Extracted lipids are subsequently dried under nitrogen pressure and phospholipid mass determined by an enzymatic assay (Boehringer).

REFERENCES AND FURTHER READING

Chinetti G, Griglio S, Antonucci M, Torra IP, Delerive P, Majd Z, Fruchart JC, Chapman J, Najib J, Staels B (1998) Activation of proliferator-activated receptors alpha and gamma induces apoptosis of human monocyte-derived macrophages. J Biol Chem 273:255573–25580

Delerive P, Furman C, Teissier E, Fruchart JC, Duriez P, Staels B (2000) Oxidized phospholipids activate PPARα in a phospholipase A2-dependent manner. FEBS Lett 471:34–38

Lee CH, Evans RM (2002) Peroxisome proliferator-activated receptor-γ in macrophage lipid homeostasis. Trends Endocr Metab 13:331–335

Vu-Dac N, Schoonjans K, Kosykh, Dallongeville J, Fruchart JC, Staels B, Auwerx J (1995) Fibrates increase human apolipoprotein A-II through activation of the peroxisome proliferators-activated receptor. J Clin Invest 96:741–750

M.8.2.2 PPARγ

PURPOSE AND RATIONALE

PPARγ is a transcription factor required for the activation of many adipose-specific genes (Vosper et al. 2002). PPARγ essentially controls the accumulation of lipids in adipocytes and many experiments have demonstrated the ability of the receptor to direct adipocyte stimulation (Rosen et al. 2000). Reginato et al. (1998) reported that prostaglandins can both promote and block adipogenesis through opposing effects on PPARγ . PPARγ is a molecular target for the thiazolidine group of insulin-sensitizing drugs (Rieusset et al. 1999). PPARγ promotes lipid clearance in the liver of mice (Memon et al. 2000).

REFERENCES AND FURTHER READING

Memon RA, Tecott LH, Nonogaki K, Beigneux A, Moser AH, Grunfeld C, Feingold KR (2000) Up-regulation of peroxisome proliferator-activated receptors (PPA-α) and PPR-γ messenger ribonucleic acid expression in the liver in murine obesity: triglitazone induces expression of PPAR-γ responsive adipose tissue-specific genes in the liver of obese mice. Endocrinology 141:4021–4031

Reginato MJ, Krakow Sl, Bailley ST, Lazar MA (1998) Prostaglandins promote and block adipogenesis through opposing effects on peroxisome proliferator-activated receptor γ. J Biol Chem 273:1855–1858

Rieusset J, Auwerx J, Vidal H (1999) Regulation of gene expression by activation of the peroxisome proliferator-activated receptor γ with rosiglitazone (BRL 49653) in human adipocytes. Biochem Biophys Res Commun 265:265–271

Rosen ED, Walkey CJ, Puigserver P, Spiegelman BM (2000) Transcriptional regulation of adipogenesis. Genes Dev 14:1293–1307

Vosper H, Khoudoli GA, Graham TL, Palmer CAN (2002) Peroxisome proliferator-activated receptor agonists, hyperlipidemia and atherosclerosis. Pharmacol Ther 95:47–62

M.8.2.2.1 Effect of PPARγ Agonists in Mice

PURPOSE AND RATIONALE

Collins et al. (2001) reported the inhibition of the formation of early atherosclerotic lesions in diabetic and nondiabetic LDL receptor-deficient mice by a PPARγ agonist.

PROCEDURE

Transendothelial Monocyte Migration

THP-1 cells, a human monocytic leukemia cell line, were added to a human aortic EC monolayer covering a gelatin-coated 8-mm porous membrane and incubated for 30 min at 37°C to facilitate their attachment. Cells were then pretreated with the ligands or vehicle (dimethyl sulfoxide) for 30 min at 37°C. Migration was induced by the addition of monocyte chemoattractant protein-1 (MCP-1, 50 ng/ml) to the lower compartment. After 90 min, non-migrating THP-1 cells and human aortic ECs were removed with a cotton tip, and the membranes were fixed and stained with the Quik-Diff Stain Set (DADE, Miami, Fla., USA) to identify migrated cells. The number of migrated cells was determined per 3320 high-power field. Experiments were performed in duplicate and were repeated at least 3 times.

Western Blots

Western immunoblots were performed (Goetze et al. 1999). Membranes were incubated with rabbit polyclonal antibodies (1:1000 dilution, New England Biolabs) that recognize either: (1) total extracellular signal-regulated kinase (ERK) or (2) ERK phosphorylated on threonine 202 and tyrosine 204.

Animals and Diets

Male LDLR2/2 mice were obtained (C57BL/6J-Ldlrtm1Her, stock No. 002207, Jackson Laboratory) and were group-housed under a 12-h light and 12-h dark regimen. At 3 months of age, the mice were randomly assigned to one of five dietary regimens: (1) chow (Harlan Teklad 8604), (2) high-fat complex carbohydrate (Research Diets), (3) high-fat complex carbohydrate with 4 g troglitazone/kg of food, (4) high fructose (Research Diets), or (5) high fructose with 4 g troglitazone /kg of food. The high-fat diet consisted of 21% fat, 20% protein, 50% carbohydrate, and 0.15% cholesterol. The high-fructose diet contained 4% fat, 16% protein, 71% fructose, and 0.15% cholesterol. Mice and feed were weighed weekly, and the rate of consumption of drug was computed. The mice were fed for a period of 12 weeks.

Metabolic Measurements

Blood samples from the retro-orbital sinus were obtained from the mice before the beginning of treatment and every month thereafter and from the abdominal vena cava at euthanasia. Mice were fasted overnight before the collection of the blood samples. Plasma glucose was measured by glucose oxidase reaction (Beckman Glucose Analyzer 2, Beckman Instruments). Plasma lipids and plasma insulin were measured. Blood pressures were obtained by using an

indirect tail-cuff method with a controlled-temperature chamber.

Vessel Preparation and Image Analysis

Mice were euthanized and perfused with 7.5% sucrose in 4% paraformaldehyde. Aortas were dissected out, split longitudinally, pinned flat in a dissection pan, and stained with Sudan IV to detect lipids and determine lesion area. Images were captured by use of a Sony 3-CCD video camera and analyzed using ImagePro image analysis software. The extent of lesion formation is expressed as the percentage of the total aortic surface area covered by lesions.

Cross Sections: Determination of Intimal Macrophage Content

The largest lesions from the aortic arch were excised and embedded in paraffin. The avidin-biotin-peroxidase complex technique for immunostaining was used. Macrophages were stained by using monoclonal antibody to CD68 (titer 1:100, KP1 clone, M0814, Dako). Non-immune serum was used as a control. Primary antibody incubations were performed in 1% BSA/2% goat serum containing PBS for 60 min. Biotinylated rabbit anti-mouse (Dako) was applied; incubation with a streptavidin-peroxidase complex followed. Peroxidase activity was detected with the use of diaminobenzidine tetrahydrochloride as a chromogen. Slides were then counterstained with hematoxylin. Images of the stained sections were analyzed by using the software described above. After tracing the intimal area to be measured with a cursor, five pixels of color, which defined the anti-CD68 stain, were sampled by the operator. The area encompassed by the pixels, which was not contiguous, in the color range for anti-CD68 was then computed automatically by the software.

EVALUATION

Statistical analysis was performed by using 2-factorial ANOVA with Student-Newman-Keuls to determine the differences between individual group means.

MODIFICATIONS OF THE METHOD

Li et al. (2000) used LDL-receptor deficient mice to study the inhibition of atherosclerosis by PPARγ ligands.

Chen et al. (2001) used apolipoprotein E knockout mice to study the inhibition of atherosclerosis by a thiazolidinedione.

Gavrilova et al. (2003) used lipoatrophic A-ZIP/F-1 mice to study the contribution of peroxisome proliferator-activated receptor γ to hepatic steatosis, triglyceride clearance, and regulation of body fat mass.

Tao et al. (2003) found antioxidative, antinitrative, and vasoprotective effects of a peroxisome proliferator-activated receptor-γ agonist in hypercholesterolemic New Zealand white rabbits.

Iwaki (2003) used C57BL/KsJ (*db+/db+*) mice to study the induction of adiponectin, a fat-derived antidiabetic and antiatherogenetic factor, by nuclear receptors.

Corti et al. (2004) performed an *in vivo* study by high-resolution magnetic resonance imaging of male New Zealand white rabbits. A selective PPARγ agonist showed an additive effect on plaque regression in combination with a statin in experimental atherosclerosis.

REFERENCES AND FURTHER READING

Chen Z, Ishibashi S, Perrey S, Osuga JI, Gotoda T, Kitamine T, Tamura Y, Okazaki H, Yahagi N, Iizuka Y, Shionoiri F, Ohashi K, Harada K, Shimano H, Nagai R, Yamada N (2001) Troglitazone inhibits atherosclerosis in apolipoprotein E-knockout mice. Pleiotropic effects on CD36 expression and HDL. Arterioscler Thromb Vasc Biol 21:372–377

Collins AR, Meehan WP, Kintscher U, Jackson S, Wakino S, Noh G, Palinski W, Hsueh WA, Law RE (2001) Troglitazone inhibits formation of early atherosclerotic lesions in diabetic and nondiabetic low density lipoprotein receptor deficient mice. Atheroscler Thromb Vasc Biol 21:365–371

Corti R, Osende JI, Fallon JT, Fuster V, Mizsei G, Jneid H, Wright SD, Chaplin WF, Badimon JJ (2004) The selective peroxisomal proliferator-activated receptor-gamma agonist has an additive effect on plaque regression in combination with simvastatin in experimental atherosclerosis. In vivo study by high-resolution magnetic resonance imaging. J Am Coll Cardiol 43:464–473

Gavrilova O, Haluzik M, Matsusue K, Cutson JJ, Johnson L, Dietz KR, Nicol CJ, Vinson C, Gonzalez FJ, Reitman ML (2003) Liver peroxisome proliferator-activated receptor γ contributes to hepatic steatosis, triglyceride clearance, and regulation of body fat mass. J Biol Chem 278:34268–34276

Goetze S, Xi XP, Kawano H, Gotlibowski T, Fleck E, Hsueh WA, Law RE (1999) PPAR gamma ligands inhibit migration mediated by multiple chemoattractants in vascular smooth muscle cells. J Cardiovasc Pharmacol 33: 798–806

Iwaki M, Matsuda M, Maeda N, Funahashi T, Matsuzawa Y, Makashima M, Shimomura I (2003) Induction of adiponectin, a fat-derived antidiabetic and antiatherogenetic factor, by nuclear receptors. Diabetes 52:1655–1663

Li AC, Brown KK, Silveste MJ, Willson TM, Paliski W, Glass CK (2000) Peroxisome proliferator-activated receptor γ ligands inhibit development of atherosclerosis in LDL-receptor deficient mice. J Clin Invest 106:523–531

Tao L, Liu HR, Gao E, Teng ZP, Lopez BL, Christopher TA, Ma XL, Batinic-Haberle I, Willette RN, Ohlstein EH, Yue TL (2003) Antioxidative, antinitrative, and vasoprotective effects of a peroxisome proliferator-activated receptor-γ agonist in hypercholesterolemia. Circulation 108:2805–2811

M.8.2.2.2 Effect of PPARγ Agonists on Gene Expression in Macrophages

PURPOSE AND RATIONALE

Hodgkinson and Ye (2003) used a combination of expression microarray and Northern blot analyses to identify target genes for peroxisome proliferator-activated receptor (PPAR)γ in RAW264.7 macrophages. PPARγ natural ligand 15-deoxy-Δ12−14 prostaglandin and synthetic ligands ciglitazone and rosiglitazone increased the expression of scavenger receptor CD36 and ATP-binding cassette transporter A1, as well as adipophilin (a lipid droplet coating protein involved in intracellular lipid storage and transport), calpain (a protease implicated in ABCA1 protein degradation), and ADAM8 (a disintegrin and metalloprotease protein involved in cell adhesion).

PROCEDURE

Cell Culture

Macrophage RAW264.3 cells were purchased from ATCC and cultured in DMEM (Sigma, Poole, UK) at 37°C in a humidified atmosphere with 95% air–5% CO_2. When cells reached ~ 80% confluence, WY14,643, 15d-PGJ2, ciglitazone, rosiglitazone, and BADGE were added to the medium as described below to give final concentrations of 100, 5, 50, 1, and 500 µM, respectively.

RNA Extraction

Total RNA from RAW264.7 macrophages was extracted using the BD Clontech Nucleobond RNA purification system (BD Clontech, Basingstoke, UK). Cells were lysed by a lysis buffer containing guanidine thiocyanate. After removing cellular proteins from the lysate, RNA was precipitated, then immobilized in a column containing silica glass fibers, and subjected to RNase-free DNase I digestion to remove genomic DNA. The RNA sample was further purified by washing and finally eluted from the column into nuclease-free water. The integrity of the RNA sample was verified by spectrophoretic analysis and formaldehyde agarose gel electrophoresis.

Microarray Filters and Hybridization

cDNA microarray nylon filters were purchased from Research Genetics. Radiolabeled cDNA probes were generated by reverse transcription of RNA extracted from rosiglitazone- or ciglitazone-treated and untreated (control) RAW264.7 macrophages using a Research Genetics GeneFilters Probe Labeling and Purification kit (Invitrogen, Paisley, UK). Briefly, 4–10 µg of total RNA was mixed with 0.4 mg of oligo(dT) and incubated at 70°C for 10 min. Then, 10 nmol each of dATP, dGTP, and dTTP, 37.5 U of AMV reverse transcriptase, and 100 µCi of [α-^{33}P]dCTP (3000 Ci/mmol; Amersham, Bucks, UK) were added, and the solution (30 µl of final volume) incubated at 42°C for 2 h. The labeled cDNA probe was then purified using spin columns supplied with the kit to remove unincorporated radioactive nucleotide. Prehybridization was carried out in 5 ml of MicroHyb buffer (Research Genetics) supplemented with poly(dA) (1 µg/ml) and denatured human Cot-1 DNA (1 µg/ml) at 42°C for 2 h. Radiolabeled cDNA probe was denatured at 100°C for 3 min and then added to the above solution, followed by hybridization at 42°C overnight. The filters were then washed twice in a solution containing 2 × SSC and 1% SDS at 50°C for 20 min and a brief wash (5 min) in a solution containing 0.5 × SSC and 1% SDS at room temperature. The filters were exposed to a low-energy phosphor storage screen, which was then scanned using a Storm phosphorimager (Molecular Dynamics), and the resultant TIFF images analyzed using Pathways 4 software (Research Genetics). The intensities of the spots were normalized to mean intensities of all spots on each filter. Normalized intensities of corresponding spots were compared between two filters. In order to check the data, the filters were stripped and re-probed with the opposite radiolabeled cDNA probe, thus a filter probed with control cDNA was stripped and probed with treated cDNA and vice versa.

Northern Blot and Hybridization

RNA was denatured in 50% (v/v) formamide and 6% (w/v) formaldehyde at 65°C for 10 min and subjected to electrophoresis on 1.5% (w/v) agarose gel in MOPS buffer [20 mM MOPS, 5 mM sodium acetate, and 1 mM EDTA (pH 7.0)] containing 1.9% (w/v) formaldehyde. Integrity and equal loading of the RNA was confirmed by observing ethidium-bromide-stained 28S and 18S mRNA bands under UV illumination. The RNA was transferred overnight to Hybond-N nylon membrane (Amersham) by capillary action and the RNA linked to the membrane by baking at 80°C for 2 h. cDNA probes for ABCA1, ADAM8, adipophilin, calpain-L3, CD36, protein phosphatase 2A non-catalytic subunit, and thymosin were generated from the IMAGE clone which had been isolated, sequenced, and verified by Research Genetics. Purified plasmid DNA was cut with the appropriate restriction enzymes and the digested insert was purified by

electrophoresis on 0.8% agarose in TAE buffer [4 mM Tris, 1 mM EDTA, and 0.0114% (v/v) acetic acid (pH 7.6)] containing 1 µg/ml ethidium bromide. The purified insert was purified from the gel using a Qiagen Gel Extraction kit (Qiagen, Crawley, UK) and 25 ng of cDNA was denatured at 95°C for 2 min and the cDNA was radiolabeled with [α-32P]dCTP by random priming using the Klenow Labeling kit as supplied by Promega. Unincorporated label from cDNA labeling was removed using a QIAquick Nucleotide Removal kit (Qiagen). Hybridizations with cDNA probes were performed with PerfectHyb (Sigma, Poole, UK) at 65°C. Prehybridization was carried in 5 ml PerfectHyb supplemented with 150 µg of denatured salmon sperm DNA (Sigma) for 2 h. Hybridization with the radiolabeled cDNA probe was carried out in the same mixture overnight. Membranes were washed twice at room temperature with 2 × SSC–0.1% SDS for 10 min followed by a 10 min wash in 0.1 × SSC–0.1% SDS. A high-stringency wash (5–10 min) was performed in 0.1 × SSC–0.1% SDS at 65°C. The membranes were then subjected to autoradiography at −70°C for between 12 h and 7 days.

EVALUATION

Autoradiographs of Northern blots were scanned and analyzed using Phoretix software.

MODIFICATIONS OF THE METHOD

Tontonoz et al. (1988) reported that PPARγ promotes the differentiation of monocytes/macrophages and the uptake of oxidized LDL.

Moore et al. (2001) reviewed the role of PPARγ in macrophage differentiation and cholesterol uptake.

Arimura et al. (2004) found that the peroxisome proliferator-activated receptor γ regulates expression of the perilipin gene in adipocytes. Perilipins are a family of proteins coating the surface of lipid droplets in adipocytes.

REFERENCES AND FURTHER READING

Arimura N, Horiba T, Imagawa M, Shimizu M, Sato R (2004) The peroxisome proliferator-activated receptor γ regulates expression of the perilipin gene in adipocytes. J Biol Chem 279:10070–10076

Hodgekinson CP, Ye S (2003) Microarray analysis of peroxisome proliferator-activated receptor γ-induced changes in gene expression in macrophages. Biochem Biophys Res Commun 308:505–510

Moore KJ, Rosen RD, Fitzgerald ML, Randow F, Andersson LP, Altshuler D (2001) The role of PPARγ in macrophage differentiation and cholesterol uptake. Nature Med 7:41–47

Tontonoz P, Nagy L, Alvarez JGA, Thomazy VA, Evans RM (1988) PPARγ promotes monocytes/macrophages differentiation and uptake of oxidized LDL. Cell 93:241–252

M.8.2.3 PPARδ

PURPOSE AND RATIONALE

Vosper et al. (2001) reported that PPARδ promotes lipid accumulation in human macrophages.

PROCEDURE

Isolation of Human Monocytes and In VitroMonocyte/Macrophage Differentiation

Human monocytes were isolated from buffy coat preparations of whole blood taken from healthy volunteers. The buffy coat was mixed with OptiprepTM (Robbins Scientific) in a ratio of 2.5:1 and then overlaid with a discontinuous OptiprepTM gradient. Following centrifugation for 25 min at 600 *g* the monocyte layer formed within the top 5–10 ml of the gradient was removed, washed with phosphate-buffered saline, and resuspended in RPMI 1640, supplemented with 2 mM glutamine and 10% human serum (Sigma). Cell viability was assessed by the ability to exclude trypan blue and was typically 95%. Monocyte purity was determined by differential counts of DiffQuik-stained (Porvair Sciences) cell preparations and was typically >95%. For monocyte-macrophage differentiation, monocytes isolated as above were resuspended in culture medium at a density of 2.5×10^6/ml and seeded into 12-well tissue culture plates; medium was changed every 48 h.

Transient Transfection

COS-1 cells were transfected by the DEAE-dextran method. The reporter construct pFABPLUC contained four copies of the peroxisome proliferator response element from the human liver FABP gene in front of the herpes simplex virus-thymidine kinase promoter, cloned immediately upstream of the cDNA encoding firefly luciferase in pGLBAS (Promega). The PPAR expression vectors contained the coding sequence for human PPARα, -δ, and -γ under the control of the enhancer/promoter of the human cytomegalovirus. PSV-Gal was co-transfected with each sample to act as an internal control for transfection. Cell lysates were prepared and luciferase and β-galactosidase activities were assayed using kits as described by the manufacturer (Promega).

Data are presented as the relative light units obtained with the luciferase assay divided by the ab-

sorbance obtained at 405 nm in the β-galactosidase assays (Luc/β-galactosidase).

Culture and Differentiation of THP-1 Cells

THP-1 cells were obtained from ATCC. Cultures were grown in RPMI supplemented with 10% heat-inactivated fetal calf serum. Differentiation was initiated by the addition of 5 ng/ml PMA in the above medium. All drugs were added in Me_2SO and were replaced at intervals of 48 h. After 4 days the cells were fixed with 0.66% paraformaldehyde then stained with Oil red O and hematoxylin. Quantification of lipid accumulation was achieved by extracting Oil red O from stained cells with isopropyl alcohol and measuring the optical density of the extract at 510 nm. The value obtained using a control culture was subtracted from the resulting values. The Oil red O absorbance was corrected by co-staining DNA with SYBR green dye (Molecular Probes) and quantified on a Labsystems FluoroSkan Ascent FL microplate fluorimeter. Cell number was determined from a standard curve.

Isolation of Stable Cell Lines

The entire coding sequence of human PPAR was subcloned, in both sense and antisense orientations, into the eukaryotic expression vector pCLDN. The resulting plasmids were transfected into THP-1 cells using a modified DEAE-dextran procedure. The cells were maintained in medium containing 1 mg/ml G418 and 10% THP-1 conditioned medium, with rigorous washing procedures to remove dead cells. This was continued until cell killing stopped and robust growth was observed.

Western Blotting

Cultures were lysed in SDS-polyacrylamide gel electrophoresis loading buffer and analyzed by Western blotting using standard procedures. PPAR antiserum was used at a 1:2000 dilution and the anti-AFAR antiserum was used at a 1:3000 dilution. A peroxidase-conjugated mouse anti-rabbit IgG antiserum (Sigma) was used as a secondary detection reagent at 1:3000 and the results were visualized using enhanced chemiluminescence (ECL+) as described by the manufacturer (Amersham Pharmacia Biotech).

Lipid Extraction and Measurement

Cultures were treated as above and then extracted with methanol/chloroform/phosphate-buffered saline (1:1:1, v/v) containing stigmasterol as an internal standard for cholesterol. The organic phase was analyzed for cholesterol with and without saponification by GC-MS using a Finnegan ThermoQuest Trace 2000. Triglycerides were quantified colorimetrically using a kit from Sigma and triolein as a standard. Protein concentrations were determined using the Bio-Rad Protein assay reagent.

Cholesterol Efflux Assays

THP-1 cells were differentiated with PMA in the absence or presence of 100 nM compound F for 3 days. PPAR SENSE cells were differentiated with PMA for 3 days. The cells were labeled with 2 µCi (40 nmol) of [4-^{14}C]cholesterol in 2 ml of medium containing 10% fetal calf serum for 3 h. ApoA1-specific efflux was determined (Oliver et al. 2001). For apoA1-independent efflux assays the cells were incubated for a further 120 h in medium containing 10% fetal calf serum.

Radioactivity release into the medium was determined by scintillation counting at 1, 4, 18, 24, 48, 72, and 120 h. All cultures incorporated similar levels (between 80 and 95%) of the labeled cholesterol.

RNA Extraction and Analysis

RNA was extracted from THP-1 cells using TRIZOL reagent as recommended by the manufacturer. cDNA was synthesized from such RNA using "You-Prime Ready-To-Go" beads from Amersham Pharmacia Biotech. TAQMANTM real time PCR analysis was applied using prepared reagents from PerkinElmer LifeSciences. The primers and probes are described elsewhere (Kliewer et al. 1992). Relative levels of mRNA were calculated using the values obtained with each target gene compared with the values obtained with the 18 S ribosomal RNA probes.

EVALUATION

All graphs and statistics were prepared using Graphpad Prism for the Macintosh v3.0 (Graphpad Inc., San Diego, Calif., USA). Non-linear regression was applied using a sigmoidal response model for the dose response to compound F in transient transfection experiments. *P*-values were calculated using a standard Student's *t*-test.

MODIFICATIONS OF THE METHOD

Wang et al. (2004) described the engineering of a mouse capable of continuous running up to twice the distance of a littermate. This was achieved by targeted expression of an activated form of PPARδ in skeletal muscle, which induces a switch to form increased numbers of type I muscle fibers. Treatment of wild-type mice with PPARδ agonist elicits a similar type I fiber gene expression profile in muscle.

Forman et al. (1997) developed a conformation-based assay that screens activators for their ability to bind to PPARα/δ and induce DNA binding. Specific fatty acids, eicosanoids, and hypolipidemic drugs are ligands for PPARα or PPARδ. Because altered fatty levels are associated with obesity, atherosclerosis, hypertension, and diabetes, PPARs serve as molecular sensors that are central to the development and treatment of these metabolic disorders.

PROCEDURE

Cell Culture and Transfection

CV-1 cells were grown and transfected (Forman et al. 1995a). The reporter construct, PPREx3 TK-LUC, contained three copies of the acyl-CoA oxidase PPRE upstream of the Herpes virus thymidine kinase promoter (Kliewer et al. 1992). Expression vectors contained the cytomegalovirus IE promoter/enhancer (pCMX) upstream of wild-type mouse PPARα, mouse PPARγ 1-ΔN (Met-105-Tyr-475), mouse PPARδ-ΔN (Leu-69-Tyr-440), mouse PPARα-G (Glu-282 Gly) (Hsu et al. 1995), or *Escherichia coli* β-galactosidase as an internal control. Cells were exposed to the compounds for 24 h and then harvested and assayed for luciferase and β-galactosidase activity. All points were performed in triplicate and varied by less than 10%. Normalized luciferase activity was determined and plotted as *n*-fold activation relative to untreated cells. Each experiment was repeated three or more times with similar results.

Electrophoretic Mobility-Shift Assays

In vitro-translated mouse PPARα (0.2 µl) and human RXRα (0.1 µl) were incubated for 30 min at room temperature with 100,000 cpm of Klenow-labeled acyl-CoA oxidase PPRE as described (Forman et al. 1995b) but with 150 mM KCl.

REFERENCES AND FURTHER READING

Forman BM, Tontonoz P, Chen J, Brun RP, Spiegelman BM, Evans RM (1995a) 15-Deoxy-$\Delta^{12,14}$-prostaglandin J_2 is a ligand for the adipocytes determination factor PPARγ. Cell 83:803–812

Forman BM, Goode E, Chen J, Oro AE, Bradley DJ, Perlmann D, Noonan DJ, Burke LT, McMorris T, Lamph WW, Evans RM, Weinberger C (1995b) Identification of a nuclear receptor that is activated by farnesol metabolites. Cell 81:687–693

Forman BM, Chen J, Evans RM (1997) Hypolipidemic drugs, polyunsaturated fatty acids, and eicosanoids are ligands for peroxisome proliferator-activated receptors. Proc Natl Acad Sci USA 94:4312–4317

Hsu MH, Palmer CN, Griffin KJ, Johnson EF (1995) A single amino acid change in the mouse peroxisome proliferator-activated receptor alpha alters transcriptional responses to peroxisome proliferators. Mol Pharmacol 48:559–567

Kliewer SA, Umesono K, Noonan DJ, Heyman RA, Evans RM (1992) Convergence of 9-cis retinoic acid and peroxisome signalling pathways through heterodimer formation of their receptors. Nature 358:771–774

Oliver WR Jr, Shenk JL, Snaith MR, Russell CS, Plunket KD, Bodkin NL, Lewis MC, Winegar DA, Sznaidman ML, Lambert MH, Xu HF, Sternbach DD, Kliewer SA, Hansen BC, Wilson TM (2001) The peroxisome proliferator-activated receptor δ promotes reverse cholesterol transport. Proc Natl Acad Sci USA 98:5306–5311

Vosper H, Patel L, Graham TL, Khoudoli GA, Hill A, Macphee CH, Pinto I, Smith SA, Suckling KE, Wolf CR, Palmer CAN (2001) The peroxisome proliferator-activated receptor δ promotes lipid accumulation in human macrophages. J Biol Chem 276:44258–44265

Wang YX, Zhang CL, Yu RT, Cho HK, Nelson MC, Bayuga-Ocampo CR, Ham J, Kang H, Evans RM (2004) Regulation of muscle fibre type and running endurance by PPARδ. PloS Biology 2:1532–1539

M.8.3 Influence of Liver X Receptor Agonists

PURPOSE AND RATIONALE

Liver X receptors (LXR) are nuclear receptors that are intracellular sensors, which regulate the expression of genes controlling cholesterol absorption, excretion, catabolism and cellular efflux in target organs including small intestine, liver and macrophages. The LXRs belong to a subgroup of nuclear receptors that are considered "metabolic receptors". Also included in this group are the PPARs and FXR (farnesol-activated receptor). The endogenous ligands for these receptors are intermediates or endproducts of metabolic pathways. The two LRXs, LRXα and LRXβ , are activated by physiological concentrations of oxidized cholesterol, such as 22(R)-hydroxycholesterol and 24(S),25-epoxycholesterol. LRXα is expressed at high levels in liver, intestine adipose tissue, and macrophages, whereas LRXβ is expressed ubiquitously (Konvanen and Pentikäinen 2003; Jaye 2003; Joseph and Tontonoz 2003). Macrophage liver XC receptors are identified as inhibitors of atherosclerosis (Tangirala et al. 2002). Liver X receptors are regarded as potential therapeutic agents for dyslipidemia and atherosclerosis (Lund et al. 2003).

REFERENCES AND FURTHER READING

Kovanen PT, Pentikäinen MO (2003) Pharmacological evidence for a role of liver X receptors in atheroprotection. FEBS Lett 536:3–5

Jaye M (2003) LXR agonists for the treatment of atherosclerosis. Curr Opin Invest Drugs 4:1053–1058

Joseph SB, Totonoz P (2003) LXRs: new therapeutic targets in atherosclerosis? Curr Opin Pharmacol 3:192–197

Lund EG, Menke JG, Sparrow CP (2003) Liver X receptor agonists as potential therapeutic agents for dyslipidemia and atherosclerosis. Arterioscler Thromb Vasc Biol 23:1169–1177

Tangirala RK, Bishoff ED, Joseph SB, Wagner BL, Walczak R, Laffitte BA, Daige CL, Thomas DA, Heyman RA, Mangelsdorf DJ, Wang X, Lusis AJ, Tontonoz P, Scholman IG (2002) Identification of liver XC receptors as inhibitors of atherosclerosis. Proc Natl Acad Sci USA 99:11896–11901

M.8.3.1 Stimulation of Cholesterol Efflux

PURPOSE AND RATIONALE

LXRs induce ATP binding cassette (ABC) transporters, e. g., ABCA1 (Costet et al. 2000) and ABCG1 (Venkateswaran et al. 2000), which are involved in the transport of cholesterol and phospholipids from cells to extracellular receptors.

Sparrow et al. (2002) described a potent synthetic LXR agonist that is more effective than 22(R)-hydroxycholesterol in inducing ABCA1 mRNA and stimulating cholesterol efflux.

PROCEDURE

Cells

Cells were cultured at 37°C in a humidified atmosphere consisting of 95% air and 5% carbon dioxide. Primary human fibroblasts were obtained from the Camden human cell repository. The cells were grown, handled, and cholesterol-loaded as described by Francis et al. (1955). Human primary hepatocytes were maintained in phenol red-free Dulbecco's modified Eagle's medium (high glucose) containing 10% charcoal-stripped FCS, 1% non-essential amino acids, 1% glutamine, 100 units/ml penicillin G, and 100 µg/ml streptomycin sulfate. Caco-2 cells were obtained from ATCC and grown in Opti-MEM containing 10% FCS, non-essential amino acids, and vitamins. THP-1 cells were obtained from ATCC and were grown in RPMI medium containing 10% FCS, 0.05 µM 2-mercaptoethanol, 1 mM sodium pyruvate, 2 mM L-glutamine, and antibiotic-antimyotic solution (100 units/ml penicillin, 0.1 µg/ml streptomycin, 0.25 µg/ml amphotericin B). THP-1 cells were differentiated into macrophages in six-well tissue culture dishes at a density of 1 million cells/well by incubation in the same medium plus 100 nM tetradecanoyl phorbol acetate for 3 days. After differentiation into macrophages, cells were used for mRNA measurements or for cholesterol efflux assays as described below. Human primary monocytes were prepared as described by Wright and Silverstein (1982) and differentiated to macrophages by culturing for 7 days in Teflon jars in RPMI 1640 medium supplemented with 12% human serum, 100 units/ml penicillin, and 100 µg/ml streptomycin sulfate. They were then plated in the same medium to initiate experiments.

Assays of Cholesterol Efflux Using [^{3}H]Cholesterol

Cells were labeled by incubation for 24 h in fresh growth medium containing [^{3}H]cholesterol (10 µCi/ml). In some experiments, cells were simultaneously labeled with [^{3}H]cholesterol and cholesterol-loaded using acetylated LDL. Following labeling with [^{3}H]cholesterol, cells were washed and incubated for an additional 24 h in serum-free media containing 1 mg/ml bovine serum albumin to allow for equilibration of [^{3}H]cholesterol with intracellular cholesterol. Cholesterol efflux was initiated by adding the indicated amount of apoA-I, usually 10 µg/ml, with or without APD, in serum-free medium. APD was added to cell culture medium from Me_2SO solutions, and control cells received an equivalent amount of Me_2SO, never exceeding 0.1%. After 24 h, media were harvested, and cells were dissolved in 1 mM HEPES, pH 7.5 containing 0.5% Triton X-100. Media were briefly centrifuged to remove non-adherent cells, and then aliquots of both the supernatants and the dissolved cells were subjected to liquid scintillation spectrometry to determine radioactivity.

Assays of Cholesterol Efflux Using Gas Chromatography-Mass Spectrometry

At the end of the 24-h efflux assay, cells and media were extracted. Cells were extracted twice (10 min with shaking each time) with 1 ml of hexane/isopropyl alcohol/water (3:2:0.1, v/v/v)/5 cm^2 of cell surface area. Media were extracted with 2.5 vols of chloroform/methanol (2:1, v/v). Internal standard [26,27-^{2}*H*_{6}]cholesterol, was added to the extracts, and the samples were taken to dryness under a stream of argon. Half of the cellular lipid extract was saponified for 1 h at 60°C in a solution of 3% KOH in 90% ethanol. One volume of water was added, and the mixture was extracted with 2 vols of hexane. The extracts of media and cellular lipids with or without saponification were taken to dryness under argon, derivatized to trimethylsilyl ethers by treatment with Sigma Sil-A for 1 h at 60°C, redissolved in hexane, and analyzed by gas chromatography/mass spectrometry. The amount of cholesterol in the original sample was determined using a standard curve.

Gas Chromatography/Mass Spectrometry

Gas chromatography/mass spectrometry was performed using a ThermoQuest GCQ instrument equipped with an RTX-5MS column (30 m × 0.25 mm inner diameter, 0.25-µm phase thickness; Restek, Bellefonte, Pa., USA). The gas chromatography program was 180°C for 1 min, followed by a temperature

gradient of 20°C/min to 290°C and a final elution at 290°C for 20 min. The injector was operated in the split mode (1:10 split), and the temperature was kept at 275°C. Helium was used as the carrier gas at a constant flow rate of 1 ml/min. The instrument was operated in the electron ionization mode with the electron energy set to 70 eV. The ion trap was used for the selected ion monitoring of *m*/*z* 458 and 464 for determination of cholesterol and [26,27-$^2H_6$]cholesterol, respectively.

Transactivation Assays

Expression constructs were prepared by inserting the ligand binding domain of human LXRα and LXRβ cDNAs adjacent to the yeast GAL4 transcription factor DNA binding domain in the mammalian expression vector pcDNA3 to create pcDNA3-LXRα/ GAL4 and pcDNA3-LXRβ/GAL4, respectively. The GAL4-responsive reporter construct, pUAS(5x)-tk-luciferase, contained five copies of the GAL4 response element placed adjacent to the thymidine kinase minimal promoter and the luciferase reporter gene. The transfection control vector, pEGFP-N1, contained the green fluorescence protein gene under the regulation of the cytomegalovirus promoter. For transient transfections, HEK-293 cells were seeded at 4×10^4 cells/well in 96-well plates in Dulbecco's modified Eagle's medium (high glucose) containing 10% FCS, 100 units/ml penicillin G, and 100 µg/ml streptomycin sulfate at 37°C in a humidified atmosphere of 5% CO_2. After 24 h, transfections were performed with LipofectAMINE (Invitrogen) according to the instructions of the manufacturer. Transfection mixes contained 0.002 µg of LXRα/GAL4 or LXRβ/GAL4 chimeric expression vectors, 0.02 µg of reporter vector pUAS(5x)-tk-luc, and 0.034 µg of pEGFP-N1 vector as an internal control of transfection efficiency. Compounds were characterized by incubation with transfected cells for 48 h across a range of concentrations in phenol red-free Dulbecco's modified Eagle's medium (high glucose) containing 10% charcoal-stripped FCS), 1% non-essential amino acids, 1% glutamine, and 100 units/ml penicillin G and 100 µg/ml streptomycin sulfate. Cell lysates were prepared from washed cells using cell lysis buffer (Promega, Madison, Wis., USA).

Measurement of mRNA Levels by Real-Time Quantitative Reverse Transcription-PCR (TaqMan)

Real-time quantitative PCR analysis was used to determine the relative levels of ABCA1 and ABCG1 mRNA. Reverse transcription and PCRs were performed according to the manufacturer's instructions. Sequence-specific amplification was detected with an increasing fluorescent signal of FAM (reporter dye) during the amplification cycle.

Amplification of the mRNA for the human 23-kDa highly basic protein, also called ribosomal protein L13a, was performed in the same reaction on all samples tested as an internal control for variations in RNA amounts. Levels of the different mRNAs were subsequently normalized to highly basic protein mRNA levels. Oligonucleotide primers and Taq-Man probes were designed using Primer Express software (Applied Biosystems) and were synthesized by Applied Biosystems. Sequences of forward primers, reverse primers, and probes (respectively) were as follows:

ABCA1, TGTCCAGTCCAGTAATGGTTCTGT, AAACGAGATATGGTCCGGATT, 6FAM-ACACCT GGAGAGAAGCTTTCAACGAGACTAACCTAMR A; *ABCG1*, TGCAATCTTGTGCCATATTTGA, CC AGCCGACTGTTCTGATCA, 6FAM-TACCACAAC CCAGCAGATTTTGTCATGGA-TAMRA; *SREBP-1c*, GGTAGGGCCAACGGCCT, CTGTCTTGGTT GTTGATAAGCTGAA. 6FAM - ATCGCGGAGCCA TGGATTGCACT - TAMRA; *HBP*, GCTGGAAGT ACCAGGCAGTGA, ACCGGTAGTGGATCTTGG CTTT, VIC-TCTTTCCTCTTCTCCTCCAGGGTGG CT-TAMRA.

EVALUATION

For Cholesterol Efflux

Cholesterol efflux is expressed as a percentage, calculated as ([^{3}H]cholesterol in medium)/([^{3}H]cholesterol in medium + [^{3}H]cholesterol in cells) × 100.

For Transactivation Assay

Luciferase activity in cell extracts was determined using luciferase assay buffer in a ML3000 luminometer (Dynatech Laboratories). Green fluorescence protein expression was determined using the Tecan Spectrofluor Plus at an excitation wavelength of 485 nm and emission at 535 nm. Luciferase activity was normalized to green fluorescence protein expression to account for any variation in efficiency of transfection.

MODIFICATIONS OF THE METHOD

Chawla et al. (2003) used null stem cell of mice to demonstrate that PPARδ is a very low-density lipoprotein sensor in macrophages.

REFERENCES AND FURTHER READING

Chawla A, Lee CH, Barak Y, He W, Rosenfeld J, Liao D, Han J, Kang H, Evans RM (2003) PPARδ is a very low-density

lipoprotein sensor in macrophages. Proc Natl Acad Sci USA 100:1268–1273
Costet P, Luo Y, Wang N, Tall AR (2000) Sterol dependent activation of the *ABC1* promotor by the liver Xrecptor/retinoid X receptor. J Biol Chem 36:28240–28245
Francis GA, Knopp RH, Oram JF (1995) Defective removal of cellular cholesterol and phospholipids by apolipoprotein A-1 in Tangier disease. J Clin Invest 96:78–87
Sparrow CP, Baffic J, Lam MH, Lund EG, Adams AD, Fu X, Hayes N, Jones AB, Macnaul KL, Ondeyka J, Singh S, Wang J, Zhou G, Moller DE, Wright SD, Menke JG (2002) A potent synthetic LXR agonist is more effective than cholesterol loading and inducing *ABCA1* mRNA and stimulating cholesterol efflux. J Biol Chem 277:10021–10027
Venkateswaran A, Repa JJ, Lobacarro JM, Bronson A, Mangelsdorf DJ, Edwards PA (2000) Human white/murine ABC8 mRNA levels are highly induced in lipid-loaded macrophages. A transcriptional role for specific oxysterols. J Biol Chem 275:14700–14707
Wright SD, Silverstein SC (1982) Tumor promoting phorbol esters stimulate C3b and C3b' receptor-mediated phagocytosis in cultured human monocytes. J Exp Med 156:1149–1164

M.8.3.2 Liver X Receptor Binding

PURPOSE AND RATIONALE

Several authors have studied the structure and function of the liver X receptors (Spencer et al. 2001; Yoshikawa et al. 2002; Hoerer et al. 2003; Yu et al. 2003; Williams et al. 2003).

Janowski et al. (1999) studied the structural requirement of ligands for the oxysterol liver X receptors LXRα and LXRβ and developed a ligand binding assay.

PROCEDURE

Ligands

Purchased ligands include the following: 9-*cis*-[20-*methyl*-^{3}H]retinoic acid (72 Ci/mmol; 1 Ci = 37 GBq) and [26,27-^{3}H(N)]-24(S),25-EC (76 Ci/mmol); 22(R,S)-HC, 25-HC, 7α-HC, 24,25-dehydrocholesterol, cholic acid, pregnenolone, 9-*cis*-retinoic acid (9cRA). Stereocontrolled syntheses for the following ligands were performed: 24(S),25-EC; 22(R)-hydroxy-24(S),25-EC; 24(R),25-EC; 22(S)-hydroxy-24(R),25-EC; 7-keto-, 7β-hydroxy-, and 7α-hydroxy-24(S),25-ECs; 24(S),25-iminocholesterol; and 22(R),24(S)-dihydroxycholesterol. The methyl ester and dimethylamide of cholenic acid were prepared from cholesterol trisnorcarboxylic acid via acid chloride by reaction with methanol and dimethylamine, respectively.

Cell Cotransfection Assays

CV-1 cell conditions and transient transfections were performed (Willy et al. 1995). Receptor expression plasmids encoding full-length human LXRβ (CMX-hLXRβ) or LXRα (CMX-hLXRα) (Willy et al. 1995) were cotransfected with a luciferase reporter plasmid [TK-CYP7a-LXRE(X3)-LUC] (Peet et al. 1998) containing three tandem copies of the sequence (gcttTG-GTCActcaAGTTCAagtta) from the rat *Cyp7a* gene (Chiang and Stroup 1994). Increasing concentrations of ligand (0.1–40 mM) were added to cells in media containing 5% lipid-depleted calf bovine serum. Transfection data were normalized to a β-galactosidase internal standard.

Data are presented as mean relative light units (RLU) from triplicate assays $\pm$ SEM. EC_{50} values generated from duplicate assays were determined by fitting the data to a sigmoidal dose–response curve (GRAPHPAD PRISM, GraphPad Software, San Diego, Calif., USA). Efficacy values represent the fraction of maximal fold activation of each compound relative to 24(S),25-EC. Fold activation was determined by dividing the maximal activation of each compound by the activation observed in the absence of compound.

Receptor Protein Purification

Polyhistidine human RXRα (His10-hRXRα) (Petty 1995), LXRα LBD or LXRβ LBD fusion proteins (His_6-hLXRα-LBD, His_6-hLXRβ-LBD) were expressed in *Escherichia coli* strain BL21(DE3) (Novagen). Cultures grown in Luria-Bertani medium were induced with 0.5 mM isopropyl β-D-thiogalactoside (IPTG) for 4 h at 25°C. Pellets were suspended in lysis buffer (250 mM NaCl, 16 mM Na_2HPO_4, 4 mM NaH_2PO_4, 1% Triton X-100, 10 mM imidazole, 200 mg of lysozyme per ml). The supernatant was incubated with Ni^{2+}-NTA agarose (Qiagen). The resin was washed twice with 20 vols of 50 mM Hepes, pH 7.5, 250 mM NaCl supplemented first with 50 mM then 75 mM imidazole. Protein was eluted with a linear 75–500 mM imidazole gradient. Peak fractions were tested for purity by SDS-PAGE, pooled, and cleared of imidazole over a PD-10 column (Pharmacia) equilibrated with 20 mM Hepes, pH 7.5, 200 mM NaCl, 2.5 mM EDTA, 5 mM DTT. Concentrations were determined by UV spectral analysis.

Ligand-Binding Assay

Scintillant-filled beads precoated with polylysine to permit protein binding (Amersham) were diluted in scintillation proximity assay (SPA) buffer [10 mM K_2HPO_4, 10 mM KH_2PO_4, 2 mM EDTA, 50 mM NaCl, 1 mM DTT, 2 mMCHAPS, 10% (vol/vol) glycerol, pH 7.1; CHAPS is 3-[(3-cholamidopropyl)dimethylammonio]-1-propanesulfonate] to a fi-

nal concentration of 10 mg/ml. Binding assays were performed in 96-well plates (Packard) in a total volume of 100 ml containing beads (0.2 mg per well) and His_6-hLXRα- LBD (600 ng per well), His_6-hLXRβ-LBD (250 ng per well), or His_6-hRXRα (250 ng per well). The amount of protein used did not deplete ligand concentrations. [^{3}H]-24(S),25-EC or [^{3}H]-9cRA was diluted in SPA buffer and added to wells for a final concentration of 25 nM or 5 nM, respectively. Competition binding assays using a single concentration of unlabeled competitor contained 25 mM 24(S),25-EC or 5 µmM9cRA. In other competition binding assays, unlabeled ligands were serially diluted in SPA buffer, then added at final concentrations ranging from 3 nM to 50 µM. Plates were shaken at 25°C for 3 h, and then radioactivity was measured with a Packard Topcount at 1 min per well. All concentrations were assayed in triplicate and the results were averaged. Values from wells void of competitor represented 100% binding.

EVALUATION

Generation of K_i Value

Competition curves were generated by non-linear regression analysis with GRAPHPAD PRISM, and apparent equilibrium dissociation constants (K_i values) were determined by using a method described by DeBlasi et al. (1989) based on the Cheng–Prusoff equation. K_i values for compounds that served as weak competitors in the assay (competition < 70% at the highest concentrations tested) are described as poor competitors. All K_i and SEM values reported are averages generated from duplicate or triplicate assays.

REFERENCES AND FURTHER READING

Chiang JY, Stroup D (1994) Identification and characterization of a putative bile-acid-responsive element in the cholesterol 7α-hydroxylase gene promoter. J Biol Chem 269:17502–17507

DeBlasi A, O'Reilly K, Motulsky HY (1989) Calculation receptor number from binding experiments using same compound as radioligand and competitor. Trends Pharmacol Sci 10:227–229

Hoerer S, Schmid A, Keckel A, Budzinski RM, Nar H (2003) Crystal structure of the human liver X receptor βligand binding domain in complex with a synthetic agonist. J Mol Biol 344:853–861

Janowski BA, Grogan MJ, Jones SA, Wisely GB, Kliewer SA, Corey EJ, Mangelsdorf DJ (1999) Structural requirements of ligands for the oxysterol liver X receptors LXRα and LXRβ. Proc Natl Acad Sci USA 96:266–271

Peet DJ, Turley SD, Ma W, Janowski BA, Lobaccaro JM, Hammer RE, Mangelsdorf DJ (1998) Cholesterol and bile acid metabolism are impaired in mice lacking the nuclear oxysterol receptor LXRα. Cell 93:693–704

Petty KJ (1995) Tissue- and cell-specific distribution of proteins that interact with the human thyroid receptorβ. Mol Cell Endocrinol 108:131–142

Spencer TA, Li D, Russel JS, Collins JL, Bledsoe RK, Consler TG, Moore LB, Galardi CM, McKee DD, Moore JT, Watson MA, Parks DJ, Lambert MH, Willson TM (2001) Pharmacophore analysis of the nuclear oxysterol receptor LXRα . J Med Chem 44:886–897

Williams S, Bledsoe RK, Collins JL, Boggs R, Lambert MH, Miller AB, Moore J, McKee DD, Moore L, Nichols J, Parks D, Watson M, Wisely B, Willson TM (2003) X-ray crystal structure of the liver X receptor β ligand binding domain. Regulation by a histidine-tryptophan twitch. J Biol Chem 278:27138–27143

Willy JP, Umesono K, Ong ES, Evans RM, Heyman RA, Mangelsdorf DJ (1995) LXR, a nuclear receptor that defined a distinct retinoid response pathway. Genes Dev 9:1022–1045

Yoshikawa T, Shimano H, Yahagi N, Ide T, Amemiya-Kudo M, Matsuzaka Z, Nakakuki M, Tomita S, Okazaki H, Tamura Y, Izuka Y, Ohashi K, Takahashi A, Sone H, Osuka JL, Gotoda T, Ishibashi S, Yamada N (2002) Polyunsaturated fatty acids suppress sterol regulatory element-binding protein 1c promoter activity by inhibition of liver X receptor (LXR) binding to LXR responsive elements. J Biol Chem 277:1705–1711

Yu L, York J, von Bergmann K, Cohen JC, Hobbs HH (2003) Stimulation of cholesterol excretion by liver X receptor agonist requires ATP-binding cassette transporter G5 and G8. J Biol Chem 15565–15570

M.8.3.3 Inhibition of Atherosclerosis by LXR Ligands

PURPOSE AND RATIONALE

Several authors studied the potential antiatherosclerotic effects of LXR ligands. Alberti et al. (2001) used LXRβ-deficient mice to study hepatic cholesterol metabolism and resistance to dietary cholesterol.

Chawla et al. (2001) reported that the nuclear receptor LXRα mediates a transcriptional cascade via PPARγ, which induces ABCA1 expression and cholesterol removal from macrophages. Ligand activation of PPARγ leads to primary induction of LXRα and to coupled induction of ABCA1. Transplantation of PPARγ null bone marrow into LDLR$^{-/-}$ mice results in a significant increase in atherosclerosis, consistent with the hypothesis that regulation of LXRα and ABCA1 expression is protective *in vivo*.

PROCEDURE

Reagents

Oxysterols were dissolved in ethanol prior to addition to cells (< 1 µl/ml).

Cell Culture, Stable Cell Lines, and RNA Analysis

THP-1 cells were cultured in RPMI 1640 supplemented with 10% fetal bovine serum or 10% lipoprotein-deficient fetal bovine serum (LPDS). ES cells were cultured in the presence of rLIF (Gibco) as described (Keller et al. 1993). Macrophage differentia-

tion was induced in ES cells in a two-stage process. Initially, ES cells were differentiated into embryoid bodies. Day 6 embryoid bodies were isolated, disaggregated, and replated in the presence of interleukin-3 and macrophage colony-stimulating factor-1 to induce differentiation of monocytes and macrophages, respectively. Total RNA was isolated using TRIzol reagent (Gibco), and Northern blot analyses were performed.

Transfection Assays

Murine LXRα and β promoters were amplified by PCR using the published genomic structure and sequence. Primers for PCR of LXR promoters were: LXRα: 5′-ATCCTGTCCCTTCTGTCC-3′ and 5′-CC TCCAGAGTCAGCGTTC-3′, and LXRβ: 5′-CAGTG AGCGCATACAGGT-3′ and 5′-TCTCCGACTCTGT TGCCC-3′ . To determine the transcription initiation site for mABCA1, 5′ RACE was performed using the 5′/3′ RACE kit (Roche) with RNA from the RAW 274 cell line and mouse liver, and the gene-specific 3′ primer (5′-CTGAGGCCAACAAGCCAT-3′). The extended RACE products were used to screen a mouse genomic library (Stratagene). Sequence analysis of the isolated clones by the Blast program revealed that the identified initiation site and 5′ regulatory region of ABCA1 were identical to the sequences deposited in GenBank (accession number AJ017356). The 2.5-kb genomic fragment of the mABCA1 promoter was cloned into a pGL3-basic vector. CV-1 cells were transfected by lipofection and assayed for reporter activity as described by Forman et al. (1995). Transfections were performed in triplicate and normalized to an internal CMX-βgal control. pCMX expression vectors for the PPARs and LXRs have been described (Kliewer et al. 1994; Willy et al. 1995).

Gel Mobility Shift Assays

Gel mobility shift assays were performed using *in vitro* translated receptors and 32P end-labeled oligonucleotides in a buffer containing 20 mM HEPES (pH 7.4), 100 mM KCl, 1 mM β-mercaptoethanol, 10% glycerol, 100 mg/ml polydI-dC, and 5 mg/ml BSA. For competition studies, an excess of unlabeled oligonucleotide was added.

Cholesterol Efflux

Cholesterol efflux assays were performed as described by Venkateswaran et al. (2000), with minor modifications. Cells were plated at 50% confluence. On day 2, cells were washed and incubated for 24 h in RPMI 1640 supplemented with 10% LPDS. Cells were labelled with [^{3}H]cholesterol (1.0 mCi/ml), either in the presence of the ACAT inhibitor (58–035; 2 µg/ml) or with acLDL (50 µg/ml) in the absence of the ACAT inhibitor. Ligands for PPARβ (BRL; 5 µM), RXR (LG268; 50 nM), or LXR (22[R]-OHC; 2.0 µg/ml) were added to the cells. To equilibrate cholesterol pools, cells were washed twice with PBS and incubated for 8 h in RPMI containing 0.2% BSA plus the ligands, but lacking radiolabeled cholesterol or acLDL. Cells were again washed with PBS and incubated in RPMI containing 0.2% BSA in the absence or presence of HDL (50 µg/ml) or apoAI (15 µg/ml), for 4 h. An aliquot of the medium was removed and centrifuged at 14,000 *g* for 2 min, and the radioactivity was determined by liquid scintillation counting. Total cell-associated radioactivity was determined by dissolving the cells in isopropanol.

The data are presented as percent HDL-specific efflux or apoAI-specific efflux, which is efflux in the presence of acceptor minus efflux in the absence of acceptor. Each assay was performed in triplicate.

Bone Marrow Transplantation

LDL-R$^{-/-}$ mice backcrossed onto the C57BL/6 background were initially obtained from Jackson Laboratories. Mice were fed a chow diet ad libitum until they were enrolled into the study. PPARg2/2ES cells were injected into C57/Bl6 blastocysts to generate PPAR$\gamma^{-/-}$ chimeric mice. The majority of the chimeric mice obtained were high-percentage chimeras. Peripheral blood, spleen, and bone marrow of PPAR$\gamma^{-/-}$ chimeras were extensively analyzed by facs analysis with antibodies directed against Ly 9.1, CD11b/CD18, F4/80, CD3, B220, and Ly 6.1 to quantify the extent of chimerism. Chimeras, which were greater than 90% null in their contribution to the monocytic/macrophage lineage, were used for bone marrow transplantation, along with wild-type control mice. In all, 24 6-week-old male LDL-R$^{-/-}$ mice were γ-irradiated with 1000 rads to eliminate the majority of their bone marrow cells. Each of the γ-irradiated mice were reconstituted via a tail vein injection with 2,000,000 bone marrow cells isolated from either PPARγ +/+ mice (designated PPARγ +/+ BMT) or PPARg 2/2 mice (designated PPARg 2/2 BMT). The mice were placed on a chow diet for 4 weeks while their marrow repopulated with the donor cells. For induction of atherosclerosis, the transplanted mice were placed on an atherogenic diet containing 15.8% (wt/wt) fat and 1.25% cholesterol (no cholate; diet 94059, Harlan Teklad) for 8 weeks. At weeks 0 (before BMT), 4, and 12, blood was drawn via

the retro-orbital plexus following an 8-h fast, and total plasma cholesterol was measured via an enzymatic assay.

Lesion Analysis and Immunohistochemistry

Atherosclerotic lesions were quantified in the aortic valve of each mouse as described by Boisvert et al. (1998). The OCT-embedded, frozen aortic valves were sectioned serially at 10 µm thickness for a total of 300 µm beginning at the base of the aortic valve, where all three leaflets are first visible. Every fourth section for a total of five sections from each animal was stained with oil red O to identify the lipid-rich lesions. The stained areas were quantified using a computer-assisted video imaging system, and the mean area of the five sections from each animal was used for comparison analysis. The mouse aortic valve lesions were analyzed immunohistochemically with the following antibodies: anti-MOMA-2 (Serotec) for detection of intimal macrophages; anti-β-galactosidase (Cappel) for detection of PPAR$\gamma^{-/-}$ cells; and anti-α-actin (Dako) for detection of smooth muscle cells in the lesion. The frozen tissue sections were blocked with 5% normal sera and incubated for 2 h at room temperature with the primary antibody (1–10 µg/ml). The sections were blocked for endogenous peroxidase activity with Peroxo-Block (Zymed, South San Francisco, Calif., USA), followed by incubation with the appropriate secondary antibody (5 µg/ml) for 1 h. The washed sections were finally incubated for 30 min with Vectastain ABC Elite solution (Vector Laboratories, Burlingame, Calif., USA), developed with 9-amino-3-ethylene-carbazole (AEC; Vector Laboratories), and counterstained with hematoxylin.

EVALUATION

Statistical analysis was performed using the Mann-Whitney *U* test, and data are expressed as mean ± SD.

MODIFICATIONS OF THE METHOD

Dressel et al. (2003) used mouse myogenic C2C12 cells to study the influence of a peroxisome proliferator-activated receptor β/δ agonist on the expression of genes involved in lipid catabolism and energy uncoupling in skeletal muscle cells.

Tanaka et al. (2003) used skeletal muscle cells of mice to study the influence of peroxisome proliferator-activated receptor δ on fatty acid β-oxidation in skeletal muscle and the metabolic syndrome.

REFERENCES AND FURTHER READING

Alberti S, Schuster G, Parini P, Feltkamp D, Diczfalusi U, Rudling M, Angelin B, Björkhem I, Pettersson S, Gustavsson JA (2001) Hepatic cholesterol metabolism and resistance to dietary cholesterol in LXRβ-deficient mice. J Clin Invest 107:565–573

Boisvert WA, Santiago R, Curtiss LK, Terkeltaub RA (1998) A leukocyte homologue of the IL-8 receptor CXCR-2 mediates the accumulation of macrophages in the aortic lesions of LDL receptor-deficient mice. J Clin Invest 101:353–345

Chawla A, Boisvert WA, Lee CH, Laffitte BH, Barak Y, Joseph SB, Liao D, Nagy L, Edwards PA, Curtiss KL, Evans RM, Tontonoz P (2001) A PPARγ-LXR-ABCA1 pathway in macrophages is involved in cholesterol efflux and atherogenesis. Mol Cell 7:161–171

Dressel U, Allen TL, Pippal JP, Rohde PR, Lau P, Muscat GEO (2003) The peroxisome proliferator-activated receptor β/δ agonist, GW501516, regulates the expression of genes involved in lipid catabolism and energy uncoupling in skeletal muscle cells. Mol Endocrinol 17:2477–2493

Forman BM, Tontonoz P, Chen J, Brun RP, Spiegelman PM, Evans RM (1995) 15-Deoxy-δ 12,14-prostaglandin J2 is a ligand for the adipocyte determination factor PPARγ. Cell 83:803–812

Keller G, Kennedy M, Papyannopoulou T, Wiles MV (1993) Hematopoietic commitment during embryonic stem cell differentiation in culture. Mol Cell Biol 13:473–486

Kliewer SA, Forman BM, Blumberg B, Ong ES, Borgmeyer U, Mangelsdorf DJ, Umesono K, Evans RM (1994) Differential expression and activation of a family of murine peroxisome receptor-activated receptors. Proc Natl Acad Sci USA 91:7355–7359

Tanaka T, Yamamoto J, Iwasaki S, Asaba H, Hamura H, Ikeda Y, Watanabe M, Mgoori K, Ioka RX, Tachibana K, Watanabe Y, Uchiyama Y, Sumi K, Iguchi H, Ito S, Doi T, Hamakubo T, Naito M, Auwerx J, Yagishawa M, Kodama T, Sakai J (2003) Activation of peroxisome proliferator-activated receptor δ induces fatty acid β-oxidation in skeletal muscle and attenuates metabolic syndrome. Proc Natl Acad Sci USA 100:15924–15929

Venkateswaran A, Laffitte BA, Joseph SB, Mak PA, Wilpitz CD, Edwards PA, Tontonoz P (2000) Control of cellular efflux by the nuclear oxysterol receptor LXRα. Proc Natl Acad Sci USA 97:12097–12102

Willy JP, Umesono K, Ong ES, Evans RM, Heyman RA, Mangelsdorf DJ (1995) LXR, a nuclear receptor that defined a distinct retinoid response pathway. Genes Dev 9:1022–1045

M.9
Safety Pharmacology of Anti-Atherosclerotic Drugs

See Herling (2006).

REFERENCES AND FURTHER READING

Herling AW (2006) Metabolism pharmacology. In: Vogel HG (ed), Hock FJ, Maas J, Mayer D (co-eds) *Drug Discovery and Evaluation – Safety and Pharmacokinetic Assays*. Springer, Berlin Heidelberg New York, Chap. I.G, pp 151–193

Chapter N
Endocrinology[1]

[1] Reviewed and amended by J. Sandow

N.1 Preface

In the development of methods for endocrine investigation, many changes have occurred since the early period of animal investigation, in which extensive surgical procedures were used to remove endocrine organs in order to study their function by deficiency symptoms, and their active principles were replaced by organ extracts and hormone preparations of increasing purity and specificity of action. Much of the classical endocrinology has now been replaced by investigations of ever increasing sophistication and specificity. Where possible, surgical procedures are discarded and avoided. Studies are performed on intact animals with a minimum of stress and interference (noninvasive procedures). One example of early noninvasive investigation is the study of adrenal gland hormone secretion, by investigation of the urinary excretion of adrenal steroids and changes induced by specific procedures.

Where surgical procedures cannot be avoided, techniques for anesthetizing animals have changed very markedly (new anesthetics have replaced ether anesthesia), animal husbandry has undergone major changes, and postoperative animal care has been standardized and optimized. Specific strains of animals with endocrine disease conditions have been developed by selection from naturally occurring genetic disorders, and increasingly detailed investigations are now available through the study of genetics and patterns of gene expression following the administration of test compounds and candidate drugs.

There is however a price to be paid for any method of increasing sophistication. The interpretation of the relevance of changes to the clinical situation (predictive relevance) becomes more difficult. As an example, in the chain of events from receptor binding of a drug, to the intracellular changes summarized as receptor signaling, and finally to the observed effects on patterns of gene expression, interpretation is much more tenuous and the pathway to understanding clinical relevance is often more difficult than it used to be. Endocrinologists will have to be careful and conservative when interpreting their findings, and often a set of coordinated investigations is needed before the complex early findings of an investigation can be unraveled. With these words of introduction, the following descriptions of methods are presented to encompass both historical and classical approaches, as well as the highly effective and specific investigation of detail now at hand.

N.1.1 Endocrine Survey

PURPOSE AND RATIONALE

The effects of steroid and peptide hormones as well as the influence of drugs on the endocrine system are detected by repeated administration of the test substances. The procedure is analogous to toxicology studies with repeated administration, however the dose range is limited to the intention of understanding physiological changes at concentrations of endogenous compounds found in the body, and concentrations of drugs which are intended for future therapeutic use (methods with intention to predict clinical effects and explain physiological regulations) (Sandow 1979). Animals are treated for at least several days to achieve equilibration of the physiological response to administration of compounds. After administration for a period of 1–4 weeks, the endocrine glands and the organs that are dependent on hormonal influences are weighed. Furthermore, the hormonal content of the endocrine glands and the blood levels of hormones are determined.

During treatment and at the time of animal sacrifice, blood samples or tissue samples may be obtained where needed for investigation and interpretation, and frequently the same treatment protocol may need to be repeated when taking samples during treatment, and when investigating the time sequence of induced changes, always with a minimum of interference and based on noninvasive procedures whenever possible.

PROCEDURE

The endocrine survey is performed using young or adult rats depending on the purpose of the investigation. Selection of this animal species is based on extensive knowledge of physiological data for organ development and hormone secretion. It is also based on the

technology for obtaining blood and urine samples with a minimum of stress to the animals. Separate groups of five to ten male and female Sprague-Dawley rats weighing 55–65 g are used (animals during development). For some compounds, groups of 200 or 300 g body weight may be required. They are treated daily over a period of 6–12 days with the test compound by the intended route (orally or by subcutaneous injections). For toxicological studies, a treatment period of 4 weeks is preferable. A similar protocol is applied for chronic toxicity studies in rats and dogs. On the day after the last application, the animals are sacrificed, weighed, and the parameters determined:

Parameter	Optional
Pituitary-adrenal axis	
Pituitary weight	Corticotropin-releasing hormone in hypothalamus
Adrenal weight	Pituitary content of adrenocorticotropin and vasopressin
Thymus weight	Adrenal content of corticosterone and aldosterone; corticosterone and aldosterone blood level; electrolyte (Na^+, K^+, Ca^{2+}, Cl^-) concentrations in serum; urinary excretion of corticosterone and aldosterone
Pituitary–gonadal axis	
Male reproduction	
Pituitary weight	LH-RH in hypothalamus
Weight of testes	Pituitary content of FSH, LH and prolactin
Weight of seminal vesicles	Blood levels of FSH, LH and prolactin
Weight of ventral prostate	Testosterone content in testes and serum
Weight of musculus levator ani	Growth hormone in pituitary and serum
Female reproduction	
Pituitary weight	LH-RH in hypothalamus
Weight of ovaries	Pituitary content of FSH, LH and prolactin
Weight of uterus	Blood levels of FSH, LH and prolactin; content of estradiol and progesterone in ovaries and serum
Pituitary–thyroid axis	
Pituitary weight	TRH in hypothalamus
Thyroid weight	Pituitary content of thyrotropin; serum content of TSH, T3 and T4

FSH Follicle-stimulating hormone, *LH* luteinizing hormone, *LH-RH* LH-releasing hormone, *TRH* thyrotropin-releasing hormone

After dissection, organ weights are recorded, and serum or plasma and the endocrine glands are stored frozen at −20°C for further determination of hormonal content. This method may include histology, in situ hybridization, etc. as required. In many instances, an investigation of patterns of gene expression can now be part of these studies, in particular when previous experience is available for the changes considered to be of relevance.

EVALUATION

The mean values of each parameter for the treated groups are compared with the values for the control group. The control group is generally treated with the solvent or vehicle required for administration of the test compound. In many cases a group of untreated animals, undergoing the same sampling procedures, is investigated in order to make certain of the physiological background for comparison.

MODIFICATIONS OF THE METHOD

Many modifications are possible; for example, extension of the treatment period up to 4 weeks in order to detect toxicological effects after long-term administration, inclusion of supplementary parameters, satellite groups. Further specific tests are necessary to clarify the mode of action.

REFERENCES AND FURTHER READING

Sandow J (1979) Toxicological evaluation of drugs affecting the hypothalamic-pituitary system. Pharmacol Ther 5:297–303

N.2 Adrenal Steroid Hormones

N.2.0.1 Adrenalectomy in Rats

PURPOSE AND RATIONALE

The classical way to evaluate hormone function is to surgically ablate the hormone-producing endocrine gland and substitute with exogenously administered substances (extracts or synthetic hormones) (Biedl 1916). Many studies on the physiological role of adrenocortical hormones and the pharmacological effects of corticosteroids were performed using adrenalectomized rats.

PROCEDURE

Sprague-Dawley or Wistar rats of either sex weighing 120–150 g are used. The dorsal fur is shaved, the rat

is anesthetized and placed on a support in order to elevate the viscera. A transverse incision about 5 mm long is made in the mid-line at the costovertebral angle. To remove the left adrenal gland, the skin is retracted to the ventral side and the lumbar muscles incised just superior and anterior to the splenic shadow. The adrenal gland now appears directly beneath the incision and no exteriorization of the kidney is necessary. The periadrenal tissue is grasped between the kidney and the adrenal by small curved forceps and the intact gland together with the periadrenal fat and the mesenteric attachments is removed in toto. The bleeding is negligible in young animals so that no vessels need be tied off.

After ablation of the left adrenal, the animal is turned around and the right gland is removed through the original skin incision. A small incision through the lumbar muscles is made just above and anterior to the prominent lumbocostal arch which is seen near the costal margin. The curved forceps are inserted over the kidney and by elevating the liver, which covers the adrenal on this side, the gland is brought into view and grasped by the forceps, removing again the intact gland with the periadrenal fat and the mesenteric attachments. The incisions made in the lumbar muscles need not exceed 3 mm in length and may be made by spreading the blades of a pair of scissors; hemostasis or closure by sutures is not necessary. The incision is closed by a skin clip. The entire procedure is done in a time sufficiently short to avoid long-acting anesthetics. The animals appear normal in every aspect within a few minutes following the operation.

It is essential to provide good postoperative care for animals after adrenalectomy, and to correct the electrolyte imbalance due to deficiency of mineralocorticoid secretion (1% sodium chloride solution in water).

REFERENCES AND FURTHER READING

Biedl A (1916) Physiologie der Nebenniere. Exstirpationsversuche. In: Biedl A (ed) Innere Sekretion. Ihre physiologischen Grundlagen und ihre Bedeutung für die Pathologie. 3rd edn., Part I. Urban and Schwarzenberg, Berlin, pp 458–491

Bomskov C (1937) Die chirurgischen Methoden der Nebennierenforschung. In Bomskov C (ed) Methodik der Hormonforschung, Vol. 1. Thieme, Leipzig, pp 467–485

Dorfman RI (1962) Corticoids. In Dorfman RI (ed) Methods in hormone research, Vol II. Bioassay. Academic Press, New York, pp 325–367

Grollman A (1941) Biological assay of adrenal cortical activity. Endocrinology 29:855–861

N.2.1
Glucocorticoid Activity

N.2.1.1
In Vitro Methods for Glucocorticoid Hormones

N.2.1.1.1
Corticoid Receptor Binding

PURPOSE AND RATIONALE

Steroid hormone receptors are intracellular metalloproteins which bind steroids with high affinity and high specificity (nuclear receptors). The lipophilic steroids enter the cell by diffusion. The binding of the hormone to its specific receptors results in a series of conformational changes, leading to an increase in affinity for specific DNA regulatory elements (steroid responsive elements). After binding, transcription of target genes is enhanced and mRNAs are produced. These mRNAs are then translocated to the cytoplasm and translated into proteins regulating cellular metabolism and initiating the cellular responses. The structure and functions of the steroid receptor superfamily have been reviewed by Carson-Jurica et al. (1990), Lazar (1991), Barnes and Adcock (1993), Distelhorst (1993), Power et al. (1993), Brinkmann (1994), Ojasoo et al. (1994, 1995), Wittliff and Raffelsberger (1995), Beato et al. (1996), and Jensen (1996). The relative binding affinities for the glucocorticoid receptor of rat liver or thymus cytosol can be measured by competitive displacement of [^{3}H]dexamethasone (Raynaud et al. 1979; Schlechte et al. 1982; Wojnar et al. 1986; Ueno et al. 1991).

PROCEDURE

A steroid receptor preparation may be obtained from rats. Male Wistar rats weighing 140–150 g are adrenalectomized under anesthesia. Two days later, the liver is excised and homogenized in a tenfold buffer containing 50 mM Tris-HCl, 1 mM EDTA, 2 mM dithiothreitol, 10 mM Na_2MoO_4, and 10% glycerol (pH 7.4). The homogenate is centrifuged for 1 h at 105,000 *g* at 4°C and collected as the supernatant fraction. The cytosol is mixed with 5 nM [^{3}H]dexamethasone in the presence or absence of appropriate concentrations of competitors and incubated for 2 h at 4°C. The reaction is terminated by the addition of hydroxyapatite in order to separate the receptor–steroid complex from the free [^{3}H]dexamethasone.

The radioactivity bound to the receptors is determined by liquid scintillation spectrometry.

EVALUATION

IC_{50} values for the receptor preparation are calculated by probit analysis.

MODIFICATIONS OF THE METHOD

Numerous modifications of the glucocorticoid receptor assay have been reported, and cloning of receptor subtypes is ongoing (Zeelen 1992; White et al. 1994). Cytosols have been prepared from rat liver, from cultured rat hepatoma cells (Rousseau and Schmit 1977), and from normal human lymphocytes (Steiner and Wittliff 1985); thymocytes, from rat thymus gland (Lefebvre et al. 1988), human leukemic lymphoid cell line, CEM C7 (Srivastava and Thompson 1990), rat lung (Druzgala et al. 1991; Hochhaus et al. 1991), human lung (Rohdewald et al. 1985), rat hippocampus (Jacobson et al. 1993) and other sources.

Differentiation of type I (mineralocorticoid) and type II (glucocorticoid) receptors has been attempted (Spencer et al. 1990; Jacobson et al. 1993).

A new affinity label for glucocorticoid receptors was described by Lopez and Simons (1991).

The solution structure of the glucocorticoid receptor DNA-binding domain has been determined (Härd et al. 1990).

Berger et al. (1992) used transient co-transfection of receptor cDNA and suitable reporter genes to study human glucocorticoid receptor function in a CV-1 mammalian cell line. A variety of natural and synthetic steroids were analyzed for their ability to activate gene expression through the human glucocorticoid receptor and to bind to extracts of cells expressing human glucocorticoid receptor cDNA. A good correlation between both *in vitro* parameters and *in vivo* anti-inflammatory activity was reported for most of the steroids tested.

Guo et al. (1995) tested the binding of various steroids to the synaptic plasma membrane, which may be a novel type of glucocorticoid receptor on neuronal membranes that is significantly different from cytosolic glucocorticoid receptors.

A general survey of steroid hormones, receptors and antagonists was given by Jensen (1996).

Teutsch et al. (1995) discussed the structure–activity correlation of hormone antagonists ("antihormones").

Yoshikawa et al. (2002) showed that the pyrazolosteroid cortivazol is a specific ligand for the glucocorticoid receptor.

REFERENCES AND FURTHER READING

Barnes PJ, Adcock I (1993) Anti-inflammatory actions of steroids: molecular mechanisms. Trends Pharmacol Sci 14:436–441

Beato M, Truss M, Chávez S (1996) Control of transcription by steroid hormones. Ann NY Acad Sci 784:93–123

Berger TS, Parandoosh Z, Perry BW, Stein RB (1992) Interaction of glucocorticoid analogues with the human glucocorticoid receptor. J Steroid Biochem Mol Biol 41:733–738

Brinkmann AO (1994) Steroid hormone receptors: activators of gene transcription. J Pediatr Endocrinol 7:275–282

Carson-Jurica MA, Schrader WR, O'Malley BW (1990) Steroid receptor family: structure and functions. Endocr Rev 11:201–220

Distelhorst CW (1993) Steroid hormone receptors. J Lab Clin Med 122:241–244

Druzgala P, Hochhaus G, Bodor N (1991) Soft drugs. 10. Blanching activity and receptor binding affinity of a new type of glucocorticoid: loteprednol etabonate. J Steroid Biochem Mol Biol 38:149–154

Guo Z, Chen YZ, Xu RB, Fu H (1995) Binding characteristics of glucocorticoid receptor in synaptic plasma membrane from rat brain. Funct Neurol 10:183–194

Härd T, Kellenbach E, Boelens R, Maler BA, Dahlman K, Freedman LP, Carlstedt-Duke J, Yamamoto KR, Gustafsson JÅ, Kaptein R (1990) Solution structure of the glucocorticoid receptor DNA-binding domain. Science 249:157–160

Hochhaus G, Druzgala P, Hochhaus R, Huang MJ, Bodor N (1991) Glucocorticoid activity and structure activity relationships in a series of some novel 17α-ether-substituted steroids: influence of 17α-substituents. Drug Design Discov 8:117–125

Jacobson L, Brooke S, Sapolsky R (1993) Corticosterone is a preferable ligand for measuring brain corticosteroid receptors: competition by RU 28362 and RU 26752 for dexamethasone binding in rat hippocampal cytosol. Brain Res 625:84–92

Jensen EV (1996) Steroid hormones, receptors, and antagonists. Ann NY Acad Sci 784:1–17

Lazar MA (1991) Steroid and thyroid hormone receptors. Endocrinol Metab Clin North Am, 20:681–695

Lefebvre P, Danze PM, Sablonniere B, Richard C, Formstecher P, Dautrevaux M (1988) Association of the glucocorticoid receptor binding with the 90K nonsteroid-binding component is stabilized by both steroidal and nonsteroidal antiglucocorticoids in intact cells. Biochemistry 27:9186–9194

Lopez S, Simons SS (1991) Dexamethasone 21-(β-isothiocyanatoethyl) thioether: a new affinity label for glucocorticoid receptors. J Med Chem 34:1762–1767

Ojasoo T, Raynaud JP, Doré JC (1994) Affiliations among steroid receptors as revealed by multivariate analysis of steroid binding data. J Steroid Biochem Mol Biol 48:31–46

Ojasoo T, Raynaud JP, Doré JC (1995) Correspondence factor analysis of steroid libraries. Steroids 60:458–469

Power RF, Conneely OM, O'Malley BW (1993) New insights into activation of the steroid hormone receptor superfamily. Trends Pharmacol Sci 13:318–323

Raynaud JP, Ojasoo T, Bouton MM, Philibert D (1979) Receptor binding as a tool in the development of new bioactive steroids. In: Ariëns EJ (ed) Drug design, Vol VIII. Academic Press, New York, pp 169–214

Rohdewald P, Möllman HW, Hochhaus G (1985) Affinities of glucocorticoids for glucocorticoid receptors in the human lung. Agents Actions 17:290–292

Rousseau GG, Schmit JP (1977) Structure-activity relationships for glucocorticoids – I: Determination of receptor binding and biological activity. J Steroid Biochem 8:911–919

Schlechte JA, Ginsberg BH, Sherman BM (1982) Regulation of the glucocorticoid receptor in human lymphocytes. J Steroid Biochem 16:69–74
Spencer RL, Young EA, Choo PH, McEwen BS (1990) Adrenal steroid type I and type II receptor binding: estimates of *in vivo* receptor number, occupancy, and activation with varying level of steroid. Brain Res 514:37–48
Srivastava D, Thompson EB (1990) Two glucocorticoid binding sites on the human glucocorticoid receptor. Endocrinology 127:1770–1778
Steiner AE, Wittliff JL (1985) A whole-cell assay for glucocorticoid binding sites in normal human lymphocytes. Clin Chem 31:1855–1860
Teutsch G, Nique F, Lemoine G, Bouchoux F, Cérède E, Goffo D, Philibert D (1995) General structure-activity correlations of antihormones. Ann NY Acad Sci 761:5–28
Ueno H, Maruyama A, Miyake M, Nakao E, Nakao K, Umezu K, Nitta I (1991) Synthesis and evaluation of anti-inflammatory activities of a series of corticosteroid 17α-esters containing a functional group. J Med Chem 34:2468–2473
White JH, McCuaig KA, Mader S (1994) A simple and sensitive high-throughput assay for steroid agonists and antagonists. Biotechnology 12:1003–1007
Wittliff LJ, Raffelsberger W (1995) Mechanisms of signal transduction: sex hormones, their receptors and clinical utility. J Clin Ligand Assay 18:211–235
Wojnar RJ, Varma RK, Free CA, Millonig RC, Karanewsky D, Lutsky BN (1986) Androstene-17-thioketals. 1st Communication: Glucocorticoid receptor binding, antiproliferative and anti-inflammatory activities of some novel 20-thiasteroids (androstene-17-thioketals). Arzneimittelforschung 36:1782–1787
Yoshikawa N, Makino Y, Okamoto K, Moromoto C, Makino I, Tanaka H (2002) Distinct interaction of cortivazol with the ligand binding domain confers glucocorticoid specificity. Cortivazol is a specific ligand for the glucocorticoid receptor. J Biol Chem 277:5529–5540
Zeelen FJ (1992) Medicinal chemistry of steroids: recent developments. In: Testa B (ed) Advances in drug research. Academic Press, London, pp 149–189

N.2.1.1.2 Transactivation and Transrepression Assays for Glucocorticoids

N.2.1.1.2.1 General Considerations

PURPOSE AND RATIONALE

The effects of glucocorticoids are mediated by both transactivation and transrepression mechanisms. Classical glucocorticoids, such as prednisolone or dexamethasone, induce both mechanisms. The desired anti-inflammatory effects are mainly mediated by repression of gene expression, whereas side-effects are predominantly mediated via transactivation (Pfahl 1993; Schäcke et al. 2002; Buttgereit et al. 2005).

REFERENCES AND FURTHER READING

Buttgereit F, Song IH, Straub RH, Burmester GR (2005) Aktueller Stand zur Entwicklung neuer Glucocortiocoidrezeptorliganden. Z Rheumatol 64:170–176
Pfahl M (1993) Nuclear receptor/AP-1 interaction. Endocr Rev 14:651–658
Schäcke H, Döcke WD, Asadullah H (2002) Mechanisms involved in the side effects of glucocorticoids. Pharmacol Ther 96:23–43

N.2.1.1.2.2 Transactivation Assay for Glucocorticoids

PURPOSE AND RATIONALE

Steroid agonistic and antagonistic properties can be evaluated by transactivation assays (Muhn et al. 1995; Fuhrmann et al. 1995, 1996). The transactivation assay assumes that steroid receptor proteins act as ligand-regulated transcriptional activators. After binding of hormone, the steroid receptor interacts with hormone responsive elements of hormone-regulated genes, thereby inducing a cascade of transcriptional events (Green and Chambon 1988). The hormone-dependent transcriptional activation can be determined in tissue culture by transfection of the steroid receptor under investigation and a reporter gene linked to a hormonally responsive promoter into cells. The transactivation assay allows determination of the agonistic and also the antagonistic potency of a given compound, by induction or inhibition of reporter gene activity (Fuhrmann et al. 1992).

PROCEDURE

Vector Construct

The expression plasmid pHGO containing the full-length coding sequence of the human glucocorticoid receptor driven from the SV 40 early promoter is prepared according to Hollenberg et al. (1985). The pMMTV-CAT plasmid containing the mouse mammary tumor virus promoter linked to a chloramphenicol acetyltransferase gene is prepared according to Cato et al. (1986).

Cell Culture and Transfections

CV-1 cells and COS-1 cells for transfection are cultured in Dulbecco's Modified Eagle's Medium (DMEM) supplemented with 10% fetal calf serum, 4 mmol/l L-glutamine, penicillin and streptomycin. Stable and transient transfections are performed using Lipofectin reagent (Gibco BRL) according to a procedure recommended by Felgner and Holm (1989), and Felgner et al. (1987). Stable transfections are carried out according to Fuhrmann et al. (1992). For transient transfection, 1×10^6 COS-1 or CV-1 cells are plated onto 100-mm dishes 1 day prior to transfection. Cells are typically about 80% confluent after 24 h.

Before transfection, cells are washed twice with 1 ml Opti-MEM (Gibco BRL) per dish. For each dish, 5 µg pHGO (hGR expression plasmid) and 5 µg pMMTV-CAT are diluted with 1 ml Opti-MEM; in addition, 50 µg Lipofectin Reagent is diluted with 1 ml Opti-MEM. Next, DNA and Lipofectin Reagent dilutions are combined in a polystyrene snap-cup tube to obtain 2 ml of transfection solution per dish, gently mixed, incubated at room temperature for 5 min, and added to the washed cells. After 5 h the transfection solution is replaced by 6 ml DMEM supplemented with 10% fetal calf serum.

To study the effect of the test hormones, transiently transfected cells are trypsinized, pooled and replated onto 60-mm dishes at a density of 4.5×10^5 per dish 24 h after transfection. Stably transfected cells are seeded onto 6-well dishes (1×10^5 cells per dish). Cells are cultured in medium supplemented with 3% charcoal-stripped fetal calf serum and the appropriate hormones for 48 h. As negative control for the reporter gene induction, cells are cultured with 1% ethanol. Transactivation assays with transiently or stably transfected cells are carried out at least three times.

CAT Assay

Transiently transfected cells and stably transfected cells are disrupted by freezing (ethanol/dry ice bath) and thawing (37°C water bath) three times. Protein concentrations of the cell extract are determined according to Bradford (1976). The CAT assay is performed according to Gorman et al. (1982). After the cells are spun for 15 min in an Eppendorf microfuge at 4°C, the supernatants are removed and assayed for enzyme activity. The assay mixture contains (in a final volume of 180 µl) 100 µl of 0.25 M Tris-hydrochloride (pH 7.5), 20 µl of cell extract, 1 µCi of [^{14}C]chloramphenicol (50 µCi/mmol; New England Nuclear), and 20 µl of 4 mM acetyl coenzyme A. Controls contain CAT (0.01 U; P.L. Biochemicals) instead of cell extract. All of the reagents except coenzyme A are pre-incubated together for 5 min at 37°C. After equilibration is reached at this temperature, the reaction is started by adding coenzyme A. The reaction is stopped with 2 ml cold ethyl acetate, which is also used to extract the chloramphenicol. The organic layer is dried and taken up in 30 µl of ethyl acetate, spotted on silica gel thin-layer plates, and run with chloroform:methanol (95:5), ascending. After autoradiography of the separated acetyl chloramphenicol forms, the spots are cut out and counted. Data are expressed as the amount of chloramphenicol acetylated by 20 µl of extract.

EVALUATION

CAT activity is calculated as percentage conversion from chloramphenicol to acetylated chloramphenicol. Concentration–response curves for CAT induction are established to determine the potency of the test hormone. Dexamethasone (10^{-10}–10^{-6} mol/l) serves as standard.

For antiglucocorticoid activity, CAT activity in the presence of 10^{-8} mol/l dexamethasone is set as 100% and relative CAT activity is calculated as a percentage of this value. Concentration–response curves for CAT inhibition are established with increasing concentrations of the steroid hormone antagonist RU 486 as the standard inhibitor.

CRITICAL ASSESSMENT OF THE METHOD

Hollon and Yoshimura (1989) examined the causes of high variability in data from enzymatic transient gene expression assays. Their results strongly suggested that variation in transfection efficacy is the major cause of data variation and can seriously compromise valid interpretation of data.

MODIFICATIONS OF THE METHOD

White et al. (1994) described a simple and sensitive high-throughput assay for steroid agonists and antagonists. A DNA cassette, containing a synthetic steroid-inducible promoter controlling the expression of a bacterial chloramphenicol acetyltransferase gene (GRE5-CAT), was inserted into an Epstein-Barr virus episomal vector which replicates autonomously in primate and human cells. This promoter/reporter system was used to generate two stably transfected human cell lines. In the cervical carcinoma cell line HeLa, which expresses high levels of glucocorticoid receptor, the GRE5 promoter is inducible over 100-fold by the synthetic glucocorticoid dexamethasone. In the breast carcinoma cell line T47D, which expresses progesterone and androgen receptors, the GRE5 promoter is inducible over 100-fold by either progesterone or dihydrotestosterone. These cell lines can be used to screen large numbers of natural and synthetic steroid agonists and antagonists in microtiter wells using a colorimetric chloramphenicol acetyltransferase assay.

Dias et al. (1998) recommended the use of CRE recombinase in mammalian cells for high throughput screening of chemical libraries to identify new receptor ligands. A translational fusion of CRE recombinase and the ligand binding domain of the human glucocorticoid receptor was transfected into mammalian cells with the LOX P/luciferase reporter gene (DeWet 1907). A stable transfected clone was isolated and

used to characterize the kinetics, ligand specificity, and dose–response to various receptor ligands.

REFERENCES AND FURTHER READING

Bradford M (1976) A rapid and sensitive method for the quantitation of microgram quantities of protein utilizing the principle of protein-dye binding. Anal Biochem 72:248–254

Cato ACB, Miksicek R, Schütz G, Arnemann J, Beato M (1986) The hormone regulatory element of mouse mammary tumor virus mediates progesterone induction. EMBO J 6:2237–2240

DeWet JR, Wood KV, deLucca M, Helinski DR, Subramani S (1987) Firefly luciferase gene: structure and expression in mammalian cells. Mol Cell Biol 7:725–737

Dias JM, Go NF, Hart CP, Mattheakis LC (1998) Genetic recombination as a reporter for screening steroid receptor agonists and antagonists. Anal Biochem 258:96–102

Felgner PL, Holm M (1989) Cationic liposome-mediated transfection. Focus 11:21–25

Felgner PL, Gadek TR, Holm M, Roman R, Chan HW, Wenz M, Northrop JP, Ringold GM, Danielsen M (1987) Lipofection: a highly efficient, lipid-mediated DNA-transfection procedure. Proc Natl Acad Sci, USA 84:7413–7417

Fuhrmann U, Bengtson C, Repenthin G, Schillinger E (1992) Stable transfection of androgen receptor and MMTV-CAT into mammalian cells: inhibition of CAT expression by antiandrogens. J Steroid Biochem Mol Biol 42:787–793

Fuhrmann U, Slater EP, Fritzemeier KH (1995) Characterization of the novel progestin gestodene by receptor binding studies and transactivation assays. Contraception 51:45–52

Fuhrmann U, Krattenmacher R, Slater EP, Fritzemeier KH (1996) The novel progestin drospirone and its natural counterpart progesterone: biochemical profile and antiandrogenic potential. Contraception 54:243–251

Gorman CM, Moffat LF, Howard BH (1982) Recombinant genomes which express chloramphenicol acetyltransferase in mammalian cells. Mol Cell Biol 2:1044–1055

Green S, Chambon P (1988) Nuclear receptors enhance our understanding of transcription regulations. Trends Genet 4:309–314

Hollenberg SM, Weinberger C, Ong ES, Cerelli G, Oro A, Lebo R, Thompson EB, Rosenfeld MG, Evans RM (1985) Primary structure and expression of a functional human glucocorticoid receptor cDNA. Nature 318:635–641

Hollon T, Yoshimura FK (1989) Variation in enzymatic transient gene expression assays. Anal Biochem 182:411–418

Muhn P, Fuhrmann U, Fritzemeier KH, Krattenmacher R, Schillinger E (1995) Drospirenone: a novel progestogen with antimineralocorticoid and antiandrogenic activity. Ann NY Acad Sci 761:311–335

White JH, McCuaig KA, Mader S (1994) A simple and sensitive high-throughput assay for steroid agonists and antagonists. Biotechnology 12:1003–1007

N.2.1.1.2.3 Transrepression Assay for Glucocorticoids

PURPOSE AND RATIONALE

The immunosuppressive and anti-inflammatory actions of glucocorticoid hormones are mediated by transrepression of activating protein-1 (AP-1) and nuclear factor kappa B (NFκB) transcription factors. Since the anti-inflammatory effects of glucocorticoids are thought to be related to repression mechanisms and the side-effects mainly to activation mechanisms, a therapeutic benefit of dissociated glucocorticoids is expected (Vayssière et al. 1997; Vanden Berghe et al. 1999; Belvisis et al. 2001; Lin et al. 2002; Tanigawa et al. 2002; Schottelius et al. 2002, Coghlan et al. 2003; Lietal 2003; Ali et al. 2004; Hochhaus 2004; Schäke et al. 2004; Smith et al. 2005; Thompson et al. 2005). Schäke et al. (2004) investigated the dissociation of transactivation from transrepression by a selective glucocorticoid receptor agonist, leading to separation of therapeutic effects from side-effects.

PROCEDURE

Receptor-Binding Assays

Cytosol preparations of Sf9 cells, infected with recombinant baculovirus coding for the human GR, MR, or PR, were used for the binding assays. After centrifugation (15 min, 600 *g*) Sf9 pellets were resuspended in 1/20 volume of 20 mM Tris-HCl, pH 7.5; 0.5 mM EDTA, 2 mM DTT, 20% glycerol, 400 mM KCl, 20 mM sodium molybdate, 0.3 µM aprotinin, 1 µM pepstatin, 10 µM leupeptin and shock frozen in liquid nitrogen. After three freeze–thaw cycles, the homogenate was centrifuged for 1 h at 100,000 *g*. The protein concentration in the resulting supernatant was between 10 and 15 mg/ml. Aliquots were stored at −40°C.

For the binding assays for GR, MR, and PR, [^{3}H]dexamethasone (≈ 20 nM), [^{3}H]aldosterone or [^{3}H]progesterone, SF9 cytosol (100–500 µg protein), test compound, and binding buffer (10 mM Tris-HCl, pH 7.4; 1.5 mM EDTA, 10% glycerol) were mixed in a total volume of 50 µl and incubated for 1 h at room temperature. Specific binding was defined as the difference between binding of [^{3}H]dexamethasone, [^{3}H]aldosterone, and [^{3}H]progesterone in the absence and presence of 10 µM unlabeled dexamethasone, aldosterone, and progesterone.

After incubation, 50 µl of cold charcoal suspension was added for 5 min, and the mixtures were transferred to microtiter filtration plates. The mixtures were filtered into Picoplates (Canberra Packard, Dreieich, Germany) and mixed with 200 µl of Microszint-40 (Canberra Packard). The bound radioactivity was determined with a Packard Top Count plate reader. The concentration of test compound giving 50% inhibition of specific binding (IC_{50}) was determined from Hill analysis of the binding curves.

Induction of Tyrosine Aminotransferase (TAT)

Induction of TAT by test compounds was determined *in vitro* in the rat liver hepatoma cell line H4-II-

EC3. Cells were grown in MEM (Life Technologies, Karlsruhe, Germany) supplemented with 10% FBS (Life Technologies), 2 mM L-glutamine (Life Technologies), and 1% NEAA (nonessential amino acids) (Life Technologies). For compound testing, cells were seeded in 96-well plates (2×10^4 cells per well) and incubated with test compounds or dexamethasone for 20 h. Cells were then lysed and TAT activity assayed as described below for hepatic TAT induction *in vivo*.

Inhibition of IL-8 Production

IL-8 synthesis was induced by stimulation of the human promyeloic cell line THP-1 with lipopolysaccharide (LPS, *Escherichia coli* serotype 0127:B8; Sigma). Cells (2.5×10^4 cells per well) were treated with 10 µg/ml LPS in the absence or presence of test compounds or dexamethasone for 18 h. IL-8 concentration was determined in the supernatant by an IL-8-specific ELISA (Beckman Coulter).

Inhibition of Monokine Secretion

Monocytic secretion of tumor necrosis factor-alpha (TNF-α) and IL-12 p70 was determined after stimulation of peripheral blood mononuclear cells from healthy donors with 1 µg/ml LPS (*E. coli* serotype 0127:B8; Sigma) and 10 ng/ml interferon-gamma 1b (IFN-γ 1b) (Imukin, Boehringer Ingelheim). After 24 h of stimulation at 37°C, 5% CO_2, in the absence or presence of different concentrations of the compounds, the concentrations of IL-12 p70 and TNF-α in culture supernatants were determined by using commercial ELISA kits from R and D Systems (IL-12 HS Immunoassays, Nivelles, Belgium) and Bio-Source International (TNF-α EASIA, Wiesbaden, Germany). The calculated IC_{50} value represents the concentration of compound giving 50% inhibition of maximal TNF-α and IL-12 p70 production.

MODIFICATIONS OF THE METHOD

Vayssière et al. (1997) described synthetic glucocorticoids that dissociate transactivation and AP-1 transrepression as being weak transactivators of tyrosine aminotransferase (TAT) in cultured liver cells but potent inhibitors of LPS-induced IL-1β secretion in the human monocytic cell line THP1.

González et al. (2000) found that glucocorticoids antagonize AP-1 by inhibiting the activation/phosphorylation of JNK without affecting its subcellular distribution.

Kagoshima et al. (2001) reported that glucocorticoid-mediated transrepression is regulated by histone acetylation and DNA methylation.

Reichardt et al. (2001) studied the repression of inflammatory responses in the absence of DNA binding by the glucocorticoid receptor using mice with a mutation in the glucocorticoid receptor, which cannot activate glucocorticoid receptor response element promoters.

De Haij et al. (2003) reported dissociation of transrepression and transactivation in the steroid responsiveness of renal epithelial cells.

Schaaf and Cidlowski (2003) investigated the importance of ligand affinity for molecular determinants of glucocorticoid receptor mobility in living cells.

Stevens et al. (2003) investigated the role of tyrosine 735 in the dissociation of steroid receptor co-activators and nuclear receptor recruitment to the human glucocorticoid receptor.

Carballo-Jane et al. (2004) recommended skeletal muscle cells as a dual system to measure glucocorticoid-dependent transactivation and transrepression of gene regulation.

Studying transactivation and transrepression activity, Koubovec et al. (2005) found that synthetic progestins used in hormone replacement therapy have different glucocorticoid agonist properties.

Eberhardt et al. (2005) reported that dissociated glucocorticoids equipotently inhibit cytokine- and cAMP-induced matrix-degrading proteases in rat mesangial cells.

REFERENCES AND FURTHER READING

Ali A, Thompson CF, Balkovec JM, Graham DW, Hammond ML, Quraishi N, Tata JR, Einstein M, Ge L, Harris G, Kelly TM, Mazur P, Pandit S, Santoro J, Sitlani A, Wang C, Williamson J, Miller DK, Thompson CM, Zaller DM, Forrest JM, Carballo-Jane E, Luell S (2004) Novel *N*-arylpyrazol[3,2-*c*]-based ligands for the glucocorticoid receptor: receptor binding and *in vivo* activity. J Med Chem 47:2441–2452

Belvisis M, Wicks SL, Battram CH, Bottoms SEW, Redford JE, Woodman P, Brown TJ, Webber SE, Foster ML (2001) Therapeutic benefit of a dissociated glucocorticoid and the relevance of *in vitro* separation of transrepression from transactivation activity. J Immunol 166:1975–1982

Carballo-Jane E, Pandit S, Santoro JC, Freund C, Luell S, Harris G, Forrest MJ, Sitlani A (2004) Skeletal muscle: a dual system to measure glucocorticoid-dependent transactivation and transrepression of gene regulation. J Steroid Biochem Mol Biol 88:191–201

Coghlan MJ, Jacobson PB, Lane B, Nakane M, Lin CW, Elmore SW, Kym PR, Luly JR, Carter GW, Turner R, Tyree CM, Hu J, Elgort M, Rosen J, Miner JN (2003) A novel anti-inflammatory maintains glucocorticoid efficacy with reduced side effects. Mol Endocrinol 17:860–689

De Haij S, Adcock JM, Bakker AC, Gobin SJP, Daha MR, van Kooten C (2003) Steroid responsiveness of renal epithelial cells. Dissociation of transrepression and transactivation. J Biol Chem 278:5091–5098

Eberhardt W, Kilz T, Akool ES, Müller R, Pfeilschifter J (2005) Dissociated glucocorticoids equipotently inhibit cytokine- and cAMP-induced matrix degrading proteases in rat mesangial cells. Biochem Pharmacol 70:433–445

González M, Jiménez B, Berciano MT, Ganzález-Sancho, Caelles C, Lafarga M, Muñoz A (2000) Glucocorticoids antagonize AP-1 by inhibiting the activation/ phosphorylation of JNK without affecting its subcellular distribution. J Cell Biol 150:1199–1207

Hochhaus G (2004) New developments in corticosteroids. Proc Am Thorac Soc 1:269–274

Kagoshima M, Wilcke T, Ito K, Tsaprouni L, Barnes PJ, Punchard N, Adcock IM (2001) Glucocorticoid-mediated transrepression is regulated by histone acetylation and DNA methylation. Eur J Pharmacol 429:327–334

Koubovec D, Ronacher K, Stubsrud E, Louw A, Hapgood JP (2005) Synthetic progestins used in HRT have different glucocorticoid agonist properties. Mol Cell Endocrinol 242:23–32

Li G, Wang S, Gelehrter TD (2003) Identification of glucocorticoid receptor domains involved in transrepression of transforming growth factor-β action. J Biol Chem 278:41779–41788

Lin CW, Nakane M, Stashko M, Falls D, Kuk J, Miller L, Huang R, Tyree C, Miner JN, Rosen J, Kym PR, Coghlan MJ, Carter G, Lane BC (2002) *trans*-Activation and repression properties of the novel nonsteroid glucocorticoid receptor ligand 2.5-dihydro-9-hydroxy-10-methoxy-2,2,4-trimethyl-5-(1-methylcyclohexen-3-yl1)-1*H*-[1]benzopyrano[3,4-*f*]quinoline (A276575) and its four stereoisomers. Mol Pharmacol 62:297–303

Reichardt HM, Tuckermann JP, Göttlicher M, Vujic M, Weih F, Angel P, Herrlich P, Schütz G (2001) Repression of inflammatory responses in the absence of DNA binding by the glucocorticoid receptor. EMBO J 20:7168–7173

Schaaf MJM, Cidlowski JA (2003) Molecular determinants of glucocorticoid receptor mobility in living cells: the importance of ligand affinity. Mol Cell Biol 23:1922–1934

Schäke H, Schottelius A, Döcke WD, Strehlke P, Jaroch S, Schmees N, Rehwinkel H, Hennekes H, Asadullah K (2004) Dissociation of transactivation from transrepression by a selective glucocorticoid receptor agonist leads to separation of therapeutic effects from side effects. Proc Natl Acad Sci USA 101:227–232

Schottelius AJ, Giesen C, Asadullah K, Fierro IM, Colgan SP, Bauman J, Guilford W, Perez HD, Parkinson JF (2002) An aspirin-triggered lipoxin A4 stable analog displays a unique topical anti-inflammatory profile. J Immunol 169:7063–7070

Smith CJ, Ali A, Balkovec JM, Graham DW, Hammond ML, Patel GF, Rouen GP, Smith SK, Tata JR, Einstein M, Ge L, Harris GS, Kelly TM, Mazur P, Thompson CM, Wang CF, Williamson JM, Miller DK, Pandit S, Santoro JC, Sitlani A, Yamin TD, O'Neill EA, Zaller DM, Carballo-Jane E, Forest MJ, Luell S (2005) Novel ketal ligands for the glucocorticoid receptor: *in vivo* and *in vitro* activity. Bioorg Med Chem Lett 15:2926–2931

Stevens A, Garside H, Berry A, Waters C, White A, Ray D (2003) Dissociation of steroid receptor coactivator and nuclear receptor recruitment to the human glucocorticoid receptor by modification of the ligand-receptor interface: the role of tyrosine 735. Mol Endocrinol 17:845–859

Tanigawa K, Nagase H, Ohmori K, Tanaka K, Miyake H, Kiniwa M, Ikizawa K (2002) Species-specific differences in the glucocorticoid receptor transactivation function upon binding with betamathasone-esters. Int Immunopharmacol 2:941–950

Thompson CF, Quraishi N, Ali A, Tata JR, Hammond ML, Balkovec JM, Einstein M, Ge L, Harris G, Kelly TM, Mazur P, Pandit S, Santoro J, Sitlani A, Wang C, Williamson J, Miller DK, Yamin TD, Thompson CM, O'Neill EA, Zaller D, Forrest MJ, Carballo-Jane E, Luell S (2005) Novel heterocyclic glucocorticoids: *in vitro* profile and *in vivo* activity. Bioorg Med Chem Lett 15:2163–2167

Vanden Berghe W, Francesconi E, de Bosscher K, Resche-Rigon M, Hageman G (1999) Dissociated glucocorticoids with an anti-inflammatory potential repress interleukin-6 gene expression by a nuclear factor-κB-dependent mechanism. Mol Pharmacol 56:797–806

Vayssière BM, Dupont S, Choquart A, Petit F, Garcia T, Marchandeau C, Gronemeyer H, Resche-Rigon M (1997) Synthetic glucocorticoids that dissociate transactivation and AP-1 transrepression exhibit anti-inflammatory activity *in vivo*. Mol Endocrinol 11:1245–1255

N.2.1.1.3 Induction of Tyrosine Aminotransferase (TAT) in Hepatoma Cells

PURPOSE AND RATIONALE

The synthesis of tyrosine aminotransferase in hepatoma tissue culture (HTC) cells (Thompson et al. 1966) can be induced by glucocorticoids (Giesent and Beck 1982; Raynaud et al. 1980; Rousseau et al. 1977). This effect can be abolished by glucocorticoid antagonists.

PROCEDURE

Hepatoma tissue culture (HTC) cells are grown in suspension to a density of about 8×18^5 cells/ml. The cells are washed 3 times at 0°C in a total volume of buffered saline equivalent to half of the culture medium. The suspension is centrifuged and cell pellets resuspended in serum-free medium containing 0.1% BSA and 0.1% $NaHCO_3$. Ethanol solutions of standard (dexamethasone) and test steroids in various concentrations are added to 10-ml aliquots of cell suspension, with the final ethanol concentration not exceeding 0.5%. After 16 h of incubation in tightly capped flasks on a rotary shaker (100 rev/min) at 37°C, the cells are harvested and tyrosine aminotransferase determined. The cells are washed twice and then disrupted with an ultrasonicator. The enzyme is assayed at 37°C by conversion of *p*-hydroxyphenylpyruvate to *p*-hydroxybenzaldehyde (Diamondstone 1966). One unit of activity represents the conversion of 1 µmol of p-hydroxyphenylpyruvate per minute.

EVALUATION

Enzyme-specific activity is expressed in milliunits of tyrosine aminotransferase/mg of cell protein. Dose–response curves are established for the standard

and the test preparation allowing the calculation of potency ratios with confidence limits.

REFERENCES AND FURTHER READING

Diamondstone TI (1966) Assay of tyrosine transaminase activity by conversion of *p*-hydroxyphenylpyruvate to *p*-hydroxybenzaldehyde. Anal Biochem 16:385–401

Giesen EM, Beck G (1982) Hormonal deinduction of tyrosine aminotransferase. Horm Metab Res 14:252–256

Neef G, Beier S, Elger W, Henderson D, Wiechert R (1984) New steroids with antiprogestional and antiglucocorticoid activities. Steroids 44:349–372

Raynaud JP, Bouton MM, Moguilewsky M, Ojasoo T, Philibert D, Beck G, Labrie F, Mornon JP (1980) Steroid hormone receptors and pharmacology. J Steroid Biochem 12:143–157

Rousseau GG, Schmit JP (1977) Structure-activity relationships for glucocorticoids – I: Determination of receptor binding and biological activity. J Steroid Biochem 8:911–919

Thompson EB, Tomkins GM, Curran JF (1966) Induction of tyrosine α-ketoglutarate transaminase by steroid hormones in a newly established tissue culture cell line. Proc Natl Acad Sci USA 56:269–303

N.2.1.1.4 Effect on T-Lymphocytes

PURPOSE AND RATIONALE

Corticosteroids as immunosuppressive agents have suppressive effects on T-lymphocyte function. Snijdewint et al. (1995) determined *in vitro* dose-dependent inhibition of Th1- and Th2-type cytokine production by various corticosteroids.

PROCEDURE

Culture Media

T-lymphocyte clones are maintained and expanded in Iscove's modified Dulbecco's medium (IMDM) supplemented with 10% pooled c-inactivated human serum and gentamicin (80 µg/ml). Experiments are performed in IMDM supplemented with 10% fetal calf serum (FCS), human transferrin (35 µg/ml), 2-mercaptoethanol (2-ME, 3.5 µg/l) and human insulin (1.75 IE/ml).

Peripheral Blood Lymphocytes and T-Lymphocyte Clones

Peripheral blood mononuclear cells are prepared from heparinized venous blood of healthy volunteers by flotation on Lymphoprep (Nycomed, 1.077 g/ml) and the peripheral blood lymphocytes are separated by centrifugation on a discontinuous Percoll density gradient. Peripheral blood lymphocytes are collected from the interface between densities 1.977 g/ml and 1.061 g/ml, washed three times in HBSS plus 2% FCS and suspended in IMDM plus 10% FCS. Isolated peripheral blood lymphocytes (0.5×10^6 cells/ml) are stimulated with CD2 mAb plus CD28 mAb (1.1000 final dilution of ascites) in the absence or presence of corticosteroids (Van der Pouw-Kraan et al. 1992). Supernatants are collected after 48 h for IFN-γ and IL-2 measurement, and after 96 h for IL-4 measurement.

T-lymphocyte clones specific to housedust mite (*Dermatophagoides pteronyssinus*) are generated from the peripheral blood and skin of atopic individuals (Van der Heijden et al. 1991). These clones are Th0 typed, capable of producing both IFN-γ and IL-4 (Kapsenberg et al. 1988). T-lymphocyte clone cells (0.5×10^6 cells/ml) are stimulated with CD2 and CD28 mAb (1.1000) plus 1 ng/ml phorbol 12-myristate 13-acetate (PMA) to induce optimal levels of cytokine production. Corticosteroids are added at the start of the stimulation and then 24 h after stimulation, supernatants are collected and stored at ≈ 20°C until cytokine production is analyzed.

Proliferation Assay and Cytokine Measurements

Proliferation by peripheral blood lymphocytes is measured 48 or 96 h after stimulation in 96-well flat-bottom culture plates using 10^4 cells/well, the last 16 h in the presence of 13 kBq (0.33 µC)/well of [^{3}H]TdR (Radiochemical Centre, Amersham, UK). The proliferation of T-lymphocyte clones (10^4 cells/well) is similarly measured after stimulation for 40 h, again the last 16 h in the presence of [^{3}H]TdR. Incorporation of [^{3}H]TdR is determined by liquid scintillation spectroscopy.

Measurement of IFN-γ and IL-4 in peripheral blood lymphocytes and T-lymphocyte clone supernatants is performed with specific solid-phase sandwich ELISA systems (Van der Pouw-Kraan et al. 1992). For quantification of IL-2 production, a commercial ELISA kit is used. IL-2R expression by T cells of peripheral blood lymphocytes is determined 48 h after stimulation by labeling with mouse anti-human CD25 mAb.

EVALUATION

Dose–response curves of inhibition of IFN-γ, IL-4 and IL-2 production as a percentage of initial values in peripheral blood lymphocytes and in different T-lymphocyte clones are established for various corticosteroids in the range of 10^{-10} to 10^{-6} M.

All measurements are performed in duplicate or triplicate. Data are expressed as mean ±SEM and differences are assessed using Student's *t*-test.

MODIFICATIONS OF THE METHOD

Mollison et al. (1999) compared a macrolactam inhibitor of T helper type 1 and T helper type 2 cytokine biosynthesis in various animal models with several steroid preparations used for topical treatment of inflammatory skin diseases.

REFERENCES AND FURTHER READING

Kapsenberg ML, Van der Pouw-Kraan T, Stiekema FEM, Schootenmeijer A, Bos JD (1988) Direct and indirect nickel-specific stimulation of T lymphocytes from patients with allergic contact dermatitis to nickel. Eur J Immunol 18:977–982

Mollison KW, Frey TA, Gauvin DM, Kolano RM, Sheets MP, Smith ML, Pong M, Nikolaidis NM, Lane BC, Trevillyan JM, Cannon J, Marsh K, Carter GW, Or Y S, Chen Y W, Hsieh GC, Luly JR (1999) A macrolactam inhibitor of T helper type 1 and T helper type 2 cytokine biosynthesis for topical treatment of inflammatory skin diseases. J Invest Dermatol 112:729–738

Snijdewint FGM, Kapsenberg ML, Wauben-Penris PJJ, Bos JD (1995) Corticoids class-dependently inhibit Th1- and Th2-type cytokine production. Immunopharmacology 29:93–101

Van der Heijden FL, Wierenga EA, Bos JD, Kapsenberg ML (1991) High frequency of IL-4-producing $CD4^+$ allergen-specific T lymphocytes in atopic dermatitis lesional skin. J Invest Dermatol 97:389–394

Van der Pouw-Kraan T, Van Kooten C, Rensink I, Aarden L (1992) Interleukin (IL)-4 production by human T cells: differential regulation of IL-4 vs. IL-2 production. Eur J Immunol 22:1237–1241

N.2.1.1.5 Inhibition of Cartilage Degradation

PURPOSE AND RATIONALE

The efficacy of glucocorticosteroids after intra-articular injection has been clearly demonstrated in several animal models of osteoarthritis (Van den Berg et al. 1992; Pelletier et al. 1995). Augustine and Oleksyszyn (1997) used *in vitro* experiments to study the inhibition of degradation in bovine cartilage explants stimulated with concomitant plasminogen and interleukin-1α by various glucocorticosteroids.

PROCEDURE

Preparation of Bovine Articular Cartilage Explants

Bovine (calf) radiocarpal joints are acquired from a local abattoir immediately after sacrifice and transported on ice. The specimens are washed thoroughly and placed on ice containing 25% Povidine (10% Povidone-iodine topical solution). The specimens are then dissected in a sterile hood using good sterile technique. Media (DMEM containing 4.5 g/l D-glucose and L-glutamine, without sodium pyruvate) is supplemented with HEPES buffer (3.57 g/l) and sodium bicarbonate (3.7 g/l), and the pH adjusted to 7.4. The medium is further supplemented with penicillin (100 U/ml), streptomycin (100 µg/ml) and 50 µg/ml L-ascorbic acid. The articulating cartilage surfaces are exposed, and the synovial fluid is wiped away with sterile gauze. A sterile cork-borer with a diameter of 3.5 mm is used to remove uniform cores of cartilage. The cores are placed in a sterile flask, washed 4 times with sterile medium, and then placed in an incubator (37°C, 5% CO_2/95% air, adequate humidity) and allowed to equilibrate for 1 h. The cartilage disks are then labeled en mass with [^{35}S]sulfate at 10 µC/ml for approximately 72–96 h, with hand-stirring every few hours. After labeling, explants are equilibrated with fresh medium (minimum of two washes before use in experiments).

Inhibition of IL-1-Induced Cartilage Degradation in Bovine Articular Cartilage in the Presence of Human Plasminogen

Individual explants are transferred to 96-well plates containing 250 µl of fresh medium per well, with or without plasminogen and IL-1α, and with or without glucocorticosteroids. A negative control consists of medium alone, while two positive controls are IL-1α alone, and plasminogen with IL-1α. All other groups contain the glucocorticosteroids along with recombinant human IL-1α (0.4 ng/ml) alone or concomitant human plasminogen (0.4 µM) plus IL-1α. Glucocorticosteroids are added in concentrations between 10 and 10,000 pM. Control and experimental explants are incubated for approximately 96 h (4 days) prior to counting a 50-µl sample of supernatant from each well. A 50-µl sample of a papain-digest of each explant is also counted.

EVALUATION

The data are expressed as percentage glycosaminoglycan release over the 4 days. The values for all groups with glucocorticosteroids present are then compared to the values for concomitant plasminogen and IL-1α without glucocorticosteroids, and percentage inhibitions are calculated. Dose–response curves are established for each glucocorticosteroid.

REFERENCES AND FURTHER READING

Augustine AJ, Oleksyszyn J (1997) Glucocorticoids inhibit degradation in bovine cartilage explants stimulated with concomitant plasminogen and interleukin-1α. Inflamm Res 46:60–64

Pelletier JP, DiBattista JA, Raynauld JP, Wilhelm S, Martel-Pelletier J (1995) The *in vivo* effects of intraarticular corticosteroid injections on cartilage lesions, stromelysin, in-

terleukin-1, and oncogen protein synthesis in experimental osteoarthritis. Lab Invest 72:578–586
Van den Berg WB, Joosten LAB, van de Loo FAJ, de Vries BJ, van der Kraan PM, Vitters EL (1992) Drug evaluation in normal and arthritic mouse patellas. In: Kuettner KE, Schleyerbach R, Peyron JG, Hascall VC (eds) Articular cartilage and osteoarthritis. Raven, New York, pp 583–595

N.2.1.2
In Vivo Methods for Glucocorticoid Hormones

N.2.1.2.1
General Considerations

Muscle work tests (early fatigue) were used in early stages of adrenal gland research (Bomskov 1937; Ingle 1944; Dorfman 1962), and their description is of historical interest. The method is based upon the fact that muscular responsiveness is lost within a few hours following the removal of the adrenal glands and can be maintained by the administration of corticosteroids. Since the 11-oxygenated steroids are quite active and compounds such as desoxycorticosterone are practically without activity, it appears that the main effect monitored is on carbohydrate metabolism.

REFERENCES AND FURTHER READING

Bomskov C (1937) Biologische Methoden der Nebennierenrindenforschung. In Bomskov C (ed) Methodik der Hormonforschung, 1. Band. Thieme, Leipzig, pp 489–534
Dorfman RI (1962) Corticoids. In: Dorfman RI (ed) Methods in hormone research, Vol II, Bioassay. Academic Press, New York, pp 325–367
Ingle DJ (1944) Physiology and chemistry of hormones. American Association for the Advancement of Science, Washington

N.2.1.2.2
Adrenal and Thymus Involution

PURPOSE AND RATIONALE

Repeated administration of corticosteroids causes central and peripheral effects on pituitary hormone content and secretion, and on adrenal weight and histology. In the immature rat, thymus involution is observed in a dose-related manner.

PROCEDURE

Groups of six to ten immature male Sprague–Dawley rats weighing 60–70 g are injected subcutaneously daily for 6 days with 0.2 ml of a homogenized suspension of different doses of the test compound in 0.5% aqueous carboxymethylcellulose solution. The standard, hydrocortisone acetate, is given in daily doses of 0.05 and 0.2 mg per animal. Controls receive the vehicle. On the 7th day, the animals are sacrificed and the adrenal and thymus weights determined.

EVALUATION

The involution of the thymus gland is a measure of the catabolic activity of the compound (metabolic effect). Involution of the adrenals is a measure of the ability of the compound to inhibit the secretion of ACTH (negative steroid feedback). Dose–response curves are established for both parameters and compared with hydrocortisone and the potency ratios are calculated.

MODIFICATIONS OF THE METHOD

The numeric test result is improved when the product of thymus and adrenal weights is calculated. Dose–response curves of the product of thymus and adrenal weights are steeper than those of each individual parameter (Laschet and Hohlweg 1960).

Inhibition of uridine incorporation into the ribonucleic acid of thymocytes has been used as a parameter for agonistic and antagonistic glucocorticoid activity (Gaignault et al. 1977).

REFERENCES AND FURTHER READING

Byrnes WW, Shipley EG (1955) Guinea pig copulatory reflex in response to adrenal steroids and similar compounds. Endocrinology 57:5–9
Dorfman RI (1962) Corticoids. In: Dorfman RI (ed) Methods in hormone research, Vol II, Bioassay. Academic Press, New York, pp 325–367
Gaignault JP, Duval D, Meyer P (1977) The relationship between glucocorticoid structure and effects upon thymocytes. Mol Pharmacol 13:948–955
Laschet U, Hohlweg W (1960) Die Testierung neuer Glucocorticoidpräparate mit dem NTP-Test. Pharmazie 15:374–377
Ringler I (1964) Activities of adrenocorticosteroids in experimental animals and man. In: Dorfman RI (ed) Methods in hormone research, Vol III, Steroidal activity in experimental animals and man. Academic Press, New York, pp 227–349

N.2.1.2.3
Eosinopenia in Adrenalectomized Mice

PURPOSE AND RATIONALE

Glucocorticoids decrease the eosinophilic cell blood count in laboratory animals as well as in humans. This effect was used to quantitate the potency of corticosteroids in adrenalectomized mice (Silber and Arcese 1964; Speirs and Meyer 1951; Tolksdorf 1959).

PROCEDURE

Male mice weighing 20–25 g (e. g., of Jax C57 Brown, subline cd strain) are adrenalectomized and maintained at 28°C with 1% sodium chloride solution in water.

Then, 15-mg pellets of desoxycorticosterone acetate are implanted at the time of operation. Steroids are dissolved in benzyl alcohol and mixed with sesame oil (1:10). Three days after operation, the mice receive 5 µg epinephrine by subcutaneous injection and 4 h later 1–6 µg of hydrocortisone (or the test substance) in 0.03 ml oil. Three doses of the unknown substance and standard are tested, using six animals per dose. Blood samples are taken from the tail before and 3 h after steroid injection. Mice with fewer than 100 eosinophils per cubic millimeter of blood before injection are discarded.

EVALUATION

The percentage decrease of eosinophil blood count after 3 h is averaged per group. From dose–response curves, potency ratios are calculated.

CRITICAL ASSESSMENT OF THE METHOD

The test is relatively simple and has the advantage of requiring little material.

REFERENCES AND FURTHER READING

Silber RH, Arcese PS (1964) Animal techniques for evaluating adrenocortical drugs. In: Nodine JH, Siegler PE (eds) Animal and clinical pharmacologic techniques in drug evaluation. Year Book Medical, Chicago, Ill., pp 542–550

Speirs RS, Meyer RK (1951) A method of assaying adrenal cortical hormones based on a decrease in circulating eosinophil cells of adrenalectomized mice. Endocrinology 48:316–326

Tolksdorf S (1959) Laboratory evaluation of anti-inflammatory steroids. Ann New York Acad Sci 82:829–835

N.2.1.2.4 Liver Glycogen Test in Rats

PURPOSE AND RATIONALE

The liver glycogen deposition test, as described by Stafford et al. (1955), is a simple and specific test for glucocorticoid activity (Dorfman 1962; Ringler 1964; Silber and Arcese 1964).

PROCEDURE

Male Sprague–Dawley rats weighing 140–160 g are adrenalectomized. They are fed stock laboratory diet and 1% sodium chloride solution. On the morning of the fourth postoperative day, food is withdrawn. On the morning of the fifth day, the drinking fluid is withdrawn and the rats are given the test compound by a single subcutaneous injection in appropriate dosages suspended in 0.5 ml sesame oil. Seven hours later, the rats are sacrificed. The livers are removed and blotted on filter paper to remove blood, weighed, dropped into flasks containing 10 ml hot 30% potassium hydroxide and digested on a hot plate. The digest is diluted to 100 ml and a 50-fold dilution of an aliquot is used for analysis.

Then, 10 ml 0.2% anthrone in 95% sulfuric acid is slowly added to 5 ml of liver digest dilution with cooling. The mixture is heated in a boiling water bath for 10 min and then placed into cold water. Optical density is measured in a spectrophotometer at 620 µm using the anthrone-reagent as blank. Calibration curves are established using glucose as standard. Groups of five animals are used for each dose and for the vehicle controls. Three doses of test compound and of standard are used to find dose–response activities. Standard doses of hydrocortisone are 0.5, 1.0, and 2.0 mg per animal subcutaneously or 1.25, 2.5, and 5.0 mg per animal orally.

EVALUATION

The amount of glycogen expressed as glucose is calculated per gram liver weight. Dose–response curves are established for each compound and for the standard in order to calculate potency ratios.

MODIFICATIONS OF THE METHOD

The method can be used to determine the time course and duration of action of derivatives such as corticosteroid esters compared to the free alcohol (Vogel 1963, 1965) and for evaluation of topical and systemic activity (Alpermann et al. 1982).

The liver glycogen deposition in the adrenalectomized mouse has been used by Dorfman et al. (1946) and by Venning et al. (1946) to evaluate glucocorticoid activity. Liver tryptophan peroxidase activity in the rat is decreased after adrenalectomy and increased after administration of corticosteroids (Knox and Auerbach 1955) indicating an early effect of corticoids.

The enzyme activity of tryptophan pyrrolase in guinea pig liver is increased by systemic administration of corticoids, but this effect is short-lived and achieved only with high subcutaneous doses (Albrecht et al. 1979). In contrast, the enzyme is markedly reduced by protracted application of corticoids to the skin (“dermatocorticoids”).

REFERENCES AND FURTHER READING

Albrecht W, Longauer JK, Weirich EG (1979) Wirkung von Dermatocorticoiden auf die Aktivität der hepatischen Tryptophanpyrrolase beim Meerschweinchen. Arch Dermatol Res 265:275–281

Alpermann HG, Sandow J, Vogel HG (1982) Tierexperimentelle Untersuchungen zur topischen und systemischen

Wirksamkeit von Prednisolon-17-ethylcarbonat-21-propionat. Arzneimittelforschung 32:633–638
Dorfman RI (1962) Corticoids. In: Dorfman RI (ed) Methods in hormone research, Vol II, Bioassay. Academic Press, New York, pp 325–367
Dorfman RI, Ross E, Shipley RA (1946) The assay of adrenal cortical material by means of a glycogen test in the adrenalectomized mouse. Endocrinology 38:178–188
Knox E, Auerbach VH (1955) The hormonal control of tryptophan peroxidase in the rat. J Biol Chem 214:307–313
Ringler I (1964) Activities of adrenocorticosteroids in experimental animals and man. In: Dorfman RI (ed) Methods in hormone research, Vol III, Steroidal activity in experimental animals and man. Academic Press, New York, pp 227–349
Silber RH, Arcese PS (1964) Animal techniques for evaluating adrenocortical drugs. In: Nodine JH, Siegler PE (eds) Animal and clinical pharmacologic techniques in drug evaluation. Year Book Medical, Chicago, Ill., pp 542–550
Stafford RO, Barnes LE, Bowman BJ, Meinzinger MM (1955) Glucocorticoid and mineralocorticoid activities of Δ^1-fluorohydrocortisone. Proc Soc Exp Biol Med 89:371–374
Venning EH, Kazmin VE, Bell JC (1946) Biological assay of adrenal corticoids. Endocrinology 38:79–89
Vogel G (1963) Intensität und Dauer der antiinflammatorischen und glykoneogenetischen Wirkung von Prednisolon und Prednisolonazetat nach oraler und subcutaner Applikation an der Ratte. Acta Endocrinol 42:85–96
Vogel HG (1965) Intensität und Dauer der Wirkung von 6α-Methylprednisolon und seinen Estern an der Ratte. Acta Endocrinol 50:621–642

N.2.1.2.5 Anti-Inflammatory Activity of Corticoid Hormones

GENERAL CONSIDERATIONS

Most of the tests described in the Sect. H.3 (anti-inflammatory activity) have been used for evaluation of corticosteroids.

The effects on acute inflammation are less suitable, [Ultraviolet erythema in guinea pigs (see H.3.2.2.1), Vascular permeability in rats (see H.3.2.2.2), Paw edema in rats (see H.3.2.2.6)], whereas the methods measuring subacute inflammation are very well suited [Granuloma pouch test in rats (see H.3.2.2.8), Cotton granuloma test in rats (see H.3.2.3.1), Glass rod granuloma test in rats (see H.3.2.3.3), Sponge implantation technique (see H.3.2.3.2)].

The molecular mechanisms of the anti-inflammatory actions of glucocorticoids were reviewed by Barnes (1998). Development of dissociated steroids which are more active in transrepression (interaction with transcription factors) than transactivation (binding to glucocorticoid response elements) as reported by Vayssiere et al. (1997) was recommended.

REFERENCES AND FURTHER READING

Barnes PJ (1998) Anti-inflammatory actions of glucocorticoids. Molecular mechanisms. Clin Sci 94:557–572
Vayssiere BM, Dupont S, Chaoquart A et al (1997) Synthetic glucocorticoids that dissociate transactivation and AP-1 transrepression exhibit anti-inflammatory activity *in vivo*. Mol Endocrinol 11:1245–1255

N.2.1.2.6 Animal Studies for Corticoid Hormone Evaluation

Several examples are presented here for the specific pharmacology of corticoids. The methods applied in some instances are the same methods as for antiphlogistic and anti-inflammatory compounds. Corticosteroids intended for systemic treatment or local application are administered daily for 3–14 days, and the pharmacological effects are determined. NMRI mice (26–28 g) or Wistar rats (140–160 g) are housed according to institutional guidelines with access to food and water ad libitum; 8–11 animals may be randomly allocated to the different treatment groups.

Croton Oil-Induced Ear Inflammation

This test is performed by local application, to reduce or prevent the effect of a local irritant. Topical application of the nonspecific contact irritant croton oil, a mixture of several phorbol esters, leads to acute inflammation characterized by edema and a mainly granulocytic cell infiltration into the skin. Swelling of the ear due to inflammation is prevented by the corticoid solution or suspension. For topical application, corticosteroids are dissolved in the same vehicle as used for croton oil and may be applied separately, or together with the irritant croton oil.

Systemic application of corticosteroids (subcutaneously) may also be performed 2 h before croton oil application. At the maximum of the inflammatory reaction, animals are killed, and ears (mice, area $\approx 1\,cm^2$) or a punch biopsy (rats, 10-mm diameter) of each ear are weighed as an indicator of edema formation. The tissue samples are then snap-frozen in liquid nitrogen in polypropylene tubes and kept at −20°C for up to 24 h (Tonelli et al. 1965; Alpermann et al. 1982; Vayssière et al. 1997).

Peroxidase Activity Assay

Peroxidase activity, as a measure for total granulocyte infiltration, may be assayed in the tissue samples by using a modification of a method described by Schottelius et al. (2002).

Induction of Tyrosine Aminotransferase (TAT) in Vivo

In a similar manner as performed *in vitro*, the induction of tyrosine aminotransferase (TAT) may be investigated *ex vivo* in tissue of treated animals. TAT in-

duction is evaluated 6 h after compound administration (subcutaneously) to juvenile rats by determination of TAT activity in liver homogenates. Animals are killed, and biopsy samples (10-mm diameter) are taken from the liver and snap-frozen. Biopsy samples are homogenized in 2 ml of homogenizing buffer (140 mM KCl in 20 mM KPO_4 buffer, pH 7.6) and centrifuged at 24,000 *g* for 20 min at 4°C. Supernatants are assayed for protein content by the BCA (bicinchoninic acid) Protein Assay Kit from Pierce. Then 20 µl of supernatant diluted 1:50 in PBS is incubated for 30 min at 37°C with 200 µl of TAT-reaction buffer (tyrosine 1.2 mg/ml or 6.6 mM/45 mM KH_2PO_4/0.06 mM pyridoxal-5′-phosphate/12 mM oxoglutaric acid, adjusted to pH 7.6 with KOH). After stopping the reaction with 10 M KOH and further incubation for 30 min, extinction was measured at 340 nm, and TAT activity is calculated in relation to 500 µg/ml total protein content. TAT induction is defined as *x*-fold increase in TAT activity measured as OD at 340 nm in comparison to the TAT activity in vehicle-treated animals (Thompson et al. 1966).

ACTH Suppression in Rats

Animals are housed under conditions of minimum stress before the study, in a quiet laboratory room. Six hours after application of compounds, animals are killed with minimum stress (decapitation in a separate room), and EDTA-anticoagulated blood is collected from the abdominal aorta. Plasma ACTH content is determined using the ACTH ^{125}I-assay system (ImmuChem Double Antibody hACTH) following the manufacturer's instructions (ICN).

The method requires considerable experience because the isolation of animals and sacrificing with a minimum of stress are difficult to achieve. Refer to pretreatment with lower doses of dexamethasone to improve this test method. Treatment with increasing doses of the corticosteroids and prednisolone as the reference standard will reduce the ACTH concentrations, such tests however have an inherently high variability of the vehicle-treated control groups (Sakakura et al. 1981; Baumann et al. 1985).

Increased Blood Glucose in Rats (Hyperglycemia Induced by Corticoids)

Animals are isolated before the study to avoid stress and fasted for 16 h. Six hours after application of compounds, animals are killed, and EDTA-treated blood is collected from the abdominal aorta to assess the corticoid-induced rise in blood glucose. Glucose in plasma is measured by colorimetric serum glucose determination by using hexokinase and glucose-6-phosphate dehydrogenase with a Hitachi 904 automatic analyzer (Roche Diagnostics).

Skin Atrophy After Chronic Corticoid Application

To assess the effect of local application on collagen composition of the skin, the test compound or the reference compound prednisolone (75 µl on a marked area of 9 cm^2 in 95% ethanol/5% isopropyl myristate) was applied daily for 19 days to the dorsal skin of nude rats (strain hr-hr, 120–140 g, Iffa-Credo). Animals were killed on day 20. Skin thickness was determined by using a specifically designed dial thickness gauge. Mean values were derived by measuring two adjacent treated skin areas. To determine skin-breaking strength of treated skin, a dorsal skin patch (5 × 5 cm) was removed. The skin patch was placed on filter paper, and two double-T-piece skin strips (50 mm long, 4 mm wide at the narrowest point) were punched in a caudal–cranial direction out of the patch. The skin strips were covered with moistened filter paper to avoid drying and were fixed with the wider ends into an apparatus developed in-house to measure skin-breaking strength. At a constant rate of stretch (200 mm/min), the force necessary to tear the skin strip was determined with a pressure sensor and was expressed as the skin-breaking strength (Alpermann et al. 1982; Vogel and Petri 1985).

Effect of Chronic Treatment on Thymus, Spleen, Adrenal, and Body Weight

To determine effects of repeated-dose corticoid treatment on body weight, animals were weighed before and after completion of treatment. Thymus, spleen, and adrenal glands were removed from animals killed after systemic or topical treatment and weighed. Organ weights are expressed as absolute values or as a percentage inhibition when compared with untreated animals (Laschet et al. 1960; Stoeck et al. 2004).

EVALUATION

For the examples given here, group means were calculated and the statistical significance of the effects of TAT, glucose induction, and ACTH suppression was assessed by using Dunnett's test. Differences between test compound and the corresponding prednisolone group (used as the reference standard) were assessed by using the Mann–Whitney test.

REFERENCES AND FURTHER READING

Alpermann HG, Sandow J, Vogel HG (1982) Tierexperimentelle Untersuchungen zur topischen und systemischen

Wirksamkeit von Prednisolon-17-ethylcarbonat-21-propionat. Arzneimittelforschung 32:633–638
Baumann JB, Girard J, Christen E, Eberle AN, Ruch W (1985) Inhibition of the ACTH adrenal response to stress by treatment with hydrocortisone, prednisolone and dexamethasone in the rat. Horm Res 21:254–260
Laschet U, Hohlweg W (1960) Die Testierung neuer Glucocorticoidpräparate mit dem NTP-Test. Pharmazie 15:374–377
Sakakura M, Yoshioka M, Kobayashi M, Takebe K (1981) Degree of inhibition of ACTH release by glucocorticoids in adrenalectomized rats. Neuroendocrinology 32:38–41
Schottelius AJ, Giesen C, Asadullah K, Fierro IM, Colgan SP, Bauman J, Guilford W, Perez HD, Parkinson JF (2002) An aspirin-triggered lipoxin A4 stable analog displays a unique topical anti-inflammatory profile. J Immunol 169:7063–7070
Stoeck M, Riedel R, Hochhaus G, Häfner D, Masso JM, Schmidt B, Hatzelamnn A, Marx D, Bundschuh DS (2004) *In vitro* and *in vivo* anti-inflammatory activity of the new glucocorticoid Ciclesonide. J Pharmacol Exp Ther 309:249–258
Thompson EB, Tomkins GM, Curran JF (1966) Induction of tyrosine α-ketoglutarate transaminase by steroid hormones in a newly established tissue culture cell line. Proc Natl Acad Sci USA 56:269–303
Tonelli G, Thibault L, Ringler I (1965) A bioassay for the concomitant assessment of the antiphlogistic and thymolytic activities of topically applied steroids. Endocrinology 77:625–630
Vayssière BM, Dupont S, Choquart A, Petit F, Garcia T, Marchandeau C, Hronemeyer H, Resche-Rigon M (1997) Synthetic glucocorticoids that dissociate transactivation and AP-1 transrepression exhibit antiinflammatory activity *in vivo*. Mol Endocrinol 11:1245–1255
Vogel HG, Petri W (1985) Comparison of various pharmaceutical preparations of prednicarbate after repeated topical administration to the skin of rats. Arzneimittelforschung 35:939–946

N.2.1.3 Effects of Steroids on Mechanical Properties of Connective Tissue

N.2.1.3.1 Breaking Strength of Bones

PURPOSE AND RATIONALE

Patients with Cushing's disease or after long-term treatment with corticosteroids have an increased susceptibility for bone fractures. The related animal tests were developed as a model for corticosteroid-induced osteoporosis, and they are of historical interest. The tests are based on changes in the mechanical properties of bone. Surprisingly, in chickens as well as in rats, short-term treatment with low and medium doses of glucocorticosteroids increased the breaking strength of bones dose-dependently whereas very high doses induced a decrease of breaking strength .

PROCEDURE

White Leghorn chicken at an age of 14 days weighing 170 ± 20 g were used. The animals were treated for 14 days by intramuscular injection of 0.2 up to 100 mg/kg cortisol (reference compound) or equivalent doses of other glucocorticoids in oily solution. At autopsy, body weight and comb weight are recorded and the femur and tibia bones from both sites are weighed. Length of bone (l) and outer diameter (D) of the diaphysis are measured using calipers. The bone is fastened on both ends, supported on edges 5 mm distant from the ends, and broken in the central portion of the diaphysis by a special device attached to an Instron-instrument. Breaking load (P) is recorded. The contralateral bone is cut at the middle of the diaphyseal shaft into rings by a small saw. Inner (d) and outer diameter (D) are measured in two perpendicular directions.

EVALUATION

Breaking strength (σ) of the hollow bones is calculated according to the technical formula for hollow cylinders:

$$\sigma = \frac{8}{\pi} \times \frac{P \times 1 \times D}{D^4 - d^4} .$$

Doses between 0.2 and 2.0 mg/kg cortisol and 0.05 and 1.0 mg/kg prednisolone show a parallel increase of breaking strength allowing the calculation of potency ratios. With higher doses, the response changes to inhibition of breaking strength. Excessive doses of 50 and 100 mg/kg cortisol, which are in the range of the LD_{50}, induce a decrease of breaking strength (Vogel 1968, 1969, 1990; Vogel and Ther 1962).

MODIFICATIONS OF THE METHOD

In young and adult rats, 10 days of treatment with cortisol and other corticosteroids induce a dose-dependent increase of breaking strength, whereas with longer treatment (30 days) a bell-shaped dose–response (increase with low doses, decrease with high doses) is seen.

REFERENCES AND FURTHER READING

Vogel G (1968) Untersuchungen zur Wirkung von Hormonen auf physikalische und chemische Eigenschaften des Binde- und Stützgewebes. Fortschr Med 86:666–668
Vogel G, Ther L (1963) Tierexperimentelle Untersuchungen über den Einfluß von Hormonen auf physikalische Eigenschaften von Knochen. Verh Dtsch Ges Pathol 47. Fischer, Stuttgart, pp 167–171
Vogel HG (1969) Zur Wirkung von Hormonen auf physikalische und chemische Eigenschaften des Binde- und Stützgewebes. Arzneimittelforschung 19:1495–1503, 1732–1742, 1790–1801, 1981–1996
Vogel HG (1990) Influence of desmotropic drugs on breaking strength and on viscoelastic properties of rat bone. Relaxation and hysteresis experiments. Acta Ther 16:109–127

N.2.1.3.2 Tensile Strength of Femoral Epiphyseal Cartilage in Rats

PURPOSE AND RATIONALE

The epiphyseal cartilage of rats is very sensitive to treatment with hormones and other desmotropic drugs. The tensile strength of the distal femoral epiphyseal plate is decreased after adrenalectomy and is restored or increased by treatment with low doses of corticosteroids.

PROCEDURE

Male Sprague-Dawley rats weighing 120 ± 10 g are treated with several doses of corticosteroids or other hormones for periods of between 1 and 14 days. After sacrifice, the hind legs are exarticulated in the hip joint and fastened at the collum femoris. Longitudinal tension always results in rupture of the distal femoral epiphyseal cartilage (Ther et al. 1963; Vogel and Ther 1964; Vogel 1969). The ultimate load of the femoral epiphyseal plate is recorded by an Instron instrument at an extension rate of 5 cm/min.

Single injections of doses between 10 and 100 mg/kg cortisol acetate or 2.5 and 40 mg/kg prednisolone acetate induce a dose-dependent increase of tensile strength up to twice the control levels after 24–48 h, which subsides after 96 h. Repeated administration up to 15 days also results in a dose-dependent increase. There is a maturation-dependent increase of tensile strength in untreated rats.

The effect of other hormones, e. g., gonadal steroids, on cartilage is much smaller than that of glucocorticosteroids.

EVALUATION

Dose–response curves for steroids can be established allowing the calculation of potency ratios in experiments with single-dose or repeated-dose administration.

REFERENCES AND FURTHER READING

Ther L, Schramm H, Vogel G (1963) Über die antagonistische Wirkung von Trijodthyronin und Progesteron auf den Prednisoloneffekt am Epiphysenknorpel. Acta Endocrinol 42:29–38

Vogel G, Ther L (1964) Über den Einfluß von einigen Hormonen auf mechanisch-physikalische Eigenschaften des Binde- und Stützgewebes. Anatom Anzeig Suppl 115:117–122

Vogel HG (1969) Zur Wirkung von Hormonen auf physikalische und chemische Eigenschaften des Binde- und Stützgewebes. Arzneimittelforschung 19:1495–1503, 1732–1742, 1790–1801, 1981–1996

N.2.1.3.3 Tensile Strength of Tail Tendons in Rats

PURPOSE AND RATIONALE

The thread-like tail tendons of rats are very suitable for studying the mechanical properties of connective tissue. They are easy to prepare and consist predominantly of collagen. Like other organs of connective tissue, such as bone, cartilage, and skin, the tensile strength of tail tendons is reduced after adrenalectomy and dose-dependently increased after short-term treatment with glucocorticosteroids (Vogel 1965, 1969).

PROCEDURE

Male Sprague-Dawley rats weighing 120 ± 10 g are treated with increasing doses of corticosteroids or other hormones for periods of between 1 and 14 days. After sacrifice, the tail is amputated at its base. The tail skin and the last few coccygeal vertebrae are removed. Single tendons are pulled out from the dorsal and ventral bundles and kept in saline solution. Tendons of the same diameter (0.25 mm) are selected with a stereomicroscope. Since the diameter of the tendons may be influenced by long-term treatment of the animals, tendons of the same vertebral insertion are tested, alternatively. For this purpose, the 10th vertebra is counted from the tail tip. All six tendons (four on the ventral and two on the dorsal side) inserting on this vertebra are removed and tested. The tendons are fixed in special clamps at a distance of 2.0 cm and immersed in physiological saline. Stress–strain curves and ultimate loads are determined with an Instron instrument with an extension rate of 5 cm/min.

A single injection of cortisol acetate (10–100 mg/kg) or prednisolone acetate (2 and 20 mg/kg) causes a dose-dependent increase of tensile strength allowing the calculation of a potency ratio of 1:4 for prednisolone versus cortisol. Repeated injections of cortisol acetate in doses between 1.0 and 50 mg/kg (s.c.) or prednisolone acetate in doses between 0.05 and 50 mg/kg (s.c.) show the same dose dependence and potency ratio. The tensile strength of tail tendons is similarly changed by treatment with gonadal steroids, depending on the dose and duration of treatment, but to a much lesser degree than by corticosteroids.

EVALUATION

For changes in mechanical properties, the potency ratios of glucocorticoids versus cortisol as the standard are calculated.

MODIFICATIONS OF THE METHOD

In addition to tensile strength, other biophysical parameters can be determined in tail tendons, such as hysteresis behavior (Vogel 1984). The ratio of energy input versus energy dissipation is calculated. Furthermore, dependence on strain rate and relaxation behavior under the influence of corticosteroids (Vogel 1989) as well as retardation (strain rate under constant load) have been studied (Vogel and Schorning 1990).

REFERENCES AND FURTHER READING

Vogel HG (1965) Intensität und Dauer der Wirkung von 6α-Methylprednisolon und seinen Estern an der Ratte. Acta Endocrinol 50:621–642

Vogel HG (1969) Zur Wirkung von Hormonen auf physikalische und chemische Eigenschaften des Binde- und Stützgewebes. Arzneimittelforschung 19:1495–1503, 1732–1742, 1790–1801, 1981–1996

Vogel HG (1984) Influence of desmotropic drugs on viscoelastic properties of rat tail tendons. Hysteresis experiments. Arzneimittelforschung 34:213–216

Vogel HG (1989) Influence of desmotropic drugs on viscoelastic properties of tail tendons in rats. Acta Ther 15:239–252

Vogel HG, Schorning M (1990) Retardation experiments in rat tail tendons. Influence of maturation and age and of desmotropic and anti-inflammatory drugs. Acta Ther 16:3–11

N.2.1.3.4 Tensile Strength of Skin Strips in Rats

PURPOSE AND RATIONALE

Clinical experience shows a decrease of skin thickness after long-term systemic or local treatment with corticosteroids (skin atrophy, thinning). The mechanical properties of human skin after treatment with corticosteroids are difficult to measure. As with other connective tissues, in animal experiments a clear increase of tensile strength of skin has been found after short-term administration of corticosteroids (Vogel 1969, 1971a, 1971b, 1974, 1981, 1986, 1993b).

PROCEDURE

Male Sprague-Dawley rats with an initial weight of 120 ± 10 g are treated with increasing doses of corticosteroids or other substances for periods of between 1 and 14 days. After sacrifice, the back of the animals is shaved and a flap of skin measuring about 5×5 cm is removed. The skin flap is placed between two pieces of plastic material with known thickness. By these means, the actual thickness of the excised skin is measured by calipers. Two dumbbell-shaped specimens are cut with a special punch in perpendicular direction to the body axis, having in the middle a width of 4 mm. They are fixed between the clamps of an Instron instrument. In the usual experiments, stress–strain curves and ultimate loads are recorded at a strain rate of 5 cm/min. From stress–strain curves, the values of ultimate load and ultimate extension are recorded. The stress–strain curves are almost linear in part, allowing the calculation of the modulus of elasticity. Tensile strength is calculated from ultimate load divided by original cross-sectional area.

Dose–response curves for 10 and 100 mg/kg cortisol acetate or 2 and 20 mg/kg prednisolone acetate show a sharp increase of ultimate load and tensile strength up to 5 days of treatment, a continuous decrease of skin thickness upon longer treatment, and a decrease of ultimate load up to 2 months of treatment, which is below controls for ultimate load, but not for tensile strength (Vogel 1970a).

EVALUATION

Dose–response curves are established for corticosteroids versus the standard cortisol and potency ratios with confidence limits are calculated.

MODIFICATIONS OF THE METHOD

With a similar method, the tensile strength of skin wounds after treatment with corticosteroids was studied in rats (Vogel 1970a, 1970b). See also Sect. P.11.4.

Strain rate influences the values of ultimate load, tensile strength and modulus of elasticity, but not the effect of corticosteroids (Vogel 1972).

In contrast to parameters indicating the strength and elasticity of collagen, the parameters indicating plasticity, such as relaxation, hysteresis, strain at constant load (creep experiments), and isorheological behavior, are less dramatically changed by corticosteroids but indicate a decrease of viscosity or an increase of stiffness.

For a more detailed description of relaxation experiments (Vogel 1973) see Sect. P.11.2.1.5; of hysteresis experiments (Vogel 1976, 1989), see Sect. P.11.2.1.6; of creep experiments (strain at constant load) (Vogel 1977, 1989), see Sect. P.11.2.1.8; of measurement of isorheological behavior (Vogel 1987, 1989), see Sect. P.11.2.1.7; and for *in vivo* experiments in rat skin (Vogel and Denkel 1985; Vogel 1989, 1993a), see Sect. P.11.3.

REFERENCES AND FURTHER READING

Vogel HG (1969) Zur Wirkung von Hormonen auf physikalische und chemische Eigenschaften des Binde-

und Stützgewebes. Arzneimittelforschung 19:1495–1503, 1732–1742, 1790–1801, 1981–1996
Vogel HG (1970a) Beeinflussung der mechanischen Eigenschaften der Haut von Ratten durch Hormone. Arzneimittelforschung 20:1849–1857
Vogel HG (1970b) Tensile strength of skin wounds in rats after treatment with corticosteroids. Acta Endocrinol 64:295–303
Vogel HG (1971a) Antagonistic effect of aminoacetonitrile and prednisolone on mechanical properties of rat skin. Biochim Biophys Acta 252:580–585
Vogel HG (1971b) Zur Wirkung von Hormonen, insbesondere Glucocorticoiden, auf die physikalischen und chemischen Eigenschaften normaler und traumatisierter Haut. Acta Endocrinol Suppl 152:19
Vogel HG (1972) Influence of age, treatment with corticosteroids and strain rate on mechanical properties of rat skin. Biochim Biophys Acta 286:79–83
Vogel HG (1973) Stress relaxation in rat skin after treatment with hormones. J Med 4:19–27
Vogel HG (1974) Correlation between tensile strength and collagen content in rat skin. Effect of age and cortisol treatment. Connect Tissue Res 2:177–182
Vogel HG (1976) Measurement of some viscoelastic properties of rat skin following repeated load. Connect Tissue Res 4:163–168
Vogel HG (1977) Strain of rat skin at constant load (creep experiments). Influence of age and desmotropic agents. Gerontology 23:77–86
Vogel HG (1981) Influence of desmotropic agents on the directional variations of mechanical properties in rat skin. Bioeng Skin 3:85–97
Vogel HG (1986) *In vitro* test systems for evaluation of the physical properties of the skin. In: Marks R, Plewig G (eds) Skin models. Models to study function and disease of skin. Springer, Berlin Heidelberg New York, pp 412–419
Vogel HG (1987) Repeated loading followed by relaxation and isorheological behaviour of rat skin after treatment with desmotropic drugs. Bioeng Skin 3:255–269
Vogel HG (1989) Mechanical properties of rat skin with aging. In: Balin AK, Kligman AM (eds) Aging and the skin. Raven, New York, pp 227–275
Vogel HG (1993a) *In vivo* recovery of repeatedly strained rat skin after systemic treatment with desmotropic drugs. Skin Pharmacol 6:103–110
Vogel HG (1993b) Strength and viscoelastic properties of anisotropic rat skin after treatment with desmotropic drugs. Skin Pharmacol 6:92–102
Vogel HG, Denkel K (1985) Influence of maturation and age, and of desmotropic compounds on the mechanical properties of rat skin *in vivo*. Bioeng Skin 1:35–54

N.2.1.4
Topical Effects of Glucocorticosteroids on Skin

N.2.1.4.1
Skin Thickness and Tensile Strength

PURPOSE AND RATIONALE

From clinical experience it is known that a decrease of skin thickness occurs after long-term local treatment with corticosteroids. The mechanical properties of human skin after treatment with corticosteroids are difficult to assess. A clear increase of tensile strength of skin after short-term local administration of corticosteroids has been found in animal experiments, whereas skin thickness decreased (Alpermann et al. 1982; Vogel and Petri 1985).

PROCEDURE

Male Sprague-Dawley rats with an initial weight of 150 ± 10 g are used. The animals are shaved before and once again during treatment. The animals are treated once daily over 10 days with various concentrations of the test compound or the standard or with fixed concentrations of the test compound in different galenical preparations. The test material is applied in a volume of 0.2 ml to an area of 4 cm^2 to the shaven back skin. The animals are kept in individual cages to avoid systemic absorption by mutual licking. Two days after the last treatment the animals are sacrificed, a flap of skin measuring about 5×5 cm is removed, and skin thickness is determined. The skin flap is placed between two pieces of plastic material with known thickness. The thickness of the excised skin is measured by calipers. Perpendicular to the body axis two dumbbell-shaped specimens are punched out. Stress–strain curves are recorded using an Instron instrument. The following parameters are determined:

- load at rupture (ultimate load)
- extension at rupture (ultimate strain)
- skin thickness
- tensile strength (ultimate load divided by cross-sectional area)
- modulus of elasticity (calculated from the straight part of the stress–strain curve).

EVALUATION

Dose–response curves are established for the parameters ultimate load, ultimate strain, skin thickness, tensile strength, and modulus of elasticity for the standard (prednisolone acetate) and the test compound allowing the calculation of potency ratios with confidence limits.

CRITICAL ASSESSMENT OF THE METHOD

In addition to corticosteroid-induced atrophy of the skin after topical application assessed by histology, mechanical parameters can be determined.

MODIFICATIONS OF THE METHOD

Kapp et al. (1977) used specially devised apparatus for rats covering the site of substance application, which

guarantees an exclusive dermal absorption and excludes oral ingestion of the steroid.

In addition to skin thickness and breaking strength, Töpert et al. (1990) determined thymus weight, water and glycosaminoglycan content in the skin of rats after topical application of steroids over 30 days.

Iwasaki et al. (1995) measured the skin atrophy in Wistar rats by locally applied clobetasol-17-propionate, a synthetic glucocorticoid, and the influence of simultaneously applied RU 486. Then, 24 h after the last application, the thickness of the skin was measured with a dial skin thickness gauge, with an accuracy of 0.01 mm. The treated skin was pinched lengthwise, and both skin surfaces were held vertically between two plastic discs of the gauge.

Hartop et al. (1978) measured transepithelial water loss (TEWL) in the skin of rats deficient in essential fatty acids (Prottey et al. 1976; Lowe and Stoughton 1977) after local treatment with corticosteroids.

Woodbury and Kligman (1992) recommended the hairless mouse as a model for assaying the atrophogenicity of topical steroids. Epidermal atrophy was determined by the number of cell layers of viable epidermis on five fields under ×400 magnification. Dermal thickness was determined under ×400 magnification. The total number of sebocytes in all visualizable sebaceous glands was counted in ten fields at ×250 magnification.

Van den Hoven et al. (1991) used the hairless mouse as a model to distinguish between local and systemic atrophogenic effects of topical steroids. Male hairless mice (strain h/h-NMRI) were treated on the left flank with test preparations once daily for 3 weeks. During this time, body weight was measured and the skinfold thickness of treated and untreated sides was determined using a graduated micrometer. On day 21, the animals were sacrificed and dermal thymidine uptake and weights of the thymus were determined.

Corticosteroid-induced skin atrophy in hairless mice can be prevented by tretinoin (Lesnik et al. 1989; Schwartz et al. 1994). In these studies, albino Skh-hairless-1 mice were treated topically twice daily with corticosteroids or in combination with tretinoin. At the end of the treatment, all mice were sacrificed and specimens of the dorsal skin were frozen for light microscopy and quantification of glycosaminoglycans, fibronectin, and collagen.

Wrench (1980) applied commercially available topical corticosteroid preparations to the proximal halves of albino mouse tail for 21 days and measured epidermal thickness by histology. All steroids caused epidermal thinning, except clobetasone butyrate.

Altmeyer and Buhles (1981) tested the anti-acanthogenic effect of topically applied steroids after long-term treatment of guinea pigs (up to 118 days) by histological measurement of epithelial thickness. For delimitation of the measuring lines, the upper boundary was taken as that between the stratum granulosum and the stratum corneum, and the lower boundary as that between the basal cell layer and the corium.

Kajita et al. (1986) tested epidermal beta-adrenergic adenylate cyclase responses in pigs after topical application of glucocorticoids. A significant increase of this receptor response was observed 24 h following topical application of potent glucocorticoid ointments. Domestic white-haired pigs were anesthetized with 30 mg/kg nembutal i.p. Four 5 × 5 cm areas were chosen and the following treatments were administered to each area: (1) topical administration of glucocorticoid ointments; (2) UVB irradiation alone (230 mJ/cm^2); (3) topical application of glucocorticoid ointments following UVB irradiation; (4) no treatment as a control. After 24 h the treated pigs were anesthetized again and skin specimens were obtained from the four areas by means of a Castroviejo keratome (Storz Instrument, St. Louis, Mo., USA) adjusted to the 0.3 mm setting. Each skin slice obtained by the Castroviejo keratome was cut into 5 × 5 cm squares, which were washed 3 times in RPMI 1640 medium and preincubated in RPMI 1640 medium for 37°C to standardize the cAMP level (Yoshikawa et al. 1975). After the preincubation, two pieces of skin squares were randomly selected and were incubated with various adenylate cyclase stimulators (Iizuka et al. 1985). The concentrations of epinephrine, adenosine, and histamine added to the incubation medium were 50 μM, 2 mM and 1 mM, respectively. The cAMP content in skin squares was measured by radioimmunoassay using a Yamasa cAMP assay kit (Yamasa Shoyu, Tokyo, Japan) after partial purification (Yoshikawa et al. 1975). The cAMP phosphodiesterase activities in skin squares were measured by the method of Adachi et al. (1976) who purified multiple forms of pig epidermal cyclic nucleotide phosphodiesterases by DEAE-cellulose column chromatography.

In vitro experiments measuring the effects of retinoids and glucocorticoids on the beta-adrenergic adenylate cyclase system of pig skin epidermis were performed by Iizuka et al. (1985).

REFERENCES AND FURTHER READING

Adachi K, Levine V, Halprin KM, Iizuka K, Yoshikawa K (1976) Multiple forms of cyclic nucleotide phosphodiesterase in pig epidermis. Biochim Biophys Acta 429:498–507

Alpermann HG, Sandow J, Vogel HG (1982) Tierexperimentelle Untersuchungen zur topischen und systemischen Wirksamkeit von Prednisolon-17-ethylcarbonat-21-propionat. Arzneimittelforschung 32:633–638
Altmeyer P, Buhles N (1981) Tolerance on corticosteroids? Guinea pig epithelium as an experimental system. Arch Dermatol Res 271:3–9
Hartop PJ, Allenby CF, Prottey C (1978) Comparison of barrier function and lipids in psoriasis and essential fatty acid-deficient rats. Clin Exp Dermatol 3:259–267
Iizuka H, Ohkuma N, Ohkawara A (1985) Effects of retinoids on the cyclic AMP system of pig skin epidermis. J Invest Dermatol 85:324–327
Iwasaki K, Mishima E, Miura M, Sakai N, Shimao S (1995) Effect of RU 486 on the atrophogenic and antiinflammatory effects of glucocorticoids in skin. J Dermatol Sci 10:151–158
Kajita S, Iizuka H, Hirokawa M, Tsutsui M, Mizumoto T (1986) Topical application of potent glucocorticoids augments epidermal beta-adrenergic adenylate cyclase response *in vivo* Acta Derm Venereol (Stockh) 66:491–496
Kapp JF, Gliwitzki B, Josefiuk P, Weishaupt W (1977) Dermale und systemische Nebenwirkungen von Fluocortinbutylester (FCB). Hautreißversuche im Vergleich mit Wirkstoffen aus Handelspräparaten. Arzneimittelforschung 27:2206–2213
Lesnik RH, Mezick JA, Capetola R, Kligman LH (1989) Topical all-trans-retinoic acid prevents corticosteroid-induced skin atrophy without abrogating the anti-inflammatory effects. J Am Acad Dermatol 21:168–190
Lowe NJ, Stoughton RB (1977) Essential fatty acid deficient hairless mouse: a model of chronic epidermal hyperproliferation. Br J Dermatol 96:155–162
Prottey C, Hartop PJ, Black JG, McCormac JI (1976) The repair of impaired epidermal barrier function in rats by the cutaneous application of linoleic acid. Br J Dermatol 94:13–21
Schröder HG, Babej M, Vogel HG (1974) Tierexperimentelle Untersuchungen mit dem lokal wirksamen 9α-Fluor-16α-methyl-17-desoxy-prednisolon. Arzneimittelforschung 24:3–5
Schwartz E, Mezick JA, Gendimenico GJ, Kligman LH (1994) *In vivo* prevention of corticosteroid-induced skin atrophy by tretinoin in the hairless mouse is accompanied by modulation of collagen, glycosaminoglycans, and fibronectin. J Invest Dermatol 102:241–246
Töpert M, Olivar A, Opitz D (1990) New developments in corticosteroid research. J Dermatol Treatment 1 [Suppl 3]:S5–S9
Van den Hoven WE, van den Berg TP, Korstanje C (1991) The hairless mouse as a model for study of local and systemic atrophogenic effects following topical application of corticosteroids. Acta Derm Venereol Suppl (Stockh) 71:29–31
Vogel HG, Petri W (1985) Comparison of various pharmaceutical preparations of prednicarbate after repeated topical administration to the skin of rats. Arzneimittelforschung 35:939–946
Woodbury R, Kligman AM (1992) The hairless mouse model for assaying the atrophogenicity of topical corticosteroids. Acta Derm Venereol Suppl (Stockh) 72:403–408
Wrench R (1980) Epidermal thinning: evaluation of commercial corticosteroids. Arch Dermatol Res 267:7–24
Yoshikawa K, Adachi K, Halprin KM, Levine V (1975) Cyclic AMP in skin: effects of acute ischemia. Br J Dermatol 92:249–254

N.2.1.4.2 Assay of Topical Glucocorticoid Activity in Transgenic Mice

PURPOSE AND RATIONALE

Katchman et al. (1995) proposed a transgenic mouse model as a biological assay of topical glucocorticosteroid potency.

PROCEDURE

A homozygous line of transgenic mice expressing 5.2 kilobases (kb) of the human elastin promoter region linked to the chloramphenicol acetyltransferase (CAT) reporter gene was developed (Hsu-Wong et al. 1994). For this purpose, 5.2 kb of human elastin 5′-flanking DNA is linked to a 0.7-kb CAT gene, followed by 0.3 kb of DNA with a polyadenylation signal. This linearized construct is injected into fertilized oocytes, and a line of transgenic mice expressing the human elastin promoter, as detected by CAT activity, is developed. These transgenic mice have no clinical phenotype and they do not express human elastin protein, as no part of the coding sequence is contained within the transgene. The human elastin promoter/CAT construct is expressed in a tissue-specific and developmentally regulated manner.

Test animals are 4- or 5-day-old hairless pups, homozygous for the transgene. In each experiment, pups of the same litter are used for comparison between glucocorticosteroid-treated and control preparations in parallel. Steroid preparations are tested by applying 0.03 g uniformly on their dorsal surface ($\approx 14\,mg/cm^2$). Control animals receive the same amount of cream base. The test animals are separated from each other and from their mothers and are sacrificed at different time points. Skin biopsy samples are removed immediately from the treated area.

For the CAT assay, skin is homogenized with a Polytron tissue homogenizer in 0.25 M TRIS hydrochloride (pH 7.5). The homogenates are freeze-thawed three times and centrifuged at 10,000 *g* for 15 min. The protein content of the supernatant is determined by a commercial kit and aliquots, containing 100 mg of protein, are assayed for CAT activity in the linear range of the assay (Gorman et al. 1982) (see Sect. N.2.1.1.2).

EVALUATION

The significance of differences between treatment groups is evaluated by Student's *t*-test.

REFERENCES AND FURTHER READING

Gorman CM, Moffat LF, Howard BH (1982) Recombinant genes which express chloramphenicol acetyltransferase in mammalian cells. Mol Cell Biol 2:1044–1051

Hsu-Wong S, Katchman SD, Ledo I, Wu M, Khillan J, Bashir MM, Rosenbloom M, Uitto J (1994) Tissue-specific and developmentally regulated expression of human elastin promoter activity in transgenic mice. J Biol Chem 269:18072–18075

Katchman SD, Del Monaco M, Wu M, Brown D, Hsu-Wong S, Uitto J (1995) A transgenic mouse model provides a novel biological assay of topical glucocorticosteroid potency. Arch Dermatol 131:1274–1278

N.2.1.4.3 Effect on Epidermal DNA Synthesis

PURPOSE AND RATIONALE

Du Vivier et al. (1978), Marshall and Du Vivier (1978), Marshall et al. (1981), and Clement et al. (1983) evaluated the local and systemic effects of topically applied corticosteroids on epidermal DNA synthesis in hairless mice.

PROCEDURE

Hairless mice of either sex, 2–4 months old, are dosed in groups of six with test preparations or control base: 0.03 ml of test drug formulation is spread over 3 cm^2 of the anterior dorsal skin. The posterior half of the dorsal surface of the animal is left untreated. Animals are injected subcutaneously with 25 mCi (methyl-^{3}H) thymidine, specific activity 5 Ci/mM, in the right thigh 1 h before being sacrificed 6 or 24 h after application of test formulation.

The neck and back skin samples, with at least 2 cm unsampled skin left between them (to avoid inclusion of treated skin in the back sample) are removed. The epidermis is separated from the dermis by placing the sample, dermis downwards, on a stainless steel plate at 57°C for 25 s. The epidermis can then easily be separated from the dermis with a scalpel blade. The epidermal samples are wrapped in aluminum foil and stored at 20°C until analysis.

Approximately 30 mg of epidermis in 5 ml of a 0.24 M sodium phosphate buffer solution, containing 8 M urea, 1% sodium lauryl sulfate and 1 mM EDTA at pH 6.8, is lysed using an ultrasonic disintegrator. DNA is extracted from the cell lysate by column chromatography using hydroxylapatite. The epidermal cell lysate is added to the hydroxylapatite column and washed with a buffer containing 0.24 M sodium phosphate and 8 M urea at pH 6.8 to remove RNA and protein. The urea is then removed with 50 ml of 0.14 M sodium phosphate buffer at pH 6.8. Double-stranded DNA, which binds to hydroxylapatite under low-salt buffer conditions, is eluted with 0.48 M sodium phosphate buffer at pH 6.8, and a 2-ml sample is collected.

The DNA concentration in the sample is determined by UV absorption at 260 nm in a spectrophotometer. Then 0.5-ml aliquots of the sample are added to 12 ml scintillation cocktail and 0.2 ml N HCl in scintillation vials. Each sample is prepared in triplicate and counted for 20 min/vial in a scintillation counter.

EVALUATION

The results are initially expressed as mean counts per minute (c.p.m.) for the vial triplets, converted to mean disintegrations per minute (d.p.m.) and the results expressed as d.p.m./μg DNA. The significance of differences between treatment groups is evaluated by Student's *t*-test.

MODIFICATIONS OF THE METHOD

Marks et al. (1973) described a method for the assay of topical corticosteroids in mice based on changes in thymidine incorporation after treatment. Sticky tape was applied five or six times to the dorsal skin of mature male hairless mice of the Harwell strain to remove the horny layer. A similar quantity of topical test preparations (about 70 mg) was applied on the stripped dorsal skin of each mouse. A dressing of cotton gauze lined with a plastic film was applied and secured with strapping, staying for periods of from 5 to 156 h. Then 4 h before sacrifice the mice were intraperitoneally injected with 0.15 ml of a 0.1% Colcemid solution together with 30 μCi of tritiated thymidine. The dorsal skin area previously treated was removed, fixed in 10% buffered formalin and stained with hematoxylin and eosin. For estimation of the mitotic index, cells in the prophase, anaphase, and metaphase stages were counted. To quantitate the labeling index, the number of labeled basal and suprabasal cells was estimated as a proportion of the total number of basal cells.

REFERENCES AND FURTHER READING

Clement M, Hehir M, Phillips H, du Vivier A (1983) The effect on epidermal DNA synthesis of a combination of topical steroid with either dithranol or tar as used for psoriasis. Br J Dermatol 109:327–335

Du Vivier A, Marshall AC, Brookes LG (1978) An animal model for evaluating the local and systemic effects of topically applied corticosteroids on epidermal synthesis. Br J Dermatol 98:209–215

Marks R, Pongsehirun D, Saylan T (1973) A method for the assay of topical corticosteroids. Br J Dermatol 88:69–74

Marshall RC, Du Vivier A (1978) Effect on epidermal DNA synthesis of the butyrate esters of clobetasone and clobetasol, and the propionate ester of clobetasol. Br J Dermatol 98:355–359

Marshall RC, Burrows M, Brookes LG, du Vivier A (1981) The effect of topical and systemic glucocorticosteroids on DNA synthesis in different tissues of the hairless mouse. Br J Dermatol 105:517–520

N.2.1.4.4 Induction of Drug-Metabolizing Enzymes

PURPOSE AND RATIONALE

Finnen et al. (1984, 1985) evaluated the effects of topical application of glucocorticosteroids on the activity of drug-metabolizing enzymes in the skin of adult hairless mice. The ability of steroid preparations to induce enzyme activity was related to their clinical potency.

PROCEDURE

Adult male and female hairless mice are treated with 0.3 g of test creams or cream base applied to the dorsal skin and rubbed in until no visible traces remain. Then 16–18 h after treatment, the animals are sacrificed, the treated area of skin removed, and placed epidermis-down on a curved surface, and subcutaneous fat and muscle are removed using a scalpel blade. Epidermis and dermis are separated by a heating technique (Thompson and Slaga 1976). The tissue is then placed in 0.1 M phosphate buffer (pH 7.4) and minced finely using surgical scissors. Scissors-minced tissue is then homogenized in ice-cold 0.1 M phosphate buffer (pH 7.4) using a Polytron homogenizer. Whole-skin homogenates are then centrifuged at 9000 *g* for 20 min and the resulting supernatant used as the source for the determination of 7-ethoxycoumarin O-deethylase (Greenlee and Poland 1978). For the determination of ethoxyresorufin O-dealkylation (Pohl and Fouts 1980) the 9000 *g* supernatants are further centrifuged at 100,000 *g* for 1 h, the resulting microsomal pellet resuspended in 0.1 M phosphate buffer (pH 7.4), and used as the enzyme source. The DNA content of the 9000 *g* pellet is estimated by the diphenylamine reaction (Burton 1956).

EVALUATION

The significance of differences between treatment groups is evaluated by Student's *t*-test.

REFERENCES AND FURTHER READING

Burton K (1956) A study on the conditions and mechanisms of the diphenylamine reaction for the colorimetric estimation of desoxyribonucleic acid. Biochem J 62:401–437

Finnen MJ, Herdman ML, Shuster S (1984) Induction of drug metabolizing enzymes in the skin by topical steroids. J Steroid Biochem 20:1169–1173

Finnen MJ, Herdman ML, Shuster S (1985) Strain differences in the induction of mono-oxygenase activity in mouse skin by topical clobetasol propionate: evidence of a role for the HR locus. J Steroid Biochem 23:431–435

Greenlee WF, Poland A (1978) An improved assay of 7-ethoxycoumarin O-deethylase activity: induction of hepatic enzyme activity in C57BL/6J and DBA/2J mice by phenobarbital, 3-methylcholanthrene and 2,3,7,8-tetrachlorodibenzo-p-dioxin. J Pharmacol Exp Ther 205:596–606

Pohl RJ, Fouts JR (1980) A rapid method for assaying the metabolisms of 7-ethoxyresorufin by microsomal subcellular fractions. Anal Biochem 107:150–155

Thompson S, Slaga TJ (1976) The effects of dexamethasone on mouse initiation skin and aryl hydrocarbon hydroxylase. Eur J Cancer 12:363–370

N.2.1.4.5 Cornea Inflammation in Rabbits

PURPOSE AND RATIONALE

Leibowitz and Kupferman (1974), Leibowitz et al. (1978, 1992) and Cantrill et al. (1975) studied the anti-inflammatory efficacy of topical corticosteroids for treatment of glaucoma in rabbits. Again, this test is purely of historical interest.

PROCEDURE

New Zealand albino rabbits weighing 1.8–2.3 kg are anesthetized for approximately 5 min with 15 mg/kg i.v. thiamylal sodium. A corneal inflammatory response is produced by intralamellar inoculation of 0.03 ml of laboratory-grade clove oil. Before the induction of corneal inflammation, the rabbits are given three intravenous inoculations of 1.85×10^6 Bq/kg of an aqueous solution of tritiated thymidine (24.79×10^{10} Bq/mol) at 24-h intervals. The intracorneal injection of clove oil is given concomitantly with the third thymidine injection, and 24 h later, therapy is initiated. A standard drop (0.05 ml) of drug is instilled hourly for a total of six doses, and then, after a lapse of 18 h, one drop is administered hourly for an additional total of seven doses.

Corticosteroid preparations are tested in different concentrations. A control group is run with each experimental trial; control rabbits are handled in the same manner as experimental rabbits, except that the control rabbits receive either prednisolone acetate (positive control) or no treatment (negative control). At autopsy, a 10-mm penetrating corneal button is removed by trephination, tissue samples are placed in a commercially available solubilizing agent (Soluene 350, Packard Instrument), 1 ml per cornea, until dissolved. The samples are counted for a minimum of 10 min, measuring the amount of radioactivity in each cornea sample.

EVALUATION

The significance of differences between treatment groups is evaluated by Student's *t*-test.

REFERENCES AND FURTHER READING

Cantrill HL, Palmberg PF, Zink HA, Waltman SR, Podos SM, Becker B (1975) Comparison of *in vitro* potency of corticosteroids with ability to raise intraocular pressure. Am J Ophthalmol 79:1012–1017

Leibowitz HM, Kupferman A (1974) Anti-inflammatory effectiveness in the cornea of topically administered prednisolone. Invest Ophthalmol 13:757–763

Leibowitz HM, Kupferman A, Stewart HR, Kimbrough RL (1978) Evaluation of dexamethasone acetate as a topical ophthalmic formulation. Am J Ophthalmol 86:418–423

Leibowitz HM, Ryan WJ, Kupferman A (1992) Comparative anti-inflammatory efficacy of topical corticosteroids with low glaucoma-inducing potential. Arch Ophthalmol 110:118–120

N.2.1.4.6 Endotoxin-Induced Uveitis in Rats

PURPOSE AND RATIONALE

Salmonella endotoxin, a lipopolysaccharide, produces uveitis 12–24 h after injection into the footpad of rats. Uveitis is characterized by miosis, iris hyperemia, increase of protein content in aqueous humor, and inflammatory cell accumulation in the anterior uvea and aqueous humor. Glucocorticoids strongly inhibit endotoxin-induced uveitis by suppressing inflammatory mediators (Cousins et al. 1982; Tsuji et al. 1997).

PROCEDURE

Female inbred Lewis rats weighing about 160 g are used. Then 500 µg/kg *Salmonella* endotoxin dissolved in saline is injected into the footpads. Twelve hours later, the animals are sacrificed and both eyes of each animal used in the experiments. The anterior chamber of the eye is punctured, using a 27-gauge needle, to collect the aqueous humor. Then 5-µl aqueous humor samples are placed into 495 µl of phosphate-buffered saline containing 1% paraformaldehyde. The number of cells in the aqueous humor is then counted using a flow cytometry system. The cell number for both eyes of each animal is averaged for statistical analysis of the results.

In topical applications, glucocorticoids are instilled (5 µl/eye) three times at 1 h before and 3 and 7 h after lipopolysaccharide injection. For systemic application, glucocorticoids are injected subcutaneously 3 h after lipopolysaccharide injection.

Total RNA is isolated from the iris-ciliary body with a mRNA purification kit (Pharmacia Biotech, Uppsala, Sweden). Each RNA sample is extracted from the pooled iris-ciliary bodies of both eyes of each animal. The extracted RNA is quantified after which 4 µg is used for DNA synthesis via polymerase chain reaction.

EVALUATION

Dunnetts's multiple comparison test was applied for statistical analysis.

Further methods for measuring local or topical activity of corticosteroids are very suitable for evaluating local corticosteroid activity, described in Sect. H.3 "Anti-inflammatory activity", such as oxazolone-induced ear edema in mice (see Sect. H.3.2.2.4) and croton-oil-induced ear edema in rats or mice (see Sect. H.3.2.2.5).

Furthermore, methods described in Chap. I "Anti-arthrotic and immunomodulatory activity", Sect. I.2.2.4 "Passive cutaneous anaphylaxis", and Sect. I.2.2.6 "Delayed type hypersensitivity are recommended as models for testing topical corticosteroid potency".

REFERENCES AND FURTHER READING

Cousins SW, Rosenbaum JT, Guss RB, Egbert PR (1982) Ocular albumin fluorophotometric quantitation of endotoxin-induced vascular permeability. Infect Immun 36:730–736

Tsuji F, Sawa K, Kato M, Mibu H, Shirasawa E (1997) The effects of betamethasone derivatives on endotoxin-induced uveitis in rats. Exp Eye Res 64:31–36

N.2.1.4.7 Croton Oil-Induced Ear Inflammation

Topical application of the nonspecific contact irritant croton oil, a mixture of several phorbol esters, leads to acute inflammation characterized by edema and a mainly granulocytic cell infiltration into the skin. For topical application, compounds are dissolved in the same vehicle as used for croton oil and are co-applied. Systemic application of compounds (s.c.) is performed 2 h before croton oil application. At the maximum of the inflammatory reaction, animals are killed, and ears (mice, area $\approx 1\,cm^2$) or a punch biopsy (rats, 10 mm diameter) are weighed as an indicator of edema formation, then snap-frozen in liquid nitrogen in polypropylene tubes and kept at –20°C for up to 24 h.

N.2.1.5 Anti-Glucocorticoid Activity

N.2.1.5.1 Adrenal and Thymus Involution

PURPOSE AND RATIONALE

The involution of thymus and adrenal glands induced by hydrocortisone can be antagonized by compounds with anti-glucocorticoid activity (Dorfmann 1962).

PROCEDURE

Groups of six to ten immature male Sprague-Dawley rats weighing 60–70 are injected subcutaneously daily for 6 days with 0.2 ml of the antagonistic test compound in 0.5% aqueous carboxymethylcellulose solution. Hydrocortisone acetate is used as the agonist in daily doses of 0.2 mg per animal. Controls receive hydrocortisone acetate only. On the seventh day, the animals are sacrificed and the adrenal and thymus weights determined.

EVALUATION

The relative weight [quotient of adrenal or thymus weight (mg) and body weight (g)] is calculated for each rat. Means of the antagonist-treated groups are compared with the means of hydrocortisone-only controls. An increase of thymus and adrenal weight relative to the hydrocortisone control indicates anti-glucocorticoid activity.

MODIFICATIONS OF THE METHOD

Inhibition of tyrosine aminotransferase induced by corticosterone or dexamethasone was used by Vincent et al. (1997) to characterize the anti-glucocorticoid properties of a novel synthetic steroid.

REFERENCES AND FURTHER READING

Dorfman RI (1962) Corticoids. In: Dorfman RI (ed) Methods in hormone research, Vol II, Bioassay. Academic Press, New York, pp 325–367

Vincent GP, Monteserin MC, Valeiro AS, Burton G, Lantos CP, Galigniana MD (1997) 21-Hydroxy-6,19-oxidoprogesterone: a novel synthetic steroid with specific antiglucocorticoid properties in the rat. Mol Pharmacol 52:749–753

N.2.2 Mineralocorticoid Activity

N.2.2.1 In Vivo Methods

N.2.2.1.1 General Considerations

Very early bioassays ("Survival tests") have been used to standardize extracts of adrenal cortex for mineralocorticoid activity (Grollman 1941; Ringler 1964; Tolksdorf et al. 1956). For evaluation of mineralocorticoid activity these tests have been replaced by bioassays measuring electrolyte excretion in the urine.

Several animal species do not survive after adrenalectomy. However, they can be kept alive by administration of mineralocorticoids. The first animal species used successfully was the adrenalectomized drake (Bülbring 1937). The methods employing adrenalectomized rats and mice (Dorfman 1962) suffered from the fact that in these species aberrant adrenal cortical tissue may occur, which is not removed by surgical adrenalectomy. In contrast, male Syrian golden hamsters weighing 50–60 g are very suitable for testing adrenocortical activity (Junkmann 1955).

REFERENCES AND FURTHER READING

Bülbring E (1937) The standardization of cortical extracts by the use of drakes. J Physiol (Lond) 89:64–80

Dorfman RI (1962) Corticoids. In: Dorfman RI (ed) Methods in hormone research, Vol II, Bioassay. Academic Press, New York, pp 325–367

Grollman A (1941) Biological assay of adrenal cortical activity. Endocrinology 29:855–861

Junkmann K (1955) Über protrahiert wirksame Corticoide. Naunyn-Schmiedebergs Arch Exp Pathol Pharmacol 227:212–213

Ringler I (1964) Activities of adrenocorticosteroids in experimental animals and man. In: Dorfman RI (ed) Methods in hormone research, Vol III, Steroidal activity in experimental animals and man. Academic Press, New York, pp 227–349

Tolksdorf S, Battin ML, Cassidy JW, McLeod RM, Warren FH, Perlman PL (1956) Adrenocortical properties of $\Delta^{1,4}$-pregnadiene-17α,21-diol-3,11,20-trione (Meticorten) and $\Delta^{1,4}$-pregnadiene-11β,17α21-triol-3,20-dione (Meticortelone). Proc Soc Exp Biol Med 92:207–214

N.2.2.1.2 Electrolyte Excretion

PURPOSE AND RATIONALE

Mineralocorticosteroids enhance sodium retention and potassium excretion. The sodium excretion in adrenalectomized rats is dose-dependently decreased. This parameter can be used to assess the mineralocorticoid activity of test compounds (Kagawa et al. 1952; Marcus et al. 1952).

PROCEDURE

Male Sprague-Dawley rats weighing 140–160 g are adrenalectomized. They are maintained on 1% sodium chloride solution. On the morning of the fourth postoperative day, food and drinking fluid are withdrawn. On the following day, each rat is given 5 ml water by stomach tube; 1 h later 5 ml of 0.9% sodium chloride solution is given orally. Test compounds are injected s.c. in 0.2 ml of vehicle suspension. Desoxycorticosterone acetate (DOCA; 1–40 µg per rat) is used as standard (reference compound). The rats are placed in metabolic cages, two rats per cage, three cages per dosage group, for 4 h, and then removed from the cages. The use of light, transient ether anesthesia in this method is obsolete. Urine volume is recorded and

in addition cages may be rinsed with a distilled water spray. Appropriate dilutions of urine are analyzed for sodium with a flame photometer. The amount of sodium excreted by each rat is calculated, and group means are expressed as percentage of excretion by control animals.

EVALUATION

Percent reduction of sodium excretion compared with controls is calculated for each dosage group. Potency ratios are calculated with reference to desoxycorticosterone acetate.

MODIFICATIONS OF THE METHOD

Simpson and Tait (1952) measured both urinary sodium and potassium and used the sodium-to-potassium ratio as an index of the electrolyte activity of corticoids. Nikisch et al. (1991) infused glucocorticoid-substituted adrenalectomized rats with saline-glucose solution containing aldosterone and measured sodium and potassium concentrations in 1-h fractions of urine. The anti-aldosterone activity was assessed by the ability of test compounds to reverse the aldosterone effect on the urinary Na/K ratio.

REFERENCES AND FURTHER READING

Kagawa CM, Shipley EG, Meyer RK (1952) A biological method for determining small quantities of sodium retaining substances. Proc Soc Exp Biol Med 80:281–285

Marcus F, Romanoff LP, Pincus G (1952) The electrolyte-excreting activity of adrenocortical substances. Endocrinology 50:286–293

Nikisch K, Beier S, Bittler D, Elger W, Laurent H, Losert W, Nishino Y, Schillinger E, Wiechert R (1991) Aldosterone antagonists. 4. Synthesis and activities of steroidal 6,6-ethylene-15,16-methylene 17-spirolactones. J Med Chem 34:2464–2468

Simpson SA, Tait JF (1952) A quantitative method for the bioassay of the effect of adrenal cortical steroids on mineral metabolism. Endocrinology 50:150–161

Souness GW, Morris DJ (1991) The "mineralocorticoid-like" actions conferred on corticosterone by carbenoxolone are inhibited by the mineralocorticoid receptor (type I) antagonist RU28318. Endocrinology 129:2451–2456

Stafford RO, Barnes LE, Bowman BJ, Meinzinger MM (1955) Glucocorticoid and mineralocorticoid activities of Δ^1-fluorohydrocortisone. Proc Soc Exp Biol Med 89:371–374

N.2.2.2 In Vitro Methods

N.2.2.2.1 Mineralocorticoid Receptor Binding

PURPOSE AND RATIONALE

Rat kidney receptor preparations and radioactively labeled aldosterone were used to test affinity for the mineralocorticoid receptor (Raynaud et al. 1975, 1979; Pasqualini and Sumida 1977; Ojasoo and Raynaud 1978; Wambach and Higgins 1971).

PROCEDURE

Kidney homogenates of adrenalectomized rats are centrifuged at 0°C for 10 min at 800 *g* in a buffer solution (10 mM Tris, 0.25 M saccharose, HCl, pH 7.4). Following addition of RU 28362 at 0.001 mM (to inhibit binding of aldosterone to the glucocorticoid receptor) the supernatant is centrifuged again at 105,000 *g* for 60 min. The supernatant (cytosol) is removed and incubated at 0°C with ^{3}H-aldosterone (5 nM) and increasing concentrations of test compounds (0–25,000 nM). Nonspecific binding is determined in the presence of 1 μM aldosterone. Free ^{3}H-aldosterone is removed from the incubation medium by charcoal-dextran absorption after 1 h or 24 h of incubation (Raynaud 1978). Following centrifugation, the concentration of receptor-bound ligand is determined in the supernatant by liquid scintillation counting.

EVALUATION

The following parameters are calculated: total binding of ^{3}H-aldosterone, nonspecific binding in the presence of 1 μM aldosterone, specific binding (= total binding–non-specific binding), % inhibition with specific binding as a percentage of the control value.

For structure–activity studies, all compounds are first tested at a single high concentration (25,000 nM) in triplicate. For those showing more than 50% inhibition a displacement curve is determined using seven to eight different concentrations of compound. The binding potency of compounds is expressed as binding affinity (RBA), relative to the standard compound (aldosterone).

MODIFICATIONS OF THE METHOD

Affinity for the mineralocorticoid receptor was tested using the cytosol of rabbit kidneys (Claire et al. 1993) or rat kidney slices (Funder et al. 1974). It is also useful to use overexpressed human mineralocorticoid receptors.

Monkey kidney COS-1 cells were transfected with plasmids containing the human mineralocorticoid receptor – cloned by Arriza et al. (1987) – and the glucocorticoid receptor for binding studies with various steroids (Rupprecht et al. 1993a, 1993b).

A survey of mineralocorticoid receptor ligands has been given by Sutano and de Kloet (1991).

Specific bioluminescent *in vitro* assays for selecting potential anti-mineralocorticoids were developed by Jausons-Loffreda et al. (1994).

Wehling (1994) found evidence for a membrane-bound mineralocorticoid receptor in human mononuclear leukocytes.

The human mineralocorticoid receptor was used by Grassy et al. (1997) to study structure–activity relationships of steroids with anti-mineralocorticoid activity.

Davioud et al. (1996) described the synthesis and biological activities of new steroidal diazoketones as potential photoaffinity labeling reagents for the mineralocorticoid receptor.

Fagart et al. (1997a) recommended [^{3}H-2]-21-diazoprogesterone as a potent photoaffinity labeling reagent for the mineralocorticoid receptor.

Fagart et al. (1997b) proposed a three-dimensional model for antagonism in the human mineralocorticoid receptor.

The biological and clinical relevance of glucocorticoid and mineralocorticoid receptors has been reviewed by Funder (1997).

Rogerson et al. (1999, 2003) studied the structural determinants of aldosterone-binding selectivity in the mineralocorticoid receptor. To characterize ligand-binding specificity, chimeras were made between the human mineralocorticoid receptor and glucocorticoid receptor ligand-binding domains. Models of the mineralocorticoid receptor ligand-binding domain bound to aldosterone and spironolactone were created based on the crystal structure of the progesterone receptor ligand-binding domain. These techniques have been used by Rogerson et al. (2004) to evaluate the differences in the determinants of eplerenone, spironolactone, and aldosterone binding to the mineralocorticoid receptor.

REFERENCES AND FURTHER READING

Arriza JL, Weinberger C, Cerelli G, Glaser TM, Handelin BL, Housman DE, Evans RM (1987) Cloning of human mineralocorticoid receptor complementary DNA: Structural and functional kinship with the glucocorticoid receptor. Science 237:268–275

Claire M, Faraj H, Grassy G, Aumelas A, Rondot A, Auzou G (1993) Synthesis of new 11β-substituted spironolactone derivatives. Relationship with affinity for mineralocorticoid and glucocorticoid receptors. J Med Chem 36:2404–2407

Davioud E, Fagart J, Souque A, Rafestin-Oblin ME, Marquet A (1996) New steroidal diazo ketones as potential photoaffinity labelling reagents for the mineralocorticoid receptor: synthesis and biological activities. J Med Chem 39:2860–2864

Fagart J, Sobrio F, Marquet A (1997a) Synthesis of [^{3}H-2]-21-diazoprogesterone as a potent photoaffinity labelling reagent for the mineralocorticoid receptor. J Labelled Compd Radiopharm 39:791–795

Fagart J, Wurtz J-M, Souque A, Hellal-Levy C, Moras D, Rafestin-Oblin M-E (1997b) Antagonism in the human mineralocorticoid receptor. EMBO J 17:3317–3325

Funder JW (1997) Glucocorticoid and mineralocorticoid receptors: biological and clinical relevance. Annu Rev Med 48:231–240

Funder JM, Feldman D, Highland E, Edelman IS (1974) Molecular modifications of anti-aldosterone compounds: effects on affinity of spironolactones for renal aldosterone receptors. Biochem Pharmacol 23:1493–1501

Grassy G, Fagart J, Calas B, Adenot M, Rafestin-Oblin ME, Auzou G (1997) Structure-activity relationships of steroids with anti-mineralocorticoid activity. Eur J Med Chem 32:869–879

Jausons-Loffreda N, Balaguer P, Auzou G, Pons M (1994) Development of specific bioluminescent *in vitro* assays for selecting potential antimineralocorticoids. J Steroid Biochem Mol Biol 49:31–38

Ojasoo T, Raynaud JP (1978) Unique steroid congeners for receptor studies. Cancer Res 38:4186–4198

Pasqualini JR, Sumida CH (1977) Mineralocorticoid receptors in target tissues. In: Pasqualini JR (ed) Receptors and mechanism of action of steroid hormones, Part II. Dekker, New York, pp 399–511

Raynaud JP (1978) The mechanism of action of antihormones. In: Jacob J (ed) Advances in pharmacology and therapeutics, Vol 1, Receptors. Pergamon, Oxford, pp 259–278

Raynaud JP, Bonne C, Bouton MM, Moguilewsky M, Philibert D, Azadian-Boulanger G (1975) Screening for antihormones by receptor studies. J Steroid Biochem 6:615–622

Raynaud JP, Ojasoo T, Bouton MM, Philibert D (1979) Receptor binding as a tool in the development of new bioactive steroids. In: Ariëns EJ (ed) Drug design, Vol VIII. Academic Press, New York, pp 169–214

Rogerson FM, Dimopoulos N, Sluka P, Chu S, Curtis AJ, Fuller PJ (1999) Structural determinants of aldosterone binding selectivity in the mineralocorticoid receptor. J Biol Chem 274:36305–36311

Rogerson FM, Yao YZ, Smith BJ, Dimopoulos N, Fuller PJ (2003) Determinants of spironolactone binding specificity in the mineralocorticoid receptor. J Mol Endocrinol 31:573–582

Rogerson FM, Yao Y, Smith BJ, Fuller PJ (2004) Differences in the determinants of eplerenone, spironolactone, and aldosterone binding to the mineralocorticoid receptor. Clin Exp Pharmacol Physiol 31:704–709

Rupprecht R, Reul JMHM, van Steensel B, Spengler D, Söder M, Berning B, Holsboer F, Damm K (1993a) Pharmacological and functional characterization of human mineralocorticoid and glucocorticoid receptor ligands. Eur J Pharmacol Mol Pharmacol Sect 247:145–154

Rupprecht R, Arriza JL, Spengler D, Reul JMHM, Evans RM, Holsboer F, Damm K (1993b) Transactivation and synergistic properties of the mineralocorticoid receptor: relationship to the glucocorticoid receptor. Mol Endocrinol 7:597–603

Sutano W, de Kloet ER (1991) Mineralocorticoid ligands: biochemical, pharmacological, and clinical aspects. Med Res Rev 11:617–639

Wambach G, Higgins JR (1978) Antimineralocorticoid action of progesterone in the rat: correlation of the effect on electrolyte excretion and interaction with mineralocorticoid receptors. Endocrinology 102:1686–1693

Wehling M (1994) Novel aldosterone receptors: specificity-conferring mechanism at the level of the cell membrane. Steroids 59:160–163

N.2.2.2.2 Transactivation Assay for Mineralocorticoids

PURPOSE AND RATIONALE

Steroid agonistic and antagonistic properties can be evaluated by transactivation assays (Muhn et al. 1995; Fuhrmann et al. 1995, 1996). The transactivation assay assumes that steroid receptor proteins act as ligand-regulated transcriptional activators. After binding of hormone, the steroid receptor acts with hormone responsive elements of hormone-regulated genes, thereby inducing a cascade of transcriptional events (Green and Chambon 1988). The hormone-dependent transcriptional activation can be determined in tissue culture by transfection of the steroid receptor under investigation and a reporter gene linked to a hormonally responsive promoter into cells. The transactivation assay allows determination of the agonistic and also of the antagonistic activity of a given compound, by either induction or inhibition of reporter gene activity (Fuhrmann et al. 1992).

PROCEDURE

Vector Construct

The expression plasmid pRShMR containing the full-length coding sequence of the mineralocorticoid receptor expressed from the long terminal repeat of the Rous sarcoma virus is prepared according to Arriza et al. (1987). The pMMTV-CAT plasmid containing the mouse mammary tumor virus promoter linked to a chloramphenicol acetyltransferase gene is prepared according to Cato et al. (1986).

Cell Culture and Transfections

CV-1 cells and COS-1 cells for transient infections are cultured in Dulbecco's Modified Eagle's Medium (DMEM) supplemented with 10% fetal calf serum, 4 mmol/l L-glutamine, penicillin and streptomycin. Stable and transient transfections are performed using Lipofectin reagent (Gibco BRL) according to a procedure recommended by Felgner and Holm (1989). Stable transfections are carried out according to Fuhrmann et al. (1992). For transient transfection, 1×10^6 COS-1 or CV-1 cells are plated onto 100-mm dishes 1 day prior to transfection. Cells are typically about 80% confluent after 24 h. Before transfection, cells are washed twice with 1 ml Opti-MEM (Gibco BRL) per dish. For each dish, 5 µg pRShMR (hMR expression plasmid) and 5 µg pMMTV-CAT are diluted with 1 ml Opti-MEM; in addition, 50 µg Lipofectin Reagent is diluted with 1 ml Opti-MEM. Next, DNA and Lipofectin reagent dilutions are combined in a polystyrene snap-cup tube to obtain 2 ml of transfection solution per dish, gently mixed, incubated at room temperature for 5 min, and added to the washed cells. After 5 h the transfection solution is replaced by 6 ml of DMEM supplemented with 10% fetal calf serum.

To study the effect of the test hormones, transiently transfected cells are trypsinized, pooled and replated onto 60-mm dishes at a density of 4.5×10^5 per dish 24 h after transfection. Stably transfected cells are seeded onto 6-well dishes (1×10^5 cells per dish). Cells are cultured in medium supplemented with 3% charcoal-stripped fetal calf serum and the appropriate hormones for 48 h. As negative control for the reporter gene induction, cells are cultured with 1% ethanol. Transactivation assays with transiently or stably transfected cells are carried out at least three times.

CAT Assay (Chloramphenicol Acetyltransferase)

Transiently transfected cells and stably transfected cells are disrupted by freezing (ethanol/dry ice bath) and thawing (37°C water bath) three times. Protein concentrations in the cell extract are determined according to Bradford (1976). The CAT assay is performed according to Gorman et al. (1982).

EVALUATION

CAT activity is calculated as percentage conversion from chloramphenicol to acetylated chloramphenicol. Concentration–response curves for CAT induction are established to demonstrate the potency of the test hormone. Aldosterone (10^{-10} to 10^{-6} mol/l) serves as standard.

For anti-mineralocorticoid activity, CAT activity in the presence of 10^{-8} mol/l aldosterone is set as 100% and relative CAT activity is calculated as a percentage of this value. Concentration–response curves for CAT inhibition are established with increasing concentrations of the antihormone.

CRITICAL ASSESSMENT OF THE METHOD

See N.2.1.1.2.

MODIFICATIONS OF THE METHOD

White et al. (1994) described a simple and sensitive high-throughput assay for steroid agonists and antagonists. A DNA cassette, containing a synthetic steroid-inducible promoter controlling the expression of a bacterial chloramphenicol acetyltransferase gene (GRE5-CAT), was inserted into an Epstein-Barr virus episomal vector, which replicates autonomously in primate and human cells. This promoter/reporter system was used to generate two stably transfected human

cell lines. In the cervical carcinoma cell line HeLa, which expresses high levels of glucocorticoid receptor, the GRE5 promoter is inducible over 100-fold by the synthetic glucocorticoid dexamethasone. In the breast carcinoma cell line T47D, which expresses progesterone and androgen receptors, the GRE5 promoter is inducible over 100-fold by either progesterone or dihydrotestosterone. These cell lines can be used to screen large numbers of natural and synthetic steroid agonists and antagonists in microtiter wells directly using a colorimetric chloramphenicol acetyltransferase assay.

Rupprecht et al. (1993a, 1993b) examined the functional agonistic and antagonistic activity of several steroids by co-transfecting human mineralocorticoid or human glucocorticoid receptor expression vectors, together with a mouse mammary tumor virus-luciferase (MTV-LUC) reporter gene into the human neuroblastoma cell line SK-N-MC. Transfections were performed using an electroporation system (Biotechnologies and Experimental Research, San Diego, Calif., USA).

Lombès et al. (1994) used a co-transfection assay in CV-1 cells to study the discrimination of aldosterone from natural and synthetic glucocorticoids by the human mineralocorticoid receptor. Cells were transfected by the calcium phosphate method with pRShMR, a plasmid that contains the entire coding sequence of the human mineralocorticoid receptor; pFC31Luc, which contains the mouse mammary tumor virus (MMTV) promoter driving the luciferase gene; pCH110 encoding the β-galactosidase as an internal transfection control; and pSP72 as plasmid carrier.

Lim-Tio et al. (1997) studied the determinants of specificity of transactivation by the mineralocorticoid or glucocorticoid receptor in three cell lines: CV-1 cells; a porcine renal epithelial cell line, LLC-PK1; a pig kidney cell strain, and RN33B; a neuronal medullary raphe cell line. The reporter gene used was MMTV-LUC (the long terminal repeat of the mouse mammary tumor virus promoter linked to the luciferase reporter gene). RSV-CAT (Rous sarcoma virus promoter-chloramphenicol acetyl transferase gene) was used as an internal control for the transfection efficacy.

REFERENCES AND FURTHER READING

Arriza JL, Weinberger C, Cerelli G, Glaser TM, Handelin BL, Housman DE, Evans RM (1987) Cloning of human mineralocorticoid receptor complementary DNA: structural and functional kinship with the glucocorticoid receptor. Science 237:268–275

Bradford M (1976) A rapid and sensitive method for the quantitation of microgram quantities of protein utilizing the principle of protein-dye binding. Anal Biochem 72:248–254

Cato ACB, Miksicek R, Schütz G, Arnemann J, Beato M (1986) The hormone regulatory element of mouse mammary tumor virus mediates progesterone induction. Embo J 6:2237–2240

Felgner PL, Holm M (1989) Cationic liposome-mediated transfection. Focus 11:21–25

Fuhrmann U, Bengtson C, Repenthin G, Schillinger E (1992) Stable transfection of androgen receptor and MMTV-CAT into mammalian cells: inhibition of CAT expression by antiandrogens. J Steroid Biochem Mol Biol 42:787–793

Fuhrmann U, Slater EP, Fritzemeier KH (1995) Characterization of the novel progestin gestodene by receptor binding studies and transactivation assays. Contraception 51:45–52

Fuhrmann U, Krattenmacher R, Slater EP, Fritzemeier KH (1996) The novel progestin drospirone and its natural counterpart progesterone: biochemical profile and antiandrogenic potential. Contraception 54:243–251

Gorman CM, Moffat LF, Howard BH (1982) Recombinant genomes which express chloramphenicol acetyltransferase in mammalian cells. Mol Cell Biol 2:1044–1055

Green S, Chambon P (1988) Nuclear receptors enhance our understanding of transcription regulations. Trends Genet 4:309–314

Lim-Tio SS, Keightley M-C, Fuller PF (1997) Determinants of specificity of transactivation by the mineralocorticoid or glucocorticoid receptor. Endocrinology 138:2537–2543

Lombès M, Kenouch S, Souque A, Farman N, Rafestin-Oblin ME (1994) The mineralocorticoid receptor discriminates aldosterone from glucocorticoids independently of the 11β-hydroxysteroid dehydrogenase. Endocrinology 135:834–840

Muhn P, Fuhrmann U, Fritzemeier KH, Krattenmacher R, Schillinger E (1995) Drospirenone: a novel progestogen with antimineralocorticoid and antiandrogenic activity. Ann NY Acad Sci 761:311–335

Rupprecht R, Reul JMHM, van Steensel B, Spengler D, Söder M, Berning B, Holsboer F, Damm K (1993a) Pharmacological and functional characterization of human mineralocorticoid and glucocorticoid receptor ligands Eur J Pharmacol Mol Pharmacol Sect 247:145–154

Rupprecht R, Arriza JL, Spengler D, Reul JMHM, Evans RM, Holsboer F, Damm K (1993b) Transactivation and synergistic properties of the mineralocorticoid receptor: relationship to the glucocorticoid receptor. Mol Endocrinol 7:597–603

White JH, McCuaig KA, Mader S (1994) A simple and sensitive high-throughput assay for steroid agonists and antagonists. Biotechnology 12:1003–1007

N.2.2.3 Anti-Mineralocorticoid Activity

N.2.2.3.1 Electrolyte Excretion

PURPOSE AND RATIONALE

The method is based on the mineralocorticoid activity of desoxycorticosterone acetate (agonists) (reference compound) reversed by spironolactone (reference antagonist) and other anti-mineralocorticoids to be evaluated (test compounds).

PROCEDURE

Male Sprague-Dawley rats weighing 140–160 g are adrenalectomized and maintained on 1% NaCl solution as drinking fluid. On the morning of the fourth postoperative day, food and drinking fluid are withdrawn. On the following day, each rat is given 5 ml water by stomach tube; 1 h later it is given 5 ml 0.9% NaCl orally and injected with 40 µg desoxycorticosterone acetate. At a separate site, the antagonistic test compound is injected s.c. in 0.2 ml of vehicle suspension. Spironolactone, 50 µg or 500 µg, is injected as the reference compound with anti-mineralocorticoid activity. Rats are placed in metabolic cages, two rats per cage, three cages per dosage group, for 4 h of urine collection. Urine volume is recorded and cages rinsed over the collection cylinders with a distilled water spray. Appropriate dilutions of collected urine are analyzed for sodium and potassium with a flame photometer.

EVALUATION

The amount of water, sodium, and potassium excreted per 100 g bodyweight is calculated. The product of water volume and sodium excretion is divided by the potassium excretion. The excretion ratios (quotient) are compared for untreated adrenalectomized rats, animals treated with DOCA, and animals treated with spironolactone

MODIFICATIONS OF THE METHOD

Anti-mineralocorticoid activity of spironolactone and its analogs has been tested in adrenalectomized golden hamsters treated simultaneously with daily injections desoxycorticosterone acetate over a period of 3 weeks (Vogel, unpublished data 1965). The mean survival of adrenalectomized animals of 4.7 days was prolonged to 13.5 days by daily subcutaneous injections of 2 mg desoxycorticosterone acetate. Additional injection of 0.5 or 1.0 mg spironolactone reduced the survival time.

Losert et al. (1985) tested the ability of several steroids with progestogenic potency to inhibit the renal actions of aldosterone in adrenalectomized, glucocorticoid-treated rats. The rats were continuously infused with an isotonic solution of low sodium content (0.05% NaCl + 5.2% glucose, 3 ml/rat per hour) supplemented with D-aldosterone (1 µg/kg per h) resulting in a long-lasting reduction in renal sodium excretion, an increase in renal potassium excretion, and hence a decrease in the urinary Na/K ratio. The test drugs were administered either subcutaneously or orally 1 h before the start of infusion. The anti-mineralocorticoid activity was judged by the increase in the aldosterone-lowered Na/K ratio in urine collected at hourly intervals up to 21 h.

Cutler et al. (1978, 1979) described a potent mineralocorticoid receptor antagonist with decreased antiandrogenic activity relative to spironolactone.

De Gasparo et al. (1987) evaluated epoxy-spironolactone derivatives for their anti-mineralocorticoid activity (Kagawa test) and their antiandrogenic and progestogenic side-effects *in vitro* and *in vivo*.

Gómez-Sánchez et al. (1990) reported the effect of intracerebroventricular infusion of mineralocorticoid antagonists on the hypertension in rats produced by chronic subcutaneous administration of aldosterone.

The evolution of aldosterone antagonists has been reviewed by Garthwaite and McMahon (2004) and Hu et al. (2005) featuring eplerenone, a molecule with improved steroid receptor selectivity and pharmacokinetic properties in humans compared with spironolactone.

The beneficial effects of eplerenone have been demonstrated in rats with myocardial infarction (Masson et al. 2004; Fraccarollo et al. 2005) and in rats with autoimmune myocarditis (Wahed et al. 2005) as well as in mice with chronic heart failure (Wang et al. 2004).

REFERENCES AND FURTHER READING

Cutler GB Jr, Pita JC Jr, Rifka SM, Menard RH, Sauer MA, Loriaux DL (1978) SC 25152: a potent mineralocorticoid antagonist with reduced affinity for the 5α-dihydrotestosterone receptor of human and rat prostate. J Clin Endocrinol Metab 447:171–175

Cutler GB Jr, Sauer MA, Lorioux DL (1979) SC 25152: a potent mineralocorticoid receptor antagonist with decreased antiandrogenic activity relative to spironolactone. J Pharmacol Exp Ther 209:144–146

De Gasparo M, Joss U, Ramjoué HP, Whitebread SE, Haenni H, Schenkel L, Kraehenbühl C, Biollaz M, Grob J, Schmidlin J, Wieland P, Wehrli HU (1987) Three new epoxy-spironolactone derivatives: characterization *in vivo* and *in vitro*. J Pharmacol Exp Ther 240:650–656

Fraccarollo D, Galuppo P, Schmidt I, Ertl G, Bauersachs J (2005) Additive amelioration of left ventricular remodeling and molecular alterations by combined aldosterone and angiotensin receptor blockade after myocardial infarction. Cardiovasc Res 67:97–105

Garthwaite SM, McMahon EG (2004) The evolution of aldosterone antagonists. Mol Cell Endocrinol 217:27–31

Gómez-Sánchez EP, Fort CM, Gómez-Sánchez CE (1990) Intracerebroventricular infusion of RU28318 blocks aldosterone-salt hypertension. Am J Physiol 258:E482–E484

Hu X, Li S, McMahon EG, Lala D, Rudolph AE (2005) Molecular mechanisms of mineralocorticoid receptor antagonism by eplerenone. Mini Rev Med Chem 5:709–718

Kagawa CM (1960) Blocking the renal electrolyte effects of mineralocorticoids with an orally active steroidal spironolactone. Endocrinology 67:125–132

Kagawa CM, Brown EA (1960) Ability of isopregnenolone-21-carboxylates to block renal effects of desoxycorticos-

terone and aldosterone in rats. Proc Soc Exp Biol Med 105:648–650
Kagawa CM, Shipley EG, Meyer RK (1952) A biological method for determining small quantities of sodium retaining substances. Proc Soc Exp Biol Med 80:281–285
Losert W, Casals-Stenzel J, Buse M (1985) Progestogens with antimineralocorticoid activity. Arzneimittelforschung 35:459–471
Losert W, Bittler D, Buse M, Casals-Stenzel J, Haberey M, Laurent H, Nikisch K, Schillinger E, Wiechert L (1986) Mespirone and other 15,16-methylene-17-spirolactones, a new type of steroidal aldosterone antagonists. Arzneimittelforschung 36:1583–1600
Masson S, Staszewsky L, Annoni G, Carlo E, Arosio B, Bai A, Calabresi C, Martinoli E, Salio M, Fiordaliso F, Scanziani E, Rudolph AE, Latini R (2004) Eplerenone, a selective aldosterone blocker, improves diastolic function in aged rats with small-to-moderate myocardial infarction. J Cardiac Failure 10:433–441
Sakauye C, Feldman D (1976) Agonist and antagonist activities of spirolactones. Clin Res 24:135A
Stafford RO, Barnes LE, Bowman BJ, Meinzinger MM (1955) Glucocorticoid and mineralocorticoid activities of Δ^1-fluorohydrocortisone. Proc Soc Exp Biol Med 89:371–374
Wahed MII, Watanabe K, Ma M, Yamaguchi K, Takahashi T, Tachikawa H, Kodame M, Aizawa Y (2005) Effects of eplerenone, a selective aldosterone blocker, on the progression of left ventricular dysfunction and remodeling in rats with dilated cardiomyopathy. Pharmacology 73:81–88
Wang D, Liu YH, Yang XP, Rhaleb NE, Xu H, Peterson E, Rudolph AE, Carretero OA (2004) Role of a selective aldosterone blocker in mice with chronic heart failure. J Cardiac Failure 10:67–73

N.3
Ovarian Hormones

N.3.0.1
Ovariectomy of Rats

PROCEDURE

Ovariectomy is performed in immature female rats weighing 40–60 g (Bomskov 1939; Emmens 1969; May 1971). Animals are anesthetized. A single transverse incision is made in the skin of the back. This incision can be shifted readily from one side to the other by traction on the skin. A small puncture is then made over the site of the ovary, which can be seen through the abdominal wall, embedded in a pad of fat. The top of a pair of fine forceps is introduced and the fat around the ovary is grasped, care being taken not to rupture the capsule around the ovary. The tip of the uterine horn is crushed with a pair of artery forceps and the ovary, together with the fallopian tube, is removed with a single cut by a pair of fine scissors. Usually, no bleeding is observed. In older rats, the tip of the uterine horn may be ligated and the ovary removed distally from the ligature. The ovary of the other side is removed in the same way. The skin wound is closed by one or two clips. The animal recovers immediately.

Ovariectomized rats are now obtained from commercial suppliers when needed, the surgical procedure however is easy to learn, and licenses for animal experimentation are readily obtained for qualified laboratory personnel.

REFERENCES AND FURTHER READING

Bomskov C (1939) Die Methoden der Ovarexstirpation (Kastration). In Bomskov C, Methodik der Hormonforschung, 2. Band, Thieme Verlag Leipzig, pp 9–18
Emmens CW (1969) Estrogens. In: Dorfman RI (ed) Methods in Hormone Research, Vol IIA, Chapter 2, Academic Press, New York and London. pp 61–120
May M (1971) Estrogenic and antiestrogenic agents. In: Turner RD, Hebborn P (eds) Screening Methods in Pharmacology. Vol II, Academic Press, New York and London. pp 85–100

N.3.1
Estrogens

N.3.1.1
In Vitro Methods

N.3.1.1.1
Estrogen Receptor Binding

PURPOSE AND RATIONALE

The nuclear receptor assays are used to estimate the estrogenic activity of test compounds. Estradiol-17β is used as the reference compound. Estrogen receptors are prepared from mouse uteri or from human endometrium. Measurements of association rates and dissociation rates at different temperatures allow evaluation of relative binding affinities (Bouton and Raynaud 1977, 1978). Binding to the cytosolic and the nuclear fractions is measured.

PROCEDURE

Cytosol Preparation

Uteri from 18-day-old female Swiss mice are removed and homogenized at 0°C in 1:50 (w/v) of 10 mM Tris-HCl (pH 7.4), 0.25 M sucrose buffer in a conical homogenizer. Human endometrium from menopausal women is frozen within 2 h of hysterectomy and stored in liquid nitrogen until use. The frozen endometrium is pulverized and homogenized in 1:5 (w/v) Tris-sucrose buffer. Homogenates are centrifuged for 1 h at 105,000 *g*.

Dextran-Coated Charcoal (DCC) Adsorption Technique

Binding is measured as follows. A 100-µl aliquot of incubated cytosol is stirred for 10 min at 0°C in a microtiter plate with 100 µl of Dextran-coated charcoal

(DCC) suspension (0.625% Dextran 80000, 1.25% charcoal Norit A) and then centrifuged for 10 min at 800 *g*. The concentration of bound steroid is determined by measuring the radioactivity in a 100-µl aliquot of supernatant.

Determination of Specific Binding in Mouse Uterus Cytosol as a Function of Steroid Concentration, Incubation Time and Temperature

Triplicate aliquots of 125 µl of cytosol are incubated with 5 or 25 nM labeled steroid (estradiol-17ß) either for 2 or 24 h at 0°C or for 2 or 5 h at 25°C in the absence (total binding) or presence (nonspecific binding) of a 100-fold excess of radio-inert steroid. Bound steroid is measured by DCC adsorption.

Measurement of Association Rate at 0°C

For this, 1 or 5 nM concentration of labeled steroid is added to cytosol maintained at 0°C. Every 5 min for 1 h after addition of the labeled steroid, a 100-µl aliquot is transferred into a 5000 nM radio-inert steroid solution in a microtiter plate to stop the reaction. Bound radioactivity is determined by DCC adsorption.

Measurement of Dissociation Rate at 25°C

Dissociation rate is measured by the isotopic dilution technique. Radio-inert steroid (2500 nM) is added to crude cytosol previously incubated with 5 nm labeled steroid for 15 h at 0°C. After different times of incubation at 25°C, 100-µl samples are treated with DCC at 0°C in order to determine bound radioactivity. Specific binding is evaluated by subtracting nonspecific binding from total binding.

Nuclear Uptake

Homogenate samples (0.5 ml; two uteri per 0.5 ml) are incubated with 2.5, 5 or 25 nM labeled steroid for 5 or 60 min at 25°C, then cooled on ice and centrifuged at 800 *g* for 10 min at 0°C. The pellet (crude nuclei) is washed 3 times with 1 ml Tris-sucrose buffer, dissolved in 0.5 ml Soluene (Packard) and counted.

Nuclear Extract Preparation

After incubation with 25 nM labeled steroid for 1 h at 25°C, the crude nuclei are resuspended in 0.5 ml Tris-sucrose buffer, to which 50 µl of 4 M KCl is added. The suspension is stirred (vortex), left for 30 min at 0°C and then centrifuged for 30 min at 105,000 *g*. The radioactivity in a 100-µl supernatant sample (nuclear extract) is counted.

EVALUATION

Relative binding affinity is calculated from the percentage of radioligand bound in the presence of competitor compared to radioligand bound in its absence, plotted against the concentration of unlabeled competing steroid. A standard curve for the competition of the unlabeled radioligand is constructed with the use of nine to ten concentrations; five or six concentrations of the competitor are tested. These are chosen to provide a linear portion of the semilog plot which crosses the point of 50% competition. From this plot, the molar concentration of unlabeled radioligand or steroid competitor is determined that reduces radioligand binding by 50%.

The relative affinity of a test compound is the ratio of unlabeled radioligand concentration to competitor concentration, at 50% competition. This ratio is multiplied by 100.

Association rate (k_{+1}) is calculated by the slope of the line

$$k_{+1}t = (2.3/E_0 - R_0)\log(E\,R_0/R\,E_0)$$

where E_0 and E represent free steroid and R_0 and R free receptor at time $t = 0$ and time t, respectively.

Dissociation rate (k_{-1}) is calculated from the slope of the line

$$k_{-1} = -2.3\log B/B_0$$

where B_0 and B represent bound steroid at time $t = 0$ and time t, respectively.

Similar studies were reported by: Raynaud et al. 1975; Clark et al. 1976; Katzenellenbogen et al. 1977; Ojasoo and Raynaud 1978; Clark et al. 1982; Mukawa et al. 1988; Smanik et al. 1989; Labrie et al. 1990; Chander et al. 1991; Dhar et al. 1994.

MODIFICATIONS OF THE METHOD

Sheep uteri were used for the preparation of cytosol by Shutt and Cox (1972).

Pons et al. (1990) described receptor binding of estrogens and anti-estrogens in the estrogen-receptor-positive breast cancer cell line MCF-7, using the firefly luciferase assay (Brasier et al. 1989) as endpoint.

Ludwig et al. (1990) described a microliter well assay for quantitative measurement of estrogen receptor binding to estrogen-responsive elements.

Hwang et al. (1992) studied the use of tetrahydrochrysenes, inherently fluorescent, which are high-affinity ligands for the estrogen receptor.

Estrogen receptor binding has also been used to study the mechanism of action of nonsteroidal anti-es-

trogens (Jordan et al. 1977; Wakeling and Slater 1980; Astroff and Safe 1988).

The sequence and expression of human estrogen receptor complementary DNA was reported by Greene et al. (1986).

Solution structure of the DNA-binding domain of the estrogen receptor has been described by Schwabe et al. (1990).

Obourn et al. (1993) studied the hormone- and DNA-binding mechanisms of the recombinant human estrogen receptor overproduced in insect cells using a baculovirus expression system.

Cloning, chromosomal localization, and functional analysis of the murine estrogen receptor β are reported by Tremblay et al. (1997).

Nichols et al. (1998) showed that agonists and antagonists differently position the C-terminus of the ligand-binding domain (helix 12) and the F domain of the estrogen receptor.

REFERENCES AND FURTHER READING

Astroff B, Safe S (1988) Comparative antiestrogenic activities of 2,3,7,8-tetrachlorodibenzo-*p*-dioxin and 6-methyl-1,3,8-trichlorodibenzofuran in the female rat. Toxicol Appl Pharmacol 95:435–443

Bouton MM, Raynaud JP (1977) Impaired nuclear translocation and regulation: a possible explanation of anti-estrogenic activity. Res Steroids 7:127–137

Bouton MM, Raynaud JP (1978) The relevance of kinetic parameters in the determination of specific binding to the estrogen receptor. J Steroid Biochem 9:9–15

Brasier AR, Tate JE, Habener JF (1989) Optimized use of the firefly luciferase assay as a reporter gene in mammalian cell lines. Bio Techniques 7:1116–1122

Chander AK, McCague R, Luqmani Y, Newton C, Dowsett M, Jarman M, Coombes RC (1991) Pyrrolidino-4-iodotamoxifen and 4-iodotamoxifen, new analogues of the antiestrogen tamoxifen for the treatment of breast cancer. Cancer Res 51:5851–5858

Clark JH, Peck J Jr, Anderson JN (1976) Estrogen-receptor binding: relationship to estrogen-induced responses. J Toxicol Environ Health 1:561–586

Clark JH, Williams M, Upchurch S, Eriksson H, Helton E, Markaverich BM (1982) Effects of estradiol-17α on nuclear occupancy of the estrogen receptor, stimulation of nuclear type II sites and uterine growth. J Steroid Biochem 16:323–328

Dhar JD, Dwivedi A, Srivastava A, Setty BS (1994) Structure activity relationship of some 2,3-diaryl-2H-1-benzopyrans to their anti-implantation, estrogenic and antiestrogenic activities in the rat. Contraception 49:609–616

Greene GL, Gilna P, Waterfield M, Baker A, Hort Y, Shine J (1986) Sequence and expression of human estrogen receptor complementary DNA. Science 231:1150–1154

Hwang KJ, Carlson KE, Anstead GM, Katzenellenbogen JA (1992) Donor-acceptor tetrahydrochrysenes, inherently fluorescent, high-affinity ligands for the estrogen receptor: binding and fluorescence characteristics and fluorometric assay of receptor. Biochemistry 31:11536–11545

Jordan VC, Dix CJ, Rowsby L, Prestwich G (1977) Studies on the mechanism of action of the nonsteroidal antioestrogen tamoxifen (I.C.I. 46,474) in the rat. Mol Cell Endocrinol 7:177–192

Katzenellenbogen BS, Ferguson ER, Lan NC (1977) Fundamental differences in the action of estrogens and antiestrogens on the uterus: comparison between compounds with similar duration of action. Endocrinology 100:1252–1259

Labrie F, Poulin R, Simard J, Zhao HF, Labrie C, Dauvois S, Dumont M, Hatton AC, Poirier D, Mérand Y (1990) Interactions between estrogens, androgens, progestins, and glucocorticoids in ZR-75–1 human breast cancer cells. Ann NY Acad Sci 595:130–148

Ludwig LB, Klinge CM, Peale FV Jr, Bambara RA, Zain S, Hilf (1990) A microliter well assay for quantitative measurement of estrogen receptor binding to estrogen-responsive elements. Mol Endocrinol 4:1027–1033

Mukawa F, Suzuki T, Ishibashi M, Yamada F (1988) Estrogen and androgen receptor binding affinity of 10β-chloro-estrenen derivatives. J Steroid Biochem 31:867–870

Nichols M, Rientjes JMJ, Stewart AF (1998) Different positioning of the ligand binding domain helix 12 and the F domain in the estrogen receptor accounts for the functional differences between agonists and antagonists. EMBO J 17:765–773

Obourn JD, Koszweski NJ, Notides AC (1993) Hormone- and DNA-binding mechanisms of the recombinant human estrogen receptor. Biochemistry 32:6229–6236

Ojasoo T, Raynaud JP (1978) Unique steroid congeners for receptor studies. Cancer Res 38:4186–4198

Pons M, Gagne D, Nicolas JC, Mehtali M (1990) A new cellular model of response to estrogens: a bioluminescent test to characterize (anti)estrogen molecules. BioTechniques 9:450–459

Raynaud JP, Bonne C, Bouton MM, Moguilewsky M, Philibert D, Azadian-Boulanger G (1975) Screening for antihormones by receptor studies. J Steroid Biochem 6:615–622

Schwabe JWR, Neuhaus D, Rhodes D (1990) Solution structure of the DNA-binding domain of the oestrogen receptor. Nature 348:458–461

Shutt DA, Cox RI (1972) Steroid and phyto-oestrogen binding to sheep uterine receptors *in vitro*. J Endocrinol 52:299–310

Smanik EJ, Calderon JJ, Muldoon TG, Mahesh VB (1989) Effect of progesterone on the activity of occupied nuclear estrogen receptor *in vitro*. Mol Cell Endocrinol 64:111–117

Tremblay GB, Tremblay A, Copeland NG, Gilbert DJ, Jenkins NA, Labrie F, Giguère V (1997) Cloning, chromosomal localization, and functional analysis of the murine estrogen receptor β. Mol Endocrinol 11:353–365

Wakeling AE, Slater SR (1980) Estrogen-receptor binding and biological activity of tamoxifen and its metabolites. Cancer Treat Rep 64:741–744

N.3.1.1.2 Transactivation Assay for Estrogens

PURPOSE AND RATIONALE

Transient transfection of a suitable cell culture with a reporter gene controlled by an estrogen-responsive element (ERE) has become a convenient assay for estrogens.

Steroid agonistic and antagonistic properties can be evaluated by transactivation assays (Muhn et al. 1995; Fuhrmann et al. 1995, 1996). The transactivation assay assumes that steroid receptor proteins act as ligand-regulated transcriptional activators. After binding of hormone, the steroid receptor interacts with hormone-responsive elements of hormone-regulated genes, thereby inducing a cascade of transcriptional events (Green and Chambon 1988).

The assay in the estrogen-receptor-positive human breast cancer cell line MCF-7, described by Meyer et al. (1994) as a rapid luciferase transfection assay for transcription activation of estrogenic drugs, has been used for evaluation of synthetic estrogen antagonists by Von Angerer et al. (1994, 1995) and Biberger and Von Angerer (1996).

PROCEDURE

MCF-7 cells used for transfection are grown in Dulbecco's Modified Essential Medium supplemented with 10% fetal calf serum, 100 U penicillin, 100 µg streptomycin and 150 mg L-glutamine in 500 ml of medium without phenol red. Shortly before confluence, the cells are washed with 10 ml of PBS. Cells are gently shaken for a few seconds with trypsin-EDTA solution (4 ml) and after removal of the solution incubated for 2 min at 37°C. After addition of 10 ml of medium, the cell suspension (0.5 ml/well) is transferred to 6-well plates containing 2 ml of medium. Cells are grown until the density of the monolayer is about 50% (1–2 days) before 2 µg of the luciferase reporter plasmid EREwtc luc, harboring the luciferase gene from *Photinus pyralis*, is added. For a successful transfection, it is necessary to generate a very fine precipitate of the DNA by subsequent dilution with 45% water, 5% M $CaCl_2$, and 50% HBS buffer and continuous shaking. After 20 min at room temperature, an opalescent solution should be obtained.

After addition of the DNA solution, the medium is removed and the cells are washed with 2 ml of PBS, followed by treatment with glycerol (15% in PBS) for 2 min. After washing with PBS, fresh medium containing the test substances is added. The maximum of luciferase expression is reached 18 h after addition of the transfection solution. At this time, the medium is removed and cells are washed with PBS. Cell lysis and quantification of luminescence is performed according to the procedure described in the luciferase assay system E1500 of PROMEGA (Serva, Heidelberg, Germany). Luminescence is measured in a luminometer Lumat LB (Berthold, Wildbad, Germany) as relative light units, which are converted into fg luciferase by a calibration curve.

EVALUATION

Dose–response curves of luciferase activity after induction by the test substances and estradiol as control (10^{-14} to 10^{-9} M) are established.

CRITICAL ASSESSMENT OF THE METHOD

See N.2.1.1.2. Variation in transfection efficacy is the major cause of data variation and needs to be controlled for valid interpretation of data.

MODIFICATIONS OF THE METHOD

With the same method as for MCF-7 cells, Von Angerer et al. (1994) and Biberger and Von Angerer (1996) transfected HeLa-cells using the estrogen expression receptors HE0, HEG0, HE15 and HEG19, together with the receptor plasmid EREwtc luc.

Bergmann et al. (1994) determined estrogenic activity by a transient transfection assay in CHO cells deficient in estrogen receptors (ER) transfected with an expression vector encoding the ER using an estrogen-responsive reporter gene construct, $(ERE)_2$-TATA-CAT, containing two estrogen-response elements linked to a TATA promoter and the chloramphenicol transferase reporter gene.

For assessing environmental chemicals for estrogenicity, Shelby et al. (1996) recommended a transcriptional activation assay in ER-transfected HeLa cells using the estrogen-responsive reporter, ERE81CAT, and the pRSV vector containing the mouse ER cDNA without the neomycin resistance cassette. Triplicate samples for each hormone concentration were harvested at 28 h post-transfection and assayed for CAT protein using the CAT-ELISA kit (Boehringer Mannheim).

Several authors used yeast for assays of estrogenicity (McDonnell et al. 1991; Pierrat et al. 1992; Kohno et al. 1994; Bush et al. 1996; Tran et al. 1996; Odum et al. 1997).

Pierrat et al. (1992) constructed yeast strains in which the *Saccharomyces cerevisiae* URA3 gene is induced by the human estrogen receptor. Promoter sequences required for both basal and activated transcription of URA3 were replaced with estrogen-response elements positioned upstream of the native TATA box. These constructs were integrated at the TRP1 locus of a yeast strain in which the natural URA3 gene has been deleted and the integrants were transformed with shuttle plasmids expressing wild-type or truncated derivatives of human estrogen recep-

tor. Transformants were assayed for growth on uracil-deficient medium plus or minus estradiol, for resistance to 5-fluoroorotic acid, and for activity of orotidine-5′-monophosphate decarboxylase, the product of the URA3 gene.

Tran et al. (1996) used the yeast strain ER(wt) expressing human estrogen receptor and an estrogen-sensitive reporter to characterize the estrogenic or anti-estrogenic activities of polynuclear aromatic hydrocarbons.

Gaido et al. (1997) described a yeast-base steroid hormone receptor gene transcription assay to evaluate estrogenic and androgenic activity. The yeasts contain two separate plasmids: (1) an expression plasmid which contains the CUP1 metallothionein promoter fused to the human estrogen receptor cDND, and (2) a receptor plasmid carrying two estrogen-response elements or a reporter plasmid carrying two copies of a progesterone/androgen-responsive element upstream of the structural gene for β-galactosidase.

Chu et al. (2004) described transrepression of estrogen receptor β signaling by nuclear factor-κB in ovarian granulosa cells.

REFERENCES AND FURTHER READING

Bergmann KE, Wooge CH, Carlson KE, Katzenellenbogen BS, Katzenellenbogen JA (1994) Bivalent ligands as probes for estrogen receptor action. J Steroid Biochem Mol Biol 49:139–152

Biberger C, Von Angerer E (1996) 2-Phenylindoles with sulfur containing side chains. Estrogen receptor affinity, antiestrogenic potency, and antitumor activity. J Steroid Biochem Mol Biol 58:31–43

Bush SM, Folta S, Lannigan DA (1996) Use of the yeast one-hybrid system to screen for mutations in the ligand-binding domain of the estrogen receptor. Steroids 61:102–109

Chu S, Nishi Y, Yanase T, Nawata H, Fuller PJ (2004) Transrepression of estrogen receptor β signaling by nuclear factor-κB in ovarian granulosa cells. Mol Endocrinol 18:1919–1928

Fuhrmann U, Slater EP, Fritzemeier KH (1995) Characterization of the novel progestin gestodene by receptor binding studies and transactivation assays. Contraception 51:45–52

Fuhrmann U, Krattenmacher R, Slater EP, Fritzemeier KH (1996) The novel progestin drospirone and its natural counterpart progesterone: biochemical profile and antiandrogenic potential. Contraception 54:243–251

Gaido KW, Leonard LS, Lovell S, Gould JC, Babal D, Portier CJ, McDonnell DP (1997) Evaluation of chemicals with endocrine modulating activity in a yeast-based steroid hormone receptor gene transcription assay. Toxicol Appl Pharmacol 143:205–212

Green S, Chambon P (1988) Nuclear receptors enhance our understanding of transcription regulations. Trends Genet 4:309–314

Kohno H, Gandini O, Curtis SW, Korach KS (1994) Anti-estrogenic activity in the yeast transcription system: estrogen receptor mediated agonist response. Steroids 59:572–578

McDonnell DP, Nawaz Z, O'Malley BW (1991) *In situ* distinction between steroid receptor binding and transactivation at a target gene. Mol Cell Biol 11:4350–4355

Meyer T, Koop R, von Angerer E, Schönenberger H, Holler E (1994) A rapid luciferase transfection assay for transcription activation and stability control of estrogenic drugs in cell cultures. J Cancer Res Clin Oncol 120:359–364

Muhn P, Fuhrmann U, Fritzemeier KH, Krattenmacher R, Schillinger E (1995) Drospirenone: a novel progestogen with antimineralocorticoid and antiandrogenic activity. Ann NY Acad Sci 761:311–335

Odum J, Lefevre PA, Tittensor S, Paton D, Routledge EJ, Beresford NA, Sumpter PJ, Ashby J (1997) The rodent uterotrophic assay: critical protocol features, studies with nonyl phenols, and comparison with a yeast estrogenicity assay. Regul Toxicol Pharmacol 25:178–188

Pierrat B, Heery DM, Lemoine Y, Losson R (1992) Functional analysis of the human estrogen receptor using a phenotypic transactivation assay in yeast. Gene 119:237–245

Shelby MD, Newbold RR, Tully DB, Chae K, Davis VL (1996) Assessing environmental chemicals for estrogenicity using a combination of *in vitro* and *in vivo* assays. Environ Health Perspect 104:1296–1300

Tran DQ, Die CF, McLachlan JA, Arnold SF (1996) The anti-estrogenic activity of selected polynuclear aromatic hydrocarbons in yeast expressing human estrogen receptor. Biochem Biophys Res Commun 229:102–108

Von Angerer E, Biberger C, Holler E, Koop R, Leichtl S (1994) 1-Carbamoylalkyl-2-phenylindoles: relationship between side chain structure and estrogen antagonism. J Steroid Biochem Mol Biol 49:51–62

Von Angerer E, Biberger C, Leichtl S (1995) Studies on heterocycle-based pure estrogen antagonists. Ann NY Acad Sci 761:176–191

N.3.1.1.3 Estrogen-Dependent Cell Proliferation

PURPOSE AND RATIONALE

Specific cell proliferation induced by estrogens is the principle of these assays. Some human breast cancer cell lines, such as MCF-7 and T47-D cells, respond to estrogens with proliferation (Zondek 1935; Eisler 1964). This effect has been used for assays of estrogenic and antiestrogenic activity (Miller and Katzenellenbogen 1983; Scholl et al. 1983; Thompson et al. 1984; Palkowitz et al. 1997; Zacharewski 1997).

PROCEDURE

MCF-7 breast adenocarcinoma cells are maintained in MEM (Minimal Essential Medium), minus phenol red (which is estrogenic at high concentrations) supplemented with 10% fetal bovine serum (FBS), 2 μM L-glutamine, 1 μM sodium pyruvate, 10 μM HEPES, nonessential amino acids and 1 mg/ml bovine insulin. Ten days prior to assay, MCF-7 cells are switched to maintenance medium supplemented with 10% dextran-coated FBS in place of 10% FBS to deplete internal stores of steroids. MCF-7 cells are

removed from maintenance flasks using cell dissociation medium [Ca^{2+}/Mg^{2+}-free HBSS (phenol red-free) supplemented with 10 µM HEPES and 2 nM EDTA]. Cells are washed twice with assay medium and adjusted to 80,000 cells/ml. Approximately 100 µl (8000 cells) is added to flat-bottomed microculture wells and incubated at 37°C in a 5% CO_2 humidified incubator for 48 h to allow for cell adherence and equilibration transfer. Serial dilutions of test compounds, or dimethylsulfoxide (DMSO) as a diluent control, are prepared in assay medium and 50 µl transferred to triplicate microcultures, followed by 50 µl assay medium for a final volume of 200 µl. After an additional 48 h incubation, microcultures are pulsed with 1 µCi [^{3}H]thymidine (specific activity 6.7 Ci/mmol) for the last 4–6 h of culture and the assay terminated by freezing at −70°C. Microcultures are then thawed and harvested using a Skatron semiautomatic cell harvester. Samples are counted by liquid scintillation using a Wallace BetaPlate β-counter.

EVALUATION

Plotting of dpm versus compound concentration is used to determine the half-maximal effective concentrations EC_{50} or inhibitory concentration IC_{50}.

REFERENCES AND FURTHER READING

Miller MA, Katzenellenbogen BS (1983) Characterization and quantitation of antiestrogen binding sites in estrogen receptor-positive and -negative human breast cancer cell lines. Cancer Res 43:3094–3100

Palkowitz AD, Glasebrook AL, Thrasher KJ, Hauser KL, Short LL, Phillips DL, Muehl BS, Sato M, Shetler PK, Cullinan GJ, Pell TR, Bryant HU (1997) Discovery and synthesis of [6-hydroxy-3-[4-[2-(1-piperidinyl)ethoxy]phenoxyl]-2-[4-hydroxyphenyl)]benzo[*b*]thiophene. A novel, highly potent selective estrogen receptor modulator. J Med Chem 40:1407–1417

Scholl SM, Huff KK, Lippman ME (1983) Antiestrogenic effects of LY117018 in MCF-7 cells. Endocrinology 112:611–617

Thompson EW, Reich R, Shima TB, Albini A, Graf J, Martin GR, Dickson MB, Lippman ME (1984) Differential growth and invasiveness of MCF-7 breast cancer cells by antiestrogens. Cancer Res 48:6764–6768

Zacharewski T (1997) *In vitro* bioassays for assessing estrogenic substances. Environ Sci Technol 31:613–623

N.3.1.2 In Vivo Methods

N.3.1.2.1 Vaginal Cornification Assay

PURPOSE AND RATIONALE

This is an early bioassay for estrogenic activity based on epithelial proliferation. The Allen-Doisy test for vaginal cornification in rodents (Allen and Doisy 1923) is based on the observations of Stockard and Papanicolaou (1917), who first reported the cyclic cornification of the vaginal epithelium in guinea pigs.

PROCEDURE

Immature female Sprague-Dawley rats weighing about 55 g are ovariectomized. They are kept for about 1 week on standard laboratory diet and water ad libitum. The test compounds are administered orally or subcutaneously in 0.5% solution of carboxymethylcellulose or in cotton seed oil injected at several doses to groups of 10–20 rats. Doses of 0.02, 0.1, and 0.5 µg estradiol per animal are used as standard. The compounds are dosed twice daily, for example, on two following days at 10:00 a.m. and 5:00 p.m. At 5:00 p.m. of the third day and at 10:00 a.m. of the fourth day vaginal smears are taken using cotton swabs moistened with saline. The smears are transferred to a glass slide and stained for 10 min with 5% aqueous methylene blue solution. They are evaluated microscopically according to the following scores:

0 diestrus smear, mainly leukocytes, few epithelia cells
1 mixture of leukocytes and epithelial cells
2 proestrus smear, nucleated or nucleated plus cornified cells
3 estrus smear, cornified cells only.

Only animals showing a score of 2 or 3 of cornification are considered to be positive.

EVALUATION

The number of positive animals in each dosage group is recorded. ED_{50} values are calculated and potency ratios compared with the standard estradiol may be determined.

MODIFICATIONS OF THE METHOD

The sensitivity of the assay is increased by local vaginal application of estrogens in ovariectomized rats or mice (Emmens 1969).

REFERENCES AND FURTHER READING

Allen E, Doisy EA (1923) An ovarian hormone. Preliminary report on its localization, extraction and partial purification, and action in test animals. J Am Med Assoc 81:819–821

Eisler M (1964) Animal techniques for evaluating sex steroids. In: Nodine JH, Siegler PE (eds) Animal and clinical pharmacologic techniques in drug evaluation. Year Book Medical Publishers, Chicago, Ill., pp 566–573

Emmens CW (1969) Estrogens. In: Dorfman RI (ed) Methods in hormone research, Vol IIA. Academic Press, New York, pp 61–120

Stockard CR, Papanicolaou GN (1917) The existence of a typical oestrus cycle in the guinea-pig – with a study of its histological and physiological changes. Am J Anat 22:225–283

Zondek B (1935) Die Brunstreaktion der Nagetiere als Testobjekt zum Nachweis des weiblichen Sexualhormones. In: Zondek B (ed) Hormone des Ovariums und des Hypophysenvorderlappens. Springer, Berlin Heidelberg New York, pp 23–33

N.3.1.2.2 Uterine Weight Assay

PURPOSE AND RATIONALE

This is an early bioassay for estrogenic activity based on myometrial/endometrial proliferation. Repeated administration of estrogens induces a dose-dependent increase of uterine weight in ovariectomized rats.

PROCEDURE

Immature female Sprague-Dawley rats weighing about 55 g are ovariectomized. Groups of five to ten animals are injected daily with several doses of the test compound or the standard (estradiol 0.03 to 0.06 µg per animal s.c.) for 7 days. The test compound is administered orally or subcutaneously in 0.5% solution of carboxymethylcellulose or in cotton seed oil. Controls receive the vehicle. On the 8th day, the animals are sacrificed and uterine weights determined.

EVALUATION

Dose–response curves are established and potency ratios are calculated, using at least two doses of test compound and oestradiol standard.

Similar studies were reported by: Zondek 1935; Junkmann 1957; Emmens 1969; Nishino et al. 1991; Van de Velde et al. 1994)

MODIFICATIONS OF THE METHOD

Rubin et al. (1951) used albino mice 23–25 days of age weighing approximately 8 g. The mice are given subcutaneous injections once daily for 3 days of an oil solution of the hormone. Then, 24 h after the last injection, the animals are sacrificed and uterine and body weights recorded. The uterine ratio is calculated by dividing uterine weight in milligrams by body weight in grams, multiplied by 100 (relative uterine weight). Two groups receive a standard preparation and two groups the unknown.

Bhakoo and Katzenellenbogen (1977) showed that one of the earliest biosynthetic tissue responses after estrogen binding in the rat uterus, the synthesis of a specific uterine protein called “induced protein”, is antagonized by progesterone.

In addition to uterus weight, Branham et al. (1993) studied luminal and glandular epithelium height in cross-sections of the uterine horns of rats by histomorphology.

Uterine peroxidase activity was proposed as a marker for estrogen action by Lyttle and DeSombre (1977) and Astroff and Safe (1991).

Odum et al. (1997) compared the rodent uterotrophic assay with a yeast estrogenicity assay.

REFERENCES AND FURTHER READING

Astroff B, Safe S (1991) 6-Alkyl-1,3,8-trichlorodibenzofurans as antiestrogens in female Sprague-Dawley rats. Toxicology 69:187–197

Bhakoo HS, Katzenellenbogen B (1977) Progesterone antagonism of estradiol-stimulated uterine ‘induced protein’ synthesis. Mol Cell Endocrinol 8:105–120

Branham W, Zehr DR, Sheehan DM (1993) Differential sensitivity of rat uterine growth and epithelium hypertrophy to estrogens and antiestrogens. Proc Soc Exp Biol Med 203:297–303

Emmens CW (1969) Estrogens. In: Dorfman RI (ed) Methods in hormone research, Vol IIA. Academic Press, New York, pp 61–120

Junkmann K (1957) Long-acting steroids in reproduction. Rec Progr Horm Res 13:389–427

Lyttle CR, DeSombre ER (1977) Uterine peroxidase as a marker of estrogen action. Proc Natl Acad Sci USA 74:3162–3166

Nishino Y, Schneider MR, Michna H, von Angerer E (1991) Pharmacological characterization of a novel oestrogen antagonist, ZK 119010, in rats and mice. J Endocrinol 130:409–414

Odum J, Lefevre PA, Tittensor S, Paton D, Routledge EJ, Beresford NA, Sumpter PJ, Ashby J (1997) The rodent uterotrophic assay: critical protocol features, studies with nonyl phenols, and comparison with a yeast estrogenicity assay. Regul Toxicol Pharmacol 25:178–188

Rubin BL, Dorfman AS, Black L, Dorfman RI (1951) Bioassay of estrogens using mouse uterine response. Endocrinology 49:429–439

Van de Velde O, Nique F, Bouchoux F, Brémaud J, Hameau MC, Lucas D, Moratille C, Viet S, Philibert D, Teutsch G (1994) RU 58 668, a new pure antiestrogen inducing a regression of human mammary carcinoma implanted in nude mice. J Steroid Biochem Mol Biol 48:187–196

Zondek B (1935) Das Wachstum des Uterus als Testobjekt zum Nachweis des weiblichen Sexualhormons (Ovarialhormon) In: Zondek B (ed) Hormone des Ovariums und des Hypophysenvorderlappens. Springer, Berlin Heidelberg New York, pp 10–16

N.3.1.2.3 Chick Oviduct Method

PURPOSE AND RATIONALE

This is an early bioassay for estrogenic activity based on proliferation of the oviduct. The weight of the oviduct of young chickens is increased dose depen-

dently by natural and synthetic estrogens (Tullner and Hertz 1956; Lerner et al. 1958; Dorfmann 1969).

PROCEDURE

Seven-day-old pullet chicks are injected subcutaneously twice daily with solutions of the test compound in various doses for 6 days. Doses between 0.02 and 0.5 µg estradiol-17β per animal serve as standard. Six to ten chicks are used for each dosage group. On the day after the last injection, the animals are sacrificed and the weights of the body and oviduct determined.

EVALUATION

The ratio oviduct weight/body weight is calculated for each animal (relative weight). Mean values are plotted as dose–response curves in order to calculate potency ratios.

MODIFICATION OF THE METHOD

The assay was used for evaluation of anti-estrogenic activity using simultaneous injection of 0.6 µg estradiol-17β 1 and the inhibitor, e. g., progestagens, and calculation of the percentage of oviduct weight in estrogen/anti-estrogen-treated animals versus the estrogen control group.

REFERENCES AND FURTHER READING

Dorfman RI (1969) Antiestrogens. In: Dorfman RI (ed) Methods in hormone research, Vol IIA. Academic Press, New York, pp 121–149

Lerner LJ, Holthaus FJ Jr, Thompson CR (1958) A non-steroidal estrogen antagonist 1-(*p*-2-diethylaminoethoxyphenyl)-1-phenyl-2-*p*-methoxyphenyl ethanol. Endocrinology 63:295–318

Tullner WW, Hertz R (1956) The effect of 17-alpha-hydroxy-11-desoxycorticosterone on estrogen-stimulated chick oviduct growth. Endocrinology 58:282–283

N.3.1.3 Anti-Estrogenic Activity

N.3.1.3.1 Antagonism of Estrogen Effect on Uterus Weight

PURPOSE AND RATIONALE

These assays are modifications of estrogen bioassays. The effect of estrogen treatment on uterine weight in ovariectomized rats was antagonized by anti-estrogenic compounds.

PROCEDURE

Immature female Sprague-Dawley rats weighing about 55 g are ovariectomized. Groups of five to ten animals are injected daily for 7 days with estradiol 0.03 to 0.06 µg per animal s.c. and various doses of the test compound or estradiol alone. The test compound is administered in 0.5% solution of carboxymethylcellulose or in cotton seed oil either orally or injected subcutaneously. On day 8, the weight of the uterus is determined and the inhibitory effect of anti-estrogenic compounds is assessed.

EVALUATION

The anti-estrogenic effect is expressed as a percentage reduction of estrogen-stimulated uterine weight by test compounds.

Similar studies were reported by: Byrnes and Shipley 1955; Dorfmann 1969; Terenius 1971; Wakeling and Bowler 1988; Levesque et al. 1991; Kangas 1992; Nique et al. 1994)

MODIFICATIONS OF THE METHOD

Three-week old female NMRI mice can be used for determination of uterus weight (Lerner et al. 1958).

The inhibition by anti-estrogens of vaginal cornification induced by estradiol can be used as the assessment parameter.

The chick oviduct weight can be adapted for the assay of anti-estrogenic activity (Tullner and Hertz 1956).

Anti-estrogenic activity may also be determined in castrated immature male rats. The animals show an increase in seminal vesicle weight when treated with 20 µg estradiol for 5 days, and the effect is counteracted by anti-estrogenic steroids (Byrnes et al. 1953).

REFERENCES AND FURTHER READING

Byrnes WW, Shipley EG (1955) Guinea pig copulatory reflex in response to adrenal steroids and similar compounds. Endocrinology 57:5–9

Byrnes WW, Stafford RO, Olson KJ (1953) Anti-gonadal hormone activity of 11α-hydroxyprogesterone. Proc Soc Exp Biol Med 82:243–247

Dorfman RI (1969) Antiestrogens. In: Dorfman RI (ed) Methods in hormone research, Vol IIA. Academic Press, New York, pp 121–149

Kangas L (1992) Agonistic and antagonistic effects of antiestrogens in different target organs. Acta Oncol 31:143–146

Lerner LJ, Holthaus FJ Jr, Thompson CR (1958) A non-steroidal estrogen antagonist 1-(*p*-2-diethylaminoethoxyphenyl)-1-phenyl-2-*p*-methoxyphenyl ethanol. Endocrinology 63:295–318

Levesque C, Merand Y, Dufour JM, Labrie C, Labrie F (1991) Synthesis and biological activity of new halo-steroidal antiestrogens. J Med Chem 34:1624–1630

Nique F, Van de Velde P, Brémaud J, Hardy M, Philibert D, Teutsch G (1994) 11β-Amidoalkoxyphenyl estradiols, a new series of pure antiestrogens. J Steroid Biochem Mol Biol 50:21–29

Terenius L (1971) Structure–activity relationships of anti-oestrogens with regard to interaction with 17β-oestradiol in

the mouse uterus and vagina. Acta Endocrinol 66:431–447
Tullner WW, Hertz R (1956) The effect of 17-alpha-hydroxy-11-desoxycorticosterone on estrogen-stimulated chick oviduct growth. Endocrinology 58:282–283
Wakeling AE, Bowler J (1988) Novel antiestrogens without partial agonistic activity. J Steroid Biochem 31:645–653

N.3.1.3.2 Aromatase Inhibition

PURPOSE AND RATIONALE

Estrogen synthesis by local action of the enzyme aromatase occurs in various tissues, and is also found in estrogen-dependent tumors (Brodie 1992). Specific aromatase (estrogen synthetase) inhibitors are potential therapeutic agent for estrogen-dependent tumors, e. g., some breast cancers. 4-Hydroxyandrostandione (4-OHA) inhibits aromatase completely but also causes destruction of the enzyme (irreversible inhibitor). Test compounds can be evaluated both *in vitro* (Häusler et al. 1989) and *in vivo* (Geelen et al. 1991). Tests are based on stimulation of estrogen biosynthesis by luteinizing hormone (LH) and inhibition of this effect by aromatase inhibitors.

PROCEDURE

For *in vitro* experiments, ovarian tissue from adult golden hamsters (*Mesocricetus auratus*) is used. Estrus cycle is monitored for at least three consecutive 4-day estrus cycles prior to the experiment. The experiments for evaluating inhibitor effects are performed with ovaries obtained from animals sacrificed on day 4 (proestrus), at the time of preferred estrogen synthesis. The ovaries are excised, freed from adhering fat tissue, and quartered. The quarters are transferred to plastic incubation flasks with 2 ml of Krebs-Ringer-bicarbonate (KBR) salt solution, pH 7.6, containing 8.4 mM glucose. The flasks are gassed with O_2/CO_2 (95%/5%), tightly closed, and placed in a shaker/water bath (37°C) for incubation of the fragments. The incubation media are replaced with fresh KBR after preincubation for 1 h.

The ovaries are further incubated for 4 h in the presence or absence of ovine LH (100 ng/ml) and inhibitors to be tested. 4-OH-Androstendione is used as standard in concentrations between 0.33 and 330 µM. At the end of the experiment, the incubation media are removed and centrifuged. In the supernatant, estrogen, progesterone, and testosterone are determined by radioimmunoassay.

EVALUATION

The results are expressed as percentage inhibition of oestradiol synthesis relative to control incubations containing 100 ng/ml LH in the absence of inhibitor. Statistical analyses are performed using Dunnetts's *t*-test.

MODIFICATIONS OF THE METHOD

Geelen et al. (1991) determined the *in vivo* aromatase activity of test compounds in hypophysectomized rats treated with the estrogen precursor dehydroepiandrosterone (DHEA) sulfate, using the inhibition of cornification of vaginal epithelium and estradiol levels in plasma as parameters. Furthermore, aromatase activity was determined in homogenized ovaries. To the supernatant, [1β-^{3}H]androst-4-ene-3,17-dione was added. Incubation was performed with a NADPH-generating system for 1 h at 37°C. Incubations were terminated by placing the tubes on ice followed by an extraction with chloroform. After phase separation by centrifugation, the aqueous phase was diluted with an equal volume of dextran-coated charcoal suspension. Following centrifugation, the ^3H_2O content was determined by liquid scintillation counting. The amount of ^3H_2O is a measure of the amount of estrogen produced.

Zaccheo et al. (1989) studied the antitumor activity of aromatase inhibitors in rats with tumors induced by 7,12-dimethylbenzanthracene (DMBA).

Wouters et al. (1993) studied the inhibition of aromatase activity in FSH-stimulated rat granulosa cells by vorozole, a selective, nonsteroidal aromatase inhibitor.

Suzuki et al. (1996) described changes in prostate volume and histopathological findings in androstenedione-treated castrated beagle dogs as a bioassay for an aromatase inhibitor.

Takahashi et al. (1997) tested the inhibition of aromatase activity in the microsomes from fresh human placentae by the amount of tritiated water released from [1β-^{3}H]androstenedione. For biological proof, the dose-dependent suppression of androstenedione-induced uterine hypertrophy in immature rats was measured.

REFERENCES AND FURTHER READING

Brodie A (1991) Aromatase and its inhibitors – an overview. J Steroid Biochem Mol Biol 40:255–261
Geelen JAA, Deckers GH, van der Wardt JTH, Loozen HJJ, Tax LJW, Kloosterboer HJ (1991) Selection of 19-(ethyldithio)-andro-4-ene-3,17-dione (ORG 30958): a potent aromatase inhibitor *in vivo*. J Steroid Biochem Mol Biol 38:181–188
Häusler A, Schenkel L, Krähenbühl C, Monnet G, Bhatnagar AS (1989) An *in vitro* method to determine the selective

inhibition of estrogen biosynthesis by aromatase inhibitors. J Steroid Biochem 33:125–131
Suzuki K, Ito K, Tamura Y, Suzuki T, Honma S, Yamanaka H (1996) Effect of an aromatase inhibitor, TZA-2209, on the prostate of androstenedione-treated castrated dogs. Prostate 28:328–337
Takahashi M, Kyo T, Karakida T, Nakagawa S, Kato M, Matsuno S, Koide Y, Sakato M, Kawashima S (1997) Potent and selective aromatase inhibitor: *in vitro* and *in vivo* studies with s-triazine derivative SEF19. Endocr Res 23:1–13
Wouters W, Van Ginckel R, Krekels M, Bowden C, De Coster R (1993) Pharmacology of vorozole. J Steroid Biochem Mol Biol 44:617–621
Zaccheo T, Giudici D, Lombard P, di Salle E (1989) A new irreversible aromatase inhibitor, 6-methylenandrosta-1,4,-diene-3,17-dione (FCE 24304): antitumor activity and endocrine effects in rats with DMBA-induced mammary tumors. Cancer Chemother Pharmacol 23:47–50

N.3.1.3.3 Anti-Estrogenic Effect on MCF-7 Breast Cancer Cells

PURPOSE AND RATIONALE

The MCF-7 cell line, derived from a pleural effusion of a malignant breast cancer, is a widely studied model for hormone-dependent human breast cancer. These cells contain functional estrogen receptors and show a pleiotropic response to estrogen which can be used to evaluate anti-estrogenic effects (Miller and Katzenellenbogen 1983; Scholl et al. 1983; Thompson et al. 1988). The MCF-7 cells proliferate and invade through an artificial basement membrane. Anti-estrogens reduce both the proliferation and invasiveness of MCF-7 cells.

PROCEDURE

MCF-7 cells are maintained in T75 flasks in IMEM (Biofluids, Rockville, Md., USA) supplemented with 2 mM glutamine and 10% fetal bovine serum. To deplete estrogen, the cells are passaged for at least 2 weeks in IMEM supplemented with 5% calf serum which has been treated sequentially with sulfatase and dextran-coated charcoal (DCC) to remove endogenous estrogen.

Estrogen and Anti-Estrogen Treatment

Cells are trypsinized, reseeded in tissue culture dishes (1×10^6 cells/10-cm-diameter Falcon dish), and allowed to adhere overnight in a humidified incubator (37°C, 5% CO_2, 95% air). The cells are treated the next day with either 17β-estradiol (10^{-9} M) or the anti-estrogen or 0.1% ethanol alone. Four days later, the cells are harvested with trypsin, washed twice in IMEM containing 0.1% BSA, counted with a Coulter cell counter and tested for chemotaxis and chemoinvasion activities.

Chemoinvasion Assay

Boyden chambers are used (Albini et al. 1987). Polycarbonate filters (12-µm pore, polyvinylpyrrolidone-free, Nucleopore) are coated with matrigel (25 µg/filter), a mixture of basement membrane components (Kleinman et al. 1986), which is dried and then reconstituted at 37°C into a solid, even layer over the surface of the filter. Fibroblast-conditioned medium, obtained by incubating confluent NIH-3T3 cells for 24 h with IMEM, is used as the chemoattractant. Cells are harvested with trypsin, washed twice with BSA/IMEM, and added to the top chamber (300,000 cells/chamber). Chambers are incubated in a humidified incubator at 37°C in 5% CO_2 in air for 6, 9, or 12 h. The cells which have traversed the matrigel and attached to the lower surface of the filter are stained with Diff-Quick (American Scientific Products) and quantitated electronically with the Optimax V image analyzer.

Chemotaxis Assay

Chemotaxis assays are performed as described for the chemoinvasion studies with the single exception that the filter surfaces are coated with 5 µg collagen IV instead of the layer of matrigel. This coats the interstices of the filters but does not form a barrier over the surface. Chemotaxis assays are performed in parallel to the chemoinvasion assays using the same cells and conditioned medium.

EVALUATION

One-way analysis of variance is performed on the data from each experiment.

REFERENCES AND FURTHER READING

Albini A, Iwamoto Y, Kleinman HK, Martin GR, Aaronson SA, Kozlowski JM, McEwan RM (1987) A rapid *in vitro* assay for quantitating the invasive potential of tumor cells. Cancer Res 47:3239–3245
Kleinman HK, McGarvey ML, Hassel JR, Star VL, Cannon FB, Laurie GW, Martin GR (1986) Basement membrane complexes with biological activity. Biochemistry 25:312–318
Miller MA, Katzenellenbogen BS (1983) Characterization and quantitation of antiestrogen binding sites in estrogen receptor-positive and -negative human breast cancer cell lines. Cancer Res 43:3094–3100
Scholl SM, Huff KK, Lippman ME (1983) Antiestrogenic effects of LY 117018 in MCF-7 cells. Endocrinology 113:611–617
Thompson EW, Reich R, Shima TB, Albini A, Graf J, Martin GR, Dickson RB, Lippman ME (1988) Differential regulation of growth and invasiveness of MCF-7 breast cancer cells by antiestrogens. Cancer Res 48:6764–6768

N.3.2 Progestional Activity

N.3.2.1 In Vitro Methods

N.3.2.1.1 Gestagen Receptor Binding

PURPOSE AND RATIONALE

Progesterone receptor preparations may be obtained from numerous sources of tissue: uteri from estrogen-primed rabbits (Ojasoo and Raynaud 1978; Boonkasemsanti et al. 1989; Phillips et al. 1990; Cook et al. 1992), castrated-estrogen-treated mice or rats (Philibert and Raynaud 1977; Li et al. 1997), MCF-7 cells derived from human breast tumor (Bergink et al. 1983; Kloosterboer et al. 1988a, 1988b, 1994), breast cancer T47D cells (Meyer et al. 1990), the quail fibroblast cell line QT6 (Schowalter et al. 1991) or human uteri obtained after hysterectomy (Jänne et al. 1976; Pollow et al. 1989a, 1989b, 1992). Tritium-labeled progesterone and R 5020 ([6,7-^{3}H]17,21-dimethyl-19-norpregna-4,9-diene-3,20-dione) are used as ligands (Moguilewsky and Raynaud 1979).

PROCEDURE

Relative Binding Affinities

Human uteri obtained after hysterectomy are snap-frozen in liquid nitrogen and stored at −80°C until use. For cytosol preparations, uterine tissues are minced and homogenized with an Ultra-Turrax at 0–4°C in ice-cold buffer composed of 10 mM KH_2PO_4, 10 mM K_2HPO_4, 1.5 mM EDTA, 3 mM NaN_3, 10% glycerol, pH 7.5 (PENG buffer). The homogenates are then centrifuged at 105,000 *g* at 4°C for 30 min. The supernatant is taken as cytosol. The cytosol preparations are incubated with ^{3}H-R 5020 as radioligand at a concentration of 8 nmol/l and increasing concentrations (1×10^{-10} to 1×10^{-5} mol/l) of the competitor steroids overnight at 4°C. Then, unbound steroids are adsorbed by incubating with 0.5 ml of DCC (0.5% Norit A, 0.05% dextran T400 in PENG buffer) for 10 min at 4°C. After centrifugation (10 min at 1500 *g* at 4°C) 0.5 ml of the supernatant is withdrawn and counted for radioactivity.

Association rate and dissociation rate are determined as described for the estrogen receptor.

EVALUATION

For calculation of **relative binding affinity**, the percentage of radioligand bound in the presence of competitor compared to that bound in its absence is plotted against the concentration of unlabeled steroid. A standard curve for the unlabeled radioligand (progesterone) is constructed with of nine to ten concentrations; five or six concentrations of the competitor are tested. The molar concentrations of unlabeled radioligand and steroid competitors that reduce radioligand binding by 50% are determined. The ratio of unlabeled radioligand and competitor for 50% competition multiplied by 100 is calculated for relative binding affinity.

Association rate (k_{+1}) is calculated by the slope of the line

$$k_{+1}t = (2.3/E_0 - R_0)\log(E\,R_0/R\,E_0)$$

where E_0 and E represent free steroid and R_0 and R free receptor at time $t = 0$ and time t, respectively.

Dissociation rate (k_{-1}) is calculated from the slope of the line

$$k_{-1} = -2.3\log B/B_0$$

where B_0 and B represent bound steroid at time $t = 0$ and time t, respectively.

MODIFICATIONS OF THE METHOD

For screening procedures homogenates of rabbit uteri may be used (Philibert et al. 1977).

The binding of the progesterone agonist R 5020 and of the progesterone antagonist RU 486 to the progesterone receptor from calf uterus was characterized by Hurd and Moudgil (1988).

A high-affinity ligand and novel photoaffinity labeling reagent for the progesterone receptor ([^{3}H]DU41165) was described by Pinney et al. (1990).

The different DNA-binding properties of the calf uterine estrogen and progesterone receptors were explained by different dimerization constants (Skafar 1991).

Mutations of the progesterone receptor were found to be responsible for species specificity and have been used for evaluation of agonistic and antagonistic activity (Benhamou et al. 1992; Garcia et al. 1992).

The complete amino acid sequence of the human progesterone receptor has been deduced from cloned cDNA by Misrani et al. (1987).

Structural requirements of the ligand and mapping of the hormone-binding site of the progestin receptor have been discussed by Ojasoo and Raynaud (1990).

Allan et al. (1992) studied conformational changes in the ligand-binding domain induced by various progestins and antiprogestins.

Collins (1994) recommended the ratio between the affinity of a compound to progesterone receptors to the

affinity to androgen receptors as a selection criterion for new oral contraceptives.

Comparative pharmacology of newer progestagens has been reviewed by Kuhl (1996).

Oñate et al. (1994) found that the DNA-binding protein HMG-1 enhances progesterone receptor binding to its target DNA sequences.

The concept of two categories of progestin antagonists based on differences in how they interact with and inactivate the progestin receptor has been discussed by Edwards et al. (1995).

Carbajo et al. (1996) studied the binding of [^{3}H]progesterone to the human progesterone receptor existing in two isoforms hPR-A and hPR-B which differ in that hPR-A lacks 164 amino acids at the amino terminus of hPR-B.

REFERENCES AND FURTHER READING

Allan GF, Leng X, Tsai SY, Weigel NL, Edwards DP, Tsai M-J, O'Malley BW (1992) Hormone and antihormone induce distinct conformational changes which are central to steroid receptor activation. J Biol Chem 287:19513–19520

Bélanger A, Philibert D, Teutsch G (1981) Regio- and stereospecific synthesis of 11β-substituted 19-norsteroids. Steroids 37:361–382

Benhamou B, Garcia T, Lerouge T, Vergezac A, Gofflo D, Bigogne C, Chambon P, Gronemeyer H (1992) A single amino acid that determines the sensitivity of progesterone receptors to RU486. Science 255:206–209

Bergink EW, van Meel F, Turpijn EW, van der Vies J (1983) Binding of progestagens to receptor proteins in MCF-7 cells. J Steroid Biochem 19:1563–1570

Boonkasemsanti W, Aedo AR, Cekan SZ (1989) Relative affinity of various progestins and antiprogestins to a rabbit myometrium receptor. Arzneimittelforschung 39:195–199

Carbajo P, Christensen K, Edwards DP, Skafar DF (1996) Binding of [^{3}H]progesterone to the human progesterone receptors: differences between individual and mixed isoforms. Endocrinology 137:2339–2346

Collins DC (1994) Sex hormone receptor binding, progestin selectivity, and the new oral contraceptives. Am J Obstet Gynecol 170:1508–1513

Cook CA, Wani MC, Lee YW, Fail PA, Petrow V (1992) Reversal of activity profile in analogs of the antiprogestin RU 486: effect of a 16α-substituent on progestional (agonist) activity. Life Sci 52:155–162

Cook CE, Lee YW, Wani MC, Fail PA, Petrow V (1994) Effects of D-ring substituents on antiprogestional (antagonist) and progestional (agonist) activity of 11β-aryl steroids. Human Reprod 9 [Suppl 1]:32–39

Edwards DP, Altmann M, DeMarzo A, Zhang Y, Weigel NL, Beck CA (1995) Progesterone receptor and the mechanisms of action of progesterone antagonists. J Steroid Biochem Mol Biol 53:449–458

Garcia T, Benhamou B, Gofflo D, Vergezac A, Philibert D, Chambon P, Gronemeyer H (1992) Switching agonistic, antagonistic, and mixed transcriptional responses to 11β-substituted progestins by mutation of the progesterone receptor. Mol Endocrinol 6:2071–2078

Hurd C, Moudgil VK (1988) Characterization of R5020 and RU486 binding to progesterone receptor from calf uterus. Biochemistry 27:3618–3623

Jänne O, Kontula K, Vihko R (1976) Progestin receptors in human tissues: concentration and binding kinetics. J Steroid Biochem 7:1061–1068

Kloosterboer HJ, Deckers GHJ, van der Heuvel MJ, Loozen HJJ (1988a) Screening for antiprogestagens by receptor studies and bioassays. J Steroid Biochem 31:567–571

Kloosterboer HJ, Vonk-Noordegraaf CA, Turpijn EW (1988b) Selectivity in progesterone and androgen receptor binding of progestagens used in oral contraceptives. Contraception 38:325–332

Kloosterboer HJ, Deckers GH, Schoonen WGEJ (1994) Pharmacology of two new very selective antiprogestagens: Org 31710 and Org 31806. Human Reprod 9 [Suppl 1]:47–52

Kontula K, Jänne O, Vihko R, de Jager E, de Visser J, Zeelen F (1975) Progesterone binding proteins: *in vitro* binding and biological activity of different steroidal ligands. Acta Endocrinol 78:574–592

Kuhl H (1996) Comparative pharmacology of newer progestagens. Drugs 51:188–215

Li F, Kumar N, TsongY-Y, Monder C, Bardin CW (1997) Synthesis and progestional activity of 16-methylene-17α-hydroxy-19-norpregn-4-ene-3,20-dione and its derivatives. Steroids 62:403–408

Meyer ME, Pornon A, Ji J, Bocquel MT, Chambon P, Gronemeyer H (1990) Agonistic and antagonistic activities of RU486 on the functions of the human progesterone receptor. EMBO J 9:3923–3932

Misrani M, Atger M, d'Auriol L, Loosfelt H, Meriel C, Fridlansky F, Guiochon-Mantel A, Galibert F, Milgrom E (1987) Complete amino acid sequence of the human progesterone receptor deduced from cloned cDNA. Biochem Biophys Res Commun 143:740–748

Moguilewsky M, Raynaud JP (1979) Estrogen-sensitive progestin-binding sites in the female rat brain and pituitary. Brain Res 164:165–175

Ojasoo T, Raynaud JP (1978) Unique steroid congeners for receptor studies. Cancer Res 38:4186–4198

Ojasoo T, Raynaud JP (1990) Steroid hormone receptors. Binding to the progestin receptor. Structural requirements of the ligand and mapping of the hormone-binding site. In: Emmet E, Hansch C (eds) Comprehensive medicinal chemistry, Vol 3. Pergamon, New York, pp 1200–1207

Oñate SA, Pendergast P, Wagner PJ, Nissen M, Reeves R, Pettijohn DE, Edwards DE (1994) The DNA-binding protein HMG-1 enhances progesterone receptor binding to its target DNA sequences. Mol Cell Biol 14:3376–3391

Philibert D, Raynaud JP (1977) Cytoplasmatic progestin receptors in mouse uterus. In: McGuire WL, Raynaud JP, Baulieu EE (eds) Progress in cancer research and therapy, Vol 4. Progesterone receptors in normal and neoplastic tissues. Raven, New York, pp 227–243

Philibert D, Ojasoo T, Raynaud JP (1977) Properties of the cytoplasmatic progestin-binding protein in the rabbit uterus. Endocrinology 101:1850–1861

Phillips A, Demarest K, Hahn DW, Wong F, McGuire JL (1990) Progestional and androgenic receptor binding affinities and *in vivo* activities of norgestimate and other progestins. Contraception 41:399–410

Pinney KG, Carlson KE, Katzenellenbogen JA (1990) [^{3}H]DU41165: A high affinity ligand and novel photoaffinity labeling reagent for the progesterone receptor. J Steroid Biochem 35:179–189

Pollow K, Juchem M, Grill HJ, Elger W, Beier S, Henderson D, Schmidt-Gollwitzer K, Manz B (1989a) Gestodene: a novel synthetic progestin-characterization of binding to receptor and serum proteins. Contraception 40:325–341

Pollow K, Juchem M, Grill HJ, Manz B, Beier S, Henderson D, Schmidt-Gollwitzer K, Elger W (1989b) ^{3}H-ZK 98,734, a new 11β-aryl substituted antigestagen: binding characteristics to receptor and serum proteins. Contraception 40:213–232

Pollow K, Juchem M, Elger W, Jacobi N, Hoffmann G, Möbus V (1992) Dihydrospirorenone (ZK 30595): a novel synthetic progestagen – characterization of binding to different receptor proteins. Contraception 46:561–574

Reel JR, Humphrey RR, Shih YH, Windsor BL, Sakowski R, Creger PL, Edgren RA (1979) Competitive progesterone antagonists: receptor binding and biological activity of testosterone and 19-nortestosterone derivatives. Fertil Steril 31:552–561

Savouret JF, Chauchereau A, Misrahi M, Lescop P, Mantel A, Bailly A, Milgrom E (1994) The progesterone receptor: biological effects of progestins and antiprogestins. Hum Reprod 9 [Suppl 1]:7–11

Schowalter DB, Sullivan WP, Maihle NJ, Dobson ADW, Conneely OM, O'Malley BW, Toft DO (1991) Characterization of progesterone receptor binding to the 90- and 70-kDa heat shock proteins. J Biol Chem 266:21165–21173

Seth NM, Bhaduri AP (1986) Progesterone binding of steroidal and nonsteroidal compounds. In: Jucker E (ed) Progress in drug research, Vol 30. Birkhäuser, Basel, pp 151–188

Skafar DF (1991) Differential DNA binding by calf uterine estrogen and progesterone receptors results from differences in oligomeric states. Biochemistry 30:6148–6154

Snyder BW, Beecham GD, Winneker RC (1989) Studies on the mechanism of action of danazole and gestrinone (R2323) in the rat: evidence for a masked estrogen component. Fertil Steril 51:705–710

Theofan G, Notides AC (1984) Characterization of the calf uterine progesterone receptor and its stabilization by nucleic acids. Endocrinology 114:1173–1179

N.3.2.1.2 Transactivation Assay for Gestagens

PURPOSE AND RATIONALE

Steroid agonistic and antagonistic properties can be evaluated by transactivation assays (Muhn et al. 1995; Fuhrmann et al. 1996). The transactivation assay assumes that steroid receptor proteins act as ligand-regulated transcriptional activators. After binding of hormone, the steroid receptor acts with hormone-responsive elements of hormone-regulated genes, thereby inducing a cascade of transcriptional events (Green and Chambon 1988).

Transactivation assays were used by several authors to test the progestional and antiprogestional activity of steroidal and nonsteroidal compounds (Sobek et al. 1994; Pathirana et al. 1995; Fuhrmann et al. 1996; Jones et al. 1996; Dijkema et al. 1998; Edwards et al. 1998; Schoonen et al. 1998; Zhi et al. 1998).

PROCEDURE

CV-1 cells (African green monkey kidney fibroblasts) are grown in Dulbecco's modified Eagle medium containing 10% charcoal resin-stripped fetal bovine serum, 2 mM glutamine, and 55 µg/ml gentamicin. Cells are maintained in an environment of 4% carbon dioxide and routinely passaged from T-255 flasks to 96-well microtiter plates (1.5×10^5 cells/well, 70% confluent) 1 day before transfection.

Cells are transiently transfected by the standard calcium phosphate co-precipitation procedure with 50 ng/well of plasmids coding for: human progesterone receptor-B (hPR-B1) and pRS-β-Gal under constitutive control and a reporter (MTV-LUC) containing a response element for the progesterone receptor. After 6 h, the medium is replaced with medium containing progesterone at concentrations between 10^{-11} and 10^{-5} M or another progestagen. After a 40-h incubation, wells are washed with phosphate-buffered saline and the cells are lysed with Triton X-100-based buffer. An aliquot of lysate (20 µl) is then transferred to Dynatech 96-well plates containing 1.6 mM ATP. LUC activity (chemiluminescence upon addition of luciferin substrate) is determined using a Dynatech ML1000 luminometer, according to the equation:

$$\text{LUC units} = \text{relative LUC unit} \times 10^4 .$$

β-Gal activity is determined from the remaining lysate in the original 96-well plates. The substrate, *o*-nitrophenol-β-galactoside, is added to the plates, followed by incubation at 37°C. The incubation is terminated by addition of sodium carbonate when the average absorbance, as determined by visual observation of the yellow product (*o*-nitrophenol), is within a standard range. Absorbance at a wavelength of 415 nm is then quantified spectrophotometrically. β-Gal rates are calculated according to the following equation:

$$\beta\text{-Gal rate} = \frac{\beta\text{-Gal absorbance} \times 10^5}{\beta\text{-Gal incubation time}} .$$

For each set of replicate wells, normalized response is calculated according the following equation:

$$\text{Normalized response} = \text{LUC units}/\beta\text{-Gal rate}$$

EVALUATION

Agonist activity is determined by examining the amount of LUC expression (normalized response). The effective concentration that produces 50% of the maximal response (EC_{50}) is quantified. The efficacy is a function of the LUC expression relative to the maximal LUC expression produced by the reference agonist, e. g., progesterone. Antagonist activity is determined by testing the amount of LUC expression in

the presence of a fixed concentration (equal to its agonist EC_{50}) of reference agonist. The concentration of test compound that inhibits the gene expression induced by the reference compound by 50% is quantified (IC_{50}). In addition, the efficacy of antagonists is determined as a function of maximal inhibition (LUC expression = basal activity).

CRITICAL ASSESSMENT OF THE METHOD

See Sect. N.2.1.1.2. for the importance of controlling transfection efficacy.

MODIFICATIONS OF THE METHOD

For transactivation studies, hPRA-A-MMTV-LUC and hPR-B-MMTV-LUC and stably co-transfected CHO cells were used by Dijekema et al. (1998) and Schoonen et al. (1998).

REFERENCES AND FURTHER READING

Dijkema R, Schoonen WEG, Teuwen R, van der Struik E, de Ries RJH, van der Kar BAT, Olijve W (1998) Human receptor A and B isoforms in CHO cells. I. Stable transfection of receptor and receptor-responsive reporter genes: transcription modulation by (anti)progestagens. J Steroid Biochem Mol Biol 64:147–156

Edwards JP, West SJ, Marschke KB, Mais DE, Gottardis MM, Jones TK (1998) 5-Aryl-1,2-dihydro-5*H*-chromeno[3,4-*f*] quinolines as potent, orally active nonsteroidal progesterone receptor agonists. The effect of D-ring substituents. J Med Chem 41:303–310

Fuhrmann U, Krattenmacher R, Slater EP, Fritzemeier KH (1996) The novel progestin drospirone and its natural counterpart progesterone: biochemical profile and antiandrogenic potential. Contraception 54:243–251

Green S, Chambon P (1988) Nuclear receptors enhance our understanding of transcription regulations. Trends Genet 4:309–314

Jones TK, Pathirana C, Goldman ME, Hamann LG, Farmer LJ, Ianiro T, Johnson MG, Bender SL, Mais DE, Stein RB (1996) Discovery of novel intracellular receptor modulating drugs. J Steroid Biochem Mol Biol 56:61–66

Muhn P, Fuhrmann U, Fritzemeier KH, Krattenmacher R, Schillinger E (1995) Drospirenone: a novel progestogen with antimineralocorticoid and antiandrogenic activity. Ann NY Acad Sci 761:311–335

Pathirana C, Stein RB, Berger TS, Fenical W, Ianiro T, Mais DE, Torres A, Goldman ME (1995) Nonsteroidal human progesterone receptor modulators from the marine alga *Cymopolia barbata*. Mol Pharmacol 47:630–635

Schoonen WGEJ, Dijkema R, de Ries RJH, Wagenaars JL, Joosten JWH, de Gooyer ME, Deckers GH, Kloosterboer HJ (1998) Human progesterone receptor A and B isoforms in CHO cells. II. Comparison of binding, transactivation and ED_{50} values of several synthetic (anti)progestagen. *in vitro* in CHO and MCF-7 cells and *in vivo* in rabbits and rats. J Steroid Biochem Mol Biol 64:157–170

Sobek L, di Lorenzo D, Oettel M, Kaufmann G (1994) Normal and stable transfected cancer cell lines: tools for a screening of progestogenic, antiprogestogenic and antiglucocorticoid substances. Methods Find Exp Clin Pharmacol 16:545–551

Zhi L, Tegley CM, Kallel EA, Marschk KB, Mais DE, Gottardis MM, Jones TK (1998) 5-Aryl-1,2-dihydrochromeno[3,4-*f*] quinolines: a novel class of nonsteroidal human progesterone receptor agonists. J Med Chem 41:291–302

N.3.2.1.3 Alkaline Phosphatase Assay

PURPOSE AND RATIONALE

Progestins induce the *de novo* synthesis of alkaline phosphatase (Di Lorenzo et al. 1991, 1993). The progestin induction of the nonspecific tissue alkaline phosphatase is not altered by other steroid hormones or synthetic analogs. This finding has been used by Sobek et al. (1994), Pathirana et al. (1995), and Li et al. (1997) to measure the progestogenic and antiprogestogenic actions in a microplate assay.

PROCEDURE

T47D cells are grown in 96-well plates to near confluence and then treated with 0.1%–0.2% alcohol (control) or steroid agonists; otherwise R 5020 plus potential antagonist for 2 days. The cells are then fixed with 3.7% formaldehyde in phosphate-buffered saline for 15 min at 15°C, washed with 200 µl phosphate-buffered saline and stored at −90°C. After thawing, each well is incubated with 100 µl *p*-nitrophenyl phosphate (1 mg pNPP/ml) in DEAM (1 M diethanolamine, pH 9.8, containing 0.5 mM $MgCl_2$, and 20 µM $ZnSO_4$). The enzyme reaction is allowed to proceed in the dark at 37°C. Formation of *p*-nitrophenol is monitored periodically at 405 nm in a microplate reader. In each microtiter plate, blanks, *p*-nitrophenol, and alkaline phosphatase standards are measured together with the samples. One unit of alkaline phosphatase is defined as the amount of enzyme capable of transforming 1 µmol of substrate in 1 min at 37°C. Enzyme assays are performed under conditions of linearity relative to the substrate and to the concentration of proteins.

EVALUATION

Progestin concentrations corresponding to half the maximal increase in alkaline phosphatase activity (ED_{50}) are calculated graphically and by computer-assisted analysis using the ImmunoFit EIA/RIA analysis software (Beckman Instruments).

REFERENCES AND FURTHER READING

Di Lorenzo D, Albertini A, Zava D (1991) Progestin regulation of alkaline phosphatase in the human breast cancer cell line T47D. Cancer Res 51:4470–4475

Di Lorenzo D, Gianni M, Savoldi GF, Ferrari F, Albertini A, Garattini E (1993) Progesterone induced expression of alkaline phosphatase is associated with a secretory phenotype in T47D breast cancer cells. Biochem Biophys Res Commun 192:1066–1072

Li F, Kumar N, TsongY-Y, Monder C, Bardin CW (1997) Synthesis and progestional activity of 16-methylene-17α-hydroxy-19-norpregn-4-ene-3,20-dione and its derivatives. Steroids 62:403–408

Pathirana C, Stein RB, Berger TS, Fenical W, Ianiro T, Mais DE, Torres A, Goldman ME (1995) Nonsteroidal human progesterone receptor modulators from the marine alga *Cymopolia barbata*. Mol Pharmacol 47:630–635

Sobek L, di Lorenzo D, Oettel M, Kaufmann G (1994) Normal and stable transfected cancer cell lines: tools for a screening of progestogenic, antiprogestogenic and antiglucocorticoid substances. Methods Find Exp Clin Pharmacol 16:545–551

N.3.2.2
In Vivo Methods

N.3.2.2.1
Clauberg (McPhail) Test in Rabbits

PURPOSE AND RATIONALE

In this historical bioassay, Clauberg (1930a, 1930b, 1930c, 1930d) first described the histological changes of the endometrium in estrogen-pretreated rabbits after administration of progestional compounds. The test was further studied by Butenandt et al. (1934) and systematically examined by McPhail (1934) who introduced scoring the changes of the endometrium.

PROCEDURE

Immature female rabbits (Yellow Silver or New Zealand strain), weighing 550–650 g, receive daily injections of 5.0 µg estradiol benzoate per animal in sesame oil solution for a period of 6 days (priming). From days 7–12 (treatment for 5 days) the test compound or standard is administered at several doses, three to four animals per group. Standard doses are: 0.02, 0.08 and 2.0 mg progesterone per day and animal s.c. in sesame oil solution, or 0.01, 0.02, and 0.04 mg medroxyprogesterone acetate orally. Controls receive either the vehicles or estradiol benzoate only. At autopsy on day 15, both horns of the uterus are removed and fixed in 10% formalin. Sections from the middle part of each uterine horn are low examined by histology.

EVALUATION

Pretreatment with oestradiol stimulates uterine weight developmental (priming), progestagens induce further proliferation and secretory transformation. The following scores are established:

0 ramification of the uterus mucosa, but no proliferation (estrogen treatment only)
1 slight proliferation of the uterus mucosa
2 medium proliferation of the uterus mucosa, slight additional ramification
3 pronounced proliferation of the uterus mucosa
4 very pronounced proliferation of the uterus mucosa, pronounced ramification.

The scores from each dosage group are averaged. Dose–response curves are constructed in order to calculate potency ratios versus the standard (progesterone). The morphological evaluation needs to be done by an experienced investigator. Preliminary experiments with standard drugs and photographical documentation of the histological findings are recommended.

Similar studies were reported by: Zondek 1935; Junkmann 1957; Elton and Edgren 1958; Miyake 1962; Wiechert and Neumann 1965

MODIFICATIONS OF THE METHOD

In order to study the prolonged activity of progestogen esters, the animals are primed with estradiol for 6 days, followed by a single subcutaneous injection of the test compound or hydroxyprogesterone caproate standard. Daily treatment with estradiol is continued and the rabbits sacrificed at increasing intervals up to 4 weeks.

McGinty et al. (1939) established a local **progestional test** which involves the direct injection of progesterone into a uterine segment. The test is performed in immature rabbits primed for 6 days with estrogen. On day 7, the uterus is exposed by laparotomy. The upper middle segment of each horn is ligated without disturbance of blood circulation. A solution of the gestagen in oil is injected into the lumen of one segment through the lower ligature, which is closed tightly after the injection. In the opposite horn, only the vehicle is injected. The animals are sacrificed 3 days later and sections of the horn are evaluated histologically according to the McPhail scores (Tayama et al. 1979).

Pincus et al. (1957) improved the quantitative aspects of the McPhail test with the planimetric measurement of the endometrial proliferation.

REFERENCES AND FURTHER READING

Butenandt A, Westphal U, Hohlweg W (1943) Über das Hormon des Corpus luteum. Hoppe-Seyler's Z Biol Chem 227:84–98

Clauberg C (1930a) Der biologische Test für das Corpus luteum-Hormon. Klin Wschr 9:2004–2005

Clauberg C (1930b) Das Hormon des Corpus luteum. Zentralbl Gynäkol 54:7–19

Clauberg C (1930c) Experimentelle Untersuchungen zur Frage eines Mäusetestes für das Hormon des Corpus luteum. Zentralbl Gynäkol 54:1154–1164
Clauberg C (1930d) Zur Physiologie und Pathologie der Sexualhormone, im besonderen des Hormons des Corpus luteum. 1. Mitteilung: Der biologische Test für das Luteohormon (das spezifische Hormon des Corpus luteum) am infantilen Kaninchen. Zentralbl Gynäkol 54:2757–2770
Elton RL, Edgren RA (1958) Biological actions of 17α-(2-methallyl)-19-nortestosterone, an orally active progestional agent. Endocrinology 63:464–472
Hebborn P (1971) Progestional agents. In: Turner RD, Hebborn P (eds) Screening methods in pharmacology, Vol II. Academic Press, New York, pp 105–119
Junkmann K (1957) Long-acting steroids in reproduction. Recent Prog Horm Res 13:389–427
McGinty DA, Anderson LP, McCollough NB (1939) Effect of local application of progesterone on the rabbit uterus. Endocrinology 24:829–832
McPhail MK (1934) The assay of progestin. J Physiol (Lond) 83:145–156
Miyake T (1962) Progestional substances. In: Dorfman RI (ed) Methods in hormone research, Vol II. Academic Press, New York, pp 127–178
Pincus G, Miyake T, Merrill AP, Longo P (1957) The bioassay of progesterone. Endocrinology 61:528–533
Tayama T, Motoyama T, Ohono Y, Ide N, Turusaki T, Okada H (1979) Local progestional and antiprogestional effects of steroids and their metabolites on the rabbit uterus. Jpn J Fertil Steril 24:48–51
Wiechert R, Neumann F (1965) Gestagene Wirksamkeit von 1-Methyl- und 1,2α-Methylen-Steroiden. Arzneimittelforschung 15:244–246
Zondek B (1935) Follikelhormon (Follikulin) und Corpus-luteum-Hormon (Progestin). In: Zondek B (ed) Hormone des Ovariums und des Hypophysenvorderlappens. Springer, Berlin Heidelberg New York, pp 162–170

N.3.2.2.2 Endometrial Carbonic Anhydrase Assay

PURPOSE AND RATIONALE

Carbonic anhydrase activity in the endometrium is increased after administration of progesterone. Carbonic anhydrase activity in the endometrium of rabbits was used for a quantitative progestin assay (Lutwak-Mann 1955; Pincus et al. 1957; Elton and Edgren 1958; Miyake and Pincus 1958; Eisler 1964).

PROCEDURE

Immature female rabbits are estrogen primed and progestin treated as described in the Clauberg test. After sacrifice of the animals, the uteri are opened longitudinally. Endometrium is dissected, weighed and homogenized with a tenfold volume in a glass homogenizer. After centrifugation, carbonic anhydrase is determined in the supernatant with the colorimetric method of Philpot and Philpot (1936) using bromothymol as indicator.

EVALUATION

Mean values of carbonic anhydrase activity/g wet tissue are calculated and potency ratios for test compound and standard established.

REFERENCES AND FURTHER READING

Eisler M (1964) Animal techniques for evaluating sex steroids. In: Nodine JH, Siegler PE (eds) Animal and clinical pharmacologic techniques in drug evaluation. Year Book Medical Publishers,, Chicago, Ill., pp 566–573
Elton RL, Edgren RA (1958) Biological actions of 17α-(2-methallyl)-19-nortestosterone, an orally active progestional agent. Endocrinology 63:464–472
Lutwak-Mann C (1955) Carbonic anhydrase in the female reproductive tract. Occurrence, distribution and hormonal dependence. J Endocrinol 13:26–38
Miyake T (1962) Progestional substances. In: Dorfman RI (ed) Methods in hormone research, Vol II. Academic Press, New York, pp 127–178
Miyake T, Pincus G (1958) Progestional activity of certain 19-norsteroids and progesterone derivatives. Endocrinology 63:816–824
Philpot FJ, Philpot J St L (1936) A modified colorimetric estimation of carbonic anhydrase. Biochem J 30:2191–2193
Pincus G Miyake T, Merrill AP, Longo P (1957) The bioassay of progesterone. Endocrinology 61:528–533

N.3.2.2.3 Deciduoma Formation

PURPOSE AND RATIONALE

This is a classical bioassay for progestagens. The deciduoma tests are based on the fact that the endometrium of the estrogen-primed, progesterone-treated rodent is sensitive to local stimuli such as scratching (Astwood 1939), chemical irritation, and electrical stimulation. The effect of local irritation produces a deciduoma, similar to the formation of a maternal placenta (Astwood 1939; Elton and Edgren 1958; Zarrow et al. 1958; Miyake 1962; Eisler 1964; Sreenivasulu 1993).

PROCEDURE

Adult female Sprague-Dawley rats weighing 200–250 g are ovariectomized and 1 week later treated with 0.5 µg estradiol/animal once daily subcutaneously for 4 days, followed by 9 days of progesterone or the test compound in various doses. The uterus is exposed on day 5 of progesterone treatment and 1.0 mg histamine dihydrochloride is injected into the lumen of one horn. The animals are sacrificed after the last treatment. Both uterine horns are removed and weighed. The degree of deciduoma formation is evaluated by the percentage increase in weight of the histamine-injected uterine horn as compared with the untreated control horn.

EVALUATION

Dose–response curves are established plotting percentage increase in weight of the treated uterus horn versus logarithm of dose of test compound and standard in order to calculate potency ratios.

REFERENCES AND FURTHER READING

Astwood EB (1939) An assay method for progesterone based on the decidual reaction in the rat. J Endocrinol 1:49–55

Eisler M (1964) Animal techniques for evaluating sex steroids. In: Nodine JH, Siegler PE (eds) Animal and clinical pharmacologic techniques in drug evaluation. Year Book Medical Publishers, Chicago, Ill., pp 566–573

Elton RL, Edgren RA (1958) Biological actions of 17α-(2-methallyl)-19-nortestosterone, an orally active progestional agent. Endocrinology 63:464–472

Miyake T (1962) Progestional substances. In: Dorfman RI (ed) Methods in hormone research, Vol II. Academic Press, New York, pp 127–178

Sreenivasulu S, Singh MM, Setty BS, Kamboj VP (1993) Effect of a pure nonsteroidal antiestrogen, CDRI-85/287, on implantation-associated histological and biochemical changes in the rat uterus. Contraception 48:597–609

Zarrow MX, Peters LE, Caldwell AL Jr (1958) Comparative potency of several progestogenic compounds in a battery of different biological tests. Ann NY Acad Sci 71:532–541

N.3.2.2.4
Pregnancy Maintenance Assay

PURPOSE AND RATIONALE

This is a historical bioassay for progestational activity. In the rat, ovariectomy performed during the first half of pregnancy terminates gestation, but ovariectomy during the second half of pregnancy does not result in abortion, because the placenta now provides estrogens and progesterone for maintenance of pregnancy. In early pregnancy, maintenance of pregnancy after ovariectomy can be achieved by sufficient exogenous progestin with and without estrogen (Stucki 1958; Miyake 1962; Eisler 1964; Hebborn 1971; Phillips et al. 1984; Kuhnz und Beier 1994).

PROCEDURE

Mature Sprague-Dawley female rats are inseminated by being placed with males overnight. Presence of sperm is assessed by vaginal lavage and, if positive, is considered to be day 1 of pregnancy. On day 8, the females are ovariectomized if found pregnant upon examination of the uterus. Test compounds are administered once daily, subcutaneously, for 13 days beginning immediately after ovariectomy. Estradiol (0.1 µg/day) is administered concomitantly with the test compound. At autopsy on day 21, the presence or absence of implantation sites, and the numbers of live embryos are recorded.

EVALUATION

Normal pregnant rats have an average of 11 implantation sites and about 10 live embryos. Maintenance of pregnancy is assessed with reference to these normal values.

MODIFICATIONS OF THE METHOD

Similar tests have been performed in rabbits (Elton and Edgren 1958), in mice (McGinty 1959), and in hamsters (Shipley 1965). In rabbits, abortion can be induced by intravenous injection of oxytocin from day 30 of pregnancy onwards. The abortifacient effect can be suppressed by progestagens.

REFERENCES AND FURTHER READING

Eisler M (1964) Animal techniques for evaluating sex steroids. In: Nodine JH, Siegler PE (eds) Animal and clinical pharmacologic techniques in drug evaluation. Year Book Medical Publishers, Chicago, Ill., pp 566–573

Elton RL, Edgren RA (1958) Biological actions of 17α-(2-methallyl)-19-nortestosterone, an orally active progestional agent. Endocrinology 63:464–472

Hebborn P (1971) Progestional agents. In: Turner RD, Hebborn P (eds) Screening methods in pharmacology, Vol II. Academic Press, New York, pp 105–119

Kuhnz W, Beier S (1994) Comparative progestational and androgenic activity of norgestimate and levonorgestrel in the rat. Contraception 49:275–289

McGinty (1959) Discussion. Fed Proc Fed Am Soc Exp Biol 18:1048–1050

Miyake T (1962) Progestional substances. In: Dorfman RI (ed) Methods in hormone research, Vol II. Academic Press, New York, pp 127–178

Phillips A, Hahn DW, Klimek S, McGuire JL (1987) A comparison of the potencies and activities of progestagens used in contraceptives. Contraception 36:181–192

Shipley EG (1965) Effectiveness of topical application of a number of progestins. Steroids 5:699–717

Stucki JC (1958) Maintenance of pregnancy in ovarectomized rats with some newer progestins. Proc Soc Exp Biol Med 99:500–504

N.3.2.3
Anti-Progestional Activity

N.3.2.3.1
Progesterone Antagonism (Anti-Progestins)

PURPOSE AND RATIONALE

The anti-progestional activity of a test compound may be determined by antagonism against the effect of progesterone in the Clauberg/McPhail assay in rabbits (N.3.2.2.1) or the McGinty test (N.3.2.2.1) and in the deciduoma formation assay in rats (N.3.2.2.3) (Miyake 1965; Tamaya et al. 1979; Oettel and Kurischko 1980; Philibert et al. 1985; Cook 1994; Teutsch and Philibert 1994).

MODIFICATIONS OF THE METHOD

Progesterone control of cervical ripening in the guinea pig and the tree shrew *Tupaja belangeri* has been used for the evaluation of progesterone antagonists (Chwalisz et al. 1991; Chwalisz 1994). The effects of progesterone antagonists on surgically induced endometriosis in rats have been studied by Stöckemann and Chwalisz (1993).

Michna et al. (1991) developed a bioassay which allows quantification of the antiproliferative potency of progesterone antagonists on the mammary gland in rats. Female Wistar rats with a body weight of 100 g were ovarectomized. One week after ovariectomy the rats were substituted with 10 µg estrone and 3 mg progesterone for 3 days. The animals in the experimental groups simultaneously received the progesterone antagonist. The animals were then sacrificed and the inguinal mammary glands dissected: the right gland for biochemical analysis (DNA), the left for morphometrical analysis. The entire inguinal mammary gland was prepared for conventional paraffin sections and stained with ferric ammonium sulfate. Microphotographs were taken in transmitted light. The number of tubulo-alveolar buds was counted in the whole mount preparations using a 40-fold magnification. In the neighborhood of the inguinal node, a square of 2.5 mm^2 was quantified and calculated for a tissue volume of 100 mm^3 in more than ten animals. The antiproliferative action of progesterone antagonists on the amount of tubulo-alveolar buds was estimated for an 80% confidence interval of mean inhibition.

CRITICAL ASSESSMENT OF THE METHOD

This method is very detailed and time-consuming, it appears to be suitable for the advanced stages of drug evaluation for anti-progestins. In contrast to the only biochemical assessment, the method provides detailed information which is also applicable to toxicological evaluations.

REFERENCES AND FURTHER READING

Chwalisz K (1994) The use of progesterone antagonists for cervical ripening and as adjunct to labor and delivery. Human Reprod 9:131–161

Chwalisz K, Hegele-Hartung C, Schulz R, Qing SS, Louton PT, Elger W (1991) Progesterone control of cervical ripening – experimental studies with the progesterone antagonists onapristone, lilopristone and mefipristone. In: Leppert PC, Woessner JF (eds) The extracellular matrix of the uterus, cervix and fetal membranes: synthesis, degradation and hormonal regulation. Perinatology, Ithaca, New York, pp 119–131

Cook CE, Lee YW, Wani MC, Fail PA, Petrow V (1994) Effects of D-ring substituents on antiprogestational (antagonist) and progestational (agonist) activity of 11β-aryl steroids. Human Reprod 9 [Suppl 1]:32–39

Michna H, Nishino Y, Schneider MR, Louton T, El Etreby MF (1991) A bioassay for the evaluation of antiproliferative potencies of progesterone antagonists. J Steroid Biochem Mol Biol 38:359–365

Miyake T, Dorfman RI (1965) Anti-progestional compounds. In: Dorfman RI (ed) Methods in hormone research, Vol IV. Academic Press, New York, pp 95–106

Oettel M, Kurischko A (1980) STS 557, a new orally active progestin with antiprogestional and contragestional properties in rabbits. Contraception 21:61–75

Philibert, D, Moguilewsky M, Mary I, Lecaque D, Tournemine C, Secchi J, Deraedt R (1985) Pharmacological profile of RU 486 in animals. In: Baulieu EE, Segal SJ (eds) The anti-progestin steroid RU 486 and human fertility control. Plenum, New York, pp 49–68

Stöckemann K, Chwalisz K (1993) Effects of the progesterone antagonists onapristone and ZK 136799 on surgically induced endometriosis in rats. Exp Clin Endocrinol 101 [Suppl 1]:59

Tamaya T, Motoyama T, Ohono Y, Ide N, Turusaki T, Okada H (1979) Local progestational and antiprogestational effects of steroids and their metabolites on the rabbit uterus. Jpn J Fertil Steril 24:48–51

Teutsch G, Philibert D (1994) History and perspectives of antiprogestins from the chemist's point of view. Human Reprod 9 [Suppl 1]:12–31

N.3.2.3.2 Luteolytic Activity of Prostaglandins

PURPOSE AND RATIONALE

Synthetic prostaglandins are used for synchronization of estrus and for treatment of anestrus caused by a persistent corpus luteum in cattle. Furthermore, synthetic prostaglandins were studied for termination of early pregnancy in humans (Karim et al. 1977; Takagi et al. 1977, 1978; Toppozada et al. 1979, Dwivedy 1979). The most useful animal model for luteolytic activity is the hamster (Gutknecht et al. 1971; Labhsetwar 1971, 1972a; Dukes et al. 1974; Bartmann et al. 1979; Galliani et al. 1984; Roy et al. 1987). The effects of prostaglandins on reproductive function in other species such as rat (Fuchs et al. 1974), mouse (Labhsetwar 1972b), and guinea pig (Blatchley and Donovan 1969) have also been studied.

PROCEDURE

Adult female golden hamsters (*Mesocricetus auratus*), weighing approximately 100 g, with regular, 4-day estrus cycles are housed under controlled light and temperature conditions and given a standard diet. They are caged with fertile males on the day before expected vaginal discharge and the next morning vaginal smears are taken. If clumps of spermatozoa are found in the smear, this day is designated as day 1 of pregnancy (see similar procedure in rats). Groups of

ten animals are treated on days 4, 5, and 6 with four different doses of standard (prostaglandin $F_{2\alpha}$) or test compound. On day 13 of pregnancy, the hamsters are sacrificed and the number of implantation scars in the uterus is counted as the parameter of luteolytic activity causing early termination of pregnancy.

EVALUATION

The luteolytic activity is expressed as the median effective dose for termination of pregnancy in 50% of the treated animals (ED_{50}).

MODIFICATIONS OF THE METHOD

The mode of action of luteolysis by prostaglandins has been studied by various authors both *in vitro* (Speroff and Ramwell 1970; O'Grady et al. 1972; Henderson and McNatty 1975; Kenny and Robinson 1986; Brambaifa 1988) and *in vivo* (Pharriss and Wyngarden 1969; Johnston and Hunter 1970; McCracken et al. 1970; Chatterjee 1973; Buhr et al. 1983; Torjesen and Aakvaag 1984, 1986).

Cao and Chan (1993) investigated the effects of oxytocin and luteal prostaglandins on the functional regression of the corpus luteum in pseudopregnant rats.

Motta et al. (1996) studied the effect of an oxytocin receptor antagonist on ovarian and uterine synthesis and release of prostaglandin $F_{2\alpha}$ in pseudopregnant rats.

Stocco and Deis (1998) examined the participation of intraluteal progesterone and prostaglandin $F_{2\alpha}$ in LH-induced luteolysis in pregnant rats.

Luteolysis by prostaglandins in the rhesus monkey has been studied by Auletta and Kelm (1994) and Auletta et al. (1995).

The ewe as a model for regulation of luteal regression has been recommended by Hoyer (1998).

REFERENCES AND FURTHER READING

Auletta FJ, Kelm LB (1994) Mechanisms controlling corpus luteum function in the rhesus monkey (*Macaca mulatta*): inhibitory action of hCG on luteolysis induced by $PGF_{2\alpha}$. J Reprod Fertil 102:215–220

Auletta FJ, Kelm LB, Schofield MJ (1995) Responsiveness of the corpus luteum of the rhesus monkey to gonadotrophin *in vitro* during spontaneous and prostaglandin $F_{2\alpha}$-induced luteolysis. J Reprod Fertil 103:107–113

Bartmann W, Beck G, Lerch U, Teufel H, Schölkens B (1979) Luteolytic prostaglandins. Synthesis and biological activity. Prostaglandins 17:301–311

Blatchley FR, Donovan BT (1969) Luteolytic effect of prostaglandin in the guinea-pig. Nature 221:1065–1066

Brambaifa N (1988) Luteolytic potency of 16-phenoxy-derivatives of prostaglandin $F_{2\alpha}$. Experientia 44:45–47

Buhr MM, Gruber MY, Riley JCM, Carlson JC (1983) The effect of prolactin pretreatment on prostaglandin $F_{2\alpha}$-associated structural changes in membranes from rat corpora lutea. Am J Obstet Gynecol 145:263–268

Cao L, Chan WY (1993) Effects of oxytocin and luteal prostaglandins on the functional regression of the corpus luteum in pseudopregnant rats. J Reprod Fertil 99:181–186

Chatterjee A (1973) Possible mode of action of prostaglandins: differential effects of prostaglandin $F_{2\alpha}$ before and after the establishment of placental physiology in pregnant rats. Prostaglandins 3:189–199

Dukes M, Russell W, Walpole AL (1974) Potent luteolytic agents related to prostaglandin $F_{2\alpha}$. Nature 250:330–331

Dwivedy I, Ray S, Grover A (1993) Present status of luteolytic agents in fertility regulation. Prog Drug Res 40:239–267

Fuchs AR, Mok E, Sundaram K (1974) Luteolytic effects of prostaglandins in rat pregnancy, and reversal by luteinizing hormone. Acta Endocrinol 76:583–596

Galliani G, Ciabatti R, Colombo G, Guzzi U, Luzzani F, Glässer A (1984) Studies on the luteolytic activity of MDL-646, a new gastroprotective PGE_1 analogue, in the hamster. Prostaglandins 27:583–590

Gutknecht GD, Wyngarden LJ, Pharriss BB (1971) The effect of prostaglandin $F_{2\alpha}$ on ovarian and plasma progesterone levels in the pregnant hamster. Proc Soc Exp Biol Med 136:1151–1157

Henderson KM, McNatty KP (1975) A biochemical hypothesis to explain the mechanism of luteal regression. Prostaglandins 9:779–797

Hoyer PB (1998) Regulation of luteal regression: the ewe as a model. J Soc Gynec Invest 5:49–57

Johnston JO, Hunter KK (1970) Prostaglandin $F_{2\alpha}$: mode of action in pregnant hamster. Physiologist 13:235

Karim SMM, Ratnam SS, Ilancheran A (1977) Menstrual induction with vaginal administration of 16,16 dimethyl trans-Δ^2-PGE_1 methyl ester (ONO 802). Prostaglandins 14:615–616

Kenny N, Robinson J (1986) Prostaglandin $F_{2\alpha}$-induced functional luteolysis: interactions of LH, prostaglandin $F_{2\alpha}$ and forskolin in cyclic AMP and progesterone synthesis in isolated rat luteal cells. J Endocrinol 111:415–423

Labhsetwar AP (1971) Luteolysis and ovulation induced by prostaglandin $F_{2\alpha}$ in the hamster. Nature 230:528–529

Labhsetwar AP (1972a) New antifertility agent – an orally active prostaglandin – ICI 74,205. Nature 238:400–401

Labhsetwar AP (1972b) Luteolytic and ovulation-inducing properties of prostaglandin $F_{2\alpha}$ in pregnant mice. J Reprod Fertil 28:451–452

McCracken JA, Glew ME, Scaramuzzi RJ (1970) Corpus luteum regression induced by prostaglandin $F_{2\alpha}$. J Clin Endocrinol Metab 30:544–546

Motta AB, Franchi AM, Faletti A, Gimeno MF (1996) Effect of an oxytocin receptor antagonist on ovarian and uterine synthesis and release of prostaglandin $F_{2\alpha}$ in pseudopregnant rats. Prostaglandins Leukot Essent Fatty Acids 54:95–100

O'Grady JP, Kohorn EI, Glass RH, Caldwell BV, Brock WA, Speroff L (1972) Inhibition of progesterone synthesis *in vitro* by prostaglandin $F_{2\alpha}$. J Reprod Fertil 30:153–156

Pharriss BB, Wyngarden LJ (1969) The effect of prostaglandin $F_{2\alpha}$ on the progesterone content of ovaries of pseudopregnant rats. Proc Soc Exp Biol Med 130:92–94

Roy R, Karanth S, Dutt A, Juneja HS (1987) Involvement of prostaglandin A1 in interrupting early pregnancy in Syrian golden hamsters. Adv Contracept 3:341–348

Speroff L, Ramwell PW (1970) Prostaglandin stimulation of *in vitro* progesterone synthesis. J Clin Endocrinol Metab 30:345–350

Stocco CO, Deis RP (1998) Participation of intraluteal progesterone and prostaglandin $F_{2\alpha}$ in LH-induced luteolysis in pregnant rats. J Endocrinol 156:253–259
Takagi S, Sakata H, Yoshida T, Nakazawa S, Fujii KT, Tominaga Y, Iwasa Y, Ninagawa T, Hiroshima T, Tomioda Y, Itoh K, Masukawa R (1977) Termination of early pregnancy by ONO-802 (16,16 dimethyl trans-Δ^2-PGE_1 methyl ester). Prostaglandins 14:791–799
Takagi S, Sakata H, Yoshida T, Den K, Fujii TK, Amemiya H, Tomita M (1978) Termination of early pregnancy by ONO-802 suppositories (16,16 dimethyl trans-Δ^2-PGE_1 methyl ester). Prostaglandins 15:913–919
Toppozada M, Warda A, Ramadan M (1979) Intramuscular 16-phenoxy PGE_2 ester for pregnancy termination. Prostaglandins 17:461–467
Torjesen PA, Aakvaag A (1984) Ovarian production of progesterone and 20α-dihydroprogesterone *in vitro* following prostaglandin $F_{2\alpha}$ induced luteolysis in the superluteinized rat. Acta Endocrinol 105:258–265
Torjesen PA, Aakvaag A (1986) Characterization of adenylate cyclase of the rat corpus luteum during luteolysis induced by a prostaglandin $F_{2\alpha}$ analogue. Mol Cell Endocrinol 44:237–242

N.4
Testicular Steroid Hormones

N.4.0.1
Castration of Male Rats (Orchiectomy)

PROCEDURE

Castration of young male rats is performed with minimal bleeding in animals weighing less than 60 g. The animal is anesthetized. A small transversal incision is made in the skin on the ventral site over the symphysis. The testis lying in the scrotum is gently pushed into the abdominal cavity. With a pair of fine forceps, the abdominal wall is opened. The epididymal fat pad, easily seen, is grasped with the forceps and the testis with the epididymis is pulled out from the wound. The ductus deferens with the testicular vessels is crushed with artery forceps and the testis together with the epididymal fad pad cut off with a pair of fine scissors. There is almost no bleeding in young animals. In older animals, ligation of the testicular vessels together with the ductus deferens may be necessary. The same procedure is performed on the other side. The skin wound is closed with one or two wound clips. The animal recovers immediately. With some skill, the operation can be performed very rapidly (Bomskov 1939).

MODIFICATIONS OF THE METHODS

Dorfman (1969) recommended removing the testes through an incision in the tip of the scrotum. In our hands, the procedure described above was preferable.

REFERENCES AND FURTHER READING

Bomskov C (1939) Chirurgische Methoden der Erforschung des Hodenhormones Die Kastration des männlichen Säugetieres. In Bomskov C (ed) Methodik der Hormonforschung, 2. Band. Thieme, Leipzig, pp 350–353
Dorfman RI (1969) Androgens and anabolic agents. In: Dorfman RI (ed) Methods in hormone research, Vol IIA. Academic Press, New York, pp 151–220

N.4.0.2
Caponizing of Cockerels (Orchiectomy)

PROCEDURE

This is a classical bioassay for androgens. White Leghorn cockerels are used for surgery at approximately 6 weeks of age. The animals, fasted 24 h prior to surgery, were anesthetized with ether and placed on their sides. An incision is made between the last two ribs, the muscle layer is divided, and the incision is pulled apart with small retractors. The testis is found close to the midline of the posterior abdominal wall, alongside the vena cava. The capsule enclosing the testis is cut and the gonad is removed. It is imperative to remove the testis intact, as fragments left behind are usually vascularized and persist, giving rise to incompletely caponized animals. The incision is closed by a suture. The contralateral testis is removed in a similar fashion (Bomskov 1939).

REFERENCES AND FURTHER READING

Bomskov C (1939) Chirurgische Methoden der Erforschung des Hodenhormones. Die Kastration des männlichen Vogels (Ka-paunisieren). In: Bomskov C (ed) Methodik der Hormonforschung, 2. Band. Thieme, Leipzig, pp 353–357
Dorfman RI (1969) Androgens and anabolic agents. In: Dorfman RI (ed) Methods in hormone research, Vol IIA. Academic Press, New York, pp 151–220

N.4.1
Androgenic and Anabolic Activity

N.4.1.1
In Vitro Methods

N.4.1.1.1
Androgen Receptor Binding

PURPOSE AND RATIONALE

Rat ventral prostate (Bonne and Raynaud 1974; Liao et al. 1974; Grover and Odell 1975; Ojasoo and Raynaud 1978; Raynaud et al. 1979; Winnecker et al. 1989; Duc et al. 1995) or mouse kidney (Isomaa et al. 1982) serve as sources for androgen receptors. Human androgen receptors have been prepared from trans-

fected COS-1 cells (Teutsch et al. 1994). Labeled androstanolone, 5α-dihydrotestosterone, testosterone, and, more recently, methyltrienolone (R 1881) have been used as radioligands.

PROCEDURE

Androgen Receptor Assay

Cytosol is prepared from ventral prostate glands of adult male rats castrated approximately 24 h before use. The tissue is homogenized in TMDG buffer (10 mM Tris, 20 mM sodium molybdate, 2 mM dithiothreitol, 10% glycerol, pH = 7.4) at room temperature using a motor-driven glass homogenizer and centrifuged at 135,000 *g* for 1 h. Aliquots of the supernatant (cytosol) are diluted to contain 40 mg tissue/ml and incubated for 1 h or overnight with [17α-methyl-^{3}H]R 1881 (methyltrienolone, 5 nM final concentration, 87 Ci/mmol, New England Nuclear) in either the absence or presence of increasing concentrations (1 nM to 10 µM) of R 1881 or test compounds. Because R 1881 binds weakly to progesterone and glucocorticoid receptors, cytosols are pretreated with 1 µM triamcinolone acetonide to block these interactions. After a 1- or 18-h incubation period, a suspension of dextran-coated charcoal (1% charcoal, 0.05% dextran T-70, 0.05% BSA) is added to the ligand-cytosol mixture and incubated for 5 min. The charcoal is removed by centrifugation at 1500 *g* for 10 min and the supernatant (protein-bound [^{3}H]R 1881) counted using 10 ml of scintillation fluid (New England Nuclear) in a liquid scintillation spectrometer.

Nuclear Androgen Receptor Exchange Assay

Ventral prostates are homogenized at 100 mg/ml in hexylene glycol buffer (1 M hexylene glycol, 1 mM $MgCl_2$, 2.0 mM dithiothreitol, 5.0 mM EGTA, 1.0 mM PIPES, pH = 7.4) using a motor-driven ground glass homogenizer. Homogenates are centrifuged at 1500 *g* for 10 min. The nuclear pellet is washed 3 times in homogenization buffer by gently resuspending the pellet in a Dounce homogenizer and centrifugation at 1500 *g* for 10 min. The washed nuclear pellet is resuspended in pyridoxal-5′-phosphate extraction buffer (20 mM sodium barbital, 5 mM pyridoxal-5′-phosphate, 5.0 mM dithiothreitol, 1.5 mM EDTA, 150 mM KCl, 20% glycerol, pH = 7.4) for 60 min at a final concentration of 60 mg tissue/ml. The extracted nuclei are centrifuged at 25,000 *g* for 30 min with the resulting supernatant being used in the same single saturating dose assay as described for prostate cytosol.

EVALUATION

Binding of test substances to the androgen receptor (receptor affinity) is quantified by calculating relative binding affinity (ratio of the molar concentration of unlabeled R 1881 to test substance required to inhibit the binding of [^{3}H]R 1881 by 50% after correction for nonspecific binding) and equilibrium inhibitory binding constant ($K_i = IC_{50}/(1 + C)/K_d$, where C = the concentration of [^{3}H]R 1881 and the K_d for R 1881 is 1.3 nM).

In the nuclear androgen receptor exchange assay treatment group means are compared to control means, using ANOVA and Dunnett's multiple comparison tests.

MODIFICATIONS OF THE METHOD

Cell assays and animal assays are described for evaluation of androgens and anti-androgens (Raynaud et.al. 1975; Liang et al. 1977; Sivelle et al. 1982; Liao et al. 1984; Traish et al. 1986; Stobaugh and Blickenstaff 1990; Christiansen et al. 1990; Humm and Schneider 1990; Neubauer et al. 1993).

Brown et al. (1981) studied anti-androgen effects on androgen receptor binding in cultured human newborn foreskin fibroblasts.

Tezón et al. (1982) studied the intracellular distribution of the androgen receptor in the rat epididymis under the influence of androgens and anti-androgens.

The use of tritiated 7α,17α-dimethyl-19-nortestosterone for the assay of androgen receptors was recommended by Schilling and Liao (1984).

Characterization and expression of a cDNA encoding the human androgen receptor was described by Tilley et al. (1989).

Hoyte et al. (1993) recommended 7α-methyl-17α-(E-2′-[^{125}I]iodovinyl)-19-nortestosterone as radioligand for the detection of the androgen receptor.

Structure–affinity relationships of various steroids structurally related to nomegestrol and progesterone for [^{3}H]testosterone binding to rat ventral prostate cytosol were reported by Botella et al. (1987).

Molecular cloning of human androgen receptor complementary cDNA has been reported by Chang et al. (1988) and Lubahn et al. (1988).

DNA-binding of androgen receptor overexpressed in COS-1 cells has been reported by Von Krempelhuber et al. (1994).

Thoth et al. (1995) studied *in vitro* binding of 16-methylated C-18 and C-19 steroid derivates to the androgen receptor using cytosol of castrated rat prostate and [^{3}H]R 1881 as radioligand.

Chang et al. (1995) reviewed the structure and function of the androgen receptor and its role in the function of the mammalian system.

The interaction of androgen receptors with the androgen-response element in intact cells was investigated by Karvonen et al. (1997).

REFERENCES AND FURTHER READING

Bonne C, Raynaud JP (1974) Mode of spironolactone anti-androgenic action: inhibition of androstanolone binding to rat prostate androgen receptor. Mol Cell Endocrinol 2:59–67

Botella J, Paris J, Lahlou B (1987) The cellular mechanism of the antiandrogenic action of nomegestrol acetate, a new 19-norprogestagen, on the rat prostate. Acta Endocrinol 115:544–550

Brown TR, Rothwell SW, Sultan C, Migeon CJ (1981) Inhibition of androgen binding in human foreskin fibroblasts by antiandrogens. Steroids 37:635–647

Chang C, Kokontis J, Liao S (1988) Molecular cloning of human and rat androgen complementary cDNA encoding androgen receptors. Science 240:324–326

Chang C, Saltzman A, Yeh S, Young W, Keller E, Lee HJ, Wang C, Mizokami A (1995) Androgen receptor: an overview. Crit Rev Eukaryotic Gene Expression 5:97–125

Christiansen RG, Bell MR, D'Ambra TE, Mallamo JP, Hermann JL, Ackerman JH, Opalka CJ, Kullnig RK, Winneker RC, Snyder BW, Batzold FH, Schane HP (1990) Antiandrogenic steroidal sulfonylpyrazoles. J Med Chem 33:2094–2100

Duc I, Botella J, Bonnet P, Fraboul F, Delansorne R, Paris J (1995) Antiandrogenic activity of nomegestrol acetate. Arzneimittelforschung 45:70–74

Grover PK, Odell WD (1975) Correlation of *in vivo* and *in vitro* activities of some naturally occurring androgens using a radioreceptor assay for 5α-dihydrotestosterone with rat prostate cytosol receptor protein. J Steroid Biochem 5:1373–1379

Hoyte RM, Brown TJ, MacLusky NJ, Hochberg RB (1993) 7a-Methyl-17α-(E-2′-[^{125}I]iodovinyl)-19-nortestosterone: a new radioligand for the detection of the androgen receptor. Steroids 58:13–23

Humm AW, Schneider MR (1990) Entwicklung nichtsteroidaler Antiandrogene: 4-Nitro-3-trifluormethyldiphenylamine. Arch Pharmacol 323:83–87

Isomaa V, Pajunen AE, Bardin CW, Jänne OA (1982) Nuclear androgen receptors in the mouse kidney: validation of a new assay. Endocrinology 111:833–843

Karvonen U, Kallio PJ, Jänne OA, Palvimo JJ (1997) Interaction of androgen receptors with androgen response element in intact cells. J Biol Chem 272:15973–15979

Liang T, Tymoczko JL, Chan KMB, Hung SC, Liao S (1977) Androgen action: receptors and rapid responses. In: Martini L, Motta M (eds) Androgens and antiandrogens. Raven, New York, pp 77–89

Liao S, Howell DK, Chang TM (1974) Action of a nonsteroidal antiandrogen, flutamide, on the receptor binding and nuclear retention of 5α-dihydrotestosterone in rat ventral prostate. Endocrinology 94:1205–1208

Liao S, Witte D, Schilling K, Chang C (1984) The use of a hydroxylapatite-filter steroid receptor assay method in the study of the modulation of androgen receptor interaction. J Steroid Biochem 20:11–17

Lubahn DB, Joseph DR, Sullivan PM, Willard HF, French FS, Wilson EM (1988) Cloning of human androgen receptor complementary cDNA and localization to the X chromosome. Science 240:327–330

Neubauer BE, Best KL, Clemens JA, Gates CA, Goode RL, Jones CD, Laughlin ME, Shaar CJ, Toomey RE, Hoover DM (1993) Endocrine and antiprostatic effects of Raloxifene (LY156758) in the male rat. Prostate 23:245–262

Ojasoo T, Raynaud JP (1978) Unique steroid congeners for receptor studies. Cancer Res 38:4186–4198

Raynaud JP, Bonne C, Bouton MM, Moguilewsky M, Philibert D, Azadian-Boulanger G (1975) Screening for anti-hormones by receptor studies. J Steroid Biochem 6:615–622

Raynaud JP, Bonne C, Bouton MM, Lagace L, Labrie F (1979) Action of a non-steroid anti-androgen, RU 23908, in peripheral and central tissues. J Steroid Biochem 11:93–99

Schilling K, Liao S (1984) The use of radioactive 7α,17α-dimethyl-19-nortesteosterone (Mibolerone) in the assay of androgen receptors. Prostate 5:581–588

Sivelle PC, Underwood AH, Jelly JA (1982) The effects of histamine H_2 receptor antagonists on androgen action *in vivo* and dihydrotestosterone binding to the rat prostate androgen receptor *in vitro*. Biochem Pharmacol 31:677–684

Stobaugh ME, Blickenstaff RT (1990) Synthesis and androgen receptor binding of dihydrotestosterone hemisuccinate homologs. Steroids 55:259–262

Teutsch G, Goubet F, Battmann T, Bonfils A, Bouchoux F, Cerede E, Gofflo D, Gaillard-Kelly M, Philibert D (1994) Non-steroidal antiandrogens: synthesis and biological profile of high-affinity ligands for the androgen receptor. J Steroid Biochem Mol Biol 48:111–119

Tezón JG, Vazquez MH, Blaquier JA (1982) Androgen-controlled subcellular distribution of its receptor in the rat epididymis: 5α-dihydrotestosterone-induced translocation is blocked by antiandrogens. Endocrinology 111:2039–2045

Thoth I, Faredin I, Mesko E, Wolfling J, Schneider G (1995) *In vitro* binding of 16-methylated C-18 and C-19 steroid derivates to the androgen receptor. Pharmacol Res 32:217–221

Tilley WD, Marcelli M, Wilson JD, McPhaul MJ (1989) Characterization and expression of a cDNA encoding the human androgen receptor. Proc Natl Acad Sci USA 86:327–331

Traish AM, Müller RE, Wotiz HH (1986) Binding of 7α,17α-dimethyl-19-nortestosterone (Mibolerone) to androgen and progesterone receptors in human and animal tissues. Endocrinology 118:1327–1333

Von Krempelhuber A, Müller F, Fuhrmann U (1994) DNA-binding of androgen receptor overexpressed in mammalian cells. J Steroid Biochem Mol Biol 48:511–516

Winneker RC, Wagner MM, Batzold FH (1989) Studies on the mechanism of action of WIN 49596: a steroidal androgen receptor antagonist. J Steroid Biochem 33:1133–1138

N.4.1.1.2 Transactivation Assay for Androgens

PURPOSE AND RATIONALE

Steroid agonistic and antagonistic properties can be evaluated by transactivation assays (Muhn et al. 1995; Fuhrmann et al. 1995, 1996). The transactivation assay assumes that steroid receptor proteins act as ligand-regulated transcriptional activators. After binding of hormone, the steroid receptor interacts with hormone-responsive elements of hormone-regulated genes, in-

ducing a cascade of transcriptional events (Green and Chambon 1988). The hormone-dependent transcriptional activation can be determined in tissue culture by transfection of the steroid receptor under investigation and a reporter gene linked to a hormonally responsive promoter into cells. The transactivation assay allows determination of the agonistic and also the antagonistic potency of a given compound, by either induction or inhibition of reporter gene activity (Fuhrmann et al. 1992).

PROCEDURE

Vector Construct

CV-1 cells are stably transfected with the rat androgen receptor and pMMTV-CAT7. The pMMTV-CAT plasmid containing the mouse mammary tumor virus promoter linked to a chloramphenicol acetyltransferase gene is prepared according to Cato et al. (1986).

Cell Culture and Transfections

The culture medium of CV-1 cells stably transfected with the rat androgen receptor and pMMTV-CAT7 is supplemented with 400 µg/ml G418 (Gibco BRL) and 5 µg/ml puromycin.

Stable and transient transfections are performed using Lipofectin reagent (Gibco BRL) according to a procedure recommended by Felgner and Holm (1989). Stable transfections are carried out according to Fuhrmann et al. (1992). For transient transfection, 1×10^6 COS-1 or CV-1 cells are plated onto 100-mm dishes 1 day prior to transfection. Cells are typically about 80% confluent after 24 h. Before transfection, cells are washed twice with 1 ml Opti-MEM (Gibco BRL) per dish. For each dish, 5 µg hAR expression plasmid and 5 µg pMMTV-CAT are diluted with 1 ml Opti-MEM; in addition, 50 µg Lipofectin Reagent is diluted with 1 ml Opti-MEM. Next, DNA and Lipofectin Reagent dilutions are combined in a polystyrene snap-cup tube to obtain 2 ml of transfection solution per dish, gently mixed, incubated at room temperature for 5 min, and added to the washed cells. After 5 h the transfection solution is replaced by 6 ml DMEM supplemented with 10% fetal calf serum.

To study the effect of the test hormones, transiently transfected cells are trypsinized, pooled and replated onto 60-mm dishes at a density of 4.5×10^5 per dish 24 h after transfection. Stably transfected cells are seeded onto 6-well dishes (1×10^5 cells per dish). Cells are cultured in medium supplemented with 3% charcoal-stripped fetal calf serum and the appropriate hormones for 48 h. Cells are cultured with 1% ethanol as a negative control for the reporter gene induction. Transactivation assays with transiently or stably transfected cells are carried out at least three times.

CAT Assay

Transiently transfected cells and stably transfected cells are disrupted by freezing (ethanol/dry ice bath) and thawing (37°C water bath) three times. Protein concentrations of the cell extract are determined according to Bradford (1976). The CAT assay is performed according to Gorman et al. (1982).

EVALUATION

CAT activity is calculated as percentage conversion from chloramphenicol to acetylated chloramphenicol. Concentration–response curves for CAT induction are established to demonstrate the potency of the test hormone. The synthetic androgen R 1881 (10^{-10} to 10^{-6} mol/l) is used as the standard.

For anti-androgenic activity, CAT activity in the presence of 0.5 nmol/l R 1881 is set as 100% and relative CAT activity is calculated as a percentage of this value. Concentration–response curves for CAT inhibition are established with increasing concentrations of the antihormone.

CRITICAL ASSESSMENT OF THE METHOD

See N.2.1.1.2.

MODIFICATIONS OF THE METHOD

Warriar et al. (1993) examined the ability of dihydrotestosterone (DHT) and various antiandrogens to stimulate or to inhibit the transcription activation of mouse mammary tumor virus-bacterial chloramphenicol acetyltransferase (MMTV-CAT) in CV-1 cells.

White et al. (1994) described a simple and sensitive high-throughput assay which can be adapted for several classes of steroid agonists and antagonists. A DNA cassette, containing a synthetic steroid-inducible promoter controlling the expression of a bacterial chloramphenicol acetyltransferase gene (GRE5-CAT), was inserted into an Epstein-Barr virus episomal vector which replicates autonomously in primate and human cells. This promoter/reporter system was used to generate two stably transfected human cell lines. In the cervical carcinoma cell line HeLa, which expresses high level of glucocorticoid receptor, the GRE5 promoter is inducible over 100-fold by the synthetic glucocorticoid dexamethasone. In the breast carcinoma cell line T47D, which expresses progesterone and androgen receptors, the GRE5 promoter is inducible over 100-fold by either progesterone or dihydrotestosterone

(DHT). These cell lines can be used to screen large numbers of natural and synthetic steroid agonists and antagonists in microtiter wells directly using a colorimetric chloramphenicol acetyltransferase (CAT) assay.

REFERENCES AND FURTHER READING

Bradford M (1976) A rapid and sensitive method for the quantitation of microgram quantities of protein utilizing the principle of protein-dye binding. Anal Biochem 72:248–254

Cato ACB, Miksicek R, Schütz G, Arnemann J, Beato M (1986) The hormone regulatory element of mouse mammary tumor virus mediates progesterone induction. EMBO J 6:2237–2240

Felgner PL, Holm M (1989) Cationic liposome-mediated transfection. Focus 11:21–25

Fuhrmann U, Bengtson C, Repenthin G, Schillinger E (1992) Stable transfection of androgen receptor and MMTV-CAT into mammalian cells: inhibition of CAT expression by antiandrogens. J Steroid Biochem Mol Biol 42:787–793

Fuhrmann U, Slater EP, Fritzemeier KH (1995) Characterization of the novel progestin gestodene by receptor binding studies and transactivation assays. Contraception 51:45–52

Fuhrmann U, Krattenmacher R, Slater EP, Fritzemeier KH (1996) The novel progestin drospirone and its natural counterpart progesterone: biochemical profile and antiandrogenic potential. Contraception 54:243–251

Gorman CM, Moffat LF, Howard BH (1982) Recombinant genomes which express chloramphenicol acetyltransferase in mammalian cells. Mol Cell Biol 2:1044–1055

Green S, Chambon P (1988) Nuclear receptors enhance our understanding of transcription regulations. Trends Genet 4:309–314

Muhn P, Fuhrmann U, Fritzemeier KH, Krattenmacher R, Schillinger E (1995) Drospirenone: a novel progestogen with anti-mineralocorticoid and antiandrogenic activity. Ann NY Acad Sci 761:311–335

Warriar N, Page N, Koutsilieris M, Govindan MV (1993) Interaction of antiandrogen-androgen complexes with DNA and transcription activation. J Steroid Biochem Mol Biol 46:699–711

White JH, McCuaig KA, Mader S (1994) A simple and sensitive high-throughput assay for steroid agonists and antagonists. Biotechnology 12:1003–1007

N.4.1.2 In Vivo Methods

N.4.1.2.1 Chicken Comb Method for Androgen Activity

PURPOSE AND RATIONALE

This is a historical bioassay based on the response of the comb of castrate cockerels (capons). The method has been used by many authors to assay androgenic activity and has been found to be extremely useful for the isolation and structural elucidation of natural androgens. Many modifications have been published (reviewed by Dorfman 1969).

PROCEDURE

Prior to assay, the surface area (sum of the length plus height of each individual comb) is determined by a millimeter rule placed directly on the comb. The capons are injected q.d. intramuscularly for 5 days consecutively with a solution or suspension of the test compound and reference animals are treated with the androgen standard in 1 ml olive oil. Then 24 h after the last injection, the combs are measured again and the growth of the comb is expressed as the sum of length and height in millimeters. Groups of eight animals are used for at least two doses of the test compound and the standard. In this method, animals can be used repeatedly.

EVALUATION

The experimental parameter is the surface area of the comb. The mean values of each group are calculated, dose–response curve for the test compound and the standard are plotted, and potency ratios are calculated where possible.

Similar studies were reported by: Gallagher and Koch 1935; Greenwood et al. 1935; Oesting and Webster 1938

MODIFICATIONS OF THE METHOD

The hormones, dissolved in oil, have been applied locally to the capon's comb instead of by injection. A greater sensitivity has been achieved with this modification (Fussgänger 1934; McCullagh and Cuyler 1939).

Newly hatched chicks of either sex have been used to study the growth of combs after systemic or local administration (Frank et al. 1942; Dorfman 1948). White Leghorn chicks are used at an age of 2–3 days. They are kept in a brooder with thermostatic control. An oily solution (0.05 ml) of the test compound or the standard is applied to the comb daily for a period of 7 days. Then 24 h after the last application, the animals are autopsied. Body weights are determined. The combs are removed by two longitudinal incisions along the base of the comb at its juncture with the scalp. The comb is freed from the scalp, touched lightly on a towel to remove blood and weighed. Dose–response curves are established.

REFERENCES AND FURTHER READING

Dorfman RI (1948) Studies on the bioassay of hormones. The assay of testosterone propionate and androsterone by a chick inunction method. Endocrinology 48:1–6

Dorfman RI (1969) Androgens and anabolic agents. In: Dorfman RI (ed) Methods in hormone research, Vol IIA. Academic Press, New York, pp 151–220

Frank RT, Klempner E, Hollander R, Kriss B (1942) Detailed description of technique for androgen assay by the chick comb method. Endocrinology 31:63–70
Fussgänger R (1934) Ein Beitrag zum Wirkungsmechanismus des männlichen Sexualhormons. Med Chem 2:194–204
Gallagher TF, Koch FC (1935) The quantitative assay for the testicular hormone by the comb-growth reaction. J Pharmacol Exp Ther 55:97–117
Greenwood AW, Blyth JSS, Callow RK (1935) Quantitative studies on the response of the capon's comb to androsterone. Biochem J 29:1400–1413
McCullagh DF, Cuyler WC (1939) The response of the capon's comb to androsterone. J Pharmacol Exp Ther 66:379–388
Oesting RB, Webster B (1938) The sex hormone excretion in children. Endocrinology 22:307–314

N.4.1.2.2 Weight of Androgen-Dependent Organs in Rats

PURPOSE AND RATIONALE

Androgens affect the development of secondary sex organs in the male rat (ventral prostate, seminal vesicles). The growth of the ventral prostate, the seminal vesicles and the musculus levator ani is dependent on the presence of male sexual hormones. Weight development of the musculus levator ani was considered to indicate anabolic activity, and weight development of the ventral prostate and seminal vesicles was considered to indicate androgenic activity (Dorfmann 1969).

PROCEDURE

Immature male Sprague-Dawley rats weighing about 55 g are orchiectomized. Animal body weight is recorded at the beginning and at the end of the experiment.

The animals are treated with test compounds by gavage (orally) in 0.5 ml 0.5% carboxymethylcellulose or by subcutaneous injection in 0.2 ml sesame oil suspension once per day over a period of 10 days. Testosterone is given in doses of 0.02, 0.1, and 0.5 mg per animal subcutaneously, and methyltestosterone orally in doses of 0.25, 1.5, and 5 mg per animal. Controls receive the respective vehicle. Ten animals are used for each group. On day 10 at autopsy, the seminal vesicles, ventral prostate, and levator ani muscle are dissected out and weighed. The seminal vesicles are squeezed and dried to remove the fluid.

Dissection of the levator ani muscle is performed after removal of the skin in the scrotal area between the base of the penis and the anus. The posterior aspect of the perineal complex is cleared of fat and connective tissue with forceps, particular care being taken to expose the constrictions at either end of the levator ani where it joins the bulbocavernosus muscle. The rectum is transected just caudad to the point where the musculus levator ani loops around it dorsally. The body of the levator ani is then freed of the rectum and is removed by incisions at the points of attachment to the bulbocavernosus muscle. The levator ani is cleared of any connective tissue and weighed to the nearest 0.1 mg.

EVALUATION

The ratio of organ weight to body weight is calculated for every animal and each organ (relative organ weights). Dose–response curves are constructed for each organ comparing the test compound with the standard in order to calculate potency ratios. An increase in the weight of seminal vesicles and ventral prostate indicates androgenic activity, whereas an increase in the weight of musculus levator ani is considered to indicate anabolic activity.

In evaluating steroids for possible use as anabolic agents, Hershberger et al. (1953) suggested the use of the levator ani:ventral prostate ratio, which is defined as the ratio of the increase in levator ani weight divided by the increase in ventral prostate weight.

The method has been useb by several authors: Korenchevsky and Dennison 1935; Eisenberg and Gordon 1950; Junkmann 1957; Kincl 1965; Eisler 1964; Dorfmann 1969; Kuhnz and Beier 1994.

REFERENCES AND FURTHER READING

Dorfman RI (1969) Androgens and anabolic agents. In: Dorfman RI (ed) Methods in hormone research, Vol IIA. Academic Press, New York, pp 151–220
Eisenberg E, Gordon GS (1950) The levator ani muscle of the rat as an index of myotrophic activity of steroidal hormones. J Pharmacol Exp Ther 99:38–44
Eisler M (1964) Animal techniques for evaluating sex steroids. In: Nodine JH, Siegler PE (eds) Animal and clinical pharmacologic techniques in drug evaluation. Year Book Medical Publishers, Chicago, Ill., pp 566–573
Hershberger LG, Shipley EG, Meyer RK (1953) Myotrophic activity of 19-nortestotestone and other steroids determined by modified levator ani muscle method. Proc Soc Exp Biol Med 83:175–180
Junkmann K (1957) Long-acting steroids in reproduction. Rec Prog Horm Res 13:389–427
Kincl FA (1965) Anabolic steroids. In: Dorfman RI (ed) Methods in hormone research, Vol IV. Academic Press, New York, pp 21–76
Korenchevsky V, Dennison M (1935) The assay of crystalline male sexual hormone (androsterone). Biochem J 29:1720–1731
Kuhnz W, Beier S (1994) Comparative progestational and androgenic activity of norgestimate and levonorgestrel in the rat. Contraception 49:275–289

N.4.1.2.3 Nitrogen Retention

PURPOSE AND RATIONALE

Anabolic agents induce positive nitrogen balance in the living organism (Polish 1964; Dorfmann 1969). Many modifications of this assay principle have evolved. Stafford et al. (1954) suggested a method involving the measurement of nitrogen excretion in the castrated rat fed a liquid diet and in nitrogen balance.

PROCEDURE

Twenty-five-day-old rats are castrated and kept untreated for 67 days, reaching about 300 g in body weight on normal laboratory diet. After 67 days, they are changed to a liquid diet, forced-feeding regime. The diet contains carbohydrates and fat, as well as casein and brewer's yeast as a nitrogen source. At the start, the rats receive 10 ml of feed per day, and this is increased to 26 ml per day. Feeding is continued for 30 days with simultaneous administration of the test drug once a day. Twenty-four-hour urine specimens are collected 3 times weekly and analyzed for total nitrogen.

EVALUATION

Indices are calculated, such as greatest daily retention, which is defined as the difference between the lowest daily nitrogen value after the beginning of treatment and the preinjection mean; the total nitrogen retention, which is the sum of the differences between the preinjection excretion and the daily values during the retention period; and the number of days in the retention period.

MODIFICATIONS OF THE METHOD

A method for the assay of anabolic steroids in the monkey (*Macaca mulatta*) has been suggested by Stucki et al. (1960). Nitrogen retention expressed as total nitrogen retained per day during the treatment period is chosen as the end point.

CRITICAL ASSESSMENT OF THE METHOD

The assay is time-consuming and labor-intensive, and its use is no longer recommended.

REFERENCES AND FURTHER READING

Dorfman RI (1969) Androgens and anabolic agents. In: Dorfman RI (ed) Methods in hormone research, Vol IIA. Academic Press, New York, pp 151–220

Polish E (1964) Clinical techniques for evaluating anabolic agents. In: Nodine JH, Siegler PE (eds) Animal and clinical pharmacologic techniques in drug evaluation. Year Book Medical Publishers, Chicago, Ill., pp 561–565

Stafford RO, Bowman BJ, Olson KJ (1954) Influence of 19-nortestosterone cyclopentyl-propionate on urinary nitrogen of castrate male rat. Proc Soc Exp Biol Med 86:322–326

Stucki JC, Forbes AD, Northam JI, Clark JJ (1960) An assay for anabolic steroids employing metabolic balance in the monkey: the anabolic activity of fluoxymesterone and its 11-keto analogue. Endocrinology 66:585–598

N.4.2 Anti-Androgenic Activity

N.4.2.0.1 General Considerations

Anti-androgens may exhibit their activity both peripherally on androgen-dependent tissues and by feedback action at a central site (Neumann et al. 1970; Mainwaring 1977; Neri 1977; Neumann et al. 1977; Raynaud et al. 1977; Neumann 1985; Moguilewski and Bouton 1988). They compete with the peripheral androgen receptors and thus inhibit the effect of endogenous or exogenous androgens. Centrally, they inhibit gonadotropin secretion and thereby diminish testosterone production by the gonads. In addition to their effects on reproduction and accessory sexual organs, anti-androgens inhibit sebum production (anti-acne drugs) and delay androgen-dependent hair loss (alopecia). The methods to detect and quantify gonadotropin inhibition are described in Sect. N.7.1.8.

Inhibition of 5α-reductase, an enzyme located in tissues such as the prostate, is one pharmacological approach to inhibit benign prostate hyperplasia in men. Such inhibitors reduced the conversion from testosterone to 5α-dihydrotestosterone (DHT).

REFERENCES AND FURTHER READING

Mainwaring WIP (1977) Modes of action of antiandrogens: a survey. In: Martini L, Motta M (eds) Androgens and antiandrogens. Raven, New York, pp 151–161

Moguilewski M, Bouton MM (1988) How the study of biological activities of antiandrogens can be oriented towards the clinic. J Steroid Biochem 31:699–710

Neri RO (1977) Studies on the biology and mechanism of action of nonsteroidal antiandrogens. In: Martini L, Motta M (eds) Androgens and antiandrogens. Raven, New York, pp 179–189

Neumann F (1985) Chemistry and pharmacology of anti-androgens. Chron Dermatol 16:557–563

Neumann F, von Berswordt-Wallrabe, Elger W, Steinbeck H, Hahn JD, Kramer M (1970) Aspects of androgen-dependent events as studied by antiandrogens. Recent Prog Horm Res 26:337–410

Neumann F, Gräf KJ, Hasan SH, Schenck B, Steinbeck H (1977) Central actions of antiandrogens. In: Martini L, Motta M (eds) Androgens and anti-androgens. Raven, New York, pp 163–177

Raynaud JP, Azadian-Boulanger G, Bonne C, Perronnet J, Sakiz E (1977) In: Martini L, Motta M (eds) Androgens and antiandrogens. Raven, New York, pp 281–293

N.4.2.1 In Vitro Methods

N.4.2.1.1 Inhibition of 5α-Reductase

PURPOSE AND RATIONALE

Testosterone is converted to 5α-dihydrotestosterone (DHT) by the enzyme 5α-reductase which is specifically localized in some androgen-responsive target tissues (e. g., prostate, seminal vesicle, epididymis, skin and sebaceous glands), whereas in other androgen-sensitive tissues, such as the skeletal muscles and the central structures, the androgenic hormone is testosterone. Inhibition of 5α-reductase provides a selective approach to androgen deprivation in DHT-target tissues, such as the prostate. The 5α-reductase inhibitors are applied in the therapy of benign prostate hyperplasia.

PROCEDURE

5α-Reductase preparations are obtainable from prostates of various species, such as human, dog, and rat.

Frozen human prostates from benign prostatic hyperplasia patients are thawed and minced with a pair of scissors. The minced tissue is homogenized in three tissue volumes of medium A (20 mM potassium phosphate, pH 6.5, containing 0.32 M sucrose, 1 mM dithiothreitol and 50 µM NADPH) with a Brinkmann Polytron and a glass-glass homogenizer. The homogenate is centrifuged at 140,000 *g* for 60 min and the pellets are washed with approximately three tissue volumes of medium A. The washed pellets are suspended at a concentration of 5–10 mg protein/ml in 20 mM potassium phosphate, pH 6.5, containing 20% glycerol and 1 mM dithiothreitol.

Dog prostatic particulates are prepared from either fresh or frozen specimens of male mature dogs as described for human prostate. The washed pellets are suspended in medium A at a concentration of 30–60 mg protein/ml.

Ventral prostates from male Sprague-Dawley rats weighing 400 g are processed as described for human prostate, except that medium A without NADPH is used throughout the procedures. NADPH prevents inactivation of human and dog 5α-reductases during the preparation, the rat enzyme however is stable without the coenzyme.

For the 5α-reductase assay, reaction solutions are prepared in duplicate tubes containing 1 µM [^{14}C]testosterone, 1 mM dithiothreitol, 40 mM buffer (potassium phosphate, pH 6.5, for the rat and for the dog enzymes; Tris-citrate, pH 5.0, for the human enzyme), prostatic particulate (1 mg protein), and NADPH (50 µM for reaction with rat enzyme, 500 µM for reaction with human and dog enzyme) in a final volume of 0.5 ml. Test compounds or standard as inhibitors are added in 5 µl ethanol at concentrations between 10^{-9} and 10^{-5} M. The control tubes receive the same volume of ethanol. The reactions for the rat and dog enzymes are started by the addition of the prostatic particulates. The human prostatic particulate is premixed with NADPH before starting the reaction. The reactions are linear for at least 1 h at 37°C. The reactions are carried out for 10–30 min and are stopped with 2 ml ethyl acetate containing testosterone, 5α-dihydrotestosterone, and androstenedione (10 µg each). After centrifugation at 1000 *g* for 5 min, the ethyl acetate phase is transferred to a tube and evaporated under nitrogen to dryness. The steroids are taken up in 50 µl ethyl acetate. The solutions are applied to Whatman LK5DF silica plates and the plates are developed in either ethyl acetate:cyclohexane (1:1) at 25°C or chloroform:methanol (96:4) at 4°C. The plates are air-dried and the chromatography is repeated. Nonradioactive steroid standards are located by UV and by spraying with 1% $CeSO_4$/10% H_2SO_4 solution followed by heating. The radioactivity profiles are determined by scanning the plates or by scraping the silica in sections and counting in a scintillation counter. 5α-Dihydrotestosterone is the only radioactive product for the rat and human enzymes. With the dog enzyme 5α-dihydrotestosterone, 3α,17β-androstanediol, androstan-3,17-dione, and androstenedione are formed. The radioactivities of the first three products are combined for the calculation of the 5α-reductase activity.

EVALUATION

IC_{50} values are calculated based on at least five dilutions of test preparations or standard.

MODIFICATIONS OF THE METHOD

The method has been useb by several authors: Bruchovsky and Wilson 1968; Corvol et al. 1975; Brooks et al. 1981; Liang et al. 1985; Rhodes et al. 1993; di Salle et al. 1993; Sudduth and Koronkowski 1993; di Salle et al. 1994

Using human genital skin fibroblasts and simian COS cells, specific inhibition of 5α-reductase type 1 has been observed (Hirsch et al. 1993).

Wennbo et al. (1997) reported that **transgenic mice** overexpressing the prolactin gene develop dramatic enlargement of the prostate gland.

Sigimura et al. (1994) described age-related changes of the prostate gland in the senescence-accelerated mouse and recommended this strain as a model of age-related changes in the prostate gland.

Neubauer et al. (1993) measured prostatic 5α-reductase in rats both *in vitro* and *ex vivo* and determined *in vivo* uptake of [^{3}H]testosterone by the prostate.

At least two isoforms of 5α-reductase have been isolated (Andersson and Russell 1990; Jenkins et al. 1992). Recombinant human prostatic 5α-reductase type I and II were expressed using the baculovirus-directed insect cell expression system (Iehlè et al. 1993).

Iehlè et al. (1995) and di Salle et al. (1998) tested synthetic 5α-reductase inhibitors against both isoforms.

Tolman et al. (1995) identified a 4-azasteroid as a scalp isoenzyme selective inhibitor.

REFERENCES AND FURTHER READING

Andersson S, Russell DW (1990) Structural and biochemical properties of cloned and expressed human and rat steroid 5α-reductases. Proc Natl Acad Sci USA 87:3640–3644

Brooks JR, Baptista EM, Berman C, Ham EA, Hichens M, Johnston DBR, Primka RL, Rasmusson G, Reynolds GF, Schmitt SM, Arth GE (1981) Response of rat ventral prostate to a new and novel 5α-reductase inhibitor. Endocrinology 109:830–836

Bruchovsky N, Wilson JD (1968) The conversion of testosterone to 5α-androstan-17β-ol-3-one by rat prostate *in vivo* and *in vitro*. J Biol Chem 243:2012–2021

Corvol P, Michaud A, Menard J, Freifeld M, Mahoudeau J (1975) Antiandrogenic effect of spirolactones: mechanism of action. Endocrinology 97:52–58

di Salle E, Giudici D, Briatico G, Ornati G, Panzeri A (1993) Hormonal effects of turosteride, a 5α-reductase inhibitor, in the rat. J Steroid Biochem Mol Biol 46:549–555

di Salle E, Briatico G, Giudici D, Ornati G, Panzeri A (1994) Endocrine properties of the testosterone 5α-reductase inhibitor turosteride (FCE 26073). J Steroid Biochem Mol Biol 48:241–248

di Salle E, Giudici G, Radice A, Zaccheo T, Ornati G, Nesi M, Panzeri A, Délos S, Martin PM (1998) PNU 157706, a novel dual type I and II 5α-reductase inhibitor. J Steroid Biochem Mol Biol 64:179–186

Hirsch KS, Jones CD, Audia JE, Andersson S, McQuaid L, Stamm NB, Neubauer BL, Pennington P, Toomey RE, Russell DW (1993) LY191704: a selective, nonsteroidal inhibitor of human steroid 5α-reductase type 1. Proc Natl Acad Sci USA 90:5277–5281

Iehlè C, Délos S, Filhol O, Martin PM (1993) Baculovirus-directed expression of human prostatic steroid 5α-reductase 1 in an active form. J Steroid Biochem Mol Biol 46:177–182

Iehlè C, Délos S, Guirou O, Tate R, Raynaud JP, Martin PM (1995) Human prostatic steroid 5α-reductase isoforms: a comparative study of selective inhibitors. J Steroid Biochem Mol Biol 54:273–279

Jenkins EP, Andersson S, Imperato-McGinley J, Wilson J, Russell DW (1992) Genetic and pharmacological evidence for more than one human steroid 5α-reductase. J Clin Invest 89:293–300

Liang T, Cascieri MA, Cheung AH, Reynolds GF, Rasmusson GH (1985) Species differences in prostatic steroid 5α-reductase of rat, dog and human. Endocrinology 117:571–579

Neubauer BL, Best KL, Blohm TR, Gates C, Goode RL, Hirsch KS, Laughlin ME, Petrow V, Smalstig EB, Stamm NB, Toomey RE, Hoover DM (1993) LY207320 (6-methylene-4-pregnene-3,20-dione) inhibits testosterone biosynthesis, androgen uptake, 5α-reductase, and produces prostatic regression in rats. Prostate 23:181–199

Rhodes L, Primka RL, Berman C, Vergult G, Gabriel M, Pierre-Malice M, Gibelin B (1993) Comparison of Finasteride (Proscar), a 5α reductase inhibitor, and various commercial plant extracts in *in vitro* and *in vivo* 5α reductase inhibition. Prostate 22:43–51

Sigimura Y, Sakurai M, Hayashi N, Yamashita A, Kawamura J (1994) Age-related changes of the prostate gland in the senescence-accelerated mouse. Prostate 24:24–32

Sudduth SL, Koronkowski MJ (1993) Finasteride: the first 5α reductase inhibitor. Pharmacotherapy 13:309–329

Tolman RL, Aster S, Bakshi RK, Bergman JP, Bull HG, Chang B, Cimis G, Dolenga MP, Durette P, Ellsworth K, Esser C, Graham DW, Hagman WK, Harris G, Kopka I, Lanza T, Patel G, Polo S, Rasmusson GH, Sahoo S, Toney JH, Von Langen D, Witzel B (1995) 4-Azasteroids as 5α-reductase inhibitors: identification of 4,7β-dimethyl-4-aza-5α-cholestan-3-one (MK-386) as a scalp isozyme selective inhibitor. Eur J Med Chem Suppl 30:311s–316s

Wennbo T, Kindblom J, Isaksson OPG, Tornell J (1997) Transgenic mice overexpressing the prolactin gene develop dramatic enlargement of the prostate gland. Endocrinology 138:4410–4415

N.4.2.2 In Vivo Methods

N.4.2.2.1 Chick Comb Method

PURPOSE AND RATIONALE

This method is now obsolete for the evaluation of anti-androgens. Several modifications of the chick comb method have been described for anti-androgens applied either systemically or locally to the comb of intact cockerels (Dorfmann 1960, 1969).

PROCEDURE

Male or female, 1- to 3-day-old White Leghorn chicks are housed at constant temperature in a heated incubator. Testosterone is incorporated into the finely ground chick starting mash at a concentration of 80 mg/kg of food to stimulate comb growth. The chicks are placed on this diet on day 1. The anti-androgen to be tested is

dissolved in sesame oil and injected for several days. At 24 hours after the last injection, the animals are sacrificed, the combs removed and blotted to remove blood, and weighed rapidly to the nearest 0.5 mg. Body weights are also determined.

EVALUATION

The results may be expressed as absolute comb weights or as milligram of comb per gram of body weight. Dose–response curves for groups treated with increasing doses of anti-androgen are plotted.

REFERENCES AND FURTHER READING

Dorfman RI (1969) Antiandrogens. In: Dorfman RI (ed) Methods in hormone research, Vol IIA. Academic Press, New York, pp 221–249

Dorfman RI, Dorfman AS (1960) A test for anti-androgens. Acta Endocrinol 33:308–316

N.4.2.2.2 Antagonism of Androgen Action in Castrated Rats

PURPOSE AND RATIONALE

In this modification, anti-androgens are administered to reduce or inhibit testosterone action's on androgen-dependent organs.

PROCEDURE

Male Sprague-Dawley rats weighing 50–70 g are orchiectomized. Starting 1 day after castration, the rats are injected once daily for 7 days with 0.15 mg testosterone propionate in 0.1 ml sesame oil (agonist action). The test compounds (anti-androgens) are dissolved in sesame oil or suspended and injected subcutaneously daily at a separate site for the same test period of 7 days. Six to ten animals are used per group. At autopsy on day 8, weights of ventral prostate, seminal vesicles and musculus levator ani as well as body weight are recorded.

EVALUATION

The organ weight to body weight ratio is calculated for each order, preferably based on relative organ weight to 100 g of body weight. The inhibition by the anti-androgen is compared with agonist action in the groups of animals receiving testosterone propionate alone. Dose–response curves may be plotted for each organ, and expressed as percentage inhibition of the agonist effect of testosterone by the anti-androgen.

MODIFICATIONS OF THE METHOD

Dorfman (1962) described an anti-androgen assay using the castrated mouse. Weights of prostate and seminal vesicles were determined after injection of the anti-androgen test compounds and simultaneous injections of 2 mg testosterone over a period of 7 days.

APPLICATIONS OF THE METHOD

The intrinsic anti-androgenic activity is an important parameter in the evaluation of the pharmacological activity of H2-receptor antagonists (Winters et al. 1979; Broulik 1980; Baba et al. 1981; Sivelle et al. 1982; Foldesy et al. 1985; Takeda et al. 1982; Neubauer et al. 1990). In general pharmacology studies, there is rarely any need for specific anti-hormonal tests. However, in toxicology studies, tests for anti-androgen activity may be warranted when the effects on the testes and androgen-dependent organs are found in repeated-dose studies.

REFERENCES AND FURTHER READING

Baba S, Paul HJ, Pollow K, Janetschek G, Jacobi GH (1981) *In vivo* studies on the antiandrogenic effects of cimetidine versus cyproterone acetate in rats. Prostate 2:163–174

Broulik PD (1980) Antiandrogenic activity of cimetidine in mice. Endokrinologie 76:118–121

Byrnes WW, Stafford RO, Olson KJ (1953) Anti-gonadal hormone activity of 11α-hydroxyprogesterone. Proc Soc Exp Biol Med 82:243–247

Christiansen RG, Bell MR, D'Ambra TE, Mallamo JP, Herrmann JL, Ackerman JH, Opalka CJ, Kullnig RK, Winnecker RC, Snyder BW, Batzold FH, Schane HP (1990) Antiandrogenic steroidal sulfonylpyrazoles. J Med Chem 33:2094–2100

Dorfman RI (1962) An anti-androgen assay using the castrated mouse. Proc Soc Exp Biol Med 111:441–443

Dorfman RI (1969) Antiandrogens. In: Dorfman RI (ed) Methods in hormone research, Vol IIA. Academic Press, New York, pp 221–249

Eviatar A, Danon A, Sulman FG (1961) The mechanism of the "push and pull" principle. V. Effect of the antiandrogen RO 2-7239 on the endocrine system. Arch Int Pharmacodyn 133:75–88

Foldesy RG, Vanderhoof MM, Hahn DW (1985) *In vitro* and *in vivo* comparisons of antiandrogenic potencies of two histamine H2-receptor antagonists, cimetidine and etintidine-HCl (42087). Proc Soc Exp Biol Med 179:206–210

Furr BJA, Valcaccia B, Curry B, Woodburn JR, Chesterson C, Tucker H (1987) ICI 176,334: a novel non-steroidal, peripherally selective antiandrogen. J Endocrinol 113:R7–R9

Neri F, Florance K, Koziol P, van Cleave S (1972) A biological profile of a nonsteroidal antiandrogen, SCH 13521 (4′-nitro-3′-trifluoromethylisobutyranilide). Endocrinology 91:427–437

Neubauer BE, Best KL, Clemens JA, Gates CA, Goode RL, Jones CD, Laughlin ME, Shaar CJ, Toomey RE, Hoover DM (1993) Endocrine and antiprostatic effects of Raloxifene (LY156758) in the male rat. Prostate 23:245–262

Neubauer BL, Goode RL, Best KL, Hirsch KS, Lin TM, Pioch RP, Probst KS, Tinsley FC, Shaar CJ (1990) Endocrine effects of a new histamine H_2-receptor antagonist, Nizatidine (LY139037), in the male rat. Toxicol Appl Pharmacol 102:219–232

Neumann F, Gräf KJ, Hasan SH, Schenck B, Steinbeck H (1977) Central actions of antiandrogens. In: Martini L, Motta M (eds) Androgens and antiandrogens. Raven, New York, pp 163–177

Randall LO, Selitto JJ (1958) Anti-androgenic activity of a synthetic phenanthrene. Endocrinology 62:693–695

Shibata K, Takegawa, S, Koizumi N, Yamakoshi N, Shimazawa E (1992) Antiandrogen. I. 2-Azapregnane and 2-oxapregnane steroids. Chem Pharm Bull 40:935–941

Sivelle PC, Underwood AH, Jelly JA (1982) The effects of histamine H_2 receptor antagonists on androgen action *in vivo* and dihydrotestosterone binding to the rat prostate androgen receptor *in vitro*. Biochem Pharmacol 31:677–684

Snyder BW, Winneker RC, Batzold FH (1989) Endocrine profile of WIN 49596 in the rat: a novel androgen receptor antagonist. J Steroid Biochem 33:1127–1132

Tagekawa S, Koizumi N, Takahashi H, Shibata K (1993) Antiandrogen. II. Oxygenated 2-oxapregnane steroids. Chem Pharm Bull 41:870–875

Takeda M, Takagi T, Yashima Y, Maneo H (1982) Effect of a new H_2-blocker, 3-[[[2-[(diaminomethylene)amino]-4-thiazoly] methyl]thio]-N^2-sulfamoyl propionamidine (YM-11170), on gastric secretion, ulcer formation and male accessory sex organs in rats. Arzneimittelforschung 32:734–737

Turner RA (1965) Anabolic, androgenic, and antiandrogenic agents. In: Turner RA (ed) Screening methods in pharmacology. Academic Press, New York, pp 244–246

Winters SJ, Banks JL, Loriaux DL (1979) Cimetidine is an antiandrogen in the rat. Gastroenterology 76:504–508

N.4.2.2.3 Anti-Androgenic Activity in Female Rats

PURPOSE AND RATIONALE

This is another historical bioassay of interest due to the design of exploring anti-androgenic activity. Neumann and Elger (1966) described a method for testing the anti-androgenic activity of compounds in immature female rats. The inhibition by the anti-androgen cyproterone of the trophic effect of testosterone on uterine and preputial growth was studied in intact as well as in castrated female rats (Neri et al. 1972; Snyder et al. 1989) .

PROCEDURE

Female Sprague-Dawley rats weighing 40–45 g are ovariectomized. One week later, the treatment is started for 12 days with daily subcutaneous injections of 0.3 mg testosterone propionate and several doses of the antagonist. Controls receive testosterone propionate only. At autopsy on day 13, the uteri and preputial glands are distracted out and weighed. The weight increase of female accessory sexual organs caused by testosterone's action is dose-dependently reduced by the anti-androgen (in this case, cyproterone). Similar results are found using intact immature female rats.

EVALUATION

Dose–response curves were established for increasing doses of the anti-androgen at a given dose of testosterone propionate or for increasing doses of testosterone propionate at a given dose of the anti-androgen, cyproterone.

CRITICAL ASSESSMENT OF THE METHOD

The method is time-consuming and was directed to the specific investigation of cyproterone and cyproterone acetate in precocious puberty and androgen-dependent disorders.

REFERENCES AND FURTHER READING

Neri F, Florance K, Koziol P, van Cleave S (1972) A biological profile of a nonsteroidal antiandrogen, SCH 13521 (4′-nitro-3′-trifluoromethylisobutyranilide). Endocrinology 91:427–437

Neumann F, Elger W (1966) Eine neue Methode zur Prüfung antiandrogen wirksamer Substanzen an weiblichen Ratten. Acta Endocrinol 52:54–62

Snyder BW, Winneker RC, Batzold FH (1989) Endocrine profile of WIN 49596 in the rat: a novel androgen receptor antagonist. J Steroid Biochem 33:1127–1132

N.4.2.2.4 Intra-Uterine Feminizing/Virilizing Effect

PURPOSE AND RATIONALE

From clinical observations as well as from experimental data (Neumann and Junkmann 1963; Neumann and Kramer 1964), it is well known that the external genitalia of female fetuses can be masculinized by tumors secreting endogenous androgens or by steroids with androgenic activity. This effect can be antagonized by an anti-androgen.

The method is of interest for assessment of reproductive toxicology.

PROCEDURE

Adult female Sprague-Dawley rats are mated and the beginning of pregnancy is determined by vaginal smears. From day 16 to day 19 of pregnancy, the antiandrogens are administered in various doses subcutaneously in sesame oil. Testosterone propionate is used in doses between 1.0 and 10.0 mg as the androgenic stimulus. The dams are sacrificed on the 20th day of pregnancy and the external genitalia of the female embryos examined. The sex of the embryos is recognized by the presence of ovaries and uterus. A dose of 10 mg

testosterone propionate leads to total masculinization of female embryos with loss of female and the appearance of male sex characteristics. The anogenital distance in female rat fetuses measured macroscopically and microscopically is dose-dependently increased by testosterone propionate. This characteristic androgen effect is diminished by an anti-androgen.

EVALUATION

The androgen-dependent decrease of the anogenital distance in female fetuses by various doses of the anti-androgen is expressed as percentage inhibition of the testosterone-induced virilization.

MODIFICATIONS OF THE METHOD

Feminization of male rats was induced by treatment of pregnant rats during the second half of gestation and of the newborn fetuses during weeks 1–3 post partum with an anti-androgen, e. g., cyproterone acetate (Neumann and Elger 1966; Nishino et al. 1988; review by Neumann 1994). A decrease of the anogenital distance in the male fetuses of anti-androgen-treated rats is expressed as percentage inhibition relative to fetuses from untreated mothers.

In feminized male rats, nipples and associated glandular tissues develop after birth as in normal female rats (Neumann and Elger 1967).

Feminization of male rats treated *in utero* was also observed with nonsteroidal anti-androgens and a 5α-reductase inhibitor (Imperato-McGinley et al. 1992).

REFERENCES AND FURTHER READING

Imperato-McGinley J, Sanchez RS, Spencer JR, Yee B, Vaughan D (1992) Comparison of the effects of the 5α-reductase inhibitor Finasteride and the antiandrogen Flutamide on prostate and genital differentiation: dose-response studies. Endocrinology 131:1149–1156

Neumann F (1994) The antiandrogen cyproterone acetate: discovery, chemistry, basic pharmacology, clinical use and tool in basic research. Exp Clin Endocrinol 102:1–32

Neumann F, Elger W (1966) Permanent changes of gonadal function and sexual behaviour as a result of early feminization of male rats by treatment with an antiandrogenic steroid. Endokrinologie 50:209–225

Neumann F, Elger W (1967) Steroidal stimulation of mammary glands in prenatally feminized male rats. Eur J Pharmacol 1:120–123

Neumann F, Junkmann K (1963) A new method for determination of virilizing properties of steroids on the fetus. Endocrinology 73:33–37

Neumann F, Kramer M (1964) Antagonism of androgenic and anti-androgenic agents in their action on the rat fetus. Endocrinology 75:428–433

Nishino Y, Schröder H, El Etreby MF (1988) Experimental studies on the endocrine side effects of new aldosterone antagonists. Arzneimittelforschung 38:1800–1805

N.4.2.2.5 Anti-Androgenic Activity on Sebaceous Glands

PURPOSE AND RATIONALE

Bioassays for topical anti-androgens are based on inhibition of sebum secretion. Sebum production is increased by endogenous or exogenous androgens in many species including humans. In the mouse (Lapière and Chèvremont 1953; Neumann and Elger 1966), the Mongolian gerbil (Mitchell 1965), and the golden hamster (Hamilton and Montagna 1950), the male sex hormone stimulates sebum production and sebaceous gland growth. Morphometric evaluation by light microscopy in the rat has shown that castration causes a large reduction in the volume of the glands (Sauter and Loud 1975). The administration of testosterone over several days produces an enlargement of the sebaceous glands. This effect is used for morphometric evaluation of topical anti-androgens.

The method is described in detail in Sect. P.9.1.

REFERENCES AND FURTHER READING

Hamilton JB, Montagna W (1950) The sebaceous gland of the hamster. I. Morphological effects of androgens on integumentary structures. Am J Anat 86:191–234

Lapière CH, Chèvremont M (1953) Modifications des glandes sébacées par des hormones sexuelles appliquées localement sur la peau de Souris. CR Soc Biol (Paris) 147:1302–1306

Mitchell OG (1965) Effect of castration and transplantation on ventral gland of the gerbil. Proc Soc Exp Biol Med 119:953–955

Neumann F, Elger W (1966) The effect of a new antiandrogenic steroid, 6-chloro-17-hydroxy-1α,2α-methylenepregena-4,6-diene-3,20-dione acetate (cyproterone acetate) on the sebaceous glands of mice. J Invest Dermatol 46:561–572

Sauter LS, Loud AV (1975) Morphometric evaluation of sebaceous gland volume in intact, castrated, and testosterone-treated rats. J Invest Dermatol 64:9–13

N.4.2.2.6 Anti-Androgenic Activity in the Hamster Flank Organ

PURPOSE AND RATIONALE

This is another bioassay preferably for topical anti-androgens. The flank organs of Syrian golden hamsters are located on each flank of the animal consisting mainly of sebaceous tissue. Like sebaceous glands in other species, these pigmented spots respond to androgens by an increase in size. This proliferation is inhibited by systemic or topical anti-androgens.

The method is described in detail in Sect. P.9.5.

N.4.2.2.7 Effect of 5α-Reductase Inhibitors on Plasma and Tissue Steroid Levels

PURPOSE AND RATIONALE

5α-Reductase inhibitors change the ratio of plasma testosterone to dihydrotestosterone (DHT) as well as the tissue concentrations particularly in the prostate tissue.

PROCEDURE

Treatment of Animals

Male Sprague-Dawley rats are treated subcutaneously with the 5α-reductase inhibitor or vehicle beginning on postnatal day 3 until the age of 4 or 7 weeks. After sacrifice, blood is withdrawn for testosterone and DHT determinations (George et al. 1989). Moreover, intraprostatic concentrations of testosterone and DHT are determined as an index of antiproliferative activity (di Salle et al. 1993).

Radioimmunoassay for Testosterone and Dihydrotestosterone

Serum testosterone and DHT are measured by radioimmunoassay (RIA) in serum or serum extracts using specific antisera without prior chromatography (Falvo and Nalbandov 1974). Serum samples of 0.5 ml may be extracted with 2 ml of freshly purified, peroxide-free diethyl ether by shaking for 60 s on a Vortex mixer. The aqueous phase is frozen at −70°C, then the ether phase containing steroids is transferred to conical test tubes, and evaporated under a stream of dry nitrogen. The dry residue is redissolved in BSA/phosphate buffer (1% BSA = bovine serum albumin) for RIA. [1,2,6,7-^{3}H]-Testosterone or [1,2,6,7-^{3}H]-dihydrotestosterone and specific antisera are added and tubes incubated over a period of 24 h at +4°C under nonequilibrium conditions. Bound hormone and free hormone are separated by adsorption on dextran-coated charcoal. The activity of each sample is determined by beta-spectrometry.

Commercially available RIA kits can be used with suitable validation.

EVALUATION

The hormone concentrations in the sample are calculated from a standard curve by a computer program (e. g., RIA-Calc, LKB), using appropriate control sera. The ratios of testosterone to DHT in rats treated with different doses of 5α-reductase inhibitors are compared with those of vehicle-treated intact control rats.

MODIFICATIONS OF THE METHOD

di Salle et al. (1998) measured prostatic concentrations of testosterone and 5α-dihydrotestosterone in rats by specific RIAs after treatment with a dual type I and II 5α-reductase inhibitor. Similar measurements of tissue testosterone:DHT ratios have been performed in dogs, in the context of pituitary down-regulation of androgen secretion by luteinizing-hormone-releasing hormone (LHRH) agonists.

REFERENCES AND FURTHER READING

di Salle E, Giudici D, Briatico G, Ornati G, Panzeri A (1993) Hormonal effects of turosteride, a 5α-reductase inhibitor, in the rat. J Steroid Biochem Mol Biol 46:549–555

di Salle E, Giudici G, Radice A, Zaccheo T, Ornati G, Nesi M, Panzeri A, Délos S, Martin PM (1998) PNU 157706, a novel dual type I and II 5α-reductase inhibitor. J Steroid Biochem Mol Biol 64:179–186

Falvo RE, Nalbandov AV (1974) Radioimmunoassay of peripheral plasma testosterone in males from eight species using a specific antibody without chromatography. Endocrinology 95:1466–1468

George FW, Johnson L, Wilson JD (1989) The effect of a 5α-reductase inhibitor on androgen physiology in the immature male rat. Endocrinology 125:2434–2438

N.5 Thyroid Hormones

N.5.0.1 General Considerations

The purpose of this section is twofold: to described the methods for determination of hormones secreted by the thyroid gland, and to described investigation of thyroid function in experimental models. For information on the hypothalamic–pituitary–thyroid system and its investigation, see the sections on anterior pituitary hormones (N.7) and hypothalamic hormones (N.9).

The thyroid gland secretes two types of hormones: the **thyroid hormones**, i. e., l-**thyroxine** (T_4), and **triiodothyronine** (T_3) which have metabolic functions and are involved in neuronal development, and the **calcitropic hormone**, **calcitonin**. The functional system for metabolic regulation subserved by the thyroid hormones is entirely different from the complex system for regulation of calcium and phosphate balance fulfilled by (thyro)calcitonin, parathormone from the parathyroid glands, and the calciferol hormones (formerly vitamin D) produced by the liver and kidneys and activated in the skin.

The main biological effects of $\mathbf{T_3}$ and $\mathbf{T_4}$ are on growth and development (e. g., maturation of tadpoles), their calorigenic effect (increase of basic metabolic rate), cardiovascular function (increased

sensitivity of the heart to catecholamines), and metabolic functions (lipid, carbohydrate, and collagen metabolism). The primary feedback effect is inhibition of thyroid-stimulating hormone (TSH) secretion. These effects can be used to test thyroid hormone analogs and metabolites. The thyroid hormones regulate iodine uptake and utilization in the thyroid, and their action can be inhibited by antithyroid drugs.

Historical bioassays rely on morphogenesis and neuronal development in **amphibia** (Biedl 1916; Pitt-Rivers and Tata 1959; Copp et al. 1962; Turner and Premachandra 1962). Thyroid hormones induce premature metamorphosis in amphibian tadpoles. Since the first observation by Gudernatsch (1913a, 1913b) this phenomenon has been studied by numerous workers with the purpose of adapting this response for the assay of thyroidal substances (Bomskov 1937). Within a short period of time, the treatment with thyroid hormones induces the transformation of the **tadpole** into a small frog with growth of limbs, lungs, and other terrestrial accoutrements, and stimulates the synthesis of enzymes mediating morphogenesis and transformation.

The **axolotl** (*Ambystoma mexicanum* or *tigrinum*) has been used as a test object to study metamorphosis induced by thyroid hormones. This animal loses the gills and forms lungs, changing the shape of its tail at the same time (Huxley and Hogben 1922; Zavadovsky and Zavadovsky 1926; Haffner 1927).

Another principle action of T_3 and T_4 is metabolic activation and increased energy expenditure. Kreitmair (1928) standardized thyroid preparations using the **weight loss of guinea pigs** after 1 week of treatment as a parameter. A guinea pig unit was defined as the dose which reduces the body weight of guinea pigs with an initial weight of 250–300 g within 7 days by at least 10%.

A different functional role is subserved by calcitonin. The **hypocalcemic hormone calcitonin** was discovered by Copp (Copp et al. 1962; Copp 1964). Calcitonin originates from parafollicular C-cells of the thyroid. Its functional antagonist is parathyroid hormone. The bioassay of calcitonin preparations is performed by assessing their ability to **lower the plasma calcium** in the rat. Assay of serum (thyro)calcitonin has a significant diagnostic role for thyroid carcinoma.

As with other hormones, research methods have progressed from bioassays of thyroid hormone action to direct measurement of the thyroid hormones (thyroxine and triiodothyronine) and their metabolites, to studies on enzymatic steps in thyroid hormone synthesis and inactivation, to the identification of thyroid hormone receptors as members of the super family of nuclear receptors, and to signaling induced by binding of thyroid hormones to their receptors.

Thyroid Hormone Receptors

Nuclear triiodothyronine binding proteins were purified and characterized by Torresanai and Anselmet (1978). Ichikawa and DeGroot (1987a, 1987b) described the purification and characterization of rat liver nuclear thyroid hormone receptors and thyroid hormone receptors in a human hepatoma cell line. Apriletti et al. (1988) reported large-scale purification of the nuclear thyroid hormone receptor from rat liver and sequence-specific binding of the receptor to DNA. Ichikawa et al. (1988) and Ichikawa and Hashizume (1991) published methods of an aqueous two-phase (dextran and polyethylene glycol) partitioning study of nuclear thyroid hormone receptors. Glucocorticoids, other steroid hormones, thyroid hormones and vitamin-derived hormones (including retinoids) all exert their effects by the regulation of hormone-responsive target genes within the cell nucleus. William and Franklyn (1994) reviewed the physiology of the steroid–thyroid hormone nuclear receptor superfamily. A nuclear hormone receptor-associated protein that inhibits transactivation by the thyroid hormone and retinoic acid receptors was described by Burris et al. (1995). Two different genes encode two different thyroid hormone receptors, thyroid hormone receptor-α and thyroid hormone receptor-β and these two thyroid hormone receptors are often co-expressed at different levels in different tissues. Chiellini et al. (1998) designed a high-affinity subtype-selective agonist ligand for the thyroid hormone receptor-β. The expression of thyroid hormone receptor isoforms in rat growth plate cartilage *in vivo* was described by Ballock et al. (1999). Yuan et al. (1998) described a component of a thyroid hormone receptor-associated protein (TRAP) co-activator complex which interacts directly with nuclear receptors in a ligand-dependent fashion. The sequence of the thyroid-hormone-response element and the recruitment of retinoid X receptors for thyroid hormone responsiveness was investigated by Wu et al. (2001).

REFERENCES AND FURTHER READING

Apriletti JW, Baxter JD, Lavin TN (1988) Large scale purification of the nuclear thyroid hormone receptor from rat liver and sequence-specific binding of the receptor to DNA. J Biol Chem 263:9409–9417

Ballock RT, Mita BC, Zhou X, Chen DH, Mink LM (1999) Expression of thyroid hormone receptor isoforms in

rat growth plate cartilage *in vivo*. J Bone Miner Res 14:1550–1556
Biedl A (1916) Das thyreo-parathyreo-thymische System. In: Biedl A (ed) Innere Sekretion. Ihre physiologischen Grundlagen und ihre Bedeutung für die Pathologie. Dritte Auflage, Erster Teil. Urban and Schwarzenberg, Berlin, pp 5–405
Bomskov C (1937) Methodik der Hormonforschung. Vol 1, Das Hormon der Schilddrüse. Thieme, Leipzig, pp 143–394
Burris TP, Nawaz Z, Tsai M-J, O'Malley BW (1995) A nuclear hormone receptor-associated protein that inhibits transactivation by the thyroid hormone and retinoic acid receptors. Proc Natl Acad Sci USA 92:9525–9529
Chiellini G, Apriletti JW, Yoshikara HA, Baxter JD, Ribeiro RCJ, Scalan TS (1998) A high-affinity subtype-selective agonist ligand for the thyroid hormone receptor. Chem Biol 5:299–306
Copp DH (1964) Parathyroids, calcitonin, and control of plasma calcium. Recent Prog Horm Res 20:59–88
Copp DH, Cameron EC, Cheney BA, Davidson AFG, Henze KG (1962) Evidence for calcitonin – a new hormone from the parathyroid that lowers calcium. Endocrinology 70:638–649
Gundernatsch JF (1913a) Feeding experiments on tadpoles. I. The influence of specific organs given as food on growth and differentiation. Roux Arch Entwicklungsmech 35:457–483
Gundernatsch JF (1913b) Feeding experiments on tadpoles. II. A further contribution to the knowledge of organs with internal secretion. Am J Anat 15:431–473
Haffner F (1927) Pharmakologische Untersuchungen mit einem deutschen Thyroxin. Klin Wschr 6:1932–1935
Huxley JS, Hogben LT (1922) Experiments on amphibian metamorphosis and pigment responses in relation to internal secretions. Proc R Soc Biol 93:36–53
Ichikawa K, DeGroot LJ (1987a) Purification and characterization of rat liver nuclear thyroid hormone receptors. Proc Natl Acad Sci USA 84:3420–3424
Ichikawa K, DeGroot LJ (1987b) Thyroid hormone receptors in a human hepatoma cell line: multiple receptor forms on isoelectric focusing. Mol Cell Endocrinol 51:135–143
Ichikawa K, Hashizume K, Miyamoto T, Nishii Y, Yamauchi K, Ohtsuka H, Yamada T (1988) Conformational transition of thyroid hormone receptor upon hormone binding: demonstration by aqueous two-phase partitioning. J Endocrinol 119:431–437
Ichikawa K, Hashizume K (1991) Use of aqueous two-phase partitioning to study thyroid hormone receptor. In: Greenstein B (ed) Neuroendocrine research methods, Vol 1. Harwood, Chur, pp 149–159
Kreitmair H (1928) Jodgehalt und Schilddrüsenwirkung. Zugleich Bekanntgabe einer biologischen Wertbestimmungsmethode für Schilddrüsenpräparate. Z Ges Exp Med 61:202–210
Pitt-Rivers R, Tata JR (1959) The thyroid hormones. Pergamon, London
Torresanai J, Anselmet A (1978) Partial purification and characterization of nuclear triiodothyronine binding proteins. Biochem Biophys Res Commun 81:147–153
Turner CW, Premachandra BN (1962) Thyroidal substances. In: Dorfman RI (ed) Methods in hormone research, Vol II. Academic Press, New York, pp 385–411
William GR, Franklyn JA (1994) Physiology of the steroid-thyroid hormone nuclear receptor superfamily. Balliéres Clin Endocrinol Metab 8:241–266
Wu Y, Xu B, Koenig RJ (2001) Thyroid hormone response element sequence and the recruitment of retinoid X receptors for thyroid hormone responsiveness. J Biol Chem 276:3929–3936
Yuan C-X, Ito M, Fondell JD, Fu Z-Y, Roeder RG (1998) The TRAP220 component of a thyroid hormone receptor-associated protein (TRAP) coactivator complex interacts directly with nuclear receptors in a ligand-dependent fashion. Proc Natl Acad Sci USA 95:7939–7944
Zavadovsky BM, Zavadovsky EV (1926) Application of the axolotl metamorphosis reaction to the quantitative assay of thyroid gland hormones. Endocrinology 10:550–559

N.5.0.2 Thyroidectomy

PURPOSE AND RATIONALE

Experiments for pharmacological evaluation of thyroid hormones and analogs were performed in thyroidectomized rats. Bomskov (1937) described the method of thyroidectomy in various animal species, such as tadpoles, frogs, birds, goats, dogs, cats, rabbits, guinea pigs, rats and mice, based on the clinical experience with thyroid resection in humans.

PROCEDURE

The thyroid in rats consists of three lobes (left, median, and right). The rat is anesthetized, e. g., with pentobarbital, and placed on a surgical table. The fur of the neck is removed with electric clippers and the area disinfected. A median skin incision of 2.0 cm length is made. On both sides large salivary glands and maxillary lymph nodes are found. They are pushed aside, making visible the musculus hyoideus covering the trachea. This muscle is split in the midline. The isthmus of the thyroid connecting both lobes is located below the thyroid cartilage. The lobes and the isthmus are separated with blunt forceps from the trachea and the blood vessels ligated. Alternatively, the thyroid can be removed by electrocauterization. In most cases, the parathyroid glands are severed by the operation, and postoperative substitution with calcium lactate 1% in drinking water is advised.

REFERENCES AND FURTHER READING

Bomskov C (1937) Die chirurgischen Methoden der Schilddrüsenforschung In: Methodik der Hormonforschung. Band 1. Georg Thieme, Leipzig, pp 143–155 Hammet 1924, 1926a, 1926b; Smith et al. 1927; Hammet 1929; Pittman et al. 1964; Grossie 1965;
Grossie J, Hendrich CE, Turner CW (1965) Comparative methods for determining biological half-life (t1/2) of L-thyroxine in normal, thyroidectomized and methimazole treated female rats. Proc Soc Exp Biol Med 120:413–415
Hammet FS (1924) Studies of the thyroid apparatus. XXVIII. The differential development of the albino rat from 75 to 150 days of age and the influence of thyro-parathy-

roidectomy and parathyroidectomy thereon. Am J Physiol 70:259–272
Hammet FS (1926a) Studies on the thyroid apparatus. XXIX. The role of the thyroid apparatus in growth. Am J Physiol 76:69–91
Hammet FS (1926b) Studies on the thyroid apparatus. The relation between age at initiation of and response of body growth to thyroid and parathyroid deficiency. Endocrinology 10:29–42
Hammet FS (1929) Thyroid and differential development. Endokrinologie 5:81–86
Pittman CS, Shinohara M, Thrasher H, McCraw EF (1964) Effect of thyroxine analogues on the peripheral metabolism of thyroxine: the half-life and pattern of elimination. Endocrinology 74:611–616
Smith PE, Greenwood CF, Foster GL (1927) A comparison in normal, thyroidectomized and hypophysectomized rats of the effects upon metabolism and growth resulting from daily injections of small amounts of thyroid extract. Am J Pathol 3:669–687

N.5.1
In Vivo Tests for Thyroid Hormones

N.5.1.1
Oxygen Consumption

PURPOSE AND RATIONALE

Basal metabolic rate, oxygen consumption and CO_2 production are increased by thyroid hormones. This has been used for diagnostic procedures in humans as well as for evaluation of thyroid hormones and their derivatives in animals (indirect calorimetry). The historical method based on survival time of mice placed individually into tightly closed glass jars (Smith et al. 1947; Basil et al. 1950; Gemmill 1953) was modified, measuring time until occurrence of convulsions. The method was based on the increase in oxygen consumption associated with the markedly increased metabolic rate at high doses of thyroid hormones.

PROCEDURE

This is a description of the now obsolete assay: mice are placed individually into 200-ml wide-necked bottles. The bottom of the bottles is covered with filter paper to soak up the urine. The bottles are tilted to an angle of 60° and rotated five times per minute in a special apparatus. The time until asphyctic seizures occur is noted. Immediately after observation of seizures, the mouse is released for recovery. Due to the defined muscle work, the time to seizures is shortened in controls to 20–30 min.

EVALUATION

Average time to seizures was calculated and dose–response curves were established.

MODIFICATIONS OF THE METHOD

Similar studies were reported by: Bomskov 1937; Lilienthal et al. 1949; MacLagan and Sheahan 1950; Reineke and Turner 1950; Anderson 1954; Heming 1964; Turner 1969

Several apparatuses have been designed to measure oxygen consumption in animals, e. g., by Holtkamp et al. (1955).

Stock (1975) described an automatic, **closed-circuit oxygen consumption apparatus** for small animals. A Perspex animal chamber is surrounded by a water jacket except for one end, which has a removable cover plate. This cover, as well as allowing access to the chamber interior, also holds the connections for the oxygen delivery line and the pressure line. For experiments involving injections, infusions, and blood sampling, catheters are passed through, and sealed into rubber bungs which are then forced into holes in the cover plate. A rubber gasket forms an airtight seal between the cover and the chamber. Within the chamber, the animal is supported on a wire grid over a layer of self-indicating soda lime and silica gel. A major determinant of sensitivity in this system is the dead space of the chamber. Chambers with internal dimensions of $20 \times 10 \times 10$ cm are suitable for animals such as mice and rats up to about 250 g body weight. Fixed volumes of oxygen are introduced into the chamber by an automatic syringe dispenser (Fisons Scientific) which draws pure oxygen from a spirometer through a drying tube filled with silica gel. When chamber pressure exceeds atmospheric by about 3 mmH_2O, the microdifferential pressure switch (KDG Instruments) inactivates the dispenser. The dispenser is reactivated when the pressure differential drops below this threshold value. The volume of oxygen dispensed is adjusted to the smallest volume that, with a single action of the syringe, will return chamber pressure to above the threshold value. The particular dispenser used in this system has the advantages of being (1) gas tight and (2) when activated will complete its pump cycle even if the chamber pressure exceeds the threshold value in midcycle. A discrete fixed volume of oxygen is delivered each time it is activated. To obtain the rate of oxygen consumption it is merely necessary to record the pump rate.

REFERENCES AND FURTHER READING

Anderson BG (1954) Potency and duration of action of triiodothyronine and thyroxine in rats and mice. Endocrinology 54:659–665
Basil B, Somers GF, Woolett EA (1950) Measurement of thyroid activity by mouse anoxia method. Br J Pharmacol 5:315–322

Bomskov C (1937) Methodik der Hormonforschung. Vol. 1, Das Hormon der Schilddrüse. Thieme, Leipzig, pp 143–394
Gemmill CL (1953) Comparison of activity of thyroxine and 3,5,3′-triiodothyronine. Am J Physiol 172:286–290
Heming AE (1964) Animal techniques for evaluating thyroid and antithyroid agents. In: Nodine JH, Siegler PE (eds) Animal and clinical pharmacologic techniques in drug evaluation. Year Book Medical, Chicago, Ill., pp 530–534
Holtkamp DE, Ochs S, Pfeiffer CC, Heming AE (1955) Determination of the oxygen consumption of groups of rats. Endocrinology 56:93–104
Lilienthal JL, Zierler KL, Folk BP (1949) A simple volumeter for measuring the oxygen consumption of small animals. Bull John Hopkins Hosp 84:238–244
MacLagan NF, Sheahan MM (1950) The measurement of oxygen consumption in small animals by a closed circuit method. J Endocrinol 6:456–463
Reineke EP, Turner CW (1950) Thyroidal substances. In: Emmens CW (ed) Hormone assay. Academic Press, New York, pp 489–511
Smith AU, Emmens CW, Parkes AS (1947) Assay of thyroidal activity by a closed vessel technique. J Endocrinol 5:186–206
Stock MJ (1975) An automatic, closed-circuit oxygen consumption apparatus for small animals. J Appl Physiol 39:849–850
Turner CW (1969) Thyroidal substances. In: Dorfman RI (ed) Methods in hormone research, Vol IIA. Academic Press, New York, pp 301–363

N.5.1.2 Inhibition of Iodine Release

PURPOSE AND RATIONALE

The thyroid gland has a high avidity for iodine, uptake of which may be measured by isotope-labeled iodine (^{131}I), in a dose-related and time-dependent manner. The release of ^{131}I from the thyroid in rats is inhibited by treatment with thyroxine (Wolff 1951), and the degree of inhibition is related to the dose administered (Perry 1951). This phenomenon was used to compare activity of thyroid hormone derivatives with the standard thyroxine.

For analytical and diagnostic purposes, direct quantitation of thyroid hormones is now achieved by methods such as radioimmunoassay and HPLC chromatography, and by measuring feedback inhibition of thyroid hormones directly via the decrease in serum TSH.

PROCEDURE

Male Sprague-Dawley rats weighing 180–240 g are fed a commercial laboratory chow without or with addition of 0.03% propylthiouracil (reference compound for thyroid peroxidase inhibition). Food is withheld 8 h before the injection of 25 μC ^{131}I or ^{125}I intraperitoneally. Radioactivity over the thyroid region of the neck is determined 40 h later (if necessary under sedation). This reading is taken as time zero and all further counts made at 24-h intervals may be expressed as a percentage of time-zero counts after correction for physical decay of the ^{131}I isotope. After the reading at time zero, the diet is changed to a feed containing 0.03% propylthiouracil, and several doses of the test preparation or the standard are injected subcutaneously at 24-h intervals up to a total of four doses. The daily loss of ^{131}I is inversely proportional to the dose of thyroid hormone.

EVALUATION

Percentage of time-zero counts after 96 h of ^{131}I remaining in the thyroid after the last of four doses is plotted against logarithm of dose. From these dose–response curves, potency ratios are calculated.

The method has been used by several authors: Reineke and Turner 1950; Anderson 1954; Turner and Premachandra 1962

CRITICAL ASSESSMENT OF THE METHOD

The assay described here was used for quantitative estimates and has now been replaced by analytical determination of thyroid hormone contents. For human drug formulations, bioequivalence studies are required when generic formulations are assessed This approach of measuring the uptake and release of labeled iodine may be modified for short-term uptake of ^{131}I or ^{125}I as a parameter of thyroid peroxidase inhibition by antithyroid drugs, and other drugs affecting thyroid function.

REFERENCES AND FURTHER READING

Anderson BG (1954) Potency and duration of action of triiodothyronine and thyroxine in rats and mice. Endocrinology 54:659–665
Perry WF (1951) A method for measuring thyroid hormone secretion in the rat with its application to the bioassay of thyroid extracts. Endocrinology 48:643–650
Reineke EP, Turner CW (1950) Thyroidal substances. In: Emmens CW (ed) Hormone assay. Academic Press, New York, pp 489–511
Turner CW, Premachandra BN (1962) Thyroidal substances. In: Dorfman RI (ed) Methods in hormone research, Vol II. Academic Press, New York, pp 385–411
Wolff J (1951) Some factors that influence the release of iodine from the thyroid gland. Endocrinology 48:284–297

N.5.1.3 Anti-Goitrogenic Activity

PURPOSE AND RATIONALE

Thyroid weight and size are controlled by the action of thyroid-stimulating hormone (TSH) on thyroid tissue. In rats, increased secretion of TSH induces thyroid enlargement and weight increase within a few

days (addressed as goiter formation). In normal animals the secretion of TSH by the pituitary is regulated by feedback of thyroid hormones. The administration of goitrogenic compounds which block thyroid hormone synthesis and/or secretion reduces the concentrations of circulating thyroid hormones (T_4/T_3) and their pituitary effect (negative feedback inhibition of TSH secretion), releasing TSH from its feedback inhibition. The TSH rise induces hyperplasia of the thyroid follicles as indicated by the dose-related increase of thyroid weight. Hyperplasia is prevented by injection of thyroxine, triiodothyronine or thyroid hormone analogs.

PROCEDURE

Male Sprague-Dawley rats weighing 150–180 g are used in groups of eight to ten animals. During the treatment period, 0.1% propylthiouracil (PTU) is added to the food or to the drinking water, in order to achieve a stable baseline of thyroid weight. Over a period of 2 weeks, the rats are treated (preferably by gavage) with various doses of the test compound or the thyroxine standard (10–40 µg/kg). PTU controls are treated with the suspension medium or saline injections only. At autopsy on day 14, the thyroid glands are dissected out and weighed rapidly to avoid evaporation loss. Thyroids may also be lyophilized first to weigh dry matter. The two- to three-fold increase of thyroid weight by PTU is reversed dose-dependently to normal values by thyroid active substances.

EVALUATION

Dose–response curves are plotted and potency ratios with confidence limits may be calculated.

MODIFICATIONS OF THE METHOD

Similar studies were reported by: Reineke et al. 1945; Pitt-Rivers and Tata 1959; Turner and Premachandra 1962; Wiberg et al. 1964; Ortiz-Caro et al. 1983; Pisarev et al. 1994

The effect of PTU-induced baseline suppression is monitored and ascertained by measuring serum TSH, T_4 and T_3. The dose-related inhibition of the TSH rise by thyroid substances is used as the parameter to assess goiter prevention.

REFERENCES AND FURTHER READING

Ortiz-Caro J, Pastor RM, Jolin T (1983) Effects of $KClO_4$ in propylthiouracil-hypothyroid rats. Acta Endocrinol 103:81–87

Pisarev MA, Krawiec L, Juvenal GJ, Bocanera LV, Pregliasco LB, Sartorio G, Chester HA (1994) Studies on the goiter inhibiting action of iodolactones. Eur J Pharmacol 258:33–37

Pitt-Rivers R, Tata JR (1959) The thyroid hormones. Pergamon, London

Reineke EP, Mixner JP, Turner CW (1945) Effect of graded doses of thyroxine on metabolism and thyroid weight of rats treated with thiouracil. Endocrinology 36:64–67

Turner CW, Premachandra BN (1962) Thyroidal substances. In: Dorfman RI (ed) Methods in hormone research, Vol II. Academic Press, New York, pp 385–411

Wiberg GS, Carter JR, Stephenson NR (1964) The effects of various goitrogens on the determination of the relative potency of thyroid by the goiter prevention assay. Acta Endocrinol 45:370–380

N.5.1.4 Tensile Strength of Connective Tissue in Rats, Modified for Thyroid Hormones

These studies are an example of evaluating the biological effect of high doses of thyroid hormones on tissues other than those involved in the increase of metabolic rate. Thyroid hormone secretion affects almost all tissues in the body, and high doses may exert unwanted effects on connective tissue.

PURPOSE AND RATIONALE

The decrease of tensile strength after a single high-dose injection of thyroid hormones is dose dependent and can be used for evaluation of thyroid hormone derivatives. Short-term treatment with corticosteroids increases the strength of connective tissue (Vogel 1969). This effect is antagonized by thyroid hormones (Ther et al. 1963; Vogel and Ther 1964). Thyroid hormones per se have a biphasic effect: short-term treatment decreases the dose-dependent tensile strength of epiphyseal cartilage, tail tendons and skin strips, whereas treatment over 10 days increases tensile strength, probably mediated by activation of endogenous adrenal secretion (similar to the effect of corticosteroid treatment).

PROCEDURE

Male Sprague-Dawley rats weighing 110 ± 10 g are injected subcutaneously with thyroid hormones (dose range of the standard L-triiodothyronine 0.1–1.0 mg/kg). After 24 h the animals are sacrificed and the tensile strength of distal femoral epiphyseal plates, tail tendons, or skin strips are tested as described in Sects. N.2.1.3.2, N.2.1.3.3, N.2.1.3.4, and P.11.2.1.1.

EVALUATION

Doses–response curves of test compounds and standard are established and potency ratios may be calculated. T_3 (L-triiodothyronine) is about 3 times more active than T_4 (levothyroxine), in accordance with its

metabolic activity. The mechanism of action of this short-term effect of thyroid hormones on connective tissue has not been explored.

REFERENCES AND FURTHER READING

Ther L, Schramm H, Vogel G (1963) Über die antagonistische Wirkung von Trijodthyronin und Progesteron auf den Prednisoloneffekt am Epiphysenknorpel. Acta Endocrinol 42:29–38

Vogel G, Ther L (1964) Über den Einfluß von einigen Hormonen auf mechanisch-physikalische Eigenschaften des Binde- und Stützgewebes. Anatom Anzeig Suppl 115:117–122

Vogel HG (1969) Zur Wirkung von Hormonen auf physikalische und chemische Eigenschaften des Binde- und Stützgewebes. Arzneimittelforschung 19:1495–1503, 1732–1742, 1790–1801, 1981–1996

N.5.2 Antithyroid Drugs

N.5.2.1 General Considerations

Antithyroid drugs interfere with synthesis, release, and/or the peripheral action of the thyroid hormone, lowering the basal metabolic rate. They are used in the treatment of thyroid disorders (hyperthyroidism). The suppression of T_4/T_3 secretion reduces thyroidal inhibition of the pituitary gland, increasing TSH secretion, and then induces the goitrogenic response. This response was used to detect antithyroid drugs and has been widely used for screening procedures. It is, however, nonspecific and may be caused by several different mechanisms, including enzyme induction of glucuronyltransferases. The goitrogenic response is of considerable interest in toxicology, because it may be produced by several compounds during early drug evaluation which modify the biosynthesis and/or inactivation of thyroid hormones in an unexpected manner.

REFERENCES AND FURTHER READING

Heming AE (1964) Animal techniques for evaluating thyroid and antithyroid agents. In: Nodine JH, Siegler PE (eds) Animal and clinical pharmacologic techniques in drug evaluation. Year Book Medical, Chicago, Ill., pp 530–534

MacKenzie CG, MacKenzie JB (1943) Effect of sulfonamides and thioureas on the thyroid gland and basal metabolism. Endocrinology 32:185–209

N.5.2.2 Inhibition of Iodine Uptake in Rats

PURPOSE AND RATIONALE

Propylthiouracil (PTU) and a wide spectrum of drugs may inhibit thyroid hormone synthesis. Some of these drugs are used to treat thyrotoxicosis. As a consequence of thyroid peroxidase inhibition, the iodine uptake by and content in the thyroid is decreased. This phenomenon is dose dependent and may occur at lower doses than those increasing thyroid weight in rats (McGinty and Bywater 1945). The historical parameter of iodine content has been replaced by measuring the uptake and release of ^{131}I.

PROCEDURE

Groups of male Wistar rats age 26–28 days, weighing 40–45 g, are placed into metabolism cages. They are fed normal diet, and potassium iodide is added to the drinking water. In one modification of the method (for toxicology studies), the test compounds or the reference standard (several concentrations) may be added to the diet over a period of 10 days, and the amount of compound ingested by each rat is then calculated from the total food consumption over 10 days and expressed in milligram daily per kilogram of body weight. After 10 days of treatment, the rats are sacrificed and the thyroids dissected free from adjacent tissue and capsule. The thyroid is weighed and iodine content determined. In daily doses of between 0.1 and 10.0 mg/kg, thiouracil decreases the iodine content of the thyroid in a dose-dependent manner. Definitely higher doses are necessary to increase thyroid weight.

EVALUATION

Dose–response curves of test compounds and reference standard are plotted, and potency ratios with confidence limits may be calculated.

MODIFICATIONS OF THE METHOD

Walker and Levy (1989) used implantable pellets of propylthiouracil to induce thyroid dysfunction in rats. Uptake of labeled iodine is measured instead of iodine content. Release of labeled iodine may be stimulated by protirelin (TRH) injection in order to assess thyroid function, or as a quantitative bioassay for the effect of the hypothalamic hormone TRH.

REFERENCES AND FURTHER READING

Astwood EB, Bissell A (1944) Effect of thiouracil on the iodine content of the thyroid gland. Endocrinology 34:282–296

McGinty DA, Bywater WG (1945) Antithyroid studies. I. The goitrogenic activity of some thioureas, pyrimidines and miscellaneous compounds. J Pharmacol Exp Ther 84:342–357

Prasad R, Srivastava PK (1993) 1-Aryl-2-amino/hydrazino-4-phenyl-1,6-dihydro-1,3,5-triazine-6-thione and related thiocarbamides/thiosemicarbazides as antithyroidal agents. Arch Pharmacol 326:963–966

Walker JS, Levy G (1989) Induction of experimental thyroid dysfunction in rats with implantable pellets of thyroxine or propylthiouracil. J Pharmacol Methods 21:223–229

N.5.2.3 Antithyroidal Effects in Animal Assays

The oxygen consumption in iodine-treated mice has been used as a bioassay, modified for antithyroid activity.

PURPOSE AND RATIONALE

The historical bioassay is based on oxygen consumption, which is increased in acutely potassium-iodide-treated mice, resulting in a decrease of asphyxiation time (thyroid activation). This effect is dose-dependently antagonized by antithyroidal compounds, and the time to convulsions is prolonged due to the reduced metabolic rate. The methods based on increased oxygen consumption after thyroid hormones (Sect. N.5.1.1) are applied.

MODIFICATIONS OF THE METHOD

Thyroid weight was an early parameter for the detection of antithyroid activity. Rabbits treated with goitrogenic compounds or fed exclusively with cabbage (Chesney et al. 1928; Marine et al. 1929) showed an up to tenfold increase of thyroid weight, histologically manifested as hyperplasia without colloid formation. These phenomena were reversed by iodine treatment (Bomskov 1937).

Goiter formation as a side-effect of non-steroidal anti-inflammatory drugs was studied by Müller et al. (1985).

REFERENCES AND FURTHER READING

Bänder A, Bauer F, Häussler A, Muschaweck R, Vogel G (1962) Pharmakologische Untersuchungen mit Isonikotinsäure-[3,3-di-(p-chlorphenyl)-propyl(1)]-amid (Präparat Hoechst 13217). Z Vet Med 9:693–704

Bomskov C (1937) Methodik der Hormonforschung. Vol 1, Das Hormon der Schilddrüse. Thieme, Leipzig, pp 143–394

Chesney AM, Clawson TA, Webster B (1928) Endemic goiter in rabbits. Incidence and characteristics. Bull Hopkins Hosp 43:261–277

Marine D, Baumann EJ, Cipra A (1929) Studies on simple goiter produced by cabbage and other vegetables. Proc Soc Exp Biol Med 26:822–824

Müller P, Löbe M, Sorger D, Ludewig R, Hambsch K (1985) Zur strumigenen Wirkung nichtsteroidaler Antirheumatika und Zytostatika. Ergebnisse experimenteller Untersuchungen. Radiobiol Radiother 26:201–206

Webster B (1934) Studies in the experimental production of simple goiter. Endocrinology 16:617–625

Weiss SR, Burns JM (1988) The effect of acute treatment with two goitrogens on plasma thyroid hormones, testosterone and testicular morphology in adult male rats. Comp Biochem Physiol 90A:449–452

N.5.3 Calcitonin

N.5.3.1 General Considerations

The calcitropic hormone (thyro)calcitonin was discovered in C-cells of the thyroid gland by Copp (Copp et al. 1962; Copp 1964, 1994). This hypocalcemic hypophosphatemic principle of the thyroid gland (Austin and Heath 1981) was designated thyrocalcitonin by Hirsch et al. (1964), Munson and Hirsch (1966), Raisz et al. (1967), and MacIntyre (1992). Its calcitropic effects on bone and kidney function are opposite to those of the parathyroid hormone. Calcitonin originates from parafollicular C-cells of the thyroid. Calcitonin secretion can be evaluated *in vitro* using the isolated perfused porcine thyroid (Pento 1985). Radioimmunoassays for calcitonin are available (Tashjian and Voelkel 1979), and species-specific methods for calcitonin determination need to be considered. Assays for calcitonin receptors have been described (Nissenson et al. 1985). Surveys on the effects of exogenous calcitonin was given by Deftos (1989); Braga (1994); Wallach et al. (1999). The biology and clinical relevance of calcitonin gene peptides has been reviewed (Reginster 1993; Silverman 2003; Zaidi et al. 1990).

REFERENCES AND FURTHER READING

Austin LA, Heath H 3rd (1981) Calcitonin: physiology and pathophysiology [review]. N Engl J Med 304(5):269–278

Braga PC (1994) Calcitonin and its antinociceptive activity: animal and human investigations 1975–1992 [review]. Agents Actions 41(3–4):121–131

Copp DH (1964) Parathyroids, calcitonin, and control of plasma calcium. Recent Prog Horm Res 20:59–88

Copp DH (1994) Calcitonin: discovery, development, and clinical application. Clin Invest Med 17:268–277

Copp DH, Cameron EC, Cheney BA, Davidson AFG, Henze KG (1962) Evidence for calcitonin – a new hormone from the parathyroid that lowers calcium. Endocrinology 70:638–649

Deftos LJ (1989) In: Azria M (ed) The calcitonins. Physiology and pharmacology. Karger, Basel, pp 67–132

Hirsch PF, Voelkel EF, Musnon PL (1964) Thyrocalcitonin: hypocalcemic hypophosphatemic principle of the thyroid gland. Science 146:412–413

MacIntyre I (1992) The calcitonin family of peptides [review]. Ann N Y Acad Sci 657:117–118

Munson PF, Hirsch RP (1966) Thyrocalcitonin. Newly recognized thyroid hormone concerned with metabolism of bone. Clin Orthopaed 49:209–215

Nissenson RA, Teitelbaum AP, Arnaud CD (1985) Assay for calcitonin receptors. Methods Enzymol 109:40–48

Pento JT (1985) A method for the evaluation of calcitonin secretion using the isolated perfused porcine thyroid. J Pharmacol Methods 13:43–51

Raisz LG, Au WYW, Friedman J, Nieman I (1967) Thyrocalcitonin and bone resorption. Studies employing a tissue culture bioassay. Am J Med 43:684–690

Reginster JY (1993) Calcitonin for prevention and treatment of osteoporosis [review]. Am J Med 95(5A):44S–47S
Silverman SL (2003) Calcitonin [review]. Endocrinol Metab Clin North Am 32(1):273–284
Tashjian A, Voelkel EF (1979) Human calcitonin: application of affinity chromatography. In: Jaffe BM, Behrman HR (eds) Methods of hormone radioimmunoassay, 2nd edn. Academic Press New York, pp 355–373
Wallach S, Rousseau G, Martin L, Azria M (1999) Effects of calcitonin on animal and *in vitro* models of skeletal metabolism. Bone. 25(5):509–16. Review.
Zaidi M, Moonga BS, Bevis PJR, Bascal ZA, Breimer LH (1990) The calcitonin gene peptides: biology and clinical relevance. Crit Rev Clin Lab Sci 28:109–174

N.5.3.2 Decrease of Serum Calcium in Rats

PURPOSE AND RATIONALE

The bioassay of calcitonin preparations is performed using their ability to lower the plasma calcium in the rat. This procedure has also been adopted by pharmacopoeias, using the International Reference Preparation for Calcitonin (porcine) consisting of freeze-dried purified pork calcitonin, and the International Reference Preparation for Calcitonin (salmon) consisting of freeze-dried purified synthetic salmon calcitonin. These assays for calcitonin quantitation, however, have now been replaced by a physicochemical method for pharmaceutical quality control. Either intravenous or subcutaneous administration can be chosen. International standards for salmon calcitonin, eel calcitonin, and the Asu^{1-7} analogue of eel calcitonin have been elaborated (Zanelli et al. 1990). A second international standard for porcine and human calcitonins has been established by an international collaborative study group based on the *in vivo* rat hypocalcemia bioassay (Zanelli et al. 1993).

PROCEDURE

Groups of at least five female Wistar rats, weighing 100–120 g, are used. Three doses of standard preparation (1, 3 and 9 mU per rat) and three doses of test preparation are injected intravenously. Then 1 h after injection, blood is withdrawn under light anesthesia. Plasma calcium is determined by flame photometry or by atomic absorption photometry.

EVALUATION

Dose–response curves of decreases in plasma calcium are established and potency ratios with confidence limits are calculated.

MODIFICATIONS OF THE METHOD

Similar studies were reported by: Kumar et.al. 1965; Munson et al. 1968; Rittel et al. 1976; Schwartz et al. 1981;Michelangeli et.al. 1983; Findlay et al. 1985; Buck and Maxl 1990; Deming et.al. 1994

Yates et al. (1990) assessed the acute hypocalcemic responses to single subcutaneous injections of calcitonin preparations in intact young male ICR Swiss mice weighing 12–20 g.

Calcitonin of the stingray and of the goldfish were characterized by Sasayama et al. (1992, 1993).

Kapurniotu and Taylor (1995) performed *in vitro* hypocalcemic assays in mice by analysis of serum calcium 1 h after subcutaneous injection of lactam-bridged analogs of human calcitonin.

REFERENCES AND FURTHER READING

British Pharmacopoeia (1988) Volume II, 1. Biological assay of calcitonin (pork). Biological assay of salcatonin. A164. HMSO, London
Buck RH, Maxl F (1990) A validated HPLC assay for salmon calcitonin analysis. Comparison of HPLC and biological assay. J Pharm Biomed Anal 8:761–769
Deming Q, Genquan S, Ruolun K (1994) Biological assay of calcitonin by blood calcium determination in rats. Chin J Pharm Anal 14:30–34
European Pharmacopoeia (1986) Monograph 471. Maisonneuve, Sainte Ruffine, France
Findlay DM, Michelangeli VP, Orlowski RC, Martin TJ (1983) Biological activities and receptor interactions of des-leu^{16} salmon and des-phe^{16} human calcitonin. Endocrinology 112:1288–1291
Findlay DM, Michelangeli VP, Martin TJ, Orlowski RC, Seyler JK (1985) Conformational requirements for activity of salmon calcitonin Endocrinology 117:801–805
Kapurniotu A, Taylor JW (1995) Structural and conformational requirements for human calcitonin activity: design, synthesis, and study of lactam-bridged analogues. J Med Chem 38:836–847
Kumar M, Slack E, Edwards A, Soliman H, Baghdiantz A, Foster GV, MacIntyre I (1965) A biological assay for calcitonin. J Endocrinol 33:469–475
Munson PL, Hirsch PF, Brewer HB, Reisfeld RA, Cooper CW, Wästhed AB, Orimo H, Potts JT Jr (1968) Thyrocalcitonin. In: Astwood EB (ed) Recent progress in hormone research, Vol 24. Academic Press, New York, pp 589–650
Rittel W, Maier R, Brugger M, Kamber B, Riniker B, Sieber P (1976) Structure-activity relationship of human calcitonin. III. Biological activity of synthetic analogues with shortened or terminally modified peptide chains. Experientia 32:246–248
Sasayama Y, Suzuki N, Oguro C, Takei Y, Takahashi A, Watanabe TX, Nakajima K, Sakakibara S (1992) Calcitonin of the stingray: comparison of the hypocalcemic activity with other calcitonins. Gen Comp Endocrinol 86:269–274
Sasayama Y, Ukawa KI, Kai-Ya H, Oguro C, Takei Y, Watanabe TX, Nakayama K, Sakakibara S (1993) Goldfish calcitonin: purification, characterization, and hypocalcemic potency. Gen Comp Endocrinol 89:189–194
Schwartz KE, Orlowski RC, Marcus R (1981) des-Ser^2 salmon calcitonin: a biologically potent synthetic analog. Endocrinology 108:831–835
Yates AJ, Gutierrez GE, Garrett IR, Mencel JJ, Nuss GW, Schreiber AB, Mundy GR (1990) A noncyclical analog of calcitonin (N^{α}-propionyl di-$ala^{1,7}$,des-leu^{19} sCT) retains

full potency without inducing anorexia in rats. Endocrinology 126:2845–2849
Zanelli JM, Gaines-Das RE, Corran PH (1990) International standards for salmon calcitonin, eel calcitonin, and the Asu[1-7] analogue of eel calcitonin: calibration by international collaborative study. Bone Miner 11:1–17
Zanelli JM, Gaines-Das RE, Corran P (1993) Establishment of the second international standards for porcine and human calcitonins: report of the international collaborative study. Acta Endocrinol 128:443–450

N.5.3.3 Effect of Calcitonin on Osteoclasts in Vitro

PURPOSE AND RATIONALE

Calcitonin acts primarily by inhibition of osteoclastic bone resorption (Friedman and Raisz 1965; Aliapoulios et al. 1966). Zaidi et al. (1990, 1994) reported the development and validation of three microbioassays for calcitonin based on calcitonin-induced inhibition of the activity of isolated osteoclasts.

PROCEDURE

Femora and tibiae are removed from newborn Wistar rats. The bones are freed from adherent soft tissues and cut across their epiphyses in HEPES-buffered Medium 199 supplemented with heat-inactivated fetal calf serum, benzyl penicillin (100 µU/ml) and streptomycin (100 µg/ml). The osteoclasts are mechanically disaggregated by curetting the bones of each rat with a scalpel blade into 1 ml medium and agitating the suspension with a pipette. Larger fragments are allowed to settle for 10 s, before the supernatant is dropped onto appropriate substrate (bone slices, plastic Petri dishes or glass coverslips).

Motility-Based System

The morphological appearance of stained osteoclasts is used as an index to assess the state of cytoplasmic activity. Osteoclasts are settled on coverslips in microtiter wells and are incubated for 20 min at 37°C. The coverslips are removed, washed with Medium 199 and placed in separate wells, each containing 100 µl medium.

Following a further incubation for 30 min (37°C), serial dilutions (tenfold) of salmon or human calcitonin or test preparations or appropriate dilutions of plasma samples are added. The cells are finally incubated for 2 h, fixed in 10% glutaraldehyde and stained with toluidine blue. The state of motility of each osteoclast on each coverslip is scored by observing the characteristic shape change these cells undergo when motility is inhibited; a motile cell is characterized by a smooth outline with increased staining intensity over all or part of its periphery, whereas a immotile cell typically shows an irregular pale outline without ruffled edges. The number of immotile cells is counted on each coverslip and expressed as a percentage of the total number of cells counted.

Cytoplasmatic Spreading System

Osteoclasts are settled in tissue culture dishes (35 mm) and are incubated at 37°C for 20 min to allow sedimentation and attachment. The cells are then washed with Medium 199 and 2 ml of the same medium is placed in each well. The dishes are placed in the incubation chamber of an inverted phase-contrast microscope. Images of the osteoclasts are recorded on a time-lapse video recorder. A tracing of their outlines is transferred through a digitizing system into a computer, programmed to measure the area within each tracing.

The outlines of each osteoclast are recorded before or after the addition of calcitonin or vehicle to the cultures. For each variable, the outline of six osteoclasts is traced after a 60-min incubation in the chamber and again 40 min following the addition of the hormone. The mean surface area covered by six osteoclasts after incubation is expressed as a percentage of the mean surface area of the osteoclasts before the addition of hormone or vehicle.

Bone Resorption System

Specimens of human femoral cortical bone are obtained from donors (patients who died without evidence of bone disease). The adherent soft tissue is removed and the bone cortex cut longitudinally into slices (0.1 mm thick). The slices are then cut into pieces (approximately 3 mm^2). They are cleaned by ultrasonication (15 min, in sterile distilled water), dehydrated by immersion in 80% aqueous ethanol for 2 h, and stored to dry at room temperature. Osteoclasts isolated in Medium 199 are dropped onto 12–16 bone slices placed in a well of an 18-mm multiwell dish. Following incubation (37°C, 15 min), slices are removed, and washed gently in Minimal Essential Medium supplemented with 10% FCS and antibiotics as described above. They are placed in separate wells, each well containing five to six slices in 900 µl medium. After further incubation (37°C, 10% humidified CO_2, 10 min), 100 µl of medium containing the test concentration of the hormone or the test solution is added. Human $PTH_{(1–34)}$ (0.1 U/ml) is used to assess functional effects of contaminating osteoblasts.

The calcitonin analogs are tested at various concentrations (tenfold dilutions). Finally, bone slices

are incubated overnight (37°C, 10% humidified CO_2, 18 h). The cells are fixed in glutaraldehyde, stained with toluidine blue and examined by transmitted light microscopy. Osteoclasts and mononuclear cells are counted. The slices are then bleached by immersion in sodium hypochlorite solution for 30 min and dehydrated in 80% aqueous ethanol. Finally, they are sputter coated with gold, randomized and examined in a scanning electronic microscope. The numbers of osteoclastic excavations, each defined by a continuous border, are counted. The area of bone surface resorbed is calculated by tracing the outline of the concavities into a digitizing tablet, linked to a microcomputer. Resorption surface areas may be expressed as a percentage of the mean of the control response.

EVALUATION

Data of each assay are analyzed using classical methods for analysis of parallel line assays. Estimates of relative potencies are calculated from parallel log dose–response lines of test preparations and a reference preparation.

Osteoclasts are mechanically disaggregated from neonatal rat long bones and dispersed at low densities on slices of devitalized bovine cartilage bone. The resulting areas of bone excavation are quantified with micrometric precision by scanning electron microscopy together with computer-assisted image analysis. These findings are used to develop a formal bioassay for calcitonin.

REFERENCES AND FURTHER READING

Aliapoulios MA, Goldhaber P, Munson PL (1966) Thyrocalcitonin inhibition of bone resorption induced by parathyroid hormone in tissue culture. Science 151:330–331

Friedman J, Raisz LG (1965) Thyrocalcitonin: inhibitor of bone resorption in tissue culture. Science 150:1465–1467

Zaidi M, Chambers TJ, Moonga BS, Oldoni T, Passarella E, Soncini R, MacIntyre I (1990) A new approach for calcitonin determination based on target cell responsiveness. J Endocrinol Invest 13:119–126

Zaidi M, Bax BE, Shankar VS, Moonga BS, Simon B, Towhidul Alam ASM, Gaines Das RE, Pazianis M, Huang CLH (1994) Dimensional analysis of osteoclastic bone resorption and the measurement of biologically active calcitonin. Exp Physiol 79:387–399

N.5.3.4 Receptor Binding and cAMP Accumulation in Isolated Cells

PURPOSE AND RATIONALE

The human breast cancer cell line T47D responds to calcitonin and its analogs by receptor binding and accumulation of cAMP. This can be used as a biological assay (Findlay et al. 1980, 1983, 1985; Grauer et al. 1992; Sexton and Hilton 1992; Blind et al. 1993).

PROCEDURE

The human breast cancer cell line T47D was originally established from a pleural effusion from an infiltrating ductal breast cancer (Horwitz et al. 1978). For binding experiments, cell monolayers are washed with 0.02% EDTA before treatment with 0.125% trypsin in 0.02% EDTA for 2 min at 37°C, addition of complete medium before centrifugation at 200 *g*, and resuspension in complete medium.

Iodination of calcitonin is performed with ^{125}I using the chloramine-T method.

For binding experiments T47D cells suspended in isotonic buffer are added to ^{125}I-labeled salmon calcitonin mixed with varying concentrations of unlabeled calcitonin or analogs and incubated at 20°C for 1 h. Nonspecific binding is assessed as the binding of ^{125}I-labeled salmon calcitonin in the presence of excess (2 µg/ml) unlabeled salmon calcitonin.

Stimulation of adenylate cyclase in intact T47D cells by calcitonin analogs is assessed by measuring [^{3}H]cAMP production in cells prelabeled with [^{3}H]adenine. Cellular ATP pools are labeled by incubation with 2,8-[^{3}H]adenine (0.5–2 µCi/ml) for 2 h at 37°C in 12-well culture dishes in RPMI 1640 medium containing 0.1% BSA. Cells are then washed twice with serum-free medium and incubated for a further 20 min in medium containing 0.1% BSA and 1 mM isobutylmethylxanthine (IBMX) before treatment with calcitonin and its analogs for 10 min at 37°C in the same buffer. Incubations are terminated by removing medium and adding 100 µl 20% trichloroacetic acid at 4°C. This is followed by 800 µl of a 5 mM solution of ATP, ADP, AMP, cAMP, and adenine. The [^{3}H]cAMP is isolated by chromatography on Dowex and alumina. Radioactivity is counted in a scintillation counter.

EVALUATION

For both parameters full dose–response curves are generated and the concentrations required for half-maximal responses are calculated.

MODIFICATIONS OF THE METHOD

Yates et al. (1990) measured stimulation of adenylate cyclase activity by calcitonin analogs in primary cultures of mouse renal cortex which were prepared according to the methods of Fukase et al. (1982) from 4-week-old ICR Swiss mice and used at confluence after 4 days of culture.

A radioreceptor assay for potency determinations of formulations of salmon calcitonin was described by Sjödin et al. (1990).

Albrandt et al. (1993) cloned two receptors with high affinity for salmon calcitonin from the nucleus accumbens region of rat brain.

Likewise, Sexton et al. (1993) identified in rats two isoforms of the calcitonin receptor, designated C1a and C1b.

Functional aspects of the isoforms C1a and C1b were discussed by Martin et al. (1995).

The calcitonin receptor isoforms C1a and C1b were localized in rat brain using *in vitro* autoradiography by Hilton et al. (1995).

Keustner et al. (1994) cloned and characterized a second form of the human calcitonin receptor from T47D cells.

Sexton et al. (1994) assayed the cloned renal porcine calcitonin receptor cDNA expressed by transient transfection in COS-1 cells or stable transfection in HEK-293 cells for interaction with calcitonin, amylin and calcitonin gene-related peptide. The results suggested that amylin may act as a natural ligand for the renal porcine calcitonin receptor.

The various pathways in signal transduction by calcitonin were discussed by Horne et al. (1994).

Houssami et al. (1994) found that different structural requirements exist for calcitonin receptor binding specificity and adenylate cyclase activation.

Suva et al. (1997) synthesized benzophenone-containing calcitonin analogs and tested them for receptor binding and stimulation of cAMP accumulation.

Povzek et al. (1997) investigated the structure–function relationship of salmon calcitonin analogs as agonists, antagonists, or inverse agonists in heterologous calcitonin receptor expression systems using two calcitonin receptor cell clones, B8-H10 and G12-E12, which express about 5 million and 25,000 C1b receptors/cell, respectively.

The location of the phosphorylation of the human calcitonin receptor by multiple kinases was studied by Nygaard et al. (1997).

REFERENCES AND FURTHER READING

Albrandt K, Mull E, Brady EMG, Herich J, Moore CX, Beaumont K (1993) Molecular cloning of two receptors from rat brain with high affinity for salmon calcitonin. FEBS Lett 325:225–232

Blind E, Raue F, Kienle P, Schroth J, Grauer A, Kabay A, Brügger P, Ziegler R (1993) Development and validation of an assay to measure bioactivity of human calcitonin *in vitro* using T47D cell membranes. Anal Biochem 212:91–97

Findlay DM, Michelangeli VP, Eisman JA, Frampton RJ, Moseley JM, MacIntyre I, Whitehead R, Martin TJ (1980) Calcitonin and 1,25-dihydroxyvitamin D_3 receptors in human breast cancer lines. Cancer Res 40:4764–4767

Findlay DM, Michelangeli VP, Orlowski RC, Martin TJ (1983) Biological activities and receptor interactions of des-leu^{16} salmon and des-phe^{16} human calcitonin. Endocrinology 112:1288–1291

Findlay DM, Michelangeli VP, Martin TJ, Orlowski RC, Seyler JK (1985) Conformational requirements for activity of salmon calcitonin. Endocrinology 117:801–805

Fukase M, Birge SJ, Rifas L, Avioli LV, Chase LR (1982) Regulation of 25 hydroxyvitamin D_3 1-hydroxylase in serum-free monolayer culture of mouse kidney. Endocrinology 110:1073–1075

Grauer A, Raue F, Reinel HH, Schneider HG, Schroth J, Kabay A, Brügger P, Ziegler R (1992) A new *in vitro* bioassay for human calcitonin: validation and comparison to the rat hypocalcemia bioassay. Bone Miner 17:65–74

Hilton JM, Chai SY, Sexton PM (1995) *In vitro* autoradiographic localization of the calcitonin receptor isoforms, C1a and C1b, in rat brain. Neuroscience 69:1223–1237

Horne WC, Shyu J-F, Chakraborty M, Baron R (1994) Signal transduction by calcitonin. Multiple ligands, receptors, and signaling pathways. Trends Endocrinol Metab 5:395–401

Horwitz KB, Zava DT, Thilager AK, Jensen EM, McGuire WL (1978) Steroid receptor analyses of nine human breast cancer cell lines. Cancer Res 38:2434–2437

Houssami S, Findlay DM, Brady CL, Martin TJ, Epand RM, Moore EE, Murayama E, Tamura T, Orlowski RC, Sexton PM (1994) Different structural requirements exist for calcitonin receptor binding specificity and adenylate cyclase activation. Mol Pharmacol 47:798–809

Kuestner RE, Elrod RD, Grant FJ, Hagen FS, Kuijper JL, Matthewes SL, O'Hara PJ, Sheppard PO, Stroop SD, Thompson DL, Whitmore TE, Findlay DM, Houssami S, Sexton PM, Moore EE (1994) Cloning and characterization of an abundant subtype of the human calcitonin receptor. Mol Pharmacol 46:246–255

Martin TJ, Findlay DM, Houssami S, Ikegame M, Rakopoulos M, Moseley JM, Sexton PM (1995) Heterogeneity of the calcitonin receptors: functional aspects in osteoclasts and other sites. J Nutr 125:2009S–2014S

Nygaard SC, Küstner RE, Moore EE, Stroop SD (1997) Phosphorylation of the human calcitonin receptor by multiple kinases in localized to the C-terminus. J Bone Miner Res 12:1681–1690

Povzek G, Hilton JM, Quiza M, Houssami S, Sexton PM (1997) Structure/function relationships of salmon calcitonin analogues as agonists, antagonists, or inverse agonists in a constitutively activated receptor cell system. Mol Pharmacol 51:658–665

Sexton PM, Hilton JM (1992) Biologically active salmon calcitonin-like peptide is present in brain. Brain Res 596:279–284

Sexton PM, Houssami S, Hilton JM, O'Keefe M, Center RJ, Gillespie MT, Darcy P, Findlay DM (1993) Identification of brain isoforms of the rat calcitonin receptor. Mol Endocrinol 7:815–821

Sexton PM, Houssami S, Brady CL, Myers DE, Findlay DM (1994) Amylin is an agonist for the renal porcine calcitonin receptor. Endocrinology 134:2103–2107

Sjödin L, Nederman T, Pråhl M, Montelius (1990) Radioreceptor assay for formulations of salmon calcitonin. Int J Pharm 63:135–142

Suva LJ, Flannery MS, Caulfileld MP, Findlay DM, Juppner G, Goldring SR, Rosenblatt M, Chorev M (1997) Design, synthesis and utility of novel benzophenone-containing calci-

tonin analogs for photoaffinity labeling the calcitonin receptor. J Pharmacol Exp Ther 283:876–884
Yates AJ, Gutierrez GE, Garrett IR, Mencel JJ, Nuss GW, Schreiber AB, Mundy GR (1990) A noncyclical analog of calcitonin (N^{α}-propionyl di-ala^{1,7},des-leu^{19} sCT) retains full potency without inducing anorexia in rats. Endocrinology 126:2845–2849

N.6 Parathyroid Hormone

N.6.0.1 General Considerations

The primary function of parathyroid hormone (PTH) is to maintain a constant concentration of Ca^{2+} in the extracellular fluid. Processes that are regulated include the absorption of Ca^{2+} from the gastrointestinal tract, the deposition and mobilization of bone Ca^{2+}, and the excretion of Ca^{2+} in urine, feces, sweat, and milk. PTH is the functional antagonist of calcitonin. The most prominent effect is to promote the mobilization of Ca^{2+} from bone. In the kidney, tubular reabsorption of Ca^{2+} is increased and tubular reabsorption of phosphate is inhibited. Clinically, idiopathic or postoperative hypoparathyroidism results in hypocalcemia followed by tetany.

PTH is used for treatment of hypoparathyroidism, and the symptoms of the disease can also be effectively antagonized by oral administration of dihydrotachysterol. A survey on the structure and function of the parathyroid gland in animals was published by Capen and Rosol (1989). The biologically active synthetic human parathyroid hormone 1–34 fragment (active sequence of PTH) is used for diagnostic testing (Mallette 1988).

An experimental model for secondary hyperparathyroidism with elevated levels of parathyroid hormone in rats has been described by Sancho et al. (1989).

Radioligand assays for parathyroid hormone receptors have been described (Habener and Potts 1976; Nissenson et al. 1985; Schneider et al. 1993).

Immunoassays for PTH are those measuring intact hormone (N-terminal, intact) and those measuring inactive fragments and partial sequences of the intact hormone (mid-region, C-terminal, polyvalent) (Endres et al. 1989). An immunochemiluminometric assay has been described by Klee et al. (1992).

Parathyroid hormone-related protein (PTHrP) was first identified and cloned from malignant tumor cells and tissues from patients with a syndrome called humoral hypercalcemia of malignancy (Moseley et al. 1987; Strewler et al. 1987; Suva et al. 1987). PTHrP-(1–34) and PTH-(1–34) act via a single species of cloned receptor (Abou-Samra et al. 1992; Schipani et al. 1993), although other studies have shown that specific receptors for each of these peptides exist (Usdin et al. 1995; Behar et al. 1996; Bergwitz et al. 1997; Yamamoto et al. 1997; Fukayama et al. 1998). PTHrP is an example of the widening array of sequences identified by molecular endocrinology, with functional characterization of their endocrine role often following after a considerable delay.

REFERENCES AND FURTHER READING

Abou-Samra AB, Jüppner H, Force T, Freeman MW, Kong XF, Schipani E, Urena P, Richards J, Bonventre JV, Potts TJ Jr, Kronenberg HM, Segre GV (1992) Expression of a common receptor for parathyroid hormone and parathyroid-related peptide from rat osteoblast-like cells: a single receptor stimulates intracellular accumulation of both cAMP and inositol triphosphates and increases intracellular calcium. Proc Natl Acad Sci USA 89:2732–2736
Behar V, Nakamoto C, Greenberg Z Bisello A, Suva LJ, Rosenblatt M, Chorev M (1996) Histidine at position 5 is the specificity "switch" between two parathyroid hormone receptor subtypes. Endocrinology 137:4217–4244
Bergwitz C, Jusseaume SA, Luck MD, Jüppner H, Gardella TJ (1997) Residues in the membrane-spanning and extracellular loop regions of the parathyroid hormone (PTH)-2 receptor determine signaling selectivity for PTH and PTH-related peptide. J Biol Chem 272:28861–28868
Capen CC, Rosol TJ (1989) Recent advances in the structure and function of the parathyroid gland in animals and the effect of xenobiotics. Toxicol Pathol 17:333–345
Endres DB, Villanueva R, Sharp CF, Singer FR (1989) Measurement of parathyroid hormone. Endocrin Metab Clin North Am 18:611–629
Fukayama S, Royo M, Sugita M, Imrich A, Chorev M, Suva LJ, Rosenblatt M, Tashjian AH Jr (1998) New insights into interactions between the human PTH/PTHrP receptor and agonist/antagonist binding. Am J Physiol 274:E297–E303
Habener JF, Potts JT (1976) Radioimmunoassay of parathyroid hormone. In: Hormones in human blood. Detection and assay. Harvard University Press, Cambridge, pp 551–588
Klee GG, Preissner CM, Schryver PG, Taylor RL, Kao PC (1992) Multisite immunochemiluminometric assay for simultaneously measuring whole-molecule and amino-terminal fragments of human parathyrin. Clin Chem 35:628–635
Mallette LE (1988) Synthetic human parathyroid hormone 1–34 fragment for diagnostic testing. Ann Intern Med 109:800–804
Moseley JM, Kubota M, Dieffenbach-Jagger H, Wettenhall REH, Kemp BE, Suva LJ, Rodda CP, Ebeling PR Hudson PJ, Zajac D, Martin TJ (1987) Parathyroid hormone-related protein purified from a human lung cancer cell line. Proc Natl Acad Sci USA 84:5048–5052
Nissenson RA, Teitelbaum AP, Arnaud CD (1985) Assay for parathyroid hormone receptors. Methods Enzymol 109:48–56
Sancho JJ, Duh Qy, Oms L, Sitges-Serra A, Hammond ME, Arnaud CD, Clark OH (1989) A new experimental model for secondary hyperparathyroidism. Surgery 106:1002–1008

Schipani E, Karga H, Karaplis AC, Potts JT Jr, Kronenberg HM, Segre GV, Abou-Samra AB, Jüppner H (1993) Identical complementary deoxyribonucleic acids encode a human renal and bone parathyroid (PTH)/PTH-related peptide receptor. Endocrinology 132:2157–2165

Schneider H, Feyen JHM, Seuwen K, Movva NR (1993) Cloning and functional expression of a human parathyroid hormone receptor. Eur J Pharmacol 246:149–155

Strewler GJ, Stern PH, Jacobs JW, Eveloff J, Klein RF, Leung SC, Rosenblatt M, Nissenson RA (1987) Parathyroid hormone-like protein from human renal carcinoma cells. Structural and functional homology with parathyroid hormone. J Clin Invest 80:1803–1807

Suva LJ, Winslow GA, Wettnehall REH, Hammonds RG, Moseley JM, Dieffenbacher-Jagger H, Rodda CP, Kemp BE, Rodriguez H, Chen EY, Hudson PJ, Martin TJ, Wood WL (1987) A parathyroid hormone-related protein implicated in malignant hypercalcemia: cloning and expression. Science 237:893–896

Usdin TB, Gruber C, Bonner TI (1995) Identification and functional expression of a receptor selectively recognizing parathyroid hormone, the PTH2 receptor. J Biol Chem 270:15455–15458

Yamamoto S, Morimoto I, Yanagihara N, Zeki K, Fujihira T, Izumi F, Yamashita H, Eto S (1997) Parathyroid hormone-related peptide-(1–34) [PTHrP-(1–34)] induces vasopressin release from the rat supraopticus nucleus *in vitro* through a novel receptor distinct from a type I or II PTH/PTHrP receptor. Endocrinology 138:2066–2072

N.6.0.2 Receptor Binding Assay for PTH

PURPOSE AND RATIONALE

In many instances, the presence of receptors is explored as the counterpart of the presence of hormonally active substances in tissues and organs. However, the presence of binding sites does not immediately indicate functional activation of the respective tissue, and there are indeed circulating "free receptors" which have been identified as subunits of fragments of "whole receptors" located in cell membranes. Cloned receptors are frequently used for advanced research, to identify compounds which might interact with functional receptors in tissues, and acquire relevance as pharmacological tools for example for high-throughput screening. Furthermore, using radioligand assays to determine the receptor affinity of PTH analogs may provide helpful structure–activity information. Three receptors that are activated by PTH have been cloned. PTH and PTHrP bind to the PTH_1 receptor, for which many studies are published (Abou-Samra et al. 1992; Uneno et al. 1992; Schipani et al. 1993; Ureña et al. 1993; Kaufmann et al. 1994; Schermer et al. 1994; Orloff et al. 1995; Usdin et al. 1995; Bergwitz et al. 1996; Gardella et al. 1996; Yasuka et al. 1996; Bergwitz et al. 1997; Bisello et al. 1997; Guo et al. 1997; Yamamoto et al. 1997; Fukayama et al. 1998; Yaghoobian and Drueke 1998).

Behar et al. (1996b) reported ligand binding in stably transfected human embryonic kidney cells, HEK-293/C-21 cells that express the hPTH/PTRrP receptor, and HEK/BP16 cells that express the hPTH2 receptor.

The PTH_2 receptor has about 50% amino acid sequence identity with the PTH_1 receptor and is not activated by PTHrP, but by a peptide isolated from bovine hypothalamus, TIP39, which is only distantly related to PTH and PTHrP (Usdin 2000).

The PTH_3 receptor has been isolated from zebrafish (Rubin and Juppner 1999).

It is part of the problem of advanced research that cloning of receptors frequently precedes the validation of physiological relevance of receptor subclasses.

PROCEDURE

Stably transfected human embryonic kidney cells, HEK-293/C-21 cells that express the hPTH/PTRrP receptor (Pines et al. 1994), and HEK/BP16 cells that express the hPTH2 receptor (Behar et al. 1996a) are maintained in DMEM supplemented with 10% FBS.

The cells are incubated with [^{131}I]PTH-(1–34) (100,000 cpm/well) with or without competing unlabeled PTH-(1–34) or other ligands in binding buffer for 2 h at room temperature. Cells are washed twice with PBS, then solubilized in 0.5 ml of 0.1 M NaOH. Aliquots are taken for determination of bound radioactivity by γ-counting.

EVALUATION

Specific binding is expressed as counts per minute bound per well (raw data) and converted to the percentage specific binding of radioligand. Affinity constants and binding capacity of these receptors in tissue may be calculated, and dose–response curves of ligands are compared as a first step towards proof of signaling and biological activity.

MODIFICATIONS OF THE METHOD

McCuiag et al. (1994) reported the molecular cloning of the gene encoding the receptor for the parathyroid hormone/parathyroid hormone-related peptide in the mouse.

Inomata et al. (1995) characterized a PTH receptor with specificity for the carboxy-terminal region of PTH-(1–84).

REFERENCES AND FURTHER READING

Abou-Samra AB, Jüppner H, Force T, Freeman MW, Kong XF, Schipani E, Urena P, Richards J, Bonventre JV, Potts TJ Jr,

Kronenberg HM, Segre GV (1992) Expression of a common receptor for parathyroid hormone and parathyroid-related peptide from rat osteoblast-like cells: a single receptor stimulates intracellular accumulation of both cAMP and inositol triphosphates and increases intracellular calcium. Proc Natl Acad Sci USA 89:2732–2736

Behar V, Pines M, Nakamoto C, Greenberg Z, Bisello A, Stueckle S, Bessalle R, Usdin TB, Chorev M, Rosenblatt M, Suva L (1996a) The human PTH2 receptor: binding and signal transduction properties of the stably expressed recombinant receptor. Endocrinology 137:2748–2757

Behar V, Nakamoto C, Greenberg Z Bisello A, Suva LJ, Rosenblatt M, Chorev M (1996b) Histidine at position 5 is the specificity "switch" between two parathyroid hormone receptor subtypes. Endocrinology 137:4217–4244

Bergwitz C, Gardella TJ, Flannery MR, Potts JT Jr, Kronenberg HM, Jüppner H (1996) Full activation of chimeric receptors by hybrids between parathyroid hormone and calcitonin. Evidence for a common pattern of ligand-receptor interaction. J Biol Chem 271:26469–26472

Bergwitz C, Jusseaume SA, Luck MD, Jüppner H, Gardella TJ (1997) Residues in the membrane-spanning and extracellular loop regions of the parathyroid hormone (PTH)-2 receptor determine signaling selectivity for PTH and PTH-related peptide. J Biol Chem 272:28861–28868

Bisello A, Nakamoto C, Rosenblatt M, Chorev M (1997) Mono- and bicyclic analogs of parathyroid hormone-related protein. 1. Synthesis and biological studies. Biochemistry 36:3293–3299

Fukayama S, Royo M, Sugita M, Imrich A, Chorev M, Suva LJ, Rosenblatt M, Tashjian AH Jr (1998) New insights into interactions between the human PTH/PTHrP receptor and agonist/antagonist binding. Am J Physiol 274: E297–E303

Gardella TJ, Luck MD, Fan M-H, Lee C (1996) Transmembrane residues of the parathyroid hormone (PTH)/PTH-related peptide receptor that specifically affect binding and signaling by agonist ligands. J Biol Chem 271:12820–12825

Guo J, Liu B, Bringhurst FR (1997) Mechanisms of homologous and heterologous desensitization of PTH/PTHrP receptor signaling in LLC-PK-1 cells. Am J Physiol 273:E383–E393

Inomata N, Akiyama M, Kubota N, Jüppner H (1995) Characterization of a novel parathyroid hormone (PTH) receptor with specificity for the carboxy-terminal region of PTH-(1–84). Endocrinology 136:4732–4740

Kaufmann M, Muff R, Born W, Fischer JA (1994) Functional expression of a stably transfected parathyroid hormone/parathyroid hormone-related protein receptor complementary DNA in CHO cells. Mol Cell Endocrinol 104:21–27

McCuiag KA, Clarke JC, White JH (1994) Molecular cloning of the gene encoding the mouse parathyroid hormone/parathyroid hormone-related peptide receptor. Proc Natl Acad Sci USA 91:5051–5055

Orloff JJ, Kats Y, Urena P, Schipani E, Vasavada RC, Philbrick WM, Behal A, Abou-Sarma A-B (1995) Further evidence for a novel receptor for amino-terminal parathyroid hormone-related peptide on keratinocytes and squamous carcinoma cell lines. Endocrinology 136:3016–3023

Pines M, Adams AE, Stueckle S, Bessalle R, Rashti-Behar V, Chorev M, Rosenblatt M, Suva LJ (1994) Generation and characterization of human kidney cell lines stably expressing recombinant human PTH/PTHrP receptor: lack of interaction with a C-terminal human PTH peptide. Endocrinology 135:1713–1716

Rubin DA, Juppner H (1999) Zebrafish express the common parathyroid hormone/parathyroid hormone-related peptide receptor (PTH1R) and a novel receptor (PTH3R) that is preferentially activated by mammalian and fugu-fish parathyroid hormone-related peptide. J Biol Chem 274:28185–28190

Schermer DT, Bradley MS, Bambino TH, Nissenson RA, Strewler GJ (1994) Functional properties of a synthetic chicken parathyroid hormone-related protein 1–36 fragment. J Bone Miner Res 9:1041–1046

Schipani E, Karga H, Karaplis AC, Potts JT Jr, Kronenberg HM, Segre GV, Abou-Samra AB, Jüppner H (1993) Identical complementary deoxyribonucleic acids encode a human renal and bone parathyroid (PTH)/PTH-related peptide receptor. Endocrinology 132:2157–2165

Uneno S, Yamamuro T, Jüppner H, Abou-Samra A-B, Keutmann HT, Potts JT Jr, Segre GV (1992) Solubilization of functional receptors for parathyroid hormone and parathyroid hormone-related peptide from clonal rat osteosarcoma cells, ROS17/2.8. Calcif Tiss Int 51:382–386

Ureña P, Kong X-F, Abou-Samra A-B, Jüppner H, Kronenberg HM, Potts JT Jr, Segre GV (1993) Parathyroid hormone (PTH)/PTH-related peptide receptor messenger ribonucleic acids are widely distributed in rat tissues. Endocrinology 133:717–623

Usdin TB (2000) The PTH_2 receptor and TIP39: a new peptide-receptor system. Trends Pharmacol Sci 21:128–130

Usdin TB, Gruber C, Bonner TI (1995) Identification and functional expression of a receptor selectively recognizing parathyroid hormone, the PTH2 receptor. J Biol Chem 270:15455–15458

Yaghoobian J, Drueke TB (1998) Regulation of the transcription of parathyroid hormone/parathyroid hormone-related peptide receptor mRNA by dexamethasone in ROS 17/2.8 cells. Nephrol Dial Transpl 13:580–586

Yamamoto S, Morimoto I, Yanagihara N, Zeki K, Fujihira T, Izumi F, Yamashita H, Eto S (1997) Parathyroid hormone-related peptide-(1–34) [PTHrP-(1–34)] induces vasopressin release from the rat supraopticus nucleus *in vitro* through a novel receptor distinct from a type I or II PTH/PTHrP receptor. Endocrinology 138:2066–2072

Yasuka T, Kawashima M, Takahashi T, Iwata A, Oka N, Tanaka K (1996) Changes in parathyroid hormone receptor binding affinity during egg laying: implication for calcium homeostasis in chicken. J Bone Miner Res 11:1913–1920

N.6.0.3
PTH Assay by Serum Calcium Increase

PURPOSE AND RATIONALE

The classical method by Collip and Clark (1925) involves measurement of the rise in serum calcium after administration of parathyroid extracts to dogs. Hamilton and Schwartz (1932) use rabbits treated with oral loads of calcium chloride. The intact rat is very insensitive to injected parathyroid hormone; however, parathyroidectomy produces an increase in sensitivity (Holtz 1937; Davies and Gordon 1953; Davies et al. 1954; Thorp 1969; Zull and Malbon 1976).

PROCEDURE

Male Wistar rats weighing 200–250 g are anesthetized with pentobarbital sodium intraperitoneally. Parathy-

roidectomy is performed by cauterization. After a recovery period of 1 week, blood is withdrawn by retroorbital puncture (baseline). Various doses of the test preparation or standard are injected subcutaneously to groups of six to ten animals. Blood samples are obtained again 21 h later. Serum calcium is determined by flame photometry. The increase of calcium 21 h after PTH injection is calculated for each animal.

EVALUATION

Mean values of the increase in serum calcium are plotted versus logarithm of dose, and potency ratios versus PTH standard may be calculated for the test compounds.

MODIFICATIONS OF THE METHOD

An increase of whole-body calcium and skeletal mass after repeated-dose treatment with parathyroid hormone in normal rats and in rats with osteoporosis induced by pregnancy and lactation under a low-calcium diet was found by Hefti et al. (1981).

Parathyroid hormone prevented bone loss and augmented bone formation in ovariectomized rats (Kalu et al. 1990; Liu and Kalu 1990).

The active sequence of PTH has been used instead of the full secreted sequence.

REFERENCES AND FURTHER READING

Collip JB, Clark EP (1925) Further studies on the physiological action of a parathyroid hormone. J Biol Chem 64:485–507

Davies BMA, Gordon AH (1953) The effect of parathyroid hormone on phosphate excretion in the rat. J Endocrinol 9:292–300

Davies BMA, Gordon AH, Mussett MV (1954) A plasma calcium assay for parathyroid hormone, using parathyroidectomized rats. J Physiol (Lond) 125:383–395

Hamilton B, Schwartz C (1932) A method for the determination of small amounts of parathyroid hormone. J Pharmacol 46:285–292

Hefti E, Trechsel U, Fleisch H, Schenk R (1981) Increase of whole-body calcium and skeletal mass in normal and osteoporotic adult rats treated with parathyroid hormone. Clin Sci 62:389–396

Holtz F (1937) Wirkstoffe der Nebenschilddrüsen. In: Heubner W, Schüller J (eds) Handbuch der experimentellen Pharmakologie, Ergänzungswerk, Vol 3. Springer, Berlin Heidelberg New York, pp 151–161

Kalu DN, Echon R, Hollis BW (1990) Modulation of ovarectomy-related bone loss by parathyroid hormone in rats. Mechan Ageing Dev 56:49–62

Liu CC, Kalu DN (1990) Human parathyroid hormone-(1–34) prevents bone loss and augments bone formation in sexually mature ovarectomized rats. J Bone Miner Res 5:973–982

Thorp RH (1969) Parathyroid hormone. In: Dorfman RI (ed) Methods in hormone research, Vol IIA. Academic Press, New York, pp 435–445

Zull JE, Malbon CC (1976) Parathyroid hormone receptors. In: Belcher M (ed) Methods in receptor research, Part II. Dekker, New York, pp 533–564

N.6.0.4
Serum Phosphate Decrease After PTH

PURPOSE AND RATIONALE

Tepperman et al. (1947) developed a method using the fall in serum inorganic phosphorus in the rat after injection of parathyroid hormone (Thorp 1962).

PROCEDURE

Male Wistar rats weighing 150–200 g are fed Purina dog chow for at least 2 weeks prior to the experiment. During the experiment only water is allowed. Blood samples (baseline and PTH stimulated, 3 h after PTH) are taken from the tail and 0.6 ml is collected from each rat into tubes, centrifuged for 10 min and 0.2-ml samples of the serum are pipetted into 6 ml of 10% trichloroacetic acid; solutions are centrifuged and 5-ml aliquots of the protein-free solution are used for the estimation of inorganic phosphorus, by the method of Fiske and Subbarow (1925) for example. Serum phosphorus is measured before and 3 h after subcutaneous administration of various doses of test preparation or standard.

EVALUATION

Dose–response curves showing a linear relationship between log dose and response are suitable for the calculation of potency ratios.

REFERENCES AND FURTHER READING

Fiske CH, Subbarow Y (1925) The colorimetric determination of phosphorus. J Biol Chem 66:375–400

Tepperman HM, L'Heureux MV, Wilhelmi AE (1947) The estimation of parathyroid hormone activity by its effect on serum anorganic phosphorus in the rat. J Biol Chem 168:151–165

Thorp RH (1962) Parathyroid hormone. In: Dorfman RI (ed) Methods in hormone research, Vol II. Academic Press, New York, pp 477–493

N.6.0.5
cAMP Release in Isolated Perfused Rat Femur

PURPOSE AND RATIONALE

This is an *in vitro* assay. The effect of parathyroid hormone and analogs on release of cAMP from adult bone can be measured in a perfusion system of isolated rat femora (Sugimoto et al. 1985; Lopez-Hilker et al. 1992).

PROCEDURE

Five-week-old Wistar rats anesthetized with pentobarbital (45 mg/kg) are heparinized and used as donors, the femora are removed. Adhering muscles are stripped from the bone. A hole with about half of the depth of the cortex is made with a fine drill at the nutrient foramen below the femoral neck. Then a 21-gauge needle is inserted into this hole and fixed by dental cement to avoid leakage of the perfusate. The bone is then placed in an apparatus for liver perfusion and perfused at a flow rate of 1 ml/5 min by a pump with Krebs-Ringer-bicarbonate, continuously gassed with 95% O_2 and 5% CO_2 and containing 1 mg/ml glucose. Once the perfused bone is assembled, the bone is allowed to equilibrate for 45 min. Samples are collected into a chilled tube for the last 5 min for determination of basal cAMP levels. Then various doses of the test preparations or the standard are infused for 5 min and serial samples are collected every 5 min. In the perfusate, cAMP is measured by radioimmunoassay.

EVALUATION

Time–response curves and dose–response curves are established allowing the calculation of potency ratios with confidence limits.

MODIFICATIONS OF THE METHOD

Nissenson et al. (1981) measured the activation of canine renal cortical plasma membrane adenylate cyclase activity produced by parathyroid hormone standard and test sera from parathyroid venous effluent of patients with primary hyperparathyroidism, in the presence of the hydrolysis-resistant GTP analog 5′-guanylimidodiphosphate.

Gundberg et al. (1995) compared the effects of parathyroid hormone and parathyroid-hormone-related protein on osteocalcin release in the isolated rat hindlimb and in intact and thyro-parathyroidectomized rats.

Saito et al. (1987) established a new biological assay system for simultaneous measurement of bone resorption and bone mineralization in **organ cultures of chick embryonic femur**. Eleven-day-old chick embryonic femur was labeled with ^{45}Ca *in vitro*. $T_{1/2}$ of calcium efflux was calculated from the sequential release of the label into the medium. Parathyroid hormone increased calcium mobilization, indicating enhanced bone resorption, whereas hydrocortisone and sodium fluoride inhibited bone resorption. Calcitonin was ineffective.

Barling et al. (1989) measured the adenylate cyclase response to parathyroid hormone in cultured rabbit marrow fibroblast cells.

Docherty and Heath (1989) used osteosarcoma cells for an *in vitro* bioassay determining cAMP formation.

REFERENCES AND FURTHER READING

Barling PM, Bennett JH, Triffitt JT, Owen ME (1989) The adenylate cyclase response to parathyroid hormone in cultured rabbit marrow fibroblastic cells. Bone Mineral 7:23–30

Docherty HM, Heath DA (1989) Multiple forms of parathyroid hormone-like proteins in a human tumor. J Mol Endocrinol 2:11–20

Gundberg CM, Fawzi MI Clough ME, Calvo MS (1995) A comparison of the effects of parathyroid hormone and parathyroid hormone-related protein on osteocalcin in the rat. J Bone Miner Res 10:903–906

Lopez-Hilker S, Martin KJ, Sugimoto T, Slatopolsky E (1992) Biological activities of parathyroid hormone (1–34) and parathyroid hormone-related peptide (1–34) in isolated perfused rat femur. J Lab Clin Med 119:738–743

Nissenson RA, Abbott SR, Teitelbaum AP, Clark OH, Arnaud CD (1981) Endogenous biologically active human parathyroid hormone: measurement by a guanyl nucleotide-amplified renal adenylate cyclase assay. J Clin Endocrinol Metab 52:840–846

Saito M, Kawashima K, Endo H (1987) The establishment of a new biological assay system for simultaneous measurement of bone resorption and bone mineralization in organ cultures of chick embryonic femur. J Pharmacobiodyn 10:487–493

Sugimoto T, Fukase M, Tsutsumi M, Imai Y, Hishikawa R, Yoshimoto Y, Fujita T (1985) Additive effects of parathyroid hormone and calcitonin on adenosine 3′,5′-monophosphate release in newly established perfusion system of rat femur. Endocrinology 117:190–195

N.6.0.6 Renal and Metatarsal Cytochemical Bioassay

PURPOSE AND RATIONALE

Cytochemical bioassays using renal and metatarsal tissue are sensitive enough to detect plasma levels of parathyroid hormone and useful for determining the agonist and antagonist activities of fragments and analogs (Chambers et al. 1978; Goltzman et al. 1980; Bradbeer et al. 1988; Loveridge et al. 1991; Zaman et al. 1991; Bourdeau et al. 1990; Wood 1992).

PROCEDURE

For the **renal cytochemical assay**, kidney segments from vitamin-D-depleted guinea pigs are maintained in non-proliferative organ culture for 5 h using Trowell's T8 medium (GIBCO). The medium is then changed for 8 min before exposure to various doses of the parathyroid hormone standard, the parathyroid hormone fragment or the analog for an additional 8 min.

In the experiments for antagonistic activities, each segment is exposed to a single concentration of hPTH-(1–84) (106 fmol/l) or to hPTH-(1–34) (255 fmol/l) in the presence or absence of the antagonist to be tested. The segments are then shock-frozen to −70°C in *N*-hexane before being sectioned at 16 µm on a cryostat. The sections are examined for glucose-6-phosphate dehydrogenase activity using specific staining. The precipitated formazane is quantified in the cells of the distal convoluted tubules by means of a microdensitometer (wavelength 585 nm). Ten readings with each of two duplicate sections are made and the results presented as the mean integrated absorbance × 100 (±SEM).

For the **metatarsal cytochemical assay**, the metatarsals of young female Wistar rats weighing 50–100 g are removed and the growth plates are isolated. Only the four longest metatarsals have growth plates large enough to be of use. The metatarsals are maintained individually in nonproliferative organ culture in 5–10 ml Trowell's T8 medium buffered to pH 7.6 in an atmosphere of 95% O_2, 5% CO_2 at 37°C for 5 h. After the culture period, the medium is removed and each metatarsal exposed to fresh medium (buffered to pH 7.6 by bubbling with a 95% O_2, 5% CO_2 mixture) containing a low priming dose of PTH (0.5 fg/ml) for 8 min, followed by exposure to known concentrations of a standard PTH preparation or various concentrations of the analog or to dilutions of plasma for 8 min. The metatarsals are then briefly dipped in a 5% solution of polyvinyl alcohol and chilled immediately in *N*-hexane to −70°C.

Each bone is sectioned at 10 µm in a cryostat. The sections are reacted for glucose-6-phosphate dehydrogenase activity in a similar way as described for the renal cytochemical assay. The activity in hypertrophic chondrocytes is linear with respect to time from 10 min, at which time there is enough formazan to be measured, up to 40 min when the density of the formazan formed is too great for a reliable linear response. The enzyme activity in each section is measured in ten individual hypertrophic chondrocytes or osteoblasts lining the metaphyseal trabeculae by scanning and integrating microdensitometry at a wavelength of 585 nm. The results are presented as the mean integrated extinction × 100 (±SE) of ten measurements from each of two sections of each metatarsal.

EVALUATION

Dose–response curves are tested for linearity and parallelism and potency ratios are calculated.

CRITICAL ASSESSMENT OF THE METHOD

The cytochemical assays are sensitive but very time-consuming when compared with other analytical methods for the detection of PTH and PTH fragments.

REFERENCES AND FURTHER READING

Bourdeau A, Manganella G, Thil-Trubert CL, Sachs C, Cournot G (1990) Bioactive parathyroid hormone in pregnant rats and fetuses. Am J Physiol 258:E549–E554

Bradbeer JN, Dunham J, Fischer JA, de Deuxchaisnes CN, Loveridge N (1988) The metatarsal cytochemical bioassay of parathyroid hormone: validation, specificity, and application to the study of pseudohypoparathyroidism type I. J Clin Endocrinol Metab 67:1237–1243

Chambers DJ, Dunham J, Zanelli JM, Parsons JA, Bitensky L, Chayen J (1978) A sensitive bioassay of parathyroid hormone in plasma. Clin Endocrinol (Oxford) 9:375–379

Goltzman D, Henderson B, Loveridge N (1980) Cytochemical bioassay of parathyroid hormone: characteristics of the assay and analysis of circulating hormonal forms. J Clin Invest 65:1309–1317

Loveridge N, Dean V, Goltzman D, Hendy GN (1991) Bioactivity of parathyroid hormone and parathyroid hormone-like peptide: agonist and antagonist activities of amino-terminal fragments as assessed by the cytochemical bioassay and *in situ* biochemistry. Endocrinology 128:1938–1946

Wood PJ (1992) The measurement of parathyroid hormone. Ann Clin Biochem 29:11–21

Zaman G, Saphier PW, Loveridge N, Kimura T, Sakakibara S, Bernier SM, Hendy GM (1991) Biological properties of synthetic human parathyroid hormone: effect of deamidation at position 76 on agonistic and antagonistic activity. Endocrinology 128:2583–2590

N.6.0.7 cAMP Accumulation in Cultured Cells

PURPOSE AND RATIONALE

Parathyroid hormone and parathyroid hormone-related protein (PTHrP) stimulate intracellular cAMP accumulation in various cell types in a dose-dependent manner; for example, in PTHrP-overexpressing ROS cells, an osteoblast-like cell line Motomura et al. (1996); in UMR106 cells, a rat osteosarcoma cell line (Oldenburg et al. 1996); in the human osteosarcoma SaOS cell line (Rodan et al. 1987; Fukayama and Tashjian 1994); in COS-7 cells transfected with the human PTH-1 (PTH/PTHrP) receptor and the human PTH-2 receptor (Bergwitz et al. 1997); or in stably transfected human embryonic kidney cells (HEK-293/C-21 cells that express the hPTH/PTRrP receptor and HEK/BP16 cells that express the hPTH2 receptor) (Behar et al. 1996b).

PROCEDURE

Stably transfected human embryonic kidney cells, HEK-293/C-21 cells that express the hPTH/PTRrP receptor (Pines et al. 1994) and HEK/BP16 cells that

express the hPTH2 receptor (Behar et al. 1996a) are maintained in DMEM supplemented with 10%FBS. For cAMP determination, C-21 or BP-16 cells are incubated in 24-well tissue plates with various peptides for 10 min in DMEM in the presence of 1 mM 3-isobutyl-1-methylxanthine. The incubation is terminated by removal of the cell culture medium and addition of perchloric acid (final concentration 30%, vol/vol). Samples are neutralized with potassium bicarbonate and acetylated with acetic anhydrate. Total cAMP values (medium plus cells) are determined by RIA. Data are presented as the percentage stimulation, from the ratio of maximal accumulated cAMP levels obtained in the presence of the highest concentration of the agonist PTH-(1–34) compared to the basal cAMP level. The accumulated cAMP levels (picomoles) are calculated per 100,000 cells. Cell number is determined in a Coulter counter.

EVALUATION

Data are presented as the triplicate mean of $([cAMP]_c/[cAMP]_{PTHmax}) \times 100$ (±SEM) or sample stimulation vs. maximal PTH induced stimulation. $[cAMP]_c$ is the concentration of cAMP accumulated in response to a given concentration of a ligand, and $[cAMP]_{PTHmax}$ is the concentration of cAMP accumulated at the maximal dose (10^{-6} M) of PTH-(1–34).

REFERENCES AND FURTHER READING

Behar V, Pines M, Nakamoto C, Greenberg Z, Bisello A, Stueckle S, Bessalle R, Usdin TB, Chorev M, Rosenblatt M, Suva L (1996a) The human PTH2 receptor: binding and signal transduction properties of the stably expressed recombinant receptor. Endocrinology 137:2748–2757

Behar V, Nakamoto C, Greenberg Z, Bisello A, Suva LJ, Rosenblatt M, Chorev M (1996b) Histidine at position 5 is the specificity "switch" between two parathyroid hormone receptor subtypes. Endocrinology 137:4217–4244

Bergwitz C, Jusseaume SA, Luck MD, Jüppner H, Gardella TJ (1997) Residues in the membrane-spanning and extracellular loop regions of the parathyroid hormone (PTH)-2 receptor determine signaling selectivity for PTH and PTH-related peptide. J Biol Chem 272:28861–28868

Fukayama S, Tashjian AH (1994) Involvement of alkaline phosphatase in the modulation of receptor signaling in osteoblasts: evidence for a difference between human parathyroid hormone-related protein and human parathyroid hormone. J Cell Physiol 158:391–397

Motomura K, Ohtsuru A, Enomoto H, Tsukazaki T, Namba H, Tsuji Y, Yamashita S (1996) Osteogenic action of parathyroid hormone-related peptide (1–141) in rat ROS cells. Endocrinol J 43:527–535

Oldenburg KR, Epand RF, D'Orfanit A, Vo K, Selick H, Epand RM (1996) Conformational studies on analogs of recombinant parathyroid hormone and their interactions with phospholipids. J Biol Chem 271:17582–17591

Pines M, Adams AE, Stueckle S, Bessalle R, Rashti-Behar V, Chorev M, Rosenblatt M, Suva LJ (1994) Generation and characterization of human kidney cell lines stably expressing recombinant human PTH/PTHrP receptor: lack of interaction with a C-terminal human PTH peptide. Endocrinology 135:1713–1716

Rodan SB, Imai Y, Thiede MA, Wesolowski G, Thompson D, Bar-Shavit Z, Shull S, Mann K, Rodan GA (1987) Characterization of a human osteosarcoma cell line (SaOS-2) with osteoblastic properties. Cancer Res 47:4961–4966

N.6.0.8 Bone Anabolic Activitym in Ovariectomized, Osteopenic Rats

PURPOSE AND RATIONALE

This is an *in vivo* bioassay which may be used for the beneficial effect of PTH on bone. Vickery et al. (1996) tested an analog of human parathyroid hormone-related protein (1–43) (hPTHrP) in ovariectomized, osteopenic rats.

PROCEDURE

Groups of 3-month-old virgin female rats are subjected to bilateral ovariectomy or sham surgery. The ovariectomized animals are treated by daily subcutaneous injections of 0, 9, 29 or 80 µg/kg of test compound or human parathyroid hormone-related protein (1–43), starting on day 17 after surgery and continuing for 21 days. On day 12 and 19 following the first day of treatment, animals are dosed intraperitoneally with 6 mg/kg of a 3.75 mg/ml solution of calcein (Sigma) in 2% sodium bicarbonate saline. Body weights are recorded, following an 18-h fast, on the last day of treatment. The animals are sacrificed immediately following the last injection and the femurs, tibiae, and L2 vertebrae are excised.

The distal part of the right femur is cut in half longitudinally after removal of the epiphysis. The bone marrow is flushed out using a stream of water. The trabecular and cortical bone are separated using a dental drill. Calcium is extracted by immersion of the trabecular bone for 3 days and the cortical bone for 5 days in 5% trichloroacetic acid. The calcium content of the extracts is determined. Measurement are expressed as mean ±SEM in units of milligrams of Ca^{2+}/distal half femur per 100 g of body weight.

For histomorphometry, the left tibiae from sham, ovariectomized and high-dose-treated rats are removed and fixed in formalin. The tibiae are cut with a diamond disc into three pieces: the proximal 1 cm, 2 cm of the diaphysis, and the distal end. The proximal and diaphyseal portions are transferred to Villanueva stain for 72 h (Villanueva and Lundin 1989). The proximal specimen is then dehydrated through increasing con-

centrations of ethanol (70%–100%), defatted in acetone, and embedded in modified methyl methacrylate. Pairs of 5-µm-thick frontal sections are prepared from the anterior aspect with a microtome. The first section is stained with a modified Masson trichrome technique (Goldner 1938) and the second left unstained.

The diaphyseal portion is also dehydrated, defatted and embedded in methyl methacrylate. Five 150-µm-thick sections are prepared, ground to 100 µm thickness, and mounted unstained.

Growth cartilage thickness is measured by finding the distance between the proximal border of the epiphyseal growth cartilage and the metaphyseal junction at 12 places spaced 0.2 mm apart.

On each slide, a rectangular window is defined as the field for evaluation. The top line is drawn under the primary spongiosa, and the second line is drawn parallel to it and 3.5 mm distally. The side lines are drawn near to, but not touching, the endocortical surface.

Histomorphometric variables are calculated for mean trabecular volume and structure (trabecular thickness, number, spacing, mineralizing surface, individual osteoblast activity, and osteoclast surface). Surface-based, bone-volume-based, and total tissue-volume-based bone formation rates are also calculated.

In the cortical bone of the tibial diaphysis, the periosteal and endocortical surfaces are measured separately. Using transmitted light at 25 × magnification, the periosteal and endo-osteal perimeters are measured. The periosteal single-labeled and double-labeled surface and endo-osteal single-labeled and double-labeled surface are measured using 160 × magnification.

Vertebral processing and electron microscopy are performed in sham, ovariectomized and compound-treated groups. The second lumbar vertebra is removed, dissected from soft tissue, and split sagittally with a diamond saw. The two halves are fixed in a mixture of glutaraldehyde and formaldehyde for 24–48 h at 4°C. The tissue is decalcified in 10% EDTA in 0.1 M cacodylate, pH 7.2, postfixed for 1.5 h in OsO_4, stained in block with uranyl acetate, dehydrated and fixed in Epon. Then 50-nm sections are cut and examined in an electron microscope. Microphotographs are printed at a final magnification of 1300 ×. Each microphotograph is overlaid with a grid with a total test line length of 2.22×10^3 µm. Each intercept of the line with the trabecular surface is scored into one of four categories, depending on the cell type adjacent to the intercept: osteoblasts, osteoclasts, lining cells, no cells. The proportion of the trabecular bone surface area covered by each cell type is estimated by pooling the pictures from each rat and summing the grid points that intersect each cell type, then dividing by the total number of intersection, excluding the "no cell" counts.

EVALUATION

The treatment groups are compared by one-way analysis of variance (ANOVA) followed by Fisher's least-significance difference test to compare each treatment group with the ovariectomized vehicle control group. For the histomorphometric determinations, the Kruskal-Wallis test is applied to assess *r* group differences. For relative surface area cell coverage estimation, the treatments are compared overall as to the proportions of osteoblasts, osteoclasts, lining cells, and no cells using one-way ANOVA.

MODIFICATIONS OF THE METHOD

Anderson et al. (1990) proposed the ovariectomized, lactating Sprague-Dawley rat as an experimental model for the rapid development of osteopenia which may be used to test the effectiveness of bone-retentive drugs, potentially useful for treating osteoporotic women. Rats were ovariectomized on day 2 postpartum and were kept on a low-calcium diet. Measurements of serum total calcium, ionic calcium, albumin and parathyroid hormone were conducted between days 4 and 21 of lactation.

REFERENCES AND FURTHER READING

Anderson JJB, Garner SC, Mar M-H, Boass A, Toverud SU, Parikh I (1990) The ovarectomized, lactating rat as an experimental model for osteopenia: calcium metabolism and bone changes. Bone Mineral 11:43–53

Goldner J (1938) A modification of the Masson trichrome technique for routine laboratory purposes. Am J Pathol 14:237–243

Vickery BH, Avnur Z, Cheng Y, Chiou SS, Leaffer D, Caulfield JP, Kimmel DB, Ho T, Krastenansky JL (1996) RS-66271, a C-terminally substituted analog of human parathyroid hormone-related protein (1–43), increases trabecular and cortical bone in ovarectomized, osteopenic rats. J Bone Miner Res 11:1943–1951

Villanueva AR, Lundin KD (1989) A versatile new mineralized bone stain for simultaneous assessment of tetracycline and osteoid seams. Stain Technol 64:129–138

N.7
Anterior Pituitary Hormones

Much of the early research on anterior pituitary hormones was performed with extracts obtained from animal pituitary glands, and with animal models for the specific analytical determination of the concentrations of anterior pituitary hormones in serum, in pituitary tissue, and in some cases by measurement of

urinary excretion, for hormones which are excreted during pregnancy, for example. Biosynthetic hormone preparations are now available for human therapy, and species-specific hormone standards are also available for numerous animal species. For an understanding of the development of endocrine research, and the approach to understanding physiology that was necessary, helpful and effective, reference is made extensively to historical methods that are no longer required. As with other fields, the receptors for hypothalamic hormones and anterior pituitary hormones have been characterized and studied, for both a better understanding of regulation, and in several cases structure–activity studies. This approach has also been very helpful in understanding how the sensitivity of the pituitary gland is regulated by both negative feedback of gonadal steroids and the impact of hypothalamic hormones.

N.7.0.1 Hypophysectomy in Rats

PURPOSE AND RATIONALE

This is a classical technique for assessment of the biological effects of pituitary hormones (Collip et al. 1933b; Burn et al. 1952; Vogel 1965; Vogel 1969b). The pituitary gland is removed entirely (anterior and posterior pituitary), the functional deficiencies are identified, and hormone preparations are injected for substitution. Due to the presence of multiple deficiencies after the operation, results by this technique are limited. The approach is of considerable historical interest but has now been replaced by more specific investigation of single hormonal systems. Various techniques of hypophysectomy have been described by Biedl (1916), Thompson (1932), Collip et al. (1933b), Anselmino and Pecharz (1935), and Bomskov (1939) in several animal species, including dog, cat, rabbit, ferret, guinea pig, rat, mouse, chicken, and frog. For some time, hypophysectomy in the rat has been applied to biological standardization of anterior pituitary hormones.

Nowadays, hypophysectomized rats may be obtained from certified suppliers who are licensed to perform the required operation, and who are experienced in postoperative handling and maintenance.

PROCEDURE

In the rat, the parapharyngeal approach is less destructive than the transauricular approach, and is preferred for bioassay. Male Wistar or Sprague-Dawley rats weighing 110–150 g are anesthetized with modern anesthetics, and placed on a surgical table in a recumbent position. The head is tilted backwards to expose the operating field, the fur is removed with electric clippers, and the field of surgery is cleaned with alcohol. A median incision is made 2.5 cm in front of the sternum. The large salivary glands and the maxillary lymph nodes are retracted, the muscles over the trachea are divided at the midline, slightly below the thyroid a hole is made in the trachea ("tracheotomy"), and tracheal mucus is removed by vacuum aspiration. The insertion of a tracheal cannula is not necessary.

A deep blunt dissection is made directly medial to the tendon of the left or right digastric muscle. The ipsilateral glossopharyngeal nerve and the blood vessels are drawn to one side, and the pharynx and trachea are drawn to the other side, for an approach to the midline of the base of the skull. For the subsequent procedure, the use of an operating microscope is recommended (stereo microscope)

The base of the skull is cleaned using small pellets of cotton-wool. The spheno-occipital suture running between both mastoid processes is exposed. From behind, the crista occipitalis runs longitudinally up to the middle of this suture. Just at this point, a small hole is drilled at the base of the skull with a dental drill, taking care to leave the surrounding sinus blood vessels intact. The pituitary is now visible as a small, lens-shaped organ. With the tip of a fine glass tube, attached to a suction device, the pituitary gland is removed by aspiration. Occasional bleeding is stopped with a cotton-wool pellet. The trachea is now cleaned by suction pump and the wound closed. Animals are placed carefully in padded recovery cages, at an ambient temperature of 20–22°C for recovery. The removal of the posterior pituitary gland causes the animals to have experimentally induced diabetes insipidus and therefore they need access to sufficient quantities of drinking water.

MODIFICATIONS OF THE METHOD

Instead of a parapharyngeal approach, the **transauricular approach** may be used (S. Jung and H. G. Vogel unpublished data) to facilitate surgery. Male rats weighing 120–150 g are anesthetized and placed on their right side. The head is fixed between the thumb and the index finger of the left hand. In the perpendicular direction, a dental drill with a diameter of 2.2 mm is introduced into the meatus acusticus externus osseus. First, the fine lamellae of the middle ear are passed. Then, the drill is directed from the external ear to the contralateral orbita. In this way, the thin inner wall of

the bulla tympani is perforated. The junction of the bulla tympanica, os occipitale and os sphenoidale is located here. A small, straight forceps is introduced to remove bone fragments, and a blunt cannula diameter 1.6 mm is introduced to remove the pituitary gland by suction. The procedure needs much more technical skill than the current pharyngeal approach, and is more destructive.

REFERENCES AND FURTHER READING

Anselmino KJ, Pecharz RI (1935) Über die Technik der Hypophysenexstirpation bei verschiedenen Versuchstieren. Z Exp Med 93:660–665

Biedl A (1916) Innere Sekretion. Ihre physiologischen Grundlagen und ihre Bedeutung für die Pathologie. Dritte Auflage, zweiter Teil. Urban and Schwarzenberg, Berlin, pp 111–126

Bomskov C (1939) Die Exstirpation der Hypophyse im Tierversuch. In: Methodik der Hormonfoschung. 2. Band, G. Thieme, Leipzig, pp 553–587

Burn JH, Finney DJ, Goodwin LG (1952) Biological standardization. Anterior lobe of the pituitary gland. Oxford University Press, Oxford, pp 268–279

Collip JB, Selye H, Thompson DL (1933a) Beiträge zur Kenntnis der Physiologie des Gehirnanhanges. Virchows Arch 290:23–46

Collip JB, Selye H, Thompson DL (1933b) Gonad-stimulating hormones in hypophysectomised animals. Nature 131:56

Loeser A, Thompson KW (1934) Hypophysenvorderlappen, Jod und Schilddrüse. Endokrinologie 14:144–150

Smith PE (1927) The disabilities caused by hypophysectomy and their repair. The tuberal (hypothalamic) syndrome in the rat. J Am Med Assoc 88:158–161

Thompson KW (1932) A technique for hypophysectomy of the rat. Endocrinology 16:257–263

Vogel HG (1965) Evaluation of synthetic peptides with ACTH-activity. Acta Endocrinol Suppl 100:34

Vogel HG (1969a) Tierexperimentelle Untersuchungen über synthetische Peptide mit Corticotropin-Aktivität. A: Vergleich mit dem III. Internationalen Standard für Corticotropin. Arzneimittelforschung 19:20–24

Vogel HG (1969b) Tierexperimentelle Untersuchungen über synthetische Peptide mit Corticotropin-Aktivität. B: Prüfung einer Depot-Zubereitung von $\beta^{1\text{-}23}$-Corticotropin-23-amidacetat. Arzneimittelforschung 19:25–27

N.7.1 Gonadotropins

N.7.1.0.1 General Considerations

Selection of assay methods depends on the study's objectives, i. e., whether it is the biological activity of gonadotropins or the quantitative response of elements in the signaling chain being assessed. The biological assays have been widely replaced by methods for receptor binding and receptor-induced response (signaling).

Follicle-stimulating hormone (FSH) and luteinizing hormone (LH) are glycoproteins which exist in multiple molecular isoforms (microheterogeneity) with different molecular weights and with different degrees of glycosylation (Ulloa-Aguirre et al. 1988; Dahl and Stone 1991). The fine differences identified by analytical methods are not relevant for the bioassay, which measures the sum of biological activities. The immunological methods provide limited information on biological activity and need to be validated for detection of the intact hormone or cross-reactivity with inactive subunits. *In vivo* animal bioassays are available (e. g., the Steelman–Pohley assay), and *in vitro* cell bioassays with a high degree of sensitivity and specific radioreceptor assays have been developed (Simoni and Nieschlag 1991). Striking differences in assay results were found when comparing estimates obtained by *in vivo* bioassays, *in vitro* cell assays, receptor-binding assays, and immunoassays with the International Standard for Pituitary FSH, when assayed in terms of the Second International Reference Preparation of Human Pituitary FSH and LH (Storring and Gaines Das 1989).

For binding assays, gonadotropin receptors of various animal species have been cloned (Poyner and Hanley 1992). Time-resolved fluoroimmunoassay for gonadotropins has been proposed by Iwasawa et al. (1994). Application of methods for detection and quantification depends on the research objective, which may be targeted to physiological functions, or to the biochemical identification of isoforms and subunits (Imse et al. 1992).

REFERENCES AND FURTHER READING

Dahl KD, Stone MP (1991) FSH isoforms, radioimmunoassays, bioassays, and their significance. J Androl 13:11–22

Imse V, Holzapfel G, Hinney B, Kuhn W, Wuttke W (1992) Comparison of luteinizing hormone pulsatility in the serum of women suffering from polycystic ovarian disease using a bioassay and five different immunoassays. J Clin Endocrinol Metab 74:1053–1061

Iwasawa A, Tomizawa KL, Wakabayashi K, Kato Y (1994) Time-resolved fluoroimmunoassay (TR-FIA) of gonadotropins. Exp Clin Endocrinol 102:39–43

Poyner DR, Hanley MR (1992) Molecular biology of peptide and glycoprotein hormone receptors. In: Braun MR (ed) Molecular biology of G-protein-coupled receptors. Birkhäuser, Boston, pp 198–232

Simoni M, Nieschlag E (1991) *In vitro* bioassays of follicle-stimulating hormone: methods and clinical applications. J Endocrinol Invest 14:983–997

Storring PL, Gaines Das RE (1989) The International Standard for pituitary FSH: collaborative study of the Standard and of four other purified human FSH preparations of differing molecular composition by bioassays, receptor assays and different immunoassay systems. J Endocrinol 123:275–293

Ulloa-Aguirre A, Espinoza R, Damian-Matsumura P, Chappel SC (1988) Immunological and biological potencies of the different molecular species of gonadotrophins. Human Reprod 3:491–501

N.7.1.1
Follicle-Stimulating Hormone (FSH)

Some of the methods described here are used for quantal assay of biological FSH activity (in animals and *in vitro*); others are used for FSH activity in samples from nonclinical and clinical studies.

N.7.1.1.1
Ovarian Weight in hCG-Primed Rats

PURPOSE AND RATIONALE

Follicle-stimulating hormone (FSH) increases the weight of ovaries in immature rats by inducing follicular maturation in a dose-related manner. This effect is greatly enhanced by simultaneous administration of a constant dose of human chorionic gonadotropin (hCG) for luteinization of the follicles, allowing the detection of low amounts of FSH (Steelman and Pohley 1953).

PROCEDURE

Immature female Sprague-Dawley rats weighing 40–45 g are treated for 3 days by subcutaneous injections of FSH (twice per day), using three doses of the standard (e. g., ovine NIH-FSH-S-9, National Institute of Health, Bethesda, Md., USA) or the test preparation (at the same dose interval). A constant amount of 25 IU hCG (Primogonyl, Schering, Berlin) is added. Hormone preparations are injected in physiological saline containing 2% gelatin. Six to eight animals are used per group. Then, 18 h after the last injection, the animals are sacrificed, then the ovaries are dissected out and weighed to the nearest 0.1 mg.

EVALUATION

Dose–response curves for standard and test compounds are plotted and potency ratios with confidence limits are calculated.

CRITICAL ASSESSMENT OF THE METHOD

The Steelman–Pohley test is rather specific for FSH. The addition of luteinizing hormone (LH), thyroid-stimulating hormone (TSH), adrenocorticotropin (ACTH), human growth hormone (hGH), or prolactin did not influence the dose–response curves of FSH (Christiansen 1972b). The method has been adopted by pharmacopoeias (e. g., British Pharmacopoeia 1988).

MODIFICATIONS OF THE METHOD

Similar studies were reported by: Evans et al. 1939; Brown 1955; Segaloff 1962; Parlow and Reichert 1963; Christiansen 1972a; Storring and Gaines 1989

Igarashi and McCann (1964) reported a bioassay for FSH in mice using an added constant dose of hCG for augmentation, and uterine weight as the endpoint.

Brown and Wells (1966) described an assay of human urinary FSH with hCG augmentation, using ovarian weight in mice as the endpoint. The method has been used by Wide and Hobson (1986) to identify the effect of the assay method used to select the most active forms of FSH from human pituitary extracts.

Lamond and Bindon (1966) recommended the use of immature hypophysectomized mice for the assay of FSH with hCG augmentation, using uterine weight as endpoint.

Gans and van Rees (1966) studied a testicular augmentation assay method for FSH. Immature male rats were hypophysectomized and on the same day the right testis was removed and weighed. Treatment with various doses of FSH together with a constant dose of 20 IU hCG was started on the next day and continued for 6 days. On the 7th day, the animals were sacrificed and the remaining left testis was removed and weighed. The difference between weights of the right and left testis in each animal was used as the endpoint.

Uberoi and Meyer (1967) used the uterine weight of the immature rat as a pituitary gonadotropin assay, with augmentation by hCG.

Results obtained with the *in vivo* bioassay (Steelman and Pohley 1953) have been compared with an *in vitro* bioassay based on estradiol production by cultured Sertoli cells, and with an FSH immunoassay by Storring et al. (1981).

REFERENCES AND FURTHER READING

British Pharmacopoeia (1988) Biological assay of menotrophin. Follicle stimulating hormone activity. Appendix XIV C. HMSO, London, p A165

Brown PS (1955) The assay of gonadotrophin from urine of non-pregnant human subjects. J Endocrinol 13:59–64

Brown PS, Wells M (1966) Observations on the assay of human urinary follicle-stimulating hormone by the augmentation test in mice. J Endocrinol 35:199–206

Christiansen P (1972a) Studies on the rat ovarian augmentation method for follicle stimulating hormone. Acta Endocrinol 70:636–646

Christiansen P (1972b) The rat ovarian augmentation method for follicle stimulating hormone. Specificity of the test. Acta Endocrinol (Kbh) 70:647–653

Evans HM, Simpson ME, Tolksdorf S, Jensen H (1939) Biological studies of the gonadotropic principles in sheep pituitary substance. Endocrinology 25:529–546

Gans E, van Rees GP (1966) Studies on the testicular augmentation assay method for follicle stimulating hormone. Acta Endocrinol 52:573–582

Igarashi M, McCann SM (1964) A new sensitive bioassay for follicle-stimulating hormone. Endocrinology 74:440–445

Lamond DR, Bindon BM (1966) The biological assay of follicle-stimulating hormone in hypophysectomized immature mice. J Endocrinol 34:365–376
Parlow AF, Reichert LE Jr (1963) Species differences in follicle-stimulating hormone as revealed by the slope in the Steelman–Pohley assay. Endocrinology 73:740–743
Segaloff A (1962) The gonadotropins. In: Dorfman RI (ed) Methods in hormone research, Vol II, Bioassay. Academic Press, New York, pp 591–608
Steelman SL, Pohley FM (1953) Assay of follicle stimulating hormone based on the augmentation with human chorionic gonadotropin. Endocrinology 53:604–616
Storring PL, Gaines Das RE (1989) The International Standard for pituitary FSH: collaborative study of the Standard and of four other purified human FSH preparations of differing molecular composition by bioassays, receptor assays and different immunoassay systems. J Endocrinol 123:275–293
Storring PL, Zaidi AA, Mistry YG, Fröysa B, Stenning BE, Diczfalusy E (1981) A comparison of preparations of highly purified human pituitary follicle-stimulating hormone: differences in the follicle-stimulating hormone potencies as determined by in-vivo bioassay, in-vitro bioassay and immunoassay. J Endocrinol 91:353–362
Uberoi NK, Meyer RK (1967) Uterine weight of the immature rat as a measure of augmentation of pituitary gonadotrophins by human chorionic gonadotrophin (HCG). Fertil Steril 18:420–428
Wide L, Hobson B (1986) Influence of the assay method used on the selection of the most active forms of FSH from the human pituitary. Acta Endocrinol 113:17–22

N.7.1.1.2 [^{3}H]Thymidine Uptake in Cultured Mouse Ovaries

PURPOSE AND RATIONALE

Follicle-stimulating hormone stimulates [^{3}H]thymidine uptake by cultured mouse ovaries in a dose-dependent manner, using the tissue-specific proliferation response of the follicles (Ryle 1971; Boggins and Ryle 1972).

PROCEDURE

Intact ovaries are obtained from 15-day-old mice. They are dissected carefully with the aid of a stereomicroscope and transferred to culture dishes. Each ovary is placed on a strip of lens tissue supported on a stainless steel mesh grid 4 mm above the floor of a plastic Petri dish and incubated in Eagle's medium supplemented with glucose and glutamine. The dishes are gassed with 5% CO_2 in air at 37°C. Three replicate dishes are used for each concentration of the standard (0.1 and 0.4 IU/ml) and of the test preparation. [^{3}H]Thymidine (0.02 µC) is added to each dish the day after the cultures are set up. Three days later the tissue is prepared for counting. Each grid is irrigated with about 5 ml saline solution. The ovary is then transferred to a counting vial and dissolved for counting the incorporated radioactivity in a liquid scintillation counter.

EVALUATION

Dose–response curves of [^{3}H]thymidine uptake are established for the standard and the test preparation, and potency ratios with confidence limits are calculated. Advantages over animal bioassays include increased specificity and a reduced requirement for a purified test preparation, which may be available only in small quantities.

CRITICAL ASSESSMENT OF THE METHOD

The [^{3}H]thymidine uptake by cultured mouse ovaries has found less acceptance than other *in vitro* methods described below.

MODIFICATIONS OF THE METHOD

Follicle cultures from mouse ovaries for the study of follicular metabolism have been described by Boland et al. (1993).

REFERENCES AND FURTHER READING

Boggins J, Ryle M (1972) An in-vitro procedure for the quantitative measurement of follicle-stimulating activity. J Endocrinol 54:355–356
Boland NI, Humpherson PG, Leese HJ, Gosden RG (1993) Pattern of lactate production and steroidogenesis during growth and maturation of mouse ovarian follicles *in vitro*. Biol Reprod 48:798–806
Ryle M (1971) The activity of human follicle-stimulating hormone preparations as measured by a response *in vitro*. J Endocrinol 51:97–107

N.7.1.1.3 Granulosa Cell Aromatase Assay in Vitro

PURPOSE AND RATIONALE

The granulosa cell aromatase assay *in vitro* is based on the principle of the *in vivo* bioassay of Steelman and Pohley (1953), in which the ovarian weight response is the result of FSH-induced follicular maturation and induced estradiol production, which stimulates ovarian growth. The co-administration of human chorionic gonadotropin (hCG) at a standard amount enhances androgen production by theca cells, which in turn provides the androgen substrate for FSH-dependent aromatase activity in granulosa cells. Hsueh et al. (1983) and Jia and Hsueh (1985) developed a sensitive *in vitro* bioassay for FSH based on the stimulation of estrogen production by cultured granulosa cells in serum-free medium containing androstenedione.

PROCEDURE

Intact Sprague-Dawley rats (21–22 days old) are implanted with Silastic capsules containing diethylstilbestrol to stimulate granulosa cell proliferation. Four

days after implantation, the animals are sacrificed and ovaries are dissected for granulosa cell collection. The ovaries are decapsulated, follicles are punctured with 27-gauge hypodermic needles, and granulosa cells are carefully expressed into McCoy's 5a medium. An aliquot is diluted with trypan blue stain, and viable cells are counted with a hemocytometer. Cells are cultured in 16-mm, 24-well culture plates for 2–3 days at 37°C in a humidified, 95% air–5% CO_2 incubator. Each well contains 5×10^4 viable cells in 0.5 ml McCoy's 5a medium supplemented with 2 mM L-glutamine, 100 U/ml penicillin, 100 µg/ml streptomycin sulfate, 10^{-7} M diethylstilbestrol (DES), 10^{-6} M androstenedione (as aromatase substrate), 0.125 mM 1-methy-3-isobutylxanthine (MIX), 1 µg/ml insulin, and 30 ng/ml hCG.

For the measurement of FSH bioactivity in serum samples, each test is performed in triplicate at three dose levels (5, 10, and 20 µl). To ensure a constant volume of 20 µl serum in the total incubation volume of 500 µl, gonadotropin-free serum is added as required. For the FSH standard curve, 4% gonadotropin-free serum is added to the culture medium. The sensitivity is increased when the serum is pretreated with 12% polyethylene-glycol (PEG, mol. wt. 8000). After a culture period of 3 days, estradiol content in the medium is measured by radioimmunoassay (RIA).

EVALUATION

RIA data are analyzed using weighted logit-log regression analysis. Calculation of FSH bioactivity in serum samples or test preparations is performed using a standard curve fitted with a second-order polynomial.

MODIFICATIONS OF THE METHOD

Dorrington et al. 1975; Hsueh et al. 1984; Jia and Hsueh 1986; Dahl et al. 1989; Fauser et al. 1989; Storring and Gaines 1989; Matzkin et al. 1990; Simoni and Nieschlag 1991; YoungLai et al. 1992

Sensitivity may be improved by using a specific response of the follicles. Beers and Strickland (1978), Wang and Leung (1983), Combarnous et al. (1984), and Thakur et al. (1990) found that FSH led to a dose-dependent increase of plasminogen activator production in cultures of rat granulosa cells. This assay has been found to be extremely sensitive: as little as 10^{-15} mol of FSH could be detected.

Ax and Ryan (1979) found that FSH dose-dependently stimulates ^{3}H-glucosamine incorporation into proteoglycans by porcine granulosa cells *in vitro*.

Bhargava et al. (1989) used normal human ovarian cells for long-term cultures. These cells produced progesterone from cholesterol or pregnenolone and estrone from androstenedione when stimulated by FSH.

REFERENCES AND FURTHER READING

Ax RL, Ryan RJ (1979) FSH stimulation of ^{3}H-glucosamine incorporation into proteoglycans by porcine granulosa cells *in vitro*. J Clin Endocrin Metab 49:646–648

Beers WH, Strickland S (1978) A cell culture assay for follicle-stimulating hormone. J Biol Chem 253:3877–3881

Bhargava G, Poretsky L, Denman H, Jandorek R, Miller LK (1989) Hormonally active long-term culture of human ovarian cells: initial characterization. Metabolism 38:195–196

Combarnous Y, Guillou F, Martinat N (1984) Comparison of *in vitro* follicle-stimulating hormone (FSH) activity of equine gonadotropins (luteinizing hormone, FSH, and chorionic gonadotropin) in male and female rats. Endocrinology 115:1821–1827

Dahl KD, Papkoff H, Hsueh AJW (1989) Effects of diverse mammalian and nonmammalian gonadotropins in a rat granulosa cell bioassay for follicle-stimulating hormone. Gen Comp Endocrinol 73:368–373

Dorrington JH, Moon YS, Armstrong DT (1975) Estradiol-17β biosynthesis in cultured granulosa cells from hypophysectomized immature rats; stimulation by follicle-stimulating hormone. Endocrinology 97:1328–1331

Fauser BCJM, Soto D, Czekala NM, Hsueh AJW (1989) Granulosa cell aromatase bioassay: changes of bioactive FSH levels in the female. J Steroid Biochem 33:721–726

Hsueh AJW, Erickson GF, Papkoff H (1983) Effect of diverse mammalian gonadotrophins on estrogen and progesterone production by cultured rat granulosa cells. Arch Biochem Biophys 225:505–511

Hsueh AJW, Adashi EY, Jones PBC, Welsh TH (1984) Hormonal regulation of the differentiation of cultured ovarian granulosa cells. Endocr Rev 5:76–127

Jia XC, Hsueh AJW (1985) Sensitive *in vitro* bioassay for the measurement of serum follicle-stimulating hormone. Neuroendocrinology 41:445–448

Jia XC, Hsueh AJW (1986) Granulosa cell aromatase bioassay for follicle-stimulating hormone: validation and application of the method. Endocrinology 119:1570–1577

Matzkin H, Homonnai ZT, Galiani D, Paz G, Dekel N (1990) Serum bioactive and immunoreactive follicle-stimulating hormone in oligozoospermic and azoospermic men: application of a modified granulosa cell bioassay. Fertil Steril 53:709–714

Simoni M, Nieschlag E (1991) *In vitro* bioassays of follicle-stimulating hormone: methods and clinical applications. J Endocrinol Invest 14:983–997

Steelman SL, Pohley FM (1953) Assay of follicle stimulating hormone based on the augmentation with human chorionic gonadotropin. Endocrinology 53:604–616

Storring PL, Gaines Das RE (1989) The International Standard for pituitary FSH: collaborative study of the Standard and of four other purified human FSH preparations of differing molecular composition by bioassays, receptor assays and different immunoassay systems. J Endocrinol 123:275–293

Thakur AN, Coles R, Sesay A, Earley B, Jacobs HS, Ekins RP (1990) A rat granulosa cell plasminogen activator bioassay for FSH in human serum. J Endocrinol 126:159–168

Wang Ch, Leung A (1983) Gonadotropins regulate plasminogen activator production by rat granulosa cells. Endocrinology 112:1201–1207

YoungLai EV, Yie SM, Yeo J (1992) Development patterns of bioactive and immunoreactive FSH in the female rabbit:

effects of ovarectomy. Eur J Obstet Gynecol Reprod Biol 46:45–49

N.7.1.1.4 Sertoli Cell Aromatase Assay in Vitro

PURPOSE AND RATIONALE

The Sertoli cell aromatase assay was first described by Van Damme et al. (1979). This *in vitro* bioassay was developed following the observation by Dorrington et al. (1975) that FSH, but not LH, stimulates estradiol production by cultured Sertoli cells from immature rats. The assay has been further improved by Ritzén et al. (1982), Shah and Ritzén (1984), and Padmanabhan et al. (1987). These assays are used to determine bioactive FSH in serum for diagnostic use, and they are also applicable for measuring the activity of FSH preparations intended for therapy.

PROCEDURE

Sertoli cells are obtained from 7- to 10-day-old male Sprague-Dawley rats. Testes are decapsulated, the testicular tissue is chopped twice, at right angles, with a mechanical tissue slicer and incubated in culture medium containing 0.03% collagenase and 0.003% trypsin inhibitor for 5–10 min at 34°C. After the initial dispersal, seminiferous tubules settle to the bottom of the incubation flask, and the medium is decanted to remove interstitial cells. The tubules are washed several times; resuspended in medium that contains collagenase, trypsin inhibitor and 0.03% DNase (to prevent clumping of cells), and then incubated for 30 min at 34°C. During incubation, dispersion of Sertoli cells is hastened by repeated aspiration with a Pasteur pipette. The resulting cell suspension is washed three times; cell number and viability are determined by counting in trypan-blue-dye-containing medium. Cells are suspended in a density of 5×10^5 viable cells/ml. One milliliter of cell suspension is transferred to each well of Falcon multiwell culture dishes (16 mm diameter, Falcon Plastics, Oxnard, Calif., USA).

Sertoli cells are cultured in medium comprised of the following constituents: 1:1 (vol/vol) mixture of Ham's F-10 nutrient mixture and Dulbecco's Modified Eagle's Medium that contains 1.2 g/l sodium bicarbonate, 20 mg/l gentamicin, and 1 mg/l amphotericin. Also included in the medium are: 1 µg/ml insulin, 5 µg/ml transferrin, 10 ng/ml epidermal growth factor, 20 pg/ml T_4, 10^{-8} M hydrocortisone, and 10^{-6} M retinoic acid. The cell cultures are incubated in this medium in a water-saturated atmosphere that consists of 95% air and 5% CO_2 at 37°C.

After an initial incubation of the cell monolayers for 72 h, the medium is removed; the cells are washed once with the medium and re-incubated in the medium described above, which contains 2.5×10^{-6} M 19-hydroxyandrostenedione, FSH standard or unknown samples at various concentrations, and 0.1 mM methylisobutylxanthine (MIX). After a 24-h incubation, the medium is aspirated and centrifuged. The resultant supernatants are stored frozen until estradiol measurement by radioimmunoassay (England et al. 1974).

EVALUATION

The results are expressed as picograms of estradiol formed per milliliter culture medium. To evaluate changes in estradiol secretion with changes in FSH concentration, regression analyses are performed. From these data, activity ratios with confidence limits are calculated.

MODIFICATIONS OF THE METHOD

Similar studies were reported by: Dorrington and Armstrong 1975; Marana et al. 1974; Storring et al. 1981; Zaidi et al. 1981; Foulds and Robertson 1983; Wide and Hobsen 1983, 1986; Khna et al. 1984; Harlin et.al. 1988; Storring and Gaines 1989; Simoni and Nieschlag 1991;

Rao and Ramachandran (1975) used isolated rat seminiferous tubule cell preparations free of Leydig cells for determination of cyclic AMP production as an *in vitro* assay for FSH.

Sairam and Manjunath (1982) used rat seminiferous tubular suspensions containing Sertoli cells, incubated them with FSH preparations and measured cyclic AMP formation as the endpoint.

REFERENCES AND FURTHER READING

Dorrington JH, Armstrong DT (1975) Follicle-stimulating hormone stimulates estradiol-17β synthesis in cultured Sertoli cells. Proc Natl Acad Sci USA 72:2677–2681

Dorrington JH, Roller NF, Fritz IB (1975) Effects of follicle-stimulating hormone on cultures of Sertoli cell preparations. Mol Cell Endocrinol 3:57–70

England BG, Niswender GD Midgley AR (1974) Radioimmunoassay of estradiol-17β without chromatography. J Clin Endocrin Metab 38:42–50

Foulds LM, Robertson DM (1983) Electrofocusing fractionation and characterization of pituitary follicle-stimulating hormone from male and female rats. Mol Cell Endocrinol 31:117–130

Harlin J, Khan SA, Diczfalusy E (1988) Molecular composition of luteinizing hormone and follicle-stimulating hormone in commercial gonadotropin preparations. Fertil Steril 46:1055–1061

Khan SA, Syed V, Fröysa B, Lindberg M, Diczfalusy E (1984) Influence of gonadectomy on isoelectrofocusing profiles of

pituitary gonadotropins in rhesus monkeys. J Med Primatol 14:177–194
Marana R, Robertson DM, Suginami H, Diczfalusy E (1979) The assay of human follicle-stimulating hormone preparations: the choice of a suitable standard. Acta Endocrinol 92:599–614
Padmanabhan V, Chappel SC, Beitins I (1987) An improved *in vitro* bioassay for follicle-stimulating hormone (FSH): suitable for measurement of FSH in unextracted human serum. Endocrinology 121:1089–1098
Rao AJ, Ramachandran J (1975) Cyclic AMP production in isolated rat seminiferous tubule cell preparations: a potential *in vitro* assay for follicle stimulating hormone. Life Sci 17:411–416
Ritzén EM, Fröysa B, Gustafsson B, Westerholm G, Diczfalusy E (1982) Improved bioassay of follitropin. Horm Res 16:42–48
Sairam MR, Manjunath P (1982) Studies on pituitary follitropin. XI. Induction of hormonal antagonistic activity by chemical deglycosylation. Mol Cell Endocrinol 28:139–150
Shah GV, Ritzén EM (1984) Validation of a bioassay for follitropin in urine samples. J Endocrinol Invest 7 [Suppl 3]:59–66
Simoni M, Nieschlag E (1991) *In vitro* bioassays of follicle-stimulating hormone: methods and clinical applications. J Endocrinol Invest 14:983–997
Storring PL, Gaines Das RE (1989) The International Standard for pituitary FSH: collaborative study of the Standard and of four other purified human FSH preparations of differing molecular composition by bioassays, receptor assays and different immunoassay systems. J Endocrinol 123:275–293
Storring PL, Zaidi AA, Mistry YG, Fröysa B, Stenning BE, Diczfalusy E (1981) A comparison of preparations of highly purified human pituitary follicle-stimulating hormone: differences in the follicle-stimulating hormone potencies as determined by in-vivo bioassay, in-vitro bioassay and immunoassay. J Endocrinol 91:353–362
Van Damme MP, Robertson DM, Marana R, Ritzén EM, Diczfalusy E (1979) A sensitive and specific *in vitro* bioassay method for the measurement of follicle-stimulating hormone activity. Acta Endocrinol 91:224–237
Wide L, Hobson BM (1983) Qualitative difference in follicle-stimulating hormone activity in the pituitaries of young women compared to that of men and elderly women. J Clin Endocrinol Metab 56:371–375
Wide L, Hobson B (1986) Influence of the assay method used on the selection of the most active forms of FSH from the human pituitary. Acta Endocrinol 113:17–22
Zaidi AA, Robertson DM, Diczfalusy E (1981) Studies on the biological and immunological properties of human follitropin: profile of two international reference preparations and of an aqueous extract of pituitary glands after electrofocusing. Acta Endocrinol 97:157–165
Zaidi AA, Fröysa B, Diczfalusy E (1982) Biological and immunological properties of different molecular species of human follicle-stimulating hormone: electrofocusing profiles of eight highly purified preparations. J Endocrinol 92:195–204

N.7.1.1.5 Receptor Binding Assay for FSH

PURPOSE AND RATIONALE

Significant differences between the receptor binding activity of FSH preparations and biological activity have been found by Marana et al. (1979), Zaidi et al. (1981), Foulds and Robertson (1983), and Burgon et al. (1993). This is attributed to measuring binding activity, which may differ from subsequent intracellular signaling. Several receptor binding assays have been described [Cheng (1975); Andersen et al. (1983) using bovine testes; Reichert (1976) using rat testes tubule tissue].

PROCEDURE

Membrane preparations from bovine testes are used according to the Cheng (1975) and Andersen et al. (1983). Fresh bovine testes or testes from rats weighing 220–280 g are decapsulated and rinsed with cold 0.025 M Tris-HCl buffer at pH 7.2, containing 0.3M sucrose, and then minced and homogenized with a Polytron homogenizer at maximum speed for 30 s at a concentration of 5 ml buffer per gram of tissue. The homogenate is first filtered through four layers, and the filtrate is again filtered through eight layers of cheesecloth. The filtrate is then centrifuged at 12,000 *g* for 30 min at 4°C. The pellet is discarded and the supernatant is further centrifuged at 100,000 *g* for 1 h at 4°C. The supernatant is discarded and the pellet resuspended in cold 0.025 M Tris-HCl buffer at pH 7.2, containing 10 mM $MgCl_2$, at a concentration of 1 ml buffer per gram of the original weight of the testis. The isolated membranes are stored at −70°C in aliquots of 10 ml per vial until use.

For assays, 12/75 mm glass disposable tubes are used. To each tube, 0.2 ml of 0.025 M Tris-HCl buffer at pH 7.2, containing 10 mM $MgCl_2$ and 0.1% BSA, 0.1 ml of standard FSH or unknown samples in the same buffer, 0.1 ml of ^{125}I-hFSH tracer labeled by the lactoperoxidase method (50,000 cpm, approximately 2 ng), and finally 0.1 ml of plasma membrane receptors of appropriate dilution (approximately 1–2 mg/ml) are added to reach a final volume of 500 µl per tube. All the above solutions are kept at 4°C before use. The tubes are then shaken vigorously and incubated at room temperature for 20 h. Following incubation, the reaction is stopped by adding 3.0 ml of cold 0.025 M Tris-HCl buffer containing 0.1% BSA. After centrifugation at 4000 rpm for 30 min, the supernatant is drained and the tip of each tube is dried. The pellet remaining at the bottom of the tube is counted in an automatic gamma counter.

EVALUATION

Specific binding (%) is defined as $(C_B - C_N) \times 100/C_T$, where C_B is the cpm bound to the testicular receptor (pellet), C_N is the nonspecific bound cpm (not

displaced by 1000-fold excess of unlabeled hFSH), and C_T is the total cpm added per tube. For standard curves, the specific binding of tracer ^{125}I-hFSH in the absence of cold hormone (6%–8% by 150–200 µg of receptor protein) is taken as 100% bound ^{125}I-hFSH, and the nonspecific bound ^{125}I-hFSH (1%–2% of the total cpm added) as the baseline. The specific binding of ^{125}I-hFSH over a range of hFSH concentrations is used for calculating a standard curve and sample concentrations.

MODIFICATIONS OF THE METHOD

The method has been used by several authors: Lee and Ryan 1973; Schwartz et al. 1973; Ketelslegers and Catt 1974; Reichert and Bhalla 1974; Calvo et. al 1986; Storring and Gaines 1989

Simoni et al. (1993a) analyzed the biological and immunological properties of the International Standard for FSH 83/575 by isoelectrofocusing and made a comparison with other FSH preparations. The results suggested that the international standard 83/575 is not fully representative of pituitary and serum FSH, and its use for calibration of immunometric methods based on monoclonal antibodies is unlikely to resolve problems of inaccuracy in the measurement of serum FSH.

Grasso et al. (1993) studied the effects of a testicular toxicant on FSH binding to membranes of cultured rat Sertoli cells, as a method in toxicology.

Wakabayashi et al. (1997) reported the cDNA cloning and transient expression of a chicken gene encoding an FSH receptor.

Simoni et al. (1993b) analyzed the molecular heterogeneity of two batches of commercially available urofollitropin by immunofluorometric assay, radioligand receptor assay and *in vitro* bioassay.

REFERENCES AND FURTHER READING

Andersen TT, Curatolo LM, Reichert LE Jr (1983) Follitropin binding to receptors in testis: studies on the reversibility and thermodynamics of the reaction. Mol Cell Endocrinol 33:37–52

Burgon PG, Robertson DM, Stanton PG, Hearn MTW (1993) Immunological activities of highly purified isoforms of human FSH correlate with *in vitro* bioactivities. J Endocrinol 139:511–518

Calvo FO, Keutmann HT, Bergert ER, Ryan RJ (1986) Deglycosylated human follitropin: characterization and effects on adenosine cyclic 3′,5′-phosphate production in porcine granulosa cells. Biochemistry 25:3938–3943

Cheng KW (1975) A radioreceptor assay for follicle-stimulating hormone. J Clin Endocrin Metab 41:581–589

Foulds LM, Robertson DM (1983) Electrofocusing fractionation and characterization of pituitary follicle-stimulating hormone from male and female rats. Mol Cell Endocrinol 31:117–130

Grasso P, Heindel JJ, Powell CJ, Reichert LE Jr (1993) Effects of mono(2-ethylhexyl)phthalate, a testicular toxicant, on follicle-stimulating hormone binding to membranes of cultured rat Sertoli cells. Biol Reprod 48:454–459

Ketelslegers JM, Catt KJ (1974) Receptor binding properties of ^{125}I-hFSH prepared by enzymatic iodination. J Clin Endocrin Metab 39:1159–1162

Lee CY, Ryan RJ (1973) Interaction of ovarian receptors with human luteinizing hormone and human chorionic gonadotropin. Biochemistry 12:4609–4619

Marana R, Robertson DM, Suginami H, Diczfalusy E (1979) The assay of human follicle-stimulating hormone preparations: the choice of a suitable standard. Acta Endocrinol 92:599–614

Reichert LE Jr (1976) Follicle-stimulating hormone: measurement by a rat testes tubule receptor assay. In: Blecher M (ed) Methods in receptor research. Part I. Dekker, New York, pp 99–118

Reichert LE, Bhalla VK (1974) Development of a radioligand receptor assay for human follicle stimulating hormone. Endocrinology 94:483–491

Schwartz S, Bell J, Rechnitz S, Rabinowitz D (1973) Binding of human FSH and its subunits to rat testes. Eur J Clin Invest 3:475–481

Simoni M, Jockenhovel F, Nieschlag E (1993a) Biological and immunological properties of the international standard for FSH 83/575: Isoelectrofocusing profile and comparison with other FSH preparations. Acta Endocrinol 128:281–288

Simoni M, Weinbauer GF, Nieschlag E (1993b) Molecular composition of two different batches of urofollitropin: analysis by immunofluorometric assay, radioligand receptor assay and *in vitro* bioassay. J Endocrin Invest 16:21–27

Storring PL, Gaines Das RE (1989) The International Standard for pituitary FSH: collaborative study of the Standard and of four other purified human FSH preparations of differing molecular composition by bioassays, receptor assays and different immunoassay systems. J Endocrinol 123:275–293

Wakabayashi N, Suzuki A, Hoshino H, Nishimori K, Mizuno S (1997) The cDNA cloning and transient expression of a chicken gene encoding a follicle-stimulating hormone receptor. Gene 197:121–127

Zaidi AA, Robertson DM, Diczfalusy E (1981) Studies on the biological and immunological properties of human follitropin: profile of two international reference preparations and of an aqueous extract of pituitary glands after electrofocusing. Acta Endocrinol 97:157–165

N.7.1.2 Luteinizing Hormone (LH) = Interstitial Cell Stimulating Hormone (ICSH)

Some of the methods described here are classical animal bioassays for LH/ICSH preparations, others are *in vitro* bioassays used in research and for clinical samples.

N.7.1.2.1 Prostate Weight in Hypophysectomized Rats

PURPOSE AND RATIONALE

The assay is based on a biological response. Injection of luteinizing hormone (ICSH) in hypophysectomized

male rats causes enlargement of the testes and the secondary sexual organs. The interstitial cells of the testes (Leydig cells) are stimulated by LH/ICSH and secrete androgens which in turn stimulate the accessory organs, such as the ventral prostate of the rat.

PROCEDURE

The method has been used by several authors: Greep et al. 1942; Segaloff et al. 1956; Segaloff 1962; British Pharmacopoeia 1988;

Immature male Sprague-Dawley rats aged 21 days are hypophysectomized. From the 2nd to the 5th day, they receive daily subcutaneous injections of two or more doses of the test preparation and the LH/ICSH standard. They are sacrificed on the 6th day. Both testes and the ventral prostate are prepared and weighed. LH/ICSH – but not FSH – induces a specific dose-dependent increase of prostate weight, whereas FSH also induces an increase of testis weight. A predominant LH activity in the test material mainly stimulates prostate weight, but not testis weight.

EVALUATION

Dose–response curves are plotted for the ventral prostate of each group of test preparation or standard allowing the calculation of activities and potency ratios with confidence limits.

REFERENCES AND FURTHER READING

British Pharmacopoeia (1988) Biological assay of menotrophin. Luteinising hormone activity. Appendix XIV C. HMSO, London, pp A165–A166

Greep RO, van Dyke HB, Chow BF (1942) Gonadotropins of the swine pituitary. I. Various biological effects of purified thylakentrin (FSH) and pure metakentrin (ICSH). Endocrinology 30:635–649

Segaloff A (1962) The gonadotropins. In: Dorfman RI (ed) Methods in hormone research, Vol II, Bioassay. Academic Press, New York, pp 591–608

Segaloff A, Steelman SL, Flores A (1956) Prolactin as a factor in the ventral prostate assay for luteinizing hormone. Endocrinology 59:233–240

N.7.1.2.2 Superovulation in Immature Rats

PURPOSE AND RATIONALE

An assay for evaluation of luteinizing hormone (LH) and the luteinizing component of human chorionic gonadotropin (hCG) was described by Zarrow et al. (1958). The sensitivity of the response is enhanced by priming with pregnant mares' serum gonadotropin (PMSG – mainly follicle-stimulating hormone activity) and by intravenous injection of the LH test preparation.

PROCEDURE

Groups of five immature female rats (Charles River strain, age 21 days) are treated with a priming dose of 30 IU of PMS to induce follicular development. Increasing doses of LH reference or test preparations are injected intravenously 56 h later, to induce ovulation. Then 24 h after the final injection, the animals are sacrificed, the fallopian tubes are removed and examined under a dissecting microscope (magnification of 40×) ϕ for the presence oocytes (ova). Ovulation is easily noted by an enlarged translucent segment of the tube, through which the ova can be seen. The segment is punctured with a dissecting needle and the entire cumulus clot containing the ova is expelled. The clump containing the oocytes is treated with hyaluronidase, and the number of ova is counted.

EVALUATION

Doses–response curves are obtained using three doses of standard/reference and test preparation for the calculation of potency ratios with confidence limits.

REFERENCES AND FURTHER READING

Zarrow MX, Cladwell AL Jr, Hafez ESE, Pincus G (1958) Superovulation in the immature rat as a possible assay for LH and HCG. Endocrinology 63:748–758

N.7.1.2.3 Ascorbic Acid Depletion of Ovaries in PMSG/hCG-Primed Rats

PURPOSE AND RATIONALE

Luteinizing hormone (LH, also known as interstitial cell stimulating hormone or ICSH) induces dose-dependent depletion of ascorbic acid in the ovaries of rats primed with pregnant mares' serum gonadotropin (PMSG) and human chorionic gonadotropin (hCG) (Parlow 1961; Parlow and Reichert 1963; Sandow et al. 1972.

PROCEDURE

Female Sprague-Dawley rats weighing 40 ± 5 g are injected with 50 IU PMSG (e. g., Anteron, Schering, Berlin) in 0.2 ml saline subcutaneously on day 1 at 3:00 p.m. On day 3, the rats receive 25 IU hCG (e. g., Primogonyl, Schering, Berlin) subcutaneously at 9:00 a.m. On day 7, three different doses of the standard (e. g., NIH LH-S-1, National Institute of Health, Bethesda, Md., USA) and the test substance are injected subcutaneously. Eight animals are used per group. Three hours later, the animals are sacrificed,

and both ovaries are removed, weighed, and homogenized for determination of ascorbic acid content.

EVALUATION

Dose–response curves for standard and test compound are plotted and activity ratios with confidence limits calculated.

REFERENCES AND FURTHER READING

Parlow AF (1961) Bio-assay of pituitary luteinizing hormone by depletion of ovarian ascorbic acid. In: Albert A (ed) Human pituitary gonadotrophins, Vol III. Thomas, Springfield, Ill., pp 1–300

Parlow AF, Reichert LE Jr (1963) Influence of follicle-stimulating hormone on the prostate assay of luteinizing hormone (LH, ICSH). Endocrinology 73:377–385

Sandow J, Schally AV, Schröder HG, Redding TW, Heptner W, Vogel HG (1972) Pharmacological characteristics of a synthetic releasing hormone LH/FSH-RH (Hoe 471). Arzneimittelforschung 22:1718–1721

N.7.1.2.4 Testosterone Production by Leydig Cells in Vitro Induced by LH

PURPOSE AND RATIONALE

Luteinizing hormone (LH) increases the biosynthesis and secretion of androgens in the Leydig cells of the testes. This can be used for an *in vitro* assay using isolated Leydig cells.

PROCEDURE

For Leydig cell isolation, male Wistar or Sprague-Dawley rats weighing 250–300 g are sacrificed, the testes removed and immediately decapsulated. Two testes are then digested with 7 ml of collagenase solution (1 mg collagenase/1 ml Gibco medium 199) at 37°C for 18 min. Plastic tubes of 40 ml capacity with tight-fitting caps are used, and are placed longitudinally in the water bath with constant shaking (75 cycles/min). After incubation, 15 ml of cold saline is added to each tube. The tubes are inverted a few times and then left at 4°C for 10 min. The supernatants are then carefully siphoned off from the top. The clear supernatant is mixed with an equal volume of 26% Ficoll/0.4% BSA/medium 199 at pH 6.5, and then centrifuged at 1500 *g* for 10 min at 4°C. The cell pellet obtained from the centrifugation is suspended in a known volume of incubation medium (Medium 199 containing 1% BSA and 0.01% lima bean trypsin inhibitor). An aliquot of the cell suspension is taken for counting in a Coulter counter, and the balance is diluted with the incubation medium giving a density of 4×10^6 cells/ml.

For each assay, 0.25 ml of the cell suspension is used. The assay is carried out in 12×75 mm plastic tubes incubated with graded doses of test compound at 37°C. Constant shaking (100 cycles/min) under a 95% O_2/5% CO_2 atmosphere for 3 h is required. At the end of the incubation, each tube is centrifuged, and the supernatant is assayed for testosterone by a radioimmunoassay (Dufau et al. 1972). The assay is carried out in triplicate and needs to be repeated at least once with different batches of donor animals.

EVALUATION

Dose–response curves are obtained with various doses of standard and test preparation to allow calculation of activities and potency ratios with confidence limits.

MODIFICATIONS OF THE METHOD

Similar studies were reported by: Van Damme et al. 1974; Dufau et al. 1976; Janszen et al. 1976; Dufau et al. 1977; Khan et al. 1984; Liu et al. 1984; Harlin et al. 1988; Stadler et al. 1989;Haavisto et al. 1990; Rodgers et al. 1992

The effect of chemically deglycosylated human chorionic gonadotropin on cAMP and testosterone production in rat Leydig cells has been used by Chen et al. (1982) for characterization.

Cultures of mouse Leydig cell tumor cells (MA10) have been used by Ascoli (1981), Whitcomb and Schneyer (1990), and Dahl and Sarkissian (1993).

REFERENCES AND FURTHER READING

Ascoli M (1981) Characterization of several clonal lines of cultured Leydig tumor cells: gonadotropin receptors and steroidogenic responses. Endocrinology 108:88–95

Bousfield GR, Liu WK, Ward DN (1989) Effects of removal of carboxy-terminal extension from equine luteinizing hormone (LH) β-subunit on LH and follicle-stimulating hormone receptor-binding activities and LH steroidogenic activity in rat testicular Leydig cells. Endocrinology 124:379–387

Chen HC, Shimohigashi Y, Dufau ML, Catt KJ (1992) Characterization and biological properties of chemically deglycosylated human chorionic gonadotropin. J Biol Chem 257:14446–14452

Dahl KD, Sarkissian A (1993) Validation of an improved *in vitro* bioassay to measure LH in diverse species. J Androl 14:124–129

Dufau ML, Catt KJ, Tsuruhara J (1972) A sensitive gonadotropin responsive system: radioimmunoassay of testosterone production by the rat testis *in vitro*. Endocrinology 90:1032–1040

Dufau ML, Pock R, Neubauer A, Catt KJ (1976) *In vitro* bioassay of LH in human serum: the rat interstitial cell testosterone (RICT) assay. J Clin Endocrinol Metab 42:958–969

Dufau ML, Tsuruhara T, Horner KA, Podesta E, Catt KJ (1977) Intermediate role of adenosine 3′:5′-cyclic monophosphate and protein kinase during gonadotropin-induced steroido-

genesis in testicular interstitial cells. Proc Natl Acad Sci USA 74:3419–3423
Haavisto AM, Dunkel L, Pettersson K, Huhtaniemi I (1990) LH measurements by *in vitro* bioassay and a highly sensitive immunofluorometric assay improve the distinction between boys with constitutional delay of puberty and hypogonadotropic hypogonadism. Pediatr Res 27:211–214
Harlin J, Khan SA, Diczfalusy E (1988) Molecular composition of luteinizing hormone and follicle-stimulating hormone in commercial gonadotropin preparations. Fertil Steril 46:1055–1061
Janszen FHA, Cooke BA, van Driel MJA, van der Molen HJ (1976) Purification and characterization of Leydig cells from rat testes. J Endocrinol 70:345–359
Khan SA, Syed V, Fröysa B, Lindberg M, Diczfalusy E (1984) Influence of gonadectomy on isoelectrofocusing profiles of pituitary gonadotropins in rhesus monkeys. J Med Primatol 14:177–194
Liu WK, Young JD, Ward BN (1984) Deglycosylated ovine lutropin: preparation and characterization by *in vitro* binding and steroidogenesis. Mol Cell Endocrinol 37:29–39
Rodgers M, Michell R, Lambert A, Peers N, Robertson WR (1992) Human chorionic gonadotropin contributes to the bioactivity of Pergonal. Clin Endocrinol 37:558–564
Stadler U, Rovan E, Aulitzky W, Frick J, Adam H, Kalla N (1989) Bioassay for determination of human serum luteinizing hormone (LH): a routine clinical method. Andrologia 21:580–583
Van Damme MP, Robertson DM, Diczfalusy E (1974) An improved *in vitro* bioassay method for measuring luteinizing hormone (LH) activity using mouse Leydig cell preparations. Acta Endocrinol 77:655–671
Whitcomb RW, Schneyer AL (1990) Development and validation of a radioligand receptor assay for measurement of luteinizing hormone in human serum. J Clin Endocrinol Metab 71:591–595

N.7.1.2.5 Receptor Binding Assay for LH

PURPOSE AND RATIONALE

LH receptors are membrane receptors that mediate the initial hormone binding step; they are suitable for structure–activity studies and *ex vivo* analysis of receptor concentration changes. Luteinizing hormone is a glycoprotein composed of an α- and a β-subunit. Carbohydrate moieties are attached to both. Removal of the carbohydrate chains reduces bioactivity but enhances receptor binding.

PROCEDURE

For the preparation of Leydig cell receptors, the partially purified Leydig cells obtained from Ficoll gradient centrifugation as described above for the testosterone formation test are used. The cell pellet obtained from the Ficoll gradient centrifugation is first washed twice with unlabeled radioligand buffer (0.1 M Tris-HCl, pH 7.4, containing 5 mM $MgCl_2$, 0.1 M sucrose, and 0.1% BSA). The pellet is resuspended in a known volume of the same buffer. An aliquot of this suspension is taken for cell counting in a Coulter counter, and the balance is homogenized in a Polytron homogenizer for 10 s to break up the cells. This prevents internalization of the hormone molecule during the binding assay. The iodination of LH is carried out according to the chloramine-T method (Liu et al. 1977). After the addition of 2.5 ng of ^{125}I-labeled LH tracer, the binding assay is carried out at 37°C for 2 h with constant shaking. The hormone–receptor complex is then separated by centrifugation and bound radioactivity is counted in a Packard gamma-counter.

EVALUATION

Competitive–inhibition curves for specific binding are established and binding capacity is calculated.

MODIFICATIONS OF THE METHOD

Similar studies were reported by: Liu et al. 1974; Catt et al. 1976; Liu et al. 1984

Lee and Ryan (1972) described specific binding of human luteinizing hormone (LH) to homogenates of luteinized rat ovaries.

Storring and Gaines-Das (1993) described the second International Standard for Human Pituitary LH. Two new batches (coded as 80/552 and 81/535) were compared with the International Reference Preparation of Human Pituitary LH for Immunoassay (IRP 68/40) by 19 laboratories in 11 countries, using *in vivo* and *in vitro* bioassays, a receptor assay and immunoassays. An activity of 35 International Units of Human Pituitary LH was assigned to the contents of each ampoule coded 80/552.

Selvaraj and Moudgal (1993) used sheep luteal membranes for an LH receptor assay capable of measuring serum LH/chorionic gonadotropin (CG) in a wide variety of species.

Chen and Bahl (1993) reported a high expression of the hormone-binding active extracellular domain (1–294) of rat lutropin receptor in *Escherichia coli*.

Jia et al. (1993) developed a LH/CG bioassay using 293 cells permanently transfected with the human LH receptor cDNA and a luciferase reporter gene driven by a cAMP-dependent promoter.

Selvaraj et al. (1996) established a radioreceptor assay for LH/CG in human sera using immortalized granulosa cells transfected with LH/CG receptor.

REFERENCES AND FURTHER READING

Catt KJ, Ketelslegers JM, Dufau ML (1976) Receptors for gonadotropic hormones. In: Blecher M (ed) Methods in receptor research. Part I. Dekker, New York, pp 175–250

Chen W, Bahl OP (1993) High expression of the hormone binding active extracellular domain (1–294) of rat lutropin receptor in *Escherichia coli*. Mol Cell Endocrinol 91:35–41
Jia XC, Perlas E, Su JGJ, Moran F, Lasley BL, Ny T, Hsueh AJW (1993) Luminescence luteinizing hormone/choriogonadotropin (LH/CG) bioassay: measurement of serum bioactive LH/CG during early pregnancy in human and macaque. Biol Reprod 49:1310–1316
Lee CY, Ryan RJ (1972) Luteinizing hormone receptors: specific binding of human luteinizing hormone to homogenates of luteinized rat ovaries. Proc Natl Acad Sci USA 69:3520–3523
Liu WK, Yang KP, Nakagawa Y, Ward DN (1974) The role of the amino group in subunit association and receptor site interaction for ovine luteinizing hormone as studied by acylation. J Biol Chem 249:5544–5550
Liu WK, Furlong NB, Ward DN (1977) Effects of β subunit acylation on lutropin receptor site binding. J Biol Chem 252:522–527
Liu WK, Young JD, Ward BN (1984) Deglycosylated ovine lutropin: preparation and characterization by *in vitro* binding and steroidogenesis. Mol Cell Endocrinol 37:29–39
Selvaraj N, Moudgal NR (1993) Development of an LH receptor assay capable of measuring serum LH/CG in a wide variety of species. J Reprod Fertil 98:611–616
Selvaraj N, Dantes A, Limor R, Golander A, Amsterdam A (1996) Establishment of an *in vitro* bioassay and radioreceptor assay for LH/CG in human sera using immortalized granulosa cells transfected with LH/CG receptor. Endocrine 5:275–283
Storring PL, Gaines-Das RE (1993) The second International Standard for Human Pituitary LH: Its collaborative study by bioassays and immunoassays. J Endocrinol 138:345–359

N.7.1.3 Other Gonadotropins

GENERAL CONSIDERATIONS

The pituitary gonadotropins are species specific and exist in various isoforms containing different carbohydrate moieties. In the treatment of infertility, they were substituted by gonadotropin preparations from human urine purified by extraction (human menopausal gonadotropin, hMG, and human chorionic gonadotropin, hCG, from urine in pregnancy), containing variable proportions of follicle-stimulating and luteinizing activity. Pituitary gonadotropins for the treatment of infertility are now obtained by biosynthesis (recombinant DNA methods). Their structure closely resembles human FSH and LH.

Human chorionic gonadotropin (*hCG*) is excreted in the urine of pregnant women, and may also be excreted by tumors, such as hydatidiform mole and chorionepithelioma. hCG is measured as a tumor marker, and for the diagnosis of early pregnancy. hCG has mainly LH-like activity. Purified preparations of hCG and hMG are tested by bioassays.

Human menopausal gonadotropin (*hMG*) is excreted in the urine of postmenopausal women. hMG has predominantly FSH-like activity and was used to induce follicular maturation.

A gonadotropin preparation previously used in therapy is *pregnant mares' serum gonadotropin* (*PMSG*). Pregnant horses secrete large amounts of pituitary gonadotropin, which is not excreted in the urine and accumulates in serum. PMSG has predominantly FSH-like activity.

N.7.1.3.1 Corpus Luteum Formation in Immature Mice (Aschheim–Zondek Test)

PURPOSE AND RATIONALE

Aschheim and Zondek (1927, 1935) injected the urine of pregnant women (containing FSH and LH activity) into immature female mice and observed the ovulation and formation of corpora lutea. This procedure was widely used as a biological pregnancy test and later replaced the hCG assays. Further studies were performed by Hamburger and Pedersen-Bjergaard (1937).

PROCEDURE

Groups of 10–20 mice, 21 days of age, are treated with 5 equal subcutaneous injections of urinary extracts over the course of 48 h. The animals are sacrificed 96 h after the first injection. The ovaries are dissected and the formation of corpora lutea is observed by examination with a lens or a stereomicroscope. Rupture of follicles is indicated by blood spots.

EVALUATION

The number of ovaries showing the formation of corpora lutea was expressed as dose–response curves.

REFERENCES AND FURTHER READING

Aschheim S, Zondek B (1927) Hypophysenvorderlappenhormon und Ovarialhormon im Harn von Schwangeren. Klin Wchschr 6:1322
Hamburger C, Pedersen-Bjergaard K (1937) The assay of gonadotropic hormones. Standardisation curves for pregnant mare's serum hormone and human pregnant urine hormone. Q J Pharm Pharmacol 10:662–676
Zondek B (1935) Die hormonale Schwangerschaftsreaktion aus dem Harn bei Mensch und Tier. In: Zondek B (ed) Hormone des Ovariums und des Hypophysenvorderlappens. Springer, Berlin Heidelberg New York, pp 534–578

N.7.1.3.2 Biological Assay of hCG in Immature Male Rats

PURPOSE AND RATIONALE

The LH-like activity of hCG can be determined by measuring the weight increase of the prostate and seminal vesicles in immature male rats.

PROCEDURE

Immature male Sprague-Dawley rats at an age between 21 and 24 days are assigned at random to six groups of at least five animals. Three doses of standard (e. g., 4, 8, and 16 IU) and corresponding doses of the test preparation are dissolved in albumin-phosphate buffer, pH 7.2, and injected subcutaneously daily over a period of 4 days. On the 5th day, the animals are sacrificed and the seminal vesicles and prostate glands are prepared and weighed.

EVALUATION

Dose–response curves of the weights of seminal vesicles and ventral prostate glands are established for standard and test preparations allowing calculation of potency ratios with confidence limits.

MODIFICATIONS OF THE METHOD

The United States Pharmacopoeia USP 23 (1995) requests standardization of hCG in immature female rats at an age of 20–23 days. The animals are injected subcutaneously with three different doses of test preparation or standard daily on 3 days consecutively. They are sacrificed on the 5th day and the uteri are prepared and weighed.

REFERENCES AND FURTHER READING

British Pharmacopoeia (1988) Biological assay of chorionic gonadotrophin. Appendix XIV C. HMSO, London, pp A164–A165

United States Pharmacopoeia USP 23 (1995) Chorionic gonadotropin. United States Pharmacopoeial Convention, Rockville, Md., pp 718–719

N.7.1.3.3 Receptor Binding Assay for hCG

PURPOSE AND RATIONALE

The initial binding step to the luteinizing hormone (LH) receptor is used for quantification; the receptors may be obtained from superovulated rat ovaries, or from other tissues. Selvaraj et al. (1996) described an *in vitro* bioassay and radioreceptor assay for LH/chorionic gonadotropin (CG) in human sera using immortalized granulosa cells transfected with the LH/CG receptor.

PROCEDURE

Ovaries from pseudopregnant rats primed with pregnant mares' serum gonadotropin (PMSG) and hCG are homogenized. The homogenates are centrifuged at 2000 *g* for 15 min and the pellets are washed 3 times with 40 mM Tris buffer and resuspended in the same buffer. The suspension is filtered through four layers of cheesecloth prior to use. Fresh 2000-*g* fraction is prepared for each experiment. Purified hCG is labeled by the chloramine-T method resulting in a specific activity of approximately 60–70 μCi/μg.

For assessment of binding to receptors, a mixture consisting of the 2000-*g* fraction (equivalent to 2.5 or 5 mg of wet ovary or 45–90 μg of protein) and $(0.1–30) \times 10^{-10}$ M labeled gonadotropin or other test substances is incubated in a final volume of 1 ml of 40 mM Tris buffer (pH 7.4) containing 0.1% BSA at 25°C for 16 h. Then 1 ml ice-cold Tris buffer is added to the medium. This is immediately filtered, with suction, through Millipore EHWP filters (pore size 0.5 μm) previously wetted with 4% BSA to reduce nonspecific binding. The adsorbed material is washed with another 10 ml of ice-cold Tris buffer. The radioactivity on the filter is measured. Binding in the presence of a large excess of unlabeled hCG (200 IU/ml) is used to assess nonspecific binding.

EVALUATION

Specific binding is calculated and dose–response curves are obtained.

MODIFICATIONS OF THE METHOD

Similar studies were reported by: Catt et al. 1972,1976; Lee and Ryan 1973; Saxena 1976; Keutmann et al. 1983.

REFERENCES AND FURTHER READING

Catt KJ, Dufau ML, Tsuruhara T (1972) Radioligand-receptor assay of luteinizing hormone and chorionic gonadotropin. J Clin Endocrinol Metab 34:123–132

Catt KJ, Ketelslegers JM, Dufau ML (1976) Receptors for gonadotropic hormones. In: Blecher M (ed) Methods in receptor research. Part I. Dekker,New York, pp 175–250

Keutmann HT, McIlroy PJ, Bergert ER, Ryan RJ (1983) Chemically deglycosylated chorionic gonadotropin subunits: characterization and biological properties. Biochemistry 22:3067–3072

Lee CY, Ryan RJ (1973) Interaction of ovarian receptors with human luteinizing hormone and human chorionic gonadotropin. Biochemistry 12:4609–4619

Saxena BB (1976) Gonadotropin receptors. In: Blecher M (ed) Methods in receptor research. Part I. Dekker, New York, pp 251–299

Selvaraj N, Dantes A, Limor R, Golander A, Amsterdam A (1996) Establishment of an *in vitro* bioassay and radioreceptor assay for LH/CG in human sera using immortalized granulosa cells transfected with LH/CG receptor. Endocrine 5:275–283

N.7.1.4
Human Menopausal Gonadotropin (hMG)

N.7.1.4.1
Biological Assay of hMG in Immature Rats

PURPOSE AND RATIONALE

The FSH-like activity of hMG can be measured by the ovarian weight response of immature rats. The LH-like activity of hMG can be determined in immature male rats by the increase of prostate and seminal vesicle weights.

PROCEDURE

Female Sprague-Dawley rats at an age between 21 and 24 days are assigned at random to six groups of at least five animals. Three doses of standard (e. g., a total dose of 1.5, 3, and 6 IU) and corresponding doses of the test preparation are dissolved in albumin-phosphate buffer, pH 7.2, and injected subcutaneously daily over a period of 3 days. On the 4th day, the animals are sacrificed and the ovaries are removed and weighed.

EVALUATION

Dose–response curves for FSH-like activity are established, and potency ratios with confidence limits may be calculated using hMG standard preparations.

REFERENCES AND FURTHER READING

British Pharmacopoeia (1988) Biological assay of menotrophin. Follicle-stimulating activity. Appendix XIV C. HMSO, London, pp A165–A166

N.7.1.5
Pregnant Mares' Serum Gonadotropin (PMSG)

N.7.1.5.1
Biological Assay of PMSG in Immature Female Rats

PURPOSE AND RATIONALE

The predominant FSH-like activity of equine gonadotropin preparations is determined by the ovarian weight response of immature rats, as described for hMG (Hamburger 1950).

REFERENCES AND FURTHER READING

Hamburger C (1950) Gonadotropins. In: Emmens CW (ed) Hormone assay. Academic Press, New York, Chap. VII, pp 173–203

N.7.1.6
Immunoassays of Gonadotropins

Immunoassays of gonadotropins are important in clinical diagnostics (RIA, ELISA and related methods). For pharmacological and biological experiments, they are measured in blood, urine, and pituitary tissue, e. g., for evaluation of gonadotropin releasing hormones (as described in Sects. N.9.2.5 and N.9.2.6). Many comparisons for results of *in vivo* and *in vitro* bioassays versus immunoassays showed significant discrepancies when expressed as the ratios of bioactive to immunoreactive LH (B/I ratio). However, there are numerous validated species-specific methods which are used for experimental endocrinology and clinical diagnosis.

Similar studies were reported by: Faiman and Ryan 1967; Wide and Hobson 1983; Ulloa-Aguire et al. 1988; Seth et al. 1989; Terouanne et al. 1989; Armbruster and Haws 1990; Wheeler 1991; Rosenfield an Helke 1992; Weiss et al. 1992; YoungLai et al. 1992; Haavisto et. al 1993.

REFERENCES AND FURTHER READING

Armbruster DA, Haws LC (1990) Assay of follitropin and lutropin by fluorescence enzyme immunoassay. J Clin Lab Anal 4:170–174

Faiman C, Ryan RJ (1967) Serum follicle-stimulating hormone and luteinizing hormone concentrations during the menstrual cycle as determined by radioimmunoassays. J Clin Endocrin Metab 27:1711–1716

Haavisto AM, Pettersson K, Bergendahl M, Perheentupa A, Roser FJ, Huhtaniemi I (1993) A supersensitive immunofluorometric assay for rat luteinizing hormone. Endocrinology 132:1687–1691

Rosenfield RL, Helke J (1992) Is an immunoassay available for the measurement of bioactive LH in serum? J Androl 13:1–10

Seth J, Hanning I, Bacon RRA, Hunter WM (1989) Progress and problems in immunoassays for pituitary gonadotrophins: evidence from the UK external quality assessment schemes, (EQAS) 1980–1988. Clin Chim Acta 186:67–82

Terouanne B, Alameddine S, Martin JL, Nicolas JC, Cristol P, Sultan C, de Paulet AC (1989) Dosage par bioluminescence de l'hormone lutéinisante dans le plasma et l'urine. Ann Biol Clin 47:15–21

Ulloa-Aguirre A, Espinoza R, Damian-Matsumura P, Chappel SC (1988) Immunological and biological potencies of the different molecular species of gonadotrophins. Human Reprod 3:491–501

Weiss P, Zech H, Schönholzer HP, Fritzsche H (1992) Abbott IMx and Serono MAIAclone assays compared for lutropin determinations in urine. Clin Chem 38:2280–2283

Wheeler MJ (1991) The radioimmunoassay of gonadotrophins. In: Greenstein B (ed) Neuroendocrine research methods, Vol 2. Harwood, Chur, pp 487–498

Wide L, Hobson BM (1983) Qualitative difference in follicle-stimulating hormone activity in the pituitaries of young women compared to that of men and elderly women. J Clin Endocrin Metab 56:371–375

YoungLai EV, Yie SM, Yeo J (1992) Development patterns of bioactive and immunoreactive FSH in the female rabbit: effects of ovarectomy. Eur J Obstet Gynecol Reprod Biol 46:45–49

N.7.1.7
Gonadotropin inhibition

N.7.1.7.1
General Considerations

Gonadotropin inhibition is suspected when, in early testing of compounds or in toxicology studies, weight reduction of gonads and the endocrine-dependent organs is found. Early tests used the physiological feedback effects of endogenous steroids in rats, e. g., the parabiosis experiment. This technique in rats was applied to the relationship between central and peripheral endocrine organs, the pituitary–gonadal axis. Basically, the deficit in gonadal steroid hormones after castration of one parabiotic partner induces increased secretion of gonadotropin which in turn stimulates hypertrophy of the gonads of the noncastrated partner. The procedure is described in detail by Byrnes and Meyer (1951); Shipley (1962). The parabiosis technique is now obsolete but was applied again a few years ago with remarkable success in the identification of the adipose tissue hormone leptin (see Sect. L.4.1).

REFERENCES AND FURTHER READING

Byrnes WW, Meyer RK (1951) The inhibition of gonadotrophic hormone secretion by physiological doses of estrogen. Endocrinology 48:133–136

Shipley EG (1962) Anti-gonadotropic steroids, inhibition of ovulation and mating. In: Dorfman RI (ed) Methods in hormone research, Vol II, Bioassay. Academic Press, New York, pp 179–274

N.7.1.7.2
Inhibition of Gonadotropin Secretion in Intact Animals

PURPOSE AND RATIONALE

The suppression of gonadotropin secretion by steroid compounds (as an example) can be detected in the endocrine survey test, described in Sect. N.1. Young rats, e. g., 80–100 g initial body weight, are treated with gonadal steroids or their derivatives to induce gonadotropin suppression by negative feedback of steroids (McGinty and Djerassi 1953; Saunders and Drill 1958; Shipley 1962). In intact rats, a reduction of gonadal weight indicates gonadotropin inhibition, whereas in castrated control groups (females or males), the weight increase of the sexual-hormone-dependent organs indicates the intrinsic estrogenic or androgenic property of the test compound.

PROCEDURE

Immature male and female Sprague-Dawley rats weighing 55–65 g or young rats 80–100 g are used. Groups of ten animals per sex and dosage group are treated daily over a period of 21 days with doses of the test compound usually by the oral or subcutaneous route. Controls receive the vehicle only. Testosterone may be used as reference compound (standard) in males and estradiol as the reference compound in females. Twenty-four hours after the last treatment, the animals are sacrificed and body weights recorded: in males, testes, seminal vesicles, ventral prostate and musculus levator ani; and in females, ovaries and uterus are dissected out and weighed. In addition, the gonadotropin content of the pituitary glands at autopsy may be determined to detect inhibition of gonadotropin synthesis.

EVALUATION

Organ weight averages are calculated for each treatment group and compared with controls. The reference steroids testosterone and estradiol suppress gonadal weight by pituitary gonadotropin inhibition (negative feedback) in intact animals, and increase gonadal weight in castrated animals by direct action. Dose–response curves can be established for the test compounds and the standard, and the relative potency of gonadotropin inhibition is calculated.

MODIFICATIONS OF THE METHOD

As an example of a classical bioassay, gonadotropin inhibition can be tested in semicastrated male rats (H. G. Vogel unpublished data, 1964). Male Sprague-Dawley rats weighing 50–60 g are orchiectomized on the left side. The testis is weighed (without epididymis and epididymal fat). Test compounds in various doses or the standard are administered subcutaneously once daily for a period of 10 days. Controls receive the vehicle only. Standard compounds may be medroxyprogesterone acetate 0.4, 2.0, and 10.0 mg per animal per day, or 17-ethinyl-19-nortestosterone acetate 0.1, 0.5, and 2.0 mg per animal per day subcutaneously.

On day 11, the animals are sacrificed and the remaining testis, the adrenals, the seminal vesicles, the ventral prostate and the musculus levator ani are dissected out and weighed. Gonadotropin suppression results in atrophy of the remaining (contralateral) testis as compared with testis weight of the untreated control. A decrease in adrenal weight indicates feedback inhibition of the pituitary–adrenal axis. The weight of seminal vesicles, the ventral prostate and the musculus levator ani indicates androgenic activity of the test

compound. Dose–response curves for the test compound and the standard as well as potency ratios are calculated.

REFERENCES AND FURTHER READING

McGinty DA, Djerassi C (1958) Some chemical and biological properties of 19-nor-17α-ethinyltetosterone. Ann NY Acad Sci 71:500–515

Saunders FJ, Drill VA (1958) Some biological activities of 17-ethynyl and 17-alkyl derivatives of 17-hydroxyestrenones. Ann NY Acad Sci 71:516–531

Shipley EG (1962) Anti-gonadotropic steroids, inhibition of ovulation and mating. In: Dorfman RI (ed) Methods in hormone research, Vol II, Bioassay. Academic Press, New York, pp 197–274

N.7.1.7.3 Inhibition of Ovulation and Luteinization

PURPOSE AND RATIONALE

These methods were used frequently in research on contraception and selection of contraceptive steroids. Described here is an assay for progestational steroids. Progestagens inhibit pituitary gonadotropin secretion and synthesis. Progestional compounds, e. g., cyproterone acetate, inhibit ovulation and corpus lutea formation in young female rats by reducing luteinizing hormone secretion.

PROCEDURE

Female rats (35 days old) are treated once daily over a period of 7 days with increasing doses of gestagens, e. g., 0.125–2.0 mg progesterone or 0.025–0.40 mg 6α-methyl-17α-acetoxy-progesterone, subcutaneously. Controls receive the vehicle only. On the 8th day, the animals are sacrificed and body weight, ovarian weight, and number of corpora lutea are recorded. Progestogens inhibit follicular maturation, ovulation, and corpus lutea formation in this assay.

EVALUATION

Dose–response curves are established for average number of corpora lutea per animal and ovarian weight.

Similar studies were reported by: Junkmann 1957; Shipley 1962; Hebborn 1971; Phillips et al. 1987; Uilenbroek 1991

MODIFICATION OF THE METHOD

Ovum count can be performed in the oviduct of immature mice or rats after treatment with low doses of estradiol (Austin and Bruce 1956; May 1971). Immature rats or mice are injected with estradiol or stilbestrol at several dose levels to initiate estrus and ovulation. Then 72 h later the animals are sacrificed, and the oviducts are removed and examined under a stereomicroscope for the presence of ova. They can be seen through the swollen translucent walls of the oviduct. The swollen part of the oviduct is punctured with dissecting needles to release the ova and count the number of ova per animal. The rate of ovulation (number of ova) is related to the dose of estrogenic compound. In a modification of the method, inhibition of the rate of ovulation induced using a standard dose of estradiol by anti-ovulatory test compounds may be determined.

Hahn et al. (1977) treated rats in diestrus with test compounds administered orally in 0.5 ml sesame oil, and again on the following day when the animals were in proestrus. The animals were sacrificed on the next day, at which time they would normally have ova in the proximal segment of the fallopian tubes. Oviducts were separately flushed with saline onto a glass microscope slide, and the condition and number of ova were noted.

Inhibition of ovulation by gestagens can be studied in rabbits (Shipley 1965). Progesterone has a time-dependent effect on ovulation (stimulating or inhibiting secretion of pituitary gonadotropins). The timing of progesterone injection relative to the anticipated time of ovulation is important. Progesterone injected less than 4 h before ovulation in rabbits facilitates ovulation. In contrast, when injected more than 4 h before the anticipated time of ovulation (Sawyer 1952), progesterone inhibits ovulation. The rabbit ovulates within a few hours after mating, after mechanical stimulation of the vagina or after an intravenous injection of copper acetate (0.3 mg/kg). Progesterone injected 24 h before induction of ovulation will prevent ovulation.

Sexually mature female rabbits weighing 3–4 kg are treated with various doses of a standard progestogen or the test compound and 24 h later an ovulation-inducing stimulus is given. The rabbits are sacrificed and the ovaries are examined 18–24 h later. The total number of ovulation points on both of the ovaries is recorded for each animal. Dose–response curves for standard and test preparations are calculated.

REFERENCES AND FURTHER READING

Austin CR, Bruce HM (1956) Effect of continuous oestrogen administration on oestrus, ovulation and fertilization in rats and mice. J Endocrinol 13:376–383

Hahn DW, Allen GO, McGuire JL (1977) The pharmacological profile of norgestimate, a new orally active progestin. Contraception 16:541–553

Hebborn P (1971) Progestional agents. In: Turner RD, Hebborn P (eds) Screening methods in pharmacology, Vol II. Academic Press, New York, pp 105–119

Junkmann K (1957) Long acting steroids in reproduction. Recent Prog Horm Res 13:389–427
May M (1971) Anovulatory agents. In: Turner RD, Hebborn P (eds) Screening methods in pharmacology, Vol II. Academic Press, New York, pp 101–104
Phillips A, Hahn DW, Klimek S, McGuire JL (1987) A comparison of the potencies and activities of progestogens used in contraceptives. Contraception 36:181–192
Sawyer CH (1952) Progesterone initially facilitates and later inhibits release of pituitary ovulating hormone in the rabbit. Fed Proc Fed Am Soc Exp Biol 11:138
Shipley EG (1962) Anti-gonadotropic steroids, inhibition of ovulation and mating. In: Dorfman RI (ed) Methods in hormone research, Vol II, Bioassay. Academic Press, New York, pp 179–274
Shipley EG (1965) Effectiveness of topical application of a number of progestins. Steroids 5:699–717
Uilenbroek JTJ (1991) Hormone concentrations and ovulatory response in rats treated with antiprogestagens. J Endocrinol 129:423–429

N.7.1.7.4 Ovary–Spleen Transplantation

PURPOSE AND RATIONALE

This is a historical assay for gonadal steroids. Venous outflow from the spleen is exclusively to the liver. The steroids secreted by an ovary grafted to the spleen do not reach the peripheral circulation; they are degraded to inactive metabolites in the liver, and cannot exert their systemic feedback inhibition. The increasing gonadotropin secretion stimulates the growth of the transplanted ovary. This effect can be diminished or prevented by systemic application of gonadal steroids. Several studies were reported by: Mardones et.al. 1956; Shipley 1962; Biskind and Biskind 1990; D'Albora et al. 1992. The method by Mardones et al. (1956) for the guinea pig and by Desclin (1959) for the rat was modified by H. G. Vogel and S. Jung (unpublished data, 1962).

PROCEDURE

Female Sprague-Dawley rats weighing 100–120 g are anesthetized. The abdominal wall is opened by an incision lateral to the linea alba. Both ovaries are removed. One ovary is freed from the capsule and connective tissue and weighed to the nearest 0.1 mg. An incision is made at the cranial end of the spleen forming a deep pocket. The decapsulated ovary is pushed into this pocket. The incision is closed, and animals are treated with daily subcutaneous injection of an estrogen (e. g., 0.01, 0.1, 1.0, and 10 µg estradiol in 0.1 ml sesame oil) or a gestagen (e. g., 0.001, 0.01, 0.1, and 1.0 mg 6α-methyl-17α-acetoxyprogesterone) for a period of 5 weeks. Controls receive the vehicle only. In controls, the weight of the ovary may increase about eightfold, from an average weight at implantation of about 10.0 mg to values around 80.0 mg.

Estradiol at doses starting from 0.1 µg and 6α-methyl-17α-acetoxyprogesterone at a dose of 1.0 mg suppress ovarian growth completely by inhibition of LH secretion. The weight of the uterus is increased by direct action of estradiol too.

EVALUATION

Dose–response curves of test compounds and reference standards are calculated.

CRITICAL ASSESSMENT OF THE METHOD

The ovary–spleen transplantation method is similar to the parabiosis experiment, with much less stress to the animals.

REFERENCES AND FURTHER READING

Biskind MS, Biskind GS (1990) Development of tumors in the rat ovary after transplantation into the spleen. Historical milestone paper. Cancer J 3:113–116
D'Albora H, Cassina MP, Barreiro JP, Sapiro R, Domínguez R (1992) Differences in follicular growth and ovulation ability in the autografted right and left ovary of hemiovarectomised prepubertal rats. Med Sci Res 20:755–757
Desclin L (1959) Action du benzoate d'oestradiol et du propionate de testostérone sur la structure de l'ovaire implanté dans la rate. Ann Endocrinol (Paris) 20:222–227
Mardones E, Iglesias R, Lipschutz A (1956) The antiluteinizing potency of five derivatives of progesterone. Endocrinology 58:212–219
Shipley EG (1962) Anti-gonadotropic steroids, inhibition of ovulation and mating. In: Dorfman RI (ed) Methods in hormone research, Vol II, Bioassay. Academic Press, New York, pp 197–274

N.7.1.7.5 Inhibition of Fertility

PURPOSE AND RATIONALE

Fertility in rats can be inhibited by treatment of females with steroids that inhibit pituitary gonadotropin secretion or compete at the progesterone receptor. The test was used for contraceptive steroids (Shipley 1962; Philibert et.al. 1985; Dhar et. al 1994).

PROCEDURE

A colony of about 100 adult female Sprague-Dawley rats weighing between 200 and 250 g is established. Daily vaginal smears are taken at noon for 5 days. Then 15 regularly cycling females in proestrus are selected and caged separately. The first drug dose is administered at 3:00 p.m. (day 1). At 5:00 p.m. two males are placed with each female. On day 2, vaginal smears are taken for sperm count at 8:00 a.m.. The sec-

ond drug dose is administered at 4:30 p.m. On day 3, vaginal smears are taken for sperm count at 8:00 a.m. again. The third drug dose is administered and sperm counts are taken at 4:30 p.m. The males are then removed. From the 4th to the 7th day the test drugs are administered in the morning. Controls receive the vehicle only. On day 9, the animals are sacrificed and the uterus examined for implantation sites.

EVALUATION

Compounds which prevent conception, as evidenced by the absence of implantation sites at autopsy, were given further consideration. Minimal effective doses preventing ovulation in all animals of a test group were determined.

REFERENCES AND FURTHER READING

Dhar JD, Dwivedi A, Srivastava A, Setty BS (1994) Structure activity relationship of some 2,3-diaryl-2H-1-benzopyrans to their anti-implantation, estrogenic and antiestrogenic activities in the rat. Contraception 49:609–616

Philibert D, Moguilewsky M, Mary I, Lecaque D, Tournemine C, Secchi J, Deraedt R (1985) Pharmacological profile of RU 486 in animals. In: Baulieu EE, Segal SJ (eds) The antiprogestin steroid RU 486 and human fertility control. Plenum, New York, pp 49–68

Shipley EG (1962) Anti-gonadotropic steroids, inhibition of ovulation and mating. In: Dorfman RI (ed) Methods in hormone research, Vol II, Bioassay. Academic Press, New York, pp 197–274

N.7.2 Prolactin

There are considerable sequence homologies in the structures of growth hormone, prolactin and placental lactogen; however, their biological activities are rather different and each hormone exerts its specific pattern of activities on tissues, with growth hormone being an anabolic hormone, and prolactin predominantly a reproductive hormone.

N.7.2.1 General Considerations

The classical procedure for the bioassay of prolactin is based on the work of Riddle et al. (1939); namely, the increase in the weight of the crop sacs of doves and pigeons. Other methods are based on the induction of secretory changes in the mammary glands of rodents. Most of these methods can now be replaced by cell-based assays using suitable cell lines responding to prolactin.

The clinical measurements rely on immunoassays (Shiu and Friesen 1976; Jacobs 1979; Jeffcoate et al. 1986). Due to the species specificity of prolactin, a special radioimmunoassay for rats was developed.

Leroy-Martin et al. (1995) reported an immunocytochemical study of human prolactin receptors using antiidiotypic antibodies in human breast cancer.

REFERENCES AND FURTHER READING

Jacobs LS (1979) Prolactin. In: Jaffe BM, Behrmann HR (eds) Methods of hormone radioimmunoassay. Academic Press, New York, pp 199–222

Jeffcoate SL, Bacon RRA, Beastall GH, Divers MJ, Franks S, Seth J (1986) Assays for prolactin: guidelines for the provision of a clinical biochemistry service. Ann Clin Biochem 23:638–651

Leroy-Martin B, Peyrat JP, Amrani S, Lorthioir M, Leonardelli J (1995) Analyse immunocytochimique des recepteurs prolactiniques (R-PRL) humains a l'aide d'anticorps antiidiotypes dans le cancers du sein humain. Ann Pathol 15:192–197

Shiu RPC, Friesen HG (1976) Prolactin receptors. In: Blecher M (ed) Methods in receptor research, Part II. Dekker, New York, pp 565–598

Riddle O, Bates RW, Dykshorn SW (1933) The preparation, identification and assay of prolactin–a hormone of the anterior pituiarity. Am J Physiol 160:191–216

N.7.2.2 Radioimmunoassay of Rat Prolactin

PURPOSE AND RATIONALE

Prolactin is a glycoprotein hormone exhibiting species specificity. For pharmacological experiments in rats, such as evaluation of gonadotropin releasing hormone activity or prolactin inhibiting factor activity, a homologous assay is necessary. The reagents for rat prolactin and guidance for the method are provided by National Pituitary Agency, USA (Jeffcoate et al. 1986).

PROCEDURE

Reagents

Standard: NIAMDD-rat-prolactin-RP-1

Antiserum: rabbit-anti-rat-prolactin (NIAMDD-S-6)

Tracer: ^{125}I-rat-prolactin (NIAMDD-I-3)

Second antibody: goat-anti-rabbit-gammaglobulin (Cat. No. OTP 14/15)

Buffer: 0.01 M-phosphate-saline/0.1% bovine serum albumin, pH 7.4

Assay Procedure

Standards: 0.03–1 ng/tube, 200 µl/tube

Antiserum: 1:4000 100 µl/tube

Tracer: specific activity 250 µCi/µg, 10,000 cpm in 100 µl/tube

Standards (or sample) are incubated with antiserum for 24 h at +4°C; the tracer is added and incubated for another 48 h. Then the second antibody (1:50), 200 µl/tube, is added, and incubated for 48 h at +4°C. Separation is performed with 1.0 ml ice-cold phosphate-buffered saline, pH 7.4, the vials spun at 1300 *g* for 15 min, the supernatant decanted, and the residue counted for 1 min in a gamma-counter.

Counting equipment required: gamma spectrometer.

EVALUATION

Data processing: standard curves and sample data are calculated by any suitable computer program, e. g., using a spline function.

REFERENCES AND FURTHER READING

Jeffcoate SL, Bacon RRA, Beastall GH, Divers MJ, Franks S, Seth J (1986) Assays for prolactin: guidelines for the provision of a clinical biochemistry service. Ann Clin Biochem 23:638–651

N.7.2.3 Pigeon Crop Method

PURPOSE AND RATIONALE

This is again a historical bioassay no longer applied. Riddle and Bates (1939) showed that the secretion of "crop milk" by pigeons and doves is initiated and maintained by a factor from the anterior pituitary of these birds that is identical to the lactogenic hormone from mammals. Suitable assay methods have been developed on this basis (Meites and Turner 1950; Segaloff 1962; Cowie and Forsyth 1995). Pigeons are exquisitely sensitive to lactogenic hormone, and the assay can be done with considerably less material than the mammalian assays. The most sensitive assay is the so-called micromethod of local intracutaneous injections of the crop sac.

PROCEDURE

Pigeons of either sex (2–3 months old), but of uniform strain, e. g., White Carneaux, are injected intramuscularly (intrapectorally) with various doses of the test preparation or the standard once daily for 4 days. On the 5th day, the birds are sacrificed. A midventral incision is made through the skin and crop wall from keel to head. The contents of the crop and the adhering crop-milk are removed. The two lateral pouches are removed, the fat cleaned from the back of the glands and the wet weight of the glands determined. Thus, the unstimulated tissue in the dorsal midline and that around the proximal and distal opening of the crop are not weighed.

EVALUATION

Mean values of at least two doses of test preparation and standard are plotted versus logarithms of doses, and the potency ratios with confidence limits calculated.

MODIFICATIONS OF THE METHOD

The micromethod is based on the observation that only a small area directly over the site of injection is stimulated when lactogenic hormone is injected intradermally over the crop sac forming a "bleb" at the site of injection. A direct comparison of the potency of two different preparations can be made by a similar injection over the other crop sac. The birds are sacrificed on the 5th day and the entire crop sacs removed and examined by transmitted light (Lyons and Page 1935).

REFERENCES AND FURTHER READING

Cowei AT, Forsyth IA (1935) Biology of prolactin. Pharmacol Ther 1:437–457

Lyons WR, Page E (1935) Detection of mammatropin in the urine of lactating women. Proc Soc Exp Biol Med 32:1049–1050

Meites J, Turner CW (1950) Lactogenic hormone. In: Emmens CW (ed) Hormone assay. Academic Press, New York, pp 237–260

Riddle O, Bates RW (1939) Sex and internal secretions, 2nd edn. Williams and Wilkins, Baltimore

Segaloff A (1962) Prolactin. In: Dorfman RI (ed) Methods in hormone research, Vol II. Academic Press, New York, pp 609–615

N.7.2.4 Lactation in Rabbits

PURPOSE AND RATIONALE

Only the rabbit and guinea pig have proven satisfactory for mammalian assays of lactogenic hormones. The assays are based on the prolactin-induced mammary growth and milk secretion of pseudopregnant animals.

PROCEDURE

Pseudopregnancy is induced in mature estrus rabbits by intravenous injection of 50 IU of human chorionic gonadotropin. On the 14th day, the rabbits are examined for the presence of well-developed mammary glands characteristic of pregnancy. Various doses of the test preparation or the standard of lactogenic hormone are injected subcutaneously once daily for 6 days. On the 7th day the animals are sacrificed and

the abdominal skin is incised in the midline and separated from the mammary gland underneath. The degree of enlargement of the glands with secretion is rated as follows:

– absence of response

+ all ducts are filled with milk

++ all ducts and most lobules are filled with milk though not greatly thickened

+++ entire gland is filled with milk

++++ mammary glands are greatly extended with milk throughout.

EVALUATION

The mean values for groups of six rabbits are compared with the values of the standard groups.

MODIFICATIONS OF THE METHOD

A more sensitive rabbit assay method is based on the ability of lactogenic hormone to act directly on mammary tissue (Lyons 1942). Small amounts of test compound are injected directly into one or more of the six milk ducts of a castrated, rabbit pretreated with estrone-progesterone. A localized lactation appears in the gland sector stimulated. A dose-dependent reaction was found. The assay is suitable for prolactin, placental lactogen and growth hormone.

REFERENCES AND FURTHER READING

Bergman AJ, Meites J, Turner CM (1940) A comparison of methods of assay of the lactogenic hormone. Endocrinology 26:716–722

Lyons WR (1942) The direct mammotropic action of lactogenic hormone. Proc Soc Exp Biol Med 51:308–311

Lyons WR, Catchpole HR (1933) Availability of the rabbit for assay of the hypophyseal lactogenic hormone. Proc Soc Exp Biol Med 31:305–309

Meites J, Turner CW (1950) Lactogenic hormone. In: Emmens CW (ed) Hormone assay. Academic Press, New York, pp 237–260

Segaloff A (1962) Prolactin. In: Dorfman RI (ed) Methods in hormone research, Vol II. Academic Press, New York, pp 609–615

N.7.3 Growth hormone (GH)

N.7.3.1 General Considerations

Growth hormone (GH) has been isolated from the pituitary glands of several species including humans and is species specific; for therapy it has been replaced by rDNA preparations. Several methods have been described for the detection and assay of GH activity (Russell 1955; Hughes 1985; Isaksson 1985; Rudd 1991).

Human GH consists of 190 amino acids with two disulfide bridges between cysteine residues. Human GH synthesis is controlled by two genes: hGH-N and hGH-V.

GH secretion is stimulated by growth-hormone-releasing hormone (see Sect. N.9.5). GH is released in a pulsatile fashion and has a half-life of about 10 min.

Receptors for GH are found in several organs, mainly in liver and muscle.

Receptor binding assays (Ilondo et al. 1991) and radioimmunoassays for GH in several animal species (Greenwood et al. 1963; Peake et al. 1978) and for somatomedins (Chochinov and Daughaday 1978) have been developed.

Amit et al. (1992) measured serum GH by radioimmunoassay and GH-binding protein by a binding assay with dextran-coated charcoal separation.

An immunoradiometric assay for Gh was described by Hofland et al. (1989).

Mertani et al. (1995) studied the cellular localization of the GH receptor/binding protein in the human anterior pituitary gland.

A high-performance receptor binding chromatography assay for GH was described by Roswell et al. (1996).

Strasburger et al. (1996) developed an immunofunctional assay for human GH (hGH). An anti-hGH monoclonal antibody recognizing binding site 2 of hGH is immobilized and used to capture hGH from the serum sample. Biotin-labeled recombinant GH-binding protein in a second incubation step forms a complex with those hGH molecular isoforms that have both binding sites for the receptor. The signal is detected after a short third incubation step with labeled streptavidin.

Functional characterization of monoclonal antibodies specific to GH receptor is described by Wang et al. (1996).

REFERENCES AND FURTHER READING

Amit T, Ish-Shalom S, Glaser B, Youdim MBH, Hochberg Z (1992) Growth-hormone-binding protein in patients with acromegaly. Horm Res 37:205–211

Chochinov RH, Daughaday WH (1978) Somatomedin A, Somatomedin C and NSILA-s. In: Jaffe BM, Behrman HR (eds) Methods of hormone radioimmunoassay. Academic Press, New York, pp 959–977

Greenwood FC, Hunter WM, Glover JS (1963) The preparation of ^{131}I-labelled human growth hormone of high specific radioactivity. Biochem J 89:114–123

Hofland LJ, van Koetsfeld PM, Verleun TM, Lamberts SWJ (1989) Glycoprotein alpha-subunit and prolactin release by cultured pituitary adenoma cells from acromegalic patients: correlation with GH release. Clin Endocrinol (Oxf) 30:601–611
Hughes JP (1985) The nature and regulation of the receptors for pituitary growth hormone. Annu Rev Physiol 47:469–482
Ilondo MM, Vanderschueren-Lodeweyckx M, DeMeyts P (1991) Measuring growth hormone activity through receptor and binding protein assays. Horm Res 36 [Suppl 1]:21–36
Isaksson OGP, Edén S, Jansson JO (1985) Mode of action of pituitary growth hormone on target cells. Annu Rev Physiol 47:483–499
Mertani HC, Pechoux C, Garcia-Caballero T, Waters MJ, Morel G (1995) Cellular localization of the growth hormone receptor/binding protein in the human anterior pituitary gland. J Clin Endocrinol Metab 80:3361–3367
Peake GT, Morris J, Buckman MT (1978) Growth hormone. In: Jaffe BM, Behrman HR (eds) Methods of hormone radioimmunoassay. Academic Press, New York, pp 327–339
Roswell EC, Mukku VR, Chen AB, Hoff EH, Chu H, McKay PA, Olson KC, Battersby JE, Gehant RL, Meunier A, Garnick ER (1996) Novel assays based on human growth hormone receptor as alternatives to the rat weight gain bioassay for recombinant human growth hormone. Biologicals 24:25–39
Rudd BT (1991) Growth, growth hormone and the somatomedins: a historical perspective and current concepts. Ann Clin Biochem 28:542–555
Russell JA (1955) Methods of detection and assay of growth hormone. In: Smith RW, Gaebler OH, Long CNH (eds) The hypophyseal growth hormone, nature and actions. McGraw-Hill, New York, pp 17–27
Strasburger CJ, Wu Z, Pflaum CD, Dressendorfer SA (1996) Immunofunctional assay of human growth hormone (hGH) in serum: a possible consensus for quantitative hGH measurement. J Clin Endocrinol Metab 81:2613–2620
Wang BS, Lumanglas AL, Bona CA, Moran TM (1996) Functional characterization of monoclonal antibodies specific to growth hormone receptor. Mol Immunol 33:1197–1202

N.7.3.2 Weight Gain in Female Rats ("Growth Plateau Rats")

PURPOSE AND RATIONALE

Female rats 6 months of age, having reached maturity, gain weight at a very slow pace; the slowing down of the growth rate is described as "plateauing". Such rats can readily be induced by growth hormone to accelerate growth and weight gain (Greenspan et al. 1950; Papkoff and Li 1962).

PROCEDURE

Groups of ten adult female rats (Long-Evans or Wistar strain), 6 months old and weighing between 220 and 280 g, are used. Only animals which fail to gain more than 10 g in a 20-day period are used. At least two doses of the hormone preparation and the standard dissolved in saline are injected subcutaneously daily over a period of up to 20 days. During this time, weight gains between 10 and 40 g can be achieved. A straight line relationship exists between the logarithm of the daily dose and the growth response by body weight increase (Marx et al. 1942).

EVALUATION

The weight gains after administration of two doses of the test preparation and of the standard are used for 2+2-point assays, and potency ratios are calculated.

CRITICAL ASSESSMENT OF THE METHOD

The test needs a relatively large amount of test material. In spite of the species specificity of growth hormone, rats respond to growth hormone from many other species over a limited time period, before developing neutralizing antibodies.

MODIFICATIONS OF THE TEST

Immature female rats hypophysectomized at 26–28 days of age can be used (Li et al. 1945; Groesbeck and Parlow 1987). Smaller amounts of test substance are necessary for weight gain than in adult rats.

A cell proliferation assay using a stable clone of the myeloid cell line FDC-P1, transfected with the full-length growth hormone receptor (FDC-P1-hGRH), was described by Roswell et al. (1996) as an alternative to the classical hypophysectomized rat weight gain bioassay.

REFERENCES AND FURTHER READING

Greenspan FS, Li CH, Simpson ME, Evans HM (1950) Growth hormone. In: Emmens CW (ed) Hormone assay. Academic Press, New York, pp 273–290
Groesbeck MD, Parlow AF (1987) Highly improved precision of the hypophysectomized female rat body weight gain bioassay for growth hormone by increased frequency of injections, avoidance of antibody formation, and other simple modifications. Endocrinology 120:2582–2590
Li CH, Evans HM, Simpson ME (1945) Isolation and properties of the anterior pituitary growth hormone. J Biol Chem 159:353–366
Marx W, Simpson ME, Evans HM (1942) Bioassay of the growth hormone of the anterior pituitary. Endocrinology 30:1–10
Papkoff H, Li CH (1962) Hypophyseal growth hormone. In: Dorfman RI (ed) Methods in hormone research, Vol II. Academic Press, New York, pp 671–704
Roswell EC, Mukku VR, Chen AB, Hoff EH, Chu H, McKay PA, Olson KC, Battersby JE, Gehant RL, Meunier A, Garnick ER (1996) Novel assays based on human growth hormone receptor as alternatives to the rat weight gain bioas-

say for recombinant human growth hormone. Biologicals 24:25–39

N.7.3.3 Tibia Test in Hypophysectomized Rats

PURPOSE AND RATIONALE

Hypophysectomy is followed by cessation of epiphyseal growth due to growth hormone deficiency. The width of the epiphyseal cartilage is markedly reduced after hypophysectomy. Administration of growth hormone to hypophysectomized rats induces a remarkable increase in the width of the epiphyseal cartilage plate.

PROCEDURE

Female rats of the Long-Evans or Sprague-Dawley strains are hypophysectomized at the age of 26–28 days. They are used for the bioassay 12–14 days after the operation. The increase of body weight during this period of time has to be less than 0.5 g per day to indicate complete hypophysectomy. Six to ten animals are used for each group of two doses of test preparation and standard. The solutions are administered intraperitoneally twice daily for 4 days.

On the 5th day, the animals are sacrificed, both tibiae are dissected free of soft tissue, and the bones split in half with a sharp razor at the proximal end in the mid-sagittal plane. The halves are washed in water for 10 min, immersed in acetone for 6 min, and washed again in water for 3 min. They are then placed in 2% silver nitrate solution for 2 min and rinsed with water. During the water rinse, they are exposed to a strong light which turns the calcified portions of the bone dark brown. The stained tibiae are the transferred to a microscopic stage and the width of the uncalcified cartilage plate, which does not stain and remains white, is measured under low power with a calibrated micrometer eyepiece. Ten individual readings are made across the epiphysis.

EVALUATION

Mean values are obtained from a total of 20 readings for each bone specimen. They are averaged for each dose group. With a 2+2-point assay, the potency ratio with confidence limits versus the standard is calculated.

CRITICAL ASSESSMENT OF THE METHOD

The test has been firmly established as a standard method for assessing growth-promoting activity. For epiphyseal measurement, morphometry may be applied.

MODIFICATIONS OF THE METHOD

Bentham et al. (1993) described a double-staining technique for the detection of growth hormone and insulin-like growth factor-1 binding to rat tibial epiphyseal chondrocytes that were incubated with biotinylated ligands with or without an excess of unlabeled ligands, followed by incubation with Vectastain ABC complex, which was then reacted with diaminobenzidine. Double staining was accomplished by carrying out the first reaction with diaminobenzidine in the presence of nickel ammonium sulfate to give a black precipitate, followed by incubation with the second ligand, then the ABC complex and finally diaminobenzidine in the absence of nickel ammonium sulfate to give a brown stain.

REFERENCES AND FURTHER READING

Bentham J, Ohlsson C, Lindahl A, Isaksson O, Nilsson A (1993) A double-staining technique for detection of growth hormone and insulin-like growth factor-1 binding to rat tibial epiphyseal chondrocytes. J Endocrinol 137:361–367

Geschwind II, Li CH (1955) The tibia test for growth hormone. In: Smith RW, Gaebler OH, Long CNH (eds) Hypophyseal growth hormone, nature and actions. McGraw-Hill, New York, pp 28–58

Greenspan FS, Li CH, Simpson ME, Evans HM (1949) Bioassay of hypophyseal growth hormone: The tibia test. Endocrinology 45:455–463

Greenspan FS, Li CH, Simpson ME, Evans HM (1950) Growth hormone. In: Emmens CW (ed) Hormone assay. Academic Press, New York, pp 273–290

Papkoff H, Li CH (1962) Hypophyseal growth hormone. In: Dorfman RI (ed) Methods in hormone research, Vol II. Academic Press, New York, pp 671–704

N.7.3.4 ^{35}S Uptake

PURPOSE AND RATIONALE

Cartilage contains glucosaminoglycans, e. g., chondroitin sulfate. The uptake of labeled sulfate into cartilage is greatly reduced after hypophysectomy and restored after growth hormone application. This phenomenon can be used as the basis of a bioassay of growth hormone activity (Collins and Baker 1960; Papkoff and Li 1962).

PROCEDURE

Female Sprague-Dawley rats are hypophysectomized at 21 days of age and used for experimentation 3 weeks later. The animals are given intraperitoneal injections of growth hormone together with radioactively labeled sulfate once daily for 4 days. Eight to ten animals are

used for at least two doses of test preparations (growth hormone derivatives) and standard. The rats are sacrificed 24 h after the last injection and the amount of radiosulfate present in the seventh rib cartilage is determined. A linear relationship exists between the uptake of radiosulfate and the hormone given over a range of 3–20 µg per day for 4 days.

EVALUATION

Mean values for each group and the potency of the test preparation versus standard calculated with confidence limits are calculated in a 2+2-point assay.

REFERENCES AND FURTHER READING

Collins EJ, Baker VF (1960) Growth hormone and radiosulfate incorporation: I. A new assay method for growth hormone. Metabolism 9:556–560

Papkoff H, Li CH (1962) Hypophyseal growth hormone. In: Dorfman RI (ed) Methods in hormone research, Vol II. Academic Press, New York, pp 671–704

N.7.3.5 Inhibition of Glucose Uptake in Adipocytes in Vitro

PURPOSE AND RATIONALE

The conversion of glucose to lipid in murine adipocytes is dose-dependently inhibited by human growth hormone (hGH). A sensitive *in vitro* bioassay was developed by Foster et al. (1993).

PROCEDURE

3T3-F442A embryonic murine fibroblasts (preadipocytes) are grown in Dulbecco's modified Eagle's medium (DMEM) containing 2 mM L-glutamine, 100 µg/ml streptomycin, 100 U/ml penicillin, and 0.1 µg/ml fungizone. The cells are plated in 60- or 100-mm plastic culture dishes at a density of 200 cells/cm^2 and grown to confluence at 37°C under a humidified atmosphere of 90% air/10% CO_2 in medium supplemented with 25 mM glucose and 10% calf serum. Medium is replaced every 2–3 days. Once confluent, the fibroblasts are converted to cells with the characteristics of adipocytes by incubation for 48 h in medium supplemented with 25 mM glucose, 10% fetal bovine serum, 0.5 mM methylisobutylxanthine, 2 µg/ml insulin, and 250 nM dexamethasone. This medium is then replaced with medium containing 10% fetal bovine serum and 2 µg/ml insulin with changes made every 2 days for 5–8 days until at least 70% of the cells have the characteristics of adipocytes as assessed by phase contrast microscopy.

For bioassays, the medium consists of DMEM containing 5.5 mM glucose, 2% BSA, 25 nM dexamethasone, 37 nM estradiol, 10 µg/l insulin, and 0.1 µCi/ml uniformly labeled [^{14}C]D-glucose. Cultures are co-incubated with increasing concentrations of 22-kDa human growth hormone (0.313–40 µg/l) as standard or test substance or medium (controls) for 24 h. For determination of hGH in patients, 100 µl or 200 µl serum is added. After incubation, the medium is removed and discarded. The cells are treated with Doles reagent (one part heptane, four parts isopropanol, 0.1 part 1 N H_2SO_4), the plates scraped, and the contents transferred to a glass tube. Lipids are extracted by the method of Dole and Meinertz (1969), and radioactivity of the lipid is determined by scintillation counting in a liquid scintillation spectrophotometer. Results are expressed as ^{14}C counts per minute per dish. Lipid accumulation in controls without hGH is taken as 100%. Logarithmic doses of 0.313–40 µg/l hGH result in a linear decrease of lipid accumulation. The assay is rather specific for 22-kDa hGH.

EVALUATION

From dose–response curves, activity ratios can be calculated.

MODIFICATIONS OF THE METHOD

Xu et al. (1995) studied the effects of GH antagonists on 3T3-F422A preadipocyte differentiation. The antagonists not only failed to induce adipose differentiation, including late marker gene expression (adipocyte protein 2), immediate early gene expression (c-fos), and tyrosine phosphorylation of intracellular proteins, but also antagonized GH-induced c-fos expression and phosphorylation of proteins of apparent molecular mass 95 kDa.

REFERENCES AND FURTHER READING

Dole V, Meinertz J (1969) Microdetermination of long chain fatty acids in plasma and tissues. J Biol Chem 235:2595–2599

Foster CM, Borondy M, Padmanabhan V, Schwartz J, Kletter GB, Hopwood NJ, Beitins IZ (1993) Bioactivity of human growth hormone in serum: validation of an *in vitro* bioassay. Endocrinology 132:2073–2082

Xu BC, Chen WY, Gu T, Ridgway D, Wiehl P, Okada S, Kopchick JJ (1995) Effects of growth hormone antagonists on 3T3-F422A preadipocyte differentiation. J Endocrinol 146:131–139

N.7.3.6 Eluted Stain Bioassay for Human Growth Hormone

PURPOSE AND RATIONALE

Ealey et al. (1988, 1995) and Dattani et al. (1993, 1995) developed an eluted stain bioassay

(ESTA) for human growth hormone (hGH). This assay is based on the production of MTT–formazan [MTT is 3-(4,5-dimethylthiazol-2-yl)-2,5-diphenyltetrazolium] by quiescent Nb2 cells under the influence of the hormone.

PROCEDURE

Rat Nb2 lymphoma cells are grown in suspension culture which consists of RPMI medium (Gibco) containing 50 U penicillin/ml, 50 µg streptomycin/ml, 2×10^{-3} M L-glutamine, 10% fetal calf serum and 10% horse serum. The cells are incubated in a humidified atmosphere of 5% CO_2/95% air at 37°C.

Prior to the bioassay of hGH, the cells are transferred to a quiescent medium, which is identical in composition to the growth medium described above except that the FCS is reduced from 10% to 1%. This slows down the rate of cell division and reduces the optical density of the unstimulated control in the subsequent ESTA bioassays by about 50%. Incubation is continued in a humidified atmosphere of 5% CO_2/95% air at 37°C for 24 h.

For the bioassay, the cells are transferred to the bioassay medium, which is the same as the growth medium but without FCS. The cells are plated out into 96-well microtiter plates, such that a final density of 2×10^5 cells/ml is obtained. Usually 50 µl of cell suspension at 4×10^4 cells/ml is added to each well. This is followed by the addition of 50 µl of various concentrations of test compound or standard (0.1–10 mU GH/l). The cells are incubated in a humidified atmosphere of 5% CO_2/95% air at 37°C for 96 h.

At the end of the bioassay incubation, the colorimetric endpoint is determined by the addition of 10 µl of MTT bromide solution (5 mg/ml in phosphate-buffered saline containing 0.1 mg/ml $CaCl_2$ and $MgCl_2 \cdot 6H_2O$, pH 7.3) to each well: incubation is continued for 40 min at 37°C in a dry incubator. During this time, activated cells reduce the yellow MTT salt to its purple formazan. After the 40-min incubation, 50 µl of 10% Triton X-100 in 0.1 M HCl is added to each well and the plate gently shaken for 30 min at room temperature. Bioassay responses of the 96 wells are quantified with a Biorad microtiter plate reader at optical densities at a test wavelength of 595 nm and a reference wavelength of 655 nm to correct for differential scattering.

EVALUATION

The determinations for all experiments are made from triplicate or quadruplicate microcultures and the results expressed as means and standard deviations. Dose–response curves for standard and test compounds are established.

MODIFICATIONS OF THE METHOD

The sensitivity of the assay can be increased by addition of ionic zinc (Dattani et al. 1993, 1995; Strasburger and Dattani 1997).

REFERENCES AND FURTHER READING

Dattani MT, Hindmarsh PC, Brook CGD, Robinson ICAF, Weir T, Marshall NJ (1993) Enhancement of growth hormone bioactivity by zinc in the eluted stain assay system. Endocrinology 1993:2803–2808

Dattani MT, Hindmarsh PC, Brook CGD, Robinson ICAF, Kopchick JJ, Marshall NJ (1995) G120R, a human growth hormone antagonist, shows zinc-dependent agonist and antagonist activity on Nb2 cells. J Biol Chem 270:9222–9226

Ealey PA, Yateman ME, Holt SJ, Marshall NJ (1988) ESTA: a bioassay system for the determination of potencies of hormones and antibodies which mimic their action. J Mol Endocrinol 1:R1–R4

Ealey PA, Yateman ME, Sandhu R, Dattani MD, Hassan MK, Holt SJ, Marshall NJ (1995) The development of an eluted stain bioassay (ESTA) for human growth hormone. Growth Regul 5:36–44

Strasburger CJ, Dattani MT (1997) New growth hormone assays: potential benefits. Acta Pediatr Suppl 412:5–11

N.7.3.7 Reverse Hemolytic Plaque Assay for Growth Hormone

PURPOSE AND RATIONALE

The reverse hemolytic plaque assay as described by Neill and Frawley (1983), Luque et al. (1986), and Smith et al. (1986) can be used to determine growth hormone (GH) secretion by dispersed rat pituitary cells (Niimi 1994a, 1994b).

PROCEDURE

Anterior pituitary lobes of male Sprague-Dawley rats weighing 200–250 g are collected and minced into approximately 1-mm^3 fragments. The pituitary cells are dispersed and transferred to a siliconized flask containing 3 mg/ml trypsin in Dulbecco's phosphate-buffered saline containing 0.1% BSA and antibiotics, and incubated in a water bath for 5 min at 37°C. After gentle trituration by a siliconized pipette, the cells are separated by centrifugation and rinsed with phosphate-buffered saline containing 2 mg/ml DNase (type I; Sigma, St. Louis, Mo., USA). The dispersed cells are separated by centrifugation and rinsed once in phosphate-buffered saline with 1.5 mg/ml trypsin inhibitor (type II-L, Sigma). The cells are washed 5 times with Dulbecco's modified Eagle's medium (DMEM) containing 0.1% BSA and resuspended. Ovine erythrocytes are coupled with staphylococcal protein A

(Sigma) in the presence of 0.9% chromium chloride in normal saline. Pituitary cells (10^6 cells/ml) are combined with an equal volume of a 30% solution of protein-A-coupled erythrocytes in DMEM containing 0.1% BSA and antibiotics. The cell mixture is infused into a poly-L-lysine coated Cunningham slide chamber and preincubated at 37°C, 95% air/5% CO_2, for 50 min. After preincubation, the chamber is rinsed in DMEM-BSA and placed in Petri dishes containing DMEM and 10% horse serum containing 1% nonessential amino acids before performing the reverse hemolytic plaque assay.

After 24 h of co-incubation, the chambers are rinsed with DMEM-BSA. Monkey anti-rat GH serum diluted 1:150 in assay medium is then infused into the chambers alone or with different secretagogues and incubated for 2 h. Plaque development is initiated by infusion of guinea pig complement (Gibco) at a final dilution of 1:40. The reaction is terminated after 0.5 h by the infusion of B-5 fixative (6 g $HgCl_2$ and 1.25 g sodium acetate in 90 ml distilled water, add 10 ml 37% formaldehyde immediately before use). The pituitary cells are stained with 0.5% toluidine blue to facilitate observation of the hemolytic plaques.

EVALUATION

In each experiment, each concentration of secretagogue or vehicle is run in duplicate, and 150–200 cells/slide are counted. Two separate experiments have to be performed. The plaque area is measured by using a calibrated ocular reticule. The area of 50 plaques per slide is measured. Statistical analysis is performed by Student's *t*-test and one-way analysis of variance.

REFERENCES AND FURTHER READING

Luque EH, Munoz de Toro M, Smith POF, Neill JD (1986) Subpopulations of lactotropes detected with the reverse hemolytic plaque assay show different responsiveness to dopamine. Endocrinology 118:2120–2124

Neill JD, Frawley S (1983) Detection of hormone release from individual cells in mixed populations using a reverse hemolytic plaque assay. Endocrinology 112:1135–1137

Niimi M, Sato M, Murao K, Takahara J, Kawanishi K (1994a) Effect of excitatory amino acid receptor agonists on secretion of growth hormone as assessed by the reverse hemolytic plaque assay. Neuroendocrinology 60:173–178

Niimi M, Sato M, Wada Y, Tamaki M, Takahara J, Kawanishi K (1994b) Analysis of growth hormone release from rat anterior pituitary cells by reverse hemolytic plaque assay: Influence of interleukin-1. Life Sci 55:1807–1913

Smith PF, Luque EH, Neill JD (1986) Detection and measurement of secretion from individual neuroendocrine cells using a reverse hemolytic plaque assay. In: Conn PM (ed) Methods in enzymology, Vol 124. Academic Press, New York, pp 443–464

N.7.3.8 Determination of Growth Hormone Isoforms by 22-kDa GH Exclusion Assay

PURPOSE AND RATIONALE

Human growth hormone exists in variety of isoforms. In the pituitary, the most abundant isoform is 22-kDa GH, while other isoforms (non-22-kDa GH) are present in variable amounts. Boguszewski et al. (1996); Strasburger and Dattani (1997) described an analytical approach that focuses on the isoforms differing from monomeric and oligomeric 22-kDa GH.

PROCEDURE

Reagents

- Recombinant 22-kDa human GH (Genotropin, Pharmacia, Uppsala, Sweden)
- 22-kDa GH-specific monoclonal antibody (MCB), (Genentech, San Francisco, Calif., USA)
- magnetic polystyrene beads coated with rat anti-mouse IgG 1 (Dynabeads M-450), (Dynal, Oslo, Norway)
- polyclonal antibody-based IRMA (Pharmacia, Uppsala, Schweden)
- assay buffer containing phosphate-buffered saline, 5 g/l BSA, 5 ml/l Tween-20, 0.1 g/l thiomerosal.

Assay Procedure

A 100-µl aliquot of serum or test solution is mixed with either 10 µl of assay buffer containing MCB (final concentration 0.3 µmol/l) or 10 µl of assay buffer without MCB. The samples are incubated for 24 h at room temperature. A 160-µl aliquot of magnetic beads coated with rat anti-mouse IgG (concentration 4×10^5 beads/µl) is added to the samples. After further incubation for 2 h at room temperature with gentle agitation in a rotator, the tubes are put in contact with a magnetic device, Dynal MPC-E (Dynal, Oslo, Norway), for 1 min. The magnetic beads with the 22-kDa GH-MCB complexes are attracted by the magnet. While the tubes are in the magnetic device, 50-µl aliquots of the supernatant are transferred to new tubes for measurement of non-22-kDa GH levels in duplicate by the polyclonal antibody-based IRMA. The same procedure is performed for samples incubated with assay buffer (without addition of MCB) to determine total GH concentration.

EVALUATION

The amount of non-22-kDa GH isoforms is expressed as a percentage of total GH concentration. The Mann-

Whitney *U* test (two-tailed) is used to compare the percentage of non-22-kDa GH isoforms between the groups. The method is an example of the increasing use of physicochemical methods to characterize the heterogeneity of hormone preparations obtained by rDNA methods.

REFERENCES AND FURTHER READING

Boguszewski CL, Hynsjö L, Johannsson G, Bengtsson BÅ, Carlsson LMS (1996) 22-kDa growth hormone exclusion assay: a new approach to measurement of non-22 kDa growth hormone isoforms in human blood. Eur J Endocrinol 135:573–582

Strasburger CJ, Dattani MT (1997) New growth hormone assays: potential benefits. Acta Pediatr Suppl 412:5–11

N.7.3.9 Steroid Regulation of Growth Hormone Receptor and GH-Binding Protein

PURPOSE AND RATIONALE

Gabrielsson et al. (1995) studied steroid regulation of growth hormone receptor (GHR) and GH-binding protein (GHPB) mRNAs in the rat. GHR and GHBP, arising from alternative splicing of the same gene, show a sexually dimorphic and GH-dependent expression pattern. Multiple alternative 5′-untranslated regions are present in GHR and GHBP transcripts in the rat, one of which, GHR_1, has been shown to be liver specific and found at higher levels in females.

PROCEDURE

Animal Treatment

For human GH treatment, groups of Wistar rats are implanted subcutaneously with osmotic minipumps delivering recombinant hGH at 200 µg/day for 7, 12, or 14 days. Steroid-treated animals are implanted subcutaneously with slow-release pellets delivering estradiol (E_2, 25 ng/day), testosterone propionate (12.5 µg/day) or corticosterone (3.5 µg/day) for up to 2 weeks. At the end of each study, animals are sacrificed and samples of blood and liver rapidly removed.

Protein Binding (GHBP) Assay

Plasma GHBP levels are measured by radioimmunoassay (RIA). Recombinant rat GHBP is used for iodination and reference preparation (Carmignac et al. 1992).

GH-Receptor-Based Assays

Liver samples are homogenized in 0.3 M sucrose containing 3 mM imidazole HCl, pH 7.4 (Carmignac et al. 1993). Samples of 100 µl (~2 mg protein) are incubated in duplicate at 22°C with radio-iodinated bovine GH (100 µl, 20,000 cpm) and 100 µl buffer (25 mM Tris-HCl, pH 7.4, containing 10 mM $CaCl_2$ and 0.1% BSA). After 2 h, 3 ml cold (4°C) buffer is added, the tubes centrifuged at 2700 *g* for 30 min, and the radioactivity in the pellets determined. Nonspecific binding is estimated in the presence of 1 µg unlabeled bovine GH and is subtracted from total binding to derive percentage specific bovine GH binding per milligram protein.

Generation of RNA Probes

Using an *in vitro* transcription kit, probes are labeled with [^{35}S]uridine triphosphate for solution hybridization assay and [^{32}P]uridine triphosphate for Northern blots and RNase protection assays. Total GHR coding region transcripts are measured using an antisense probe corresponding to a 423-nucleotide (nt) *Nco*I-*Kpn*I fragment (nt 989–1411) of the λ1 clone of the rGHR inserted into the pT7T318U vector. This sequence spans the transmembrane domain and part of the intracellular domain of the GHR and is not present in GHBP mRNA. Total GHBP transcripts are determined using a 46-nt oligonucleotide probe complementary to the alternate splice sequence encoding the GHBP hydrophilic tail. This probe does not detect GHR transcripts. GHR_1-containing transcripts are measured using a probe complementary to this 5′-UTR alternative exon sequence.

Northern Blots

Total RNA is prepared using the method of Chomczynski and Saachi (1987). RNA is run overnight on a 2.2 M formaldehyde/3-*N*-morpholine propanesulfonic acid agarose gel, transferred to a Nylon membrane and cross-linked using a Stratalinker (Strategene, La Jolla, Calif., USA). Membranes are prehybridized for 2–4 h at 60–65°C in 50% formamide, 5× SSC (1× SSC = 0.15 M NaCl, 0.015 M Na citrate, pH 7.0), 5× Denhardt's solution, 50 mM Na_2HPO_4, 0.2% sodium dodecyl sulfate (SDS), 250 µg/ml salmon sperm DNA, and 100 µg transfer RNA/ml, and incubated with ^{32}P-labeled probe [$(1–3)\times10^6$ cpm/ml] at the same temperature in 50% formaldehyde, 5× SSC, 1× Denhardt's solution, 20 mM Na_2HPO_4, 0.2% SDS, 10% dextran, 100 µg/ml salmon sperm DNA, and 100 µg tRNA/ml. After washing (60°C and 20 min/wash, starting at 3× SSC/0.1% SDS and reducing to 0.3× SSC/0.1% SDS) membranes are exposed to X-ray film with intensifying screens at −80°C or are detected by phosphorimaging.

Solution Hybridization Assays

Hepatic mRNAs are quantified by solution hybridization after the method of Möller et al. (1991). Liver is homogenized in 10 mM Tris-HCl, pH 7.5, containing 1% SDS and 5 mM EDTA, after proteinase K digestion. Total nucleic acids (TNAs) are extracted with phenol/chloroform, precipitated with ethanol, and the pellets dissolved in 0.2 × 10 mM Tris-HCl, pH 7.5, containing 1% SDS and 5 mM EDTA. For each assay, 10–100 µg TNAs is hybridized in duplicate with ^{35}S-labeled RNA probes (20,000–30,000 cpm) at 50°C overnight in 40 µl, 21 mM Tris-HCl buffer, pH 7.5, containing 600 mM NaCl, 4.5 mM EDTA, 7.5 mM dithiothreitol, 0.1% SDS, and 25% formamide. Standard tubes contain known quantities of target RNA, transcribed from the sense strand of the appropriate plasmid and quantified by absorption at 260 nm.

After digestion with RNase A (40 µg) and RNase T_1 (2 µg) protected fragments are precipitated with 10% trichloroacetic acid, are collected by filtration (GF/C paper, Whatman), detected by scintillation counting, and expressed as specific mRNA levels (attomoles per µg TNA).

RNase Protection Assay

Total RNA (20 µg) is hybridized under the same conditions as above, except that a ^{32}P-labeled probe (500,000 cpm) is used. After overnight incubation at 50°C, the samples are treated with 300 µl of a solution of 10 mM Tris, pH 7.5, 5 MM EDTA, and 300 mM NaCl, containing RNase A (40 µg/ml) and RNase T_1 (2 µg/ml), for 30 min at room temperature. After incubation with 50 µg proteinase K and 20 µl 10% SDS for 15 min at 37°C, samples are extracted with phenol/chloroform and ethanol precipitated with 10 µg tRNA as carrier. The pellets are dissolved in gel-loading buffer (10 mM EDTA and 1 mg/ml bromophenol blue in 80% formamide), denatured at 85°C for 4 min, and run on an 8 M urea/6% polyacrylamide gel. Detection is by autoradiography or phosphorimaging.

EVALUATION

Data are calculated as mean ±SEM. Differences between treatment groups are assessed using Student's *t*-test, or analysis of variance followed by Student-Newman-Keul's or Dunnett's tests.

MODIFICATIONS OF THE METHOD

Nilsson et al. (1995) described the expression of functional growth hormone receptors in cultured human osteoblast-like cells.

To measure the absolute number of mRNA molecules encoding the growth hormone receptor in human tissue, Martini et al. (1995) developed a quantitative polymerase chain reaction assay.

REFERENCES AND FURTHER READING

Carmignac D, Well T, Carlsson L, Clark RG, Robinson ICAF (1992) Growth hormone (GH)-binding protein in normal and GH-deficient dwarf rats. J Endocrinol 135:447–457

Carmignac D, Gabrielsson BG, Robinson ICAF (1993) Growth hormone binding protein in the rat: effects of gonadal steroids. Endocrinology 133:2445–2452

Chomczynski P, Saachi N (1987) Single step method for RNA isolation by acid guanidinium thiocyanate-phenol-chloroform extraction. Anal Biochem 162:156–159

Gabrielsson BG, Carmignac DF, Flavell DM, Robinson ICAF (1995) Steroid regulation of growth hormone (GH) receptor and GH-binding protein messenger ribonucleic acids in the rat. Endocrinology 136:209–217

Martini JF, Villares SM, Nagano M, Delehaye-Zervas MC, Eymard B, Kelly PA, Postel-Vinay MC (1995) Quantitative analysis by polymerase chain reaction of growth hormone receptor gene expression in human liver and muscle. Endocrinology 136:1355–1360

Möller C, Arner P, Sonnenfeld T, Norstedt G (1991) Quantitative comparison of insulin-like growth factor mRNA levels in human and rat tissues analyzed by a solution hybridization assay. J Mol Endocrinol 7:213–222

Nilsson A, Swolin D, Enerback S, Ohlsson C (1995) Expression of functional growth hormone receptors in cultured human osteoblast-like cells. J Clin Endocrinol Metab 80:3483–3488

N.7.4
Adrenocorticotropin (ACTH)

N.7.4.1
Adrenal Ascorbic Acid Depletion

PURPOSE AND RATIONALE

This is now a historical assay, which however has been used extensively for standardization of ACTH preparations. The administration of pituitary adrenocorticotropic hormone (ACTH) is followed by a decrease in the amount of ascorbic acid present in the adrenals. The depletion of adrenal ascorbic acid is a function of the dose of ACTH administered. This relationship was used for a quantitative assay of ACTH by Sayers et al. (1948). The method has been selected for standardization of ACTH by several Pharmacopoeias, e. g. The United States Pharmacopeia USP 23 (1995), Deutsches Arzneibuch (1986) and British Pharmacopoeia (1988). Furthermore, the test has been used for evaluation of synthetic corticotropin analogs (Geiger et al. 1964; Vogel 1965, 1969a, 1969b). A similar test is used for luteinizing hormone action in the rat ovary.

PROCEDURE

Male Wistar rats weighing between 100 and 200 g are hypophysectomized 1 day prior to the test. The range of weights in any one test should not exceed 15 g. For one test with three doses of test preparation and standard, at least 36, preferably 60, hypophysectomized rats are necessary.

Solutions

Five units of the International Standard for corticotropin (Bangham et al. 1962) or an amount of test preparation supposed to contain about 5 units are dissolved in 0.25 ml of 0.5% phenol solution and diluted with 8.1 ml of 15% gelatin solution. In this way, 0.5 ml contains 300 mU ACTH. Then 3 ml of this solution is diluted with 6.0 ml gelatin solution (to prevent adsorption to glassware), resulting in 100 mU ACTH per 0.5 ml. Then 3 ml of this solution is again diluted with 6.0 ml gelatin solution, resulting in a content of 33 mU ACTH per 0.5 ml.

The hypophysectomized rats are randomly distributed to six groups. Each rat receives subcutaneously 0.5 ml of one of the various concentrations of test preparation or standard. Three hours after injection, the animals are anesthetized, both adrenals removed, freed from extraneous tissue and weighed. The rats are sacrificed and the skull opened to verify completeness of hypophysectomy.

The adrenals are homogenized in 4% trichloroacetic acid and the ascorbic acid determined according to the method of Roe and Kuether (1943). Other methods have been described.

ASCORBIC ACID DETERMINATION

Reagents

First 100 mg L-ascorbic acid is dissolved in 100 ml 4% trichloroacetic acid and 20 ml of this solution is diluted with 4% trichloroacetic acid to achieve a 0.2% ascorbic acid solution; 2 ml of this solution is diluted with 4% trichloroacetic acid to achieve a 0.02% ascorbic acid solution. Sulfuric acid (85%) is obtained by adding 900 ml concentrated sulfuric acid to 100 ml distilled water. Then 2 g dinitrophenylhydrazine is dissolved in 100 ml of 9 N H_2SO_4 (75 ml distilled water and 25 ml concentrated sulfuric acid), and 6 g thiourea is dissolved in 100 ml distilled water.

Calibration

Trichloroacetic acid (4%) is added to 0.0, 0.5, 1.0, 2.0, 3.0, 4.0, 6.0, and 8.0 ml of the 0.02% ascorbic acid solution and 1.0, 1.5, and 2.0 ml of the 0.2% ascorbic acid solution to reach a final volume of 8.0 ml. Then 100 mg charcoal is added to each sample and thoroughly mixed by shaking for 1 min. After 5 min the solutions are filtered. An aliquot of 0.1 ml of the 6% thiourea solution is added to 2.0 ml of the filtrate followed by 0.5 ml dinitrophenylhydrazine solution. The mixture is shaken and heated for 45 min at 57°C in a water bath. The solutions are placed in an ice-cold water bath and with further cooling 2.5 ml of the 85% sulfuric acid is added. The calibration curve is established at a wavelength of 540 µm using the solutions without ascorbic acid as blank.

Preparation of the Adrenals

Both adrenals are homogenized in glass tubes containing 200 mg purified sand and 8.0 ml of 4% trichloroacetic acid. The reagents are added as described for the calibration curve.

EVALUATION

The potency ratio including confidence limits is calculated with the 3+3-point assay.

MODIFICATIONS OF THE METHOD

The original method, as described by Sayers et al. (1948), used intravenous administration of ACTH and the difference of ascorbic acid in the left adrenal before injection and the right adrenal 1 h after injection as endpoint. Different values of the activity of synthetic peptides versus the International Standard resulted from different ways of administration (Vogel 1965).

The ascorbic acid depletion test can also be performed in dexamethasone-blocked rats. However, different potency ratios of synthetic corticotropin analogs have been found than in hypophysectomized rats (Vogel 1969a). The difference most likely depends on the dexamethasone blocking dose.

Other authors, including British Pharmacopoeia (1988) and Deutsches Arzneibuch (1986), use the 2,6-dichlorophenol-indophenol method for determination of ascorbic acid.

The glands are homogenized in 2.5% metaphosphoric acid with the addition of a small quantity of washed sand. With additional 2.5% metaphosphoric acid a final volume of 10 ml is reached. Then 5 ml of the filtrate is added to 5 ml indophenol acetate solution, and the absorbance of the mixture is read immediately in a photometer with a 520 µm filter. The indophenol acetate solution is prepared by dissolving 15 mg of 2,6-dichlorophenol-indophenol in 500 ml distilled water and dissolving 22.65 g sodium acetate·$3H_2O$ in 500 ml distilled water and mixing equal volumes.

A cytochemical bioassay of corticotropin was described by Chayen et al. (1976).

REFERENCES AND FURTHER READING

Bangham DR, National Institute for Medical Research, London (1962) The third international standard for corticotropin and an international working standard for corticotropin. Acta Endocrinol 40:552–554

British Pharmacopoeia (1988) Vol II. HMSO, London, pp A166–167

Chayen J, Daly JR, Loveridge N, Bitensky L (1976) The cytochemical bioassay of hormones. Recent Prog Horm Res 32:33–79

Deutsches Arzneibuch (1986) 9. Ausgabe, V.2.2.2. Deutscher Apotheker, Stuttgart, p 49

Fisher JD (1962) Adrenocorticotropin. In: Dorfman RI (ed) Methods in hormone research, Vol II. Academic Press, New York, pp 641–669

Geiger R, Sturm K, Vogel G, Siedel W (1964) Synthetische Analoge des Corticotropins. Zur Bedeutung der aminoterminalen Sequenz Ser-Tyr-Ser für die adrenocorticotrope Wirkung. Z Naturforsch 19b:858–860

Inouye K, Otsuka H (1987) ACTH: structure–function relationship. In: Li CH (ed) Hormonal proteins and peptides, Vol XIII. Academic Press, New York, pp 1–29

Rerup C (1957) The subcutaneous assay of corticotrophin A. Acta Endocrinol 25:17–32

Rerup C (1958) The subcutaneous assay of corticotrophin A. II. The replacement of gelatine by saline. Acta Endocrinol 28:300–310

Roe JH, Kuether CA (1943) The determination of ascorbic acid in whole blood and urine through the 2,4-dinitrophenylhydrazine derivative of dehydroascorbinic acid. J Biol Chem 147:399–407

Sayers MA, Sayers G, Woodbury LA (1948) The assay of adreno-corticotropic hormone by the adrenal ascorbic acid-depletion method. Endocrinology 42:379–393

Schuler W, Schär B, Desaulles P (1963) Zur Pharmakologie eines ACTH-wirksamen, vollsynthetischen Polypeptids, des β^{1}–^{24}-Corticotropins, Ciba 30920-Ba, Synacthen. Schweiz Med Wschr 93:1027–1030

The United State Pharmacopeia USP 23 (1995) Corticotropin injection. The United States Pharmacopeial Convention, Rockville, Md., pp 426–428

Vogel HG (1965) Evaluation of synthetic peptides with ACTH-activity. Acta Endocrinol Suppl 100:34

Vogel HG (1969a) Tierexperimentelle Untersuchungen über synthetische Peptide mit Corticotropinaktivität. A: Vergleich mit dem III. Internationalen Standard für Corticotropin. Arzneimittelforschung 19:20–24

Vogel HG (1969b) Tierexperimentelle Untersuchungen über synthetische Peptide mit Corticotropinaktivität. B: Prüfung einer Depot-Zubereitung von $\beta^{1\text{-}23}$-Corticotropin-23-amidacetat. Arzneimittelforschung 19:25–27

N.7.4.2 Corticosterone Blood Levels in Dexamethasone-Blocked Rats

PURPOSE AND RATIONALE

Corticotropin activity can be measured by the increase of corticosterone in venous blood of hypophysectomized rats (no longer required) or dexamethasone-blocked rats. The test can be used to measure time–response curves of corticotropin analogs or depot preparations (Vogel 1969a, 1969b). The sensitivity can be increased by determining corticosterone in adrenal venous blood after cannulation of the adrenal vein (Retiene et al. 1962).

PROCEDURE

Male Sprague-Dawley rats weighing 150–200 are injected subcutaneously 24 h and 1 h prior to subcutaneous injection of the ACTH preparation or the standard with 5 mg/kg dexamethasone in oily solution. Eight rats are used for each dose of test preparation or standard. At increasing time intervals after ACTH injection, the rats are anesthetized with 60 mg/kg pentobarbital i.p. and blood is withdrawn by venipuncture (alternatively by retro-orbital puncture). Next, 1 ml plasma is diluted with 2 ml distilled water and extracted (washed) with 5 ml petrol ether to remove the lipids. The petrol ether is discarded and 2 ml of the water layer is extracted twice with 5 ml methylene chloride by vigorous shaking for 15 min. The methylene chloride phase is separated by centrifugation. Both methylene chloride extracts are unified and shaken with 1 ml ice-cold 0.1 N NaOH. The water phase is immediately removed and the methylene chloride extracts dried by addition of dry sodium sulfate. A 5-ml aliquot of the methylene chloride extract is mixed with 5 ml of the fluorescence reagent (7 parts concentrated sulfuric acid, 3 parts 96% ethanol, v/v). After vigorous shaking, the methylene chloride phase is removed and fluorescence is measured with primary filters of 436 µm and secondary filters of 530–545 µm. For calibration, concentrations of 0, 20, 50, 100, and 250 µg/ml corticosterone are treated identically and measured in each assay.

EVALUATION

Using three doses of test compound and standard, potency ratios with confidence limits can be determined for each time interval with the 3+3-point assay giving evidence for the duration of action (Vogel 1969a, 1969b).

MODIFICATIONS OF THE METHOD

Pekkarinen (1965) used fluorometric corticosteroid determinations in guinea pigs resulting in highly deviating activity ratios of synthetic and commercial corticotrophins as compared with the international working standard of ACTH.

The contemporary method for the determination of the corticosterone concentration in serum is radioim-

munoassay, requiring much smaller blood samples and reducing the stress to the animals very markedly.

REFERENCES AND FURTHER READING

Fisher JD (1962) Adrenocorticotropin. In: Dorfman RI (ed) Methods in hormone research, Vol II. Academic Press, New York, pp 641–669

Pekkarinen A (1965) Bioassay of corticotrophin preparations with the international working standard on living guinea pigs. Acta Endocrinol Suppl 100:35

Retiene K, Ditschuneit H, Fischer M, Kopp K, Pfeiffer EF (1962) Corticotropin-Bestimmung anhand des Corticosteron-Anstieges im Nebennieren-Venenblut hypophysektomierter Ratten. Vergleich von Dexamethasonblockade und Hypophysektomie. Acta Endocrinol 41:211–218

Sandow J, Geiger R, Vogel HG (1977) Pharmacological effects of a short chain ACTH-analogue. Naunyn-Schmiedebergs Arch Pharmacol 297 [Suppl II]:162

Schuler W, Schär B, Desaulles P (1963) Zur Pharmakologie eines ACTH-wirksamen, vollsynthetischen Polypeptids, des β^{1}–^{24}-Corticotropins, Ciba 30920-Ba, Synacthen. Schweiz Med Wschr 93:1027–1030

Staehelin M, Barthe P, Desaulles P (1965) On the mechanism of the adrenal gland response to adrenocorticotropic hormone in hypophysectomized rats. Acta Endocrinol 50:55–64

Vogel HG (1965) Evaluation of synthetic peptides with ACTH-activity. Acta Endocrinol Suppl 100:34

Vogel HG (1969a) Tierexperimentelle Untersuchungen über synthetische Peptide mit Corticotropinaktivität. A: Vergleich mit dem III. Internationalen Standard für Corticotropin. Arzneimittelforschung 19:20–24

Vogel HG (1969b) Tierexperimentelle Untersuchungen über synthetische Peptide mit Corticotropinaktivität. B: Prüfung einer Depot-Zubereitung von $\beta^{1\text{-}23}$-Corticotropin-23-amidacetat. Arzneimittelforschung 19:25–27

N.7.4.3 In Vitro Corticosteroid Release

PURPOSE AND RATIONALE

An *in vitro* assay of corticotropin was described by Saffran and Schally (1955). This test has been modified by Van der Vies (1957) and subsequently used by several authors (Staehelin et al. 1965; Vogel 1969a, 1969b).

PROCEDURE

Solutions

"Double Ringer" solution is prepared as follows:

4.50%	(w/v) sodium chloride	200.0 ml
5.75%	potassium chloride	8.0 ml
6.10%	calcium chloride	6.0 ml
10.55%	monopotassium phosphate	2.0 ml
19.10%	magnesium sulfate	2.0 ml
	double distilled water up to	545.0 ml

Final solution:

54.0 ml	double Ringer
26.0 ml	1% glucose solution (freshly prepared)
29.0 ml	double distilled water
21.0 ml	1.3% $NaHCO_3$ solution which has been gassed with carbon dioxide at room temperature for 1 h

The final solution is gassed with a mixture of 95% O_2 and 5% CO_2 for 10 min.

Preparation of Adrenals

Male Sprague-Dawley rats ($n = 20$) weighing 150–200 g are anesthetized with 50 mg/kg pentobarbital sodium i.p. applying as little handling stress as possible. The adrenals are removed and freed of connective tissue, taking care that the adrenals are not damaged. Each adrenal is carefully cut into four quarters with fine scissors. The eight quarters from each rat are randomly distributed to 20 preweighed incubation vessels filled with 1.5 ml of final solution. The flasks are mounted on Warburg manometers or placed into a suitable shaking water bath and are gassed under continuous shaking for 1 h with a mixture of 95% O_2 and 5% CO_2 at 38°C (= preincubation period).

The flasks are removed from the bath at the end of the preincubation period. The medium is aspirated as much as possible by means of a small tube attached via a collection bottle to the vacuum line. A 1.4-ml aliquot of fresh medium is added to each flask.

To five vessels each of the following solutions are added:

- 10.0 mU/0.1 ml ACTH standard
- 50.0 mU/0.1 ml ACTH standard
- 10.0 mU/0.1 ml test preparation
- 50.0 mU/0.1 ml test preparation
- 50.0 mU/0.1 ml medium (control)

The vessels are again incubated and gassed with a mixture of 95% O_2 and 5% CO_2 at 38°C under continuous shaking for 2 h. Then 1-ml aliquots of the medium in each vessel are transferred to carefully cleaned glass-stoppered tubes containing 2 ml methylene chloride. The tubes are vigorously shaken for 1 min and centrifuged for 5 min. The methylene chloride phase is transferred with a long needle and a syringe to a quartz micro-cuvette and readings are taken at 225, 240, and 255 µm.

Dry weight of the adrenals is determined by heating the incubations vessels to 150°C for 2 h.

EVALUATION

Extinction values are calculated for the maximum of absorption (Allen 1950) according to the formula:

$$E = E_{240} - \frac{E_{225} + E_{255}}{2}$$

The potency ratios are calculated with the 2+2-point assay.

MODIFICATIONS OF THE METHOD

Saffran et al. (1971) described a flow-through system for the study of adrenocortical function by rat tissue *in vitro*, in which the fluorometric measure of corticosterone is completely automated.

Corticosterone is now conveniently determined by RIA or by a high-performance liquid chromatography (HPLC) method.

REFERENCES AND FURTHER READING

Allen WM (1950) A simple method for analyzing complicated absorption curves, of use in the colorimetric determination of urinary steroids. J Clin Endocrinol 10:71–83

Bangham DR, Musset MV, Stack-Dunne MP (1962) The third international standard for corticotrophin and an international working standard for corticotrophin. Acta Endocrinol 40:552–554

Buckingham JC, Cover PO, Gillies GE (1991) Biological and radioimmunometric assay methods for the determination of corticotrophin. In: Greenstein B (ed) Neuroendocrine research methods, Vol 2. Harwood, Chur, pp 601–613

Fisher JD (1962) Adrenocorticotropin. In: Dorfman RI (ed) Methods in hormone research, Vol II. Academic Press, New York, pp 641–669

Rerup C (1958) The subcutaneous assay of corticotrophin A. II. The replacement of gelatine by saline. Acta Endocrinol 28:300–310

Saffran M, Schally AV (1955) *In vitro* bioassay of corticotropin: modification and statistical treatment. Endocrinology 56:512–532

Saffran M, Matthews EK, Pearlmutter F (1971) Analysis of the response to ACTH by rat adrenal in a flowing system. Recent Prog Horm Res 27:607–630

Schuler W, Schär B, Desaulles P (1963) Zur Pharmakologie eines ACTH-wirksamen, vollsynthetischen Polypeptids, des $\beta^{1\text{-}24}$-Corticotropins, Ciba 30920-Ba, Synacthen. Schweiz Med Wschr 93:1027–1030

Staehelin M, Barthe P, Desaulles P (1965) On the mechanism of the adrenal gland response to adrenocorticotropic hormone in hypophysectomized rats. Acta Endocrinol 50:55–64

Tesser GI, Schwyzer R (1966) Synthese des 17,18-Diornithin-β-corticotropin-(1-24)-tetracosapeptides, eines biologisch aktiven Analogons des adrenocorticotropen Hormones. Helvet Chim Acta 49:1013–1022

Van der Vies (1957) Experience with an assay of adrenocorticotropic hormone based on the steroid output of rat adrenals *in vitro*. Acta Physiol Pharmacol Neerl 5:361–384

Vogel HG (1969a) Tierexperimentelle Untersuchungen über synthetische Peptide mit Corticotropinaktivität. A: Vergleich mit dem III. Internationalen Standard für Corticotropin. Arzneimittelforschung 19:20–24

Vogel HG (1969b) Tierexperimentelle Untersuchungen über synthetische Peptide mit Corticotropinaktivität. B: Prüfung einer Depot-Zubereitung von $\beta^{1\text{-}23}$-Corticotropin-23-amidacetat. Arzneimittelforschung 19:25–27

N.7.4.4 Thymus Involution

PURPOSE AND RATIONALE

This is a classical indirect bioassay based on the steroid response of the target organ and its effect. Administration of corticotropin decreases thymus weight (due to inducing corticosterone secretion), followed by an increase of adrenal weight (Hayashida and Li 1952; Thing 1953; Thompson and Fisher 1953; Fischer 1962). Young rats respond with an involution of the thymus gland to graded doses of corticotropin (Rerup 1958). A similar assay is used for adrenal steroids.

PROCEDURE

Sprague-Dawley or Wistar rats of either sex, 7–10 days of age, weighing 10–15 g are used. Littermates are preferred. The animals are distributed at random to three groups of the standard and three to five groups of the unknown sample. The ACTH standard or test compounds are injected at different doses once daily subcutaneously for 3 days. Twenty-four hours after the last injection, the animals are sacrificed, the thymus dissected out and weighed to the nearest 0.1 mg. The response is expressed as the average of the individual values for each dose level.

EVALUATION

Dose–response curves are established and potency ratios calculated using a 3+3-point assay.

MODIFICATIONS OF THE METHOD

The numerical sensitivity of the assay can be increased using the quotient between the increase of the weight of the adrenals and the decrease of the weight of the thymus gland (Hohlweg et al. 1960) (ratio adrenal weight increase/thymus weight decrease).

Male Wistar rats at an age of about 3 weeks weighing 18–22 g are injected three times daily at 4-h intervals over 3 days with the test preparation or the standard dissolved in 10% gelatin solution. The animals are sacrificed 18 h after the last injection and the adrenals and the thymus gland removed and weighed.

The ratio of adrenal weight to thymus weight provides a steep dose–response curve.

REFERENCES AND FURTHER READING

Fisher JD (1962) Adrenocorticotropin. In: Dorfman RI (ed) Methods in hormone research, Vol II. Academic Press, New York, pp 641–669

Hayashida T, Li CH (1952) Enhancement of adrenocorticotropic hormone activity by alum in normal 21-day old rats. Endocrinology 50:187–191

Hohlweg W, Laschet U, Dörner G, Daume E (1960) Der NTQ-Test, eine einfache Testierungsmethode für Corticotropin- und Depot-Corticotropin-Präparate. Acta Endocrinol 35:501–507

Rerup C (1958) The thymus involution assay of corticotrophin A. Acta Endocrinol 29:93–101

Thing E (1953) The thymus involution test for ACTH. Acta Endocrinol 13:343–352

Thompson RE, Fisher JD (1953) Correlation of preparative history and method of assay of corticotropin with clinical potency. Endocrinology 52:496–509

N.7.4.5 Receptor Binding Assay for ACTH

PURPOSE AND RATIONALE

As for other hormones, receptors have been used as the test preparations for comparison of the binding affinities of adrenocorticotropin peptides using a cloned mouse adrenocorticotropin receptor expressed in a stably transfected HeLa cell line (Kapas et al. 1996). Such assays measure the initial membrane binding but not strictly the biological activation, e. g., of adrenal cells or melanocytes.

PROCEDURE

Hela cells are seeded into 12-well culture plates at a density of 10^6 cells/well. On the 2nd day of culture, the cells are washed as follows: 2 × in 1 ml of ice-cold 0.9% NaCl, 1 × in 1 ml of ice-cold glycine (50 mM glycine, 100 mM NaCl, pH 3.0) for 5 min, 2 × in 0.5 ml of ice-cold 0.9% NaCl. Cells are then incubated for 60 min at 20°C with increasing concentrations of nonradioactive ACTH or various ACTH analogs and the reactions initiated on the addition of [^{125}I-iodotyrosyl^{23}]ACTH[1-39] (2000 Ci/mmol; final concentration 0.1 pmol/l) in DMEM. At the end of the incubation, the medium is removed and the cells washed three times with 0.9% NaCl and then dissolved in 0.5 M NaOH/0.4% sodium deoxycholate. Each point is determined in triplicate, and the radioactivity is measured using a gamma-counter. Specific binding is determined by subtracting from the total binding the radioactivity associated with cells in the presence of 10^{-5} M nonradioactive ACTH.

EVALUATION

Binding parameters are determined using a computer-assisted calculation, e. g., the LIGAND program (Munson and Rodbard 1980).

MODIFICATIONS OF THE METHOD

Penhoat et al. (1993) reported the identification and characterization of corticotropin receptors in bovine and human adrenals by covalent cross-linking of radiolabeled ACTH with the bifunctional cross-linking agent disuccinimidyl suberate to cultured bovine adrenal fasciculata reticular cells and to crude plasma membrane fractions prepared from both human and bovine adrenals.

Lebrethon et al. (1994) and Penhoat et al. (1995) studied the regulation of ACTH receptor mRNA and binding sites by ACTH and angiotensin II in cultured human and bovine adrenal fasciculata cells.

Picard-Hagen et al. (1997) found that glucocorticoids enhance corticotropin receptor mRNA levels in ovine adrenocortical cells.

Zavyalov et al. (1995) described the receptor binding properties of peptides corresponding to the ACTH-like sequence of human pro-interleukin-1$_\alpha$.

Naville et al. (1996, 1997) developed a stable expression model in order to characterize the human ACTH receptor by binding studies and functional coupling to adenylate cyclase.

Schioth et al. (1996) described the pharmacological distinction of the ACTH receptor from other melanocortin receptors in the mouse adrenocortical cell line Y1.

Moreover, melanocortin receptors do not have a binding epitope for ACTH beyond the sequence of alpha-melanocyte-stimulating hormone (Schioth et al. 1997).

CRITICAL ASSESSMENT OF THE METHOD

Binding affinities are determined for structure–activity studies, and the results need to be assessed and confirmed for biological relevance using an assay for the biological response of tissues *in vitro*, and/or the biological effects in animals. These methods are also useful for assessing the sensitivity of hormone-responsive tissues from animals previously treated (adaptive response).

REFERENCES AND FURTHER READING

Kapas S, Cammas FM, Hinson JP, Clark AJL (1996) Agonistic and receptor binding properties of adrenocorticotropin peptides using the cloned mouse adrenocorticotropin re-

ceptor expressed in a stably transfected HeLa cell line. Endocrinology 137:32901–3294
Lebrethon MC, Naville D, Begeot M, Saez JM (1994) Regulation of corticotropin receptor number and messenger RNA in cultured human adrenocortical cells by corticotropin and angiotensin II. J Clin Invest 93:1828–1833
Munson PJ, Rodbard D (1980) Ligand, a versatile computerised approach for characterization of ligand binding systems. Anal Biochem 107:220–239
Naville D, Penhoat A,. Barjhoux L, Jaillard C, Fontanay S, Saez J, Durand P, Begeot M (1996) Characterization of the human ACTH receptor gene and *in vitro* expression. Endocr Res 22:337–348
Naville D, Barjhoux L, Jaillard C, Saez JM, Durand P, Begeot M (1997) Stable expression of normal and mutant human ACTH receptor. Study of ACTH binding and coupling to adenylate cyclase. Mol Cell Endocrinol 129:83–90
Penhoat A, Jaillard C, Saez M (1993) Identification and characterization of corticotropin receptors in bovine and human adrenals. J Steroid Biochem Mol Biol 44:21–27
Penhoat A, Lebrethon MC, Begeot M, Saez JM (1995) Regulation of ACTH receptor mRNA and binding sites by ACTH and angiotensin II in cultured human and bovine adrenal fasciculata cells. Endocr Res 21:157–168
Picard-Hagen N, Penhoat A, Hue D, Jaillard C, Durand P (1997) Glucocorticoids enhance corticotropin receptor mRNA levels in ovine adrenocortical cells. J Mol Endocrinol 19:29–36
Schioth HB, Chhajlani V, Muceniece R, Klusa V, Wikberg JES (1996) Major pharmacological distinction of the ACTH receptor from other melanocortin receptors. Life Sci 59:797–801
Schioth HB, Muceniece R, Larsson M, Wikberg JES (1997) The melanocortin 1, 3, 4 or 5 receptors do not have a binding epitope for ACTH beyond the sequence of alpha-MSH. J Endocrinol 155:73–78
Zavyalov VP, Maiorov VA, Safonova NG, Navolotskaya EV, Volodina EY, Abromov VM (1995) Receptor binding properties of the peptides corresponding to the ACTH-like sequence of human pro-Interleukin-1$_\alpha$. Immunol Lett 46:125–128

N.7.5
Thyrotropin (TSH)

N.7.5.1
General Considerations

The thyroid-stimulating hormone (TSH) can be determined by bioassays (effects on the thyroid gland and secretion of thyroid hormones) and its concentration can be measured by immunoassays, as with other polypeptide hormones (Utiger 1979; Meinhold et al. 1994; Spencer 1994). TSH receptors have been identified and their functional regulation has been described (Vassart and Dumontl 1992).

Large-scale synthesis of recombinant human thyrotropin has been reported (Cole et al. 1993; Hussain et al. 1996). The role of the thyrotropin receptor has been reviewed by Vassart and Dumont (1992). Castagiola et al. (1992) described a binding assay for thyrotropin receptor autoantibodies using the recombinant receptor protein. A brain-derived TSH receptor has been cloned and expressed (Bockmann et al. 1997), in accordance with the developmental effects of TSH in the fetus and newborn. Binding characteristics of antibodies to the TSH receptor were described by Oda et al. (1998).

REFERENCES AND FURTHER READING

Bockmann J, Winter C, Wittkowski W, Kreutz MR, Böckers TM (1997) Cloning and expression of a brain-derived TSH receptor. Biochem Biophys Res Commun 238:173–1780
Castagiola A, Swillens S, Niccoli P, Dumont JE, Vassart G, Ludgate M (1992) Binding assay for thyrotropin receptor autoantibodies using the recombinant receptor protein. J Clin Endocrinol Metab 75:1540–1544
Cole ES, Lee K, Lauziere K et al (1993) Recombinant human thyroid stimulating hormone: development of a biotechnology product for detection of metastatic lesions of thyroid carcinoma. Biotechnology 11:1014–1024
Hussain A, Zimmerman CA, Boose JA, Froulich J, Richardson A, Horowitz RS, Collins MT, Lash RW (1996) Large scale synthesis of recombinant human thyrotropin using methotrexate amplification: chromatographic, immunological, and biological characterization. J Clin Endocrinol Metab 81:1184–1188
Meinhold H, Altmann R, Bogner U, Finke R, Schleusener H (1994) Evaluation of various immunometric TSH assays. Exp Clin Endocrinol 102:23–26
Oda Y, Sanders J, Roberts S, Maruyama M, Kato R, Perez M, Petersen VB, Wedlock N, Furmaniak J, Smith RB (1998) Binding characteristics of antibodies to the TSH receptor. J Mol Endocrinol 20:233–244
Spencer CE (1994) Further developments in TSH technology. Exp Clin Endocrinol 102:12–22
Utiger RD (1979) Thyrotropin. In: Jaffe BM, Behrman HR (eds) Methods of hormone radioimmunoassay. Academic Press, New York, pp 315–325
Vassart G, Dumont JE (1992) The thyrotropin receptor and the regulation of thyrocyte function and growth. Endocr Rev 13:569–611

N.7.5.2
Thyroid Histology

PURPOSE AND RATIONALE

Hypophysectomy results in atrophy of the thyroid gland, which is reversed by administration of thyrotropin. In the thyroid of normal young guinea pigs (Junkmann and Schoeller 1932; McGinty and McCullough 1936) or chicks (Jones 1939) characteristic histological changes are observed after administration of thyrotropin, associated with an increase of thyroid weight (goitrogenic response). In classical bioassays, these findings were the basis for standardizing by biological units (Turner 1950, 1969).

PROCEDURE

Male guinea pigs weighing 180–200 g are injected once daily on 4 days successively. Thyroids are re-

moved on the 6th day, weighed, and embedded for histological examination. Administration of thyrotropic hormone is followed by colloid resorption, increased vascularity, and increased epithelial cell height. Several regions of the thyroid are examined histologically. Alternatively, computer-assisted morphometry may be used. Rating scores are defined between +1 and +4.

EVALUATION

The rating scores are averaged and compared between test preparation and standard.

REFERENCES AND FURTHER READING

Jones MS (1939) A study of thyrotropic hormone in clinical states. Endocrinology 24:665–671

Junkmann K, Schoeller W (1932) Über das thyreotrope Hormon des Hypophysenvorderlappens. Klin Wschr 11:1176–1177

McGinty DA, McCullough NB (1936) Thyrotropic hormone in non-pituitary tissue. Proc Soc Exp Biol Med 35:24–26

Turner CW (1950) Thyrotropic hormone. In: Emmens CW (ed) Hormone assay. Academic Press, New York. pp 215–235

Turner CW (1969) Thyrotropic hormone. In: Dorfman RI (ed) Methods in hormone research, Vol IIA. Academic Press, New York, pp 515–565

N.7.5.3 Iodine Uptake

PURPOSE AND RATIONALE

This is a bioassay for thyroid activation related to the initial step of thyroid-stimulating hormone (TSH) action (Turner 1950, 1962, 1969). The uptake of iodine (trapping) as well as the release of the newly formed iodinated thyroid hormones is under the control of thyrotropin (and in animal assays, under control of hypothalamic thyrotropin-releasing hormone, TRH). As a consequence, the uptake of ^{131}I and the release of ^{131}I-labeled thyroxin are increased after administration of TSH. A method using ^{131}I release in mice has been described by McKenzie (1958) and modified by Sakiz and Guillemin (1964).

PROCEDURE

Female mice weighing 10–15 g are kept in a temperature-controlled room and fed a low-iodine diet for 10 days. They are then injected intraperitoneally with 1.5 µC ^{131}I, followed 5 h later by 10 µg L-T_4 subcutaneously. After 24 h they receive a second injection of 5 µg L-T_4 and are used 48 h after the last injection. Under ether anesthesia 0.25 ml blood is withdrawn from the jugular vein into a heparinized syringe. Various doses of the test preparation or standard TSH are injected by the same route in 0.3 ml volume. Two hours later, again under ether anesthesia, a second 0.25-ml sample is taken, and the radioactivity measured. The increase of radioactivity in the blood samples is dependent on the dose of TSH.

EVALUATION

A 4-point assay technique is used with six observations for each of two doses of the standard and of the unknown preparation.

MODIFICATIONS OF THE METHOD

Depletion of ^{131}I from the thyroids of chicken was used as the endpoint for a TSH assay by Bates and Cornfield (1957).

REFERENCES AND FURTHER READING

Bates RW, Cornfield J (1957) An improved assay method for thyrotropin using depletion of I^{131} from the thyroid of day-old chicks. Endocrinology 60:225–238

McKenzie JM (1958) The bioassay of thyrotropin in serum. Endocrinology 63:372–382

Sakiz E, Guillemin R (1964) On a method for calculation and analysis of results in the McKenzie assay for thyrotropin. Proc Soc Exp Biol Med 115:856–860

Turner CW (1950) Thyrotropic hormone. In: Emmens CW (ed) Hormone assay. Academic Press, New York, pp 215–235

Turner CW (1962) Thyrotropic hormone. In: In: Dorfman RI (ed) Methods in hormone research, Vol II. Academic Press, New York, pp 617–639

Turner CW (1969) Thyrotropic hormone. In: In: Dorfman RI (ed) Methods in hormone research, Vol IIA. Academic Press, New York, pp 515–565

N.7.5.4 TSH Bioassay Based on cAMP Accumulation in CHO Cells

PURPOSE AND RATIONALE

Indirect cell assays measure the activation of protein kinase A (PKA) through adenylcyclase. Several cell assays for thyrotropin using cultured FRTL-5 cells have been described (Vitti et al. 1986; Nissim et al. 1987; Horimoto et al. 1989). Persani et al. (1993) reported a cell assay for human thyrotropin using measurement of cAMP accumulation on Chinese hamster ovary (CHO) cells transfected with the recombinant TSH receptor.

PROCEDURE

Cells of the CHO-R strain JP-09 are cultured in Petri dishes in RPMI-1640 medium supplemented with 1 mM glutamine and 10% fetal calf serum. In these cells TSH biological activity is evaluated by measuring cAMP production. Cells are harvested from Petri dishes using a Trypsin-EGTA mixture and seeded in 96-well plates (10,000 cells/well). Cells are fed with fresh RPMI-1640 medium 24 h after seeding.

The assay is run after 48 h. After washing, 100 µl of TSH standard or samples diluted in hypotonic or isotonic medium containing 0.4% BSA, 10 mM HEPES, and 0.5 mM isobutylmethylxanthine, are incubated for 2 h at 37°C. Three different dilutions of immunoconcentrated TSH are bioassayed in triplicate, as are TSH preparations. cAMP is measured in nonacetylated samples by an RIA method using a commercial polyclonal anti-cAMP antibody (Vitti et al. 1986).

EVALUATION

Dose–response curves or single-point comparisons are used for potency or activity estimates.

REFERENCES AND FURTHER READING

Horimoto M, Nishikawa M, Yoshikawa N, Inada N (1989) A sensitive and practical bioassay for thyrotropin using cultured FRTL-5 cells: assessment of bioactivity for serum TSH in patients with chronic renal failure. Acta Endocrinol 121:191–196

Nissim M, Lee KO, Petrick PA, Dahlberg PA, Weintraub BD (1987) A sensitive thyrotropin (TSH) bioassay on iodide uptake in rat FRTL-5 thyroid cells: comparison with the adenosine 3′,5′-monophosphate response to human serum TSH and enzymatically deglycosylated bovine and human TSH. Endocrinology 121:1278–1287

Persani L, Tonacchera M, Beck-Peccoz P, Vitti P, Mammoli C, Chiovato L, Elisei R, Faglia G, Ludgate M, Vassart G, Pinchera A (1993) Measurement of cAMP accumulation on Chinese hamster ovary cells transfected with the recombinant human TSH receptor (CHO-R): a new bioassay for human thyrotropin. J Endocrin Invest 16:511–519

Vitti P, Chiovato L, Ceccarelli P, Lombardi A, Novaes M Jr, Fenci GF, Pinchera A (1986) Thyroid-stimulating antibody mimics thyrotropin in its ability to desensitize the adenosine 3′,5′-monophosphate response to acute stimulation in continuously cultured rat thyroid cells (FRT-L5). J Clin Endocrinol Metab 63:454–458

N.7.6 Hormones Related to TSH

N.7.6.1 General Considerations

These hormonal factors are now characterized by molecular cloning. One of the characteristic symptoms of thyroid activation (Graves' or Basedow disease) is exophthalmos. A dissociation of the exophthalmos-producing activity from the TSH activity has been found (Dobyns and Steelman 1953). Moreover, time–response curves for TSH activity from the serum of patients with hyperthyroidism differed from those of the standard TSH, giving evidence for the presence of an abnormal factor, long-acting thyroid-stimulating factor (LATS). Bioassays for these factors have been developed (Ludgate 1999). TSH receptor stimulating antibodies have also been identified and suitable animal models have been investigated (diCerbo and Corda 1999; DeFelice et al. 2004).

REFERENCES AND FURTHER READING

De Felice M, Postiglione MP, Di Lauro R (2004) Minireview: thyrotropin receptor signaling in development and differentiation of the thyroid gland: insights from mouse models and human diseases. Endocrinology 145(9):4062–4027

Di Cerbo A, Corda D (1999) Signaling pathways involved in thyroid hyperfunction and growth in Graves' disease. Biochimie 81(5):415–424

Dobyns BM, Steelman SL (1953) The thyroid stimulating hormone of the anterior pituitary as distinct from the exophthalmos producing substance. Endocrinology 52:705–711

Ludgate M (1999) Animal model of thyroid-associated orbitopathy. Exp Clin Endocrinol Diabetes 107 [Suppl 5]:S158–S159

N.7.6.2 Assay of Exophthalmos-Producing Substance (EPS) in Fishes

PURPOSE AND RATIONALE

Some TSH fractions were reported to produce more exophthalmos than others (Dobyns and Steelman 1953). A second fraction containing exophthalmos-producing substance (EPS) could be separated (Brunish et al. 1962). The activity of this substance was demonstrated in fishes.

PROCEDURE

Fundulus heteroclitus Linn., the common Atlantic minnow, has been found to be the suitable animal model (Albert 1945; Sobonya and Dobyns 1967; Turner 1969). Other fish species, such as *Carassius auratus* (the common gold fish; Haynie et al. 1962) and *Cyprinus carpio* (der Kinderen et al. 1960), were also used but gave less reliable results (Sobonya and Dobyns 1967). *Fundulus heteroclitus* Linn., common Atlantic minnows, 8–10 cm in length, are kept in a tank of running tap water at 10°C in winter and 18°C in summer. Before treatment the intercorneal distance is measured with Vernier calipers to the nearest of 0.1 mm. The test compound and the standard are injected intraperitoneally at various, but at least two, doses. To avoid loss of fluids by the intraperitoneal injection route, the needle is inserted into the cloaca, through the rectum, over the pelvic girdle, and into the peritoneal cavity for a distance of about 1.2 cm. The volume of fluid injected should be 0.1–0.5 ml. The effect of the hormone is to cause protrusion of the eyeballs. The intercorneal distance is measured again after 24, 48, and 72 h. The increase in proptosis is expressed

as a percentage of the intercorneal distance found at the beginning of the test.

EVALUATION

The increases of intercorneal distance after each dose are averaged and activity ratios with confidence limits calculated from the 2+2-points assay.

REFERENCES AND FURTHER READING

Albert A (1945) The biochemistry of the thyrotropic hormone. Ann NY Acad Sci 50:466–490

Brunish R, Hayashi K, Hayashi J (1962) Purification and properties of exophthalmos-producing substance. Arch Biochem Biophys 98:135–141

der Kinderen PJ, Houtstra-Lanz M, Schwarz F (1960) Exophthalmos-producing substance in human serum. J Clin Endocrin Metab 20:712–718

Dobyns BM, Steelman SL (1953) The thyroid stimulating hormone of the anterior pituitary as distinct from the exophthalmos producing substance. Endocrinology 52:705–711

Haynie TP, Winzler RJ, Matovinovic J, Carr EA Jr, Beierwaltes WH (1962) Thyroid-stimulating and exophthalmos-producing activity of biochemically altered thyrotropin. Endocrinology 71:782–789

Sobonya RE, Dobyns BM (1967) Comparisons of the responses of native Ohio fish and two species of salt-water Fundulus to the exophthalmos-producing substance (EPS) of the pituitary gland. Endocrinology 80:1090–1096

N.7.6.3 Assay of Long-Acting Thyroid-Stimulating Factor (LATS) in Mice

PURPOSE AND RATIONALE

This is a modification of the TSH assay to assess the late onset of action of LATS. In the assay of McKenzie (1958) (see N.7.5.3), mice previously injected with ^{131}I show a maximum increase in serum ^{131}I after an interval of 2–3 h when TSH is administered. In the assay of serum from thyrotoxic patients, Adams (1958) noted that the maximum response in guinea pigs did not occur until after 16 h. The abnormal responses to thyrotoxicosis sera suggested the presence of an additional factor different from TSH.

PROCEDURE

Mice maintained on a low-iodine diet for 10 days are injected with 15 µC ^{125}I and 10 µg Na L-T_4. Four days later, 0.1 ml of blood is obtained by retro-orbital puncture immediately before the injection of the test substance 2 and 9 h later. Radioactivity in the blood is then measured. By definition, radioactivity which is maximal after 2 h is indicative of TSH, whereas LATS causes a maximal increase at 9 h.

EVALUATION

The increases of radioactivity after 2 and 9 h are compared and evaluated by statistical methods.

MODIFICATIONS OF THE ASSAY

Ikeda and Nagataki (1983) and Ikeda et al. (1984) used male DDY mice weighing 15 g. They were fed a low-iodine diet for 14 days and then injected daily with 1 µg of 3,5,3′-triiodothyronine (T_3) s.c. and given T_3 (5 µg/ml) ad libitum in drinking water until sacrifice. From the 5th day of T_3 treatment they were injected i.p. with 0.25 ml of LATS-positive serum for 9 days. Groups of five mice were sacrificed before, 1, 3, 5, 7, and 9 days after the first injection of LATS. Then 1 µCi (0.5 ml) of Na [^{131}I] was administered i.p. 1 h before sacrifice. Thyroid lobes were excised, weighed, and radioactivity was measured by a gamma counter. Immediately before injection of Na [^{131}I], approximately 60 µl of blood was collected from the orbital plexus with heparinized capillary tubes and centrifuged at 12,000 rpm for 3 min. T_4 concentrations in serum were determined by radioimmunoassay.

Ealey et al. (1984, 1985) developed a sensitive cytochemical bioassay for thyroid stimulators, using reference preparations of thyrotropin and LATS. Thyroid stimulators cause changes in lysosomal membrane permeability within the thyroid follicular cells of guinea pigs, which can be monitored by measuring increased intralysosomal enzyme activity (in the case of this assay, naphthylamidase), with a chromogenic substrate leucine-2-naphthylamide, which itself does not readily permeate the lysosomal membrane in unstimulated cells.

REFERENCES AND FURTHER READING

Adams DD (1958) The presence of an abnormal thyroid-stimulating hormone in the serum of some thyrotoxic patients. J Clin Endocrinol Metab 18:699–712

Ealey PA, Marshall NJ, Ekins RP (1984) Further studies on the response of a cytochemical bioassay to thyroid stimulators, using reference preparations of thyrotropin and long acting thyroid stimulator. J Endocrinol Invest 7:25–28

Ealey PA, Valente WA, Ekins RP, Kohn LD, Marshall NJ (1985) Characterization of monoclonal antibodies raised against solubilized thyrotropin receptors in a cytochemical bioassay for thyroid stimulators. Endocrinology 116:124–131

Ikeda H, Nagataki S (1983) Lack of refractoriness to stimulation with long acting thyroid stimulator of thyroid hormone synthesis and thyroid hormone secretion in mice *in vivo*. Acta Endocrinol 102:392–395

Ikeda H, Chiu SC, Kuzuya N, Uchimura H, Nagataki S (1984) Effects of *in vivo* triiodothyronine and long acting thyroid stimulator (LATS) administration on the *in vitro* thyroid cAMP response to thyrotrophin and LATS. Acta Endocrinol 106:193–198

McKenzie JM (1958) The bioassay of thyrotropin in serum. Endocrinology 63:372–382

N.8
Posterior Pituitary Hormones

N.8.0.1
General Considerations

Oxytocin and vasopressin were the first hormones isolated from the posterior pituitary lobe (Dale and Laidlaw 1912; Hogben et al. 1924; Fromherz 1926; Schaumann 1937). Vasopressin has antidiuretic activity and, at higher doses, hypertensive effects as well as endocrine functions (Hedge and Huffman 1987) and effects on the central nervous system (Gash et al. 1987), which are however outside the scope of this chapter. In terms of bioassays, the antidiuretic activity is the main parameter. Many analogs of vasopressin have been synthesized resulting in selective agonists and antagonists (Vogel and Hergott 1963; Allison et al. 1987; Mah and Hofbauer 1987; Manning et al. 1987). Different types of vasopressin receptors have been identified: V_1 (V_{1a}, V_{1b}) and V_2-receptors (Jard et al. 1976, 1986; Fahrenholz et al. 1988; Walker et al. 1988; Burnatowska-Hledin and Spielman 1989). Research on the vasopressin analogs has provided several compounds of clinical utility, and antagonists of vasopressin are now increasingly explored for several indications, including nonpeptide vasopressin antagonists (Mayinger and Hensen 1999; Serradeil-Le Gal et al. 2002; Greenberg and Verbalis 2007; Urban et al. 2007).

The use of bioassays in the evaluation of these vasopressin and oxytocin analogs has been reviewed (Liard 1988; Chan et al. 2000).

Oxytocin receptors have been described in several organs, such as uterus, mammary gland and CNS (Soloff 1976; Hruby and Chow 1990).

The synthesis and development of several orally active, nonpeptide oxytocin antagonists have been reported (Bell et al. 1998; Kuo et al. 1998).

Radioimmunoassays are available for both oxytocin (Kagan and Glick 1978) and vasopressin (Glick and Kagan 1978).

REFERENCES AND FURTHER READING

Allison NL, Albrightson-Winslow CR, Brooks DP, Stassen FL, Huffman WF, Stote RM, Kinter LB (1987) Species heterogeneity and antidiuretic activity of hormone antagonists: what are the predictors? In: Gash DM, Boer GJ (eds) Vasopressin. Principles and properties. Plenum, New York, pp 207–214

Bell IM, Erb JM, Freidinger RM, Gallicchio SN, Guare JP, Guidotti MT, Halpin RA, Hobbs DW, Homnick CF, Kuo MS, Lis EV, Mathre DJ, Michelson SR, Pawluczyk JM, Pettibone DJ, Reiss DR, Vickers S, Williams PD, Woyden CJ (1998) Development of orally active oxytocin antagonists: studies on 1-(1-(4-[1-(2-methyl-1-oxidopyridin-3-ylmethyl)piperidin-4-yloxy]-2-methoxybenzoyl)-4-yl)-1,4-dihydrobenz[d][1,3]oxazin-2-one (L-372,662) and related pyridines. J Med Chem 41:2146–2163

Burnatowska-Hledin MA, Spielman WS (1989) Vasopressin V_1 receptors on the principal cells of the rabbit cortical collecting tubule. J Clin Invest 83:84–89

Chan WY, Wo NC, Stoev ST, Cheng LL, Manning M (2000) Discovery and design of novel and selective vasopressin and oxytocin agonists and antagonists: the role of bioassays. Exp Physiol 85 [Spec No]:7S–18S

Dale H, Laidlaw J (1912) A method for standardising pituitary (infundibular) extracts. J Pharmacol Exp Ther 4:73–95

Fahrenholz F, Kojro E, Jans D (1988) Renal and hepatic vasopressin receptor proteins: identification and strategies for purification. In: Cowley AW Jr, Liard JF, Ausiello DA (eds) Vasopressin: cellular and integrative functions. Raven, New York, pp 27–32

Fromherz K (1926) Bemerkungen zur Auswertung von Hypophysenextrakt am Meerschweinchenuterus. Naunyn-Schmiedebergs Arch Exp Path Pharmakol 113:113–123

Gash DM, Herman JP, Thomas GJ (1987) Vasopressin and animal behavior. In: Gash DM, Boer GJ (eds) Vasopressin. Principles and properties. Plenum, New York, pp 517–547

Glick SM, Kagan A (1978) Vasopressin. In: Jaffe BM, Behrman HR (eds) Methods of hormone radioimmunoassay. Academic Press, New York, pp 341–351

Greenberg A, Verbalis JG (2006) Vasopressin receptor antagonists. Kidney Int. 69(12):21–30

Hedge GA, Huffman LJ (1987) Vasopressin and endocrine function. In: Gash DM, Boer GJ (eds) Vasopressin. Principles and properties. Plenum, New York, pp 435–475

Hogben LT, Schlapp W (1924) Studies on the pituitary. III. The vasomotor activity of pituitary extracts throughout the vertebrate series. Q J Exp Physiol 14:229–258

Hogben LT, Schlapp W, Macdonald AD (1924) Studies on the pituitary IV. Quantitative comparison of pressor activity. Q J Exp Physiol 14:301–318

Hruby VJ, Chow MS (1990) Conformational and structural considerations in oxytocin-receptor binding and biological activity. Annu Rev Pharmacol Toxicol 30:501–534

Jard S, Bockaert J, Rajerison R (1976) Vasopressin receptors. In: Blecher M (ed) Methods in receptor research, Part II. Dekker, New York, pp 667–703

Jard S, Gaillard RC, Guillon G, Marie J, Schoenenberg P, Muller AF, Manning M, Sawyer WH (1986) Vasopressin antagonists allow demonstration of a novel type of vasopressin receptor in the rat adenohypophysis. Mol Pharmacol 30:171–177

Kagan A, Glick SM (1978) Oxytocin. In: Jaffe BM, Behrman HR (eds) Methods of hormone radioimmunoassay. Academic Press, New York, pp 327–339

Kuo MS, Bock MG, Freidinger RM, Guidfotti MT, Lis EV, Pawluczyk JM, Perlow DS, Pettibone DJ, Quigley AG, Reiss DR, Williams PD, Woyden CJ (1998) Nonpeptide oxytocin antagonists: potent, bioavailable analogs of L-371,257 containing A 1-R-(pyridyl)ethyl ether terminus. Bioorg Med Chem Lett 8:3081–3086

Liard JF (1988) Vasopressin antagonists and their use in animal studies. Kidney Int Suppl 26:S43–S47

Mah SC, Hofbauer KG (1987) Pharmacological studies with the vasopressin (V_2) antagonist d(CH_2)$_5$-D-Tyr(Et)V AVP: acute and chronic effects in Sprague-Dawley and Brattleboro rats. In: Gash DM, Boer GJ (eds) Vasopressin. Principles and properties. Plenum, New York, pp 201–206

Manning M, Bankowski K, Sawyer WH (1987) Selective agonists and antagonists of vasopressin. In: Gash DM, Boer GJ

(eds) Vasopressin. Principles and properties. Plenum, New York, pp 335–368
Mayinger B, Hensen J (1999) Nonpeptide vasopressin antagonists: a new group of hormone blockers entering the scene. Exp Clin Endocrinol Diabetes 107(3):157–165
Serradeil-Le Gal C, Wagnon J, Valette G, Garcia G, Pascal M, Maffrand JP, Le Fur G (2002) Nonpeptide vasopressin receptor antagonists: development of selective and orally active V1a, V2 and V1b receptor ligands. Prog Brain Res 139:197–210
Schaumann W (1937) Wirkstoffe des Hinterlappens der Hypophyse. Handbuch exper Pharmakol, Vol 3. Springer, Berlin Heidelberg new York, pp 61–150
Soloff MS (1976) Oxytocin receptors in the mammary gland and uterus. In: Blecher M (ed) Methods in receptor research, Part II. Dekker, New York, pp 511–531
Urban JD, Clarke WP, von Zastrow M, Nichols DE, Kobilka B, Weinstein H, Javitch JA, Roth BL, Christopoulos A, Sexton PM, Miller KJ, Spedding M, Mailman RB (2007) Functional selectivity and classical concepts of quantitative pharmacology. J Pharmacol Exp Ther 320(1):1–13
Vogel G, Hergott J (1963) Pharmakologische Untersuchungen über O-Methyl-tyrosin^2-lysin^8-Vasopressin. Arzneimittelforschung 13:415–421
Walker BR, Childs ME, Adams EM (1988) Direct cardiac effects of vasopressin: role of V_1- and V_2-vasopressinergic receptors. Am J Physiol 255:H261–H265

N.8.1 Oxytocin

N.8.1.1 Isolated Uterus

PURPOSE AND RATIONALE

Several authors, such as Dale and Laidlaw (1912), Fromherz (1926), Glaubach and Molitor (1932), Lipschitz and Klar (1933), and Simon (1933), used the isolated uterus of virgin guinea pigs as a sensitive test for determination of oxytocin activity. The isolated uterus of the rat (Holton 1948) is less sensitive but, in contrast to the guinea pig, the rat uterus shows no spontaneous contractions in solutions with low calcium and glucose concentrations. Historically, the method has been adopted by several pharmacopoeias, e. g., by the British Pharmacopoeia (1988). The United States Pharmacopeia 23 (1995) uses the isolated guinea pig uterus for determination of oxytocin activity in vasopressin preparations. Physicochemical assays are now used for standardizing drug content, instead of the biological responses.

PROCEDURE

Female Sprague-Dawley or Wistar rats weighing 120–200 g are used. At 18–20 h prior to the assay, the rat is injected i.m. with 100 µg of estradiol benzoate for priming (receptor induction). Immediately before the assay the rat is tested for estrogen-induced epithelial proliferation by vaginal smear. One horn of the uterus is suspended in an organ bath containing a solution of the following composition:

Sodium chloride	6.62 g/l
Potassium chloride	0.45 g/l
Calcium chloride	0.07 g/l
Sodium hydrogen carbonate	2.56 g/l
Disodium hydrogen orthophosphate	0.29 g/l
Sodium dihydrogen orthophosphate	0.03 g/l
Magnesium chloride	0.10 g/l
D-Glucose	0.50 g/l

The bath temperature is maintained at 32°C, a temperature at which spontaneous contractions of the uterus are abolished and the preparation maintains its sensitivity. The solution is bubbled with a mixture of 95% O_2 and 5% CO_2. The preparation is loaded with 1–2 g and the contractions recorded using a Statham transducer and a polygraph. Two doses of the standard preparation are added, ranging usually between 10 and 50 µU/ml organ bath. The preparation examined is diluted in such a way to obtain responses on the addition of two doses similar to those obtained with the standard preparation. The ratio between the two doses of the preparation being examined should be the same as that between the two doses of the standard preparation. The two doses of the standard preparation and the two doses of the preparation being examined are given according to a randomized block or a Latin square design and at least six to eight responses to each are recorded. The doses should be recorded at regular intervals of 3–5 min depending on the rate of recovery of the muscle.

EVALUATION

The activity and potency ratios with confidence limits are calculated from the 2+2-points assay.

MODIFICATIONS OF THE METHOD

The isolated rat uterus is also used to test spasmolytic activity of various drugs against oxytocin as spasmogen. Liebmann et al. (1993) used the rat uterus to test the pharmacological and molecular actions of the bradykinin B_2 receptor antagonist, Hoe 140.

The method described by Schübel and Gehlen (1933) using the **uterus of cats** 2–4 days after partum is of historical interest only.

In addition to the isolated rat uterus, Berde et al. (1957) used the **rat uterus *in situ***, the **cat uterus *in***

vitro, and the **cat uterus *in situ*** for evaluation of synthetic analogs of oxytocin.

Murray and Miller (1960) observed characteristic post-ural changes in rats following administration of oxytocin to unanesthetized rats described as "cramping" which was dose-dependent in estrogen-pretreated animals.

An *in vitro* **hen oxytocic assay** was designed by Munsick et al. (1960). Muscle strips of the uterine portion of the oviduct of laying hens are dissected and suspended in a van Dyke-Hastings solution containing 0.15 mM calcium, 0.5 mM magnesium and 100 mg% glucose. The strips are 2–3 cm long and 2–3 mm wide. The solution is gassed with oxygen containing 5% carbon dioxide and maintained at a temperature of 43°C. These conditions are necessary to prevent spontaneous contractions.

The **isolated uterus from immature guinea pigs** was used for evaluation of oxytocin activity by Fromherz (1926) and by Vogel and Hergott (1963).

Guissani et al. (1995) and Pettibone et al. (1996) reported the effect of oxytocin antagonists in **pregnant rhesus monkeys** *in vivo*.

REFERENCES AND FURTHER READING

Berde B, Doepfner W, Konzett H (1957) Some pharmacological actions or four synthetic analogues of oxytocin. Br J Pharmacol 12:209–214

Berde B, Cerletti A, Konzett H (1959) The biological activity of a series of peptides related to oxytocin. In: Caldeyro-Barcia, Heller H (eds) Oxytocin: Intern Sympos Montevideo. Pergamon, London

Boissonnas RA (1960) The chemistry of oxytocin and vasopressin. In: Schachter M (ed) Polypeptides which affect smooth muscles and blood vessels. Pergamon, London, pp 7–19

Boissonnas RA, Guttmann St, Berde B, Konzett H (1961) Relationships between the chemical structures and the biological properties of the posterior pituitary hormones and their synthetic analogues. Experientia 1:377–390

British Pharmacopoeia, Vol II (1988) Biological assay of oxytocin. Appendix XIV C: A171. HMSO, London

Burn HJ, Finney DJ, Goodwin LG (1952) Biological standardization, 2nd edn, 2nd impression. Oxford University Press, Oxford

Dale H, Laidlaw J (1912) A method for standardising pituitary (infundibular) extracts. J Pharmacol Exp Ther 4:73–95

Fromherz K (1926) Bemerkungen zur Auswertung von Hypophysenextrakt am Meerschweinchenuterus. Naunyn-Schmiedebergs Arch Exp Pathol Pharmakol 113:113–123

Glaubach S, Molitor H (1932) Vergleich der Auswertungsmethoden von Gesamtextrakten des Hypophysenhinterlappens am isolierten Meerrschweinchenuterus und an der Diuresehemmung von Hunden, Ratten und Mäusen. Naunyn-Schmiedebergs Arch Exp Pathol Pharmakol 166:243–264

Guissani DA, Jenkins SL, Mecenas CA, Owiny JR, Wentwort RA, Winter JA, Derks JB, Honnebier MBOM, Nathanielz PW (1995) The oxytocin (OT) antagonist Atosiban (ATO) prolongs gestation in the rhesus monkey. J Soc Gynecol Invest 2:265

Holton P (1948) A modification of the method of Dale and Laidlaw for the standardization of posterior pituitary extract. Br J Pharmacol 3:328–334

Kruse J (1986) Oxytocin: pharmacology and clinical application. J Fam Pract 23:473–479

Liebmann C, Nawrath S, Ludwig B, Paegelow I (1993) Pharmacological and molecular actions of the bradykinin B_2 receptor antagonist, Hoe 140 in the rat uterus. Eur J Pharmacol 235:183–188

Lipschitz W, Klar F (1933) Die Abhängigkeit der Wirkung uteruserregender Mittel (Histamin und Ergotamin) von Konzentration und Reaktionstemperatur. Naunyn-Schmiedebergs Arch Exp Path Pharmakol 174:223–244

Munsick RA, Sawyer WH, van Dyke HB (1960) Avian neurohyophyseal hormones: pharmacological properties and tentative identification. Endocrinology 66:860–871

Murray WJ, Miller JW (1960) Oxytocin-induced "cramping" in the rat. J Pharmacol Exp Ther 128:372–379

Pettibone DJ, Guidotti MT, Harrell CM, Jasper JR, Lis EV, O'Brien JA, Reiss DR, Woyden CJ, Bock MG, Evans BE, Freidinger RM, Williams DP, Murphy MG (1996) Progress in the development of oxytocin antagonists for use in preterm labor. Adv Exp Biol Med 395:601–612

Schaumann W (1937) Wirkstoffe des Hinterlappens der Hypophyse. Handbuch exper Pharmakol, Vol 3. Springer, Berlin Heidelberg New York, pp 61–150

Schübel K, Gehlen W (1933) Eine neue, zuverlässige Methode zur Standardisierung von Hypophysen-Hinterlappenextrakten. Naunyn-Schmiedebergs Arch Exp Pathol Pharmakol 173:633–641

Simon A (1933) The secretion of the posterior lobe of the hypophysis after the administration of drugs. J Pharmacol 49:375–386

Thorp RH (1962) Posterior pituitary hormones. In: Dorfman RI (ed) Methods in hormone research, Vol II. Academic Press, New York, pp 495–516

Thorp RH (1969) Posterior pituitary hormones. In: Dorfman RI (ed) Methods in hormone research, Vol IIA. Academic Press, New York, pp 457–480

United States Pharmacopeia 23 (1995) Vasopressin injection. The United States Pharmacopeia 23. United States Pharmacopoeial Convention, Rockville, Md, pp 1622–1623

Van Dyke HB, Adamsons K, Engel SL (1955) I. Pituitary hormones. Aspects of the biochemistry and physiology of the neurohyophyseal hormones. Recent Prog Hormone Res 11:1–41

Vogel G, Hergott J (1963) Pharmakologische Untersuchungen über O-Methyl-tyrosin^2-lysin^8-Vasopressin. Arzneimittelforschung 13:415–421

N.8.1.2 Chicken Blood Pressure

PURPOSE AND RATIONALE

Oxytocin induces a transient fall in blood pressure in chicken and other birds. This effect can be used as an assay for oxytocin (Coon 1939). The method has been modified by Munsick et al. (1960) and accepted by pharmacopoeias; for example, the United States Pharmacopeia 23 (1995a, 1995b) uses the chicken blood pressure method for determination of oxytocin activity

with three doses of standard and test preparation and calculation of the activity ratio with confidence limits.

PROCEDURE

White Leghorn chickens weighing 1.2–2.0 kg are anesthetized by intravenous injection with 200 mg/kg sodium phenobarbital via the brachial vein. The ischiadic artery is exposed by removing the feathers from the outer surface of the left thigh, and an incision 7–8 cm long is made in the skin, parallel to and about 1.5 cm below the femur, exposing the gluteus primus muscle. The lower edge of this incision is retracted to expose the edge of the gluteus primus muscle overlying the semitendinosus muscle. The edge is then freed for the length of the incision, and when the free edge is lifted, the ischiadic artery, the ischiadic vein, and the crural vein can be seen lying along the edge of the semitendinosus muscle. The gluteus primus muscle is cut at right angles near the proximal end of the incision and the resulting flap deflected and secured to the upper thigh. A length of the ischiadic artery and the crural vein are dissected free and the artery is cannulated. The cannula is connected to a Statham pressure transducer. Blood pressure should be between 100 and 120 mmHg. The crural vein is cannulated for injections of the test preparations. Intravenous injection of oxytocin induces in chickens an immediate, transient fall in blood pressure. Doses of the standard are chosen which are followed by a decrease of blood pressure of between 20 and 40 mmHg. The required doses normally lie between 20 and 100 mU.

Two doses of the standard and two doses of the test preparations are injected according to a randomized block or to a Latin square design and at least six to eight responses to each should be recorded. The interval between injections should be constant and lies between 3 and 10 min, depending on the rate at which the blood pressure returns to normal.

EVALUATION

The responses to each dose are averaged and potency ratios with confidence limits calculated from the 2+2-points assay.

REFERENCES AND FURTHER READING

British Pharmacopoeia, Vol II (1988) Biological assay of oxytocin. Appendix XIV C:A171. HMSO, London

Coon JM (1939) A new method for the assay of posterior pituitary extracts. Arch Int Pharmacodyn Ther 62:79–99

DuVigneaud V, Fitt PS, Bodanszky M, O'Connell M (1960) Synthesis and some pharmacological properties of a peptide derivative of oxytocin: glycyloxytocin. Proc Soc Exp Biol Med 104:653–656

Munsick RA, Sawyer WH, van Dyke HB (1960) Avian neurohyophyseal hormones: pharmacological properties and tentative identification. Endocrinology 66:860–871

Thorp RH (1962) Posterior pituitary hormones. In: Dorfman RI (ed) Methods in hormone research, Vol II. Academic Press, New York, pp 495–516

Thorp RH (1969) Posterior pituitary hormones. In: Dorfman RI (ed) Methods in hormone research, Vol IIA. Academic Press, New York, pp 457–480

United States Pharmacopeia 23 (1995a) Design and analysis of biological assays. The United States Pharmacopeial Convention, Rockville, Md., pp 1705–1715

United States Pharmacopeia 23 (1995b) Oxytocin injection. The United States Pharmacopeial Convention, Rockville, Md., pp 1148–1149

Van Dyke HB, Adamsons K, Engel SL (1955) I. Pituitary hormones. Aspects of the biochemistry and physiology of the neurohyophyseal hormones. Recent Prog Hormone Res 11:1–41

N.8.1.3 Milk Ejection in the Lactating Rabbit or Rat

PURPOSE AND RATIONALE

A sensitive bioassay for the estimation of oxytocin was described by van Dyke et al. (1955). This test makes use of the milk-ejecting properties of oxytocin.

PROCEDURE

A rabbit in the first or second week of lactation is anesthetized with urethane and pentobarbital. Usually, artificial respiration is not necessary. One jugular vein is cannulated for injections. One of the six ducts in a nipple of the rabbit is cannulated with a hypodermic needle and connected with a Statham strain gauge transducer. Two doses of the standard and the test preparation are injected according to a randomized block or to a Latin square design and at least six to eight responses to each should be recorded. The interval between injections should be constant at 3 min.

EVALUATION

The responses of each dose are averaged and potency ratios with confidence limits calculated from the 2+2-points assay.

MODIFICATIONS OF THE METHOD

The British Pharmacopoeia (1988) recommends the measurement of milk-ejection pressure in the lactating rat. A lactating rat weighing about 300 g in the 3rd to 21st day after parturition is anesthetized by pentobarbitone sodium. The trachea is cannulated. One jugular or femoral vein is cannulated for injection of the test preparations. The tip of one lower inguinal teat is excised and a polyethylene tube with an external diameter of 0.6 mm is inserted to a depth sufficient to ob-

tain appropriate measurement of pressure into the primary teat duct which opens onto the cut surface and is tied firmly in place with a ligature. The cannula is connected with a suitable strain gauge pressure transducer for recording on a polygraph.

Tindal and Yokoyama (1962) recommended the use of guinea pigs using essentially a similar procedure, but the injection is made into the internal saphenous artery after ligation of the main branches supplying the limb. In the guinea pig the mammary glands are supplied with blood from the external pudendal arteries, which branch from the internal saphenous artery just as they enter the legs.

REFERENCES AND FURTHER READING

Berde B, Cerletti A (1957) Démonstration expérimentale de l'action de l'ocytocine sur la glande mammaire. Gynaecologia 144:275–278

British Pharmacopoeia, Vol II (1988) Biological assay of oxytocin. Appendix XIV C:A171. HMSO, London

Munsick RA, Sawyer WH, van Dyke HB (1960) Avian neurohyophyseal hormones: pharmacological properties and tentative identification. Endocrinology 66:860–871

Thorp RH (1962) Posterior pituitary hormones. In: Dorfman RI (ed) Methods in hormone research, Vol II. Academic Press, New York, pp 495–516

Thorp RH (1969) Posterior pituitary hormones. In: Dorfman RI (ed) Methods in hormone research, Vol IIA. Academic Press, New York, pp 457–480

Tindal JS, Yokoyama A (1962) Assay of oxytocin by the milk-ejection response in the anesthetized lactating guinea pig. Endocrinology 71:196–202

van Dyke (1959) Some features of the pharmacology of oxytocin. In: Caldeyro-Barcia, Heller H (eds) Oxytocin: Intern Sympos Montevideo. Pergamon, London, pp 48–67

van Dyke HB, Adamsons K Jr, Engel SL (1955) Aspects of the biochemistry and physiology of the neurohypophyseal hormones. Recent Prog Hormone Res 11:1–41

N.8.1.4 Oxytocin Receptor Determination

The family of the vasopressin and oxytocin receptors has been studied very intensely (Peter et al. 1995) in order to obtain evidence for new indications, and to determine the specific regions in each receptor subtype and the associated effector systems for the G-protein-linked subtypes (Thibonnier et al. 1998).

PURPOSE AND RATIONALE

Premature labor and pre-term delivery is an important cause of death among infants and a major cause of newborn and child morbidity. Strong evidence exists that oxytocin and catecholamines are involved in the spontaneous uterine contractions which bring about premature delivery. Development of oxytocin antagonists is believed to be of therapeutic value for the prevention of pre-term labor (Manning et al. 1995; Chan et al. 1996).

In vitro binding to the oxytocin receptor is used as the first step in the characterization of potential oxytocin antagonists (Pettibone et al. 1990, 1991, 1993a, 1993b, 1996; Evans et al. 1993; Manning et al. 1995; Freidinger and Pettibone 1997; Pettibone and Freidinger 1997).

PROCEDURE

Uterine tissue is taken from nonpregnant adult Sprague-Dawley rats pretreated (18–24 h) with diethylstilbestrol (300 µg/kg, i.p.) and mammary tissue from lactating rats (4–14 days of lactation). The tissues are homogenized in 10 mM Tris containing 1 mM EDTA and 0.5 mM dithiothreitol, pH 7.4 and centrifuged at 48,000 *g* for 30 min at 4°C. The resulting pellets from mammary/uterine tissue are resuspended in 50 mM Tris/5 mM $MgCl_2$/0.1% BSA (pH 7.4) and centrifuged again to produce the final pellet. Competition studies are conducted at equilibrium for 60 min at 22°C using 1 nM [^{3}H]OT (30–60 Ci/mmol, New England Nuclear, Boston, Mass., USA) in the following buffer: 50 mM Tris/5 mM $MgCl_2$/0.1% BSA (pH 7.4). Nonspecific binding (5%–10% of total binding) is determined using 1 µM unlabeled oxytocin. IC_{50} values are calculated from the linear regression analysis of log concentration of inhibitor versus percentage inhibition of specific binding. Saturation binding studies are conducted at equilibrium using a 100-fold range of radioligand concentrations (i. e., 0.1–10 nM) and analyzed by a nonlinear regression program (McPherson 1985a, 1985b). The binding reactions are initiated by the addition of the tissue preparation (final protein concentrations, 100–200 µg protein/ml) and terminated by rapid filtration through Skatron glass fiber filters using a Skatron cell harvester system (Model 7019, Skatron, Sterling, Va., USA).

EVALUATION

Inhibition constants (K_i) are calculated for each compound from three to six separate IC_{50} determinations ($K_i = IC_{50} / [1 + c / K_d]$) using mean dissociation constants (K_d) obtained from saturation binding assays.

MODIFICATIONS OF THE METHOD

Maggi et al. (1994) used cultured Hs 805.Ut (corpus uteri, normal, human) cells or cells obtained from women in the early follicular or late luteal phase to study binding of antagonists at the human oxytocin receptor.

Pak et al. (1994) compared the binding affinity of oxytocin antagonists to human and rat oxytocin receptors and correlated the results with the rat oxytocic bioassay.

Species differences in central oxytocin receptor gene expression were investigated by Young et al. (1996).

Cloning and expression of the rhesus monkey oxytocin receptor was reported by Salvatore et al. (1998).

Molecular cloning and functional characterization of the oxytocin receptor from a rat pancreatic cell line (RINm5F) was reported by Jeng et al. (1996).

Elands et al. (1987) and Klein et al. (1995) recommended selective radioligands for the oxytocin receptor for the structure–activity research directed to receptor subtypes.

REFERENCES AND FURTHER READING

Chan WY, Wo NC, Cheng LL, Manning M (1996) Isosteric substitution of Asn^5 in antagonists of oxytocin and vasopressin leads to highly selective and potent oxytocin and V_{1a} receptor antagonists: new approaches for the design of potential tocolytics for preterm labor. J Pharmacol Exp Ther 277:999–1003

Elands J, Barberis C, Jard S, Tribollet E, Dreifuss JJ, Bankowski K, Manning M, Sawyer WH (1987) ^{125}I-labelled d(CH_2)$_5$[Tyr(Me)^2,Thr^4,Tyr-NH_2^{9}]OTV. A selective oxytocin receptor ligand. Eur J Pharmacol 147:197–207

Evans BE, Lundell GF, Gilbert KF, Bock MG, Rittle KE, Carroll LA, Williams PD, Pawluczyk JM, Leighton JL, Young MB, Erb JM, Hobbs DW, Gould NP, DiPardo RM, Hoffman JB, Perlow DS, Whitter WL, Veber DF, Pettibone DJ, Clineschmidt BV, Anderson PS, Freidinger RM (1993) Nanomolar-affinity, non-peptide oxytocin receptor antagonists. J Med Chem 36:3993–4005

Freidinger RM, Pettibone DJ (1997) Small molecule ligands for oxytocin and vasopressin receptors. Med Res Rev 17:1–7

Jeng YJ, Lolait SJ, Strakova Z, Chen C, Copland JA, Mellman D, Hellmich MR, Soloff MS (1996) Molecular cloning and functional characterization of the oxytocin receptor from a rat pancreatic cell line (RINm5F). Neuropeptides 30:557–565

Klein U, Jurzak M, Gerstberger R, Fahrenholz F (1995) A new tritiated oxytocin receptor radioligand – synthesis and application for localization of central oxytocin receptors. Peptides 16:851–857

Maggi M, Fantoni G, Baldi E, Cioni A, Rossi S, Vanelli GB, Melin P, Åkerlund M, Serio M (1994) Antagonists for the human oxytocin receptor: an *in vitro* study. J Reprod Fertil 101:345–352

Manning M, Cheng LL, Klis A, Stoev S, Przybylski J, Bankowski K, Sawyer WH, Barberis C, Chan WY (1995) Advances in the design of selective antagonists, potential tocolytics and radioiodinated ligands for oxytocin receptors. In: Ivell R, Russell J (eds) Oxytocin. Plenum, New York, pp 559–584

McPherson GA (1985a) KINETIC, EBDA, LIGAND, LOWRY: a collection of radioligand binding analysis programs. Elsevier, Amsterdam

McPherson GA (1985b) Analysis of radioligand binding experiments. A collection of computer programs for the IBM PC. J Pharmacol Meth 14:213–228

Pak SC, Bertoncini D, Meyer W, Scaunas D, Flouret G, Wilson R Jr (1994) Comparison of binding affinity of oxytocin antagonists to human and rat oxytocin receptors their correlation to the rat oxytocic bioassay. Biol Reprod 51:1140–1144

Peter J, Burbach H, Adan RA, Lolait SJ, van Leeuwen FW, Mezey E, Palkovits M, Barberis C (1995) Molecular neurobiology and pharmacology of the vasopressin/oxytocin receptor family. Cell Mol Neurobiol 15(5):573–595

Pettibone DJ, Freidinger RM (1997) Discovery and development of non-peptide antagonists of peptide hormone receptors. Biochem Soc Trans 25:1051–1057

Pettibone DJ, Woyden CJ, Totaro JA (1990) Identification of functional oxytocin receptors in lactating rat mammary gland *in vitro*. Eur J Pharmacol Mol Pharmacol Sect 188:235–242

Pettibone DJ, Clineschmidt BV, Lis EV, Reiss DR, Totaro JA, Woyden CJ, Bock MG, Freidinger RM, Tung RD, Veber DF, Williams DP, Lowensohn (1991) *In vitro* pharmacological profile of a novel structural class of oxytocin antagonists. J Pharmacol Exp Ther 256:304–308

Pettibone DJ, Clineschmidt BV, Guidotti MT, Lis EV, Reiss DR, Woyden CJ, Bock MG, Evans BE, Freidinger RM, Hobbs DW, Veber DF, Williams PD, Chiu SHL, Thompson KL, Schorn TW, Siegl PKS, Kaufman MJ, Cukierski MA, Haluska GJ, Cook MJ, Novy MJ (1993a) L-368,899, a potent orally active oxytocin antagonist for potential use in preterm labor. Drug Dev Res 30:129–142

Pettibone DJ, Clineschmidt BV, Kishel MT, Lis EV, Reiss DR, Woyden CJ, Evans BE, Freidinger RM, Veber DF, Cook MJ, Haluska GJ, Novy MJ, Lowensohn (1993b) Identification of an orally active, nonpeptidyl oxytocin antagonist. J Pharmacol Exp Ther 264:308–314

Pettibone DJ, Guidotti MT, Harrell CM, Jasper JR, Lis EV, O'Brien JA, Reiss DR, Woyden CJ, Bock MG, Evans BE, Freidinger RM, Williams DP, Murphy MG (1996) Progress in the development of oxytocin antagonists for use in preterm labor. Adv Exp Biol Med 395:601–612

Salvatore CA, Woyden CJ, Guidotti MT, Pettibone DJ, Jacobson MA (1998) Cloning and expression of the rhesus monkey oxytocin receptor. J Recept Signal Transduction Res 18:15–24

Thibonnier M, Conarty DM, Preston JA, Wilkins PL, Berti-Mattera R. (1998) Molecular pharmacology of human vasopressin receptors. Adv Exp Biol 449:251–276

Young LJ, Hout B, Nilsen R, Wang Z, Insel TR (1996) Species differences in central oxytocin receptor expression: comparative analyses of promoter sequences. J Neuroendocrinol 8:777–783

N.8.2 Vasopressin

N.8.2.1 Hereditary Vasopressin Deficiency in Rats (Brattleboro Strain)

This bioassay is based on an animal strain with genetic deficiency of vasopressin synthesis. Patients with diabetes insipidus excrete large amounts of very diluted urine and need a high fluid intake. This disorder is

due to a lack of vasopressin. A similar syndrome has been found in Brattleboro rats. In the rare nephrogenic form, the vasopressin receptors are defective (Sokol and Valtin 1982; Nyunt-Wai and Laycock 1990; Szot and Dorsa 1992). Vasopressin is also considered to be a modulator in the central nervous system in particular learning and memory processes. Therefore, many studies on learning and memory have been performed with this strain of rats. Valtin et al. (1965) found very little vasopressin in hypothalami and pituitaries of homozygous Brattleboro rats.

Schmale and Richter (1984) and Schmale et al. (1984) found a single base deletion in the vasopressin gene as the cause of diabetes insipidus in Brattleboro rats. The mutant vasopressin gene is transcribed but the message is not efficiently translated. Spontaneous hypertensive rats crossbred with Brattleboro rats inherit the mutated vasopressin gene (McCabe et al. 1988). The abnormal quinine drinking aversion in the Brattleboro rat with diabetes insipidus can be reversed by a vasopressin agonist (Laycock et al. 1994)

For testing aquaretic effects in Brattleboro rats see C.1.2.1.

MODIFICATIONS OF THE METHOD (OTHER DIABETES INSIPIDUS MODELS)

Similar studies werer reported by: Byrnes et al. 1953; Randall and Selitto 1958; Eviatar et al. 1961; Turner 1965; Dorfmann 1969; Neri et al. 1972; Neumann et al. 1977; Furr et al. 1987; Snyder et al. 1989; Christiansen et al. 1990; Shibata et al. 1992; Neubauer et al. 1993; Tagekawa et al. 1993

Several other animal models of diabetes insipidus have been developed and characterized (Herman et al. 1986; Grant 2000; Lloyd et al. 2005; Petersen 2006) for the understanding of pathophysiology, for explanation of genetic deficiencies, and to validate the animal models based on substitution of vasopressin deficiency.

REFERENCES AND FURTHER READING

Grant FD (2000) Genetic models of vasopressin deficiency. Exp Physiol 85::203S–209S

Herman JP, Sladek CD, Hansen CT, Gash DM (1986) Characterization of a new rodent model of diabetes insipidus: the Roman high avoidance rat homozygous for diabetes insipidus. Neuroendocrinology 43(3):340–347

Laycock JF, Chatterji U, Seckl JR, Gartside IB (1994) The abnormal quinine drinking aversion in the Brattleboro rat with diabetes insipidus is reversed by the vasopressin agonist DDAVP: a possible role for vasopressin in the motivation to drink. Physiol Behav 55:407–412

Lloyd DJ, Hall FW, Tarantino LM, Gekakis N (2005) Diabetes insipidus in mice with a mutation in aquaporin-2. PLoS Genet 1(2):e20

McCabe JT, Almasan K, Lehmann E, Hänze J, Lang RE, Pfaff DW, Ganten D (1988) Vasopressin gene expression in hypertensive, normotensive, and diabetes insipidus rats. Clin Exp Theor Pract A10 [Suppl 1]:131–142

Nyunt-Wai V, Laycock JF (1990) The pressor response to vasopressin is not attenuated by hypertonic NaCl in the anaesthetized Brattleboro rat. J Physiol (Lond) 430:35P

Petersen MB (2006) The effect of vasopressin and related compounds at V1a and V2 receptors in animal models relevant to human disease. Basic Clin Pharmacol Toxicol 99(2):96–103

Schmale H, Richter D (1984) Single base deletion in the vasopressin gene is the cause of diabetes insipidus in Brattleboro rats. Nature 308:705–709

Schmale H, Ivell R, Breindl M, Darmer D, Richter D (1984) The mutant vasopressin gene from diabetes insipidus (Brattleboro) rats is transcribed but the message is not efficiently translated. EMBO J 3:3289–3293

Sokol HW, Valtin H (eds) (1982) The Brattleboro rat. Ann NY Acad Sci 394

Szot P, Dorsa DM (1992) Cytoplasmatic and nuclear vasopressin RNA in hypothalamic and extrahypothalamic neurons of the Brattleboro rat: an *in situ* hybridization study. Mol Cell Neurosci 3:224–236

Valtin H, Sawyer WH, Sokol HW (1965) Neurohypophyseal principles in rats homozygous and heterozygous for hypothalamic diabetes insipidus (Brattleboro strain). Endocrinology 77:701–706

N.8.2.2 Vasopressor Activity

PURPOSE AND RATIONALE

Vasopressin activity can be determined by the increase of blood pressure observed after surgical or pharmacological elimination of the central and peripheral nervous regulation of the cardiovascular system. Dekansky (1952) described a quantitative assay of vasopressin in anesthetized rats after blockade of other pressor substances by dibenamine (pithed rat).

PROCEDURE

A male Wistar rat weighing about 300 g is anesthetized by subcutaneous injection of 1.75 g/kg urethane. After 45–60 min, the trachea is cannulated with a polyethylene tube of 2.5 mm diameter. One femoral vein is cannulated for injections and the carotid artery for measuring blood pressure with a Statham transducer. The central and peripheral nervous systems, including both vagi and associated sympathetics, are left intact. No artificial respiration is necessary. Heparin (2000 U/kg) is injected through the venous cannula and washed through with saline. [Dibenamine *N*-(2-chloroethyl)dibenzylamine hydrochloride] is injected twice intravenously with an interval of 10 min at a dose of 1 mg/kg. The blood pressure stabilizes at a basal level of about 50 mmHg. Small doses of vasopressin induce an increase in blood pressure which is depen-

dent on the dose. Two doses of vasopressin standard (approximately 3–5 mU) and two doses of test preparation are injected repeatedly (usually 6 times) using a Latin square design. The doses are injected at intervals of 10–15 min.

EVALUATION

The responses of each dose are averaged and potency ratios calculated from the 2+2-points assay.

MODIFICATIONS OF THE METHOD

One of the first recommendations for standardizing posterior pituitary extract was by measuring blood pressure in anesthetized dogs (Hamilton 1912).

Vogel and Hergott (1963), studying the properties of a synthetic vasopressin analog, described a method in decerebrate rabbits previously used in this laboratory for standardization of posterior pituitary extracts. Rabbits weighing 2–3 kg were anesthetized by slow intravenous injection of butallylonal. The trachea is cannulated and the cannula connected with a respiration pump. One femoral vein is cannulated for injection of the test compounds. One carotid artery is cannulated for measurement of blood pressure with a Statham transducer. For chemical decapitation, the head of the anesthetized rabbit is bent forwards and a needle introduced into the foramen occipitale magnum, and then 0.5 ml of 30% trichloroacetic acid is injected. Artificial respiration is started immediately. Blood pressure is stabilized at a level of 30–40 mmHg. Two doses of standard and of test preparation are injected according to a Latin square design. The method has been proven to be very sensitive.

The British Pharmacopoeia (1988) recommends the intravenous injection of 10 mg/kg of the α-adrenoreceptor blocking agent phenoxybenzamine hydrochloride 18 h prior to the experiment to stabilize the blood pressure at a low level. USP 23 (1995a, 1995b) uses two doses of standard and test preparation in the phenoxybenzamine-blocked rat for calculation of vasopressin activity with confidence intervals in vasopressin and oxytocin preparations.

Knape and van Zwieten (1988) used the pithed rat to study vasoconstrictor activity of vasopressin after pretreatment with various drugs.

REFERENCES AND FURTHER READING

Altura BM, Altura BT (1984) Actions of vasopressin, oxytocin, and synthetic analogs on vascular smooth muscle. Fed Proc 43:80–86

British Pharmacopoeia, Vol II (1988) Biological assay of argipressin. Appendix XIV C:A172–A173. HMSO, London

Dekansky J (1952) The quantitative assay of vasopressin. Br J Pharmacol 7:567–572

DuVigneaud V, Fitt PS, Bodansky M, O'Conell MO (1960) Synthesis and some pharmacological properties of a peptide derivative of oxytocin: glycyloxytocin. Proc Soc Exp Biol Med 104:653–656

Hamilton HC (1912) The pharmacological assay of pituitary preparations. J Am Pharm Assoc Am Pharm Assoc 1:1117–1119

Knape JTA, van Zwieten PA (1988) Vasoconstrictor activity of vasopressin in the pithed rat. Arch Int Pharmacodyn Ther 291:142–152

Sawyer WH (1961) Neurohypophyseal hormones. Pharmacol Rev 13:225–277

Thorp RH (1969) Posterior pituitary hormones. In: Dorfman RI (ed) Methods in hormone research, Vol IIA. Academic Press, New York, pp 457–480

USP 23 (1995a) Design and analysis of biological assays. The United States Pharmacopeial Convention, Rockville, Md., pp 1705–1715

USP 23 (1995b) Vasopressin injection. The United States Pharmacopeial Convention, Rockville, Md., pp 1622–1623

Van Dyke HB, Adamsons K, Engel SL (1955) I. Pituitary hormones. Aspects of the biochemistry and physiology of the neurohypophyseal hormones. Recent Prog Hormone Res 11:1–41

Vogel G, Hergott J (1963) Pharmakologische Untersuchungen über O-Methyl-tyrosin^2-lysin^8-Vasopressin. Arzneimittelforschung 13:415–421

N.8.2.3 Antidiuretic Activity in the Conscious Rat

PURPOSE AND RATIONALE

For some period of time, it was uncertain whether vasopressin and adiuretin are the same or separate hormones. Special tests for antidiuretic activity in water-loaded rats were developed (Burn 1931) and adopted by pharmacopoeias. Vasopressin analogs show considerable dissociation of vasopressive and antidiuretic activities (Vogel and Hergott 1963).

PROCEDURE

Wistar or Sprague-Dawley rats weighing between 140 and 250 g of either sex are used. The range of weights in any one test should not exceed 50 g. Not less than 2 days before testing the preparation, the rats have to be accustomed to the metabolism cage by carrying out a preliminary test. All animals are injected with 0.1 ml saline solution per 100 g body weight instead of the test preparations given in the main test. Any rat that shows signs of stress or undue excitement or that has abnormally low or high rate of urine excretion should not be used in the main test. Food and water are withheld during each test but access is allowed between the tests. The rats are assigned at random to four groups,

each no less than four animals, and are weighed and marked for identification purposes. By stomach tube each rat receives a volume of water warmed to approximately 37°C and equivalent to 5% of the animal's body weight. Each rat is placed in a separate cage for collection of urine. Then 30 min later, the volume excreted by each rat is recorded and a second volume of tap water equal to the volume of urine together with a further volume equivalent to 3% of the animal's body weight is administered. This provides a total water load equivalent to 8% of the animal's body weight.

Using a different group of rats and two dilutions of the preparation to be examined and of the standard preparation, immediately after administration of the second dose of water, each rat is injected subcutaneously with a volume of the appropriate dilution equivalent to 0.1 ml per 100 g body weight. The urine passed during the first 5 min after injection is discarded and the volumes collected at intervals of 15 min are noted until a volume greater than 30% of the total water load is excreted.

EVALUATION

The responses of each dose are averaged and activity ratios with confidence limits are calculated from the 2+2-points assay.

MODIFICATIONS OF THE METHOD

Hydrated **conscious dogs** have been used to test the antidiuretic activity of vasopressin by van Dyke et al. (1955).

REFERENCES AND FURTHER READING

British Pharmacopoeia, Vol II (1988) Biological assay of desmopressin. Appendix XIV D:A173. HMSO, London

Burn JH (1931) Estimation of the antidiuretic potency of pituitary (posterior lobe) extract. Q J Pharm 4:517–529

Schaumann W (1937) Wirkstoffe des Hinterlappens der Hypophyse. Handbuch exper Pharmakol, Vol 3. Springer, Berlin Heidelberg New York, pp 61–150

Thorp RH (1962) Posterior pituitary hormones. In: Dorfman RI (ed) Methods in hormone research, Vol II. Academic Press, New York, pp 495–516

Thorp RH (1969) Posterior pituitary hormones. In: Dorfman RI (ed) Methods in hormone research, Vol IIA. Academic Press, New York, pp 457–480

Van Dyke HB, Adamsons K, Engel SL (1955) I. Pituitary hormones. Aspects of the biochemistry and physiology of the neurohypophyseal hormones. Recent Prog Horm Res 11:1–41

Vogel G, Hergott J (1963) Pharmakologische Untersuchungen über O-Methyl-tyrosin^2-lysin^8-Vasopressin. Arzneimittelforschung 13:415–421

N.8.2.4 Antidiuretic Activity in the Rat in Ethanol Anesthesia

PURPOSE AND RATIONALE

This is a sensitive bioassay often reported for vasopressin analogs, which has been applied extensively but is no longer required due to the availability of other methods (e. g., Brattleboro rats). Ethanol suppresses the secretion of endogenous antidiuretic hormone (van Dyke and Ames 1951). Sensitive methods measuring urine output in ethanol-induced anesthesia were described (Dicker 1953; Dettelbach 1958; Munsick et al. 1960; Berde and Cerletti 1961), whereby the water load is automatically kept constant.

PROCEDURE

Female Sprague-Dawley rats weighing 200–250 g are spayed 7–10 days prior to use in order to eliminate the effect of gonadal steroids on the response to a water load. Each animal is given a 5-ml gavage of tepid tap water. At 3-day intervals thereafter, the water load is increased by 1-ml increments until a 10-ml level is reached. The day before an assay is to be performed, two or three animals are selected and given a 10-ml gavage of 2% ethanol. The animals are fasted overnight but are allowed free access to water. On the test day, they are placed into individual metabolism cages for water loading and anesthetizing. Each rat receives 5% of its body weight of warm 12%–15% ethanol by stomach tube. This induces anesthesia within a few minutes. After 45 min the same volume of 2% ethanol is again given by gavage. After 1 h the bladder is emptied by suprapubic pressure and the total urine output is measured.

The animal with the largest volume is selected and the water load calculated as the total volume administered less the volume excreted. The load on this animal is now increased to between 6% and 8% of its body weight with warm 2% ethanol. Then the urinary bladder is catheterized. Polyethylene tubing is inserted into the rat's stomach. A femoral vein is cannulated for injections. The hind legs are secured to the operation table, while the front legs are left free. Assays are started when urine flow reaches a steady level of at least 50 µl/min. The catheter from the bladder is connected to an apparatus consisting of two Woulff bottles. Urine is directed through the catheter into the first Woulff bottle, displacing fluid into the second Woulff bottle. The second bottle is filled with 0.5% NaCl solution in 50% ethanol to reduce the size of the drops. Each drop activates an impulse counter. The drops are collected in a small glass reservoir and led by means

of polyethylene tubing to the urine metering pipette. When the fluid level in this tube rises and makes contact with an adjustable needle electrode near the top, another pipette which is calibrated to the same volume empties a solution of 5% glucose in 2% ethanol through the gavage tube into the rat's stomach. By these means a constant water load is maintained.

The animals produce urine at a relatively steady rate for 3–5 h. Intravenous injections of vasopressin produce characteristic changes (decreased rate of urine flow), which begin usually within 2 min and subside in most instances within 15 min. The range in which the assay of antidiuretic activities is useful is between 2 and 64 μU/injection.

EVALUATION

Antidiuretic potency is calculated as the log ratio of the volume excreted in 5 min preceding injection to the volume excreted in the 5 min beginning 1 min after injection. Dose–response relationships are established for the standard and the test preparation and potency ratios are calculated.

MODIFICATIONS OF THE METHOD

Berde and Cerletti (1961) placed the rat anesthetized with ethanol on a balance. The water loss due to urine excretion and perspiratio insensibilis is replaced automatically using a solution of 5% glucose in 2% ethanol.

REFERENCES AND FURTHER READING

Berde B, Cerletti A (1961) Über die antidiuretische Wirkung von synthetischem Lysin-Vasopressin. Helv Physiol Acta 19:135–150

Dettelbach HR (1958) A method for assaying small amounts of antidiuretic substances with notes on some properties of vasopressin. Am J Physiol 192:379–386

Dicker SE (1953) A method for the assay of very small amounts of antidiuretic activity with a note on the antidiuretic titer of rats' blood. J Physiol (Lond) 122:149–157

Munsick RA, Sawyer WH, van Dyke HB (1960) Avian neurohypophyseal hormones: pharmacological properties and tentative identification. Endocrinology 66:860–871

van Dyke HB, Ames RG (1951) Alcohol diuresis. Acta Endocrinol 7:110–121

N.8.2.5 Spasmogenic Activity of Vasopressin in the Isolated Guinea Pig Ileum

PURPOSE AND RATIONALE

The ileum of the guinea pig has been found to be quite sensitive to vasopressin (Simon 1933; Schaumann 1937; Vogel and Hergott 1963). This is a direct effect on smooth muscle similar to the pressor effect. This test is not specific for vasopressin.

PROCEDURE

Pieces of guinea pig ileum are suspended in an organ bath according to the Magnus' technique (see J.4.3.1). Two different doses of the test preparation and of the standard are applied according to a Latin square design and the contractions measured using a strain gauge transducer. Four to six doses of each solution are measured.

EVALUATION

The responses of each dose are averaged and activity ratios with confidence limits are calculated from the 2+2-points assay.

REFERENCES AND FURTHER READING

Schaumann W (1937) Wirkstoffe des Hinterlappens der Hypophyse. Handbuch exper Pharmakol, Vol 3. Springer, Berlin Heidelberg New York, pp 61–150

Simon A (1933) The secretion of the posterior lobe of the hypophysis after the administration of drugs. J Pharmacol 49:375–386

Vogel G, Hergott J (1963) Pharmakologische Untersuchungen über O-Methyl-tyrosin^2-lysin^8-Vasopressin. Arzneimittelforschung 13:415–421

N.8.2.6 Vasopressin Receptor Determination

PURPOSE AND RATIONALE

As in other areas of drug research, when specific receptor preparations became available for *in vitro* research, those identifying new vasopressin-like compounds (in structure–activity studies) turned to new methods with high specificity and capacity, replacing the cumbersome bioassays. Tests for receptor affinity are also used in "receptor screens" for the general pharmacology of new drug candidates, to predict their spectrum of activities.

Arginine vasopressin exerts its action through three membrane-bound G-protein-coupled receptor subtypes (V_{1a}, renal V_2 and V_3). The vasopressin-induced antidiuresis (via V_2 receptors coupled to aquaporins) helps maintain plasma osmolality and salt (NaCl) balances. The human V_1, V_2 and V_3 (V_{1b}) receptors and water-selective membrane proteins (aquaporins) in the kidney have been cloned, and receptor signaling has been characterized in detail (Thibonnier et al. 1998).

Pharmacological characterization of the human vasopressin receptor subtypes stably expressed in Chi-

nese hamster ovary cells was reported by Tahara et al. (1998).

Selective nonpeptide vasopressin antagonists (without agonistic activity) have been shown to be aquaretic agents in animals and humans. The development and therapeutic indications of orally active vasopressin receptor antagonists were reviewed by Thibonnier (1998), as were the postreceptor signaling mechanisms for the vasopressin receptor subtypes.

Serradeil-Le Gal et al. (1993, 1994a) studied the biochemical and pharmacological properties of a nonpeptide antagonist on rat and human vasopressin V_{1a} receptors, to explore the possibility of using centrally acting derivatives for indications in neuropharmacology.

PROCEDURE

Tissue samples from human uterus, adrenals, kidneys, and pituitaries are collected in conformity with national ethical rules. Uterus, adrenal, and kidney samples are immediately chilled in cold saline. Membranes are prepared within 3 h after collection. Pituitaries are collected within 6 h after death and immediately frozen in liquid nitrogen. Bovine kidneys can be obtained from a local slaughterhouse. Rat mammary tissue is taken from 19-day Sprague-Dawley pregnant rats.

For human adrenal membrane preparations, pieces of adrenal glomerulosa zone are suspended in a cold buffer (10 mM Tris-HCl, pH 7.4, 3 mM $MgCl_2$, 1 mM EDTA, 250 mM sucrose, 1 mM phenylmethylsulfonyl fluoride, PMSF) and fragmented using a glass/glass Dounce homogenizer. The homogenate is filtered through glass wool and centrifuged for 15 min at 1500 *g* at 4°C. The pellet is incubated for 15 min in ice-cold hypotonic buffer (10 mM Tris-HCl, pH 7.4, 3 mM $MgCl_2$, 1 mM EDTA, and 1 mM PMSF) and kept on ice to allow cell lysis. Lysed cells are recovered by centrifugation at 1500 *g* for 15 min at 4°C, homogenized using a loose-fitting Dounce homogenizer in hypotonic buffer supplemented with 40% glycerol, and stored at −20°C. Before experiments, glycerol is eliminated by washing the membranes in glycerol-free hypotonic buffer.

For preparation of hypophyseal membranes, frozen entire pituitary glands are rapidly thawed at 37°C in isotonic buffer supplemented with 0.1 mM PMSF, and the adenohypophyses are separated. Adenohypophyseal membranes are prepared as described above for adrenal membranes.

For rat mammary gland membrane preparations, tissues are minced and homogenized in 50 mM 10% (wt/vol) buffer A Tris-HCl, pH 7.4, 320 mM sucrose, and 0.5 mM dithiothreitol and centrifuged at 900 *g* for 15 min; the pellet is resuspended in buffer A and centrifuged as above. The two 900-*g* supernatants are filtered through cheesecloth and centrifuged at 70,000 *g* for 20 min. The pellet is washed with buffer B containing 50 mM Tris-HCl, pH 7.4, and 10 mM $MgCl_2$. Finally, the 70,000-*g* washed pellet is suspended in buffer B at a final concentration of ∼ 8 mg protein/ml and stored in aliquots in liquid nitrogen.

V_{1a} binding assays using ^{125}I linear AVP antagonist on human adrenal membranes, myometrial membranes from nonpregnant uterus, or platelet membranes are performed using an incubation medium (200 µl) containing 10 mM Tris-HCl, pH 7.4, 3 mM $MgCl_2$, 1 mg/ml bovine serum albumin (BSA), 0.05 mg/ml soy bean trypsin inhibitor, 0.5 mg/ml bacitracin, 0.1 mM PMSF, 0.5 mM EDTA, 10–60 pM ^{125}I-AVP linear antagonist, and increasing amounts of test compound. The reaction is started by the addition of membranes (10–40 µg/assay) that are incubated at 30°C for 45 min. The reaction is stopped by adding 3 ml of ice-cold filtration buffer (10 mM Tris HCl, pH 7.4, and 3 mM $MgCl_2$) followed by filtration through GF/C Whatman glass microfiber filters that have been soaked for at least 5 h in a solution containing 10 mg/ml BSA. Filters are washed five times with 3 ml of filtration buffer and counted for radioactivity by gamma spectroscopy. Nonspecific binding is determined in the presence of 0.3 µM unlabeled iodinated AVP linear antagonist or 1 µM AVP.

EVALUATION

The IC_{50} value is defined as the concentration of inhibitor required to obtain 50% inhibition of the specific binding. Inhibition constant (K_i) values are calculated from the IC_{50} values using the Cheng and Prusoff equation. Data for equilibrium binding (K_d, B_{max}), competition experiments (IC_{50} n_{Hill}), and kinetic constants (k_{obs}, k_1) are analyzed using an iterative nonlinear regression program (Munson and Rodbard 1980).

MODIFICATIONS OF THE METHOD

A receptor assay for arginine-vasopressin is described by Gopalakrishnan et al. (1986).

Pearlmutter et al. (1985) characterized a specific binding site for arginine-vasopressin in particulate membranes from rat aorta.

Pávó et al. (1993) reported the synthesis and binding characteristics of two sulfhydryl-reactive probes for vasopressin receptors.

Serradeil-Le Gal et al. (1994b) tested the effect of a nonpeptide vasopressin V_{1a} vasopressin antagonist on the binding and mitogenic activity of vasopressin in Swiss 3T3 cells.

Yatsu et al. (1997) tested the vasopressin antagonistic activities of a nonpeptide dual vasopressin V_{1a} and V_2 receptor antagonist on V_{1a} receptors in dog platelets and on V_2 receptors in dog kidney homogenates.

Ogawa et al. (1996) and Tahara et al. (1997a) tested V_{1a} receptor binding in homogenates of rat liver and V_2 receptor binding in rat kidney.

Barberis et al. (1995) characterized a linear radioiodinated vasopressin antagonist as an excellent radioligand for vasopressin V_{1a} receptors.

Radioligands for vasopressin V_1 receptors were described by Elands et al. (1988) and by Kelly et al. (1989).

Ala et al. (1997) reported the properties of a radioiodinated antagonist for human vasopressin V_2 and V_{1a} receptors and recommended this ligand for further studies on human vasopressin V_2 receptor localization and characterization, when used with a selective vasopressin V_{1a} ligand.

Howl and Wheatley (1995) found species heterogeneity in the characteristics of V_{1a} receptors and in the expression of hepatic V_{1a} receptors.

Thibonnier et al. (1994) reported molecular cloning, sequencing, and functional expression of a cDNA encoding the human V_{1a} vasopressin receptor.

Carnazzi et al. (1997) described photoaffinity labeling of the rat V_{1a} vasopressin receptor using a linear azidopeptidic antagonist.

Phalipou et al. (1997) studied the peptide-binding domains of the human V_{1a} vasopressin receptor with a photoactivatable linear peptide antagonist.

DDAVP (1-desamino-8-D-arginine vasopressin), which is considered to be a standard V_2 vasopressin receptor-selective agonist, was found to act also as an agonist at the V_{1b} vasopressin receptor (Saito et al. 1997).

Tahara et al. (1997b) investigated the effects of a nonpeptide V_{1a} and V_2 vasopressin receptor antagonist in binding and functional studies of rat vascular smooth muscle cells.

Tahara et al. (1998) expressed three subtypes of human arginine-vasopressin receptors, hV_{1a}, hV_{1b}, and hV_2, in Chinese hamster ovary cells and characterized them by [^{3}H]AVP binding. In addition, the coupling of the expressed receptor protein to a variety of signal transduction patterns was investigated.

REFERENCES AND FURTHER READING

Ala Y, Morin D, Mahé E, Cotte N, Mouillac B, Jard S, Barberis C, Tribollet E, Dreifuss JJ, Sawyer WH, Wo N C, Chan WY, Kolodziejczyk AS, Chen LL, Manning M (1997) Properties of a new radioiodinated antagonist for human vasopressin V_2 and V_{1a} receptors. Eur J Pharmacol 331:285–293

Albright JD, Chan PS (1997) Recent advances in the discovery of vasopressin antagonists: peptide and nonpeptide V_{1a} and V_2 receptor antagonists. Curr Pharm Des 3:615–632

Barberis C, Ballestre MN, Jard S, Tribollet E, Arsenijevic Y, Dreifuss JJ, Bankowski K, Manning M, Chan WY, Schlosser SS, Holsboer F, Elands J (1995) Characterization of a novel linear radioiodinated vasopressin antagonist: an excellent radioligand for vasopressin V_{1a} receptors. Neuroendocrinology 62:135–146

Carnazzi E, Aumelas A, Phalipou S, Mouillac B, Guillon G, Barberis C, Seyer R (1997) Efficient photoaffinity labeling of the rat V_{1a} vasopressin receptor using a linear azidopeptidic antagonist. Eur J Biochem 247:906–913

Elands J, Barberis C, Jard S, Lammek B, Manning M, Sawyer WH, de Kloet ER (1988) ^{125}I-d(CH_2)$_5$[Tyr(Me)^2, Tyr(NH_2)^9]AVP: iodination and binding characteristics of a vasopressin receptor ligand. FEBS Lett 229:251–255

Gaillard RC, Schoeneberg P, Favrod-Coune CA, Muller AF, Marie J, Bockaert J, Jard S (1984) Properties of rat anterior pituitary vasopressin receptors: relation to adenylate cyclase and the effect of corticotropin-releasing factor. Proc Natl Acad Sci USA 81:2907–2911

Gopalakrishnan V, Triggle CR, Sulakhe PV, McNeill JR (1986) Characterization of a specific, high affinity [^{3}H]arginine^8 vasopressin-binding site in liver microsomes from different strains of rats and the role of magnesium. Endocrinology 118:990–997

Howl J, Wheatley M (1995) Molecular pharmacology of V_{1a} vasopressin receptors. Gen Pharmacol 26:1143–1152

Kelly JM, Abrahams JM, Phillips PA, Mendelsohn FAO, Grzonka Z, Johnston CI (1989) [^{125}J]-[d(CH_2)$_5$,Sar^7]AVP: a selective ligand for V_1 vasopressin receptors. J Recept Res 9:27–41

Munson PV, Rodbard D (1980) Ligand: a versatile computerized approach for characterization of ligand-binding systems. Anal Biochem 107:220–239

Nitschke R, Fröbe U, Greger R (1991) Antidiuretic hormone acts via V_1 receptors on intracellular calcium in the isolated perfused rabbit cortical thick ascending limb. Pflügers Arch 417:622–632

Ogawa H, Yamashita H, Kondo K, Yamamura Y, Miyamoto H, Kan K, Kitano K, Tanaka M, Nakaya K, Nakamura S, Mori T, Tominaga M, Yabuuchi Y (1996) Orally active, nonpeptide vasopressin V_2 receptor antagonists: A novel series of 1-[4-(benzoylamino)benzoyl]-2,3,4,5-tetrahydro-1H-benzazepines and related compounds. J Med Chem 39:3547–3555

Pávó I, Kojro E, Fahrenholz F (1993) Synthesis and binding characteristics of two sulfhydryl-reactive probes for vasopressin receptors. FEBS Lett 316:59–62

Pearlmutter AF, Szkrybalo M, Pettibone G (1985) Specific arginine vasopressin binding in particulate membranes from rat aorta. Peptides 6:427–431

Phalipou S, Cotte N, Carnazzi E, Seyer R, Mahe E, Jard S, Barberis C, Mouillac B (1997) Mapping peptide-binding domains of the human V_{1a} vasopressin receptor with a photoactivatable linear peptide antagonist. J Biol Chem 272:26936–26944

Saito M, Tahara A, Sugimoto T (1997) 1-Desamino-8-d-arginine vasopressin (DDAVP) as an agonist on V_{1b} vasopressin receptor. Biochem Pharmacol 53:1711–1717

Serradeil-Le Gal C, Wagnon J, Garcia C, Laccour C, Guiraudou P, Christophe B, Villanova G, Nisato D, Maffrand JP, Le Fur G, Guillon G, Cantau B, Barberis C, Trueba M, Ala Y, Jard S (1993) Biochemical and pharmacological properties of SR 49059, a new, potent, nonpeptide antagonist of rat and human vasopressin V_{1a} receptors. J Clin Invest 92:224–231

Serradeil-Le Gal, Raufaste D, Marty E, Garcia C, Maffrand JP, Le Fur G (1994a) Binding of [^{3}H]SR49059, a potent non-peptide vasopressin antagonist, to rat and human liver membranes. Biochem Biophys Res Commun 199:353–369

Serradeil-Le Gal, Bourrié B, Raufaste D, Carayon P, Garcia C, Maffrand JP, Le Fur G, Casellas P (1994b) Effect of a new, potent, non-peptide vasopressin V_{1a} vasopressin antagonist, SR 49059, on the binding and the mitogenic activity of vasopressin on Swiss 3T3 cells. Biochem Pharmacol 47:633–641

Tahara A, Tomura Y, Wada K I, Kusayama T, Tsukada J, Takanashi M, Yatsu T, Uchida W, Tanaka A (1997a) Pharmacological profile of YM087, a novel potent nonpeptide vasopressin V_{1a} and V_2 receptor antagonist, *in vitro* and *in vivo*. J Pharmacol Exp Ther 282:301–308

Tahara A, Tomura Y, Wada K I, Kusayama T, Tsukada J, Ishii N, Yatsu T, Uchida W, Tanaka A (1997b) Effect of YM087, a potent nonpeptide vasopressin antagonist on vasopressin-induced hyperplasia and hypertrophy of cultured vascular smooth muscle cells. J Cardiovasc Pharmacol 30:759–766

Tahara A, Saito M, Sugimoto T, Tomura Y, Wada K, Kusayama T, Tsukuda J, Ishii N, Yatsu T, Uchida W, Tanaka A (1998) Pharmacological characterization of the human receptor subtypes stably expressed in Chinese hamster ovary cells. Br J Pharmacol 125:1463–1470

Thibonnier M (1998) Development and therapeutic indications of orally-active vasopressin receptor antagonists. Expert Opin Investig Drugs 7:729–740

Thibonnier M, Auzan C, Madhun Z, Wilkins P, Berti-Mattera L, Clauser E (1994) Molecular cloning, sequencing, and functional expression of a cDNA encoding the human V_{1a} vasopressin receptor. J Biol Chem 269:3304–3310

Thibonnier M, Berti-Mattera LN, Dulin N, Conarty DM, Mattera R (1998) Signal transduction pathways of the human V1-vascular, V2-renal, V3-pituitary vasopressin and oxytocin receptors. Prog Brain Res 119:147–161

Yatsu T, Tomura Y, Tahara A, Wada K, Tsukada J, Uchida W, Tanaka A, Takenaka T (1997) Pharmacological profile of YM087, a novel nonpeptide dual vasopressin V_{1a} and V_2 receptor antagonist, in dogs. Eur J Pharmacol 321(2):225–230

N.9 Hypothalamic Hormones

N.9.1 Thyrotropin-Releasing Hormone (TRH)

N.9.1.1 General Considerations

Hypothalamic regulatory hormones are used in diagnostic procedures and for therapy, usually modified by chemical synthesis to enhance activities (Reichlin et al. 1976). The existence of regulators of anterior pituitary function, postulated many years ago (Bargmann 1949; Scharrer and Scharrer 1954), was experimentally demonstrated for the first time by Saffran and Schally (1955) in experiments utilizing hypothalamic and neurohypophyseal extracts. TRH was the first hypothalamic hormone whose chemical structure was elucidated (Bøler et al. 1969; Schally et al. 1970). Its main use is as a diagnostic instrument in thyroid disorders, pituitary tumors, and infertility.

Cloning, characterization, and transcriptional regulation of the TRH gene are reviewed by Wilber and Ai-Hua-Xu (1998).

Pekary (1998) discussed the physiological role of TRH-enhancing peptide (Ps4) which results from proteolytic processing of prepro-TRH.

Effects of TRH and its analogs in the CNS not related to the release of thyroid-stimulating hormone (TSH) (extrapituitary effects) have been found, indicating perhaps other therapeutic indications (Metcalf 1983; Flohé et al. 1983; Nemeroff et al. 1984; Horita et al. 1986; Horita 1998).

Radioimmunoassays for TRH are available (Bassiri et al. 1978).

Furukawa et al. (1980) reported the local effects of TRH on the isolated small intestine and tenia coli of the guinea pig. This effect could be related to the local release of catecholamines.

REFERENCES AND FURTHER READING

Bargmann W (1949) Über die neurosekretorische Verknüpfung von Hypothalamus und Neurohypophyse. Z Zellforsch Mikroskop Anat 34:610–634

Bassiri RM, Dvorak J, Utiger RD (1978) Thyrotropin-releasing hormone. In: Jaffe BM, Behrman HR (eds) Methods of hormone radioimmunoassay. Academic Press, New York, pp 45–56

Bøler J, Enzmann F, Folkers K (1969) The identity of chemical and hormonal properties of the thyrotropin releasing hormone and pyroglutamyl-histidyl-proline amide. Biochem Biophys Res Comm 37:705–710

Flohé L, Bauer K, Friderichs E, Günzler WA, Hennies HH, Herrling S, Lagler F, Otting F, Schwertner E (1983) Biological effects of degradation-stabilized TRH analogues. In: Griffiths EC, Bennett GW (eds) Thyrotropin-releasing hormone. Raven, New York, pp 327–340

Furukawa K, Nomoto T, Tonoue T (1980) Effects of thyrotropin releasing hormone (TRH) on the isolated small intestine and taenia coli of the guinea pig. Eur J Pharmacol 64:279–287

Horita A (1998) An update on the CNS actions of TRH and its analogs. Life Sci 62:1443–1448

Horita A, Carino MA, Lai H (1986) Pharmacology of thyrotropin-releasing hormone. Ann Rev Pharmacol Toxicol 26:311–332

Metcalf (1983) The neuropharmacology of TRH analogues. In: Griffiths EC, Bennett GW (eds) Thyrotropin-releasing hormone. Raven, New York, pp 315–326

Nemeroff CB, Kalivas PW, Golden RN, Prange AJ (1984) Behavioral effects of hypothalamic hypophysiotropic hormones, neurotensin, substance P and other neuropeptides. Pharmacol Ther 24:1–56
Pekary AE (1998) Is Ps4 (prepro-TRH$^{160-169}$) more than an enhancer for thyrotropin-releasing hormone? Thyroid 8:963–968
Reichlin S, Saperstein R, Jackson IMD, Boyd III AE, Patel Y (1976) Hypothalamic hormones. Annu Rev Physiol 38:389–424
Saffran M, Schally AV (1955) The release of corticotrophin by anterior pituitary tissue *in vitro*. Can J Biochem Physiol 33:408–415
Schally AV, Nair RMG, Barrett JF, Bowers CY, Folkers K (1970) The structure of hypothalamic thyrotropin-releasing hormone [abstract]. Fed Proc 29:47
Scharrer E, Scharrer B (1954) Hormones produced by neurosecretory cells. Recent Prog Horm Res 10:183–240
Wilber JF, Ai-Hua-Xu (1998) The thyrotropin-releasing hormone gene 1998: cloning, characterization, and transcriptional regulation in the central nervous system, heart and testis. Thyroid 8:897–901

N.9.1.2 TRH Receptor Binding Assays

PURPOSE AND RATIONALE

Thyrotropin-releasing hormone (TRH) receptors from mouse (Straub et al. 1990; Jones et al. 1996), from rat (Sellar et al. 1993), and from men (Duthie et al. 1993; Matre et al. 1993; Yamada et al. 1993; Hinuma et al. 1994) have been expressed and characterized. Two isoforms have been identified (de la Peña et al. 1992; Lee et al. 1995). Constitutive activity of native TRH receptors has been demonstrated by Jinsi-Parimoo and Gershengorn (1997). Molecular and cellular biology of TRH receptors has been reviewed by Vassart and Dumont (1992) and by Gershengorn and Osman (1996).

TRH receptors have been localized in the pituitary gland (hypothalamic control of thyroid-stimulating hormone secretion), and in other brain regions (extrapituitary effects), which have been extensively explored but not resulted in therapeutic applications (Burt and Taylor 1983). TRH receptors can be determined by binding of [^{3}H]MeTRH (Taylor and Burt 1981; Sharif and Burt 1983; Jarowska-Feil et al. 1995; Yamada et al. 1995) or [^{3}H](3-Me-His^2)TRH (Simasko and Horita 1982).

TRH receptor affinity methods can be applied to the investigation of molecules which might interact with these receptors (Faden et al. 2005; Colson and Gershengorn 2006), and to the quantitate the description of receptor changes *ex vivo* after therapy.

PROCEDURE

Pooled tissue samples are homogenized in a sodium phosphate buffer (20 mM, pH 7.4) and centrifuged at 30,000 *g* for 30 min. The resultant pellets are washed twice by means of resuspension and centrifugation. The washed membranes are dispersed in fresh buffer and are used for the TRH receptor binding assay.

The membranes are incubated in 250 µl of the total volume with 0.5–8 nM of [^{3}H]MeTRH (NEN, sp. act. 62.8 Ci/mmol), in the presence or absence of 10 µM of TRH for 5–6 h at 0°C (in a water-ice bath). The receptor-bound and free [^{3}H]MeTRH are separated by rapid filtration through a glass fiber filter GF/B (Whatman) under reduced pressure (Harvester-Brandel). The trapped receptor-bound radioactivity is determined by liquid scintillation spectrometry (Beckman). The amount of specifically bound [^{3}H]MeTRH is expressed as fmoles per mg of protein.

EVALUATION

The data are subjected to the 6-point Scatchard analysis. The receptor density (B_{max}) and apparent dissociation constant (K_d) are determined.

MODIFICATIONS OF THE METHOD

Sun et al. (1998) described cloning and characterization of the chicken TRH receptor.

REFERENCES AND FURTHER READING

Burt DR, Taylor RL (1983) TRH receptor binding in CNS and pituitary. In: Griffiths EC, Bennett GW (eds) Thyrotropin-releasing hormone. Raven, New York, pp 71–83
Colson AO, Gershengorn MC (2006) Thyrotropin-releasing hormone analogs. Mini Rev Med Chem 6(2):221–226
de la Peña P, Delgado LM, del Camino D, Barros F (1992) Two isoforms of the thyrotropin-releasing hormone receptor generated by alternative splicing have indistinguishable functional properties. J Biol Chem 267:23703–23708
Duthie SM, Taylor PL, Anderson L, Cook J, Eidne KA (1993) Cloning and functional characterization of the human TRH receptor. Mol Cell Endocrinol 95:R11–R15
Faden AI, Knoblach SM, Movsesyan VA, Lea PM 4th, Cernak I (2005) Novel neuroprotective tripeptides and dipeptides. Ann N Y Acad Sci 1053:472–481
Gaudreau P, Boulanger L, Abribat T (1992) Affinity of human growth hormone-releasing factor (1–29)NH_2 analogues for GRF binding sites in rat adenopituitary. J Med Chem 35:1864–1869
Gershengorn MC, Osman R (1996) Molecular and cellular biology of thyrotropin-releasing hormone receptors. Physiol Rev 76:175–171
Han B, Tashjian AH Jr (1995) Importance of extracellular domains for ligand binding in the thyrotropin-releasing hormone receptor. Mol Endocrinol 9:1708–1719
Hinuma S, Hosoya M, Ogi K, Tanaka H, Nagai Y, Onda H (1994) Molecular cloning and functional expression of human thyrotropin-releasing hormone (TRH) receptor gene. Biochim Biophys Acta 1219:251–259
Jarowska-Feil L, Budziszewska B, Lason W (1995) The effect of single and repeated morphine administration on the level of thyrotropin-releasing hormone and its receptors in the rat brain. Neuropeptides 29:343–349

Jinsi-Parimoo A, Gershengorn MC (1997) Constitutive activity of native thyrotropin-releasing hormone receptors revealed using a protein kinase C-responsive reporter gene. Endocrinology 138:1471–1475
Jones KE, Brubaker JH, Chin WW (1996) An alternative splice variant of the mouse TRH receptor mRNA is the major form expressed in the pituitary gland. J Mol Endocrinol 16:197–204
Lee TW, Eidne KA, Milligan G (1995) Signalling characteristics of thyrotropin releasing hormone (TRH) receptor isoforms. Biochem Soc Trans 23:115
Lefrancois L, Gaudreau P (1994) Identification of receptor binding pharmacophores of growth hormone-releasing factor in rat adenopituitary. Neuroendocrinology 59:363–370
Matre V, Karlsen HE, Wright MS, Lundell I, Fjeldheim ÅK, Gabrielsen OS, Larhammar D, Gautvik KM (1993) Molecular cloning of a functional human thyrotropin releasing hormone receptor. Biochem Biophys Res Commun 195:179–185
Mayo KE (1992) Molecular cloning and expression of a pituitary-specific receptor for growth hormone-releasing hormone. Mol Endocrinol 6:1734–1744
Sellar RE, Taylor PL, Lamb RF, Zabavnik J, Anderson L, Eidne KA (1993) Functional expression and molecular characterization of the thyrotrophin-releasing hormone receptor from rat and anterior pituitary gland. J Mol Endocrinol 10:199–206
Sharif NA, Burt RD (1983) Rat brain TRH receptors: kinetics, pharmacology, distribution and ionic effects. Regul Pept 7:399–411
Simasko SM, Horita A (1982) Characterization and distribution of ^{3}H-(3MeHis^{2})thyreotropin releasing hormone receptors in rat brain. Life Sci 30:1793–1799
Straub RE, Frech GC, Joho RH, Gershengorn MC (1990) Expression cloning of a cDNA encoding the mouse pituitary thyrotropin-releasing-hormone receptor. Proc Natl Acad Sci USA 87:9514–9518
Sun YM, Millar RP, Ho H, Gershengorn MC, Illing N (1998) Cloning and characterization of the chicken thyrotropin-releasing hormone receptor. Endocrinology 139:3390–3398
Taylor RL, Burt DR (1981) Properties of [^{3}H](3-Me-His^{2})TRH binding to apparent TRH receptors in the sheep central nervous system. Brain Res 218:207–217
Vassart G, Dumont JE (1992) The thyrotropin receptor and the regulation of thyrocyte function and growth. Endocr Rev 13:569–611
Yamada M, Monden T, Satoh T, Satoh N, Murakami M, Iriuchijima T, Karegawa T, Mori M (1993) Pituitary adenomas of patients with acromegaly express thyrotropin-releasing hormone receptor messenger RNA: cloning and functional expression of the human thyrotropin-releasing hormone receptor gene. Biochem Biophys Res Commun 195:737–745
Yamada M, Iwasaki T, Satoh T, Monden T, Konaka S, Murakami M, Iriuchijima T, Mori M (1995) Activation of the thyrotropin-releasing hormone (TRH) receptor by a direct precursor of TRH, TRH-Gly. Neurosci Lett 196:109–112

N.9.1.3 Release of ^{131}I from Thyroid Glands of Mice

PURPOSE AND RATIONALE

An animal bioassay method for TRH utilizes iodine-deficient mice, treated with ^{131}I, codeine, and 1 µg thyroxin (Redding et al. 1966; Bowers et al. 1967; Redding and Schally 1969). This is a historical test based on the effect of thyroid hormone release by TRH (indirect bioassay). The rise in radioactivity in blood 2 h after injection of the TRH preparations is proportional to the effect of TSH released by TRH. It needs to be assessed whether the extract being tested is free of TSH contamination.

PROCEDURE

Weanling mice of the Swiss-Webster strain weighing 15 g are fed a low-iodine diet and given distilled water for 10 days. At time zero, 4 µC Na^{131}I, 1 µg thyroxin, and 1 mg codeine phosphate are injected subcutaneously. Codeine is given again subcutaneously at 24, 30, and 48 h after time zero and then 2 h after the fourth injection of codeine, blood is taken from the orbital venous sinus. The test preparation or TRH standard is injected intravenously at increasing doses (0.01, 0.03, 0.09 µg/mouse), and 2 h later, a second blood sample is taken from the orbital venous sinus. The response is obtained by the increase of radioactivity from the first to the second blood sample (Δcpm).

EVALUATION

Dose–response curves are established for the test preparation and standard in order to calculate potency ratios with confidence limits.

MODIFICATIONS OF THE METHOD

TRH also stimulates release of TSH and subsequently of ^{131}I in rats pretreated with Na^{131}I and 5 µg thyroxin (Yamakazi et al. 1963).

TRH increases plasma TSH levels in thyroidectomized rats pretreated with 1 µg of T_3 (Bowers et al. 1965). This assay is based on enhanced TSH secretion after eliminating the feedback of thyroid hormones. The baseline is then lowered by T_3 pretreatment to provide a wider range for stimulation by TSH. Rats weighing 350–400 g are surgically thyroidectomized. After 1–3 months, 1 µg of L-triiodothyronine Na is given intraperitoneally; 2 h later urethane is given subcutaneously; approximately 1 h later 1.5 ml blood is removed from the jugular vein and the TRH preparation is administered intravenously. Another 1.5 ml blood is removed 15 min later. Heparin is added to the blood and TSH levels in plasma are assayed by release of ^{131}I from the mouse thyroid (McKenzie 1958) (see N.7.5.3). Results are recorded as mean change in blood ^{131}I levels in five mice.

TRH produces a significant depletion of pituitary TSH content in mice (Bowers et al. 1967). Swiss-Webster strain mice are treated as described for de-

termination of blood ^{131}I radioactivity. Two hours after administration of TRF, the animals are decapitated and the pituitaries immediately removed. Pituitaries of each group of five mice are combined and homogenized in 5 ml of 0.01 M acetic acid which contains 0.9% NaCl. TSH is determined according to McKenzie (1958) (see N.7.5.3). Today, this has been replaced by radioimmunoassay determination of pituitary TSH content.

REFERENCES AND FURTHER READING

Bøler J, Enzmann F, Folkers K (1969) The identity of chemical and hormonal properties of the thyrotropin releasing hormone and pyroglutamyl-histidyl-proline amide. Biochem Biophys Res Commun 37:705–710

Bowers CY, Schally AV (1970) Assay of thyrotropin-releasing hormone. In: Hypophysiotropic hormones of the hypothalamus: assay and chemistry. Williams and Wilkins, Baltimore, Md., pp 74–89

Bowers CR, Redding TW, Schally AV (1965) Effect of thyrotropin releasing factor (TRF) of ovine, bovine, porcine and human origin on thyrotropin release *in vitro* and *in vivo*. Endocrinology 77:609–616

Bowers CY, Schally AV, Reynolds GA, Hawley WD (1967) Interactions of L-trijodothyronine and thyrotropin-releasing factor on the release and synthesis of thyrotropin from anterior pituitary gland of mice. Endocrinology 81:741–747

Bowers CY, Lee KL, Schally AV (1968) Effect of actinomycin D on hormones that control the release of thyrotropin from the anterior pituitary glands of mice. Endocrinology 82:303–310

McKenzie JM (1958) The bioassay of thyrotropin in serum. Endocrinology 63:372–382

Redding TW, Schally AV (1967) Depletion of pituitary thyrotropic hormone by thyrotropin releasing factor. Endocrinology 81:918–921

Redding TW, Schally AV (1969) Studies on the thyrotropin-releasing hormone (TRH) activity in peripheral blood. Proc Soc Exp Biol Med 131:420–425

Redding TW, Bowers CY, Schally AV (1966) An *in vivo* assay for thyrotropin releasing factor. Endocrinology 79:229–236

Schally AV, Bowers CY, Redding TW (1966) Purification of thyrotropic hormone-releasing hormone from bovine hypothalamus. Endocrinology 78:726–732

Schally AV, Arimura A, Bowers CY, Kastin AJ, Sawano S, Redding TW (1968) Hypothalamic neurohormones regulating anterior pituitary function. Recent Prog Horm Res 24:497–588

Schally AV, Redding TW, Bowers CY, Barrett JF (1969) Isolation and properties of porcine thyrotropin-releasing hormone. J Biol Chem 244:4077–4088

Yamakazi E, Sakiz E, Guillemin R (1963) An *in vivo* bioassay for TSH-releasing factor. Experientia 19:480–481

N.9.1.4 Release of TSH from Rat Anterior Pituitary Glands in Vitro

PURPOSE AND RATIONALE

The *in vitro* bioassay method of Saffran and Schally (1955a, 1955b), developed for detecting corticotropin-releasing factor (CRF) activity, has been modified to measure TRH activity *in vitro* (Guillemin et al. 1963; Bowers et al. 1965; Schally and Redding 1967).

PROCEDURE

Male Sprague-Dawley rats weighing 150–200 g serve as donors. After removal, each pituitary is cut in half, transferred to a 15-ml beaker containing 1.5 ml Krebs-Ringer bicarbonate medium with 200 mg% glucose and incubated for three 60-min periods. The media used in the first two incubations are discarded. At the beginning of the third incubation period, various amounts of test preparation or TRH standard are added to individual beakers. At the end of the third incubation period the media from both control and experimental beakers are carefully freed of pituitary tissue. The media are then assayed by RIA for content of TSH.

EVALUATION

Dose–response curves are established for test preparation and standard allowing calculation of potency ratios with confidence limits.

MODIFICATIONS OF THE METHOD

For the assay of TRH analogs, cultures of enzymatically dispersed anterior pituitary cells from rats can be used instead of pituitary halves (Vale et al. 1972).

Barros et al. (1986) studied the effect of TRH on cultured GH3 rat anterior pituitary cells using the whole-cell voltage-clamp technique.

REFERENCES AND FURTHER READING

Barros F, Kaczorowski GJ, Katz GM, Vandlen RL, Reuben JP (1986) Application of whole-cell voltage clamp in the study of neuroendocrine cells. In: Electrophysiological techniques in pharmacology. Liss, New York, pp 149–168

Bowers CY, Schally AV (1970) Assay of thyrotropin-releasing hormone. In: Hypophysiotropic hormones of the hypothalamus: assay and chemistry. Williams and Wilkins, Baltimore, Md., pp 74–89

Bowers CR, Redding TW, Schally AV (1965) Effect of thyrotropin releasing factor (TRF) of ovine, bovine, porcine and human origin on thyrotropin release *in vitro* and *in vivo*. Endocrinology 77:609–616

Guillemin R, Vale W (1970) Bioassays of the hypophysiotropic hormones: *in vitro* systems. In: Hypophysiotropic hormones of the hypothalamus: assay and chemistry. Williams and Wilkins, Baltimore, Md., pp 21–35

Guillemin R, Yamazaki E, Gard D, Jutisz M, Sakiz E (1963) *In vitro* secretion of thyrotropin (TSH): stimulation by a hypothalamic peptide. Endocrinology 73:564–572

Jeffcoate SL, Linton EA, Lira O, White N (1983) Age-dependent changes in the brain content, enzymic inactivation, and hypophysiotropic action of TRH in the rat. In: Griffiths EC, Bennett GW (eds) Thyrotropin-releasing hormone. Raven, New York, pp 145–155

McKenzie JM (1958) The bioassay of thyrotropin in serum. Endocrinology 63:372–382
Saffran M, Schally AV (1955a) The release of corticotrophin by anterior pituitary tissue *in vitro*. Can J Biochem Physiol 33:408–415
Saffran M, Schally AV (1955b) *In vitro* bioassay of corticotropin: modification and statistical treatment. Endocrinology 56:512–532
Schally AV, Redding TW (1967) *In vitro* studies with thyrotropin releasing factor. Proc Soc Exp Biol Med 126:320–325
Vale W, Grant G, Amoss M, Blackwell R, Guillemin R (1972) Culture of enzymatically dispersed anterior pituitary cells: functional validation of a method. Endocrinology 91:562–572

N.9.1.5
TSH and Prolactin Release by TRH in Rats

In bioassays for TRH activity based on the release of TSH measured by radioimmunoassay it was found in many species investigated, and also in clinical testing of humans, that the injection of TRH causes the dose-proportional release of prolactin. This test is suitable for biological activity of TRH, e. g., in domestic animals, and also for the clinical investigation of prolactin secretion in humans.

PROCEDURE

The TRH test in rats is performed in a minimally invasive manner, and when animals have been previously treated it is done 24 h after the last dosing on the following morning. The test dose is a subcutaneous injection of 1 µg/kg body weight synthetic TRH followed by blood sampling in unanesthetized rats 30 min later. Blood sampling may be performed by retro-orbital puncture.

For extended studies on pituitary responsiveness, it is also possible to use a very specific TRH test blocking basal TSH by injection of levothyronine (L-T_3, 1 µg/rat s.c.) 18 h before the test. The following morning, the TRH dose is injected intravenously followed by blood sampling at 15 min or (in anesthetized rats) after 15 and 30 min.

EVALUATION

The usual procedure for evaluation is to compare the TSH concentration in control animals and treated animals (drug treatment or physiological manipulation), to calculate group means, and to evaluate the significance of difference by appropriate statistical tests, where necessary by performing analysis of variance (ANOVA).

The individual response of the animals may be assessed by comparing the basal TSH concentration before the TRH test injection, and the TSH increments at increasing dose intervals after TRH stimulation.

MODIFICATIONS OF THE METHOD

The TRH test is useful in rats and in other animal species. The test dose may be administered by intravenous injection or preferably by subcutaneous injection; nasal application should also be considered (a considerably higher TRH dose is required, and this test can be performed in dogs).

Several analytical methods are available to determine the serum concentrations of TSH and prolactin, both from commercial suppliers and for research applications (Fraglia 1998; Markianos et al. 1996; Katznelson 1998; Fail et al. 1999; Hashizume et al. 2005; Koch et al. 2006). For human diagnostic applications, highly sensitive TSH tests based on measuring only the basal concentrations have replaced the diagnostic TRH test in many instances. Methods are increasingly sensitive, and, for a review, refer to the web site "thyroidmanager" (Spencer 2004).

REFERENCES AND FURTHER READING

Faglia G (1998) The clinical impact of the thyrotropin-releasing hormone test. Thyroid 8(10):903–908
Fail PA, Anderson SA, Friedman MA (1999) Response of the pituitary and thyroid to tropic hormones in Sprague-Dawley versus Fischer 344 male rats. Toxicol Sci 52(1):107–121
Hashizume T, Sasaki T, Nonaka S, Hayashi T, Takisawa M, Horiuchi M, Hirata T, Kasuya E (2005) Bovine posterior pituitary extract stimulates prolactin release from the anterior pituitary gland *in vitro* and *in vivo* in cattle. Reprod Domest Anim 40(2):184–189
Katznelson L, Riskind PN, Saxe VC, Klibanski A (1998) Prolactin pulsatile characteristics in postmenopausal women. J Clin Endocrinol Metab 83(3):761–764
Koch A, Hoppen HO, Dieleman SJ, Kooistra HS, Gunzel-Apel AR (2006) Effects of the dopamine agonist cabergoline on the pulsatile and TRH-induced secretion of prolactin, LH, and testosterone in male beagle dogs. Theriogenology 65(8):1666–1677
Markianos M, Lykouras L, Stefanis C (1996) Prolactin and TSH responses to TRH and to ECT in pre- and postmenopausal women with major depression. Biol Psychiatry 40(5):403–406
Spencer C (2004) Human diagnostic procedures, refer to website [] Assay of thyroid hormones and related substances, last revised by C. Spencer, 2004

N.9.2
Luteinizing Hormone Releasing Hormone (LH-RH)

N.9.2.1
General Considerations

Gonadotropin secretion is controlled by the hypothalamic peptide luteinizing hormone releasing hormone (LH-RH), which stimulates the release of FSH and LH.

The discovery of the structure of LH-RH then led to the synonym of gonadotropin releasing hormone (Gn-RH) and identification of its receptors followed (Conn et al. 1986). The search for a specific FSH-releasing factor has continued (McCann et al. 1993) but so far has remained elusive. LH-RH is secreted in a pulsatile fashion (Levine et al. 1991). This is not relevant to the bioassays, which use LH-RH injections as well as infusion for several hours. Radiolabeling and photoaffinity labeling of Gn-RH receptors have been described (Perrin et al. 1982; Hazum and Keinan 1983). LH-RH bioactivity is determined *in vitro* on pituitary cells and *in vivo* by its effects on ovulation, spermatogenesis, and other gonadal parameters (McCann 1970; Steelman 1970). Radioimmunoassays and radioreceptor assays are available (Nett and Niswender 1979). Many studies of rats and primates showed that prolonged administration of LH-RH agonists results in a decrease of LH and gonadal hormones to castrate levels (Sandow et al. 1978, 1980; Akhtar et al. 1983; Weinbauer et al. 1987, 1990).

Short- and long-term effects on pituitary–gonadal function in neonatal and adult female rats treated with gonadotropin-releasing hormones have been analyzed by Trimino et al. (1993).

The Food and Drug Administration (FDA) recommendations for preclinical testing of Gn-RH analogs, including pharmacology, pharmacokinetics and toxicology, are published by Raheja and Jordan (1994).

REFERENCES AND FURTHER READING

Akhtar FB, Marshall GR, Wickings EJ, Nieschlag E (1983) Reversible induction of azoospermia in rhesus monkeys by constant infusion of a gonadotropin-releasing hormone agonist using osmotic minipumps. J Clin Endocrinol Metab 56:534–540

Conn PM, Staley D, Harris C, Andrews WV, Gorospe WC, McArdle CA, Huckle WL, Hansen J (1986) Mechanism of action of gonadotropin releasing hormone. Annu Rev Physiol 48:495–513

Hazum E, Keinan D (1983) Gonadotropin releasing-hormone receptors: photoaffinity labeling with an antagonist. Biochem Biophys Res Commun 110:116–123

Levine JE, Bauer-Dantoin AC, Besecke LM, Conaghan LA, Legan SJ, Meredith JM, Strobl FJ, Urban JH, Vogelsong KM, Wolfe AM (1991) Neuroendocrine regulation of the luteinizing hormone-releasing hormone pulse generator in the rat. Recent Prog Horm Res 47:97–153

McCann SM (1970) Bioassay of luteinizing hormone-releasing hormone. In: Hypophysiotropic hormones of the hypothalamus: assay and chemistry. Williams and Wilkins, Baltimore, Md., pp 90–102

McCann SM, Marubayashi U, Sun HQ, Yu WH (1993) Control of follicle-stimulating hormone and luteinizing hormone release by hypothalamic peptides. Ann N Y Acad Sci USA 687:55–59

Nett TM, Niswender GD (1979) Gonadotropin-releasing hormone. In: Jaffe BM, Behrman HR (eds) Methods of hormone radioimmunoassay. Academic Press, New York, pp 57–75

Perrin M, Haas H, Rivier JE, Vale WW (1982) GnRH binding to rat anterior pituitary membrane homogenates: comparison of antagonists and agonists using radiolabeled antagonist and agonist. Mol Pharmacol 23:44–51

Raheja KL, Jordan A (1994) FDA recommendations for preclinical testing of gonadotropin releasing hormone (GnRH) analogues. Regul Toxicol Pharmacol 19:168–175

Sandow J, von Rechenberg W, Jerzabek G, Stoll W (1978) Pituitary gonadotropin inhibition by a highly active analog of LHRH. Fertil Steril 30:205–209

Sandow J, von Rechenberg W, Jerzabek G (1980) Hypothalamic-pituitary-testicular function in rats after supraphysiological doses of a highly active LHRH analogue (buserelin). Acta Endocrinol 94:489–497

Steelman SL (1970) The determination of the follicle-stimulating hormone-releasing factor (FSH-RF) In: Hypophysiotropic hormones of the hypothalamus: assay and chemistry. Williams and Wilkins, Baltimore, Md., pp 103–114

Trimino E, Pinilla L, Aguilar E (1993) Pituitary-gonadal function in neonatal and adult female rats treated with gonadotropin-releasing hormone agonists and antagonists. Short- and long-term effects. Acta Endocrinol 129:251–259

Weinbauer GF, Respondek M, Themann H, Nieschlag E (1987) Reversibility of long-term effects of GnRH agonist administration on testicular histology and sperm production in the nonhuman primate. J Androl 8:319–329

Weinbauer GF, Behre HM, Nieschlag E (1990) Contraceptive studies with GnRH analogs in men and non-human primates. In: Bouchard P, Haour F, Franchimont P, Schatz B (eds) Recent progress in GnRH and gonadal peptides. Elsevier, Amsterdam, pp 181–194

N.9.2.2 LH-RH Receptor Assays

PURPOSE AND RATIONALE

LH-RH (Gn-RH) interacts with a membrane receptor which belongs to the G-protein-coupled receptor family. The LH-RH-R is encoded by a single-copy gene consisting of three exons and two introns. Consistent with its site of action, LH-RH-R mRNA has been found in the brain, pituitary, gonads, placenta, as well as in tumor tissue and tumor cell lines (Jennes and Conn 1994). Binding to LH-RH receptors in rat pituitary membranes has been studied for LR-RH agonists and antagonists. Furthermore, the time course of downregulation of LH-RH receptors was followed (Halmos et al. 1996).

PROCEDURE

Receptor binding of LH-RH is determined using a sensitive *in vitro* ligand competition assay based on binding of radiolabeled buserelin or [D-Trp^6]LH-RH to rat anterior pituitary membrane homogenates (Halmos et al. 1993, 1996; Szöke et al. 1994). Membrane homogenates containing 40–80 µg of protein are incubated in triplicate with 60,000–75,000 cpm

(≈ 0.15 nM) [^{125}I][D-Trp^6]LH-RH as radioligand and with increasing concentrations (10^{-12}–10^{-6} M) of nonradioactive peptides in a total volume of 150 µl of binding buffer. At the end of the incubations, 125-µl aliquots of suspension are transferred to the top of 1 ml of ice-cold binding buffer containing 1.5% bovine serum albumin in siliconized polypropylene microcentrifuge tubes (Sigma). The tubes are centrifuged at 12,000 *g* for 3 min at 4°C. Supernatants are aspirated, and the bottoms of the tubes containing the pellet are cut off and assayed in a gamma-counter. Protein concentration is determined by the method of Bradford (1976) using a BioRad protein assay kit.

EVALUATION

Specific ligand-binding capacities and affinities are calculated by the computerized curve-fitting program of Munson and Rodbard (1980) as modified by McPherson (1985). To determine the types of receptor binding, dissociation constants (K_d values), and the maximal binding capacity (B_{max}), LH-RH binding data are also analyzed by the Scatchard method. Statistical significance is assessed by Duncan's new multiple range test.

MODIFICATIONS OF THE METHOD

Flanagan et al. (1998) recommended ^{125}I-[His^5,Tyr^6]-Gn-RH as the radioligand for analysis of mutant Gn-RH receptors.

Perrin et al. (1982) compared binding of radiolabeled antagonists and antagonists of gonadotropin-releasing hormone to rat anterior pituitary membrane homogenates.

Fekete et al. (1989) reviewed the role of receptors for LH-RH, somatostatin, prolactin, and epidermal growth factor in rat and human prostate cancers and in benign prostate hyperplasia.

Cloning, sequencing, and expression of the human gonadotropin-releasing hormone receptor are published by Kakar et al. (1992).

Marheineke et al. (1998) characterized the human gonadotropin-releasing hormone receptor heterologously produced using the baculovirus/insect cell and the semliki forest virus systems.

The binding kinetics of a long-acting gonadotropin-releasing hormone antagonist to rat LH-RH receptors were studied by Li et al. (1994).

Lovejoy et al. (1995) determined the receptor binding of gonadotropin-releasing hormone analogs in bovine pituitary membrane preparations.

The cDNA encoding the receptor for LH-RH was isolated from a human pituitary cDNA library and heterologously expressed in the murine fibroblast cell line LTK$^-$ by Beckers et al. (1995).

Tsutsumi et al. (1995) investigated the role of altered receptor biosynthesis in agonist-induced receptor downregulation in αT_3-1 cells, a mouse gonadotrope cell line.

Beckers et al. (1997) characterized gonadotropin-releasing hormone analogs by a cellular luciferase reporter gene assay. The assay is based on a fusion of the c-fos immediate-early gene promoter to *Photinus pyralis* luciferase (LUC) as reporter gene, stably transfected in murine LTK$^-$ cells expressing the human GnRH receptor. Transcription of endogenous c-fos and fos–Luc fusion gene are transiently induced quite similarly by fetal calf serum and a superagonistic Gn-RH analog. The reporter gene was used to monitor agonist-induced signaling via the human Gn-RH receptor. Whereas Luc activity was induced in a dose-dependent manner by Gn-RH or an agonistic analog, different antagonistic peptides completely inhibited this stimulation.

The current state of knowledge is reviewed by Cheng and Leung (2005), Kakar et al. (2004) and Millar et al. (2004) for domestic animals and for the human, including the description of two separate types of the gonadotropin-releasing hormone receptor (Gn-RH-I and II), and the increasing complexity of Gn-RH receptor-mediated signaling.

CRITICAL ASSESSMENT OF THE METHODS

There is an ever-increasing complexity of the extensive results of the application of LH-RH (Gn-RH) receptor methods, which may be to structure–activity studies with LHRH analogs, to elucidating species-specific regulation in domestic animals and in humans, or to the measurement of adaptive changes of the LH-RH receptor concentrations in physiology, in pharmacological experiments, and in the pathophysiology of human disease. Numerous approaches have been described based on ligand binding to receptors extracted from tissue, to cloned receptor proteins, and based on direct measurement of the receptor protein concentrations.

REFERENCES AND FURTHER READING

Beckers T, Marheineke K, Reiländer H, Hilgard P (1995) Selection and stable characterization of mammalian cell lines with stable over-expression of human pituitary receptors for gonadoliberin. Eur J Biochem 231:535–543

Beckers T, Reiländer H, Hilgard P (1997) Characterization of gonadotropin-releasing hormone analogs based on a sensitive cellular luciferase reporter gene assay. Anal Biochem 251:17–23

Bradford M (1976) A rapid and sensitive method for the quantitation of microgram quantities of protein utilizing the principle of protein-dye binding. Anal Biochem 72:248–254
Cheng CK, Leung PC (2005) Molecular biology of gonadotropin-releasing hormone (GnRH)-I, GnRH-II, and their receptors in humans. Endocr Rev 26(2):283–306
Fekete M, Redding TW, Comaru-Schally AM, Pontes JE, Connelly RW, Srkalovic G, Schally AV (1989) Receptors for luteinizing hormone-releasing hormone, somatostatin, prolactin, and epidermal growth factor in rat and human prostate cancers and in benign prostate hyperplasia. Prostate 14:191–208
Flanagan CA, Fromme BJ, Davidson JS, Millar RP (1998) A high affinity gonadotropin-releasing hormone (GnRH) tracer, radioiodinated at position 6, facilitates analysis of mutant GnRH receptors. Endocrinology 139:4115–4119
Halmos G, Rekasi Z, Szoke B, Schally AV (1993) Use of radioreceptor assay and cell superfusion system for *in vitro* screening of analogs of growth hormone-releasing hormone. Receptor 3:87–97
Halmos G, Schally AV, Pinski J, Vadillo-Buenfil M, Groot K (1996) Down-regulation of pituitary receptors for luteinizing hormone-releasing hormone (LH-RH) in rats by the LH-RH antagonist Cetorelix. Proc Natl Acad Sci USA 93:2398–2402
Jennes L, Conn PM (1994) Gonadotropin releasing hormone and its receptors in brain. Front Neuroendocrinol 15:51–77
Kakar SS, Musgrove LC, Devor DC, Sellers JC, Neill JD (1992) Cloning, sequencing, and expression of human gonadotropin releasing hormone (GnRH) receptor. Biochem Biophys Res Commun 189:289–295
Kakar SS, Malik MT, Winters SJ, Mazhawidza W (2004) Gonadotropin-releasing hormone receptors: structure, expression, and signaling transduction. Vitam Horm 69:151–207
Leung PCK, Peng C (1996) Gonadotropin-releasing hormone receptor: gene structure, expression and regulation. Biol Sig 5:63–69
Li SL, Vuagnat B, Gruaz NM, Eshkol A, Sizonenko PC, Aubert ML (1994) Binding kinetics of the long-acting gonadotropin-releasing hormone (GnRH) antagonist Antide to rat pituitary GnRH receptors. Endocrinology 134:45–52
Lovejoy DA, Corrigan AZ, Nahorniak CS, Perrin MH, Porter J, Kaiser R, Miller C, Pantoja D, Craig AG, Peter RE, Vale WW, Rivier JE, Sherwood NM (1995) Structural modifications of non-mammalian gonadotropin-releasing hormone (GnRH) isoforms: design of novel GnRH analogues. Regul Pept 60:99–115
Marheineke K, Lenhard T, Haase W, Beckers T, Michel H, Reilander H (1998) Characterization of the human gonadotropin-releasing hormone receptor heterologously produced using the baculovirus/insect cell and the semliki forest virus systems. Cell Mol Neurobiol 18:509–524
McPherson GA (1985) KINETIC, EBDA, LIGAND, LOWRY: a collection of radioligand binding analysis programs. Elsevier Science, Amsterdam
Millar RP, Lu ZL, Pawson AJ, Flanagan CA, Morgan K, Maudsley SR (2004) Gonadotropin-releasing hormone receptors. Endocr Rev 25(2):235–275
Munson PJ, Rodbard D (1980) Ligand, a versatile computerised approach for characterization of ligand binding systems. Anal Biochem 107:220–239
Nagy A, Schally AV, Armatis P, Szepeshazi K, Halmos G, Kovacs M, Zarandi M, Groot K, Miazaki M, Jungwirth A, Horvath J (1996) Cytotoxic analogs of luteinizing hormone-releasing hormone containing doxorubicin or 2-pyrrolidinodoxorubicin, a derivative 500–1000 more potent. Proc Natl Acad Sci USA 93:7269–7273
Perrin MH, Haas Y, Rivier JE, Vale WW (1982) Gonadotropin-releasing hormone binding to rat pituitary membrane homogenates. Comparison of antagonists and antagonists using radiolabeled antagonist and agonist. Mol Pharmacol 23:44–51
Pinski J, Lamharzi N, Halmos G, Groot K, Jungwirth A, Vadillo-Buenfil M, Kakar SS, Schally AV (1996) Chronic administration of the luteinizing hormone-releasing hormone (LHRH) antagonist cetrorelix decreases gonadotrope responsiveness and pituitary LHRH receptor messenger ribonucleic acid levels in rats. Endocrinology 137:3430–3436
Szöke B, Horváth J, Halmos G, Rékási Z, Groot K, Nagy A, Schally AV (1994) LH-RH analogue carrying a cytotoxic radical is internalized by rat pituitary cells *in vitro*. Peptides 15:359–366
Tsutsumi M, Laws SC, Rodic V, Sealfon SC (1995) Translational regulation of the gonadotropin-releasing hormone receptor in αT_3-1 cells. Endocrinology 136:1128–1136

N.9.2.3 LH Release in the Ovariectomized Estrogen–Progesterone-Blocked Rat

PURPOSE AND RATIONALE

Ramirez and McCann (1963) recommended the ovariectomized, estrogen–progesterone-blocked rat (OEP rat) as a highly sensitive test model for LH-releasing activity. The gonadotropin content of the pituitary is increased after ovariectomy, due to reduced feedback inhibition through the absence of gonadal steroids. Basal secretion is then acutely lowered to a stable baseline by estrogen–progesterone blockade, whereas the amplitude for stimulation of LH secretion is augmented. The increase in plasma LH levels in donor rats after injection of LH-RH previously determined by bioassay in recipient rats is now conveniently measured by RIA. Since natural and synthetic LH-RH releases both gonadotropins (Schally et al. 1971b), merely stimulation of LH is necessary for routine LH-RH assay.

PROCEDURE

Female Sprague-Dawley rats weighing 150–200 are ovariectomized. They are kept in a light- and temperature-controlled animal room at 24°C and are fed commercial rat chow and tap water ad libitum. Tests are performed 1–3 months after ovariectomy. Three days prior to the assay, the rats receive 50 µg estradiolbenzoate and 25 mg progesterone in sesame oil by the transmuscular-subcutaneous route. For the assay, the rats are anesthetized by subcutaneous injection of 0.6 ml/100 g of 25% urethane solution. Changing to a new anesthetic will require validation of the effect of that anesthetic on sensitivity of the test. Various doses of the test compound or the standard

are injected intravenously into the jugular vein. After 10 min, 4–6 ml blood is withdrawn by cardiac puncture from each donor allowing the separation of 2 ml plasma.

In the original method, bioassayable LH was measured by the ovarian ascorbic acid depletion (OAAD) method according to Parlow and Reichert (1963) (see also N.7.1.2.3). Immature female Sprague-Dawley rats are injected on day 1 at 3:00 p.m. with 50 IU pregnant mares' serum gonadotropin (PMSG) in 0.2 ml saline subcutaneously. On day 3, the rats receive at 9:00 a.m. 25 IU human chorionic gonadotropin (hCG) subcutaneously. On day 7, three different doses of the standard (e. g., NIH LH-S-1, National Institute of Health, Bethesda, Md., USA) or the 2 ml of plasma from the OEP rats is injected intravenously. Eight animals are used per group. Three hours later, the animals are sacrificed, both ovaries are prepared, weighed, and homogenized for determination of ascorbic acid content. The LH activity in OEP plasma, as measure by OAAD, is expressed in terms of NIH-LH-S16 standard.

Furthermore, LH activity in the plasma of OEP rats is measured by radioimmunoassay. OEP rats are anesthetized with 25% urethane intraperitoneally. Blood is withdrawn by retro-orbital puncture. Then various doses of the test preparation or the standard are injected intravenously. After 10 min blood is withdrawn by cardiac puncture. Radioimmunoassays of LH are carried out by the double-antibody method of Niswender et al. (1968).

EVALUATION

Dose–response curves are established for the standard and the test preparation of LH-RH measured by bioassayable LH in OEP plasma as well as for RIA of the LH level in plasma, allowing the calculation of potency ratios with confidence limits. Furthermore, time–response curves can be established by RIA determination of plasma LH levels in OEP rats.

MODIFICATIONS OF THE METHOD

Instead of OEP rats, normal Male Sprague-Dawley rats can be used for measurement of the time course of release of LH after injection of LH-RH or LH-RH derivatives (Arimura et al. 1972). Male Sprague-Dawley rats weighing 120–150 g are anesthetized with 0.6 ml/100 g body weight of 25% urethane solution subcutaneously. After 30 min 0.8 ml blood is withdrawn from the jugular vein, and immediately substituted by the same volume of Haemaccel solution. The LH-RH preparation is injected subcutaneously in 1% gelatine-saline. Blood is withdrawn at hourly intervals up to 6 h, each time being substituted with Haemaccel solution. LH in plasma is determined by the double-antibody method of Niswender et al. (1968) and follicle-stimulating hormone according to the method of Daane and Parlow (1971).

REFERENCES AND FURTHER READING

Arimura A, Schally AV (1970) Progesterone suppression of LH-releasing hormone-induced stimulation of LH release in rats. Endocrinology 87:653–657

Arimura A, Schally AV (1971) Augmentation of pituitary responsiveness to LH-releasing hormone (LH-RH) by estrogen. Proc Soc Exp Biol Med 136:290–293

Arimura A, Debeljuk L, Schally AV (1972) Stimulation of FSH release *in vivo* by prolonged infusion of synthetic LH-RH. Endocrinology 91:529–532

Daane TA, Parlow AF (1971) Periovulatory patterns of rat follicle stimulating hormone and luteinizing hormone during normal estrous cycle: effects of pentobarbital. Endocrinology 88:653–663

Monahan MW, Amoss MS, Anderson HA, Vale W (1973) Synthetic analogs of the hypothalamic luteinizing hormone releasing factor with increased agonist and antagonist properties. Biochemistry 12:4616–4620

Niswender GD, Midgley AR Jr, Monroe SE, Reichert LE Jr (1968) Radioimmunoassay for rat luteinizing hormone with antiovine LH serum and ovine LH-^{131}I. Proc Soc Exp Biol Med 128:807–811

Parlow AF, Reichert LE Jr (1963) Influence of follicle-stimulating hormone on the prostate assay of luteinizing hormone (LH, ICSH). Endocrinology 73:377–385

Ramirez VD, McCann SM (1963) A highly sensitive test for LH-releasing activity: the ovarectomized, estrogen progesterone-blocked rat. Endocrinology 73:193–198

Sandow J, Vogel HG (1972) Studies on the *in vivo* inactivation of synthetic LH-RH. Serono Foundation Conference, Acapulco (Mexico), p 21

Sandow J, Enzmann F, Schröder HG, Vogel HG (1972a) Inactivation of LH-RH by the plasma of various species. Naunyn Schmiedebergs Arch Exp Path Pharmakol 274: R95

Sandow J, Schally AV, Schröder HG, Redding TW, Heptner W, Vogel HG (1972b) Pharmacological characteristics of a synthetic releasing hormone LH/FSH-RH (Hoe 471). Arzneimittelforschung 22:1718–1721

Sandow J, Seeger K, Vogel HG (1972c) A long-acting preparation of synthetic LH/FSH-releasing hormone. In: Kaskarelis D (ed) Third European Conference on Sterility, Athens 1972

Sandow J, von Rechenberg W, Jerzabek G (1976) The effect of LH-RH, prostaglandins and synthetic analogues of LH-RH on ovarian metabolism. Eur J Obstet Gynec Reprod Biol 6:185–190

Schally AV, Arimura A, Baba Y, Nair RMG, Matsuo H, Redding TW, Debeljuk L (1971a) Isolation and properties of the FSH and LH-releasing hormone. Biochem Biophys Res Commun 43:393–399

Schally AV, Arimura A, Kastin AJ, Matsuo H, Baba Y, Redding TW, Nair RMG, Debeljuk L (1971b) Gonadotropin-releasing hormone: one polypeptide regulates secretion of luteinizing and follicle-stimulating hormones. Science 173:1036–1038

N.9.2.4 Gonadotropin Release From Anterior Pituitary Cells

PURPOSE AND RATIONALE

Anterior pituitaries can be used directly, kept in culture or used for cell lines (Mittler and Meites 1964, 1966; Mittler et al. 1970; Sandow et al. 1972b) in order to study the synthesis and release of gonadotropins in response to LH-RH.

PROCEDURE

Female Sprague-Dawley rats weighing 100–150 g are used as donors. Each anterior pituitary is removed and cut into four to six pieces of approximately equal size. The cultures are performed in sterile disposable plastic Petri dishes each containing 3 ml medium consisting of 9 parts Difco medium 199 and 1 part of newborn calf serum; 25 U/ml penicillin and 25 µg/ml streptomycin are added. In each dish, the explants are supported at the gas interface. An atmosphere of 95% oxygen and 5% carbon dioxide and a temperature of 36°C are maintained. The opposite sides of the same pituitaries provide matched control and experimental preparations. The pituitaries are incubated for a total time of 5 days. After the first 2 days, the medium is removed and discarded. Fresh medium is then added with the LH-RH solutions. Approximately 12 h after the first change of medium and addition of LH-RH, media are removed and frozen. Fresh medium with LH-RH is again added; this procedure is repeated until six samples of medium representing the last 3 days of culture are obtained. Media are assayed for LH content by radioimmunoassay according to Niswender et al. (1968) and for FSH content according to Parlow and Reichert (1963).

EVALUATION

Using various concentrations of test preparation and LH-RH standard dose–response curves are obtained allowing the calculation of potency ratios with confidence limits.

CRITICAL ASSESSMENT OF THE METHOD

These methods do not reflect the time course of release found *in vivo* but are useful for potency estimates.

MODIFICATIONS OF THE METHOD

Instead of pituitary halves for the assay of LH-RH as well as for the assay of TRF and its analogs, cultures of enzymatically dispersed anterior pituitary cells from rats can be used (Vale et al. 1972; Martin and Sattler 1979).

Loughlin et al. (1981) used perifused pituitary cultures as a model for LH-RH regulation of LH secretion.

O'Connor and Lapp (1984) studied the effect of pulse frequency and duration of exposure to LH-RH in anterior pituitary cells attached to Cytodex I beads.

The functional integrity of anterior pituitary cells separated by a density gradient has been studied (Scheikl-Lenz et al. 1985).

The receptor binding ability of different agonists and antagonists of LH-RH to rat pituitary and human breast cancer membranes was studied by Fekete et al. (1989).

Vigh and Schally (1984) and Csernus and Schally (1991) described in detail a cell superfusion system consisting of a Sephadex column with dispersed pituitary cells. The LH response of anterior pituitary cells to a 3-min exposure to various concentrations of LH-RH at 30-min intervals as well as the growth hormone (GH) response to human GH-releasing hormone resulted in excellent dose–response curves. The effect of GH-releasing hormone was inhibited by somatostatin. Likewise, the effect of LH-RH was inhibited by pretreatment with LH-RH antagonists.

REFERENCES AND FURTHER READING

Buckingham JC, Cover PO (1983) Biological assay of luteinizing hormone-releasing hormone (gonadorelin). J Pharmacol Meth 9:239–247

Csernus VJ, Schally AV (1991) The dispersed cell superfusion system. In: Greenstein B (ed) Neuroendocrine research methods, Vol 1. Harwood Academic, Chur, pp 71–109

Fekete M, Bajuz S, Groot K, Csernus VJ, Schally AV (1989) Comparison of different agonists and antagonists of luteinizing hormone-releasing hormone for receptor binding ability to rat pituitary and human breast cancer membranes. Endocrinology 124:946–955

Haviv F, Fitzpatrick TD; Swenson RE, Nichols CJ, Mort NA, Bush EN, Diaz G, Bammert G, Nguyen A, Rhutasel NS, Nellans HG, Hoffman DJ, Johnson ES, Greer J (1993) Effect of *N*-methyl substitution of peptide bonds in luteinizing hormone-releasing hormone agonists. J Med Chem 36:363–369

Loughlin JS, Badger TM, Crowley WF Jr (1981) Perifused pituitary cultures: a model for LHRH regulation of LH secretion. Am J Physiol 240:E591–E596

Martin JE, Sattler C (1979) Developmental loss of the acute inhibitory effect of melatonin on the *in vitro* pituitary luteinizing hormone and follicle-stimulating hormone response to luteinizing hormone-releasing hormone. Endocrinology 105:1007–1012

Mittler JC, Meites J (1964) *In vitro* stimulation of pituitary follicle-stimulating-hormone release by hypothalamic extract. Proc Soc Exp Biol Med 117:309–313

Mittler JC, Meites J (1966) Effects of hypothalamic extract and androgen on pituitary FSH release *in vitro*. Endocrinology 78:500–504

Mittler JC, Arimura A, Schally AV (1970) Release and synthesis of luteinizing hormone and follicle-stimulating hormone in

pituitary cultures in response to hypothalamic preparations. Proc Soc Exp Biol Med 133:1321–1325
Niswender GD, Midgley AR Jr, Monroe SE, Reichert LE Jr (1968) Radioimmunoassay for rats luteinizing hormone with antiovine LH serum and ovine LH-^{131}I. Proc Soc Exp Biol Med 128:807–811
O'Connor JL, Lapp CA (1984) Luteinizing hormone releasing hormone of fixed pulse frequency and duration. A simplified system for studying the effect of varying pulse concentration on LH release from Cytodex I attached anterior pituitary cells. J Pharmacol Meth 11:195–205
Parlow AF, Reichert LE Jr (1963) Influence of follicle-stimulating hormone on the prostate assay of luteinizing hormone (LH, ICSH). Endocrinology 73:377–385
Sandow J, Schally AV, Redding TW, Heptner W, Vogel HG (1972a) LH-release by a synthetic decapeptide LH/FSH-RH. Naunyn Schmiedebergs Arch Exp Pathol Pharmakol 274:R96
Sandow J, Schally AV, Schröder HG, Redding TW, Heptner W, Vogel HG (1972b) Pharmacological characteristics of a synthetic releasing hormone LH/FSH-RH (Hoe 471). Arzneimittelforschung 22:1718–1721
Schally AV, Mittler JC (1970b) Failure of putrescine and other polyamines to promote FSH release *in vitro*. Endocrinology 86:903–908
Scheikl-Lenz B, Markert C, Sandow J, Träger L, Kuhl H (1985) Functional integrity of anterior pituitary cells separated by a density gradient. Acta Endocrinol 109:25–31
Schröder HG, Geiger R, Enzmann F, Heptner W, Vogel HG (1972) Effect of synthetic LH/FSH-RH on the release of FSH in the rat. Naunyn Schmiedebergs Arch Exp Pathol Pharmakol 274:R93
Vale W, Grant G, Amoss M, Blackwell R, Guillemin R (1972) Culture of enzymatically dispersed anterior pituitary cells: functional validation of a method. Endocrinology 91:562–572
Vigh S, Schally AV (1984) Interaction between hypothalamic peptides in a superfused pituitary cell system. Peptides 5:241–247

N.9.2.5 Radioimmunoassay of Rat LH

PURPOSE AND RATIONALE

Luteinizing hormone is a glycoprotein hormone exhibiting species specificity. For pharmacological experiments in rats, such as evaluation of gonadotropin-releasing hormone activity, a homologous assay is necessary. The reagents are provided by the National Pituitary Agency, Bethesda, Md. The assay procedure is similar to the standard operating procedure proposed by the National Pituitary Agency, USA.

PROCEDURE

Reagents

Standard:	NIH-rat-LH-RP 1
Antiserum:	rabbit-anti-rat-S 9
Tracer:	^{125}I-rat-LH-I 6
Second antibody:	Behring goat-anti-rabbit-gamma-globulin, (Behring, Cat. No. OTOP 14/15)
Buffer:	0.01 M phosphate-saline pH 7.4

Standard and samples are dissolved in 1% bovine serum albumin, tracer in 0.1% bovine serum albumin, and antiserum in EDTA-PBS (1:350 normal rabbit serum as carrier).

Assay

Standards:	0.25–62.5 ng/tube, 200 µl/tube
Antiserum:	1:20,000 100 µl/tube
Tracer:	specific activity 120 µCi/µg, 8000 cpm in 100 µl/tube

Standards (or sample) are incubated with antiserum and tracer for 48 h at +4°C, the second antibody 1:50 (200 µl/tube) is added, and incubated for 24 h at +4°C. Separation is performed with 1.0 ml ice-cold phosphate-buffered saline pH 7.4, the vial spun at 1300 *g* for 15 min, the supernatant decanted, and the residue counted for 1 min in a gamma-counter.

EVALUATION

Data processing: standard curves and sample data are calculated on a computer program using a spline function.

Quality control parameters

Limit of detection:	0.36 ng per tube
Standard curve (ED_{80}–ED_{50}–ED_{20}):	1.31-4.56-15.74 ng per tube
Inter-assay CV (15 assays):	20.9%
Intra-assay CV:	lt; 15%

REFERENCES AND FURTHER READING

Daane TA, Parlow AF (1971) Periovulatory patterns of rat serum follicle stimulating hormone and luteinizing hormone during the normal estrous cycle: effects of pentobarbital. Endocrinology 88:653–663
Niswender GD, Midgley AR Jr, Monroe SE, Reichert LE Jr (1968) Radioimmunoassay for rat luteinizing hormone with antiovine LH serum and ovine LH-^{131}I. Proc Soc Exp Biol Med 128:807–811
Seki K, Seki M, Yoshihara T, Maeda H (1971) Radioimmunoassays for rat follicle stimulating and luteinizing hormones. Endocrinol Jpn 18:477–485

N.9.2.6 Radioimmunoassay of Rat Follicle-Stimulating Hormone (FSH)

PURPOSE AND RATIONALE

Follicle-stimulating hormone (FSH) is a glycoprotein hormone exhibiting species specificity. For pharmaco-

logical experiments in rats, such as evaluation of gonadotropin-releasing hormone activity, a homologous assay is necessary. The reagents and the procedure are provided by the National Pituitary Agency, Bethesda, Md. The assay procedure is similar to the standard operating procedure proposed by the National Pituitary Agency, USA.

PROCEDURE

Reagents

Standard:	NIAMDD-rat-FSH-RP-1
Antiserum:	rabbit-anti-rat-FSH (NIAMDD-S-9)
Tracer:	^{125}I-rat-FSH (e. g. NIAMDD-I-4)
Second antibody:	Behring goat-anti-rabbit-gamma-globulin, (Behring, Cat. No. OTOP 14/15)
Buffer:	0.01 M-phosphate-saline/0.1% bovine serum albumin, pH 7.4

Assay

Standards:	6.25–1600 ng/tube, 200 µl/tube
Antiserum:	1:2000 100 µl/tube
Tracer:	specific activity 200 µCi/µg, 10,000 cpm in 100 µl/tube

Standards (or sample) are incubated with antiserum and tracer for 72 h at +4°C, the second antibody 1:50, 200 µl/tube, is added, and incubated for 48 h at +4°C. Separation is performed with 1.0 ml ice-cold phosphate-buffered saline pH 7.4, the vial spun at 1300 *g* for 15 min, the supernatant decanted, and the residue counted for 1 min in a gamma-counter.

EVALUATION

Data processing: standard curves and sample data are calculated on a computer program using a spline function.

REFERENCES AND FURTHER READING

Beastall GH, Ferguson KM, O'Reilly DSTJ, Seth J (1987) Assays for follicle stimulating hormone and luteinizing hormone: guidelines for the provision of a clinical biochemistry service. Ann Clin Biochem 24:246–262

Midgley AR (1967) Radioimmunoassay for human follicle-stimulating hormone. J Clin Endocrinol Metab 27:295–299

N.9.2.7 Measurement of Ascorbic Acid Depletion in Ovaries of Pseudopregnant Rats

PURPOSE AND RATIONALE

The assay for LH-RH and LH-RH analogs can be performed in one step in pseudopregnant immature female rats using the biological response of the luteinized ovaries to gonadotropins released by the test compounds. Pseudopregnancy is induced in immature female Sprague-Dawley rats by treatment with gonadotropins. Numerous corpora lutea are formed after ovulation. On days 7–8 after the start of treatment the corpora lutea are very sensitive to endogenous or exogenous gonadotropins. Stimulation of steroid synthesis, mainly progesterone, is seen, associated with dose-dependent ascorbic acid depletion in the ovaries. The activity of LH-RH and LH-RH analogs can be determined by the decrease of ovarian ascorbic acid concentration, or the increase in progesterone secretion. Ascorbic acid depletion is a sensitive parameter for the endogenous gonadotropin release in the animals.

PROCEDURE

Immature female Sprague-Dawley rats weighing 35–45 g are pretreated with 50 IU pregnant mares' serum gonadotropin (PMSG) followed by an injection of 25 IU human chorionic gonadotropin (hCG) on the third day. On day 7 or 8, they are injected intramuscularly or subcutaneously with the test preparation or the LH-RH standard in 0.1 ml 1% gelatine-saline. Eight animals are used for each of three doses of the test preparation and standard. One hour later, the ovaries are dissected out, homogenized, and ascorbic acid is determined according to the method of Mindlin and Butler (1938) by photometry.

EVALUATION

Dose–response curves of ascorbic acid depletion are obtained for the test preparation and standard allowing the calculation of potency ratios with confidence limits.

MODIFICATION OF THE METHOD

The method has been adopted as a biological assay of gonadorelin with some modifications by pharmacopoeias, e. g., the British Pharmacopoeia (1988).

CRITICAL ASSESSMENT OF THE METHOD

Classical bioassays of the kind described here are now rarely applied for standardizing LH-RH (gonadorelin) due to the complexity of the biological method. They are being replaced by analytical methods of high specificity and sensitivity, e. g., high-performance liquid chromatography (HPLC) which has been compared with the biological assay and found to be suitable for standardization (see current versions of the British Pharmacopoeia). Standard preparations for gonadorelin (LH-RH, Gn-RH) and for LH-RH analogs

may be obtained from the suppliers (pharmaceutical companies); they are no longer prepared by the National Institute for Biological Standards and Control (NIBS, UK).

REFERENCES AND FURTHER READING

British Pharmacopoeia (1988) Biological assay of gonadorelin. Appendix XIV C, p A166. HMSO, London

Mindlin RL, Butler AM (1938) The determination of ascorbic acid in plasma; a macromethod and a micromethod. J Biol Chem 122:673–686

Parlow AF, Reichert LE Jr (1963) Influence of follicle-stimulating hormone on the prostate assay of luteinizing hormone (LH, ICSH). Endocrinology 73:377–385

Ramirez VD, McCann SM (1963) A highly sensitive test for LH-releasing activity: the ovarectomized, estrogen progesterone-blocked rat. Endocrinology 73:193–198

Sandow J, Schally AV, Redding TW, Heptner W, Vogel HG (1972a) LH-release by a synthetic decapeptide LH/FSH-RH. Naunyn Schmiedebergs Arch Exp Pathol Pharmakol 274:R96

Sandow J, Schally AV, Schröder HG, Redding TW, Heptner W, Vogel HG (1972b) Pharmacological characteristics of a synthetic releasing hormone LH/FSH-RH (Hoe 471). Arzneimittelforschung 22:1718–1721

Sandow J, von Rechenberg W, Jerzabek G (1976) The effect of LH-RH, prostaglandins and synthetic analogues of LH-RH on ovarian metabolism. Eur J Gynec Reprod Biol 6:185–190

N.9.2.8 Progesterone Production in Pseudopregnant Rats

PURPOSE AND RATIONALE

Pseudopregnancy is induced in immature rats by pretreatment with gonadotropins. Numerous corpora lutea are formed after ovulation that are sensitive to endogenous gonadotropins released by LH-RH or LH-RH analogs on days 6–8 after treatment. By measurement of plasma progesterone, the steroidogenic activity of LH-RH analogs can be determined (Sandow et al. 1976).

PROCEDURE

Immature female Sprague-Dawley rats weighing 35–45 g are pretreated with 50 IU pregnant mares' serum gonadotropin (PMSG) followed by an injection of 25 IU human chorionic gonadotropin (hCG) on the third day. They are injected intramuscularly with LH-RH or the LH-RH analog on days 6, 7, or 9 between 8 and 10 a.m. Eight animals are used for each of three doses of test preparation and standard. Blood samples are collected 1 h after treatment. Plasma samples of equal volume are extracted with peroxide free diethylether. The ether phase containing progesterone is evaporated and the sample re-dissolved in BSA-phosphate buffer. Tritium-labeled progesterone and a specific antiserum against progesterone are added and incubated over a period of 24 h at 4°C. Bound hormone and free hormone are separated by absorption on Dextran-coated charcoal. The activity of the sample is determined in a scintillation cocktail containing Triton-X.

EVALUATION

Dose–response curves for progesterone concentrations are established for the test preparation and standard, allowing the calculation of potency ratios with confidence limits.

REFERENCES AND FURTHER READING

Sandow J, von Rechenberg W, Jerzabek G (1976) The effect of LH-RH, prostaglandins and synthetic analogues of LH-RH on ovarian metabolism. Eur J Obstet Gynec Reprod Biol 6:185–190

N.9.2.9 Induction of Ovulation in Rabbits

PURPOSE AND RATIONALE

Ovulation can be induced in mature rabbits by injection of LH-RH after initial priming. This is a modified assay for LH release, which was applied to hypothalamic extracts containing LH-RH activity (Sandow et al. 1972).

PROCEDURE

Six unmated, mature female rabbits (Himalayan strain) weighing 1.0–1.2 kg are used for each dose of standard or test preparation. Follicular maturation is induced by eight subsequent daily subcutaneous injections of LH-RH or the LH-RH analog to be tested in 0.2 ml 1% gelatine-saline. Then 48 h after the last injection, ovulation is induced by administering a fourfold to tenfold higher dose of the peptide in 0.2 ml subcutaneously. After 24 h, the animals are sacrificed, the ovaries weighed, and ovulation is determined by counting the numbers of follicles ovulated in the ovaries, as defined by local bleeding.

EVALUATION

At least two doses of test preparation and standard are used in order to establish dose–response curves, allowing the calculation of potency ratios with confidence limits.

MODIFICATIONS OF THE METHOD

Schröder et al. (1972) and Sandow and Hahn (1973) described changes in the ovary transplanted to the anterior eye chamber in the rabbit enabling the direct ob-

servation of ovulation. This method is also applicable to steroids and prostaglandins.

CRITICAL ASSESSMENT OF THE METHODS

Classical assays such as the eye–ovary transplant have provided excellent morphological information about changes of the ovary during drug treatment. They are however becoming increasingly obsolete because of other methods which are much less invasive, and their use should be considered only as an exception.

REFERENCES AND FURTHER READING

Sandow J, Hahn M (1973) Influence of steroid hormones on the response to LH-RH in the ovary-eye-transplant of the rabbit. Acta Endocrinol Suppl 173:82

Sandow J, Schally AV, Redding TW, Heptner W, Vogel HG (1972) LH-release by a synthetic decapeptide LH/FSH-RH. Naunyn Schmiedebergs Arch Exp Pathol Pharmakol 274:R96

Schröder HG, Seeger K, Vogel HG (1972) The effect of synthetic LH-RH on induction of ovulation near puberty. Abstract Serono Foundation Conference, Acapulco (Mexico) 29.6.–1.7.1972

N.9.2.10 Induction of Superovulation in Immature Rats

PURPOSE AND RATIONALE

Immature female rats (24–26 days of age) do not show vaginal cycles before the onset of puberty. Treatment with pregnant mares' serum gonadotropin (PMSG) induces follicular maturation, followed by spontaneous ovulation 2 days later. Spontaneous ovulation can be blocked by barbiturates (e. g., phenobarbital) acting on the hypothalamus, and is overcome by exogenous LH-RH. The rats ovulate due to the release of endogenous gonadotropins. After hypophysectomy, no ovulatory activity is observed in the absence of the pituitary (Sandow et al. 1972).

PROCEDURE

Immature female Sprague-Dawley rats weighing 55–65 g are injected on day 1 with 10 IU PMSG subcutaneously. Following this pretreatment, the animals will ovulate spontaneously on day 3 between 2:00 and 4:00 p.m. Spontaneous ovulation is blocked by phenobarbital 4 mg/kg at 1:00 p.m. One hour later, the ovulatory peptide, dissolved in 1% gelatine/saline, is injected intravenously. Controls are treated with 1 or 2 IU human chorionic gonadotropin (hCG); negative controls, with gelatine-saline only. Eight rats are used for control groups and various doses of LH-RH or the LH-RH analog. On the next day, the rats are sacrificed at 11:00 a.m. and the oviducts are dissected and stained with Patent blue. The number of ova is counted under a microscope.

EVALUATION

A dose-dependent increase in the number of ova per rat is observed after LH-RH due to LH release and after hCG by direct action on the ovary. The effect of LH-RH analogs is compared with the effects of hCG. Minimal effective doses for LH release can be calculated.

REFERENCES AND FURTHER READING

Sandow J, Schally AV, Redding TW, Heptner W, Vogel HG (1972) LH-release by a synthetic decapeptide LH/FSH-RH. Naunyn Schmiedebergs Arch Exp Pathol Pharmakol 274:R96

N.9.2.11 Inhibition of Experimentally Induced Endometriosis

PURPOSE AND RATIONALE

This is an example of a disease model in animals designed to mimic treatment of an experimentally induced pathological condition. Endometriosis-like lesions can be induced in female rats by autotransplantation of endometrium under the renal capsule (Sakata et al. 1990; Mizutani et al. 1995). This method was used to compare the effect of steroid-induced suppression by a LH-RH analog after chronic administration (pituitary inhibition).

PROCEDURE

Under anesthesia laparotomy is performed in 9-week-old female Sprague-Dawley rats. The left uterine horn is resected and opened by a longitudinal incision. The endometrium is dissected from the myometrium. Then a 5×5 mm section of the endometrium is grafted under the capsule of the left kidney of the same animal. Two weeks later, the attachment and the viability of the endometrial explant are examined by a second laparotomy, the length, width, and height of the explant are measured, and the volume is then calculated. The criterion for a viable graft is fluid accumulation around the lesion. The rate of induction of endometriosis is more than 80%. Animals with endometriosis (with body weights of approximately 250 g) are randomly divided into treatment groups of ten animals each. Gonadotropin-releasing hormone agonists are injected at doses of 15 or 30 µg/kg subcutaneously daily for 3 weeks. A third laparotomy is performed 3 weeks after the beginning of the experiment. The presence of

fluid accumulation and the size of the endometrial explant are examined. The explant is excised and fixed in 10% formalin for histological evaluation.

EVALUATION

The evaluation of treatment on the regression of lesions in experimental endometriosis is analyzed statistically with the χ^2 test.

REFERENCES AND FURTHER READING

Mizutani T, Sakata M, Terakawa N (1995) Effects of gonadotropin-releasing hormone agonists, nafarelin, buserelin, and leuprolide, on experimentally induced endometriosis in the rat. Int J Fertil 40:106–111

Sakata M, Terakawa N, Mizutani T, Tanizawa O, Matsumoto K, Terada N, Sudo K (1990) Effects of danazol, gonadotropin-releasing hormone agonist and a combination of danazol and gonadotropin-releasing hormone agonist on experimental endometriosis. Am J Obstet Gynecol 163:1679–1684

N.9.3 LH-RH Antagonistic Activity

N.9.3.1 Testosterone Suppression in Rats

PURPOSE AND RATIONALE

LH-RH antagonists suppress endogenous secretion of LH and testosterone in adult male rats after a single subcutaneous injection, and after repeated dosing (Loy 1994).

PROCEDURE

Groups of eight adult male Wistar rats weighing 200–250 g are injected subcutaneously with various doses of the test compound or a reference LH-RH antagonist dissolved in 5% mannitol solution. Four hours later, rats are decapitated and blood is collected from the trunk. Serum is separated in a refrigerated centrifuge (10 min at 3000 *g*), and stored frozen at −20°C until assay.

Radioimmunoassay for Testosterone

Serum testosterone is measured by radioimmunoassay in serum extracts using a specific antiserum without prior chromatography, or by direct assay in serum depending on the method. Serum samples of 0.5 ml are extracted with 2 ml of freshly purified, peroxide-free diethylether by shaking for 60 s on a Vortex-type mixer. The aqueous phase is frozen at −70°C, and the ether phase containing testosterone is transferred to conical test tubes, and evaporated under a stream of dry nitrogen. The dry residue is re-dissolved in BSA/phosphate buffer (BSA = 1% bovine serum albumin) for RIA. [1,2,6,7-^{3}H]Testosterone (New England Nuclear NET 367) and a specific antiserum (AS-781, Behringwerke, Marburg, Germany) are added and incubated over a period of 24 h at +4°C under nonequilibrium conditions. Bound hormone and free hormone are separated by adsorption on Dextran-coated charcoal by incubation for 30 min at +4°C and centrifugation at 3000 *g* for 15 min. Then 500 µl of supernatant is transferred into minivials and scintillation cocktail is added. Radioactivity is determined in a beta-counter (Falvo and Nalbandov 1974).

EVALUATION

The hormone levels in the sample are calculated from a standard curve by means of a computer program, using appropriate control sera. Using various doses of standard and test preparation dose–response curves can be established, allowing calculation of potency ratios with confidence limits. Alternatively, minimum effective doses can be calculated from comparisons with controls. Using different time intervals, e. g., 4, 8, and 24 h, the duration of the effect can be evaluated.

MODIFICATIONS OF THE METHOD

Testosterone suppression can be measured in several animal species, e. g., dogs and marmoset monkeys, or cynomolgus monkeys (Habenicht et al. 1990).

Ayalon et al. (1993) tested the potency of the LH-RH antagonist on the pituitary–gonadal system of female castrated and intact ovulating rats.

Reissmann et al. (1996) investigated the antitumor and hormone-suppressive effect of the LH-RH antagonist cetrorelix in the model of DMBA-induced mammary carcinoma (DMBA is 7,12-dimethylbenz[a]anthracene) in female rats and by testosterone determination in normal male rats.

Danz (1995) studied the effect of a gonadotropin-releasing hormone antagonist on androgen-binding protein production and its distribution among the epididymis, seminiferous tubule fluid, testicular interstitial fluid, and blood in rats.

Fallest et al. (1995) studied the transcriptional regulation of the rat luteinizing hormone β (rLHβ) gene through the use of **transgenic mice** bearing a region of the rLHβ gene linked to a luciferase (LUC) reporter gene. The postgonadectomy rise in pituitary rLHβLUC activity in females and males was blocked by daily administration of the Gn-RH antagonist antide.

Rivier et al. (1996) synthesized and evaluated many Gn-RH analogs and established a dose–response re-

lationship between Gn-RH antagonists and pituitary suppression.

CRITICAL ASSESSMENT OF THE METHOD

Structure–activity studies on LH-RH antagonists are based on screening for receptor affinity, and receptor-associated signaling for high-throughput assays. They need to be followed up by confirmation of biological activity, and for quantitation of structure–activity assessment, the assays described here have been eminently suitable for extended compound screening, although the estimates obtained need to be checked for their relevance against the results from intact animals. Suppression of testosterone secretion is one of the preferred methods of confirmation.

REFERENCES AND FURTHER READING

Ayalon D, Farhi Y, Comaru-Schally AM, Schally AV, Eckstein N, Vagman I, Limor R (1993) Inhibitory effect of a highly potent antagonist of LH releasing hormone (SB-7) on the pituitary-gonadal axis in the intact and castrated rat. Neuroendocrinology 58:153–159

Danz BJ (1995) The effects of a gonadotropin-releasing hormone antagonist on androgen-binding protein distribution and other parameters in the adult male rat. Endocrinology 136:4004–4011

Fallest PC, Trader GL, Darrow JM, Shupnik MA (1995) Regulation of rat luteinizing hormone β gene expression in transgenic mice by steroids and a gonadotropin-releasing hormone antagonist. Biol Reprod 55:103–109

Falvo RE, Nalbandov AV (1974) Radioimmunoassay of peripheral plasma testosterone in males from eight species using a specific antibody without chromatography. Endocrinology 95:1466–1468

Habenicht UF, Schneider MR, El Etreby MF (1990) Effect of the new potent LHRH antagonist Antide. J Steroid Biochem Mol Biol 37:937–942

Loy RA (1994) The pharmacology and the potential applications of GnRH antagonists. Curr Opin Obstet Gynecol 6:262–268

Reissmann T, Klenner T, Deger W, Hilgard P, McGregor GP, Voigt K, Engel J (1996) Pharmacological studies with Cetrorelix (SB-75), a potent antagonist of luteinizing hormone-releasing hormone. Eur J Cancer 32A:1574–1579

Rivier J, Jiang G, Lahrichi SL, Porter J, Koerber SC, Rizo J, Corrigan A, Gierasch L, Hagler A, Vale W, Rivier C (1996) Dose relationship between GnRH antagonists and pituitary suppression. Hum Reprod 11 [Suppl 3]:133–147

N.9.3.2 Antiovulatory Activity in Rats

PURPOSE AND RATIONALE

The rat antiovulatory assay (AOA) was widely used for LH-RH antagonists. Immature female rats (24–26 days of age) are primed with pregnant mares' serum gonadotropin (PMSG) to induce follicular maturation, followed by spontaneous ovulation 2 days later. The endogenous hypothalamic LH-RH discharge can be blocked by barbiturates (e. g., phenobarbital) to prevent spontaneous ovulation (see Sect. N.9.2.10). For antiovulatory activity, a test dose of 800 ng exogenous LH-RH is administered together with increasing doses of the LH-RH antagonist. The antagonist will then inhibit the LHRH-induced gonadotropin release. The test measures the dose of LH-RH antagonist required to inhibit the effect of a standard dose of LH-RH.

PROCEDURE

Immature female Wistar rats weighing 55–65 g are injected on day 1 at 9:00 a.m. with 10 IU PMSG subcutaneously. This priming induces follicular maturation and estradiol secretion. A spontaneous, endogenous LH discharge is observed on day 3 between 2:00 and 4:00 p.m.. The release of LH and spontaneous ovulation is blocked by intraperitoneal injection of phenobarbital 4 mg/kg on day 3 at 1:00 p.m.. The LH-RH antagonist is administered in various doses subcutaneously, intraperitoneally or intravenously 30 min before phenobarbital injection. Two hours later, a standard dose of 800 ng LH-RH is injected subcutaneously to induce ovulation. Control groups receive phenobarbital only (negative control) or phenobarbital and 800 ng LH-RH (positive control). Six to eight rats are used for control groups and various doses of the LH-RH antagonist. On the next day, the rats are sacrificed at 9:00 a.m. Both ovaries are prepared and weighed. The oviducts are dissected and stained with Patent blue. The number of ova is counted under a microscope. An effective dose of antagonist prevents LH-RH-induced ovulation.

EVALUATION

A dose-dependent suppression of induced ovulation is observed after the LH-RH antagonist. ID_{50} values can be calculated for various LH-RH antagonists according to the procedure of Litchfield-Wilcoxon. Minimal effective doses which fully suppress ovulation in each animal are calculated.

MODIFICATIONS OF THE METHOD

De la Cruz et al. (1975) described the blockade of the preovulatory LH surge in **hamsters** by an inhibitory analog of LH-RH.

Kovács et al. (1993) found that in ovariectomized and normally cycling rats antiovulatory doses of antagonists of LH-RH inhibit LH and progesterone but not follicle-stimulating hormone (FSH) and estradiol release.

Evaluation of biological activities of new LH-RH antagonists in male and female rats was reported by Pinski et al. (1993).

Rivier et al. (1995) tested a series of gonadotropin-releasing hormone antagonists in the rat antiovulatory assay.

Pinski et al. (1995) evaluated the optical isomers of the LH-RH antagonist Cetrorelix in ovulation inhibition in rats and in suppression of LH levels.

REFERENCES AND FURTHER READING

Bowers CY, Humphries J, Wasiak T, Folkers K, Reynolds GA, Reichert LE Jr (1980) On the inhibitory effects of luteinizing hormone-releasing hormone analogs. Endocrinology 106:674–683

Corbin A, Beattie CW (1975) Inhibition of the pre-ovulatory proestrus gonadotropin surge, ovulation and pregnancy with a peptide analogue of luteinizing hormone releasing hormone. Endocr Res Commun 2:1–23

De la Cruz A, Coy DH, Schally AV, Coy EJ, de la Cruz KG, Arimura A (1975) Blockade of the pre-ovulatory LH surge in hamsters by an inhibitory analog of LH-RH (38855). Proc Soc Exp Biol Med 149:576–579

Deckers GHJ, DeGraaf JH, Kloosterboer HJ, Loozen HJJ (1992) Properties of a potent LHRH antagonist (ORG 30850) in female and male rats. J Steroid Biochem Mol Biol 42:705–712

Deghenghi R, Boutignon F, Wüthrich P, Lenaerts V (1993) Antarelix (EP 24332) a novel water soluble LHRH antagonist. Biomed Pharmacother 47:107–110

Kovács M, Koppán M, Mezö I, Teplán I, Flerkó B (1993) Antiovulatory doses of antagonists of LH-RH inhibit LH and progesterone but not FSH and estradiol release. J Neuroendocrinol 5:603–608

Litchfield JT, Wilcoxon F (1949) A simplified method for evaluating dose-effect experiments. J Pharmacol Exp Ther 96:99

McRae GI, Vickery BH, Nestor JJ Jr, Bremner WJ, Badger TM (1984) Biological activity of a highly potent LHRH antagonist. In: Vickery BH, Nestor JJ Jr, Hafez ESE (eds) LHRH and its analogs. Contraceptive and therapeutic applications. MTP, Boston, Mass., pp 137–151

Pinski J, Yano T, Janaky T, Nagy A, Juhasz A, Bokser L, Groot K, Schally AV (1993) Evaluation of biological activities of new LH-RH antagonists (T-series) in male and female rats. Int Peptide Protein Res 41:66–73

Pinski J, Schally AV, Yano T, Groot K, Srkalovic G, Serfozo P, Reissmann T, Bernd M, Deger W, Kutscher B, Engel J (1995) Evaluation of the *in vitro* and *in vivo* activity of the L-, D,L- and D-Cit^6 forms of the LH-RH antagonist Cetrorelix (SB-75). Int J Peptide Protein Res 43:410–417

Rivier C, Rivier J, Perrin M, Vale W (1983) Comparison of the effect of several gonadotropin releasing hormone antagonists on luteinizing hormone secretion, receptor binding and ovulation. Biol Reprod 29:374–378

Rivier JE, Jiang G, Porter J, Hoeger CA, Craig AG, Corrigan A, Vale W, Rivier CL (1995) Gonadotropin-releasing hormone antagonists: novel members of the azaline B family. J Med Chem 38:2639–2662

Sandow J, Schally AV, Redding TW, Heptner W, Vogel HG (1972) LH-release by a synthetic decapeptide LH/FSH-RH. Naunyn Schmiedebergs Arch Exp Pathol Pharmakol 274:R96

Vilches-Martinez JA, Coy DH, Coy RJ, Arimura A, Schally AV (1976) Comparison of the anti-LH/FSH-RH and antiovulatory activities of [D-Phe^2,D-Leu^6]-LH-RH and [D-Phe^2,D-Ala^6]-LH-RH. Endocr Res Commun 3:231–241

Yardley JP, Foell TJ, Beattie CW, Grant NH (1975) Antagonism of luteinizing hormone release and of ovulation by an analog of the luteinizing hormone-releasing hormone. J Med Chem 18:1244–1247

N.9.3.3 Effect of Repeated Administration of LH-RH Antagonists in Rats

PURPOSE AND RATIONALE

Repeated administration of LH-RH antagonists reduces the testosterone secretion in serum and the tissue content in the testes, and it also decreases the weight of testosterone-dependent organs, such as prostate and seminal vesicles. Moreover, pituitary LH content is decreased and the secretory capacity of the testes for testosterone is diminished. The effects are similar to those after supraphysiological doses of LH-RH agonists (paradoxical antifertility effects).

PROCEDURE

Male Wistar rats with an initial weight between 150 and 200 g are housed under standard conditions. They are treated with daily injections of the LH-RH antagonist for a period of 7 days up to 4 weeks. Alternatively, the LH-RH antagonist can be administered subcutaneously by infusion via minipumps or other routes of administration. Animals receiving the vehicle serve as controls, and rats castrated at the beginning of the experiment may be included for maximum inhibition. At the end of the treatment period, the animals are sacrificed 4 h after the last administration. Blood is collected for testosterone determination by radioimmunoassay. The androgen-dependent organs, testes, epididymides, ventral prostate, and seminal vesicles are dissected and weighed to the nearest 0.1 mg. The testes are decapsulated and incubated with 250 mU human chorionic gonadotropin (hCG) in order to determine the secretory capacity for testosterone. The testosterone tissue content is determined in the supernatant fraction of a testicular homogenate in the absence of hCG (unstimulated testis), and after 3 h of incubation of the contralateral testis with hCG (stimulated testis). Pituitary glands are dissected and the anterior lobe is frozen at −20°C for determination of LH by rat-specific radioimmunoassay (Sect. N.9.2.5). LH receptors in anterior pituitary homogenate are measured by binding of ^{125}I-buserelin *in vitro*.

EVALUATION

The effects of various doses of the LH-RH antagonist after various time intervals on the different parameters mentioned above are compared with values from intact controls and castrated animals. Significant differences compared to controls at the 95% level are calculated by Dunnett's test.

MODIFICATIONS OF THE METHOD

These are mainly models for contraceptive applications and tumor suppression using LH-RH antagonists.

Kangasniemi et al. (1996) used a combined treatment with a Gn-RH antagonist and an antiandrogen (flutamide) to suppress spermatogenesis in mice. Despite this effect, the treatment did not enhance recovery from spermatogenesis produced by a 10-Gy dose of radiation.

Sinha-Hikim and Swerdloff (1993, 1994) examined the time course of suppression and recovery of spermatogenesis and its relationship to the temporal changes in circulating levels of gonadotropin and testosterone and intratesticular testosterone levels after cessation of treatment with a potent Gn-RH antagonist.

REFERENCES AND FURTHER READING

Debeljuk L, Maines VM, Coy DH, Schally AV (1983) Effect of a powerful antagonist of LH-RH on testicular function in prepubertal male rats. Arch Androl 11:89–93

Habenicht UF, Schneider MR, El Etreby MF (1990) Effect of the new potent LHRH antagonist Antide. J Steroid Biochem Mol Biol 37:937–942

Kangasniemi M, Dodge K, Pemberton AE, Huhtaniemi I, Meistrich ML (1996) Suppression of mouse spermatogenesis by a gonadotropin-releasing hormone antagonist and antiandrogen. Failure to protect against radiation-induced damage. Endocrinology 137:949–955

Rivier C, Vale W, Rivier J (1983) Effects of gonadotropin hormone agonists and antagonists on reproductive functions. J Med Chem 26:1545–1550

Sinha-Hikim AP, Swerdloff RS (1993) Temporal and stage-specific changes in spermatogenesis after gonadotropin deprivation by a potent gonadotropin-releasing hormone antagonist treatment. Endocrinology 133:2161–2170

Sinha-Hikim AP, Swerdloff RS (1994) Time course of recovery of spermatogenesis and Leydig cell function after cessation of gonadotropin-releasing hormone antagonist treatment in the adult rat. Endocrinology 134:1627–1634

N.9.3.4 Inhibition of Gonadotropin Release From Anterior Pituitary Cultures

PURPOSE AND RATIONALE

The same methods as described for studying the stimulation of gonadotropin release by LH-RH agonists (Sect. N.9.2.3, N.9.2.4) can be used for assessment of LH-RH antagonists.

PROCEDURE

Anterior pituitaries of young adult Sprague-Dawley rats are digested with collagenase for 1 h followed by a mechanical dispersion. The resulting cell suspension from 1.5 pituitaries, containing mostly small clusters of cells, is then sedimented together with a suspension of Sephadex G-10 (Sigma) and packed into 6.6-mm columns. Tissue culture medium 199 (Sigma) with supplements, equilibrated with 95% air/5% carbon dioxide, is perfused through the columns at a flow rate of 0.33 ml/min. After an overnight recovery period, during which the baseline stabilizes and the cells regain their full responsiveness, the samples to be tested are introduced through a four-way valve. During a 9-h experimental period, 180 1-ml fractions are collected. The system is standardized with 3-min exposures to 100 mM potassium chloride or 3 nM LH-RH. The compounds are introduced in various concentrations, generally for 3–9 min (time of one to three fractions), at 30-min intervals. Rat LH levels are measured from aliquots (50 µl) of the collected medium effluent by radioimmunoassay. As a standard, rat LH-RP2 reference standard is used. Repeated stimulation with 3 nM LH-RH for 3 min at 30-min intervals results in a pulsatile LH release.

EVALUATION

The suppression of pulsatile LH release due to repeated administration of LH-RH by antagonists is evaluated.

MODIFICATIONS OF THE METHOD

Krummen et al. (1991) assessed the direct effects of testosterone in primary cultures of pituitary cells.

A special long-term superfusion system was developed by Rékási et al. (1993) in order to evaluate the effects of cytotoxic compounds linked to LH-RH analogs on different types of rat pituitary cells. LH, growth hormone and prolactin were determined simultaneously in the effluent.

REFERENCES AND FURTHER READING

Bowers CY, Humphries J, Wasiak T, Folkers K, Reynolds GA, Reichert LE Jr (1980) On the inhibitory effects of luteinizing hormone-releasing hormone analogs. Endocrinology 106:674–683

Csernus VJ, Schally AV (1992) Evaluation of luteinizing hormone-releasing hormone antagonistic activity *in vitro*. Proc Natl Acad Sci USA 89:5759–5763

Ding YQ, Huhtaniemi I (1989) Human serum LH inhibitor(s): behaviour and contribution to *in vitro* bioassay of LH using dispersed mouse Leydig cells. Acta Endocrinol 121:46–54

Haviv F, Fitzpatrick TD; Swenson RE, Nichols CJ, Mort NA, Bush EN, Diaz G, Bammert G, Nguyen A, Rhutasel NS,

Nellans HG, Hoffman DJ, Johnson ES, Greer J (1993) Effect of *N*-methyl substitution of peptide bonds in luteinizing hormone-releasing hormone agonists. J Med Chem 36:363–369

Haviv F, Fitzpatrick TD, Nichols CJ, Bush EN, Diaz G, Bammert G, Nguyen AT, Johnson ES, Knittle J, Greer J (1994) *In vitro* and *in vivo* activities of reduced-size antagonists of luteinizing hormone-releasing hormone. J Med Chem 37:701–705

Humphries J, Wan YP, Folkers K (1978) Inhibitory analogues of the luteinizing hormone-releasing hormone having D-aromatic residues in positions 2 and 6 and variation in position 3. J Med Chem 21:120–123

Krummen LA, Wilfinger WW, Baldwin DM (1991) Primary culture of pituitary cells and assessment of the direct effects of testosterone on pituitary function *in vitro*. In: Greenstein B (ed) Neuroendocrine research methods. Harwood, Chur, pp 57–69

Labrie F, Ferland L, Lagace L, Drouin J, Asselin J, Azadian-Boulanger G, Raynaud P (1977) High inhibitory activity of RU 5020, a pure progestin, at the hypothalamic-hypophyseal level on gonadotropin secretion. Fertil Steril 28:1104–1112

McRae GI, Vickery BH, Nestor JJ Jr, Bremner WJ, Badger TM (1984) Biological activity of a highly potent LHRH antagonist. In: Vickery BH, Nestor JJ Jr, Hafez ESE (eds) LHRH and its analogs. Contraceptive and therapeutic applications. MTP, Boston, Mass., pp 137–151

Rékási Z, Szöke B, Nagy A, Groot K, Rékási ES, Schally AV (1993) Effect of luteinizing hormone-releasing hormone analogs containing cytotoxic radicals on the function of rat pituitary cells: tests in a long term superfusion system. Endocrinology 132:1991–2000

Vale W, Grant G, Rivier J, Monahan M, Amoss M, Blackwell R, Burgus R, Guillemin R (1972) Synthetic polypeptide antagonists of the hypothalamic luteinizing hormone releasing factor. Science 176:933–934

N.9.3.5 Anti-Tumor Effect of LH-RH Antagonists

PURPOSE AND RATIONALE

LR-RH antagonists were found to inhibit experimental tumors in rats and mice.

PROCEDURE

To induce mammary carcinomas, female rats are each given a single dose of DMBA (dimethylbenzanthracene) at the age of 50 days. The first mammary tumors can be detected 20–30 days later. The tumor weight is determined by palpation, comparing the volume of each tumor to that of preformed Plasticine models. The tumor weight is calculated by multiplication of the model weight by a factor which takes account of the specific weights of Plasticine and tumor tissue. After the total tumor mass per animal has reached about 1 g, the animals are randomly divided into treatment groups. At least eight animals are used per group. The rats are treated for 3 weeks with different subcutaneous doses of LH-RH antagonists or vehicle. The experiment is terminated at the end of the 3rd week from the initiation of the experiment. Histological examination of the tumors is performed.

EVALUATION

The change in tumor volume is calculated on the basis of individual responses. For determination of the mitotic index, 4000 cells are considered in each tumor.

MODIFICATIONS OF THE METHOD

Reduction of tumor weight in female BDF_1 mice bearing MXT mammary adenocarcinomas after treatment for 3 weeks with a LH-RH antagonist was reported by Szende et al. (1990).

Inhibition of MIA PaCa-2 human pancreatic xenografts in nude mice by a LH-RH antagonist was reported by Radulovic et al. (1993).

The involvement of insulin-like growth factors in growth regulation of the Ishikawa endometrial tumor cell line and the possible interference by LH-RH analogs was evaluated by Kleinman et al. (1993).

Pinski et al. (1994) investigated the effects of treatment with a LH-RH antagonist and a LH-RH agonist in Copenhagen rats bearing the anaplastic androgen-independent Dunning R-3327-AT-1 prostatic adenocarcinoma implanted orthotopically into the ventral lobes of prostate glands.

Vincze et al. (1994) tested the anti-tumor effect of the gonadotropin-releasing hormone antagonist MI-1544 *in vitro* on human breast cancer lines and *in vivo* on xenografts in immunosuppressed mice.

Manetta et al. (1995) reported the *in vitro* and *in vivo* inhibitory effects of a LH-RH antagonist against a panel of human ovarian carcinomas.

The effects of LH-RH and a LH-RH antagonist on cell growth and production of hCG and cAMP in JAR human chorioncarcinoma cells were examined *in vitro* by Horváth et al. (1995).

CRITICAL ASSESSMENT OF THE METHOD

In many instances, research is now based on assessing and confirming the anti-apoptotic activity of tumor-inhibiting compounds, e. g., methods based on thymidine incorporation to assess tissue proliferation may be considered. In the case of LH-RH antagonists the use of biological systems based on transplanted tumors in animals reflects the suppression of pituitary hormone release followed by reduced secretion of gonadal steroids. Testing the effect on experimental tumors in animals is a recommended procedure for obtaining confirmation of the clinical potential of application.

REFERENCES AND FURTHER READING

Horváth JE, Ertl T, Qin T, Groot K, Schally AV (1995) LH-RH and its antagonist Cetrorelix inhibit growth of JAR human chorioncarcinoma cells *in vitro*. Int J Oncol 6:969–975

Kleinman D, Roberts CT Jr, LeRoith D, Schally AV, Levy J, Sharoni Y (1993) Regulation of endometrial cancer cell growth by insulin-like growth factors and the luteinizing hormone-releasing hormone antagonist SB-75. Regul Peptide 48:91–98

Manetta A, Gamboa-Vujicic G, Paredes P, Emma D, Liao S, Leong L, Asch B, Schally AV (1995) Inhibition of growth of human ovarian cancer in nude mice by luteinizing hormone-releasing hormone antagonist Cetrorelix (SB-75). Fertil Steril 63:282–287

Pinski J, Reile H, Halmos G, Groot K, Schally AV (1994) Inhibitory effects of analogues of luteinizing hormone-releasing hormone on the growth of androgen-independent Dunning R-3327-AT-1 rat prostate cancer. Int J Cancer Res 59:51–55

Radulovic S, Comaru-Schally AM, Milovanovic S, Schally AV (1993) Somatostatin analogue RC-160 and LH-RH antagonist SB-75 inhibit growth of MIA RaCa-2 human pancreatic cancer xenografts in nude mice. Pancreas 8:88–97

Reissmann T, Klenner T, Deger W, Hilgard P, McGregor GP, Voigt K, Engel J (1996) Pharmacological studies with Cetrorelix (SB-75), a potent antagonist of luteinizing hormone-releasing hormone. Eur J Cancer 32A:1574–1579

Szende B, Srkalovic G, Groot K, Lapis K, Schally AV (1990) Growth inhibition of mouse MXT mammary tumor by the luteinizing hormone-releasing hormone antagonist SB-75. J Natl Cancer Inst 82:513–517

Vincze B, Plyi I, Daubner D, Kalnay A, Mezo G, Hudecz F, Szekerke M, Teplan I, Mezo I (1994) Antitumour effect of a gonadotropin-releasing hormone antagonist (MI-1544) and its conjugate on human breast cancer lines and their xenografts. J Cancer Res Clin Oncol 20:578–584

N.9.4 Corticotropin-Releasing Hormone (CRH)

N.9.4.1 General Considerations

A hypothalamic factor inducing release of corticotropin (ACTH) from pituitaries was the first of the hypothalamic releasing hormones identified using *in vitro* bioassays (Saffran and Schally 1955; Guillemin and Rosenberg 1955). A common pre-pro-hormone, opiomelanocortin, was identified as the source of corticotropins and endorphins. Much later, the structure of a 41-residue ovine hypothalamic peptide stimulating the secretion of corticotropin and β-endorphin was identified (Vale et al. 1981), followed by elucidation of the structure of human CRH (Shibahara et al. 1983) and of other species, such as porcine corticotropin-releasing factor (CRF; Patthy et al. 1985) and equine CRF (Livesey et al. 1991). Reviews are given by Brodish (1979), Rivier and Plotsky (1986), and Taylor and Fishman (1988), Vigh et al. (1982), Koob (1999). Conformational differences between ovine and human CRH were detected using circular dichroism, Fourier transform infrared spectroscopy, nuclear magnetic resonance (NMR) and dynamic light scattering (Dahte et al. 1996).

The binding sites of immunoreactive CRH in the rat ovary and its potential physiological role were studied by Mastorakos et al. (1993).

Studies on CRF receptors in the pituitary have been performed (Wynn et al. 1983; Millan et al. 1987). Investigations into the general pharmacological properties of human CRH did not reveal any considerable side-effects (Andoh et al. 1994).

Derivatives with agonistic and antagonistic properties have been synthesized and tested (Rivier et al. 1984; Kornreich et al. 1992; Chen et al. 1996; Schulz et al. 1996; Webster et al. 1996; Arai et al. 1998).

The role of CRH in inflammatory processes was investigated by Webster et al. (1998).

Non-mammalian peptides sauvagine (from frog) and **urotensin** 1 (from fish) have approximately 50% sequence homology with CRF and share *in vitro* and physiological actions characteristic of CRF (Rivier et al. 1983). A mammalian urotensin-like peptide (named **urocortin**) with partial sequence identity with urotensin 1 and CRF has been identified in rat (Vaughn et al. 1995) and human (Donaldson et al. 1995) tissues. The mouse and human urocortin genes have been isolated and characterized (Zhao et al. 1998).

A **corticotropin-releasing factor binding** *protein (CRFBP)* was isolated and is thought to be an important modulator of CRF in both the CNS and the periphery (Behan et al. 1995; Petraglia et al. 1996; Cortright et al. 1997; Hobel et al. 1999). CRFBP levels rise at 30–35 weeks of pregnancy and dramatically decrease at 38–40 weeks. *In vitro*, CRFBP inhibits the ACTH-releasing properties of CRF.

Cortright et al. (1995) described a mouse brain CRH-binding protein (CRHBP) highly homologous to human and rat CRHBPs, but distinct from the CRH receptor.

Stenzel-Poore et al. (1996) described **transgenic mice** with CRH overproduction that induces behavioral changes that parallel the stress syndrome. Van Gaalen et al. (2002, 2003) reported anxiety-like behavior and reduced attention in mice overproducing CRH in an operant five-choice serial task, which taxes sustained and divided attention.

Bale et al. (2002) found that mice deficient for both CRF receptor 1 (CRFR1) and CRFR2 have an impaired stress response and display sexually dichotomous anxiety-like behavior.

REFERENCES AND FURTHER READING

Andoh K, Kimura T, Saeki I, Tabata R, Yamazaki S, Eguchi J, Hanazuka M, Horii D, Munt PL, Davis AS, Templetom D, Algate DR, Takahashi K (1994) General pharmacological properties of human corticotropin-releasing hormone corticorelin (human). Arzneimittelforschung 44:715–726

Arai K, Ohata H, Shibasaki T (1998) Non-peptidic corticotropin-releasing hormone receptor type 1 antagonist reverses restraint stress-induced shortening of sodium pentobarbital-induced sleeping time of rats: evidence that an increase in arousal induced by stress in mediated through CRH receptor type 1. Neurosci Lett 255:103–106

Bale TL, Picetti R, Contarino A, Koob GF, Vale WW, Lee KF (2002) Mice deficient for both corticotropin-releasing factor receptor 1 (CRFR1) and CRFR2 have an impaired stress response and display sexually dichotomous anxiety-like behavior. J Neurosci 22:193–199

Behan DP, De Souza EB, Lowry PJ, Potter E, Sawchenko P, Vale WW (1995) Corticotropin releasing factor (CRF) binding protein: a novel regulator of CRF and related peptides. Front Neuroendocrinol 16:362–382

Brodish A (1979) Control of ACTH secretion by corticotropin-releasing factor(s). Vitam Horm 37:111–152

Chen C, Dagnino R, De Souza EB, Grigoriadis DE, Huang CQ, Kim KI, Liu Z, Moran T, Webb TR, Whitten JP, Xie YF, McCarthy JR (1996) Design and synthesis of a series of non-peptide high-affinity human corticotropin-releasing factor receptor antagonists. J Med Chem 399:4358–4360

Cortright DN, Nicoletti A, Seasholtz AF (1995) Molecular and biochemical characterization of the mouse brain corticotropin-releasing hormone-binding protein. Mol Cell Endocrinol 111:147–157

Cortright DN, Goosens KA, Lesh JS, Seasholtz AF (1997) Isolation and characterization of the rat corticotropin-releasing hormone (CRH)-binding protein gene: transcriptional regulation by cyclic adenosine monophosphate and CRH. Endocrinology 138:2098–2108

Dahte M, Fabian H, Gast K, Zirwr D, Winter R, Beyermann M, Schumann M, Bienert M (1996) Conformational differences of ovine and human corticotropin releasing hormone: a CD, IR, NMR and dynamic light scattering study. Int J Peptide Protein Res 47:383–393

Donaldson DJ, Sutton SW, Perrin MJ, Corrigan AZ, Lewis KA, Rivier JE, Vaughn JM, Vale WW (1995) Urocortin, a mammalian neuropeptide related to fish urotensin 1 and to corticotropin-releasing factor. Nature 378:287–292

Guillemin R, Rosenberg B (1955) Humoral hypothalamic control of anterior pituitary: a study with combined tissue cultures. Endocrinology 57:599–607

Hobel CJ, Arora CP, Korst LM (1999) Corticotropin-releasing hormone and CRH-binding protein. In: Sandman CA, Chronwall BM, Strand FL, Flynn FW, Beckwith B, Nachman RJ (eds) Neuropeptides. Structure and function in biology and behavior. Ann N Y Acad Sci 897:54–65

Koob GF (1999) Stress, corticotropin-releasing factor, and drug addiction. In: Sandman CA, Chronwall BM, Strand FL, Flynn FW, Beckwith B, Nachman RJ (eds) Neuropeptides. Structure and function in biology and behavior. Ann N Y Acad Sci 897:27–45

Kornreich WD, Galyean RG, Hernandez JF, Craig AG, Donaldson CJ, Yamamoto G, Rivier C, Vale W, Rivier J (1992) Alanine series of ovine corticotropin releasing factor (oCRF): a structure–activity relationship study. J Med Chem 35:1870–1876

Livesey JH, Carne A, Irvine CHG, Ellis J, Evans MJ, Smith R, Donald RA (1991) Structure of equine corticotropin releasing factor. Peptides 12:1437–1440

Mastorakos G, Webster EL, Friedman TC, Chrousos GP (1993) Immunoreactive corticotropin-releasing hormone and its binding sites in the rat ovary. J Clin Invest 92:961–968

Millan M, Samra ABA, Wynn C, Catt KJ, Aguilera G (1987) Receptors and actions of corticotropin-releasing hormone in the primate pituitary gland. J Clin Endocrinol Met 64:1036–1041

Patthy M, Horvath J, Mason-Garcia M, Szoke B, Schlesinger DH, Schally AV (1985) Isolation and amino acid sequence of corticotropin-releasing factor from pig hypothalami. Proc Natl Acad Sci USA 82:8762–8766

Petraglia F, Florio P, Gallo R, Salvestroni C, Lombardo M, Genazzani AD, Di Carlo C, Stomati M, D'Ambrogio G, Artini PG (1996) Corticotropin-releasing factor-binding protein: origins and possible functions. Horm Res 45:187–191

Rivier CL, Plotsky PM (1986) Mediation by corticotropin releasing factor (CRF) of adenohypophyseal hormone secretion. Annu Rev Physiol 48:475–494

Rivier C, Rivier J, Lederis K, Vale WW (1983) ACTH releasing activity of ovine CRF, sauvagine and urotensin 1. Regul Pept 5:139–143

Rivier J, Rivier C, Vale W (1984) Synthetic competitive antagonists of corticotropin-releasing factor: effect on ACTH secretion in the rat. Science 224:889–891

Saffran M, Schally AV (1955) The release of corticotrophin by anterior pituitary tissue *in vitro*. Can J Biochem Physiol 33:408–415

Schulz DW, Mansbach RS, Sprouse J, Braselton JP, Collins J, Corman M, Dunaikis A, Faraci S, Schmidt AW, Seeger T, Seymour P, Tingley III FD, Winston EN, Chen YL, Heym J (1996) CP-154-526: a potent and selective nonpeptide antagonist of corticotropin releasing factor receptors. Proc Natl Acad Sci USA 93:10477–10482

Shibahara S, Morimoto Y, Furutani Y, Notake M, Takahashi H, Shimizu S, Horikawa S, Numa S (1983) Isolation and sequence analysis of the human corticotropin-releasing factor precursor gene. EMBO J 2:775–779

Stenzel-Poore MP, Duncan JE, Rittenberg MB, Bakke AC, Heinrichs SC (1996) CRH overproduction in transgenic mice. Behavioral and immune system modulation. Ann N Y Acad Sci 780:36–48

Taylor AL, Fishman LM (1988) Medical progress: corticotropin-releasing hormone. New Engl J Med 319:213–222

Vale W, Spiess J, Rivier C, Rivier J (1981) Characterization of a 41-residue ovine hypothalamic peptide that stimulates secretion of corticotropin and β-endorphin. Science 213:1394–1397

Van Gaalen MM, Stenzel-Poore MP, Holsboer F, Steckler T (2002) Effects of transgenic overproduction on CRF on anxiety-like behaviour. Eur J Neurosci 15:2007–2015

Van Gaalen MM, Stenzel-Poore M, Holsboer F, Steckler T (2003) Reduced attention in mice overproducing corticotropin-releasing hormone. Behav Brain Res 142:69–79

Vaughn J, Donaldson C, Bittencourt J, Perrin MH, Lewis K, Sutton S, Chan R, Turnbull AV, Lovejoy D, Rivier C, Rivier J, Sawchenko PE, Vale WW (1995) Urocortin, a mammalian neuropeptide related to fish urotensin 1 and to corticotropin-releasing factor. Nature 378:287–292

Vigh S, Merchenthaler I, Torres-Aleman I, Suieras-Diaz J, Coy DH, Carter WH, Petrusz P, Schally AV (1982) Corticotropin releasing factor (CRF): immunocytochemical localization and radioimmunoassay (RIA). Life Sci 31:2441–2448

Webster EL, Lewis DB, Torpy DJ, Zachman EK, Rice KC, Chrousos GP (1996) *In vivo* and *in vitro* characterization

of antalarmin, a nonpeptide corticotropin releasing hormone (CRH) receptor antagonist; suppression of pituitary ACTH release and peripheral inflammation. Endocrinology 137:5747–5750
Webster LE, Torpy DJ, Elenkov IJ, Chrousos GP (1998) Corticotropin-releasing hormone and inflammation. Ann N Y Acad Sci 840:21–32
Wynn PC, Aguilera G, Morell J, Catt KJ (1983) Properties and regulation of high-affinity pituitary receptors for corticotropin-releasing factor. Biochem Biophys Res Commun 110:602–608
Zhao L, Donaldson CJ, Smith GW, Vale WW (1998) The structure of the mouse and human urocortin genes (Ucn and UCN). Genomics 50:23–33

N.9.4.1.1 Central Effects and Actions of CRH

In some contrast to the initial conception of a hypothalamic factor regulating adrenocortical function, research on CRH, related CRF peptides and nonpeptidic compounds interacting with the CRH receptors, has established for CRH both a central role and important peripheral effects. In keeping with knowledge about the effects of neurohypophyseal hormones and steroids on brain functions, memory and learning, a similar role has been established for CRH (Croiset et al. 2000). In the process of establishing these functions, the presence of CRF receptors in the central nervous system and other tissues has been a starting point for investigations (reviewed by De Souza 1995; Perrin and Vale 1999; Eckard et al. 2002). As in other areas, specific animal models are now focusing on mutant mice for the prediction and confirmation of function (Contarino et al. 1999). Bruijnzeel and Gold (2005) have reviewed the role of CRF-like peptides in various forms of drug dependence, both to elucidate mechanisms and to explore potential therapies (Chatzaki et al. 2006). In keeping with the functional effect on the pituitary–adrenal system, involvement of CRH in the stress response has been addressed by Smith and Vale (2006), and the synthesis of CRF receptor antagonists may offer therapeutic potential in central disorders related to anxiety, psychiatric disorders, stress, and drug dependence (Valdez 2006).

Effects on the gastrointestinal tract of CRH have been described by several groups (Martinez and Tache 2006, 2007; Tache and Bonaz 2007).

Vergoni and Bertolini (2000) and Doyon et al. (2004) have suggested a functional role in the central regulation of appetite and body weight, by interaction with the melanocortin system.

Based on its interaction with CRH receptors, indications for modulation of synaptic transmission have also been found with CRH (Orozco-Cabal et al. 2006), which has parallels with the newly discovered functional role of LH-RH (GnRH),. Cardiovascular effects have been described and assigned to CRH receptors (Nazarloo et al. 2006). The existence of a CRH-like placental corticotropin-releasing factor has been confirmed even though the functional role remains elusive (Fadalti et al. 2000).

REFERENCES AND FURTHER READING

Bruijnzeel AW, Gold MS (2005) The role of corticotropin-releasing factor-like peptides in cannabis, nicotine, and alcohol dependence. Brain Res Brain Res Rev 49(3):505–528
Chatzaki E, Minas V, Zoumakis E, Makrigiannakis A (2006) CRF receptor antagonists: utility in research and clinical practice. Curr Med Chem 13(23):2751–2760
Contarino A, Heinrichs SC, Gold LH (1999) Understanding corticotropin releasing factor neurobiology: contributions from mutant mice. Neuropeptides 33(1):1–12
Croiset G, Nijsen MJ, Kamphuis PJ (2000) Role of corticotropin-releasing factor, vasopressin and the autonomic nervous system in learning and memory. Eur J Pharmacol 405(1–3):225–234
De Souza EB (1995) Corticotropin-releasing factor receptors: physiology, pharmacology, biochemistry and role in central nervous system and immune disorders. Psychoneuroendocrinology 20(8):789–819
Doyon C, Moraru A, Richard D (2004) The corticotropin-releasing factor system as a potential target for antiobesity drugs. Drug News Perspect 17(8):505–517
Eckart K, Jahn O, Radulovic J, Radulovic M, Blank T, Stiedl O, Brauns O, Tezval H, Zeyda T, Spiess J (2002) Pharmacology and biology of corticotropin-releasing factor (CRF) receptors. Receptors Channels 8(3–4):163–77
Fadalti M, Pezzani I, Cobellis L, Springolo F, Petrovec MM, Ambrosini G, Reis FM, Petraglia F (2000) Placental corticotropin-releasing factor. An update. Ann N Y Acad Sci 900:89–94
Martinez V, Tache Y (2006) CRF1 receptors as a therapeutic target for irritable bowel syndrome. Curr Pharm Des 12(31):4071–4088
Nazarloo HP, Buttrick PM, Saadat H, Dunn AJ (2006) The roles of corticotropin-releasing factor-related peptides and their receptors in the cardiovascular system. Curr Protein Pept Sci 7(3):229–239
Orozco-Cabal L, Pollandt S, Liu J, Shinnick-Gallagher P, Gallagher JP (2006) Regulation of synaptic transmission by CRF receptors. Rev Neurosci 17(3):279–307
Perrin MH, Vale WW (1999) Corticotropin releasing factor receptors and their ligand family. Ann N Y Acad Sci 885:312–328
Smith SM, Vale WW (2006) The role of the hypothalamic-pituitary-adrenal axis in neuroendocrine responses to stress. Dialogues Clin Neurosci 8(4):383–895
Tache Y, Bonaz B (2007) Corticotropin-releasing factor receptors and stress-related alterations of gut motor function. J Clin Invest 117(1):33–40
Valdez GR (2006) Development of CRF1 receptor antagonists as antidepressants and anxiolytics: progress to date. CNS Drugs 20(11):887–896
Vergoni AV, Bertolini A (2000) Role of melanocortins in the central control of feeding. Eur J Pharmacol 405(1–3):25–32

N.9.4.2 In Vitro Assay for CRH Activity

PURPOSE AND RATIONALE

The first *in vitro* assay procedures to detect CRF activity (Saffran and Schally 1955; Saffran et al. 1955) were based on incubation of rat anterior pituitary halves with the test substances in bicarbonate-buffered, oxygenated medium at 38°C for 1 h in the presence of 0.0004 M DL-arterenol and 0.004 M ascorbate followed by measurement of ACTH release into the medium by incubation with adrenal tissue and determination of corticosterone (a two-stage bioassay where a biological product of CRH action is determined by a quantitative biological response). Guillemin and Rosenberg (1955) used pituitary tissue culture from rat and dog and determined ACTH activity in the medium by the *in vivo* ascorbic acid depletion method in the rat according to Sayers (1954) (see Sect. N.7.4.1). The assay was later considerably simplified by using ACTH radioimmunoassay (RIA). Several modifications of these procedures have been used (Schally et al. 1968; Yasuda et al. 1982). Most investigators used rat pituitary cell cultures (Giguère and Labrie 1982; Giguère et al. 1982; Aguilera et al. 1983; Bilezikjan and Vale 1983; Vale et al. 1983a, 1983b; Patthy et al. 1985), while pituitary segments have been used by Antoni et al. (1983) and by Widmaier and Dallman (1984).

PROCEDURE

Anterior pituitaries are obtained from adult Sprague-Dawley rats, cut into small pieces and incubated in a Dubnoff incubator for 45 min at 37°C in 10 ml of oxygenated Medium 199 (GIBCO) containing 0.5% collagenase, 0.25% BSA, and 50 µg/ml gentamicin. The fragments can be easily dispersed mechanically into single cells by repeated suction and expulsion from a pipette. The cell suspension is centrifuged at room temperature for 10 min at 100 *g*. The cell pellet is then resuspended in 1.0 ml of medium and divided into four equal volumes. Each volume (containing about 5×10^6 cells) is mixed with 0.5 ml Sephadex G-15 which has been equilibrated previously with oxygenated medium. The mixture of pituitary cells and Sephadex is transferred into four chambers of a superfusion apparatus (Vigh and Schally 1984; Evans et al. 1988; Czernus and Schally 1991) consisting of a number of 1-ml plastic syringe barrels (modified by cutting off their distal end) mounted vertically in a Plexiglas holder which is kept at 37°C by circulating water. Each barrel is fitted with plungers at both ends. Holes are drilled in the plungers to accommodate plastic tubing. The lower plunger is covered with a small piece of 30-µm-pore nylon net to keep the Sephadex beads from escaping. The "pores" between the beads are small enough to prevent the pituitary cells from escaping and large enough to allow unrestricted flow of medium through the column. The upper plunger tubing is used for directing the flow through the chamber from the medium reservoir. The flow through the system is controlled by a multichannel peristaltic pump which is placed after the superfusion chamber. Thus, the system is operated by suction with negative pressure.

The cells are perfused overnight with Medium 199 (Gibco) at a flow rate of 20 ml/h. The samples are administered every 30 min for 3 min and 1-ml fractions are collected at 3-min intervals. Synthetic CRF at 0.2 and 2 mM is used as standard. The corticotropin released into the medium is measured by a specific RIA for corticotropin.

EVALUATION

Dose–response curves are established for test preparation and standard allowing the calculation of potency ratios with confidence limits.

REFERENCES AND FURTHER READING

Aguilera G, Harwood JP, Wilson JX, Morell J, Brown JH, Catt KJ (1983) Mechanism of action of corticotropin-releasing factor and other regulators of corticotropin release in rat pituitary cells. J Biol Chem 258:8039–8045

Antoni FA, Holmes MC, Jones MT (1983) Oxytocin as well as vasopressin potentiate ovine CRF *in vitro*. Peptides 4:411–415

Bilezikjan LM, Vale WW (1983) Glucocorticoids inhibit corticotropin-releasing factor-induced production of adenosine 3′,5′-monophosphate in cultured anterior pituitary cells. Endocrinology 113:657–662

Czernus V, Schally AV (1991) The dispersed cell superfusion system. In: Greenstein B (ed) Neuroendocrine research methods. Harwood Academic, London, pp 66–102

Evans MJ, Brett JT, McIntosh RP, McIntosh JEA, McLay JL, Livesey JH, Donald RA (1988) Characteristics of the ACTH response to repeated pulses of corticotrophin-releasing factor and arginine vasopressin *in vitro*. J Endocrinol 117:387–395

Giguère V, Labrie F (1982) Vasopressin potentiates cyclic AMP accumulation and ACTH release induced by corticotropin-releasing factor (CRF) in rat anterior pituitary cells in culture. Endocrinology 111:1752–1754

Giguère V, Labrie F, Côte J, Coy DH, Sueiras-Diaz J, Schally AV (1982) Stimulation of cyclic AMP accumulation and corticotropin release by synthetic ovine corticotropin-releasing factor in rat anterior pituitary cells: site of glucocorticoid action. Proc Natl Acad Sci USA 79:3466–3469

Guillemin R, Rosenberg B (1955) Humoral hypothalamic control of anterior pituitary: a study with combined tissue cultures. Endocrinology 57:599–607

Patthy M, Horvath J, Mason-Garcia M, Szoke B, Schlesinger DH, Schally AV (1985) Isolation and amino acid sequence

of corticotropin-releasing factor from pig hypothalami. Proc Natl Acad Sci USA 82:8762–8766
Saffran M, Schally AV (1955) The release of corticotrophin by anterior pituitary tissue *in vitro*. Can J Biochem Physiol 33:408–415
Saffran M, Schally AV, Benfey BG (1955) Stimulation of the release of corticotropin from the adenohypophysis by a neurohypophyseal factor. Endocrinology 57:439–444
Sayers MA, Sayers G, Woodbury LA (1948) The assay of adreno-corticotropic hormone by the adrenal ascorbic acid-depletion method. Endocrinology 42:379–393
Schally AV, Arimura A, Bowers CY, Kastin AJ, Sawano S, Redding TW (1968) Hypothalamic neurohormones regulating anterior pituitary function. Recent Prog Horm Res 24:497–588
Vale W, Rivier C, Brown MR, Spiess J, Koob G, Swanson L, Bilezikjan L, Bloom F, Rivier J (1983a) Chemical and biological characterization of corticotropin releasing factor. Recent Prog Horm Res 39:245–270
Vale W, Vaughan J, Yamamoto G, Bruhn T, Douglas C, Dalton D, Rivier C, Rivier J (1983b) Assay of corticotropin releasing factor. Methods Enzymol 103:565–577
Vigh S, Schally AV (1984) Interaction between hypothalamic peptides in a superfused pituitary cell system. Peptides 5 [Suppl I]:241–247
Widmaier EP, Dallman MF (1984) The effects of corticotropin-releasing factor on adrenocorticotropin secretion from perifused pituitaries *in vitro*: rapid inhibition by glucocorticoids. Endocrinology 115:2368–2374
Yasuda N, Greer MA, Aizawa T (1982) Corticotropin-releasing factor. Endocr Rev 3:123–140

N.9.4.3 In Vivo Bioassay of CRH Activity

PURPOSE AND RATIONALE

Munson and Briggs (1955) described an assay using rats pretreated with morphine and pentobarbital. Many modifications for a reliable *in vivo* bioassay of CRH activity have been tested including rats with hypothalamic lesions (Schally et al. 1968; Yasuda et al. 1982). Arimura et al. (1967) described an assay for corticotropin-releasing factor (CRF) using rats treated with morphine, chlorpromazine, dexamethasone and pentobarbital. This assay has been further improved by Graf et al. (1985).

PROCEDURE

Male Sprague-Dawley rats weighing about 200 g are maintained on a 12:12 h light:dark cycle at constant temperature for at least 5 days before use. On the day of the experiment, the rats are prepared with an initial single subcutaneous injection of a mixture of chlorpromazine (10 mg/kg) and morphine sulfate (20 mg/kg) followed after 75 min by pentobarbital (25 mg/kg) intraperitoneally. Then 60 min after the injection of pentobarbital, various doses of test substances or standard or vehicle (0.9% NaCl, 1% BSA, 0.1% ascorbic acid) are injected into an exposed jugular vein. Blood samples (0.5 ml) are collected in heparinized syringes immediately before and 30 min after injection of test substances. The blood is transferred to chilled polypropylene tubes containing EDTA (1.0 mg) and aprotinin (Trasylol, 50 µl) and centrifuged (2000 *g*, 15 min 4°C). Plasma samples are stored at −20°C for corticosterone assay using a cross-reacting cortisol RIA that also measures corticosterone, the main corticoid secreted by rats, or a corticosterone RIA.

EVALUATION

Data for CRH activity of experimental groups are evaluated by analysis of variance or covariance followed by Duncan's multiple range test.

REFERENCES AND FURTHER READING

Arimura A, Saito T, Schally AV (1967) Assays for corticotropin-releasing factor (CRF) using rats treated with morphine, chlorpromazine, dexamethasone and nembutal. Endocrinology 81:235–245
Graf MV, Kastin AJ, Fischman AJ (1985) Interaction of arginine vasopressin and corticotropin releasing factor demonstrated with an improved bioassay. Proc Soc Exp Biol Med 179:303–308
Munson PL, Briggs FN (1955) The mechanism of stimulation of ACTH secretion. Recent Prog Horm Res 11:83–117
Rivier C, Brownstein M, Spiess J, Rivier J, Vale W (1982) *In vivo* corticotropin-releasing factor-induced secretion of adrenocorticotropin, β-endorphin, and corticosterone. Endocrinology 110:272–278
Schally AV, Arimura A, Bowers CY, Kastin AJ, Sawano S, Redding TW (1968) Hypothalamic neurohormones regulating anterior pituitary function. Recent Prog Horm Res 24:497–588
Yasuda N, Greer MA, Aizawa T (1982) Corticotropin-releasing factor. Endocr Rev 3:123–140

N.9.4.4 Collection of Hypophyseal Portal Blood in Rats

PURPOSE AND RATIONALE

Worthington (1966), Porter and Smith (1967), Gibbs (1984), and Sarkar and Minami (1991) described methods to collect hypophyseal portal blood in rats. These methods can be used to measure the changes in secretion of several hypothalamic hormones under the influence of various factors.

Gibbs and Vale (1982), Gibbs (1985a), and Plotsky and Sawchenko (1987) studied the effect of various conditions on hypophyseal portal plasma levels of corticotropin-releasing factor (CRF) and arginine vasopressin.

Luteinizing hormone-releasing hormone (LHRH) was determined by Ching (1982), Sarkar (1987), Petraglia et al. (1987); thyrotropin releasing hormone (TRH) by Fink et al. (1982); growth-hormone-releas-

ing hormone (GH-RH) by Plotsky and Vale (1985); β-endorphin by Sarkar and Yen (1985); neuropeptide Y by Sutton et al. (1988); vasoactive intestinal peptide by Sarkar (1989); vasopressin and oxytocin by Gibbs (1984); and dopamine and epinephrine by Ben-Jonathan et al. (1977), and Gibbs (1985b).

PROCEDURE

Pentobarbital-anesthetized rats are placed on an isothermal heating pad in a stereotactic instrument. After cannulation of the trachea, the animals are mechanically ventilated. The base of the skull is exposed by a transpharyngeal approach, and the basisphenoid bone is drilled away. The dura is cut and deflected, the rat is heparinized, and, after the stalk is cut, a polyethylene cannula filled with saline is placed over the hypophyseal stalk for collection of blood. The cannula leads to an ice bath, and the distal end of the tubing ends in a fraction collector where portal blood is collected by gravity flow at a rate of about 10 µl/min.

EVALUATION

Portal plasma concentrations of CRH, LHRH, TRH, GH-RH, β-endorphin, neuropeptide Y, vasoactive intestinal peptide, vasopressin and oxytocin, and catecholamines were determined after various treatments and compared with control periods of spontaneous secretion.

MODIFICATIONS OF THE METHOD

Cowell et al. (1991) described *in vitro* models for examination of the mechanisms controlling the secretion of hypothalamic hormones.

REFERENCES AND FURTHER READING

Ben-Jonathan N, Oliver C, Weiner HJ, Mical RS, Porter JC (1977) Dopamine in hypophyseal portal plasma of the rat during the estrus cycle and throughout pregnancy. Endocrinology 100:452–458

Ching M (1982) Correlative surges of LHRH, LH and FSH in pituitary stalk plasma and systemic plasma of rat during proestrus. Effects of anesthetics. Neuroendocrinology 34:279–285

Cowell M, Cover PO, Gillies GE, Buckinham JC (1991) *In vitro* models for the examination of the mechanisms controlling the secretion of hypothalamic hormones. In: Greenstein B (ed) Neuroendocrine research methods, Vol 1, Harwood Academic, Chur, pp 111–130

Fink G, Koch Y, Ben Aroya N (1982) Release of thyrotropin releasing hormone into hypophyseal portal blood is high relative to other neuropeptides and may be related to prolactin secretion. Brain Res 234:186–189

Gibbs DM (1984) Collection of pituitary portal blood: a methodologic analysis. Neuroendocrinology 38:97–101

Gibbs DM (1985a) Measurement of hypothalamic corticotropin-releasing factors in hypophyseal portal blood. Fed Proc 44:203–206

Gibbs DM (1985b) Hypothalamic epinephrine is released into hypophyseal portal blood during stress. Brain Res 335:360–364

Gibbs DM, Vale W (1982) Presence of corticotropin releasing factor-like immunoreactivity in hypophyseal portal blood. Endocrinology 111:1418–1420

Petraglia F, Sutton S, Vale W, Plotsky P (1987) Corticotropin-releasing factor decreases plasma luteinizing hormone levels in female rats by inhibiting gonadotropin-releasing hormone release into hypophyseal-portal circulation. Endocrinology 120:1083–1088

Plotsky PM, Vale W (1985) Pattern of growth hormone-releasing factor and somatostatin secretion into hypophyseal-portal circulation of the rat. Science 230:461–463

Plotsky PM, Sawchenko PE (1987) Hypophyseal-portal plasma levels, median eminence content, and immunohistochemical staining of corticotropin-releasing factor, arginine vasopressin, and oxytocin after pharmacological adrenalectomy. Endocrinology 120:1361–1369

Porter JC, Smith KR (1967) Collection of hypophyseal stalk blood in rats. Endocrinology 81:1182–1185

Sarkar DK (1987) *In vivo* secretion of LHRH in ovarectomized rats is regulated by a possible autofeedback mechanism. Neuroendocrinology 45:510–513

Sarkar DK (1989) Evidence for prolactin feedback action on hypothalamic oxytocin, vasoactive intestinal peptide and dopamine secretion. Neuroendocrinology 49:520–524

Sarkar DK, Minami S (1991) Pituitary portal blood collection in rats. A powerful technique for studying hypothalamic hormone secretion. In: Greenstein B (ed) Neuroendocrine research methods, Vol 1. Harwood Academic, Chur, pp 235–248

Sarkar DK, Yen SSC (1985) Changes in β-endorphin-like immunoreactivity in pituitary portal blood during the estrus cycle and after ovarectomy in rats. Endocrinology 116:2075–2079

Sutton SW, Mitsugi N, Plotsky PM, Sarkar DK (1988) Neuropeptide Y (NPY): a possible role in the initiation of puberty. Endocrinology 123:2152–2154

Worthington WC (1966) Blood samples from the pituitary stalk of the rat: method of collection and factors determining volume. Nature 210:710–712

N.9.4.5 CRH Receptor Determination

PURPOSE AND RATIONALE

CRH mediates its effects through high-affinity receptors identified and characterized by radioreceptor studies. Cellular signaling was measured by stimulation of adenyl cyclase in membrane fractions of rat brain, pituitary, and spleen (Grigoriadis et al. 1993; Hauger and Aguliera 1993). Cloning studies indicate the existence of at least two types of mammalian receptor (De Souza et al. 1998; Steckler and Holsboer 1999; Dautzenberg and Hauger 2002). The CRF_1 receptor has been cloned from several species including human (Chen et al. 1993; Castro et al. 1996; Di Blasio et al. 1997; Grammatopoulos and Hillhouse 1998), mouse

(Vita et al. 1993), and rat (Perrin et al. 1993). Species homologies are 98% identical over the full length of 415 amino acids.

There are three isoforms of the CRF_2 receptor: the $CRF_{2(a)}$ receptor, which has been cloned from both rat (Lovenberg et al. 1995) and human (Liaw et al. 1996), is a 411-amino-acid protein which shares approximately 70% identity with the CRF_1 receptor; the $CRF_{2(b)}$ receptor isoform has been cloned from rat (Lovenberg et al. 1995), mouse (Stenzel et al. 1995), and human (Kostich et al. 1996) and is 431 amino acids in length, differing from the $CRF_{2(a)}$ receptor in that the first 34 amino acids in the N-terminus are replaced by 54 different amino acids; the $CRF_{2(c)}$ receptor has been identified in human brain (Sperle et al. 1997; Kostich et al. 1998).

[^{125}I]Sauvagine binding to CRH_2 receptors was characterized by Rominger et al. (1998).

CRH in plasma is mostly bound to the corticotropin-releasing hormone-binding protein (CRH-BP) and is therefore inactive except for the free fraction. CRH-BP is predominantly produced by the liver and distributed and expressed differently from the CRH receptors (Cortright et al. 1995; Zhao et al. 1997).

Rhode et al. (1996) used whole brains of Wistar rats for the CRH receptor assay.

PROCEDURE

Whole brains of male Wistar rats weighing 220–250*g* are homogenized with a Teflon-glass homogenizer (10 strokes at 800 rpm) in 0.32 M sucrose, 50 mM Tris/HCl (pH 7.2), 10 mM $MgCl_2$, 2 mM EGTA, and 0.15 mM bacitracin at 50 mg wet weight per milliliter. After centrifugation at 1000 *g* for 5 min, the supernatant is centrifuged at 26,000 *g* for 20 min. The pellet is resuspended in 50 mM Tris/HCl (pH 7.2), 10 mM $MgCl_2$, 2 mM EGTA, adding 0.15 mM bacitracin and 0.0015% aprotinin (assay buffer), and again centrifuged. The pellet is suspended in assay buffer containing 0.32 M sucrose and stored at −20°C. All steps are carried out at 4°C. Protein concentrations are determined by the method of Bradford (1976) using BSA as standard.

Then, 100 µg of membrane preparation in 300 µl assay buffer is incubated in quadruplicate with 0.1 nM [^{125}I]Tyr-oCRH in the absence and presence of 12 different concentrations (0.2 nM up to 1 µM) of unlabeled peptides at 25°C for 2 h. Nonspecific tracer binding is determined in the presence of 1 µM ovine CRH (oCRH). At the end of incubation, 3 ml of ice-cold assay buffer without inhibitors (containing 0.01% Triton X-100) is added to the assay tube and the samples are immediately filtered through GF/C filter discs (Whatman), presoaked for 2 h in 0.1% polyethylenimine using a Brandel-Harvester. The incubation tubes and filters are then washed with 3 ml cold washing buffer. Triton X-100 in this buffer strongly reduces nonspecific tracer binding. Radioactivity retained on the filter is measured by gamma-counting.

EVALUATION

Receptor affinities (K_{ass}, $K_d = 1/K_{ass}$) and capacities (B_{max}) are estimated using the nonlinear least-squares curve fitting program RADLIG (BIOSOFT, Cambridge, UK) and a K_d of 0.48 nM for the binding of the tracer peptide as determined from tracer saturation curves.

MODIFICATIONS OF THE METHOD

Schulz et al. (1996) used P2 membranes from human neuroblastoma IMR32 cells to test receptor binding of a selective nonpeptide antagonist of corticotropin-releasing factor (CRF).

Webster et al. (1996) used rat frontal cortex, pituitary, cerebellum, and heart tissue for *in vitro* characterization of antalarmin, a nonpeptide CRH receptor antagonist.

Grigoriadis et al. (1996) recommended ^{125}I-tyro-sauvagine as a high-affinity radioligand for the pharmacological and biochemical study of human CRF 2α receptors.

Differences between normal and adenomatous pituitary corticotrophs in the labeling characteristics of CRH receptors were reported by Abs et al. (1997).

Rabadan-Diehl et al. (1997) studied the role of glucocorticoids and hypothalamic factors in the regulation of pituitary CRH receptor mRNA and CRH during adrenalectomy in rats.

The differential regulation of hypothalamic pituitary CRH receptors during the development of adjuvant-induced arthritis in rats was reported by Aguilera et al. (1997).

Grammatopoulos and Hillhouse (1998) reported the solubilization and biochemical characterization of the human myometrial CRH receptor.

The interaction between glucocorticoids and CRH in the regulation of the pituitary CRH receptor has been studied in rats by Ochedalski et al. (1998).

The multiple actions of CRF on neuroendocrine and behavioral functions were examined using high-affinity, nonpeptide antagonists (Lundkvist et al. 1996).

Wei et al. (1998) described analogs of CRH and urocortin with selective activity at CRH_1 and $CRH_{2\beta}$ receptors.

Perrin et al. (1999) used an agonist, urocortin, and an antagonist, astressin, as radioligands for characterization of CRF receptors.

REFERENCES AND FURTHER READING

Abs R, Smets G, Vauquelin G, Verhelst J, Mahler C, Verlooy J, Stevenaert A, Wouters L, Borgers M, Beckers A (1997) ^{125}I-Tyr^0-hCRH labeling characteristics of corticotropin-releasing hormone receptors: differences between normal and adenomatous pituitary corticotrophs. Neurochem Int 30:291–297

Aguilera G, Jessop DS, Harbuz MS, Kiss A, Lightman SL (1997) Differential regulation of hypothalamic pituitary corticotropin releasing hormone receptors during development of adjuvant-induced arthritis in the rat. J Endocrinol 153:185–191

Bradford MM (1976) A rapid and sensitive method for the quantitation of microgram quantities of protein utilizing the principle of protein-dye binding. Anal Biochem 72:248–254

Castro MG, Morrison E, Perone MJ, Brown OA, Murray CA, Ahmed I, Perkins AV, Europe-Finner G, Lowenstein PR, Linton EA (1996) Corticotropin-releasing hormone receptor type 1: generation and characterization of polyclonal antipeptide antibodies and their localization in pituitary cells and cortical neurones *in vitro*. J Neuroendocrinol 8:521–531

Chen R, Lewis KA, Perrin MH, Vale WW (1993) Expression cloning of a human corticotropin-releasing-factor receptor. Proc Natl Acad Sci USA 90:8967–8971

Cortright DN, Nicoletti A, Seasholtz AF (1995) Molecular and biochemical characterization of the mouse brain corticotropin-releasing hormone-binding protein. Mol Cell Endocrinol 111:147–157

Dautzenberg FM, Hauger RL (2002) The CRF peptide family and their receptors: yet more partners discovered. Trends Pharmacol Sci 22:71–77

De Souza EB, Grigoriadis DE, Vale WW (1998) Corticotropin-releasing factor receptors. In: Girdlestone D (ed) The IUPHAR compendium of receptor characterization and classification. IUPHAR Media, London, pp 134–138

Di Blasio AM, Giraldi FP, Vigano P, Petraglia F, Vignali M, Cavagnini F (1997) Expression of corticotropin-releasing hormone and its R1 receptor in human endometrial stroma cells. J Clin Endocrinol Metab 85:1594–1597

Grammatopoulos D, Hillhouse EW (1998) Solubilization and biochemical characterization of the human myometrial corticotropin-releasing hormone receptor. Mol Cell Endocrinol 138:185–198

Grigoriadis DE, Heroux JA, De Souza EB (1993) Characterization and regulation of corticotropin-releasing factor receptors in the central nervous, endocrine and immune system. In: Chadwick DJ, Marsh J, Ackrill K (eds) Ciba Foundation symposium 172. Wiley, Chichester, pp 85–107

Grigoriadis DE, Liu XJ, Vaughn J, Palmer SF, True CD, Vale WW, Ling N, De Souza EB (1996) ^{125}I-Tyro-sauvagine: a novel high affinity radioligand for the pharmacological and biochemical study of human corticotropin releasing factor 2α receptors. Mol Pharmacol 50:679–686

Hauger RL, Aguilera G (1993) Regulation of pituitary corticotropin releasing hormone (CRH) receptors by CRH: interaction with vasopressin. Endocrinology 133:1708–1714

Kostich W, Chen A, Sperle K, Horlick RA, Patterson J, Largent BL (1996) Molecular cloning an expression analysis of human CRH receptor type 2 α and β isoforms. Soc Neurosci Abstr 22:609

Kostich W, Chen A, Sperle K, Largent BL (1998) Molecular Identification and Analysis of a Novel Human Corticotropin-Releasing Factor (CRF) Receptor: The $CRF_{2\gamma}$ Receptor. Mol Endocrinol 12:1077–1085

Liaw CW, Lovenberg TW, Barry G, Oltersdorf T, Grigoriadis DE, De Souza EB (1996) Cloning and characterization of the human corticotropin-releasing factor-2 receptor complementary deoxyribonucleic acid. Endocrinology 137:72–77

Lovenberg TW, Liaw CW, Grigoriadis DE, Clevenger W, Chalmers DT, De Souza EB, Oltersdorf T (1995) Cloning and characterization of a functionally distinct corticotropin-releasing factor receptor subtype from rat brain. Proc Natl Acad Sci USA 92:838–840

Lundkvist J, Chai Z, Teheranian R, Hasanvan H, Bartfai T, Jenck F, Widmer U, Moreau JL (1996) A non peptide corticotropin releasing factor antagonist attenuated fever and exhibits anxiolytic-like activity. Eur J Pharmacol 309:195–200

Ochedalski T, Rabdan-Diehl C, Aguilera G (1998) Interaction between glucocorticoids and corticotropin releasing hormone (CRH) in the regulation of the pituitary CRH receptor *in vivo* in rats. J Neuroendocrinol 10:363–369

Perrin MH, Donaldson CJ, Chen R, Lewis KA, Vale WW (1993) Cloning and functional expression of a rat brain corticotropin releasing factor (CRF) receptor. Endocrinology 133:3058–3061

Perrin MH, Sutton SW, Cervini LA, Rivier JE, Vale WW (1999) Comparison of an agonist, urocortin, and an antagonist, astressin, as radioligands for characterization of corticotropin-releasing factor receptors. J Pharmacol Exp Ther 288:729–734

Rabadan-Diehl C, Makara G, Kiss A, Zelena D, Aguilera G (1997) Regulation of pituitary corticotropin releasing hormone (CRH) receptor mRNA and CRH during adrenalectomy: role of glucocorticoids and hypothalamic factors. J Neuroendocrinol 9:689–697

Rhode E, Furkert J, Fechner K, Beyermann M, Mulvany MJ, Richter RM, Denef C, Bienert M Berger H (1996) Corticotropin-releasing hormone (CRH) receptors in the mesenteric small arteries of rats resemble the (2)-subtype. Biochem Pharmacol 52:829–833

Rominger DH, Rominger CM, Fitzgerald LW, Grzanna R, Largent BL, Zaczek R (1998) Characterization of [^{125}I]sauvagine binding to CRH_2 receptors: membrane homogenate and autoradiographic studies. J Pharmacol Exp Ther 286:459–468

Schulz DW, Mansbach RS, Sprouse J, Braselton JP, Collins J, Corman M, Dunaikis A, Faraci S, Schmidt AW, Seeger T, Seymour P, Tingley III FD, Winston EN, Chen YL, Heym J (1996) CP-154-526: a potent and selective nonpeptide antagonist of corticotropin releasing factor receptors. Proc Natl Acad Sci USA 93:10477–10482

Sperle K, Chen A, Kostich W, Largent BL (1997) CRH_2: a novel CRH_2 receptor isoform found in human brain. Soc Neurosci Abstr 23:689

Steckler T, Holsboer F (1999) Corticotropin-releasing hormone receptor subtypes and emotion. Biol Psychiatry 46:1480–1508

Stenzel P, Kesterson R, Yeung W, Cone RD, Rittenberg MB, Stenzel-Poore MP (1995) Identification of a novel murine

receptor for corticotropin-releasing hormone expressed in the heart. Mol Endocrinol 9:637–645
Vita N, Laurent P, Lefort S, Chalon P, Lelias JM, Kaghad M, Le FG, Caput D, Ferrara P (1993) Primary structure and functional expression of mouse pituitary and human brain corticotropin releasing factor receptors. FEBS Lett 335:1–5
Webster EL, Lewis DB, Torpy DJ, Zachman EK, Rice KC, Chrousos GP (1996) *In vivo* and *in vitro* characterization of antalarmin, a nonpeptide corticotropin releasing hormone (CRH) receptor antagonist: suppression of pituitary ACTH release and peripheral inflammation. Endocrinology 137:5747–5750
Wei ET, Thomas HA, Christian HC, Buckingham JC, Kishimoto T (1998) D-amino acid substituted analogs of corticotropin-releasing hormone (CRH) and urocortin with selective agonist activity at CRH_1 and $CRH_{2\beta}$ receptors. Peptides 19:1183–1190
Zhao XJ, Hoheisel G, Schauer J, Bornstein SR (1997) Corticotropin-releasing hormone-binding protein and its possible role in neuroendocrinological research. Horm Metab Res 29:373–378

N.9.4.6 CRF Receptor Antagonists

PURPOSE AND RATIONALE

Studies with CRF antagonists indicate a role for CRF in certain psychiatric diseases and drug addiction (Koob 1999). This is in line with the known clinical psychotropic effects of corticotropin and glucocorticoids at elevated doses.

Various truncations of agonist peptides with deletions of the first 8–11 amino-terminal amino acid residues have resulted in potent peptide antagonists (Rivier et al. 1984; Hernandez et al. 1993; Miranda et al. 1994; Schulz et al. 1996). Several nonpeptide CRF receptor antagonists have been described (Griebel et al. 1998; Okuyama et al. 1999; Habib et al. 2000; Gully et al. 2002; Griebel et al. 2002; Heinrichs et al. 2002; Grigoriadis 2003; Gutman et al. 2003). Receptor autoradiography was performed in treated rats by Heinrichs et al. (2002) and Gutman et al. (2003).

PROCEDURE

Brains from treated rats are sectioned at the level of the prefrontal cortex and lateral septum to determine CRF_1 and CRF_2 receptor binding, respectively. The prefrontal cortex has been shown via *in situ* hybridization to express predominantly CRF_1 receptors, whereas the lateral septum expresses CRF_2 receptors in rodents (Van Pett et al. 2000). After the behavior experiments, 15-µm-thick rat brain sections containing the prefrontal cortex and the lateral septum are sectioned at approximately −20°C, mounted on Superfrost Plus Slides and stored at −80°C until the assay. *Ex vivo* CRF receptor autoradiography is performed on 15-µm-thick rat brain sections. Sections are removed from the −80°C freezer and allowed to warm up to room temperature in a desiccator. Brain sections are fixed for 2 min in 0.1% paraformaldehyde, pH 7.5, followed by a 15-min incubation in assay buffer (50 mM Tris, 10 mM $MgCl_2$, 2 mM EGTA, 0.1% bovine serum albumin, 0.1 mM bacitracin, and 0.1% aprotinin, pH 7.5). Triplicate slides containing adjacent brain sections are incubated in one of three conditions:

1. 0.1 nM radiolabeled ^{125}I-sauvagine to determine total binding at both the CRF_1 and CRF_2 receptor subtypes;
2. 0.1 nM radiolabeled ^{125}I-sauvagine + 1 µM of a specific CRF_1 receptor antagonist to be tested, to determine CRF_2 receptor-specific binding; or
3. 0.1 nM radiolabeled ^{125}I-sauvagine + 1 µM unlabeled sauvagine to determine nonspecific binding.

After a 2-h incubation, unbound radioligand is removed by two 5-min rinses in ice-cold phosphate-buffered saline + 1% bovine serum albumin on a rotating platform at 60 rpm, followed by two brief dips in ice-cold distilled, deionized H_2O. Slides are then rapidly dried using a cold air blow dryer and exposed to Kodak Biomax MR film with ^{125}I-microscale standards (Amersham Biosciences) for 80–90 h.

Images from the receptor autoradiography films are digitized with a CCD-72 (Dage-MTI, Michigan City, Ind., USA) image analysis system equipped with a Nikon camera. Semiquantitative analysis is performed using AIS software (version 4.0, Imaging Research, St. Catherines, ON, Canada). Optical densities are calibrated against co-exposed ^{125}I-microscale standards and expressed in terms of nanocuries per gram of tissue equivalent.

EVALUATION

CRF_1-receptor-specific binding is calculated as total binding minus CRF_2 receptor binding, and CRF_2 receptor-specific binding is calculated as CRF_2 receptor binding minus nonspecific binding. Receptor binding data are expressed as a percentage of the control values. The percentage of binding is subtracted from 100 to estimate percentage of occupancy by the antagonist relative to vehicle-treated rats. In all cases, three to four sections are matched at the rostrocaudal level and used to produce a single value for each animal. Significant differences are evaluated by one- or two-tailed *t* tests or one-way ANOVA followed by Student-Newman-Keuls post hoc analysis.

REFERENCES AND FURTHER READING

Griebel G, Perrault G, Sanger DJ (1998) Characterization of the behavioral profile of the non-peptide CRF receptor antagonist CP-154,526 in anxiety models in rodents. Comparison with diazepam and bispirone. Psychopharmacology 138:55–66

Griebel G, Simiand J, Steinberg R, Jung M, Gully D, Roger P, Geslin M, Scatton B, Maffrand JP, Soubrie P (2002) 4-(2-Chloro-4-methoxy-5-methylphenyl)-N-[(1S)-2-cyclopropyl-1-(3-fluoro-4-methylphenyl)ethyl]5-methyl-N-(2-propynyl)-1, 3-thiazol-2-amine hydrochloride (SSR125 543A), a potent and selective corticotrophin-releasing factor(1) receptor antagonist. II. Characterization in rodent models of stress-related disorders. J Pharmacol Exp Ther 301:333–345

Grigoriadis DE (2003) Corticotropin-releasing factor receptor antagonists: potential novel therapies for human disease. Cell Transmissions 19:3–19

Gully D, Geslin M, Serva L, Fontaine E, Roger P, Lair C, Darre V, Marcy C, Rouby PE, Simiand J, Guitard J, Gout G, Steinberg R, Rodier D, Griebel G, Soubrie P, Pascal M, Pruss R, Scatton B, Maffrand JP, Le Fur G (2002) 4-(2-Chloro-4-methoxy-5-methylphenyl)-N-[(1S)-2-cyclopropyl-1-(3-fluoro-4-methylphenyl)ethyl]5-methyl-N-(2-propynyl)-1,3-thiazol-2-amine hydrochloride (SSR125543A): a potent and selective corticotrophin-releasing factor(1) receptor antagonist. I. Biochemical and pharmacological characterization. J Pharmacol Exp Ther 301:322–332

Gutman DA, Owens MJ, Skelton KH, Thrivikraman KV, Nemeroff CB (2003) The corticotropin-releasing factor$_1$ receptor antagonist R121919 attenuates the behavioral and endocrine responses to stress. J Pharmacol Exp Ther 304:874–880

Habib KE, Weld KP, Rice KC, Puskas J, Champoux M, Listwak S, Webster EL, Atkinson AJ, Schulkin J, Contoreggi C, Chrousos GP, McCann SM, Suomi SJ, Higley JD, Gold PW (2000) Oral administration of a corticotrophin-releasing hormone receptor antagonist significantly attenuates behavioral, neuroendocrine, and autonomic responses to stress in primates. Proc Natl Acad Sci USA 97:6079–6084

Heinrichs SC, De Souza EB, Schulteis G, Lapsansky JL, Grigoriadis DE (2002) Brain penetrance, receptor occupancy and antistress *in vivo* efficacy of a small molecule corticotropin releasing factor type 1 receptor selective antagonist. Neuropsychopharmacology 27:194–202

Hernandez JF, Kornreich W, Rivier C, Miranda A, Yamamoto G, Andrews J, Taché Y, Vale W, Rivier J (1993) Synthesis and relative potencies of new constrained CRF antagonists. J Med Chem 36:2860–2867

Koob GF (1999) Stress, corticotropin-releasing factor, and drug addiction. Ann N Y Sci 897:27–45

Kostich WA, Chen A, Largent BL (1998) Molecular identification and analysis of a novel human corticotrophin-releasing factor (CRF) receptor: the $CRF_{2(\gamma)}$ receptor. Mol Endocrinol 12:1077–1085

Miranda A, Koerber SC, Gulyas J, Lahrichi SL, Craig AG, Corrigan A, Hagler A, Rivier C, Vale W, Rivier J (1994) Conformationally restricted competitive antagonists of human/rat corticotropin-releasing factor. J Med Chem 37:1450–1459

Okuyama S, Chaki S, Kawashima N, Suzuki Y, Ogawa S, Nakazato A, Kumagai T, Okubo T, Tomisawa K (1999) Receptor binding behavioral, and electrophysiological profiles of nonpeptide corticotrophin-releasing factor subtype 1 receptor antagonists CRA1000 and CRA1001. J Pharmacol Exp Ther 289:926–935

Rivier J, Rivier C, Vale W (1984) Synthetic competitive antagonists of corticotropin-releasing factor: effect on ACTH secretion in the rat. Science 224:889–891

Schulz DW, Mansbach RS, Sprouse J, Braselton JP, Collins J, Corman M, Dunaikis A, Faraci S, Schmidt AW, Seeger T, Seymour P, Tingley III FD, Winston EN, Chen YL, Heym J (1996) CP-154-526: a potent and selective nonpeptide antagonist of corticotropin releasing factor receptors. Proc Natl Acad Sci USA 93:10477–10482

Van Pett K, Viau V, Bittecourt JC, Chan RK, Li HY, Arias C, Prins GS, Perrin M, Vale W, Sawchenko PE (2000) Distribution of MRNAs encoding CRF receptors in brain and pituitary of rat and mouse. J Comp Neurol 428:191–212

N.9.5 Growth-Hormone-Releasing Hormone (GH-RH)

N.9.5.1 General Considerations

The discovery of the growth-hormone-releasing hormone (GH-RH) by physiological experiments, and the isolation and purification of the hormonal principle are reviewed elsewhere (Reichlin et al. 1976; Krulich and Fawcett 1977; Ling et al. 1985; Frohman and Jansson 1986; Gelato and Merriam 1986; Grossman et al. 1986; Thorner et al. 1986; Frohman et al. 1986; Muller 1987; Vance 1990). The initial studies on analogs of GH-RH raised expectations that therapy by GH injections might be replaced by GH-RH therapy (Dean and Friesen 1986). It was however found that infusions and high-dose treatment with GH-RH reduced to the response of GH release, in a similar manner as described for the gonadotropin receptors, due to receptor adaptation (Catt et al. 1980).

The comparative endocrinology of hypothalamic control of GH secretion by GH-RH, and the presence of GH-RH receptors in animal species have been explored for mammalian and nonmammalian animal species (Ukena et al. 2006; Lee et al. 2007).

REFERENCES AND FURTHER READING

Catt KJ, Harwood JP, Clayton RN, Davies TF, Chan V, Katikineni M, Nozu K, Dufau ML (1980) Regulation of peptide hormone receptors and gonadal steroidogenesis. Recent Prog Horm Res 36:557–662

Dean HJ, Friesen HG (1986) Growth hormone therapy in Canada: end of one era and beginning of another. Can Med Assoc J 135(4):297–301

Frohman LA, Jansson JO (1986) Growth hormone-releasing hormone. Endocr Rev 7(3):223–253

Frohman LA, Downs TR, Chomczynski P, Frohman MA (1990) Growth hormone-releasing hormone: structure, gene expression and molecular heterogeneity. Acta Paediatr Scand Suppl 367:81–86

Gelato MC, Merriam GR (1986) Growth hormone releasing hormone. Annu Rev Physiol 48:569–591

Grossman A, Savage MO, Besser GM (1986) Growth hormone releasing hormone [review]. Clin Endocrinol Metab 15(3):607–627
Krulich L, Fawcett CP (1977) The hypothalamic hypophysiotropic hormones. Int Rev Physiol 16:35–92
Lee LT, Siu FK, Tam JK, Lau IT, Wong AO, Lin MC, Vaudry H, Chow BK (2007) Discovery of growth hormone-releasing hormones and receptors in nonmammalian vertebrates. Proc Natl Acad Sci USA 104(7):2133–2138
Ling N, Zeytin F, Bohlen P, Esch F, Brazeau P, Wehrenberg WB, Baird A, Guillemin R (1985) Growth hormone releasing factors. Annu Rev Biochem 54:403–423
Muller EE (1987) Neural control of somatotropic function. Physiol Rev 67(3):962–1053
Reichlin S, Saperstein R, Jackson IM, Boyd AE 3rd, Patel Y (1976) Hypothalamic hormones. Annu Rev Physiol 38:389–424
Thorner MO, Vance ML, Evans WS, Blizzard RM, Rogol AD, Ho K, Leong DA, Borges JL, Cronin MJ, MacLeod RM et al (1986) Physiological and clinical studies of GRF and GH. Recent Prog Horm Res 42:589–640
Ukena K, Koda A, Yamamoto K, Iwakoshi-Ukena E, Minakata H, Kikuyama S, Tsutsui K (2006) Structures and diverse functions of frog growth hormone-releasing peptide (fGRP) and its related peptides (fGRP-RPs): a review. J Exp Zoolog A Comp Exp Biol 305(9):815–821
Vance ML (1990) Growth-hormone-releasing hormone. Clin Chem 36(3):415–420

N.9.5.2 Radioreceptor Assay of Growth Hormone-Releasing Hormone

PURPOSE AND RATIONALE

As for other polypeptide hormones, GH-RH receptors may be used for quantification and potency estimates of relative binding affinities. Several agonistic and antagonistic analogs of human GH-RH (hGH-RH) have been synthesized by various groups of investigators. The clinical and basic aspects of GH-releasing peptides are reviewed by Argente et al. (1996).

In vitro assays with pituitary cells have been used for screening the biological activity of hGH-RH analogs prior to their evaluation *in vivo* (Heiman et al. 1985; Kovacs et al. 1988; Campbell et al. 1991). A careful determination of binding activities of the peptides to specific GH-RH receptors provides important data for the design of more active analogs. Several studies demonstrated that the radioligand, [His^1-, ^{125}I-Tyr^{10},Nle^{27}]-hGH-RH(1-32)NH_2, binds specifically to a single class of receptors in rat pituitary cells and homogenates, and can be used for radioreceptor assay (Campbell et al. 1991; Seifert et al. 1985a, 1985b; Struthers et al. 1989). The use of a radioreceptor assay for *in vitro* screening of analogs of GH-RH was described by Halmos et al. (1993).

PROCEDURE

Pituitaries from male Sprague-Dawley rats (250–300 g) are used to prepare crude membranes. Immediately after decapitation, anterior pituitaries are removed, rinsed with cold saline, and homogenized in 5 times their volume of homogenization buffer (50 mM Tris-HCl, 5 mM EDTA, 5 mM $MgCl_2$, 30 µg/ml bacitracin, pH 7.4) on ice using an Ultra-Turrax homogenizer at maximal speed. The homogenate is centrifuged at 500 *g* for 10 min at 4°C. The supernatant containing the crude membrane fraction is again centrifuged at 70,000 *g* for 50 min at 4°C. The pellet is washed twice by resuspending in ice-cold homogenization buffer and spinning. The final pellet is resuspended in homogenization buffer and stored at −70°C until used for the receptor binding studies. Protein concentration is determined by the method of Bradford (1976) using a commercially available protein assay kit.

[His^1,^{125}I-Tyr^{10},Nle^{27}]hGH-RH(1-32)NH_2 is iodinated by the chloramine-T method (Greenwood et al. 1963). The receptor binding assay is carried out for 60 min in GH-RH binding buffer (50 mM Tris-HCl, 5 mM EDTA, 5 mM $MgCl_2$, 1% BSA, 30 µg/ml bacitracin, pH 7.4) at 24°C. For saturation binding analyses, 50–150 µg membrane homogenates are incubated in duplicate with a least six concentrations of radioligand, ranging from 0.005 to 0.35 nM in the presence or absence of excess unlabeled peptide (1 µM) in a final volume of 300 µl. Incubation is terminated by immersing siliconized borosilicate tubes in ice water, transferring 270 µl of the suspension into cold siliconized polypropylene microfuge tubes, and centrifuging at 12,000 *g* for 2 min at 4°C, and aspirating the supernatants. To reduce the nonspecific binding, 500 µl/tube of GH-RH binding buffer is added and the tubes recentrifuged. The washing step is repeated and the supernatant again aspirated. Finally, the bottoms of the tubes, containing the pellet, are cut off and counted for radioactivity in a gamma-counter.

In the competition experiments, which also include the specificity experiments, 50–100 µg of membrane homogenates are incubated in duplicate with 0.10–0.15 nM radioligand plus various concentrations of nonradioactive analogs and other peptides (10^{-12}–10^{-6} M).

EVALUATION

Percent specific binding is plotted against the log concentration of competitors. The curves are compared at the 50% specific binding levels (IC_{50}). The ligand-PC and McPherson computerized curve fitting pro-

grams of Munson and Rodbard (1980) are used to analyze competition and saturation data. To determine the types of receptor binding, dissociation constants (K_d) and the maximal binding capacity of receptors (B_{max}), and the saturation binding data are also analyzed by the Scatchard method.

MODIFICATIONS OF THE METHOD

Carrick et al. (1995) described a rapid and sensitive binding assay for GH releasing factor (GRF). Human embryonic kidney (HEK293) cells and rat pituitary tumor (GH_4C_1) cells were transfected with the porcine GRF receptor cDNA. Stably expressing cell lines are referred to as 293-P2 and GH_4-P1, respectively. GH_4C_1 cells transfected with somatostatin receptor subtype 2 are called GH_4-R2.20 and HEK293 cells transfected with somatostatin receptor subtype 5 are called 293-R5.2. GH_4-P1 and 293-R5.2 were derived by the calcium phosphate method of transfection and 293-P2 and GH_4-R2.20 using lipofectamine. For binding assays, cells were removed from culture dishes by the addition of phosphate-buffered saline containing 1 mM EDTA and cell membrane fractions prepared. Membrane pellets were suspended in 25 mM Tris, pH 7.4, plus protease inhibitors, aliquoted and stored at −80°C. The binding assay consisted of approximately 25 pM radiolabeled ligand in the presence or absence of unlabeled ligand in assay buffer (50 mM HEPES, pH 7.4, 5 mM $MgCl_2$, 2 mM EGTA) and cell membranes (2–10 µg). The total assay volume of 200 µl included wheat-germ-agglutinin-coated SPA beads at a concentration of 1 mg/assay, and for GRF binding, 0.05 mg/ml alamethicin (Sigma St. Louis, Mo., USA); 96-well plates were used for most assays. Assays were agitated on a plate shaker for 3 h. Samples were counted on a Wallac Microbeta Counter for 1 min per sample. The conventional binding assay was performed (Mayo 1992), except that following binding and centrifugation the membranes were washed in 0.5 ml binding buffer, centrifuged, and counted.

Abribat et al. (1990) and Gaudreau et al. (1992) developed a binding assay for GH-RH in rat pituitaries. Using this technique, Lefrancois and Gaudreau (1994) tried to identify the receptor-binding pharmacophores of GH-RH in rat pituitaries.

Hassan et al. (1995) developed a competitive binding assay using cloned porcine GH-RH receptors in order to study structure–activity relationships.

Kaijkowsi et al. (1997) investigated GH-RH receptor structure and activity using yeast expression technologies.

Muccioli et al. (1998) characterized specific binding sites for synthetic GH secretagogs (sGHS) on membranes from pituitary gland and different human brain regions using a peptidyl sGHS (Tyr-Ala-hexarelin) which has been radio-iodinated to high specific activity at the Tyr residue.

REFERENCES AND FURTHER READING

Abribat T, Boulanger L, Gaudreau P (1990) Characterization of [^{125}I-Tyr^{10}] human growth hormone-releasing factor (1-44)-amide binding to rat pituitary: evidence of high and low affinity classes of sites. Brain Res 528:291–299

Argente J, Garcia-Segura LM, Pozo J, Chowen JA (1996) Growth hormone-releasing peptides: clinical and basic aspects. Horm Res 46:155–159

Bradford MM (1976) A rapid and sensitive method for the quantitation of microgram quantities of protein using the principle of protein-dye binding. Anal Biochem 72:248–254

Campbell RM, Lee Y, Rivier J, Reimer EP, Felix AM, Mowles TF (1991) GRF analogs and fragments: correlation between receptor binding and structure. Peptides 12:569–574

Carrick TA, Bingham B, Eppler CM, Baumbach WR, Zysk JR (1995) A rapid and sensitive binding assay for growth hormone releasing factor. Endocrinology 136:4701–4704

Gaudreau P, Boulanger L, Abribat T (1992) Affinity of human growth hormone-releasing factor (1-29)NH_2 analogues for GRF binding sites in rat adenopituitary. J Med Chem 35:1864–1869

Greenwood FC, Hunter WH, Glower JS (1963) The preparation of ^{125}I labeled growth hormone of high specific activity. Biochemistry 89:114–123

Halmos G, Rekasi Z, Szoke B, Schally AV (1993) Use of radioreceptor assay and cell superfusion system for *in vitro* screening of analogs of growth hormone-releasing hormone. Receptor 3:87–97

Hassan HA, Hsiung HM, Zhang X Y, Smith DP, Smiley DL Heinman ML (1995) Characterization of growth hormone-releasing hormone (GH-RH) binding to cloned porcine GH-RH receptor. Peptides 16:1469–1473

Heiman Ml, Nekola MV, Murphy WA, Lance VA, Coy DH (1985) An extremely sensitive *in vitro* model for elucidating structure-activity relationships of growth hormone-releasing factor analogs. Endocrinology 116:410–415

Kaijkowsi EM, Price LA, Pausch MH, Young KH, Ozenberger BA (1997) Investigation of growth hormone releasing hormone receptor structure and activity using yeast expression technologies. J Recept Signal Transduct Res 17:1–3

Kovacs M, Gulyas J, Bajusz S, Schally AV (1988) An evaluation of intravenous, subcutaneous, and *in vitro* activity of new agmatine analogs of growth hormone-releasing hormone hGH-RH(1-29)NH_2. Life Sci 42:27–35

Lefrancois L, Gaudreau P (1994) Identification of receptor binding pharmacophores of growth hormone-releasing factor in rat adenopituitary. Neuroendocrinology 59:363–370

Mayo KE (1992) Molecular cloning and expression of a pituitary-specific receptor for growth hormone-releasing hormone. Mol Endocrinol 6:1734–1744

Muccioli G, Ghè C, Ghigo MC, Papoti M, Arvat E, Boghen MF, Nilsson MHL, Deghengi R, Ong H, Ghigo E (1998) Specific receptors for synthetic GH secretagogues in the human brain and pituitary gland. J Endocrinol 157:99–106

Munson PJ, Rodbard D (1980) A versatile computerized approach for characterization of ligand-binding systems. Anal Biochem 107:220–239

Seifert H, Perrin M, Rivier J, Vale W (1985a) Binding sites for growth hormone releasing factor on rat pituitary cells. Nature 313:487–489
Seifert H, Perrin M, Rivier J, Vale W (1985b) Growth hormone-releasing factor binding sites in rat anterior pituitary membrane homogenates. Modulation by glucocorticoids. Endocrinology 117:424–426
Struthers RS, Perrin MH, Vale W (1989) Nucleotide regulation of growth hormone-releasing factor binding to rat pituitary receptors. Endocrinology 124:24–29

N.9.5.2.1 Growth Hormone Release from Rat Pituitaries in Vitro

PURPOSE AND RATIONALE

For testing of pituitary cell stimulation, isolated pituitary glands or cell cultures may be used. Antagonism by adding somatostatin, for example, is tested in the presence of a standard concentration of GH-RH. Human GH-RH has the structure of a 44-amino-acid amide, which was isolated from human endocrine tumors and later confirmed as a hypothalamic hormone. The effect of GH-RH analogs can be tested on isolated rat pituitaries measuring GH release. This test system avoids the interference of counter-regulatory somatostatin secretion, which limits the duration of GH release *in vivo*.

PROCEDURE

The pituitaries of male Sprague-Dawley rats weighing about 100 g are quickly removed after decapitation. The posterior lobe is discarded and the anterior lobe is divided into two halves by a midsagittal cut. Five bisected hemipituitaries are incubated in plastic vials containing 4 ml TCM 199 with 0.1% BSA, 15 µg/ml penicillin, and 25 µg/ml streptomycin. The vials are gassed with 95% O_2 and 5% CO_2. After 30 min of control incubation, the medium is changed and various doses of standard and test substances are added for an incubation of 90 min. GH content in the medium and in the pituitaries is determined by a specific radioimmunoassay (Schalch and Reichlin 1966).

EVALUATION

Dose–response curves are established for standard and test compounds measuring GH release into the medium and GH depletion from the pituitaries allowing calculation of potencies ratios with confidence limits.

MODIFICATIONS OF THE METHOD

Superfused pituitary cells may be used measuring activity and duration of effect, as well as interaction of stimulatory and inhibitory factors. Growth-hormone-releasing factor from tumors in human pancreas and from rat hypothalami as well as analogs of GH-RH were evaluated in a superfused pituitary cell system (Vigh and Schally 1984; Czernus and Schally 1991; Halmos et al. 1993), see also Sect. N.9.4.2, *in vitro* assay for CRH activity. Anterior pituitaries of two young adult male Sprague-Dawley rats were digested with 0.5% collagenase CLS2 (Worthington) for 50 min. After incubation, the fragments were digested into cell clusters (5–40 cells) by mechanical dispersion, and then transferred onto two columns and allowed to sediment simultaneously with 0.8 ml Sephadex G-10. The dead volume of the system was set to 1 ml. Medium 199 containing BSA (2.5 g/l), $NaHCO_3$ (2.2 g/l) and gentamicin sulfate (85 µg/ml) was equilibrated with a mixture of 95% air and 5% CO_2 and used as the culture medium. The medium was pumped at a flow rate of 0.33 ml/min. During an overnight recovery period, the baseline stabilized and the cells regained their full responsiveness. The samples were then infused through a four-way valve at 5×10^{-10} M concentration for 3 min (1 fraction) at 45-min intervals. Rat GH was determined by double-antibody radioimmunoassay.

The same system was used by Rekasi and Schally (1993) and Kovács et al. (1996a) to evaluate the activity of GH-RH antagonists. For determination of the antagonistic activity, the cells were exposed to 10^{-8}, 10^{-7}, and 10^{-6} M GH-RH antagonist simultaneously with 10^{-9} M GH-RH or to 10^{-6} M GH-RH antagonist combined with 100 mM KCl (controls for potassium-stimulated GH secretion) for 3 min. After 30 min, the duration of the inhibitory effect of GH-RH antagonist was also tested by repeated 3-min infusions of 10^{-9} M GH-RH.

Using this system with pituitaries of **transgenic mice** overexpressing the human GH-RH gene, Kovacs et al. (1997) evaluated the effects of GH-RH antagonists.

In addition to growth hormone release, Horváth et al. (1995) determined cAMP release from superfused rat pituitary cells stimulated by GH-RH.

GH release was determined using cultured rat pituitary cells (Brazeau et al. 1982; Perkins et al. 1983; Scheikl-Lenz et al. 1985). Pituitary cells were prepared by enzyme dispersion with collagenase, DNase and pancreatin. The cells were cultured for 3 days in microbiological Petri dishes in Dulbecco's modified essential medium with 20 mM HEPES, 15% fetal calf serum, 100 mU/ml penicillin-G and 100 µg/ml streptomycin at 37°C and 10% CO_2.

Cheng et al. (1993) tested time- and dose-dependent GH release by a nonpeptidyl GH secretagogue in rat pituitary cells.

Sanchez-Hormigo et al. (1998) tested GH-releasing hexapeptide, one of several synthetic GH secretagogues, on GH secretion from cultured porcine somatotropes.

Kovács et al. (1996b) measured the effects of chronic administration of a GH-RH agonist on body weight, tibia length and tail length in growth-hormone-deficient (monosodium-glutamate-lesioned) rats.

Jacks et al. (1996) evaluated an orally active GH secretagogue in dogs. Serum GH levels were dose-dependently increased after oral and intravenous administration. Moreover, an increase of insulin-like growth factor and serum cortisol was found.

REFERENCES AND FURTHER READING

Brazeau P, Ling N, Böhlen P, Esch F, Ying SY, Guillemin R (1982) Growth hormone releasing factor, somatocrinin, releases pituitary growth hormone *in vitro*. Proc Natl Acad Sci USA 79:7909–7013

Cheng K, Chan WWS, Butler B, Wie L, Smith RG (1993) A novel non-peptidyl growth hormone secretagogue. Horm Res 40:109–115

Czernus V, Schally AV (1991) The dispersed cell superfusion system. In: Greenstein B (ed) Neuroendocrine research methods. Harwood Academic, London, pp 66–102

Daughaday WH, Peake GT, Machlin LJ (1970) Assay of growth hormone releasing factor. In: Hypophysiotropic hormones of the hypothalamus: assay and chemistry. Williams and Wilkins, Baltimore, Md., pp 151–170

Gelato MC, Merriam GR (1986) Growth hormone releasing hormone. Annu Rev Physiol 48:569–591

Halmos G, Rekasi Z, Szoke B, Schally AV (1993) Use of radioreceptor assay and cell superfusion system for *in vitro* screening of analogs of growth hormone-releasing hormone. Receptor 3:87–97

Horváth JE, Groot K, Schally AV (1995) Growth hormone-releasing hormone stimulates cAMP release from superfused rat pituitary cells. Proc Natl Acad Sci USA 92:1856–1860

Jacks T, Smith R, Judith F, Schleim K, Frazier E, Chen H, Krupa D, Hora D Jr, Nargund R, Patchett A, Hickey G (1996) MK-0677, a potent, novel, orally active growth hormone (GH) secretagogue: GH, insulin-like growth factor I, and other hormonal responses in beagles. Endocrinology 137:5284–5289

Kovács M, Zarándi M, Halmos G, Groot K, Schally AV (1996a) Effects of acute and chronic administration of a new potent antagonist of growth hormone-releasing hormone in rats: mechanism of action. Endocrinology 137:5364–5369

Kovács M, Halmos G, Groot K, Izdebski J, Schally AV (1996b) Chronic administration of a new potent agonist of growth hormone-releasing hormone induces compensatory linear growth in growth hormone-deficient rats: mechanism of action. Neuroendocrinology 64:169–176

Kovács M, Kineman RD, Schally AV, Zarándi M, Groot K, Frohman LA (1997) Effects of antagonists of growth hormone-releasing hormone (GHRH) on GH and insulin-like growth factor I levels in transgenic mice overexpressing the human GHRH gene, an animal model of acromegaly. Endocrinology 138:4536–4542

Ling N, Zeytin F, Böhlen P, Esch F, Brazeau P, Wehrenberg WB, Baird A, Guillemin R (1985) Growth hormone releasing factors. Annu Rev Biochem 54:403–423

Perkins SN, Evans WS, Thorner MO, Cronin MJ (1983) Beta-adrenergic stimulation of growth hormone release from perifused rat anterior pituitary cells. Neuroendocrinology 37:473–475

Rekasi Z, Schally AV (1993) A method for evaluation of activity of antagonistic analogs growth hormone-releasing hormone in a superfusion system. Proc Natl Acad Sci USA 90:2146–2149

Sanchez-Hormigo A, Castano JP, Torronteras R, Malagon MM, Ramirez JL, Gracia-Navarro F (1998) Direct effect of growth hormone (GH)-releasing hexapeptide (GHRP-6) and GH-releasing factor (GRF) on GH secretion from cultured porcine somatotropes. Life Sci 63:2079–2088

Schalch DS, Reichlin S (1966) Plasma growth hormone concentration in the rat determined by radioimmunoassay: influence of sex, pregnancy, lactation, anesthesia, hypophysectomy and extrasellar pituitary transplants. Endocrinology 79:275–280

Scheikl-Lenz B, Markert C, Sandow J, Träger L, Kuhl H (1985) Functional integrity of anterior pituitary cells separated by a density gradient. Acta Endocrinol 109:25–31

Varga JL, Schally AV, Scernus VJ, Zarandi M, Halmos G, Groot K, Rekasi Z (1999) Synthesis and biological evaluation of antagonists of growth hormone-releasing hormone with high and protracted *in vivo* activities. Proc Natl Acad Sci USA 96:692–697

Vigh S, Schally AV (1984) Interaction between hypothalamic peptides in a superfused pituitary cell system. Peptides 5 [Suppl I]:241–247

N.9.5.2.2 Long-Term Pituitary Cell Culture

Long-term-cultured pituitary cells have been used extensively to study the response of GH secretion and synthesis. Roh et al. (2006) applied this principle to the investigation of priming by GH-RH and by synthetic secretagogues derived from ghrelin. They found that low doses of GHRP-2 and GH-RH were suitable for priming somatotrope cells in culture for subsequent stimulation by GH-RH and ghrelin.

Studies *in vitro* using long-term cell cultures have shown that priming with low doses of GH-RH enhances the subsequent response to the stimulation with GH-RH analogs. Fintini et al. (2005) have used a new animal model for the assessment of GH secretion, the GH-deficient GH-RH-knockout (GH-RH-KO) mouse model. The found that priming with the non-GH-RH secretagogue derived from the gastrointestinal peptide ghrelin augmented the subsequent response to a GH-RH analog.

REFERENCES AND FURTHER READING

Fintini D, Alba M, Schally AV, Bowers CY, Parlow AF, Salvatori R (2005) Effects of combined long-term treatment

with a growth hormone-releasing hormone analogue and a growth hormone secretagogue in the growth hormone-releasing hormone knock out mouse. Neuroendocrinology 82(3–4):198–207

Roh SG, Doconto M, Feng DD, Chen C (2006) Differential regulation of GH-RH-receptor and GHS-receptor expression by long-term *in vitro* treatment of ovine pituitary cells with GHRP-2 and GH-RH. Endocrine 30(1):55–62

N.9.5.3 GH-RH Bioassay by Growth Hormone Release in Rats

PURPOSE AND RATIONALE

Releasing activity can be determined by plasma GH stimulation after intravenous or subcutaneous injection of GH-RH in rats.

PROCEDURE

Male Sprague-Dawley rats weighing about 100 g are anesthetized by fractionated subcutaneous injections of 0.7 ml/kg of 25% urethane solution. The jugular vein is cannulated. Various doses of GH-RH test preparations or standard are injected intravenously in 0.2 ml 1% gelatin/saline. After 15 min blood samples are collected for determination of GH by a specific radioimmunoassay (Schalch and Reichlin 1966). The plasma concentration is expressed in terms of NIAMD-rat-GH-RP-1.

As a modification also suitable for testing other releasing hormones, e. g., by subcutaneous application, a double-barreled polyethylene catheter is implanted into the jugular vein, with one lumen being used for blood sampling and the second small lumen being used to keep the catheter open by heparin infusion into the tip of the collection catheter. Blood is continuously withdrawn by a peristaltic pump and fractions of 500 µl heparinized blood are collected at intervals of 10 min. To compensate for blood losses, the erythrocyte fraction of four to eight consecutive plasma samples is reinfused in a plasma expander (Haemaccel 3.5%) via a femoral vein. Before treatment, two 2-min samples are collected, and, after injection, two 2-min samples are collected again, followed by sampling intervals of 10 min for up to 3 h. GH is determined by a specific radioimmunoassay (Schalch and Reichlin 1966).

EVALUATION

Using several doses of standard and test preparation dose–response curves are established, allowing calculation of the potency ratio with confidence limits. Time–concentration curves after subcutaneous or, for example, intranasal application allow the duration of action to be evaluated.

MODIFICATIONS OF THE METHOD

Wehrenberg and Ling (1983) and Wehrenberg et al. (1985) determined the *in vivo* biological potency of rat and human GH-releasing factor and fragments of human GH-releasing factor in swivel-cannulated, conscious, freely moving rats and in cannulated anesthetized rats.

REFERENCES AND FURTHER READING

Schalch DS, Reichlin S (1966) Plasma growth hormone concentration in the rat determined by radioimmunoassay: influence of sex, pregnancy, lactation, anesthesia, hypophysectomy and extrasellar pituitary transplants. Endocrinology 79:275–280

Wehrenberg WB, Ling N (1983) *In vivo* biological potency of rat and human growth hormone-releasing factor and fragments of human growth hormone-releasing factor. Biochem Biophys Res Commun 115:525–530

Wehrenberg WB, Baird A, Zeytin F, Esch F, Böhlen P, Ling N, Ying SY, Guillemin R (1985) Physiological studies with somatocrinin, a growth hormone releasing factor. Annu Rev Pharmacol Toxicol 25:463–483

N.9.5.4 GH-RH Analogs

Many studies have been performed with synthetic GH-RH analogs, starting with the active sequence GHH (1–29), and proceeding to more powerful compounds, which were explored in domestic animals (Bhatti et al. 2006), and tested for their therapeutic potential in clinical studies (Doi et al. 2004; Furuta et al. 2004; Veldhuis et al. 2005).

REFERENCES AND FURTHER READING

Bhatti SF, Duchateau L, Van Ham LM, De Vliegher SP, Mol JA, Rijnberk A, Kooistra HS (2006) Effects of growth hormone secretagogues on the release of adenohypophyseal hormones in young and old healthy dogs. Vet J 172(3):515–525

Doi N, Hirotani C, Ukai K, Shimada O, Okuno T, Kurasaki S, Kiyofuji T, Ikegami R, Futamata M, Nakagawa T, Ase K, Chihara K (2004) Pharmacological characteristics of KP-102 (GHRP-2), a potent growth hormone-releasing peptide. Arzneimittelforschung 54(12):857–867

Furuta S, Shimada O, Doi N, Ukai K, Nakagawa T, Watanabe J, Imaizumi M (2004) General pharmacology of KP-102 (GHRP-2), a potent growth hormone-releasing peptide. Arzneimittelforschung 54(12):868–880

Veldhuis JD, Patrie JM, Frick K, Weltman JY, Weltman AL (2005)Administration of recombinant human GH-RH-1,44-amide for 3 months reduces abdominal visceral fat mass and increases physical performance measures in postmenopausal women. Eur J Endocrinol 153(5):669–677

N.10
Other Peptide Hormones

N.10.1
Melatonin

N.10.1.1
General Considerations

The role of melatonin as a neurotransmitter, a hormone, and a possible therapeutic agent has been a matter of controversy (Brainard 1978; Reiter 1991; Hajak et al. 1996; Huether 1996; Jansen et al. 2006) ever since melatonin was isolated and identified as *N*-acetyl-5-methoxytryptamine by Lerner et al. (1958) and characterized by Axelrod and Wurtman (1966). Melatonin is synthesized and released by the pineal gland and has been shown to play a key role in the regulation of mammalian circadian rhythms and reproductive functions (Reiter 1991; Arendt et al. 1995; DiBella and Gualano 2006). Melatonin is also produced in extrapineal sites, such as the retina (Lundmark et al. 2006), the Harderian glands, and the gut (Huether 1993, 1994; Messner et al. 2001). It should however be noted that methods for the identification of peptides and neurotransmitters have reached extremely high levels of sensitivity; as a consequence, their presence in a tissue does not necessarily indicate that a relevant physiological function is subserved in that organ or tissue. Melatonin is synthesized from 5-hydroxytryptamine (5-HT) by a two-step biochemical pathway (Reiter 1991). Initially, 5-HT is acetylated to produce *N*-acetylserotonin, which is subsequently *O*-methylated to form melatonin.

REFERENCES AND FURTHER READING

Arendt J, Deacon S, English J, Hampton S, Morgan L (1995) Melatonin and adjustment to phase shift. J Sleep Res 4:74–79

Axelrod J, Wurtman RJ (1966) The formation, metabolism and some actions of melatonin, a pineal gland substance. Res Publ Assoc Res Nerv Ment Dis 43:200–211

Brainard GC (1978) Pineal research: the decade of transformation. J Neural Transm Suppl 3–10

DiBella L, Gualano L (2006) Key aspects of melatonin physiology: thirty years of research. Neuro Endocrinol Lett 27(4):425–432

Hajak G, Rodenbeck A, Hardeland R, Hüther G (1996) Melatonin: Vom Stiefkind der Hormonforschung zur Goldmarie der Vermarktungsstrategen. TW Neurologie Psychiatrie 10:384–390

Huether G (1993) The contribution of extrapineal sites of melatonin synthesis to circulating melatonin levels in higher vertebrates. Experientia 49:665–670

Huether G (1994) Melatonin synthesis in the gastrointestinal tract and the impact of nutritional factors on circulating melatonin. Ann NY Acad Sci 719:146–158

Huether G (1996) Melatonin as an antiaging drug: between facts and fantasy. Gerontology 42:87–96

Jansen SL, Forbes DA, Duncan V, Morgan DG (2006) Melatonin for cognitive impairment [review]. Cochrane Database Syst Rev CD003802

Lerner AB, Case JD, Takahashi Y, Lee Y, Mori W (1958) Isolation of melatonin, the pineal gland factor that lightens melanocytes. J Am Chem Soc 81:2587

Lundmark PO, Pandi-Perumal SR, Srinivasan V, Cardinali DP (2006) Role of melatonin in the eye and ocular dysfunctions. Vis Neurosci 23(6):853–862

Messner M, Huether G, Lorf T, Ramadori G, Schwörer H (2001) Presence of melatonin in the human hepatobiliary-gastrointestinal tract. Life Sci 69:543–551

Reiter RJ (1991) Pineal melatonin: cell biology of its synthesis and of its physiological interactions. Endocr Rev 12:151–180

N.10.1.2
Melatonin Receptor Binding

PURPOSE AND RATIONALE

The activity of melatonin is mediated through high-affinity G-protein-coupled receptors. Two human melatonin receptor subtypes, hMT1 and hMT2, have been cloned (Reppert et al. 1994, 1995; Browning et al. 2000; Dubocovich et al. 2001). A third melatonin-binding site named MT_3 has been described as the human homolog of cytoplasmatic quinone reductase 2 (Nosjean et al. 2000, 2001).

Audinot et al. (2003) described the evaluation of selective ligands of human cloned MT_1 and MT_2 receptors. Binding affinities were determined using [2-^{125}I]-melatonin. Methods for the measurement of melatonin and melatonin derivatives (Middleton 2006) and for the melatonin receptor ligands (Zlotos 2005) have been reviewed

PROCEDURE

Membrane Preparations

HEK.293 and CHO-K1 cell lines stably expressing the hMT_1 or hMT_2 receptor are grown to confluence, harvested in phosphate buffer containing 2 mM EDTA and centrifuged at 1000 *g* for 5 min (4°C). The resulting pellet is suspended in 5 ml Tris/HCl, pH 7.4, containing 2 mM EDTA and homogenized using a Kinematica polytron. The homogenate is then centrifuged (20,000 *g*, 30 min, 4°C), and the resulting pellet is suspended in 75 mM Tris/HCl, pH 7.4, containing 2 mM EDTA and 12.5 mM $MgCl_2$. Aliquots of membrane preparations are stored in binding buffer (Tris/HCl 50 mM, pH 7.4, 5 mM $MgCl_2$) at −80°C until use.

[2-^{125}I]Melatonin Binding Assay

Membranes are incubated for 2 h at 37°C in binding buffer (Tris/HCl 50 mM, pH 7.4, 5 mM $MgCl_2$) in

a final volume of 250 µl containing [2-^{125}I]melatonin (200 pM) for competition experiments using CHO cells and 25 or 200 pM, respectively, for MT_1 and MT_2 receptors expressed in HEK cells. Nonspecific binding is defined with 10 µM melatonin. The reaction is stopped by rapid filtration through GF/B unifilters, followed by three successive washes with ice-cold buffer.

EVALUATION

Data are analyzed using the program PRISM (GraphPad Software, San Diego, Calif., USA). For saturation assays, the density of binding sites (B_{max}) and the dissociation constant of the radioligand (K_D) are calculated according to the method of Scatchard. For competition experiments, inhibition constants are calculated according to the Cheng-Prusoff equation. For the correlation analysis of pK_i values, the Pearson product moment correlation coefficient is employed.

MODIFICATIONS OF THE METHOD

Receptor binding assays have been used to evaluate new melatonin receptor ligands (Depreux et al. 1994; Dubocovich et al. 1997a; Charton et al. 2000a, 2000b; Nonno et al. 2000).

Dubocovich et al. (1997b) used **rabbit retina membranes** for binding studies with [2-^{125}I]melatonin.

Nonno et al. (2000) and Audinot et al. (2003) used the **[^{35}S]GTPγS binding assay** to evaluate the functional activity of agonists and antagonists. Membranes were prepared as for the [2-^{125}I]melatonin binding assay. Together with test drugs, they were diluted in binding buffer (20 mM HEPES, pH 7.4, 100 mM NaCl, 3 mM $MgCl_2$, 3 µM GDP) in the presence of 20 µg/ml saponin in order to enhance the agonist-induced stimulation level. For agonist tests, incubation was started by the addition of 0.1 nM [^{35}S]GTPγS to membranes and ligands, and carried on for 60 min at room temperature in a final volume of 250 µl. To test for antagonistic activity, membranes were preincubated for 30 min with melatonin (30 nM or 3 nM for hMT_1 and hMT_2 receptors, respectively) and several concentrations of the tested compound. The reaction was started by the addition of 0.1 nM [^{35}S]GTPγS and followed by a 60-min incubation. Nonspecific binding was assessed using nonradiolabeled GTPγS (10 µM). All reactions were stopped by rapid filtration through GF/B unifilters presoaked with distilled water, followed by three successive washes with ice-cold buffer.

Data were analyzed using the program PRISM to yield EC_{50} and E_{max} values for agonists. Antagonist potencies were expressed as K_B with $K_B = IC_{50}/1+([ago]/EC_{50}ago)$, where IC_{50} is the inhibitory concentration of antagonist that gives 50% inhibition of [^{35}S]GTPγS binding in the presence of a fixed concentration of agonist ([ago]) and the EC_{50}ago is the EC_{50} of the agonist when tested alone. I_{max} (maximal inhibitory effect) was expressed as a percentage of that observed with melatonin, 30 nM and 3 nM ([ago]) for hMT_1 and hMT_2 receptors, respectively.

REFERENCES AND FURTHER READING

Audinot V, Mailliet F, Lahaye-Brasseur C, Bonnaud A, Le Gall A, Amossé C, Dromaint S, Rodriguez M, Nagel N, Galizzi JP, Malpaux B, Guillaumet G, Lesieur D, Lefoulon F, Renard P, Delagrange P, Boutin JA (2003) New selective ligands of human cloned MT_1 and MT_2 receptors. Naunyn-Schmiedebergs Arch Pharmacol 367:553–561

Browning C, Beresford I, Fraser N, Giles H (2000) Pharmacological characterization of human recombinant mt_1 and MT_2 receptors. Br J Pharmacol 129:877–886

Charton I, Mamai A, Bennejean C, Renard P, Delagrange P, Morgan PJ, Howell HE, Gourdel-Martin ME, Viaud MC, Guillaumet G (2000a) Synthesis and biological activity of new melatonin receptor ligands. Pharm Pharmacol Commun 6:49–60

Charton I, Mamai A, Bennejean C, Renard P, Howell HE, Guardiola-Lamaître B, Delagrange P, Morgan PJ, Viaud MC, Guillaumet G (2000b) Substituted oxygenated heterocycles and thio-analogues: synthesis and biological evaluation as melatonin ligands. Bioorg Med Chem 8:105–114

Depreux P, Lesieur D, Mansour HA, Morgan P, Howell HE, Renard P, Caignard DH, Pfeiffer B, Delagrange P, Guardiola B, Yous S, Demarque A, Adam G, Andrieux J (1994) Synthesis and structure-activity relationships of novel naphthalenic and bioisosteric related amidic derivatives as melatonin receptor ligands. J Med Chem 37:3231–3239

Dubocovich ML, DelPedro A, Masana MI (1997a) The efficacy of melatonin receptor analogues is dependent on the level of human melatonin receptor subtype expression. Chronobiol Int 14:45

Dubocovich ML, Masana MI, Iacob S, Sauri DM (1997b) Melatonin receptor antagonists that differentiate between the human Mel_{1a} and Mel_{1b} recombinant subtypes are used to assess the pharmacological profile of the rabbit retina ML_1 presynaptic heteroreceptor. Naunyn-Schmiedebergs Arch Pharmacol 355:365–375

Dubocovich ML, Cardinali DP, Delagrange P, Krause DN, Strosberg D, Sugden D, Yocca FD (2001) Melatonin receptors. The IUPHAR compendium of receptor characterization and classification. IUPHAR Media, London, pp 270–277

Middleton B (2006) Measurement of melatonin and 6-sulphatoxymelatonin. Methods Mol Biol 324:235–254

Nonno R, Lucini V, Spadoni G, Pannacci M, Croce A, Esposti D, Balsamini C, Tarzia G, Fraschini F, Stankow BM (2000) A new melatonin receptor ligand with mt_1-agonist and MT_2-antagonist properties. J Pineal Res 29:234–240

Nosjean O, Ferro M, Cogé F, Beauverger P, Henlin JM, Lefoulon F, Fauchère JL, Delagrange P, Canet E, Boutin JA (2000) Identification of the melatonin binding site *MT*$_3$ as the quinone reductase 2. J Biol Chem 275:31311–31317

Nosjean O, Nicolas JP, Klupsch F, Delagrange P, Canet E, Boutin JA (2001) Comparative pharmacological studies of melatonin receptors: MT1, MT2 and *MT3*/QR2. Tissue distribution of *MT3*/QR2. Biochem Pharmacol 61:1369–1379

Reppert SM, Waever DR, Ebisawa T (1994) Cloning and characterization of a mammalian melatonin receptor that mediates reproductive and circadian responses. Neuron 13:1177–1185

Reppert SM, Godson C, Mahle CD, Waever DR, Slaugenhaupt SA, Gusella JF (1995) Molecular characterization of a second melatonin receptor expressed in human retina and brain: the Mel_{1b} melatonin receptor. Proc Natl Acad Sci USA 92:8734–8738

Zlotos DP (2005) Recent advances in melatonin receptor ligands. Arch Pharm (Weinheim) 338(5–6):229–247

N.10.1.3 In Vitro Assay of Melatonin: Inhibition of Forskolin-Stimulated cAMP Accumulation

PURPOSE AND RATIONALE

Reppert et al. (1995), Browning et al. (2000), and Charton et al. (2000a, 2000b) used the inhibition of forskolin-stimulated cAMP accumulation for characterization of melatonin receptors and evaluation of synthetic derivatives.

PROCEDURE

Generation of CHO-mt_1 and CHO-MT_2 Cells

Clones representing the sequence of the human mt1 receptor are amplified using degenerate primers based on the sequence of the *Xenopus laevis* melatonin receptor (Ebisawa et al. 1994). Cloning was in pBluescript (Strategene, La Jolla, Calif., USA). The human MT_2 sequence is cloned in a similar manner using the sequence described by Reppert et al. (1995). The sequences encoding the receptor are cloned into the mammalian vector pcDNA3 (Invitrogen) and introduced into CHO cells by conventional calcium phosphate precipitation techniques, which are then placed under G418 selection (1 mg/ml). Cell lines, which give the greatest melatonin-induced inhibition of cAMP accumulation, are chosen for further studies.

cAMP Assays

The assay is performed using 96-well plates in a final assay volume of 200 µl. Confluent CHO-mt_1 and CHO-MT_2 cells are incubated at 37°C with DMEM-F12, containing 300 µM isobutylmethylxanthine to inhibit phosphodiesterase activity. Following a 60-min incubation, agonist (0.01 pM to 100 µM) is added. After 60 min, forskolin (30 µM) is added and cells are incubated for a further 15 min. For antagonist experiments, melatonin is co-incubated with luzindole (0.1–100 µM) for 60 min prior to the addition of forskolin. The reaction is terminated by removal of media and addition of ice-cold ethanol (100 µl) for 30 min at 4°C. Ethanol samples are evaporated and cAMP concentrations determined by [^{125}I]cAMP scintillation proximity assay (Amersham).

EVALUATION

cAMP data are fitted with a four-parameter logistic equation to determine pIC_{50} values and Hill coefficients. Drug responses are expressed as percentage inhibition of forskolin-stimulated cAMP. The potency ratio is defined as the ratio of the EC_{50} of the drug relative to that of melatonin determined in the same experiment.

MODIFICATIONS OF THE METHOD

Morgan et al. (1989) and Conway et al. (2000) studied inhibition of cAMP production in cultures of ovine pars tuberalis cells by melatonin.

Furthermore, Conway et al. (2000) characterized the human melatonin mt_1 and MT_2 receptors using the **CRE-luciferase reporter assay**. HEK293 cells expressing human melatonin mt_1 and MT_2 receptors were cultured to ~ 80% confluence at which time they were co-transfected with the plasmids pGL3 (CRE2-TK) and pcDOR8 (Barrett et al. 1994) using the lipid transfection reagent FuGENE™ 6 (Boehringer Mannheim). Cells were cultured for 24 h post-transfection before being washed with phosphate-buffered saline (pH 7.4), recovered in phenol-red-free Dulbecco's modified Eagle medium (supplemented with 10% fetal calf serum) and seeded as 50-µl aliquots (5×10^4 cells) into white 96-well tissue culture plates. Following a further 24-h incubation, drug treatments were added in a 5.6 µl volume to triplet wells, and plates were left to incubate overnight (16 h). The level of expressed luciferase was measured by the addition of 50 µl of Constant Light Signal Reagent (Boehringer Mannheim) to each well, and plates were briefly placed in the dark (30 min, room temperature) before being quantified an a Packard LumiCount™ Reader (1 s per well). Where experiments were designed to measure drug-mediated dose–response effects, a control melatonin dose–response study was always included. Data from the triplet wells were averaged and the control data normalized from a value of 100 (no melatonin) to a value of 0 (maximum response, 10^{-5} M melatonin). Data obtained from other drug treatments were normalized relative to the control values determined in that experiment. All experiments were performed on three or more separate occasions, and mean values ± SEM determined.

IC_{50} values and apparent efficacies were calculated by fitting a four-parameter logistic curve through the

mean normalized data. For antagonists, pA_2 values were determined by performing Schild analysis.

REFERENCES AND FURTHER READING

Barrett P, MacDonald A, Helliwell R, Davidson G, Morgan P (1994) Cloning and expression of a new member of the melanocyte-stimulating hormone receptor family. J Mol Endocrinol 12:203–213

Browning C, Beresford I, Fraser N, Giles H (2000) Pharmacological characterization of human recombinant mt_1 and MT_2 receptors. Br J Pharmacol 129:877–886

Charton I, Mamai A, Bennejean C, Renard P, Delagrange P, Morgan PJ, Howell HE, Gourdel-Martin ME, Viaud MC, Guillaumet G (2000a) Synthesis and biological activity of new melatonin receptor ligands. Pharm Pharmacol Commun 6:49–60

Charton I, Mamai A, Bennejean C, Renard P, Howell HE, Guardiola-Lamaître B, Delagrange P, Morgan PJ, Viaud MC, Guillaumet G (2000b) Substituted oxygenated heterocycles and thio-analogues: synthesis and biological evaluation as melatonin ligands. Bioorg Med Chem 8:105–114

Conway S, Canning SH, Howell HE, Mowat ES, Barrett P, Drew JE, Delagrange P, Lesieur D, Morgan PJ (2000) Characterization of human melatonin mt_1 and MT_2 receptors by CRE-luciferase reporter assay. Eur J Pharmacol 390:15–24

Ebisawa T, Karne S, Lerner MR, Reppert SM (1994) Expression cloning of a high-affinity melatonin receptor from *Xenopus* dermal melanophores. Proc Natl Acad Sci USA 91:6133–6137

Morgan PJ, Lawson W, Davidson G, Howell HE (1989) Melatonin inhibits cyclic AMP production in cultures ovine pars tuberalis cells. J Mol Endocrinol 3:R5–R8

Reppert SM, Godson C, Mahle CD, Waever DR, Slaugenhaupt SA, Gusella JF (1995) Molecular characterization of a second melatonin receptor expressed in human retina and brain: the Mel_{1b} melatonin receptor. Proc Natl Acad Sci USA 92:8734–8738

N.10.1.4 Dopamine Release from Rabbit Retina

PURPOSE AND RATIONALE

Dubocovich et al. (1997) compared the pharmacological profile of the rabbit retina ML_1 presynaptic heteroreceptor that mediates the calcium-dependent release of dopamine to that of the human Mel_{1a} and Mel_{1b} recombinant melatonin receptors, and determined potencies of melatonin receptor agonists and antagonists.

PROCEDURE

Albino rabbits (2.5–3.5 kg) maintained on a 14-h/10-h light/dark cycle are sacrificed by decapitation during the light cycle. Retinal pieces are incubated in Krebs solution gassed with 95%O_2 and 5%CO_2 for 20 min at 37°C in the presence of 0.1 μM [^{3}H]dopamine (specific activity 55 Ci/mol). The pieces of retina are washed in Krebs solution at 37°C and placed in glass superfusion chambers between a pair of platinum electrodes 30 mm apart. Retinal tissue is superfused at 1 ml/min with Krebs solution (37°C) containing (*S*−*R*)-sulpiride (0.1 μM) to block D_2 dopamine autoreceptors, beginning 60 min after the onset of superfusion, i. e., when the spontaneous outflow of radioactivity has leveled off. Samples of the superfusate are collected by means of a fraction collector at 4-min intervals. Tritium release from retinal tissue is elicited by field stimulation using 2-min-duration (3 Hz, 20 mA, 2 ms) pulses that are delivered from platinum electrodes by a Grass stimulator. During stimulation, pulses are monitored on an oscilloscope. In each experiment two periods of field stimulation are applied at 60 min and 100 min after the incubation with [^{3}H]dopamine. Samples of the superfusate are collected before, during, and after the period of stimulation. Drugs are added to the perfusion medium either 40 min before the first or 20 min before the second stimulation period. At the end of the experiment, the retinal tissue contained in each chamber is solubilized in 0.5 ml TS-1 (Research Products Int., Elk Grove, Ill., USA) and the tritium content is determined by liquid scintillation counting.

EVALUATION

The outflow of radioactivity in each sample is expressed as the percentage of total tissue radioactivity determined to be present at the beginning of each sample collection period: total tritium released per sample divided by total tritium present in the tissue all multiplied by 100 (Dubocovich 1985). Results are expressed as the ratio of the overflow during the second and first periods of field stimulation within the same experiments.

REFERENCES AND FURTHER READING

Dubocovich ML (1985) Characterization of a retinal melatonin receptor. J Pharmacol Exp Ther 234:395–401

Dubocovich ML, Masana MI, Iacob S, Sauri DM (1997) Melatonin receptor antagonists that differentiate between the human Mel_{1a} and Mel_{1b} recombinant subtypes are used to assess the pharmacological profile of the rabbit retina ML_1 presynaptic heteroreceptor. Naunyn-Schmiedebergs Arch Pharmacol 355:365–375

N.10.1.5 Effect on Xenopus Melanophores

PURPOSE AND RATIONALE

TeckTeh and Sugden (1998) examined the potency of melatonin receptor ligands using the pigment aggregation response in a clonal line of *Xenopus laevis* melanophores.

PROCEDURE

Culture of Xenopus laevis melanophores

A clonal line of *Xenopus laevis* melanophores (M. Lerner, University of Texas) is grown in diluted (0.7 ×) L-15 medium (Sigma) containing 20% heat-inactivated fetal calf serum, penicillin (100 IU/ml) and streptomycin (100 µg/ml). The medium is first conditioned by *Xenopus laevis* fibroblasts (Daniolos et al. 1990).

Microtiter plate assays

Melanophores are seeded into flat-bottomed 96-well microtiter plates and grown in conditioned L-15 medium at 24°C for 2–4 days until cell density is $(6–8) \times 10^4$ cells/well. For the 4–18 h before using melanophores, condition medium is replaced with 0.7 × L-15 medium; pigmented granules remain fully dispersed in this medium. Agonist potency is determined by measuring the redistribution of pigment granules within the melanophores by quantitating the change in absorbance of the cells at 630 nm on a Biotek microtiter plate reader. The fractional change in absorbance $(1 - [A_f/A_i]$, where A_i is the initial absorbance before drug addition and A_f is the final absorbance 1 h after drug treatment) is calculated for each concentration of drug tested.

EVALUATION

Concentration–response data are plotted and EC_{50} values are determined using the ALLFIT program (De Lean et al. 1978) with the four-parameter logistic equation:

$$Y = [A - D]/[1 + (X/C)B] + D$$

where X is the concentration of the analog, Y is the fractional change in absorbance, A is the maximal absorbance in the absence of the analog, B is the slope factor, C is the concentration of the analog producing half of the maximal response (EC_{50}) and D is the minimal absorbance. The response to each drug is measured in six independent experiments. Antagonistic potency (pA_2) is determined by constructing concentration–response curves to melatonin in the absence or presence of varying concentrations (1–100 µM) of each antagonist.

REFERENCES AND FURTHER READING

Danilolos A, Lerner AB, Lerner MR (1990) Action of light on frog pigment cells in culture. Pigment Cell Res 3:38–43

TeckTeh M, Sugden D (1998) Comparison of the structure-activity relationships of melatonin receptor agonists and antagonists: lengthening the *N*-acyl side-chain has differing effects on potency on *Xenopus* melanophores. Naunyn-Schmiedebergs Arch Pharmacol 358:522–528

N.10.1.6 Vasoconstrictor Activity of Melatonin

PURPOSE AND RATIONALE

Evans et al. (1992), Ting et al. (1997), and Delagrange et al. (1999) used the vasoconstrictor action of melatonin in the tail artery of juvenile Wistar rats to evaluate melatonin agonists and antagonists. Two different recording systems, the Halpern pressure myograph (Halpern et al. 1984) and the Halpern–Mulvany wire myograph, were compared.

PROCEDURE

Male juvenile (3–4 weeks old, weighing 55–100 g) Wistar rats are housed in a 12-h light/dark cycle. They are sacrificed 1–2 h after lights on by decapitation. The ventral artery of the tail is dissected and placed onto a dissecting disc in gassed, modified Krebs-Henseleit solution. The blood vessel is carefully cleaned from fat and connective tissues with the aid of a dissecting microscope and divided into ring segments of 2–3 mm length. Ring segments are suspended between two supporting jaws in a stainless steel chamber of a Mulvany–Halpern wire myograph and allowed to equilibrate for 30 min. The preparations are bathed in Krebs-Henseleit solution maintained at 34 ± 1°C and gassed with 95% O_2/5% CO_2. Tension is applied by adjusting the micrometer connected to one of the supporting jaws, while an isometric transducer connected to the other jaw measures force. An initial tension of 0.2–0.5 g is applied. Then the preparations are allowed to relax to 0.1–0.4 g weight. Vessels are contracted with 60 mM KCl to assess tissue viability and provide a reference contracture for subsequent data analysis. A stimulator is used to deliver 5-s trains of electrical pulses (10–20 V, 3 ms pulse width) at a frequency of 2–3 Hz every 4–5 min. The voltage and the frequency of the field stimulation are adjusted at the beginning of each experiment to obtain 20%–35% of the KCl response. Concentration–responses curves are constructed for melatonin and test compounds. For experiments with putative antagonists, these agents are added 20 min before the construction of a dose–response curve for melatonin.

EVALUATION

Isometric tension responses are expressed as a percentage of the enhancement in response to the predrug of

neurogenic contractions. The sensitivity of the preparations is assessed as the negative logarithm of the concentration required to produce 50% of the maximum response (pEC_{50}) after the agonist concentration–effect ($E/[A]$) data are fitted to the formula:

$$E = \alpha[A]^n/([A]^n + [A_{50}]^n)\,,$$

where E is the response, α is the asymptote, $[A]$ is the agonist concentration, n is the gradient of the $E/[A]$ curve and $[A_{50}]$ is the midpoint of the $E/[A]$ curve (Black et al. 1985). $[A_{50}]$ values represent agonist concentration giving 50% of the maximum responses and are shown as the negative logarithm (pEC_{50}). The maximum response of each analog is expressed as a ratio of the maximum response to melatonin (E_{max}) obtained in segments from the same animal. For the antagonistic experiments, the agonist concentration ratio (CR) is determined in each experiment. The CR is the ratio of EC_{50}values in the presence and absence of antagonist. Differences between mean values are compared using either paired or unpaired Student's t-test (two tailed) and are considered statistically significant if $P < 0.05$.

MODIFICATIONS OF THE METHOD

Viswatanan et al. (1997) reported that melatonin receptors mediate **contraction of rat cerebral artery**. Male Sprague-Dawley rats (7–8 weeks old) were sacrificed by decapitation and their brains quickly removed and kept in ice-cold Krebs-Ringer buffer aerated with 95% O_2/5% CO_2. The posterior communicating artery, between the point at which the internal carotid artery joins and the middle cerebral artery originates, is dissected from the base of the brain, kept in ice-cold Krebs-Ringer buffer, cleaned of excess connective tissue, and transmitted to a vessel chamber filled with cold Krebs-Ringer buffer. Both ends of the artery are mounted on glass cannulas (100 µm diameter) and secured using 10–0 surgical silk sutures. The cannulas at the proximal and distal ends of the artery are connected to pressure transducers. The artery is perfused with oxygenated Krebs-Ringer buffer using a servo system. The intraluminal pressure of the artery is gradually increased to 60 mmHg by increasing the flow rate of the Krebs-Ringer buffer. The transmural pressure within the artery segment is maintained at 60–65 mmHg, a pressure chosen because it approximates the non-neurogenic pressure exerted on arterial blood vessels in rats. The chamber is superfused with oxygenated Krebs-Ringer buffer maintained at 37°C. The lumen diameter of the artery is continuously measured using a video electronic analyzer. The preparation is equilibrated for 45–60 min and during this interval it develops the myogenic tone.

Increasing concentrations (10^{-12}–10^{-6} M) of melatonin are administered through the perfusion buffer, without washout, at regular intervals of 5 min, and the lumen diameter is recorded continuously. Changes in lumen diameter are measured and expressed as percentage contraction.

REFERENCES AND FURTHER READING

Black JW, Leff P, Shankley NP (1985) An operational model of pharmacological agonism: the effect of E/[A] curve shape on agonist dissociation constant estimation. Br J Pharmacol 84:561–571

Delagrange P, Ting KN, Kopp C, Lahaye C, Lesieur D, Weibel L, Bennejean C, Renard R, Retton MC (1999) *In vitro* and *in vivo* antagonist properties of S 22153, a new melatonin ligand. Fundament Clin Pharmacol 13:253

Evans BK, Mason R, Wilson VG (1992) Evidence for direct vasoconstriction activity of melatonin in 'pressurized' segments of isolated caudal artery from juvenile rats. Naunyn-Schmiedebergs Arch Pharmacol 346:362–365

Halpern W, Osol G, Coy GS (1984) Mechanical behavior of pressurized *in vitro* prearteriolar vessels determined with a video system. Ann Biochem Engin 12:463–479

Ting KN, Dunn WR, Davies DJ, Sugden D, Delagrange P, Guardiola-Lamaître B, Scalbert E, Wilson VG (1997) Studies on the vasoconstrictor action of melatonin and putative melatonin receptor ligands in the tail artery of juvenile Wistar rats. Br J Pharmacol 122:1299–1306

Viswatanan M, Scalbert, Delagrange P, Guardiola-Lamaître B, Saavedra JM (1997) Melatonin receptors mediate contraction of rat cerebral artery. NeuroReport 8:3847–3849

N.10.1.7 Melatonin's Effect on Firing Rate of Suprachiasmatic Nucleus Cells

PURPOSE AND RATIONALE

Ying et al. (1996) studied the effects of drugs related to melatonin on neuronal firing activity in the suprachiasmatic nucleus, intergeniculate leaflet, and other brain areas in anesthetized Syrian hamsters. The suprachiasmatic nucleus of the hypothalamus functions as the dominant pacemaker for behavioral and physiological circadian rhythms in mammals (Moore 1983; Meijer and Reitveld 1989). Photic information required for entrainment to lighting cycles reaches the suprachiasmatic nucleus through a direct projection from the retina, and, via an indirect pathway, the geniculohypothalamic tract, originating in the retinorecipient intergeniculate leaflet of the geniculate nuclei (Zhang and Rusak 1989). The firing rates are suppressed by melatonin and its analogs, whereas antagonists reverse this effect (Ying et al. 1996; Liu et al. 1997).

PROCEDURE

Male Syrian hamsters weighing 100–140 g are kept in a photoperiod with 14 h of light beginning at 05:00 a.m. for at least 2 weeks before being used. The animals are anesthetized with 25% urethane (2 g/kg i.p.) and given subcutaneous injections of Robinul (3-hydroxy-1,1-dimethylpyrrolidinium bromide α-cyclopentylmandelate, A.H. Robins; 2%, 0.1–0.2 ml/animal) to reduce congestion of the respiratory tract during anesthesia. Hamsters are mounted in a stereotaxic apparatus and body temperature is maintained at 37°C throughout the experiment. A hole is drilled in the skull overlying the suprachiasmatic nucleus or intergeniculate leaflet region, with the aid of a magnifier. Special care is taken to avoid bleeding caused by damage to the superior sagittal sinus. The eyelids contralateral to the recording site are retracted with sutures and the eye is covered with mineral oil to prevent dehydration after the pupils are dilated with a topical application of 1% atropine sulfate. Electrodes are aimed at the suprachiasmatic nucleus using stereotaxic coordinates (0.2–0.6 mm anterior to the bregma, 0.2–0.35 mm lateral to the midline, and 7.6–7.8 mm ventral to the cortical surface), with the upper incisor bar 2 mm below the interaural line. Electrodes aimed at the hippocampus, dorsal lateral geniculate nucleus and intergeniculate leaflet are inserted 1.4–1.6 mm posterior to the bregma, 3.3–3.8 mm lateral to the midline, and 2.0–4.5 mm ventral to the cortical surface. The animal is maintained in a darkened room except during light pulses or while repositioning the electrodes.

Five-barrel glass micropipettes are prepared (Ying et al. 1993) with the recording barrel filled with fast green (Sigma) at a sub-saturated concentration in 2 M NaCl. One barrel is filled with 2 M NaCl for automatic current balancing. The other barrels are filled with melatonin hydrochloride, or metergoline, or test compound.

For intraperitoneal injections of doses between 0.5 and 10 mg/kg, melatonin and test compounds are dissolved in dimethylsulfoxide (DMSO) and further diluted with saline. For iontophoretic studies, test compounds are used in 5 mM concentrations.

Single-unit extracellular recordings are made from 15:00 to 20:00 hours, overlapping both projected light and dark phases of the daily illumination cycle in the colony room. Contralateral whole-retinal illumination is conveyed to the eye from a tungsten-halogen lamp using fiber optics and a computer-controlled shutter. Photically responsive neurons are identified and recorded during sustained light presentations (typically 1–2 min). Cells are identified as photically responsive or light sensitive if their firing rates are consistently increased or suppressed by >30% by sustained, whole-retinal illumination.

EVALUATION

A computer program controls data acquisition, light exposures and iontophoretic applications of drugs. Agonist effects are defined as repeatable changes relative to predrug firing rates of >20% at some dose of the drug. In order to compare the effects of melatonin and test compounds, agonist potencies are expressed as ED_{50}values, the doses required to produce half-maximal effects. The impact of an agonist is expressed as the proportion of the effect of an agonist that is reversed by the co-application of the antagonist; i. e., the difference between the agonist effects in the absence and the presence of the antagonist, divided by the agonist effect alone, and expressed as a percentage.

REFERENCES AND FURTHER READING

Liu C, Weaver DR, Jin X, Sherman LP, Pieschl RL, Gribkoff VR, Reppert SM (1997) Molecular dissection of two distinct actions of melatonin on the suprachiasmatic circadian clock. Neuron 19:91–102

Meijer JH, Reitveld WJ (1989) Neurophysiology of the suprachiasmatic circadian pacemaker in rodents. Physiol Rev 69:671–707

Moore RY (1983) Organization and function of a central nervous system circadian oscillator: the suprachiasmatic nucleus. Fed Proc 42:2783

Ying SW, Zhang DX, Rusak B (1993) Effect of serotonin agonists and melatonin on photic responses of hamster geniculate leaflet neurons. Brain Res 628:8–16

Ying SW, Rusak B, Delagrange P, Mocaër E, Renard P, Guardiola-Lamaître B (1996) Melatonin analogues as agonists and antagonists in the circadian system and other brain areas. Eur J Pharmacol 296:33–46

Zhang DX, Rusak B (1989) Photic sensitivity of geniculate neurons that project to the suprachiasmatic nuclei of the contralateral geniculate. Brain Res 504:161–164

N.10.1.8 Melatonin's Effect on Circadian Rhythm

PURPOSE AND RATIONALE

Melatonin induces phase shifts of circadian rhythms through an action within the suprachiasmatic nucleus of the hypothalamus (Benloucif and Dubocovich 1996; MacArthur et al. 1997; Dubocovich et al. 1998; Delagrange et al. 1999). Competitive melatonin receptor antagonists block phase shifts of circadian rhythms of electrical activity and neuronal firing within the suprachiasmatic nucleus, suggesting that these phys-

iological responses are mediated through activation of melatonin receptors. Dubocovich et al. (1998) tested phase shifts of running activity in C3H/HeN mice induced by melatonin and antagonists. From these data, the authors concluded that selective MT_2 melatonin receptor antagonism is necessary to block melatonin-mediated phase advances of circadian rhythms.

PROCEDURE

Male C3H/HeN mice (5–6 weeks old) are housed in groups of five and maintained in temperature- and humidity-controlled rooms. Food and water are provided at libitum. Animals are maintained for 2 weeks on a 12-h/12-h light/dark cycle (300 lux at the level of the cage) and are then transferred to constant and complete darkness in individual cages ($18 \times 30 \times 12$ cm) equipped with activity wheels. Mice are kept under constant darkness for 3 weeks to stabilize the free-running activity rhythm (TAU = mean duration of the free running circadian period). The animals are treated on 3 days consecutively at circadian time 10 (CT10). (CT12 = onset of activity). CT10 is estimated from the TAU value for each day. Each mouse is treated with vehicle, or melatonin (0.3, 0.9, 3.0, 9.0, or 30 µg melatonin per animal) or the antagonist to be tested at various dosages. Each mouse receives one treatment every 3 weeks and a total of four treatments. All treatments are performed under a dim red light (15 W, Kodak 1A filter) with illuminance of less than 3 lux.

Rhythms of wheel-running activity are measured with a magnetic microswitch, which detects revolutions of the running wheel and is on line with a computer (Benloucif and Dubocovich 1996). Data are collected using the Dataquest III hardware and software package and analyzed with the assistance of TAU software (Mini-mitter, Sunriver, Ore., USA) The exact circadian time of the pulse is determined after treatment from the onset of steady-state activity on the day of the pulse. Aligning the TAU guide by eye over the steady-state activity onsets of free-running activity for 7–10 days before the pulse and from day 4 to 14 after the pulse assesses phase shifts.

EVALUATION

Phase shifts induced by treatment are measured in hours as the difference between the steady-state pre- and post-pulse activity onsets, using the TAU program ruler. Differences between vehicle/melatonin and antagonist/melatonin-treated groups are assessed for each melatonin dose by analysis of variance, followed by pairwise comparison when indicated.

REFERENCES AND FURTHER READING

Benloucif S, Dubocovich ML (1996) Melatonin and light induce phase shifts of circadian rhythms in the C3H/HeN mouse. J Biol Rhythms 11:113–125

Delagrange P, Ting KN, Kopp C, Lahaye C, Lesieur D, Weibel L, Bennejean C, Renard R, Retton MC (1999) *In vitro* and *in vivo* antagonist properties of S 22153, a new melatonin ligand. Fundament Clin Pharmacol 13:253

Dubocovich ML, Yun K, Al-Ghoul WM, Benloucif S, Masana MI (1998) Selective MT_2 melatonin receptor antagonists block melatonin-mediated phase advances of circadian rhythms. FASEB J 12:1211–1220

MacArthur JJ, Hunt AE, Gilette MU (1997) Melatonin action and signal transduction on the rat suprachiasmatic circadian clock: activation of protein kinase C at dusk and dawn. Endocrinology 138:627–634

N.10.1.9 Melatonin's Effect on Neophobia in Mice

PURPOSE AND RATIONALE

Kopp et al. (1999a) studied the effects of melatonin on neophobic responses in different strains of mice. Melatonin counteracted avoidance responses to an unfamiliar environment in BALB/c and C3H/He mice, but not in C5BL/6 mice. In this experimental situation, animals can move freely in simultaneously presented familiar and unfamiliar places (Hughes 1968).

Delagrange et al. (1999) and Kopp et al. (1999b) tested the effects of a melatonin antagonist on the neophobia-reducing properties of melatonin in BALB/c mice.

PROCEDURE

Male BALB/c mice at an age of 10 weeks are housed in groups of five in standard cages with food and water available ad libitum under controlled conditions at a 12-h light:12-h dark cycle with lights on at 01:00 hours, so that the animals can observed under dim red light in their active period.

The observation apparatus consists of a rectangular polyvinylchloride box ($30 \times 20 \times 20$ cm), covered with Plexiglas and subdivided into six equal square units ($10 \times 10 \times 20$ cm), which are all interconnected by small holes located at the floor level. It can be divided in half lengthwise by closing a temporary partition. The apparatus is kept in the mouse room. The experimenter always stands next to the box at the same place. Approximately 24 h before testing each animal is randomly placed in one-half of the apparatus with the temporary partition in place, to be familiarized with it. The floor of this half only is covered with sawdust, and the animal has unlimited access to food and water during 24 h of the familiarization period. At

the end of this period, the temporary partition between the familiar and unfamiliar compartment is removed and the animal then observed for 10 min. Measures are taken of the number of approach responses followed by avoidance reaction toward the unfamiliar places (attempts), the time spent in the unfamiliar compartment (time), the total number of square units entered (locomotion), and the total number of rears made by the animals (rears).

Mice are treated either with saline (controls) or with 1 mg/kg melatonin, or with various doses of the antagonist, or combinations thereof.

EVALUATION

Data are treated with either an analysis of variance (ANOVA) followed by Newman-Keuls a posteriori *t*-test, if groups come from a population with homogeneous standard deviations, or with a Kruskal-Wallis nonparametric ANOVA test followed by Mann-Whitney tests if groups come from a population with heterogeneous standard deviations.

REFERENCES AND FURTHER READING

Delagrange P, Ting KN, Kopp C, Lahaye C, Lesieur D, Weibel L, Bennejean C, Renard R, Retton MC (1999) *In vitro* and *in vivo* antagonist properties of S 22153, a new melatonin ligand. Fundament Clin Pharmacol 13:253

Hughes RN (1968) Behaviour of male and female rats with a free choice of two environments differing in novelty. Anim Behav 16:92–96

Kopp C, Vogel E, Rettori MC, Delagrange P, Guardiola-Lamaître B, Misslin R (1999a) Effects of melatonin on neophobic responses in different strain of mice. Pharmacol Biochem Behav 63:521–526

Kopp C, Vogel E, Rettori MC, Delagrange P, Renard P, Lesieur D, Misslin R (1999b) Antagonistic effects of S22153, a new mt1 and MT2 receptor ligand, on the neophobia-reducing properties of melatonin in BALB/c mice. Pharmacol Biochem Behav 64:131–136

N.10.2
Melanophore Stimulating Hormone

The early investigations of the pigmentary effects of corticotropin, melanotropin and related peptides derived from the pro-opiomelanocortin family were focused on the control of pigmentary and adrenocortical function (Slominski and Wortsman 2000; Millington 2006). With increasing knowledge and more sophisticated methodology, this role has now been considerably extended (Boehm et al. 2006), including actions on energy balance (Fehm et al. 2004; Butler 2006; Nargund et al. 2006), actions on the cardiovascular system and kidney function (Humphreys 2007), erectile dysfunction (Hadley and Dorr 2006), and even antimicrobial properties (Catania et al. 2006). The pigmentary action of MSH analogs is being commercialized (Hadley and Dorr 2006).

The early studies on synthetic MSH-derived peptide analogs have been considerably extended, with therapeutic applications in view for the control of appetite, and anti-obesic compounds of the future.

REFERENCES AND FURTHER READING

Boehm M, Schiller M, Luger TA (2006) Non-pigmentary actions of alpha-melanocyte-stimulating hormone–lessons from the cutaneous melanocortin system [review]. Cell Mol Biol 52(2):61–68

Butler AA (2006) The melanocortin system and energy balance. Peptides 27(2):281–290

Catania A, Colombo G, Rossi C, Carlin A, Sordi A, Lonati C, Turcatti F, Leonardi P, Grieco P, Gatti S (2006) Antimicrobial properties of alpha-MSH and related synthetic melanocortins. Sci World J 6:1241–1246

Fehm HL, Born J, Peters A (2004) Glucocorticoids and melanocortins in the regulation of body weight in humans. Horm Metab Res 36(6):360–364

Hadley ME, Dorr RT (2006) Melanocortin peptide therapeutics: historical milestones, clinical studies and commercialization. Peptides 27(4):921–230

Humphreys MH (2007) Cardiovascular and renal actions of melanocyte-stimulating hormone peptides. Curr Opin Nephrol Hypertens 16(1):32–38

Millington GW (2006) Proopiomelanocortin (POMC): the cutaneous roles of its melanocortin products and receptors. Clin Exp Dermatol 31(3):407–412

Nargund RP, Strack AM, Fong TM (2006) Melanocortin-4 receptor (MC4R) agonists for the treatment of obesity. J Med Chem 49(14):4035–4043 PMID: 16821763

Slominski A, Wortsman J (2000) Neuroendocrinology of the skin. Endocr Rev 21(5):457–487

N.10.2.1
Skin Darkening in Whole Amphibia

PURPOSE AND RATIONALE

MSH (melanocyte-stimulating hormone or melanotropin) is also called melanophore expanding hormone, based on the microscopical observation of expansion of melanocytes in amphibia (Landgrebe and Waring 1950, 1962; Sandow et al. 1977; Inouye and Ozsuka 1987). Several amphibia species can be used, such as *Xenopus laevis*, *Rana temporaria* or *R. esculenta*, or *Hyla arborea*. Hypophysectomized animals are more sensitive than intact ones. Numerous corticotropin analogs have MSH activity based on a common peptide core shared with MSH. The structure of two melanocyte-stimulating hormones has been elucidated: α-MSH containing 13 amino acids, and β-MSH containing 18 amino acids.

Hunt (1995) reviewed the role of MSH as a regulator of human melanocyte physiology.

PROCEDURE

The pretest conditions require adaptation for blanching of the skin, e. g., by keeping the animals on a white background prior to the assay. *Xenopus laevis* or *Rana temporaria* are kept in single cages at 16°C under humid conditions. Injections of various doses of the test preparation or the standard are given into the dorsal lymph sac. After 1 h, the webs between the digits of the hind limbs are investigated under a stereomicroscope, the eyepiece of which is fitted with a photoelectric cell, the other being available for microscopic examination. The state of melanophore expansion can be assessed by direct visual examination and recorded in terms of an arbitrary melanophore index, or by modern methods of morphometry.

EVALUATION

For test preparation and standard, dose–response curves can be established and potency ratios calculated.

REFERENCES AND FURTHER READING

Hunt G (1995) Melanocyte-stimulating hormone: a regulator of human melanocyte physiology. Pathobiology 63:12–21

Inouye K, Otsuka H (1987) ACTH: Structure-function relationship. In: Li CH (ed) Hormonal proteins and peptides, Vol XIII. Academic Press, New York, pp 1–29

Landgrebe FW, Waring H (1950) Biological assay of the melanophore expanding hormone from the pituitary. In: Emmens CW (ed) Hormone assay. Academic Press, New York, pp 141–171

Landgrebe FW, Waring H (1962) Melanophore-expanding activity. In: Dorfman RI (ed) Methods in hormone research, Vol II. Academic Press, New York, pp 517–558

Sandow J, Geiger R, Vogel HG (1977) Pharmacological effects of a short chain ACTH-analogue. Naunyn Schmiedebergs Arch Pharmacol 297 [Suppl II]:162

N.10.2.2 Assay in Isolated Amphibian Skin

PURPOSE AND RATIONALE

Melanophores in isolated pieces of pale amphibian skin (from background-adapted animals or those maintained in MSH-free medium) expand within a short period of time after immersion in a MSH-containing buffer. Subsequent immersion of the skin in fresh saline results in contraction of the melanophores (Trendelenburg 1926; Jores 1933; Landgrebe and Waring 1950). Several methods using isolated amphibian skin have been described using either light absorption or light reflection (Landgrebe and Waring 1962). These methods are historical and have been replaced by using cell cultures of melanocytes.

PROCEDURE

For studies on light absorption, the skin of *Rana temporaria* or *R. esculenta* is used. Before sacrificing the donor animal and dissecting the isolated skin, it is important to submit the living animal to varying white and black backgrounds under overhead illumination of a light source of 100 W, so that the melanophores can expand and contract before operation. The areas most suitable for use in this technique are from the thighs. Before using the skin for an actual assay, each piece should be immersed in a sufficiently concentrated MSH solution to expand the melanophores almost but not quite fully. The skin is then washed with saline until the melanophores are fully contracted again and in a suitable condition for the test. This usually takes about 45 min. A piece of skin is mounted in a cell which holds the skin stretched and enables it to be immersed in saline or test solution. It is placed in position on the stage of a binocular microscope. An eyepiece is used for visual observation and a photoelectric cell is attached to the other connected directly to a sensitive galvanometer. Various concentrations of the test preparation or the standard are added. At least six skin pieces are used for each concentration of test preparation or standard. Galvanometer readings and readings of the melanophore index are taken simultaneously every 10–15 min until the maximum response is elicited, usually in 30–45 min.

EVALUATION

Assessment of potency is made from the readings of the melanophore index and from the light absorbed, which is recorded as a percentage of the light originally passing through the skin, and is plotted against the log concentration.

CRITICAL ASSESSMENT OF THE METHOD

The methods were originally developed to standardize extracts with (pigmentary) MSH activity by the use of a bioassay. They are still necessary for evaluating compounds for biological MSH activity since not only natural ACTH but also synthetic peptides, such as $\beta^{1\text{-}24}$-corticotropin (Schuler et al. 1963) or $\beta^{1\text{-}23}$-corticotropin-23-amide (Vogel 1965, 1969), possess MSH activity.

MODIFICATIONS OF THE METHOD

Measurement of light reflection by skin pieces, instead of light absorption, was used by Shizume et al. (1954).

In **cell-based assays**, Siegrist and Eberle (1986), Bagutti and Eberle (1993), and Sahm et al. (1993, 1996) used cultured mouse B16 melanoma cells in

a sensitive *in situ* melanoma assay to study the structure–activity relationship of melanocyte-stimulating hormone peptides. B16 cells were seeded at a density of 2500 cells per well in 96-well microtest culture plates. After 24 h the cells were incubated in the presence of serial dilutions of MSH peptides for 3–5 days. The melanin released into the medium of each well was then determined spectrophotometrically at a wavelength of 405 nm using an automatic microplate reader calibrated against synthetic melanin.

Sahm et al. (1994, 1996) measured release of ^3H_2O into the medium from [3′,5′-^{3}H]L-tyrosine by tyrosinase in B16 mouse melanoma cells after incubation with α-MSH analogs.

MSH assays have also been used to study the factors regulating the release of MSH (**MRF**) or inhibiting the release of MSH (**MIF**) (Kastin et al. 1969; Celis et al. 1971).

REFERENCES AND FURTHER READING

Bagutti C, Eberle AN (1993) Synthesis and biological properties of a biotinylated derivative of $ACTH_{1-17}$ for MSH receptor studies. J Receptor Res 13:229–244

Celis ME, Taleisnik S, Walter R (1971) Regulation of formation and proposed structure of the factor inhibiting the release of melanocyte-stimulating hormone. Proc Natl Acad Sci USA 68:1428–1433

Kastin AJ, Viosca A, Schally AV (1969) Assay of mammalian MSH release-regulating factors. Proceedings of the Workshop Conference: Hypophysiotropic Hormones of the Hypothalamus: Assay and Chemistry. Tucson, Arizona

Landgrebe FW, Waring H (1950) Biological assay of the melanophore expanding hormone from the pituitary. In: Emmens CW (ed) Hormone assay. Academic Press, New York, pp 141–171

Landgrebe FW, Waring H (1962) Melanophore-expanding activity. In: Dorfman RI (ed) Methods in hormone research, Vol II. Academic Press, New York, pp 517–558

Sahm UG, Olivier GWJ, Branch SK, Moss SH, Pouton CW (1993) Influence of α-MSH terminal amino acids on binding affinity and biological activity in melanoma cells. Peptides 15:441–446

Sahm UG, Olivier GWJ, Branch SK, Moss SH, Pouton CW (1994) Synthesis and biological evaluation of α-MSH analogues substituted with alanine. Peptides 15:1297–1302

Sahm UG, Olivier GWJ, Branch SK, Moss SH, Pouton CW (1996) Receptor binding affinities and biological activities of linear and cyclic melanocortins in B16 murine melanoma cells expressing the native MC_1 receptor. J Pharm Pharmacol 48:197–200

Schuler W, Schär B, Desaulles P (1963) Zur Pharmakologie eines ACTH-wirksamen, vollsynthetischen Polypeptids, des b1-24-Corticotropins, Ciba 30920-Ba, Synacthen. Schweiz Med Wschr 93:1027–1030

Shizume K, Lerner AB, Fitzpatrick TB (1954) *In vitro* bioassay for the melanocyte stimulating hormone. Endocrinology 54:553–560

Siegrist W, Eberle AN (1986) *In situ* melanin assay for MSH using mouse B16 melanoma cells in culture. Anal Biochem 159:191–197

Trendelenburg P (1926) Weitere Versuche über den Gehalt des Liquor cerebrospinalis an wirksamen Substanzen des Hypophysenhinterlappens. Naunyn Schmiedebergs Arch Exp Pathol Pharmakol 114:255–261

Vogel HG (1965) Evaluation of synthetic peptides with ACTH-Activity. Acta Endocrinol Suppl 100:34

Vogel HG (1969) Tierexperimentelle Untersuchungen über synthetische Peptide mit Corticotropinaktivität. A: Vergleich mit dem III. Int. Standard für Corticotropin. Arzneimittelforschung 19:20–24

N.10.2.3 Binding to the Melanocortin Receptor

PURPOSE AND RATIONALE

Much of the initial work on the biological effects of hormones has been expanded by using cloned subclasses of receptors for identification of more specific ligand compounds. A family of five MSH receptor subclasses for the melanocortic peptides has been identified (Chhajlani and Wikberg 1992; Chhajlani et al. 1993; Gantz et al. 1993b; Schiöth et al. 1997a, 1988a; Strand 1999). The melanocortin MC_1 receptor is expressed in melanocytes and melanoma cells and binds α-MSH with high affinity. The MC_1 receptor plays an important role in skin and fur pigmentation in a variety of vertebrates (Cone et al. 1996). The melanocortin MC_2 receptor (i. e., the ACTH receptor) has a well-defined function in steroid production in the adrenal gland (Schiöth et al. 1996a). The melanocortin MC_3 receptor is found in the hypothalamus, the brain, and in the placenta, gut tissues and the heart (Gantz et al. 1993a; Desarnaud et al. 1994; Sahm et al. 1994). The melanocortin MC_4receptor (Schiöth et al. 1996b, 1998b) has been found to affect feeding in rodents and may be important for weight homeostasis (Fan et al. 1997; Huszar et al. 1997). The melanocortin MC_5 receptor is primarily located in various peripheral tissues but has also been found in the brain (Labbé et al. 1994; Fathi et al. 1995).

Schiöth et al. (1997b, 1998a) described binding of synthetic MSH analogs to the human melanocortin receptor subtypes.

Melanocortin-4 receptor antagonists increase food uptake in rats (Kask et al. 1998a, 1998b; Skuladottir et al. 1999).

PROCEDURE

Expression of Receptor Clones

The human melanocortin MC_1 and human melanocortin MC_5 receptors are cloned into the expression vector pRc/CMV (Invitrogen). The human melanocortin MC_3 and human melanocortin MC_4 receptors were cloned into the expression vector

pCMV/neo. For receptor expression COS-1 cells are grown in Dulbecco's modified Eagle's medium with 10% fetal calf serum. Eighty percent confluent cultures are transfected with the DNA mixed with liposomes in serum-free medium. After transfection, the serum-free medium is replaced by serum-containing medium and the cells are cultivated for 48 h. Cells are then scraped off, centrifuged and used for radioligand binding.

Binding Studies

The transfected cells are washed with binding buffer (Schiöth et al. 1995) and distributed into 96-well non-culture-coated plates, which are centrifuged and the binding buffer is removed. The cells are then immediately incubated in the well plates for 2 h at 37°C with 0.05 ml binding buffer in each well containing a constant concentration of [125I]NDP (= [Nle^4-D-Phe^7]α-MSH) and appropriate concentrations of the competing unlabeled ligand. After incubation the cells are washed with 0.2 ml of ice-cold binding buffer and detached from the plates with 0.2 ml of 0.1 M NaOH. Radioactivity is counted by a gamma-counter.

EVALUATION

Data are analyzed by fitting to formulas derived from the law of mass action. The method is generally referred to as computer modeling. K_d values for [125I]NDP are calculated (Schiöth et al. 1995, 1996a). The binding assays are performed in duplicate and repeated three times.

MODIFICATIONS OF THE METHOD

Adan et al. (1994) compared the behavioral effects of melanocortins with binding data on MC_3 and MC_4 receptors.

Sahm et al. (1996) studied receptor binding affinities and biological activities of linear and cyclic melanocortins in B16 murine melanoma cells expressing the native MC_1 receptor.

Quillan and Sadée (1996) searched for peptide ligands that cross-react with melanocortin receptors and found several peptides with previously unrecognized agonistic or antagonistic activity on amphibian and human melanocortin receptors.

Peng et al. (1997) compared the actions of C-terminally modified melanocortin peptides at rodent MC_1 and MC_3 receptors.

Bagutti et al. (1993) recommended [^{111}In]DTPA-labeled (where DTPA is diethylenetriaminopentaacetic acid) analogs of α-MSH as ligands for the detection of MSH receptors *in vitro* and *in vivo*.

Erskine-Grout et al. (1996) described functional photoaffinity-labeled, biotinylated and fluorescent probes for the melanoma MC_1 receptor.

REFERENCES AND FURTHER READING

Adan RAH, Cone RD, Burbach JPH, Gispen WH (1994) Differential effects of melanocortin peptides on neural melanocortin receptors. Mol Pharmacol 46:1182–1190

Bagutti C, Stolz B, Albert R, Bruns C, Pless J, Eberle AN (1993) [^{111}In]DTPA-labeled analogues of α-MSH for the detection of MSH receptors *in vitro* and *in vivo*. Ann NY Aced Sci 680:445–447

Chhajlani V, Wikberg JES (1992) Molecular cloning of a novel human melanocyte stimulating hormone receptor cDNA. FEBS Lett 309:417–420

Chhajlani V, Muceniece R, Wikberg JES (1993) Molecular cloning of a novel human melanocortin receptor. Biochem Biophys Res Commun 195:866–873

Cone RD, Lu D, Koppula S, Vage DI, Klungland H, Boston B, Chen W, Orth DN, Pouton C, Kesterson RA (1996) The melanocortin receptors: agonists, antagonists, and the hormonal control of pigmentation. Recent Prog Horm Res 51:287–317

Desarnaud F, Labbe O, Eggerickx D, Vassart G, Parmentier M (1994) Molecular cloning, functional expression and pharmacological characterization of a mouse melanocortin receptor gene. Biochem J 299:367–373

Erskine-Grout ME, Olivier GWJ, Lucas P, Sahm UG, Branch SK, Moss SH, Notarianni LJ, Pouton CW (1996) Melanocortin probes for the melanoma MC_1 receptor: synthesis, receptor binding and biological activity. Melanoma Res 6:89–94

Fan W, Boston BA, Kesterson RA, Hruby VJ, Cone RD (1997) Role of melanocortin neurons in feeding and agouti obesity syndrome. Nature 386:165–168

Fathi Z, Iben LG, Parker RM (1995) Cloning, expression, and tissue distribution of a fifth melanocortin receptor subtype. Neurochem Res 20:107–113

Gantz I, Konda Y, Tashiro T, Shimoto Y, Miwa H, Munzert G, Watson SJ, Del Valle J, Yamada T (1993a) Molecular cloning of a novel melanocortin receptor. J Biol Chem 268:8246–8250

Gantz I, Miwa H, Konda Y, Shimoto Y, Tashiro T, Watson SJ, Del Valle J, Yamada T (1993b) Molecular cloning, expression, and gene location of a fourth melanocortin receptor. J Biol Chem 268:15174–15179

Huszar D, Lynch CA, Fairchild-Huntress V, Dunmore JH, Fang Q, Berkemeier RL, Gu W, Hesterson RA, Boston BA, Cone RD, Smith FJ, Campfield LA, Burn P, Lee F (1997) Targeted disruption of the melanocortin-4 receptor results in obesity in mice. Cell 88:131–141

Kask A, Rago L, Mutulis F, Pahkla R, Wikberg JES, Schioth HB (1998a) Selective antagonist for the melanocortin-4 receptor (HS014) increases food uptake in free-feeding rats. Biochem Biophys Res Commun 245:90–93

Kask A, Mutulis F, Muceniece R, Pahkla R, Mutule I, Wikberg JS, Rago L, Schioth HB (1998b) Discovery of a novel superpotent and selective melanocortin-4 receptor antagonist (HS024): evaluation *in vitro* and *in vivo*. Endocrinology 139:5006–5014

Labbé O, Desarnaud F, Eggerickx D, Vassart G, Parmentier M (1994) Molecular cloning of a mouse melanocortin 5 receptor gene widely expressed in peripheral tissues. Biochemistry 93:4543–4549

Peng PJ, Sahm UG, Doherty RVM, Kinsman RG, Moss SH, Pouton CW (1997) Binding and biological activity of C-terminally modified melanocortin peptides: a comparison of their actions at rodent MC_1 and MC_3 receptors. Peptides 18:1001–1008

Quillan JM, Sadée W (1996) Structure-based search for peptide ligands that cross-react with melanocortin receptors. Pharm Res 13:1624–1630

Sahm UG, Qarawi MA, Olivier GWJ, Ahmed AHR, Branch SK, Moss SH, Pouton CW (1994) The melanocortin (MC3) receptor from rat hypothalamus: photoaffinity labelling and binding of alanine-substituted analogues. FEBS Lett 350:29–32

Sahm UG, Olivier GWJ, Branch SK, Moss SH, Pouton CW (1996) Receptor binding affinities and biological activities of linear and cyclic melanocortins in B16 murine melanoma cells expressing the native MC_1 receptor. J Pharm Pharmacol 48:197–200

Schiöth HB, Muceniece R, Wikberg JES, Chhajlani V (1995) Characterization of melanocortin receptor subtypes by radioligand binding analysis. Eur J Pharmacol 288:311–317

Schiöth HB, Chhajlani V, Muceniece R, Klusa V, Wikberg JES (1996a) Major pharmacological distinction of the ACTH receptor from other melanocortin receptors. Life Sci 59:797–801

Schiöth HB, Muceniece R, Wikberg JES (1996b) Characterization of the melanocortin 4 receptor by radioligand binding. Pharmacol Toxicol 79:161–165

Schiöth HB, Muceniece R, Larsson M, Mutulis F, Szardenings M, Prusis P, Lindeberg G, Wikberg JES (1997a) Binding of cyclic and linear MSH core peptides to the melanocortin receptor subtypes. Eur J Pharmacol 319:369–373

Schiöth HB, Müceniece R, Mutulis F, Prusis P, Lindeberg G, Sharma SD, Hruby VJ, Wikberg JE (1997b) Selectivity of cyclic [D-Nal^7] and D-Phe^7] substituted MSH analogues for the melanocortin receptor subtypes. Peptides 18:1009–1013

Schiöth HB, Mutulis F, Muceniece R, Prusis P, Wikberg JES (1998a) Selective properties of C- and N-terminals and core residues of the melanocyte-stimulating hormone on the binding to the human melanocortin receptor subtypes. Eur J Pharmacol 349:359–366

Schiöth HB, Mutulis F, Muceniece R, Prusis P, Wikberg JES (1998b) Discovery of novel $melanocortin_4$ receptor selective MSH analogues. Br J Pharmacol 124:75–82

Skuladottir GV, Jonsson L, Skarphedinsson JO, Mutulis F, Muceniece R, Raine A, Mutule I, Helgason J, Prusis J, Wikberg JES, Schioth HB (1999) Long term orexigenic effect of a novel melanocortin-4 receptor selective antagonist. Br J Pharmacol 126:27–34

Strand FL (1999) New vistas for melanocortins. finally an explanation for their pleiotropic function. In: Sandman CA, Chronwall BM, Strand FL, Flynn FW, Beckwith B, Nachman RJ (eds) Neuropeptides. Structure and function in biology and behavior. Ann N Y Acad Sci 897:1–16

N.10.3 Melanocortin Peptides

The melanocortin system refers to a set of hormonal, neuropeptidergic, and paracrine signaling pathways that are defined by components that include the five G-protein-coupled melanocortin receptors; peptide agonists derived from the pro-opiomelanocortin preprohormone precursor; and the endogenous antagonists, agouti and agouti-related protein (Gantz and Fong 2003; Cone 2006). This group of regulatory peptides was explored in the context of understanding regulation of body weight development, and finding specific anti-obesic compounds (Bjorbaek and Hollenberg 2002; Della-Fera and Baile 2005; Padwal and Majumdar 2007). As with the leptin research, there are also indications for the central regulation of thermogenesis by melanotropin peptides (Myers 2004; Fan et al. 2005). The subclasses of melanocortin receptors involved in these several functions have been characterized, and the MC4 receptor is of particular interest (Garcia-Borron et al. 2005; Adan and van Dijk 2006; Adan et al. 2006; Getting 2006). Structure–activity studies on the melanocortin agonists and antagonists have provided further tools for detailed investigation (Cai et al. 2005) by modification of the natural ligands, and by the search for small molecule ligands (Todorovic and Haskell-Luevano 2005). Not surprisingly, the research on body weight regulation has also provided indications for the pathophysiology of cachexia (DeBoer and Marks 2006a, 2006b).

Interactions of the hypothalamic–pituitary–thyroid axis with the central melanocortin system have been investigated and reviewed (Martin et al. 2006).

There has also been considerable interest in the regulation of immune responses and inflammation by melanocortin peptides (Maaser et al. 2006), based on the established relationship of α-MSH and inflammation (Eves et al. 2006; Lin and Fisher 2007).

REFERENCES AND FURTHER READING

Adan RA, van Dijk G (2006) Melanocortin receptors as drug targets for disorders of energy balance. CNS Neurol Disord Drug Targets 5(3):251–261

Adan RA, Tiesjema B, Hillebrand JJ, la Fleur SE, Kas MJ, de Krom M (2006) The MC4 receptor and control of appetite. Br J Pharmacol 149(7):815–827

Bjorbaek C, Hollenberg AN (2002) Leptin and melanocortin signaling in the hypothalamus. Vitam Horm 65:281–311

Cai M, Mayorov AV, Ying J, Stankova M, Trivedi D, Cabello C, Hruby VJ (2005) Design of novel melanotropin agonists and antagonists with high potency and selectivity for human melanocortin receptors. Peptides 26(8):1481–1485

Cone RD (2006) Studies on the physiological functions of the melanocortin system. Endocr Rev 27(7):736–749

Deboer MD, Marks DL (2006a) Cachexia: lessons from melanocortin antagonism. Trends Endocrinol Metab 17(5):199–204

DeBoer MD, Marks DL (2006b) Therapy insight: use of melanocortin antagonists in the treatment of cachexia in chronic disease. Natl Clin Pract Endocrinol Metab 2(8):459–466

Della-Fera MA, Baile CA (2005) Roles for melanocortins and leptin in adipose tissue apoptosis and fat deposition. Peptides 26(10):1782–1787
Eves PC, MacNeil S, Haycock JW (2006) alpha-Melanocyte stimulating hormone, inflammation and human melanoma. Peptides 27(2):444–452
Fan W, Voss-Andreae A, Cao WH, Morrison SF (2005) Regulation of thermogenesis by the central melanocortin system. Peptides 26 (10):1800–1813
Gantz I, Fong TM (2003) The melanocortin system. Am J Physiol 284(3):E468–E474
Garcia-Borron JC, Sanchez-Laorden BL, Jimenez-Cervantes C (2005) Melanocortin-1 receptor structure and functional regulation. Pigment Cell Res 18(6):393–410
Getting SJ (2006) Targeting melanocortin receptors as potential novel therapeutics. Pharmacol Ther 111(1):1–15
Lin JY, Fisher DE (2007) Melanocyte biology and skin pigmentation. Nature 445(7130):843–850
Maaser C, Kannengiesser K, Kucharzik T (2006) Role of the melanocortin system in inflammation. Ann N Y Acad Sci 1072:123–134
Martin NM, Smith KL, Bloom SR, Small CJ (2006) Interactions between the melanocortin system and the hypothalamo-pituitary-thyroid axis. Peptides 27(2):333–339
Myers MG Jr (2004) Leptin receptor signaling and the regulation of mammalian physiology. Recent Prog Horm Res 59:287–304
Padwal RS, Majumdar SR (2007) Drug treatments for obesity: orlistat, sibutramine, and rimonabant. Lancet 369(9555): 71–77
Todorovic A, Haskell-Luevano C (2005) A review of melanocortin receptor small molecule ligands. Peptides 26(10):2026–2036

N.10.4 Relaxin

N.10.4.1 General Considerations

Relaxin is a peptide hormone originally prepared from sow ovaries. The hormone acts on collagen and induces increased flexibility of the pelvic girdle of guinea pigs. In mice, the length of the interpubic ligament is increased. Moreover, relaxin inhibits spontaneous uterine motility. In addition to its effects on the reproductive tract, relaxin exerts hemodynamic effects (Coulson et al. 1996). The actions of relaxin as a pleiotropic hormone were reviewed by Bani (1997).

The therapeutic relevance of relaxin in humans is still open to debate (Schwabe and Büllesbach 1994; Goldsmith et al. 1995).

The primary structure of relaxin is highly homologous to insulin. Unlike insulin, the structure of which is remarkably well conserved among the vertebrates, relaxin sequences can vary by more than 50% between different species (Evans et al. 1993; Layden and Tregear 1996). Despite these large variations, most relaxins have very similar biological activities in animal test systems, probably because the receptor binding region of the B chain, in contrast to the rest of the molecule, is highly conserved between species.

Relaxin of various species has been synthesized (Büllesbach and Schwabe 1993; Wade et al. 1994).

Synthetic human relaxin has been characterized by high-performance liquid chromatography (Canova-Davis et al. 1990).

Klonisch et al. (1999) determined the nucleic acid sequence of canine **preprorelaxin** using reverse transcription polymerase chain reaction (PCR) and rapid amplification of cDNA ends-PCR. Canine preprorelaxin consists of 534 base pairs encoding a protein of 177 amino acids with a signal peptide of 25 amino acids, a B domain of 35 amino acids, a C domain of 93 amino acids, and an A domain of 24 amino acids.

The **relaxin-like factor (RLF)** is described as a member of the insulin/relaxin/insulin-like growth factor family that is expressed predominantly in the reproductive system, with greatest expression in the Leydig cells of the testis (Pusch et al. 1996; Zarreh-Hoshyari-Khah et al. 1999).

Several **bioassays** have been used for relaxin, such as the pubic symphysis method in guinea pigs and mice, inhibition of uterine motility in rats, and stimulation of interstitial collagenase activity in cultured uterine cervical cells from guinea pigs (see below).

Taylor and Clark (1989, 1992a, 1992b) developed a **reverse hemolytic plaque assay** which allows the quantitative analysis of relaxin secreted by single porcine luteal cells.

Radioimmunoassays for relaxin were described by Sherwood (1979), Jockenhövel et al. (1991), and Steinetz et al. (1996). Lucas et al. (1989) developed an enzyme-linked immunoassay to study human relaxin in human pregnancy and in pregnant rhesus monkeys.

REFERENCES AND FURTHER READING

Bani D (1997) Relaxin: a pleiotropic hormone. Gen Pharmacol 28:13–22
Büllesbach EE, Schwabe C (1993) Mouse relaxin: synthesis and biological activity of the first relaxin with an unusual cross-linking pattern. Biochem Biophys Res Commun 196:311–319
Canova-Davis E, Baldonado IP, Teshima GM (1990) Characterization of chemically synthesized human relaxin by high-performance liquid chromatography. J Chromatogr 508:81–96
Coulson CC, Thorp Jr JM, Mayer DC, Cefalo RC (1996) Central hemodynamic effects of recombinant human relaxin in the isolated, perfused rat heart model. Obstet Gynecol 87:610–612
Evans BA, John M, Fowler KJ, Summers RJ, Crink M, Shine J, Tregear GW (1993) The mouse relaxin gene: nucleotide sequence and expression. J Mol Endocrinol 10:15–23

Goldsmith LT, Weiss G, Steinetz BG (1995) Relaxin and its role in pregnancy. Endocrinol Metab Clin North Am 24:171–186
Jockenhövel F, Peterson MA, Johnston PD, Swerdloff RS (1991) Directly iodinated rat relaxin as a tracer for use in radioimmunoassays. Eur J Clin Chem Clin Biochem 29:71–75
Klonisch T, Hombach-Klonisch S, Froehlich C, Kauffold J, Steger K, Steinetz BG, Fischer B (1999) Canine preprorelaxin: nucleic acid sequence and localization within the canine placenta. Biol Reprod 60:551–557
Layden SS, Tregear GW (1996) Purification and characterization of porcine prorelaxin. J Biochem Biophys Methods 31:69–80
Lucas C, Bald LN, Martin MC, Jaffe RB, Drolet DW, Mora-Worms M, Bennett G, Chen AB, Johnston PD (1989) An enzyme-linked immunoassay to study human relaxin in human pregnancy and in pregnant rhesus monkeys. J Endocrinol 120:449–457
Pusch W, Balvers M, Ivell R (1996) Molecular cloning and expression of the relaxin-like factor from the mouse testis. Endocrinology 137:3009–3013
Schwabe C, Büllesbach EE (1994) Relaxin: structures, functions, and nonevolution. FASEB J 8:1152–1160
Sherwood OD (1979) Relaxin. In: Jaffe BM, Behrman HR (eds) Methods of hormone radioimmunoassay. Academic Press, New York, pp 785–886
Steinetz BG, Büllesbach EE, Godsmith LT, Schwabe C, Lust G (1996) Use of synthetic canine relaxin to develop a rapid homologous radioimmunoassay. Biol Reprod 54:1252–1260
Taylor MJ, Clark CL (1989) Analysis of relaxin release by cultured porcine luteal cells using a reverse hemolytic plaque assay: effects of arachidonic acid, cyclo- and lipoxygenase blockers, phospholipase A_2, and melittin. Endocrinology 125:1389–1397
Taylor MJ, Clark CL (1992a) Basic fibroblast growth factor inhibits basal and stimulated relaxin secretion by cultured luteal cells: analysis by reverse hemolytic plaque assay. Endocrinology 130:1951–1956
Taylor MJ, Clark CL (1992b) Discordant secretion of relaxin by individual porcine large luteal cells: quantitative analysis by a reverse hemolytic plaque assay. J Endocrinol 134:77–83
Wade JD, Layden SS, Lambert PF, Kakouris H, Tregear GW (1994) Primate relaxin: synthesis of gorilla and rhesus monkey relaxins. J Protein Chem 13:315–321
Zarreh-Hoshyari-Khah MR, Einspanier A, Ivell R (1999) Differential splicing and expression of the relaxin-like factor gene in reproductive tissues of the marmoset monkey (*Callithrix jacchus*). Biol Reprod 60:445–453

N.10.4.2 Relaxin Bioassay by Pubic Symphysis Method in Guinea Pigs

PURPOSE AND RATIONALE

Experimental relaxation of the pubic symphysis of the spayed guinea pig was described as early as 1929 by Hisaw. The relaxation of the symphysis after relaxin administration is determined by manual palpation.

PROCEDURE

Virgin female guinea pigs of mixed strains weighing 300–400 g are used. Prior to the assay, the animals have to be primed with estrogen and relaxin. Estrogen priming consists of one subcutaneous injection per week of 5 µg of estradiol cyclopentylpropionate in 0.1 ml of sesame oil. Relaxin priming is accomplished by administering 20 µg of relaxin standard in 1 ml saline subcutaneously once a week on day 5 after the estrogen injection.

Six hours after relaxin administration the symphysis of the animal is palpated. The animal is held head down, ventral side away, between the thighs of the seated observer. The sciatic crests and symphysis pubis are firmly grasped between the thumbs and forefingers so that the two halves of the pelvis may be moved back and forth alternately. If the pubic symphysis is rigid at this time, the estrogen and relaxin priming are continued weekly until marked mobility of the symphysis is observed. The increased flexibility is transient: the peak response occurs at 6 h and subsides 12–24 h after injection. Mobility responses are estimated subjectively and scored on an arbitrary scale of 0–6. "Zero" indicates no detectable flexibility of the pubic symphysis, whereas "6" represents extreme softening. Scoring should be performed by the same investigator throughout a study.

One week after an animal has responded positively to 20 µg of relaxin standard, it is added to the assay colony. Before assay time, all eligible animals are mixed and divided into groups of 10–20 each. On the day of the experiment, all animals are palpated before injection. Only those with no symphyseal movement are used. Two doses of test preparation and two doses of standard are injected subcutaneously to different groups. Six hours later, two operators palpate and score each animal.

EVALUATION

The scores are averaged and a median score calculated. The activity of an unknown preparation is determined by comparison with the dose–response curve of concomitantly administered relaxin standard.

MODIFICATIONS OF THE METHOD

Steinetz and Lust (1994) reported that the relaxin-induced pubic symphyseal relaxation in guinea pigs is inhibited by treatment with glycosaminoglycan polysulfates or pentosan polysulfate. The authors recommended the guinea pig symphysis assay for relaxin as a novel rapid screening test for compounds with potential chrondroprotective activity.

REFERENCES AND FURTHER READING

Hisaw FL (1929) The corpus luteum hormone. I. Experimental relaxation of the pelvic ligaments of the guinea pig. Physiol Zool 2:59–79

Kroc RL, Steinetz BG, Beach VL, Stasilli NR (1956) Bioassay of relaxin extracts in guinea pigs and mice, using a reference standard. J Clin Endocrinol Metab 16:966

Kroc RL, Steinetz BG, Beach VL (1959) The effects of estrogens, progestagens, and relaxin in pregnant and nonpregnant laboratory rodents. Ann NY Acad Sci 75:942–980

Steinetz BG, Lust G (1994) Inhibition of relaxin-induced pubic symphyseal 'relaxation' in guinea pigs by glycosaminoglycan polysulfates and pentosan polysulfate. Agents Actions 42:74–80

Steinetz BG, Beach VL, Kroc RL (1969a) Relaxin. In: Dorfman RI (ed) Methods in hormone research, Vol II. Academic Press, New York, pp 559–589

Steinetz BG, Beach VL, Kroc RL (1969b) Bioassay of relaxin. In: Dorfman RI (ed) Methods in hormone research, Vol IIA. Academic Press, New York, pp 481–513

N.10.4.3 Relaxin Bioassay in Mice

PURPOSE AND RATIONALE

An increase in length of the interpubic ligament in mice can be used as a bioassay for relaxin. Other methods used include X-ray measurement of pubic separation (Hall 1948; Dorfman et al. 1953) and direct measurement of interpubic ligament (Kroc et al. 1959; Steinetz et al. 1960, 1969a, 1969b).

PROCEDURE

Virgin female mice (e. g., NMRI strain) weighing 18–20 g are used for the assay. Twenty mice are employed for each of three dose levels of standard and test preparation. On day zero each mouse is primed with a single subcutaneous injection of 5 µg estradiol cyclopentylpropionate in 0.1 ml sesame oil. On day 7, the test preparation and the standard are injected subcutaneously. At 18–24 h later, the mice are sacrificed, the abdominal cavities are opened, and uteri are examined for evidence of estrogen priming. Mice exhibiting threadlike uteri are discarded. The anal and vulval areas are then cut away with scissors, and the upper half of the body is cut off to prevent subsequent bleeding at the pubic symphysis. The bony birth canal is freed of skin, vagina, and rectum, and fascia are cleaned off the symphysis pubis. The pelvis is placed on a binocular microscope fitted with a calibrated ocular micrometer. A transilluminating device consisting of a U-shaped lucite rod is affixed to the microscope. The tip of the rod is beveled to direct light vertically through the exposed pubic ligament. The feet of the carcass are grasped between the thumb and index finger, applying a slight lateral traction.

The shortest distance between the edges of the pubes is measured, using the ocular micrometer. Micrometer readings are then converted to millimeters.

EVALUATION

Mean values of length of interpubic ligament, expressed in millimeters, are plotted versus logarithm of dose. From dose–response curves activity ratios with confidence limits versus the standard are calculated.

MODIFICATIONS OF THE METHOD

Bullesbach and Schwabe (1996) tested rat relaxin and synthetic analogs in the mouse symphysis pubis assay for structure–activity relationships.

Samuel et al. (1998) studied the effects of relaxin, pregnancy and parturition on collagen metabolism in the **rat** pubic symphysis. During pregnancy and particularly during birth, there was a significant reduction of tissue wet and dry weight, which coincided with an increase in water content and a significant reduction of overall collagen content.

REFERENCES AND FURTHER READING

Bullesbach EE, Schwabe C (1996) The chemical synthesis of rat relaxin and the unexpectedly high potency of the synthetic hormone in the mouse. Eur J Biochem 241:533–537

Dorfman RI, Marsters RW, Dinerstein J (1953) Bioassay of relaxin. Endocrinology 52:204–214

Hall K (1948) Further notes on the action of oestrone and relaxin on the pelvis of the spayed mouse, including a single-dose test of potency of relaxin. J Endocrinol 5:314–321

Kroc RL, Steinetz BG, Beach VL (1959) The effects of estrogens, progestagens, and relaxin in pregnant and nonpregnant laboratory rodents. Ann NY Acad Sci 75:942–980

Samuel CS, Coghlan JP, Bateman JF (1998) Effects of relaxin, pregnancy and parturition on collagen metabolism in the rat pubic symphysis. J Endocrinol 159:1178–125

Steinetz BG, Beach VL, Kroc RL, Stasilli NR, Nussbaum RE, Nemith PJ, Dunn RK (1960) Bioassay of relaxin using a reference standard: a simple and reliable method utilizing direct measurement of interpubic ligament formation in mice. Endocrinology 67:102–115

Steinetz BG, Beach VL, Kroc RL (1969a) Bioassay of relaxin. In: Dorfman RI (ed) Methods in hormone research, Vol IIA. Academic Press, New York, pp 481–513

Steinetz BG, Beach VL, Kroc RL (1969b) Relaxin. In: Dorfman RI (ed) Methods in hormone research, Vol II. Academic Press, New York, pp 559–589

N.10.4.4 Inhibition of Uterine Motility

PURPOSE AND RATIONALE

This is one of the historical assays based on a nonspecific biological response. Its application and reliability depend on the state of purification of relaxin preparations. Relaxin specifically inhibits the spontaneous motility of estrogen-dominated uterus *in vivo* and *in*

vitro (Downing and Hollingsworth 1993). Wiqvist and Paul (1958) proposed a relaxin assay based on inhibition of motility of the rat uterus *in vitro* (Steinetz et al. 1969).

PROCEDURE

The donors (female Sprague-Dawley or Wistar rats weighing 150–180 g) are ovariectomized and primed with 2 µg estradiol daily for 3 days. On day 4, uterine horns are removed, bisected, and suspended in Locke's solution gassed with 1% CO_2 in O_2 at a temperature of 37.5 ± 0.5°C. The contractions are recorded using a Statham transducer and a polygraph. A symmetrical 4-point assay is adopted with twofold dose increments of standard and test preparation. Responses consisting of slowing down the contraction frequency up to total suppression of the contractions are classified visually and assigned score values of 1–3. All four test doses (two doses each of standard and test preparation) are run simultaneously on the four uterine segments obtained from each rat.

EVALUATION

Mean values of scores are calculated for each dose. Potency ratios with confidence limits are calculated from the 2+2-point assay.

MODIFICATIONS OF THE METHOD

Felton et al. (1953) described a test for relaxin activity using the inhibition of uterine contraction in anesthetized guinea pigs *in vivo*.

Inhibition of spontaneous and prostaglandin-driven myometrial activity by relaxin in anesthetized rats was reported by Porter et al. (1979).

Downing and Sherwood (1985) studied the influence of relaxin on uterus contractility and on cervical distensibility in different stages of pregnancy in the rat.

Del Angel Meza et al. (1991) measured the effect of relaxin on uterine and ileum tissue of rats *in vivo* and *in vitro*.

Vu et al. (1993) tested the activity of a recombinant prorelaxin in an *in vitro* bioassay in CHO cells. Human uterine endometrial cells were treated with various dilutions of conditioned medium and the amounts of intracellular cAMP produced were determined by radioimmunoassay.

REFERENCES AND FURTHER READING

Del Angel Meza AR, Beas-Zárate C, Alfaro FL, Morales-Villagran A (1991) A simple biological assay for relaxin measurement. Comp Biochem Physiol 99 C:35–39

Downing SJ, Hollingsworth M (1993) Action of relaxin on uterine contractions. A review. J Reprod Fertil 99:275–282

Downing SJ, Sherwood OD (1985) The physiological role of relaxin in the pregnant rat. III. The influence of relaxin on cervical distensibility. Endocrinology 116:1215–1220

Felton LC, Frieden EH, Bryant HH (1953) The effects of ovarian extracts upon activity of the guinea pig uterus *in situ*. J Pharmacol Exp Ther 107:160–164

Porter DG, Downing SJ, Bradshaw JMC (1979) Relaxin inhibits spontaneous and prostaglandin-driven myometrial activity in anaesthetized rats. J Endocrinol 83:183–192

Steinetz BG, Beach VL, Kroc RL (1969) Bioassay of relaxin. In: Dorfman RI (ed) Methods in hormone research, Vol IIA. Academic Press, New York, pp 481–513

Vu AL, Green CB, Roby KF, Soares MJ, Fei DTW, Chen AB, Kwok SCM (1993) Recombinant porcine prorelaxin produced in Chinese hamster ovary cells is biologically active. Life Sci 52:1055–1061

Wiqvist N, Paul KG (1958) Inhibition of the spontaneous uterine motility *in vitro* as a bioassay of relaxin. Acta Endocrinol 31:135–146

N.10.4.5 Relaxin Assay by Interstitial Collagenase Activity in Cultured Uterine Cervical Cells

PURPOSE AND RATIONALE

As an example of the changing approach in assay methods, Mushayandebvu and Rajabi (1995) provided evidence for a biological response suitable for *in vitro* assay. Relaxin is involved in cervical dilatation by stimulating interstitial collagenase, a key enzyme involved in this process. Human recombinant relaxin induces a dose-dependent increase of collagenase activity in cultured guinea pig cervical cells.

PROCEDURE

Abdominal hysterectomy is performed in anesthetized female Hartley guinea pigs under aseptic conditions. The cervix is excised and washed three times in Hank's balanced salt solution (HBSS) containing penicillin G sodium (100 U/ml), streptomycin sulfate 100 µg/ml), and amphotericin B (1.25 µg/ml). The cervix is cut into 2- to 4-mm pieces and digested in Dulbecco's modified Eagle's medium (DMEM) containing bacterial collagenase type A1 (0.5 mg/ml) and DNase type 1 (0.05 mg/ml) at 37°C. The digested mixture is filtered once every 15–30 min through a nylon monofilament with a pore size of 400 µm. Following each filtration, separated cells are collected by centrifugation at 365 *g* for 10 min at room temperature followed by a resuspension in DMEM containing 10% heat-inactivated fetal calf serum (FCS). Cells are washed twice with HBSS; this is followed by resuspension in DMEM containing 10%

penicillin G sodium (100 U/ml), streptomycin sulfate 100 µg/ml), and amphotericin B (1.25 µg/ml). The unfiltered material is redigested and the process is repeated until the cervical tissue is completely digested.

Cells are plated in 24-well plates at 1×10^5 cells per well in 500 µl of medium containing 10% FCS and antibiotics and then are incubated in a humidified atmosphere of 5% CO_2 in air at 37°C. After 4 days all viable cells are adhered. Culture medium and unattached cells are removed and fresh medium is added. At confluency (5–7 days), culture medium is removed, cells are washed once with HBSS, and serum-free DMEM containing antibiotics is added. The cells are treated with recombinant human relaxin (1–1000 ng/ml) at 0, 24, and 48 h. Culture media are collected at 96 h from initial treatment with the appropriate controls and frozen immediately at −20°C until assayed for collagenase activity (Dean and Woessner 1985; Rajabi et al. 1988, 1991).

Enzyme samples [up to 100 µl in assay buffer: 50 mM Tris HCl (pH 7.5), 0.2 M NaCl, 10 mM $CaCl_2$, 0.02% sodium azide, 0.035% Brij-35] are incubated with 10 µl of [^{3}H]telopeptide-free collagen substrate [specific activity 3.1×10^6 cpm/mg collagen at 2.24 mg/ml, in 50 mM Tris HCl (pH 7.6), 0.3 M NaCl] in 1.5-ml microfuge tubes. Aminophenylmercuric acetate (0.5 mM) is used to activate procollagenase; 1,10-phenanthroline (1 mM) is added to inhibit collagenase and serves as blank control for nonspecific collagenolysis. After 18–48 h of incubation at 29°C, the reaction is terminated by addition of EDTA to a final concentration of 40 mM. Collagenase cleavage products are further digested by trypsin and chymotrypsin in the presence of BSA (10 mg/ml assay buffer) for 2 h at 29°C. The undigested [^{3}H]telopeptide-free substrate is precipitated in 10% trichloroacetic acid at 0°C for 30 min followed by centrifugation at 18,000 *g* at 4°C for 30 min. A 100-µl aliquot of the supernatant is mixed in 5 ml Aquasol scintillation fluid and counted in a liquid scintillation counter.

EVALUATION

The percentage digestion is calculated as the total cpm in the supernatant minus cpm in the 1,10-phenanthroline blanks divided by original counts in the [^{3}H]telopeptide-free substrate (in 100 µl of 10% trichloroacetic acid in assay buffer) × 100. One milliunit of collagenase is defined as the amount of collagenase that digests 1 ng of collagen in 1 min at 29°C.

All results are presented as the mean ±SEM of three separate experiments. Statistical analysis is performed by Student's *t*-test for paired observations and by one-way ANOVA for multiple observations.

REFERENCES AND FURTHER READING

Dean DD, Woessner JF Jr (1985) A sensitive specific assay for tissue collagenase using telopeptide-free ^{3}H-acetylated collagen. Anal Biochem 148:174–181

Mushayandebvu TI, Rajabi MR (1995) Relaxin stimulates interstitial collagenase activity in cultured uterine cervical cells from nonpregnant and pregnant but not immature guinea pigs; estradiol-17β restores relaxin's effect in immature cervical cells. Biol Reprod 53:1030–1037

Rajabi MR, Dean DD, Beydoun SN, Woessner JF Jr (1988) Elevated tissue levels of collagenase during dilatation of uterine cervix in human parturition. Am J Obstet Gynecol 159:971–976

Rajabi MR, Solomon S, Poole AR (1991) Biochemical evidence of collagenase-mediated collagenolysis as a mechanism of cervical dilatation in the guinea pig at parturition. Biol Reprod 45:764–772

N.10.4.6 Relaxin Receptor Binding

PURPOSE AND RATIONALE

Using a monocomponent, high specific activity, carrier-free porcine relaxin tracer [^{125}I], Yang et al. (1992) demonstrated relaxin receptors in the symphysis pubis, uterus, and ovary of mice. A linear Scatchard plot suggested the presence of only one kind of receptor and a dissociation constant of 5×10^{-10} M.

PROCEDURE

Crude membranes are prepared from uterine horns of estrogen-primed mice. The tissues are homogenized three times for 10 s with a Polytron homogenizer. The homogenate is centrifuged at 700 *g* for 10 min, and the supernatants are recovered and recentrifuged twice at the same speed. Thereafter, the supernatants are centrifuged at 10,000 *g* for 30 min. The crude membrane pellets are washed with HEPES buffer, centrifuged again, the resuspended in 200–500 µl water, and aliquots are removed for Lowry protein estimates.

The crude membrane suspension is diluted to 3 mg/ml protein with binding buffer (25 mM HEPES, 0.14 M NaCl, 5.7 mM KCl, 1.6 mM $CaCl_2$, 0.025 mM $MgCl_2$, 1.5 mM $MnCl_2$, 1% BSA, 2.8 mM glucose, 0.2 mM phenylmethylsulfonylfluoride, 80 mg/l soybean trypsin inhibitor, pH 7.5). The assay is initiated by adding this to 120 µl crude membranes (300 µg protein) with and without 0.2 µg unlabeled relaxin. At the end of the incubation period, 1 ml HEPES buffer, containing 1% BSA, is added, and bound and free relaxin are separated by three successive washings and centrifugations.

EVALUATION

The tubes are analyzed for radioactivity in a Minigamma 400 (LKB, Rockville, Md., USA). Duplicates are run for each experimental point, and experiments are repeated several times.

MODIFICATIONS OF THE METHOD

The control of relaxin secretion and relaxin receptors by relaxin was studied by Bryant-Greenwood et al. (1982).

Relaxin receptors in the myometrium of rats and pigs were studied by Mercado-Simmen et al. (1982a, 1982b).

Fluoresceinylthiocarbamyl relaxin was prepared by Segaloff and Gabbard (1982) for the demonstration of relaxin receptors.

Experiments by Büllesbach and Schwabe (1988) suggested a unique site for the interaction of relaxin with its uterine and symphyseal receptors.

Using a ^{32}P-labeled human relaxin, Osheroff and Phillips (1991) localized relaxin binding sites in rat uterus, cervix, and brain.

The receptor binding site of human relaxin II was studied by Büllesbach et al. (1992).

Min and Sherwood (1996) identified specific cell types that contain relaxin receptors in various organs of pregnant pigs.

REFERENCES AND FURTHER READING

Bryant-Greenwood GD, Greenwood FC, Mercado-Simmen R, Weiss T, Yamamoto S, Ueno M, Arakaki R (1982) Relaxin secretion and relaxin receptors: the linkages. Ann NY Acad Sci 380:100–110

Büllesbach EE, Schwabe C (1988) On the receptor binding site of relaxin. Int J Peptide Protein Res 32:361–367

Büllesbach EE, Yang S, Schwabe C (1992) The receptor binding site of human relaxin II. A dual prong-binding mechanism. J Biol Chem 267:22957–22960

Mercado-Simmen RC, Bryant-Greenwood GD, Greenwood FC (1982a) Relaxin receptor in the rat myometrium: regulation by estrogen and relaxin. Endocrinology 110:220–226

Mercado-Simmen RC, Goodwin B, Ueno MS (1982b) Relaxin receptors in the myometrium and cervix of pig. Biol Reprod 26:120–128

Min G, Sherwood OD (1996) Identification of specific relaxin-binding cells in the cervix, mammary glands, nipples, small intestine, and skin of pregnant pigs. Biol Reprod 55:1243–1252

Osheroff PL, Phillips HS (1991) Autoradiographic localization of relaxin binding sites in rat brain. Proc Natl Acad Sci USA 88:6413–6417

Segaloff A, Gabbard RB (1982) Preparation of fluoresceinylthiocarbamyl relaxin for the demonstration of relaxin receptors. Ann NY Acad Sci 380:198–199

Yang S, Rembiesa B, Büllesbach EE, Schwabe C (1992) Relaxin receptors in mice: demonstration of ligand binding in symphyseal tissues and uterine membrane fragments. Endocrinology 130:179–185

N.10.5 Calcitonin Gene-Related Peptide

N.10.5.1 General Considerations

In relation to the established traditional hormone definition, many new polypeptides have been identified by molecular biology and characterized by receptor binding and *in vitro* systems, while their definitive function is not yet assigned. Calcitonin-gene-related peptide (CGRP) is an example of this rapid development and change in approach by applying new methods. CGRP is a 37-amino-acid neuropeptide which was first identified as a product of the calcitonin gene by alternative splicing (Amara et al. 1982). This original peptide is referred to as α-CGRP; a second gene, unrelated to calcitonin, produces β-CGRP (Amara et al. 1985). These two forms are closely related in both rat and humans, and are widely distributed throughout most parts of the nervous system. CGRP shares about 50% identity with another 37-amino-acid peptide, amylin (Rink et al. 1993). CGRP shows weak but significant homology with adrenomedullin, a 52-amino-acid peptide (Kitamura et al. 1993). Several forms of CGRP have been sequenced: α- and β-CGRP from rat and humans, and single variants from sheep, pig, chick, salmon, and the laughing frog, *Rana ridibunda* (Poyner 1997). The calcitonin/CGRP gene is expressed in specific cell types of both the endocrine and nervous systems. The gene is alternatively spliced to yield mRNA encoding calcitonin in thyroid C-cells or the neuropeptide CGRP in a subset of central and peripheral neurons (Amara et al. 1982; Morris et al. 1984; Born and Fischer 1993). The rat as well as the human calcitonin/CGRP gene consists of six exons. The calcitonin mRNA contains exons 1–4 with a poly(A) tail at exon 4 whereas CGRPα includes exons 1, 2, 3, 5, and 6 with a poly(A) tail at exon 6 (Van Rossum et al. 1997).

α- and β-CGRP display several biological activities, including peripheral and cerebral vasodilatation, a blood-pressure-lowering effect, cardiac acceleration, regulation of calcium metabolism, reduction of intestinal motility, regulation of glucose metabolism, stimulation of pancreatic enzyme secretion, diminution of appetite, reduction of growth hormone release, influence on inflammation and nociception, and inhibition of interleukin-2 production (Poyner 1992, 1997; Wang et al. 1992; Wimalawansa 1996).

Nuki et al. (1994) compared the vasodilatory activity of chicken calcitonin gene-related peptide with human α-CGRP and rat CGRP in the precontracted mesenteric vascular bed of rats (see Sect. A.8.2.5).

Wisskirchen et al. (1998) tested agonists of calcitonin gene-related peptide, homologs, and antagonists in rat isolated pulmonary artery (see Sect. A.1.2.1) and rat deferens (see Sect. A.1.2.3).

Tomobe et al. (1998) found that the vasodilatation in isolated superior mesenteric arteries by calcitonin gene-related peptide was significantly larger in spontaneously hypertensive rats than in normal Wistar–Kyoto rats.

In order to elucidate the mechanism of endogenous CGRP release in peripheral vasodilatation, Brain et al. (1993) used a multiple site ^{133}Xe clearance technique.

Raddino et al. (1997) studied the mechanism of action of human calcitonin gene-related peptide in rabbit heart and human mammary arteries.

Champion et al. (1997) analyzed the responses of human synthetic adrenomedullin and calcitonin gene-related peptides in the hindlimb vascular bed of the cat (see Sect. A.8.2.1).

Castellucci et al. (1993) investigated the vasodilator activity of CGRP in the rat isolated and perfused kidney.

McMurdo et al. (1997) investigated the effect of the calcitonin gene-related peptide receptor antagonist $CGRP^{8-37}$ on blood flow in the knee joint of anesthetized rats. Synovial blood flow was measured in both exposed and intact skin-covered knees by Laser Doppler perfusion imaging.

Sakai et al. (1998) found a synergism of calcitonin gene-related peptide with the blood-pressure-lowering effect of adenosine.

Preibisz (1993) reported beneficial effects of CGRP infusions in patients with congestive heart failure and in subjects with neurological deficits after surgical treatment of subarachnoid hemorrhage.

Cadieux et al. (1999) described bronchoprotector properties of calcitonin gene-related peptide in guinea pig and human airways. Calcitonin gene-related peptide inhibited substance-P-induced bronchoconstriction *in vivo* and *in vitro*.

Smith et al. (1993) tested the ability of C-terminally truncated fragments of human α-calcitonin gene-related peptide to stimulate amylase secretion from guinea pig pancreatic acini and to relax precontracted mesenteric arteries (see Sect. A.1.2.9).

Meini et al. (1995) investigated the propagation of impulses in the guinea pig ureter and its blockade by calcitonin gene-related peptide. Furthermore, Maggi et al. (1995) studied the mechanisms of the inhibitory effect exerted by calcitonin gene-related peptide on the spontaneous activity of the guinea pig isolated renal pelvis.

Protective effects of calcitonin gene-related peptide in different experimental models of gastric ulcers (reserpine-induced gastric lesions, ethanol-induced gastric lesions, gastric damage and acid secretion in pylorus-ligated rats) were reported by Clementi et al. (1993).

The role of nitric oxide in the anti-ulcer activity of calcitonin gene-related peptide was investigated by Clementi et al. (1994a).

Evangelista and Renzi (1997) investigated the protective role of endogenous and exogenous calcitonin gene-related peptide in water immersion stress-induced gastric ulcers in rats.

Li et al. (1997) determined the ability of analogs of human α-calcitonin gene-related peptide to stimulate amylase secretion from guinea pig pancreatic acini (see Sect. J.7.0.10) and to relax isolated porcine coronary arteries precontracted with 20 mM KCl (see Sect. A.3.1.3).

Calcitonin gene-related peptide acutely augments the contractile response of skeletal muscle to both direct and indirect stimulation as studied in the isolated rat diaphragm by Fleming et al. (1993).

Dumont et al. (1997) used the isolated guinea pig heart (see Sect. A.3.1.2) and the isolated rat vas deferens (see Sect. A.1.2.3) for *in vitro* bioassays of CGRP agonists and antagonists.

Poyner et al. (1999) found a concentration-dependent inhibition of the electrically stimulated twitch response of guinea pig vas deferens by calcitonin gene-rated peptide, amylin and adrenomedullin (see Sect. A.1.2.3).

The role of calcitonin gene-related peptide in the protection of capsaicin-induced gastric mucosal hyperemia in rats was studied by Merchant et al. (1994).

Clementi et al. (1994b) studied the anti-inflammatory activity of calcitonin gene-related peptide in cutaneous inflammation induced by Croton oil, arachidonic acid, tetradecanoylphorbol acetate or cantharidin.

Schaible (1996) investigated the role of tachykinins and calcitonin gene-related peptide in the spinal mechanisms of nociception and in the induction and maintenance of inflammation-evoked hyperexcitability in spinal cord neurons.

The development of tolerance to spinal morphine analgesia in rats was prevented by a calcitonin gene-related peptide receptor antagonist (Menard et al. 1996).

Lutz et al. (1997) investigated the anorectic effects of CGRP and amylin in rats chronically cannulated in the lateral brain ventricle.

Specific calcitonin gene-related peptide receptors were characterized in hamster pancreatic cells (Barakat et al. 1993).

In doses of 25–200 µg/kg i.p., CGRP decreased food intake in mice, suggesting a role for CGRP as a satiety factor (Morley et al. 1996).

CGRP inhibits insulin-stimulated glycogen synthesis in rat skeletal muscle (Leighton and Cooper 1988).

Chatzipantelli et al. (1996) described the lipolytic actions of calcitonin gene-related peptide.

Howitt and Poyner (1997) determined the effects of a series of agonists and antagonists on the calcitonin gene-related peptide receptor of cultured rat L6 skeletal myocytes.

Kurz et al. (1995) studied the receptors of calcitonin gene-related peptide in the rat thymus and suggested that CGRP is a paracrine thymic mediator that may influence the differentiation, maturation, and proliferation of thymocytes.

REFERENCES AND FURTHER READING

Amara SG, Jonas V, Rosenfeld MG, Ong ES, Evans RM (1982) Alternative RNA processing in calcitonin gene expression generates mRNAs encoding different polypeptide products. Nature (Lond) 289:240–244

Amara SG, Arriza JI, Swanson LW, Evans RM, Rosenfeld MG (1985) Expression in brain of a messenger RNA encoding a novel neuropeptide homologous to calcitonin gene-related peptide. Science 229:1094–1097

Barakat A, Rosselin G, Marie J-C (1993) Characterization of specific calcitonin gene-related peptide receptors present in hamster pancreatic β-cells. Biosci Rep 13:221–231

Born W, Fischer A (1993) Calcitonin gene products: molecular biology, chemistry, and actions. Handb Exp Pharmacol 107:569–616

Brain SD, Hughes SR, Cambridge H, O'Driscoll G (1993) The contribution of calcitonin gene-related peptide (CGRP) to neurogenic vasodilator responses. Agents Actions 38 [Special Issue I]:C19–C21

Cadieux A, Monast NP, Pomerleau F, Fournier A, Lanoue C (1999) Bronchoprotector properties of calcitonin gene-related peptide in guinea pig and human airways: effect of pulmonary inflammation. Am J Respir Crit Care Med 159:235–243

Castellucci A, Maggi CA, Evangelista S (1993) Calcitonin gene-related peptide $(CGRP)_1$ receptor mediates vasodilation in the rat isolated and perfused kidney. Life Sci 53:PL153–PL158

Champion HC, Akers DL, Santiago JA, Lambert DG, McNamara DB, Kadowitz PJ (1997) Analysis of the responses to human synthetic adrenomedullin and calcitonin gene-related peptides in the hindlimb vascular bed of the cat. Mol Cell Biochem 176:5–11

Chatzipantelli K, Goldberg RB, Howard GA, Roos BA (1996) Calcitonin gene-related peptide is an adipose-tissue neuropeptide with lipolytic actions. Endocrinol Metab 3:235–242

Clementi G, Amico-Roxas M, Caruso A, Cutuli VMC, Maugeri S, Prato A (1993) Protective effects of calcitonin gene-related peptide in different experimental models of gastric ulcers. Eur J Pharmacol 238:101–104

Clementi G, Caruso A, Prato A, De Bernardis E, Fiore CE, Amico-Roxas M (1994a) A role of nitric oxide in the anti-ulcer activity of calcitonin gene-related peptide. Eur J Pharmacol 256:R7–R8

Clementi G, Amico-Roxas M, Caruso A, Cutuli VMC, Prato A, Maugeri S, de Bernardis E, Scapagnini U (1994b) Effects of CGRP in different models of mouse ear inflammation. Life Sci 54:119–124

Dumont Y, Fournier A, St-Pierre S, Quirion R (1997) A potent and selective $CGRP_2$ agonist, $[Cys(Et)^{2,7}]$hCGRPα: comparison in prototypical $CGRP_1$ and $CGRP_2$ *in vitro* bioassays. Can J Physiol Pharmacol 75:671–676

Evangelista S, Renzi D (1997) A protective role for calcitonin gene-related peptide in water-immersion stress-induced gastric ulcers in rats. Pharmacol Res 35:347–350

Fleming NW, Lewis BK, White DA, Dretchen KL (1993) Acute effects of calcitonin gene-related peptide on the mechanical and electrical responses of the rat hemidiaphragm. J Pharmacol Exp Ther 265:1199–1204

Howitt SG, Poyner DR (1997) The selectivity and structural determinants of peptide antagonists at the CGRP receptor of rat, L6 myocytes. Br J Pharmacol 121:1000–1004

Kitamura K, Kanagawa K, Kawamoto M, Ichiki Y, Nakamura S, Matsuo H, Ato T (1993) Adrenomedullin, a novel hypotensive peptide isolated from human phaeochromocytoma. Biochem Biophys Res Commun 192:553–560

Kurz V, von Gaudecker B, Kranz A, Krisch B, Mentlein R (1995) Calcitonin gene-related peptide and its receptor in the thymus. Peptides 16:1497–1503

Leighton B, Cooper GJS (1988) Pancreatic amylin and calcitonin gene-related peptide cause resistance to insulin in skeletal muscle. Nature 335:632–634

Li J, Matsuura JE, Waugh DJJ, Adrian TE, Abel PW, Manning MC, Smith DD (1997) Structure–activity studies on position 14 of human α-calcitonin gene-related peptide. J Med Chem 40:3071–3076

Lutz TA, Rossi R, Althaus J, Del Prete E, Scharrer E (1997) Evidence for a physiological role of central calcitonin gene-related peptide (CGRP) receptors in the control of food intake in rats. Neurosci Lett 230:159–162

Maggi CA, Giuliani S, Santicioli P (1995) CGRP inhibition of electromechanical coupling in the guinea-pig isolated rat pelvis. Naunyn Schmiedebergs Arch Pharmacol 352:529–537

McMurdo L, Lockhart JC, Ferrell WR (1997) Modulation of synovial blood flow by the calcitonin gene-related peptide (CGRP) receptor antagonist, $CGRP^{8-37}$. Br J Pharmacol 121:1075–1080

Meini S, Santicioli P, Maggi CA (1995) Propagation of impulses in the guinea-pig ureter and its blockade by calcitonin gene-related peptide (CGRP). Naunyn Schmiedebergs Arch Pharmacol 351:79–86

Menard DP, Van Rossum D, Kar S, St Pierre S, Sutak M, Jhamandas K, Quirion R (1996) A calcitonin gene-related peptide antagonists prevents the development of tolerance to spinal morphine analgesia. J Neurosci 16:2342–2351

Merchant NB, Dempsey DT, Grabowski MW, Rizzo M, Ritchie WP Jr (1994) Capsaicin-induced gastric mucosal hyperemia and protection: the role of calcitonin gene-related peptide. Surgery 116:419–425

Morley JE, Farr SA, Flood JF (1996) Peripherally administered calcitonin gene-related peptide decreases food intake in mice. Peptides 17:511–516

Morris HR, Panico M, Etienne T, Tippins J, Girgis SI, MacIntyre I (1984) Isolation and characterization of human calcitonin gene-related peptide. Nature 308:746–748

Nuki C, Kawasaki H, Takasaki K, Wada A (1994) Structure-activity study of chicken calcitonin gene-related peptide (CGRP) on vasorelaxation in rat mesenteric resistance vessels. Jpn J Pharmacol 65(2):99–105
Poyner DR (1992) Calcitonin-gene-related peptide: multiple actions, multiple receptors. Pharmacol Ther 56:23–51
Poyner DR (1997) Molecular pharmacology of receptors for calcitonin-gene-related peptide, amylin and adrenomedullin. Biochem Soc Trans 25:1032–1036
Poyner DR, Taylor GM, Tomlinson AE, Richardson AG, Smith DM (1999) Characterization of receptors for calcitonin gene-related peptide and adrenomedullin on the guinea pig vas deferens. Br J Pharmacol 126:1276–1282
Preibisz JJ (1993) Calcitonin gene-related peptide and regulation of human cardiovascular homeostasis Am J Hypertens 6:434–450
Raddino R, Pela G, Manca C, Barbagallo M, D'Aloia A, Passeri M, Visioli O (1997) Mechanism of action of human calcitonin gene-related peptide in rabbit heart and human mammary arteries. J Cardiovasc Pharmacol 29:463–470
Rink TJ, Beaumont K, Koda J, Young AA (1993) Structure and biology of amylin. Trends Pharmacol Sci 14:113–118
Sakai K, Saito K, Akima M (1998) Synergistic effect of calcitonin gene-related peptide on adenosine-induced vasodepression in rats. Eur J Pharmacol 344:153–159
Schaible H-G (1996) On the role of tachykinins and calcitonin gene-related peptide in the spinal mechanisms of nociception and in the induction and maintenance of inflammation-evoked hyperexcitability in spinal cord neurons (with special reference to nociception in joints). In: Kumazawa T, Kruger L, Mizumura K (eds) Progress in brain research, Vol 113. Elsevier Science, Amsterdam, pp 423–441
Smith DD, Li J, Wang Q, Murphy RF, Adrian TE, Elias Y, Bockman CS, Abel PW (1993) Synthesis and biological activity of C-terminally truncated fragments of human α-calcitonin gene-related peptide. J Med Chem 36:2536–2541
Tomobe YI, Ishikawa T, Goto K (1998) Enhanced endothelium-independent vasodilator response to calcitonin gene-related peptide in hypertensive rats. Eur J Pharmacol 35:351–355
Van Rossum D, Hanisch UK, Quirion R (1997) Neuroanatomical localization, pharmacological characterization and functions of CGRP, related peptides and their receptors. Neurosci Biobehav Rev 21:649–678
Wang F, Millet I, Bottomly K, Vignery A (1992) Calcitonin gene-related peptide inhibits interleukin 2 production by murine T lymphocytes. J Biol Chem 267:21052–21057
Wimalawansa SJ (1996) Calcitonin gene-related peptide and its receptors: molecular genetics, physiology, pathophysiology, and therapeutic potentials. Endocr Rev 17:533–585
Wisskirchen FM, Burt RP, Marshall I (1998) Pharmacological characterization of CGRP receptors of the rat pulmonary artery and inhibition of twitch responses f the rat deferens. Br J Pharmacol 123:1673–1683

N.10.5.2 Receptor Binding of CGRP

PURPOSE AND RATIONALE

Calcitonin gene-related peptide receptors are localized in many tissues, such as brain, heart, spleen, blood vessels, liver, lung, and kidney (Born and Fischer 1993; Muff et al. 1995). They are abundant in the brain, and the pattern is similar in the rat, pig, cow, sheep, and humans (Wimalawansa and El-Kholy 1993, 1996).

Multiple CGRP receptors (subclasses) have been observed: based on pharmacological properties they are divided into at least two subtypes and denoted as $CGRP_1$ and $CGRP_2$ (Dennis et al. 1989, 1991; Quirion 1992; Poyner 1997). CGRP-(8-37), which lacks seven terminal amino acid residues, is a selective antagonist of $CGRP_1$ receptors, whereas the linear analog of CGRP, diacetoamidomethyl cysteine CGRP (Cys[ACM2,7]CGRP), is a selective agonist of $CGRP_2$ receptors.

An atypical CGRP subtype has been reported (Dennis et al. 1991; Van Rossum 1997).

A sensitive and specific radioreceptor assay for calcitonin gene-related peptide was described by Wimalawansa (1989).

PROCEDURE

For membrane preparation, tissue samples, e. g., dissected brain areas from rats, are placed in 10 vols of ice-cold 50 mM Tris-HCl buffer (pH 7.4) containing 0.32 M sucrose, 0.5 mM dithiothreitol, and 5 mM EDTA. After centrifugation of the homogenate at 100 *g* for 10 min, the resultant pellet is rehomogenized with 5 vols of fresh buffer and recentrifuged. The pellet is discarded and the supernatants are pooled and recentrifuged at 30,000 *g* for 45 min at 4°C. The resulting crude membrane pellet is resuspended in 5 vols of assay buffer (50 mM Tris-HCl, 10 mM KCl, 3 mM sodium azide, and 200 IU/ml aprotinin) and recentrifuged at 30,000 *g* for a further 45 min. This procedure is repeated twice with fresh assay buffer. Protein concentrations are determined and adjusted to 1–2 mg/ml. The samples are frozen on dry ice and stored at −70°C until radioligand binding studies.

For radioligand binding studies, [^{125}I]CGRP (25 pM, ~5 fmol containing ~20,000 cpm/tube) is incubated with various membrane preparations (150–200 µg/ml membrane protein in an incubation medium of 200 µl) in the presence of 200 IU/ml aprotinin and 0.2% heat-inactivated BSA at 4°C for 120 min in polypropylene microcentrifuge tubes in a shaking water bath. At the end of the incubation period, 700 µl of chilled assay buffer is added and immediately centrifuged at 11,000 *g* for 2 min in a refrigerated microcentrifuge. The supernatant is discarded and the resulting membrane pellet is rewashed and the radioactivity remaining in the pellet is counted.

EVALUATION

Specific binding is calculated by subtracting the [^{125}I]CGRP binding in the presence of unlabeled

CGRP. Results are expressed as fmol of [^{125}I]CGRP bound/mg membrane protein.

MODIFICATIONS OF THE METHOD

Van Rossum et al. (1994) described the binding profile of a selective calcitonin gene-related peptide receptor antagonist ligand, [^{125}I-Tyr]hCGRP$_{8-37}$, in rat brain and peripheral tissues.

Muff et al. (1992) reported that the calcitonin gene-related peptide receptor in a human neuroblastoma cell line (SK-N-MC) is clearly different from the calcitonin receptor in a human breast carcinoma cell line (T47D).

Aiyar et al. (1996) described a cDNA encoding the calcitonin gene-related peptide type 1 receptor. Stable expression in human embryonic kidney 293 (HEK 293) cells produced specific high-affinity binding sites for CGRP that displayed pharmacological and functional properties very similar to those of the native human CGRP$_1$ receptor.

Poyner et al. (1999) characterized the receptors for calcitonin gene-related peptide and adrenomedullin on the guinea pig vas deferens.

Juaneda et al. (2000) reviewed the molecular pharmacology of CGRP and related peptide receptor subtypes.

Schindler and Doods (2002) described binding properties of the nonpeptide CGRP receptor antagonist radioligand, [^{3}H]BIBN4096BS.

REFERENCES AND FURTHER READING

Aiyar N, Rand K, Elshourbagy NA, Zeng Z, Adamou JE, Bergma DJ, Li Y (1996) A cDNA encoding the calcitonin gene-related peptide type 1 receptor J Biol Chem 271:11325–11329

Born W, Fischer JA (1993) Calcitonin gene products: molecular biology, chemistry, and actions. Handb Exp Pharmacol 107:569–616

Dennis T, Fournier A, St. Pierre S, Quirion R (1989) Structure-activity profile of calcitonin gene-related peptide in peripheral and brain tissues. Evidence for receptor multiplicity. J Pharmacol Exp Ther 251:718–725

Dennis T, Fournier A, Guard S, St. Pierre S, Quirion R (1991) Calcitonin gene-related peptide (hCGRP alpha) binding sites in nucleus accumbens. Atypical structural requirements and marked phylogenetic differences. Brain Res 539:59–66

Juaneda C, Dumont Y, Quirion R (2000) The molecular pharmacology of CGRP and related peptide receptor subtypes. Trends Pharmacol Sci 21:432–438

Muff R, Stangl D, Born W, Fischer JA (1992) Comparison of a calcitonin gene-related peptide receptor in a human neuroblastoma cell line (SK-N-MC) and a calcitonin receptor in a human breast carcinoma cell line (T47D). Ann N Y Acad Sci 657:106–116

Muff R, Born W, Fischer JA (1995) Receptors for calcitonin, calcitonin gene related peptide, amylin, and adrenomedullin. Can J Physiol Pharmacol 73:963–967

Poyner DR (1997) Molecular pharmacology of receptors for calcitonin-gene-related peptide, amylin and adrenomedullin. Biochem Soc Trans 25:1032–1036

Poyner DR, Taylor GM, Tomlinson AE, Richardson AG, Smith DM (1999) Characterization of receptors for calcitonin gene-related peptide and adrenomedullin on the guinea pig vas deferens. Br J Pharmacol 126:1276–1282

Quirion R, van Rossum D, Dumont Y, St. Pierre S, Fournier A (1992) Characterization of CGRP$_1$ and CGRP$_2$ receptor subtypes. Ann NY Acad Sci 657:88–105

Schindler M, Doods HN (2002) Binding properties of the novel, non-peptide CGRP receptor antagonist radioligand, [^{3}H]BIBN4096BS. Eur J Pharmacol 442:187–193

Van Rossum D, Ménard DP, Fournier A, St-Pierre S, Quirion R (1994) Binding profile of a selective calcitonin gene-related peptide (CGRP) receptor antagonist ligand, [^{125}I-Tyr]hCGRP$_{8-37}$, in rat brain and peripheral tissues. J Pharmacol Exp Ther 269:846–853

Van Rossum D, Hanisch UK, Quirion R (1997) Neuroanatomical localization, pharmacological characterization and functions of CGRP, related peptides and their receptors. Neurosci Biobehav Rev 21:649–678

Wimalawansa SJ (1989) A sensitive and specific radioreceptor assay for calcitonin gene-related peptide. J Neuroendocr 1:15–18

Wimalawansa SJ (1996) Calcitonin gene-related peptide and its receptors: molecular genetics, physiology, pathophysiology, and therapeutic potentials. Endocr Rev 17:533–585

Wimalawansa SJ, El-Kholy AA (1993) Comparative study of distribution and biochemical characterization of brain calcitonin gene-related peptide receptors in five different species. Neuroscience 54:513–519

N.10.6 Inhibin

N.10.6.1 General Considerations

Inhibin is a gonadal dimeric glycoprotein that has an inhibitory effect on the secretion of follicle-stimulating hormone by the pituitary gland. The existence of a nonsteroidal gonadal hormone was described by McGullagh as early as 1932. The hormone was isolated and purified from human seminal plasma, ram rete testis fluid, and from bovine follicular fluid (Franchimont et al. 1979, 1989; Robertson et al. 1986; Vale et al. 1986; De Kretser and Robertson 1989). After the determination of the full structure of bovine (Forage et al. 1986) and human (Mason et al. 1986; Stewart et al. 1986; Tierney et al. 1990) inhibin, it was found that inhibin shares structural homology with a family of glycoproteins which includes Mullarian inhibiting substance, transforming growth factor-β, follistatin, activin, and bone morphogenic proteins (Robertson 1991; Moore et al. 1994). Inhibin is a disulfide-linked dimer of an α-subunit and a structurally related β-subunit, either β_A or β_B (Robertson et al. 1992). Inhibin A and inhibin B are related dimeric

protein hormones and endocrine regulators of the reproductive axis which show differing patterns during the period of follicular development (Woodruff et al. 1996).

Clinically, inhibin determination may have uses in reproductive medicine and oncology; the diagnosis of some forms of cancer including granulosa cell tumors, cystadenocarcinoma of the ovary and hydatidiform mole and in the physiology and pathology of pregnancy including placental function (Halvorson and DeCherney 1996).

An International Standard for Porcine Inhibin was described by Gaines Das et al. (1992). An International Standard for human recombinant inhibin was established by Rose and Gaines Das (1996).

Tio et al. (1994) purified gonadotropin surge-inhibiting factor (GnSIF), a monomeric polypeptide that shares some biological activities with inhibin, from Sertoli cell-enriched medium.

REFERENCES AND FURTHER READING

De Kretser DM, Robertson DM (1989) The isolation and physiology of inhibin and related proteins. Biol Reprod 40:33–47

Forage RG, Ring JM, Brown RW et al (1986) Cloning and sequence analysis of cDNA species coding for the two subunits of inhibin from bovine follicular fluid. Proc Natl Acad Sci USA 83:3091–3095

Franchimont P, Verstraelen-Proyard J, Hazee-Hagelstein MT, Renard Ch, Demoulin A, Bourguignon JP, Hustin J (1979) Inhibin: from concept to reality. In: Munson PL, Diczfalusy E, Glover J, Olson RE (eds) Vitamins and hormones. Advances in research and applications, Vol 37. Academic Press, New York, pp 243–302

Franchimont P, Hazee-Hagelstein MT, Jaspar JM, Charlet-Renard C, Demoulin A (1989) Inhibin and related peptides: mechanisms of action and regulation of secretion. J Steroid Biochem 32:193–197

Gaines Das RE, Rose M, Zanelli JM (1992) International collaborative study by *in vitro* bioassays of the first International Standard for porcine inhibin. J Reprod Fertil 96:803–814

Halvorson LM, DeCherney AH (1996) Inhibin, activin, and follistatin in reproductive medicine. Fertil Steril 65:459–469

Mason AJ, Niall HD, Seeburg PH (1986) Structure of two human ovarian inhibins. Biochem Biophys Res Commun 135:957–964

McGullagh DR (1932) Dual endocrine activity of the testes. Science 76:19–20

Moore A, Krummen LA, Mather JP (1994) Inhibins, activins, their binding proteins and receptors: interactions underlying paracrine activity in the testis. Mol Cell Endocrinol 100:81–86

Robertson DM (1991) Transforming growth factor-β/inhibin family. Baillières Clin Endocrinol Metab 5:615–634

Robertson DM, Giacometti MS, de Kretser DM (1986) The effects of inhibin purified from bovine follicular fluid in several *in vitro* pituitary culture systems. Mol Cell Endocrinol 46:29–36

Robertson DM, Foulds LM, Prosk M, Hedger MP (1992) Inhibin/activin β-subunit monomer: isolation and characterization. Endocrinology 130:1680–1687

Rose MP, Gaines Das RE (1996) International collaborative study by *in vitro* bioassays and immunoassays of the first international standard for inhibin, human recombinant. Biologicals 24:1–18

Stewart AG, Millborrow HM, Ring JM, Crowther CE, Forage RG (1986) Human inhibin genes: genomic characterization and sequencing. FEBS Lett 206:329–334

Tierney ML, Goss NH, Tomkins SM, Kerr DB, Pitt DE, Forage RG, Robertson DM, Hearn MTW, de Kretser DM (1990) Physicochemical and biological characterization of recombinant human inhibin A. Endocrinology 126:3268–3270

Tio S, Koppenaal D, Bardin CW, Cheng CY (1994) Purification of gonadotropin surge-inhibiting factor from Sertoli cell-enriched medium. Biochem Biophys Res Commun 199:1229–1236

Vale W, Rivier C, Hsueh AJW, Campen C, Meunier H, Bicsak T, Vaughan J, Corrigan A, Bardin W, SawchenkoP, Petraglia F, Yu J, Plotsky P, Spiess J, Rivier J (1986) Chemical and biological characterization of inhibin family of proteins. Recent Prog Horm Res 44:1–34

Woodruff TK, Besecke LM, Groome N, Draper LB, Schwartz NB, Weiss J (1996) Inhibin A and inhibin B are inversely correlated to follicle-stimulating hormone, yet are discordant during the follicular phase of the rat estrus cycle, and inhibin A is expressed in a sexually dimorphic manner. Endocrinology 137:5463–5467

N.10.6.2 In Vitro Bioassay for Inhibin

PURPOSE AND RATIONALE

Several modifications of *in vitro* bioassays for inhibin have been used to establish the International Standard for porcine inhibin (Gaines Das et al. 1992) and for human recombinant inhibin (Rose and Gaines Das 1996). Mason et al. (1996) used rat anterior pituitary cells for characterization and determination of the biological activities of noncleavable high-molecular-weight forms of inhibin A and activin A.

PROCEDURE

Anterior pituitary cells are prepared from adult male rats and added to 48-well cluster plates at an initial density of 75,000 cell per 0.4 ml of medium per well. Cultures are preincubated in DMEM-Ham's F12 (1:1) medium with bicarbonate supplemented with nonessential amino acids, antibiotics (100 U/ml penicillin, 100 pg/ml streptomycin, and 250 ng/ml fungizone), and 10% charcoal-stripped FBS. Two days later, the cells are washed, and the medium is replaced with serum-free medium supplemented with antibiotics and recombinant human inhibin A (20–100 pM) as standard. Cultures are incubated with test samples for 65–72 h, after which the samples of medium are collected and stored at −20°C until assayed for follicle-stimulating hormone (FSH) by radioimmunoassay (RIA) using goat second antibody precipitation with

the following reagents (NIDDK): rat FSH-RP-2, rat FSH-I-8 iodinated using Iodogen, and anti-rat FSH-S-11 primary antiserum. Each sample for bioassay is tested at least twice in independent cell cultures to confirm the observations.

EVALUATION

Characteristics of the concentration–response curve, including the maximum effect and medium inhibitory concentration (IC_{50}), are computed using the Allfit program (Munson and Rodbard 1980).

MODIFICATIONS OF THE METHOD

Robertson et al. (1991) studied *in vivo* the FSH-suppressing activity of human recombinant inhibin A in the serum of male and female rats.

Wreford et al. (1994) studied the age dependence of gonadotropin-suppressing activity of human recombinant inhibin in the serum of male rats.

Simpson et al. (1992) induced bilateral cryptorchism in adult male Sprague Dawley rats under ether anesthesia by cutting the gubernaculum of both testes, translocating the testes to the abdominal cavity and ligating the inguinal canal to prevent redescent of the testes into the scrotum. After 28 days, Sertoli cell cultures from these rats were prepared and inhibin secretion in response to follicle-stimulating hormone (FSH) was measured.

Brown et al. (1991) investigated the effects of inhibin-rich porcine follicular fluid administration on serum bioactive and immunoreactive FSH concentrations and compensatory testosterone secretion in hemicastrated adult rats.

Hertan et al. (1999) used primary cultures of ovine anterior pituitary cells for bioassays of inhibin and identified high-affinity binding sites for inhibin using iodinated recombinant human 31-kDa inhibin.

Jakubowiak et al. (1989) found similar effects of inhibin and cycloheximide on gonadotropin release in superfused rat pituitary cell cultures.

Demura et al. (1996) studied the levels of inhibin α, β_A and β_B subunit mRNAs by a quantitative reverse transcription-polymerase chain reaction and the changes in their levels caused by adding inhibin α, β_A and β_B subunit mRNA antisense oligonucleotides and inhibin A, activin A or gonadotropin-releasing hormone (GnRH) to cultured rat anterior pituitary cells.

Robertson et al. (1996) investigated the specificity of several immunoassay methods in terms of their ability to detect the range of inhibin forms found in plasma and their relationship to bioactivity.

A commercially available enzyme-linked immunosorbent assay (ELISA) for inhibin A (Serotec, Oxford) was used by several authors (Wenstrom et al. 1997; Blumenfeld et al. 1998; Wallace et al. 1998). Magoffin and Jakimiuk (1998) used specific and sensitive two-site enzyme-linked immunosorbent assays for determination of inhibin A, inhibin B, and activin A.

An *in vitro* method has been developed by Allenby et al. (1991) for culturing isolated seminiferous tubules from adult rats for 1–3 days and optimized on the basis of the secretion of immunoactive inhibin under basal conditions and after maximal stimulation with rat FSH or dibutyryl cAMP. Inhibin was measured using a double-antibody radioimmunoassay based on an antibody generated in a sheep to the 1–26 sequence (plus gycine^{27}tyrosine^{28}) of the N-terminus of the α-subunit of porcine 32-kDa inhibin. The effect of three known testicular toxicants (meta-dinitrobenzene, nitrobenzene, and methoxy acetic acid) on these cultures was assessed.

Knight et al. (1991) described the development of a two-site immunoradiometric assay for dimeric inhibin using antibodies against chemically synthesized fragments of the α and β subunit. Knight and Muttukrishna (1994) described the measurement of dimeric inhibin using a modified two-site immunoradiometric assay specific for oxidized (Met O) inhibin.

REFERENCES AND FURTHER READING

Allenby G, Foster PMD, Sharpe RM (1991) Evaluation of changes in the secretion of immunoreactive inhibin by adult rat seminiferous tubules *in vitro* as an indicator of early toxicant action on spermatogenesis. Fundam Appl Toxicol 16:710–724

Blumenfeld Z, Ritter M, Shen-Orr Z, Shariki K, Ben-Shahar M, Haim N (1998) Inhibin A concentrations in the sera of young women during and after chemotherapy for lymphoma: correlation with ovarian toxicity. Am J Reprod Immunol 39:33–40

Brown JL, Dahl KD, Chakraborty PK (1991) Effects of follicular fluid administration on serum bioactive and immunoreactive FSH concentrations and compensatory testosterone secretion in hemicastrated adult rats. J Androl 12:221–225

Demura R, Suzuki T, Tajima S, Kubo O, Yoshimoto T, Demura H (1996) Inhibin α, β_A and β_B subunit messenger ribonucleic acid levels in cultured rat pituitary: studies by a quantitative RT-PCR. Endocr J 43:403–410

Gaines Das RE, Rose M, Zanelli JM (1992) International collaborative study by *in vitro* bioassays of the first International Standard for porcine inhibin. J Reprod Fertil 96:803–814

Hertan R, Farnworth PG, Fitzsimmons KL, Robertson DM (1999) Identification of high affinity binding sites for inhibin on ovine pituitary cells in culture. Endocrinology 140:6–12

Jakubowiak A, Janecki A, Steinberger A (1989) Similar effects of inhibin and cycloheximide on gonadotropin release in superfused pituitary cell cultures. Biol Reprod 41:454–463

Knight PG, Muttukrishna S (1994) Measurement of dimeric inhibin using a modified two-site immunoradiometric assay specific for oxidized (Met O) inhibin. J Endocrinol 141:417–425
Knight PG, Groome M, Beard AJ (1991) Development of a two-site immunoradiometric assay for dimeric inhibin using antibodies against chemically synthesized fragments of the α and β subunit. J Endocrinol 129:R9–R12
Magoffin DA, Jakimiuk AJ (1998) Inhibin A, inhibin B and activin A concentrations in follicular fluid from women with polycystic ovary syndrome. Hum Reprod 13:2693–2698
Mason AJ, Farnworth PG, Sullivan J (1996) Characterization and determination of the biological activities of noncleavable high molecular weight forms of inhibin A and activin A. Mol Endocrinol 10:1055–1065
Munson PJ, Rodbard D (1980) Ligand, a versatile computerised approach for characterization of ligand binding systems. Anal Biochem 107:220–239
Robertson DM, Prisk M, McMaster JW, Irby DC, Findlay JK, de Kretser DM (1991) Serum FSH-suppressing activity of human recombinant inhibin A in male and female rats. J Reprod Fertil 91:321–328
Robertson D, Burger HG, Sullivan J, Cahir N, Groome N, Poncelet E, Franchimont P, Woodruff T, Mather CP (1996) Biological and immunological characterization of inhibin forms in human plasma. J Clin Endocrinol Metab 81:669–676
Rose MP, Gaines Das RE (1996) International collaborative study by *in vitro* bioassays and immunoassays of the first international standard for inhibin, human recombinant. Biologicals 24:1–18
Simpson BJB, Hedger MP, de Kretser DM (1992) Characterisation of adult Sertoli cell cultures from cryptorchid rats: inhibin secretion in response to follicle-stimulating hormone. Mol Cell Endocrinol 87:167–177
Wallace EM, Crossley JA, Ritoe SC, Aitken DA, Spencer K, Groome NP (1998) Evolution of an inhibin A ELISA method: implications for Down's syndrome screening. Ann Clin Biochem 35:656–664
Wenstrom KD, Owen J, Chu DC, Boots L (1997) Elevated second-trimester dimeric inhibin A levels identify Down syndrome pregnancies. Am J Obstet Gynecol 177:992–996
Wreford NG, O'Connor AE, de Kretser DM (1994) Gonadotropin-suppressing activity of human recombinant inhibin in the male rat is age dependent. Biol Reprod 50:1066–1071

N.10.7 Activin

N.10.7.1 General Considerations

Activin is a pluripotent growth factor that was originally isolated based on its ability to stimulate follicle-stimulating hormone (FSH), but is now known to have other important roles during development, erythropoiesis, inflammation, and wound healing (De Paolo 1997). Three types of activin, formed by dimerization of two inhibin-β subunits β_A and β_B, are termed activin A ($\beta_A\beta_A$), activin AB ($\beta_A\beta_B$) and activin B ($\beta_B\beta_B$) (Ling et al. 1986; Vale et al. 1986; Mason et al. 1989; Nakamura et al. 1992). In addition, a third β-subunit (β_C) has been identified (Hötten et al. 1995; Loveland et al. 1996). Lee et al. (1989) suggested that, in the testis, the Leydig cells secrete activin and the Sertoli cells produce inhibin, or a combination of both. As members of the transforming growth factor beta (TGF-β) family, the activins are involved in a diverse range of physiological processes, including the regulation of FSH biosynthesis and secretion (Mason 1988; MacConnell et al. 1999), steps in embryonic development (Thomsen et al. 1990), spermatogonial mitosis (Mather et al. 1990) and erythroid differentiation (Eto et al. 1987). Activin acts via a family of activin receptor subunits that includes one type I (Act RI or ALK-2) and two homologous type II (IIA and IIB) subunits (Dalkin et al. 1996; Hashimoto et al. 1998).

REFERENCES AND FURTHER READING

Dalkin AC, Haisenleder DJ, Yasin M, Gilrain JT, Marshall JC (1996) Pituitary activin receptor subtypes and follistatin gene expression in female rats: differential regulation by activin and follistatin. Endocrinology 137:548–554
De Paolo LV (1997) Inhibins, activins, follistatins: the saga continues. Proc Soc Exp Biol Med 214:328–339
Eto Y, Tsuji T, Takezawa M, Takano S, Tokagawa Y, Shibai H (1987) Purification and characterization of erythroid differentiation factor (EDF) isolated from human leukemia cell line THP-1. Biochem Biophys Res Commun 142:1095–1103
Hashimoto O, Yamato K, Koseki T, Ohguchi M, Ishisaki A, Shoji H, Nakamura T, Hayashi Y, Sugino H, Nishihara T (1998) The role of activin type I receptors in activin A-induced growth arrest and apoptosis in mouse B-cell hybridoma cells. Cell Signal 10:743–749
Hötten G, Neidhardt H, Schneider C, Pohl J (1995) Cloning of a new member of the TGF-β family: a putative new activin β_C chain. Biochem Biophys Res Commun 206:608–613
Lee W, Mason AJ, Schwall R, Szonyi E, Mather JP (1989) Secretion of activin by interstitial cells in the testis. Science 243:396–398
Ling N, Ying SY, Ueno N, Shimasaki S, Etsch F, Hott M, Guillemin R (1986) Pituitary FSH is released by a homodimer of the beta subunit from the two forms of inhibin. Nature 321:779–782
Loveland KL, McFarlane JR, de Kretser DM (1996) Expression of activin β_C subunit mRNA in reproductive tissue. J Mol Endocrinol 17:61–65
MacConnell LA, Lawson MA, Mellon PL, Roberts VJ (1999) Activin A regulation of gonadotropin-releasing hormone synthesis and release *in vitro*. Neuroendocrinology 70:246–254
Mason AJ (1988) Structure and recombinant expression of human inhibin and activin. In: Nonsteroidal gonadal factors: physiological roles and possibilities in contraceptive development. Jones Institute, Norfolk, Va., pp 1–19
Mason AJ, Berkemeier LM, Schmelzer CH, Schwall RH (1989) Activin B: precursor sequences, genomic structure and *in vitro* activities. Mol Endocrinol 3:1352–1358

Mather JP, Attie KM, Woodruff DK, Rice GC, Phillips DM (1990) Activin stimulates spermatogonial proliferation in germ-Sertoli cell cocultures from immature rat testis. Endocrinology 127:3206–3214

Nakamura T, Asashima M, Eto Y, Takio K, Uchiyama H, Moriya M, Ariizumi T, Yashiro T, Sugino K, Titani K, Sugino H (1992) Isolation and characterization of native activin B. J Biol Chem 267:16385–16389

Thomsen G, Woolf T, Whitman M, Solkol S, Vaughan J, Vale W et al (1990) Activins are expressed early in *Xenopus* embryogenesis and can induce axial mesoderm and anterior structures. Cell 63:485–493

Vale W, Rivier J, McClintock R, Corrigan A, Woo W, Karr D, Spiess J (1986) Purification and characterization of an FSH releasing protein from porcine ovarian follicular fluid. Nature 321:776–779

N.10.7.2 In Vitro Bioassay for Activin

PURPOSE AND RATIONALE

In vitro bioassays for activin have been developed using the production of follicle-stimulating homone (FSH) from cultured pituitary cells (Robertson et al. 1992), the accumulation of hemoglobin in K562 erythroleukaemia cells (Schwall and Lai 1991), and the ability to induce mesoderm tissue in animal cap explants of *Xenopus* (De Winter et al. 1992). One of the sites of production of activin A is the bone marrow (Shao et al. 1992; Yamashita et al. 1992; Uchimaru et al. 1995). Brosh et al. (1995) found that the mouse plasmacytoma cell line MPC-11 (Laskov and Scharff 1970) was exquisitely sensitive to inhibition by activin A without being influenced by a variety of other cytokines and growth factors. On this basis, Phillips et al. (1999) evaluated the MPC-11 cell line as the basis for an *in vitro* bioassay for activin.

PROCEDURE

MPC-11 plasmacytoma cells are cultured in Dulbecco's modified Eagle's medium supplemented with 10% fetal calf serum, 24 mM bicarbonate, L-glutamine, nonessential amino acids and Pen-strep in a 95% air/5% CO_2atmosphere at 37°C, and passaged at 1×10^6 cells/25 cm^2 flask every second day. For experiments, 100 µl cell suspension is added to 96-well plates at a density of 1000 viable cells/well in culture medium containing 25 µM β-mercaptoethanol. Activin, other test reagents and sera (100 µl/well) are added to the cultures diluted in phosphate buffer (pH 7.4) containing 6.5 mM Na_2HPO_4, 1.5 mM KH_2PO_4, 0.14 M NaCl, 0.01% BSA and Pen-strep. Cells are cultured in the presence of test reagents for 2 days; on the third day 25 µl [^{3}H]thymidine (0.25 µCi/25 µl, 6.7 Ci/mmol) is added to each well and 24 h later the cells harvested and thymidine incorporation assessed. Proliferation of MCP-11 cells, as measured by thymidine incorporation, is inhibited by increasing doses of activin A or activin B, whereas follistatin, inhibin A, LH, and interleukin-1β are ineffective.

EVALUATION

All test preparations, including activin standards and sera, are assayed in quadruplicate, and experiments are repeated at least twice. Relative bioactivity and parallelism are assessed using parallel-line bioassay statistics.

MODIFICATIONS OF THE METHOD

Mesoderm induction assays in *Xenopus* were used by Wuytens et al. (1999). *Xenopus* embryos were obtained by *in vitro* fertilization. They were maintained in 10% Normal Amphibian Medium and staged according to Nieuwkoop and Faber (1967). Animal pole regions were dissected from mid-blastula (stage 8) embryos and cultured in 75% Normal Amphibian Medium containing 0.1% bovine serum albumin and wild-type or mutant activin (2.5 ng/ml). A preliminary assessment of mesoderm induction was based on the elongation of the animal caps. Animal pole regions were then frozen on dry ice, and expression of the mesoderm-specific gene Brachyury (Xbra) was assessed by RNase protection analysis.

LaPolt et al. (1989) examined the effects of purified porcine activin on inhibin secretion and messenger RNA levels in cultured granulosa cells obtained from immature, estrogen-treated rats. Western blot analyses performed with affinity-purified antisera to inhibin α- and β_A-subunits revealed that treatment with either FSH or activin increased the secretion of inhibin $\alpha\beta$ dimer, with a further increase after co-treatment.

Attardi and Miklos (1990) examined the effect of purified recombinant human activin A on steady-state levels of mRNAs for the gonadotropin subunits in pituitary cell cultures prepared from adult male rats.

Carroll et al. (1991) used rat anterior pituitary cells *in vitro* and determined the apparent half-life of FSHb mRNA in the presence and absence of recombinant human activin A after addition of actinomycin D.

Demura et al. (1993) measured follistatin-free activin and inhibin in the culture medium of porcine granulosa cells by a competitive protein binding assay and N-fragment RIA, respectively. Both activin and inhibin were secreted under the control of FSH and LH.

Miyamoto et al. (1999) investigated the effect of activin A on secretion of LH, FSH, and prolactin by fe-

male cultured rat pituitary cells at the single-cell level by means of the cell immunoblot assay. Anterior pituitary cells were preincubated with or without activin A for 24 h, after which they were monodispersed and immediately used for cell immunoblot assay.

Peng et al. (1999) examined the expression of activin receptor mRNAs in human ovary and placenta. Primers specific for two type-I and two type-II receptors (ActR-I, Act-RI_B, ActR-II, and Act-RII_B) were used in polymerase chain reaction to amplify cDNAs prepared from granulosa-luteal cells, placental tissues, and trophoblast cells.

Liu et al. (1996) measured release of immunoreactive activin A from cultured rat anterior pituitary cells by a specific radioimmunoassay.

Shintani et al. (1991) developed a radioimmunoassay for the measurement of activin A, which is identical to erythroid differentiation factor.

For measurement of activin in biological fluids by radioimmunoassay, McFarlane et al. (1996) added sodium deoxycholate, Tween 20 and sodium dodecyl sulphate as dissociating agents in order to remove interference by follistatin.

Knight et al. (1996) developed a two-site enzyme immunoassay for the determination of total activin A concentrations in serum and follicular fluid.

Saito et al. (1991) developed an assay method for activin-binding protein, which exploits its high affinity for sulfated polysaccharides, and used this method to investigate the production of activin-binding protein by rat ovarian granulosa cells *in vitro*.

REFERENCES AND FURTHER READING

Attardi B, Miklos J (1990) Rapid stimulatory effect of activin-A on messenger RNA encoding the follicle-stimulating hormone b-subunit in pituitary cell cultures. Mol Endocrinol 4:721–726

Brosh N, Sternberg D, Honigswachs-Sha'anani J, Lee BC, Shav-Tal Y, Tzehoval E, Shulman LM, Toledo J, Hacham Y, Carmi P, Jiang W, Sasse J, Horn F, Burstein Y, Zipori D (1995) The plasmacytoma growth inhibitor restrictin-P is an antagonist of interleukin 6 and interleukin 11. Identification as a stroma-derived activin A. J Biol Chem 270:29594–29600

Carroll RS, Corrigan AZ, Vale W, Chin WW (1991) Activin stabilizes follicle-stimulating hormone-beta messenger ribonucleic acid levels. Endocrinology 129:1721–1726

Demura R, Suzuki T, Tajima S, Mitsuhashi S, Odagiri E, Demura H (1993) Activin and inhibin secretion by cultured porcine granulosa cells is stimulated by FSH and LH. Endocr J 40:447–451

De Winter JP, Timmermann MA, Vanderstichele HMJ, Klaij IA, Grootenhuis AJ, Rommerts FFG, de Jong FH (1992) Testicular Leydig cells *in vitro* secrete only inhibin α-subunits, whereas Leydig cell tumors can secrete bioactive inhibin. Mol Cell Endocrinol 83:105–115

Knight PG, Muttukrishna S, Groome NP (1996) Development and application of a two-site enzyme immunoassay for the determination of 'total' activin-A concentrations in serum and follicular fluid. J Endocrinol 148:267–279

LaPolt PS, Soto D, Su J-G, Campen CA, Vaughan J, Vale W, Hsueh AJW (1989) Activin stimulation of inhibin secretion and messenger RNA levels in cultured granulosa cells. Mol Endocrinol 3:1666–1673

Laskov R, Scharff MD (1970) Synthesis, assembly, and secretion of gamma globulin by mouse myeloma cells. I. Adaptation of the Mervin plasma cell tumor-11 to culture, cloning and characterization of gamma globulin subunits. J Exp Med 131:515–541

Liu ZH, Shintani Y, Wakatsuki M, Sakamoto Y, Harada K, Zhang CY, Saito S (1996) Regulation of immunoreactive activin A secretion from cultured rat anterior pituitary cells. Endocr J 43:39–44

McFarlane JR, Foulds LM, Pisciotta A, Robertson DM, de Kretser DM (1996) Measurement of activin in biological fluids by radioimmunoassay, utilizing dissociating agents to remove the interference of follistatin. Eur J Endocrinol 134:481–489

Miyamoto S, Irahara M, Ushigoe K, Kuwahara A, Sugino H, Aono T (1999) Effects of activin on hormone secretion by single female rat pituitary cells: analysis by cell immunoblot assay. J Endocrinol 161:375–382

Nieuwkoop PD, Faber J (1967) Normal table of *Xenopus laevis*. Daudlin, Amsterdam

Peng C, Ohno T, Loo Yee Koh, Chen VTS, Leung PCK (1999) Human ovary and placenta express messenger RNA for multiple activin receptors. Life Sci 64:983–994

Phillips DJ, Brauman JN, Mason AJ, de Kretser DM, Hedger MP (1999) A sensitive and specific *in vitro* bioassay for activin using a mouse plasmacytoma cell line, MPC-11. J Endocrinol 162:111–116

Robertson DM, Foulds LM, Prisk M, Hedger MP (1992) Inhibin/activin β-subunit monomer: isolation and characterization. Endocrinology 130:345–351

Saito S, Nakamura T, Titani K, Sugino H (1991) Production of activin-binding protein by rat granulosa cells *in vitro*. Biochem Biophys Res Commun 176:413–422

Schwall RH, Lai C (1991) Erythroid differentiation assays for activin. Methods Enzymol 198:340–346

Shao L, Frigon NL Jr, Sehy DW, Yu AL, Lofgren J, Schwall R, Yu J (1992) Regulation of production of activin A in human marrow stromal cells and monocytes. Exp Hematol 20:1235–1242

Shintani Y, Takada Y, Yamasaki R, Saito S (1991) Radioimmunoassay for activin A/EDF. Method and measurement of immunoreactive A/EDF levels in various biological materials. J Immunol Methods 137:267–274

Uchimaru K, Motokura T, Takahashi S, Sakurai T, Asano S, Yamashita T (1995) Bone marrow stromal cells produce and respond to activin A: interactions with basic fibroblast growth factor and platelet-derived growth factor. Exp Hematol 23:613–618

Wuytens G, Verschueren K, de Winter JP, Gajendran N, Beek L, Devos K, Bosman F, de Waele P, Andries M, van den Eijnden-van Raaij AJM, Smith JC, Huylebroeck D (1999) Identification of two amino acids in activin A that are important for biological activity and binding to the activin type II receptors. J Biol Chem 274:9821–9827

Yamashita T, Takahashi S, Ogata E (1992) Expression of activin A/erythroid differentiation factor in murine bone marrow stromal cells. Blood 79:304–307

N.10.8
Follistatin

N.10.8.1
General Considerations

Follistatin is a monomeric glycosylated polypeptide chain which was identified from bovine and porcine follicular fluids on the basis of its inhibition of pituitary follicle-stimulating hormone secretion (Robertson et al. 1987; Ueno et al. 1987; Ying et al. 1987; Bohnsack et al. 2000). Follistatin exerts its inhibitory effect on FSH secretion by neutralizing activin activity (Namakura et al. 1990; Shimonaka et al. 1991; De Winter et al. 1996). Follistatin is able to bind and neutralize the actions of many members of the transforming growth factor-β family of proteins and plays a significant role during organogenesis (Patel 1998). There are two main forms of mature mammalian follistatin which occur as a result of alternative modes of precursor mRNA splicing, giving core proteins of 315 amino acids and the carboxy-truncated variant of 288 amino acids. Further variants in the molecular weight of mature follistatin occur as a result of varying degrees of glycosylation (Inouye et al. 1991; Sugino et al. 1993).

REFERENCES AND FURTHER READING

Bohnsack BL, Szabo M, Kilen SM, Tam DH, Schwartz HB (2000) Follistatin suppresses steroid-enhanced follicle-stimulating hormone release *in vitro* in rats. Biol Reprod 62:636–641

De Winter JP, ten Dijke P, de Vries CJM, van Achterberg TAE, Sugino H, de Waele P, Huylebroeck D, Verschueren K, van den Eijnden-van Raaij AJM (1996) Follistatins neutralize activin bioactivity by inhibition of activin binding to its type II receptors. Mol Cell Endocrinol 116:105–114

Inouye S, Guo Y, de Paolo L, Shimonaka M, Ling N, Shimasaki S (1991) Recombinant expression of human follistatin with 315 and 288 amino acids: chemical and biological comparison with native porcine follistatin. Endocrinology 129:815–822

Namakura T, Takio K, Eto Y, Shibai H, Titani K, Sugino H (1990) Activin-binding protein from rat ovary is follistatin. Science 247:836–838

Patel K (1998) Follistatin. Int J Biochem Cell Biol 30:1087–1093

Robertson DM, Klein R, de Vos FL, McLachlan RI, Wettenhall REH, Hearn MTW, Burger HG, de Kretser DM (1987) The isolation of polypeptides with FSH suppressing activity from bovine follicular fluid which are structurally different to inhibin. Biochem Biophys Res Commun 149:744–749

Shimonaka M, Inouye S, Shimasaki S, Ling N (1991) Follistatin binds to both activin and inhibin through the common beta-subunit. Endocrinology 128:3313–3315

Sugino K, Kurosawa N, Nakamura T, Takio K, Shimasaki S, Guillemin R (1993) Molecular heterogeneity of follistatin, an activin-binding protein. J Biol Chem 268:15579–15587

Ueno N, Ling N, Ying SY, Esch F, Shimasaki S, Guillemin R (1987) Isolation and partial characterization of follistatin: a single-chain, monomeric protein that inhibits the release of follicle-stimulating hormone. Proc Natl Acad Sci USA 84:8282–8286

Ying SY, Becker A, Swanson G, Tan P, Ling N, Esch F, Ueno N, Shimasaki S, Guillemin R (1987) Follistatin specifically inhibits pituitary follicle-stimulating hormone release *in vitro*. Biochem Biophys Res Commun 149:133–139

N.10.8.2
Immunoassay for Follistatin

PURPOSE AND RATIONALE

Evans et al. (1998) developed an ultra-sensitive two-site enzyme immunoassay for human follistatin.

PROCEDURE

Female Balb/c mice are immunized subcutaneously with 20 µg recombinant human follistatin rh-FS288 in an emulsion with complete Freund's adjuvant. The immunization is repeated on two further occasions at monthly intervals in complete Freund's adjuvant, before finally boosting intravenously with rh-FS288 (total 100 µg in saline). The spleen is removed and the splenocytes are fused to Sp2/0 myeloma cells using polyethylene glycol following a standard fusion protocol (Galfre and Milstein 1981). Hybridoma supernatants are screened on a 96-well plate coated with rh-FS288 (0.2 µg/ml in sodium bicarbonate buffer, pH 9.4). Positive clones are expanded and recloned in methyl cellulose. The supernatants from these clones are titrated against rh-FS288 (0.2 µg/ml) under a standard ELISA protocol (Groome et al. 1995). On the basis of these experiments, clones are selected (29/9 and 17/2) and isotoped with a commercial kit. The clones are grown to produce ascitic fluid in pristane-primed BALB/c mice. Purification of IgG is carried out using protein-G affinity chromatography.

Antibody to a selected clone (29/9) diluted in 0.2 M sodium bicarbonate buffer, pH 9.4, is coated by simple absorption onto 96-well ELISA plates overnight at room temperature (10 µg/ml). The following day, the plates are banged to dryness on paper toweling, then 100 µl of dry coat reagent per well is added to the plates. After a 1-h incubation at room temperature the plates are banged to dryness and stored in a sealed box.

Both standard (rh-FS288) and samples are diluted in dissociation solution (84 mmol/l sodium deoxycholate, 3.4% Tween 20, 1% BSA, 5% mouse serum in PBS). Standards are prepared by serially diluting the stock rh-FS288 to give a high standard of 2500 pg/ml and a low standard of 19.53 pg/ml.

Duplicate 50-µl amounts of standard or test samples are added to wells on the plate, which is then sealed

and incubated overnight stationary at room temperature in a sealed moist box. The following day, the plate is washed and to each well is added 50 µl of approximately 1 µg/ml of Fab fragment of clone 17/2, which has previously been coupled to alkaline phosphatase by heterobifunctional chemistry (Ishikawa et al. 1983). This is diluted in Tris conjugate buffer: 1% BSA in 25 mM Tris-HCl, pH 7.5, containing 0.15 M NaCl and 0.5% Tween 20. After a 2-h incubation in a moist chamber at room temperature, the plate is washed thoroughly, and banged to dryness on paper toweling. Alkaline phosphate substrate (50 µl) is added to each well and the plate incubated for 2 h stationary at room temperature. Amplifier solution (50 µl) is then added to each well and the ensuing chromogenic reaction is stopped by adding 0.4 M HCl (50 µl/well) once color begins to develop in the zero analyte wells and the top standard has an absorbance of approximately 1.8. The well absorbencies are read at 490 nm with a reference wavelength set at 620 nm using a microplate reader.

EVALUATION

To determine whether dose–response relationships of serially diluted standard and test samples are identical (parallel), the slope values (± 95% confidence intervals) of log-transformed data for each response curve are compared by linear regression. The curves are deemed to be parallel if the slopes (± 95% confidence intervals) are found to overlap.

MODIFICATIONS OF THE METHOD

Nakamura et al. (1992) investigated the effect of follistatin on activin-induced granulosa cell differentiation in freshly harvested granulosa cells from diethylstilbestrol-treated rats. Activin induced a remarkable change in granulosa cellular morphology from elongated fibroblast-like to round cells, which was prevented by follistatin.

Xiao et al. (1992) studied the effects of activin and follistatin on FSH receptors and differentiation of cultured rat granulosa cells *in vitro*.

DePaolo et al. (1991) determined FSH and LH levels by RIA in the serum of ovariectomized rats and compared *in vivo* the FSH-suppressing activity of follistatin and inhibin.

REFERENCES AND FURTHER READING

DePaolo LV, Shimonaka M, Schwall RH, Ling N (1991) *In vivo* comparison of the follicle-stimulating hormone-suppressing activity of follistatin and inhibin in ovariectomized rats. Endocrinology 128:668–674

Evans LW, Muttukrishna S, Groome NP (1998) Development, validation and application of an ultra-sensitive immunoassay for human follistatin. J Endocrinol 156:275–282

Galfre G, Milstein C (1981) Preparation of monoclonal antibodies: strategies and procedures. In: Langone JJ, Vunakis HV (eds) Methods in enzymology. Academic Press, New York, pp 3–36

Groome NP, Illingworth PJ, O'Brien M, Priddle J, Weaver K, McNeilly AS (1995) Quantification of inhibin pro-αC-containing forms in human serum by a new ultrasensitive two-site enzyme-linked immunosorbent assay. J Clin Endocrinol Metab 80:2926–2932

Ishikawa A, Imagawa M, Hashida S, Yoshitake S, Hamaguchi Y, Ueno T (1983) Enzyme labeling of antibodies and their fragments for enzyme immunoassay and immunocytochemistry. J Immunoassay 4:209–327

Nakamura T, Hasegawa Y, Sugino K, Kogawa K, Titani K, Sugino H (1992) Follistatin inhibits activin-induced differentiation of rat follicular granulosa cells *in vitro*. Biochim Biophys Acta 1135:103–109

Xiao S, Robertson DM, Findlay JK (1992) Effects of activin and follicle-stimulating hormone (FSH)-suppressing protein/follistatin on FSH receptors and differentiation of cultured rat granulosa cells. Endocrinology 131:1009–1016

N.10.9
Further Peptide Hormones Discussed in Chapters Related to the Respective Indications

Further peptide hormones are discussed in chapters related to the respective indications such as:

Chapter A Cardiovascular activity

A.1.1.12.1 Inhibition of Angiotensin-Converting Enzyme *in Vitro*
A.1.1.12.2 Inhibition of Neutral Endopeptidase (Neprilysin)
A.1.1.14 Angiotensin
A.1.1.15 Renin
A.1.1.17 Endothelin
A.1.1.17.6 Endothelin-Converting Enzyme
A.1.1.26 Adrenomedullin
A.1.1.28 Urotensin
A.1.1.29 Apelin

Chapter E Psychotropic and Neurotropic Activity

E.5.1.16 Neurotensin

Chapter F Drug Effects on Learning and Memory

F.2.0.10 Nerve Growth Factor (Cultured Neurons/Astroglial Cells)

Chapter H Analgesic, Anti-Inflammatory, and Anti-Pyretic Activity

H.1.1.6 Nociceptin
H.1.1.7 Vasoactive Intestinal Polypeptide (VIP) and Pituitary Adenylate Cyclase-Activating Peptide (PACAP)

H.2.0.7 Antagonism to Nerve Growth Factor
H.3.1.2 Bradykinin
H.3.1.3 Substance P and the Tachykinin Family
H.3.1.3.3 Neurokinin
H.3.1.7 Cytokines
H.3.1.7.3 Interleukin-1 Antagonists
H.3.1.7.4 Interleukin-1-β Converting Enzyme
H.3.1.7.5 Nuclear Factor-κB
H.3.1.8 TNF-Alpha
H.3.1.9 Interferon Receptors
H.3.1.10 Peroxisome Proliferator-Activated Receptors

Chapter J Activity on the gastrointestinal Tract
J.3.1.6 Gastrin
J.3.1.8 Gastrin Releasing-Peptide/ Bombesin/Neuromedin
J.3.1.9 Bombesin
J.7.0.6 Somatostatin
J.7.0.8 Secretin
J.7.0.10 Cholecystokinin

Chapter K Antidiabetic Activity
K.3 Insulin and Insulin-Like Activity
K.4.0.1 Glucagon
K.4.0.3 Glucagon-Like Peptide I
K.4.0.4 Insulin-Like Growth Factors/Somatomedin
K.4.0.5 Amylin

Chapter L Anti-Obesity Activity
L.3.2.2 Uncoupling Protein
L.4.0.1 Agouti-Related Protein
L.4.0.1 Melanin Concentrating Hormone (MCH)
L.4.0.1 Cocaine- and Amphetamine- Regulated Transcript (CART)
L.4.0.1 Resistin
L.4.1 Leptin
L.4.2 Neuropeptide Y
L.4.3 Orexin
L.4.4 Galanin
L.4.5 Adipsin
L.4.6 Ghrelin

Chapter M Anti-Atherosclerotic Activity
M.8 Peroxisome Proliferator-Activated Receptors (PPARs) and Liver X Receptors (LXRs)

Chapter O
Ophthalmologic Activity[1]

[1] Review and contributions by B. Schultz and W.H. Vogel.

O.1 Introduction

Ocular pharmacology shares many methods with other indications and treatment of other organs. Therefore, in many instances, the reader has to be referred to other sections, such as:

- neovasculrization of the cornea to Sect. A.8.3.4,
- topical anesthesia of the cornea to Sect. G.1.3.1,
- influence on α- and β-adrenoreceptors in the mouse iris to Sect. A.1.3.24,
- *in vitro* determination of carbonic anhydrase inhibition to Sect. C.1.1.1,
- electroretinogram in diabetic hyperglycemia and galactosemia to Sect. K.8.1.5,
- effect of streptomycin induced cataract to Sect. K.8.1.6,
- effect on galactose feeding-induced cataract to Sect. K.8.1.7,
- effect on naphthalene induced cataract to Sect. K.8.1.8,
- immunological methods to Sect. I.2.2.16.

Nevertheless, ocular pharmacology is a special issue, which justifies a special chapter in this book.

O.2 Intraocular Pressure

O.2.1 Acute Measurement of Intraocular Pressure

PURPOSE AND RATIONALE

For evaluation of drugs, intraocular pressure is measured in normal animals or in animals with experimental glaucoma.

PROCEDURE

New Zealand white rabbits, weighing 2.0–2.5 kg, are acclimated to the laboratory environment at least

one day prior to experimentation. Intraocular pressure (IOP) measurements consist of topically administering one drop (approximately 50 µl) of a short-acting local anesthetic (Ophthaine 0.5%) directly on the eyes of an unrestrained rabbit. Approximately 40–45 s following local anesthetic administration, an IOP reading for each eye is taken for 10 s and recorded as mm Hg. IOP is determined by applanation pneumotonometry using an Alcon pneumotonograph modified for the rabbit eye (Vareilles et al. 1977).

On the day of the experiment, two baseline IOP measurements are determined and designated as $P_1$and P_2, respectively. The P_1 measurement is recorded 30 min prior to drug administration while the P_2 measurement occurs just prior drug or placebo administration. The P_2 measurement is designated as IOP at zero time and is used as the baseline control value for determination of percent reduction in pressure. Thus, a baseline is determined for each rabbit studied.

Immediately following the P_2 measurement, the appropriate concentration of drug or vehicle is administered topically to the right eye of 5 rabbits. This is done by placing three successive 20 µl additions directly onto the eye at two- or three-minute intervals. In addition, during drug application, the lower eyelid is held so that excess fluid is collected in the exposed conjunctival sac. Simultaneously, the left eye receives vehicle with the same regimen as the drug-treated right eye. The vehicle (control) treatment is to monitor potential contralateral ocular effects. Following drug or vehicle treatment, IOP measurement are taken at the following time periods: 0.5; 1.0; 1.5; 2.0; 3.0; 4.0; 5.0 and 6.0 h.

EVALUATION

The *IOP* of each rabbit eye for each time period is initially recorded in mm Hg. However, to account for initial *IOP* differences among rabbits, the changes in mm Hg are normalized by converting to percent reduction in outflow pressure (*ROP*).The *ROP* is calculated according to an equation proposed by Mishima (1981):

$$\%\,ROP = (Po - Pe/Po - Ep) \times 100$$

where *Po* is the *IOP* reading in mm Hg at zero time, *Pe* is the experimental *IOP* reading at the appropriate time following drug or vehicle administration and *Ep* is the episcleral venous pressure taken as a constant of 10 mm Hg. The percent *ROP* for each rabbit at each time period is recorded and grouped to determine a mean percent *ROP* for each time period as well as the duration of action. The overall activity of the drug based on the mean percent *ROP* for five rabbits is categorized as follows:

% reduction in outflow pressure	activity
10.1–20.0	slight
20.1–40.0	moderate
>40	marked

MODIFICATIONS OF THE METHOD

Rowland et al. (1981) studied circadian rhythm in intraocular pressure using repeated tonometry in **rabbits**.

Santafé et al. (1997) studied the hypotensive effects of topically applied calcium-antagonists on intraocular pressure in conscious rabbits using a manual applanation tonometer calibrated by direct manometry.

Okada et al. (1995) studied the *IOP* response to different doses of intravitreally injected endothelin-1 in rabbits using a pneumatotonometer.

Drago et al. (1997) studied the effect of repeated administration of combinations of beta-blockers with pilocarpine on *IOP* and heart rate in conscious rabbits.

Chidlow et al. (1999) investigated the effect of topical application of a HT_{1A} receptor agonist on *IOP* in normotensive rabbits using an applanation tonometer.

Goldblum et al. (2000) studied the effect of an acetylcholinesterase inhibitor on *IOP* in normotensive rabbits using a TonoPen XL.

The effect of various carbonic anhydrase inhibitors on *IOP* pressure was measured by several authors, such as Supuran et al. 1999; Briganti et al. (2000).

Burke and Potter (1986) studied the ocular effects of a relatively selective $\alpha 2$ agonist in cats, rabbits and monkeys. Intraocular pressure was measured using an Alcon pneumatonometer, and pupil diameter under constant illumination using a pupillometer. Furthermore, cat nictitating membrane responses were recorded after injections via the lingual artery into the right external artery supplying the nictitating membrane.

Moore et al. (1995) described long-term non-invasive measurement of *IOP* in the **rat** eye. Rats were anesthetized with short-acting isoflurane inhalant and *IOP* was determined by averaging 15 valid individual readings with a TonoPen 2 tonometer.

Krishna et al. (1995) studied the circadian rhythm of *IOP* in Lewis rats using a TonoPen 1 tonometer.

Diurnal variations of *IOP* in the eyes of awake male brown Norway rats were measured by Moore et al. (1996) using a TonoPen XL tonometer.

Cabrera et al. (1999) found no significant difference of *IOP* in four strains of rats using conscious, unsedated animals.

Jia et al. (2000) determined the diurnal *IOP* response of Brown Norway rat eyes after sclerosis of the aqueous humor outflow pathways and its relationship to optic nerve damage. Hypertonic saline was injected into a single episcleral vein and *IOP* measured in both the light and dark phases of the circadian cycle in awake animals.

John et al. (1997) developed a method to measure *IOP* in living **mice** of genetically different mouse strains. Eyes of anesthetized mice were cannulated with a very fine fluid-filled glass micro-needle. The micro-needle was connected to a pressure transducer and the pressure signal was analyzed with a computer system.

Miller and Rhaesa (1996) evaluated the effect of a topical α_2-agonist on *IOP*, pupil size and heart rate in normal **cats**.

Bhattacherjee et al. (1999) trained domestic adult cats to accept topical ocular drug administration and pneumotonometry. Cats received either various corticosteroids or vehicle topically to both eyes three times a day for approximately 28 days. The increase of *IOP* was found to depend on the concentration and structure of the corticosteroid.

Gelatt et al. (1997) evaluated the effects of locally applied pilocarpine preparations on *IOP* and pupil size in glaucomatous Beagle **dogs**.

Peterson et al. (1996) compared readings with the Tono-Pen, a handheld applanation tonometer based on the Mackay-Mark principle, with *IOP* measured manometrically after anterior chamber cannulation through the peripheral cornea with a 26-gauge needle connected to a vertically adjustable reservoir and a pressure transducer in cynomolgus **monkeys**.

For *in vitro* determination of carbonic anhydrase inhibition see C.1.1.1.

REFERENCES AND FURTHER READING

Bhattacherjee P, Peterson CA, Spellman JM, Graff G, Yanni JM (1999) Pharmacological validation of a feline model of steroid-induced ocular hypertension. Arch Ophthalmol 117:361–361

Briganti F, Tilli S, Mincione G, Menabuoni L, Supuran CT (2000) Carbonic anhydrase inhibitors. Metal complexes of 5-(2-chlorophenyl)-1,3,4-thiadiazole-2 sulfonamide with topical intraocular pressure lowering properties: The influence of metal ions upon the pharmacological activity. J Enzyme Inhibit 15:185–200

Burke JA, Potter DE (1986) Ocular effects of a relatively selective $\alpha 2$ agonist (UK-14, 304–18) in cats, rabbits and monkeys. Curr Eye Res 5:665–676

Cabrera CL, Wagner LA, Schork MA, Bohr DF, Cohan BE (1999) Intraocular pressure measurement in the conscious rat. Acta Ophthalmol Scand 77:33–36

Chidlow G, Nash MS, De Santi LM, Osborne NN (1999) The 5-HT_{1A} receptor agonist 8-OH-DPAT lowers intraocular pressure in normotensive NZW rabbits. Exp Eye Res 69:587–593

Drago F, Emmi I, Marino V (1997) Effects of beta-blockers association with pilocarpine on rabbit intraocular pressure and heart rate. Pharmacol Res 35:299–302

Gelatt KN, Mackay EO, Gelatt JK, Stengard-Ollies K, Aza J (1997) Effects on intraocular pressure and pupil size in glaucomatous beagles after topical pilocarpine instilled with standard (pH 5) and buffer-tip (pH 7) droptainers. J Ocul Pharmacol Ther 13:95–104

Goldblum D, Garweg JG, Bohnke M (2000) Topical rivastigmine, a selective acetylcholinesterase inhibitor, lowers intraocular pressure in rabbits. J Ocul Pharmacol Ther 16:29–35

Jia L, Cepurna WO, Johnson EC, Morrison JC (2000) Patterns of intraocular pressure elevation after aqueous humor outflow obstruction in rats. Invest Ophthalmol Vis Sci 41:1380–1385

John SW, Hagaman JR, MacTaggart TE, Peng L, Smithes O (1997) Intraocular pressure in inbred mouse strains. Invest Ophthalmol Vis Sci 38:249–253

Krishna R, Mermoud A, Baerveldt G, Minckler DS (1995) Circadian rhythm of intraocular pressure: a rat model. Ophthalmic Res 27:163–167

Miller PE, Rhaesa SL (1996) Effects of topical administration of 0.5% apraclonidine on intraocular pressure, pupil size, and heart rate in clinically normal cats. Am J Vet Res 57:83–86

Mishima S (1981) Clinical pharmacokinetics of the eye. Invest Ophthalmol Vis Sci 21:504–541

Moore CG, Epley D, Milne ST, Morrison JC (1995) Long-term non-invasive measurement of intraocular pressure in the rat eye. Curr Eye Res 14:711–717

Moore CG, Johnson EC, Morrison JC (1996) Circadian rhythm of intraocular pressure in the rat. Curr Eye Res 15:185–191

Okada K, Sugiyama K, Haque MS, Taniguchi T, Kitazawa Y (1995) The effects of endothelin-1 on intraocular pressure and pupillary diameter in rabbits. Jpn J Ophthalmol 39:233–241

Peterson JA, Kiland JA, Croft MA, Kaufman PL (1996) Intraocular pressure measurement in cynomolgus monkeys. Tono-Pen versus manometry. Invest Ophthalmol Vis Sci 37:1197–1199

Rowland JM, Potter DE, Reiter RJ (1981) Circadian rhythm in intraocular pressure: a rabbit model. Curr Eye Res 1:169–173

Santafé J, Martínez de Ibarreta MJ, Segarra J, Melena J (1997) A long-lasting hypotensive effect of topical diltiazem on the intraocular pressure in conscious rabbits. Naunyn-Schmiedeberg's Arch Pharmacol 355:645–650

Supuran CT, Scozzafava A, Menabuoni L, Mincione F, Briganti F, Mincione G (1999) Carbonic anhydrase inhibitors. Part 71. Synthesis and ocular pharmacology of a new class of water-soluble, topically effective intraocular pressure lowering sulfonamides incorporating picolinoyl moieties. Eur J Pharm Sci 8:317–328

Vareilles P, Conquet P, Le Douarec JC (1977) A method for the routine intraocular pressure (*IOP*) measurement in the rabbit: Range of *IOP* variations in this species. Exp Eye Res 24:369–375

0.2.2 Measurement of Intraocular Pressure by Telemetry

PURPOSE AND RATIONALE

McLaren et al. (1996), Pericot et al. (1996), Schnell et al. (1996) published methods to measure intraocular pressure by telemetry in conscious, unrestrained rabbits.

PROCEDURE

Telemetric Pressure Transducers

The implantable pressure monitors (Model TA11PA-C40; Data Sciences International, St. Paul, MN) are cylindrical, measure 25 mm in length and 15 mm in diameter, and weigh approximately 9 g. They contain a pressure transducer, a short-range amplitude modulation radiotransmitter, and a battery in a biocompatible case. Pressure is conducted to the transducer through a fluid-filled polyurethane catheter that is 15 cm long and 0.7 mm in diameter. The 3-mm distal tip of the catheter couples the transducer to the surrounding fluid; it is modified with a thin flexible wall, and the end is filled with a biocompatible gel. The thin wall conducts transient pressure changes, whereas the gel prevents mixing of the fluid in the catheter with the surrounding biological fluid and conducts slow pressure changes.

The transmitter broadcasts an amplitude modulation signal to two antenna and receiver assemblies mounted inside the animal's cage.

Implant Surgery

The transducers are implanted in rabbits weighing 2 to 3.5 kg by using aseptic conditions under anesthesia with intramuscular injections of 50 mg/kg ketamine and 5 mg/kg xylazine. A 4-cm midline incision is made on the dorsal neck and connective tissue and muscle layer over the vertebral column and between the scapulae are blunt dissected to form a pocket to contain the transducer capsule. This area is covered with moist gauze while the eye is prepared to receive the catheter.

The right eye is used in all experiments. Eyelids are retracted with an infant lid speculum, and a 7-0 silk suture is placed through the mid-corneal stroma approximately 3 mm from the superior limbus. The two ends are weighted to maintain downward rotation of the globe. The conjunctiva is opened 2 to 3 mm temporal to the superior rectus muscle and gently dissected free of the sclera back to the supertemporal orbital rim.

A 10 cm, 17-gauge catheter needle is inserted through the conjunctival opening, advanced to the orbital rim, and pushed through the orbital fascia into the subcutaneous space just behind the orbital rim. It is advanced carefully under the skin to the top of the skull and back between the ears until the tip emerges from the opening at the back of the neck. The needle is flushed with sterile saline to remove any tissue or blood it has collected.

The transducer is dipped in an antibiotic solution (1000 U/ml bacitracin and 10 mg/ml neomycin in Ringer's solution) and is placed in the pocket formed earlier in the neck. The tip of the cannula is then inserted into the bore of the 17-gauge needle and advanced carefully as far as possible. The needle is withdrawn and removed from the conjunctival opening, leaving the transducer catheter along its path. Approximately 2 cm of the catheter is left extending through the conjunctival opening.

The anterior edge of the conjunctival flap is reflected forward, and the sclera over the trabecular meshwork is scraped with a sharp, rounded blade until the trabecular meshwork is visible as a dark streak. A 21-gauge needle is inserted through this thinned tissue into the anterior chamber and withdrawn, and the anterior chamber is refilled through the same opening with Healon. The catheter is grasped with a tube forceps and is inserted through the opening into the anterior chamber. The tip is advanced to approximately mid pupil. Care is taken not to touch the corneal endothelium.

The catheter is secured to the sclera with three 9-0 or 10-0 nylon sutures. Each is tied securely around the catheter three times and its ends passed through the sclera before they are tied together. One 8-0 silk suture is also tied tightly three times around the catheter to promote formation of granulation tissue. The catheter is pulled gently back toward the transducer to remove the excess loop in the orbit.

The capsule is anchored in the pocket on the neck. Again, care is taken, not to nick or make any sharp bends in the catheter. The muscle layer and the skin are closed so that the entire transducer and the catheter assembly are located internally.

For measurement of intraocular pressure lowering drugs, ocular hypertension caused by injection of 5% glucose is used. The rabbits are left undisturbed for 30 min before the beginning of telemetric intraocular pressure measurements. One measurement is recorded every 15 s for 5 s with a sampling rate of 250 Hz. Fifty µl of test solution or saline are instilled into the conjunctival sac of the implanted eye and intraocu-

lar pressure is recorded for the next 60 min. A sterile 5% glucose solution (20 ml/kg) is then injected into the marginal vein of the ear. Intraocular pressure is recorded for the next 40 min. All studies are performed using a cross-over protocol. A wash-out period of 5 days is allowed between experiments.

EVALUATION

For statistical analysis, the average values of data collected over the time period of interest are calculated for individual animals. For comparisons within groups, statistical analysis is performed on averaged date using two-tailed Student's *t*-test for paired data or unpaired test for unpaired data.

MODIFICATIONS OF THE METHOD

Pericot et al. (1996) induced chronic ocular hypertension by a single injection of α-chymotrypsin into the posterior ocular chamber of rabbits anesthetized by an intramuscular injection of 35 mg/kg ketamine and 4 mg/kg xylazine. Continuous intraocular pressure was measured by telemetry and the effects of timolol, dorzolamide, and epinephrine. The transmitter of a miniaturized radiotelemetry system was implanted into rabbits, and its catheter was tunneled subcutaneously to the superior conjunctival sac and inserted into the midvitreous.

Dinslage et al. (1998) recorded the effects of tonometry, handling, water drinking, and instillation of topical ophthalmic medications on *IOP* by telemetry in rabbits for several months during each 24-h day/night cycle.

McLaren et al. (1999) measured the effects of topical ibopramine and epinephrine on the circadian rhythm of *IOP* in undisturbed rabbits by telemetry.

REFERENCES AND FURTHER READING

Dinslage S, McLaren J, Brubaker R (1998) Intraocular pressure in rabbits by telemetry. II: effect of animal handling end drugs. Invest Ophthalmol Vis Sci 39:2485–2489

McLaren JW, Brobaker RF, Fitz-Simon JS (1996) Continuous measurement of intraocular pressure by telemetry. Invest Ophthalmol Vis Sci 37:966–975

McLaren JW, Bachman LA, Brubaker RF (1999) Comparison of effects of topical ibopramine and epinephrine on the circadian rhythm of intraocular pressure of the rabbit eye as measured by telemetry. J Ocul Pharmacol Ther 15:107–116

Pericot CL, Schnell CR, Debon C, Hariton C (1996) Continuous intraocular pressure measurement by telemetry in alpha-chymotrypsin-induced glaucoma model in the rabbit: Effects of timolol, dorzolamide, and epinephrine. J Pharmacol Toxicol Meth 36:223–238

Schnell CR, Debon C, Pericot CL (1996) Measurement of intraocular pressure by telemetry in conscious, unrestrained rabbits. Invest Ophthalmol Vis Sci 37:958–965

0.3 Aqueous Humor Flow Rate

PURPOSE AND RATIONALE

Aqueous humor flow rate can be determined by ocular fluorophotometry (Ogidigben et al. 1993, 1994).

PROCEDURE

New Zealand White rabbits weighing 2.5–4 kg of either sex are used. For unilateral sympathectomy, the animals are anesthetized with a dose of ketamine/xylazine (44/8 mg/kg i.v.). Through a midline incision in the neck, the cervical sympathetic nerve trunk is isolated from both the vagus and the common carotid artery by blunt dissection. To be sure that the isolated nerve is the sympathetic trunk, it is electrically stimulated with a square-wave pulse of 4 Hz (0.7-ms duration, 5-s train) at 4 V with a bipolar electrode connected to a Grass SD9 stimulator; dilatation of the rabbit's pupil is satisfactory confirmation of nerve isolation. The preganglionic sympathetic trunk and superior cervical ganglion are severed and removed. During 1–2 weeks post surgery, sympathetically denervated eyes of rabbits are examined for persistent miosis and ptosis.

The corneas of adult rabbits are treated bilaterally by instilling 2% fluorescein topically, 1 drop every 5 min for a period of 30 min (Brubaker 1989). Subsequently, fluorescein concentrations in the cornea and anterior chamber are measured using a Fluorotron Master (Coherent Medical Inc., Palo Alto, CA). Basal aqueous humor flow rates are established both in sympathetically denervated and normal eyes. In the following week, groups of rabbits are treated bilaterally with the test drug or with vehicle. Fluorometry recordings are started 30 min after drug or vehicle administration, and subsequent recordings are made every hour for a total of 5 h.

EVALUATION

Student's *t*-tests for paired data are used to evaluate drug-induced changes.

CRITICAL ASSESSMENT OF THE METHOD

The study in hemi-sympathectomized animals allows the separation of direct drug effects from effects exerted via the sympathetic nervous system

MODIFICATIONS OF THE METHOD

According to Yablonski et al. (1978), the acute decrease in intraocular pressure caused by timolol can be explained entirely by its effect on the aqueous humor flow.

The effect of various compounds on aqueous humor inflow into the posterior chamber of the **rabbit** eye can be used to determine the mechanism of action and to compare the potency of *IOP* lowering compounds. Aqueous humor production is indirectly quantified in the New Zealand white rabbit by means of the *IOP* recovery rate assay of Vareilles and Lotti (1981). After a control pneumotonographic *IOP* measurement, a 20% NaCl solution is infused i.v. into the marginal ear vein of a rabbit at a rate of 1 ml/min for 10 min using an infusion pump. The hypertonic saline infusion causes a rapid and marked fall in *IOP* with a peak reduction occurring 15 min after the start of infusion. Thereafter, the pressure gradually returns to normal over the ensuing 120 min in normal rabbits. Compounds under study are solubilized in a suitable vehicle. Sixty min prior to NaCl infusion, the drugs are instilled directly onto both eyes as three successive 20 µl drops with each drop separated by two or three min. Following the NaCl infusion, the intraocular pressures of both eyes are measured at 5, 10, 15, 30, 60, 90 and 120 min and then every 30 min until *IOP* recovers to preperfusion values. The mean of the *IOP* for the 2 eyes is recorded and plotted against time. The *IOP* recovery rate is then expressed as the slope of the *IOP* recovery line calculated from the points 15 min from the start of NaCl infusion to the ensuing 120 min by means of the least squares method. The difference in slope and percentage change between control and that produced by experimental compounds are analyzed using an unpaired Student's *t*-test. A compound which lowers *IOP* by reducing aqueous humor flow will exhibit a prolonged *IOP* recovery rate as evidenced by a shallow slope compared to that produced by vehicle.

Taarnhøj et al. (1990) reported calibration of measurements *in vivo* of fluorescein in the rabbit cornea. The quenching was measured by four different techniques: (1) by elution of fluorescein, (2) by elution of albumin, (3) by polarization of fluorescence, and (4) by spectrofluorometry. Quenching of fluorescence of fluorescein in the rabbit cornea can be explained by the interaction of fluorescein and albumin in the cornea.

Burke and Schwartz (1996) surveyed the preclinical data on aqueous humor flow and intraocular pressure of brimonidine.

Beilin et al. (2000) characterized the *IOP* lowering activity and possible mechanism of action of a synthetic, non-psychotropic cannabinoid after i.v. administration in rabbits measuring *IOP* by pneumatonometry, aqueous humor inflow rate by fluorophotometry, blood pressure and heart rate by a computerized physiograph system connected to the central ear artery.

Mermoud et al. (1996) established methods to determine normal outflow facility using anterior chamber infusion with constant pressure and aqueous humor production by a technique of dilution with FITC-albumin in Lewis **rats**.

Tian et al. (1997) determined the effects of adenosine agonists on intraocular pressure with an minified Goldmann applanation tonometer and aqueous humor dynamics by fluorophotometry in cynomolgus **monkeys**.

REFERENCES AND FURTHER READING

Beilin M, Neumann R, Belkin M, Green K, Bar-Ilan A (2000) Pharmacology of the intraocular pressure (*IOP*) lowering effect of systemic dexanabinol (HU-211), a non-psychotropic cannabinoid. J Ocul Pharmacol Ther 16:217–230

Brubaker RF (1989) Measurement of aqueous flow by fluorophotometry. In: Ritch R, Shields MB, Krupin R (eds) The glaucomas. CV Mosby Co., St. Louis, pp 337–344

Burke J, Schwartz M (1996) Preclinical evaluation of brimonidine. Surv Ophthalm 41, Suppl 1:S9–S18

Mermoud A, Baerfelder G, Minckler DS, Prata JA, Rao NA (1996) Aqueous humor dynamics in rats. Graefe's Arch Clin Exp Ophthalmol 234, Suppl 1:S198–203

Ogidigben M, Chu TC, Potter DE (1993) Ocular hypotensive action of a dopaminergic (DA_2) agonist, 2,10,11-trihydroxy-N-n-propylnoraporphine. J Pharmacol Exp Ther 267:822–827

Ogidigben M, Chu TC, Potter DE (1994) Ocular actions of moxonidine: a possible role for imidazoline receptors. J Pharmacol Exp Ther 269:897–904

Taarnhoj J, Schlecht L, McLaren JW, Brubaker RF (1990) Calibration of measurements *in vivo* of fluorescein in the cornea. Exp Eye Res 51:113–118

Tian B, Gabelt BT, Crosson CE, Kaufman PL (1997) Effects of adenosine agonists on intraocular pressure and aqueous humor dynamics in cynomolgus monkeys. Exp Eye Res 64:979–989

Vareilles P, Lotti VJ (1981) Effects of timolol on aqueous humor dynamics in the rabbit. Ophthalm Res 13:72–79

Yablonski ME, Zimmerman TJ, Waltman SR, Becker B (1978) A fluorophotometric study of the effect of timolol on aqueous humor dynamics. Exp Eye Res 27:135–142

0.4 Experimental Glaucoma

0.4.1 Alpha-Chymotrypsin Induced Glaucoma in Rabbits

PURPOSE AND RATIONALE

Sears and Sears (1974) induced glaucoma in rabbits by intraocular injection of alpha-chymotrypsin. Several other animal models resembling glaucoma in human beings have been reviewed (Gelatt 1977).

PROCEDURE

Male New Zealand rabbits weighing about 2 kg are pretreated with 10 mg/kg i.p. indomethacin to prevent the otherwise immediate onset of inflammation and

then slightly anesthetized with pentobarbital to eliminate any nystagmus. The right eye is anesthetized topically with 2% lidocaine. The anterior chamber is cannulated with a 30-gauge needle attached to a reservoir set at a pressure of 25 mm Hg. Then a second cannula, 32-gauge, is introduced into the anterior chamber near the limbus and directed to the posterior chamber through the pupil. A sterile isotonic saline solution (0.5 ml) containing 150 units of alpha-chymotrypsin is irrigated through the cannula into the posterior chamber. Care is taken to avoid the injection of any enzyme into the corneal stroma. Both cannulae are then removed without significant loss of aqueous humor. The eyes are examined at daily intervals for the first week, then on alternate days for the second week, and then weekly for the duration of the experiments. Intraocular pressure is measured with a tonometer adapted for rabbit eyes.

Treatment with drugs is performed before and after surgery.

EVALUATION

Intraocular pressure of animals treated with alpha-chymotrypsin and those treated additionally with drugs is expressed as mean ± SEM and compared statistically with untreated controls using ANOVA followed by Student's *t*-test.

MODIFICATIONS OF THE METHOD

Melena et al. (1998a) measured the effect of topical dihydroergocristine on *IOP* in alpha-chymotrypsin-induced ocular hypertensive **rabbits** with a pneumatonometer.

Drago et al. (1997) measured the effects of beta-blockers combined with pilocarpine on rabbit intraocular pressure. Experimental increase of intraocular pressure was induced by a subconjunctival injection of betamethasone-21-phosphate (4 mg/ml) in both eyes every week for 4 weeks. The intraocular pressure was measured in conscious rabbits using an electronic pneumotonometer after surface anesthesia with one drop of 0.4% benoxinate solution.

Melena et al. (1997) induced ocular hypertension in rabbits by weekly subconjunctival injection of a betamethasone suspension into the left eye and measured *IOP* with a manometrically calibrated pneumatonograph.

With the same method, Melena et al. (1998b) measured the effect of topical diltiazem on the rise of *IOP* and the effect on established ocular hypertension.

Santafe et al. (1999) induced ocular hypertension in rabbits by oral administration of 60 ml/kg tap water and measured the effect of topical diltiazem on *IOP*.

Balaban et al. (1997) studied the mechanisms of vasopressin effects on intraocular pressure in anesthetized **rats** after cannulation of the anterior chamber of the eye and infusions of artificial cerebrospinal fluid or arginine vasopressin solutions.

Mermoud et al. (1994) described an animal model of uveitic glaucoma. Uveitis was induced in Lewis rats by injection of S-antigen.

Morrison et al. (1998) produced scarring of the aqueous humor outflow pathways by unilateral episcleral vein injections of hypertonic saline in Brown Norway rats and measured *IOP* and optical nerve damage after topical treatment with artificial tears, 0.5% betaxolol, or 0.5% apraclonidine.

Ueda et al. (1998) described an experimental glaucoma model in the rat induced by laser trabecular photo-coagulation after an intracameral injection of India ink.

Gu et al. (2000) induced experimental glaucoma in the right eyes of Wistar albino rats by intracameral injection of India ink followed by laser trabecular photocoagulation 4 days later. The left eye served as control. Drugs were injected intraperitoneally just before trabecular photocoagulation. Five days later, 3% fast blue was injected into both superior colliculi. The eyes were enucleated another 3 days later and flat mounts of the retinas were prepared. Labeled ganglion cells were counted in the area 1 mm away from the optical disc.

Wang et al. (1997) induced glaucoma in one eye of cynomolgus **monkeys** by repeated argon laser photocoagulation or diode photocoagulation of the mid-trabecular meshwork to study the effects of 5-methylurapidil.

Schmidt et al. (1998) induced glaucoma in rhesus monkeys by 2–3 laser treatments of one eye and measured *IOP*, ocular pulse amplitude and peak pulse blood volume after treatment with anti-glaucoma drugs.

Serle et al. (1998) studied the effect of prostanoid derivates on *IOP* and aqueous humor flow rates in cynomolgus monkeys with unilateral laser-induced glaucoma.

REFERENCES AND FURTHER READING

Balaban CD, Palm DE, Shikher V, Searles RV, Keil LC, Severs WB (1997) Mechanisms for vasopressin effects on intraocular pressure in anesthetized rats. Exp Eye Res 65:517–531

Caprioli J (1985) The pathogenesis and medical management of glaucoma. Drug Dev Res 6:193–215

Drago F, Emmi I, Marino V (1997) Effects of beta-blockers association with pilocarpine on rabbit intraocular pressure and heart rate. Pharmacol Res 35:299–302
Gelatt KN (1977) Animal models for glaucoma. Invest Ophthalmol 16:592–596
Gu Z, Yamamoto T, Kawase C, Matsubara M, Kawase K, Sawada A, Kitazawa Y (2000) Nippon Ganka Gakkai Zasshi 104:11–16
Friedland BR, Maren TH (1984) Carbonic anhydrase: Pharmacology of inhibitors and treatment of glaucoma. In: Pharmacology of the Eye. Handbook Exp Pharmacol 69:279–309
Melena J, Santafe J, Segarra J (1997) Betamethasone-induced ocular hypertension in rabbits. Methods Find Exp Clin Pharmacol 19:553–558
Melena J, Santafe J, Segarra J (1998a) The effect of topical dihydroergocristine on the intraocular pressure in alpha-chymotrypsin-induced ocular hypertensive rabbits. Methods Find Exp Clin Pharmacol 20:861–867
Melena J, Santafe J, Segarra J (1998b) The effect of topical diltiazem on the intraocular pressure in betamethasone-induced ocular hypertensive rabbits. J Pharmacol Exp Ther 284:278–282
Mermoud A, Baerveldt G, Mickler DS, Wu GS Rao NA (1994) Animal model of uveitic glaucoma. Graefe's Arch Clin Exp Ophthalmol 232:553–560
Morrison JC, Nylander KB, Lauer AK, Cepurna WO, Johnson E (1998) Glaucoma drops control intraocular pressure and protect optic nerves in a rat model of glaucoma. Invest Ophthalmol Vis Sci 39:526–531
Santafe J, Martinez de Ibarreta MJ, Segarra J, Melena J (1999) The effect of topical diltiazem on ocular hypertension induced by water loading in rabbits. Gen Pharmacol 32:201–205
Schmidt KG, von Ruckmann A, Eisenmann D, Stegmann DY, Mittag TW (1998) Peak pulse blood volume and topical antiglaucoma drugs in rhesus monkeys with experimental open angle glaucoma. (Pulsgipfelblutvolumen und topische Antiglaukomatosa bei Rhesusaffen mit experimentellem Offenwinkelglaukom.) Klin Monatsbl Augenheilkd 213:341–346
Serle JB, Podos SM, Kitazawa Y, Wang RF (1998) A comparative study of latanoprost (Xalatan) and isopropyl unoprostone (Rescula) in normal and glaucomatous monkey eyes. Jpn J Ophthalmol 42:95–100
Sears D, Sears M (1974) Blood-aqueous barrier and alpha-chymotrypsin glaucoma in rabbits. Am J Ophthalm 77:378–383
Ueda J, Sawaguchi S, Hanyu T, Yaoeda K, Fukuchi T, Abe H, Ozawa H (1998) Experimental glaucoma model in the rat induced by laser trabecular photocoagulation after an intracameral injection of India ink. Jpn J Ophthalmol 42:337–344
Wang RF, Lee PY, Mittag TW, Podos SM, Serle JB (1997) Effect of 5-methylurapidil, an α_{1a}-adrenergic antagonist and 5-hydroxytryptamine$_{1a}$ agonist, on aqueous humor dynamics in monkeys and rabbits. Curr Eye Res 16:769–775

0.4.2 Episcleral Venous Occlusion Induced Glaucoma in Rats

PURPOSE AND RATIONALE

The importance of trabecular and uvosceral outflow for the treatment of glaucoma has been underlined by Woodward and Gil (2004). Shareef et al. (1995), Sawada & Neufeld (1999), Neufeld et al. (1999) described a rat model of chronic elevated intraocular pressure.

PROCEDURE

Male Wistar rats weighing about 250 g are anesthetized with a mixture of 80 mg/kg ketamine and 12 mg/kg xylazine given intraperitoneally. All ocular surgical manipulations are unilateral, the contralateral eye serving as control. A 2-mm-long incision through the conjunctiva and Tenon's capsule is made on the limbal periphery of the eye. Two radial relaxing incisions are made at the edges of the initial incision. The tissue is recessed posteriorly exposing the underlying extraocular muscle, which is isolated and anchored by a suture to expose the underlying episcleral vein. The episcleral veins are identified by their location (slightly deeper than the ocular muscles), relative immobility, larger caliber, branching pattern, the darker blood contained and their communication with a limbal venous plexus. In contrast, the arteries travel a relatively straight course and communicate with a single perilimbal artery. In most cases, four episcleral veins are noted. By manipulating the anchored muscles, a hand-held cautery is applied to the veins. After ocular surgery, the eyes are treated with an antibiotic ointment.

Immediately after surgery, intraocular pressure rises from 12 mm Hg up to at least 20 mm Hg, remaining at this level for months.

This model is used more recently to study biochemical changes during elevated intraocular pressure and/or to study effects of drugs for antiglaucoma effects. Neufeld et al. (1999) treated a group of rats with aminoguanidine, a relatively selective inhibitor of nitric-oxide synthase 2 in the drinking water for 6 months. Tsai (2005) studied the effects of erythropoietin and the preservation of ganglion cells during glaucoma. Sarup (2005) reported on the effects of dorzolamide and timolol on glaucomatous eyes. Guo (2006) studied the effects of glutamate on glaucoma.

EVALUATION

Once a week, each animal is anesthetized (xylazine/ketamine) and intraocular pressure is determined bilaterally using a pneumotonometer. On any given eye, three to five tonometer readings are taken and averaged. On a given day, mean ± SD is derived for all control and surgical eyes. Significant differences between surgical and control eyes are determined by χ^2 analysis with Student's t test for independent means

for each day on which measurements are performed. Furthermore, IOP between treated and non-treated animals is compared.

MODIFICATIONS OF THE METHOD

WoldeMussie et al. (2001, 2002) induced chronic ocular hypertension in rats using laser photocoagulation with a blue-green argon laser.

REFERENCES AND FURTHER READING

Guo L, Salt TE, Maass A, Luong V, Moss SE, Fitzke FW, Cordeiro MF (2006) Assessment of neuroprotective effects of glutamate, modulation on glaucoma-related retinal ganglion cell apoptosis in vivo. Invest Ophthalmol Vis Sci 47:626–33

Neufeld AH, Sawada A, Becker B (1999) Inhibition of nitric-oxide synthase 2 by aminoguanidine provides neuroprotection of retinal ganglion cells in a rat model of chronic glaucoma. Proc Natl Acad Sci USA96:9944–0048

Sarup V, McEwan GC, Thompson C, Patil KA, Sharma SC (2005) Dorzolamide and timolol saves retinal ganglion cells in glaucomatous adult rats. J Ocul Pharmacol Ther 21:454–462

Sawada A, Neufeld AH (1999) Confirmation of the rat model of chronic, moderately elevated intraocular pressure. Exp Eye Res 69:525–531

Shareef SR, Garcia-Valenzuela E, Salierno A, Walsh J, Sharma SC (1995) Chronic ocular hypertension following episcleral venous occlusion in rats. Exp Eye Res 61:179–182

Tsai JC, Wu L, Worgu B, Forbes M, Cao J (2006) Intravitreal administration of erythropoietin and preservation of retinal ganglion cells in an experimental rat model of glaucoma. Curr Eye Res 30:1025–1031

WoldeMussie E, Ruiz G, Wijono M, Wheeler LA (2001) Neuroprotection of retinal ganglion cells by brimonidine in rats with laser-induced chronic ocular hypertension. Invest Ophthalmol Vis Sci 42:2849–2855

WoldeMussie E, Yoles E, Schwartz M, Ruiz G, Wheeler LA (2002) Neuroprotective effect of Memantine in different retinal injury models in rats. J Glaucoma 11:474–480

Woodward DA, Gil DW (2004) The inflow and outflow of antiglaucoma drugs. Trends Pharmacol Sci 25:238–241

0.4.3 Photocoagulation Induced Glaucoma in Monkeys

PURPOSE AND RATIONALE

Lee et al. (1985), Woodward et al. (2003) used a method originally described by Gaasterland and Kupfer (1974) for the production of sustained, elevated intraocular pressure in the rhesus monkey by repeated, circumferential argon laser photocoagulation of the mid-trabecular meshwork.

PROCEDURE

Cynomolgus or rhesus monkeys are anesthetized with systemic pentobarbital and placed at the slit lamp delivery system of the argon laser. Both eyes are treated with topical proparacaine 0.5% and photocoagulated using a modified Koeppe-type gonioscopy lens with hydroxypropylmethylcellulose as the filling fluid. Approximately 200 laser applications are made to each eye, aimed at the middle of the trabecular meshwork, using a 50 µbeam diameter, 0.2 to 0.5 second duration and 0.4 to 0.8 watts of power. Slit lamp and fundus examination are repeated every 5 to 8 days.

Drugs are applied locally as solutions with a drop size of 50 µl. Intraocular pressure is recorded in 6-h diurnal curves at 9:30 a.m., 10:00 a.m., 10:30 a.m., 11:30 a.m., 12:30 p.m., 1:30 p.m., 2:30 p.m., and 3:30 p.m. The baseline diurnal curve serves as control and is made 1 or 2 days before the experimental diurnal curve. On the experimental day, baseline intraocular pressure is measured at 9:30 a.m. The test drugs are administered to both eyes of the monkey immediately after the 9:30 a.m. measurement.

This procedure has also been applied by Kielczewski et al. (2005).

EVALUATION

The intraocular pressures on the treated day are compared to that of the control day. Alternatively, the differences in intraocular pressures at intervals after therapy between the treated and control day measurements are compared to the initial (0 hour) differences between the treated and control day values.

REFERENCES AND FURTHER READING

Chan HH, Leung MC, So KF (2005). Electroacupuncture provides a new approach to neuroprotection in rats with induced glaucoma (2005) J Altern Complement Med 11:315–322

Gaasterland D, Kupfer C (1974) Experimental glaucoma in the rhesus monkey. Invest Ophthalmol 13:455–457

Lee PY, Podos SM, Howard-Williams JR, Severin CH, Rose AD, Siegel MJ (1985) Pharmacological testing in the laser-induced monkey glaucoma model. Curr Eye Res 4:775–781

Kielczewski JL, Pease ME, Quigley HA (2005) The effect of experimental glaucoma and optic nerve transection on amacrine cells in the rat retina.. Invest Ophthalmol Vis Sci 46:3188–3196

Woodward DF, Kraus AHP, Chen J, Liang Y, Li C, Protzman CE, Bogardus A, Chen R, Kedzie KM, Krauss HA, Gil DW, Kharlamb A, Wheller LA, Babusis D, Welty D, Tang-Liu DDS, Cherukury M, Andrews SW, Burk RM, Garst ME (2003) Pharmacological characterization of a novel antiglaucoma agent, Bimatoprost (AGN 192024). J Pharmacol Exp Ther 305:772–785

Woodward DA, Gil DW (2004) The inflow and outflow of antiglaucoma drugs. Trends Pharmacol Sci 25:238–241

0.5 Local Anesthesia of the Cornea

PURPOSE AND RATIONALE

Surface anesthesia of the cornea is a prerequisite for ophthalmic surgery. Sigmund Freund studied the phar-

macological actions of cocaine and Carl Koller introduced cocaine in 1884 into clinical practice as a topical anesthetic. In pharmacology, following the pioneering work of Sollmann (1918), block of the rabbit corneal reflex as described by Régnier (1923) has become a standard test method for evaluating local anesthetics (Quevauviller 1971; Muschaweck et al. 1986). A detailed description of methods to evaluate the activity of compounds for surface anesthesia is given in Sect. G.1.3.1.

REFERENCES AND FURTHER READING

Muschaweck R, Habicht R, Rippel R (1986) Lokalanaesthetica. In: Ehrhart G, Ruschig H (eds) Arzneimittel. Entwicklung – Wirkung – Darstellung. Verlag Chemie GmbH, Weinheim. pp 1–44

Quevauviller A (1971) Experimental methods for comparing local anesthetic activity. In: Radouco-Thomas (ed) International Encyclopedia of Pharmacology and Therapeutics. Section 8: Local Anesthetics (Lechat P, Section editor) Vol I, Pergamon Press, Oxford New York, pp 291–318

Régnier MJ (1923) Essai de mesure de l'anesthésie produite sur les terminaisons nerveuses de la cornée par les anesthésiques locaux. Comparaison des pouvoirs anesthésiques de la cocaïne, de la novocaïne et de la stovaïne. C R hebd Scéances Acad Sci 177:558–560

Sollmann T (1918) Comparison of activity of local anesthetics. IV. Anesthesia of rabbit's cornea. J Pharmacol Exp Ther 11:17–25

0.6 Experimental Cataract Formation

PURPOSE AND RATIONALE

Cataract formation can be induced experimentally by various procedures, such as

- **streptomycin** treatment (see Sect. K.8.1.6),
- **galactose feeding** (see Sect. K.8.1.7),
- **naphthalene** treatment (see Sect. K.8.1.8).

Another procedure to induce experimental cataract is treatment of young rats with **selenite**. A review of this model was given by Shearer et al. (1997). Oštádalová et al. (1978) induced cataract by administration of a single dose of sodium selenite to suckling rats.

PROCEDURE

Male Wistar rats are used. On the 2nd day of life, the sucklings are divided in such a way that 8 males were kept with one mother. On the 10th day of life (i. e., when they are in absolute nutritive dependence of the mother) a single dose of 0.02 M solution of Na_2SeO_3 is administered s.c. to 5 experimental groups receiving 5, 10, 20, 40 and 60 µmoles/kg, respectively. The first control group receives s.c. a 0.02 M solution of a sulphur compound (Na_2SO_3), i. e., an element homologous with selenium, at a dose of 60 µmoles/kg. As reference group, 2-months-old male rats are used to which a 0.02 M solution of Na_2SeO_3 is administered s.c. in an amount of 20 µmoles/kg. Mothers of the sucklings as well as the group of adult males, are fed on a standard laboratory diet with water ad libitum. All animals are checked daily and the experiment is terminated 20 days after the treatment.

Cataracts in the sucklings are visible by the naked eye after the opening of their eyes, i. e., on the 14–16th day of life. The opacity is yellowish-white, localized in the center of the lens (nuclear cataract). Two forms are observed: permanent cataracts, persisting through the whole experimental period, and intermittent cataracts, which disappear after some time and reappear after a certain delay. Doses of 40 and 20 µmoles/kg are mostly associated with permanent cataract, the dose of 10 µM/kg causes an uneven distribution of both types of cataracts. The cataractogenic effect is not found in adult animals.

EVALUATION

Dose-dependence of the incidence of cataracts is evaluated using the χ^2-test.

MODIFICATIONS OF THE METHOD

Anderson et al. (1988) observed massive cortical cataract 15–30 days after a single injection of an overdose of sodium selenite into 14-day-old rats.

Watanabe and Shearer (1989) studied the release of crystallins from the lens into aqueous an vitreous humor in rats with a selenite overdose cataract.

Huang et al. (1991) studied DNA damage, repair, and replication in selenite-induced cataract in rat lens.

Huang et al. (1992) observed cataract formation in lenses from rat receiving multiple, low doses of sodium selenite.

Kelley et al. (1993) demonstrated a marked reduction in alpha-crystallin chaperone activity by calpain II in selenite cataract induced in young rats.

Zhao and Shichi (1998) tested the prevention of cataract and other ocular tissue damage induced by injection of 350 mg/kg **acetaminophen** and induction of cytochrome P450 in C57BL/6 mice.

Kojima et al. (1996), Shui et al. (1997) studied cataract formation in Brown Norway rats treated with X-ray irradiation and **corticosteroids** using slit lamp microscopy, photography with a Scheimpflug camera and scanning electron microscopy.

Hatano and Kojima (1996) induced cataract in Brown Norway rats by **UV-B irradiation** and pretreatment with **l-buthionine sulfoximine**.

Ishida et al. (1997) treated adult rats with oral doses of 0.2, 1 or 5 mg/kf **FK506 (tacrolimus)** over 13 weeks. In the highest dose, cataract development was observed.

Cataract formation in **transgenic mice** was studied by Mitton et al. (1996) and by Cammarata et al. (1999).

REFERENCES AND FURTHER READING

Anderson RS, Trune DR, Shearer TR (1988) Histologic changes in selenite cortical cataract. Invest Ophthalm Vis Sci 29:1418–1427

Cammarata PR, Zhou C, Chen G, Singh I, Reeves RE, Kuszak JR, Robinson ML (1999) A transgenic animal model of osmotic cataract. Part 1: over-expression of bovine Na^+/myo-inositol cotransporter in lens fibers. Invest Ophthalmol Vis Sci 40:1727–1737

Hatano T, Kojima M (1996) UV-b-induced cataract model in brown-Norway rat eyes combined with preadministration of buthionine sulfoximine. Ophthalmic Res 28, Suppl 2:54–63

Holmen JB, Ekesten B, Lundgren B (1999) Naphthalene-induced cataract model in rats: A comparative study between slit and retroillumination images, biochemical changes and naphthalene dose and duration. Curr Eye Res 19:418–425

Huang LL, Hess JL, Bunce GE (1991) DNA damage, repair, and replication in selenite-induced cataract in rat lens. Curr Eye Res 9:1041–1050

Huang LL, Zhang CY, Hess JL, Bunce GE (1992) Biochemical changes and cataract formation in lenses from rat receiving multiple, low doses of sodium selenite. Exp Eye Res 55:671–678

Ishida H, Mitamura T, Takahashi Y, Hisatomi A, Fukuhara Y, Murato K, Ohara K (1997) Cataract development induced by repeated oral dosing with FK506 (tacrolimus) in adult rats. Toxicology 123:167–175

Kelley MJ, David LL, Iwasaki N, Wright J, Shearer TR (1993) alpha-Crystallin chaperone activity is reduced by calpain II *in vitro* and in selenite cataract. J Biol Chem 268:18844–18849

Kojima M, Shui YB, Murano H, Sasaki K (1996) Inhibition of steroid-induced cataract in rat eyes by administration of vitamin-E ophthalmic solution. Ophthalmic Res 28, Suppl 2:64–71

Mitton KP, Kamiya T,. Tumminia SL, Russell P (1996) Cysteine protease activated by expression of HIV-1 protease in transgenic mice. MIP26 (aquaporin-0) cleavage and cataract formation *in vivo* and *ex vivo*. J Biol Chem 271:31803–31806

Oštádalová, Babický A, Obenberger J (1978) Cataract induced by administration of a single dose of sodium selenite to suckling rats. Experientia 34:222–223

Shearer TR, Ma H, Fukiage C, Azuma M (1997) Selenite nuclear cataract: Review of the model. Mol Vis 3:8–20

Shui YB, Vrensen GF, Kojima M (1997) Experimentally induced steroid cataract in the rat: a scanning electron microscopic study. Surv Ophthalmol 42, Suppl 1:S127–S132

Watanabe H, Shearer TR (1989) Lens crystallins in aqueous an vitreous humor in selenite overdose cataract. Curr Eye Res 8:479–486

Zhao C, Shichi H (1998) Prevention of acetaminophen-induced cataract by a combination of diallyl disulfide and N-acetylcysteine. J Ocul Pharmacol Ther 14:345–355

0.6.1 N-Methyl-N-Nitrosourea Cataract Induction Sprague-Dawley Rats

PURPOSE AND RATIONALE

Cataracts can be induced in rats by injection of N-methyl-N-nitrosourea (MNU). Yoshizawa et al. (2000) utilized a direct acting alkylating agent to induce cataractous lesions in neonatal stage of critical development. Longstanding evidence of lenticular tissue susceptibility to N-methyl-N-nitrosourea (Murthy et al. 1972, 1979, Roy et al., 1989, and Smith et al. 1988) and retinal tissue susceptibility to N-methyl-N-nitrosourea (Nakajima et al. 1996, Nambu et al. 1997, Taomoto et al. 1998, Yuge et al. 1996) has been documented.

PROCEDURE

Chemical and dose formulation were prepared as follows. N-Methyl-N-nitrosourea(MNU) was purchased from Nacalai Tesque (Kyoto) and kept at −20°C in the dark. Just before use, MNU solution was dissolved in physiological saline containing 0.05% acetic acid. A total of 254 rats (male: 120, female 134) received a single IP injection of 100 mg/kg body weight of MNU at 0 (day of birth), 5, 10, 15, or 20 days of age. For sequential observation the rats treated on days 0 and 5 (groups 1 and 2, respectively were killed 1, 2, 3, 5, 7, or 14 days after dosing. Those treated on days 10, 15, and 20 (groups 3, 4, and 5, respectively) were euthanized 3, 7, 14, and 30 days after dosing. The rats were observed daily for clinical signs and 8 (group 1) or 4 (groups 2–5) randomly selected rats were weighed on each examination day and euthanized. At each time point, 4 untreated rats were euthanized for comparison.

At necropsy, bilateral eyeballs were macroscopically examined and quickly removed using an operation microscope K-280 (Konan, Tokyo and complete necropsy was done on all animals.

Acquired tissue was fixed and processed. At each time point 1 eye was fixed overnight in 10% neutral buffered formalin, and the other was fixed either in Davidson solution (2 eyes of each group, in methacarn methanol:chloroform:acetic acid, 6:3:1, 2 or 4 eyes of each group), or in 2.5% glutaraldehyde solution (2 eyes of group 1). The formalin-, Davidson-, and methacarn-fixed tissues were routinely processed for paraffin embedding and stained with hematoxylin and eosin (HE), and selective sections were used for TUNEL staining. Lenses from day 0 MNU-treated rats (group 1) as well as age-matched untreated rats, prefixed in 2.5% glutaraldehyde solution, were postfixed

in 2% OsO_4 and processed for Luveak-812 embedding. One-micrometer thick sections stained with toluidine blue were used to locate areas for electron microscopy. Ultrathin sections stained with uranyl acetate and lead citrate were examined with uranyl acetate and lead citrate were examined with a Hitachi H-600 electron microscope (Hitachi, Tokyo).

EVALUATION

Cataractous lesions are examined by immunohistochemical analysis, in situ detection of apoptosis, DNA fragmentation and Western blotting of Bcl-2 and Bax Proteins, Caspase – 3/CPP 32 Protease activity assay, and cataract index. Immunohistochemical detection of 7-Methyldeoxyguanosine (7-mdGua) adducts was performed to detect DNA methylamine adducts. Per methods from Sato et al. (1986) eyes from sacrificed rats were fixed in acetone methylbenzoate xylene (Amex) and processed for paraffin embedding. Per methods by Ozaki et al. (1993), deparaffinized sections treated with 0.05 N sodium hydroxide in 40% ethanol for 15 seconds, and 1% nonfat milk in phosphate-buffered saline for 1 hour and then exposed to primary antibody (× 1,000) at 4°C overnight. Immunohistochemistry was carried out using a labeled streptavidin biotin kit (Dako, Carpineteria, CA). 3,3′-Diaminobenzidine tetrahydrochloride (DAB, Wako Pure Chemicals, Osaka) was used for antigen visualization.

In situ detection of apoptosis by TUNEL was carried out using an apoptosis detection kit (Apop-Tag, Oncor, Gaithersburg, MD). Cells with fragmented nuclei in HE-stained sections correlated well with the TUNEL-positive cells. The apoptotic index (number of fragmentation nuclei per whole nuclei × 100) was determined in HE-stained sections and compared among groups. A total of approximately 300 lens epithelial cells located in the germinative zone were counted.

DNA fragmentation was compared with apoptotic methods. The genomic DNA was isolated from the excised lenses (each sample contained 8 whole rat lens with the use of a SepaGene kit (Sanko, Tokyo) based on the guanidine thiocyanate extraction procedure. Per methods from Nambu et al. (1998) an equal amount of DNA sample (10 µg/lane) was subjected to electrophoresis on a horizontal 0.8% agarose gel containing ethidium bromide and visualized under ultraviolet illuminations.

Western Blotting of Bcl-2 and Bax proteins was performed to detect downregulation and upregulation, respectively as a downstream expression within the apoptotic cascade. Lenses were minced and homogenized in PBS (-). The homogenate was sonicated 3 times and centrifuged at 14,000 × *g* for 30 minutes. Per methods by Laemmli (1970) the supernatant was diluted with lysis buffer, and tissue extracts containing 50 µg of total protein were subjected to 12% SDS-PAGE. Proteins were blotted to nitrocellulose membrane (Bio-Rad, Hercules, CA). After the nonspecific protein binding had been blocked with 5% nonfat dry milk in PBS for 30 minutes, blots were incubated at 4°C overnight in antimous/rat Bax (PharMingen, CA. × 200 dilution in PBS with 1% BSA) or anti-Bcl-2 (PharMingen, CA, × 200) antibody. After being washed 3 times in buffer containing 1% Triton × 100, blots were incubated for 30 minutes in EnVision + (× 20, Dako Glostrup) and treated with DAB for color development. The density of each band was evaluated by computer-associated scanner densitometry (NIH image).

Caspase-3/CPP 32 Protease activity assay was used to examine for CPP-32 activation after lens epithelial cells and to differentiate a-nucleated lens fibers (Ishizaki et al. 1998). Caspase 3 activity of lenses was assayed using caspase 3/CPP32 colorimetric protease assay kit (MBL, Nagoya). Same protein samples used for western blotting were homogenized in 500 µl of lysis buffer, and homogenates were centrifuged at 10,000 × *g* for 1 minute. Supernatants were prepared to 100 µg protein/50 µl lysis buffer, and 50 µl were added to reaction buffer and incubated for 2 hours at 37°C with 200 µM DEVD (Asp-Glu-Val-Asp)-p NA substrate (MBL, Nagoya). Reactions were monitored in a microplate reader at an excitation wave length of 405 nm.

Cataract index was assigned to determine severity of cataract. In routinely prepared HE-stained tissue sections, bilateral eye specimens were evaluated based on the presence of the following 7 items: 1) lens epithelial apoptosis, 2) lens epithelial desquamation 3) multilayered spindle epithelium, 4) lens fiber swelling, 5) liquefaction/vacuolar change, 6) calcification and 7) bizarre nuclei of lens fiber cells. Each item was arbitrarily scored as absent (point 0), slight (point 1), moderate (point 2), severe (point 3), and very severe (point 4). The cataract index was the sum of each score.

MODIFICATIONS OF THE METHOD

Kiuchi et al. (2002) altered the age at injection and confirmed presence of cataracts by histological methods. Cataract was induced by single intraperitoneal injection of N-methyl-N-nitrosourea in 15-day-old Sprague-Dawley (Jcl:SD) rats. Threshold dose

of MNU required for cataract induction in a 3–4 week time period was 70 mg/kg. Males and females were both equally affected. Mature cataract was confirmed histologically by degeneration, swelling, vacuolation, liquefaction of the lens fibers and formation of Morgagni-like water vacuoles.

Miki et al. (2006) used the model to compare the effects of differences in gender and gonadal status on the occurrence of N-methyl-N-nitrosourea induced cataract and retinopathy in Lewis rats. Ovary-intact, ovariectomized, testis-intact and testectomized rats were used for the study. Castration was performed at 36 days of age, 50 mg/kg MNU was administered intraperitoneally at 50 days of age and lens and retinal changes were evaluated at 260 days of age (210 days after MNU injection). Results were assessed by cataract index and retinal damage ratio.

Kiuchi et al. (2003) adapted cataract model to examine retinal degeneration following single injection of 60 mg/kg body weight of N-methyl-N-nitrosourea into Sprague-Dawley rats. Retinal degeneration was confirmed by electroretinogram (ERG) recordings and morphometric analysis of retinal thickness and damaged retinal area. For ERG, animals were dark-adapted for 12 hours and prepared under dim red light. ERGs were recorded with a gold wire loop on the cornea using 1% tetracaine topical anesthesia and a drop of 1% methylcellulose. A gold wire electrode was placed on the sclera 1 mm from the temporal limbus. Ground electrode was placed on the ear. Signals were bandpass amplified using a computer-assisted signal averaging system. Scotopic ERG responses averaged with a stimulus interval of 3 to 60 seconds and 20–30 scotopic responses were averaged with a stimulus interval of 1 second. Strobe flash stimuli were presented in a Ganzfeld bowl (Model GS2000; LACE Electronica sel via marmiccilo, Pisa, Italy). Immediately after ERG animals were sacrificed and morphometric analysis was completed. Tissues were fixed and processed as above. Then, color images of stained sections were obtained as PICT files with a Fujix HC-2000 high-resolution digital camera (Fujifilm, Tokyo, Japan). Brightness and contrast of each image file were uniformly enhanced using Adobe Photoshop version 4.0 and images were analyzed using NIH imaging freeware. Total retinal thickness (from the internal limiting membrane to the pigment epithelium) and photoreceptor cell thickness (thickness of the outer nuclear layer and photoreceptor layer were measured and the photoreceptor ratio (photoreceptor cell thickness/total retinal thickness × 100) was calculated as described by Yoshizawa et al. (2000). Measurements were taken at the posterior pole (approximately 200 µm on either side of the optic nerve). Area of retinal damage was determined from sections prepared at megaloscopic magnification and color images obtained as PICT files using high- resolution digital slide scanner (Dimage Scan Multi: Minolta, Tokyo, Japan. Entire length of retinal and length of damaged area were measured on brightness and contrast enhanced images. Damaged area was defined as the presence of fewer than 4 photoreceptor cells in the outer nuclear layer and the retinal damage ratio was defined as length of damaged retina/length of whole retina × 100.

CRITICAL ASSESSMENT OF THE METHOD

Most animal models cause more or less complete opacification whereas human cataracts start as many focal points in different lens layers. Human lens layers include: anterior capsule, cortex, nucleus, and posterior capsule. Age related human lenticular cataractous changes are localizable in these layers and termed capsular opacities, anterior cortical cataracts, nuclear sclerosis and posterior subcapsular cataracts respectively.

REFERENCES AND FURTHER READING

Ishizaki Y, Jacobson MD, Raff MC (1998) A role for caspases in lens fiber differentiation. J Cell Biol 140:153–158

Kiuchi K, Kondo M, Ueno S, Moriguchi K, Yoshizawa K, Miyake Y, Matsumura M, Tsubura A (2003) Functional rescue of N-methyl-N-nitrosourea-induced retinopathy by nicotinamide in Sprague-Dawley rats. Curr Eye Res 26:355–362

Kiuchi K, Yoshizawa K, Moriguchi K, Tsubura A (2002) Rapid induction of cataract by a single intraperitoneal administration of N-methyl-N-nitrosourea in 15-day-old Sprague-Dawley (Jcl:SD) rats. Exp Toxic Pathol 54:181–186

Laemmli UK (1970) Cleavage of structural proteins during the assembly of the head of bacteriophage. Nature 227:680–685

Miki K, Yoshizawa K, Shikata N, Yuri T, Matsuoka Y, Tsubura A (2006) Effects of Gender and Gonad Status on N-methyl-N-nitrosourea-induced cataractogenesis and retinopathy in Lewis Rats. In Vivo 20:5–10

Murthy ASK, Vawter GF, Kopito L, Rossen E (1972) Retinal atrophy and cataract in rats following administration of N-methyl-N-nitrosourea. Proc Soc Exp Biol Med 139:84–87

Murthy ASK, Vawter GF, Peterson RA (1979) Ocular lesions and neoplasms in wistar rats after a single injection of N-methyl-N-nitrosourea. Toxicol Lett 4:439–447

Nakajima M, Yuge K, Senzaki H, Shikata N, Miki H, Uyama M, Tsubura A (1996) Photoreceptor apoptosis induced by a single systemic administration of N-methyl-N-nitrosourea in the rat retina. Am J Pathol 148:631–641

Nambu H, Yoshizawa K, Yang J, Yamamoto D, Tsubura A (1998) Age-specific and dose-dependent retinal dysplasia and degeneration induced by a single intraperitoneal administration of N-methyl-N-nitrosourea to rats. J Toxicol Pathol 11:127–131

Nambu H, Yuge K, Nakajima M, Shikata N, Takashi K, Miki H, Uyama M, Tsubura A (1979) Morphologic characteristics

of N-methyl-N-nitrosourea-induced retinal degeneration in C57BL mice. Pathol Int 47:377–383
Ozaki K, Kato T, Asamoto M, Wild CP, Montesano R, Nagao S, Iwase T, Matsumoto K, Tsuda H (1993) Decreased dimethylnitrosamine-induced O6- and N7-methyldeoxyguanosine levels correlate with development and progression of lesions in rat hepatocarcinogenesis. Jpn J Cancer Res 84:1245–1251
Roy B, Fujimoto N, Watanabe H, Ito A (1989) Induction of cataract in methylnitrosourea treated Fischer (F244) rats. Hiroshima J Med Sci 38:95–98
Sato Y, Mukai K, Watanabe S, Goto M, Shimosato Y (1986) The AmeX method: Simplified technique of tissue processing and paraffin embedding with improved preservation of antigens for immuno-staining. Am J Pathol 125:431–435
Smith SB, O'Brien PJ (1988) Biochemical characterization of retinal protein and phospholipids synthesis in mice exposed transplacentally to N-methyl-N-nitrosourea. Exp Eye Res 47:713–725
Taomoto M, Nambu H, Senzaki H, Shikata N, Oishi Y, Fujii T, Miki H, Uyama M, Tsubura A (1998) Retinal degeneration induced by N-methyl-N-nitrosourea in Syrian golden hamsters. Graefe's Arch Clin Exp Ophthalmol 236:688–695
Yoshizawa K, Oishi Y, Nambu H, Yamamoto D, Yang J, Senzaki H, Miki H, Tsubura A (2000) Cataractogenesis in Neonatal Sprague-Dawley Rats by N-Methyl-N-Nitrosourea. Toxicologic Pathology 28(4):555–564
Yoshizawa K, Yang J, Senzaki H, Uemura Y, Kiyozuka Y, Shikata N, Oishi Y, Miki H, Tsubura A (2000) Caspase-3 inhibitor rescues N-methyl-N-nitrosourea-induced retinal degeneration in Sprague-Dawley rats. Exp Eye Res 71:629–635
Yuge K, Nambu H, Senzaki H, Nakano I, Miki H, Uyama M, Tsubura A (1996) N-methyl-N-nitrosourea-induced photoreceptor apoptosis in the mouse retina. In Vivo 10:483–488

0.6.2 TGFβ Cataract Induction in Wistar Rats

PURPOSE AND RATIONALE

Hales et al. (1999) used TGFβ normally secreted by transforming cells to stimulate growth of normal cells for cataract induction. Previous studies by Lui et al. (1994) and Hales et al. (1994) reported that TGFβ specifically stimulates growth of lens epithelial cells evidenced by aberrant morphologic and molecular changes that mimic those documented in some forms of human cataract.

PROCEDURE

Male Wistar rats were killed at 15 weeks, one at 6 weeks and one at 12 weeks. Per methods by Schulz et al. (1996), following euthanizing, eyes were removed and placed in culture dishes containing Medium 199 (Trace Biosciences, Sydney, Australia) with BSA and antibiotics.

EVALUATION

Both eyes from four rats were fixed whole for routine histology to determine the influence of TGFβ on all ocular tissues. Lenses removed from remaining eyes as whole lens cultures then examined for the presence of opacities and photographed. Representative lenses and whole eyes were fixed in Carnoy's (1:3 acetic acid: ethanol) and processed for routine histology and immunolocalization. Briefly, entire lenses and whole eyes were serially sectioned and collected onto subbed glass slides. Every fifth slide was stained with hematoxylin-eosin (HE)and sections were examined for evidence of plaque formation and/or fiber deterioration. Sections corresponding to those that displayed histological changes were used for immunolocalization of β-crystallin and the extra cellular matrix proteins laminin and type I collagen. Nuclei were counterstained (Hoechst 33258; Boehringer-Mannheim, La Jolla, CA).

Photographed lenses were examined for displaying loss of clarity and changes in cellular architecture. Cell rupture of fibers if evident would be a result of needle tip penetration of capsule rather than an alteration induced by TGFβ.

Micrographs of lenses were assessed for transparency. Lack of transparency was detectable as the presence of distinct subcapsular opacities toward the anterior and/or posterior poles of the lens, or a generalized more diffuse clouding involving the cortical fiber cells.

Histological examination of serial sections compared controls vs. TGFβ eyes. Control eyes maintained a normal lens equator and bow zone and eyes injected with TGFβ revealed the characteristic appearance of lens equator and bow zone disruption histologically. An abnormal finding in eyes injected with TGFβ may also be evidenced by nucleated fiber cells in the lens cortex and extending toward the posterior pole. Mikuni (1980) and Vrensen (1995) have recognized that severe disruption of the ordered arrangement of nuclei at the rat lens equator and in the bow region as well as rat lenses that atypically retain their nuclei beyond the bow region resemble the changes in lenses associated with human cortical cataract. Finally, cataractous growth from TGFβ injected eyes was viewed for their tendency to lose their uniform curvature, as depicted by an undulating capsule.

HE stained sections were observed for plaque formation. Positive plaque formation is demonstrated in slides containing subscapsular plaques with cells appearing rounded and containing large, dense nuclei or others present with matrix deposits where cells appear flattened and slightly elongated except for a layer of epithelial-like cells beneath the matrix deposits.

Immunolocalization following previous methods established by Hales et al. (1995) was performed on HE stained sections that were histologically positive for abnormalities. Sections were assessed immunologically for deposits of laminin and type I collagen by reactivity with laminin.

MODIFICATIONS OF THE METHOD

Fujinaga (1990) conducted long-term observations on 180 Wistar male rats to demonstrate similarities between the senile Wistar rat cataract and the human senile cataract. Other variables under study included agents thought to slow the progression of cataracts. Rats were initially classified into six groups (control, vitamin E diet, ARI, EPC eye drops, catalin eye drops and reduced catalin eye drops) to study the effects of the agents on the cataract. Effects of anti-cataract agents were investigated using cultured lens epithelial cells.

REFERENCES AND FURTHER READING

Fujinaga Y (1990) Cataract— -clinic and pathology. Nippon Ganka Gakkai Zasshi;94:903–27

Hales AM, Chamberlain CG, Dreher B, McAvoy JW (1999) Intravitreal injection of TGFβ induces cataract in rats. Invest Ophthalmol and Vis Sci;40:3231–3236

Hales AM, Chamberlain CG, McAvoy JW (1995) Cataract induction in lenses cultured with transforming growth factor-β. Invest Ophthalmol Vis Sci 36:1709–1713

Hales AM, Chamberlain CG, Murphy CR, McAvoy JW (1999) Estrogen protects lenses against cataract induced by TGFβ. J Exp Med 185:273–280

Hales AM, Schulz MW, Chamberlain CG, McAvoy JW (1994) TGFβ induces lens cells to accumulate α-smooth muscle actin, a marker for subcapsular cataracts. Cur Eye Res 13:885–890

Liu J, Hales AM, Chamberlain CG, McAvoy JW (1994) Induction of cataract-like changes in rat lens epithelial explants by transforming growth factor-β. Invest Ophth Vis Sci;35:388–401

Mikuni I (1980) Histological comparison of senile posterior subcapsular cortical cataract and experimental posterior subcapsular cortical cataract induced by vincristine sulfate. Tokai J Exp Clin Med 5:243–250

Schulz MW, Chamberlain CG, McAvoy JW (1996) Inhibition of transforming growth factor-β induced cataractous changes in lens explants by ocular media and α-2-macroglobulin. Invest Ophth Vis Sci 37:1509–1519

Vrensen G (1995) Aging of the human eye lens: a morphological point of view. Comp Biochem Physiol 111:519–532

0.6.3 Diabetic Cataract Formation in Sprague Dawley Rats

PURPOSE AND RATIONALE

Diabetic cataract formation was induced in rats by injection of streptozocin. Takamura et al. (2001) employed the diabetic cataract model to study apoptosis in lens epithelial cells.

PROCEDURE

Sprague-Dawley rats that were three weeks old were intraperitonealy injected with 0.1 mg/g bodyweight of streptozotocin (Sigma, St. Louis, MO, USA) to prepare a rat diabetes model. All rats weighed 50 g. Every other week between 4 and 12 weeks of age the lens anterior capsule was excised for subsequent epithelial proliferation studies. A total of 60 rats were used; twelve rats were used each time. Diabetic inclusion criteria were defined as a blood glucose level of 200 mg/dL or higher, which was measured twice: One week after streptozotocin administration and prior to excision of the anterior capsules. Rats were sacrificed with ether anesthesia and the eyeballs were immediately extracted, incised at the posterior lens capsular side, and the anterior capsules with lens epithelial cells were obtained.

Once the rat diabetes model was established, immunostaining of proliferating cell nuclear antigen (PCNA)was performed. This is an index of nuclear DNA synthesis. Each sample was fixed in 0.1M phosphate buffer (pH 7.4) containing methanol for anti-PCNA immunohistochemical analysis.

To perform immunohistochemical staining of PCNA the avidin-biotin complex method (ABC method) was applied. ABC method utilizes a Histofine SAB-PO(M) kit (Nichirei, Tokyo) and anti-PCNA monoclonal antibody (mouse monoclonal antibody NC012; Novocastra Lab, Newcastle, UK) as the primary antibody. Samples without treatment with anti-PCNA monoclonal antibody represented the negative control in each staining. Light microscopy via a differential interference prism (Olympus, Tokyo) was completed to observe fragments.

EVALUATION

Diabetic cataracts of the anterior lens capsules are examined by immunohistochemical analysis. Sprague-Dawley rats injected with streptozotocin can serve as a model for the formation of diabetic cataracts and studying lens epithelial apoptosis. In the absence of high glucose levels the non-diabetic lens epithelial cells survive independently of signals from other cells and produce a factor that inhibits cell death or apoptosis (Ishizaki et al. (1993), Raff et al. (1993).

MODIFICATIONS OF THE METHOD

Gavrieli et al. (1992) observed lens epithelial proliferation and detected an amount of fragmented DNA rep-

resenting apoptotic cell bodies by using the TUNEL method. In this method, diabetic cataracts are induced as above and the anterior capsule is excised as above. Then each sample was fixed in 0.1M phosphate buffer (pH 7.4) containing 4% paraformaldehyde for the Terminal deoxynucleotidyl transferase (TdT-mediated dUTP-biotin nick end labeling (TUNEL) method for immunohistochemical analysis. Specimens of anterior capsule were then extended on glass slides and treated with 10-fold diluted proteinase K (DAKO, Glostrup, Denmark). ApopDETEK (DAKO) was used for TdT reaction, and Horseradish Peroxidase-DAB in situ Detection System (DAKO) was used for reaction of biotin-labeled dUTP with peroxidase-avidin complex. Samples without treatment with TdT represented the negative control in each staining.

Umemura et al. (1996) extended the duration of sample fixation and concentration of proteolytic enzymes. This may increase the ratio of TUNEL-positive cells to whole fragments which would improve the relationship between the types of cataract and diabetes. The results show that DNA is fragmented over time in fixed preparations so that an increased duration may be necessary.

Hegde et al. (2003) investigated the suitability of using CD-1 mice, a species known to have low lens aldose reductase activity as a streptozotocin diabetic cataract induced model. The mice were injected with streptozotocin and blood glucose evaluated seven days post injection. Diabetic inclusion criteria were defined as a blood glucose level of 300–400 mg/dL or higher. Animals were examined by direct ophthalmoscopy, slit lamp examination and Scheimpflug photography. Additionally morphological studies were performed to view multilayered and numerous nucleated cells in the superficial anterior cortex.

Lee et al. (1994, 1999) compared diabetic cataract formation in transgenic mice that overexpress aldose reductase. The entire 1.4-kb cDNA from a human AR (hAR) clone with 36-bp 5′ and 325-bp 3′ untranslated regions (16) was released from the Bluescript vector by Xba 1 and EcoRV digests and inserted into the Xba I and Msc I site of the pCAT-Basic vector (Promega) that contains the simian virus 40 splice site and poly (A) sequence. A single intraperitoneal injection of streptozotocin at a dose of 200 mg/kg of body weight induced hyperglycemia. Lenses were examined through a dilated pupil. The study showed that these transgenic mice that overexpress aldose reductase in their lens epithelial cells were found to become susceptible to the development of diabetic and galactose cataracts.

REFERENCES AND FURTHER READING

Gavrieli Y, Sherman Y, Ben-Sasson SA (1992) Identification of programmed cell death in situ via specific labeling of nuclear DNA fragmentation. J Cell Biol 119:493–501

Hegde KR, Henein MG, Varma SD (2003) Establishment of the mouse as a model animal for the study of diabetic cataracts. Ophthalmic Res 35:12–18

Ishizaki Y, Voyvodic JT, Vrne JB, Ralt MC (1993) Control of lens epithelial cell survival. J Cell Biol 121:899–908

Lee AYW, Chung SK, Chung SSM (1995) Demonstration that polyol accumulation is responsible for diabetic cataract by the use of transgenic mice expressing the aldose reductase gene in the lens. Proc Natl Acad Sci USA 92:2780–2784

Lee AYW, Chung SSM (1999) Contributions of polyol pathway to oxidative stress in diabetic cataract. FASEB J 13:23–30

Raff MC, Barres BA, Burne JF, Coles HS, Ishizaki Y, Jacobson MD (1993) Programmed cell death and the control of cell survival: lessons from the nervous system. Science 262:695–700

Takamura Y, Sugimoto Y, Kubo E, Takahashi Y, Akagi Y (2001) Immunohistochemical Study of apoptosis of lens epithelial cells in human and diabetic rat cataracts. Jpn J Ophthalmol 45:559–563

Umemura S, Yasuda M, Osamura RY, Kawarada Y, Sugiyanna T, Tsutsami Y (1996) Enhancement of TdT-mediated dUTP biotin nick end-labeling (TUNEL) method using mung bean nuclease, a single-stranded DNA digestion enzyme. J Histochem Cytochem 44:125–32

0.6.4 Cataract Formation in Knock Out Mice

PURPOSE AND RATIONALE

Cataract formation was studied in genetically altered mice to detect factors influencing cataract origination and progression. Brady et al. (1997) studied the influence of αA-crystallin (αA), a dominant protein in the lens, on cataract initiation and development.

PROCEDURE

αA Gene knockout mice were generated as follows. A λ phage clone spanning 16 kb of the αA locus was isolated from a 129Sv mouse genomic library (Stratagene). A targeting vector was constructed by placing the following pieces of DNA, in the given order, into the plasmid pBluescript (Pro-mega): a 9-kb NotI/AatII restriction fragment encompassing the 5′ flanking region and first nine nucleotides of the αA coding region, the phosphoglycerate kinase neomycin phosphotransferase (PGK/neo) expression cassette from the vector pPNT (24) in opposite transcriptional orientation to the αA gene, a 1.3-kb XhoI/XmnI restriction fragment containing most of the first intron and part of the second exon of the αA gene in the same orientation as the αA promoter fragment, and the PGK/herpes simplex virus thymidine kinase expression cassette of pPNT in the same orientation as the aA sequences. In addition, to ensure that no protein-encoding transcripts

could be produced by the disrupted allele, a double-stranded oligonucleotide containing translation termination codons in all three reading frames as well as a copy of the αA polyadenylylation signal was inserted between the 5′ αA sequence and the PGK/neo cassette. Linearized knockout plasmid DNA (30 mg) was electroporated into 4×10^7 J1 embryonic stem cells derived from 129Sv mice. Cell lines established from 192 colonies surviving double selection with the neomycin analogue G418 and ganciclovir were analyzed by PCR for homologous recombination at the αA locus. Correctly targeted embryonic stem cells, confirmed by Southern blot analysis, were injected into C57BL/6 blastocysts and then implanted into pseudopregnant CD1 female mice. Chimeric males were mated to 129Sv or B6D2F1 females, and heterozygous offspring identified by PCR were interbred to produce mice homozygous for the αA knockout allele.

Mice that were homozygous for the disrupted allele produced no detectable αA in their lenses. Initially, the αA-deficient lenses appeared structurally normal, but they were smaller than the lenses of wild-type littermates. Later on, the lenses developed an opacification that started in the nucleus and progressed to a general opacification with age.

EVALUATION

Eyes were examined by slit lamp, histo-and immunochemistry and protein analyses. It is suggested that such knock-out mice can serve as a model for studying the formation and drug treatment of cataracts.

REFERENCES AND FURTHER READING

Brady JP, Garland D, Duglas-Tabor Y, Robinson WG Jr, Groome A, Wawrousek EF (1997) Targeted disruption of the mouse αA-crystallin gene induces cataract and cytoplasmatic inclusion bodies containing the small heat shock protein αB-crystallin. Proc Natl Acad Sci USA 94:884–889

0.7 Models of Eye Inflammation

0.7.1 Allergic Conjunctivitis

PURPOSE AND RATIONALE

Allergic conjunctivitis is a common clinical condition that resembles immediate hypersensitivity reactions in the nose, airways, and skin in many aspects. Allergic conjunctivitis is regarded as a mast cell-mediated disease: a similar array of inflammatory mediators, mostly histamine, is released, and the conjunctiva is responsive to many of these inflammatory mediators.

Trocme et al. (1986), Fukushima et al. (1997), Iwamoto et al. (1999) induced allergic blepharoconjunctivitis in rats by immunization with ovalbumin. Keane-Myers et al. (1999) sensitized and challenged mice by local application of a cat dander extract. Ragweed pollen was used for sensitization of mice by Merayo-Lloves et al. (1996), Hu et al. (1998), Magone et al. (1998, 2000).

PROCEDURE

An extract of ragweed pollen is prepared. Ragweed is defatted with acetone and extracted with 50 mM Tris buffer overnight. The extract is then dialyzed against PBS for 48 h, filtered, and stored at 4°C until use. Protein concentration is determined with Coomassie plus protein assay. The ragweed extract is biotinylated. An $Al(OH)_3$ gel (alum) is prepared, centrifuged for 15 min at 1000 rpm and stored at 4°C. Ragweed and alum are mixed at a concentration of 50 µg ragweed in 5 mg of alum 40 min before immunization. On day 0 mice are anesthetized with methoxyflurane during the injection of ragweed and alum in one hind footpad. On day 10, conjunctivitis is induced by topical application of 1.5 mg ragweed suspended in 10 ml phosphate buffered saline, pH 7.2, into each eye. Two groups of control mice are either not immunized or immunized with alum alone; both groups are challenged with the same dose of ragweed on day 10. The animals are sacrificed 20 min and 3, 6, 12, 24, 48, and 72 h after topical ragweed administration.

Animals are examined clinically for signs of immediate hypersensitivity response 20 min after the topical application of ragweed. Chemosis, conjunctival redness, lid edema, and tearing were each graded on a 0–3+ scale. The total score consists of the sum of scores in each of these four categories.

For histology, the eyes are enucleated with the attached lids and intact conjunctiva and immediately fixed in 4% glutaraldehyde for 30 min and then transferred to 4% formaldehyde for at least 24 h before processing. The tissue is embedded in methyl acrylate, serially sectioned and stained. The numbers of infiltrating neutrophils, eosinophils, goblet cells, and mast cells in one section are counted. Immunohistochemical staining is performed with rat primary antibodies using an avidin-biotin-peroxidase complex technique. Macrophages and lymphocytes in one section of the conjunctiva are assessed.

EVALUATION

All results are presented as mean ±SE. Comparisons between immunized mice, drug treated mice

and controls are made with the two-sided Student's *t*-test.

MODIFICATIONS OF THE METHOD

Hu S et al. (1998) compared effectiveness and molecular pharmacological mechanisms of antiallergic agents on experimental conjunctivitis induced by ragweed in SWR/J mice. Allergic conjunctivitis was evaluated by scoring of the clinical signs and histopathology. mRNA expression of interleukin 1β, IL-6 and tumor necrosis factor α was analyzed by reverse transcription polymerase chain reaction techniques.

Woodward et al. (1995) studied the pruritogenic and inflammatory effects of prostanoids in the conjunctiva in **guinea pigs** and counted the scratching episodes by the hind limb.

Reichel et al. (1998) established a simple model of **conjunctival wound healing** in the mouse eye. Four week old BABL/c mouse eyes were studied over a 14 day period. Surgical procedure under general anesthesia involved a blunt dissection of the conjunctiva performed by injection of 25 µl of phosphate buffered saline via a 27 gauge needle into one eye, while the was used as control.

REFERENCES AND FURTHER READING

Allansmith MR, Baird RS, Ross RN, Barney NP, Bloch KJ (1989) Ocular anaphylaxis induced in the rat by topical application of compound 48/80. Dose response and time course study. Acta Ophthalmol (Copenh.) 67:145–153

Doherty MJ, Easty DL (1989) Inflammatory and immunological cell profiles in a rat model of conjunctival immediate hypersensitivity. Clin Exp Allergy 19:449–455

Fujino Y, Mochizuki M, Chan CC, Raber J, Kotake S, Gery I (1991) FK506 treatment of S-antigen induced uveitis in primates. Curr Eye Res 10:679–690

Fukushima A, Yoshida H, Iwamoto H, Yoshida O, Ueno H (1997) The role of cellular immunity both in the induction and effector phases of allergic blepharoconjunctivitis (EAC) in rats. Exp Eye Res 65:631–637

Hu S, Merayo-Lloves J, Zhao T, Foster CS (1998) Comparative effectiveness and molecular pharmacological mechanisms of antiallergic agents on experimental conjunctivitis in mice. J Ocular Pharmacol Ther 14:67–74

Iwamoto H, Yoshida H, Fukushima A, Ueno H (1999) Inhibitory effects of FK506 on the development of allergic/immune-mediated blepharoconjuntivitis in Lewis rats by systemic but not topical administration. Graefe's Arch Clin Exp Ophthalmol 237:407–414

Keane-Myers AM, Miyazaki D, Liu G, Dekaris I, Ono S, Dana MR (1999) Prevention of allergic eye disease by treatment with IL-1 receptor antagonist. Invest Ophthalmol Vis Sci 40:3041–3046

Li Q, Luyo D, Hikita N, Whitcup SM, Chan CC (1996) Compound 48/80-induced conjunctivitis in the mouse: Kinetics, susceptibility, and mechanism. Int Arch Allergy Immunol 109:277–285

Magone MT, Chan C-C, Rizzo LV, Kozhich AT, Whitcup SM (1998) A novel murine model of allergic conjunctivitis. Clin Immunol Immunopathol 87:75–84

Magone MT, Whitcup SM, Fukushima A, Chan CC, Silver PB, Rizzo LV (2000) The role of IL-12 in the induction of late-phase cellular infiltration in a murine model of allergic conjunctivitis. J Allergy Clin Immunol 105:299–308

Merayo-Lloves J, Calonge M, Foster CS (1995) Experimental model of allergic conjunctivitis to ragweed in the guinea pig. Curr Eye Res 14:487–494

Merayo-Lloves J, Zhao TZ, Dutt JE, Foster CS (1996) A new murine model of allergic conjunctivitis and effectiveness of nedocromil sodium. J Allergy Clin Immunol 97:1129–1140

Reichel MB, Cordeiro MF, Alexander RA, Cree IA, Bhattacharya SS, Khaw PT (1998) New model of conjunctival scarring in the mouse eye. Br J Ophthalmol 82:1072–1077

Trocme SD, Trocme MC, Bloch KJ, Allansmith MR (1986) Topically induced ocular anaphylaxis in rats immunized with egg albumin. Ophthalmic Res 18:68–74

Woodward DF, Spada CS, Nieves AL (1989) Eye models of inflammation. Pharmacological Models in the Control of Inflammation. Alan R. Liss, Inc. pp 233–253

Woodward DF, Nieves AL, Hawley SB, Joseph R, Merlino GF, Spada CS (1995) The pruritogenic and inflammatory effects of prostanoids in the conjunctiva. J Ocular Pharmacol 11:339–347

0.7.2 Corneal Inflammation

PURPOSE AND RATIONALE

Unlike the conjunctiva, the cornea is an avascular tissue. The cornea serves three major functions: protection, refraction and light transmission. Corneal inflammatory diseases usually result from injury and infection rather than from allergic disorders. Models involving chemical or mechanical injury, therefore, directly mimic clinically encountered situations.

Leibowitz and Kupferman (1974) induced inflammatory response by the injection of clove oil directly into the corneal stroma, resulting in the chemotactic attraction of large numbers of polymorphonuclear leukocytes.

PROCEDURE

New Zealand albino rabbits of either sex are anesthetized with 15 mg/kg i.v. sodium thiamylal. A corneal inflammatory response is produced in both eyes by the interlaminar inoculation 0.03 ml of laboratory grade clove oil centrally with a 30-gauge needle attached to a tuberculin syringe. All animals receive two intravenous injections of 0.05 mCi/kg of tritiated thymidine (0.7 Ci/mM) 24 h apart. The second thymidine injection is given 24 h prior to the induction of the corneal inflammatory response. Therapy is initiated immediately after the intracorneal injection of clove oil consisting of one drop (0.05 ml) of test compound or standard every hour for a total of 6 doses. One h later, the animals are sacrificed under anesthesia and a 10 mm penetrating corneal button is removed by

trephination. The tissue samples are solubilized with a commercially available solubilizing agent (Soluene, Packard Instruments Corp.). The samples are counted in a scintillation counter for 10 min and the amount of radioactivity in each cornea documented.

EVALUATION

The data from individually treated eyes are expressed as percent change in radioactivity relative to their own untreated control eyes. These differences are averaged to determine a mean value for each treatment group. Statistical comparisons are performed by standard methods including random block analysis.

MODIFICATIONS OF THE METHOD

Neovascularization of the rabbit cornea has been used by several authors to study inhibition of angiogenesis (see Sect. A.8.3.4).

Alio et al. (1994, 1995) studied the relative effectiveness of nonsteroidal anti-inflammatory drugs versus corticosteroids and of antioxidants in the topical treatment of experimental acute corneal inflammation induced by corneal alkali burn in rabbits. The corneal inflammatory response was evaluated by Luminol-enhanced chemiluminescence, ultrasonic pachymetry, and computer-assisted analysis of the area of corneal ulceration.

Laria et al. (1997) evaluated combined non-steroidal therapy in experimental corneal injury. A corneal alkali burn was induced in New Zealand white rabbits by applying 1-N NaOH filter paper on the central axis of the right cornea for 30 s. The inflammatory index, area and perimeter of the wounded corneal zone, and corneal transparency were evaluated after 5 days treatment.

A similar method was used by Ozturk et al. (2000).

Sonoda et al. (1998) studied inhibition of corneal inflammation by the topical use of Ras farnesyltransferase inhibitors. The central corneas of BALB/c **mice** were cauterized with silver nitrate. Clinical signs and neovascularization were evaluated.

REFERENCES AND FURTHER READING

Alio JL, Ayala MJ, Mulet ME, Artola A, Ruiz JM (1994a) Topical treatment of experimental acute corneal inflammation by dexamethasone and nonsteroidal drugs. Ophthalmic Res 26:87–94

Alio JL, Ayala MJ, Mulet ME, Artola A, Ruiz JM, Belot J (1994b) Antioxidant therapy in the treatment of experimental acute corneal inflammation. Ophthalmic Res 27:136–143

Laria C, Alio JL, Ruiz-Moreno JM (1997) Combined non-steroidal therapy in experimental corneal injury. Ophthalmic Res 29:145–153

Leibowitz HM, Kupferman A (1974) Anti-inflammatory effectiveness in the cornea of topically administered prednisolone. Invest Ophthalmol 13:757–763

Ozturk F, Kurt E, Cerci M, Emiroglu L, Inan U, Turker M, Ilker S (2000) The effect of propolis extract in experimental chemical corneal injury. Ophthalmic Res 32:13–18

Sonoda K, Sakamoto T, Yoshikawa H, Ashizuka S, Ohshima Y, Kishihara K, Nomoto K, Ishibashi T, Inomata H (1998) Inhibition of corneal inflammation by the topical use of Ras farnesyltransferase inhibitors: selective inhibition of macrophage localization. Invest Ophthalmol Vis Sci 39:2245–2251

0.7.3 Auto-Immune Uveitis in Rats

PURPOSE AND RATIONALE

The mechanisms of certain types of uveitis have been studied in animals involving autoimmunity. Uveitis has been produced in guinea pigs following injections with homologous uveal tissue.

PROCEDURE

Hartley strain guinea pigs, weighing 400–500 g, are injected at 0, 1, 2, 5, and 8 weeks with a 10% suspension of homologous retina emulsified in Freund's complete adjuvant. The retinas are obtained by dissection of freshly removed eyes of either normal albino or pigmented guinea pigs and stored frozen at –50°C. Each animal receives 0.2 ml of this emulsion at a time, the first injection being administered intradermally into both hind foot-paws, and the remainder of the series given intramuscularly. Groups of 6 animals receive the test drug or the vehicle orally. Control animals receive similar injections of saline. The severity of the uveal inflammation can be clinically evaluated by slit lamp examination. The animals are sacrificed and the eyes are examined histologically.

EVALUATION

The incidence of uveitis is recorded by histological means as percentage of treated animals.

MODIFICATIONS OF THE METHOD

Highly purified bovine retinal S antigen in complete Freund's adjuvant was injected subcutaneously in **guinea pigs** to induce experimental autoimmune uveitis (Liversidge et al. 1987; Mahlberg et al. 1987).

Cultured retinal pigment epithelial cells from guinea pigs were used by Liversidge et al. (1988).

Experimental autoimmune uveitis has been induced in **rats** (Nussenblatt et al. 1981; Chan et al. 1984, 1987; Mochizuki et al. 1985; Fujino et al. 1988).

Experimental autoimmune uveoretinitis was in-

duced in Lewis rats by injection of very high doses of bovine opsin (Brockhuyse et al. 1987).

Melanin-associated antigen from the iris and ciliar body was used to induce experimental autoimmune anterior uveitis in male Lewis rats by Bora et al. (1995).

Ramanathan et al. (1996) found that recombinant IL-4 aggravates experimental autoimmune uveoretinitis in Lewis rats.

Hanashiro et al. (1997) injected various doses of either lipopolysaccharide or the lipid A region of the lipopolysaccharide into the foot pad of an inbred strain of Lewis rats and compared the inflammation patterns by assessing the protein concentrations and the inflammatory cell content in the aqueous humor.

Merino et al. (1998) reported that lipoteichoic acid from *Staphylococcus aureus* injected into the foot pad of Lewis rats induced a strong ocular inflammation between 24 and 30 h after injection.

Hikita et al. (1995) evaluated the effects of topical FK506 on endotoxin-induced uveitis in the Lewis rat.

Tsuji et al. (1997) investigated the effects of systemically and topically applied betamethasone derivatives on endotoxin-induced uveitis in female Lewis rats.

McMenamin and Crewe (1995) studied kinetics and phenotype of the inflammatory cell infiltrate and the response of the resident tissue macrophages and dendritic cells in the iris and ciliary body in endotoxin-induced uveitis in Lewis rats.

Uchio et al. (1997) achieved suppression of actively induced experimental autoimmune uveoretinitis in rats by $CD4^+$ T cells.

Egwuagu et al. (1999) found in transgenic Lewis rats that expression of interferon-gamma in the lens exacerbates anterior uveitis and induces degenerative changes in the retina.

Immunogenic uveitis in **rabbits** was studied by Kaswan and Kaplan (1988).

Jamieson et al. (1989) sensitized rabbits to bovine serum proteins and then challenged intravitreally to induce an uveitis. They recommended this procedure as a model for anti-inflammatory drug screening.

Whitcup et al. (1996) produced endotoxin-induced uveitis in **mice** by injecting 200 µg *Salmonella typhimurium* endotoxin diluted in 0.1 ml sterile saline into one hindpad.

Geiger et al. (1994) reported that transgenic mice expressing IFN-gamma in the retina develop inflammation in the eye and photoreceptor loss.

REFERENCES AND FURTHER READING

Bora NS, Kim MC, Kabeer NH, Simpson SC, Tandhasetti MT, Cirrito TP, Kaplan AD, Kaplan HJ (1995) Experimental autoimmune anterior uveitis: Induction with melanin-associated antigen from the iris and ciliar body. Invest Ophthalmol Vis Sci 36:1056–1066

Brockhuyse RM, Kuhlmann EC, van Vugt AHM, Winkens HJ (1987) Immunological and immunopathological aspects of opsin-induced uveoretinitis. Graefe's Arch Clin Exp Ophthalmol 225:45–49

Caspi RR, McAllister CG, Gery I, Nussenblatt RB (1988) Differential effects of cyclosporins A and G on functional activation of a T-helper-lymphocyte line mediating experimental autoimmune uveoretinitis. Cell Immunol 113:350–360

Chan CC, Palestine AG, Nussenblatt RB (1984) Cyclosporine-induced alterations of humoral response in experimental autoimmune uveitis. Invest Ophthalmol Vis Sci 25:867–870

Chan CC, Caspi R, Mochizuki M, Diamantstein T, Gery I, Nussenblatt RB (1987) Cyclosporine and dexamethasone inhibit T-lymphocyte MHC class II antigens and IL-2 receptor expression in experimental autoimmune uveitis. Immunol Invest 16:319–331

de Kozak Y, Sakai J, Thillaye B, Faure JP (1982) S antigen-induced experimental autoimmune uveo-retinitis in rats. Curr Eye Res 1:327–337

Egwuaga CE, Mahdi RM, Chan CC, Sztein J, Li W, Smith JA, Chepelinski AB (1999) Expression of interferon-gamma in the lens exacerbates anterior uveitis and induced retinal degenerative changes in transgenic Lewis rats. Clin Immunol 91:196–205

Fujino Y, Okumura A, Nussenblatt RB, Gery I, Mochizuki M (1988) Cyclosporine-induced specific unresponsiveness to retinal soluble antigen in experimental autoimmune uveoretinitis. Clin Immunol Immunopathol 46:234–248

Geiger K, Howes E, Gallina M, Huang XJ, Travis GH, Sarvetnik N (1994) Transgenic mice expressing IFN-gamma in the retina develop inflammation in the eye and photoreceptor loss. Invest Ophthalmol Vis Sci 35:2667–2681

Hanashiro RK, Fujino Y, Gugunfu, Samura M, Takahashi T, Masuda K (1997) Synthetic lipid A-induced uveitis and endotoxin-induced uveitis: a comparative study. Jpn J Ophthalmol 41:355–361

Hikita N, Chan CC, Whitcup SM, Nussenblatt RB, Mochizuki M (1995) Effects of topical FK506 on endotoxin-induced uveitis (EIU) in the Lewis rat. Curr Eye Res 14:209–214

Jamieson L, Meckoll-Brinck D, Keller N (1989) Characterized and predictable rabbit uveitis model for antiinflammatory drug screening. J Pharmacol Meth 21:329–338

Kaswan RL, Kaplan HJ (1988) Comparison of the efficacy of unilateral, bilateral, and oral cyclosporine in experimental immunogenic uveitis in rabbits. Transplant Proc 20, Suppl 4:149–157

Liversidge J, Thompson AW, Sewell HF, Forrester JV (1987) EAU in the guinea pig: inhibition of cell-mediated immunity and Ia antigen expression by cyclosporine A. Clin exp Immunol 69:591–600

Liversidge J, Thomson AW, Sewell HF, Forrester JV (1988) Cyclosporine A, experimental autoimmune uveitis, and major histocompatibility class II antigen expression of cultured retinal pigment epithelial cells. Transplant Proc 20, Suppl 4:163–169

McMenamin PG, Crewe J (1995) Endotoxin-induced uveitis. Kinetics and phenotype of the inflammatory cell infiltrate and the response of the resident tissue macrophages and dendritic cells in the iris and ciliary body. Invest Ophthalmol Vis Sci 36:1949–1959

Mahlberg K, Uusitalo H, Uusitalo R, Palkama A, Tallberg T (1987) Suppression of experimental autoimmune uveitis in

guinea pigs by ethylenediamine tetra-acetic acid, corticosteroids and cyclosporin. J Ocul Pharmacol 3:199–210
Merino G, Fujino Y, Hanshiro RK (1998) Lipoteichoic acid as an inducer of acute uveitis in the rat. Invest Ophthalmol Vis Sci 39:1251–1256
Mochizuki M, Nussenblatt RB, Kuwabara T, Gery I (1985) Effects of cyclosporine and other immunosuppressive drugs on experimental autoimmune uveoretinitis in rats. Invest Ophthalmol Vis Sci 26:226–232
Nordmann JP, de Kozak Y, Le Hoang P, Faure JP (1986) Cyclosporine therapy of guinea-pig autoimmune uveitis induced with autologous retina. J Ocul Pharmacol 2:325–333
Nussenblatt RB, Rodrigues MM, Wacker WB, Cevario SJ, Salinas-Carmona MC (1981) Inhibition of experimental autoimmune uveitis in Lewis rats. J Clin Invest 67:1228–1231
Ramanathan S, de Kozak Y, Saoudi A, Goureau O, Van der Meide PH, Druet P, Bellon B (1996) Recombinant IL-4 aggravates experimental autoimmune uveoretinitis in rats. J Immunol 157:2209–2215
Smith-Lang L, Glaser RL, Miller ST, Weimer LK, Robertson SM, Aoki KR, Yanni JM (1992) Efficacy of novel immunomodulators leflunomide and rapamycin in autoimmune uveitis. FASEB J 6:A1048, Part 1
Tsuji F, Sawa K, Kato M, Mibu H, Shirasawa E (1997) The effects of betamethasone derivatives on endotoxin-induced uveitis in rats. Exp Eye Res 64:31–36
Uchio E, Kijima M, Ishioka M, Tanaka SI, Ohno S (1997) Suppression of actively induced experimental autoimmune uveoretinitis by $CD4^+$ T cells. Graefe's Arch Clin Exp Ophthalmol 235:97–102
Wacker WB, Lipton MM (1965) Experimental allergic uveitis: homologous retina as uveitigenic antigen. Nature 206:253–254
Wacker WB, Lipton MM, Ongchua FE (1964) Antibody production in the guinea pig to homologous uvea. Proc Soc Exp Biol Med 117:150–154
Whitcup SM, Rizzo LV, Lai JC, Hayashi S, Gazzinelli R, Chan C-C (1996) IL-12 inhibits endotoxin-induced inflammation in the eye. Eur J Immunol 26:995–999

0.7.4 Ocular Inflammation Induced by Paracentesis

PURPOSE AND RATIONALE

Paracentesis stimulates prostaglandin PGE_2 and $PGF_{2\alpha}$ release into the anterior chamber of the eye which can be inhibited by antiinflammatory agents (Miller et al. 1973; Kulkarni and Srinivasan 1985).

PROCEDURE

New Zealand white rabbits (2.0 to 2.5 kg) are anesthetized with a 50:50 mixture of xylazine (20 mg/kg) and ketamine (100 mg/kg) i.m. Test compounds are topically administered by placing three drops (about 60 µl) on each eye. The eyes are then taped shut to prevent drying. One hour after compound or vehicle administration, inflammation is induced by paracentesis. For each rabbit, the aqueous humor from both eyes is combined to form the "Pre" sample. Three more drops of compound or vehicle are again administered to each eye and the eyes taped shut. Another one-hour period is allowed to elapse, enough time for the aqueous humor to build back up in the eye. Paracentesis is performed a second time and the aqueous humor from both eyes is combined to form the "Post" sample. Prior to this second paracentesis, the general appearance of the eye is rated on a scale of 1 to 3, based on the following criteria: 1 = clear, relatively normal appearance; 2 = opaque, some protein accumulation in the anterior chamber; 3 = very cloudy, protein accumulates in clumps in the anterior chamber, hyperemia, swelling. This rating gives some indication of the extent of inflammation and correlates with the amount of prostaglandin accumulation. Prostaglandins are measured in 10 µl of aqueous humor from the "Pre" and "Post" samples by RIA.

EVALUATION

The amount of prostaglandin present is determined according to the standard curve supplied with each RIA kit. The extent of inflammation is determined by the magnitude of increase in prostaglandin levels in the "Post" versus the "Pre" sample. Dose-response curves for inhibition by test drug and standard are established.

MODIFICATIONS OF THE METHOD

Struck et al. (1995) studied the effects of non-steroidal anti-inflammatory drugs on inflammatory reactions. The right eye of rabbits was burned with alkali (0.25 M sodium hydroxide). The animal were treated with eye drops containing a cyclooxygenase inhibitor and a leukotriene antagonist. Hyperemia of the limbal vessels, corneal vascularization, the number of PMNLs in the cornea and the prostacyclin level in the anterior chamber of the eye served as criteria.

REFERENCES AND FURTHER READING

Kulkarni PS, Srinivansan BD (1985) Comparative *in vivo* inhibitory effects of nonsteroidal antiinflammatory agents on prostaglandin synthesis in rabbit ocular tissue. Arch Ophthalmol 103:103–106
Miller JD, Eakins KE, Atwal M (1973) The release of PGE_2-like activity in aqueous humor after paracentesis and its prevention by aspirin. Invest Ophthalmol 12:939–942
Struck HG, Giessler S, Giessler C (1995) Effect of non-steroidal anti-inflammatory drugs on inflammatory reaction. An animal experiment study. (Zum Einfluß nichtsteroidaler Antiphlogistika auf die Entzündungsreaktion. Eine tierexperimentelle Studie.) Ophthalmologe 92:849–853
Unger WG, Cole DF, Hammond B (1975) Disruption of the blood-aqueous barrier following paracentesis in the rabbit. Exp Eye Res 20:255–270

0.7.5 Ocular Inflammation by Lens Proteins

PURPOSE AND RATIONALE

Ocular inflammation can be induced by lens proteins which can be prevented by lipoxygenase inhibitors (Miyano and Chiou 1984; Chiou and Chiou 1985; Chang and Chiou 1989).

PROCEDURE

New Zealand albino rabbits are anesthetized by i.m. injection of 25 mg/kg ketamine hydrochloride and 5 mg/kg xylazine. The anesthesia is maintained by injection of 12.25 mg/kg ketamine and 2.5 mg/kg xylazine every hour throughout the experiment. After the animals are deeply anesthetized, 50 µl of the drug is topically applied to one eye and the other eye receives 50 µl of the solvent. One hour after the application of the drug, 25 µl of lens protein (30 mg/ml, prepared according to Miyano and Chiou 1984) is injected intracamerally with a 27 1/2 gauge needle; extreme care is taken to avoid contact with the iris. Fifteen min after injection of lens proteins, 14 mg/kg of fluorescein is infused through the marginal ear vein at a rate of 1 ml/min. The inflammation which occurs in the eyes of the rabbits is measured by quantifying the amount of fluorescein leakage into the anterior chamber using a fluorophotometer. Measurements are taken at various intervals after injection of lens proteins. At the end of experiments, the animals are sacrificed by an overdose of pentobarbital sodium. Fluorescence measurements are done at 30, 60, 90, 120, 180, 240 and 300 min intervals.

EVALUATION

The concentration of fluorescein in the anterior chamber is determined by taking the average of three values in each of the fluorometric measurements. The results are analyzed by using a paired *t*-test with *P*-values of less than 0.05 as statistically significant.

MODIFICATIONS OF THE METHOD

Augustin et al. (1996) evaluated the effects of allopurinol in lens induced uveitis by morphological methods and compared these effects with those of steroids and a combination of both drugs biochemically and morphologically.

REFERENCES AND FURTHER READING

Augustin AJ, Spitznas M, Sekundo W, Koch F, Lutz J, Meller D, Grus FH, Wegener A, Blumenroder SH (1996) Effects of allopurinol and steroids on inflammation and oxidative tissue damage in experimental lens induced uveitis: a biochemical and morphological study. Br J Ophthalmol 80:451–457

Chang MS, Chiou GCY (1989) Prevention of lens protein-induced ocular inflammation with cyclooxygenase and lipoxygenase inhibitors. J Ocul Pharmacol 5:353–360

Chiou L, Chiou G (1984) Ocular anti-inflammatory action of a lipoxygenase inhibitor in the rabbit. J Ocul Pharmacol 1:383–389

Miyano K, Chiou G (1984) Pharmacological prevention of ocular inflammation induced by lens proteins. Ophthalmic Res 16:256–263

0.7.6 Proliferative Vitreoretinopathy in Rabbits

PURPOSE AND RATIONALE

Injection of cultured fibroblast cells into the rabbit vitreous results in a condition that mimics the features of proliferative vitreoretinopathy in man (Algvere and Kock 1976; Sugita et al. 1980; Ophir 1982). Proliferative vitreoretinopathy is a complication of severe eye injury or retinal detachment and is a major cause of failure in retinal reattachment surgery. Because of its simplicity and reproducibility, Wiedemann et al. (1984) proposed this model in rabbits as screening model for antiproliferative drugs.

PROCEDURE

Dermal fibroblasts are obtained from skin explants of young rabbits which are prepared by excising a 1 × 1 cm area of dorsal skin and scraping it thoroughly with a scalpel blade to remove hair and subcutaneous fat. The explants are rinsed in sterile PBS, minced finely, and placed in 35-mm Petri dishes containing 200 µl of Dulbecco's medium supplemented with 20% heat-inactivated fetal calf serum, 50 µg/ml garamycin, and 5 µg/ml fungizone. When cells begin to grow, tissue pieces and medium are removed and 2 ml of fresh medium is added. When cells have grown to confluence, they are passaged into 75-cc flasks by rinsing with 1 ml of PBS and incubating with 1 ml of 0.25% trypsin/0.02% EDTA for 5–10 min at room temperature. Subsequent to the initial passage, cells are split at a 1:4 ratio upon reaching confluence. For injection into the vitreous, confluent cells from the third to tenth passage are trypsinized with 0.25% trypsin/0.02% EDTA, centrifuged at 500–600 g, washed twice with the medium, then resuspended in the medium and allowed to stand for 10–15 min to let cell clumps settle. The number of cells in suspension is determined using a Coulter counter. Tuberculin syringes are filled with 600 µl of cell suspension, which allows five injections in 0.01 ml steps.

Pigmented rabbits of either sex weighing 2–3 kg are anesthetized with 2.0–2.5 ml of a 1:1 Rompun-ketamine mixture. The eyes are dilated using one drop of 10% Neo-Synephrine, 1% Mydriacyl, and 1% atropine. Only one eye of each animal in injected using an operating microscope. Fifty thousand, 100000 or 250,000 cells in a total volume of 0.1 ml medium are injected into the posterior portion of the midvitreous through a 27-gauge needle 5 mm from the corneoscleral limbus at the superonasal quadrant. The test drug or the vehicle is injected as a second injection through the same entrance site and is delivered to the same place in the vitreous. Both injections have to be done slowly to prevent posterior retinal holes or deformation of the injected cells by shearing forces. The needle is withdrawn slowly to prevent leakage of vitreous from the wound. A paracentesis is performed to equilibrate the intraocular pressure after the second injection. An ointment containing antibiotics and atropine is applied at the end of the procedure.

EVALUATION

The development of proliferative vitreoretinopathy in the injected eyes is followed by indirect ophthalmoscopy; the appearance of membranes and detachment is documented by fundus photography.

MODIFICATIONS OF THE METHOD

A survey of eye models of inflammation including conjunctivitis, corneal responses to injurious stimuli, uveitis models, and retinal diseases has been presented by Woodward et al. (1989).

Retinopathy in **rats** resembling lesions seen in human retinopathy of prematurity could be provoked in newborn rats by exposure to 80% O_2 for the first 5 days of life (Ricci et al. 1995, 2000).

Hikchi et al. (1996) described an experimental model of ocular inflammation induced by intravitreal injection of interleukin 1 beta in rabbits.

REFERENCES AND FURTHER READING

Algvere P, Kock E (1976) Experimental fibroplasia in the rabbit vitreous. Retinal detachment induced by autologous fibroblasts. Albrecht von Graefe's Arch Klin Exp Ophthalmol 199:215–222

Hikichi T, Ueno N, Chakrabarti B, Trempe CL (1996) Vitreous changes during ocular inflammation induced by interleukin 1 beta. Jpn J Ophthalmol 40:297–302

Ophir A, Blumenkranz MS, Claflin A (1982) Experimental intraocular proliferation and neovascularization. Am J Ophthalmol 94:450–457

Ricci B, Minicucci G, Manfredi A, Santo A (1995) Oxygen-induced retinopathy in the newborn rat: effects of hyperbarism and topical administration of timolol maleate. Graefe's Arch Clin Exp Ophthalmol 233:226–230

Ricci B, Ricci F, Maggiano N (2000) Oxygen-induced retinopathy in the newborn rat: morphological and immunohistological findings in animals treated with topical timolol maleate. Ophthalmologica 214:136–139

Sugita G, Tano Y, Machemer L, Abrams G, Claflin A, Florentino G (1980) Intravitreal autotransplantation of fibroblasts. Am J Ophthalmol 89:121–130

Wiedemann P, Sorgente N, Ryan SJ (1984) Proliferative vitreoretinopathy: The rabbit cell injection model for screening of antiproliferative drugs. J Pharm Meth 12:69–78

Woodward DF, Spada CS, Nieves AL (1989) Eye models of inflammation. In: Pharmacological Methods in the Control of Inflammation. Alan R. Liss, Inc., pp 233–253

O.8 Safety Pharmacology of Drugs with Ophthalmologic Activity

See Schulz (2006).

REFERENCES AND FURTHER READING

Schultz BL (2006) Ocular toxicity tests.In: Vogel HG, Hock FJ, Maas J, Mayer D (eds) Drug Discovery and Evaluation – Safety and Pharmacokinetic Assays, Chapter I.M. Springer-Verlag, Berlin Heidelberg New York, pp 255–318

Chapter P
Pharmacological Models in Dermatology

P.1 Skin Sensitization Testing

P.1.1 Guinea Pig Maximization Assay

PURPOSE AND RATIONALE

A variety of methods are available for the prospective identification of skin sensitizing chemicals. The methods that have been used are the Draize rabbit irritancy test (Draize et al. 1944; Phillips et al. 1972), the occluded guinea pig patch test (Buehler 1965), and the guinea pig maximization test (Magnusson and Kligman 1969; Magnusson 1980). The guinea pig maximization test is an adjuvant sensitization test requiring intradermal injections of the test substance, in combination with Freund's complete adjuvant, which stimulates non-specifically the immune system of treated animals, enhancing their ability to respond to sensitizing chemicals.

PROCEDURE

Groups of 15–20 guinea pigs (Hartley strain) are used. On day 0 an area of 4 × 6 cm over the shoulder region is clipped short with an electric clipper. Three pairs of intradermal injections are made simultaneously, so that on each side of the midline there are two rows of injections each. The injection sites are just within the boundaries of the 2 × 4 cm patch, which is applied one week later. Injections are (1) 0.1 ml Freund's adjuvant alone, (2) 0.1 ml test material, and (3) 0.1 ml test material in Freund's adjuvant. Control animals are given the same injections but without the test agent, i. e. Freund's adjuvant and vehicle.

On day 7, the same area over the shoulder region is again clipped and shaved with an electric razor. The test agent in petrolatum is spread over a 2 × 4 cm filter paper in an even, rather thick layer or, if liquid, to saturation. The patch is covered by an overlapping, impermeable plastic adhesive tape. This in turn is firmly secured by an elastic adhesive bandage, which is wound

around the torso of the animal. The dressing is left in place for 48 h. Control animals are exposed to the vehicle without the test agent in the same way as the experimental group.

On day 21, in experimental and control animals the flanks are shaved on both sides on an area of 5 × 5 cm each. Filter paper pieces, 2 × 2 cm, are sealed to the flanks for 24 h with the same occlusive bandage as for topical induction: (1) left side: patch with the test agent in the highest non-irritant concentration. The same vehicle as for topical induction is used; (2) right side: path with the vehicle.

On day 23, reading is made 24 h after removing of the patches. By then, skin irritation due to the occlusive dressing has usually faded.

EVALUATION

If the challenge reactions in the experimental group clearly outweigh those in the control group, the agent is regarded to be a sensitizer. To grade the substances according to the percentage of animals sensitized, the substances are divided into 5 classes, ranging from weak (grade I) to extreme (grade V) sensitizers (Kligman 1966).

MODIFICATIONS OF THE METHOD

Improvement of the classical guinea pig maximization test was proposed by several authors: Maurer et al. (1980a), Shillaker et al. (1989), Botham (1992), Kashima et al. (1993), Basketter et al. (1995), Frankild et al. (1996), Vohr et al. (2000), Steiling et al. (2001).

Maurer et al. (1980b) developed a model for the evaluation of the photocontact allergenic potential in the guinea pig. Four days before the induction period, Pirbright white guinea pigs were shaved on the back skin and chemically depilated. During the 3-week initial induction period, the animals were treated epicutaneously four times a week with the test drug. Four days before the challenge at week 6 the skin was again chemically depilated. During the challenge periods at weeks 6 and 9, the animals were treated for 3 days consecutively with the test drug. To stimulate the immunological reactivity, the guinea pigs received four intradermal injections of Freud adjuvant/saline 1:1. After each application, the animals were irradiated for 15 min with a Osram Xenon 6000 W UV lamp. The intensity of erythematous reactions was evaluated according to the Draize scoring scale.

A predictive assay for contact allergens using human skin explant cultures has been described by Pistoor et al. (1996).

Use of **transgenic animals** to investigate drug hypersensitivity has been proposed by Moser et al. (2001).

REFERENCES AND FURTHER READING

Basketter DA Scholes EW Chamberlain M Barrat MD (1995) An alternative strategy to the use of guinea pigs for the identification of skin sensitization hazard. Food Chem Toxicol 33:1051–1056

Botham PA (1992) Classification of chemicals as sensitizers based on new test methods. Toxicol Lett 64–65, Spec No165–171

Buehler EV (1965) Delayed contact hypersensitivity in the guinea pig. Arch Dermatol 91:171–177

Draize JH Woodard G Calvery HO (1944) Methods for the study of irritation and toxicity of substances applied topically to the skin and mucous membranes. J Pharmacol Exp Ther 82:377–390

Frankild S Basketter DA Andersen KE (1996) The value and limitations of rechallenge in the guinea pig maximization test. Contact Dermatitis 35:135–140

Kashima R Oyake Y Okada J Ikeda Y (1993) Studies of new short-period methods for delayed contact hypersensitivity assay in the guinea pig. I. Development and comparison with other methods. Contact Dermatitis 28:235–242

Kligman AM (1966) The identification of contact allergens by human assay. III. The maximization test: a procedure for screening and rating contact sensitizers. J Invest Dermatol 47:393–409

Magnusson B (1980) Identification of contact sensitizers by animal assay. Contact Dermatitis 6:46–50

Magnusson B Kligman AM (1969) The identification of contact allergens by animal assay. The guinea pig maximization test. J Invest Dermatol 52:268–276

Maurer T Weirich EG Hess R (1980a) The optimization test in the guinea pig in relation to other predictive sensitization methods. Toxicology 15:163–171

Maurer T Weirich EG Hess R (1980b) Evaluation of the photocontact allergenic potential of 6-methylcoumarin in the guinea pig. Contact Dermatitis 6:275–278

Moser R Quesniaux V Ryffel B (2001) Use of transgenic animals to investigate drug hypersensitivity. Toxicology 158:75–83

Phillips L Steinberg M Maibach HI Akers WA (1972) A comparison of rabbit and human skin response to certain irritants. Toxicol Appl Pharmacol 21:369–382

Pistoor FHM Rambukkana A Kroezen M Lepoittevin JP Bos JD, Kapsenberg ML Das PK (1996) Novel predictive assay for contact allergens using human skin explant cultures. Am J Pathol 149:337–343

Shillaher RO Bell GM Hogson JT Padgham MD (1989) Guinea pig maximization test for skin sensitization: the use of fewer test animals. Arch Toxicol 63:283–288

Steiling W Basketter D Berthold K Butler M Garrigue JL Kimber I Lea L, Newsome C Roggeband R Stropp G Waterman S Wiemann C (2001) Skin sensitization testing – new perspectives and recommendations. Food Chem Toxicol 39:293–301

Vohr HW Blümel J Blotz A Homey B Ahr HJ (2000) An intralaboratory validation of the integrated model for the differentiation of skin reactions (IMDS): discrimination between (photo)allergic and (photo)irritant skin reactions in mice. Arch Toxicol 73:501–509

P.1.2 Popliteal Lymph Node Hyperplasia Assay

PURPOSE AND RATIONALE

The popliteal lymph node assay in mice or rats has been recommended as a tool for predicting allergies (Kammuller et al. 1989; Bloksma et al. 1995; Koch et al. 2000; Pieters 2001). Moreover, the inhibition of popliteal lymph node hyperplasia can be measured (Schorlemmer et al. 1998; Mollison et al. 1999). The test can be used to study compounds potentially effective in allergic eczema

PROCEDURE

Spleens from Brown-Norway rats are harvested aseptically, splenocytes expressed by compression with a hemostat in Dulbecco's phosphate buffered saline (DPBS), red blood cells lysed with Tris (0.16 M) buffered in ammonium chloride (0.17 M) buffer, washed twice (400 *g*), irradiated (20 Gy), washed in DPBS, and suspended in DPBS at 5×10^7 cells per ml. On day 0, recipient Lewis rats are injected subcutaneously into the plantar surface of the right hindpaw with 0.1 ml of the splenocyte suspension. Compounds are dissolved in an appropriate vehicle and dosed daily, 2 ml/kg, on days 0–3. Recipients are sacrificed on day 4 and popliteal lymph nodes (PLN) from both hind limbs from vehicle control rats, or the right popliteal lymph node from drug-treated rats, are dissected free and weighed individually on a microbalance (Mollison et al. 1993). The average weight of PLN from the left leg of vehicle-treated animals is used as background.

EVALUATION

Percent inhibition is calculated using the following formula:

$$100 - \frac{PLN_{\text{exp.}} - PLN_{\text{mean left}}}{PLN_{\text{mean right}} - PLN_{\text{mean left}}} \times 100$$

$PLN_{\text{exp.}}$ = experimental PLN weight

$PLN_{\text{mean left}}$ = mean vehicle control left PLN weight

$PLN_{\text{mean right}}$ = mean vehicle control right PLN weight

ED_{50} values are derived by simultaneous least square regressive analysis.

REFERENCES AND FURTHER READING

Bloksma N Kubicka-Muanyi M Schuppe HC Gleichmann E Gleichmann H (1995) Predictive immunotoxicological test systems: suitability of the popliteal lymph node assay in mice and rats. Crit Rev Toxicol 25:369–396

Kammuller ME Thomas C De Bakker JM Bloksma N Seinen W (1989) The popliteal lymph node assay in mice to screen for the immune disregulating potential of chemicals – a preliminary study. Int J Immunopharmacol 11:293–300

Koch E Jaggy H Chatterjee SS (2000) Evidence for immunotoxic effects of crude Ginkgo biloba L. leaf extracts using the popliteal lymph node assay in the mouse. In J Immunopharmacol 22:229–236

Mollison KW Fey TA, Krause RA Thomas VA Mehta AP Luly JR (1993) Comparison of FK-506, rapamycin, ascomycin and cyclosporine in mouse models of host-versus-graft disease and heterotopic heart transplantation. Ann NY Acad Sci 685:55–57

Mollison KW Fey TA, Gauvin DM Kolano RM Sheets MP Smith ML Pong M Nikolaidis NM Lane BC Trevillyan JM Cannon J Marsh K Carter GW Or Y-S, Chen Y-W, Hsieh GC Luly JR (1999) A macrolactam inhibitor of T helper type 1 and T helper type 2 cytokine biosynthesis for topical treatment of inflammatory skin diseases. J Invest Dermatol 112:729–738

Pieters R (2001) The popliteal lymph node assay: a tool for predicting allergies. Toxicology 158:65–69

Schorlemmer HU Kurrle R Schleyerbach R (1998) A77–1726, leflunomide's active metabolite, inhibits *in vivo* lymphoproliferation in the popliteal lymph node assay. Int J Immunotherapy 14:205–211

P.1.3 Local Lymph Node Assay

PURPOSE AND RATIONALE

More recently, the local lymph node assay in mice has been recommended for measurement of allergenic potency (Kimber and Weisenberger 1989; Kimber et al. 1995; Kimber 2001; Basketter and Scholes 1992; Basketter et al. 2001).

PROCEDURE

Groups of mice (CBA strain), weighing 20–25 g, receive topical applications of the test chemical on the dorsum of both ears, once a day for three consecutive days. In standard analyses, three concentrations of the test material are evaluated together with the relevant vehicle control. Five days after the initiation of exposure, all mice receive an intravenous injection of [^{3}H]-labeled thymidine into their tail vein. Five hours later, animals are sacrificed and draining auricular lymph nodes excised. A single cell suspension of lymph node cells is prepared by gentle mechanical disaggregation and the cells are washed and resuspended in trichloroacetic acid for at least 12 h at 4°C. Precipitates are resuspended in trichloroacetic acid and transferred to an appropriate scintillation fluid. The incorporation by draining lymph node cells of [^{3}H]-labeled thymidine is measured by ß-scintillation counting and recorded as mean disintegrations per min (dpm).

EVALUATION

For each concentration of the test material a stimulation index (*SI*) is derived relative to the concurrent vehicle control. Those chemicals that at one or more test concentrations induce a *SI* of three or greater are classified as skin sensitizers.

Dose-response curves are plotted in order to provide information on the relative potencies of skin sensitizers. The concentration of the test chemical required to produce a stimulation index (*SI*) of three (named *EC3* value) is calculated using the formula:

$$EC3 = c + [(3 - d)/(b - d) \times (a - c)]$$

where the data points lying immediately above and below the *SI* value of three on the dose-response plot have the coordinates (a,b) and (c,d), respectively.

MODIFICATIONS OF THE METHOD

On the basis of a modified local lymph node assay, Homey et al. (1997) analyzed immunosuppressive effects of topically applied drugs. On four consecutive days, NMRI mice were treated on the dorsal surfaces of both ears with increasing concentrations of test compound. During the last three days, the mice received in addition the contact sensitizer, oxazolone (1%). On day 5, draining auricular lymph nodes were removed in order to assess lymph node cell counts and perform flow cytometric analysis of lymph cell subpopulations.

Hariya et al. (1998) developed a non-radioactive endpoint in a modified local lymph node assay.

REFERENCES AND FURTHER READING

Basketter DA Scholes EW (1992) Comparison of the local lymph node assay with the guinea pig maximization test for the detection of a range of contact allergens. Food Chem Toxicol 30:65–69

Basketter DA Gerberick GF Kimber I (2001) Measurement of allergic potency using local lymph node assay. Trends Pharmacol Sci 22:264–265

Hariya T Hatao M Ichikawa H (1998) Development of a non-radioactive endpoint in a modified local lymph node assay. Food Chem Toxicol 37:L 87–93

Homey B Schuppe HC Assmann T Vohr HW Lauerma AI Ruzicka T Lehman P (1997) A local lymph node assay to analyse immunosuppressive effects of topically applied drugs. Eur J Pharmacol 325:199–207

Kimber I (2001) The local lymph node assay and potential application to the identification of drug allergens. Toxicology 158:59–64

Kimber I Weisenberger C (1989) A murine local lymph node assay for the identification of contact allergens. Assay development and results of an initial validation study. Arch Toxicol 63:274–282

Kimber I Hilton J Dearman RJ Gerberick GF Ryan CA Basketter DA Scholes EW Ladics GS Loveless SE House RV (1995) An international evaluation of the murine local lymph node assay and comparison of modified procedures. Toxicology 103:63–73

P.2 Experimental Dermatitis

Several methods involving skin reactions are discussed in other chapters, such as:

- Ultraviolet erythema in guinea pigs (H.3.2.2.1),
- Vascular permeability (H.3.2.2.2),
- Oxazolone-induced ear edema (H.3.2.2.4),
- Croton-oil ear edema in rats and mice (H.3.2.2.5),
- Spontaneous autoimmune diseases in animals (I.2.2.1),
- Passive cutaneous anaphylaxis (I.2.2.4),
- Arthus type immediate hypersensitivity (I.2.2.5),
- Delayed type hypersensitivity (I.2.2.6),
- Reversed passive Arthus reaction (I.2.2.7),
- Acute graft versus host disease (I.2.2.15),
- SLE-like disorder in MRL/lpr mice (I.2.2.16),
- Inhibition of allogenic transplant rejection (I.2.2.20).

P.2.1 Spontaneous Dermatitis

P.2.1.1 NC/Nga Mouse as Model for Atopic Dermatitis

The NC/Nga mouse has been recommended as a model for atopic dermatitis (Matsuda et al. 1997; Tsudzuki et al. 1997; Suto et al. 1999; Vestergaard et al. 1999, 2000; Kotani et al. 2000; Aioi et al. 2001; Kohara et al. 2001). When kept in specific pathogen free conditions, it remains healthy, but when kept in non-sterile conditions, it spontaneously develops a disease resembling atopic dermatitis at the age of 6–7 weeks. The level of IgE in the blood gradually increases to very high levels, and peaks at the age of 16–18 weeks (Matsuda et al. 1997). This enhanced IgE production has been attributed to an increased sensitivity of the B cell to the CD40 ligand and to IL-4, which is the result of enhanced phosphorylation of Janus kinase 3, a feature found also in atopic dermatitis (Matsumoto et al. 1999). At 16–18 weeks, the mice develop dry skin, and, gradually, nodular lesions, which in turn become crusted wounds. The lesions are pruritic and they are located on the back, the neck, the ears and the face. Biophysical parameters show impairment of water retention and barrier function. The amount of ceramide in the skin decreases significantly (Aioi et al. 2001).

Histologically, the skin lesions in the NC/Nga mice are characterized by hyperkeratosis and parakeratosis, which resemble the lichenified lesions observed in atopic dermatitis patients. In the dermis, an infiltration is found, similar to that seen in atopic dermatitis patients, containing lymphocytes, eosinophils, mast cells and macrophages, in addition to a large population of dendritic cells (Vestergaard et al. 1999).

The lesions in the NC/Nga mouse improve after treatment with tacrolimus hydrate (FK506) ointment (Hiroi et al. 1998) and also with topical steroids (Vestergaard et al. 1999). Both treatments reverse the changes in the skin, block the expression of inflammatory cytokines and decrease the serum levels of IgE.

FURTHER DERMATITIS MODELS

Iwasaki et al. (2001) recommended atopic NC/Nga mice as a model for allergic asthma: after immunization with ovalbumin, severe allergic responses were elicited by a single intranasal challenge.

Arai et al. (2004) showed that a prostanoid DP_1 receptor agonist inhibits the pruritic activity in NC/Nga mice with atopic dermatitis.

Mihara et al. (2004) described the vital role of the itch-scratch response in development of spontaneous dermatitis in NC/Nga mice. Capsaicin-sensitive sensory nerves of these mice were ablated by neonatal capsaicin treatment. Scratching behavior was almost completely prevented in these mice and the development of dermatitis and elevation of the serum IgE level were significantly suppressed.

Ohmura et al. (2004) studied the involvement of substance P in scratching behavior in a picrylchloride-induced dermatitis model in NC/Nga mice.

Takano et al. (2004) evaluated the antipruritic effects of several agents on scratching behavior by NC/Nga mice.

Takaoka et al. (2005, 2006) tested the expression of IL-31 gene transcripts in NC/Nga mice with atopic dermatitis. The expression of IL-31 mRNA in the skin of NC/Nga mice with scratching behavior was significantly higher than that in NC/Nga mice without scratching behavior.

Further animal models for atopic dermatitis were described, such as the NOA (Naruto Research Institute Otsuka Atrichia) mouse (Natori et al. 1999; Watanabe et al. 1999). The mice develop ulcerative skin lesions with accumulation of mast cells and increased serum IgE.

A spontaneous mutation characterized by chronic proliferative dermatitis in C57BL mice was described by HogenEsch et al. (1993).

Barton et al. (2000) reported that mice lacking the transcription factor ReIB develop T cell-dependent skin lesions similar to human atopic dermatitis.

Herz et al. (1998) developed a human-SCID mouse model to analyze the possible role of bacterial superantigens in human allergic immune responses under *in vivo* conditions.

Hossen et al. (2005) described the effect of loratadine on atopic-dermatitis-associated pruritus in ICR and hairless mice.

Sonkoly et al. (2006) described IL-31 as a new link between T cells and pruritus in atopic skin inflammation.

Chan et al. (2001) reported that the expression of IL-4 in the epidermis of **transgenic mice** results in a pruritic inflammatory skin disease. The mice spontaneously develop a skin disease reproducing all key features of human atopic dermatitis, including xerosis, conjunctivitis, inflammatory skin lesions, *Staphylococcus aureus* infection, histopathology of chronic dermatitis with T cell, mast cell, macrophage-like mononuclear cell, and eosinophil infiltration, and elevation of total serum IgE and IgG1.

Konishi et al. (2002) demonstrated in IL-18-transgenic mice that IL-18 contributes to the spontaneous development of atopic dermatitis-like inflammatory skin lesion independently of IgE/stat6 under specific pathogen-free conditions.

REFERENCES AND FURTHER READING

Aioi A Tonogaito H Suto H Hamada K Ra CR, Ogawa H Maibach H Matsuda H (2001) Impairment of skin barrier function in NC/Nga Tnd mice as a possible model for atopic dermatitis. Br J Dermatol 144:12–18

Arai I Takano N Hashimoto Y Futaki N Sugimoto M Takahashi N Inoue T Nakaike S (2004) Prostanoid DP_1 receptor agonist inhibits the pruritic activity in NC/Nga mice with atopic dermatitis. Eur J Pharmacol 505:229–235

Barton D Hogen-Esch H Weih F (2000) Mice lacking the transcription factor ReIB develop T cell-dependent skin lesions similar to human atopic dermatitis. Eur J Immunol 30:2323–2332

Chan LS Robinson N Xu L (2001) Expression of interleukin-4 in the epidermis of transgenic mice results in a pruritic inflammatory skin disease: an experimental animal model to study atopic dermatitis. J Invest Dermatol 117:977–983

Herz U Schnoy N Borelli S Weigl L Käsbohrer U Daser A Wahn U Köttgen E Ranz H (1998) A human-SCID mouse model for allergic immune response. Bacterial superantigen enhances skin inflammation and suppresses IgE production. J Invest Dermatol 110:224–231

Hiroi J Sengoku T Morita K Kishi S Sato S Ogawa T Tsudzuki M Wada A Esaki K (1998) Effect of tacrolimus hydrate (FK506) ointment on spontaneous dermatitis in NC/Nga mice. Jpn J Pharmacol 76:175–183

HogenEsch H Gijbels MJ Offerman E van Hooft J van Bekkum DW Zurcher C (1993) A spontaneous mutation

characterized by chronic proliferative dermatitis in C57BL mice. Am J Pathol 143:972–982
Hossen MA Fujii Y Ogawa M Takubo M Tsumuro T Kamei C (2005) Effect of loratadine on mouse models of atopic dermatitis associated pruritus. Int Immunopharmacol 5:1331–1336
Iwasaki T Tanaka A Itakura A Yamashita N Ohta K Matsuda H Onuma M (2001) Atopic NC/Nga mice as a model for allergic asthma: severe allergic responses by single intranasal challenge with protein antigen. J Vet Med Sci 63:413–419
Kohara Y Tanabe K Matsuoka K Kanda N Matsuda H Karasuyama H Yonekawa H (2001) A major determinant quantitative-trait locus responsible for atopic dermatitis-like skin lesions in NC/Nga mice is located on chromosome 9. Immunogenetics 53:15–21
Konishi H Tsutsui H Murakami T Yumikura-Futatsugi S Yamanaka KI Tanaka M Iwakura Y Suzuki N Takeda K Akira S Nakanishi K Mizutani H (2002) IL-18 contributes to the spontaneous development of atopic dermatitis-like inflammatory skin lesion independently of IgE/stat6 under specific pathogen-free conditions. Proc Natl Acad Sci USA 99:11340–11345
Kotani M Matsumoto M Fujita A Higa S Wang W Suemura M Kishimoto T Tanaka T (2000) Persimmon leaf extract and astragalin inhibit development of dermatitis and IgE elevation in NC/Nga mice. J Allergy Clin Immunol 106:159–166
Matsuda H Watanabe N Geba GP Sperl J Tsudzuki M Hiroi J Matsumoto M Ushio H Saito S Askenase PW Ra C (1997) Development of atopic dermatitis-like skin lesion with IgE hyperproduction in NC/Nga mice. Int Immunol 9:461–466
Matsumoto M Ra C, Kawamoto K Sato H Itakura A Sawada J Ushio H Mitsuishi K Hikasa Y Matsuda H (1999) IgE hyperproduction through enhanced tyrosine phosphorylation of Janus kinase 3 in NC/Nga mice, a model for human atopic dermatitis. J Immunol 162:1056–1063
Mihara K Kuratani K Matsiu T Nakamura M Yokota K (2004) Vital role of the itch-scratch response in development of spontaneous dermatitis in NC/Nga mice. Br J Dermatol 151:335–345
Natori K Tamari M Watanabe O Onouchi Y Shiomoto Y Kubo S Nakamura Y (1999) Mapping of a gene responsible for dermatitis in NOA (Naruto Research Institute Otsuka Atrichia) mice, an animal model of allergic dermatitis. J Hum Genet 44:372–376
Ohmura T Hayashi T Satoh Y Konomi A Jung B Satoh H (2004) Involvement of substance P in scratching behaviour in an atopic dermatitis model. Eur J Pharmacol 491:191–194
Sonkoly E Muller A Lauerma AI Pivarsci A Soto H Kemeny L Alenius H Dieu-Nosjean MC Meller S Rieker J Steinhoff M Hoffmann TK Ruzicka T Zlotnik A Homey B (2006) IL 31: a new link between T cells and pruritus in atopic skin inflammation. J Allergy Clin Immunol 117:411–417
Suto H Matsuda H Mitsuishi K Hira K Uchida T Unno T Ogawa H Ra C (1999) NC/Nga mice: a mouse model for atopic dermatitis. Int Arch Allergy Immunol 120, Suppl 1:70–75
Takano N Arai I Hashimoto Y Kurachi M (2004) Evaluation of antipruritic effects of several agents on scratching behavior by NC/Nga mice. Eur J Pharmacol 452:159–165
Takaoka A Arai I Sugimoto M Yamaguchi A Tanaka M Nakaike S (2005) Expression of IL-31 gene transcripts in NC/Nga mice with atopic dermatitis. Eur J Pharmacol 516:180–181
Takaoka A Arai I Sugimoto M Honma Y Futaki N Nakamura A Nakaike S (2006) Involvement of IL-31 on scratching behavior in NC/Nga mice with atopic-like dermatitis. Exp Dermatol 15:161–167
Tsudzuki M Watanabe N Wada A Nakane Y Hiroi J Matsuda H (1997) Genetic analyses for dermatitis and IgE hyperproduction in the NC/Nga mouse. Immunogenetics 47:88–90
Vestergaard C Yoneyama H Murai M Nakamura K Tamaki K Yoshie O Irimura T Mizutani H Matsushima K (1999) Overproduction of Th2-specific chemokines in NC/Nga mice exhibiting atopic dermatitis-like lesions. J Clin Invest 104:1097–1105
Vestergaard C Yoneyama H Matsushima K (2000) The NC/Nga mouse: a model for atopic dermatitis. Mol Med Today 6:209–210
Watanabe O Natori K Tamari M Shiomoto Y Kubo S Nakamura Y (1999) Significantly elevated expression of PF4 (platelet factor 4) and eotaxin in the NOA mouse, a model of atopic dermatitis. J Hum Genet 44:173–176

P.2.1.2 Motheaten Mice

Mice homozygous for the autosomal recessive motheaten (me) or the allelic viable motheaten (me^v) mutations develop severe and early-age onset of systemic autoimmune and inflammatory disease (Green and Shultz 1975; Shultz et al. 1984; Shultz 1988; Kovarik et al. 1994; Su et al. 1998). These mice show arthritis, patchy dermatitis and hemorrhagic pneumonitis; the latter is considered to be the cause of the early death of me and me^v mice at the age of 3 and 9 weeks, respectively.

Homozygous me^v mice are identified first at the age of 3–4 days by focal depigmentation of the skin, followed by patchy absence of hair and by necrotic lesions on paws, tail and ears.

REFERENCES AND FURTHER READING

Green MC Shultz LD (1975) Motheaten, an immunodeficient mutant of the mouse. I. Genetics and pathology. J Hered 66:250–258
Kovarik J Kuntz L Ryffel B Borel JF (1994) The viable motheaten (me^v) mouse – a new model for arthritis. J Autoimmun 7:575–588
Shultz LD (1988) Pleiotropic effects of deleterious alleles in the "motheaten" locus. Curr Top Microbiol Immunol 137:216–222
Shultz LD Coman DR Bailey CL Beamer WG Sidman CL (1984) "Viable motheaten", a new allele in the motheaten locus. Am J Pathol 116:179–192
Su X, Zhou T Yang P Edwards CK III, Mountz JD (1998) Reduction of arthritis and pneumonitis in motheaten mice by soluble tumor necrosis factor receptor. Arthr Rheum 41:139–149

P.2.1.3 Spontaneous Erythema in Hairless Rats

The hairless rat (WBN/Kob-*Ht*) is a dominant mutant derived from the Wistar strain. With an incidence rate of about 4% in both male and female animals, at an age of 20 weeks an erythema appears spontaneously

on the dorsal skin, gradually becoming widespread and progressive in nature (Iwamoto et al. 1997; Tani et al. 1998). Histopathologically, erythema is characterized by dermatitis induced by an immunological reaction. Areas of erythema in the skin were decreased by treatment with dexamethasone (1 mg/kg) or cyclosporine (25 or 50 mg/kg) injected subcutaneously every other day for 2 weeks. The results suggested that erythema on the hairless rat could be used as an animal model of spontaneous dermatitis.

MODIFICATIONS OF THE METHOD

Atopic dermatitis-like symptoms were reported in hypomagnesaemic hairless rats by Chavaz et al. (1984) and Neckermann et al. (2000).

REFERENCES AND FURTHER READING

Chavaz P Faucher F Saurat JH (1984) Dermatosis of hairless rats fed with a hypomagnesic diet – pathology and immunology. Dermatologica 169:105–111

Iwamoto S Nakayama H Yasoshima A Doi K (1997) Hydrogen peroxide-induced dermatitis in WBN/Kob-Ht rats. Exp Anim 46:147–151

Neckermann G Bavandi A Meingassner JG (2000) Atopic dermatitis-like symptoms in hypomagnesaemic hairless rats are prevented and inhibited by systemic or topical SDT ASM 981. Br J Dermatol 142:669–679

Tani S Noguchi M Hosada Y Sugibayasi K Morimoto Y (1998) Characteristics of spontaneous erythema appeared in hairless rats. Exp Anim 47:253–256

P.2.1.4 Spontaneous Atopic Dermatitis in Dogs

PURPOSE AND RATIONALE

Atopic dermatitis is a known chronic inflammatory skin disease in dogs (Scott et al. 2001).

Olivry et al. (2001) characterized the inflammatory infiltrate during IgE-mediated late phase reactions in the skin of normal and atopic dogs with *Dermatophagoides farinae*-induced allergy.

Nuttall et al. (2002) studied the expression of Th1, Th2 and immunosuppressive gene transcripts in canine atopic dermatitis and found over-production of IL-4. Canine atopic dermatitis was proposed as a possible animal model of human atopic dermatitis.

REFERENCES AND FURTHER READING

Nuttall TJ Knight PA McAleese SM Lamb JR Hill PB (2002) Expression of Th1, Th2 and immunosuppressive gene transcripts in canine atopic dermatitis. Clin Exp Allergy 32:789–795

Olivry T Dunston SM Murphy KM Moore PF (2001) Characterization of the inflammatory infiltrate during IgE-mediated late phase reactions in the skin of normal and atopic dogs. Vet Dermatol 12:49–58

Scott DW Miller WH Griffin C (eds) (2001) Skin immune system and allergic skin disease. In: Muller & Kirk's small animal dermatology. Saunders, Philadelphia, Pa., pp 534–666

P.2.2 Contact Dermatitis

P.2.2.1 Contact Hypersensitivity in Animals

PURPOSE AND RATIONALE

The phenomenon of contact hypersensitivity in animals is thought to mirror atopic dermatitis or eczema in patients (Corsini et al. 1979; Cooper 1994; Leung 1997).

P.2.2.1.1 Contact Hypersensitivity in Mice

PROCEDURE

CD1 mice are sensitized on the shaved abdomen with 20 µl of 0.5% 2,4-dinitrofluorobenzene (DNFB) in a vehicle consisting of 95% acetone/5% olive oil on days 0 and 1. On day 5, groups of 10 mice are challenged with 0.2% DNFB with or without co-dissolved drug, 10 µl on both the internal and external surface of both ears. Mice are sacrificed 24 h post-challenge, and a 7 mm diameter circle punched from each ear is weighed immediately on a microbalance.

EVALUATION

The mean earplug weight from naïve mice challenged with 0.2% DNFB are used as background control.

Percent inhibition is calculated using the following formula:

$$100 - \frac{\text{plug}_{\text{exp.}} - \text{plug}_{\text{mean naïve}}}{\text{plug}_{\text{mean sens.}} - \text{plug}_{\text{mean naïve}}} \times 100$$

$\text{plug}_{\text{exp.}}$ = experimental ear plug weight

$\text{plug}_{\text{mean naïve}}$ = mean naïve ear plug weight

$\text{plug}_{\text{mean sens.}}$ = mean sensitized vehicle control plug weight

ED_{50} values are derived by simultaneous least square regressive analysis.

MODIFICATIONS OF THE METHOD

Lowe et al. (1977) used oxazolone-sensitized Swiss Webster **mice** to evaluate anti-inflammatory properties

of a prostaglandin antagonist, a corticosteroid and indomethacin in experimental contact dermatitis.

Studies in mice on allergic contact dermatitis were performed by Ek and Theodorsson (1990), Fraginals et al. (1990), Katayama et al. (1990), Lavaud et al. (1991), Trenam et al. (1991), Stanley et al. (1991), Maguire (1996), and Corsini and Galli (1998).

Grabbe et al. (1995) showed that removal of the majority of epidermal Langerhans cells by topical or systemic steroid application enhances the effector phase of contact hypersensitivity in BALB/c mice.

Koyama et al. (1998) used tenascin-C knockout mice and studied the effect on dinitrofluorobenzene-induced dermatitis.

Meingassner et al. (1997) sensitized female NMRI mice on the shaved abdomen with 50 µl of oxazolone (2% in acetone). After 7 days, they were challenged with 10 µl of 2% (for topical testing) or 0.5% (for systemic testing) oxazolone on the inner surface of the right ear. Compounds were tested topically by a single application of 10 µl ethanolic solution to the challenge site, 30 min after challenge. Compounds were tested for systemic activity by administration of a single subcutaneous injection immediately after challenge or by two oral doses (2 h before and immediately after challenge). The unchallenged left ears served as normal controls. Dermatitis was evaluated from the difference in pinnal weight, which was taken as a measure of inflammatory edema 24 h after challenge.

Traidl et al. (1999) reported inhibition of allergic contact dermatitis to dinitrochlorobenzene (DNCB) but not to oxazolone in interleukin-4-deficient mice.

Morita et al. (1999) reported that fur mites induce dermatitis associated with IgE hyperproduction in NC/Kuj mice. Four-week-old NC/Kuj mice were kept together with NC mice infected with fur mite (*Myocoptes musculinus*) for 2 weeks in isolated clean rooms and thereafter separated. Serum IgE levels were determined and the skin examined histologically.

Matsuoka et al. (2001) described a mouse model of the atopic eczema/dermatitis syndrome by repeated application of a crude extract of house-dust mite *Dermatophagoides farinae*. The mites were cultured in a mixture of mouse diet and dried yeast in culture flasks. A crude extract in PBS was applied to the shaved back of NC/Nga mice or BALB/c mice three times a week for 8 weeks. In the NC/Nga group, dryness and scaling appeared on the skin, and scratching behavior increased at the second week in the treated group. Skin erosion and hemorrhage occurred in the fourth week. The epidermis thickened and deepened into the upper dermis, in which mast cells were highly accumulated, corresponding with the skin lesions of atopic eczema/dermatitis syndrome in patients.

Matsui and Nishikawa (2002) used female specific-pathogen-free BALB/c mice at an age of 6–8 weeks. The animals were barrier-disrupted by repeated applications of adhesive cellophane tape prior to percutaneous sensitization by topical administration of 100 µl of a solution of house dust mite antigen. Seven days after the sensitization, the mice were challenged on the shaved dorsal skin near the ear by subcutaneous injection of 10 µl of mite antigen or lipoteichoic acid from *Staphylococcus aureus* for elicitation of localized skin inflammation. The cytokine response in the dorsal skin was investigated by reverse transcription-polymerase chain reaction and immunohistological analysis.

Spergel et al. (1998) reported that epicutaneous sensitization with ovalbumin induced localized allergic dermatitis and hyper-responsiveness to methacholine after single exposure to aerosolized antigen in mice.

Spergel et al. (1999) used mice with targeted deletions of IL-4, IL-5, and interferon-γ cytokine genes to assess the role of these cytokines in a murine model of allergic dermatitis elicited by epicutaneous sensitization with ovalbumin.

Laouini et al. (2003) used IL-$10^{-/-}$ mice to examine the role of IL-10 in a mouse model of allergic dermatitis induced by epicutaneous sensitization with ovalbumin on tape-stripped skin.

Takeshita et al. (2004) underlined the essential role of MHC II-independent $CD4^+$ T cells, IL-4 and STAT6 in contact hypersensitivity induced by fluorescein isothiocyanate in the mouse and recommended fluorescein-isothiocyanate-induced contact hypersensitivity as a suitable animal model for atopic dermatitis.

Sasakawa et al. (2001) induced atopic dermatitis-like lesions by topical application of mite antigens in NC/Nga mice. Extracts of mite antigen were injected repeatedly at the ventral side of the ear. Clinical symptoms and thickness of the ear were measured. On day 18, blood and submandibular lymph nodes were collected to measure plasma immunoglobulins and to perform histochemical analysis.

Heishi et al. (2003) performed gene expression analysis of atopic dermatitis-like skin lesions induced in NC/Nga mice by mite antigen stimulation under specific pathogen-free conditions. Mite Extract-Dp (LSL Japan) was injected intradermally into the right and left pinnae and into the skin of NC/Nga of BALB/c mice in two places once per 3 days, and the clinical symptoms and the ear thickness were measured. On day 14 or 28, plasma IgE was determined. Further-

more, mRNA transcripts in pinnae were analyzed using real-time quantitative PCR.

Food hypersensitivity plays a pathogenic role in patients with atopic dermatitis (Sicherer and Sampson 1999).

Li et al. (2001) reported a murine model of atopic dermatitis associated with food hypersensitivity. Female C3H/HeJ mice were sensitized orally to cow's milk or peanut with cholera toxin adjuvant and then subjected to low-grade allergen exposure. Histologic examination of skin lesions, allergen-specific Ig levels, and allergen-induced T-cell proliferation were studied. Treatment of the eruption with topical corticosteroids led to decreased pruritus and resolution of the cutaneous eruption.

P.2.2.1.2 Contact Hypersensitivity in Rats

Meingassner et al. (1997) sensitized female Sprague Dawley rats by application of 80 µl of 2% 2,4-dinitrofluorobenzene (DNFB, dissolved in acetone, DMSO and olive oil 50:10:38 v/v/v), applied in 20 µl volumes to the inner surface of both ear lobes and to both shaved inguinal regions on day 1. Allergic contact dermatitis was elicited with 30 µl of 0.5% DNFB applied to the test sites of ≈15 mm in diameter on both shaved flanks on day 12. Animals were treated twice by gavage 2 h before and immediately after challenge. Dermatitis was evaluated by measuring the thickness of the lifted skin fold at the test sites with a spring-loaded micrometer (Schnelltaster, Kröplin, Germany) before challenge and 24 h after challenge.

P.2.2.1.3 Contact Hypersensitivity in Guinea Pigs

Guinea pigs, six per group, are sensitized on the dorsal surface of one ear pinna with 50 µl of 10% DBFB in 50% acetone: 50% olive oil on day 0, and then on the opposing ear on day 1. On day 5, animals are shaved and challenged with 0.5% 1-chloro-2,4-dinitrochlorobenzene (DNCB) with or without co-dissolved drug, 15 µl per site, 4.8 µl per cm^2, on the dorsolateral surface (Hsieh et al. 1996). Naïve animals are challenged with DNCB and serve as non-specific controls. The response is scored visually in a blinded fashion 24 h after challenge (0: no change; 0.5: questionable erythema; 1: faint or scattered erythema; 2: mild, confluent erythema; 3: moderate erythema without edema or induration; 4: strong erythema with uniform induration or edema; 5: severe erythema with induration or edema, plus ulceration). Data are calculated as for mouse contact hypersensitivity.

Rosenqvist et al. (1991) studied the effects of cilazaprilat and enalaprilat on experimental dermatitis in guinea pigs.

Boyera et al. (1992) tested repeated application of dinitrochlorobenzene to the ears of sensitized guinea pigs as an animal model for contact eczema in humans.

The effect of a topical preparation of mycophenolic acid on experimental allergic contact dermatitis of guinea pigs induced by dinitrofluorobenzene was described by Shoji et al. (1994).

P.2.2.1.4 Contact Hypersensitivity in Pigs

Groups of 6–12 pigs are sensitized with 10% DNFB in acetone/DMSO/olive oil (45:5:50 by volume) to the shaved outer aspect of both ears and bilateral sites of the lower abdomen, 100 µl per site, on day 0, with a second application of 5% DNFB to the internal pinna and the lower thorax on day 3. On day 9, pigs are restrained on a webbed canvas cart and the test area carefully shaved with an electric clipper. A pilot challenge with 0.1, 0.15, and 0.2% DNCB in acetone/olive oil (95:5 by volume), 3.8 µl per cm^2, is used to determine conditions for obtaining submaximal average response in each animal cohort. Pigs are scored by a blinded observer, 24 h post-challenge on a scale from 0 to 4 (0: no change; 0.5: questionable erythema; 1: faint or scattered erythema; 2: moderate erythema without induration or edema; 3: strong erythema with focal areas of edema or induration: 4: extreme erythema with uniform induration or edema). Pigs having a mean DNCB control score <1.5 are excluded (Hsieh et al. 1997). Based on their pilot response on day 10, animals are stratified into two groups having comparable mean scores, challenged on duplicate sites with DNCB in 95:5, with or without co-dissolved drug, and scored on day 11. Scores for each challenge site are compared with the average of the control spots treated with DNCB alone on the same pig, and expressed as percentage inhibition.

Bilski and Thomson (1984) recommended allergic contact dermatitis in the domestic pig as a model for evaluating the topical anti-inflammatory activity of drugs and their formulations.

Meingassner and Stütz (1992) sensitized female domestic pigs with a 10% solution of DNFB dissolved in 50% acetone, 10% dimethylsulfoxide (DMSO) and 30% olive oil applied in volumes of 100 µl onto both auricles (medial aspects) and groins on day 1. The ani-

mals were exposed again on the lateral aspects of both auricles to 100 µl of 2% DNFB on day 4. Challenge was performed with a 1% DNFB solution (without DMSO) on day 12 by applying 20 µl epicutaneously to each of 24 test sites (2 cm diameter) arranged in four craniocaudal lines on the dorsolateral back of each animal. The test sites were treated twice (0.5 and 6 h after challenge) with 20 µl of solutions of active compound or drug vehicle. Evaluation of the treatment-related effects was performed at the peak inflammatory response which was 24 h after challenge. Each test site was evaluated visually for (1) intensity, (2) extent of erythema, and (3) consistency using arbitrary scores from 0 to 4. In addition, skin changes were biophysically characterized by measuring microvascular perfusion (PeriFlux PF3 Laser Doppler Perfusion Monitor) and reflective color measurement (Minolta Chroma Meter CR 200).

Vana and Meingassner (2000) described morphologic and immunohistochemical features of experimentally induced contact dermatitis in **Göttingen minipigs**.

REFERENCES AND FURTHER READING

Bilski AJ Thomson DS (1984) Allergic contact dermatitis in the domestic pig. A new model for evaluating the topical anti-inflammatory activity of drugs and their formulations. Br J Dermatol 111, Suppl 27:143

Boyera N Cavey D Bouclier M Burg G Rossio P Hensby C (1992) Repeated application of dinitrochlorobenzene to the ears of sensitized guinea pigs; a preliminary characterization of a potential new animal model for contact eczema in humans. Skin Pharmacol 5:184–188

Cooper KD (1994) Atopic dermatitis: recent trends in pathogenesis and therapy. J Invest Dermatol 102:128–137

Corsini E Galli CL (1998) Cytokines and irritant contact dermatitis. Toxicol Lett 102–103:277–282

Corsini AC Bellucci SB Costa MG (1979) A simple method of evaluating delayed type hypersensitivity in mice. J Immunol Meth 30:195–200

Ek L, Theodorsson E (1990) Tachykinins and calcitonin gene-related peptide in oxazolone-induced allergic contact dermatitis in mice. J Invest Dermatol 94:761–763

Fraginals R Lepoittevin JP Benezra C (1990) Sensitizing capacity of three methyl alkanesulphonates: a murine *in vivo* and *in vitro* model of allergic contact dermatitis. Arch Dermatol Res 282:455–458

Grabbe S Steinbrink K Steinert M Luger TA Schwarz T (1995) Removal of the majority of epidermal Langerhans cells by topical or systemic steroid application enhances the effector phase of murine contact hypersensitivity. J Immunol 155:4207–4217

Heishi M Imai Y Katayama H Hashida R Ito M, Shinagawa A Sugita Y (2003) Gene expression analysis of atopic dermatitis-like skin lesions induced in NC/Nga mice be mite antigen stimulation under specific pathogen-free conditions. Int Arch Allergy Immunol 132:356–363

Hsieh GC Kolano RM Andrews JW (1996) Immunosuppressant effects on improved guinea pig contact hypersensitivity (CH) model: induction with DNFB and elicitation with DNCB. FASEB J 10:A1221

Hsieh GC Kolano RM Gauvin DM (1997) Development of a swine contact hypersensitivity (CH) model – sensitization with DNFB and elicitation with DNCB for evaluating topical inhibitors. J Invest Dermatol 108:671

Katayama I Tanei R Yokozeki H Nishioka K Dohi Y (1990) Induction of eczematous skin reaction in experimentally induced hyperplastic skin of BALB/c mice by monoclonal anti-DNP IgE antibody: Possible implications for skin lesion formation in atopic dermatitis. Int Arch Allergy Appl Immunol 93:148–154

Koyama Y Kusubata M Yoshiki A Hiraiwa N Ohashi T Irie S Kusukabe M (1998) Effect of tenascin-C deficiency on chemically induced dermatitis in the mouse. J Invest Dermatol 111:930–935

Laouini D Alenius H Bryce P Oettgen H Tsitsikov E Geha RS (2003) IL-10 is critical for Th2 response in a murine model of allergic dermatitis. J Clin Invest 112:1058–1066

Lavaud P Rodrigue F Carre C Touvay C Mencia-Huerta JM Braquet P (1991) Pharmacological modulation of picryl chloride-induced contact dermatitis in the mouse. J Invest Dermatol 97:101–105

Leung DM (1997) Atopic dermatitis: immunobiology and treatment with immune modulators. Clin Exp Immunol 107:25–30

Li XM, Kleiner G Huang CK Lee SY, Schofield B Soter NA Sampson HA (2001) Murine model of atopic dermatitis associated with food hypersensitivity. J Allergy Clin Immunol 107:693–702

Lowe NJ Virgadamo F Stoughton RB (1977) Anti-inflammatory properties of a prostaglandin antagonist, a corticosteroid and indomethacin in experimental contact dermatitis. Br J Dermatol 96:433–438

Maguire HC (1996) Cyclophosphamide and interleukin-12 synergistically upregulate the acquisition of allergic contact dermatitis in the mouse. Arch Derm Venereol 76:277–279

Matsui K Nishikawa A (2002) Lipoteichoic acid from *Staphylococcus aureus* induces Th2-prone dermatitis in mice sensitized percutaneously with allergen. Clin Exp Allergy 32:783–788

Matsuoka H Maki N Yoshida S Arai M Wang J Oikawa Y Ikeda T Hirota N Nakagawa H Ishii A (2001) A mouse model of the atopic eczema/dermatitis syndrome by repeated application of a crude extract of house-dust mite *Dermatophagoides farinae*. Allergy 58:139–145

Meingassner JG Stütz A (1992) Immunosuppressive macrolides of the type FK 506: a novel class of topical agents for treatment of skin diseases? J Invest Dermatol 98:851–855

Meingassner JG Grassberger M Fahrngruber H Moore HD Schuurman H Stütz A (1997) A novel anti-inflammatory drug, SDZ ASM 981, for the topical and oral treatment of skin diseases*: in vivo* pharmacology. Br J Dermatol 137:568–576

Morita E Kaneko S Hiragun T Shindo H Tanaka T Furukawa T Nobukiyo A Yamamto S (1999) Fur mites induce dermatitis associated with IgE hyperproduction in an inbred strain of mice, NC/Kuj. J Dermatol Sci 19:37–43

Rosenqvist U Persson K Lindgren BR Andersson RG (1991) Effects of cilazaprilat and enalaprilat on experimental dermatitis in guinea pigs. Pharmacol Toxicol 68:404–407

Sasakawa T Higashi Y Sakuma S Hirayama Y Sasakawa Y Ohkubo Y Goto T Matsumoto M Matsuda H (2001) Atopic dermatitis-like lesions induced by topical application of mite antigens in NC/Nga mice. Int Arch Allergy Immunol 126:239–247

Shoji Y Fukumura T Kudo M Yanagawa A Shimada J Mizushima Y (1994) Effect of topical preparation of mycophe-

nolic acid on experimental allergic contact dermatitis of guinea pigs induced by dinitrofluorobenzene. J Pharm Pharmacol 46:643–646
Sicherer SH Sampson HA (1999) Food hypersensitivity and atopic dermatitis: pathophysiology, epidemiology, diagnosis and management. J Allergy Clin Immunol 104:114–122
Spergel JM Mizoguchi E Brewer JP Martin TR Bhan AK Geha RS (1998) Epicutaneous sensitization with protein antigen induced localized allergic dermatitis and hyperresponsiveness to methacholine after single exposure to aerosolized antigen in mice. J Clin Invest 101:1614–1622
Spergel JM Mizoguchi E Oettgen H Bhan AK Geha RS (1999) Roles of T_H1 and T_H2 cytokines in a murine model of allergic dermatitis. J Clin Invest 103:11034–1111
Stanley PL Steiner S Havens M Tramposch KM (1991) Mouse skin inflammation induced by multiple topical applications of 12-O-tetradecanoylphorbol-13-acetate. Skin Pharmacol 4:262–271
Takeshita K Yamasaki T Akira S Gantner F Bacon KB (2004) Essential role of MHC II-independent $CD4^+$ T cells, IL-4 and STAT6 in contact hypersensitivity induced by fluorescein isothiocyanate in the mouse. Int Immunol 16:685–695
Traidl C Jugert F Krieg T Merk H Hunzelmann N (1999) Inhibition of allergic contact dermatitis to DNCB but not to oxazolone in interleukin-4 deficient mice. J Invest Dermatol 112:476–482
Trenam CW Dabbagh AJ Morris CJ Blake DR (1991) Skin inflammation induced by reactive oxygen species (ROS): an *in vivo* model. Br J Dermatol 125:325–329
Vana G Meingassner JG (2000) Morphologic and immunohistochemical features of experimentally induced contact dermatitis in Göttingen minipigs. Vet Pathol 37:565–580

P.2.2.2 Non-Immunologic Contact Urticaria

PURPOSE AND RATIONALE

Contact urticaria is defined as a wheal-and flare reaction, appearing shortly after certain substances contact intact skin and disappearing within some hours, leaving normal appearing skin. Contact urticaria is divided into two main types, immunologic and non-immunologic (Maibach and Johnson 1975). Immunologic contact urticaria is mediated at least partially by specific IgE antibodies attached to mast cell membranes. Vasoactive substances, released from mast cells, elicit erythema and edema of the skin. Non-immunologic contact urticaria appears only on the contact area without previous sensitization. Specific antibodies against the causative substance are not found in serum. Lahti and Maibach (1984) investigated the suitability of the guinea pig for studies on non-immunologic contact urticaria.

PROCEDURE

Female Hartley strain guinea pigs weighing 350–500 g are used. Fifty µl of test substances is applied with a micropipette to both sides of the earlobe. One ear of the animal is challenged with the contact urticant, while the other ear serves as control with ethyl alcohol. Earlobe thickness is measured three times on four different sites using a string micrometer with round touching plates, 6 mm in diameter. The string of the instrument is adjusted so that the moving plate does not squeeze the tissue, but stops at once when it reaches the surface of the ear. The mean of 12 measurements is recorded as the pre-application thickness. All measurements after application of the test substance are performed once on the same four sites, and the mean is recorded as the post-application thickness.

The thickness of the ear is measured 5 min after application, and then every 10 min during the first h, every 15 min during the second, and every 30 min during the third h.

EVALUATION

The differences between post-application and pre-application values are recorded and plotted as time-response and dose-response curves.

MODIFICATIONS OF THE METHOD

Lauerma et al. (1997) used the trimellitic anhydride-sensitive mouse as an animal model for contact urticaria. BALB/c mice were sensitized with trimellitic anhydride by topical applications and treated with glucocorticosteroids, antihistaminics, or non-steroidal anti-inflammatory drugs. Ears were challenged with trimellitic anhydride and ear thickness was measured at baseline and 1, 2, 4, 8, and 24 h after challenge. Trimellitic anhydride caused a biphasic ear swelling response. However, there was also an early swelling by trimellitic anhydride in non-sensitized mice, suggesting that non-immunological as well as immunological mechanisms contribute to early swelling by trimellitic anhydride.

Irritant contact dermatitis was induced in mice by the application of 20 µl 0.01% A23187 (calcium ionophore) or 0.005% PMA (phenyl mercuric acetate) to both aspects of the right pinnae which were treated simultaneously (A23187) or after 30 min (PMA) with the test compound or vehicle (Meingassner and Stütz 1992). Topical efficacy was assessed by determination of the differences in weight of both auricles of treated and untreated mice 7.5 h (A23187) or 6 h (PMA) after application of the irritants.

REFERENCES AND FURTHER READING

Lathi A Maibach HI (1984) An animal model of nonimmunologic contact urticaria. Toxicol Appl Pharmacol 76:219–234
Lauerma AI Fenn B Maibach HI (1997) Trimellitic anhydride-sensitive mouse as an animal model for contact urticaria. J Appl Toxicol 17:357–360

Maibach HI Johnson HL (1975) Contact urticaria syndrome. Contact urticaria to diethyltoluamide (immediate-type hypersensitivity). Arch Dermatol 111:426–434
Meingassner JG Stütz A (1992) Anti-inflammatory effects of macrophilin-interacting drugs in animal models of irritant and allergic contact dermatitis. Int Arch Allergy Immunol 99:486–489

P.2.3
Immunological Models of Atopic Dermatitis

P.2.3.1
Mononuclear Cells from Atopic Dermatitis Donors

PURPOSE AND RATIONALE

Rühl et al. (2003) studied the effects of PPAR-α and PPAR-β ligands on immunoglobulin synthesis and cytokine production by peripheral blood mononuclear cells from normal donors and patients with atopic dermatitis.

PROCEDURE

Peripheral blood mononuclear cells were isolated from buffy coats of non-allergic healthy donors and atopic dermatitis patients by Ficoll Hypaque (D = 1.077) separation (350 *g*, 30 min, room temperature). B cells were purified by magnetic cell sorting using anti-CD19-coupled magnetic beads. Then 4×10^8 peripheral blood mononuclear cells in 800 µl PBS + 20 nM ethylenediaminetetraacetic acid + 0.2% bovine serum albumin + 15 µl Beriglobin (Chinon Bering, Marburg, Germany) were incubated for 10 min in ice, followed by addition of 200 µl conjugated beads (1.5 ratio) and 10 min of incubation at 4°C. After several washings, CD19-positive B cells were selected by magnetic positive selection with LS^+ column, and the cells were then resuspended in medium and counted. The same procedure was done for the purification of T cells and monocytes, respectively, using anti-CD3 and anti-CD14 coupled magnetic beads.

Peripheral blood mononuclear cells and purified B cells (10^6 cells per ml) were cultured in RPMI 1640 culture medium supplemented with L-glutamine (2 mM), penicillin (100 U per ml), streptomycin (100 µg/ml) and 10% heat inactivated fetal calf serum. All cell cultures were carried out at 37°C in humidified air and 5% CO_2 atmosphere.

For the immunoglobulin assays, immunoplates (Nunc, Wiesbaden, Germany) were coated overnight at 4°C with the isotope-specific anti-human Ig-Fc antibodies diluted in 0.1 M bicarbonate buffer. Blocking was performed by adding 2% bovine serum albumin/Tris-buffered saline for 1 h, followed by several washings. Supernatants and internal standard were then added to the wells and incubated in duplicate for 2 h. After several washes, the alkaline phosphatase-conjugated antibodies (IgA, IgG and IgM) or biotinylated anti-IgE MoAb was added. For IgE, plates were incubated for another hour with alkaline-phosphatase-conjugated streptavidin. Following the final reaction with phosphatase substrate (Sigma, Dreieich, Germany), plates were read in a microplate ELISA reader at 405 nm, and the amount of immunoglobulin was calculated according to the standard curve. Cytokines were determined by ELISA assays.

EVALUATION

Wilcoxon's signed rank test for matched pairs was performed to compare the results within the donor groups.

MODIFICATIONS OF THE METHOD

Furthermore, Rühl et al. (2003) performed *in vivo* experiments in ovalbumin-sensitized female NMRI mice confirming the *in vitro* findings and showing that the IL-4-mediated immune response was inhibited in PPAR-activator-treated mice.

Sperhake et al. (1998) studied the effects of recombinant human soluble interleukin-4 receptor on interleukin-4/staphylococcal enterotoxin B-stimulated peripheral mononuclear cells from patients with atopic eczema.

Hong et al. (2003) demonstrated the PPARγ-dependent anti-inflammatory action of rosiglitazone in human monocytes. Furthermore, it was shown that the suppression of tumor necrosis factor α (TNFα) secretion is not mediated by phosphatase and tensin homolog (PTEN) regulation.

REFERENCES AND FURTHER READING

Hong G Davis B Khattoon N Baker SF Brown J (2003) PPARγ-dependent anti-inflammatory action of rosiglitazone in human monocytes: suppression of TNFα secretion is not mediated by PTEN regulation. Biochem Biophys Res Commun 303:782–787
Rühl R, Dahten A Schweigert FJ Herz U Worm M (2003) Inhibition of IgE-production by peroxisome proliferator-activated ligands. J Invest Dermatol 121:757–764
Sperhake K Neuber K Enssle K Ring J (1998) Effects of recombinant human soluble interleukin-4 receptor on interleukin-4/staphylococcal enterotoxin B-stimulated peripheral mononuclear cells from patients with atopic eczema. Br J Dermatol 139:784–790

P.2.3.2
The SCID-hu Skin Mouse as Model for Atopic Dermatitis

PURPOSE AND RATIONALE

Severe combined immunodeficiency (SCID) mice have a defect in the antigen recombinant system that prevents the development of mature B and T lymphocytes (Bosma et al. 1983) and therefore renders these mice tolerant to xenografts of human cells and tissues.

Carballido et al. (2000, 2003), Biedermann et al. (2002, 2004), Igney et al. (2004) and Lametschwandtner et al. (2004) reported the establishment of an *in vivo* mouse model that allows monitoring of human T cell migration into human skin. This model is based on the use of SCID mice transplanted with human skin (SCID-hu Skin mice). Adoptively transferred human T helper (Th)2 cells obtained from atopic dermatitis skin lesions or peripheral blood T cells selectively migrate to the human skin grafts of these SCID mice in response to defined chemokines locally injected in the human skin grafts. Homing of human T cells into the human skin on SCID-hu Skin mice is a specific process since it only occurs in response to chemokine ligands that are specific for the chemokine receptors expressed on the migrating T cells.

PROCEDURE

Generation of SCID-hu Skin Mice

Human adult skin is obtained from breast or abdominal reduction surgery. The skin is perfused with cell culture media containing penicillin and streptomycin and fat tissues are removed. Subsequently, full thickness skin is trimmed at the dermal side to obtain skin biopsy samples containing the full epidermis, the papillary dermis, and part of the reticular dermis. This skin tissue is cut into pieces of approximately 10×10 mm and kept at 4°C in cell culture media until use. C.B-17/GbmsTac-*Prkdc*^{scid} *Lyst*^{bg} mice (M&B, Ry, Denmark, herein referred to as SCID mice) are anesthetized by i.p. injection of a solution containing ketamine and xylazine and their backs shaved. Subsequently, two pieces of skin of the same size as the human grafts are removed from the back of the mice and replaced by human skin pieces, which are fixed at their edges using surgical glue. At the end of the procedure, the human grafts are covered with a polyvinyl bandage to prevent scratching and to facilitate tissue engraftment. After transplantation, the human grafts undergo a period of human keratinocyte hyperproliferation resulting in the formation of hyperkeratotic crusts. During this process, human skin grafts fuse with the adjacent mouse skin. About 5 weeks after transplantation, the crusts fall off and reveal a skin tissue containing all the characteristic structures of normal human skin including a network of newly grown vessels connecting the graft with the underlying mouse tissues.

Generation and characterization of human T cells for skin homing studies in vivo

Th lymphocytes selected for *in vivo* migration studies in SCID-hu Skin mice are isolated from human atopic skin lesions in order to obtain Th cells with optimal skin homing potential. Human Th cell lines are grown from biopsies of **atopic dermatitis** patients challenged with house dust mite (HDM) antigens (Carballido et al. 1997). Th cell clones are isolated from the HDM-specific lines by limiting dilution and maintained by repeated stimulation with irradiated allogenic human peripheral blood mononuclear cells (PBMC) and phytohaem agglutinin (PHA), followed by expansion with human IL-2.

Atopic dermatitis is an inflammatory skin disease in which skin-infiltrating allergen-specific Th2 cells play a crucial role (Robert and Kupper 1999). Accordingly, the majority of the human Th cell clones isolated from atopic skin biopsy samples are of the polarized Th2 phenotype. These cells produce large amounts of IL-4, IL-5 and IL-13 but low or undetectable levels of IL-2 and IFN-γ. All Th cells express CLA LFA-1 and CCR4. Based on these results and the observation that CCL22 (macrophage-derived chemokine, MDC) is abundantly produced in atopic dermatitis skin lesions, CCL22 is selected as a relevant ligand for the evaluation of skin-specific migration of human Th cells in the SCID-hu Skin mouse model. In order to demonstrate that CCL22 induces Th2 cell activation, Th2 clones are loaded with Fluo-4acetoxymethyl ester (Fluo-4/AM, Molecular Probes, Eugene, Ore., USA). Following the addition of CCL22 (300 ng/ml), changes in fluorescence intensity are analyzed every 5 s using a FACScan FL-1 channel (Becton Dickinson, San Jose, Calif., USA) (Biedermann et al. 2002). Comparable results were obtained with CCL17 (thymus-activation-regulated chemokine, TARC), which is the other ligand for CCR4 and is also abundantly expressed in atopic dermatitis lesions. These results demonstrate the relevance of CCL17 and CCL22 interactions with CCR4 for activation of Th2 cells derived from atopic dermatitis skin lesions. In addition, human peripheral T cells are analyzed for their skin homing capacity in SCID-hu Skin mice. PBMC are isolated from healthy volunteers.

Recruitment of Human Th Cells to Human Skin Grafts in SCID-hu Skin Mice

To evaluate the potential of selected chemokines to recruit atopic-dermatitis-derived human Th2 cells and peripheral blood T cells to human skin *in vivo*, 1.5×10^8 Th2 cells or PBMC are adoptively transferred (i.p.) into SCID mice which have been previously transplanted (6–8 weeks) with two pieces of human skin (SCID-hu Skin mice). Following Th cell transfer, 300 ng of CCL22, CXCL10 (IFN-γ-inducible

protein of 10 kDa, IP-10), or vehicle control is injected intradermally (i.d.) in the human skin grafts of the SCID-hu Skin mice. On day 8, mice are sacrificed and human skin grafts are harvested and processed into single-cell suspensions using a mechanical tissue disaggregator. These cell suspensions are stained with human anti-CD3, anti-CD4 or anti-CD45 mAb conjugated to FITC and PE (Becton Dickinson) and analyzed in the FACScan. CCL22 effectively recruits human Th2 cells into human skin grafts of SCID-hu Skin mice, whereas CXCL10 is ineffective. These data are consistent with the expression of CCR4 on atopic-dermatitis-derived Th2 cells, whereas CXCR3, which is the receptor for CXCL10, is not expressed on these cells. Furthermore, treatment of Th2 cells prior transfer into SCID mice with *Bordetella pertussis* toxin, an inhibitor of G-protein-coupled receptors, completely abolishes the migratory capacity of these Th2 cells indicating the requirement of an intact chemokine receptor signaling pathway (Biedermann et al. 2002). It has to be noted that CCR4-mediated human skin homing of Th2 cells is not restricted to CCL22 since the alternative CCR4-ligand, CCL17, also induces Th2 migration to human skin grafts, although to a lesser degree than CCL22.

Similarly to Th2 cells, T cells present in human PBMC can also be recruited into human skin grafts of SCID-hu Skin mice. These T cells migrate in response to both CCL22 and CXCL10 chemokines (300 ng injected i.d. into human skin), which is consistent with CCR4 and CXCR3 expression on these cells. Peripheral blood T cells also express functional CCR2, since the T cells migrate into human skin in response to the CCR2 ligand CCL2. From these data it can be concluded that both skin-derived Th2 cells and peripheral blood T cells can be recruited into human skin grafts provided that these T cells express the chemokine receptors specific for the recruiting chemokine.

Inhibition of Human T Cell Migration into Human Skin of SCID-hu Skin Mice

The present SCID-hu Skin mouse model has been validated for measuring various inhibitors of human T cell rolling, extravasation and migration *in vivo*. It was shown that inhibition of CLA/E-Selectin interactions using an E-Selectin-specific mAb or a low molecular weight (LMW) E-Selectin-specific antagonist strongly inhibited CCL22-mediated Th2 cell migration into the skin (Biedermann et al. 2002). Similarly, anti-LFA-1 mAbs administered at 5 mg/kg at day 1 prior to Th2 cell transfer and on day 4 strongly inhibits Th2 cell migration into the human skin. Th2 cell migration in response to CCL22 is also inhibited in a dose-dependent fashion by LMW LFA-1 inhibitors, given daily p.o. starting on the day of T cell transfer.

CRITICAL ASSESSMENT OF THE METHOD

This mechanistic model allows analysis of the relevant steps involved in human T-lymphocyte migration into inflamed skin. In addition, it can be used for preclinical testing of drug candidates that are highly selective for human target molecules associated with the different steps of T cell migration in an environment that resembles the physiologic or pathologic conditions occurring in humans. The model allows the study of chemotactic responses of human cells toward specific, intracutaneously administered chemokines and testing of specific antagonists of human Th cell migration *in vivo*.

REFERENCES AND FURTHER READING

Biedermann T Schwärzler C Lametschwandtner G Thoma G Carballido-Perrig N Kund J de Vries JE Rot A, Carballido JM (2002) Targeting CLA/E-Selectin interactions prevents CCR4 mediated recruitment of human Th2 memory cells to human skin in vivo. Eur J Immunol 32:3171–3180

Biedermann T Röcken M Carballido JM (2004) TH1 and TH2 lymphocyte development and regulation of TH cell-mediated immune responses of the skin. J Invest Dermatol Symposium Proc 9:5–14

Bosma GC Custer RP Bosma MJ (1983) A severe combined immunodeficiency mutation in the mouse. Nature 301:527–530

Carballido JM Aversa G Kaltoft K Cocks BG Punnonen J Yssel H Thestrup-Pedersen K de Vries JE (1997) Reversal of human allergic T helper 2 responses by engagement of signaling lymphocytic activation molecule. J Immunol 159:4316–4321

Carballido JM Namikawa R Carballido-Perrig N Antonenko S Roncarolo MG de Vries JE (2000) Generation of primary antigen-specific human T- and B-cell responses in immunocompetent SCID-hu mice. Nature Med 6:103–106

Carballido JM Biedermann T Schwärzler C de Vries (2003) The SCID-hu skin mouse as a model to investigate selective chemokine mediated homing of human T-lymphocytes to the skin in vivo. J Immunol Meth 273:125–135

Igney FH Asadullah K Zollner TM (2004) Techniques: species' finest blend – humanized mouse models in inflammatory skin disease research. Trends Pharmacol Sci 25:543–549

Lametschwandtner G Biedermann T Schwärzler C Günther C Kund J Fassl S Hinteregger S Carbadillo-Perrig N Szabo SJ Glimcher LH Carbadillo JM (2004) Sustained T-bet expression confers polarized human TH2 cells with TH1-like cytokine production and migratory capacities. J Allergy Clin Immunol 113:987–994

Robert C Kupper TS (1999) Inflammatory skin diseases, T cells, and immune surveillance. N Engl J Med 341:1817

P.3 Pruritus Models

P.3.1 Pruritus and Scratching Behavior in Mice

PURPOSE AND RATIONALE

Pruritus is a common feature of many skin disorders. Since its pathogenesis in largely unknown, proper treatment is not available. The development of new treatments is hampered by the lack of animal models for studying pruritus (Woodward et al. 1985). Kuraishi et al. (1995) have proposed that pruritogenic but not algesiogenic agents stimulate the scratching activity in mice. Scratching is usually registered by counting the number of scratches from direct visual observation or from a video recording (Gmerek and Cowan 1983; Larsen et al. 1994; Thomas et al. 1994). Elliott et al. (2000) developed a method, which allows the automated registration of the scratching activity of the hind legs of mice for periods longer than 24 h.

PROCEDURE

Mice with chronic proliferative dermatitis (cpdm/cpdm mice), a spontaneous mutation of C57BL/Ka mice showing a skin disorder accompanied by severe scratching (Gijbels et al. 1996, 2000), at an age of 6–12 weeks or normal C57BL/Ka mice treated subcutaneously with 100 µg/mouse compound 48/80 or 3 mg/mouse histamine hydrochloride, are used.

Metal rings made of soft 1-mm-diameter aluminum wire are placed around both hind legs of the animal just above the ankle. The ring has to be of sufficient diameter that it is just free enough to rotate around the limb. Mice are housed individually in cages (12 × 18 × 13 cm), which are placed on a scratch detection unit consisting of a plastic outer casing containing the circuit board, and, inset into the top, four ferrite rods with copper coils.

As the mouse scratches, the movement of the metal rings (fitted around its hind legs) in the field generated by the coils elicits a signal that can be transformed into peaks of different frequencies using fast Fourier transformation. Data are downloaded to memory every 3 s, filtered and a power spectrum constructed. The power spectrum is analyzed for a scratch pattern every 1.5 s. Scratching is routinely classified as a signal that gives rise to peaks with maximal amplitudes of around 200 mV and frequencies greater than 15 Hz. The amplitude of general motor activity peaks (movement from bedding using hind limbs, drinking from water bottle) is usually greater than 500 mV and at frequencies of less than 10 Hz. In order to obtain the best discrimination between scratching and general motor activity, any contribution to the scratch frequencies of high energy/low frequency peaks is filtered out by setting the upper detection limit at 0.5 mV for scratching.

EVALUATION

Data are expressed as mean ± SEM Statistical analysis is performed by one-way analysis of variance followed by Student's *t*-test.

MODIFICATIONS OF THE METHOD

Inagaki et al. (2002, 2003) used new apparatus, MicroAct, to study mechanisms in the induction of scratching behavior in BALB/c mice by compound 48/80. A small magnet (1 mm in diameter, 3 mm long) was inserted subcutaneously in both hind paws under ether anesthesia. The mouse with magnets was placed in an observation chamber (11 cm in diameter, 18 cm high), which was surrounded by a round coil. The electric current induced in the coil by the movement of magnets attached to the hind paws was amplified and recorded. Characteristic waves reflecting scratching behavior were detected by a computer.

Brash et al. (2005) designed a repetitive movement detector used for automatic monitoring and quantification of scratching in mice. The system is based on a sensitive force transducer positioned below a recording platform holding a lightweight recording box in which the animal is placed. A programmed microcontroller is used to discriminate between non-specific movement, grooming behavior, and scratching movements made by the animal's hind limb. Following subdermal injections of histamine receptor agonists into the neck of a mouse, dose-related scratching occurred which was detected and quantified.

Larsen et al. (1994) studied the influence of ultraviolet irradiation on scratching behavior in hairless mice. Especially the wavelengths 315–330 nm were more itch provoking than erythemogenic.

Several authors used the model of **compound 48/80-induced scratching behavior** in mice. Sugimoto et al. (1998) studied the effects of histamine H_1 receptor antagonists on compound 48/80-induced scratching behavior in mice. Rojavin et al. (1998) investigated the antipruritic effect of millimeter waves in mice treated with compound 48/80. Inagaki et al. (2002) studied the mechanisms of induction of scratching behavior in BALB/c mice by compound 48/80. Shinmei et al. (2004) studied the effect of Brazilian propolis on scratching behavior induced by compound 48/80 and histamine in mice. Oliveira et al. (2004) re-

ported suppression of the scratching behavior induced by dextran 40 and compound 48/80 by treatment with pentacyclic triterpenoids. Inagaki et al. (1999, 2000) studied the participation of histamine H_1 and H_2 receptors in passive cutaneous anaphylaxis-induced scratching behavior in ICR mice and evaluated anti-scratch properties of drugs in BBLB/c, ICR, and ddY mice treated with dinitrofluorobenzene painting.

Hossen et al. (2003) reported involvement of histamine H_3 receptors in scratching behavior in mast-cell-deficient mice.

The involvement of the μ- and κ-opioid system in scratching behavior was investigated by Tohda et al. (1997), Kamei and Nagase (2001), and Umeuchi et al. (2003, 2005).

Tan-No et al. (2000) reported that intrathecally administered spermine produces scratching, biting, and licking behavior in mice.

Hansson et al. (2002) described a model of chronic itchy dermatitis in transgenic mice with epidermal overexpression of stratum corneum chymotryptic enzyme.

Andoh and Kuraishi (2002) described inhibitory effects of azelastine on the substance P-induced itch-associated response in mice.

Umeuchi et al. (2005) tested spontaneous scratching behavior in MRL/*lpr* mice, a possible model for pruritus in autoimmune diseases, and antipruritic activity of a κ-opioid receptor agonist and recommended MRL/*lpr* mice scratching behavior as a suitable model of pruritus that occurs in autoimmune diseases.

REFERENCES AND FURTHER READING

Andoh T Kuraishi Y (2002) Inhibitory effects of azelastine on substance P-induced itch-associated response in mice. Eur J Pharmacol 436:235–239

Brash HM McQueen DS Christie D Bell JK Bond SM Rees JL (2005) A repetitive movement detector used for automatic monitoring and quantification of scratching in mice. J Neurosci Methods 142:107–114

Elliott GR Vanwersch RAP Bruijnzeel PLB (2000) An automated method for registering and quantifying scratching activity in mice. Use for drug evaluation. J Pharmacol Toxicol Meth 44:453–459

Gijbels MJ Zurcher C Krall G Elliott GR HogenEsch H Schijff G Savelkoul HF Bruijnzeel PL (1996) Pathogenesis of skin lesions in mice with chronic proliferative dermatitis (cpdm/cpdm). Am J Pathol 148:941–950

Gijbels MJ Elliott GR HogenEsch H Zurcher C van den Hoven A Bruijnzeel PL (2000) Therapeutic interventions with mice with chronic proliferative dermatitis (cpdm/cpdm). Exp Dermatol 9:351–358

Gmerek DE Cowan A (1983) An animal model for preclinical screening of systemic antipruritic agents. J Pharmacol Meth 10:107–112

Hansson L Backman A Ny A, Edlund M Ekholm E Ekstrand-Hammarstrom B Tornell J Wallbrandt P Wennbo H Egelrud T (2002) Epidermal overexpression of stratum corneum chymotryptic enzyme in mice: a model of chronic itchy dermatitis. J Invest Dermatol 118:444–449

Hossen MA Sugimoto Y Kayasuga R Kamei C (2003) Involvement of histamine H_3 receptors in scratching behaviour in mast cell-deficient mice. Br J Dermatol 149:17–22

Inagaki N Nakamura N Nagao M Musoh K Kawasaki H Igeta K Nagai H (1999) Participation of histamine H_1 and H_2 receptors in passive cutaneous anaphylaxis-induced scratching behavior in ICR mice. Eur J Pharmacol 367:361–371

Inagaki N Nagao M Nakamura N Kawasaki H Igeta K Musoh K Nagai H (2000) Evaluation of anti-scratch properties of oxatomide and epinastine in mice. Eur J Pharmacol 400:73–79

Inagaki N Igeta K Kim JF, Nagao M Shiraishi N Nakamura N Nagai H (2002) Involvement of unique mechanisms in the induction of scratching behavior in BALB/c mice by compound 48/80. Eur J Pharmacol 448:175–183

Inagaki N Igeta K Shiraishi N Kim JF, Nagao M Nakamura N Nagai H (2003) Evaluation and characterization of mouse scratching behavior by a new apparatus, MicroAct. Skin Pharmacol Appl Skin Physiol 16:165–175

Kamei J Nagase H (2001) Norbinaltorphimine, a selective κ-opioid receptor antagonist, induces an itch-associated response in mice. Eur J Pharmacol 418:141–145

Kuraishi Y Nagasawa T Hayashi K Satoh M (1995) Scratching behavior induced by pruritogenic but not algesiogenic agents in mice. Eur J Pharmacol 275:229–233

Larsen J Hædersdal M Wulf HC (1994) Scratching and ultraviolet irradiation: an experimental animal model. Photodermatol Photoimmunol Photomed 10:38–41

Oliveira FA Lima-Junior RCP Cordeiro WM Vieira-Júnior GM Chaves MH Almeida FRC Silva RM Santos FA Rao VSN (2004) Pentacyclic triterpenoids, α,β-amyrins, suppress the scratching behavior in a mouse model of pruritus. Pharmacol Biochem Behav 78:719–725

Rojavin MA Cowan A Radzievsky AA Ziskin MC (1998) Antipruritic effect of millimeter waves in mice: evidence of opioid involvement. Life Sci 18:251–257

Shinmei Y Hossen MA Okihara K Sugimoto H Yamada H Kamei C (2004) Effect of Brazilian propolis on scratching behavior induced by compound 48/80 and histamine in mice. Int Immunopharmacol 4:1431–1436

Sugimoto Y Umakoshi K Nojiri N Kamei C (1998) Effects of histamine H_1 receptor antagonists on compound 48/80-induced scratching behavior in mice. Eur J Pharmacol 351:1–5

Tan-No K, Taira A Wako K Niijima F Nakagawaai O Tadano T Sakurada C Sakuarda T Kisara K (2000) Intrathecally administered spermine produces the scratching, biting and licking behaviour in mice. Pain 86:55–61

Thomas DA Dubner R Ruda MA (1994) Neonatal capsaicin treatment in rats results in scratching behavior with skin damage: potential model of non-painful dysesthesia. Neurosci Lett 171:101–104

Tohda C Yamaguchi T Kuraishi Y (1997) Intracisternal injection of opioids induces itch-associated response through μ-opioid receptors in mice. Jpn J Pharmacol 74:77–82

Umeuchi H Togashi Y Honda T Nakao K Okano K Tanaka T Nagase H (2003) Involvement of central μ-opioid system in the scratching behavior in mice and the suppression of it by the activation of κ-opioid system. Eur J Pharmacol 477:29–35

Umeuchi H Kawashima Y Aoki CA Kurakawa T Nakao K Itoh M Kikuchi K Kato T Okano K Gershwin ME Miyakawa H (2005) Spontaneous scratching behavior in MRL/*lpr* mice, a possible model for pruritus in autoim-

mune diseases, and antipruritic activity of a novel κ-opiod receptor agonist nalfurafine hydrochloride. Eur J Pharmacol 518:133–139
Woodward DF Conway JL Wheeler LA (1985) Cutaneous itching models. In: Models in Dermatology, Karger, Basel, pp 157–163

P.3.2 Pruritic Dermatitis in Other Species

Gmerek and Cowan (1983) described an animal model for preclinical screening of systemic antipruritic agents in **rats**. Bombesin induces dose-related excessive scratching when administered intracerebroventricularly (i.c.v.) to rats. Scratching elicited by 0.10μg bombesin i.c.v. was monitored with the help of a microcomputer.

Thomas and Hammond (1995) found that microinjections of morphine into the rat medullary dorsal horn produces a dose-dependent increase in facial scratching in Sprague Dawley rats.

Thomsen et al. (2001) proposed scratch induction in the rat by intradermal serotonin as a model of pruritus. Several compounds (histamine, compound 48/80, kallikrein, trypsin, papain, substance P and PAF) were injected into the rostral back of rats. Only serotonin induced excessive scratching at the site of injection. The model was recommended for research and development of antipruritics of the non-histaminic type.

De Castro Costa (1987) tested scratching behavior in arthritic rats; Thomsen et al. (2002), in hairless rats; Ozaki et al. (2005), in beige rats with IgE hyperproduction.

Hayashi et al. (2001) studied the effects of a histamine H_1 antagonist on cutaneous hyperpermeability and scratching behavior induced by poly-L-arginine in rats.

Noshima and Carstens (2003) described quantitative assessment of directed hind limb scratching behavior in Sprague Dawley rats after intradermal injection of serotonin into the nape of the neck.

Gingold and Bergasa (2003) found that a cannabinoid agonist increases nociception threshold in rats with cholestasis secondary to bile duct resection. The model was recommended when testing compounds for treatment of pruritus due to cholestasis.

Minami and Kamei (2004) published a chronic model for evaluating the itching associated with allergic conjunctivitis in rats. After subcutaneous and local sensitization with egg albumin, scratching behavior was observed after instillation of egg albumin into the eyes.

Butler et al. (1983) described pruritic dermatitis in asthmatic basenji-greyhound **dogs**, which was manifested as lichenified plaques and as inflammatory nodules and papules. The authors recommended this disease as a model for human atopic dermatitis.

Osifo (1991) used a dog model to study structure–activity relationships in the pruritogenicity of chloroquine and amodiaquine metabolites.

Patterson and Harris (1981) reported chronic pruritic dermatitis in asthmatic **rhesus monkeys**.

Ko and Naughton (2000) described an experimental itch model in rhesus monkeys.

Holden et al. (2003) found in this model that activation of κ-opioid receptors inhibits pruritus evoked by subcutaneous or intrathecal administration of morphine.

REFERENCES AND FURTHER READING

Butler JM Peters JE Hirshman CA White CR Margolin LB Hanifin JM (1983) Pruritic dermatitis in asthmatic basenji-greyhound dogs: a model for human atopic dermatitis. J Am Acad Dermatol 8:33–38
De Castro Costa M Gybels J Kupers R Van Hees J (1987) Scratching behavior in arthritic rats: a sign of chronic pain or itch? Pain 29:123–131
Gingold AR Bergasa NV (2003) The cannabinoid agonist WIN 55,212–2 increases nociception threshold in cholestatic rats: implications for the pruritus of cholestasis. Life Sci 73:2741–2747
Gmerek DE Cowan A (1983) An animal model for preclinical screening of systemic antipruritic agents. J Pharmacol Methods 10:107–112
Hayashi K Kaise T Ohmori K Ishii A Karasawa A (2001) Effects of olopatadine hydrochloride on the cutaneous hyperpermeability and the scratching behavior induced by poly-L arginine in rats. Jpn J Pharmacol 87:167–170
Holden MC Lee H, Song MS Sobczyk-Kojiro K Mosberg HI Kishioka S Woods JH Naughton NN (2003) Activation of κ-opioid receptors inhibits pruritus evoked by subcutaneous or intrathecal administration of morphine in monkeys. J Pharmacol Exp Ther 305:173–179
Ko M-C, Naughton NN (2000) An experimental itch model in monkeys: characterization of intrathecal morphine-induced scratching and antinociception. Anesthesiology 92:792–805
Minami K Kamei C (2004) A chronic model for evaluating the itching associated with allergic conjunctivitis in rats. Int Immunopharmacol 4:101–108
Noshima H Carstens E (2003) Quantitative assessment of directed hind limb scratching behavior as a rodent itch model. J Neurosci Methods 126:137–143
Osifo NG (1991) Structure activity relationships in the pruritogenicity of chloroquine and amodiaquine metabolites in a dog model. J Dermatol Sci 2:92–96
Ozaki K Matsuura T Narama I (2005) Characterization of spontaneous dermatitis in beige rats with IgE hyperproduction. Int Arch Allergy Immunol 136:73–82
Patterson R Harris K (1981) Chronic pruritic dermatitis in asthmatic monkeys: a subhuman primate analogue of atopic dermatitis? Int Arch Allergy Appl Immunol 64:332–337

Thomas DA Hammond DL (1995) Microinjections of morphine into the rat medullary dorsal horn produces a dose dependent increase in facial scratching. Brain Res 695:267–270
Thomsen JS Petersen MB Benfeldt E Jensen SB Serup J (2001) Scratch induction in the rat by intradermal serotonin: a model of pruritus. Acta Dermatol Venereol 81:250–254
Thomsen JS Benfeldt E Serup J (2002) Suppression of spontaneous scratching in hairless rats by sedatives but not by antipruritics. Skin Pharmacol Appl Skin Physiol 15:218–224

P.4 Psoriasis Models

P.4.1 General Considerations

Several authors reviewed the experimental models for psoriasis (Krueger and Jorgensen 1990; Boehncke 1997; Nickoloff 1999; Rosenberg et al. 1999; Schön 1999; Mizutani et al. 2003). In addition to studies in animals, various *in vitro* investigations were carried out with autopsy material from human psoriatic lesions. Several studies were devoted to the T-cell hypothesis of psoriasis (Bos and de Rie 1999). Lymphocytes may change epidermal growth homeostasis, leading to increased keratinocyte proliferation and abnormal differentiation of these apoptotic cells that end their life cycle as corneocytes.

REFERENCES AND FURTHER READING

Boehncke WH (1997) Psoriasis im Tiermodell. Hautarzt 48:707–713
Bos JD, de Rie MA (1999) The pathogenesis of psoriasis: immunological facts and speculations. Immunology Today 20:40–46
Krueger GG Jorgensen CM (1990) Experimental models for psoriasis. J Invest Dermatol 95:56S–58S
Mizutani H Yamanaka K Konishi H Murakami T (2003) Animal models of psoriasis and pustular psoriasis. Arch Dermatol Res 295 [Suppl1]:S67–S68
Nickoloff BJ (1999) Animal models of psoriasis. Expert Opin Invest Drugs 8:393–401
Rosenberg EW Noah PW Skinner RB Jr (1999) Animal models of psoriasis. J Invest Dermatol 113:427
Schön MP (1999) Animal models of psoriasis – what can we learn from them? J Invest Dermatol 112:405–410

P.4.2 In Vitro Studies with Isolated Cells

P.4.2.1 Cultured Keratinocytes

PURPOSE AND RATIONALE

Cultured keratinocytes have been used to study the pathogenesis of psoriasis (Mils et al. 1994; Bata-Csörgö et al. 1993, 1995a, b; Ockenfels et al. 1996; Nylander-Lundqvist and Egelrud 1997a, b; Nylander-Lundqvist et al. 1998; Konger et al. 1998; Szabo et al. 1998; Dimon-Gadal et al. 2000; Karvonen et al. 2000; Segaert et al. 2000; Ting et al. 2000) and to evaluate antipsoriatic drugs (Chapman et al. 1990; Ockenfels et al. 1995; Medalie et al. 1996; Lin et al. 1999; Diaz et al. 2000; Farkas et al. 2001). Sampson et al. (2001) tested the *in vitro* keratinocyte antiproliferant effect of *Centella asiatica* extract and triterpenoid saponins.

PROCEDURE

The medium (FDMEM) consists of Dulbecco's Modified Eagle Medium supplemented with 10% fetal bovine serum (FBS), 1% penicillin and 2% streptomycin.

SVK-14 keratinocytes (Taylor-Papadimitriou et al. 1982) are cultured in FDMEM medium in flasks at 10% CO_2 and 37°C. When confluent, cells are washed with magnesium- and calcium-free phosphate buffered saline (PBS). PBS is decanted and cells detached by adding 5 ml of trypsin (0.05%) in EDTA (0.02%). PBS is added to a volume of 50 ml. The cell pellet obtained by centrifugation (1000 *g*, 5 min) is re-suspended in 10 ml of FDMEM. Cell counts in the final suspension are determined using a haemocytometer, and the cell density is adjusted to 25000/ml with FDMEM.

For microtiter assays, cells (5000 in 200 µl medium) are inoculated into the inner wells of 96-well plates. The outer edge wells of the plate contain 200 µl of 10% fetal bovine serum in PBS. After 24 h at 37°C, 10% CO_2, plating medium is replaced with FDMEM containing test material or standard in 200 µl. Standard substances are: madecassoside (50 nM–5 mM), asiaticoside (100 nM–10 mM), dissolved in methanol, and dithranol (0.33–170 µM) dissolved on DMSO. Each sample concentration is tested with 6 replicates on each of three separate plates. Cells exposed to FDMEM alone provide 100% growth control. Cells are incubated for 7 days at 37°C, 10% CO_2 prior to carrying out the sulphorhodamine B assay.

For the sulphorhodamine B (SRB) assay (Skehan et al. 1990), cells are fixed by layering 100 µl of ice-cold 50% trichloroacetic acid on top of the growth medium. Cells are incubated at 4°C for 1 h, after which plates are washed 5 times with cold water, excess water drained off and the plates left to dry in air. SRB stain (50 µl; 0.4% in 1% acetic acid) (Sigma) is added to each well and left in contact with the cells for 10 to 30 min after which they are washed with 1% acetic acid, rinsing 4 times until only the dye adhering to the cells is left. The plates are dried and 100 µl of 10 mM Tris buffer added to each well to solubilize the dye. The plates are shaken gently for 5 in on a plate reader

and the absorbance is read at 550 nm using a Titertek Multiscan MCC/340 II plate reader.

EVALUATION

Mean optical density (OD ± SD) is calculated for each concentration from the six replicate wells in a single plate. The data is used to plot a dose response curve from which IC_{50} values ± SD are obtained.

MODIFICATIONS OF THE METHOD

Fogh et al. (1993) described an *ex vivo* skin model. Keratomized psoriatic skin samples were incubated in the presence of the calcium ionophore a23187 and arachidonic acid for 45 min at 37°C. After extraction of lipids, eicosanoids were determined by reversed-phase high-performance liquid chromatography in combination with specific radioimmunoassays.

Hager et al. (1999) described long-term culture of murine epidermal keratinocytes.

Hanley et al. (1998) found that the differentiation of keratinocytes in cultures from human foreskin was stimulated by activators of the nuclear hormone receptor peroxisome proliferator-activated receptor α (PPARα).

Rivier et al. (1998) reported differential expression of PPAR subtypes during the differentiation of human keratinocytes. When normal human keratinocytes were induced to differentiate by shifting the culture medium to a high Ca^{2+} concentration, the expression of PPARα and PPARγ mRNA was increased, whereas that of PPARδ remained unchanged. In lesional compared with unlesional psoriatic epidermis, the expression of PPARα and PPARγ was reduced, indicating that these two subtypes are tightly linked in the epidermal differentiation process.

Naik et al. (1999) found that human keratinocytes constitutively express interleukin-18 and secrete biologically active interleukin-18 after treatment with pro-inflammatory mediators and dinitrochlorobenzene.

Muga et al. (2000) reported that 8S-lipoxygenase products activate PPARα and induce differentiation in murine keratinocytes. Transgenic mice with 8S-lipoxygenase targeted to keratinocytes were generated through the use of a loricrin promoter. In cultured keratinocytes, PPARα was identified as a crucial component of keratin-1 induction through transient transfection with expression vectors for PPARα, PPARγ, and a dominant negative PPAR as well as through the use of known PPAR agonists.

Ellis et al. (2000) found that ligands for PPARγ inhibit keratinocyte proliferation. Troglitazone improved psoriasis and showed normalization in these models of proliferative skin disease.

Kömüves et al. (2000) studied keratinocyte differentiation in hyperproliferative epidermis and found that topical application of PPARα activators restores tissue homeostasis.

Rosenfield et al. (2000) reviewed PPARs and skin development.

Sakamoto et al. (2000) described activation of human PPAR subtypes by pioglitazone.

Tan et al. (2001) studied the roles of PPARβ/δ in the keratinocyte's response to inflammation. The authors showed by the use of cultures of primary keratinocytes from wild-type and PPAR$\beta/\delta^{-/-}$ mice that inflammatory signals, such as tumor necrosis factor α (TNFα) and interferon β (INFβ), induce keratinocyte differentiation. The proinflammatory cytokines initiate the production of endogenous PPARβ/δ ligands, which are essential for PPARβ/δ activation and action.

Thuillier et al. (2002) found inhibition of PPAR-mediated murine keratinocyte differentiation by lipoxygenase inhibitors. The effect was mediated primarily through PPARα and PPARγ.

Zhou et al. (2002) performed genetic analysis of four novel PPARγ splice variants in monkey macrophages.

Hong et al. (2003) described PPARγ-dependent anti-inflammatory action of rosiglitazone in human monocytes, whereby the suppression of TNFα secretion is not mediated by Lipid phsophatase PTEN regulation.

Kojo et al. (2003) evaluated human PPAR subtype selectivity of a variety of anti-inflammatory drugs based on a novel assay for PPARδ (β).

Kuenzli and Saurat (2003) reviewed the role of PPARs in cutaneous biology.

Westergaard et al. (2003) studied expression and localization of PPARs and nuclear factor κB in normal and lesional psoriatic skin.

Gosh et al. (2004) found disruption of transformation growth factor signaling and profibrotic responses in normal skin fibroblasts by PPARγ.

REFERENCES AND FURTHER READING

Bata-Csörgö Z, Hammerberg C Voorhees JJ Cooper KD (1993) Flow cytometric identification of proliferative subpopulations within normal epidermis and the localization of the primary hyperproliferative population in psoriasis. J Exp Med 178:1271–1281

Bata-Csörgö Z, Hammerberg C Voorhees JJ Cooper KD (1995a) Intralesional T-lymphocyte activation as a mediator of psoriatic epidermal hyperplasia. J Invest Dermatol 105:895–945

Bata-Csörgö Z, Hammerberg C Voorhees JJ Cooper KD (1995b) Kinetics and regulation of human keratinocyte stem cell

growth in short-term primary *ex vivo* culture. Cooperative growth factors from psoriatic lesional T lymphocytes stimulate proliferation among psoriatic uninvolved, but not normal, stem keratinocytes. J Clin Invest 93:317–327

Chapman ML Dimitrijevivh SD Hevelone JC Goetz D Cohen J Wise G Gracy RW (1990) Inhibition of psoriatic cell proliferation in *in vitro* skin models by amiprilose hydrochloride. *In vitro* Cell Dev Biol 26:991–996

Diaz BV Lenoir MC Ladoux A Frelin C Demarchez M Michel S (2000) Regulation of vascular endothelium growth factor expression in human keratinocytes by retinoids. J Biol Chem 275:642–650

Dimon-Gadal S Gerbaud P Thérond P Guibourdenche J Anderson WB Evain-Brion D Raynaud F (2000) Increased oxidative damage to fibroblasts in skin with and without lesions in psoriasis. J Invest Dermatol 114:984–989

Ellis CN Varani J Fisher GJ Zeigler ME Pershadsingh HA Benson SC Chi Y, Kurtz TW (2000) Troglitazone improves psoriasis and normalizes models of proliferative skin disease. Ligands for peroxisome proliferator-activated receptor-γ inhibit keratinocyte proliferation. Arch Dermatol 136:609–616

Farkas A Kemény L, Szöny BJ, Bata-Csörgö Z, Pivarcsi A Kiss M Széll M, Koreck A Dobozy A (2001) Dithranol upregulates IL-10 receptors on the cultured human keratinocyte cell line HaCaT. Inflamm Res 50:44–49

Fogh K Iversen L Herlin T Kragballe K (1993) Modulation of eicosanoid formation by lesional skin of psoriasis: an *ex vivo* skin model. Acta Derm Venereol 73:191–193

Gosh AK Bhattacharyya S Lakos G Chen SJ Mori Y Varga J (2004) Disruption of transformation growth factor signaling and profibrotic responses in normal skin fibroblasts by peroxisome proliferator-activated receptor-γ. Arthritis Rheum 50:1305–1318

Hager B Bickenbach JR Fleckman P (1999) Long-term culture of murine epidermal keratinocytes. J Invest Dermatol 112:971–976

Hanley K Jiang Y He SS, Friedman M Elias PM Bikle DD Williams ML Feingold KR (1998) Keratinocyte differentiation is stimulated by activators of the nuclear hormone receptor PPARγ. J Invest Dermatol 110:368–375

Hong G Davis B Khattoon N Baker SF Brown J (2003) PPARγ-dependent anti-inflammatory action of rosiglitazone in human monocytes: suppression of TNFα secretion is not mediated by PTEN regulation. Biochem Biophys Res Commun 303:782–787

Karvonen SL Korkiamäki T, Ylä-Outinen H Nissinen M Teerikangas H Pummi K Karvonen J Peltonen J (2000) Psoriasis and altered calcium metabolism: downregulated capacitative calcium influx and defective calcium-mediated signaling in cultured psoriatic keratinocytes. J Invest Dermatol 114:693–700

Kojo H Fukagawa M Tajima K Suzuki A Fujimura T Aramori I Hayashi KI Nishimura S (2003) Evaluation of human peroxisome-activated receptor (PPAR) subtype selectivity of a variety of anti-inflammatory drugs based on an novel assay for PPARδ (β). J Pharmacol Sci 93:347–355

Kömüves LG Hanley K Man MQ, Elias PM Williams ML Feingold KR (2000) Keratinocyte differentiation in hyperproliferative epidermis: topical application of PPARα activators restore tissue homeostasis. J Invest Dermatol 115:361–367

Konger RL Malaviya R Pentland AP (1998) Growth regulation of primary human keratinocytes by prostaglandin E receptor EP_2 and EP_3 subtypes. Biochim Biophys Acta/Mol Cell Res 1401:221–234

Kuenzli S Saurat JH (2003) Peroxisome proliferator-activated receptors in cutaneous biology. Br J Dermatol 149:229–236

Lin X, Wilkinson DI Huang T Farber EM (1999) Experimental studies on topoisomerase inhibitor camptothecin as an antipsoriatic agent. Chin Med J 112:504–508

Medalie DA Eming SA Tompkins RG Yarmush ML Krueger GG Morgan JR (1996) Evaluation of human skin reconstituted from composite grafts of cultured keratinocytes and human acellular dermis transplanted to athymic mice. J Invest Dermatol 107:121–127

Mils V Basset-Seguin N Moles JP Tesniere A Leigh I Guilhou JJ (1994) Comparative analysis of normal and psoriatic skin both *in vivo* and *in vitro*. Differentiation 58:77–86

Muga SJ Thuillier P Pavone A Rundhaug JE Boeglin WE Jisaka M Brash AR Fischer SM (2000) 8S-Lipoxygenase products activate peroxisome-activated receptor α and induce differentiation in murine keratinocytes. Cell Growth Differ 11:447–454

Naik SM Cannon G Burbach GJ Singh SR Swerlick RA Wilcox JN Ansel JC Caughman SW (1999) Human keratinocytes constitutively express interleukin-18 and secrete biologically active interleukin-18 after treatment with pro-inflammatory mediators and dinitrochlorobenzene. J Invest Dermatol 131:766–772

Nylander-Lundqvist E Egelrud T (1997a) Biologically active, alternatively processed interleukin-1β in psoriatic scales. Eur J Immunol 27:2165–2171

Nylander-Lundqvist E Egelrud T (1997b) Formation of active IL-1β from pro-IL-1β catalyzed by stratum corneum chymotryptic enzyme *in vitro*. Acta Derm Venereol (Stockh) 77:203–206

Nylander-Lundqvist E Companjen AR Prens EP Egelrud T (1998) Biological activity of human epidermal interleukin-1beta: comparison with recombinant human interleukin-1beta. Eur Cytokine Netw 9:41–46

Ockenfels HM Nussbaum G Schultewolter T Burger PM Goos M (1995) Cyclosporin A FK506, and dithranol after tyrosine-specific protein phosphorylation in HaCaT keratinocytes. Arch Dermatol Res 287:304–309

Ockenfels HM Wagner SM Keim-Maas C Funk R Nussbaum G Goos M (1996) Lithium and psoriasis: cytokine modulation of cultured lymphocytes and psoriatic keratinocytes by lithium. Arch Dermatol Res 288:173–178

Rivier M Safonova I Lebrun P Griffith CEM Ailhaud G Michel S (1998) Differential expression of peroxisome proliferator-activated receptor subtypes during the differentiation of human keratinocytes. J Invest Dermatol 111:1116–1121

Rosenfield RL Deplewski D Greene ME (2000) Peroxisome proliferator-activated receptors and skin development. Horm Res 54:269–274

Sakamoto J Kimura H Moriyama S Odaka H Momose Y Sugiyama Y Sawada H (2000) Activation of human peroxisome proliferator-activated receptor (PPAR) subtypes by pioglitazone. Biochem Biophys Res Commun 278:704–711

Sampson JH Raman A Karlsen G Navsaria H Leigh IM (2001) *In vitro* keratinocyte antiproliferant effect of *Centella asiatica* extract and triterpenoid saponins. Phytomedicine 8:230–235

Segaert S Garmyn M Degreef H Bouillon R (2000) Suppression of vitamin D receptor and induction of retinoid X receptor a expression during squamous differentiation of cultured keratinocytes. J Invest Dermatol 114:494–501

Skehan P Storeng R Scudiero D Monks A McMahon I Vistica D Warren JT Bokesch H Kenney S Boyd MR (1990) New colorimetric cytotoxicity assay for anticancer-drug screening. J Natl Cancer Inst 82:1107–112

Szabo SK Hammerberg C Yoshida Y Bata-Csörgö Z, Cooper KD (1998) Identification and quantitation of interferon-

gamma producing T cells in psoriatic lesions: localization to both $CD4^+$ and $CD8^+$ subsets. J Invest Dermatol 111:1072–1078

Tan NS, Michalik L Noy N, Yasmin R Pacot C Heim M Flühmann B Desvergne B Wahli W (2001) Critical roles of PPARβ/δ in keratinocyte response to inflammation. Genes Dev 15:3263–3277

Taylor-Papadimitriou J Purkis P Lane BE McKay L, Chang SE (1982) Effects of SV40 transformation on the cytoskeleton and behavioural properties of human keratinocytes. Cell Differ 11:169–180

Thuillier P Brash AR Kehrer JP Stimmel JB Leesnitzer LM Yang P Newman RA Fischer SM (2002) Inhibition of peroxisome proliferator-activated receptor (PPAR)-mediated keratinocyte differentiation by lipoxygenase inhibitors. Biochem J 366:901–910

Ting KM Rothaupt D McCormick TS Hammerberg C Chen G Gilliam AC Stevens S Culp L Cooper KD (2000) Overexpression of the oncofetal Fn variant containing the EDA splice-in segment in the dermal-epidermal junction of psoriatic uninvolved skin. J Invest Dermatol 114:706–711

Westergaard M Henningsen J Johansen C Rasmussen S Svendsen ML Jensen UB Schrøder HD Stacls B Iversen L Bolund R Kragballe K Kristiansen K (2003) Expression and localization of peroxisome proliferator-activated receptors and nuclear factor κB in normal and lesional psoriatic skin. J Invest Dermatol 121:1104–1117

Zhou J Wilson KM Medh JD (2002) Genetic analysis of four novel peroxisome proliferator activated receptor-γ splice variants in monkey macrophages. Biochem Biophys Res Commun 293:274–283

P.4.2.2 Effect on T Lymphocytes

PURPOSE AND RATIONALE

Psoriasis vulgaris is considered as an inflammatory cell-mediated autoimmune disorder (Uyemura et al. 1993; Gottlieb et al. 1994; Bata-Csörgö et al. 1995; Austin et al. 1999). Lesional skin T cells contribute pro-inflammatory/type 1 (T1) cytokines to initiate and maintain the cell-mediated keratinocyte hyperplasia in inflammatory lesions. Atopic dermatitis is characterized by the presence of Th2 cell and their respective cytokines (Cooper 1994; Leung 1997). A therapeutic agent down-regulating both Th1 and Th2 cytokine production would be desirable (Mollison et al. 1999; Santamaria et al. 1999).

PROCEDURE

Human Mixed Leukocyte Reaction (MLR) Assay

Fifty milliliters of sodium heparinized blood, obtained from normal, unrelated donors, is mixed with an equal volume of Dulbecco's phosphate buffered saline (DPBS). Peripheral blood mononuclear cells (PBMC) are isolated by density centrifugation at 400 *g* over Histopaque-1077. A sufficient number of PBMC are washed three times in RPMI-1640 medium and used as responder cells. The remaining PBMC (stimulator cells) are washed as above and treated with 25 µg/ml mitomycin C for 30 min at 37°C in an atmosphere of 5% CO_2 and 100% humidity and then washed three times with RPMI-1640 medium. The stimulator cells are pooled at $0.5–1.0 \times 10^6$ cells per ml per donor in RPMI-1640 medium. Cells are cultured in medium consisting of RPMI-1640 supplemented with 4 mM L-glutamine, 500 µM 2-mercaptoethanol, 10% fetal bovine serum, 25 units/ml penicillin, and 25 µg/ml streptomycin. Mixed leukocyte reactions are performed in 96 well flat-bottom plates (Corning, Acton MA) in a final volume of 220 µl, containing 20 µl of culture medium with or without test compound or standard (ascomycin, purified from a fermentation of *Streptomyces hygroscopicus* ssp. *ascomyceticus* ATCC 14891 and characterized according to Or et al. 1993), 100 µl of responder cells (1×10^6 cells per ml) and 100 µl of stimulator cells ($2–4 \times 10^6$ cells per ml). Cultures are incubated at 37°C in an atmosphere of 5% CO_2 and 100% humidity for 4 days. On day 4, 0.5 µCi of [^{3}H]thymidine is added to each well during the last 6 h of culture. Cultures are harvested onto glass-fiber mats using a 96 well harvester. [^{3}H]Thymidine uptake is measured by direct β-counting using a Matrix 9600 β-counter (Packard, Meriden, CT).

Inhibition of IL-2 Production in Human Whole Blood and PBMC

Fifty milliliters of venous blood from normal donors is drawn into tubes containing sodium heparin. Twenty-five milliliters of blood is used directly. PBMC are isolated from the remaining sample as described above and cultured at 1×10^6 cells per ml with supplemented RPMI-1640. Whole blood or PBMC are induced to secrete IL-2 with 50 ng PMA per ml plus 1 µg ionomycin per ml. Immunosuppressive potency of test compound vs. standard is determined by measuring the inhibition of IL-2 secretion. Assays are performed in 96 well flat-bottom plates in a volume of 210 µl, which includes 190 µl of whole blood or PBMC (1×10^6 cells per ml), 10 µl of PMA (1 µg/ml) and ionomycin (20 µg/ml) mixture and 10 µl of serially diluted test compound. Plasma or tissue culture supernatants are collected 24 h later and IL-2 concentrations determined by ELISA.

Porcine MLR Assay

Fifty milliliters of sodium heparinized venous blood is drawn from pigs and diluted with an equal volume of 0.9% saline. PBMC are isolated by density centrifugation for preparation of responder and stimulator cells as described above. MLR are performed as described for human MLR using 100 µl of responder

cells (2×10^6 cells per ml) and 100 µl of stimulator cells ($0.5–4 \times 10^6$ cells per ml).

Rat MLR Assay

Popliteal, inguinal, and mesenteric lymph nodes from newly sacrificed Lewis rats and spleens from Brown Norway rats are aseptically removed. Single cell suspensions of splenocytes and lymphocytes are prepared using forceps and a hemostat to macerate the tissues. Red blood cells in the splenocyte suspension are lysed by 2 min incubation at ambient temperature in red blood cell lysis buffer containing 0.14 M NH_4Cl in 0.0167 M Tris-HCl, pH 7.2. Responder cells from Lewis rat lymph nodes and stimulator cells from Brown Norway rat spleens are washed three times in RPMI-1640 medium and then sedimented at 400 *g* for 10 min. Stimulator cells are prepared as for human, and the assay is conducted in serum-free AIM-V medium supplemented with 1% Antibiotic-Antimycotic solution and 50 µM 2-mercaptoethanol, using an optimized cell ratio of 100 µl of responder cells (2×10^6 cells per ml) and 100 µl of stimulator cells ($1–2 \times 10^6$ cells per ml) and an incubation period of 4 days.

Mouse MLR Assay

Spleens are aseptically removed from newly sacrificed C_3H(C_3H/HeNCrIBR) and BALB/c mice. Splenocytes are prepared and the assay conducted as for rat, using an optimized cell ratio of 100 µl of responder cells (4×10^6 cells per ml) and 100 µl of stimulator cells (1×10^6 cells per ml).

Concanavalin A-Induced Guinea Pig Lymphocyte Proliferation Assay

Spleens are aseptically removed from newly sacrificed guinea pigs. Single cell suspensions of splenocytes are prepared as for rat using 4 min incubation in lysis buffer to remove red blood cells. Splenocytes are washed three times in RPMI-1640 medium and adjusted to 6.25×10^5 cells per ml in culture medium consisting of RPMI-1640 supplemented as described for human MLR. Concanavallin A-induced proliferation reactions are performed in a volume of 200 µl, containing 20 µl of culture medium with or without test compound or standard, 160 µl of guinea pig splenocytes and 20 µl concanavallin A (20 µg/ml). Cultures are incubated for 3 days, pulse labeled on the last day with [^{3}H]thymidine, harvested and counted as described.

Inhibition of Cytokine Secretion

Serially diluted test compound or standard is added to 96 well plates with PBMC in RPMI-1640 medium at 1×10^6 cells per ml. PMA and ionomycin are added to effect 10 ng per ml and 500 ng per ml concentrations, respectively. Supernatants from these cultures are collected 24 h later after centrifugation and stored at –80°C until use. Concentrations of IL-2 and IFN-γ in the supernatants are determined by ELISA. For assessing inhibition of IL-4 and IL-5 secretion in T cells by the test compound, $CD4^+$ cells are isolated from PBMC using a T cell subset enrichment column (RandD Systems, Minneapolis, MN). Purified $CD4^+$ cells are cultured with serially diluted test compound and PMA at 10 ng per ml in plates previously coated with 100 ng per ml solution of anti CD3 antibody (Immunotech, Westbrook, ME). Supernatants are collected after centrifugation 40 h later. IL-4 and IL-5 concentrations in the supernatants are determined by ELISA.

EVALUATION

Dose response curves for test compound and standard are established and IC_{50} values for inhibition calculated.

MODIFICATIONS OF THE METHOD

Gillitzer et al. (1996) studied neutrophil migration in psoriatic lesions as a model for neutrophil chemotaxis.

Kunstfeld et al. (1997) investigated the migration of inflammatory T cells from psoriasis through superficial vascular plexus and through deep vascular plexus endothelium. Superficial and deep plexus human skin was placed separately into SCID mice.

REFERENCES AND FURTHER READING

Austin LM Ozawa M Kikuchi T Walters IB Krueger JG (1999) The majority of epidermal T cells in psoriasis vulgaris lesions can produce type 1 cytokines, interferon γ, interleukin-2, and tumor necrosis factor-α, defining TC1 (cytotoxic T lymphocyte) and TH1 effector populations: a type 1 differentiation bias in also measured in circulating blood T cells in psoriatic patients. J Invest Dermatol 113:752–759

Bata-Csörgö Z, Hammerberg C Voorhees JJ Cooper KD (1995) Intralesional T-lymphocyte activation as a mediator of psoriatic epidermal hyperplasia. J Invest Dermatol 105:895–945

Cooper KD (1994) Atopic dermatitis: recent trends in pathogenesis and therapy. J Invest Dermatol 102:128–137

Gillitzer R Ritter U Spandau U Goebeler M Brocker EB (1996) Differential expression of GROα and IL-8 mRNA in psoriasis. A model for neutrophil migration and accumulation *in vivo*. J Invest Dermatol 107:778–782

Gottlieb S Johnson R Gilleaudeau P Woodworth T Nylen P Gottlieb AB Krueger JG (1994) A specific lymphocyte toxin (DAB389IL-2) reversed epidermal keratinocyte activation in psoriasis. J Invest Dermatol 102:531

Kunstfeld R Lechleitner S Groper M Wolff K Petzelbauer P (1997) HECA-453^+ T cells migrate through superficial vas-

cular plexus but not through deep vascular plexus endothelium. J Invest Dermatol 108:343–348
Leung DM (1997) Atopic dermatitis: immunobiology and treatment with immune modulators. Clin Exp Immunol 107:25–30
Mollison KW Fey TA, Gauvin DM Kolano RM Sheets MP Smith ML Pong M Nikolaidis NM Lane BC Trevillyan JM Cannon J Marsh K Carter GW Or Y-S, Chen Y-W, Hsieh GC Luly JR (1999) A macrolactam inhibitor of T helper type 1 and T helper type 2 cytokine biosynthesis for topical treatment of inflammatory skin diseases. J Invest Dermatol 112:729–738
Or YS, Clark RF Xie Q, McAlpine J Whittern DN Henry R Luly JR (1993) The chemistry of ascomycin: Structure determination and synthesis of pyrazole analogues. Tetrahedron 49:8771–8786
Santamaria LF Torres R Giménez-Arnau AM Giménez-Camarasa JM Ryder H Palacios JM Beleta J (1999) Rolipram inhibits staphylococcal enterotoxin B-mediated induction of the human skin-homing receptor on T lymphocytes. J Invest Dermatol 113:82–86
Uyemura K Yamamura M Fivenson DF Modlin RK Nickoloff BJ (1993) The cytokine network in lesional and lesion-free psoriatic skin is characterized by a T-helper cell-mediated response. J Invest Dermatol 101:701–705

P.4.3
Psoriasis Models in Normal Animals

P.4.3.1
Mouse Tail Model for Psoriasis

PURPOSE AND RATIONALE

The mouse-tail test was introduced by Jarrett and Spearman (1964). The model is based on the induction of orthokeratosis in those parts of the adult mouse-tail, which have normally a parakeratotic differentiation. Quantification of orthokeratosis was achieved by morphometric evaluation of the scales with the aid of a semiautomatic evaluation unit (Bosman et al. 1992; Bosman 1994; Sebök et al. 1996).

PROCEDURE

Male albino NMRI mice weighing 25–27 g are used.

The tails are treated locally with 0.1 ml ointment applied to the proximal part of the tail. For the contact time of 2 h a plastic cylinder is slipped over the tail and fixed with adhesive tape. At the end of contact time the cylinders are removed and the tails washed. Animals are treated once daily, 5 times a week, for 2 weeks. Five to 8 animals are used per dosage group. Two hours after the last treatment the animals are sacrificed and the tails prepared histologically (fixation in 4% formalin, paraplastic embedding). Longitudinal sections of about 5 µm thickness are prepared and stained with hematoxylin-eosin.

The epidermal thickness is measured as the distance between the dermo-epidermal borderline and the beginning of the horny layer. Five measurements per animal are made in each of 10 scales. Out of these 50 measurements the mean for the individual animals is calculated.

The sections are examined for the presence of a granular layer or isolated granular cells induced in the previously parakeratotic skin areas (10 sequential scales per animal). The measurements are carried out at the border of the scale with a semiautomatic image evaluation unit (VIDS III, AI TEKTRON). The distances are obtained in pixels (1 pixel = 1.2120 µm).

Quantitative values of orthokeratosis are obtained by measuring the length of the granular layer per scale (A) and the whole scale length (B). The whole scale length is defined as the length of the scale lying between two adjacent hair follicles, beginning and ending at the turning point between hair follicle and scale. Percent keratosis is calculated by the formula:

$$(A/B) \times 100\,.$$

EVALUATION

Ten sequential scales per animal are measured and the results given in % orthokeratosis per scale. Five to 8 animals are taken for one drug concentration or control group. Thus 50–80 individual orthokeratosis values are obtained per test group. Mean and standard error of the mean are calculated per animal and per group. From the individual orthokeratosis values per dosage group (50–80 scales) a frequency distribution is constructed. Therefore the values (ranging from 0 to 100% orthokeratosis) are grouped into classes with a constant class interval of 10% (class 1: 0–10%; class 2: 10.1–20%; class 10: 90.1–100% orthokeratosis). The frequency per class is calculated in %:

$$\text{class frequency} = \frac{\text{no. of scales in the class}}{\text{total no. of scales}} \times 100\,.$$

For every class the cumulative frequency is constructed by adding the frequencies of all foregoing classes.

Due to a non-Gaussian distribution of the orthokeratotic values (100% is the maximal effect), the Mann-Whitney U-test is used.

The efficacy of test compounds on epidermal differentiation is calculated from the mean length of orthokeratosis after treatment with the substrate (Ok_s) and with salicylic acid as control (Ok_c) using the formula:

$$(Ok_s - Ok_c)/(100 - Ok_c) \times 100\,.$$

MODIFICATIONS OF THE METHOD

Nagano et al. (1990) studied the effect of tumor necrosis factor in the mouse-tail model of psoriasis.

Beyaert et al. (1992) induced a psoriasiform inflammatory reaction in mice by subcutaneous injection of a combination of tumor necrosis factor and lithium chloride.

Sebök et al. (2000) used the mouse tail test to compare tazarotene, a receptor-specific retinoid, with the classical topical antipsoriatic compound dithranol.

Worm et al. (2001) studied the effects of retinoids on *in vitro* and *in vivo* IgE production in ovalbumin-sensitized BALB/c mice.

Several studies were performed in **guinea pigs** (Miller and Ziboh 1990; Kumar et al. 1992; Maini et al. 1999). Tuzun et al. (1993) reported psoriasis lesions in guinea pigs receiving propranolol; however, their results could not be confirmed by Wolf et al. (1994).

REFERENCES AND FURTHER READING

Beyaert R Schulze-Osthoff K van Roy F, Fiers W (1992) Synergistic induction of interleukin-6 by tumor necrosis factor and lithium chloride in mice: possible role in the triggering and exacerbation of psoriasis by lithium treatment. Eur J Immunol 22:2181–2184

Bosman B (1994) Testing of lipoxygenase inhibitors, cyclo-oxygenase inhibitors, drugs with immunomodulating properties and some reference antipsoriatic drugs in the modified mouse tail test, an animal model of psoriasis. Skin Pharmacol 7:324–334

Bosman B Matthiessen T Hess V Friderichs E (1992) A quantitative method for measuring antipsoriatic activity of drugs by the mouse tail test. Skin Pharmacol 5:41–48

Jarrett A Spearman RIG (1964) Psoriasis. In Taverner D Trounce J (eds) Histochemistry of the Skin. London University Press

Kumar S Malick AW Meltzer NM Mouskountakis JD Behl CR (1992) Studies of *in vitro* skin permeation and retention of a leukotriene antagonist from topical vehicles with a hairless guinea pig model. J Pharm Sci 81:631–634

Mani I Iversen L Ziboh VA (1999) Evidence of nuclear PVK/MAP-kinase cascade in guinea pig model of epidermal hyperproliferation. J Invest Dermatol 112:42–48

Miller CC Ziboh VA (1990) Induction of epidermal hyperproliferation by topical n-3 polyunsaturated fatty acids on guinea pig skin linked to decreased levels of 13-hydroxyoctadecadienoic acid (13-HODE). J Invest Dermatol 94:353–358

Nagano K Hori K Nagane T Sugarawa T Ohishi J Hayashi H Watanabe N Niitsu Y (1990) Effect of tumor necrosis factor in the mouse-tail model of psoriasis. Arch Dermatol Res 282:459–462

Sebök B, Szabados T Kerényi M Schneider I Mahrle G (1996) Effect of fumaric acid, its dimethylester, and topical antipsoriatic drugs on epidermal differentiation in the mouse tail model. Skin Pharmacol 9:99–103

Sebök B, Bonnekoh B Kerenyi M Gollnick H (2000) Tazarotene induces epidermal cell differentiation in the mouse tail test used as an animal model for psoriasis. Skin Pharmacol Appl Skin Physiol 13:285–291

Tuzun B Tuzun Y Gurel N Tuzuner N Altug T Buyukdevrim S (1993) Psoriasis lesions in guinea pigs receiving propranolol. Int J Dermatol 32:133–134

Wolf R Shechter H Brenner S (1994) Induction of psoriasiform changes in guinea pig by propranolol. Int J Dermatol 33:811–814

Worm M Herz U Krah JM Renz H Henz BM (2001) Effects of retinoids on in vitro and in vivo IgE production. Int Arch Allergy Immunol 124:233–236

P.4.3.2 Rat Ultraviolet Ray B Photodermatitis Model for Psoriasis

PURPOSE AND RATIONALE

Rat ultraviolet ray B photodermatitis has been proposed as an experimental model of psoriasis vulgaris by Nagakuma et al. (1995).

PROCEDURE

Male Wistar rats weighing around 300 g are used. Hair on the dorsal skin is clipped and carefully shaved. An area (1.5 × 2.5 cm) on one side of the flank is irradiated for 15 min (1.5 J/cm^2) at a vertical distance of 20 cm with UV-B lamps. A biphasic erythema is observed. Immediately after irradiation, initial faint erythema appears, disappearing within 30 min. The second phase of erythema starts 6 h after the irradiation and gradually increases, peaking between 24 and 48 h. The color is brownish-red, and the reaction is confined to the exposed area with a sharp boundary. By 48–72 h after irradiation, dark-brown scale is formed on the erythematous lesion. Pieces of the scale are relatively thick. The scale separates and the erythema decreases daily. The skin sites return to normal about 10 days after irradiation.

The irradiated rats are sacrificed after various time intervals by decapitation under ether anesthesia. Skin biopsies are taken immediately, fixed in 10% formalin and embedded in paraffin. Tissue sections (4 µm thick) are stained with hematoxylin and eosin. The numbers of the keratinocyte layers, including the basal layer, are counted by direct microscopy.

For DNA labeling (Morimoto et al. 1991), 20 mg/kg 5-bromo-2-deoxyuridine (BrdU) is administered i.p. 8 h before decapitation. Frozen tissue sections (8 µm) are prepared with a cryostat. The sections are then fixed in acetone for 10 min, 4% paraformaldehyde containing 1% $CaCl_2$ (pH 7.0) for 10 min and 1% glutaraldehyde for 5 min. After fixation, sections are digested with 0.006% pepsin in 10 mM HCl for 10 min at 37°C, and incubated in 4 M HCl for 30 min at ambient temperature to denature DNA. They are then incubated with anti-BrdU mouse monoclonal antibody and then

with alkaline phosphatase-conjugated anti-mouse IgG sheep IgG antibody. Antibody-binding sites are visualized with naphthol and fast red at pH 9 in the dark. The number of labeled as well as unlabeled cells at the epidermal basal layer or outer root sheath cell layers of the hair follicles are counted in five high-power fields to a total of at least 100 cells. The intensity of BrdU incorporation is demonstrated as a labeling index (%) with the following formula:

$$\text{labeling index} = \frac{\text{no. of labelled cells}}{\text{total cell no. counted}} \times 100$$

EVALUATION

Chronological changes of thickness of keratinocytes at the epidermis and the hair follicles as well as of DNA labeling indices are plotted as time-response curves.

MODIFICATIONS OF THE METHOD

Kippenberger et al. (2001) found that activators of peroxisome proliferator-activated receptors (PPARs) protect human skin from ultraviolet-B-light induced inflammation. In an *in vitro* model with human keratinocytes inflammation was mimicked by irradiation with ultraviolet light. Activators of PPARα were shown to reverse ultraviolet-B-light-mediated expression of inflammatory cytokines.

REFERENCES AND FURTHER READING

Kippenberger S Loitsch SM Grundmann-Kollmann M Simon S Dang TA Hardt-Weinelt K Kaufmann R Bernd A (2001) Activators of peroxisome proliferator-activated receptors protect human skin from ultraviolet-B-light induced inflammation. J Invest Dermatol 117:1430–1436

Morimoto Y Saga K Bando M Takahashi M (1991) *In vitro* DNA synthesis of keratinocytes in normal human skin, seborrhoeic keratosis, Bowen's disease and basal cell carcinoma. Br J Dermatol 125:9–13

Nagakuma H Kambara T Yamamoto T (1995) Rat ultraviolet ray B photodermatitis: an experimental model of psoriasis vulgaris. Int J Exp Pathol 76:65–73

P.4.4 Hyperproliferative Epidermis in Hairless Mice

PURPOSE AND RATIONALE

Epidermal differentiation and barrier development *in vivo* are influenced by nuclear hormone receptors (Hanley et al. 1997, 1998, 1999; Kömüves et al. 1998; Rosenfield et al. 2000; Smith et al. 2001a, 2001b; Kuenzli and Saurat 2003a, 2003b). Kömüves et al. (2000) studied the effect of PPARα activators on keratinocyte differentiation in hyperproliferative epidermis in hairless mice.

PROCEDURE

Subacute epidermal hyperproliferation is induced by repeated barrier abrogation with acetone treatment (Denda et al. 1996). Animals are treated twice a day with acetone until the transepidermal water loss reaches 8–10 mg per cm^2 per h (measured on four to five different spots) as determined by an electrolyte water analyzer.

Chronic epidermal hyperproliferation due to essential fatty acids deficiency is achieved by feeding an isocaloric diet free of essential fatty acids after weaning for 2–3 months (Man et al. 1993).

To test the effect of PPARα activators, mice are treated on one flank side with solutions of the drug dissolved in propylene glycol/ethanol (3/7) twice a day for 3 days. After sacrifice, tissues are collected for histology, *in situ* hybridization, or immunohistochemistry.

EVALUATION

Data are presented as mean ± SEM. Statistical differences are determined using Student's *t*-test.

REFERENCES AND FURTHER READING

Denda M Wood LC Emami S Calhoun C Brown BE Elias PM Feingold KR (1996) The epidermal hyperplasia associated with repeated barrier disruption by acetone treatment or taps stripping cannot attributed to increased water loss. Arch Dermatol Res 288:230–238

Hanley K Jiang Y Crumrine D Bass NM Appel R Elias PM Williams ML Feingold KR (1997) Activators of the nuclear receptors PPARa and FXR accelerate the development of the fetal epidermal permeability barrier. J Clin Invest 100:705–712

Hanley K Jiang Y He SS, Friedman M Elias PM Bikle PM Williams ML Feingold KR (1998) Keratinocyte differentiation is stimulated by activators of the nuclear hormone receptor PPARα. J Invest Dermatol 110:368–375

Hanley K Kömüves LG Bass NM He SS, Jian Y Crumrine D Appel R Friedman M Bettencort J Min K, Elias PM Williams ML Feingold KR (1999) Fetal epidermal differentiation and barrier development in vivo is accelerated by nuclear hormone receptor activators. J Invest Dermatol 113:788–795

Kömüves LG Hanley K Jiang Y Elias PM Williams ML Feingold KR (1998) Ligands and activators of nuclear hormone receptors regulate epidermal differentiation during fetal rat skin development. J Invest Dermatol 111:429–433

Kömüves LG Hanley K Man MQ, Elias PM Williams ML Feingold KR (2000) Keratinocyte differentiation in hyperproliferative epidermis: application of PPARα activators restores tissue homeostasis. J Invest Dermatol 115:361–367

Kuenzli S Saurat JH (2003a) Peroxisome-proliferator-activated receptors in cutaneous biology. Br J Dermatol 149:229–236

Kuenzli S Saurat JH (2003b) Effect of topical PPARβ/δ and PPARγ agonists on plaque psoriasis. Dermatology 206:252–256

Man MQ, Feingold KR Elias PM (1993) Exogenous lipids influence permeability barrier recovery in acetone-treated murine skin. Arch Dermatol129:728–738

Rosenfield RL Deplewski D Greene ME (2000) Peroxisome proliferator-activated receptors and skin development. Horm Res 54:269–274
Smith KJ Dipreta E Skelton H (2001a) Peroxisomes in dermatology. Part I. J Cutan Med Surg 5:231–243
Smith KJ Dipreta E Skelton H (2001b) Peroxisomes in dermatology. Part II. J Cutan Med Surg 5:315–322

P.4.5 Psoriatiform Skin Diseases in Spontaneous Mice Mutations

PURPOSE AND RATIONALE

Nearly 100 mouse mutations have been described as causing some type of abnormality of the skin or hair. These include "asebia", a mildly hyperkeratotic disorder with sebaceous gland hyperplasia, "ichthyosis", an example of abnormal hair growth associated with hyperkeratosis, "rhino" and "hairless", two related examples of congenital follicular malformations, and "flaky skin", a potential animal model of eruptive psoriasis.

REFERENCES AND FURTHER READING

Sundberg PJ Beamer WG Shultz LD Dunstan RW (1990) Inherited mouse mutations as models of human adnexal, cornification, and papulosquamous dermatoses. J Invest Dermatol 95:62S–63S

P.4.5.1 Flaky Skin (*fsn*) Mouse

PURPOSE AND RATIONALE

Flaky skin (*fsn*) is an autosomal recessive mouse mutation that causes pathologic changes in the skin, yielding a papulosquamous disease resembling human psoriasis (Sundberg et al. 1993). In addition, this mutation, assigned to distal chromosome 17, causes anemia and gastric forestomach hyperplasia (Beamer et al. 1995).

The *fsn* mutation arose spontaneously in the A/J inbred strain at The Jackson Laboratory (Beamer et al. 1986). Psoriasiform skin lesions are first evident as focal epidermal hyperplasia and inflammation at 2 weeks of age. These lesions become confluent and diffuse by 3–4 weeks of age and are associated with marked dermal infiltration of lymphocytes and small numbers of neutrophils and macrophages. Mast cell numbers increase significantly in the dermis from 2 weeks of age onward. Diffuse dermal neovascularization accompanies these cutaneous changes (Sundberg et al. 1997). Systemic lesions include progressive and massive papillomatosis of the stratified squamous epithelium of the forestomach, hyperplasia and dysplasia of the glandular stomach, increased apoptosis of cecal enterocytes, renal glomerulopathy associated with inflammatory cell infiltrates and fibrosis around the portal triads in the liver, splenomegaly due to massive erythropoiesis, and granulomatous lymphadenitis.

Scanning microscope examination (Morita et al. 1995) reveals a greatly thickened epidermis, and sparsity of hairs and scale accumulations in the epidermal surface. Hair shafts have conspicuous pits, striations, and exophytic protrusions. Nails are bent at a 90-degree angle with surface irregularities and accumulation of scale at the nail base. Transmission electron microscopic examination shows increased epidermal thickness, mitochondrial aberrations, and intraepidermal invasion by neutrophils. Keratin abnormalities are detected using immunocytochemical staining for profilaggrin. At the dermal-epidermal junction, numerous macrophages and mast cells are seen in close proximity to focal dissolutions of the basement membrane. A high density of collagen fibers and cellular infiltrates are evident in the papillary dermis.

Besides lymphadenopathy and mast cell accumulation, elevated serum IgE levels (>7000 fold increase compared with normal littermates), autoimmunity (evidenced by glomerulonephritis with immune complex deposition in the kidneys), are observed in flaky skin mutant mice (Pelsue et al. 1998).

Peripheral lymph nodes of adult mutant (*fsn/fsn*) mice were found to contain almost 10-fold more leukocytes than peripheral lymph nodes from phenotypically normal littermates. Analysis of peripheral lymph node cells using mAbs and flow cytometry revealed that this predominantly lymphoid hyperplasia is characterized by approximately equivalent increases of $CD3^+$ T cells and $C19^+$ B cells (Abernethy et al. 2000a). A dysregulated expression of CD69 and IL-2 receptor alpha and beta chains was found on $CD8^+$ T lymphocytes (Abernethy et al. 2000b). Expression and function of IL-1 beta is increased in psoriasiform skin lesions of flaky skin (*fsn/fsn*) mice (Schön et al. 2001).

However, neutrophils also played a critical role of for the generation of psoriasiform skin lesions in flaky skin mice (Schön et al. 2000). Intraperitoneal injection of the neutrophil-depleting RB6–85C monoclonal antibody resulted in a dramatic reduction of the epidermal thickness.

Similar to active human psoriatic lesions, an increase of epidermal growth factor receptors was observed in *fsn/fsn* mice (Nanney et al. 1996).

Sundberg et al. (1994a) transplanted full-thickness skin grafts from flaky skin mice on the dorsal skin

of genetically athymic nude (*nu/nu*) mice. The grafts maintained the psoriatiform phenotype of the donors.

Backcrosses to different mouse strains suggested several modifier genes affecting the *fsn* phenotype (Sundberg et al. 1994b). As cyclosporine A, in contrast to glucocorticoids, was not effective when used for topical or systemic treatment of *fsn* lesions, it seems that there is no immunologic basis for these lesions. Therefore, it remains uncertain whether the flaky skin mouse can be used to test potential therapeutic compounds.

REFERENCES AND FURTHER READING

Abernethy NJ Hagan C Tan PL, Birchall NM Watson JD (2000a) The peripheral lymphoid compartment is disrupted in flaky skin mice. Immunol Cell Biol 78:5–12

Abernethy NJ Hagan C Tan PL, Watson JD (2000b) Dysregulated expression of CD69 and IL-2 receptor alpha and beta chains on $CD8^+$ T lymphocytes in flaky skin mice. Immunol Cell Biol 78:596–602

Beamer W Maltais L Bernstein S (1986) Disturbed iron metabolism in flaky skin (*fsn*) mutant mice. The Jackson Lab Ann Report 1986:92

Beamer WG Pelsue SC Shultz LD Sundberg JP Barker JE (1995) The flaky skin (*fsn*) mutation in mice: map localization and description of the anemia. Blood 86:3220–3226

Morita K Hogan ME Nanney LB King LE Manabe M Sundberg JP (1995) Cutaneous ultrastructural features of the flaky skin (*fsn*) mouse mutation. J Dermatol 22:385–395

Nanney LB Sundberg JP King LE (1996) Increased epidermal growth factor receptor in *fsn/fsn* mice. J Invest Dermatol106:1169–1174

Pelsue SC Schweitzer PA Schweitzer IB Christianson SW Gott B Sundberg JP Beamer WG Shultz LD (1998) Lymphadenopathy, elevated serum IgE levels, autoimmunity, and mast cell accumulation in flaky skin mutant mice. Eur J Immunol 28:1379–1388

Schön M, Denzer D Kubitza RC Ruicka T Schön MP (2000) Critical role of neutrophils for the generation of psoriasiform skin lesions in flaky skin mice. J Invest Dermatol 114:976–983

Schön M, Behmenburg C Denzer D Schön MP (2001) Pathogenic function of IL-1 beta in psoriasiform skin lesions of flaky skin (*fsn/fsn*) mice. Clin Exp Immunol 123:505–510

Sundberg JP Boggees D Sundberg BA Beamer WG Shultz LD (1993) Epidermal dendritic cell populations in the flaky skin mutant mouse. Immunol Invest 22:389–401

Sundberg JP Dunstan RW Roop DR Beamer WG (1994a) Full-thickness skin grafts from flaky skin mice to nude mice: maintenance of the psoriatiform phenotype. J Invest Dermatol 102:781–788

Sundberg JP Boggess D Shultz LD Beamer WG (1994b) The flaky skin (*fsn*) chromosome? In: Sundberg JD (ed) Handbook of Mouse Mutations with Skin, Hair and Abnormalities. Boca Raton: CRC Press, pp 253–268

Sundberg JP France M Boggess D Sundberg BA Jenson AB Beamer WG Shultz LD (1997) Development and progression of psoriasiform dermatitis and systemic lesions in the flaky skin (*fsn*) mouse mutant. Pathobiology 65:271–286

P.4.5.2 Asebia (*ab/ab*) Mouse

PURPOSE AND RATIONALE

The asebia mouse was first described by Gates and Kasarek (1965) as hereditary absence of sebaceous glands. The asebia mouse represents a spontaneous mutation in BALB/c mice leading to hyperplasia of the epidermis and chronic inflammatory dermal changes, including enhanced cellularity, edema and elevated mast cell numbers (Josefowicz and Hardy 1978; Brown and Hardy 1988). The circadian rhythms in cell proliferation are suppressed in the chronically hyperproliferative epidermis of the asebia mouse (Brown et al. 1988a). UVB radiation as well as anthralin and tar with UVB further stimulate proliferation in the already hyperproliferative epidermis of the asebia mouse (Brown et al. 1988b, 1989). The gene for the enzyme stearyl-CoA desaturase 1, which is expressed in sebaceous glands, is disrupted in the asebia mouse (Parimoo et al. 1999; Zheng et al. 1999; Miyazaki et al. 2000). Besides Sdc1 and Sdc2, Zheng et al. (2001) identified Scd3 – a novel gene of the stearoyl-CoA desaturase family with restricted expression in the skin. Since T cell and neutrophil infiltrates are not observed in asebia mice, a pathogenesis distinct from psoriasis has been suggested (Schön 1999).

Asebia-2J (Scd1(ab2J)): a new allele and a model for scarring alopecia was described by Sundberg et al. (2000).

REFERENCES AND FURTHER READING

Brown WR Hardy MH (1988) A hypothesis on the cause of chronic epidermal hyperproliferation in asebia mice. Clin Exp Dermatol 13:74–77

Brown WR Furukawa RD Ramsay CA (1988a) Circadian rhythms are suppressed in hyperproliferative mouse epidermis. Cell Tissue Kinet 21:159–167

Brown WR Rogozinski TT Ramsay CA (1988b) Anthralin and tar with UVB increase epidermal cell proliferation in asebia mice. Clin Exp Dermatol 13:248–251

Brown WR Furukawa RD Ramsay CA (1989) UVB radiation further stimulates proliferation in the already hyperproliferative epidermis of the asebia mouse. Arch Dermatol Res 281:366–367

Gates AH Kasarek M (1965) Hereditary absence of sebaceous glands in the mouse. Science 148:1471–1473

Josefowicz WJ Hardy MH (1978) The expression of the gene asebia in the laboratory mouse. I. Epidermis and dermis. Genet Res 31:53–65

Miyazaki M Kim YC, Gray-Keller MP Attie AD Ntambi JM (2000) The biosynthesis of hepatic cholesterol esters and triglycerides in impaired in mice with a disruption of the gene for stearoyl-CoA desaturase 1. J Biol Chem 275:30132–30138

Oran A Marshall JS Kondo S Paglia D McKenzie RC (1997) Ciclosporin inhibits intracellular adhesion molecule-1 ex-

pression and reduces mast cell numbers in the asebia model of chronic skin inflammation. Br J Dermatol 136:519–526
Parimoo S Zheng Y Eilertsen K Ge L, Prouty S Sundberg J Stenn K (1999) Identification of a novel SCD gene and expression of the SCD gene family in mouse skin. J Invest Dermatol Symp Proc 1999 Dec 4:320–322
Schön MP (1999) Animal models of psoriasis – what can we learn from them? J Invest Dermatol 112:405–410
Sundberg JP Boggess D Sundberg BA Eilertsen K Parimoo S Filippi M Stenn K (2000) Asebia-2J (Scd1(ab2J)): a new allele and a model for scarring alopecia. Am J Pathol 156:2067–2075
Zheng Y Eilertsen KJ Ge L, Zhang L Sundberg JP Prouty SM Stenn KS Parimoo S (1999) Scd1 is expressed in sebaceous glands and is disrupted in the asebia mouse. Nat Genet 23:268–270
Zheng Y Prouty SM Harmon A Sundberg JP Stenn KS Parimoo S (2001) Scd3 – a novel gene of the stearoyl-CoA desaturase family with restricted expression in the skin. Genomics 71:182–191

P.4.6 Psoriasiform Skin Diseases in Genetically Modified Animals

PURPOSE AND RATIONALE

Based on expression in inflammatory skin disorders, several factors, such as cytokines, are considered to play a crucial role in the pathogenesis of psoriasis and other skin diseases. Transgenic animals are tools to analyze these factors (Meyer 1990; Rothnagel et al. 1990; Sellheyer 1996; Rosenberg et al. 1999).

Bullard et al. (1996) described a polygenic mouse model of psoriasiform skin disease in **CD18-deficient mice**. CD18 deficiency in patients results in recurrent microbial infections, leukocytosis, impaired wound healing, failure of granulocyte emigration, and lack of pus formation (Anderson et al. 1995). A hypomorphic mutation for CD18 was introduced by Wilson et al. (1993) into mice with homocygotes displaying mild leukocytosis, an impaired response to chemically induced peritonitis, and delays in transplantation rejection. When this CD18 mutation was crossed back onto PL/J strain of mice, the development of an inflammatory skin disorder was observed (Bullard et al. 1996). The disease is characterized by erythema, hair loss, and the development of crusts. The histopathology reveals hyperplasia of the epidermis, subcorneal microabscesses, orthohyperkeratosis, parakeratosis, and lymphocyte exocytosis similar to human psoriasis and other hyperproliferative skin disorders. The dermatitis rapidly resolved after subcutaneous administration of dexamethasone.

Dermal infiltrates of macrophages/monocytes within the dermis of clinically uninvolved skin were seen in transgenic mice with epidermal overexpression of K14/IL-1α, suggesting a role of IL-1α for macrophage attraction (Groves et al. 1995). In severely affected animals, inflammation reactions occur that are characterized by a mixed inflammatory infiltrate, and by acanthosis and parakeratosis. **IL-1α transgenic mice** support a primary role of IL-1α as an inducer of cutaneous inflammation, which may be helpful for clarifying pathogenesis of psoriasis.

Wilson et al. (1990) reported that expression of the **BNLF-1 oncogene** of Epstein-Barr virus in the skin of transgenic mice induces hyperplasia and aberrant expression of keratin 6.

Cook et al. (1997, 1999) found that overexpression of the heparin-binding EGF-related ligand amphiregulin in the epidermis of transgenic mice induces a psoriasis-like cutaneous phenotype. **Transgenic mice with a K14 enhancer/promoter-driven amphiregulin gene** targeted to the epidermis displayed a macroscopic phenotype that included extensive areas of scaling and erythematous skin with marked alopecia. Histological examination revealed hyperkeratosis, focal parakeratosis, acanthosis, mixed leukocytic infiltration that included both CD3-positive T cells in the dermis and epidermis, and a tortuous vasculature.

Two completely opposite phenotypes were observed in **mice expressing K10/BMP-6** (bone morphogenetic protein-6, a member of the TGF-β superfamily) within the epidermis (Blessing et al. 1996). Whereas keratinocyte proliferation was severely reduced in animals with strong and homogenous expression of the transgene, weaker and patchy expression led to marked hyperproliferation.

Rodriguez-Villanueva et al. (1998) reported that **human keratin-1.bcl-2 mice** aberrantly express keratin 6, exhibit reduced sensitivity to keratinocyte cell death induction, and are sensible to skin tumor formation.

The concept of vascular endothelial growth factor (VEGF) being an important angiogenic factor in psoriatic skin (Detmar et al. 1994) was supported by **transgenic mice with constitutive epidermal K14/VEGF expression**. These animals exhibited dilated and contorted dermal microvessels (Detmar et al. 1998). There was also an increased number of dermal mast cells, and leukocyte adhesion and extravasation was enhanced in VEGF transgenic mice. The transgenic delivery of VEGF to mouse skin results in a profound inflammatory condition with many of the cellular and molecular features of psoriasis, including the characteristic vascular changes, epidermal alterations, and inflammatory infiltrates. These symptoms can be effectively reversed by the addition of VEGF Trap, a potent VEGF antagonist (Xia et al. 2003). VEGF-A also promoted lym-

phatic vessel proliferation and enlargement. Combined systemic treatment with blocking antibodies against VEGF receptor-1 (VEGFR-1) and VEGFR-2 potently inhibited inflammation and also decreased lymphatic vessel size (Kunstfeld et al. 2004).

Klement et al. (1996) found that **IκBα deficiency** results in a sustained NF-κB response and widespread dermatitis in mice.

Seitz et al. (1998) reported that alterations on NF-κB function in transgenic epithelial tissue demonstrate a growth inhibitory role for **NF-κB**.

To determine the role of κB-α deficient immunocytes in the pathogenesis of skin disease in adult mice, Chen et al. (2000) utilized the RAG2-deficient blastocyst complementation system to generate **RAG2–/–, IκB-α–/– chimeras**. These animals display a psoriasiform dermatitis characterized by hyperplastic epidermal keratinocytes and dermal infiltration of immunocytes, including lymphocytes. Skin grafts transferred from diseased chimeras to recipient nude mice produce hyperproliferative epidermal keratinocytes in response to stimulation.

Transgenic mice overexpressing suprabasal integrins α_2, α_5, and β_1 demonstrate a phenotype similar to psoriasis with cycles of flaking and inflamed skin, suggesting that disrupted keratinocyte integrin-ligand interactions may play a role in hyperproliferative states (Carroll et al. 1995).

Robles et al. (1996) found that **expression of cyclin D1 in epithelial tissue** of transgenic mice results in epidermal hyperproliferation and severe thymic hyperplasia.

Carroll et al. (1997) used the **involucrin promoter to overexpress** IFN$_\gamma$ in the suprabasal layers of transgenic mouse epidermis. The mice exhibited striking hypopigmentation of the hair due to reduction of DOPA-positive melanocytes. Severely affected mice had reddened skin, growth retardation, hair loss, and flaky skin lesions. The skin was characterized by a dermal infiltrate of T lymphocytes and macrophages/monocytes.

When **scid/scid mice were reconstituted with MHC-matched, but minor histocompatibility mismatched CD4$^+$/CD45RB^{hi}T lymphocytes**, almost all of the animals developed skin lesions similar to human psoriasis within 4–8 weeks after transfer (Schön et al. 1997). The psoriatiform skin lesions did not develop in recipients of unfractionated splenocytes or CD4$^+$/CD45RB^{lo} T cells, indicating that T cell dysregulation is the primary pathogenic factor in this model. When recipients of CD4$^+$/CD45RB^{hi} T cells were treated with either cyclosporine A or UVB irradiation, the psoriasiform lesions were dramatically improved demonstrating that immunosuppressive therapies are efficacious. The model was proposed as a T cell initiated murine model of inflammatory skin lesions (Schön and Parker 1997).

Mann et al. (1993) found that mice with a **null mutation of the TGF-a gene** have abnormal skin architecture, wavy hair, and curly whiskers and often develop corneal inflammation.

Turksen et al. (1992) described psoriasiform changes in the skin of transgenic mice with **overexpression of interleukin 6**.

Guo et al. (1993) reported that targeting expression of **keratinocyte growth factor** to keratinocytes elicits striking changes in epithelial differentiation in transgenic mice.

Hong et al. (1999) showed that IL-12, independently of IFN-gamma, plays a crucial role in the pathogenesis of a murine psoriasis-like disorder. Only a few *scid/scid* mice develop skin lesions when CD4$^+$/CD45RB^{hi} are transferred alone. Coadministration of LPS plus IL-12 or staphylococcal enterotoxin B in *scid/scid* mice one day after **CD4$^+$/CD45RB^{hi}cell transfer** greatly enhances disease penetrance and severity.

Schön et al. (2000) reported a cutaneous inflammatory disorder in **integrin alpha E (CD103)-deficient mice**. Skin inflammation correlated with alpha E deficiency in mice with a mixed 129/Sv × BALB/c background.

Transgenic rats expressing human HLA-B27 and β_2-microglobulin develop psoriasiform skin changes as part of a multi-organ inflammatory disease (Hammer et al. 1990). In the most severely affected lines, psoriasiform lesions first occurred at about 20 weeks of life and were observed in 10% to 80% of animals. Male appeared to be more prone to skin changes than females (Taurog et al. 1993, 1994, 1999). Similar to human pathogenesis, T cells seem to be the most important factor in HLA-B27 transgenic rats (Breban et al. 1996).

REFERENCES AND FURTHER READING

Anderson DC Kishimoto TK Smith CW (1995) In: Scriver CR Beaudet AL Sly WS, Valle D (eds) Leukocyte Adhesion Deficiency and Other Disorders of Leukocyte Adherence and Motility. McGraw-Hill, New York, pp 3955–3994

Blessing M Schirmacher P Kaiser S (1996) Overexpression of bone morphogenetic protein-6 (BMP-6) in the epidermis of transgenic mice: Inhibition of stimulation of proliferation depending on the pattern of transgene expression and formation of psoriatic lesions. J Cell Biol 135:227–239

Breban M Fernandez-Sueiro JL Richardson JA Hadavand RR Maika SD Hammer RE Taurog JD (1996) T cells, but not

thymic exposure to HLA-B27 are required for the inflammatory disease of HLA-B27 transgenic rats. J Immunol 156:794–803
Bullard DC Scharffetter-Kochanek K McArthur MJ Chosay JG McBride ME Montgomery CA Beaudet AL (1996) A polygenic mouse model of psoriasiform skin disease in CD18-deficient mice. Proc Natl Acad Sci 93:2116–2121
Carroll JM Rosario RM Watt FM (1995) Suprabasal integrin expression in the epidermis of transgenic mice results in developmental defects and a phenotype resembling psoriasis. Cell 83:957–968
Carroll JM Crompton T Seery JP Watt FM (1997) Transgenic mice expressing IFN$_\gamma$ in the epidermis have eczema, hair hypopigmentation, and hair loss. J Invest Dermatol 108:412–422
Chen C-L, Yull FE Cardwell N Singh N Strayhorn WD Nanney LB Kerr LD (2000) RAG2–/–, IκB-α–/– chimeras display a psoriasiform skin disease. J Invest Dermatol 115:1124–1133
Cook PW Piepkorn M Clegg CH Plowman GD Demay JM Brown JR Pittelkow MR (1997) Transgenic expression of human amphiregulin gene induces a psoriasis-like phenotype. J Clin Invest 100:2286–2294
Cook PW Pittelkow MR Piepkorn M (1999) Overexpression of amphiregulin in the epidermis of transgenic mice induces a psoriasis-like cutaneous phenotype. J Invest Dermatol 113:860
Detmar M Brown LF Claffey KP (1994) Overexpression of vascular permeability factor/vascular endothelial growth factor and its receptors in psoriasis. J Exp Med 180:1141–1146
Detmar M Brown LF Schön MP (1998) Increased microvascular density and enhanced leukocyte rolling and adhesion in the skin of VEGF transgenic mice. J Invest Dermatol 111:1–6
Groves RW Mizutani H Kieffer JD Kupper TS (1995) Inflammatory skin disease in transgenic mice that express high levels of interleukin 1α in basal epidermis. Proc Natl Acad Sci USA 92:11874–11878
Guo L, Yu QC, Fuchs B (1993) Targeting expression of keratinocyte growth factor to keratinocytes elicits striking changes in epithelial differentiation in transgenic mice. EMBO J 12:973–986
Hammer RE Maika SD Richardson JA Tang JP Taurog JD (1990) Spontaneous inflammatory disease in transgenic rats expressing HLS-B27 and human β_2m: an animal model of HLA-B27 associated human disorders. Cell 63:1099–1112
Hong K Chu A, Ludviksson BR Berg EL Ehrhardt RO (1999) IL-12, independently of IFN-gamma, plays a crucial role in the pathogenesis of a murine psoriasis-like disorder. J Immunol 162:7480–7491
Klement JF Rice NR Car BD (1996) I$\kappa B\alpha$ deficiency results in a sustained NF-κB response and widespread dermatitis in mice. Mol Cell Biol 16:2341–2349
Kunstfeld R Hirakawa S Hong YK Schacht V Lange-Asschenfeldt B Velasco P Lin C, Fiebiger E Wei X, Wu Y, Hicklin D Bohlen P Detmar M (2004) Induction of cutaneous delayed-type hypersensitivity reactions in VEGF-A transgenic mice results in chronic skin inflammation associated with persistent lymphatic hyperplasia. Blood 104:1048–1057
Mann GB Fowler KJ Gabriel A (1993) Mice with a null mutation of the TGF-a gene have abnormal skin architecture, wavy hair, and curly whiskers and often develop corneal inflammation. Cell 73:249–261
Meyer LJ (1990) Psoriasis: the application of genetic technology and mapping. J Invest Dermatol 95:5S–6S
Robles AJ Larcher F Whalin RB (1996) Expression of cyclin D1 in epithelial tissue of transgenic mice results in epidermal hyperproliferation and severe thymic hyperplasia. Proc Natl Acad Sci USA 93:7634–7638
Rodriguez-Villanueva J Greenhalgh D Wang X-J, Bundman D Cho S, Delhedde M Roop D McDonnell TJ (1998) Human keratin-1.*bcl*-2 mice aberrantly express keratin 6, exhibit reduced sensitivity to keratinocyte cell death induction, and are sensible to skin tumor formation. Oncogene 16:853–863
Rosenberg EW Noah PW Skinner RB Jr (1999) Animal models of psoriasis. J Invest Dermatol 113:427
Rothnagel JA Longley MA Bundman D Greenhalgh DA Dominey AM Roop DR (1990) Targeting gene expression to the epidermis of transgenic mice: potential applications to genetic skin disorders. J Invest Dermatol 95:59S–81S
Schön MP, Parker CM (1997) A T cell initiated murine model of inflammatory skin lesions. Retinoids Lipid-Soluble Vitamins Clin Pract 13:128–131
Schön MP, Detmar M Parker CM (1997) Murine psoriasis-like disorder induced by naive CD4$^+$ T cells. Nat Med 3:183–188
Schön MP, Schön M, Warren HB Donohue JP Parker CM (2000) Cutaneous inflammatory disorder in integrin alpha E (CD103)-deficient mice. J Immunol 165:6583–6589
Seitz CS Lin Q, Deng H Khavari PA (1998) Alterations on NF-κB function in transgenic epithelial tissue demonstrates a growth inhibitory role for NF-κB. Proc Natl Acad Sci USA 95:2307–2312
Sellheyer K (1996) Transgene Mäuse als Modelle für Hautkrankheiten. Hautarzt 47:475–476
Taurog JD Maika SD Simmons WA Breban M Hammer RE (1993) Susceptibility to inflammatory disease in HLA-B27 transgenic rat lines correlates with the levels of B27 expression. J Immunol 150:4168–4178
Taurog JD Richardson JA Croft JT (1994) The germfree state prevents development of gut and joint inflammatory disease in HLA-B27 transgenic rats. J Exp Med 180:2359–2364
Taurog JD Maika SD Satumtira M Dorris ML McLean IL Yanagisawa H Sayad A Stagg AJ Fox GM, Le-O'Brien A Rehman M Zhou M Weiner AL Splawski JB Richardson JA Hammer RE (1999) Inflammation disease in HLA-B27 transgenic rats. Immunol Rev 169:209–223
Turksen K Kupper T Degenstein L Williams I Fuchs E (1992) Interleukin 6: insights to its function by overexpression in transgenic mice. Proc Natl Acad Sci USA 89:5068–5072
Wilson JB Weinberg W Johnson R Yuspa S Levine AJ (1990) Expression of the BNLF-1 oncogene of Epstein-Barr virus in the skin of transgenic mice induces hyperplasia and aberrant expression of keratin 6. Cell 61:1315–1327
Wilson RW Ballantyne CM Smith CW Montgomery C Bradley A O'Brien WE Beaudet AL (1993) Integrin beta 2: Gene targeting yields a CD18-mutant mouse for study of inflammation. J Immunol 151:1571–1578
Xia YP, Li B, Hylton D Detmar M Yancopoulos GD Rudge JS (2003) Transgenic delivery of VEGF to mouse skin leads to an inflammatory condition resembling human psoriasis. Blood 102:161–168

P.4.7
Xenotransplantation of Human Psoriatic Skin

PURPOSE AND RATIONALE

Xenotransplantation models for psoriasis involve the transfer of human psoriatic skin to animals. First stud-

ies were performed by transplantation of involved psoriatic and non-psoriatic human skin onto congenitally athymic (nude) mice (Krueger et al. 1975, 1985; Baker et al. 1992). More recently, human psoriatic skin grafts were transplanted onto SCID mice (Nickoloff et al. 1995; Boehncke et al. 1994, 1997, 1999; Gilhar et al. 1997; Sugai et al. 1998; Dam et al. 1999; Raychaudhuri et al. 2001) allowing screening of anti-psoriatic drugs.

PROCEDURE

Keratome biopsies ($7 \times 2 \times 0.05$ cm containing both dermis and epidermis) are obtained from clinically symptomless skin of patients with psoriasis or from psoriatic plaques. Prior to the procedure, the skin is defined and infiltrated with 1% lidocaine and epinephrine 1:200. The full-thickness skin biopsy is dissected into 12 grafts. CB-17 SCID mice at an age of 6–8 weeks are anesthetized with an i.p. injection of 1.56 mg phenobarbital before transplantation of the human xenografts on the flank area. The grafts are sutured with absorbable 6–0 Vicryl Rapid suture and covered with Xeroform dressings for one week. Animals transplanted with the psoriatic plaque are then randomized into groups receiving PBS as negative controls or 0.15 mg cyclosporine A or the test compound intradermally into the xenografts. Within 4 weeks, the animals are sacrificed by CO_2 asphyxiation and 4 mm punch biopsies are obtained from each xenograft. Biopsies are fixed in 10% neutral-buffered formalin for paraffin embedding.

EVALUATION

A semiquantitative scale is used to indicate the extent of new vessel formation (angiogenesis) that can be seen between the xenograft and the underlying fascia muscularis. A calibrated eyepiece microscope is used for estimating the epidermal thickness in the vertical sections. Statistical differences are calculated using Student's *t*-test for multiple comparisons.

MODIFICATIONS OF THE METHOD

Using this model, Raychaudhuri et al. (2004) found that a high-affinity nerve growth factor receptor blocker improves psoriasis.

Nickoloff et al. (1995) studied severe combined immunodeficiency mouse and human psoriatic skin chimeras. Autologous blood-derived $CD4^+$ cells injected into symptomless transplanted psoriatic skin engrafted onto SCID mice produced full-fledged psoriatic lesions (Wrone-Smith and Nickoloff 1996; Sugai et al. 1998; Nickoloff and Wrone-Smith 1999; Nickoloff et al. 1999; Nickoloff 2000).

Yamamoto et al. (1998) studied the effects of superantigen-driven peripheral blood mononuclear cells on the persistence of psoriasiform epidermis and on the cytokine gene expression of grafted psoriatic skin. Staphylococcal enterotoxin B-stimulated peripheral blood mononuclear cells from psoriatic patients were repeatedly injected under the grafted full-thickness involved psoriatic skin onto severe combined immunodeficient mice. A persistence of the psoriasiform epidermis was found after 5 weeks. E-selectin expression was observed on endothelial cells in the upper epidermis of the mice.

Tissue specificity of E- and P-selectin ligands in Th1-mediated chronic inflammation was studied by Chu et al. (1999).

Zeigler et al. (2001) used the human psoriatic skin-SCID mouse transplant model to compare the effect of antibody to CD11a with ciclosporin and clobetasol propionate.

Zollner et al. (2002) used a SCID-hu model and found that proteosome inhibition reduces superantigen-mediated T cell activation and the severity of psoriasis.

Boyman et al. (2004) presented an animal model in which skin lesions developed spontaneously when symptomless prepsoriatic human skin was engrafted onto AGR129 mice, deficient in type I and type II interferon receptors, and for the recombination activating gene 2. Upon engraftment, resident human T cells in prepsoriatic skin underwent local proliferation.

REFERENCES AND FURTHER READING

Baker BS Brent L Valdimarsson H Powles AV Al-Imara L (1992) Is epidermal cell proliferation in psoriatic skin grafts on nude mice driven by T-cell cytokines? Br J Dermatol 126:105–110

Boehncke WH Stery W Hainzl A Scheffold W Kaufmann R (1994) Psoriasiform architecture of murine epidermis overlying human psoriatic dermis. Arch Dermatol Res 286:325–330

Boehncke WH Zollener TM Dressel D Kaufmann R (1997) Induction of psoriasiform inflammation by a bacterial superantigen in the SCID-hu xenogenic transplantation model. J Cutan Pathol 24:1–7

Boehncke WH Kock M Hardt-Weinelt K Wolter M Kaufmann R (1999) The SCID-hu xenogenic transplantation model allows screening of antipsoriatic drugs. Arch Dermatol Res 291:104–106

Boyman O Hefti HP Conrad C Nickoloff BJ Suter M Nestle FO (2004) Spontaneous development of psoriasis in a new animal model shows an essential role for resident T cells and tumor necrosis factor-$\alpha\alpha$. J Exp Med 199:731–736

Chu A, Hong K Berg EL Ehrhardt RO (1999) Tissue specificity of E- and P-selectin ligands in Th1-mediated chronic inflammation. J Immunol 163:5086–5093

Dam TN, Kang S Nickoloff BJ Voorhees JJ (1999) 1α,25-Dihydrocalciferol and cyclosporine suppress induction and promote resolution of psoriasis in human skin grafts transplanted on to SCID mice. J Invest Dermatol 113:1082–1089
Gilhar A David M Ullmann Y Berkutski T Kalish RS (1997) T-lymphocyte dependence of psoriatic pathology in human psoriatic skin grafted to SCID mice. J Invest Dermatol 109:283–288
Krueger GG Manning DD Malouf J Ogden B (1975) Long-term maintenance of psoriatic human skin on congenitally athymic (nude) mice. J Invest Dermatol 64:307–312
Krueger GG Wojciechowski ZJ Burton SA Gilhar A Huether SE Leonard LG Rohr DU Petelenz TJ Higuchi WI Pershing LK (1985) The development of a rat/human skin flap served a defined and accessible vasculature on a congenital athymic (nude) rat. Fundam Appl Toxicol 5:S112–S121
Nickoloff BJ (2000) The search for pathogenic T cells and the genetic basis of psoriasis using a severe combined immunodeficient mouse model. Cutis 65:110–114
Nickoloff BJ Wrone-Smith T (1999) Injection of pre-psoriatic skin with $CD4^+$ cells induces psoriasis. Am J Pathol 155:145–158
Nickoloff BJ Kunkel SL Burdick M Strieter RM (1995) Severe combined immunodeficiency mouse and human psoriatic skin chimeras. Am J Pathol 146:580–588
Nickoloff BJ Wrone-Smith T Bohnisch B Porcelli SA (1999) Response of murine and normal human skin to injection of allogenic blood-derived immunocytes: Detection of T cells expressing receptors typically present on natural killer cells, including CD94, CD158, and CD161. Arch Dermatol 135:546–552
Raychaudhuri SP Dutt S Raychaudhuri SK Sanyal M Farber EM (2001) Severe combined immunodeficiency mouse – human skin chimeras: a unique animal model for the study of psoriasis and cutaneous inflammation. Br. J Dermatol 144:931–939
Raychaudhuri SP Sanyal M Weltman H Kundu-Raychaudhuri S (2004) K252, a high-affinity nerve growth factor receptor blocker, improves psoriasis: an in vivo study using the severe combined immunodeficient mouse-human skin model. J Invest Dermatol 122:812–819
Schön MP (1999) Animal models of psoriasis – what can we learn from them? J Invest Dermatol 112:405–410
Sugai J Iizuka M Kawakubo Y Ozawa A Ohkido M Ueyama Y Tamaoki M Inokuchi S Shimamura K (1998) Histological and immunocytochemical studies of human psoriatic lesions transplanted onto SCID mice. J Dermatol Sci 17:85–92
Yamamoto T Matsuuchi M Katayama I Nishioka K (1998) Repeated subcutaneous injection of staphylococcal enterotoxin B-stimulated lymphocytes retains epidermal thickness of psoriatic skin graft onto severe combined immunodeficient mice. J Dermatol Sci 17:8–14
Wrone-Smith T Nickoloff BJ (1996) Dermal injection of immunocytes induces psoriasis. J Clin Invest 98:1878–1887
Zeigler M Chi Y, Tumas DB Bodary S Tang H Varani J (2001) Anti-CD11a ameliorated disease in the human psoriatic skin-SCID mouse transplant model: comparison of antibody to CD11a with cyclosporin A and clobetasol propionate. Lab Invest 81:1253–1261
Zollner TM Podda M Pien C Elliott PJ Kaufmann R Boehncke WH (2002) Proteosome inhibition reduces superantigen-mediated T cell activation and the severity of psoriasis in a SCID-hu model. J Clin Invest 109:671–679

P.5
Scleroderma Models

P.5.1
Scleroderma Models in Chicken

Scleroderma is an autoimmune disorder which occurs in the severe systemic form, a localized scleroderma (morphoea) and as lichen sclerosus et atrophicus. Chickens of the University of California line 200 (**UCD-200 chickens**) developed an inherited inflammatory fibrotic disease, closely resembling human progressive systemic sclerosis (scleroderma) (Gershwin et al. 1981; Van de Water et al. 1984; Boyd et al. 1991; Gruschwitz et al. 1991, 1993; Herold et al. 1992; Needleman 1992; Brezinscheck et al. 1993; Ausserlechner et al. 1997; Nguyen et al. 2000). An acute inflammatory stage started at an age of about 60 days after hatching, leading to fibrosis with fast progression with severe lymphocytic infiltration and excessive accumulation of collagen in skin and internal organs. A sequential increase of type VI, type I and type II procollagen transcripts and a progressive increase of autoantibodies to histone, to ssDNA and to dsDNA was found.

A further strain of chickens with progressive systemic sclerosis (UCD 206) has been identified (Duncan et al. 1995; Sgonc et al. 1995).

Worda et al. (2003) analyzed the apoptosis-inducing effect of anti-endothelial cell antibodies in systemic sclerosis by the chorionallantoic membrane assay.

REFERENCES AND FURTHER READING

Ausserlechner MJ Sgonc R Dietrich R Wick G (1997) Altered procollagen mRNA expression during the progression of avian scleroderma. Mol Med 3:654–662
Boyd RL Wilson TJ Van de Water J Haapanen LA Gershwin ME (1991) Selective abnormalities in the thymic microenvironment associated with avian scleroderma, an inherited fibrotic disease of L200 chicken. J Autoimmunol 4:369–380
Brezinschek HP Gruschwitz M Sgone R Moormann S Herold M Gershwin ME Wick G (1993) Effects of cytokine application on glucocorticoid secretion in an animal model for systemic scleroderma. J Autoimmun 6:719–733
Duncan MR Berman B Van de Water J Boyd RL Wick G Gershwin ME (1995) Mononuclear cells isolated from fibrotic skin lesions in avian scleroderma. Int Arch Allergy Immunol 107:519–526
Gershwin ME Abplanalp JJ Castles RM Ikeda J van de Water J Eklund J Haynes D (1981) Characterization of a spontaneous disease of white leghorn chickens resembling progressive systemic sclerosis (scleroderma). J Exp Med 153:1640–1659
Gruschwitz MS Moormann S Kromer G Sgonc R Gietrich H Boeck G Gershwin ME Boyd R Wick G (1991) Phenotypic analysis of skin infiltrates in comparison with peripheral blood lymphocytes, spleen cells and thymocytes in early avian scleroderma. J Autoimmun 4:577–593

Gruschwitz MJS Shoenfeld Y Krupp M Gershwin ME Penner E Brezinscheck HP Wick G (1993) Antinuclear antibody profile in the UCD line 200 chickens: a model for progressive systemic sclerosis. Int Arch Allergy 100:307–313
Herold M Brezinschek HP Gruschwitz M Dietrich H Wick G (1992) Investigations of ACTH responses of chickens with autoimmune disease. Gen Comp Endocrinol 88:186–198
Needleman BW (1992) Immunologic aspects of scleroderma. Curr Opin Rheumatol 4:862–868
Nguyen VA Sgonc R Dietrich M Wick G (2000) Endothelial injury in internal organs of University of California at Davis line 200 (UCD 200) chickens, an animal model for systemic sclerosis (scleroderma). J Autoimmun 14:143–149
Sgonc R Dietrich R Gershwin ME Colombatti A Wick G (1995) Genomic analysis of collagen and endogenous virus loci in the UCD-200 and 206 lines of chickens, animal models of scleroderma. J Autoimmunol 8:763–770
Van de Water J Gershwin ME Aplanalp H Wick G van der Mark K (1984) Serial observations and definition of mononuclear cell infiltrates in avian scleroderma, an inherited fibrotic disease of chickens. Arthr Rheum 27:807–815
Worda M Sgong R Dietrich H Niederegger H Sundick RS Gershwin ME Wick G (2003) In vivo analysis of the apoptosis-inducing effect of anti-endothelial cell antibodies in systemic sclerosis by the chorionallantoic membrane assay. Arthritis Rheum 48:2605–2614

P.5.2 Scleroderma Models in Mice

Jimenez and Christner (2002) gave a survey on murine animal models of systemic sclerosis.

The **tight-skin mouse** is regarded as an experimental model for scleroderma (Walker et al. 1990; Muryoi et al. 1992; Delany and Brinkerhoff 1993; Kasturi et al. 1993, 1994; Wallace et al. 1994; Pablos et al. 1995; Frondoza et al. 1996). This mutant mouse develops autoantigens specific for scleroderma target tissues. The tight-skin disease was first discovered in 1967 at the Jackson Laboratory in the B10.D2(58N)/Sn mouse strain. The disease occurred spontaneously. Green et al. (1976) have identified the tsk locus and shown it to be linked to pallid locus. The tight skin character is transmitted as an autosomal dominant trait and homozygous tsk/tsk mice die *in utero*. The striking feature of the disease is the presence of thickened skin, firmly bound to subcutaneous and deep muscular tissue, with excessive accumulation of collagen in skin and internal organs (Menton et al. 1978; Osborn et al. 1983). Synthesis and accumulation of type I collagen is markedly increased (Jimenez et al. 1986; Ong et al. 1998). Biochemical studies have shown that the prolyl hydroxylase and glycosaminoglycan content of the affected tissue is increased (Ross et al. 1987).

Dermal fibrosis in the tight-skin mouse was reduced after local application of halofuginone, an inhibitor of collagen type I synthesis (Pines et al. 2001).

Additionally, the **tight skin 2 mouse** has been described as an animal model of scleroderma displaying cutaneous fibrosis and mononuclear cell infiltration (Christner et al. 1995, 1996; Wooley et al. 1998; Sgonc et al. 1999).

Bleomycin-induced scleroderma in genetically mast cell deficient **WBB6F1-W/W^V mice** was described as an animal model of sclerotic skin (Yamamoto et al. 1999a–d, 2000; Yamamoto and Nishioka 2001, 2002; Yamamoto 2002).

Murine sclerodermatous graft-versus-host disease is considered as a model for human scleroderma (Claman 1990; Schiltz et al. 1994; McCormick et al. 1999; Zhang et al. 2002, 2003; Atamas and White 2003). Fibrosis in sclerodermatous graft-versus-host disease is driven by infiltrating TGF-β_1-producing mononuclear cells. Zhang et al. (2002) characterized the origin and types of cutaneous effector cells, the cytokine and chemokine environments, and the effects of anti-TGF-β antibodies on skin fibrosis, immune cell activation markers, and collagen and cytokine synthesis.

Dong et al. (2002) transplanted skin from scleroderma patients to SCID mice and investigated the skin xenografts for factors downstream of TGF-β. Deficient expression of Smad7 was found as a putative molecular defect in scleroderma.

A syndrome resembling human systemic sclerosis (scleroderma) in **MRL/lpr mice lacking interferon-receptor** was described by Le Hir et al. (1999).

REFERENCES AND FURTHER READING

Atamas SP White B (2003) The role of chemokines in the pathogenesis of scleroderma. Curr Opin Rheumatol 15:772–777
Christner PJ Peters J Hawkins D Siracusa LD Jiménez SA (1995) The tight skin 2 mouse. An animal model of scleroderma displaying cutaneous fibrosis and mononuclear cell infiltration. Arthr Rheum 38:1791–1798
Christner PJ Siracusa LD Hawkins DF McGrath R Betz JK Ball ST Jiménez SA Peters J (1996) A high resolution linkage map of the tight skin 2 (Tsk2) locus: a mouse model for scleroderma (SSc) and other cutaneous fibrotic diseases. Mamm Genome 7:610–612
Claman HN (1990) Mast cells and fibrosis. The relevance to scleroderma. Rheum Dis Clin North Am 16:141–151
Delany AM Brinkerhoff CE (1993) The synthetic retinoid (4-hydoxyphenyl) retinamide decreases collagen expression *in vitro* and in the tight-skin mouse. Arthr Rheumatol 36:983–993
Dong C Zhu S, Wang T Yoon A Li Z, Alvarez RJ ten Dijke P White B Wigley FM Goldschmidt-Clermoont PJ (2002) Deficient Smad7 expression. A putative molecular defect in scleroderma. Proc Natl Acad Sci USA 99:3908–3913
Frondoza C Jones L Rose NR Hatakeyama A Phelps R Bona C (1996) Silicone does not potentiate development of the scleroderma-like syndrome in tight sin (TSK/+) mice. J Autoimmun 9:473–483

Green MC Sweet HO Bunker LE (1976) Tight-skin, a new mutation of the mouse causing excessive growth of connective tissue and skeleton. Am J Pathol 82:493–512
Jimenez SA Williams CJ Meyers JC Basey R (1986) Increased collagen biosynthesis and increased expression of type I and type II pro-collagen genes in tight-skin (TASK) mouse fibroblasts. J Biol Chem 261:657–662
Jimenez SA Christner OJ (2002) Murine animal models of systemic sclerosis. Curr Opin Rheumatol 14:671–680
Kasturi KN Dalan C Saitoh Y Muryoi T Bona CA (1993) Tight-skin mouse autoantibody repertoire: Analysis of V_H and V_K usage. Mol Immunol 30:969–978
Kasturi KN Shibata S Muryoi T Bona CA (1994) Tight-skin mouse an experimental model for scleroderma. Int Rev Immunol 11:253–271
Kasturi KN Hatakeyama A Murai C Gordon R Phelps RG Bona CA (1997) B-cell deficiency does not abrogate development of cutaneous hyperplasia in mice inheriting the defective fibrillin-1 gene. J Autoimmun 10:505–517
Le Hir M, Martin M Haas C (1999) A syndrome resembling human systemic sclerosis (scleroderma) in MRL/lpr mice lacking interferon-γ (IFNγ) receptor (MRL/lpr$\gamma R^{-/-}$). Clin Exp Immunol 115:281–287
McCormick LL Zhang Y Tootell E Gilliam AC (1999) Anti-TGFß treatment prevents skin and lung fibrosis in murine sclerodermatous graft-versus-host disease: a model for human scleroderma. J Immunol 163:5693–5699
Menton DN Hess RA Lichenstein JR Eisen AJ (1978) The structure and tensile properties of the skin of tight-skin mutant mice. J Invest Dermatol 70:4–10
Muryoi T Andre-Schwartz J Saitoh Y Daian C Hall B Dimitriu-Bona A Schwartz RS Bona CA Kasturi KN (1992) Self-reactive repertoire of tight skin (TSK/+) mouse: Immunological and molecular characterization of anti-cellular autoantibodies. Cell Immunol 144:43–54
Ong C, Wong C Roberts CR The HS, Jirik FR (1998) Anti-IL-4 treatment prevents dermal collagen deposition in the tight-skin mouse model of scleroderma. Eur J Immunol 28:2619–2629
Osborn TG Bauer NE Ross SC (1983) The tight-skin mouse: physical and biochemical properties of the skin. J Rheumatol 10:793–796
Pablos JL Everett ET Harley R LeRoy EC, Norris JS (1995) Transformation growth factor ß$_1$ and collagen gene expression during postnatal skin development and fibrosis in the tight-skin mouse. Lab Invest 72:670–678
Pines M Domb A Ohana M Inbar J Genina O Alexiev R Nagler A (2001) Reduction in dermal fibrosis in the tight-skin (Tsk) mouse after local application of halofuginone. Biochem Pharmacol 62:1221–1227
Ross SC Osborn TG Dorner RW Juckner J (1987) Glycosaminoglycan composition of tight-skin and control mouse skins. J Rheumatol 14:295–298
Schiltz PM Giorno RC Calman HN (1994) Increased ICAM-1 expression in the early stages of murine chronic graft-versus-host disease. Clin Immunol Immunopathol 71:136–1141
Sgonc R Dietrich H Sieberer C Wick G Christner PJ Jiménez SA (1999) Lack of endothelial cell apoptosis in the dermis of tight skin 1 and tight skin 2 mice. Arthr Rheum 42:581–584
Walker M Harley R Leroy EC (1990) Ketotifen prevents skin fibrosis in the tight skin mouse. J Rheumatol 17:57–59
Wallace VA Kondo S Kono T Xing Z Timms E Furlonger C Keystone E Gauldie J Sauder DN Mak TW (1994) A role of $CD4^+$ T cells in the pathogenesis of skin fibrosis in tight skin mice. Eur J Immunol 24:1463–1466
Wooley PH Sud S, Langendorfer A Calkins C Christner PJ Peters J Jiménez SA (1998) T cells infiltrating the skin of Tsk2 scleroderma-like mice exhibit T cell receptor bias. Autoimmunity 27:91–98
Yamamoto T (2002) Animal model of sclerotic skin induced by bleomycin: a clue to the pathogenesis of and therapy for scleroderma? Clin Immunol 102:209–216
Yamamoto T Nishioka K (2001) Animal model of sclerotic skin. IV: induction of dermal sclerosis by bleomycin is T cell independent. J Invest Dermatol 117:999–1001
Yamamoto T Nishioka K (2002) Animal model of sclerotic skin. V: increased expression of α-smooth muscel actin in fibroblastic cells in bleomycin-induced scleroderma. Clin Immunol 102:77–83
Yamamoto T Takagawa S Katayama I Nishioka K (1999a) Anti-sclerotic effect of transforming growth factor β antibody in a mouse model of bleomycin-induced scleroderma. Clin Immunol 92:6–13
Yamamoto T Takagawa S Katayama I Yamazaki K Hamazaki Y Shinkai H Nishioka K (1999b) Animal model of sclerotic skin. I: Local injections of bleomycin induce sclerotic skin mimicking scleroderma. J Invest Dermatol 112:456–462
Yamamoto T Takahashi Y Takagawa S Katayama I Nishioka K (1999c) Animal model of sclerotic skin. II. Bleomycin induced scleroderma in genetically mast cell deficient WBB6F1-W/W^V mice. J Rheumatol 26:2628–2634
Yamamoto T Takagawa S Katayama I Mizushima Y Nishioka K (1999d) Effect of superoxide dismutase on bleomycin-induced dermal sclerosis: implications for the treatment of systemic sclerosis. J Invest Dermatol 113:843–847
Yamamoto T Kuroda M Nishioka K (2000) Animal model of sclerotic skin. III: histopathological comparison of bleomycin-induced scleroderma in various mice strain. Arch Dermatol Res 292:535–541
Zhang Y McCormick LL Desai SR Wu C, Gilliam AC (2002) Murine scleroderma graft-versus-host disease, a model for human scleroderma: cutaneous cytokines, chemokines, and immune cell activation. J Immunol 168:3088–3098
Zhang Y McCormick LL Gilliam AC (2003) Latency-associated peptide prevents skin fibrosis in murine graft-versus-host disease, a model of human scleroderma. J Invest Dermatol 121:713–719

P.6 Pemphigus Models

P.6.1 Experimentally Induced Pemphigus in Mice

PURPOSE AND RATIONALE

Pemphigus is defined as a group of spontaneously occurring disorders of skin and mucosae in which blisters and erosions form within the epidermis due to loss of intercellular contact (Marks 1987). Pemphigus occurs also spontaneously in domestic animals, such as dogs, cats, and horses (Hurvitz 1980; Scott et al. 1983; Sueki et al. 1997). Various attempts were made to study experimentally induced pemphigus in mice (Buschard et al. 1981; Takahashi et al. 1985; Anhalt et al. 1986a, b; Rock et al. 1990; Juhasz et al. 1993; Allbritton et al. 1997; Koch et al. 1997; Fan et al. 1999;

Mahoney et al. 1999; Amagai et al. 2000; Zillikens et al. 2001, Rädisch et al. 2002; Hashimoto 2003).

Fan et al. (1999) screened four strains of female mice (BALB/c, DBA/1, SJL/J, and HRS/J) for their ability to produce pathogenic anti-desmoglein 3 antibodies. Only BLB/c mice immunized with full length desmoglein 3 can produce pathogenic antibodies capable of causing acantholysis in human foreskin in culture and blistering in neonatal mice.

PROCEDURE

Six- to 8-week-old female BALB/c, DBA/1, SJL/J, and HRS/J are immunized four times with 20 µg/mouse of purified desmoglein 3 protein in CFA (on days 1, 10, 20, and 30), four times with 20 µg/mouse of extracellular domain of desmoglein 3 (on days 40, 50, 60, and 70), and twice with 20 µg/mouse of refolded desmoglein 3 (on days 80 and 90), then they are boosted twice more with 20 µg/mouse of extracellular domain of desmoglein 3 in IFA by i.p. inoculation (on days 97 and 104). Control groups of mice are similarly immunized with BSA.

IGs from 10 ml of pooled serum from mice immunized with desmoglein 3 are precipitated with 40% ammonium sulfate, dialyzed against PBS twice, lyophilized, and reconstituted in water to 1 ml. One hundred µl of the reconstituted antibodies/mouse is injected into neonatal BALB/c mice.

EVALUATION

Mice are examined 18–24 h post injection for blister formation. Cross sections containing the blister and comparable areas in control animals are biopsied and frozen sections are prepared for routine histological examination.

MODIFICATIONS OF THE METHOD

Amagai et al. (2000) and Ohyama et al. (2002) developed an active autoimmune disease model for pemphigus using autoantigen knockout mice.

Xu et al. (2001) characterized BALB/c mice B lymphocyte autoimmune responses to skin basement membrane component type XVII collagen, the target antigen of the autoimmune skin disease bullous pemphigoid. The mice were immunized with peptides of the human and/or the murine-equivalent BPAg2 pathogenic NC16A domain.

Using keratinocytes from plakoglobin knockout mice, Caldelari et al. (2001) studied the role of the Armadillo protein plakoglobin in pemphigus vulgaris.

Nguyen et al. (2004) reported that pemphigus vulgaris IgG and methylprednisolone exhibit reciprocal effects on keratinocytes. The therapeutic effects of methylprednisolone may be due to both the upregulated synthesis and the post-translational modifications of keratinocyte adhesion molecules.

REFERENCES AND FURTHER READING

Allbritton JI Nousari HC Anhalt GJ (1997) Anti-epiligrin (laminin 5) cicatricial pemphigoid. Br J Dermatol 137:992–996

Amagai M Tsunoda K Suzuki H Nishifuji K Koyasu S Nishikawa T (2000) Use of autoantigen-knockout mice in developing an active autoimmune disease model for pemphigus. J Clin Invest 105:625–631

Anhalt GJ Patel HP Labib RS Diaz LA Proud D (1986a) Dexamethasone inhibits plasminogen activator activity in experimental pemphigus *in vivo* but does not block acantholysis. J Immunol 136:113–117

Anhalt GJ Till GO Diaz LA Labib RS Patel HP Eaglstein NF (1986b) Defining the role of complement in experimental pemphigus vulgaris in mice. J Immunol 137:2835–2840

Buschard K Dabelsteen E Bretlau P (1981) A model for the study of autoimmune diseases applied to pemphigus: transplants of human oral mucosa to athymic nude mice binds pemphigus antibodies *in vivo*. J Invest Dermatol 76:171–173

Caldelari R de Bruin A Baumann D Suter MM Bierkamp C Balmer V Müller E (2001) A central role for the Armadillo protein plakoglobin in the autoimmune disease pemphigus vulgaris. J Cell Biol 153:823–834

Fan J-L, Memar O McCormick DJ Prabhakar BS (1999) BALB/c mice produce blister-causing antibodies upon immunization with a recombinant human desmoglein 3. J Immunol 163:6228–6235

Hashimoto T (2003) Recent advances in the study of the pathophysiology of pemphigus. Arch Dermatol Res 295 [Suppl1]:S2–S11

Hurvitz AI (1980) Animals model of human disease: pemphigus vulgaris. Am J Pathol 98:861–864

Juhasz I Lazarus GS Murphy GF Shih I-M, Hertyn M (1993) Development of pemphigus vulgaris-like lesions in severe combined immunodeficiency disease mice reconstituted with lymphocytes from patients. J Clin Invest 92:2401–2407

Koch PJ Mahoney MG Ishikawa H Pulkkinen L Uitto J Shultz L Murphy GF Whitaker-Menezes D Stanley JR (1997) Targeted disruption of the pemphigus vulgaris antigen (desmoglein 3) gene in mice causes loss of keratinocyte adhesion with a phenotype similar to pemphigus vulgaris. J Cell Biology 137:1091–1102

Mahoney MG Wang ZH Stanley JR (1999) Pemphigus vulgaris and pemphigus foliaceus antibodies are pathogenic in plasminogen activator knockout mice. J Invest Dermatol 113:22–25

Marks R (1987) Skin Disease in Old Age. Martin Dunitz Ltd., London

Memar O Christensen B Rajaraman S Goldblum R Tyring SK Brysk MM McCormick DJ el-Zaim H Fan JL, Prabhakar BS (1996) Induction of blister-causing autoantibodies by a recombinant full-length, but not the extracellular, domain of the pemphigus vulgaris antigen (desmoglein 3). J Immunol 157:3171–3177

Nguyen VT Arredondo J Chernyavsky Ai, Kitajima Y Pittelkow M Grando SA (2004) Pemphigus vulgaris IgG and methylprednisolone exhibit reciprocal effects on keratinocytes. J Biol Chem 279:2135–2146

Ohyama M Amagai M Tsunoda K Ota T, Koasu S Hata J Umezawa A Nishikawa T (2002) Immunologic and histopathologic characterization of an active disease mouse model for pemphigus vulgaris. J Invest Dermatol 118:199–204

Rädisch T Riechers R Hertl M (2002) The humanized SCID mouse model to study HLA class II-linked autoimmunity to desmoglein 3 in pemphigus vulgaris. Br J Dermatol 146:189–193

Rock B Labib RS Diaz LA (1990) Monovalent Fab' immunoglobulin fragments from endemic pemphigus foliaceus auto-antibodies reproduce the human disease in neonatal Balb/c mice. J Clin Invest 85:296–299

Scott DW Manning TO Smith CA Lewis RM (1983) Pemphigus and pemphigoid in dogs, cats, and horses. Ann N Y Acad Sci 420:353–360

Sueki H Shanley K Goldschmidt MH Lazarus GS Murphy GF (1997) Dominantly inherited acantholysis in dogs, simulating human benign familial chronic pemphigus (Hailey-Hailey disease). Br J Dermatol 136:190–196

Takahashi Y Patel HP Labib RS Diaz LA Anhalt GJ (1985) Experimentally induced pemphigus vulgaris in neonatal BLB/c mice: a time-course study of clinical, immunological, ultrastructural, and cytochemical changes. J Invest Dermatol 84:41–46

Xu L, Robinson N Miller SD Chan LS (2001) Characterization of BALB/c mice B lymphocyte autoimmune responses to skin basement membrane component type XVII collagen, the target antigen of autoimmune skin disease bullous pemphigoid. Immunol Lett 77:10–111

Zillikens D Schmidt E Reimer S Chimanovitch I Hardt-Weinelt K Rose C Bröcker EB Kock M Boehncke WH (2001) Antibodies to desmogleins 1 and 3, but not to BP 180, induce blisters in human skin grafted onto SCID mice. J Pathol 193:117–124

P.7
Ichthyosis Vulgaris Models

P.7.1
Experimentally Induced Ichthyosis in Mice

PURPOSE AND RATIONALE

Ichthyosis vulgaris is a heterogeneous autosomal skin disease characterized by dry, scaly skin, mild hyperkeratosis, and a decreased or absent granular layer that either lacks, or contains morphologically abnormal, keratohyalin granula (Anton-Lamprecht and Hofbauer 1972). Both the skin of ichthyosis vulgaris patients and keratinocytes cultured from affected individuals exhibit reduced or absent profilaggrin mRNA and protein levels (Sybert et al. 1985). The symptoms and the genetics of the ichthyotic (*ic/ic*) mouse were described by Spearman (1960), Green et al. (1974), Jensen and Esterly (1977), Holbrook (1989). Presland et al. (2000) demonstrated loss of normal profilaggrin and filaggrin in flaky tail (*ft/ft*) mice and proposed this as an animal model for the filaggrin-deficient skin disease ichthyosis vulgaris.

Elias et al. (1983) and Chung et al. (1984) induced ichthyosis in the hairless mouse by treatment with diazacholesterol and used this as an assay for comparative potency of topical retinoids.

PROCEDURE

Male hairless mice, 2–3 months old, are fed either a normal laboratory diet supplemented with 60 mg/kg/day of 20,25-diazacholesterol or normal laboratory diet. Diazacholesterol blocks the conversion of Δ^{24}-reduction of desmosterol to cholesterol (Anderson and Martt 1965), and as a result desmosterol accumulates in stratum corneum lipids rather than cholesterol. Ichthyotic changes generally become apparent after 8–12 weeks and are most pronounced over the back and tail. With the exception of some reduction in body weight in comparison with controls, the animals appear healthy. Since the tail manifests the most exaggerated scaling, this site is used for topical drug applications. As the animals become ichthyotic, the daily dose of diazacholesterol can be lowered to 30 mg/kg and maintained at that level.

The test substances (retinoids) are first solubilized in a small volume of dimethyl sulfoxide and then dissolved in Cremophore EL. A volume of ~100 µl of each test substance is applied once daily to circumscribed areas of the tail. Treatment groups consist of 3 animals each, and each animal serves as its own control. The drop is first placed on an investigator's gloved index fingers and then spread evenly around a designated band of the tail. Each animal is treated with two concentrations of the test drug. The most proximal and most distal portions of the tail are left untreated as control regions. Applications are continued for 2 weeks. At three- or four-day intervals, and at the termination of the experiment, the clinical response is graded from 0 to 4+, with 0 indicating no response and 4+ indicating removal of all visible scale, leaving a glistening surface.

Prior to biopsy, the skin surface is coated with a thin film of flexible collodion to prevent fragmentation during frozen sectioning. Perpendicular sections of biopsy samples are stained with aqueous 8-anilino-2-naphthalene sulfonic acid, which on fluorescence microscopy depict selectively stratum corneum hydrophobic membrane domains.

EVALUATION

Both control and drug-treated sections are measured in a double-blind manner. The mean and SE from a minimum of five separate regions are tabulated. Significant differences are determined by Student's *t*-test.

MODIFICATIONS OF THE METHOD

Harlequin ichthyosis (ichq): a juvenile lethal mouse mutation with ichthyosiform dermatitis was described by Sundberg et al. (1997).

Shultz et al. (2003) described mutations at the mouse ichthyosis locus within the lamin B receptor gene as a single gene model for human Pelger-Huet anomaly.

Knox and Lister-Rosenoer (1998) described an infantile ichthyosis in **rats** and proposed this as a new model of hyperkeratotic skin disease.

REFERENCES AND FURTHER READING

Anderson PC Martt JM (1965) Myotonia and keratoderma induced by 20,25-diazacholesterol. Arch Dermatol 92:181–187

Anton-Lamprecht I Hofbauer M (1972) Ultrastructural distinction of autosomal dominant ichthyosis vulgaris and X-linked recessive ichthyosis. Humangenetik 15:261–264

Chung J-C, Law MYL, Elliott ST Elias PM (1984) Diazacholesterol-induced ichthyosis in the hairless mouse. Assay for comparative potency of topical retinoids. Arch Dermatol 120:342–347

Elias PM Lampe MA Chung JC Williams ML (1983) Diazacholesterol-induced ichthyosis in the hairless mouse. I. Morphologic, histochemical, and lipid biochemical characterization of a new animal model. Lab Invest 48:565–577

Green MC Alpert BN Mayer TC (1974) The site of action of the ichthyosis locus (*ic*) in the mouse as determined by dermal-epidermal recombinations. J Embryol Exp Morphol 32:715–724

Holbrook KA (1989) Ichthyosis, inherited, skin mouse (ic/ic). In Jones TC Mohr U Hunt RD (eds) Integument and Mammary Glands. Monographs on Pathology of Laboratory Animals. Springer-Verlag, Heidelberg, pp 223–229

Jensen JE Esterly NB (1977) The ichthyosis mouse: histologic, histochemical, ultrastructural, and autoradiographic studies of interfollicular epidermis. J Invest Dermatol 68:23–31

Knox WE Lister-Rosenoer LM (1998) Infantile ichthyosis in rats: a new model of hyperkeratotic skin disease. J Hered 69:391–394

Nirunsuksiri W Presland RB Brumbaugh SG Dale BA Fleckman P (1995) Decreased profilaggrin expression in ichthyosis vulgaris is a result of selectively impaired post-transcriptional control. J Biol Chem 270:871–876

Presland RB Boggess D Lewis SP Hull C Fleckman P Sundberg JP (2000) Loss of normal profilaggrin and filaggrin in flaky tail (*ft/ft*) mice: an animal model for the filaggrin-deficient skin disease ichthyosis vulgaris. J Invest Dermatol 115:1072–1081

Shultz LD Lyons BL Burzenski LM Gott B Samuels R Schweitzer PA Dreger C Herrmann H Kalscheuer V Olins AL Olins DE Sperling K Hoffmann K (2003) Mutations at the mouse ichthyosis locus are within the lamin B receptor gene: a single gene model for human Pelger-Huet anomaly. Hum Mol Genet 12:61–69

Spearman RJ (1960) The skin abnormality of "ichthyosis", a mutant of the house mouse. J Embryol Exp Morphol 8:387–395

Sundberg JP Boggess D Hogan ME Sundberg BA Rourk MH Harris B Johnson K Dunstan RW Davisson MT (1997) Harlequin ichthyosis (ichq): a juvenile lethal mouse mutation with ichthyosiform dermatitis. Am J Pathol 151:293–310

Sybert VP Dale BA Holbrook KA (1985) Ichthyosis vulgaris: identification of a defect in syntheses of filaggrin correlated with an absence of keratohyline granules. J Invest Dermatol 84:191–194

P.8 Xeroderma Models

P.8.1 Experimentally Induced Xeroderma in Mice

PURPOSE AND RATIONALE

Xeroderma pigmentosum is an autosomal recessive disorder characterized by hyperphotosensitivity and multiple cancers in association with abnormal DNA repair (Robbins et al. 1974; Satokata et al. 1992). Xeroderma pigmentosum group A (XPA) gene-deficient mice cannot repair UV-induced DNA damage and easily develop skin cancers by UV-irradiation (Nakane et al. 1995; Miyauchi-Hashimoto et al. 1996, 1999). Kuwamoto et al. (2000) tested the involvement of enhanced prostaglandin E_2 production in the photosensitivity in Xeroderma pigmentosum group A model mice and the influence of a prostaglandin synthesis inhibitor.

PROCEDURE

XPA gene-deficient homogeneous mice, age 8–12 weeks, are used (Nakane at al 1995). The UVB source consists of a bank of fluorescent sunlamps with an emission spectrum from 270 to 375 nm, peaking at 305 nm. The mice are anesthetized by i.p. injection of phenobarbital to keep them immobile during exposure. The ears are irradiated with 250 mJ per cm^2 of UVB. Immediately after irradiation, the test drug (20 µl of 1% solution of the prostaglandin synthesis inhibitor indomethacin) is applied to the ears. Ear thickness is measured with a dial thickness gauge immediately before irradiation and 1–4 days after irradiation. The amounts of PGD_2, PGE_2, and PGF_{2a} in mouse ears at 0, 24, 48, and 72 after UVB irradiation are determined by enzyme immunoassay.

EVALUATION

Student's *t*-test is employed to determine the statistical difference between means.

MODIFICATIONS OF THE METHOD

De Boer et al. (1999) described a mouse model for the DNA repair/basal transcription disorder trichothiodystrophy, revealing cancer predisposition.

Sun et al. (2003) described a genetic mouse model carrying the nonfunctional xeroderma pigmentosum group G gene. A disrupted XPG allele was generated by insertion of neo cassette sequences into exon 3 of the XPG gene by using embryonic stem dell techniques.

REFERENCES AND FURTHER READING

De Boer J van Steeg H Berg RJ Garssen J de Witt J van Oostrum CT Beems RB van der Horst GT van Kreijl CF de Gruijl FR Bootsma D Hoeijmakers JK Weeda G (1999) Mouse model for the DNA repair/basal transcription disorder trichothiodystrophy reveals cancer predisposition. Cancer Res 59:3489–3494

Kuwamoto K Miyauchi-Hashimoto H Tanaka K Eguchi M Inui T Urade Y Horio T (2000) Possible involvement of enhanced prostaglandin E_2 production in the photosensitivity in Xeroderma pigmentosum group A model mice. J Invest Dermatol 114:241–246

Miyauchi-Hashimoto H Tanaka K Horio T (1996) Enhanced inflammation and immunosuppression by ultraviolet radiation in xeroderma pigmentosum group A (XPA) model. J Invest Dermatol 107:343–348

Miyauchi-Hashimoto H Okamoto H Tanaka K Horio T (1999) Ultraviolet radiation-induced suppression of natural killer cell activity is enhanced in xeroderma pigmentosum group A (XPA) model mice. J Invest Dermatol 112:965–970

Nakane H Takeuchi S Yuba S Saijo M Nakatsu Y Murai H Nakatsuru Y Ishikawa T Hirota S Kitamura Y (1995) High incidence of ultraviolet-B- or chemical-carcinogen-induced skin tumors in mice lacking the xeroderma pigmentosum group A gene. Nature 337:165–168

Robbins JH Kraemer KH Lutzner MA Festoff BW Coon HG (1974) Xeroderma pigmentosum: an inherited disease with sun sensitivity, multiple cutaneous neoplasms, and abnormal DNA repair. Ann Intern Med 80:221–248

Satokata I Tanaka K Okada Y (1992) Molecular basis of group A xeroderma pigmentosum: a missense mutation and two deletions located in a zinc finger consensus sequence of the XPAC gene. Hum Genet 88:603–607

Sun XZ, Harada YN Zhang R Cui C, Takahashi S Fukui Y (2003) A genetic mouse model carrying the nonfunctional xeroderma pigmentosum group G gene. Congenit Anom Kyoto 43:133–139

P.9 Vitiligo Models

P.9.1 Vitiligo in Mice

PURPOSE AND RATIONALE

A **mouse model for vitiligo** was described by Lerner et al. (1986), designated C57BL/6J-vit/vit. The vitiligo mouse has congenital dorsal and ventral white spots as well as progressive replacement of pigmented hairs with each spontaneous molt or after plucking.

Sidman et al. (1996) described pigment epithelial and retinal phenotypes in the vitiligo mivit, mutant mouse.

Tang et al. (1997) studied abnormalities of the electroretinogram in relation to histopathological findings in vitiligo mutant mice.

Iwamoto et al. (1991) established a mouse model for melanoma in which metallothionein/ret transgenic mice express the ret oncogene fused to the metallothionein promoter. Lengagne et al. (2004) reported the occurrence of spontaneous vitiligo in this animal model for human melanoma.

REFERENCES AND FURTHER READING

Iwamoto T Takahashi M Ito M, Hamatani K Ohbayashi M Wajjwalku W Isobe K Nakashima I (1991) Aberrant melanogenesis and melanocyte tumor development in transgenic mice theat carry a metallothionein/ret fusion gene. EMBO J 10:3167–3175

Lengagne R Le Gal FA, Garcette M Fiette L Ave P, Kato M Briand JP Massot C Nakashima I Renia L Guillet JG Prevost-Blondel A (2004) Spontaneous vitiligo in an animal model for human melanoma: role of tumor-specific $CD8^+$ T cells. Cancer Res 64:1496–1501

Lerner AB Shiohara T Boissy RE Jacobson KA Lamoreux ML Moellmann GE (1986) A mouse model for vitiligo. J Invest Dermatol 87:299–304

Sidman RL Kosaras B Tang M (1996) Pigment epithelial and retinal phenotypes in the vitiligo mivit, mutant mouse. Invest Ophthalmol Vis Sci 37:1097–1115

Tang M Pawlyk BS Kosares B Berson EL Sidman RL (1997) ERG abnormalities in relation to histopathological findings in vitiligo mutant mice. Exp Eye Res 65:215–222

P.9.2 Smyth Line Chickens

PURPOSE AND RATIONALE

Smyth et al. (1981) developed a mutant line of chickens (DAM line) that is charactereized by a high incidence of spontaneous, postnatal, cutaneous amelanosis as a result of an autoimmune phenomenon (Smyth 1989). An intrinsic melanocyte defect, characterized by melanosomes with abnormal irregular surfaces, predisposes these chickens to the pigment disorder (Boissy et al. 1986). Both B cell and T cell compartments of the immune system are involved in the pathology of the disease (Lamont et al. 1982; Erf et al. 1995). Melanocyte-specific antibodies have been detected in the serum of Smyth line chickens (Austin et al. 1992). These autoantibodies cross-react with mouse and human melanocytes and are able to bind pigment within tissues (Searle et al. 1993). Mammalian tyrosinase-related protein-1 is recognized by autoantibodies from vitiligous Smyth chickens (Austin and Boissy 1995). The Smyth chicken model for spontaneous autoimmune vitiligo shows various incidences and degrees of alopecia ranging from alopecia areata-like to universalis-like integumental changes (Smyth and McNeil 1999). Sreekumar et al. (2000) analyzed

the effect of endogenous viral genes in the Smyth line chicken model for autoimmune vitiligo. Erf et al. (2001) reported a strong connection between herpes virus infection and the expression of autoimmune vitiligo in Smyth line chickens. Sreekumar et al. (2001) performed molecular characterization of the Smyth chicken sublines and their parental controls by restriction fragment length analysis and DNA fingerprint analysis. Wang and Erf (2003, 2004) investigated the melanocyte-specific cell-mediated immune response in vitiliginous Smyth line chickens and studied apoptosis in feathers of Smyth line chickens with autoimmune vitiligo.

REFERENCES AND FURTHER READING

Austin LM Boissy RE (1995) Mammalian tyrosinase-related protein-1 is recognized by autoantibodies from vitiligous Smyth chickens. An avian model for human vitiligo. Am J Pathol 146:1529–1541

Austin LM Boissy RE Jacobson BS Smyth JR Jr (1992) The detection of melanocyte autoantibodies in the Smyth chicken model of vitiligo. Clin Immunol Immunopathol 64:112–120

Boissy RE Moellmann G Trainer AT Smyth JR Jr, Lerner AB (1986) Delayed-amelanotic (DAM or Smyth) chicken: melanocyte dysfunction in vivo and in vitro. J Invest Dermatol 86:149–156

Erf GF, Trejo-Skalli AV Smyth JR Jr (1995) T cells in regenerating feathers of Smyth line chickens with vitiligo. Clin Immunol Immunopathol 76:120–126

Erf GF, Bersi TK Wang X Sreekumar GP Smyth JR Jr (2001) Herpesvirus connection in the expression of autoimmune vitiligo in Smyth line chickens. Pigment Cell Res 14:40–46

Lamont SJ Boissy RE Smyth JR Jr (1982) Humoral immune response and expression of spontaneous postnatal vitiligo in DAM chicken. Immunol Commun 11:121–127

Searle EA Austin LM Boissy YL Zhao H Nordlund JJ Boissy RE (1993) Smyth chicken melanocyte autoantibodies: cross-specific recognition, in vivo binding, and plasma reactivity of the antiserum. Pigment Cell Res 6:145–157

Smyth JR Jr (1989) The Smyth line chicken: a model for autoimmune vitiligo. Crit Rev Poult Biol 1:1–19

Smyth JR Jr, McNeil M (1999) Alopecia areata and universalis in the Smyth chicken model for spontaneous autoimmune vitiligo. J Invest Dermatol Symp Proc 4:211–215

Smyth JR Jr, Boissy RE Fite KV (1981) The DAM chicken: a model for sponateaous postnatal cutaneous and ocular amelanosis. J Hered 72:150–156

Sreekumar GP Smyth JR Jr, Ambady S Ponce de Leon FA (2000) Analysis of the effect of endogenous viral genes in the Smyth line chicken model for autoimmune vitiligo. Am J Pathol 156:1099–1107

Sreekumar GP Smyth JR Jr, Ponce de Leon FA (2001) Molecular characterization of the Smyth chicken sublines and their parental controls by RFLP and DNA fingerprint analysis. Poult Sci 80:1–5

Wang X Erf GF (2003) Melanocytew-specific cell mediated immune response in vitiliginous Smyth line chickens. J Autoimmun 21:149–160

Wang X Erf GF (2004) Apoptosis in feathers of Smyth line chickens with autoimmune vitiligo. J Autoimmun 22:21–30

P.10 Erythropoietic Protoporphyria

P.10.1 General Considerations

PURPOSE AND RATIONALE

Erythropoietic protoporphyria (EPP) is an inherited disease that is associated with deficiency of the last enzyme of heme biosynthesis, ferrochelatase, which catalyzes the insertion of ferrous iron into protoporphyrin. Ferrochelatase deficiency is accompanied by photosensitivity syndrome (Bottomley et al. 1975; Cox 1997; Lim and Cohen 1999). It is characteristically manifested by a severe burning pain associated with edema and erythema within a few minutes of exposure to visible light (Cox 1997). Some of these symptoms are related to the extravasation of intravascular contents, such as blood plasma, caused by pronounced damage to endothelial cells (Brun and Sandberg 1991). The defect in ferrochelatase results in accumulation of protoporphyrin (Bottomley et al. 1975; Cox 1997; Lim and Cohen 1999), which may be produced in immature red blood cells, released into the plasma, and accumulate in the cell membranes of endothelial cells due to its hydrophobicity (Brun and Sandberg 1991).

REFERENCES AND FURTHER READING

Bottomley SS, Tanaka M, Everett MA (1975) Diminished erythroid ferrochelatase activity in protoporphyria. J Lab Clin Med 86:126–131

Brun A, Sandberg S (1991) Mechanisms of photosensitivity in porphyric patients with special emphasis on erythropoietic protoporphyria. J Photochem Photobiol B Biol 10:285–302

Cox TM (1997) Erythropoietic protoporphyria. J Inher Metab Dis 20:258–269

Lim HW, Cohen JL (1999) The cutaneous porphyrias. Semin Cutan Med Surg 18:285–292

P.10.2 Animal Models for Erythropoietic Protoporphyria

PURPOSE AND RATIONALE

Many animal models on erythropoietic protoporphyria are published. Berenson et al. (1992) described a new model of protoporphyric hepatopathy using protoporphyrin overload in unrestrained rats.

Most studies have been performed using mice (Gschnait et al. 1975; Konrad et al. 1975; Cantoni et al. 1983; Tanaka et al. 1993; Libbrecht et al. 2003; Bellingham et al. 1995) described experimental murine protoporphyria induced by griseofulvin. Smith et al. (1997) induced protoporphyria by the orally active iron chelator 1,2-diethyl-3-hydroxypyridin-4-one in C57BL/10ScSn mice.

Many authors (Boulechfar et al. 1993; De Verneul et al. 1995; Meerman et al. 1999; Fontanellas et al. 2001; Abitbol et al. 2005; Han et al. 2005; Navarro et al. 2005) have used genetically altered mice with a recessive inherited ferrochelatase deficiency, originally described by Tutois et al. (1991). Magness et al. (1998) analyzed the human ferrochelatase promoter in transgenic mice.

Pawliuk et al. (2005) reported prevention of murine erythropoietic protoporphyria-associated skin photosensitivity and liver disease by dermal and hepatic ferrochelatase.

Takeshita et al. (2004) performed an L-band electron spin resonance (ESR) study to investigate *in vivo* oxygen radical generation in the skin of the protoporphyria mouse model with visible light exposure.

PROCEDURE

Chemiluminescence techniques have been used to detect $^1O_2$ and O_2^{*-} using the emission of $^1O_2$ itself or a chemiluminescent probe (Khan 1981; Nakano et al. 1986). As the luminescence arising from reactive oxygen species is usually very weak compared with the irradiating light, it is technically hard to evaluate reactive oxygen species generation during photodynamic reactions using this method. *In vivo* generation of reactive oxygen species was detected in the skin in erythropoietic protoporphyria disease during irradiation with light, using a technique other than chemiluminescence.

In vivo electron spin resonance (ESR) spectroscopy was used operating at low microwave frequencies as an alternative to chemiluminescence techniques. This technique has enabled the non-invasive measurement of durable free radicals, including a nitroxyl radical, in living experimental animals (Subczynski et al. 1986; Bacic et al, 1989; Ishida et al. 1989; Ferrari et al, 1990; Utsumi et al. 1993). The nitroxyl radical loses its ESR signal on reaction with transient free radicals, such as $^*OH$ and O_2^{*-} (Takeshita et al. 2004). Free radical reactions were evaluated in various animal models, including hyperoxia (Miura et al. 1992), ischemia–reperfusion (Utsumi et al. 1993), X-ray irradiation (Miura et al. 1997), and streptozotocin-induced diabetes (Sano et al. 1998) using L-band (1–1.2 GHz) and 300 MHz ESR spectrometers with a nitroxyl radical probe (a spin probe). In these experiments, the disease model animal was set in the loop-gap resonator of the ESR spectrometer. Loop-gap type resonators are unsuitable for measuring radicals in the skin of experimental animals, because they detect radicals distributed throughout the body. By contrast, a surface-coil-type resonator (surface resonator) has been used to measure radicals in limited positions, such as the skin (Bacic et al. 1989; Swartz et al. 1994; Kuppusamy et al. 1998; He et al. 2001; Fuchs et al. 1997). Furthermore, ESR measurement with a surface resonator does not interfere with light irradiation, since only the single-turn coil portion of the resonator is attached to the skin.

This study used ESR with a surface resonator to detect *in vivo* ROS generation with light exposure in the skin of griseofulvin-induced protoporphyria model mice, a standard model for EPP (Gschnait et al. 1975; Konrad et al. 1975; Wolff et al. 1975; Plosch et al. 2002).

REFERENCES AND FURTHER READING

Abitbol M Bernex F Puy H, Jouault H Deybach JC Guénet JL Montagutelli X (2005) A mouse model provides evidence that genetic background modulates anaemia and liver injury in erythropoietic protoporphyria. Am J Physiol 288:G1208–G1216

Bacic G, Nilges MJ, Magin RL, Walczak T, Swartz HM (1989) *In vivo* localized ESR spectroscopy reflecting metabolism. Magn Reson Med 10:266–272

Bellingham RMA Gibbs AH de Matteis F Lian LY Roberts GCK (1995) Determination of the structure of an N-substitutes protoporphyrin from the livers of griseofulvin-fed mice. Biochem J 307:505–512

Berenson MM Kimura B Samowitz Q Bjorkman D (1992) Protoporphyrin overload in unrestrained rats: biochemical and histopathological characterization of a new model of protoporphyric hepatopathy. Int J Exp Ther 73:665–673

Boulechfar S Lamoril J Montagutelli X Guénet JL Deybach JC Nordmann Y Dailey H Grandchamp B de Verneuil H (1993) Ferrochelatase structural mutant (*Fech*^{m1Pas}) in the house mouse. Genomics 16:645–648

Cantoni L di Padova C Rovagnati P Ruggierie R Dal Fiume D Tritapepe R (1983) Bile secretion and liver microsomal mixed function oxidase system in mice with griseofulvin-induced hepatic protoporphyria. Toxicology 27:27–39

De Verneul H Ged C, Boulechfar S Moreau-Gaudry F (1995) Porphyrias: animal models and prospects for cellular and gene therapy. J Bioenerg Biomembr 27:239–248

Ferrari M, Colacicchi S, Gualtieri G, Santini MT, Sotgiu A (1990) Whole mouse nitroxide free radical pharmacokinetics by low frequency electron paramagnetic resonance. Biochem Biophys Res Commun 166:168–173

Fontanellas A Mendez M Mazurier F Cario-Andre M Navarro S Ged C, Taine L Géronimi F Richard E Moreau-Gaudry F Ed SR, de Verneuil H (2001) Successful therapeutic effect in a mouse model of erythropoietic protoporphyria by partial genetic correction and fluorescence-based selection of hematopoietic cells. Gene Ther 8:618–626

Fuchs J, Groth N, Herrling T, Zimmer G (1997) Electron paramagnetic resonance studies on nitroxide radical 2,2,5,5-tetramethyl-4-piperidine-1-oxyl (TEMPO) redox reactions in human skin. Free Radic Biol Med 22:967–976

Gschnait F Konrad K Honoigsmann H Denk H Woilff K (1975) Mouse model for protoporphyria. I. The liver and hepatic protoporphyrin crystals. J Invest Dermatol 65:290–299

Han AP, Flemong MD Chen JJ (2005) Heme-regulated eIF2α kinase modifies phenotypic severity in murine models of

erythopoietic protoporphyria and β-thalassemia. J Clin Invest 115:1562–1570
He G, Samouilov A, Kuppusamy P, Zweier JL (2001) *In vivo* EPR imaging of the distribution and metabolism of nitroxide radicals in human skin. J Magn Reson 148:155–164
Ishida S, Kumashiro H, Tsuchihashi N, Ogata T, Ono M, Kamada H, Yoshida E (1989) *In vivo* analysis of nitroxide radicals injected into small animals by L-band ESR technique. Phys Med Biol 34:1317–1323
Khan AU (1981) Direct spectral evidence of the generation of singlet molecular oxygen ($^1\Delta_g$) in the reaction of potassium superoxide with water. J Am Chem Soc 103:6516–6517
Konrad K Honigsmann H Gschnait F Wolff K (1975) Mouse model for protoporphyria. II. Cellular and subcellular events in the photosensitivity flare of the skin. J Invest Dermatol 65:300–310
Kuppusamy P, Wang P, Shankar RA, Ma L, Trimble CE, Hsia CJC, Zweier JL (1998) *In vivo* topical EPR spectroscopy and imaging of nitroxide free radicals and polynitroxyl-albumin. Magn Reson Med 40:806–811
Libbrecht L, Meerman L Kuipers F Roskams T Desmet V Jansen P (2003) Liver pathology and hepatocarcinogenesis in a long-term mouse model of erythropoietic protoporphyria. J Pathol 199:191–200
Magness ST Tugores A Diala ES Brenner DA (1998) Analysis of the human ferrochelatase promoter in transgenic mice. Blood 92:320–328
Meerman L Koopen NR Bloks V Van Goor H Havinga R Wolthers BG Kramer W Stengelin S Muller M Kuipers F Jansen PL (1999) Biliary fibrosis associated with altered bile composition in a mouse model of erythropoietic protoporphyria. Gastroenterology 117:696–705
Miura Y, Utsumi H, Hamada A (1992) Effect of inspired oxygen on *in vivo* redox reaction of nitroxide radicals in whole mice. Biochem Biophys Res Commun 182:1108–1114
Miura Y, Hamada A, Utsumi H (1995) *In vivo* ESR studies of antioxidant activity on free radical reaction in living mice under oxidative stress. Free Radic Res 22:209–214
Miura Y, Anzai K, Urano S, Ozawa T (1997) *In vivo* electron paramagnetic resonance studies on oxidative stress caused by x-irradiation in whole mice. Free Radic Biol Med 23:533–540
Nakano M, Sugioka K, Ushijima Y, Goto T (1986) Chemiluminescence probe with Cypridina luciferin analog, 2-methyl-6-phenyl-3,7-dihydroimidazo[1,2-a]pyrazin-3-one, for estimating the ability of human granulocytes to generate O_2^-. Anal Biochem 159:363–369
Navarro S del Hoyo P Campos Y Abitbol M Morán-Jiménez MJ García-Bravo M Pilar Ochoa P Grau M Montagutelli X Frank J Garesse R Arenas J Enríquez de Salamanca R Fontanellas A (2005) Increased mitochondrial respiratory chain enzyme activities correlate with minor extent of liver damage in mice suffering from erythropoietic protoporphyria. Exp Dermatol 14:26–33
Pawliuk R Tighe R Wise RJ Mathews-Roth MM Leboulch P (2005) Prevention of murine erythropoietic protoporphyria-associated skin photosensitivity and liver disease by dermal and hepatic ferrochelatase. J Invest Dermatol 124:256–262
Plosch T, Bloks VW, Baller JF, Havinga R, Verkade HJ, Jansen PL, Kuipers F (2002) Mdr P-glycoproteins are not essential for biliary excretion of the hydrophobic heme precursor protoporphyrin in a griseofulvin-induced mouse model of erythropoietic protoporphyria. Hepatology 35:299–306
Sano T, Umeda F, Hashimoto T, Nawata H, Utsumi H (1998) Oxidative stress measurement by *in vivo* electron spin resonance spectroscopy in rats with streptozotocin-induced diabetes. Diabetologia 41:1355–1360
Smith AG Clothier B Francis JE Gibbs AH de Matteis F Hider RC (1997) Protoporphyria induced by the orally active iron chelator 1,2-diethyl-3-hydroxypyridin-4-one in C57BL/10ScSn mice. Blood 89:1045–1051
Subczynski WK, Lukiewicz S, Hyde JS (1986) Murine *in vivo* L-band ESR spin-label oximetry with a loop-gap resonator. Magn Reson Med 3:747–754
Swartz HM, Liu KJ, Goda F, Walczak T (1994) India ink: potential clinically applicable EPR oximetry probe. Magn Reson Med 31:229–232
Takeshita K, Hamada A, Utsumi H (1999) Mechanisms related to reduction of radical in mouse lung using an L-band ESR spectrometer. Free Radic Biol Med 26:951–960
Takeshita K Takajo T Hirata H Ono M, Utsumi H (2004) *In vivo* oxygen radical generation in the skin of the protoporphyria mouse model with visible light exposure. an L-band ESR study. J Invest Dermatol 122:1463–1470
Tanaka K Ohgami T Nonaka S (1993) Experimental murine protoporphyria induced by griseofulvin (GF). the relationship between hepatic porphyrin levels and liver function test values in mice treated with GF. J Dermatol 20:545–553
Tutois S Montagutelli X Da Silva V Jouault H Rouyer-Fessard P Leroy-Viard K Guénet JL Nordmann Y Beuzard Y Deybach JC (1991) Erythropoietic protoporphyria in the house mouse – a recessive inherited ferrochelatase deficiency with anemia, photosensitivity, and liver-disease. J Clin Invest 88:1730–1736
Utsumi H, Takeshita K, Miura Y, Masuda S, Hamada A (1993) *In vivo* ESR measurement of radical reaction in whole mice. Influence of inspired oxygen and ischemia–reperfusion injury on nitroxide reduction. Free Radic Res Commun 19:S219–S225
Wolff K, Wolff-Schreiner E, Gschnait F (1975) Liver inclusions in erythropoietic protoporphyria. Eur J Clin Invest 5:21–26

P.11 Acne Models

P.11.1 Activity on Sebaceous Glands of Rats

PURPOSE AND RATIONALE

Bioassays for topical antiandrogens are based on inhibition of sebum secretion. Sebum production is increased by endogenous or exogenous androgens in many species including humans. In the mouse (Lapière and Chèvremont 1953; Neumann and Elger 1966), the Mongolian gerbil (Mitchell 1965), and the golden hamster (Hamilton and Montagna 1950), the male sex hormone stimulates sebum production and sebaceous gland growth. Morphometric evaluation by light microscopy in the rat has shown that castration causes a large reduction in the volume of the glands (Sauter and Loud 1975). The administration of testosterone over several days produces an enlargement of the sebaceous glands. Early transformations, which take place in the morphology of the organelles in sebaceous cells, can be observed by electron microscopy. In the cyto-

plasm of intermediate cells a large number of vesicular elements derived from the smooth endoplasmic reticulum is formed, participating in the synthesis of lipids which appear as droplets of varying size (Karasek 1968; Morohashi 1968). Following an increase of lipid droplets, the cells increase in size, become totally differentiated and are pushed towards the apex of the gland where they break up and release their content (sebum) into the infundibulum. This effect is used for morphometric evaluation of topical anti-androgens.

PROCEDURE

Groups of 5 adult male Sprague-Dawley rats weighing 180–220 g are shaved in the interscapular area. Twenty-four hours later, the test preparation or the standard (cyproterone acetate) is applied locally to the shaved area at increasing doses (0.05, 0.5, and 5 mg/cm^2) in 20 µl ethanol. The treatment is continued for three weeks. Controls receive ethanol only. The animals are sacrificed 24 h after the last administration. Pieces of skin from the interscapular region are excised and processed for evaluation by electron microscopy. The volume density of the smooth endoplasmic reticulum vesicles is measured.

EVALUATION

Dose-response curves are established for volume density of vesicles of the smooth endoplasmic reticulum after various doses of antiandrogen and testosterone standard in order to calculate activity ratios. Statistical comparison with untreated controls allows calculation of threshold doses.

MODIFICATIONS OF THE METHOD

Ebling and Petrow (1993) tested 19-Aldehydo-4-androstene-3,17-dione, an estrogen precursor that inhibits sebaceous secretion in ovariectomized testosterone-treated rats.

De Young et al. (1984, 1985) described intradermal injection of *Propionibacterium acnes* as a model of inflammation relevant to acne. Intradermal injection of killed *P. acnes* into the rat ear induces a chronic acne-like inflammation characterized by edema and cell infiltration of several months' duration, formation of comedones, hypersensitization, and transepithelial elimination.

Shamoto et al. (1999) investigated the dermal histology and the regional draining superficial lymph node of a new mutant strain of hairless rats (ISh). The homocygote ISh rat was characterized as having naked and wrinkled skin. The comedo-like casts in the skin resembled human acne.

REFERENCES AND FURTHER READING

De Young LM Young JM Ballaron SJ Spires DA Puhvel SM (1984) Intradermal injection of Propionibacterium acnes: a model of inflammation relevant to acne. J Invest Dermatol 83:394–398

De Young LM Spires DA Ballaron SJ Cummins CS Young JM Allison AC (1985) Acne like chronic inflammatory activity of Propionibacterium acnes preparations in an animal model: correlations with ability to stimulate the reticular endothelial system. J Invest Dermatol 85:255–258

Ebling FJG Petrow V (1993) 19-Aldehydo-4-androstene-3,17-dione: An estrogen precursor that inhibits sebaceous secretion in a rat model. J Invest Dermatol 101, Suppl 1:121S–123S

Hamilton JB Montagna W (1950) The sebaceous gland of the hamster. I. Morphological effects of androgens on integumentary structures. Am J Anat 86:191–234

Karasek J (1968) The ultrastructure of the sebaceous gland of the rat. Folia Morphol (Praha) 16:272–276

Lapière CH, Chèvremont M (1953) Modifications des glandes sébacées par des hormones sexuelles appliquées localement sur la peau de Souris. CR Soc Biol (Paris) 147:1302–1306

Lecaque D Secchi J (1982) Ultrastructural changes of sebaceous glands in castrated and testosterone-treated male rats. Cell Tissue Res 226:621–628

Mitchell OG (1965) Effect of castration and transplantation on ventral glands of the gerbil. Proc Soc Exp Biol Med 119:953–955

Morohashi M (1968) An electron microscope study of the sebaceous glands, with special reference to the effect of sexual hormones. Jpn J Dermatol Ser B 78:133–152

Neumann F Elger W (1966) The effect of a new antiandrogenic steroid, 6-chloro-17-hydroxy-1α,2α-methylenepregena-4,6-diene-3,20-dione acetate (cyproterone acetate) on the sebaceous glands of mice. J Invest Dermatol 46:561–572

Sauter LS Loud AV (1975) Morphometric evaluation of sebaceous gland volume in intact, castrated, and testosterone-treated rats. J Invest Dermatol 64:9–13

Shamoto M Shinzato M Qian B Hosokawa S Ishibashi M (1999) Paracortical hyperplasia of superficial lymph nodes in a new mutant strain of hairless rats (ISh): a lesion similar to dermatopathic lymphadenopathy. Pathol Int 49:305–309

P.11.2 Activity on Sebaceous Glands of the Fuzzy Rat

PURPOSE AND RATIONALE

Fuzzy rats, a genetic mutant between hairless and haired albino rats, exhibit sexual dimorphism in the skin (Ferguson et al. 1979). A brown-colored, thick seborrhoeic coating on the entire back is characteristic of male rats while the female rats show clear skin with white fuzzy hairs. In male rats the hair follicles resemble human sebaceous follicles associated with hyperplastic glandular lobules, dilatation and micro-comedo (Plewig and Kligman 1975). Castration caused a reduction in size of the sebaceous glands and ducts, and a testosterone implant in castrated rats resurrected glandular hyperplasia and ductal dilatation (Uno et al. 1990).

This rodent model for androgen-dependent hyperplasia of the sebaceous glands is useful for the study of many pharmacological aspects, comprising the rate of percutaneous absorption, stability, and affinity to target organs of the testing compounds and selection of adequate vehicles for topical application (Ye et al. 1997).

PROCEDURE

Peripubertal male fuzzy rats at an age of 25 days weighing about 40 g are kept in single cages at a temperature of 24°C and a 12-h light-and-dark cycle. They are divided into several groups for local treatment with 5α-reductase inhibitors or androgen receptor antagonists. One group serving as control is castrated at an age of 25 days in anesthesia. Approximately 0.5 ml of a 1% solution of test compounds dissolved in 30% propylene glycol, 50% alcohol and 20% water are applied to the other groups in a 4 × 4 cm area on the lower back once per day 5 days per week. Vehicle solution alone is applied to the control and castrate groups. After 8 weeks of treatment, the animals are euthanized by anesthesia with ketamine HCl, 100 g/ml, xylazine HCl, 120 g/ml, acepromazine, 5 g/ml, 1 ml/kg intramuscularly.

Photographs of the backs are taken pre-treatment and every 2 weeks after the start of treatment.

Eight weeks after starting treatment, the animals in all groups are given an intraperitoneal injection of 200 mg/kg bromodeoxyuridine 2 h before euthanasia. A blood sample is then collected from the right ventricle of the heart under anesthesia with the ketamine-xylazine-acepromazine mixture. After euthanasia with an overdose of the same anesthesia solution, fresh skin tissues are taken by a punch (4 mm diameter) from the marked area of the back and immediately incubated with EDTA solution for the split-skin preparation. The rest of the skin in the marked area is cut and fixed with 10% neutral buffered formalin solution for morphometric analysis of the sebaceous glandular lobules. The ventral lobes of the prostate are dissected and the weight is measured.

For morphometric analysis of the sebaceous glands, the size of sebaceous glandular lobules is first determined. Using formalin-fixed skin, small skin samples are taken by punch (4 mm diameter) and serial frozen sections (40 µm thick), horizontal to the epidermal surface, are cut and collected in water-filled wells. Four to five free-floating sections containing sebaceous glandular lobules are selected and stained with 1% osmium and 2.5% potassium dichromate solution for 2–3 min. The sections are washed with distilled water and mounted on a glass slide with aqua mount. Darkly stained globular lobules are distinctively seen under the microscope or on microvideo images. The largest lobular area in each glandular image is measured by a computer-assisted microimage apparatus, using a program of image analysis.

Split preparations of the pilosebaceous organ are used to measure the size of the sebaceous lobule and duct, and the number of DNA synthesis sebocytes. Fresh skin samples, 4 mm punched, are incubated with 17 mM EDTA in phosphate buffer (0.1 M, pH 7.4) for 2 h at 27°C. The pilosebaceous organs attached to the epidermis are manually split from the dermis. Following fixation with 10% buffered formalin, free-floating split tissues are stained by the immunocytochemical method, using a monoclonal antibody against bromodeoxyuridine with the avidin-biotin complex method.

On viewing the split tissue under a stereomicroscope, the sebaceous glandular lobules with a duct attached to the follicular shaft are clearly visible. After mounting on a slide glass, these *in situ* images of the sebaceous glands are observed on a computer monitor with a microvideo apparatus, and the area of the lobes, the diameter of the duct and number of bromodeoxyuridine-stained nuclei in the sebocytes are measured.

EVALUATION

Group data are expressed as means ± standard error. The results are analyzed using the *t*-test.

MODIFICATIONS OF THE METHOD

Marit et al. (1995) presented anatomical and physiological parameters of the fuzzy rat, collected for each sex at five ages, including histological and clinical biochemical profiles, organ and body weights, and a characterization of gross and histopathological findings.

Yourick and Bronaugh (2000) studied percutaneous penetration and metabolism of 2-nitro-*p*-phenylendiamine in human and fuzzy rat skin.

Salcido et al. (1995) described an animal model and computer-controlled surface pressure delivery system for the production of pressure ulcers. A method for inducing dermal pressure lesions on the fuzzy rat was developed using a computer-controlled displacement column, which produced a constant tissue interface pressure.

REFERENCES AND FURTHER READING

Ferguson FG Irving GW III, Stedham MA (1979) Three variants of hairlessness association with albinism in the laboratory rat. Lab Anim Sci 29:459–465

Marit GB Young SM Hadick CL (1995) Anatomic and physiologic characterization of the WF/PmWp-"fz" (fuzzy) rat. Lab Anim Sci 45:184–190
Plewig G Kligman AM (1975) Acne: Morphogenesis and Treatment. Springer, Berlin, Heidelberg
Salcido R Fisher SB Donofrio JC Bieschke M Knapp C Liang R LeGrand EK Carney JM (1995) An animal model and computer-controlled surface pressure delivery system for the production of pressure ulcers. J Rehab Res Dev 32:149–161
Uno H, Fors TD Packard SM Bazzano GS Kligman AM (1990) Androgen-dependent activity of the sebaceous gland and the effect of topical tretinoin in fuzzy rats. J Invest Dermatol 94:587
Ye F, Imamura K Imanishi N Rhodes L Uno H (1997) Effects of topical antiandrogen and 5-alpha-reductase inhibitors on sebaceous glands in male fuzzy rats. Skin Pharmacol 10:288–297
Yourick JJ Bronaugh RL (2000) Percutaneous penetration and metabolism of 2-nitro-*p*-phenylendiamine in human and fuzzy rat skin. Toxicol Appl Pharmacol 166:13–23

P.11.3 Activity on Ear Sebaceous Glands of Syrian Hamsters

PURPOSE AND RATIONALE

The ear sebaceous glands of the Syrian hamster have been proposed as a model system for human sebaceous glands because of the similarities in morphology and in turnover time (Hamilton and Montagna 1950; Plewig and Luderschmidt 1977). As an androgen-sensitive structure, the ear sebaceous glands have been used to determine the effect of antiandrogenic compounds by the use of histoplanimetry on projections of sagittal sections of the ear (Luderschmidt and Plewig 1977). Matias and Orentreich (1983) developed a stripped skin planimetric method to measure the ear sebaceous gland areas in Syrian golden hamsters.

Seki et al. (1995) determined the effects of topically applied spironolactone on androgen stimulated sebaceous glands in the hamster pinna.

PROCEDURE

Adult female Syrian golden hamsters, 9–10 weeks of age and 110–120 g in weight, are kept at constant temperature and humidity and fed commercially prepared hamster food and water. The hamsters are divided at random into three groups. Testosterone propionate (80 µg dissolved in 1 ml sesame oil) is administered to two groups every other day over a two weeks period to stimulate androgen responses. Hamsters in the third group are injected with 1 ml sesame oil only as controls. The hamsters receive once daily applications of 0.1 g of a colorless clear hydrophilic gel preparation of 5% spironolactone, containing ethanol and isopropyl alcohol on the ventral side of the right pinna for two weeks. The left side is left untreated as control. On day 15, 4 mm punch biopsy specimens from each hamster are obtained from the central region of the bilateral pinnae where sebaceous glands are most developed.

The sebaceous gland size is measured by the whole mount technique (Motoyoshi 1988). After the biopsy specimens are immersed in physiological saline at 4°C for 18 h, cartilages are removed. Then, each specimen is immersed in 2 N NaBr at 37°C for one hour, and the epidermis is peeled off with fine forceps. The obtained dermis sheet containing sebaceous glands is stained with Susan III and mounted on a glass slide.

EVALUATION

An area of five or more sebaceous glands, including all the sebaceous acini attached to one pilosebaceous unit in each biopsy specimen, is measured with a computerized image analyzer (Olympus CIA-102) and shown as a mean value ± standard deviation ($mm^2/100$). The values are compared using Student's paired *t*-test.

MODIFICATIONS OF THE METHOD

Gollnick (1990, 1992) evaluated azelaic acid proposed for acne treatment, using comedo formation in the hamster ear model and recommended it as a new substance in the spectrum of antiacne agents.

Matias and Gaillard (1995) studied the local inhibition of sebaceous gland growth in the ventral ear pinna of sexually mature male Syrian hamsters by topically applied androgen receptor inhibitors.

Seki and Morohashi (1993) investigated the effect of some alkaloids, flavonoids and triterpenoids on the lipogenesis of sebaceous glands of the hamster ear. Lipogenesis was assayed by determining ^{14}C incorporation into sebaceous lipids extracted from the sebaceous glands, which were incubated with ^{14}C-acetate.

Morgan et al. (1993) studied the occurrence of zinc-induced synthesis of metallothionein in skin after topical application of the anti-acne drug Zineryt lotion in hamster ears. The dinitrophenyl hapten-sandwich immunohistochemical method involving a monoclonal anti-metallothionein antibody was used to detect and localize zinc-binding metallothionein in the treated and untreated hamster skin.

Burkhart et al. (2000) studied the effects of benzoyl peroxide on lipogenesis in sebaceous glands using the flank organs of female golden Syrian hamsters.

REFERENCES AND FURTHER READING

Burkhart CG Butcher C Burkhart CN Lehmann P (2000) Effects of benzoyl peroxide on lipogenesis in sebaceous glands using an animal model. J Cutan Med Surg 4:138–141

Gollnick H (1990) A new therapeutic agent: Azelaic acid in acne treatment. J Dermatol Treat 1, Suppl. 3:S23–S28
Gollnick HPM (1992) The C-9-dicarbonic azelaic acid – a new substance in the spectrum of antiacne agents. Dermatol Monatsschr 178:143–152
Hamilton JB Montagna W (1950) The sebaceous gland of the hamster. I. Morphological effects of androgens on integumentary structures. Am J Anat 86:191–234
Luderschmidt C Plewig G (1977) Effect of cyproterone acetate and carboxylic acid derivates on the sebaceous glands of the Syrian hamster. Arch Dermatol Res 258:185–191
Matias JR Orentreich N (1983) The hamster ear sebaceous glands. I. Examination of the regional variation by stripped skin planimetry. J Invest Dermatol 81:43–46
Matias JR Gaillard M (1995) Local inhibition of sebaceous gland growth by topically applied RU 58841. Ann NY Acad Sci 761:56–65
Morgan AJ Lewis G Van den Hoven WE Akkerboom PJ (1993) The effect of zinc in the form of erythromycin-zinc complex (Zineryt) and zinc acetate on metallothionein expression and distribution in hamster skin. Br J Dermatol 129:563–570
Motoyoshi K (1988) Whole mount technique: An improved hamster ear model to evaluate pharmacologic effects on sebaceous glands. J Dermatol (Tokyo) 15:252–256
Plewig G Luderschmidt C (1977) Hamster ear model for sebaceous glands. J Invest Dermatol 68:171–176
Seki T Morohashi M (1993) Effect of some alkaloids, flavonoids and triterpenoids, contents of Japanese-Chinese traditional herbal medicine, on the lipogenesis of sebaceous glands. Skin Pharmacol 6:56–60
Seki T Toyomoto T Morohashi M (1995) Effects of topically applied spironolactone on androgen stimulated sebaceous glands in the hamster pinna. J Dermatol 22:233–237

P.11.4
Activity on Ear Sebaceous Glands of Rabbits

PURPOSE AND RATIONALE

Several authors used the rabbit ear model to study comedo formation (Weirich and Longauer 1974; Mills and Kligman 1975; Motoyoshi 1983a; Kligman 1989; Ito et al. 1985, 1991; Maeda 1991) in order to assess the comedogenicity of cosmetics, toiletries and drugs and to evaluate potential anti-acne drugs. Sebaceous follicles in the inner surface of rabbit ears are sensitive to many substances called comedogenes, which, when applied topically, induce comedo formation. This comedo induction takes place after about 2 weeks of repeated topical application of a chemical comedogen such as 1% coal tar, 50% oleic acid, or 50% tetradecane.

PROCEDURE

Male rabbits weighing 2.5–3.5 kg are used. Tetradecane, testosterone, and dimethyl sulfoxide are separately inuncted on rabbit pinnas once a day for 4 weeks. The pinnas are biopsied on days 1, 3, 7, and 28. Untreated pinnas and squalene-treated pinnas serve as controls. Three-dimensional images of sebaceous glands are reconstructed from their serial histological sections using a computer-image analysis system.

EVALUATION

The volumes of the sebaceous glands, the number of acini, and the volume of individual acini are compared between groups.

MODIFICATIONS OF THE METHOD

Motoyoshi (1983b) studied the correlation between surface microscopy and dermal histology in tetradecane-induced comedones in rabbit ear skin.

Kligman and Kligman (1994) used the rabbit ear to assay the comedogenic potentialities of an array of known tumorigens. Complete carcinogens and some tumor promoters were invariably strongly comedogenic at concentrations of 1.0% and below. The rabbit ear model was recommended to be an easy and reliable way to screen for carcinogenicity.

REFERENCES AND FURTHER READING

Ito M, Motoyoshi K Suzuki M Sato Y (1985) Sebaceous gland hyperplasia on rabbit pinna induced by tetradecane. J Invest Dermatol 85:249–254
Ito M, Ikeda K Yokoyama H Motoyoshi K Sato Y Hashimoto K (1991) Stereographic and sterometric study of sebaceous gland hyperplasia in rabbit pinnas induced by topically applied substances. J Invest Dermatol 97:85–90
Kligman AM (1989) Improved procedure for assessing acnegenicity (comedogenicity) in the rabbit ear model. J Toxicol Cutaneous Ocul Toxicol 8:395–410
Kligman AM Kligman LH (1994) Carcinogens show comedogenic activity: a potential animal screen for tumorigenic substances. Cancer Lett 87:171–178
Maeda T (1991) An electron microscopic study of experimentally-induced comedo and effects of vitamin A acid on comedo formation. J Dermatol 18:397–407
Mills OH Kligman AM (1975) Assay of comedolytic agents in the rabbit ear. In: Maibach HI (ed) Animal Models in Dermatology. pp 176–183, Churchill Livingstone, New York
Motoyoshi K (1983a) Enhanced comedo formation in rabbit ear skin by squalene and oleic acid peroxides. Br J Dermatol 109:191–198
Motoyoshi K (1983b) The correlation between surface microscopy and dermal histology in tetradecane-induced comedones in rabbit ear skin. Br. J Dermatol 108:573–579
Weirich EG Longauer J (1974) Topographical differences in the development and reactivity of the auricular sebaceous glands of the rabbit. II. Communication: Histometric studies of the activity if the sebaceous glands. Dermatologica 149:23–28

P.11.5
Activity on the Hamster Flank Organ

PURPOSE AND RATIONALE

The flank organs of Syrian golden hamsters are located on each flank of the animal consisting mainly of sebaceous tissue. Like sebaceous glands in other species,

these pigmented spots respond to androgens by an increase in size. This proliferation is inhibited by systemical or topical anti-androgens.

PROCEDURE

Female Syrian golden hamsters (*Mesocricetus auratus*), weighing 80–110 g are kept at constant temperature on a commercial diet and water ad libitum. They are castrated 24 h prior to the experiment. The costovertebral region is shaved; the horny layer is stripped the day prior to the tes and then every 3 days. For stimulation, animals receive a subcutaneous dose of 250 µg testosterone propionate in 25 µl peanut oil in the dorsal neck fold, for three weeks (weekdays only or continually). On the same days, the anti-androgen dissolved in water/ethanol (1:4, v/v) is applied locally to the left flank organ at increasing doses, using a micropipette under a continuous air stream to enhance the evaporation of the solvent. At least 5 animals are used per group. Controls receive vehicle only, and another group, testosterone propionate only. After treatment the animals are sacrificed under ether anesthesia. The 2 major perpendicular axes of the pigmented spot overlying each flank organ are measured and multiplied to obtain the surface area index. The flank organs are excised and divided into two halves along the major axis, immediately fixed in 10% formalin and embedded in paraffin. The 5 µm-thick sections are stained with haematoxylin-eosin. Sebaceous glands and hairs are measured in the first 2 sections of each half of the specimen, using a semiautomatic computerized image analyzer. The sebaceous gland area in each field is quantified in square millimeters. The diameter of all the hair under each flank organ is measured in micrometers.

EVALUATION

The local (topical) anti-androgenic activity of the test compound is estimated by the ability to inhibit the effects in the ipsilateral treated flank organ whereas the systemic activity is evaluated by the inhibition on the untreated contralateral flank organ. The values for surface area index, sebaceous gland area, and average of diameter of the hairs on the flank organ of the treated left and the untreated right side are compared for anti-androgen-treated animals with controls using two-way analysis of variance and *t*-test.

MODIFICATIONS OF THE METHOD

Wuest and Lucky (1989) studied the differential effect of testosterone on pigmented spot, sebaceous glands and hair follicles in the Syrian hamster flank organ.

Noto et al. (1991) quantified the antiandrogenic activity of topically applied canrenoic acid in the hamster flank organ. The flank organs of female Syrian hamsters were stimulated by subcutaneous administration of testosterone propionate. Sebaceous glands and hair follicles were measured by a computerized image analyzer. Using this method, the same authors (Noto et al. 1992) compared the activity of some topical antiandrogens.

Aricò et al. (1993) found no antiandrogenic effects of topical bifonazole on sebaceous glands and hair in the hamster flank organ.

Lucky et al. (1995) studied the autoradiographic localization of tritiated dihydrotestosterone in the flank organ of the albino hamster.

Foreman et al. (1984) found that in the hairless hamster, progesterone can antagonize dihydrotestosterone-mediated hypertrophy of the sebaceous gland.

CRITICAL ASSESSMENT OF THE METHOD

The relevance of the hamster flank organ model to man has been challenged by Franz et al. (1989).

REFERENCES AND FURTHER READING

Aricò M, Noto G Pravatà G, Bongiorno MR (1993) Lack of antiandrogenic effects of topical bifonazole on sebaceous glands and hairs in the hamster flank organ. Skin Pharmacol 6:52–55

Battmann T Bonfils A Branche C Humbert J Goubet F Teutsch G Philibert D (1994) RU 58841, a new specific topical antiandrogen: a candidate of choice for the treatment of acne, androgenic alopecia and hirsutism. J Steroid Biochem Mol Biol 48:55–60

Chakrabarty K Ferrari RA Dessingue OC Beyler AL Schane HP (1980) Mechanism of action of 17α-propyltestosterone in inhibiting hamster flank organ development. J Invest Dermatol 74:5–8

Ferrari RA Chakrabarty K Beyler AL Wiland J (1978) Suppression of sebaceous gland development in laboratory animals by 17α-propyltestosterone. J Invest Dermatol 71:320–323

Foreman MI Devitt H Clanachan I (1984) Inhibition of dihydrotestosterone-mediated hamster sebaceous gland hypertrophy by progesterone. Br J Dermatol 110:185–186

Franz TJ Lehman PA Pochi P Odland GF Olerud J (1989) The hamster flank organ model: Is it relevant to man? J Invest Dermatol 93:475–479

Kaszynski E (1983) The stimulation of hair growth in the flank organ of female hamsters by subcutaneous testosterone propionate and its inhibition by topical cyproterone acetate. Dose-response studies. Br J Dermatol 109:565–569

Lucky AW Eisenfeld AJ Visintin I (1995) Autoradiographic localization of tritiated dihydrotestosterone in the flank organ of the albino hamster. J Invest Dermatol 84:122–125

Noto G Pravatà G, Bongiorno MR Bosco M Aricò M (1991) Topical canrenoic acid. Quantification of the antiandrogenic activity in the hamster flank organ. Int J Dermatol 30:810–813

Noto G Pravatà G, Bongiorno MR Bosco M Aricò M (1992) Comparison of the activity of some topical antiandrogens. Ann Ital Dermatol Clin Sper 46:17–21

Orentreich N Matias JR Malloy V (1984) The local antiandrogenic effect of the intracutaneous injection of progesterone in the flank organ of sexually mature male Syrian golden hamsters. Arch Dermatol Res 276:401–405
Voigt W Hsia SL (1973) The antiandrogenic action of 4-androstene-3-one-17beta-carboxylic acid and its methyl ester on hamster flank organ. Endocrinology 92:1216–1222
Weissmann A Bowden J Frank B Horwitz SN Frost P (1984) Morphometric studies of the hamster flank organ: An improved model to evaluate pharmacologic effects on sebaceous glands. J Invest Dermatol 82:522–525
Weissmann A Bowden J Frank BL Horwitz SN Frost P (1985) Antiandrogenic effect of topically applied spironolactone on the hamster flank organ. Arch Dermatol 121:57–62
Wuest PA Lucky AM (1989) Differential effect of testosterone on pigmented spot, sebaceous glands and hair follicles in the Syrian hamster flank organ. Skin Pharmacol 2:103–113

P.11.6
Activity on the Skin of the Rhino Mouse

PURPOSE AND RATIONALE

The Rhino mouse has been widely used as an experimental acne model to evaluate topically active comedolytic and anti-keratinizing agents (Kligman and Kligman 1979; Ashton et al. 1984; Mezick et al. 1984; Chatelus et al. 1989; Bernerd et al. 1991; Bouclier et al. 1991; Tramposch et al. 1992; Zheng et al. 1993; Sundberg 1994; Fort-Lacoste et al. 1999).

Rhino mice are hairless mutants with a rhinoceros-like appearance, which carry the rhino gene, a recessive allele of the hairless gene ($hr^{rh}hr^{rh}$) (Howard 1941). This recessive mutation on chromosome 14 results in a mouse with wrinkled skin devoid of body hair by age of 25 days. At that time, the end of the first hair cycle, the follicular papillae fail to follow the regressing hair follicles and become isolated in the dermis. The papillae do not re-associate with the follicular epithelium to initiate a new hair follicle cycle. The upper remnants of the hair follicles are filled with sloughed, cornified cells and form utriculi with a small sebaceous gland at their base, resembling an open comedone. The Rhino skin becomes progressively loose, forming folds and ridges, due to the expansion of the surface, secondary to abortive hair follicles filling with cornified debris. The utriculi progressively enlarge, forming pillory cysts (pseudocomedones), which are dilated follicular infundibula filled with cornified debris (Mann 1971). The dermal cysts of the rhino mouse develop into unopened sebaceous glands (Bernerd et al. 1996).

Seiberg et al. (1997) studied the effects of trypsin on apoptosis, utriculi size and skin elasticity in the rhino mouse. González et al. (2000) measured the effect of graduated local doses of all-*trans* retinoic acid applied to the skin of rhino mice with fluorescence excitation spectroscopy and compared the data with histological findings.

PROCEDURE

Seven-weeks old female rhino mice ($hr^{rh}hr^{rh}$) obtained from Charles River Laboratories are divided into groups receiving graduated doses of test compound (all-*trans* retinoic acid) dissolved in an ethanol/propylene glycol mixture (70:30) or the solvent as controls. The solution is applied once per day in doses of 100 µl on the entire dorsal skin, for 5 consecutive days each week, for a total period of 2 weeks. Animals in all groups are sacrificed 24 h after the last treatment and biopsies are obtained immediately following sacrifice. Fluorescence excitation spectra are collected from dorsal skin on a daily basis during treatment. During the measurements, the animals are sedated with inhalation of methoxyflurane.

Fluorescence excitation spectra are obtained *in vivo* with a fluorescence spectrophotometer (SkinSkan, SPEX, Edison NJ) equipped with a 450 W Xenon lamp, double monochromators on the excitation and emission, a photomultiplier detector (R928P, Hamamatsu, Japan) connected to a single photon counting system and a bifurcated quartz fiber bundle (Model 1950; SPEX Ind., Edison, NJ) for light delivery and collection. The individual fibers are 100 µm in diameter and are randomly arranged to form a bundle 6 mm in diameter. The resolution is 4 nm, the intensity of the excitation radiation is in the range of 1–20 mW/cm^2, and the total delivered radiation dose is below the erythema threshold. Each fluorescence measurement consists of a set of eight serial excitation spectra collected by positioning the emission monochromator from 340 to 480 nm in increments of 20 nm and scanning the excitation monochromator from 260 to within 20 nm of the emission monochromator setting. Light from the excitation monochromator is focused into one leg of the bifurcated fiber bundle. The other leg of the fiber bundle is focused into the input of the emission monochromator. The joined end of the fiber bundle is brought into direct contact with the skin site measured. Care is taken to clean properly the fiber bundle end with an alcohol swab between measurements on different animals and that gentle pressure is applied to the animals during measurement.

Significant changes are observed in the fluorescence spectra as a result of the application of comedolytic agents. The first peak, located approximately at

295 nm, which is related to tryptophan, increases significantly, whereas the second peak at 340–370 nm, which is attributed to collagen links, exhibits a dramatic decrease.

For histology, skin samples approximately 5 mm in diameter are obtained from the skin of each animal following sacrifice, from the mid-line of the anterior portion of the skin. All specimens are fixed in 10% buffered formaldehyde for 24 h, and later embedded in paraffin. Tissue sections 5 µm thick are cut perpendicularly to the epidermal surface and stained with hematoxylin and eosin for light microscopic examination. For each animal, the epidermal and dermal thickness, utriculi diameter, and number of capillaries containing more than 5 erythrocytes are assessed with a micrometer eyepiece adapted to a microscope (Leitz SM-LUX, Ernst Leitz, Wetzlar, Germany) using a 40× objective for the measurement of epidermal and dermal thickness, and utriculi diameter, and a 20× objective for the count of dilated capillaries.

EVALUATION

Time-response curves and dose-response curves of the changes of fluorescence spectra are established compared with the changes of histological data.

MODIFICATIONS OF THE METHOD

In addition to image analysis, Seiberg et al. (1997) tested the effects of trypsin on skin elasticity and elastin expression in the Rhino mouse.

Beehler et al. (1995) studied gene expression of retinoic acid receptors and cellular retinoic acid-binding proteins in rhino and hairless mouse skin.

Imakado et al. (1995) found that targeting expression of a dominant-negative retinoic acid receptor (RAR) mutant in the epidermis of transgenic mice results in loss of barrier function.

Feng et al. (1997) reported that suprabasal expression of a dominant-negative RXR alpha mutant in transgenic mouse epidermis impairs regulation of gene transcription and basal keratinocyte proliferation by RAR-selective retinoids.

González et al. (1997) investigated DNA ploidy changes in rhino mouse skin after treatment with all-*trans* retinoic acid and retinol.

Petersen et al. (1984) developed an animal model using human face skin onto the nude mouse to study human sebaceous glands. The effects of androgens were evaluated.

Lesnik et al. (1992) reviewed agents that cause enlargement of sebaceous glands in hairless mice.

REFERENCES AND FURTHER READING

Ashton RE Connor MJ Lowe NJ (1984) Histologic changes in the skin of the rhino mouse ($hr^{rh}hr^{rh}$) induced by retinoids. J Invest Dermatol 82:632–635

Beehler BC Chen S Tramposch KM (1995) Gene expression of retinoic acid receptors and cellular retinoic acid-binding proteins in rhino and hairless mouse skin. Arch Dermatol Res 287:488–493

Bernerd F Ortonne JP Bouclier M Chatelus A Hensby C (1991) The rhino mouse model: the effects of topically applied *all*-trans retinoids acid and CD271 on the fine structures of the epidermis and utricle wall of pseudocomedones. Arch Dermatol Res 6:692–696

Bernerd F Schweizer J Demarchez M (1996) Dermal cysts of the rhino mouse develop into unopened sebaceous glands. Arch Dermatol Res 288:586–595

Bouclier M Chatelus A Ferracin J Delain C Shroot B Hensby CN (1991) Quantification of epidermal histological changes induced by topical retinoids and CD271 in the rhino mouse model using a standardized image analysis technique. Skin Pharmacol 4:65–73

Chatelus A Caron JC Shroot B Eustache J Hensby C (1989) Structure-activity relationships between different retinoids using the topical Rhine mouse comedolytic model. In: Reichert U Shroot B (eds) Pharmacology and the Skin. Vol 3, pp 144–148, Karger Basel

Feng X Peng ZH Di W, Li XY, Rochette-Egly C Chambon P Voorhees JJ Xiao JH (1997) Suprabasal expression of a dominant-negative RXR alpha mutant in transgenic mouse epidermis impairs regulation of gene transcription and basal keratinocyte proliferation by RAR-selective retinoids. Genes Dev 11:59–71

Fort-Lacoste L Verscheure Y Tisne-Versailles J Navarro R (1999) Comedolytic effect of topical retinaldehyde in the rhino mouse model. Dermatology 199, Suppl 1:33–35

González S Alcaraz MW Díaz F, Flotte TJ Pérez de Vargas I Anderson RR Kollias N (1997) DNA ploidy changes in rhino mouse skin by all-*trans* retinoic acid and retinol. Skin Pharmacol 10:135–143

González S Zonios G Nguyen BC Gillies R Kollias N (2000) Endogenous skin fluorescence is a good marker for objective evaluation of comedolysis. J Invest Dermatol 115:100–105

Howard A (1941) "Rhino" an allele of hairless in the mouse. J Hered 31:467–470

Imakado S Bickenbach JR Bundman DS Rothnagel JA Attar PS Wang XJ Walczak VR Wisniewski S Pote J Gordon JS (1995) Targeting expression of a dominant-negative retinoic acid receptor mutant in the epidermis of transgenic mice results in loss of barrier function. Genes Dev 9:317–328

Kligman LH Kligman AM (1979) The effect in rhino mouse skin of agents which influence keratinization and exfoliation. J Invest Dermatol 73:354–358

Lesnik RH Kligman LH Kligman AM (1992) Agents that cause enlargement of sebaceous glands in hairless mice. I. Topical substances. Arch Dermatol Res 284:100–105

Mann SH (1971) Hair loss and cysts formation in hairless and rhino mutant mice. Anat Rec 170:485–500

Mezick JA Bhatia MC Capetola RJ (1984) Topical and systemic effects of retinoids on horn-filled utriculus size in the rhino mouse. A model to quantify "antikeratinizing" effects of retinoids. J Invest Dermatol 83:110–113

Petersen MJ Zone JJ Frueger GG (1984) Development of a nude mouse model to study human sebaceous gland physiology and pathophysiology. J Clin Invest 74:1358–1365

Seiberg M Siok P Wisniewski S Cauwenbergh G Shapiro SS (1997) The effects of trypsin on apoptosis, utriculi size

and skin elasticity in the Rhino mouse. J Invest Dermatol 109:370–376
Sundberg JP (1994) The hairless and rhino mutations, chromosome 14. In: Sundberg JP (ed) Handbook of Mouse Mutations with Skin and Hair Abnormalities. CRC Press, Boca Raton, FL, pp 291–312
Tramposch KM Nair X Gendimenico GJ Tetrault GB Chen S Kiss I Whithing G Bonney RJ (1992) The pharmacology of a novel topical retinoid, BMY 30123: comparison with tretinoin. J Pharm Pharmacol 44:379–386
Zheng P Gendimenico GJ Mezick JA Kligman AM (1993) Topical *all*-trans retinoic acid corrects the follicular abnormalities in the rhino mouse. An ultrastructural study. Acta Dermatol Venereol 73:97–101

P.11.7 Activity on the Skin of the Mexican Hairless Dog

PURPOSE AND RATIONALE

The Mexican hairless dog has been recommended as a model for the comedolytic and morphogenic activity of retinoids and other anti-acne agents (Loux et al. 1974; Schwartzman et al. 1996; Kimura and Doi 1996). A semilethal mutation of an autosomal dominant 'L' gene produces an animal with multiple developmental defects, including poor dentition, early degeneration of the thymus, hairlessness and numerous comedones (Yankell et al. 1970a; González-Diddi et al. 1971; Goto et al. 1987; Fukuda et al. 1991). The Mexican hairless dog is nearly bald, with sparse, flimsy hair most abundant on the limbs and head. In most hairy species, the primary hair is surrounded by 7 to 10 accessory hairs. In this species, the follicles are mainly single and not in clusters. The skin is tan-colored. A brownish, waxy material unevenly coats the surface; this can be removed easily by soap and lipid solvents. A great number of comedones cover the surface, and these are nearly all of the open variety. The majority is rather small (a few millimeters in diameter), and may be viewed as horn-filled shallow invaginations. Scattered among these, especially on the face, neck and thighs, are larger, black-tipped open comedones. These are hard, deep, horny impactions, which are expelled with difficulty. A few small, closed comedones occur on the neck and lateral aspect of the chest.

Papulopustules are rare, and are found mainly on the metacarpus and metatarsus. They apparently do not develop from the rupture of comedones as in humans. Thus, this animal mimics human acne only with regard to comedones. These, unlike the human variety, do not originate from pre-existing sebaceous follicles. They arise de novo, and completely lack sebaceous glands.

PROCEDURE

About 1-year-old female animals are used. Areas of 4–5 cm^2 on the dorsolateral aspects of the trunk are treated once daily (5 working days) for 14 weeks with test formulations or tretinoin formulations (0.025–0.1%) as standard.

Biopsies are taken from each site under local anesthesia at 5 weeks and again at 14 weeks.

EVALUATION

The clinical picture and the histology of biopsies are compared before, during, and after treatment.

MODIFICATIONS OF THE METHOD

Yankell et al. (1970b) used the Mexican hairless dog for sunscreen recovery studies.

Hunziker et al. (1978) compared percutaneous penetration of benzoic acid, progesterone and testosterone between Mexican hairless dogs and man.

Matsumura et al. (1992) described a burn wound-healing model in the hairless descendant of the Mexican hairless dog.

REFERENCES AND FURTHER READING

Fukuda K Koizumi N Imamaura K (1991) Microscopic observations of skin and lymphoid organs in the hairless dog derived from the Mexican hairless dog. Exp Anim 40:69–76
González-Diddi M Place V Ortega E Gallegos AJ (1971) Histological study of the skin of the Tepeitzcuintli Mexican hairless dog. Arch Invest Med (Mex.) 2:127–134
Goto N Imamura K Miura Y Ogawa T Hamada H (1987) The Mexican hairless dog, its morphology and inheritance. Jikken Dobutso 36:87–90
Hunziker N Feldmann RJ Maibach H (1978) Animal models of percutaneous penetration: comparison between Mexican hairless dogs and man. Dermatologica 156:79–88
Kimura T Doi K (1996) Spontaneous comedones on the skin of hairless descendants of Mexican hairless dogs. Exp Anim 45:377–384
Loux JJ DePalma PD Yankel RM (1974) Testing antiacne agents in the Mexican hairless dog. J Soc Cosmet Chem 25:473–479
Matsumura H Yoshizawa N Kimura T Watanabe K Gibran MS Engrav LH (1992) A burn wound healing model in the hairless descendant of the Mexican hairless dog. J Burn Care Rehabil 18:306–312
Schwartzman RM Kligman AM Duclos DD (1996) The Mexican hairless dog as a model for the comedolytic and morphogenic activity of retinoids. Br J Dermatol 134:64–70
Yankell SL Schwartzman AM Resnik B (1970a) Care and breeding of the Mexican hairless dog. Am Ass Lab Anim Sci 20:940–945
Yankell SL Khemani L Dolan MM (1970b) Sunscreen recovery studies in the Mexican hairless dog. J Invest Dermatol 55:31–33

P.11.8 In Vitro Sebocyte Model

PURPOSE AND RATIONALE

Cultured human sebocytes have been used by several authors to study sebum formation and to evaluate po-

tential anti-acne drugs (Zouboulis et al. 1991a, b, 1993, 1994, 1998; Rosenfield 1989; Doran and Shapiro 1990; Doran et al. 1991; Akamatsu et al. 1993; Guy et al. 1996a, b; Rosenfield et al. 1998; Wauben-Penris et al. 1998; Tsukada et al. 2000; Fritsch et al. 2001).

PROCEDURE

Human sebaceous glands are isolated from facial skin and seeded on monolayer 3T3 cells (Xia et al. 1989). Primary sebocyte cultures are derived from the periphery of the gland lobules and are maintained to confluence before subcultivation. All experiments are performed using secondary sebocyte cultures, which consist of cells undergoing sebocytic differentiation.

Human sebocytes are seeded in 96-well culture plates at a concentration of 10^4 cells/well and are left to attach for 2 days at 37°C with 5% CO_2 in culture medium consisting of Dulbecco's modified Eagle's medium and Ham's F12 medium (1:1) supplemented with 8% fetal calf serum, 2% human serum, 10 ng/ml epidermal growth factor, 10^{-9} M cholera toxin, 3.4 mM L-glutamine, 100 IU/ml penicillin, and 100 µg/ml streptomycin. The medium is then aspirated, and serum-free keratinocyte basal medium (KBM) (Clonetics, San Diego, CA) without additives, supplemented with steroids, e. g., testosterone (10^{-8}–10^{-5} M), 5a-dihydrotestosterone (10^{-8}–10^{-5} M), or spironolactone (10^{-12}–10^{-7} M) or their combinations are added to 6 wells at each concentration. KBM is concomitantly added to another 6 wells serving as controls. The plates are incubated at 37°C for 10 days before evaluation. KBM with and without compounds is changed every 2 days.

Cell numbers of treated human sebocytes in 96-well culture plates are assessed over 9 days by counting single-cell suspensions in Neubauer chambers and compared with the absolute fluorescence units (AUF) of parallel wells obtained using the 4-methylumbelliferyl heptanoate (MUH)-fluorescence assay (Stadler et al. 1989). This assay is based on the hydrolysis of the fluorogenic substrate MUH by esterases of proliferating cells. A stock solution of 10 mg/ml MUH is prepared in DMSO and kept frozen at –20°C until use. On the day of assessment, KBM is removed, and the cells are washed twice with phosphate-buffered saline without Ca^{2+} and Mg^{2+} (pH 7.2). The MUH stock solution is diluted in phosphate-buffered saline up to 100 µg/ml, and 100 µl of the final solution is added to each well. The plates are then incubated for 30 min at 37°C and read automatically on a Titertek Fluoroscan II (Flow, Meckenheim, Germany).

EVALUATION

The results are given as absolute fluorescence units using 355-nm excitation and 460-nm emission filters. Statistical significance of the differences between the means is assessed by Student's *t*-test.

REFERENCES AND FURTHER READING

Akamatsu H Zouboulis CC Orfanos CE (1993) Spironolactone directly inhibits proliferation of cultured human facial sebocytes and acts antagonistically to testosterone and 5-alpha-dihydrosterosterone *in vitro*. J Invest Dermatol 100:660–662

Doran TI Shapiro SS (1990) Retinoid effects on sebocyte proliferation. Methods Enzymol 190:334–338

Doran TI Baff R Jacobs P Pacia E (1991) Characterization of human sebaceous cells *in vitro*. J Invest Dermatol 96:341–348

Fritsch M Orfanos CE Zouboulis CC (2001) Sebocytes are the key regulators of androgen homeostasis in human skin. J Invest Dermatol 116:793–800

Guy R, Green MR Kealey T (1996a) Modeling acne *in vitro*. J Invest Dermatol 106:176–182

Guy R, Ridden C Kealey T (1996b) The improved organ maintenance of the human sebaceous gland: modeling *in vitro* the effects of epidermal growth factor, androgens, estrogens, 13-cis retinoic acid, and phenol red. J Invest Dermatol 106:454–460

Rosenfield RL (1989) Relationship of sebaceous cell stage to growth in culture. J Invest Dermatol 92:751–754

Rosenfield RL Deplewski D Kentsis A Ciletti N (1998) Mechanisms of androgen induction of sebocyte differentiation. Dermatology 196:43–46

Stadler R Detmar M Stephanek K Bangemann C Orfanos CE (1989) A rapid fluorometric assay for the determination of keratinocyte proliferation *in vitro*. J Invest Dermatol 93:532–534

Tsukada M Schröder M Roos TC Chandraratna RA Reichert U Merk HF Orfanos CE Zouboulis CC (2000) 13-cis retinoic acid exerts its specific activity on human sebocytes through selective intracellular isomerization to all-trans retinoic acid and binding to retinoic acid receptors. J Invest Dermatol 115:321–327

Wauben-Penris PJ Cerneus DP van den Hoven WE Leuven PJ den Brok JH Hall DW (1998) Immunomodulatory effects of tretinoin in combination with clindamycin. J Eur Acad Dermatol Venereol 11, Suppl 1:S2–S7

Xia L, Zouboulis ChC, Detmar M Mayerda-Silva A Stadler R Orfanos CE (1989) Isolation of human sebaceous glands and cultivation of sebaceous gland-derived cells as an *in vitro* model. J Invest Dermatol 93:315–321

Zouboulis CC Xia LQ, Detmar M Bogdanoff B Giannakopoulos G Gollnick H Orfanos CE (1991a) Culture of human sebocytes and markers of sebocytic differentiation *in vitro*. Skin Pharmacol 4:74–83

Zouboulis CC Korge B Akamatsu H Xia LQ, Schiller S Gollnick H Orfanos CE (1991b) Effects of 13-cis-retinoic acid, all-trans-retinoic acid, and acitrecin on the proliferation, lipid synthesis and keratin expression of cultured human sebocytes *in vitro*. J Invest Dermatol 96:792–797

Zouboulis CC Korge BP Mischke K Orfanos CE (1993) Altered proliferation, synthetic activity, and differentiation of cultured human sebocytes in the absence of vitamin A and their modulation by synthetic retinoids. J Invest Dermatol 101:628–633

Zouboulis CC Krieter A Gollnick H Mischke D Orfanos CE (1994) Progressive differentiation of human sebocytes *in*

vitro is characterized by increasing cell size and altering antigen expression and is regulated by culture duration and retinoids. Exp Dermatol 3:151–160
Zouboulis CC Xia L, Akamatsu H Seltmann H Fritsch M Hornemann S Ruhl R Chen W Nau H, Orfanos CE (1998) The human sebocyte culture model provides new insights into development and management of seborrhoea and acne. Dermatology 196:21–31

P.12 Skin Mycosis

P.12.1 General Considerations

PURPOSE AND RATIONALE

Fungal infections of the skin account for a large number of consultations to general practitioners and dermatologists. They are caused by dermatophytes, such as Trichophyton rubrum, Trichophyton tonsurans, Trichophyton mentagrophytes, Microsporum canis, Epidermophyton floccosum, Microsporum gypseum, and Trichophyton verrucosum. (Sinski and Kelley 1991).

Most fungal skin infections, such as tinea pedis and tinea cruris, respond to topical therapy, although widespread or chronic infections that do not respond to local measures may require systemic treatment, for example with griseofulvin, ketoconazole or terbinafine. Traditional topical products such as compound benzoic acid ointment (Whitfield's ointment) and tolnaftate preparations have largely been superseded by other topical-active antifungal agents, such as the imidazoles (e. g. clotrimazole, miconazole or econazole) or hydroxypyridones (e. g. ciclopirox), which are well tolerated and rapidly effective (Gupta et al. 1994). Fungal infections also affect the appendices, such as hair and nails. To evaluate antifungal agents not only the antimicrobial spectrum, but also the penetration plays a decisive role.

REFERENCES AND FURTHER READING

Gupta AK Sauder DN Shear NH (1994) Continuing medical education. Antifungal agents: An overview. Part I and II. J Am Acad Dermatol 30:677–698, 911–933
Sinski JT Kelley LM (1991) A survey of dermatophytes from human patients in the United States from 1985–187. Mycopathologica 114:117–126

P.12.2 In Vitro Inhibitory Activity

PURPOSE AND RATIONALE

In vitro tests are performed to investigate whether the test compound in comparison to standards covers the most relevant pathogens of dermal mycoses. The test conditions are rendered more difficult by addition of protein since the main infection site for fungi is the horny layer of the epidermis, which has a high protein content.

PROCEDURE

The studies are performed by means of conventional serial dilution procedures in test medium without and with addition of 4% bovine albumin. The test medium is Sabouraud dextrose broth containing 1% Neopeptone Difco (Difco Laboratories, Detroit, Mich., USA) and 2% glucose. The basic medium is sterilized in an autoclave at 121°C for 15 min. The pH is adjusted to 6.5 with 1 N NaOH. The medium containing albumin is sterilized by filtration through a membrane filter. For preparation of the test series, the inhibiting substances are dissolved in methanol and then rapidly diluted with slightly warmed test medium, so that series with a continuous dilution factor of 2 are obtained: 125–0.03 µg/ml in medium without protein, 500–1 µg/ml in medium with protein. Each test tube contains 3 ml. The test organisms are various strains of dermatophytes (*Trichophytum mentagrophytes*, *T. rubrum*, *T. verrucosum*, *T. equinum*, *T. gallinum*, *Microsporum canis*, *Microsporum gypseum*) and yeasts (*Candida albicans*, *Ca. tropicalis*, *Ca. pseudotropicalis*, *Ca. krusei*, *Ca. parapsilosis*, *Ca. lipolytica*, *Ca. brumpti*, *Ca. utilis*, *Torulopsis glabrata*). The organisms are pre-cultured on a modified Grütz agar at 28°C for periods of 1–4 weeks. The suspensions are adjusted by photometry that about 10^5 microconidia of dermatophytes and 10^4 yeast cells per ml are obtained in each inoculated test tube. The minimal inhibitory concentrations are measured after 14 days incubation at 28°C.

EVALUATION

The percentage of strains of *Trichophytum mentagrophytes*, *Trichophytum rubrum*, and *Candida albicans* is plotted against dilution steps for each test compound with and without albumin and IC_{50} values are calculated.

REFERENCES AND FURTHER READING

Dittmar W Lohaus G (1973) HOE296, a new antimycotic compound with a broad antimicrobial spectrum. Arzneim Forsch/Drug Res 23:670–674
Dittmar W Grau W Raether W Schrinner E Wagner WH (1981) Mikrobiologische Laboruntersuchungen mit Ciclopiroxolamin. (Microbiological laboratory studies with ciclopriroxolamine) Arzneim Forsch/Drug Res 31:1317–1322

P.12.3 In Vivo Activity in the Guinea Pig Trichophytosis Model

PURPOSE AND RATIONALE

The guinea pig trichophytosis model has been used by several authors to evaluate antimycotic compounds (Millberger and Gillert 1973; Dittmar et al. 1981; Plempel et al. 1983; Petranyi et al. 1987; Schaude et al. 1990; Garcia Rafanell et al. 1992; Arika et al. 1993).

PROCEDURE

Male albino guinea pigs (Pirbright White), bred mycosis-free, weighing 450–550 g are fed Altromin pellets and tap water ad libitum. On both sides of the back, areas of 5 × 12 cm are shorn to a fur length of 1 mm. Three areas with a diameter of 3 mm are inoculated with a pipette on either side. Per injection site, 10^4 spores of *Trichophyton mentagrophytes* 2114 in 0.05 ml suspension in physiological saline solution are inoculated. Three days after inoculation, infections with redding and scale formations are observed. From days 3–7 after the infection, 1 ml of the test preparation or standard is applied onto the right animal sides and rubbed in once daily. The diameters (mm) of all alopecias are measured with a ruler 3.5 weeks after the infection.

EVALUATION

The values of alopecias, separated according to the treated group and animal side, are determined and statistically evaluated using Duncan's new multiple range test.

REFERENCES AND FURTHER READING

Arika T Hase T Yokoo M (1993) Anti-Trichophyton mentagrophytes activity and percutaneous permeation of butenafine in guinea pigs. Antimicrob Agents Chemother 37:363–365

Dittmar W Grau W Raether W Schrinner E Wagner WH (1981) Mikrobiologische Laboruntersuchungen mit Ciclopiroxolamin. (Microbiological laboratory studies with ciclopriroxolamine) Arzneim Forsch/Drug Res 31:1317–1322

Garcia Rafanell J Dronda MA Merlos M Forn J Torres JM Zapatero MI Basi N (1992) *In vitro* and *in vivo* studies with flutrimazole, a new imidazole derivative with antifungal activity. Arzneim Forsch/Drug Res 42:836–840

Millberger HJ Gillert KE (1973) Induction of chronic trichophytosis in small experimental animals for testing antimycotics. II Effect of triamcinolone acetonide in experimental guinea pig trichophytosis. Z Hautkr 48:637–6421

Petranyi G Meingassner JG Mieth H (1987) Activity of terbinafine in experimental fungal infections of laboratory animals. Antimicrob Agents Chemother 31:1558–1561

Plempel M Regel E Büchel KH (1983) Antimycotic efficacy of bifonazole *in vitro* and *in vivo*. Arzneim Forsch/Drug Res 33:517–524

Schaude M Petranyi G Ackerbauer H Meingassner JG Mieth H (1990) Preclinical antimycotic activity of SDZ-485: a new orally and topically effective triazole. J Med Vet Mycol 28:445–454

P.12.4 Skin Penetration

PURPOSE AND RATIONALE

Cutaneous pathogenic fungi like dermatophytes or Candida ssp. present a particular affinity for the stratum corneum. Therefore the bioavailability of antimycotic drugs in the thick horny layer of the skin is an important element of treatment success. These studies can be performed in human cadaver skin (Dittmar 1981; Kligmann et al. 1987; Hänel et al. 1988)

PROCEDURE

Skin pieces, measuring 10 × 12 cm are removed from the back of corpses not later than 24 h after death. The subcutis is removed and the skin piece divided 3 to 5 parts. The edges (4 mm) of each individual piece are then taped with Tesa-film (adhesive tape) and the remaining surface is treated with the antimycotic compound. 0.05 ml of compound preparation or solution is rubbed into the skin for 10 s. For a period of one h, the pieces are placed on water agar, allowing for free admission of air. After this time, the compound is carefully wiped off with filter paper and water.

The skin area treated with the antimycotic is then stripped with Tesa-film tape as follows: (A) one third of the area remains unstripped; (B) one third of the area is stripped three times; (C) one third of the area is stripped six times. Then each piece of skin is placed into a Petri dish, which is heated in a water bath to 52°C for 15 min. The epidermis is removed from all the skin pieces, which are then placed on slides (with the base turned upwards) and put into the upper parts of plastic Petri dishes. Each of the epidermis pieces is inoculated in 20 sites with a microconidia suspension of the dermatophyte Trichophyton mentagrophytes 109-FHM 1a. The spores had been rinsed off from three-week-old slant cultures, using distilled water. Approximately 50–100 viable spores are deposited at each inoculation site.

The upper parts of the Petri dishes (containing the slides with the epidermis pieces) are then covered with the bottom parts of Petri dishes, which contain 2% aqueous agar for producing a wet chamber. Holes in the covers serve to avoid excess humidity in the chamber. The chambers are incubated at 28°C for 5 days. The fungal growth is recorded daily according to a three points score system.

EVALUATION

Growth is evaluated by visual scoring from days 2–5 after inoculation and calculation of AUCs from growth curves.

Inhibition values (%) are calculated according to the formula:

$$\text{inhibition} = \frac{\text{growth on controls} - \text{growth after treatment}}{\text{growth on contols} \times 100}$$

MODIFICATIONS OF THE METHOD

Ceschin-Roques et al. (1991) performed penetration studies on excised skin from the back of slaughtered pigs.

REFERENCES AND FURTHER READING

Ceschin-Roques CG Hänel H Pruja-Bougaret SM Lagarde I Vandermander J Michel G (1991) Ciclopirox cream 1%: *In vitro* and *in vivo* penetration into the stratum corneum. Skin Pharmacol 4:95–99

Dittmar W (1981) Zur Penetration und antimyzetischen Wirksamkeit von Ciclopiroxolamin in verhorntem Körpergewebe. (Penetration and antifungal activity of ciclopirox olamine in hornified tissue.) Arzneim Forsch/Drug Res 31:1353–1356

Hänel H Raether W Dittmar W (1988) Evaluation of fungicidal action and in a skin model considering the influence of penetration kinetics of various standard antimycotics. Ann NY Acad Sci 544:329–337

Kligman AM McGinley KJ Foglia A (1987) An *in vitro* human skin model for assaying topical drugs against dermatophytic fungi. Acta Derm Venereol (Stockh) 67:243–248

P.13 Biomechanics of Skin

P.13.1 General Considerations

Several attempts were made to describe the mechanical properties of skin by mathematical models (Ridge and Wright 1965; Harkness 1971; Hirsch and Sonnerup 1968; Jamison et al. 1968; Viidik 1968, 1969, 1973, 1979; Frisén et al. 1969a, b; Veronda and Westman 1970; Danielson 1973; Soong and Huang 1973; Wilkes et al. 1973; Jenkins and Little 1974; Lanir and Fung 1974; Vogel 1976, 1986; Barbanel and Evans 1981; Barbanel et al. 1978; Lanir 1979; Barbanel and Payne 1980; Burlin 1980, 1981; Fung 1981; Sanjeevi 1982; Potts and Breuer 1983).

Most of these authors used models derived from studies in polymers (Ferry 1970). The simplest mechanical model analogous to a viscoelastic system is a spring combined with a dashpot, either in series (**Maxwell element**) or in parallel (**Voigt or Kelvin element**). Combinations of these elements were used to explain the mechanical phenomena in connective tissue, such as stress-strain behavior, relaxation and mechanical recovery, hysteresis and creep phenomena (Jamison et al. 1968; Frisén et al. 1969a, b; Hirsch and Sonnerup 1968; Vogel 1976, 1993; Riedl and Nemetscheck 1977; Vogel and Hilgner 1979; Viidik 1968, 1969, 1973, 1977, 1979). Larrabee (1986), Larrabee and Sutton (1986).

Larrabee and Galt (1986) reviewed the theoretical and experimental mechanics of skin and soft tissue and proposed a mathematical model of skin deformation based on the finite element method. A finite element based method to determine the properties of planar soft tissue was also described by Flynn et al. (1998).

Unfortunately none of these models has been found to be sufficient to describe all properties of human and animal skin including the mechanical history before measurement and the time-dependence during measurement. There is no comprehensive and unequivocally accepted model to describe completely the biorheology of skin. Therefore, several methods are used in order to get insight into the physical properties of skin.

REFERENCES AND FURTHER READING

Barbanel JC Evans JH (1977) The time-dependent mechanical properties of skin. J Invest Dermatol 69:318–320

Barbanel JC Payne PA (1981) *In vivo* mechanical testing of dermal properties. Bioeng Skin 3:8–38

Barbanel JC Evans JH Jordan MM (1978) Tissue mechanics. Eng Med 7:5–9

Burlin TE (1980) Towards a standard for *in vivo* testing of the skin subject to uniaxial extension. Bioeng Skin 2:37–40

Burlin TE (1981) Towards a standard for *in vivo* testing of the skin subject to biaxial extension. Bioeng Skin 3:47–49

Danielson DA (1973) Human skin as an elastic membrane. J Biomechanics 6:539–546

Ferry JD (1970) Viscoelastic Properties of Polymers. 2nd edn. John Wiley & Sons. Inc., New York, London, Sydney, Toronto

Frisén M, Mägi M, Sonnerup M Viidik A (1969a) Rheological analysis of soft collagenous tissue. Part I: Theoretical considerations. J Biomechanics 2:13–20

Frisén M, Mägi M, Sonnerup M Viidik A (1969b) Rheological analysis of soft collagenous tissue. Part II: Experimental evaluation and verification. J Biomechanics 2:21–28

Flynn DM Peura GD Grigg P Hoffman AH (1998) A finite element based method to determine the properties of planar soft tissue. J Biomech Eng 120:202–210

Fung YC (1981) Biomechanics. Mechanical properties of living tissue. Springer, New York

Harkness RD (1971) Mechanical properties of skin in relation to its biological function and its chemical components. In: Elden HR (ed) Biophysical Properties of the Skin. Wiley-Interscience, New York, pp 393–436

Hirsch C Sonnerup L (1968) Macroscopic rheology in collagen material. J Biomechanics 1:13–18

Jamison CE Marangoni RC Glaser AA (1968) Viscoelastic properties of soft tissue by discrete model characterization. J Biomechanics 1:33–46
Jenkins RB Little RW (1974) A constitutive equation for parallel-fibered elastic tissue. J Biomechanics 7:397–402
Lanir Y (1979) A structural theory for The homogeneous biaxial stress-strain relationships in flat collagenous tissue. J Biomechanics 12:423–436
Lanir Y Fung YC (1974) Two-dimensional properties of rabbits skin. II. Experimental results. J Biomechanics 7:171–182
Larrabee WF Jr (1986) A finite element model of skin deformation. I. Biomechanics of skin and soft tissue: a review. Laryngoscope 96:399–405
Larrabee WF Jr, Galt JA (1986) A finite element model of skin deformation. III. The finite element model. Laryngoscope 96:413–419
Larrabee WF Jr, Sutton D (1986) A finite element model of skin deformation. II. An experimental model of skin deformation. Laryngoscope 96:406–412
Potts RO Breuer MM (1983) The low-strain, viscoelastic properties of skin. Bioeng Skin 4:105–114
Ridge MD Wright V (1965) The rheology of skin. A bioengineering study of the mechanical properties of human skin in relation to its structure. Br. J Dermatol 77:639–649
Riedl H Nemetscheck Th (1977) Molekularstruktur und mechanisches Verhalten von Kollagen. Sitzungsberichte der Heidelberger Akademie der Wissenschaften. Mathematisch-naturwissenschaftliche Klasse. pp 216–248
Sanjeevi R (1982) A viscoelastic model for the mechanical properties of biological materials. J Biomechanics 15:107–109
Soong TT Huang WN (1973) A stochastic model for biological tissue elasticity in simple elongation. J Biomechanics 6:451–485
Veronda DR Westman RA (1970) Mechanical characterization of skin – finite deformations. J Biomechanics 3:111–124
Viidik A (1968) A rheological model for uncalcified parallel-fibred collagenous tissue. J Biomechanics 1:3–11
Viidik A (1969) The aging of collagen as reflected in its physical properties. In: Engel A Larsson T (eds) Aging of Connective and Skeletal Tissue. Thule International Symposia, Nordiska Bokhandels Förlag, Stockholm, pp 125–152
Viidik A (1973) Functional properties of collagenous tissues. In: Hall DA Jackson DS (eds) International Review of Connective Tissue Research. Vol 6, Acad Press, New York, London, pp 127–215
Viidik A (1977) Thermal contraction – Relaxation and dissolution of rat tail tendon collagen in different ages. Akt Gerontol 7:493–498
Viidik A (1979) Connective tissues – possible implications of the temporal changes for the aging process. Mech Ageing Dev 9:267–285
Vogel HG (1976) Tensile strength, relaxation and mechanical recovery in rat skin as influenced by maturation and age. J Med 2:177–188
Vogel HG (1986) *In vitro* test systems for evaluation of the physical properties of skin. In: Marks R Plewig G (eds) Skin Models. Springer-Verlag, Berlin, Heidelberg, New York, Tokyo, pp 412–419
Vogel HG (1993) Mechanical measurements in assessing aging. In: Frosch PJ Kligman AM (eds) Noninvasive Methods for the Quantification of Skin Functions. An Update on Methodology and Clinical Applications. Springer-Verlag Berlin, Heidelberg, New York, pp 145–180
Vogel HG Hilgner W (1979) The "step phenomenon" as observed in animal skin. J Biomechanics 12:75–81
Wilkes GL Brown IA Wildnauer RH (1973) The biomechanical properties of skin. In: Fleming D (ed) Critical Reviews in Bioengineering. CRC

P.13.2
In Vitro (ex Vivo) Experiments

P.13.2.1
Stress-Strain Behavior

P.13.2.1.1
Measurement of Skin Thickness, Ultimate Load, Tensile Strength, Ultimate Strain and Modulus of Elasticity

PURPOSE AND RATIONALE

Animal experiments are preferable when studying the biomechanical properties of the dermis, since only in animals can the values at higher extension degrees be studied, *ex vivo* or *in vivo* under anesthesia, whereas studies in humans are limited by pain threshold or to tests in cadaver skin. Skin thickness, ultimate load, tensile strength, ultimate strain and ultimate modulus of elasticity are the most informative parameters, which describe the mechanical properties of the dermis.

PROCEDURE

Groups of at least 10 male Sprague-Dawley rats with an initial weight of 120 ± 5 g are treated subcutaneously or orally with test drugs or saline. The duration of treatment is usually 5 days; however, for special studies treatment can be prolonged up to 3 months. The animals are sacrificed under anesthesia. The back skin is shaved and a flap of 5×5 cm removed. Subcutaneous fat is removed from the skin flaps. The sample is placed between two pieces of plastic material with known thickness. In this way, **skin thickness** can be measured reliably by calipers with an accuracy of 0.1 mm. Perpendicular to the body axis two dumbbell shaped specimens with a width of 4 mm in the middle of the sample are punched out (Vogel 1969, 1970, 1989, 1993a). The samples are kept in Peteri dishes until testing at room temperature on filter paper soaked with saline solution. The specimens are fixed between the clamps of an INSTRON instrument a at gauge length of 30 mm. All measurements are carried out within at least 1 h. For long lasting test procedures, such as relaxation or cyclic loading, the samples are wrapped with saline soaked filter paper (Vogel 1976a, b 1989, 1993a, b).

Stress-strain curves are registered at an extension rate of 5 cm/min, showing a characteristic shape. During low strain values, there is a gradual increase of load; the curve has a concave part. The stress-strain curve ascends according to an exponential func-

tion (Vogel and Hilgner 1977). Afterwards an almost straight part is reached indicating the dependence on Hook's law. At this part the **ultimate modulus of elasticity** (Young's modulus) can be calculated (increase of load divided by the cross sectional area). Then some yielding of the curve occurs which ends in a sudden break of the specimen. This point indicates **ultimate strain** and **ultimate load**.

EVALUATION

From ultimate load divided by the cross sectional area (specimen width times original skin thickness measured at the beginning of the experiment), **tensile strength** can be calculated. The mean values of skin thickness, ultimate strain, ultimate load, tensile strength, and modulus of elasticity of treated animals are compared with controls using ANOVA and Student's *t*-test.

CRITICAL ASSESSMENT OF THE METHOD

The parameters: **skin thickness, ultimate strain, ultimate load, tensile strength, and modulus of elasticity** are influenced by many factors, such as hormones and desmotropic drugs. The most pronounced changes are seen after glucocorticosteroids, both after systemic and local application (Vogel 1969, 1970, 1974a). Several studies were performed on age dependence of mechanical parameters in rat skin. Ultimate load, tensile strength and modulus of elasticity show a very sharp increase during puberty, a maximum at 12 months and a slight decrease thereafter (Vogel et al. 1970; Vogel 1976b, 1978, 1983, 1988, 1989, 1993a). Studies on age dependence show a similar pattern for skin thickness, ultimate load, tensile strength, ultimate extension, modulus of elasticity, hysteresis, relaxation, creep behavior and biochemical data both in animals and men (Holzmann et al. 1971; Vogel 1987a, b).

Therefore, extrapolations from animal studies to behavior of human skin are justified.

However, due to the anatomical conditions (haired skin in animals) the biomechanics of the epidermis can be studied better in human experiments than in animals.

MODIFICATIONS OF THE METHOD

Measurement of skin thickness, ultimate strain, ultimate load, tensile strength, and modulus of elasticity can be used in the evaluation of topical corticosteroids (Schröder et al. 1974; Alpermann et al. 1982; Vogel and Petri 1985).

Similarly, Töpert et al. (1990) measured skin atrophy and tensile strength of skin after 30 days local administration of corticosteroids in rats.

Oxlund and Manthorpe (1982) found an increase of strength and a decrease of extensibility of skin strips after long-term glucocorticoid treatment of rats. In agreement with studies by Vogel (1974b, 1978), these results were explained by a change in collagen cross-linking pattern.

Jørgensen et al. (1989) found a dose-dependent increase of mechanical strength in intact rat skin after treatment with biosynthetic human growth hormone.

Andreassen et al. (1981) studied the biomechanical properties of skin in rats with streptozotocin-induced diabetes. An increased stiffness and strength was found: maximal stiffness was increased by 20% and the strain rate at maximum stress was decreased by 10%.

Oxlund et al. (1980) found that the stiffness of rat skin was increased in the early postpartum period. This increase was also found in adrenalectomized animals.

Foutz et al. (1992) studied the effects of freezing on mechanical properties of rat skin.

Among desmotropic drugs, *lathyrogenic* compounds, such as amino-acetonitrile, and *D-penicillamine* decrease ultimate load, tensile strength without major influence on skin thickness (Vogel 1971a, b, 1974a). A decrease of the strength of skin strips in rats after treatment with D-penicillamine was also found by Fiedrich et al. (1975) and by Oxlund et al. (1984).

A dose-dependent increase of tensile strength in skin after treatment with was found with **non-steroidal anti-inflammatory drugs** (Vogel 1977).

Strain rate influences the values of ultimate load, tensile strength and modulus of elasticity, but not the effect of age and of corticosteroids (Vogel 1972b). Changes in tensile strength are correlated with the content of insoluble collagen (Vogel 1974b).

Fry et al. (1964) prepared skin rings from the lower part of the leg in rats and studied the age-dependence of the mechanical properties.

Nimni et al. (1966) measured tensile strength of excised skin samples in rabbits during aging.

Pan et al. (1998) studied ultrasound, viscoelastic and mechanical properties in rabbit skin, including stress relaxation, creep and Young's modulus as a function of strain.

Lofstrom et al. (1973) described circadian variations of tensile strength in the skin of two inbred strains of mice.

The effect of radiation therapy on mechanical properties of skin was studied in mice by Hutton et al. (1977) and by Spittle et al. (1980).

Schneider et al. (1988) measured tensiometric properties in guinea pig skin from flaps of normal dor-

sal skin and after implantation of an ovoid **tissue expander** filled for four days with saline.

Belkoff et al. (1995) studied the mechanical properties of skin in pigs after subcutaneous implantation and inflation of silicone tissue expanders.

Mustoe et al. (1989) compared the effects of a conventional tissue expansion regimen of 6 weeks with an accelerated regimen of 2 weeks in a model in dogs and measured skin thickness, elasticity, creep and stress relaxation.

REFERENCES AND FURTHER READING

Alpermann HG Sandow J Vogel HG (1982) Tierexperimentelle Untersuchungen zur topischen und systemischen Wirksamkeit von Prednisolon-17-ethylcarbonat-21-propionat. Arzneim Forsch/Drug Res 32:633–638

Andreassen TT Seyer-Hansen K Oxlund H (1981) Biomechanical changes in connective tissue induced by experimental diabetes. Acta Endocrinol (Copenh) 98:432–436

Belkoff SM Naylor EC Walshaw R Lanigan E Colony L Haut RC (1995) Effect of subcutaneous expansion on the mechanical properties of porcine skin. J Surg Res 58:117–123

Foutz TL Stone EA Abrams CF Jr (1992) Effects of freezing on mechanical properties of rats skin. Am J Vet Res 53:788–792

Friedrich L Wuppermann D Zimmermann F (1975) Einfluss hoher Dosen von D-Penicillamin und Paramethason auf die mechanischen Eigenschaften des Bindegewebes der Ratte. Arch Dermatol Forsch 252:161–166

Fry P, Harkness MLR Harkness RD (1964) Mechanical properties of the collagenous framework of skin in rats of different ages. Am J Physiol 206:1425–1429

Holzmann H Korting GW Kobelt D Vogel HG (1971) Prüfung der mechanischen Eigenschaften von menschlicher Haut in Abhängigkeit von Alter und Geschlecht. Arch Klin Exp Derm 239:355–397

Hutton WC Burlin TE Ranu HS (1977) The effect of split dose radiations on the mechanical properties of the skin. Phys Med Biol 22:411–421

Jørgensen PH Andreassen TT Jørgensen KD (1989) Growth hormone influences collagen deposition and mechanical strength in intact rat skin. A dose-response study. Acta Endocrin (Copenh) 120:767–772

Lofstrom DE Felts WJL Halberg F (1973) Circadian variation in skin tensile strength of two inbred strains of mice. Intern J Chronobiology 1:259–267

Mustoe TA Bartell TH Garner WL (1989) Physical, biochemical, histologic, and biochemical effects of rapid versus conventional expansion. Plast Reconstr. Surg 83:787–691

Nimni ME de Guia E Bavetta LA (1966) Collagen, hexosamine and tensile strength of rabbit skin during aging. J Invest Dermatol 47:156–158

Oxlund H Manthorpe R (1982) The biochemical properties of tendon and skin as influences by long term glucocorticoid treatment and food restriction. Biorheology 19:631–641

Oxlund H Rundgren A Viidik A (1980) The influence of adrenalectomy on the biomechanical properties of collagenous structures of rats in the post-partum phase. Acta Obstet Gynecol Scand 59:453–458

Oxlund H Adreassen TT Junker P Jensen PA Lorenzen I (1984) Effect of D-penicillamine on the mechanical properties of aorta, muscle tendon and skin in rats. Atherosclerosis 52:243–252

Pan L, Zan L, Foster FS (1998) Ultrasonic and viscoelastic properties of skin under transverse mechanical stress *in vitro*. Ultrasound Med Biol 24:995–1007

Schneider MS Borkow JE Cruz IT Marangoni RD Shaffer J Grove D (1988) The tensiometric properties of expanded guinea pig skin. Plastic Reconstr Surg 81:398–405

Schröder HG Babej M Vogel HG (1974) Tierexperimentelle Untersuchungen mit dem lokal wirksamen 9-Fluor-16-methyl-17-desoxy-prednisolon. Arzneimittel-Forsch. 24:3–5

Spittle RF Ranu HS Hutton WC Challoner AV Burlin TE (1980) A comparison of different treatment regimens on the visual appearance and mechanical properties of mouse skin. Br J Radiol 53:697–702

Töpert M Olivar A Opitz D (1990) New developments in corticosteroid research. J Dermatol Treatment 1, Suppl 3:S5–S9

Vogel HG (1969) Zur Wirkung von Hormonen auf physikalische und chemische Eigenschaften des Binde- und Stützgewebes. Arzneim Forsch/Drug Res 19:1495–1503, 1732–1742, 1790–1801, 1981–1996

Vogel HG (1970) Beeinflussung der mechanischen Eigenschaften der Haut von Ratten durch Hormone. Arzneim Forsch/Drug Res 20:1849–1857

Vogel HG (1971) Antagonistic effect of aminoacetonitrile and prednisolone on mechanical properties of rat skin. Biochim Biophys Acta 252 3:580–585

Vogel HG (1972a) Effects of D-penicillamine and prednisolone on connective tissue in rats. Connective Tiss Res 1:283–289

Vogel HG (1972b) Influence of age, treatment with corticosteroids and strain rate on mechanical properties of rat skin. Biochim Biophys Acta 286:79–83

Vogel HG (1974a) Organ specificity of The effects of D-penicillamine and of lathyrogen (aminoacetonitrile) on mechanical properties of connective and supporting tissue. Arzneimittel-Forsch. 24:157–163

Vogel HG (1974b) Correlation between tensile strength and collagen content in rat skin. Effect of age and cortisol treatment. Connective Tiss Res 2:177–182

Vogel HG (1976a) Measurement of some viscoelastic properties of rat skin following repeated load. Connective Tiss Res 4:163–168

Vogel HG (1976b) Tensile strength, relaxation and mechanical recovery in rat skin as influenced by maturation and age. J Med 2:177–188

Vogel HG (1977) Mechanical and chemical properties of various connective tissue organs in rats as influenced by nonsteroidal antirheumatic drugs. Connective Tiss Res 5:91–95

Vogel HG (1978) Influence of maturation and age on mechanical and biochemical parameters of connective tissue of various organs in the rat. Connective Tiss Res 6:161–166

Vogel HG (1983) Effects of age on the biomechanical and biochemical properties of rat and human skin. J Soc Cosmet Chem 34:453–463

Vogel HG (1987a) Age dependence of mechanical and biochemical properties of human skin. Part I: Stress-strain experiments, skin thickness and biochemical analysis. Bioeng Skin 3:67–91

Vogel HG (1987b) Age dependence of mechanical and biochemical properties of human skin. Part II: Hysteresis, relaxation, creep and repeated strain experiments. Bioeng Skin 3:141–176

Vogel HG (1988) Age-dependent mechanical and biomechanical changes in the skin. Bioeng Skin 4:75–81

Vogel HG (1989) Mechanical properties of rat skin with aging. In: Balin AK Kligman AM (eds) Aging and the Skin. Raven Press, New York, pp 227–275

Vogel HG (1993a) Mechanical measurements in assessing aging. In: Frosch PJ Kligman AM (eds) Noninvasive Meth-

ods for the Quantification of Skin Functions. An Update on Methodology and Clinical Applications. Springer-Verlag Berlin, Heidelberg, New York, pp 145–180
Vogel HG (1993b) Strength and viscoelastic properties of anisotropic rat skin after treatment with desmotropic drugs. Skin Pharmacol 6:92–102
Vogel HG Hilgner W (1977) Analysis of the low part of stress-strain curves in rat skin. Influence of age and desmotropic drugs. Arch Derm Res 258:141–150
Vogel HG Petri W (1985) Comparison of various pharmaceutical preparations of prednicarbate after repeated topical administration to the skin of rats. Arzneim-Forsch/Drug Res 35:939–946
Vogel HG Kobelt D Korting GW Holzmann H (1970) Prüfung der Festigkeitseigenschaften von Rattenhaut in Abhängigkeit von Alter und Geschlecht. Arch klin exp Derm 239:296–305

P.13.2.1.2 Measurement of Mechanical Properties at Low Extension Degrees

PURPOSE AND RATIONALE

At low strain values, stress-strain curves of skin samples show a gradual increase of load, the curve has a concave part. The stress-strain curve ascends according to an exponential function (Vogel and Hilgner 1977).

PROCEDURE

Groups of at least 10 male Sprague-Dawley rats with an initial weight of 120 ± 5 g are treated subcutaneously or orally with test drugs or saline. The animals are sacrificed under anesthesia; the back skin is shaved and a flap of 5×5 cm removed. Subcutaneous fat is removed from the skin flaps. The sample is placed between two pieces of plastic material with known thickness to measure skin thickness by calipers. Perpendicular to the body axis two dumb-bell shaped specimens with a width of 4 mm in the middle of the sample are punched out (Vogel 1969, 1970, 1981, 1989, 1993). The specimens are fixed between the clamps of an INSTRON instrument at a gauge length of 30 mm. An extension rate of 5 cm/min is chosen. Tension is registered at 2, 5, 10, 20, 30, 40, 50, 60, 70, 80 and eventually 90% elongation. The registration is started with high sensitivity and switched to one tenth of the sensitivity in order to register the steep end of the curve.

EVALUATION

During registration with high sensitivity, the curve reaches an almost straight part. At this part, a tangent is drawn which is used for calculation of E_2. The distance from the start to the cross-point of this tangent with the baseline is measured and denominated as extension until the first rise (D). The angle between the tangent and the baseline is halved. At the cross-point with the stress-strain curve another tangent is drawn and used for calculation of E_1. At the second part of the curve registered with low sensitivity a further tangent is drawn for calculation of E_3, which is identical to the ultimate modulus of elasticity.

Mean values for $\boldsymbol{E_1}$, $\boldsymbol{E_2}$, $\boldsymbol{E_3}$, and ultimate stress of skin strips from treated animals are compared with controls using Student's t-test.

MODIFICATIONS OF THE METHOD

Belkoff and Haut (1991) developed a structural model to evaluate the changing microstructure of maturing rat skin.

Foutz et al. (1994) developed a phenomenological model to characterize the non-linear portion of stress-strain curves of rat skin.

REFERENCES AND FURTHER READING

Belkoff SM Haut RC (1991) A structural model to evaluate the changing microstructure of maturing rat skin. J Biomech 24:711–720
Foutz TL Abrams CF Jr, Stone EA Thrall DE (1994) Characterization of the non-linear loading curve of rat skin. Front Med Biol Eng 6:187–197
Vogel HG (1969) Zur Wirkung von Hormonen auf physikalische und chemische Eigenschaften des Binde- und Stützgewebes. Arzneim Forsch/Drug Res 19:1495–1503, 1732–1742, 1790–1801, 1981–1996
Vogel HG (1970) Beeinflussung der mechanischen Eigenschaften der Haut von Ratten durch Hormone. Arzneim Forsch/Drug Res 20:1849–1857
Vogel HG (1981) Mechanical properties of rat skin at high and low loads. Influence of age and desmotropic drugs. In: Marks R Payne PA (eds) Bioengineering and the Skin. Proceedings of the European Soc. for Dermatological Research Symposium, held at the Welsh National School of Medicine, Cardiff, 19–21 July 1979. MTP Press Limited 1981, pp 79–101
Vogel HG (1989) Mechanical properties of rat skin with aging. In: Balin AK Kligman AM (eds) Aging and the Skin. Raven Press, New York, pp 227–275
Vogel HG (1993) Mechanical measurements in assessing aging. In: Frosch PJ Kligman AM (eds) Noninvasive Methods for the Quantification of Skin Functions. An Update on Methodology and Clinical Applications. Springer-Verlag Berlin, Heidelberg, New York, pp 145–180
Vogel HG Hilgner W (1977) Analysis of the low part of stress-strain curves in rat skin. Influence of age and desmotropic drugs. Arch Derm Res 258:141–150

P.13.2.1.3 Step Phenomenon

PURPOSE AND RATIONALE

Analysis of the low parts of the stress-strain curve revealed a "step"-phenomenon (Vogel and Hilgner 1977, 1979a, b; Vogel 1988). If samples obtained perpendicular to the body axis are extended, a gradual increase of load is observed at low degrees of extension,

which is suddenly interrupted by a decrease of the registered curve. Then the curve increases again, being interrupted by a second or third step.

PROCEDURE

Groups of 10 male Sprague-Dawley rats with an initial weight of 120 ± 10 g are treated subcutaneously or orally with test drugs or saline. The animals are sacrificed under anesthesia, the back skin is shaved and a flap of 5 × 5 cm removed. Subcutaneous fat is removed from the skin flaps. The sample is placed between two pieces of plastic material with known thickness to measure skin thickness by calipers. Perpendicular to the body axis two dumb-bell shaped specimens with a width of 4 mm in the middle of the sample are punched out. The ends of the skin strips are fixed in the clamps of an INSTRON instrument resulting in a gauge length of 30 mm. The specimen is stretched with a strain rate of 50 mm/min. The first part of the stress-strain curve is registered with 10 times higher amplification than the second part. The steps are evaluated as follows.

EVALUATION

Tangents to the curves are drawn before and after each step. Then a vertical line is drawn in the middle of the step. The distance between the cross-points of this line with the tangents is measured and calculated as stress loss (ΔS). Furthermore, in the middle of each vertical line a horizontal line is drawn. The distance between the cross-point with the curves is measured and calculated as elongation due to the step (ΔE). Total stress loss is calculated by adding all values of ΔS and dividing by the number of specimens.

If this parameter is considered not only by itself but also in connection with tensile strength it can be calculated as percentage of ultimate stress (= % of breaking strength). In addition, the stress value, which would have been achieved without the step (= value *S*) and the elongation at which the step occurred (= value *E*) is registered. If stress loss at one step is multiplied with the elongation at this point, an indication of work loss is achieved (value ΔS times *E*). Taking into account the corresponding parameters indicating total work input (ultimate stress times ultimate strain), the relative work loss can be calculated.

Furthermore, elongation gain due to the steps is calculated by adding all values of ΔE and by dividing by the number of specimens.

Mean values of these parameters from treated animals are compared with controls using Student's *t*-test.

CRITICAL ASSESSMENT OF THE METHOD

The step phenomenon can be explained by the different orientation of collagen fibers in the dermis and by the presence of a muscular layer in rat skin. The muscular fibers are in a direction longitudinal to the body axis. If samples are obtained perpendicular to the body axis, the muscle bundles are cut transversally. In further studies the muscle layer was removed in one specimen and compared with a control still having the muscle layer. Investigation of the directional variation showed that the step phenomenon is mainly due to the muscular layer oriented longitudinal to the body axis and the connective tissue between the muscle bundles, whereas the anisotropic behavior of extensibility and ultimate strain is caused by the directional variation of the collagenous bundles in the dermis.

MODIFICATIONS OF THE METHOD

The step phenomenon could also be found in creep experiments (Vogel and Hilgner 1979b).

REFERENCES AND FURTHER READING

Vogel HG (1988) Further studies on directional variations and the "step-phenomenon" in rat skin depending on age. Bioeng. Skin 4:297–309

Vogel HG Hilgner W (1977) Analysis of the low part of stress-strain curves in rat skin. Influence of age and desmotropic drugs. Arch Derm Res 258:141–150

Vogel HG Hilgner W (1979a) The "step phenomenon" as observed in animal skin. J Biomechanics 12:75–81

Vogel HG Hilgner W (1979b) Influence of age and of desmotropic drugs on the step phenomenon observed in rat skin. Arch Dermatol Res 264:225–241

P.13.2.1.4 Anisotropy of Skin

PURPOSE AND RATIONALE

As is the case with human skin indicated by Langer's lines (Langer 1861; Gibson et al. 1969; Wright 1971; Stark et al. 1977; Daly 1982), the skin of rats exhibits **directional differences** (Hussein 1972, 1973; Vogel and Hilgner 1979a, b; Vogel 1981, 1983a, 1985a, b, 1988; Belkoff and Haut 1991). Stress-strain curves of rat skin showed a different shape if excised perpendicularly or longitudinally to the body axis. Directional variations of mechanical parameters in rat skin were studied depending on maturation and age (Vogel 1981).

PROCEDURE

Male Sprague-Dawley rats are used at different age groups from 1 week up to 24 months. Young animals (1, 2 and 3 weeks) are delivered with their mothers from the breeder. Each age group is randomly divided

into 2 blocks which are assigned as "perpendicular to body axis" or "longitudinal to body axis". The animals are sacrificed under anesthesia, the back skin is shaved and a flap of 5×5 cm removed. Subcutaneous fat is removed from the skin flaps. The sample is placed between two pieces of plastic material of known thickness to measure skin thickness by calipers. From each rat two dumb-bell shaped specimens with a width of 4 mm in the middle of the sample are punched out either perpendicular or longitudinal to the body axis, allowing a gauge length between the clamps of an INSTRON instrument of 30 mm. Stress-strain curves are measured at a strain rate of 50 mm/min, whereby the first part of the curve is registered with 10-fold amplification. Besides ultimate values, the extension is measured at given load interval for each curve:

0. 05, 0. 1, 0. 2, 0. 5, 1, 2, 10, 20, and 50 N

and at given stresses:

0. 01, 0. 02, 0. 05, 0. 1, 0. 5, 1, 2, 5, and 10 N/cm^2.

EVALUATION

Each parameter is measured longitudinal and perpendicular to the body axis. The mean values are statistically compared within each age group using Student's *t*-test.

At low loads, extension is higher in the longitudinal than in the perpendicular direction. The situation is reversed at medium and high stress values. Ultimate extension shows remarkable differences between longitudinal and perpendicular samples. Specimens obtained perpendicular to the body axis showed an increase during maturation, a maximum at 4 months of age and a decrease during further aging. The behavior of samples obtained longitudinal to the body axis was quite different. After an initial rise a maximum was found at 3 weeks. Afterwards a slight decrease was noted. Between 1 and 4 weeks all values of ultimate extension were significantly higher in samples punched out longitudinally to the body axis; between 4 and 12 months they were considerably lower (Vogel 1981).

CRITICAL ASSESSMENT OF THE METHOD

The data indicate the importance of directional variations in all studies of biomechanics of skin.

MODIFICATIONS OF THE METHOD

Directional variations of rat skin were also found in hysteresis experiments (Vogel 1983a) and in relaxation experiments (Vogel 1985a).

Directional variations of the stress-strain curves were also described in the skin of tight-skin mutant mice (Menton et al. 1978).

REFERENCES AND FURTHER READING

Belkoff SM Haut RC (1991) A structural model used to evaluate the changing microstructure of maturing rat skin. J Biomech 24:711–720

Daly CH (1982) Biomechanical properties of dermis. J Invest Dermatol 79:17s–20s

Gibson T Stark H Evans JH (1969) Directional variation in extensibility of human skin *in vivo*. J Biomechanics 2:201–204

Hussein MAF (1972) The orientation of connective tissue fibers in rat skin. Acta Anat 82:549–564

Hussein MAF (1973) Skin cleavage lines in the rat. Eur Surg Res 5:73–79

Langer K (1861) Zur Anatomie und Physiologie der Haut. I. Über die Spaltbarkeit der Cutis. Sitzungsberichte der Akademie in Wien 44:19–46

Menton DN Hess RA Lichtenstein JR Eisen AZ (1978) The structure and tensile properties of the skin of tight-skin (Tsk) mutant mice. J Invest Dermatol 70:4–10

Stark HL Strath PD Eng C, Mech MI Aust MIE (1977) Directional variations in the extensibility of human skin. Br J Plastic Surg 30:195–114

Vogel HG (1981) Directional variations of mechanical parameters in rat skin depending on maturation and age. J Invest Dermatol 76:493–497

Vogel HG (1983a) Effects of age on the biomechanical and biochemical properties of rat and human skin. J Soc Cosmet Chem 34:453–463

Vogel HG (1983b) Age dependence of viscoelastic properties in rat skin. Directional variations in stress-strain and hysteresis experiments. Bioengin Skin 4:136–155

Vogel HG (1985a) Age dependence of viscoelastic properties in rat skin; directional variations in relaxation experiments. Bioeng Skin 1:157–174

Vogel HG (1985b) Repeated relaxation and determination of the isorheological point in skin strips of rats as influenced by maturation and ageing. Bioeng Skin 1:321–335

Vogel HG (1988) Further studies on directional variations and the "step-phenomenon" in rat skin depending on age. Bioeng. Skin 4:297–309

Vogel HG Hilgner W (1979a) The "step phenomenon" as observed in animal skin. J Biomechanics 12:75–81

Vogel HG Hilgner W (1979b) Influence of age and of desmotropic drugs on the step phenomenon observed in rat skin. Arch Dermatol Res 264:225–241

Wright V (1971) Elasticity and deformation of skin. In: Elden HR (ed) Biophysical Properties of Skin. Wiley Interscience, New York, pp 437–449

P.13.2.1.5 Relaxation Phenomenon

PURPOSE AND RATIONALE

In the relaxation experiment the viscous properties of rat skin are measured (Vogel 1973, 1976a, b, 1983, 1985, 1993a, b).

PROCEDURE

Groups of 10 male Sprague-Dawley rats with an initial weight of 120 ± 10 g are treated subcutaneously

or orally with test drugs or saline. The animals are sacrificed in anesthesia, the back skin is shaved and a flap of 5 × 5 cm removed. Subcutaneous fat is removed from the skin flaps. The sample is placed between two pieces of plastic material with known thickness to measure skin thickness by calipers. Perpendicular to the body axis two dumb-bell shaped specimens with a width of 4 mm in the middle of the sample are punched out.

Skin strips are fastened between the clamps of an INSTRON instrument and extended with the high strain rate of 1000 mm/min up to 20% extension. This extension is kept constant for 5 min. The chart speed is initially 1000 mm/min, then 10 mm/min. In this way, the **initial tension** and the **stress values at 0.001, 0.01, 0.1, 1, and 5 min** can be measured. Due to relaxation, the stress values drop down roughly with the logarithm of time.

Furthermore, the **residual stress** after 5 min relaxation period is measured and calculated as percentage of the original stress. After 5 min the sample is returned to 90% of the original strain, for example, from 20% to 18%. The stress following such unloading is recorded and again calculated as percentage of the original stress. Immediately after unloading, the measured stress values rise again spontaneously, which is called **mechanical recovery**. Mechanical recovery is calculated as percentage of initial tension and as percentage of stress after unloading. The relaxation experiment is repeated with increasing degrees of extension of 40%, 60%, 80% and eventually 100% until the specimen breaks.

EVALUATION

For each sample, the relaxation is calculated according to the formula

$$\sigma(t) = A_1 + A_2 \times \log t$$

resulting in two constants (A_1 and A_2) for each sample whereby A_1 is the stress at $t = 0$, and A_2 the slope of the relaxation curve.

The **ratio between the constants A_1 and A_2** has to be considered as the most characteristic parameter of the relaxation experiment.

The means of these parameters are compared between treated animals and controls using Student's *t*-test.

MODIFICATIONS OF THE METHOD

In studies of age dependence in rats skin, a definitive decrease of the **ratio A_2/A_1** was found at 40% and 60% extension degrees indicating a decrease of plasticity with age. Mechanical recovery, as an indicator of secondary elasticity, was better in old animals at medium extension degrees than in young individuals. Stress relaxation was decreased after corticosteroids and increased after thyroid hormones and D-penicillamine (Vogel 1973, 1993a, b).

Purslow et al. (1998) suggested that relaxation processes within the collagen fibers or at the fiber-matrix interface might be responsible for the viscoelastic behavior of skin.

REFERENCES AND FURTHER READING

Purslow PP Wess TJ Hukins DW (1998) Collagen orientation and molecular spacing during creep and stress-relaxation in soft connective tissue. J Exp Biol 201:135–142

Vogel HG (1973) Stress relaxation in rat skin after treatment with hormones. J Med 4:19–27

Vogel HG (1976a) Measurement of some viscoelastic properties of rat skin following repeated load. Connective Tiss Res 4:163–168

Vogel HG (1976b) Tensile strength, relaxation and mechanical recovery in rat skin as influenced by maturation and age. J Medicine 7:177–188

Vogel HG (1983) Effects of age on the biomechanical and biochemical properties of rat and human skin. J Soc Cosmet Chem 34:453–463

Vogel HG (1985) Age dependence of viscoelastic properties in rat skin; directional variations in relaxation experiments. Bioeng Skin 1:157–174

Vogel HG (1993a) Mechanical measurements in assessing aging. In: Frosch PJ Kligman AM (eds) Noninvasive Methods for the Quantification of Skin Functions. An Update on Methodology and Clinical Applications. Springer-Verlag Berlin, Heidelberg, New York, pp 145–180

Vogel HG (1993b) Strength and viscoelastic properties of anisotropic rat skin after treatment with desmotropic drugs. Skin Pharmacol 6:92–102

P.13.2.1.6 Hysteresis Experiments

PURPOSE AND RATIONALE

In the hysteresis experiment not only the elastic but also the viscous properties of skin are measured (Vogel 1978, 1983).

PROCEDURE

Groups of 10 male Sprague-Dawley rats with an initial weight of 120 ± 10 g are treated for 10 days subcutaneously or orally with test drugs or saline. The animals are sacrificed under anesthesia, the back skin is shaved and a flap of 5 × 5 cm removed. Subcutaneous fat is removed from the skin flaps. The sample is placed between two pieces of plastic material of known thickness to measure skin thickness by calipers. Perpendicular to the body axis two dumb-bell shaped specimens

with a width of 4 mm in the middle of the sample are punched out.

Using the INSTRON instrument, the samples are stretched up to a given extension degree (e. g., 20%) with an extension rate of 20 mm/min. When the given extension is achieved the crosshead is immediately moved back to the starting position with the same velocity. From the upward curve the stress and the modulus of elasticity at the end of the loading phase at the given strain indicating the elastic properties can be measured. When the sample is unstretched the unloading curve shows a different pattern reaching the baseline much earlier than the curve left it during the upward phase. From this point the **residual extension** can be measured. Immediately after the first hysteresis cycle, the experiment is repeated up to an extension degree of 30%, than to 40% and 50% and finally up to 60%.

EVALUATION

By planimetry of the area below the upward curve the **energy input** and of the area between the hysteresis loop the **energy dissipation** can be calculated as well as the **ratio between energy dissipation and energy input** at each hysteresis cycle indicating the viscous properties. Stress and modulus of elasticity at the end of the hysteresis loop, energy input, energy dissipation and the ratio between energy dissipation and energy input at each hysteresis cycle are compared between treated animals and controls using Student's *t*-test.

MODIFICATIONS OF THE METHOD

In rat skin, a maximum of the ratio between energy dissipation and energy input was found at 30% to 40% extension. This ratio is influenced by age. At low extension degrees there was an increase with age, whereas at high extension degrees an age-dependent decrease was noted. The ratio dissipation/input was slightly decreased by prednisolone, but definitively increased by D-penicillamine (Vogel 1993b).

REFERENCES AND FURTHER READING

Vogel HG (1976a) Measurement of some viscoelastic properties of rat skin following repeated load. Connective Tiss Res 4:163–168

Vogel HG (1978) Age dependence of mechanical parameters in rat skin following repeated strain. Akt. Gerontol. 8:601–618

Vogel HG (1983) Age dependence of viscoelastic properties in rat skin. Directional variations in stress-strain and hysteresis experiments. Bioeng Skin 4:136–155

Vogel HG (1993) Strength and viscoelastic properties of anisotropic rat skin after treatment with desmotropic drugs. Skin Pharmacol 6:92–102

P.13.2.1.7 Isorheological Point

PURPOSE AND RATIONALE

Buss et al. (1976) demonstrated the determination of the isorheological point to be a valuable parameter for the mechanics of connective tissue. This method has been modified and elaborated for the skin strips of rats (Vogel 1984, 1985, 1987).

PROCEDURE

Groups of 20 male Sprague-Dawley rats with an initial weight of 120 ± 10 g are treated subcutaneously or orally with test drugs or saline. The groups are divided randomly into groups of 10 animals for examination of skin samples either perpendicular or longitudinal to the body axis. The animals are sacrificed under anesthesia, the back skin is shaved and a flap of 5×5 cm removed. Subcutaneous fat is removed from the skin flaps. The sample is placed between two pieces of plastic material with known thickness to measure skin thickness by calipers. Two dumb-bell shaped specimens with a width of 4 mm in the middle of the sample are punched out.

Being fastened between the clamps of an INSTRON instrument, the specimen is expanded rapidly up to 2 N and the corresponding strain is measured. Keeping this strain constant, the load decay (relaxation) is measured for 5 min. Then the sample is again loaded up to 2 N and a second relaxation period of 5 min is evaluated. In the third cycle, the sample is unloaded to 50% of the load observed after the 5-min relaxation period in the second cycle. The phenomenon of **mechanical recovery** is observed. With the crosshead driven up and down, the point is sought where neither immediate relaxation nor mechanical recovery can be observed. The load and strain at this point define the **isorheological point**, which is characterized by the fact that under isometric conditions, the measured load is constant for several minutes. Increasing and decreasing the load by 10% produces a saw-tooth-shaped curve from which the **modulus of elasticity at the isorheological point** can be calculated. The same procedure is performed at higher initial loads such as 10 N and 50 N. The product of percentage of strain multiplied by stress at the isorheological point indicates energy density.

EVALUATION

The means of these parameters are compared between treated animals and controls using Student's *t*-test.

The values showed a decrease during maturation, a minimum at 12 months and an increase during senescence. In studies with desmotropic compounds, the decreased viscosity after treatment with prednisolone acetate was more evident at the isorheological points than at the ultimate values. Likewise, the higher extensibility after treatment with D-penicillamine was indicated more clearly by the isorheological points than by the ultimate strain.

REFERENCES AND FURTHER READING

Buss V Lippert H Zech M Arnold G (1976) Zur Biomechanik menschlicher Sehnen: Zusammenhänge von Relaxation und Spannungsrückgewinn. Arch Orthop Unfall-Chir 86:169–182

Vogel HG (1984) Messung der Relaxation und des isorheologischen Punkts an Hautstreifen von Ratten. Zeitschr Rheumatol 43, Suppl. 1:46–47

Vogel HG (1985) Repeated relaxation and determination of the isorheological point in skin strips of rats as influenced by maturation and ageing. Bioeng Skin 1:321–335

Vogel GH (1987) Repeated loading followed by relaxation and isorheological behaviour of rat skin after treatment with desmotropic drugs. Bioeng. Skin 3:255–269 (1987)

P.13.2.1.8 Creep Experiments

PURPOSE AND RATIONALE

In creep experiments, viscous behavior of skin is studied. The strain under constant load is also denominated as retardation behavior. (Vogel 1977, 1987).

PROCEDURE

Groups of 10 male Sprague-Dawley rats with an initial weight of 120 ± 10 g are treated for 10 days subcutaneously or orally with test drugs or saline. The animals are sacrificed under anesthesia, the back skin is shaved and a flap of 5×5 cm removed. The sample is placed between two pieces of plastic material with known thickness to measure skin thickness by calipers. Perpendicular to the body axis three dumb-bell shaped specimens with a width of 4 mm in the middle of the sample are punched out.

In a special apparatus, skin specimens are suddenly loaded with 100, 200 or 500 g and the extension degree measured. An immediate extension occurs which is followed by a slow and almost continuous creep being measured as **ultimate extension rate**. Furthermore, **extension achieved after 1 h** is registered.

EVALUATION

The means of these parameters are compared between treated animals and controls using Student's *t*-test.

An age-dependent decrease of these parameters was found in rat and human specimens indicating a decrease of viscosity or plasticity with maturation and age. Ultimate extension rate was decreased by prednisolone and increased by D-penicillamine.

REFERENCES AND FURTHER READING

Vogel HG (1977) Strain of rat skin at constant load (creep experiments). Influence of age and desmotropic agents. Gerontology 23:77–86

Vogel HG (1987) Age dependence of mechanical and biochemical properties of human skin. Part II: Hysteresis, relaxation, creep and repeated strain experiments. Bioeng Skin 3:141–176

P.13.2.1.9 Repeated Strain

PURPOSE AND RATIONALE

By the method of using repeated strain, mainly the viscous properties of skin are measured (Vogel and Hilgner 1978; Vogel 1987).

PROCEDURE

Groups of 10 male Sprague-Dawley rats with an initial weight of 120 ± 10 g are treated for 10 days subcutaneously or orally with test drugs or saline. The animals are sacrificed under anesthesia, the back skin is shaved and a flap of 5×5 cm removed. The sample is placed between two pieces of plastic material with known thickness to measure skin thickness by calipers. Perpendicular to the body axis two dumb-bell shaped specimens with a width of 4 mm in the middle of the sample are punched out.

Skin specimens are fastened between the clamps of an INSTRON instrument, extended with a strain rate of 100 mm/min up to 20% extension and immediately unloaded followed by further cycles with the same strain rate and extension degree. The peak of the second cycle is considerably lower than the first, followed by a further decrease in the next cycles. The number of cycles is counted until the stress value is only one half of that of the first cycle. Immediately afterwards, the degree of extension is increased to 30%. Again the number of cycles is counted until the stress value was only one half of that of the first cycle. In this way, the **number of cycles indicating the half-life of tension** due to relaxation is counted at each step of 20%, 30%, 40%, 50%, 50%, 70%, 80%, 90% and eventually 100% extension. The number of cycles decreased from the first step (20%) to the third step (40%) and increased continuously until the last step. This increase was almost an exponential function of the number of steps.

EVALUATION

The means of the number of cycles indicating the half-life of tension due to relaxation at each step are compared between treated animals and controls using Student's *t*-test.

The parameters measured with this method are influenced by several factors: An increase was noted from an age of 1 month up to 24 months. The values were decreased by D-penicillamine and increased by prednisolone treatment. Again this method showed that plasticity of skin is decreased by age and by corticosteroids and increased by D-penicillamine.

MODIFICATIONS OF THE METHOD

Lafrance et al. (1998) tested mechanical properties of human skin equivalents submitted to cyclic forces. The *in vitro* production of disk-shaped (25.4 mm diameter) skin equivalents was based on the culture, under submerged conditions, of keratinocytes seeded on anchorage-based dermal equivalents, a human type I+III collagen gel supplemented with elastin and glycosaminoglycans. The specimens were submitted to quasi-static ramp-deflection cycles induced by means of an actuated hemispherical head. The effects of repeated loading were studied by monitoring the indentation load versus deflection and the relaxation of load over 1000 s.

REFERENCES AND FURTHER READING

Lafrance H Yahia L'H Germain L Auger FA (1998) Mechanical properties of human skin equivalents submitted to cyclic forces. Skin Res Technol 4:228–236

Vogel HG (1987) Age dependence of mechanical and biochemical properties of human skin. Part II: Hysteresis, relaxation, creep and repeated strain experiments. Bioeng Skin 3:141–176

Vogel HG Hilgner W (1978) Viscoelastic behaviour of rat skin after repeated and stepwise increased strain. Bioeng Skin 1:22–33

P.13.2.1.10 Correlation Between Biomechanical and Biochemical Parameters

PURPOSE AND RATIONALE

Mechanical parameters of skin, such as skin thickness, ultimate load, tensile strength, ultimate strain and ultimate load of elasticity as well as hysteresis, relaxation, isorheological point, creep behavior and values after repeated strain are clearly dependent on maturation and age. They are also influenced by drugs, such as corticosteroids and desmotropic compounds. Therefore, it was of interest to elucidate the correlations of these parameters with biochemical values such as collagen content, collagen fraction, glycosaminoglycans, and elastin (Vogel 1973, 1976, 1980, 1987, 1988).

PROCEDURE

Mechanical Parameters

Male Sprague Dawley rats are sacrificed under anesthesia; the back skin is shaved and a flap of 5 × 5 cm removed. Subcutaneous fat is removed from the skin flaps. The sample is placed between two pieces of plastic material with known thickness to measure skin thickness by calipers. Perpendicular to the body axis two dumbbell-shaped specimens with a width of 4 mm in the middle of the sample are punched out. The specimens are fixed between the clamps of an INSTRON instrument at a gauge length of 30 mm. An extension rate of 5 cm/min is chosen. Tension is recorded at 2, 5, 10, 20, 30, 40, 50, 60, 70, 80 and eventually 90% elongation. The recording starts with high sensitivity and is switched to one-tenth of the sensitivity in order to record the steep end of the curve. Stress-strain curves are determined at an extension rate of 5 cm/min, showing a characteristic shape. During low strain values, there is a gradual increase of load; the curve has a concave part. The stress-strain curve ascends according to an exponential function (Vogel and Hilgner 1977). Afterwards an almost straight part is reached indicating the dependence on Hook's law. At this part the ultimate modulus of elasticity (Young's modulus) can be calculated (increase of load divided by the cross-sectional area). Then some yielding of the curve occurs, which ends in a sudden break of the specimen. This point indicates ultimate strain and ultimate load.

Biochemical Parameters

Total collagen content was measured as mg hydroxyproline/g wet weight of skin according to the method of Stegemann (1958). Collagen was further analyzed according to solubility at 4°C.

Fraction I	soluble in 0.15 mol NaCl solution
Fraction II	soluble in 0.5 mol NaCl solution
Fraction II	soluble in citrate buffer solution
Fraction IV	insoluble.

Glycosaminoglycan content and the fractions hyaluronic acid, chondroitin sulfates and heparan sulfate were determined by column chromatography. The results were expressed as glucuronic acid per g wet weight. Glucuronic acid was determined according to Bitter and Muir (1960).

Elastin was determined according to Naum and Morgan (1973). The specimen was homogenized in deep-frozen state. A sample of 50 mg was extracted with 0.15 M NaCl solution, later on twice by 5 M guanidine hydrochloride solution at 25°C. After hydrolyzation in an autoclave at 1 atm excess pressure for 45 min, the residue was digested with 0.01% elastase solution (Elastase, Merck, Darmstadt) at 37°C for 2 h. Bovine ligamentum nuchae was used as standard. Elastin was determined in the supernatant as protein according to Lowry et al. (1951). Results were expressed as mg elastin per g wet weight.

EVALUATION

A clear correlation between tensile strength and the content of insoluble collagen was found in all studies for age dependence and the effect of corticosteroids and desmotropic compounds such as D-penicillamine (correlation coefficient 0.9901; Vogel 1974). The values of glycosaminoglycans and of elastin showed age-related dependence and changes after drug treatment, but no significant correlation with the mechanical parameters.

MODIFICATIONS OF THE METHOD

Oxlund et al. (1988) studied the role of elastin in the mechanical properties of rat skin. They concluded that elastin plays a role in the mechanical behavior of rat skin at small stress values and small deformations.

REFERENCES AND FURTHER READING

Bitter T Muir H (1960) A modified uronic acid carbazole raction. Anal Biochem 4:330–334

Lowry OH Rosenbrough NJ Farr AL Randall RJ (1951) Protein measurement with the Folin phenol reagent. J Biol Chem 193:265

Naum Y Morgan TE (1973) A microassay for elastin. Anal Biochem 53:392–396

Oxlund H Manschot J Viidik A (1988) The role of elastin in the mechanical properties of skin. J Biomech 21:213–218

Stegemann H (1958) Mikrobestimmung von Hydroxyprolin mit Chloramin-T und p-Dimethylaminobenzaldehyd. Hoppe-Seylers Z Physil Chemie311:41–45

Vogel HG (1973) Attempts to correlate tensile strength of skin to solubility of collagen Proceedings of the Workshop Conference HOECHST Schloss Reisensburg 21–22 April 1972. International Congress Series No. 264, EXCERPTA MEDICA Amsterdam (1973)

Vogel HG (1974) Correlation between tensile strength and collagen content in rat skin. Effect of age and cortisol treatment. Connect Tissu Res 2:177–182

Vogel HG (1976) Altersabhängige Veränderungen der mechanischen und biochemischen Eigenschaften der Cutis bei Ratten. Aktuelle Gerontologie 6:477–487

Vogel HG (1980) Influence of maturation and aging on mechanical and biochemical properties of connective tissue in rats. Mech Ageing Dev 14:283–292

Vogel HG (1987) Age dependence of mechanical and biochemical properties of human skin Part I: Stress-strain experiments, skin thickness and biochemical analysis Bioeng. Skin 3:67–91

Vogel HG (1988) Age-dependent mechanical and biomechanical changes in the skin Bioeng. Skin 4:75–81

Vogel HG Hilgner W (1977) Analysis of the low part of stress-strain curves in rat skin. Influence of age and desmotropic drugs. Arch Dermatol Res 258:141–150

P.13.2.2 Thermocontraction

PURPOSE AND RATIONALE

If collagenous material such as skin or tendon is heated in a water bath, thermocontraction occurs. This phenomenon was already described by Wöhlisch (Wöhlisch and du Mesnil de Rochemont 1927; Wöhlisch 1932). Verzár and other authors used the phenomenon of thermocontraction of tendons and skin strips extensively to study the ageing process (Verzár 1955, 1957; Lerch 1951; Rasmussen et al. 1964; Boros-Farkas and Everitt 1967; Viidik 1969, 1977, 1979; Vogel 1969). With increasing temperature, a sudden increase of isometric force is found, which is followed by a decrease. To evaluate this phenomenon, either the **shrinkage temperature** or the **stress at and above the shrinkage temperature** can be measured. Furthermore, the decrease of sample strength can be measured.

PROCEDURE

Groups of 10 male Sprague-Dawley rats with an initial weight of 120 ± 10 g are treated for 10 days subcutaneously or orally with test drugs or saline. The animals are sacrificed under anesthesia, the back skin is shaved and a flap of 5×5 cm removed. The sample is placed between two pieces of plastic material with known thickness to measure skin thickness by calipers. Perpendicular to the body axis two dumb-bell shaped specimens with a width of 4 mm in the middle of the sample are punched out.

The samples are attached to the clamps of a specifically modified INSTRON instrument which allows the submersion of the test specimen into a beaker filled with 0.9% saline solution. This solution is kept at 58°C or 60°C by a thermostat. Immediately after immersion, the exerted tension is measured and the **maximum of tension** and **time until maximal tension** are recorded.

EVALUATION

The means of these parameters are compared between treated animals and controls using Student's *t*-test.

MODIFICATIONS OF THE METHOD

Joseph and Bose (1962) tested the shrinkage temperature of skin in newborn rats, at 10 months and 2 years and found an increase from 51.2°C to 61.1°C.

Alain et al. (1977, 1980) tested pieces of dorsal skin of rats. Temperature of maximum tension was decreased from birth to 1 month, and then very slowly increased with age. A rapid relaxation was observed in young rats and in non-senescent adult rats.

Rundgren (1976) found changes of thermal contractility in skin of young and old female rats, and also changes due to repeated pregnancies.

Blackett and Hall (1980) found an increase of thermal shrinkage temperature in two strains of mice during the aging period.

Danielsen (1981) determined thermal stability measured as area shrinkage without tension during heating for membranes of collagen fibrils, reconstituted from solutions of highly purified rat skin collagen.

Allain et al. (1980) built a device, which measured not only hydrothermal shrinking but also swelling in rat skin.

Le Lous et al. (1982a, b, 1983), Flandin et al. (1984) applied the technique of differential scanning calorimetry to evaluate the denaturation process of collagen in rat skin.

REFERENCES AND FURTHER READING

Allain JC Bazin S le Lous M Delaunay A (1977) Pathologie expérimentale – Variations de la contraction hydrothermique de la peau du rat en fonction de l'âge des animaux. C R Acad Sci, Paris 284:1131–1134

Allain JC Le Lous M Cohen-Solal L Bazin S Maroteaux P (1980) Isometric tensions developed during the hydrothermal swelling of rat skin. Connective Tiss Res 7:127–133

Blackett AD Hall DA (1980) The action of vitamin E on the ageing of connective tissues in the mouse. Mech Ageing Dev 14:305–316

Boros-Farkas M Everitt AV (1967) Comparative studies of age tests on collagen fibers. Gerontologia 13:37–49

Danielsen CC (1981) Thermal stability of reconstituted collagen fibrils. Shrinkage characteristics upon *in vitro* maturation. Mech Ageing Dev 15:269–278

Flandin F Buffevant C Herbage D (1984) A differential scanning calorimetry analysis of the age-related changes in the thermal stability of rat skin collagen. Biochim Biophys Acta 791:205–211

Joseph KT Bose SM (1962) Influence of biological ageing on the stability of skin collagen in albino rats. In: Ramanathan N (ed) Collagen. pp 371–393, Interscience, New York

Lerch H (1951) Über Wärmeschrumpfungen des Kollagengewebes. Gegenbaur's morphol Jahrb 90:206–220

Le Lous M Flandin F Herbage D Allain JC (1982a) Influence of collagen denaturation on the chemorheological properties of skin, assessed by differential scanning calorimetry and hydrothermal isometric tension measurement. Biochim Biophys Acta 717:295

Le Lous M Allain JC Cohen-Solal L Maroteaux P (1982b) The rate of collagen maturation in rat and human skin. Connective Tiss Res 9:253–262

Le Lous M Allain JC Cohen-Solal L Maroteaux P (1983) Hydrothermal isometric tension curves from different connective tissues. Role of collagen genetic types and noncollagenous components. Connective Tiss Res 11:199–206

Rasmussen DM Wakim KG Winkelmann RK (1964) Effect of aging on human dermis: studies of thermal shrinkage and tension. In: Montagna W (ed) Advances in Biology of Skin. Vol 6:151–162

Rundgren A (1976) Age changes of connective tissue in the rat as influenced by repeated pregnancies. Akt Gerontol 6:15–18

Verzár F (1955) Veränderungen der thermoelastischen Kontraktion von Haut und Nerv bei alternden Tieren. Experientia (Basel) 11:230–231

Verzár F (1957) The ageing of connective tissue. Gerontologica 1:363–378

Viidik A (1969) The aging of collagen as reflected in its physical properties. In: Engel A Larsson T (eds) Aging of Connective and Skeletal Tissue. Thule International Symposia, Nordiska Bokhandels Förlag, Stockholm, pp 125–152

Viidik A (1977) Thermal contraction – Relaxation and dissolution of rat tail tendon collagen in different ages. Akt Gerontol 7:493–498

Viidik A (1979) Connective tissues – possible implications of the temporal changes for the aging process. Mech Ageing Dev 9:267–285

Vogel HG (1969) Zur Wirkung von Hormonen auf physikalische und chemische Eigenschaften des Binde- und Stützgewebes. Arzneim Forsch/Drug Res 19:1495–1503, 1732–1742, 1790–1801, 1981–1996

Wöhlisch E (1932) Die thermischen Eigenschaften der faserig strukturierten Gebilde des tierischen Bewegungsapparates. Ergebn Physiol 34:406–493

Wöhlisch E du Mesnil de Rochemont (1927) Die Thermodynamik der Wärmeumwandlung des Kollagens. Z Biol 85:406

P.13.3 In Vivo Experiments

P.13.3.1 Stress-Strain Curves in Vivo

PURPOSE AND RATIONALE

In contrast to studies in human beings, animal experiments allow measurement of mechanical properties both *in vivo* under anesthesia and later on *in vitro* (*ex vivo*) at the same site. For this purpose, special methods had to be developed (Barbanel and Payne 1981; Vogel 1981a, b, 1982; Vogel and Denkel 1982, 1985; Denkel 1983).

PROCEDURE

Groups of 10 male Sprague-Dawley rats with an initial weight of 120 ± 10 g are treated for 10 days subcutaneously or orally with test drugs or saline.

The rats are anesthetized with 60 mg/kg Nembutal i.p. The back skin is shaved mechanically. Skin thick-

ness is measured by use of calipers on an elevated skin fold. Four small (14 × 14 mm) metal plates bearing a hook are used as tabs and are glued on the skin in both longitudinal and perpendicular direction at a distance of 25 mm with a cyanoacrylate preparation. An operation table is mounted on the crosshead of an INSTRON instrument. The table can be turned to allow stretching of the skin in both perpendicular and longitudinal directions relative to the body axis. The anesthetized animals are fastened by their legs to the operation table. A triangle is attached to the load cell. At the end of the triangle, threads are fastened which are conducted by reels and hooked to the tabs. The cross head is moved down manually until the threads are stretched, however, no tension is measured yet. Then the crosshead is driven downwards with a rate of 50 cm/min, what means that the actual extension rate is 100 cm/min. The load is measured only to limited values in order to prevent damage of the skin. In each rat the stress-strain curve is recorded in both directions whereby the order (first longitudinal or first perpendicular) is changed from animal to animal. In this way, the influence of the first extension on the results of the second extension is eliminated. Stress-strain curves are recorded up to an elongation of 80%. Modulus of elasticity is calculated from the almost straight part of the curve.

EVALUATION

Average stress-strain curves with standard deviations are plotted for each treatment group perpendicular and longitudinal to the body axis. The stress values and the values for modulus of elasticity of the treated groups are compared with controls using Student's *t*-test.

CRITICAL ASSESSMENT OF THE METHOD

In spite of similar conditions, differences between the stress-strain curves from *in vitro* and *in vivo* experiments were found. These findings confirmed the statements of other authors (Barbanel and Payne 1981; Wijn 1980) of the importance of tab distance and tab geometry (Vogel 1981b). Analysis of the data showed that the higher the ratio of distance between the tabs to the area below the tabs, the higher were the stress values. These findings can be explained by the fact that skin consists of several layers. Only the upper layer (epidermis) is fastened to the tabs in the *in vivo* experiment. The forces transmitted to the lower layers are transmitted by a larger area if the area under the tabs is larger. The lower layer can slide over a larger area and is therefore less extended resulting in lower stress values. No sliding is possible if the sample is fastened from both sides as it is performed in the *in vitro* experiments. Taking into account all experimental conditions including the strain rate, the *in vivo* results are comparable with those obtained *in vitro*. This holds true for the age-dependence as well as for the influence of desmotropic compounds (Vogel and Denkel 1985).

MODIFICATIONS OF THE METHOD

Cook et al. (1977) compared tension/extension ratio curves *in vivo* and *in vitro* in **rats** using the suction-cup method. Baker et al. (1988) described an apparatus for testing mechanical properties of normal and irradiated **pig** skin *in vivo.* In this system, the pads were attached to the skin of the pig rump with double-sided tape. They were moved apart at a predetermined rate using a motorized unit. Force was assessed using a S-shaped, center point, double beam load cell mounted on a movable crosshead. Displacement of the pads was measured using a floating core linear variable displacement transducer. Using this system, Baker et al. (1989) studied the effect of single doses of X-rays on the mechanical properties of pig skin *in vivo*.

Zeng et al. (2001) studied the biorheological characteristics of skin after expansion in **dogs**.

REFERENCES AND FURTHER READING

Baker MR Bader DL Hopewell JW (1988) An apparatus for testing of mechanical properties of skin *in vivo*: Its application to The assessment of normal and irradiated pig skin. Bioeng Skin 4:87–103

Baker MR Bader DL Hopewell JW (1989) The effect of single doses of X rays on the mechanical properties of pig skin *in vivo*. Br J Radiol 62:830–837

Barbanel JC Payne PA (1981) *In vivo* mechanical testing of dermal properties. Bioeng Skin 3:8–38

Cook T Alexander H Cohen M (1977) Experimental method for determining the 2-dimensional mechanical properties of living human skin. Med Biol Eng Comput 15:381–390

Denkel K (1983) Vergleich rheologischer Parameter *in vivo* und *in vitro* an der Rückenhaut der Ratte. Ingenieurarbeit Frankfurt-Hoechst

Vogel HG (1981a) Attempts to compare "*in vivo*" and "*in vitro*" measurement of mechanical properties in rat skin. Bioeng Skin 3:39–46

Vogel HG (1981b) Comments on the paper by Barbenel and Payne '*In vivo*' mechanical testing of dermal properties". Bioeng Skin 3:53–56

Vogel HG (1982) Mechanical properties of rat skin as compared by *in vivo* and *in vitro* measurement. Bioeng Skin 3:198–209

Vogel HG Denkel K (1982) Methodological studies on biomechanics of rat skin comparing *in vivo* and *in vitro* results. Bioeng Skin 4:71–79

Vogel HG Denkel K (1985) Influence of maturation and age, and of desmotropic compounds on the mechanical properties of rat skin *in vivo*. Bioeng Skin 1:35–54

Wijn PFF (1980) The alinear viscoelastic properties of human skin *in vivo* for small deformations. Proefschrift ter Verkri-

jging van de Graad von Doctor in de Wiskunde en Natuurwetenschappen an de Katholieke Universiteit te Nijmegen
Zeng Y Huang K Xu C, Zhang J Sun G (2001) Biorheological characteristics of skin after expansion. Biorheology 38:367–378

P.13.3.2 Repeated Strain in Vivo

PURPOSE AND RATIONALE

A special method has been developed to study the mechanical properties of rat skin after repeated strain *in vivo* and the course of recovery during different time intervals (Denkel 1983; Vogel and Denkel 1985; Vogel 1988).

PROCEDURE

Male Sprague-Dawley rats with an initial weight of 120 ± 10 g are treated for 10 days subcutaneously or orally with test drugs or saline. Groups of 10 animals are used for each time interval tested and for the two directions of testing.

Tabs are fastened on the shaved back skin of anesthetized rats with a distance of 25 mm either perpendicular or longitudinal to the body axis with a cyanoacrylate preparation. With an extension rate of 100 mm/min, the skin is extended 30 times for a 50% strain under anesthesia. Load is recorded and stress calculated by dividing load by skin thickness measured from a skin fold obtained with calipers. The 1st, 5th, 10th, 20th, 25th and 30th cycles are recorded with faster paper speed in order to facilitate the evaluation of modulus of elasticity and stress values. Modulus of elasticity is calculated from the upper part of the stress-strain curve. The area under the curve of 30 cycles is evaluated by computerized calculation according to Simpson's formula (Hütte 1915; Denkel 1983; Vogel 1988).

EVALUATION

Average curves of stress vs. number of cycles with standard deviations are plotted for each treatment group perpendicular and longitudinal to the body axis. The stress values and the values for modulus of elasticity of the treated groups are compared with controls using Student's *t*-test.

CRITICAL ASSESSMENT OF THE METHOD

Stress values decreased after repeated loading approximately with the logarithm of number of cycles. Stress values and the area under the curve were higher perpendicular than longitudinal to the body axis, as found in other *in vivo* experiments (Vogel and Denkel 1985). During the experiment, modulus of elasticity increased in both directions from the first to the fifth cycle. This may be explained by the so-called "conditioning" of connective tissue (Nemetscheck et al. 1980). From the 5th to the 30th cycle, a decay of modulus of elasticity approximately with the logarithm of number of cycles was noted. The area under the curve calculated from stress values resembled closely the pattern of initial stress, indicating that this value dominates for the area under the curve and that the decay is only of secondary importance.

REFERENCES AND FURTHER READING

Denkel K (1983) Vergleich rheologischer Parameter *in vivo* und *in vitro* an der Rückenhaut der Ratte. Ingenieurarbeit Frankfurt-Hoechst "Hütte" Des Ingenieurs Taschenbuch (1915) Berlin, Verlag von Wilhelm Ernst & Sohn, Vol II, pp 630–631
Nementscheck T Riedl H Jonak R Nementscheck-Gansler H Bordas J Koch MHJ Schilling V (1980) Die Viskoelastizität parallelsträhnigen Bindegewebes und ihre Bedeutung für die Funktion. Virchow's Arch 386:125–151
Vogel HG (1988) Restitution of mechanical properties of rat skin after repeated strain. Influence of maturation and ageing. Bioeng. Skin 4:343–359
Vogel HG Denkel K (1985) Influence of maturation and age, and of desmotropic compounds on the mechanical properties of rat skin *in vivo*. Bioeng Skin 1:35–54

P.13.3.3 In Vivo Recovery After Repeated Strain

PURPOSE AND RATIONALE

A method was developed to study the *in vivo* recovery of mechanical properties of rat skin after repeated strain (Denkel 1983; Vogel and Denkel 1985; Vogel 1988, 1990, 1993a, b). Full recovery, i. e., ***restitutio ad integrum***, can be observed only by doing *in vivo* experiments but not by *in vitro* experiments.

PROCEDURE

Male Sprague-Dawley rats with an initial weight of 120 ± 10 g are treated for 10 days subcutaneously or orally with test drugs or saline. Groups of 10 animals are used for each time interval tested and for the two directions of testing.

As in the experiment of repeated strain, tabs are fastened on the shaved back skin of anesthetized rats with a distance of 25 mm either perpendicular or longitudinal to the body axis with a cyanoacrylate preparation. With an extension rate of 100 mm/min, the skin is extended 30 times for a 40% strain under anesthesia. Load is recorded and stress calculated by dividing load by skin thickness measured from a skin fold obtained with calipers. The 1st, 5th, and 30th cycles are recorded with faster paper speed in order to facilitate

the evaluation of modulus of elasticity and stress values. Modulus of elasticity is calculated from the upper part of the stress-strain curve. The area under the curve of 30 cycles is evaluated by computerized calculation according to Simpson's formula (Hütte 1915; Denkel 1983; Vogel 1988).

After the first run the animals are returned to their cages with the tabs still in position. A second run of repeated strain is applied after different time intervals at 1, 6, and 16 h. The stress values in the second run are definitively lower than in the first run.

When calculated as percentage of the first run, the differences diminish with extended time intervals. By this *in vivo* method not only the mechanical recovery, which can also be observed *in vitro*, but also the biological recovery, i. e., the restitutio ad integrum, can be measured. Almost full recovery is found after 16 h.

EVALUATION

Average curves of stress vs. number of cycles with standard deviations are plotted for each treatment group perpendicular and longitudinal to the body axis. The stress values and the values for modulus of elasticity of the treated groups are compared with controls using Student's *t*-test. Stress of the first and 30th cycle as well as the area under the curve at the second run are expressed as percentage of the first run after the 1, 6, or 16 h interval. Furthermore, the hours to reach certain percent levels up to 100% are calculated for the stress values during the first cycle and the area under the curve both longitudinally and perpendicularly to the body axis.

CRITICAL ASSESSMENT OF THE METHOD

In the late phase of recovery, an even better restitutio ad integrum was found in animals treated with 300 mg/kg p.o. D-penicillamine or 10 mg/kg s.c. prednisolone acetate. In contrast to other biomechanical parameters, the restoration process was found to be barely influenced by treatment with desmotropic compounds.

Surprisingly, in studies on age dependence restitutio ad integrum was the fastened in old animals. The ability of the dermis to reconstitute the fibrous structure is apparently not influenced negatively by age.

REFERENCES AND FURTHER READING

Denkel K (1983) Vergleich rheologischer Parameter *in vivo* und *in vitro* an der Rückenhaut der Ratte. Ingenieurarbeit Frankfurt-Hoechst "Hütte" Des Ingenieurs Taschenbuch (1915) Berlin, Verlag von Wilhelm Ernst & Sohn, Vol II, pp 630–631

Vogel HG (1988) Restitution of mechanical properties of rat skin after repeated strain. Influence of maturation and ageing. Bioeng. Skin 4:343–359

Vogel HG (1990) Restitutio ad integrum der mechanischen Eigenschaften von Rattenhaut nach wiederholter Dehnung. Einfluß von Reifung und Alterung. Z Gerontol 23:126–127

Vogel HG (1993a) *In vivo* recovery of repeatedly strained rat skin after systemic treatment with desmotropic drugs. Skin Pharmacol 6:103–110

Vogel HG (1993b) Mechanical measurements in assessing aging. In: Frosch PJ Kligman AM (eds) Noninvasive Methods for the Quantification of Skin Functions. An Update on Methodology and Clinical Applications. Springer-Verlag Berlin, Heidelberg, New York, pp 145–180

Vogel HG Denkel K (1985) *In vivo* recovery of mechanical properties in rat skin after repeated strain. Arch Derm Res 277:484–488

P.13.4 Healing of Skin Wounds

PURPOSE AND RATIONALE

Healing of skin wounds is a multiphasic process. The effect of drugs on the healing process was studied by measuring the mechanical strength at various time intervals after incision of the skin (Vogel 1970).

PROCEDURE

Groups of 10 to 20 male Sprague-Dawley rats weighing 120 ± 5 g are used for each dosage or control and for each test interval. Under anesthesia the dorsal skin is shaved and an approximately 3 cm long incision is made down to the fascia in a cranio-caudal direction in the dorso-lumbar region. Immediately afterwards, the wound is closed with wound clips. The rats are treated subcutaneously with test drugs beginning on the day of surgery. The clips are removed the day before the tensile strength is tested or on the 10th post-operative day at the latest.

For the measurement of wound tensile strength, the rats are sacrificed under anesthesia on days 3, 6, 9, or 12 after surgery. Wound clips are fastened *in situ* on each side of the incision and connected by means of threads with the load cell and the crosshead of an INSTRON-Instrument. Stress-strain curves are recorded at an extension rate of 5 cm/min. **Dehiscence of the wound** results in a sudden drop of the registered load. For experiments up to 3 weeks, bell-shaped skin strips are punched and tensile strength is tested, as described for evaluation of tensile strength in normal skin.

EVALUATION

Mean values of tensile strength of skin wounds in drug treated groups at each time interval are compared with controls using Student's *t*-test. To visualize the influ-

ence of drugs on the healing process, the changes following treatment with drugs are expressed as percentage of vehicle treated controls.

A dose-dependent decrease following treatment with corticosteroids is found after immediate postoperative treatment and a dose-dependent increase in prolonged experiments. This data serve as comparative parameters for new test compounds

MODIFICATIONS OF THE METHOD

Many authors measured tensile strength of skin wound to follow the course of wound healing under various conditions. Most experiments were performed in **rats** (Struck et al. 1967; Corps 1969; Holm-Pedersen and Zederfeldt 1971; Holm-Pedersen and Viidik 1972a, b; Andreassen et al. 1977; Andreassen and Oxlund 1987; Greenwald et al. 1993; Seyer-Hansen et al. 1993; Jyung et al. 1994; Adamson et al. 1996; Brunius and Ahren 1996; Oxlund et al. 1996; Paul et al. 1997; Taylor et al. 1997; Quirinia and Viidik 1991, 1998; Canturk et al. 1999; Gupta et al. 1999), with some of them also using the INSTRON-Instrument (Phillips et al. 1993; Maxwell et al. 1998; Jimenez and Rampy 1999; Kim and Pomeranz 1999).

A biphasic effect of corticosteroids on wound healing in rats was also found by Oxlund et al. (1979).

Forslund et al. (2006) published a comparative dose–response study of cartilage-derived morphogenetic protein (CDMP)-1, -2 and -3 for tendon healing in rats.

Furthermore, **mice** (Butler et al. 1991; Celebi et al. 1994; Kashyap et al. 1995; Vegesna et al. 1995; Gonul et al. 1998; Matsuda et al. 1998), **guinea pigs** (Bernstein et al. 1991; Drucker et al. 1998; Silverstein and Landsman 1999), **rabbits** (Sandblom 1957; Wu and Mustoe 1995; Pandit et al. 1998, 1999; Knabl et al. 1999; Xia et al. 1999), **dogs** (Howes et al. 1929; Al Sadi and Gourley 1977; Scardino et al. 1999), **pigs** (Langrana et al. 1983; Higashiyama et al. 1992; Chang et al. 1998; Fung et al. 1999) or **Yukatan miniature pigs** (Van Dorp et al. 1998) were used.

Using PPARα, β and γ mutant mice, Michalik et al. (2001) demonstrated that PPARα and β are important for the rapid epithelialization of a skin wound and that each of them plays a specific role in this process. PPARα is mainly involved in the early inflammatory phase of the healing, whereas PPARβ is implicated in the control of keratinocyte proliferation.

PPARβ is discussed as a target for wound healing drugs (Tan et al. 2003).

Smith et al. (2001a, 2001b) discussed the role of peroxisomes in dermatology.

In some studies simultaneously polyvinyl alcohol sponges were implanted in which collagen accumulation was determined (Albina et al. 1993; Schaffer et al. 1996; Koshizuka et al. 1997; Bitar 1998; DaCosta et al. 1998; Witte et al. 1998).

Ågren and Mertz (1994) found excessive granulation tissue formation and retarded wound contraction in wounds in tight-skin mice.

Kyriakides et al. (1999) reported accelerated wound healing in mice with a disruption of the thrombospondin 2 gene.

REFERENCES AND FURTHER READING

Adamson B Schwarz D Klugston P Gilmont R Perry L Fisher J Lindblad W Rees R (1996) Delayed repair: The role of glutathione in a rat incisional wound model. J Surg Res 62:159–164

Ågren MS Mertz PM (1994) Are excessive granulation tissue formation and retarded wound contraction due to decreased collagenase activity in wounds in tight-skin mice? Br J Dermatol 131:337–340

Albina JE Gladden P Walsh WR (1993) Detrimental effects of an ω_3 fatty acid-enriched diet on wound healing. J Parenter Enter Nutr 17:519–521

Al Sadi HI Gourley IM (1997) Simplified method for studying mechanical properties of healing linear skin wounds in the dog. Am J Vet Res 38:903–906

Andreassen TT Fogdestam I Rundgren Å (1977) A biomechanical study of healing of skin incisions in rats during pregnancy. Surg Gynecol Obstet 145:175–178

Andreassen TT Oxlund H (1987) The influence of experimental diabetes and insulin treatments on the biochemical properties of rat skin incisional wounds. Acta Chir Scand 153:405–409

Bernstein EF Harisiadis L Solomon G Norton J Sollberg S Uitto J Glatstein E Glass J Talbot T Russo A Mitchel JB (1991) Transforming growth factor-β improved healing of radiation-impaired wounds. J Invest Dermatol 97:430–434

Bitar MS (1998) Glucocorticoid dynamics and impaired wound healing in diabetes mellitus. Am J Pathol 152:547–554

Brunius U Ahren C (1996) Healing during the cicatrization phase of skin incisions closed by non-suture technique. A tensiometric and histologic study in the rat. Acta Chir Scand 135:289–295

Butler PEM Barry-Walsh C Curren B Grace PA Leader M Bouchier Hayes D (1991) Improved wound healing with a modified electrosurgical electrode. Br J Plast Surg 44:495–499

Canturk NZ Vural B Esen N Canturk Z Oktay G Kirkali G Solakoglu S (1999) Effects of granulocyte-macrophage colony-stimulating factor on incisional wound healing in an experimental diabetic rat model. Endocr Res 25:105–116

Celebi N Erden N Gonul B Koz M (1994) Effects of epidermal growth factor dosage forms on dermal wound strength in mice. J Pharm Pharmacol 46:386–387

Chang HS Hom DB, Agarwal RP Pernell K Manivel JC Song C (1998) Effect of basic fibroblast growth factor on irradiated porcine skin flaps. Arch Otolaryngol Head Neck Surg 124:307–312

Corps BV (1969) Wound contracture in the hooded rat in relation to skin tension lines and design of injury. Br J Plast Surg 22:44–47

DaCosta ML Regan MC Al Sader M Leader M Bouchier-Hayes D (1998) Diphenylhydantoin sodium promotes early and marked angiogenesis and results in increased collagen deposition and tensile strength in healing wounds. Surgery 123:287–293

Drucker M Cardenas E Arizti P Valenzuela A Gamboa A Kerstein MD (1998) Experimental studies on the effect of lidocaine on wound healing. World J Surg 22:394–398

Forslund C Rueger D Aspenberg P (2006) A comparative dose-response study of cartilage-derived morphogenetic protein (CDMP)-1, -2 and -3 for tendon healing in rats. J Orthop Res 21:617–621

Fung LC Mingin GC Massicotte M Felsen D Poppas DP (1999) Effects of temperature on thermal injury and wound strength after photothermal wound closure. Laser Surg Med 25:295–290

Gonul B Soylemezoglu T Babul A Celebi N (1998) Effect of epidermal growth factor dosage forms on mice full-thickness skin wound zinc levels and relation to wound strength. J Pharm Pharmacol 50:641–644

Greenwald DP Shumway S Zachary LS LaBarbera M Albear P Temaner M Gottlieb LJ (1993) Endogenous versus toxin-induced diabetes in rats: A mechanical comparison of two skin wound-healing models. Plast Reconstr. Surg 91:1087–1093

Gupta A Jain GK Raghubir R (1999) A time course study for the development of an immunocompromised wound model, using hydrocortisone. J Pharmacol Toxicol Meth 41:183–187

Higashiyama M Hashimoto K Takada A Fujita K Kido K Yoshikawa K (1992) The role of growth factor in wound healing. J Dermatol 19:676–679

Holm-Pedersen P Zederfeldt B (1971) Strength development of skin incisions in young and old rats. Scand J Plast Reconstr. Surg 5:7–12

Holm-Pedersen P Viidik A (1972a) Maturation of collagen in healing wounds in young and old rats. Scand J Plast Reconstr. Surg 6:16–23

Holm-Pedersen P Viidik A (1972b) Tensile properties and morphology of healing wounds in young and old rats. Scand J Plast Reconstr. Surg 6:24–35

Howes EL Sooy JW Harvey SC (1929) The healing of wounds as determined by their tensile strength. J.A.M.A 92:42–45

Jiminez PA Rampy MA (1999) Keratinocyte growth factor-2 accelerates wound healing in incisional wounds. J Surg Res 81:238–242

Jyung RW Mustoe TA Busby WH Clemmons DR (1994) Increased wound-breaking strength induced by insulin-like growth factor I in combination with insulin-like growth factor binding protein-1. Surgery 115:233–239

Kashyap A Beezhold D Wiseman J Beck WC (1995) Effect of povidone iodine dermatologic ointment on wound healing. Am Surg 61:486–491

Kim LR, Pomeranz B (1999) The sympathomimetic agent, 6-hydroxydopamine, accelerates cutaneous wound healing. Eur J Pharmacol 376:257–264

Knabl JS Bauer W Andel H Schwendenwein I Dado PF Mittlbock M Romer W Choi MS Horvat R Meissl G Frey M (1999) Progression of burn wound depth by systemic application of a vasoconstrictor: an experimental study with a new rabbit model. Burns 25:715–721

Koshizuka S Kanazawa K Kobayashi N Takazawa I Waki Y Shibusawa H Shumiya S (1997) Beneficial effects of recombinant human insulin-like growth factor-I (IGF-I) on wound healing in severely wounded senescent mice. Surg Today 27:946–952

Kyriakides TR Tam JWY, Bornstein P (1999) Accelerated wound healing in mice with a disruption of the thrombospondin 2 gene. J Invest Dermatol 113:782–787

Langrana NA Alexander H Strauchler I Metha H Ricci J (1983) Effect of mechanical load in wound healing. Ann Plast Surg 10:200–208

Matsuda H Koyama H Sato H Sawada J Itakura A Tanaka A Matsumoto M Konno K Ushio H Matsuda K (1998) Role of nerve growth factor in cutaneous wound healing: Accelerating effects in normal and healing-impaired diabetic mice. J Exp Med 187:297–306

Maxwell GL Soisson AP Brittain PC Harris R Scully T (1998) Tissue glue as an adjunct to wound healing in the porcine model. J Gynecol Tech

Michalik L Desvergne B Tan NS, Basu-Modak S Escher P Rieusset J Peters JM Kaya G Gonzales FJ Zakany J Metzger D Chambon P Duboule D Wahli W (2001) Impaired skin wound healing in peroxisome proliferator-activated receptor PPARα and PPARβ mutant mice. J Cell Biol 154:799–814

Oxlund H Fogdestam I Viidik A (1979) The influence of cortisol on wound healing of the skin and distant connective tissue response. Surg Gynecol Obstet 148:867–880

Oxlund H Christensen H Seyer-Hansen M Andreassen TT (1996) Collagen deposition and mechanical strength of colon anastomoses and skin incisional wounds of rats. J Surg Res 66:25–30

Pandit A Ashar R Feldman D Thompson A (1998) Investigation of acidic fibroblast growth factor delivered through a collagen scaffold for the treatment of full-thickness skin defects in a rabbit model. Plast Reconstr Surg 101:766–775

Pandit A Ashar R Feldman D (1999) The effect of TGF-β delivered through a collagen scaffold on wound healing. J Invest Surg 12:89–100

Paul RG Tarlton JF Purslow PP Sims TJ Watkins P Marshall F Ferguson JM Bailey AJ (1997) Biomechanical and biochemical study of a standardized wound healing model. Int J Biochem Cell Biol 29:211–220

Phillips LG Abdullah KM Geldner PD Dobbins S Ko F, Linares HA Broemeling LD Robson MC (1993) Application of basic fibroblast growth factor may reverse diabetic wound healing impairment. Ann Plast Surg 31:331–334

Quirinia A Viidik A (1991) The influence of age on the healing of normal and ischemic incisional skin wounds. Mech Ageing Dev 58:221–232

Quirinia A Viidik A (1998) The effect of recombinant basic fibroblast growth factor (bFGF) in fibrin adhesive vehicle on the healing of ischemic and normal incision skin wounds. Scand J Plast Reconstr. Surg Hand Surg 32:9–18

Sandblom P (1957) Wundheilungsprobleme, mit Reißfestigkeitsmethoden untersucht. Langenbeck's Arch Dtsch Z Chir 287:469–480

Scardino MS Swaim SF Morse BS Sartin MA Wright JC Hoffman CE (1999) Evaluation of fibrin sealants in cutaneous wound closure. J Biomed Mater Res 48:315–321

Schaffer MR Tantry U Gross SS Wasserkrug HL Barbul A (1996) Nitric oxide regulates wound healing. J Surg Res 63:237–240

Seyer-Hansen M Andreassen TT Jørgensen PH Oxlund H (1993) Influence of biosynthetic human growth hormone on the biomechanical strength development in skin incisional wounds of diabetic rats. Eur Surg Res 25:162–168

Silverstein RJ Landsman AS (1999) The effects of a moderate and a high dose of vitamin C on wound healing in a controlled guinea pig model. J Foot Ankle Surg 38:333–338

Smith KJ Dipreta E Skelton H (2001a) Peroxisomes in dermatology. Part I. J Cutan Med Surg 5:231–243

Smith KJ Dipreta E Skelton H (2001b) Peroxisomes in dermatology. Part II. J Cutan Med Surg 5:315–322
Struck H Schink W Hernández-Richter J Moll W (1967) Eine Apparatur zur Bestimmung der Wundfestigkeit *in vivo*. Zschr Ges Exp Med 142:87–94
Tan NS, Michalik L Desvergne B Wahli W (2003) Peroxisome proliferator-activated receptor (PPAR)-β as a target for wound healing drugs. What is possible? Am J Clin Dermatol 4:523–530
Taylor DL Schafer SA Nordquist R Payton ME Dickey DT Bartels KE (1997) Comparison of high power diode laser with the Nd:YAG laser using in situ wound strength analysis of healing cutaneous incisions. Lasers Surg Med 21:248–254
Van Dorp AG Verhoeven MC Koerten HK Van der Nat van der Meij TH Van Blitterswijk CA Ponec M (1998) Dermal regeneration in full-thickness wounds in Yukatan miniature pigs using a biodegradable copolymer. Wound Repair Regen 6:556–568
Vegesna V McBride WH Taylor JGM Withers HR (1995) The effect of interleukin 1β or transforming growth factor β on radiation impaired murine skin wound healing. J Surg Res 59:600–704
Vogel HG (1970) Tensile strength of skin wounds in rats after treatment with corticosteroids. Acta Endocrin 64:295–303
Witte MB Thornton FJ Kiyama T Efron DT Schulz GS Moldawer LL Barbul A Hunt TK (1998) Metalloproteinase inhibitors and wound healing: A novel enhancer of wound strength. Surgery 124:464–470
Wu L, Mustoe TA (1995) Effect of ischemia on growth factor enhancement of incisional wound healing. Surgery 117:570–576
Xia YP, Zhao Y Marcus J Jimenez PA Ruben SM Moore PA Khan F Mustoe TA (1999) Effects of keratinocyte growth factor-2 (KGF-2) on wound healing in an ischaemia-impaired rabbit ear model and on scar formation. J Pathol 188:431–438

P.14 Protection Against UV Light

PURPOSE AND RATIONALE

The mechanical parameters' skin thickness, ultimate strain, ultimate load, tensile strength and modulus of elasticity were used to evaluate the effects of UV-irradiation and the prevention of skin damage in hairless mice (Alpermann and Vogel 1978; Vogel et al. 1981).

PROCEDURE

Female hairless mice (strain mutant h/h) with an initial weight of 20 ± 2 g are used. Groups of 20 animals are treated topically with 0.025 ml of the sunscreen product or the base. One other group is not treated topically, but irradiated. A further group is neither treated nor exposed to UV-B.

A special light source (Osram Ultra-Vitalux No. 2) is used. This light source is almost free from UV-C. For UV exposure groups of 5, mice are immobilized under a fine wire net of 14×14 cm at a distance of from the lamp, resulting in an irradiation energy of 14 mW/cm^2 for UV-B and 33 mW/cm^2 for UV-A. Irradiation is performed once a day except Saturday and Sunday during 4 weeks. Exposure time is 45 s in the first week, 60 s in the second, 90 s in the third, and 120 s in the fourth week. The animals are sacrificed umder anesthesia 72 h after the last irradiation. A flap of back skin is removed, skin thickness measured by use of calipers and two dumb-bell shaped samples punched with a width of 4 mm in the middle of the specimen. Stress-strain curves are recorded with an INSTRON-instrument at a strain rate of 5 cm/min. Ultimate load and ultimate strain are recorded and tensile strength as well as ultimate modulus of elasticity are calculated.

Furthermore, samples of skin are deep-frozen for chemical analysis of collagen and soluble collagen fractions as well as of elastin (Vogel 1978).

EVALUATION

The mean data from animals treated with sunscreen products are compared with those of animals treated with ointment base, irradiated and non irradiated controls using ANOVA and Student's *t*-test.

MODIFICATIONS OF THE METHOD

The effect of UV-irradiation on skin has been studied by several authors both in man and in animals.

Wolska (1974) recommended the hairless mouse as an experimental model for evaluating the effectiveness of sunscreen preparations.

Cook et al. (1979) investigated the changes in the mechanical properties of intact **guinea pig** skin resulting from ultra-violet irradiation.

Lowe and Breeding (1986) evaluated several sunscreen preparations by UVB irradiation of mice. Sunscreen solutions were applied to the back of 5–8 weeks old female skh/HR-1 mice one h before irradiation with FS40 sunlamps. Epidermal DNA synthesis assay was used to measure sunscreen efficacy. The amount of UVB required to achieve a 50% suppression of radiolabelled thymidine incorporation in treated and untreated mice was compared as a ratio to determine the protective factor. Furthermore, epidermal ornithine decarboxylase activity was determined by measuring the release of $^{14}CO_2$ from L-[1-^{14}C]ornithine 24 h after a single UVB exposure. Edema was estimated by the increase in double skin fold thickness measured by a caliper at 24 h post irradiation.

Benrath et al. (1995) reported that substance P and nitric oxide mediate wound healing of ultraviolet photodamaged skin in **rats**.

Muizzudim et al. (1998) studied the effect of topical application of antioxidants and free radical scavengers on protection of hairless mouse skin, exposed to

suberythemal doses of ultraviolet B three times a week, and measured epidermal thickness by microscopy.

Fullerton and Keiding (1997) quantified UV-B induced erythema in depilated Hartley-strain albino male guinea pigs and compared the results with a tristimulus colorimeter (Minolta ChromaMeter CR-200) and two spectrophotometers (Minolta Spectrophotometer CM-508i and CM-2002). With the tristimulus colorimeter the color is expressed in a three-dimensional color space, which simulates the perception of color by the human eye.

Nishimori et al. (2001) described degenerative alterations of dermal collage fiber bundles in photodamaged human skin and UV-irradiated hairless mouse skin and the effects on decreasing skin mechanical properties and appearance of wrinkles.

Oba and Edwards (2006) studied the relationships between changes in mechanical parameters of the skin, wrinkling, and destruction of dermal fiber bundles caused by photoaging on hairless mice irradiated with UVB light.

Further description of ultraviolet erythema in animals see Sect. H. 3.2.2.1.

REFERENCES AND FURTHER READING

Alpermann H Vogel HG (1978) Effect of repeated ultraviolet irradiation on skin of hairless mice. Arch Derm Res 262:1:15–25

Benrath J Zimmermann M Gillardon F (1995) Substance P and nitric oxide mediate wound healing of ultraviolet photodamaged rat skin: effect for an effect of nitric oxide on keratinocyte proliferation. Neurosci Lett 200:17–20

Cook D Mitchell R Darr D (1979) Changes in the mechanical properties of intact guinea pig skin resulting from ultraviolet irradiation. Bioeng Skin 2:13

Fullerton A Keiding J (1997) A comparison between a tristimulus colorimeter (Minolta ChromaMeter CR-200) and two spectrophotometers (Minolta Spectrophotometer CM-508i and CM-2002). Quantification of UV-B induced erythema in a hairless guinea pig model. Skin Res Technol 3:237–241

Harber LC Armstrong RB Ichikawa H (1982) Current status of predictive animal models for drug photoallergy and their correlation with drug photoallergy in humans. J Natl Cancer Inst 69:237–244

Lowe NJ Breeding J (1986) Sunscreen evaluation by mouse spectrophotometric and human assays. In: Marks R Plewig G (eds) Skin Models. Springer-Verlag Berlin Heidelberg, pp 34–41

Muizzudim N Shakoori AR Marenus KD (1998) Effect of topical application of antioxidants and free radical scavengers on protection of hairless mouse skin exposed to chronic doses of ultraviolet B. Skin Res Technol 4:200–204

Nishimori Y Edwards C Pearse A Matsumoto K Kawai M Marks R (2001) Degenerative alterations of dermal collage fiber bundles in photodamaged human skin and UV-irradiated hairless mouse skin: possible effects on decreasing skin mechanical properties and appearance of wrinkles. J Invest Dermatol 117:1458–1463

Oba A, Edwards C (2006) Relationships between changes in mechanical parameters of the skin, wrinkling, and destruction of dermal fiber bundles caused by photoaging. Skin Res Technol 12:28–288

Vogel HG (1978) Influence of maturation and age on mechanical and biochemical parameters of connective tissue of various organs in the rat. Conn Tiss Res 6:161–166

Vogel HG Alpermann HG Futterer E (1981) Prevention of changes after UV-irradiation by sunscreen products in skin of hairless mice. Arch Dermatol Res 270:421–428

Wolska H (1974) The hairless mouse as an experimental model for evaluating the effectiveness of sunscreen preparations. J Soc Cosmet Chem 25:639–644

P.15 Transepidermal Water Loss (TEWL)

PURPOSE AND RATIONALE

The physical basis for the measurement of transepidermal water loss (TEWL) is the diffusion law discovered by A. Fick in 1855.

$$dm/dt = -D \times A \times dp/dx$$

where:

A = surface (m^2),

m = water transported (g),

t = time (h),

D = diffusion constant ($= 0.0877\ g/m \times h \times mm\ Hg$),

p = vapor pressure of the atmosphere (mm Hg),

x = distance from skin surface to point of measurement.

Most of the recent studies are performed with commercially available instruments, such as Tewameter TM 210, Courage and Khazaka, Cologne, Germany, Evaporimeter EP1, Servo Med AB, Vallingby, Sweden, primarily designed for the used in human beings.

Several studies were performed in **rats**, e. g., in hairless rats (Doucet et al. 1991; Vanbever et al. 1998), neonatal rats (Wickett et al. 1995), in rats with experimentally induced condition of essential fatty acid deficiency (Basnayake and Sinclair 1956; Prottey et al. 1976; Hartop et al. 1976, 1978; Penneys 1992; Yamaguchi et al. 1998; Meguro et al. 2000), **hairless mice** (Grubauer et al. 1989; Mortz et al. 1997; Sato et al. 1998), essential fatty acid deficient hairless mice (Menton 1968; Lowe and Stoughton 1977), platelet-type 12-lipoxygenase deficient mice (Johnson et al. 1999), keratin 10 deficient mice (Jensen et al. 2000), **guinea pigs** (Frosch et al. 1993; Fuchs et al. 1998; Sagiv et al. 2000), **pigs** (Zhao and Singh (1999) **Yucatan micro-swine** (Gendimenico et al. 1995).

Löffler et al. (2001) evaluated irritant skin reaction in mice by measurement of auricular transepithelial water loss.

PROCEDURE

BALB/c mice aged 10–16 weeks are sensitized on day 0 by applying 50 µl 2,4-dinitro-flurobenzene (DNFB) solution (0.5% diluted in acetone/olive oil 4:1) to the shaved dorsal neck region. On day 5, the dorsal surface of one ear is challenged by applying 10 µl DNFB 0.3%; the other side is treated by acetone/olive oil alone.

Transepithelial water loss is measured with an evaporimeter (Tewameter TM 210, Courage and Khazaka, Cologne, Germany) with a measuring cylinder into which the whole ear of the mouse can be placed. The measurements are performed under isofluoran inhalation anesthesia. Measurements are performed before and 24 h after challenge.

EVALUATION

The comparison between the treated and untreated ears is calculated by the Wilcoxon test. The comparison between the tested groups is calculated by the Kruskal-Wallis *H*-test, after the Mann-Whitney *U*-test.

REFERENCES AND FURTHER READING

Basnayake V Sinclair HM (1956) The effects of deficiency of essential fatty acids upon the skin. In: Popjak E de Breton E (eds) Biochemical Problems of Lipids. Butterworth Scientific Publications, London, pp 476–484

Doucet O Tidjani A Venecie PY Bismuth H Marty JP (1991) Transepidermal water loss modifications in rats and humans treated with ciclosporin. Skin Pharmacol 4:84–88

Frosch PJ Schulze-Dirks A Hoffmann M Axthelm I Kurte A (1993) Efficacy of skin barrier creams. (I) The repetitive irritation test (RIT) in the guinea pig. Contact Dermatitis 28:94–100

Fuchs J Groth N Herrling T (1998) Cutaneous tolerance to nitroxide free radicals and nitrone spin traps in the guinea pig. Toxicology 126:33–40

Gendimenico GJ Liebel FT Fernandez JA Mezick JA (1995) Evaluation of topical retinoids for cutaneous pharmacological activity in Yucatan microswine. Arch Dermatol Res 287:675–679

Grubauer G Elias PM Feingold KR (1989) Transepithelial water loss; the signal for recovery of barrier structure and function. J Lipid Res 30:323–333

Hartop PJ Prottey C (1976) Changes in transepithelial water loss and the composition of epidermal lecithin after applications of pure fatty acid triglycerides to skin of essential fatty acid-deficient rats. Br J Dermatol 95:255–264

Hartop PJ Allenby CF Prottey C (1978) Comparison of barrier function and lipids in psoriasis and essential fatty acid-deficient rats. Clin Exp Dermatol 3:259–267

Jensen JM Schütze S Neumann C Proksch E (2000) Impaired cutaneous permeability barrier function, skin hydration, and sphingomyelinase activity in keratin 10 deficient mice. J Invest Dermatol 115:708–713

Johnson EN Nanney LB Virmani J Lawson JA Funk CD (1999) Basal transepidermal water loss is increased in platelet-type 12-lipoxygenase deficient mice. J Invest Dermatol 112:861–865

Löffler H Hoffmann R Happle R Effendy I (2001) Murine auricular transepithelial water loss – a novel approach for evaluating irritant skin reaction in mice. Clin Exp Dermatol 26:196–200

Lowe NJ Stoughton RB (1977) Essential fatty acid deficient hairless mouse: a model of chronic epidermal hyperproliferation. Br J Dermatol 96:155–162

Meguro S Arai Y Masukawa Y Uie K, Tokimitsu I (2000) Relationship between covalently bound ceramides and transepithelial water loss (TEWL). Arch Dermatol Res 292:463–468

Menton DN (1968) The effects of essential fatty acid deficiency in the skin of the mouse. Am J Anat 122:337

Mortz CG Andersen KE Halkier-Sorensen L (1997) The efficacy of different moisturizers on barrier recovery in hairless mice evaluated by non-invasive bioengineering methods. A model to select the potentially most effective product. Contact Dermatitis 36:297–301

Penneys NS (1992) Animal models for testing topical corticosteroid potency: A review and some suggested approaches. Int J Dermatol 31, Suppl 1:6–8

Prottey C Hartop PJ Black JG McCormac JI (1976) The repair of impaired epidermal barrier function in rats by the cutaneous application of linoleic acid. Br J Dermatol 94:13–21

Sagiv AE Ingber A Dikstein S (2000) A novel *in vivo* model in guinea pigs for dry skin syndrome. Skin Res Technol 6:37–42

Sato J Denda M Ashida Y Koyama J (1998) Loss of water from the stratum corneum induces epidermal DNA synthesis in hairless Mice. Arch Dermatol Res 290:634–637

Vanbever R Fouchard D Jadoul A De Morre N Préat V, Marty JP (1998) *In vivo* noninvasive evaluation of hairless rat skin after high-voltage pulse exposure. Skin Pharmacol Appl Skin Physiol 11:23–34

Wickett RR Nath V Tanaka R Hoath SB (1995) Use of continuous electrical capacitance and transepithelial water loss measurements for assessing barrier function in neonatal rat skin. Skin Pharmacol 8:179–185

Yamaguchi H Yamamoto A Watanabe R Uchiyama N Fujii H Ono T, Ito M (1998) High transepithelial water loss induces fatty acid synthesis and cutaneous fatty acid-binding protein expression in rat skin. J Dermatol Sci 17:205–213

Zhao K Singh J (1999) *In vitro* percutaneous absorption enhancement of propranolol hydrochloride through porcine epidermis by terpenes/ethanol. J Controlled Release 62:359–366

P.16 Skin Hydration

PURPOSE AND RATIONALE

Techniques to characterize the barrier function of the skin include a number of noninvasive methods to measure moisture content and loss through the skin surface. One of these measurements is the determination of skin hydration using a method known as corneometry (Bilchmann and Serup 1988). This technique determines the capacitance of the skin due to its behavior as a dielectric medium and assesses a 10- to

20-µm thickness of the stratum corneum. The method has been compared with other techniques (Van Neste 1991; Fluhr et al. 2001) and applied to evaluate dermatological and cosmetic products in human volunteers (Zuang et al. 1997; Singh et al. 2001; Yilmaz and Borchert 2006).

Jensen et al. (2000) studied skin hydration in keratin-10-deficient mice. Kappes et al. (2004) used this method to investigate the quality of human xenografts on SCID mice. Hester et al. (2004) evaluated this method in dogs.

PROCEDURE

Normal adult dogs (female Beagle and male houndcross dogs) were used. Hair was clipped from the left inguinal region of each dog 1 week before measurements to minimize any effects of recent hair clipping. Because hair grows sparsely in the inguinal region, only a minimal amount of clipping was necessary. To measure skin hydration, a Corneometer 825 meter (Courage Khazaka Electronics) was used. Animals were gently restrained in a right-lateral recumbency on a padded floor and were given time to relax so that movements could be minimized during data collection. The probes were held in place manually, and readings were taken for 20 s each. The data were stored electronically using a laptop computer and appropriate software. Values representing an average of at least ten determinations were used to calculate average values.

EVALUATION

Statistical analyses were conducted by repeated-measures ANOVA for main time-and-breed effects and time × breed interactions with Tukey' multiple comparisons performed at P values <0.05.

REFERENCES AND FURTHER READING

Bilchmann CW Serup J (1988) Assessment of skin moisture. Measurement of electric conductance, capacitance and transepidermal water loss. Acta Derm Venereol 68:284–290

Fluhr JW Kuss O Diepgen T Lazzerini S Pelosi A Gloor M Berardesca E (2001) Testing for irritation with a multifactorial approach: comparison of eight non-invasive measuring techniques on five different irritation types. Br J Dermatol 145:696–703

Hester SL Rees CA Kennis RA Zoran DL Bigley KE Wright AS Kirby NA Bauer JE (2004) Evaluation of corneometry (skin hydration) and transepidermal water loss. Measurements in two canine breeds. J Nutr 134:2110S–2113S

Jensen JM Schütze S Neumann C Proksch E (2000) Impaired cutaneous permeability barrier function, skin hydration, and sphingomyelinase activity in keratin 10 deficient mice. J Invest Dermatol 115:708–713

Kappes U Schliemann-Willers S Bankova L Heinemann C Fischer TW Ziemer M Schubert H Norgauer J Fluhr JM Elsner P (2004) The quality of human xenografts on SCID mice: a noninvasive bioengineering approach. Br J Dermatol 151:971–976

Singh J Gross M Sage B Davis HT Maibach HI (2001) Regional variations in skin barrier function and cutaneous irritation due to iontophoresis in human subjects. Food Chem Toxicol 39:1079–1086

Van Neste D (1991) Comparative study of normal and rough human skin hydration in vivo: evaluation with four different instruments. J Dermatol Sci 2:119–124

Yilmaz E Borchert HH (2006) Effect of lipid-containing, positively charged nanoemulsions on skin hydration, elasticity and erythema – an in vivo study. Int J Pharmaceutics 307:232–238

Zuang V Rona C Distante F Barardesca E (1997) The use of a capacitance device to evaluate the hydration of human skin. J Appl Cosmetol 15:95–102

P.17
Influence on Hair Growth

PURPOSE AND RATIONALE

Several mutations affecting hair growth or quality have been reported in the laboratory mouse (Holland 1988), among them "alopecia" (Dicke 1955); "alopecia periodica" (Tutikawa 1952); "crinkled" (Falconer et al. 1951); "frizzy" (Falconer and Snell 1952); "fuzzy" (Mann 1964); "rhino" (Mann 1971); "naked" (Raphael et al. 1982); "nude" (Flenagen 1966; Buhl et al. 1990; Militzer 2001); "ragged" (Slee 1962); androchronogenetic alopecia (AGA) mouse (Matias et al. 1989); aging C3H/HeJ mice (Sundberg et al. 1994); SPF-ASH mice (Shimada et al. 1994); "nackt" (Benavides et al. 1998); transgenic mice overexpressing homeobox gene MSX-2 (Jiang et al. 1999). Kligman (1988, 1998) used the Skh-hairless mouse as a model for evaluating promoters of hair growth.

PROCEDURE

Six litters of Skh-hairless-1 albino mice with 5–8 animals are housed, with their mothers, in individual plastic cages. Food and water are supplied ad libitum. Beginning at 1 week of age, topical treatment is applied: two litters dorsal application of low dose (e. g., 0.2% minoxidil), two litters dorsal application of high dose, two litters abdominal application of high dose. Application is performed once daily five times a week at a rate of 20 µl/cm^2 of skin using a digital micropipette. Two control litters receive no treatment. All treatment continue for up to 17 weeks, after which mice are sacrificed and grossly examined for signs of toxicity.

Mice are observed daily for hair growth and weighed each week. Photographs are taken when hair growth appears to be maximum. At the time of maxi-

mal hair growth, two or three representative neonates from the treated and untreated groups are sacrificed for skin biopsies; all remaining mice continue on treatment to asses the extent of a third pelage. Biopsy specimens are fixed in formalin and stained with hematoxylin and eosin.

EVALUATION

In transverse sections, all active hair matrices or viable follicles, which contain keratin zed hairs located in the subcutis, are counted. Fourteen to 16 contiguous fields are examined over a surface distance of 1 cm at 250× magnification. Mean values of the groups are compared using Student's *t*-test.

MODIFICATIONS OF THE METHOD

De Brouwer et al. (1997) studied the effects of a nonsteroidal anti-androgen on human hair production by balding scalp grafts maintained in testosterone-conditioned **nude mice**. Samples of balding human scalp were grafted on to the left flank of nude mice (bal/c, nu/nu). All mice received a topical application of 300 µg/10 µl testosterone propionate on the non-grafted flank. Testosterone conditioning started 5–7 weeks after grafting and went on until the end of the experiment, once daily 5 days a week. Anti-androgen/placebo treatment was started before hair production was visible. Hair production potential was assessed according the number and diameter of the hairs.

A hair loss mutation on mouse chromosome 19, called **scraggly**, was described by Herron et al. (1999).

Several authors studied **chemotherapy-induced alopecia in mice, rats and rabbits** (Powis and Kooistra 1987; Paus et al. 1994a, b; Cece et al. 1996; Sredni et al. 1996).

The **Dundee experimental bald rat (DEBR)** was used as model for alopecia areata (Oliver and Lowe 1995; McElwee et al. 1997).

Kimura (1996) underlined the usefulness of studies in **hairless descendants of Mexican hairless dogs** in dermatological science.

The **balding stumptail macaque** is recommended as a model for androgenetic alopecia (Brigham et al. 1988; Diani et al. 1995; Pan et al. 1998).

The stimulating effect of drugs on hair growth has been studied using *in vitro methods.*

Kurata et al. (1996) investigated the effect of hypertrichotic agents on follicular from macaque and human skin and nonfollicular cells (normal keratinocytes and dermal fibroblasts) *in vitro*. Minoxidil induced a significant increase in all follicular cells in a dose-specific manner, whereas nonfollicular cells showed no response.

Lachgar et al. (1996) found inhibitory effects of bFGF, VEGF and minoxidil on collagen synthesis by cultured hair dermal papilla cells from rat vibrissa follicles.

Boyera et al. (1997) described biphasic effects of minoxidil on the proliferation and differentiation of normal human keratinocytes obtained form microdissected hairs of from plucked hairs. Minoxidil stimulated human keratinocyte proliferation at micromolar doses, while antiproliferative, pro-differentiative and partially cytotoxic effects were observed with millimolar concentrations.

Sato et al. (1999) reported that minoxidil increases 17β-hydroxysteroid dehydrogenase and 5a-reductase of cultured human dermal papilla cells from balding scalp.

REFERENCES AND FURTHER READING

Benavides F Giordano M Fiette L Brunialti ALB Palenzuela NM Vanzulli S Baldi P Schmidt R Pasqualini CD Guénet JL (1998) Nackt (*nkt*), a new hair loss mutation of the mouse with associated CD4 deficiency. Immunogen 49:413–419

Boyera N Galey I Bernard BA (1997) Biphasic effects of minoxidil on the proliferation and differentiation of normal human keratinocytes. Skin Pharmacol 10:206–220

Brigham PA Cappas A Uno H (1988) The stumptailed macaque as a model for androgenic alopecia: Minoxidil analyzed by the use of the folliculogram. Clinics Dermatol 6:177–187

Buhl AE Waldon DJ Miller BF Brunden MN (1990) Differences in activity of minoxidil and cyclosporin A on hair growth in nude and normal mice. Comparison of *in vivo* and *in vitro* studies. Lab Invest 62:104–107

Cece R Cazzaniga S Morelli D Sfondrini L Bignotti M Menard S Colnaghi MI Balsari A (1996) Apoptosis of hair follicle cells during doxorubicin-induced alopecia in rats. Lab Invest 75:601–609

De Brouwer B Tételin C Leroy T Bonfils A van Neste D (1997) A controlled study of the effects of RU58841, a non-steroidal antiandrogen, on human hair production by balding scalp grafts maintained in testosterone-conditioned nude mice. Br J Dermatol 137:699–702

Diani AR Shull KL Brunden MN (1995) The penetration enhancer SEPA augments stimulation of scalp hair by topical minoxidil in the balding stumptail macaque. Skin Pharmacol 8:221–228

Dicke MM (1955) Alopecia, a dominant mutation in the house mouse. J Hered 46:31–34

Falconer DS Snell GD (1952) Two new hair mutants, rough and frizzy, in the house mouse. J Hered 43:53–57

Falconer DS Fraser AS King JWB (1951) The genetics and development of "crinkled", a new mutant in the house mouse. J Genet 50:324–344

Flenagen SP (1966) Nude, a new hairless gene with pleiotropic effects in the mouse. Genet Res 8:295–309

Herron BJ Bryda EC Heverly SA Collins DN Flaherty L (1999) Scraggly, a new hair loss mutation on mouse chromosome 19. Mamm Genome 10:864–849

Holland JM (1988) Animal models of alopecia. Clin Dermatol 6:159–162

Jiang T-X, Liu Y-H, Widelitz RB Kundo RKL Maxson RE Chuong CM (1999) Epidermal dysplasia and abnormal hair follicles in transgenic mice overexpressing homeobox gene MSX-2. J Invest Dermatol 113:230–237
Kimura T (1996) Studies on the development of hairless descendants of Mexican hairless dogs and their usefulness in dermatological science. Exp Anim 45:1–13
Kligman LH (1988) The hairless mouse as a model for evaluating promoters of hair growth. Clin Dermatol 6:163–168
Kligman LH (1996) The hairless mouse model for photoaging. Clinics Dermatol 14:183–195
Kligman AM, Kligman LH (1998) A hairless mouse model for assessing the chronic toxicity of topically applied chemicals. Food Chem Toxicol 36:867–878
Kurata S Uno H, Allen-Hoffmann BL (1996) Effect of hypertrichotic agents on follicular and nonfollicular cells *in vitro*. Skin Pharmacol 9:3–8
Lachgar S Charvéron M Bouhaddioui N Neveux Y Gall Y Bonafé JL (1996) Inhibitory effects of bFGF, VEGF and minoxidil on collagen synthesis by cultured hair dermal papilla cells. Arch Dermatol Res 288:469–473
Mann SJ (1964) The hair of fuzzy mice. J Herd 55:121–123
Mann SJ (1971) Hair loss and cyst formation in hairless and rhino mutant mice. Anat Rec 170:485–500
Matias JR Malloy V Orentreich N (1989) Animal models of androgen-dependent disorders of the pilosebaceous apparatus. I. The androchronogenetic alopecia (AGA) mouse as a model for male-pattern baldness. Arch Dermatol Res 281:247–253
McElwee KJ Rushton DH Trachy R Oliver RF (1997) Topical FK506: a potent immunotherapy for alopecia areata? Studies using the Dundee experimental bald rat model. Br J Dermatol 137:491–497
Militzer K (2001) Hair growth pattern in nude mice. Cells Tissues Organs 168:285–294
Oliver RF Lowe JGB (1995) Oral cyclosporin A restores hair growth in the DEBR rat model for alopecia areata. Clin Exp Dermatol 20:127–131
Pan HJ, Wilding G Uno H, Inui S Goldsmith L Messing E Chang C (1998) Evaluation of RU58841 as an anti-androgen in prostate PC3 cells and a topical anti-alopecia agent in the bald scalp of stump-tailed macaques. Endocrine 9:39–43
Paus R Handjiski B Czarnetzki BM Eichmüller S (1994a) A murine model for inducing and manipulating hair follicle regression (catagen): effects of dexamethasone and cyclosporin A. J Invest Dermatol 103:143–147
Paus R Handjiski B Eichmüller S Czarnetzki BM (1994b) Chemotherapy-induced alopecia in mice. Induction by cyclophosphamide, inhibition by cyclosporine A and modulation by dexamethasone. Am J Pathol 144:719–734
Powis G Kooistra KL (1987) Doxorubicin-induced hair loss in the Angora rabbit: a study of treatments to protect against hair loss. Cancer Chemother Pharmacol 20:291–296
Raphael KA Chapman RE Frith PA (1982) The structure of hair and follicles in mice carrying the naked (N) gene. Genet Res 39:139–148
Sato T Tadokoro T Sonada T Asada Y Itami S Takayasu S (1999) Minoxidil increases 17ß-hydroxysteroid dehydrogenase and 5a-reductase of cultured human dermal papilla cells from balding scalp. J Dermatol Sci 19:123–125
Shimada T Tashiro M Kanzaki T Noda T Murakami T Takiguchi M Mori M Yamamura K Saheki T (1994) Normalization of hair growth in sparse fur-abnormal skin and hair (SPF-ASH) mice by introduction of the rat ornithine transcarbamylase (OTC) gene. J Dermatol Sci 7, Suppl: S27–S32
Shirai A Ikeda J-I, Kawashima S Tamaoki T Kamiya T (2001) KF19418, a new compound for hair growth promotion *in vitro* and *in vivo* mouse models. J Dermatol Sci 25:213–218
Slee J (1962) Development morphology of the skin and hair follicles in normal and "ragged" mice. J Embryol Exp Morphol 10:507–529
Sredni B Xu R-H, Albeck M Gafter U Gal R, Shani A Tichler T Shapira J Bruiderman I Catane R Kaufman B Whisnant JK Mettinger KL Kalechman Y (1996) The protective role of the immunomodulator AS101 against chemotherapy-induced alopecia. Studies in human and animal models. Int J Cancer 65:97–103
SundbergJP, Cordy WR King LE Jr (1994) Alopecia areata in aging C3H/HeJ mice. J Invest Dermatol 102:847–856
Tutikawa K (1952) Studies on an apparently new mutant, "alopecia periodica" found in the mouse. Ann Rep Nat Inst Genet Jap 3:9–10
Van der Veen, Hebeda KM de Bruijn HS Star WM (1999) Photodynamic effectiveness and vasoconstriction in hairless mouse skin after topical 5-aminolevulinic acid and single- or two-fold illumination. Photochem Photobiol 70:921–929

P.18
Cutaneous Microcirculation

P.18.1
General Considerations

PURPOSE AND RATIONALE

Various techniques are used to determine cutaneous blood flow, such as radioactive microspheres, xenon clearances, plethysmography, laser Doppler velocimetry (Flagrell 1986; Guy et al. 1985), reflectance spectrophotometry (Kimura et al. 1988; Kakizoe et al. 1992).

REFERENCES AND FURTHER READING

Flagrell B (1986) Clinical studies of skin microcirculation. Klin Wochenschr 64:943–946
Guy RH, Tur E, Maibach H (1985) Optical techniques for monitoring cutaneous microcirculation. Int J Dermatol 24:88–94
Kakizoe E Kobayashi Y Shimoura K Hattori K Jidoi J (1992) Real-time measurement of microcirculation of skin by reflectance spectrophotometry. J Pharmacol Toxicol Meth 28:175–180
Kimura T Tsushima N Nakayama R Yoshizaki S Otsiji K Shinohara M (1988) Effects of prostaglandin E_1 on the microcirculation of skin in the arteriosclerosis obliterans. J Jpn Coll Angiol 28:177–181

P.18.2
Laser Doppler Velocimetry

PURPOSE AND RATIONALE

Laser Doppler velocimetry and laser Doppler flowmetry are essentially identical procedures. With these methods, light is transmitted from a helium-neon laser source in the instrument to the skin via an optical fiber. The laser provides light of single frequency (wave-

length 632.9 nm) and allows the Doppler effect to be exploited. The incident radiation enters the skin tissue and is multiply scattered and reflected by non-moving components and by the mobile red blood cells that are encountered as the radiation penetrates to a depth of 1–1.5 mm. A portion of scattered/reflected incident radiation exits the skin and is collected by second or third optical fibers that carry the light back to the instrument. The returning radiation falls on a photodetector and is converted to an electrical signal. Stationary skin tissue reflects and backscatters light at the same frequency as the incident source. Erythrocytes moving with certain velocity, however, reflect radiation that is slightly frequency-shifted, the shift increasing with increasing velocity.

Hirkaler and Rosenberger (1989) described simultaneous two-probe laser Doppler velocimetric assessment of topically applied drugs as a simple, noninvasive method for the determination of cutaneous blood flow in anesthetized rats.

PROCEDURE

Male Sprague-Dawley rats (400–500 g) are anesthetized with urethane (1.6 g/kg), the abdominal region carefully clipped and the remaining hair removed with a commercially available depilatory. Phthalate buffer (pH 4.0) is gently applied to neutralize the effects of the depilatory cream. The rat is placed on its back and allowed to stabilize for approximately 15 min. Cutaneous blood flow is measured using two standard Medpacific LD 5000 capillary perfusion monitors and probes (1.9 cm diameter). The probes are modified to allow application of the drug without removal of the probe. This is achieved by enlarging the center opening of the adhesive pad to 1 cm, which creates a drug well of approximately 5 µl vol. The drug is introduced through a short length of polyethylene tubing (PE10) held in place by the adhesive pad and placed slightly off center to avoid interference with the sensing device.

The modified probes are attached to the lower abdominal region of the rat, approximately 1–2 cm from the midline. Cutaneous blood flow is recorded continuously from 30 min prior to drug application and for 5 h post-dosing. Various doses of standard (0.015 to 0.75 mg/kg minoxidil) or test compound or control vehicle (propylene glycol 15%, ethyl alcohol 65%, water 20%) are applied. At the end of the experiment, the animals are sacrificed.

EVALUATION

Post-dosing values are expressed as % change from control and analyzed using Student's paired *t*-test.

MODIFICATIONS OF THE METHOD

Knight et al. (1987) measured microvascular blood flow by a laser Doppler flow meter in **rabbit** epigastric island flaps made ischemic for various intervals of time.

REFERENCES AND FURTHER READING

Guy RH, Tur E, Maibach H (1985) Optical techniques for monitoring cutaneous microcirculation. Int J Dermatol 24:88–94

Hirkaler GM Rosenberger LB (1989) Simultaneous two-probe laser Doppler velocimetric assessment of topically applied drugs in rats. J Pharmacol Meth 21:123–127

Knight KR Collopy PA O'Brien BM (1987) Correlation of viability and laser Doppler flowmetry in ischemic flaps. J Surg Res 43:444–451

P.18.3 Measurement of Skin Microcirculation by Reflectance Spectroscopy

PURPOSE AND RATIONALE

Kimura et al. (1988), Kakizoe (1992) developed reflectance spectrophotometric measurement to analyze the microcirculation of the skin in real time. The light reflected from the skin tissue containing information about hemoglobin, the injected dye, and other data, is continuously analyzed into the relative absorption spectrum and the changes in relative absorption values at specific wavelengths are used as indices of oxyhemoglobin content and capillary permeation.

PROCEDURE

Male Wistar rats weighing 300–400 g are anesthetized with pentobarbital (40 mg/kg i.p.). The skin of the back is shaved and the hair removed by a commercial hair remover. A polyethylene catheter (PE10) is inserted into the femoral artery to measure blood pressure on a polygraph. An other catheter is inserted into the femoral vein for injection of drugs or Evans blue.

To obtain the relative absorption spectra, a spectro-multi-channel-photodetector system (MCPD 110; Otsuka Electronics Co., Ltd., Osaka, Japan) is used. White light (halogen lamp 150 W) is projected onto the skin through an optical fiber. The light reflected from the skin is transmitted to the detector system via another optical fiber. The positions of the optical fibers are fixed independently. Each fiber is attached to a steel arm on the stand, and the height of the arms is adjusted so that the top of the fibers can be in gentle contact with surface of the skin. The angles of the fibers are adjusted so that the relative absorbance spectrum with the best peaks of oxyhemoglobin can be obtained. The reflected light is passed through a slit and illuminated

on the grating surface to obtain the spectrum. Following amplification by an image intensifier, the component wavelengths are sampled by photodiode array in a short time interval. The relative absorbance spectra from the skin against the spectra for the white light are obtained at wavelengths ranging from 450 to 643 nm, arranging the initial relative absorbance at 640 nm to zero. The sampling time is 50 ms. The average of 10 measurements is indicated at 1-s intervals on the output unit. The spectrum at a point of time and time-dependent changes in relative absorbance values at selected wavelength are shown on the display and registered by an X-Y recorder.

After achieving a steady state under anesthesia, the relative absorbance spectrum is obtained from the skin, and two peaks ate wavelength of about 540 and 577 nm, corresponding to those of oxyhemoglobin, are observed. The relative absorbance spectrum is measured at the posterior part of the back near the backbone because the shape is relatively flat in this region and it is easy to fix the optical fibers.

To standardize the changes in oxyhemoglobin content in skin tissue, graduated doses of noradrenaline are injected intravenously and the effect on relative absorbance is measured.

To measure the content of oxyhemoglobin and permeation of the capillaries at the same time, 1.5 ml/kg 0.05% Evans blue solution is injected intravenously 10 min before measurement. Histamine (0.3–100 µg/50 µl/site) is injected intradermally into the skin of the back, and measurement is started 1 min after the injection. The changes in the relative absorbance values at 540 nm, an absorption peak in the oxyhemoglobin spectrum, and at 610 nm, an absorption peak in the Evans blue spectrum, are measured for 15 min, and the absorption values at baseline and the point of maximum change are compared.

EVALUATION

Results are expressed as mean ± SEM. Comparisons are made using the Student's *t*-test or Mann-Whitney's *U*-test.

MODIFICATIONS OF THE METHOD

Hertel (1986, 1992) measured cutaneous microcirculation in the pinnal of conscious rats. Erythrocyte flow velocities were measured by the 'flying spot technique' (Tyml and Ellis 1982) and the diameters of the capillaries were measured from a monitor with a ruler.

Da Costa et al. (1992) measured the fluctuations in the diameter of selected arterioles in the cutaneous microcirculation of **Syrian golden hamster** dorsal skin flap chambers. These ranged in size between 10 and 70 µm at different branching order sites, before burn, at the same site after burn and after injection of drugs.

REFERENCES AND FURTHER READING

Da Costa R Aggarwal SJ Diller KR Baxter CR (1992) The effects of epinephrine, iboprofen, and tetrachlorodecaoxide on cutaneous microcirculation in thermally injured hamsters. J Burn Care Rehabil 13:396–402

Hertel RF (1986) Microcirculatory measurements in the same conscious rats (WKY and SHR) during the first year from birth. Microcirculation, Endothelium and Lymphatics 3:75–87

Hertel RF (1992) Potassium channel activation improves blood flow pattern of conscious rats in cutaneous microcirculation. Clin Exp Pharmacol Physiol 19:243–248

Kakizoe E Kobayashi Y Shimoura K Hattori K Jidoi J (1992) Real-time measurement of microcirculation of skin by reflectance spectrophotometry. J Pharmacol Toxicol Meth 28:175–180

Kimura T Tsushima N Nakayama R Yoshizaki S Otsiji K Shinohara M (1988) Effects of prostaglandin E_1 on the microcirculation of skin in the arteriosclerosis obliterans. J Jpn Coll Angiol 28:177–181

Tyml K Ellis CG (1982) Evaluation of the flying spot technique as a television method for measuring red cell velocity in microvessels. Int J Microcirc Clin Exper 11:145–155

P.19
Isolated Perfused Skin Flap

PURPOSE AND RATIONALE

Riviere et al. (1986) and Riviere and Monteiro-Riviere (1991) described the isolated perfused porcine skin flap as an *in vitro* model for percutaneous absorption and cutaneous toxicology studies. This group has used the model for various purposes (Riviere et al. 1995; Vaden et al. 1996; Baynes et al. 1997; Inman et al. 2003; Monteiro–Riviere et al. 2003).

PROCEDURE

Weanling female Yorkshire pigs weighing 20–30 kg are acclimated for 1 week prior to the study. The pigs are housed on elevated floors and provided water and 15% protein pig and sow pellets ad libitum.

The isolated perfused porcine skin flap is a single, axial pattern tubed skin flap obtained from the ventral abdomen of female weanling swine. Two flaps per pig, each lateral of the ventral midline, may be obtained in a single surgical procedure. The surgery involves two steps: creation of the flap in stage I and harvest in stage II. Pigs weighing approximately 20–30 kg are pre-medicated with atropine sulfate and xylazine hydrochloride, induced with ketamine hydrochloride, and inhalation anesthesia is maintained with halothane. Each pig is prepared for routine

surgery in the caudal abdominal and inguinal region and a 4 × 12 cm area of skin is demarcated. Following incision and scalpel dissection of the subcutaneous tissue, the caudal incision is apposed, sutured, and the tubed skin flap edges trimmed of fat and closed. Two days later, a second surgical procedure is used to cannulate the artery and harvest each of these skin flaps. The isolated perfused porcine skin flap is then transferred to a custom-designed temperature- and humidity-regulated perfusion chamber. A computer monitors perfusion pressure, flow, pH, and temperature. The flaps are perfused for 1 h prior to dosing with a modified Krebs/Ringer bicarbonate buffer (pH 7.4) containing bovine serum albumin, glucose, penicillin G amikacin, and heparan, during which 1.0-ml arterial and 3.0-ml venous samples are collected to assess glucose utilization. Once flap viability is confirmed, the perfusion is interrupted and each flap is removed from the chamber. Flap perfusion is resumed, with the venous perfusate sampled every 15 min for the first 2 h and every 30 min thereafter for the 8-h duration. Absorption is defined as the total amount of radioactivity detected in the perfusate over an 8-h perfusion period and expressed in units of % of applied radioactivity or mass absorbed. Penetration is defined as the sum of total radioactivity found in the perfusate (absorption), stratum corneum, fat and dosed skin samples. Penetration is the maximum amount of test compound that could be absorbed into the systemic circulation if all test compounds within the skin ultimately were absorbed over a prolonged period of time. Penetration is also relevant to the direct toxic effect within the skin.

EVALUATION

Total recovery is calculated as the sum of penetration plus the amount of radioactivity found in the washing samples. All data are expressed as mean ± standard error of the mean (SEM). The significant differences ($P < 0.05$) across each set of treatments are determined by ANOVA in PC SAS (SAS Institute, Cary, N.C., USA; version 8.01). Significant differences ($P < 0.05$) between each mean and paired nonaqueous counterpart are determined using a Student's *t*-test.

MODIFICATIONS OF THE METHOD

Pickens et al. (1994) studied the effect of extended perioperative pentoxifylline on random skin flap survival in Yorkshire pigs.

Skin flap models have been described for several animal species, mostly in **rats** (Hahn et al. 1993; Stadelmann et al. 1998; Yenidunya et al. 1998; Cottler et al. 1999; Yang and Morris 1999; Jones et al. 2001; Oksar et al. 2001; Lay et al. 2003; Mittermayer et al. 2003; Ozkan et al. 2004; Agaoglu and Siemionow 2005; Ulusal et al. 2005; Hosnuter et al. 2006). Lineaweaver et al. (2004) described the influence of vascular endothelium growth factor and surgical delay on survival of the transverse rectus abdominis myocutaneous flap in rats. The model is based on the right abdominis rectus muscle as carrier and inferior epigastric vessels as vascular pedicle. Following induction of general anesthesia, the abdominal regions were shaved, and a rectangle measuring 3 × 8 cm was drawn onto the upper abdominal area of the rats. The borders of the skin paddle of the proposed transverse rectus abdominis myocutaneous flap were cut down to deep fascia. The branches of both superficial epigastric vessels joining the flap were ligated and cut. Both rectus abdominis muscles were divided at the superior border of the skin paddle. The superior deep epigastric vessels of both rectus abdominis muscles were divided. The skin incision was then closed using 4–0 nylon sutures.

Barker et al. (1989) and Minh et al. (2002) described skin flap models in **mice**.

Degner et al. (1996) described a medial saphenous fasciocutaneous free flap in **dogs**.

Teunissen et al. (2004) evaluated the primary critical ischemia time for the deep circumflex iliac cutaneous flap in **cats**.

Bristol et al. (1991) reported preparation and metabolic parameters of an isolated perfused skin flap in **horses**.

REFERENCES AND FURTHER READING

Agaoglu G Siemionow M (2005) Combined semimembranosus muscle and epigastric skin flap: a new model of composite-free flap in the rat. Ann Plast Surg 55:310–315

Barker JH Hammersen F Bondar I Galla TJ Menger MD Gross W Messmer K (1989) Direct monitoring of nutritive blood flow in a failing skin flap: the hairless mouse ear skin-flap model. Plast Reconstr Surg 84:303–313

Baynes RE Monteiro-Riviere NA Qiao GL Riviere JE (1997) Cutaneous toxicity of the benzidine dye direct red 28 applied as mechanistically-defined chemical mixtures (MDCM) in perfused porcine skin. Toxicol Lett 93:159–169

Bristol DG Riviere JE Monteiro-Riviere NA Bowman KF Rogers RA (1991) The isolated perfused equine skin flap. Preparation and metabolic parameters. Vet Surg 20:424–433

Cottler PS Gampper TJ Rodeheaver GT Skalak TC (1999) Evaluation of clinically applicable exsanguination treatments to alleviate venous congestion in an animal skin flap model. Wound Repair Regen 7:187–195

Degner DA Walshaw R Lanz O Rosenstein D Smith RJ (1996) The medial saphenous fasciocutaneous free flap in dogs. Vet Surg 25:105–113

Hahn EW Peschke P Mason RP Babcock EE Antich PP (1993) Isolated tumor growth in a surgically formed skin pedicle

in the rat: a new tumor model for NMR studies. Magn Res Imaging 11:1007–1017
Hosnuter M Kargi E Peksoy I Babuccu O Payasli C (2006) An ameliorated skin flap model in rats for experimental research. J Plast Reconstr Aesthet Surg 59:299–303
Inman AO Still KR Jederberg WW Carpenter RL Riviere JE Brooks JD Monteiro-Riviere NA (2003) Percutaneous absorption of 2,6-di-*tert*-butyl-4-nitrophenol (DBNP) in isolated perfused porcine skin. Toxicol Vitro 17:289–292
Jones M Zhang F Blain B Guo M, Cui D, Dorsett-Martin W Lineaweaver WC (2001) Influence of recipient-bed isolation on survival rates of skin-flap transfer in rats. J Reconstr Microsurg 17:653–658
Lay IS, Hsieh CC Chiu JH Shiao MS Lui WY, Wu CW (2003) Salvianolic acid B enhances in vitro angiogenesis and improves skin flap survival in Sprague-Dawley rats. J Surg Res 115:279–285
Lineaweaver WC Lei MP, Mustain W Oswald TM Cui D, Zhang F (2004) Vascular endothelium growth factor, surgical delay, and skin flap survival. Ann Surg 239:866–875
Minh TC Ichioka S Harii K Shibata M Ando J Nakatsuka T (2002) Dorsal bipedicled island skin flap: a new flap model in mice. Scand J Plast Reconstr Surg Hand Surg 36:262–267
Mittermayer R Valentini D Fitzal F Hallstrom S Gasser H Redl H (2003) Protective effect of a novel NO-donor on ischemia/reperfusion injury in a rat epigastric flap model. Wound Repair Regen 11:3–10
Monteiro–Riviere NA Baynes RE Riviere JE (2003) Pyridostigmine bromide modulates topical irritant-induced cytokine release from human epidermal keratinocytes and perfused porcine skin. Toxicology 183:15–28
Oksar HS Coskunfirat OK Ozgentas HE (2001) Perforator-based flap in rats: a new experimental model. Plast Reconstr Surg 108:125–131
Ozkan O Coskunfirat OK Ozgentas HE Dikici MB (2004) New experimental flap model in the rat: free flow-through epigastic flap. Microsurgery 24:454–458
Pickens JP Rodman SM Wetmore SJ (1994) The effect of extended perioperative pentoxifylline on random skin flap survival. Am J Otolaryngol 15:358–369
Riviere JE Monteiro-Riviere NA (1991) The isolated perfused porcine skin flap as an *in vitro* model for percutaneous absorption and cutaneous toxicology. Crit Rev Toxicol 21:329–344
Riviere JE Bowman KF Monteiro-Riviere NA Dix LP, Carver MP (1986) The isolated perfused porcine skin flap (IPPSF). I. A novel *in vitro* model for percutaneous absorption and cutaneous toxicology studies. Fundam Appl Toxicol 7:444–353
Riviere JE Brooks JD Williams PL Monteiro-Riviere NA (1995) Toxicokinetics of topical sulfur mustard penetration, disposition, and vascular toxicity in isolated perfused porcine skin. Toxicol Appl Pharmacol 135:25–34
Stadelmann WK Hess DB Robson MC Greenwald DP (1998) Aprotinin in ischemia-reperfusion injury: flap survival and neutrophil response in a rat skin flap model. Microsurgery 18:354–361
Teunissen BD Walshaw R Hauptman JG Degner DA Jackson AH (2004) Evaluation of primary critical ischemia time for the deep circumflex iliac cutaneous flap in cats. Vet Surg 33:440–445
Ulusal BG Ulusal AE Yazar S Chang CH Hung LM Wei FC (2005) Pectoral skin flap as a reliable and simple model for vascularized composite skin transplantation research. J Reconstr Microsurg 21:187–190
Vaden SL Page RL Riviere JE (1996) An in vitro-in vivo validation of the isolated tumor and skin flap preparation as a model of cisplatin delivery to tumors. J Pharmacol Toxicol Meth 35:173–177
Yang D Morris SF (1999) An extended dorsal island skin flap with multiple vascular territories in the rat: a new skin flap model. J Surg Res 87:164–170
Yenidunya MO Tsukagoshi T Morioka D Hosaka Y (1998) An axial-pattern skin flap in the rat. J Reconstr Microsurg 14:383–386

P.20
Safety Assays in Skin Pharmacology

For safety assays in skin pharmacology, see Maibach (2006).

REFERENCE

Maibach H (2006) Safety assays in skin pharmacology. In: Vogel HG (ed), Hock FJ Maas J Mayer D (co-eds) *Drug Discovery and Evaluation – Safety and Pharmacokinetic Assays*. Springer, Berlin Heidelberg New York, Chap. I.P, pp 365–383

Chapter Q
Guidelines for the Care and Use of Laboratory Animals[1]

[1] By A.W. Herling, J. Maas, K. Seeger (1st edition), revised by U. Albus (2nd and 3rd edition).

Q.1 Regulations for the Care and Use of Laboratory Animals in Various Countries

See Table Q.1 on the following page.

Q.2 Techniques of Blood Collection in Laboratory Animals

Q.2.1 Introduction

Blood is collected from laboratory animals for various scientific purposes, for example, to study the effects of a test drug on various constituents, such as hormones, substrates, or blood cells. In the field of pharmacokinetics and drug metabolism, blood samples are necessary for analytical determination of the drug and its metabolites. Blood is also needed for some *in vitro* assays using blood cells or defined plasma protein fractions.

The techniques for blood collection depend on specific factors which differ from one experiment to the other. There is a difference between terminal and non-terminal blood collection techniques. The conditions of blood collection at the end of an experiment which includes death of the animal (terminal experiment) are completely different (anesthesia, volume of blood)

Table 1 Regulations for the care and use of laboratory animals

Country, Institutions	Legislation
Australia National Health and Medical Research Council	Australia is governed by a national Government, six State Governments, and two Territory Governments. Animal welfare within Australia is a State/Territory responsibility.
Commonwealth Scientific and Industrial Research Organisation	The Australian Animal Welfare Strategy (AAWS) from 2005
Australian Agricultural Council	http://www.daff.gov.au/ http://www.animallaw.info/
Austria Ministry of Agriculture	Bundesgesetz über den Schutz der Tiere (TSchG), BGBl. I Nr. 118/2004 http://www.vu-wien.ac.at/vetrecht/TSchG%20BGBl.pdf
Belgium	In 1991 the provisions of the ETS 123 convention were enacted in the Belgian legislation through the "Law of 18 October 1991 approving the European Convention on protection of vertebrate animals used for Experimental or other Scientific Purposes and its Annexes A and B done at Strasbourg on 18 March 1986". In 1994 the "Royal Decree of 14 November 1993 related to the protection of experimental animals" was enacted.
Canada	Canadian Council on Animal Care http://www.animallaw.info
China (Peoples Republic of China)	Regulations for the Administration of Affairs Concerning Experimental Animals, Nov. 1988
State Science and Technology Commission, Beijing	Implementing Regulations of the Administration on Medical Experiments on Animals, June 1989 http://www.nal.usda.gov/awic/legislat/internat.htm http://www.animallaw.info/
Denmark	LBK (Lovbekendtgørelse) nr. 726 af 9. sept. 1993: Bekendtgørelse om lov om dyreforsøg A minor change has been added to the above about animals that are released in connection to an experiment: • LOV nr. 386. 6 juni 1991 (animal protection law) • LOV nr. 1081 af 20. dec. 1995: Lov om ændring af lov om dyreforsøg • BEK (Bekendtgørelse) nr. 332 af 18. maj 1990: Bekendtgørelse om fremskaffelse af dyr til forsøg • BEK nr. 27 af 22. jan. 1996: Bekendtgørelse om ændring af bekendtgørelse om fremskaffelse af dyr til forsøg • BEK nr. 716 af 1. aug. 1994: Bekendtgørelse om forretningsorden for Rådet for Dyreforsøg • BEK nr. 333 af 18. maj 1990: Bekendtgørelse om forsøgdyrs pasning of opstaldning of om udryddelsestruede og vildtlevende dyr til forsøg m.v. • BEK nr. 739 af 6. dec. 1988: Bekendtgørelse over og indberetning om dyreforsøg Legislation revised in 1993 in conformity with EU directives http://www.retsinfo.dk/
European Union	Council of Minister's Directive 86/609/EEC (1986) on the Approximation of Laws, Regulations and Administrative Provisions of the Member States Regarding the Protection of Animals Used for Experimental and other Scientific Purposes http://europa.eu.int/ European Convention for the Protection of Vertebrate Animals used for Experimental and other Scientific Purposes. December 15, 1990 http://www.uku.fi/laitokset/vkek/Sopimus/convention.html
Federal Republic of Germany	Neufassung des Tierschutzgesetzes vom 18. Mai 2006
Ministry for Food, Agriculture and Forestry	Richtlinie vom 24. November 1986 zur Annäherung der Rechts- und Verwaltungsvorschriften der Mitgliedstaaten zum Schutz der für Versuche und andere wissenschaftliche Zwecke verwendeten Tiere (86/609/EWG) Gesetz zu dem Europäischen Übereinkommen vom 18. März 1986 zum Schutz der für Versuche und andere wissenschaftliche Zwecke verwendeten Wirbeltiere vom 11. Dezember 1990 http://www.bml.de/ and http://www.uni-giessen.de/tierschutz/

Table 1 (continued)

Country, Institutions	Legislation
Finland	Act on Animal Protection (247/1996, amend. 1194/1996 and 594/1998), Statute on Animal Protection (396/1996, amend. 402/1998), Statute on the Transport of Animals (491/1996, amend. 1398/1997 and 955/1998) and Statute on Animal Experimentation (1076/1985, amend. 395/1996)http://www.nca-nl.org/
France	No uniform national animal welfare law, but several decrees. "Loi à la protection de la nature", 10 juillet 1976 "Décret aux expériences pratiquées sur les animaux" 19 octobre 1987 Arrêtés interministériels (3 arrêtés), 19 avril 1988 http://www.nca-nl.org/
Italy	Legislative Decree no. 116 of January 27, 1992, enforcing European Recommendations contained in Directive 86/609/EEC Specific Law of October 12, 1993 http://www.nca-nl.org/
Ireland Department of Agriculture and Food	Cruelty to Animals Act, 1876 European Communities (Amendment of Cruelty to Animals Act, 1876) Regulations, 1994 http:/www.agriculture.gov.ie/
Japan Prime Minister authorized to set standards for minimum pain provision	Law Concerning the Protection and Control of Animals (Law No. 105, October 1, 1973, revised June 15, 2005) http://www.alive-net.net/english/en-law/L3-outline.html
New Zealand Animal Welfare Advisory Committee (AWAC), established in 1989 by the Minister of Agriculture	Animal Welfare act 1999, Commenced January 1, 2000 http://rangi.knowledge-basket.co.nz/gpacts/public/text/1999/an/142.html The codes of recommendations and minimum standards for the welfare of animals, endorsed as a national code on 25 May 1995 http://www.maf.govt.nz/mafnet/profile/legislation/
Netherlands Minister of Health, Welfare and Sport	Dutch experiments on animals act entered into force on 5 February 1997 http://www.nca-nl.org/
Norway Ministry of Agriculture	Norwegian Animal Welfare Act, 1974 New version of June 16, 1995 http://www.dyrebeskyttelsen.no/english/law.shtml
Republic of Czechia Czech National Assembly	"Law for the Protection of Animals" no 246 Sb, 15. April 1992, inclusive the amendments no. 162 Sb, 19. May 1993 http://www.nca-nl.org/
South Korea 1. Ministry of Agriculture, Fishery and Forestry 2. Ministry of Health and Welfare	1. "Animal Protection Act", May 1991 2. "Pharmaceutical Affairs Law" Korean Good Laboratory Practice Guidelines for Breeding and Caretaking of Test Animals
Spain	Real Decreto 223/1988 http://www.boe.es
Sweden The Swedish National Board for Laboratory Animals (CFN) Ministry of Agriculture, Stockholm	National Board for Laboratory Animals Ordinance Amending the Board's Ordinance (LSFS 1988:45, as last amended by SFS 1998:1344 of October 22, 1998) Containing Regulations and General Recommendations Concerning Ethical Examinations of the Use of Laboratory Animals for Scientific Purposes, etc. http://www.nca-nl.org/
Switzerland	"Tierschutzgesetz vom 9. März 1978 (TSchG), under revision in 2006 "Tierschutzverordnung", 27. Mai 1981 http://www.bvet.admin.ch/
Taiwan Council of Agriculture; In future: Provincial/ Municipal Governments	Taiwan Animal Protection Law, November 4, 1998. Very generally, so that additional regulations are going to be required. http://www.gio.gov.tw/info/98html/aplaw.htm

Table 1 (continued)

Country, Institutions	Legislation
United Kingdom	"Protection of Animals Act", 1991 "Animals (Scientific Procedures) Act", 1986 http://scienceandresearch.homeoffice.gov.uk/animal-research/legislation/
U.S.A. U.S. Department of Agriculture, Animal and Plant Health Inspection Service (APHIS), Animal Care (AC)	Guide for the Care and Use of Laboratory Animals, January 1996 http://www.nap.edu/readingroom/books/labrats/ The Animal Welfare Act, signed into law in 1966, amended four times (1970, 1976, 1985, 1990), can be found in United States Code, Title 7, Sections 2131 to 2156 http://www.nal.usda.gov/awic/legislat/usdaleg1.htm
Most countries	Local ethical commisions at universities and other institutions of biomedical research Useful Internet-links on international animal protection: http://www.nca-nl.org/ http://www.animallaw.info/ http://www.nal.usda.gov/awic/legislat/internat.htm http://www.uni-giessen.de/tierschutz/

from those of single or repeated blood collections from a conscious animal. Terminal blood collection under anesthesia allows the use of techniques which are not acceptable for non-terminal blood collections.

Q.2.2 Aspects of Animal Welfare

Minimizing any pain and distress in laboratory animals during the procedure have to be as important as achieving the desired experimental results. This is important not only for humanitarian reasons but also as part of good scientific practice. Blood collection may be stressful to the animal due to the handling and the discomfort associated with a particular technique. Many biochemical and physiological changes are associated with stress which affect the results, e. g. increases in the blood levels of catecholamines, prolactin and glucocorticosteroids can influence certain metabolic parameters, such as glucose, as well as the counts of erythrocytes, white cells, and packed cell volume. Therefore, stress should be reduced to an absolute minimum if it is not possible to avoid it at all, this is not only in the interest of animal welfare but also in the interest of good science to obtain representative data. To minimize stress during blood collection, e. g. from dogs or cats, it may be helpful for the animal as well as for the operator first to do some dummy runs and provide rewards to the animal.

During non-terminal blood collection it is important not to withdraw too much blood which could reduce total blood volume and lead to false results. A reduced total blood volume is accompanied by a reduced hemoglobin content and oxygen transport capacity (Gainer et al. 1955) as well as by a fall in blood pressure, and an increase in the concentrations of stress-related hormones. It may be further accompanied by other factors such as necrosis of the gastric mucosa.

The welfare of the individual animal should not be endangered by removal of too large a volume of blood or by too frequent collections. This may be the case more often when small laboratory animals, e. g. mice, gerbils, rats or hamsters are used. In these cases the study protocol should be adapted to use more animals to minimize distress for the individual animal.

Q.2.3 Total Blood Volume

The total blood volume is very difficult to determine (McGuill et al. 1989) and depends on species, sex, age and health as well as nutritional condition. Total blood volume is smaller in larger animals than in smaller animals of the same species in relation to body weight. It is also smaller in older and obese animals compared to normal weight and young animals. Total circulating blood volume is in the range of 55–70 ml/kg body weight.

Q.2.4 Terminal Blood Collection

Terminal blood collection represents (i) exsanguination as a single process of blood removal to collect as much blood as possible and (ii) multiple blood sampling during a terminal experiment under general anesthesia. Basically, exsanguination should only be performed after the animal has been rendered unconsciuos by another method, e. g. physical stunning or general anesthesia. This is due to the fact that stress occurs

with extreme hypovolemia and accessing deeper blood vessels causes pain. Due to the anesthetized condition of the animal and the terminal nature of the experiment, methods can be used for exsanguination which can never be recommended for non-terminal blood collections with recovery of the animal. These include

- blood withdrawal from the V. cava caudalis or the aorta after laparatomy when as much blood as possible should be removed in a sterile manner,
- exsanguination after decapitation, incision of the jugular vein or carotid artery or techniques in the slaughterhouse, when a non-sterile collection is possible,
- retro-orbital bleeding of smaller laboratory animals like mice, gerbils, hamsters and rats which can also be a method of exsanguination.

Q.2.5 Non-terminal Blood Collection

Non-terminal blood collections can be differentiated into single and multiple blood withdrawals. Possible peripheral veins for blood withdrawal are listed in Table Q.2.

Q.2.5.1 Single Blood Removal

A single withdrawal of up to 15% of total blood volume does not influence the well-being of the animal. However, the removal of 15 to 20% might be accompanied by side effects such as fall in cardiac output or blood pressure. Haemorrhagic shock can be induced by the withdrawal of 30–40% of total blood volume and the loss of 40% causes mortality in up to 50% of pigs and rats (McGuill et al. 1989).

A single removal of up to 15% of total blood volume may be repeated after 3–4 weeks from normal and healthy animals with no detectable adverse effects. This does not mean that the animal does not experience any adverse effects, but it does not show any.

Symptoms of hypovolaemic shock are fast pulse, pale mucous membranes, hyperventilation and a subnormal body temperature including cold skin and extremities. In these animals therapeutic intervention consists of volume substitution with warm isotonic intravenous infusion.

Q.2.5.2 Multiple Blood Removal

Multiple withdrawal of blood samples should not exceed 1% of total blood volume every 24 h (0.6 ml/kg/d). More frequent withdrawals and/or removal of larger volumes of blood causes anemia.

Symptoms of anemia are pale mucous membranes of the conjunctiva or inside the mouth, intolerance to exercise and an increased respiratory rate in cases of severe anemia. Anemia can be easily detected by de-

Table 2 Blood vessels for venous blood withdrawal

Species	V. coccygica + tt	V. auricularis	Orbital venous	V. jugularis	V. cephalica V. saphena	V. femoralis	V. mammarica
Mouse	cc + cc	–	a	–	–	–	–
Gerbil	cc + cc	–	aa	a	–	–	–
Hamster	–	—	aa	a	–	–	–
Rat	ccc + cc	–	a	aa	–	–	–
Guinea pig	–	c	–	a	–	–	–
Rabbit	–	ccc	–	c	–	–	–
Cat	–	–	–	aa/c	ccc	cc	–
Dog	–	–	–	ccc	ccc	a	–
Rhesus monkey	–	–	–	aa/c	ccc	cc	–
Pig	–	iii	–	iii/cc(cvc)	–	–	–
Sheep	–	–	–	ccc	c	– c	–
Goat	–	–	–	ccc	c	–	– c
Cattle	cc	c	–	ccc	c	–	– cc
Horse	–	–	–	ccc	–	–	–

c/cc/ccc conscious animal, c/i/a possible alternative, i/ii/iii immobilized animal, – not recommended or impossible, a/aa/aaa anaesthetized animal, cvc cranial vena cava, ccc/iii/aaa recommended route, tt amputation tail tip, cc/ii/aa acceptable route repetition of letters indicates the preferred condition

termination of erythrocyte cell count and packed cell volume (haematocrit), hemoglobin level as well as reticulocyte count in a blood sample. In case of anemia the animal should be treated with iron and vitamin B12 and should be monitored for the above mentioned blood parameters during therapy until normal values are reached again.

Q.2.6
Technical Aspects of Blood Removal

A common method in mice and rats for collecting up to 0.1 ml capillary blood is to remove the tip of the tail. For repeated blood sampling the blood clot on the tail has to be removed to get fresh capillary blood. This method is sufficient for multiple blood collections to determine, e. g. blood glucose or total radioactivity after the administration of radiolabeled drugs. In tailless animals such as guinea pigs and hamsters, cardiac puncture under general anesthesia may be the preferred technique.

Blood collections from larger animals will preferably be performed from a superficial vein. The person holding the animal and raising the vein plays a key role in collecting blood without undue stress to the animal by talking to and stroking the animal. Some animals, e. g. dogs and some primates, may be trained to present a limb for blood removal without the use of any physical restraint.

It is important to locate the vessel accurately before insertion of the needle or the catheter. In most cases obstruction of the venous return is necessary for distension of the vessel and to successfully insert the needle. The bore of the needle should be as large as possible to ensure rapid blood withdrawal with minimal risk of blood clotting within the needle. When the sample is taken too quickly by a syringe, the vein will collapse. After the needle has been withdrawn, continuous pressure should be applied immediately to the puncture site and maintained for at least 30 s. The animal should be monitored 15 min later to check for after-bleeding.

Q.2.6.1
Permanent Venous Cannulation

For multiple blood collections a permanent venous access by chronic cannulation is often recommended. In most cases, particularly in rats, it is necessary to restrain the animal in harnesses or jackets to prevent it from damaging or removing the cannula. In these cases the signs of stress are often apparent by an increase in serum levels of stress hormones. However, a few days after implantation of catheters, hormone levels are normal in restrained rats (Tsukamoto et al. 1984; Wiersma and Kastelijn 1985). Such animals are usually housed alone and the tethering restricts normal movements such as lying on the back and rolling over. Such restrictions may be considered as potential sources of stress. This can be prevented by having the catheter exit the back of the animal for only 2 cm and capping it with a steel needle. At the time of the experiment, a longer catheter is attached for blood collections.

A simple device for serial blood collection has been described by Sir-Petermann et al. (1995).

One has to balance very carefully the distress and discomfort of the individual animal with a permanent cannulation under restraint conditions for a longer period with multiple blood samplings without permanent cannulation. In the first case, multiple values from the same animal can be obtained showing perhaps individual differences among a group of animals. In the latter case it may be necessary to use a larger number of animals but there is less discomfort for the individual animal.

Short-term cannulation (less than a day) of a peripheral blood vessel in larger animals is easy to perform. A butterfly needle can be inserted under aseptic conditions and multiple blood samples can readily be collected. Long-term cannulation (longer than two days) in larger and smaller animals often presents complications such as blockage of the cannula by thrombi. The infusion and administration of substances via the permanent cannula are much easier than the removal of blood. Thrombi attached to the end of the cannula function as a one-way valve. Clotting can be prevented by repeatedly filling the catheter with saline containing heparin.

Q.2.6.2
Retro-Orbital Bleeding

Blood sampling by orbital puncture is a controversial technique. The puncture of the orbital venous plexus is often performed in tailless animals, e. g. hamsters. This technique is also used in rats and mice, when larger volumes are required which cannot be obtained from the tail vein. Basically, retro-orbital bleeding should always be performed under anesthesia. Pasteur pipettes, micropipettes or microcapillary tubes are used and pushed with a rotating movement through the conjunctiva laterally, dorsally or medially of the eye to the back wall of the orbit. In general, inflammatory reactions can be seen histologically in the puncture

track four days after punction. After 4 weeks the lesions have healed without detectable scars (van Herck et al. 1992). However severe side-effects such as retro-orbital haematoma with subsequent pressure on the eye cannot be completely excluded. This pressure can damage the optical nerve. The animal may be unable to close its eye. Bleeding from the orbital venous plexus should only be performed with recovery of the animal in exceptional circumstances when there is no other method available. The technique should be performed only by a well-trained staff and only one eye should be used.

Q.2.6.3
Cardiac Puncture

The collection of blood by cardiac puncture has been performed in guinea pigs, gerbils and hamsters. In these species it is difficult to collect blood by alternative methods except retro-orbital bleeding. In general, cardiac puncture should be performed under general anesthesia with atropine as premedication to prevent cardiac arrhythmia. If cardiac puncture is used for a non-terminal blood withdrawal with recovery, the animal has to be separated from other animals until it is fully conscious. It should be carefully watched for adverse effects and sacrificed if found in distress due to complications like bleeding into the pericardium or into the thorax.

REFERENCES AND FURTHER READING

Commission of the European Communities (1993) Recommendations for euthanasia of experimental animals, Final report

First Report of the BVA/FRAME/RSPCA/UFAW Joint Working Group on Refinement, Removal of blood from laboratory mammals and birds. Laboratory Animals (1993) 27:1–22

Gainer JL, Lipa MJ, Ficenec MC (1995) Hemorrhagic shock in rats. Laboratory Animal Science 45:169–172

McGuill MW, Rowan AN (1989) Biological effects of blood loss: implications for sampling volumes and techniques. ILAR News 31:5–18

Sir-Petermann T, Recabarren SE, Bittl A, Jäger W, Zimmermann U, Wildt L (1995) A simple device for serial blood collection in human subjects and animals. Exp Clin Endocrinol 103:398–401

Tsukamoto H, Reidelberger RD, French SW, Largman C (1984) Long-term cannulation model for blood sampling and intragastric infusion in the rat. Am J Physiol 247 (Regulatory Integrative Comp Physiol 16):R595–R599

van Herck H, Baumans V, van der Craats NR, Hesp APM, Meijer GW, van Tintelen G, Walvoort HC, Beynen AC (1992) Histological changes in the orbital region of rats after orbital puncture. Laboratory Animals 26:53–58

Wiersma J, Kastelijn J (1985) A chronic technique for high frequency blood sampling/transfusion in the freely behaving rat which does not affect prolactin and corticosterone secretion. J Endocr 107:285–292

Q.3
Anesthesia of Experimental Animals[2]

Q.3.1
Introduction

In biomedical research, experiments should only be done with a conscious animal if it is not possible to do the study in an anesthetized one. Anesthetic conditions should always be chosen to exclude stress, discomfort and pain for the animal which could have negative influences on the pharmacological results and reproducibility of the data. Therefore, an experimental design causing minimal discomfort to the animal is always preferable. This is important not only for humanitarian reasons but also for good scientific practice.

Many pharmacological experiments are performed under anesthesia:

- terminal experiments under anesthesia followed by euthanasia,
- experiments under anesthesia with recovery at the end of the study, and
- experiments in which an animal is surgically prepared under anesthesia and continuation of the experiment occurs with the conscious animal after recovery.

Generally, two possibilities exist for immobilization of aggressive animals and to prevent escape: (i) physical restraint (e. g. immobilization cages or immobilization tubes) and (ii) chemical restraint with anesthetic compounds. As a rule of thumb it is recommended to use physical restraint for animal studies in which no anesthesia would be used in comparable studies in man. Physical restraint can be used for short and painless interventions like administration of substances or blood sampling from a vein.

In general, physical restraint produces fear, distress and anxiety in experimental animals with the result of stress symptoms which could affect the results of the study. To minimize pain for the animals, to obtain correct and reproducible results and to protect the handlers from aggression by the animals, it is often necessary to use chemical restraint. However, the chemical used can affect the biochemistry or physiology of the animal.

It is possible to anesthetize special areas of the animal (local anesthesia) or the whole animal (general anesthesia). Local anesthesia plays only a minor role

[2] By J. Maas, A.W. Herling, K. Seeger (first edition), revised by U. Albus (2nd and 3rd edition).

for experimental animals as compared to general anesthesia.

Q.3.2 Local Anesthesia

Local anesthesia is the regional and reversible elimination of pain with chemical compounds. Circulatory, pulmonary and renal functions are not disturbed and the animals are conscious. Surface anesthesia has to be distinguished from the anesthesia produced after a local injection. The most common compounds for surface anesthesia are tetracaine and proparacaine. Procaine, butanilicaine, lidocaine, mepivacaine and etidocaine are commonly used injectable local anesthetics. Local anesthesia is only recommended for gentle and calm animals (cattle, sheep). For most laboratory animals, general anesthesia is the method of choice.

Q.3.3 General Anesthesia

Q.3.3.1 Preparation

It is very important to check the general condition of the animal prior to anesthesia. This check should include a clinical examination (inspection, auscultation, palpation) of the animal concerned. Sometimes it could be useful to perform a few laboratory tests, e. g. hematocrit, hemoglobin, pH-value of blood and acid/base parameters.

Those animals with a vomiting reflex should be fasted prior to anesthesia. Most animal species should be fasted for a period of at least 12 h but pigs and cattle for at least 24 h. Water can be offered during the fasting period ad libitum.

Q.3.3.2 Premedication

Premedication is recommended prior to anesthesia for easier administration of the anesthetic and for elimination of side effects of the anesthetic used, such as disturbing autonomic reflexes.

Q.3.3.2.1 Hydration and Base Excess

Based on hematocrit, hemoglobin and erythrocyte values, the hydration of the animal should be normalized prior to anesthesia. Infusions of glucose or Ringer solution can be used for this purpose. To check the success of the treatment repeated determinations of the above mentioned values are necessary.

In cases of acidosis (pH of blood < 7.36), treatment of the animals with $NaHCO_3$ is recommended. If measurement of base excess is possible, the amount of $NaHCO_3$ can be determined from the following formula:

$$\text{Dose } NaHCO_3 \text{ (ml)} = \text{g body weight} \times \text{base excess}/0.6$$

Q.3.3.2.2 Atropine

To avoid cardiopulmonary problems and to decrease saliva production, atropine should be administered intramuscularly prior to general anesthesia. The recommended dose varies considerably and is usually between 0.05 and 0.1 mg/kg body weight. Cats and rodents have a higher activity of atropine-esterase in the liver, and these species need higher amounts of atropine (up to 0.25 mg/kg).

Q.3.3.2.3 Sedation and Pain Elimination

Indications for sedation and elimination of pain are to calm the animals and to stabilize the autonomic nervous system.

For sedation the following compounds are used:

- minor tranquilizers without autonomic effects:
- meprobamate, diazepam,
- major tranquilizers with autonomic side effects:
- propionyl-promazine, acetylpromazine, azaperone, dehydrobenzperidol, xylazine, detamidone.

Anaesthesia does not necessarily lead to analgesia (elimination of pain). Although general anaesthesia produces loss of consciousness and pain isnot perceived, the noxious stimuli will be transmitted to the CNS and will develop central hypersensitivity, leading to a postoperative heightened perception. To reduce the degree of central hypersensitivity analgesics have to be administered before noxious stimulation begins (preemptive analgesia). Analgesia should also reduce or eliminate peripheral inflammation, which aggravates central hypersensitivity.

For analgesia, the opioids used are mainly:

- methadone, meperidine, fentanyl.

In most species (dog, rabbit, guinea pig) a sedative effect is to be observed after administration of these compounds. In other species (pig, cat) an excitatory effect can occur.

Minor tranquilizers, major tranquilizers and analgesic compounds are often used in common with anes-

Table 3 Anesthesia of experimental animals (values are in mg/kg)

Species	Premedication	Sedation	Short anaesthesia	Medium anaesthesia	Long anaesthesia
Rat	Atropine (0.2 s.c.)	Diazepam (2.5 i.m.)	Alfentanyle + Etomidate (0.03 + 2 i.m.) or Inhalation (Isoflurane)	Xylazine + Ketamine (5 + 100 i.m.) or Pentobarbitone (50 i.p.)	Xylazine + Ketamine (16 + 100 i.m.) or Urethane (1500 i.m.)
Mouse	Atropine (0.1–0.25 s.c.)	Diazepam (5 i.p.)	Alfentanyle + Etomidate (0.03 + 2 i.m.) or Inhalation (Isoflurane)	Xylazine + Ketamine (5 + 100 i.m.) or Pentobarbitone (50 i.p.)	Xylazine + Ketamine (16 + 100 i.m.)
Hamster	Atropine (0.1–0.2 s.c.)	Diazepam (5 i.p.)	Inhalation (Isoflurane)	Xylazine + Ketamine (5 + 50 i.m.) or Pentobarbitone (35 i.p.)	Xylazine + Ketamine (10 + 200 i.m.)
Guinea pig	Atropine (0.1–0.2 s.c.)	Diazepam (2.5–5 i.m.)	Inhalation (Isoflurane)	Xylazine + Ketamine (2 + 80 i.m.)	Xylazine + Ketamine (4 + 100 i.m.) or Pentobarbitone + Chloralhydrate (30 i.p. + 300 i.v.)
Rabbit	Atropine (0.1–0.2 s.c.)	Diazepam (1–5 i.m.)	Inhalation (Isoflurane)	Xylazine + Ketamine (5 + 25–80 i.m.)	Xylazine + Ketamine (5 + 100 i.m.) or Pentobarbitone + Chloralhydrate (30 i.p. + 300 i.v.)
Cat	Atropine (0.05–0.2 s.c.)	Diazepam (0.2–1 i.m.)	Acetylpromazine (0.5–1 i.v./i.m.) or Propionylpromazine (0.5–1 i.v.) or Xylazine (2 i.m.)	Xylazine + Ketamine (2 + 10 i.m.) or Ketamine (5 i.v.) or Inhalation (Isoflurane)	Pentobarbitone (35 i.v./i.p.)
Dog	Atropine (0.05 s.c.)	Xylazine (3 i.m.) or Acetylpromazine (0.5 i.m.) or Propionylpromazine (0.5 i.m.) or Droperidol (1 i.m.) or Diazepam (1 i.m.)	Thiopental (17 i.v.) or Metomidate + Fentanyl (4 + 0.005 i.m.) or Alfentanil + Etomidat (0.03 + 1 i.m.) or Inhalation/Intubation (Isoflurane)	Xylazine + Methadone (2 + 1 i.m.) or Xylazine + Ketamine (2 + 10 i.m.) or comb. with Diazepam (0.6 i.m.) or Propionylpromazine + Methadone (0.5 + 1 i.v.) or Acetylpromazine + Methadone (0.5 + 0.5–1 i.v.)	Pentobarbitone (30 i.v.) or Xylazine + Ketamine (2 + 15 i.m.) or Intubation (Isoflurane)
Pig		Azaperone (1–2 i.m.) or Chlorpromazine (1–2 i.m.)	Thiopental (10 i.v; 5% solution)	Azaperone + Metomidate (0.05–5 + 2.5–5 i.m. + i.v./i.p.) or Tiletamine + Zolazepam + Xylazine (2 + 2 + 0.5–1 i.m.)	Pentobarbitone (10–25 i.v.)
Sheep Goat		Xylazine (0.05–0.1 i.m.) or Diazepam (2 i.m.)	Xylazine + Ketamine (1–2 + 5–10 i.m.) or Thiopental (7.5–10 i.v.)	Pentobarbitone (20–30 i.m.)	Ketamine after pretreatment with Xylazine/ketamine 3–4 h or Intubation (Isoflurane)
Monkey[a]	Atropine (0.05–0.1 s.c.)	Diazepam (1.0 i.m.) or Xylazine (1–2 i.m.) or Ketamine (10–30 i.m.)	Inhalation/Intubation (Isoflurane)	Xylazine + Ketamine (2 + 10 i.m.)	Pentobarbitone (20–30 i.v./i.p.) or Intubation (Isoflurane)

[a] Anaesthesia of monkeys depends very much on the monkey species.

thetics. A compilation of such combinations is summarized in Table Q.3.

Q.3.3.3
Course of Anesthesia

The animal has always to be observed very carefully during anesthesia. Various systems can be checked with technical equipment, e. g. circulatory system (heart rate, pulse, blood pressure, ECG, peripheral perfusion, temperature) or pulmonary system (respiratory rate).

A very important procedure during anesthesia is the determination of the depth of anesthesia. There are four stages of anesthesia:

I. Stage of analgesia (from the first effect to unconsciousness):
   - heart and respiratory rate increase, normal dilation of pupils.

II. Stage of excitation (from the beginning of unconsciousness to the start of regular respiration): respiration irregular, dilated pupils, increased motor reflexes, nystagmus, opisthotonus.

III. Stage of tolerance (from the beginning of regular respiration to the termination of spontaneous respiration):
   This stage is divided into four steps:
   A) regular respiration, narrow pupils, most reflexes present
   B) skeletal muscles relaxed, narrow pupils, no eyelid reflex, corneal reflex present, flat respiration, good analgesia.
      This is the optimal stage of anesthesia for surgery
   C) only corneal reflex present, respiration very flat, pupils dilated
   D) no reflexes, respiration very flat, pupils very dilated

IV. Stage of asphyxia (after termination of the spontaneous diaphragmatic respiration):

V. no reflexes, no respiration: danger of death, immediate use of antidotes is necessary to prevent death.

By using combinations of different anesthetics – mainly by using combinations with muscle relaxing agents – the reactions of animals will differ from this scheme.

Q.3.3.4
Routes of General Anesthesia

In general, there are two different routes to induce general anesthesia: (i) injection and (ii) inhalation anesthesia. Sometimes combinations of both routes are used. The decision for one or the other route depends on the animal species, the purpose of the study and the necessity of control during anesthesia.

Q.3.3.4.1
Injection

By using this route of anesthesia the narcotic compound is dissolved in a liquid. The route of administration can be intravenous, intramuscular, subcutaneous or intraperitoneal. The mostly frequently used compounds are mentioned below:

Barbiturates

There are three groups of barbiturates: long acting, short acting and very short acting barbiturates. For laboratory animals short and very short acting barbiturates are used predominantly (sodium pentobarbitone, thiopental, hexobarbital).

Barbiturates are metabolized in the liver and mainly excreted via the bile. They are very fat soluble.Their short duration of action is caused by a distribution into adipose tissue. Fat represents a large compartment for these compounds with a relatively slow excretion. This can lead to prolongation of the narcotic effects after repeated dosing. The dosing of barbiturates should be adjusted according to the observed reactions of the individual animal as there are individual differences due to age, body weight, size, fat content and general condition of the animal. Barbiturates are not analgesic and should not be given without opioids.

Chloralhydrate

Chloralhydrate is a relatively old soporific compound. By using it for anesthesia cardiovascular side effects are often observed. The range of dosing is very narrow. Its use for laboratory animals is therefore limited. Intraperitoneal injections in rats can lead to paralysis of the ileus.

Combinations of Analgesic with Neuroleptic Compounds

This method is often used for dogs and rodents. Strong analgesics (morphine, methadone, meperidine, fentanyl) are combined with neuroleptics like phenothiazine, acetylpromazine or butyrophenone. The anaesthesia can be rapidly terminated by available antagonists.

Ketamine

Ketamine is a neuroleptic compound with a very fast onset of action following intramuscular administration. It can be used for nearly all species. A side effect of this compound is an increased tonus of skeletal

muscles but this can be prevented by the simultaneous administration of xylazine or diazepam.

Hypnotic Agents

Hypnotics are compounds which produce a very deep sleep without analgesia (metomidate). Therefore combination with neuroleptic compounds is recommended (e. g. combination azaperone with metomidate for pigs). As a single compound, metomidate can only cause anesthesia in birds.

Xylazine

Xylazine is frequently used for anesthesia in combination with other substances (Table Q.3). As a single compound it is only used to produce anesthesia in cattle.

Urethane

Urethane was formerly used as a hypnotic agent, It can, at the appropriate dose, produce a long acting (about 10 h) anesthesia in rats. Urethane is liver toxic and therefore its use is limited to some pharmacological models in which liver metabolism is of no importance. Due to its carcinogenic properties it should not be used anymore.

The important criteria of anesthesia are sedation, unconsciousness, analgesia and relaxation. These cannot be achieved with a single compound. Therefore, a combination of different compounds is necessary. The most common combinations for different species are listed in Table Q.3 with respect to the duration of anesthesia: short (up to 30 min), medium (up to 120 min) and long anesthesia (longer than 120 min).

Q.3.3.4.2 Inhalation

Inhalation anesthesia is more common for the bigger laboratory animals such as dogs, cats, sheep, goats and monkeys. However, it has gained an increased importance in small laboratory animals like rodents. The advantages of this form of anesthesia are the possibilities of controlling exactly the depth of anesthesia and of fast management of complications.

The parts of an inhalation system include:

- Bottle with oxygen (blue bottles)
- Valve to regulate pressure (reduces the pressure of the oxygen-bottle)
- Flowmeter (monitors the gas flow to the animal)
- Evaporator (evaporation of liquid anesthetic compounds)
- Oxygen-bypass (fast supply of oxygen to the animal in case of need)
- Tube to the system

Different techniques are used for laboratory animals:

Technique of Insufflation

Administration of anesthetic compounds is performed via a mask. Expiration occurs into the air of the room. Advantages are the simple procedure without valves and CO_2-absorber, and the very small dead volume of the system. Disadvantages are the waste of compounds, drying of the trachea of the animals, the impossibility of checking the respiration volume and the expiration of narcotic compounds into the room air (jeopardy to the staff).

Open System

Inspired and expired gases are separated by a valve. The inspired air consists of the fresh mixture of gases. The expiration reaches completely the atmosphere. The "Stephen slater" is the most used system of this group. It is recommended for smaller animals.

Half-Closed and Closed Systems

In closed systems all of the expired air passes to a CO_2 absorber. The CO_2 is removed chemically and the air is inspired again with newly evaporated anesthetic compounds mixed with oxygen. In a half-closed system, part of the expired air reaches the atmosphere. Advantages of closed systems include the economic benefit, the decrease of fluid and body heat loss from the animal and no risk to the laboratory staff. Disadvantages are the necessity to change the absorber every 8–10 h during anesthesia, the production of heat and the increase of resistance to breathing.

Summary

If it is possible inhalation should be done by intubating the animal. The risk of aspiration of stomach contents with the danger of an aspiration pneumonia can then be minimized. It is very important to use a tube with the correct diameter and length. An animal should be unconscious for intubation (see Table Q.3). In order to avoid gulp or cough reflexes it is recommended to administer succinylcholine, a muscle relaxant. Atropine can also be administered to decrease saliva production. Generally, all methods of injection anesthesia mentioned (Table Q.3) can be combined with an inhalation method. Such a "balanced anesthesia" is recommended for long and highly sophisticated operations.

Compound	Conc. with N_2O/O_2 (%)	Conc. without N_2O/O_2 (%)	MAC
Methoxyflurane	0.4–1	3.5	0.23
Isoflurane	1.0–2.5	1.5–3.5	1.4
Enflurane	0.5–1.5	2	2.2

MAC: minimal alveolar concentration for an anesthetic effect.

Table 4 Inhalation compounds and their characteristics

Q.3.3.4.3 Inhalation Compounds

The inhalation mixture has to include 21% oxygen. Sometimes it is better to administer 33% oxygen. Isoflurane, methoxyflurane and enflurane are widely used compounds for inhalation anesthesia. Ether is not longer recommended for anesthesia, due to the hazard of explosion and fire and because it is highly irritating to the respiratory tract. By using a mixture of N_2O and O_2 the amount of the evaporated compounds can be reduced drastically (Table Q.4).

Q.3.3.5 Termination of Anesthesia

Inhalation anesthesia can be stopped by removing the supply of evaporated compounds. To hasten the elimination of anesthetic compounds, the concentration of oxygen in the system can be increased for a period of five min.

The elimination of injected compounds is difficult to influence. It may be possible to accelerate metabolism of the anesthetic by using agents which stimulate metabolism in the liver and excretion by the kidney.

It is very important to check the body temperature of the animal during and after anesthesia. In cases of low body temperature the use of heating lamps or pads is necessary. After termination of anesthesia the animals go through the same phases as mentioned above but in the reverse order (tolerance, excitation, analgesia).

During anesthesia it might be necessary to stimulate respiration or circulation. Stimulatory agents for respiration are doxapram, pentamethylentetrazole, nikethamide, methetarimide, lobeline or micoren. Stimulatory agents for circulation are adrenaline, effortil, dopamine and ephedrine. The application of pure oxygen via a mask is also recommended during an injection anesthesia. Antidotes to morphine and its derivatives are morphine-antagonists like naloxone. Yohimbine is an antagonist of xylazine. The antidote for diazepam is flumazenil. There are no direct antagonists for ketamine and barbiturates.

Q.3.4 Postoperative Analgesia

To effectively reduce pain in animals a pain assessment has to be made using behavior, stress response etc. Pain assessment will be facilitated by

- a good knowledge of the species specific behaviors of the animal being assessed
- a knowledge and comparison of the individual animal's behaviour before and after the onset of pain (eg pre- and post-operatively)
- the use of palpation or manipulation of the affected area and assessment of the responses obtained
- examination of the level of function of the affected area: e. g. leg use following injury or limb surgery, together with a knowledge of any mechanical interference with function
- the use of analgesic regimens or dose rates that have been shown to be effective in controlled clinical studies, and evaluation of the change in behaviour this brings about
- a knowledge of the non-specific effects of any analgesic, anaesthetic or other drugs that have been administered

Analgesics can be broadly divided into two groups, the opioids or narcotic analgesics and the non-steroidal anti-inflammatory drugs (NSAID). Clinical pain involves several pathways, mechanisms and transmitter systems. To provide the most effective pain relief, drugs of different classes should be applied, acting on different parts of the pain system, for example combining opioids and NSAIDs.

REFERENCES AND FURTHER READING

Alpert M, Goldstein D, Triner L (1982) Technique of endotracheal intubation in rats. Lab Anim 32:78–79

Erhard W, Scherer M, Greiner C, Blümel G (1985) Methods of low term anaesthesia in the rat. Z Versuchstierkunde 27:84

Flecknell PA (1996) Laboratory Animal Anaesthesia. Academic Press

Guedel AE (1951) Inhalation Anaesthesia. MacMillan, New York

Kohn DF, Wixson SK, White WJ, Benson GJ (1997) Anesthesia and Analgesia in Laboratory Animals, Academic Press,

Sawyer DC (1983) The Practice of Small Animal Anaesthesia. W.B. Saunders, Philadelphia

Van Pelt LF (1977) Ketamine and Xylazine for surgical anaesthesia in rats. J Am Vet Med Assoc 171:842–844

Q.4 Euthanasia of Experimental Animals[3]

Q.4.1 Introduction

Biomedical research needs animals. This is most obvious in case of *in vivo* animal experiments. However, for other scientific purposes, e. g. *in vitro* studies, biological material is also necessary to study enzymes, membranes, receptors, cells, tissues, or organs which are obtained from dead animals. Therefore, animals have to be sacrificed in biomedical laboratories (i) at the end of an *in vivo* experiment, (ii) during experiments where sacrifice of the animals is not part of the study but must be done when pain, distress and suffering exceed acceptable levels or if it is likely for the animal to remain in pain or distress after cessation of the experiment, and (iii) to provide biological material for *in vitro* studies.

The following remarks are a summary of the*Recommendations for Euthanasia of Experimental Animals* of the *Commission of the European Communities* (1993) and the *Guidelines for Skillful and Human Euthanasia of Laboratory Animals* (1993) of Switzerland.

Q.4.2 Euthanasia

Euthanasia means a gentle death and should be regarded as an act of a human method of sacrificing an animal with a minimum of physical and mental suffering. The method of euthanasia should be appropriate for the species and the age of the animals. The method should be painless, avoid excitement and achieve rapid unconsciousness and death. Additionally, the method should be reliable, reproducible and irreversible.

Prior to euthanasia, it is important to recognize symptoms of fear, distress and anxiety; these symptoms are species specific. Depending on the species these symptoms may include distress vocalisation, attempts to escape, aggression, freezing, salivation, urination and defecation. Distress vocalization and release of certain odors or pheromones by a frightened animal may cause anxiety in other animals housed nearby. In this context it has to be stressed that many vocalisations of animals are in a range of frequencies which are out of the human hearing range. Therefore, animals should not be present during euthanasia of other animals, especially of their own species. If possible, an animal should not be killed in a room where other animals are housed, in particular in case of a bloody method of euthanasia, e. g. decapitation.

Euthanasia usually requires some physical control over the animals. Suitable control minimizes pain, distress, fear and anxiety in the animal and depends on animal species, size, state of domestication and method of euthanasia. Gentle handling, stroking and talking to the animal during euthanasia often have a calming effect on many animals. The use of sedating and immobilising drugs may be necessary in those cases, where capture or restraint may cause pain, injury or anxiety to the animal.

The person performing euthanasia is the most relevant factor during sacrificing an animal in order to cause a minimum of pain, fear and distress. A suitable method of euthanasia can be extremely harmful to the animal if it is badly performed. All persons performing euthanasia should be well trained, demonstrate professionalism and be sensitive to the value of animal life.

After euthanasia it is essential to confirm death. Signs of death are cessation of heartbeat and respiration, and absence of reflexes. Death must be guaranteed by exsanguination or removal of the heart, destruction of the brain, decapitation, evisceration or the presence of rigor mortis.

Methods for euthanasia of laboratory animals can be separated into physical and chemical methods.

Q.4.2.1 Physical Methods Recommended for Euthanasia of Laboratory Animals

Physical methods are stunning (concussion, electrical stunning, and stunning with a captive bolt), cervical dislocation, decapitation, and microwave irradiation. The different methods of stunning as well as cervical dislocation cause a rapid loss of consciousness which must be followed immediately by a method to force and guarantee death of the animal.

Concussion may be sufficient in smaller animals, e. g. rodents, to achieve unconsciousness and is performed by a blow to the head. Electrical stunning is a common method in the slaughterhouse predominantly for pigs. Only specific equipment must be used for this method either in the slaughterhouse or in laboratory. Stunning with a captive bolt is also a common and an effective method for larger animals in the slaughterhouse to achieve unconsciousness. Adapted equipment can also be used for larger rabbits in biomedical labo-

[3] By A.W. Herling (1st edition), revised by U. Albus (2nd and 3rd edition).

ratories. The correct localisation of the captive bolt is important in order to achieve immediate destruction of the brain. Cervical dislocation destroys the brainstem but the large vessels to the brain are often intact. All these methods have to be followed immediately by an act to force and guarantee death, e. g. exsanguination, removal of the heart or destruction of the brain.

During the decapitation process the head is separated from the neck which causes an immediate interruption of the blood circulation to the brain and a fall in blood pressure in the brain with subsequent loss of consciousness. This is valid only for warm-blooded animals. In cold-blooded vertebrates it is recommended to stun the animals prior to decapitation due to their higher resistance against anoxia. For decapitation of smaller laboratory animals specific guillotines have been developed.

Euthanasia by microwave irradiation is used by neurobiologists for fixation of brain metabolites without destruction of brain anatomy. Only specific equipment developed for this purpose must be used (no domestic microwave ovens). It is essential to localize correctly the microwave beam onto the brain of the animal.

Q.4.2.2 Chemical Agents Recommended for Euthanasia of Laboratory Animals

Many chemicals can cause death due to their toxicity, but only a few are recommended for euthanasia. The most suitable chemicals for euthanasia are certain anesthetics in overdose. In this case, the anaesthetic agent causes unconsciousness, followed by death.

Volatile anesthetics such as halothane, enflurane, isoflurane and methoxyflurane should only be used in a gas scavenging apparatus. Carbon dioxide at high concentrations of 80 to 100% causes unconsciousness within a few seconds.

Injectable anesthetics, predominantly barbiturates such as sodium pentobarbitone, are the most widely used and the most appropriate agents for euthanasia for most animals. Three times the anesthetic dose causes generally rapid unconsciousness and death. Intravenous injection is the most reliable and rapid route. Intraperitoneal injection may also be used in smaller rodents but it needs more time for death to occur. The intracardial and intrapulmonal administration can only be recommended in unconscious animals, because it is painful and, in the case of intracardial injection, difficult to perform successfully on the first attempt.

The agent T61 is a mixture of a local anesthetic, a hypnotic and a curariform component. It is used only intravenously. Due to the curareform component it is not allowed in some countries but it has been demonstrated that unconsciousness and neuromuscular blockade occur simultaneously in dogs and rabbits. Nevertheless, prior sedation should be performed if possible.

Q.4.2.3 Methods and Agents Not to Be Used for Euthanasia of Laboratory Animals

Physical methods not to be used for euthanasia are exsanguination, rapid freezing, pithing, decompression, hyperthermia, hypothermia, asphyxia, drowning and strangulation. Chemicals not to be used are carbon monoxide, nitrogen, nitrous oxide, cyclopropane, chloroform, trichloethylene, hydrogen cyanide, magnesium sulfate, potassium chloride, nicotine, strychnine, chloral hydrate, and ethanol. Some of the above mentioned chemicals are not recommended for euthanasia because they are extremely noxious and dangerous to the experimenter.

Neuromuscular blocking agents such as curare, succinylcholine or suxamethonium which do not cause rapid unconsciousness prior to death should also not be used. Ketamine is a very good anesthetic with a wide therapeutic safety margin for most animal species. Therefore, it is unsuitable for euthanasia.

However, non-acceptable methods of euthanasia can be used if animals are anaesthetized or rendered insensible and unconscious by a recommended method. This is used for, e. g. exsanguination, rapid freezing, and pithing. Exsanguination must not be performed in sight or smell of other animals. Rapid freezing is important to minimize enzymatic processes prior to subsequent biochemical determinations in tissues and organs. Pithing is a quick method of brain destruction achieved by insertion of a needle through the foramen magnum.

Q.4.2.4 Recommended Methods for Euthanasia for Specific Animal Species

Mouse

- Decapitation
- Cervical dislocation with subsequent exsanguination
- Euthanasia within a 80% carbon dioxide atmosphere
- Euthanasia within an atmosphere of suitable volatile anesthetics
- Sodium pentobarbitone at a dose of 150 mg/kg i.p.

Rat

- Concussion, cervical dislocation (both with subsequent exsanguination), and decapitation, conducted only by well trained persons
- Euthanasia within a 80% carbon dioxide atmosphere
- Euthanasia within an atmosphere of suitable volatile anesthetics
- Sodium pentobarbitone at a dose of 100 mg/kg i.v. or 150 mg/kg i.p.
- Microwave irradiation

Hamster

- Decapitation; conducted only by well trained persons
- Euthanasia within a 80% carbon dioxide atmosphere
- Euthanasia within an atmosphere of suitable volatile anesthetics
- Sodium pentobarbitone at a dose of 300 mg/kg i.p.

Guinea Pig

- Concussion (with subsequent exsanguination), and decapitation; conducted only by well trained persons
- Euthanasia within a 80% carbon dioxide atmosphere
- Euthanasia within an atmosphere of suitable volatile anesthetics
- Sodium pentobarbitone at a dose of 150 mg/kg i.p.

Rabbit

- Stunning with captive bolt
- Concussion (with subsequent exsanguination); conducted only by well trained persons
- Sodium pentobarbitone at a dose of 120 mg/kg i.v.
- T61 at a dose of 0.3 ml/kg strictly i.v. via a catheter

Cat

- Sodium pentobarbitone at a dose of 100 mg/kg i.v. or 200 mg/kg i.p.
- T61 at a dose of 0.3 ml/kg strictly i.v. via a catheter; it is recommended to anesthetize the animal beforehand with 20–30 mg/kg ketamine i.m. or 1–2 mg/kg xylazine plus 10 mg/kg ketamine i.m.

Dog

- Sodium pentobarbitone at a dose of 100 mg/kg i.v.
- T61 at a dose of 0.3 ml/kg strictly i.v., it is recommended to anesthetize the animal beforehand with 1–2 mg/kg xylazine plus 10 mg/kg ketamine i.m.

Ferret

- Sodium pentobarbitone at a dose of 120 mg/kg i.p.

Cattle, Sheep, Goat, Horse, Pig

- Sodium pentobarbitone at a dose of 100 mg/kg i.v.; for larger animals prior sedation is recommended (Xylazin).
- All other acceptable methods which are used for slaughtering

Primate

- Sodium pentobarbitone at a dose of 100 mg/kg i.v.; it is recommended to anaesthetize the animal beforehand with 1–2 mg/kg xylazine plus 10 mg/kg ketamine i.m.
- T61 at a dose of 0.3 ml/kg strictly i.v., it is recommended to anesthetize the animal beforehand with xylazine/ketamine i.m.

REFERENCES AND FURTHER READING

Commission of the European Communities (1993) Recommendations for euthanasia of experimental animals. Final report

Erhard W, Scherer M, Greiner C, Blümel G (1985) Methods of low term anaesthesia in the rat. Z

Federal Veterinary Office, Switzerland (1993) Guidelines for skillful and human euthanasia of laboratory animals

Hellebrekers LS, Baumans V, Bertens APMG, Hartman W (1990) On the use of T61 for euthanasia of domestic and laboratory animals; an ethical evaluation. Laboratory Animals 24:200–204

Rowan A (1992) More on decapitation and scientific research. Science and Animal Care, Vol. No 3.3

Index

A

B

C

D

E

F

G

H

I

J

K

L

M

N

O

P

Q

R

S

T

U

V

W

X

Y

Z